ANGEWANDTE CHEMIE
International Edition in English
Volume 30 · Number 1
January 1991
Pages 1–112

Representation in Chemistry

By Roald Hoffmann* and Pierre Laszlo*

Modes of Representation

If you look in old chemistry books
you see
all those line cuts
of laboratory experiments
in cross-section.
The sign for water
is a containing line, the meniscus
(which rarely curls up the walls of the beaker),
and below it
a sea
of straight horizontal dashes
carefully unaligned vertically.
Every cork or rubber stopper
is cutaway.
You can see inside
every vessel
without reflections, without getting wet,
and explore every kink
in a copper condenser.
Flames are outlined cypresses
or a tulip at dawn,
and some Klee arrows
help to move gases and liquids the right way.
Sometimes a disembodied hand
holds up a flask.
Sometimes there is an unblinking observer's eye.

Around 1920
photoengraving
became economically feasible
and took over.
Seven-story distillation columns
(polished up for the occasion),
like giant clarinets,
rose in every text, along
with heaps of chemicals, eventually in color.
Suddenly
water and glass, all reflection
became difficult.
One had to worry about light,
about the sex
and length of dress or cut of suit
of the person sitting at the controls of this impressive
instrument.
Car models and hairstyles
dated the books more
than the chemistry in them.
Around that time
teachers noted a deterioration
in the students' ability to follow
a simple experimental procedure.

Roald Hoffmann[54]

1. Introduction

Chemical structures are among the trademarks of our profession, as surely chemical as flasks, beakers, and distillation columns. When someone sees one of us busily scribbling formulas or structures, he has no trouble identifying a chemist. Yet these familiar objects, which accompany our work from start to end, from the initial doodlings (Fig. 1) to the final polished artwork in a publication (Fig. 2), are deceptively simple. They raise interesting and difficult questions about representation. It is the intent of this article to reflect upon molecular graphics.

We are hooked on these little diagrams, aren't we? Yet what are they? Are they representations of reality, just a

[*] Prof. R. Hoffmann
Department of Chemistry, Cornell University
Ithaca, NY 14850 (USA)
Prof. P. Laszlo
Laboratoire de Chimie, Ecole Polytechnique
F-91128 Palaiseau Cedex (France)

 © VCH Verlagsgesellschaft mbH, W-6940 Weinheim, 1991 0570-0833/91/0101-0001 $ 3.50+.25/0

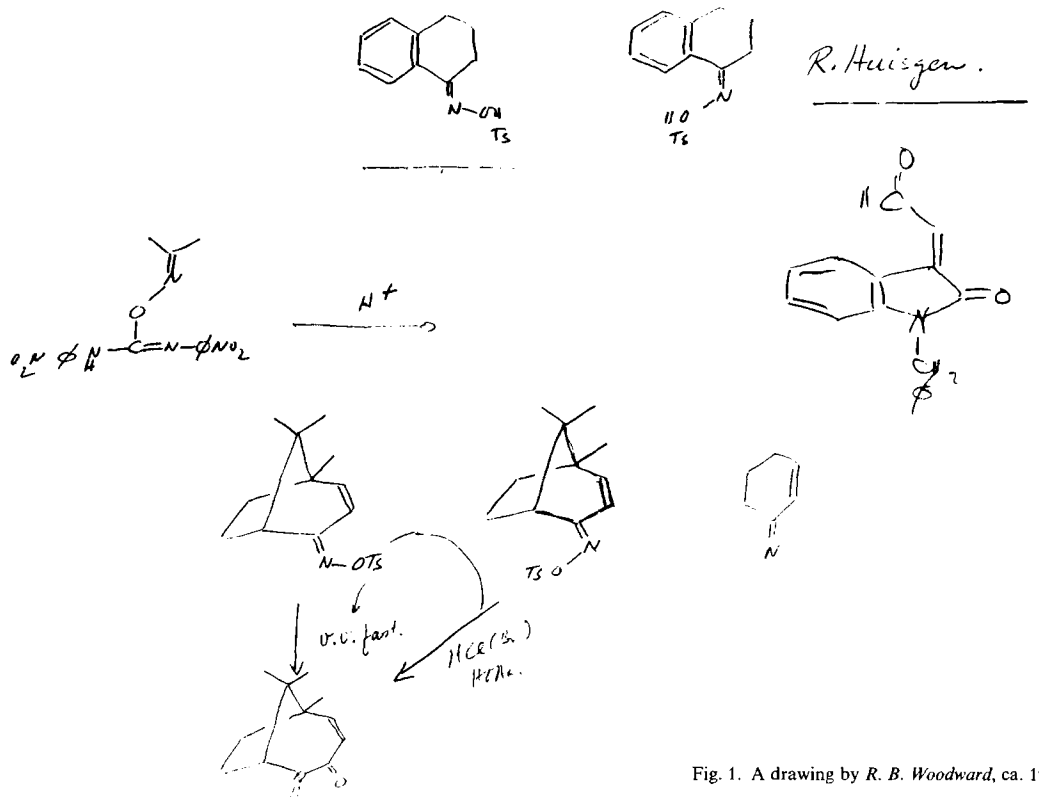

Fig. 1. A drawing by *R. B. Woodward*, ca. 1966, in the course of a discussion.

simplified two-dimensional version of the models that can be built from interpretation of X-ray diffraction patterns of a molecular crystal—in a word, are they *realistic*? A look at a few papers by others (not ours or yours, of course) will show how far short of realism these structures fall. They mix convention and realism in the most innocent manner. Take the case of the bicyclo[2.2.1]heptane skeleton (**1**).

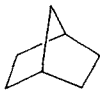

1

Roald Hoffmann was born on July 18, 1937, in Zloczow, Poland. Having survived the war, he came to the U.S. in 1949, and studied chemistry at Columbia University and Harvard University (Ph.D. 1962). Since 1965 he has been at Cornell University, where he is now the John A. Newman Professor of Physical Science. He has received many of the honors of his profession, including the 1981 Nobel Prize in Chemistry (shared with Kenichi Fukui). "Applied theoretical chemistry" is the way Roald Hoffmann likes to characterize the particular blend of computations stimulated by experiment and the construction of generalized models, of frameworks for understanding, that is his contribution to chemistry. Roald Hoffmann also writes essays and poems. Two of his poetry collections, "The Metamict State" (1987) and "Gaps and Verges" (1990), have been published by the University Presses of Florida. He also is the presenter of a television course, "The World of Chemistry", which began to be aired on many U.S. educational television stations in the fall of 1990.

Pierre Laszlo was born on August 15, 1938, in Algiers. He went to school in Grenoble, Rio de Janeiro, and Paris and studied science at the Sorbonne (Ph.D. 1965 with E. Lederer) and Princeton (research associate, 1962–1963, with P. von R. Schleyer). After a postdoctoral appointment at Orsay, he became Assistant Professor at Princeton (1966–1970). Since 1970, he has been Professor of Physical Organic Chemistry at the Université de Liège (Belgium). In addition, he has been a professor at the Ecole Polytechnique in Palaiseau (France) since 1986. Pierre Laszlo has been a guest professor at numerous universities and has received a number of awards, including the Prix Biennal de la Sociéte Chimique de Belgique (1981). His main areas of research are NMR spectroscopy, carrier-bound reagents, and physical organic chemistry. He has published roughly 200 papers and is also the author or editor of seven books. His hobby is the translation of Petrarca's poems into French. In addition, he writes literary criticism.

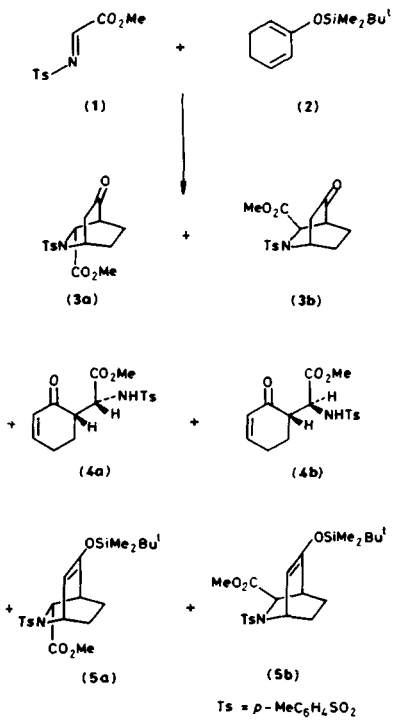

The results of a systematic variation of solvent, temperature, and Lewis acid on the outcome of the reaction of (**1**) with (**2**) resemble the pattern reported for the trimethylsilyl analogue of (**2**), but with several important differences. Firstly, the *exo*/*endo* ratio of bicyclic adducts derived from (**2**) is greater than that for the trimethylsilyl analogue, and secondly, there is a corresponding greater preference for (**4a**) over (**4b**). Under certain low temperature conditions only cyclohexenone products (**4a,b**) and no bicyclic products were obtained. Hydrolysis of the hindered bicyclic silyl enol ether (**5a**) under relatively forcing conditions (AcOH–THF, 50 °C) barely produced any retro-Michael product (**4b**). These observations are consistent with (**3a**) and (**5a**) being derived from a [2 + 4] transition state in which the unfavourable steric interaction between the *N*-tosyl and t-butyldimethylsilyl groups is minimised,[5] while (**4a**) is derived from an open transition state in which the bulky silyl substituent avoids the steric clash with the ester group of the imine (**1**). Thus the proposed mechanism (c) in the previous paper,[1] involving a dual pathway explanation[6] for the origin of bicyclic and monocyclic products, seems to be supported in the present study.

We thank the S.E.R.C. for supporting this work, Merck, Sharp and Dohme, Harlow for a CASE award (A. B. T.), and Clare College for financial support (T. N. B.) and the award of the Denman Baynes Studentship (A. B. T.).

Received, 11th May 1988; Com. 8/01856A

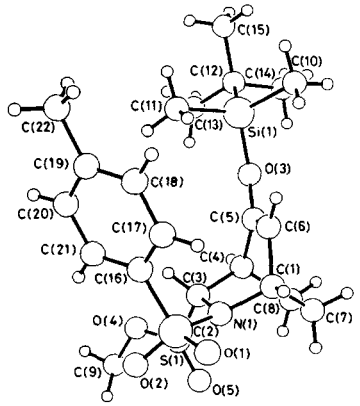

Figure 1. The structure of the *exo* silyl enol ether (**5a**).

References

1 T. N. Birkinshaw, A. B. Tabor, A. B. Holmes, P. Kaye, P. M. Mayne, and P. R. Raithby, preceding communication.
2 W. G. Dauben and R. A. Bunce, *J. Org. Chem.*, 1982, **47**, 5042.
3 F. Brisse, D. Thoraval, and T. H. Chan, *Can. J. Chem.*, 1986, **64**, 739.
4 A. J. Kirby, 'The Anomeric Effect and Related Stereoelectronic Effects at Oxygen,' Springer-Verlag, Berlin, 1983; K. L. Brown, L. Damm, J. D. Dunitz, A. Eschenmoser, R. Hobi, and C. Kratky, *Helv. Chim. Acta*, 1978, **61**, 3108; L. I. Kruse, C. W. DeBrosse, and C. H. Kruse, *J. Am. Chem. Soc.*, 1985, **107**, 5435 and references cited therein.
5 S. M. Weinreb and R. R. Staib, *Tetrahedron*, 1982, **38**, 3087.
6 S. J. Danishefsky, E. Larson, D. Askin, and N. Kato, *J. Am. Chem. Soc.*, 1985, **107**, 1246.

Fig. 2. A page (the second of two) from an article: T. N. Birkinshaw, A. B. Tabor, A. B. Holmes, P. R. Raithby ("Imino Diels-Alder Reaction of 2-*t*-Butyldimethylsilyloxycyclohexadiene: Isolation of an Azabicyclo[2.2.2]octene Silyl Enol Ether Adduct"), *J. Chem. Soc. Chem. Commun. 1988*, 1601.

This commonly seen, supposedly three-dimensional representation actually sports an inverted perspective, the vanishing point being not in back, where it should be, but on the viewer's side. Most chemical drawings eschew obvious primitive artistic stratagems for communicating three-dimensionality; they float in a world of their own.

Perhaps they are "art", then, an abstraction from reality of the essence of norbornanes. If so, it's interesting to reflect on what kind of art they are. This is part of what we will do.

Perhaps chemical drawings do not need to be realistic representations because they are symbols, signs, that in a chemist's mind are reconstructed into the three-dimensional structure, or at least the ball-and-stick model. Chemical structures are then part of a chemical language. What is interesting about language (it doesn't matter whether it is German or English or ...) is that (1) despite its impreciseness, people communicate with it and (2) it, language, inevitably brings us complications, ambiguities and richnesses that we did not expect. Or perhaps that we subconsciously intended.

We both studied chemistry at a time when elongated benzene rings (**2a**) went out of fashion. Two arguments can be made about this iconic upheaval. True, the old way did not prevent incredible progress in synthetic organic chemistry, nor the perceptive theorizing of *Hückel*. On the other hand, the new and assuredly more accurate representation by a

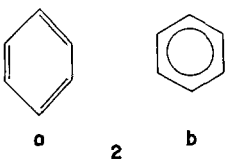

regular hexagon (**2b**) did not serve only a cosmetic and PR purpose for the novel, powerful physical organic and theoretical chemistries associated with names such as *Saul Winstein* and *Charles Coulson*. It beaconed a change of focus, however subtle. This was the same time, remember, when conformational analysis came into general use. After decades of estrangement, structural chemistry and reactivity studies were coming back under the same roof. The writing of a structure is not innocent. It is ideology-laden. It carries, besides its face value, another message; in this case, the modern reunification of the theoretical and the experimental.

The ability to see a conformation behind a constitution, so that the set of symbols **3** is understood by an organic chemist as **4**, engages two types of skills. The imagination, the visual ability to perceive a shape in three-dimensional space runs second to *translation*. To go from the first, "flat" set of symbols, to the second, "skewed" set of symbols is equivalent to switching from one language (the word "science") to another

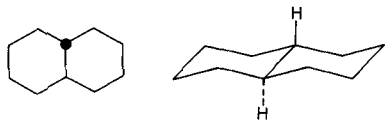

3 4

(the word "Wissenschaft"). This example drives home how much of a linguistic component there is in the thought processes of chemists, as activated by these small sketches that we call chemical structures. Part of our paper deals explicitly with chemical structures as constituting a language.

2. The Shapes of Molecules and How They Are Communicated

When we wish to probe something which is so ingrained in us that it is second nature (as the structural formula is), it is useful to put oneself outside. Imagine telling someone intelligent, attentive, and sympathetic, but someone who is not a chemist, about structure and its communication in our science. Here is what we might say:[1]

Shape matters in chemistry. Two molecules as subtly different from each other as a left hand is from a right, may have quite different physical, chemical, and biological properties. Thus, the mirror image of carvone, the main component of oil of spearmint, smells of caraway. The arrangement of atoms in space is not just a laboratory curiosity, it can be a matter of life or death. Thalidomide, a sedative of the early sixties, was responsible for thousands of fetal malformations in Europe. The pharmaceutical marketed was a mixture of left- and right-handed mirror image molecules. One form was teratogenic, causing malformation, its mirror image was not. Had this been known at the time, great anguish and human loss could have been prevented.[2]

Molecules are made up of atoms. (Forgive us, chemist friends; we're still continuing our hypothetical monologue directed at the nonchemist.) But molecular structure is not just the identity of the atoms. Or even how they are connected up, those elemental atomic building blocks within the molecule. At the operative level of modern chemistry, structure means the three-dimensional arrangement of atoms in space.[3] It is a graph, at the very least, a three-dimensional set of points connected by lines called bonds.

It is critical that chemists easily communicate this structural information among themselves. Via what's at hand, which are two-dimensional media—paper, a screen. The information is complex—many atoms, many bonds, a richness of geometrical structure. The information is at some important level inherently graphic—it is essentially a shape to be drawn. And now we come to the crux of the matter. The group of professionals to whom this visual, three-dimensional information is essential are not talented (any more, any less) at transmitting such information. Chemists are not selected, do not select themselves, for their profession on the basis of their artistic talents. Nor are they trained in basic art technique. The authors' ability to draw a face so that it looks like a face atrophied at age ten.

So how do they do it, how do we do it? With ease, almost without thinking, but, as we will see, with much more ambiguity than we, the chemists, think there is. The process is *representation*, a symbolic transformation of reality. It is both *graphic* and *linguistic*. It has a *historicity*. It is *artistic* and *scientific*. The representational process in chemistry is a shared code of this subculture.

Let us begin our look at the process by a look at the outcome. This was shown in Figure 2, a typical page from a modern chemical article. The substantial amount of graphic content just stares one in the face. There are little pictures here. Lots of them. But the intelligent observer who is not a chemist is likely to be stymied. He finds himself in a situation analogous to that of *Roland Barthes* on his first visit to Japan, beautifully described in his "The Empire of Signs".[4] What do these signs mean? We know that molecules are made of atoms, but what is one to make of a polygon such as structure **5**, here representing a white, waxy medicinal

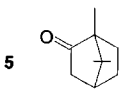

5

compound with a penetrating aroma, camphor?[*] Only one familiar atomic symbol, O for oxygen, emerges.

Well, it's a shorthand. Just as the military man gets tired of saying Commander in Chief, South Pacific Operations, and writes CICSPO, so the chemist tires of writing all those carbons and hydrogens, ubiquitous elements that they are, and draws the carbon skeleton. Every vertex and endpoint that is not specifically labeled otherwise in structural representation **5** of camphor is carbon. Since the valence of carbon (the number of bonds it forms) is typically four, chemists privy to the code will know how many hydrogens to put at each carbon. The polygon drawn above is in fact a graphic shorthand for structure **6**.

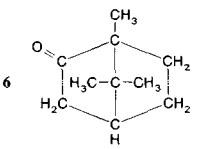

6

But is **6** the true structure of the molecule of camphor? Yes and no. At some level it is. At another level the chemist wants to see the three-dimensional picture, and so draws **7**. At still

[*] A further story needs to be told of camphor. We picked this molecule as one recognizable to the public, but carrying within it minimal complexities of representation. One of us (*R. H.*), having forgotten its structure, checked it in a textbook, then specified to some friends the geometry needed to produce the beautiful drawings of camphor in this paper. Every one of them was the mirror image of what you see, which is the naturally occurring, dextrorotatory material (1*R*,4*R* in configuration)! That we had the wrong absolute configuration was pointed out to us by a careful reader, *Ryoji Noyori*, the 1990 Baker Lecturer at Cornell. A literature search then revealed the wrong configuration disported by many, if not most textbooks, the Merck Index, and numerous literature papers, such as the important one by *G. M. Whitesides* and *D. W. Lewis*, (*J. Am. Chem. Soc* 92 (1970) 6979) on the use of an NMR shift reagent to determine enantiomeric purity. The structure is correctly given in the Sigma, Aldrich, and Fluka catalogues and the references to the assignment may be found in the following handbook: W. Klyne, J. Buckingham: *Atlas of Stereochemistry, Vol. 1*, Chapman and Hall, London 1978, p. 85.

7

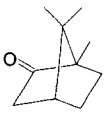

another level, he or she wants to see the "real" interatomic distances, that is, the molecule drawn in its correct proportions. Such critical details are available, with a little money, a little work, by a technique called X-ray crystallography. And so we have a drawing **8**, likely to have been produced by a computer.[5]

8

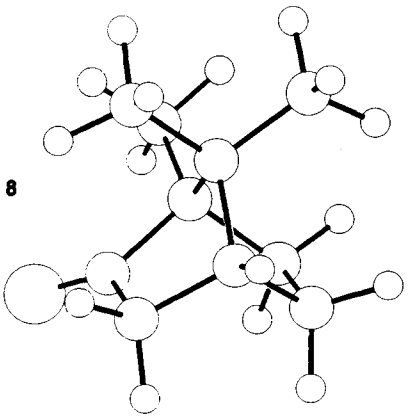

This is a view of a so-called ball-and-stick model, perhaps the most familiar representation of a molecule in this century. The sizes of the balls representing the carbon, hydrogen, and oxygen atoms are somewhat arbitrary. A more "realistic" representation of the volume that the atoms actually take up is given by the "space-filling" model **9**. Note that in

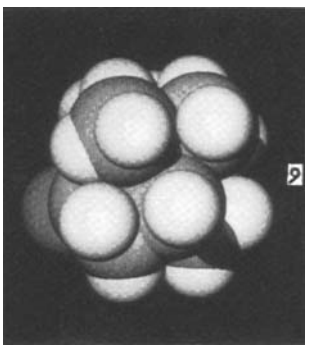

9 the positions of the atoms, better said of their nuclei, become obscured. And neither **8** or **9** is portable. It cannot be sketched by a chemist in the 20 seconds that a slide typically remains on a screen in the rapid-fire presentation of the new and intriguing by a visiting lecturer.

The ascending (descending?) ladder of complexity in representation hardly stops here. Along comes the physical chemist to remind his or her organic colleagues that the atoms are not nailed down in space, but moving in near harmonic motion around those sites. The molecule vibrates; it doesn't have a static structure. Another chemist comes and says: "You've just drawn the positions of the nuclei. But chemistry is in the electrons, you should draw out the chance of finding them at a certain place in space, the electronic distribution." As one tries to do in **10** and **11**.

10

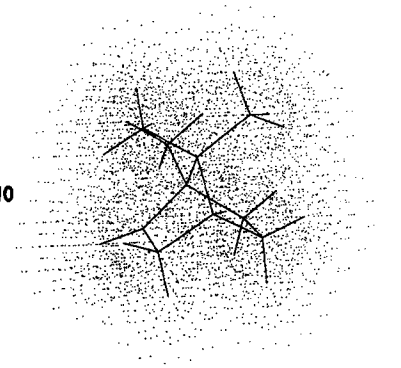

We could go on. The literature of chemistry does. But let's stop and ask: Which of these representations, **5** through **11**, is right? Which *is* the molecule? Well, all are, and none is. Or, to be serious—all of them are models, representations suitable for some purposes, not for others.[6] Sometimes just the name "camphor" will do. Sometimes the formula, $C_{10}H_{16}O$, suffices. Often it's the structure that's desired, and something like **5** or **7** is fine. At other times one requires **8** or **9**, or even **10** or **11**.[7]

11

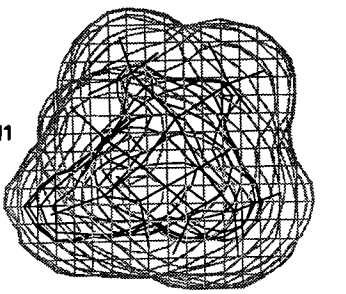

Naive realism asserts that chemical formulas resemble reality: they do. It is possible to obtain pictures of benzene rings by physical means. They look, sometimes, like the benzene rings of the chemist (**2**). Sometimes they don't. The scientist who thinks that now, with scanning tunneling microscopy (STM), one can finally see atoms in molecules, has a shock coming when he or she looks at an STM image of graphite.[8] Half the hexagonal lattice atoms are highlighted in the image, half not. For good reasons. Seeing and believing have a complex relationship to each other. These (the benzene rings of the chemist) are rough approximations. They stand not unlike a metaphor to the molecular object represented.

Let us fix on the *typical* level of presentation (of Figures 1 and 2), that of a polygon (**5**) or a three-dimensional idealization of it (**7**). But what *are* these curious constructions, these drawings, filling the pages of a scientific paper? We now ask the question from the point of view of an artist or draftsman. They're not isometric projections, certainly not photo-

graphs. Yet they're obviously attempts to represent in two dimensions a three-dimensional object for the purpose of communicating its essence to some remote reader.

The clues to three-dimensionality in these drawings are minimal. Some are conventional: here and there (one example in **7**), there is a line "cut" to establish that some piece of the structure is in front of another, that is, **12** instead of **13**.

12 **13**

This is hardly a modern invention, something that one must learn at the Ecole des Beaux Artes. Figure 3 shows one of the cave paintings from Lascaux.[9] Note the treatment of the legs of the bisons as they go into the body. Now smart chemists should be able to do what cavemen 15 000 years ago did, shouldn't they? Too often they don't bother.

Fig. 3. Two bisons from the Lascaux Cave. Reproduced from J. Vouvé, J. Brunet, P. Vidal, J. Marsal: *Lascaux en Périgord Noir*, Pierre Fanlac, Périgeux 1982, p. 31. Reproduced with permission of the publishers.

Scattered about in the drawings of Figures 1 and 2 are sundry wedges and dashed lines. These are pieces of a visual code, simple in conception: a solid line is in the plane of the paper, a wedge in front, a dashed line in back. Thus, **14**

14

shows several views, all quite recognizable to chemists, of the tetrahedral methane molecule, CH_4. The tetrahedron is the single most important geometrical figure in chemistry. (Be patient, colleagues, think of telling your father-in-law about what you are doing.)

Describing this notation may be enough to make these structures rise from the page for some people, but the neural networks that control representation are effectively etched in, for life, when one handles (in human hands, not in a computer) a ball-and-stick model of the molecule while looking at its picture.

A glance at the more complicated molecules of Figure 2 shows that the wedge-dash convention is not applied consistently. Most compounds have more than a single plane of interest; what's behind one plane may be in front of another. So the convention is almost immediately used unsystematically, the author or lecturer choosing to emphasize the plane he or she thinks important. The result is a cubist perspective, a kind of Hockney photocollage.[10] The molecule is certainly seen, but may not be seen as the scientist thinks (in a dogmatic moment) that it is seen. It is represented as he chooses to see it, nicely superimposing a human illogic on top of an equally human logic.

They're floating in space, curiously unframed, these representations. You search in vain for a set of reference planes, a chair, a figure to orient you. But these are not given. The reader must decode the three-dimensionality with little help. Mind you it's not that difficult—there is an innate drive to see things as three-dimensional. Witness the difficulty we have in seeing the pattern of connected rhomboids, **15**, as flat.[11a]

15

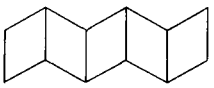

Let us now come out of the didactic monologue. The hypothetical nonchemist, if he or she has persevered, has now partaken of the knowledge (prejudices?) that the chemist has about structures. We can proceed together.

The question remains: what do these chemical structures represent? How are they drawn and read? *Philostratus* tells, much mythologized, the story of *Apollonius of Tyana*, a Pythagorean who lived around the time of Christ. In a dialogue with a disciple *Apollonius* explores what painting is. It's done to make a likeness, to imitate. But what about cloud shapes in the sky, read by us as horses or bulls? Are those also imitations? *Apollonius* and his disciple agree that these are but chanced configurations, that it is we who interpret those shapes, give them meaning. He continues: "But does this not mean that the art of imitation is twofold? One aspect of it is the use of hands and mind in producing imitations, another aspect the producing of likenesses with the mind alone... I should say that those who look at works of painting and drawing must have the imitative faculty and that no one could understand the painted horse or bull unless he knew what such creatures are like."[11b]

Knowing is not an unproblematical concept. How does that three-dimensional structure unfold in its full glory in the mind of a chemist? As we said, the direct images produced by contemporary techniques such as scanning tunneling microscopy or electron microscopy (and these are not so "direct" on close examination) are few. Secondary knowledge, through X-ray crystallography, microwave spectroscopy, or electron diffraction, is experienced still by only a small number of specialists. For most of us it is the real, physical handling of models that sets the stage—the analogy to seeing *Apollonius*' bull or horse in the first place. Or looking at many pictures of molecules drawn by others, assimilating

thereby the set of conventions shared by chemists. It's much like art, and we will return to this below.

3. History, Media

How did the chemists' way of seeing and drawing evolve? One can choose a starting point for chemistry almost at will, and ours will be *Lavoisier*. In his time, the end of the 18th century, there were no chemical structures of type **5–11**. The idea of an element was just taking form; the symbols for these elements were still not codified. The results of chemical experiments could be perfectly well communicated in words and, especially after *Lavoisier*, with numbers.

Illustrations figure importantly in *Lavoisier*'s work, nevertheless. They are often the illustrations of his experimental equipment, of glass and metal containers, gauges, barometers, all exquisitely detailed. A plate from *Lavoisier*'s 1789 classic "Traité Elementaire de Chimie" is shown in Figure 4.[12a] The appeal of these illustrations is in large part due to their creator: Mme. *Lavoisier, Marie Anne Pierrette Paulze*. Her original sketches, as well as her corrections of these engravings, are available. Mme. *Lavoisier* was an accomplished artist, a student of *David*.[12b]

The media available to the scientific communication process of the time were quite circumscribed. In lecture presentations it was the voice, demonstrations,and blackboard and chalk. Illumination levels were low. In printed presentations one had, aside from normal typesetting possibilities, woodcuts and engravings, usually copperplate.

When did it become essential to communicate three-dimensional chemical information? By the middle of the 19th century there arose some pressure to represent the ways

The reaction is easily understood by the following diagram, in which the atoms

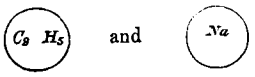

are supposed to be capable of changing places by turning round upon the central point A.

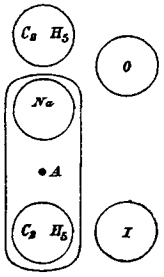

It is clear that we thus get $\begin{matrix}C_2H_5\\C_2H_5\end{matrix}$O and NaI. The circles are merely used to separate off the atoms or units of comparison. To express the corresponding decomposition of iodide of ethyle by hydrate of potash, forming alcohol, we should replace the ethyle of the sodium-compound by hydrogen, and the same change of place between sodium and ethyle forms $\begin{matrix}H\\C_2H_5\end{matrix}$O (alcohol) and Na I.

Fig. 5. An excerpt from an article by A. W. Williamson ("On Etherification"), *J. Chem. Soc. London 4* (1852) 229. The original runs across two pages.

atoms were linked to each other. Figure 5 shows a page from a crucial 1852 paper by *A. W. Williamson*.[13] Note the illustration, presumably engraved, and the way chemists of the time tried to represent, within the linear confines of a printed text, that in ordinary alcohol, ethanol, one has C_2H_5 group and H atom connected to an oxygen. We see here the beginnings of the tension between the medium and the content.

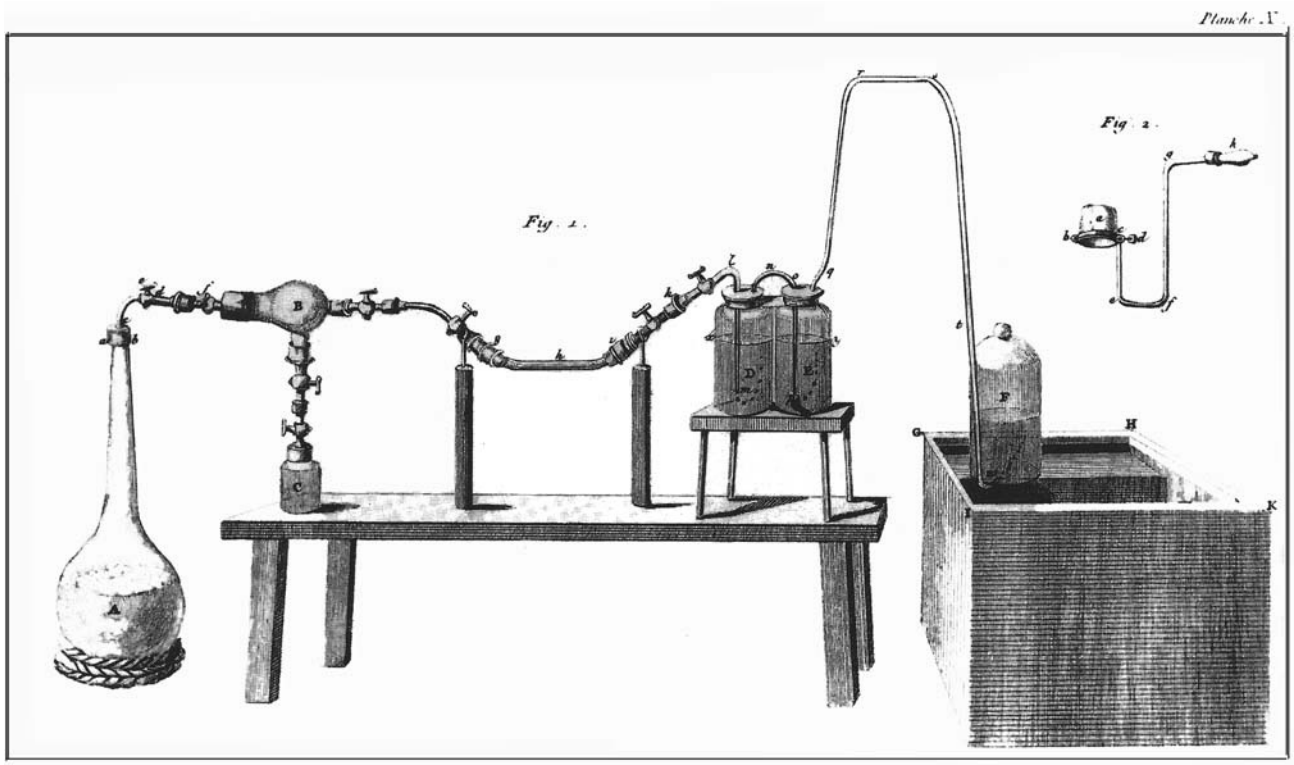

Fig. 4. Plate X from *A. Lavoisier*'s classic "Traité Elementaire de Chimie" (Cuchet, Paris 1789). The drawing is by Mme. *Lavoisier*.

The content, incidentally, is fascinating, in that it reveals a struggle to give structure to and withhold it from the molecular formula.

The study of optical isomerism led *L. Pasteur* to the remarkable insight that the still unseen microscopic molecules must be in some way three-dimensional and left- or right-handed.[14] It seems in retrospect almost strange that it took another quarter of a century for a correct model to take shape. But so it did, in 1874, in the tetrahedral carbon atom of *J. H. van't Hoff* and *J. A. Le Bel*.[15] Structure **16** reproduces one of *van't Hoff*'s original drawings.

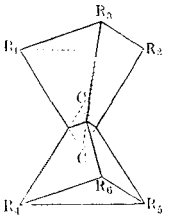

16

A carbon lies at the middle of each tetrahedron. *Van't Hoff* was led to this model some forty years before any one "saw", even indirectly, the disposition of atoms in space in a molecule. *N. J. Turro* in a perceptive article addressing some of the same issues discussed here, has aptly called the tetrahedral carbon atom "a triumph of topological thinking".[16]

The increased reliance of chemists upon molecular formulas derived much from the example of another pivotal 19th-century figure, *Kekulé*. As a teenager, *Kekulé* had hesitated between two professions, architecture and chemistry. His strong leanings for the former showed up in his routine building of molecular models, which he would display in his lectures. He would make projections onto planar screens of these models and use these projections as graphic formulas in his publications.

With the contributions of *Kekulé*, *van't Hoff*, and many others, the structural theory of organic chemistry evolved apace, and by 1890, one hundred years ago, it was clear that one needed the capability to set in print quasi-three-dimensional drawings of type **7**.

There was no problem in doing so on a blackboard. But the printing media were not up to it, at least not at the budgetary levels appropriate to mass dissemination of a scientific journal. Photography had been around for a good part of the century, but it also had not yet affected the routine printing process. Nor did it *ever* subsequently make an impact on the communication of chemical structures. This is worth a digression relevant to the question of what one is trying to communicate in these drawings, which we will take later.

Engraving still remained the technique of choice in the printing process of a hundred years ago. It was expensive to set lines at an angle. So if a journal had to set the molecule of norbornane, C_7H_{12}, the "skeleton" of camphor, it was represented as **17** rather than **18**. This was done not only in 1890, but until 1950, even when engraving was replaced by photogravure.

The policies of journals, their economic limitations, and the available technology put constraints not only on what is printed, but also on how we *think* about molecules. Now everyone (in chemistry) knew since 1874 that carbon was "tetrahedral", that its four bonds pointed to the corners of tetrahedron. Molecular models were available or could be relatively easily built. Yet we suspect that the image or icon of norbornane that a typical chemist had in his mind around 1925 was **17** and not **18**. The chemist is conditioned by what

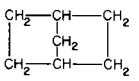

17

18

he or she sees in a journal or textbook—an image—and might have been moved to act, in synthesizing a derivative of this molecule, for instance, by that unrealistic image.[17] And yet *G. Komppa* did synthesize it![18]

Maybe it's not that different from the way we approach romance in our lives, equipped with a piecewise reliable set of images from novels and movies.

4. Chemical Representation as Language

Most, if not all, scientists make use of visual imagery for problem-solving, in order to sort out and organize information, to find analogies, to think.[19, 20] But chemists are unusual among scientists (though they share this with the architects) in having an iconic vernacular, that of the formulas.

A chemical formula is like a word. It purports to identify, to single out the chemical species it stands for. Chemical formulas embody the ancient dictum (going back, as far as teaching is concerned, to the Czech *Comenius* at the time of the Renaissance): "One thing, one word."[21] Indeed, chemical systematics takes great care to avoid ambiguous situations; we have nomenclatures that deal with every conceivable type of isomerism.

A first problem is easily discarded. When we refer to a familiar object in the outside world by its name, we project a measure of personal experience into the identification. If I say "dog", I cannot help forming a fleeting mental image of a furry or fiery quadruped, wagging its tail or baring its teeth, in between a friend and a threat.[22] The trivial names of chemicals, which often have been with us for centuries, are no different, even when imbued with outdated knowledge that has leached out: sulfuric acid, potash, albumin, *azote*, etc.

This brings up a second, more serious problem. Chemistry is a mature science. It has shed to a large extent its childhood habit of going no further than a phenomenological description of bulk properties, at the macroscopic level (that of sensory perceptions), accompanied by an apt denomination (such as "potash"—because the compound was first found, literally, in pot ash).

Chemistry has become a microscopic science. Explanations nowadays go routinely, paradigmatically from the microscopic scale to the observable: from the way the electrons are distributed in a dye molecule to its color; from the de-

tailed shape of a molecule and of the electrostatic potential around it to its pharmacological activity; from bond energies to the superior tensile strength of Kevlar.

Such a seminal characteristic of chemical sciences was noted already at the time of the Enlightenment. The entry for "chemistry" in the *Encyclopédie* by *Diderot* and *D'Alembert* points out that chemists (but not the Newtonian physicists of the time, who explained everything with central forces acting on material points) are wont to posit invisible and intangible entities or qualities to explain observations. They are forced to do so by the smallness of their particles. We are still under a similar constraint, even though "images" of some molecules and of some atoms have become available very recently. Indeed we know our building blocks, molecules, much better. But it remains a long, long way from the molecular scale to the macroscopic world of the senses. We still have to represent molecules, and chemists have to do so as much as other people. And we tend to represent to ourselves atoms *as if* they were normal objects in our everyday experience: with a size, with a certain hardness or softness, with measurable attractions to other atoms or to electrons, and so on. This is a little naive, unavoidable, and endearing—not unlike a belief in angels in past centuries.

We made earlier (last sentence in Section 3) the same point. Humans delude themselves with mental constructs projected upon reality, often deemed as "realism". Chemistry, in like manner, is a mix of a molecular engineering, based on extrapolations from the macroscopic to the microscopic, and a science, coming to grasp directly with the microscopic. The puritans among us wish to get rid of the former, and they push for our minds to handle abstractions only, as in mathematics. Thus, they tend to measure our understanding of the physical world by its secession from everyday experience. While we have a great deal of respect for such an inclination, a constant temptation to most scientists one would think, we are not such purists ourselves. The needs of communication and teaching are one, circumstantial, reason. A second, and more potent, reason is the centrality of semirealistic representations to chemical thought. This is the central theme in our discussion.

What we have is a fascinating philosophical quandary, and an instance of quasi-circular reasoning,[23] too. The above cited quantities—the size of an electronic cloud in an atom, the atom's *electronegativity*—are neither derivable from first principles[24] nor are they observables. They, these Platonic archetypes, have evolved slowly among chemists, in an inductive manner, from experimental determinations; and we attempt to *deduce* from them in turn consequences, for objects in the physical world only very slightly different from those that formed the basis for the formulation of these qualities. This feature is one of the major hurdles for students learning chemistry. Our discipline is a curious mix of empirical observation *and* abstract reasoning. This is not unlike music—but it parts chemistry from the rigor of pure mathematics. Students brought up on deductive logic have a hard time with chemistry!

True, chemical formulas have been severed from subjective life experiences to a considerable extent, much more so than words such as "dog", "automobile", or "contraception". Yet, despite such an excision, chemical structures retain a strong connection with sensory experiences; by contrast with such mundane words, they carry an essential *representational* component.

Let us elaborate some on this interesting paradox. As *Ferdinand de Saussure* pointed out, in one of his fundamental insights, the *word–thing* relationship is that of the *signifier* to the *signified*; and a key notion is that of the *arbitrariness* of the signifier.[25] When we say "dog" (or "Hund" or "cachorro"), each of these terms has been selected more or less randomly in the history of the language. It could have been a "snark" or a "livel" or a "rop" in English, who knows! The word "dog" has settled into its niche (forgive the pun) in the common language by way of the numerous cross-relations it bears with other words in the dictionary (such as "leash", "dogfood", "bitch", or "seeing eye"). We flesh out a word because we cannot help loading it with our private empirical experience, just as we do with atoms. But in actuality the word is a total fabrication. It could have been an entirely different choice.[26]

With this reminder, we return to this paradox: formulas forsake reality in a sense, and they aim to stand for reality in another. Indeed, chemical structures differ from words in the normal language because they combine symbolic and representational (iconic) values. Take the case of the molecule of natural gas, methane, drawn above in structure **14**. The various types of strokes in **14** indicate *both* connection of the carbon with the hydrogens via chemical bonds (the symbolic statement) and whether the bond butts out of the plane of the paper, or recedes from the viewer to the backside (the representational or geometric statement). The chemical formula is trying to signify a lot with the utmost economy in graphics. It aims at portraying accurately the connectivity of atoms—the nearest-neighbor relationships as stemming from chemical bonds—and the geometry.

Thus, we can state the second problem with chemical formulas: they are in between *symbols* and *models*. This hybrid status is an uneasy one. These two poles pull formulas toward opposite and sometimes incompatible requirements.

As models, chemical formulas ought to be reliable and accurate representations of what one might term "molecular reality" (we shall return to this useful figment of the collective psyche of chemists). As symbols, they ought to be arbitrary, to a large extent. This is reflected, to give an all-too-familiar example, in the use of a capital O to represent an oxygen atom: behind this universal convention, there is an assumption of transferability (an oxygen atom *here* is very much like an oxygen atom *there*) which is not that easy to put on a firm theoretical basis. An oxygen atom free of a molecule is indistinguishable from any other oxygen atom. But inside a molecule, a ketone oxygen is very different from an ether one.

Words of a common language are highly ambiguous. Take the word "representation" itself. It can mean either the act of representing or the result of such a mental or physical action. In the latter sense, a representation can be a description, according to this or that framework: representations are theory-laden. In a closely related sense a representation will refer to the worldview, to the *style* of whoever makes it; this is the more subjective meaning of representation. In yet another meaning (that of the poet, for instance), a representation is an epiphany; making the represented object be under our very eyes, whereas it truly is absent. This is representa-

tion as illusion. Not to mention yet other meanings, such as in the diplomatic lingo, where representations are a protest and a rebuke. Strings of words, as arranged in a poem, any text for that matter, have also a plurality of meanings. Hermeneutics strives to enrich the reading of a text by associating to the more obvious and mundane meaning a deeper meaning as well.[27]

Is the world of chemistry and chemical structures unambiguous, characterized by one drawing, one molecule? To some extent chemistry is such, because it is "a sign imprinted in matter", as *J.-M. Lehn* has called it.[28] The instructions for making aspirin work here as well as in Montevideo and Karaganda. The article reporting the synthesis of a new drug perhaps needs translation, but in another sense it doesn't, for it is understood around the world, it is infinitely paraphrasable. Chemical structures, chemical formulas are the signing tools of this language.

But in another way the graphic language of chemistry is quite ambiguous. We've seen clear evidence for this in the plurality of answers given for camphor to the simple question: What is the structure of the molecule? It could be argued that once drawn, no matter how drawn, the single molecule "camphor" enters the mind of the chemist. But as we will see later, how a molecule is thought about and subsequently manipulated in the material world is very much influenced by the way we carry it around in our minds.

A chemical formula is at once a metaphor, a model (in the sense of a technical diagram), and a theoretical construct. A chemical formula is part pure imagination, part inference. It is an attempt to depict the real by manipulation of symbols, just as language enables us to talk about the world and about ourselves by combining arbitrary utterances. The simile cannot be pushed too strongly. In a deep philosophical sense, calling something an "acid" and calling something else "red" are identical mental operations. Likewise, referring to "ethanol" or "reserpine" is akin to talking about "Rockefeller Center" or about the "Eiffel Tower".

"Acid" and "red" are ill-defined but most useful concepts relating to everyday experiences. Conversely, "ethanol" and "Eiffel Tower" are defined unambiguously, but they need not be commonplace objects, they are cultural objects in the widest sense.

One of the points *C. P. Snow* made in his "Two Cultures" lecture was precisely that we should give equal status—that the value judgments had to be either suspended or commensurate—for two cultural objects such as, say, the novels of *Jane Austen* on one hand and the structure of DNA or the second law of thermodynamics on the other.

If "ethanol" is in a similar mental category as "Eiffel Tower", the chemical formula of ethanol stands to it not unlike a dictionary definition for "Eiffel Tower": a chemical formula is a concise paraphrase, in a half-symbolical, half-iconic language, of some of the attributes of an object, so that the object can be properly and unambiguously identified, that is, differentiated from like objects (Eiffel Tower as distinguished from the Madeleine or the Centre Pompidou; ethanol as distinct from ethane or from acetic acid).

Language and chemical representation, besides their joint use of names, have other similarities. They share use of invariant elements. Many words and most chemical compounds are just that, compounds, put together by association of structural fragments. There is deep similarity between a word such as "one-upmanship" and a "chemical word" such as C_6H_5-CH_2-CO-OH. In the latter case, just as in the former, the structural fragments (phenyl, methylene, carbonyl, hydroxy) are stable semes: to a first approximation they retain their basic meaning whatever the nature of the other modules they are connected with.

Chemistry is the science of change, of transformations. Every science starts with axioms about the integrity of certain of its objects. The mechanical engineer believes in the integrity of a steel girder. The cell biologist believes in the integrity of chloroplasts or mitochondria: he or she is convinced that these organelles are interchangeable, playing identical roles in one cell or in another.

For chemistry, it is crucial to make sense of change by constraining it to occur between well-defined states. Invariance and its equivalent, transferability, are basic assumptions to chemistry. At each level of understanding (or complexity), the lower units are set as invariant: starting with atoms, going on to the simple structural fragments such as the above (C_6H_5, CH_2, CO, OH), on to simple molecules, further on to chains or polymers, the helices of proteins and nucleic acids, and so forth.

The concept of transferability goes back, beyond *Dalton*'s atoms, to the Lavoisier revolution: "Rien ne se perd, rien ne se crée." By a quirk of scientific history, his use of the balance made *Lavoisier* discover the physical law of mass conservation; but the linguistic bent he had inherited from *Condillac* made him give a *linguistic* expression to it. *Lavoisier* founded modern chemical language on the explicit analogy to natural language. No wonder that chemical formulas, to this day, retain an important linguistic component.

It is possible to set up a formal relationship between chemistry and language; an intriguing initial step in this direction has already been taken by *H. W. Whitlock, Jr.*[29] In the terminology of *Chomsky*, a language is defined by a set of symbols (a vocabulary) from which strings (sentences) may be generated by a set of productions or transformations (rules for making changes).[30] The identification of symbols with chemical elements or those simple structural fragments (CH_2, CO, OH) we have alluded to above, and of productions with chemical reactions, is obvious. *Whitlock* interestingly shows that a certain problem in organic synthesis may be approached by analyzing it in the context of formal language.[31]

The shared productivity of language, formal or natural, with chemistry applies also to the realm of what has not yet been said, or written, or synthesized. There exist rules, for instance such that we have the competence to pronounce a word that we have never heard: "a roor", "to roat", "the poot". Likewise, we can write utopian formulas for (so far) unknown chemical species (e.g., **19**–**21**). This serves quite often as an inducement to try and prepare them.

19

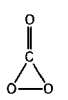

20

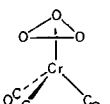

21

These structures, waiting impatiently to be made, have for chemists the incongruous look, both attractive and shocking, of a novel object deemed by some as an impossibility: not unlike a first look at a laser printer in action, or a monorail train levitating above its magnetized track, a Stealth bomber, or a town-size space station.

This is a strong analogy, that of language and chemistry. Its tiny area of invalidity is homonymies ("rapt" and "wrapped"). They don't occur in chemistry, or very seldom: "*periodic* table" and "*periodic* acid", linguistic look-alikes, in fact, are easily told apart from the context and pronunciation.

Thus both languages, the natural and the chemical, witness an evolution of meaning, from so-called nonsense to highly significant statements. Even though it does not build upon known ("domesticated") words, and it invents instead new ("wild") words, the "Jabberwocky" poem by *Lewis Carroll* makes sense because of its impeccable syntax, which lets the imagination of the reader both be charmed by the word-play and invests some of the words with meaning, by way of various associations. Chemistry has likewise its wild species (benzyne, tetrahedrane, or **19**–**21** above), besides its more usual bottled samples. In fact most of the molecules of chemistry, wild dreams or not, are invented, synthesized. They were not on earth before.

Chemical representation is also language-like when dealing with the class of transformations known as chemical reactions. In an important sense, chemistry is the skillful study of symbolic transformations applied to graphic objects, the formulas. There are one-to-one correspondences between compounds and formulas. Likewise, it is possible to specify unequivocally the transform from one compound to another. If one thinks of chemical compounds as nodes in an infinite and multidimensional grid, then the connecting lines in such a network are the transforms. Chemistry has thus two facets, structural when the focus is static, on the points in the grid; and dynamic when what is examined is the interconversion along the edges in the network. There are strict rules about *rewriting* formulas to express transforms; not unlike rules of musical composition.

Chemical transforms are the analogues of action sentences in natural language. The parallel is illustrated by **22**.

subject substrate	transitive verb reagent	object product

22

An example of the former is "John saws a log". An example of the latter is "the aldehyde is reduced by sodium borohydride to the alcohol".

Just as action sentences carry subordinates as modifiers, to provide information about time, location, quantity, manner, so the chemical equation is wont to specify the solvent, the reaction temperature, the reaction time, the yield of product, etc.

In another sense, this parallel is too general. The product molecules in a chemical reaction contain the same atoms as the reactants, but reconnected in a different way. The relationship of subject and object is different—except in a category of sentences having a pronominal (or reflexive) verb. Sentences such as "Jane washes herself" or "John admires himself in the mirror" are somewhat like statements about chemical transforms. Funny that chemical equations come so close to psychological statements!

In *Goethe*'s 1809 novel "Die Wahlverwandtschaften" (Elective Affinities), a by-then outdated theory of chemical combination powers a work of fiction.[32] The actions and emotions of the characters of this work embody (and probe critically) the way some people thought molecules behave. One wishes one were able to point today to a similarly inspired literary text. The closest one comes is *Primo Levi*'s remarkable memoir "The Periodic Table", or some chapters in his novel "The Monkey's Wrench". Nevertheless, it is interesting to reflect on the deep morphological resemblance of chemistry and, if not life, at least language.

In the foregoing, the parallel between chemical formulas and everyday language may have appeared rather artificial and a little forced. We can defend it nevertheless with an anecdote.

One of us was visiting recently the office of Professor *C. Tamm*, at the University of Basel. The conversation turned to a structure of a complex natural product, inscribed on the blackboard and recently elucidated in Professor *Tamm*'s laboratory. As an aside, one of us said: "The way I read this structure starts with the six-membered ring, goes on to the *spiro* junction with the five-membered ring, etc." Professor *Tamm* agreed. We discovered in this manner that we shared the same vision of this particular molecule. Both of us were going around this complex network (bonds and atoms) in well-nigh identical manners—obviously a result of our training.

It is thus our contention that chemical formulas are read according to conventional sequences. Recent research in neuropsychology teaches indeed that mental patterns do not spring up whole. They are built up gradually, a part at a time; and the parts, it is found, are visualized in roughly the same order as they are typically drawn. With respect to the two types of tasks (retrieval of archival shapes and coordination of shapes into a mental image), the two brain hemispheres play different roles.[33, 34]

The opposite viewpoint is a necessary complement. As *Verbrugge* indicates, discussing the example of *Kekulé*'s architectural formulas, his ring structure for benzene, and the oscillation of benzene between the two equivalent ring forms, "scientific understanding develops only when we are prepared to reshape our representation systems in fundamental ways."[35]

We submit that the combined pressures of (1) the learning, early on, of chemical nomenclature, (2) incessant on-the-job confrontations with formulas through seminars, the reading of publications, the handling of molecular models, and (3) the demands of communication with other chemists have built this largely unconscious and stereotyped collective way of seeing. Probably art historians act the same; it is quite possible, even likely that two specialists of Quattrocento painting will both scan a picture in much the same ways.

Let us now explore the opposite viewpoint. Because perception of chemical shapes is so stereotyped, conversely to be able to see a structure in a novel way can be extremely fruitful. Chemistry shares with poetry its notion of elegance, its mission so to say. This is to discover new relations between

objects. Very often, the elegance of a key step in a series of chemical transformations is rooted in the perception of a nonobvious connection between parts of the molecular object. More generally, it would repay the student of psychological invention to take a close look at flowsheets, the sequence of molecules made and transformed, in synthesis of natural products. Indeed, the synthetic elaboration of complex chemical structures offers fascinating glimpses into the creative process, in the doing. In the hands of a master craftsman such as *R. B. Woodward*, structural fragments experience what are to the mind—that of the conceiver as well as that of the reader—genuine *Gestalt* shifts, from one part of the synthesis to another. By studying the Woodward syntheses in detail, one can just see him turning a molecule over in this mind, and seeing some of its elements from new angles. The changes of the structures in the course of a Woodward synthesis are metaphors of creativity.[36] They exploit the plurality of meanings embodied in a chemical structure. We submit that it may be difficult to move closer to the creative imagination in action.[37]

A final point, made to us by *H. Hopf*.[38] Chemistry is full of representations other than graphic ones—take the various spectra, IR, NMR, photoelectron, all different (the medium is the message; in German the plotter is even called "Schreiber"). Their music (the tones, overtones and harmonics of spectroscopy) carry incredible dynamic detail far beyond the static structure. Some (NOESY plots) claim to embody the same informational content as conformational drawings. It's a wondrous multitude of representational imagery out there, artists/scientists working in so many media to capture the essence of the real.

5. But Is It Art...

Art or the reaction to it, the aesthetic response, has never been easy to define. There are so many forms of pleasing human creation, so many constructed objects or patterns evoking emotional reactions. Cognizant of the complexity and venerable history of aesthetics, let us hazard a definition.[39, 40] While it is one contestable in all of its parts, perhaps it touches on most of the qualities of what we've chosen to call art. Then we will examine representation in chemistry as it measures up against this definition.

Let's call Art those symbolic acts or creations of human beings which aspire to the extraction from the complex realm of Nature, or the equally involved world of the emotions, of some aspect of the essence of these worlds. Art functions by communication of a symbol, meant to convey information and/or evoke an emotional response.

The essential components of the aesthetic system are (1) the creator—painter, composer, photographer, writer, dancer, (2) the audience—both that perceived in the creator's mind and the real one, the viewers, (3) the set of symbols by which communication takes place—the watercolor, sound waves, and images evolving in time, a text, (4) the act of communication itself—to an audience that is present (watching a dance, listening to a cantata) or absent (reading a novel).

If this definition sounds too rational, too "scientific", devoid of the gut emotional response we should like good art to hit us with, so be it. *Nelson Goodman* argues persuasively that "in aesthetic experience the *emotions function cognitively*", that feeling is knowing. He goes on to examine the usual attributes of art (that the aesthetic is directed to no practical end, that it gives immediate satisfaction, that in art inquiry is a means of obtaining satisfaction, etc., all of these existing as marks of art mainly by contrasting them with an opposite attributed to science), and he finds them wanting. He says: "... the difference between art and science is not that between feeling and fact, intuition and inference, delight and deliberation, synthesis and analysis, sensation and cerebration, concreteness and abstraction, passion and action, mediacy and immediacy, or truth and beauty, but rather a difference in domination of certain specific characteristics of symbols."[41]

To return to the question heading this section: are chemical structures art? It seems clear that they possess all the components of the "aesthetic system". Structural formulas are symbols created by one chemist (or several) to communicate information to others. The drawing of the structure of camphor is certainly a symbolic motion, a communication of an essence—the arrangement in space of the atoms of this molecule. Some might call it just a sketch, an information-reducing stratagem by someone not able or willing to compute and show others the all-important electron density around the nuclei. *That* electron density is the real molecule; the structural formula—well, that's "just a poor representation".

Of course, that simple structural drawing is more. It is the appropriate tool, the model fitting the occasion. Indeed, it's the extraction from the complexity (of something so simple as a molecule!) of one aspect of its essence. It certainly conveys information, that structure. And, in the few careful readers of the paper, the structure may even evoke an emotional response, a wonder that it was made, jealousy of the man or woman who made it first.

Does it matter that the aesthetic response will be provoked instantly only in the minds of those initiated to the chemical structure code? We don't think so. To be sure one has to be taught to understand the chemists' ways of signing. But it's not that difficult. Responses of the population at large to abstract art, or some primitive tribal groups to realistic Western art, have not been, are not likely to be, immediately appreciative.

The chemical structure is an artistic construct because it is a transformation of a model of reality (note the secondhand if not nth-hand relationship to the real) for the purpose of communication. Neither chemistry texts nor anatomy books are much illustrated with photographs. There are some photographs, to be sure. But by and large a photograph (and we certainly don't wish to imply that photography is mere representation; it is far from that) contains too much detail. What one wants to communicate is the essence needed for the moment. One wants to teach, to evoke a response. Drawings, with their artistically selected detail, are much better for that purpose.[42]

The symbolic nature of the chemical formula, the fact that chemists know that a hexagon stands for a ring of carbon atoms that in turn is much, much smaller, the implicit knowledge that that hexagon is *not* an enlarged photograph of the ring, all that symbolic distancing of course enhances the

metaphorical nature of the chemical discourse. Structures are not what they stand for; they stand for what they are not.

But is it art? Having argued that chemical representations, such as structural formulas, share all the symptoms of art, let us take the opposite tack, at least for a while.

Just as it is impossible to ignore the artist and his audience, the mental set of both, so it is impossible to put out of mind the context of a picture or a scientific illustration. And chemical structures, in particular, are often really part of the text. Oh, they may have artistic value or expressive power on their own. One could mount a good art exhibit around them. But their function, their organizing referent, is the text.

By way of illustration, Figure 6 shows the beginning of a paper written by one of us.[43] Note four little drawings in the first two paragraphs. They are typically floating in midair, typically using the wedge–dash–line notation. The structures are numbered boldface, and referred to specifically in the text. In fact they are part of the text, and that they are referenced to (by their boldface numbers) even in the middle of a sentence, confirms this role. In one chain (labeled **2** in Fig. 6) the units of five telluriums are related by a so-called screw axis, whereas in another chain (labeled **3** in Fig. 6) they are simply translated, one relative to the other. All that could have been said in words. But it was easier to draw a picture. So a structure was born.

Actually, the motives of the representation are not so simple here. The authors use the pictures not only to save space. They are also plumbing strategies to capture their audience. These tellurium compounds are not immediately interesting to everyone in chemistry. Specialization is a plague in any field of scholarship. The geometries of the tellurium structures are difficult to see. Since in science, as everywhere else, what we do not understand we are afraid of, what we do not understand we find uninteresting, the authors are using the visual appeal (and density of explanatory power) of a drawing to inform, to pull in, to attract, to seduce. Still another motive: It is the "style" of one of the authors (*R. H.*) to decorate his papers with such drawings. He is establishing a visual signature.

Still another argument against assigning full artistic value to a chemical structure is that it is not, to use *Goodman*'s terminology, "replete".[44] Not every stroke in the representation matters; the lines could be a different color, the molecule readily recognizable as what it is even if drawn from a somewhat different viewpoint. This is in contrast to a Goya etching, which, were similar changes made in it, would be another Goya etching, a different work of art, or at the very least a different "êtat".[45] To put it in another way, the chemical structure addresses the inherent paraphrasability of scientific knowledge (paraphrase as one of the (few) differentiations of art and science has been persuasively forwarded by *G. Stent*[46]). It's the same molecule, intended to be the same, perceived to be the same. But what if the slightly different representation enters the unusual mind, prompting an experiment untried before? The icon powers the iconoclast.

Perhaps another way to approach the artistic content of chemical drawings is to think of their relationship to various visual art genres. For instance, we see a similarity between chemical structures and what has been called, not without controversy, primitive art. Tribal art, be it of Australian aborigines or an Eskimo clan, often appears schematic to us, deficient in perspective. That's our problem, for to the native group which shares the culture that informs that art, the representation may be highly accurate and perceptive. So it is with chemical drawings—their perspective may be inadequate, their representation artistically unsophisticated. But they tell a concise story to the chemical reader. Like primitive images or sculptures, chemical drawings will usually distort a view if the viewers' ability to clearly *classify* an object is enhanced by that distortion. So if it is important to show that someone owns six sheep, the sheep will be posed so that they are distinct, and clearly seen as sheep. A deity will be represented by its symbolic attributes so that we cannot confuse it with any other.

The iconic representation of camphor (see drawing **7**) is simplified and distorted (compare with **9** or **11**) so as to allow us to identify the molecule, to trigger a connection in the

The recent literature contains a number of examples of a square-planar tellurium structural unit which may formally be defined as Te_5^{n-} (1). In some cases such as Rb_2Te_5[1] and Cs_2Te_5[2]

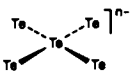

1

the stoichiometry clearly defines the cnarge on the unit as 2−. In these instances the unit is the basic building block of a one-dimensional anionic chain. In Cs_2Te_5 the Te_5^{n-} units are screw axis related (2) while in Rb_2Te_5 the Te_5^{n-} units are related by translation (3).

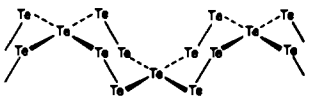

2

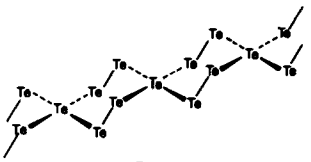

3

For most of the other cases in which the Te_5^{n-} unit appears, the attribution of a particular charge to the unit is more ambiguous. For instance, on K_2SnTe_5,[3] the unit again appears embedded in a one-dimensional chain (4) but the Te_5^{n-} units alternate

4

with tetrahedral Sn in making up the chain. Formally, at least, the square-planar units could still be considered Te_5^{2-} if the tin is Sn(0), but the Te–Sn bond length of 2.74 Å is almost identical with the sum of the tetrahedral covalent radii (2.72 Å) given by Pauling.[4] This suggests a formal oxidation state of 4+ for the Sn and a net charge of 6− on the Te_5^{n-} unit.

Fig. 6. The beginning of a paper, "Hypervalent Tellurium in One-dimensional Extended Structures Containing Te_5^{n-} Units": J. Bernstein, R. Hoffmann, *Inorg. Chem. 24* (1985) 4100. The original runs across three columns in the journal.

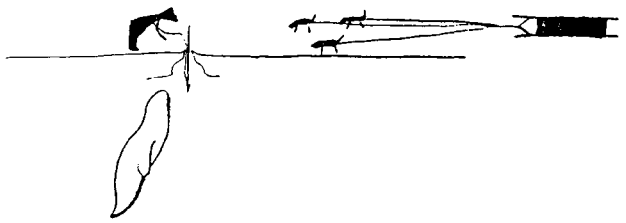

Fig. 7. An Aivilik drawing of a seal hunt. From E. Carpenter: *Eskimo Realities*, Holt, Rinehart and Winston, New York 1973, p. 117. Reproduced with permission of the publishers.

mind. The Aivilik drawing (Fig. 7[47]) of seal hunting through the ice rearranges space (top view of sled, side view, X-ray, of hunter, ice, and seal) and time (the seal approaching, the harpoon already thrown) so as to render visible, in all its richness, the hunt.

Something similar occurs in the pictorial language of chemists. If a piece of a molecule, some functionality such as an aldehyde group is essential, even if it is hidden behind another part of the molecule, it will be brought forward without much regard to faithfulness of representation.

There is still another anthropological point of contact. In some cultures knowing the true name of an object or a person forms a special bond, even gives power. So it is in chemistry. Knowing the "name" of a compound, which means its structure, gives the chemist tremendous power over the molecule. A range of its properties, its behavior are implied by that structure.

Guy Ourisson, in a perceptive article that deals with many of the same issues we have discussed, identified the chemical structure as an ideogram or pictogram, a symbol that represents an idea or object directly.[7] This point was also made by *R. Etiemble*. He makes the analogy to Chinese characters, and perhaps one could also do so productively to Egyptian hieroglyphs. Like the character, the chemical sign enters the conscience of a chemist directly. All its meanings are attached, and the chemist manipulates that little picture mentally in a multiplicity of ways. The chemical structure implies not only a molecule but its physical, chemical, even biological properties.

Rudolf Hoppe has prefaced one of his review articles with stimulating reflections on the symbolic language of the chemist; his graphics are admirably chosen; they more than hint at the convergence of *la pensée sauvage* and the language of chemistry.[48]

Fig. 8. An illustration from a book by *Tove Jansson* (Tove Jansson: *Moominsummer Madness*, Henry Z. Walck, New York 1955, p. 53). Reproduced with permission of the publishers.

The drawing of chemical structures also has a kinship with caricature and comic strips. If one examines a successful cartoon or schematic book illustration closely one finds that a wide spectrum of emotion—grief, terrible anger, ecstasy—is communicated in just a few strokes of a pen. Think of the Dr. Seuss books, *Jean de Brunhoff*'s Babar, *Hergé*'s Tintin books, *Tove Jansson*'s Moomintrolls (see Fig. 8[49]), or *Walt Disney*'s numerous cartoon characters. And not just for children. *Gombrich* discusses the effect of caricature perceptively, arguing that we "accept the grotesque and simplified partly because its lack of elaboration guarantees the absence of contradictory clues".[50] In examining a work of art we look at the information in it, and unconsciously seek relationships. It's not the absolute flux of light entering our eye from a painted white spot that makes us see it as brightly lit, it is its differentiation from neighboring patches of paint.

The act of viewing is collaborative (between painter and viewer) and forgiving. We always create space, in our minds, when we see a two-dimensional representation. And we elaborate the information, interpolating our experience to fill out what is omitted. At least providing there are no contradictory clues, no signals to tell us that we are wrong. Caricatures or cartoons (or if those are not "serious" enough, take a Goya or Picasso etching) work by providing the appropriate minimal information.

So do chemical structures. The chemist's mind is very tolerant. It will accept both **23** and **24** as representations of an eclipsed ethane. It will read the substituent attached at lower left to the six-membered ring in **25** through **28** as a methyl group. It will fill in the missing three-dimensional background required to make these molecules come to life; it will geometrize the floating world of these little symbols.

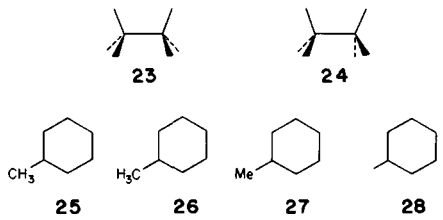

In any case, the drawing does not exist by itself, but is an integral part of the text. It is as if the chemist invented a new language, part text, part the tactile sense that is behind the model-building that is behind the ability of a chemist to reconstruct a molecule in his or her mind from such minimal information. We are pushed back to the logic of language. And in another way, to viewing the combined text–structure complex as an art form.

Note added in proof (July 1990): The reader's attention is directed to two recent contributions: *Stephen T. Weininger*, Worcester Polytechnic Institute, explores in an important, well-documented lecture-essay a semiotic perspective on chemistry.[51] And *Pier-Luigi Luisi* and *Richard M. Thomas*, ETH Zürich, make a number of comments similar to ours (and many original ones) in an article on pictographic communication in chemistry and biology.[52] There is also a beautiful discussion of the language of chemistry in two recently translated essays by *Primo Levi*.[53]

We've benefited much from the critical comments of Kurt Mislow, Hearne Pardee, Noel Carroll, Vivian Torrence, Gilles-Gaston Granger, and Henning Hopf. The assistance of Dennis Underwood, Donald Boyd, and Laura Linke is also gratefully acknowledged, as are the photographs of Stephen R. Singer, the drawings of Jane Jorgensen and Elisabeth Fields, and the typing of Joyce Barrows. A slightly different version of this essay has appeared in Diogène, Paris.

Received: July 21, 1989
supplemented: August 2, 1990 [A 800 IE]
German version: *Angew. Chem. 103* (1991) 1

[1] For a general introduction to molecules we might direct that hypothetical listener to the beautiful book by *P. W. Atkins* (P. W. Atkins: *Molecules*, Scientific American Library, New York 1987).

[2] The story is more complicated. It seems that, if one subjects the harmless form to physiological conditions, it transforms into a mixture of mirror images, one harmful, one not. See *Chem. Br. 25* (1989) 259.

[3] The precise definition of molecular structure is still a subject of debate in chemistry. See, for instance, R. D. Brown, *Chem. Br. 24* (1988) 770; R. G. Woolley, *J. Amer. Chem. Soc. 100* (1978) 1073; and the articles by *Mislow* and *Turro* cited below.

[4] R. Barthes: *L'Empire des Signes*, Skira, Geneva 1980; English: *The Empire of Signs*, Hill and Wang, New York 1982; German: *Das Reich der Zeichen*, Suhrkamp, Frankfurt am Main 1981.

[5] Not really. What we have is a human being guiding a tool, which in turn was programmed by other human beings, not to speak of it being built by still other ones and their tools. I am grateful to *Dennis Underwood* and *Don Boyd* for their help with structures **8**–**11**.

[6] For methodological discussions of how models are used in chemistry see C. J. Suckling: K. E. Suckling, C. W. Suckling, *Chemistry Through Models*, Cambridge Univ. Press, Cambridge 1978; C. Trindle, *Croat. Chim. Acta 57* (1984) 1231; J. Tomasi, *J. Mol. Struct. (Theochem). 179* (1988) 273. And for the different meanings of "model" see the amusing comment by *N. Goodman* in *Languages of Art*, 2nd ed., Hackett, IN, USA, 1976, p. 171.

[7] That there are many ways to look at a molecule's structure is, of course, well known to the chemical community; we are not saying anything new here. See, for instance, G. Ourisson, *Actual. Chim. 1986*, 41.

[8] H. Mizes, S. Park, W. A. Harrison, *Phys. Rev. B 36* (1977) 4491; G. Binnig, H. Fuchs, C. Gerber, H. Rohrer, E. Stoll, E. Tosatti, *Europhys. Lett. 1* (1986) 32.

[9] J. Vouvé, J. Brunet, P. Vidal, J. Marsal: *Lascaux en Périgord Noir*, Pierre Fanlac, Périgeux 1982, p. 31.

[10] For an introduction to *David Hockney*'s neocubist perspective, see D. Hockney: *Cameraworks*, A. A. Knopf, New York 1984; German: D. Hockney: *Cameraworks*, Kindler, Munich 1984.

[11] a) E. H. Gombrich, *Art and Illusion*, 2nd ed., Bollingen Series, Princeton Univ. Press, Princeton 1961, p. 262; German: E. H. Gombrich: *Kunst und Illusion. Zur Psychologie der bildlichen Darstellung*, Belser, Stuttgart 1986. See also the comments of *R. Thom* (R. Thom: *Stabilité Structurelle et Morphogenese*, 2nd ed., Intereditions, Paris 1977; English: *Structural Stability and Morphogenesis*, W. A. Benjamin, Reading 1975) on the inherently geometrical in our minds. b) F. Philostratus, *Life of Apollonius of Tyana*, Book II, Chap. 22, Macmillan, New York 1912, I, 175–179; German: *Appollonius von Tyana*, Artemis, Zürich 1983. We owe this story to *E. H. Gombrich* (*Art and Illustion* (see above) pp. 181–182.

[12] a) A. Lavoisier, *Traité Elementaire de Chimie*, Cuchet, Paris 1789. b) J. Brody, *New Sci. 119* (1987), 24–31 December, p. 19. The originals of many of Mme. *Lavoisier*'s drawings and her annotations on proofs of the etchings are in the collection of the History of Science Library at Cornell University.

[13] A. W. Williamson, *Q. J. Chem. Soc. London 4* (1852) 229.

[14] For a beautifully reasoned "epistemological note on chirality", the propertiy of molecules existing in such nonsuperimposable mirror image forms, see K. Mislow, P. Bickart, *Isr. J. Chem. 15* (1976/1977) 1. An important point in their discussion is the distinction between geometric figures or models (where the notion of chirality is well-defined) and real molecules, where it is fuzzy, depending upon conditions of measurement.

[15] J. H. van't Hoff, *Voorstel tot uitbredning der tegenwoordig...*, J. Greven, Utrecht 1874; English: *The Arrangement of Atoms in Space*, 2nd ed., Longman, Green and Co., London 1898. J. A. Le Bel, *Bull. Soc. Chim. Fr. 22* (1874) 337. *Le Bel* and *van't Hoff* infused their independent and quasi-simultaneous discovery with quite distinct yet complementary world views. Their scientific approaches differed, and, as far as we can appreciate, so did their *themata* (in the sense of *G. Holton*) and their impact on what came after. See on this point, of great interest to philosophers of science: J. Weyer, *Angew. Chem. 86* (1974) 604; *Angew. Chem. Int. Ed. Engl. 13* (1974) 591; F. G. Riddell, M. J. T. Robinson, *Tetrahedron 30* (1974) 2001; R. G. Grossman, *J. Chem. Ed. 66* (1989) 30; S. F. Mason, *Topics Stereochem. 9* (1976) 1; O. B. Ramsay (Ed.), *van't Hoff-Le Bel Centennial*, American Chemical Society, Washington 1975.

[16] N. J. Turro, *Angew. Chem. 98* (1986) 872; *Angew. Chem. Int. Ed. Engl. 25* (1986) 882.

[17] The gift for seeing structures in space with one's eyes, and the cognate imaginative prowess of seeing them with the mind's eye, are important components of creativity for a chemist. And perhaps not only for chemists. For instance, mathematicians still discuss, since *Hadamard*'s pioneering study of mathematical creativity (K. Hadamard, *The Psychology of Invention in the Mathematical Field*, Princeton Univ. Press, Princeton 1945) whether iconic representations are involved in the thought processes of mathematicians (A. Muir, *the Mathematical Intelligencer 10* (1988) 33). If one were to rely on the example of chemists, the answer to this much-debated question would have to be "Yes, of course!".

[18] G. Komppa, *Ber. Dtsch. Chem. Ges. 41* (1908) 4470.

[19] See R. R. Hoffman: "Some Implications of Metaphor for Philosophy and Psychology of Science" in R. Dirven, W. Paprotte (Eds.): *The Ubiquity of Metaphor*, John Benjamin, Amsterdam 1985.

[20] We take the view that such figures of speech as the metaphor, should be seen as cognitive tools, and not as deviations with respect to the prosaic norm. See D. Sperber, D. S. M. Wilson: *Relevance: Communication and Cognition*, Blackwell, Oxford/Harvard Univ. Press, Cambridge, MA, USA, 1986.

[21] J. A. Comenius: *Orbis Sensualium Pictus*, Michael Endter, Nüremberg 1658.

[22] We have not succumbed to the nominalist fallacy! We have elected our Fido example because the view, admittedly restricted and restrictive, of language as nomenclature is precisely that embodied in the language of chemistry. *Saussure*, with his idea of signs as uniting a signifier and a signified, swept off the illusory notion of language as nomenclature for objects. The word "dog" refers, not to a real object, but to an attribute shared by several different entities.

[23] Circular reasoning is not all bad. Elsewhere one of us makes a sort of a case for its utility in real chemistry: R. Hoffmann, *Amer. Sci. 75* (1988) 182.

[24] Though actually some convincing progress has been made in this direction. See R. G. Parr, *Ann. Rev. Phys. Chem. 34* (1983) 631.

[25] J. Culler: *Ferdinand de Saussure* (revised ed.), Cornell Univ. Press, Ithaca, NY, USA, 1986.

[26] *K. Mislow* brought to our attention in this context the story *Feynman* tells of how his father taught him the difference between knowing the name of something and knowing something: R. P. Feyman: *What do You Care What Other People Think?*, W. W. Norton, New York 1988, pp. 13, 14.

[27] P. Ricoeur in D. Ihde (Ed.): *The Conflict of Interpretation*, Northwestern Univ. Press, Evanston, IL, USA 1974.

[28] J.-M. Lehn, *Traduire 116* (1983) 62.

[29] H. W. Whitlock, Jr. in W. T. Wipke, W. J. Howe (Eds.): *Computer-Assisted Organic Synthesis* (ACS Symp. Ser. 61), American Chemical Society, Washington, D.C. 1977, p. 60. We thank *K. Mislow* for reminding us of this work.

[30] N. Chomsky in R. D. Luce, R. R. Bush, E. Galanter (Eds.): *Handbook of Mathematical Psychology, Vol. 2*, Wiley, New York 1963, p. 323; N. Chomsky: *Cartesian Linguistics*, Harper & Row, New York 1966.

[31] See also D. I. Cooke-Fox, G. H. Kirby, J. D. Rayner, *J. Chem. Inf. Comput. Sci. 29* (1989) 101, 106, 112.

[32] J. W. von Goethe: *Die Wahlverwandtschaften*, Insel Taschenbücher, Frankfurt am Main 1972; English: *Elective Affinities*, F. Ungar Publ., New York 1962.

[33] See S. M. Kosslyn, *Science (Washington D.C.) 240* (1988) 1621.

[34] For an illuminating series of articles on biological aspects of aesthetics see I. Rentscher, B. Herzberger, D. Epstein (Eds.): *Beauty and the Brain*, Birkhäuser, Basel 1988.

[35] R. R. Verbrugge, *Ann. N. Y. Acad. Sci. 433* (1984) 167.

[36] We have had the privilege of reading in manuscript a remarkable psychobiography of *R. B. Woodward*, written by his daughter, *Crystal Woodward*. Some of the observations on science, creativity, and art that *Ms. Woodward* makes in her study are similar to ours. One of us (*P.L.*) alludes elsewhere to the relationship, which *C. Woodward* explores in detail, that operates between molecular models and molecules, on one hand, and the "transitional objects" of *D. W. Winnicott*, on the other hand, in a book "La Parole des Choses", to be published.

[37] For a presentation of the marvels of organic synthesis, see N. Anand, J. S. Bindra, S. Ranganathan: *Art in Organic Synthesis*, 2nd ed., Wiley, New York 1988; E. J. Corey, X.-M. Cheng: *The Logic of Chemical Synthesis*, Wiley, New York 1989.

[38] H. Hopf, Universität Braunschweig, private communication.

[39] To get a feeling for the complexity of definitions and the range of opinions in this field, see M. C. Beardsley: *Aesthetics*, 2nd ed., Hackett, IN, USA, 1981.

[40] Related to this section are a series of articles one of us has written on "Molecular Beauty". This is a kind of anthropological study of the objects chemists admit as possessing aesthetic value: R. Hoffmann, *Amer. Sci. 76* (1988) 389, 604; *77* (1989) 177, 330.

[41] N. Goodman: *Languages of Art*, 2nd ed., Hackett, IN, USA, 1976, p. 264.
[42] See, in this context, the article by C. Rose-Innes, *New Sci.*, 7 January 1988, p. 42.
[43] J. Bernstein, R. Hoffmann, *Inorg. Chem. 24* (1985) 4100.
[44] See [41], pp. 229, 230.
[45] This point was made to us by *H. Pardee*, for whose comments on this paper we're grateful.
[46] G. Stent: *Engineering and Science* (California Institute of Technology), September 1985, p. 9; Nobel Symposium, Royal Swedish Academy of Sciences, 1986, private communication.
[47] For an insightful, beautifully presented account of Eskimo ways of seeing and representing, see E. Carpenter: *Eskimo Realities*, Holt, Rinehart and Winston, New York 1973. We're grateful to *Vivian Torrence* for bringing this book to our attention.
[48] R. Hoppe, *Angew. Chem. 92* (1980) 106; *Angew. Chem. Int. Ed. Engl. 19* (1980) 110.
[49] T. Jansson: *Moominsummer Madness*, Henry Z. Walck, New York 1955, p. 53.
[50] E. H. Gombrich: *Art and Illusion* (see [11], Chap. 10; E. Kris, E. H. Gombrich in E. Kris (Ed.): *Psychoanalytic Explorations in Art*, International Univ. Press, New York 1952, Chap. 7.
[51] S. I. Weininger: "Contemplating the Finger: a Semiotic Perspective on Chemistry," Society for Literature and Science, 3rd Annual Conference, 24 September 1989, Univ. of Michigan.
[52] P.-L. Luisi, R. M. Thomas, *Naturwissenschaften 77* (1990) 67.
[53] P. Levi: *Other People's Trades*, Summit Books, New York 1989; Italian: *L'Altrui Mestiere*, Giulo Einaudi Editore, 1985.
[54] R. Hoffmann: *Gaps and Verges*, University of Central Florida Press, Orlando, FL, USA, 1990, p. 55.

Missing issues?

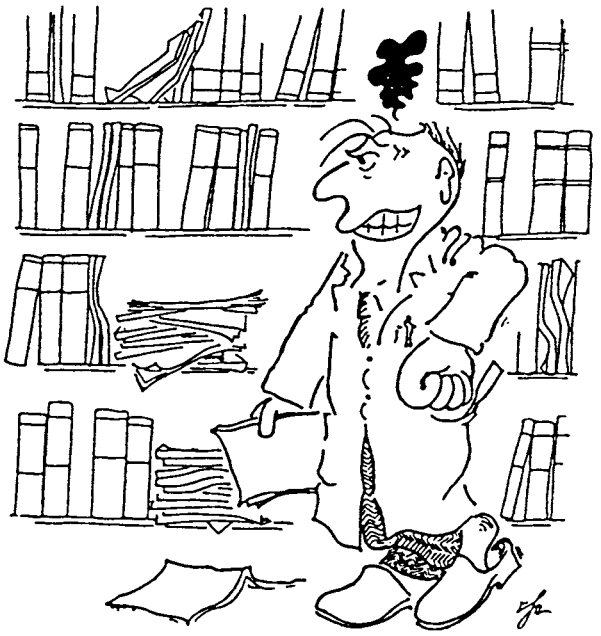

No problem with a personal subscription to „Angewandte Chemie". Your own copy to read when you want, where you want. Subscribe today!

Just phone or fax

VCH

USA: Tel. (800) 422-8824, Fax (305) 428-8201
Rest of the world: Tel. (06201) 602216, Fax (06201) 602328

Structure and Molecular Stacking of Anthocyanins—Flower Color Variation

By Toshio Goto and Tadao Kondo*

In 1913 *Willstätter* made the striking observation that the same pigment can give rise to different colors. Thus, the same pigment, cyanin, is found in the blue cornflower and in the red rose. *Willstätter* attributed the variety of flower colors to different pH values in solution. Indeed, anthocyanin changes its color with pH; it appears red in acidic, violet in neutral, and blue in basic aqueous solution. *Willstätter*'s pH-theory for explaining flower color variation is still to be found in major text books of organic chemistry. Very recently, however, reinvestigation has disclosed that the color variation and stabilization of anthocyanins in aqueous solution could have other causes, namely self-association, copigmentation and intramolecular sandwich-type stacking. The stacking would be mainly brought about by intermolecular or intramolecular hydrophobic interaction between aromatic nuclei such as anthocyanidins, flavones and aromatic acids. In addition, hydrogen bonds and charge transfer interactions may also be involved. The most interesting molecular complexes of anthocyanins are the metalloanthocyanins such as commelinin and protocyanin (blue cornflower pigment). These seemingly pure blue complexes each consist of six anthocyanin and six flavone molecules and two metal ions; their molecular weight is nearly 10000. A structure is proposed for commelinin.

1. Introduction[1-6]

1.1. Controversy about Blue Flower Colors

Beautiful flower colors are in greater part due to anthocyanins. Research into the chemistry of anthocyanins first began around 1913 with investigations by *Willstätter*, who had just finished his famous work on chlorophyll. He determined the structure of cyanin, which had been isolated from the blue cornflower, *Centaurea cyanus*.[7] Within a few years thereafter he had determined the structures of most of the important anthocyanin aglycons, the anthocyanidins, which are responsible for the color of the anthocyanins.

Like litmus, anthocyanin changes its color with changing pH: in strongly acidic medium it appears orange to red in color, whereas in weakly acidic to neutral solutions it appears purple to violet. The blue color can be produced only in alkaline solutions.

Willstätter attributed the variety of flower colors to variation in pH in the flower cell sap. Indeed, he had isolated cyanin[7] from blue cornflower as well as from red rose. *Shibata*,[8] a Japanese botanist, questioned this theory of pH-value for explaining the blue flower color, for it was hardly conceivable that flower cell sap could be alkaline.[9] Instead, he proposed, in 1919,[8] a metal-complex theory, according to which the blue color is produced by complexation of anthocyanins with metal ions such as magnesium ions. As experimental evidence he mentioned, inter alia, the reduction of flavones with magnesium and acid in non-aqueous media, which leads to a blue complex of anthocyanin and magnesium. *Everest*, one of *Willstätter*'s collaborators, strongly opposed this theory without offering any experimental evidence to the contrary. Since then the theory fell into oblivion, until it was resurrected in 1957 by *Hayashi*, a former co-worker of *Shibata*. *Hayashi* isolated[10,11] a blue-colored anthocyanin, commelinin, in crystalline form from deep-blue flower petals of *Commelina communis* (Fig. 1, left) and reported[7] that it consists of two molecules each of an anthocyanin (awobanin **A**), and a flavone (flavocommelin **F**),[12] and one atom each of magnesium[13,14] and potassium. This pigment is so stable that its blue color does not immediatly alter upon changing the pH from 7 to 1. *Hayashi* et al. explained its color and stability in terms of a 1:4 coordination complex of magnesium and flavonoids (**A** + **F**), as shown in Figure 2 (top).[15] He named such a metal complex of anthocyanin metalloanthocyanin. However, *Bayer*[16] opposed this explanation, since, in contrast to iron(III) or aluminum ions, magnesium ions generally do not form stable chelates with anthocyanins.

In 1958, *Bayer*[17] isolated another blue metalloanthocyanin named protocyanin from the blue cornflower *Centaurea cyanus* (Fig. 1, right). He reported that it contained 19.2% cyanin and about 80% of a polysaccharide as well as ferric and aluminum ions (MW ca. 6200). He proposed a structure for it in which the trivalent metal ions coordinatively bind two cyanin molecules and a polygalacturonic acid (Fig. 2, bottom).[16,18] *Hayashi* et al. reported[19] that the protocyanin that they had isolated, yielded, on hydrolysis, cyanin, a flavone, a polysaccharide, and a polypeptide, as well as iron, magnesium, and potassium ions, but not aluminum ions. *Asen* and *Jurd*[20] isolated from blue cornflower a blue pigment, which, according to their analysis, was an iron complex of four molecules of cyanin and three molecules of a flavone glucoside. Since they thought that it differed markedly from protocyanin they named it

[*] Dr. T. Kondo
Chemical Instrument Center, Nagoya University
Chikusa, Nagoya 464 (Japan)
Prof. Dr. T. Goto (deceased)
Faculty of Agriculture, Nagoya University
Chikusa, Nagoya 464 (Japan)

Fig. 1. Left: *Commelina communis* (left: cultivar; right: wild). Middle: Purple flower variant of *Commelina communis*. Right: Cornflower *Centaurea cyanus*.

cyanocentaurin, but *Osawa*[21] later concluded that it was identical with *Hayashi*'s protocyanin.

Commelinin and protocyanin show two surprising properties that distinguish them from other anthocyanin pigments; they are not dialyzable, and, upon electrophoresis at pH 4–6, they migrate to the anode, thus indicating that they are high molecular weight, negatively charged pigments.[22]

In 1931, *Robinson* et al.[23] suggested a "copigmentation effect" of flavones and tannins. The effect produces a bathochromic shift of the visible absorption band of anthocyanins. The copigmentation, however, occurs only in aqueous solutions, is nonstoichiometric, and gives, at most, a bluish-violet and never the pure blue color of commelinin and protocyanin.

1.2. Controversy about the Stabilization of Anthocyanins

Numerous anthocyanins have been isolated from flowers, fruits and leaves, but relatively few anthocyanidins, the, aglycons of anthocyanins, have been found. The main anthocyanidins found in nature are pelargonidin, cyanidin, peonidin, delphinidin, petunidin, and malvidin (Fig. 3). The most widely spread anthocyanins are anthocyanidin 3-glucosides and 3,5-diglucosides.[24] In strongly acidic media (pH below 2.5), anthocyanins form stable flavylium ions, whose color is usually orange or red. When an acidic solution of an anthocyanin is neutralized to pH 4 to 6, the violet anhydrobase is formed first, but it decolorizes rapidly to form a pseudobase by hydration (Fig. 4).[4, 25–29] Since

Toshio Goto was born in Gifu (Japan) in 1929. He graduated from Nagoya University in 1952 and became a member of the staff in the Department of Chemistry of the University in 1954. From 1957 through 1959 he worked with professor L. F. Fieser in the Department of Chemistry at Harvard University. He received his Ph.D. from Nagoya University in 1960 and was promoted to Associate Professor in 1961. In 1966 he transferred to the Department of Agricultural Chemistry as a Professor of Organic Chemistry. His main research interests included the determination of the structure of and total synthesis of biologically active or functionally interesting natural products such as marine toxins, nucleosides, and gangliosides, and the chemistry of bioluminescence and flower color variation. In August 1990 Professor Goto suffered a fatal heart attack.

Tadao Kondo was born in Nagoya (Japan) in 1941. He graduated from Gifu Pharmaceutical College in 1965 and continued his studies in the Department of Agricultural Chemistry of the University of Nagoya. After obtaining his M.Sc. and joining the teaching staff of the Department in 1969, he finally gained his Ph.D. in 1973. He then joined Professor R. U. Lemieux's group and worked as a post-doc in the Department of Chemistry at the University of Alberta, Canada, in the period 1973–1975. In 1979 he moved to the Chemical Instrument Center, Nagoya University, as a Research Associate. His major research fields are the synthesis of nucleosides and gangliosides, and the chemistry of flower color variation.

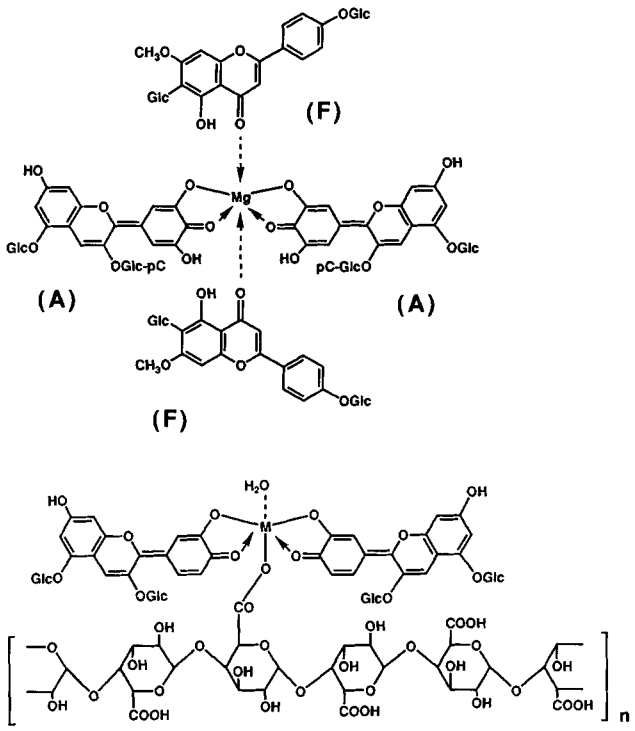

Fig. 2. Top: Structure of commelinin proposed by *Hayashi* et al. [15] (1970). A: awobanin 5; F: flavocommelin 3. Bottom: structure of protocyanin proposed by *Bayer* et al. [16] (1966). pC = *p*-hydroxycinnamoyl.

flower cell sap is usually weakly acidic, anthocyanins cannot be stable in the cell sap if there is no additional stabilizing effect.

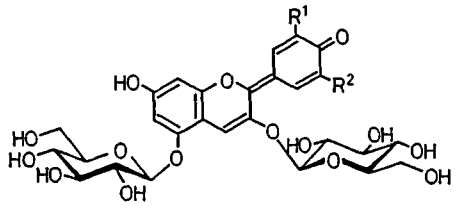

R^1	R^2	Anthocyanin	Aglycon
H	H	pelargonin	pelargonidin
OH	H	cyanin	cyanidin
OCH_3	H	peonin	peonidin
OH	OH	delphin	delphinidin
OCH_3	H	petunin	petunidin
OCH_3	OCH_3	malvin	malvidin

Fig. 3. Structure of common anthocyanins.

The copigmentation has some stabilizing effect as well as a bathochromic effect on anthocyanins. Polyphenols such as flavones and tannins have copigmentation effects, which have long been attributed to hydrogen bonding between the host compound and the copigment used.[30-32]

Another stabilizing mechanism was suggested by *Asen* et al.[30] in 1972: the self-association of anthocyanins. It was based on the observation that, at pH 3.16, the absorbance of cyanidin 3,5-diglucoside at λ_{max} increased 300 times when the concentration was increased from 10^{-4} M to 10^{-2} M (100 times), suggesting a self-association of the anthocyanin in the form of the flavylium ions.[6] Similarly, the shape of the visible absorption spectrum changed when a solution of a delphinidin derivative at pH 6.6 was diluted from 8×10^{-3} M to 8×10^{-5} M; the absorbance ratio $A_{624\ nm}/A_{540\ nm}$ changed from 0.58 to 1.10, i.e. the solution became intense blue.[33]

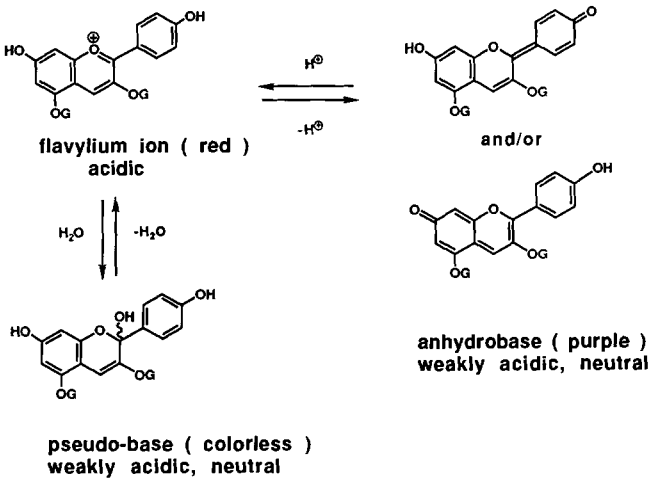

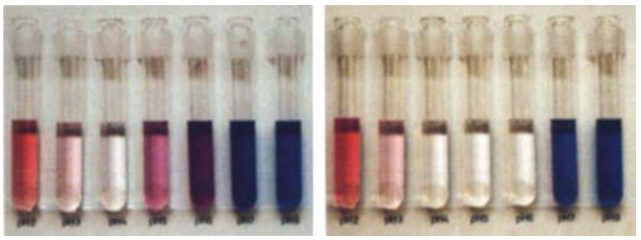

Fig. 4. Top: Change in structure of an anthocyanin in aqueous solution as a function of pH (G = sugar residue). Bottom left: Malvin in water (5×10^{-5} M) at several pH values; just after dissolving. Bottom right: Malvin in water (5×10^{-5} M) at several pH values; 2 hours after dissolving.

Raising the temperature produced a similar change. This suggested that dilution or heating caused dissociation of associated anthocyanins. Indeed, the concentration of anthocyanins in vivo reaches as high as 2.4×10^{-2} M.[34, 35]

1.3. Controversy about Horizontal Stacking (Hydrogen Bonding) and Vertical Stacking (Hydrophobic Interaction)

Numerous workers have considered self-association and copigmentation as being very likely; however, the association has in greater part been attributed to hydrogen bonding between hydroxy and carbonyl groups on the aromatic nuclei and sugar moieties to form horizontally stacked molecules.[30, 32, 36]

On studying the molecular assembly of commelinin, the blue pigment obtained from *Commelina communis*, we already alluded, as long ago as 1976,[37, 38] to a vertical stacking of anthocyanin and flavone molecules by hydrophobic interaction between the aromatic nuclei, a stacking which is further stabilized by superimposed hydrophilic sugar moieties. This concept was supported by *Sweeny* et al.[39] Then, convincing evidence was obtained for a vertical self-

association of anthocyanin anhydrobases in neutral solution by means of circular dichroism and ^{1}H-NMR spectroscopic measurements (Section 2). Copigmentation phenomena such as the association between anthocyanin and flavone were analyzed similarly (Section 4). Flavone itself was also found to self-stack vertically (Section 3). Although intermolecular associations such as self-association and copigmentation are destroyed by dilution, very stable anthocyanins have been found recently in dilute neutral aqueous solutions. All of these stable anthocyanins contain two or more aromatic acyl moieties in a molecule. We and *Brouillard* proposed a sandwich-type vertical stacking of an anthocyanidin nucleus and two aromatic acyl moieties, and have reported some experimental evidence supporting this mechanism (Section 7).

Metalloanthocyanins such as commelinin and protocyanin have proven to be very complicated molecules. We have shown that they consist of six molecules each of anthocyanin and flavone with two metal ions; their molecular weight is nearly 10000. Unlike in the case of copigmentation their molecular assembly is stoichiometric. We attribute this arrangement in the metalloanthocyanins to self-association and copigmentation as well as to the complexation of metal ions (Section 5).

Thus, the stability and color variation of anthocyanins in aqueous solutions is mainly due to vertical, hydrophobic stacking (and/or charge transfer interaction) of aromatic nuclei in flavonoids and aromatic acids. The stacking may be further assisted by hydrogen bonding in the hydrophilic sugar moieties superposed on the stacks.

2. Self-Association of Anthocyanins

Although some indications of a self-association of flavylium ions in acidic solutions had been reported before, it was *Hoshino, Matsumoto*, and *Goto* who were first able to demonstrate the self-association of anthocyanin anhydrobases in neutral solution, by means of circular dichroism[40-42] and ^{1}H-NMR measurements.[43] Thus, the CD curves of typical anthocyanidin 3,5-diglucosides were found to show a large negative exciton-type Cotton effect in the visible absorption band region when the anthocyanins (in the form of their flavylium chlorides) are dissolved in a neutral buffer (pH 7.0) in fairly high concentration (Fig. 5, top). At least two anthocyanidin chromophores must stack vertically in a left-handed screw axis to cause this type of split bands. This finding is supported by theoretical calculations using the method of CD exciton-type chirality.[44] The magnitudes of $[\theta]$ are strongly intensified when the concentration is increased, indicating enhanced formation of stacked molecules in the more concentrated solutions.

Shifting of the visible spectra towards shorter wavelengths due to formation of the chiral aggregates is also observed at pH 7.0. The self-association of the delphin anhydrobase produces a remarkable hypsochromic shift in the visible spectrum (Fig. 5, top) as well as a large Cotton effect.[42] This indicates that the stability and color variation of these anthocyanins in flower petals are derived at least in part from self-association. The vertical stacking was also supported by ^{1}H-NMR spectral analyses.[43] The hypsochromic shift of malvin in aqueous solution is not only due to simple self-association. At pH 7.0 the anhydrobase and its anion are in equilibrium, and self-association suppresses ionization of the anhydrobase, thus giving rise to a hypsochromic shift.[45]

Cyanin and pelargonin behave abnormally.[46] The negative exciton-type Cotton curve formed at first gradually transforms into a large positive exciton-type Cotton curve with an unsymmetrical shape (Fig. 5, bottom). It was concluded therefrom that these anthocyanins gradually form a suspension of insoluble particles, which are responsible for the curve. Since these anhydrobases are sparingly soluble in water, highly aggregated particles are expected to be formed. In some flowers, pigment crystals were detected in the cell sap.[33,47-49] An X-ray structure analysis showed that pelargonidin bromide stacks vertically.[50]

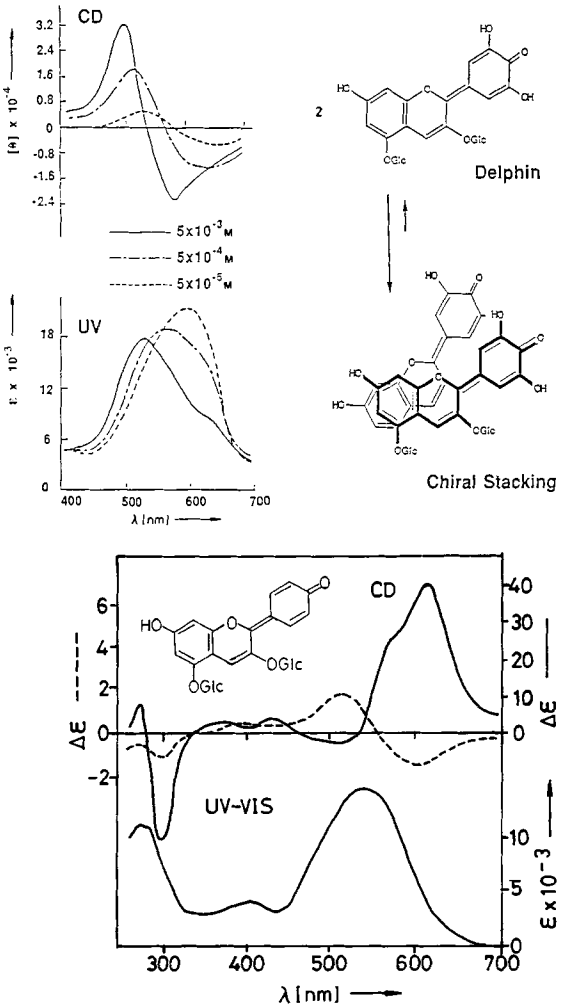

Fig. 5. Top: Dependence of CD and electronic spectra of delphin on concentration in water at pH 7.0. Bottom: UV/VIS and CD spectra of pelargonin (7×10^{-4} M) in 0.05 M phosphate buffer at pH 7.27. CD spectra: --- 2 min after dissolving; — insoluble particles formed by aging. Electronic spectrum: — 2 min after dissolving.

3. Self-Association of Flavones[51]

In aqueous solution, both the CD spectra and the UV spectra of the flavone flavocommelin depend on its concen-

tration (Figure 6, top). When the concentration increases to 5×10^{-3} M, fairly large exciton-type Cotton curves are observed, indicating that the flavone molecules are chirally self-associated in aqueous solutions at high concentrations. Such a stacking can also be supported by the decreasing absorbance in the UV spectrum and from the temperature dependence of CD and UV spectra. In contrast in DMSO solutions, no Cotton effect on the CD and no change in the

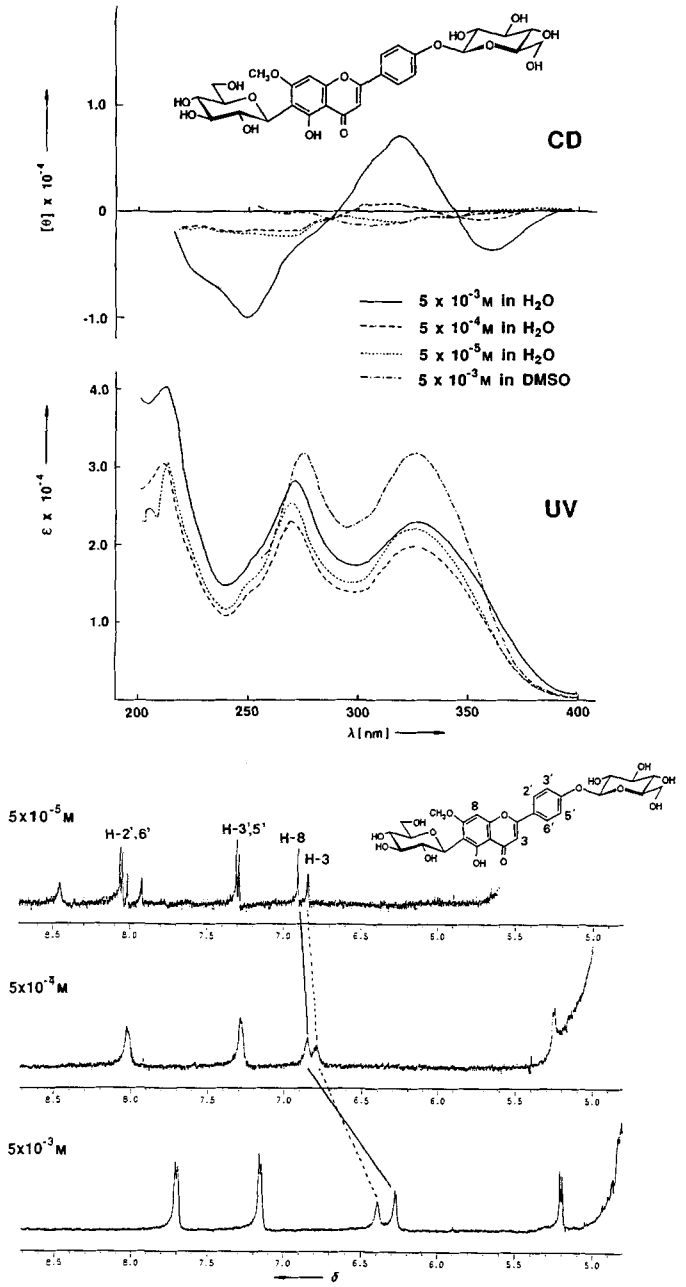

Fig. 6. Top: CD and UV spectra of flavocommelin **3** in water at pH 5.7 and in DMSO. Bottom: Concentration dependence on the ^{1}H-NMR signals of flavocommelin in D_2O at 30 °C.

UV spectra are observed at concentrations as high as 5×10^{-3} M. The NMR spectra also support assumption of such a stacking. The signals corresponding to the ring protons are all shifted toward higher fields when the concentration of the solution is increased (Fig. 6, bottom), whereas very little change is observed in the signal of the anomeric protons at $\delta = 0.04$, indicating that the aromatic rings are stacked vertically, so that the aromatic ring protons of a molecule are shielded by the aromatic rings of other molecules.

4. Copigmentation of Flavones with Anthocyanins

Since *Robinson* and *Robinson*[23] discovered the copigmentation effect in 1931 there have been many papers[6, 21, 27, 30, 33–35, 44, 52–62] reporting this phenomena between anthocyanin and flavone or other polyphenols. The copigmentation[21] depends on the type and concentration of the anthocyanin, on the type and concentration of the flavone, and on the pH and temperature of the solution. Anthocyanins which contain an aromatic acyl group form a much stabler copigmentation complex with flavones[53, 63] than unacylated anthocyanins, but anthocyanins having two or more aromatic acyl groups are stabilized by intramolecular sandwich-type stacking (Section 7) rather than by copigmentation. A copigmentation is possible both with the flavylium ion as well as the anhydrobase. It proceeds non-stoichiometrically only in solution, giving at best a bluish-purple color, and never producing a pure blue color.[44] Copigmentation not only causes a bathochromic shift of the visible absorption maximum of anthocyanin but also results in a large increase in absorptivity (stabilization) (Fig. 7, top).

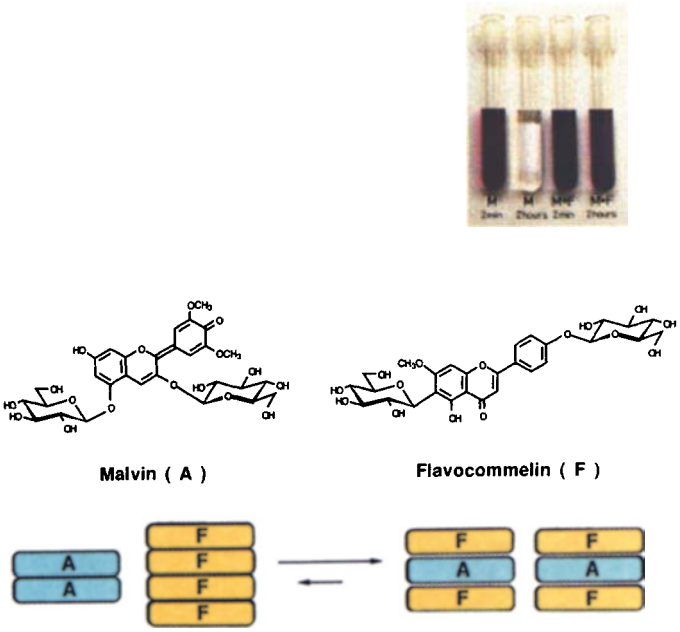

Fig. 7. Top: Copigmentation of flavocommelin and malvin in water at pH 6.0 (malvin: 5×10^{-5} M; flavocommelin: 5×10^{-4} M). Bottom: Copigmentation effect of flavocommelin on malvin.

The copigmentation effect had long been explained in terms of hydrogen bonding between the host compound and the copigment used to produce horizontal stacking.[30–32, 36] We proposed[37, 38, 64] that copigmentation in aqueous solution arises from hydrophobic stacking between the aromatic nuclei of anthocyanin and flavone (vertical

stacking; charge transfer interaction[65] could also play a role) (Fig. 7, bottom). This hydrophobic stacking could be further stabilized by the hydrophilic sugar moieties covering them (hydrogen bonding). As an example, the mechanism of color development in the purple flower of *Commelina communis* is described.[66]

The purple flowering variant of *Commelina communis* (Fig. 1, middle) differs from the common blue flower (see Section 5).[67] The fact that also flowers with multicolored petals, e.g. half blue and half purple have been found, would indicate that a close relationship must exist between the blue and the purple pigments. Two anthocyanins, **1** and **2**, as well as flavocommelin **3** are found in the purple petals, whereas the blue petals contain malonylawobanin **4** and flavocommelin **3**.

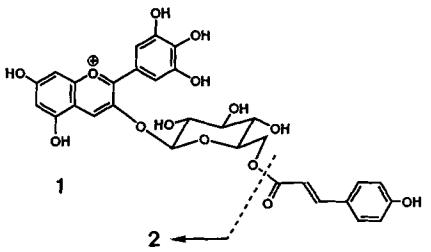

3-*O*-[6-*O*-(*p*-hydroxycinnamoyl)-β-D-glucopyranosyl]delphinidin (**1**) and 3-*O*-(β-D-glucopyranosyl)delphinidin (**2**) from the purple flower of *Commelina communis*.

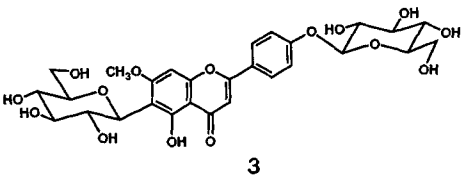

Flavocommelin (**3**) from *Commelina communis*.

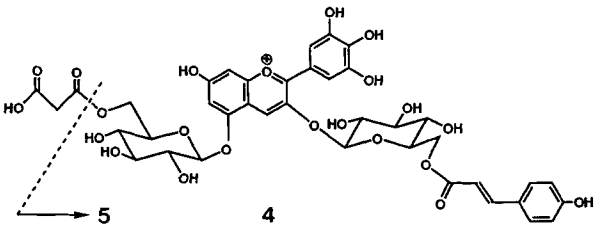

Malonylawobanin **4** and awobanin **5** from the blue flower of *Commelina communis*.

Press juice from the purple petals has an absorption maximum in the visible range at 580 nm, while, at the same pH (pH 5.8) the absorption maxima of the anthocyanins **1** and **2** appear at 530 and 540 nm, respectively, suggesting copigmentation with the flavone, flavocommelin. The addition of three equivalents of flavocommelin **3** shifts the absorption maximum of **1** and **2**, about 30 and 40 nm to a longer wave lengths, respectively. The intensities of the absorptions are also increased considerably in the presence of the flavone, whereas Cotton effects in the CD spectrum of the anthocyanins are decreased. The visible spectrum of the press juice of purple petals coincides well with that of a mixture containing the anthocyanins, **1** and **2**, and the flavocommelin **3** (Fig. 8), thus indicating that the purple color of the

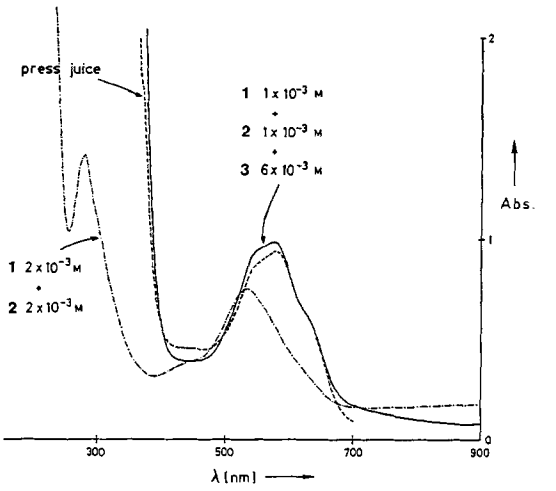

Fig. 8. Copigmentation effect of flavocommelin **3** on the anthocyanins **1** and **2**, to reproduce the in vivo purple color of *Commelina communis* variant. ---: press juice from purple petals, pH 5.8; -·-·-: **1** and **2** in 0.02 M acetate buffer, pH 5.8; ——: **1**, **2**, and **3** in 0.02 M acetate buffer, pH 5.8.

petals is produced by copigmentation of anthocyanins **1** and **2** and flavocommelin **3**. The disappearance of the Cotton effect in the visible region suggests a sandwich-type vertical stacking by hydrophobic interaction. A charge transfer interaction between the anthocyanin and the flavone could contribute to the bathochromic effect.

5. Metalloanthocyanins: Commelinin and Protocyanin[44]

5.1. Structure of Components

Up to now only two metalloanthocyanins have been isolated: commelinin and protocyanin. The pigment of the *Hydrangea* might also belong to this group.[59, 60]

Since commelinin moves towards the anode upon electrophoresis,[22, 68] it must have a negative charge. This was very difficult to explain, since neither awobanin (**A**) **5** nor flavocommelin (**F**) **3** has a negative charge, nor does the magnesium ion. The problem was finally solved, however, when it was discovered that the true anthocyanin present in the flower is malonylawobanin (**M**) **4**,[69, 70] which contains a malonic acid residue. Hence, awobanin (**A**) **5** is an artifact produced during extraction.

Willstätter et al. isolated cyanin **7** from cornflower petals.[7] It was believed to be the anthocyanin component of the blue pigment, protocyanin; however, we[71] and *Takeda*[72] found that the true anthocyanin is succinylcyanin **6**, which, similarly to malonylawobanin **4**, also contains a carboxy group. In 1974, *Asen* et al.[73] isolated a flavone from cornflower petals, and they established its structure as apigenin-4′-*O*-glucoside-7-*O*-glucuronide **9**, but it was also found to be an artifact. The true flavone **8** proved to have an additional malonic acid residue in the molecule.[72] Pink flowers of *C. cyanus* contain succinylpelargonin **10**,[74] while crimson flowers of the same species contain malonylcyanin **11** and succinylcyanin **6**[75] (Fig. 1, right).

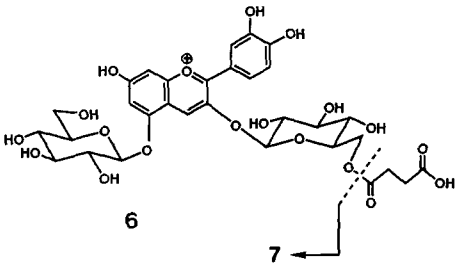

Succinylcyanin **6** and cyanin **7** from the blue flower of *Centaurea cyanus*.

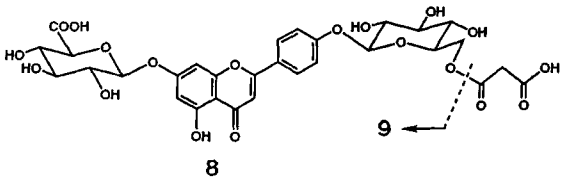

The malonylflavone **8** and *Asen*'s flavone **9** from *Centaurea cyanus*.

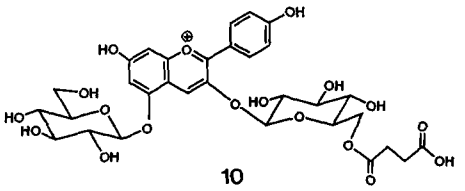

Succinylpelargonin **10** from the pink flower of *Centaurea cyanus*.

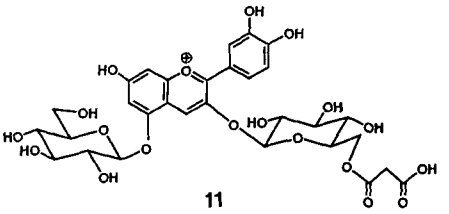

Malonylcyanin **11** from the crimson flower of *Centaurea cyanus*.

5.2. Molecular Composition of the Metalloanthocyanins

Hayashi and *Takeda*[15] reported that commelinin consists of two molecules each of awobanin (**A**) **5** and flavocommelin (**F**) **3**, and one atom each of magnesium[76] and potassium; high molecular components such as polysaccharides and polypeptides could not be detected. These authors proposed a coordinated complex of magnesium and four flavonoid molecules (Fig. 2, top). Later, we[69] found that the actual anthocyanin involved is malonylawobanin (**M**) **4**.

On electrophoresis an aged commelinin sample mysteriously gave several blue spots (Fig. 9, right).[22,69] We found that commelinin obtained from fresh petals and that synthesized from **M**, **F** and magnesium ions produced only the spot that moved fastest, and that pigments prepared from **M**, **A**, **F**, and magnesium ions produced seven blue spots at the same intervals (Fig. 9, left). Commelinin synthesized from **A**, **F**, and magnesium ions gave only the spot that moved the slowest. This finding indicated that commelinin must contain six molecules each of **M** and **F** per molecule (MW about 9500).[77] The molecular weight determined by analytical ultracentrifugation was around 10 000.

Bayer et al.[16] and *Hayashi* et al.[19] independently described protocyanin as a complex of cyanin, a flavone, polysaccharides and/or polypeptides, and metal ions such as Fe and Al (*Bayer*), or Fe and Mg (*Hayashi*). *Bayer* proposed a structure containing polygalacturonic acid (Fig. 2, bottom), in which two anthocyanins and the polysaccharide chelate a metal ion.

We[44] obtained natural protocyanin free of macromolecular substances. It consisted of succinylcyanin **6**, the malonylflavone **8**, and Fe and Mg ions. A pigment reconstructed from the above components was identical with the natural pigment and contained about six molecules each of succinylcyanin **6** and the malonylflavone **8**, and one atom each of Fe and Mg; thus the composition is very similar to that of commelinin, suggesting a similar overall structure.

5.3. Evidence of Flavonoid Stacking in Commelinin

In commelinin, malonylawobanin molecules self-associate chirally, as is evident from the large exciton-type Cotton effect in the visible absorption band (Fig. 10, top).[44] Stacking between the anthocyanidin and flavone nuclei was apparent from ^{1}H-NMR spectrum of commelinin (Fig. 10, middle), in which some nuclear Overhauser effects were observed between protons of the anthocyanidin and the flavone, suggesting the crossing arrangement of **M** and **F** as shown in Fig. 10 (bottom).[78] The ^{1}H-NMR spectrum (Fig. 10, middle) reveals that six molecules each of **M** and **F** reside in the same environment, thus suggesting a cyclic arrangement such as cyclo(-**MMFFMMFFMMFF**-) of the twelve flavonoids. Strong evidence of vertical stacking of

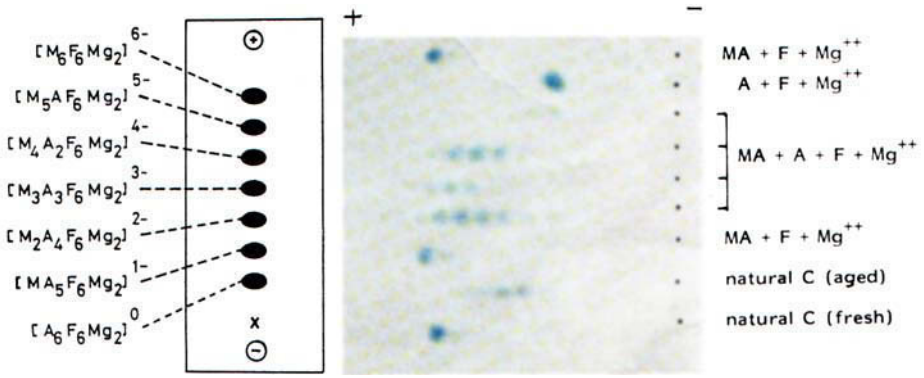

Fig. 9. Left: Schematic representation of the electrophoresis of commelinin and commelinin-like pigments. Right: Electrophoresis of natural and synthetic commelinin and commelinin-like pigments. Conditions: cellulose acetate sheet, 0.02 M acetate buffer at pH 5.7. M = malonylawobanin **4**; F = flavocommelin **3**; A = awobanin **5**; C = commelin (ageing: one year at room temperature).

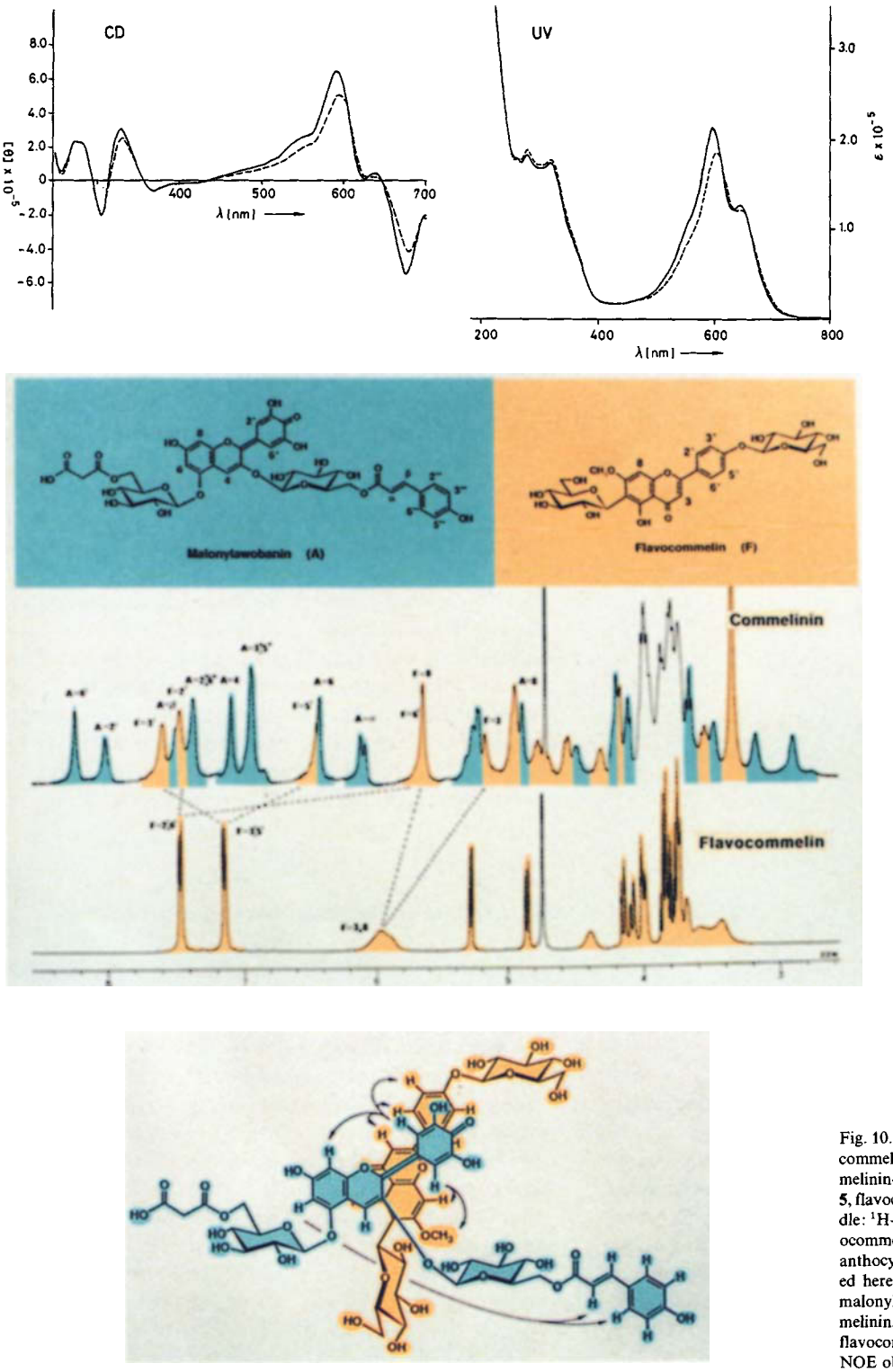

Fig. 10. Top: CD and UV/VIS spectra of commelinin. —— commelinin; --- commelinin-like pigment obtained from awobanin **5**, flavocommelin **3**, and magnesium ion. Middle: ^{1}H-NMR spectra of commelinin and flavocommelin in D_2O. (By way of exception the anthocyanidin malonylawobanin is abbreviated here as **A**.) Bottom: Stacking pattern of malonylawobanin and flavocommelin in commelinin. Blue: malonylawobanin **4**; yellow: flavocommelin **3** (arrows indicate negative NOE observed between protons of **4** and **3**).

flavocommelin with other aromatic nuclei is obtained from the large high-field shifts of the aromatic proton signals of flavocommelin in commelin (Fig. 10, bottom).[78]

5.4. Gross Structure of Commelinin

It is well known that anthocyanins having *o*-dihydroxy groups on the B-ring form a blue chelate complex with trivalent metal ions such as iron(III) and aluminum(III); in contrast, divalent magnesium is not capable of forming such a complex.[16] *Hayshi* and *Takeda*[15] proposed, a priori, a structure for commelinin (Fig. 2, top) in which magnesium ion chelates with the *o*-dihydroxy group in the B-ring of awobanin (**A**) **5**. In order to establish the essential binding sites for the magnesium ions, we have examined whether commelinin-like pigment can be produced from modified components (Fig. 11, top left). Neither the malonyl and *p*-hydroxycinnamoyl groups of malonylawobanin (**M**) **4** nor the hydroxy group on C-5 of flavocommelin (**F**) **3** are essen-

tial. Since at least the *o*-dihydroxy group in the B-ring is necessary in order to obtain a similar type of complex, it could be that the metal ion chelates to this position.[44]

Crystals of commelinin[15] and the cadmium analogues of commelinin[13] have been prepared by *Hayashi* and *Takeda*, and subjected to X-ray crystallographic analyses by *Y. Saito* et al.[79] A complete structural analysis could not be accomplished, but the following crystal data were obtained: trigonal, space group $P321$, $a = 31.251$ Å, $c = 33.675$ Å, $Z = 12(?)$ (**AF** as one unit), $V = 28.529$ Å^3. This crystal has a threefold symmetry axis; the commelinin molecule must therefore have a three-fold symmetry.

6. Structure of Polyacylated Anthocyanins

6.1. General

Although numerous natural anthocyanins have been reported, little is yet known about their structures, since the structure determinations have thus far mainly been carried out by hydrolysis or oxidative degradation to fragments. Thus, as little is known about the configuration at the anomeric center and ring size of the sugar moieties as about the binding sites of the acyl groups in anthocyanins and the configuration of the double bond in the case of the cinnamic

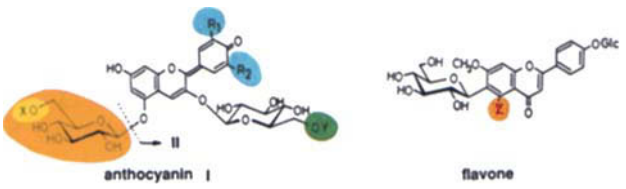

		R^1	R^2	X [a]	Y [b]		Z	Complexation
4	I	OH	OH	Mal	pC	3	OH	yes (commelinin)
5	I	OH	OH	H	pC	3	OH	yes
	I	OH	H	Mal	pC	3	OH	yes
	I	H	H	Mal	pC	3	OH	no
4	I	OH	OH	Mal	pC		OCH_3	yes
	I	OH	H	H	Suc	3	OH	yes
	II	OH	OH	–	pC	3	OH	no
	II	OH	OH	–	H	3	OH	no

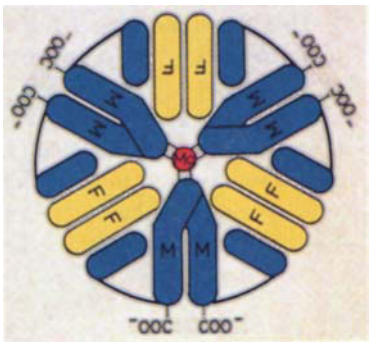

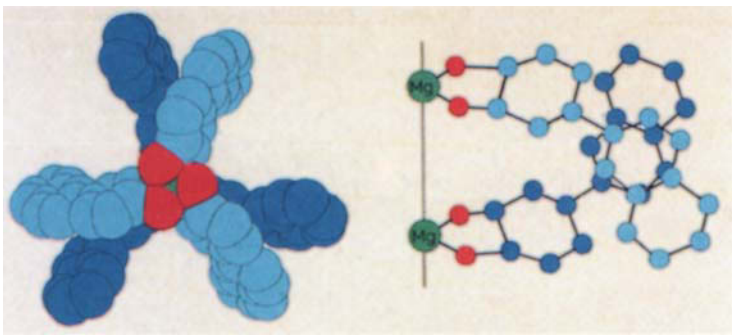

Fig. 11. Top left: Formation of commelinin-like complexes in presence of magnesium ion. Top right: A proposed gross structure of commelinin (another magnesium ion is under the magnesium ion shown, and two magnesium ions have an octahedral structure). **M**: malonylawobanin **4**; **F**: flavocommelin **3**. Bottom: Arrangement of six anthocyanidin skeletal frameworks, in the commelinin molecule. Left: View along the *c*-axis; right: view perpendicular to the c-axis. Based on a rough analysis of the X-ray crystallographic data.

Considering these crystal data and the above-mentioned findings, we proposed the structure shown in Figure 11 (top right) for commelinin.[1,44] The composition $[M_6F_6Mg_2]^{6\ominus}$ can be fulfilled by placing three M_2F_2 units around the *c*-axis and two magnesium atoms at the center. Two copigmented **MF** units are stacked chirally by hydrophobic interaction between the two anthocyanin molecules to form the **FMMF** unit; an intense exciton type Cotton band indicates chiral stacking of the two anthocyanins. Three **FMMF** units are doubly linked by chelation with two magnesium ions. A more detailed stacking form of the anthocyanidin nuclei is proposed in Figure 11 (bottom left and right), which we assumed from a very crude analysis[1] of the X-ray data recorded by *Y. Saito* et al.[79]

acid derivatives. ^{1}H-NMR and mass spectrometric analyses would seem most promising for elucidation of the structures of complex natural anthocyanins, but such investigations were not reported until 1978, when we first published the ^{1}H-NMR spectra of acylated anthocyanins.[70,80,81] The difficulty in obtaining analyzable NMR spectra may lie in the conventional purification method for anthocyanins.

Accurate molecular weight determination by mass spectrometry is also important for the elucidation of the structure of complex anthocyanins, since small components that show no NMR signals might be overlooked if the molecular weight is not known. Anthocyanin-flavylium salts are, however, highly polar compounds and do not readily give a molecular ion in their EI mass spectra. The molecular weight

(1113) of gentiodelphin was first determined by field desorption (FD) mass spectrometry in 1982.[82] Fast atom bombardment (FAB) mass spectrometry was then found best for observing the molecular ion, as reported by *N. Saito* et al.[83] and us[84] in the case of platyconin **13** (*m/z* 1421). Mass spectrometry enabled discovery of the presence of malonic acid in the anthocyanin **4** from *Commelina communis*.[69] The methylene protons in the malonic acid moiety are easily exchangeable with deuterium in acidic deuterium oxide or deuteriomethanol; hence the malonic acid moiety is difficult to detect by means of ^{1}H-NMR spectroscopy.[85]

In the conventional extraction method using methanolic hydrochloric acid the malonyl group in the anthocyanins is very likely to hydrolyze.[86] The finding of malonylawobanin **4** and succinylcyanin **6** discussed in Section 5.1 stimulated a reinvestigation of the structures of the natural anthocyanins that have so far been reported. *Harborne* reinvestigated natural anthocyanins by electrophoresis, since malonated anthocyanins exist as zwitterions at around pH 4.4. He and *Boardley*[87] (see also Ref. [88]) examined flowers of 81 species belonging to 27 plant families and found that zwitterionic anthocyanins occur in half of the samples; in particular, almost all species in the Compositae and the Labiatae gave a positive test. *Takeda* et al.[89] detected some dimalonated anthocyanins from Compositae by means of FAB mass spectrometry. Thus, zwitterionic anthocyanins widely occur in nature. Natural polyacylated anthocyanins, whose structure and stereochemistry have mainly been determined by us, are presented in the following sections.

6.2. Anthocyanins Polyacylated with Cinnamic Acid Derivatives

Cinnamic acid derivatives such as *p*-coumaric acid (4-hydroxycinnamic acid), caffeic acid (3,4-dihydroxycinnamic acid) and ferulic acid (4-hydroxy-3-methoxycinnamic acid) are very common in polyacylated anthocyanins. We have determined the complete structure of several such complex pigments as shown below.

Gentiodelphin **12**[82] obtained from *Gentiana makinoi* (Fig. 12, left) has two caffeylglucoside groups at the C-5 and C-3′ positions, while platyconin **13**[84] (for isolation, see Ref. [90, 91]) obtained from the Chinese bellflower *Platycodon grandiflorum* (Fig. 12, middle) has a long chain glucosylcaffeylglucosylcaffeylglucoside at the 7-position, which is a rare position to be glycosylated. Cinerarin **14**[92] (for isolation see Refs. [93–95]), obtained from the garden cineraria *Senecio cruentus* (Fig. 12, right), has a more complicated structure of this type; it has three caffeylglucosyl units in addition to a malonylglucosyl moiety at C-3. Heavenly blue anthocyanin (HBA) **15**, isolated[96,97] from blue flowers of a morning glory *Ipomoea tricolor* (Fig. 13, left), has a branched chain containing three glucosylcaffeic acid moieties at C-3; two moieties have a glucose unit in the *m*-position of the caffeic acid and one on the *p*-position.[98–101] The anthocyanins **16–18**, each with two cinnamic acid derivatives, have been found in the red cabbage, *Brassica oleracea*.[102,103] (see also Ref. [104]). Interestingly, one of the acids is attached at the 2-position of a glucose unit instead of

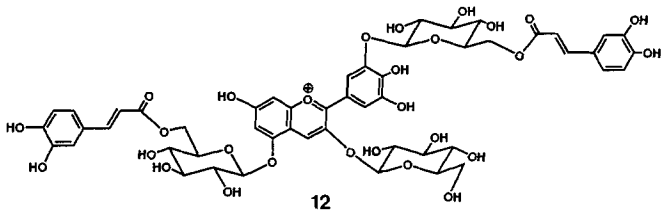

12

Gentiodelphin **12** from *Gentiana makinoi*.

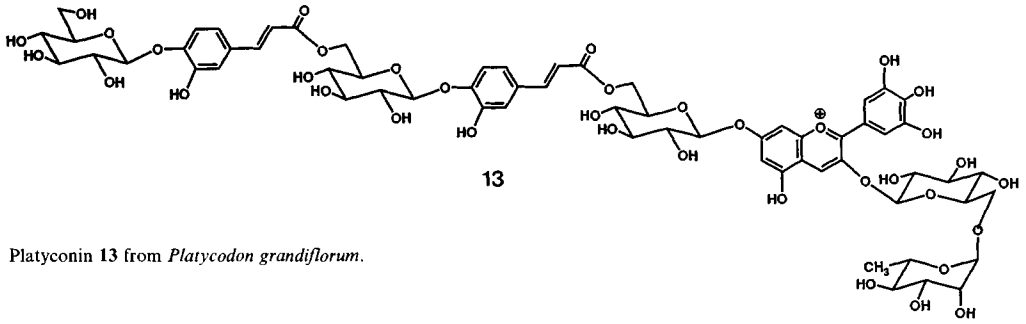

13

Platyconin **13** from *Platycodon grandiflorum*.

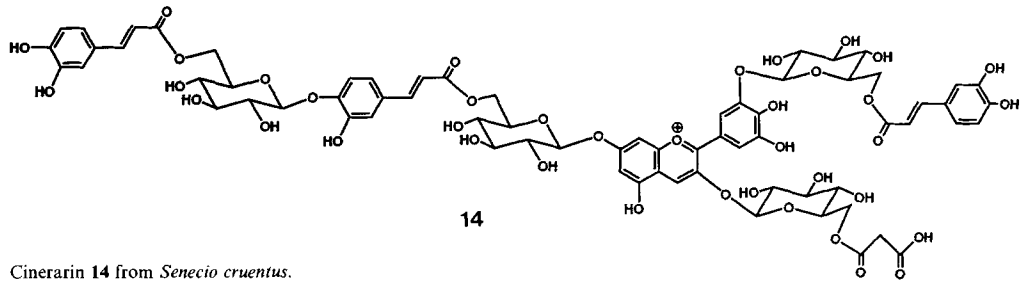

14

Cinerarin **14** from *Senecio cruentus*.

Fig. 12. Left: Autumn bellflower *Gentiana makinoi*. Middle: Chinese bellflower *Platycodon grandiflorum*. Right: Cineraria *Senecio cruentus*.

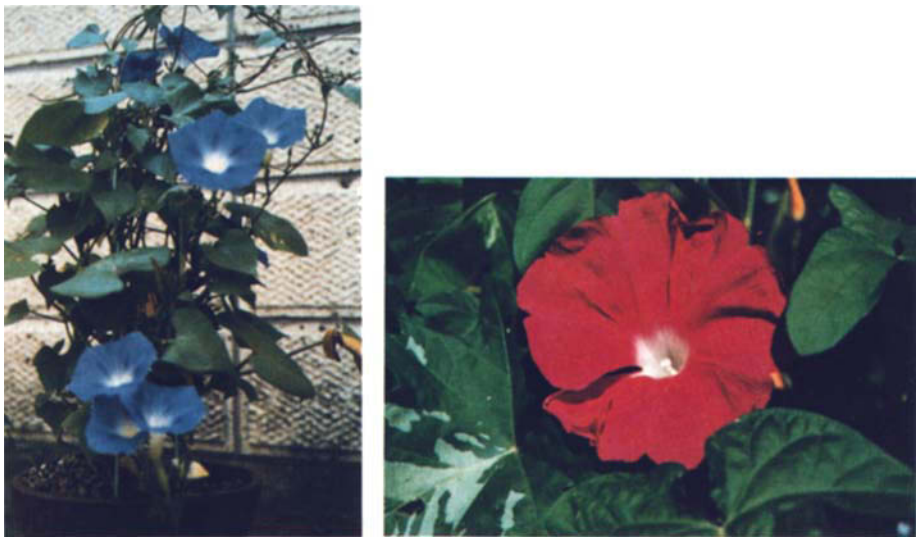

Fig. 13. Left: Morning glory *Ipomoea tricolor* 'Heavenly Blue'. Right: Morning glory *Iponoea nil* 'Scarlet O'Hara'.

the usual 6-position, and anthocyanins containing one of three different acids—*p*-coumaric, ferulic, and sinapic acid—coexist.

Zebrinin **19**,[105] obtained from *Zebrina pendula* (Fig. 14, left), has four caffeyl groups; two groups are bound to an arabinose unit. It is interesting that lobelinin B **21**[106] (for isolation, see Ref. [107]) from *Lobelia erinus* (Fig. 14, right) has four different acyl glucosides on the cyanidin: *p*-coumaric, caffeic, ferulic, and malonic acids are bound to different sugar moieties (cf. lobelinin A **20**)! Recently, similar type

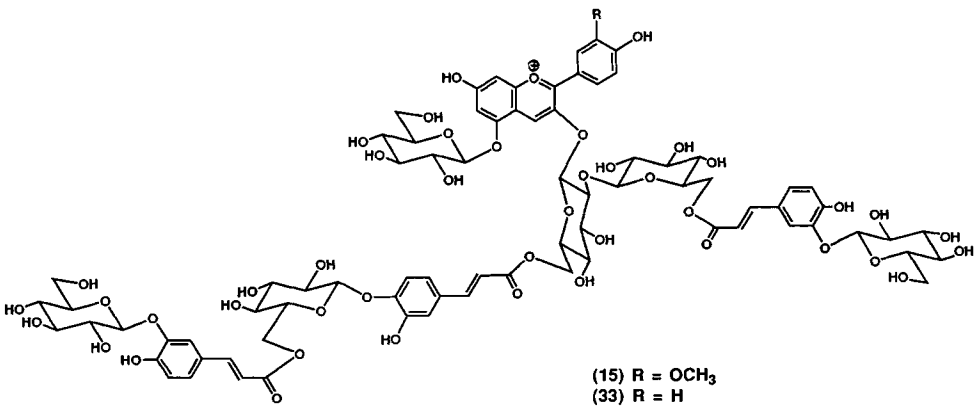

Heavenly blue anthocyanin (HBA) **15** and Scarlet O'Hara anthocyanin **33** from *Ipomoea tricolor* and *I. nil*, respectively.

(15) R = OCH_3
(33) R = H

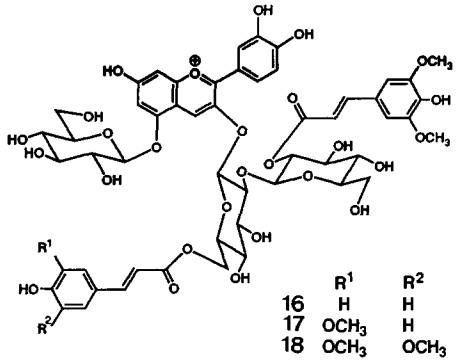

Three diacylated anthocyanins **16**–**18** from *Brassica oleracea*.

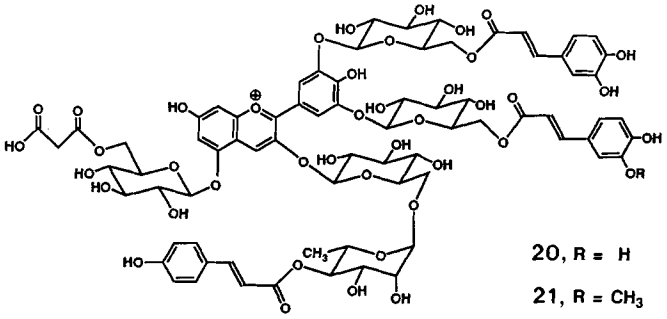

Lobelinin A **20** and lobelinin B **21** from *Lobelia erinus*.

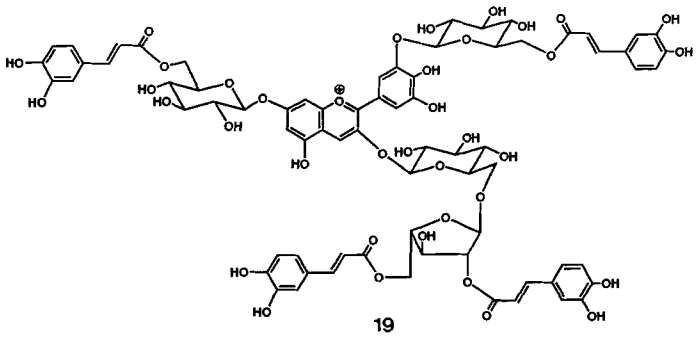

Zebrinin **19** from *Zebrina pendula*.

pigments, ternatin A1 **22** and ternatin B1 from *Clitoria ternatea*, were reported by *Terahara* et al.[108] and *Kondo* et al.,[109] respectively.

Curiously, the 3-phenylpropenoic acid derivatives in the anthocyanins are predominantly in the *E* configuration, i.e.

6.3. Anthocyanins Polyacylated with Benzoic Acid Derivatives

Delphinium flower is widely cultivated as one of the most famous horticultural plants in the world. In 1915, *Willstätter*[113] isolated a pigment, delphinin, from the petals of *Delphinium consolide* and suggested the structure as bis(*p*-hydroxybenzoyl)diglucosyldelphinidin. At that time very few anthocyanins with benzoic acid derivatives as acyl components were known. In 1964, however, *Harborne*[86] reported that the presence of a *p*-hydroxybenzoyl group in this molecule is doubtful. Later, *Asen* et al. reported an anthocyanin isolated from the larkspur "Dark Blue Supreme" to be delphinidin 3-[bis(*p*-hydroxybenzoyl)glucosylglucoside],[33] and an anthocyanin from flowers of the biennial bellflower, *Campanula sp.* "Rose" to be pelargonidin 3-[bis(*p*-hydroxybenzoyl)rutinoside-7-glucoside].[114] From violet flowers of

Fig. 14. Left: *Zebrina pendula*. Right: *Lobelia erinus*.

are present as cinnamic acid derivatives.[110, 111] The reason for this is still unclear. In the case of monoacylated anthocyanins, however, derivatives with *Z*-configuration may be formed.[111, 112]

the *Delphinium hybridum* "Black Night" (Fig. 15, left) we[115] isolated the anthocyanin violdelphin **23**. It contains two molecules of *p*-hydroxybenzoic acid, but has a structure completely different from those reported above. The

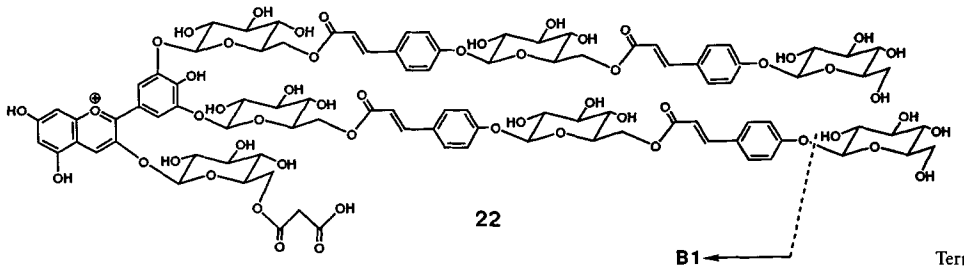

Ternatin A1 **22** and B1 from *Clitoria ternatea*.

Fig. 15. Left: *Delphinium hybridum* 'Black Night'. Middle: *Salvia splendens*. Right: *Slavia farinacea*.

blue flowers of *Delphinium* furnished a more complicated anthocyanin which has two more *p*-hydroxybenzoylglucosyl units than **23**.

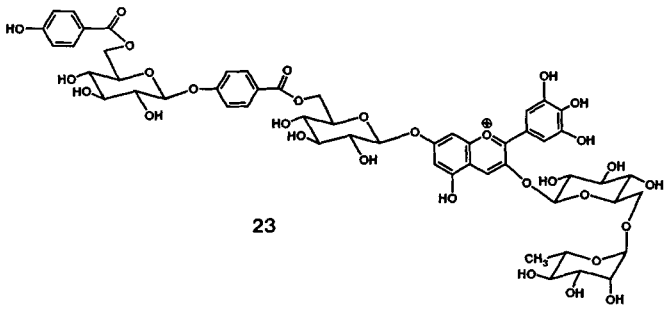

23

Violdelphin **23** from the violet flower of *Delphinium hybridum*.

6.4. Anthocyanins Polyacylated with Malonic Acid

Willstätter and *Bolton*[116] reported that salvianin isolated from *Salvia coccinea* consists of pelargonidin diglucoside acylated with malonic acid. *Karrer* and *Widmer*[117, 118] isolated monardaein from *Monarda didyma*, which they considered to be identical with salvianin and composed of pelargonidin diglucoside acylated with two molecules of malonic acid and one molecule of *p*-coumaric acid. Contrary to the above results neither *Harborne*[86] nor *Birkofer* et al.[119] could find malonic acid in any of these anthocyanins.

We found that monardaein (**30**)[120] indeed contains two molecules of malonic acid. We have also examined scarlet, purple, and blue flowers of *Salvia* (Fig. 15, middle).[121] In scarlet petals of *s. splendens* we found salvianin **24**,[122] monodemalonylsalvianin **25**, monardaein **30**, and monodemalonylmonardaein **31** (ratio of yields, 8:4:2:1). Purple petals of *s. splendens* gave salviadelphin (**26**), monodemalonylsalviadelphin (**27**), bisdemalonylsalviadelphin (**28**), and dimalonylawobanin (**32**) (5:4:1:1). Similarly, blue petals of *S. farinacea* (Fig. 15, right) gave malonylawobanin **4** and salviamalvin **29** (2:1).

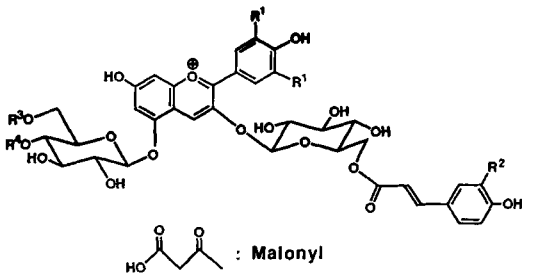

: Malonyl

	R^1	R^2	R^3 [a]	R^4 [a]		Color
24	H	OH	Mal	Mal	salvianin	scarlet
25	H	OH	Mal	H		scarlet
26	OH	OH	Mal	Mal	salviadelphin	purple
27	OH	OH	Mal	H		purple
28	OH	OH	H	H		purple
29	OCH_3	H	Mal	H	salviamalvin	blue
30	H	H	Mal	Mal	monardaein	scarlet
31	H	H	Mal	H		scarlet
32	OH	H	Mal	Mal		purple
4	OH	H	Mal	H	malonylawobanin	blue

[a] Mal = Malonyl.

Anthocyanins **24**–**32** from scarlet, purple, and blue flowers of *Salvia*.

Very interestingly, the difference in color of the scarlet, purple, and blue petals of *Salvia* not only arises from the difference in the anthocyanidin nuclei (pelargonidin, delphinidin, and malvidin; cf. Fig. 3) but also from the difference in pH in the petals: pH 5.6 in scarlet petals, pH 6.1 in purple petals, and pH 7.0 in blue petals.

7. Intramolecular Sandwich-type Stacking of Polyacylated Anthocyanins

In 1971 *N. Saito* et al.[90] found that platyconin **13** is unusually stable in neutral or weakly acidic aqueous solu-

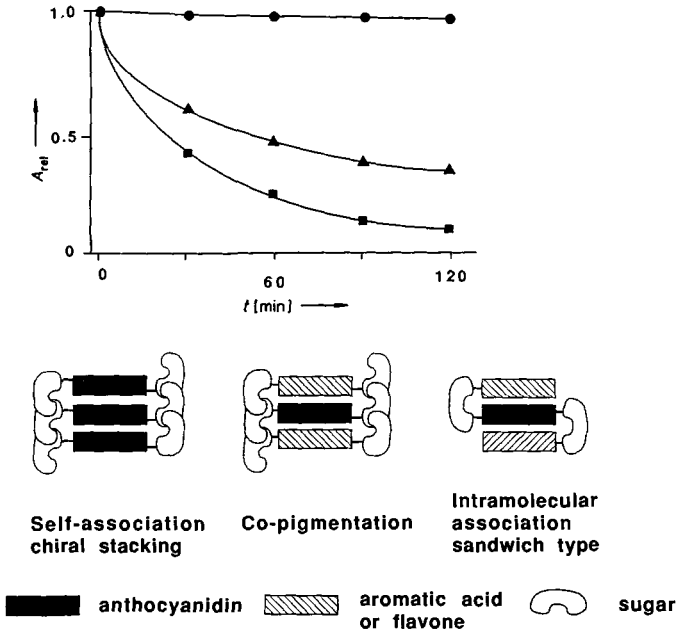

Fig. 16. Top: Approximate representation of the stability of anthocyanins (5×10^{-5} M) in water at pH 6.5. ●–●: Anthocyanins having two or more moieties of cinnamic acid derivative(s); ▲–▲: anthocyanins having one moiety of a cinnamic acid derivative; ■–■: anthocyanins having no acyl moiety. Bottom: Schematic representation of three stacking types. Dark rectangle: anthocyanidin; light rectangle: flavone or aromatic acid; Kidney-shaped symbol: sugar.

tions. Then, a few of the stable anthocyanins listed in Section 6.2 were found.[94, 107, 108] These anthocyanins contained two or more cinnamic acid derivatives. Removal of the acyl groups by hydrolysis made the anthocyanin unstable (Fig. 16, top). Such an effect had been attributed to hydrogen bonding between the phenolic hydroxyl groups in the anthocyanidin and the aromatic acids.[93] We[82, 84] and *Brouillard*,[27, 64, 123] on the other hand, were of the opinion that diacylated anthocyanins must be stabilized by a sandwich-type stacking (Fig. 16, bottom) caused by hydrophobic interaction between the anthocyanidin ring and the two aromatic acyl groups, as suggested in the case of copigmentation[37] and self-association.[40]

Evidence supporting this hypothesis has been obtained from ^{1}H-NMR spectra. Careful nuclear Overhauser effect (NOE) measurements on heavenly blue anthocyanin (HBA) **15** showed several long-range NOE's (Fig. 17, top), indicating a folded conformation for HBA.[44] A comparison of the ^{1}H-NMR data of HBA with those of methyl glucosylcaffeate showed that: the proton signals on the two caffeic acid residues, which are close to the anthocyanidin nucleus of HBA, exhibited large upfield shifts, whereas the signals of the third caffeic acid residue, which is distant from the anthocyanidin, showed only small shifts (Fig. 17, top). This indicates that two of the aromatic acyl groups are stacked parallel with the anthocyanidin nucleus. The CD curve showed a strong Cotton effect near the absorption of the acyl groups (ca. 349 nm), whereas no exciton-type splitting was observed in the visible region.

Figure 17 (bottom) shows an intramolecular sandwich-type stacking model of HBA **15**. Such stacking protects the HBA molecule from attack by water to form the pseudobase, thus stabilizing the flavylium ion as well as the anhydro base. The blue color of the petals is caused by an increase in the pH of the cell sap to 7.5,[124, 125] an unusually high pH (Fig. 18). The red morning glory, "Scarlet O'Hara" (*Ipomoea nil*) (Fig. 13, right), has an anthocyanin **33** that differs from HBA **15** only by lacking a methoxy group on the B-ring,[78] but the color is quite different because the pH of the cell sap is lower (pH 6.1).

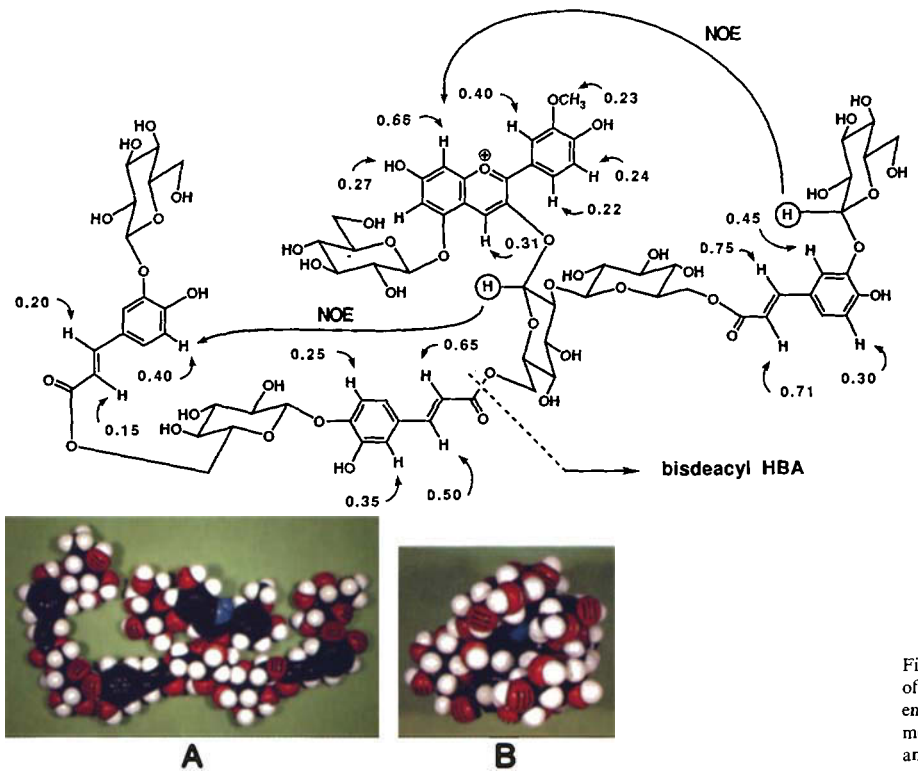

Fig. 17. Top: Long-range NOE's and upfield shifts of proton signals in the ^{1}H-NMR spectrum of heavenly blue anthocyanin **15** in acidic deuteriomethanol. Bottom: CPK models of heavenly blue anthocyanin **15**. A: extended form; B: stacked form.

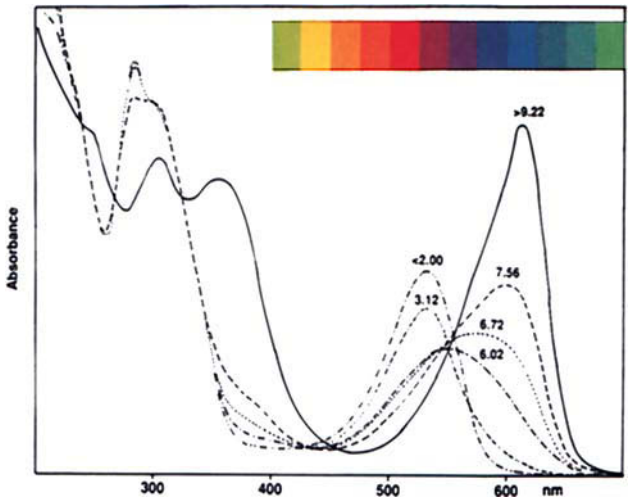

Fig. 18. Electronic spectra of heavenly blue anthocyanin **15** in aqueous solutions at several pH's (the rainbow colors show only approximate spectra).

A detailed conformational analysis of gentiodelphin **12** was carried out using the coupling constants and NOE data of the ^{1}H-NMR spectra (Figure 19, top). Unlike HBA, gentiodelphin does not assume a sandwich-type conformation (Fig. 19, bottom).[75] Despite this gentiodelphin **12** is fairly stable in aqueous solution (Fig. 20). The reason why gentiodelphin is so stable, however, awaits further clarification.

8. Summary and Outlook

Simple anthocyanins are not stable in dilute aqueous solutions; they are stabilized by vertical stacking of aromatic rings between anthocyanins (self-association), anthocyanins and phenols such as flavones (copigmentation), or intramolecularly between anthocyanidins and their aromatic acid residues (intramolecular sandwich-type stacking) by hydrophobic interactions (Fig. 21, top). Such stackings are further

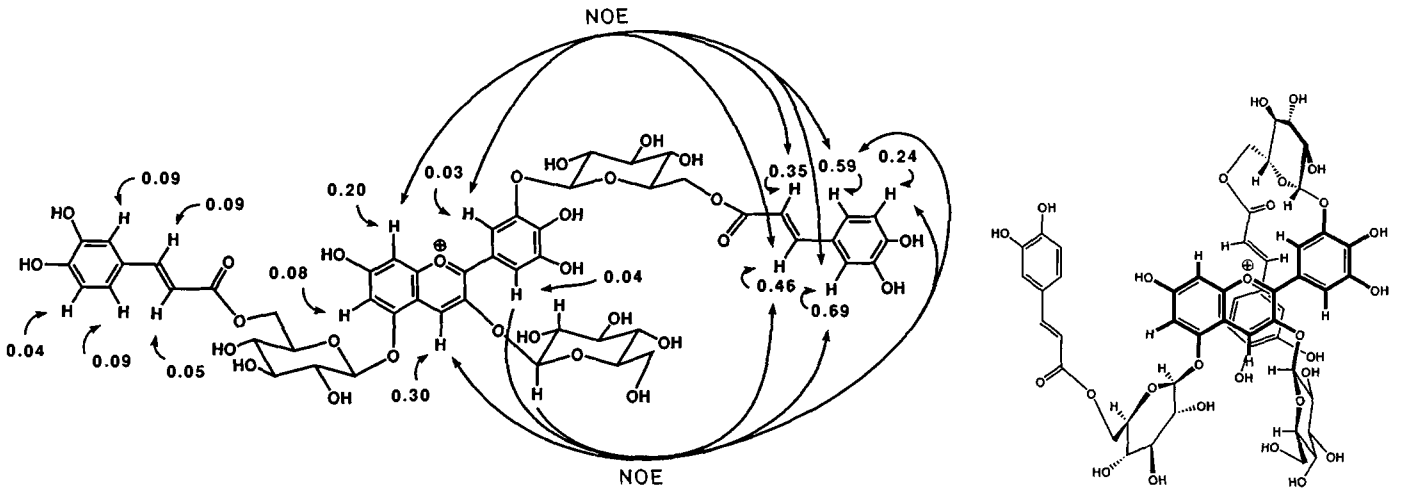

Fig. 19. Left: Long-range NOE's and upfield shifts of proton signals in the ^{1}H-NMR spectrum of gentiodelphin **12**. Right: A stacked conformation of gentiodelphin **12**.

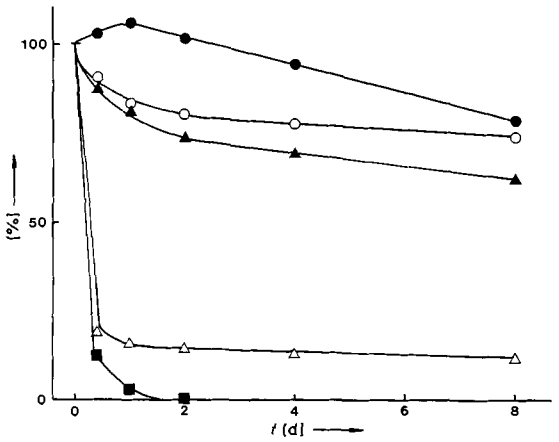

Fig. 20. Stability of acylated anthocyanins (5×10^{-5} M) in aqueous solutions at pH 6.5. ●–● lobelinin A **20**, ○–○ gentiodelphin **12**, ▲–▲ HBA **15**, △–△ bisdeacyl-HBA, ■–■ awobanin **5**.

stabilized by a superposed layer of hydrophilic sugar moieties (hydrogen bonding). Attack by a water molecule at C-2 of the anthoycanidin nucleus is prevented by the stacked moities since hydration would result in conversion of the sp^2-hybridized carbon atom C-2 into a sp^3-hybridized carbon atom (Fig. 21, bottom). The presence of such stackings has been detected in vivo by means of CD,[126] and resonance Raman spectra.[127, 128]

In the case of metalloanthocyanins, metal ions chelate with anthocyanin molecules, which, in turn, stack with flavone molecules. A cyclic arrangement of twelve flavonoids (six anthocyanins and six flavones) centered by metal ions has been proposed. Commelinin has two magnesium ions in the center of twelve flavonoid molecules arranged symmetrically, but, remarkably, two different metal ions are involved in protocyanin. Is it possible that two different metal ions exist in a symmetrical arrangement similar

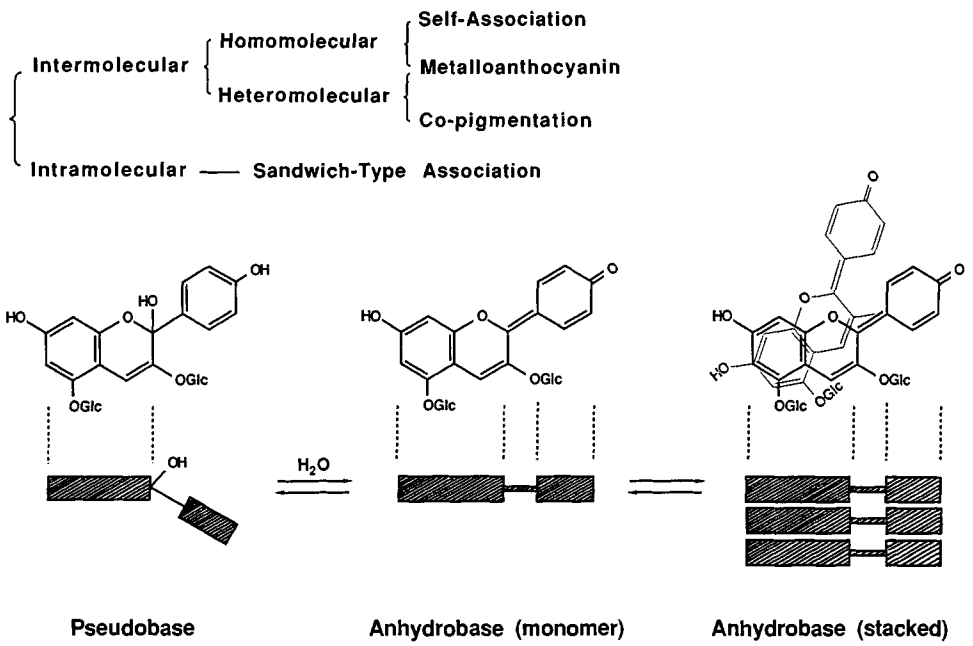

Fig. 21. Top: Stabilization mechanisms of anthocyanin. Bottom: Stacking of anthocyanin anhydrobase molecules prevents hydration, and thus formation of the pseudobase.

to that of commelinin? This interesting problem will be solved only by X-ray analysis of the complex molecules. Now, the X-ray analysis of commelinin is in progress.

Polyacylated anthocyanins are suggested to be stabilized by sandwich-type stacking of two aromatic acyl moieties on and under the anthocyanidin nucleus, as is evident from the ^{1}H-NMR data of HBA **15**. In the case of gentiodelphin **12**, however, only one aromatic acyl group can be stacked on the anthocyanidin nucleus; nevertheless it shows a similar stability to that of HBA. Further studies, in particular a detailed analysis of the molecular recognition, are necessary in order to clarify these stabilization mechanisms.

Received: March 19, 1990 [A 799 IE]
German version: *Angew. Chem. 103* (1991) 17

[1] T. Goto, *Prog. Chem. Org. Nat. Prod. 52* (1987) 158.
[2] J. B. Harborne, R. J. Grayer in J. B. Harborne (Ed.): *The Flavonoids*, Advances in Research since 1980, Chapman and Hall, Londonf 1988, p. 1
[3] G. Hrazdina in J. B. Harborne, T. Mabry (Eds.): *The Flavonoids*, Chapman and Hall, London 1982, p. 135.
[4] R. Brouillard in P. Markakis (Ed.): *Anthocyanins as Food Colors*, Academic Press, New York 1982, p. 1.
[5] R. Brouillard in J. B. Harborne (Ed.): *The Flavonoids*, Advances in Research since 1980, Chapman and Hall, London 1988, p. 525–538.
[6] C. F. Timberlake, P. Bridle in J. Walford, (Ed.): *Developments in Food Colours, Vol. 1*, Applied Science Publishers, London 1980, p. 115.
[7] R. Willstätter, A. E. Everest, *Justus Liebigs Ann. Chem. 401* (1913) 189.
[8] K. Shibata, Y. Shibata, I. Kasiwagi, *J. Am. Chem. Soc. 41* (1919) 208.
[9] K. Shibata, K. Hayashi, T. Inosaka, *Acta Phytochim. 15* (1949) 17.
[10] K. Hayashi, Y. Abe, S. Mitsui, *Proc. Jpn. Acad. 34* (1958) 373.
[11] S. Mitsui, K. Hayashi, S. Hattori, *Proc. Jpn. Acad. 35* (1959) 169.
[12] K. Takeda, S. Mitsui, K. Hayashi, *Bot. Mag. Tokyo 79* (1966) 578.
[13] K. Takeda, *Proc. Jpn. Acad. Ser. B. 53* (1977) 257.
[14] K. Takeda, K. Hayashi, *Proc. Jpn. Acad. Ser. B. 53* (1977) 1.
[15] K. Hayashi, K. Takeda, *Proc. Jpn. Acad. 46* (1970) 535.
[16] E. Bayer, H. Egeter, A. Fink, K. Nether, K. Wegmann, *Angew. Chem. 78* (1966) 834; *Angew. Chem. Int. Ed. Engl. 5* (1966) 791.
[17] E. Bayer, *Chem. Ber. 91* (1958) 1115.
[18] E. Bayer, K. Nether; H. Egeter, *Chem. Ber. 93* (1960) 2871.
[19] K. Hayashi, N. Saito, K. Mitsui, *Proc. Jpn. Acad. 37* (1961) 393.
[20] S. Asen, L. Jurd, *Phytochemistry 6* (1967) 577.
[21] Y. Osawa in P. Markakis (Ed.): *Anthocyanins as Food Colors*, Academic Press, New York 1982, p. 41.
[22] Y. Osawa, M. Koizumi, N. Saito, *Phytochemistry 10* (1971) 1591.
[23] G. M. Robinson, R. Robinson, *Biochem. J. 25* (1931) 1687.
[24] J. B. Harborne in T. W. Goodwin, (Ed.): *Chemistry and Biochemistry of Plant Pigments, Vol. 1*, 2nd edit., Academic Press, New York 1976, p. 736.
[25] R. Brouillard, B. Delaporte, *J. Am. Chem. Soc. 99* (1977) 8461.
[26] R. Brouillard, J.-E. Dubois, *J. Am. Chem. Soc. 99* (1977) 1359.
[27] R. Brouillard, J.-M. H. Chahime, *J. Am. Chem. Soc. 102* (1980) 5375.
[28] R. Brouillard, G. A. Iacobucci, J. G. Sweeny, *J. Am. Chem. Soc. 104* (1982) 7585.
[29] A. Cheminat, R. Brouillard, *Tetrahedron Lett. 27* (1986) 4457.
[30] S. Asen, R. N. Stewart, K. H. Norris, *Phytochemistry 11* (1972) 1139.
[31] T. C. Sommers, M. E. Evans, *J. Sci. Food Agric. 30* (1979) 623.
[32] L.-J. Chen, G. Hrazdina, *Phytochemistry 20* (1981) 297.
[33] S. Asen, R. N. Stewart, K. H. Norris, *Phytochemistry 14* (1975) 2677.
[34] S. Asen, K. H. Norris, R. N. Stewart, *J. Am. Soc. Hortic. Sci. 96* (1971) 770.
[35] N. Ishikura, K. Yoshitama, *J. Plant Physiol. 115* (1984) 171.
[36] M. Williams, G. Hrazdina, *J. Food Sci. 44* (1979) 66.
[37] T. Goto, T. Hoshino, S. Takase, *Tetrahedron Lett. 1979*, 2905.
[38] T. Goto, T. Hoshino, S. Takase, *20th Symposium on the Chemistry of Natural Products* (Japan), Symposium papers, pp. 59–66 (1976).
[39] J. G. Sweeny, M. M. Wilkinson, G. A. Iacobucci, *J. Agric. Food Chem. 29* (1981) 563.
[40] T. Hoshino, U. Matsumoto, T. Goto, *Tetrahedron Lett. 21* (1980) 1751.
[41] T. Hoshino, U. Matsumoto, N. Harada, T. Goto, *Tetrahedron Lett. 22* (1981) 3621.
[42] T. Hoshino, U. Matsumoto, T. Goto, *Phytochemistry 20* (1981) 1971.
[43] T. Hoshino, U. Matsumoto, T. Goto, N. Harada, *Tetrahedron Lett. 23* (1982) 433.
[44] T. Goto, H. Tamura, T. Kawai, T. Hoshino, N. Harada, T. Kondo, *Ann. N. Y. Acad. Sci. 471* (1986) 155.
[45] T. Hoshino, T. Goto, *Tetrahedron Lett. 31* (1990) 1593.
[46] T. Goto, H. Tamura, T. Kondo, *Tetrahedron Lett. 28* (1987) 5907.
[47] R. C. Pecket, C. J. Small, *Phytochemistry 19* (1980) 2571.
[48] V. Hemleben, *Z. Naturforsch. C. 36* (1981) 925.
[49] N. Ishikura, *Iden 35* (1981) 38.
[50] N. Saito, K. Ueno, *Heterocycles 23* (1985) 2709.
[51] T. Goto, K. Yoshida, M. Yoshikane, T. Kondo, *Tetrahedron Lett. 31* (1990) 713.
[52] S. Asen, R. N. Stewart, K. H. Norris, *Phytochemistry 10* (1971) 171.
[53] S. Asen, R. N. Stewart, K. H. Norris, D. R. Hassie, *Phytochemistry 9* (1970) 619.
[54] L. Jurd, S. Asen, *Phytochemistry 5* (1966) 1263.
[55] P. Scheffeldt, G. Hrazdina, *J. Food Sci. 43* (1978) 517.
[56] Y. Yazaki, *Bot. Mag. Tokyo 89* (1976) 45.

[57] C. F. Timberlake in J. Friend, M. J. C. Rhodes (Eds.): *Recent Advances in the Biochemistry of Fruit and Vegetables,* Academic Press, New York 1981–1982, p. 221.
[58] S. Asen, R. Griesbach, *J. Am. Soc. Hortic. Sci. 108* (1983) 845.
[59] K. Takeda, R. Kubota, C. Yagioka, *Phytochemistry 24* (1985) 1207.
[60] K. Takeda, M. Kariuda, H. Itoi, *Phytochemistry 24* (1985) 2251.
[61] C. F. Timberlake, *Food Chem. 5* (1980) 69.
[62] R. Brouillard, G. Hazza, Z. Saad, A. M. Albrecht-Gary, A. Cheminat, *J. Am. Chem. Soc. 111* (1989) 2604.
[63] T. Hoshino, U. Matsumoto, T. Goto, *Phytochemistry 19* (1980) 663.
[64] R. Brouillard, *Phytochemistry 22* (1983) 1311.
[65] S. Ootani, *Rep. Inst. Breeding Res. Tokyo Univ. Agric.* (1973) Suppl. 1.
[66] K. Yoshida, M. Yoshikane, T. Kondo, T. Goto, unpublished results.
[67] Y. Osawa, N. Saito, T. Kawai, *Meiji-Gakuin Ronso 156* (1970) 1.
[68] Y. Osawa, M. Koizumi, N. Saito, T. Kawai, *Meiji-Gakuin Ronso 159* (1970) 187.
[69] T. Goto, T. Kondo, H. Tamura, S. Takase, *Tetrahedron Lett. 24* (1983) 4863.
[70] T. Kondo, H. Tamura, S. Takase, T. Goto, *Nippon Kagaku Kaishi 1986,* 1571.
[71] H. Tamura, T. Kondo, Y. Kato, T. Goto, *Tetrahedron Lett. 24* (1983) 5749.
[72] K. Takeda, S. Tominaga, *Bot. Mag. Tokyo 96* (1983) 359.
[73] S. Asen, R. M. Horowitz, *Phytochemistry 13* (1974) 1219.
[74 K. Takeda, Ch. Kumegawa, J. B. Harborne, R. Self, *Phytochemistry 27* (1988) 1228.
[75] K. Yoshida, T. Kondo, T. Goto, unpublished results.
[76] K. Takeda, T. Fujii, M. Iida, *Phytochemistry 23* (1984) 879.
[77] H. Tamura, T. Kondo, T. Goto, *Tetrahedron Lett. 27* (1986) 1801.
[78] T. Kondo, K. Yoshida, T. Goto, unpublished results.
[79] Y. Saito, M. Ito, S. Oba, unpublished results.
[80] T. Goto, S. Takase, T. Kondo, *Tetrahedron Lett. 1978,* 2413.
[81] P. Bridle, R. S. T. Loeffler, C. F. Timberlake, R. Self, *Phytochemistry 23* (1984) 2968.
[82] T. Goto, T. Kondo, H. Tamura, H. Imagawa, A. Iino, K. Takeda, *Tetrahedron Lett. 23* (1982) 3695.
[83] N. Saito, C. F. Timberlake, O. G. Tucknott, I. A. S. Lewis, *Phytochemistry 22* (1983) 1007.
[84] T. Goto, T. Kondo, H. Tamura, K. Kawahori, *Tetrahedron Lett. 24* (1983) 2181.
[85] R. M. Horowitz, S. Asen, *Phytochemistry 28* (1989) 2531.
[86] J. B. Harborne, *Phytochemistry 3* (1964) 151.
[87] J. B. Harborne, M. Boardley, *Z. Naturforsch. C 40* (1985) 305.
[88] J. B. Harborne, *Phytochemistry 25* (1986) 1887.
[89] K. Takeda, J. B. Harborne, R. Self, *Phytochemistry 25* (1986) 1337.
[90] N. Saito, Y. Osawa, K. Hayashi, *Phytochemistry 10* (1971) 445.
[91] N. Saito, Y. Osawa, K. Hayashi, *Bot. Mag. Tokyo 85* (1972) 105.
[92] T. Goto, T. Kondo, T. Kawai, H. Tamura, *Tetrahedron Lett. 25* (1984) 6021.
[93] K. Yoshitama, K. Hayashi, *Bot. Mag. Tokyo 87* (1974) 33.
[94] K. Yoshitama, K. Hayashi, K. Abe, H. Kakisawa, *Bot. Mag. Tokyo 88* (1975) 213.
[95] N. Ishikura, E. Yamamoto, *Nippon Nogei Kagaku Kaishi 54* (1980) 637.
[96] N. Ishikura, M. Shimizu, *Kumamoto J. Sci. Biol. 12* (1975) 41.
[97] A. B. Pomilio, J. F. Sproviero, *Phytochemistry 11* (1972) 2323.
[98] T. Goto, T. Kondo, H. Imagawa, I. Miura, *Tetrahedron Lett. 22* (1981) 3213.
[99] T. Goto, T. Kondo, H. Imagawa, S. Takase, M. Atobe, I. Miura, *Chem. Lett. 1981,* 883.
[100] T. Goto, H. Imagawa, T. Kondo, *Heterocycles 17* (1982) 355.
[101] T. Kondo, T. Kawai, H. Tamura, T. Goto, *Tetrahedron Lett. 28* (1987) 2273.
[102] E. Idaka, K. Suzuki, H. Yamakita, T. Ogawa, T. Kondo, T. Goto, *Chem. Lett. 1987,* 145.
[103] E. Idaka, H. Yamakita, T. Ogawa, T. Kondo, M. Yamamoto, T. Goto, *Chem. Lett. 1987,* 1213.
[104] G. Hrazdina, H. Iredale, L. R. Mattick, *Phytochemistry 16* (1977) 297.
[105] E. Idaka, T. Ogawa, T. Kondo, T. Goto, *Agric. Biol. Chem. 51* (1987) 2215.
[106] T. Kondo, J. Yamashiki, K. Kawahori, T. Goto, *Tetrahedron Lett. 30* (1989) 6055.
[107] K. Yoshitama, *Phytochemistry 16* (1977) 1857.
[108] N. Saito, K. Abe, T. Honda, C. F. Timberlake, P. Bridle, *Phytochemistry 24* (1985) 1583; N. Terahara, N. Saito, T. Honda, K. Toki, *Tetrahedron Lett. 30* (1989) 5305; N. Terahara, N. Saito, T. Honda, K. Toki, Y. Osajima, *ibid. 31* (1990) 2921.
[109] T. Kondo, M. Ueda, T.Goto, *Tetrahedron 46* (1990) 4749.
[110] L. Birkofer, C. Kaiser, W. Koch, M. Donike, D. Wolf, *Z. Naturforsch. B 18* (1963) 631.
[111] K. Yoshida, T. Kondo, K. Kameda, T. Goto, *Agric. Biol. Chem. 54* (1990) 1745.
[112] T. Kondo, H. Tamura, K. Yoshida, T. Goto, *Agric. Biol. Chem. 53* (1989) 797.
[113] R. Willstätter, W. Mieg, *Justus Liebigs Ann. Chem. 408* (1915) 61.
[114] S. Asen, R. N. Stewart, K. H. Norris, *Phytochemistry 18* (1979) 1251.
[115] T. Kondo, K. Oki, K. Yoshida, T. Goto, *Chem. Lett. 1990,* 137.
[116] R. Willstätter, E. K. Bolton, *Justus Liebigs Ann. Chem. 412* (1917) 113.
[117] P. Karrer, R. Widmer, *Helv. Chim. Acta 11* (1928) 837.
[118] P. Karrer, R. Widmer, *Helv. Chim. Acta 12* (1929) 292.
[119] L. Birkofer, C. Kaiser, M. Donike, W. Koch, *Z. Naturforsch. B 20* (1965) 424.
[120] T. Kondo, Y. Nakane, H. Tamura, T. Goto, *Tetrahedron Lett. 26* (1985) 5879.
[121] T. Kondo, M. Yoshikane, K. Yoshida, T. Goto, *Tetrahedron Lett. 30* (1989) 6729.
[122] F. A. Tomas-Barberom, J. B. Harborne, R. Self, *Phytochemistry 26* (1987) 2759.
[123] R. Brouillard, *Phytochemistry 20* (1981) 143.
[124] S. Asen, R. N. Stewart, K. H. Norris, *Phytochemistry 16* (1977) 1118.
[125] N. Ishikura, *Kumamoto J. Sci. Biol. 15* (1981) 29.
[126] T. Hoshino, *Phytochemistry 25* (1986) 829.
[127] R. Brouillard, *Phytochemistry 22* (1983) 1311.
[128] J.-C. Marlin, A. Statoua, R. Brouillard, *Phytochemistry 24* (1985) 1575.

Polyoxometalate Chemistry: An Old Field with New Dimensions in Several Disciplines

By Michael T. Pope* and Achim Müller*

Inorganic metal–oxygen cluster anions form a class of compounds that is unique in its topological and electronic versatility and is important in several disciplines. Names such as *Berzelius, Werner,* and *Pauling* appear in the early literature of the field. These clusters (so-called isopoly- and heteropolyanions) contain highly symmetrical core assemblies of MO_x units (M = V, Mo, W) and often adopt quasi-spherical structures based on Archimedean and Platonic solids of considerable topological interest. Understanding the driving force for the formation of high-nuclearity clusters is still a formidable challenge. Polyoxoanions are important models for elucidating the biological and catalytic action of metal–chalcogenide clusters, since metal–metal interactions in the oxo clusters range from very weak (virtually none) to strong (metal–metal bonding) and can be controlled by choice of metal (3d, 4d, 5d), electron population (degree of reduction), and extent of protonation. Mixed-valence vanadates, in particular, show novel capacities for unpaired electrons, and the magnetic properties of these complexes may be tuned in a stepwise manner. Many vanadates also act as cryptands and clathrate hosts not only for neutral molecules and cations but also for anions, whereby a remarkable "induced self-assembly process" often occurs. Polyoxometalates have found applications in analytical and clinical chemistry, catalysis (including photocatalysis), biochemistry (electron transport inhibition), medicine (antitumoral, antiviral, and even anti-HIV activity), and solid-state devices. These fields are the focus of much current research. Metal–oxygen clusters are also present in the geosphere and possibly in the biosphere. The mixed-valence vanadates contribute to an understanding of the extremely versatile geochemistry of the metal. The significant differences between the chemistry of the polyoxoanions and that of the thioanions of the same elements is of relevance to heterogeneous catalysis, bioinorganic chemistry, and veterinary medicine.

Ubi materia, ibi geometria.

Mundus participat quantitate, et mens hominis...
nihil rectius intelligit, quam ipsas quantitates, quibus percipiendis factus videri potest.[**]
Johannes Kepler

1. Introduction and Historical Background

The chemistry of molybdenum (VI), tungsten (VI), and vanadium (V) in aqueous solution is dominated by the formation of polyoxoanions,[1] as exemplified by Equations (a) and (b).

$$8\,H^{\oplus} + 7[WO_4]^{2\ominus} \longrightarrow [W_7O_{24}]^{6\ominus} + 4\,H_2O \quad (a)$$

$$23\,H^{\oplus} + [HPO_4]^{2\ominus} + 12[MoO_4]^{2\ominus} \longrightarrow [PMo_{12}O_{40}]^{3\ominus} + 12\,H_2O \quad (b)$$

This behavior has long been recognized; in the earliest systematic investigation of molybdenum chemistry, *Berzelius*[2] noted the formation of yellow (heteropolyanion) products from the reaction of molybdate with phosphate or arsenate and the subsequent ready formation (which has important consequences) of the blue (mixed-valence) derivatives. The first heteropolytungstates were discovered and characterized by *Marignac* in 1862. During the next 70 years, polyoxometalates were intensively investigated, and hundreds of such compounds are described in the Gmelin volumes published in the 1930s.[3, 4] In his famous book, *Neuere Anschauungen auf dem Gebiete der Anorganischen Chemie* (1909), *A. Werner* proposed structures for the species ("Iso- und Heteropolysäuren und Heteropolysalze"). A remarkable sentence is: "Wahrscheinlicher ist aber, daß die einzelnen Kerne der mehrkernigen Anionen viel inniger, d. h. nicht nur durch ein, sondern durch mehrere Sauerstoffatome miteinander verbunden sind"[***] (anticipation of edge- and face-sharing of polyhedra!). *Pauling,* with his instinct for an important class of compounds, proposed structures that were based on corner-sharing of MO_6 octahedra,[5] but it was not until 1933, when *Keggin* reported the structure of the heteropoly acid $[H_3PW_{12}O_{40}]\cdot 6\,H_2O$ (by analysis of 32 powder X-ray lines),[6] that the importance of more compact

[*] Prof. M. T. Pope
Department of Chemistry, Georgetown University
Washington, DC 20057 (USA)
[*] Prof. Dr. A. Müller
Fakultät für Chemie der Universität
Postfach 8640, W-4800 Bielefeld 1 (FRG)

[**] Wherever there is geometry, there is structure.
The world works quantitatively, and the human mind... does not understand anything better than the quantities themselves. Man even seems to have been created in order to comprehend quantities.

[***] "But it is more likely that the individual [metal] atoms of multinuclear anions are connected together, not through one, but through several oxygen atoms."

 © VCH Verlagsgesellschaft mbH, W-6940 Weinheim, 1991 0570-0833/91/0101-0034 $ 3.50+.25/0

edge-shared polyhedral arrangements was revealed. Further progress was slow; a review published in 1971[7] listed only 25 X-ray investigations, most of low quality. Subsequent developments in X-ray crystallographic hardware and software have altered this picture considerably; in 1987/88, for example, some 66 structures were published. During the last 20 years, spectroscopic methods such as Raman and one- and two-dimensional metal and ^{17}O NMR spectroscopy have flourished[8–14] and these, in combination with precise electrochemical measurements (see, for example, Refs. [15,16]) and new analytical techniques such as fast atom bombardment (FAB) mass spectrometry,[17] have enabled the important links between solid and solution structure to be established. New classes of structures with often unexpected reactivity and applications are still being characterized. The number of heteropolymolybdate and -tungstate anions is immense; more than 70 different heteroelements, with "coordination numbers" ranging from 3 to 12, have been confirmed and, for many of these (e.g., P/Mo pair species), dozens of stoichiometries and structures are known.

The present article aims to highlight some of the more interesting and important recent results and to indicate some of the directions and challenges of future research. Polyoxometalates form a class of inorganic compounds that is unmatched in terms of molecular and electronic structural versatility, reactivity, and relevance to analytical chemistry, catalysis, biology, medicine, geochemistry, materials science, and topology.

2. Problems of Nomenclature

The nomenclature of polyoxometalates involves two considerations: a name for the class as a whole and the systematic nomenclature of individual species.

The names "isopoly" and "heteropoly" for species such as those formed in Equations (a) and (b), respectively, are unsatisfactory for at least two reasons: not only is "homo" a more usual antonym for "hetero", but the distinction between the two groups is wholly artificial and could lead to solecisms such as "mixed isopolyanion" to describe species such as β-$[Mo_6V_2O_{26}]^{6\ominus}$ (isostructural with the isopolymolybdate β-$[Mo_8O_{26}]^{4\ominus}$) and the consideration of $[(H_2)W_{12}O_{40}]^{6\ominus}$ (which is chemically and structurally equivalent to a heteropolyanion like $[SiW_{12}O_{40}]^{4\ominus}$) as an isopolyanion. Names such as "polyoxoanions" and "polyoxometalates" have been used more recently, but it is important with a field as venerable as this, with a vast early literature, that changes in nomenclature not be made lightly. However, we favor the gradual introduction of a name such as "metal–oxygen clusters", which can be used for the field as a whole and which emphasizes the presence of *metal* centers. The word cluster in inorganic chemistry has hitherto been applied to species in which there are strong as well as weak metal–metal interactions (cf. "iron–sulfur clusters"). This seems appropriate for the present field, since, as we shall see, polyoxometalates exhibit the whole range of metal–metal interactions, from extremely weak to very strong.

The question of systematic nomenclature, which is important for information retrieval, has been addressed by IUPAC.[18] The names must take into account a labeling system for the metal atoms and may also require one for the oxygens if ambiguity is to be avoided in certain cases. The resulting names are almost never used in normal scientific intercourse, since they are very long and cumbersome—for example, 1.4,1.9,2.5,2.6,3.7,3.8,4.10,5.10,6.11,7.11,8.12,9.12-dodeca-μ-oxo-μ_{12}-(tetraoxophosphato-$O^{1,4,9}$,$O^{2,5,6}$,$O^{3,7,8}$,$O^{10,11,12}$)tetrakis[tri-μ-oxo-tris(oxomolybdate)](3−) for α-$[PMo_{12}O_{40}]^{3\ominus}$.

Michael T. Pope was born in Exeter, England, in 1933 and received B.A. and Ph.D. degrees in Chemistry at Oxford University in 1954 and 1957 under the supervision of R. J. P. Williams. He was introduced to the field of heteropolyanion chemistry during postdoctoral research with Louis C. W. Baker at Boston University. In 1962, following a three-year period with Laporte Industries in England, he went to Georgetown University as Assistant Professor. He has been Full Professor at Georgetown since 1973 and is currently Department Chairman. His research interests center around all aspects of the reactivity, structures, and applications of polyoxometal clusters.

Achim Müller was born in Detmold in 1938 and received the Ph.D. degree (1965) and habilitation (1967) at the University of Göttingen under the supervision of O. Glemser. He has worked on problems of molecular physics (theory of mass influence on molecular constants), vibrational spectroscopy (matrix isolation spectroscopy, band contour analysis, resonance Raman effect, metal isotope effects), bioinorganic chemistry (biological N_2 fixation by free-living microorganisms as well as model compounds), and molecular metal oxide and sulfide complexes and clusters (synthesis, geochemical relevance, electronic and molecular structure, topological aspects, and use in heterogeneous catalysis). He has published 30 reviews in these areas and is now Full Professor of Inorganic Chemistry at the University of Bielefeld.

3. Structures: Variety Based on Highly Symmetrical Core Assemblies

That molybdenum(VI) and tungsten(VI) are polyoxoanion formers par excellence is clearly the result both of a favorable combination of ionic radius and charge and of accessibility of empty d orbitals for metal–oxygen π bonding.[1b] Other elements and oxidation states possess these attributes to a greater or lesser degree. Polyoxoanions of vanadium (V), niobium (V), and tantalum (V) are also known. Other possibilities exist with hexavalent Tc, Re, Ru and Os, pentavalent Cr, Mo, W, Tc, and Re, and tetravalent Ti, V, Cr, Mo, and W.[1b] The extent to which some of these occur is discussed below. As we shall see, the relevant 3d-element chemistry is different, and the situation with vanadium is, so far, unique in the whole field of cluster chemistry. Structures may also include VO_5 units, and quite a number of paramagnetic fully reduced (V^{IV}) and mixed-valence species are known. These species are discussed in Section 7.

Rather than attempting to catalogue all known polyoxometalates, we illustrate here some of their major structural features and their architecture. We exclude the purely "tetrahedral" polyvanadates ($[V_2O_7]^{4\ominus}$, *cyclo*-$[V_4O_{12}]^{4\ominus}$, etc.), since their structural and acid-base chemistry is very similar to that of the corresponding phosphates, although we note in passing that such oligomers may play an important role in biochemical processes.[19] We also exclude, mainly for reasons of space, the emerging structural variety of oxo-alkoxo molybdate and vanadate oligomers.[20, 21]

Polyoxometalate structures are governed by two general principles:

1. Each metal atom occupies an MO_x coordination polyhedron (most commonly an octahedron or square pyramid) in which the metal atoms are displaced, as a result of M–O π bonding, towards those polyhedral vertices that form the surface of the structure.
2. Structures with MO_6 octahedra that contain three (or more) free vertices are, in general, not observed (*Lipscomb*[22]).

It follows from the first principle that the metal atoms M are never located at inversion centers, although other octahedrally coordinated *hetero*atoms may not be so restricted: contrast, for example, the isostructural anions $[W_7O_{24}]^{6\ominus}$ (C_{2v} symmetry with "central" W^{VI})[23] and $[MnW_6O_{24}]^{8\ominus}$ (D_{3d} symmetry with "central" Mn^{IV}).[24]

The second principle, the Lipscomb restriction, has been rationalized in terms of the strong *trans* influence of the terminal M–O bonds, which facilitates dissociation of neutral $\{MO_3\}$ from the cluster.[25] However, the stability of some mononuclear *fac*-trioxo complexes, such as $[MoO_3(tacn)]$ and $[WO_3(tacn)]$ (tacn = *N,N',N''*-triazacyclononane), in aqueous solution[26] suggests that this restriction is not absolute. Indeed, two anti-Lipscomb polyoxomolybdate structures have recently been characterized.[27, 28] Such structures are likely to remain uncommon, however, since the terminal oxygens of the $\{MoO_3\}$ groups are more strongly basic/nucleophilic[26] than those of $\{MoO_2\}$ and $\{MoO\}$ and will therefore offer sites for further polymerization.

3.1. Quasi-Spherical Structures Derived from Assemblies of MO_6 Octahedra and Based on Regular (Platonic) Solids

Three compact, highly symmetrical ("parent") clusters of MO_6 octahedra are shown in Figures 1–3. An important principle is that each cluster retains the symmetry of its central oxygen polyhedron: a tetrahedron (Fig. 1), an octahedron (Fig. 2), and an icosahedron (Fig. 3). The parent clusters form a convenient starting point for the discussion of many other polyoxometalate structures, which can be regarded as "derivatives".

The $\{(XO_4)(M_{12}O_{36})\}$ parent structure ("Keggin"; Fig. 1) is adopted by many polyoxometalates. Some of the possibilities for derivative structures are shown in Scheme 1. The very high formation tendency of Keggin fragments is particularly noteworthy: self-assembly of a cluster of T_d symmetry

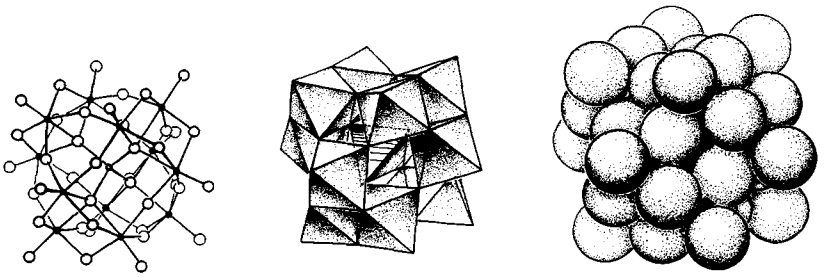

Fig. 1. $\{XM_{12}O_{40}\}$ (T_d) parent structure: the Keggin ion in bond, polyhedral, and space-filling representations.

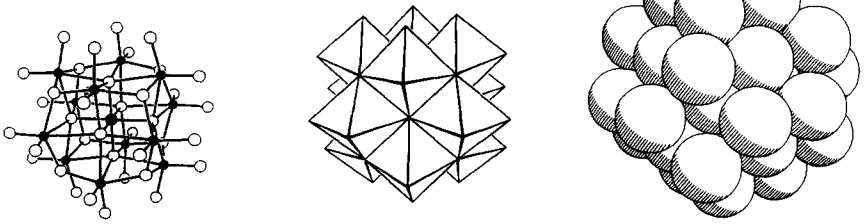

Fig. 2. $\{XM_{12}O_{38}\}$ (O_h) parent structure in bond, polyhedral, and space-filling representations.

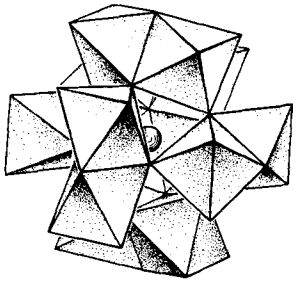

Fig. 3. $\{XM_{12}O_{42}\}$ (I_h) parent structure in polyhedral representation.

lanthanide and actinide cations. Although polyanions with this structure can function as ligands (see Section 6), no lacunary or capped versions have yet been reported.

3.2. Quasi-Cyclic Structures

Some polyoxometalates are topologically based on cyclic arrangements of polyhedra. Figure 5 shows a simple example. Such structures may be viewed as neutral rings of corner-sharing distorted MO_4 tetrahedra to which the heteroatom

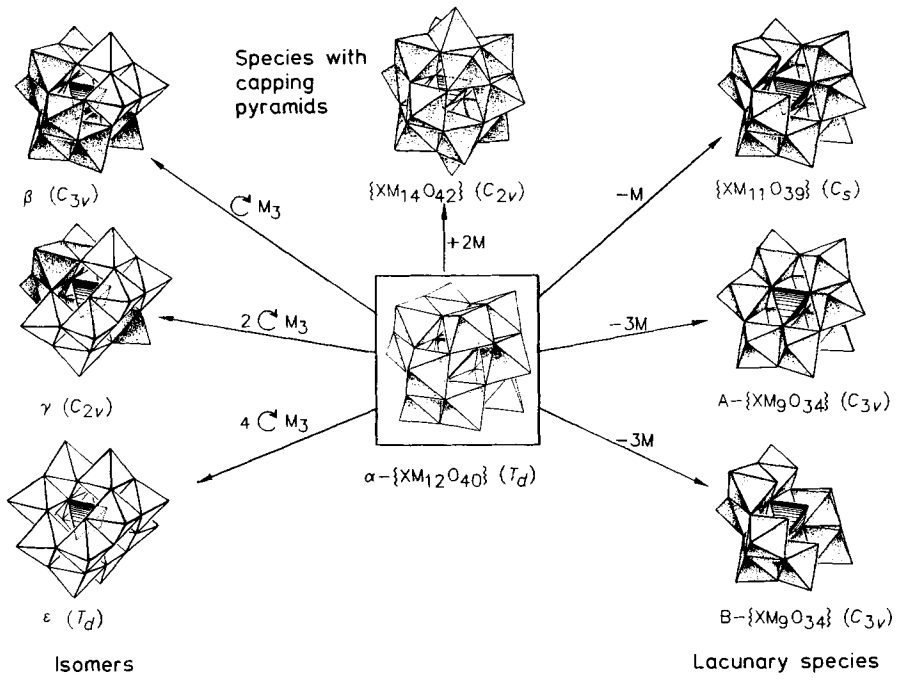

Scheme 1. The $\{(XO_4)(M_{12}O_{36})\}$ parent ("Keggin") structure and its relationship to some known capped, deficient (lacunary), and isomeric versions. The three isomeric structures are obtained by rotation (C_6) of one, two, or four M_3 groups by 60°.

from 12 units of T_d symmetry occurs even when there is no central tetrahedral nucleus, as exemplified by Equation (c).

$$12[WO_4]^{2\ominus} + 18H^{\oplus} \longrightarrow [(H_2)W_{12}O_{40}]^{6\ominus} + 8H_2O \qquad (c)$$

For reasons that are not clear at present, but which are probably electrostatic in origin, the $\{(XO_6)(M_{12}O_{32})\}$ parent structure (Fig. 2), with O_h symmetry, has not yet been observed for a discrete polyoxometalate. However, as Scheme 2 shows, several derivatives, such as the mixed-valence mineral sherwoodite, $[AlV_{14}O_{40}]^{9\ominus}$ (compare also the relevant model in Section 7), are known. Note that all structures in this scheme are based entirely upon edge-sharing MO_6 octahedra and may be considered as fragments of a cubic closest packing of oxygen atoms.[29-31]

There are also other edge-shared clusters that are not, strictly speaking, pieces of the parent structure shown in Figure 2. An important example is the $\{M_6O_{19}\}$ unit, which has complete O_h symmetry (Fig. 4).

The $\{(XO_{12})(M_{12}O_{30})\}$ parent structure (Fig. 3) is known only for a handful of heteropolymolybdates of tetravalent

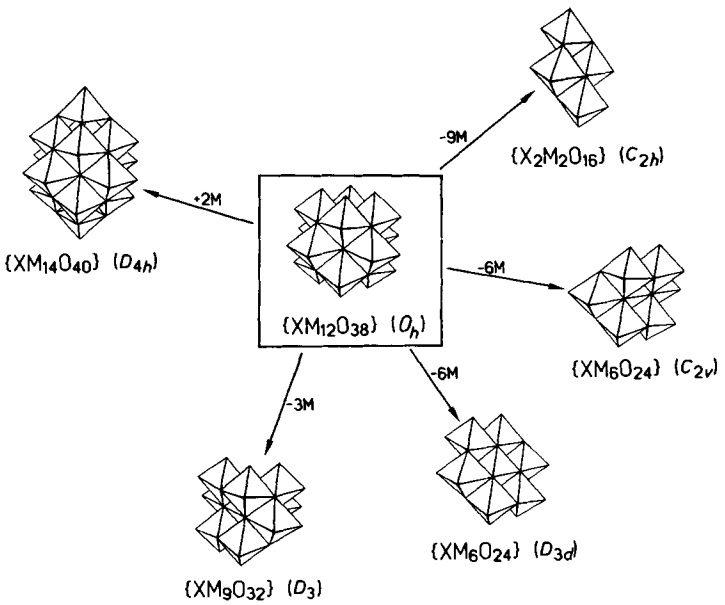

Scheme 2. The $\{(XO_6)(M_{12}O_{32})\}$ parent structure and its relationship to some known capped ("sherwoodite") and deficient versions.

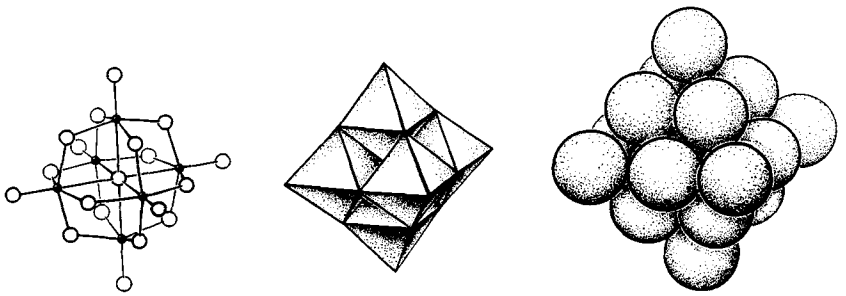

Fig. 4. $\{M_6O_{19}\}$ structure in bond, polyhedral, and space-filling representations. This structure is well-known for M = Mo, W, Nb, Ta, and recently, as bi- and tetracapped derivatives [32–34], for V.

tetrahedra are attached by additional, relatively weak bonds.[35] Much of the reactivity and fluxionality of these anions in solution is thereby understandable.[36–37]

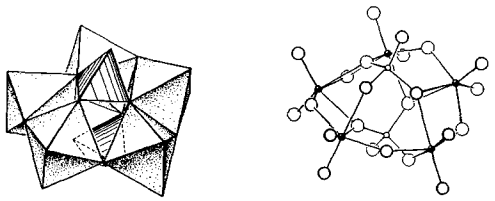

Fig. 6. Structure of $[(PO_4)_2Mo_5O_{15}]^{6\ominus}$ in polyhedral and bond representations

A more complex example of this type of structure is provided by the very large isopolymolybdate anion $[Mo_{36}O_{112}(H_2O)_{16}]^{8\ominus}$.[38] The structure consists of identical Mo_{17} "halves" linked by two MoO_6 octahedra. Each half may be viewed as an $\{Mo_7O_{24}\}$ unit (of C_{2v} symmetry, see Scheme 2) that is encircled by a ring of ten corner-sharing distorted MoO_4 tetrahedra. Relatively weak bonds to oxygens of the enclosed $\{Mo_7O_{24}\}$ units and to hydrate water molecules complete six-coordination for each of the exterior molybdenum atoms.

4. Formation and Solution Behavior

It is appropriate to consider formation and solution properties together, since these topics are intimately related. The majority of polyoxometalates have been formed and studied in aqueous solution[39a] and a recent compilation of typical syntheses is available.[39b] However, nonaqueous syntheses have also been developed.[8] Equations (a) and (b) (Section 1) show that aqueous solutions of these species can act as high-capacity buffers.

As shown in Figure 6, several species may be in equilibrium, depending on the pH. The compound isolated in crystalline form may not necessarily be the one with the highest abundance. In addition, as will be shown in Section 5, many polyoxometalates are unequaled in their "electron reservoir" properties. Coupled or uncoupled proton- and electron-transfer chemistry therefore underlies many realized and potential applications. A further significant general property of polyoxometalates is their solubility (in the presence of appropriate counterions) in solvents ranging in polarity from dimethyl sulfoxide to benzene.[40] The solubility of such complexes in anhydrous solvents extends their chemistry to include the reactions of organometallic species[11c,41,42] as well as other kinds of reactivity such as atom- and group-transfer processes.[43,44] Underlying all aspects of the chemistry of polyoxometalates is their extreme thermal robustness and stability against oxidants. In Section 9, we touch upon some of the diverse applications that have been reported; a complete survey is beyond the scope of the present article.

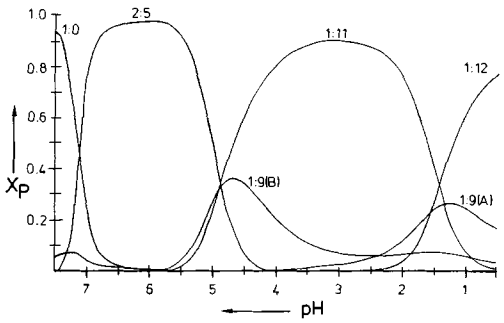

Fig. 6. Distribution diagram for species present in fresh solutions containing $[MoO_4]^{2\ominus}$ and $[HPO_4]^{2\ominus}$ in a molar ratio of 12:1 at different pH values (3.0 M $NaClO_4$ medium). Curves are labeled with the ratio of P:Mo in each complex. Differences in the extent of protonation of the complexes are not distinguished [15].

5. Electronic Structures: Mixed-Valence Species, Intramolecular Electron Transfer, Ring Currents, and Electron-Storage Properties

The electronic structures of "oxidized" (d^0) polymolybdates and polytungstates may to first order be extrapolated from those of the individual MO_6 octahedra from which they are constructed. Although the actual environment of the metal atoms is of lower symmetry in most cases, MO_6 octahedra in polyoxometalates fall into two classes, "mono-oxo" (C_{4v}) and "*cis* dioxo" (C_{2v}), based on the number of terminal M–O bonds. We earlier labeled these as types I and II, respectively.[45] In the absence of in-plane π bonding, the LUMO for type I octahedra is a nominally nonbonding, mainly metal-centered ("d_{xy}") orbital, whereas the LUMO for type II octahedra is strongly antibonding with respect to the terminal M–O bonds. Polyoxometalates constructed of type I octahedra, of which the Keggin structure is a prime example, are therefore easily reduced to mixed-valence species (heteropoly "blues" and "browns") which retain the overall architecture of the oxidized anions. This result can

also be understood from extended Hückel[46] and Xα[47] calculations, which show that, as expected, the density of states in the LUMO (a "d_{xy} band" that has some oxygen contribution and is responsible for the intervalence charge-transfer (IVCT) transitions) increases, and the HOMO-LUMO gap decreases, with aggregation of MO_6 octahedra. On the other hand, type II polyoxometalates are reduced irreversibly and with more difficulty to complexes that have not yet been identified. The following summary refers only to reductions of type I species.

Cyclic voltammograms of molybdate and tungstate Keggin anions, and indeed of all type I polyoxometalates, display sequences of reversible one- or two-electron reductions (see, for example, Fig. 7), which yield deeply colored mixed-valence species ("heteropoly blues"). Electronic spectra of the reduced polyoxometalates show intensity-enhanced d–d bands in the visible and IVCT bands in the near-IR regions. Depending on the acidity of the solution and the polyanion charge, the reductions involve addition either of single electrons or simultaneously of pairs of electrons and protons.[48]

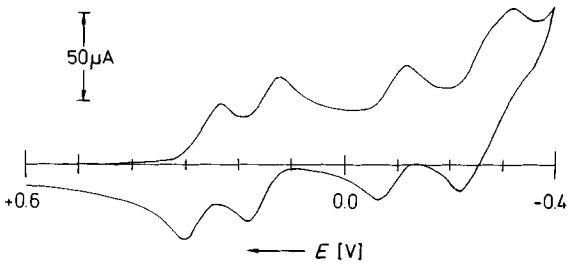

Fig. 7. Cyclic voltammogram of α-$[PMo_{12}O_{40}]^{3\ominus}$ in 0.1 M HCl (50% H_2O/EtOH) showing sequence of five reversible two-electron reductions.

For the paramagnetic one-electron-reduced anions, ESR and ^{17}O NMR spectroscopy demonstrate that the unpaired electron is weakly trapped at low temperatures, but undergoes rapid hopping (intramolecular electron transfer) at room temperature (class II mixed-valence behavior according to the well-known classification of *Robin* and *Day*;[49-52] see Fig. 8). Anions generated by two-electron (and four-electron) reduction are ESR-silent, but ^{17}O and ^{183}W NMR spectra show that the additional electrons are fully delocalized (on the NMR time scale) at room temperature and generate "ring currents" analogous to those produced by the π electrons of benzene.[55-58] Two structural studies of two-electron-reduced anions, α-$[H_2AsMo_{12}O_{40}]^{3\ominus}$[28] and α-$[H_2CoW_{12}O_{40}]^{6\ominus}$,[59] have been reported; both revealed crystallographically disordered anions of T_d symmetry, so that no conclusions about possible valence trapping could be drawn from interatomic distances.

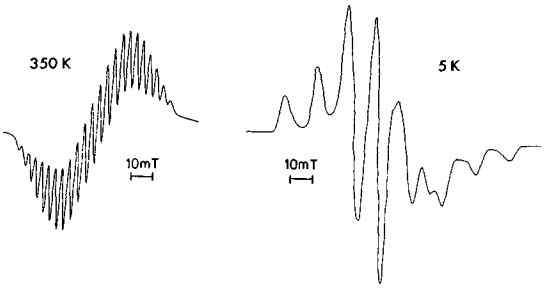

Fig. 8. ESR spectra of α-$[P_2W_{15}V^{IV,V}_3O_{62}]^{10\ominus}$ containing a trigonal "mixed-valence V_3 unit". Note the interaction of the unpaired electron with three equivalent V nuclei ($I = 7/2$, 22 hyperfine lines) at 350 K and with a single V nucleus (8 parallel and 8 perpendicular hyperfine lines) at 5 K [53, 54].

Reduction of Keggin anions beyond the two-electron stage leads to modest changes in electronic and molecular structure, although the reductions remain chemically reversible. For the molybdates, some of the bridging oxygens become protonated and a four-electron-reduced β-Keggin structure is stabilized [Eq. (d)]. Electronic and NMR spectra of these complexes, together with two X-ray structural determinations, suggest that complete valence averaging involving at least six of the Mo atoms has occurred.[28, 58, 60]

$$\alpha\text{-}[PMo_{12}O_{40}]^{3\ominus} + 4\,e + 3\,H^{\oplus} \longrightarrow \beta\text{-}[H_3PMo^{V}_{12}O_{40}]^{4\ominus} \quad (d)$$

With tungstates, on the other hand, protonated $W^V_6W^{VI}_6$ (blue) polyanions undergo intramolecular disproportionation to $W^{IV}_3W^{VI}_9$ (brown) species. In the latter, terminal oxygens have become protonated to form water molecules coordinated to W^{IV} atoms occcupying adjacent edge-sharing octahedra of the Keggin structure[61-63] (Fig. 9). The W^{IV} atoms are linked by metal–metal bonds as in the aqua cation $[W_3O_4(aq)]^{4\oplus}$. Subsequent reductions lead to conversion of the remaining W atoms to W^{IV} (for studies in solution, see Ref. [61]). According to the simple principles treating M_3 clusters of the early transition elements,[64, 65] each W^{IV}_3 triad (of C_{3v} symmetry) in the 24-electron-reduced cluster can formally accept an additional two electrons into a nonbonding a_1 orbital [Eq. (e)] (cf. Ref. [65]), so that an astonishing *32-electron reduction of the Keggin anion* can be demonstrated. The Keggin structure is completely restored upon reoxidation.[61]

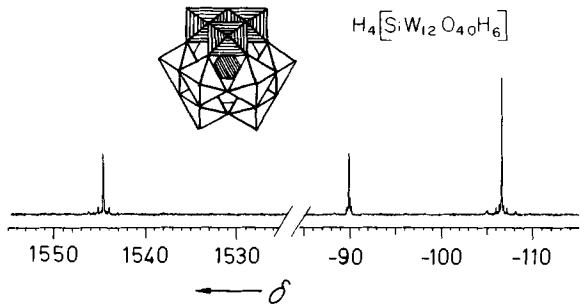

Fig. 9. ^{183}W NMR spectrum of $[SiW_{12}O_{40}H_6]^{4\ominus}$ showing resonances for W^{IV} ($\delta = +1545$) and W^{VI} ($\delta = -90, -107$). The magnitudes of the W···W coupling constants derived from the satellites at the base of each line establish that the W^{IV} atoms occupy an edge-shared triad (cross-hatched) [63].

$$(1a_1)^2(1e)^4(2a_1)^0 \longrightarrow (1a_1)^2(1e)^4(2a_1)^2 \quad (e)$$

6. Polyoxometal Systems as Unique Ligands: Multianion Clusters, Cryptates, and Clathrates

Polyoxometalate anions can act as ligands that are unique in two respects: topology and electron-acceptor ability due

to the reducibility of the metal centers. Several types of physical measurements support the acceptor nature of polyoxometalate ligands:

1. Electrochemical investigations show that such "ligands" are easily reduced.
2. The electronic spectra contain low-energy metal-to-ligand absorption bands (e.g., for Cu^{I} in $[CuW_{12}O_{40}]^{7\ominus}$[66] and Ce^{III} in $[CeMo_{12}O_{42}]^{9\ominus}$[67]), comparable to the bands found for thiometalate complexes.
3. The ESR-derived value of the Fermi contact term for the unpaired electron of V^{IV} in $[XM_{11}VO_{40}]^{x\ominus}$ (M = W, Mo) is reduced (electron delocalization is greater in the molybdates[68]).
4. The ^{183}W NMR isotropic shifts reveal delocalization of unpaired spin density of Co^{II} onto W atoms in α-$[CoW_{12}O_{40}]^{6\ominus}$.[69]

Two modes of complex formation with polyoxometalate ligands can be distinguished: (1) "complete" (plenary) structures binding metal cations via surface terminal and bridging oxygen atoms; (2) "defect" (lacunary) structures enclosing cations in the vacancies.

Complexes of the first kind are favored if the polyoxometalate has a high charge, more than one oxygen atom is coordinated to the external cation, and the reactions are carried out in nonaqueous solutions. Examples of such complexes include the weak and labile complexes of Mn^{II} and Eu^{III} with $[(H_2)W_{12}O_{40}]^{6\ominus}$ acting as a monodentate ligand through a terminal oxygen atom,[70] species such as $[UMo_{12}O_{42}\{Ni(H_2O)_3\}_2]^{4\ominus}$[71] with the anion of Figure 3 acting as a tridentate ligand through three adjacent terminal oxygen atoms, and complexes like $[(CpTi(SiW_9V_3O_{40})]^{4\ominus}$[72] in which three adjacent bridging oxygen atoms of a Keggin anion function as donors to the Ti atom.

Complexes with lacunary polyoxometalate structures as ligands are of great variety and are exceedingly numerous.[1b, 73] The vacancy created by the nominal loss of an MO_6 octahedron (equivalent to stoichiometric loss of $MO^{n\oplus}$) from, for example, a Keggin anion, represents a binding site that is pentadentate, as in $[(SiW_{11}O_{39})Co(H_2O)]^{6\ominus}$ ("octahedral" Co^{II}), or tetradentate, as in $[(PW_{11}O_{39})Cu]^{5\ominus}$ ("square-planar" Cu^{II}) and $[(PW_{11}O_{39})_2Ce]^{10\ominus}$ ("square antiprismatic" Ce^{IV}). Some of the possible reactions of such complexes are summarized in Scheme 3.

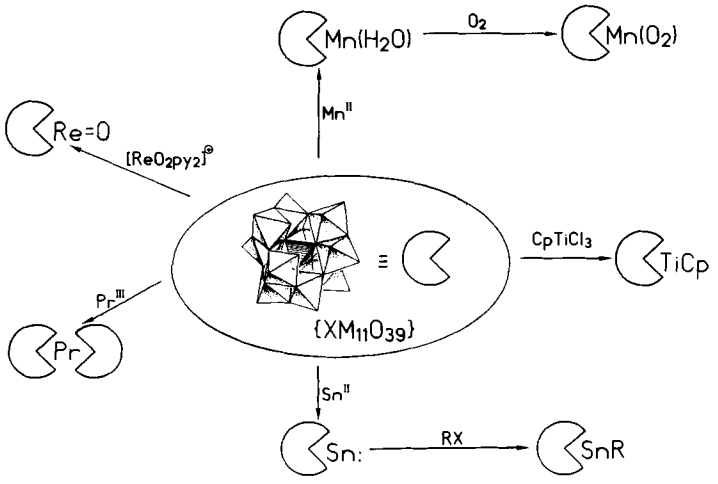

Scheme 3. Some examples of the many possible reactions of lacunary Keggin anions [151–156].

Complex anions such as $[(SiW_{11}O_{39})M]^{n\ominus}$ have been viewed and used as inorganic analogues of metalloporphyrins,[43, 74] but with several differences and advantages. (1) The inorganic polyoxometalate ligand is not susceptible to oxidative degradation and is thermally more robust than porphin or other macrocyclic ligands. (2) Owing to the oxygen donor atoms, complexes of 3d cations are of high-spin type. (3) The acceptor properties of the oxometalate ligand are dependent on its reducibility and can be modified by metal replacement or by partial reduction. (4) In general, the electron population on metal and ligand is considerably more variable than for the metalloporphyrins.

Derivatives of lacunary polyoxometalates in which more than one metal atom has been lost, for example, the XM_9 complexes of Scheme 1 (three vacancies), present a range of structures, reactions, and potential applications. Their chemistry is still in the early stages of development.

Reconstituted Keggin-like structures are possible (e.g., β-$[SiW_9O_{37}\{Co(H_2O)\}_3]^{10\ominus}$[40] and γ-$[PW_{10}O_{38}(VO)_2]^{5\ominus}$.[75] These are soluble well-defined species, which serve as models of transition-metal oxide surfaces.

Alternatively, lacunary anion fragments may assemble into larger clusters, either directly [Eq. (f)] or, more commonly, with the incorporation of metal ion linkers. Three of the many possible examples are shown in Figure 10. Other compounds of this type include unusual groupings of adjacent paramagnetic metal centers (e.g., $Fe_4^{III}C_2^{II}$[78]).

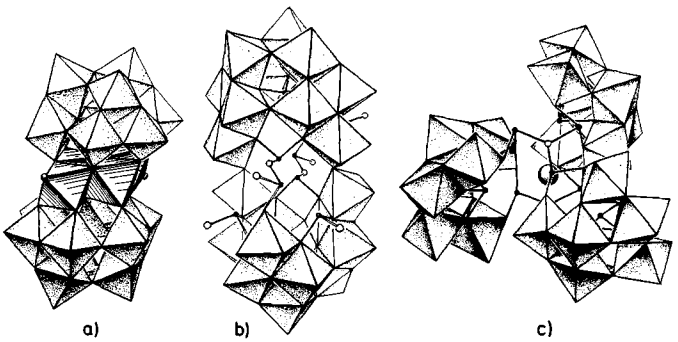

Fig. 10. Structures of three polyoxometalates assembled from Keggin fragments: a) $[Co_4(H_2O)_2(PW_9O_{34})_2]^{10\ominus}$ [79]; b) $[As_{10}Mo_{24}O_{90}]^{14\ominus}$ [28]; c) $[(Na)(Sb_3O_7)_2(SbW_7O_{24})_3]^{18\ominus}$ ("HPA-23") [80].

$$2\,[PMo_9O_{31}(H_2O)_3]^{3\ominus} \longrightarrow [P_2Mo_{18}O_{62}]^{6\ominus} + 6\,H_2O^{[15]} \qquad (f)$$

$[P_8W_{48}O_{184}]^{40\ominus}$ ($\triangleq$ 4 "P_2W_{12}" from $[P_2W_{18}O_{62}]^{6\ominus}$)[76]
$[P_5W_{30}O_{110}]^{15\ominus}$ ($\triangleq$ 5 "PW_6" from $[PW_{12}O_{40}]^{3\ominus}$)[77]

Many of the larger multianion clusters have structures that permit the inclusion of cations or anions. The central sodium ion in the tungstoantimonate of Figure 10 is readily exchangeable with other mono- or divalent cations (compare with crown ether complexes),[81] but in some other cases, such as $Na^{\oplus}$ in $[(Na)H_2W_{18}O_{56}F_6]^{7\ominus}$[82] and $NO_3^{\ominus}$ in

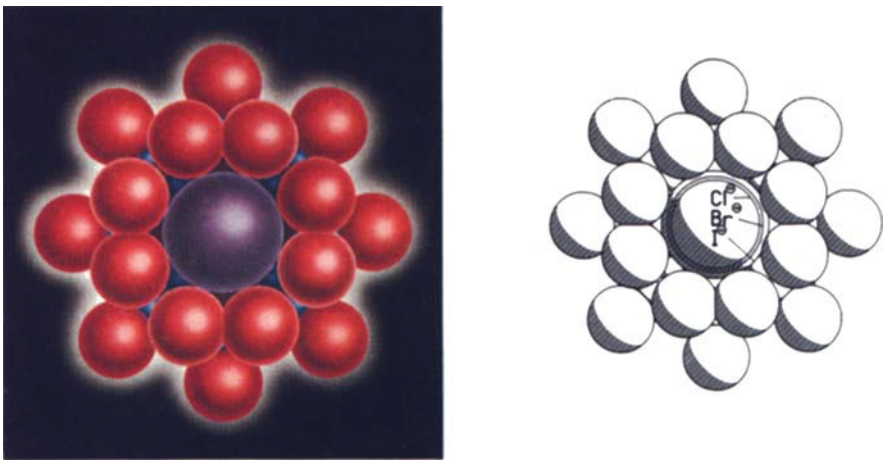

a) b)

Fig. 11. Structure of a hemisphere of a species containing the $\{V_{18}O_{42}\}$ shell viewed along the virtual S_8 axis: a) $I^{\ominus}$ (violet), V (blue), O (red); b) with $Cl^{\ominus}$, $Br^{\ominus}$, $I^{\ominus}$ [85].

$[(NO_3)Cu_3(PW_9O_{34})_2]^{13\ominus}$,[83] the encrypted ions are tightly bound and therefore inert.

There is a fine distinction between *cryptates* and *clathrates*. The examples given in the preceding paragraph are probably best thought of as cryptates, since the enclosed ions have reasonably well-defined bonding interactions with the polyanion. Recent work has identified polyoxometalate inclusion compounds or clathrates in which the host–guest interaction is much weaker: for example, $[V_{12}O_{32}(CH_3CN)]^{4\ominus}$[84] and $[H_4V_{18}O_{42}(X)]^{9\ominus}$ (X = I, Br, Cl[85]; see Fig. 11). These compounds demonstrate that charge, as well as shape- and size-selectivity, can be important factors in the synthesis and possible reactivity of polyoxometalates (for the template effect of the enclosed anion, see Ref. [87] and Section 7).

7. Reduced Polyoxovanadates: A New Class of Metal–Oxygen Clusters

Although only two large V^V isopolyanions, $[V_{10}O_{28}]^{6\ominus}$[86] and $[V_{12}O_{32}]^{4\ominus}$,[84] are known, several V^{IV}-containing species have been isolated recently (Table 1). Their chemistry is different from that of the Mo and W anions, since, for example, the metal–metal interactions are not very marked (in contrast, spin pairing is preferred in reduced clusters of the 4d and 5d metals[56, 58]). Nearly all ratios of V^{IV} to V^V can be observed: V–O clusters are possible with as few as *two* $V^{IV}(d^1)$ centers (uncoupled or very weakly coupled spins) to as many as *eighteen* V^{IV} (d^1) centers (antiferromagnetically coupled with no V–V bonds). In clusters with small numbers of spins, the spins are found as far apart as possible. The magnetic moment per V^{IV} center decreases (indicating that spin–spin coupling increases) with increasing numbers of spins or V^{IV} centers (which necessarily come into closer contact) in a nearly continuous manner, a unique situation for metal cluster compounds[87] (Table 1). The coordination geometries at the V centers are also highly variable (tetrahedral (V^V), square-pyramidal (V^{IV}, V^V), octahedral (V^{IV}, V^V), and trigonal-bipyramidal (V^V)) and lead to structures unknown for Mo and W.

"Hollow spheres" with "cryptand/clathrate" properties may be formed by linking VO_5 pyramids. The spherical cluster shells $\{V_{18}O_{42}\}$ and $\{V_{15}O_{36}\}$[88–90] have the hitherto virtually unknown property of encapsulating negatively charged ions, even those with significantly different radii (as in the species $[H_4V_{18}O_{42}(X)]^{9\ominus}$, X = I, Br, Cl[85]). The anion serves as a template for the cluster shell, which can be widely varied in an "induced self-assembly" manner. The template itself can be formed from the reaction solution, leading, for example, to the generation of a cluster ($\{V_4O_4\}O_4$ cube) inside a cluster ($V_{30}O_{74}$ shell; cf. synthesis of the unusual mixed-valence species $[V_{34}O_{82}]^{10\ominus}$).[87]

Table 1. Vanadium–oxygen clusters with varying numbers of V^{IV} d^1 centers and spin–spin coupling (most of them with the O_{24} rhombicuboctahedron of the Keggin structure) [87].

Anion	Structure	V^{IV} centers	μ [h]	Ref.
$[V_{14}AsO_{40}]^{7\ominus}$	[a]	2	1.77	[87]
$[V_{12}O_{36}(AsOH)_3(AsO_4)]^{7\ominus}$	[b]	4	1.75	[87]
$[V_{12}As_8O_{40}(HCO_2)]^{3\ominus}$	[c, g]	6	1.75	[87]
$[V_{12}As_8O_{40}(HCO_2)]^{5\ominus}$	[c, g]	8	1.39	[87]
$[V_{12}As_8O_{40}(H_2O)]^{4\ominus}$	[c, g]	8	1.38	[87]
$[V_{15}O_{36}(Cl)]^{6\ominus}$	[d]	8	1.38	[90]
$[V_{18}O_{42}(SO_4)]^{8\ominus}$	[e, g]	12	1.14	[89]
$[V_{14}As_8O_{42}(SO_3)]^{6\ominus}$	[f, g]	14	1.20	[87]
$[V_{15}As_6O_{42}(H_2O)]^{6\ominus}$	[f, g]	15	1.08	[157]
$[V_{18}O_{42}H_4(I)]^{9\ominus}$	[e, g]	18	1.06	[85]

[a] Sherwoodite type. [b] Three-fourths of an AsV_{12} ε-Keggin-type structure capped with three VO and three AsOH groups. [c] Derivative of the "extended Keggin" V_{18} species (Fig. 12) in which $As_2O^{4\oplus}$ groups have replaced some of the twelve "original" VO groups and two of the six "extra" VO groups are missing. [d] $\{V_{15}O_{36}\}$ shell illustrated in Figure 13. [e] Shown in Figure 14. [f] As [c] but with no missing VO groups. [g] Rhombicuboctahedron spanned by 24 oxygen atoms as in the Keggin structure. [h] Magnetic moment per V^{IV} center at room temperature in μ_B.

Starting with the hypothetical $\{V_{12}O_{36}\}$ "Keggin" shell of cubic symmetry, VO groups can be added (according to the capped species of Scheme 1) to the six equivalent (100) square faces of the rhombicuboctahedron formed by the 24 oxygen atoms (thereby generating the $\{V_{18}O_{42}\}$ structure), or $As_2O^{4\oplus}$ groups can replace some of the "original" VO groups above the other 12 equivalent (110) square faces[85]

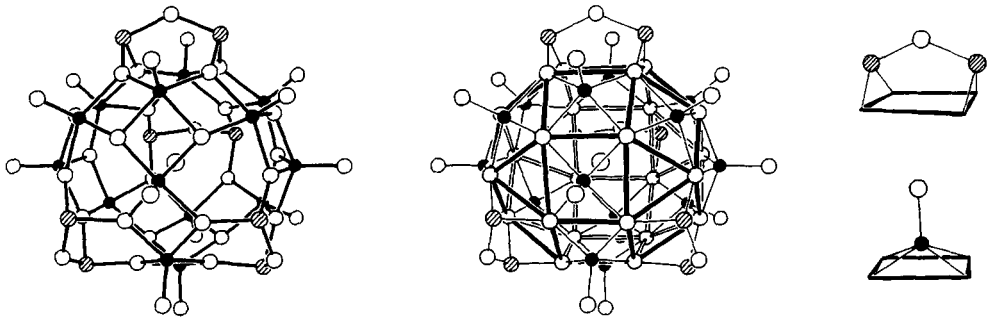

Fig. 12. Structure of $[V_{14}As_8O_{42}(H_2O)]^{4\ominus}$ and demonstration of the capping of the faces of the rhombicuboctahedron by VO and $As_2O^{4\oplus}$ groups [87].

(Fig. 12 and Table 1; see also Section 8). The complexation of, for example, $VO^{2\oplus}$, by a lacunary Keggin anion (Scheme 3), is analogous. Furthermore, binding of $(RX)_2O^{4\oplus}$ (X = Si, Ge) groups to (oxidized) lacunary Keggin anions was proposed[153] to occur in exactly the same fashion as that now demonstrated for $As_2O^{4\oplus}$ and the reduced vanadate clusters.

Other interesting and structurally unique mixed-valence species are the ellipsoidal cluster $[V_{19}O_{41}(OH)_9]^{8\ominus}$[91] (12 $V^{IV}O_6$ octahedra, 7 $V^{V}O_4$ tetrahedra, including a central group), $[AsV_{14}O_{40}]^{7\ominus}$[87] (12 $V^{V}O_6$ octahedra and 2 $V^{IV}O_5$ square pyramids, model for the mineral sherwoodite), $[V_{10}O_{26}]^{4\ominus}$[92] (8 $V^{V}O_4$ tetrahedra, 2 $V^{IV}O_5$ square pyramids), $[V_{15}As_6O_{42}(H_2O)]^{6\ominus}$ (which has D_3 symmetry and is a derivative of the V_{18} species, Table 1), and $[V_{15}O_{36}(CO_3)]^{7\ominus}$[85] (Fig. 13). The anion $[V_{19}O_{41}(OH)_9]^{8\ominus}$

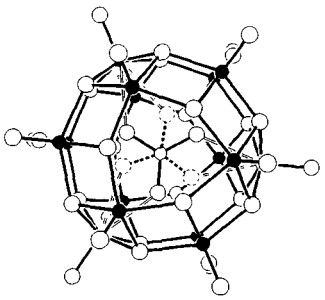

Fig. 13. Structure of $[V_{15}O_{36}(CO_3)]^{7\ominus}$ [85].

provides a molecular model for the magnetic properties of VO_2, since it contains six rather short V–V vectors and the singlet state is still highly populated at (for the magnetochemist) rather high temperatures.[87]

8. Topological Considerations

Egli è scritto in lingua matematica, e i caratteri son triangoli, cerchi, ed altre figure geometriche, senza i quali mezi è impossibile a intenderne umanamente parola...[*]

Galileo Galilei

Topology describes the properties of geometrical elements that are unchanged by reversible single-valued and continuous mappings.[93, 94] The most obvious connection to crystallography and chemistry is that crystals grow as convex polyhedra and that, in species of the type AX_n, the X atoms can form a (coordination) polyhedron. In addition, space-filling arrangements, in which small polyhedra are interconnected by vertex-, edge-, and face-sharing, are of importance for the subject considered here.

The important polyhedra are mostly *regular* (Platonic), with all vertices equivalent and all faces of the same type, and *semiregular* (Archimedean), where only the first condition is fulfilled.[95] Polyoxometalate chemistry is governed by these types of polyhedra, the vertices being defined by oxygen and/or metal atoms (Table 2; see also Section 3). Such "global" polyhedra may be distorted owing to the influence of a lower-symmetry central unit, as in the Keggin-type species.

The tendency of the oxygens to form space-filling assemblies (perhaps even closest-packed) of polyhedral domains, and of the metal atom centers to form polyhedra with mini-

[*] "[The greatest book of philosophy, which is the universe itself,] is written in the language of mathematics, and the letters are triangles, circles, and other geometrical figures, without whose help it is impossible for a human being to understand a single word."

Table 2. Polyhedra (M_x,O_y) spanned by metal and oxygen atoms of polyoxometalates.

x	Polyhedron	Point group [a]	y	Polyhedron	Point group [a]	Example	Ref.
6	octahedron	O_h	12	cuboctahedron	O_h	$[Mo_6O_{19}]^{2\ominus}$	[158]
12	icosahedron	I_h (T_h)	12 [b]	icosahedron	I_h	$[Mo_{12}O_{42}(Ce)]^{8\ominus}$	[159, 1b]
12	truncated tetrahedron	T_d	12 [b]	cuboctahedron	O_h (T_d)	$[Mo_{12}O_{34}(HOAsO_3)_4]^{4\ominus}$	[166]
12	cuboctahedron	O_h (T_d)	24	rhombicuboctahedron	O_h (T_d)	$[Mo_{12}O_{36}(PO_4)]^{3\ominus}$ (α-Keggin)	[161]
12	anticuboctahedron [c]	D_{3h} (C_{3v})				$[W_{12}O_{36}(SiO_4)]^{4\ominus}$ (β-Keggin [d])	[162]
12	truncated tetrahedron	T_d				$[V_{12}O_{40}Mn_3H_3]^{5\ominus}$ [e] (ε-Keggin [f])	[163]
12	cuboctahedron	O_h (D_{4h})				sherwoodite core [g] $[V_{14}O_{40}(Al)]^{9\ominus}$	[164]
			24	rhombicuboctahedron	O_h (T_d)	$[V_{18}O_{42}(SO_4)]^{8\ominus}$	[89]
			24	"14th Archimedean solid" [h]	D_{4d}	$[H_4V_{18}O_{42}(X)]^{9\ominus}$ (X = Cl, Br, I)	[85]

[a] Real symmetry due to systematic distortion in parentheses. [b] Inner shell of oxygen atoms. [c] Not an Archimedean solid; it can be derived from the cuboctahedron by a 60° rotation of one triangle (see [d]). [d] Derived from the α-Keggin isomer by a 60° rotation of one $\{M_3O_{13}\}$ unit (see Scheme 1). [e] Symmetry reduced to C_{3v} by Mn and H atoms. The polycation $[Al_{12}(OH)_{24}(H_2O)_{12}(AlO_4)]^{7\oplus}$ is a hydroxo cluster with this structure [165]. [f] Derived from the α-Keggin isomer by 60° rotations of all $\{M_3O_{13}\}$ units (see Scheme 1). [g] Figure 2. [h] Not an Archimedean solid; it can be derived from the rhombicuboctahedron by a 45° rotation of one hemisphere.

mization of Coulombic repulsions, seems obvious but is not completely understood.

Two compounds with the same $\{V_{18}O_{42}\}$ fragment form an illustrative example. The 24 oxygen atoms of the spherical shells of $[H_4V_{18}O_{42}(X)]^{9\ominus}$ and $[H_9V_{18}O_{42}(VO_4)]^{6\ominus}$ form corners of convex polyhedra (with idealized sides of equal length). The first structure forms the so-called 14th Archimedean solid[96] (also called pseudo-rhombicuboctahedron; its vertices are not equivalent, but each one is surrounded by three squares and one triangle in an equal way). This can be converted into the rhombicuboctahedron (one of the usual 13 Archimedean solids) by a 45° rotation of the upper hemisphere. The latter polyhedron (but with a tetrahedral distortion induced by the central VO_4 unit) is formed by the corresponding 24 oxygens of the second polyvanadate anion[85] (Fig. 14).

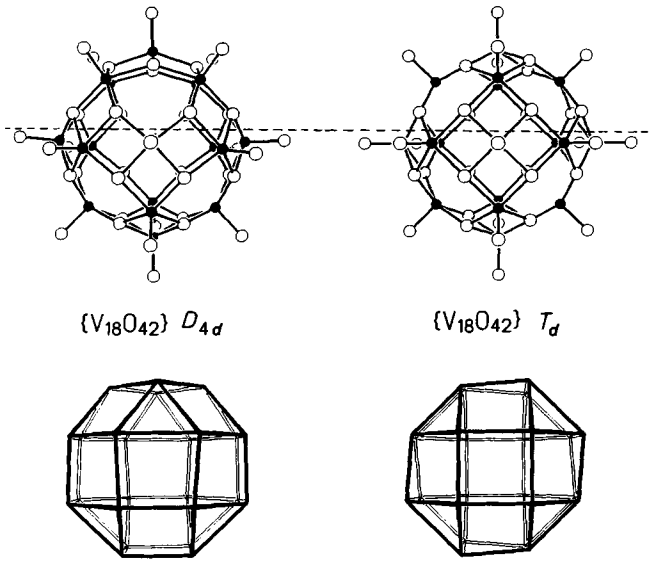

Fig. 14. Comparison of the structures of the $\{V_{18}O_{42}\}$ shells of $[H_4V_{18}O_{42}(X)]^{9\ominus}$ and $[H_9V_{18}O_{42}(VO_4)]^{6\ominus}$ (black = V, white = O), which can be interconverted by C_8 rotation of a hemisphere (marked by dotted line), and the demonstration of the so-called 14th Archimedean solid [96] and the rhombicuboctahedron, respectively, spanned by the 24 bridging oxygen atoms of these two anions [85].

An aspect relevant to chemistry and based on capping by VO or $As_2O^{4\oplus}$ groups of the two sets of O_4-square faces of the rhombicuboctahedron of the Keggin anion was mentioned in Section 7.

9. Applications

The applications of polyoxometalates are mainly based on their unique properties, including size, mass, electron- and proton-transfer/storage abilities, thermal stability, lability of "lattice oxygen", high Brønsted acidity of the corresponding acids. An additional advantage is the fact that heteropoly acids can be separated and enriched by extraction into organic solvents.

9.1. Analytical and Clinical Chemistry

Polyoxometalates have long been used for detection, separations, and quantitation, based particularly on properties such as (1) their high molecular weights, (2) their electrochemical activity and reducibility to form colored species, and (3) the variety of elements that can be incorporated. Consequently, many different types of analytical methods can be used for a variety of purposes. Some 26 elements can be determined through heteropolymolybdate formation alone.[97]

The earliest[98] and still probably the most widely used application has been the determination of P and Si either gravimetrically or by physical methods after reduction to heteropoly blues. Recent examples include simultaneous determination of P, Si, Ge, and As by differential-pulse anodic voltammetry,[99] chromatographic (HPLC) separations,[100] and measurement of nanomolar concentrations of silica in seawater.[101]

Many pharmaceuticals and biological samples are routinely determined using polyoxometalates.[102] The ability of polyoxometalates to coagulate proteins and to precipitate organic molecules like alkaloids is important in this connection. Their use in clinical chemistry and in the analysis of drug preparations, pesticides, and other biologically active molecules was reviewed recently.[102] Some examples are shown in Table 3. The methods involve reduction to mixed-valence blues (uric acid determination,[103] Lowry protein determination[104]) or selective precipitation (cholesterol, low-density (LDL) and high-density lipoprotein (HDL) separations[105]).

Table 3. Use of heteropolymolybdates to analyze biomaterials [a].

Sample	Substance	Polyanion used	Method [b]
Whole blood	Si	$SiMo_{12}$ blue	S
Blood serum	Si	$SiMo_{12}$ blue	S
Blood, urine	As	$AsMo_{12}$ blue	S, N
Biosolutions	uric acid	$SiMo_{12}$ blue	S
	uric acid	PMo_{12}	G
Cell nuclei	histones	PMo_{12} blue	S
Animal tissues	nialamide [c]	PMo_{12} in ethanol	TLC
	cocaine	PMo_{12} in ethanol	TLC
	amidopyrine	$SiMo_{12}$	G

[a] Abstracted from [102]. [b] S, spectrophotometry; N, nephelometry; G, gravimetry; TLC, thin layer chromatography. [c] Antidepressive.

The use of polytungstates, long employed as imaging agents, for electron microscopy has recently been improved with the development of organic derivatives of these anions[106, 107] that permit highly selective labeling.

9.2. Catalysis and Photocatalysis

Heteropolyanions are widely used as oxidation catalysts as well as acid catalysts. They are also excellent model systems for investigating several fundamental problems of catalysis.

The basic reversible redox reactions involved in substrate oxidations are shown in Equations (g) and (h), where

$[HPA]_{ox}$ and $[HPA]_{red}$ signify the oxidized and reduced forms of a heteropolyanion. Such catalysts can be used, for instance, in the formation of carboxylic acids from the corresponding aldehydes, as well as in the dehydrogenation of alcohols, aldehydes, and carboxylic acids to form C=C and C=O bonds.

$$[HPA]_{ox} + \text{substrate} + i\,H^{\oplus} \rightleftarrows H_i[HPA]_{red} + \text{oxidized substrate} \quad (g)$$

$$H_i[HPA]_{red} + i/4\,O_2 \rightleftarrows [HPA]_{ox} + i/2\,H_2O \quad (h)$$

Heterogeneous catalytic oxidation processes involving well-characterized polyoxometalates have been reviewed:[108-110] among the more important are the commercial vapor-phase oxidation of methacrolein to methacrylic acid (80000 tons per year)[111] and methane oxidation.[112] Synthesis of new bifunctional catalysts from polyoxometalates (e.g., $[(Ph_3P)_2Rh(CO)]_4[SiW_{12}O_{40}]$, which can be used for sequential hydroformylation and oxidation of olefins) is a recent development.[113]

Homogeneous oxidative catalytic activity[114] has been demonstrated for both thermal[115] and photochemical dehydrogenation and H_2 evolution from RX-type (e.g., X = CH_2OH, COOH) species, including water-splitting processes,[116-118] and for oxygen transfer to alkanes.[119] Polymolybdovanadates have been used as reoxidants in Wacker chemistry (oxidation of alkenes, coupling of aromatics) and may themselves be reoxidized with oxygen[120] [Eqs. (i) and (j)].

$$Pd^0 + [HPA]_{ox} + 2H^{\oplus} \longrightarrow Pd^{II} + H_2[HPA]_{red} \quad (i)$$

$$H_2[HPA]_{red} + 1/2\,O_2 \longrightarrow [HPA]_{ox} + H_2O \quad (j)$$

Use of the heteropolyanion instead of the normal $CuCl_2$ oxidant avoids corrosion by HCl. Table 4 summarizes some catalyzed oxidation reactions.

Table 4. Some oxidation reactions catalyzed by polyoxometalates [a].

Reaction	Catalyst [b]	T [°C]	Yield [%]
Isobutene → methacrylonitrile	"$Mo_{10}PBi_3Fe_6K_{0.06}$"	420	74
Butene → maleic anhydride	"$Mo_{12}PBi_{0.36}Mn_{0.52}$"	400	63
Butadiene → furan	$(NH_4)_3[PMo_{12}O_{40}]$	350	21
Crotonaldehyde → furan	$[PMo_{12}O_{40}]^{3\ominus}$	350	40
Methacrolein → methacrylic acid	Mo-P-V-Cu, As, Bi, Cs	280–340	70–80
Isobutyric acid → methacrylic acid	$[PMo_{10}V_2O_{40}]^{5\ominus}$	310	70
Phenol → catechol, hydroquinone	$[PW_{12}O_{40}]^{3\ominus}/H_2O_2$	80	82

[a] Abstracted from [108]. Examples mostly from the patent literature. [b] Formula or approximate composition of catalyst.

The $V^{IV}/V^V/O$ polyoxometalate system is important for understanding the "V_2O_5" Contact Process catalyst for oxidation of SO_2. The catalyst is a melt formed from V_2O_5 and $NaVO_3$ and, during turnover, contains V^{IV} centers according to ESR studies[121,122] and therefore very probably contains mixed-valence polyvanadates. Similar species should also be involved in the Stretford Process for removal of H_2S from fossil fuel gas[123] [Eq. (k)].

$$HS^{\ominus} + 2\,V^V \longrightarrow \{S\} + 2\,V^{IV} + H^{\oplus} \quad (k)$$
(overall reaction: $H_2S + 1/2\,O_2 \longrightarrow S + H_2O$)

Polyoxometalate surfaces are models for metal oxide surfaces and the oxidation activity can be understood in terms of the loss of surface oxygen atoms and delocalization of the remaining electrons over several metal atoms under relatively mild conditions [schematically according to [Eq. (l)].

$$\{M^{n\oplus}-O\} \longrightarrow \{M^{(n-2)\oplus} - \square\} + O \quad (l)$$

Acid catalysis by heteropoly acids can nicely be related to the known data on their acidity. Compounds of the type $H_x[XM_{12}O_{40}]$ with the Keggin structure are strong polybasic acids. In the crystal lattice there are nonlocalized protons that rapidly exchange with the protons of the crystal water molecules of the so-called secondary structure and with the protons localized on the μ_2-bridging oxygen atoms of the polyanions. In aqueous solution the compounds are strong acids, which are often completely dissociated. Upon reduction, the anion basicity increases and, consequently, the anion has a tendency to become protonated [see Eqs. (i) and (j)]. Although heteropoly acids are more expensive than mineral acids like sulfuric and hydrochloric acid, they have the advantages of being nonvolatile, odorless, and thermally stable. They can be used in homogeneous acid catalysis as well as in heterogeneous catalysis using supports like silica gel or activated charcoal at temperatures of approximately 300 °C.

Since the acid centers are considered to be at the bridging oxygens on the anion's surface, knowledge of the electronic structures, as well as electron density studies, are of critical importance (see Section 5).

Table 5. Heteropolyanion acid-catalyzed reactions [a].

Reaction	Catalyst [b]	T [°C]	Activity ratio [c]
Homogeneous			
Propene → isopropanol	PMo_{12}, PW_{12}	150	2–4
Phenylacetylene → acetophenone	PMo_{12}, PW_{12}	60	>10
Heterogeneous			
Isopropanol → propene	PW_{12}	150	100
2-methylpropene, methanol → methyl *tert*-butyl ether	PMo_{12}, PW_{12}/SiO_2	90	300
Methacrylic acid → propene	PW_{12}, SiW_{12}	240	4

[a] Abstracted from [108]. [b] $[H_nXM_{12}O_{40}]$ abbreviated as XM_{12}. [c] Ratio of the catalytic activity of the heteropoly acid to that of mineral acids and silica-alumina for homogeneous and heterogeneous systems, respectively.

Currently, in what is probably the most important catalytic application, industrial production of 2-propanol, 2-butanol, and *tert*-butanol by liquid-phase hydration of the corresponding olefins [e.g., Eq. (m)] is catalyzed by tungstophosphoric acid. Table 5 gives an overview of different acid-catalyzed reactions.

$$CH_2 = CHCH_3 + H_2O \longrightarrow CH_3CH(OH)CH_3 \quad (m)$$

The most widely used industrial catalysts are probably those for hydrodesulfurization (HDS), hydrodenitrification (HDN), and hydrodemetalation (HDM) of fossil fuels (see, e.g., Refs. [124–126]). In most cases these catalysts contain,

before promotion, polymolybdate species (probably heptamolybdates) on an alumina support[125] and, in the promoted form, a "cobalt polymolybdate". Catalytic activity has been related to the form of polymolybdate used in impregnation of the alumina support.[125]

9.3. Solid-State Applications: Electronic and Protonic Conductors

Many of the solution properties of polyoxometalates are also observed in the crystalline salts and free acids, since the large anions tend to have very weak attractions for countercations and solvate molecules. In particular, the electron- and proton-transfer characteristics are often retained in the solid state. Crystalline acids of Keggin anions such as $H_3[PW_{12}O_{40}]\cdot 21H_2O$ are protonic conductors,[127] and proton-conducting films have been described.[128] The same types of acids have been used as solid electrolytes for fuel cells.[129] Electrochromic[130] and ion-selective electrodes have also been reported. An example of the latter, sensitive to ammonium ions, is based on compressed pellets of ammonium 12-molybdophosphate in polystyrene.[131] Insoluble molybdophosphate salts have also long been used and are commercially available as cation-exchange materials.[132] They are especially valuable for highly radioactive solutions that destroy organic resins. The use of polyoxometalates as inorganic electron-acceptor components in charge-transfer salts[133a] and of polytungstates as sources of inorganic resist materials[133b] demonstrate other recent applications in materials science.

9.4. Medicine: Antitumoral, Antiviral, and Antiretroviral Activity

Many polyoxometalate salts have been shown to be biologically active. Such activity includes highly selective inhibition of enzyme function,[134-136] in vitro and in vivo antitumoral activity,[137] antiviral activity (e.g., against rabies[138] and scrapie, the sheep version of "mad cow disease"[139]), and antiretroviral activity (e.g., against HIV infections, connected with AIDS, SAIDS[134]). One particular heteropolytungstate (HPA-23, see Fig. 10) has been used for treatment of AIDS patients in France. Research in this field is particularly vigorous.

Reasons for biological activity may include ionic size and shape (blocking of the CD4 plasmamembrane receptors of T4 lymphocytes for the interaction with the gp 120 envelope glycoprotein of HIV?), electron-transfer and -reservoir properties (i.e., inhibition of biological electron transfer[140]), and stability (or nonlability) at micromolar concentrations and physiological pH (particularly true for large polytungstates, but also, surprisingly, for some molybdates and vanadates).

10. Occurrence in the Geo- and Biospheres

The geochemistry of vanadium is particularly diverse.[141-143] Three oxidation states are detectable, and two (IV, V) are stable in the normal range of geological environments. Consequently, a bewildering variety of interesting minerals, including many mixed-valence ones, are known (e.g., the heteropolyanion-containing sherwoodite;[142, 143] see Scheme 2). There are also several minerals (e.g., pascoite, hummerite) that contain the isopoly decavanadate anion, $[V_{10}O_{28}]^{6\ominus}$.[142, 143] The oxidized and mixed-valence minerals are presumably formed by weathering of the primary postmagmatic ore montroesite, (V,Fe)O(OH).[142, 143] The geochemical situation corresponds to the variety of mixed-valence vanadium clusters (Section 7).

As expected, molybdenum and tungsten do not form such a variety of mixed-valence minerals. There is only one known related (amorphous) oxidic species, ilsemannite, a blue mixed-valence molybdenum mineral.[142]

Little is known about the aggregation of $MO_4^{n\ominus}$ (M = V, Mo, W) anions in the biosphere, bearing in mind the low concentrations under physiological conditions. The mononuclear species are important for uptake and transport of the elements V, Mo, and W. Mo is an essential trace element for most, if not all, organisms, and V and Mo are involved in biological nitrogen fixation. The Mo storage protein[144] in *Azotobacter vinelandii* possibly contains an apoprotein with an isopolymolybdate core, since the release of Mo can easily be controlled by pH variation.

11. Thiometalates Are Different

The early transition elements discussed here also form thiometalates of the type $[MS_4]^{n\ominus}$ with d^0 configurations and polymeric species. Their chemistry is relevant for different biological processes (e.g., nitrogen fixation or the Cu–Mo antagonism of ruminants) and for their use as catalysts in industrial processes (e.g., HDS, see Section 9.2).

The very large differences in the chemistry between mononuclear oxo- and thioanions, $[MX_4]^{n\ominus}$, can be attributed to the following properties of the thioanions:[145-147]

1. The HOMO–LUMO difference is very small.
2. They are less basic than the oxoanions.
3. They exhibit strong electron-withdrawing properties as ligands.
4. They undergo intramolecular redox reactions ($S^{2\ominus}$ oxidation, M reduction) upon protonation [e.g., Eq. (n)] or heating [e.g., Eq. (o)]

$$[Mo^{VI}O_2S_2]^{2\ominus} \longrightarrow [Mo^{V}_2O_2S_2(S_2)_2]^{2\ominus} \quad (n)$$

$$[W^{VI}S_4]^{2\ominus} \longrightarrow [W^{IV}S(W^{VI}S_4)_2]^{2\ominus} \quad (o)$$

5. Metal sulfides, with reduced metal centers, are easily and irreversibly precipitated from aqueous solution.

The following differences in the chemistry of the polynuclear thioanions result:

1. Coordination numbers of the metal centers are in general smaller (4, 5) as a result of the larger S atom.
2. There is a tendency towards the formation of smaller aggregates.
3. Lower oxidation states of the metal atoms tend to be favored as a result of facile intramolecular redox pro-

cesses. Exceptions involve Nb and Ta, which are difficult to reduce (see, for example, the hexanuclear thioanions[148]).

4. $S_n^{2\ominus}$ (mainly $S_2^{2\ominus}$) ligands are frequently present.
5. Thiometalate complexes almost always exist with mononuclear ligands (e.g., $[Ni(WS_4)_2]^{2\ominus}$), although it has been possible to replace oxygen by sulfur to a very limited extent in polyoxometalates (e.g., $[NbW_5O_{18}S]^{3\ominus}$[149]).

12. Epilogue

Savoir pour prévoir[*]
Auguste Comte

The molecular metal–oxygen clusters of the early transition elements are remarkable for their topology and electronic structures (electron-, proton-, and oxygen-reservoir properties). Although the first compounds of this type were reported over 150 years ago, new types of clusters continue to be discovered.

It will be important to understand the high tendency for self-assembly of the "spherical" species in terms of close-packing of oxygens and minimal metal–metal repulsions. A predictable direction for future research will be exploitation of the unique property of these species, namely, that metal–metal interactions can be varied from extremely weak (but nonzero[150]), through weak (antiferromagnetic coupling), to strong (metal–metal bonding) by stepwise reduction of the cluster without changing its topology. It should be kept in mind that metal–oxygen, as well as metal–sulfur, clusters play an important role in the biosphere and in catalysis.

That some species may be used to model n-type semiconducting oxides and indeed other solid-state processes and that others display reactivity with respect to oxygen-transfer processes (e.g., those catalyzed by enzymes like the Mo-containing oxygen transferases, but also selective oxidation processes) are additional factors that have not gone unnoticed and will continue to stimulate research. The characterization of the different electron-transfer components in the photosynthesis system, for example, is of importance and heteropolyanions can be of help as artificial electron acceptors (see, for instance, Ref. [102]).

The possible impact for further medical applications is difficult to predict, and research in this area (e.g., related to HIV replication) is still being carried out in several institutions. The reasons for the versatile biological functions need further clarification.

Michael T. Pope thanks the Alexander von Humboldt Foundation for a Senior Scientist Award and Georgetown University for a sabbatical leave, during which this article was prepared, as well as the National Science Foundation, the Petroleum Research Fund, administered by the American Chemical Society, and ARCO Chemical Corporation for research support. Achim Müller thanks the Deutsche Forschungsgemeinschaft, the Fonds der Chemischen Industrie, and the Westfälisch-Lippische Universitätsgesellschaft for financial support. We are both deeply indebted to our co-workers, whose names appear in the references, for their friendship, enthusiasm, hard work, and insights, and to our colleagues for valuable discussions. We particularly thank Dr. Howard T. Evans, Jr., for permission to use many of his structural illustrations, Michael Penk for his skills in preparing several polyhedral diagrams, and Chaoying Rong for recording the cyclic voltammogram shown in Figure 7.

Received: July 18, 1990 [A 802 IE]
German version: *Angew. Chemie 103* (1991) 56

[*] Know in order to predict.

[1] a) P. Souchay: *Ions Minéraux Condensés*, Masson, Paris 1969; b) M. T. Pope: *Heteropoly and Isopoly Oxometalates*, Springer, New York 1983; c) V. W. Day, W. G. Klemperer, *Science (Washington, DC) 228* (1985) 533; d) M. T. Pope in G. Wilkinson, R. D. Gillard, J. A. McCleverty (Eds.): *Comprehensive Coordination Chemistry, Vol. 3*, Pergamon, Oxford 1987, p. 1023. More specialized reviews are cited in the text.
[2] J. J. Berzelius, *Poggendorffs Ann. Phys. Chem. 6* (1826) 369, 380.
[3] *Gmelin Handbuch der Anorganischen Chemie*, Verlag Chemie, Berlin; System-No. 53 (Molybdän) 1935; System-No. 54 (Wolfram) 1933.
[4] The history of these compounds and the hypotheses for their structures are extensively discussed (more than 15 pages in the chapter entitled "Über die Komplexnatur und die Besonderheiten der Polysäuren") in F. Hein: *Chemische Koordinationslehre*, S. Hirzel, Leipzig 1950.
[5] L. Pauling, *J. Am. Chem. Soc. 51* (1929) 2868.
[6] J. F. Keggin, *Nature (London) 131* (1933) 908; *Proc. R. Soc. London Ser. A 144* (1934) 75.
[7] H. T. Evans, Jr., *Perspect. Struct. Chem. 4* (1971) 1.
[8] J. Fuchs, *Z. Naturforsch. B 28* (1973) 389.
[9] M. Filowitz, R. K. C. Ho, W. G. Klemperer, W. Shum, *Inorg. Chem. 18* (1979) 93.
[10] R. Acerete, C. F. Hammer, L. C. W. Baker, *J. Am. Chem. Soc. 101* (1979) 267.
[11] P. J. Domaille, *J. Am. Chem. Soc. 106* (1984) 7677.
[12] C. J. Besecker, W. G. Klemperer, D. J. Maltbie, D. A. Wright, *Inorg. Chem. 24* (1985) 1027.
[13] T. L. Jorris, M. Kozik, N. Casan-Pastor, P. J. Domaille, R. G. Finke, W. K. Miller, L. C. W. Baker, *J. Am. Chem. Soc. 109* (1987) 7402.
[14] M. A. Leparulo-Loftus, M. T. Pope, *Inorg. Chem. 26* (1987) 2112.
[15] L. Pettersson, I. Andersson, L.-O. Öhman, *Inorg. Chem. 25* (1986) 4726.
[16] K. H. Tytko, G.Baethe, J. J. Cruywagen, *Inorg. Chem. 24* (1985) 3132.
[17] K. S. Suslick, J. C. Cook, B. Rapko, M. W. Droege, R. G. Finke, *Inorg. Chem. 25* (1986) 241.
[18] See appendix of [1 b] and Y. Jeannin, M. Fournier, *Pure Appl. Chem. 59* (1987) 1529.
[19] D. C. Crans, E. M. Willging, S. R. Butler, *J. Am. Chem. Soc. 112* (1990) 427.
[20] L. Ma, S. Liu, J. Zubieta, *J. Chem. Soc. Chem. Commun. 1989*, 440.
[21] Q. Chen, S. Liu, J. Zubieta, *Inorg. Chem. 28* (1989) 4433; *Angew. Chem. 102* (1990) 100; *Angew. Chem. Int. Ed. Engl. 29* (1990) 70.
[22] W. N. Lipscomb, *Inorg. Chem. 4* (1965) 132.
[23] K. G. Burtseva, T. S. Chernaya, M. I. Sirota, *Dokl. Akad. Nauk SSSR 243* (1978) 104; *Sov. Phys. Dokl. (Engl. Transl.) 23* (1978) 784.
[24] V. S. Sergienko, V. N. Molchanov, M. A. Porai-Koshits, *Koord. Khim. 5* (1979) 936; *Sov. J. Coord. Chem. (Engl. Transl.) 5* (1979) 740.
[25] See [1 b], p. 130.
[26] P. Schreiber, K. Wieghardt, B. Nuber, J. Weiss, *Polyhedron 8* (1989) 1675.
[27] L. Ma, S. Liu, J. Zubieta, *Inorg. Chem. 28* (1989) 175.
[28] A. Müller, E. Krickemeyer, M. Penk, V. Wittneben, J. Döring, *Angew. Chem. 102* (1990) 85; *Angew. Chem. Int. Ed. Engl. 29* (1990) 88. The $\{MoO_3\}$-containing species is mentioned in footnote [5].
[29] D. L. Kepert, *Inorg. Chem. 8* (1969) 1556.
[30] P. B. Moore, *Neues Jahrb. Mineral. Abh. 120* (1974) 205.
[31] H.-J. Lunk, S. Schönherr, *Z. Chem. 27* (1987) 157.
[32] H. K. Chae, W. G. Klemperer, V. W. Day, *Inorg. Chem. 28* (1989) 1423.
[33] Y. Hayashi, Y. Ozawa, K. Isobe, *Chem. Lett. 1989*, 425.
[34] Q. Chen, J. Zubieta, *Inorg. Chem. 29* (1990) 1456.
[35] V. W. Day, M. F. Fredrich, W. G. Klemperer, W. Shum, *J. Am. Chem. Soc. 99* (1977) 952.
[36] a) S. H. Wasfi, W. Kwak, M. T. Pope, K. M. Barkigia, R. J. Butcher, C. O. Quicksall, *J. Am. Chem. Soc. 100* (1978) 7786; b) P. R. Sethuraman, M. A. Leparulo, M. T. Pope, F. Zonnevijlle, C. Brévard, J. Lemerle, *ibid. 103* (1981) 7665.
[37] W. G. Klemperer, C. Schwartz, D. A. Wright, *J. Am. Chem. Soc. 107* (1985) 6941.
[38] B. Krebs, I. Paulat-Böschen, *Acta Crystallogr. Sect B 38* (1982) 1710.
[39] a) See, e.g., K.-H. Tytko, O. Glemser, *Adv. Inorg. Chem. Radiochem. 19* (1976) 239; b) "Early Transition Metal Polyoxoanions", *Inorg. Synth. 27* (1990) Chap. 3, p. 71.

[40] D. E. Katsoulis, M. T. Pope, *J. Am. Chem. Soc. 106* (1984) 2737.
[41] B. Krebs in A. Müller, E. Diemann (Eds.): *Transition Metal Chemistry*, Verlag Chemie, Weinheim 1981, p. 91.
[42] D. J. Edlund, R. J. Saxton, D. K. Lyon, R. G. Finke, *Organometallics 7* (1988) 1692.
[43] D. E. Katsoulis, M. T. Pope, *J. Chem. Soc. Chem. Commun. 1986*, 1186.
[44] K. Piepgrass, M. T. Pope, *J. Am. Chem. Soc. 111* (1989) 753.
[45] M. T. Pope, *Inorg. Chem. 11* (1972) 1973.
[46] A. Müller, V. Wittneben, unpublished.
[47] K. Eguchi, T. Seiyama, N. Yamazoe, S. Katsuki, H. Taketa, *J. Catal. 111* (1988) 336.
[48] M. T. Pope in D. B. Brown (Eds.): *Mixed-Valence Compounds, NATO ASI Ser. C*, Reidel, Dordrecht 1980, p. 365.
[49] J. P. Launay, M. Fournier, C. Sanchez, J. Livage, M. T. Pope, *Inorg. Nucl. Chem. Lett. 16* (1980) 257.
[50] C. Sanchez, J. Livage, J. P. Launay, M. Fournier, Y. Jeannin, *J. Am. Chem. Soc. 104* (1982) 3194.
[51] M. Kozik, C. F. Hammer, L. C. W. Baker, *J. Am. Chem. Soc. 108* (1986) 7627.
[52] K. Piepgrass, J. N. Barrows, M. T. Pope, *J. Chem. Soc. Chem. Commun. 1989*, 10.
[53] S. P. Harmalker, M. A. Leparulo, M. T. Pope, *J. Am. Chem. Soc. 105* (1983) 4286.
[54] H. So, C. W. Lee, D. Lee, *Bull. Korean Chem. Soc. 8* (1987) 384.
[55] L. P. Kazanskii, M. A. Fedotov, I. V. Potapova, V. I. Spitsyn, *Dokl. Adad. Nauk SSSR 244* (1979) 372; *Dokl. Chem. (Engl. Transl.) 244* (1979) 36.
[56] M. Kozik, C. F. Hammer, L. C. W. Baker, *J. Am. Chem. Soc. 108* (1986) 2748.
[57] M. Kozik, N. Casan-Pastor, C. F. Hammer, L. C. W. Baker, *J. Am. Chem. Soc. 110* (1988) 7697.
[58] J. N. Barrows, M. T. Pope, *Adv. Chem. Ser. 226* (1990) 403.
[59] N. Casan-Pastor, *Ph.D. Thesis*, Georgetown University, Washington, DC, 1988; *Diss. Abstr. Int. B 50* (1989) 1397.
[60] J. N. Barrows, G. B. Jameson, M. T. Pope, *J. Am. Chem. Soc. 107* (1985) 1771.
[61] J. P. Launay, *J. Inorg. Nucl. Chem. 38* (1976) 807.
[62] Y. Jeannin, J. P. Launay, M. A. Seid Sedjadi, *Inorg. Chem. 19* (1980) 2933.
[63] K. Piepgrass, M. T. Pope, *J. Am. Chem. Soc. 109* (1987) 1586.
[64] F. A. Cotton, *Inorg. Chem. 3* (1964) 1217.
[65] A. Müller, R. Jostes, F. A. Cotton, *Angew. Chem. 92* (1980) 921; *Angew. Chem. Int. Ed. Engl. 19* (1980) 875.
[66] D. R. Wexell, M. T. Pope, *Chem. Commun. 1971*, 886.
[67] L. McKean, M. T. Pope, *Inorg. Chem. 13* (1974) 747.
[68] J. J. Altenau, M. T. Pope, R. A. Prados, H. So, *Inorg. Chem. 14* (1975) 417.
[69] R. Acerete, N. Casan-Pastor, J. Bas-Serra, L. C. W. Baker, *J. Am. Chem. Soc. 111* (1989) 6049.
[70] K. Piepgrass, *Ph. D. Thesis*, Georgetown University, Washington, DC, 1989; *Diss. Abstr. Int. B 50* (1990) 5059.
[71] M. A. Petrukhina, V. M. Ionov, A. E. Prozorovskii, V. N. Molchanov, I. V. Tat'yanina, E. A. Torchenkova, *Koord. Khim. 14* (1988) 1519; *Sov. J. Coord. Chem. (Engl. Transl.) 14* (1988) 855.
[72] R. G. Finke, B. Rapko, P. J. Domaille, *Organometallics 5* (1986) 175.
[73] T. J. R. Weakley, *Struct. Bonding (Berlin) 18* (1974) 131.
[74] C. L. Hill, R. B. Brown, Jr., *J. Am. Chem. Soc. 108* (1986) 536.
[75] P. J. Domaille, R. L. Harlow, *J. Am. Chem. Soc. 108* (1986) 2108.
[76] R. Contant, A. Tézé, *Inorg. Chem. 24* (1985) 4610.
[77] M. H. Alizadeh, S. P. Harmalker, Y. Jeannin, J. Martin-Frère, M. T. Pope, *J. Am. Chem. Soc. 107* (1985) 2662.
[78] S. H. Wasfi, A. L. Rheingold, G. F. Kokoszka, A. S. Goldstein, *Inorg. Chem. 26* (1987) 2934.
[79] H. T. Evans, C. M. Tourné, G. F. Tourné, T. J. R. Weakley, *J. Chem. Soc. Dalton Trans. 1986*, 2699.
[80] J. Fischer, L. Ricard, R. Weiss, *J. Am. Chem. Soc. 98* (1976) 3050.
[81] M. Michelon, G. Hervé, M. Leyrie, *J. Inorg. Nucl. Chem. 42* (1980) 1583.
[82] T. L. Jorris, *Ph.D. Thesis*, Georgetown University, Washington, DC, 1987; *Diss. Abstr. Int. B 49* (1989) 2639; T. L. Jorris, M. Kozik, L. C. W. Baker, *Inorg. Chem. 29* (1990) 4584.
[83] W. H. Knoth, P. J. Domaille, R. L. Harlow, *Inorg. Chem. 25* (1986) 1577.
[84] V. W. Day, W. G. Klemperer, O. M. Yaghi, *J. Am. Chem. Soc. 111* (1989) 5959.
[85] A. Müller, M. Penk, R. Rohlfing, E. Krickemeyer, J. Döring, *Angew. Chem. 102* (1990) 927; *Angew. Chem. Int. Ed. Engl. 29* (1990) 926.
[86] H. T. Evans, Jr., *Inorg. Chem. 5* (1966) 967.
[87] A. Müller et al., unpublished results; A. Müller, J. Döring, M. I. Khan, V. Wittneben, *Angew. Chem. 103* (1991), in press; *Angew. Chem. Int. Ed. Engl. 30* (1991), in press; A. Müller, J. Döring, H. Bögge, *J. Chem. Soc. Chem. Commun.*, in press; A. Müller, R. Rohlfing, H. Bögge, J. Döring, M. Penk, *Angew. Chem. 103* (1991), in press; *Angew. Chem. Int. Ed. Engl. 30* (1991), in press.
[88] G. K. Johnson, E. O. Schlemper, *J. Am. Chem. Soc. 100* (1978) 3645.
[89] A. Müller, J. Döring, H. Bögge, E. Krickemeyer, *Chimia 42* (1988) 300.
[90] A. Müller, E. Krickemeyer, M. Penk, H.-J. Walberg, H. Bögge, *Angew. Chem. 99* (1987) 1060; *Angew. Chem. Int. Ed. Engl. 26* (1987) 1045.
[91] A. Müller, M. Penk, E. Krickemeyer, H. Bögge, H.-J. Walberg, *Angew. Chem. 100* (1988) 1787; *Angew. Chem. Int. Ed. Engl. 27* (1988) 1719.
[92] A. Bino, S. Cohen, C. Heitner-Wirguin, *Inorg. Chem. 21* (1982) 429.
[93] H. von Mangoldt, K. Knopp: *Höhere Mathematik, Bd. 4*, S. Hirzel, Stuttgart 1990.
[94] V. G. Boltjanskij, V. A. Efremovic: *Anschauliche Kombinatorische Topologie*, Vieweg, Wiesbaden 1986.
[95] J. Šaškin, A. Šaškin: *Ecken, Flächen, Kanten*, Harri Deutsch, Frankfurt am Main 1989.
[96] N. W. Johnson, *Can. J. Math. 18* (1966) 169.
[97] G. A. Parker: *Analytical Chemistry of Molybdenum*, Springer, New York 1983.
[98] F. Osmond, *Bull. Soc. Chim. Fr. 47* (1887) 745.
[99] A. G. Fogg, N. K. Bsebsu, B. J. Birch, *Talanta 28* (1981) 473.
[100] M. Braungart, H. Rüssel, *Chromatographia 19* (1984) 185.
[101] M. A. Brzezinski, D. M. Nelson, *Mar. Chem. 19* (1986) 139.
[102] E. N. Semenovskaya, *Zh. Anal. Khim. 41* (1986) 1925; *J. Anal. Chem. USSR (Engl. Transl.) 41* (1986) 1339.
[103] M. L. Matheke, G. Kessler, K. M. Chan, *Clin. Chem.* (Winston-Salem, NC) *33* (1987) 2109.
[104] G. Legler, C. M. Müller-Platz, M. Mentges-Hettkamp, G. Pflieger, E. Jülich, *Anal. Biochem. 150* (1985) 278.
[105] G. R. Warnick, C. Mayfield, J. Benderson, J. S. Chen, J. J. Albers, *Am. J. Clin. Pathol. 78* (1982) 718.
[106] J. F. W. Keana, M. D. Ogan, Y. Lü, M. Beer, J. Varkey, *J. Am. Chem. Soc. 107* (1985) 6714.
[107] J. F. W. Keana, Y. Wu, G. Wu, *J. Org. Chem. 52* (1987) 2571.
[108] M. Misono, *Catal. Rev. Sci. Eng. 29* (1987) 269.
[109] J. B. Moffat, *Chem. Eng. Commun. 83* (1989) 9.
[110] M. Misono, T. Okuhara, N. Mizuno, *Stud. Surf. Sci. Catal. 44* (1989) 267.
[111] E. M. Serwicka, J. B. Black, J. B. Goodenough, *J. Catal. 106* (1987) 23.
[112] S. Ahmed, J. B. Moffat, *Appl. Catal. 40* (1988) 101.
[113] A. R. Siedle, R. A. Newmark, W. B. Gleason, R. P. Skarjune, K. O. Hodgson, A. L. Roe, V. W. Day, *Solid State Ionics 26* (1988) 109; A. R. Siedle, R. A. Newmark, K. A. Brown-Wensley, R. P. Skarjune, L. C. Haddad, K. O. Hodgson, A. L. Roe, *Organometallics 7* (1988) 2078.
[114] I. V. Kozhevnikov, *Usp. Khim. 56* (1987) 1417; *Russ. Chem. Rev. (Engl. Transl.) 56* (1987) 811.
[115] R. Neumann, M. Lissel, *J. Org. Chem. 54* (1989) 4607.
[116] C. L. Hill, D. A. Bouchard, *J. Am. Chem. Soc. 107* (1985) 5148.
[117] E. Papaconstantinou, *Chem. Soc. Rev. 18* (1989) 1.
[118] T. Yamase, *Polyhedron 5* (1986) 79.
[119] M. Faraj, C. L. Hill, *J. Chem. Soc. Chem. Commun. 1987*, 1487.
[120] I. V. Kozhevnikov, K. I. Matveev, *Appl. Catal. 5* (1983) 135.
[121] C. N. Kenney, *Catalysis (London) 3* (1980) 123.
[122] I. M. Campbell: *Catalysis at Surfaces*, Chapman & Hall, New York 1988.
[123] A. J. Moyes, J. S. Wilkinson, *The Chemical Engineer 1974*, 84.
[124] A. Müller, E. Diemann, F.-W. Baumann, *Nachr. Chem. Tech. Lab. 36* (1988) 18; H. Topsøe, B. S. Clausen, N.-Y. Topsøe, P. Zeuthen in D. L. Trimm, S. Akashah, M. Absi-Halabi, A. Bishara (Eds.): *Catalysts in Petroleum Refining 1989*, Elsevier, Amsterdam 1990.
[125] H. Knözinger, *Proc. Int. Congr. Catal. 9th 5* (1988) 20, and references cited therein.
[126] T. Butz, C. Vogdt, A. Lerf, H. Knözinger, *J. Catal. 116* (1989) 31.
[127] A. Hardwick, P. G. Dickens, R. C. T. Slade, *Solid State Ionics 13* (1984) 345.
[128] M. Tatsumisago, T. Minomi, *J. Am. Ceram. Soc. 72* (1989) 484.
[129] O. Nakamura, *Prog. Batteries Sol. Cells 4* (1982) 230.
[130] T. Shimidzu, A. Ohtani, M. Aiba, K. Honda, *J. Chem. Soc. Faraday Trans. 1 84* (1988) 3941.
[131] Yu. G. Vlasov, M. S. Miloshova, P. P. Antonov, E. A. Bychkov, A. Ya. Efa, *Elektrokhimiya 19* (1983) 1049.
[132] J. van R. Smit, *Nature (London) 181* (1958) 1530.
[133] a) L. Ouahab, M. Bencharif, D. Grandjean, *C. R. Acad. Sci. Ser. 2 307* (1988) 749; b) H. Okamoto, T. Iwayanagi, K. Mochiji, H. Umezaki, T. Kudo, *Appl. Phys. Lett. 49* (1986) 298.
[134] D. Dormont, B. Spire, F. Barre-Sinoussi, L. Montagnier, J. C. Chermann, *Ann. Inst. Pasteur/Virol. 136 E* (1985) 75.
[135] E. G. DeMaster, R. A. Mitchell, *Biochem. Arch. 3* (1987) 301.
[136] R. H. Glew, M. S. Czuczman, W. F. Diven, R. L. Berens, M. T. Pope, D. E. Katsoulis, *Comp. Biochem. Physiol. B 72* (1982) 581.
[137] T. Yamase, H. Fujita, K. Fukushima, *Inorg. Chim. Acta 151* (1988) 15.
[138] F. Bussereau, M. Picard, J. Blancou, P. Sureau, *Acta Virol. (Engl. Ed.) 32* (1988) 33.
[139] R. H. Kimberlin, C. A. Walker, *Arch. Virol. 78* (1983) 9.
[140] G. Chottard, M. Michelon, M. Hervé, G. Hervé, *Biochim. Biophys. Acta 916* (1987) 402.
[141] W. E. Petrascheck, W. Pohl: *Lagerstättenlehre*, Schweizerbart'sche Verlagsbuchhandlung, Stuttgart 1982.
[142] H. J. Rösler: *Lehrbuch der Mineralogie*, Verlag für Grundstoffindustrie, Leipzig, 2nd ed., 1981.

[143] H. T. Evans, Jr., S. Landergren: "Vanadium" in K. H. Wedepohl (Ed.): *Handbook of Geochemistry, Vol. II/2*, Springer, Berlin 1978.
[144] P. T. Pienkos, W. J. Brill, *J. Bacteriol. 145* (1981) 743.
[145] A. Müller, *Polyhedron 5* (1986) 323; A. Müller, E. Diemann, R. Jostes, H. Bögge, *Angew. Chem. 93* (1981) 957; *Angew. Chem. Int. Ed. Engl. 20* (1981) 934.
[146] A. Müller, E. Diemann in G. Wilkinson, R. D. Gillard, J. A. McCleverty (Eds.): *Comprehensive Coordination Chemistry, Vol. 2*, Pergamon, Oxford 1987, Chap. 16.1.
[147] See [146], Chap. 16.3.
[148] J. Sola, Y. Do, J. M. Berg, R. H. Holm, *J. Am. Chem. Soc. 105* (1983) 7784.
[149] W. G. Klemperer, C. Schwartz, *Inorg. Chem. 24* (1985) 4459.
[150] That polyoxometalates form at all is evidence of metal–metal interactions. The observation of small (< 50 Hz) W–W NMR coupling constants is a further argument.
[151] D. E. Katsoulis, M. T. Pope, *J. Chem. Soc. Dalton Trans. 1989*, 1483.
[152] R. K. C. Ho, W. G. Klemperer, *J. Am. Chem. Soc. 100* (1978) 6772.
[153] W. H. Knoth, *J. Am. Chem. Soc. 101* (1979) 759.
[154] G. S. Chorghade, M. T. Pope, *J. Am. Chem. Soc. 109* (1987) 5134.
[155] R. D. Peacock, T. J. R. Weakley, *J. Chem. Soc. A 1971*, 1836.
[156] F. Ortéga, M. T. Pope, *Inorg. Chem. 23* (1984) 3292.
[157] A. Müller, J. Döring, *Angew. Chem. 100* (1988) 1789; *Angew. Chem. Int. Ed. Engl. 27* (1988) 1721.
[158] O. Nagano, Y. Sasaki, *Acta Crystallogr. Sect. B 35* (1979) 2387.
[159] D. D. Dexter, J. V. Silverton, *J. Am. Chem. Soc. 90* (1968) 3589.
[160] T. Nishikawa, Y. Sasaki, *Chem. Lett. 1975*, 1185.
[161] H. D'Amour, R. Allmann, *Z. Kristallogr. Kristallgeom. Kristallphys. Kristallchem. 143* (1976) 1.
[162] K. Y. Matsumoto, A. Kobayashi, Y. Sasaki, *Bull. Chem. Soc. Jpn. 48* (1975) 3146.
[163] H. Ichida, K. Nagai, Y. Sasaki, M. T. Pope, *J. Am. Chem. Soc. 111* (1989) 586.
[164] H. T. Evans, Jr., J. A. Konnert, *Am. Mineral. 63* (1978) 863.
[165] G. Johansson, *Ark. Kemi 20* (1963) 305, 321.

Enantioselective Addition of Organometallic Reagents to Carbonyl Compounds: Chirality Transfer, Multiplication, and Amplification**

New Synthetic Methods (83)

By Ryoji Noyori* and Masato Kitamura

Nucleophilic addition of organometallic reagents to carbonyl substrates constitutes one of the most fundamental operations in organic synthesis. Modification of the organometallic compounds by chiral, nonracemic auxiliaries offers a general opportunity to create optically active alcohols, and the catalytic version in particular provides maximum synthetic efficiency. The use of organozinc chemistry, unlike conventional organolithium or -magnesium chemistry, has realized an ideal catalytic enantioselective alkylation of aldehydes leading to a diverse array of secondary alcohols of high optical purity. A combination of dialkylzinc compounds and certain sterically constrained β-dialkylamino alcohols, such as (−)-3-*exo*-dimethylaminoisoborneol [(−)-DAIB], as chiral inducers affords the best result (up to 99% *ee*). The alkyl transfer reaction occurs via a dinuclear Zn complex containing a chiral amino alkoxide, an aldehyde ligand, and three alkyl groups. The chiral multiplication method exhibits enormous chiral amplification: a high level of enantioselection (up to 98%) is attainable by use of DAIB in 14% *ee*. This unusual nonlinear effect is a result of a marked difference in chemical properties of the diastereomeric (homochiral and heterochiral) dinuclear complexes formed from the dialkylzinc and the DAIB auxiliary. This phenomenon may be the beginning of a new generation of enantioselective organic reactions.

1. Introduction

Chirality is a major phenomenon in Nature, and molecular asymmetry in particular is playing a crucial role in science and technology. A variety of significant biological functions emerge through molecular recognition, which requires strict matching of chirality. Nonracemic molecules will also contribute to the creation of advanced materials possessing unique physical properties. Accordingly enantioselective synthesis of chiral organic compounds is an important task allotted to synthetic chemists. Asymmetric catalysis using chiral metal complexes, among others, provides a general, powerful tool in this context.[1]

The carbon–carbon bond forming reaction, together with oxidation, reduction, and functional group transformation, is one of the most fundamental operations for constructing organic molecules. Addition of organometallic reagents to carbonyl compounds is among the most common reactions for this purpose, complementary to reduction of aldehydes or ketones, and provides a reliable way to form alcoholic products. Organometallic chemistry dates back to the discovery of organozinc compounds by *Frankland* in 1849.[2] Although this pioneering achievement was deeply appreciated, the significance of organozinc chemistry remained somewhat underestimated, at least in terms of synthetic utility. The Reformatsky reaction[3] and Simmons–Smith reaction[4] utilize Zn metal but, in simple alkylation to carbonyl compounds, organozinc compounds were replaced by Grignard reagents (discovered 50 years later)[5] and organolithium compounds (developed by *Wittig* and *Gilman*[6] among others), owing perhaps to their higher generality, higher reactivity, and easier manipulation. Recently, the chemistry of organoboron, -aluminum, -titanium, -lanthanide compounds, etc. has been further developed with the hope of obtaining high selectivities. The enantioselective version of the reaction between organometallic reagents and carbonyl compounds which leads to optically active alcohols is desirable because of its general synthetic importance.

A nonracemic, chiral environment can be introduced into organometallic compounds in two ways (Fig. 1). One is the coordination of aprotic chiral solvents or complexing agents to the metallic center, and the other is the modification of the organometallic reagent by protic chiral ancillaries, such as alcohols or amines, to give organometallic alkoxides or amides, respectively. The molecular structures of various main-group organometallic compounds having neutral and anionic ligands have been studied by X-ray crystallographic analysis and spectroscopic methods, revealing that the steric and electronic properties of the ligands significantly affect the structures, including configuration, metal coordination number, and bond polarity.[7–9] Many organometallic compounds form labile molecular associates, so the aggregation state responsible for the reaction may be different from that of the ground-state structure. The organometallic compounds are amphiphilic in nature: the nucleophilicity of the carbon moiety and Lewis acidity of the metallic center cooperate in the alkyl transfer reaction. Thus chiral ligands per-

Fig. 1. Enantioselective addition of organometallic reagents to carbonyl compounds. L* = neutral or anionic chiral ligand

[*] Prof. Dr. R. Noyori, Dr. M. Kitamura
Department of Chemistry, Nagoya University
Chikusa, Nagoya 464-01 (Japan)

[**] Parts of this review were presented by *R. N.* during his Merck-Schuchardt lecture series in the Federal Republic of Germany in May 1989.
Ar represents aryl substituents in this article.

turb the structure and stability of the transition state in many ways.

In the last two decades, a number of highly enantioselective alkylation reactions of carbonyl compounds have been developed by proper combination of organometallic reagents and well-designed chiral ancillaries. So far most selective reactions have used a chiral auxiliary in a stoichiometric or an excess amount, but it has been our hope to realize a catalytic asymmetric induction. In this respect, a number of unexpected, nonclassical aspects have been observed with the classical organozinc chemistry. This review describes the historical background and our personal account of this research.[10-13] The subject is limited to simple alkylation or arylation reactions. The chemistry using structurally more elaborate carbon nucleophiles, such as metal enolates or allylic metal compounds, is not included.

2. Stoichiometric Asymmetric Alkylation

2.1. Reaction with Organometallic Reagents Modified by Aprotic Chiral Ligands

The curtain on enantioselective alkylation of aldehydes was raised in 1940 by *Betti* and *Lucchi* who claimed the first successful use of Grignard reagents and a chiral tertiary amine.[14] The Bologna chemists reported that the reaction of benzaldehyde and methylmagnesium iodide in the presence of *N,N*-dimethylbornylamine gave, in 73% yield, 1-phenylethanol showing an optical rotation of 0.30°. However, two years later *Tarbell* and *Paulson*, who were unable to reproduce this result, concluded that the optically active alcohol had not been produced although a neutral optically active impurity was formed by the reaction.[15] The original concept remained valid, however: certain chiral complexing agents are able to effect enantioselective addition of organometallic compounds to aldehydes.

Cohen and *Wright* reported in 1953 that the reaction of ethyl 2-oxo-2-phenylacetate with 1.6 equivalents of ethylmagnesium chloride and (2*R*,3*R*)-dimethoxybutane in benzene yielded ethyl 2-hydroxy-2-phenylbutanoate in 5% *ee* and in 37% yield.[16] Multidentate ethers such as dimethoxybutane, hexa(*O*-methyl)mannitol, or penta(*O*-methyl)arabitol are more effective than unidentate chiral ethers.[17] Table 1 outlines the development of this type of chemistry.

In the late 1960's we became interested in the use of (−)-sparteine **1**, a naturally occurring tertiary diamine, and noticed a 22% *ee* in the reaction of benzaldehyde and ethylmagnesium bromide.[18] Organolithium reagents were less sensitive than Grignard reagents to the presence of this chiral ligand. *Seebach* studied systematically the effects of multidentate ligands[19] and attained 52% *ee* in the reaction of benzaldehyde and *n*-butyllithium aided by an amino ether **2**.[19d] Ultimately, *Mazaleylat* and *Cram* accomplished 95% *ee* in the same alkylation using the chiral diamine ligand **3** having three C_2 axes.[20] A strong solvent effect was observed and use of diethyl ether at −120°C gave the best *ee*

Ryoji Noyori, born in Kobe, Japan in 1938, completed his undergraduate study in 1961 and the Master's degree in 1963 at Kyoto University, and immediately became an instructor in Professor H. Nozaki's laboratory at the same university. While at Kyoto he earned his Ph.D. degree in 1967. Appointed as an associate professor at the Department of Chemistry of Nagoya University in 1968, he was promoted to his current position in 1972. Noyori did his postdoctoral work with Professor E. J. Corey at Harvard University in 1969–1970. His research interests have been mainly in the exploitation of new synthetic methods, particularly on the basis of organometallic chemistry and their application. Noyori discovered a variety of asymmetric syntheses including enantioselective catalyses using BINAP (p,p'-(1,1'-binaphthyl-2,2'-diyl)bis(diarylphosphane)) chemistry, which have enormous utility. His organometallic methodologies have opened truly efficient routes to terpenes, vitamins, β-lactam antibiotics, alkaloids, prostaglandins, carbohydrates, nucleic acids, etc. Noyori's contribution has been recognized by a number of awards and honors, which include the Chemical Society of Japan Award (1985), the Centenary Medal and Lectureship from the Royal Society of Chemistry (1989), the Fluka Prize (1989), the Naito Foundation Research Prize (1989), the Toray Science & Technology Prize (1990).

Masato Kitamura was born in Nagoya in 1956 and studied agricultural chemistry at Nagoya University where he completed his doctoral work on total synthesis of maytansine under the direction of Professors T. Goto and M. Isobe. In 1983 he was a postdoctoral fellow with Professor G. Stork (Columbia University) and then joined the Noyori group as an assistant professor. He is a recipient of the Chemical Society of Japan Award for Young Chemists (1989).

Table 1. Chiral ligand aided enantioselective addition of organometallic reagents to carbonyl compounds.

Chiral ligand (equiv.)	Reagent (equiv.)	Substrate (equiv.)	Optical yield, configuration	Ref.
(1)	C_2H_5MgCl (1)	$C_6H_5COCO_2C_2H_5$ (0.64)	5, –	[16]
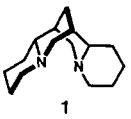 (1) **1**	C_2H_5MgBr (1)	C_6H_5CHO (0.8)	22, (*R*)	[18]
(+)- (1)	C_6H_5MgBr (0.22)	*t*-C_4H_9CHO (0.33)	11, –	[22]
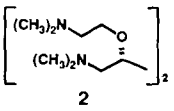 (1) **2**	*n*-C_4H_9Li (0.55)	C_6H_5CHO (0.5)	52, (*S*)	[19d]
(–)- 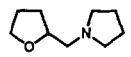 (1)	CH_3Li (0.83)	C_6H_5CHO (0.75)	19, –	[23]
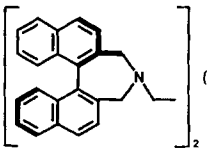 (1) **3**	*n*-C_4H_9Li (0.88)	C_6H_5CHO (0.24)	95, (*R*)	[20]
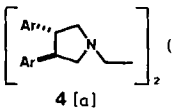 (1) **4** [a]	1-$C_{10}H_7MgBr$ (0.83)	C_6H_5CHO (0.33)	75, (*S*)	[21]

[a] Ar = 3,5-xylyl.

value. Similar diamine ligands, such as **4**, containing two *trans*-2,4-diarylpyrrolidine units were effective for asymmetric addition of arylmagnesium bromides to aldehydes, providing the corresponding alcohols in up to 75% *ee*.[21]

2.2. Reaction with Organometallic Reagents Modified by Protic Chiral Auxiliaries

This strategy, though now widely utilized, was found rather recently. Since the importance of molecular aggregates in organometallic reactions was not correctly recognized, most synthetic chemists considered that the reaction of organolithiums or Grignard reagents of type RMgX and protic compounds formed, by eliminating an alkane, metallic compounds with no alkylation ability. In 1969, however, *Inch* et al. demonstrated that, in the presence of an α-D-glucofuranose derivative **5** containing a free hydroxyl group (Table 2), methylmagnesium bromide reacts with cyclohexyl phenyl ketone (alcohol:CH_3MgBr:ketone = 1:1.75:0.5) to afford the corresponding alcohol in 70% *ee* and in 95% chemical yield.[24] This reaction probably involves a multi-

Table 2. Enantioselective reactions of chirally modified organometallic reagents and carbonyl compounds.

Chiral auxiliary (equiv.)		Reagent (equiv.)	Substrate (equiv.)	*ee* [%], configuration	Ref.
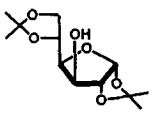 **5**	(1)	CH_3MgBr (1.75)	$C_6H_5COC_6H_{11}$ (0.5)	70, (*R*)	[24]
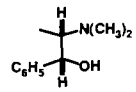 **6**	(1)	$(C_2H_5)_2Mg$ (1)	*t*-C_4H_9CHO (0.75)	20, (*R*)	[25]
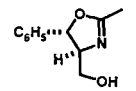 **7**	(1)	CH_3MgBr (1.75)	$C_6H_5COC_2H_5$ (0.5)	25, (*S*)	[29]
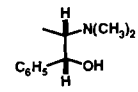 **6**	(–)	$(CH_3)_2CuLi$ (–)	C_6H_5CHO (–)	16.5, (*R*)	[26]
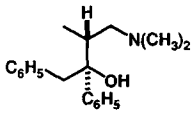 **8**	(1)	$(n\text{-}C_4H_9)_4AlLi$ (1)	$C_6H_5COCO_2CH_3$ (0.95)	43, –	[28]
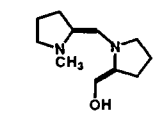 **9**	(1)	*n*-C_4H_9Li (1.68)	C_6H_5CHO (0.25)	95, (*S*)	[30]
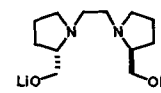	(1)	*n*-C_4H_9Li (0.67)	C_6H_5CHO (0.33)	36, (*R*)	[35]
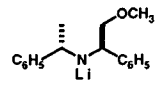 **10**	(1)	*n*-C_4H_9Li (0.68)	C_6H_5CHO (0.25)	90, (*S*)	[40]
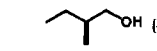	(–)	$CH_3Li/TiCl_4$ (–)	C_6H_5CHO (–)	8, (*S*)	[32a]
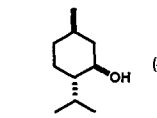	(–)	$(CH_3)_2Ti(O\text{-}i\text{-}C_3H_7)_2$ (–)	C_6H_5CHO (–)	13.5, (*S*)	[32b]
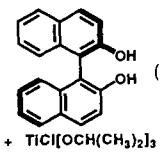 (*R*)-**11**	(1)	C_6H_5MgBr (1)	1-$C_{10}H_7CHO$ (0.77)	>98, –	[33]
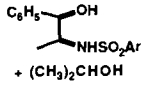 **12**	(1)	$(CH_3)_4Ti$ (1)	*o*-$NO_2C_6H_4CHO$ (0.91)	90, (*R*)	[34]
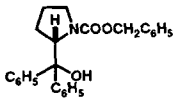	(1)	$(CH_3)_2Ti(O\text{-}i\text{-}C_3H_7)_2$ (1)	C_6H_5CHO (0.33)	54.1, (*R*)	[36]

nuclear magnesium compound containing methyl group(s) and a sugar alkoxide.

Later, the influence of chiral amino alcohols such as *N*-methylephedrine **6**[25-27] and Darvon alcohol **8**[28] or chiral dihydrooxazoles such as **7**[29] was examined in alkylations using Grignard reagents, organocuprates, organoaluminates, etc. *Mukaiyama* attained 95% *ee* in the reaction of benzaldehyde and *n*-butyllithium in the presence of a proline-derived diamine, **9**, in a 1:1 mixture of dimethoxymethane and dimethyl ether at −123 °C.[30] The reaction using lithium trimethylsilylacetylide also proceeded in 92% optical yield and was used for the synthesis of corticoids.[31]

Chirally modified organotitanium compounds are also useful.[32] *Seebach* et al., after extensive experimentation, found that aromatic aldehydes are arylated with organotitanium compounds generated in situ from enantiomerically pure 2,2′-dihydroxy-1,1′-binaphthyl **11** (binaphthol), chlorotriisopropoxytitanium and aryl Grignard reagents in THF to give the diaryl alcohols in greater than 98% *ee* in some cases.[33] *Reetz* et al. noted that *N*-sulfonylated derivatives of norephedrine, such as **12**, are good chiral ligands for modification of methyltitanium reagents, which effect alkylation of aromatic aldehydes to form (*R*)-alcohols in ca. 90% *ee*.[34] ^{1}H and ^{13}C NMR spectra of the titanium reagent showed a multitude of peaks not in line with a single monomeric or dimeric species. The results of several representative examples of reactions with reagents modified by chiral ligands are given in Table 2.

2.3. Reaction with Lithium/Magnesium Binary Reagents Modified by Binaphthol

A high level of enantioselection, based on ligand-directed chirality transfer, is obtained by careful combination of chiral auxiliaries, carbonyl compounds, and organic groups (alkyl, aryl, etc.), as exemplified in Section 2.2. A general method did not exist. The chemical and optical yields of reactions using organolithium or -magnesium compounds often vary depending on the reaction conditions, the ratio chiral ligand: alkylmetal :substrate, the way the chiral reagents were prepared, etc.

The use of excess amounts of chiral sources (usually 4 equivalents or more) over carbonyl substrates is imperative in many cases in order to achieve a high level of enantioselective addition, although the titanium reagents were usually utilized with only 1 to 1.3 equivalents of chiral auxiliaries.[33] This can be a result of the competition between achiral and chiral alkylating agents present in the reaction system, leading to products with varying selectivities and at different rates. Therefore, the creation of a single highly reactive species possessing excellent chiral recognition ability is crucial in achieving a stereoselective reaction. A readily available Li/Mg binary organometallic agent **13** (Fig. 2, empirical formula) is advantageous for this purpose: coordinatively saturated tetrahedral lithium and magnesium can avoid the complication of reagents by polymerization or aggregation, and the C_2 chiral bidentate modifier can minimize the number of the reactive species.[33, 37] The two kinds of metals may play specific roles as alkyl donor and carbonyl activator, which results in high reactivity.

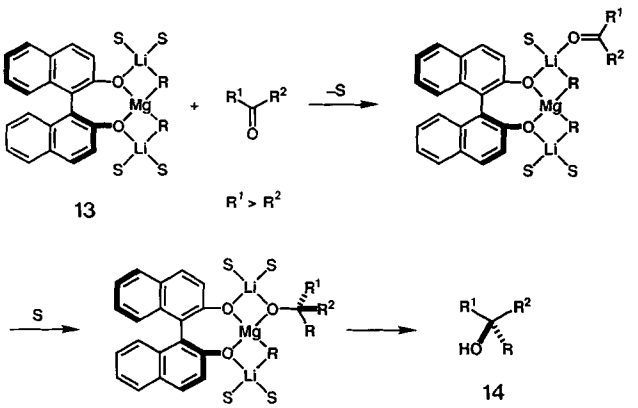

Fig. 2. Enantioselective addition of binaphthol modified Li/Mg binary organometallic agents to carbonyl compounds. S = solvent.

Thus the ethylating agent, (*S*)-**13** (R = ethyl), possessing two homotopic ethyl groups, was prepared by treatment of enantiomerically pure (*S*)-binaphthol (*S*)-**11** dissolved in THF with 2 equivalents of *n*-butyllithium, and then with 1 equivalent of diethylmagnesium at −78 °C. And indeed, the golden-yellow homogeneous reagent (0.074 M) reacted with 1 equivalent of benzaldehyde at −100 °C for 1 h in a 1:1 mixture of THF and dimethoxyethane (DME) to form (*S*)-1-phenyl-1-propanol (**14**, R = ethyl, R^1 = phenyl, R^2 = H) in 92% *ee* and 93% yield. As exemplified in Table 3, a variety of aromatic or aliphatic aldehydes were alkylated in greater than 80% optical yield with the alkyl or phenyl reagents using a 1:1 stoichiometry (not an excess).[11]

Table 3. Enantioselective reactions of the Li/Mg reagent, (*S*)-**13**, with carbonyl compounds $R^1R^2C{=}O$ [a].

Organometallic R in (*S*)-**13**	R^1	R^2	Product Yield [%]	*ee* [%]	Configuration
C_2H_5	C_6H_5	H	93	92	*S*
C_2H_5	p-$CH_3OC_6H_4$	H	98	83	*S*
C_2H_5	$C_6H_5CH_2CH_2$	H	40	85	*S*
C_2H_5	n-C_6H_{13}	H	86	85	*S*
C_2H_5	c-C_6H_{11}	H	68	84	[b]
n-C_4H_9	C_6H_5	H	98	88	[b]
C_6H_5	1-$C_{10}H_7$	H	89	82	[b]
C_2H_5	C_6H_5	CH_3	57	45	[b]

[a] The reaction was carried out at −100 °C in a 1:1 THF–DME mixture. [b] Not determined.

A 0.074 M [D_8]THF solution of di-*O*-lithiobinaphthol, prepared by mixing (*S*)-**11** and *n*-butyllithium in a 1:2 mole ratio followed by recrystallization from THF–hexane, exhibited a broad ^{7}Li NMR signal at $\delta = -0.25$ (LiCl in [D_8]THF as external reference, half-width $\nu_{1/2} = 14$ Hz at 20 °C). The aromatic protons also gave broad NMR signals. However, addition of 1 equivalent of diethylmagnesium to this solution sharpened the signals to a great extent (Fig. 3).

The ^{1}H NMR spectra of the ethylating agent **13** (R = ethyl) revealed a very sharp, single triplet and quartet due to the methyl and methylene protons at $\delta = 1.32$ and −0.92, respectively, at temperatures ranging from 20 to −50 °C.[38] The ^{7}Li NMR spectrum, measured at 20 °C,

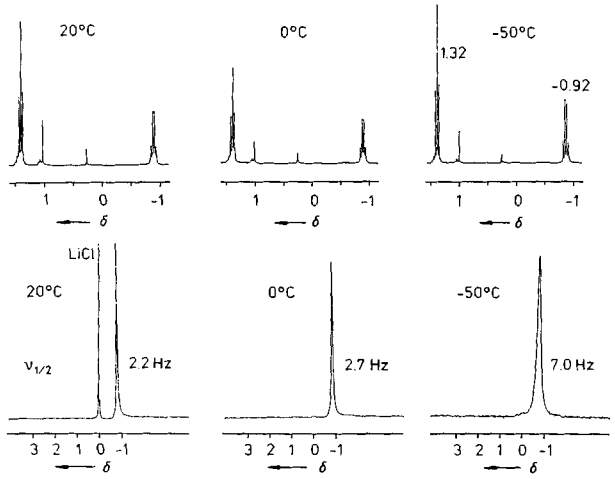

Fig. 3. ^{1}H (top, THF as internal standard) and ^{7}Li NMR spectra (bottom, LiCl in [D_8]THF as external standard) of the Li/Mg ethylating agent **13** (R = C_2H_5, S = [D_8]THF, 0.074 M [D_8]THF solution) at 20, 0, and -50 °C.

showed a single signal ($\nu_{1/2}$ = 2.2 Hz) at $\delta = -0.96$, and this signal was broadened at -50 °C ($\delta = -0.98$, $\nu_{1/2}$ = 7.0 Hz). Obviously some equilibration such as exchange of the coordinated THF molecules exists, but such a dynamic effect does not affect the magnetic environment of the ethyl protons to any great extent. Upon addition of benzaldehyde the spectrum became complicated, giving several new broad ^{7}Li signals at lower field. Notably, however, the original $\delta = -0.98$ signal due to **13** remained, though with decreased intensity, during the alkylation reaction.

The degree of enantioselection in alkylations with **13** was little affected by the extent of conversion of the starting materials. The ethylation of benzaldehyde using 4 equivalents of (*S*)-**13** (R = ethyl) afforded the same enantioselectivity (*S*/*R* = 96:4) as 1 equivalent, while the reaction with half an equivalent of the reagent resulted in decrease in the selectivity, *S*/*R* = 91:9 (90% yield). The resulting alkylmetal alkoxide products may cause adverse enantioselective alkylation.[39]

The enantioselectivity of the ethylation of benzaldehyde varies from 66% to 92% *ee* on changing the reaction temperature from 20 to -100 °C. Plotting of ln(*S*/*R*) as a function of $1/T$ shows direct proportionality, and from the line slope the difference in activation energy of the alkylation leading to the *S* and *R* alcohols is calculated to be 1.3 kcal/mol. This linearity suggests the participation of a single chiral reagent in the enantioselective alkylation over this temperature range. A further increase of enantioselectivity is expected by decreasing the reaction temperature, but the freezing of the reaction media prohibits such experiments. A possible transition state giving the *S* alkoxide product is illustrated by the structure **15** (naphthalene rings are omitted in **15a**).

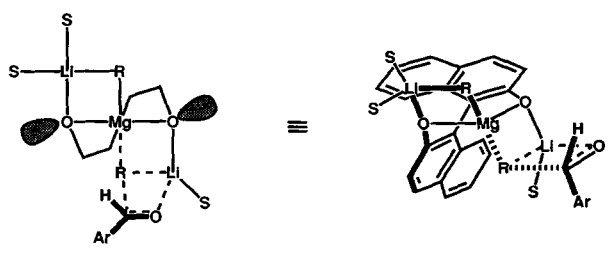

15a **15b**

The reaction with (*S*)-**13** provides one of the most effective ways to alkylate carbonyl compounds in an enantioselective manner, but it is still based on stoichiometric chirality transfer; the preparation of optically active alcohols suffers from the necessity of using an equimolar amount of binaphthol.

3. Catalytic Enantioselective Alkylation

3.1. The Concept

Reactivity of organometallic compounds is profoundly affected by neutral or anionic heteroatom auxiliaries. In certain cases, addition of a chiral auxiliary could enhance the reactivity and at the same time control the stereochemical outcome in an absolute sense. Catalytic asymmetric alkylation is the obvious ideal and Figure 4 presents a possible pathway to this ultimate goal, where addition of dialkylmetal, R_2M, to a prochiral carbonyl substrate is achieved by a catalytic amount of protic chiral auxiliary, HX*. Actually the metallic compounds are not simple monomers as formulated but usually exist as aggregates or in forms associated with other molecules.[9]

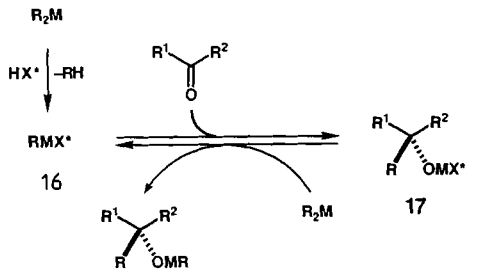

Fig. 4. Enantioselective alkylation catalyzed by protic auxiliary HX*. M = metallic species. X* = chiral heteroatom ligand.

In order to obtain a high degree of enantioselection in this scheme, the chiral anionic ligand X* must possess a suitable three-dimensional structure which clearly differentiates between the diastereomeric transition states of the alkyl delivery step, **16** → **17**. In addition, several kinetic conditions are to be satisfied to achieve catalytic asymmetric induction. First, the rate of the alkylation by the chirally modified organometallic **16** should substantially exceed that of the reaction of the original achiral reagent R_2M. Second, ligand X* must be readily detached from the initially formed metal alkoxide **17** by the action of the alkyl donor or carbonyl substrate to establish the catalytic cycle. These are key issues for obtaining a high turnover efficiency and an excellent chiral bias. These considerations also apply to the reaction using aprotic modifiers.

Although a wide array of well-shaped chiral auxiliaries or ligands are now accessible, the kinetic requirements described above are not easily secured by use of conventional organolithium or -magnesium compounds. *Cram* has found

that reaction of *n*-butyllithium and benzaldehyde in the presence of 0.77 mol% of a chiral diamine with binaphthyl skeleton gives 1-phenyl-1-pentanol in 7% *ee*.[20] *Hogeveen* has also observed a rate-enhancing effect in the same reaction system, resulting in production of 1-phenyl-1-pentanol in 19% *ee* by employing 2.4 mol% of the chiral lithium amide **10** prepared from (*S*)-α-methylbenzylamine (Table 2).[40] The rate of the catalyzed chiral reaction appears to exceed the uncatalyzed alkylation rate considerably, but the factor is too small to provide a synthetically useful turnover.

3.2. Amino Alcohol Promoted Alkylation with Diorganozinc Compounds

Among the various organometallic compounds diorganozinc acts as an ideal alkyl donor for catalytic asymmetric alkylation. In ordinary hydrocarbon or ethereal solvents, dialkylzinc compounds do not react with aldehydes. When dimethylzinc or diethylzinc, for instance, is mixed with benzaldehyde in toluene at or below room temperature, a yellow coloration occurs owing to reversible donor-acceptor complexation.[41] However, no chemical reaction, or even change in the ^{1}H NMR spectrum, is observed. At elevated temperatures ethylation does take place, but very slowly.

There have been several trials using dialkylzinc for the catalytic asymmetric alkylation of benzaldehyde. In the presence of Pd^{II} or Co^{II} complexes of (1*R*)-camphorquinone oxime, the reaction is accelerated to some extent and the ethylation product is obtained with 40–60% *ee*.[42a] In 1984 *Oguni* and *Omi* reported that certain β-amino alcohols also catalyze ethylation of benzaldehyde.[42b] For example, the reaction occurs in toluene at 24°C in the presence of 2 mol% of (*S*)-leucinol, giving after 48 h (*R*)-1-phenyl-1-propanol (*R*)-**18** in 48.8% *ee* and 96% yield. However, other simple amino alcohols are less efficient. In this first successful example, the *ee* value was not satisfactory and the reaction was slow.

In view of the prime significance of "ligand acceleration"[43] in the scenario outlined in Figure 4, we have screened a variety of bidentate protic auxiliaries and aprotic ligands in the hope of obtaining greater acceleration of the nucleophilic alkylation.[10, 13] Figure 5 illustrates the results of the reaction of benzaldehyde and diethylzinc in a

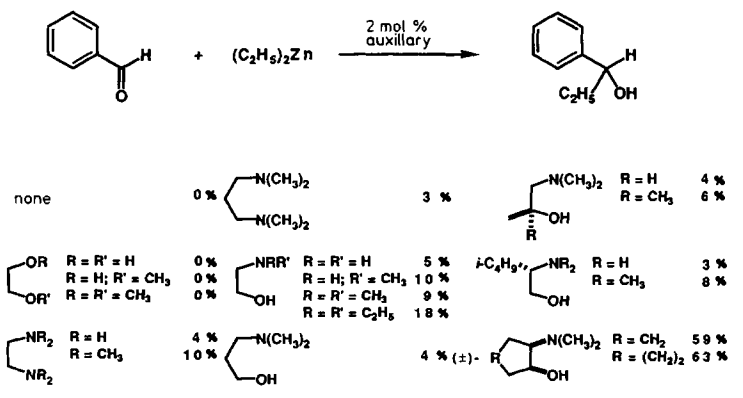

Fig. 5. Yields of ethylation of benzaldehyde with diethylzinc in the presence of 2 mol% of auxiliary in toluene at 0°C for 1 h.

1:1.2 mole ratio performed in toluene containing 2 mol% of various additives at 0°C for 1 h. Aprotic additives such as *N,N,N',N'*-tetramethylethylenediamine are also effective as promoters, and the efficiency appears highly dependent on the structures and substitution patterns. β-Dialkylamino alcohols act better than the corresponding *N*-monoalkyl or non-alkylated compounds. *N,N*-Dimethylleucinol is ca. three times more reactive than leucinol itself, where the acidic proton on the nitrogen may cause complications. Further impressive rate enhancement has been obtained with sterically constrained α,β-disubstituted β-dialkylamino alcohols: some cyclic compounds proved to be 10 to 100 times more effective than simple α-amino acid derived alcohols. Later, simple acyclic β-dialkylamino alcohols possessing a bulky α-substituent were found to be equally efficient.[13, 44]

In 1986 we reported for the first time a highly enantioselective alkylation[10] catalyzed by (−)-3-*exo*-(dimethylamino)isoborneol [(−)-DAIB **19**],[45] a camphor-derived, sterically congested, chiral β-dialkylamino alcohol (Fig. 6).

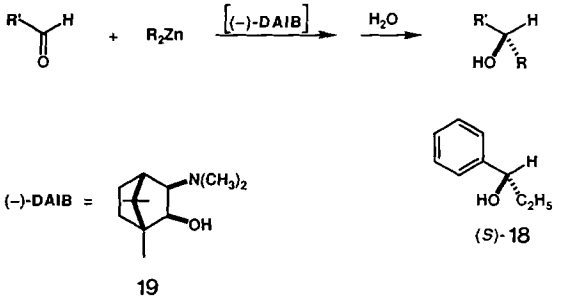

Fig. 6. DAIB-promoted enantioselective addition of dialkylzinc compounds to aldehydes. R = alkyl; R' = aryl, alkenyl, alkyl

In the presence of 2 mol% of (−)-DAIB, for example, the reaction of benzaldehyde and diethylzinc proceeds rapidly in toluene at 0°C, and after 6 h the alcohol (*S*)-**18** is obtained in 98% *ee* and in 97% yield. With the isomer of **19**, (+)-3-*endo*-(dimethylamino)borneol **20**, the *R* alcohol in 95% *ee* is obtained.[46]

A range of alkylating agents and aldehydes can be used for the DAIB-catalyzed enantioselective reaction. Dimethyl-, diethyl-, and other simple dialkylzinc agents are equally employable: methylation of benzaldehyde proceeds considerably more slowly than other alkylations, but gives an *ee* of greater than 90%; alcohols of type **21** are derived from substituted benzaldehydes; the reaction of furan-2-carbaldehyde and di-*n*-pentylzinc forms synthetically useful (*S*)-**22** in greater than 95% *ee*.[13, 47] Use of ferrocenecarbaldehyde leads to optically active **23**, a key compound for the synthesis of a wide range of chiral ferrocene derivatives.[13] Certain α,β-unsaturated or aliphatic aldehydes can also be alkylated in an enantioselective manner, in which case the *ee*'s of the products **24** are highly influenced by the substrate structures. Addition of di-*n*-pentylzinc to (*E*)-3-tributylstannylpropenal affords **25** with *S*/*R* = 93:7, a chiral building block of the three-component coupling prostaglandin synthesis.[48]

Thus DAIB satisfies the conditions of an ideal chiral auxiliary that results in high reactivity and excellent stereoselectivity. Our first report[10] was followed by publication of a

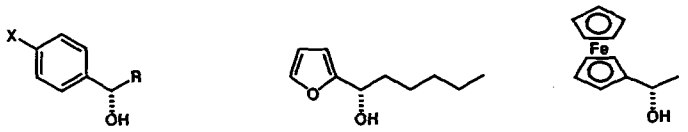

21a: R = CH_3, X = H
b: R = C_2H_5, X = H
c: R = C_2H_5, X = Cl
d: R = C_2H_5, X = CH_3O
e: R = n-C_4H_9, X = H
f: R = C_2H_5, X = C_6H_5CO
g: R = n-C_4H_9, X = C_6H_5CO

(*S*)-**22**

23

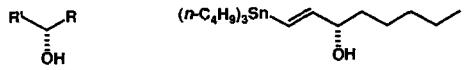

24, R = alkyl
R' = alkenyl, alkyl

25

series of related work,[49-52] and now a number of chiral β-amino alcohols can be used for enantioselective alkylation. Some successful examples are compiled in Table 4. The reaction of racemic 2-phenylpropanal and diethylzinc in the presence of (2*R*)-(−)-1-diisopropylamino-3,3-dimethyl-2-butanol proceeds with 5.4:1 enantiomer discrimination.[53] We see a rather good correlation between reactivity and enantioselectivity: high enantioface selection is obtained with a fast reaction.[13] β-Dialkylamino alcohols **26**–**33**, among others, are highly effective catalysts. *Fréchet* et al. was able to immobilize DAIB on polystyrene supports to facilitate recovery and recycling of the chiral catalyst, although this lowered the reaction rate.[50a] Polymer-bound ephedrine acts similarly.[50a, 51j] Some immobilized β-imino alcohols also act as catalysts.[50b] Certain γ-dialkylamino alcohol derivatives such as **36**, as well as divinylzinc, can also be used (see Table 5).[54]

Reactivity is increased by some functional groups near to the carbonyl group, but enantioselectivity is often diminished, probably because heteroatom coordination to the Zn atom facilitates the uncatalyzed achiral pathway. For instance, benzyloxyacetaldehyde or propyl pyruvate is readily ethylated with diethylzinc, even without amino alcohols, but the product is racemic. *n*-Butyl acetoacetate and acetophenone are not alkylated under the standard conditions. However, alkylation of γ- or δ-keto esters proceeds to give the corresponding hydroxy esters in optically active form.[51l] *p*-Benzoylbenzaldehyde, a keto aldehyde, is ethylated chemoselectively giving the optically active secondary alcohol **21f** without alkylating the keto group.[51m]

The choice of solvents is important. In the DAIB-catalyzed ethylation of benzaldehyde, nonpolar solvents such as toluene, hexane, ether, or their mixtures give the most satisfactory results. The reaction in THF is sluggish and the *ee* of product **18** is only 91% (98% in toluene and 99% in a 1:1 mixture of toluene and ether). The enantioselectivity of the ethylation is virtually not affected by DAIB concentration. With regard to the temperature effect, the optical yield of **18** in toluene is decreased from 98% at −20 to 0 °C to less than 95% at 50 °C.[58] With some other amino alcohol catalysts, opposite temperature effects on the selectivity have been observed.[51d]

Some other active catalysts include certain tridentate diamino alcohols,[51b] amido alcohols,[54] γ-amino alcohols,[51d, 54] secondary amino alcohols,[55] and lithium,[51b, g, i] titanium,[56] and boron[57] salts of the appropriate amino alcohols, amines, or sulfonamides, etc. These examples are summarized in Table 5.

A major byproduct of the reaction of benzaldehyde and diethylzinc is benzyl alcohol, whose yield increases with increasing aldehyde/alkylzinc ratio. The ethylation product, ethylzinc 1-phenyl-1-propanoxide, tends to react slowly with benzaldehyde, forming propiophenone and ethylzinc benzyloxide. Alkyl–Zn moieties do reduce aldehydes but are not a main source of hydrides, since the reaction using dimethylzinc also forms benzyl alcohol after aqueous workup, together with acetophenone. Diisobutylzinc, however, reduces benzaldehyde, owing to the enhanced β-hydrogen reactivity.[50a]

3.3. Mechanism of the Amino Alcohol Catalyzed Alkylation

3.3.1. *Transition State Models*

It is worth pointing out that the stoichiometry of the aldehyde, dialkylzinc, and DAIB auxiliary has marked effects on the reactivity[10] (Table 6). The reaction of benzaldehyde and diethylzinc does not occur in toluene at 0 °C without DAIB and, notably, no alkylation takes place with *an equimolar amount* of DAIB either. Remarkably, however, *a catalytic quantity* of DAIB promotes smooth alkylation. In other words, a complex formed from equimolar amounts of a dialkylzinc and DAIB by elimination of an alkane can not alkylate benzaldehyde despite the presence of an alkyl–Zn bond, but nevertheless does catalyze alkylation with dialkylzinc present in excess. This phenomenon clearly indicates that two Zn atoms per aldehyde are responsible for the alkyl transfer reaction. This view is also consistent with the result of a matrix isolation experiment using polymer-bound DAIB as an auxiliary.[50a]

The exact mechanism of alkyl transfer from organometallic species to carbonyl compounds remains to be elucidated. However, various bimetallic transition state models such as **37**–**39** (see page 58) can explain why the highly enantioselective alkylation generates an *S* configuration.

The first is the bicyclic transition state **37**.[12] The reaction occurs from the mixed-ligand dinuclear zinc complex **40**, where DAIB structure is simplified. A number of positional isomers and stereoisomers are possible for the product-forming dinuclear complex, but the formulated structure **40** is appropriate from an electronic basis for the promotion of the alkyl transfer. In going from the ground state to the transition state, electrophilicity of the aldehyde and nucleophilicity of the alkyl group must be enhanced. As easily seen from the polar limiting structure **40b**, this electronic requirement is satisfied best by this molecular assembly. The more Lewis acidic DAIB-chelated Zn_A accommodates the aldehyde substrate, increasing the electrophilicity at the carbon atom, and the bridging alkyl rather than the terminal alkyls

Table 4. Enantioselective addition of diorganozinc compounds to aldehydes catalyzed by β-amino alcohols [a].

Amino alcohol	Aldehyde	R_2Zn	Alcoholic product			Ref.
			Yield [%]	*ee* [%]	Configuration	
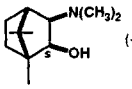 (−)-**19**	C_6H_5CHO	$(CH_3)_2Zn$	59	91	*S*	[10]
	C_6H_5CHO	$(C_2H_5)_2Zn$	98	99 [b]	*S*	[10]
	C_6H_5CHO	$(C_2H_5)_2Zn$	97	98	*S*	[10]
	C_6H_5CHO	$(n\text{-}C_4H_9)_2Zn$	88	95	*S*	[13]
	$p\text{-}ClC_6H_4CHO$	$(C_2H_5)_2Zn$	86	93	*S*	[10]
	$p\text{-}CH_3OC_6H_4CHO$	$(C_2H_5)_2Zn$	96	93	*S*	[10]
	furan-2-carbaldehyde	$(n\text{-}C_5H_{11})_2Zn$	80	>95	*S*	[13]
	5-methylfuran-2-carbaldehyde	$(C_2H_5)_2Zn$	91	97	[c]	[47]
	ferrocenecarbaldehyde	$(CH_3)_2Zn$	60	81	*S*	[13]
	$(E)\text{-}C_6H_5CH=CHCHO$	$(C_2H_5)_2Zn$	81	96	*S*	[10]
	$(E)\text{-}(n\text{-}C_4H_9)_3SnCH=CHCHO$	$(n\text{-}C_5H_{11})_2Zn$	84	85	*S*	[11]
	$C_6H_5CH_2CH_2CHO$	$(C_2H_5)_2Zn$	80	90	*S*	[10]
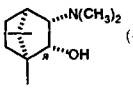 (+)-**19**	C_6H_5CHO	$(C_2H_5)_2Zn$	94	98	*R*	[13]
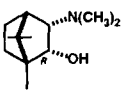 **20**	C_6H_5CHO	$(C_2H_5)_2Zn$	88	95	*R*	[46]
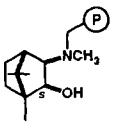 **26**	C_6H_5CHO	$(C_2H_5)_2Zn$	91	92	*S*	[50a]
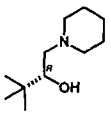 **27**	C_6H_5CHO	$(C_2H_5)_2Zn$	95	98	*R*	[13]
	$(E)\text{-}CH_3CH=CHCHO$	$(C_2H_5)_2Zn$	90	90	*R*	[13]
	$(E)\text{-}C_6H_5CH=CHCHO$	$(C_2H_5)_2Zn$	86	84	*R*	[13]
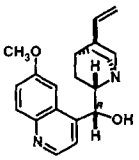 **28**	$o\text{-}C_2H_5OC_6H_4CHO$	$(C_2H_5)_2Zn$	72	92	[c]	[49]
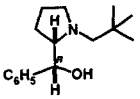 **29**	C_6H_5CHO	$(C_2H_5)_2Zn$	100	100	*R*	[51f]
	$C_6H_5CH_2CH_2CHO$	$(C_2H_5)_2Zn$	100	86	*R*	[51f]
	$c\text{-}C_6H_{11}CHO$	$(C_2H_5)_2Zn$	100	86	*R*	[51f]
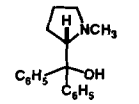 **30**	C_6H_5CHO	$(C_2H_5)_2Zn$	100	99.5 [d]	*S*	[51f]
	$C_6H_5COC_6H_4CHO$	$(C_2H_5)_2Zn$	99	93	*S*	[51m]
	$(CH_3)_3SiC\equiv CCHO$	$(C_2H_5)_2Zn$	67	78	[c]	[51k]
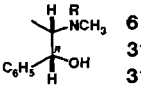 **6**, R = CH_3	C_6H_5CHO	$(C_2H_5)_2Zn$	81	81	*R*	[51d]
31a, R = $i\text{-}C_3H_7$	C_6H_5CHO	$(C_2H_5)_2Zn$	72	80	*R*	[51a]
31b, R = $CH_2C_6H_5$	C_6H_5CHO	$(C_2H_5)_2Zn$	91	86	*R*	[50a]
31c, R = CH_2(P)	C_6H_5CHO	$(C_2H_5)_2Zn$	96	80	*R*	[50a]
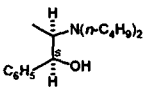 **32**	C_6H_5CHO	$(C_2H_5)_2Zn$	100	90	*S*	[51h]
	$n\text{-}C_6H_{13}CHO$	$(C_2H_5)_2Zn$	95	88	*S*	[51h]
	$n\text{-}C_6H_{13}CHO$	$(CH_3)_2Zn$	70	100	*S*	[51h]
	$C_6H_5CH_2CH_2CHO$	$(C_2H_5)_2Zn$	94	95	*S*	[51h]
	$(CH_3)_2CHCH_2CHO$	$(C_2H_5)_2Zn$	92	93	*S*	[51h]
	$C_6H_5COC_6H_4CHO$	$(C_2H_5)_2Zn$	84	91	*S*	[51m]
	$C_2H_5OCO(CH_2)_2CHO$	$(C_2H_5)_2Zn$	90	92	*S*	[51l]
	$C_2H_5OCO(CH_2)_3CHO$	$(C_2H_5)_2Zn$	87	95	*S*	[51l]
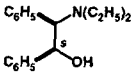 **33**	C_6H_5CHO	$(C_2H_5)_2Zn$	93	94	*S*	[13]
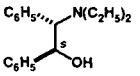 **34**	C_6H_5CHO	$(C_2H_5)_2Zn$	97	81	*S*	[13]
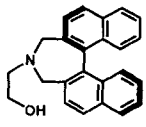 **35**	C_6H_5CHO	$(C_2H_5)_2Zn$	71	49	*S*	[13]

[a] Most of the reactions were carried out at 0 °C in toluene or hexane. Details are found in the original papers. [b] Ether–toluene mixture as solvent. [c] Not determine [d] Lithium alkoxide of the amino alcohol was used.

Table 5. Catalytic enantioselective addition of diorganozinc reagents to aldehydes [a].

Catalyst	Aldehyde	R_2Zn	Yield [%]	Alcoholic product *ee* [%]	Configuration	Ref.
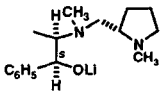	C_6H_5CHO	$(C_2H_5)_2Zn$	68	95	*S*	[51 b]
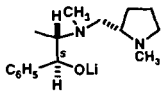	C_6H_5CHO	$(C_2H_5)_2Zn$	85	85	*S*	[51 b]
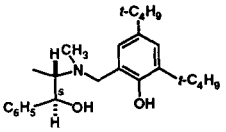	C_6H_5CHO	$(C_2H_5)_2Zn$	93	86	*S*	[51 c]
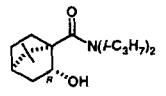	C_6H_5CHO	$(C_2H_5)_2Zn$	68	91	*R*	[54]
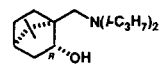	C_6H_5CHO	$(C_2H_5)_2Zn$	35	82	*R*	[54]
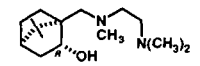	C_6H_5CHO	$(C_2H_5)_2Zn$	85	92	*S*	[54]
	C_6H_5CHO	$(n\text{-}C_3H_7)_2Zn$	85	92	*S*	[54]
	C_6H_5CHO	$(CH_2{=}CH)_2Zn$	96	87	*S*	[54]
36	$n\text{-}C_5H_{11}CHO$	$(CH_2{=}CH)_2Zn$	90	>96	*R*	[54]
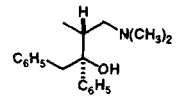	C_6H_5CHO	$(C_2H_5)_2Zn$	66	87	*R*	[51 d]
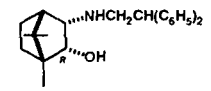	C_6H_5CHO	$(C_2H_5)_2Zn$	83	97	*R*	[55]
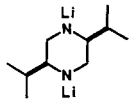	C_6H_5CHO	$(C_2H_5)_2Zn$	68	92	*R*	[51 g]
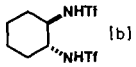 [b]	C_6H_5CHO	$(C_2H_5)_2Zn/Ti(O\text{-}i\text{-}C_3H_7)_4$	98	99	*S*	[56]
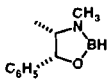	C_6H_5CHO	$(C_2H_5)_2Zn$	>85	95	*R*	[57]
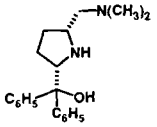	C_6H_5CHO	$(C_2H_5)_2Zn$	>95	94	*S*	[51 n]
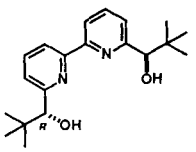	C_6H_5CHO	$(C_2H_5)_2Zn$	94	97	*R*	[51 o]

[a] Most of the reactions were carried out at $-30\,^{\circ}C$ to room temperature in toluene or hexane. Details are given in the original papers. [b] Tf = Trifluoromethanesulfonate.

acts as the migrating group. Although the electron density of the bridging R in the ground state is slightly lower than that of the terminal R, the $Zn-R_{bridging}$ bond is more polarizable than the $Zn-R_{terminal}$ linkage.

The folded bicyclic transition structure **37** features a tricoordinate structure of the migrating R group. This postulate is based on the ab initio molecular orbital calculations by *Schleyer, Houk*, and co-workers on the vapor-phase addition

Table 6. Effect of the benzaldehyde:diethylzinc:(−)-DAIB molar ratio on the yield of (*S*)-**18** [a].

Ratio C_6H_5CHO:$(C_2H_5)_2Zn$:(−)-DAIB			(*S*)-1-phenyl-1-propanol Yield [%]	*ee* [%]
1	1	0	0	–
1	1	1	1	0
1	2	2	0	–
1	2	1	88	98
2	2	1	49	96
100	50	1	48	98
50	50	1	97	98

[a] All reactions were carried out under argon at 0°C in degassed anhydrous toluene.

of dimeric methyllithium to formaldehyde.[59] The reaction is thought to involve transfer of a bridged methyl via a related planar bicyclic transition state **41**. This transition structure is considered to be very early on the reaction coordinate and the distance between the carbonyl carbon and the incoming methyl is quite large. The trajectory of attack by the carbon nucleophile is controlled by the lithium ion, and the reacting Li–CH_3 bond is elongated to a great extent. The aggregation state of the reactive alkyllithium species in solution has been a matter of controversy,[60] but it seems to be the consensus that dimers are the reacting entities in ethereal solvents. In THF *n*-butyllithium exists mainly as a tetramer, but the dimer is much more reactive.[61] Monomeric species are not detected in THF.

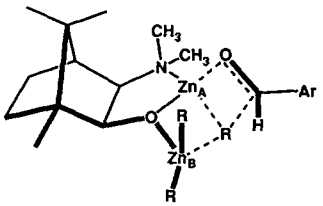

37

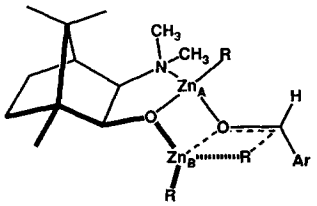

38

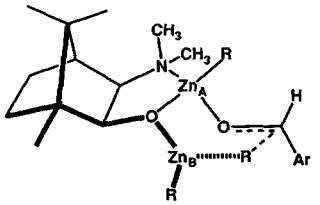

39

The bicyclic transition state **38** could give an alternative explanation for the stoichiometry and stereochemistry of the organozinc reaction.[50a] Such a mechanism involving transfer of a terminally located R to the electrophilically activated, bridged carbonyl carbon[62] was first suggested by *Mole* et al. for the reaction of trimethylaluminum and benzophenone.[63] The *Pasynkiewicz–Sliwa* type bimetallic assembly **39**, postulated by *Corey* and *Hannon*,[51c] is also in full accord with the experimental findings. This transition state model, originally proposed for the reaction of trimethylaluminum and propiophenone,[64] is characterized by the monocyclic, six-centered structure.

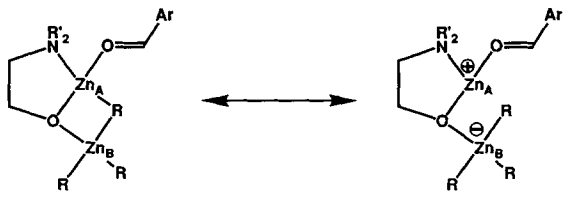

40a **40b**

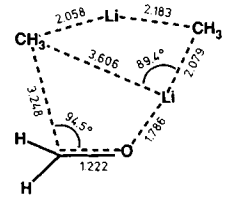

41

3.3.2. The Sense of the Asymmetric Induction

A survey of the stereochemical outcome observed with a range of chiral β-amino alcohols as promoters (Table 4) is outlined in Figure 7.

The bicyclic transition state model of type **37** correctly predicts the absolute configuration of the products. The general sense of the asymmetric induction is controlled primarily by the chirality of the stereodetermining bicyclic intermediates, **42** and **43**.[12] The *S*-configurated Zn alkoxide is derived from **42** which possesses *S*-Zn and *S*-O bridgehead atoms, while the *R* alkoxide is obtained from the *R*-Zn, *R*-O enantiomer **43**. As illustrated by the diastereomeric transition structures **44** and **45** arising from **42**, the kinetic stereochemical bias is provided by a nonbonded repulsion between the carbonyl substituents, Ar and H, and a terminal R group attached to Zn_B. The *S*-generating geometry **44** is obviously preferable to the *R*-forming transition state **45**. The relative stabilities of the chiral bicyclic structures are influenced by substituents at the α and β positions, in accord with the general sense of Figure 7, as well as by the nitrogen substituents. The α*S* or β*R* configuration shows a preference for **42**, whereas **43** is stabilized by the enantiomeric α*R* or β*S* configuration of the auxiliary.

The degree of the enantioselection depends on the bulkiness of the substituents at the α carbon and, indeed, β-dialkyl-

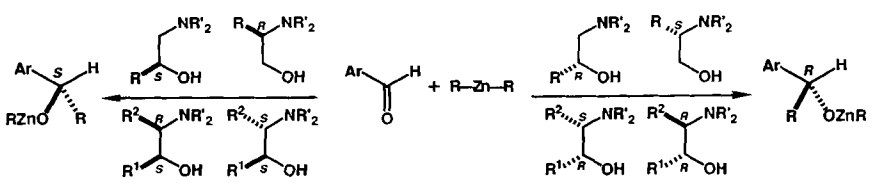

Fig. 7. General sense of asymmetric induction with a β-dialkylamino alcohol catalyst.

amino-α-*tert*-butylethanol **27** results in up to 98% *ee* in the ethylation of benzaldehyde.[113] As is seen in (−)-DAIB, the *αS, βR* (or *αR, βS*) configuration, generating *cis*-α,β-disubstitution in the five-membered chelate complexes, is the most desirable, because the directing effects of the vicinal substituents cooperate in keeping a single chiral integrity **42** (or **43**), which presents very clear facial bias in the alkyl transfer step. With *trans*-α,β-disubstitution in the Zn chelate, the directing effects offset each other, but the α stereogenic center is more influential than the β center. In the ethylation of benzaldehyde, the diastereomeric amino alcohols, **33** and **34**, deliver the same asymmetric orientation, with higher enantioselectivity in the case of **33** (94% *ee* vs 81% *ee*, see Table 4).[113] A similar tendency is observed with (1*R*,2*S*)-*N*-ethylephedrine and (1*R*,2*R*)-*N*-ethylpseudoephedrine (77% *ee* vs 72% *ee*).[65] In addition, bulky alkyl groups at the nitrogen atom tend to increase the enantioselectivity.[113]

With **35**, i.e., an (*S*)-binaphthyl moiety is the only chiral element, the ethylation of benzaldehyde proceeds in 49% optical yield (Table 4). Thus *αS* configurated β-dialkylamino alcohols always afford *S*-enriched alkylation products, while *αR* auxiliaries lead predominantly to *R* products. No exceptions have been seen in the enantioselective alkylation of benzaldehyde,[66] at least in those with a high level of stereoselection. The steric, not electronic, origin of the stereoselectivity agrees with the consistently high optical yields gained with a variety of benzaldehydes possessing electronically different substituents. Other aldehydes behave similarly. In summary, stereochemical information from the backbone of the chiral auxiliary defines the chirality of the bridgehead atoms in the stereodetermining bicyclic intermediates **42** and **43**, which in turn is transmitted to the aldehyde ligand by an alkyl transfer reaction (via **44** and **45**). Direct steric interaction between carbonyl substituents and α- or β-substituents of chiral auxiliaries is unimportant.

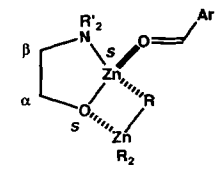

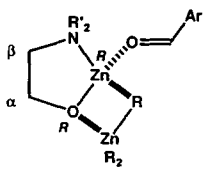

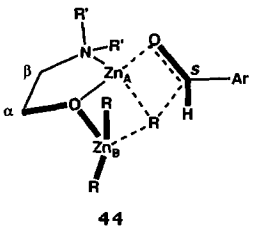

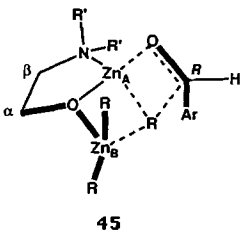

The same arguments on the substituent effects apply to the transition state models of the types **38**[50a] and **39**.[51c] Now with the *αS* configurated amino alcohol ancillaries, the *S*-generating transition states **46** and **48** are favored over the diastereomeric *R* transition states, **47** and **49**, which suffer

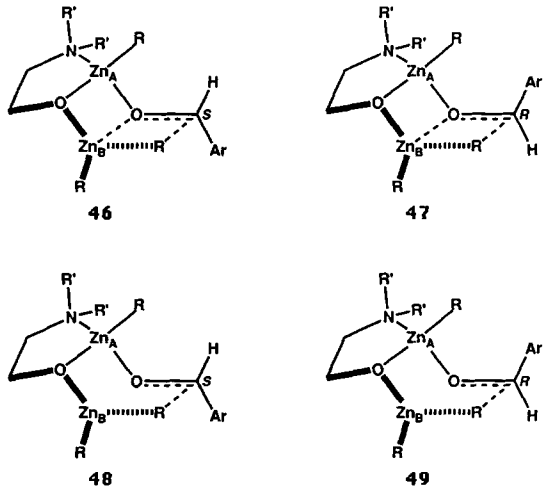

significant nonbonded repulsion between Ar and the Zn_A-linked R group.[67, 68]

3.3.3. The Reaction Pathway

On the basis of ^1H NMR studies, single-crystal X-ray analysis, molecular weight (MW) determination of certain key intermediates, alkyl scrambling experiments, kinetic measurement, etc., we have postulated the catalytic cycle of Figure 8 for the amino alcohol accelerated alkylation by dialkylzinc compounds.[112] The scheme has a soft energy surface and compounds **50**–**53** are in dynamic equilibrium.

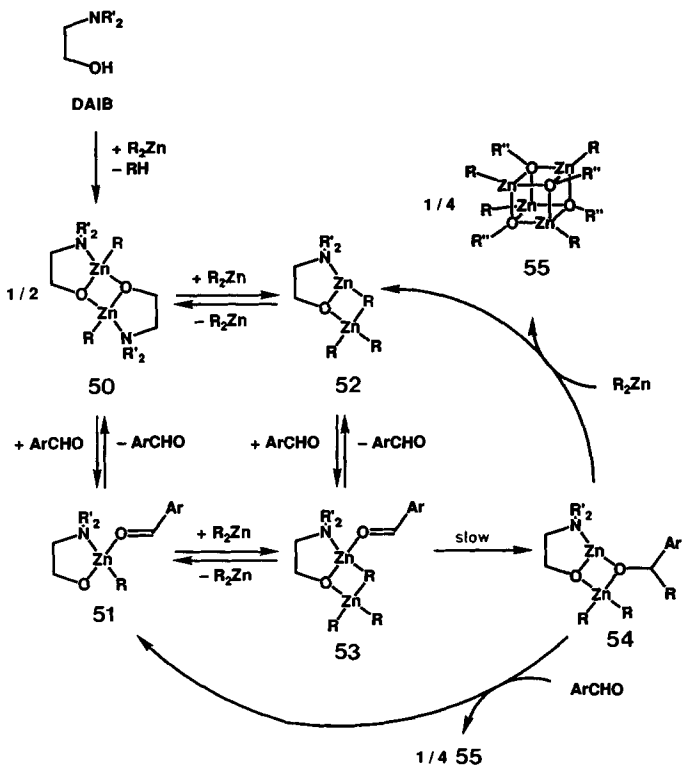

Fig. 8. Catalytic cycle of the DAIB-catalyzed enantioselective alkylation of benzaldehyde with dialkylzinc compounds R_2Zn. Ar = C_6H_5, R′ = CH_3, R″ = $CH(C_6H_5)R$.

In addition, alkylzinc compounds are generally flexible in nature and readily undergo interconversion with many other structural isomers by intra- or intermolecular processes: only entities with a significant contribution in the reaction are formulated in the scheme. The structural study has been done mainly by using dimethylzinc, because the methylzinc intermediates fluctuate less than the other alkyl analogues and are hence easier to monitor.

The proposed reaction pathways in Figure 8 are supported by many lines of structural information. The following phenomenona are to be noted:

1) The ^{1}H NMR spectrum of a 1:1 mixture of benzaldehyde and dimethyl- or diethylzinc in [D_8]toluene at room temperature gives only the independent signals of each component. The signals are sharp and no appreciable change in chemical shift is observed. No chemical reaction takes place under such conditions.

2) Reaction of (−)-DAIB and dimethylzinc in a 1:1 mole ratio in toluene evolves methane and produces only one dimeric compound, **50** (R = CH_3), among three possible stereoisomers. This complex possesses a dinuclear structure both in hydrocarbon solution and in the solid state, as substantiated by cryoscopic MW determination in benzene, ^{1}H and ^{13}C NMR measurements, and single-crystal X-ray analysis. The detailed structure will be given in Section 3.5 ((2*S*,2′*S*)-**50** (R = CH_3) in Fig. 11).

3) Complex **50** contains Zn–alkyl moieties but cannot alkylate aldehydes. However, the complex acts as a catalyst precursor. Such dimers are perhaps in equilibrium in toluene with a small amount of a coordinately unsaturated monomeric species **60**, which possesses a trigonal Zn atom, in accord with the fact that the MW decreases with decreasing concentration. This view is also supported by the results obtained with a polymer-bound DAIB **26**.[50a]

4) The dinuclear framework of **50** (R = CH_3) is ruptured spontaneously upon addition of 1 equivalent of benzaldehyde, leading to the mononuclear complex **51**. The ^{1}H NMR spectrum at 0 °C shows a broad aldehydic proton signal.[69] This process is reversible and would occur mainly via **60** by a dissociative mechanism. The unsaturated Zn atom in the trigonal monomer **60** accepts the donor aldehyde molecule to form a tetrahedral complex **51**.[68] MW measurement reveals that the position of the equilibrium is dependent on the **50**:aldehyde ratio.

5) The monomeric mixed ligand complex **51** is still unable to undergo alkyl transfer. The aldehyde ligand in **51** (R = C_2H_5; Ar = C_6H_5) is very slowly reduced, giving benzyl alcohol after hydrolysis. As noted in Section 3.2, only dialkylzinc compounds present in excess to DAIB or **50** can deliver alkyl groups to aldehydes.

6) Dimethylzinc also breaks the dimeric structure of **50** to give new fluctuant dimeric complexes such as **52**, exhibiting only one Zn–CH_3 signal in the ^{1}H NMR spectrum in a 25 to − 50 °C temperature range.

7) This process is also reversible as judged by MW measurement. The compound **52** (R = C_2H_5) and its isomers have dinuclear Zn structures and no sign of the occurrence of higher aggregates is observed in a 52 to 170 mM concentration range.

8) When 1 equivalent of benzaldehyde is introduced to the dinuclear complex **52** (R = CH_3) in toluene at 0 °C, a new dynamic system containing **53** is formed. The same equilibrating mixture is obtained by the reaction of the mononuclear complex **51** and dimethylzinc in a 1:1 ratio. The presence of a rapid equilibrium, **51**⇄**53**⇄**52**, is indicated by its broad ^{1}H NMR spectrum giving a single broad Zn–CH_3 signal.

9) The alkyl-transfer step, **53**→**54**, is slow. Upon standing, a 0.5:1:1 molar mixture of **50** (R = CH_3), dimethylzinc, and benzaldehyde at 20 °C slowly yields an alkoxide assignable to **54** (MW unknown). The ^{1}H NMR spectrum shows a doublet at δ = 1.93 and a quartet at δ = 5.36 due to methyl and methine protons of the bridged alkoxide, as well as a broad singlet at δ = − 0.17 due to Zn–CH_3.

10) The newly generated complex **54** (R = CH_3) is rather stable under these conditions and, over a period of several days, is converted slowly to the cubic Zn alkoxide tetramer **55** (R = CH_3) and catalyst precursor **50**. The tetrameric nature of **55** has been ascertained by cryoscopic MW measurement. Interestingly, **54** upon exposure to benzaldehyde or dimethylzinc undergoes instantaneous decomposition to **55**, completing the catalytic cycle.

Rates of the alkylation reaction are dependent on the nature of the alkyl groups. In accord with the fluctuating nature of the Zn intermediates, when two different dialkylzincs, R^1_2Zn and R^2_2Zn, are utilized in the DAIB-catalyzed reaction, a statistical distribution of the possible alkylation products, **56** and **57**, is observed (Fig. 9).[70]

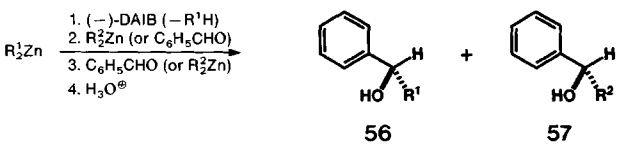

Fig. 9. Alkyl scrambling experiment.

As illustrated in Table 7, the product ratio **56**/**57** is determined only by the ratio of the two alkyl groups and their relative reactivities (CH_3:C_2H_5:*n*-C_4H_9 = 1:20:8). It is not

Table 7. Product distribution in the reaction of R^1_2Zn, R^2_2Zn, benzaldehyde, and (−)-DAIB in a 1:1:1:1 molar ratio [a].

Dialkylzincs		Product ratio		
R^1	R^2	$C_6H_5CH(OH)R^1$ **56**	$C_6H_5CH(OH)R^2$ **57**	rel. reactivity R^1/R^2
CH_3	C_2H_5	2	93	1/21
C_2H_5	CH_3	76 [b]	8 [c]	19/1
C_2H_5	*n*-C_4H_9	44	35	2.5/1
C_2H_5 [d]	*n*-C_4H_9	41	32	2.6/1
C_2H_5 [e]	*n*-C_4H_9	38	32	2.4/1
n-C_4H_9	C_2H_5	14	68	1/2.4
n-C_4H_9 [d]	C_2H_5	13	66	1/2.5
n-C_4H_9 [e]	C_2H_5	14	67	1/2.4

[a] R^1_2Zn was first added to a toluene solution of (−)-DAIB at 30 °C, and after 15 min R^2_2Zn was added. After the mixture was stirred for 10 min and cooled to 0 °C, benzaldehyde was added. The mixture was stirred at 0 °C for 6 h, quenched with water, and analyzed by high pressure liquid chromatography. All reactions produced 3–14% of benzyl alcohol. [b] (*S*)-Product in 98% *ee*. [c] (*S*)-Product in 94% *ee*. [d] R^2_2Zn was added to the initially formed R^1Zn complex and the mixture was stirred at −78 °C. Then benzaldehyde was added. [e] Benzaldehyde was added to the R^1Zn complex prior to addition of R^2_2Zn (see Fig. 9).

influenced by the order or conditions, such as temperature (30 to −78 °C), of the mixing of benzaldehyde and the second alkylzinc to the initially formed dimeric DAIB-chelated complex **50**. The low migratory aptitude of the methyl group is consistent with the slow reaction using dimethylzinc, which may be attributed to relatively high stability of the methyl bridged dinuclear intermediates. The sense and degree of asymmetric induction in the competitive experiments are also identical with those of the independent reactions.

The mechanism of Figure 8 fully agrees with the kinetic data obtained by the DAIB-aided ethylation of benzaldehyde in toluene at 0 °C. Under standard catalytic conditions, the reaction is first order in (−)-DAIB but zero-order in diethylzinc and benzaldehyde. The rate is only affected by aldehyde concentrations when they are lower than 0.3 M. The kinetic results also agree with the presence of the equilibrium described in Figure 8 (complexes **50**–**53**) and, importantly, indicate that the alkyl transfer is occurring intramolecularly from the dinuclear mixed-ligand complex **53**. The result convincingly dismisses the possibility of any bimolecular mechanisms such as a reaction between the DAIB-modified organozinc species and free benzaldehyde, or nucleophilic attack of a free dialkylzinc to benzaldehyde complexed with a DAIB-chelated Zn Lewis acid. The ^{1}H NMR study also supports this interpretation. Since the degree of enantioselection is decreased from $S:R = 99:1$ to less than 97.5:2.5[58] by raising the reaction temperature from −20 to 50 °C, the alkyl-transfer step **53**→**54** via **37** is the turnover-limiting, as well as the stereo-determining step.

3.4. Origin of the Catalyst Efficiency

The efficient catalytic enantioselective reaction is a result of the combination of the stereo-regulating ability of the well-shaped amino alcohols and the appropriate kinetics. At least three factors are suitably coupled to achieve the ideal catalytic system.

The first is the structure/reactivity profile of organozinc compounds. Monomeric dialkylzinc compounds which have an sp-hybridized linear geometry at Zn (**58**) are inert to aldehydes, because the alkyl–metal linkage is rather nonpolar.[71] However, the bond polarity can be enhanced by creating a bent geometry **59**, where the Zn atom uses orbitals having a higher p character. A coordinatively unsaturated

58 **59**

X = alkyl, N, O, halogen etc.

bent compound **59**, particularly with an electronegative substituent, has a strong donor character at the alkyl group and acceptor character at the Zn atom. Such auxiliary-induced structural perturbation increasing the reactivity toward carbonyl substrates is attained by amino alcohols such as DAIB (the argument is simplified because the actual reactive species has a dinuclear structure).

The second important factor is the tendency of the alkylzinc alkoxide product **54** to form the cubic tetrameric structure **55**, which is removed from the reaction system. The tetramer **55** neither alkylates aldehydes nor acts as a catalyst: The reaction of diethylzinc and benzaldehyde in the presence of the homologue of **55** formed from enantiomerically pure (*S*)-1-phenyl-1-ethanol gave, after 12 h at 0 °C, 1-phenyl-1-propanol in only 2.2% yield.[39] *Fréchet's* matrix isolation experiment, in which filtration of the DAIB-bound polymer before hydrolysis did not affect the yield of the alkylation product, demonstrates that the final Zn alkoxides, which are soluble in hydrocarbon, do not bind to the chiral ligands.[50a]

Third, the use of sterically congested chiral auxiliaries is essential for obtaining high reactivity. DAIB upon reaction with organozinc compounds forms the dimeric compound **50**. By contrast, 2-dimethylaminoethanol, which possesses a similar but sterically noncongested structure, is known to give trimeric alkylzinc alkoxides of type **61**.[72] This is the origin of the great rate enhancement for the congested compound, because the dimer dissociates more readily into the reactive monomer **60** than the trimer does. Furthermore,

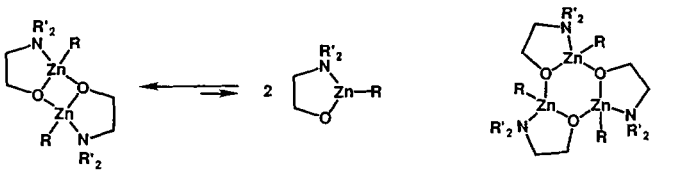

50 **60** **61**, R = CH_3, C_2H_5; R' = CH_3

DAIB-derived **52** or its isomers are dinuclear in nature, whereas tetranuclear complexes are formed by mixing diethylzinc and less congested amino alcohols, such as 2-dimethylamino-3-methyl-1-butanol, 3-dicyclohexylamino-2-propanol, and 2-dimethylamino-1-phenylethanol, in a 2:1 molar ratio.[73]

3.5. Chiral Amplification

A number of nonclassical aspects have emerged in the amino alcohol aided enantioselective alkylation, but perhaps the most striking is the far from linear relationship between *ee* values of the chiral auxiliaries and the alcoholic products. The reaction catalyzed by DAIB[11] or *Oguni's* **27**[44] in a low *ee* leads to the alkylation products in *ee*'s which are very close to those obtained with the enantiomerically pure auxiliaries. The chirality amplifying phenomenon[74] is clearly seen in Figure 10, which shows the *ee*'s of the *S* alcohols as a function of the *ee* of DAIB auxiliary. Typically, the reaction of benzaldehyde and diethylzinc promoted by 8 mol% of (−)-DAIB in 15% *ee* in toluene at 0 °C gives rise to (*S*)-**18** in 95% *ee* and 92% yield.

We have disclosed that the extreme convex deviation from a linear correlation results from a marked difference in chemical properties of the diastereomeric dinuclear complexes of type **50** formed from dialkylzinc and the DAIB auxiliary.[12] When enantiomerically pure (−)-DAIB is mixed with a stoichiometric quantity of dimethylzinc in

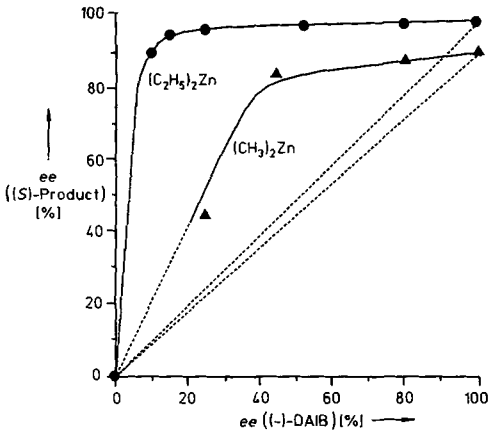

Fig. 10. The *ee* of the alkylation product as a function of the *ee* of DAIB. • 0.42 M $(C_2H_5)_2Zn$, 0.42 M C_6H_5CHO, 34 mM (−)-DAIB in toluene at 0 °C. ▲ 0.47 M $(CH_3)_2Zn$, 0.49 M C_6H_5CHO, 47 mM (−)-DAIB in [D_8]toluene at 32 °C.

toluene at room temperature, a single dimeric complex, (2*S*,2′*S*)-**50** (R = CH_3), is formed quantitatively. The stereochemistry elucidated by single crystal X-ray analysis is given in Figure 11 (top). The structure is characterized by chiral C_2 symmetry. The central Zn_2O_2 four-membered ring is "*endo*-fused" to the adjacent DAIB-Zn five-membered rings because of the sterically demanding bornane backbone. The central 5/4/5 tricyclic structure has *syn* geometry. The simple ^1H and ^{13}C NMR spectra indicate magnetic equivalency for the two DAIB moieties of the complex in solution. The cryoscopic MW measurement also suggests a dimeric structure in benzene, but the concentration effect indicates a tendency of (2*S*,2′*S*)-**50** (R = C_2H_5) to dissociate into the monomer (2*S*)-**60**.

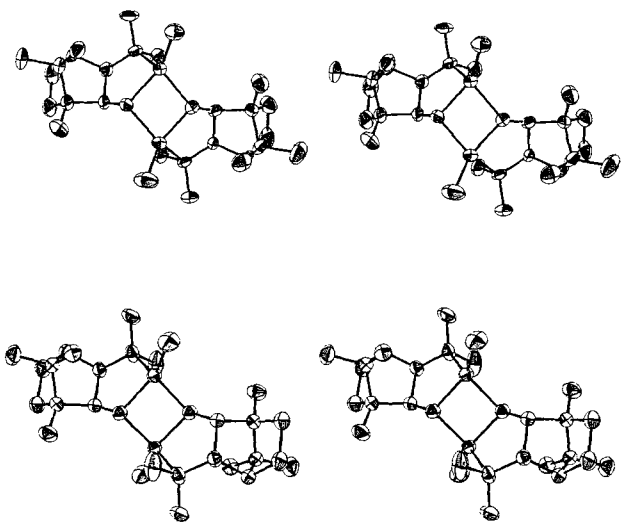

Fig. 11. Stereoview of (2*S*,2′*S*)-**50** (R = CH_3) (top) and (2*S*,2′*R*)-**50** (R = CH_3) (bottom).

Interestingly, an equimolar mixture of (2*S*,2′*S*)-**50** (R = CH_3) and the enantiomer (2*R*,2′*R*)-**50** in toluene is instantaneously converted to a new dinuclear Zn compound. The same complex is obtained by the reaction of racemic DAIB and dimethylzinc in a 1:1 mole ratio. This dinuclear complex, (2*S*,2′*R*)-**50** (R = CH_3), is a *meso* compound and possesses achiral C_i symmetry. The ^1H and ^{13}C NMR spectra are simple because of the degeneracy of the structure. The dimeric nature has been proven by MW measurement of the ethyl derivative, as the methylzinc complex has low solubility in aromatic hydrocarbons and hence MW measurement at high concentration is difficult. The single-crystal X-ray analysis (Fig. 11, bottom) of (2*S*,2′*R*)-**50** (R = CH_3) indicates that the Zn_2O_2 four-membered ring is *endo*-fused to the DAIB-Zn chelate rings, as in its chiral counterpart, but the central 5/4/5-fused tricyclic moiety has an *anti* configuration.

Thus what we have seen is strict matching of chirality or, in other words, accurate enantiomer recognition, leading to the thermodynamic situation outlined in Figure 12. Mono-

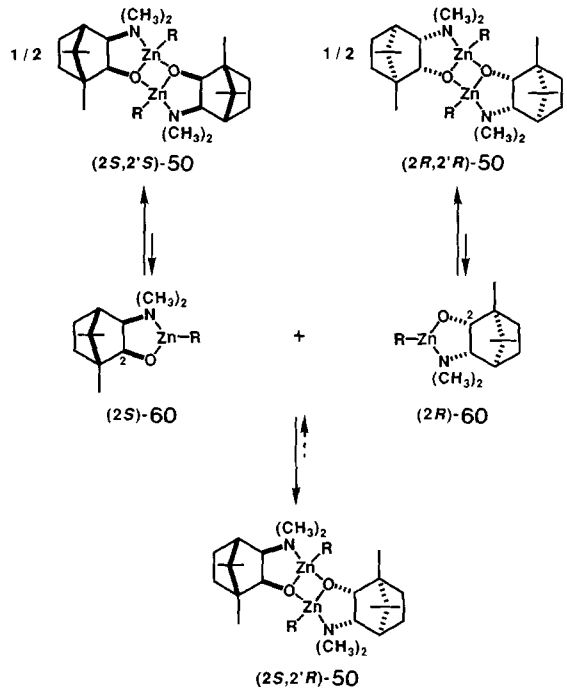

Fig. 12. Enantiomer recognition of the chiral trigonal Zn compounds **60**.

meric (2*S*)-**60** and (2*R*)-**60** are catalytically active chiral complexes derived from a dialkylzinc and (−)- or (+)-DAIB, respectively. Homochiral or heterochiral interaction between these monomers leads to the chiral dimeric complexes, (2*S*,2′*S*)-**50** and (2*R*,2′*R*)-**50**, or the *meso* dinuclear complex, (2*S*,2′*R*)-**50**, which is diastereomeric to the other two. In our system the heterochiral complex (2*S*,2′*R*)-**50** is overwhelmingly more stable than the homochiral dimers (2*S*,2′*S*)- and (2*R*,2′*R*)-**50**. When racemic DAIB is reacted with dimethylzinc in a 1:1 ratio in toluene, (2*S*,2′*R*)-**50** (R = CH_3) is produced exclusively, without forming diastereomer (2*S*,2′*S*)- and (2*R*,2′*R*)-**50**. A 1:1 mixture of (2*S*,2′*S*)- and (2*R*,2′*R*)-**50** (R = CH_3) in toluene is also instantaneously and quantitatively transformed to the more stable (2*S*,2′*R*)-**50** by way of the monomers, (2*S*)- and (2*R*)-**60**.

The chemical properties of the diastereomeric complexes, (2*S*,2′*R*)-**50** and (2*S*,2′*S*)- or (2*R*,2′*R*)-**50** are surprisingly different. The *meso* compound, (2*S*,2′*R*)-**50** (R = CH_3), is not

affected by the addition of 1 equivalent of dimethylzinc, benzaldehyde, or their mixtures. The ^{1}H NMR spectrum in toluene (Fig. 13b) exhibits only independent signals of these three components: the unchanged dinuclear complex and dimethylzinc afford separate Zn–CH_3 signals and benzaldehyde gives a sharp aldehyde signal.

The behavior of the chiral (2*S*,2′*S*)-**50** is, however, entirely different (Fig. 13c,d). As described in Section 3.3.3, the dimeric structure is ruptured instantaneously on exposure to equimolar amounts of dimethylzinc and benzaldehyde, establishing a dynamic equilibrium among complexes **50**–**53** (Fig. 8). In the ^{1}H NMR spectrum (Fig. 13d), a single Zn–CH_3 signal and a broad aldehydic proton are observed, consistent with this view. In addition, a small amount of **54** (R = CH_3) is starting to emerge.

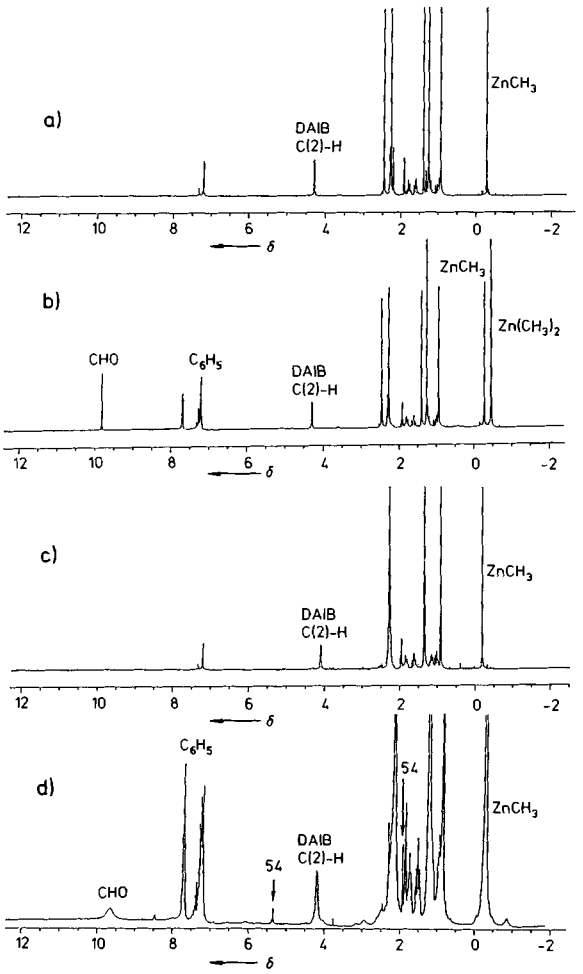

Fig. 13. ^{1}H NMR spectra of the dinuclear catalyst precursors and their mixtures with dimethylzinc and benzaldehyde in [D_8]toluene at 25 °C. a) (2*S*,2′*R*)-**50** (R = CH_3). b) 0.5:1:1 (2*S*,2′*R*)-**50**/$(CH_3)_2Zn$/C_6H_5CHO mixture. c) (2*S*,2′*S*)-**50** (R = CH_3). d) 0.5:1:1 (2*S*,2′*S*)-**50**/$(CH_3)_2Zn$/C_6H_5CHO mixture.

The ^{1}H NMR study using *stoichiometric* amounts of dimethylzinc, DAIB auxiliary, and benzaldehyde has thus shed light on the difference between the chiral and *meso* dinuclear complexes of type **50**: the homochiral complexes are very reactive in the presence of dialkylzincs and aldehydes, while the heterochiral isomer is unreactive. Notably, however, under the standard *catalytic* conditions, both enantiomerically pure DAIB and the racemate do promote alkylation, but the difference in rate of these independent reactions is not large enough to explain the great chiral amplification. For example, in the ethylation using 34 mM DAIB, 0.42 M diethylzinc, and 0.42 M benzaldehyde in toluene at 0 °C, the reaction with (−)-DAIB is merely 14-times faster than that with (±)-DAIB. On the other hand, the reaction catalyzed by (−)-DAIB in 15% *ee* under the same conditions affords the ethylation product in 95% *ee*, indicating the rate difference in the chiral and achiral pathways is about 171. The independent and competitive figures are not the same.

A refined explanation of such a phenomenon is provided by considering the difference in kinetic behavior. Figure 14 illustrates the kinetic profiles of the ethylation using (−)-DAIB and racemic DAIB. The rate of the reaction using

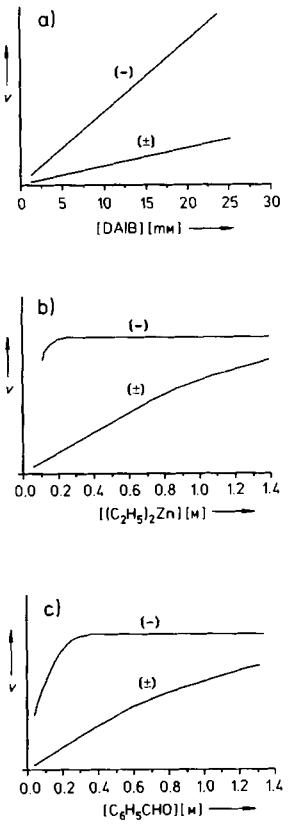

Fig. 14. Kinetic profiles of the reaction of benzaldehyde and diethylzinc catalyzed by (−)- and racemic DAIB. a) The plot of the initial rate as a function of DAIB concentration (0.41 M $(C_2H_5)_2Zn$, 0.41 M C_6H_5CHO). b) The plot of the initial rate as a function of $(C_2H_5)_2Zn$ concentration (2.1 mM DAIB, 0.33 M C_6H_5CHO). c) The plot of the initial rate as a function of C_6H_5CHO concentration (2.1 mM DAIB, 0.33 M $(C_2H_5)_2Zn$).

pure (−)-DAIB, as described above, is not affected by the concentration of diethylzinc and benzaldehyde under the ordinary conditions. By sharp contrast, the rate of the (±)-DAIB catalyzed reaction is profoundly influenced by the dialkylzinc and aldehyde concentrations, where some bimolecular reaction between (2*S*,2′*R*)-**50** and dialkylzinc or benzaldehyde may be involved. Therefore, the rate difference of the reaction with (−)- and (±)-DAIB becomes more

significant with lower concentrations of dialkylzincs and aldehyde substrates. In other words, with given concentrations of an organozinc and aldehyde, the larger rate difference is obtained with higher auxiliary concentration.

Such different kinetic behavior results in a marked dependence of the degree of nonlinearity on DAIB concentration. Figure 15 shows nonlinearity in the ethylation aided by (−)-DAIB in 14% *ee* [(−)/(+) = 57:43], where all reaction parameters except for DAIB concentration are fixed. Evi-

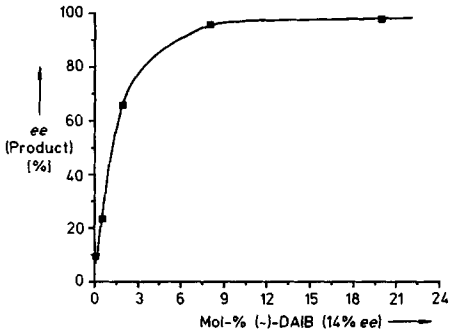

Fig. 15. Effect of auxiliary concentration on the nonlinearity in the ethylation of benzaldehyde aided by (−)-DAIB in 14% *ee* (0.42 M $(C_2H_5)_2Zn$, 0.42 M C_6H_5CHO, toluene, 0 °C).

dently, a chiral catalyst system and achiral one are working competitively in the alkylation. When the reaction is carried out with 0.5 mol% of the partially resolved DAIB, the turnover difference is only twofold, giving the alcohol in 24% *ee*, but with the use of 20 mol% of the catalyst, the product is obtained in 98% *ee*. In the latter case, the turnover efficiency of the chiral catalyst system becomes even more than 600 times greater than that of the coexisting achiral catalyst system.[75]

Thus we can conclude that the emergence of the intriguing nonlinearity is a result of conspicuous differences in the properties of the diastereomeric complexes, (2*S*,2′*S*)- or (2*R*,2′*R*)-**50** and (2*S*,2′*R*)-**50**. The origin of the nonlinear effect is basically the differences in the stability of these complexes, but the difference in the kinetic behavior is also important for evaluating the degree of chiral amplification. When partially resolved DAIB is employed as auxiliary, the chiral and achiral dinuclear complexes are generated in a thermodynamically controlled ratio. All the minor enantiomer, within the limit of NMR accuracy, is converted to the thermodynamically stable *meso* dinuclear complex, (2*S*,2′*R*)-**50**, while the major enantiomer, present in excess, forms the less stable chiral counterpart. The latter possesses a greater tendency to dissociate into the active monomer **60**, thereby exhibiting a much higher turnover efficiency. The difference in stability is understood by comparing the relative steric congestion of the central *syn* and *anti* 5/4/5 tricyclic ring systems. The crystalline structures of these complexes (Fig. 11) indicate that the dihedral angle of the five- and four-membered rings in the *syn* isomer, (2*S*,2′*S*)-**50** (R = CH_3), is substantially larger (ca. 20°) than in the less congested *anti* isomer, (2*S*,2′*R*)-**50** (R = CH_3).

4. Diastereomeric Interactions of Enantiomers

Diastereomeric interaction of the enantiomeric organozinc compounds has played a key role in the unusual chiral amplification. Although chirality recognition is a general phenomenon, a systematic investigation of interactions between *enantiomers* possessing an identical molecular constitution has not been made. This section deals with some examples related to this effect.

Enantiomer recognition is a fundamental principle in crystal lattice formation, giving racemates or conglomerates, and multilayer interactions.[76] Such effects are also noted during sublimation. *Kwart* and *Hoster* found that evacuation of partially resolved **62** causes loss of optical activity owing to sublimation of the enantiomorph in excess leaving behind the less volatile racemate.[77] Some samples represented enrichment from a starting level of 6% optical purity to 74%. Similarly optical purity of mandelic acid could be enhanced or reduced, depending on the optical purity of the starting material.[78]

Paquette et al. found spontaneous resolution by sublimation of racemic chiral alcohol **63**.[79] Thus evacuation of **63** to 20 Torr at 20 °C for several days gave a crystal of the sublimed material, whose X-ray analysis confirmed its single mirror image form. Because the individual needles were clustered and never very large, several crystals were removed together for optical rotation measurements. Consequently there was some mixing of the two mirror image forms. Nevertheless, the sublimed crystals possessed optical activity, while the residual material did not. Interestingly, optical purity of the precipitates formed by titration of nonracemic **64** with hydrochloric acid was lower than that of original **64**.[80]

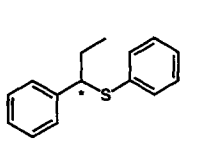

62

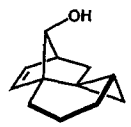

63

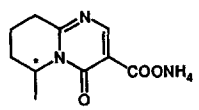

64

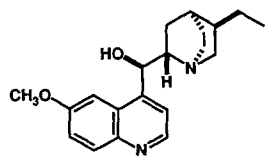

65

Liquid crystals are extremely sensitive to optically active compounds.[81] Upon mixing enantiomeric cholesteric liquid crystals, a nematic phase could form.

Enantiomer recognition in solution may be interpreted by a simple symmetry argument. Under certain conditions, enantiomers can form homochiral or heterochiral associates which can be differentiated by achiral methods. Although such associates in solution are usually labile, their presence was clearly shown by *Horeau* et al., who found that *ee* and optical purity determined by rotation value, in general, need not be in linear relationship.[82] The existence of such effects has also been suggested by slight differences in nonoptical

properties such as dielectric constants,[83] boiling points,[84] and IR spectra.[85]

Uskoković noted that the ^{1}H NMR spectra of optically pure dihydroquinine **65** and of its racemate are significantly different when taken at the same concentration in $CDCl_3$.[86] The spectrum of the partially resolved **65** affords two sets of peaks whose areas are proportional to the relative amount of each enantiomer. These facts can be rationalized by considering the solute-solute interactions of the enantiomers.

In a like manner, the ^{1}H NMR spectra of optically active, but optically impure, samples of methylphenylphosphinic anilide and related analogues exhibit distinct signals for the *P*-methyl groups in the *R* and *S* enantiomers, which may be ascribed to the molecular association through hydrogen bonding as illustrated by **66** (homochiral, favored) and **67** (heterochiral, unfavored).[87] Similar NMR nonequivalence of the enantiomers has been noted for some substituted succinic acids and rather complex compounds having both phosphorus and carbon chiral centers.[88] The organotin compounds derived from partially resolved 2,3-butanediol and dibutyltin oxide are shown by an ^{1}H NMR study to form a mixture composed of *meso* dimer **68** and chiral dimer **69**. This diastereomeric relationship may be used for the optical enrichment of the diol from 75% *ee* to 98% *ee*.[89]

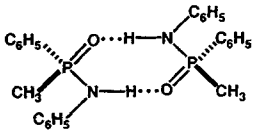

66

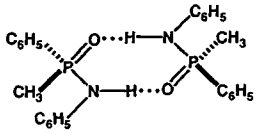

67

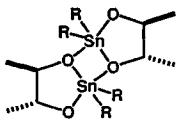

68

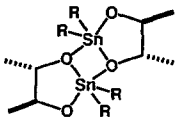

69

R = *n*-C_4H_9

The diastereomeric self-assemblies are even separable in special environments. Thus chromatography of partially resolved enantiomers can cause depletion or enrichment in enantiomers on achiral stationary phases with an achiral mobile phase: *Cundy* and *Crooks* first resolved ^{14}C-labeled nicotine **70** into its enantiomers with high-performance liquid chromatography on Partisil ODS and SCX through coinjection with optically active nicotine.[90] When the diamide **71** (84% optical purity) was subjected to chromatography on Kieselgel 60 using a mixture of hexane and ethyl acetate as eluent, the elute had lower optical purity

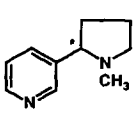

70

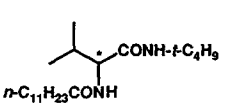

71

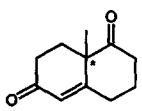

72

than the starting material (30% yield, 46% optical purity), and the latter fractions contained **71** with an average 90% optical purity.[91] Under some conditions, optical enrichment from 60% to greater than 99.8% was attained. *Dreiding* et al. found that chromatography of a nonracemic mixture of the enantiomeric diketone **72** with achiral stationary phase (silica gel) and mobile phase (4:1 hexane–ethyl acetate) furnishes fractions which differ in *ee*.[92]

By use of aminopropyl silica gel as the stationary phase and a hexane–2-propanol mixture as the mobile phase, chromatography of binaphthol **11** with only 33% *ee* leads to a distinct separation into two signals.[93] The excess enantiomer is eluted first and then the racemate. The separation factor is improved on increasing the *ee* and the amount loaded. In a like manner, excess enantiomers of the chiral NMR shift reagents **73** and **74**, the tranquilizer chloromezanone, and the benzodiazepine camazepane can be separated.

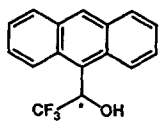

73

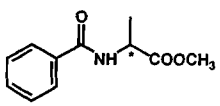

74

The solution-phase enantiomer recognition results in various intriguing stereochemical outcomes in organic reactions:

1) In 1974, *Touboul* and *Dana* reported an amazing selectivity in the controlled potential electrochemical reduction of the enone **75**.[94] While the dimerization of optically pure (+)-**75** or its enantiomer gave solely the *cis-threo-cis* diol (+)- and (−)-**76**, respectively, racemic **75** behaved similarly to lead to racemic **76** and to no other possible diastereomer.

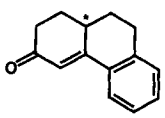

75

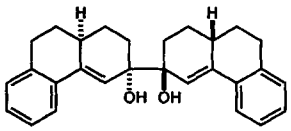

76

2) Reductive dimerization of camphor **77** under McMurry's conditions gives the stereoisomers, **78**, **79** (and

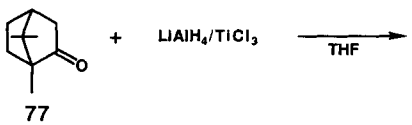

77

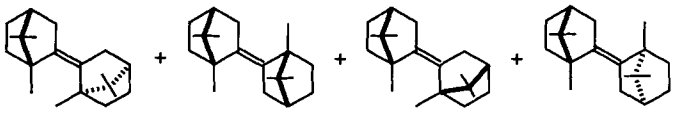

78 79 80 81

77	78 (1*R*,1'*R* + 1*S*,1'*S*)	79 (1*R*,1'*R* + 1*S*,1'*S*)	80 (1*R*,1'*S*)	81 (1*R*,1'*S*)
1*R*	34.8	65.2	—	—
1*R*,1*S*	24.3	40.6	8.9	26.2

Fig. 16. Reductive dimerization of camphor **77**. Product ratios in %.

their enantiomers), **80**, and **81**. *Wynberg* and *Feringa* noticed that the reaction of racemic camphor prefers homochiral dimerization (total 64.9%) over the diastereomeric heterochiral coupling (35.1%).[95]

3) Oxidative dimerization of the chiral phenol **82** affords the chiral dimers **83** and **84** (and their enantiomers) and the *meso* dimer **85**, whereby a significant difference in diastereoselectivity is seen between the reactions of the enantiomerically pure and racemic substrate.[95] The reaction of (*S*)-**82** produces (*S,S*)-**83** exclusively, while the dimerization of racemic **82** lacks stereoselectivity. In the latter case, some indirect enantiomer effect assists the production of **84**, which is absent in the former reaction.

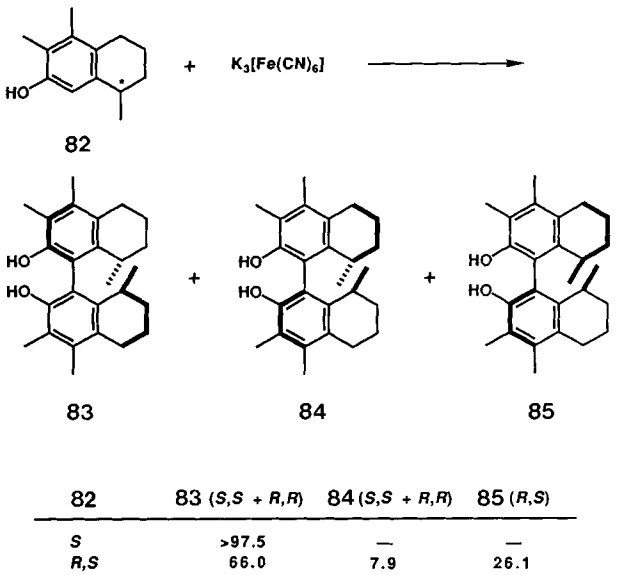

Fig. 17. Oxidative dimerization of the chiral phenol **82**. Yields in %.

4) A striking stereospecificity was observed by *Gladysz* et al. in the intermolecular coupling of a rhenium–carbene species.[96] Crossover experiments using the enantiomerically configurated metal complexes **86** and **87** showed that the reaction proceeds through strict enantiomer self-recognition to form only homochiral coupling products, **88** and **89** (Fig. 18).

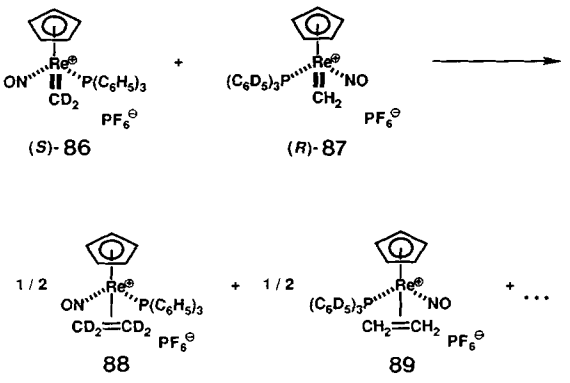

Fig. 18. Coupling of carbene ligands. The dots represent further rhenium complexes.

A considerable departure from the linear relationship between the *ee* of a chiral auxiliary and the extent of the asymmetric induction has also been observed in certain catalytic reactions:

1) *Kagan, Agami,* and their co-workers reported some interesting examples.[97] First, oxidation of *p*-tolyl methyl sulfide **90** with *tert*-butyl hydroperoxide was effected in the presence of titanium tetraisopropoxide modified with enantiomerically pure (+)-diethyl tartrate (DET) to afford the (*R*)-sulfoxide **91** in 85% *ee*, whereas use of tartrate ancillary in 50% *ee* gave the product not in 42.5% *ee* as expected when linearity is assumed, but in only 19% *ee* (catalytic conditions), or 33% *ee* (stoichiometric conditions).

2) The Sharpless oxidation of geraniol **92** using enantiomerically pure DET gave the epoxide **93** in 94% *ee*. The optical yield drops to 70% *ee* by using the auxiliary with 50% *ee*. This value is considerably higher than the *expected* 47% *ee* (Fig. 19, center).

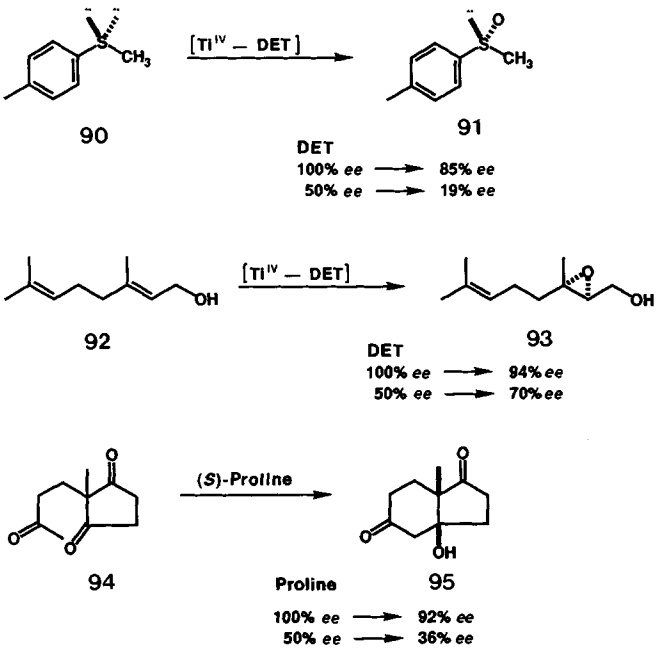

Fig. 19. Examples of the nonlinear effect in asymmetric catalysis.

3) The Hajos–Wiechert intramolecular aldol reaction of triketone **94** to **95** also exhibits a nonlinear relationship between the enantiomeric purity of the (*S*)-proline catalyst and the enantioselectivity.[98] With the partially resolved amino acid, the cyclization gave the product in an *ee* lower than the anticipated value. On the basis of the kinetic study, these results have been interpreted in terms of the involvement of two chiral auxiliary molecules in the stereodetermining steps.[98b]

The enantioselective addition of organozincs to prochiral aldehydes discussed in Sections 3.2 and 3.3 presents an extreme example of such a phenomenon. By virtue of the catalytic nature of the reaction together with the conspicuous difference in the chemical properties of the homochiral and heterochiral *catalyst dimers*, the nonlinear effect has led to unprecedentedly high chiral amplification. This molecular

mechanism may be related to the mechanism of chirality amplification in nature.[74]

5. Outlook

Since the discovery in 1966 of asymmetric cyclopropanation of olefines with diazoalkanes, catalyzed by a chiral Schiff base/Cu^{II} complex,[99] a variety of homogeneous asymmetric reactions using metal complex catalysts and prochiral substrates have been developed. Most of the enantioselective organometallic reactions (defined as transformations involving metal–carbon or –hydrogen bonds) rely on transition metal chemistry, but chiral multiplication can also be achieved by main group elements.[43a, 100] This article has presented some aspects of this subject. Addition of organometallic compounds to carbonyl substrates is one of the most fundamental synthetic reactions. Although asymmetric synthesis with chirally modified organomagnesium or lithium reagents has some 50 years of history, it was only 10 years ago when a level of enantioselection greater than 90% was accomplished on the basis of stoichiometric chirality transfer. Now this domain is growing continuously, and particularly over the last five years there has been great progress in the catalytic reaction. We have realized the highly stereoselective reaction (in some cases 99% *ee*) using organozinc compounds and a catalytic quantity of chiral auxiliary, which at the same time exhibits chiral amplification. The mechanism has now been elucidated at the molecular level. This achievement, however, marks only the beginning of this important area, which is yet to be fully explored. The organozinc chemistry is intriguing, but the scope of the reaction is still limited. The procedure can be applied to a variety of organozinc compounds having primary alkyl groups, but not to the secondary and tertiary compounds, which are too unstable because of alkene elimination. Furthermore, we have not looked closely at reactions using highly functionalized organometallic reagents or substrates, which might be useful for the synthesis of complex natural products or their artificial analogues. Thus a general method for enantiofacial and selective alkylation or arylation still remains elusive. Further development of versatile methods using other metal elements is strongly desired, and we hope that the principles described here will be helpful.

In scientific research a rational approach to problems is obviously ideal, although in reality major breakthroughs in this field have been obtained mainly by serendipity or through trial-and-error improvements of the existing systems. A large body of information has accumulated in organometallic chemistry, but the level of our structural and mechanistic understanding, particularly in the supramolecular chemistry,[9] still remains primitive. Unifying views on the structure-reactivity relationship or reliable selection rules have not appeared. However, we are quite optimistic: chemists' intuition coupled with logical designing and keen insight will continue to generate a series of versatile stereoselective organic reactions along this line.

Finally, we would emphasize that asymmetric catalysis is a four-dimensional chemistry. Stereochemical differentiation is crucially important but not enough. As illustrated above, high efficiency is obtained only by combining the ideal three-dimensional structure (x,y,z) and appropriate kinetics (t).

The author (R. N.) was exceedingly honored with the Merck-Schuchardt lectureship, (FRG), and indeed enjoyed the memorable lecture tour in May, 1989. We would like to thank Messrs. M. Okada, S. Suga, and K. Kawai, our students at Nagoya who made sustained intellectual and experimental efforts to elucidate the new chemistry described in this article. Valuable discussions with Professor N. Oguni at Yamaguchi University are also appreciated. This work was supported financially by Specially Promoted Research (No. 62065005) from the Japanese Government, the Ministry of Education, Science and Culture of Japan.

Received: February 12, 1990 [A 801 IE]
German Version: *Angew. Chem. 30* (1990) 34

[1] For the present state of asymmetric carbon–carbon bond formation catalyzed by metal complexes, see: R. Noyori, M. Kitamura in R. Scheffold (Ed.): *Modern Synthetic Methods*, Springer, Berlin 1989, pp. 115–198.
[2] E. Frankland, *Ann. Chem. Pharm. 71* (1849) 171–213.
[3] M. W. Rathke, *Org. React. (NY) 22* (1975) 423–460.
[4] H. E. Simmons, T. L. Cairns, S. A. Vladuchick, *Organic Reactions 20* (1973) 1–132.
[5] V. Grignard, *C. R. Hebd. Sceances Acad. Sci. 130* (1900) 1322; *Chem. Zentralbl. 1900 II*, 33.
[6] G. Wittig, U. Pockels, H. Droge, *Chem. Ber. 71* (1938) 1903; H. Gilman, A. L. Jacoby, *J. Org. Chem. 3* (1938) 108–119; H. Gilman, W. Langham, A. L. Jacoby, *J. Am. Chem. Soc. 61* (1939) 106–109.
[7] W. E. Lindsell in G. Wilkinson, F. G. A. Stone, E. W. Abel (Eds.): *Comprehensive Organometallic Chemistry, Vol. 1*. Pergamon, New York 1982, p. 155–252.
[8] A. W. Langer: *Polyamine-Chelated Alkali Metal Compounds (Adv. Chem. Ser. 130* (1974)).
[9] D. Seebach, *Angew. Chem. 100* (1988) 1685; *Angew. Chem. Int. Ed. Engl. 27* (1988) 1624–1654.
[10] M. Kitamura, S. Suga, K. Kawai, R. Noyori, *J. Am. Chem. Soc. 108* (1986) 6071–6072.
[11] R. Noyori, S. Suga, K. Kawai, S. Okada, M. Kitamura, *Pure Appl. Chem. 60* (1988) 1597–1606.
[12] M. Kitamura, S. Okada, S. Suga, R. Noyori, *J. Am. Chem. Soc. 111* (1989) 4028–4036.
[13] R. Noyori, S. Suga, K. Kawai, S. Okada, M. Kitamura, N. Oguni, M. Hayashi, T. Kaneko, Y. Matsuda, *J. Organomet. Chem. 382* (1990) 19–37.
[14] M. Betti, E. Lucchi, *Boll. Sci. Fac. Chim. Ind. Bologna 1/2* (1940) 2–5; *Chem. Abstr. 34* (1940) 2354.
[15] D. S. Tarbell, M. C. Paulson, *J. Am. Chem. Soc. 64* (1942) 2842–2844.
[16] H. L. Cohen, G. F. Wright, *J. Org. Chem. 18* (1953) 432–446.
[17] N. Allentoff, G. F. Wright, *J. Org. Chem. 22* (1957) 1–6; W. French, G. F. Wright, *Can. J. Chem. 42* (1964) 2474–2479; C. Blomberg, J. Coops, *Recl. Trav. Chim. Pays-Bas 83* (1964) 1083–1095.
[18] H. Nozaki, T. Aratani, T. Toraya, *Tetrahedron Lett. 1968*, 4097–4098; H. Nozaki, T. Aratani, T. Toraya, R. Noyori, *Tetrahedron 27* (1971) 905–913.
[19] a) D. Seebach, H. Dörr, B. Bastani, V. Ehrig, *Angew. Chem. 81* (1969) 1002–1003; *Angew. Chem. Int. Ed. Engl. 8* (1969) 982; b) D. Seebach, H.-O. Kalinowski, B. Bastani, G. Crass, H. Daum, H. Dörr, N. P. DuPreez, V. Ehrig, W. Langer, C. Nüssler, H.-A. Oei, M. Schmidt, *Helv. Chim. Acta 60* (1977) 301–325; c) D. Seebach, W. Langer, *ibid. 62* (1979) 1701–1709; d) D. Seebach, G. Crass, E.-M. Wilka, D. Hilvert, E. Brunner, *ibid. 62* (1979) 2695–2698.
[20] J.-P. Mazaleylat, D. J. Cram, *J. Am. Chem. Soc. 103* (1981) 4585–4586.
[21] K. Tomioka, M. Nakajima, K. Koga, *Chem. Lett. 1987*, 65–68.
[22] D. C. Iffland, J. E. Davis, *J. Org. Chem. 42* (1977) 4150–4151.
[23] J. K. Whitesell, B.-R. Jaw, *J. Org. Chem. 46* (1981) 2798–2799.
[24] T. D. Inch, G. J. Lewis, G. L. Sainsbury, D. J. Sellers, *Tetrahedron Lett. 1969*, 3657–3660.
[25] J.-P. Battioni, W. Chodkiewicz, *Bull. Soc. Chim. Fr. 1972*, 2068–2069.
[26] J. S. Zweig, J. L. Luche, E. Barreiro, P. Crabbé, *Tetrahedron Lett. 1975*, 2355–2358.
[27] G. Boireau, D. Abenhaim, J. Bourdais, E. Henry-Basch, *Tetrahedron Lett. 1976*, 4781–4782.

[28] D. Abenhaim, G. Boireau, B. Sabourault, *Tetrahedron Lett. 21* (1980) 3043–3046.
[29] A. I. Meyers, M. E. Ford, *Tetrahedron Lett. 1974*, 1341–1344.
[30] T. Mukaiyama, K. Soai, T. Sato, H. Shimizu, K. Suzuki, *J. Am. Chem. Soc. 101* (1979) 1455–1460.
[31] W. S. Johnson, B. Frei, A. S. Gopalan, *J. Org. Chem. 46* (1981) 1512–1513.
[32] a) B. Weidmann, L. Widler, A. G. Olivero, C. D. Maycock, D. Seebach, *Helv. Chim. Acta 64* (1981) 357–361; b) M. T. Reetz, R. Steinbach, B. Wenderoth, J. Westermann, *Chem. Ind. (London) 1981*, 541–542.
[33] D. Seebach, A. K. Beck, S. Roggo, A. Wonnacott, *Chem. Ber. 118* (1985) 3673–3682.
[34] M. T. Reetz, T. Kükenhöhner, P. Weinig, *Tetrahedron Lett. 27* (1986) 5711–5714.
[35] L. Colombo, C. Gennari, G. Poli, C. Scolastico, *Tetrahedron 38* (1982) 2725–2727.
[36] H. Takahashi, A. Kawabata, K. Higashiyama, *Chem. Pharm. Bull. 35* (1987) 1604–1607.
[37] R. Noyori, I. Tomino, Y. Tanimoto, M. Nishizawa, *J. Am. Chem. Soc. 106* (1984) 6709–6716; R. Noyori, I. Tomino, M. Yamada, M. Nishizawa, *ibid. 106* (1984) 6717–6725.
[38] ^{1}H NMR of $(C_2H_5)_2Mg$ (270 MHz, [D$_8$]THF, 20 °C, THF as internal standard) $\delta = 1.27$ (t, $J = 8.1$ Hz), -0.71 (q, $J = 8.1$ Hz).
[39] A. H. Alberts, H. Wynberg, *J. Am. Chem. Soc. 111* (1989) 7265–7266.
[40] M. B. Eleveld, H. Hogeveen, *Tetrahedron Lett. 25* (1984) 5187–5190.
[41] J. G. Noltes, J. W. G. van der Hurk, *J. Organomet. Chem. 3* (1965) 222–228; K. H. Thiele, H. Rau, *Z. Anorg. Allg. Chem. 353* (1967) 127.
[42] a) N. Oguni, T. Omi, Y. Yamamoto, A. Nakamura, *Chem. Lett. 1983*, 841–842; b) N. Oguni, T. Omi, *Tetrahedron Lett. 25* (1984) 2823–2824.
[43] a) E. J. Corey, R. K. Bakshi, S. Shibata, *J. Am. Chem. Soc. 109* (1987) 5551–5553; b) E. N. Jacobsen, I. Markó, W. S. Mungall, G. Schröder, K. B. Sharpless, *J. Am. Chem. Soc. 110* (1988) 1968–1970.
[44] N. Oguni, Y. Matsuda, T. Kaneko, *J. Am. Chem. Soc. 110* (1988) 7877–7878.
[45] A. H. Beckett, N. T. Lan, G. R. McDonough, *Tetrahedron 25* (1969) 5689–5692, 5693–5702; R. A. Chittenden, G. H. Cooper, *J. Chem. Soc. C 1970*, 49–54; A. Daniel, A. A. Pavia, *Bull. Soc. Chim. Fr. 1971*, 1060–1073; M. T. Reetz, T. Zierke, *Chem. Ind. (Dekker) 17* (1988) 663; for preparation of enantiomerically pure DAIB, see ref. [13].
[46] M. Kitamura, S. Okada, R. Noyori, unpublished results.
[47] A. van Oeveren, W. Menge, B. L. Feringa, *Tetrahedron Lett. 30* (1989) 6427–6430.
[48] R. Noyori, M. Suzuki, *Angew. Chem. 96* (1984) 854–882; *Angew. Chem. Int. Ed. Engl. 23* (1984) 847–876; M. Suzuki, A. Yanagisawa, R. Noyori, *J. Am. Chem. Soc. 107* (1985) 3348–3349; Y. Morita, M. Suzuki, R. Noyori, *J. Org. Chem. 54* (1989) 1785–1787; R. Noyori, *Chem. Br. 25* (1989) 883–888.
[49] A. A. Smaardijk, H. Wynberg, *J. Org. Chem. 52* (1987) 135–137.
[50] a) S. Itsuno, J. M. J. Fréchet, *J. Org. Chem. 52* (1987) 4140–4142; b) S. Itsuno, Y. Sakurai, K. Ito, T. Maruyama, S. Nakahama, J. M. J. Fréchet, *ibid. 55* (1990) 304–310.
[51] a) P. A. Chaloner, S. A. R. Perera, *Tetrahedron Lett. 28* (1987) 3013–3014; b) E. J. Corey, F. J. Hannon, *ibid. 28* (1987) 5233–5236; c) *ibid. 28* (1987) 5237–5240; d) G. Muchow, Y. Vannoorenberghe, G. Buono, *ibid. 28* (1987) 6163–6166; e) K. Soai, A. Ookawa, K. Ogawa, T. Kaba, *J. Chem. Soc. Chem. Commun. 1987*, 467–468; f) K. Soai, A. Ookawa, T. Kaba, K. Ogawa, *J. Am. Chem. Soc. 109* (1987) 7111–7115; g) K. Soai, S. Niwa, Y. Yamada, H. Inoue, *Tetrahedron Lett. 28* (1987) 4841–4842; h) K. Soai, S. Yokoyama, K. Ebihara, T. Hayasaka, *J. Chem. Soc. Chem. Commun. 1987*, 1690–1691; i) K. Soai, M. Nishi, Y. Ito, *Chem. Lett. 1987*, 2405–2406; j) K. Soai, S. Niwa, M. Watanabe, *J. Org. Chem. 53* (1988) 927–928; k) K. Soai, S. Niwa, *Chem. Lett. 1989*, 481–484; l) K. Soai, S. Yokoyama, T. Hayakawa, K. Ebihara, *56th Annu. Meet. Chem. Soc. Jpn.* (Kyoto, Japan 1988), Paper 1XIIB34; m) K. Soai, M. Watanabe, M. Koyano, *J. Chem. Soc. Chem. Commun. 1989*, 534–536; n) E. J. Corey, P. Yuen, F. J. Hannon, D. A. Wierda, *J. Org. Chem. 55* (1990) 784–786; o) C. Bolm, M. Zehnder, D. Bur, *Angew. Chem. 102* (1990) 206–208; *Angew. Chem. Int. Ed. Engl. 29* (1990) 205–207.
[52] D. A. Evans, *Science (Washington) 240* (1988) 420–426.
[53] M. Hayashi, H. Miwata, N. Oguni, *Chem. Lett. 1989*, 1969–1970.
[54] W. Oppolzer, R. N. Radinov, *Tetrahedron Lett. 29* (1988) 5645–5648.
[55] K. Tanaka, H. Ushio, H. Suzuki, *J. Chem. Soc. Chem. Commun. 1989*, 1700–1701.
[56] M. Yoshioka, T. Kawakita, M. Ohno, *Tetrahedron Lett. 30* (1989) 1657–1660; H. Takahashi, T. Kawakita, M. Yoshioka, S. Kobayashi, M. Ohno, *ibid. 30* (1989) 7095–7098.
[57] N. N. Joshi, M. Srebnik, H. C. Brown, *Tetrahedron Lett. 30* (1989) 5551–5554.
[58] Reaction of diethylzinc and benzaldehyde in toluene containing 2 mol% (−)-DAIB at 50 °C for 2 min gave the (*S*)-1-phenyl-1-propanol in 94.6% *ee* and 70.2% yield. The blank experiment without (−)-DAIB afforded the racemic alcohol in 0.3% yield, indicating that the *S*/*R* ratio in the DAIB catalyzed reaction at 50 °C was at most 97.5:2.5. The previously recorded value 94.5:5.5, obtained by the 1.5 h reaction [11–13], ignores the participation of the uncatalyzed reaction and hence should be revised.
[59] E. Kaufmann, P. von R. Schleyer, K. N. Houk, Y.-D. Wu, *J. Am. Chem. Soc. 107* (1985) 5560–5562.
[60] T. L. Brown, *Adv. Organomet. Chem. 3* (1965) 365; *J. Organomet. Chem. 5* (1966) 191; S. G. Smith, L. F. Charbonneau, D. P. Novak, T. L. Brown, *J. Am. Chem. Soc. 94* (1972) 7059–7063; L. F. Charbonneau, S. G. Smith, *J. Org. Chem. 41* (1976) 808–812; M. A. Al-Aseer, S. G. Smith, *ibid. 49* (1984) 2608–2613; M. A. Al-Aseer, B. D. Allison, S. G. Smith, *ibid. 50* (1985) 2715–2719.
[61] J. F. McGarrity, C. A. Ogle, *J. Am. Chem. Soc. 107* (1985) 1805–1810; J. F. McGarrity, C. A. Ogle, Z. Brich, H.-R. Loosli, *ibid. 107* (1985) 1810–1815.
[62] For coordination of phosphoryl oxygen to two lithium ions see K. Jens, J. Kopf, N. P. Lorenzen, E. Weiss, *Chem. Ber. 121* (1988) 1201–1202.
[63] E. A. Jeffery, T. Mole, J. K. Saunders, *Aust. J. Chem. 21* (1968) 649–657; E. A. Jeffery, T. Mole, *ibid. 23* (1970) 715–724; see also D. S. Matteson, *Organomet. Chem. Rev. Sect. A 4* (1969) 263–305.
[64] S. Pasynkiewicz, E. Sliwa, *J. Organomet. Chem. 3* (1965) 121–128.
[65] P. A. Chaloner (University of Sussex), personal communication.
[66] Certain γ-amino alcohols [54] or β-monoalkylamino alcohols showed opposite selectivities. For example, ethylation of benzaldehyde in the presence of **36**, gives (*S*)-1-phenyl-1-propanol in 92% *ee*. In *Chaloner*'s report [51a], the structure is not really meant to be a Fischer projection, and the results quoted there are indeed for (1*R*,2*S*)-ephedrines and not pseudoephedrine derivatives.
[67] T. J. LePage, K. B. Wiberg, *J. Am. Chem. Soc. 110* (1988) 6642–6650.
[68] M. T. Reetz, M. Hüllmann, W. Massa, S. Berger, P. Rademacher, P. Heymanns, *J. Am. Chem. Soc. 108* (1986) 2405–2408.
[69] ^{1}H NMR spectrum of **51** in [D$_8$]toluene at 0 °C gave a singlet at $\delta = 6.2$ with 10–20% intensity of aldehydic proton signal, which may be assignable to the hemiacetal proton of **I**. An analogous observation was made in the reaction of *n*-butyllithium with benzaldehyde at − 85 °C [61], giving compound **II** with the hemiacetal proton signal at $\delta = 5.74$, or in the reaction of tetrakis(dialkylamido)titanium with aldehydes at −78 °C [M. T. Reetz, B. Wenderoth, R. Peter, *J. Chem. Soc. Chem. Commun. 1983*, 406].

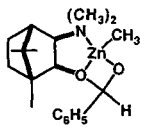

I

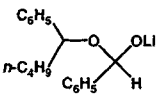

II

[70] A different conclusion was drawn in ref. [50a] and [54].
[71] J. Boersma in G. Wilkinson, F. G. A. Stone, E. W. Abel (Eds.): *Comprehensive Organometallic Chemistry, Vol. 2*, Pergamon, New York 1982, p. 823–862.
[72] G. E. Coates, D. Ridley, *J. Chem. Soc. A* (1966) 1064–1069.
[73] Y. Matsuda, T. Tokumitsu, N. Oguni, *34th Symp. Organomet. Chem.* (Kyoto, Japan 1987), PB 205.
[74] S. Mason, *Chem. Soc. Rev. 17* (1988) 347–359.
[75] The calculation was made by assuming the product *ee* to be over 97%.
[76] J. Jacques, A. Collet, S. H. Wilen: *Enantiomers, Racemates, and Resolutions*, Wiley, New York 1981.
[77] H. Kwart, D. P. Hoster, *J. Org. Chem. 32* (1967) 1867–1870.
[78] D. L. Garin, D. J. C. Greco, L. Kelley, *J. Org. Chem. 42* (1977) 1249–1251.
[79] L. A. Paquette, C. J. Lau, *J. Org. Chem. 52* (1987) 1634–1635.
[80] E. Fogassy, F. Faigl, M. Ács, *Tetrahedron 41* (1985) 2841–2845.
[81] G. Solladié, R. G. Zimmermann, *Angew. Chem. 96* (1984) 335; *Angew. Chem. Int. Ed. Engl. 23* (1984) 348–362.
[82] A. Horeau, J. P. Guetté, *Tetrahedron 30* (1974) 1923–1931.
[83] R. J. W. Le Févre, F. Maramaba, *J. Chem. Soc. 1952*, 235–240.
[84] C. J. MacGinn, *J. Phys. Chem. 65* (1961) 1896–1897.
[85] a) W. Walden, C. Zimmermann, A. Kolbe, H. Pracejus, *Tetrahedron 33* (1977) 419–421; b) W. C. Herndon, S. P. Vincenti, *J. Am. Chem. Soc. 105* (1983) 6174–6175.
[86] T. Williams, R. G. Pitcher, P. Bommer, J. Gutzwiller, M. Uskoković, *J. Am. Chem. Soc. 91* (1969) 1871–1872.
[87] M. J. P. Harger, *J. Chem. Soc. Perkin Trans. 2 1977*, 1882–1887; *ibid. 1978*, 326–331.
[88] M. I. Kabachnik, T. A. Mastryukova, E. I. Fedin, M. S. Vaisberg, L. L. Morozov, P. V. Petrovsky, A. E. Shipov, *Tetrahedron 32* (1976) 1719–1728.
[89] A. Shanzer, J. Libman, H. E. Gottlieb, *J. Org. Chem. 48* (1983) 4612–4617.

[90] K. C. Cundy, P. A. Crooks, *J. Chromatogr. 281* (1983) 17–33.
[91] R. Charles, E. Gil-Av, *J. Chromatogr. 298* (1984) 516–520.
[92] W.-L. Tsai, K. Hermann, E. Hug, B. Rohde, A. S. Dreiding, *Helv. Chim. Acta 68* (1985) 2238–2243.
[93] R. Matusch, C. Coors, *Angew. Chem. 101* (1989) 624; *Angew. Chem. Int. Ed. Engl. 28* (1989) 626–627.
[94] E. Touboul, G. Dana, *C. R. Seances Acad. Sci. Ser. C 278* (1974) 1063–1064. However, reductive dimerization of a related cyclic ketone failed to give such stereoselectivity. See L. A. Paquette, I. Itoh, W. B. Farnham, *J. Am. Chem. Soc. 97* (1975) 7280–7285.
[95] H. Wynberg, B. Feringa, *Tetrahedron 32* (1976) 2831–2834.
[96] J. H. Merrifield, G.-Y. Lin, W. A. Kiel, J. A. Gladysz, *J. Am. Chem. Soc. 105* (1983) 5811–5819.
[97] C. Puchot, O. Samuel, E. Duñach, S. Zhao, C. Agami, H. B. Kagan, *J. Am. Chem. Soc. 108* (1986) 2353–2357.
[98] a) C. Agami, J. Levisalles, C. Puchot, *J. Chem. Soc. Chem. Commun. 1985*, 441–442; b) C. Agami, *Bull. Soc. Chim. Fr. 1988*, 499–507.
[99] H. Nozaki, S. Moriuti, H. Takaya, R. Noyori, *Tetrahedron Lett. 1966*, 5239; H. Nozaki, H. Takaya, S. Moriuti, R. Noyori, *Tetrahedron 24* (1968) 3655.
[100] A number of *organic* reactions are catalyzed by chiral Lewis acids, for example, a) K. Maruoka, T. Itoh, T. Shirasaka, H. Yamamoto, *J. Am. Chem. Soc. 110* (1988) 310–312; b) K. Narasaka, M. Inoue, T. Yamada, *Chem. Lett. 1986*, 1967–1968; c) K. Mikami, M. Terada, T. Nakai, *J. Am. Chem. Soc. 111* (1989) 1940–1941; d) E. J. Corey, R. Imwinkelried, S. Pikul, Yi B. Xiang, *ibid. 111* (1989) 5493–5495.

Missing issues?

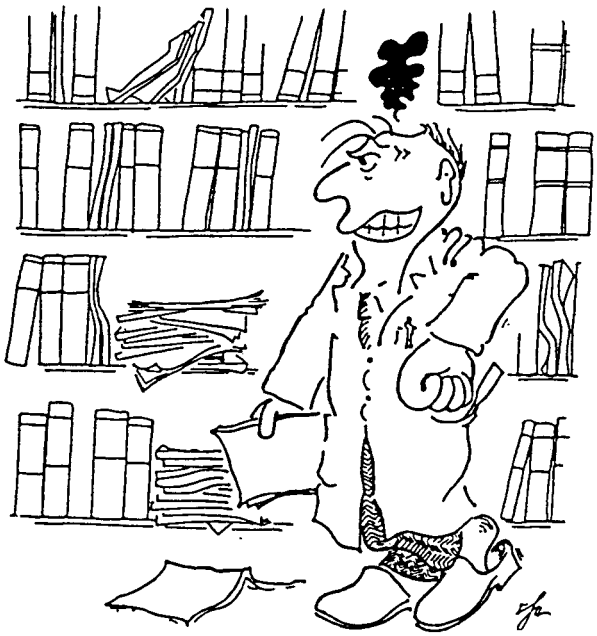

No problem with a personal subscription to „Angewandte Chemie". Your own copy to read when you want, where you want.
Subscribe today!

Just phone or fax

VCH

USA: Tel. (800) 422-8824, Fax (305) 428-8201
Rest of the world: Tel. (06201) 602216, Fax (06201) 602328

The Third Allotropic Form of Carbon

By *J. Fraser Stoddart**

From Fiction to Fact. Every so often something happens in science that is extremely simple and immensely satisfying. The harvesting of C_{60} in the late summer of last year by *Krätschmer* and his associates[1] from a rather special brew of soot has vindicated the inspired structural proposal—the celebrated truncated icosahedron with the ultimate symbol (I_h) in point group symmetry that also happens to grace the familiar pattern displayed on regulation soccer balls—advanced away back in the mid-80s by *Kroto* and his collaborators[2] for a compound they dubbed buckminsterfullerene, molecules of which they had clearly observed by time-of-flight mass spectrometry following vaporization of graphite by laser evaporation.

Prior knowledge by most in the field of the autumnal announcement[1] in *Nature* heralded a flurry of activity in numerous research laboratories around the world. Now that sample tube quantities of this new race of carbon compounds are available, this third allotropic form of carbon promises to create chemistry and aid and abet applications around it every bit as rich as those associated with the ubiquitous and rare allotropes—graphite and diamond, with their diversely distinctive properties and distinctly diverse uses.

Harvesting the Soot. At present, access to milligram quantities of C_{60}, and its rugby ball counterpart, C_{70} (Fig. 1) depends on perfecting simultaneously two separate arts—firstly, isolating fullerene-rich soot in gram quantities, apparently best achieved when graphite rods of uniform particle size are evaporated by resistive heating under a partial atmosphere of an inert gas like helium[1] or argon[3] and then, secondly, effecting the demanding chromatographic separation of C_{60} from C_{70}, both of which are to be found in boiling benzene extracts of the soot. The top yield reported for this harvest at the onset of winter was a remarkable 14% by *Diederich* and his team at UCLA[4] who have employed a battery of chromatographic and spectroscopic techniques to show that their soot is 85:15, C_{60}:C_{70}. Although chromatography has been executed with modest success using hexane as the eluant on both alumina[3,4] and silica gel,[5] fractional sublimation[1,6] at very high temperatures (ca. 600 °C) under vacuum from an inert atmophere should be amenable to the large scale manufacture of this new product line of carbon. It is surely only a matter of time until both physical and chemical means of isolation are perfected to a point where kilograms of C_{60}, C_{70}, and other homologues, can be stored in bottles. And there is promise[5] of even better things to come—the preparation of C_{60} and C_{70} starting from precursors other than graphite.

Believing is Seeing. Both C_{60} and C_{70} are highly colored crystalline solids that are sparingly soluble in common organic solvents, giving rise to solutions with pinkish-to-red hues to them. The UV-VIS spectra of C_{60} both neat[1] and in solution[3,4] reveal three, if not four, broad bands of considerable intensities in the UV that correspond roughly with the allowed transitions predicted by theory for the molecule.

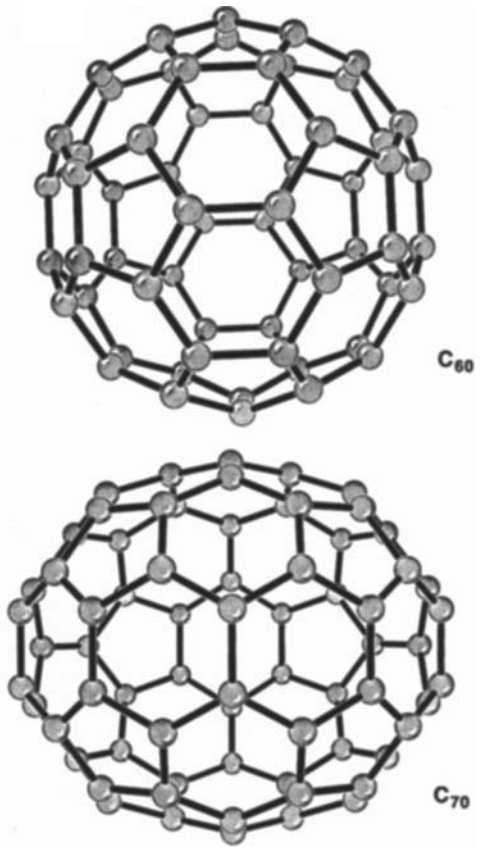

Fig. 1. Drawings of the proposed molecular structures for C_{60} (top) and C_{70} (bottom). Reproduced by permission of Professor *F. Diederich*, Los Angeles.

The chemical world awaits a detailed single crystal X-ray diffraction analysis of the structure of C_{60} or C_{70}, or more likely perhaps, of a derivative in the first instance. In the meantime, X-ray diffraction studies[1] on micrometer sized hexagonal platelets of C_{60}, with unit cell parameters of 10.02 and 16.36 Å, correspond closely to a simple hexagonal close packing of disordered spherical molecules.[7] These days STM is all the rage for seeing images of molecules very often sitting on a surface of graphite! Late in December two reports appeared in which the imaging of C_{60} and the slightly taller C_{70} with a scanning tunnelling microscope is described.[8]

Seeing is Believing. The weight of the spectroscopic evidence for the structures proposed[2] for C_{60} and C_{70} is overwhelming. There is agreement from at least four camps[1,3,5,9] that the four strongest bands for C_{60} in conventional KBr pellets of soot extracts in various states of purification appear at 1430, 1182, 577, and 527 cm^{-1}. Almost identical spectra were observed[9] from argon and krypton matrices deposited on gold substrates, indicating that the solid state absorptions are close to the gas phase ones.

[*] Prof. J. F. Stoddart
School of Chemistry, University of Birmingham
Edgbaston, GB-Birmingham B15 2TT (UK)

 © VCH Verlagsgesellschaft mbH, W-6940 Weinheim, 1991 0570-0833/91/0101-0070 $ 3.50+.25/0

The findings[1, 3, 5] of mass spectrometry are equally convincing. Both the EI and FAB methods reveal strong molecular ions at m/z 720 and 840 for C_{60} and C_{70}, respectively. The EIMS shows[5] the expected isotopic distribution patterns with the $[M+1]^{\oplus}$ intensities for C_{60} and C_{70}, 61% and 67%, respectively, of the $M^{\oplus}$ peak. Interestingly, the $C_{60}^{2\oplus}$ ion is detected[5] in appreciable quantities when EI spectra are run at high (70 eV) ionization energies, confirming the amazing stability of the C_{60} carbon cage.

Since C_{60} has I_h symmetry, all its carbon atoms are equivalent. Thus, the ^{13}C NMR spectrum should display one, and only one, signal. It does.[3-6] In a C_6D_6 solution, the single peak is observed at $\delta = 143.2$ (Fig. 2). For C_{70}, with its D_{5h}

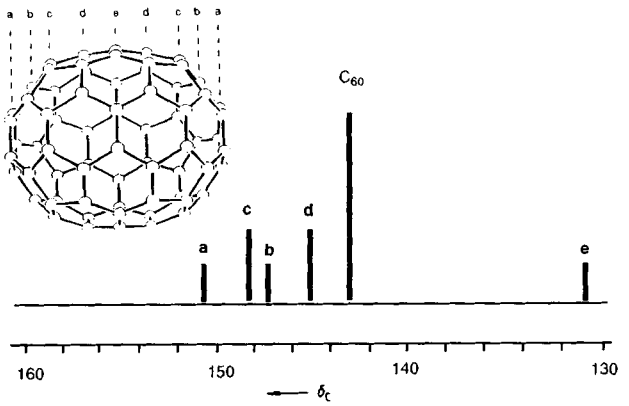

Fig. 2. A ^{13}C NMR line spectrum of a mixture of C_{60} and C_{70}. The five sets (a–e) of identical carbon atoms lie in the vertical planes as indicated on the inset schematic diagram of C_{70}. The assignments are those given in [3]. The schematic diagram is reproduced by permission of Professor *H. W. Kroto*, Brighton.

symmetry, we should observe five signals—two, both with twice the intensities of the other three. Indeed, when a long 20 second pulse delay was used[5] to make allowances for the relatively long T_1 values, the ^{13}C NMR spectrum, also recorded in a C_6D_6 solution (Fig. 2), revealed[5] peaks at $\delta = 150.7$ (a), 147.4 (b), 148.1 (c), 145.4 (d) and 130.9 (e) in the ratio of 10:10:20:20:10 as expected for C_{70}.

The Proof of the Pudding is in the Eating. Now that C_{60} and C_{70} exist as authentic crystalline samples, can any chemistry be done with them? The answer is yes according to *Smalley* et al.[9] They have found that C_{60} undergoes a Birch reduction [Eq. (a)] to give a product, which is a mixture of

$$C_{60} \underset{\text{DDQ/Toluene}}{\overset{\text{Li/liquid NH}_3\text{/tBuOH}}{\rightleftharpoons}} C_{60}H_{36} \qquad \text{(a)}$$

isomers with the molecular formula $C_{60}H_{36}$. The fact that treatment of this hydrogenated product with 2,3-dichloro-5,6-dicyano-1,4-benzoquinone (DDQ) in toluene produces a substance indistinguishable from authentic buckminsterfullerene demonstrates that the reduction of C_{60} is fully reversible, indicating that no alteration occurs to the carbon skeleton of the molecule during its Birch reduction.

In CH_2Cl_2 with nBu$_4$NBF$_4$ as the supporting electrolyte, C_{60} undergoes electrochemical reduction in two waves at -610 mV and -1000 mV relative to the normal hydrogen electrode [Eq. (b)]. This electrochemical behavior[10] suggests that stable salts based on C_{60} as either an anion or dianion might be on the cards.

$$C_{60} \underset{-e}{\overset{+e}{\rightleftharpoons}} C_{60}^{\ominus} \underset{-e}{\overset{+e}{\rightleftharpoons}} C_{60}^{2\ominus} \qquad \text{(b)}$$

The photophysical properties of C_{60} have also been studied recently. It is a potential generator of singlet oxygen.[11]

From Fact to Fiction. Confronted with molecules as pretty and as fascinating as C_{60} and C_{70}, the human imagination starts to run riot. Will they behave as the ultimate in lubricants, i.e. as molecular ball-bearings? The materials science of carbon is on the move again.

Then, smaller molecules and ions, which can no doubt be trapped inside the carbon cages, are expected to have a rather unique chemistry. One can also envisage the introduction of holes and even trap doors into the surfaces of the carbon cages, leading to the possibility of dialysis at the molecular level or the controlled slow release of bioactive molecules. The pharmaceutical and agrochemical industries should not be disinterested in the post-Columbus chemistry of carbon.

And then, there is the prospect of doing outer and inner sphere chemistry, particularly with transition metals. To what extent can chemical species that are imprisoned, not only covalently but also mechanically inside fullerenes, influence their optical and redox properties? Can much larger fullerenes,[12] like C_{540}, be made and can one be assembled onion-like inside another? Surely the scientists who are fortunate enough to find themselves bang in the middle of this bonanza will be limited only by their imaginations for some considerable time to come.

[1] W. Krätschmer, L. D. Lamb, K. Fostiropoulos, D. R. Huffman, *Nature (London) 347* (1990) 354.

[2] H. W. Kroto, J. R. Heath, S. C. O'Brien, R. F. Curl, R. E. Smalley, *Nature (London)* 318 (1985) 162. It should be noted that C_{60} was first predicted by *E. Osawa (Kagaku (Kyoto) 25* (1970) 85 (In Japanese)).

[3] R. Taylor, J. P. Hare, A. K. Abdul-Sada, H. W. Kroto, *J. Chem. Soc. Chem. Commun. 1990*, 1423. Chromatography on alumina using a 8 × 60 cm column with hexane/toluene (98:5 for C_{60} and 80:20 for C_{70}) as eluant is the very best method, according to *F. Diederich* (personal communication). In this way, 400 mg of the C_{60}/C_{70} mixture can be separated. See also [4].

[4] P.-M. Allemand, A. Koch, F. Wudl, Y. Rubin, F. Diederich, M. M. Alvarez, S. J. Anz, R. L. Whetten, *J. Am. Chem. Soc. 113* (1991), in press.

[5] H. Ajie, M. M. Alvarez, S. J. Anz, R. D. Beck, F. Diederich, K. Fostiropoulos, D. R. Huffman, W. Krätschmer, Y. Rubin, K. E. Schriver, D. Sensharma, R. L. Whetten, *J. Phys. Chem. 94* (1990) 8630.

[6] R. D. Johnson, G. Meijer, D. S. Bethune, *J. Am. Chem. Soc. 112* (1990) 8983.

[7] According to *F. Diederich* (personal communication), pure C_{60} crystallizes in a cubic f-centered close packing. The hexagonal packing is preferred by pure C_{70} as well as by the conglomerate.

[8] R. J. Wilson, G. Meijer, D. S. Bethune, R. D. Johnson, D. D. Chambliss, M. S. de Vries, H. E. Hunziker, H. R. Wendt, *Nature (London) 348* (1990) 621; J. L. Wragg, J. E. Chamberlain, H. W. White, W. Krätschmer, D. R. Huffman, *ibid. 348* (1990) 623.

[9] R. E. Haufler, J. Conceicao, L. P. F. Chibante, Y. Chai, N. E. Byrne, S. Flanagan, M. M. Haley, S. C. O'Brien, C. Pan, Z. Xiao, W. E. Billups, M. A. Ciufolini, R. H. Hauge, J. L. Margrave, L. J. Wilson, R. F. Curl, R. E. Smalley, *J. Phys. Chem. 94* (1990) 8634.

[10] *Three* observable reversible reductions have been identified in CH_2Cl_2 by *F. Diederich* et al. [4]. C_{70} exhibits the same cyclic volammetry behavior as C_{60}.

[11] J. W. Arbogast, A. P. Darmanyan, C. S. Foote, F. Diederich, R. L. Whetten, Y. Rubin, *J. Phys. Chem. 95* (1991), in press. **Warning**: In a letter to *Chem. Eng. News* (December 17, 1990 issue, page 2), *C. S. Foote* et al. warn researchers to take precautions against skin contact and breathing of the dusts, at least until the physiological properties of the material have been better characterized.

[12] H. W. Kroto, *Science (Washington D.C.) 242* (1988) 1139.

Molecular Systems with Perfect Metal Structure

By *Georg Süss-Fink* *

Lord Lewis and his research group at the University of Cambridge have taken a spectacular step on the road from molecular clusters to metallic structures. They have synthesized the dianionic transition-metal cluster $[Os_{20}(CO)_{40}]^{2\ominus}$, whose metal framework represents a perfect tetrahedral cubic-close-packed metal core. This cluster anion, crystallized as its tetrabutylphosphonium salt, is remarkable for the aesthetics of its molecular structure.

The last two decades have witnessed a very rapid expansion in the chemistry of transition-metal complexes containing more than two metal atoms. *F. A. Cotton* proposed that such complexes be termed "clusters".[1] They are oligonuclear systems generally consisting of a framework of metal atoms held together by intermetallic bonds and surrounded by a shell of terminal or bridging ligands.

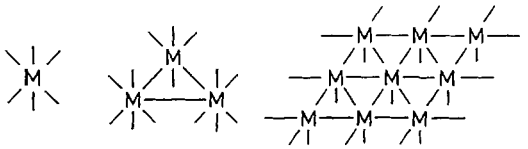

mononuclear oligonuclear polynuclear

As oligonuclear species, metal clusters occupy a no-man's-land between mononuclear metal complexes on the one side and polynuclear metal surfaces on the other, and thus between typical homogeneous and typical heterogeneous catalysts. Starting from the notion of *P. Chini*[2] that clusters represent molecular metal fragments containing chemisorbed species on their peripheries, *J. Lewis* et al.[3] and *E. L. Muetterties*[4] related transition-metal clusters to catalysis: On the one hand, transition-metal clusters can serve as molecular models for poorly understood heterogeneous catalysts. On the other hand, they might function as unconventional homogeneous catalysts. Furthermore, the pioneering work of *G. Schmid*[5] on superclusters has awakened hope that they might allow metal particles of defined size to be prepared, a possibility of great interest not only for chemistry but also for physics and materials science. The chemistry of transition-metal clusters has received considerable impulse from these potential applications. A basic understanding of the formation and properties of metal cores is expected to emerge in this area of research.

The large transition-metal clusters—containing up to 42 metal atoms—observed during the last two decades exhibit diverse structures, which have been established by X-ray diffraction techniques.[6] For very large clusters with 55 or more metal atoms, electron microscopy has proved particularly useful.[5] Whereas the structures of smaller clusters can be explained largely in terms of electronic factors (i.e., they obey the noble-gas rule or the skeletal electron pair theory), the frameworks of larger metal clusters are governed primarily by geometric factors (i.e, their metal atoms are as close packed as possible).

Now, the research group of *Lord Lewis* has reported a new cluster that strikingly illustrates the transition from molecular structures to compact metal structures. The trinuclear cluster $[Os_3(CO)_{10}(NCCH_3)_2]$ decomposes in an unclear fashion upon vacuum pyrolysis at 300 °C and 10^{-3} Torr. Extraction of the decomposition residue affords the dianion $[Os_{20}(CO)_{40}]^{2\ominus}$, together with other lower-nuclearity clusters. The dianion can be crystallized as its tetrabutylammonium salt.[7]

A single-crystal X-ray analysis reveals that the dianion has a metal framework consisting of 20 cubic-close-packed osmium atoms arranged to form a perfect tetrahedron. The symmetry of the ligand shell, consisting of 40 terminal carbonyl groups, corresponds to that of the metal framework.

The new cluster $[Os_{20}(CO)_{40}]^{2\ominus}$ should be compared with the cluster $[HNi_{38}Pt_6(CO)_{48}]^{5\ominus}$, described in 1985 by *G. Longoni* et al.[8] (Fig. 1). Whereas the metal lattice of the

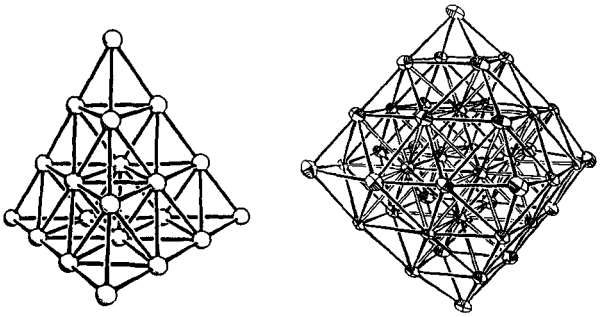

Fig. 1. Tetrahedral section of a cubic close packing (ccp) in $[Os_{20}(CO)_{40}]^{2\ominus}$ (left) and an octahedral section of a ccp in $[HNi_{38}Pt_6(CO)_{48}]^{5\ominus}$ (right).

latter corresponds to an octahedral section of a cubic-close-packed array of metal atoms, the osmium framework of the former represents a tetrahedral section. It should be noted, however, that metallic osmium crystallizes as a hexagonal-close-packed structure, whereas the osmium atoms in $[Os_{20}(CO)_{40}]^{2\ominus}$ are cubic close packed.

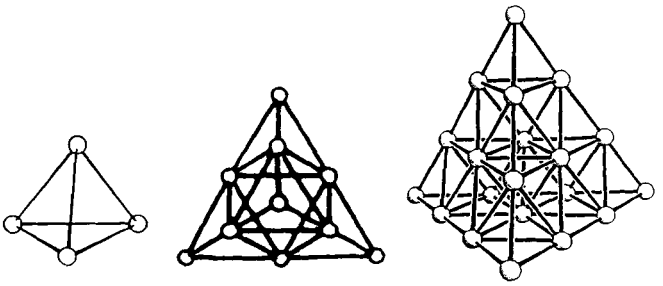

Fig. 2. Gradual growth of the tetrahedron on going from four ($[H_2Os_4(CO)_{12}]^{2\ominus}$) to ten ($[Os_{10}C(CO)_{24}]^{2\ominus}$) to twenty metal atoms ($[Os_{20}(CO)_{40}]^{2\ominus}$).

[*] Prof. Dr. G. Süss-Fink
Institut de Chimie, Université de Neuchâtel
Avenue de Bellevaux 51, CH-2000 Neuchâtel (Switzerland)

Still another comparison emerges: In the series of metal clusters with tetrahedral symmetry, $[H_2Os_4(CO)_{12}]^{2\ominus}$ [9] and $[Os_{10}C(CO)_{24}]^{2\ominus}$ [10] were the first two clusters containing two and three osmium atoms, respectively, on the edges of the tetrahedron. The new cluster $[Os_{20}(CO)_{40}]^{2\ominus}$, which has four osmium atoms on the edges of a face-centered tetrahedron, readily fits into this series (Fig. 2). Thus, gradual tetrahedral growth is possible on going from molecular clusters to metallic structures.

[1] F. A. Cotton, *Quart. Rev. 20* (1966) 389.
[2] P. Chini, *Inorg. Chim. Acta Rev. 2* (1968) 31.
[3] B. F. G. Johnson, J. Lewis, *Pure Appl. Chem. 44* (1975) 43.
[4] E. L. Muetterties, *Bull. Soc. Chim. Belg. 84* (1975) 959.
[5] G. Schmid, *Nachr. Chem. Tech. Lab. 35* (1987) 249.
[6] D. M. P. Mingos in D. F. Shriver, H. D. Kaesz, R. D. Adams (Eds.): *The Chemistry of Metal Cluster Complexes*, VCH Publishers, New York 1990.
[7] A. J. Amaroso, L. H. Gade, B. F. G. Johnson, J. Lewis, P. R. Raithby, W.-T. Wong, *Angew. Chem. 103* (1991) 102; *Angew. Chem. Int. Ed. Engl. 31* (1991) 107.

VCH Index Library

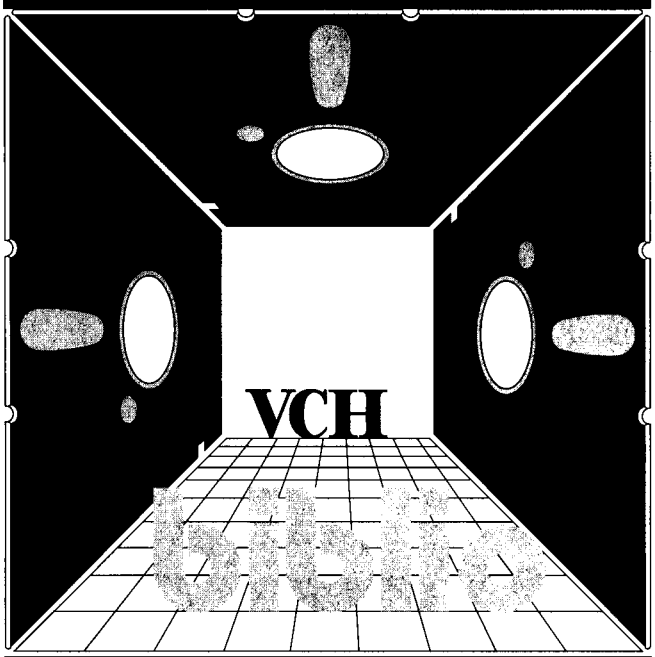

The electronic index comes with the search module of the literature-management program, VCH Biblio. You can use this index on all PCs running with MS-DOS.

ANGEWANDTE CHEMIE
International Edition in English

Soon available

At the press of a button

The annual index of "Angewandte" is soon available on 5 1/4" and 3 1/2" diskettes.

Yearly updates will keep this invaluable electronic library complete. You can search the cumulative contents in mere seconds.

Price: ca. DM 34.00 plus shipping and handling.

Special news! In honor of the 30th anniversary of "Angewandte Chemie I.E." the cumulative index will also be available on diskette.

VCH
Software
P.O. Box 101161
D-6940 Weinheim

VCH

Communications may be submitted in English *or* in German. Further details regarding the submission of communications can be found in the "Notice to Authors" reproduced in the January issue of the journal. Copies thereof may be obtained from the editorial office upon request.

Dynamic HPLC: A Method for Determining Rate Constants, Energy Barriers, and Equilibrium Constants of Molecular Dynamic Processes**

By *Jaume Veciana** and *Maria I. Crespo*

Dynamic spectroscopic (NMR, ESR, IR) experiments are extensively used for the study of molecular dynamic processes and the determination of their kinetic parameters.[1] By contrast, such studies are rather uncommon in chromatography despite its importance in chemistry.[2-5] The simplest dynamic chromatographic experiment involves two resolvable species that are interconvertible on the separation time scale (minutes). In this case, the temperature and flow-rate dependence of the chromatographic profiles can be observed. Although various examples of such behavior have been reported[3-6] and the basic theory describing a dynamic chromatographic experiment has largely been developed,[3,4,7] a general method for evaluating the kinetic parameters of the molecular dynamic processes is still lacking. The methods so far reported either suffer from practical limitations[8] or are unrealistic.[9]

The method described here, based on a simulation procedure, permits the determination of the rate constants, energy barriers, and equilibrium constants of interconversion processes occurring during HPLC separation. This method, which is called D-HPLC (dynamic HPLC) in analogy to the well-known DNMR method, has proved effective and readily applicable to several kinds of interconversions (enantiomerizations, conformational changes), detectors (spectrophotometer, polarimeter), and stationary phases (reversed phases, chiral phases), including those giving rise to either linear (Gaussian or ideal peaks) or nonlinear (skewed peaks) chromatographic processes.

Using stochastic models, *Giddings* et al.[2] theoretically analyzed the spatial distribution of two species at a given time in a chromatographic separation (TLC), where the two species, A and B, undergo slow reversible first-order interconversions. In this analysis, the authors assumed that the apparent rate constants of the overall forward and reverse reactions, $\vec{k}$ and $\overleftarrow{k}$, respectively, are smaller than those of the purely chromatographic processes (partition, adsorption, etc.), so that the species in the mobile phase (A, B) are, at any time, in equilibrium with the bound species (A_b, B_b) in the stationary phase (Scheme 1a).

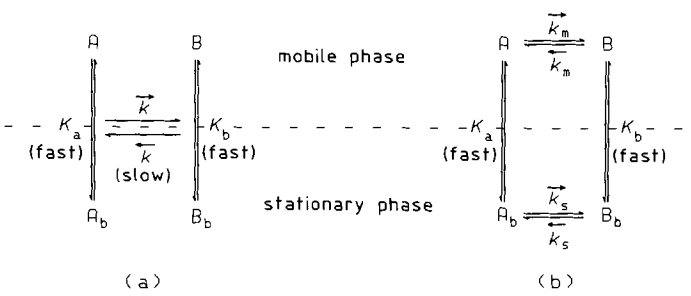

Scheme 1. Equilibria involved in the chromatographic separation of two interconverting species, A and B: a) simulated equilibria; b) actual equilibria.

The corresponding temporal distribution at the end of a chromatographic column (GC, HPLC) is readily obtainable from the spatial distribution by a simple mathematical transformation.[7b] An explicit function[10] describing the chromatographic profiles of a D-HPLC experiment may then be derived by determining the time dependence of the probability density functions of all the molecular dynamic events that occur during the chromatographic separation. This is done by using the proper temporal distribution function that takes into account the kinetics of mass transfer of the species between the mobile and the stationary phases. Depending on the degree of linearity of the chromatographic process, the temporal distribution function can be equated to either a normalized Gaussian function (for symmetric peaks in linear chromatography) or a normalized exponentially modified Gaussian function (for skewed peaks in nonlinear chromatography).[11] Figure 1 shows the time dependence of the probability density functions for all the molecular dynamic events occurring in a linear chromatographic process. Thus, simulation of the chromatograms of any D-HPLC experi-

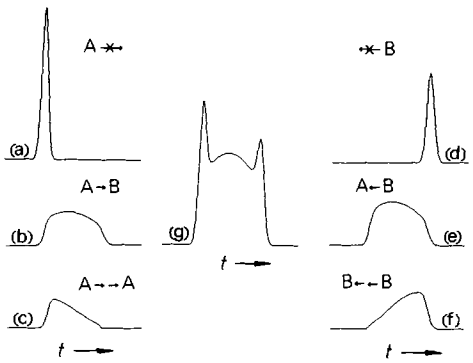

Fig. 1. Theoretical curves corresponding to the time dependence of the probability density functions of all the molecular dynamic events occurring in a linear chromatographic separation of two interconverting species, A and B. Curves were calculated using $t_A = 12.5$ min, $t_B = 16.25$ min, $N_A = 4000$, $N_B = 5000$, $\varepsilon_B/\varepsilon_A = 1.0$, $C_B^0/C_A^0 = 1.0$ [12], and $\vec{k} = \overleftarrow{k} = 1.7 \times 10^{-3}\ s^{-1}$. a) The curve corresponding to the fraction of species that are injected as A and do not suffer any conversion during the chromatography. b) The fraction of species that are injected as A and are detected as B. c) The fraction of species that are injected as A and, after undergoing more than one reaction, are finally detected as A. d)–f) The theoretical curves corresponding to the molecular dynamic events of the species that are injected as B. g) The calculated chromatographic profile generated by combination of these theoretical curves.

[*] Dr. J. Veciana, Dipl.-Eng. Chem. M. I. Crespo
Instituto de Ciències de Materiales-C.I.D., C.S.I.C.
Jordi Girona, 18–26, E-08034 Barcelona (Spain)

[**] This work was supported by the C.I.C. y T. (Grant No. MAT 88-0268). We acknowledge Dr. *C. Rovira* (C.S.I.C) for her comments and Dr. *J. Badenas* for his computer assistance.

ment can be accomplished by using, as trial parameters, the apparent rate constants ($\vec{k}$ and $\overleftarrow{k}$) and the chromatographic parameters of the two interconverting species (retention times, t_A and t_B; theoretical plate numbers, N_A and N_B; and asymmetry factors, τ_A and τ_B[12]), provided that the injected molar ratio of the two species, C_B^0/C_A^0, and the relative response of the detector, $\varepsilon_B/\varepsilon_A$, are known. In such a way, the values of $\vec{k}$ and $\overleftarrow{k}$ best describing the dynamic behavior of the studied system can be determined.[13]

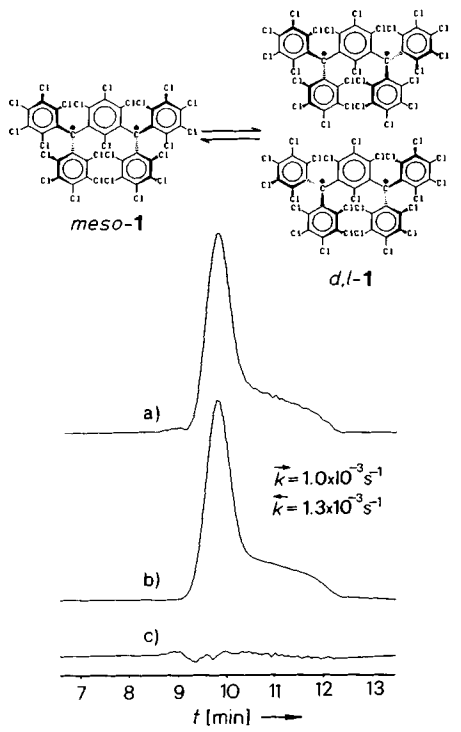

Fig. 2. Resolution versus diastereomerization in a D-HPLC experiment involving diradical **1**. a) Experimental chromatogram: C_{18} reversed-phase column, 12.5 cm × 0.46 cm (inner diameter); $T = 45\,^{\circ}C$; eluent CH_3CN/THF (88:12); flow rate 1 mL min^{-1}; dead time 1.07 min; UV detector at 383 nm; amount of sample, ca. 1 μg. b) Simulated chromatogram: $t_A = 9.8$ min, $t_B = 12.1$ min, $N_A = 1800$, $N_B = 3000$, $\varepsilon_B/\varepsilon_A = 1.0$, and $C_B^0/C_A^0 = 0.02$ [12] c) Residuals: (a) − (b).

Figures 2 and 3 show the excellent agreements achieved in the simulation of two representative examples of two series of D-HPLC experiments performed at different temperatures and using distinct eluent flow rates.[14] Although the apparent rate constants determined by this method need not be equal (see below) to the rate constants of the processes occurring in the mobile and the stationary phases (Scheme 1b), in practice we have found only small differences between them.[15] Therefore, the apparent rate constants may be used to determine the approximate energy barrier[16] for the molecular dynamic process in question. Using the apparent forward rate constants given in Figures 2 and 3, we have found $\Delta G^{\ddagger}_{317} = 96.0 \pm 0.2$ kJ mol^{-1} for **1** and $\Delta G^{\ddagger}_{268} = 80.4 \pm 0.2$ kJ mol^{-1} for **2**. These values are in agreement with those measured by independent techniques: $\Delta G^{\ddagger}_{317} = 97 \pm 2.5$ kJ mol^{-1} (direct equilibration of *meso*-**1** in CH_3CN/THF, 70/30[17]) and $\Delta G^{\ddagger}_{268} = 82 \pm 3$ kJ mol^{-1} (DNMR spectroscopy[18] of racemic **2**[19] in hexachlorobutadiene/$(CD_3)_2SO$, 1/1).

The apparent rate constants determined by the D-HPLC method are in fact related to those involved in the mobile

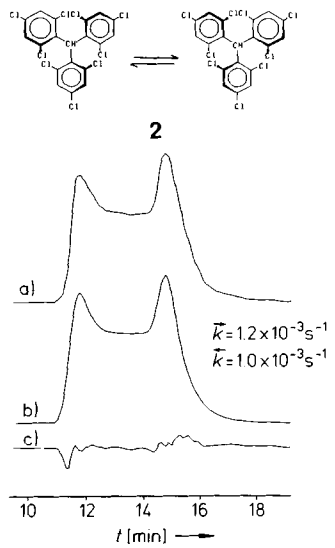

Fig. 3. Chiral resolution versus enantiomerization in a D-HPLC experiment involving racemic **2**. a) Experimental chromatogram: column, (+)-poly(triphenylmethylmethacrylate), 25 cm × 0.46 cm (inner diameter); $T = -5\,^{\circ}C$; eluent, methanol; flow rate, 0.5 mL min^{-1}; dead time 2.97 min; UV detector at 254 nm; amount of sample, ca. 1 μg. b) Simulated chromatogram: $t_A = 11.4$ min, $t_B = 14.7$ min, $N_A = 2300$, $N_B = 3400$, $\tau_A = 0.47$, $\tau_B = 0.60$, $\varepsilon_B/\varepsilon_A = 1.0$, and $C_B^0/C_A^0 = 1.0$ [12] (A = (−)-**2**, B = (+)-**2**). c) Residuals: (a) − (b).

phase ($\vec{k}_m$ and $\overleftarrow{k}_m$ and in the stationary phases ($\vec{k}_s$ and $\overleftarrow{k}_s$) by Equations (a) and (b), where k'_A and k'_B are the capacity

$$\vec{k} = (\vec{k}_m + k'_A\vec{k}_s)/(1 + k'_A) \quad \text{(a)}$$

$$\overleftarrow{k} = (\overleftarrow{k}_m + k'_B\overleftarrow{k}_s)/(1 + k'_B) \quad \text{(b)}$$

factors of the two species.[20] The principle of microscopic reversibility[21] and Equations (a) and (b) allow Equation (c) to be derived. Equation (c) relates the apparent rate con-

$$\vec{k}/\overleftarrow{k} = K_m t_B/t_A \quad \text{(c)}$$

stants to the equilibrium constant in the mobile phase, $K_m = \vec{k}_m/\overleftarrow{k}_m$. Therefore, this simulation method also allows a direct determination of the K_m constants. The equilibrium constants calculated from Equation (c) for compounds **1** and **2** are $K_m = 0.62 \pm 0.05$ and $K_m = 0.93 \pm 0.08$, respectively. These values agree with the experimentally determined equilibrium constant for **1**, $K_m = 0.66 \pm 0.04$,[17] and that expected for a chiral compound such as **2** in an achiral solvent, $K_m = 1$.[18]

The positive results described here validate the simulation method and also show that Scheme 1a does not violate the principle of microscopic reversibility. In addition, excellent results have also been obtained with this simulation method for other families of compounds (triarylmethyl radicals, helicenes, triptycenes, thioamides), chiral stationary phases (triacetylcellulose), and detectors (polarimeter).[22]

The D-HPLC method thus represents a new way to study molecular dynamic processes which has some limitations and advantages with respect to other classical methods. The main limitation arises from the use of apparent rate constants instead of those for the processes actually occurring in the chromatographic phases. However, such a limitation does not have a serious influence on the determination of precise energy barriers, which differ by less than 2 kJ mol^{-1} from those determined by independent techniques. The principal advantages of this method come from the versatility,

availability, and analytical scale of the HPLC technique. This method is especially suitable to the study of processes with activation energies ranging from 65 to 105 kJ mol^{-1}, since such processes are difficult to study by DNMR experiments and direct equilibration techniques. Furthermore, it also permits a complete kinetic study to be performed using insignificant amounts (nanograms) of samples without cumbersome previous enrichments being required.

Received: March 23, 1990
revised: September 17, 1990 [Z 3872 IE]
German version: *Angew. Chem. 103* (1991) 85

CAS Registry numbers: **1**, 127316-84-1; **2**, 105633-27-0.

[1] J. Sandström: *Dynamic NMR Spectroscopy*, Academic, London 1982; K. U. Ingold, J. C. Walton, *Acc. Chem. Res. 22* (1989) 8; F. W. Grevels, J. Jache, W. E. Klotzbücher, C. Krüger, K. Seevogel, Y.-H. Tsay, *Angew. Chem. 99* (1987) 960; *Angew. Chem. Int. Ed. Engl. 26* (1987) 885; and references cited therein.

[2] J. C. Giddings, *J. Chromatogr. 3* (1960) 443.

[3] a) V. Schurig, W. Bürkle, *J. Am. Chem. Soc. 104* (1982) 7573; b) W. Bürkle, H. Karfunkel, V. Schurig, *J. Chromatog. 288* (1984) 1.

[4] W. R. Melander, H.-J. Lin, C. Horváth, *J. Phys. Chem. 88* (1984) 4527.

[5] A. Mannschreck, H. Zinner, N. Pustet, *Chimia 43* (1989) 165.

[6] Representative articles dealing with this topic: M. Lebl, V. Gut, *J. Chromatogr. 260* (1983) 478; A. Eiglsperger, F. Kastner, A. Mannschreck, *J. Mol. Struct. 126* (1985) 421; M. Moriyasu, C. Yamagami, A. Kato, Y. Hashimoto, N. Takao, *Bull. Chem. Soc. Jpn. 59* (1986) 1539, and earlier papers; A. Mannschreck, D. Andert, A. Eiglsperger, E. Gmahl, H. Buchner, *Chromatographia 25* (1988) 182; A. Mannschreck, L. Kießl, *ibid. 28* (1989) 263.

[7] For this purpose, three different theoretical models have been used: stochastic model: a) see [2]; b) R. Kramer, *J. Chromatog. 107* (1975) 241; c) E. Cremer, R. Kramer, *ibid. 107* (1975) 253; d) S. Endo, A. Wado, *Biophys. Chem. 18* (1983) 291; discontinuous plate model: e) J. Kallen, H. W. Heilbronner, *Helv. Chim. Acta. 43* (1960) 489; f) see [3b]; continuous flow model: g) S. H. Langer, J. Y. Yurback, J. E. Patton, *Ind. Eng. Chem. 61*(1969) 11; h) see [4].

[8] Most of them deal with linear chromatographic processes: see [3b] and [4]. Methods that treat nonlinear chromatographic processses require either external standards or one of the interconverting species in the pure state: see J. Jacobson, W. R. Melander, G. Vaisnys, C. Horváth, *J. Phys. Chem. 88* (1984) 4536; R. Hanai, S. Endo, A. Wada, *Biophys. Chem. 25* (1986) 27.

[9] M. Moriyasu, K. Kawanishi, A. Kato, Y. Hashimoto, M. Sigiura, T. Sai, *Bull. Chem. Soc. Jpn. 58* (1985) 3351.

[10] The explicit function describing the chromatographic profile of a D-HPLC experiment, as well as the program for the computer simulation of the chromatographic profiles, will be supplied by the authors on request.

[11] J. P. Foley, J. G. Dorsey, *J. Chromatogr. Sci. 22* (1984) 40.

[12] For the species with intermediate apparent retention times. ($t_A < t' < t_B$), the mean values $N' = (N_A + N_b)/2$ and $\tau' = (\tau_A + \tau_B)/2$ were used. Other kinds of dependence do not produce any significant change in the chromatographic profiles.

[13] The reproducibility of $\vec{k}$ and $\overleftarrow{k}$ values obtained with this simulation method is around 4%. This value was determined by studying the mutual influence of the chromatographic (t, N, and τ) and kinetic ($\vec{k}$ and $\overleftarrow{k}$) parameters on the agreement between the simulated and the experimental profiles.

[14] The apparent rate constants determined from the simulation of chromatograms for D-HPLC experiments performed at a constant temperature and using different eluent flow rates were always in agreement and showed a standard deviation of approximately 8%. This result, together with that described in [13], indicates that the precision of the simulation method is around 8%.

[15] The largest difference between $\vec{k}$ (or $\overleftarrow{k}$) and $\vec{k}_m$ (or $\overleftarrow{k}_m$) values observed for the diastereomerization of **1** corresponds to 35% of $\vec{k}_m$, which can be considered of small account; see [16]. Such close agreement is due to the presence of short-range and weak interactions between the species and the mobile and stationary phases.

[16] Deviations of the rate constant even larger than 50% of its exact value give rise to errors of approximately 2% in the associated energy barrier determined from the Eyring equation.

[17] This $\Delta G^{\neq}$ value was calculated from $\Delta H^{\neq}[meso \rightarrow d \text{ (or } l)] = 91 \pm 2.5$ kJ mol^{-1}, $\Delta S^{\neq}[meso \rightarrow d \text{ (or } l)] = -24 \pm 10$ J mol^{-1} K^{-1}, taking into account the statistical correction of the entropy by a factor of $R \ln 2$: J. Veciana, C. Rovira, M. I. Crespo, O. Armet, V. M. Domingo, F. Palacio, *J. Am. Chem. Soc.* in press.

[18] J. Veciana, M. I. Crespo, 1st Int. Symp. on Separation of Chiral Molecules, Paris 1988. This $\Delta G^{\neq}$ value was calculated from the thermodynamic parameters of the process determined by the simulation of ^{1}H NMR spectra (D-NMR 4, QCPE no. 466, University of Indiana) of **2** in the temperature range 335–383 K.

[19] O. Armet, J. Veciana, C. Rovira, J. Riera, J. Castañer, E. Molins, J. Rius, C. Miravitlles, S. Olivella, J. Brichfeus, *J. Phys. Chem. 91* (1987) 5608.

[20] Capacity factors are related to the equilibrium constants of distribution (or partition) by $K = \beta k'$, where β is the phase ratio: see C. F. Poole, S. A. Schuette: *Contemporary Practice of Chromatography*, Elsevier, Amsterdam 1984.

[21] The principle of microscopic reversibility in Scheme 1b takes the following form: $k'_B/k'_A = K_B/K_A = \vec{k}_m\vec{k}_s/\overleftarrow{k}_m\overleftarrow{k}_s$ (see [3b, 4].

[22] We thank to Prof. *A. Mannschreck* and his group (Universität Regensburg) for permitting us to analyze several of their D-HPLC experiments with this method.

Thermally Irreversible Photochromic Liquid Crystal Polymers**

By *Ivan Cabrera, Achim Dittrich*, and *Helmut Ringsdorf**

Photochromism has always been something of a curiosity, while liquid crystals (LCs), though once mere chemical rarities, have already found widespread application in displays and many other electrical and electrooptical devices. Materials which combine both properties in a molecular entity should, therefore, be considered as chemical curiosities with many potential applications. Indeed, photochromic LC-polymers have already found use, e.g., as nonlinear optical materials[1] or for optical information storage.[2, 3] The holographic information storage in LC-polymers with azobenzene side groups[3] is based on the *trans-cis* isomerization of these groups. This tranformation causes a local reorientation of the mesogenic groups, which results in a variation of the refractive index. Thus a phase hologram can be formed. Photochromic LC-polymers containing spiropyran side groups have also been prepared.[4] Since these materials offer the possibility of controlling with light and temperature the formation of the three primary colors, they may be used in display and information storage technologies.

A disadvantage in all these polymers, however, is that the colored form of the photochrome is not thermally stable even at room temperature. Therefore, the color formation and related molecular reorientations upon which the recording of information is based are not permanent. In this communication, the first LC-polymers with thermally irreversible photochromic properties are reported. The materials are copolymers with mesogenic and photochromic fulgimide ((*E*)-2-[1-(2,5-dimethyl-3-furyl)ethylidene]-3-isopropylidenesuccinimide) side groups. They do not show any thermochromic behavior, in contrast to other photochromic compounds mentioned above, because their photochromic units are thermally stable up to 100 °C.

The synthesis, isomerization and electrocyclization of the photochromic (*E*)-2-[1-(2,5-dimethyl-3-furyl)ethylidene]-3-isopropylidenesuccinic anhydride (fulgide) have been studied in detail by *Heller* et al.[5] They have shown that its photochromic properties result from a conrotatory photocyclization to the 7,7a-dihydrobenzofuran (7,7a-DHBF) derivative, which undergoes the reverse process on exposure to visible light [Eq. (a)].

[*] Prof. H. Ringsdorf, Dr. I. Cabrera, Dipl. Chem. A. Dittrich
Institut für Organische Chemie der Universität
J.-J.-Becher-Weg 18–20, W-6500 Mainz (FRG)

[**] This research was supported by the Alexander von Humboldt Foundation with a fellowship (*I.C.*) and by the NEDO project (*A.D.*) (NEDO = New Energy and Industrial Technology Development Organization).

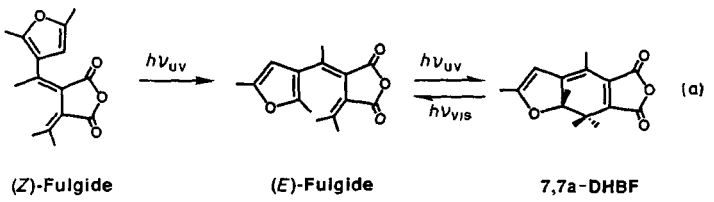

Fulgimide-containing LC-polymers were synthesized according to Scheme 1. Furyl-fulgimide **1** was prepared by treatment of an *(E)*/*(Z)* fulgide mixture with ammonia in acetone solution.[6, 7] A Mitsunobu reaction[8] was used for

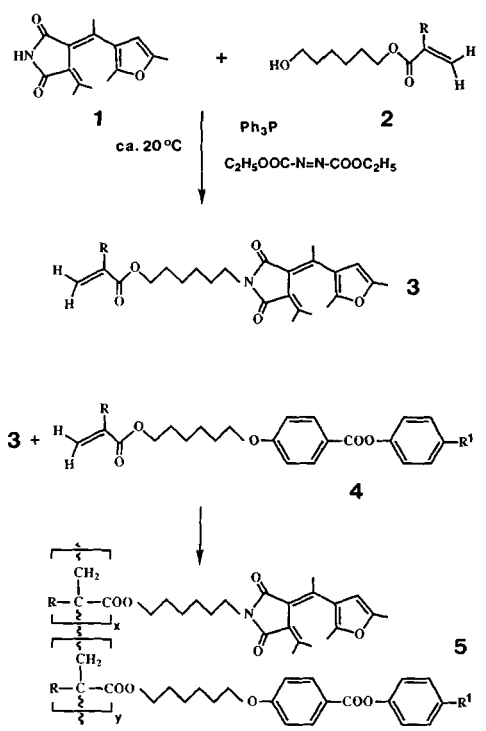

Scheme 1. Synthesis of LC-polymers with fulgimide side groups. Acrylate (**a**): R = H, R^1 = CN; methacrylate (**b**): R = CH_3, R^1 = OCH_3.

the preparation of the acrylate- and methacrylatefulgimide monomers **3** from **1**, which on radical copolymerization with the mesogenic monomers **4** led to the desired LC-copolymers **5**. For both the acrylate-(**5a**) and methacrylate-copolymers (**5b**) the clearing point of the mesophase decreases with increase of the fulgimide content. The phase diagrams are given in Figure 1.

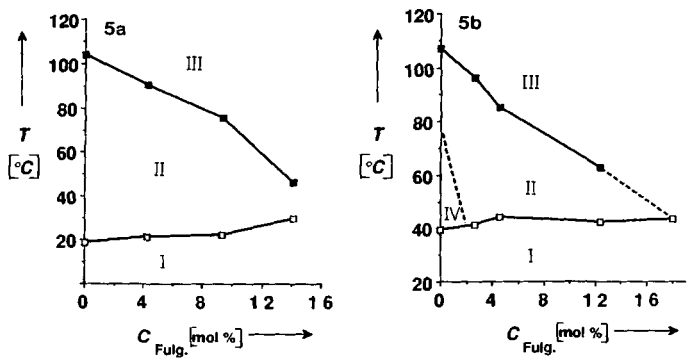

Fig. 1. Effect of the number of fulgimide side groups on the phase transitions of copolyacrylates **5a** and copolymethacrylates **5b**. I = glassy, II = nematic, III = isotropic, IV = smectic

The photochemical ring closure of the fulgimide groups on irradiation at λ = 366 nm and the reverse decoloration on irradiation with visible light (λ > 475 nm) can be clearly followed by UV-visible spectroscopy as a function of the time of irradiation. Characteristic changes in the absorption spectrum of the copolymers in solution and in an oriented filmare given in Figure 2. A homeotropically oriented film of a

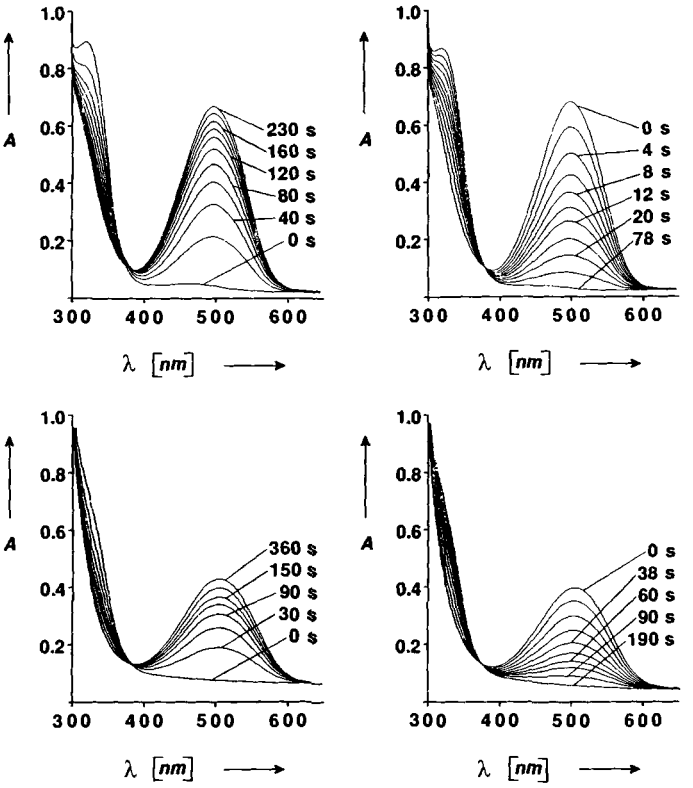

Fig. 2. Coloration on ring closure (λ = 366 nm) (left) and decoloration on ring opening (λ > 475 nm) (right) of a copolyacrylate **5a** (9.4 mol% of fulgimide groups) as a function of irradiation time *t*. Top: in toluene; bottom: homeotropically oriented film. *A* = Absorption in arbitrary units.

copolyacrylate was prepared by heating the polymer to the isotropic state followed by slow cooling of the material in an electric field.

Comparison of the spectra obtained in solution (Fig. 2 top) with those of the oriented film (Fig. 2 bottom) indicates that there is a bathochromic shift of the absorption maximum from 496 nm in solution to 506 nm in the film. In both cases, however, the existence of isosbestic points as well as exactly linear absorption difference diagrams[9] conclusively demonstrate the first-order character of the photoreactions (Fig. 3).

The photocolored form of the fulgimide side groups shows complete thermal stability at room temperature. Figure 4 demonstrates this for a copolymethacrylate **5b**. When a UV-irradiated film is kept in the dark, the absorption maximum in the visible does not change at all.

An interesting feature of the photochromic LC-polymers reported here, in contrast to the previously synthesized systems, is that one can clearly study the effect of each of the photochromic groups on the meso phase. In fact, polarizing

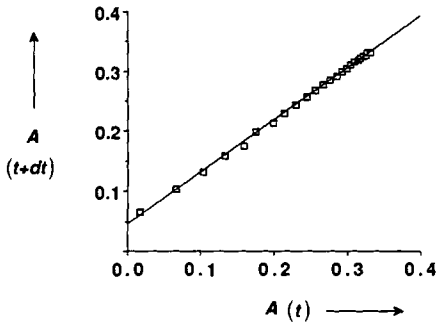

Fig. 3. Absorption at time $t + dt$ vs absorption at time t for the photoreaction from the open to the closed photochromic form in toluene (λ_{max} = 496 nm; copolyacrylate **5a** with 9.4 mol % fulgimide groups).

microscope observations have already revealed that irradiation of the materials with UV light leads to a higher clearing point of the meso phase. This suggests that the dihydrobenzofuran side groups (colored form) distort the parallel arrangement of the molecules in the meso phase less that the fulgimide groups.

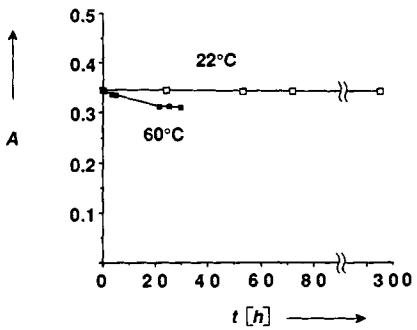

Fig. 4. Thermal stability of the colored form of the fulgimide groups in a copolymethacrylate **5b** with 2.5 mol % fulgimide content at 22 °C and 60 °C. A UV-irradiated film was used.

To test the possibility of recording optical information, a film of a photochromic polymer was covered with a standard photomask and irradiated with UV light (λ = 366 nm). The optically stored image of the mask could be observed with the polarizing microscope. Moreover, preliminary experiments have already shown that holographic patterns can be stored in the materials described here. The exact contribution of amplitude and phase effects is currently being investigated.

Experimental Procedure

1 was prepared by reaction of (*E*)/(*Z*)-2-[1-(2,5-dimethyl-3-furyl)ethylidene]-3-isopropylidenesuccinic anhydride with ammonia in acetone solution [6, 7]. 6-Hydroxyhexylacrylate **2a** (R = H) and 6-hydroxyhexylmethacrylate **2b** (R = CH_3) were synthesized as described in reference [10].

Typical example of the procedure for **3a** and **3b**: 0.115 g of **1**, 0.157 g of triphenylphosphane and 0.108 g of **2a** were dissolved in dry THF. To this a solution of azodicarboxylate (0.108 g) in dry THF was added. A trace of *p*-benzoquinone was also added to inhibit polymerization. The mixture was stirred for 14 hours in the dark. Afterwards the solvent was removed under vacuum and the product purified by flash chromatography (petrol ether: ethyl acetate 12:1). Yields: **3a** 40.4% **3b** 29.3% (based on **1**); oily compounds.

All compounds have been characterized by IR, ^{13}C and ^1H NMR spectroscopy. **3a**: ^1H NMR ($CDCl_3$, 400 MHz): δ = 6.33 (m; *Z*-H of CH_2=), 6.06 (t; H_2C=C*H*), 5.87 (s; furan-H), 5.78 (m; *E*-H of CH_2=), 4.11 (t; H_2C-OOC), 3.55 (t; CH_2-N), 2.54 (s; CH_3-C=), 2.28 (s; *Z*-CH_3 of $(CH_3)_2C$=), 2.20 (s; furan-5-CH_3), 1.94 (s; furan-2-CH_3), 1.64, 1.37 (m; N-CH_2-(CH_2)$_4$-CH_2-OOC), 1.28 (s; *E*-CH_3 of $(CH_3)_2C$=). **3b**: ^1H NMR ($CDCl_3$, 400 MHz): δ = 6.06 (m; *Z*-H of CH_2=), 5.88 (s; furan-*H*), 5.52 (m; *E*-H of CH_2=), 4.10 (t; CH_2-OOC), 3.55 (t; CH_2-N), 2.54 (s; CH_3-C=), 2.28 (s; *Z*-CH_3 of $(CH_3)_2C$=); 2.21 (s; furan-5-CH_3); 1.95 (s; furan-2-CH_3); 1.91 (t; H_2C=CCH_3), 1.64, 1.37 (m; N-CH_2-(CH_2)$_4$-CH_2-OOC), 1.28 (s; *E*-CH_3 of $(CH_3)_2C$=).

The mesogenic monomers **4** were prepared by standard methods [11, 12]. The copolymers **5** were prepared by polymerization of the monomer (20–30 percent in THF solution) with 1.2 mol % of 2,2'-azobis(isobutyronitrile) at 55 °C. The polymers were precipitated in methanol, purified by reprecipitation and dried under vacuum at room temperature. The yields of the polymers (20–70%) depended substantially on the concentration of fulgimide monomer. The higher the concentration the lower the polymer yield. The composition of the polymers was determined by NMR spectroscopy. Typical molecular weights, determined by gel permeation chromatography, are 5000 for copolyacrylates **5a** and 14000 for copolymethacrylates **5b**.

Received: July 5, 1990 [Z 4053 IE]
German version: *Angew. Chem. 103* (1991) 106

[1] S. Ytzchaik, G. Berkovic, V. Krongauz, *Adv. Mater. 2* (1990) 33.
[2] C. B. McArdle in C. B. McArdle (Ed): *Side Chain Liquid Crystal Polymers*, Blackie and Son, Glasgow 1989, p. 357.
[3] M. Eich, J. H. Wendorff, B. Reck, H. Ringsdorf, *Makromol. Chem. Rapid Commun. 1987*, 59.
[4] I. Cabrera, V. Krongauz, H. Ringsdorf, *Angew. Chem. 99* (1987) 1204; *Angew. Chem. Int. Ed. Engl. 26* (1987) 1178.
[5] P. J. Darcy, H. G. Heller, P. J. Strydom, J. Whittall, *J. Chem. Soc. Perkin Trans. 1 1981*, 202.
[6] H. G. Heller (Aberystwyth, Wales), personal communication.
[7] S. Goldschmidt, R. Riedle, A. Richardt, *Justus Liebigs Ann. Chem. 604* (1957) 121.
[8] O. Mitsunobu, M. Wada, T. Sano, *J. Am. Chem. Soc. 94* (1972) 679.
[9] G. Mauser, *Z. Naturforsch. B 23* (1968) 1025.
[10] W. Kreuder, *Diplomarbeit*, Universität Mainz 1982.
[11] M. Portugall, H. Ringsdorf, R. Zentel, *Makromol. Chem. 183* (1982) 2311.
[12] H. Finkelmann, H. Ringsdorf, W. Siol, J. Wendorff in A. Blumstein (Ed): *Mesomorphic Order in Polymers (ACS Symp. Ser. 74* (1978) 22).

Selective Halogenation at Primary Positions of Cyclomaltooligosaccharides and a Synthesis of Per-3,6-anhydro Cyclomaltooligosaccharides

By *Andrée Gadelle* and *Jacques Defaye**

6-Deoxyhalo cyclomaltooligosaccharides are of interest as reactive intermediates for the modification of solubility and inclusion properties of cyclomaltooligosaccharides.[1, 2] A main route to these derivatives involves the displacement of acylated 6-sulfonates by a halide salt. However, the direct sulfonylation at primary positions of cyclomaltooligosaccharides, although well documented, does not usually proceed with high yield and selectivity,[1, 3, 4] and the displacement is furthermore not a quantitative process.[5] An improved access to such derivatives was introduced by *Takeo* et al.,[6] who obtained per-6-bromo-6-deoxy cyclomaltooligosaccharides by direct bromination of the cyclic oligosaccharides with methanesulfonyl bromide in DMF. This halogenation procedure, which presumably involves the in situ formation of a brominated dimethylammonium bromide and is then related to the more general activation process of alcohols toward nucleophilic displacements by

[*] Dr. J. Defaye, Dr. A. Gadelle
Département de Recherche Fondamentale
Laboratoires de Chimie et CNRS (SDI 5509)
Centre d'Etudes Nucléaires de Grenoble
BP 85 X, F-38041 Grenoble (France)

Vilsmeier–Haack complexes,[3, 7] was found, in our case, to result in some methanesulfonylation when applied to amylose.[8] Subsequent modification, which involved the use of pure crystalline Vilsmeier bromide, prepared from triphenylphosphane and bromine in DMF, resulted in the formation, in high yield and purity, of 6-bromo-6-deoxyamylose.[8] Extension of this reaction to the preparation of 6-deoxyhalo cyclomaltooligosaccharides and their conversion into per-3,6-anhydro derivatives is now described.

Isolation of a Vilsmeier iodide, from the reaction of iodine and triphenylphosphane in DMF does not proceed as easily as for the corresponding bromide,[8] and iodination reactions were conducted in situ. When either cyclomaltohexaamylose **1** or cyclomaltoheptaamylose **2** was allowed to react in DMF containing triphenylphosphane and iodine at 80 °C for 15 h and the solution further treated with sodium methoxide to destroy the formate esters formed in the reaction, per-6-deoxy-6-iodo cyclomaltooligosaccharides **3** and **4**, which were suitable for use without further purification, were obtained in 80% and 88% yields, respectively. Their structures were inferred from fast atom bombardment mass spectrometry (FABMS), which gave the expected protonated molecular ions at *m/z* 1633.6 (**3**) and 1904.7 (**4**) and which were shifted to 1671.5 by the addition of potassium iodide (**3**) and to 1926.7 with sodium iodide (**4**). Both compounds gave six signals in their ^{13}C NMR spectra. The C-6 signals were found at high field, in agreement with the inductive effect of the iodine atom. A further structural confirmation for **4** came from its conversion into its known tetradecaacetate.[5]

The versatility of the reagent for the preparation of 6-deoxyhalo cyclomaltooligosaccharides is further exemplified by the preparation of heptakis(6-bromo-6-deoxy)cyclomaltoheptaamylose[6] **5** by reaction of **2** with bromine and triphenylphosphane in DMF under similar conditions.

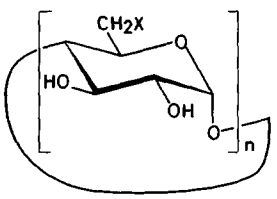

1 X = OH n = 6
2 X = OH n = 7
3 X = I n = 6
4 X = I n = 7
5 X = Br n = 7

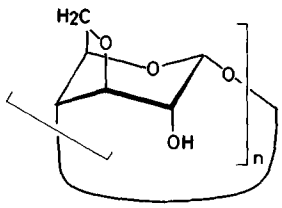

6 n = 6
7 n = 7

3,6-Anhydroamylose was previously obtained in high yield from the reaction of 6-bromo-6-deoxyamylose with base.[8] It is water-soluble and its ability to bind with fatty acids is attributed to a partial helical conformation.[8] It was then of interest to prepare, for comparison, closely related cyclic structures. Interestingly, although mono-[9], di-[10] and tri-3,6-anhydro[11] cyclomaltooligosaccharides were already described, per(3,6-anhydro)cyclomaltoheptaose **7** has only quite recently been reported from the corresponding heptakis(6-*O*-*p*-tosyl) derivative.[12] The ready availability of per-6-deoxyhalo derivatives **3** and **4** now makes the access to such structures quite easy. **6** and **7** were prepared by treatment of the respective 6-iodo derivatives **3** and **4** with aqueous sodium hydroxide in DMSO. Anhydro cyclomaltooligosaccharides were recovered from the reaction after partial neutralization by addition of dry ice, and ultrafiltration against water. Confirmation of the structures **6** and **7** came from FABMS, which gave signals at *m/z* 887 and 1031 for the sodium species. In the ^{13}C NMR spectra of **6** and **7**, the signal for C-3 was shielded in both derivatives by $\delta = 2.5$ relative to the unmodified cyclomaltooligosaccharide signal, whereas that of C-6 was deshielded by $\delta = 7.7-7.8$, in agreement with data found for methyl 3,6-anhydro-α-D-glucopyranoside.[13] The D-glucopyranose units in **6** and **7** must have the alternative $^1C_4$ conformation.

In preliminary experiments, the per-3,6-anhydro cyclomaltooligosaccharides **6** and **7** were more soluble in water than the corresponding cyclomaltooligosaccharides. They were also appreciably soluble in methanol.

Experimental Procedure

3 and **4**: To a stirred solution of triphenylphosphane (21 g, 80 mmol) and iodine (20.2 g, 80 mmol) in DMF (80 mL) was added either **1** or **2** (4.32 g, 26.6 mole equiv.) and the solution was stirred at 80 °C for 15 h. It was then concentrated under vacuum to half the volume and the pH adjusted to 9–10, by the addition of sodium methoxide in methanol (3 M, 30 mL), with simultaneous cooling. The solution was kept at room temperature for 30 min to destroy the formate esters formed in the reaction, after which it was poured into ice water (1.5 L). The precipitate was collected by filtration to yield either **3** (5.8 g, 80% from **1**) or **4** (6.41 g, 88% from **2**) [14].

3: m.p. 227 °C (dec.); $[\alpha]_D^{25} + 95°$ ($c = 1.3$, DMF); ^{13}C NMR (50 MHz, $(CD_3)_2SO$, DMSO): $\delta = 101.8$ (C-1), 86.3 (C-4), 72.3 (C-5), 71.8 (C-3), 70.8 (C-2), 9.3 (C-6); FABMS (VG-ZAB-SEQ, dithioerythritol–dithiothreitol 1:4 *p*/*p*–KI): *m/z* 1671.5 ([*M* + K]$^\oplus$, 90%), 1633.6 ([*M* + H]$^\oplus$, 24), 1545.6 ([*M*HK − I]$^\oplus$, 100), 1418.7 ([*M*H_2K − 2I]$^\oplus$, 95), 1292.8 ([*M*H_3K − 3I]$^\oplus$, 76). Correct elemental analysis (C,H,I).

4: m.p. 235 °C (dec.); $[\alpha]_D^{25} + 66.1°$ ($c = 1.15$, DMF); ^{13}C NMR (50 MHz, $(CD_3)_2SO$, DMSO): $\delta = 102.3$ (C-1), 86.1 (C-4), 72.3 (C-3, C-5), 71.2 (C-2), 9.6 (C-6); FABMS (glycerol–thioglycerol–NaI): *m/z* 1926.7 ([*M* + Na]$^\oplus$, 100%), 1904.7 ([*M* + H]$^\oplus$, 21), 1800.9 ([*M*HNa − I]$^\oplus$, 71). Correct elemental analysis (C,H,I). Pyridine–Ac_2O acetylation of **4** yielded crystalline peracetylated heptakis(6-deoxy-6-iodo)cyclomaltoheptaose (69%), m.p. 180 °C (from Me_2CO–EtOH), $[\alpha]_D^{25} + 83.3°$ (*c* 1.2, $CHCl_3$); from [5]: m.p. 172–177 °C, $[\alpha]_D^{24} + 84°$ ($c = 0.1$, MeOH).

5: The experimental description was analogous to that of **3** and **4** except that bromine (4 mL, 80 mmol) was used instead of iodine. Yield 5.57 g (93%) [14].

5: m.p. 214 °C (dec.); $[\alpha]_D^{25} + 78.1°$ ($c = 1.76$, DMF). Correct elemental analysis (C,H,Br). From [6]: m.p. 205–206 °C (dec.), $[\alpha]_D^{25} + 98°$ ($c = 1$, pyridine).

6 and **7**: To a stirred solution of either **3** or **4** (1 g) in DMSO (30 mL) at 60 °C, was added aqueous sodium hydroxide (M, 6 mL) and the mixture was stirred for 6 h at 60 °C. The solution was cooled, dry ice was added in small portions, and the solvent was removed under vacuum. The solid residue was dissolved in water (150 mL), purified by ultrafiltration (Amicon 8200 device fitted with an Amicon Diaflo YCO5 membrane) against water for 24 h, and freeze-dried. Yield: **6** (405 mg, 75% from **3**). **7**: (502 mg, 88% from **4**) [14, 15].

6: m.p. 258 °C (EtOH aq.); $[\alpha]_D^{25} + 13°$ ($c = 0.72$, H_2O); ^{13}C NMR (50 MHz, D_2O, Me_2CO): $\delta = 97.6$ (C-1), 77.2 (C-4), 73.7 (C-5), 71.0 (C-3), 68.5 (C-6), 68.2 (C-2); FABMS (dithioerythritol–dithiothreitol–NaI): *m/z* 887 ([*M* + Na]$^\oplus$, 100%). Correct elemental analysis (C,H).

7: m.p. 289 °C (EtOH aq.); $[\alpha]_D^{25} - 10°$ ($c = 0.76$, H_2O); ^{13}C NMR (50 MHz, $(CD_3)_2SO$, DMSO): $\delta = 97.7$ (C-1), 76.9 (C-4), 73.6 (C-5), 70.9 (C-3), 68.4 (C-2, C-6); FABMS (glycerol–thioglycerol–NaI): *m/z* 1031 ([*M* + Na]$^\oplus$, 100%), 1053 ([*M* + 2Na − H]$^\oplus$, 58%), 1075 ([*M* + 3Na − 2H]$^\oplus$, 12%). Correct elemental analysis (C,H).

Received: June 20, 1990
revised: October 9, 1990 [Z 4027 IE]
German version: *Angew. Chem. 103* (1991) 94

CAS Registry numbers:
1, 10016-20-3; **2**, 7585-39-9; **3**, 131105-41-4; **4**, 30754-23-5; **4** (tetradecaacetate), 123155-24-8; **5**, 53784-83-1; **6**, 131105-39-0; **7**, 131105-40-3.

[1] A. P. Croft, R. A. Bartsch, *Tetrahedron 39* (1983) 1417–1474.
[2] J. Defaye, A. Gadelle, A. Coste-Sarguet, R. Darcy, N. Lynam, *5th Int. Symp. Cyclodextrins* (Paris 1990), abstract p. 90.
[3] J. Boger, R. J. Corcoran, J. M. Lehn, *Helv. Chim. Acta 61* (1978) 2190–2218.
[4] A. Lipták, P. Fügedi, Z. Szurmai, J. Imre, P. Nánási, J. Szejtli in J. Szejtli (Ed.): *1st Proc. Int. Symp. Cyclodextrins* (Budapest 1981), D. Reidel, Dordrecht 1981, pp. 275–287.
[5] F. Cramer, G. Mackensen, K. Sensse, *Chem. Ber. 102* (1969) 494–508.

[6] K. Takeo, T. Sumimoto, T. Kuge, *Staerke 24* (1974) 111–118.
[7] J. B. Lee, T. J. Nolan, *Can. J. Chem. 44* (1966) 1331–1334; J. B. Verheyden, J. G. Moffatt, *J. Org. Chem. 37* (1972) 2289–2299; B. Castro, Y. Chapleur, B. Gross, C. Selve, *Tetrahedron Lett. 1972*, 5001–5004.
[8] De-Pei Lu, C. E. Ballou, J. Defaye, A. Dell, *Carbohydr. Res. 160* (1987) 171–184.
[9] K. Fujita, H. Yamamura, T. Imoto, I. Tabushi, *Chem. Lett. 1988*, 543–546.
[10] K. Fujita, H. Yamamura, T. Imoto, T. Fujioka, K. Mihashi, *J. Org. Chem. 53* (1988) 1943–1947.
[11] K. Fujita, T. Tahara, T. Koga, *Chem. Lett. 1989*, 821–824; K. Fujita, T. Tahara, H. Yamamura, T. Imoto, T. Koga, T. Fujioka, K. Mihashi, *J. Org. Chem. 55* (1990) 877–880.
[12] P. Ellwood, J. F. Stoddart, *5th Int. Symp. Cyclodextrins* (Paris 1990), abstract p. 74; see also the following communication: P. R. Ashton, P. Ellwood, I. Staton, J. F. Stoddart, *Angew. Chem. 103* (1991) 96; *Angew. Chem. Int. Ed. Engl. 30* (1991) 80.
[13] K. Bock, C. Pedersen, *Adv. Carbohydr. Chem. Biochem. 41* (1983) 27–66.
[14] Yields for **3**–**7** are based on isolated pure compounds.
[15] Compounds **6** and **7** are homogeneous in HPLC (Perkin Elmer LC/500 chromatograph, C_{18} bonded silica column, elution with water, refractometric detection).

Synthesis and Characterization of Per-3,6-anhydro Cyclodextrins**

By *Peter R. Ashton, Paul Ellwood, Ian Staton,* and *J. Fraser Stoddart**

Cyclodextrins (CDs) are a class of cyclic oligosaccharides composed commonly of 6 (α-CD), or 7 (β-CD), α(1 → 4)-linked D-(+)-glucopyranose units. They have been widely investigated on account of their ability to form inclusion complexes with a wide variety of substrates.[1] The structures of the CDs have been extensively studied both in the solid state[2] and in solution.[3, 4] These investigations have established unambiguously that the D-glucopyranose residues adopt the expected $^4C_1$ chair conformation and that the gross structures of the molecules are those of truncated cones.[2] All the hydroxyl groups are located on the exteriors of the cones, making them somewhat hydrophilic, whereas the interiors of the cavities are relatively hydrophobic because they are lined with the H-3 and H-5 methine protons.

Many researchers have sought to change the structures and properties of CDs by chemical modification.[5] Although this research has led to a great deal of extremely elegant work, the majority of the chemical modifications to date have not resulted in significant perturbations of the gross structural features of the CD molecules. As a consequence, CDs have become trapped in something of a "structural straightjacket". Recently, however, a number of chemical modifications which could release CDs from this "structural straightjacket" have been achieved.[6, 7] In this paper, we wish to report another key chemical modification, namely per-3,6-anhydration. Examination of space-filling molecular models of, for example, per(3,6-anhydro)-β-CD indicates that the cavity of this derivative is dominated by the glucosidic pyranose ring and free hydroxyl oxygen atoms. Thus, the per-3,6-anhydro CDs constitute, potentially, a completely new class of CD-derived molecular receptor.

[*] Dr. J. F. Stoddart, P. R. Ashton, P. Ellwood, I. Staton
Department of Chemistry, The University
Sheffield S3 7HF (UK)

[**] Presented in part at the Royal Society of Chemistry Carbohydrate Group Spring Meeting, Cardiff, UK, 25–28 March 1990, at the Fifth International Symposium on Cyclodextrins, Paris, France, 27–30 March 1990, and at the Smith Kline Beecham Pharmaceutical Research Symposium on "Chirality in Drug Design and Synthesis", Cambridge, UK, 27–28 March 1990. This work was supported by the Science and Engineering Research Council and the Johnson Matthey Technology Centre in the United Kingdom.

Among carbohydrates in general, 3,6-anhydro derivatives of pyranose sugars are well known.[8] Usually, such derivatives are prepared by base treatment of pyranose derivatives carrying a good leaving group at C-6 and a *syn*-hydroxyl group at C-3. *Fujita* et al.[9] were the first to report 3,6-anhydration in CD systems. However, to date only partial anhydro ring formation has been achieved.[10]

Our initial attempt to synthesize the per-3,6-anhydro derivatives **3** and **4** of α-CD and β-CD involved (Scheme 1, R = H) the use of the per-6-*O*-tosyl derivatives **1** and **2**, respectively. These tosylates were first reported by *Lehmann* et al.[11] in 1954; since then, modifications to the original procedure have been reported by *Umezawa* et al.,[12] *Cramer* et al.,[13] and *Breslow* et al.[14] However, despite the extensive amount of research on **1** and **2**, analytical data for them are scarce.[15] In addition, only *Umezawa* et al.[12] give details of a chromatographic procedure for the purification of per(6-*O*-tosyl)-α-CD **1**. The other researchers[11, 13, 14] all used recrystallization as the means of purification. Thus, we suspected that the established literature procedures yield mixtures and not pure compounds. All the crude reaction products obtained in the present study were subjected to careful chromatography followed by a detailed analysis with a battery of physical methods.

Purification and analysis by HPLC, FABMS and NMR spectroscopy did indeed show that the reaction products of tosylations of both α-CD and β-CD contained mixtures of over- and under-tosylated derivatives, as well as the desired axially symmetrical derivatives **1** and **2**.[16] As expected[17] however, the reaction mixture obtained from α-CD was considerably more complicated than that obtained from β-CD: only sufficient pure **1** was isolated to permit its full characterization,[16] whereas sufficient pure **2** was isolated to allow the reaction illustrated in Scheme 1 (R = H) to be attempted. By

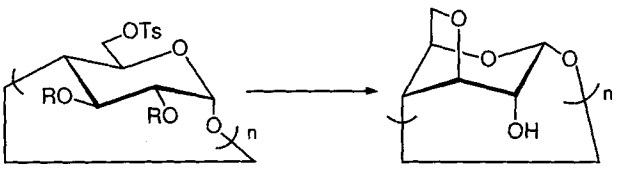

R = H, n = 6 **1** n = 6 **3**
R = H, n = 7 **2** n = 7 **4**
R = Bz, n = 6 **5**

Scheme 1. The synthesis of per-3,6-anhydro CDs **3** and **4** from the corresponding per-6-*O*-tosyl derivatives **1**, **2** and **5**. R = H: $NaOH/H_2O$; R = Bz: $Et_3N/CH_3OH/H_2O$

suspending the pure tosylate **2** in 1 M aqueous sodium hydroxide solution and stirring the reaction mixture for 2 days at 60 °C, per(3,6-anhydro)-β-CD **4** was isolated in 44% yield after reverse phase chromatography.[18] The ^1H and ^{13}C NMR spectra of the pure material were recorded in both D_2O and CD_2Cl_2 solutions. The vicinal H-H coupling constants obtained from the ^1H NMR spectra confirmed that the D-glucopyranose residues are locked in the $^1C_4$ chair conformation. However, the ^1H NMR chemical shifts and $[\alpha]_D$ values were different in the two solvents, which suggests that the gross conformation of the molecule is exhibiting some solvent dependence. In addition, a ^{13}C INEPT NMR spectrum was recorded in D_2O and an accurate value (164 Hz) of $^1J_{CH}$ was obtained for the anomeric position. This value is consistent[19] with an axial orientation for the

anomeric proton; thus the presence of the anhydro-D-glucose units with their $^1C_4$ chair conformation is confirmed (Scheme 2). The FABMS of pure per(3,6-anhydro)-β-CD **4** showed a pseudo molecular ion corresponding to a mono-

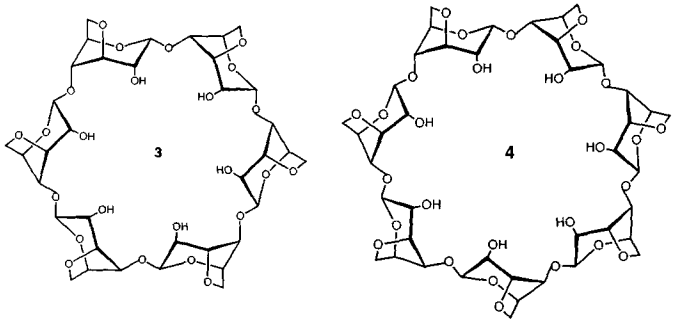

Scheme 2. Structures of **3** and **4**.

sodium adduct and further ions consistent with disodium and sodium/potassium adducts.[20] Single crystals suitable for X-ray crystallography were obtained by the vapor diffusion of methanol into an aqueous solution of **4**, and the full structural solution has not yet been achieved,[21] although a full set of X-ray data has been collected.

In view of the difficulties experienced in isolating large quantities of pure per(6-*O*-tosyl)-α-CD **1**, an alternative method of synthesizing per(3,6-anhydro)-α-CD **3** was developed using per (2,3-*O*-benzoyl-6-*O*-tosyl)-α-CD **5** as the key synthetic precursor (Scheme 1, R = Bz). This derivative was prepared according to the procedure described by *Lehn* et al.[17] Suspending **5** in $Et_3N/CH_3OH/H_2O$[22] and refluxing for 4 days gave eventually a clear solution. Neutralization with hydrochloric acid, followed by removal of the CH_3OH/H_2O under vacuum afforded a white solid. The FABMS of this white solid showed a base peak at *m/z* 966 corresponding to the triethylammonium adduct of **3**. Reverse phase chromatography with extensive recycling was necessary in order to isolate a small quantity of pure **3**. The ^1H and ^{13}C NMR spectra of this material were recorded in D_2O, and vicinal H-H coupling constants again indicate that the anhydro glucose residues were in the $^1C_4$ chair conformation (Scheme 2). The FABMS of the pure compound now showed molecular ion adducts corresponding to $[M + 2Na - H]^{\oplus}$ and $[M + K]^{\oplus}$, as well as the expected monosodium adduct.[20]

The development[23] of synthetic and chromatographic procedures for the preparation of the pure per-3,6-anhydro CDs **3** and **4** provides the opportunity to investigate their ability to form inclusion complexes.

Experimental Procedure

3: **5** [17] (50 mg, 0.016 mmol) was suspended in $Et_3N/CH_3OH/H_2O$ (1:5:1 v/v) (7 mL) and heated under reflux for 4 days. The resulting solution was then cooled and neutralized with hydrochloric acid (ca. 0.1 M). The solvents were removed under vacuum to give a white residue. HPLC using a Technicol Reverse Phase Column and CH_3OH/H_2O (1:4 v/v) as eluant afforded pure **3**. (3 mg, 22%); m.p. 236–237 °C; (Found: C 47.7; H 5.29% (material was very hygroscopic); *m/z* 887 $[M + Na]^{\oplus}$, 904 $[M + K]^{\oplus}$, 909 $[M + 2Na - H]^{\oplus}$. $(C_6H_8O_4)_6$ requires C 50.0; H 5.55%; *M* 864); $[\alpha]_D$ + 10 (*c* = 0.25, H_2O); δ_H (250 MHz, D_2O): 3.87 (6H, dd, $J_{1,2}$ = 4, $J_{2,3}$ = 5 Hz), 3.98 (6H, dd, $J_{5,6b}$ = 3, $J_{6a,6b}$ = 11.5 Hz), 4.24 (6H, d, $J_{6a,6b}$ = 11.5 Hz), 4.31 (6H, dd, $J_{3,4}$ = 5.5, $J_{4,5}$ = 2 Hz), 4.39 (6H, t, $J_{2,3}$, $J_{3,4}$ = 5 Hz), 4.56 (6H, m), 5.24 (6H, d, $J_{1,2}$ = 3 Hz). δ_C (63 MHz, D_2O): 68.4 (C-2), 68.8 (C-6), 71.3 (C-3), 74.0. (C-5), 77.5 (C-4), 98.0 (C-1).

4: **2** (20 mg, 0.009 mmol) was suspended in aqueous NaOH solution (2 mL of a 1 M solution) and the reaction mixture was stirred at 50 °C for 2 days. The clear solution was neutralized with hydrochloric acid (0.1 M) and the H_2O was removed under vacuum to leave a white residue. The desired compound was isolated by reverse phase HPLC. Thus, injecting a H_2O/CH_3OH (3:2 v/v) solution of the white residue onto a Dynamax C-18 Reverse Phase Preparative Column, and eluting with this solvent system afforded pure **4**. (4 mg, 44%); m.p. 226–227 °C; (Found: C 48.7; H 5.76% (material was very hygroscopic); *m/z* (positive ion FABMS) 1031 $[M + Na]^{\oplus}$, 1053 $[M + 2Na - H]^{\oplus}$, 1069 $[M + Na + K - H]^{\oplus}$. $(C_6H_8O_4)_7$ requires C 50.0; H 5.55%, *M* 1008). $[\alpha]_D$ 0 (*c* = 0.6, D_2O), $[\alpha]_D$ − 33 (*c* = 0.4, CH_2Cl_2); δ_H (250 MHz, D_2O): 3.94 (7H, br, dd, $J_{1,2}$ = 3.5, $J_{2,3}$ = 5 Hz), 4.03 (7H, dd, $J_{5,6b}$ = 3, $J_{6a,6b}$ = 11.5 Hz), 4.29 (7H, d, $J_{6a,6b}$ = 11.5 Hz), 4.36 (7H, dd, $J_{3,4}$ = 5, $J_{4,5}$ = 2 Hz), 4.46 (7H, t, $J_{2,3}$, $J_{3,4}$ = 5 Hz), 4.63 (7H, m), 5.31 (7H, d, $J_{1,2}$ = 3 Hz); δ_H (250 MHz, CD_2Cl_2): 3.89 (7H, br, dd, $J_{1,2}$ = 3.5, $J_{2,3}$ = 5 Hz), 3.95 (7H, dd, $J_{5,6b}$ = 2.5, $J_{6a,6b}$ = 11 Hz), 4.17 (7H, d, $J_{6a,6b}$ = 11 Hz), 4.19 (7H, dd, $J_{3,4}$ = 5, $J_{4,5}$ = 2.5 Hz), 4.38 (7H, t, $J_{2,3}$, $J_{3,4}$ = 5 Hz), 4.54 (7H, t, $J_{4,5}$, $J_{5,6b}$ = 2.5 Hz), 5.19 (7H, d, $J_{1,2}$ = 3 Hz). δ_C (63 MHz, D_2O): 68.0 (C-2), 68.6 (C-6), 71.0 (C-3), 73.8 (C-5), 76.5 (C-4), and 97.5 (C-1).

Received: June 20, 1990;
revised: October 19, 1990 [Z 4028IE]
German version: *Angew. Chem. 103* (1991) 96

CAS Registry numbers:
1, 21884-25-3; **2**, 23734-54-5; **3**, 131105-39-0; **4**, 131105-40-3; **5**, 68715-48-0.

[1] J. Szejtli: *Cyclodextrin Technology*, Kluwer Academic Publishers, Dordrecht, 1988.
[2] W. Saenger in J. L. Atwood, J. E. D. Davies, D. D. MacNicol (Eds.): *Inclusion Compounds, Vol. 2*, Academic Press, London 1984, p. 231 and references cited therein.
[3] R. J. Bergeron in J. L. Atwood, J. E. D. Davies, D. D. MacNicol (Eds.): *Inclusion Compounds, Vol. 2*, Academic Press, London 1984, p. 391.
[4] Y. Yamamoto, Y. Inoue, *J. Carbohydr. Chem. 8* (1989) 29.
[5] A. P. Croft, R. A. Bartsch, *Tetrahedron 39* (1983) 1417.
[6] M. Mori, Y. Ito, T. Ogawa, *Tetrahedron Lett. 30* (1989) 1273; *Carbohydr. Res. 192* (1989) 131.
[7] K. Fujita, Y. Egashira, T. Imoto, T. Fujioka, K. Mihashi, T. Tahara, T. Koga, *Chem. Lett. 1989*, 429; K. Fujita, T. Tahara, H. Sasaki, Y. Egashira, T. Shingu, T. Imoto, T. Koga, *ibid. 1989*, 917.
[8] R. D. Guthrie, in W. Pigman, D. Horton (Eds.): *The Carbohydrates Vol. 1A*, Academic Press, New York 1972, p. 423.
[9] K. Fujita, H. Yamamura, T. Imoto, I. Tabushi, *Chem. Lett. 1988*, 543.
[10] For a recent example see: K. Fujita, T. Tahara, H. Yamamura, T. Imoto, T. Koga, T. Fujioka, K. Mihashi, *J. Org. Chem. 55* (1990) 877.
[11] Von W. Lautsch, R. Wiechert, H. Lehmann, *Kolloid-Ztg. 135* (1954) 134.
[12] S. Umezawa, K. Tatsuta, *Bull. Chem. Soc. Jpn. 41* (1968) 464.
[13] F. Cramer, G. Mackensen, K. Sensse, *Chem. Ber. 102* (1969) 494.
[14] R. Breslow, M. F. Czarniecki, J. Emert, H. Hamaguchi, *J. Am. Chem. Soc. 102* (1980) 762.
[15] The principal researchers in this field (see [11–14]) report only varying combinations of m.p.'s, $[\alpha]_D$ values and microanalytical results. In addition, the actual numerical values reported for these data differ.
[16] A full paper, which includes full details of the chromatographic procedures used for the purification of the per-6-*O*-tosyl derivatives, and their analytical data, is in preparation.
[17] J. Boger, R. J. Concoran, J.-M. Lehn, *Helv. Chim. Acta. 61* (1978) 2190.
[18] The relative simplicity of the crude reaction mixture after the tosylation of β-CD led us to investigate the possibility of using the recrystallized but impure reaction product as the starting material for the per-3,6-anhydration. Such a procedure did indeed afford pure **4** because the subsequent chromatographic purification of the per(3,6-anhydro)-β-CD is straightforward. Therefore, we recommend using impure starting tosylate routinely to obtain large quantities of **4**. A similar investigation in the case of the α-CD derivatives was unsuccessful on account of the large number of asymmetrical 3,6-anhydro derivatives produced.
[19] J. A. Schwarz, A. S. Perlin, *Can. J. Chem. 50* (1972) 3667; A. Parfondry, N. Cyr, A. S. Perlin, *Carbohydr. Res. 59* (1977) 299.
[20] In our experience (for example, see P. R. Ashton, J. F. Stoddart, R. Zarzycki, *Tetrahedron Lett. 29* (1988) 2103), the FABMS of chemically modified cyclodextrins with *m*-nitrobenzyl alcohol as matrix gives only one pseudomolecular ion—a sodium adduct. Unlike the parent CDs and the majority of chemically modified CDs, the per-3,6-anhydro CDs **3** and **4** have cavities dominated by oxygen atoms, and therefore constitute a better binding environment for metal ions.
[21] Crystal data: monoclinic, a = 10.223(3), b = 41.213(12), c = 13.738(4) Å, β = 111.54(2)°, V = 5284 Å^3, $P2_1$, Z = 4 (2 crystallographically independent molecules). Full three-dimensional diffraction data have been collected and the structural solution is being attempted currently (A. M. Z. Slawin, D. J. Williams, unpublished results).
[22] K. Tsuzi, Y. Nakajima, T. Watanabe, M. Matsumoto, *Tetrahedron Lett. 1978*, 989; S. V. Ley, F. Sternfield, S. Taylor, *ibid. 28* (1987) 225.
[23] When we had completed the research reported in this communication, we discovered that **3** and **4** had also been prepared by *J. Defaye* et al. at the same time using a slightly different synthetic procedure; see the preceeding communication: A. Gadelle, J. Defaye, *Angew. Chem. 103* (1991) 94; *Angew. Chem. Int. Ed. Engl. 30* (1991) 78.

Aggregation of Aza Crown Ethers by Metalation: Synthesis and Crystal Structure of 1-Lithio-1,7-diaza[12]crown-4—The First Lithiated Crown Ether**

By *Donald Barr, David J. Berrisford, Luis Méndez, Alexandra M. Z. Slawin, Ronald Snaith,* J. Fraser Stoddart,* David J. Williams,** and *Dominic S. Wright*

There is much current interest[1, 2] in lithium amide reagents whose $Li^{\oplus}$ centers are complexed by functional groups inherent to the amide residue, in contrast with the more usual "external" complexation provided by added Lewis bases. The interest is concerned mainly with the precise structures of these reagents both in the solid state and in solution as well as with how these structures govern their subsequent reactions with organic substrates. Elsewhere in alkali-metal chemistry, neutral macrocyclic ligands (crowns, cryptands, etc.) are widely used, normally to encapsulate $M^{\oplus}$ ions and to separate them from their anions.[3] Here, we report our first attempt at merging these two strands of alkali-metal coordination chemistry—namely, the results of monolithiating a diaza crown ether (**1**) containing NH units. The ensuing ligand must be both the anion and the complexant such that, taken together with the $Li^{\oplus}$ center, a single entity is formed. It seemed likely that the $Li^{\oplus}$ ion in the product, **2**, would be unusually accessible to added organic substrates. X-ray diffraction studies showed that the lithiation product **2** is present in the solid state as the dimeric structure **3**.[4–6]

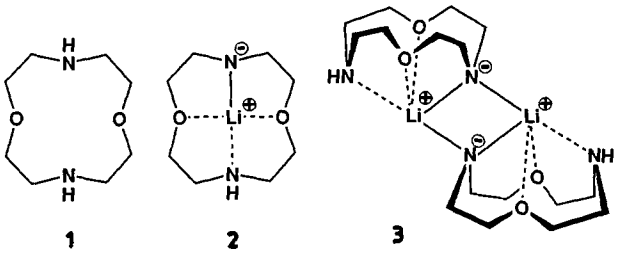

1 **2** **3**

Reaction of macrocycle **1**[7, 8] with *n*BuLi (1 molar equivalent) in the presence of 1 molar equivalent of $OP(NMe_2)_3$ (HMPA) afforded a compound with the empirical formula **2**. (The bulk product contained only traces[9] of HMPA). The crystal structure reveals that **2** forms a dimer **3** (Fig. 1). In each monomeric unit, the $Li^{\oplus}$ ion is bonded to its $N^{\ominus}$ center (2.111(4) Å), to the intact NH center (2.186(4) Å), and to both O atoms (2.258(4), 2.327(3) Å). Dimerization is due to interaction of the $Li^{\oplus}$ ion of each monomer with the $N^{\ominus}$ center of the other monomer (N-Li, 1.996(4) Å). To accommodate this interaction, each $Li^{\oplus}$ ion is displaced markedly from its "own" crown ether (by 0.94 Å) and becomes five-coordinate; this is an unusual—but not unknown—coordination[2] for $Li^{\oplus}$. The four-membered Li_2N_2 ring is planar and rhombic with transannular Li···Li' and N(7)···N(7') distances of 2.476(6) and 3.28(1) Å, respectively. The Li–N(7)-Li' angle is 74.1(2)°. All the other angles at each N are close to tetrahedral. To our knowledge, **3** is the first example[10, 11] of an oligomeric $Li^{\oplus}$–crown ether complex, to be characterized fully in the solid state; **3** is atypical, however, since the crown ether is anionic.

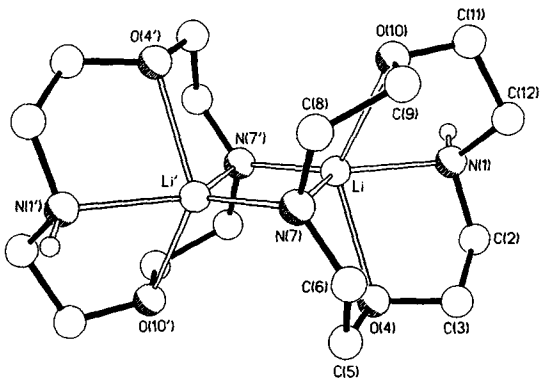

Fig. 1. The structure of **3** in the crystal. The hydrogen atoms, with the exception of those on N(1) and N(1'), have been omitted for clarity. The torsional angles in the macrocycle, starting with that about the N(1)–C(2) bond and proceeding clockwise, are 81, −167, 59, −160, 83, 59, −166, 78, 59, −161, 82, and 56° (average estimated standard deviation 0.2°).

MNDO calculations[12] have been used to probe the structural features of **3**. The results of calculations on four model species are summarized in Table 1. For monomeric **2**, it was assumed initially that the $Li^{\oplus}$ ion was in the heteroatom plane of the crown ether with the CH_2 units mutually eclipsed. The optimized geometry, freely refined, shows the $Li^{\oplus}$ ion bonded to all four heteroatoms. To achieve this situation, the $Li^{\oplus}$ ion is displaced 0.79 Å above the idealized N_2O_2 plane, the N–H bond is twisted away from the Li–N(H) bond, and the CH_2 groups become staggered. The $Li^{\oplus}$···crown ether displacement is typical for five-coordi-

Table 1. The results of MNDO calculations on monomeric **2**, on a model for HMPA-complexed monomeric **2**, and on two models for dimeric **3**.

Species	ΔH_f° [kcal mol^{-1}]	$\Delta H_{coord.}^\circ$ [kcal mol^{-1}]	N/O–Li bond lengths within the crown ether complex [Å]			
			$N^{\ominus}$-Li	N(H)···Li	O···Li	Li···O_2N_2 [i]
2, monomer	−92.8	–	1.933	2.263	2.222	0.79
2 · OPH_3	−99.9 [a]	−17.1	2.063	2.332	2.263 [b] 2.269	0.99
2 · $H_2N'Li'$	−128.6 [c]	−43.7	2.247 [d]	2.372	2.291 2.302	1.12
2 · $H_2N'Li'$ · NH_3 · $2H_2O$	−266.9 [e]	−35.3	2.173 [f]	2.416 [g]	2.308 [h] 2.310	1.11

[a] ΔH_f° of OPH_3, +9.97 kcal mol^{-1}. [b] H_3PO···Li, 2.093 Å. [c] ΔH_f° of H_2NLi, +7.94 kcal mol^{-1}. [d] $N^{\ominus}$–Li distances outside the crown ether complex [Å]: $N^{\ominus}$-Li' 2.061, $(H_2N')^{\ominus}$-Li' 1.995, $(H_2N')^{\ominus}$-Li 2.134. [e] ΔH_f° of $H_2NLi \cdot NH_3 \cdot 2H_2O$ (O and N atoms refined in the same symmetry as in monomer **2**), −138.8 kcal mol^{-1}. [f] $N^{\ominus}$–Li distances outside the crown ether complex [Å]: $N^{\ominus}$-Li 2.301, $(H_2N')^{\ominus}$-Li 2.185, $(H_2N')^{\ominus}$-Li 2.085. [g] H_3N-Li' 2.372 Å. [h] H_2O-Li' 2.373 Å. [i] Distance to the mean crown plane.

[*] Dr. J. F. Stoddart, Dr. D. J. Berrisford, L. Méndez
Department of Chemistry, The University
GB-Sheffield S3 7HF (UK)
Dr. R. Snaith, Dr. D. Barr, Dr. D. S. Wright
University Chemical Laboratory, Lensfield Road
GB-Cambridge CB2 1EW (UK)
Dr. D. J. Williams, A. M. Z. Slawin
Chemical Crystallography Laboratory
Department of Chemistry, Imperial College
GB-London SW7 2AY (UK)

[**] This work was supported by the Science and Engineering Research Council (UK), by the Spanish Ministerio de Educación y Ciencia (FPI Grant for *L.M.*), and by Gonville and Caius College, Cambridge (Research Fellowship for *D.S.W.*).

nate $Li^{\oplus}$ complexes (i.e., ones with $Li^{\oplus}$–anion contacts; cf. 0.85 Å in the solid-state structure of ([12]crown-4)LiSCN[11] and 0.79 Å in that of (dibenzo[14]crown-4)LiSCN[13]).

A complex of the monomer, $2 \cdot OPH_3$, was also examined. Again the structure was freely refined, with no symmetry restrictions. The important findings are (1) that the complexation energy is rather small (-17.1 kcal mol^{-1}), (2) that all the bonds between $Li^{\oplus}$ and the heteroatoms of the crown ether lengthen as expected compared with the distances found in uncomplexed **2**, and (3) that the $Li^{\oplus}$ ion moves further out (to 0.99 Å) of the crown plane. As a preliminary model for dimeric **3**—the association state found by X-ray diffraction—an H_2N'-*Li'* unit was contacted with the $N^{\ominus}$–$Li^{\oplus}$ edge of monomeric **2**. After optimization, the resulting association energy (a mean of -21.9 kcal mol^{-1} expressed per mole of Li) is somewhat larger than the complexation energy found for the monomeric $2 \cdot OPH_3$ adduct. This implies that the $Li^{\oplus}$ ion in this system prefers to achieve fivefold coordination by such association rather than by bonding a complexant. This is perhaps relevant to the experimental observation that HMPA is not incorporated—at least, stoichiometrically—in the dimeric product **3**. In the calculated $2 \cdot H_2N'Li'$ structure, the $Li^{\oplus}$ ion of the crown ether is "lifted" even further out of the plane to 1.12 Å. In addition, the $N^{\ominus}$–Li distance lengthens markedly compared with the values in monomeric **2** and in $2 \cdot OPH_3$. Thus, the complexed $Li^{\oplus}$ ion moves to a much more central position above the crown ether. In a final calculation, an attempt was made to mimic a species more closely related to the dimeric structure found for **3** in the solid state. In this species, whose optimized structure is shown in Figure 2, one NH_3 and two H_2O ligands were attached to the $Li'^{\oplus}$ ion of $2 \cdot H_2N'Li'$. The

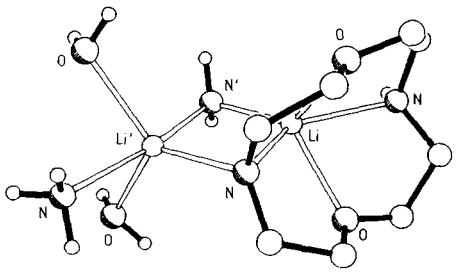

Fig. 2. The MNDO-optimized structure of $2 \cdot H_2N'Li' \cdot 2H_2O \cdot NH_3$ as viewed side-on.

calculated association energy of the two units (monomer **2** plus $H_2N'Li' \cdot NH_3 \cdot 2H_2O$) is a mean of -17.6 kcal mol^{-1} expressed per mole of Li. The $Li^{\oplus}$ ion of the crown ether is less central than in $2 \cdot H_2N'Li'$. The $N^{\ominus}$–*Li'* bond lengthens since the $Li'^{\oplus}$ ion now bears NH_3 and H_2O ligands, and thus the $N^{\ominus}$–Li bond shortens. Once more, however, the complexed $Li^{\oplus}$ ion is found to be raised markedly above the mean plane of the crown ether (by 1.11 Å). Thus, the results of the MNDO calculations agree reasonably well with the experimental findings principally in demonstrating (1) the deprotonation of a crown ether induces a strong preference for association of the metalated product and (2) that, to effect such association, the metal ion needs to move considerably further away from the plane of its "own" crown ether.

The results of this preliminary investigation raise several possibilities which are being explored: (1) Since **3** is still an amine containing an active NH function, further lithiation should be feasible, thus giving polymers,[14] or, by introduction of neutral donors to satisfy the extra metal ion, higher oligomers. (2) Although electronically well-satisfied, the five-coordinate $Li^{\oplus}$ centers in **3** remain sterically open to attack by added organic substrates (e.g., ketones). (3) The second metal[15] need not be a $Li^{\oplus}$ ion, so that mixed-metal $(crown)^{2\ominus}/Li^{\oplus} \cdot M^{\oplus}$ species could be synthesized. A particularly interesting aspect of the structure is that the dimerization caused by deprotonation requires additional displacement of the $Li^{\oplus}$ ion from the crown plane. A consequence of these structural features may be to allow incorporation of larger $M^{\oplus}$ ions (e.g., $Na^{\oplus}$, $K^{\oplus}$), which would normally not fit into the crown, or even of $M^{2\oplus}$ ions (e.g., $Mg^{2\oplus}$), possibly leading to cyclization products, "$(N \cdot crown \cdot N\text{-}Mg)_n$".

Experimental Procedure

2: The aza crown ether **1** [7, 8] (177 mg, 1.02 mmol), in a stirred solution of dry THF (3 mL), was lithiated under N_2 by addition of 1 molar equivalent of a 1.6 M solution of *n*BuLi in hexane (0.63 mL). This reaction yielded a white precipitate. *Addition of 1 molar equivalent of HMPA (0.18 mL) in THF* (3 mL), followed by heating under reflux, gave a clear solution from which crystals started to grow after 1 h at room temperature. The air-sensitive solid was filtered off, dried in vacuo, and transferred to a drybox under N_2. Yield (first batch of crystals) 71 mg, 39%; m.p. 105 °C (dec.). ^{1}H NMR (360.14 MHz, $C_6D_5CD_3$, 25 °C): $\delta = 2.13$ (1H, br. s, NH), 2.89 (8H, br. s, $4 \times CH_2$), 3.67 (8H, t, $4 \times CH_2$) [9]. ^{7}Li NMR (139.96 MHz, $C_6D_5CD_3$, δ relative to PhLi): δ (25 °C) = -0.54 (br. s), δ (-90 °C) = -0.50 (sharper s) (both ^{7}Li peaks have small shoulders, probably as a result of partial hydrolysis). Single crystals suitable for X-ray crystallography were sealed under N_2 in Lindemann tubes prior to data collection.

Received: August 15, 1990 [Z 4136 IE]
German version: *Angew. Chem. 103* (1991) 97

[1] D. Barr, D. J. Berrisford, R. V. H. Jones, A. M. Z. Slawin, R. Snaith, J. F. Stoddart, D. J. Williams, *Angew. Chem. 101* (1989) 1048; *Angew. Chem. Int. Ed. Engl. 28* (1989) 1044, and references therein.

[2] For reviews of organolithium structural chemistry, including amidolithium species, see: W. N. Setzer, P. von R. Schleyer, *Adv. Organomet. Chem. 24* (1985) 353; D. Seebach *Angew. Chem. 100* (1988) 1685; *Angew. Chem. Int. Ed. Engl. 27* (1988) 1624.

[3] P. P. Power, *Acc. Chem. Res. 21* (1988) 147.

[4] Nicolet R3m diffractometer, ω scans, $Cu_{K\alpha}$ radiation (graphite monochromator). The structure was solved by direct methods and refined anisotropically. Further details of the crystal structure investigation can be obtained from the Cambridge Crystallographic Data Centre, University Chemical Laboratory, Lensfield Road, Cambridge CB2 1EW (England). Any request should be accompanied by the full literature citation of this communication.

[5] Crystal data for **3**: monoclinic, $a = 9.442(1)$, $b = 8.729(1)$, $c = 12.882(2)$ Å, $\beta = 109.56(1)°$, $V = 1000$ Å^3, space group $P2_1/n$, $Z = 2$ (the molecule is disposed about a center of symmetry), $\varrho = 1.20$ g cm^{-3}, $\mu(Cu_{K\alpha}) = 6$ cm^{-1}, 1181 independent observed reflections with $|F_o| > 3\sigma|F_o|$, $2\theta \leq 116°$, refined to $R = 0.039$, $R_w = 0.044$.

[6] There are weak interdimer N-H···O hydrogen bonds between N(1) and O(10) of a symmetrically related dimer (and likewise for N(1)'-H···O(10)). *N(1)···O(10)*, 3.14; *H(1)···O(10)*, 2.18 Å; N-H···O angle 166°.

[7] B. Dietrich, J. M. Lehn, J. P. Sauvage, J. Blanzat, *Tetrahedron 29* (1973) 1629; D. J. Cram, S. P. Ho, C. B. Knobler, E. Maverick, K. N. Trueblood, *J. Am. Chem. Soc. 108* (1986) 2989.

[8] Anhydrous **1** was purified by sublimation (90 °C, 0.05 Torr Hg), m.p. 88–88.5 °C (83–84 °C [7]). Analytical and spectroscopic data were in agreement with the literature information.

[9] ^{1}H NMR spectroscopic analysis indicates the presence of approximately one HMPA ligand per five $Li^{\oplus}$ ions in part of the bulk crystalline sample. However, there is no evidence that the single crystal used for structural analysis contains similar amounts of HMPA. The maximum residual electron density in the final ΔF map 0.14 e Å^{-3}.

[10] The monolithiation of **1** has been previously reported (P. L. Anelli, F. Montanari, S. Quici, *J. Org. Chem. 50* (1985) 3453) as an intermediate step in the synthesis of [1.1.1]cryptates, but no isolation or characterization of the lithium amide was mentioned. Treatment of monoaza[18]crown-6 with KH has been shown to afford a potassium amide which acts as a self-solvating base for a number of reactions, including 1,2-eliminations (G. W. Gokel, B. J. Garcia, *Tetrahedron Lett. 1977*, 317; R. A. Bartsch, D. K. Roberts, *ibid. 1977*, 321). Not unrelated structurally are the aminoalanes obtained on reaction of organoaluminum species with macrocycles (e.g., 1,4,8,11-tetraazacyclotetradecane, cyclam) and open-chain tetradentate

amines (G. H. Robinson, S. A. Sangokoya, *J. Am. Chem. Soc. 109* (1987) 6852; *Organometallics 7* (1988) 1453; G. H. Robinson, A. D. Rae, C. F. Campana, S. K. Byram, *ibid. 6* (1987) 1227; G. H. Robinson, S. A. Sangokoya, F. Moise, W. T. Pennington, *ibid. 7* (1988) 1887; S. A. Sangokoya, F. Moise, W. T. Pennington, M. F. Self, G. H. Robinson, *ibid. 8* (1989) 2584; G. H. Robinson, M. F. Self, S. A. Sangokoya, W. T. Pennington, *J. Am. Chem. Soc. 111* (1989) 1520).

[11] All the known complexes of $Li^{\oplus}$ with neutral crown ethers are monomers, usually with the $Li^{\oplus}$ ion separated from its anion, though occasionally with $Li^{\oplus}$–anion contacts (e.g., [12]crown-4-LiSCN; P. Groth, *Acta Chem. Scand. 35* (1981) 463). See also S. M. Doughty, J. F. Stoddart, H. M. Colquhoun, A. M. Z. Slawin, D. J. Williams, *Polyhedron 4* (1985) 567; I. Goldberg in S. Patai, Z. Rappoport (Eds.): *Crown Ethers and Analogs*, Wiley Interscience, Chichester 1989; p. 207]. Binuclear (as opposed to dimeric) complexes of dications with neutral crown ethers are known for the heavier alkali-metal cations and very large crown ethers (e.g., dibenzo[30]crown-10 · $(NaNCS)_2$, J. D. Owen, M. R. Truter, *J. Chem. Soc. Dalton Trans. 1979*, 183). In the context of metalated crown ethers, the closest analogies to **3** for which X-ray structural data are available are (1) a benzene sulfonate crown ether species containing a $C_6H_3SO_3^{\ominus}Li^{\oplus} \cdot H_2O$ unit wherein the $Li^{\oplus}$ ion is bonded to only two of the crown ether oxygens, with loose association being effected by intermolecular $SO_3^{\ominus} \cdots H_2O$ hydrogen bonding (J. van Eerden, M. Skowronska-Ptasinka, P. D. J. Grootenhuis, S. Harkema, D. N. Reinhoudt, *J. Am. Chem. Soc. 111* (1989) 700), and (2) a MgBr benzo crown ether containing a $C_6H_3^{\ominus}$ $(MgBr)^{\oplus}$ unit in which the $Mg^{2\oplus}$ ion is coordinated to all four oxygen centers, the complex remaining monomeric (P. R. Markies, O. S. Akkerman, F. Bickelhaupt, W. J. J. Smeets, A. L. Spek, *J. Am. Chem. Soc. 110* (1988) 4284).

[12] M. S. J. Dewar, W. Thiel, *J. Am. Chem. Soc. 99* (1977) 4899; W. Thiel, *QCPE No. 438*, Vol. 2 (1982) 63; M. S. J. Dewar, C. H. Reynolds, *J. Comput. Chem. 2* (1985) 140. We thank Dr. *T. Clark* (Universität Erlangen-Nürnberg) for the use of his MNDO program, Dr. *R. Amos* (Cambridge) for much computational assistance, and Professor *P. von R. Schleyer* (Universität Erlangen-Nürnberg) for some helpful discussions.

[13] G. Shoham, W. N. Lipscomb, U. Olsher, *J. Chem. Soc. Chem. Commun. 1983*, 208.

[14] Attempts to isolate a dilithiathed crown ether complex have, to date, invariably resulted in the rapid formation of insoluble oligomeric materials. Further studies are in progress.

[15] Mixed-metal crown ether complexes should have interesting properties as superbases (A. Mordini, E. Ben Rayana, C. Margot, M. Schlosser, *Tetrahedron 46* (1990) 2401; C. Margot, M. Rizzolio, M. Schlosser, *ibid. 46* (1990) 2411; C. Margot, H. Matsuda, M. Schlosser, *ibid. 46* (1990) 2425, and references therein).

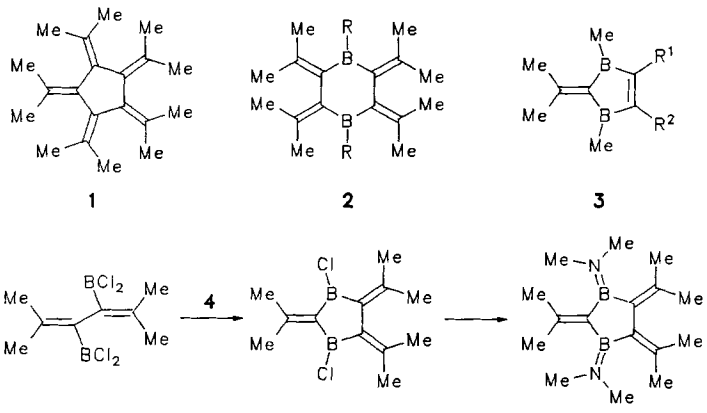

Scheme 1. Synthesis of 1,3-dibora[5]radialenes **6** from 3,4-bis(dichlorboryl)-2,5-dimethyl-2,4-hexadiene **5** and 2-methyl-1,1-bis(trimethylstannyl)propene **4** [5]. **6a**: 3,4-dilithio-2,5-dimethyl-2,4-hexadiene [4], $B(OMe)_3$, TMEDA, 0 °C → 3,4-bis(dimethoxyboryl)-2,5-dimethyl-2,4-hexadiene, 48%, b.p. 85 °C/5 torr; OCH_3Cl exchange with BCl_3 → **5**, 72%, b.p. 65 °C/0.6 torr; ring closure of **5** with **4**, pentane → **6a**, 40%, b.p. 80 °C/10^{-3} torr. **6b**: **6a**, 2 MeLi, − 50 °C, pentane → **6b**, 90%, b.p. 70 °C/10^{-3} torr. **6c**: **6a**, 2 Me_3SiNMe_2, *n*-hexane, 70 °C → **6c**, 92%, b.p. 85 °C/10^{-3} torr, m.p. 75 °C (ether, − 20 °C).

Synthesis, Structure, and Rearrangement of 1,3-Dibora[5]radialenes**

By *Markus Enders, Albrecht Krämer, Hans Pritzkow*, and *Walter Siebert**

Dedicated to Professor Max Schmidt on the occasion of his 65th birthday

Radialenes are of interest in many respects because of their reactivity and electronic structure.[1] Metal-catalyzed oligomerizations of cumulenes on nickel(0)[1, 2] have recently enabled simple syntheses of [4]- and [6]radialenes, and the decamethyl[5]radialene **1** could be obtained for the first time via $(Me_2C=CBr)_2CuLi$.[3] Despite the numerous heteroradialenes reported in the literature, thus far only one boron-containing radialene has been documented. We report here the synthesis of the 1,3-dibora[5]radialene **6** from the versatile diene **5** (Scheme 1). Attempts to synthesize **6** from 3,4-dilithio-2,5-dimethyl-2,4-hexadiene and $Me_2CC=CC(BClR)_2$ analogously to the route leading to 1,4-dibora[6]radialene **2** ($R = CMe_3$, NPh_2) described by *Maercker* et al.[4] failed. We therefore examined the reaction of bis(trimethylstannyl)propene **4**[5] with 3,4-bis(dichloroboryl)-2,5-dimethyl-2,4-hexadiene **5**, and indeed obtained the dibora[5]radialene **6a** in 40% yield. Substitution of the chlorine atoms in the yellow distillable **6a** by methyllithium leads to the light yellow octamethyl derivative **6b**; with Me_3SiNMe_2 the bis(dimethylamino) compound **6c** isoelectronic with **1** is formed.

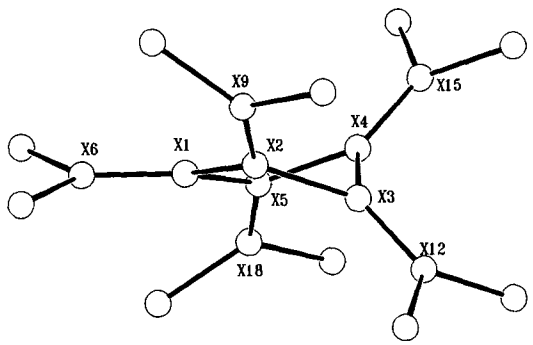

Fig. 1. Molecular structure of **6c**. The two independent molecules have approximately the same conformation, with a twofold axis through X1 and the midpoint of X3–X4. Averaged distances [Å] (standard deviation 0.005 Å): X1-X2(X5) 1.587, X1-X6 1.401, X3-X4 1.586, X3(X4)-X12(X15) 1.368, X2(X4)-X3(X5) 1.546 (individual values 1.522, 1.549, 1.566), X2(X5)-X9(X18) 1.353.

The constitution of **6a–c** follows from the spectroscopic data (Table 1); the X-ray structure analysis[6] of **6c** shows that the five-membered ring is not planar, but has the half-chair conformation (Fig. 1). The expected differences in the lengths of the C–C and B–C bonds in the ring and the exocyclic C=C and B=N bonds are small. According to MNDO calculations[7] several conformers are possible, all of which are half-chair shaped and thus have a similar struc-

[*] Prof. Dr. W. Siebert, Dipl.-Chem. M. Enders, Dr. A. Krämer, Dr. H. Pritzkow
Anorganisch-chemisches Institut der Universität
Im Neuenheimer Feld 270, W-6900 Heidelberg (FRG)

[**] This work was supported by the Deutsche Forschungsgemeinschaft (SFB 247), by the Fonds der Chemischen Industrie, and by BASF AG (Ludwigshafen).

ture and the same spatial demand. The result of the X-ray structure analysis can be explained in terms of a superposition of several conformers and therefore does not provide any accurate information about the bond lengths and angles.

Prolonged heating (10 d/110 °C) of **6b** in toluene leads, because of steric interaction of the neighboring dimethylmethylene groups, to a mixture of substances, from which the 1,3-diborafulvene **3b** (R^1 = MeC=CH_2, R^2 = $CHMe_2$) is isolated in 64% yield.[8] The formation of **3b** as a result of

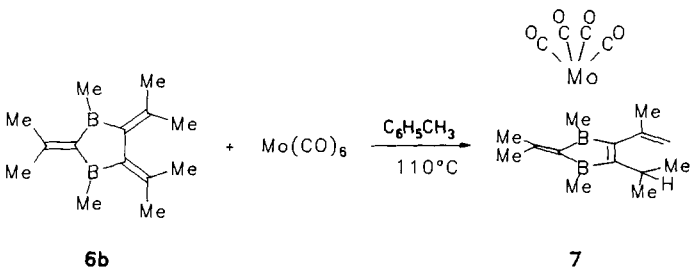

6b **7**

Scheme 2. Synthesis of the tetracarbonyl(1,3-diborapentafulvene)molybdenum complex **7**: **6b** and $Mo(CO)_6$ in toluene, 110 °C, 4 h → orange **7**, column chromatography (SiO_2, hexane), 85%, m.p. 77 °C (hexane, − 20 °C).

a sigmatropic 1,5-H-shift proceeds much more rapidly in the presence of metal complex fragments: Reaction with hexacarbonylmolybdenum in toluene (110 °C) leads within a few hours to formation of the 1,3-diborafulvenemolybdenum complex **7** (Scheme 2), which was also characterized by an X-ray structure analysis.[9]

1,3-Dibora[5]radialenes **6** are thus excellent educts for the synthesis of unsymmetrically substituted 1,3-diborafulvenes **3**. Furthermore, they have great potential for the synthesis of novel carbaboranes (by hydroboration) and metallacarbaboranes (by hydrometalation).

Table 1. ^{1}H-, ^{11}B- and ^{13}C-NMR data of **6a**, **6b**, **6c** and **7**.

6a: ^{1}H NMR ($CDCl_3$): δ = 1.67 (s, 6H), 2.17 (s, 6H), 2.44 (s, 6H). ^{11}B NMR ($CDCl_3$): δ = 60.5. ^{13}C NMR (C_6D_6): δ = 23.4 (CH_3C), 25.7 (CH_3C), 28.5 (CH_3C), 146.1 (C_{exo}), 185.1 (C_{exo}), 153 (br, C_{ring})

6b: ^{1}H NMR ($CDCl_3$): δ = 1.20 (s, 6H, BCH_3), 1.66 (s, 6H), 1.99 (s, 6H), 2.21 (s, 6H). ^{11}B NMR ($CDCl_3$): δ = 72.3. ^{13}C NMR ($CDCl_3$): δ = 11.9 (BCH_3), 23.7 (CH_3C), 24.5 (CH_3C), 28.2 (CH_3C); 153 (br, C_{ring}), 137.5 (C_{exo}), 172.7 (C_{exo})

6c: ^{1}H NMR (C_6D_6): δ = 1.73 (s, 6H), 1.83 (s, 6H), 1.85 (s, 6H), 2.68 (s, 6H, NCH_3), 2.74 (s, 6H, NCH_3). ^{11}B NMR (C_6D_6): δ = 42.5. ^{13}C NMR (C_6D_6): δ = 23.4 (CH_3C), 25.2 (CH_3C), 27.7 (CH_3C), 42.4 (NCH_3), 42.6 (NCH_3), 145.1 (C_{exo}), 129.3 (C_{exo}), 148 (br, C_{ring})

7: ^{1}H NMR (C_6D_6): δ = 0.91 (s, 3H, BCH_3), 1.02 (s, 3H, BCH_3), 1.15 (d, 3H, ^3J(H,H) = 7.0 Hz), 1.25 (d, 3H, ^3J(H,H) = 7.0 Hz), 1.66 (s, 3H), 1.69 (s, 3H), 1.85 (m, 3H), 2.48 (sept., 1H, ^3J(H,H) = 7.0 Hz), 4.61 (m, 1H), 5.01 (m, 1H). ^{11}B NMR (C_6D_6): δ = 37.7. ^{13}C NMR (C_6D_6): 1.3 (BCH_3), 2.2 (BCH_3), 23.7, 25.7, 26.0, 28.3, 28.5 (each CH_3C), 31.2 ($CH(CH_3)_2$), 112 and 148 (br, C_{ring}), 115.0 (CH_2), 143.7 (C_{exo}), 153.0 (C_{exo}), 210.9, 211.8, 212.0, 217.0 (each CO)

Received: July 17, 1990;
supplemented: September 27, 1990 [Z 4070 IE]
German version: *Angew. Chem. 103* (1991) 80

CAS Registry numbers:
3b, 131193-62-9; **4**, 103670-41-3; **5**, 131193-59-4; **6a**, 131193-60-7; **6b**, 131193-61-8; **6c**, 131193-63-0; **7**, 131235-83-1; $B(OMe)_3$, 121-43-7; $Mo(CO)_6$, 13939-06-5; 3,4-dilithio-2,5-dimethyl-2,4-hexadiene, 96445-43-1; 3,4-bis(dimethoxyboryl)-2,5-dimethyl-2,4-hexadiene, 131193-58-3.

[1] M. Iyoda, S. Tanaka, H. Otani, M. Nose, M. Oda, *J. Am. Chem. Soc. 110* (1988) 8494.
[2] G. Wilke, *Angew. Chem. 100* (1988) 189; *Angew. Chem. Int. Ed. Engl. 27* (1988) 185; L. Stehling, G. Wilke, *ibid. 97* (1985) 505 and *24* (1985) 248.
[3] M. Iyoda, H. Otani, M. Oda, Y. Kai, Y. Baba, N. Kasai, *J. Chem. Soc. Chem. Commun. 1986*, 1794.
[4] A. Maercker, W. Brieden, T. Schmidt, H. D. Lutz, *Angew. Chem. 101* (1989) 477; *Angew. Chem. Int. Ed. Engl. 28* (1989) 477.
[5] T. N. Mitchell, W. Reimann, *Organometallics 5* (1986) 1991.
[6] **6c**: space group $C2/c$, a = 32.117(20), b = 15.036(10), c = 11.994(7) Å, β = 106.73(5)°; V = 5547 Å^3, Z = 12 (two independent molecules, one in a special position, twofold axis); 2384 observed reflections ($I > 2\sigma_I$, four circle diffractometer, Mo_{K_α}, ω-scan); refinement: non-hydrogen atoms anisotropic, methyl groups as rigid groups with a common isotropic temperature factor for the H atoms of each molecule. The ring atoms (and the atoms of the exocyclic double bonds) were partially refined as C,B or as average from B and C (and C,N or as average from C and N). R = 0.051, R_w = 0.064 (319 parameters). Further details of the crystal structure investigation are available on request from the Fachinformationszentrum Karlsruhe, Gesellschaft für wissenschaftlich-technische Information mbH, W-7514 Eggenstein-Leopoldshafen 2 (FRG) on quoting the depository number CSD-54966, the names of the authors, and the journal citation.
[7] C. W. von der Lieth, Heidelberg private communication 1990.
[8] B.p. (83 °C/0.6 torr. ^{1}H-NMR (C_6D_6): δ = 1.09 (s, 3H, BCH_3), 1.17 (d, 6H, ^3J(HH) = 7.0 Hz, $CH(CH_3)_2$), 1.19 (s, 3H, BCH_3), 1.80 (m, 3H, CH_2=CCH_3), 1.95 (s, 6H, $C(CH_3)_2$), 3.03 (sept, 1H, $CH(CH_3)_2$), 4.56, 5.01 (each 1H, m, CH_2=CCH_3). ^{11}B-NMR (C_6D_6): δ = 71.8. ^{13}C-NMR (C_6D_6): δ = 7, 9 (br, BCH_3), 22.5, 24.1, 26.4 (each CH_3), 31.4 ($CH(CH_3)_2$), 109.5 (C = CH_2), 146.7/154.4 (= $C(CH_3)_2$/H_2C = CCH_3), C_{ring} not found.
[9] The coordination of the molybdenum and the bending in the 1,3-diborafulvene ligand are consistent with the results for the complex **3a** · $Mo(CO)_4$ obtained from **3a** (R^1 = R^2 = Et) and $Mo(CO)_6$ [10]. IR (ν(CO), hexane): 1936.0 cm^{-1} (vs), 1951.0 (vs), 1959.5 (m), 2039.0 (s).
[10] V. Schäfer, H. Pritzkow, W. Siebert, *Chem. Ber. 122* (1989) 401.

Synthesis of a Novel Macrobicyclic Cavity Possessing Six Convergent Hydroxyl Groups and Acting as a Siderophore

By *Jean Louis Pierre*,* *Paul Baret* and *Giselle Gellon*

Naturally occurring and synthetic ferric ion chelators, like siderophores, are currently of great interest because of their biochemical role in microorganisms[1, 2] and plants,[2] their potential applications in the treatment of iron overload disease,[3, 4] and their use both as NMR contrast agents[5] for the imaging of organs and tumors in the human body[4] and as anticancer drugs.[1, 6] The natural and synthetic siderophores containing catecholate or hydroxamate donor groups are not ideal drugs (desferrioxamine B, for example, needs to be infused for 6–12 h per day because of its very short half-life in the body; catecholates are air sensitive); thus it is a stimulating challenge to synthesize new families of such molecules.

The pioneering work of *Vögtle* et al.,[7] *Raymond* et al.,[8] and *Martell* et al.[9] suggested to us the ultimately successful synthesis of macrobicyclic siderophores which contain 2,2'-dihydroxybiphenyl groups. Incorporation of three such subunits in a macrobicycle effectively produces six convergent phenolate groups as potential coordination sites; in addition, with such groups the often observed facile oxidation of the subunit (e.g. catechol group) may be attenuated.

The synthesis of the bicapped ligand **1a** was carried out by the high-dilution technique, as well as in high yield through a template reaction. The methyl-protected macrobicyclic derivative **1b** was obtained from the tripodal precursor **2b** by high-dilution (benzene) route in 25% yield. Removal of the

[*] Prof. J. L. Pierre, Prof. P. Baret, and Mrs. G. Gellon
L.E.D.S.S. Equipe Chimie biomimétique
Université Joseph Fourier
B.P. 53X, F-38041 Grenoble Cédex (France)

methyl protecting groups (BBr_3, $CHCl_3$) then gave **1a** in 70% yield. The ^1H and ^{13}C NMR spectra of **1a** (in D_2O/NaOD) and of **1b** (in $CDCl_3$) reflect the symmetry of the molecules. The methoxyl groups are magnetically equivalent in **1b**, but in the open-chain triester precursor **2b**, two

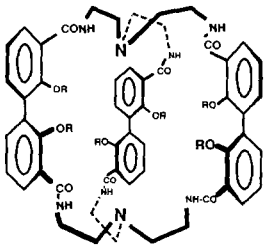

1a: R = H
1b: R = Me

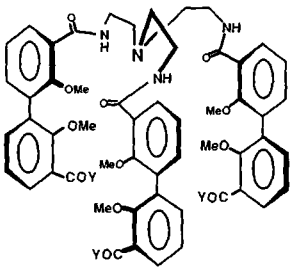

2a: Y = Cl
2b: Y = OMe

methoxy signals at lower field than the corresponding resonance for **1b** are observed. The FAB (Fast Atom Bombardment) mass spectra of **1a** and **1b** exhibit the characteristic $[M + H]^{\oplus}$ peaks.

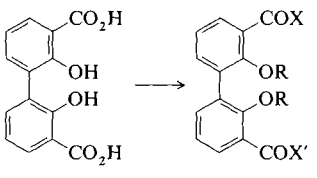

3 **4**

4a: R = Me; X = X′ = OMe
4b: R = Me; X = Cl, X′ = OMe
4c: R = CH_2Ph; X = X′ = OH
4d: R = CH_2Ph; X = X′ = O–N(succinimide)
4e: R = H; X = X′ = O–N(succinimide)
4f: R = H; X = X′ = $N(Me)_2$

Scheme 1.

The template synthesis was performed through the key compound **4e** (Scheme 1) by using the elegant procedure of *Raymond*.[10] The template-reaction step (**4e**, $N(CH_2CH_2NH_2)_3$ (tren), $FeCl_3$, Et_3N, DMF, 4-dimethylaminopyridine) gave the red ferric complex of **1a** in nearly quantitative yield. The colorless product **1a** obtained on demetalation ($Na_2S_2O_4$, HCl, DMSO) was identical to that secured from the stepwise synthesis. The ferric complex could be prepared from **1a** through an exchange procedure involving ferric acetylacetonate;[11] this method avoided the initial basic conditions required for dissolving the chelator. The FAB mass spectrum of the complex corroborated the 1:1 stoichiometry $[M - 4H + Fe]$. The UV/VIS spectrum of the iron(III) complex of **1a** in acetonitrile solution showed an absorption ($\lambda_{max} = 464$ nm, $\varepsilon \approx 870$), similar to that observed with compound **4f**. Competition experiments in water at pH 11.5 between **1a** and either EDTA or desferrioxamine-B attest the great stability of the Fe^{III} complex with this new ligand. The UV/VIS absorption curve of a solution containing equimolecular amounts of EDTA and **1a** is similar to that of the pure Fe^{III} complex of **1a**. With desferrioxamine B, the absorption ($\lambda = 430$ nm) is shifted to longer wavelength ($\lambda = 460$ nm) upon addition of **1a**.

The determination of stability constants and protonation constants is in progress, as are electrochemical, biochemical and structural studies.

Experimental Procedure

The derivatives of **4** are defined in Scheme 1. **3** was obtained from dibenzofuran: a) *s*-BuLi, TMEDA, Et_2O; b) CO_2; c) $H_3O^{\oplus}$; d) NaOH/KOH fusion; e) $H_3O^{\oplus}$ (overall yield = 83%).

4e was obtained from **3**: a) $PhCH_2Br$, K_2CO_3, acetone; b) NaOH, methanol; c) $H_3O^{\oplus}$; d) *N*-hydroxysuccinimide, dicyclohexylcarbodiimide, dioxane; e) H_2/Pd-C, dichloromethane (overall yield = 41%).

The podand **2b** was prepared from **4b**: tren, Et_3N, THF; 76%; **4b** was obtained from **3** via **4a**: a) Me_2SO_4, K_2CO_3, acetone; b) NaOH 1 eq., methanol; c) $H_3O^{\oplus}$; d) $SOCl_2$ (overall yield = 45%).

The macrocycle **1a** was recrystallized from methanol/ether; **1b** was purified by chromatography (silica gel, CH_2Cl_2/$iPrNH_2$).

1a: ^1H NMR (300 MHz, D_2O, NaOD): $\delta = 8.02$ (d, $J = 7.4$ Hz, 6H, Ar-H4), 7.43 (d, $J = 7.4$ Hz, 6H, Ar-H6), 6.87 (t, $J = 7.4$ Hz, 6H, Ar-H5), 3.85 (m, br, 12H, CH_2NH), 3.26 (m, br, 12H, CH_2N); ^{13}C NMR (75 MHz, D_2O, NaOD): $\delta = 169.8$ (C = O), 159.5 (Ar-C2), 134.8, 130.6, 128.6, 119.7, 117.1 (Ar-C1, 3, 4, 5, 6), 51.1 (NHC), 37.0 (NC); MS(FAB): *m/z* 1007. Correct C, H analyses.

1b: ^1H NMR (300 MHz, $CDCl_3$): $\delta = 7.94$ (dd, $J = 7.6$, 1.8 Hz, 6H, Ar-H4), 7.7 (m, br, 6H, NH), 7.25 (dd, $J = 7.6$, 1.8 Hz, 6H, Ar-H6), 7.15 (t, br, $J = 7.6$ Hz, 6H, Ar-H5), 3.53 (m, br, 12H, CH_2NH), 3.14 (s, 18H, CH_3O), 2.84 (m, br, 12H, CH_2N); ^{13}CNMR (75 MHz, $CDCl_3$): $\delta = 165.4$ (C = O), 156 (ArC2), 134.3, 132.2, 131.6, 126.8, 124.6 (ArC1,3,4,5,6), 61.8 (CH_3O), 53.3 (NHC), 37.7 (NC); MS (FAB): m/z 1091. Correct C, H analyses.

2b: ^1H NMR (300 MHz, $CDCl_3$): $\delta = 8.08$ (m, br, 3H, NH), 8.01 (dd, $J = 7.7$, 1.8 Hz, 3H, Ar-H4), 7.82 (dd, $J = 7.7$, 1.8 Hz, 3-H, Ar-H4′), 7.47, 7.45 (dd, superimposed, $J = 7.7$, 1.8 Hz, 6H, Ar-H6,6′), 7.22 (t, $J = 7.7$ Hz, 3H, Ar-H5′), 7.20 (t, $J = 7.7$ Hz, 3H, Ar-H5′), 3.93 (s, 9H, CO-OMe), 3.55 (m, br, 6H, CH_2NH), 3.51 (s, 9H, OMe), 3.47 (s, 9H, OMe) 2.86 (m, br, 6H, CH_2N); ^{13}C NMR (75 MHz, $CDCl_3$): $\delta = 166.6$ (HNC = O), 165.6 (OC = O), 157.4 (ArC2), 155.8 (ArC2′), 135.3, 134.7, 132.7, 131.5, 131.3, 131.2, 126.8, 125.4, 124.3, 123.6, (ArC1,3,4,5,6,1′,3′,4′,5′,6′), 61.8 (CH_3O), 61.5 (CH_3O), 53.5 (NHC), 52.3 (CH_3OCO), 37.8 (NC); MS (FAB), *m/z* 1041. Correct C, H analyses.

Received: July 25, 1990 [Z 4090 IE]
German version: *Angew. Chem. 103* (1991) 75

CAS Registry numbers:
1a, 131179-11-8; **1b**, 131179-12-9; **2b**, 131179-13-0; **3**, 105595-68-4; **4e**, 131179-14-1.

[1] V. Braun, G. Winkelmann, *Prog. in Clin. Biochem. and Med. 5* (1988) 67.
[2] R. C. Hider, *Struct. Bond. (Berlin) 58* (1984) 25.
[3] A. E. Martell, W. F. Anderson, D. G. Badman (Eds.): *Development of Iron Chelators for Clinical Use*, Elsevier Holland, New York 1981.
[4] A. E. Martell (Ed.): *Inorganic Chemistry in Biology and Medicine, A.C.S. Symp. Ser. 140* (1980).
[5] R. C. Brasch, H. J. Weinman, G. E. Webey, *Am. J. Roentgenol. 142* (1984) 625.
[6] E. D. Weinberg, *Physiol. Rev. 64* (1984) 65.
[7] P. Stutte, W. Kiggen, F. Vögtle, *Tetrahedron 43* (1987) 2065.
[8] K. N. Raymond, T. J. Mac Murry, T. M. Garrett, *Pure Appl. Chem. 60* (1988) 545 and references cited therein.
[9] Y. Sun, A. E. Martell, *J. Am. Chem. Soc. 111* (1989) 8023.
[10] T. J. Mac Murry, S. J. Rodgers, K. N. Raymond, *J. Am. Chem. Soc. 109* (1987) 3451.
[11] J. B. Dionis, H. B. Jenny, H. H. Peter, *J. Org. Chem. 54* (1989) 5623.

Enzymatic Synthesis of Chiral C_4 Building Blocks from *meso*-Tartaric Acid

By *Hans Jürgen Bestmann** and *Ulrich Christian Philipp*

The use of optically active (*R,R*)- and (*S,S*)-tartaric acids as chiral starting compounds for a diversity of syntheses is well documented.[1] In contrast, the conversion of *meso*-tartaric acid into chiral building blocks has so far remained an unsolved problem, if one disregards an earlier resolution of the monomethyl ester with strychnine (without determination of the absolute configuration)[2] and an enzymatic hydrolysis of the dimethyl ester to the monomethyl ester with moderate *ee* value (48%).[3]

[*] Prof. Dr. H. J. Bestmann, Dr. U. C. Philipp
Institut für Organische Chemie der Universität Erlangen-Nürnberg
Henkestrasse 42, W-8520 Erlangen (FRG)

By reaction of maleic esters **1** with potassium permanganate in aqueous solution we have prepared isomer-free *meso*-tartaric acid ester, protected the OH groups in various ways, and subjected the compounds **2** so obtained to a screening with several enzymes. Of the results, we describe here only the most favorable.[4]

meso-Dimethoxysuccinic acid dimethyl ester **2** ($R^1 = R^2 = CH_3$) is hydrolyzed by porcine liver esterase [as porcine liver-acetone powder (PLAMP)[5, 6] in 0.1 N phosphate buffer at pH = 7 in the presence of 20% methanol] at the pro-*S* ester group to give (+)-**4** with an *ee* value of 90.5% and a chemical yield > 90%.[7] In contrast, lipase from *Candida cylindrecea* (CCL, sigma type VII), in the absence of methanol, attacks the pro-*R* ester group. (−)-**4** is obtained with an *ee* value of 92.5% in a yield of > 90%. The determination of the absolute configuration of (+)-**4** and (−)-**4** was accomplished by application of the Freudenberg shift principle[8] by comparison of the change in molecular rotation during the transition from *R,R*-2,3-dimethoxysuccinic acid dimethyl ester to the corresponding (*R,R*)-monoester with the signs of the rotation of (+)-**4** and (−)-**4**. The *ee* values were determined by gas chromatography of the diastereomeric (*S*)-1-phenylethylamides, which were prepared from (+)-**4** and (−)-**4** and (*S*)-1-phenylethylamine by reaction with propanephosphinic acid anhydride and *N*-methylmorpholine[9] in methylene chloride.

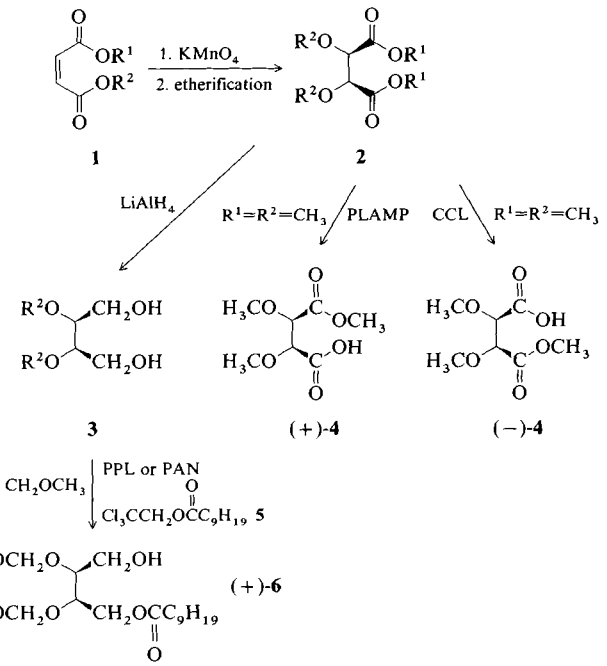

In addition, we have converted the diesters **2** with lithium aluminum hydride into the diols **3** and again carried out a screening—in this case of the enzymatic nonacylation—the following result being the most favorable: by reaction of the readily cleavable acetalic methoxymethyl protecting group in **3** ($R^2 = CH_2OCH_3$) with 2,2,2-trichloroethyl deconoylate **5** in the presence of PPL or pancreatin from porcine pancreas (PAN, Fluka), an acylation of the pro-*R*-CH_2OH group leads to (+)-**6**.[10] The *ee* value is 95% and the chemical yield 90%. The determination of the absolute configuration of (+)-**6** was achieved by conversion into D-(−)-erythrose in three steps: (+)-**6** was converted with pyridinium chromate (PDC) into the aldehyde **7** (brownish oil), which, without further purification was hydrolyzed with PPL at pH = 7 in phosphate buffer to the mixture of diastereomers **8** (colorless liquid, purified by chromatography on silica gel 60 with petroleum ether/ether 1:1, $[\alpha]_D = +9.00$, $c = 1.3$, in $CHCl_3$). Reaction of **8** with HCl/methanol afforded D-(−)-

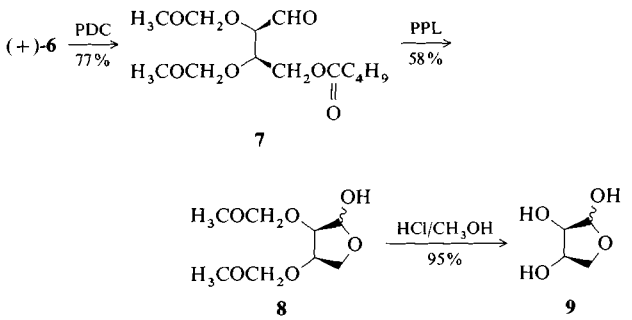

erythrose, whose rotation, ^{1}H-NMR spectrum, and TLC retention time (mixed chromatogram) were identical with authentic material. The *ee* value of (+)-**6** was determined via the diastereomeric Mosher effect.[11]

Experimental Procedure

All experiments were carried out on the 10 mmol scale.

Enzymatic hydrolysis: The diester **2**, $R^1 = R^2 = CH_3$ (10 mmol) was dissolved, emulsified or suspended in 0.1 N phosphate buffer (pH = 7.0, 30 mmol) and treated with 500 U of the enzyme. During the reaction, the temperature and pH value were kept constant [thermostat and autotitrator (1.00 N NaOH), respectively]. The reaction mixture was worked-up when the reaction had come to a standstill, i.e. when no more sodium hydroxide was titrated. The mixture was first saturated with NaCl and continually extracted with ether at pH = 7.0 to remove any diester **2** that had been formed. The semiester was then continually extracted at pH = 4.0 (autotitrator, 2 N H_2SO_4). Finally, the organic phase was dried with $MgSO_4$ and freed from ether. The product could be used for further reactions without additional purification.

(+)-**6**: A mixture of 2.10 g of diol **3**, $R^2 = CH_2$-O-CH_3, 12 mL of 2,2,2-trichloroethyl decanoylate, and 2.0 g of PPL in 100 mL of anhydrous THF was stirred for 5 d at room temperature in the dark. The enzyme was then filtered off and the clear solution freed of THF. The residue was then subjected to column chromatography (silica gel 60; eluent: 1. petroleum ether/ether/triethylamine 200:100:1; 2. ether/triethylamine 200:1). Yield: 3.27 g (90%).

Received: July 30, 1990;
revised: October 24, 1990 [Z 4100 IE]
German version: *Angew. Chem. 103* (1991) 78

CAS Registry nmumbers:
2, 62182-40-5; **3** ($R^2 = CH_2OMe$), 131433-75-5; (−)-**4**, 131353-68-9; (+)-**4**, 127319-79-3; (+)-**6**, 131353-69-0; **7**, 131353-70-3; **8** (stereoisomer 1), 131353-71-4; **8** (stereoisomer 2), 131353-72-5; D-(−)-erythrose, 583-50-6.

[1] D. Seebach, E. Hungerbühler in R. Scheffold (Ed.): *Modern Synthetic Methods, Vol. 2*, Wiley, New York 1980, p. 91; D. Seebach, H. O. Kalinowski, B. Bastani, G. Crass, H. Daum, H. Dörr, N. P. DuPreez, V. Ehrig, W. Lauger, C. Nüssler, H. A. Oei, M. Schmidt, *Helv. Chim. Acta 60* (1977) 301; G. Adam, D. Seebach, *Synthesis 1988*, 373; H. J. Bestmann, T. Moenius, *Angew. Chem. 98* (1986) 10; *Angew. Chem. Int. Ed. Engl. 25* (1986) 994; H. J. Bestmann, D. Roth, *ibid. 102* (1990) 95 and *29* (1990) 90.

[2] W. Marckwald, L. Karczag, *Ber. Dtsch. Chem. Ges. 42* (1909) 1518.

[3] C. Tamm, P. Mohr, S. Waespe-Sarcevic, *Helv. Chim. Acta 66* (1983) 2501.

[4] Concerning the asymmetrization of other *meso* compounds with enzymes cf. [3] and J. B. Jones, I. J. Jacovac, *Org. Synth. 63* (1985) 10; M. Kunihara, K. Kamiyama, S. Kobayashi, M. Ohno, *Tetrahedron Lett. 26* (1985) 5831; G. M. Whitesides, C. H. Wong, *Angew. Chem. 97* (1985) 617; *Angew. Chem. Int. Ed. Engl. 24* (1985) 617.

[5] B. Zerner, D. J. Horgan, J. K. Storps, E. C. Webb, *Biochemistry 8* (1969) 2000; D. Seebach, M. Eberle, *Chimia 1986*, 315.

[6] The results with the more expensively purified porcine liver esterase (PLE) offered no advantages. Regarding enzymatic reactions with PLE, cf. M. Ohno, M. Otsuka, *Org. React. 37* (1989) 1.

[7] (+)-**4**: m.p. 55 °C; IR (KBr): $\tilde{\nu} = 1760$, 1730 cm^{-1} (CO); ^{1}H NMR (400 MHz, $CDCl_3$): $\delta = 3.54$, 3.57 (2s, H, $CHOCH_3$), 3.80 (s, 3H,

CO_2CH_3), 4.28 (AB, J_1 = 13.7 Hz, J_2 = 3.0 Hz, 2H, C*H*), 9.61 (s, 1H, COOH); ^{13}C NMR (25.2 MHz, $CDCl_3$): δ = 52.2 (CO_2CH_3), 59.3, 59.5 ($CHOCH_3$) 81.2 (CH), 168.9 (CO_2CH_3), 172.4 (COOH); MS: *m/z* 192 ($M^{\oplus}$); $[\alpha]_D$ = + 6.25° (*c* = 7.2, $CHCl_3$).

[8] K. Freudenberg, *Ber. Dtsch. Chem. Ges. 66* (1933) 177; J. H. Brewster, *J. Am. Chem. Soc. 81* (1959) 5475, 5483, 5493; K. Freudenberg, F. Brauns, H. Siegel, *Ber. Dtsch. Chem. Ges. 56* (1923) 193; K. Freudenberg, L. Markert, *ibid. 58* (1925) 1753; K. Freudenberg, *Monatsh. Chem. 85* (1954) 537; D. H. R. Barton, W. Klyne, *Chem. Ind. (London) 1948*, 755.

[9] H. J. Kleiner, H. Wissmann, *Angew. Chem. 92* (1980) 129; *Angew. Chem. Int. Ed. Engl. 19* (1980) 133.

[10] (+)-**6**: oil (purified chromatographically on silicagel 60, eluted with petroleum ether/ether 2:1); IR: $\tilde{\nu}$ = 1735 cm^{-1} (CO); ^{1}H NMR (60 MHz, $CDCl_3$): δ = 0.85 (t, 3H, CH_2CH_3), 1.00–1.90 (m, 14H, $(CH_2)_7$), 2.35 (t, 2H, $COCH_2$), 3.20 (s, OH), 3.40 (s, 6H, OCH_3), 3.60–4.60 (m, 6H, $CHCH_2$), 4.75 (s, 4H, OCH_2O); ^{13}C NMR (25.2 MHz, $CDCl_3$): δ = 13.9, 22.5, 24.7, 29.1, 29.2, 31.7, 34.0 (7 signals, C_9H_{19}), 55.6 (CH_3O), 61.7 (CH_2OH), 63.1 (CH_2OCO), 74.5 ($CHCH_2OCO$), 79.0 ($CHCH_2OH$), 96.2, 96.6 (OCH_2O), 173.4 (CO); $[\alpha]_D$ = + 19.2° (*c* = 2.2, methanol).

[11] H. S. Mosher, J. A. Dale, D. L. Dull, *J. Org. Chem. 34* (1969) 2543.

Molecular and Ionic Hydrogen Isocyanide (CNH) Adducts with N-H···O- and "Super-Short" N-H···N-Hydrogen Bridges: Metal-Stabilized Hydrogen Bisisocyanides**

By *Eberhard Bär, Joachim Fuchs, Dirk Rieger, Francisco Aguilar-Parrilla, Hans-Heinrich Limbach,* and *Wolf P. Fehlhammer**

Short and super-short hydrogen bonds, particularly as occur in homonuclear molecule-ion associates AHA$^{\ominus}$ (A$^{\ominus}$ = anion base, e.g. Hal$^{\ominus}$) and BHB$^{\oplus}$ (B = neutral base, e.g. N-heterocycle), are currently a subject of intensive theoretical and experimental investigations.[1] Interest in H-bridged *cyanide* and *hydrogen cyanide* systems[2] may well originate from their capability of spontaneous aggregation and self-condensation to give biologically relevant secondary products $[HCN]_n$ (n, e.g., 2, 5(adenine),[3] and greater) rather than from mere bonding aspects. This property is in turn closely coupled with the question of chemical evolution.[4, 5]

Hydrogen isocyanide (HNC), which has only recently been discovered in interstellar clouds, is also connected with prebiotic organic synthesis.[6] We discovered the marked tendency of this acid to form hydrogen bonds during an attempted preparation of $[Cr(CO)_5CNH]$ in THF, when instead the sublimable (!) etherate **1** was obtained. On the strength of this finding we carried out directed syntheses of further adducts with cyclic ethers (e.g. **2**) and crown ethers (**3**, **4**), which selectively take up one or two hydrogen isocyanide complex molecules, respectively.[7] In the case of **2** we determined X-ray crystallographically an N(H)···O distance of 2.877(11) Å,[8] whose very small difference from the sum of the van-der-Waals radii of nitrogen and oxygen (2.93 Å) is indicative of only a weak H bond. Due to the low quality of the intensity data, however, this value should be regarded with some reservation.

We expected to find stronger hydrogen bonding in adducts of the (at least formally) symmetric type AHA$^{\ominus}$ **5** (A$^{\ominus}$ = $[Cr(CN)(CO)_5]^{\ominus}$), which should be formed from pentacarbonyl(hydrogen isocyanide)chromium and its conjugate base. It has long been known that such structural units are present in the crystal lattice of "cyanometallic acids" and determine their coordination polymeric structure.[9] The N(H)···N distances in this type of bridge are very short; the shortest distance measured so far is that in the highly symmetric, three-dimensionally H-cross-linked $H_3[Co(CN)_6]$ (2.582(4) Å).[10] In this connection, the prediction of a surprisingly high stability for $[NCHCN]^{\ominus}$[2c] warrants attention, which might even be surpassed by the stability of the "iso form" $[CNHNC]^{\ominus}$.[11]

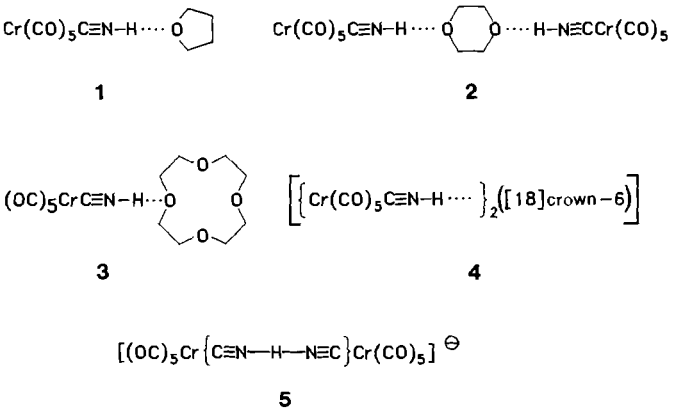

Indeed, yellow (**5a**, $ER_4 = NEt_4$) or colorless (**5b**, $ER_4 = AsPh_4$) products having all the properties required of the *metal-stabilized hydrogen bisisocyanide ion* **5** crystallize from ether-layered CH_2Cl_2-solutions of equimolar amounts of $[Cr(CO)_5CNH]$ and $(ER_4)[Cr(CN)(CO)_5]$. In the first place, the ν(NH) absorption bands are broadened and shifted to long wavelengths such as to develop an absorption continuum which superimposes the IR region from about 1800 to 300 cm^{-1}. Also the downfield shifts of the ^{1}H-NMR signals of the hydrogen bridge protons (δ = 11.2 (**5a**), 11.9 (**5b**)), which are larger than those of the NH···O adducts **1**–**4** by a good 2 ppm, point to strong hydrogen bonding. That the hydrogen bonds, moreover, are symmetrical, is indicated by the appearance of only one set of ^{13}C-NMR res-

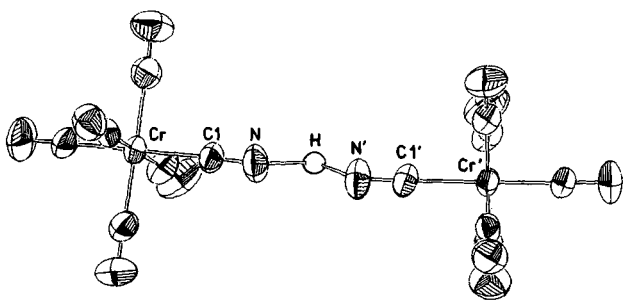

Fig. 1. Structure of **5** in crystals of **5b** (ORTEP, ellipsoids at the 50% probability level). Space group $P2/n$, a = 11.295(2), b = 6.817(1), c = 24.476(6) Å, β = 100.85(1)°, V = 1850.9 Å^3, Z = 2; 2824 measured reflections, 2552 observed ($I > 2\sigma(I)$), 271 refined parameters, R = 0.056 (R_w = 0.054). Selected bond lengths [Å] and angles [°]: Cr–C(O)$_{trans}$ 1.847(6), Cr–C(O)$_{cis}$ (average value) 1.894, Cr–C1 2.012(6), C1–N 1.167(8), N···N' 2.569(7); Cr–C1–N 178.8(5). The H position taken from the difference Fourier synthesis and refined (y coordinate) is associated with a high temperature factor and is therefore not reliable (cf. text).

[*] Prof. Dr. W. P. Fehlhammer, Dr. E. Bär, Prof. Dr. J. Fuchs, D. Rieger
Institut für Anorganische und Analytische Chemie der Freien Universität
Fabeckstrasse 34–36, W-1000 Berlin 33 (FRG)
F. Aguilar-Parrilla, Prof. Dr. H.-H. Limbach
Institut für Physikalische Chemie der Universität Freiburg (FRG)

[**] Chemistry of Hydrogen Isocyanide, Part 7. This work was supported by the Deutsche Forschungsgemeinschaft, the Fonds der Chemischen Industrie, and the Graduiertenkolleg "Synthese und Strukturaufklärung niedermolekularer Verbindungen.—Part 6: D. Rieger, F. E. Hahn, W. P. Fehlhammer, *J. Chem. Soc. Chem. Commun. 1990*, 285.

onance signals ($\delta = 157.4$ s (CN), 216.5 CO_{cis}), 219.1 (CO_{trans}) and by the band-deficient IR and Raman spectra.

The X-ray structure analysis of **5b** (Fig. 1)[12] confirms the strong bridge bond: the N(H)···N distance of 2.569(7) Å is even less than that in $H_3[Co(CN)_6]$. Since the bridge H-atom could not be localized with certainty, however, the question of its symmetrical arrangement had to remain open for the time being. In any case, no decision can be made as to whether the bridge H atom moves in a single or a double minimum potential, because of the crystallographic symmetry element (C_2) coinciding with the bridge midpoint.[13, 10b]

The method of choice for obtaining detailed information about proton motions in NH···N hydrogen bridges is currently high-resolution solid-state ^{15}N-CPMAS-NMR spectroscopy (^1H cross polarization (CP), sample rotation about the magic angle (MAS)) with ^1H decoupling.[14] The spectra[15] of the reference compounds $[Cr(CO)_5C^{15}NH]$ and $NnPr_4$ $[Cr(C^{15}N)(CO)_5]$ measured at 25 °C each show one singlet, at $\delta \approx 135$ and 273, respectively. In contrast, the two nitrogen atoms of ^{15}N-labeled **5b** (= **5b'**) give rise to only *one* line at $\delta = 193$ ($\nu_{1/2} = 38.5$ Hz), i.e. they are (as to be expected from the X-ray structure analysis of **5b**) chemically equivalent. The value of $\delta = 193$ is reconcilable both with a symmetrical double minimum potential with small energy barrier as well as with a single minimum potential for the proton motion. Surprisingly, however, two signals are observed at $\delta = 209$ ($\nu_{1/2} = 50.2$ Hz) and 178 ($\nu_{1/2} = 53.5$ Hz) in the case of **5a'** (= ^{15}N-labeled **5a**). This means that the established chemical equivalence of the two nitrogen atoms in **5b'** does not apply here due to interactions between the ions; the average distances between the bridge H-atom and the two nitrogen atoms are no longer identical. Measurements at several temperatures showed that the signal splitting observed in the case of **5a'**, in contrast to that of other NH···N hydrogen bridges perturbed by intermolecular interactions, is temperature independent. We regard this as a first indication that the proton motion in **5a** is a result of an unsymmetrical single minimum potential.

The handicap of an enforced crystal symmetry (see **5b**) does not apply in the heterodinuclear *neutral* adduct **6** (diphos = bis(diphenylphosphino)ethane, for which one

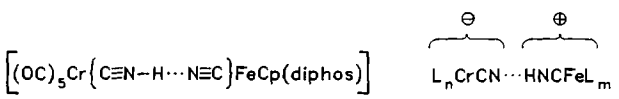

6 **7**

naturally does not expect an ideally symmetrical H-bridge either. Nevertheless, it is surprising at first sight, how asymmetrically the unequivocally established bridge H-atom here is located between the very close cyano N atoms (Fig. 2).[12] In view of the charge separation, which should effect a shift of the bridge H-atom in the direction of the iron atom (see **7**), the structural variety of the hydrogen bisisocyanide **6** contrary to **5** does not, however, seem unlikely. Both the asymmetry and the strength of this NH···N bond are also reflected in the IR and NMR spectra of **6**, which show markedly separated ν(CN) bands [(Nujol): $\tilde{\nu} = 2122$ s, 2070 w cm^{-1}] and CN signals [$\delta(^{13}C) = 156.9$ (s, CrCN), 161.7 (t, $J = 30.5$ Hz, FeCN)] besides the characteristic NHN absorption continuum ($\tilde{\nu} = 1300-300\ cm^{-1}$) and downfield shift ($\delta(^1H) = 11.4$).

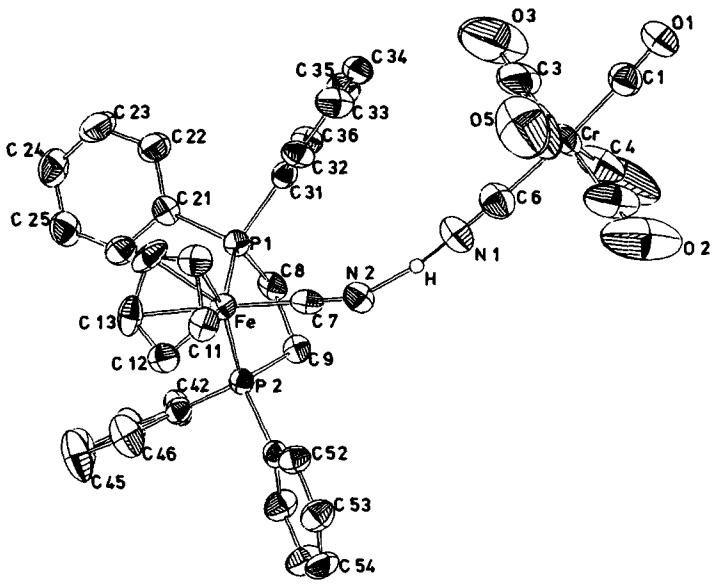

Fig. 2. Molecular structure of **6** (ORTEP), ellipsoids at the 50% probability level). Space group $P\bar{1}$, $a = 8.919(2)$, $b = 15.617(4)$, $c = 15.809(5)$ Å, $\alpha = 111.68(2)$, $\beta = 101.88(2)$, $\gamma = 96.49(2)°$, $V = 1958.65$ Å^3, $Z = 2$; 4950 measured reflections, 4188 observed ($I > 2\sigma(I)$), 593 refined parameters, $R = 0.062$ ($R_w = 0.064$). Selected bond lengths [Å] and angles [°]: Cr–C1 1.846(11), Cr–$C(O)_{cis}$ (mean value) 1.854, Cr–C6 2.025(12), C6-N1 1.155(15), N1-H 1.17(14), H-N2 1.40(14), N1···N2 2.557(12), N2-C7 1.164(11), C7-Fe 1.855(9); Fe-C7-N2 177.9(6), C7-N2-H 157(4), N2-H-N1 171(9), H-N1-C6 178(5), N1-C6-Cr 178.5(8).

Experimental Procedure

3: Freshly sublimed $[Cr(CO)_5CNH]$ [17] (0.22 g, 1.00 mmol) was dissolved in ca. 5 mL of [12]crown-4, the excess ether removed in a vacuum, and the residue reprecipitated from CH_2Cl_2/*n*-hexane at −20 °C. There remained 265 mg (67%) of colorless crystals which melt without decomposition at 50 °C. IR (polyoil): $\tilde{\nu}$ [cm^{-1}] = 3200–2400 s, br. (NH···O) 2123, 2077 m, 2053 m–s, 1946 vs, br. (ν(CN) + ν(CO)); Raman (CH_2Cl_2): $\tilde{\nu}$ [cm^{-1}] = 2094 m,sh,p, 2088 s,p, 2036 s,p, 1993 s,dp, 1943 m,br.,dp (ν(CN) + ν(CO)); 270-MHz ^1H NMR ($CDCl_3$, 25 °C): $\delta = 9.2$ (s, br., NH···O), 3.6 (s, 16H, CH_2). sh = shoulder, p = polarized, dp = depolarized.

5b: A solution of $AsPh_4[Cr(CN)(CO)_5]$ (0.60 g, 1.00 mmol) in CH_2Cl_2 (20 mL) was filtered through a cellulose filter and added dropwise to a solution of freshly sublimed $[Cr(CO)_5CNH]$ (0.22 g, 1.00 mL) in CH_2Cl_2 (20 mL). The reaction solution was then carefully layered with ca. 30 mL of diethyl ether and cooled to −78 °C. A pale yellow solid was formed (0.45 g, 55% yield; m.p. 103 °C (decomp.)), which was collected on a glass frit and dried in a stream of argon.

6: A solution of $[Cr(CO)_5CNH]$ (220 mg, 1.00 mmol) and [Fe(CN)(Cp)diphos] [18] (545 mg, 1.00 mmol) in CH_2Cl_2 (20 mL) was layered with petroleum ether (40–60 °C). On cooling to −20 °C orange-red crystals were formed in about 80% yield. M.p. 150 °C (decomp.).

All the new compounds gave correct elemental analyses.

Received: October 4, 1990 [Z 4114 IE]
German version: *Angew. Chem. 103* (1991) 88

CAS Registry numbers:
2, 131130-23-9; **3**, 131105-42-5; **5a**, 131105-43-6; **5b**, 131105-45-8; **6**, 131105-44-7; $[Cr(CO)_5CNH]$, 15040-33-2; $NEt_4[Cr(CN)(CO)_5]$, 82675-16-9; $AsPh_4[Cr(CN)(CO)_5]$, 131105-46-9; [Fe(CN)(Cp)diphos], 70460-15-0; [12]crown-4, 294-93-9.

[1] Cf., e.g. a) J. Emsley, D. J. Jones, J. Lucas, *Rev. Inorg. Chem. 3* (1981) 105; b) B. S. Ault, *Acc. Chem. Res. 15* (1982) 103; c) D. Mootz, K. Bartmann, *Angew. Chem. 100* (1988) 424; *Angew. Chem. Int. Ed. Engl. 27* (1988) 391; d) H. J. Berthold, W. Preibsch, E. Vonholdt, *ibid. 100* (1988) 1581 and *27* (1988) 1527.

[2] a) M. Meot-Ner, *J. Am. Chem. Soc. 100* (1978) 4694; b) G. L. Johnson, L. Andrews, *ibid. 105* (1983) 163; c) J. W. Larson, T. B. McMahon, *Inorg. Chem. 23* (1984) 2029.

[3] F. Seel, M. von Blon, A. Dessauer, *Z. Naturforsch. B37* (1982) 820.

[4] K. Dose, H. Rauchfuss: *Chemische Evolution und der Ursprung lebender Systeme*, Wissenschaftliche Verlagsgesellschaft, Stuttgart 1975, p. 105f.
[5] J. P. Ferris, W. J. Hagan, Jr., *Tetrahedron 40* (1984) 1093.
[6] a) G. Winnewisser, *Top. Curr. Chem. 99* (1981) 39; b) D. W. McPherson, M. L. McKee, P. B. Shevlin, *J. Am. Chem. Soc. 105* (1983) 6493.
[7] Diverse $[Cr(CO)_5CNH]$ adducts with acyclic diethers are reported in a patent: R. E. Maginn, US Pat. 3136798 (1964), Ethyl Corporation, New York, NY.
[8] Crystallographic data of **2**: STOE four-circle diffractometer, $Cu_{K\alpha}$ radiation, nickel filter; monoclinic; space group $P2_1/n$; $a = 17.376(3)$, $b = 10.742(3)$, $c = 5.898(1)$ Å; $\beta = 94.54(2)°$; $\varrho_{calc} = 1.59$, $\varrho_{exp} = 1.58$ g cm^{-3}; $Z = 2$. 1293 independent reflections, 1134 observed ($F > 2\sigma(F)$). For the refinement however, only reflections with odd l and the (specially scaled) equatorial reflections were used, since the crystal was twinned, and, for $l = 2n$, the h,k,l reflections of one twin coincided with the $h + l/2$, $-k,-l$ reflections of the other. $R = 0.075$.
[9] a) D. F. Evans, D. Jones, G. Wilkinson, *J. Chem. Soc. 1964*, 3164; W. Beck, H. Smedal, *Z. Naturforsch. B 20* (1965) 109; c) H. U. Güdel, *J. Chem. Phys. 56* (1972) 4984.
[10] a) R. Haser, B. Bonnet, J. Roziere, *J. Mol. Struct. 40* (1977) 177; b) similarly short and even slightly shorter N(H)···N distances are found in the proton sponges. However, in this case they are *intra*molecular H-bridges: H. A. Staab, T. Saupe, *Angew. Chem. 100* (1988) 895; *Angew. Chem. Int. Ed. Engl. 27* (1988) 865; cf. also R. W. Alder, *Chem. Rev. 89* (1989) 1215.
[11] CNH is an essentially stronger proton donor than HCN: P. Kollman, J. McKelvey, A. Johansson, S. Rothenberg, *J. Am. Chem. Soc. 97* (1975) 955.
[12] **5b(6)**: STOE four-circle diffractometer, $Cu_{K\alpha}$ ($Mo_{K\alpha}$) radiation, $5° \leq 2\theta \leq 120°$ ($4° \leq 2\theta \leq 50°$); ω scan; structure solutions by direct methods. Programs used: X-ray 76, Multan-77, ORTEP. Further details of the crystal structure investigations are available on request from the Fachinformationszentrum Karlsruhe, Gesellschaft für wissenschaftlich-technische Information mbH, W-7514 Eggenstein-Leopoldshafen 2 (FRG), on quoting the depository number CSD-54867, the names of the authors, and the journal citation.
[13] Cf. A. Novak, *Struct. Bonding (Berlin) 18* (1974) 177.
[14] Cf. J. A. S. Smith, B. Wehrle, F. Aguilar-Parrilla, H.-H. Limbach, M. C. Foces-Foces, F. H. Cano, J. Elguero, A. Baldy, M. Pierrot, M. M. T. Khurshid, J. B. Larcombe-McDuall, *J. Am. Chem. Soc. 111* (1989) 7304, and references cited therein.
[15] The ^{15}N-CPMAS-NMR spectra were recorded with a Bruker CXP100 spectrometer (proton resonance frequency 90.02 MHz) and a CPMAS probe head manufactured by Doty-Scientific, Columbia, USA. Rotation frequency of the 7-mm rotor between 2.5 and 3.5 kHz. Spectra free of rotation sidebands were thus obtained. The chemical shifts of the ^{15}N nuclei are referred to external $^{15}NH_4Cl$.
[16] For example: H.-H. Limbach, B. Wehrle, H. Zimmermann, R. D. Kendrick, C. S. Yannoni, *J. Am. Chem. Soc. 109* (1987) 929; B. Wehrle, H. Zimmermann, H.-H. Limbach, *Ber. Bunsenges. Phys. Chem. 91* (1987) 941; B. Wehrle, H. Zimmermann, H.-H. Limbach, *J. Am. Chem. Soc. 110* (1988) 7014.
[17] W. P. Fehlhammer, W. A. Herrmann, K. Öfele in G. Brauer (Ed.): *Handbuch der Präparativen Anorganischen Chemie, Vol. III*, 3rd Edit., Ferdinand Enke Verlag, Stuttgart 1981.
[18] G. J. Baird, S. G. Davies, *J. Organomet. Chem. 262* (1984) 215.

Formation of a *trans*-1,2,4,5-Tetraphosphatricyclo-[3.1.0.0^{2,4}]hexane by [2+2] Cyclodimerization of a 3*H*-Diphosphirene**

By *Edgar Niecke*,* *Rainer Streubel*, and *Martin Nieger*

Diazirines exist only in the 3*H* form **II** [1,2] and are widely used as precursors of electrophilic carbenes.[2] On the other hand, only the 1*H* isomer **III**, which corresponds to **I** and was recently obtained by phosphanediyl transfer starting from a halogen(silyl)phosphane and a phosphaalkyne,[3] is known for the homologous phosphorus compounds. Our investigations in this area were motivated by the possibility of preparing a 3*H*-diphosphirene **IV**, isomeric to **III**, in a corresponding way from an α-bifunctional 1,2-diphospha-2-propene(halogen(silyl)phosphinomethylenephosphane).

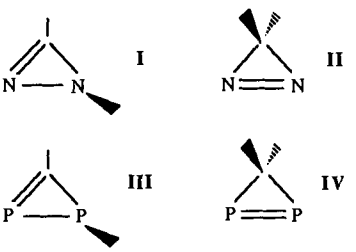

Reaction of the persilylated 1,2-diphospha-2-propene **1**[4] with hexachloroethane under mild conditions[5] results in elimination of chlorotrimethylsilane and formation of a product having the analytical composition of diphosphirene **5** but twice its molecular mass. The spectroscopic data all indicate the formation of the tricyclic system **6**, a cyclodimer of **5**.

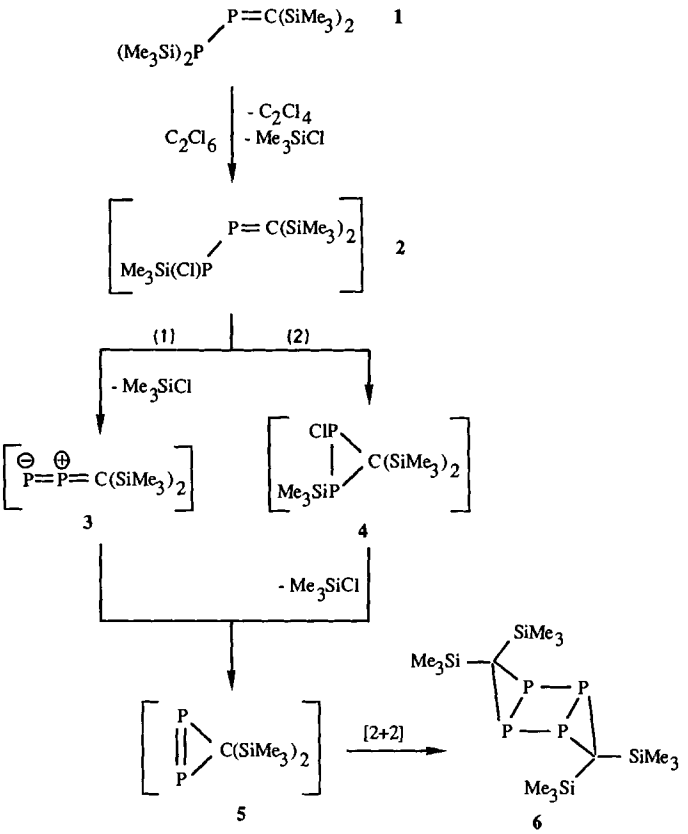

Two pathways are conceivable for the formation of the diphosphirene intermediate **5**: (1) an α elimination of chlorotrimethylsilane from the 1,2-diphospha-2-propene intermediate **2** to give **3**, the diphospha analogue of a diazaalkane, followed by cycloisomerization of **3** to afford **5**—an isomerization similar to the vinylcarbene/cyclopropene rearrangement;[6] (2) a 1,2-chloro shift accompanied by cyclization to give the β-functional diphosphirane **4**, which subsequently loses chlorotrimethylsilane to yield **5**. The recently observed diphospha-2-propene/diphosphirane isomerization[7] makes the second pathway equally plausible. The reaction step leading from **5** to **6** is typical of diphosphenes with *Z* configurations;[8] for cyclopropene, this process is thermodynamically favored and can be initiated by catalysts.[9]

[*] Prof. Dr. E. Niecke, Dr. R. Streubel, Dr. M. Nieger
Anorganisch-chemisches Institut der Universität
Gerhard-Domagk-Strasse 1, W-5300 Bonn 1 (FRG)

[**] This work was supported by the Fonds der Chemischen Industrie.

The constitution of **6** was established by elemental analysis, the mass spectrum,[10] the relatively high-field position of the ^{31}P NMR signal ($\delta = -87.6$), and the appearance of two sets of pseudoquintets for the trimethylsilyl groups in the ^{1}H and ^{13}C NMR spectra.[11] The expected steric crowding of the molecule in *syn* form with two silyl groups in "flagpole" position, as well as the resulting repulsion between the lone pairs on the phosphorus atoms, favors an *anti* conformation for **6**. Its existence was confirmed by an X-ray structure analysis[12] (Fig. 1).

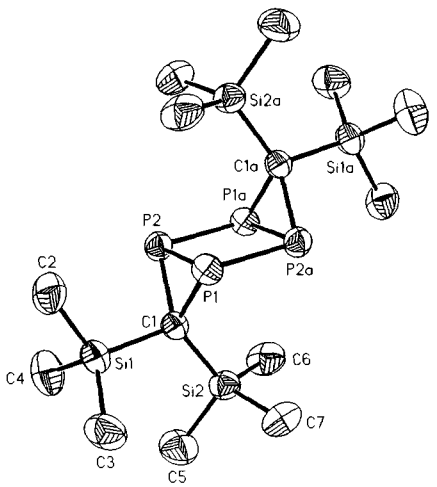

Fig. 1. Molecular structure of **6**. Important bond lengths [pm] and angles [°]: P1-P2 220.4(1), P1-P2a 224.5(1), P1-C1 187.1(3), P2-C1 187.3(3), C1-Si2 189.8(3), C1-Si1 192.4(3); P1-P2-P1a 90.2(1), P2-P1-P2a 89.8(1), P1-P2-C1, 53.9(1), P2-P1-C1 54.0(1), P1-C1-P2 72.1(1), C1-P1-P2a 102.0(1), C1-P2-P1a 102.3(1), P2-C1-Si1 104.8(1), P2-C1-Si2 129.0(1), P1-C1-Si1 106.3(1), P1-C1-Si2 121.4(1); Interplanar angle between the P1–P2–P1a–P2a and P1–P2–C1 planes 105°; angle between the P1–P2–C1 plane and the C1–Si2 bond 135°.

The molecule possesses C_1 symmetry in the solid state. The bonding in the diphosphirane framework, which exhibits an interplanar angle of 105° with respect to the planar P_4 framework,[13] is similar to that in the correspondingly substituted 1,2,3-triphosphabicyclo[1.1.0]butanes.[14] However, the two P–P distances (220.4(1) and 224.5(1) pm) are significantly different; the longer distance points to the formation of the cycloadduct from two molecules of **5**. Also noteworthy are the P–C–Si_{endo} angles (129.0(1) and 121.4(1)°), which are larger than the P–C–Si_{exo} angles (104.8(1) and 106.3(1)°). Two distinctly different C1–Si distances (192.4(3) and 189.8(3) pm) are therefore found.

Further investigations are necessary to determine to what extent this finding can be interpreted in terms of a polarization of the molecular structure toward formation of a diphosphiranylium ion in the solid state. The same holds true for the possible complex stabilization of the 3*H*-diphosphirene **5**.

Received: August 14, 1990 [Z 4134 IE]
German version: *Angew. Chem. 103* (1991) 103

CAS Registry numbers:
1, 114032-10-9; **6**, 130830-95-4; C_2Cl_6, 67-72-1.

[1] a) S. R. Paulsen, *Angew. Chem. 72* (1960) 781; b) A 1*H*-diazirine was recently assumed on the basis of NMR spectroscopy as an intermediate in a nitrilimine/diazaoalkane rearrangement. M. Granier, A. Baceiredo, H. Grützmacher, H. Pritzkow, G. Bertrand, *ibid. 102* (1990) 671; *Angew. Chem. Int. Ed. Engl. 29* (1990) 659.

[2] Reviews: a) M. Regitz: *Diazoalkane*, Thieme Stuttgart 1977; b) C. Wentrup, *Methoden Org. Chem. (Houben Weyl; Carbene und Carbine)* 4th ed.

[3] E. Niecke, R. Streubel, M. Nieger, D. Stalke, *Angew. Chem. 101* (1989) 1708; *Angew. Chem. Int. Ed. Engl. 28* (1989) 1673.

[4] K. Dunker, *Dissertation*, Universität Bonn 1986.

[5] *Experimental Procedure:* **6**: A solution of hexachloroethane (0.8 g, 3.2 mmol) in 2.5 mL of toluene was added dropwise to a solution of **1** (1.2 g, 3.2 mmol) in 2.5 mL of toluene at 0 °C. The resulting reaction mixture was stirred for 2 h at 0 °C and then for 4 h at 35 °C. After removal of the volatiles under vacuum, the remaining oily product, 95% of which is **6**, was dissolved in a small amount of *n*-pentane and crystallized at −80 °C. Yield 0.23 g (32%) of an orange-red product. M.p. 143–145 °C.

[6] Reviews: a) W. M. Jones, U. H. Brinker in A. P. Marchand, R. E. Lehr (Eds.): *Pericyclic Reactions, Vol. 1*, Academic Press, New York 1977, p. 126; b) B. Halton, M. G. Banwell in Z. Zappoport (Ed.): *The Chemistry of the Cyclopropenyl Group*, Wiley, New York 1987, p. 1231.

[7] R. Streubel, E. Niecke, *Chem. Ber. 123* (1990) 1245; R. Streubel, *Dissertation*, Universität Bonn 1990.

[8] E. Niecke, B. Kramer, M. Nieger, *Angew. Chem. 101* (1989) 217; *Angew. Chem. Int. Ed. Engl. 28* (1989) 215.

[9] P. Binger, H. M. Büch, *Top. Curr. Chem. 135* (1987) 88.

[10] MS (70 eV): *m/z* 440 ($M^{\oplus}$, 15%), 425 ($M^{\oplus}$ − Me, 2), 367 ($M^{\oplus}$-$SiMe_3$, 2), 221 ($M^{\oplus}/2$ + H, 4), 73 ($SiMe_3^{\oplus}$, 100).

[11] ^{1}H NMR (80 MHz, C_6D_6, 25 °C, TMS): $\delta = 0.10$ (m_c, 18H, $J_{eff} = 0.9$ Hz; $SiMe_3$), 0.64 (m_c, 18H, $J_{eff} = <0.2$ Hz; $SiMe_3$). $^{13}C\{^{1}H\}$ NMR (100 MHz, C_6D_6, 25 °C, TMS): $\delta = 0.2$ (m_c, $J_{eff} = 3.7$ Hz; SiC_3), 7.2 (m_c, $J_{eff} = 2.4$ Hz; SiC_3); the signals for the ring C atoms could not be identified.

[12] X-ray structure analysis of **6** ($C_{14}H_{36}Si_4P_4$): $M_r = 440.7$; yellow crystals ($0.3 \times 0.3 \times 0.4$ mm); space group $P2_1/n$ (No. 14); $a = 651.6(1)$, $b = 1151.5(2)$, $c = 1695.1(3)$ pm, $\beta = 97.00(1)°$; $V = 1.262$ nm^3; $Z = 2$; $\varrho_{calcd} = 1.16$ g cm^{-3}; $\mu(Mo_{K\alpha}) = 0.48$ mm^{-1}; 2213 symmetry-independent reflections ($2\theta_{max} = 50°$), of which 1837 with $F > 4\sigma(F)$ were used for structure solution (direct methods) and refinement (100 parameters); P, Si, and C atoms refined anisotropically, H atoms (localized by difference electron density determination) refined with a "riding" model. $R = 0.040$ ($R_w = 0.044$, $w^{-1} = \sigma^2(F) + 0.0005\,F^2$). Further details of the crystal structure investigation may be obtained from the Fachinformationszentrum Karlsruhe, Gesellschaft für wissenschaftlich-technische Information mbH, W-7514 Eggenstein-Leopoldshafen 2 (FRG), on quoting the depository number CSD-54796, the names of the authors, and the journal citation.

[13] A planar P_4 framework is also present in the [2+2] cyclodimer of a 1,2-dihydro-1-azatriphosphete: E. Niecke, O. Altmeyer, M. Nieger, F. Knoll, *Angew. Chem. 99* (1987) 1299; *Angew. Chem. Int. Ed. Engl. 26* (1987) 1250.

[14] a) R. Appel, B. Niemann, M. Nieger, *Angew. Chem. 100* (1988) 957; *Angew. Chem. Int. Ed. Engl. 27* (1988) 957; b) E. Niecke, O. Altmeyer, M. Nieger, *J. Chem. Soc. Chem. Commun. 1988*, 945.

Metal Carbonyl Complexes of Sapphyrins**

By *Anthony K. Burrell, Jonathan L. Sessler,* Michael J. Cyr, Ellen McGhee*, and *James A. Ibers**

Sapphyrin is a 22 π-electron pentapyrrolic "expanded porphyrin".[1] It has an N-center radius of about 2.7 Å. Consequently, one can anticipate a rich organometallic chemistry of sapphyrins, a chemistry that should differ from that of the smaller tetrapyrrolic porphyrins. Nevertheless, only a few metal complexes have been reported[1a] and these involve

[*] Prof. J. L. Sessler, Dr. A. K. Burrell, M. J. Cyr
Department of Chemistry, University of Texas
Austin, TX 78712 (USA)
Prof. J. A. Ibers, E. McGhee
Department of Chemistry, Northwestern University
Evanston, IL 60208 (USA)

[**] This work was supported by the Texas Advanced Research Program (*J. L. S.*, grant number 1581) and by the NIH (*J. A. I.*, Grant HL 13157). *J. L. S.* also thanks the NSF for a Presidential Young Investigator Award (1986), the Alfred P. Sloan Foundation for a Research Fellowship (1989–1991), and the Camille and Henry Dreyfus Foundation for a Teacher-Scholar Award (1988–1922). *J. L. S., A. K. B.*, and *M. J. C.* are grateful to Prof. *E. Vogel*, Cologne, for the gift of a bipyrrole sample used to prepare sapphyrin **1a**.

primarily first-row transition metals with characterization limited to visible spectroscopy and mass spectrometry. The paucity of metal complexes of sapphyrin probably results from the difficulties associated with its preparation. We recently reported a convenient synthesis for sapphyrin,[2] which has enabled us to initiate studies of its organometallic chemistry. We expected second- and third-row transition metals to be the most promising for initial study, with metal carbonyls being particularly attractive owing to their successful use in the porphyrin series.[3]

When $[\{RhCl(CO)_2\}_2]$ and $[IrCl(CO)_2(py)]$ were allowed to react with the free-base sapphyrin macrocycles, H_3sap[4] (**1**), no evidence for "in-plane" products was obtained (Scheme 1). However, a wide variety of new complexes did result. For instance, addition of 0.5 equivalent of $[\{RhCl(CO)_2\}_2]$ or 1 equivalent of $[IrCl(CO)_2(py)]$ to a solution of **1** in CH_2Cl_2 containing a small amount of NEt_3[5] affords $[Rh(CO)_2(H_2sap)]$ (**2**) or $[Ir(CO)_2(H_2sap)]$ (**3b**).[6] During isolation and purification, **2** and **3b** are protonated to form the cationic complexes $[Rh(CO)_2(H_3sap)]^{\oplus}$ (**4**) and $[Ir(CO)_2(H_3sap)]^{\oplus}$ (**5b**).[6] The structures shown for **4** and **5b** (Scheme 1) were anticipated on spectroscopic grounds and were confirmed in a crystal structure determination of $[Ir(CO)_2(H_3sap)]Cl$[7] (Fig. 1). The ^1H NMR spectrum of **4**, for instance, indicates the presence of an unsymmetrical system. Four methyl signals along with four *meso*-proton signals are evident in the $\delta = 4.11-3.68$ and $\delta = 11.44-10.98$ regions, respectively. In addition, the three pyrrolic NH protons appear as three distinct signals at high field ($\delta = -2.60$, -2.71, -3.22), as would be expected for such an unsymmetrical protonated complex.

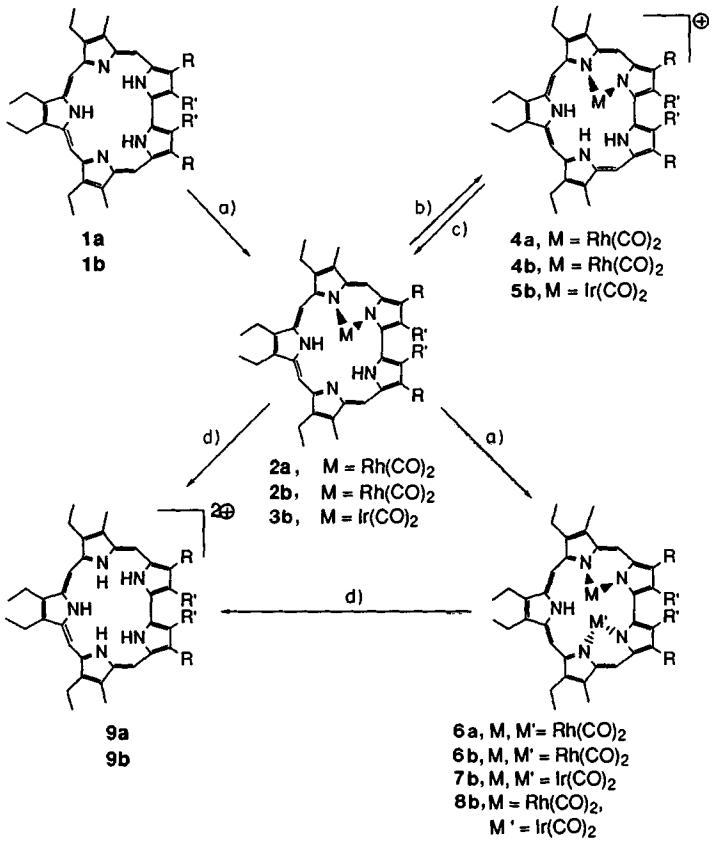

Scheme 1. Synthesis of sapphyrin complexes. a) $[\{RhCl(CO)_2\}_2]$, NEt_3 or $[IrCl(CO)_2(py)]$, NEt_3; b) silica gel; c) NEt_3; d) HCl. **a**, R = $CH_2CH_2CH_3$, R' = H; **b**, R = CH_2CH_3, R' = CH_3.

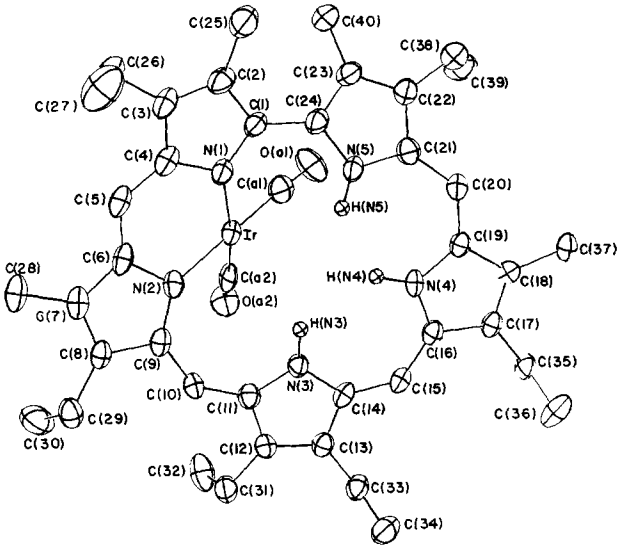

Fig. 1. Structure of $[Ir(CO)_2(H_3sap)]^{\oplus}$ (**5b**-Cl). The labeling scheme is shown. Here and in Figure 2 the 50% ellipsoids are shown, and all hydrogen atoms, save those in the core, are omitted for the sake of clarity.

Treatment of **2** with a further molar equivalent of $[\{RhCl(CO)_2\}_2]$ or reaction of **1** with an excess of $[\{RhCl(CO)_2\}_2]$ gives $[\{Rh(CO)_2\}_2(Hsap)]$ (**6**).[6] Similar chemistry in the iridium system leads to **7b**. An interesting feature of this step-by-step addition of metals is that the formation of a heterobimetallic complex is easily achieved. Either addition of $[IrCl(CO)_2(py)]$ to **2** or of $[\{RhCl(CO)_2\}_2]$ to **3b** results in the rapid formation of $[\{Ir(CO)_2\}\{Rh(CO)_2\}(Hsap)]$ (**8b**).[6] The structures shown for the complexes **6**–**8** (Scheme 1) were determined by spectroscopic means and were confirmed by a crystal structure determination of **6a** (Fig. 2).[8]

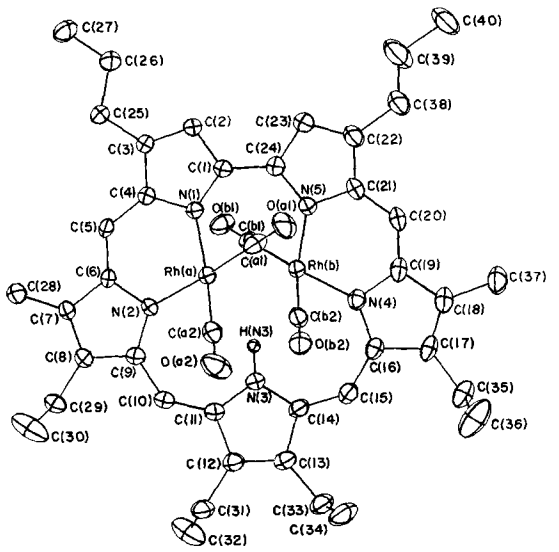

Fig. 2. Structure of $[\{Rh(CO)_2\}_2(Hsap)]$ (**6a**).

During the course of the reaction converting **1** into **4** via **2**, the position of the Soret-like band in the UV/VIS spectrum changes from approximately 450 nm to about 480 nm. The resultant changes in the ^1H NMR spectrum are again

consistent with the proposed structure, notably the return to C_2 symmetry. The addition of a second rhodium dicarbonyl fragment and formation of **6** causes this Soret-like band to shift still further to the red, to about 500 nm. The structures of **5b**-Cl and **6a** (Fig. 1 and 2, respectively) are similar to those of $[\{Rh(CO)_2\}_2(OEP)]$[9] and $[\{Rh(CO)_2\}_2(NMC)]$ (NMC = *N*-methylcorrole)[10] in that each metal center bridges an imine and an amine nitrogen atom. The Rh–N distances range from 2.061(4) to 2.081(4) Å, the Ir–N distances from 2.064(5) to 2.091(6) Å. The general geometry around the metal atoms is thus approximately square-planar, with the metal planes at an angle of roughly 47° to the plane of the sapphyrin. The sapphyrin plane is considerably ruffled, with the pyrrole rings distorted in such a way that the nitrogen atoms N1 and N2 are bent towards Rh(a) and Ir and the nitrogen atoms N4 and N5 are bent towards Rh(b). Maximum and average deviations from the N_5C_{24} plane are −0.425 and 0.264/0.054 Å, respectively, for Rh and −0.398(6) and 0.765(8)/0.206 Å, respectively, for Ir.

All of the sapphyrin complexes discussed here, with the exception of **2a** and **4a**,[6] show remarkable stability. The relatively high ν(CO) values indicate that at least one of the carbonyl groups bound to the rhodium center in either **4** or **6** should be easily displaced. To date, however, we have not seen any indication of either photolytic or thermal loss of CO from either **4** or **6**. Also, all of the coordination compounds reported here display much lower reactivity under oxidizing conditions (e.g., methyl iodide or acetic anhydride).[11] Reagents such as HCl cleave the metals to form protonated sapphyrins (**9**). Iodine reacts only slowly with **6** or **7**, removing one of the metal carbonyl moieties to afford **3** and **5b**, respectively. Furthermore, in preliminary studies we have found that complex **6** acts as an efficient homogeneous catalyst for the hydrogenation of alkenes.[12]

Experimental Procedure

5b: Sapphyrin **1b** (50 mg, 0.08 mmol) was dissolved in dichloromethane (15 mL) containing triethylamine (0.5 mL). $[IrCl(CO)_2(py)]$ (30 mg, 0.08 mmol) was added and the solution stirred at room temperature for 12 h. The solvent was removed in vacuo and the residue taken up in dichloromethane. Filtration through Celite, followed by chromatographic purification on silica gel using dichloromethane/methanol (9:1) as the eluent, gave the cationic iridium complex **5b** (62 mg) in 81% yield. Recrystallization from dichloromethane–methanol then gave analytically pure product (73% recovery). ^{1}H NMR (300 MHz, $CDCl_3$, 25 °C, TMS): δ = 11.41 (s, 1H; *meso*), 11.15 (s, 1H; *meso*), 10.96 (s, 2H; *meso*), 4.55 (m, 8H; CH_2), 4.32 (m, 4H; CH_2), 4.09 (s, 3H; Me), 3.89 (s, 3H; Me), 3.83 (s, 3H; Me), 3.74 (s, 3H; Me), 2.16 (m, 12H; CH_3), 2.10 (m, 3H; CH_3), 1.74 (m, 3H; CH_3), −2.67 (s, 1H; NH), −2.96 (s, 1H; NH), −3.29 (s, 1H; NH). IR (KBr): ν[cm^{-1}] = 2044 (vs), 1967 (vs) (CO), 3156(w), 3100(w), 3114(w) (NH). MS (FAB): *m/z* 884 ($M^{\oplus}$), 819 ($M^{\oplus}$ − CO). VIS (CH_2Cl_2) λ_{max} (lgε) = 360 (4.23), 484 (5.62), 596 (3.00), 638 (3.60), 694 (3.96), 715 (3.94) nm. Correct elemental analysis (C,H,N).

6a: Sapphyrin **1a** (50 mg, 0.08 mmol) was dissolved in dichloromethane (15 mL) containing triethylamine (0.5 mL). $[\{RhCl(CO)_2\}_2]$ (40 mg, 0.1 mmol) was added and the solution stirred at room temperature for 12 h. The solvent was removed in vacuo and the residue taken up in dichloromethane. Filtration through Celite, followed by chromatographic purification on silica gel using dichloromethane as the eluent, afforded the dirodium complex **6a** (67 mg) in 88% yield. ^{1}H NMR (300 MHz, $CDCl_3$, 25 °C, TMS): δ = 11.34 (s, 2H; *meso*), 11.06 (s; 2H, *meso*), 10.20 (s, 2H; β-pyrrolic), 4.76 (m, 4H; CH_2), 4.65 (m, 4H; CH_2), 4.78 (m, 4H; CH_2), 4.04 (s, 6H; Me), 2.64 (m, 4H; CH_2), 2.24 (t, 12H; CH_3, J = 7.3) 1.37 (t, 12H; CH_3, J = 7.4), −3.54 (s, 1H; NH). IR (KBr): ν[cm^{-1}] = 2060, 1996 (CO), 3215 (NH), MS (FAB): *m/z* 917 ($M^{\oplus}$). VIS (CH_2Cl_2): λ_{max} (lgε) = 372 (4.65), 428 (4.68), 499 (5.32), 593 (3.08), 643 (3.74), 700 (5.74) nm. Correct elemental analyses (C,H,N)

Received: August 8, 1990 [Z 4125 IE]
German version: *Angew. Chem. 103* (1991) 83

CAS Registry numbers:
2a, 131154-66-0; **2b**, 131154-67-1; **3b**, 131154-68-2; **4a**, 131154-69-3; **4b**, 131154-70-6; **5b**, 131154-71-7; **6a**, 131178-14-8; **6b**, 131178-15-9; **7b**, 131178-16-0; **8b**, 131178-17-1; **9a**, 131154-64-8; **9b**, 131154-65-9; $\{Rh(CO)_2\}_2$, 14523-22-9; $[IrCl(CO)_2(py)]$, 15682-58-3; cyclohexene, 110-83-8.

[1] a) V. J. Bauer, D. L. J. Clive, D. Dolphin, J. B. Paine, III, F. L. Harris, M. M. King, J. Loder, S.-W. C. Wang, R. B. Woodward, *J. Am. Chem. Soc., 105* (1983) 6429; b) M. J. Broadhurst, R. Grigg, A. W. Johnson, *J. Chem. Soc., Perkin Trans. 1 1972*, 2111.

[2] J. L. Sessler, M. J. Cyr, V. Lynch, E. McGhee, J. A. Ibers, *J. Am. Chem. Soc. 112* (1990) 2810.

[3] a) D. Cullen, E. M. Jun, T. S. Srivastava, M. Tsutsui, *J. Chem. Soc. Chem. Commun. 1972*, 584; b) E. B. Fleischer, R. Thorp, D. Venerable, *ibid. 1969*, 475; c) J. P. Collman, C. E.Barnes, P. N. Swepston, J. A. Ibers, *J. Am. Chem. Soc. 106* (1984) 3500; d) B. R. James, D. V. Stynes, *ibid. 94* (1972) 6225; e) H. Ogoshi, J.-I. Setsune, T. Omura, Z.-I. Yoshida, *ibid. 97* (1975) 6461; f) R. Grigg, J. Trocha-Grimshaw, V. Viswantha, *Tetrahedron Lett. 1976*, 289; g) H. Ogoshi, J.-I. Setsune, Z.-I. Yoshida, *J. Organomet. Chem. 159* (1978) 317; h) T. S. Srivastava, E. B. Fleischer, *J. Am. Chem. Soc. 92* (1970) 5518; i) M. Tsutsui, C. P. Hrung, *ibid. 95* (1973) 5777; j) D. Ostfeld, M. Tsutsui, C. P. Hrung, D. C. Conway, *ibid. 93* (1971) 2548.

[4] OEP = 2,3,7,8,12,13,17,18-octaethylporphyrinato dianion, sap = either 8,12,13,17-tetraethyl-7,18-dimethyl-3,22-dipropylsapphyrinato trianion or 3,8,12,13,17,22-hexaethyl-2,7,18,23-tetramethylsapphyrinato trianion.

[5] If this reaction is monitored by UV spectroscopy, an intermediate complex can be observed with a Soret-like absorption band at 462 nm. This complex is relatively stable in the absence of oxygen, but contact with air results in its immediate destruction and formation of **2**.

[6] All new compounds with the exception of **2a** and **4a**, which proved to be much less stable than **2b** and **4b**, were characterized completely by NMR, IR, and UV/VIS spectroscopy and by microanalysis. Compounds **2a** and **4a** were only characterized spectroscopically.

[7] **5b**-Cl: $C_{42}H_{49}ClIrN_5O_2$; C_{2h}^5-$P2_1/a$; Z = 4 in a cell of dimensions a = 16.994(6), b = 13.980(4), c = 17.402(5) Å, β = 111.80(2)° at 160 K. Data collected with filtered $Cu_{K\alpha}$ radiation on a CAD4 diffractometer to 75° in θ; 8152 unique observations, 5427 with $F_0^2 > 3\sigma(F_0^2)$. All hydrogen atom positions were idealized (C, N–H = 0.95 Å) and each hydrogen atom was given an isotropic thermal parameter 1 Å^2 larger than that of the atom to which it is bonded. Final model involved anisotropic refinement of all non-hydrogen atoms, 460 variables, $R(F_0^2)$ = 0.079; for $F_0^2 > 3\sigma(F_0^2)$, $R(F)$ = 0.047.

[8] **6a** · 1/2 CH_2Cl_2: $C_{44}H_{47}N_5O_4Rh_2$ · 1/2 CH_2Cl_2; C_i^1-$P\bar{1}$; Z = 2 in a cell of dimensions a = 10.678(2), b = 11.719(2), c = 18.981(6) Å, α = 103.77(2), β = 90.19(2), γ = 113.61(2)° at 160 K. Data collected with filtered $Cu_{K\alpha}$ radiation on a CAD4 diffractometer to 75° in θ; 8619 unique observations, 6536 with $F_0^2 > 3\sigma(F_0^2)$. All hydrogen atom positions were idealized (C, N-H = 0.95 Å) and each hydrogen atoms was given an isotropic thermal parameter 1 Å^2 larger than that of the atom to which it is bonded. Final model involved anisotropic refinement of all non-hydrogen atoms, 511 variables, $R(F_0^2)$ = 0.071; for $F_0^2 > 3\sigma(F_0^2)$, $R(F)$ = 0.045. The solvent is poorly defined. Further details of the crystal structure investigations are available on request from the Director of the Cambridge Crystallographic Data Centre, University Chemical Laboratory, Lensfield Road, GB-Cambridge CB21EW (UK), on quoting the full journal citation.

[9] A. Takenaka, Y. Sasada, H. Ogoshi, T. Omura, Z.-I. Yoshida, *Acta. Crystallogr. Sect. B31* (1975) 1.

[10] A. M. Abeysekera, R. Grigg, J. Trocha-Grimshaw, V. Viswanatha, T. J. King, *J. Chem. Soc. Perkins Trans. 1 1979*, 2184.

[11] a) A. M. Abeysekera, R. Grigg, J. Trocha-Grimshaw, V. Viswanatha, *J. Chem. Soc. Perkins Trans. 1 1977*, 36; b) *ibid. 1977*, 1395.

[12] Ten equivalents of cyclohexene were successfully converted into cyclohexane by treatment with hydrogen (100 kPa) for 12 hours in the presence of **6a**. There was no decomposition or change in the sapphyrin sample which was obtained from the same batch of crystals as that used for the X-ray structure determination.

Unsaturated Tin Compounds: Generation and Reactivity of $Me_2Sn{=}C(SiMe_3)_2$ and $Me_2Sn{=}N(SitBu_2Me)$**

By *Nils Wiberg** and *Sham-Kumar Vasisht*

Dedicated to Professor Edwin Hengge on the occasion of his 60th birthday

The simple route to the thermally labile silaethene **1**[1] and germaethene **2**,[2] found by us some time ago, motivated us

[*] Prof. Dr. N. Wiberg, Prof. Dr. S.-K. Vasisht
Institut für Anorganische Chemie der Universität
Meiserstrasse 1, W-8000 München 2 (FRG)

[**] Unsaturated Compounds of Silicon and Its Group Homologues, Part 37. Part 36: N. Wiberg, H. Schuster, *Chem. Ber. 124* (1991), in press.

to attempt the preparation of the stannaethene **3**, a further example of an unsaturated tin compound, by a corresponding route involving "thermal salt elimination" (the first stannaethene was synthesized by *A. Berndt* et al.[3]).

Indeed, **3** was generated similarly to **1** and **2** as shown in Scheme 1, via intermediate **4** (E = Sn), by dropwise addition of a solution of phenyllithium to a solution of the dibromo compound **6** (E = Sn) in diethyl ether at $-100\,^{\circ}C$; at low temperatures, **3** is a short-lived species that dimerizes to give **5** (E = Sn).

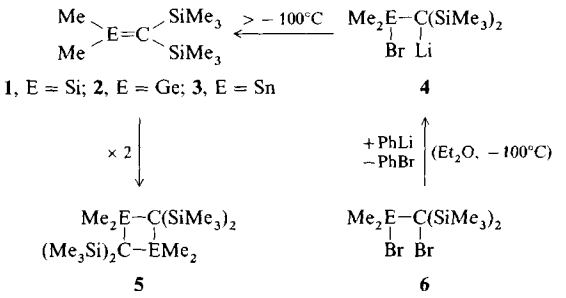

Scheme 1. Generation of sila-, germa-, and stannaethenes **1**–**3**.

The intermediacy of stannaethene **3** was established by trapping of the unsaturated compound. Addition of PhLi to a solution of **6** (E = Sn) in ether in the presence of 2,3-dimethylbutadiene (DMB) or azido(di-*tert*-butyl)methylsilane resulted in formation of the [2 + 4] cycloadduct **7** or the [2 + 3] cycloadduct **8**, respectively, of stannaethene **3** (Scheme 2). As already observed for **1** and **2**, the silyl azide is a better trapping reagent than DMB. This is shown by the following observations: (1) Dimer **5** is formed together with **7** even when a 20-fold excess of DMB is used, whereas [2 + 3] cycloaddition with the azide is quantitative.[4] (2) When PhLi is added dropwise to a solution of **6** (E = Sn) in the presence or absence of DMB (but not in the presence of tBu$_2$MeSiN$_3$), the addition product **9** (Scheme 2), formed from PhLi and **3**, is also obtained. This also means that **4** (Scheme 1) slowly decomposes even at $-100\,^{\circ}C$ to stannaethene **3**, which is trapped by PhLi (**9** was identified, after protolysis, as **10a** and, after bromination, as **10b**).

The [2 + 3] cycloadduct **8** formed from **3** and tBu$_2$MeSiN$_3$, undergoes [2 + 3] cycloreversion at slightly raised temperature to give stannanimine **11** and bis(trimethylsilyl)diazomethane. The intermediacy of imine **11**, which dimerizes to **12** in the absence of other reactants, was also shown by trapping reactions. In the presence of DMB in excess or of tBu$_2$MeSiN$_3$, the ene reaction product **13** or the [2 + 3] cycloadduct **14**, respectively, is formed. Compound **14**, in turn, is a precursor of **11** and decomposes upon warming in the presence of DMB to form **12** and **13**. Thus, trapping with tBu$_2$MeSiN$_3$ allows stannanimine **11** to be "stored".

The silaethene **1**[1] and the germaethene **2**,[2] generated by treatment of **6** with PhLi as shown in Scheme 1, as well as the silanimine and germanimine Me$_2$E = N(SiMetBu$_2$)[5] generated, via a [2 + 3] cycloadduct, by treatment of **1** and **2**, respectively, with tBu$_2$MeSiN$_3$, react with DMB and tBu$_2$MeSiN$_3$ in a basically analogous fashion to **3** and **11**, respectively.[6–8] Only gradual differences are observed. Thus, ethenes **1**–**3** and DMB undergo not only [2 + 4] cycloadditions but also ene reactions; however, the amount of Diels–Alder reaction product decreases from about 80% to practically 0% on going from **1** to **2** to **3**[9] (in the reaction of the imine Me$_2$E = N(SiMetBu$_2$) with DMB, only ene reaction occurs). Moreover, the metastability of the [2 + 3] cycloadducts of **1**–**3** with tBu$_2$MeSiN$_3$ with respect to first-order [2 + 3] cycloreversion increases in the series **1**-, **2**-, **3**-cycloadduct. This finding can be explained by, for example, an increase in the energy of the imine in the order silan-, german-, stannanimine. The fact that the chemical behavior of the unsaturated tin compounds **3** and **11** is analogous to that of the corresponding silicon and germanium compounds indicates that the bonding in these systems is similar.[10, 11]

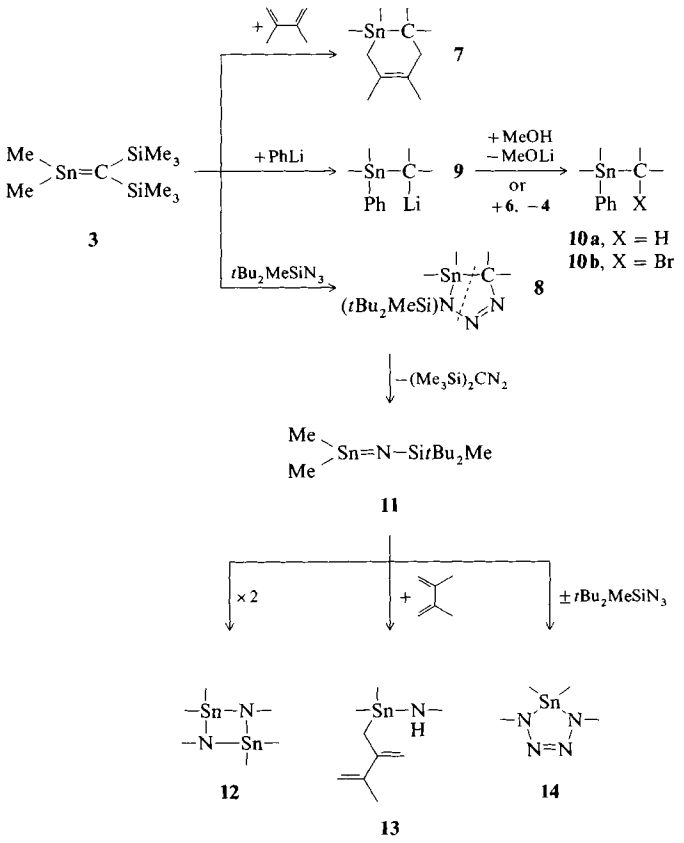

Scheme 2. Generation of the stannanimine **11** as well as reactions of **3** and **11** (the Me, SiMe$_3$, and SiMetBu$_2$ groups on Sn, C, and N are partly omitted for clarity).

Experimental Procedure

The NMR spectra were recorded at the following frequencies: ^{1}H 89.55 and 270.166 MHz, ^{13}C 22.49 and 67.936 MHz, ^{29}Si 33.35 and 53.674 MHz, ^{119}Sn 33.35 and 100.682 MHz.

6 (E = Sn): BuLi (55.0 mmol) in 30 mL of hexane was added over 4 h to a solution of (Me$_3$Si)$_2$CBr$_2$ (17.27 g, 54.3 mmol) [12] in 80 mL of Et$_2$O at $-100\,^{\circ}C$. Me$_3$SnCl (11.00 g, 55.0 mmol) in 20 mL of Et$_2$O was then added over 1 h at $-78\,^{\circ}C$ (quantitative formation of (Me$_3$Si)$_2$(Me$_3$Sn)CBr. ^{1}H NMR: $\delta = 0.201$ (2 SiMe$_3$), 0.271 (SnMe$_3$)). LiBr was removed by filtration and Et$_2$O and hexane were replaced by 60 mL of CH$_2$Cl$_2$. The reaction mixture was then added dropwise at room temperature to a solution of Br$_2$ (54.0 mmol, 2.80 mL) in 20 mL of CH$_2$Cl$_2$. The reaction mixture was allowed to stand for 12 h and the CH$_2$Cl$_2$ and MeBr were then removed by distillation. Sublimation at 60–70 °C/10^{-4} mbar afforded 22.4 g (47.9 mmol; 89%) of colorless, crystalline **6** (E = Sn), m.p. 144 °C; correct elemental analysis (C, H). ^{1}H NMR (C$_6$D$_6$): $\delta = 0.248$ (2SiMe$_3$), 0.651 (SnMe$_2$). ^{13}C{^{1}H} NMR (C$_6$D$_6$): $\delta = 1.506$ (2SiMe$_3$), 1.923 (SnMe$_2$), 33.31 (CBr). ^{29}Si NMR (C$_6$D$_6$): $\delta = 7.45$. ^{119}Sn NMR (C$_6$D$_6$): $\delta = 58.82$. MS (70 eV): m/z 468 ($M^{\oplus}$).

5 (E = Sn), **7**, **10**: PhLi (3.30 mmol) in 1 mL of C$_6$H$_6$ and 6 mL of Et$_2$O was added over 3 h to a solution of **6** (E = Sn) (1.50 g, 3.20 mmol) in 25 mL of Et$_2$O ($-100\,^{\circ}C$) (A) or **6** (E = Sn) (1.50 g, 3.20 mmol) and DMB (32.0 mmol, 3.6 mL)

in 10 mL of Et_2O. After warming to room temperature and addition of MeOH, the solution contained—according to the ^1H NMR spectrum—90% **5** (E = Sn), 5% **10a** and 5% **10b** in case (A) and 60% **5** (E = Sn), 10% **7**, 5% **10a**, and 25% **10b** in case (B). The products were separated by preparative HPLC (retention times: **10a** < **10b** < **7** < **5**).

5 (E = Sn): Colorless crystals, characterized by comparison with an authentic sample [13]. **7**: Colorless crystals, correct elemental analysis (C, H). ^1H NMR (C_6H_6): $\delta = 0.125$ ($2SiMe_3$), 0.234 ($SnMe_2$), 1.400 (CH_2Sn), 1.696 ($2CH_3$), 2.453 (CH_2). $^{13}C\{^1H\}$ NMR (C_6D_6): $\delta = -5.780$ ($SnMe_2$), 2.015 ($2SiMe_3$), 9.719 (CSi_2), 17.11 (CH_2Sn), 22.83 ($2CH_3$), 36.09 (CH_2), 127.2/129.2 (C=C). ^{29}Si NMR (C_6D_6): $\delta = 3.358$. ^{119}Sn NMR (C_6D_6): $\delta = 5.271$. MS (70 eV): *m/z* 390 ($M^{\oplus}$).

10a: Colorless liquid. ^1H NMR (C_6D_6): $\delta = -0.458$ (CH), 0.084 ($2SiMe_3$), 0.364 ($SnMe_2$), phenyl multiplet. $^{13}C\{^1H\}$ NMR (C_6D_6): $\delta = -6.064$ ($SnMe_2$), 0.215 (CH), 3.349 ($2SiMe_3$), 136.2/143.8 (Ph). ^{29}Si NMR (C_6D_6): $\delta = 1.575$. ^{119}Sn NMR (C_6D_6): $\delta = -23.67$. MS (70 eV): *m/z* 371 ($M^{\oplus} - Me$).

10b: Colorless, liquid, correct elemental analysis (C, H). ^1H NMR (C_6D_6): $\delta = 0.137$ ($2SiMe_3$), 0.459 ($SnMe_2$), phenyl multiplet. $^{13}C\{^1H\}$ NMR (C_6D_6): $\delta = -5.485$ ($SnMe_2$), 1.587 ($2SiMe_3$), 30.58 (CBr), 136.8/142.8 (Ph). ^{29}Si NMR (C_6D_6): $\delta = 5.909$. ^{119}Sn NMR (C_6D_6): $\delta = -21.46$. MS (70 eV): *m/z* 464 ($M^{\oplus}$).

8: PhLi (4.36 mmol) in 2 mL of C_6H_6 and 10 mL of Et_2O was added dropwise over 3 h to a solution of **6** (E = Sn) (2.04 g, 4.36 mmol) and tBu_2MeSiN_3 (3.60 g, 17.6 mmol) in 15 mL of Et_2O at −78 °C. The reaction mixture was allowed to warm to room temperature and the LiBr and solvent were removed. Recrystallization of the reaction mixture from pentane afforded 1.80 g (3.50 mmol; 80%) of colorless, crystalline **8**. M.p. 116 °C. Correct elemental analysis (C, H). ^1H NMR (C_6D_6): $\delta = 0.068$ (SiMe), 0.112 ($2SiMe_3$), 0.359 ($SnMe_2$), 1.142 ($SitBu_2$). $^{13}C\{^1H\}$ NMR (C_6D_6): $\delta = -5.78$ ($SnMe_2$), −0.843 (SiMe), 1.140 ($2SiMe_3$), 15.54 (CSi_2), 21.11 ($2CMe_3$), 28.80 ($2CMe_3$). ^{29}Si NMR (C_6D_6): $\delta = 0.012$ ($2SiMe_3$), 12.77 ($SiMetBu_2$). ^{119}Sn NMR (C_6D_6): $\delta = 64.88$. MS (70 eV): *m/z* 450 ($M^{\oplus} - tBu$).

12, 13, 14: Compound **8** (0.25 g, 0.50 mmol) was heated in 0.5 mL of C_6D_6 (A), in 0.5 mL of C_6D_6 containing 5 mmol (0.6 mL) of DMB (B), or in 0.5 mL of C_6D_6 containing 0.63 g (3.36 mmol) of tBu_2MeSiN_3 (C) for 20 h at 60 °C. According to the ^1H NMR spectrum of the reaction solution, 100% **12** (A), 100% **13** (B), or 60% **14**/40% **12** (C) were present in addition to $(Me_3Si)_2CN_2$ (^1H NMR: $\delta = 0.074$) [14]. Compounds **12**, **13**, and **14**/**12** remain as residue after distillative removal of solvent and $(Me_3Si)_2CN_2$ under high vacuum. Compounds **14** and **12** can be separated by fractional crystallization from Et_2O (1st fraction: **14**). **12**: Colorless solid. ^1H NMR (C_6D_6): $\delta = -0.100$ ($2SiMe$), 0.545 ($2SnMe_2$), 1.040 ($2SitBu_2$). $^{13}C\{^1H\}$ NMR (C_6D_6): $\delta = -3.141$ ($2SiMe$), 5.018 ($2SnMe_2$), 21.01 ($4CMe_3$), 29.12 ($4CMe_3$). ^{29}Si NMR (C_6D_6): $\delta = 5.113$. ^{119}Sn NMR (C_6D_6): $\delta = 140.1$. MS (70 eV): *m/z* 583 ($M^{\oplus} - tBu$).

13: Colorless oil. ^1H NMR (C_6D_6): $\delta = 0.011$ (SiMe), 0.199 ($SnMe_2$), 1.055 ($SitBu_2$), 1.823 (CH_3), 2.054 (CH_2Sn), 4.900 ($2H_2C=$). $^{13}C\{^1H\}$ NMR (C_6D_6): $\delta = -5.969$ (SiMe), −4.824 ($SnMe_2$), 20.74 (CH_3), 22.94 (CMe_3), 28.53 (CH_2Sn), 28.60 (CMe_3), 109.7/113.4 ($2H_2C=$), 143.7/146.4 ($2C=$). ^{29}Si NMR (C_6D_6): $\delta = 10.71$. ^{119}Sn NMR (C_6D_6): $\delta = 42.60$. MS (70 eV): *m/z* 503 ($M^{\oplus}$).

14: Colorless crystals, decomposition at 160 °C. ^1H NMR (C_6D_6): $\delta = -0.021$ ($2SiMe$), 0.337 ($SnMe_2$), 1.121 ($2SitBu_2$). $^{13}C\{^1H\}$ NMR (C_6D_6): $\delta = -4.938$ ($2SiMe$), 0.001 ($SnMe_2$), 21.05 ($4CMe_3$), 28.70 ($4CMe_3$). ^{29}Si NMR (C_6D_6): $\delta = 11.75$. ^{119}Sn NMR (C_6D_6): $\delta = 41.50$. MS (70 eV): *m/z* 520 ($M^{\oplus}$).

Received: August 16, 1990 [Z 4139 IE]
German version: *Angew. Chem. 103* (1991) 105

CAS Registry numbers:
3, 130984-20-2; **5** (E = Sn), 54008-66-1; **6** (E = Sn), 130984-22-4; **7**, 130984-23-5; **8**, 130984-24-6; **10a**, 130984-25-7; **10b**, 130984-26-8; **11**, 130984-27-9; **12**, 130984-28-0; **13**, 130984-29-1; **14**, 130984-30-4; DMB, 513-81-5; tBu_2MeSiN_3, 103457-88-1; $(Me_3Si)_2CBr_2$, 29955-10-0; Me_3SnCl, 1066-45-1; $(Me_3Si)_2(Me_3Sn)CBr$, 130984-21-3.

[1] N. Wiberg, G. Preiner, *Angew. Chem. 89* (1977) 343; *Angew. Chem. Int. Ed. Engl. 16* (1977) 328; N. Wiberg, G. Preiner, O. Schieda, G. Fischer, *Chem. Ber. 114* (1981) 3505.
[2] N. Wiberg, C.-K. Kim, *Chem. Ber. 119* (1986) 2966.

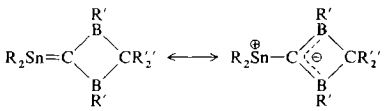

[3] A. Berndt, H. Meyer, G. Baum, W. Massa, S. Berger, *Pure Appl. Chem. 59* (1987) 1011, and references cited therein. The C_2Sn-CB_2 unit is strongly twisted from the planarity required for a "true" stannaethene (twist angle ca. 60°).
[4] On the other hand, tBu_3SiN_3, which is much more bulky than tBu_2MeSiN_3, does not trap **3**, generated from **6** and PhLi.
[5] N. Wiberg, P. Karampatses, C.-K. Kim, *Chem. Ber. 120* (1987) 1203, 1213.
[6] N. Wiberg, G. Preiner, O. Schieda, *Chem. Ber. 114* (1981) 3518.
[7] N. Wiberg, C.-K. Kim, *Chem. Ber. 119* (1986) 2980.
[8] N. Niberg, G. Preiner, P. Karampatses, C.-K. Kim, K. Schurz, *Chem. Ber. 120* (1987) 1357.
[9] Isobutene also does not trap **3** generated from **6** and PhLi.
[10] N. Wiberg, G. Wagner, J. Riede, G. Müller, *Organometallics 6* (1987) 32.
[11] G. Reber, J. Riede, N. Wiberg, K. Schurz, G. Müller, *Z. Naturforsch. B44* (1989) 786.
[12] N. Wiberg, G. Preiner, O. Schieda, *Chem. Ber. 114* (1981) 2087.
[13] D. Seyferth, J. L. Lefferts, *J. Organomet. Chem. 116* (1976) 257.
[14] D. Seyferth, T. J. Flood, *J. Organomet. Chem. 29* (1971) 5.

On the Differing Lewis Basicity of In^I Compared with Sn^{II} in Molecular Indium-Tin and Thallium-Tin Alkoxides**

By *Michael Veith** and *Klaus Kunze*

In the thallium-tin alkoxide **1**,[1] which we synthesized for the first time some years ago, each of the two metal atoms has a lone pair. Therefore, **1** could act as a double Lewis base toward electrophilic metal centers, whereby both Sn and Tl

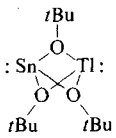

1

can engage in bonding. When **1** is allowed to react thermally or photochemically with chromium or molybdenum hexacarbonyl in excess, however, only the monoadduct **2** or **3**, respectively, is obtained, as shown in Equation (a).

$$[Sn(OtBu)_3Tl] + [M(CO)_6] \xrightarrow[-CO]{\Delta T \text{ or } h\nu} [(CO)_5M-Sn(OtBu)_3Tl] \quad (a)$$

1 → **2**, M = Cr; **3**, M = Mo

An X-ray structure analysis (Fig. 1 and Table 1) confirms that the tin atom in **3** is bonded to the molybdenum atom.

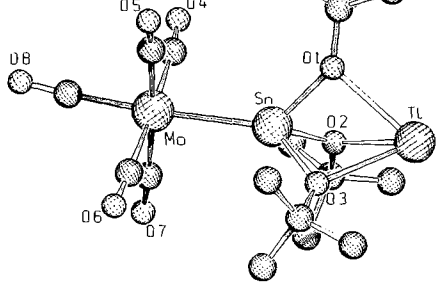

Fig. 1. Molecular structure of **3** [8] determined by X-ray analysis [2, 9]. The unlabeled spheres are carbon atoms; hydrogen atoms are omitted. The Mo-Sn···Tl angle is 178.9(1)°.

[*] Prof. Dr. M. Veith, Dr. K. Kunze
Institut für Anorganische Chemie der Universität
Im Stadtwald 1, W-6600 Saarbrücken (FRG)

[**] Chemistry of Alkoxystannates, Part 6. This work was supported by the Deutsche Forschungsgemeinschaft and the Fonds der Chemischen Industrie. We thank Prof. *P. Jutzi* for recording the ^{119}Sn NMR spectra. Part 5: M. Veith, J. Hans, L. Stahl, P. May, V. Huch, A. Sebald, *Z. Naturforsch.*, in press.

Table 1. Results of the X-ray structure analyses of **3**, **4**, **8**, and **10** [2].

	4	**3**	**8**	**10**
Crystal system	hexagonal	monoclinic	orthorhombic	monoclinic
Space group	$P6_3/m$	$P2_1/n$	*Pnma*	$P2_1/n$
Z	2	4	4	4
a [Å]	9.867(9)	9.952(8)	15.11(1)	10.51(1)
b [Å]	9.867(9)	17.59(1)	14.17(1)	30.30(2)
c [Å]	11.21(1)	15.11(1)	15.76(1)	10.748(7)
Angle [°]	$\gamma = 120$	$\beta = 100.20(7)$	–	$\beta = 107.36(7)$
In-O [Å] (Tl-O)	2.413(4)	2.557(15)	2.141(6)	2.21(1)
Sn-O [Å]	2.032(4)	2.017(9)	2.122(9)	2.07(1)
Sn-Mo [Å]	–	2.770(2)	2.761(1)	–
Sn-Cr [Å]	–	–	–	2.636(3)
In-Mo [Å]	–	–	2.742(1)	2.734(2)
O-In-O [°] (O-Tl-O)	66.7(1)	63.9(8)	73.2(3)	70.6(5)
O-Sn-O [°]	81.5(1)	84.2(9)	74.0(3)	76.6(5)
In···Sn [Å] (Tl)	3.200(3)	3.298(1)	3.078(1)	3.087(2)
R value	0.037	0.062	0.058	0.068

Compared with the starting compound **1** (Sn-O = 2.023(9), Tl-O = 2.595(7), and Tl···Sn = 3.306(2) Å[1]), all metal–oxygen distances are slightly shortened; the distance between thallium and tin is decreased. Characteristic of the monoadducts **2** and **3** are the high CO wave numbers ($\nu(A_1^{1b})$ bands) and a strong downfield shift of the ^{119}Sn NMR signals relative to those of compound **1** ($\Delta\delta = 97.04$; Table 2). Even under drastic conditions (large excess of metal carbonyl, higher temperature, longer reaction time), no complex fragment becomes bonded to the thallium atom of **2** or **3**.

We therefore attempted to replace thallium by its homologue indium. The desired compound **4** may be obtained starting either from **1** or from the sodium salt $[\{Na(OtBu)_3Sn\}_2]$[3] in a heterogeneous reaction with InBr [Eq. (b)].

$$\left.\begin{array}{l}[Tl(OtBu)_3Sn]\ \mathbf{1}\\ 1/2[\{Na(OtBu)_3Sn\}_2]\end{array}\right\} \xrightarrow[-TlBr/-NaBr]{+InBr} [In(OtBu)_3Sn]\ \mathbf{4} \qquad (b)$$

Toluene, used as solvent, apparently causes partial dissolution of InBr via formation of an arene complex.[4] The monomeric product **4**, like **1**, is soluble in nonpolar solvents, exhibits a similar ^{119}Sn absorption (Table 2), and forms isotypic crystals (Table 1). According to an X-ray structure analysis, **4** has a distorted bipyramidal InO_3Sn structure with In and Sn in apical positions and the three oxygens in equatorial positions. Compared with **1**, the indium atom is closer to the O_3 plane than the thallium atom, as expected; the distances to the oxygen atoms lie in the normal range (see also indium 2,4,6-tris(trifluoromethyl)phenoxide[5]).

Reaction of **4** with $[Cr(CO)_6]$ or $[Mo(CO)_6]$ in THF either thermally or photochemically in analogy to Equation (a) likewise results in formation of monoadducts **5** and **6**, respectively. Use of an excess of the metal carbonyl or longer reaction times results in further reaction to give the diadducts **7** and **8**, respectively [Eq. (c)].

$$[In(OtBu)_3Sn]\ \mathbf{4} \xrightarrow[-CO]{+[M(CO)_6]\ (\Delta T \text{ or } h\nu)} [Sn(OtBu)_3In-M(CO)_5]\ \begin{array}{l}\mathbf{5},\ M = Cr\\ \mathbf{6},\ M = Mo\end{array} \xrightarrow[-THF]{+[M(CO)_5(thf)]} [(CO)_5M-Sn(OtBu)_3In-M(CO)_5]\ \begin{array}{l}\mathbf{7},\ M = Cr\\ \mathbf{8},\ M = Mo\end{array} \qquad (c)$$

In contrast to **2** and **3**, the transition-metal atoms in **5** and **6** are not coordinated to the tin atom but rather to the indium atom. This is revealed by the upfield shift of the ^{119}Sn NMR signal (**6**: $\Delta\delta = -95.96$) compared with that of **4** and by the wave numbers of the $\nu(A_1^{1b})$ stretching band, which indicate a different electron density *trans* to the CO group (see Table 2).

This is shown especially clearly on going from the monoadducts **5** and **6** to the diadducts **7** and **8**. The second $\nu(A_1^{1b})$ bands due to the $M(CO)_5$ units on tin lie in the absorption region observed for compounds **2** and **3** (Table 2).

The result of an X-ray structure analysis of **8** is shown in Figure 2. The four metal atoms Mo, Sn, In, and Mo are

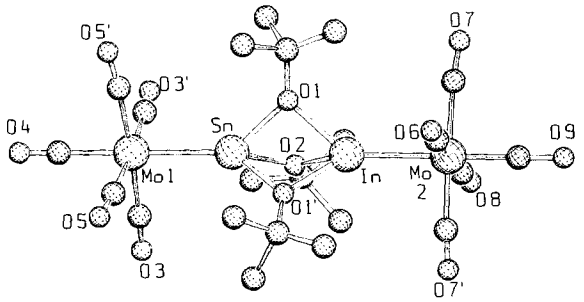

Fig. 2. Molecular structure of **8** [2] (atoms labeled as in Fig. 1). The stacked arrangement of the $Mo(CO)_5$ groups is clearly shown.

arranged nearly linearly (Mo-Sn-In = 174.2°, Mo-In-Sn = 178.8°), with metal single bonds between Mo and In and between Mo and Sn (distances in Table 1); as found in the starting compound **4**, In and Sn are bridged by three *tert*-butoxy groups. The coordination of $Mo(CO)_5$ units on indium and tin results in withdrawal of electron density from indium, so that the In–O distance is significantly less than that in **4**. The electron density on Sn is increased to a comparable extent; that is, the Sn–O distances are longer than those in free **4**. If the whole molecule is considered, however, **4** acts as an electron donor toward the $Mo(CO)_5$ units, since the In···Sn distance in **8** is less than that in **4** by 0.122 Å (Table 1).

The preferential coordination of the fragments $[Cr(CO)_5]$ and $[Mo(CO)_5]$ to indium in the monoadducts can be ex-

Table 2. ^{1}H and ^{119}Sn NMR data (δ values in benzene) and CO wave numbers [cm^{-1}] for compounds **1**–**10**.

	$\delta(^1H)$	$\delta(^{119}Sn)$	$\nu(A_1^{1b})$	ν (other CO)
$[Tl(OtBu)_3Sn]$ **1**	1.32	−78.72 [a]	–	–
$[In(OtBu)_3Sn]$ **4**	1.37	−77.27	–	–
$[Tl(OtBu)_3Sn\text{-}Cr(CO)_5]$ **2**	1.31	–	2060 (m)	1970 (sh) 1920 (vs)
$[Tl(OtBu)_3Sn\text{-}Mo(CO)_5]$ **3**	1.31	+18.32	2070 (m)	1980 (sh) 1930 (vs)
$[Sn(OtBu)_3In\text{-}Cr(CO)_5]$ **5**	1.23	–	2033 (m)	1968 (w) 1913 (vs)
$[Sn(OtBu)_3In\text{-}Mo(CO)_5]$ **6**	1.23	−173.23	2051 (m)	1925 (vs)
$[(CO)_5Cr\text{-}Sn(OtBu)In\text{-}Cr(CO)_5]$ **7**	1.27	–	2058 (m) 2041 (m)	1975 (sh) 1925 (vs, br)
$[(CO)_5Mo\text{-}Sn(OtBu)_3In\text{-}Mo(CO)_5]$ **8**	1.28	–	2069 (m) 2050 (m)	1965 (s) 1915 (vs, br)
$[(CO)_5Cr\text{-}In(OtBu)_3Sn\text{-}Mo(CO)_5]$ **9**	1.28	–	2069 (m) 2033 (m)	1978 (sh) 1950 (vs) 1930 (vs) 1912 (vs)
$[(CO)_5Mo\text{-}In(OtBu)_3Sn\text{-}Cr(CO)_5]$ **10**	1.28	–	2059 (m) 2051 (m)	1975 (sh) 1930 (vs) 1912 (vs)

[a] $J(^{205,203}Tl\text{-}Sn) = 1293$ Hz.

 © VCH Verlagsgesellschaft mbH, W-6940 Weinheim, 1991 0570-0833/91/0101-0096 $ 3.50+.25/0

ploited chemically. As shown in Equations (d) and (e) reaction of **5** and **6** with the THF adduct of the corresponding metal pentacarbonyl affords the positional isomers **9** and **10**, respectively, which contain four different metal atoms.

$$\underset{\mathbf{5}}{[(CO)_5Cr-In(OtBu)_3Sn]} + [Mo(CO)_5(thf)] \xrightarrow[-THF]{} \underset{\mathbf{9}}{[(CO)_5Cr-In(OtBu)_3Sn-Mo(CO)_5]} \quad (d)$$

$$\underset{\mathbf{6}}{[(CO)_5Mo-In(OtBu)_3Sn]} + [Cr(CO)_5(thf)] \xrightarrow[-THF]{} \underset{\mathbf{10}}{[(CO)_5Mo-In(OtBu)_3Sn-Cr(CO)_5]} \quad (e)$$

Compounds **9** and **10** are clearly distinguished by their CO wave numbers (Table 2) and crystal data (Table 1).[6] The X-ray structure analysis of **10** (Fig. 3, Table 1) again reveals

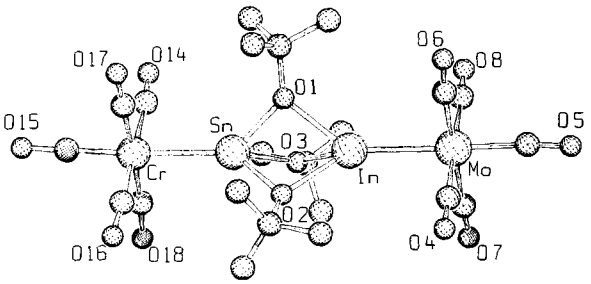

Fig. 3. Molecular structure of **10** [2]. In contrast to **8**, the $M(CO)_5$ groups are arranged in an eclipsed fashion.

an almost linear arrangement of the metal atoms (Mo-In···Sn = 178.1(1)°, Cr-Sn···In = 179.7(1)°). Interchange of the Sn and In positions in the structure analysis leads here and for **8** to poorer U values. As found for **8**, addition of $[M(CO)_5]$ fragments to **4** results in a decrease in the separation of the main-group metals (Δd = 0.113 Å) and a charge shift from indium to tin. However, owing to the shorter Cr–Sn bond compared with the Mo–Sn bond in **8**, the charge shift is less pronounced.

Experimental Procedure

4: $[Tl(OtBu)_3Sn]$ (1.0 mmol) [1] or $[\{Na(OtBu)_3Sn\}_2]$ (0.5 mmol) [3] was stirred with indium(I) bromide (1.4 mmol) in 15 mL of toluene at 110 °C for 5 or 40 h, respectively. The insoluble material, which may contain some indium, was removed by filtration and the filtrate was concentrated. Sublimation of the residue at 30 °C/10^{-2} Torr afforded 0.42 g (92%) or 0.41 g (90%), respectively, of **4**; m.p. 41 °C.

2, **3**, and **5**–**10**: A stirred solution of **1** or **4** and $[Cr(CO)_6]$ or $[Mo(CO)_6]$ in toluene was heated to reflux. Alternatively, the metal carbonyl was first photolyzed in THF and then allowed to react with **1** or **4** in toluene. Preparation of **9** and **10** starts with **5** and **6**, respectively, whose synthesis must be carried out with exact molar ratios of starting materials. All of the compounds were purified by sublimation or recrystallization and gave correct elemental analyses (C, H, metal).

Received: August 27, 1990 [Z 4155 IE]
German version: *Angew. Chem. 103* (1991) 92

CAS Registry numbers:
1, 83437-08-5; **2**, 131010-15-6; **3**, 131010-16-7; **4**, 131010-17-8; **5**, 131010-18-9; **6**, 131010-19-0; **7**, 131010-20-3; **8**, 131010-21-4; **9**, 131010-22-5; **10**, 131010-23-6; $[Cr(CO)_6]$, 13007-92-6; $[Mo(CO)_6]$, 13939-06-5; $[Na(OtBu)_3Sn]$, 105803-03-0; $[Cr(CO)_5(thf)]$, 15038-41-2; $[Mo(CO)_5(thf)]$, 53248-43-4; In, 7440-74-6; Mo, 7439-98-7; Cr, 7440-47-3; Sn, 7440-31-5.

[1] M. Veith, R. Rösler, *Angew. Chem. 94* (1982) 867; *Angew. Chem. Int. Ed. Engl. 21* (1982) 858.

[2] Further details of the crystal structure investigations of **3**, **4**, **8**, and **10** may be obtained from the Fachinformationszentrum Karlsruhe, Gesellschaft für wissenschaftlich-technische Information mbH, W-7514 Eggenstein-Leopoldshafen 2 (FRG), on quoting the depository number CSD-54897, the names of the authors, and the journal citation.

[3] M. Veith, R. Rösler, *Z. Naturforsch. B41* (1986) 1071.

[4] H. Schmidbaur, *Angew. Chem. 97* (1985) 893; *Angew. Chem. Int. Ed. Engl. 24* (1985) 893.

[5] M. Scholz, M. Noltemeyer, H. W. Roesky, *Angew. Chem. 101* (1989) 1419; *Angew. Chem. Int. Ed. Engl. 28* (1989) 1383.

[6] Compound **9** forms orthorhombic crystals, space group *Pnma*, a = 14.93(2), b = 14.33(2), c = 15.46(2) Å.

[7] M.p., b.p., yield: **2**, 104 °C, 40 °C/10^{-3} Torr, 50%; **3**, 107 °C, 45 °C/10^{-3} Torr, 70%; **5**, 101 °C, 44 °C/10^{-3} Torr, 50%; **6**, 103 °C, 50 °C/10^{-3} Torr, 25%; **7**, 148 °C (dec.), –, 80%; **8**, 150 °C (dec.), –, 64%; **9**, 143 °C (dec.), –, 58%; **10**, 145 °C (dec.), –, 75%.

[8] E. Keller, SCHAKAL-86, Universität Freiburg 1986.

[9] G. M. Sheldrick, SHELX-86 (Program for Crystal Structure Determination), Universität Göttingen 1986.

Efficient Stereoselective Total Synthesis of Denticulatins A and B**

By *Marc W. Andersen, Bernhard Hildebrandt,* and *Reinhard W. Hoffmann**

The stereoselective synthesis of natural products of polyketide origin, particularly those which contain the stereotriad D, remains a challenge to the preparative chemist.[1] Among such substances are the denticulatins **3**,[2] two polypropionates isolated from *Siphonaria*, whose biological significance remains unclear. Denticulatin is a polyhydroxy-polyketo compound and exists in the form of a semiacetal. For the synthesis of the denticulatins it is of interest whether open-chain precursors such as **2** cyclize to the correct denticulatin isomer **3**, as well as whether other semiacetals such as **1** isomerize to the desired product (Scheme 1).

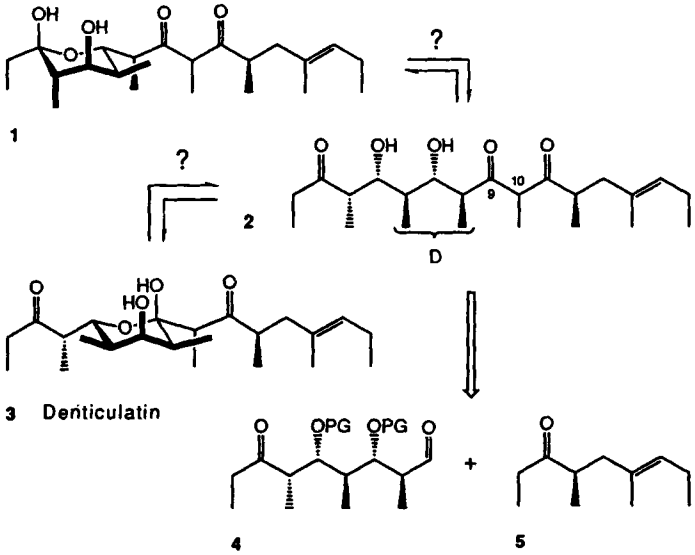

Scheme 1. Possible synthetic routes to denticulatin. PG = protecting group.

[*] Prof. Dr. R. W. Hoffmann, M. W. Andersen, M.Sc., Dr. B. Hildebrandt
Fachbereich Chemie der Universität
Hans-Meerwei-Strasse, W-3550 Marburg (FRG)

[**] This work was supported by the Deutsche Forschungsgemeinschaft and the Fonds der Chemischen Industrie. We thank Prof. Dr. *J. Faulkner*, San Diego, USA, and Dr. *M. Garson*, Wollongong, Australia, for spectra and samples of natural denticulatin. Our thanks also go to Miss *Sonja Wissner*, Miss *Sabine Gärtner*, and Mr. *Georg Dahmann* for assistance with the experiments.

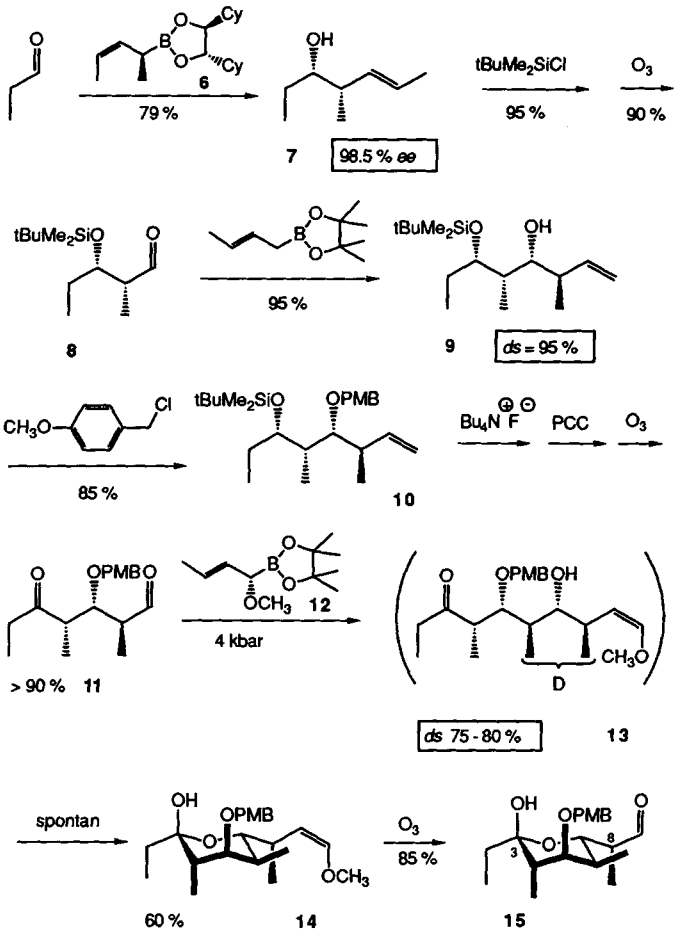

Scheme 2. Synthesis of the building block **15**, which serves as synthetic equivalent for **4** (Scheme 1). PMB = *para*-methoxybenzyl.

Ziegler and *Becker*[3] have recently synthesized **3** for the first time by cyclization of *open-chain* educts. We describe here a shorter route to the denticulatins via the semiacetal **1**.

The synthetic concept, like that of *Ziegler*'s, involves a coupling between C9 and C10. The actual improvement exemplified by our method, however, lies in the rapid synthesis of the building block **4** via three stereoselective allylboration reactions. The carbon chain from C1 to C9 is thereby synthesized, similarly as in the biogenesis, by linkage of propionaldehyde synthetic equivalents (Scheme 2). Accordingly, in the first step, propionaldehyde was extended with the reagent **6** providing the *syn*-alcohol **7** with high stereo- and enantioselectivity.[4] Protection of the OH group and subsequent ozonolysis furnished the aldehyde **8**, previously obtained via a more circuitous route.[5] We have already reported on the *anti*-diastereoselective chain extension of **8** by crotylboration, leading to **9** with substrate control of the diastereoselectivity, and on alcohol protection to give **10**.[5] Conversion of the C-3 alcohol function to the required ketone oxidation state was carried out by desilylation of **10** and oxidation with pyridinium chlorochromate (PCC). Ozonolysis then gave the ketoaldehyde **11**.

The next step was considered the most challenging aspect of the synthesis, namely, the chain extension with formation of the stereotriad D, a step which requires an effective reagent control of the diastereoselectivity. The α-methoxycrotylboronate reagent successfully used for this purpose in preliminary experiments[6] also proved useful here. In view of the high asymmetric induction originating from the aldehyde **11**, which actually favors formation of the undesired diastereomer, a selectivity of 75–80% in favor of the mismatched pair product **13** is still acceptable. The δ-hydroxyketone **13** cyclized spontaneously to the semiacetal **14**, ozonolysis of which led to the aldehyde **15**. This represents the key building block **4**, which can be prepared in 26% yield in ten steps by our synthesis.

The other required fragment, ketone **5**, was obtained from the allyl alcohol **16**[7] by Claisen rearrangement to the acid **17** and subsequent reaction with ethyllithium (Scheme 3). The constitution and configuration of **5** were checked by comparison with a sample prepared according to *Enders* et al.[3, 8] The ketone **5** was converted with Hünig base/9BBN-OTf into the enol borinate **18**. The (*Z*)-configuration of the enol double bond was verified by transformation[9] of **18** into the corresponding silyl enol ether, which showed the characteristic C4 signal at $\delta = 37.6$ in the ^{13}C-NMR spectrum. Addition of **18** to the aldehyde **15** gave, besides the

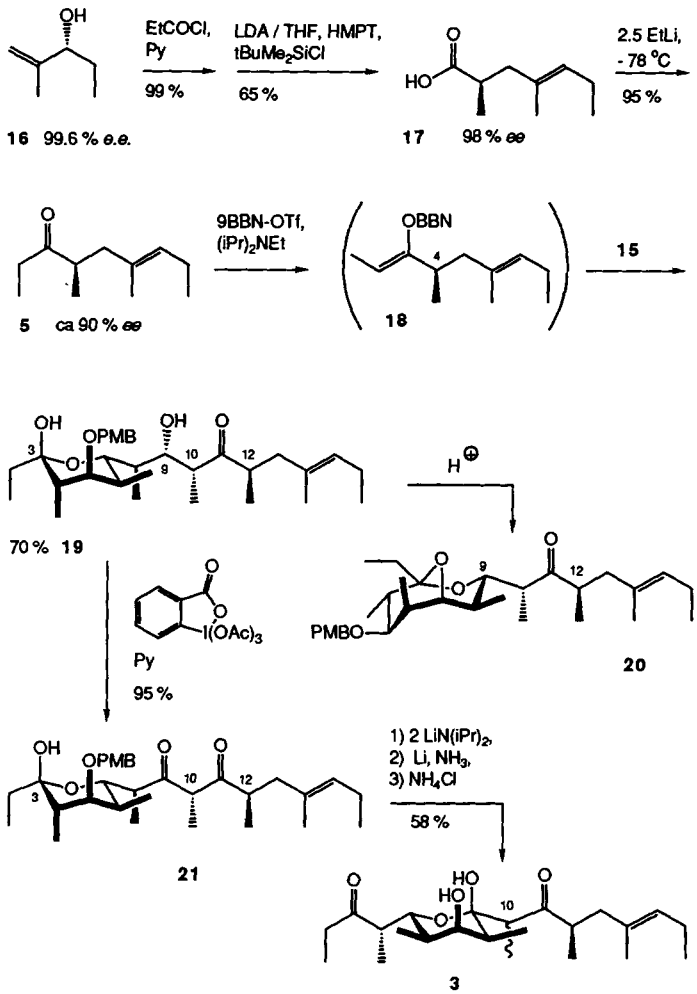

Scheme 3. Synthesis of the second building block **5** and subsequent reactions leading to denticulatin. Natural denticulatin also exists as a C10 epimer mixture. LDA = lithium diisopropylamide, HMPT = hexamethylphosphoric triamide, 9BBN = 9-borabicyclo[3.3.1]nonane, OTf = trifluoromethanesulfonate.

main product **19**, ca. 20% of another stereoisomer. This results from a partial racemization of the ketone **5** occurring during its distillation or during the formation of **18**. This follows from the condensation of racemic **5** with the aldehyde **15** affording with a 4:1 selectivity the above mentioned by-product, which must therefore be 12-*epi*-**19**.

Addition of **18** to **15** occurred with selective (>90%) formation of the *anti*-Cram isomers **19** (and 12-epi-**19**); this became clear after the bicyclization of **19** to **20** initiated by traces of acid: ^{1}H-NMR data (NOE values and coupling constants) of **20** confirm the chair/boat conformation of the bicycle and its relative configuration at C9. This also holds true for the product derived from 12-epi-**19**.

The completion of the synthesis had to take into account the sensitivity of **19** and the succeeding compounds towards acid. Oxidation of the C9 hydroxy group to give the latent triketone **21** was accomplished with the Dess-Martin periodinane[10] in the presence of pyridine. Compound **21** is thereby obtained as a stereoisomer that is uniform at C10 (cf. Ref. [3]).

Up to this reaction step a selective synthesis of the denticulatin A (with α-configuration at C10) seems possible. Numerous attempts to cleave the PMB group at C5 oxidatively or by hydrogenation failed because of the lability of the denticulatins. We therefore had to forfeit the stereochemistry at C10: after deprotonation at C10 the PMB group could be cleaved with lithium in ammonia, resulting in a 1:1 mixture of the denticulatins A and B. These were identified on the basis of their ^{13}C-NMR and ^{1}H-NMR spectra. The rotation $[\alpha]_D^{21} = -33.3$ ($c = 0.42$, $CHCl_3$) corresponds to that of the natural denticulatins [A = −30.7 ($c = 1.49$, $CHCl_3$); B = −26.4 ($c = 0.39$, $CHCl_3$)].[2] The spectroscopic data of the compounds **15**, **19** and **21** are summarized in Table 1.

The conversion of **21** into **3** confirms that the initially formed semiacetal **1** spontaneously isomerized to denticulatin **3**, whereby the number of axial residues on the respective semiacetal ring decreases.

Received: August 28, 1990 [Z 4159 IE]
German version: *Angew. Chem. 103* (1991) 90

Table 1. Spectroscopic data of the compounds **15**, **19**, and **21**. ^{1}H NMR (400 MHz, $CDCl_3$, TMS); ^{13}C NMR (75 MHz, $CDCl_3$). All the compounds are oils.

15: ^{1}H NMR: $\delta = 9.70$ (d, $J = 2.74$ Hz, 1H; C9-H), 7.22 (d, $J = 8.66$ Hz, 2H; Aryl-H), 6.85 (d, $J = 8.68$ Hz, 2H; Aryl-H), 6.00 (s, 1H; C3-OH), 4.65 (d, $J = 10.91$ Hz, 1H; CH_a-Aryl), 4.35 (d, $J = 10.91$ Hz, 1H; CH_b-Aryl), 3.94 (dd, $J = 11.24$, 2.15 Hz, 1H; C7-H), 3.76 (s, 3H; OMe), 3.43 (dd=t, $J = 2.83$, 1H; C5-H), 2.46 (ddq=tq, $J = 6.96$, 2.44 Hz, 1H; C8-H), 2.08 (dq, $J = 7.16$, 2.68 Hz, 1H; C4-H), 1.90 (ddq, $J = 11.10$, 6.75, 3.02 Hz, 1H; C6-H), 1.50 (m, 2H; C2-H,H′), 1.20 (d, $J = 6.71$ Hz, 3H; C8-Me), 0.93 (d, $J = 7.44$ Hz, 3H; C4-Me), 0.88 (d, $J = 6.93$ Hz, 3H; C6-Me), 0.86 (t, $J = 6.61$ Hz, 3H; C2-Me); ^{13}C-NMR (assigned by ^{1}H-^{13}C correlation): $\delta = 205.4$(C9), 159.7(Aryl), 129.8(Aryl), 129.2(Aryl), 114.0(Aryl), 99.4(C3), 84.2(C5), 72.5(C7), 72.0($\underline{C}H_2$Aryl), 55.3(OMe), 47.5(C8), 36.0(C4), 31.2(C2), 31.1(C6), 13.7(C4-Me), 13.5(C6-Me), 11.4(C8-Me), 6.8(C1-Me); Elemental analysis for $C_{20}H_{30}O_5$: calcd. C 68.54, H 8.63; found. C 68.52, H 8.72

19: ^{1}H NMR δ: = 7.18 (d, $J = 8.64$ Hz, 2H; Aryl-H), 6.80 (d, $J = 8.72$ Hz, 2H; Aryl-H), 5.98 (s, 1H; C3-OH), 5.06 (t, $J = 5.97$ Hz, 1H; C15-H), 4.60 (d, $J = 10.96$ Hz, 1H; CH_a-Aryl), 4.30 (d, $J = 10.95$ Hz, 1H; CH_b-Aryl), 4.04 (ddd, $J = 8.59$, 2.58, 2.35 Hz, 1H; C9-H), 3.70 (s, 3H; OMe), 3.66 (dd, $J = 11.06$, 2.77 Hz, 1H; C7-H), 3.34 (t, $J = 2.77$ Hz, 1H; C5-H), 3.22 (d, $J = 2.60$ Hz, 1H; C9-OH), 2.82 (dq, $J = 7.04$, 14.06 Hz, 1H; C12-H), 2.68 (dq, $J = 7.12$, 2.26 Hz, 1H; C10-H), 2.24 (dd, $J = 14.01$, 7.24 Hz, 1H; C13-H_a), 2.21 (ddq, $J = 11.01$, 6.82, 3.19 Hz, 1H; C6-H), 2.04 (dq, $J = 7.12$, 2.77 Hz, 1H; C4-H), 1.90 (m, 2H; C10-H_a,H_b), 1.86 (dd, J =13.74, 6.14 Hz, 1H; C13-H_b), 1.72 (ddq, $J = 8.50$, 7.02, 2.75 Hz, 1H; C8-H), 1.52 (s, 3H; C14)-Me, 1.46 (m, 2H; C2-H,H′), 0.99 (d, $J = 7.02$ Hz, 3H; C10-Me), 0.96 (d, $J = 6.86$ Hz, 3H; C12-Me), 0.87 (d, $J = 7.09$ Hz, 3H; C8-Me), 0.87 (t, $J = 7.32$ Hz, 3H; C1-Me), 0.863 (d, $J = 7.09$ Hz, 3H; C4-Me), 0.856 (d, $J = 6.70$ Hz 3H; C6-Me), 0.84 (t, $J = 7.57$ Hz, 3H; C17-Me); ^{13}C-NMR (assignment by ^{1}H-^{13}C correlation): δ = 219.0(C11), 159.5(Aryl), 131.3(Aryl), 129.7(Aryl), 129.5(C15), 129.3(C14), 113.9(Aryl), 99.3(C3), 85.0(C5), 74.1(C7), 72.3($\underline{C}H_2$Aryl), 71.9(C9), 55.2(OMe), 47.3(C10), 43.3(C13), 43.1(C12), 36.8(C8), 36.0(C4), 32.7(C6), 31.4(C2), 21.2(C10), 16.5(Cx8,12), 15.7(C14-Me), 14.1(C6-Me), 14.0(C4-Me), 13.8(C17-Me), 8.4(C10-Me), 6.8(C1-Me); MS (EI): *m/z* calcd. for $C_{31}H_{48}O_5$ (M^+-H_2O) 500.3503. found 500.3495

21: ^{1}H NMR: $\delta = 7.24$ (d, $J = 8.59$ Hz, 2H; Aryl-H), 6.88 (d, $J = 8.69$ Hz, 2H; Aryl-H), 6.00 (s, 1H; C3-OH), 5.12 (bt, $J = 5.86$ Hz, 1H; C15-H), 4.66 (d, $J = 10.94$ Hz, 1H; CH_a-Aryl), 4.38 (d, $J = 10.92$ Hz, 1H; CH_b-Aryl), 4.04 (q, $J = 6.98$ Hz, 1H; C10-H), 3.93 (dd, $J = 10.96$, 3.61 Hz, 1H; C7-H), 3.81 (s, 3H; OMe), 3.40 (dd=t, $J = 2.80$ Hz, 1H; C5-H), 2.88 (dq, $J = 6.95$, 14.14 Hz, 1H; C12-H), 2.76 (dq, $J = 3.84$, 7.11 Hz, 1H; C8-H), 2.38 (ddq, $J = 10.95$, 6.81, 2.80 Hz, 1H; C6-H), 2.26 (dd, $J = 13.51$, 6.83 Hz, 1H; C13-H), 2.08 (dq, $J = 7.16$, 2.45 Hz, 1H; C4-H), 1.91 (m, 3H; C13-H, C16-H,H′), 1.59 (s, 3H; C14-Me), 1.58 (m, 2H; C2-H,H′), 1.23 (d, $J = 6.80$ Hz, 3H; C8-Me), 1.22 (d, $J = 6.90$ Hz, 3H; C10-Me), 1.04 (d, $J = 6.80$ Hz, 3H), 0.80-0.95 (m, 12H); ^{13}C-NMR: $\delta = 211.1$(C9), 208.3(C11), 159.6(Aryl), 131.1(Aryl), 129.8(Aryl), 129.6(C15), 129.2(C14), 113.9(Aryl), 99.6(C3), 84.7(C5), 72.4 x 2($\underline{C}H_2$-Aryl, C7), 58.9(C10), 55.3(OMe), 49.1(C8), 43.6(C12), 43.4(C13), 35.8(C4), 32.0(C2), 31.3(C6), 21.2(C16), 16.5(C12-Me), 15.9(C14-Me), 14.2, 13.9, 13.6, 13.2, 13.0, 6.9(C1-Me); MS (EI): *m/z* calcd. for $C_{31}H_{46}O_5$ (M^+- H_2O) 498.3345. found 498.3342

[1] R. W. Hoffmann, *Angew. Chem. 99* (1987) 503; *Angew. Chem. Int. Ed. Engl. 26* (1987) 489.
[2] J. E. Hochlowski, D. J. Faulkner, G. K. Matsumoto, J. Clardy, *J. Am. Chem. Soc. 105* (1983) 7413.
[3] F. E. Ziegler, M. R. Becker, *J. Org. Chem. 55* (1990) 2800.
[4] R. W. Hoffmann, K. Ditrich, G. Köster, R. Stürmer, *Chem. Ber. 122* (1989) 1783.
[5] R. W. Hoffmann, S. Dresely, B. Hildebrandt, *Chem. Ber. 121* (1988) 2225.
[6] R. W. Hoffmann, S. Dresely, *Tetrahedron Lett. 28* (1987) 5303.
[7] L. E. Overman, N.-H. Lin, *J. Org. Chem. 50* (1985) 3669.
[8] D. Enders, U. Baus, *Liebigs Ann. Chem. 1983*, 1439.
[9] D. A. Evans, J. V. Nelson, E. Vogel, T. R. Taber, *J. Am. Chem. Soc. 103* (1981) 3099.
[10] D. B. Dess, J. C. Martin, *J. Org. Chem. 48* (1983) 4155.

Catalytic and Stoichiometric Enantioselective Addition of Diethylzinc to Aldehydes Using a Novel Chiral Spirotitanate **

By *Beat Schmidt* and *Dieter Seebach**

The enantioselective addition of diethylzinc to aldehydes, catalyzed by chiral amino alcohols, has become a sport in organic synthesis, generating a number of unusual achievements.[1-5] We report here another record: it is possible, with the same catalyst, to obtain either enantiomer in an excess of up to 99.5:0.5 by simply changing the reaction conditions.

In the course of our work on the use of chiral titanates[6-8] for the addition of nucleophiles to carbonyl groups, we have prepared the spirotitanate **1**. A colorless, spectroscopically and analytically pure, crystalline compound, **1** is stable in air for many hours and exists as a monomer in solution. This spirotitanate is prepared from the corresponding diol derived from (*R*,*R*)-tartaric acid[9-13] and tetraethyl titanate by azeotropic distillation of ethanol with toluene followed by removal of the solvent in vacuo. We

[*] Prof. Dr. D. Seebach, Dipl.-Chem. B. Schmidt
Laboratorium für Organische Chemie der
Eidgenössischen Technischen Hochschule
ETH-Zentrum, Universitätstrasse 16, CH-8092 Zürich (Switzerland)

[**] The results described herein are part of the proposed dissertation of B. S.

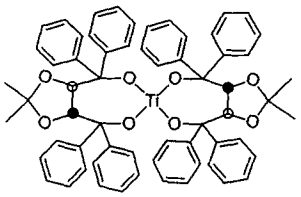

1

tested **1** for the enantioselective activation of aldehydes on addition of diethylzinc. Details of the execution of the reaction and of the current results are shown in equations 1 and 2, as well as in Table 1. The enantiomeric ratios listed have been determined by ^{19}F NMR spectroscopy of the Mosher esters.

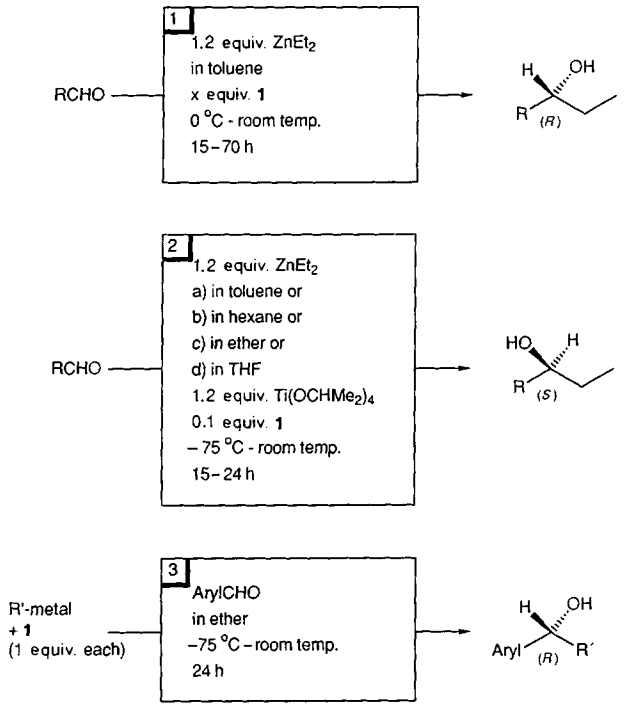

The addition of 0.05–2.0 equivalents of **1** to a mixture (1.2:1) of diethyzinc[14] and anisaldehyde in toluene leads to the (*R*)-alcohol (up to 99:1). However, if the concentration of **1** is held constant at 0.1 equivalents and an additional 1.2 equivalents of tetraisopropyl titanate are added at low temperature, the (*S*)-alcohol is formed in excess (97:3). Under these conditions (RCHO:Ti(O*i*Pr)$_4$:1 = 1:1.2:0.1) we have also tested some other aromatic, as well as saturated and α,β-unsaturated aliphatic aldehydes and have found that the (*S*)-alcohol always predominates (≥ 9:1). Moreover, unlike in the previously published enantioselective activations of Et_2Zn, the hydrocarbon solvent can be replaced by diethyl ether or even tetrahydrofuran. Finally we investigated whether titanate **1** can also be used for the enantioselective addition of methyllithium and Grignard reagents to aldehydes via a chiral ate-complex[10, 15] (see Equation 3 and Table 1). This is indeed possible and the stereochemical outcome is reversed again: the (*R*)-alcohol is formed from anisaldehyde with a selectivity of 96:4.

These findings are remarkable for the following reasons: a) the reaction is an exclusively Lewis acid mediated addition of diethylzinc to aldehydes (no amino alcohol or amide is added); b) the induction achieved by the use of the bulky chiral spirotitanate is reversed, rather than "diluted", by the addition of a tenfold excess of achiral titanate; c) donor solvents such as ether may be used without detrimental effects.

Table 1. Results of enantioselective alkyl transfer reactions mediated by the spirotitanate **1** as shown in equations 1–3.

Method		Aldehyde	Formula	Product Yield [%]	*R/S*
1	x = 0.05	Anisaldehyde	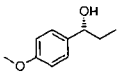	33	91:9
	x = 0.1			15	91:9
	x = 1.0			42	95:5
	x = 2.0			89	99:1
2	a	Heptanal	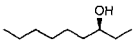	75	4:96
	a	3-Phenyl-propanal	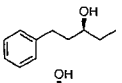	85	9:91
	b	Isobutyr-aldehyde		44	3:97
	a	Cyclohexane carbaldehyde		67	9:91
	a	Cinnamic aldehyde	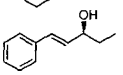	89	2:98
	a	Benzaldehyde		75	0.5:99.5
	c			62	1:99
	d			63	9:91
	a	Anisaldehyde	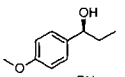	86	3:97
	a	*p*-Bromobenz-aldehyde	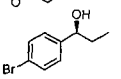	88	5:95
	a	Thiophene-1-carbaldehyde		75	3:97
3	MeLi	Benzaldehyde	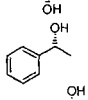	65	95:5
	MeLi	Anisaldehyde	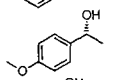	53	96:4
	MeMgI	Benzaldehyde		46	81:19
	MgBr	Benzaldehyde	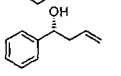	50	80:20

These results are of general significance for enantioselective synthesis,[16] and we hope soon to be able to explain the observed effects.[17]

Experimental Procedure

Spirotitanate: The spirotitanate **1**, prepared as described above from highly pure starting materials, should not contain more than 10% of the free diol for use in the reactions. It is insoluble in ether and can be washed with this solvent.

Catalytic reactions: Upon completion of the reaction (20 mL solvent/10 mmol aldehyde/1 mmol **1**), 10 mL of saturated NH_4Cl and 30–50 mL Et_2O are added, and the solution is stirred for 30 min. The solution is then filtered through celite, dried (saturated NaCl solution, then Na_2SO_4), and concentrated. Low molecular weight products are purified by flash chromatography through a short column (hexane/Et_2O 3:1) to remove unreacted aldehyde, toluene, and

traces of a light yellow impurity. The alcohol is obtained from the resulting residue by kugelrohr vacuum distillation.

Stoichiometric reactions: The diol, prepared as above until after the drying stage, is precipitated by the addition of pentane to the ether solution and filtered (this may need to be repeated). The resulting solution is concentrated and the residue is distilled either directly, or after chromatography, as described above. Recovery of the diol (m.p. 190–192 °C, $[\alpha]_D^{20} = -68.5$ ($c = 1$, $CHCl_3$)) [6c]: By recrystallization from ether/pentane; hydrolysis of the dioxolane ring was not observed in the experiments described here.

Received: September 3, 1990 [Z 4164]
German version: *Angew. Chem. 103* (1991) 100

[1] For a compilation of references: R. C. Larock: *Comprehensive Organic Transformations*, VCH, New York, Weinheim 1989, pp. 566–567.
[2] M. Kitamura, S. Suga, K. Kawai, R. Noyori, *J. Am. Chem. Soc. 108* (1986) 6071; for the mechanism: M. Kitamura, S. Okada, S. Suga, R. Noyori, *ibid. 111* (1989) 4028.
[3] K. Soai, A. Ookawa, T. Kaba, K. Ogawa, *J. Am. Chem. Soc. 109* (1987) 7111.
[4] M. Yoshioka, T. Kawakita, M. Ohno, *Tetrahedron Lett. 30* (1989) 1657.
[5] E. J. Corey, P. W. Yuen, F. J. Hannon, D. A. Wierda, *J. Org. Chem. 55* (1990) 784.
[6] a) B. Weidmann, L. Widler, A. G. Olivero, C. D. Maycock, D. Seebach, *Helv. Chim. Acta 64* (1981) 357; b) D. Seebach, A. K. Beck, S. Roggo, A. Wonnacott, *Chem. Ber. 118* (1985) 3673; c) D. Seebach, A. K. Beck, R. Imwinkelried, S. Roggo, A. Wonnacott, *Helv. Chim. Acta 70* (1987) 954.
[7] Reviews: a) B. Weidmann, D. Seebach, *Angew. Chem. 95* (1983) 12–26; *Angew. Chem. Int. Ed. Engl. 22* (1983) 31–45; b) D. Seebach, B. Weidmann, L. Widler in R. Scheffold (Ed.): *Modern Synthetic Methods, Vol. 3*, Salle + Sauerländer, Aarau/Wiley, New York 1983, pp. 217–353; c) D. Seebach, A. K. Beck, M. Schiess, L. Widler, A. Wonnacott, *Pure Appl. Chem. 55* (1983) 1807–1822; d) D. Seebach in J. Streith, H. Prinzbach, G. Schill (Eds.): *Organic Synthesis an Interdisciplinary Challenge (IUPAC Symp. Org. Synth. 5th)*, Blackwell, Oxford 1985, pp. 77–99.
[8] Work of other authors: a) M. T. Reetz: *Organotitanium Reagents in Organic Synthesis*, Springer, Berlin 1985, chapter 5.5; M. T. Reetz, T. Kükenhöhner, P. Weinig, *Tetrahedron Lett. 77* (1986) 5711; b) R. O. Duthaler, P. Herold, S. Wyler-Helfer, M. Riediker, *Helv. Chim. Acta 73* (1990) 659 (Part 5 of "Enantioselective Syntheses with Titanium-Carbohydrate-Complexes") and earlier publications in this series.
[9] Originally prepared by A. K. Beck, ETH Zürich, November 1982, and A. Wonnacott, Masters Thesis, ETH Zürich 1983; Experimental procedure for preparation of the diol: [6c, 7b]; earlier applications for nucleophilic additions: [6c, 7].
[10] Use of the diol for chiral titanium-ate-complexes: [7c] and H. Takahashi, A. Kawabata, H. Niwa, K. Higashiyama, *Chem. Pharm. Bull. 36* (1988) 803.
[11] Use of similar diol for the preparation of chiral titanium Lewis acids employed in enantioselective Diels–Alder reactions: [6c, 11a]; cyanohydrin addition: [11b]; ene reactions: [11c]. a) K. Narasaka, N. Iwasawa, M. Inoue, T. Yamada, T. Yamada, M. Nakashima, J. Sugimori, *J. Am. Chem. Soc. 111* (1989) 5340; b) K. Narasaka, T. Yamada, H. Minamikawa, *Chem. Lett. 1987*, 2073; c) K. Mikami, M. Terada, T. Nakai, *J. Am. Chem. Soc. 112* (1990) 3949.
[12] a) Application of the diol for the preparation and solid-phase reactions of inclusion compounds: F. Toda, K. Mori, *J. Chem. Soc. Chem. Commun. 1989*, 1245 and many other publications of the group of Prof. Toda. b) X-ray-structures of clathrates from the diol and amines: E. Weber, N. Dörpinghaus, I. Goldberg, *ibid. 1988*, 1566.
[13] Since our first publications [7, 9] on the application of the diol, the hydroxy(diphenyl)methyl group has been successfully employed as part of numerous chiral auxiliaries: [3, 5, 11, 12], and a) E. J. Corey, R. K. Bakshi, *Tetrahedron Lett. 31* (1990) 611 and earlier papers cited therein; b) M. Braun, R. Devant, *ibid. 25* (1984) 5031. Reviews: M. Braun, *Angew. Chem. 99* (1987) 24; *Angew. Chem. Int. Ed. Engl. 26* (1987) 24; detailed description for the Braun method: R. Devant, U. Mahler, M. Braun, *Chem. Ber. 121* (1988) 397.
[14] The diol alone furnished in this reaction yields of $\leq 10\%$ and enantiomeric ratios of $\leq 3:1$ (L. Behrendt, ETH Zürich, hitherto unpublished results).
[15] J.-T. Wang, X. Fan, X. Feng, Y.-M. Qian, *Synthesis 1989*, 291.
[16] Other, more or less obvious applications and modifications of **1** are currently under intensive investigation in our laboratories.
[17] Until now, there has been no time for mechanistic studies; we know, however, from NMR studies, that mixing of a $CHCl_3$ solution of **1** with $Ti(OCHMe_2)_4$ at room temperature leads to exchange of the RO ligands, presumably with formation of a monocyclic titanate with two Me_2CHO groups on titanium! In other cases of enantioselectively catalyzed Et_2Zn additions, detailed mechanistic proposals have been made [2, 4, 5].

$Th_6Br_{15}H_7$—Stabilization of a Th_6Br_{12} Cluster by Seven Hydrogen Atoms

By *Arndt Simon*,* *Fred Böttcher*, and *Jeremy Karl Cockcroft*

The formation of cluster compounds of thorium was observed for the first time during attempts to prepare reduced thorium bromides. Their formation requires the presence of a third element, which, as interstitial atoms, stabilizes the cluster.[1] These compounds are, on the one hand, structurally closely related with corresponding compounds of zirconium[2, 3] and niobium,[4] and, on the other, they form hitherto unknown types of clusters. Thus, the compounds $Th_6Br_{14}C$ and $Th_6Br_{15}M$ with Th_6Br_{12} clusters were obtained, which are stabilized by a C or M atom (M = Mn, Fe,Co,Ni) in the center of the octahedral Th_6 unit.[5] In contrast, the central units in compounds of the type $Th_{12}Br_{29}N_6A_y$ (A = Li–Rb; $y = \leq 1$) consist of twelve closely packed Th atoms.[6]

The incorporation of an interstitial H atom in the M_6 octahedron was first demonstrated years ago in HNb_6I_{11}.[7] In a corresponding attempt to stabilize the Th_6Br_{12} cluster by hydrogen we obtained a remarkable result. The reaction of Th and $ThBr_4$ under H_2[8] led, inter alia, to black, cubic crystals, an X-ray structure analysis of which[10] revealed an arrangement of the Th and Br atoms as in Nb_6F_{15}.[11] Th_6Br_{12} clusters are linked to one another via Br atoms facing all six vertices of the octahedra according to $Th_6Br^i_{12}Br^{a-a}_{6/2}$ (via linear Br^{a-a} bridges!). Two such interpenetrating skeletons form a body-centered structure. Neutron diffraction diagrams of the deuteriated powder confirmed the analytically determined, surprisingly high hydrogen content of the compound.[10] Seven D atoms[12] are statistically distributed over the eight face centers of the Th octahedron. As shown in Figure 1 the D atoms do not lie in the interior of the octahedron but about 22 pm from the triangular faces. This displacement can easily be explained in terms of the electrostatic repulsion between the hydride-like bonded H atoms; the D–D distance (205.0 pm) is very short, comparable with the assumed shortest H–H distances in Th_4H_{15}.[13]

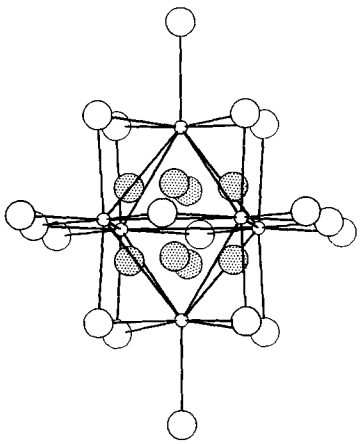

Fig. 1. Metal clusters in $Th_6Br_{15}D_7$ (small circles Th, large open circles Br, hatched circles D with 7/8 occupation). Shortest distances pm from neutron diffraction data: d(Th–Th) = 386.1(2), d(Th–D) = 223.8(2), octahedra edges $d(Th–Br^i) = 294.5(1)$, octahedra apices $d(Th–Br^{a-a}) = 295.8(1)$, d(D–D) = 205.0(3). The D atoms are surrounded by an almost trigonal planar array of Th atoms. The Th–Th distance is slightly shorter than in the compounds MTh_6Br_{15} with M = Fe, Co (d(Th–Th) = 391.8(2)).

[*] Prof. Dr. A. Simon, Dr. F. Böttcher, Dr. J. K. Cockcroft
Max-Planck-Institut für Festkörperforschung
Heisenbergstrasse 1, W-7000 Stuttgart 80 (FRG)

The additional occupation of the face centers of the M_6 octahedron of a M_6X_{12} cluster is observed for the first time in $Th_6Br_{15}H_7$; this type of occupation is already known for systems with condensed clusters. In the compounds ZrXH (X = Cl, Br)[14] and $LnXH_2$[15] two H atoms assume positions in opposite faces of elongated trigonal antiprisms of M atoms (d(D–D) = 220 pm in the case of ZrBrD and 298 pm in the case of $TbBrD_2$).

The number of bonding orbitals in the $Th_6Br_{12}H_7$ cluster is the same as in the hypothetical empty Th_6Br_{12} cluster: bonding H–Th interactions merely lead to a lowering of individual orbital energies; the antibonding combinations lie above the HOMO-LUMO gap. Thus, the electron balance for $Th_6Br_{15}H_7$ ($6\times4-15+7=16$) corresponds exactly to that for a complete occupation of all bonding cluster orbitals (for comparison Nb_6F_{15}: $6\times5-15=15$). The metal–metal bonding in the (empty) M_6X_{12} cluster is best described in terms of closed three-center two-electron bonds in all eight faces of the M_6 octahedron[16] and provides a clear picture of the bonding contribution of the H atoms. Seven of these multicenter bonds are reinforced by the mixing of the 1s function of the respective H atom in the center of the bond and by the additional electron of each H atom, so that finally there are seven four-center two-electron bonds and one three-center two-electron bond.

Since the electron balance already varies in the case of empty clusters (e.g. $Ta_6Cl_{12}^{n\oplus}$ with n = 2–4, corresponding to 16 to 14 electrons in M–M bonding states[17]) and can be further decreased in clusters with interstitial atoms (e.g. $Sc_7Cl_{12}B$ corresponding to 12 electrons[18]), it is to be expected that the hydrogen content in $Th_6Br_{15}H_7$ is variable. Further investigations are currently under way.

Received: September 3, 1990 [Z 4165 IE]
German version: *Angew. Chem. 103* (1991) 79

CAS Registry numbers:
$Th_6Br_{15}H_7$, 131104-16-0; $Th_6Br_{15}D_7$, 131130-13-7.

[1] A. Simon, *Angew. Chem. 100* (1988) 163; *Angew. Chem. Int. Ed. Engl. 27* (1988) 159.
[2] R. P. Ziebarth, J. D. Corbett, *Acc. Chem. Res. 22* (1989) 256.
[3] F. Rogel, J. Zhang, M. W. Payne, J. D. Corbett *Adv. Chem. Ser. 226* (1990) 379.
[4] H. Schäfer, H. G. Schnering, *Angew. Chem. 76* (1964) 833.
[5] F. Böttcher, A. Simon, R. K. Kremer, H. Buchkremer-Hermanns, J. K. Cockcroft, *Z. Anorg. Allg. Chem.*, in press.
[6] A. Simon, F. Ueno, F. Böttcher, T. Braun, unpublished.
[7] A. Simon, *Z. Anorg. Allg. Chem. 355* (1967) 295.
[8] Procedure: 708 mg of $ThBr_4$ and 182 mg of ThH_2 were heated in a sealed Ta capsule (protected by a quartz glass ampoule from oxidation) for 3 d at 100 °C. Finally the unopened Ta capsule was tempered for 1 d under 1 atm of H_2 at 680 °C. The X-ray diagram of the reaction product showed cubic symmetry of $Th_6Br_{15}H_x$ with a few very weak extraneous lines. The analytical determination of the H content (combustion in O_2, determination as H_2O) yielded $5.5 \le x \le 5.7$. For the neutron diffraction, a sample b was used which was originally prepared for other purposes (4320 mg $ThBr_4$, 687 mg Th, Ta capsule in quartz glass ampoule, 0.5 d 1000 °C, three weeks 640 °C, finally annealed in Ta capsule for 3 d at 680 °C in 1 atm D_2). The X-ray investigation showed the simple diagram of $Th_6Br_{15}D_x$ besides the line-rich (therefore weak) diagram of $ThBr_{3.5}D_{0.17}$ [9]. The analytical determination of the D content gave $x \approx 5.8$ for the corresponding portion of $Th_6Br_{15}D_x$.
[9] F. Böttcher, *Dissertation*, Universität Stuttgart 1990.
[10] Space group $Im\bar{3}m$ 229); $Z = 2$. a) Single crystal (X-ray structure analysis): $P2_1$ diffractometer, $Mo_{K\alpha}$, $\lambda = 71.069$ pm; $a = 1140.7(1)$ pm; 1228 reflections, 245 symmetry independent, 243 with $F_0 \ge 3\sigma(F_0)$; absorption correction with ψ scan; $R = 0.049$, $R_w = 0.041$ (anisotropic); $\varrho_{calcd} = 5.83\ g\ cm^{-3}$; x parameter: Th(12e)0.2402(4), Br1(24h)0.2560(2), Br2(6b)0.5. b) Powder (neutron diffraction): D1A diffractometer ILL Grenoble, $\lambda = 191.10$ pm; ca. 5 g (sample b) in quartz glass tube; $a = 1137.61(1)$ pm; Rietveld refinement for the $Th_6Br_{15}D_x$ portion, $R_{wp} = 0.075$, $R_{exp} = 0.048$; x parameter: Th 0.2400(1), Br1 0.2582(1), D(16f)0.0901(2); S.O.F.$_D$ = 0.88(1) corresponding to $Th_6Br_{15}D_{7.0}$. Further details of the crystal structure investigation are available on request from the Fachinformationszentrum Karlsruhe, Gesellschaft für wissenschaftlich-technische Information mbH, W-7514 Eggenstein-Leopoldshafen 2 (Germany) on quoting the depository number CSD-54881, the names of the authors, and the journal citation.
[11] H. Schäfer, H. G. von Schnering, K.-J. Niehues, H. G. Nieder-Vahrenholz, *J. Less-Common Met. 9* (1965) 95.
[12] The weak diamagnetism in the temperature range 60–300 K corresponds to 7 H atoms in the cluster.
[13] W. H. Zachariasen, *Acta Crystallogr. 6* (1953) 393.
[14] S. D. Wijeyesekera, J. D. Corbett, *Solid State Common. 54* (1985) 657.
[15] H. Mattausch, A. Simon, K. Ziebeck, *J. Less-Common Met. 113* (1985) 149.
[16] O. K. Andersen, unpublished.
[17] J. H. Espenson, R. E. McCarley, *J. Am. Chem. Soc. 88* (1966) 1063.
[18] S.-J. Hwu, J. D. Corbett, *J. Solid State Chem. 64* (1986) 331.

The Reduction of the NbX_5/AlX_3 System with Aluminum in the Presence of Aromatic Hydrocarbons: An Approach to Niobium(II), Niobium(I), and Niobium(0) Organometallics**

By *Fausto Calderazzo*, Guido Pampaloni, Lucia Rocchi, Joachim Strähle* and *Klaus Wurst*

In memoriam Fausto Ungari

Since the pioneering work by *E. O. Fischer* and *F. Röhrscheid*,[1] who reported the isolation of the hexamethylbenzene (hmb) complexes $[Nb_3Cl_6(\eta^6\text{-hmb})_3]^{n\oplus}$ (n = 1,[1] n = 2[2]) and $Nb_2Cl_4(\eta^6\text{-hmb})_2$[1] by low temperature hydrolysis of the unknown primary reaction products of the $Al/AlX_3/NbX_5$/arene system, this method has seldom been used for the preparation of low-valent niobium organometallics. To the best of our knowledge, only the metal vapor technique is available[3] for the preparation of the bis-arene complexes of niobium(0). In this paper, we report the identification of the primary reaction products in the $Al/AlX_3/NbX_5$/arene system, the further reaction to bis(1,3,5-trimethylbenzene)niobium(0) ([Nb(mes)$_2$]), and some new chemistry of [Nb(mes)$_2$].

The synthesis of the primary reaction products (**1**) is summarized in Equation (a). Compounds **1** have been isolated in moderate yields (30–50%) as dark brown solids sensitive to oxygen and moisture. We assume for these niobium(II)

$$NbX_5 + Al + AlX_3 + \text{arene} \longrightarrow \underset{\mathbf{1}}{[Nb(\eta^6\text{-arene})(AlX_4)_2]} \qquad \text{(a)}$$

X = Cl, arene = benzene, hmb; X = Br, arene = hmb

derivatives a halo-bridged structure of the type already established by X-ray diffractometry for the corresponding titanium(II) complexes,[4] $[\eta^6\text{-arene})Ti\{(\mu\text{-}X)_2(AlX_2)\}_2]$, and by chemical and spectroscopic data for the similar zirconium(II) species.[5]

[*] Prof. F. Calderazzo,* Dr. G. Pampaloni, Dr. L. Rocchi
Dipartimento di Chimica e Chimica Industriale,
Sezione di Chimica Inorganica
Università di Pisa
Via Risorgimento 35, I-56126 Pisa (Italy)
Prof. Dr. J. Strähle, Dipl. Chem. K. Wurst
Institut für Anorganische Chemie der Universität
Auf der Morgenstelle 18
W-7400 Tübingen (FRG)

[**] This work was supported by the Consiglio Nazionale delle Ricerche (C.N.R. Roma) and by the Ministero dell'Università e della Ricerca Scientifica e Tecnologica (MURST).

Treatment of **1** (X = Br, arene = hmb) with tetrahydrofuran at room temperature gives compound **2** [Eq. (b)].

$$2[Nb(\eta^6\text{-hmb})(AlBr_4)_2] \xrightarrow[\sim 20\,^\circ C]{THF} \underset{\mathbf{2}}{[Nb_2Br_4(\eta^6\text{-hmb})_2]} + 4\,AlBr_3 \qquad (b)$$

Preliminary results of an X-ray diffractometric experiment on a single crystal of **2**, showed a dimeric centrosymmetric structure with four bridging bromides and a Nb–Nb distance of 2.760(2) Å, suggestive, together with the 18-electron count, of a single niobium–niobium bond.[6] Compound **1** (arene = hmb, X = Br) is oxidized by water at about $-30\,^\circ C$ giving a 50% yield of the trinuclear compound $[Nb_3Br_6(\eta^6\text{-hmb})_3]Br$.[2]

The primary reaction product of $Al/AlX_3/NbX_5$/1,3,5-trimethylbenzene (mes) system was not isolated; however, the crude reaction mixture, still containing unreacted aluminum, was treated with tetrahydrofuran (THF) or 1,2-dimethoxyethane (DME) at temperatures as low as $-15\,^\circ C$. Under these conditions, further reduction occurs and $Nb(mes)_2$ is obtained in 30–50% yields [see reaction sequence (c)]. This represents the first synthesis of a niobium(0) derivative which does not require the use of the vapor-metal technique.

$$NbCl_5 \xrightarrow[2)\ DME,\ -15\,^\circ C]{1)\ Al/AlCl_3/mes} [Nb(mes)_2] \qquad (c)$$

The redox reactivity of $[Nb(mes)_2]$ in the presence of carbon monoxide has been investigated in some detail. $[Nb(mes)_2]$ reacts with CO in *n*-heptane at room temperature, the reaction time depending on the pressure of carbon monoxide (48 h at atmospheric pressure, 24 h at 5 atm, 10 h at 50 atm), to give the green $[Nb(mes)_2(CO)][Nb(CO)_6]$ in substantially quantitative yields [Eq. (d)]. Thus, the chemistry of $[Nb(mes)_2]$ parallels that of the corresponding

$$2[Nb(mes)_2] + 7\,CO \longrightarrow [Nb(mes)_2(CO)][Nb(CO)_6] + 2\,mes \qquad (d)$$

vanadium(0) system,[7] except that vanadium requires more drastic conditions: $[V(mes)_2]$ does not react appreciably with CO under the conditions used for $[Nb(mes)_2]$. The hexacarbonylvanadate(−1) and the tetraphenylborate salts of the bis(mesitylene)carbonylniobium(I) cation have been obtained by oxidation of $[Nb(mes)_2]$ with $V((CO)_6$ and (N,N'-Me_2-4,4′-bipyridyl)$(BPh_4)_2$ under CO. When the oxidation of $[Nb(mes)_2]$ by (N,N'-Me_2-4,4′-bipyridyl)$(BPh_4)_2$ was performed under argon in THF, $[Nb(mes)_2(thf)]BPh_4$ was isolated in high yields.

$[Nb(mes)_2]$ has been reported[8] to be reduced to the $[Nb(mes)_2]^\ominus$ anion by potassium in DME. We have observed that $[Nb(mes)_2]$ is not affected by $[CoCp^*_2]$ ($Cp^* = (\eta^5$-$C_5Me_5)$) in toluene under argon, but it slowly reacts under CO at atmospheric pressure to give high yields of $[Co(Cp^*)_2][Nb(CO)_6]$ [Eq. (e)]. This suggests that the presumably fast electron transfer occurs on a partially carbonylated product of niobium(0).

$$[Nb(mes)_2] + 6\,CO + [CoCp^*_2] \longrightarrow [CoCp^*_2][Nb(CO)_6] + 2\,mes \qquad (e)$$

Experimental Procedure

$[Nb(mes)_2]$: A suspension of Al powder (5.7 g, 211 mmol), sublimed $AlCl_3$ (4.69 g, 35.2 mmol) and sublimed $NbCl_5$ (9.45 g, 35.0 mmol) in mesitylene (40 mL) was stirred at room temperature for 15 h and at 120–130 °C for 4 h. The reaction mixture consisted of two brown liquid layers. Under vigorous stirring. DME (50 mL) was slowly added (30 min) to the reaction mixture cooled to $-15\,^\circ C$. After the addition was complete, *n*-heptane (50 mL) was added and the deep red suspension was stirred at room temperature for 15 h. After filtration, the red filtrate was dried at 30–40 °C/10^{-2} torr and the residue treated with *n*-heptane (50 mL). The solution was filtered and evaporated to dryness under vacuum at room temperature, and the residue treated with *n*-heptane (5 mL) which partially dissolved the solid. After cooling to $-78\,^\circ C$, $[Nb(mes)_2]$ (5.03 g, 43% yield) was obtained as dark brown microcrystals.

$[Nb(mes)_2(CO)][Nb(CO)_6]$: A solution of $[Nb(mes)_2]$ (1.02 g, 3.1 mmol) in *n*-heptane (100 mL) was introduced into a glass autoclave (Büchi, Uster, Switzerland) and stirred for 24 h under CO at a pressure of 5 atm. The bright green solid was filtered, dried under vacuum at room temperature and identified as $[Nb(mes)_2(CO)][Nb(CO)_6]$ (0.64 g, 67% yield). Analysis: Found: CO 31.1, Nb 28.9; Calcd. for $C_{25}H_{24}Nb_2O_7$: CO 31.5, Nb 29.3. IR (THF): $\tilde{\nu}$ [cm^{-1}] = 1990 m, 1889 m(sh), 1859 vs.

Received: September 4, 1990 [Z 4168]
German version: *Angew. Chem. 103* (1991) 109

CAS Registry numbers:
1 (arene = benzene, X = Cl), 131078-97-2; **1** (arene = hmb, X = Cl), 131078-98-3; **1** (arene = hmb, X = Br), 131078-99-4; **2**, 131079-00-0; hmb, 87-85-4; mes, 108-67-8; $NbCl_5$, 10026-12-7; $NbBr_5$, 13478-45-0; $AlCl_3$, 7446-70-0; $AlBr_3$, 7727-15-3; $[V(CO)_6]$, 14024-00-1; $[Nb_3Br_6(\eta^6\text{-hmb})_3]Br$, 37328-49-7; $[Nb(mes)_2]$, 68088-96-0; $[Nb(mes)_2(CO)][Nb(CO)_6]$, 131079-02-2; $[Nb(mes)_2(thf)]BPh_4$, 131079-04-4; $[CoCp^*_2][Nb(CO)_6]$, 131079-05-5; $[CoCp^*_2]$, 74507-62-3; (4,4′-Me_2bipyridyl)$(BPh_4)_2$, 80777-50-0; Al, 7429-90-5; benzene, 71-43-2.

[1] E. O. Fischer, F. Röhrscheid, *J. Organomet. Chem. 6* (1966) 53.
[2] M. R. Churchill, S. W. Y. Chang, *J. Chem. Soc., Chem. Commun. 1974*, 248; R. B. King, D. M. Braitsch, P. N. Kapoor, *J. Am. Chem. Soc. 97* (1975) 60; S. Z. Goldberg, B. Spivack, G. Stanley, R. Eisenberg, D. M. Braitsch, J. S. Miller, M. Abkowitz, *ibid. 99* (1977) 110; F. Stollmaier, U. Thewalt, *J. Organomet. Chem. 222* (1981) 227.
[3] F. G. N. Cloke, M. L. H. Green, *J. Chem. Soc. Dalton Trans. 1981*, 1938.
[4] U. Thewalt, F. Österle, *J. Organomet. Chem. 172* (1979) 317; U. Thewalt, F. Stollmaier, *ibid. 228* (1982) 149; S. I. Troyanov, V. B. Rybakov, *Metalloorg. Khim. 1* (1988) 1280; *ibid. 2* (1989) 1382.
[5] F. Calderazzo, S. Pallavicini, G. Pampaloni, *J. Chem. Soc. Dalton Trans. 1990*, 1813.
[6] C. E. Holloway, M. Melník, *J. Organomet. Chem. 303* (1986) 1, and references cited therein; F. A. Cotton, M. P. Diebold, W. J. Roth, *J. Am. Chem. Soc. 109* (1987) 5506.
[7] F. Calderazzo, R. Cini, *J. Chem. Soc. A 1965*, 818.
[8] J. A. Bandy, K. Prout, F. G. N. Cloke, H. C. deLemos, J. M. Wallis, *J. Chem. Soc. Dalton Trans. 1988*, 1475.

Stereoselective Synthesis of Vicinal Diamines**

By *Manfred T. Reetz,* Ralf Jaeger, Ralf Drewlies,* and *Marcus Hübel*

Although vicinal diamines are a synthetically, biologically, and medicinally important class of compounds,[1] there is still no general procedure for diastereoselective synthesis of these compounds in enantiomerically pure form.[1, 2] Here we report on two methods that transform amino acids **1** selectively into either diamines **5** or **9**, having a new stereogenic center.

To synthesize diamines **5** of (*S,S*) configuration, the *N,N*-dibenzylamino aldehydes **2**,[3] readily accessible from amino acids **1**, were converted under standard conditions (benzylamine/CH_2Cl_2/$MgSO_4$, 0°, 4 h) into the corresponding *N*-benzyl aldimines **3** (90–95% yield). Because Grignard-like additions to simple aliphatic aldimines are notoriously difficult owing to competing α deprotonation,[4] such C–C bond

[*] Prof. Dr. M. T. Reetz, Dipl.-Chem. R. Jaeger, R. Drewlies, Dipl.-Chem. M. Hübel
Fachbereich Chemie der Universität
Hans-Meerwein-Strasse, W-3550 Marburg (FRG)

[**] This work was supported by the Deutsche Forschungsgemeinschaft (SFB 260 and Leibniz-Programm) and the Fonds der Chemischen Industrie.

formation was not expected to be facile in the case of aldimines **3**. In fact, the method based on R_2CuLi in the presence of BF_3 failed[4g] (< 15% adducts), as did the use of Grignard reagents in several solvents and of alkyllithium compounds in THF. In *ether*, on the other hand, MeLi and *n*-BuLi add diastereoselectively with formation of the chelation-controlled[5] adducts **5** (Scheme 1, Table 1). The reason for the poor yield in the case of MeLi was unclear and led us to try the less basic organocerium reagents.[6] Indeed, acceptable results were obtained with the combination *n*BuLi/$CeCl_3$ (Table 1), but not with MeLi/$CeCl_3$! This problem was solved by use of the more reactive Me_3Ce.[7] Organolithium and -cerium reagents add without accompanying racemization.

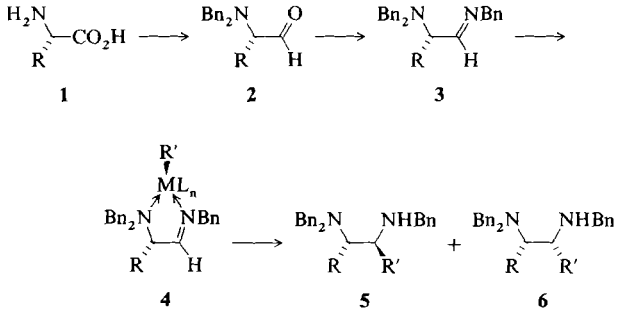

Scheme 1. Bn = CH_2Ph.

Table 1. Stereoselective additions to aldimines **3**.

R	Reagent[a]	Yield [%]	**5**:**6**
Me	*n*BuLi	54	86: 14
Me	*n*BuLi/$CeCl_3$	71	88: 12
Bn	MeLi	40	>95: <5
Bn	MeLi/$CeCl_3$	28	>95: <5
Bn	3 MeLi/$CeCl_3$	78	>95: <5
Bn	3 MeLi/$LaCl_3$	63	>95: <5
Bn	3 MeLi/$YbCl_3$	40	>95: <5
Bn	*n*BuLi	80	93: 7
Bn	*n*BuLi/$CeCl_3$	84	93: 7
Me_2CH	*n*BuLi	85	93: 7
Me_2CH	*n*BuLi/$CeCl_3$	80	89: 11
Me_2CHCH_2	*n*BuLi	77	82: 18
Me_2CHCH_2	*n*BuLi/$CeCl_3$	86	82: 18
Me_2CHCH_2	*n*BuLi/$LaCl_3$	83	83: 17
$Bn_2N(CH_2)_3$	*n*BuLi	76	87: 13

[a] All reactions [14a] were carried out in ether at −78 °C with subsequent warming to room temperature.

We postulate the intermediacy of chelates **4**, which are attacked preferentially from the sterically less shielded side. This contrasts with addition of RLi and RLi/$CeCl_3$ to the corresponding aldehydes **2**, which undergo > 90% non-chelation-controlled reactions.[3] Thus, α-amino aldimines of type **3** are much better chelating agents than aldehydes **2**. This is presumably due to the stronger N–metal bond compared with an O–metal bond and to the (*E*) configuration of the C–N double bond, which makes only *syn* complexation possible.

In order to reverse the direction of diastereoselectivity, it seemed necessary to weaken the donor strength of the nitrogen atoms of the α-amino aldimines to the point where effective chelation no longer pertains. This was accomplished by the replacement of the benzyl group on the aldimine nitrogen by the electron-withdrawing tosyl group. The *N*-tosyl derivatives **7** were prepared by the Weinreb procedure[8] and allowed to react in situ with Grignard reagents. Indeed, the non-chelation-controlled adducts **9** were preferentially formed (Scheme 2, Table 2). This result is consistent with the Felkin–Anh model[5, 9a] or with possible ground-state phenomena.[9b]

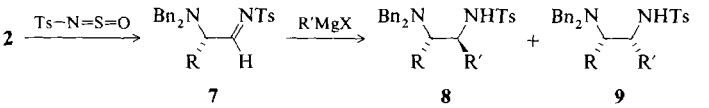

Scheme 2.

Table 2. Stereoselective additions to aldimines **7**.

R	Reagent	Yield [%]	**8**:**9**
Me	MeMgBr	90	11: 89
Me	EtMgBr	89	<5: >95
Me	*n*-BuMgCl	76	15: 85
Me	PhMgCl	89	8: 92
Me	CH_2=$CHMgBr$	85	6: 94
Me	CH_2=$CHCH_2MgCl$	71	6: 94
Bn	MeMgBr	95	7: 93
Bn	EtMgBr	72	9: 91
Bn	*n*-BuMgCl	71	10: 90
Bn	PhMgCl	82	6: 94
Bn	CH_2=$CHMgBr$	79	6: 94
Bn	CH_2=$CHCH_2MgCl$	86	<5: >95
Me_2CH	MeMgBr	91	7: 93
Me_2CH	EtMgBr	86	6: 94
Me_2CH	*n*-BuMgCl	61	6: 94
Me_2CH	PhMgCl	88	<5: >95
Me_2CH	CH_2=$CHMgBr$	69	8: 92
Me_2CH	CH_2=$CHCH_2MgCl$	57	8: 92
Me_2CHCH_2	MeMgBr	72	<5: >95
Me_2CHCH_2	EtMgBr	76	8: 92
Me_2CHCH_2	*n*-BuMgCl	80	10: 90
Me_2CHCH_2	PhMgCl	70	6: 94
Me_2CHCH_2	CH_2=$CHMgBr$	75	<5: >95

The assignment of the configuration of the adducts **5** was made possible by selective deprotection of **5** (R = Bn; R′ = *n*Bu) with H_2/Pd-black[3] to give **10** followed by cyclization to give the urea derivative **11**. The NOE difference spectrum indicated a *trans* arrangement of the two alkyl moieties at the stereogenic centers. Complete debenzylation—for example, to give the free diamine **12**—was accomplished with the Pearlman catalyst according to the method of *Yoshida* et al (Scheme 3).[10] Compound **12** was acylated on both amino groups by treating it with an excess of (+)-3,3,3-trifluoro-2-methoxy-2-phenylpropionyl chloride according to the method of *Mosher*.[11] The bis-acylated adduct shows a single set

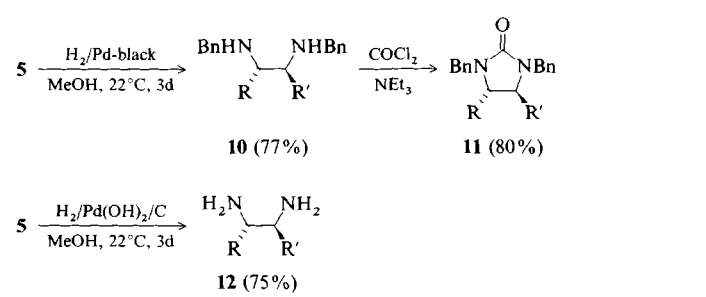

Scheme 3. **10**, **11**, R = Bn, R′ = *n*Bu; **12**, R = Me_2CH, R′ = *n*Bu.

of signals in the ^1H, ^{13}C, and ^{19}F NMR spectra—proof that the synthesis and reactions of the aldimine proceed without racemization (*ee* > 98%). The *N*-tosylamine **9** could also be selectively deprotected. For example, **9** (R = Bn; R′ = Me) was transformed into **13** by treatment with Pearlman catalyst and then cyclized to give the urea derivative **14** having a *cis* arrangement of groups on the stereogenic centers (Scheme 4). Compound **13** was acylated on the NH_2 groups according to the Mosher method[11] and also proved to be optically pure (*ee* > 98%). The tosyl group in **9** was selectively removed by treatment with sodium naphthalide (dimethoxyethane (DME), 6 h, 22 °C)[12] or with sodium in liquid ammonia (−40 °C, 4 h)[13] (81–86% yields), affording product **15**. The free amine **16** was prepared by debenzylation. Such regioselective deprotection is of importance for further reactions at one or the other nitrogen atom.

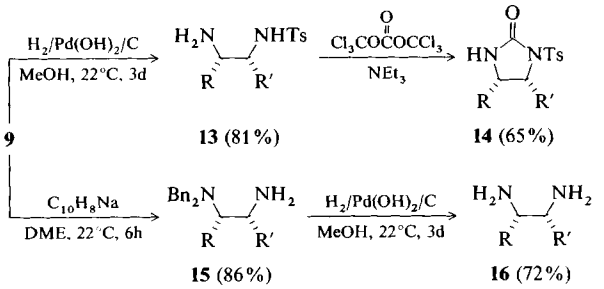

Scheme 4. R = Bn, R′ = Me.

The reactions leading to vicinal diamines **5** and **12** or **9** and **16** are stereoselective, proceed without racemization, and are simple to carry out.[14] Since many amino acids are also accessible in the (*R*) form,[15] it is also possible to prepare the enantiomeric vicinal diamines.

Received: September 6, 1990 [Z 4169 IE]
German version: *Angew. Chem. 103* (1991) 76

CAS Registry numbers:
2 (R = Me), 111060-63-0; **2** (R = Bn), 111060-64-1; **2** (R = Me_2CH), 111060-66-3; **2** (R = Me_2CHCH_2), 111060-65-2; **3** (R = Me), 130984-39-3; **3** (R = CH_2Ph), 130984-40-6; **3** (R = Me_2CH), 130984-41-7; **3** (R = Me_2CHCH_2), 130984-42-8; **3** (R = $Bn_2N(CH_2)_3$)), 130984-43-9; **5** (R = Me, R′ = Bn), 130984-44-0; **5** (R = Bn, R′ = Me), 130984-46-2; **5** (R = Bn, R′ = Bn), 130984-47-3; **5** (R = Me_2CH, R′ = Bn), 130984-49-5; **5** (R = Me_2CHCH_2, R′ = Bn), 130984-51-9; **5** (R = $Bn_2N(CH_2)_3$, R′ = Bn), 130984-53-1; **6** (R = Me, R′ = Bn), 130984-45-1; **6** (R = Bn, R′ = Bn), 130984-48-4; **6** (R = Me_2CH, R′ = Bn), 130984-50-8; **6** (R = Me_2CHCH_2, R′ = Bn), 130984-52-0; **6** (R = $Bn_2N(CH_2)_3$, 130984-54-2; **7** (R = Me), 130984-55-3; 7 (R = Bn), 130984-56-4; 7 (R = Me_2CH), 131010-14-5; **7** (R = Me_2CHCH_2), 130984-57-5; **8** (R = Me, R′ = Me), 130984-58-6; **8** (R = Me, R′ = Ph), 130984-62-2; **8** (R = Bn, R′ = Me), 130984-66-6; **8** (R = Bn, R′ = Et), 130984-68-8; **8** (R = Bn, R′ = Bu), 130984-70-2; **8** (R = Me_2CH, R′ = Me), 130984-75-7; **8** (R = Me_2CH, R′ = CH = CH_2), 130984-80-4; **8** (R = Me_2CHCH_2, R′ = Et), 130984-84-8; **8** (R = Me_2CHCH_2, R′ = Bn), 130984-86-0; **8** (R = Me, R′ = Bn), 130984-97-3; **9** (R = Me, R′ = Me), 130984-59-7; **9** (R = Me, R′ = Et), 130984-60-0; **9** (R = Me, R′ = Bn), 130984-61-1; **9** (R = Me, R′ = Ph), 130984-63-3; **9** (R = Me, R′ = CH = CH_2), 130984-64-4; **9** (R = Me, R′ = CH_2−CH = CH_2), 130984-65-5; **9** (R = Bn, R′ = Me), 130984-67-7; **9** (R = Bn, R′ = Et), 130984-69-9; **9** (R = Bn, R′ = Bu), 130984-71-3; **9** (R = Bn, R′ = Ph), 130984-72-4; **9** (R = Bn, R′ = CH = CH_2), 130984-73-5; **9** (R = Bn, R′ = CH_2 − CH = CH_2), 130984-74-6; **9** (R = Me_2CH, R′ = Me), 130984-76-8; **9** (R = Me_2CH, R′ = Et), 130984-77-9; **9** (R = Me_2CH, R′ = Bu), 130984-78-0; **9** (R = Me_2CH, R′ = Ph), 130984-79-1; **9** (R = Me_2CH, R′ = CH = CH_2), 130984-81-5; **9** (R = Me_2CH, R′ = CH_2 = $CHCH_2$), 130984-82-6; **9** (R = Me_2CHCH_2, R′ = Me), 130984-83-7; **9** (R = Me_2CHCH_2, R′ = Et), 130984-85-9; **9** (R = Me_2CHCH_2, R′ = Bu), 130984-87-1; **9** (R = Me_2CHCH_2, R′ = Ph), 130984-88-2; **9** (R = Me_2CHCH_2, R′ = CH = CH_2), 130984-89-3; **10**, 130984-90-6; **11**, 130984-91-7; **12**, 130984-92-8; **13**, 130984-93-9; **14**, 130984-94-0; **15**, 130984-95-1; **16**, 130984-96-2; T_5N = S = O, 4104-47-6.

[1] Vicinal diamines as ligands in metal-induced stereoselective reactions: a) E. J. Corey, *Pure Appl. Chem. 62* (1990) 1209; K. Tomioka, M. Nakajima, Y. Iitaka, K. Koga, *Tetrahedron Lett. 29* (1988) 573; T. Mukaiyama, *Tetrahedron 37* (1981) 4111; W. Zhang, J. L. Loebach, S. R. Wilson, E. N. Jacobson, *J. Am. Chem. Soc. 112* (1990) 2801; M. Tokles, J. K. Snyder, *Tetrahedron Lett. 27* (1986) 3951; b) as natural products: I. Uchida, N. Shigematsu, M. Ezaki, M. Hashimoto, *Chem. Pharm. Bull. 33* (1985) 3053; E. Atherton, J. Meienhofer, *Hoppe-Seyler's Z. Physiol. Chem. 354* (1973) 689; H. Kohn, N. Zein, *J. Am. Chem. Soc. 105* (1983) 4105; M. Marx, F. Marti, J. Reisdorff, R. Sandmeier, S. Clark, *ibid. 99* (1977) 6754; c) in *cis*-platinum analogues used in chemotherapy: S. J. Lippard, *Pure Appl. Chem. 59* (1987) 731; A. Pasini, F. Zunino, *Angew. Chem. 99* (1987) 632; *Angew. Chem. Int. Ed. Engl. 26* (1987) 615; J. Reedijk, *Pure Appl. Chem. 59* (1987) 181; d) as ligands in technetium-99 chelate compounds for tumor contrasting: S. Kasina, A. R. Fritzberg, D. L. Johnson, D. Eshima, *J. Med. Chem. 29* (1986) 1933.

[2] a) Synthesis of racemic vicinal diamines: H. Kohn, S.-H. Jung, *J. Am. Chem. Soc. 105* (1983) 4106; P. N. Becker, R. G. Bergmann, *Organometallics 2* (1983) 787; A. O. Chong, K. Oshima, K. B. Sharpless, *J. Am. Chem. Soc. 99* (1977) 3420; E. J. Roskamp, S. F. Pedersen, *ibid. 109* (1987) 3153; E. J. Enholm, D. C. Forbes, D. P. Holub, *Synth. Commun. 20* (1990) 981; P. Mangeney, A. Tejero, A. Alexakis, F. Grosjean, J. Normant, *Synthesis 1988*, 255; D. S. Jones, A. Srinivasan, S. Kasina, A. R. Fritzberg, D. W. Wilkening, *J. Org. Chem. 54* (1989) 1940; W. Chamchaang, A. R. Pinhas, *ibid. 55* (1990) 2531; J. Altmann, M. Grinberg, M. Wilchek, *Liebigs Ann. Chem. 1990*, 339; H. Natsugari, R. R. Whittle, S. M. Weinreb, *J. Am. Chem. Soc. 106* (1984) 7867; C. Betschart, B. Schmidt, D. Seebach, *Helv. Chim. Acta 71* (1988) 1999; G. Buono, C. Triantaphylides, G. Pfeiffer, F. Petit, *Synthesis 1982*, 1030;; K. Osowska-Pacewicka, A. Zwierzak, *Synthesis 1990*, 505; b) special optically active vicinal diamines: J. Zhu, J. C. Quirion, H.-P. Husson, *Tetrahedron Lett. 30* (1989) 5137; E. Bruni, G. Cardillo, M. Orena, S. Sandri, C. Tomasini, *Tetrahedron Lett. 30* (1989) 1679.

[3] M. T. Reetz, M. W. Drewes, A. Schmitz, *Angew. Chem. 99* (1987) 1186; *Angew. Chem. Int. Ed. Engl. 26* (1987) 1141.

[4] a) G. Stork, S. Dowd, *J. Am. Chem. Soc. 85* (1963) 2178; b) R. W. Layer, *Chem. Rev. 63* (1963) 489; c) J. Huet, *Bull. Soc. Chim. Fr. 1964*, 952; d) D. Mea-Jacheest, A. Horeau, *Bull. Soc. Chim. Fr. 1968*, 4571; e) A. Hosomi, H. Araki, H. Sakurai, *J. Am. Chem. Soc. 104* (1982) 2081; f) F. E. Scully, *J. Org. Chem. 45* (1980) 1515; g) M. Wada, K. Sakurai, K. Akiba, *Tetrahedron Lett. 25* (1984) 1079; h) J. Yamada, H. Sato, Y. Yamamoto, *Tetrahedron Lett. 30* (1989) 5611.

[5] a) Review on chelation- and non-chelation-controlled reactions of chiral alkoxycarbonyl compounds: M. T. Reetz, *Angew. Chem. 96* (1984) 542; *Angew. Chem. Int. Ed. Engl. 23* (1984) 556; b) additions to α-alkoxyhydrazones and imines: D. A. Claremon, P. K. Lumma, B. T. Philipps, *J. Am. Chem. Soc. 108* (1986) 8265; R. D. Clark, Jahangir M. Souchet, J. R. Kern, *J. Chem. Soc. Chem. Commun. 1989*, 930.

[6] a) T. Imamoto, N. Takiyama, K. Nakamura, T. Hatajima, Y. Kamija, *J. Am. Chem. Soc. 111* (1989) 4392; b) S. E. Denmark, T. Weber, D. Piotrowski, *ibid. 109* (1987) 2224.

[7] Synthesized from three equivalents of MeLi and one equivalent of $CeCl_3$. Practically nothing is known about the structure of the organocerium compounds. We thank Prof. *S. E. Denmark*, University of Illinois, Urbana, IL, for extensive discussions.

[8] J. Siko, S. M. Weinreb, *J. Org. Chem. 55* (1990) 393.

[9] a) N. T. Anh, *Top. Curr. Chem. 88* (1980) 145; b) M. T. Reetz, *Pure Appl. Chem. 60* (1988) 1607.

[10] K. Yoshida, S. Nakajima, T. Wakamatsu, Y. Ban, M. Shibasaki, *Heterocycles 27* (1988) 1167.

[11] J. A. Dale, D. L. Dull, H. S. Mosher, *J. Org. Chem. 34* (1969) 2543.

[12] P. Wriede, L. B. Gortler, A. Waring, A. Battisti, S. Bank, W. D. Closson, S. Ji, *J. Am. Chem. Soc. 89* (1967) 5311.

[13] R. C. Roemmle, H. Rapoport, *J. Org. Chem. 53* (1988) 2367.

[14] a) General procedure for additions to **3**: A solution containing 1 mmol of an aldimine **3** in 10 mL of anhydrous ether was allowed to react under an inert atmosphere with 1.3 mmol of an alkyllithium reagent at −78 °C. After 1 h, the reaction mixture was allowed to warm to room temperature and stirred for 1–2 h; in the case of the aldimine obtained from ornithine (R = $Bn_2N(CH_2)_3$), the reaction time was increased to 4 d. Aqueous workup and chromatography on silica gel (petroleum ether/ethyl acetate 2:1) afforded diamines **5** (Table 1); b) General procedure for additions to **7**: An aldehyde **2** (2 mmol) in 2 mL of anhydrous dichloromethane was added to a solution of *N*-sulfinyl-*p*-toluenesulfonamide (600 mg, 2.8 mmol) [8] in 10 mL of anhydrous dichloromethane at room temperature under an inert atmosphere. The reaction mixture was stirred for 2–3 h (exception: **7** (R = Me_2CH), 48 h) and 6 mmol of a Grignard reagent was

then added at 22–30 °C. After 1 h, the reaction mixture was worked up with 50 mL of saturated NaCl solution and extracted twice with ethyl acetate. The combined organic extracts were dried over $MgSO_4$ and evaporated. Chromatography on silica gel (petroleum ether/ethyl acetate 2:1) afforded adducts **9** (Table 2); c) General procedure for single debenzylation of **5**: Pd-black (ca. 50–100 mg) was added to a solution of 20 mL of methanol and 1 mL of formic acid. Diamine **5** (0.5–2 mmol) was dissolved in a small amount of methanol (2–5 mL) and added dropwise to the above solution. The reaction mixture was stirred for 1–3 d at room temperature under 1 atm of H_2. After filtration to remove Pd-black and removal of the solvent by distillation, a 75–85% yield of diamine **10** was obtained: d) General procedure for triple debenzylation of **5**: The catalyst [10] $Pd(OH)_2/C$ was dried for 24 h at 60 °C over P_2O_5 prior to use. $Pd(OH)_2/C$ (50–100 mg) was then added to a solution of diamine **5** (0.5–2 mmol) in anhydrous methanol and the mixture was stirred for 3 d under 1 atm of H_2. After filtration over Celite to remove the catalyst and removal of the solvent by distillation, a 70–90% yield of the completely debenzylated diamine **12** was obtained.

[15] R. M. Williams: *Synthesis of Optically Active Alpha-Amino Acids*, Pergamon, Oxford 1989.

2,4,6-Triaryl-1,3,5λ^3-diazaphosphinines

By *Gottfried Märkl** and *Christian Dörges*

Dedicated to Professor Karl Dimroth on the occasion of his 80th birthday

The N/P electronegativity difference causes a dramatic change in the reactivity of 1,2λ^3-[2] and 1,4λ^3-azaphosphinines[1] compared with that of λ^3-phosphinines. The 1,3λ^3-azaphosphinines,[3] for which a mesomeric interaction between the heteroatoms is not possible, have proven useful, for example, as building blocks for the synthesis of functionally substituted λ^3-phosphinines.[4] It therefore seemed especially interesting to investigate how the heteroatom effects in diaza-λ^3-phosphinines reinforce or compensate each other. Of the diaza-λ^3-phosphinines **1**–**6**, homologous to triazines, only a derivative of 1,2,4λ^3-diazaphosphinine **4** (see below) has been described.[5]

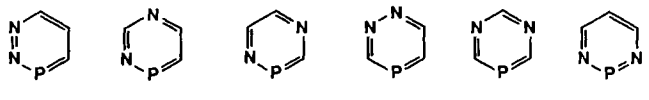

1 **2** **3** **4** **5** **6**

Some years ago, we were able to transform the 3-azapyrylium salts **7**, described by *R. R. Schmidt* et al.,[6] into the 1,3λ^3-azaphosphinines **8**[3] by O/P exchange with $P(SiMe_3)_3$.[7] This synthesis parallels the formation of λ^3-phosphinines[8] by O/P exchange with $P(SiMe_3)_3$ and of 1,3λ^3-azaphospholes[9] and 1,2,4λ^3-diazaphospholes[10] from the corresponding oxonium salts.

This O/P exchange was unsuccessful with the readily accessible 2,4,6-triaryl-3,5-diazapyrylium salts **9**, $X^{\ominus} = SnCl_5^{\ominus}$,

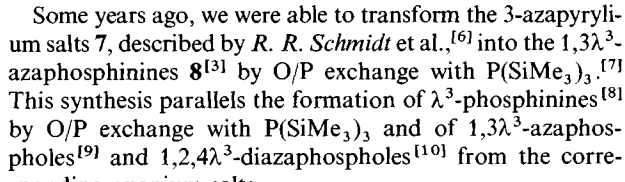

7

[*] Prof. Dr. G. Märkl, Dipl.-Chem. C. Dörges
Institut für Organische Chemie der Universität
Universitätsstrasse 31, W-8400 Regensburg (FRG)

which *R. R. Schmidt* et al. prepared in a straightforward and elegant fashion by reaction of aroyl chlorides and aryl nitriles with $SnCl_4$. The salts obtained by reaction of the $SnCl_5^{\ominus}$ salts with NH_4PF_6, NaI, or $NaClO_4$ in anhydrous acetonitrile also do not undergo O/P exchange either with $P(SiMe_3)_3$ or with $P(CH_2OH)_3$[11] or PH_3[12] (this behavior corresponds to that of the corrseponding azapyrylium salts **7**). Likewise, the fluoroborates **9**, $X = BF_4^{\ominus}$, obtained in 80–90% yield by reaction of **9**, $X = SnCl_5^{\ominus}$, with $AgBF_4$, react with $P(SiMe_3)_3$ in CH_3CN to give an undefined mixture of products. However, reaction in refluxing benzene for 24 h affords, after chromatographic workup (silica gel 60, toluene), pale yellow, crystalline products, which, according to the analytical and spectroscopic data, are the 1,3,5λ^3-diazaphosphinines **10** (Table 1).

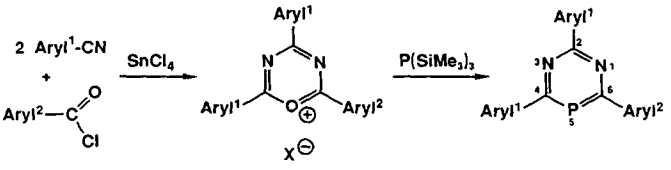

9 **10**

9, **10**: **a**, $Aryl^1 = Aryl^2 = C_6H_5$; **b**, $Aryl^1 = Aryl^2 = 4\text{-}CH_3C_6H_4$; **c**, $Aryl^1 = Aryl^2 = 4\text{-}ClC_6H_4$; **d**, $Aryl^1 = C_6H_5$, $Aryl^2 = 4\text{-}ClC_6H_4$; **e**, $Aryl^1 = 4\text{-}ClC_6H_4$, $Aryl^2 = C_6H_5$; **f**, $Aryl^1 = 4\text{-}ClC_6H_4$, $Aryl^2 = 4\text{-}CH_3C_6H_4$; **g**, $Aryl^1 = 4\text{-}CH_3C_6H_4$, $Aryl^2 = 4\text{-}ClC_6H_4$; $X^{\ominus} = SnCl_5^{\ominus}$, $PF_6^{\ominus}$, $I^{\ominus}$, $ClO_4^{\ominus}$, $BF_4^{\ominus}$.

The mass spectra of diazaphosphinines **10** show that they decompose into their components R-C≡P and R-C≡N; the mass spectra of the unsymmetrically substituted derivatives indicate that scrambling of the radical cations occurs (for

Table 1. Yields and physical data for **10a**.

10a: Yield 6%; m.p. 146–147.5 °C, (CH_2Cl_2/EtOH), MS (70 eV): *m/z* 326 ($M^{\oplus}$, 10%), 223 ([*M*-PhCN]$^{\oplus}$, 1.3), 120 ([PhC≡P]$^{\oplus}$, 100%). ^{31}P NMR ($CDCl_3$): $\delta = 140.3$ [for comparison: 1,3λ^3-azaphosphinine **2**, Aryl = C_6H_5: $\delta = 163.0$[3]; 2,4,6-triphenyl-λ^3-phosphinine: $\delta = 172.0$[11]. UV (CH_2Cl_2): λ_{max} [nm] (ε) = 294 (26600) [for comparison: 1,3λ^3-azaphosphinine **2**, Aryl = C_6H_5 (*n*-hexane): $\lambda_{max} = 289$ (28000), 344 (sh, 4900)[3]; 2,4,6-triphenyl-λ^3-phosphinine (CH_3OH): $\lambda_{max} = 278$ (41000), 314 (12600)[11]. ^{13}C NMR ($CDCl_3$): $\delta = 200.3$ (d, ^1J(P,C) = 69.3 Hz, C-4,6), 161.7 (d, ^3J(P,C) = 23.2 Hz, C-2) [for comparison: 1,3λ^3-azaphosphinine **2**, Aryl = C_6H_5[3]; $\delta = 191.5$ (d, ^1J(P,C) = 69.3 Hz, C-2), 180.5 (d, ^3J(P,C) = 52.6 Hz, C-4), 119.8 (d, ^2J(P,C) = 10.1 Hz, C-5), 157.1 (d, ^1J(P,C) = 18.3 Hz, C-6); 2,4,6-triphenyl-λ^3-phosphinine[14]: $\delta = 172.9$ (d, ^2J(P;C) = 51.7 Hz, C-2), 132.4 (d, ^3J(P,C) = 12.2 Hz, C-3), 145.2 (d, ^4J(P,C) = 13.8 Hz, C-4)]

10b: Yield 5.1%; m.p. 184–185 °C (CH_2Cl_2/EtOH). MS (70 eV): *m/z* 368 ($M^{\oplus}$, 15%), 134 ([4-$CH_3C_6H_4C{\equiv}P]^{\oplus}$, 100). ^{31}P NMR: $\delta = 135$ UV (CH_2Cl_2): λ_{max} [nm] (ε) = 298 (27.400)

10c: Yield 5.3%; m.p. 194–195 °C (CH_2Cl_2/EtOH). MS (70 eV): *m/z* 428 ($M^{\oplus}$, 65%), 154 ([4-$ClC_6H_4C{\equiv}P]^{\oplus}$, 100), 119 ([PhC≡P]$^{\oplus}$, 17). ^{31}P NMR: $\delta = 140.2$ UV (CH_2Cl_2): λ_{max} [nm] (ε) 290 (30000)

10d: Yield 5.6%; m.p. 166–167 °C (CH_2Cl_2/EtOH). MS: *m/z* 360 ($M^{\oplus}$, 20%), 154 ([4-$ClC_6H_4C{\equiv}P]^{\oplus}$, 80), 120 ([$C_6H_5C{\equiv}P]^{\oplus}$, 100), 103 ([$C_6H_5C{\equiv}N]^{\oplus}$, 3). ^{31}P NMR ($CDCl_3$): $\delta = 139.7$ UV (CH_2Cl_2): λ_{max} [nm] (ε) = 295 (31.700)

10e: Yield 5.8%; Fp = 180–183 °C (CH_2Cl_2/EtOH). MS: *m/z* 394 ($M^{\oplus}$, 10%), 154 ([4-$ClC_6H_4C{\equiv}P]^{\oplus}$, 65); 120 ([$C_6H_5C{\equiv}P]^{\oplus}$, 100). ^{31}P NMR ($CDCl_3$): $\delta = 140.8$ UV (CH_2Cl_2): λ_{max} [nm] (ε) = 294 (29.500)

10f: Yield 6.0% Fp = 180–182 °C (CH_2Cl_2/EtOH) MS: *m/z* 408 ($M^{\oplus}$, 32%), 388 (67%), 368 (23%), 154 ([4-$ClC_6H_4C{\equiv}P]^{\oplus}$, 27), 134 ([4-$CH_3C_6H_4C{\equiv}P]^{\oplus}$, 65), 119 ([$C_6H_4C{\equiv}P]^{\oplus}$, 100). ^{31}P NMR ($CDCl_3$): $\delta = 139.1$ UV (CH_2Cl_2): λ_{max} [nm] (ε) = 304 (29.000). ^{13}C NMR ($CDCl_3$): $\delta = 200.2$ (77.4 Hz, C-4), 199.0 (77.3 Hz, C-6), 161.9 (20.9 Hz, C-2)

10g: Yield 6.6% Fp = 185–186 °C (CH_2Cl_2/EtOH). MS: *m/z* 388 ($M^{\oplus}$, 20%), 154 ([4-$ClC_6H_4C{\equiv}P]^{\oplus}$, 100), 134 ([4-$CH_3C_6H_4C{\equiv}P]^{\oplus}$, 64), 119 ([$C_6H_4C{\equiv}P]^{\oplus}$, 9). ^{31}P NMR ($CDCl_3$): $\delta = 136.1$. UV (CH_2Cl_2): λ_{max} [nm] (ε) = 296 (35.000). ^{13}C NMR ($CDCl_3$):$\delta = 200.4$ (69.2 Hz, C-4), 199.2 (68.9 Hz, C-6), 160.8 (21.2 Hz. C-2)

example, the molecular ion peaks of **10b** and **10g** are also observed in the mass spectrum of **10f**).

Besides the 1,2,4λ^3-diazaphosphinine **11**, obtained by reaction of 2-*tert*-butyl-1-chloro-3-phenylphosphirene with lithio-*tert*-butyldiazomethane, only the 1,2,4λ^5-diazadihydrophosphinine **12**[15] and several 1,2,4λ^5-diazaphosphinines of type **13**[16] have been described so far. The synthesis

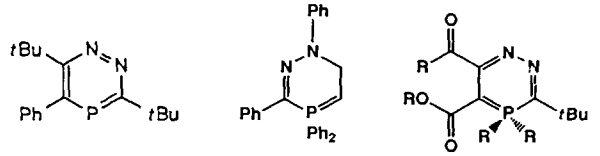

11 **12** **13**

of the 1,3,5λ^3-diazaphosphinines **10** thus provides the first general route to λ^3-phosphinines containing two nitrogen atoms in the ring.

Preliminary investigations into the chemistry of the 1,3,5λ^3-diazaphosphinines **10** have revealed striking similarities with the reactivity of the 1,3λ^3-azaphosphinines **8**. In contrast to λ^3-phosphinines, which react only with highly reactive alkyne dienophiles (F_3C-C≡C-CF_3, NC-C≡C-CN) at 100 °C (sealed tube) to form heterobarrelenes,[17] diazaphosphinines **10** undergo a "domino" reaction in refluxing toluene with all alkyne dienophiles so far investigated to give the tri- and pentasubstituted λ^3-phosphinines **17** via the heterobarrelenes **14**, the 1,3λ^3-azaphosphinines **15**, and the heterobarrelenes **16**. Starting from **10**, only the fragments phosphorus and aryl-C^6 of the original diazaphosphinine are present in **17**. Thus, diazaphosphinines **10** can be formally regarded as synthons for P≡C-Aryl.

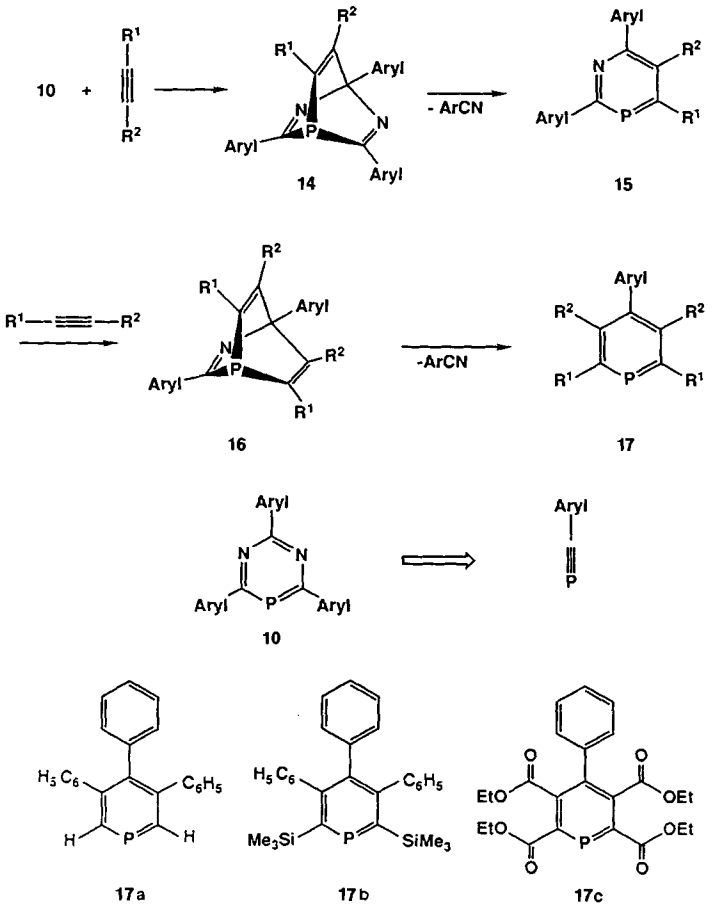

14 **15** **16** **17** **10** **17a** **17b** **17c**

In this way, the pentasubstituted λ^3-phosphinines **17a**–**17c** have so far been synthesized by reaction of **10a** with phenylacetylene, 1-phenyl-2-trimethylsilylacetylene, and diethyl acetylenedicarboxylate, respectively.

Received: August 2, 1990 [Z 4108 IE]
German version: *Angew. Chem. 103* (1991) 82

CAS Registry numbers:
9a (X = $BF_4^\ominus$), 131068-92-3; **9a** (X = $SnCl_5^\ominus$), 749-55-3; **9b** (X = $BF_4^\ominus$), 131068-94-5; **9b** (X = $SnCl_5^\ominus$), 131104-18-2; **9c** (X = $BF_4^\ominus$), 131068-95-6; **9c** (X = $SnCl_5^\ominus$), 809-87-0; **9d** (X = $BF_4^\ominus$), 131068-96-7; **9d** (X = $SnCl_5^\ominus$), 131079-07-7; **9e** (X = $BF_4^\ominus$), 131068-97-8; **9e** (X = $SnCl_5^\ominus$), 131079-08-8; **9f** (X = $BF_4^\ominus$), 131068-99-0; **9f** (X = $SnCl_5^\ominus$), 131079-09-9; **9g** (X = $BF_4^\ominus$), 131069-01-7; **9g** (X = $SnCl_5^\ominus$), 131079-10-2; **10a**, 131069-02-8; **10b**, 131069-03-9; **10c**, 131069-04-0; **10d**, 131069-05-1; **10e**, 131069-06-2; **10f**, 131079-06-6; **10g**, 131069-07-3; **17a**, 131068-08-4; **17b**, 131069-09-5; **17c**, 131069-10-8; $P(SiMe_3)_3$, 15573-38-3; phenylacetylene, 536-74-3; 1-phenyl-2-trimethylsilylacetylene, 2170-06-1; diethyl acetylenedicarboxylate, 762-21-0.

[1] G. Märkl, D. Matthes, *Angew. Chem. 84* (1972) 1069; *Angew. Chem. Int. Ed. Engl. 11* (1972) 1019.
[2] C. Bourdieu, A. Foucaud, *Tetrahedron Lett. 28* (1987) 4673.
[3] G. Märkl, G. Dorfmeister, *Tetrahedron Lett. 28* (1987) 1093.
[4] G. Märkl, C. Dörges, Th. Riedl, F.-G. Klärner, C. Lodwig, *Tetrahedron Lett. 32* (1990) 4589; see also G. Märkl, S. Dietl, *ibid. 29* (1988) 539.
[5] M. Regitz, Kaiserslautern (FRG), personal communication.
[6] a) R. R. Schmidt, *Chem. Ber. 98* (1965) 334, 3892; b) R. R. Schmidt, D. Schwille, U. Sommer, *Justus Liebigs Ann. Chem. 723* (1969) 111.
[7] G. Becker, W. Hölderich, *Chem. Ber. 108* (1975) 2484.
[8] G. Märkl, F. Lieb, A. Merz, *Angew. Chem. 79* (1967) 475; *Angew. Chem. Int. Ed. Engl. 6* (1967) 458.
[9] G. Märkl, G. Dorfmeister, *Tetrahedron Lett. 27* (1986) 4419.
[10] G. Märkl. S. Pflaum, *Tetrahedron Lett. 27* (1986) 4415; *ibid. 28* (1987) 1511.
[11] G. Märkl, *Angew. Chem. 78* (1966) 907; *Angew. Chem. Int. Ed. Engl. 5* (1966) 846.
[12] G. Märkl, F. Lieb, A. Merz, *Angew. Chem. 79* (1967) 947; *Angew. Chem. Int. Ed. Engl. 6* (1967) 944.
[13] G. Märkl, S. Dietl, *Tetrahedron Lett. 29* (1988) 535.
[14] T. Bundgaard, H. J. Jakobsen, K. Dimroth, H. H. Pohl, *Tetrahedron Lett. 1974*, 3179.
[15] G. Märkl, *Angew. Chem. 77* (1965) 1109; *Angew. Chem. Int. Ed. Engl. 4* (1965) 1023 and especially p. 1124.
[16] T. Facklam, O. Wagner, H. Heydt, M. Regitz, *Angew. Chem. 102* (1990) 316; *Angew. Chem. Int. Ed. Engl. 29* (1990) 314.
[17] G. Märkl, F. Lieb, *Angew. Chem. 80* (1969) 702; *Angew. Chem. Int. Ed. Engl. 7* (1968) 733.

$(n\mathrm{Bu}_4\mathrm{P})_2[\mathrm{Os}_{20}(\mathrm{CO})_{40}]$, a Thermolytically Generated High-Nuclearity Cluster with a Tetrahedral Cubic-Close-Packed Metal Core**

By *Angelo J. Amoroso, Lutz H. Gade, Brian F. G. Johnson, Jack Lewis,* Paul R. Raithby,* and *Wing-Tak Wong*

The structures and properties of metal cores containing tens or hundreds of metal atoms are of considerable interest not only in their role as model systems in surface sciences[1] but also due to their postulated, and in some cases proven, unusual catalytic and physicochemical behavior.[2] However, little is known about the detailed kinetic and thermodynamic constraints that influence the buildup of either large clusters or small colloidal metal particles.[3]

[*] Prof. Lord Lewis, A. J. Amoroso, L. H. Gade, Dr. B. F. G. Johnson, Dr. P. R. Raithby, W.-T. Wong
University Chemical Laboratory
Lensfield Road, GB-Cambridge, CB2 1EW (UK)

[**] We acknowledge the financial support of the British Council (FCO-Kurt Hahn Scholarship to *L.H.G.*), the Royal Commission for the Exhibition of 1851, and the U.K. Committee of Vice Chancellors and Principals (*W.-T.W.*), and the SERC (*A.J.A.*).

A powerful method for the synthesis of binary high-nuclearity carbonyl clusters containing metals of the iron triad has been the thermolytic generation of metal carbonyl fragments which combine to generate an array of clusters containing between 4 and > 20 metal atoms.[4] In these thermolyses certain atom numbers are found to dominate the product distributions, thereby allowing highly selective syntheses of these species under the appropriate reaction conditions. For osmium clusters, the generation of metal cores containing 4, 6, 10, and, as reported here, 20 metal atoms appears to be particularly favored. With the exception of the hexaosmium clusters, these atom numbers correspond to the series of "magic" numbers 4, 10, and 20 associated with molecular tetrahedra of edge lengths 2 (atoms), 3, and 4 and therefore represent a gradual buildup of cubic-close-packed cores with an overall tetrahedral symmetry. While the structures and chemistry of the first two members of this series (e.g., $[H_2Os_4(CO)_{12}]^{2\ominus}$ [5] and $[Os_{10}C(CO)_{24}]^{2\ominus}$ [6]) have been extensively studied, it is only the recent reinvestigation of the vaccum pyrolysis (10^{-3} Torr, 300 °C) of the osmium cluster **1** that has led to the isolation of the dianion **2** and the characterization of the $Os_{20}^{\ominus}$ tetrahedron.

$[Os_3(CO)_{10}(NCCH_3)_2]$ **1**

$[Os_{20}(CO)_{40}]^{2\ominus}$ **2**

The cluster dianion **2**, which may be isolated as its $(Ph_3P)_2N^{\oplus}$, $(nBu_4P)^{\oplus}$, or $(Me_4N)^{\oplus}$ salt, is formed in 20% yield along with $[Os_{10}C(CO)_{24}]^{2\ominus}$, $[Os_{17}(CO)_{36}]^{2\ominus}$,[7] and a number of lower-nuclearity fractions (Os_4, Os_5). The stoichiometry of the compound was initially established by FAB mass spectrometry.[8] The simplicity of the ν(CO) absorption band pattern in the IR spectrum indicated a highly symmetrical cluster geometry.[9] This was confirmed by a single-crystal X-ray structure analysis of its $(nBu_4P)^{\oplus}$ salt (Fig. 1a), which established the hitherto unobserved metal core geometry (Fig. 1b).[10] The metal polyhedron may be derived from that of $[Os_{10}X(CO)_{24}]^{2\ominus}$ (X = H_4, C) by addition of a further planar triangular layer of ten osmium atoms. This kind of skeletal geometry has been the object of a number of theoretical studies related to the abundant M_{20} clusters in supersonic beams of alkali-metal vapors.[11] Simple electron-counting rules would demand a higher skeletal electron count for a tetrahedral Os_{20} species than that obtained on the basis of the formulation put forth in this paper. However, neither the crystal structure analysis nor IR, ^1H NMR or ^{13}C NMR spectroscopy[9] has revealed the presence of interstitial atoms (C,H) in the four octahedral or eleven tetrahedral cavities of the core. Moreover, for a molecular mass of this magnitude the FAB mass spectra obtained are not unambiguous in determining the presence of interstitial hydrogen or even carbon atoms.

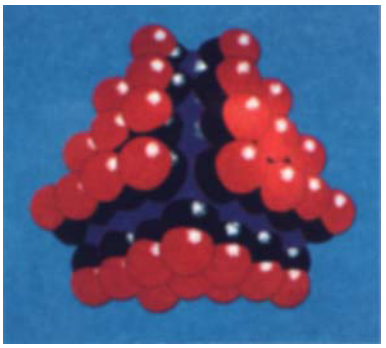

Fig. 2. Space-filling model of **2** showing the monolayer of CO on the surface of the metal core.

The mean metal–metal distances (2.786(5), 2.747(3), 2.678(8) Å for the Os atoms surrounding the three different types of tetrahedral cavities and 2.746(4) Å for the octahedral cavities) are similar to those in the recently characterized dianion $[Os_{17}(CO)_{36}]^{2\ominus}$, which is also a binary cluster with unoccupied interstitial sites.[7] The four Os atoms of the unique tetrahedron at the center of the cluster (shaded in Figure 1b) have the highest metal–metal connectivity and an

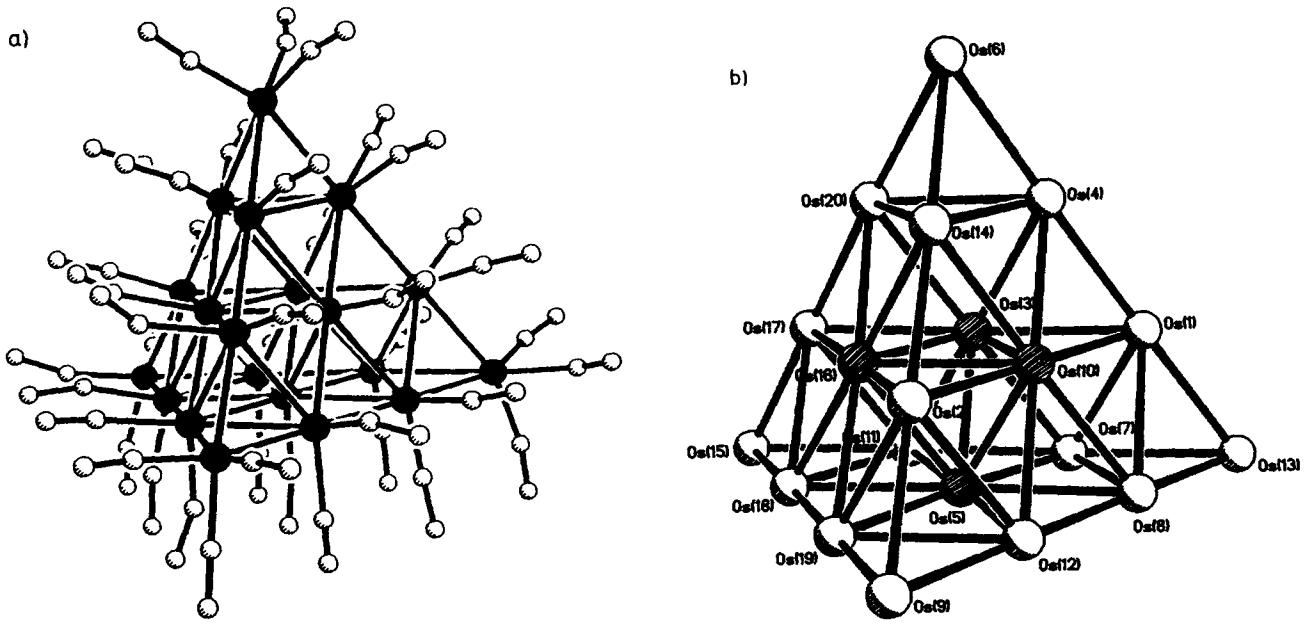

Fig. 1. a) Molecular structure of the dianion $[Os_{20}(CO)_{40}]^{2\ominus}$ (**2**). b) Structure of the Os_{20} metal core.

average bond distance of 2.678(8) Å, approaching that observed for the bulk metal (2.6754 Å).[12]

The symmetry of the core is matched by that of the CO ligand shell in which there are 40 terminal CO ligands in three chemically distinct environments (Fig. 2). The coordination of CO to the cluster surface is similar to that observed for chemisorbed carbon monoxide on the (111) surface of cubic-close-packed metals.

Preliminary cyclovoltammetric studies of the cluster have revealed a rich electrochemistry[13] which reflects the increased density of accessible oxidation states for large metal particles in comparison to the smaller clusters studied so far.[14]

Experimental Procedure

A 180-mL Carius tube was filled with a suspension of 1 g of **1** [15] in 30 mL of CH_2Cl_2. The solvent was evaporated under reduced pressure and the solid evenly distributed over the interior surface of the tube, which was then sealed at 10^{-3} Torr. The precursor compound was pyrolyzed at 300 °C for 70 h to yield a brown-black powder which was initially sparingly soluble in acetone. Heating under reflux in a mixture of 100 mL of acetone and 30 mL of methanol in the presence of $[(Ph_3P)_2N]Cl$ (1.2 g) for 20 h resulted in almost complete dissolution of the solid. The deep brown solution was filtered (ca. 100 mg of insoluble material) and the filtrate evaporated to dryness. After the removal of surplus $[(Ph_3P)_2N]Cl$ by extraction with methanol, the residue was redissolved in 25 mL of acetone and separated by thin layer chromatography (silica gel) using acetone/hexane (60/40) as eluent. Apart from the neutral low-nuclearity fractions moving near the solvent front ($R_f = 0.9$, ca. 100 mg of Os_4 and Os_5 clusters), the major fractions were $[(Ph_3P)_2NOs_{17}(CO)_{36}]$ ($R_f = 0.65$, brown, 73 mg (7%)), $[(Ph_3P)_2N]_2[Os_{10}C(CO)_{24}]$ ($R_f = 0.60$, red, 350 mg (29%)), and $[(Ph_3P)_2N]_2[Os_{20}(CO)_{40}]$ (**2**) ($R_f = 0.4$, brown-green, 200 mg (20%)). Other minor fractions, including the baseline, accounted for ca. 100 mg of material. The $(nBu_4P)^{\oplus}$ salt of **2** was obtained through cation metathesis with $(nBu_4P)Cl$ and crystallized by slow evaporation of a solution of the salt in acetone/methanol (2/1).

Received: September 21, 1990 [Z 4197 IE]
German version: *Angew. Chem. 103* (1991) 102

[1] a) E. L. Muetterties, T. N. Rhodin, E. Band, C. F. Brucker, W. R. Pretzer, *Chem. Rev. 79* (1979) 91; b) G. Ertl in B. C. Gates, L. Guczi, H. Knözinger (Eds.): *Metal Clusters in Catalysis*, Elsevier, Amsterdam 1986, p. 575.

[2] a) J. M. Thomas, *Pure Appl. Chem. 60* (1988) 1517; b) R. F. Marzke, *Catal. Rev.-Sci. Eng. 19* (1979) 43; c) D. C. Johnson, R. E. Benfield, P. P. Edwards, W. J. H. Nelson, M. D. Vargas, *Nature (London) 314* (1985) 231.

[3] a) M. R. Hoare, P. Pal, *Nature (London) Phys. Sci. 236* (1972) 35; b) *Adv. Phys. 24* (1975) 645; c) P. Chini, *J. Organomet. Chem. 200* (1980) 51; d) P. Fayet, M. J. McGlinchey, L. H. Wöste, *J. Am. Chem. Soc. 109* (1987) 1733; e) G. Schmid, *Struct. Bonding (Berlin) 62* (1985) 51; f) P. J. Bailey, *Ph.D. Thesis*, University of Cambridge 1990.

[4] M. D. Vargas, J. N. Nicholls, *Adv. Inorg. Chem. Radiochem. 30* (1986) 123.

[5] B. F. G. Johnson, J. Lewis, P. R. Raithby, G. M. Sheldrick, G. Süss, *J. Organomet. Chem. 162* (1978) 179.

[6] P. F. Jackson, B. F. G. Johnson, J. Lewis, W. J. H. Nelson, M. McPartlin, *J. Chem. Soc. Dalton Trans. 1982*, 2099.

[7] E. Charalambous, L. H. Gade, B. F. G. Johnson, J. Lewis, M. McPartlin, H. R. Powell, *J. Chem. Soc. Chem. Commun. 1990*, 688.

[8] The negative ion FAB mass spectra of the salts of dianionic clusters display a characteristic peak pattern: dianion, monoanion, (dianion + cation), and, in exceptional cases, (dianion + 2 × cation). For **2**, the most abundant isotopomers were found at *m/z* 2467 dianion; simulated 2464, 4937 (monoanion; simulated 4929), 5186 (dianion + $(nBu_4P)^{\oplus}$; simulated 5197), 5450 (dianion + 2 × $(nBu_4P)^{\oplus}$; simulated 5462).

[9] IR (CH_2Cl_2): $\tilde{\nu}$ [cm^{-1}] = 2045 (s), 2002 (s), 1955 (w); no absorption bands for an interstitial carbide observed between 500 and 800 cm^{-1} ($Me_4N^{\oplus}$ salt, CsI disk). ^{13}C NMR (100.6 MHz, [D_6] acetone, 295 K): $\delta = 158.0$ (12 CO), 179.5 (4 CO), 179.8 (24 CO); no carbide resonances observed between $\delta = 350$ and 480. A set of up to six paramagnetically shifted ^{13}CO signals may appear between $\delta = 55$ and 310, depending on the treatment of the sample before recording of the spectra.

[10] Crystal data for $(nBu_4P)_2[Os_{20}(CO)_{40}]$: triclinic, space group $P\bar{1}$, $a = 14.094(5)$, $b = 16.539(8)$, $c = 22.650(9)$ Å, $\alpha = 105.93(1)$, $\beta = 101.78(1)$, $\gamma = 90.21(1)°$, $M = 5443.2$, $V = 4960(4)$ Å^3, $Z = 2$, $\varrho_{calcd} = 3.645$ g cm^{-3}, $F(OOO) = 4748$, $Mo_{K\alpha}$ radiation, $\lambda = 0.71069$ Å, $\mu(Mo_{K\alpha}) = 256.47$ cm^{-1}. The structure was solved by a combination of direct methods and difference Fourier techniques and refined by the block-matrix least-squares method. All osmium atoms were refined anisotropically, while the carbonyl ligands were refined independently at a later stage. No attempt to refine the $(nBu_4P)^{\oplus}$ has been made. 6210 reflections (corrected for absorption and decay), 2891 observed reflections with $F > 3\sigma(F)$ with $5° < 2\theta < 38°$, $R = 0.072$, $R_w = 0.065$. Further details of the crystal structure investigation can be obtained from the Director of the Cambridge Crystallographic Data Centre, University Chemical Laboratory, Lensfield Rd, Cambridge CB2 1EW (UK). Any request should be accompanied by the full literature citation for this communication.

[11] a) D. M. P. Mingos, Z. Lin, *Chem. Phys. 137* (1989) 15; b) P. Fantucci, K. Koutecky in G. Benedek, T. P. Martin, G. Pacchioni (Eds.): *Elemental and Molecular Clusters*, Springer, Berlin 1988, p. 125; c) W. D. Knight, K. Clemenger, W. A. de Heer, W. A. Saunders, M. Y. Chou, M. L. Cohen, *Phys. Rev. Lett. 52* (1984) 2141; d) M. L. Cohen, M. Y. Chou, W. D. Knight, W. A. de Heer, *J. Phys. Chem. 91* (1987) 3141.

[12] R. C. Weast (Ed.): *Handbook of Chemistry and Physics*, 70th ed., CRC Press, Boca Raton, FL, USA 1989/1990, p. F 189.

[13] A. J. Amoroso, L. H. Gade, B. F. G. Johnson, J. Lewis, W.-T. Wong, unpublished results.

[14] a) M. H. Barley, S. R. Drake, B. F. G. Johnson, J. Lewis, *J. Chem. Soc. Chem. Commun. 1987*, 1657; b) S. R. Drake, B. F. G. Johnson, J. Lewis, R. C. S. McQueen, *J. Chem. Soc. Dalton Trans. 1987*, 1051.

[15] B. F. G. Johnson, J. Lewis, D. A. Pippard, *J. Chem. Soc. Dalton Trans. 1981*, 407.

Book Reviews are written by invitation from the editor. Suggestions for books to be reviewed and for book reviewers are welcome. Publishers should send brochures or (better) books to the following address: Redaktion Angewandte Chemie, Postfach 101161, W-6940 Weinheim, Federal Republic of Germany. The editor reserves the right of selecting which books will be reviewed. Uninvited books not chosen for review will not be returned.

High Pressure Chemical Synthesis. Edited by *J. Jurczac* and *B. Baranowski*. Elsevier, Amsterdam 1989. x, 507 pp., hardcover DFl 320.00.—ISBN 0-444-88187-5

Formerly, in the good old days, when one believed that one had acquired sufficient knowledge it was usual to sit down and write a book. Nowadays, when it seems that there is no longer anyone who has a complete grasp of a subject unaided, one persuades one's scientific friends to write something for a field which has now reached an advanced stage of development and has great future potential (or alternatively, a publisher or a "series editor" organizes this). From this there then emerges a book, the parts of which are in many cases better than the whole.

"High Pressure Chemical Synthesis", edited by *J. Jurczac* and *B. Baranowski* of the Polish Academy of Sciences in Warsaw, is a multi-author book. In its 13 chapters (plus an introduction by the editors) the 18 authors report their experiences in the area of high pressure chemical (?) synthesis. The fact that more than half the authors (10) as well as the editors belong to the Polish Academy of Sciences is an indication of the importance attached there to the use of "pressure" to assist chemical reactions. There is certainly some justification for this, even though it remains true that the bunsen burner, compared with the high pressure autoclave or press, is a cheaper item of apparatus. The merit of the idea behind this book, and the achievement of its editors, is that it deals with such reactions (and processes) that require pressure to proceed usefully or even to occur at all.

In the introduction the editors point out that the earth itself is a unique high pressure laboratory for the synthesis of many inorganic substances (minerals). However, this is probably also true for the area of organic syntheses. Accordingly, the range of topics covered in this multi-author book is very wide.

Only four chapters are concerned with inorganic substances: ultrahard materials, diamond, cubic boron nitride (*O. Fukunaga*, Tokyo), metal nitrides, mainly III-V semiconductors, but also molybdenum nitrides (*S. Porowski, I. Grzegory* and *J. Jun*, Warsaw), (transition) metal hydrides (*B. Baranowski* and *S. M. Filipek*, Warsaw), oxides of iron, cobalt and nickel in higher oxidation states (*G. Demazeau*, Bordeaux). These chapters only deal with the classes of substances that are of technological interest; many aspects, such as fluorides, sulfides, and solid state reactions and phase transformations at high pressures are not covered at all.

The other nine chapters are concerned with organic chemistry (including biochemistry and biological chemistry). In the chapters on open-chain systems (*N. S. Isaacs*, Reading) and (carbo-)cyclic systems (*J. W. Scheeren*, Nijmegen), as also in the following chapters, the effects of pressure on the reaction rate are clearly seen as negative contributions to the activation volume and reaction volume. The contribution on monosaccharides (*A. Golebiowski, J. Jurczac* and *S. Pikul*, Warsaw) examines the effects of pressure on the regio- and stereoselectivity of organic reactions. The following chapters are concerned with β-lactams and other N-heterocycles prepared by cycloadditions and -condensations (*M. Chmielewski* and *J. Jurczak*, Warsaw), cryptands and other host molecules (*J. Jurczak* and *M. Pietraszkiewicz*, Warsaw), organic syntheses using organometallic reagents or catalysts (*J. Jurczak*, Warsaw and *A. Rahm*, Bordeaux), and materials of biological interest, amino acids and enzyme-catalyzed reactions (*Y. Taniguchi*, Kyoto). *G. Luft* (Darmstadt) then deals with polymers, an area of special technological importance in which the advantages of high pressures are particularly evident. Next *G. Jenner* (Strasbourg) discusses C_1 chemistry, i.e. the synthesis of basic chemicals from carbon monoxide and hydrogen, another area of great technological promise which is only accessible through the use of high pressures and catalysts.

Each chapter is constructed on the lines of a review article, and thus includes an adequate number of references to the original literature. The extensive author index (24 pp.) is an aid to finding relevant papers in cases where the names of the authors signify something to the reader. The subject index too is undoubtedly useful. The book contains a total of 507 pages, reproduced from many different typewriters and PC printers (a form which is not aesthetically appealing, and is also inappropriate in the age of compatible computers). It is definitely more in the nature of a volume of a review journal than a textbook, each chapter having been written for the specialist rather than for the reader seeking an overview of high pressure synthesis. Also, regrettably, the high price will be an obstacle to this very useful work reaching a wide readership; however, it can be recommended without reservation to well-funded libraries for their "progress reports" sections.

Gerd Meyer [NB 1069 IE]
Institut für Anorganische Chemie
der Universität Hannover (FRG)

Sensors—A Comprehensive Survey. Series editors: *W. Göpel, J. Hesse* and *J. N. Zemel*. VCH Verlagsgesellschaft, Weinheim. **Vol. 1: Fundamentals and General Aspects.** Edited by *T. Grandke* and *W. H. Ko*. 1989. xxxiii, 641 pp., hardcover DM 350.00 (subscription price: DM 290.00).—ISBN 3-527-26767-0; **Vol. 5: Magnetic Sensors.** Edited by *R. Boll* and *K. J. Overshott*. 1989. xii, 513 pp., hardcover DM 350.00 (subscription price: DM 290.00).—ISBN 3-527-26771-9

If one can believe the forecasts of leading market research agencies, the field of sensors has an enormous development potential with annual growth rates running into two figures. Owing to the central importance of sensors in measurement and control and their vital role in automated processes, a new key technology has grown up in this area. The function of sensors in general is to provide information. The more information one has on the state of a system, the more precisely can one model the system and predict its behavior, and

 © VCH Verlagsgesellschaft mbH, W-6940 Weinheim, 1991 0570-0833/91/0101-0110 $ 3.50+.25/0

the more effectively control its operation. Without a highly developed sensor technology it is impossible to be at the forefront of measurement and control technology and to manufacture high-technology products. VCH has just published the first two volumes of an eight-volume handbook on sensors, which sets out to describe the most important types of sensors and to present a comprehensive survey of the latest developments in this fast-moving field. The handbook is thus very much in tune with current trends and with the economic importance of such measuring devices.

The eight volumes deal with the following topics: 1. Fundamentals and General Aspects, 2/3. Mechanical Sensors, 4. Thermal Sensors, 5. Magnetic Sensors, 6. Optical Sensors, 7/8. Chemical and Biochemical Sensors. Following the appearance of Volumes 1 and 5 the editors and publishers are to be congratulated on a series which is (up to now) turning out very well. The authors engaged for the work are acknowledged experts, and they have generally covered the literature up to 1988/89 in their respective special fields. Unnecessary overlapping of subject matter, which is often an annoying feature of multi-author works, has been largely avoided. Where overlapping does occur, a different point of view is presented, thereby adding significantly to the description.

The first chapter of Volume 1 deals with the general principles of sensors, definitions, sensor characteristics and models, and includes useful information on the design of integrated-circuit chips and their encapsulation. Chapter 2 is concerned with the basic technology used in manufacturing modern sensors. The practically-orientated descriptions of the manufacture of integrated circuit chips, of thin-film and thick-film technologies, and of integrated optics are impressively good, and will provide newcomers to the field with some detailed know-how. Chapter 3 deals with sensor interfaces, including signal processing and data treatment. The suggested approaches to sensors or sensor arrays that are self-correcting undoubtedly represent a good way of obtaining improved reliability in the measurement of physical quantities. However, in the field of trace analysis of gases by chemical sensors, a method which is only used in low concentration ranges and is therefore very susceptible to trouble, so that it is seldom possible to identify all trace substances or to rule out their presence, the computation method described as a way of correcting for inadequate chemical selectivity only works with a little luck on one's side, to use the words of one of the authors of this volume. The disastrous results obtained in comparative trace analysis trials on the same sample using instruments from different manufacturers or based on different principles speak for themselves, and regularly illustrate the dangers of underestimating the difficulties of trace analysis problems. The final chapter of Volume 1 describes some typical applications of sensors, including examples of their use in automobiles, in domestic equipment, for process control in the chemical industry and in power-station technology, for environmental protection purposes, for medical technology, and for aerospace applications, together with indications of other potential uses. Although some of the contributions here seem rather trivial from the analytical chemist's viewpoint, they will serve to impress on non-specialist readers the many different types of sensors that are still waiting to be developed.

Volume 5 contains twelve articles on magnetic sensors, starting from the basic physical principles and continuing through to trends for the future. The subjects of the individual articles are: magnetogalvanic, magnetoresistive and magnetoelastic sensors, fluxgate sensors, inductive loop sensors, Wiegand and pulse-wire sensors, superconducting quantum interference devices (SQUIDs), and applications for each of these types of devices.

This monograph, written by authors drawn from both industry and universities, is a highly informative work, even for the non-specialist. It describes in a compact form all the modern magnetic sensors that are of practical importance. It also makes easy reading, not least because of the excellent standard of presentation of this series, in which the numerous figures and tables greatly facilitate finding the required information. Also extremely useful are the references to the most recent published work, dissertations, company reports and other material.

If the remaining volumes turn out to be equally well edited and competently written, the result will be a series that no library should be without. This standard work can be recommended unreservedly for scientists in the fields of chemistry, electronics, process technology and measurement and control technology. A more up-to-date review of such quality in a rapidly developing field is unlikely to be found anywhere.

Karl Cammann [NB 1089 IE]
Lehrstuhl für Analytische Chemie
der Universität Münster (FRG)

Photochemistry on Solid Surfaces. (Series: Studies in Surface Science and Catalysis, Vol. 47). Edited by *M. Anpo* and *T. Matsuura*. Elsevier, Amsterdam 1989. xx, 585 pp., hardcover DFl 360.00.—ISBN 0-444-87413-5

In the Elsevier series "Studies in Surface Science and Catalysis", which began in 1975, Volume 47 "Photochemistry on Solid Surfaces" has now appeared under the editorship of *M. Anpo* and *T. Matsuura*. This work must be compared with the review article "Radiation and Photoeffects at Gas/Solid Interfaces" by *J. Cunningham*, which appeared five years earlier in *Comprehensive Chemical Kinetics, Vol. 19* (also published by Elsevier). The present volume sets out to give a review of the latest developments in photochemistry on solid surfaces. This field is in fact developing very rapidly, especially with regard to high-technology industrial applications, which according to the editors are now profiting from a major governmental research project in Japan. To help stimulate further progress in this area, 69 authors have been engaged to report on this many-faceted field, which they have done in 35 articles grouped in 9 chapters with a total of 581 pages. The preponderance here of Japanese (52%) and North American (29%) authors should not be allowed to obscure the fact that European workers have made and continue to make fundamental contributions in this area; in many of the articles the European contributions are underrepresented in the literature citations, and of course this imbalance is not corrected when one refers back to the earlier review. Despite this, the volume is also of interest to European research workers as a means of keeping informed about work in Japan and North America, although more complete information is, of course, available from CAS-ONLINE and from data banks on patents.

Following a short introductory chapter (13 pages), Chapter 2 (104 pages) discusses time-resolved fluorescence spectroscopy, the spectroscopy of transient absorbed species, laser flash photolysis at solid surfaces, excimer formation on silica gel surfaces, and photoacoustic measurements on adsorbed species. The descriptions of the techniques and of the types of information that can be expected from them are elucidated by numerous block diagrams, by presentation of

the basic equations, and by diagrams which are mainly redrawn from earlier publications.

In Chapter 3 (77 pages) specific surface effects on photochemical reactions are discussed. Most of these are free radical reactions, which can be carried out on surfaces of glass, silica gel, semiconductors and metal oxides at various temperatures. The presence of defects with electron acceptor properties can cause chemiluminescence.

New developments in organic photochemistry at solid surfaces are described in Chapter 4 (57 pages). Surfaces that can function as electron transfer partners include those of zeolites, micelles and organic crystals.

Chapter 5 (62 pages) is devoted to inorganic photochemistry at solid surfaces. Metal complexes and metal carbonyls can be illuminated on low temperature matrices, crystal surfaces, porous Vycor glass or silica gel; metal oxides and metal carbonyl catalysts are prepared on supports.

Chapter 6 (36 pages) gives a short introduction to the industrially important processes of photodeposition and photoablation on solid surfaces (often using lasers). These high-technology applications (e.g. in microelectronics) have not been adequately covered here. In this area especially, extensive industrial research and development programs are under way in Europe, e.g. the ESPRIT project (European Strategic Programme for Research and Development in Information Technologies), which go far beyond those reported in this book.

Similarly in Chapter 7 (65 pages) on photochemistry at semiconductor surfaces, it is not possible in so few pages to do justice to the topic. Although the chapter offers some useful thoughts on fractal surfaces, area-selective illumination, photoluminescence of CdS and fluorescence of adsorbed dyes, it is advisable to first obtain an overview of the topic by looking through the published proceedings of major international conferences on photochemistry, which usually contain numerous contributions on photoelectrochemistry.

The application of photochemistry to optical information storage media such as laser-CDs is an area of great importance, which is treated in Chapter 8 (50 pages). The topics that are sketchily covered here include IR-absorbing dyes for DRAW disks, photoinduced phase transitions in liquid crystals, and the application of surface reactions of polymers in lithography. Here again it is regrettable that European laser research is not represented.

Finally Chapter 9 (97 pages) deals with photochemistry in crystals (very briefly, and restricted to ketones), liquid crystals, chiral crystals (absolute asymmetric syntheses), and proteins (picosecond dynamics, energy transfer). The book ends with a subject index (15 double-column pages).

Thus the book is a collection of short articles which exemplify most aspects of the field described by the title, but these are not of a genuine review character. In fact many of the individual topics are covered elsewhere in monographs.

The book is likely to be useful to libraries as an aid to the newcomer entering the field and as a source of ideas for the specialist in his more advanced research. Although it does not cover every topic, it provides an indication of the breadth of this rapidly developing field of research. Future publications of this type should have their subject matter more precisely defined, and should also include contributions from industry.

The economies made by the publishers through reproducing typescripts in (more or less) camera-ready form are unfortunately not reflected in the price; at DFl 360, despite the use of glossy paper, it is too expensive, especially for individual purchasers.

Gerd Kaupp [NB 1078 IE]
Fachbereich Chemie
der Universität Oldenburg (FRG)

Registered names, trademarks, etc. used in this journal, even when not marked as such, are not to be considered unprotected by law.

© VCH Verlagsgesellschaft mbH, W-6940 Weinheim, 1991. – Printed in the Federal Republic of Germany by Konrad Triltsch Druck- und Verlagsanstalt Würzburg.

All rights reserved (including those of translation into foreign languages). No part of this issue may be reproduced in any form — by photoprint, microfilm, or any other means — nor transmitted or translated into a machine language without written permission from the publishers. Only single copies of contributions, or parts thereof, may be made for personal use. This journal was carefully produced in all its parts. Nevertheless, authors, editors and publisher do not warrant the information contained therein to be free of errors. Readers are advised to keep in mind that statements, data, illustrations, procedural details or other items may inadvertently be inaccurate.

Valid for users in the USA: The appearance of the code at the bottom of the first page of an article (serial) indicates the copyright owner's consent that copies of the article may be made for personal or internal use, or for the personal or internal use of specific clients. This consent is given on the condition, however, that the copier pay stated per-copy fee through the Coypright Clearance Center, Inc. (CCC), for copying beyond that permitted by Sections 107 or 108 of the U.S. Copyright Law. This consent does not extend to other kinds of copying, such as copying, for general distribution, for advertising or promotional purposes, for creating new collective works, or for resale. For copying from back volumes of this journal see 'Permissions to Photo-Copy: Publisher's Fee List' of the CCC.

Editorial office: Postfach 10 11 61, W-6490 Weinheim, Federal Republic of Germany, Telephone (06201) 60 23 15, Telex 465 516 vchwh d, Telefax (06201) 602 328, E-Mail Z16@DHDURZ2 in Earn Bitnet.

Editor: *Peter Gölitz*

Associate editors: *D. I. Loewus, K. J. Schneider, A. Stimson.* **Editorial assistant:** *E. Schweikart*

Publishers: VCH Verlagsgesellschaft mbH. (Managing Directors: *Hans Dirk Köhler, Dr. Hardy G. Sehrt.*), Pappelallee 3, W-6940 Weinheim, Federal Republic of Germany.

Advertising office (Advertising Manager *R. J. Roth*): Postfach 10 11 61, W-6940 Weinheim, Federal Republic of Germany, Telephone (0 62 01) 60 61 36, Telex 467 155, Telefax (0 62 01) 606 156.

ANGEWANDTE CHEMIE
International Edition in English
Volume 30 · Number 2
February 1991
Pages 113–216

Towards the Chemical Synthesis of Proteins

By Ernst Bayer*

The chemical total synthesis of proteins using solid supports has made great progress. It is therefore becoming a reality what *E. Fischer* already predicted in 1902[**]: "I foresee the time when physiological chemistry... is able to prepare synthetic enzymes." The synthesis of peptides of up to 20 amino acids by the well-established solid-phase procedure on polymeric supports (SPPS) has made great progress through the development of newer supports. At the same time, methods have emerged which facilitate the separation and characterization of peptides, thus allowing optimization of the synthesis of pure materials. The new supports which enable one to synthesize peptides by a rapid continuous flow procedure are characterized by hydrophilicity, beads of approximately equal size, similar swelling properties in the solvents used for peptide synthesis, and stability at high pressure. With graft copolymers of weakly cross-linked polystyrene and linear polyethylene glycol (PEG), the synthetic cycle for coupling of one amino acid can routinely be reduced to 10–20 min with a concomitant higher yield. With beads of monodispersed graft copolymer of 10 μm diameter, a synthetic cycle can, in principle, be shortened to 1–5 min. By utilizing this high-speed solid-phase procedure, larger peptides up to the size of proteins could also be prepared in a few hours. With newer mass spectroscopic methods such as ion-spray mass spectrometry, peptides of up to a molecular mass of 100 kDa can be characterized, and with the advent of capillary electrophoresis, another very efficient separation tool, besides HPLC, is at our disposal.

1. Introduction

The chemical synthesis of peptides has made great progress in the last two decades. Peptide synthesis has proven indispensable for the structural elucidation of many recently isolated natural products having a peptide structure such as hormones, neuropeptides, and antibiotics, which very often could be isolated in only minute quantities. Investigation of the structure–activity relationships of biologically active peptides also demands the synthesis of many analogues of a given peptide. Peptide synthesis has moreover become an indispensable research tool in immunology. Thus, the synthesis of overlapping peptide sequences is essential for epitope characterization and antibody formation.

The advances made in the chemical synthesis of peptides would not have been possible without the availability of the method of solid-phase peptide synthesis (SPPS) introduced by *Merrifield*.[1–3] Experts outside the field of peptide chemistry erroneously gained the impression that every peptide could be synthesized on a routine basis in this way, yet this notion even gains more support when one considers the possibility of peptide synthesis using fully automated synthesizers. It is therefore not surprising that since the introduction of SPPS it has been predicted that the chemical synthesis of proteins would become a routine matter. Table 1 shows several selected examples of reports concerning the solid-phase synthesis of proteins in the last 20 years.

[*] Prof. Dr. E. Bayer
Institut für Organische Chemie der Universität
Auf der Morgenstelle 18, W-7400 Tübingen (FRG)

[**] Cited from *Nobel Lectures—Chemistry 1901–1921*, Elsevier, Amsterdam 1966, p. 34.

 © VCH Verlagsgesellschaft mbH, W-6940 Weinheim, 1991 0570-0833/91/0202-0113 $ 3.50+.25/0

Table 1. Attempted syntheses of naturally occurring proteins by SPPS.

Protein	Number of amino-acid residues	Year	Authors
Ferredoxin	55	1968	*Bayer, Hagenmaier, Jung* [133]
Ribonuclease A	124	1969	*Gutte, Merrifield* [134]
Cytochrome c	104	1969	*Sano, Kurihara* [135]
Growth hormone	188	1970	*Li, Yamashiro* [136]
Ribonuclease T_1	104	1972	*Izumiya* [138]
Lysozyme	129	1973	*Sharp* et al. [137]

Considering the purity criteria which govern the areas of organic and pharmaceutical synthetic chemistry, it becomes obvious that none of the protein syntheses listed in Table 1 furnish, with certainty, a pure product. In the period 1969–1973 numerous publications appeared regarding protein synthesis, but the mere fact and the recognition that the purity criteria were often not fulfilled resulted in a large reduction of the number of publications appearing thereafter. The aim to achieve a reliable synthesis of long polypeptides has therefore still not been realized. Nonetheless, it is worthwhile aiming for this goal. After all, the synthesis of pure and biologically active small peptides by SPPS furnishes a lot of information regarding the structure-activity relationships of these compounds. Similar results could be expected from the same studies on proteins, if a reliable synthesis were possible.

One question that is often posed, is whether preparing proteins via gene technology renders their chemical synthesis superfluous. But as long as a reliable chemical synthesis is not possible this question remains purely hypothetical. It is also obvious that in the case of syntheses involving non-coded amino acids, or in the case of the subsequent derivatization of proteins, the chemical synthesis could represent an easier procedure. Substitution of genetically coded amino acids by non-protein amino acids in small peptides often produces surprising biological activities; the same effects can be expected in the case of proteins. Above all, specific introduction of ^{13}C-labeled amino acid residues in the active centers of proteins and subsequent NMR investigation regarding the mechanism of action is only possible by the chemical synthesis. The biotechnological and chemical syntheses can therefore supplement each other and the new science of protein engineering[4–6] could gain impetus by the successful synthesis of long chain peptides. It is therefore important to assess the state of the art of automated peptide synthesis and to survey the trends of future developments.

2. Principles of the Merrifield Peptide Synthesis

In principle, solid-phase peptide synthesis follows the strategy of the stepwise assembly of peptides by consecutive coupling of amino acids. This procedure, with the use of low molecular mass *C*-terminal carboxy protecting groups, has long been known in peptide chemistry,[7] but has found less widespread application than the classical coupling of fragments.[8–10] It has also long been known that the stepwise synthesis should be carried out from the *C*-terminal to the *N*-terminal end;[11,12] since only in this way can the danger of racemization be largely circumvented. Furthermore, the stepwise synthesis using low-molecular *C*-terminal protecting groups finds less application simply because the sparing solubility of one of the coupling partners does not permit a homogeneous reaction. Carrying out the synthesis as a heterogeneous reaction in such cases is also unpromising due to the poor filterability of the reaction mixture.

Merrifield's ingenious idea was to employ an insoluble and filterable polymeric support such as cross-linked polystyrene which functions at the same time as the carboxy protecting group for the *C*-terminal amino acid. Thus, the N^{α}-protected *C*-terminal amino acid is attached to the chloromethylated polystyrene-divinylbenzene as shown in Scheme 1. After removal of the N^{α}-protection, the next N^{α}-protected amino acid is coupled and the process is repeated until the entire desired peptide is assembled on the polymeric support. The advantage of this procedure is that a large excess of coupling components and additive reagents can be employed which will be easily separated from the polymer-bound peptide by simple filtration. Consequently, the laborious and cumbersome purification of intermediate peptides, a process typical of the classical solution synthesis, is avoided and results in a tremendous saving of time.

Originally, dicyclohexylcarbodiimide was proposed as the coupling reagent, but many other suitable coupling proce-

Ernst Bayer, born March 24, 1927 in Ludwigshafen/Rhein, studied chemistry at the Universities of Heidelberg and Freiburg. After completing his Diploma in 1952 he continued his studies at the Max-Planck-Institut für Medizinische Forschung, Heidelberg, where he gained his doctorate in 1954 for research on hemovanadium under the supervision of Richard Kuhn. After his habilitation in 1958 at Karlsruhe, he remained there as Dozent until 1962. In 1962 he was offered and accepted a Professorship at the University of Tübingen, and, except for a short spell as Robert A. Welch Professor at the University of Huston (February 1967–April 1970), has remained there ever since. In 1978 he received the Tswett medal of the Soviet Academy of Sciences and the British A.J.P. Martin award, in 1981 the Max Bergmann medal, in 1985 the American Tswett award, in 1989 the Distinguished Service Cross 1st Class of the Federal Republic of Germany, and in 1990 the Richard Kuhn medal of the German Chemical Society. Since 1982 he has been chairman of the advisory board for environmentally relevant existing chemicals. His scientific interests include natural products chemistry, peptide synthesis, separation methods, natural metal complexes, polymer chemistry, catalysis, and enantiomeric analysis.

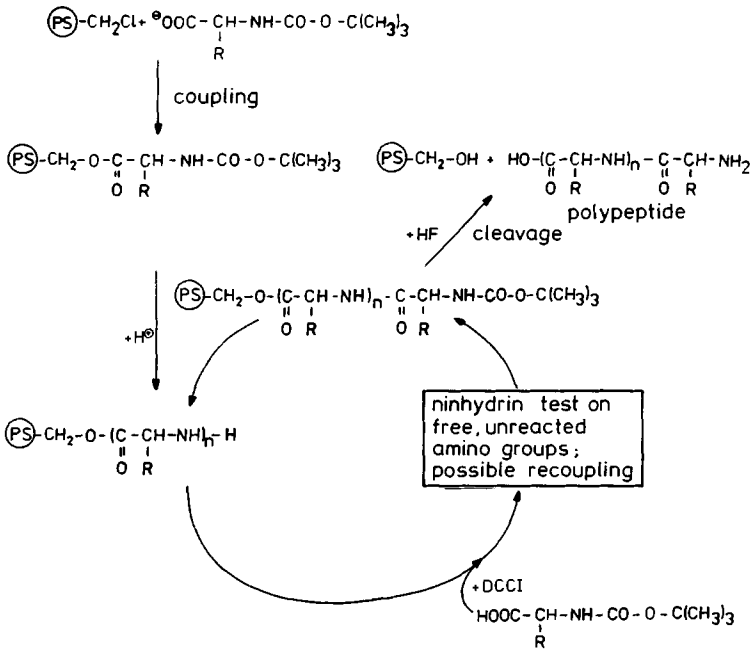

Scheme 1. Standard cycle for solid phase peptide synthesis after *Merrifield*. PS = polystyrene cross-linked with 0.5–1% DVB; DCCI = dicyclohexylcarbodiimide.

dures, e.g. with active esters or anhydrides can also be used.[13 - 20] Besides the chloromethyl group originally proposed for the anchoring of the *C*-terminal amino acid on the polymer, in the meantime many other anchoring agents have been introduced.[13, 21 - 28]

Even today, *Merrifield*'s original strategy using the benzyl ester anchor and the acid labile *tert*-butyloxycarbonyl group for amino protection is widely employed. The protection of the trifunctional amino acids follows principally the known methods in peptide chemistry and is well-documented in the literature.[9, 13, 29 - 35]

After completion of the synthesis, the peptide is detached from the support. In the Merrifield strategy, strong acids or anhydrous HF are used for the cleavage of peptides from the polymer. Under these conditions the side-chain protecting groups are simultaneously removed and free peptides are obtained. Owing to standardization of the steps involved, the solid-phase synthesis can easily be automated. In fact automatic peptide synthesizers have already been developed and are commercially available.[31, 36 - 38]

3. Problems in the Synthesis of Pure Peptides

Like all other ingenious ideas, SPPS also has its short comings. Thus, it very soon became obvious that the fact that the growing peptide chain always remains on the polymer not only has advantages (facile separation), for, in principle, a multistep synthesis without purification of the intermediates can only yield a pure product if every reaction step proceeds unequivocally and quantitatively. However, which organic reaction can always be claimed to proceed quantitatively? Also in peptide synthesis the occurrence of some side reactions should be taken into account, such as, e.g., detachment of the protecting groups of trifunctional amino acids and additional reactions of the third functional groups (carboxy, amino and hydroxy), racemization, rearrangements, and cyclizations.

The by-products thus formed can then react further and remain together with the growing peptide chain on the polymeric support until the end of the synthesis. Yet even if the side reactions can be avoided, a complete peptide coupling and amino deprotection in every cycle is highly unlikely in the heterogeneous reactions that take place on polymeric beads. Polymer matrix effects as well as the formation of rigid conformations can also drastically lower the yield. The effects of these conformational changes are well documented in the literature.[38 - 46] Above all, the formation of β-folded structures in the case of peptides with 6–20 amino acid residues can often lead to an abrupt termination of the synthesis before the desirable end product is obtained. Even if a statistical yield of 99.5% is obtained in every coupling and deprotection reaction, the problem of the so-called truncated and failure sequences remains unresolved.[47 - 52] As an example the synthesis of a pentapeptide A–B–C–D–E is given in Figure 1. The truncated sequences arise if the polymer-

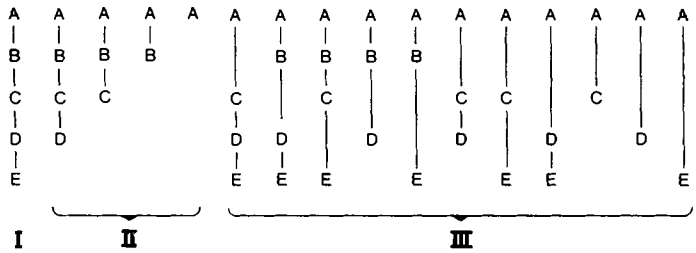

Fig. 1. Truncated **II** and failure sequences **III** obtained by solid-phase synthesis of a pentapeptide A-B-C-D-E **I**.

bound peptide no longer reacts in a synthetic step. They possess, in principle, the correct sequence. But because of conformational changes, an end group which has not reacted in one or several coupling steps can again become accessible at a later stage. Therefore as the peptide grows, a binominally increasing number of failure sequences will be produced. These peptides with failure sequences, which are chemically related to the desired end product, are extremely difficult to separate. It has been demonstrated that such failure sequences are also produced during otherwise successful syntheses.[47 - 54] Besides chromatographic procedures, the more recent spectroscopic methods such as FAB (fast atom bombardment) and ion-spray MS can also be used for the detection of failure sequences. Figure 2 shows the detection of such failure sequences of a synthetic heptadecapeptide, directly after its cleavage from a polymeric support.

Assuming a 95% yield in every coupling and amino deprotection step in the synthesis of ribonuclease with 124 amino acids, the product can only be obtained in 0.0002% yield, whereas, concomitantly a 15-fold amount of peptides containing one less amino acid is produced. It is therefore obvious that the synthesis of a peptide using the original conditions of SPPS would be possible only under very fortunate circumstances. Only if the yield is improved through optimization of the conditions, is there a chance to prepare

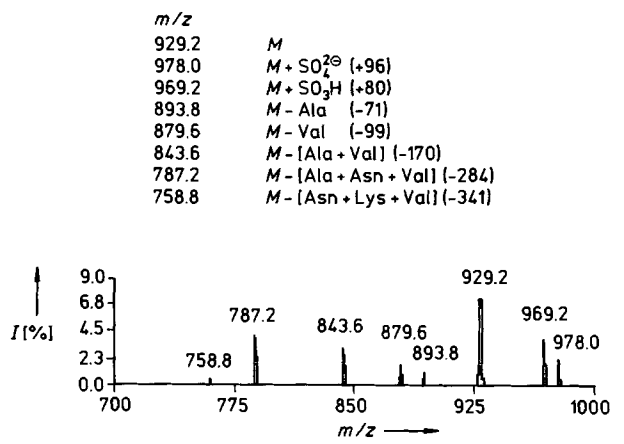

Fig. 2. Ion-spray mass spectrum of the 17-residue peptide H-Ala-Val-Leu-Gly-His-Asp-Glu-Ala-Ala-Tyr-Ser-Lys-Asn-Arg-Arg-Ala-Val-OH *M* directly after its cleavage from the polymeric support. Besides the heptadecapeptide, $m/z = 929.2$, there exist five peptides with failure sequences. The m/z values are valid for the ions of the composition given on the right, which, in each case were determined as diprotonated species.

a long chain peptide with the correct structure in high yield and in pure form. With a 99.5% yield in every step of a ribonuclease synthesis, the main product could be obtained in 29% yield, whereas the sequences with one less amino acid are produced in 36% yield. In the case of shorter peptides the percentage of failure sequences is lower and chromatographic separation is easier. Nevertheless, the synthesis of small peptides in pure form was a difficult task in the early days of SPPS. Only after the development of an efficient separation procedure by HPLC (high performance liquid chromatography) in the 1970s, did SPPS become so successful. The application of HPLC for the separation of peptides was first mentioned in the literature in 1973.[55, 56] Today there is rarely a publication in which HPLC is not used for the final purification of a peptide synthesized on a solid support. It was therefore essential to have access to a new reliable separation method in order to promote the polymer supported synthesis of peptides of up to about 20 amino acids.

The separation of proteins by conventional HPLC is far less feasible. On the one hand, in the case of long chain polypeptides the number and the amount of difficultly separable peptides with similar sequences increase exponentially, and, on the other, many stationary phases are not suitable for proteins. Therefore, the development of newer separation and characterization techniques is absolutely necessary to guarantee a reliable protein synthesis. The correlation between synthesis and separation methods will be discussed in more detail in Section 6.

4. Optimization of the Polymeric Support

Without de-emphasizing the importance of optimizing SPPS by correct choice of the protecting groups, the anchor for binding the *C*-terminal amino acid, and the strategy of the synthesis, it is quite evident that an optimization of the polymeric support could contribute most fundamentally to the improvement of SPPS. Polystyrene is a relatively hydrophobic matrix and therefore not the best choice for the hydrophilic peptides. Furthermore, steric factors and a lack of kinetic equivalence of the functional groups play a certain role in the case of cross-linked polymers. Since SPPS involves heterogeneous reactions, lowering the dependence on diffusion is important. The varied reactivity of the functional groups in cross-linked polystyrene has been demonstrated by *Rudinger* et al. [57] as well as by *Andreatta* et al.[58]

4.1. Liquid Phase Synthesis

The matrix effect of the cross-linked polymer and the heterogeneous reaction can be avoided if a linear and soluble polymer is used. This goal was achieved by *Shemyakin, Ovchinnikov* et al.[59] who used linear polystyrene, and by *Bayer* and *Mutter* et al.[60, 66] who employed linear polyethylene glycol. Linear polystyrene is very easily cross-linked and difficult to handle. More suitable is polyethylene glycol (PEG), which, owing to its good solubility in many organic solvents, can solubilize even otherwise insoluble peptides.

A synthetic cycle using the liquid-phase procedure is shown in Scheme 2. The couplings are carried out in homogeneous solution. Kinetic investigations have shown[67] that amino acid-PEG esters have the same coupling rates as the low molecular mass amino acid esters (Table 3). Diffusion phenomena play no role in this technique. Instead of the simple filtration used in SPPS, membrane filtration is employed in this procedure. This is possible because polymer-bound peptides ($M_r = 3-20$ kDa) and the low molecular mass reagents show considerable differences in molecular size. Recrystallization of the peptide-PEGs can also be used as a valuable alternative procedure for purification purposes.[64]

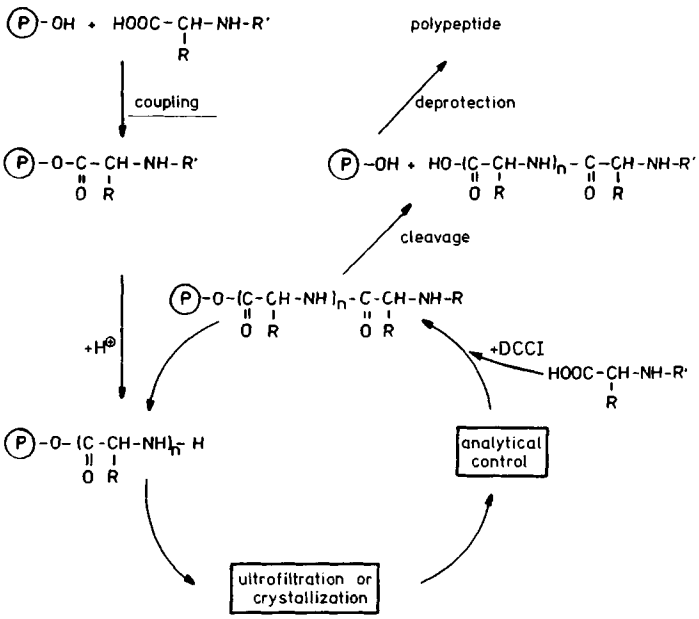

Scheme 2. Standard cycle for liquid phase peptide synthesis [60–66].

A noticeable advantage of the liquid-phase method is the possibility of carrying out a better analytical control of the reaction, since now also spectroscopic methods such as

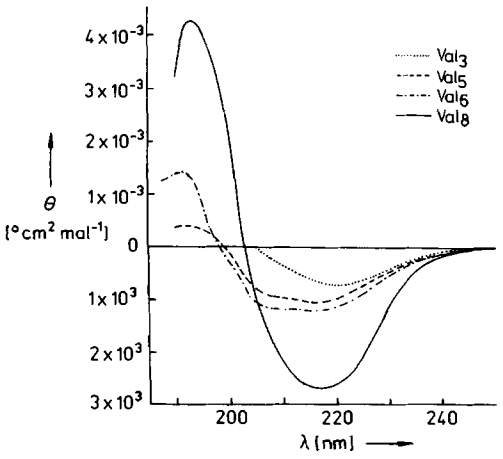

Fig. 3. CD Spectra of Boc-(L-Val)$_n$-Gly-PEG in trifluoroethanol. n = 3 and 5 (random coil); n = 6, 15% β-structure; n = 8, 100% β-structure.

NMR and CD can routinely be applied. This method has been employed the widest to study the changes in folding during the stepwise peptide synthesis.[65, 68 - 70] Figure 3 shows such an investigation by means of CD-spectroscopy during the stepwise synthesis of polyvaline.[71] Figure 4 presents the NMR spectrum of a PEG-bound sequence of insulin.[72]

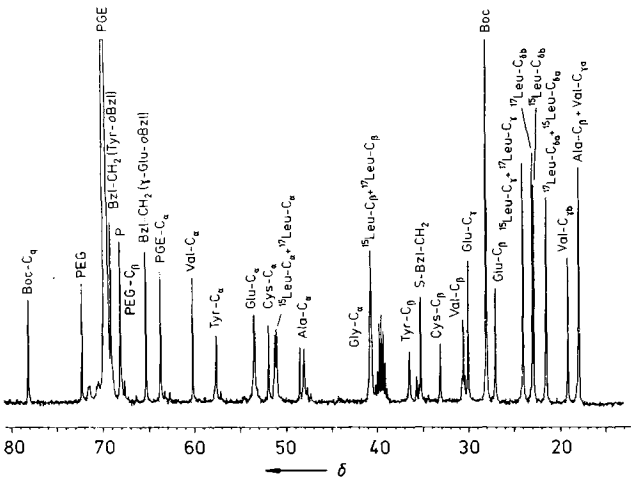

Fig. 4. Aliphatic region of the ^{13}C-NMR signals of the polyethylene glycol-bound octapeptide, which corresponds to the insulin B13–20 fragment. Measurement in suspension.

The disadvantages of liquid phase synthesis are, however, the problem of automation and the time-consuming operations.[73] Membrane filtration often takes very long, and for the crystallization process the product must be precipitated, washed, and redissolved. These operations practically render an untroublesome automation impossible. Moreover, the solubilization by PEG is unsatisfactory in the case of longer peptides.

4.2. Polyacrylamides as Polymeric Supports

Polyacrylamides, which are more hydrophilic than polystyrene, were introduced as polymeric supports in peptide syntheses by *Atherton* and *Sheppard* et al.[32, 74 - 76] Poly(*N*,*N*-dimethylacrylamide) has a polarity similar to peptides and swells much better than polystyrene in the solvents which are commonly used in peptide synthesis, e.g. dimethylformamide (DMF). A good swelling of the polymeric support is essential for the free access of functional groups to the polymer, specially to the micropores. The less the reaction space is restricted by the polymeric matrix, the more favorable become the reaction conditions. At about the same time, *Carpino* and *Han*[77] described the use of the fluorenylmethoxycarbonyl (Fmoc) group for protection of the amino function. The Fmoc group can be cleaved with alkalies such as piperidine and can therefore be used in conjunction with acid labile protecting groups. Compared to the solely acid labile Boc group, the Fmoc group furnishes decisive improvements. Its UV absorption also opens up the possibility of spectroscopically monitoring the peptide synthesis. Regarding corrosion of the automated peptide synthesizers, treatment with alkalies is more preferable than treatment with acids. The increased scope of the strategy in the case of the alkaline cleavage is also appreciable.

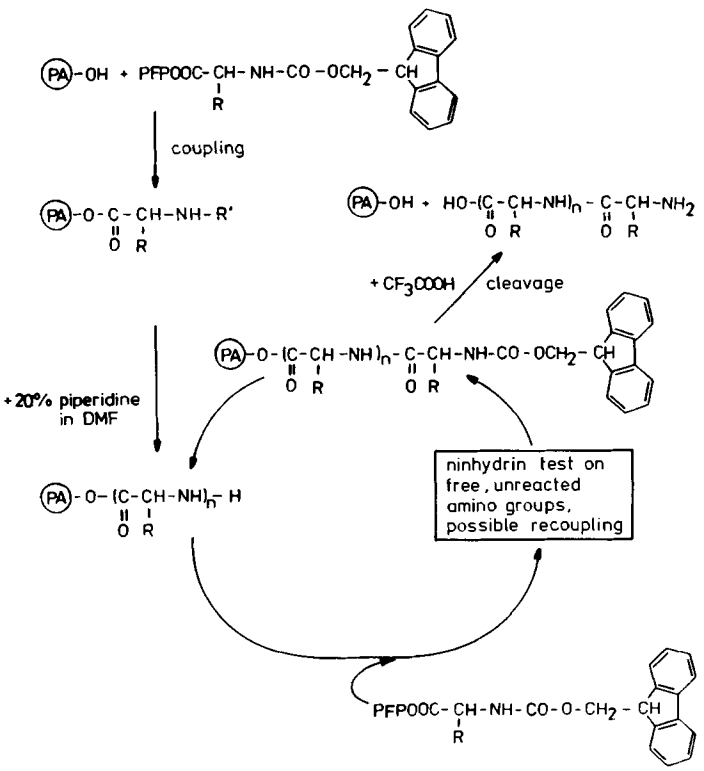

Scheme 3. Standard cycle for solid-phase method on polyacrylamide gel using Fmoc strategy. PA = copoly(dimethylacrylamidebis(acryloyl)ethylenediamine-acryloylsarcosine methyl ester) + linker. PFP = pentafluorophenyl.

For these reasons, the polyacrylamide gel and Fmoc strategy have found wider use in Europe than the original *Merrifield* strategy. Scheme 3 depicts a peptide synthesis on poly(*N*,*N*-dimethylacrylamide) using the Fmoc strategy.

4.3. Hydrophilic Tentacle Polymers

As mentioned in Section 4.1, PEG is very compatible with peptides. It is soluble in water and in almost all organic

solvents with the exception of aliphatic hydrocarbons and diethyl ether. PEG was shown to be a valuable support for peptide syntheses using the liquid-phase method. The main difficulty encountered, however, was the separation of PEG-bound peptide from the reagents in the homogeneous phase. It was therefore justifiable to believe that this problem could be circumvented by immobilizing long chain PEGs on an insoluble polymer, thus combining the advantages of SPPS and the liquid phase method.

Since cross-linking of the linear polyethylene glycol would restrict the mobility of the polymer chains, an attempt was made to graft it on an insoluble matrix. Inorganic solids such as silica gels could not be considered, because modified silica gels are not stable enough under the conditions of repeated alkaline and acidic treatment which are usually employed during the peptide synthesis. The simplest immobilization procedure would be the coupling of one of the hydroxy groups of PEG to chloromethylated polystyrene according to a classical ether synthesis.[78, 79] The main problem of this procedure, however, is that when long PEG chains (>800 Da) are used, the yields are unsatisfactory. Moreover, both terminal hydroxy groups react with chloromethyl groups, so that the polystyrene is additionally cross-linked. Consequently, the number of free hydroxy groups will be reduced with concomitant lowering of the capacity of the graft copolymer for binding to peptides.

By means of anionic polymerization of ethylene oxide, PEG chains of unlimited size can be immobilized on cross-linked polystyrene beads containing hydroxy functional groups.[80 - 86] This article describes in summary the preparation, properties, and application of graft copolymers for the first time. Preferably the potassium salt of poly(styryl-methyltetraethylene glycol ether), which is present in the form of an open crown ether, is used for the synthesis (Scheme 4). When carrying out this grafting reaction, functionalized polystyrene beads of any degree of porosity can be employed. If nonporous beads are used, the ethylene oxide can only be grafted on the surface. In this case, the polyoxyethylene chains extend outwards from the matrixlike tentacles. Such polymers are of interest as stationary phases for HPLC; however, they are not suitable for peptide syntheses, since their peptide loading is too low. For peptide and nucleotide syntheses, graft copolymers based on porous polystyrene are more interesting.

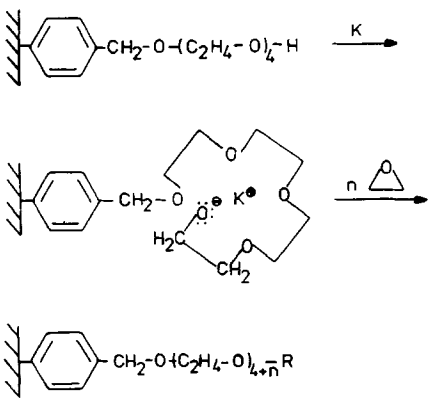

Scheme 4. Synthesis of graft copolymers from cross-linked PS and linear PEG. R = H, K.

Graft copolymers with PEG chains of about 3000 Da have proven optimal. These copolymers contain about 70% of linear PEG and only about 30% of cross-linked polystyrene matrix. The properties of these polymers are therefore largely determined by the PEG portion of the molecules. This is demonstrated, in particular, by the swelling properties. Table 2 shows a comparison of the swelling factors of the polystyrene-polyethylene glycol graft copolymers and polystyrene in several solvents. The graft copolymers swell in all solvents which dissolve PEG.

Table 2. Comparison of the swelling factors of polystyrene (PS) cross-linked with 1% DVB with those of a graft copolymer of polyethylene glycol (M = 3300 Da) and PS (PS-PEG).

Solvent	PS	PS-PEG
Water	–	2.5
MeOH	0.95	2.5
EtOH	1.05	1.2
CH_2Cl_2	5.2	3.0
Toluene	5.3	3.1
DMF	3.5	3.2
CH_3CN	2.0	3.0
THF	5.5	3.4
Dioxane	4.8	3.7
Ether	2.5	1.1

A good solvation leads to a high degree of mobility of the PEG chains and the peptides bound to them. This mobility can be demonstrated by ^{13}C-NMR relaxation time measurements.[87] Figure 5 shows that the ^{13}C-NMR relaxation times T_1 of peptides which are bound to polystyrene are lower than those of peptides which are bound to PEG or to graft copolymers, whereas those of the peptides bound to the last two supports are about the same. Both the PEG chain as well as the peptides bound to it give rise to sharp NMR

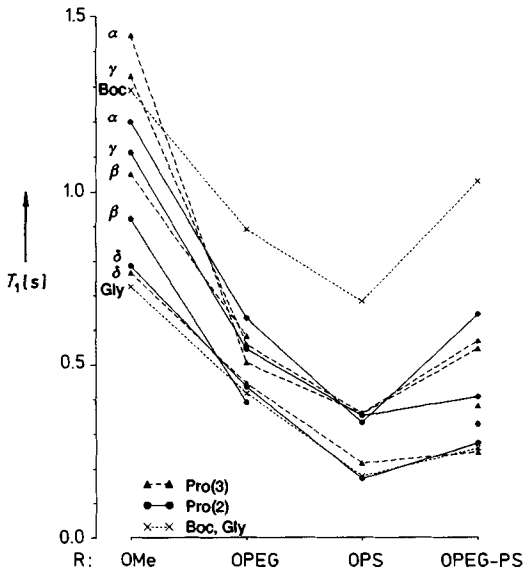

Fig. 5. ^{13}C-NMR relaxation time T_1 of the free (R = OMe) and of the polymer-bound tripeptides Boc-Gly-Pro(2)-Pro(3)-R.

signals such as are normally not expected from measurements on solid materials in suspensions. On the other hand, in solvents such as ether, which do not solvate PEG, wide NMR signals typical of the measurements on solids in suspensions are obtained.

We can therefore distinguish between a solvated tentacle conformation and a non-solvated knäuel conformation of the graft copolymer as shown schematically in Figure 6. For

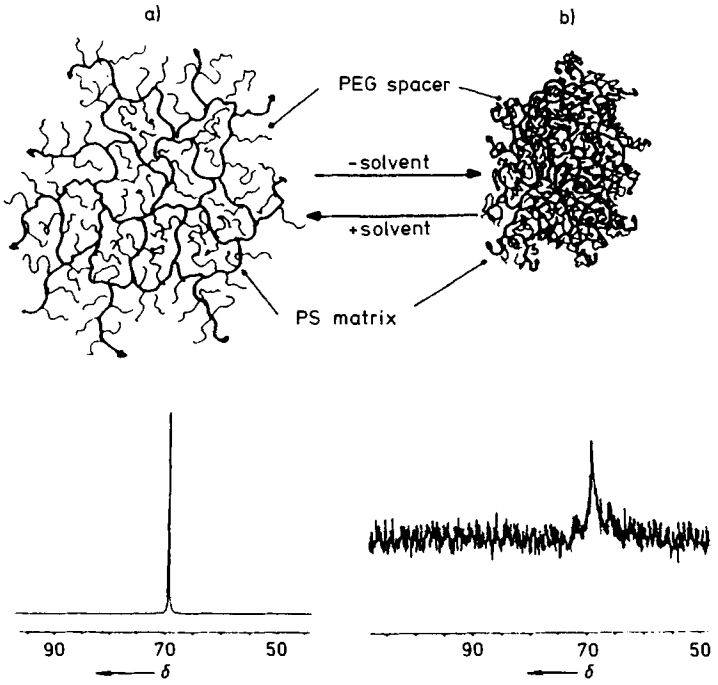

Fig. 6. Top: Conformations of the graft copolymers PS and PEG. Bottom: The respective ^{13}C-NMR spectra of a) folded and solvated form, sharp NMR signals in spite of the measurement in suspension; b) Knäuel conformation in contact with nonsolvating solvents; usual signal broadening of the solid state.

this reason, such polymers have received the trivial name tentacle polymers.[88] Figure 7 shows the homogeneous distribution of the PEG chains on the surface and in the interior of the polymer bead. Under the conditions used in the electron microscopic investigation, the graft copolymers exist in

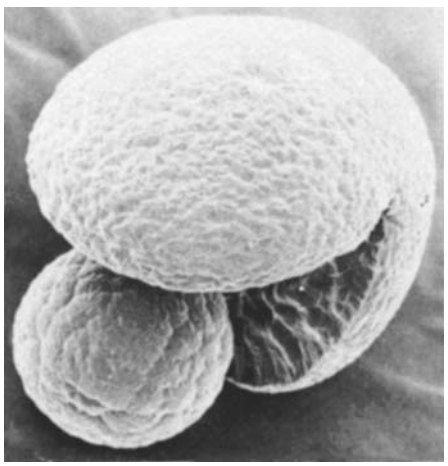

Fig. 7. Electron micrograph of the graft copolymer of PS and PEG 1 mm ≈ 3.227 μm.

the knäuel conformation. A remarkable feature is the observed comparable swelling factors of the tentacle polymers in different solvents (Table 2). This enables the packing of columns with the graft copolymer for continuous flow peptide syntheses in columns, since no change in the packing occurs on applying different solvents during the synthesis. The swelling factors also remain unchanged as the peptide chain grows.

A further property of the copolymer rarely observed in other polymers can promote its use in continuous flow peptide synthesis: due to the solvation, the PEG-PS beads are stable under pressures up to 200 bars, the condition under which relatively high flow rates can be achieved. This in turn shortens the time required for a coupling cycle. The advantages of the continuous flow synthesis will be discussed again in Section 5.

Since, according to NMR investigations, the mobility of the PEG chains of the graft copolymers is about the same as the mobility of free PEGs, it can be assumed that these copolymers after being solvated, behave like a homogeneous phase. The same conclusion can be reached by considering the rate constants of peptide coupling on the graft copolymer which have the same order of magnitude as those of the liquid phase synthesis (Table 3). According to these exami-

Table 3. Comparison of the rate constants k of coupling glycine active esters to polyethylene glycol glycine (PEG-Gly) in solution and to polystyrene-poly(ethyleneglycolglycine) graft copolymers (PS-PEG-Gly). The numbers represent M_r of the PEG chains.

Polymeric support	k[mol^{-1} · s^{-1}]	meq Gly/g polymer [a]
PS-PEG-2000-Gly	0.37	0.20
PS-PEG-3300-Gly	0.32	0.12
PS-PEG-5700-Gly	0.29	0.08
PEG-2000-Gly	0.16	0.49
PEG-4000-Gly	0.17	0.38
PEG-6000-Gly	0.13	0.27
Glycine ethyl ester	0.12	

[a] meq. = milliequivalents.

nations, tentacle polymers are suitable as hydrophilic supports for a rapid peptide synthesis.

4.4. Monodispersed Tentacle Polymers

So far, diffusion phenomena have not adequately been taken into account in the optimization of peptide syntheses, although they are of prime importance for shortening the duration of the synthetic cycles. Since the reactions are heterogeneous, the particle diameter plays a decisive role in all the diffusion processes. As the particle diameter gets larger, the contribution of diffusion becomes more extensive. The commercially available resins that are used for a Merrifield SPPS are polydispersed, i.e., they have a wide particle size distribution, e.g. 10–200 μm. It is obvious that the duration of the synthesis is determined by the largest particles. These also contain a relatively higher number of functional groups in comparison to the small particles, as shown in Figure 8. A

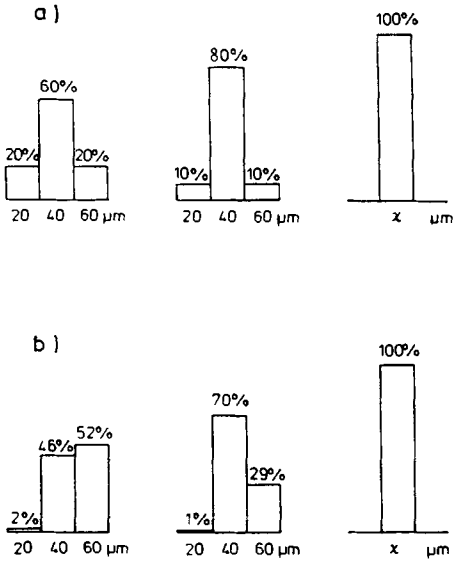

Fig. 8. Arbitrary size distributions of the polydispersed polymeric beads (a) and calculated percentage of the functional groups in the polymeric beads with different diameters (b). χ: arbitrary size of monodispersed beads.

considerable shortening of the duration of a synthetic cycle would therefore be possible, if monodispersed and uniform particles with as small a diameter as possible were available. Most of the polymerization procedures, however, lead to polydispersed materials.

Following a detailed study of diffusion processes, *Ugelstad* et al.[89, 90] investigated the essential parameters for the preparation of monodispersed polystyrene beads. Using this as a basis, the preparation of monodispersed and cross-linked polystyrene beads with diameters of 5–20 µm was elaborated. First of all, a "seed" is prepared in a two-step reaction (Scheme 5) in a homogeneous solution using an initiator.[91] In order to obtain particles with equal diameters, it is important to produce the seed in a short time and

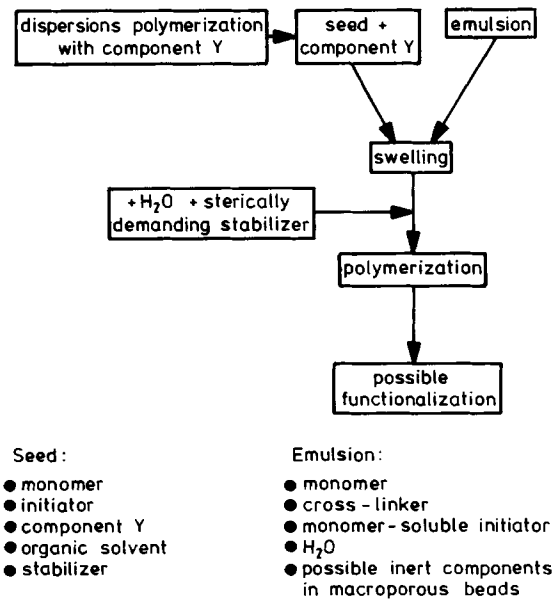

Scheme 5. Two-step process for the synthesis of monodispersed, cross-linked polystyrene.

to work in the presence of bulky stabilizers which suppress the formation of aggregations and micelles. The particles of the seed are still not cross-linked; they are then brought into an aqueous emulsion of the monomeric styrene, the cross-linker divinylbenzene, and the initiator. In a diffusion-controlled process in the presence of water-soluble and sterically hindered stabilizers, the seed becomes swollen and cross-linked (Figure 9). Figure 10 shows the monodispersed and

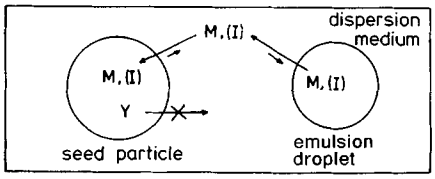

Fig. 9. Swelling of the monodispersed seed. M = monomer, I = initiator; Y = component Y.

cross-linked polystyrene beads thus obtained. The deviations in the diameters are less than 2%, e.g. 10 ± 0.02 µm. If one compares these polymers with the other customary resins with a broad distribution of molecular size, it is immediately evident that for the first time large molecules with such a uniform molecular structure and size can be prepared, which otherwise only nature is able to produce. These monodispersed and cross-linked polystyrene beads can now be functionalized and used as supports for peptide synthesis.

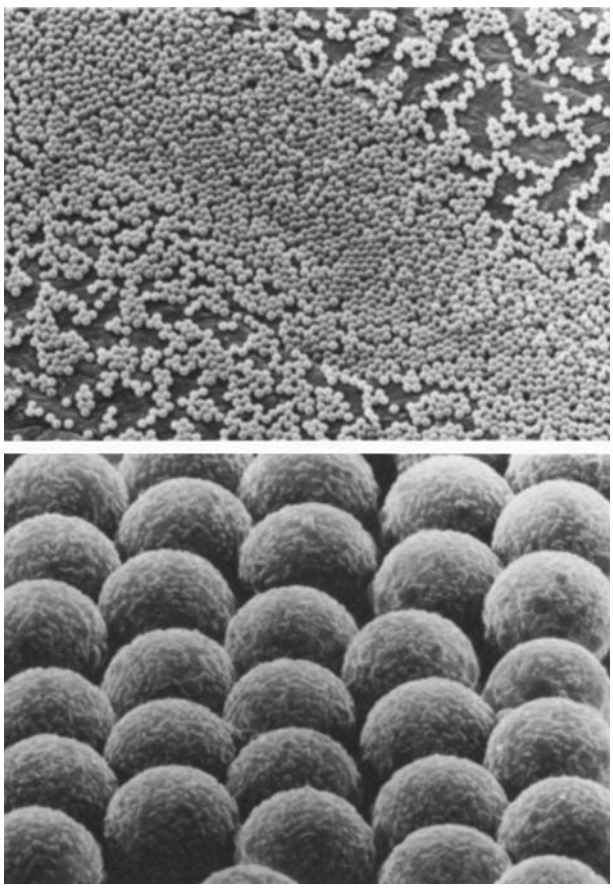

Fig. 10. Electron micrographs of the monodispersed polystyrene (top, 1 mm ≈ 1.424 µm) and of the graft copolymer of PS and PEG (bottom, 1 mm ≈ 0.420 µm).

It is also possible to graft PEG chains to these beads, as already described in Section 4.3. Figure 10 (bottom) shows an example of such monodispersed graft copolymers. Under the conditions used in the electron microscopic investigation the PEG chains of the above polymers exist in ordered spherical forms.

With these pressure-stable and hydrophilic polymeric supports, we can minimize the diffusion problems of the solid-phase synthesis. Moreover, the new supports cannot only be used for the synthesis of peptides and nucleotides, but also as stationary phase for HPLC.[92]

5. Continuous Flow Synthesis

Tentacle polymers are pressure stable and show almost equal swelling factors in different solvents. These two properties make them suitable for column packings and for carrying out continuous peptide syntheses with high flow rates. As a consequence, tentacle polymers distinguish themselves from all other polymers. A continuous flow synthesis has advantages over the batch synthesis recommended by *Merrifield. Bayer, Halasz* et al. already described the first continuous flow synthesis on chemically modified silica gel supports as long ago as 1970.[73] They demonstrated that a shorter time was required for a cycle and at the same time the peptide synthesized showed a higher purity. For the synthesis of longer peptide chains, however, the modified silica gels are not chemically stable enough.

Later, pellicular resins were used for the continuous synthesis.[94] Because of the low pressure-stability and different swelling factors, the usual supports cannot be used. Therefore, *Frank* and *Gausepohl* employed loosely packed cartridges of different polymeric gels for the continuous flow synthesis.[95] *Atherton, Sheppard* et al. polymerized polydimethylacrylamide gels on kieselguhr and successfully employed the material obtained for continuous flow syntheses using an automated synthesizer.[96, 97] Kieselguhr is, however, not a spherical support as can be seen from the electron micrograph of a polydimethylacrylamide polymerized in kieselguhr (Fig. 11), which in comparison to the graft copolymer in Figure 10, is clearly a characteristically more heterogeneously distributed polymer.

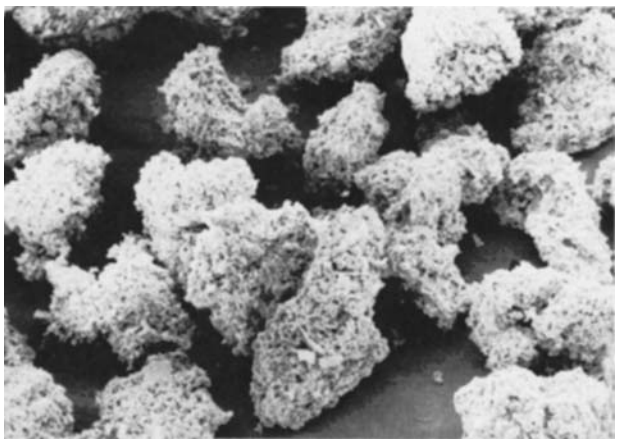

Fig. 11. Electron micrograph of polyacrylamide-kieselguhr supports.

The graft copolymers of cross-linked polystyrene and polyethylene glycol show pressure stability, similar swelling behavior in different solvents, chemical stability, spherical form, and equal bead size. All of these properties are prerequisite for a rapid peptide synthesis by the continuous flow method. Since its introduction, it has been shown on many occasions that this procedure is superior to the normal batch-wise synthesis.

An essential advantage of the continuous flow method is that the excess of coupling components and solvents normally used in SPPS can be drastically reduced. Moreover, the coupling and deprotection reactions can be monitored by UV measurements at the inlet and outlet of the column. In this respect the UV active protecting groups such as Fmoc are especially suitable.

The lowering of the excess of reagents compared to that in the batch-wise method results from carrying out the reaction in a continuous flow. When a relatively highly concentrated solution of the coupling components is allowed to pass through the column a concentration profile develops, as shown in Figure 12 (right). Since only a relatively small region of the functional polymer (support) comes in contact with the coupling components while the reagent flows through the column, the excess of reagents in every column segment is larger than would have been the case if the reagents had been in contact with the total support. The narrower the coupling components band, the larger the excess of reagents in a given column segment. Hence, the reaction can proceed more completely, and the content of peptides with statistical failure sequences will be lowered. A typical spectrophotometric monitoring of a synthetic cycle is shown in Figure 13a.

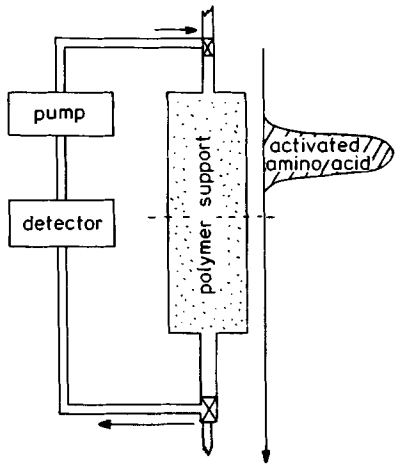

Fig. 12. Moving band of the coupling components in the reaction vessel during continuous flow synthesis.

When using polymeric beads having a diameter of about 80 μm, the cycle for coupling one amino acid lasts about 6–15 min. Even if double couplings are used, a peptide with 30 amino acid residues can be synthesized in a few hours. By employing the already available tentacle polymers with a diameter of 8 μm, the time required for the coupling cycle can be further reduced by a factor of ten, i.e. to 1–2 min. For

these short times, however, there are no synthesizers available. Continuous monitoring of the synthesis also allows the detection of difficult coupling steps, which for example are caused by conformational effects. This effect is specially evident during the cleavage of amino protecting groups, as it is symbolized by appearence of a strong tailing. Thus, it is possible to distinguish the difficult coupling steps which can be avoided in a subsequent optimized synthesis. Figure 13 shows the course of a synthetic cycle with the normal coupling time and another one which has been slowed down by such conformational influences (Fig. 13 b).[*] Therefore, before the actual synthesis is carried out, it is advisable to perform a so-called preview synthesis on a small scale and to follow the course of the reaction spectroscopically, and to investigate the peptide analytically.

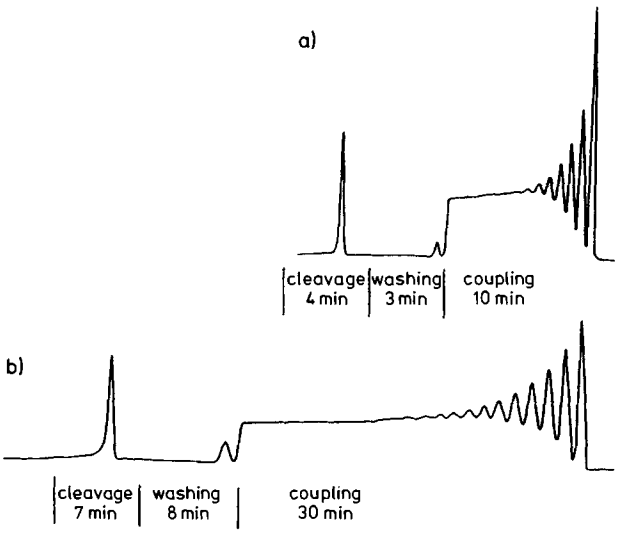

Fig. 13. Continuous UV spectroscopic monitoring of a) the coupling and cleavage reactions of a cycle of continuous flow synthesis on the tentacle polymeric support and b) of the slower reaction due to the formation of a β-folded structure.

Since the time required to perform a total synthesis with the new polymers is very short, it will be rewarding to spare the time for a preview synthesis. By performing a preview synthesis, the difficult coupling steps will be identified and the strategy for the main synthesis can accordingly be changed. This can be achieved, e.g., by changing the solvents, using a higher temperature, choosing other protecting groups or overcoming the difficult steps by coupling small peptides instead of single amino acids. Through further developments of the spectrophotometric control of the continuous flow synthesis, future synthesizers could eventually be able to determine the coupling time and the necessity of post-coupling reactions automatically, i.e. they could be intelligent and self-regulating machines.

[*] Note added in proof: *D. Seebach* has reported in a recent review (*Angew. Chem. 102* (1990) 1363; *Angew. Chem. Int. Ed. Engl. 29* (1990) 1320) (therein p. 1379 and 1337, respectively), that the synthesis of critical sequences proceeds with higher coupling yields on graft copolymers of polystyrene and polyethylene glycol in comparison to the classical polystyrene support using solvents containing LiX.

6. Analytical Control and Purification

The application of carrier-synthesis for the preparation of proteins is naturally dependent on reliable procedures to separate and characterize the synthesized products. Thus, SPPS became an established procedure only after the introduction of efficient HPLC.

The first applications of HPLC to the separation and characterization of synthetic peptides were reported at the 15th European Peptide Symposium in 1973.[55, 56] Since then, HPLC has been the main, and unfortunately also often the only, method of characterization. In the literature, the occurrence of a single HPLC peak is often uncritically interpreted as an indication of a single entity, and almost with no exception, the purity of a product is ascertained by a simple integration and comparison of the peak areas without considering the discrepancy between the specific UV extinction of different peptides. The possible error sources concerning the purity, which are due to neglecting the response factors of the UV detectors, should at least be mentioned.

Since the presence of impurities due to failure sequences can always be suspected, despite optimization of the synthetic methods, it does not suffice to carry out only HPLC and amino acid analysis to characterize the products. Reversed-phase HPLC characterizes peptides according to their hydrophobic interactions, whereby small parts of the peptides are often responsible for the interaction.[98 - 100] Reversed-phases are not suitable for differentiating peptides according to their different acidity, basicity, and molecular size. Therefore, for a complete characterization, an electrophoretic or ion-exchange chromatographic separation (characterization based on the charge) and a size exclusion chromatographic separation (characterization based on the molecular size) must also be carried out. Multidimensional chromatography enables optimal separations using different separation mechanisms.[101 - 103]

Besides employing chromatographic procedures, it is strongly recommended that spectroscopic methods such as mass spectrometry or NMR spectroscopy also be used for the characterization. In the field of synthetic peptide chemistry, for peptides up to 20 amino acids there is an arsenal of separation and characterization methods which one can draw on to ensure that the desired goal of the synthesis is attained.

However, in the case of large peptides and proteins, whose reliable chemical syntheses are still a thing of the future, many of the methods suitable for peptides, remain inapplicable. For example, during the HPLC of proteins on modified silica gels, the molecules are often denatured,[104, 105] and the mass spectroscopic characterization of proteins by the conventional methods (EI, FAB and CI) is not always possible.

With respect to the synthesis of proteins, and parallel to the continuing developments of support (carrier) synthesis, new methods have fortunately been introduced for the separation and mass spectroscopic identification of large peptides. These methods are expected to give the same impetus to the support synthesis of proteins as was given by HPLC to the synthesis of peptides via SPPS.

Numerous new stationary phases have now been developed for the rapid separation of proteins, and they show a

higher mechanical and chemical stability than the ordinary reversed-phase materials. Particularly worth mentioning are: the pellicular resins, in which a functionalized monomer is polymerized on a solid inorganic support such as silica gel,[106-109] and the tentacle polymers described in Sections 4.3 and 4.4, which are also pressure stable.[110] Figure 14 shows a rapid separation of proteins on such supports. A further automated separation procedure which has appeared on the horizon is capillary electrophoresis.[111-118] This method matches HPLC with regard to

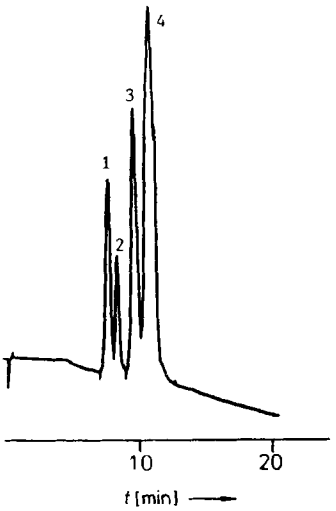

Fig. 14. Fast separation of proteins on monodispersed TentaGel (13 μm); 1 = ribonuclease, 2 = insulin, 3 = lysozyme, 4 = albumin. Gradient from 0.1% trifluoroacetic acid (TFA) in H_2O to 0.1% TFA in H_2O: acetonitrile 20:80 in 20 min; 1.5 mL min^{-1}, column 60 × 4.6 mm, UV detection at λ = 210 nm.

separation efficiency, speed, and ease of handling, and will certainly find a similarly broad spectrum of applications. Capillary zone electrophoresis (CZE) in open capillaries with diameters of 40–100 μm, and lengths of 20–80 cm can easily attain theoretical plates of 100 000, which is normally achieved by capillary gas chromatography. Since in essence, capillary zone electrophoresis separates molecules according to their charges it will complement reversed-phase HPLC, which is based on hydrophobic interaction.

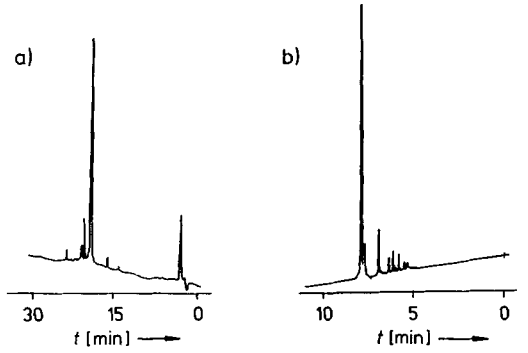

Fig. 15. Separation of a peptide a) using HPLC and b) capillary electrophoresis CE. HPLC: reversed-phase C_{18} column 250 × 4.6 mm, gradient water/acetonitrile. CE: quartz capillary, chemically modified with Chirasil-Val, 500 μm × 400 mm, 100 mM phosphate buffer, pH = 2.5; 15 kV. UV detection at λ = 200 nm (a and b).

Peptides which appear to be pure according to HPLC, show further impurities upon subjection to capillary electrophoresis, as shown in Figure 15.[116] Now it becomes apparent that "orthogonal" separation techniques, and not only reversed-phase HPLC, must be applied to establish the purity of peptides. For nucleotide separation, CZE is already a well-established method. In the case of protein separation, unmodified capillaries are not suitable; this is due to the adsorption of proteins on the quartz surface, a problem that can be circumvented by deactivating the surface with a coating of polymer. Sharp peaks as in Figure 16 are then obtained for the separation on quartz capillary inactivated by a coating of PEG.[118]

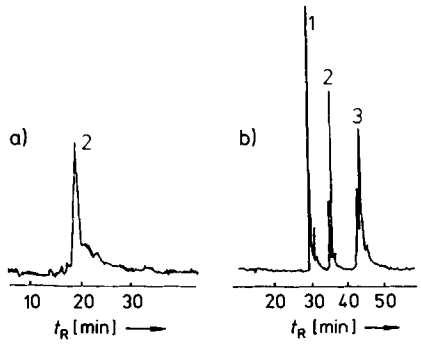

Fig. 16. CE-separation of a protein mixture (1 = lysozyme, 2 = trypsin, 3 = chymotrypsinogen) a) on an unmodified capillary, b) on a PEG-impregnated capillary. a) 0.01 M KH_2PO_4 buffer, pH = 6.8. b) 0.05 M KH_2PO_4 buffer, pH = 4.1 (after Ref. [118]).

Parallel to the development of these new separation methods, mass spectroscopy has penetrated into the field of protein chemistry, but so far only for proteins with molecular masses of up to 120 000 Da. Besides FAB and plasma desorption ionization, the ion-spray method should be mentioned.[119, 120, 127, 128] In this method, the solution containing the sample to be analyzed is pumped through a sprayer which is kept at high voltage in order to form a mist of highly charged droplets. The droplets contain both positive and

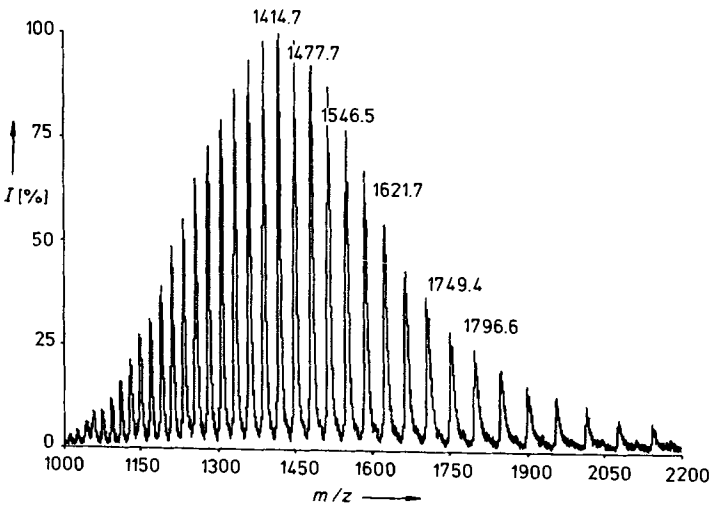

Fig. 17. Ion-spray mass spectrum of pig serum albumin, M = 66 439 Da. The peak at m/z = 1796.6 corresponds to 37 times positively charged protein (SCIEX mass spectrometer).

negative ions with ions of one polarity being predominant. As the solvent evaporates, the electrical field at the surface of the droplets increases due to the decreasing radius. If the droplets evaporate far enough, a critical field is reached at which ions are emitted from the surface, ejected into a gas phase and enter the mass analyzer. Since peptides and proteins contain basic amino acids such as arginine and lysine, they can develop multiple charges. The m/z values of these multiply charged ions lie, even in the case of proteins, in the range of a quadrupole mass spectrometer. Figure 17 shows, e.g., the mass spectrum of a protein recorded by this method.[116] Since the first step of ion-spray mass spectroscopy is the formation of a mist of the substance to be analyzed from the solution under atmospheric pressure, it is possible to couple an ion-spray MS to a HPLC or a CZE instrument. With such an arrangement, a new dimension for the investigation of macromolecular natural products is obtained.[116, 121, 122] Figure 18 shows the separation of

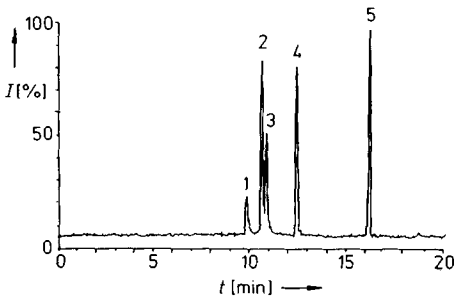

Fig. 18. Coupled capillary electrophoresis/ion-spray mass spectrometry of dynorphins [121]: 1 = Tyr-Gly-Gly-Phe-Leu-Arg-Arg-Ile-Arg, 2 = Tyr-Gly-Gly-Phe-Leu-Arg-Arg, 3 = Tyr-Gly-Gly-Phe-Leu-Arg-Arg-Ile, 4 = Tyr-Gly-Gly-Phe-Leu-Arg, 5 = Tyr-Gly-Gly-Phe-Leu. Quartz capillary 100 μm × 100 cm. Buffer: acetonitrile/30 mM ammonium acetat = 50/50, pH = 4.8; SCIEX mass spectrometer, total ion stream.

dynorphins by coupled CZE/ion-spray MS. For peak 5 in Figure 18 a separation efficiency of about 250 000 theoretical plates could be calculated. Figure 19a shows the ion-spray mass spectrum of the dynorphin giving rise to peak 5 in Figure 18.[121] Using tandem mass spectrometry, it is possible to determine the peptide sequence from the $(M + H)^{\oplus}$ peak (Fig. 19b).

7. Examples of Syntheses on the Tentacle Polymers

The practical application of tentacle polymers will be illustrated by way of example with the synthesis of two polypeptides, and the importance of the novel analytical procedures for the control and optimization of the synthesis will be dealt with in detail. As a model, a rapid preview synthesis of the HIV-1 protease sequence 59–99 is described. The course of the synthesis was monitored by analytical methods.

7.1. Tentacle Polymer-Peptides for the in vivo Formation of Antibodies

The prediction of epitopes for the formation of antibodies and the synthesis of these epitopes are nowadays indispens-

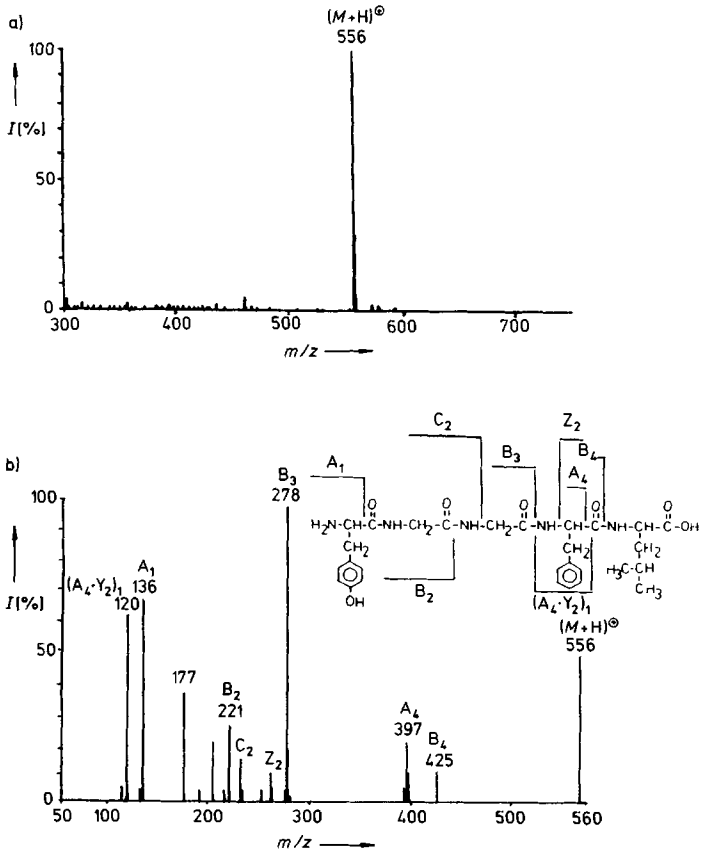

Fig. 19. Mass spectra to peak 5 in Figure 18. a) Ion-spray MS. b) Daughter ion spectrum to peak in (a) [121] for sequence analysis.

able tools in immunology. A multitude of overlapping peptides is required for a dependable prediction. Conjugates of peptides with carriers such as serum albumin or lipopeptides are employed in immunization.[123–125] It would now constitute a tremendous step forward methodologically, if the peptides did not need to be cleaved from the polymeric support, and in place of a conjugate, they could be directly applied for the in vivo and in vitro immunization and production of antibodies. Owing to the compatibility of the PEG chains with biological systems, the tentacle polymers are said to be suitable in this respect.

In order to verify this hypothesis, an epitope region of the hemophilus influenzae P6 protein, corresponding to the sequence 115–131, was synthesized on TentaGel, and for comparison, also on PEG.[126] The synthesis of the sequence H_2N-Ala-Val-Leu-Gly-His-Asp-Glu-Ala-Ala-Tyr-Ser-Lys-Asn-Arg-Ala-Val-OH was carried out according to the Fmoc strategy with the following side-chain protecting groups: Mtr for Arg, Boc for Lys, Trt for His, *t*Bu for Ser, O*t*Bu for Glu, O*t*Bu for Asp, and ONp for Asn (Mtr = 4-methoxy-2,3,6-trimethylbenzylsulfonyl, Trt = triphenylmethyl, *t*Bu = *tert*-butyl, O*t*Bu = *tert*-butyl ester, ONp = nitrophenyl ester).

Figure 20 shows the ion-spray mass spectrum of the PEG peptide. It is interesting to note that the exact molecular mass distribution of the peptide-polymer can be determined with a single mass spectrum, whereas otherwise it could be achieved only indirectly by means of exclusion chromatography and standard substances. The difference in the individual peaks of the mass spectrum of the fourfold protonated polymer-peptide $(M + 4H)^{3\oplus}$ with an average molecular

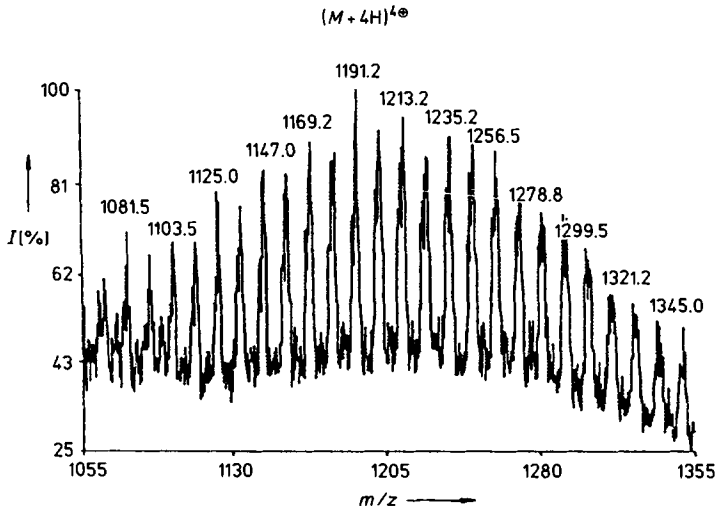

Fig. 20. Ion-spray mass spectrum of the $(M + 4H)^{4\oplus}$ peak of the PEG peptide A-V-L-G-H-D-E-A-A-Y-S-K-N-R-R-A-V-PEG_{3000}. The peptide was synthesized by the liquid-phase procedure. Average molecular mass 4850.9 (SCIEX mass spectrometer).

mass of 4850 corresponds exactly to one fourth of the molecular mass of the CH_2-CH_2-O-monomeric unit.

For immunization, the soluble PEG peptide as well as the immobilized PEG peptide were administered to mice, and, after four weeks, serum samples were taken for the determination of antibodies, using the ELISA test. The titers of the ELISA in Figure 21 show that the polymer peptides form

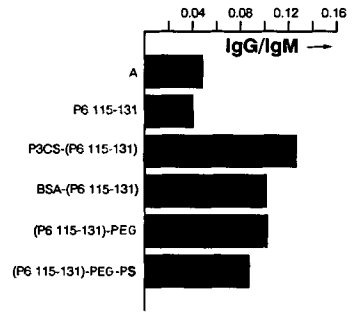

Fig. 21. ELISA titers of the serums after immunization with different conjugates of the sequence 115–131 of hemophilus influenza P6 protein [126]. G = goat; M = mouse; A = negative control.

antibodies as nicely as the serum albumin conjugate BSA-(PG 115–131).[126]

7.2. Preview-Synthesis of the Sequence 59–99 of HIV-1 Protease

It is interesting to carry out the chemical synthesis of HIV-1 protease, which is required for activation of the aids virus, since the amino acids of the active center can be specifically labeled with ^{13}C and inhibition studies can be carried out using NMR. The two critical cysteine residues, which have been substituted by less critical ones in an attempted synthesis by *Kent* et al.[131] are located at positions 67 and 95.

Sequence 59–99 of the HIV-1 protease was synthesized on a TentaGel support using the rapid continuous flow procedure (Scheme 6). By applying the preview-synthesis mode and subsequent characterization of the by-products, it could easily be established which couplings presented difficulties and the synthetic strategy could be optimized according to these

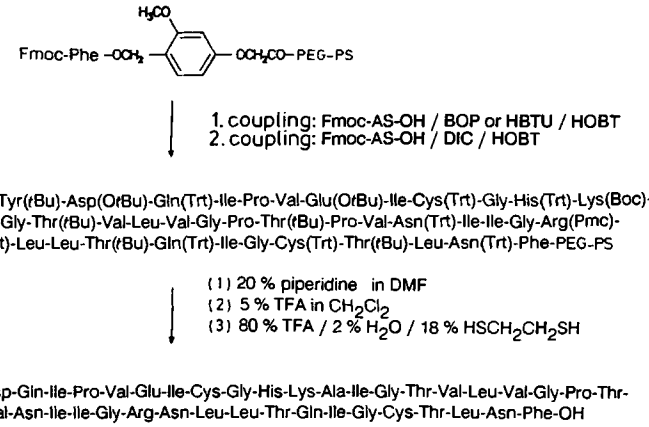

Scheme 6. Scheme of the synthesis of the HIV-1 protease sequence. BOP = benzotriazol-1-yloxytris(dimethylamino)phosphonium hexafluorophosphate; HOBT = hydroxybenzotriazole; HBTU = *O*-benzotriazol-1-yl-*N*,*N*,*N*',*N*'-tetramethyluronium hexafluorophosphate; DIC = diisopropylcarbodiimide; AA = amino acid.

findings. This synthesis furnished a crude material with a complex composition as shown by the chromatogram in Figure 22. The structures of the major by-products could be assigned on the basis of their molecular masses obtained on

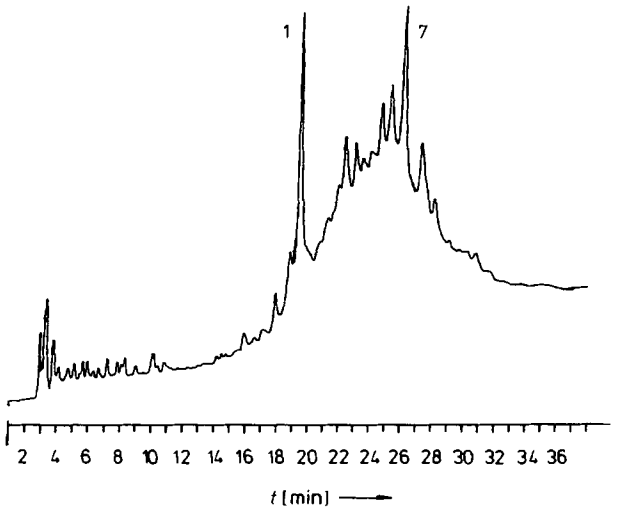

Fig. 22. HPL chromatogram of the crude product of sequence 59–99 of HIV-1 protease after its cleavage from the polymeric support. Column 250 × 4.6 mm, Nucleosil 100 C18, 5 µm. Mobile phase water/acetonitrile/0.1% TFA. Gradient, acetonitrile from 25% to 50%. 1 = failure sequence; 7 = HIV protease sequence 59–99.

direct injection into an ion-spray spectrometer and without any previous separation (Fig. 23). The retention times of the desired main product and of the by-products could be ascertained exactly by HPLC with single-ion monitoring

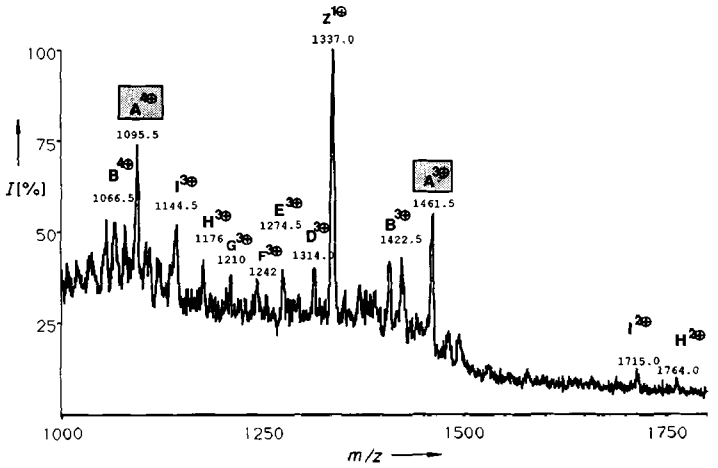

(Fig. 24). Thus, the fraction of the HIV-1 protease sequence (A) could be isolated in the pure form by HPLC, as is shown by the mass spectrum in Figure 25.

The by-products were identified using a coupled HPLC/tandem mass spectrometer. By this means, the structural elucidation of the by-products requires only as much time as running a HPLC chromatogram, i.e., about 30 min. Figure 26 shows the fragmentation scheme of a by-product determined by tandem mass spectrometry; the structure of the by-product could be assigned unequivocally. The most important by-products are shown in Figure 27. From this synthesis it was learned that, due to the formation of rigid conformations, the couplings of the residue 91 (Thr) up to the residue 82 (Val) took place in low yields. In the subsequent couplings, the reactions were complete and no failure sequences were observed. It is interesting to note that failure sequences are formed in which up to nine amino acids are missing in a chain. Even though the aim of the synthesis, i.e., preparation of pure HIV-1 protease sequence, was already achieved in this preview synthesis, a larger amount of the peptide for the inhibition studies could be obtained by opti-

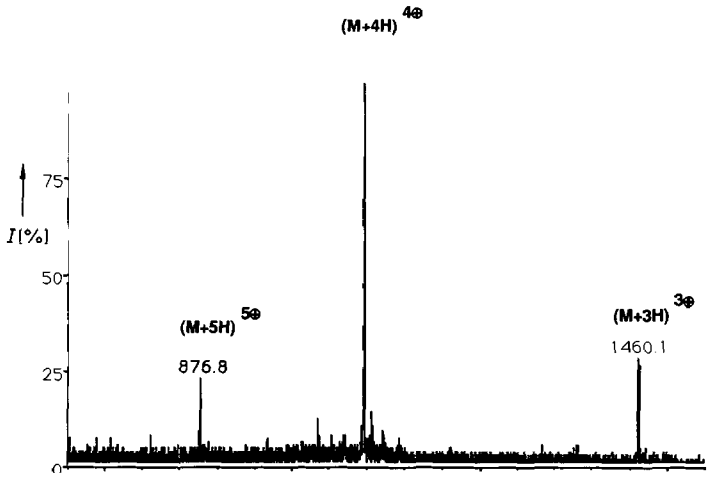

Fig. 25. Ion-spray mass spectrum of the isolated pure HIV-1 protease sequence 59–99. Molecular mass was found to be 4377.8 ± 1.

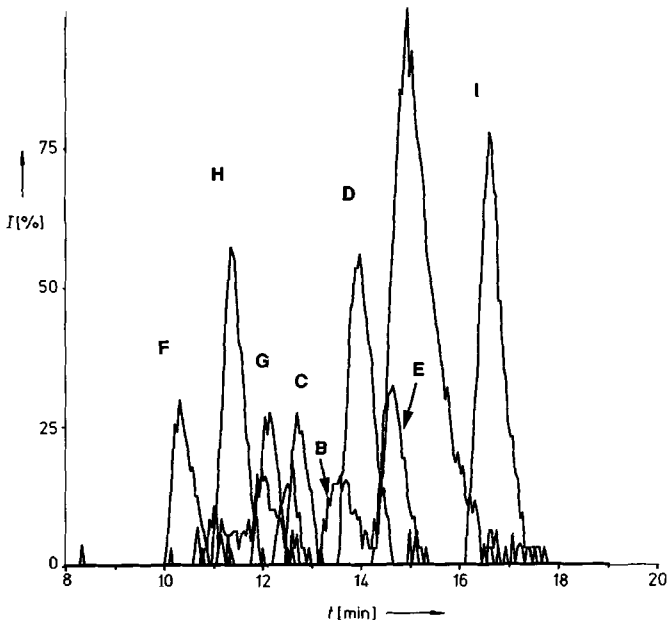

8. Outlook

By employing new polymeric supports for peptide synthesis under the conditions of continuous flow, it became possible to synthesize long chain polypeptides in a matter of a few days. As shown, the required time to carry out a cycle can even be shortened further to 1–2 min by using 8 μm supports.

New analytical methods such as capillary electrophoresis and ion-spray mass spectroscopy as well as continuous monitoring of the synthesis by means of UV spectroscopy allow one to recognize the difficult sequences and failures likely to be encountered in the course of synthesis. Hence the hitherto "black box" of the support synthesis becomes fully transparent and permits optimization of the critical steps. By judicially sparing a little time, one can carry out a small scale preview synthesis. Exact analytical investigations enable the problems of a synthesis to be recognized and thus help in choosing the strategy to be adopted in the main synthesis. In this way a purer peptide can be assembled on the polymer and the unsuccessful or troublesome final purifications which frequently are encountered can be circumvented. The

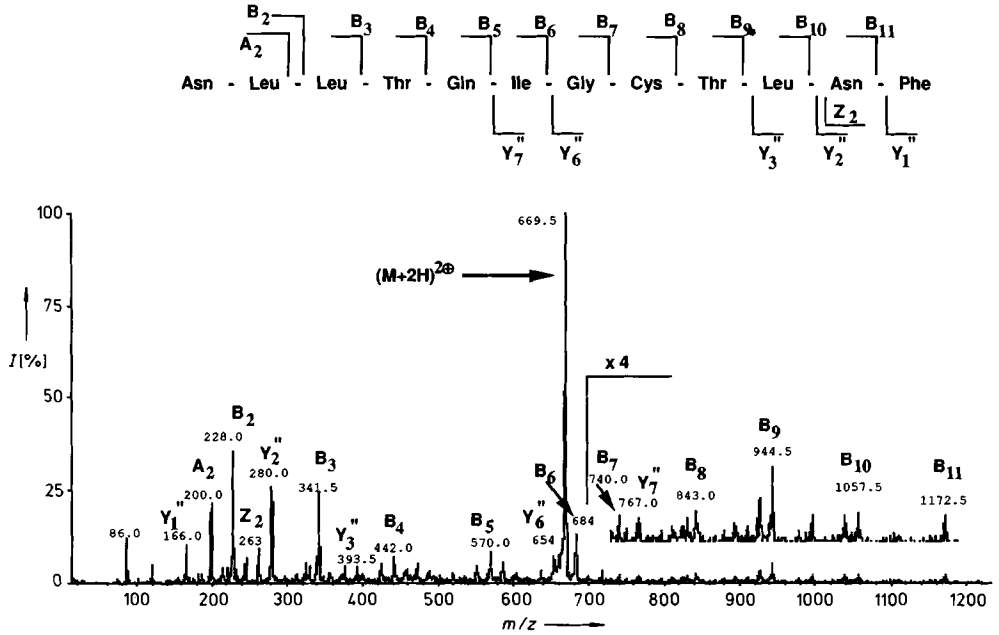

Fig. 26. MS/MS fragmentation scheme of the failure sequence peptide Z.

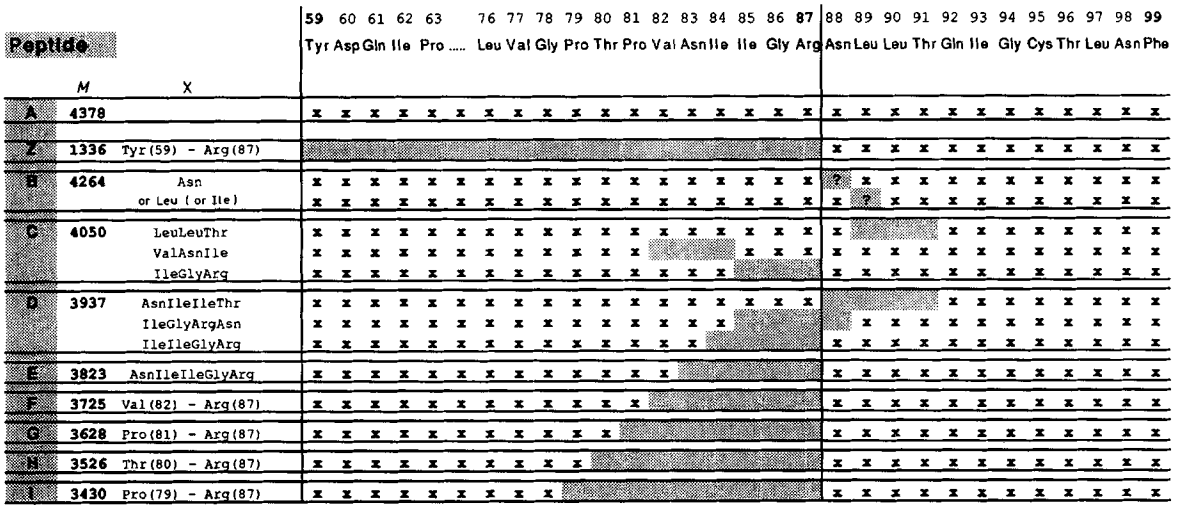

Fig. 27. Failure sequence peptides of the crude product in the synthesis of the HIV-1 protease sequence 59–99 A. X = deleted amino acids.

continuous flow procedure can also be carried out more easily than the normal batch procedure on a large scale. By carrying out pilot syntheses, we have prepared proteins with up to 120 amino acid residues such as HIV-1 protease, [129, 130] human insulin, metallothionein, [129] as well as cardiodilatin [132] on the tentacle polymers. Through these syntheses, the critical steps were analytically ascertained, and the strategy for the optimized syntheses were established.

These investigations show unambiguously that proteins up to a molecular mass of over 10000 Da can be prepared synthetically, and that analytical methods for purity verification are at our disposal. It depends primarily on future developments of the supports and the analytical methods as to whether it will be possible to use this procedure for the synthesis of even larger proteins. For an understanding of the biological activities of proteins, the already accessible synthetic fields provide valuable information and consequently contribute to resolving the remaining secret correlations of structure and biological activity in nature.

The work presented in this article and carried out in the laboratory at Tübingen could never have been achieved without the committed collaboration of many generations of young chemists. That the names of merely a few may be emphasized in no way detracts from the significance of the accomplishments of the other co-workers mentioned in the literature section. To be mentioned here are Professors G. Jung, H. Hagenmaier, W. Voelter, W. Parr, H. Eckstein, and Dr. B. Hemmasi, who in the years 1966–1973, above all, contributed to the first attempt to synthesize peptides up to the size of apoferrodoxin on a solid support. They also carried out investigations regarding the problem of failure sequences. The liquid-phase method was developed between 1971 and 1976 in collaboration with Professor M. Mutter. All the above associates now command

their own fields of peptide chemistry and have successfully accomplished outstanding works. Dr. Uhmann, Dr. Frank, Dr. Hupe and Mr. Nicholson have contributed to the development of HPLC and the gas chromatographic detection of racemization. Recently, the development of monodispersed and of polyethyleneglycol-polystyrene supports was realized in association with Dr. W. Rapp. The syntheses of longer polypeptides were performed in collaboration with Mr. Zhang.

Thanks are due to all the sponsors of this work: The State of Baden-Württemberg, the Deutsche Forschungsgemeinschaft, the Fonds der Chemischen Industrie; the Bundesminister für Forschung und Technologie; Hoffmann La Roche, Basel, Hoechst AG (Frankfurt) Diamalt AG (München) and BACHEM USA.

Received: May 21, 1990 [A 804 IE]
German version: *Angew. Chem. 103* (1991) 117
Translated by Dr. *B. Hemmasi*, Tübingen (FRG)

[1] R. B. Merrifield, *Fed. Proc. Fed. Am. Soc. Exp. Biol. 21* (1962) 412.
[2] R. B. Merrifield, *J. Am. Chem. Soc. 85* (1963) 2149.
[3] R. B. Merrifield, *Biochemistry 3* (1964) 1385.
[4] E. T. Kaiser, *Angew. Chem. 100* (1988) 945; *Angew. Chem. Int. Ed. Engl. 27* (1988) 913.
[5] E. T. Kaiser, F. J. Kezdy, *Annu. Rev. Biophys. Biophys. Chem. 16* (1987) 561.
[6] M. Mutter, S. Vuilleumier, *Angew. Chem. 101* (1989) 551; *Angew. Chem. Int. Ed. Engl. 28* (1989) 535.
[7] M. Bodanszky, *Ann. N. Y. Acad. Sci. 88* (1960) 655.
[8] R. Schwyzer, P. Sieber, *Nature (London) 199* (1963) 172.
[9] E. Wünsch, *Angew. Chem. 83* (1971) 773; *Angew. Chem. Int. Ed. Engl. 10* (1971) 786.
[10] E. Gross, J. Meienhofer (Eds.): *The Peptides: Analysis, Synthesis, Biology*, Academic Press, New York 1975.
[11] M. Bodanszky, M. A. Ondetti: *Peptides Synthesis*, Interscience, New York 1966, p. 162.
[12] K. Hofmann, P. G. Katsoyannis in H. Neurath (Ed.) *The Proteins, Vol. 1*, 2nd Edit., Academic Press, New York 1963.
[13] G. Barany, R. B. Merrifield in [10], p. 100.
[14] S. Moore, A. Felix, J. Meienhofer, C. W. Smith, R. Walter, *J. Med. Chem. 20* (1977) 495.
[15] T. Wieland, C. Birr, F. Flor, *Angew. Chem. 83* (1971); *Angew. Chem. Int. Ed. Engl. 10* (1971) 336.
[16] H. Hagenmaier, H. Frank, *Hoppe-Seyler's Z. Physiol. Chem. 356* (1972) 1973.
[17] E. Atherton, D. L. Clive, R. C. Sheppard, *J. Am. Chem. Soc. 97* (1975) 6584.
[18] R. B. Merrifield, *Endeavour 24* (1965) 3.
[19] K. Kovács, B. Penke in H. Hanson, H. D. Jakubke (Eds.): *Peptides 1972*, North-Holland, Amsterdam 1973, p. 187.
[20] M. Bodanszky, K. W. Funk, *J. Org. Chem. 38* (1973) 1296.
[21] R. L. Letsinger, M. J. Kornet, V. Mahadevan, D. M. Jerina, *J. Am. Chem. Soc. 86* (1964) 5163.
[22] a) E. Bricas (Eds.): *Peptides 1968*, North-Holland, Amsterdam 1968; b) F. Weygand in [22a], p. 183.
[23] S. S. Wang, R. B. Merrifield, *J. Am. Chem. Soc. 91* (1969) 6488.
[24] E. Bayer, E. Breitmaier, G. Jung, W. Parr, *Hoppe-Seyler's Z. Physiol. Chem. 352* (1971) 759.
[25] R. C. Sheppard, B. J. Williams, *J. Chem. Soc. Chem. Commun. 1982*, 587.
[26] F. Albericio, G. Barany, *Int. J. Pept. Protein Res. 30* (1987) 206.
[27] M. S. Bernatowicz, S. B. Daniels, H. Köster, *Tetrahedron Lett. 30* (1989) 4645.
[28] H. Rink, *Tetrahedron Lett. 28* (1987) 3787.
[29] E. Wünsch, *Methoden Org. Chem.* (Houben-Weyl) 44th Edit. 15 (1974) 1.
[30] H.-D. Jakubke, H. Jeschkeit: *Aminosäuren, Peptide, Proteine*, Verlag Chemie, Weinheim 1982.
[31] J. M. Stewart, J. D. Young: *Solid Phase Peptide Synthesis*, Freeman, San Francisco 1969.
[32] E. Atherton, R. C. Sheppard: *Solid Phase Peptide Synthesis, a Practical Approach*, Oxford University Press, Oxford 1989.
[33] M. Bodanszky, *The Practice of Peptide Synthesis*, Springer, Berlin 1984.
[34] C. Birr, *Aspects of the Merrifield Peptide Synthesis*, Springer, Berlin 1979.
[35] R. Geiger in H. Tschesche (Ed.): *Modern Methods in Protein Chemistry, Vol. 2*, de Gruyter, Berlin 1985, p. 399.
[36] R. B. Merrifield, *Adv. Enzymol. 32* (1969) 221.
[37] A. Loffet, J. Close in [22a], p. 189.
[38] A. Dryland, R. C. Sheppard, *J. Chem. Soc. Perkin Trans. 1 1968*, 125.
[39] M. Mutter, V. N. R. Pillai, H. Anzinger, E. Bayer, C. Toniolo in K. Brunfeldt (Ed.): *Peptides 1980*, Scriptor, Copenhagen 1981, p. 660.
[40] C. M. Deber, V. J. Hruby, K. D. Kopple (Eds.): *Peptides Structure and Function*, Pierce Chem. Co., Rockford, Il, USA 1985.
[41] S. B. H. Kent in [40], p. 407.
[42] E. Atherton, R. C. Sheppard in [40], p. 415.
[43] A. G. Ludwick, L. W. Jelinski, D. Live, A. Kintanar, J. J. Dumais, *J. Am. Chem. Soc. 108* (1986) 6493.
[44] C. Toniolo, G. M. Bonora, E. P. Heimer, A. M. Felix, *Int. J. Pept. Protein Res. 30* (1987) 232.
[45] V. N. R. Pillai, M. Mutter, *Acc. Chem. Res. 14* (1981) 122.
[46] M. Gausepohl, W. Frank, W. Rapp, E. Bayer, unpublished.
[47] E. Bayer, H. Eckstein, K. Hägele, W. A. König, W. Brüning, H. Hagenmaier, W. Parr, *J. Am. Chem. Soc. 92* (1970) 1735.
[48] E. Bayer, H. Hagenmaier, G. Jung, W. A. König in [22a], p. 162.
[49] E. Bayer in B. Weinstein, S. Laude (Eds.): *Peptides, Chemistry and Biochemistry*, Marcel Dekker, New York 1970.
[50] E. Bayer, *Chem. Labor Betr. 20* (1969) 193.
[51] E. Bayer, H. Hagenmaier, G. Jung, W. Parr, H. Eckstein, P. Hunziker, R. E. Sievers in E. Nesvabada (Ed.): *Peptides 1969*, North-Holland, Amsterdam 1971, p. 65.
[52] E. Bayer, P. Hunziker, M. Mutter, R. E. Sievers, R. Uhmann, *J. Am. Chem. Soc. 94* (1972) 265.
[53] H. Hagenmaier, *Tetrahedron Lett. 1974*, 283.
[54] B. W. Erickson, R. B. Merrifield, *J. Am. Chem. Soc. 95* (1973) 3757.
[55] a) J. Wolman (Ed.): *Peptides 1973*, Wiley, New York 1973; b) E. Bayer in [55a], p. 247.
[56] M. Goodman in [55a], p. 250.
[57] V. Gut, J. Rudinger in [22a], p. 185.
[58] R. H. Andreatta, H. Rink, *Helv. Chim. Acta 56* (1973) 1205.
[59] M. N. Shemyakin, Y. A. Ovchinnikov, A. A. Kiryushkin, I. V. Kozhevnikova, *Tetrahedron Lett. 1965*, 2323.
[60] E. Bayer, *Nachr. Chem. Tech. 20* (1972) 495.
[61] M. Mutter, H. Hagenmaier, E. Bayer, *Angew. Chem. 83* (1971) 883; *Angew. Chem. Int. Ed. Engl. 10* (1971) 811.
[62] E. Bayer, M. Mutter, *Nature (London) 237* (1972) 512.
[63] M. Mutter, E. Bayer in E. Gross, J. Meienhofer (Eds.): *The Peptides, Vol. 2*, Academic Press, New York 1970, p. 285.
[64] M. Mutter, E. Bayer, *Angew. Chem. 86* (1974) 101; *Angew. Chem. Int. Ed. Engl. 13* (1974) 149.
[65] E. Bayer, M. Mutter, *Chem. Ber. 107* (1974) 1344.
[66] M. Mutter, R. Uhmann, E. Bayer, *Justus Liebigs Ann. Chem. 1975*, 901.
[67] E. Bayer, M. Mutter, R. Uhmann, J. Polster, H. Mauser, *J. Am. Chem. Soc. 96* (1974) 7333.
[68] M. Mutter, *Macromolecules 10* (1977) 1413.
[69] M. Mutter, F. Maser, K.-H. Altmann, C. Toniolo, G. M. Bonora, *Biopolymers, 24* (1985) 1057.
[70] M. Mutter, H. Mutter, E. Bayer, *Pept. Chem. Struct. Biol. Proc. Am. Pept. Symp. 5th 1977*, 403.
[71] M. Mutter, *Tetrahedron Lett. 1978*, 2843.
[72] W. Schoknecht, K. Albert, G. Jung, E. Bayer, *Liebigs Ann. Chem. 1982*, 1514.
[73] E. Bayer, M. Mutter, G. Holzer, *Pept. Chem. Struct. Biol. Proc. Am. Pept. Symp. 4th 1975*, 425.
[74] E. Atherton, M. J. Gait, R. C. Sheppard, B. J. Williams, *Biorg. Chem. 8* (1979) 351.
[75] E. Atherton, J. Holder, M. Meldal, R. C. Sheppard, R. M. Valerio, *J. Chem. Soc. Perkin Trans. 1 1988*, 2887.
[76] E. Atherton, C. J. Logan, R. C. Sheppard, *J. Chem. Soc. Perkin Trans. 1 1981*, 538.
[77] L. A. Carpino, G. Y. Han, *J. Am. Chem. Soc.* 92 (1970) 5748; *J. Org. Chem. 37* (1972) 3404.
[78] A. Warshavsky, R. Kaliv, A. Doshe, H. Berkovitz, A. Patchornik, *J. Am. Chem. Soc. 101* (1979) 4249.
[79] E. Tsuchida, H. Nishide, N. Shimidazu, A. Yamada, M. Keneko, *Makromol. Chem. Rapid Commun. 2* (1981) 621.
[80] E. Bayer, B. Hemmasi, K. Albert, W. Rapp, M. Dengler in V. J. Hruby, D. H. Rich (Eds.): *Peptides: Structure and Function*, Pierce Chem. Comp., Rockford, Il, USA 1983, p. 87.
[81] E. Bayer, W. Rapp, DE-A 3714258 (1988).
[82] E. Bayer, M. Dengler, B. Hemmasi, *Int. J. Pept. Protein Res. 25* (1985) 178.
[83] E. Bayer, W. Rapp in W. Voelter, E. Bayer, Y. A. Ovchinnikov, V. I. Ivanov (Eds.): *Chemistry of Peptides and Proteins*, de Gruyter, Berlin 1986, p. 3.
[84] E. Bayer, H. Hellstern, H. Eckstein, *Z. Naturforsch. C 42* (1987) 455.
[85] W. Rapp, *Dissertation*, Universität Tübingen 1985.
[86] W. Rapp, L. Zhang, R. Häbich, E. Bayer in G. Jung, E. Bayer (Eds.): *Peptides 1988*, de Gruyter, Berlin 1989, p. 199.
[87] E. Bayer, K. Albert, H. Willisch, W. Rapp, B. Hemmasi, *Macromolecules 23* (1990) 1937.

[88] Tentacle polymers are supplied as TentaGel® by Rapp Polymere, Tübingen. Germany.
[89] J. Ugelstad, P. C. Mork, *Adv. Colloid Interface Sci. 13* (1980) 101.
[90] F. K. Hansen, J. Ugelstad, *J. Polym. Sci. 16* (1978) 1953; *ibid. 17* (1979) 3033.
[91] E. Bayer, W. Rapp, unpublished.
[92] E. Bayer, *10th Int. Symp. Column Liquid Chromatogr. 1980* (San Francisco), Abstract 504.
[93] E. Bayer, G. Jung, I. Halasz, I. Sebestian, *Tetrahedron Lett. 1970*, 4503.
[94] R. P. W. Scott, K. K. Chan, P. Kucna, P. Zolty, *J. Chromatogr. Sci. 9* (1971) 577.
[95] R. Frank, H. Gausepohl in H. Tscheche (Eds.): *Modern Methods in Protein Chemistry, Vol. 3*, de Gruyter, Berlin 1988, p. 41.
[96] E. Atherton, E. Brown, R. C. Sheppard, *J. Chem. Soc. Chem. Commun. 1981*, 1151.
[97] A. Dryland, R. C. Sheppard, *J. Chem. Soc. Chem. Commun. 1986*, 125.
[98] M. T. W. Hearn, *Methods Enzymol. 104* (1984) 190.
[99] R. A. Houghton, J. M. Ostresh, *Biochromatography 2* (1986) 80.
[100] B. Pfleiderer, K. Albert, K. D. Lork, K. K. Unger, H. Brückner, E. Bayer, *Angew. Chem. 101* (1989) 336; *Angew. Chem. Int. Ed. Engl. 28* (1989) 327.
[101] G. Schomburg, F. Wecke, F. Müller, M. Oreans, *Chromatographia 16* (1982) 87.
[102] J. F. K. Huber, presented at ANAKON, Baden-Baden, May 1987.
[103] H. Hulpke, U. Werthmann, *Chromatographia 13* (1980) 395.
[104] S.-L. Wu, A. Figueroa, B. L. Karger, *J. Chromatogr. 371* (1986) 3.
[105] S. Shaltiel, *Methods Enzymol. 104* (1984) 69.
[106] C. Horvath, B. A. Preiss, S. R. Lipsky, *Anal. Chem. 39* (1967) 1422.
[107] K. K. Unger, G. Jilge, J. N. Kinkel, M. T. W. Hearn, *J. Chromatogr. 359* (1986) 61.
[108] I. Mazsaroff, M. A. Rounds, F. F. Regnier, *J. Chromatogr. 411* (1987) 452.
[109] L. Varády, K. Kalghatgi, C. Horvath, *J. Chromatogr. 458* (1988) 207.
[110] E. Bayer, W. Rapp, *14th Int. Symp. Column Liquid Chromatogr. 1990* (Boston).
[111] J. W. Jorgenson, K. D. Lukacs, *Science (Washington) 222* (1983) 266.
[112] J. W. Jorgenson, K. D. Lukacs, *Anal. Chem. 53* (1981) 1298.
[113] A. S. Cohen, A. Paulus, B. L. Karger, *Chromatographia 24* (1987) 15.
[114] S. Hjerten, M.-D. Zhu, *J. Chromatogr. 327* (1985) 157.
[115] A. Chrambach, M. J. Dann, B. J. Radola, *Advances in Electrophoresis, Vol. 2*, VCH, Weinheim 1988.
[116] E. Bayer in H. Tscheche (Ed.): *Modern Methods in Protein Chemistry, Vol. 4*, p. 133, W. de Gryter, Berlin 1990.
[117] K. A. Gobb, M. Novotny, *Anal. Chem. 61* (1989) 2226; P. D. Grossmann, J. C. Colburn, H. H. Lauer, R. G. Nielsen, R. M. Riggin, G. S. Sittampalam, E. C. Richard, *ibid. 61* (1989) 1186.
[118] G. J. M. Bruin, J. P. Chang, R. H. Kuhlmann, K. Zegers, J. C. Kraak, H. Poppe, *J. Chromatogr. 471* (1989) 429.
[119] A. P. Bruins, T. R. Covey, J. D. Henion, *Anal. Chem. 59* (1987) 2642.
[120] S. F. Wong, C. K. Meng, J. B. Fenn, *J. Phys. Chem. 92* (1988) 546.
[121] Anonymus, 1989. The API III Book. Edited by SCIEX, Division of MDS Health Group Ltd., Toronto, Canada.
[122] E. D. Lee, T. R. Covey, W. Muck, J. D. Henion, *J. Chromatogr. 458* (1988) 313.
[123] H. Zeppezauer, W. Rapp, E. Bayer, unpublished.
[124] K.-H. Wiesmüller, G. Jung, G. Hess, *Vaccine 7* (1989) 29.
[125] K. Deres, H. Schild, K.-H. Wiesmüller, G. Jung, H.-G. Rammansee, *Nature (London) 342* (1989) 561.
[126] E. Bayer, W. Rapp, L. Zhang, A. Beck-Sickinger, K. Deres, K.-H. Wiesmüller, G. Jung, unpublished.
[127] R. D. Smith, J. A. Loo, C. G. Edmonds, C. J. Barringa, H. R. Udseth, *Anal. Chem. 62* (1990) 882.
[128] I. Jardine, *Nature (London) 345* (1990) 747.
[129] E. Bayer, W. Rapp, L. Zhang, unpublished.
[130] E. Bayer, W. Rapp, L. Zhang, *21st Europ. Pept. Symp. 1990* (Barcelona).
[131] J. Schneider, S. B. H. Kent, *Cell 54* (1988) 363.
[132] W. Rapp, K. Nokihara, 21st Europ. Pept. Symp. 1990 (Barcelona).
[133] E. Bayer, H. Hagenmaier, G. Jung, *Tetrahedron 24* (1968) 4853.
[134] B. Gutte, R. B. Merrifield, *J. Am. Chem. Soc. 91* (1969) 1348.
[135] S. Sano, M. Kurihara, *Hoppe Seyler's Z. Physiol. Chem. 350* (1969) 1183.
[136] C. H. Li, D. Yamashiro, *J. Am. Chem. Soc. 92* (1970) 7608.
[137] J. Sharp, A. B. Robinson, M. D. Kamen, *J. Am. Chem. Soc. 95* (1973) 6097.
[138] N. Izumiya, M. Waki, T. Kato, M. Ono, H. Aoyagi, N. Mitsuyasu in J. Meienhofer (Ed.): *Chemistry and Biology of Peptides*, Ann Arbor Science Publ., Ann Arbor, MI, USA 1972, p. 269.

Bryophytes, a Source of Biologically Active, Naturally Occurring Material?

By Hans Dietmar Zinsmeister*, Hans Becker, and Theophil Eicher.

Chemical studies of the plant category of mosses (bryophytes) were neglected for a long time. They have now been shown to be a storehouse of naturally occurring materials, including some with novel chemical structures. Many of these materials display considerable biological activity. Investigations are hampered frequently by too small amounts of plant material. The resulting low yields of components are then generally inadequate to permit testing for biological activity. In vitro culture and appropriate chemical synthesis on a preparative scale are being undertaken to overcome this difficulty.

1. Introduction

Many bioactive substances from bacteria, fungi, lichens, and plants are invaluable to humanity and are sometimes used extensively in medicine. Thus a large proportion of medicaments on the German market are genuine or modified naturally occurring compounds.[1] It is tacitly assumed that plant compounds are derived almost entirely from higher plants, without questioning whether components of lower plants, such as bryophytes, could also serve as sources of bioactive material. The foreword of a textbook of pharmacy published in 1985[2] contains the quotation "only few types of living material have been excluded from procedures providing medicaments and other products of pharmaceutical interest—the bryophytes are an example of these". This appears to give a clear answer to the above question. Closer examination of this plant group reveals, however, that this statement will have to be revised in the future.

The plant group of the bryophytes is first considered briefly here: They represent an independent branch of the plant world, with about 20000 species, mostly terrestrial. This is about five percent of the estimated total of 400000 plant species in the world. Morphologically they occupy a position intermediate between the thallophytes and the cormophytes. From the taxonomic point of view they are divided into three classes:[3b, 4]

- Hornworts (Anthocerotae)
- Liverworts (Hepaticae)
- Mosses (Musci or Bryatae)

The hornworts always adopt simple thallus forms, that is, with little differentiation into distinct tissue systems, but there are liverworts with ground-hugging, thallus vegetation forms, as well as those with a small stem, prostrate or erect, bearing simple leaves without midrib. Almost without exception the mosses fall into the small stem and small leaf types, often with notable morphological differentiation.

[*] Prof. Dr. H. D. Zinsmeister
Fachrichtung 13.1 Botanik der Universität des Saarlandes
W-6600 Saarbrücken
Prof. Dr. H. Becker
Fachrichtung 12.3 Pharmakognosie und Analytische Phytochemie der Universität
W-6600 Saarbrücken
Prof. Dr. T. Eicher
Fachrichtung 11.2 Organische Chemie der Universität
W-6600 Saarbrücken

The bryophytes[5] are in general prostrate but can become somewhat conspicuous through the formation of green "mats", as encountered in moorland and woods. The largest moss, up to 70 cm tall, is a species of *Dawsonia*; the smallest, sometimes not even half a millimeter in height, is an *Ephemerum* species. A so-called generation change occurs in the development cycle of a bryophyte. The bryophyte plant itself, as encountered in nature, is the haploid gametophyte, providing masculine and feminine sexual cells. These fuse to the zygote, which develops into the sporophyte, the second generation. The sporophyte is, however, not an individual in the full sense but remains attached to the gametophyte during its life and is represented by the often clearly visible spore capsule. Haploid spores develop in it through meiosis (reductive division). They germinate to green thallus protonema on which "buds" form, which grow into new, haploid bryophytes. The bryophytes are a group of plants which appeared very early in the earth's history. Fossilized bryophytes have been found from the Upper Devonian period, about 300 million years ago. In contrast, flowering plants can be traced back only to the Cretaceous time, about 100 million years ago.

Bryophytes grow predominantly in relatively shady and moist places, even though there are "wizards of survival" among them as far as the ability to withstand drying out is concerned. Such bryophytes are termed xerophytic (xeros = dry; phytein = grow). They can keep alive for a very long time in the air-dried state. It was possible to "reawaken" the moss *Anoectangium compactum* after 19 years in a herbarium! Some bryophytes also set up records in resistance to extremes of temperature. For example, some species are found at high altitudes where ground temperatures of 70 °C have been measured. Their demands for light are far more modest than those of flowering plants, whose limits for propagation lie at about 2% of full daylight. Bryophytes tolerate down to 0.1% and are thus able to penetrate into deep recesses.

Bryophytes are found everywhere except in the oceans and regions of extreme desert. Their species are most prevalent in tropical mountain and rain forests (Fig. 1). There they prefer the epiphytic form of life, that is, they grow on other plants, such as trees, covering trunks and branches with a smooth layer or hanging down from them in meter lengths. Even leaves can be covered with moss growth.

Biomasses of up to 100 g dry weight per square meter can be attained in such biotopes. They profit there from their

Fig. 1. Epiphytic mosses and liverworts in tropical mountain forest (2800 m altitude) near Quito, Ecuador. Left: *Macromitrium guatemalense*; right (hanging): *Frullania brasiliense*. Photography: Prof. R. Mues.

general ability to take up water and nutrients with the whole vegetation body and to store considerable amounts of water. Some liverworts have developed parts of their leaves into water sacs; others, for example the peat mosses which form the peat moors, possess special cells for water storage. Measurements on various bryophytes have shown that they are able to store water in amounts up to eight times their dry weight. Their important regulatory function in the water cycle in nature depends mainly on this.

2. Components of Bryophytes

2.1. General Remarks

The chemical analysis of bryophytes was neglected for a long time. Even though analyses were performed in the previous century,[6, 7] it was not until the last two decades that biologists, chemists and pharmacists began to take an interest in the chemistry of this fascinating group of plants. This long period of neglect can be attributed principally to the difficulties of acquiring larger amounts of bryophyte material and the laborious workup procedures for obtaining the pure substances. The bryophyte plants, often only a few centimeters large, have to be cleaned with great care to avoid a mixture of species and to prevent extracting parts of higher plants embedded in the moss cushions. A stereomicroscope frequently has to be used for this.

In the last twenty years rapid and unexpected progress has been made in the chemical investigation of bryophyte com-

Hans Dietmar Zinsmeister was born in Munich in 1935, studied biology there at the Ludwig Maximilian University from 1954–1959, completing his doctorate with L. Brauner. After an assistantship at the Botanical Institute of the University of Munich and a research year as NATO-fellow with L. J. Audus in London, he obtained his 'Habilitation' in Botany in 1965. He was guest professor at the Munich Campus of the University of Maryland until 1968 and has been Professor of Botany at the University of the Saarland since 1972 and also Director of the Botanical Garden there since 1982. His main research fields are the phytochemistry of bryophytes and the cyanogenesis of nutritional plants, including the physiological and chemotaxonomic aspects.

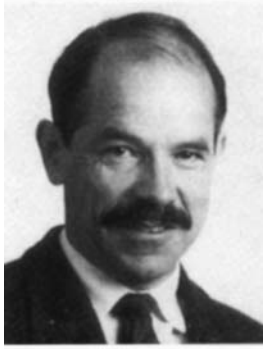

Hans Becker was born in Neustadt/W in 1940, studied pharmacy from 1961 to 1964 in Mainz and obtained his doctorate in 1970 at the Botanical Institute in Karlsruhe under E. Sprecher with a comparative work on the secondary metabolism of plants and callus cultures. He acquired his 'Habilitation' in 1973 in Pharmaceutical Biology and was professor from 1973–1986 at the Institute of Pharmaceutical Biology in Heidelberg. He has been professor of Pharmacognosy and Analytical Phytochemistry at the University of the Saarland since 1987. His fields of work concern secondary metabolism in callus cultures and bryophytes. Besides his research activities he is co-author of several books.

Theophil Eicher was born in Heidelberg in 1932, studied chemistry at the University of Heidelberg from 1952–1957 and received his doctorate there under G. Wittig. After a postdoctoral year in R. Breslow's group at Columbia University in New York, he worked as research assistant in Heidelberg and Würzburg, where he obtained his 'Habilitation' in 1967. In 1974 he was appointed associate professor at the Institute of Organic Chemistry of the University of Hamburg and in 1976 full professor at the Department of Chemistry of the University of Dortmund. Since 1982 he has been professor at the Department of Chemistry of the University of the Saarland. His research activities include the synthetic aspects of the chemistry of cyclopropenones and triafulvenes, and natural products. He is co-author of several books and received the literature award of the Fonds der Chemischen Industrie in 1982 together with L.-F. Tietze.

ponents, especially the secondary metabolites.[8] This has been helped by the progressive refinement of analytical techniques, so that today only a few milligrams substance suffice for characterization of the structures of natural products. Nevertheless, the components of, at the most, only 5% of known species have been studied. The results obtained up to now reveal an astonishing, latent store of new and rare, naturally occurring compounds, including new structural types. Compared to the other bryophyte categories, the liverworts are the best investigated.

The basic compound classes found, such as minerals, carbohydrates, proteins, nucleic acids, lipids, and the organic acids which participate in fundamental metabolic processes, admittedly show close similarities to those in other, in particular higher, plants, but distinct differences have also been found. For instance, polyunsaturated C-20 and C-22 fatty acids are widely found in bryophytes. Although they also occur in algae and ferns, they are absent from seed plants.[9, 10] Fatty acids containing an acetylenic bond (e.g. eicosa-11,14-dien-8-inoic acid, **1**) have also been isolated from liverworts and mosses.[11–13] The high content of arachidonic acid (**2**), found in some bryophyte species, also deserve mention. Thus the total lipid fraction of cell cultures of the moss *Leptobryum pyriforme* was reported to contain 20% arachidonic acid.[14] Another interesting report is of the discovery in some moss species of substances similar to prostaglandins.[15]

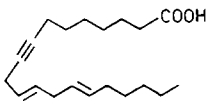

1

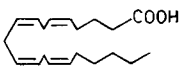

2

Numerous secondary metabolites have been isolated from mosses recently. The results have been summarized in various review articles.[9, 16, 17] Table 1 contains a survey of the classes of secondary metabolites found so far in bryophytes; distinct differences between liverworts, hornworts and mosses are evident. According to our present state of knowledge, phenolic and isoprenoid components predominate in all bryophytes. It is striking that nitrogen-containing secondary products have been found only occasionally, for example, two prenylated indole derivatives from *Riccardia* species (liverwort), namely the 6- and 7-(3-methyl-2-butenyl)indoles, **3** and **4**.[18]

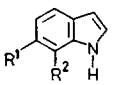

3: R^1 = , R^2 = H

4: R^1 = H, R^2 =

Cyanoglucosides, common in higher plants, occur only rarely in bryophytes. Hydrocyanic acid could be identified unequivocally in only one (*Dicranum scoparium*) of 80 investigated moss and liverwort species.[19]

Table 1. Important secondary components.

Compound Class	Liverworts	Mosses	Hornworts
Terpenes			
monoterpenes	+	+	
sesquiterpenes	+		+
diterpenes	+	+	+
triterpenes	+	+	
tetraterpenes	+	+	+
Steroids	+	+	+
Prenylquinones	+	+	
Phenols			
benzoic acid derivatives	+	+	
cinnamic acid derivatives	+	+	+
bibenzyl derivatives	+		
bis(bibenzyl) derivatives	+		
phenol ethers	+		
alkylphenols	+		
flavonoids	+	+	
acylflavonoids	+	+	
isoflavonoids		+	
biflavonoids		+	
flavone and isoflavone dimers		+	
chalcone derivatives	+		
aurones	+	+	
sphagnorubins		+	
lignanes			+
Alkaloids	+		
Cyanoglycosides		+	
Tetrapyrroles	+	+	+
s-Acrylates	+		
Azulenes	+		
Naphthalene derivatives	+		
Phenanthrene derivatives	+		
Cyclophanes		+	
Vitamins	+	+	

2.2. Phenolic Components

Flavonoids dominate at present among the phenolic compounds. They have been found in just about half of the liverwort and moss species hitherto examined for their presence (600 and 300 species, respectively).[20]

2.2.1. Flavonoids

This compound class is represented by an especially high number of flavones. They are often present as *C*-glycosides, e.g. tricetin-6,8-di-*C*-glucopyranoside (**5**), tricetin-6-arabino-8-glucopyranoside (**6**), apometzgerin-6,8-di-*C*-arabinopyranoside (**7**), and tricin-6,8-di-*C*-arabinopyranoside (**8**).

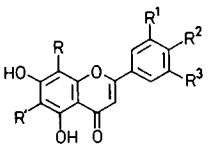

5: R^1–R^3 = OH; R,R′ = β-D-glucopyranosyl
6: R^1–R^3 = OH; R = β-D-glucopyranosyl; R′ = α-L-arabinopyranosyl
7: R^1, R^2 = OCH_3; R^3 = OH; R,R′ = α-L-arabinopyranosyl
8: R^1, R^3 = OCH_3; R^2 = OH; R,R′ = α-L-arabinopyranosyl
9: R^1, R^3 = H; R^2 = OH; R = β-D-(2-*O*-ferulyl)glucopyranosyl; R′ = α-L-arabinopyranosyl

Mention should be made also of some *O*- and *O,C*-glucosides, such as apometzgerin-7-*O*-glucuronide (**10**),[21] iso-

furcatain-7-*O*-β-D-glucopyranoside (**11**),[22] isoorientin-3′-*O*-sophoroside (**12**),[23] and the flavonoid-*O*-triglycoside, diosmetin-7-*O*-(2,4-di-*O*-α-L-rhamnopyranosyl)-β-D-glu-

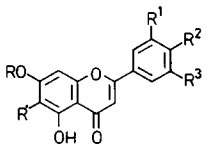

10: R^1,R^2 = OCH_3; R^3 = OH; R = β-D-glucuronyl; R′ = H
11: R^1,R^3 = H; R^2 = OH; R = β-D-glucopyranosyl; R′ = α-L-rhamnopyranosyl
12: R^1 = *O*-sophorosyl; R^2 = OH; R^3,R,R′ = H

copyranoside (**13**), of unusually branched structure and isolated from two moss species.[24, 25] Acylated flavonoids are not rarely encountered in bryophytes, for example, feruloylisoschaftoside (**9**), diosmetin-7-*O*-glucoside-6″-malonyl ester (**14**), and orobol-7-*O*-glucoside-6″-malonyl ester (**15**).[26, 27]

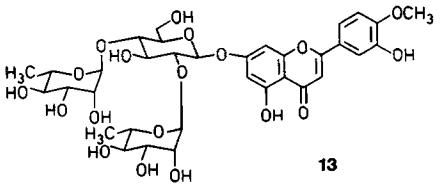

13

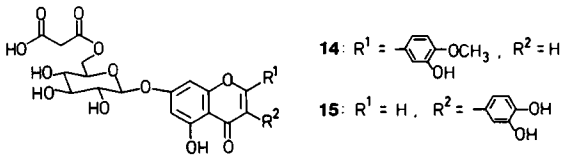

14: R^1 = , R^2 = H
15: R^1 = H , R^2 =

Biflavonoids appear to be restricted to mosses but are widespread there. New types of compound are, for example, bryoflavone (**16**), heterobryoflavone (**17**), philonotisflavone (**18**), and dicranolomin (**19**); the first two contain one flavone and one isoflavone unit.[28–30]

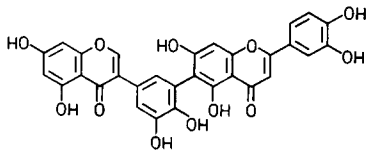

16

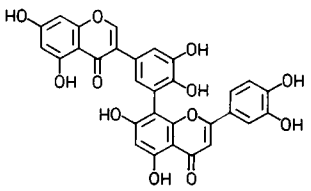

17

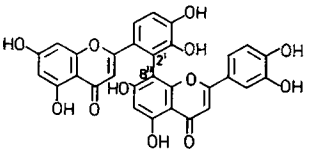

18

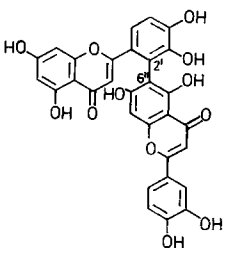

19

Flavonols and particularly anthocyanidins seem to be rarer. So far, the only representatives of the latter which have been isolated are the two 3-deoxyanthocyans of the luteolinidin type, from *Bryum* species (Musci),[31] although red to violet coloured bryophyte organs are encountered.

2.2.2. *Other Phenolic Components*

The structural variants of bibenzyl and bis(bibenzyl) in liverworts are especially remarkable in this connection.[16, 32] Examples of the former are lunularic acid (**20**), brittonin (**21**) and the related system **22**, prenylbibenzyl (**23**) and its geranyl analogue (**24**), and the radulanins A and F (**25** and **26**).

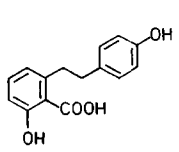

20

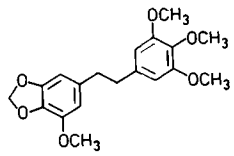

21

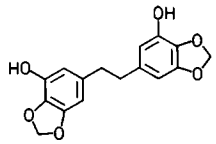

22

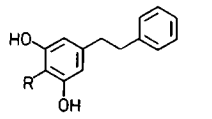

23: R =
24: R = 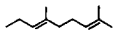

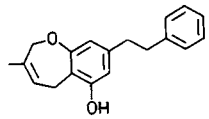

25

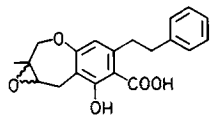

26

Examples of the bis(bibenzyl) compounds are the perrottetins E–G (**27**–**29**), the marchantins A, C and I (**30**–**32**), the riccardins B and C (**33** and **34**), and plagiochin D (**35**).

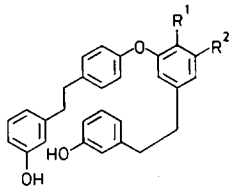

27: R^1 = OH; R^2 = H
28: R^1,R^2 = OH
29: R^1 = OCH_3, R^2 = OH

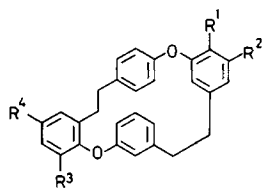

30: R^1–R^3 = OH; R^4 = H
31: R^1,R^3 = OH; R^2,R^4 = H
32: R^1–R^3 = H; R^4 = OCH_3

No examples of structures of these types are yet known in the other bryophyte classes. The sphagnorubins A–C (**36**–**38**), red cell wall coloring materials containing a phenanthrene nucleus, have been found in peat mosses (Musci).[33]

Two new types of naphthalene derivative have recently been discovered: 6,7-dihydroxy-4-(3,4-dihydroxyphenyl)-

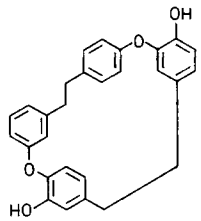

33

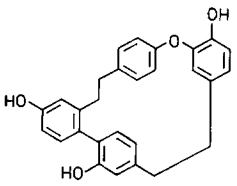

34

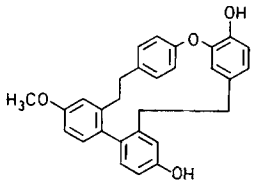

35

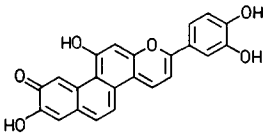

36

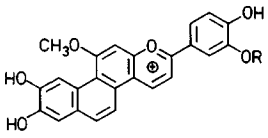

37 : R=H
38 : R=CH_3

naphthalene-2-carboxylic acid (**39**) in *Pellia*,[34] and scapaniapyrone (**40**) in *Scapania undulata*.[35] The first lignanes to be discovered in bryophytes, megacerosic and anthocerosic acids (**41**, **42**), were from hornwort species which, in contrast to the mosses and liverworts, appear to produce no flavonoids.[36] The occurrence of rosmarinic acid (**43**), built up from two caffeic acid units, also deserves mention. It is found widely in higher plants and has pharmacological significance.[36]

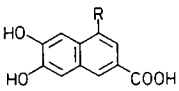

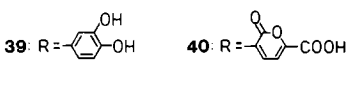

39: R= 40: R=

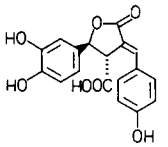

41

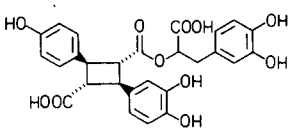

42

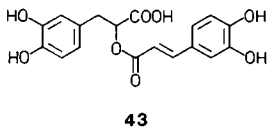

43

Although many intermediate and end products of the secondary metabolism of bryophytes are known, only very meagre information is available about their biogenesis and the enzyme systems involved. For example, in phenylpropane metabolism only three enzymes have up to now been reported. They are phenylalanine ammoniumylase (Hepaticae, Musci), cinnamic acid 4-hydroxylase (*trans* cinnamic acid 4-monoxygenase; Hepaticae), and cinnamyl alcohol dehydrogenase (Musci).[37]

2.3. Isoprenoids

Especially interesting in this compound class are the terpenes, which are numerous especially in liverworts and occur in many structural variants. They constitute an important part of the essential oils, which are contained in their own individual oil bodies (Fig. 2).

Fig. 2. Oil bodies in cells of *Jungermannia obovata* Nees (Hepaticae), ca. 1000 x. Photography: Prof. R. Mues.

2.3.1. Monoterpenes

Many liverworts have a characteristic, strong odour, due mainly to very volatile monoterpenes. By 1983, 25 different monoterpenes had been detected.[17] These are almost entirely compounds known also in higher plants. They have mostly been identified through GC–MS, so that their optical rotations are known in only a few cases. (+)-Bornyl acetate and (−)-β-sabinene have been isolated from *Wiesnerella denudata* and *Conocephalum conicum*.[38] (+)-Bornyl ferulate and (−)-limonene have also been isolated from the latter as optically active components.[39] Recently we succeeded in isolating (−)-limonene from *Ricciocarpos natans*.[40] A substance with intense fragrance has been isolated from *Lophocolea heterophylla*.[41] A mossy scent was still clearly noticeable when 0.05–0.08 mg of it, eluted from the GC column, was expanded into a volume of about 40 m^3. Its empirical formula was given as $C_{12}H_{20}O$;[41] the structural elucidation has not yet been carried out. *Lophocolea cuspidata* also contains a powerful fragrance similar to pine needles, which can still be detected even when the culture preparation vessel is closed with a cottonwool plug.[42] Tamariscol (**44**), a sesquiterpene from *Frullania tamarisci*[43]

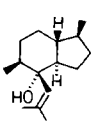

44

and other liverwort species, has a "mysterious, sweet-mossy and woody" fragrant note and has been patented as a perfume.[44]

2.3.2. *Sesquiterpenes*

The sesquiterpenes form the largest group of terpenes hitherto found in liverworts.[16,17] Of the approximately 50 different types found in the liverworts, some have been isolated only from this plant class. These include the barbatanes (gymnomitranes), pinguisanes, the 2,3-secoaromadendranes, myltaylanes and vitranes. Some of these typical liverwort components are described briefly here. Gymnomitrol (**45**) was first detected in 1972 in *Gymnomitrion obtusum*.[45] Derivatives have been subsequently found which contain a hydroxyl group exclusively or additionally in the 9-position.[46,47]

Pinguisanes are widely distributed in species of the liverwort genera *Porella, Lejeunea, Ptilidium*, and *Aneura*. It may be necessary to revise some pinguisane structures, because the structure of one of the reference compounds, pinguisanin, has been altered from **46** to **47**, after comprehensive experimental work on the nuclear Overhauser effect (NOE).[48]

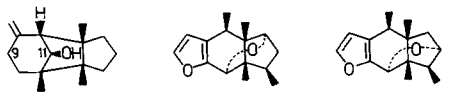

45 **46** **47**

Some 2,3-secoalloaromadendranes, such as plagiochilin A (**48**)[49] show a striking similarity to the monoterpenoid valepotriates; for example, valtrate (**49**),[50] isolated from Valerianaceae and discussed as the potential active substance of valerian. The ^{13}C NMR data of some of the 2,3-secoalloaromadendranes were tabulated in 1981.[51] Two sesquiterpene alcohols with a hitherto unknown carbon skeleton, myltaylenol and cyclomyltaylenol (**50** and **51**), have been isolated from *Mylia taylorii*.[52,53]

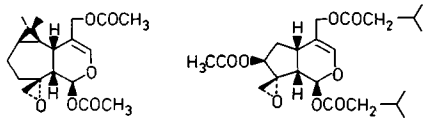

48 **49**

50 **51**

A crystalline derivative could be prepared from **50** for X-ray structure analysis by oxidizing the exomethylene to a keto group and esterifying the alcohol. With the aid of the circular dichroism (CD) spectrum, the absolute configuration of this norbornan-2-one derivative could be elucidated. The same liverwort contained many additional unusual sesquiterpenes.[54]

Vitrenal (**52**), from the liverwort *Lepidozia vitrea*, is a spiro compound, which could have been formed by ring-closure of isobicyclogermacrenal (**53**) found in the same species.[55]

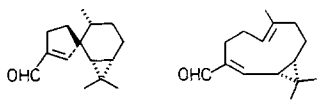

52 **53**

Many sesquiterpenes found in liverworts are enantiomers of the corresponding compounds from higher plants (see table in [17]). Any potential biological activity of these compounds can therefore be tested with both enantiomers.

2.3.3. *Diterpenes*

In contrast to mono- and sesquiterpenes, diterpenes occur in both mosses and liverworts, although more frequently in the latter.[17,56] Phytol has been found relatively frequently in open-chain diterpenes.[57,40] It is, however, unclear whether this is a real component or an artifact from chlorophyll during workup. Isophytol[58] and geranylgeraniol[59] are further aliphatic diterpenes.

Carbocyclic diterpenes from bryophytes can, for the most part, be classified with the carbon skeletons described for compounds found in plants and marine organisms. Some examples of each basic skeleton type are presented here. Further examples can be found in review articles.[16,17,56] Diterpenes with carbon skeletons hitherto not encountered elsewhere have also been detected in bryophytes. Labdane derivatives (basic skeleton **54**) have been isolated from various liverwort species. *Jungermannia rosulans* yielded 3-oxolabda-8,14-dien-13-ol and its isomer, 3-oxolabda-8(17),14-dien-13-ol,[60] and the liverwort *Porella perrottetiana*, trans-(5*R*,7*S*,8*S*,9*S*,10*S*)-labda-12,14-diene-7,8-diol.[61] A series of further labdane derivatives has been described more recently.[62-64] Among the different structures, which are remarkable for their variety of oxidation states, is the new compound **55**, described by the authors as a "novel rearranged labdane".[62] Its angular methyl groups and the C-6 side chain are each displaced by one C-atom in the labdane ring structure.

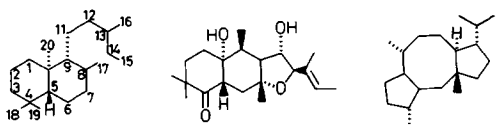

54 **55** **56**

Dolabellanes (basic structure **56**) are diterpenes with a tricyclic carbon skeleton. They were first isolated in 1971, from species of the liverwort genus *Barbilophozia*.[65] Their structure, established through spectroscopic data and chemical reactions, has been confirmed by X-ray structure analysis.[66] Dolabellanes have since also been found in the liver-

worts *Chandonanthus setiformis*[67] and *Odontoschisma denudatum*.[68]

The carbon skeleton of the sacculatanes has so far been found only in liverworts. It is closely similar to the drimane skeleton of the sesquiterpenes. Both these compound classes display similar substitution patterns. Thus, sacculatal (**57**), isolated from various liverworts, corresponds formally to polygodial (**58**), shortened by one isoprene unit. It is interesting that sacculatal has a pungent taste, whereas the 9-epimer, isosacculatal, does not possess this property.[16] Altogether, four perrottetianal derivatives from various liverwort species have been described.[69, 70] We were recently able to isolate from cultures of *Fossombronia pusilla* the derivative 8-hydroxy-8,9-dihydroperrottetianal A (**61**), in addition to the perrottetianals A and B (**59** and **60**).[71]

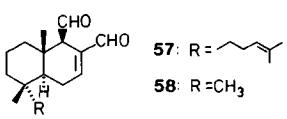

57: R =

58: R = CH_3

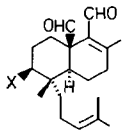

59: X = H

60: X = OH

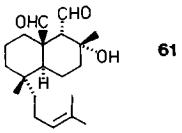

61

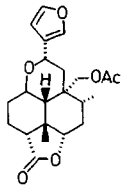

62

Gymnocolin (**62**), a bitter-tasting diterpenoid, has been isolated from *Gymnocolea inflata*.[72] This was the first example in liverworts of a clerodane, known from higher plants. Further examples of this diterpene class have been detected in, among others, *Anastrepta orcadensis*,[73] *Scapania bolanderi*,[74] and *Pleurozia acinosa*.[75]

A short time ago we were able to isolate from *Anastrophyllum minutum* six diterpenes (**63**–**68**) belonging to a new structural type, sphenolobane.[76]

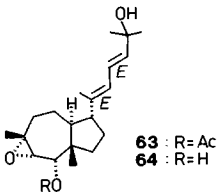

63: R = Ac
64: R = H

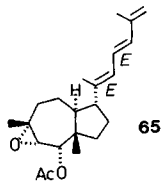

65

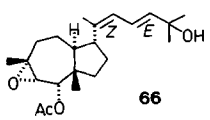

66

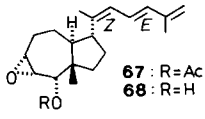

67: R = Ac
68: R = H

Tricyclic diterpenes from liverworts can contain four different carbon skeletons: *ent*-pimarane, pimarane, abietane and fusicoccane.[56] The fusicoccane type had been found only in microorganisms[78] before its discovery in *Plagiochila acanthophylla japonica*.[77] Recently we detected two new spiro compounds, plagiospirolides A and B (**69** and **70**), in *Plagiochila moritziana*. These are derived formally through

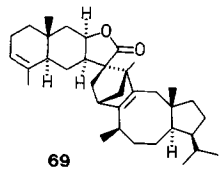

69

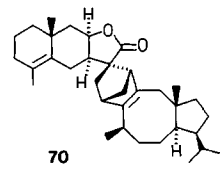

70

Diels–Alder cycloaddition of a fusicoccane with a sesquiterpene methylenelactone of the eudesmane type.[79]

Tetracyclic diterpenes encountered have been of the *ent*-kaurane structural type, widespread in higher plants, and the verrucosanes and neoverrucosanes (basic structures **71** and **72**) detected so far only in liverworts. The verrucosanes were

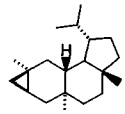

71

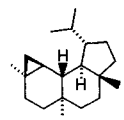

72

first isolated from *Mylia verrucosa*[80] and subsequently also from other liverworts;[56] the neoverrucosanes were found only associated with verrucosanes in *Mylia verrucosa*[80] and *Scapania bolanderi*.[74]

2.3.4. Triterpenes and Phytosterols

The triterpenoids found in bryophytes can be subdivided into the following carbon skeletal types:[17] α-amyrane, fernane, friedelane, D-friedooleanane, hopane, lupane, neohopane, and serratane. The most frequently encountered triterpene is 22(29)-hopene (**73**).

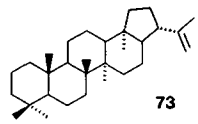

73

Exhaustive investigation has been made of the configuration at C-24 of the 24-methyl- and 24-ethylsterols in mosses.[81] Evidently 24β-alkylsterols dominate in algae and fungi but 24α-alkylsterols in higher plants. Bryophytes appear to take an intermediate position; the two epimeric 24-methylcholesterols occur in bryophytes in an α:β ratio ranging from 1:4 to 4:1.

3. Biologically Active Substances from Bryophytes

Even though bryophytes have not yet formally become important as medicinal or toxic plants,[82] preparations from them have indeed been used, notably in the Chinese and North American Indian folk medicine.[83] For example, as long ago as 1590 the Chinese *Ri* reported the diuretic properties of two mosses and the hair-growth-stimulating action of the ash of the maidenhair moss. North American Indians made use of pastes and ointments derived from mosses for treating wounds. During the first World War both the Ger-

mans and the Allies apparently took advantage of the special absorptive and antibiotic properties of *Sphagnum* species (peat mosses) for making bandage material. Furthermore, forest workers in Canada, North America and Europe have been known for a long time to be susceptible to contact dermatitis, which could be traced to epiphytically growing liverworts of the genus *Frullania*. The observation that many bryophytes are neither eaten by animals nor attacked by pest organisms has led to speculation about endogenous protective agents. It is also noteworthy that viruses have not yet been found in bryophytes.[84]

Nowadays many moss components are known to be responsible for various biological activities (Table 2). Several of these display many quite different bioactivities. A small selection of bioactive compounds produced by bryophytes is given here.

Table 2. Biological activities of bryophyte components.

1. Allergenic effect
2. Cytotoxic and cytostatic action
3. Cardiotonic activity
4. Carcinogenic action
5. Anti-inflammatory action
6. Vasopressin antagonism
7. Liberation of peroxide
8. Antibacterial activity
9. Toxicity toward fungi
10. Antifeedant activity
11. Prophylaxis against pest organisms
12. Toxicity toward molluscs
13. Toxicity toward molluscs
14. Growth regulation and plant development
15. Enzyme inhibition

Some sesquiterpene lactones, such as the two frullanolide enantiomers (**74** and *epi*-**74**) are the compounds from *Frullania* species which cause the contact dermatitis.[85-87] The allergenic action has been traced to the α-methylene-γ-butyrolactone ring. A series of new, naturally occurring compounds from bryophytes show appreciable cytotoxic and cytostatic properties (Table 3); examples are: 4-epiarbusculin (**75**), oxyfrullanolide (**76**), 8α-acetoxyzaluzanin C (**77**), diplophyllin (**78**) and (+)-epoxyfrullanolide (**79**). The

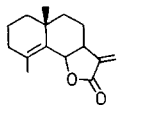

74

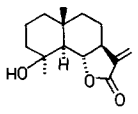

75

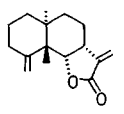

76

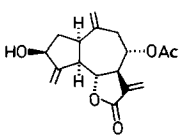

77

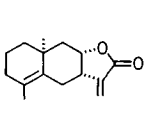

78

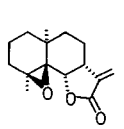

79

maytansinoside, 15-methoxyansamitocin P-3 (**80**), isolated from two moss species,[88] showed a powerful antitumor activity in the mouse-P-338-lymphocyte-leukemia-cell test

Table 3. Some cytostatic compounds from liverworts.

Compound	Structure	ED_{50} in ppm[a]
4-epiarbusculin A	**75**	0.5
oxyfrullanolide	**76**	0.8
8α-acetoxyzaluzanin C	**77**	1.6
diplophyllin	**78**	2.1
(+)-epoxyfrullanolide	**79**	2.65
marchantin A	**30**	8.39
riccardin B	**33**	10.0
perrottetin E	**27**	12.5

[a] Test system: KB cell cultures, ED_{50} values according to [32].

(IC_{50}: 2×10^{-5} ppm[87]). Its activity exceeds by a factor of 100 that of doxorubicin (formerly adriamycin), which has been employed successfully in various cancer cases.[89] However, only microgram amounts of this compound have been isolated so far from 20 kilograms of bryophyte sample. The furanosesquiterpene norpinguisone (**81**), from species of the liverwort genus *Porella*,[116] is toxic toward the mould *Aspergillus niger*.

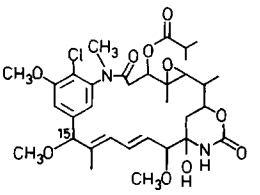

80

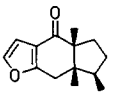

81

The sesquiterpene aldehyde (−)-isobicyclogermacrenal (**53**), from *Lepidozea vitrea* (Hepaticae), inhibits the growth of roots and leaves of rice seedlings in the concentration range from 1.1×10^{-3} M to 2.3×10^{-4} M.[90] In contrast, the diterpene acetate gymnocolin (**62**), from *Gymnocolea inflata* (Hepaticae), promotes the germination of wheat seeds in 10^{-6} to 10^{-7} M concentration.[91] The bibenzyl derivative lunularic acid (**20**), found in all liverworts subsequently studied (about 80)[92] very probably plays a decisive role in growth regulation and development in this class of bryophyte. The information about the occurrence of this substance in algae in the relevant literature is conflicting; it has been sought in vain in hornworts, mosses, and lichens, and there is only one example as yet of a seed plant containing it. Some of its derivatives (esters, amides) show molluscicidal activity.[93]

Sacculatal (**57**) possesses a potent piscicidal activity. Individual killie fish (a carplike species), *Orizia latipes*, are killed within two hours by solutions of 0.4 ppm.[94] The same compound is also highly active as a tumor provoker.[95] The sesquiterpene hemiacetal, plagiochilin A (**48**), from various *Plagiochila* species (Hepaticae) is a most powerful antifeedant. Concentrations of only 1–10 ng cm^{-2} were sufficient in the „Choice-Test" for the cotton plant pest, a butterfly species called the „African army worm". This is about 10 to 100 times more active than similarly functioning substances from higher plants.[116] The bis(bibenzyl), marchantin A (**30**), isolated from various *Marchantia* species,[116] shows

Table 4. Antibacterial activity of marchantin A (**30**) (according to[32], modified).

Bacterial species	Min. inhibiting concentration (ppm)
Acinetobacter calcoaceticus	6.25
Alcaligenes faecalis	100
Bacillus cereus	12.5
Bacillus megaterium	25
Bacillus subtilis	25
Cryptococcus neoformans	12.5
Enterobacter cloacae	100
Escherichia coli	100
Proteus mirabilis	100
Pseudomonas aeruginosa	100
Salmonella typhimurium	100
Staphylococcus aureus	3.13–25

distinct antibacterial activity toward some types of bacteria (Table 4). The furanosesquiterpene ricciocarpin A (**82**), from *Ricciocarpos natans*, is strongly toxic toward the water snail, *Biomphalaria glabrata*, known to be a bilharzia carrier.[93]

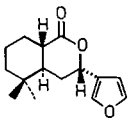

82

4. In Vitro Culture of Bryophytes

In addition to the difficulties of acquiring large amounts of bryophytes, there is the problem that many of them are spread over wide areas and occur only in small populations. The bryophyte growth sites, especially in the tropics, are often accessible only with difficulty. This frequently impedes the collection of a particular species in amounts sufficient for isolating and testing components for potential biological and pharmacological activity. Field cultivation of bryophytes similar to that of useful and medicinal plants is not practicable; even if the required ecological conditions were created, mixed populations would result.

A highly promising way out of this impasse is the use of in vitro culture of the bryophytes. They can be grown in vitro on suitable nutrient media, under aseptic conditions, as surface or submersed cultures. Although this technique has been known for higher plants since 1939, it was first employed relatively late for bryophytes (for a review, see [96]). Originally the cultures were used to answer morphological and physiological questions, but since the beginning of the eighties also to test for the possible formation of secondary metabolites.[14, 97–102]

Bryophyte cultures offer effectively the same advantages as in vitro cultures of higher plants.[103] Plants from all climatic zones can be grown in cultures. A comparatively constant production of material can be achieved through controlled culture conditions. Herbicides and insecticides are not needed, so that it is in general an environmentally favorable method.

Bryophyte cultures have additional advantages: The plants, often only a few millimeters large, can be cultivated easily, even in differentiated form, in fermenters. Since the bryophyte plant itself is haploid, it is possible to select mutants relatively rapidly.[104] Many bryophyte species are available in nature in such tiny amounts that in vitro culture is the only way of obtaining larger quantities of plant material. An example of this is the liverwort *Fossombronia pusilla*, which is just a few millimeters in size; a brief description is given here of its in vitro culture: A small cushion (about 5 g fresh material weight) with spore capsules was collected in August 1987. Starting with these spore capsules, an in vitro culture was set up according to the general plan (Fig. 3) on a mineral salt medium,[105] 2% in sugar, at 23 °C, and in permanent illumination (4500 Lux) (stages e–g in Fig. 3). The liverwort can be cultivated also in a liquid medium.

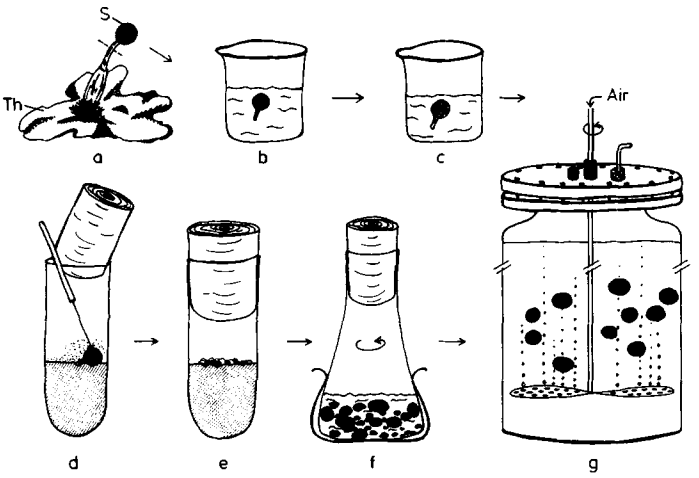

Fig. 3. Sketch of the layout of a liverwort in vitro culture:
a) liverwort with spore capsule (S = spore capsule, Th = thallus)
b) surface sterilization of the capsule
c) washing with sterilized water
d) placing the spores on the sterile agar medium
e) preliminary culture on agar medium of the small liverwort plants formed
f) "liquid culture" in an erlenmeyer flask (220 ml)
g) culture in 5-L fermenters

However, these cultures grew only when 12.5 μg L^{-1} vitamin B_{12} were introduced. A nutrition experiment with ^{57}Co-tagged B_{12} showed that a considerable fraction of the vitamin was taken up by the cultures.[71] Starting from two spores and after only one year, 1 kg *F. pusilla* plant was harvested (Fig. 4). The cultures also grow in 5-L fermenters. The cultures yield the same substances (see Section 2.3.3) as the plants in nature, as shown by a qualitative TLC and GC comparison.[14, 97–102]

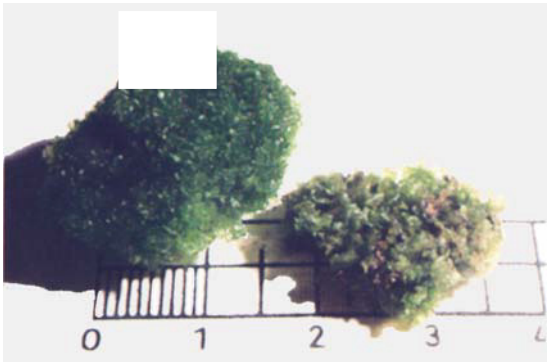

Fig. 4. *Fossombronia pusilla* (L). Nees, left: grown in an in vitro culture; right: grown under natural conditions. Photography: Prof. R. Mues.

Another good example of the efficacy of in vitro culture of bryophytes is certainly *Ricciocarpos natans*, a thallus liverwort of amphibious life mode. The thalli float like duckweed on the surface of ponds, ditches, and stagnant water stretches. The species is rare in Central Europe and is dying out as a result of water pollution. Consequently this bryophyte cannot be collected in adequate amounts; furthermore, it is usually contaminated with algae, a grave handicap to the isolation of material. In vitro cultures of *Ricciocarpos natans* on a mineral salt nutrient medium, 1% in sucrose, show the sigmoid growth curve, typical for microorganisms (see Fig. 5). The weight of fresh material increased eightfold

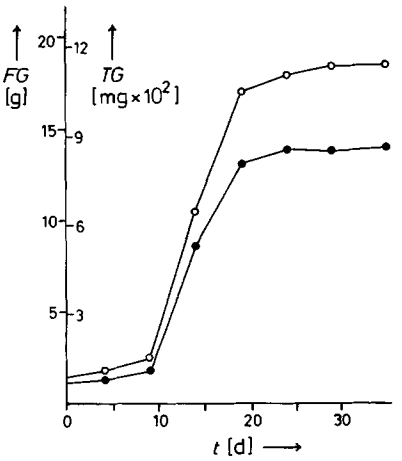

Fig. 5. Growth of the sterile culture of *Ricciocarpos natans*. Nutrient medium: modified B5 medium according to *Gamborg*: 1% sucrose, permanent irradiation of 2000 Lux; 22 °C. ○ fresh weight (g/flask); ● dry weight (mg/flask). Each point is the mean of five parallel culture preparations.

during 10 days of this logarithmic growth phase. This clearly surpasses the growth under natural conditions. A chromatographic comparison showed that the same pattern of components was produced both under natural conditions and in the in vitro culture.[40] Ricciocarpins A and B (**82** and **83**), ricciofuranol (**84**), cuprenolide (**85**), and cuprenolidol (**86**), all hitherto unknown structures, were isolated from the cultures.[40]

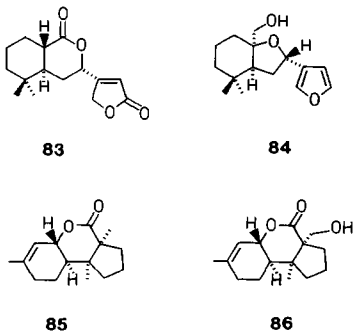

These two examples show that in vitro cultures furnish bryophytes in amounts sufficient to permit isolation of the components. Up to now, the chromatograms of the components from the plants in the cultures agree with those from the plants growing freely in nature.

5. Syntheses of Bryophyte Components

5.1. General Remarks

Chemical synthesis is very important for acquiring the natural products on a larger scale and for independent elucidation of structures. Despite the large number and variety of the bryophyte components hitherto isolated and structurally classified, comparatively little is known about syntheses of these naturally occurring compound classes. The investigations undertaken on representative examples in the domains of the phenolic and the nonphenolic components have centered on new types of structure and stereochemical aspects and, above all, on important biological activities. The aim of our own work is primarily the development of efficient and versatile syntheses on preparative scale.

5.2. Phenolic Components

5.2.1. Bibenzyl Derivatives

Lunularic acid (**20**) has been synthesized in a number of ways.[106] Syntheses with good yields[107] start from 6-methylsalicylate (**87**)[108], whereby the 6-methyl group is converted into the bibenzyl unit by either metalation/alkylation or bromination/Wittig reaction/hydrogenation via the methyl ether (**88**), or acetate (**89**). The organometallic route (**88** → **90** → **20**) gives a total yield of 50% of lunularic acid in three stages and on a 5–10 g scale, the Wittig reaction route (**89** → **92** → **94** → **95** → **20**), 75% acid in five stages and on a 100 g scale. The Wittig reaction of **92** with *p*-benzyloxy-

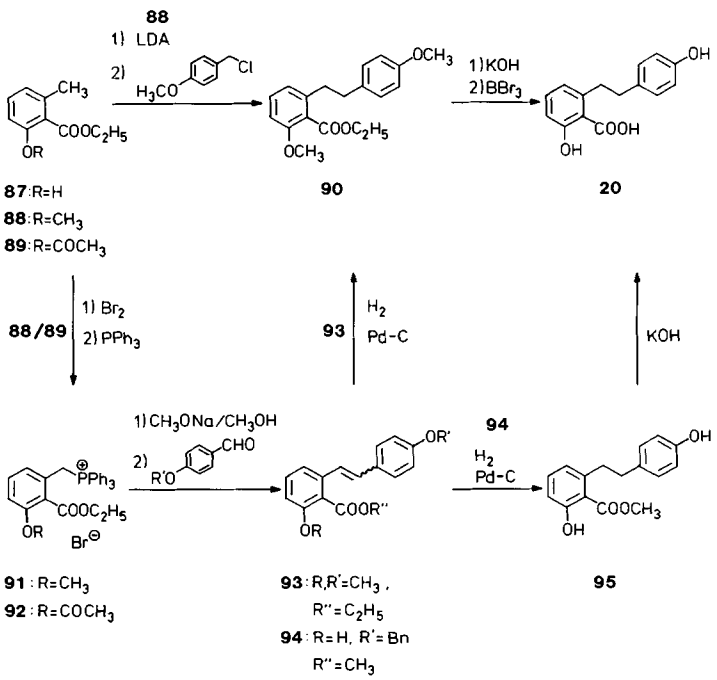

benzaldehyde to **94** is accompanied by transesterification and deacetylation and is virtually quantitative.

The stilbene-*o*-carboxylate esters (**93**/**94**) are useful intermediates for synthesizing hydrangenol derivatives. Thus the *rac*-hydrangenol (**98**) is obtained in an overall yield of 70% from the ester (**94**) by hydrolysis, acid-catalyzed cyclization of the carboxylic acid (**96**) and catalytic debenzylation of the lactone (**97**).[109]

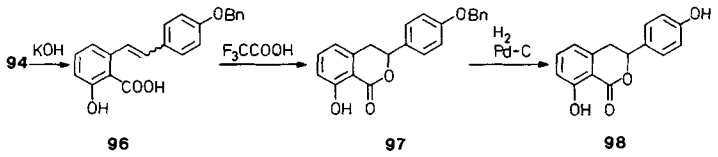

96 **97** **98**

The prenylbibenzyl derivative (**99**),[110] its (decarboxylated) analogues (**23** and **24**), and the perrottetins A and D (**100** and **101**) are related structurally to lunularic acid (**20**). Starting material for the synthesis of **99**[111] is the bis-*O*-acetylated ester of orsellinic acid (**102**). It is converted to the bibenzyl intermediate **103** in a reaction sequence analogous to that for lunularic acid (see above); the prenylbibenzyl derivative **99** is obtained by prenylation with α,α-dimethylallyl alcohol in the presence of $ZnCl_2$ as catalyst, followed by saponification of the ester.

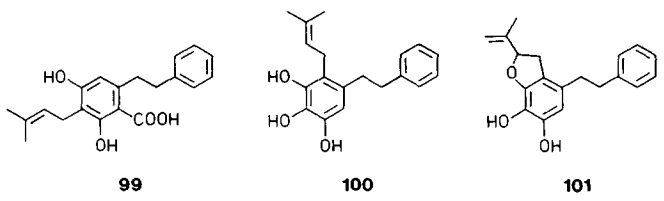

99 **100** **101**

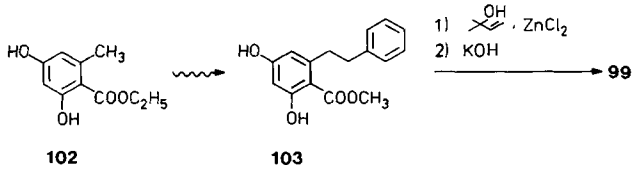

102 **103**

The key compound for synthesis of the amorfrutin analogues **23** and **24**[112] is 5-(β-phenylethyl)resorcinol (**104**). It is easily available in the methyl- or methoxymethyl(MOM)-protected form (**105** or **106**) from β-resorcylaldehyde.[113] The γ,γ-dimethylallyl or geranyl side chain is introduced by regioselective metalation of the 2-position with n-butyllithium and alkylation with the appropriate bromides. Removal of the blocking group (3% HCl in ethanol) from the MOM compound (**107**) leads to **23** or **24**, whereas deprotection of the dimethyl ether (**108**, R′ =) by means of BBr_3 and cyclization via the allyl side chain (forming **110**) using NaH/*N*,*N*-dimethylaniline splits off only one methyl group (forming **109**).

The perrottetins A and D (**100** and **101**) can be obtained in analogous reaction sequences from the dibenzyl derivatives **111** and **112**, accessible from 3,4,5-trimethoxybenzaldehyde.[114]

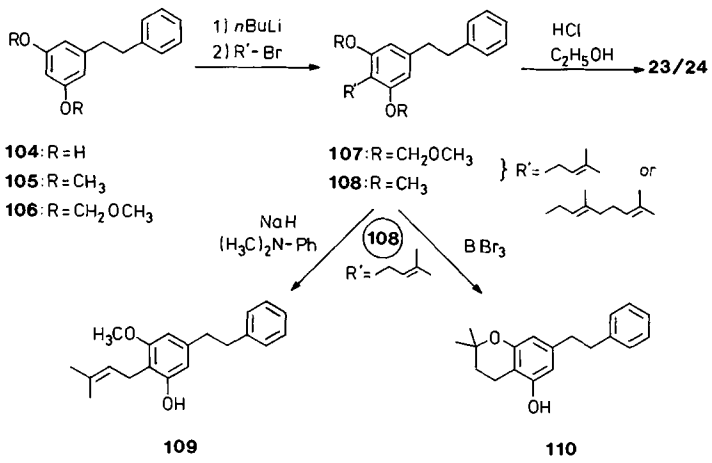

109 **110**

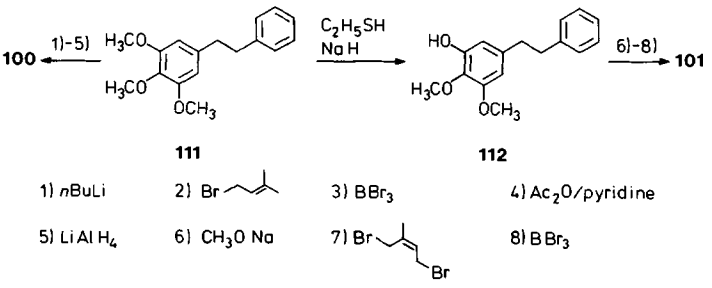

5.2.2. *Bis(bibenzyl) Derivatives*

The perrottetins E, F and G (**27**–**29**) are acyclic bis(bibenzyl) derivatives. Perrottetin E (**27**) is derived formally—perhaps also biogenetically[16]—from lunularin (**113**), the decarboxylation product of lunularic acid (**20**), through oxidative O–C coupling of the *p*-substituted hydroxyphenyl radicals.

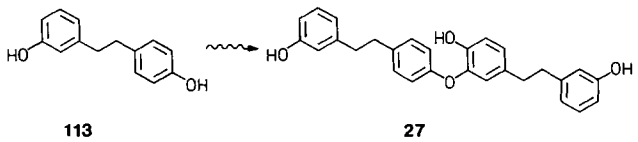

113 **27**

Several syntheses are known for the perrottetins E–G.[115–117] The usual principle is to construct suitably substituted 4,3′-diphenyl ether derivatives such as **114** and **115**. These are subjected to double Wittig or Horner reactions and subsequent hydrogenation which permits formation of the *m*-hydroxyphenyl side chain in OH-protected form; the perrottetins **27**–**29** are then obtained on removing the blocking group.

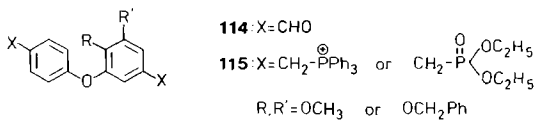

The compounds **114** and **115** can be synthesized by first forming the diphenyl ether through an S_NAr reaction of phenolates with aromatic halides activated by *o*-NO_2, and then transforming -NO_2 to -H; this has proved to be superior preparatively to direct Ullmann coupling. The example of the synthesis of perrottetin E (**27**) may be taken, in which the desired molecule is obtained in 35% overall yield in six stages.[117]

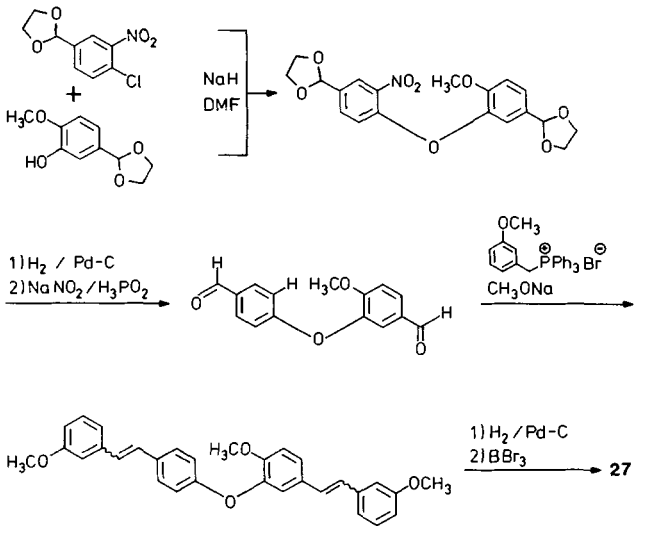

The cyclic bis(bibenzyl) derivatives of the marchantin, riccardin and plagiochin types deserve special mention. They can occur in many forms with a variety of substituents on both the benzene nucleus and ethylidene bridge.[114] A plausible hypothesis for their biogenesis considers cyclization of open-ring precursors, such as perrottetins, through intramolecular phenol oxidation, accompanied by C–O or C–C linkage of the terminal *m*-hydroxyphenyl units.[16] In this way the macrocyclic diphenyl ethers, marchantin C, riccardins B and C, and plagiochin D can be correlated biogenetically with perrottetin E (**27**).

Syntheses of the marchantins A (**30**)[118,119] and I (**32**)[120] and the riccardins B (**33**)[119,121] and C (**34**)[122] have been described. The synthesis of marchantin A (**30**), given below, illustrates the possibility of building up the cyclic bis(bibenzyl) compounds via the scheme developed for perrottetin synthesis. This makes use of a selectively protected (β-phenylethyl)-substituted diphenyl ether unit containing a free phenolic OH group (such as **116**), which is coupled with another diphenyl ether unit through an S_NAr reaction (**116** → **117**); the macrocycle is then closed by an intramolecular Horner reaction (**118** → **30**).[123]

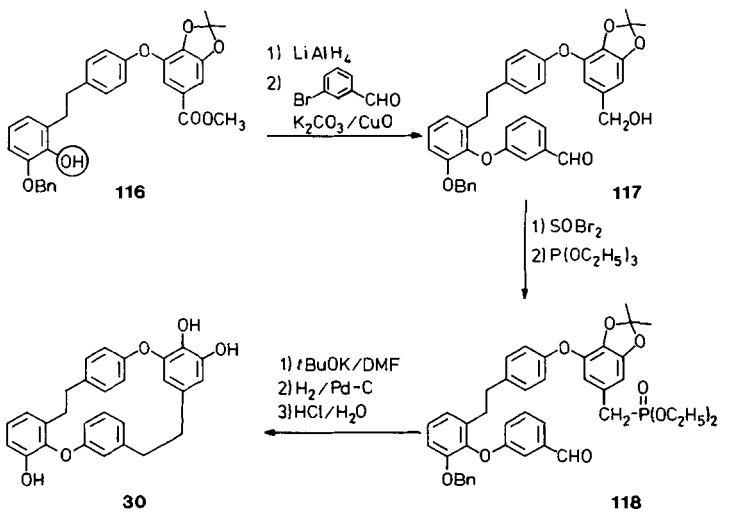

5.2.3. *Flavonoids*

Tricetin (**119**) and its *O*-methylated derivatives apometzgerin (**120**), tricin (**121**) and selgin (**122**), which occur in bryophytes as aglycones of *O*- and *C*-glycosides, can be synthesized on the preparative scale in good yields.[124,125]

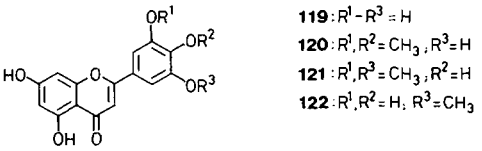

One route is via a Baker–Venkataraman transformation of protected *o*-aroyloxyacetophenones to *o*-hydroxydibenzoylmethanes, followed by acid-catalyzed cyclization; the other involves direct oxidative (with selenium dioxide) ring closure of chalcones to yield flavones, as illustrated in the following synthesis of apometzgerin (**120**).[125]

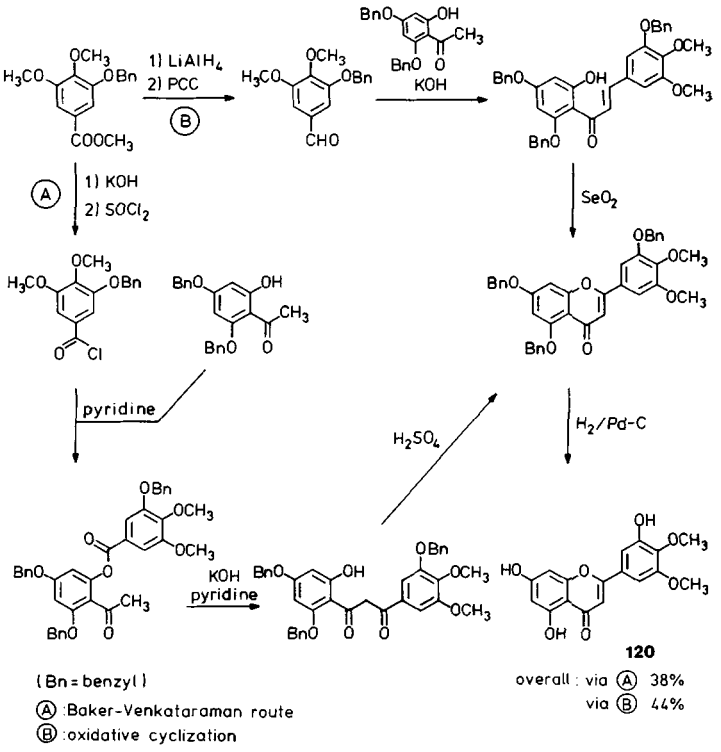

5.2.4. *Other Phenolic Components*

The 6,7-dihydroxy-4-(3,4-dihydroxyphenyl)naphthalene-3-carboxylic acid (**39**) is a representative of a new class of

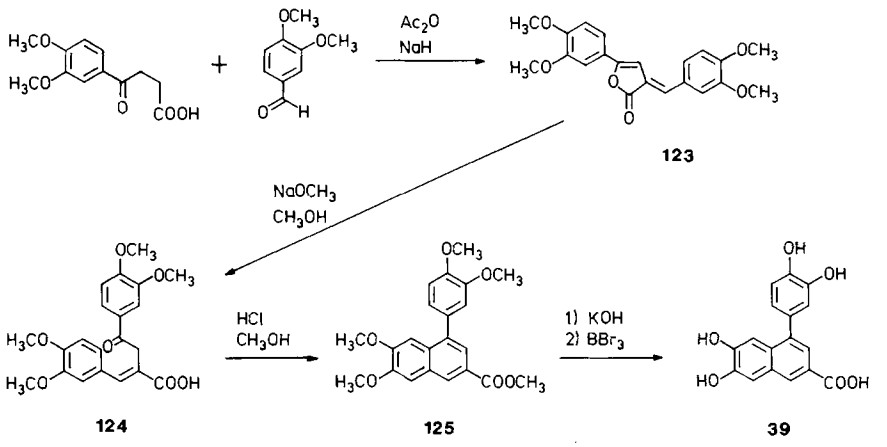

phenolic bryophyte components (see Section 2.2.2). Its structure has been confirmed by independent synthesis: The butenolide (**123**) was converted by base into the open-chain α,β-unsaturated acid (**124**), which was then cyclized through an intramolecular S_EAr reaction to the ester (**125**); the acid (**39**) was obtained by hydrolysis of the ester and demethylation with BBr_3.

The starting material for the synthesis of rosmarinic acid (**43**) (Scheme 1, first carried out by us[126]) is β-(3,4-methylenedioxy)-α-acetamidocinnamic acid (**126**), which is conveniently available from piperonal through azlactone synthesis and subsequent partial hydrolysis. Further hydrolysis with 1 N HCl converts **126** (present almost entirely in the enol form) to the α-ketoacid (**128**), which is hydrogenated to piperonyllactic acid (**129**). *N,N'*-Diisopropyl-*O*-(β-trimethylsilylethyl)isourea transforms **129** into the β-trimethylsilyl ester (**130**), the free hydroxyl function of which is esterified with *O,O*-dibenzylcaffeic acid (**131**) according to the DCC (dicyclohexylcarbodiimide) method. The silylated ester group in (**132**) is split off using tetra-*n*-butylammonium fluoride, and the phenol protective group removed by BBr_3. Alternatively the α-ketoacid (**128**) can be obtained by the Corey–Seebach method[127] from **127**, through an alkylation reaction with 1,3-dithiane-2-carboxylic acid.

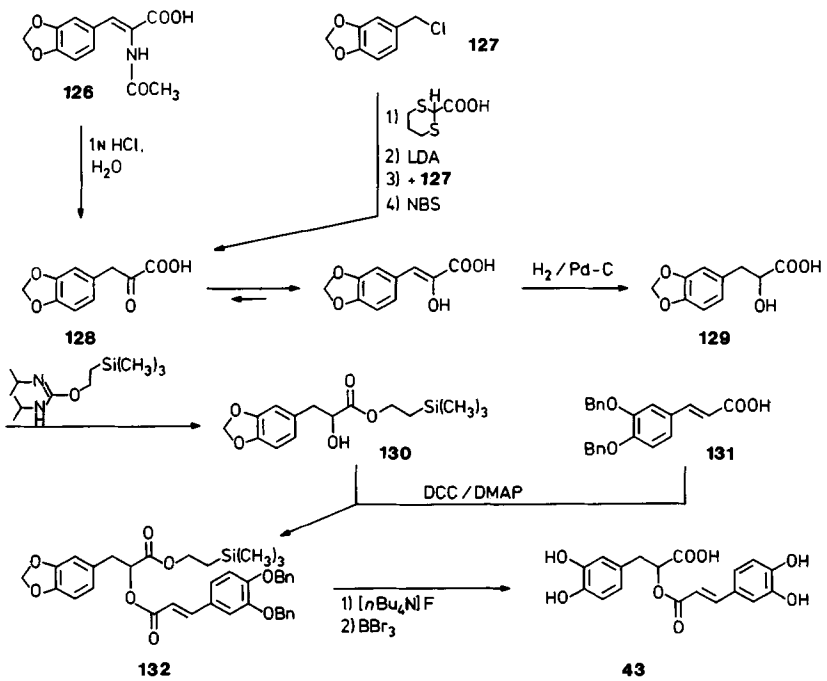

Scheme 1. NBS = *N*-bromosuccinimide, LDA = lithium diisopropylamide, DCC = dicyclohexylcarbodiimide, DMAP = 4-dimethylaminopyridine.

5.3. Isoprenoids

Numerous sesquiterpene and diterpene systems isolated from bryophytes have special structural or stereochemical features, or biological activities. This has attracted the attention of chemists interested in syntheses. Examples are the sesquiterpenes anastreptene (**140**), taylorione (**145**), chiloscyphone (**155**), ricciocarpin A (**82**), and the diterpenes sacculatal (**57**) and perrottetianal A (**59**).

5.3.1. *Sesquiterpenes*

(−)-9-Anastreptone (**139**) can be built up from the starting material, (−)-carone (**133**).[128] The silylenol ether of the carone (**134**) is subjected to Robinson annulation with 3-penten-2-one, using $TiCl_4/Ti(OiPr)_4$ as catalyst. Subsequent treatment with HCl/ethanol opens the three-membered ring to yield an epimeric mixture of chloroenones (**136**) (76:24 mixture, separable by fractional crystallization). Restoring the ring with NaH yields the epimeric enones **135**, which can be transformed into the dienone **138** in two ways, namely, oxidation of the dienol silyl ether **137** with $Pd(OAc)_2$/*p*-benzoquinone, or direct dehydrogenation with $C_6H_5IO_2$/phenylseleninic anhydride. Irradiation in methanol leads via a stereoselective di-π-methane rearrangement to a single product, (−)-9-anastreptenone (**139**) ($[\alpha]_D^{20} = -235$ (c = 0.11 in $CHCl_3$)). A similar reaction sequence converts (+)-carone into the (+)-enantiomer of **139**. So far it has not been possible to reduce the anastreptenones to the hydrocarbons.

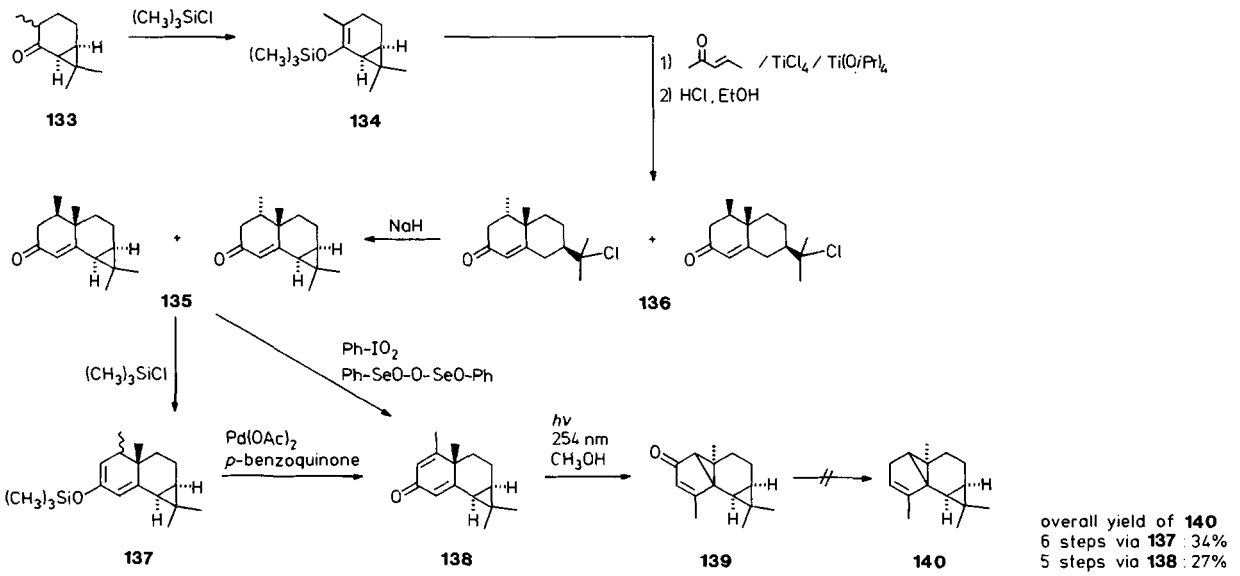

(−)-Taylorione (**145**) has been obtained in a 17-stage partial synthesis, starting from (−)-Δ^3-carene (**141**).[129] The key compound is the chiral aldehyde **142** (S = MOM). This yields the desired product **145** via chain lengthening (to **143**), intramolecular aldol condensation (to **144**), and finally Wittig olefination and oxidation.

The racemic aldehyde **142** (S = tetrahydropyran, THP)[130] can be obtained in 15% overall yield in a simple sequence of six stages, beginning with 5-hexin-2-ol **146** (**146** → **142**, S = THP). This represents a total synthesis of the racemic naturally occurring compound **145**. The route to total synthesis of the chiral natural product can be accomplished via diazoacetic ester reactions[132] of the *cis* olefin

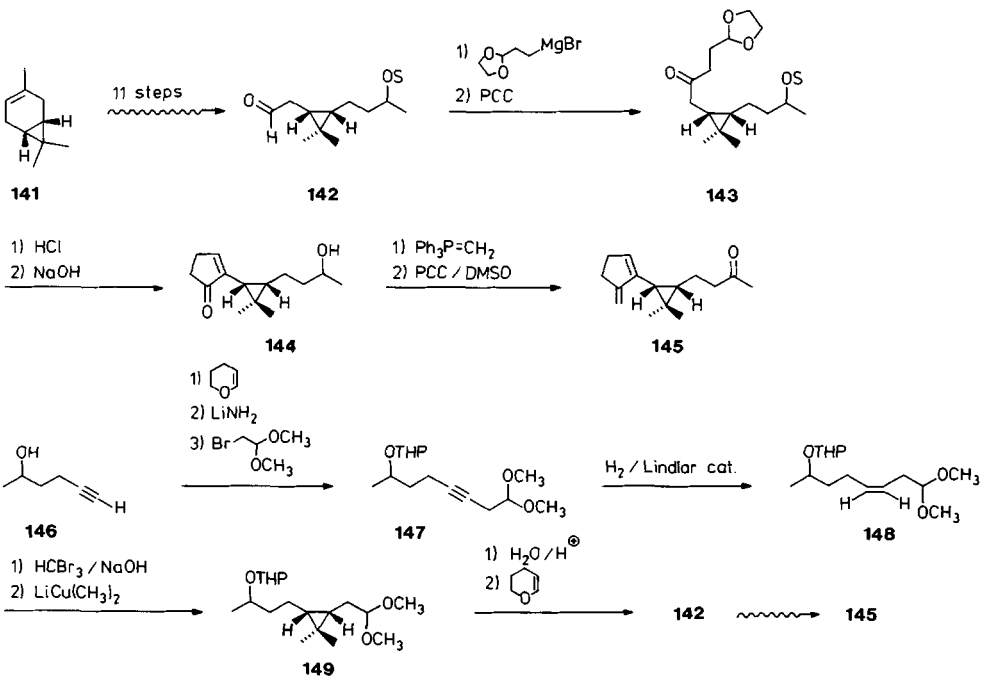

148, analogously to the synthesis of the *ent*-chrysanthemic acid.[131]

The bicyclic α-methylene ketone chiloscyphone (**155**)[133] has been built up in a multistage reaction sequence, beginning with 3,4-dimethyl-2-cyclohexen-1-one (**150**).[134] 1,4-Addition of vinyl cuprate to **150** furnishes the cyclohexanone **151** with the desired *cis* stereochemistry of the vicinal

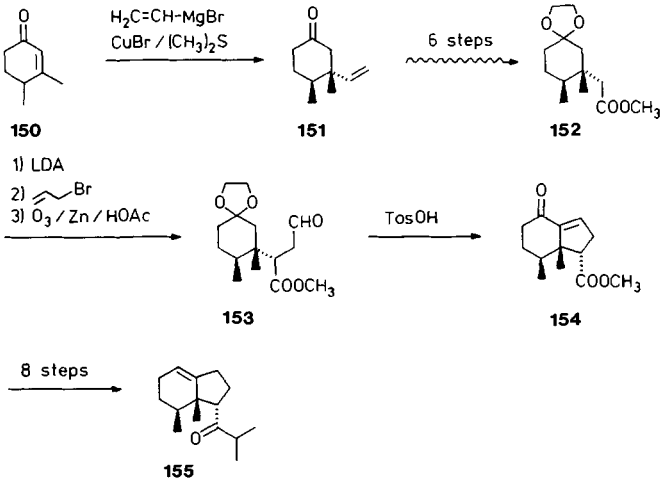

methyl groups. The vinyl group in **151** is converted into $-CH_2COOCH_3$ (→**152**) and then a C^2 aldehyde side chain is introduced into the α-position to the ester function by alkylation with allyl bromide/lithium diisopropylamide (LDA) and subsequent ozonolysis. After deprotection, the aldehyde **153** undergoes an intramolecular aldol condensation to the bicycloenone **154**. This can be separated from its C-6 epimer and yields the naturally occurring compound **155** after further conventional transformations.

Ricciocarpin A (**82**) has been obtained as racemate via two synthetic routes. In route 1[135] allyllithium is added to the enol ether of 6,6-dimethyl-2-formylcyclohexanone (**156**). Hydrolysis of the product yields the 2-allyl-substituted cyclohexenaldehyde (**157**), which is oxidized with $NaClO_2$ to the corresponding carboxylic acid. Its conjugated double bond is then selectively reduced with sodium in liquid ammonia. The saturated acid **158** is esterified with diazomethane, and subsequent ozonolysis converts it into the ester aldehyde, to which β-furyllithium is added to give the carbinol ester epimers **159**. Subsequent hydrolysis in a basic medium yields a mixture of lactone stereoisomers, from which *rac*-ricciocarpin A (**82**) can be isolated as the main product.

In route 2[136] dimethylcyclohexenylmethanol (**160**) is converted into the acid (**161**) by a [3,3]-sigmatropic Claisen orthoester reaction, followed by saponification. The acid chloride derivative is treated with tris-*n*-butyl-β-furylstannane in the presence of benzylchlorobis(triphenylphosphine)palladium in hexamethylphosphoric triamide to yield the furylketone **162** (pallescensone, natural product from *Pictyodendrilla cavernosa*[137]). Hydroboration/reduction with 9-borabicyclo[3.3.1]nonane (9-BBN) gives the diol **163** in a stereocontrolled way. Its oxidation by pyridinium dichromate (PDC) yields the ketocarboxylic acid **164** of *trans* configuration. The sterically uniform *trans* form of *rac*-ricciocarpin A (**82**) is furnished by reducing the acid **164** with sodium borohydride.

5.3.2. *Diterpenes*

(−)-Sacculatal (**57**) has been synthesized from the chiral dione **165** as starting material.[138]. The saturated carbonyl function of **165** is first converted selectively into a ketal and an allyl side chain introduced at C-4 by reductive alkylation (→**166**). Oxygen removal at C-3 (**166** → **167**) is accomplished by reducing the carbonyl group, converting the secondary alcohol into the dithiocarbonate and performing radical fission of the dithiocarbonate with tributyl stannane according

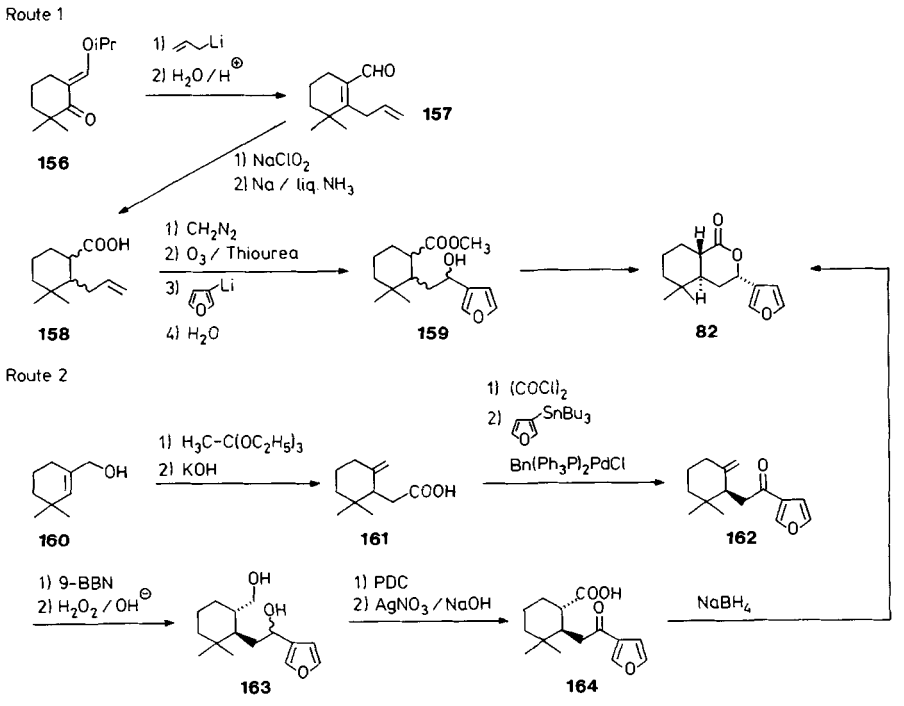

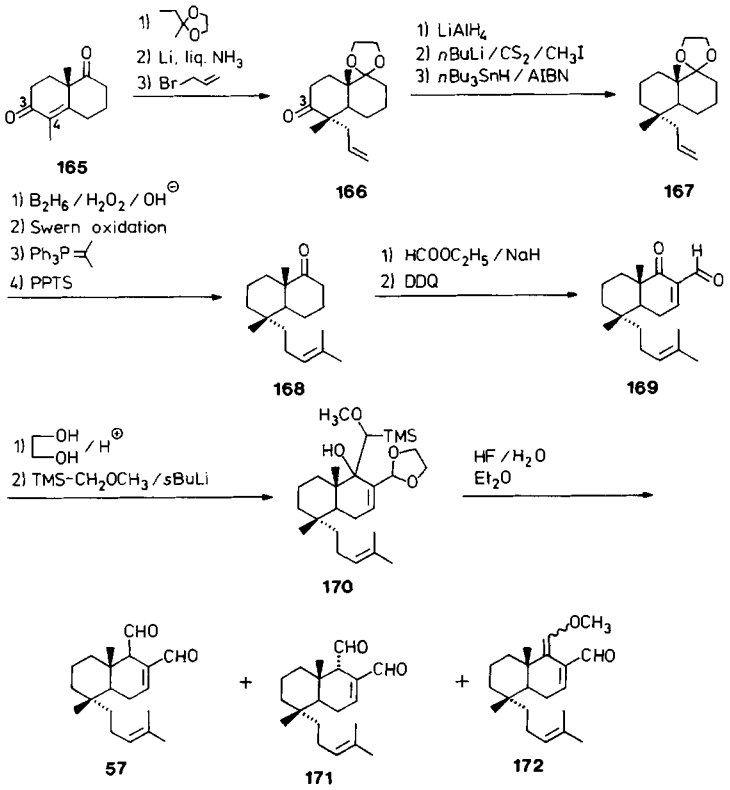

to the method of *Barton*. The decalone (**168**) is the key compound for the synthesis. It is derived from **167** by building up the C-4 homoprenyl side chain (through hydroboration, Swern oxidation and a Wittig reaction of the aldehyde thus obtained with $Ph_3P{=}CH(CH_3)_2$ and ketal fission with pyridinium *p*-toluenesulphonate (PPTS). The two formyl groups of sacculatal are introduced by Claisen condensation with formate, dehydrogenation with 2,3-dichloro-5,6-dicyano-*p*-benzoquinone (DDQ), protection of the aldehyde function in **169** and addition of methoxy-(trimethylsilyl)-methyllithium. The intermediate **170** thereby attained is hydrolysed, but not selectively. In addition to sacculatal (**57**, 26%), isosacculatal **171** (16%) and the *E*/*Z*-isomeric enol ethers **172** (20%) are obtained.

latal synthesis, into the decalone **174**, functionalized at the angular substituent. Compound **174** is then α-methylated conventionally (Claisen condensation with diethyl carbonate, and Krapcho fission of the methylated β-ketoester) and the angular CH_2OR group oxidized to the protected aldehyde group (**175** → **176**). The second aldehyde group is introduced by adding dichloromethyllithium to **176**, eliminating water and hydrolyzing to **177**. The desired end product **59** is then obtained by deblocking with pyridinium *p*-toluenesulphonate.

6. Résumé and Further Prospects

The present state of research in the chemistry of bryophytes can be summarized as follows:

1. Bryophytes constitute a notable reserve of rare and structurally new natural products.
2. Many such substances display marked biological activity.
3. In vitro cultures of bryophytes produce numerous secondary metabolites. They thus offer promising possibilities of providing larger amounts of plant material and also of components.
4. Chemical syntheses enable many bryophyte constituents to be obtained on a preparative scale. This is essential for broad biological screening. Furthermore, interesting biological activities may be shown by synthesized modified natural products and intermediates.

The question posed in the title "are bryophytes a source of biologically active material?" can consequently be answered with a clear "yes". It appears quite possible that, in the future, bryophyte components or products derived from them, can be used in pharmacological and agricultural chemical domains, or in food technology and the cosmetic industry. In our experience bryophyte constituents offer a rich field for combined research by biologists, pharmacists and chemists. This has led to the foundation in Saarbrücken of an interdisciplinary working group, "Chemistry and Biology of the Bryophytes", and also to close cooperation with BASF in Ludwigshafen on a project supported by the Bun-

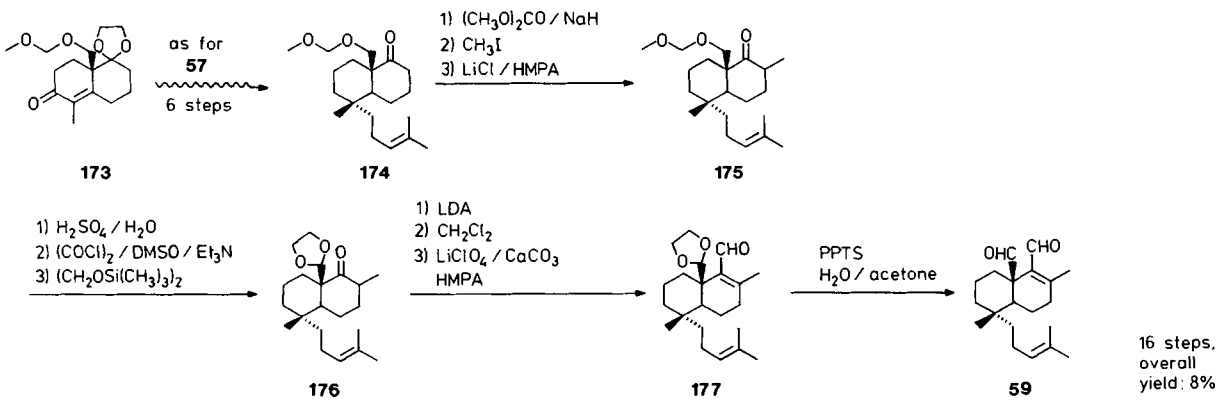

The synthesis of (+)-perrottetianal A (**59**)[139] follows the same scheme. The protected chiral dione **173**, obtainable in a multistage synthesis,[140] is transformed, as in the sacculatal synthesis, into the decalone **174**, functionalized at the angular substituent. Compound **174** is then α-methylated conventionally (Claisen condensation with diethyl carbonate, and Krapcho fission of the methylated β-ketoester) and the angular CH_2OR group oxidized to the protected aldehyde group (**175** → **176**). The second aldehyde group is introduced by adding dichloromethyllithium to **176**, eliminating water and hydrolyzing to **177**. The desired end product **59** is then obtained by deblocking with pyridinium *p*-toluenesulphonate.

desministerium für Forschung und Technologie (BMFT, Federal Ministry for Research and Technology). The main points of future research are, in addition to present aims,

principally the preparation of auto- and heterotrophic tissue cultures up to the technical scale, and research on the biogenesis of bryophyte component compounds.

Our sincere thanks are due to all scientific co-workers in the participating research groups for their dedicated experimental work. Further, we wish to thank Mrs. Christine Zehren, Mrs. Uta Krienke, and Mr. Alois Etringer for their work on the figures. We are grateful also to Mrs. Christel Allmann for preparing the manuscript, to Prof. Dr. R. Mues for the use of his colour photographs and to Prof. M. Ashworth for undertaking the translation into English.

We are especially indebted to the BASF Agricultural Field Station in Limburgerhof for their effective cooperation and energetic encouragement. For financial support we thank the BMFT.

Received: February 1, 1990 [A 805 IE]
German version: *Angew. Chem. 103* (1990) 134
Translated by Professor M. Ashworth, Saarbrücken

[1] *Rote Liste, Verzeichnis von Fertigarzneimitteln der Mitglieder des Bundesverbandes der Pharmazeutischen Industrie e.V.*, Editio Cantor, Aulendorf 1990.
[2] G. Schneider: *Pharmazeutische Biologie*, 2nd Edit., Bibliographisches Institut, Mannheim 1985.
[3] a) R. M. Schuster (Ed.): *New Manual of Bryology*, Hattori Bot. Lab. Nichinan, Miyazaki, Japan. b) R. M. Schuster in [3a], *Vol. 2*, 1984, p. 892.
[4] R. M. Schuster in [3a]; *Vol. 2*, 1984, p. 1071.
[5] D. H. C. Richardson: *The Biology of Mosses*, Blackwell, Oxford 1981, p. 1.
[6] E. Treffner (Beiträge zur Chemie der Laubmoose) *Dissertation*, Universität Dorpat 1881.
[7] H. Reinsch, *Jahrbuch Pract. Pharm. 10* (1845) 298.
[8] H. D. Zinsmeister, R. Mues, *GIT Fachz. Lab. 31* (1987) 499.
[9] R. Hegnauer: *Bryophyta* in R. Hegenauer (Ed.): *Chemotaxonomie der Pflanzen, Vol. VII*, Birkhäuser, Basel 1986, p. 374.
[10] a) H. D. Zinsmeister, R. Mues (Eds.): *Bryophytes: Their Chemistry and Chemical Taxonomy (Annu. Proc. Phytochem. Soc. Eur. 29)* Clarendon, Oxford 1990; b) P. Karunen in [10a], p. 121.
[11] G. Kohn, A. Vierengel, O. Vandekerkhove, E. Hartmann, *Phytochemistry 26* (1987) 2101.
[12] G. Kohn, S. Demmerle, O. Vandekerkhove, E. Hartmann, P. Beutelmann, *Phytochemistry 26* (1987) 2271.
[13] G. Kohn, O. Vandekerkhove, E. Hartmann, P. Beutelmann, *Phytochemistry 27* (1988) 1049.
[14] E. Hartmann, P. Beutelmann, O. Vandekerkhove, R. Euler, G. Kohn, *FEBS Lett. 198* (1986) 51.
[15] T. K. Ichikawa, K. Yamada, M. Namikawa, K. Sakai, K. Kondo, *J. Hattori Bot. Lab. 56* (1984) 209.
[16] Y. Asakawa, *Prog. Chem. Org. Nat. Prod. 42* (1982) 1.
[17] S. Huneck in [3a] *Vol. 1*, 1983, p. 1.
[18] V. Benezová, Z. Samek, V. Herout, F. Šorm, *Collect. Czech. Chem. Commun. 34* (1969) 582.
[19] H. D. Zinsmeister, B. Marx, unpublished results.
[20] R. Mues, H. D. Zinsmeister, *J. Hattori Bot. Lab. 64* (1988) 109.
[21] R. Mues, G. Leidinger, V. Lauck, H. D. Zinsmeister, T. Koponen, K. R. Markham, *Z. Naturforsch. C41* (1986) 971.
[22] K. R. Markham, R. Theodor, R. Mues, H. D. Zinsmeister, *Z. Naturforsch. C* 37 (1982) 562.
[23] P. Freitag, R. Mues, C. Brill-Fess, M. Stoll, H. D. Zinsmeister, K. R. Markham, *Phytochemistry 25* (1986) 669.
[24] B.-G. Österdahl, *Acta Chem. Scand. Ser. B 32* (1978) 714.
[25] R. Becker, R. Mues, H. D. Zinsmeister, H. Herzog, H. Geiger, *Z. Naturforsch. C41* (1986) 507.
[26] R. Theodor, H. D. Zinsmeister, R. Mues, K. R. Markham, *Phytochemistry 19* (1980) 1695.
[27] W. Stein, S. Anhut, H. D. Zinsmeister, R. Mues, W. Barz, J. Köster, *Z. Naturforsch. C40* (1985) 469.
[28] H. Geiger, M. Bokel, *Z. Naturforsch. C44* (1989) 559.
[29] K. R. Markham, O. M. Andersen, E. S. Viotto, *Phytochemistry 27* (1988) 1745.
[30] H. Geiger, W. Stein, R. Mues, H. D. Zinsmeister, *Z. Naturforsch. C42* (1987) 863.
[31] E. Nilsson, G. Bendz in G. Bendz, J. Santesson (Eds.): *Chemistry in Botanical Classification (Nobel Symp. 25)* Academic, New York 1973, p. 117.
[32] Y. Asakawa in [10a], p. 369.
[33] R. Mentlein, E. Vowinkel, *Liebigs Ann. Chem. 1984*, 1024.
[34] M. Rischmann, R. Mues, H. Geiger, H. J. Laas, T. Eicher, *Phytochemistry 28* (1989) 867.
[35] R. Mues, S. Huneck, J. D. Connolly, D. S. Rycroft, *Tetrahedron Lett. 29* (1988) 6793.
[36] R. Takeda, J. Hasegawa, K. Sinozaki in [10a], p. 201.
[37] H. Rudolph in [10a], p. 227.
[38] Y. Asakawa, R. Matsuda, T. Takemoto, *Phytochemistry 19* (1980) 567.
[39] C. L. Suire, Y. Asakawa, M. Toyota, T. Takemoto, *Phytochemistry 21* (1982) 349.
[40] G. Wurzel, H. Becker, *Phytochemistry 29* (1990) 2565.
[41] V. Herout, *Flavour and Fragrance J. 1* (1985) 43.
[42] H. Becker, unpublished results.
[43] J. D. Connolly, L. J. Harrison, D. S. Rycroft, *Tetrahedron Lett. 25* (1984) 1401.
[44] Y. Asakawa, JP-B 228 409 (1985); EP-B 0 185 921 (1986); JP-B 53 273 (1986); JP-B 126 013 (1986); US-A 4 659 509 (1987).
[45] J. D. Connolly, A. E. Harding, I. M. S. Thornton, *J. Chem. Soc. Chem. Commun. 1972*, 1320.
[46] R. M. S. C. Morais, L. J. Harrison, H. Becker, *J. Chem. Res. Synop. 1988*, 380.
[47] M. Toyota, F. Nagashima, Y. Asakawa, *Phytochemistry 27* (1988) 2161.
[48] Y. Asakawa, J. D. Connolly, C. O. Fakunle, D. S. Rycroft, M. Toyota, *J. Chem. Res. Synop. 1987*, 82.
[49] Y. Asakawa, M. Toyota, T. Takemoto, *Tetrahedron Lett. 1978*, 1553.
[50] H. Becker, S. Charadej, P. W. Thies, E. Finner, *Planta Med. 1984*, 245.
[51] A. Matsuo, K. Atsumi, K. Nadaya, M. Nakayama, S. Hayashi, *Phytochemistry 20* (1981) 1065.
[52] D. Takaoka, A. Matsuo, J. Kuramoto, M. Nakayama, S. Hayashi, *J. Chem. Soc. Chem. Commun. 1985*, 483.
[53] D. Takaoka, H. Tani, A. Matsuo, *J. Chem. Res. Synop. 1988*, 130–131.
[54] L. J. Harrison, H. Becker, *Phytochemistry 28* (1989) 1261.
[55] A. Matsuo, S. Uto, H. Nozaki, M. Nakayama, S. Hayashi, *J. Chem. Soc. Chem. Commun. 1980*, 1220.
[56] V. Herout in [10a], p. 83.
[57] I. Beneš, N. Beizaee, T. Vaňek, J. Váňa, V. Herout, *Phytochemistry 20* (1981) 2438.
[58] I. Beneš, T. Vaňek, M. Buděšinský, *Collect. Czech. Chem. Commun. 47* (1982) 1873.
[59] C. Liljenberg, P. Karunen, *Physiol. Plant. 44* (1978) 369.
[60] A. Matsuo, M. Nakayama, S. Hayashi, T. Seki, T. Amakawa, *Bryophytorum Bibl. 13* (1978) 321.
[61] Y. Asakawa, N. Tokunaga, M. Toyota, S. Hattori, A. Mizutani, *J. Hattori Bot. Lab. 46* (1979) 67.
[62] S. Huneck, J. D. Connolly, L. J. Harrison, R. Joseph, W. R. Phillips, D. S. Rycroft, G. Ferguson, M. Parvez, *J. Chem. Res. Synop. 1986*, 162.
[63] Y. Asakawa, M. Toyota, A. Cheminat, *Phytochemistry 25* (1986) 2555.
[64] C.-L. Wu, F. F. Wey, C. C. Hsieh, *Chemistry (Beijing) 40* (1982) 121.
[65] S. Huneck, K. H. Overton, *Phytochemistry 10* (1971) 3279.
[66] S. Huneck, G. A. Baxter, A. F. Cameron, J. D. Connolly, L. J. Harrison, W. R. Phillips, D. S. Rycroft, G. A. Sim, *J. Chem. Soc. Perkin Trans. 1 1986*, 809.
[67] S. Huneck, K. Schreiber, *J. Hattori Bot. Lab. 39* (1975) 215.
[68] A. Matsuo, K. Kamio, K. Kohama, K. Yoshida, J. D. Connolly, G. A. Sim, *Phytochemistry 27* (1988) 1153.
[69] Y. Asakawa, M. Toyota, T. Takemoto, *Phytochemistry 18* (1979) 1681.
[70] Y. Asakawa, M. Toyota, Z. Taira, T. Takemoto, K. Kida, Y. Ichikawa, *24th Symp. Chem. Terp. Essent. Oils and Arom., Koriyama, Japan, Symp. Papers 1980*, 221.
[71] M. Sauerwein, H. Becker, *Planta Med. 56* (1990) 339.
[72] S. Huneck, Y. Asakawa, Z. Taira, A. F. Cameron, J. D. Connolly, D. S. Rycroft, *Tetrahedron Lett. 24* (1983) 115.
[73] J. D. Connolly, *Rev. Latinoamer. Quim. 12* (1981) 121.
[74] A. Matsuo, K. Atsumi, M. Nakayama, *Z. Naturforsch. B39* (1984) 1281.
[75] C.-L. Wu, Y. Asakawa, *Phytochemistry 27* (1988) 940.
[76] J. Beyer, H. Becker, M. Toyota, Y. Asakawa, *Phytochemistry 26* (1987) 1085.
[77] T. Hashimoto, M. Tori, Z. Taira, Y. Asakawa, *Tetrahedron Lett. 26* (1985) 6473.
[78] K. D. Barrow, D. H. R. Barton, E. Chain, F. E. Ohnsorge, R. P. Sharma, *J. Chem. Soc. Perkin Trans. 1 1973*, 1590.
[79] J. Spörle, H. Becker, H. P. Gupta, M. Veith, V. Huch, *Tetrahedron 45* (1989) 5003.
[80] A Matsuo, H. Nozaki, M. Nakayama, S. Hayashi, D. Takaoka, *J. Chem. Soc. Chem. Commun. 1978*, 198.
[81] P.-L. Chiu, G. W. Patterson, G. P. Fenner, *Phytochemistry 24* (1985) 263.
[82] H. Becker, G. Wurzel, *Pharm. Unserer Zeit 16* (1987) 152.
[83] H. Ando, A. Matsuo in M. Schultze-Motel (Ed.): *Advances in Bryology, Vol. 2*, J. Cramer, Vaduz 1984, p. 135.

[84] F. Nienhaus: *Viren, Mykoplasmen and Rickettsien* (UTB No. 1361), Ulmer, Stuttgart 1985, p. 16.
[85] H. Knoche, G. Ourisson, G. W. Perold, J. Foussereau, J. Maleville, *Science 166* (1969) 239.
[86] B. M. Hausen: *Allergiepflanzen, Pflanzenallergene*, Ecomed, Landsberg/Lech 1988, p. 127.
[87] Y. Asakawa in [10a], p. 371.
[88] K. Sakai, T. Ichikawa, K. Yamada, M. Yamashita, M. Tanimoto, A. Hikata, Y. Iyuin, K. Kondo, *J. Nat. Prod. 51* (1988) 845.
[89] H. Wagner: *Pharmazeutische Biologie, Bd. 2: Drogen und ihre Inhaltsstoffe, 4. Aufl.*, G. Fischer, Stuttgart 1988, p. 402.
[90] A. Matsuo, H. Nozaki, N. Kubota, S. Uto, N. Nakayama, *J. Chem. Soc. Perkin Trans. 1 1984*, 203.
[91] S. Huneck, K. Schreiber, *J. Hattori Bot. Lab. 39* (1975) 215.
[92] J. Gorham, *Phytochemistry 16* (1977) 249.
[93] G. Wurzel, H. Becker, T. Eicher, K. Tiefensee, *Planta Med. 56* (1990) 421.
[94] Y. Asakawa, H. L. J. Harrison, M. Toyota, *Phytochemistry 24* (1985) 261.
[95] Y. Asakawa, *Rev. Latinoamer. Quim. 14* (1984) 109.
[96] S. Huneck, *The Bryological Times 38* (1986) 1.
[97] R. Takeda, K. Katoh, *Planta 151* (1981) 525.
[98] R. Takeda, K. Katoh, *J. Am. Chem. Soc. 105* (1983) 4056.
[99] R. Takeda, K. Katoh, *Bull. Chem. Soc. Jpn. 56* (1983) 1256.
[100] S. Abe, Y. Ohta, *Phytochemistry 22* (1983) 1917.
[101] H. Rudolph, J. Samland, *Phytochemistry 24* (1985) 745.
[102] H. Becker in [10a], p. 339.
[103] E. Teuscher, *Pharmazie 26* (1973) 6.
[104] C. D. Knight, D. J. Cove, P. J. Boyd, N. W. Ashton in J. M. Glime (Ed.): *Methods in Bryology (Proc. Bryol. Meth. Workshop*, Mainz) Hattori Botanical Laboratory, Nichihan, Miyazaki, Japan 1988, p. 47.
[105] O. L. Gamborg, R. A. Müller, K. Ojima, *Exp. Cell Res. 50* (1968) 151.
[106] Y. Arai, T. Kamikawa, T. Kubota, J. Masuda, R. Yamamoto, *Phytochemistry 12* (1973) 2279; S. Huneck, K. Schreiber, *ibid. 16* (1977) 1013; T. Hashimoto, M. Tori, Y. Asakawa, *ibid. 27* (1988) 109.
[107] T. Eicher, K. Tiefensee, R. Pick, *Synthesis 1988*, 525.
[108] F. M. Hauser, S. A. Pogany, *Synthesis 1980*, 814.
[109] M. Günes, *Dissertation*, Universität des Saarlandes 1991.
[110] The 4-*O*-methyl ether of **14** is known as amorfrutin A and the corresponding methyl ether with a 3-geranyl side chain as amorfrutin B: L. A. Mitscher, Y. M. Park, A. Al-Shamma, P. B. Mudson, T. Maas, *Phytochemistry 20* (1981) 781.
[111] R. Dönig, *Diplomarbeit*, Universität des Saarlandes 1990.
[112] K. Tiefensee, *Dissertation*, Universität des Saarlandes 1988.
[113] R. Pick, unpublished results, Universität des Saarlandes 1989.
[114] M. Tori in [10a], p. 411.
[115] M. Toyota, M. Tori, K. Takikawa, Y. Shiobara, M. Kodama, Y. Asakawa, *Tetrahedron Lett. 26* (1985) 6097.
[116] G. Mezey-Vándor, M. Nógrády, V. P. Novikov, A. Wiszt, M. Kajtár-Peredy, *Liebigs Ann. Chem. 1989*, 401.
[117] M. Walter, *Dissertation*, Universität des Saarlandes 1990.
[118] M. Kodama, Y. Shiobara, K. Matsumura, H. Sumitomo, *Tetrahedron Lett. 26* (1985) 877.
[119] M. Kodama, Y. Shiobara, H. Sumitomo, K. Matsumura, M. Tsukamoto, C. Harada, *J. Org. Chem. 53* (1988) 72.
[120] Z. Dienes, M. Nógrády, B. Vermes, M. Kajtár-Peredy, *Liebigs Ann. Chem. 1989*, 1141.
[121] M. Nógrády, B. Vermes, M. Kajtár-Peredy, *Tetrahedron Lett. 28* (1987) 2899.
[122] A. Gottsegen, M. Nógrády, B. Vermes, M. Kajtár-Peredy, E. Bihátsi-Karsai, *Tetrahedron Lett. 29* (1988) 5039.
[123] Ring formation through modified Wurtz reaction is also possible; cf. [120].
[124] T. Eicher in [10a], p. 209.
[125] H. J. Laas, *Dissertation*, Universität des Saarlandes 1988.
[126] B. Albert, *Dissertation*, Universität des Saarlandes 1989.
[127] M. Ott, *Diplomarbeit*, Universität des Saarlandes 1990.
[128] K. Massonne, *Diplomarbeit*, Universität des Saarlandes 1987.
[129] M. Nakayama, S. Ohira, S. Shinke, Y. Matsushita, A. Matsuo, S. Hayashi, *Chem. Lett. 10* (1979) 1245.
[130] A. Speicher, *Diplomarbeit*, Universität des Saarlandes 1989.
[131] T. Aratani, Y. Yoneyoshi, T. Nagase, *Tetrahedron Lett. 1977*, 2599.
[132] A. Speicher, T. Eicher, unpublished results.
[133] S. Hayashi, A. Matsuo, T. Matsuura, *Tetrahedron Lett. 1969*, 1599; A. Matsuo, *Tetrahedron 28* (1972) 1203; J. D. Connolly, L. J. Harrison, D. S. Rycroft, *J. Chem. Soc. Chem. Commun. 1982*, 1236.
[134] M. Tori, T. Hasebe, Y. Asakawa, *Chem. Lett. 1988*, 2059; see also: K. G. Gerling, H. Wolf, *Tetrahedron Lett. 26* (1985) 1293.
[135] M. Herrmann, *Dissertation*, Universität des Saarlandes 1990.
[136] K. Massonne, *Dissertation*, Universität des Saarlandes 1990.
[137] R. C. Cambie, P. E. Craw, *J. Nat. Prod. 50* (1987) 948; Synthesis of the racemate: R. Baker, I. F. Cottrell, P. D. Ravenscroft, C. I. Swain, *J. Chem. Soc. Perkin Trans. 1 1985*, 2463.
[138] H. Hagiwara, H. Uda, *Bull. Chem. Soc. Jpn. 62* (1989) 624.
[139] H. Hagiwara, H. Uda, *J. Chem. Soc. Chem. Commun. 1987*, 1351.
[140] Y. Tamai, Y. Mizutani, H. Hagiwara, H. Uda, N. Harada, *J. Chem. Res. Synop. 1985*, 148.

The Bioinorganic Chemistry of Vanadium

By Dieter Rehder*

Vanadium is a trace element that plays an important, perhaps essential and general role in the regulation of enzymatic phosphorylations. Several forms of life, including the fly agaric toadstool (*Amanita muscaria*) and certain sea squirts (ascidians), are able to concentrate vanadium. In other organisms vanadium is part of the active site of some enzymes. Well-studied examples are the nitrogen-fixing bacterium *Azotobacter* and various seaweeds that use vanadate-dependent peroxidases to synthesize halogenated organic compounds. Despite its importance as a "biometal" both in primitive, prokaryotic organisms (*Azotobacter*) and in the highly organized ascidians, which represent an early stage in the evolution of vertebrates, the bioinorganic chemistry of vanadium is still in its infancy. Just as young, but undergoing explosive development, is the chemistry of model compounds for vanadium-containing biomolecules, a domain of the bioinorganic coordination chemist, who almost daily discovers compounds with new and surprising structural features. This article reviews this fascinating area of bioinorganic chemistry.

1. Introduction

Vanadium occurs with an abundance of 0.014% in the earth's crust and thus, though more widely dispersed, is as common as zinc, whose extensive biological function has been known much longer. The vanadium concentration in the oceans, where life evolved, is only 50 nM. However, some groups of aquatic organisms can accumulate vanadium. Among these are many members of an order of tunicates, the Ascidiacea (sea squirts), which concentrate vanadium to 0.15 M in specialized blood cells.[1] The first specific vanadate-dependent enzyme, a haloperoxidase, was isolated from the knobbed wrack (a marine brown alga).[2] The ability to accumulate vanadium is not restricted to marine life, however, as is shown by the discovery in lichen of a haloperoxidase with vanadium at the active site[3] and by the isolation of a vanadium compound of low molecular weight (amavadin) in the toadstool *Amanita muscaria* and other species of the genus *Amanita*.[4, 5] Above-average vanadium content is found in fossil matter[6a] such as crude oil, coal, and carbonaceous fossils, in bituminous rock, and in limestone sediments (cf. Table 1). The early work of *Treibs* showed[6b] that the vanadium found there is mostly in the form of vanadium porphyrins, which probably arose through secondary processes.

The biological significance of vanadium was recognized as early as 1904 through its fungostatic effect on yeasts.[7] The significant concentrations of vanadium in ascidians led shortly thereafter to the first proposals for its biological function.[8] *Henze*, who published his studies of vanadium in the blood of ascidians in 1911, assumed that "Hämovanadin" had an oxygen transport function. Although such a function was later refuted, there is still no consensus on the actual role of vanadium in ascidians. During the following decades, sporadic reports of possible biochemical functions for vanadium appeared. That vanadium is essential in chlorophyll synthesis[9] and in the growth of rats and chickens[10, 11] has been known since the beginning of the seventies. The inhibition of ribonuclease by vanadium was also reported during this period.[12] General acceptance of vanadium as a biometal was assisted by the discovery in 1977 that it inhibited the Na,K ATPase (sodium-potassium pump).[13] Since then several reviews on the "new biochemistry of vanadium" have appeared.[14–20] Only in recent years did vanadium become interesting to bioinorganic chemistry, when it became clear that this element is present at the active site of enzymes. Two such enzymes are known today: the above-mentioned haloperoxidases in sea algae and lichens[2, 3, 21] and the nitrogenases in the nitrogen-fixing bacterium *Azotobacter*, which incorporates vanadium only (instead of molybdenum) into the corresponding cofactor when molybdenum is deficient or after genetic manipulation.[22] Besides a Mo and V nitrogenase, an iron nitrogenase, free of these two metals, is often—but not always[23a]—coded in the nitrogen-fixing microorganism.[23b–d] The significant role that vanadium can play in the reduction of N_2 to NH_3 was already proved half a century ago by *Bortels'* comprehensive series of investigations into *Azotobacter*,[24] but was apparently forgotten thereafter.

Similar to molybdenum, vanadium assumes an exceptional position among the biometals in that both its anionic and

Table 1. Distribution of vanadium [a].

Sample	Concentration	Ref.
Seawater (Pacific)	1.6 $\mu g L^{-1}$; 35 nM	[27]
Fresh water	1.3 $\mu g L^{-1}$	[27a]
Carbon-containing sediments of marine origin (e.g., shale, limestone)	up to 100 $mg kg^{-1}$	[28a, b]
Basalt and igneous rock	150 $mg kg^{-1}$	[28c]
Coal, crude oil	up to 1 $g kg^{-1}$ [b]	[30]
Ascidians	up to 2 $g kg^{-1}$	
Other vertebrates	0.4 $mg kg^{-1}$	[32]
Cow's milk	0.2–10 $\mu g L^{-1}$	[33b]
Tissue (human)	0.1–1 μM	[34]
Invertebrates	0.5–2.5 $mg kg^{-1}$	[32]
Fly agaric (*Amanita muscaria*)	up to 1 $g kg^{-1}$	[4b]
Brown algae	2 $mg kg^{-1}$	[32a]
Other plant material	0.1–5 $mg kg^{-1}$	[28c, 32, 33a]

[a] Average values relative to dry weight (whenever applicable). [b] Some crude oils (e.g., Venezuelan petroleum) contain significantly more vanadium.

[*] Prof. Dr. D. Rehder
Institut für Anorganische und Angewandte Chemie der Universität
Martin-Luther-King-Platz 6,
W-2000 Hamburg 13 (FRG)

cationic forms can participate in biological processes. The anionic form, vanadate(v), strongly resembles phosphate; the inhibitory, stimulatory, and regulatory functions with respect to phosphohydrolases and phosphotransferases, as well as the interesting toxicological and pharmacological effects of vanadate, are probably attributable to this similarity. In three fundamental points, however, vanadate differs from phosphate: (1) At physiological pH values monovanadate exists in the diprotonated form, $H_2VO_4^{\ominus}$, in contrast to the monoprotonated form of phosphate, $HPO_4^{2\ominus}$, which has two negative charges. Furthermore, vanadate tends to form oligovanadates, although not at the usual physiological concentrations. (2) Vanadium shows a pronounced tendency to use its energetically favorable d orbitals to form compounds with coordination numbers 5, 6, and 7. With diols, for example, vanadium undergoes not only esterification but can also—in contrast to phosphate—extend its coordination geometry from a tetrahedron to a tetragonal pyramid or trigonal bipyramid.[25] (3) Vanadate is easily reduced under physiological conditions. In the oxidation states III and IV, cationic species are preferentially formed. Thus, vanadium can behave as a transition metal and, as such, replaces other metal ions in enzymes and enters into complex reactions with potential ligand systems. The formation of vanadyl porphyrins during the generation of fossil matter from plants and animals is an example of this; vanadyl porphyrins have also been identified in vivo.[26]

The biological function of vanadium is a result of these features, which I shall expand upon individually in Section 3. Besides the ability of vanadium to assume various oxidation states, its coordination chemistry plays a central role in the interaction with biomolecules. The challenge to the bioinorganic chemist lies in preparing model compounds and in characterizing both biogenetic and biomimetic vanadium compounds; this area will be covered in greater detail in Section 4. First, however, a few aspects of the aqueous chemistry of vanadium will be addressed in order to provide the prerequisites for understanding the role of vanadium in biological processes.

2. The Aqueous Chemistry of Vanadium

Of the common oxidation states of vanadium, only V^{III}, V^{IV}, and V^{V} are involved in physiological systems; V^{II} reduces water to hydrogen, as the compilation of standard electrochemical potentials[29] in Table 2 shows. V^{IV} is easily oxidized to V^{V} under aerobic conditions, possibly according to Equation (a).

$$4\,VO^{2\oplus} + O_2 + 2\,H_2O \longrightarrow 4\,VO_2^{\oplus} + 4\,H^{\oplus} \qquad (a)$$

More recent investigations indicate that autoxidation and formation of $O_2^{\ominus}$ (hyperoxide) must also be considered in neutral medium. Hyperoxide either exists alongside vanadate(v) or reacts further to give peroxovanadyl, $V(O_2)^{2\oplus}$.[31] On the other hand, V^{V} is easily reduced by organic matter to V^{IV}. V^{III} and V^{IV} are found in the vanadocytes of certain tunicates[35a,b] and V^{IV} is found in amavadin in *Amanita muscaria*.[4,36] XANES (X-ray absorption near edge structure) data suggest an oxidation state of between II and IV for vanadate-containing nitrogenases.[37] V^{V} is present in seawater, in the exoplasm of tunicates, and in vanadate-dependent peroxidases. The action of vanadium as a phosphate antagonist is directly attributable to V^{V} and probably also indirectly to the facile change to V^{IV}. The ions listed in Table 2, with the exception of $H_2VO_4^{\ominus}$, exist only in strongly acidic media; however, they can be stabilized by complexation even under physiological conditions. This is particularly true for $VO^{2\oplus}$; its stable complexes with proteins, for example, have formation constants of $10^7-10^9\ M^{-1}$.[38]

Table 2. Electrochemical potentials [a].

Redox pair	Standard potential [V]
$H_2VO_4^{\ominus} + 4H^{\oplus} + e \rightleftarrows VO^{2\oplus} + 3H_2O$	1.31
$O_2 + 4H^{\oplus} + 4e \rightleftarrows 2H_2O$	1.23
$VO_2^{\oplus} + 2H^{\oplus} + e \rightleftarrows VO^{2\oplus} + H_2O$	0.99; 1.016(2) [b]
$VO^{2\oplus} + 2H^{\oplus} + e \rightleftarrows V^{3\oplus} + H_2O$	0.34; 0.309(2) [b]
$V^{3\oplus} + e \rightleftarrows V^{2\oplus}$	−0.25
$NAD^{\oplus} + 2H^{\oplus} + 2e \rightleftarrows NADH + H^{\oplus}$ [c]	−0.34
$2H^{\oplus} + 2e \rightleftarrows H_2$; pH 7	−0.42

[a] If not otherwise indicated, the data are taken from standard tables. [b] In 1 M NaCl [30]. [c] NAD = nicotine adenine dinucleotide.

The V^{V} species present in aqueous medium, which depend on both the pH and the vanadium concentration, have been largely identified by potentiometric[39,40] and combined potentiometric/^{51}V NMR spectroscopic studies.[41] The regions in which the different vanadates exist within the pH interval 5–9 and at two total-vanadate concentrations, c(V),

Dieter Rehder, born in 1941 in Hamburg, studied chemistry in Hamburg from 1961 to 1967 (Ph.D. thesis, 1970, under the supervision of R. Nast). After a stay in Kingston, Jamaica (1972–1975; with the German Volunteer Service), he returned to Hamburg as "Hochschulassistent" and attained his Habilitation in 1979. He has been a full professor since 1984. His research programs encompass organometallic and hydrido compounds of the (early) transition metals, the inorganic biochemistry of vanadium, and magnetic resonance spectroscopy of metal nuclei.

are shown in Figure 1, together with the ^{51}V NMR spectrum at pH 7.6. In the more restricted physiological range (pH $= 7 \pm 1$) and at high enough $c(V)$, the species found are dihydrogen orthovanadate (V_1''), dihydrogen divanadate (V_2''), and *cyclo*-tetravanadate (V_4), -pentavanadate (V_5), and (at higher ionic strengths) -hexavanadate (V_6). A trivanadate appears not to be present.[41] At pH 6.3, the orange or yellow

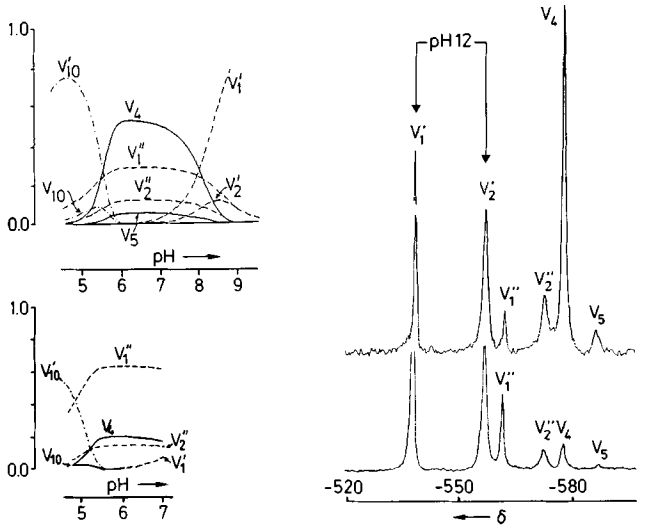

Fig. 1. Left: Regions in which vanadates exist in physiological pH range when the total concentration $c(V)$ is 1.25 mM (top) and 0.31 mM (bottom). In the former case the dominant species is $V_4O_{12}^{4\ominus}$ (V_4), in the latter $H_2VO_4^{\ominus}$ (V_1''). Right: This also becomes clear from the relative integral intensities of the ^{51}V NMR signals of the vanadates. The spectra were recorded at 94.7 MHz in H_2O/D_2O 2/1 (internal standard vanadate ($c(V) = 0.74$ M) at pH 12; 0.17 M NaCl (physiological ionic strength); 0.1 M Hepes buffer, pH = 7.6) for $c(V) = 1.5$ mM (top) or $c(V) = 0.37$ mM (bottom). At pH 12 and $c(V) = 0.74$ M, only V_1' and V_2' are observed. $V_1' = HVO_4^{2\ominus}$, $V_2' = HV_2O_7^{3\ominus}$, $V_2'' = H_2V_2O_7^{2\ominus}$, $V_5 = V_5O_{15}^{5\ominus}$, $V_{10} = V_{10}O_{28}^{6\ominus}$, $V_{10}' = HV_{10}O_{28}^{5\ominus}$. For further details on the left side of the figure, see [41a] and [41c].

(depending on the dilution) monohydrogen decavanadate (V_{10}') also occurs. This mixture of vanadates is often named metavanadate. At $c(V) < 10^{-4}$ M (e.g., in seawater), virtually the only species present is monovanadate, which undergoes a rapid protonation equilibrium [Eq. (b)].

$$H_2VO_4^{\ominus} \rightleftharpoons HVO_4^{2\ominus} + H^{\oplus} \qquad (b)$$

In contrast, exchange between vanadates of differing nuclearity is slow. The chemical shift of the ^{51}V NMR signal, $\delta(^{51}V)$, is dependent on the position of the equilibrium and therefore on pH according to Equation (c), which may be

$$pH = pK_a + \log(\delta_2 - \delta_{obs})/(\delta_{obs} - \delta_1) \qquad (c)$$

used to determine the pH of, for instance, biological systems [$\delta_1 = \delta(HVO_4^{2\ominus}) = -537.7$, $\delta_2 = \delta(H_2VO_4^{\ominus}) = -561.7$ (relative to $VOCl_3$), $pK_a(H_2VO_4^{\ominus}) = 8.16$[42]]. V^V occurs as orthovanadate, $VO_4^{3\ominus}$, above pH 12. (For information on the oxosulfidovanadates(V), which are of potential interest for the genesis of vanadium-containing nitrogenases, see Ref. [43].)

Peroxovanadate(V) has been mentioned in connection with therapies for cancer[44] and diabetes (see Section 3.1); furthermore, such species possibly play a role in the halogenation of organic compounds by vanadate-dependent peroxidases. In the pH range 5–9 the following anions were identified by Raman,[45a] ^{17}O NMR,[45b] and ^{51}V NMR[45] spectroscopy: *cis*-$[VO_2(O_2)_2(H_2O)]^{3\ominus}$, $[V_2O_3(O_2)_4]^{4\ominus}$ (or its protonated form), $[VO(OH)(O_2)_2(H_2O)]^{2\ominus}$, and $[VO(O_2)_2(H_2O)]^{\ominus}$ (formulated as in Ref. [45a]). The $\delta(^{51}V)$ values of the peroxo compounds lie between $\delta = -690$ and -760 and are thus clearly higher than those of the simple vanadates; all these compounds may therefore easily be observed in the same solution after it has been treated with H_2O_2.

Of special relevance to the phosphate/vanadate antagonism is the formation of the anions $H_xPVO_7^{(4-x)\ominus}$ ($x = 1,2$) and $HVP_2O_{10}^{4\ominus}$, which are analogous to pyro- and triphosphate. These mixed anhydrides have been identified in the pH range 6.7–8.0 by ^{51}V NMR spectroscopy and are more susceptible to hydrolysis into the individual components than divanadate by a factor of 10; however, they are 10^6 times more stable than pyrophosphate.[42a] The formation constant for the formation of $H_2PVO_7^{2\ominus}$ from hydrogen vanadate and hydrogen phosphate is 25 M^{-1}. In acid medium, furthermore, several "triphosphate complexes" of $VO_2^{\oplus}$ (e.g., $[VO_2(HP_3O_{10})]^{3\ominus}$) have been identified by spectroscopic means.[42b]

The free cations $[V(H_2O)_6]^{3\oplus}$, $[VO(H_2O)_5]^{2\oplus}$, and $[VO_2(H_2O)_4]^{\oplus}$ are of lesser importance, as they exist only in more strongly acidic medium. V^{III} forms a sparingly soluble precipitate of vanadium oxide at pH > 2.2. The blue cation $[VO(H_2O)_5]^{2\oplus}$ is in equilibrium with its deprotonated form $[VO(OH)(H_2O)_4]^{\oplus}$, which becomes the dominant species around pH 6. In addition, a dimer, probably $[\{VO(H_2O)_4\}_2(\mu\text{-}OH)_2]^{2\oplus}$, can be observed. In this pH range, however, the precipitation of sparingly soluble vanadyl hydroxide, $VO(OH)_2$, begins. Vanadate(IV) forms in strongly alkaline solution.

3. The Biological Role of Vanadium

3.1. Physiological Effects and Medical Applications

Vanadium poisoning is known to occur in particular by inhalation of vanadium-rich dust and its symptoms resemble those of influenza.[33b] But an etiological role in manic-depressive psychosis has also been attributed to vanadium.[33c] The MAK value (maximum workplace concentration—German standard) for V_2O_5 dust, which can occur especially in the vicinity of large-scale furnaces and has a direct toxicological effect on lung parenchyma, is 0.01 mg m^{-3}.[46] When vanadium is administered intravenously, the tolerance level is very low: although 5.6 mg kg^{-1} body weight can be well tolerated, 11.2 mg kg^{-1}, for example, leads to serious health disorders.[33b] The LD_{50} value in animal experiments is a few milligrams per kilogram.[47] Oral intake is less hazardous, mainly because only 2% of the vanadium is resorbed. Vanadium levels of 1 mg kg^{-1} in food are considered acceptable.[19] The bones, liver, and kidneys retain vanadium with a biological half-life of 20–100 h. The excretion takes place mainly through the urine,[33b] probably as V^{IV} coordinated, for example, to transferrin.

Many of the effects of vanadium are due to inhibition or stimulation of enzymes that participate in phosphate metabolism. This subject has been reviewed several times[15-19] and selected examples will be treated below. Not only monovanadate but also decavanadate and the oligovanadates which exist at physiological pH (Fig. 1) can bind to tissue, as is shown, for example, by the binding of vanadate to the Ca ATPase of the sarcoplasmic reticulum (SR).[48b] As a rule, the regulatory effect of vanadium slowly diminishes owing to its reduction to $VO^{2\oplus}$. V^{V} and V^{IV} (for which the effect is more pronounced) form complexes with a large number of biogenic ligands.[54a, b] Table 3 lists some formation constants. Some of these complexes can be reduced or oxidized reversibly. The redox potentials for selected examples show (Table 4) that a reduction from V^{V} to V^{IV} can take place under physiological conditions with, for example, NADH ($E^{\circ} = -0.34$ V) or glutathione ($E^{\circ} = -0.23$ V). Under aerobic conditions, $VO^{2\oplus}$ catalyzes the oxidation of NADH and NADPH via vanadium(v) intermediates and $O_2^{\ominus}$.[31] In oxidation state V or IV, vanadium binds to serum albumin[53b, 64-66] and, more efficiently, to transferrin[53, 67, 68] (the latter also coordinates V^{III}[69]). Vanadotransferrin probably is the actual form in which vanadium is transported in the more highly organized organisms. Vanadium enters into the cell cytoplasm as vanadate via the same channels through which phosphate is translocated; in erythrocytes the transport paths are the same as those for chloride and hydrogen carbonate.[70] Inside the cell, vanadate is slowly reduced by glutathione to $VO^{2\oplus}$, which can bind to the protein mantle of ferritins and thereby be temporarily "stored".[67]

Table 3. Formation constants $K[M^{-1}]$ of selected V^{IV} and V^{V} complexes with biogenic or related ligands.

Ligand	K [a]	Ref.
V^{V} (as $HVO_4^{2\ominus}$)		
Oxalate	13	[49a]
Lactate	0.54	[49a]
Salicylate	1.7	[49b]
Glycol	0.34	[49c]
Mannose	24	[50]
Ribose	230	[50]
Adenosine monophosphate	5.4–19.6 [b]	[51]
Uridine	130	[51]
Inosine	685	[52a]
Picolinate	200	[51]
H-Gly-His-OH	113	[52a]
H-Gly-Asp-OH	49	[52b]
H-Gly-His-Lys-OH	11	[52a]
Glutathione	$10^{4.2}$	[54a]
Glutathione disulfide	$10^{3.26}$	[55]
H-Gly-Gly-Gly-OH	200	[54b]
Ribonuclease T_1	145	[52a]
Acid phosphatase	$10^{4.8}$	[54b]
Serum albumin	$600-10^{3.3}$	[53b, 54a, 54b]
Serum transferrin	$10^{6.5}$	[53a]
V^{IV} (as $VO^{2\oplus}$)		
Phosphate	$10^{4.3}$	[54a]
Triphosphate	$10^{9.87}$	[57]
Adenosine monophosphate	$10^{5.1}$	[54a]
Adenosine triphosphate	$10^{5.9}/10^{6.7}$	[54a/57]
Creatine phosphate	$10^{3.6}$	[54a]
Glutamic acid	$10^{3.4}$	[54a]
Serine	$10^{5.7}$	[56a]
Alanine	$10^{6.9}$	[56b]
H-Gly-Gly-Gly-OH	$10^{4.6}$	[54b]
Ascorbic acid	$10^{3.3}$	[54a]
Citric acid	$10^{4.0}$	[54a]
Glutathione	501	[54a]
Serum albumin	$10^{3.1}$	[54a]

[a] The data hold for 1:1 complexes. Complexes of a different composition are in many cases also observed. [b] Dependent on pH (8.0–6.5).

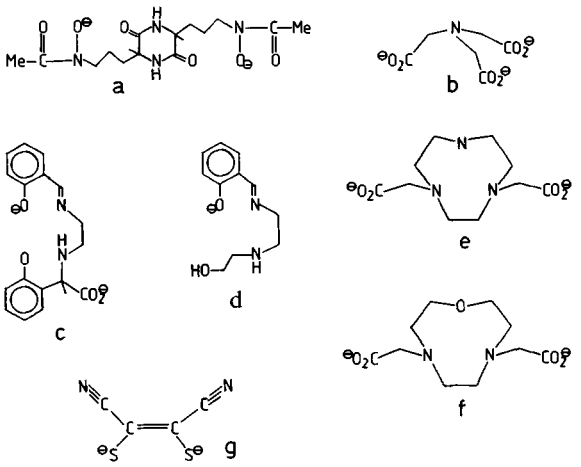

Table 4. Redox potentials of some V^{V}/V^{IV} pairs with organic ligands **a**–**g**.

Redox pair [a]	E° [V]	Medium	Ref.
$VO(L)OH + H^{\oplus} + e \rightleftharpoons VOL + H_2O$ L = rhodotorulate(2−), **a**	0.51	H_2O, pH 4–7	[58]
$VO_2L^{2\ominus} + 2H^{\oplus} + e \rightleftharpoons VO_2L(H_2O)^{\ominus}$ L = nitrilotriacetate(3−), **b**	0.105	H_2O, pH 6	[59]
$VOL + e \rightleftharpoons VOL^{\ominus}$, L = ehgs(3−), **c**	0.531	H_2O	[60]
	0.380	MeOH	[60]
	0.311	MeCN	[60]
V^{V}/VOH(L)acac, L = Hshed(1−), **d**	0.740	MeOH	[61]
$VOL^{\oplus} + e \rightleftharpoons VOL$, L = tcda(2−), **e**	0.827	MeCN	[62]
$VOL^{\oplus} + e \rightleftharpoons VOL$, L = docda(2−), **f**	1.022	MeCN	[62]
$VL_3^{\ominus} + e \rightleftharpoons VL_3^{2\ominus}$, L = dcdt(2−), **g**	0.85	MeCN	[63]

[a] The boldface letters refer to the structures shown above the table. Rhodotorulic acid is a naturally occurring dihydroxamic acid. Abbreviations: ehgs = *N*-[2-(*o*-salicylideneamino)ethyl](*o*-hydroxyphenyl)glycine; acac = acetylacetonate (1−); H_2shed = *N*-salicylidene-*N*'-(2-hydroxyethyl)ethylenediamine; tcad(2−) = 1,4,7-triazacyclononane-*N*,*N*'-diacetate; docda(2−) = 1-oxa-4,7-diazacyclononane-*N*,*N*'-diacetate; dcdt(2−) = 1,2-dicyanoethylene-1,2-dithiolate.

Vanadium compounds of therapeutic importance are listed in Figure 2. The unspecific, pharmacological effects of vanadium compounds include the lowering of cholesterol and glucose levels, a diuretic and natriuretic[71a] (weight-reducing) effect, the contraction of blood vessels, and the enhancement of the oxygen affinity of hemoglobin and myoglobin.[71b, c] The latter effect is probably due to the decrease in the concentration of 2,3-diphosphoglycerate in erythrocytes, a result of the vanadium-mediated stimulation of the 2,3-diphosphoglycerate phosphatase activity of phosphoglycerate mutase. This has led to the suggestion that vanadate be used for the symptomatic treatment of sickle-cell anemia.[71c]

Vanadium (e.g., vanadate, **1**, in Fig. 2) has a direct cardial effect, similar to digitalis. Possible reasons include the inhibition of the Na,K ATPase and the stimulation of adenylate cyclase[72] in particular, as well as the inhibition of the Ca ATPase of the sarcoplasmic reticulum.[17a] The mechanism

of inhibition of ATPases by vanadium is explained in Section 3.2. Noteworthy is the insulin-mimetic effect of **1**[73] and peroxovanadate(v)[74] (**2**), which is reminiscent of the role of chromium and the chromium-containing glucose tolerance factor. A corresponding effect of $VO^{2\oplus}$[75] is disputed.[17a] Diabetic rats which were fed vanadate in drinking water displayed a normal glucose concentration in the blood.[73c] The arguments for and against the various hypotheses for the insulin-like action of vanadate have been summarized.[76a] A plausible mechanism assumes that vanadate activates the phosphorylation of a tyrosine group of the insulin receptor (a tyrosine kinase). Recently an unspecific increase in the phosphorylation of protein tyrosine in the presence of vanadate was reported.[76b] But even a vanadylation of this tyrosine kinase by vanadate has been implicated in the insulin-mimetic effect. The observation that phenol and *N*-acetyltyrosine ethyl ester form esters with vanadate that are several orders of magnitude more stable than those with phosphate supports this hypothesis.[76c]

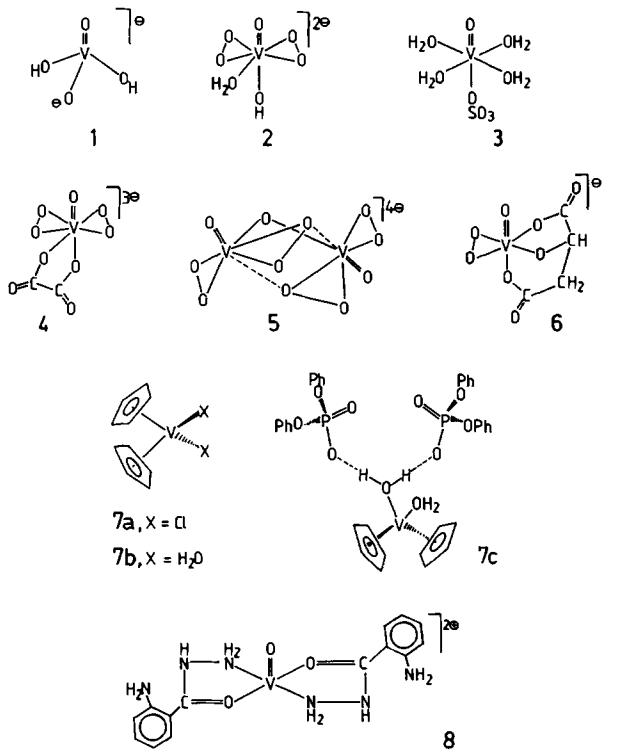

Fig. 2. Vanadium compounds which have been discussed in connection with therapeutic applications and have already proved to be active in animal tests. Compound **1** is a vasocontractor, lowers the cholesterol level, and has a diuretic and natriuretic effect; **1**, **2**, and **3** have insulin-mimicking functions; **3**–**7** show a carcinoma-inhibitive effect (**7a** is the administered and **7b** the active form). Compound **7c** is a model compound (simplified sketch) for the interaction of **7** with nucleotides. The hydrazine complex **8** has a higher activity against tuberculosis mycobacteria than the ligand itself, which is used in therapy [78d]. Compounds **1**, **3**–**5**, **6**, **7a**, and **7b** are also structurally characterized.

Several vanadium compounds have been studied with respect to their cytostatic activity. The peroxovanadate(v) complexes **4**–**6** show antitumor activity in certain forms of leukemia when administered at doses of 4.5–11.5 mg kg^{-1} body weight (i.e., just below the toxic level). An internal redox process in which V^{IV} and $O_2^{\ominus}$ are formed has been held responsible for this activity.[44] V^{IV}, administered as vanadyl sulfate (**3**) in the diet, inhibits in rats the formation of mammary carcinoma induced by methyl nitrosourea.[77a] This is interesting inasmuch as $VO^{2\oplus}$ is distinctly less toxic than V^{V}. The first step in the inhibition of carcinogenesis by vanadium could be its transfer as $VO^{2\oplus}$-transferrin to the neoplastic tissue, which is particularly rich in transferrin receptors.[67] Another interesting fact is that with bleomycin, an antibiotic used in cancer chemotherapy, $VO^{2\oplus}$ forms a stable complex,[77b] which may be considered a "supercancerostatic" agent.

A bifunctional complex is also formed between the antitumor antibiotic anthracycline and vanadocene dichloride (**7a**).[77c] Complex **7a**, like other cyclopentadienyl complexes of transition metals, has long been regarded as a potential cytostatic.[78a,b] Under physiological conditions, **7a** forms the aqua complex **7b**, analogous to cisplatin. With the phosphate groups of nucleotides it forms labile outer-sphere complexes with V–P distances of around 600 pm (calculated from ^{31}P NMR data), in good agreement with the results from the X-ray diffraction analysis of the model compound **7c** (Fig. 2).[78c] The formation of a labile complex between the stable complex **7b** and nucleotides contrasts with the behavior of cisplatin, which forms a stable bond to the endocyclic N atoms of the nucleotide bases. Moreover, cisplatin influences the hydrogen bonding between base pairs of DNA, whereas **7b** does not.

3.2. Functional, Unspecific Vanadium Compounds

3.2.1. The Interaction between Vanadate and Enzymes

Inorganic vanadate ($V_i = H_2VO_4^{\ominus}$) can probably be assigned an exogenic regulatory function with respect to enzymes that are involved in the widest sense in phosphorylations. In the previous sections this aspect has been mentioned repeatedly; I intend now to examine well-studied examples more closely. At the available concentrations of 10^{-6} to 10^{-7} M, both exogenic vanadate(v) and intracellular $VO^{2\oplus}$ are able to enter into bonding interactions with numerous biological molecules. Examples are phosphoglucomutase,[54c] alkaline and acid phosphatase, oligopeptides, and enzyme substrates such as citrate, malate, and glycerate.[54a] Reports have also appeared on the in vitro inhibition of enzymes by di-[79a] and tetravanadate[79b] at higher (toxic) concentrations. V^{IV} can also function as an inhibitor of, for example, glucose-6-phosphate dehydrogenase from baker's yeast[79c] and the ATPases of skeletal muscle membrane.[79d] As a rule, however, the slow reduction of V^{V} to V^{IV} in cells, which *Willsky* et al. studied in vivo for *Saccharomyces cerevisiae* (brewer's yeast) using ^{51}V NMR and ESR spectroscopy,[80a–c] is regarded as a detoxification process.

A long-known and thoroughly studied example of enzyme inhibition is the blocking of the Na-K pump (Na,K ATPase) by vanadate.[13, 16, 79e–g, 81] The Na-K pump transports $Na^{\oplus}$ out of and $K^{\oplus}$ into cells. This is an active translocation; the energy required is provided by the hydrolysis of ATP to ADP and phosphate ($P_i = HPO_4^{2\ominus}$). The bond breaking (and the accompanying ion transport) is catalyzed by an

ATPase that is an integral part of the cell membrane and that is active only in the presence of $Mg^{2\oplus}$. The ATPase can exist in two different conformations, E_1 and E_2, which are sensitized for the acceptance of $Na^{\oplus}$ and $K^{\oplus}$, respectively. These processes are represented in Figure 3. During the change from E_1 to E_2 the enzyme is phosphorylated [E_1(P)]. After the release of P_i, vanadate inhibits the enzyme by bonding to the vacated pocket to give [E_2(K, V, Mg)]. Vanadate is very tightly bound: the reverse reaction, [E_2(V)]$\rightarrow E_2 + V_i$, takes place at a rate of 0.32 h^{-1}.[81a, b] The complex formation constant K is 2.4×10^8 M^{-1}.[81c] There exists another coordination possibility with lower affinity ($K = 1.9 \times 10^6$ M^{-1}), which plays no role in inhibition. The reason for the tight bond may be that vanadate forms, in contrast to phosphate, stable five-coordinate complexes, in this case a bidentate coordination with the carboxylate group of an aspartate residue. $H^{\oplus}$-translocating ATPases for which no E(P) transition state has been found are insensitive to vanadate. Desferrioxamine B, a tris(hydroxamate), can rapidly reactivate vanadium-inhibited ATPases; vanadate forms a stable complex with this siderophore.[80d]

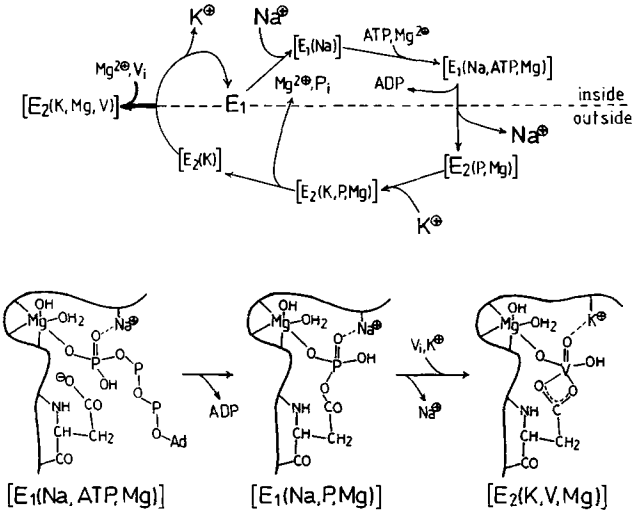

Fig. 3. Top: Schematic representation of the transport of $Na^{\oplus}$ and $K^{\oplus}$ (coupled to the hydrolysis of ATP) through the cell membrane and the inhibition of this process by vanadate(v). E represents the enzyme ATPase. The scheme is based on [80c]. Bottom: The inclusion of vanadate into the enzyme is represented in a simplified manner insofar as the binding site for vanadate is not identical with that of highest affinity for ATP. $V_i = H_2VO_4^{\ominus}$, $P_i = HPO_4^{2\ominus}$.

Vanadate(v) is also an effective inhibitor of ribonucleases. Well-investigated examples include RNase A from bovine pancreas[82] and RNase T_1 from the mold *Aspergillus oryzae*.[52a, 83, 84] RNase T_1 catalyzes the specific hydrolysis of the phosphodiester bonds of RNA at the 3′ position of guanosine. As in other enzymatic cleavages of the P–O bond, the transition state postulated is a pentavalent phosphorus in trigonal-bipyramidal geometry (cf. Fig. 4a).[83] The function of vanadate in this inhibition has been traced to the blocking of the recognition site of the enzyme for the substrate (RNA). In the case of RNase T_1, this site contains histidine, arginine, and glutamate. Model studies on histidine and glutamate with di- and tripeptides showed that an interaction between vanadate and the peptide bond occurs.[52] RNase T_1

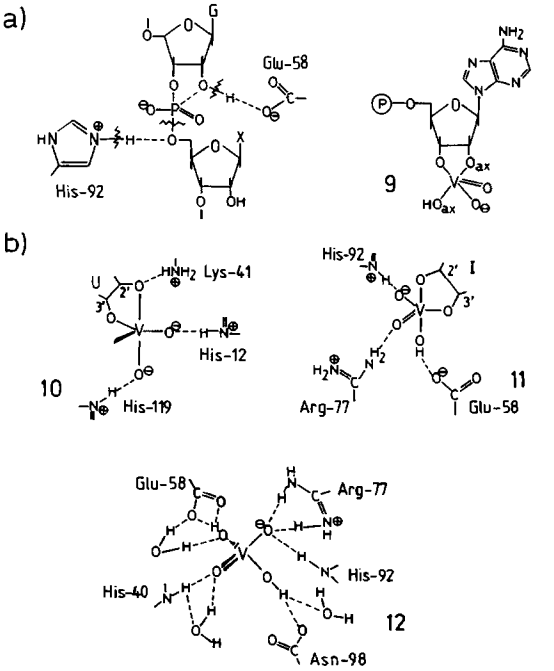

Fig. 4. Coordination of vanadate to ribonucleases. **a)** The (postulated) transition state for the enzymatic phosphodiester cleavage [83b]. The cleavage occurs at the sites marked with zigzag lines. Dashed lines are bonds after cleavage. Compound **9** is a vanadate–AMP complex that models the transition state [50, 51]. **b)** Schematic representation of the complexes formed from vanadate and RNase A + uridine (**10**) [82b], RNase T_1 + inosine (**11**) [52a], and RNase T_1 (**12**) [84].

forms a relatively weak complex ($K = 145(30)$ M^{-1}) with vanadate. An increase in the stability is observed in the ternary complex, not only for RNase T_1/vanadate/inosine ($K = 1.5 \times 10^5$ M^{-2}),[52a] but also for RNase A/vanadate/

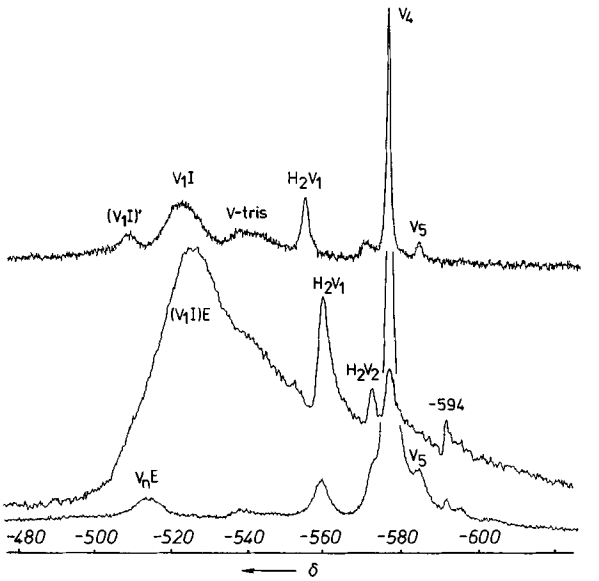

Fig. 5. 94.7-MHz ^{51}V NMR spectra of vanadate in ribonuclease-containing solutions (Tris buffer, pH 7.8; Tris = tris(hydroxymethyl)aminomethane). The broad signals are from the complexes vanadate/RNase T_1 (V_1E; cf. **12** in Fig. 4), and inosine/vanadate/RNase T_1 ($(V_1I)E$; cf. **11** in Fig. 4); the signal at $\delta = -541$ is from a complex of vanadate and Tris. $(V_1I)'$ is a ternary complex formed between vanadate, inosine, and Tris [184]. The middle spectrum reflects the significant increase in complexation of monovanadate in ternary compared with binary systems (cf. [52a]). For the abbreviations for the sharp resonances, which correspond to free vanadates, see the legend of Fig. 1. Concentrations: $c(V) = 12.8$ mM, c(enzyme) $= 5.5$ mM, c(inosine) $= 10.9$ mM.

uridine.[82] The characteristics of these complexes correspond to those of binary complexes of vanadate with nucleosides or nucleotides (compare compound **9** in Fig. 4 and the ^{51}V NMR spectra in Fig. 5), for which it is assumed that cyclic ester formation involves coordination of vanadate across the 2′ and 3′ positions of ribose with formation of a trigonal-bipyramidal environment about V^V.[50, 51] That this coordination geometry also occurs in the case of ternary complexes with RNase A and RNase T_1 (Fig. 4b, **10** and **11**) is supported by neutron diffraction[82b] and ^{51}V NMR studies.[52a] Recently an X-ray diffraction analysis of the binary complex of vanadate with RNase T_1 showed that tetrahedral $H_2VO_4^{\ominus}$ is hydrogen-bonded into the active site of the enzyme.[84]

3.2.2. Vanadium in Photosynthesis

That vanadium is also an essential trace element for green plants was known as early as 1953.[85] Vanadate increases oxygen production by stimulating photosystem I in the chloroplasts of single-cell green algae (*Chlorella, Scenedesmus*).[85, 86a] Simultaneously, the production of biomass and chlorophyll (and other leaf pigments) increases.[9b, 14, 86] It is particularly noticeable that the stress symptoms in algae cultivated under iron-deficiency conditions can be suppressed completely by vanadate. This led to the suggestion that vanadium centers might be involved in redox catalysts.[86a] Better documented is the function of vanadium in chlorophyll production: vanadate and V^{IV} (perhaps only the latter, since reduction of vanadium is probable) are capable of a nonenzymatic catalysis of the formation of δ-aminolevulinic acid (ALA).[86b] ALA plays a central role as a precursor in the biosynthesis of chlorophyll. It is formed from 4,5-dioxyvaleric acid (DOVA) and alanine (Ala) by transamination in the presence of pyridoxal phosphate (PLP). Alanine is transformed into pyruvate (PA) [Eq. (d)]. A Schiff base acts as

$$\text{Ala} + \text{DOVA} \xrightarrow{\text{PLP, } V_i} \text{ALA} + \text{PA} \qquad \text{(d)}$$

intermediate in this transamination and the formation of a complex at least with V^{IV} of type **13** is considered responsible for the efficacy of vanadium.[86b]

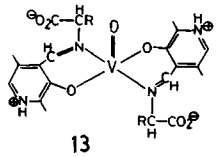

13

Besides stimulation of photosynthesis, vanadium can also inhibit it under certain circumstances. This is suggested by studies on the deactivation of the carboxylase activity of ribulose-1,5-diphosphate carboxylase/oxygenase in the presence of vanadium during irradiation.[87a] The enzymatic carboxylation of ribulose-1,5-diphosphate is the initial step in carbon fixation. The deactivation is attributed to photooxidation of serine by vanadium in the active site of the enzyme.

3.2.3. Vanadium in the Blood of Ascidians

Ascidians (sea squirts), which are sessile organisms belonging to the tunicates (Urochorda), are found worldwide in the tidal zones of oceans. Many of them are capable of concentrating vanadium to 10^7 times the level in seawater in specialized blood cells, the vanadocytes. Other types accumulate iron instead of vanadium. The vanadium concentration in the vanadocytes is 0.15 M; in special vanadium-containing vacuoles in the vanadocytes, the vanadophores, it can reach 1 M. The vanadium is absorbed as vanadate(v) into the exoplasm. There are at least five morphologically distinguishable types of vanadocytes, which correspond to different maturation stages and take up vanadium to different extents (the highest concentration of V is found in the so-called signet-ring cells). Depending on the ascidian suborder, chiefly V^{IV} (Aplousobranchia) or V^{III} (Phleobranchia) is present.[35a, c] This view is supported by both magnetic[87b] and chemical evidence. For instance, complexes **14**[35a] and **15**[35c] (Fig. 6) have been identified after external application of bipyridine or acetylacetonate.

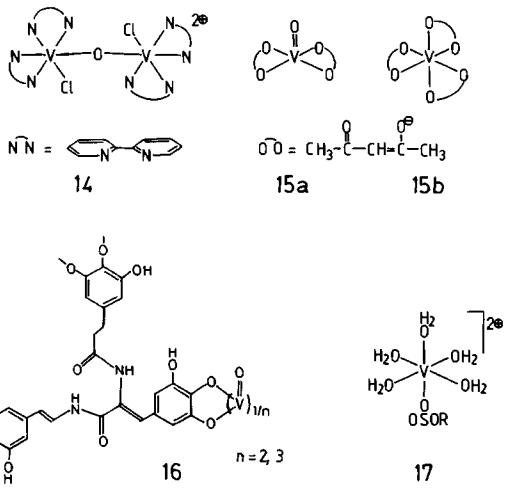

14 15a 15b 16 17

Fig. 6. Vanadium complexes considered in connection with the vanadocytes of ascidians. Compounds **14** and **15** could be identified when the vanadocytes were exposed externally to bipyridine or acetylacetonate [35a]. The V–O–V angle in **14** is 173.5°; the two halves of the molecule are twisted 61.6° relative to one another [35c]. Compound **16** possibly plays a decisive role in the construction of the tunicae of ascidians [1] (for catecholate complexes as models, see **58** and **59** in Fig. 13, Section 4.2). Compound **17** can occur in concentrated sulfuric acid [89b].

Even the more recent investigations on ascidians[35, 88, 89a] have not been able to answer two of the most interesting questions on the biochemistry of vanadium. They involve, on the one hand, the function of vanadium and, on the other, its coordination environment and the closely related question of the pH within the vanadophores. Among the functions mentioned are participation in the construction of the tunica, toxicity for foraging enemies, a store for redox equivalents, and an antidote against oxygen starvation.[88a] At present the most popular is the first function, according to which vanadium acts as a mediator (in the sense of a template effect) in the construction of the polymeric structure of the material of the tunica. This thesis is supported by the fact that the pigments (the so-called tunichromes)[89a, b] in certain

vanadocytes (the morula cells) also participate in the construction of the tunica. Tunichromes are hydroxy-DOPA-containing di- and tripeptides (DOPA = 3,4-dihydroxyphenylalanine) that form very stable complexes such as **16** with $VO^{2\oplus}$.[11] Another $VO^{2\oplus}$-coordinating compound isolated from the vanadocytes, vanadobin, contains a reducing sugar, but is otherwise not further characterized.[88b, 89c] A further possibility is the coordination of $VO^{2\oplus}$ or V^{III} to a glycoprotein that corresponds to ferreascidin. Ferreascidin (M = 10000 g mol^{-1}) contains a high percentage of tyrosine and DOPA, which complex Fe^{III} in iron-accumulating ascidians[90] and are also good ligands for vanadium.

Whether vanadium in the vanadocytes or vanadophores is in fact bonded to tunichrome, vanadobin, or another organic ligand is not definite and is tied up with the unsolved problem of pH within the cell structures, pH values of between 1.8 and 7.2 have been measured by diverse methods and in a great variety of cell fractions. Only with reference to the literature (e.g., Refs. [35a, b] and [88b]) can one sift through the data. Naked vanadium(III) can exist only below pH 3 (cf. Section 2); when the acid medium is sulfuric acid it occurs as $[V(H_2O)_5OSO_3]^{\oplus}$ (perhaps also as $[V(H_2O)_5OSO_2R]^{2\oplus}$;[89b] **17** in Fig. 6). This is the form postulated on the grounds of, among others, EXAFS (extended X-ray absorption fine structure)[91] and ESR studies.[92a, b] Recent experiments[92c] on *Ascidia ceratodes*, in which the distribution of ^{14}C-labeled dimethylamine and the acid 5,5-dimethyloxazolidine-2,4-dione between the intra- and extracellular blood-cell matter was analyzed, gave a pH of 7.1(2) for the cytoplasm of morula cells and 5.0(2) for the vacuoles. Since between 50 and 90% of vanadium is present as V^{III} in these cases, a stabilization by complexation must take place.

3.3. Coordination Compounds with Biogenic Ligands

3.3.1. Vanadyl Porphyrins in Fossil Matter

The high vanadium content (up to 4%) in petroleum, oil shales, bituminous limestone, and similar materials of marine origin,[28a, b, 93a, 94, 95] in which the organic fractions arise as a rule from the fossilization of planktonic organisms and/or bacterial activity in the initial stages of fossilization, raised early on the question of the source of the vanadium.[6] Quite high vanadium contents are also measured in fossilized terrestrial plants (e.g., between 0.4 and 0.7% in fossilized mosses[95a]). Regardless of the origin, vanadium occurs in such material chiefly in the form of vanadyl ($VO^{2\oplus}$) porphyrins,[38, 93a, 94b] which only occur in the smallest quantities in living organisms.[26b, 96] Consequently, vanadium must have been incorporated into the porphyrins through secondary processes (transmetalation). Although the so-called geoporphyrins bear, in the main, no simple biosynthetic relationship to the naturally occurring porphyrins, chlorophyll (e.g., from green algae and chlorophyll-containing bacteria) was presumably the original porphyrin compound.[93a, 97] This assumption is supported by the isolation and structural characterization of vanadyl porphyrin **18**.[93b] Whether the vanadium is of biotic or abiotic origin is an open question. In view of the information in the previous section, a biotic origin for at least part of the vanadium may be considered likely. But plausible arguments have also been aired for abiotic sources, especially from volcanic ashes.[94a]

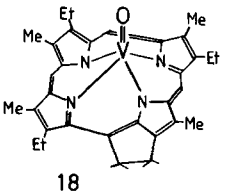

18

The generally accepted assumption that vanadyl porphyrins are indigenous components of petroleum has recently been opposed by the suggestion that these pigments were extracted out of the sedimentary stratum (e.g., shaley limestone) by the percolation of younger petroleum fractions and thereby concentrated in the petroleum.[95b] This migration theory was also advanced earlier by *Goldschmidt*.[6a]

3.3.2. Nucleotides, Nucleosides, Sugar, and Phosphate

The coordination behavior of vanadium with respect to these molecules has potential significance in connection with competitive processes in the regulation of the activity of, for example, the ATPases and ribonucleases (Section 3.2.1) as well as with regard to the cancerostatic action of vanadate (Section 3.1). Both V^{V} and V^{IV} are capable of reacting with the phosphate groups and/or the sugar alcohol groups of nucleotides. The complexes formed with vanadate(v) may be conceived as mixed anhydrides or esters of the hypothetical orthovanadic acid. The nitrogen functions of the bases are coordinated only in exceptional cases.

Sugars and nucleosides react with vanadate(v) to form cyclic esters, which are derived from mono- and divanadate and in which the vanadium is probably coordinated in a trigonal-bipyramidal fashion. With nucleosides, bonding takes place with the hydroxyl groups at C2′ and C3′ of ribose and leads to stable five-membered ring chelates. Examples are the esters **19** and **20**.[50a, 51, 52a, 82b] β-Mannopyranoside forms the bicyclic ester **21** with vanadate.[50a]

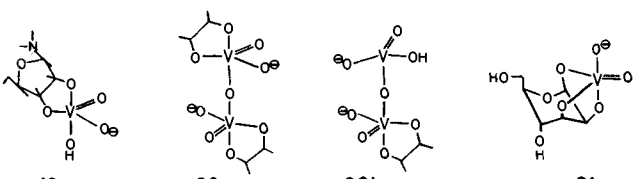

19 20a 20b 21

Nucleotides can also bind to vanadate through their phosphate residues. AMP reacts in this way with $H_2VO_4^{\ominus}$. In addition to compounds of type **19** (cf. also **9** of Fig. 4) and **20a**,[51] principally the mixed anhydrides "AVP" (**22**) and "AV_2P",[50a, 51] analogous to ADP and ATP, are formed. These undergo rapid exchange equilibria with their components AMP, $H_2VO_4^{\ominus}$, and $H_2V_2O_7^{2\ominus}$.[51] Similar mixed anhy-

drides are also formed with ribose 5-phosphate[50b] and phosphate itself[42] (Section 2).

The formation constants for 1:1 complexes of V^V with nucleotides are of an order of magnitude between 1 and $10^3\ M^{-1}$; their existence has been established chiefly by spectrophotometric, potentiometric, and ^{51}V NMR spectroscopic techniques. $VO^{2\oplus}$ shows a more pronounced tendency to coordinate such ligands (cf. Table 3), so that in many cases complexes could be isolated,[57, 98a-c] even if not characterized by X-ray structure determination. Structure proposals in

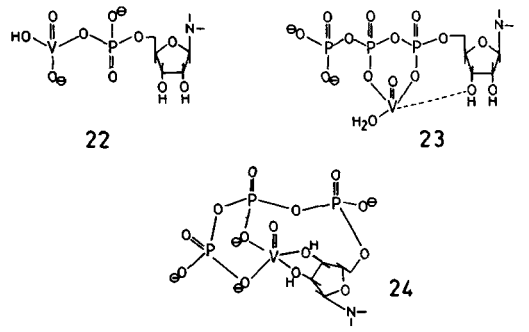

these cases are also based on spectroscopic data.[57, 98c, d, 99] $VO^{2\oplus}$ forms 1:1 compounds[57] in acid medium with triphosphate and a blue 1:1 complex in the acidic to neutral region with ATP, in which the vanadyl ion probably bonds to two oxygen atoms of the triphosphate residue as well as to one or two hydroxyl groups of ribose (**23** and **24**).[99]

3.3.3. Amavadin—a Vanadium Compound from Fly Agaric

The concentrations of vanadium in some types of *Amanita* and related fungi[5] are remarkably high, whereby fly agaric (*Amanita muscaria*) contains by far the highest concentration (up to $325\ mg\,kg^{-1}$ dry weight), mainly in the bulb. Isolated from this toadstool is a vanadium(IV) compound of exceptional stability, amavadin, for which no biological function is known. As the compound is reversibly oxidizable (E° in $H_2O = 0.78$ V), a function as redox catalyst is conceivable.[36b] Amavadin was originally formulated as the pentacoordinate vanadyl complex $[VO(H_2L)_2]$ (**25**) with H_3L = *N*-hydroxy-2,2′-iminodipropionic acid.[100a] Recently the composition $[VL_2]^{2\ominus}$ (**26**) was assigned to it, where L

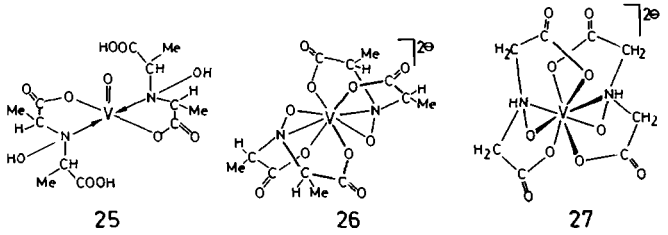

is coordinated through the hydroxylamido function and both carboxylate functions according to spectroscopic evidence.[36c] The argument presented for structure **26** rests partly on the lack of a short V=O bond in the EXAFS spectrum.[100b] The bond lengths for the V=O group lie typically between 155 and 165 pm, but can also be stretched up to 180 pm as in complex **61a** (Fig. 13).[101] The structure proposal **26** is supported by X-ray diffraction analysis of the complex **27**, which contains the very similar ligand *N*-hydroxyiminodiacetate.[102]

3.3.4. Vanadate-Dependent Haloperoxidases from Sea Algae and Lichen

Vanadate-dependent nonheme bromo/iodoperoxidases (V-PO) were discovered in 1983 by *Vilter* in the knobbed wrack (*Ascophyllum nodosum*)[2] and later, especially by the research group of *Wever* in Amsterdam, not only in *Ascophyllum*[21a, 103a, b] but also in other marine brown algae (*Laminaria* and *Chorda*),[21b, c] in marine red algae (*Ceramium, Corallina*),[21d, 103c, d] and in a terrestrial lichen (*Xanthoria parietina*).[3] An overview of the state of the investigations to 1987 is given in Ref. [104]. The best-studied isoenzyme from *A. nodosum* has a molecular mass of $105\,000\ g\,mol^{-1}$. Conspicuously high (ca. 25%) is the content of acidic amino acids. In its active state V-PO contains two V^V per molecule.[66] It is not known whether the two vanadium centers cooperate. The holoenzyme can be rendered inactive by dialysis against EDTA/citrate buffer (EDTA = ethylenediaminetetraacetate(2−)) and the activity restored with $H_2VO_4^\ominus$. Reduction of V^V to V^{IV} by dithionite also diminishes the enzyme activity. V-PO catalyzes the bromination and iodination of organic substrates by H_2O_2 (or peroxides) in the presence of inorganic bromide or iodide according to Equation (e).

$$RH + X^\ominus + H_2O_2 + H^\oplus \longrightarrow RX + 2H_2O \qquad \text{(e)}$$

The process possibly involves a hypohalite intermediate, which acts either directly or via HOX as the actual halogenating agent.[103e, f] In favor of such a mechanism is the V-PO-catalyzed, in vitro bromination of barbituric acid[103g] and the in vitro formation of hypoiodite from iodide and peroxovanadium(V).[105] A hypohalite intermediate is also likely when one considers that disproportionation of H_2O_2 to O_2 and H_2O is catalyzed by V-PO only in the presence of $Br^\ominus$ or $I^\ominus$.[106]

As many of the often quite complicated organic halogen compounds found in seaweeds exhibit antibiotic activity, it is generally suspected that vanadate-dependent peroxidases (and also their "normal" companion peroxidases) from the algae have a function, among others, in counteracting bacterial attack. As sea algae also produce considerable amounts of simple, volatile brominated hydrocarbons (e.g., $CHBr_3$), and indeed in quantities equal to the industrial production (ca. 10^4 tons per year), a geological and topically significant role in the regulation of the stratospheric ozone layer may be attributed to them.[108]

Ideas about the coordination environment around vanadium have been deduced from ^{51}V NMR,[66, 107] X-ray absorption (XAS),[109, 110] ESR,[111] and electron spin echo envelope modulation (ESEEM) spectra,[112] both on the native V^V-PO (XAS, Fig. 7, top, and NMR) and on the species obtained by reduction with dithionite, V^{IV}-PO (XAS, ESR,

ESEEM). Common to all suggestions (**A**, **B**, and **C** in Fig. 7, bottom) is a coordination number of at least 5 for vanadium, the presence of a vanadyl group, and an environment of ligands with mainly *O*-ligands as donor groups. Substrates such as halide ($Br^{\ominus}$, $I^{\ominus}$) probably cause an increase in coordination number,[66, 107] while reduction causes a decrease.[110] Candidates for oxygen-containing functional groups are carboxylate residues of glutamate or aspartate and OH groups of tyrosine or serine. The participation of esterlike bonds is suggested by the short V–O bond length of 172 pm, which was found by XAS in the EXAFS region for one of the V–O bonds in native V-PO[109a] (**A** in Fig. 7).

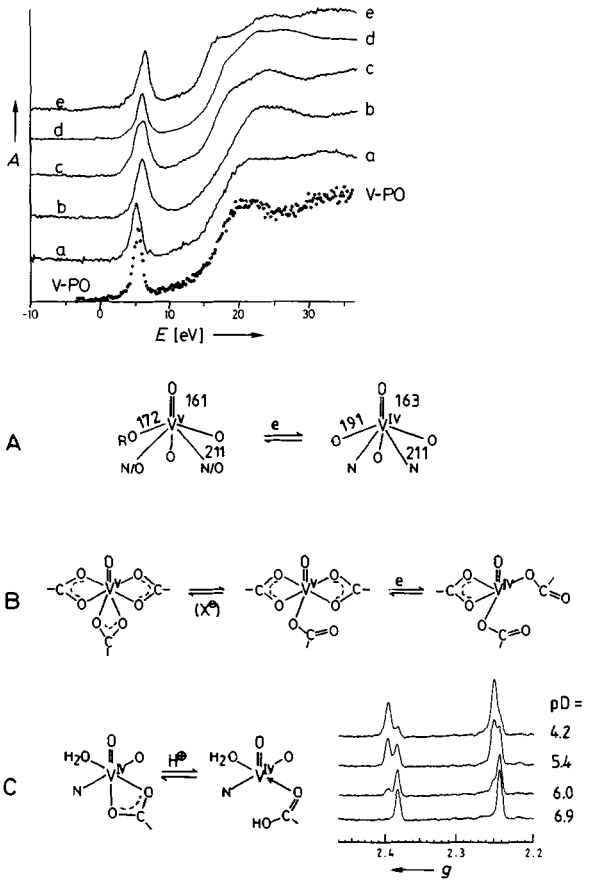

Fig. 7. Top: 2.5-GeV XAS spectra (XANES region) of vanadate(v) haloperoxidase (V-PO) from *Ascophyllum nodosum* (bottom spectrum) and some model compounds ($a = [VO(O_2)_2(oxalate)]^{3\ominus}$, $b = [VO(O_2)(oxalate)_2]^{3\ominus}$, $c = [VO_2(oxalate)_2]^{3\ominus}$, $d = [VO(O_2)(H_2O)dipicolinate]^{\ominus}$, $e = [VO_2(edta)_2]^{3\ominus}$ [110]. The zero of the energy scale is defined by vanadium metal (5465 eV absolute). The position and half-height width of the white band ("1s→3d"), the uniformity of the rise in the absorption edge, and the position of the K edge (1s→4p) of the spectrum of V-PO agree well with the corresponding characteristics of the oxo-peroxo-oxalato complexes. Bottom: Structural proposals for the prosthetic group in vanadate-dependent peroxidases, deduced from spectroscopic investigations. **A** based on EXAFS [109], **B** on XANES [110] and ^{51}V NMR [66, 107], and **C** on ESR [111] and electron spin echo [112] investigations on reduced peroxidase. The pD dependence for the $m_I = -7/2$ and 5/2 lines of the ESR signal for the holoenzyme in D_2O reveals a change in the coordination sphere of vanadium, which can be traced to a protonation/deprotonation equilibrium. The spectrum is reproduced from [111] with permission. With regard to **B**, compare also the model compound **48** in Fig. 12, Section 4.2.

Such a short single bond length is typical for vanadyl esters.[113] Furthermore, ESR studies of reduced V-PO show that both a protonatable ligand (Glu, Asp, or His) and H_2O are involved in the coordination to vanadium[111] (compare the pH dependence of the *g* value for the $m_I = -7/2$ resonance in the ESR spectrum, Fig. 7, **C**). The coordination of an *N*-donor ligand (histidine), at least in V^{IV}-PO, is suggested in particular by an ESEEM study.[112]

3.3.5. *Vanadium Nitrogenase*

Besides the usual molybdenum nitrogenase (Mo-Nase), another with vanadium as active center (V-Nase) was discovered only a few years ago in the nitrogen-fixing bacteria *Azotobacter chroococcum* and *A. vinelandii*. It is activated by molybdenum deficiency.[22] Also, certain mutants of *Azotobacter*, in which the genetic information for encoding Mo-Nase is missing, can reduce atmospheric nitrogen with V-Nase.[23a, 114, 115] Other microorganisms besides *Azotobacter* are capable of synthesizing the alternative nitrogenase, namely the cyanobacterium *Anabaena variabilis*[116] and probably also *Clostridium pasteurianum*.[117] It is interesting that, when it grows in Mo-deficient media, the hydrogen bacterium *Xanthobacter autotrophicus* accumulates vanadium as well. As the ESR spectra show, however, V^{IV} is not a component of a nitrogenase in this microorganism.[118]

The progress of the research into V-Nase has been summarized recently in two review articles.[119] The enzyme resembles its Mo analogue in the construction and structure of the prosthetic groups, as well as in its functions: It consists of a FeV protein with a molecular mass of 240 000 g mol^{-1} (six subunits as against four in the Mo-Nase)[23a, 115] and an

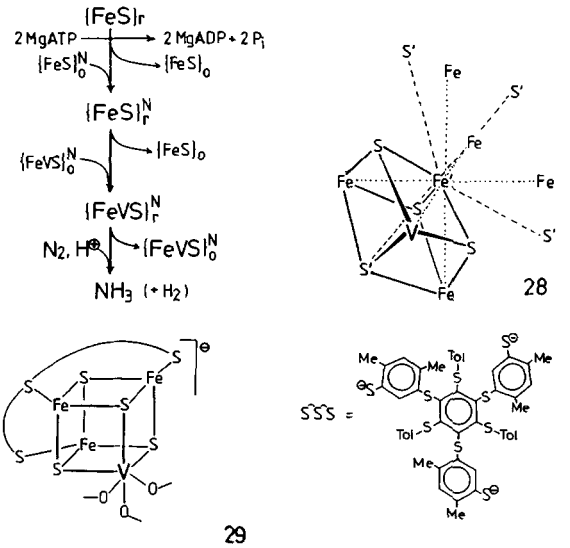

Fig. 8. Simplified representation of the electron-transfer processes during nitrogen fixation by vanadate nitrogenase (top left) as well as of the FeV cofactor (**28**, according to [124a]) and of the model compound **29** for the VFe_3S_4 cluster in the cofactor [125]. {FeS} is an iron protein of the type [4Fe-4S]-ferredoxin; $\{FeS\}^N$ and $\{FeVS\}^N$ are components of the FeV protein. The indices "r" and "o" refer to the reduced and oxidized forms, respectively. In the case of **28**, the cubane-like VFe_3S_4 unit (solid lines) is represented as part of a larger metal-sulfur cluster, a "superstructure" deduced from EXAFS data; Fe', in a corner position of the cubane, is octahedrally surrounded by five Fe and one V (dotted lines). All iron ions are tetrahedrally coordinated by sulfur; this is indicated by dashed lines for $Fe'(S')_4$. V can achieve octahedral coordination through two ligand functions not belonging to the cluster. In model **29**, V carries, in addition to the three $S^{2\ominus}$ ligands, three O ligands (e.g., DMSO or DMF) or N ligands. Tol = p-$CH_3C_6H_4$.

iron protein (a 4Fe-4S ferredoxin). From the FeV protein, which contains 2 V, about 23 Fe, and 20 sulfide S atoms,[114] the actual iron-vanadium (FeV) cofactor can by extracted with dimethylformamide (DMF). It contains V, Fe, and sulfide S atoms in the ratio 1:6:5.[120]

The mechanistic route of nitrogen fixation is shown in abbreviated form in Fig. 8 (top left). At each electron-transfer process from Fe to the FeV protein, two molecules of Mg-ATP are hydrolyzed.[121a] In contrast to the Mo-Nase, which uses 25% of the electron flux to reduce two $H^{\oplus}$ to H_2, the enzymatic reduction by V-Nase requires about 50% of the reduction equivalents in this side reaction.[121b] Another difference is that the reduction of C_2H_2 by Mo-Nase stops at C_2H_4, whereas the reduction by V-Nase can proceed to C_2H_6.[117]

According to data from the XANES region of the XAS spectrum, the oxidation number of V lies between II and IV.[37] (See Ref. [122] for the general problem of determining the oxidation number from XANES parameters.) From the ESR spectrum of the reduced form of V-Nase, a spin state of $S = 3/2$ is determined for vanadium.[123] The weak intensity of the white band in the XANES range suggests a (distorted) octahedral rather than a tetrahedral environment for vanadium. These results are corroborated by EXAFS studies, which yield the parameters in Table 5.

Table 5. EXAFS data for the FeV cofactor in the vanadium nitrogenase.

Ligand atom (V-XAS) [a]	Number		Distance [pm]	
S	3(1)	3–4	231(3)	233(3)
Fe	3(1)	3(1)	275(3)	276(3)
O or N	ca. 3	2–3	215(3)	215(3)
(Fe-XAS) [b]				
S	3		224	
V	1		290	
Fe	2		265	

[a] The values for number and distance were taken from [124a, b] (left column) and [124c] (right column). [b] Values from [127d].

This data indicates that a VFe_3S_4 cluster is part of the FeV cofactor. Furthermore, a long Fe–Fe distance of 369 pm[124d] reveals an additional long-range order in the cluster. The structure proposal **28** (Fig. 8) follows from these results. It may be compared with the corresponding FeMo cofactor and also, according to the XAS data, with the VFe_3S_4 cluster in the model compound **29**.[128]

3.3.6. *Transferrin and Related Proteins*

Already in Section 3.1 the significance of the transferrins (Tf) in the transport of V^V, V^{IV}, and also V^{III} was mentioned (see also Ref. [126]). At this point, details about the coordination of vanadium to these and related proteins will be presented. The reader is referred to the review by *Chasteen*[38] for studies of further vanadium–protein complexes and, for other selected examples of proteins with enzyme character, to the previous sections. In addition, Table 3 includes several formation constants of V–protein complexes.

Vanadium is present in blood serum as V^V and also as V^{IV} and bonds tightly to Tf in both oxidation states (complex formation constants are around $10^{6.5}$ M^{-1} [127]). The affinity of serum albumin for V^{IV} is comparable;[53b] V^V, on the other hand, is bonded only weakly to albumin. A maximum of two V per Tf are taken up; the two not quite equivalent binding sites on the C and N termini of human apo-Tf could be distinguished using both ^{51}V NMR (for V^V)[68] and ESR (for V^{IV}) techniques.[67]

As a result of coupling of an unpaired electron with the nuclear spin of ^{51}V (7/2), either an eight-line system or, for axial symmetry (which occurs as a rule in $VO^{2\oplus}$ complexes), two sets of overlapping eight-line systems appear in the ESR spectrum. As example, Figure 9 (top) shows the X-band

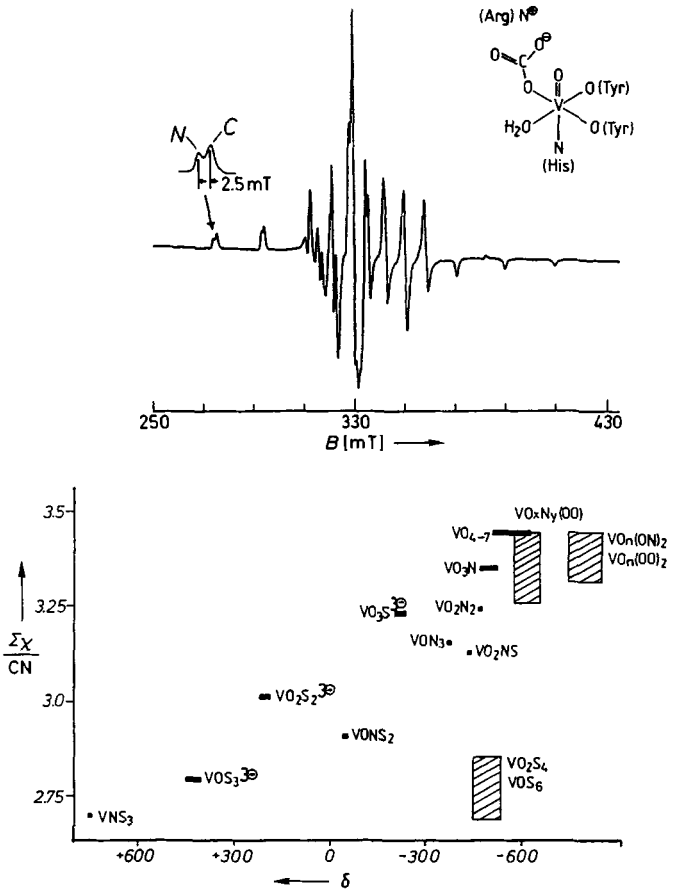

Fig. 9. Top: The X-band ESR spectrum of the divanadyl complex of human serum transferrin [$(VO^{2\oplus})_2$-Tf] at 77 K and pH 7.4 (Hepes/hydrogen carbonate buffer). $c(V) = 0.36$ mM, c(protein) = 0.18 mM. The expanded signal ($m_I = -7/2$) shows a splitting due to the different binding centers for $VO^{2\oplus}$ (N or C terminus). The structure proposal (top right) corresponds to the present state of knowledge for the coordination sphere of a Tf-bonded metal ion and is consistent with ESR data. The spectrum is reproduced from [67] with permission. Bottom: Relationship between $\delta(^{51}V)$ (standard $VOCl_3$) and the sum of the electronegativities of the ligand functions coordinated to V, Σ_χ, divided by the coordination number CN [107]. Shaded columns indicate complexes that contain strained ring structures ($OO^{2\ominus}$, $R_2NO^{\ominus}$, $CO_2^{\ominus}$, $CS_2^{\ominus}$). O, N, and S represent ligands which coordinate via these ligands to the vanadium. (OO) and (ON) are peroxo or hydroxylamido ligands.

ESR spectrum of the complex which is formed from $VO^{2\oplus}$ and human serum transferrin and in which such anisotropy is clearly observed. It is interesting that the $m_I = -7/2$ resonance reveals a further splitting, which is attributed to the two slightly different binding centers (N and C termini).[67]

In Table 5 are listed the ESR parameters (g factors and hyperfine coupling constants A) of some vanadyl compounds; they show that at least the differentiation between N- and O-coordination can become problematic. The ESR spectrum of $(VO_2^{\oplus})_C$-Tf (C-terminal attachment) corresponds to a vanadyl complex with octahedral geometry and is consistent with the ligand sphere sketched in Figure 9.[67] The participation of tyrosine in the coordination is confirmed by the appearance of a corresponding charge-transfer (CT) band in V^{III}-Tf, a compound which is surprisingly stable (e.g., towards atmospheric oxygen).[69]

Table 6. ESR parameters of selected vanadyl complexes.

Ligand	Coordination [a]	$g_{\parallel}/g_{\perp}$ [b]	$A_{\parallel}/A_{\perp}$ [c]	Ref.
Water	O_6	1.938/1.986	178/70	[154d]
Oxalate	O_6	1.941/1.978	171/62	[38]
Carbonate	O_6	1.941/1.978	168/57	[128a]
Catecholate	$O_{6/5}$	1.97 [d]	107 [e]	[128b]
Peroxidase from *A. nodosum*	unknown	1.948/1.979 [f]	160/50	[111]
Carboxipeptidase A (bovine)	N_2O_n	1.944/1.978	166/61	[128c]
Serum transferrin (rat)	N_2O_4	1.937/1.868	168/95	[67]
2-Methyloxine	N_2O_3	1.941/1.985 [g]	157/53 [g]	[128d]
Benzimidazole on support [h], pH 5	N_2O_4	1.943/1.988	170/61	[128e]
Imidazole, pH 7	$N_{3/4}O_{1/2}$ [i]	1.952/1.981	162/57	[128e]
Etioporphyrin	N_4O	1.948/1.987	159/52	[128e]

[a] In some cases the number of donor O- and N-ligands is assumed from preliminary structures. [b] $g_{\parallel}$ refers to the axis in which the vanadyl oxygen is found. [c] Hyperfine coupling constants in 10^{-4} cm^{-1}. [d] Isotropic factor $g_o = 1/3(g_{\parallel} + 2g_{\perp})$. [e] Isotropic hyperfine coupling constant $A_0 = 1/3(A_{\parallel} + 2A_{\perp})$. [f] The spectrum is not strictly axial. The deviation for $g_{\perp}$ (1.979), $g_{xx} - g_{yy}$, is 0.01. [g] The rhombic distortion in the tetragonal plane of this complex is reflected in $g_{xx} - g_{yy} = 0.005$ and $A_{xx} - A_{yy} = 4.2 \times 10^{-4}$ cm^{-1}. [h] Cf. **76** in Fig. 15. [i] The complex has, according to [128f], the composition $[VO(im)_3(H_2O)]^{2\oplus}$ and tetragonal-pyramidyl geometry.

^{51}V NMR spectroscopy has shown itself to be a useful method of characterizing V^V-containing biological and biomimetic systems.[129a, b] The chemical shifts of V^V-Tf ($\delta = -529.5$ and -531.5 relative to $VOCl_3$)[68] correspond to a complex with a coordination number of 5 or 6 and O/N-coordination with oxygen ligand dominance.[107, 129c] As in all d^0 systems, the δ values of V^V complexes also show an "inverse dependence" on the electronegativity χ for the ligand function bonded to vanadium; that is, the shielding of the ^{51}V nucleus increases with increasing χ and decreases with increasing polarizability α. The δ/χ correlation is shown in Figure 9 (bottom) for biorelevant ligand functions (S,N,O). Furthermore, the V^V compounds show a dependence of the δ values on steric factors, in that the shielding also increases with increasing bulkiness of the ligands and with any ring strain in chelate systems (three- and four-membered rings). We have systematically examined the steric effect, which can also be used, for example, to distinguish diastereomers, in the complexes $[VO(oxine)_2OR]$[101] (oxine = 8-hydroxyquinoline).

The transferrin-related proteins in milk (lactoferrin) and in the whites of bird eggs (ovotransferrin, conalbumin) also coordinate vanadium.[130] In the case of human lactoferrin, two $VO^{2\oplus}$ (at the C- and N-terminal ends) are taken up. Moreover, the coordination of a third vanadyl ion to an unspecific binding site on the surface of the protein close to the C terminus can be identified.[130a] Polarographic investigations on conalbumin similarly show two distinguishable binding sites with a coordination capacity of 1 and 16 V per molecule and formation constants of $10^{5.5}$ and $10^{3.1}$. The bonding to vanadate(v) is presumably due to the ion-pair interactions between vanadate and protonated nitrogen functions of amino acid side chains (histidine or arginine).[130c]

4. Model Complexes

In biological systems the available ligand atoms are sulfur (sulfide, thiolate), nitrogen (amide and amine), and oxygen (oxide, hydroxide, water, alcoholate, phenolate, carboxylate, hydroxamate, hydroxylamide). In the case of vanadium there are examples of all above-mentioned ligand types. Thus, vanadium is bonded to, among others, sulfide in vanadium nitrogenase and probably to carboxylate and $OR^{\ominus}$ (perhaps also to histidine) in vanadate-dependent haloperoxidase. For amavadin the coordination to the O atoms of carboxylate and hydroxylamide groups may be considered proven. The bonding to proteins like transferrin and ATPase occurs through O- and N-functions from side chains, but possibly also involves peptide bonds. Vanadium can adopt the coordination number (CN) 4–8 and thus form tetrahedral (CN = 4), tetragonal-pyramidal or trigonal-bipyramidal (CN = 5), octahedral or trigonal-prismatic (CN = 6), pentagonal-bipyramidal or capped trigonal-prismatic (CN = 7), and dodecahedral (CN = 8) complexes. In the selection of model compounds I have restricted myself to "modern" bioinorganic aspects of the coordination chemistry of vanadium: (1) systems with S-ligands as well as ligands with N_2 groups (nitrogenase models), (2) complexes with carboxylate, alcoholate, phenolate, and hydroxamate ligands, and (3) histidine-modeling ligands. Some of the complexes described in the following discussion (e.g., the polynuclear carboxylato complexes or compounds with tridentate nitrogen ligands) have—as yet—no immediate relevance to biomolecules; nevertheless, they are considered here to illustrate, among other features, the parallels to the bioinorganic chemistry of iron[131a] and of manganese.[131b]

4.1. Model Compounds for Vanadium Nitrogenase

One should distinguish here between compounds which approximate the structure of the vanadium center of the FeV cofactor, in that sulfur ligands are involved in the construction of the coordination sphere (structural models), and those which contain N_2 and ligands derived therefrom and as such have potential functional character. The following vanadium complexes containing S-ligands do not only have the character of model compounds for nitrogenase; they are, like the cysteine-ester complex **35a** (Fig. 10), also of interest in improving the understanding of the role of vanadate in the activation of the serine sulfhydrase (enzymatic transformation of cysteine into serine + H_2S).[132a]

Counted among the structural models is the cubane cluster **29** already introduced in Figure 9a, which probably reproduces the central component of the FeV cofactor fairly accurately and is related to corresponding models for the FeMo cofactor. The compounds in Figure 10 (ordered according to decreasing oxidation number for vanadium) reflect the variety with respect to oxidation number, coordination geometry, and nuclearity that one also meets in the still young field of vanadium-sulfur coordination chemistry. Particularly interesting in the light of the possible function of vanadium in the nitrogenase as electron-transfer agent are the mixed-valence complexes **33** (V^{V}/V^{IV}) and **38a** (V^{IV}/V^{III}). Complex **38a** contains in the V_3S_4 nucleus a *nido* cluster, which is derived from the corresponding *closo* structure of a V_4S_4 cubane like **38b**. Complex **38a** can be reversibly reduced and oxidized in MeCN in a one-electron process [Eq. (f), edt = ethanedithiolate (2−)].[136b] The one-electron oxidation of **36** and **39** in MeCN yields mixed-valence complexes too.

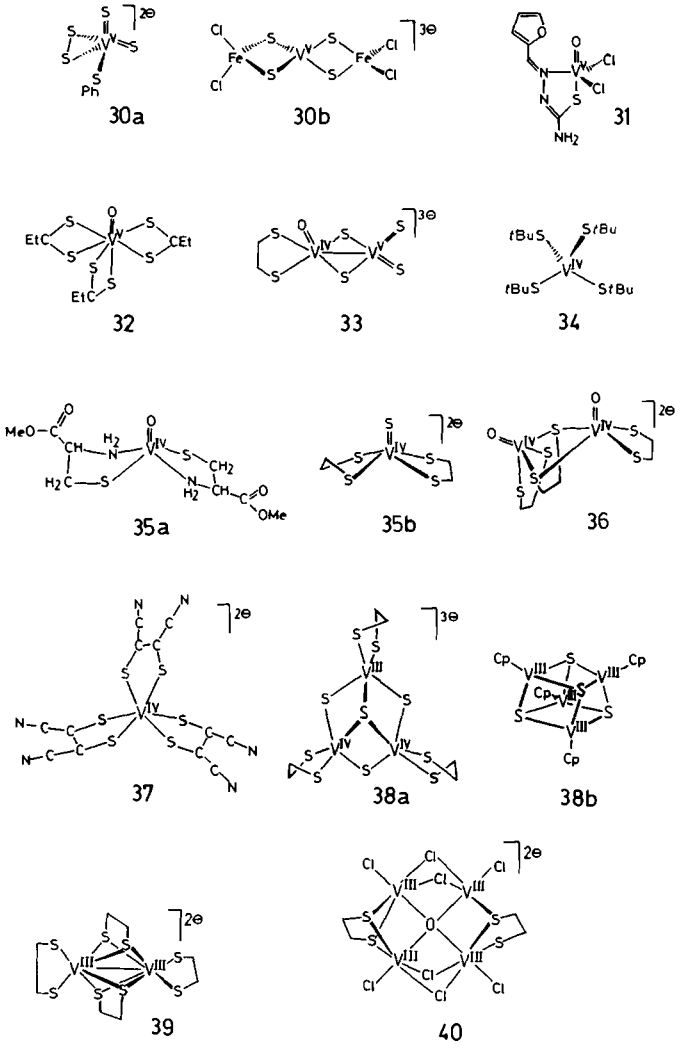

Fig. 10. Coordination compounds of vanadium with sulfur ligands as structural models for the iron-vanadium cofactor of vanadium nitrogenases. The molecular structures were, with the exception of **31**, determined by X-ray diffraction analysis. For clarity some structures have been reproduced somewhat idealized from the original literature. Sources: **30a** and **33** [132c], **30b** [132d], **31** [133], **32** [134], **34** and **36** [135], **35a** [132b], **35b** [136a], **37** [63], **38a** [136b], **38b** [136d], **39** [137], **40** [137c]. Compounds **37** and **39** show an arrangement for the VS_6 unit that lies between a trigonal prism and an antiprism (= octahedron).

$$[V_3S_4(edt)_3]^{4\ominus} \overset{-1.51\ V}{\rightleftharpoons} [V_3S_4(edt)_3]^{3\ominus} \overset{-0.63\ V}{\rightleftharpoons} [V_3S_4(edt)_3]^{2\ominus} \quad (f)$$

38a

Potential functional models are collected in Figure 11. The series **41** and **42** describe both the dinitrogen complexes (**41a** exists only in gas matrix[138a]) and the complexes with reduced ligands (hydrazine and ammonia); nothing is known about a direct transformation of **41a**/**42a** into **41b**/**42b** or **41c**/**42c**. In contrast, it was already shown almost two decades ago that N_2 is reduced in alkaline solutions containing $V^{2\oplus}$ and $Mg^{2\oplus}$, depending on the conditions, either to N_2H_4 (100 bar, 293 K) or to NH_3 (0.9 bar, 343 K).[141a] At pH values around 4.5, N_2 is reduced to N_2H_4 by the system $V^{2\oplus}/HO_2C(CH_2)_nCO_2H$ (n = 5, 6). The postulated intermediate, a binuclear complex with bridging carboxylate, keeps the two V centers together and thus allows the end-on bridging coordination of N_2.[141b] A binuclear μ-N_2 complex of V^{II}, **43**,[142] has recently been characterized structurally.

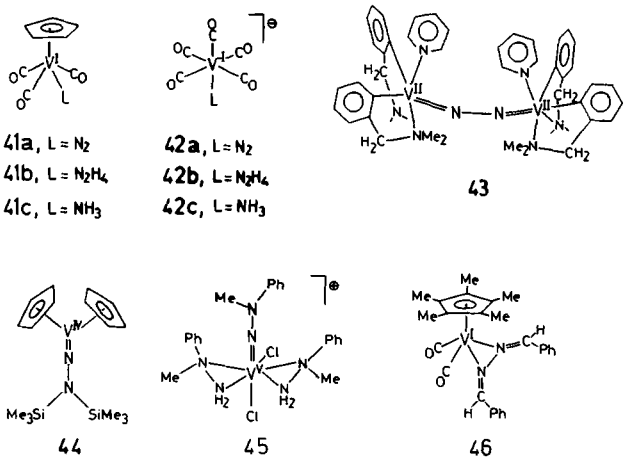

	d(NN) [pm]	d(VN) [pm]	(VNN) [°]
43	122.8(4)	183.3(3)	171.4(3)
44	136.9(9)	166.6(6)	180
45 $[NNMePh]^{2\ominus}$	129.5(17)	169.6(24)	174.4(19)
η^2-NH_2NMePh	144.8	210	
46	140.0(12)	201.9(5)	

Fig. 11. Vanadium complexes with N_2 and other *N-N* ligands; potential functional models for vanadium nitrogenases. Sources: **41a** [138a], **41b** [140a], **41c** [139a], **42a** [138b], **42b** [140b], **42c** [139b, c], **43** [142], **44** [143], **45** [144], **46** [140b].

Bond lengths approach that of a formulation with the hydrazido(4−) ligand; the magnetic behavior of the compound and the easy exchange of N_2 for CO and alkyne suggest a N_2 complex. As a first reduction step in the nitrogen fixation, intermediates with diimide, isodiimide/hydrazide(2−), and hydrazine are discussed. To the rare examples of such complexes belong **44**, **45**, and also the diazine complex **46**. The bond lengths and angles listed below indicate that the end-on-bonded ligands in complexes **44** and **45** are isodiimine and hydrazido(2−) ligands, respectively.

4.2. Carboxylato, Hydroxamato, Alkoxo, and Aryloxo Complexes

Mono-, di-, hydroxo-, and aminocarboxylates form, in the main, weak complexes with vanadate(v) and $VO^{2\oplus}$ in aqueous systems (see Table 3). Isolation is often only possible from organic solvents. Complexes of V^V with carboxylates that have no other functional groups available are generally mononuclear (**47** and **48** in Fig. 12) and have typical coordination numbers of 6 or 7. As was shown in example **48** with η^2 coordination of the pivalate ligand (for the model character of this compound for vanadate-dependent peroxidases, compare with **B** in Fig. 7), CN 7 is only partly achieved in solution.[147] When a binuclear V^V carboxylate is formed, as in the case of the citrate complex **49**, the vanadium centers are connected by an additional function, here the deprotonated hydroxyl group of citric acid. The bridging by $O^{2\ominus}$, known from the oligovanadates(v), appears to be reserved for the mixed-valence carboxylato complexes (**50**, V_5^V/V^{IV}; **51**, V^V/V_4^{IV}) and species with vanadium(IV) (**52**). *Casey* et al. referred early on to the "polymeric" nature of $VO^{2\oplus}$ carboxylates;[152] their "island" structures could only be unraveled by X-ray analyses. A further characteristic of these complexes is the bidentate bridging function of the carboxylato ligands. With multifunctional ligands such as tartrate, oxalate, and malonate, V^{IV} can form both bi- (**53**) and mononuclear (**54**) complexes. Carboxylate functions operate here as in the V^V complex **49** only in a monodentate fashion. The cluster **51** can undergo irreversible and reversible redox processes [Eq. (g)].[149]

$$V_5^{IV} \xleftarrow{+e} V^V V_4^{IV} \underset{}{\overset{-e,\ 0.68\ V}{\rightleftharpoons}} V_2^V V_3^{IV} \xrightarrow{-e} V_3^V V_2^{IV} \qquad \text{(g)}$$

The investigation of $VO^{2\oplus}$ complexes in solution has also been successfully performed by ^1H ENDOR spectroscopy (ENDOR = electron nuclear double resonance). This method, in which the frequencies of irradiation are those of selected transitions in the ESR spectrum of an axial molecule (e.g., the components at $m(I)_{\parallel} = -5/2$ and $m(I)_{\perp} = -3/2$), enables, through the determination of hyperfine coupling constants A_H, conclusions to be drawn about the distance d(H-V) of the ligand proton coupled with the unpaired electron on the vanadium center and therefore also about the mode of coordination of the ligand. In this manner it could be shown, for example, that galacturonic acid coordinates at pH < 4 via the carboxylate group (Fig. 12, bottom, **55a**), in the physiological pH range via carboxylate and the deprotonated OH group on C4 (**55b**), and in strongly alkaline medium via two alkoxy oxygens (**55c**).[154a] Some data are listed in Figure 12. For comparison, ENDOR data for $[VO(H_2O)_5]^{2\oplus}$ [154c] and the V^{IV}–catecholate complex **58** (Fig. 13) have been included. These data agree well with those based on the bonding parameters from X-ray structure determinations.

In connection with the inhibition of enzymes (e.g., ribonucleases, ATPases), the CN 5 of vanadium is of interest, because vanadate, in contrast to its antagonist phosphate, forms stable complexes after expansion of its coordination sphere (from a tetrahedral geometry). These complexes are models for the transition state in phosphodiester hydrolysis.

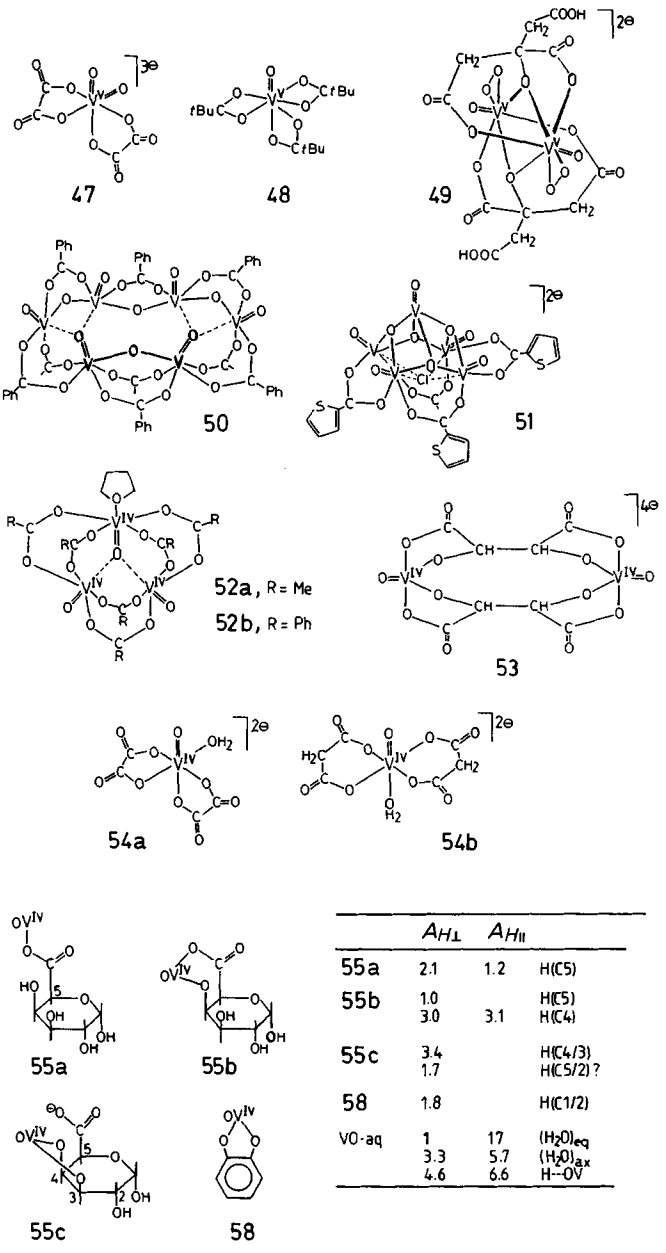

	$A_{H\perp}$	$A_{H\parallel}$	
55a	2.1	1.2	H(C5)
55b	1.0		H(C5)
	3.0	3.1	H(C4)
55c	3.4		H(C4/3)
	1.7		H(C5/2)?
58	1.8		H(C1/2)
VO-aq	1	17	$(H_2O)_{eq}$
	3.3	5.7	$(H_2O)_{ax}$
	4.6	6.6	H--OV

Fig. 12. Top: Complexes of V^V and V^{IV} with carboxylato ligands, in which exclusively *O*-donation occurs (**47**–**54b**). Sources: **47** [145], **48** and **50** [= $V^{IV}V_5^VO_4(\mu\text{-}O)_4(\mu_3\text{-}O)_2(\mu\text{-}O_2Ph)_8$] [147], **49** [148], **51** [= $V_3^{IV}V_2^VO_5(\mu_3\text{-}O)_4\mu_4\text{-}Cl(\mu\text{-}tca)_4$; Htca = thiophene-2-carboxylic acid] [149], **52a** [150a], **52b** (with THF twisted 90° relative to the O = V-O axis) [150b], **53** [151], **54a** [146a], **54b** [146b]. Bottom: ^1H ENDOR results and structure proposals for complexes of $VO^{2\oplus}$ with galacturonic acid (**55** [154a]), catechol (**58** [154b]), and water (VO-aq = $[VO(H_2O)_5]^{2\oplus}$ [154c]. For the structure of **58**, see Fig. 13. Coupling constant data $A(H)$ in MHz.

CN 5 is achieved in **53** (trigonal bipyramidal), in the apical vanadium of complex **51** (tetragonal pyramidal), and in the V_4 subunit of complex **50** (between trigonal bipyramidal and tetragonal pyramidal). Further examples may be found in the previous sections and in Figures 13 (**56**–**58**) and 14 (**64a**). Compounds **56** and **57** are the only structurally well-characterized triesters $VO(OR)_3$ of tetraoxovanadic (orthovanadic) acid. They occur as dimers for R = Me and as monomers for R = C_2H_4Cl (and probably for all other R), which however associate into larger aggregates in the solid state and also in solution[113] (in Fig. 13 this is indicated by dashed lines). The V–OR bond in these two esters and the

ester bond in **60** are conspicuously short (175–186 pm; V–O single bonds otherwise lie around 200 pm, V=O double bonds between 155 and 165 pm), which has been discussed as evidence for an ester bond in native vanadate-dependent peroxidase (Fig. 7, **A**). The catecholate complexes **58** and **59**, as well as the hydroxamate complexes **60**–**62**, are noteworthy in that catecholates and hydroxamates are the most important function carriers of the siderophores produced by bacteria and fungi and are possibly also active in the mobilization of vanadium, similar to that of $Fe^{3\oplus}$, out of inorganic extracellular depots. Kinetic investigations into complexation of aromatic diols by vanadate(v) and its reduction to V^{IV} were performed by *Ferguson* and *Kustin*.[156]

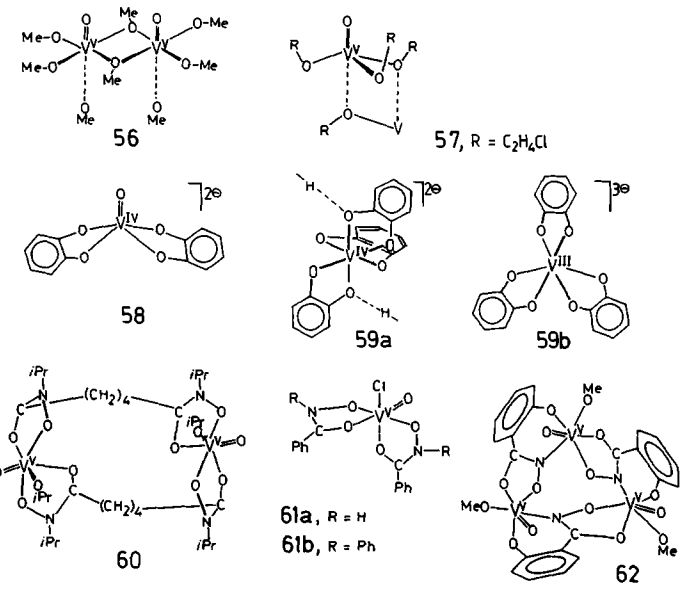

Fig. 13. Vanadium complexes with alkoxo, aryloxo, and hydroxamato ligands. Sources: **56** [153], **57** [113], **58** and **59** [128b], **60** and **61a** [58], **61b** [101], **62** [155]. The dashed lines in **56** and **57** imply bonding interactions with neighboring molecules. **59a** is octahedral, but shows considerable distortions from ideal octahedral geometry, for which hydrogen bonds (dashed lines) from the counterion $HNEt_3^{\oplus}$ to the phenolate oxygens may be held responsible. In the potassium salt of complex **59b** the trigonal torsion angle is 45.6°. The V=O double bond in **61a** is normal at 159.1 pm; in **61b**, however, it is unusually long (180.1(4) pm).

Structurally characterized complexes of vanadium with simple amino acids appear not to exist. Cysteine methyl ester forms with $VO^{2\oplus}$ the complex **35a** (Fig. 10) with *N,S*-coordination. Histidine (in connection with $VO^{2\oplus}$)[158] and various dipeptides studied by us (in connection with $H_2VO_4^{\ominus}$; see, for instance, **63** in Fig. 14), which contain freely available carboxylate groups, tend to avoid the coordination with the carboxylate oxygen. In contrast, *N,O*-coordination occurs with more complex aminocarboxylates and related ligands. Examples are the complexes with picolinate (1–) **64a**, dipicolinate(2–) **64b**, nicotinate(1–) **65**, EDTA **66** and **67**, and triazacyclononane-*N,N*-diacetate(2–/1–) **68**, shown in Figure 14. Compound **68a** can be reversibly oxidized to **68b** (Table 4).

N,O-coordination of a different kind, namely exclusively or additionally from Schiff base functions plus $OR^{\ominus}$, is displayed by the complexes **69** (here, an acetate group of EDTA is replaced by the hydroxyethyl group), as well as by **70**–**74**.

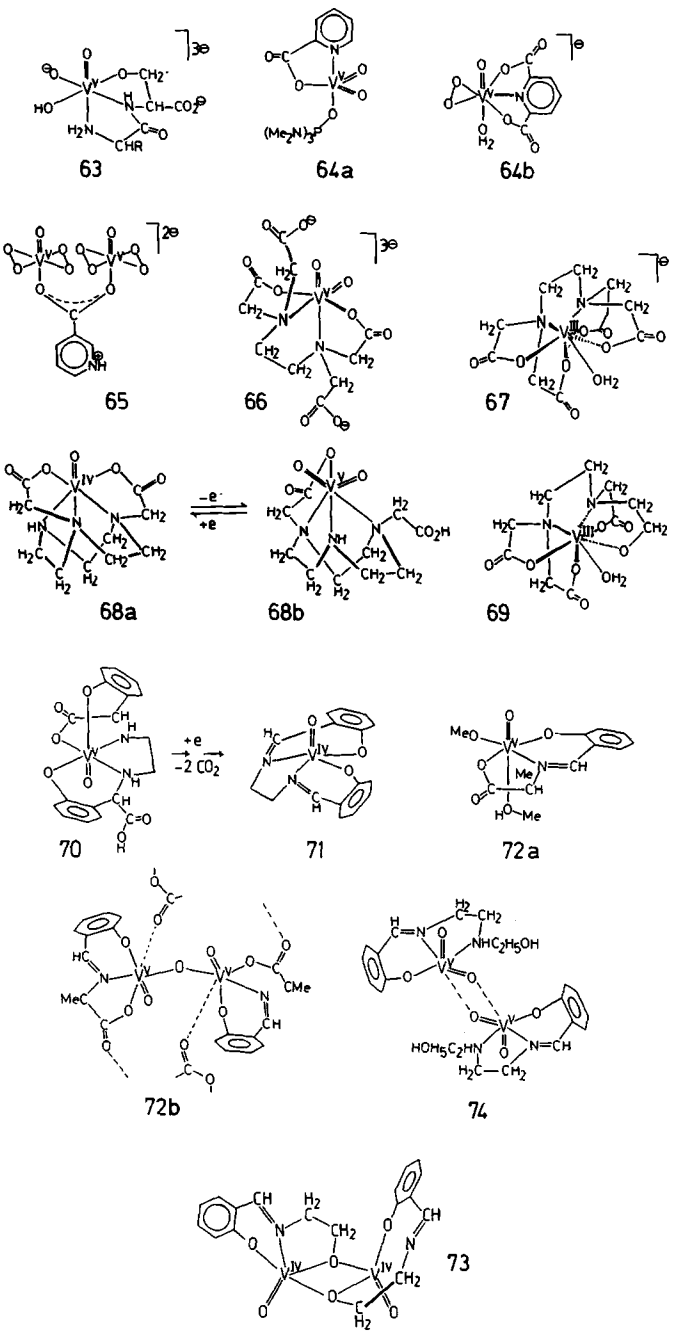

Fig. 14. Complexes with *O,N*-donor ligands. Sources: **63** [52], **64a** [157a], **64b** [157b], **65** [159], **66** [160], **67** [161], **68** [62], **69** [162], **70** [60, 163b], **71** [163a], **72a** and **72b** [165a], **73** [165b], **63**, **65**, and **70** are structure proposals. Compounds **67** and **69** have the geometry of twisted trigonal prisms with the aqua ligands in capping positions. The decarboxylation of **70** takes place in two steps and with the participation of an intermediate with V^{III}. Compound **72b** is, as the dashed lines (= weak bonding interactions) show, associated with a second dimeric unit to form a tetranuclear complex.

Complex **70**, which contains the ligand ethylenebis(hydroxyphenyl)glycine, decarboxylates under suitable conditions to the salen complex **71**[60, 163b, c] (salen is the double Schiff base formed from two molecules of salicylaldehyde and ethylenediamine). This unusual oxidative (with respect to the ligand) decarboxylation is a notable model for the decarboxylation of *S*-adenosylmethionine by vanadate(v), a reaction that takes place in the presence of pyridoxal phosphate at vanadate concentrations as low as 10^{-7} M via the formation of a Schiff base complex[164] (see also Section 3.2.2).

The ligand in **72a** and **72b** is the Schiff base formed from salicylaldehyde and alanine. The low magnetic moment of **73** (1.53 μ_B) allows conclusions to be drawn about the antiferromagnetic interaction between the two-alkoxo-bridged V centers (d(V-V) = 306.8(4) pm). Oxidation by air transforms **73** into a dimeric V^V complex.

4.3. Histidine-Modeling Ligands

Histidine (imidazolylalanine) as component of a protein matrix is capable of coordinating biometals such as $Zn^{2\oplus}$, $Cu^{\oplus/2\oplus}$, $Fe^{2\oplus/3\oplus}$, and $Mn^{2\oplus/3\oplus/4\oplus}$ and is also mentioned in connection with the coordination of $VO^{2\oplus}$ in transferrin and (reduced) vanadate-dependent haloperoxidase (V^{IV}-PO). Histidine itself complexes vanadate(v) only weakly.[52a, 158] ESR spectra of model compounds such as **75** and **76** (Fig. 15) show a similarity to that of V^{IV}-PO (compare also the data in Table 6, Section 3.3.6) inasmuch as they give similar g factors and hyperfine coupling constants and furthermore correspond to the total habitus (i.e., they display in principle an axial spectrum), but they reveal the significant rhombic distortion in the plane (splitting of $g_{\|}$) as well.

The coordination of three histidine residues in Fe-hemerythrin and Cu-hemocyanin, for example, has stimulated the recent development of the coordination chemistry with suitable tridentate *N*-ligands, and vanadium is no exception. Particularly noteworthy are 1,4,7-triazacyclononane and its derivatives[62] (cf. **68** in Fig. 14, **80** and **81** in Fig. 15), hydrotris(3,5-dimethylpyrazolyl)borate[167, 168] (pz; **77** and **78** in Fig. 15), the hexadentate tetrakis(2-pyridylmethyl)ethylenediamine, which additionally joins doubly OH-bridged $VO^{2\oplus}$ centers with one another (**79** in Fig. 15), and the Schiff base in **82**, which also presents six *N*-functions in a binuclear, OR-bridged complex. Compound **77** is formed by oxidation with air (and other reactions) from a precursor containing V^{III} and can be reversibly oxidized in DMF to a species containing V^V [Eq. (h)].

$$[pzV^{III}Cl_2(dmf)] \xrightarrow{O_2} \underset{\mathbf{77}}{[pzV^{IV}OCl(dmf)]} \underset{+e,\ 1.18\ V}{\overset{-e}{\rightleftharpoons}} \text{"p-}V^{V}\text{"} \qquad \text{(h)}$$

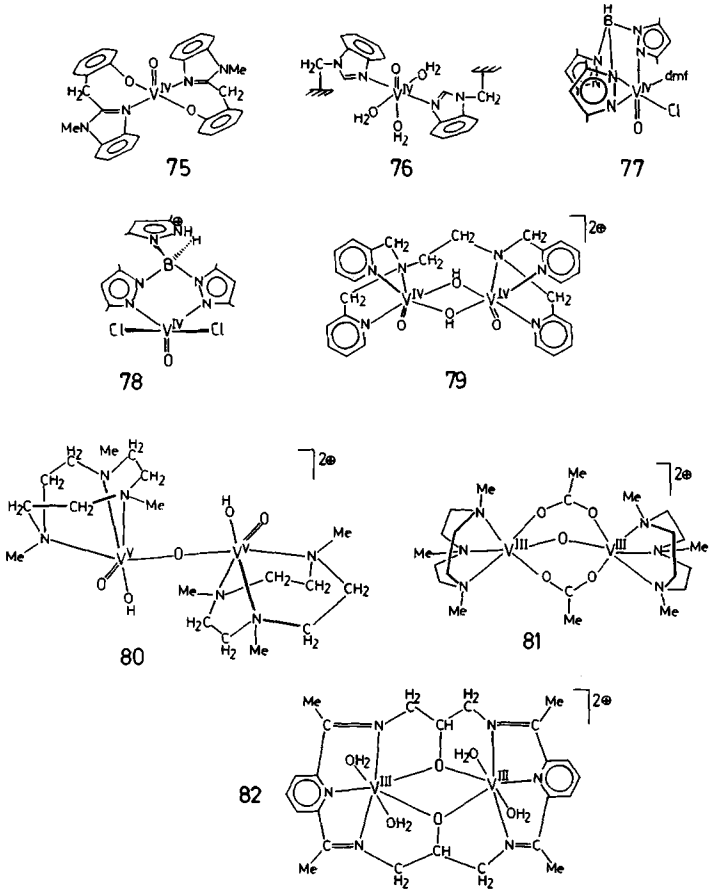

Fig. 15. Vanadium complexes with ligands that model the coordination to histidine. Compare also **68** in Fig. 14. Sources: **75** [166], **76** [128e] (benzimidazole is bonded to a support), **77** and **78** [167], **79** [169], **80** [170], **81** [171], **82** [172]. Compounds **75** and **76** are preliminary structure proposals. In **81** the V–O–V angle is 130.2° (usually the V–O–V unit is approximately linear; see, e.g., **14** in Fig. 6). The aqua ligands in **82** are in apical positions, the O of the μ-alkoxo group in trigonal-planar surroundings.

Addendum

Section 2: The kinetic exchange pathways between monovanadate and oligovanadates have been studied at pH 8.6 by ^{51}V–^{51}V exchange spectroscopy (EXSY). The dimer is mainly formed from two monomers, and dimer–monomer exchange is fast. The main pathway for tetramer formation is the reaction between two monomers and a dimer (a labile linear trimer may be involved); the pentamer forms either from tetramer and monomer (low c(V)) or from two tetramers.[174]

Sections 3.1 and 3.2: Several recent experiments cast new light on the vanadate species responsible for enzyme inhibition. Oligomers probably have a more potential role in this respect than recognized previously.[175, 176] Monovanadate *and* oligovanadates coordinate to myosin and its subfragment 1, and it has been suggested that photocleavage of the subfragment occurs only when tetravanadate is bound.[177] New results are also available on the metabolism of vanadate(v) (mainly detoxification through reduction to V^{IV}): Vanadate(v) is reduced by nonprotein thiols related to glutathione[178] and by dihydroxyacetone.[179] In the latter case, the half-life of $H_2VO_4^{\ominus}$ is 20 min. Reduction is about 75 times slower than ester formation (between vanadate and dihydroxyacetone). V^V is restored on contact with O_2.[179] $VO^{2\oplus}$ has been shown to stimulate O_2 evolution by photosystem II particles inactivated by removal of $Ca^{2\oplus}$.[180]

The use of appropriate ^{48}V complexes (such as [^{48}V]vanadylpheophorbide[181]) for tumor imaging by positron emission tomography (PET) is a promising new development in the medical application of vanadium.

Section 3.3: $VO^{2\oplus}$ complexed to ribonucleic acid reacts with hydrogen peroxide in a Fenton-like manner to produce OH radicals.[182] The interaction of vanadate with mononucleosides, ADP, and ATP was investigated by multinuclear NMR spectroscopy. Among the compounds formed are the mixed anhydrides AMPV, $AMPV_2$, and ADPV.[183] The main component of the complexes generated from vanadate(v) and inosine (and other nucleosides) in aqueous solution is binuclear and contains two ligands, with the vanadium centers in a trigonal-bipyramidal array.[184]

The accumulation and chemistry of vanadium (in the form of amavadin) in the fly agaric toadstool has been reviewed.[185] Electrochemical data suggest that the role of

amavadin is that of an electron-transfer catalyst or mediator. A plausible, though hypothetical, assumption is that amavadin is a component of a primitive oxidase.[185]

A ^{51}V NMR study on vanadate-dependent bromo/iodoperoxidase from *Ascophyllum nodosum* has revealed that, in addition to the active site (where V^V is tightly bound), there are unspecific, low-affinity binding sites on the protein for vanadate. These have been modeled with Gly-Tyr and Phe-Glu.[186] While vanadate-dependent peroxidases are usually found in the cell wall (between cortex and medulla) of the algae, peroxidases have now also been isolated from the protoplasts of seaweeds belonging to the genus *Laminaria*.[187] Vanadium and iron are constituents of a nonheme peroxidase from the marine red alga *Corallina vancouveriensis*.[188] In the absence of substrate, the system peroxidase/H_2O_2/$Br^{\ominus}$ evolves singlet oxygen.[188]

A supplementary EXAFS study of the FeV cofactor in vanadium nitrogenase, employing Fe as the back-scatterer, supports the view that the structural similarity of FeV and FeMo cofactors includes the long-range order and a mixed Fe/M second shell.[189]

Section 4: V^{IV} in an environment of eight sulfur functions is present in the binuclear (d(V-V) = 280 pm) and diamagnetic complex $\{V(S_2CMe)_2\}(\mu\text{-}S_2)_2$.[190] Functional models for vanadium nitrogenase, *cis*/*trans*-$[V(N_2)_2p_4]^{\ominus}$ and $[V(N_2)p_5]^{\ominus}$ (the p_n are oligodentate phosphane ligands), have been characterized by ^{51}V and ^{15}N NMR and by IR. The compounds are stable at ambient temperatures; part of the N_2 is reductively protonated to $NH_4^{\oplus}$ in the presence of HCl.[191]

Several new vanadium complexes serving as potential models for vanadium binding in biological systems have been reported. Among these are the pseudo-octahedral "bare" (i.e., without the V=O group) complexes $V^{III}L$, $[V^{IV}L]^{\oplus}$, and $[V^{V}L]^{2\oplus}$, with L a triazacyclononane derivative carrying phenoxy groups at the nitrogens and coordinating through three N and three O atoms. The three complexes can be reversibly interconverted by cyclovoltammetry.[192] Other complexes of interest that have been structurally characterized are $[V^{V}O(N,N')$-(pentane-3-ol)bis(salicylaldimine)][193] and $[V^{V}OCl(pinacolate)]_2$.[194] An ENDOR investigation into the systems $VO^{2\oplus}$/salicylic acid and $VO^{2\oplus}$/2,3-dihydroxybenzoic acid has shown that dihydroxybenzoic acid behaves, depending on the pH, either as a catecholic or as a salicylic ligand.[195] An EPR study of the aqueous $VO^{2\oplus}$/catecholate system has revealed the formation of 1:1, 1:2, and 1:3 (metal:ligand) complexes.[196]

The first comprehensive book on vanadium in biological systems has appeared, covering biochemical, chemical, and methodological aspects of the biochemistry of vanadium (cf. Ref. [129b]). In two additional reviews, emphasis is laid on V-PO and vanadium in ascidians[197] and on the latter aspect only.[198]

5. Concluding Remarks

The high abundance of vanadium in fossil matter of animal and plant origin as against its comparatively low concentration in most organisms today (Table 1) prompts the question whether vanadium was formerly more intensively used and whether the present groups of organisms which still accumulate vanadium (Ascidiacea, *Amanita*) are not in a certain sense living fossils. Similarly, the question arises whether those enzymes which still contain vanadium in the active site (haloperoxidases, nitrogenases) are not in fact handed-down function carriers which have not bowed to evolutionary pressure. In this regard, it is interesting to note that only the phylogenetically older subdivisions of the Ascidiacea show high vanadium contents, while the younger take up preferentially or exclusively iron.[88c, 188] Furthermore, peroxidases containing iron are more wide-spread than vanadate-dependent peroxidases and even among these there are apparently examples which contain iron besides vanadium[103d] or which conduct their enzymatic activity with iron as well as vanadium.[173] Points of intersection in the vanadium and iron metabolisms are probable.[18, 86a] After all, nitrogen-fixing organisms fall back on vanadium (or iron), only when no molybdenum is available. All this appears to indicate that, in the course of evolution, nature has found better solutions with other metals for many types of functions. Considering these premises, the chances of discovering further vanadium compounds with specific functions in nature should be judged with skepticism (possibly the search for such compounds among the geologically oldest groups of organisms such as the archaebacteria and the zymogenic species of the genus *Clostridium* would be successful). Undisputed is the fact that the dual nature of vanadium—on the one hand, in anionic form (as vanadate(v)) a competitor of phosphate in its metabolism and, on the other, in cationic form (as $VO^{3\oplus}$, $VO_2^{\oplus}$, $VO^{2\oplus}$, and $V^{3\oplus}$) a transition-metal ion which can interact with biogenic ligands (including proteins)—enables this element to serve many regulatory tasks in the organism.

The work of my own group, cited in the list of references, would not have been possible without the dedicated assistance of my co-workers, whom I would like to thank. The Deutsche Forschungsgemeinschaft, the Fonds der Chemischen Industrie, and the Freie und Hansestadt Hamburg have been generous in supporting this research. My particular thanks are due to those colleagues whose cooperation made the joint work on enzymes possible. These are above all Dr. Vilter, Institut für Pharmazeutische Biologie der Universität Bonn (work on peroxidase) and Prof. Saenger and his group, Institut für Kristallographie der Freien Universität Berlin (work on ribonuclease). I thank Prof. Achim Müller, Universität Bielefeld, for the critical perusal of the manuscript and lively discussions.

Received: February 9, 1990;
addendum: October 31, 1990 [A 803 IE]
German version: *Angew. Chem. 103* (1991) 152
Translated by *Dr. Karen J. Schneider*, Frankfurt am Main (FRG)

[1] E. M. Oltz, R. C. Bruening, M. J. Smith, K. Kustin, K. Nakanishi, *J. Am. Chem. Soc. 110* (1988) 6162.
[2] a) H. Vilter, *Bot. Mar. 26* (1983) 429, 451; b) H. Vilter, *Phytochemistry 23* (1984) 1387.
[3] H. Plat, B. E. Krenn, R. Wever, *Biochem. J. 248* (1987) 277.
[4] H. Kneifel, E. Bayer, *Angew. Chem. 85* (1973) 542; *Angew. Chem. Int. Ed. Engl. 12* (1973) 508.
[5] a) H.-U. Meisch, J. A. Schmitt, W. Reinle, *Z. Naturforsch. C33* (1978) 1; b) *Naturwissenschaften 66* (1979) 620.
[6] a) B. Mason, C. B. Moore: *Grundzüge der Geochemie*, Enke, Stuttgart 1985, p. 265; b) A. Treibs, *Justus Liebigs Ann. Chem. 517* (1935) 172.
[7] T. Bokorny, *Chem. Ztg. 28* (1904) 596.
[8] M. Henze, *Hoppe-Seyler's Z. Physiol. Chem. 72* (1911) 494.

[9] a) H.-U. Meisch, H.-J. Bielig, *Arch. Microbiol. 105* (1975) 77; b) H.-U. Meisch, H. Benzschawel, H.-J. Bielig, *ibid. 114* (1977) 67.
[10] L. L. Hopkins, Jr., H. E. Mohr, in W. Merz, W. E. Cornatzer (Eds.): *Newer Trace Elements in Nutrition*, Dekker, New York 1971, p. 195.
[11] K. Schwarz, D. B. Milne, *Science (Washington DC) 174* (1971) 426.
[12] R. N. Lindquist, J. L. Lynn, G. E. Lienhard, *J. Am. Chem. Soc. 95* (1973) 8762.
[13] a) L. C. Cantley, Jr., L. Josephson, R. Warner, M. Yanagisawa, C. Lechene, G. Guidotti, *J. Biol. Chem. 252* (1977) 7421; b) L. Josephson, L. C. Cantley, Jr., *Biochemistry 16* (1977) 4572.
[14] H.-U. Meisch, H.-J. Bielig, *Basic Res. Cardiol. 75* (1980) 413.
[15] K. Lee, *Adv. Environ. Sci. Technol. 13* (1983) 155.
[16] O. Hansen, *Acta Pharmacol. Toxicol. Suppl. 52* (1983) 1.
[17] a) K. Kustin, *Comments Inorg. Chem. 2* (1982) 1; b) K. Kustin, G. C. McLeod, T. R. Gilbert, Le B. R. Briggs, 4th, *Struct. Bond. Berlin 53* (1983) 139; c) D. W. Boyd, K. Kustin, Adv. *Inorg. Biochem. 6* (1984) 311.
[18] N. D. Chasteen, *Struct. Bond. Berlin 53* (1983) 105.
[19] R. Wennig, N. Kirsch, in H. G. Seiler, H. Sigel, A. Sigel (Eds.): *Handbook on Toxicity of Inorganic Compounds*, Dekker, New York 1988, p. 749.
[20] E. Erdman, K. Werdan, W. Krawietz, W. Schmidt, H. Scholz, *Biochem. Pharmacol. 33* (1984) 945.
[21] a) E. de Boer, Y. van Kooyk, M. G. M. Tromp, H. Plat, R. Wever, *Biochim. Biophys. Acta 869* (1986) 48; b) E. de Boer, M. G. M. Tromp, H. Plat, G. E. Krenn, R. Wever, *ibid. 872* (1986) 104; c) P. Jordan, B. Kloareg, H. Vilter, *FEBS Lett.*, in press; d) B. E. Krenn, H. Plat, R. Wever, *ibid. 912* (1987) 287.
[22] a) B. J. Hales, E. E. Case, J. E. Morningstar, M. F. Dzeda, L. A. Mauterer, *Biochemistry 25* (1986) 7251; b) R. L. Robson, R. R. Eady, T. H. Richardson, R. W. Miller, M. Hawkins, J. R. Postgate, *Nature (London) 322* (1986) 388.
[23] a) R. L. Robson, P. R. Woodley, R. N. Pau, R. R. Eady, *EMBO J. 8* (1989) 1217. b) K. Schneider, A. Müller, *Eur. J. Biochem.*, in press. c) For a discussion on this issue, see also A. Müller, R. Jostes, E. Krickemeyer, H. Bögge, *Naturwissenschaften 74* (1987) 388, and J. Erfkamp, A. Müller, *Chem. Unserer Zeit 24* (1990) 267. d) D. Sellmann, W. Soglowek, F. Knoch, M. Moll, *Angew. Chem. 101* (1989) 1244; *Angew. Chem. Int. Ed. Engl. 28* (1989) 1271.
[24] H. Bortels, *Zentralbl. Bakteriol. Parasitenk. Infektionskr., Abt. 2, 95* (1936/37) 13.
[25] M. J. Gresser, A. S. Tracey, *J. Am. Chem. Soc. 108* (1986) 1935.
[26] a) L. C. Cantley, Jr., P. Aisen, *J. Biol. Chem. 254* (1979) 1781; b) I. G. Macara, K. Kustin, L. C. Cantley, Jr., *Biochim. Biophys. Acta 629* (1980) 95.
[27] a) T. Shimizu, K. Ichikawa, M. Masayuki, Y. Shijo, *Bunseki Kagaku 38* (1989) 201; b) H. Michabata, T. Terada, N. Anada, K. Yamakawa, T. Numakunai, *Biol. Bull. (Woods Hole, Mass.), 171* (1986) 672.
[28] a) P. I. Premović, *Geochim. Cosmochim. Acta 48* (1984) 873; b) P. I. Premović, L. S. Jovanović, G. B. Popović, N. Z. Pavlović, M. S. Pavlović, *J. Serb. Chem. Soc. 53* (1988) 427; c) L. L. Hopkins, *Geochem. Environ. 2* (1977) 93; d) D. H. Maylotte, J. Wong, R. L. S. Peters, W. S. Lytle, R. B. Greegor, *Science (Washington DC) 214* (1981) 554.
[29] All data on electrochemical potentials in this article are quoted relative to the standard hydrogen electrode for the redox pairs Ox. + $ne \rightleftharpoons$ Red.
[30] S. Orecchio, V. Romano, R. Zingales, *J. Chem. Res. (S) 1989*, 14, 335.
[31] S. Liochev, I. Fridovich, *Arch. Biochem. Biophys. 255* (1987) 274.
[32] a) H. J. M. Bowen: *Trace Elements in Biochemistry*, Academic, New York 1966, p. 241; b) D. Bertrand, *Bull. Am. Mus. Nat. Hist. 94* (1954) 409.
[33] a) F. W. Oehme (Ed.): *Toxicity of Heavy Metals in the Environment*, Dekker, New York 1978, Part 1; b) R. Seeger, H.-G. Neumann, *Dtsch. Apoth. Ztg. 125* (1985) 405; c) D. A. T. Dick, E. G. Dick, G. J. Naylor, *J. Physiol. (London) 310* (1981) 24.
[34] I. G. Macara, *Trends Biochem. Sci. 5* (1980) 92.
[35] a) S. G. Brand, C. J. Hawkins, A. T. Marshall, G. W. Nette, D. L. Parry, *Comp. Biochem. Physiol. B 93* (1989) 425; b) S. Lee, K. Kustin, W. E. Robinson, R. B. Frankel, K. Spartalian, *J. Inorg. Biochem. 33* (1988) 183; c) S. G. Brand, N. Edelstein, C. J. Hawkins, G. Shalimoff, M. R. Snow, E. R. T. Tiekink, *Inorg. Chem. 29* (1990) 434.
[36] a) P. Krauß, E. Bayer, H. Kneifel, *Z. Naturforsch. B39* (1984) 829; b) M. A. Nawi, T. L. Riechel, *Inorg. Chim. Acta 136* (1987) 33; c) E. Bayer, E. Koch, G. Anderegg, *Angew. Chem. 99* (1987) 570; *Angew. Chem. Int. Ed. Engl. 26* (1987) 545.
[37] J. M. Arber, B. R. Dobson, R. R. Eady, P. Stevens, S. S. Hasnain, C. D. Garner, B. E. Smith, *Nature (London) 325* (1987) 372.
[38] N. D. Chasteen, *Biol. Magn. Reson. 3* (1981) 53.
[39] K. H. Tytko, J. Mehmke, *Z. Anorg. Allg. Chem. 503* (1983) 67.
[40] A. A. Ivakin, L. D. Kurbatova, M. V. Kruchinina, N. I. Medvedeva, *Z. Neorg. Khim. 31* (1986) 388; *Russ. J. Inorg. Chem. Engl. Transl. 31* (1986) 219.
[41] a) L. Pettersson, B. Hedman, I. Andersson, N. Ingri, *Chem. Scr. 22* (1983) 254; b) L. Pettersson, I. Andersson, B. Hedman, *ibid. 25* (1985) 309; c) L. Pettersson, B. Hedman, A.-M. Nenner, I. Andersson, *Acta Chem. Scand. Ser. A 39* (1985) 499.
[42] a) M. J. Gresser, A. S. Tracey, K. M. Parkinson, *J. Am. Chem. Soc. 108* (1986) 6229; b) A. A. Ivakin, L. D. Kurbatova, *Z. Neorg. Khim. 29* (1984) 2538. The data for the pK_a of $H_2VO_4^{\ominus}$ vary, according to source, method of determination, and composition of the medium, from 7.9 to 8.3. The value in [42a] was determined by ^{51}V NMR and is valid for an ionic strength of 1 M (KCl).
[43] A. T. Harrison, O. W. Howarth, *J. Chem. Soc. Dalton Trans. 1986*, 1405.
[44] C. Djordjevic, G. L. Wampler, *J. Inorg. Biochem. 25* (1985) 51.
[45] a) N. J. Campbell, A. C. Dengel, W. P. Griffith, *Polyhedron 8* (1989) 1379; b) A. T. Harrison, O. W. Howarth, *J. Chem. Soc. Dalton Trans. 1985*, 1173; c) A. P. Makarov, A. E. Gekhman, Y. M. Nekidelov, E. P. Talzi, O. Ya. Polotnyuk, K. I. Zamarev, I. I. Moiseev, *Bull. Acad. Sci. USSR, Div. Chem. Sci. (Engl. Transl.) 34* (1985) 1764.
[46] T. G. Faulkner-Hudson: *Vanadium. Toxicology and Biological Significance*. Elsevier, Amsterdam 1964.
[47] Kühn-Birett: *Merkblätter gefährliche Arbeitsstoffe*, ecomed. Landsberg/Lech 1986, Vol. 7, 29. Supplement.
[48] C. Coan, D. J. Scales, A. J. Murphy, *J. Biol. Chem. 261* (1986) 10394.
[49] a) A. S. Tracey, M. J. Gresser, K. M. Parkinson, *Inorg. Chem. 26* (1987) 629; b) B. Galeffi, A. S. Tracey, *ibid. 28* (1989) 1726; c) A. S. Tracey, M. J. Gresser, *ibid. 27* (1988) 1269.
[50] a) C. F. G. C. Geraldes, M. M. C. A. Castro, *J. Inorg. Biochem. 35* (1989) 79; b) *ibid.*, in press.
[51] A. S. Tracey, M. J. Gresser, S. Liu, *J. Am. Chem. Soc. 110* (1988) 5869.
[52] a) D. Rehder, H. Holst, R. Quaas, W. Hinrichs, U. Hahn, W. Saenger, *J. Inorg. Biochem. 37* (1989) 141; b) D. Rehder, *Inorg. Chem. 27* (1988) 4312.
[53] a) W. R. Harris, C. J. Carrano, *J. Inorg. Biochem. 22* (1984) 201; b) N. D. Chasteen, J. K. Grady, C. E. Holloway, *Inorg. Chem. 25* (1986) 2754.
[54] a) B. R. Nechay, L. B. Nanninga, P. S. E. Nechay, *Arch. Biochem. Biophys. 251* (1986) 128; b) D. C. Crans, R. L. Bunch, L. A. Theisen, *J. Am. Chem. Soc. 111* (1989) 7997; c) M. D. Percival, K. Doherty, M. J. Gresser, *Biochemistry 29* (1990) 2764.
[55] M. D. Cohen, A. C. Sen, C.-I. Wei, *Inorg. Chim Acta 138* (1987) 91.
[56] a) J. C. Pessoa, L. F. V. Boas, R. D. Gillard, *Polyhedron 8* (1989) 1173; b) J. C. Pessoa, L. F. V. Boas, R. D. Gillard, R. J. Lancashire, *ibid. 7* (1988) 1245.
[57] R. Cini, G. Giorgi, F. Laschi, M. Sabat, A. Sabatini, A. Vacca, *J. Chem. Soc., Dalton Trans. 1989*, 575.
[58] D. C. Fisher, S. J. Barclay-Peet, C. A. Balfe, K. N. Raymond, *Inorg. Chem. 28* (1989) 4399.
[59] R. Meier, G. Werner, M. Otto, *Collect. Czech. Chem. Commun. 54* (1989) 64.
[60] J. A. Bonadies, C. J. Carrano, *J. Am. Chem. Soc. 108* (1986) 4088.
[61] X. Li, M. S. Lah, V. L. Pecoraro, *Inorg. Chem. 27* (1988) 4657.
[62] A. Neves, W. Walz, K. Wieghardt, B. Nuber, J. Weiss, *Inorg. Chem. 27* (1988) 2484.
[63] G.-E. Matsubayashi, K. Akiba, T. Tanaka, *Inorg. Chim. Acta 157* (1989) 195.
[64] H. Sakurai, M. Nishida, K. Kida, M. Koyama, J. Takada, *Inorg. Chim. Acta 138* (1987) 149.
[65] H. Sakurai, M. Nishida, M. Koyama, J. Takada, *Biochim. Biophys. Acta 924* (1987) 562.
[66] H. Vilter, D. Rehder, *Inorg. Chim. Acta 136* (1987) L7.
[67] N. D. Chasteen, E. M. Lord, H. J. Thompson, J. K. Grady, *Biochim. Biophys. Acta 884* (1986) 84.
[68] A. Butler, H. Eckert, *J. Am. Chem. Soc. 111* (1989) 2802.
[69] I. Bertini, G. Canti, C. Luchinat, *Inorg. Chim. Acta. 67* (1982) L21.
[70] L. C. Cantley, M. Resh, G. Guidotti, *Nature (London) 272* (1978) 552.
[71] a) J. Meyerovitch, Y. Shechter, S. Amir, *Physiol. Behav. 45* (1989) 1113; b) J. L. Vives-Corons, J. M. Jou, A. Ester, M. Ibars, J. Carreras, R. Bartrons, F. Climent, S. Grisolia, *Biochem. Biophys. Res. Commun. 103* (1981) 111; c) H. Sakurai, T. Goda, S. Shimomura, *ibid. 107* (1982) 1349; d) P. J. Stankiewicz, M. J. Gresser, A. S. Tracey, L. F. Hass, *Biochemistry 26* (1987) 1264.
[72] K. Greeff, *Herz/Kreislauf 11* (1979) 501.
[73] a) G. R. Dubyak, A. Kleinzeller, *J. Biol. Chem. 255* (1980) 5306; b) A. Green, *Biochem. J. 238* (1986) 663; c) C. E. Heyliger, A. G. Tahiliani, J. H. McNeill, *Science (Washington DC) 227* (1985) 1474.
[74] a) S. Kadota, I. G. Fantus, G. Deragon, H. J. Guyda, B. Hersh, B. I. Posner, *Biochem. Biophys. Res. Commun. 147* (1987) 259; b) I. G. Fantus, S. Kadota, G. Deragon, B. Foster, B. I. Posner, *Biochemistry 28* (1989) 8864.
[75] a) Y. Shechter, S. J. D. Karlish, *Nature (London) 284* (1980) 556; b) S. Ramanadham, J. J. Mongold, R. W. Brownsey, G. H. Cros, J. H. McNeill, *Am. J. Physiol. 257* (1989) H 904.
[76] a) M. J. Gresser, A. S. Tracey, P. J. Stankiewicz, *Adv. Protein Phosphatases 4* (1987) 35; b) K. M. Lerea, N. K. Tonks, E. G. Krebs, E. H. Fischer, J. A. Glomset, *Biochemistry 28* (1989) 9286; c) A. S. Tracey, M. J. Gresser, *Proc. Natl. Acad. Sci. USA 83* (1986) 609.
[77] a) H. J. Thomson, N. D. Chasteen, L. D. Meeker, *Carcinogenesis (London) 5* (1984) 849; b) L. Banci, A. Dei, D. Gatteschi, *Inorg. Chim. Acta 67* (1982) L53; c) A. Moustatih, M. M. L. Fiallo, A. Garnier-Suillerot, *J. Med. Chem. 32* (1989) 336.
[78] a) P. Köpf-Maier, H. Köpf, *Z. Naturforsch. B34* (1979) 805; b) M. S. Murthy, J. H. Toney, L. N. Rao, L. Y. Kuo; T. J. Marks, *Proc. Am. Assoc.*

Cancer Res. 27 (1986) 279; c) J. H. Toney, C. P. Brock, T. J. Marks. *J. Am. Chem. Soc. 108* (1986) 7263; d) A. Maiti, S. Ghosh, *J. Inorg. Biochem. 36* (1989) 131.

[79] a) M. D. Cohen, A. S. Sen, C.-I. Wei, *Inorg. Chim. Acta 138* (1987) 179; b) F. Vyskocil, J. Teisinger, H. Dlouha, *Biochem. Biophys. Res. Commun. 100* (1981) 982; c) D. C. Crans, C. M. Simone, A. K. Saha, R. H. Glew, *ibid. 165* (1989) 246; d) R. C. Crans, E. M. Willging, S. R. Butler, *J. Am. Chem. Soc. 112* (1990) 427; e) G. H. Bond, P. M. Hudgins, *Biochemistry 18* (1979) 325; f) E. T. Wallick, L. K. Lane, A. Schwartz, *J. Biol. Chem. 254* (1979) 8107; g) O. Hansen, *Biochem. Biophys. Acta 692* (1982) 187.

[80] a) G. R. Willsky, D. A. White, B. C. McCabe, *J. Biol. Chem. 21* (1984) 13273; b) G. R. Willsky, S. F. Dosch, *Yeast 2* (1986) 77; c) G. R. Willsky, J. O. Leung, P. von Offermann, Jr., E. K. Plotnick, S. F. Dosch, *J. Bacteriol. 164* (1985) 611; d) A. Butler. S. M. Parsons, S. K. Yamagata, R. I. de la Rosa, *Inorg. Chim. Acta 163* (1989) 1. The formation constant in 0.5 M $HClO_4$ is $10^{6.8}$ M^{-1} (I. Baltnić, M. Biruš, M. Pribanić, *Croat. Chem. Acta. 60* (1987) 279).

[81] a) R. Smith, K. Zinn, L. C. Cantley, *J. Biol. Chem. 255* (1980) 9852; b) C. T. Carilli, R. A. Farley, D. Perlman, L. C. Cantley, *ibid. 257* (1982) 5601; c) L. C. Cantley, Jr., L. G. Cantley, L. Josephson, *ibid. 253* (1978) 7361.

[82] a) A. Wlodawer, M. Miller, L. Sjölin, *Proc. Natl. Acad. Sci. USA 80* (1983) 3628; b) B. Borah, C.-W. Chen., W. Egan, M. Miller, A. Wlodawer, J. S. Cohen, *Biochemistry 24* (1985) 2058.

[83] a) U. Heinemann, W. Saenger, *Nature (London) 299* (1982) 27; b) U. Heinemann, W. Saenger, *J. Biomol. Struct. Dyn. 1* (1983) 523; c) W. Saenger, R. Arni, M. Maslowska, A. Pähler, U. Heinemann, in D. Moras, J. Drenth, B. Strandlberg, D. Suck, K. Wilson (Eds.): *Crystallography in Molecular Biology,* Plenum, New York 1987.

[84] D. Kostrewa, H.-W. Choe, U. Heinemann, W. Saenger, *Biochemistry 28* (1989) 7592.

[85] a) D. I. Arnon, G. Wessel, *Nature (London) 172* (1953) 1039; b) O. Warburg, G. Krippahl, W. Buchholz, *Z. Naturforsch. B10* (1955) 422.

[86] a) L. Becker, H.-U. Meisch, in G. Akoyunoglou (Ed.): *Photosynthesis II. Electron Transport and Photophosphorylation,* Balaban Int. Science Services, Philadelphia 1981; b) H.-U. Meisch, H. Hoffmann, W. Reinle, *Z. Naturforsch. C33* (1978) 623; c) R. J. Porra, H.-U. Meisch, *Trends Biochem. Sci. 9* (1984) 99.

[87] a) S. N. Mogel, B. A. McFadden, *Biochemistry 28* (1989) 5423; b) In *Ascidia nigra* of the Phleobranchia, V^{III} has been shown directly to be the dominant vanadium species by using SQUID measurements (susceptibility measurements with a superconducting quantum interference device) (S. Lee, K. Kustin, W. E. Robinson, R. B. Frankel, K. Spartalian, *J. Inorg. Biochem. 33* (1988) 183); the magnetic properties resemble those of the catecholate complex **59b**, Fig. 13 in Section 4.2.

[88] a) M. J. Smith, *Experientia 45* (1989) 452; b) H. Michibata, *Zool. Sci. 6* (1989) 639; c) J. H. Swinehart, W. R. Biggs, D. J. Halko, N. C. Schroeder, *Biol. Bull (Woods Hole Mass.) 146* (1974) 302.

[89] a) E. M. Oltz, S. Pollack, T. Delohery, M. J. Smith, M. Ojika, S. Lee, K. Kustin, K. Nakanishi, *Experientia 45* (1989) 186; b) I. G. Macara, G. C. McLeod, K. Kustin, *Biochem. J. 181* (1979) 457; c) H. Michibata, T. Miyamoto, H. Sakurai, *Biochem. Biophys. Res. Commun. 141* (1986) 251.

[90] a) L. C. Dorsett, C. J. Hawkins, J. A. Grice, M. F. Lavin, P. M. Merefield, D. L. Perry, I. L. Ross, *Biochemistry 26* (1987) 8078; b) C. J. Hawkins, S. W. Taylor, *Abstr. 27th Int. Conf. Coord. Chem.* (1989), Broadbeach, Queensland, Australien.

[91] P. Frank, B. Hedman, R. M. K. Carlson, T. A. Tyson, A. L. Roe, K. O. Hodgson, *Biochemistry 26* (1987) 4975.

[92] a) P. Frank, R. M. K. Carlson, K. O. Hodgson, *Inorg. Chem. 25* (1986) 470; b) S. G. Brand, C. J. Hawkins, D. L. Parry, *ibid. 26* (1987) 627; c) S. Lee, K. Nakanishi, K. Kustin, *Biochim. Biophys. Acta,* in press.

[93] a) E. W. Baker, S. E. Palmer in D. Dolphin (Ed.): *The Porphyrins I,* Academic, New York 1978, p. 485; b) R. C. Pettersen, *Acta Crystallogr. Sect. B25* (1969) 2527.

[94] a) P. I. Premović, M. S. Pavlović, N. Z. Pavlović, *Geochim. Cosmochim. Acta 50* (1986) 1923; b) B. B. Garrett, W. M. Gulick, Jr., *J. Chem. Soc. Faraday Trans. 179* (1983) 1733.

[95] a) H.-U. Meisch, W. Reinle, *Naturwissenschaften 68* (1981) 569; b) P. I. Premović in R. Rodriguez-Clemente, Y. Tardy (Eds.): *Geochemistry and Mineral Formation in the Earth Surface, Proc. Int. Meet.* Granada (1986) p. 431.

[96] L. C. Cantley, Jr., P. Aisen, *J. Biol. Chem. 254* (1979) 1781.

[97] A. Treibs, *Justus Liebigs Ann. Chem. 510* (1936) 42; *ibid. 517* (1936) 172.

[98] a) S. L. Berger, C. S. Birkenmeier, *Biochemistry 18* (1979) 5143; b) A. Terron, V. Moreno, *Inorg. Chim. Acta 56* (1981) L57; c) S. B. Etcheverry, E. G. Ferrer, E. J. Baran, *Z. Naturforsch. B44* (1989) 1355; d) G. Urretavizcaya, E. J. Baran, *ibid. 42* (1987) 1537.

[99] a) H. Sakurai, T. Goda, S. Shimomura, *Biochem. Biophys. Res. Commun. 108* (1982) 474; b) H. Sakurai, T. Goda, S. Shimomura, T. Yoshimura, *ibid. 104* (1982) 1421.

[100] a) H. Kneifel, E. Bayer, *J. Am. Chem. Soc.* 108 (1986) 3075; b) E. Bayer, H. Kneifel, *Abstr. 27th Int. Conf. Coord. Chem. (1989) Broadbeach,* Queensland, Australia.

[101] C. Weidemann, P. Priebsch, D. Rehder, *Chem. Ber. 122* (1989) 235.

[102] M. A. A. F. de C. T. Carrondo, M. T. L. S. Duarte, J. C. Pessoa, J. A. L. Silva, J. J. R. F. de Silva, M. C. T. A. Vaz, L. F. Vilas-Boas, *J. Chem. Soc. Chem. Commun. 1988,* 1158.

[103] a) B. E. Krenn, M. G. M. Tromp, R. Wever, *J. Biol. Chem. 265* (1989), in press; b) N. Itoh, Y. Izumi, H. Yamada, *J. Biol. Chem. 261* (1986) 5194; c) B. E. Krenn, Y. Izumi, H. Yamada, R. Wever, *Biochim. Biophys. Acta 998* (1989) 63; d) H. Yu, J. W. Whittaker, *Biochem. Biophys. Res. Commun. 160* (1989) 87; e) R. Wever, H. Plat, E. de Boer, *Biochim. Biophys. Acta 830* (1985) 181; f) E. de Boer, R. Wever, *J. Biol. Chem. 263* (1988) 12326; g) M. C. R. Franssen, J. D. Jansma, H. C. van der Plas, E. de Boer, R. Wever, *Bioinorg. Chem. 16* (1988) 352.

[104] R. Wever, B. E. Krenn, E. de Boer, H. Offenberg, H. Plat, in T. E. King, H. S. Mason, M. Morrison (Eds.): *Oxidases and Related Redox Systems, Proc. 4th. Int. Symp.* Portland (Oregon); Liss, New York 1987, p. 477.

[105] F. Secco, *Inorg. Chem. 19* (1980) 2722.

[106] R. R. Everett, A. Butler, *Inorg. Chem. 28* (1989) 393.

[107] D. Rehder, H. Vilter, A. Duch, W. Priebsch, C. Weidemann, *Recl. Trav. Chim. Pays-Bas 106* (1987) 408.

[108] R. Wever, *Nature (London) 335* (1988) 501.

[109] a) J. M. Arber, E. de Boer, C. D. Garner, S. S. Hasnain, R. Wever, *Biochemistry 28* (1989) 7968; b) B. Hedman, K. O. Hodgson, C. D. Garner, in S. S. Hasnain (Ed.): *Biophysics and Synchroton Radiation,* Horwood, in press.

[110] J. Hormes, U. Kuetgens, R. Chauvistre, W. Schreiber, N. Anders, H. Vilter, D. Rehder, C. Weidemann, *Biochim. Biophys. Acta 956* (1988) 293.

[111] E. de Boer, K. Boon, R. Wever, *Biochemistry 27* (1988) 1629.

[112] E. de Boer, C. P. Keijzers, A. A. K. Klaassen, E. J. Reijerse, D. Collison, C. D. Garner, R. Wever, *FEBS Lett. 235* (1988) 93.

[113] W. Priebsch, D. Rehder, *Inorg. Chem. 29* (1990) 3013; b) S. L. Chandha, K. Uppal, *Indian J. Chem. Sect. A 29* (1990) 80.

[114] R. R. Eady, R. L. Robson, T. H. Richardson, R. W. Miller, M. Hawkins, *Biochem. J. 244* (1987) 197.

[115] R. L. Robson, P. R. Woodley, R. N. Pau, R. R. Eady, *EMBO J. 8* (1989) 1217.

[116] A. F. Yakunin, Chan Van Ni, I. N. Gogotov, *Dokl. Akad. Nauk. SSSR 307* (1989) 1269. An alternative nitrogenase is also formed by *A. azollae* under Mo-deficient conditions: Chan Van Ni, A. F. Jakunin, I. N. Gogotov, *ibid. 109* (1989) 1480.

[117] M. J. Dilworth, R. R. Eady, R. L. Robson, R. W. Miller, *Nature (London) 327* (1987) 167.

[118] A. Müller, K. Schneider, J. Erfkamp, V. Wittneben, E. Diemann, A. N. Eaton, *Naturwissenschaften 75* (1988) 625.

[119] a) R. R. Eady, *BioFactors 1* (1988) 111; b) R. R. Eady, *Polyhedron 8* (1989) 1695.

[120] B. E. Smith, R. R. Eady, D. J. Lowe, C. Gormal, *Biochem. J. 250* (1988) 299.

[121] a) R. N. F. Thorneley, N. H. J. Bergström, R. R. Eady, D. J. Lowe, *Biochem. J. 257* (1989) 789; b) R. W. Miller, R. R. Eady, *ibid. 256* (1988) 429.

[122] C. Weidemann, D. Rehder, U. Kuetgens, J. Hormes, H. Vilter, *Chem. Phys. 136* (1989) 405. The energy of the white band, a pre-edge structure, (the so-called 1s → 3d transition), is generally correlated with the coordination charge, which is made up of the oxidation number of V and the ionicities of the V–L bonds. This association suggests that, for vanadium complexes with the same or a similar construction for the coordination sphere, the K → 3d transitions for V^V lie at higher energies than those for V^{IV}. The trend indeed confirms this. [J. Wong, F. W. Lytle, R. P. Messmer, H. D. Maylotte, *Phys. Rev. B: Condens. Matter 30* (1984) 5596; K.-H. Hallmeier, R. Szargan, G. Werner, R. Meier, N. A. Sheromov, *Spectrochim. Acta Part A42* (1986) 841]. Nevertheless, geometric factors such as distortions in octahedral complexes (bent octahedral axis, unequal bond lengths in the octahedral plane, vanadium outside the octahedral plane) can have distinctly greater effects than differences in oxidation number. For V^{IV} complexes, we have found energies of the white band between 4.3 and 5.8 eV, for V^V complexes between 4.6 and 6.2.

[123] a) R. R. Eady, R. L. Robson, T. H. Richardson, R. W. Miller, M. Hawkins, *Biochem. J. 244* (1987) 197; b) J. E. Morningstar, B. J. Hales, *J. Am. Chem. Soc. 109* (1987) 6854; c) B. J. Hales, A. E. True, B. M. Hoffman, *ibid. 111* (1989) 8519; d) see also the Mo-X_α-calculations for $Fe_3VS_4(SH)_6^{4\ominus}$. A. Müller, V. Wittneben, *J. Mol. Struct. THEOCHEM,* in press.

[124] a) C. D. Garner, J. M. Arber, I. Harvey, S. S. Hasnain, R. R. Eady, B. E. Smith, E. de Boer, R. Wever, *Polyhedron 8* (1989) 1649; b) J. M. Arber, B. R. Dobson, R. R. Eady, S. S. Hasnain, C. D. Garner, T. Matsushita, M. Nomuras, B. E. Smith, *Biochem. J. 258* (1989) 733; c) G. N. George, C. L. Coyle, B. J. Hales, S. P. Cramer, *J. Am. Chem. Soc. 110* (1988) 4057; d) I. Harvey, J. M. Arber, R. R. Eady, B. E. Smith, C. D. Garner, S. S. Hasnain, *Biochem. J. 266* (1990) 929.

[125] a) J. A. Kovacs, R. H. Holm, *J. Am. Chem. Soc. 108* (1986) 340; b) J. A. Kovacs, R. H. Holm, *Inorg. Chem. 26* (1987) 711; c) S. Ciurli, R. H. Holm, *ibid. 28* (1989) 1685.

[126] I. Bertini, C. Luchinat, L. Messori, *J. Inorg. Biochem. 25* (1985) 57.
[127] W. R. Harris, C. J. Carrano, *J. Inorg. Biochem. 22* (1984) 201.
[128] a) R. Meier, G. Werner, R. Kirmse, J. Stach, L. Dunsch, *Z. Anorg. Allg. Chem.* (1990), in press; b) S. R. Cooper, Y. B. Koh, K. N. Raymond, *J. Am. Chem. Soc. 104* (1982) 5092; c) R. J. DeKoch, D. J. West, J. C. Cannon, N. D. Chasteen, *Biochemistry 13* (1974) 4347; d) D. Collison, B. Gahan, F. E. Mabbs, *J. Chem. Soc. Dalton Trans. 1987,* 111; e) O. P. Shvoeva, G. P. Kuchava, G. A. Evtikova, V. K. Belyaeva, G. V. Myasoedova, I. N. Marov, *Z. Neorg. Khim. 34* (1989) 844; *Russ. J. Inorg. Chem. 34* (1989) 472; f) T. Bora, M. Devi, *Indian J. Chem. Sect. A27* (1988) 1097.
[129] a) General literature on ^{51}V NMR spectroscopy: D. Rehder, *Bull. Magn. Reson. 4* (1982) 33; *Magn. Reson. Rev. 9* (1984) 125; *Chimia 40* (1986) 186; D. Rehder, in J. Mason (Ed.): *Multinuclear NMR,* Plenum, New York 1987, Chapter 19; b) Applications to biological systems: D. Rehder, in N. D. Chasteen (Ed.): *Vanadium in Biological Systems,* Kluwer, Dordrecht 1990, Chapter 10; c) W. Priebsch, D. Rehder, *Inorg. Chem. 24* (1985) 3058.
[130] a) J. Mazurier, J.-M. Lhoste, J. Montreuil, G. Spik, *Biochim. Biophys. Acta 745* (1983) 44; b) California State University Report 1986, *Energy Res. Abstr. 12* (1987), Abstr. No. 10078; c) S. M. Ashraf, W. U. Malik, *J. Inorg. Biochem. 35* (1989) 1.
[131] a) S. J. Lippard, *Angew. Chem. 100* (1988) 353; *Angew. Chem. Int. Ed. Engl. 28* (1988) 344; b) K. Wieghardt, *Angew. Chem. 101* (1989) 1179; *Angew. Chem. Int. Ed. Engl. 29* (1989).
[132] a) H.-U. Meisch, S. Kappesser, *Biochim. Biophys. Acta 925* (1987) 234; b) H. Sakurai, Z.-E. Taira, N. Sakai, *Inorg. Chim. Acta 151* (1988) 85. For electrochemistry of $VO^{2\oplus}$ complexes with cysteine esters, see M. D. Sifri, T. L. Riechel, *ibid. 142* (1988) 229; c) J. K. Money, J. R. Nicholson, J. C. Huffman, G. Christou, *Inorg. Chem. 25* (1986) 4072; d) Y. Do, E. D. Simhon, R. H. Holm, *ibid. 24* (1985) 4635.
[133] N. Kanoongo, R. Singh, J. P. Tandon, *Transition Met. Chem. (London) 12* (1987) 271.
[134] G. Gattow, G. Kiel, H. Sayin, *Z. Anorg. Allg. Chem. 498* (1983) 85. Further xanthogenato complexes are described in, for example: A. L. Doadrio-Villarejo, C. V. Ragel, A. Doadrio, *An. Quim. 81* (1985) 309 and 374.
[135] G. Christou, D. Heinrich, J. K. Money, J. R. Rambo, J. C. Huffman, K. Folting, *Polyhedron 8* (1989) 1723.
[136] a) J. K. Money, J. C. Huffman, G. Christou, *Inorg. Chem. 24* (1985) 3297; b) J. K. Money, J. C. Huffman, G. Christou, *ibid. 27* (1988) 507; c) J. R. Rambo, J. C. Huffman, G. Christou, *J. Am. Chem. Soc. 111* (1989) 8027; d) S. A. Duraj, M. T. Andras, B. Rither, *Polyhedron 8* (1989) 2763.
[137] a) D. Szeymies, B. Krebs, G. Henkel, *Angew. Chem. 95* (1983) 903; *Angew. Chem. Int. Ed. Engl. 22* (1983) 885; b) J. R. Dorfman, R. H. Holm, *Inorg. Chem. 22* (1983) 3179.
[138] a) R. B. Hitam, A. J. Rest, *Organometallics 8* (1989) 1598; b) K. Ihmels, D. Rehder, *Chem. Ber. 118* (1985) 895.
[139] a) G. M. Brown, L. Maya, *Inorg. Chem. 28* (1989) 2007; b) D. Rehder, *J. Organomet. Chem. 37* (1972) 303; c) F. P. Warnock, S. B. Philson, J. E. Ellis, *J. Chem. Soc. Chem. Commun. 1984,* 893.
[140] a) C. Woitha, D. Rehder, *J. Organomet. Chem. 353* (1988) 315; b) C. Woitha, U. Behrens, V. Vergopoulos, D. Rehder, *ibid. 393* (1990) 97.
[141] a) A. Shilov, N. Denisov, O. Efimov, N. Shuvalov, N. Shuvalova, A. Shilova, *Nature (London) 231* (1971) 460. b) B. Folkesson, R. Larsson, *Acta Chem. Scand. Ser. A33* (1979) 347.
[142] J. J. H. Ederna, A. Meetsma, S. Gambarotta, *J. Am. Chem. Soc. 111* (1989) 6878.
[143] M. Veith, *Angew. Chem. 88* (1976) 384; *Angew. Chem. Int. Ed. Engl. 15* (1976) 387.
[144] J. Bultitude, L. F. Larkworthy, D. C. Povey, G. W. Smith, J. R. Dilworth, G. J. Leigh, *J. Chem. Soc. Chem. Commun. 1986,* 1748.
[145] R. Stomberg, *Acta Chem. Scand. Ser. A40* (1986) 168.
[146] a) R. E. Oughtred, E. S. Raper, H. M. M. Shearer, *Acta Crystallogr. Sect. B32* (1976) 82; b) A. Pajunen, S. Pajunen, *ibid. 36* (1980) 2425.
[147] D. Rehder, W. Priebsch, M. von Oeynhausen, *Angew. Chem. 101* (1989) 1295; *Angew. Chem. Int. Ed. Engl. 28* (1989) 1221.
[148] C. Djordjevic, M. Lee, E. Sinn, *Inorg. Chem. 28* (1989) 719.
[149] D. D. Heinrich, K. Folting, W. E. Streib, J. C. Huffman, G. Christou, *J. Chem. Soc. Chem. Commun. 1989,* 1411.
[150] a) D. Rehder, W. Priebsch, U. Behrens, unpublished: The complex **52a**, crystallizes in the orthorhombic space group *Pcmn* with the following cell parameters: $a = 891.0(3)$, $b = 1458.3(5)$, $c = 1913.7(9)$ pm; $V = 2486.6 \times 10^6$ (pm)^3; $Z = 4$. Selected distances [pm] and angles [°]: V-O(μ_3) 162.6(17), 235.1(15), and 240.4(19); V=O(*exo*) 151.9(18) and 158.9(15); V-O(THF) 219.9(18); V-O(carboxylato) 198.2 (averaged); V-O(μ_3)-V 121.9(8), 121.2(10), and 117.0(8). The vanadium atoms are octahedrally coordinated and lie, together with the μ_3-O, the O of THF, and the *exo* vanadyl oxygen atom, on the crystallographic mirror plane; b) F. A. Cotton, G. E. Lewis, G. N. Mott, *Inorg. Chem. 21* (1982) 3127.
[151] J. G. Forrest, C. K. Prout, *J. Chem. Soc. A 1967,* 1312.
[152] A. T. Casey, B. S. Morris, E. Sinn, J. R. Thackeray, *Aust. J. Chem. 25* (1972) 1195.
[153] C. N. Caughlan, H. M. Smith, K. Watenpaugh, *Inorg. Chem. 12* (1966) 2131.
[154] a) M. Branca, G. Micera, A. Dessi, H. Kozlowski, *J. Chem. Soc. Dalton Trans. 1989* 1283; b) M. Branca, G. Micera, A. Dessi, *ibid.,* 1289; c) H. van Willigen, *J. Magn. Reson. 39* (1980) 37; d) H. van Willigen, T. K. Chandrasekhar, *J. Am. Chem. Soc. 105* (1983) 4232.
[155] V. L. Pecoraro, *Inorg. Chim. Acta 155* (1989) 171.
[156] J. H. Ferguson, K. Kustin, *Inorg. Chem. 18* (1979) 3349.
[157] a) H. Mimoun, L. Saussine, E. Daire, M. Postel, J. Fischer, R. Weiss, *J. Am. Chem. Soc. 105* (1983) 3101; b) R. E. Drew, F. W. B. Einstein, *Inorg. Chem. 12* (1973) 829.
[158] L. Casella, M. Gullotti, A. Pintar, S. Colonna, A. Manfredi, *Inorg. Chim. Acta 144* (1988) 89.
[159] C. Djordjevic, B. C. Puryesr, N. Vuletic, C. J. Abelt, S. J. Sheffield, *Inorg. Chem. 27* (1988) 2926.
[160] W. R. Scheidt, R. Countryman, J. L. Hoard, *J. Am. Chem. Soc. 93* (1971) 3878.
[161] M. Shimoi, Y. Saito, H. Ogino, *Chem. Lett. 1989,* 1675.
[162] H. Ogino, M. Shimoi, Y. Saito, *Inorg. Chem. 28* (1989) 3596.
[163] a) M. Pasquali, F. Marchetti, C. Floriani, M. Cesari, *Inorg. Chem. 19* (1980) 1198; b) J. A. Bonadies, C. J. Carrano, *ibid. 25* (1986) 4358; c) X. Li, V. L. Pecoraro, *ibid. 28* (1989) 3403.
[164] S. Colombatto, M. A. Grillo, *Int. J. Biochem. 17* (1985) 657.
[165] a) K. Nakajima, M. Kojima, K. Toriumi, K. Saito, J. Fujita, *Bull. Chem. Soc. Jpn. 62* (1989) 760; b) C. J. Carrano, C. M. Nunn, R. Quan, J. A. Bonadies, V. L. Pecoraro, *Inorg. Chem. 29* (1990) 944.
[166] L. J. Calviou, D. Collison, C. D. Garner, F. E. Mabbs, M. A. Passand, M. Pearson, *Polyhedron 8* (1989) 1835.
[167] E. Kime-Hunt, K. Spartalian, M. DeRusha, C. M. Nunn, C. J. Carrano, *Inorg. Chem. 28* (1989) 4392.
[168] D. Collison, F. E. Mabbs, M. A. Passand, K. Rigby, W. E. Cleland, Jr., *Polyhedron 8* (1989) 1827.
[169] A. Neves, K. Wieghardt, B. Nuber, J. Weiss, *Inorg. Chim. Acta 150* (1988) 183.
[170] P. Knopp, K. Wieghardt, B. Nuber, J. Weiss, W. S. Sheldrick, *Inorg. Chem. 29* (1990) 363.
[171] M. Köppen, G. Fresen, K. Wieghardt, R. M. Llusar, B. Nuber, J. Weiss, *Inorg. Chem. 27* (1988) 721.
[172] J. C. Dutton, G. D. Fallon, K. S. Murray, *J. Chem. Soc. Chem. Commun. 1990,* 64.
[173] R. R. Everett, A. Butler, *Inorg. Chem. 28* (1989) 393.
[174] D. C. Crans, C. D. Rithner, L. A. Theisen, *J. Am. Chem. Soc. 112* (1990) 2901.
[175] D. C. Crans, C. M. Simone, A. K. Saha, R. H. Glew, *Biochem. Biophys. Res. Commun. 165* (1989) 246.
[176] D. C. Crans, E. M. Willging, S. R. Butler, *J. Am. Chem. Soc. 112* (1990) 427.
[177] a) C. R. Cremo, G. T. Long, J. C. Grammer, *Biochemistry 29* (1990) 7982; b) I. Ringel, Y. M. Peyser, A. Muhlrad, *ibid.* 9091.
[178] X. Shi, X. Sun, N. S. Dalal, *FEBS Lett. 271* (1990) 185.
[179] D. G. Drueckhammer, J. R. Durrwachter, R. L. Pederson, D. C. Crans, L. Daniels, C.-H. Wong, *J. Org. Chem. 54* (1989) 70.
[180] C. J. Lockett, C. Demetriou, J. H. A. Nugent, *NATO Adv. Study Inst. Ser., Ser. A,* 1989, 168.
[181] K. Iwai, T. Ido, R. Iwata, M. Kawamura, S. Kimura, *Nucl. Med. Biol. 16* (1989) 783.
[182] A. J. Carmichael, *FEBS Lett. 261* (1990) 165.
[183] C. F. G. C. Geraldes, M. M. C. A. Castro, *J. Inorg. Biochem.* (1990), in press.
[184] A. S. Tracey, J. Jaswal, M. J. Gresser, D. Rehder, *Inorg. Chem. 29* (1990) 4283.
[185] J. J. R. Frausto da Silva, *Chem. Speciation Bioavailability 1* (1989) 139.
[186] D. Rehder, H. Holst, W. Priebsch, H. Vilter, *J. Inorg. Biochem. 40* (1990), in press.
[187] P. Jordan, B. Kloareg, H. Vilter, *J. Plant Physiol.* (1990), in press.
[188] R. R. Everett, J. R. Kanofsky, A. Butler, *J. Biol. Chem. 265* (1990) 4908.
[189] I. Harvey, J. M. Arber, R. R. Eady, B. E. Smith, C. D. Garner, S. S. Hasnain, *Biochem. J. 266* (1990) 929.
[190] S. A. Duraj, M. T. Andras, P. A. Kibala, *Inorg. Chem. 29* (1990) 1232.
[191] C. Woitha, D. Rehder, *Angew. Chem. 102* (1990) 1495; *Angew. Chem. Int. Ed. Engl. 29* (1990) 1438.
[192] U. Auerbach, B. S. P. C. della Vedova, K. Wieghardt, B. Nuber, J. Weiss, *J. Chem. Soc. Chem. Commun. 1990,* 1004.
[193] J. C. Dutton, K. S. Murray, E. R. T. Tiekink, *Inorg. Chim. Acta 166* (1989) 5.
[194] D. C. Crans, R. A. Felty, M. M. Miller, *J. Am. Chem. Soc. 113* (1991), in press.
[195] M. Branca, G. Micera, A. Dessi, *J. Chem. Soc. Dalton Trans. 1990,* 457.
[196] M. Branca, G. Micera, A. Dessi, D. Sanna, K. N. Raymond, *Inorg. Chem. 29* (1990) 1586.
[197] R. Wever, K. Kustin, *Adv. Inorg. Chem. 35* (1990) 81.
[198] K. Kustin, W. E. Robinson, M. J. Smith, *Invertebr. Reprod. Dev. 17* (1990) 129.

Highly-Reduced Metal Carbonyls

By *Wolfgang Beck* *

Anionic carbonyl complexes (carbonylmetalates) contain metals with formal negative oxidation numbers and constitute one of the most important classes of compounds in organometallic chemistry. Since the first systematic studies of carbonylmetalates by *Hieber* et al.[1] these compounds have proven to be valuable starting compounds for the synthesis of a variety of—even multinuclear—metal carbonyls and their derivatives.[2] They are also used in organic synthesis.[3]

The first anionic carbonyl complexes $[HFe(CO)_4]^{\ominus}$ and $Fe(CO)_4^{2\ominus}$ were obtained by reaction of $Fe(CO)_5$ with alkaline hydroxide solutions[4] (Hieber base reaction).

$$Fe(CO)_5 + 3\,OH^{\ominus} \longrightarrow [HFe(CO)_4]^{\ominus} + CO_3^{2\ominus} + H_2O$$

Kruck et al.[5] interpreted the mechanism of this reaction in terms of an attack by hydroxide at the C atom of a CO ligand with elimination of carbon dioxide.

The simplest and most straightforward entry to carbonylmetalates is via the reduction of metal carbonyls, usually with alkali metals, whereby a CO-ligand (two-electron donor) is formally replaced by two electrons or a metal–metal bond is reductively cleaved.

$$Fe(CO)_5 + 2\,Na \longrightarrow Na_2[Fe(CO)_4] + CO$$

$$[(OC)_5Re\text{–}Re(CO)_5] + 2\,Na \longrightarrow 2\,Na[Re(CO)_5]$$

Pioneering work by *Behrens*[6] in 1941 already showed that this reduction is effectively carried out in liquid ammonia. Using the 18e rule a series of mononuclear neutral and anionic carbonyl complexes results in which the central atom in each case has a noble gas electron configuration (Table 1).

Table 1. Mononuclear neutral and anionic carbonyl complexes with noble gas electron configuration [a].

Metal		Structure: tetrahedral	trigonal-bipyramidal	octahedral
Ni		$Ni(CO)_4$		
Co,Rh,Ir	$M(CO)_3^{3\ominus}$	$M(CO)_4^{\ominus}$		
Fe,Ru,Os		$M(CO)_4^{2\ominus}$	$M(CO)_5$	
Mn,Re		$M(CO)_4^{3\ominus}$	$M(CO)_5^{\ominus}$	$M(CO)_6^{\oplus}$
Cr,Mo,W	$(M(CO)_3^{6\ominus}$	$M(CO)_4^{4\ominus}$	$M(CO)_5^{2\ominus}$	$M(CO)_6$
V,Nb,Ta		$(M(CO)_4^{5\ominus})$	$M(CO)_5^{3\ominus}$	$M(CO)_6^{\ominus}$
Ti,Zr,Hf		$(M(CO)_4^{6\ominus})$	$(M(CO)_5^{4\ominus})$	$M(CO)_6^{2\ominus}$

[a] Derivatives of the compounds quoted in parentheses are known.

The compounds within a column are iso-structural. The anions in the same row are each derived from the one on the right by replacement of a CO-ligand by two electrons.

Recently, *Ellis* et al.[7] were able to prepare new, highly reduced, i.e. three- and four-fold negatively charged metal carbonyls ("Ellis compounds") by a series of impressive experimentally demanding and systematically planned studies. A few years ago one would scarcely have thought of the existence of anions such as $Cr(CO)_4^{4\ominus}$!

Synthesis: Highly-reduced metal carbonyls and their derivatives were prepared by *Ellis* et al. with alkali metals or alkali metal naphthalenides as reducing agents in liquid ammonia, in hexamethylphosphoric triamide, or even in THF. Singly charged anions or metal carbonyls with donor ligands (amines, phosphanes) were employed as starting compounds (see, e.g., Ref. [8,9]).

$$Na[M(CO)_6] + 2\,Na \longrightarrow Na_3[M(CO)_5] + CO \quad (M = V,Nb,Ta)$$

$$[M(CO)_4(tmeda)] + 4\,Na \longrightarrow Na_4[M(CO)_4] \quad (M = Cr,Mo,W)$$

$$Na[M(CO)_5] + 2\,Na \longrightarrow Na_3[M(CO)_4] + CO \quad (M = Mn,Re)$$

$$Na[Co(CO)_4] + 2\,Na \longrightarrow Na_3[Co(CO)_3] + CO$$

The synthesis of hexacarbonyltitanate, -zirconate, and -hafnate(− II), the first stable binary carbonyls of elements of group 4, was achieved, inter alia, by reductive carbonylation of $[M(CO)_4L]$ with potassium naphthalenide as reducing agent in the presence of cryptands:[10]

$$[M(CO)_4L] + 2\,KC_8H_{10} \xrightarrow{\text{cryptand, CO}} [K(\text{cryptand})]_2[M(CO)_6] + 2\,C_8H_{10} + L$$

$(L = H_3CC(CH_2PMe_2)_3,\ M = Ti, Zr, Hf)$

The titanium and zirconium compounds are also accessible under similar conditions directly from the metal tetrachlorides. The "exhaustively" reduced carbonylmetalates $M(CO)_4^{5\ominus}$ (M = V,Nb,Ta), $M(CO)_4^{6\ominus}$ (M = Ti,Zr,Hf) and $M(CO)_3^{6\ominus}$ (M = Cr,Mo,W) have not yet been characterized; *Ellis* et al., however, have been able to isolate their corresponding triphenylstannyl derivatives (see below).

Properties and reactivity: The solvent-free salts of the tri- and tetraanionic carbonylmetalates are, as expected, strong reducing agents; they are extremely pyrophoric. The isolated salts $Na_4[M(CO)_4]$ (M = Cr,Mo,W) or $Cs_3[Ta(CO)_5]$ can explode under argon (!), even without external interference. The extremely sensitive compounds were therefore mostly employed in situ.

Carbonylmetalates, e.g. $Cr(CO)_5^{2\ominus}$ can reduce CO_2.[11]

$$Cr(CO)_5^{2\ominus} + 2\,CO_2 \longrightarrow Cr(CO)_6 + CO_3^{2\ominus}$$

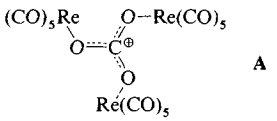

A

Such a reaction is possibly responsible for the unexpected formation of the novel μ_3-carbonato-bridged complex **A**, which is formed along with the hydride $[(OC)_5ReIr(H)(CO)_3Re(CO)_5]$ from $Ir(CO)_3^{3\ominus}$ and $[(C_2H_4)Re(CO)_5]^{\oplus}$ on exposing the reaction solution to air.[12]

The protonation of carbonylmetalates is one of their most important reactions and usually leads to hydrido complexes.

[*] Prof. Dr. W. Beck
Institut für Anorganische Chemie der Universität
Meiserstrasse 1, W-8000 München 2 (FRG)

 © VCH Verlagsgesellschaft mbH, W-6940 Weinheim, 1991 0570-0833/91/0202-0168 $ 3.50+.25/0

$$Fe(CO)_4^{2\ominus} + 2H^{\oplus} \longrightarrow [H_2Fe(CO)_4]$$

$$Re(CO)_4^{3\ominus} + 2H^{\oplus} \longrightarrow [H_2Re(CO)_4]^{\ominus}$$

$V(CO)_5^{3\ominus}$ reacts with NH_4Cl in liquid ammonia with H_2-elimination ($H^{\oplus}$ as oxidizing agent) and formation of $[V(CO)_5NH_3]^{\ominus}$; the ammonia in this anion can be readily replaced by stronger donor ligands L (isocyanide, phosphane).

$$V(CO)_5^{3\ominus} + 2H^{\oplus} \xrightarrow[-H_2]{NH_3} [V(CO)_5NH_3]^{\ominus} \xrightarrow[-NH_3]{+L} [V(CO)_5L]^{\ominus}$$

Carbonylmetalates react as nucleophiles with alkyl and aryl halides, affording access to the important class of organometallic complexes containing a metal–carbon σ-bond.

$$Re(CO)_5^{\ominus} + CH_3I \xrightarrow[-I^{\ominus}]{} [(OC)_5Re-CH_3]$$

Corresponding reactions can also be carried out with the highly reduced $Re(CO)_4^{3\ominus}$ anion (H_3COTos = methyl *p*-toluenesulfonate:[8]

$$Re(CO)_4^{3\ominus} + CH_3OTos \xrightarrow[-OTos^{\ominus}]{} [H_3CRe(CO)_4]^{2\ominus} \longrightarrow [(H_3C)_2Re(CO)_4]^{\ominus}$$

As we have already been able to show, protonation of $[(H_3C)_2Re(CO)_4]^{\ominus}$ with tetrafluoroboric acid affords the doubly coordinatively unsaturated $Re(CO)_4^{\oplus}$,[13a] a useful organometallic Lewis acid[13b] for reactions with nucleophiles.

$$[(H_3C)_2Re(CO)_4]^{\ominus} + 2H^{\oplus} \longrightarrow Re(CO)_4^{\oplus} + 2CH_4$$

In our studies we have used carbonylmetalates as nucleophiles for additions to coordinated unsaturated hydrocarbons. The addition of carbonylmetalates to unsaturated hydrocarbons in cationic complexes has proven to be a direct and rational method for the synthesis of numerous hydrocarbon-bridged complexes.[14]

$$[(OC)_5Re(C_2H_4)]^{\oplus} + Os(CO)_4^{2\ominus} + [(C_2H_4)Re(CO)_5]^{\oplus} \xrightarrow{(CO)_4} (OC)_5Re(CH_2)_2Os(CH_2)_2Re(CO)_5$$

Highly reduced metal carbonyls are especially useful for the synthesis of multinuclear complexes with metal–metal bonds between main-group and subgroup elements, which, e.g., are formed by reaction with chlorotriphenylstannane or chlorotriphenylphosphinegold.

$$Cr(CO)_4^{4\ominus} + 3ClSnPh_3 \xrightarrow[-3Cl^{\ominus}]{} [(OC)_4Cr(SnPh_3)_3]^{\ominus}$$

$$V(CO)_5^{3\ominus} + 3ClAuPPh_3 \xrightarrow[-3Cl^{\ominus}]{} (OC)_5V(AuPPh_3)_3$$

According to the studies of *Ellis* et al. triphenylstannyl derivatives of almost all highly reduced metal carbonyls are known.

$[Co(CO)_3(SnPh_3)_2]^{\ominus}$ ($\triangleq Co(CO)_3^{3\ominus}$), $[W(CO)_3(SnPh_3)_4]^{2\ominus}$ ($\triangleq W(CO)_3^{6\ominus}$),

$(OC)_4Zr(SnPh_3)_4]^{2\ominus}$ ($\triangleq Zr(CO)_4^{6\ominus}$), $[Ti(CO)_5(SnPh_3)_2]^{2\ominus}$ ($\triangleq Ti(CO)_5^{4\ominus}$).

The multinuclear complexes have interesting structures containing transition metals with high coordination numbers. The synthesis, structure, and dynamic behavior of $(Ph_3Sn)_4M(CO)_4^{2\ominus}$ (M = Zr, Hf) in solution is described in this issue of "Angewandte Chemie".[7]

Investigations on highly reduced metal carbonyls also led *Ellis* et al. to novel carbonyl compounds of the early transition metals.[15] Thus, the CO-richest derivative of the hitherto unknown $Ti(CO)_7$ could be synthesized with the structurally characterized $[Ti(CO)_5(Me_2PCH_2CH_2PMe_2)]$.

Finally, the bonding situation in these unusual carbonylmetalates should be briefly discussed. The high negative charge leads to strong metal–CO π-backbonding; the negative charge is distributed over the antibonding π^*-CO orbitals corresponding to $M=C=O \leftrightarrow {}^{\oplus}M\equiv C-O^{\ominus}$.

With increasing negative charge the C-O bond is weakened, as shown by the wave numbers of the CO vibrations (Table 2).

Table 2. CO vibration frequencies of binary metal carbonyls.

Metal carbonyl	$\tilde{\nu}$ (CO) [cm^{-1}]	Metal carbonyl	$\tilde{\nu}$ (CO) [cm^{-1}]
$Mn(CO)_6^{\oplus}$	2090	$Ni(CO)_4$	2050
$Cr(CO)_6$	1980	$Co(CO)_4^{\ominus}$	1890
$V(CO)_6^{\ominus}$	1860	$Fe(CO)_4^{2\ominus}$	1790
$Ti(CO)_6^{2\ominus}$	1750	$Mn(CO)_4^{3\ominus}$	1670
		$Cr(CO)_4^{4\ominus}$	1460

The position of the CO bands of tetracarbonylchromate(– IV) corresponds almost to that of a C–O single bond, i.e. the CO group can be formulated as a carbyne ligand.

Summarizing, it can be stated that these remarkable compounds with metal atoms in the lowest known oxidation states have enriched the chemistry of metal carbonyls considerably.[16] Further interesting results can be expected.

German version: *Angew. Chem. 103* (1991) 173

[1] W. Hieber, W. Beck, G. Braun, *Angew. Chem. 72* (1960) 795; *Angew. Chem. Int. Ed. Engl. 1* (1961) 65. W. Hieber, *Adv. Organomet. Chem. 8* (1970) 1.

[2] J. E. Ellis, *J. Organomet. Chem. 86* (1975) 1.

[3] Cf., e.g., *Collman*'s reagent $Na_2Fe(CO)_4$ for the synthesis of aldehydes and ketones. $[HFe(CO)_4]^{\ominus}$ finds many uses in organic syntheses and catalysis (J.-J. Brunet, *Chem. Rev. 90* (1990) 1041).

[4] W. Hieber, F. Leutert, *Naturwissenschaften 19* (1931) 360; *Z. Anorg. Allg. Chem. 204* (1932) 145.

[5] T. Kruck, M. Höfler, M. Noack, *Chem. Ber. 99* (1966) 1153.

[6] H. Behrens, *Adv. Organomet. Chem. 18* (1980) 1.

[7] Part 29 of Highly Reduced Organometallic Compounds: J. E. Ellis, K.-M. Chi, A.-J. DiMaio, S. R. Frerichs, J. R. Stenzel, A. L. Rheingold, B. S. Haggerty, *Angew. Chem. 103* (1991) 196; *Angew. Chem. Int. Ed. Engl. 30* (1991) 194 and earlier communications.

[8] G. F. P. Warnock, L. C. Moodie, J. E. Ellis, *J. Am. Chem. Soc. 111* (1989) 2131.

[9] J. E. Ellis, P. T. Barger, M. L. Winzenburg, G. F. Warnock, *J. Organomet. Chem. 383* (1990) 521.

[10] J. E. Ellis, K.-M. Chi, *J. Am. Chem. Soc. 112* (1990) 6022.

[11] G. R. Lee, J. M. Maher, N. J. Cooper, *J. Am. Chem. Soc. 109* (1987) 2956.

[12] J. Breimair, C. Robl, W. Beck, *J. Organomet. Chem.*, in press.

[13] a) E. Lippmann, W. Beck, unpublished; b) W. Beck, K. Sünkel, *Chem. Rev. 88* (1988) 1405.

[14] W. Beck, B. Niemer, J. Breimair, J. Heidrich, *J. Organomet. Chem. 372* (1989) 79; W. Beck, B. Niemer, B. Wagner, *Angew. Chem. 101* (1989) 1699; *Angew. Chem. Int. Ed. Engl. 28* (1989) 1705.

[15] J. E. Ellis, *Polyhedron 8* (1989) 1611.

[16] *Note added in proof:* A detailed review on "Highly Reduced Metal Carbonyl Anions" has been published (J. E. Ellis, *Adv. Organomet. Chem. 31* (1990) 1.

Ultramicroelectrodes—a New Dimension in Electrochemistry?

By *Jürgen Heinze**

Metal electrodes with extremely small dimensions, in the μm range, have been used for voltammetric and polarographic measurements for some time now. They were originally developed for biological and medical research.[1] The electrochemists initially paid little attention to ultramicroelectrodes, in the firm belief not only that the current would diminish with decreasing electrode surface area and thus present measurement problems, but also that no significant differences would exist between the properties of large and small electrodes. Only through the works of *M. Fleischmann* et al. at the beginning of the eighties was it finally clear that a decrease in the surface area of the electrode not only effects quantitative changes, but also results in unusual qualitative effects. In 1981 *R. M. Wightman* reported, in one of the first comprehensive reviews, on the properties and perspectives of microvoltammetric electrodes.[2] The steadily growing interest in ultramicroelectrodes since that time primarily results from the fact that their employment based on well-established measuring principles (as apply in voltammetry or chronoamperometry) opens up new possibilities for the investigation of electrode reactions and electron transfer processes.

Which then are the new properties that make this type of electrode so attractive? One generally speaks of ultramicroelectrodes when the expansion of the inherently small diffusion layer on the time scale of the experiment is "greater" than the characteristic dimensions of the electrode. In the case of a spherical electrode such a characteristic is its radius or diameter, in the case of a band electrode the width, and in the case of the frequently employed disk electrodes, again the radius. Relatively large diffusion layers develop a few seconds after current starts passing through electrodes with characteristic dimensions below 20 μm. The originally planar diffusion field transforms into a (hemi)cylindrical or a (hemi)spherical diffusion field (see Fig. 1 bottom). As a consequence substantially more electroactative particles reach the electrode per unit time and surface area than in the case of a pure planar diffusion. On the other hand, the ever-increasing volume in a prescribed solid angle dictates that in time the flow of particles in and out of unit volume becomes stationary. The mass transport coefficient m, which is a measure of the rate of transport of particles in the stationary diffusion layer is, in a spherical field, inversely proportional to the radius of the electrode ($m = D/r$[cm s^{-1}], D = diffusion coefficient, r = electrode radius); as a result the diffusion rate at extremely small electrodes can be unusually large.

In practice this means, in the case of ultramicroelectrodes, that despite overall decreasing currents, the current densities increase by several orders of magnitudes compared to those in the case of a conventional large-surface-area electrode. The ratio between faradaic and capacitive current is drastically improved and opens up interesting analytical applications. Current densities of up to 70 A cm^{-2} have been reported. Moreover, in contrast to cyclic voltammetry (CV) (Fig. 1, left), one observes the formation of stationary current-voltage curves analogous to the *polarograms* obtained with the dropping mercury electrode or the rotating electrode (Fig. 1, right). Theoretical studies confirm that the transition from the transient state to the stationary state can be described by a parameter $\sigma = (Da^{-1}r^{-2})^{1/2}$, where $a = vRT\,n^{-1}\,F^{-1}$ is the normalized scan rate in the CV experiment. At $\sigma = 0$ the limiting case for normal planar diffusion ($r \rightarrow \infty$) is given by the typical transient voltammogram (Fig. 1, top left), whereas above $\sigma > 1$ the stationary state develops (Fig. 1, top right). Large σ values, usually coupled with small electrode radii, imply high transport coefficients m and thus also high current densities. Since the rate of transport of the electroactive particles in the diffusion layer increases with decreasing electrode radius, this process in the case of extremely small electrodes is as rapid, or more rapid, than heterogeneous charge transfer, i.e. a change from a diffusion-controlled to a kinetically-controlled process occurs. The resulting stationary current-voltage curves shift and change their shape compared to those for a diffusion-controlled process, which indicates thermodynamic (Nernst) equilibrium at the electrodes (Fig. 1). Ultramicroelectrodes are therefore a very elegant new tool for the determination of kinetic parameters in fast heterogeneous charge-transfer reactions. Kinetic data for rapid homogeneous chemical processes can also be determined thus, but, owing to the number of electrons transferred, only if the diffusion-limited current is dependent on the homogeneous kinetics e.g. in three-step *e*lectrochemical, *c*hemical, *e*lectrochemical (ECE) but not in EC processes.[3]

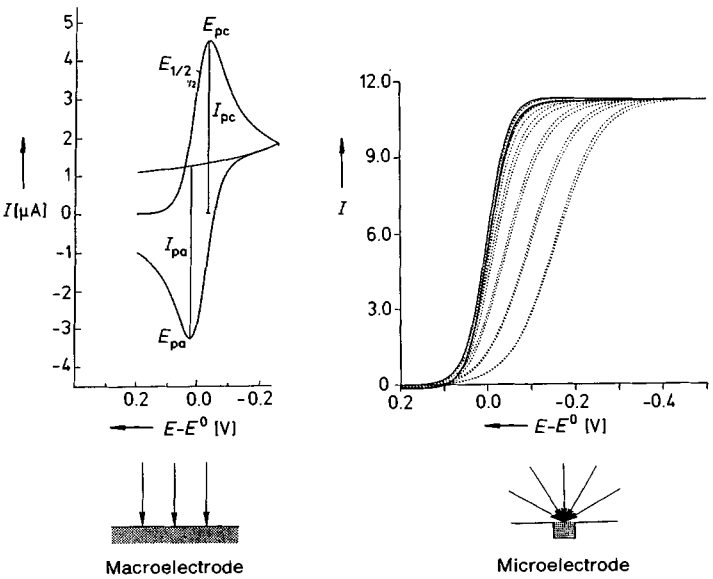

Fig. 1. Left: conventional cyclic voltammogram during measurements with macroelectrodes ($\sigma = 0$, planar diffusion field); right: steady-state cyclic voltammograms for a spherical ultramicroelectrode ($\sigma = 11.1$, $D = 1 \times 10^{-6}$ cm^2 s^{-1}, $r = 0.5$ μm, (hemi)spherical diffusion field); k_s^0: (—) > 100, (– – –) 1.1, 0.35, 0.11, 0.035, 0.011, 0.0035, 0.0011 cm s^{-1}. At $k_2^0 > 100$ cm s^{-1} and a mass transport coefficient of $m = 0.2$ cm s^{-1} the electrode process is diffusion-controlled. For $k_2^0 \leq 0.2$ cm s^{-1} the process switches to kinetic control and the steady-state voltammograms shift on the potential axis with a small change in shape. k_s^0 can be determined with the aid of theory from the shift of the curves. [11]

[*] Prof. Dr. J. Heinze
Institut für Physikalische Chemie der Universität
Alberstrasse 21, W-7800 Freiburg (FRG)

The unusually small currents from ultramicroelectrodes in the nA and pA range means that largely undistorted current-voltage curves can be measured, even at the high electrolyte resistances met with in almost electrolyte-free or in poorly conducting media, e.g. in benzene, in the solid or in the gas phase. Thus, for the first time electrochemical data can be obtained under the conditions common in spectroscopy.[4] Moreover, in cyclic voltammetry the small *IR* effect for current passage through microelectrodes permits the use of extremely high scan rates. In standard experiments with normal electrodes, scanning rates of between 0.05 $V s^{-1}$ and 0.2 $V s^{-1}$ are the rule, whereas with the new technique values of over 1 000 000 $V s^{-1}$ are achieved.[5] This means that in a voltammetric experiment, rate constants of electron-transfer-induced chemical reactions of up to 10^7 s^{-1} (1st order) or 10^9 $M^{-1} s^{-1}$ (2nd order) and heterogeneous standard rate constants of up to ca. 1 $cm s^{-1}$ can be measured. In this connection fast-sweep cyclic voltammetry can be regarded as an alternative to steady-state voltammetry, the former being preferred for mechanistic investigations.

Aside from the novel methodological aspects which ultramicroelectrodes offer, their size is a further argument in favor of their exploitation. In neurophysiology they are used for voltammetric in vivo measurements in single cells; in lithography they serve for the generation of microstructures in the nm range. Further applications are seen in electrochemical scanning tunneling microscopy and in sensors.[6]

Theoretical and experimental studies have shown that the specific qualities of ultramicroelectrodes improve only with decreasing electrode radii. Nevertheless, it has so far not been possible to utilize the full potential of such electrodes. This is primarily due to the fact that only shielded electrodes with radii of down to 5 μm were commercially available. Electrodes with radii down to 0.1 μm were produced exclusively by a few specialists and only in small numbers worldwide.

A group of scientists at CALTEC under the leadership of *N. S. Lewis* has now apparently made a breakthrough in the further miniaturization of microelectrodes.[7] They have succeeded in preparing ultramicroelectrodes (the authors speak of *nanodes*) with radii of 1 nm (= 10 Å). The procedure comprises two steps: Pt wires with a diameter of 0.5 mm were first electrochemically etched and then drawn at a precisely prescribed rate through a glass melt, the temperature of which was adjusted exactly to within 10 °C between 1250 and 1370 °C. During the drawing process the etched Pt tip was drawn out and simultaneously covered with glass. Of 200 electrodes prepared in this way 50% had radii of less than 0.1 μm, and some 10% of even 1–10 nm. With a radius of 1 nm the platinum surface is formed from ca. only 40 Pt atoms.

The extremely small surface areas of such "disk" electrodes ensure that within a few μ seconds a hemispherical diffusion field is formed in which the transport coefficients m of the diffusion can be up to 100 $cm s^{-1}$. Thus, for the first time, there is the possibility of determining heterogeneous diffusion rate constants whose values are orders of magnitude greater than 1 $cm s^{-1}$ from the shift and change of shape of steady-state voltammograms (cf. Fig. 1). Indeed, in measurements with nanodes ($r = 1-2$ nm) the authors could determine k_s^0 values of 79 ± 44 cm^{-1} and 220 ± 120 $cm s^{-1}$ for a series of redox pairs, e.g. $[Ru(NH_3)_6^{\ominus}]^{2/3\oplus}$ (H_2O, 0.5 M KCl) and ferrocene ($Fc^{0/\oplus}$) (CH_3CN, 0.3 M nBu_4NClO_4). For the reduction of methylviologen ($MV^{2\oplus/\oplus}$), even fully reversible steady-state curves were obtained with nanodes (= 2.2 nm). This confirms that the total electrode reaction is diffusion-controlled, despite the high transport rates, and that Nernst equilibrium must exist at the electrodes. An estimation of the heterogeneous rate constant gave a minimum value of over 170 ± 80 $cm s^{-1}$. Such high standard rate constants have never been measured. A comparison of this value with the values predicted by the electron transfer theory of *Marcus*[7] shows surprisingly good agreement. Measurements of heterogeneous rate constants by classical electrochemical methods had hitherto mostly furnished significantly lower values, which threw doubt on the reliability of the theoretical predictions. Apparently the high-transport rates hinder the formation of passivating films, which thwart reproducible measurements of heterogeneous rate constants considerably, and naturally lead to low values depending upon the thickness of the passivation layer. The authors have several arguments against objections and criticisms. The assumption that quantum or double-layer effects and migration effects already lead to the observed signals with a 1 nm electrode, is refuted by the fact that Nernst behavior is always observed independently of the electrode size in very rapid redox reactions, whereas, in the case of slow electron transfer, kinetic waves are obtained as expected, already with "larger" electrodes (1 nm $\leqq r \leqq$ 5 nm). Also the assumption that several domains one underneath the other are formed with metallic surfaces during the preparation of the electrodes cannot apply, since the electrode radii in the individual domains would then have to be even smaller than 1 nm. Finally, as always with new methods, good agreement with the results of other methods of measurements is quoted.

Nevertheless, the measuring technique, about which information is only indirectly accessible in the publication, cannot be problem-free. Especially critical in the case of small currents (ca. 1–2 pA) are ripple and noise effects, which cannot be eliminated with standard measuring equipment. Finally, the theory of diffusion at these electrodes is complicated and has been worked out in detail only for simple redox processes not complicated by homogeneous reactions. However, the development of efficient numerical methods[9] also promises remedies here, so that no major hurdles should stand in the way of a routine application of this new dimension in electrochemistry.

[1] Y. H. Lee, G. T. Tsao, *Adv. Biochem. Eng. 13* (1979) 36–86.
[2] R. M. Wightman, *Anal. Chem. 53* (1981) 1125 A.
[3] M. Fleischmann, F. Lasserre, J. Robinson, D. Swan, *J. Electranal. Chem. 177* (1984) 97; M. Fleischmann, F. Lasserre, J. Robinson, *ibid. 177* (1984) 115.
[4] A. Bond, M. Fleischmann, J. Robinson, *J. Electroanal. Chem. 168* (1984) 299.
[5] C. P. Andrieux, P. Hapiot, J.-M. Saveant, *Electroanalysis 2* (1990) 183.
[6] P. A. Broderick, *Electroanalysis 2* (1990) 241; D. H. Craston, S. W. Lin, A. J. Bard, *J. Electrochem. Soc. 135* (1988) 785; P. Lustenberger, H. Rohrer, R. Christoph, H. Siegenthaler, *J. Electroanal. Chem. 243* (1988) 225.
[7] R. M. Penner, M. J. Herben, T. L. Longin, N. S. Lewis, *Science 250* (1990) 1118.
[8] R. A. Marcus, *J. Phys. Chem. 67* (1963) 853.
[9] J. Heinze, M. Störzbach, *Ber. Bunsenges. Phys. Chem. 90* (1986) 1043.
[10] R. M. Wightman, *Electronal. Chem. 15* (1989) 267–353.
[11] A. M. Bond, K. B. Oldham, C. G. Zoski, *J. Electroanal. Chem. 245* (1988) 71.

Communications may be submitted in English *or* in German. Further details regarding the submission of communications can be found in the "Notice to Authors" reproduced in the January issue of the journal. Copies thereof may be obtained from the editorial office upon request.

Synthesis of a Highly Amphoteric *s*-Indaceno[1,2,3-*cd*:5,6,7-*c'd'*]diphenalene: Switching between Diatropism and Paratropism Due to Changes in Oxidation Level**

By *Ichiro Murata,* Shigeru Sasaki, Kay-Uwe Klabunde, Jiro Toyoda,* and *Kazuhiro Nakasuji*

Dedicated to Professor Tetsuo Nozoe on the occasion of his 88th (Beiju) birthday

We have successfully used the phenalenyl group as a crucial unit for the construction of highly amphoteric hydrocarbons such as 1,2-bis(phenalen-1-ylidene)ethane,[1] 1,2-bis(phenalen-1-ylidene)ethene,[2] and pentaleno[1,2,3-*cd*:4,5,6-*c'd'*]diphenalene (PDPL).[3] In addition to these hydrocarbons, *s*-indaceno[1,2,3-*cd*:5,6,7-*c'd'*]diphenalene (IDPL, **1**) is also expected to be a highly amphoteric hydrocarbon, since the neutral state of **1** will be destabilized by the unfavorable electronic contribution of a nonaromatic *s*-indacene system[4] and the redox states $\mathbf{1}^{2\oplus}$, $\mathbf{1}^{\bullet\oplus}$, $\mathbf{1}^{\bullet\ominus}$, and $\mathbf{1}^{2\ominus}$ will be substantially stabilized by the formation not only of two terminal phenalenyl segments but also of a central benzene structure with loss of the *s*-indacene conjugation (Fig. 1). We now report the synthesis of **12**, a diisopropyl derivative of **1**, and switching between diatropism and paratropism due to changes in oxidation level.

We chose dibromoacenaphthyleno[1,2-*k*]fluoranthene (**4**) as a key intermediate which might be converted in a straightforward fashion into the final skeleton. Diels–Alder reaction of 5-bromoacenaphthylene (**2**)[5] and 3-bromo-7,9-diisopropylcyclopent[*a*]acenaphthylen-8-one (**3**),[6] followed by decarbonylation and aromatization with *p*-chloranil, afforded an isomeric mixture of the 3,10- and 3,11-dibromo compounds **4**.[7] The formation of two regioisomeric dibromides at this stage was not of long-range consequence, since they converged to a single symmetrical product in the final stage

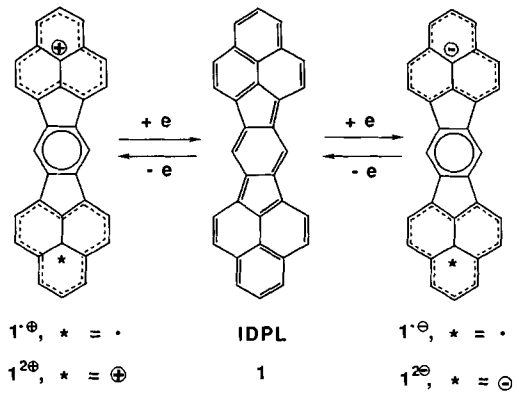

Fig. 1. Expected redox behavior of **1**.

(**11**→**12**). Conversion of dibromide **4** to the bis(bromomethyl) derivative **7** was performed by the usual method. Compound **7** was transformed into the bispropionic acid **9** by the Schlessinger two-carbon elongation procedure.[8]

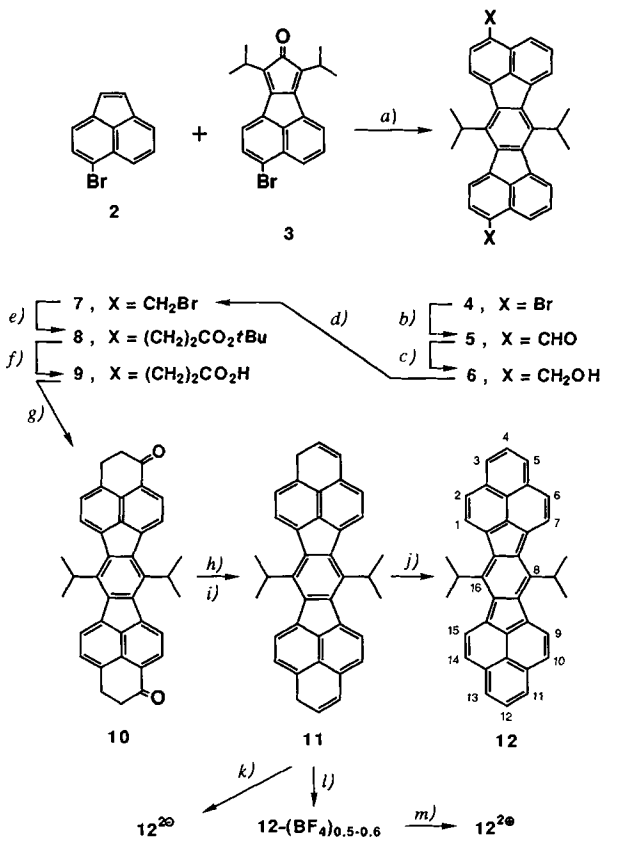

Scheme 1. Synthesis of **12**, $\mathbf{12}^{2\oplus}$, and $\mathbf{12}^{2\ominus}$. Reaction conditions: a) **2** (1.4 equiv.) + **3** (1 equiv.), reflux, xylene, 3 h, then *p*-chloranil (1.2 equiv.), xylene, reflux 2 h, 74%. b) *n*BuLi (2.8 equiv.), DME, −60 °C, 1.5 h, then PhN(CH$_3$)CHO (4.9 equiv.), −50 → −40 °C, 1.5 h, 49%. c) NaBH$_4$ (2.2 equiv.), EtOH, reflux 2 h, 96%. d) PBr$_3$ (2.5 equiv.), benzene, reflux, 15 min, 80%. e) *n*BuLi, (CH$_3$)$_2$CHNH$_2$ (1.2 equiv.), CH$_3$CO$_2$*t*Bu (1.6 equiv.), THF, −78 °C, then **7** (0.34 equiv.), 2 h, 93%. f) Cat. *p*-TosOH, benzene, 1.5 h, 97%. g) Excess SOCl$_2$, reflux, 40 min, then AlCl$_3$ (9 equiv.), CH$_2$Cl$_2$, −78 → −40 °C, 5 h, 78%. h) NaBH$_4$ (3 equiv.), CH$_2$Cl$_2$ + EtOH, room temperature, 2 h. i) Cat. β-C$_{10}$H$_7$SO$_3$H, benzene, reflux, 15 min, 55%. j) *p*-Chloranil (1.14 equiv.), benzene, room temperature, 20 min, then reflux 25 min, 81%. k) K mirror, under vacuum, [D$_8$]THF, −78 °C, 1 week. l) Ph$_3$CBF$_4$ (4.5 equiv.), CH$_2$Cl$_2$, 74%. m) Conc. D$_2$SO$_4$.

[*] Prof. Dr. I. Murata, S. Sasaki, Dr. K.-U. Klabunde [+]
Department of Chemistry, Faculty of Science
Osaka University
Toyonaka, Osaka 560 (Japan)
Dr. J. Toyoda, Prof. Dr. K. Nakasuji
Institute for Molecular Science
Myodaiji, Okazaki 444 (Japan)

[+] Present adress:
E. Merck AG, Frankfurter Strasse 250, W-6100 Darmstadt (FRG)

[**] This work was supported by a Grant-in-Aid for Scientific Research on Priority Areas (No. 01648003) from the Ministry of Education, Science and Culture, Japan. We thank Professor *Jun-ichi Aihara* for the ring current calculations. *K.-U. K.* thanks the Japan Society for the Promotion of Science for a postdoctoral fellowship.

Friedel–Crafts cyclization of **9** gave the diketone **10**, which was converted into the dihydro compound **11** through a reduction–dehydration sequence. Dehydrogenation of **11** with *p*-chloranil in benzene provided the desired **12** as a green crystalline solid.[9]

Investigation of the electrochemical behavior of **12** by cyclic voltammetry[10] revealed two reversible reduction waves ($E_1^{red} = -0.48$ V, $E_2^{red} = -1.07$ V) and two irreversible oxidation waves ($E_1^{ox} = 0.62$ V, $E_2^{ox} = 0.84$ V). If we adopt the span of the oxidation and reduction potentials, $E^{sum} = E^{ox} + (-E^{red})$, as an experimental measure of the amphotericity of a molecule, diisopropyl-IDPL **12** may be considered a highly amphoteric hydrocarbon,[11] although $E_1^{sum} = 1.10$ V observed for **12** is slightly greater than that of PDPL ($E_1^{sum} = 0.99$ V).[3] Interestingly, the E_2^{sum} value (1.91 V for **12**) is smaller than that of PDPL (2.19 V).[3] This finding suggests substantial stabilities for both the doubly charged species $\mathbf{12}^{2\oplus}$ and $\mathbf{12}^{2\ominus}$.

Unexpectedly, treatment of the dihydro compound **11** with excess trityl tetrafluoroborate in dichloromethane afforded, instead of the mono- or dication salts, a radical-cation salt with nonstoichiometric composition, **12**-$(BF_4)_{0.5-0.6}$[12] in 74% yield, which, on dissolution in concentrated D_2SO_4, gave the dication $\mathbf{12}^{2\oplus}$ as a dark blue solution. On the other hand, the dianion $\mathbf{12}^{2\ominus}$ could be generated as a bluish purple solution when **11** was treated with potassium mirror[13] under vacuum at −78 °C for a week. The ^{1}H NMR chemical shifts for the three redox states $\mathbf{12}^{2\oplus}$, **12**, and $\mathbf{12}^{2\ominus}$ are compared in Table 1.[14] The most striking

Table 1. ^{1}H NMR chemical shifts for $\mathbf{12}^{2\oplus}$, **12**, and $\mathbf{12}^{2\ominus}$.

Proton	$\mathbf{12}^{2\oplus}$ [a]	**12** [b]	$\mathbf{12}^{2\ominus}$ [c]
CH_3	1.47	1.49 1.50 [d]	2.09
CH	3.40	3.67	5.45
H-1, 7, 9, 15	7.60	7.11 7.20 [d]	8.39
H-2, 6, 10, 14	8.22	6.99 7.01 [d]	6.95
H-3, 5, 11, 13	8.25	7.09	7.01
H-4, 12	7.50	6.95	7.14

[a] Measured in D_2SO_4 at 60 °C, 400 MHz. [b] Measured in CS_2 + [D_6]acetone (4:1) at −80 °C, 500 MHz. [c] Measured in [D_8]THF at 0 °C, 400 MHz. [d] Nonequivalence of these protons is presumably due to the restricted rotation of two isopropyl groups. Indeed, the spectra of $\mathbf{12}^{2\oplus}$, **12**, and $\mathbf{12}^{2\ominus}$ are temperature-dependent.

feature is that, despite the shielding caused by the two negative charges, the isopropyl protons (both CH_3 and CH), as well as the protons at the 1-, 7-, 9-, and 15-positions of $\mathbf{12}^{2\ominus}$, unexpectedly appear at lower field than those of the corresponding protons in the dication $\mathbf{12}^{2\oplus}$. Nevertheless, the chemical shifts of the remaining ring protons of $\mathbf{12}^{2\ominus}$ are comparable to those of the neutral species **12**. These findings clearly suggest the effect of a diamagnetic ring current in the dianion $\mathbf{12}^{2\ominus}$, which possesses a conjugated periphery of 30 π electrons. This aromatic system is only weakly perturbed by the inner two double bonds.[15] In contrast, the dication $\mathbf{12}^{2\oplus}$, which corresponds to a two-electron oxidation state of the highly amphoteric hydrocarbon **12**, exhibits paratropism, even though it has 4n + 2 π electrons both in the whole molecule (30 π) and in the periphery (26 π).

London–McWeeny ring current calculations,[16] based on the Hückel approximation, were performed on the parent systems $\mathbf{1}^{2\oplus}$, **1**, and $\mathbf{1}^{2\ominus}$. They suggest that the IDPL dianion $\mathbf{1}^{2\ominus}$ should have pronounced diamagnetic ring currents mainly along the periphery of the molecule,[15] whereas the IDPL dication $\mathbf{1}^{2\oplus}$ should show strong and weak paratropism at the central *s*-indacene and the terminal benzene rings, respectively. Currently, we are studying the intriguing solid-state properties of **12** and **12**-$(BF_4)_{0.5-0.6}$.

Received: August 16, 1990 [Z 4138 IE]
German version: *Angew. Chem. 103* (1991) 198

[1] K. Nakasuji, K. Yoshida, I. Murata, *J. Am. Chem. Soc. 104* (1982) 1432–1433.
[2] K. Nakasuji, K. Yoshida, I. Murata, *Chem. Lett. 1982*, 969–970.
[3] K. Nakasuji, K. Yoshida, I. Murata, *J. Am. Chem. Soc. 105* (1983) 5136–5137.
[4] K. Hafner, *Angew. Chem. 75* (1963) 1041–1050; *Angew. Chem. Int. Ed. Engl. 3* (1964) 165–173; K. Hafner, K. H. Häfner, C. König, M. Kreuder, G. Ploss, G. Schulz, E. Strum, K. H. Vöpel, *ibid. 75* (1963) 35–46 and *2* (1963) 123; K. Hafner, H.-P. Krimmer, *ibid. 92* (1980) 202–204 and *19* (1980) 199–201; K. Hafner, B. Stowasser, H.-P. Krimmer, S. Fischer, M. C. Böhm, H. J. Lindner, *ibid. 98* (1986) 646–648 and *25* (1986) 630–632.
[5] G. P. Petrenko, E. N. Tel'nyuk, *Zh. Org. Khim. 2* (1966) 722–727. Compound **2** was synthesized starting from 5-bromoacenaphthene by acetoxylation (Pb_3O_4/HOAc, 81%), hydrolysis (KOH/MeOH-H_2O, 98%) and dehydration (*p*-TosOH/benzene, 86%).
[6] Compound **3** was prepared by the reaction of 5-bromoacenaphtylene-1,2-dione (F. Dewhurst, P. K. J. Shah, *J. Chem. Soc. C 1970*, 1737–1740) with 2,6-dimethyl-4-heptanone (KOH/THF-MeOH, then H_2SO_4 in acetone, 57%).
[7] All new compounds have been characterized spectroscopically and by elemental analysis and/or mass spectrometry.
[8] R. J. Cregge, J. L. Herrmann, C. S. Lee, J. E. Richman, R. H. Schlessinger, *Tetrahedron Lett. 1973*, 2425–2428.
[9] Compound **12**: dark green crystalline solid (from benzene–hexane) m.p. > 300 °C. UV/VIS (benzene): λ_{max} [nm] (lg ε) = 344 (4.44), 359 (4.60), 401 (3.60), 440 (3.39), 484 (2.80), 528 (2.79), 576 (3.01), 762 (4.78).
[10] Measured versus SCE in DME with 0.1 M Et_4NClO_4 as supporting electrolyte at −40 °C under argon, Pt working electrode $v = 500$ mV s^{-1}.
[11] Recently, highly amphoteric nonhydrocarbon molecules have been reported: T. Takahashi, T. Suzuki, *J. Am. Chem. Soc. 111* (1989) 5483–5485.
[12] This stable radical-cation salt was obtained as a dark purple solid with a nonstoichiometric composition: **12**-$(BF_4)_{0.5-0.6}$. Elemental analysis: found C 85.54, H 5.47; calcd for $C_{38}H_{28}(BF_4)_{0.6}$, C 85.04, H 5.26%; $C_{38}H_{28}(BF_4)_{0.5}$, C 86.44, H 5.34%. The formation of **12**-$(BF_4)_{0.5-0.6}$ bears a close parallel to the fact that treatment of 1-cyano-6-methylthiophenalene with trityl perchlorate afforded a paramagnetic cation salt having a nonstoichiometric ratio of the components: (1-cyano-6-methylthiophenalenyl)$_1$$(ClO_4)_{0.7}$: K. Nakasuji, M. Yamaguchi, I. Murata, K. Yamaguchi, T. Fueno, H. Ohya-Nishiguchi, T. Sugano, M. Kinoshita, *J. Am. Chem. Soc. 111* (1989) 9265–9267.
[13] Potassium metal reduction was performed according to the procedure given in the literature: K.-U. Klabunde, K. Müllen, H. Vogler, *Tetrahedron 43* (1987) 1183–1196.
[14] For super-charged polycyclic ions, see: M. Rabinovitz, I. Willner, A. Minsky, *Acc. Chem. Res. 16* (1983) 298–304, and references therein.
[15] J. R. Platt, *J. Chem. Phys. 22* (1954) 1448–1455. Since the HMO calculations on **1** reveal a nodal plane through the central six carbon atoms in the LUMO of the IDPL system, the molecular orbital that accommodates two additional electrons in the dianion $\mathbf{1}^{2\ominus}$ is of pure peripheral nature.
[16] F. London, *J. Phys. Radium 8* (1937) 397–409; R. McWeeny, *Mol. Phys. 1* (1958) 311–325.

Tetra-*tert*-butyltetraboratetrahedrane

By Theo Mennekes, Peter Paetzold, Roland Boese,* and Dieter Bläser*

Davan and *Morrison*[1] obtained the glassy compound B_4R_4 (R = *t*Bu), which contains extremely deshielded boron

[*] Prof. Dr. P. Paetzold, T. Mennekes
Institut für Anorganische Chemie der Technischen Hochschule
Templergraben 55, W-5100 Aachen (FRG)
Dr. R. Boese, D. Bläser
Institut für Anorganische Chemie der Universität-Gesamthochschule
Universitätsstrasse 5–7, W-4300 Essen (FRG)

atoms ($\delta(^{11}B) = 135.1$),[2] by reaction of LiR with tetrachlorotetraboratetrahedrane, B_4Cl_4. *Klusik* and *Berndt*[3] reduced di-*tert*-butyldichlorodiborane(4), Cl–B(R)–B(R)–Cl, with Na/K alloy to generate mostly a radical anion, $[B_4R_4]^{\cdot\ominus}$, which they investigated by ESR spectroscopy and to which they assigned a four-membered ring structure. The reaction solution showed a ^{11}B NMR signal at $\delta = 135.7$, presumably due to the uncharged molecule B_4R_4. The structure of B_4R_4 was previously unknown, although its formation from the tetrahedrane B_4Cl_4 points to a tetrahedral structure; however, the interconvertibility of the tetrahedrane and cyclobutadiene structures of the carbon analogues C_4R_4[4] made the cyclobutadiene structure a possibility for B_4R_4 as well.

We have now reduced RBF_2 in pentane with Na/K alloy (M) and thereby obtained B_4R_4 as a yellow solid in 79% yield [(Eq. (a)].

$$12\,RBF_2 + 8\,M \rightarrow B_4R_4 + 8\,M[RBF_3] \qquad (a)$$

The NMR spectra of our product in $CDCl_3$ display only one NMR signal for each element: $\delta(^1H) = 1.00$ (s), $\delta(^{11}B) = 135.4$, $\delta(^{13}C) = 28.2$ (q); the NMR signal of the B-bonded ^{13}C atom, which, as expected, is very broad, could not be resolved. A broad UV absorption with a maximum at 282.8 nm ($\varepsilon = 5012$, in isooctane) is responsible for the yellow color.

The X-ray structure analysis (Fig. 1) revealed that B_4R_4 is indeed a tetrahedrane.[5] The molecular symmetry C_2 of the central B_4C_4 framework deviates only slightly from the ideal T_d symmetry: the values for the B–B bond lengths (1.699(6)–1.714(4) Å) the angles in the cluster triangles (59.5(2)–60.4(2)°), and the angles between the edges of the polyhedron and the B–C bonds (143.5(2)–146.8(1)°, ideal value 144.74°) lie within narrow ranges. In the tetrahedrane B_4Cl_4 (point group in the crystal: D_{2d}), the two different B–B distances (1.69(4) and 1.71(4) Å) lie in the same range as those in B_4R_4.[6] The molecules B_4R_4 and C_4R_4,[7] which certainly are structurally analogous in the gas phase, also exhibit similarities in the crystalline modifications isolated and characterized in each case.[8] Thus, the vibrational amplitudes in the central B_4C_4 and C_4C_4 frameworks are relatively small and nearly isotropic, whereas they are large and strongly anisotropic for the twelve peripheral C atoms. Conformational interactions between the *t*Bu groups are less important in B_4R_4, since the mean B–B distance of 1.707 Å is significantly larger than the mean C–C distance of 1.485 Å in the C_4 tetrahedron. We therefore ascribe the anisotropic vibrations of the methyl groups of B_4R_4 to normal torsional vibrations around the B–C axis. In our opinion, an "enantiomeric disorder", which, in the case of C_4R_4, could change a structure of near T symmetry to one of near T_d symmetry, is ruled out for B_4R_4.

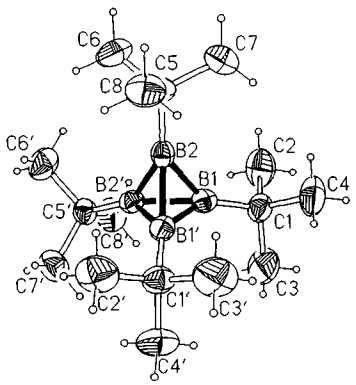

Fig. 1. Molecular structure of B_4tBu_4. The C_2 axis is perpendicular to the B1–B1′ and B2–B2′ bonds. Selected distances [Å] and angles [°] (standard deviations in parentheses): B1-B1′ 1.699(6), B2-B2′ 1.705(6), B1-B2 1.708(4), B1-B2′ 1.714(4), B1-C1 1.570(4), C1-C2 1.537(4), C1-C3 1.538(4), C1-C4 1.536(4), B2-C5 1.576(4), C5-C6 1.543(4), C5-C7 1.527(4), C5-C8 1.530(4); B2-B1-B1′ 60.4(2), B2-B1-B2′ 59.8(2), B1′-B1-B2′ 60.1(2), B1-B2-B1′ 59.5(2), B1-B2-B2′ 60.3(2), B1′-B2-B2′ 59.9(2), B2-B1-C1 145.0(2), B1′-B1-C1 143.9(1), B2′-B1-C1 145.2(2), B1-B2-C5 143.9(2), B1′-B2-C5 143.5(2), B2′-B2-C5 146.8(1).

Although the B_4 framework of B_4R_4 is less shielded than the smaller C_4 framework of C_4R_4, B_4R_4 is unusually inert for an organoboron compound with strained B–B bonds. It may be handled for short periods in the air without decomposition, it is insoluble in water and is not attacked by water at the surface, it cannot be hydrogenated with H_2 in the presence of Pd on carbon in toluene, and it does not react with CO or 3-hexyne in toluene, nor with PMe_3 in hexane.

B_4R_4 crystallizes from toluene, but the single crystals decompose when the mother liquor is removed. The structure analysis could be carried out, however, with a crystal embedded in toluene. A so-called diamond–square–diamond rearrangement, in which opposite edges of the tetrahedron undergo planarization to form a square followed by the reverse process from the opposite edges of the square, can hardly be the cause of the instability of the crystal. This planarization involves a HOMO–LUMO crossing, which, according to an ab initio calculation for the parent B_4H_4 exhibits an activation energy of 85 kcal mol^{-1}.[9]

The formation of B_4R_4 according to Equation (a) probably proceeds via an intermediate, F–B(R)–B(R)–F, which gives either a diborane(2), RB=BR, or a longer-chained compound $F-(BR)_n-F$ (n = 3,4) and then the product. If, instead of RBF_2, $R'BCl_2$, containing the extremely bulky group $R' = (Me_3Si)_3C$, is treated with Na/K alloy, then R′B = BR′ is presumably formed as intermediate. This species does not dimerize, but rather is stabilized by double C–H insertion into the B–B bond.[10]

Experimental Procedure

Tetra-*tert*-butyltetraboratetrahedrane: Na/K alloy (1/3; 9.50 g) was added at room temperature to a solution of *tert*-butyldifluoroborane (15.0 g) [11] in 50 mL of pentane. The resulting exothermic reaction caused the mixture to reflux for 10 min. The precipitated salts were collected by filtration at room temperature and washed with 2 × 5 mL of pentane. The filtrate was evaporated to dryness and the residue sublimed at 80 °C/0.005 Torr into a receptacle cooled with liquid nitrogen to afford 2.52 g of pure product.

Received: August 20, 1990 [Z 4140 IE]
German version: *Angew. Chem. 103* (1991) 199

CAS Registry numbers:
B_4tBu_4, 78694-48-1; $tBuBF_2$, 119366-59-5.

[1] T. Davan, J. A. Morrison, *J. Chem. Soc. Chem. Commun. 1981*, 250.
[2] B. Wrackmeyer, *Annu. Rep. NMR Spectrosc. 20* (1988) 61.
[3] H. Klusik, A. Berndt, *J. Organomet. Chem. 234* (1982) C17.
[4] G. Maier, *Angew. Chem. 100* (1988) 317; *Angew. Chem. Int. Ed. Engl. 27* (1988) 309.
[5] A single crystal of B_4R_4 was grown in a capillary from a saturated toluene solution by using focused IR radiation; $a = 14.686(7)$, $b = 14.830(10)$, $c = 9.434(7)$ Å, $\beta = 95.98(5)°$, $V = 2043(2)$ Å^3, $Z = 4$, $\varrho_{calcd} = 0.883$ g cm^{-3}, $C2/c$ (No. 15); measuring temperature 190 K; measuring range $3 \le 2\theta \le 50°$; 1539 unique reflections, 958 of which were observed with $F_o \ge 4\sigma(F)$; anisotropic temperature factors for the non-hydrogen

[6] B. Wrackmeyer, *Angew. Chem. 91* (1979) 865; *Angew. Chem. Int. Ed. Engl. 18* (1979) 790.
[7] G. Maier, *Angew. Chem. 86* (1974) 491; *Angew. Chem. Int. Ed. Engl. 13* (1974) 425.
[8] G. Maier, H. Pfriem, U. Schäfer, R. Matusch, *Angew. Chem. 102* (1990) 1519; *Angew. Chem. Int. Ed. Engl. 29* (1990) 1501.
[9] M. Bühl, P. v. R. Schleyer, *J. Am. Chem. Soc. 112* (1990) 2440.
[10] H. Nöth, H. Pommerening, *Angew. Chem. 92* (1980) 481; *Angew. Chem. Int. Ed. Engl. 19* (1980) 482.
[11] H. Nöth, H. Pommerening, *Angew. Chem. 92* (1980) 482; *Angew. Chem. Int. Ed. Engl. 19* (1980) 482.

atoms; 97 refined parameters, $R = 0.0568$, $Rw = 0.0513$. Further details of the crystal structure investigation may be obtained from the Fachinformationszentrum Karlsruhe, Gesellschaft für wissenschaftlich-technische Information mbH, W-7514 Eggenstein-Leopoldshafen 2 (FRG), on quoting the depository number CSD-320147, the names of the authors, and the journal citation.

[6] M. Atoji, W. N. Lipscomb, *Acta Crystallogr. 6* (1953) 547.

[7] G. Maier, S. Pfriem, U. Schäfer, R. Matusch, *Angew. Chem. 90* (1978) 552; *Angew. Chem. Int. Ed. Engl. 17* (1978) 520.

[8] H. Irngartinger, A. Goldmann, R. Jahn, M. Nixdorf, H. Rodewald, G. Maier, K.-D. Malsch, R. Emrich, *Angew. Chem. 96* (1984) 967; *Angew. Chem. Int. Ed. Engl. 23* (1984) 993.

[9] D. A. Kleier, J. Bicerano, W. N. Lipscomb, *Inorg. Chem. 19* (1980) 216.

[10] T. Mennekes, P. Paetzold, R. Boese, *Angew. Chem. 102* (1990) 909; *Angew. Chem. Int. Ed. Engl. 29* (1990) 899.

[11] R. Boese, P. Paetzold, A. Tapper, R. Ziembinski, *Chem. Ber. 122* (1989) 1057.

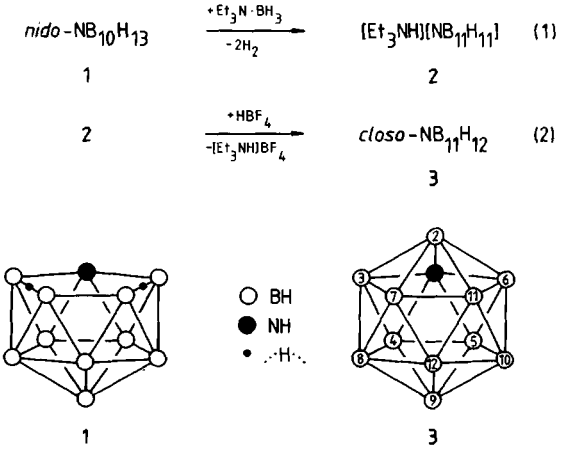

closo-Azadodecaborane, $NB_{11}H_{12}$ **

By *Jens Müller, Jan Runsink*, and *Peter Paetzold**

Rhombohedrally distorted B_{12} icosahedra are the building blocks of elemental boron, anions with exact icosahedral symmetry are found in solutions of $Na_2[B_{12}H_{12}]$, and well-known examples of the three isomeric dicarbadodecaboranes $C_2B_{10}H_{12}$ are heterododecaboranes containing discrete neutral icosahedral units. The carbon atoms in the latter compounds represent the most electronegative element of coordination number 6 found in molecules. Is it possible to incorporate the still more electronegative element nitrogen as a heteroatom into an icosahedral framework isoelectronic to $C_2B_{10}H_{12}$ and $B_{12}H_{12}^{2\ominus}$ to give a compound with the composition $NB_{11}H_{12}$?

We have repeatedly attempted to carry out such a synthesis in analogy to that of 1,2-$C_2B_{10}H_{12}$, which involves closure of the open *arachno* structure of $B_{10}H_{12}L_2$ (L = Lewis base) by incorporation of the two C atoms of acetylene. Unfortunately, use of iminoboranes[1] such as MeB≡NMe, isoelectronic to acetylene, has been unsuccessful. The iminoboranes undergo oligomerization more rapidly than reaction with $B_{10}H_{12}L_2$. However, our recent preparation of *nido*-$NB_{10}H_{13}$ (**1**)[2] opened up the possibility of closing the *nido* framework of **1** with a BH fragment.[3] Addition of BH_3 to **1** should result in comproportionation of two of the hydridic H atoms of BH_3 with the two protonic bridging H atoms of **1** to give H_2.

Indeed, the open cluster borane **1** can be closed by treatment with an excess of $Et_3N{\cdot}BH_3$ at 140 °C [Eq. (1)]. The initial product was the ionogenic compound **2**, however, formed in quantitative yield.[4] Reaction of **2** with HBF_4 affords the corresponding acid **3**, our target molecule, as a sublimable, colorless solid[5] [Eq. (2)].

The constitution of **3** was established by NMR spectroscopy. Three ^{11}B NMR doublets in a ratio of 5:5:1[5] are indicative of a B_{11} framework with fivefold symmetry and 11 terminal H atoms. The 2D ^{11}B–^{11}B NMR spectrum confirms that a set of five equivalent B atoms (B7 to B11) is bonded to a second such set (B2 to B6) as well as to a single B atom (B12) on the C_5 axis. Moreover, no cross-peak, which would have indicated a bond between B12 and the atoms B2 to B6, is observed. The coupling constants $J_{BH} = 177$, 147, and 150 Hz for B2 to B6, B7 to B11, and B12, respectively, reveal that the B–H bonds in proximity to the N atom are stronger than the others. For *closo*-1-methyl-1-phosphadodecaborane, $MePB_{11}H_{11}$, which is comparable to **3**, the corresponding coupling constants (164, 150, and 150 Hz)[6] show the same trend. The overlapping quartets for the three kinds of H atoms cannot be resolved in the ^1H NMR spectrum; however, their chemical shifts[5] may be determined from the three cross-peaks in the 2D ^{11}B-^1H NMR spectrum. The *N*-bonded H atom gives rise to a 1:1:1 triplet in the ^1H NMR spectrum with $J_{NH} = 62.5$ Hz, a consequence of the symmetrical charge distribution around the ^{14}N atom on the C_5 axis.

The title compound is thus the first cluster molecule containing a sixfold coordinated N atom in the framework.

Experimental Procedure

3: Compound **1** (0.50 g) [2] was dissolved in triethylamine-borane (1.00 g) and the resulting solution was heated at 140 °C for 3.5 h. Removal of the excess $Et_3N{\cdot}BH_3$ in vacuum affords the NMR-spectroscopically pure product **2**, which was dissolved in 5 mL of a 54% solution of HBF_4 in diethyl ether. The solution was extracted with 5 × 20 mL of toluene and the combined toluene extracts were evaporated to dryness. Sublimation of the residue at 50 °C/0.001 Torr gave 0.25 g (47%) of **3**.

Received: August 24, 1990 [Z 4150 IE]
German version: *Angew. Chem. 103* (1991) 201

CAS Registry numbers:
1, 131179-98-1; **2**, 131180-01-3; **3**, 131179-99-2; $Et_3N \cdot BH_3$, 1722-26-5; HBF_4, 16872-11-0.

[*] Prof. Dr. P. Paetzold, J. Müller
Institut für Anorganische Chemie der Technischen Hochschule
Templergraben 55, W-5100 Aachen (FRG)
Dr. J. Runsink
Institut für Organische Chemie der Technischen Hochschule
Templergraben 55, W-5100 Aachen (FRG)

[**] This work was supported by the Deutsche Forschungsgemeinschaft.

[1] P. Paetzold, *Adv. Inorg. Chem. 31* (1987) 123.

[2] J. Müller, P. Paetzold, R. Boese, *Heteroatom Chem. 1* (1990) 461.

[3] N. N. Greenwood, J. H. Morris, *Proc. Chem. Soc. 1963*, 338; J. S. Beck, A. P. Kahn, L. G. Sneddon, *Organometallics 5* (1986) 2552.

[4] **2**: NMR spectra in CD_2Cl_2 at 25 °C; ^1H NMR (300 MHz, TMS): $\delta = 1.28$ (t, $J = 7.2$ Hz, 9H; CH_3), 1.79 and 1.98 (H on B2 to B11 and H on B12, respectively; measured and assigned as cross-peaks in the 2D ^{11}B-^1H NMR spectrum), 3.08 (q, $J = 7.2$ Hz with d, $J = 5.0$ Hz, 6H; CH_2), 7.6 (broad, 1H; NH). ^{11}B NMR (96.23 MHz, $Et_2O{\cdot}BF_3$): $\delta = -10.3$ (d, $J = 147$ Hz, 10 B; B2 to B11), -1.0 (d, $J = 137$ Hz, 1 B; B12).

[5] **3**: NMR spectra in C_6D_6 at 25 °C; ^1H NMR (300 MHz, TMS): $\delta = 1.91$, 2.46, 3.19 (H on B2 to B6, on B7 to B11, on B12; for measurement and assignment, see [4]), 2.95 (t; NH). ^{11}B NMR (96.23 MHz, $Et_2O{\cdot}BF_3$): $\delta = -11.9$ (d, $\nu_{1/2} = 55$ Hz; B7 to B11), -9.8 (d, $\nu_{1/2} = 106$ Hz; B2 to B6), 2.7 (d; B12). $^{14}N\{^1H\}$ NMR (5.79 MHz, CH_3NO_2): $\delta = -282$ ($\nu_{1/2} = 78$ Hz). IR(CCl_4): $\tilde{\nu}$ [cm^{-1}] = 3299 (NH), 2622, 2579 (BH).

[6] T. D. Getmen, H.-B. Deng, L.-Y. Hsu, S. G. Shore, *Inorg. Chem. 28* (1989) 3612.

Radical Cation Salts of 1,3,6,8-Tetrakis(methylthio)-pyrene—New Easily Accessible Compounds with High Electrical Conductivity and Excellent Stability**

By *Gerhard Heywang** and *Sigmar Roth*

Dedicated to Professor Rudolf Gompper on the occasion of his 65th birthday

The discovery of the charge-transfer complex formed from tetracyanoquinodimethane (TCNQ) and tetrathiafulvalene (TTF)[1] gave new impetus to the studies begun in the fifties[2] on electrically conducting radical cation salts, which led to the superconducting complexes of bis(ethylenedithio)tetrathiafulvalene (BEDT-TTF).[3] Disadvantages are the long-winded syntheses of the donor molecules (TTF, five steps with overall yield of 55%;[4,5] BEDT-TTF, five steps with overall yield of 35%[6]), and the low stability of the radical cation salts (for example, the halogen complexes of pyrene and perylene cannot be stored[7]).

The search for novel sulfur-containing donor components led to the compounds **1**–**3**.[8–10] The overall yield of the many-step synthesis lies here, as in most cases, below 12%. We now report the title compound, donor ligand **4**, a component easily accessible in large quantities. The radical cation salts from **4** are characterized by a high electrical conductivity and good thermal stability.

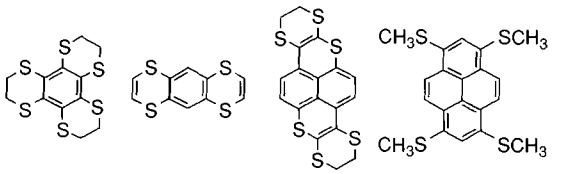

1 **2** **3** **4**

The halogenation of pyrene leads in quantitative yield to 1,3,6,8-tetrahalopyrene,[11] which reacts with sodium methyl sulfide in aprotic solvents to tetrakis(methylthio)pyrene (**4**) with optimal yields of 98%. Electrocrystallization of **4** in the presence of suitable electrolytes gives the radical cation salts **5a**–**c**, with powder conductivities between 10^{-1} and 10^{-2} S cm^{-1}.

Compound **5a** shows single crystal conductivities of 300 to 677 S cm^{-1}, which increase with decreasing temperature. Because of the high mechanical stress of the four point probe, the temperature dependence of the conductivity measurements could only be followed to 260 K.

The reaction of **4** with iodine affords **5d** (pressed pellet, without pressure 5–10 S cm^{-1}). The temperature dependence of the single crystal conductivity is shown in Figure 1. The conductivity increases continually with decreasing temperature till $T = 46$ K, even though a steplike function, in which the conductivity of each successive step is lower than the previous step, is obtained. Our interpretation is that these steps result from microcracks in the crystal, because in one particular crystal the original room-temperature conductivity was reproducible in spite of many such steps in the temperature dependence curve.

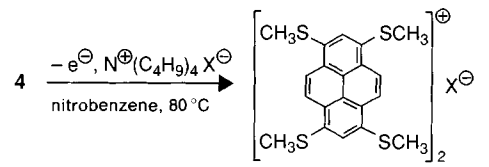

5a X = ClO_4 [4.7 × 10^{-2} S cm^{-1}]
5b X = BF_4 [2.5 × 10^{-2} S cm^{-1}]
5c X = PF_6 [3.7 × 10^{-2} S cm^{-1}]

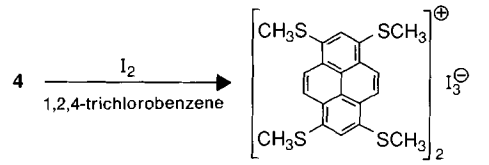

5d

The function of ln σ vs $1/T$ between 46 K and 10 K is strictly linear. The activation energy calculated from such a plot is $kT_0 = 0.011$ eV at $T_0 = 130$ K. For most transitions induced by an electron–phonon interaction, the temperature condition $T_0 = 3.5\ T_1$ holds.[12] This requirement is satisfied relatively well for **5d**.

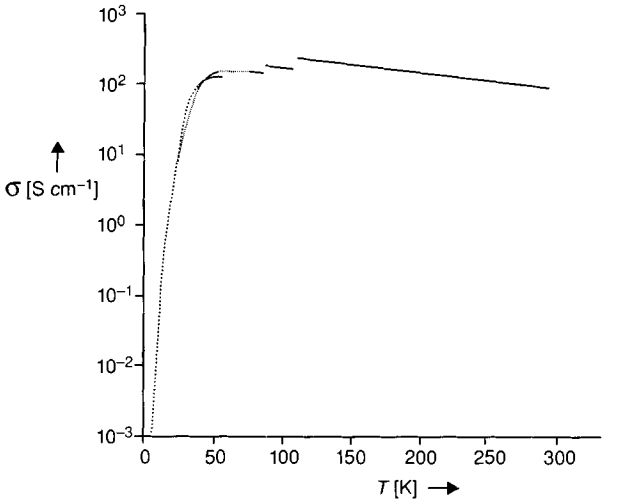

Fig. 1. Temperature dependence of the electrical conductivity of the complex **5d**, measured on a crystal (needle) 0.4 mm long. The crystal broke at 60 K on repetition. Where fewer measurements were made, the line is dotted.

Whereas the TTF–iodine complex decomposes at 180 °C and the corresponding BEDT–TTF complex at 220 °C through reaction of the iodine ion with the donor component, compound **5d** reacts back to **4** above 245 °C by loss of iodine. That the four methylthio substituents are responsible for this stabilizing effect is confirmed by comparison with the iodine complex of the 1,6-bis(methylthio)pyrene described earlier[13] (halfwave potential: 0.96 V[14]), which loses about 1% iodine per day at room temperature (initial conductivity of a pressed pellet is 10^{-2} S cm^{-1}). Cyclovoltammetry yields a potential of $E_1 = 0.65$ V vs Ag/AgCl for **4**.[15] The new radical cation salts probably owe their high stability to the favorable redox potential as well as to the symmetry of **4**.

[*] Dr. G. Heywang
ZF-FKH, Geb. Q18
Bayer AG
W-5090 Leverkusen
Dr. S. Roth
Max-Planck-Institut für Festkörperforschung, Stuttgart

[**] This work was supported by the Bundesministerium für Forschung und Technologie (Kennzeichen 3M 4022 9).

Diverse radical cation salts of **4** may also be prepared with oxidizing agents such as H_2O_2 and $KMnO_4$ in the presence of suitable anions in aqueous medium to which small amounts of tetrahydrofuran and sulfuric acid have been added. Compound **5a** prepared in the presence of $NaClO_4$ with these oxidizing agents shows the same powder conductivity as the electrochemically prepared sample. Table 1 shows that

Table 1. Comparison of the single crystal conductivities σ [S cm^{-1}] of radical cation salts.

Anion	Cation			
	TTF	BEDT-TTF	**3**	**4**
$I_3^{\ominus}$	100–450 [16]	60–250 [17, 18] 10–50 [20] [a]	42 [19]	110
$ClO_4^{\ominus}$	10^{-5} [21] [b]	33 [22]		300–677

[a] First values represent the α modification, second values the β modification. [b] Conductivity of a pressed pellet.

the radical cation salts of the donor components **4** have the highest single crystal conductivities.

Experimental Procedure

4: 46.6 g of 1,3,6,8-tetrabromopyrene[11] was added in small portions to 29 g of sodium methyl sulfide in 800 mL dimethylformamide in a 2-L three-necked flask and allowed to react for 15 h at 100 °C. Thereafter 800 mL of water was added, and the yellow precipitate was filtered, washed with methanol and dried under vacuum. Yield: 31.5 g (91%). In *N,N'*-dimethyl-2-imidazolidinone at room temperature the yield of **4** is 98%. M.p. 270 °C; IR (KBr): ν[cm^{-1}]: 1595, 1484, 1440, 1280, 1225, 1096, 1008, 968, 848, 819; satisfactory elemental analysis (C,H,S); ^{1}H NMR (200 MHz, D_2SO_4, 20 °C, TMS): δ = 2.60 (s, 12H, S-CH_3), 6.90 (s, 2H, -CH=), 8.36 (s, 4H, -HC=CH-).

5a: In a 100-mL electrolysis cell with two platinum electrodes one centimeter apart, a solution of 386 mg (1 mmol) **4** and 1.71 g (5 mmol) tetrabutylammonium perchlorate in 100 mL nitrobenzene was electroyzed at 80 °C for 24 h with a current of 1.5 mA. A cell potential of 1.6 V was observed. At the anode 186 mg of up to 1 mm long, black, lustrous crystals of **5a** form (42.5% yield, current efficiency 16%). M.p. 230° (decomp); satisfactory elemental analysis (C, H, S, Cl); IR (KBr): ν[cm^{-1}]: 1095 ($ClO_4^{\ominus}$); ESR: g = 2.0094 ($\nu_{1/2}$ = 14.5 G), 0.004 spins per complex (reference: "strong pitch" from Bruker). The X-ray structure of **5a** was determined [23].

5d: To a solution of 772 mg (2 mmol) of **4** in 10 mL of 1,2,4-trichlorobenzene at 120 °C was added a solution of 508 mg (2 mmol) iodine in 10 mL of 1,2,4-trichlorobenzene. Black crystals with a golden luster separated immediately. The solution was cooled and filtered by suction. The crystals were washed with methylene chloride. The quantitative yield (1.15 g) was obtained. Satisfactory elemental analysis (C, H, S, I); IR (KBr): no bands; ESR: g = 2.0054 ($\nu_{1/2}$ = 14 G), 0.007 spins per complex (reference "strong pitch" from Bruker); for X-ray structure of **5d** see [23].

Received: August 23, 1990 [Z 4147 IE]
German version: *Angew. Chem. 103* (1991) 201

CAS Registry numbers:
4, 127942-56-7; **5a**, 127942-68-1; **5d**, 127942-79-4; sodium methyl sulfide, 5188-07-8; 1,3,6,8-tetrabromopyrene, 128-63-2; tetrabutylammonium perchlorate, 1923-70-2.

[1] W. E. Hatfield: *Molecular Metals*, Plenum, New York 1979.
[2] H. Akamatu, H. Inokuchi, Y. Matsunaga, *Bull. Soc. Chim. Jpn. 29* (1956) 213.
[3] H. Urayama, H. Yamochi, G. Saito, K. Nozawa, T. Sugano, M. Kinoshita, S. Sato, K. Oshima, A. Kawamoto, J. Tanaka, *Chem. Lett. 1988*, 55.
[4] L. R. Melby, H. D. Hartzler, W. A. Sheppard, *J. Org. Chem. 39* (1974) 2456; for an eight-step synthesis, see [5].
[5] K. Lerstrup, I. Johannsen, M. Jorgensen, *Synth. Met. 27* (1988) B9.
[6] K. S. Varma, A. Bury, N. J. Harris, A. E. Underhill, *Synthesis 1987*, 837.
[7] J. Kommandeur, F. R. Hall, *J. Chem. Phys. 34* (1961) 129.
[8] R. Lapouyade, J.-P. Morand, *J. Chem. Soc. Chem. Commun. 1987*, 223.
[9] T. Nabeshima, S. Iwata, N. Furukawa, K. Morihashi, O. Kikuchi, *Chem. Lett. 1988*, 1325.
[10] K. Nakasuji, M. Sasaki, T. Kotani, I. Murata, T. Enoki, K. Imaeda, H. Inokuchi, A. Kawamoto, J. Tanaka, *J. Am. Chem. Soc. 109* (1987) 6970.
[11] H. Vollmann, H. Becker, M. Correll, H. Streeck, *Liebigs Ann. Chem. 531* (1937) 1.
[12] D. Jérome, H. J. Schulz, *Adv. Phys. 31* (1982) 299.
[13] A. Zweig, A. H. Maurer, B. G. Roberts, *J. Org. Chem. 32* (1967) 1322.
[14] The polarographic halfwave potential vs. SCE corresponds to a cyclovoltammetric potential of E_1 ± 0.04 V. J. Heinze, personal communication 1990.
[15] We thank Prof. *J. Heinze*, Universität Freiburg, for the cyclovoltammetry measurements.
[16] R. J. Warmak, T. A. Callcott, C. R. Watson, *Phys. Rev. B12* (1975) 3336.
[17] K. Bender, K. Dietz, H. Endres, H. W. Helberg, I. Henning, H. J. Keller, H. W. Schäfer, D. Schweitzer, *Mol. Cryst. Liq. Cryst. 107* (1984) 45.
[18] K. Bender, I. Henning, D. Schweitzer, K. Dietz, H. Endres, H. J. Keller, *Mol. Cryst. Liq. Cryst. 108* (1984) 359.
[19] K. Nakasuji, T. Kotzani, I. Murata, A. Kawamoto, J. Tanaka, T. Enoki, K. Imaeda, H. Inokuchi, *Synth. Met. 19* (1987) 385.
[20] E. B. Yagubskii, I. F. Schegolev, V. N. Laukhin, P. A. Kononovich, M. V. Kartsovnik, A. V. Zvarykina, L. I. Buravov *Sov. Phys. JEPT Lett. 39* (1984) 12; *Chem. Abstr. 100* (1984) 113119x.
[21] E. I. Zhilyaeva, R. N. Lyubovskaya, N. L. Khidekel, *Dokl. Akad. Nauk. SSSR 269* (1983) 121.
[22] H. Inokuchi, *Angew. Chem. 100* (1988) 1817; *Angew. Chem. Int. Ed. Engl. 27* (1988) 1747. This complex has the formula $(BEDT\text{-}TTF)_2ClO_4 \cdot 0.5\ Cl_2CHCH_2Cl$.
[23] G. Heywang, S. Roth, L. Born, *Synth. Met.*, in press.

β-Lithio Ketone Enolates: Generation and Reactions with Electrophiles**

By *Hiroyuki Nakahira, Ilhyong Ryu,* Masanobu Ikebe, Nobuaki Kambe*, and *Noboru Sonoda**

It is known that β-lithio ketones (**1**) are hardly any use in C–C bond-forming reactions because of their ready isomerization to the more stable lithium cyclopropoxides **2** (eq. 1).[1] Thus, synthetic equivalents of **1**, the β-acyl carbanion, have been extensively studied.[2] We suspected that such a bond-forming process could be more conveniently performed with the enolate form (**3**) of β-lithio ketones (**1**). Reaction via intermediate **3** has the added advantage that a nucleophilic site at the α-position is available, which would allow the sequential β- and α-dialkylation of ketones (eq. 2). Although several dilithio species related to **3** having anion-stabilizing substituents in the β-position have been reported to date,[3] the simplest, unfunctionalized dilithio species **3** itself has remained unexplored.[4, 5] We now report an efficient method for the generation of β-lithio ketone enolates (**3**) from β-trialkylstannyl ketones (**5**)[6] and their use as α,β-acyl dicarbanions (eq. 3).

Deprotonation of β-stannyl ketone (**5a**) by lithium diisopropylamide (LDA) in THF afforded the *Z*-form enolate selectively. The subsequent treatment of the enolate with *n*BuLi at −78 to 0 °C for 30 min resulted in Li-Sn exchange to furnish β-lithio ketone enolate **3a** with complete retention of the stereochemistry. Further reaction with Me_3SiCl provided **6a** in 91% yield (*E*/*Z* = 0/100, see also Table 1). On the other hand, enolate formation on deprotonation of **5b** by LDA lacked both regio- and stereoselectivity. However, the use of lithium bis(trimethylsilyl)amide led to selective gener-

[*] Dr. I. Ryu, Prof. Dr. N. Sonoda, H. Nakahira, M. Ikebe, Dr. N. Kambe
Department of Applied Chemistry, Faculty of Engineering,
Osaka University,
Suita, Osaka 565 (Japan)

[**] This work was supported in part by Grant in Aid for Scientific Research from the Japanese Ministry of Education, Science, and Culture.

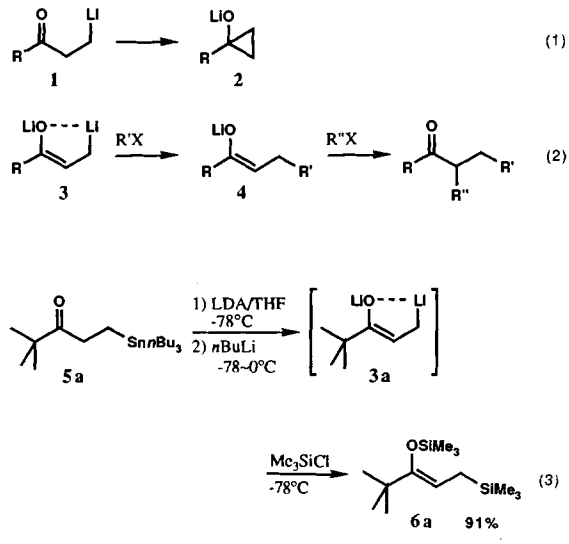

ation of (*Z*)-enolate, which was then subjected to Li-Sn exchange to give β-lithio ketone (*Z*)-enolate **3b** (Table 1, entry 4). As shown in Table 1 entry 8, β-lithio ketone enolate **3d**, which has a homoallyl structure, could also be generated by regioselective deprotonation of **5d** with LDA followed by Li-Sn exchange. In this case, however, a prolonged time (3 h) was required for the complete conversion to **3d**. Li-Sn exchange in the (*E*)-enolate of β-stannyl ketone was extremely slow, which suggests that stabilization arising from intramolecular five-membered ring complexation is a crucial factor for this exchange.

In accord with our premise (eq. 2) β-alkylation of **3** with alkyl bromides took place more rapidly than α-alkylation, allowing the direct conversion to β-alkylated enolates (**4**). Thus, treatment of **3a** with 1-bromopentane at −78 to −20 °C for 1 h followed by proton quenching gave the β-alkylated ketone **7** in 71% yield (entry 2). Similarly, the β-allylated ketone **9** was prepared by treatment with prenyl bromide (−78 °C, 5 min) in 53% yield (entry 5). β-Alkylated enolates (**4**) can undergo a number of useful transformations developed for metal enolates.[7] Further treatment with Me_3SiCl after β-alkylation of **3b** provided β-alkylated (*Z*)-enol silyl ether **10** in 68% yield (entry 6). The β-alkylation/α-allylation sequence leading to **8** was also successful (entry 3). Important spectroscopic data for compounds **6**–**10** are collated in Table 2.

Table 1. Generation of β-lithio ketone enolates (**3**) and their reactions with electrophiles[a].

Entry	Substrate **5**	β-Lithio ketone enolate **3**	Electrophile (equiv.) conditions	Product (yield [%]) [b]
1	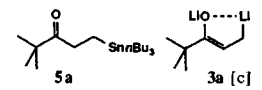 **5a**	**3a** [c]	Me_3SiCl (3.0) −78 °C, 30 min	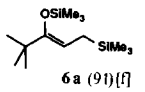 **6a** (91)[f]
2			1) $nC_5H_{11}Br$ (3.0) −78~−20 °C, 1 h 2) H_2O	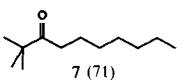 **7** (71)
3			1) $nC_5H_{11}Br$ (3.0) −78~−20 °C, 1 h 2) $CH_2{=}CHCH_2Br$ (3.0) [g] −78~25 °C, 1 h	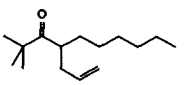 **8** (70)
4	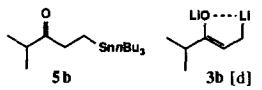 **5b**	**3b** [d]	Me_3SiCl (3.0) −78 °C, 30 min	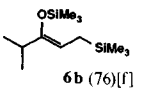 **6b** (76)[f]
5			1) $(CH_3)_2C{=}CHCH_2Br$ (3.0) −78 °C, 5 min 2) H_2O	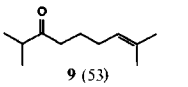 **9** (53) (3) [h]
6			1) $nC_5H_{11}Br$ (3.0) −78~−20 °C, 1 h 2) Me_3SiCl (2.0) −78 °C, 15 min	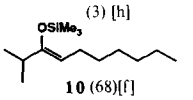 **10** (68)[f]
7	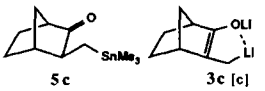 **5c**	**3c** [c]	Me_3SiCl (3.0) −78 °C, 30 min	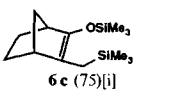 **6c** (75)[i]
8	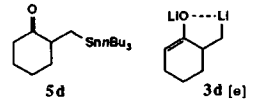 **5d**	**3d** [e]	Me_3SiCl (3.0) −78 °C, 30 min	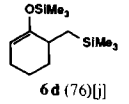 **6d** (76)[j]

[a] Carried out on 1 mmol scale in THF (5 mL). [b] Isolated by flash chromatography. [c] LDA, −78 °C, 2 h/*n*BuLi, −78 to 0 °C, 30 min. [d] LiN($SiMe_3$)$_2$, −78 °C, 5 h/*n*BuLi, −78 to 0 °C, 30 min. [e] LDA, −78 °C, 15 min/*n*BuLi, −78 to 0 °C, 3 h. [f] *E*:*Z* = 0:100. [g] HMPA (0.5 mL) was added. [h] The value in parentheses refers to the yield of S_N2' product. [i] Yield determined by GC. [j] The regioisomeric purity ≥ 98% (by GC analysis of the crude mixture).

Table 2. Spectroscopic data for **6a**–**d** and **7**–**10**[a].

6a: IR (neat): $\tilde{\nu}$[cm^{-1}] = 1656 (C=C); ^{1}H NMR (270 MHz, $CDCl_3$): δ = −0.02 (s, 9H), 0.22 (s, 9H), 1.03 (s, 9H), 1.29 (d, J = 8.2 Hz, 2H), 4.51 (t, J = 8.2 Hz, 1H); ^{13}C NMR (68 MHz, $CDCl_3$): δ = −1.79, 1.19, 15.68, 28.73, 36.31, 98.81, 157.02; *m/z* 258 ($M^{\oplus}$, 38%), 185 (100).
6b: IR (neat): $\tilde{\nu}$[cm^{-1}] = 1664 (C=C); ^{1}H NMR (600 MHz, $CDCl_3$): δ = −0.01 (s, 9H), 0.19 (s, 9H), 1.02 (d, J = 6.7 Hz, 6H), 1.31 (d, J = 8.6 Hz, 2H), 2.16 (m, 1H), 4.43 (dt, J = 0.6 and 8.6 Hz, 1H); *m/z* 244 ($M^{\oplus}$, 45%), 171 (100).
6c: IR (neat): $\tilde{\nu}$[cm^{-1}] = 1656 (C=C); ^{1}H NMR (270 MHz, $CDCl_3$): δ = 0.01 (s, 9H), 0.19 (s, 9H), 1.07–1.64 (m, 8H), 2.51, 2.58 (s, s, 1H each); ^{13}C NMR (68 MHz, $CDCl_3$): δ = −0.98, 0.64, 14.27, 26.21, 26.26, 45.29, 45.39, 45.61, 118.04, 150.22; *m/z* 268 ($M^{\oplus}$, 8%), 73 (100).
6d: IR (neat): $\tilde{\nu}$[cm^{-1}] = 1711 (C=C); ^{1}H NMR (270 MHz, $CDCl_3$): δ = 0.01 (s, 9H), 0.17 (s, 9H), 0.43 (dd, J_{vic} = 10.7 Hz, J_{gem} = 15.0 Hz, 1H), 0.38–0.47 (m, 1H), 1.06 (dd, J_{vic} = 3.3 Hz, J_{gem} = 15.0 Hz, 1H), 1.18–1.52 (m, 2H), 1.74–1.99 (m, 1H), 1.89–2.03 (m, 2H), 2.04–2.17 (m, 1H), 4.75 (t, J = 3.7 Hz, 1H); ^{13}C NMR (68 MHz, $CDCl_3$): δ = −0.71, 0.37, 19.96, 20.28, 24.22, 31.29, 35.05, 102.88, 154.91; *m/z* 256 ($M^{\oplus}$, 24%), 73 (100).
7: IR (neat): $\tilde{\nu}$[cm^{-1}] = 1707 (C=O); ^{1}H NMR (270 MHz, $CDCl_3$): δ = 0.87 (t, J = 6.7 Hz, 3H), 1.13 (s, 9H), 1.27 (m, 8H), 1.57 (m, 2H), 2.46 (t, J = 7.3 Hz, 2H); ^{13}C NMR (68 MHz, $CDCl_3$): δ = 14.05, 22.59, 23.94, 26.39, 29.15, 29.29, 31.71, 36.42, 44.07, 216.10; *m/z* 184 ($M^{\oplus}$, 15%), 57 (100).
8: IR (neat): $\tilde{\nu}$[cm^{-1}] = 1703, 1640 (C=O/C=C); ^{1}H NMR (270 MHz, $CDCl_3$): δ = 0.86 (t, J = 6.5 Hz, 3H), 1.12 (s, 9H), 1.23–1.58 (m, 10H), 2.03–2.33 (m, 2H), 2.90–2.97 (m, 1H), 4.95–5.03 (m, 2H), 5.61–5.74 (m, 1H); ^{13}C NMR (68 MHz, $CDCl_3$): δ = 14.04, 22.59, 26.37, 27.63, 29.49, 31.69, 32.30, 36.93, 44.38, 45.37, 116.48, 136.30, 218.34; *m/z* 224 ($M^{\oplus}$, 1%).
9: IR (neat): $\tilde{\nu}$[cm^{-1}] = 1712, 1674 (C=O/C=C); ^{1}H NMR (270 MHz, $CDCl_3$): δ = 1.06 (d, J = 7.0 Hz, 6H), 1.57 (s, 3H), 1.58 (m, 2H), 1.67 (s, 3H), 1.96 (m, 2H), 2.41 (t, J = 7.3 Hz, 2H), 2.57 (m, 1H), 5.06 (t, J = 7.0 Hz, 1H); ^{13}C NMR (68 MHz, $CDCl_3$): δ = 17.74, 18.32, 23.95, 25.74, 27.52, 39.79, 40.85, 123.95, 132.26, 214.93; *m/z* 168 ($M^{\oplus}$, 29%), 82 (100).
10: IR (neat): $\tilde{\nu}$[cm^{-1}] = 1669 (C=C); ^{1}H NMR (600 MHz, $CDCl_3$): δ = 0.19 (s, 9H), 0.88 (t, J = 6.9 Hz, 3H), 1.03 (d, J = 6.7 Hz, 6H), 1.27–1.30 (m, 8H), 1.96–1.98 (m, 2H), 2.12–2.17 (m, 1H), 4.45 (dt, J = 0.6 and 6.9 Hz, 1H); ^{13}C NMR (68 MHz, $CDCl_3$): δ = 0.68, 14.08, 20.78, 22.66, 25.56, 29.19, 29.99, 31.83, 34.40, 105.70, 155.60; *m/z* 242 ($M^{\oplus}$, 12%), 171 (100).

[a] Elemental analyses or high-resolution mass spectra were obtained for all new compounds.

The high efficiency of the synthesis steps via the β-lithio ketone enolates (**3**), coupled with the simplicity of the experimental procedure, makes this reaction route a promising tool for α,β-functionalization of ketones.

Experimental

Typical procedure (Table 1, entry 2): **5a** (403 mg, 1.0 mmol) was added to a cooled solution (−78 °C) of LDA—prepared from diisopropylamine (0.184 mL, 1.3 mmol) and *n*BuLi (1.58 M hexane solution, 0.76 mL, 1.2 mmol)—in THF (5 mL), and the solution was stirred for 2 h at −78 °C. *n*BuLi (1.58 mL, 2.5 mmol) was added by syringe. The reaction mixture was allowed to warm to 0 °C and stirred for 30 min. Thereafter it was cooled again to −78 °C, and 1-bromopentane (453 mg, 3.0 mmol) was added. The mixture was allowed to warm to −20 °C and stirred for 1 h. Dilution with ether followed by washing with water, drying ($MgSO_4$), concentration, and flash chromatography (SiO_2, *10% ether in pentane*) gave **7** *(130 mg, 71%)*.

Received: August 28, 1990 [Z 4197 IE]
German version: *Angew. Chem. 103* (1990) 178

CAS Registry numbers:
3a, 131435-69-3; **3b**, 131435-70-6; **3c**, 131435-71-7; **3d**, 131435-72-8; **5a**, 97782-58-6; **5b**, 129266-32-6; **5c**, 131435-61-5; **5d**, 97782-59-7; **6a**, 131435-62-6; **6b**, 131435-64-8; **6c**, 131435-67-1; **6d**, 131435-68-2; **7**, 61759-36-2; **8**, 131435-63-7; **9**, 131435-65-9; **10**, 131435-66-0; $C_5H_{11}Br$, 110-53-2; $(CH_3)_2C=CHCH_2Br$, 870-63-3.

[1] a) D. P. G. Hamon, R. W. Sinclair, *J. Chem. Soc. Chem. Commun. 1968*, 890; b) C. S. Shiner, A. H. Berks, A. M. Fisher, *J. Am. Chem. Soc. 110* (1988) 957.

[2] Reviews: a) D. Seebach, *Angew. Chem. 91* (1979) 259; *Angew. Chem. Int. Ed. Engl. 18* (1979) 239; b) N. H. Werstiuk, *Tetrahedron 39* (1983) 205; c) J. C. Stowell, *Chem. Rev. 84* (1984) 409; d) D. Hoppe, *Angew. Chem. 96* (1984) 930; *Angew. Chem. Int. Ed. Engl. 23* (1984) 932; e) T. A. Hase (Ed.): *Umpoled Synthons*, Wiley, New York 1987.

[3] For α,β-dianions of ketones bearing the anion-stabilizing substituents $(RO)_2P(O)$- [a], aryl [b, c], PhS- [d], vinyl [e, f], or divinyl [g] see: a) R. Goswami, *J. Am. Chem. Soc. 102* (1980) 5973; b) C.-L. Mao, C. R. Hauser, M. L. Miles, *ibid. 89* (1967) 5303; c) B. M. Trost, L. H. Latimer, *J. Org. Chem. 42* (1977) 3212; d) K. Ramig, M. Bhupathy, T. Cohen, *ibid. 54* (1989) 4404; e) D. Seebach, M. Pohmakotr, *Tetrahedron 37* (1981) 4047; f) D. Seebach, M. Pohmakotr, C. Schregenberger, B. Weidmann, R. S. Mail, S. Pohmakotr, *Helv. Chim. Acta 65* (1982) 419; g) I. T. Badejo, R. Karaman, N. W. I. Lee, E. C. Lutz, M. T. Mamanta, J. L. Fry, *J. Chem. Soc. Chem. Commun. 1989*, 566.

[4] For unfunctionalized α,α- and α,α′-dianions of ketones, see: a) C. J. Kowalski, M. L. O'Dowd, M. C. Burke, K. W. Fields, *J. Am. Chem. Soc. 102* (1980) 5411; b) C. J. Kowalski, G. S. Lal, *ibid. 108* (1986) 5356; c) J. S. Hubbard, T. M. Harris, *ibid. 102* (1980) 2110.

[5] An approach to unfunctionalized dianions **3** based on deprotonation of (1-phenyl)allyloxy anions was first reported by *Dimmel* et al., but their system suffered from rapid β-protonation, see: D. R. Dimmel, W. Y. Fu, S. B. Gharpure, *J. Org. Chem. 41* (1976) 3092. For a recent study involving deprotonation in potassium allyloxide systems, see: T. Cuvigny, M. Julia, L. Jullien, C. Roland, *Tetrahedron Lett. 28* (1987) 2587.

[6] a) H. Nakahira, I. Ryu, A. Ogawa, N. Kambe, N. Sonoda, *Organometallics 9* (1990) 277; b) I. Ryu, S. Murai, N. Sonoda, *J. Org. Chem. 51* (1986) 2389.

[7] Reviews: a) J. d'Angelo, *Tetrahedron 32* (1976) 2979; b) L. M. Jackman, B. C. Lange, *ibid. 33* (1977) 2737; c) R. L. Augustine (Ed.): *Carbon-Carbon Bond Formation, Vol. 2*, Marcel Dekker, New York 1979.

$K_2[Al_{12}iBu_{12}]$, a Compound with Al_{12} Icosahedra**

By *Wolfgang Hiller, Karl-Wilhelm Klinkhammer, Werner Uhl,** and *Jürgen Wagner*

The reduction of chlorodiisobutylaluminum with potassium to give the corresponding tetraisobutyldialuminum(*Al-Al*) was first described in 1976.[1, 2] However, the proposed structure was essentially based on only a deuterolysis experiment in which the amount of liberated D_2 was measured; isolation of the pure compound has not yet been achieved. The only compound with an Al–Al bond so far characterized spectroscopically and by crystal structure analysis is tetrakis[bis(trimethylsilyl)methyl]dialuminum(*Al-Al*) (**1**).[3]

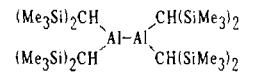

1

The reaction mentioned above, which was carried out in *n*-hexane, results in formation of a brown precipitate consisting mostly of potassium chloride. Extraction of this precipitate with toluene, however, gives a low but reproducible yield of a further product, which crystallizes at −30 °C as dark red octahedra. The crystal structure determination showed that this product was dipotassium *closo*-dodecaisobutyldodecaaluminate, $K_2[Al_{12}iBu_{12}]$ (**2**), in which Al_{12} icosahedra are present (Fig. 1). The crystals of **2** contain toluene, which is completely removed over several hours under vacuum (10^{-3} Torr) at room temperature. However, the crystals thereby become brittle and break upon even gentle handling. We obtained single crystals suitable for X-ray diffraction analysis by drying the crystals under vacuum at −30 °C; their composition was approximately $K_2Al_{12}iBu_{12} \cdot 1.2\ C_7H_8$ according to integration of the ^1H NMR spectrum. Whereas, under normal conditions, **2** completely decomposes within 30 min upon exposure to an X-ray beam, the diffraction pattern can be measured at −65 °C without any significant change in the intensities of the control reflections.

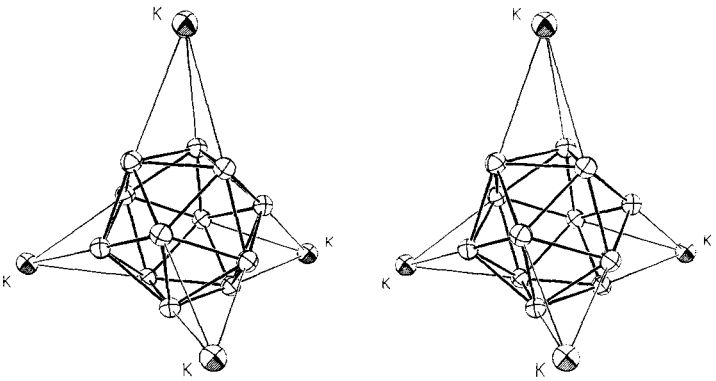

Fig. 1. Stereoscopic drawing of the Al_{12} icosahedron (thermal ellipsoids at 30% probability). For clarity, only the Al and K atoms are shown. Selected bond lengths [pm] and angles [°]: Al-Al 267.9(5), 268.0(4), 269.6(5), K-Al 400.4(3); Al-Al-Al 59.8(1), 60.0, 60.4(2).

Compound **2** crystallizes in the centrosymmetric cubic space group $Fd\bar{3}$ with eight formula units per unit cell.[4] There are three slightly different bond lengths between the aluminum atoms of the icosahedron (267.9(5), 268.0(4), and 269.6(5) pm). Moreover, the bond angles between the triangular sides, which exhibit a maximum deviation of 0.4° from the ideal value of 60°, are consistent with nearly undistorted icosahedral symmetry. The Al–Al bonds are only slightly longer than that in the Al_2 compound **1** (266.0 pm).[3]

A potassium atom lies on a threefold axis above each of four faces of the icosahedron and is coordinated by three α-C atoms of isobutyl groups. As shown in Figure 2, each potas-

[*] Dr. W. Uhl, K.-W. Klinkhammer, J. Wagner
Institut für Anorganische Chemie der Universität
Pfaffenwaldring 55, W-7000 Stuttgart 80 (FRG)
Dr. W. Hiller
Institut für Anorganische Chemie der Universität Tübingen

[**] This work was supported by the Deutsche Forschungsgemeinschaft and the Fonds der Chemischen Industrie.

sium atom bridges two icosahedra, so that its coordination number is six with respect to carbon (C1), resulting in formation of a trigonal antiprism. Thus, the solid-state structure consists of a three-dimensional network in which the icosahedral centers are surrounded tetrahedrally by potassium atoms and the cations are coordinated by the Al_{12} clusters in a linear fashion in analogy to a part structure of Cu_2O.[5] The K–C distance (323 pm) is consistent with the standard value reported in the literature.[6] Two values can be distin-

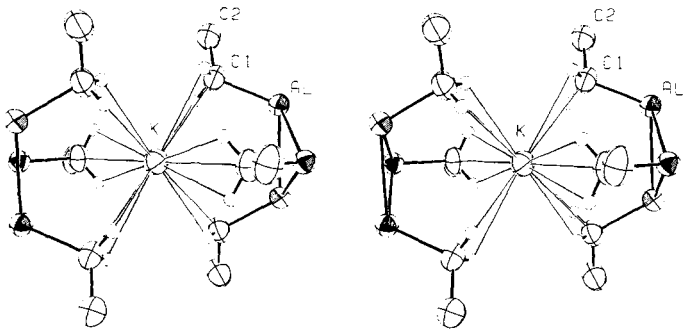

Fig. 2. Stereoscopic drawing of the environment of the potassium ions (thermal ellipsoids at 30% probability). For clarity, the methyl groups (C21 and C22) and the hydrogen atom H21 on C2 are omitted. Important distances [pm] and angles K-Cl 322.6(9), Al-C1 199.9(9), C1-C2 153(1); C1-K-C1 180.0, 86.8(2) (2×), 93.2(2) (2×), Al-C1-K 97.3(3), Al-C1-C2 117.5(7).

guished in crystalline methylpotassium:[7] short contacts with a mean value of 298.5 pm, where the lone pair of the carbanion is directed toward the cations, and longer contacts of 337 pm through C–H σ bonds, which correspond more closely to the bonding in **2**. Shorter distances between potassium and carbon than those in **2** are also observed from the powder data for the structure of potassium tetramethylaluminate (315, 348 pm) and -gallate (294, 352 pm).[8] The hydrogen atoms on the bridging C1 are 272 and 296 pm from the potassium atom. A comparable interaction between potassium and C-H σ bonds was recently found in potassium{dichlorobis[bis(trimethylsilyl)methyl]aluminate}.[9] The Al–C bond length (199.9 pm) is considerably shorter than that usually found for bridged systems and lies in the widespread region of Al–C single bonds. In agreement with the K–C–Al bridge discussed here, the IR spectrum exhibits broad bands for the Al–C and C–C stretching modes.

In the framework made up of potassium atoms and Al_{12} icosahedra, channels extending parallel to the face diagonals are formed and incorporate crystal toluene. However, the toluene molecules are so strongly disordered that their positions cannot be completely determined. For a maximum residual electron density of 0.5 $eÅ^{-3}$, only the position of a six-membered ring fragment could be determined and then refined by restriction of the bond lengths. Its influence on the *R* value and standard deviation is small, however. We are currently attempting to obtain a derivative of **2** that allows us to circumvent this disorder.

Compound **2** is surprisingly stable in air; it remains crystalline for about 2 h without noticeable change, but then a colorless substance, presumably $Al(OH)_3$, begins to grow on the crystal. Under inert atmosphere, **2** is thermally stable to about 150 °C, above which rapid decomposition occurs with deposition of aluminum.

Compound **2** corresponds to $[B_{12}H_{12}]^{2\ominus}$ in its cluster structure and number of valence electrons and, like that compound, obeys the Wade rules for a *closo* structure. $K_2[B_{12}H_{12}]$ crystallizes in the cubic space group $Fm\bar{3}$, but displays a different arrangement of anions and cations with a potassium ion coordinated by 24 hydrogen atoms.[10]

Experimental Procedure

All operations were carried out under purified argon in dry solvents. Chlorodiisobutylaluminum (8.5 g, 48 mmol) was dissolved in 40 mL of *n*-hexane and treated with potassium (1.9 g, 48 mmol). The resulting reaction mixture was stirred for three days at 0 °C and for one day at room temperature. It was then filtered and the residue was treated with 40 mL of toluene. Concentration of the solution thereby obtained to roughly one-third of its initial volume and cooling to −30 °C resulted in formation of dark red crystals of **2**, which were dried under 10^{-3} Torr at room temperature. Yield: 62 mg (1.5% based on Al). Dec. (under argon) at 150 °C. ^1H NMR (60 MHz, C_6D_6): δ = 2.35 (m; CH), 1.40 (d, *J* (H,H) = 6.2 Hz; CH_3), 0.60 (d, *J* (H,H) = 6.4 Hz; CH_2). $^{13}C\{^1H\}$ NMR (62.896 MHz, C_6D_6): δ = 30.9 (CH), 28.8 (CH_3), 17.1 (CH_2). IR (Nujol; CsBr disc) [cm^{-1}]: $\tilde{\nu}$ = 1330 (s), 1315 (s, δCH_3), 1250 (w), 1210 (m), 1165 (s, br., ϱCH_3), 1070 (w), 1045 (w), 1020 (s ν(as)CC), 950 (m), 920 (m), 840 (m), 820 (s, br.), 780 (sh, ν(s)CC), 730 (s), 700 (s), 670 (s, br.), 610 (s, br. νAlC), 560 (w), 490 (w), 470 (m), 440 (m), 400 (m), 375 (m δCC, δAlC (νAlAl?)). A Raman spectrum could not be recorded.

Received: September 10, 1990 [Z 4173 IE]
German version: *Angew. Chem. 103* (1991) 182

CAS Registry numbers:
2, 131513-79-6; $ClAl(iBu)_2$, 1779-25-5.

[1] H. Hoberg, S. Krause, *Angew. Chem. 88* (1976) 760; *Angew. Chem. Int. Ed. Engl. 15* (1976) 694.
[2] M. A. Miller, E. P. Schram, *Organometallics 4* (1985) 1362.
[3] W. Uhl, *Z. Naturforsch. B 43* (1988) 1113.
[4] Crystal structure analysis: CAD4 diffractometer, $Mo_{K\alpha}$ radiation; graphite monochromator, $T = -65$ °C; VAXSDP and SHELXTL programs; cubic, space group $Fd\bar{3}$; a = 2639.3(7) pm; V = 18 385 $Å^3$; Z = 8; $\mu = 2.4 \times 10^2$ m^{-1}; crystal dimensions 0.6 × 0.5 × 0.5 mm; θ-2θ scan; 591 unique reflections > 4σ(*F*); 74 refined parameters; H atoms refined as rigid groups with ideal distances and angles and common *U* values; other atoms refined anisotropically; high-angle refinement; disordered toluene: C atoms refined with bond-length restrictions based on an ideal model and with constant *U* values; R_w = 0.083; R = 0.089. Further details of the crystal structure investigation may be obtained from the Fachinformationszentrum Karlsruhe, Gesellschaft für wissenschaftlich-technische Information mbH, W-7514 Eggenstein-Leopoldshafen 2 (FRG), on quoting the depository number CSD-54909, the names of the authors, and the journal citation.
[5] B. G. Hyde, S. Andersson: *Inorganic Crystal Structures*, Wiley, New York 1990, p. 12.
[6] C. Schade, P. von R. Schleyer, *Adv. Organomet. Chem. 27* (1987) 169.
[7] E. Weiss, T. Lambertsen, B. Schubert, J. K. Cockroft, *J. Organomet. Chem. 358* (1988) 1.
[8] R. Wolfrum, G. Sauermann, E. Weiss, *J. Organomet. Chem. 18* (1969) 27; see also: G. Hencken, E. Weiss, *ibid. 73* (1974) 35.
[9] W. Uhl, *Z. Naturforsch. B 45* (1990) 1349.
[10] J. A. Wunderlich, W. N. Lipscomb, *J. Am. Chem. Soc. 82* (1960) 4427.

Double Stereodifferentiation in Carbohydrate Coupling Reactions: The Mismatched Interaction of Donor and Acceptor as an Unprecedented Factor Governing the α/β Ratio of Glycoside Formation**

By *Nynke M. Spijker* and *Constant A. A. van Boeckel**

One century after the first glycoside syntheses of *Michael*[1] and *Fischer*,[2] the stereochemical outcome (α/β ratio) of carbohydrate coupling reactions is still difficult to control. The best-established method for stereoselective car-

[*] Dr. C. A. A. van Boeckel, Drs. N. Spijker
Akzo Pharma Division,
Organon Scientific Development Group
P.O. Box 20, NL-5340 BH Oss (The Netherlands)

[**] We wish to thank Mr. *G. N. Wagenaars* for recording the NMR spectra

bohydrate coupling reactions, the Koenigs–Knorr procedure (1901),[3] is based on the participation of a group at C-2 of the glycosyl donor to direct the 1,2-*trans* glycosidic bond formation. Although the experimental conditions of this procedure have been revised progressively,[4] the basic principle of neighboring group participation has not been obliterated.[5]

Another breakthrough was realized by *Lemieux* et al.[6] and *Paulsen* et al.[7] in the seventies. They demonstrated that coupling reactions of various glycopyranoside donors under "in situ anomerization" conditions lead to 1,2-*cis*-glycosidic bonds. Furthermore, for the preparation of 1,2-*cis* glycosidic bonds in D-manno- and L-rhamnopyranosides other methods[8] have been introduced which use insoluble silver salt promoters.

The yield and the stereochemical outcome of the coupling strategies outlined above are frequently unsatisfactory. For this reason much attention has been paid to additional factors that may act on glycosylations, such as the type of the leaving group at the anomeric center (e.g. bromide,[7] fluoride,[9] thioether,[10] imidate,[11] or pentenyl ether[12]), the promoter,[7] the substituents at the carbohydrates,[7, 13] the solvent, and the temperature. Although these studies provided much empirical knowledge to improve glycosylations, carbohydrate chemists are still confronted with coupling reactions that proceed in low yields and give poor α/β ratios.

leading to the α-bond. That the stereochemical outcome (α/β ratio) of an interglycosidic bond formation may be affected by unfavorable steric interactions in either the α- or β-transition state, can be corroborated by applying the principle of double stereodifferentiation.[15] When stereochemical interactions between a chiral carbohydrate donor and a chiral carbohydrate acceptor are a dominant factor during the formation of the interglycosidic bond, we expect different α/β ratios in coupling reactions of L- and D-donors with a D- or L-acceptor respectively, because sterically matched and sterically mismatched pairs are possible in the individual transition states (i.e. L-α-D, L-β-D/D-α-D, D-β-D and their mirror images).

To substantiate this hypothesis we performed coupling reactions of the easily accessible 2,3,4-tri-*O*-benzoyl-6-deoxy-α-D-galactopyranosyl bromide (**6**)[16] and its L-isomer (**7**) (derived from L-fucose) with glycosyl acceptor **2** (Scheme 2).

Reaction of the D-glycopyranosyl bromide **6** with **2** in the presence of silver trifluoromethanesulfonate and 2,6-di-*tert*-butylpyridine, under the conditions described above, afforded the α-coupled disaccharide **8α** in 58% yield and the β-coupled product **8β** in 29% yield (α/β ratio: 2/1), whereas the coupling of the L-glycopyranosyl bromide (**7**) with **2** under the same conditions gave only 7% yield of **9α** and 61% of **9β** (α/β ratio: 1/8.4).[17]

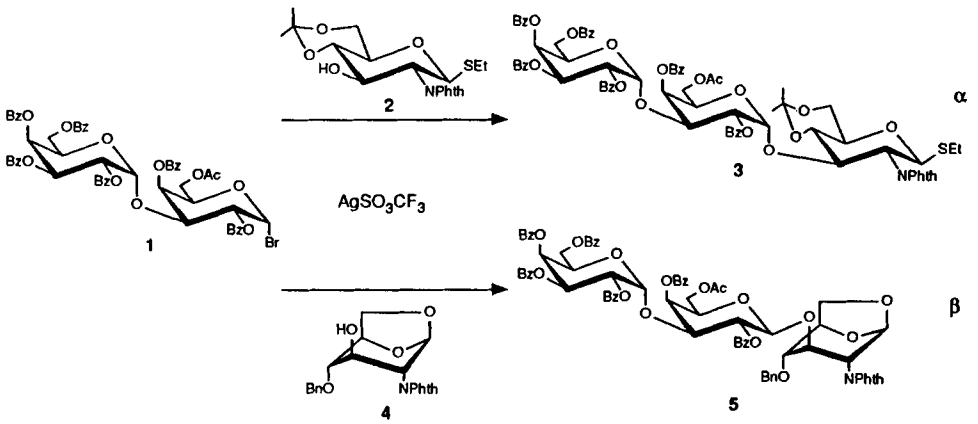

Scheme 1. Bz = benzoyl, Bn = benzyl, Ac = acetyl, Phth = phthaloyl, Et = ethyl.

We now report a most intriguing example of a carbohydrate coupling with an unexpected stereochemical outcome. The coupling between donor **1** and acceptor **2** in dichloromethane in the presence of silver trifluoromethanesulfonate, 2,6-di-*tert*-butylpyridine (0.8 equiv) and molecular sieves 4 Å gave after 20 minutes at − 50 °C *exclusively* α-coupled product **3**[14] in 23% yield (Scheme 1). Thus, although a participating group is present at C-2 of donor **1** to direct the β-glycoside formation in the synthesis of the oligosaccharide Galα(1-3)Galβ(1-3)GlcNAc, only the α-interglycosidic bond was formed.

Which factor outweighs the well-established β-directing effect of the benzoyl participating group? Even other activating groups at the anomeric center of **1** (e.g. fluoride, imidate), and different promoters (e.g. silver silicate) did not lead to the expected β-glycoside formation.

We reasoned that severe steric hindrance between the donor **1** and acceptor **2** occurs in the transition state leading to the β-interglycosidic bond, but not in the transition state

These results clearly demonstrate the influence of double stereodifferentiation on the α/β ratio of this coupling reac-

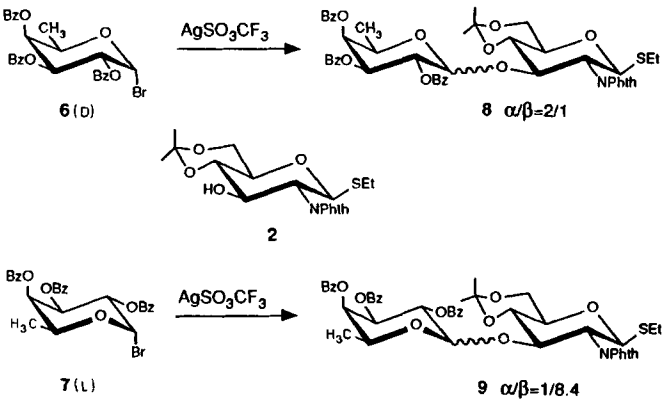

Scheme 2.

tion. Furthermore the glycosidic bonds of the products do not isomerize (anomerization) under the applied reaction conditions (the solution may become slightly acidic). Thus donor **6** and acceptor **2** apparently form a mismatched pair in the transition state leading to the β-glycoside because of disfavorable steric interactions, whereas donor **7** and acceptor **2** form a matched pair during the formation of the β-coupled product. Molecular modeling shows (Fig. 1) that during the formation of the β-glycoside considerable steric hindrance arises between the phthalimido group of **2** and the benzoyl ester at C-2 of **6** (D), but not between the phtalimido group of **2** and **7** (L). On contemplating these results we can explain the unexpected stereochemical outcome of the coupling reaction between **1** and **2** in terms of a mismatched pair for the β-glycoside transition state. The undesired α-glycoside **3** is then formed through an intermediate oxocarbenium ion[6, 7] in which the benzoyl group does not participate.

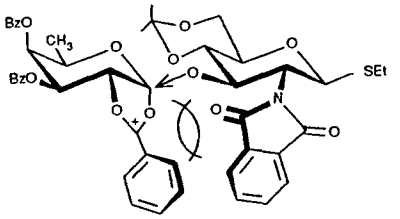

6(D)+**2**
mismatched pair

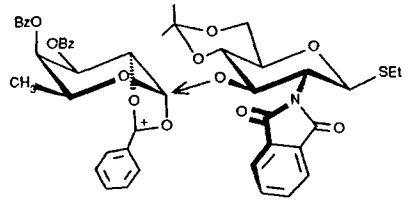

7(L)+**2**
matched pair

Fig. 1. During the formation of the β-glycoside, considerable steric hindrance arises between the phthalimido group of **2** and the benzoyl ester of **6**(D), but not between **2** and **7**(L).

We now reasoned that to synthesize the β-glycosidic bond of the oligosaccharide Galα(1-3)Galβ(1-3)GlcNAc a glycosyl acceptor has to be used that does not form a sterically mismatched pair during β-coupling with donor **1**. To this end, we used 1,6-anhydrosugar **4**[18] as glycosyl acceptor, because its hydroxyl group is oriented differently towards the bulky protecting groups than the hydroxyl group of **2**. Thus, **1** was coupled with **4** in the presence of silver trifluoromethanesulfonate and 2,6-di-*tert*-butylpyridine (Scheme 1). Indeed, in this glycosylation only β-coupled trisaccharide **5**[19] was formed, in 75% yield. Since the hydroxyl group of **4** is not intrinsically more reactive than that of **2**,[20] the difference in yield and α/β ratio of the two coupling reactions has to be attributed to the fact that a mismatched pair is formed in the transition state of the β-coupling between **2** and **1**, but not in the β-coupling of **4** with **1**.

To get more insight into the influence of double stereodifferentiation on α/β ratios of carbohydrate coupling reactions, we performed a glycosylation in which two *enantiomeric* glycosyl acceptors are individually coupled with a D-glycosyl donor. Thus, reaction of 6-*O*-acetyl-2,3,4-tri-*O*-benzyl-α-D-glucopyranosyl bromide (**10**)[21] with 1,2:5,6-di-*O*-isopropylidene-D-glucofuranose (**11**) in the presence of silver trifluoromethanesulfonate and 2,6-di-*tert*-butylpyridine (in situ anomerization conditions) afforded the α- and β-coupled disaccharides in 70% and 16% yield respectively (α/β ratio: 4.5/1), while coupling of the same donor (**10**) with the L-acceptor (**12**)[22] under the same conditions gave the α- and β-coupled products in 47% and 24% yield respectively (α/β ratio: 2/1) (Scheme 3).

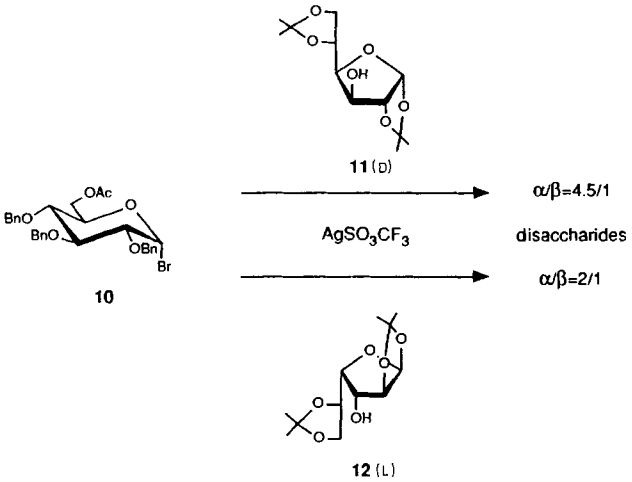

Scheme 3.

In another example the effect of double stereodifferentiation was less pronounced. Coupling of 2,3,4-tri-*O*-benzyl-6-deoxy-α-D-galactopyranosyl bromide[23] with 1,6-anhydro-2,4-di-*O*-benzyl-β-D-galactopyranose[24] in the presence of silver silicate aluminate[25] gave the α- and β-coupled disaccharides in 12% and 75% yield respectively (α/β ratio: 1/6.5), while coupling of the L-glycosyl bromide with the same aglycon afforded the α- and β-coupled dimers in 14% and 57% yield respectively (α/β ratio: 1/4). Apparently in this example other factors, like the substituents at the donor and type of promoter, play a more important role.

In conclusion, the unfavorable steric interaction between a glycosyl donor and acceptor in the transition state leading to either the α- or β-interglycosidic bond may strongly influence the stereochemical outcome (α/β ratio) of glycosylations. When unexpected α/β ratios in glycosylations are obtained, a sterically mismatched interaction in the transition state leading to the desired glycosidic bond has to be considered. These interactions may be foreseen by molecular modeling studies of the α- and β-glycosides. To reduce unfavorable steric interactions, protecting groups can be replaced by sterically less demanding ones, the conformation of the carbohydrate unit (mostly the aglycon) may be altered (e.g. through the formation of anhydro sugars), and in oligosaccharide synthesis the building block strategies can be adapted. A more systematic study of matched and mismatched pairs during interglycosidic bond formation will improve our understanding of oligosaccharide synthesis, which still relies on trial and error.

Received: August 28, 1990 [Z 4162]
German version: *Angew. Chem. 103* (1990) 179

[1] A. Michael, *Am. Chem. J. 1* (1879) 305.
[2] E. Fischer, *Ber. Dtsch. Chem. Ges. 26* (1893) 2400.
[3] W. Koenigs, E. Knorr, *Ber. Dtsch. Chem. Ges. 34* (1901) 957.

[4] a) F. Bochkov, G. E. Zaikov: *Chemistry of the O-Glycosidic Bond*, Pergamon, Oxford 1979; b) B. Helferich, K. Weis, *Chem. Ber. 89* (1956) 314.
[5] Despite the presence of a participating group at C-2, sometimes α-glycosides or α/β mixtures are formed. a) This paper b) M. E. Chacon-Fuertes, M. Martin-Lomas, *Carbohydr. Res. 43* (1975) 51–56 c) S. Sato, Y. Ito, T. Nukada, Y. Nakahara, T. Ogawa, *ibid. 167* (1987) 197.
[6] R. U. Lemieux, K. B. Hendriks, R. V. Stick, K. James, *J. Am. Chem. Soc. 97* (1975) 4056.
[7] H. Paulsen, *Angew. Chem. 94* (1982) 184; *Angew. Chem. Int. Ed. Engl. 21* (1982) 155.
[8] a) N. K. Kochetkov, V. I. Torgev, N. N. Malysheva, S. A. Shasshov, *Tetrahedron 36* (1980) 1099; b) H. Paulsen, W. Kutscker, O. Lockhoff, *Chem. Ber. 114* (1981) 3233.
[9] J. L. Randall, K. C. Nicolaou, *ACS Symp. Ser 88* (1988) 13.
[10] P. Fügedi. P. J. Garegg, H. Lönn, T. Norberg, *Glycoconjugate J. 4* (1987) 97.
[11] R. R. Schmidt, *Angew. Chem. 98* (1986) 213; *Angew. Chem. Int. Ed. Engl. 25* (1986) 212.
[12] D. R. Mootoo, P. Konradsson, B. Fraser-Reid, *J. Am. Chem. Soc. 111* (1989) 8540.
[13] N. M. Spijker, H. Zuurmond, P. Westerduin, C. A. A. van Boeckel, *Recl. Trav. Chim. Pays-Bas 108* (1989) 360.
[14] Compound **3**: ^{1}H NMR (360 MHz, C_6D_6, TMS) $\delta = 5.61$ (d, $J = 10.6$ Hz, 1H; H-1), 6.59 (d, $J = 3.5$ Hz, 1H; H-1'), 6.03 (d, $J = 3.6$ Hz, 1H; H-1''); ^{13}C NMR ($CDCl_3$): $\delta = 81.73$ (C-1), 95.89, 92.70 (C-1', C-1''). The only other two products that were isolated consisted of the hydrolysis product of **1** and the remaining **2**.
[15] S. Masamune, W. Choy, J. S. Petersen, L. R. Sita, *Angew. Chem. 97* (1985) 1; *Angew. Chem. Int. Ed. Engl. 24* (1985) 1.
[16] Compounds **6** and **7** were prepared by benzoylation of 6-deoxy-D (or L for **7**)-galactose (benzoylchloride/pyridine) and subsequent treatment with $TiBr_4$.
[17] ^{1}H NMR (360 MHz, $CDCl_3$, TMS) of **8α**: $\delta = 5.35$ (d, $J = 10.3$ Hz, 1H; H-1), 5.77 (d, $J = 3.9$ Hz, 1H; H-1'); **8β**: $\delta = 5.26$ (d, $J = 10.3$, 1H; H-1), 5.03 (d, $J = 8.0$ Hz, 1H; H-1'); **9α**: $\delta = 5.19$ (d, $J = 10.3$ Hz, 1H; H-1), 5.20 (d, $J = 3.8$ Hz, 1H; H-1'); **9β**: $\delta = 5.45$ (d, $J = 10.4$ Hz, 1H; H-1), 4.82 (d, $J = 7.5$ Hz, 1H; H-1').
[18] Compound **4** was prepared from 1,6:2,3-di-anhydro-4-*O*-benzyl-β-D-mannopyranose using the procedure described in H. Paulsen, A. Bünsch, *Carbohydr. Res. 100* (1982) 143.
[19] ^{1}H NMR (360 MHz, $CDCl_3$, TMS) of **5**: $\delta = 5.48$ (d, $J = 0.5$ Hz, 1H; H-1), 5.11 (d, $J = 8.0$ Hz, 1H; H-1'), 5.66 (d, $J = 3.7$ Hz, 1H; H-1'').
[20] In an experiment compounds **4** and **2** were acetylated at 0 °C using a pyridine/acetic anhydride mixture (3/1, v/v). Compound **2** was fully acetylated in 2.30 h, while 2.45 h was required for the acetylation of **4**.
[21] J. M. Fréchet, C. Schuerch, *J. Am. Chem. Soc. 94* (1972) 604.
[22] Compound **12** was prepared from (commercially available) L-glucose using the procedure described in R. L. Whistler, M. L. Wolfrom: *Methods in Carbohydrate Chemistry II*, Academic, New York 1963, p. 320.
[23] U. Spohr, R. U. Lemieux, *Carbohydr. Res. 174* (1988) 211.
[24] H. Paulsen, O. Lockhoff, *Chem. Ber. 114* (1981) 3079.
[25] C. A. A. van Boeckel, T. Beetz, A. Kock-van Dalen, H. van Bekkum, *Recl. Trav. Chim. Pays-Bas 106* (1987) 596.

Biogenesis of the Carbon Skeleton of Glycerinopyrin: A New Biosynthetic Pathway for Pyrroles**

By *Monika Schönewolf* and *Jürgen Rohr**

The structure of glycerinopyrin **1**, a metabolite of *Streptomyces violaceus* (strain FH-S 1081), was recently elucidated.[11] The small natural product attracted our interest in particular regarding the biosynthesis of its methyl-branched five-membered nitrogen heterocycle. This structural element has been found in nature only once before, namely in the trail marker pheromone **2** of the Texan leaf-cutting ant *Atta texana* (Buckley),[2, 3] which also is the closest natural relative of **1**. A saturated compound of this structural type, 3-hydroxy-4-methylproline[4–6] (HMP) **3**, occurs in some cyclopeptide antibiotics including echinocandin B[7, 8] and mulundocandin.[9] Herein we report for the first time the biogenesis of such a type of nitrogen heterocycle from which emerges a novel biosynthetic pathway of general significance.

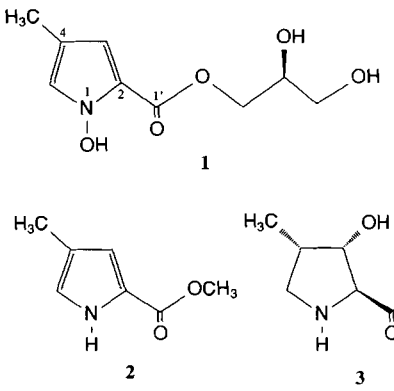

That the side chain of **1** derives from glycerol (the major source of carbon of the fermentation medium) seemed to be obvious and could be demonstrated by a feeding experiment with 0.144 mol L^{-1} [1,1,3,3-$^2H_4$]-glycerol, which resulted in an approximately 20% incorporation into **1** (Table 1).[10]

Three biogenetic hypotheses were considered for synthesis of the methyl-substituted 2-pyrrolecarboxylic acid moiety (Fig. 1): 1) a [5 + 1] assemblage of proline, hydroxyproline or ornithine and one carbon from the C_1-pool (usually the *S*-CH_3 group of methionine), 2) a [3 + 3] condensation of a metabolite of the glycolysis cascade and an amino acid derived therefrom, e.g. pyruvate and alanine (or serine), and 3) a [6 + 0] formation from leucine.

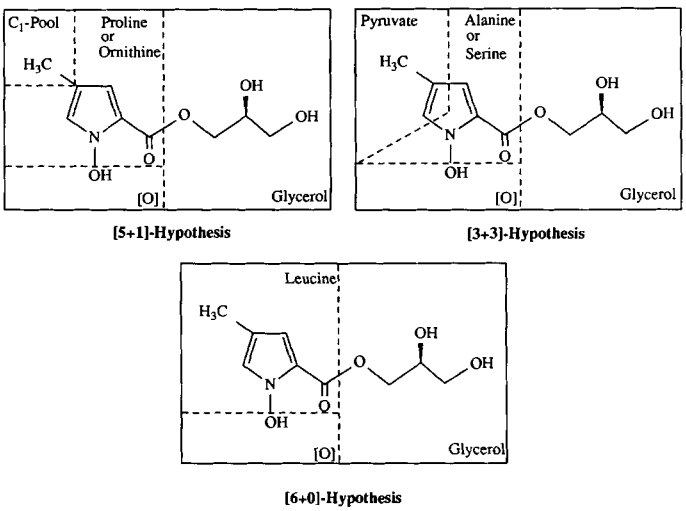

Scheme 1. Biogenesis hypotheses for glycerinopyrin **1**

Feeding experiments with [S^{13}CH$_3$]methionine and [1-^{13}C]alanine (also convertible into pyruvate by transamination) did not result in remarkable incorporations into **1** (Table 1). Hence the first hypothesis was considered unlikely, and the second one was ruled out. Administration of [1-^{13}C]acetate showed a 1.4% specific enrichment[10] of the

[*] Dipl.-Chem. M. Schönewolf and Dr. J. Rohr
Institut für Organische Chemie der Universität,
Tammannstrasse 2, W-3400 Göttingen (FRG)

[**] This work was supported by the Deutsche Forschungsgemeinschaft, the Fonds der Chemischen Industrie, and NATO. We thank Hoechst AG (Frankfurt/M., Germany) for generous gifts of chemicals.

1′-position of glycerinopyrin **1** (Table 1), a result which also ruled out the first hypothesis: If ornithine or proline were the precursor of the 2-pyrrolecarboxylic acid building block of **1**, an enrichment of C-5 in **1** would have been expected according to the metabolization of [1-^{13}C]acetate via the citric acid cycle into [5-^{13}C]α-ketoglutaric acid (precursor of ornithine and proline).[11, 12] The acetate feeding experiment also could be interpreted as an indication of the leucine hypothesis, i.e. the third hypothesis, since acetate is the source of C-1 and C-2 of leucine during its biosynthesis,[12] which is in accordance with the enrichment of C-1′ found in **1**. Finally, the third hypothesis could be proven correct by a feeding experiment with D,L-[1-^{13}C]leucine: 99% specific incorporation[10] into glycerinopyrin **1** (enrichment of C-1′, Table 1) shows leucine to be an immediate precursor of its 4-methyl-2-pyrrolecarboxylate moiety.

Table 1: Incorporation experiments with *Streptomyces violaceus*.

Precursor[a]	Amount [mmol]	Time[b] [h]	Incorporation[10] in **1** [%]	Labeled atom(s) in **1**
[1,1,3,3-$^{2}H_4$]glycerol, 99% ^{2}H	144	41	20	3′-H_2, 5′-H_2
L-[*S*-$^{13}CH_3$]methionine, 97% ^{13}C	1.005	46, 52	–	–
[1-^{13}C]D,L-alanine, 99% ^{13}C	5.612	45, 52	–	–
sodium[1-^{13}C]acetate, 99% ^{13}C	6.095	12–48, every 3	1.4	C-1′
D,L-[1-^{13}C]leucine, 99% ^{13}C	6.984	42, 46, 52	99[c]	C-1′

[a] See experimental. [b] After inoculation. [c] As a reason for this unusually high specific incorporation of leucine it is probable that the liberation of this amino acid from the fermentation medium (caseine peptone) and/or its endogenous de novo synthesis, respectively, is shut off due to the large amount of added leucine.

Our findings revealed that the biogenetic source of the entire carbon skeleton derives from only two building blocks, namely glycerol as precursor of the alcohol component of the natural ester, and—as an interesting and novel result—the amino acid leucine as precursor of the 4-methyl-2-pyrrolecarboxylic acid component (Scheme 2). The latter

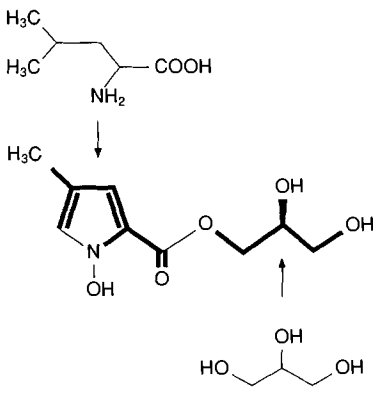

Scheme 2. Biogenesis of the carbon skeleton of glycerinopyrin **1** from leucine and glycerol

constitutes a new biosynthetic pathway for natural pyrroles in addition to the known laevulinic acid pathway, which leads to porphobilinogen (precursor of all porphyrin systems), the formation of the antibiotic pyrrolnitrin from tryptophan, and the synthesis from proline/hydroxyproline.[13–16] The novel pathway described here is probably also responsible for the formation of the pheromone **2**[2, 3] and of the amino acid HMP **3**.[4–6] Furthermore, it is an extension of nature to chemical syntheses of HMP **3** and to recently published pyrrole syntheses.[5, 6, 17–19] The two alternative mechanisms which are plausible for the formation of the pyrrole ring require a diastereoselective derivatization of one of the methyl groups of leucine. This could be achieved by an oxidation to the aldehyde or epoxide, which can be nucleophilically attacked by the α-amino group. There is a certain parallel to an oxidation in the recently discovered interconversion of leucine into hydroxymethylglutaryl(HMG)-CoA, where an oxidation of one of the methyl groups of leucine to a carboxyl group (though after its conversion into isovaleric acid via transamination and decarboxylation) is an essential initiation reaction.[20, 21] A terminal functionalization of intact leucine is so far unknown. The other alternative would be an amination (in the manner of the ornithine biosynthesis[12]) followed by a ring closure reaction of the generated amino group with the 2-keto group of the (earlier) transaminated leucine, in analogy with the biosynthesis of the 2-piperidinecarboxylic acid moiety of virginiamycin from lysine.[22] Investigation of the ring closure mechanism of the 4-methyl-2-pyrrolecarboxylate residue of **1** requires the synthesis of several postulated labeled intermediates.

Experimental

General: see Ref. [1]. Feeding experiments: The labeled compounds were dissolved in sterile water and added (in one or more equal portions) to the growing 1L-culture (1L-fermentor, type Biostat M, B. Braun, Melsungen, Germany) of *Streptomyces violaceus*[1]; pH changes were immediately corrected by addition of sterile 0.5 M HCl and 0.5 M NaOH, respectively (see also Table 1). In the case of the feeding experiment with [1,1,3,3-$^{2}H_4$]glycerol; the initial fermentation was carried out with 2% instead of 3% glycerol; the decrease in amount of unlabeled glycerol until the feeding was estimated by the dry cell weight.

Labeled compounds: The ^{13}C-labeled compounds were obtained from CIL (Cambridge Isotope Laboratories, Cambridge, Mass., USA), the deuterated glycerol was synthesized [23] via oxidation of diethyl malonate with lead tetraacetate ($PbOAc_4$) and reduction of the diethyl-2-*O*-acetylmalonate with lithium aluminum deuteride ($LiAlD_4$, 99% D, obtained from Zentralinstitut für Isotopen- und Strahlenforschung, Akademie der Wissenschaften, Leipzig, Germany).

Received: September 21, 1990 [Z 4198 IE]
German version: *Angew. Chem. 103* (1991) 211

CAS Registry numbers:
1, 129966-44-5; leucine, 61-90-5; glycerol, 56-81-5; 1H-pyrrole, 109-97-7.

[1] M. Schönewolf, S. Grabley, K. Hütter, R. Machinek, J. Wink, A. Zeeck, J. Rohr, *Liebigs Ann. Chem.*, in press.
[2] J. H. Tumlinson, J. C. Moser, R. M. Silverstein, R. G. Brownlee, J. M. Ruth, *Nature (London) 234* (1971) 348.
[3] P. E. Sonnet, J. C. Moser, *J. Agric. Food Chem. 20* (1972) 1191.
[4] G. Koyama, *Helv. Chim. Acta 57* (1974) 2477.
[5] N. Kurokawa, Y. Ohfune, *J. Am. Chem. Soc. 108* (1986) 6041.
[6] J. Mulzer, R. Becker, E. Brunner, *J. Am. Chem. Soc. 111* (1989) 7500.
[7] F. Benz, F. Knüsel, J. Nüesch, H. Treichler, W. Voser, R. Nyfeler, W. Keller-Schierlein, *Helv. Chim. Acta 57* (1974) 2459.
[8] C. Keller-Juslén, M. Kuhn, H. R. Loosli, T. J. Petcher, H. P. Weber, A. von Wartburg, *Tetrahedron Lett. 1976*, 4147.
[9] K. Roy, G. C. Reddy, T. Mukhopadhyay, B. N. Ganguli, K. P. R. Desikan, Indian IN 162 032 (1988); *Chem. Abstr. 111* (1989) 152145z.
[10] Incorporations were calculated according to: A. I. Scott, C. A. Townsend, K. Okada, M. Kajiwara, R. J. Cushley, P. J. Whitman, *J. Am. Chem. Soc. 96* (1974) 8069. The incorporation of [1,1,3,3-$^{2}H_4$]glycerol was estimated by ^{2}H NMR spectroscopy relative to the internal standard of the 4-CH_3-group (natural ^{2}H abundance) in **1**.
[11] H. G. Schlegel in P. Präve, U. Faust, W. Sittig, D. A. Sukatsch (Eds.): *Handbuch der Biotechnologie, 3rd ed.*, R. Oldenbourg Verlag, München 1987, p. 63.

[12] G. Gottschalk: *Bacterial Metabolism*, 2nd ed., Springer, Berlin 1986, p. 43.
[13] D. Shemin, *Naturwissenschaften 57* (1970) 185.
[14] B. Franck, *Angew. Chem. 91* (1979) 453; *Angew. Chem. Int. Ed. Engl. 18* (1979) 429.
[15] A. R. Battersby, *Nat. Prod. Rep. 4* (1987) 77.
[16] C.-J. Chang, H. G. Floss, D. J. Hook, J. A. Mabe, P. E. Manni, L. L. Martin, K. Schröder, T. L. Schieh, *J. Antibiot. 34* (1981) 555.
[17] W. Flitsch, M. Hohenhorst, *Liebigs Ann. Chem. 1990*, 397.
[18] V. Dragisich, C. K. Murray, B. P. Warner, W. D. Wulff, D. C. Yang, *J. Am. Chem. Soc. 112* (1990) 1251.
[19] H. Bertschy, A. Meunier, R. Neier, *Angew. Chem. 102* (1990) 828; *Angew. Chem. Int. Ed. Engl. 29* (1990) 777.
[20] F. Van Middlesworth, M. N. Beremand, T. A. Isbell, D. Weisleder, *J. Org. Chem. 55* (1990) 1237.
[21] P. Anastasis, I. Freer, K. H. Overton, D. Picken, D. S. Rycroft, S. B. Singh, *J. Chem. Soc. Perkin Trans. 1 1987*, 2427.
[22] J. W. Reed, M. B. Purvis, D. G. I. Kingston, A. Biot, F. Gosselé, *J. Org. Chem. 54* (1989) 1161.
[23] A. Murray III, D. L. Williams: *Organic Syntheses with Isotopes, Part I*, Interscience, New York 1958, p. 931.

Alkyl- and Arylrhenium Trioxides**

By *Wolfgang A. Herrmann,* Carlos C. Romao, Richard W. Fischer, Paul Kiprof,* and *Claude de Méric de Bellefon*

The β-hydrogen elimination is a preferred pathway for the decomposition of metal alkyls and accounts for the notorious instability of ethyl complexes and other complexes containing β-hydrogen atoms.[1, 2] Although a voluminous ligand sphere often guarantees kinetic stability,[3] little was previously known about its effect on the chemistry of hypervalent metals.[4] In particular, coordinatively unsaturated alkyl complexes (alkyl $\neq$ methyl) were not expected to be isolable.

Here we show that this assumption is wrong by describing well-characterized derivatives of the 14-electron complex methylrhenium trioxide (**1**).[5] Whereas reactions of rhenium oxides with tin, mercury, and aluminum alkyls led to decomposition, treatment of dirhenium heptaoxide with diethylzinc resulted in formation of ethylrhenium trioxide (**2a**) in over 60% yield [Eq. (a)]. However, maintaining an exact stoichiometry and suitable temperature is crucial to the success of the reaction.[6] The reaction proceeds quantitatively with precipitation of pure white zinc perrhenate from the THF solution.

$$2\,Re_2O_7 + ZnR_2 \xrightarrow{THF} \underset{\mathbf{2a-d}}{2[R\text{-}ReO_3]} + [Zn(ReO_4)_2(thf)_2] \qquad (a)$$

Ethylrhenium trioxide forms colorless crystals, which melt at $-21\,^{\circ}C$ to give a clear, air- and moisture-stable liquid. Since **2a** vaporizes rapidly at room temperature, isolation and handling require low temperatures. The complex survives the conditions of conventional gas chromatography. It exhibits an unexpectedly high thermal stability. Even in the absence of coordinating solvents, **2a** is stable at room temperature, only decomposing slowly at about 60 °C. However, β-hydrogen elimination is not the major pathway of decomposition. Instead, the spectrum of products determined by GC/MS analysis indicates that the decomposition occurs via radical pathways (comparable amounts of ethylene, ethane, and butene isomers; Re–C bond cleavage). The considerably better stability in solvents such as benzene and THF points to the involvement of intermolecular processes in the decomposition.

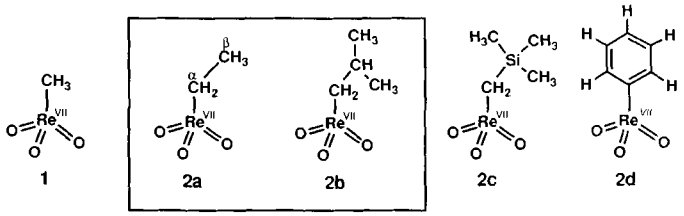

Isobutylrhenium trioxide (**2b**) and trimethylsilylmethylrhenium trioxide (**2c**) may be obtained similarly. They, too, are characterized by high volatility and thermal stability. The decomposition of the isobutyl derivative **2b** at 120 °C affords mainly isobutenes together with a small amount of isobutane. The silaneopentyl complex **2c** melts at 30 °C without decomposition, but then decomposes—surprisingly faster than **2a**!—with preferential loss of tetramethylsilane and formation of much ethylene and propene (!) along with a small amount of methane.

The likewise new phenylrhenium trioxide (**2d**) is formed according to Equation (a) as a colorless substance,[6] which decomposes slowly at room temperature, but rapidly and quantitatively at higher temperatures, to give biphenyl. Solutions of **2d** in solvents such as hexane are more stable (in the dark) than in the solid state, but readily decompose upon exposure to light with formation of a deep blue precipitate (presumably rhenium oxides) and biphenyl.

The organic rhenium oxides **2a–d** were characterized by complete elemental analysis and by IR and NMR (^1H, ^{13}C, ^{17}O) spectroscopy as well as mass spectrometry.[6] The ^{17}O NMR spectra, in particular, reveal the electron-shifting effects of the groups in **2a–c** compared with the parent compound **1**. The synthetic route is generalizable and exploits the formation of sparingly soluble zinc perrhenate via dismutation of Re_2O_7 to "$[ReO_3]^{\oplus}$" and $[ReO_4]^{\ominus}$ [Eq. (a)].

Since crystals of the solvent-free complexes **2a–d** were not suitable for X-ray structure analyses (soft consistency), we synthesized the quinuclidine adducts of ethyl- and silaneopentylrhenium trioxide[7] and characterized them structurally (Fig. 1).[8]

These base adducts **3a** and **3c** form quantitatively upon mixing of the components, thereby revealing the pronounced Lewis acidity of the coordinatively unsaturated rhenium(VII) centers in **2**. The framework geometry in both cases is nearly undistorted trigonal-bipyramidal (D_{3h} symmetry distorted toward C_{3v} symmetry) with unusual bond lengths between the metal center and the neighboring atoms. Neither the X-ray structure nor the spectroscopic data provide evidence for the interaction of β- or γ-hydrogen atoms with the metal centers or with the oxo ligands (e.g., hydrogen bridges), as observed, for example, in the complex $[(C_2H_5)TiCl_3(dmpe)]$,

[*] Prof. Dr. W. A. Herrmann, Prof. Dr. C. C. Romao [+], R. W. Fischer, P. Kiprof, Dr. C. de Méric de Bellefon [++]
Anorganisch-chemisches Institut der Technischen Universität München
Lichtenbergstrasse 4, W-8046 Garching (FRG)

[+] Visiting scientist from the Centro de Tecnologia e Quimica e Biologica, Oeiras, Portugal (1990).

[++] Visiting scientist from the Université Louis Pasteur, Strasbourg (Alexander von Humboldt Fellow, 1990/91).

[**] Multiple Bonds between Main-Group Elements and Transition Metals, Part 92. This work was supported by the Fonds der Chemischen Industrie and by Hoechst AG. Part 91: I. A. Degnan, J. Behm, M. R. Cook, W. A. Herrmann, *Inorg. Chem.*, in press.

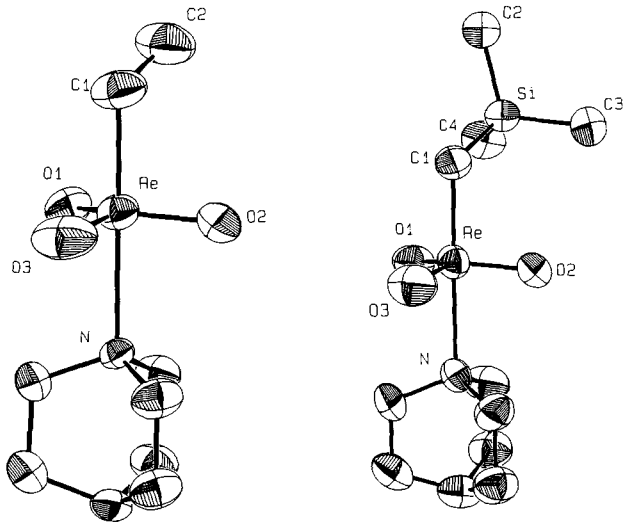

Fig. 1. Molecular structures of the quinuclidine adducts of **2a** (left) and **2c** (right) (ORTEP drawings). Selected bond lengths [pm] and angles [°]: **3a:** Re-C1 210.5(4), Re-O1 170.7(3), Re-O2 169.6(3), Re-O3 170.3(4), Re-N 240.7(3), C1-C2 151.3(6); Re-C1-C2 112.5(4), O1-Re-O2 118.1(1), C1-Re-N 179.5(2), O1-Re-N 84.4 (1). **3c:** Re-C1 209.2(4), Re-O1 168.8(3), Re-O2 169.4(3), Re-O3 169.8(4), Re-N 243.2(3), C1-Si 190.0(5); C1-Re-N 178.1(1), C1-Re-O1 98.4(1), C1-Re-O2 96.1(1), C1-Re-O3 97.2(2), O1-Re-O2 119.7(2), O1-Re-O3 118.2(2), O1-Re-N 83.4(1), Re-C1-Si 117.7(3). Further details of the crystal structure investigations may be obtained from the Fachinformationszentrum Karlsruhe, Gesellschaft für wissenschaftlich-technische Information mbH, W-7514 Eggenstein-Leopoldshafen 2 (FRG), on quoting the depository number CSD-54943, the names of the authors, and the journal citation.

dmpe = bis(dimethylphosphino)ethane (agostic interactions).[2b, d]

Sixfold coordination can be achieved by reaction of **2a–c** with ethylenediamine and analogous chelating ligands. For example, **2c**·$H_2NCH_2CH_2NH_2$ forms air- and moisture-stable yellow crystals [$\tilde{\nu}$(ReO) = 924 (vs), 911 (vs) cm^{-1} (KBr)], which, as expected, are thermally more stable than base-free **2c**. Treatment of **2a** with *diethylzinc in excess* results in smooth formation of the new Re^{VI} binuclear complex $[\{(\sigma\text{-}C_2H_5)_2ReO_2\}_2]$.[9]

The synthesis of the neopentyl complex **2e** proved extremely difficult according to the method described above.

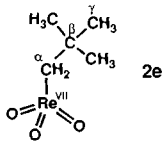

2e

Although the compound is indeed formed at −60 °C, it decomposes with loss of neopentane upon warming above −40 °C and, especially rapidly, at room temperature (solvent participation). Finally, we obtained only indirect evidence for the existence of the *tert*-butyl complex **2f**: Even at −90 °C, reaction of Re_2O_7 and $Zn(t\text{-}C_4H_9)_2$ in THF solution gives a mixture of products that indicates the formation and decomposition of **2f** according to Equation (b).[12]

$$2\,[(CH_3)_3C\text{-}ReO_3] \longrightarrow 2\,ReO_3 + H_2C{=}C(CH_3)_2 + HC(CH_3)_3 \qquad (b)$$

2f

The results described here counter the widespread and well-supported notion that coordinatively unsaturated alkyl complexes containing β-hydrogen atoms readily decompose. Furthermore, ethyl- and isobutylrhenium trioxide are the first examples of coordinatively unsaturated alkyl complexes of the oxo series with β-H atoms. Reaction (a) should also allow functionalized groups R to be attached to highly oxidized metal centers to give compounds such as $C_6H_5C{\equiv}C\text{-}ReO_3$,[10] which provide the prerequisites for the direct control of metal oxide reactivity for catalytic purposes.[11] Furthermore, these results clearly reveal once more how little we know about stability and decomposition pathways of hypervalent organometallic compounds.

Received: September 24, 1990 [Z 4199 IE]
German version: *Angew. Chem. 103* (1991) 183

[1] Reviews: a) P. J. Davidson, M. F. Lappert, R. Pearce, *Chem. Rev. 76* (1976) 213; b) R. R. Schrock, G. W. Parshall, *ibid. 76* (1976) 243; c) A. Yamamoto: *Organotransition Metal Chemistry*, Wiley-Interscience, New York 1986, pp. 286–294.

[2] $RTiX_3$ compounds: a) K.-H. Thiele, *Pure Appl. Chem. 30* (1972) 575; b) Z. Dawoodi, M. L. H. Green, V. S. B. Mietwa, K. Prout, *J. Chem. Soc. Chem. Commun. 1982*, 802; c) G. J. Erskine, N. B. Vanstone, J. D. McCowan, *Inorg. Chim. Acta 75* (1983) 159; d) N. Koga, S. Obara, K. Morokuma, *J. Am. Chem. Soc. 106* (1984) 4625.

[3] Examples: a) $[Cr(C_2H_5)_4]$ (unstable, unknown), $[Cr(t\text{-}C_4H_9)_4]$ (stable; W. Kruse, *J. Organomet. Chem. 42* (1972) C39), $[Cr\{CH_2C(CH_3)_2C_6H_5\}_4]$ (stable; W. Gramlich, K. Pfefferkorn, *ibid. 61* (1973) 247); b) $[Ti(CH_3)_4]$ (unstable), $[Ti(CH_3)_4(bpy)]$ (stable), $[Ti(1\text{-norbornyl})_4]$ (stable).

[4] In the series of organometallic oxides of the type R_aMO_b, stable ethyl complexes (R = C_2H_5) are unknown. Thus, $[(CH_3)_4OsO]$ is a stable compound in the gas phase, whereas $[(C_2H_5)_4OsO]$ decomposes above −60 °C to *n*-butane, ethane, ethylene, and reduced osmium oxides: W. A. Herrmann, S. J. Eder, P. Kiprof, K. Rypdal, P. Watzlowik, unpublished results 1990.

[5] a) W. A. Herrmann, J. G. Kuchler, J. K. Felixberger, E. Herdtweck, W. Wagner, *Angew. Chem. 100* (1988) 420; *Angew. Chem. Int. Ed. Engl. 27* (1988) 394; b) W. A. Herrmann, J. G. Kuchler, G. Weichselbaumer, E. Herdtweck, P. Kiprof, *J. Organomet. Chem. 372* (1989) 351.

[6] *Experimental Procedure:* A solution of sublimed Re_2O_7 (489 mg, 1 mmol) in 15 mL of THF (< 1 ppm H_2O) was treated at dry-ice temperature with exactly 0.5 mmol of ZnR_2 (1 M solution in THF). The colorless stirred solution was warmed to −5 °C (R = C_2H_5), −30 °C (R = *i*-C_4H_9), or 20 °C (R = $CH_2Si(CH_3)_3$, C_6H_5). The THF was evaporated in vacuo, and the residue was extracted with cold (!) *n*-pentane. The yellow extract was filtered through a cannula and concentrated to about 10 mL at −30 °C under vacuum. Cooling the solution to dry-ice temperature afforded colorless crystals, which were dried under high vacuum at −30 °C. Yield 60–70%. Gas chromatogram (HP A-5890): fused silica, HP-1, 50 m, 200 kPa He, 120/180 °C 20° C/min, 180/200 °C 40° C/min: t_R = 7.23 min. **2a**: Colorless crystals from *n*-pentane, m.p. −21 °C. IR (CS_2): $\tilde{\nu}$ [cm^{-1}] = 996 (m), 961 (vs), 950 (s), 927 (m). IR (gas phase): $\tilde{\nu}$[cm^{-1}] = 970 (vs). ^1H NMR (400 MHz): δ = 2.19 (*t*, 3H; CH_3), 3.66 (q, 2H; CH_2) (CD_2Cl_2, −20 °C); δ = 1.29 (t, 3H; CH_3), 2.31 (q, 2H; CH_2) (C_6D_6, 20 °C). $^{13}C\{^1H\}$ NMR (100.5 MHz, C_6D_6, 20 °C): δ = 18.20 (CH_3), 36.56 (CH_2). EI-MS (70 eV): *m/z* 264 ($M^{\oplus}$, rel. int. 1%), 236 ($[M - C_2H_4]^{\oplus}$, 100%), correct isotopic pattern. **2b**: Colorless crystals from *n*-pentane (−80 °C), colorless liquid at room temperature. IR (CS_2): $\tilde{\nu}$[cm^{-1}] = 994 (w-m), 962 (vs). ^1H NMR (400 MHz, C_6D_6, 20 °C): δ = 0.54 (d, 6H, ^2J(H,H) = 6.7 Hz; CH_3), 2.42 (d, 2H, ^2J(H,H) = 6.1 Hz; CH_2), 1.91 (tq, 1H; CH); $^{13}C\{^1H\}$ NMR (100.5 MHz, C_6D_6, 20 °C): δ = 24.08 (CH_3), 31.48 (CH_2), 52.15 (CH); EI MS (70 eV): *m/z* 292 ($M^{\oplus}$, rel. int. 1%), 291 ($[M - H]^{\oplus}$, ca. 30%), 277 ($[M - CH_3]^{\oplus}$, 100%). **2c**: Colorless crystals from *n*-pentane, m.p. 30 °C, slow dec. at room temperature; the crystals turn black in water. IR (CS_2): $\tilde{\nu}$[cm^{-1}] = 990 (s), 965 (vs), 957 (vs), 925 (m); ^1H NMR (400 MHz, C_6D_6, 20 °C): δ = −0.16 (s, 9H; CH_3), 1.60 (s, 2H; CH_2). ^{13}C NMR (100.5 MHz, C_6D_6, 20 °C): δ = −0.74 (q, ^1J(C,H) = 120 Hz; CH_3), 34.35 (t, ^1J(C,H) = 125 Hz, CH_2). ^{17}O NMR (54.2 MHz, *n*-pentane, 20 °C): δ = 808 (standard; ext. H_2O, δ = 0); for comparison: δ = 835 for CH_3ReO_3 in *n*-pentane. EI MS (70 eV): *m/z* 322 ($M^{\oplus}$, rel. int. 1%), 307 ($[M - CH_3]^{\oplus}$, 100%). **2d**: Colorless, crystalline powder from *n*-pentane, m.p. = 45 °C. IR (KBr): $\tilde{\nu}$[cm^{-1}] = 986 (m), 956 (vs); ^1H NMR (400 MHz, CD_2Cl_2, 20 °C): δ = 7.87 (d, 2H, ^3J(H,H) = 7.9 Hz; *o*-C_6H_5), 7.69 (t, 1H, ^3J(H,H) = 7.3 Hz; *p*-C_6H_5), 7.63 (t, 2H; *m*-C_6H_5). $^{13}C\{^1H\}$ NMR (100.5 MHz, CD_2Cl_2, 20 °C): δ = 155.5 (ReC), 142.5 (*o*-C_6H_5), 135.5 (*p*-C_6H_5), 130.4 (*m*-C_6H_5). EI MS (70 eV): *m/z* 312 ($M^{\oplus}$, rel. int. 4%), 154 ($C_{12}H_{10}$, 100%).

[7] **2a** · quinuclidine, orange, air-stable crystals, m.p. = 109 °C (dec.). IR (KBr): $\tilde{\nu}$[cm^{-1}]: 922 (vs). **2c** · quinuclidine: lemon-yellow crystals, m.p. 135 °C. ^1H NMR (400 MHz, C_6D_6, 20 °C): δ = 0.15 (s, 9H; CH_3), 1.48 (s,

2H; $ReCH_2$), 0.90/2.25 (2m, 2×6H; CCH_2), 1.17 (m, 1H; CH). $^{13}C\{^1H\}$ NMR (100.5 MHz, C_6D_6, 20°C): $\delta = -0.16$ ($SiCH_3$), 35.81 ($SiCH_2$), 20.81 (CH), 25.76/47.41 (CCH_2); IR: $\tilde{\nu}$ [cm^{-1}] = 926 (vs) (CS_2), 922 (vs) (KBr); FD MS (*n*-pentane): *m/z* 433 ($M^{\oplus}$).

[8] **2a** · quinuclidine: Orange columns from CS_2 solution (−25°C), 0.51 × 0.15 × 0.10 mm; systematic absences: *h0l* (*h* + *l* = 2*n* + 1); *0k0* (*k* = 2*n* + 1); space group: monoclinic, $P2_1/n$ (Int. Tab. No. 14); *a* = 664.3(3), *b* = 881.1(4), *c* = 2009.1(9) pm, $\beta = 98.98(2)°$, $V = 1161 \times 10^6$ pm^3; *Z* = 4; $F_{000} = 712$; $\varrho_{calcd} = 2.141$ g cm^{-3}; Enraf-Nonius CAD-4, $Mo_{K\alpha}$ ($\lambda = 71.073$ pm), graphite monochromator; $T = 23 \pm 3$°C; measuring range $2.0 < \theta < 25.0°$; ω scan; 1900 unique reflections with $I > 0.0$ used for refinement; $R = 0.034$; $R_w = 0.018$; GOF = 1.889. Direct methods, difference Fourier technique; empirical absorption correction, $\mu = 105.9$ cm^{-1}, nine reflections; decomposition −11.2% in 34 h, anisotropic correction. Hydrogen atom positions were calculated (*d*(C-H) = 95 pm) and included in the structure factor calculation, but not refined. Anomalous dispersion was taken into consideration. Shift/error: <0.01 in the last cycle of the refinement; residual electron density: +0.90 e_o $Å^{-3}$ at 75 pm and −1.07 e_o $Å^{-3}$ at 74 pm from the rhenium atom. **2c** · quinuclidine: Yellow cubes from *n*-pentane (25°C); 0.56 × 0.30 × 0.21 mm; systematic absences: *h0l* (*l* = 2*n* + 1); *0k0* (*k* = 2*n* + 1); space group, monoclinic, $P2_1/c$ (Int. Tab. No. 14); *a* = 667.7 (3), *b* = 2065.8(4), *c* = 1140.9(7) pm, $\beta = 96.42(2)°$, $V = 1564 \times 10^6$ pm^3; *Z* = 4; $F_{000} = 840$; $\varrho_{calcd.} = 1.837$ g cm^{-3}; Enraf-Nonius CAD-4, $Mo_{K\alpha}$ ($\lambda = 71.073$ pm), graphite monochromator; $T = 23 \pm 3$°C; measuring range: $2.0 < \theta < 25.0°$; 2429 unique reflections ($I > 0.0$); $R = 0.039$; $R_w = 0.021$; GOF = 1.848. Patterson methods, difference Fourier technique; empirical absorption correction, $\mu = 79.5$ cm^{-1}, eight reflections; 23.1% decomposition, corrected. Hydrogen atom positions were calculated (*d*(C-H) = 95 pm) and included in the structure factor calculation, but not refined. Anomalous dispersion was taken into consideration. Shift/error: < 0.01 in the last cycle of the refinement; residual electron density: +0.64 e_o $Å^{-3}$ at 100 pm and −0.80 e_o $Å^{-3}$ at 90 pm from the rhenium atom.

[9] W. A. Herrmann, C. C. Romao, P. Kiprof, J. Behm, M. R. Cook, M. Taillefer, *J. Organomet. Chem.*, in press.

[10] W. A. Herrmann, S. J. Eder, unpublished results 1990.

[11] W. A. Herrmann, *J. Organomet. Chem. 382* (1990) 1.

[12] Note added in proof (Jan. 15, 1991): Further studies have shown that radical-type degradation pathways (e.g., Re–C bond cleavage) are of importance and are connected with the stability of the radicals R·; for example, **2f** eliminates butene and isobutane [Eq. (b)], but also large amounts of 2.2.3.3-tetramethylbutane. The system $Re_2O_7/Zn(CH_2C_6H_5)_2$ yields a little toluene and much bibenzyl at −80°C (compare decomposition of **2d**). Cyclopentadienylrhenium trioxide, $[(C_5H_5)ReO_3]$, is stable under ordinary conditions, representing the first C_5H_5 complex of a metal in an oxidation state greater than 5 (W. A. Herrmann, M. Taillefer, C. de Méric de Bellefon, unpublished results, 1990).

Triisopropylamine: A Sterically Overcrowded Molecule with a Flattened NC_3 Pyramid and a "p-Type" Nitrogen Electron Pair**

By *Hans Bock,** *Ilka Goebel, Zdenek Havlas, Siegfried Liedle,* and *Heinz Oberhammer*

Dedicated to Jean-Marie Lehn

The "ammonia clock", the time standard based on the flip-flop of the 37-pm-high NH_3 pyramid within 4.2×10^{-11} s, is a textbook example of molecular dynamics[1a] and especially of nonclassical tunneling in a double minimum potential.[1b, c] The gas-phase structure and other characteristic molecular properties of NH_3, such as its enthalpy of inversion $\Delta H^{\ddagger}_{inv}$ and its first vertical ionization energy IE^{v}_{1}, are dramatically changed on substitution (Table 1).

Table 1. X–N–X bond angle α, inversion enthalpy $\Delta H^{\ddagger}_{inv}$, and vertical first ionization energy IE^{v}_{1} of ammonia and selected derivatives NX_3 [3].

X =	H	CH_3	CF_3	F
α [°]	106.6	110.9	117.9	102
$\Delta H^{\ddagger}_{inv}$ [kJ mol^{-1}]	24.5	31.4	?	ca. 250
IE^{v}_{1} [eV]	10.85	8.44	12.52	13.83

Considerable flattening or even planarity is observed when X = SF_5, C_3F_7, SiH_3, $Si(CH_3)_3$, GeH_3, or SCF_3;[2] the smallest inversion barriers are found in derivatives H_2NX containing a π-acceptor substituent like X = CHO, CN, or NO_2 ($\Delta H^{\ddagger}_{inv} = 4.6$, 8.5, or 11.3 kJ mol^{-1}, respectively[1b]) and the lowest ionization potentials are measured for the fluctuating amine $N(CH_2SiR_3)_3$ (R = CH_3; 7.66 eV)[3f] and the rigid molecule azabicyclo[3.3.3]dodecane (7.13 eV[3g]). These tremendous electronic ($\Delta IE^{v}_{1} = 6.6$ eV) and/or steric ($\Delta\alpha = 18°$) substitution effects (Table 1) on a dynamic center with an electron pair, as well as supporting quantum-chemical calculations,[4] have aroused our curiosity concerning the molecular properties of triisopropylamine, which is accessible by a three-step synthesis[5] [Eq. (a)].

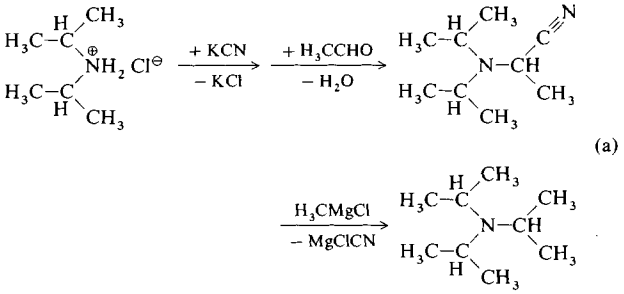

(a)

The expectations are fulfilled (Fig. 1A). The photoelectron spectrum exhibits a "lone" ionization band at only 7.18 eV, which is assigned by MNDO calculations[4c, d] to a flattened radical-cation ground state, $\tilde{X}(^2A)$, with dominant N-electron-pair contribution.[6] The cyclovoltammogram (Fig. 1B) in aprotic THF solution ($c_{H^{\oplus}} < 1$ ppm) indicates a reversible one-electron oxidation at +0.71 V;[7] that is, the usual oxidative cleavage of the α hydrogens of trialkylamines to give the respective immonium ions $R_2\overset{\oplus}{N}{=}CR'_2$ takes place not at all or only slowly. The ESR signal pattern of the radical cation (Fig. 1C), generated with SbF_5/CH_2Cl_2, consists of an ^{14}N triplet with $a_N = 1.946$ mT and an intensity of 1:1:1, centered around g = 2.0035;[8] possible couplings have to be confined within the line width of 0.367 mT. These experimental findings are in satisfactory agreement with MNDO open-shell calculations,[4d] which predict as global minimum for $((H_3C)_2HC)_3N^{\cdot\oplus}$ a C_{3h} structure with the H–C bonds in the NC_3 plane.

The surprising molecular properties of triisopropylamine (Fig. 1),[6-8] as well as the geometry-optimized approxima-

[*] Prof. Dr. H. Bock, Dipl.-Chem. I. Göbel, Dr. Z. Havlas
Institut für Anorganische Chemie der Universität
Niederurseler Hang, W-6000 Frankfurt am Main (FRG)
Prof. Dr. H. Oberhammer, Dipl.-Chem. S. Liedle
Institut für Physikalische und Theoretische Chemie der Universität
Auf der Morgenstelle 8, W-7400 Tübingen (FRG)

[**] Structures of Sterically Overcrowded and Charge-Perturbed Molecules Part 5, as well as Gas-Phase Structures of Flattened Amines, Part 4. This work was supported by the Deutsche Forschungsgemeinschaft, the Fonds der Chemischen Industrie, the Alexander von Humboldt-Stiftung (*Z. H.*), and the States of Hessen and Baden-Württemberg. Part 4: H. Bock, K. Ruppert, Z. Havlas, D. Fenske, *Angew. Chem. 102* (1990) 1095; *Angew. Chem. Int. Ed. Engl. 29* (1990) 1042. Parts 1–3: [2a–c].

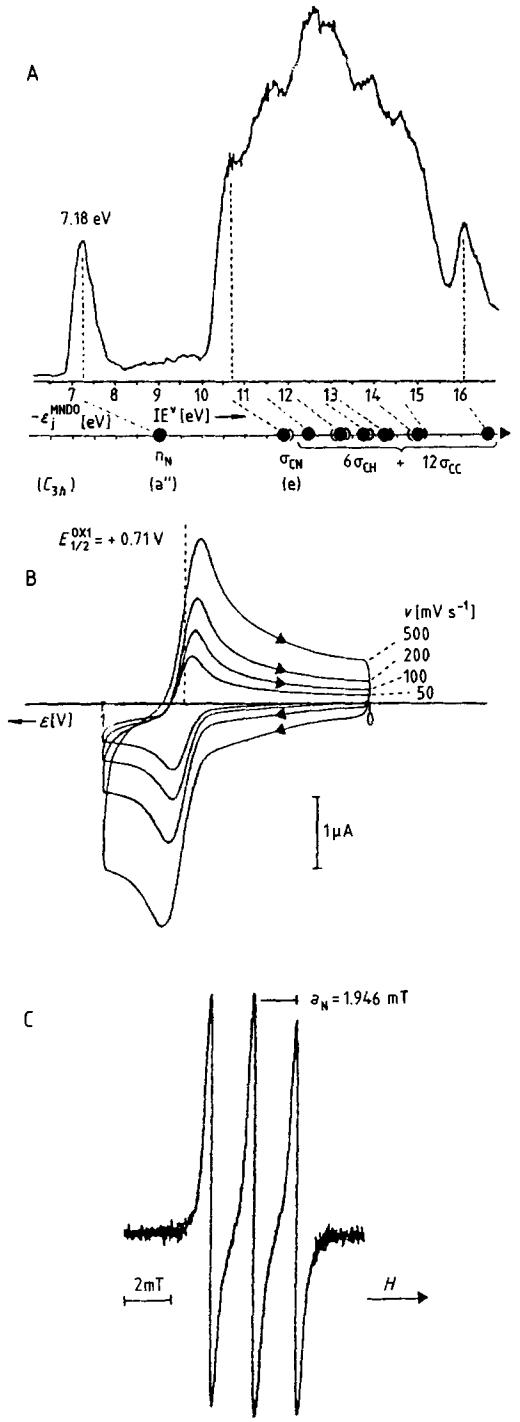

Fig. 1. Selected measurement results for triisopropylamine: A) He(I) PE spectrum at 6 to 16.5 eV and its assignment by Koopmans' correlation with MNDO eigenvalues. B) Cyclovoltammograms in THF/0.1 M $Bu_4N^{\oplus}ClO_4^{\ominus}$ at 243 K (glassy carbon electrode) vs. Ag/AgCl; scan rate $\nu = 50$ to 500 mV s^{-1}). C) ESR spectrum of the radical cation generated by SbF_5/CH_2Cl_2, at 180 K (cf. [5]).

tive calculations,[4] suggest a molecular structure with a flattened NC_3 skeleton, which can be experimentally verified by gas-phase electron diffraction[9] (Fig. 2).

Analysis of the radial distribution function (Fig. 2), calculated by Fourier transformation of the diffraction intensities,[9a] results in a molecular structure of approximate C_3 symmetry. For the "least-squares" analysis of the diffraction intensities, local C_{3v} symmetry for all methyl groups and C_s symmetry for the isopropyl groups, as well as equal C–H bond distances, were assumed. The experimental values for the C–N–C bond angles 119.2(3)°, which correspond to a tilting of 5.2(11)° out of the NC_3 plane, and for the C–N–C′–H′ dihedral angles (5.0(18)°) exhibit only small deviations from a planar C_{3h} configuration of the $N(CH)_3$ unit with C-N-C = 120° and C-N-C′-H′ = 0°. Because deviations of this magnitude are typically caused by both low-frequency "out-of-plane" vibrations of the NC_3 skeleton and torsional vibrations of the isopropyl groups around the N–C bonds, the result of the gas-phase electron diffraction study (cf. Ref. [9c]) corresponds to an equilibrium structure of triisopropylamine with a trigonal-planar amino nitrogen (Fig. 2). Surprisingly, moreover, the C–N bond distance of 146 pm is comparable to that in trimethylamine, which is pyramidal.[3a] Obviously, and in agreement with quantum-chemical calculations,[4] a bond lengthening requires higher energies than the flattening of the molecular skeleton.

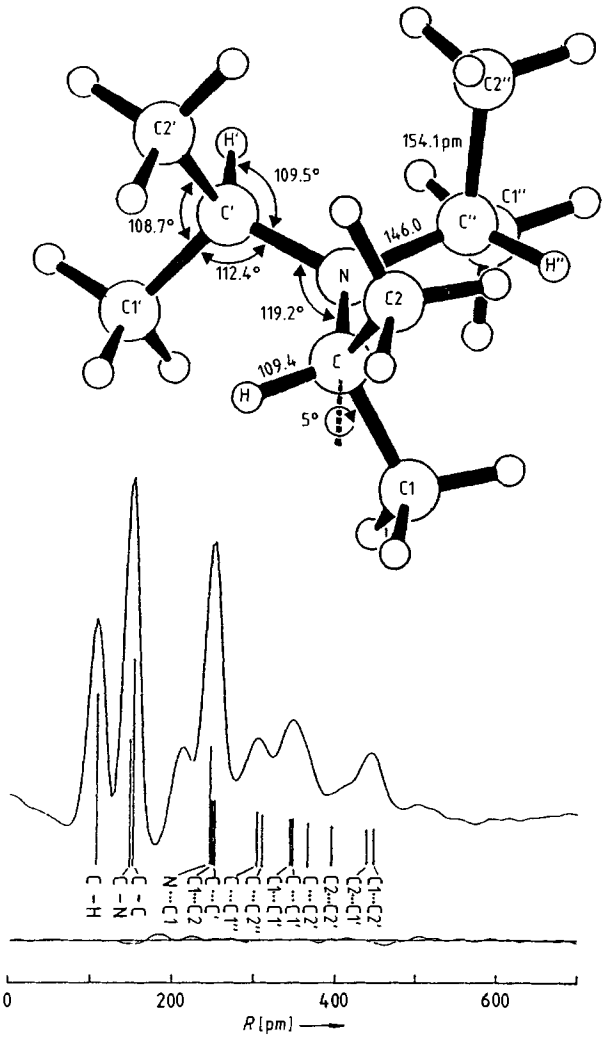

Fig. 2. Gas-phase structure of triisopropylamine and the respective radial distribution function from the electron diffraction.

According to a careful literature search,[2] triisopropylamine is thus the first trialkylamine for which a flattening of the NC_3 pyramid and, concomitantly, the formation of a p-type nitrogen electron pair could be verified by structure determination. This experimental finding not only allows the

rationalization of all measurement data (Fig. 1),[5-8] but is additionally supported by approximative quantum-chemical calculations using different methods[4a] (Table 2).

The experimentally determined structure parameters are satisfactorily embraced by the calculated approximative values.[4b,c] The dipole moment μ should be only small and the charge distribution (q_μ values, compare formula in Table 2) is polarized, according to the differing effective nuclear charges, from the rather negative nitrogen center to the positive isopropyl groups. The low inversion enthalpies[4f] estimated by MNDO FORCE and AM1 calculations for different C–N–C angles, however, suggest a rather weakly pronounced double minimum potential for triisopropylamine.[1]

Table 2. Experimental and calculated molecular properties of triisopropylamine (square brackets: charges q_μ according to AM 1).

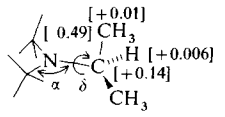

	Experiment	MM3	MNDO	AM1
α [°]	119.2	117.9	120.0	116.3
δ [°]	5.0	4.8	0	6.7
d_{CN} [pm]	146.0	145.8	147.4	145.7
μ [D]		0.02	0	0.76
ΔH_{inv} [kJ mol^{-1}]				9.6

In the meantime, the salt $[(H_3C)_2HC)_3N^{\oplus}H][SbCl_6^{\ominus}]$ has been prepared.[10a] Its structural characterization is planned, as are also the measurement of the proton affinity of triisopropylamine[10b] and single-crystal structure determinations of other sterically overcrowded alkylamino derivatives.[10c]

Received: July 6, 1990 [Z 4094 IE]
Delayed at authors' request.
German version: *Angew. Chem. 103* (1991) 193

CAS Registry numbers:
$((H_3C)_2HC)_3N$, 3424-21-3; $((H_3C)_2HC)_3N^{\cdot\oplus}$, 130248-90-7.

[1] a) N. Wiberg: *Hollemann-Wiberg, Lehrbuch der Anorganischen Chemie*, 91st–100th ed., de Gruyter, Berlin 1985, p. 551 f.; the inversion frequency $\nu = 2.38 \times 10^{10}$ s^{-1} corresponds to a tunneling barrier of 12.6 kJ mol^{-1}, that is, approximately to half of the thermodynamic barrier ($\Delta H^{\neq}_{inv} = 24.5$ kJ mol^{-1}); b) J. M. Lehn, *Fortschr. Chem. Forsch. 15* (1970) 311; c) K. Mislow, *Angew. Chem. 82* (1970) 453; *Angew. Chem. Int. Ed. Engl. 9* (1970) 400.

[2] X–N–X bond angle α in a) $(F_5S)_3N$ 119.7°: J. B. Nielsen, J. S. Thrasher, K. D. Robinson, S. G. Bott, H. Zhang, J. L. Atwood, P. Zylka, H. Oberhammer, *J. Am. Chem. Soc.*, in press; b) $(F_7C_3)N$ 120°: H. G. Mack, H. Oberhammer, *J. Mol. Struct. 197* (1989) 239; c) $(F_3C)_3N$ 117.9°: H. Bürger, H. Niepel, G. Pawelke, H. Oberhammer, *ibid. 54* (1979) 159; d) $(H_3Si)_3N$ 119.7°: B. Beagley, A. R. Conrad, *Trans. Faraday Soc. 66* (1970) 2740; e) $(H_3Si)_2NCH_3$ 125.4° (Si-N-Si) and 117.3° (Si-N-C) 117.3°: C. Glidewell, D. W. H. Rankin, A. G. Robiette, G. M. Sheldrick, *J. Mol. Struct. 4* (1969) 215; f) $(R_3Si)_3N$ (R = H,CH$_3$) 120°: D. G. Anderson, D. W. H. Rankin, H. E. Robertson, G. Gundersen, R. Seip, *J. Chem. Soc. Dalton Trans. 1990*, 161; g) $(H_3Ge)_3N$ 120°: C. Glidewell, D. W. H. Rankin, A. G. Robiette, *J. Chem. Soc. A 1970*, 2935; h) $(F_3CS)_3N$ 118.8°: C. J. Marsden, L. S. Bartell, *J. Chem. Soc. Dalton Trans. 1977*, 1582.

[3] a) Structural data: cf. the compilation in A. F. Wells: *Structural Inorganic Chemistry*, 5th ed., Clarendon Press, Oxford 1987, pp. 361 and 793 as well as [2]; b) $\Delta H^{\neq}_{inv}$ values: cf. [1]; c)–g) ionization energies: c) K. Kimura, S. Katsumata, Y. Achiba, T. Yamazaki, S. Iwata: *Handbook of He(I) Photoelectron Spectra*, Halstead Press, New York 1981; d) H. Bürger, G. Pawelke, R. Dammel, H. Bock, *J. Fluorine Chem. 19* (1982) 565; e) H. Baumgärtel, H.-W. Jochims, E. Rühl, H. Bock, R. Dammel, J. Minkwitz, R. Nass, *Inorg. Chem. 28* (1989) 943 and references cited therein; f) H. Bock, W. Kaim, M. Kira, H. Osawa, H. Sakurai, *J. Organomet. Chem. 164* (1979) 295; g) for example, R. W. Alder, R. J. Arrowsmith, A. Casson, B. Sessions, E. Heilbronner, B. Kovacs, H. Huber, M. Taagepera, *J. Am. Chem. Soc. 103* (1981) 6137, or the summarizing discussion: S. F. Nelsen, *J. Org. Chem. 49* (1984) 1891, and references cited in each article, especially D. H. Aue, H. M. Webb, M. T. Bowers, *J. Am. Chem. Soc. 97* (1975) 4136.

[4] a) The molecule $C_9H_{21}N$ possesses 31 atoms and, accordingly, 87 degrees of freedom (C_1). In order to avoid an expensive ab initio calculation employing a basis set sufficient to cover the rather small energy differences, therefore, the force field program MM2 and the semiempirical SCF programs closed and open shell MNDO, as well as AM1, have been used as different or differently parametrized calculation procedures. b) The approximative results obtained for the structural data of the almost—or according to MNDO—planar triisopropylamine, as well as its small dipole moment and its low inversion enthalpy (Table 2), are comparable. For the steric repulsion component, a value of 93 kJ mol^{-1} was estimated by MM2. c) The first vertical ionization energy was calculated to be 9.08 eV by MNDO and 8.83 eV by AM 1, corresponding to deviations from Koopmans' theorem ($IE_i^v = -\varepsilon_i^{SCF}$) of 1.9 and 1.65 eV, respectively. These, values are larger than usual and demonstrate, together with the more closely corresponding values for the pyramidal NH_3 ($IE_1^v = 10.85$ eV [3c]; MNDO, 11.91 eV; AM1, 10.42 eV) that trigonal-planar nitrogen centers are less well covered by the parametrization (cf., e.g., M. J. S. Dewar, W. Thiel, *J. Am. Chem. Soc. 99* (1977) 4970). With respect to the charge of the radical cation ground state, predominantly located at the N center ($[c_{1,N}^{MNDO}]^2 = 0.7$), however, also the electronic relaxation on electron expulsion should be rather small. d) Concomitantly, a MNDO open-shell calculation predicts a planar radical cation with spin populations $\varrho_N = 0.082$, $\varrho_{C,\alpha} = 0.009$, and $\varrho_{C,\beta} = 0.019$. e) According to MNDO FORCE calculations, the IR spectrum should show the following intense bands ($\tilde{\nu}$ [cm^{-1}] for $\langle\mu\rangle^2 > 0.25$; vibrational mode in square brackets; irreducible representation for C_3 in parentheses): 3274 [80,81] (e) and 3260 [74,73] (e), CH_3 stretch; 1535 [66,65] (e), N(CH) in-plane bending; 1494 [61] (a), CCH bending; 1369 [44,45] (e), $N(CH)_3$ in-plane bending; 1348 [41] (a), $N(CH)_3$ out-of-plane bending and 480 [18] (a), NC_3 out-of-plane. For the rotation of the isopropyl groups around the N-C bonds, a barrier of comparable height (523 cm^{-1} ≙ 6.5 kJ mol^{-1}) as that for the inversion, was calculated. f) The inversion enthalpies (Table 2) were estimated either from the N inversion vibration or from the difference in the AM 1 enthalpies of formation for the C–N–C angles of 116.3° and 120°. Accordingly, and with the necessary caution with respect to the approximation used, triisopropylamine should possess a shallow double minimum potential, each minimum corresponding to 116.3°. The barrier of 9.6 kJ mol^{-1} calculated for the saddle point at 120° would then be above the inversion mode of 480 cm^{-1} ≙ 5.9 kJ mol^{-1} and below most of the other vibrational modes ($\tilde{\nu} > 780$ cm^{-1}). g) In the meantime, *R. Ahlrichs* (Universität Karlsruhe) has begun performing ab initio calculations with increasingly improved basis sets, which so far confirm most of the above results and especially a zero-point mode in the region of the double minimum saddle point.

[5] F. Kuffner, W. Koechlin, *Monatsh. Chemie 93* (1962) 476. Synthesis (cf. *I. Göbel, Diplomarbeit*, Universität Frankfurt 1989): Diisopropylamine (4.25 mL, 0.3 mol) was neutralized with concentrated HCl and the resulting, stirred solution was then treated dropwise with a saturated aqueous solution of KCN (0.3 mol) and, after coooling to 0 °C, acetaldehyde (16.9 mL, 0.3 mol). The organic phase, as well as the ether extracts of the aqueous phase saturated with K_2CO_3, were dried over Na_2SO_4 and fractionally distilled at about 10 Torr. At a column head temperature of 58 °C, 17.4 g (37.6%) of α-diisopropylaminopropionitrile was isolated. The product (9 g, 58 mmol) was dissolved in 25 mL of dry ether at 25 °C and treated dropwise under Ar with an ether solution (100 mL) of H_3CMgCl (prepared from 4.9 g of Mg and gaseous CH_3Cl with addition of five drops of 1,2-dibromoethane). After 30-min reflux, the solution was poured on ice and neutralized with aqueous NaOH. Fractional distillation in vacuo (b.p. 47 °C/14 Torr) of the ether phase, dried over Na_2SO_4, yielded 3.74 g (45%) of $N(CH(CH_3)_2)_3$ ($n^{20} = 1.4141$) ^{1}H NMR (270 MHz, $CDCl_3$, 25 °C, TMS): $\delta = 0.9$–1.04 (d, 18H, CH_3), 2.96–3.4 (sept, m 3H, CH). MS: *m/z* 143 ($M^{\oplus}$), 128 ($M^{\oplus}$ – Me), 100 ($M^{\oplus}$ – *i*Pr), 86–84 ($M^{\oplus}$ – *i*Pr – Me), 70 ($M^{\oplus}$ – *i*Pr – 2 Me), 57 ($M^{\oplus}$ – 2 *i*Pr)). UV (diethyl ether): $\tilde{\nu}_m = 41\,670$ and $47\,900$ cm^{-1}.

[6] The known [3g] regression $IE_1^v(NR_3) = 8.92 - 0.129\,\Sigma n_{eff}$, on inserting n_{eff} (R = Me) = 1 and n_{eff} (R = *i*Pr) = 2.87, yields the following differences between estimated and experimental vertical first n_N ionization energies: Me_3N 0.09 eV, Me_2NiPr 0.09 eV, $MeiPr_2N$ 0.17 eV, $NiPr_3$ 0.62 eV. The latter value is found to be outside the regression line and in accord with a flattening of the NC_3 skeleton [4].

[7] All reversibility criteria are largely fulfilled: $\Delta E = 66$ mV, $i_{pa}/i_{pc} = 1.08$, "steady state" cycles (Abb. 1B). Trialkylamines without α hydrogens, such as 9-*tert*-butyl-9-azabicyclo[3.3.1]nonane, are also reversibly oxidized (S. F. Nelsen, C. R. Kessel, *J. Chem. Soc. Chem. Commun. 1977*, 490). These results suggest that the three C–H bonds of the title compound are located in the NC_3 skeletal plane (symmetry C_{3h}).

[8] Radical cations of amines $R^3N^{\cdot\oplus}$ are often generated by γ-irradiation of their perchlorates $(H_4N^{\oplus}ClO_4^{\ominus})$: T.Cole, *J. Chem. Phys. 35* (1961) 1169;

J. S. Hydet, E. S. Freeman, *J. Phys. Chem. 65* (1961) 1636) or by UV photolysis of suitable adducts ($(H_3C)_3N{\cdot}Cl_2$: Y. L. Chow, W. C. Danen, S. F. Nelsen, D. H. Rosenblatt, *Chem. Rev. 78* (1978) 244) and are usually short-lived. An exception is again 9-*tert*-butyl-9-azabicyclo[3.3.1]nonane, the radical cation of which in CH_2Cl_2, like that of trisopropylamine, is persistent over hours. The skilled help of Dr. *R. Baur* (Universität Frankfurt) in recording the ESR spectrum (Abb. 1 C) is gratefully acknowledged.

[9] a) The diffraction intensities were determined using a KD-GZ gas diffractograph at camera distances of 25 and 50 cm and an acceleration voltage of 60 kV. Temperature of the sample and the inlet nozzle were 25 °C; the camera pressure was 1.5×10^{-5} mbar. The photo plates were evaluated by the usual methods (H. Oberhammer, W. Gombler, H. Willner, *J. Mol. Struct. 70* (1981) 273) and the diffraction intensities in the s regions (20–180 nm^{-1} as well as 80–350 nm^{-1}) were used for the structure determination. b) The intensities were multiplied by a diagonal weight matrix and literature scattering amplitudes and phases applied (J. Haase, *Z. Naturforsch. 25A* (1970) 936). c) The following geometry parameters were obtained from the diffraction analysis (cf. Fig. 2) ([pm] and [°]; error tolerances, 3σ values with possible scaling error of 0.1% for bond lengths): C–N 146.0(5), C–C 154.1(3), C–H 109.4(4); C–N–C 119.2(3), C–C–C 108.7(12), C–C–N 112.4, C–C–H 109.0(6), N–C–H 109.5 (not refined), C–N–C′–H′ 5.0(18). The following interatomic distances (cf. Fig. 2) and vibrational amplitudes (without nonbonding distances to hydrogens) were determined: C–H 109 and 7.9(3), C–N 146 and 4.9 (not refined), C–C 154 and 5.9(3); N···C1 249, C1···C2 250, C···C′ 252 and each 8.2(2), C···C1″ 305, C···C2″ 312 and each 12.1(11), C1···C1′ 346, C···C1′ 349 and each 12.2(11), C···C2′ 370 and 9.5(19), C2···C2′ 396 and 16.9(38), C2···C1′ 441, C1···C2′ 452 and each 10.6(25).

[10] a) H. Bock, I. Göbel, unpublished. In 1-azabicyclo[3.3.3]undecane hydrochloride, the C–N–C angle is still 116° (A. H.-J. Wang, R. J. Missavage, S. R. Byrn, I. C. Paul, *J. Am. Chem. Soc. 94* (1972) 7100). b) The proton affinities for tri(*n*-propyl)amine and 1-azabicyclo[3.3.3]undecane of 988 and 977 kJ mol^{-1} differ only slightly [3g]. c) A single-crystal structure determination of tetrakis(dimethylamino)ethene at −30 °C (H. Bock, H. Borrmann, K. Ruppert, A. Simon, unpublished) also verifies largely flattened NC_3 pyramids.

Luminescence Properties of $Eu^{3\oplus}$ and $Tb^{3\oplus}$ Complexes of Branched Macrocyclic Ligands Containing Four 2,2′-Bipyridine Units**

By *Vincenzo Balzani,* Jean-Marie Lehn,* Jan van de Loosdrecht, Andrea Mecati, Nanda Sabbatini,* and *Raymond Ziessel*

An important research theme in the field of macrocyclic chemistry is the design of ligands capable of forming stable and strongly luminescent lanthanide complexes to be used as new luminescent materials and as labels for biological applications.[1–10] In such complexes the ligands must play three important roles: they must absorb light, transfer excitation energy to the lanthanide ion, and shield the lanthanide ion from interaction with solvent (water) molecules which deactivate the luminescent excited state. Previous investigations[1–4, 8] have shown that the 2,2′-bipyridine (bpy) chromophoric group may be used as a building block to design multidentate ligands which satisfy the above requirements. The synthesis of the branched macrocyclic ligands **1a** and **1b**, which contain four bpy units, has been reported recently.[11] Here we describe the luminescent properties of the novel $Eu^{3\oplus}$ and $Tb^{3\oplus}$ complexes of **1a** and the $Eu^{3\oplus}$ complex of **1b**.

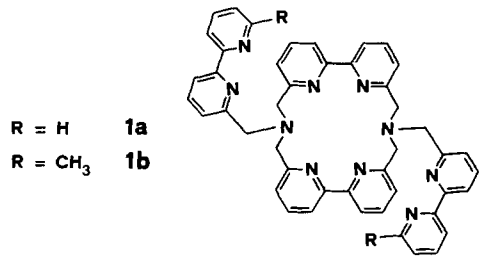

[Eu-**1a**]$Cl_3 \cdot 2H_2O$ was prepared by mixing equimolar amounts of **1a** (suspension in CH_2Cl_2/MeOH 5:1) and $EuCl_3 \cdot 6H_2O$ (solution in MeOH). Heating the mixture at 80 °C for one hour caused the solid to dissolve. The solvent was then removed under vacuum and the pale yellow residue was dissolved in MeOH. Slow diffusion of Et_2O resulted in precipitation of the complex. The same experimental procedure was used to prepare [Tb-**1a**]$Cl_3 \cdot 2H_2O$ and [Eu-**1b**]$Cl_3 \cdot 2H_2O$. The complexes were characterized by elemental analysis, NMR spectroscopy, and FAB mass spectrometry.[12] Absorption spectra, luminescence spectra, and luminescence lifetimes were measured as previously described.[8]

Solutions of [Eu-**1a**]$Cl_3 \cdot 2H_2O$ in methanol or water exhibited identical absorption spectra, which did not change even after several days. For [Tb-**1a**]$Cl_3 \cdot 2H_2O$ and [Eu-**1b**]$Cl_3 \cdot 2H_2O$, the absorption spectra in methanol solution were different from those in aqueous solution. Furthermore, in methanol solution no spectral change was observed, whereas in water the absorption spectra changed with time for a few hours until they became similar to those obtained for methanol solution. The reason why [Tb-**1a**]$Cl_3 \cdot 2H_2O$ and [Eu-**1b**]$Cl_3 \cdot 2H_2O$ are unstable in aqueous solution was not investigated, and the luminescence properties of these two complexes have only been studied in methanol solutions.

The absorption spectra of the complexes are characterized by the high-intensity ligand-centered (LC) bands of the coordinated bpy units. The wavelengths and molar absorption coefficients of the most intense band are as follows: [Eu-**1a**]$^{3\oplus}$, $\lambda_{max} = 312$ nm, $\varepsilon = 36\,000\ M^{-1}cm^{-1}$ (in H_2O) and $38\,000\ M^{-1}cm^{-1}$ (in CH_3OH); [Eu-**1b**]$^{3\oplus}$, $\lambda_{max} = 299$ nm, $\varepsilon \approx 39\,000\ M^{-1}cm^{-1}$, with another peak of comparable intensity present at 292 nm (CH_3OH); [Tb-**1a**]$^{3\oplus}$, $\lambda_{max} = 312$ nm, $\varepsilon \approx 44\,000\ M^{-1}cm^{-1}$ (CH_3OH). The molar absorption coefficients of the LC bands in these complexes are thus higher than those of the previously studied [Eu ⊂ bpy · bpy · bpy]$^{3\oplus}$ and [Tb ⊂ bpy · bpy · bpy]$^{3\oplus}$ cryptates,[3, 8] because of the presence of one more bpy unit.

Excitation of the complexes in their LC absorption bands resulted in the well-known, structured luminescence of the lanthanide ion, with the highest energy peak at 17 300 cm^{-1} for $Eu^{3\oplus}$ ($^5D_0 \rightarrow {}^7F_0$ transition) and 20 490 cm^{-1} for $Tb^{3\oplus}$ ($^5D_4 \rightarrow {}^7F_6$ transition). Corrected excitation spectra in the near-UV region closely matched the absorption spectra.

Luminescence lifetimes and quantum yields obtained under various experimental conditions are gathered in Table 1, where analogous data concerning the bpy · bpy · bpy cryptates[3, 8] are also shown for comparison purposes.

The luminescence lifetime of [Eu-**1a**]$^{3\oplus}$ in H_2O is much higher than that of [Eu ⊂ bpy · bpy · bpy]$^{3\oplus}$, whereas the lifetime in D_2O is almost the same for the two complexes.

[*] Prof. Dr. V. Balzani, Dr. J. van de Loosdrecht, Dr. A. Mecati, Prof. Dr. N. Sabbatini
Dipartimento di Chimica dell'Università
via Selmi 2, I-40126 Bologna (Italy)
Prof. Dr. J.-M. Lehn, Dr. R. Ziessel
Institut Le Bel, Université Louis Pasteur
4, rue Blaise Pascal, F-67000 Strasbourg (France)

[**] This work was supported by the Consiglio Nazionale delle Ricerche (Progetto Finalizzato Chimica Fine II), the Ministero della Pubblica Istruzione, the Centre National de la Recherche Scientifique (URA 422), and ORIS-Industrie. We wish to thank *V. Cacciari* for technical assistance, *M. Foyentin* and *G. Mathis* (ORIS-Industrie, France) for preliminary lifetime measurements of the complexes [Eu-**1a**]$^{3\oplus}$ and [Tb-**1a**]$^{3\oplus}$.

Table 1. Luminescence data [a].

Complex	Solvent	Lifetime [ms] [b]		Quantum yield [c]
		300 K	77 K	300 K
[Eu-**1a**]$^{3\oplus}$	H_2O	1.5	1.8	0.1
	D_2O	1.9	1.9	0.2
	CH_3OH	1.2	1.3	0.1
	CH_3OD	1.7	1.9	0.2
[Eu-**1b**]$^{3\oplus}$	CH_3OH	1.0	1.3	0.01
	CH_3OD	1.8	2.0	0.01
[Eu ⊂ bpy · bpy · bpy]$^{3\oplus}$ [d]	H_2O	0.34	0.81	0.02
	D_2O	1.7	1.7	0.1
[Tb-**1a**]$^{3\oplus}$	CH_3OH	1.1	2.0	0.14
	CH_3OD	1.2	2.9	0.35
[Tb ⊂ bpy · bpy · bpy]$^{3\oplus}$ [d]	H_2O	0.33	1.7	0.03
	D_2O	0.43	3.8	–

[a] Excitation in the ligand-centered band at approximately 300 nm. [b] Experimental error ≤ 10%. [c] Experimental error ≈ 30%. [d] From [3] and [8].

This shows that the $Eu^{3\oplus}$ ion is much better protected by **1a** towards the interaction with water molecules. Use of the empirical equation proposed by *Horrocks*[13] and the experimental lifetimes at 300 K in H_2O and D_2O solutions revealed that no water molecule is present in the first coordination sphere of the metal ion in [Eu-**1a**]$^{3\oplus}$, whereas about 2.5 water molecules are present in the case of [Eu ⊂ bpy · bpy · bpy]$^{3\oplus}$.[3] The efficient shielding offered by **1a** to the metal ion towards solvent interaction is also shown by the lifetime data of [Eu-**1a**]$^{3\oplus}$ in CH_3OH and CH_3OD. These results indicate that, as expected from the examination of space-filling models, the metal ion can be enclosed in the macrocyclic ring of **1a** and then encapsulated by the two branches of the ligand. This shielding effect is most likely present also in [Tb-**1a**]$^{3\oplus}$, but for this complex fast metal-to-ligand back energy transfer could explain why the lifetime is practically the same in CH_3OH and CH_3OD.[14]

Comparison of the lifetime values for [Eu-**1a**]$^{3\oplus}$ and [Eu-**1b**]$^{3\oplus}$ in methanol shows that the metal ion is almost equally shielded by the two ligands. However, the luminescence quantum yield is much smaller for [Eu-**1b**]$^{3\oplus}$, probably because the two methyl substituents in **1b** prevent a close approach of some bpy units to the metal and therefore reduce the energy-transfer efficiency from the ligand-centered to the metal-centered excited states. This hypothesis is supported by the presence of a residual ligand-centered phosphorescence (λ_{max} = 470 nm, 77 K) for [Eu-**1b**]$^{3\oplus}$.

The higher luminescence quantum yield exhibited by [Eu-**1a**]$^{3\oplus}$ compared with [Eu ⊂ bpy · bpy · bpy)]$^{3\oplus}$ in H_2O at 300 K cannot be entirely accounted for by the better shielding offered in **1a** towards interaction of the excited metal ion with solvent molecules. In fact, the quantum yield is higher by a factor of 5 whereas the lifetime is higher only by a factor of about 2. Furthermore, the quantum yield is higher also in D_2O, where the shielding effect does not play any role. These results show that the energy-transfer efficiency from the ligand-centered to the luminescent metal-centered level is larger (approximately by a factor of 2) for [Eu-**1a**]$^{3\oplus}$. For the analogous $Tb^{3\oplus}$ complexes no conclusion can be drawn in this regard because of the lack of directly comparable data and the presence of metal-to-ligand back energy transfer.[14]

In conclusion, in the $Eu^{3\oplus}$ and $Tb^{3\oplus}$ complexes of **1a** the presence of four bpy units provides a very high molar absorption coefficient and an excellent protection towards the deactivating action of water on the luminescent excited state. Furthermore, in [Eu-**1a**]$^{3\oplus}$ the ligand-to-metal energy-transfer efficiency is higher than in [Eu ⊂ bpy · bpy · bpy]$^{3\oplus}$. For these reasons, the $Eu^{3\oplus}$ and $Tb^{3\oplus}$ complexes of **1a** are strongly luminescent species, superior to the previously investigated[1–3, 8] bpy · bpy · bpy cryptates. Thus, [Eu-**1a**]$^{3\oplus}$ is a promising luminescent label even in aqueous solution. Functionalization of the bpy units[15] should make possible the coupling of this complex to biological substrates.

Received: September 26, 1990 [Z 4205 IE]
German version: *Angew. Chem. 103* (1991) 186

CAS Registry numbers:
[Eu-**1a**]Cl_3, 131457-98-2; [Tb-**1a**]Cl_3, 131457-99-3; [Eu-**1b**]Cl_3, 131458-00-9.

[1] B. Alpha, J.-M. Lehn, G. Mathis, *Angew. Chem. 99* (1987) 269; *Angew. Chem. Int. Ed. Engl. 26* (1987) 266.
[2] B. Alpha, V. Balzani, J.-M. Lehn, S. Perathoner, N. Sabbatini, *Angew. Chem. 99* (1987) 1310; *Angew. Chem. Int. Ed. Engl. 26* (1987) 1266.
[3] N. Sabbatini, S. Perathoner, V. Balzani, B. Alpha, J.-M. Lehn in V. Balzani (Ed.): *Supramolecular Photochemistry*, Reidel, Dordrecht, The Netherlands, 1987, p. 187.
[4] G. Blasse, G. J. Dirkens, N. Sabbatini, S. Perathoner, J.-M. Lehn, B. Alpha, *J. Phys. Chem. 92* (1988) 2419.
[5] F. Nicolò, D. Plancherel, G. Chapuis, J. C. Bünzli, *Inorg. Chem. 27* (1988) 3518.
[6] M. Pietraszkiewicz, S. Pappalardo, P. Finocchiaro, A. Mamo, J. Karpiuk, *J. Chem. Soc. Chem. Commun. 1989*, 1907.
[7] J.-M. Lehn, M. Pietraszkiewicz, J. Karpiuk, *Helv. Chim. Acta 73* (1990) 106.
[8] B. Alpha, R. Ballardini, V. Balzani, J.-M. Lehn, S. Perathoner, N. Sabbatini, *Photochem. Photobiol. 52* (1990) 299.
[9] R. C. Holz, S. L. Klakamp, C. A. Chang, W. DeW. Horrocks, Jr., *Inorg. Chem. 29* (1990) 2651.
[10] N. Sabbatini, M. Guardigli, A. Mecati, V. Balzani, R. Ungaro, E. Ghidini, A. Casnati, A. Pochini, *J. Chem. Soc. Chem. Commun. 1990*, 878.
[11] R. Ziessel, J.-M. Lehn, *Helv. Chim. Acta 73* (1990) 1149.
[12] FAB mass spectrometry (nitrobenzyl alcohol matrix): *m/z*: [Eu-**1a**]$Cl_3 \cdot 2H_2O$: 953.0 $[M-Cl]^{\oplus}$, 918.1 $[M-2Cl]^{\oplus}$, 882.2 $[M-3Cl]^{\oplus}$; [Tb-**1a**]$Cl_3 \cdot 2H_2O$: 959.1 $[M-Cl]^{\oplus}$, 924.1 $[M-2Cl]^{\oplus}$, 888.2 $[M-3Cl-H]^{\oplus}$; [Eu-**1b**]$Cl_3 \cdot 2H_2O$: 981.0 $[M-Cl]^{\oplus}$, 946.1 $[M-2Cl]^{\oplus}$, 911.2 $[M-3Cl]^{\oplus}$.
[13] W. DeW. Horrocks, Jr., D. R. Sudnick, *Acc. Chem. Res. 14* (1981) 384.
[14] For a thorough discussion of back energy transfer in $Tb^{3\oplus}$–bpy complexes, see [8].
[15] B. Alpha, E. Anklam, R. Deschenaux, J.-M. Lehn, M. Pietraskiewicz, *Helv. Chim. Acta 71* (1988) 1042.

A Short and Flexible Enantioselective Synthesis of the Didemnenones**

By *Heike Bauermeister, Hartmut Riechers, Dietmar Schomburg, Peter Washausen,* and *Ekkehard Winterfeldt**

Till now Caribbean tunicates have primarily been a source of cyclic peptide derivatives, but recently *Lindquist* et al. described the isolation and structure elucidation of a cyclopentenone derivative with tumor-inhibiting properties.[1] This material proved to be a mixture of the epimeric lactols

[*] Prof. Dr. E. Winterfeldt, H. Bauermeister,
Institut für Organische Chemie der Universität
Schneiderberg 1 B, W-3000 Hannover 1
Dr. H. Riechers,
BASF AG, W-6700 Ludwigshafen
Dr. D. Schomburg, Dr. P. Washausen,
GBF-Gesellschaft für Biotechnologische Forschung mbH,
Mascheroder Weg 1, W-3000 Braunschweig

[**] Financial support by the Deutsche Forschungsgemeinschaft is gratefully acknowledged. Abbreviations used: LDA = Li*N*iPr_2, TBDMS = Si*t*BuMe_2, DBU = 1,8-diazabicyclo[5.4.0]undec-7-ene, NOE = nuclear Overhauser enhancement, DIBAH = Al*i*Bu_2H.

7a and **7b**, which could, however, be converted into the nicely crystalline α methyl ether **7c** for characterization and comparison.[1, 2] Although these are comparatively small molecules they are packed with functionality and contain two functional groups that are both considered to be responsible for biological activity: the cyclopentenone moiety, which is a strong acceptor group, and the unsaturated lactol, which under slightly acidic conditions, for instance in tumor cells, could give rise to an oxonium derivative, or on oxidation could yield the corresponding unsaturated lactone with well-established acceptor properties. These are certainly the main reasons for the present synthetic interest in this field.[2, 3] In both the known syntheses of the didemnenones the stereoselective construction of the exocyclic butadiene system represents the crucial and complicated step. We now report a flexible, stereoselective synthesis in which the unsaturated lactone **6** is an important intermediate.

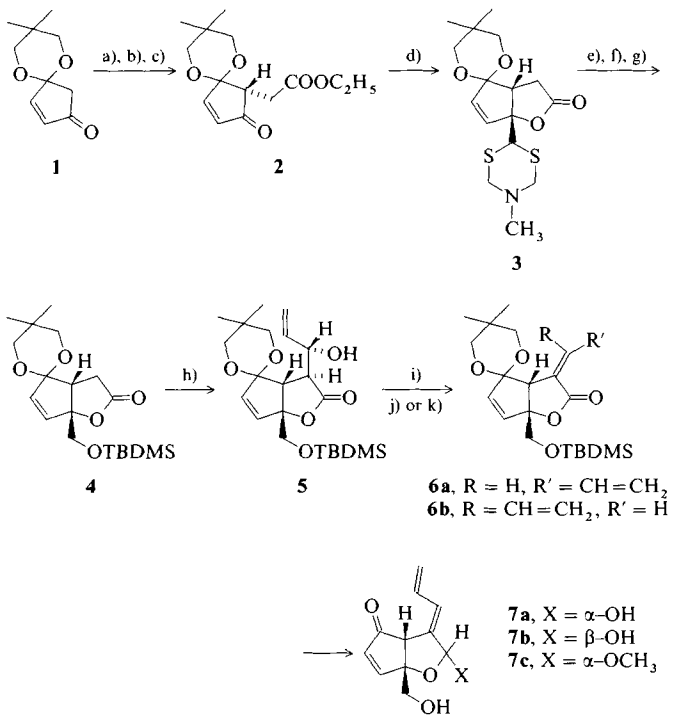

Scheme 1. Reagents and conditions: a) THF, LDA, −78 °C, 30 min; b) THF, ICH_2COOEt, −78 °C, 30 min (a + b 65%); c) Lipomod PC, H_2O, phosphate buffer (pH = 7), 27 °C, 32 h (17%, 91% *ee*); d) THF, dithiazine, *n*BuLi, −78 °C, 1 h (55%); e) $MeCN/H_2O$, HgO, $HgO/HgCl_2$, room temperature, 30 min; f) MeOH, $NaBH_4$, 0 °C, 10 min; g) CH_2Cl_2, TBDMSCl/imidazole, 1–2 h (e + f + g 65%); h) THF, LDA, acrolein, −78 °C, 45 min (73%); i) CH_2Cl_2, CH_3SO_2Cl, Et_3N, room temperature, 15 min (100%); j) THF, $KN(SiMe_3)_2$, −78 °C, 15 min (50%); k) CH_2Cl_2, DBU, room temperature, 1 h (100%).

Starting from monoketal **1**, which is easily prepared from the corresponding diketone[4] by conventional techniques, we obtained *rac*-ketoester **2** on alkylation with ethyl iodoacetate. A subsequent kinetic resolution with the commercially available lipase Lipomod PC[5] led to pure (*R*)-ester **2** in 35% yield. Thioketal **3** was generated from this ketone with high diastereoselectivity (exclusive β approach), and served extremely well for an X-ray structure determination, as the sulfur atoms allowed the determination of the absolute configuration by computational techniques.[6]

Subsequent oxidative hydrolysis, borohydride reduction, and conventional silylether formation gave rise to lactone **4**, which underwent aldol addition with high diastereoselectivity. The configuration of **5** was assigned on the basis of the *Zimmerman–Traxler* transition state. As expected for this set of configurations, mesylate elimination with DBU in dichloromethane (E_2 type, *anti* elimination) gave rise to **6a** as the main reaction product (**6a**:**6b** = 10:1). For E_{1cB} elimination conditions (*syn* elimination) we chose $KN(SiMe_3)_2$ as a strong base at low temperature and indeed obtained mainly **6b** (**6b**:**6a** = 3:1). The configuration of both lactones could easily be assigned by conventional NMR chemical shift observations (influence of the carbonyl group) and NOE experiments. DIBAH reduction and deprotection gave rise to the *iso*didemnenones from **6a**, while **6b** generated the mixture of the epimeric didemnenones, which as reported by *Lindquist* et al.[1] could be transformed into the stable α methyl ether **7c**. This was identical to the natural product derivative.[7]

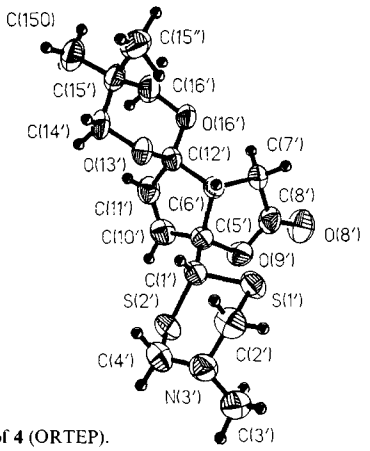

Fig. 1. X-ray crystal structure of **4** (ORTEP).

Our synthesis leads to both stereoisomers at the exocyclic double bond from a common homochiral intermediate (**5**) by simply changing the conditions of the elimination process. As this leads to the lactones, which are then reduced to the corresponding lactols, four stereoisomers are available for testing the biological activity. The influence of the double bond configuration as well as of the oxidation status of the lactone moiety on the biological activity can thus be determined.

Received: July 26, 1990
Revised version: October 29, 1990 [Z 4096]
German version: *Angew. Chem. 103* (1990) 207

CAS Registry numbers:
1, 129822-78-2; **2**, 131407-11-9; **3**, 131407-12-0; **4**, 131407-13-1; **5**, 131407-14-2; **6a**, 131407-15-3; **6b**, 131487-47-0; **7a**, 131487-88-2; **7b**, 131486-48-1; **7c**, 131486-49-2.

[1] N. Lindquist, W. Fenical, D. F. Sesin, C. M. Ireland, G. D. Van Duyne, C. J. Forsyth, L. Clardy, *J. Am. Chem. Soc. 110* (1988) 1308.
[2] C. J. Forsyth, J. Clardy, *J. Am. Chem. Soc. 112* (1990) 3497.
[3] T. Sugahara, T. Ohike, M. Soejima, S. Takano, *J. Chem. Soc. Perkin Trans. 1 1990*, 1824.
[4] H. E. Baumgarten (Ed.): *Organic Syntheses, Coll. Vol. V*, Wiley, New York 1973, p. 414.
[5] Available from Biocatalysts Ltd., Mid Glamorgan, U.K.
[6] Further details of the X-ray structural analysis can be requested from the Fachinformationszentrum Karlsruhe, Gesellschaft für wissenschaftlich-technische Information mbH, W-7514 Eggenstein-Leopoldshafen 2, on quoting the depository number CSD-54832, the authors, and the full journal quotation.
[7] NMR spectra of the natural product as well as of methyl ether **7c** were kindly provided by *Dr. Lindquist* and his colleagues.

Functional Modeling of Ni,Fe Hydrogenases: A Nickel Complex in an *N,O,S* Environment.**

By *Marc Zimmer**, *Gayle Schulte*, *Xiao-Liang Luo*, and *Robert H. Crabtree**

Hydrogenases containing both nickel and iron[1] catalyze H_2/D exchange,[2] but their physiological role is H_2 oxidation.[1] There is circumstantial evidence in favor of a Ni site for H_2 binding.[2c] Various ESR signals coupled to ^{61}Ni ($I = \frac{3}{2}$) are found for ^{61}Ni, Fe hydrogenases,[2a,c] but the oxidation state assignment for some of these (nickel(I) or (III)) is controversial.[2,c-e] Exposure to O_2 deactivates the enzymes, but they may be reductively activated to give the 'ready' form.[2c] Little is known about the ligand environment, but extended X-ray absorption fine structure (EXAFS) data suggest that three[3] to four[4] sulfurs are coordinated to Ni, while ESR data only show one.[5] Very few Ni^I or Ni^{III} *S*-donor complexes are known;[6,7] most Ni^{III} species have highly noninnocent ligands,[8,9] form dimers,[10,11] or decompose to disulfides.[12,13] Recently some interesting Ni^{III} thiolates were isolated.[14] We now report an *N,O,S*-donor Ni^{II} complex that is octahedral in the solid state but square planar in solution, can be reduced to an air-stable Ni^I form, and, like hydrogenase itself, catalyzes H_2/D exchange. This is the first nickel-containing hydrogenase model system which is functional for isotopic exchange. The previous ones, the Os and Ru porphyrins of *Collman* et al.,[15a] and the Pd(salen) (salen = bis(salicylidene)ethylenediamine) systems of *Olivé* et al.[15b] did not contain physiologically relevant metals.

We screened a large number of *S*-donor Ni complexes for activity and find H/D exchange only for $[NiL_2]Cl_2$ (**1**) (L = *o*-C_6H_4(OH)CH=N-NHCSNH_2) which is formed by refluxing $NiCl_2$ with L[16,17] in ethanol for two hours and crystallizes as dark green plates in 81% yield. An X-ray crystal structure of **1** · EtOH (Fig. 1) shows a pseudooctahedral dicationic complex.[18] Both ligands are in the phenol, rather than the phenolate form. The magnetic moment in the solid state is 1.98 B.M. (1.83×10^{-23} J T^{-1}), significantly lower than the spin-only value.[19a] The Ni–S bonds are short (2.386(3) Å and 2.362(3) Å vs. 2.45–2.55 Å in typical Ni^{II} octahedral species[19b]), consistent with significant $R_2N^{\oplus}$=C–$S^{\ominus}$ character for the ligand. The long Ni–O(Aryl) bonds (2.143(6) and 2.091(6) Å), are further evidence for protonated phenols.[19b]

In solution the complex is diamagnetic, as shown by the Evans method[20] and the normal ^1H NMR spectrum. This suggests that the complex has lost one or two ligands. Similar behavior has been observed for Ni^{II} complexes of thiourea.[21] The long Ni–O(Aryl) bond and the position of the phenol resonances (intensity: 2) almost unshifted from the free ligand (-O*H* at $\delta = 9.90$) suggest that both phenol groups dissociate (Scheme 1).

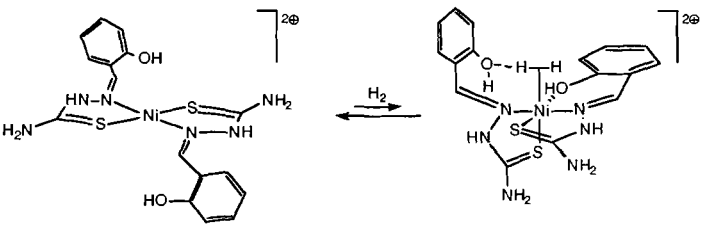

3

Scheme 1. Probable structure of the dication **1** in solution. **3**: Proposed catalytic intermediate for hydrogen activation.

Reduction of **1** electrochemically ($E > -1.05$ V, scan speed = 100 mV s^{-1}; $I_a/I_c = 1.64$; $\Delta E = 0.098$ V, quasi reversible)[22] or with $NaBH_4$ (irreversible) produces a Ni^I species (**2**) which is stable in air (ESR) for hours. Ni^I is unusual in an S environment and no air-stable examples are known. Neither the ligand itself nor $[ZnL_2]SO_4$ reacts with $NaBH_4$, suggesting that ligand L is not reduced under these conditions. Nickel is the predominant site of reduction as shown by the ESR spectrum in dimethylformamide (DMF) (Fig. 2,

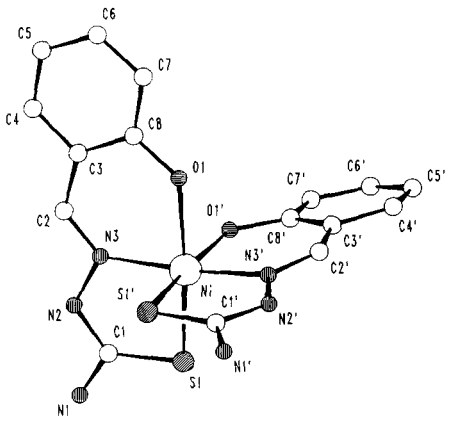

Figure 1. Structure of the Ni-salicylaldehyde thiosemicarbazone cation [18] (selected Ni–L bond lengths [Å]: S1, 2.39; S1', 2.36; N3, 2.02; N3', 2.01; O1, 2.14; O1', 2.09).

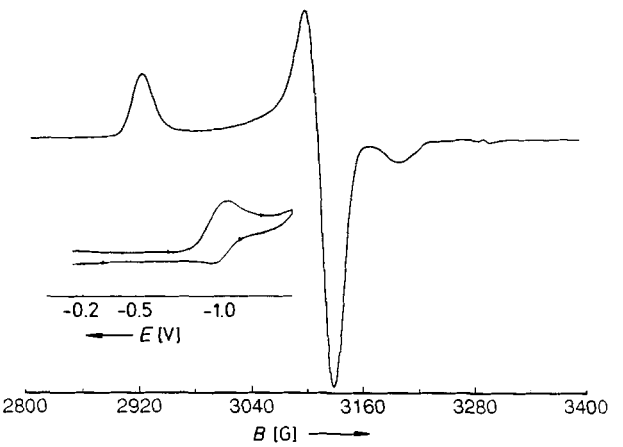

Figure 2. Frozen solution (7 K) of X band ESR spectrum ($\nu = 9.0519$ GHz) of **2**. Insert: Cyclic Voltammogram of **1** [22].

$g = 2.25$, 2.12, and 2.06),[23] which is consistent with an axially distorted Ni^I species. The reduced forms of the analogous Ni complexes which lack the phenol groups,[24]

[*] Prof. Dr. R. Crabtree, G. Schulte, X.-L. Luo
Yale Chemistry Dept.
225 Prospect Street, New Haven, CT 06511-8118 (USA)
Prof. M. Zimmer,
Chemistry Department, Connecticut College
New London, CT 06320 (USA)

[**] This research was supported by the National Institutes of Health. We thank Prof. *G. W. Brudvig* for discussions, and Ms. *C. A. Buser* and Dr. *J. Bocarsly* for obtaining ESR spectra.

four coordinate **4**, and five coordinate **5** have identical $g_\perp$ and $g_\parallel$ to **2**. UV-vis spectra show that **5** does not disproportionate to **1** and **4**. The Ni^I complexes are therefore four-coordinate with an N_2S_2 environment.

$[Ni(C_6H_5CH{=}N\text{-}NHCSNH_2)_2]Cl_2$ **4**

$[Ni(C_6H_4OHCH{=}N\text{-}NHCSNH_2)(C_6H_5CH{=}N\text{-}NHCSNH_2)]Cl_2$ **5**

We looked at D_2/H exchange with ethanol-OH protons catalyzed by **1**. Exposure to D_2 (1 atm) gave H/D exchange, especially in the presence of promoters like HI or HBF_4. A 0.1 M solution of **1** in a dimethyl sulfoxide/ethanol mixture (90:10) gave 7.5 turnovers[25] of H/D exchange after five minutes at 25 °C and 1 atm pressure of D_2. Deuteriation of the EtOH proton was followed by ^2D NMR by monitoring the EtO*D* resonance at $\delta = 4.15$ versus C_6D_6 as standard. The catalytic activity disappeared after 7.5 turnovers. Neither **4** nor **5** promotes H/D exchange, so both phenolic OH groups are required for activity. A possible catalytic intermediate is **3**,[26] in which one phenol group is bound to the nickel, and the other forms a hydrogen bond with H_2 (Scheme 1). Hydrogen bonding may increase the affinity of the complex for H_2 and promote exchange (Scheme 2).

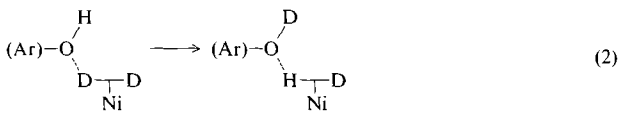

(2)

Scheme 2.

This work reveals some unusual features of Ni chemistry in an *S*-donor environment. A stable Ni^I species is formed from **1** on reduction. In solution, ligand dissociation leads to a species which interacts with D_2 and promotes H/D exchange. Compound **1** is thus a functional model for hydrogenases.

Received: August 15, 1990 [Z 4135 IE]
German version: *Angew. Chem. 103* (1990) 205

CAS Registry numbers:
1, 52637-24-8; **1** · EtOH, 131564-04-0; **2**, 131457-27-7; **4**, 51341-69-6; **5**, 131457-23-3; L, 5351-90-6; $[Ni(C_6H_5CH{=}NNHCSNH_2)_2]^{\oplus}$, 131457-24-4; $[Ni(C_6H_4OHCH{=}NNHCSNH_2)(C_6H_5CH{=}NNHCSNH_2)]^{\oplus}$, 131457-25-5; $[NiL(EtOH)]^{2\oplus}$, 131457-26-6; hydrogenase, 9035-82-9.

[1] a) G. Fauque, H. D. Peck, Jr., J. J. G. Moura, B. H. Huynh, Y. Berlier, D. V. DerVartanian, M. Teixeira, A. E. Przybyla, P. A. Lespinat, I. Moura, J. LeGall, *FEMS Microbiol. Rev. 54* (1988) 299; b) I. N. Gogotov, *Biochimie 68* (1986) 181; c) R. P. Hausinger, *Microbiol. Rev. 51* (1987) 22; d) C. T. Walsh, W. H. Orme-Johnson, *Biochemistry 26* (1987) 4901.
[2] a) P. A. Lespinat, Y. Berlier, G. Fauque, M. Czechowski, B. Dimon, J. LeGall, *Biochimie 68* (1986) 55; b) D. V. DerVartanian, H. J. Kruger, H. D. Peck, Jr., J. LeGall, *Rev. Port. Quim. 27* (1985) 70; c) R. Cammack, V. M. Fernandez, K. Schneider in J. R. Lancaster, Jr. (Ed.): *Bioinorganic Chemistry of Nickel*, VCH, Weinheim 1988, p. 167; d) J. J. G. Moura, M. Teixeira, I. Moura, J. LeGall, *ibid.* p. 191; e) J. W. Van Der Zwaan, S. P. J. Albracht, R. D. Fontijn, E. C. Slater, *FEBS Lett. 179* (1985) 271.
[3] P. A. Lindahl, N. Kojima, R. P. Hausinger, J. A. Fox, B. K. Teo, C. T. Walsh, W. H. Orme-Johnson, *J. Am. Chem. Soc. 106* (1984) 3062.
[4] R. A. Scott, S. A. Wallin, M. Czechowski, D. V. DerVartanian, J. LeGall, H. D. Peck, Jr., I. Moura, *J. Am. Chem. Soc. 106* (1984) 6864.
[5] S. P. J. Albracht, A. Kroger, J. W. von der Zwaan, G. Unden, R. Bocher, H. Mell, R. D. Fontijn, *Biochim. Biophys. Acta 874* (1986) 116.
[6] H.-J. Kruger, R. H. Holm, *Inorg. Chem. 26* (1987) 3645.
[7] a) A. A. G. Tomlinson, *Coord. Chem. Rev. 37* (1981) 221; b) K. Nag, A. Chakravorty, *ibid. 33* (1980) 87; c) A. G. Lappin, A. McAuley, *Adv. Inorg. Chem. 32* (1988) 241; d) C. L. Coyle, E. I. Stiefel in [2c], p. 1.
[8] E. I. Stiefel, J. H. Waters, E. Billig, H. B. Gray, *J. Am. Chem. Soc. 87* (1965) 3016.
[9] A. H. Maki, N. Edelstein, A. Davidson, R. H. Holm, *J. Am. Chem. Soc. 86* (1964) 4580.
[10] H.-J. Kruger, R. H. Holm, *Inorg. Chem. 28* (1989) 1148.
[11] W. Tremel, M. Kriege, B. Krebs, G. Henkel, *Inorg. Chem. 27* (1988) 3886.
[12] M. Kumar, R. O. Day, G. J. Colpas, M. J. Maroney, *J. Am. Chem. Soc. 111* (1989) 5974.
[13] M. Handa, M. Mikuriya, H. Okawa, *Chem. Lett. 1989*, 1663.
[14] a) S. Fox, Y. Wang, A. Silver, M. Millar, *J. Am. Chem. Soc. 112* (1990) 3218; b) H.-J. Krueger, R. H. Holm, *J. Am. Chem. Soc. 112* (1990) 2955.
[15] a) J. P. Collmann, P. S. Wagenknecht, R. T. Hembre, N. S. Lewis, *J. Am. Chem. Soc. 112* (1990) 1294; b) G. Henrici-Olivé, S. Olivé, *J. Mol. Catal. 1976*, 121.
[16] S. Purohit, A. P. Koley, L. S. Prasad, P. T. Manoharan, S. Ghosh, *Inorg. Chem. 28* (1989) 3735.
[17] A. V. Ablov, N. V. Gerbeleu, *Russ. J. Inorg. Chem. (Engl. Transl.) 10* (1965) 624.
[18] Monoclinic, space group $P2_1/n$ (No. 14), $a = 14.865(4)$, $b = 9.474(2)$, $c = 18.619(2)$ Å; $\beta = 110.05(1)°$, $V = 2463.2(9)$ Å^3, $Z = 4$ for $d_{calc.} = 1.526$ g cm^{-3}; 5162 unique reflections were collected on a automated diffractometer ($Mo_{K\alpha}$ radiation, $\lambda = 0.71069$ Å). The structure was solved using the Patterson method. A total of 289 parameters were refined to a final $R = 0.044$, $R_w = 0.046$, using 2639 reflections. Further details of the crystal structure investigation are available on request from the Director of the Cambridge Crystallographic Data Centre, University Chemical Laboratory, Lensfield Road, GB-Cambridge CB21EW (UK), on quoting the full journal citation.
[19] a) Nickel(II) thiourea complexes with magnetic moments ranging from 0.6 to 2.5 B.M. ($0.56-2.32 \times 10^{-23}$ J T^{-1}) have been reported in [19b]; b) L. Sacconi, F. Mani, A. Bencini in G. Wilkinson, (Ed.): *Comprehensive Coordination Chemistry*, Pergamon, New York 1987.
[20] D. F. Evans, *J. Chem. Soc. 1959*, 2003.
[21] C. Furlani, T. Tarantelli, P. Riccieri, *J. Inorg. Nucl. Chem. 33* (1971) 1389.
[22] A solution of **1** (5 mM in 0.1 M n-$Bu_4N(ClO_4)$/DMF) was reduced by controlled potential electrolysis using a Pt basket working electrode, a Pt wire auxiliary electrode and an SCE reference. Current integrated for 0.92 e mol^{-1} of **1**. Potential vs. SCE, with $E_{1/2} = 0.48$ V for $Fc^{\oplus}$/Fc (Fc = ferrocene) in DMF. No Ni^{II}/Ni^{III} wave was seen.
[23] Frozen DMF solution (7 K), X Band ESR spectrum ($\nu = 9.0519$ GHz.)
[24] **5** was made by refluxing the ligand with $NiCl_2$ in EtOH for 2 h. **4** was made by refluxing 1 equiv of the tridentate ligand with $NiCl_2$ as above, to give [NiL(EtOH)], followed by refluxing with 1 equiv of the bidentate ligand.
[25] No H/D exchange was observed in a variety of control experiments (L alone; $NiCl_2$ alone; L with $H^{\oplus}$; $NiCl_2$ with $H^{\oplus}$ and $[ZnL_2]$ alone); 2 turnovers were observed in absence of a promotor.
[26] An H_2 complex is a plausible intermediate because no dicationic first row metal is sufficiently π basic to lead to oxidative addition of H_2 and [Ir(7,8-benzoquinolinate)$(PPh_3)_2H(\eta^2H_2)]^{\oplus}$ is an extemely effective catalyst [26b] for H/D exchange between EtOH and D_2. b) A. Albeniz, D. M. Heinekey, R. H. Crabtree, unpublished results.

Eight-Coordinate Metal Carbonyls Containing Only Monodentate Ligands. Syntheses and Structural Characterization of $[nPr_4N]_2[(Ph_3Sn)_4M(CO)_4]$, M = Zr, Hf**

By *John E. Ellis,* Kai-Ming Chi, Anthony-J. DiMaio, Scott R. Frerichs, Jason R. Stenzel, Arnold L. Rheingold,* and *Brian S. Haggerty*

Until the recent synthesis of the hexacarbonylmetalates(2−) of zirconium[1, 2] and hafnium,[1] only η^5- or η^6-bonded ligands such as η^5-C_5H_5, η^5-C_5Me_5,[3, 4] and η^6-1,3,5-tri-*tert*-butylbenzene[5] and bi- or tridentate ligands

[*] Prof. J. E. Ellis, K.-M. Chi, Dr. A.-J. DiMaio, S. R. Frerichs, J. R. Stenzel
Department of Chemistry, University of Minnesota
Minneapolis, MN 55455 (USA)
Prof. A. L. Rheingold[+], B. S. Haggerty
Department of Chemistry, University of Delaware
Newark, DE 19716 (USA)
[+] X-ray structure analyses

[**] Highly Reduced Organometallics, Part 29. This work was supported by the U.S. National Science Foundation and the Petroleum Research Fund administered by the American Chemical Society. Part 28: [1].

such as η^2-1,2-bis(dimethylphosphino)ethane[6] and η^3-1,1,1-tris(dimethylphosphinomethyl)ethane[7] were known to stabilize carbonyls of these elements. We now wish to report on an unprecedented class of carbonyls of Zr and Hf which contain only the triphenylstannyl ligand as the stabilizing group. These complexes, which formally contain divalent zirconium or hafnium, are dianions of the composition $[(Ph_3Sn)_4M(CO)_4]^{2\ominus}$ (**1**, M = Zr; **2**, M = Hf). They are the first examples of eight-coordinate metal carbonyls containing only monodentate ligands.

The synthetic procedure is summarized in Equation (a) ($C_{10}H_8$ = naphthalene; further details are given under *Experimental Procedure*). Trimethylphosphane must be present

$$MCl_4 \cdot 2THF + 2NaC_{10}H_8 \xrightarrow{4PMe_3,\ 4Ph_3SnNa,\ CO} Na_2[(Ph_3Sn)_4M(CO)_4] + 2C_{10}H_8 \quad (a)$$

M = Zr, Hf.

during these reductions or the carbonylation step fails. Although the exact role of the phosphane in this synthesis is not understood, *Cloke* and *Green* previously established that PMe_3 was crucial in the synthesis and stabilization of the first bis-arene compounds of Zr^0 and Hf^0.[8] Attempts to prepare $[(Ph_3Sn)_4Ti(CO)_4]^{2\ominus}$ by this procedure resulted instead in the formation of the known Ti^0 species $Na_2[(Ph_3Sn)_2Ti(CO)_5]$[9] and Ph_6Sn_2. Cation exchange with Et_4NBr and $n Pr_4NCl$ provided salts which could easily be crystallized in pure form.

IR spectra of the tetraalkylammonium salts in CH_3CN or as mineral oil mulls of crystalline solids displayed one intense band in the ν(CO) region at about 1880 cm^{-1}.[10] ^1H, ^{13}C, and ^{119}Sn NMR spectra of the anions were independent of the counterion and in accord with the assigned compositions.[11] Corresponding ^{13}C and ^{119}Sn NMR spectra of the 99% enriched ^{13}CO compounds established that they were fluxional tetrastannyl tetracarbonyls.[12] Independent evidence for the presence of four equivalent tin atoms in **2** in solution was obtained from the ^{119}Sn NMR spectrum of the unenriched hafnium dianion, which showed, after prolonged spectral acquisition time (ca. 12 h) at 50 °C, a 1:10:1 apparent triplet with $J(^{117}Sn\text{-}^{119}Sn) = 1100 \pm 50$ Hz.[13]

The molecular structure of **1** is shown in Figure 1 and has a metal–ligand coordination core ($ZrSn_4C_4$) consisting of a dodecahedron of D_{2d} symmetry, characterized by interpenetrating tetrahedra of carbonyl and triphenylstannyl groups.[14] The Ph_3Sn units form an elongated tetrahedron (A sites), while the carbonyl groups form a substantially flattened tetrahedron (B sites) to minimize interligand repulsions.[15] A stereoview of the isostructural hafnium complex **2** emphasizes the relatively high symmetry of these dodecahedral species (Fig. 2). Selected interatomic distances

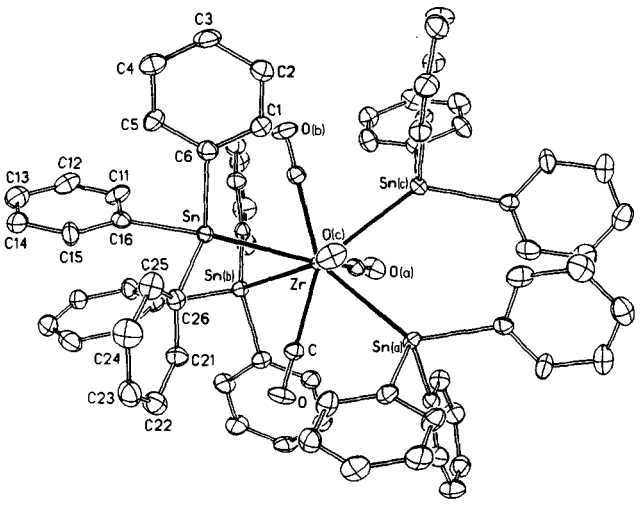

Fig. 1. Molecular structure of **1**. For important bond lengths and angles, see Table 1.

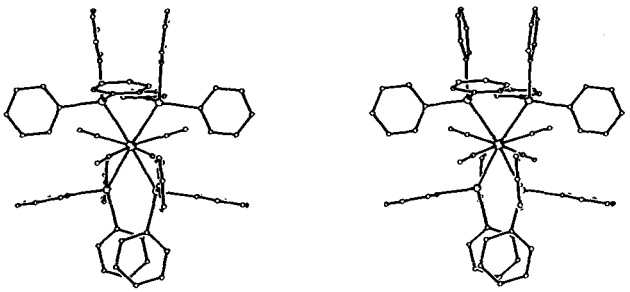

Fig. 2. Stereoview of **2** looking down the $S_4(\bar{4})$ axis.

and angles for **1** and **2** are shown in Table 1 and appear to be within normal limits. Also, cations are well separated from anions in the crystalline lattice. As expected on the basis of previous studies on isostructural zirconium and hafnium complexes,[16] the carbon and tin bonds to hafnium are somewhat shorter than corresponding bonds to zirconium. Prior to this work, $[(\eta\text{-toluene})_2Hf(SnMe_3)_2]$[17] was the only example of a structurally characterized compound containing heavier group 4 metal–tin bonds. These Hf–Sn bonds

Table 1. Selected bond lengths [Å] and angles [°] for **1** and **2**.

	Zr (**1**)	Hf (**2**)
Bond lengths		
M-C	2.232(5)	2.162(12)
M-Sn	3.086(1)	3.063(1)
C-O	1.155(6)	1.189(16)
Sn-(*ipso*)C (mean)	2.22(2)	2.22(1)
Bond angles		
M-C-O	177.9(4)	176.8(4)
Sn-M-Sn(a)	125.7(1)	125.6(1)
Sn-M-Sn(b)	80.3(1)	80.5(1)
C-M-C(a)	93.6(1)	94.0(2)
C-M-C(b)	151.1(3)	149.2(6)
C-M-Sn	89.4(1)	88.1(3)
C-M-Sn(a)	66.0(1)	66.6(3)
C-M-Sn(b)	68.2(1)	68.2(3)
C-M-Sn(c)	142.0(1)	143.3(3)

are appreciably shorter (2.953(1) Å) than those in **2**, perhaps due to a less crowded environment about hafnium in the bis-arene complex. Although the M–C bonds in **1** and **2** are somewhat longer than corresponding ones found in $[(C_5Me_5)_2M(CO)_2]$ (Zr-C = 2.145(9), Hf-C = 2.14(2) Å),[18] they are quite similar in length to those observed recently for the octahedral $[M(CO)_6]^{2\ominus}$ (Zr-C = 2.210(4), Hf-C = 2.178(3) Å).[1] The metal carbonyl units are close to being linear. Average Sn–M–Sn(b) and C–M–C(b) angles for **1** and **2** are 80.4(2) and 150(1)°, respectively, giving dodecahedral shape parameters of 40.2° for θ_A(Sn) and 75° for θ_B(C).[15] These data are typical of dodecahedral geometries.[19]

Whether similar carbonyl complexes of the group 3 metals can be prepared and isolated is currently under investigation.

Experimental Procedure

In a typical synthesis of **2**, a cold solution (−60 °C) of $NaC_{10}H_8$ (1.30 g, 8.6 mmol) in 80 mL of 1,2-dimethoxyethane (DME) was added by cannula to a mechanically stirred solution/slurry of $HfCl_4 \cdot 2THF$ (2.0 g, 4.3 mmol) and PMe_3 (1.8 mL, 18 mmol) in 70 mL of DME at −60 °C. Addition of a cold solution (−60 °C) of $NaSnPh_3$ (6.42 g, 17.2 mmol) in 100 mL of DME to the resulting red-brown solution caused the color to change rapidly to a deep green. Argon was replaced by CO (1 atm) and the reaction mixture was stirred under CO for 12 h, while slowly warming to room temperature, to give a deep red solution. After filtration and cation exchange (with Et_4NBr), a red solid was obtained upon addition of excess ethanol. Recrystallization of the product from CH_3CN–toluene provided deep purple crystals (5.1 g, 61%), which gave satisfactory analyses (C, H, Sn) for **2** as a bis-tetraethylammonium salt. Similar yields (50–60%) were obtained for the $n Pr_4N^{\oplus}$ salt (correct C, H analyses). The same procedure consistently provided lower yields (25–45%) of satisfactorily pure **1** as $Et_4N^{\oplus}$ and $nPr_4N^{\oplus}$ salts (C, H, Sn analyses). These substances are stable indefinitely under nitrogen at room temperature and decompose without melting above 150 °C. Spectroscopic data for the anions as $Et_4N^{\oplus}$ or $nPr_4N^{\oplus}$ salts are essentially identical and are shown only for the $Et_4N^{\oplus}$ compounds [10–12]. The 99% enriched ^{13}CO complexes were prepared by the same procedure with suitably enriched CO. X-ray quality crystals were obtained by slow diffusion of diethyl ether into an acetonitrile solution of the $nPr_4N^{\oplus}$ salts at 0 °C over a 3–5-day period. Suitable crystals could not be obtained with the less soluble $Et_4N^{\oplus}$ salts.

Received: October 5, 1990 [Z 4230 IE]
German version: *Angew. Chem. 103* (1991) 196

CAS Registry numbers:
[Na]-**1**, 131323-19-8; [Et_4N]-**1**, 131323-22-3; [nPr_4N]-**1**, 131323-25-6; [Na]-**2**, 131323-20-1; [Et_4N]-**2**, 131323-24-5; [nPr_4N]-**2**, 131323-26-7; $ZrCl_4 \cdot 2THF$, 21959-01-3; $HfCl_4 \cdot 2THF$, 21959-05-7; Ph_3SnNa, 42451-63-8; Sn, 7440-58-6; Hf, 7440-31-5; Zr, 7440-67-7.

[1] J. E. Ellis, K.-M. Chi, *J. Am. Chem. Soc. 112* (1990) 6022.
[2] K.-M. Chi, S. R. Frerichs, S. B. Philson, J. E. Ellis, *Angew. Chem. 99* (1987) 1203; *Angew. Chem. Int. Ed. Engl. 26* (1987) 1190.
[3] B. A. Kelsey, J. E. Ellis, *J. Chem. Soc. Chem. Commun. 1986*, 331; B. A. Kelsey, J. E. Ellis, *J. Am. Chem. Soc. 108* (1986) 1344. See also D. J. Sikora, D. W. Macomber, M. D. Rausch, *Adv. Organomet. Chem. 25* (1986) 318.
[4] S. R. Frerichs, J. E. Ellis, *J. Organometal. Chem. 359* (1989) C41.
[5] F. G. N. Cloke, M. F. Lappert, G. A. Lawless, A. C. Swain, *J. Chem. Soc. Chem. Commun. 1987*, 1667.
[6] B. K. Stein, S. R. Frerichs, J. E. Ellis, *Organometallics 6* (1987) 2017; R. P. Beatty, S. S. Wreford, *Inorg. Chem. 18* (1979) 3139.
[7] D. W. Blackburn, K.-M. Chi, S. R. Frerichs, M. L. Tinkham, J. E. Ellis, *Angew. Chem. 100* (1988) 408; *Angew. Chem. Int. Ed. Engl. 27* (1988) 437.
[8] F. G. N. Cloke, M. L. H. Green, *J. Chem. Soc. Chem. Commun. 1979*, 127.
[9] K.-M. Chi, S. R. Frerichs, J. E. Ellis, *J. Chem. Soc. Chem. Commun. 1988*, 1013.
[10] IR(CH_3CN): $\tilde{\nu}$[cm^{-1}] = 1886 (s, br Zr-CO), 1877 (s, br Hf-CO), 1843 (s, br Zr-^{13}CO (99%)), 1835 (s, br Hf-^{13}CO (99%)).
[11] Signals due to cations are not given. ^1H NMR (300 MHz, CD_3CN, 20 °C, TMS): **1** and **2**: δ = 7.4–6.9: (m, Ph_3Sn). $^{13}C\{^1H\}$ NMR (75 MHz): **1**: δ = 242.0 (s, CO), 154.7, 139.0, 127.5, 126.2 (Ph_3Sn). **2**: δ = 239.7 (s, CO), 154.3, 139.7, 127.4, 126.3 (Ph_3Sn). $^{119}Sn\{^1H\}$ NMR (112 MHz, Me_4Sn): **1**: δ = 337 (s, $W_{1/2}$ = 6 Hz). **2**: δ = 301 (s, $W_{1/2}$ = 8 Hz).
[12] Signals due to cations are not given. $^{13}C\{^1H\}$ NMR (75 MHz, CD_3CN, 50 °C, TMS): **1**: δ = 242.0 (pseudoquintet, CO, $^2J(^{119}Sn, ^{117}Sn\text{-}^{13}C)$ = 100 Hz); **1**: δ = 239.7 (pseudoquintet, CO, $^2J(^{119}Sn, ^{117}Sn\text{-}^{13}C)$ = 93 Hz). The pseudoquintet has relative intensities of approximately 1:6:16:6:1. These relative intensities are in satisfactory agreement with the calculated ones of 1:7:19:7:1 for the most intense five lines of nonets arising from four magnetically equivalent tin groups coupled to ^{13}C, assuming identical $J(^{115,117,119}Sn\text{-}^{13}C)$ values and a total relative abundance of NMR-active Sn nuclei of 16.54%. The outermost four lines of the nonets were too low in intensity for detection. $^{119}Sn\{^1H\}$ NMR (112 MHz, CD_3CN, 50 °C, Me_4Sn): **1**: δ = 337 (binomial quintet, $^2J(^{119}Sn\text{-}^{13}C)$ = 102 Hz); **2**: δ = 300 (binomial quintet, $^2J(^{119}Sn\text{-}^{13}C)$ = 93 Hz). Below 40 °C (**1**) or 50 °C (**2**), the ^{13}C and ^{119}Sn NMR signals broaden and become strongly temperature-dependent. For further details see K.-M. Chi, *Ph.D. Thesis*, University of Minnesota, 1988.
[13] *Rudolph* et al. previously established that "triplet" ^{119}Sn resonances with relative intensities of 1:6.25:1, 1:8.3:1, or 1:12.5:1 are expected from ^{117}Sn–^{119}Sn coupling for a cluster containing five, four, or three equivalent tin atoms, respectively. The observed $J(^{117}Sn\text{-}^{119}Sn)$ value of 1224 Hz for the naked metal cluster $Sn_4^{2\ominus}$ is very similar to the corresponding value we observed for $[(Ph_3Sn)_4Hf(CO)_4]^{2\ominus}$. See: R. W. Rudolph, W. L. Wilson, R. C. Taylor, *J. Am. Chem. Soc. 103* (1983) 2480.
[14] Crystal data for [nPr_4N]-**1**: tetragonal, $P\bar{4}2_1c$ (No. 114), a = 15.339(3), c = 19.045(3) Å, V = 4482(1) Å, Z = 2, ϱ_{calcd} = 1.46 g cm^{-3}, $\mu(Mo_{K\alpha})$ = 12.7 cm^{-1}, T = 293 K. Of 4339 data collected (two octants, $h \le k$, Nicolet R3m, $4° \le 2\theta \le 50°$), 4105 were independent and 3490 were observed ($3\sigma F_0$). Zr resides on a $\bar{4}$ site, and N on a twofold axis; the asymmetric unit consists of 1/4 of the structural formula. At convergence, $R(F)$ = 2.86, $R(wF)$ = 3.61. The phenyl rings were constrained to rigid hexagons. One of the propyl groups contained a disordered β carbon atom at two sites (C35 and C37). The Rogers handedness test confirms the correctness of the reported enantiomorph. All other non-hydrogen atoms were anisotropically refined; hydrogen atoms were idealized. SHELXTL software, Nicolet, Madison, WI (USA). [nPr_4N]-**2**: a = 15.322(2), c = 19.042(3) Å, V = 4470(1) Å^3, Z = 2, ϱ_{calcd} = 1.53 g cm^{-3}, $\mu(Mo_{K\alpha})$ = 23.8 cm^{-1}, T = 293 K. Of 2577 data collected (one octant, $+h \le +k \le +l$, Nicolet R3m, $4° \le 2\theta \le 52°$), 2440 were independent and 2114 were observed ($4\sigma F_0$). Refinement was initialized from the coordinates of the isomorphous zirconium salt. At convergence, $R(F)$ = 5.09, $R(wF)$ = 5.69. Further details of the crystal structure analysis are available on request from the Director of the Cambridge Crystallographic Data Centre, University Chemical Laboratory, Lensfield Road, GB-Cambridge CB2 1EW (England), on quoting the full journal citation.
[15] J. L. Hoard, J. V. Silverton, *Inorg. Chem. 2* (1963) 235.
[16] F. A. Cotton, G. Wilkinson: *Advanced Inorganic Chemistry*, 5th ed., J. Wiley, New York 1988, pp. 776–778.
[17] F. G. N. Cloke, K. P. Cox, M. L. H. Green, J. Bashkin, K. Prout, *J. Chem. Soc. Chem. Comm. 1981*, 117.
[18] D. J. Sikora, M. D. Rausch, R. D. Rogers, J. L. Atwood, *J. Am. Chem. Soc. 103* (1981) 1265.
[19] S. J. Lippard, *Prog. Inorg. Chem. 8* (1967) 109.

Synthesis of Nonstabilized Phosphaalkynes by Vacuum Gas-Solid HCl Elimination

By *J. C. Guillemin, T. Janati, P. Guenot, P. Savignac,* and *J. M. Denis**

Phosphaalkynes have recently proved useful as building blocks in synthesis.[1] The stabilized derivatives bearing tertiary or secondary alkyl groups are efficiently prepared by base-induced elimination of hexamethyldisiloxane from the corresponding α-trimethylsiloxy *P*-trimethylsilylphosphaalkenes.[2] However, with the exception of $HC{\equiv}P$ and $CH_3C{\equiv}P$, which are obtained in low yield by flash vacuum thermolysis of the corresponding dichlorophosphanes,[3] no efficient method is available to synthesize other nonstabilized phosphaalkynes. Recently we have shown that (dichloromethyl)phosphane can be regarded as a synthetic equivalent of $HC{\equiv}P$.[4] We now report that $HC{\equiv}P$ and other nonstabilized phosphaalkynes can be easily synthesized from the corresponding (dichloroalkyl)phosphanes by vacuum gas-solid HCl elimination (VGSR).[5]

Halogen–metal exchange between **1** and *n*BuLi in the presence of LiCl and subsequent acid hydrolysis or alkylation led to (dichloroalkyl)phosphonates **2**.[6] We observed a cleaner reaction and better yields with diisopropyl ester **1** in place of the diethyl ester **1** (R = Et) used previously.

$$Cl_3CP(O)(OR)_2 \xrightarrow[2)\ R^1X,\ THF,\ -80°C]{1)\ n\text{BuLi/LiCl, THF, } -85°C} R^1Cl_2CP(O)(OR)_2$$

1 **2**

R = *i*Pr
a, R^1 = H; **b**, R^1 = Me; **c**, R^1 = Et; **d**, R^1 = *n*Bu; **e**, $R^1 = Me_3Si$

[*] Dr. J. M. Denis, Dr. J. C. Guillemin, Dipl.-Chem. T. Janati
Groupe de Physicochimie Structurale, URA CNRS N° 704
Université des Rennes 1, F-35042 Rennes (France)
Dr. P. Guenot
CRMPO, Université de Rennes 1, F-35042 Rennes (France)
Dr. P. Savignac
DCPH, Ecole Polytechnique, F-91128 Palaiseau (France)

The chemoselective reduction of phosphonate **2** to **3** was critical: the best results were obtained with $AlHCl_2$ as an electrophilic reducing agent in diethyl ether at low temperature.[7] To avoid polymerization, phosphane **3** must be quickly purified by distillation. Phosphonate **1** could also be reduced in this way to give **3f** (R^1 = Cl).

$$\underset{\textbf{2a–2e}}{R^1Cl_2CP(O)(OR)_2} \xrightarrow[Et_2O,\ -80°C]{AlHCl_2} \underset{\textbf{3a–3e}}{R^1Cl_2CPH_2}$$

Purified (dichloroalkyl)phosphanes **3** can be stored for several weeks in a refrigerator (5 °C) in the presence of a small amount of hydroquinone. The stability of **3** at room temperature depends on the substituents: **3e** and **3f** decompose in a few hours, but **3b**–**3d** can be kept for several days. The parent compound **3a** cleanly isomerized, probably via a twofold HCl elimination/addition, into the corresponding dichlorophosphane CH_3PCl_2. Phosphanes **3** were characterized by ^1H, ^{13}C, and ^{31}P NMR spectroscopy as well as by high-resolution mass spectrometry (HRMS) (Table 1).

Table 1. Selected spectroscopic data for (dichloroalkyl)phosphanes **3** (*J* in Hz).

3	R^1	δ^1H [a]	$\delta^{31}P$ (^1J(PH)) [a]	$\delta^{13}C$ (^1J(CP)) [a]	*m/z* of $M^{\oplus}$ found (calcd)
a	H	6.19	−78 (199)	61.6 (26)	115.935 (115.9349)
b	Me	2.45	−46 (196)	80.3 (25)	129.951 (129.9506)
c	Et	2.40 (CH_2)	−56 (197)	86.1 (26)	143.967 (143.9662)
d	*n*Bu	2.41 (CH_2)	−53 (197)	85.2 (26)	137.028 (137.0287) [b]
e	Me_3Si	0.32 (CH_3)	−79 (195)	73.9 (30)	187.974 (187.9745)
f	Cl		−12 (200)	89.8 (42)	149.895 (149.8960)

[a] $CDCl_3$, TMS, room temperature. [b] $(M-Cl)^{\oplus}$

Owing to the acidity of the two hydrogens bonded to the phosphorus atom, dehydrochlorination of **3** readily occurred in a VGSR sequence using K_2CO_3 as a solid base.[5] The first HCl elimination was performed at 200 °C, but the transient chlorophosphaalkenes **4** polymerized even at low temperature. Complete HCl elimination takes place at 350 °C.[8] The phosphaalkynes **5** were collected by a standard procedure[5] and characterized by NMR and IR spectroscopy and by mass spectrometry (Table 2). As an example, compound **5b** was obtained from 0.018 mol of **3b** in 60% yield (see *Experimental Procedure*).

$$\underset{\textbf{3}}{R^1Cl_2CPH_2} \xrightarrow[VGSR]{K_2CO_3} \underset{\textbf{4}}{\left[\begin{array}{c} R^1 \\ \diagdown \\ Cl \end{array} C{=}P{\sim}H\right]} \xrightarrow[VGSR,\ 350°C]{K_2CO_3} \underset{\textbf{5}}{R^1{-}C{\equiv}P}$$

For **5a**, **5b**, and **5e**, the NMR data are in good agreement with the reported values;[3b, 11] for the new compounds **5c**, **5d**, and **5f**, the data are consistent with the structures. A ^{31}P NMR high-field signal for **5f** was also observed for $FC{\equiv}P$ ($\delta = -205$).[12] Phosphaalkynes **5** can be kept for several hours or days under neutral atmosphere in a dilute THF solution (see Table 2). This stability, higher than previously reported, can be explained by their good purity. We have also obtained in low yield the chlorophosphaalkyne **5f** in the flash vacuum thermolysis products of $ClCH_2PCl_2$ heated at 850 °C.[13]

Experimental Procedure

Caution: All the reactions were carried out under nitrogen in a well-ventilated hood, since (dichloroalkyl)phosphanes and phosphaalkynes are pyrophoric compounds.

3a–3d, 3f: $LiAlH_4$ (1.33 g, 3.5×10^{-2} mol) in freshly distilled diethyl ether (100 mL) was introduced into a 250-mL three-necked flask. The mixture was cooled to −80 °C and $AlCl_3$ (14.0 g, 1.05×10^{-1} mol) quickly added. The suspension was allowed to warm to 10 °C, then cooled again to −80 °C. The phosphonate (2.5×10^{-2} mol) in diethyl ether (25 mL) was added dropwise at a rate to maintain the temperature under −70 °C. At the end of the addition, the mixture was allowed to warm to 10 °C. The volatile products were condensed into a cold trap. Most of the ether was then distilled off at atmospheric pressure (the oil bath temperature must be maintained below 70 °C). The flask containing the concentrated solution (about 10 mL) was cooled to −67 °C and evacuated for 20 min (10^{-2} mbar) to remove traces of solvent. Distillation of the residue in vacuo led to the pure phosphane (yield ca. 50%).

3e: The reduction was performed under the conditions reported above. To avoid polymerization of **3e** on heating, $NaHCO_3$ (5 g) was added at room temperature to the stirred decanted solution. After 5 min, the solution was filtered under nitrogen and distilled in vacuo. Compound **3e** was condensed as a white solid into a cold trap (−40 °C) while diethyl ether was removed (yield 70%, mp > 60 °C (dec.)).

5b *(VGSR)* [5]: Dried K_2CO_3 (150 g), ground into a fine powder with a laboratory mill, was introduced into a VGSR reactor (pyrex tube, l = 80 cm, inner diameter 4.0 cm), then horizontally distributed between two pads of glass wool separated by 60 cm. The reactor, fitted to a cold trap (77 K) bearing a Schlenk flask at the bottom, was heated to 350 °C [8]. Dichlorophosphane **3b** (2.4 g, 1.83×10^{-2} mol) was then slowly vaporized in vacuo (1 g per hour) through the reactor. The trap was disconnected from the reactor and vacuum pump by closing stopcocks and allowed to warm to room temperature while phosphaalkyne **5b** (0.64 g, 1.1×10^{-2} mol) was condensed into the Schlenk flask previously cooled to 77 K (yield 60%).

Analytical samples of phosphaalkynes **5a–5f**:

The general procedure described above was modified: the solvent (THF or $CDCl_3$), introduced between reactor and trap, was condensed with **5** (ca. 1.4×10^{-3} mol) into the cold trap. Transfer of the solution into the Schlenk flask was performed at atmospheric pressure under dry nitrogen.

Received: July 19, 1990 [Z 4074 IE]
German version: *Angew. Chem. 103* (1991) 191

CAS Registry numbers:
2a, 55696-11-2; **2b**, 56798-07-3; **2c**, 131352-03-9; **2d**, 131323-80-3; **2e**, 131323-81-4; **2f**, 88020-45-5; **3a**, 125750-80-3; **3b**, 131323-82-5; **3c**, 131323-83-6; **3d**, 131323-84-7; **3e**, 131323-85-8; **3f**, 131323-86-9; **5a**, 6829-52-3; **5b**, 67517-97-9; **5c**, 131323-87-0; **5d**, 131323-88-1; **5e**, 75192-38-0; **5f**, 52323-02-1.

Table 2. Selected spectroscopic data, yields and stabilities for phosphaalkynes **5** (*J* in Hz).

5	R^1	δ^1H [a]	$\delta^{31}P$ [a]	$\delta^{13}C$ (^1J(C, P)) [a]	$\tilde{\nu}_{CP}$ [cm^{-1}]	*m/z* of $M^{\oplus}$ found (calcd)	Yield [b] [%]	Half-life [c]
a	H	2.90 [d]	−32 [d]	158.0 (56) [e]	1267 [f]	43.9818 [g] (43.98159)	80	6 h
b	Me	2.20 [h]	−61 [h]	170.8 (49) [e]	1559 [i]	57.9972 (57.99724)	80	>7 d
c	Et	2.30 (CH_2)	−62	177.0 (44)	1552 [j]	72.0131 (72.01289)	80	>7 d
d	*n*Bu	2.38 (CH_2)	−59	176.4 (43)	1545 [j]	100.044 (100.0442)	70	>7 d
e	Me_3Si	0.07 (CH_3)	+99 [k]	201.9 (13) [k]	1572 [l]	116.021 (116.0211)	65	1 d
f	Cl		−116	126.4 (17)	1460 [l]	77.9425 [g] (77.94262)	60	10 h

[a] $CDCl_3$, TMS, room temperature. [b] All the reactions were carried out on an analytical scale (2×10^{-3} mol of **3**) and the yields were determined by ^{31}P NMR spectroscopy with an internal reference. [c] 2–5% in THF solution at 20 °C. [d] Lit.: $\delta^1H = 2.90$, $\delta^{31}P = -32$ [3b]. [e] See [3b]. [f] Film, 77 K; lit.: 1279 [9]. [g] Tandem VGSR-HRMS [5b]. [h] Lit.: $\delta^1H = 2.20$, $\delta^{31}P = -60$ [3b]. [i] See [10]. [j] CCl_4, room temperature. [k] Lit.: $\delta^{31}P = +96$, $\delta^{13}C = 201.4(14)$ [11]. [l] Film, 77 K.

[1] a) J. F. Nixon, *Chem. Rev. 88* (1988) 1327; b) M. Regitz, P. Binger, *Angew. Chem. 100* (1988) 1541; *Angew. Chem. Int. Ed. Engl. 27* (1988) 1484; c) M. Regitz, *Chem. Rev. 90* (1990) 191.
[2] G. Becker, G. Gresser, W. Uhl, *Z. Naturforsch. B36* (1981) 16; W. Rösch, U. Hees, M. Regitz, *Chem. Ber. 120* (1987) 1645.
[3] a) T. A. Cooper, H. W. Kroto, J. F. Nixon, O. Ohashi, *J. Chem. Soc. Chem. Commun. 1980*, 333; b) B. Pellerin, J. M. Denis, J. Perrocheau, R. Carrié, *Tetrahedron Lett. 27* (1986) 5723; c) E. P. O. Fuchs, M. Hermesdorf, W. Schnurr, W. Rösch, H. Heydt, M. Regitz, *J. Organomet. Chem. 338* (1987) 329; d) M. J. Hopkinson, H. W. Kroto, J. F. Nixon, N. P. C. Simmons, *Chem. Phys. Lett. 42* (1976) 460; e) M. Hermesdorf, M. Birkel, H. Heydt, M. Regitz, *Phosphorus Sulfur Silicon Relat. Elem. 46* (1989) 31.
[4] J. C. Guillemin, M. Le Guennec, J. M. Denis, *J. Chem. Soc. Chem. Commun. 1989*, 988; J. M. Denis, J. C. Guillemin, M. Le Guennec, *Phosphorus Sulfur Silicon Relat. Elem. 49 & 50* (1990) 317.
[5] Other VGSR experiments: a) B. De Corte, J. M. Denis, N. De Kimpe, *J. Org. Chem. 52* (1987) 1147; J. C. Guillemin, J. M. Denis, *Tetrahedron 44* (1988) 4431; S. Lacombe, B. Pellerin, J. C. Guillemin, J. M. Denis, G. Pfister-Guillouzo, *J. Org. Chem. 54* (1989) 5958; b) L. Wazneh, J. C. Guillemin, P. Guenot, J. M. Denis, Y. Vallée, *Tetrahedron Lett. 29* (1988) 5899.
[6] D. Seyferth, R. S. Marmor, *J. Organomet. Chem. 59* (1973) 237; P. Savignac, M. Dreux, P. Coutrot, *Tetrahedron Lett. 1975*, 609; P. Savignac, J. Petrova, M. Dreux, P. Coutrot, *Synthesis 1975*, 535; P. Coutrot, C. Laurenco, J. F. Normant, P. Perriot, P. Savignac, J. Villieras, *ibid. 1977*, 615.
[7] We have successfully used $AlHCl_2$ in the chemoselective reduction of other α-functionalized phosphonates: J. L. Cabioch, B. Pellerin, J. M. Denis, *Phosphorus Sulfur Silicon Relat. Elem. 44* (1989) 27; J. L. Cabioch, J. M. Denis, *J. Organomet. Chem. 377* (1989) 227.
[8] For **3f**, the solid base was heated to 230 °C to minimize decomposition.
[9] T. E. Gier, *J. Am. Chem. Soc. 83* (1961) 1769; J. M. Garneau, A. Cabana, *J. Mol. Spectrosc. 87* (1981) 490.
[10] K. Ohno, Y. Yamamoto, H. Matsuura, H. Murata, *Chem. Lett. 1984*, 413.
[11] R. Appel, A. Westerhaus, *Tetrahedron Lett. 22* (1981) 2159.
[12] H. Eshtiagh-Hosseini, H. W. Kroto, J. F. Nixon, S. Brownstein, J. R. Morton, K. F. Preston, *J. Chem. Soc. Chem. Commun. 1979*, 653.
[13] B. Pellerin J. M. Denis, unpublished results. The ^{31}P chemical shift of **5f** ($\delta = 3.4$ [1 c]) obtained in a low-temperature NMR analysis of the thermolysis products of $ClCH_2PCl_2$ seems erroneous.

The reaction of **1** with the silver complex $Ag(OClO_3)(tht)$ (tht = tetrahydrothiophene) leads to the cationic complex **4**. Since tht is a readily displaceable ligand in gold complexes, **4** is a precursor for other cationic gold(II) complexes. For example, the cationic **5** is formed on addition of pyridine. Complexes **4** and **5** are the first cationic binuclear gold(II) complexes.

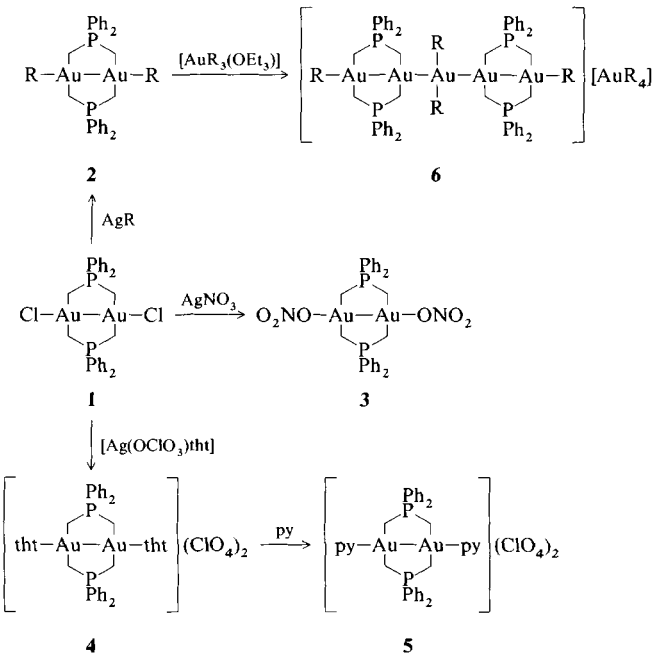

Scheme 1. Reactions of the binuclear gold(II) complex **1**. R = C_6F_5; tht = tetrahydrothiophene.

A Mixed-Valent Pentanuclear Gold Complex Containing a Linear $Au_5^{9\oplus}$ Chain**

By *Rafael Usón,* Antonio Laguna, Mariano Laguna, Josefina Jiménez* and *Peter G. Jones**

In 1988 we reported $[\{Au(CH_2)_2PPh_2\}_2Au(C_6F_5)_3]$,[1] the first oligonuclear gold complex with a gold(I)-gold(III) bond unsupported by covalent bridges. Here we report the synthesis and structure of a pentanuclear gold complex that has a linear chain of gold atoms in different oxidation states, $[Au^{III}]_2$-Au^{I}-$[Au^{III}]_2$. The central gold(I) atom, also unsupported by any covalent bridges, is linked to two gold(II) atoms.

Our starting complex is binuclear bridged **1** (Scheme 1), which is a good precursor for cationic and neutral binuclear gold(II) complexes. Complex **1** reacts with silver salts $Ag(C_6F_5)$ or $AgNO_3$ to afford the neutral complexes **2** (80% yield) or **3**[2] respectively. Complex **2** has been prepared by *Fackler* et al.[3] by a different method in slightly lower yield (62%).

The reaction of **2** with $[Au(C_6F_5)_3(OEt_2)]$ in the ratio 1:1 in dichloromethane led surprisingly to the pentanuclear cationic complex **6**, which possesses very unusual features. A stoichiometric formulation for the process is given in equation (a). The mother liquor after crystallization of **6** contains $C_{12}F_{10}$ (by ^{19}F NMR spectroscopy) together with unidentified products.

$$2\,\mathbf{2} + 2[AuR_3(OEt_2)] \longrightarrow \mathbf{6} + C_{12}F_{10} + 2\,Et_2O \qquad \text{(a)}$$
$$R = C_6F_5$$

Crystals of **6** suitable for X-ray studies were obtained from dichloromethane/petroleum ether as equidimensional red prisms. The crystals contain solvent, and thus had to be handled under inert oil to prevent cracking. The structure[4] of the cation of **6** is shown in Figure 1. Its backbone is a linear chain of five gold atoms (Au–Au–Au bond angles 176.3(1), 180°), all of which have square planar coordination geometry (maximum deviation from ideal angles 5.7°). The central atom Au1 lies on the symmetry centre $\frac{1}{4},\frac{1}{4},0$; the bond lengths are Au1–Au2 2.755(1), Au2–Au3 2.640(1) Å (cf. 2.769(1) Å across the eight-membered ring, 2.572(1) Å terminal in $[\{Au(CH_2)_2PPh_2\}_2Au(C_6F_5)_3]$).[1] The $[Au(C_6F_5)_4]^{\ominus}$ anion (not shown) lies with its Au atom (Au4) on the twofold axis $0,y,\frac{1}{4}$.

The assignment of oxidation states to the gold atoms of the pentanuclear cation is problematic. If the central atom Au1 is regarded as gold(I) in an anionic $[Au(C_6F_5)_2]^{\ominus}$ moiety, formed by reduction of the original gold(III) in $[Au(C_6F_5)_3(OEt_2)]$ by the two of $C_6F_5^{\ominus}$ leaving groups (one

[*] Prof. Dr. R. Usón, Dr. A. Laguna, Dr. M. Laguna, Josefina Jiménez, Departamento de Química Inorgánica, Instituto de Ciencia de Materiales de Aragón, Universidad de Zaragoza-C.S.I.C., 50009 Zaragoza, Spain
[*] Prof. Dr. P. G. Jones, Institut für Anorganische und Analytische Chemie der Technischen Universität, Hagenring 30, W-3300 Braunschweig (FRG)
[**] This work was supported by the Dirección General de Investigación Científica y Técnica (PB88-0075) and the Fonds der Chemischen Industrie.

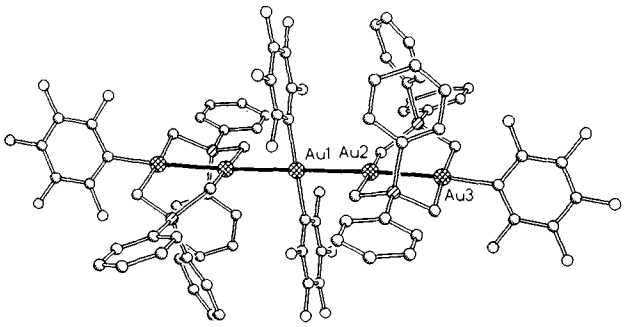

Fig. 1. The centrosymmetric cation of **6** in the crystal. Radii are arbitrary; H atoms omitted for clarity. Au–C bond lengths: at Au1 2.07 Å; Au2 2.10,2.10 Å; Au3 2.10,2.10 Å; and Au4 (not shown) 2.06,2.06 Å (estimated standard deviations 0.01 Å).

from each original gold(II) atom in **2**), then complex **6** is the first example of square planar gold(I). We prefer this description, but there is an alternative possibility: if Au1 is gold(III), part of a cationic $[Au(C_6F_5)_2]^{\oplus}$ moiety, then Au2 should be gold(I) and Au3 gold(II), again an unprecedented situation.

Received: September 6, 1990 [Z 4171]
German version: *Angew. Chem. 103* (1990) 190

[1] R. Usón, A. Laguna, M. Laguna, M. T. Tartón, P. G. Jones, *J. Chem. Soc. Chem. Commun. 1988*, 740.

[2] All the reported complexes were satisfactorily characterized by elemental analysis (C,H,N,Au) and IR spectroscopy. NMR spectra in $CDCl_3$: **2**: $\delta(^1H) = 7.96-7.26$ (m, 20H, Ph), 164 (d, 8H, CH_2, $^2J(P,H) = 9.8$ Hz); $\delta(^{31}P) = 43.3$ (s); $\delta(^{19}F) = -121.17$ (m, *o*-F), -160.96 (t, *p*-F), -161.79 (m, *m*-F). **3**: $\delta(^1H) = 7.58-7.26$ (m, 20H, Ph), 1.84 [d, 8H, CH_2, $J(P,H)$ 10.12 Hz]; $\delta(^{31}P) = 35.39$ (s). **4**: $\delta(^1H) = 7.7-7.32$ (m, 20H, Ph), 1.84 [d, 8H, CH_2, $J(P,H) = 11.53$ Hz], 2.99 (m, 8H, tht), 1.96 (m, 8H, tht); $\delta(^{31}P) = 41.7$ (s). **5**: $\delta(^1H) = 8.17-7.30$ (m, 30H, Ph, py), 1.87 [d, 8H, CH_2, $J(P,H) = 11.23$ Hz]; $\delta(^{31}P) = 39.7$ (s). **6**: $\delta(^1H) = 7.52-7.27$ (m, 40H, Ph), 2.07 [d, 8H, CH_2, $J(P,H) = 13.8$ Hz), 1.33 [d, 8H, CH_2, $J(P,H) = 11.2$ Hz]; $\delta(^{31}P) = 35.5$ (s, br); $\delta(^{19}F) = -117.27$ (m, 4F, *o*-F); -121.86 (m, 8F, *o*-F), -123.75 (m, 4F, *o*-F), -157.47 (t, 2F, *p*-F), -159.71 (t, 2F, *p*-F), -161.91 (t, 4F, *p*-F), -160.85 (m, 4F, *m*-F), -162.43 (m, 4F, *m*-F), -163.84 (m, 8F, *m*-F).

[3] H. H. Murray, J. P. Fackler, Jr., L. C. Porter, D. A. Briggs, M. A. Guerra, R. J. Lagow, *Inorg. Chem. 26* (1987) 357.

[4] Crystal data: $C_{104}H_{56}F_{40}P_4Au_6 \cdot xCH_2Cl_2$, monoclinic, $C2/c$, $a = 23.557(8)$, $b = 22.228(7)$, $c = 24.149(9)$ Å, $\beta = 112.03(3)°$, $V = 11722$ Å^3, $Z = 4$, $T = 178$ K, $R = 0.042$ for 6555 unique observed reflections. Further details of the crystal structure investigation may be obtained from the Fachinformationszentrum Karlsruhe, Gesellschaft für wissenschaftlich-technische Information mbH, W-7514 Eggenstein-Leopoldshafen 2 (FRG), on quoting the depository number CSD-54941, the names of the authors, and the journal citation.

$Li_4[FeN_2]$: A Nitridoferrate(II) with Anions Isosteric with CO_2. A Defect Variant of the Li_3N Type Structure.**

By *Axel Gudat, Rüdiger Kniep** and *Albrecht Rabenau*

Nitridoferrates were not well known up to now. Although *Frankenberger* et al.[1] prepared Li_3FeN_2 already in 1928 from Li_3N and elemental iron in a nitrogen atmosphere, the crystal structure was only determined in 1990 and proved to be a nitridoferrate(III), with infinite one-dimensional chains of tetrahedral $[FeN_2]^{3\ominus}$ units ($^1_\infty[FeN_{4/2}]^{3\ominus}$) isosteric with SiS_2.[2] Only recently nitridoferrates(III) with the anions $[FeN_3]^{6\ominus}$ isosteric with $[CO_3]^{2\ominus}$ were found in the ternary systems Ca-Fe-N and Ba-Fe-N:[3] $(Ca_3N)_2[FeN_3]$[4] and $Ba_3[FeN_3]$.[5] Now we report the synthesis of a nitridoferrate(II), which contains $[FeN_2]^{4\ominus}$ units isosteric with CO_2.

Nitridoferrates are a structural link in the series of lithium and alkali earth nitridometalates of transition metals studied thus far. Nitridometalates of transition metals with group numbers smaller than eight contain isolated tetrahedral anions, $[MN_4]^{n\ominus}$, where the metal is in its highest, or at least a high, oxidation state, for example $Li_7[V^VN_4]$,[6] $Li_6[Cr^{VI}N_4]$,[7] $Li_7[Mn^VN_4]$,[8] $Ba_3[Mo^{VI}N_4]$ and $Ba_3[W^{VI}N_4]$.[9] As 32-electron systems the tetrahedral anions $[MN_4]^{n\ominus}$ are related to the ortho acid anions (oxo anions). The partial anion structures of the nitridoferrates also satisfy isosteric principles; however, the transition metal frequently shows a tendency to form smaller coordination numbers (CN): CN = 4 for Fe^{III} in $Li_3[FeN_2]$, CN = 3 for Fe^{III} in $Ba_3[FeN_3]$ and CN = 2 for Fe^{II} in $Li_4[FeN_2]$. The low oxidation state and the linear coordination of iron in the anions $[FeN_2]^{4\ominus}$ establishes the bridge to the low valent nitridoniccolates, which also have a coordination number of two and anion structures $^1_\infty[NiN^{n\ominus}_{2/2}]$ (for example, $Ba[NiN]$,[10] $Sr_3[Li_3(NiN)_4]$[11] and $(Ba_8N)[NiN]_6$[12]).

Besides the thermodynamically stable $Li_3[FeN_2]$,[2] the ternary Li-Fe-N system also incorporates metastable phases[13, 14] formed by fast cooling or quenching the melt. In order to prepare $Li_4[FeN_2]$ we melted lithium (99%; Ventron; cut under argon) in an iron crucible (ST 37 K) under vacuum and allowed it to react with nitrogen (5.0; Oxysorb, $p(N_2) = 100-800$ mbar), while continually increasing the temperature to 900 °C. The melt was kept at this temperature for 5 h and then shocked into a water-cooled iron crucible inverted shortly before over the reaction vessel. The products obtained thus are sensitive to hydrolysis and have a dark metallic luster. Besides Li_3N, $Li_3[FeN_2]$, and amorphous phases, they consist of up to 80% of metastable mixed crystal phases of the Li_3N structure type[15–17] and its superstructure variants. The composition of the mixed crystal phases lies between $Li_2[(Li_{1-x}Fe_x)N]$ $(0 \le x \le 1)$ and $Li_2[(Li_{1-3x}Fe_x)N]$ $(0 \le x \le 0.33)$; that of the superstructure variants is $Li_4Fe_xN_2$ $(x = 1.0-1.04)$. Single crystals of $Li_4[FeN_2]$ were isolated under dry paraffin as orthogonal prisms from the quenched reguli.

The crystal structure of $Li_4[FeN_2]$[18] (Fig. 1) may be described as a defect type of the Li_3N-type structure[15, 16] $(Li_2Fe_{0.5}\square_{0.5}N)$, in which the Li_2N layers are linked by linearly coordinated iron(II). The orthorhombic unit cell results from the ordered distribution of Fe^{II} between the Li_2N layers. The identity period along [001] is twice as big as that of Li_3N. The anion partial structure of $Li_4[FeN_2]$ consists of isolated, CO_2-isosteric $[FeN_2]^{4\ominus}$ dumb-bells (16-electron system) with Fe–N bond lengths of 186(1) pm (Li–N bond lengths within the $^1_\infty[LiN_{2/2}]$ chains in Li_3N: 193.8(1) pm[16]). These bond lengths are longer than Fe^{III}–N bonds where CN = 3 (in $(Ca_3N)_2[FeN_3]$,[4] 177 (2) and in $Ba_3[FeN_3]$,[5] 173 (1) pm) and clearly shorter where CN = 4 ($Li_3[FeN_2]$,[2] 195 (1) pm). The shortest known Fe–N bond (166.1(1) pm) occurs in the tetraphenylporphyrinato complex $[(tpp)Fe]_2N$ within the linear Fe-N-Fe bridges.[19] In contrast to Li_3N the Li_2N layers in $Li_4[FeN_2]$ are slightly corrigated (deviation from an ideal plane ± 2.05 (5) pm). The average Li–N distance within the layers is 214 (2) pm and is only slightly

[*] Prof. Dr. R. Kniep,[+] Dipl.-Chem. A. Gudat, Prof. Dr. A. Rabenau (dec.)
Max-Planck-Institut für Festkörperforschung
Heisenbergstrasse 1, W-7000 Stuttgart 80 (FRG)

[+] Permanent address:
Eduard-Zintl-Institut der Technischen Hochschule
Hochschulstrasse 10, W-6100 Darmstadt (FRG)

[**] This research was supported by the Fonds der Chemischen Industrie and by the Freunde der Technischen Hochschule Darmstadt.

longer than 210.6 (1) pm for the Li_3N structure[16]; the lithium ions within these planar layers are responsible for the remarkably high ion conductivity of Li_3N[20].

The formation of $Li_4[FeN_2]$ by quenching or rapid cooling from the melt is consistent with a metastable character at least under normal conditions. Already in 1949 *Sachsze* and *Juza*[17] noticed that mixed crystal phases of the Li_3N type $(Li_{1-x}M_x)$ $[Li_2N]$ are obtained from Li_3N and the transition metals M = Co, Ni, Cu under nitrogen at temperatures between 500 and 600 °C (i.e. probably from solid–gas reactions), but only $Li_3[FeN_2]$ when M = Fe.[1, 2] By quenching the melt such mixed crystal phases for M = Fe are formed besides primary crystallization products with an orthorhombic superstructure of the Li_3N type (*Cmmm*; $a = 741.3$ (2), $b = 1283.4$ (4), $c = 753.7$ (2) pm) in which the Li_2N layers are linked exclusively via iron–nitrogen contacts. In contrast to $Li_4[FeN_2]$ (Fig. 1), the iron positions are only partly occupied, so that besides isolated FeN_2 dumb-bells, chains of $^1_\infty[Fe_xN_{2/2}]$ $(x < 1)$ are also formed, which run parallel to the [001] direction. Several room-temperature structure investigations performed on one of the orthorhombic crystals (chemical composition from the first crystal structure analysis: $Li_4Fe_{1.04}N_2$) revealed continual place-changing of the iron atoms while the Li_2N layers were preserved. Over a long period this topotactic reaction leads finally to the formation of $Li_4[FeN_2]$ under polysynthetic twinning and secretion of the minimal excess of iron at the grain boundaries. Thus no single crystals of $Li_4[FeN_2]$ could be isolated and the crystal structure determination was carried out with a triplet crystal.[18–20]

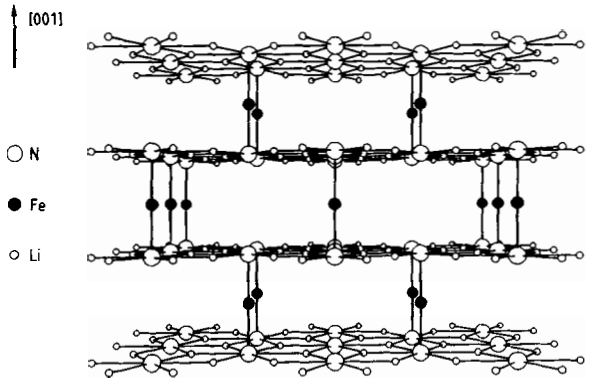

Fig. 1. Section of the crystal structure of $Li_4[FeN_2]$

Received: September 27, 1990 [Z 4207 IE]
German version: *Angew. Chem. 103* (1991) 217

CAS Registry numbers:
$Li_4[FeN_2]$, 131323-27-8; $Li_4Fe_{1.04}N_2$, 131378-93-3; lithium, 7439-93-2; iron, 7439-89-6; nitrogen, 7727-37-9.

[1] W. Frankenburger, L. Andrussow, F. Dürr, *Z. Elektrochem. 34* (1928) 632.
[2] A. Gudat, R. Kniep, A. Rabenau, W. Bronger, U. Ruschewitz, *J. Less-Common Met. 161* (1990) 31.
[3] P. Höhn, *Diplomarbeit*, Technische Hochschule Darmstadt 1990.
[4] G. Cordier, P. Höhn, R. Kniep, A. Rabenau, *Z. Anorg. Allg. Chem.*, in press.
[5] P. Höhn, R. Kniep, A. Rabenau, *Z. Kristallogr.*, in press.
[6] R. Juza, W. Gieren, J. Haug, *Z. Anorg. Allg. Chem. 300* (1959) 61.
[7] A. Gudat, S. Haag, R. Kniep, A. Rabenau, *Z. Naturforsch. B45* (1990) 111.
[8] R. Juza, E. Anschütz, H. Puff, *Angew. Chem. 71* (1959) 161.
[9] A. Gudat, P. Höhn, R. Kniep, A. Rabenau, *Z. Naturforsch. B*, in press.
[10] A. Gudat, S. Haag, R. Kniep, A. Rabenau, *J. Less-Common Met. 159* (1990) L29.
[11] A. Gudat, R. Kniep, A. Rabenau, *Z. Anorg. Allg. Chem.*, in press.
[12] A. Gudat, W. Milius, S. Haag, R. Kniep, A. Rabenau, *J. Less-Common Met.*, in press.
[13] A. Gudat, S. Haag, R. Kniep, A. Rabenau, *32nd IUPAC Congress* (Stockholm 1989), Abstract 407, p. 84.
[14] A. Gudat, *Dissertation*, Universität Düsseldorf 1990.
[15] E. Zintl, G. Brauer, *Z. Elektrochem. 41* (1935) 102.
[16] A. Rabenau, H. Schulz, *J. Less-Common Met. 50* (1976) 155.
[17] W. Sachsze, R. Juza, *Z. Anorg. Allg. Chem. 259* (1949) 278.
[18] $Li_4[FeN_2]$: structure determination and crystallographic data: orthorhombic, *Immm*; $a = 371.0$ (1), $b = 641.3$ (4), $c = 753.6$ (2) pm; $Z = 2$; 472 measured, 139 independent reflections; $R = 0.072$. Philips PW 1100 single crystal diffractometer; $Mo_{K\alpha}$, 300 K. Solution of structure on a triplet crystal[20]; relationship of the triplet units (nonoverlapping reflections of layers *hk*1 and *hk*3) 1:0.5:0.4. Further details of the crystal structure investigation may be obtained from the Fachinformationszentrum Karlsruhe, Gesellschaft für wissenschaftlich-technische Information mbH, W-7514 Eggenstein-Leopoldshafen 2 (FRG) on quoting the depository number CSD-55008, the names of the authors and the journal citation.
[19] W. R. Scheidt, D. A. Summerville, I. A. Cohen, *J. Am. Chem. Soc. 98* (1976) 6623.
[20] A. Rabenau, *Solid State Ionics 6* (1982) 277.
[21] W. R. Busing, K. O. Martin, H. D. Levy: Program system SFLS (a modified version of the classic program, ORFLS, for the refinement of crystal structures); extended version: M. Eitel, H. Bärnighausen, Universität Karlsruhe 1986.

Synthesis of the 2,3-Epoxy-2,3-dihydro-2,3-dimethylbenzo[*b*]furan, the Proposed Ultimate Mutagen of the Benzofuran Dioxetanes**

By *Waldemar Adam,* Lazaros Hadjiarapoglou, Thomas Mosandl, Chantu R. Saha-Möller*, and *Dieter Wild*

Furans can be metabolized by mixed function oxidases[1] into epoxides and these in turn are usually responsible for cellular damage. A well-known case is the potent mutagen and carcinogen aflatoxin B_1, a 2,3-dihydrofuran derivative, whose ultimate DNA-binding metabolite is the epoxide. The latter was recently prepared and shown to be a potent mutagen[2]. Since 2,3-dimethylbenzo[*b*]furan is used as a flavoring ingredient in foods,[3] we have been concerned with the possibility that its epoxide may induce DNA damage. In contrast to the reasonably stable 2,3-dihydrofuran epoxides,[2, 4] to date no furan epoxides have been isolated or detected; attempted epoxidation, even at low temperatures, afforded complex product mixtures.[5] Herein, we report the synthesis of the first benzofuran epoxides **2** by two independent routes (Scheme 1), one involving epoxidation of the benzofurans **1** with dimethyldioxirane and the other involving deoxygenation of the benzofuran dioxetane **3a** with dimethyl sulfide. Moreover, we implicate the benzofuran epoxides **2** as the ultimate compounds responsible for the high mutagenic activity in the *Salmonella typhimurium* strain TA 100 observed with benzofuran dioxetanes **3**;[6] these are the first dioxetanes which exhibit potent mutagenicity. We postulate that

[*] Prof. Dr. W. Adam, Dr. L. Hadjiarapoglou, Dr. T. Mosandl, Dr. C. R. Saha-Möller
Institut für Organische Chemie der Universität
Am Hubland, W-8700 Würzburg (FRG)
Dr. D. Wild
Institut für Pharmakologie und Toxikologie
der Universität Würzburg (FRG)

[**] Financial support of this work by the Deutsche Forschungsgemeinschaft (SFB 172 "Molekulare Mechanismen kanzerogener Primärveränderungen") and the Wilhelm-Sander-Stiftung is gratefully appreciated.

the in situ deoxygenation of polycyclic arene and heteroarene dioxetanes with formation of reactive epoxides may contribute significantly to cellular DNA damage.[7]

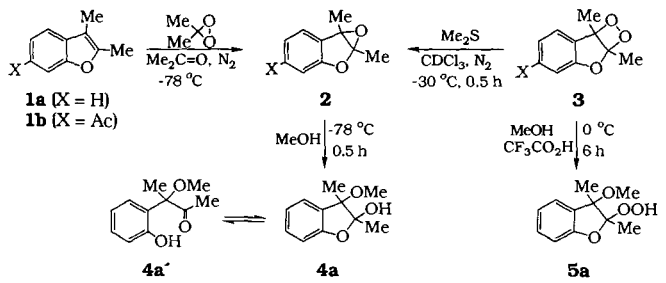

Scheme 1.

On treatment of a 0.22 M solution of benzofuran **1a** with stoichiometric amounts of a 0.05 M solution of [D_6]dimethyldioxirane in [D_6]acetone at $-78\,^{\circ}C$,[8] ^{13}C-NMR monitoring revealed after 0.5 h that the olefinic resonances of **1a** at $\delta = 109.7$(s) and 150.3(s) were replaced by the characteristic epoxide resonances for **2a** at $\delta = 66.9$(s) and 95.1(s). Analogous results were observed on reaction of the benzofuran **1b** with dimethyldioxirane to give the corresponding epoxide **2b** [^{13}C NMR ([D_6]acetone): $\delta = 66.5$ (s, C-3), 95.9 (s, C-2)]. The epoxide **2a** was also obtained on treatment of a 0.337 M solution of benzofuran dioxetane **3a** with stoichiometric amounts of a 0.337 M solution of dimethyl sulfide in $CDCl_3$ at $-30\,^{\circ}C$.[9] On warming the epoxide solutions above $0\,^{\circ}C$, complete decomposition resulted within 0.5 h.

The chemical reactivity of the epoxide **2a** manifested itself in the formation of the adduct **4a** (Scheme 1); complete conversion was observable 0.5 h after addition of methanol at $-78\,^{\circ}C$ (Scheme 1). The semiacetal **4a** was isolated in 95% yield as a *cis/trans* mixture; present in tautomeric equilibrium with the hydroxyketone (**4a**:**4a'** = 87:13).[10] In contrast, the dioxetane **3a** was stable towards methanol under these conditions; however, in the presence of traces of CF_3COOH complete methanolysis took place within 6 h at ca. $0\,^{\circ}C$ to give hydroperoxide **5a**[10] (Scheme 1). Similar reactivity differences were observed towards water as nucleophile.

These chemical transformations illustrate the labile character of the novel benzofuran epoxides **2**, and particularly their propensity to serve as alkylating agents. As expected, they also induced mutations in *Salmonella typhimurium* strain TA 100, a strain mutating especially in response to alkylation and pyrimidine dimerization in DNA. Incubation of Salmonella bacteria with epoxide **2a** (0.1–1 mM for 0.5 h) led to a linear, dose-dependent increase of revertants; the specific mutagenic activity was calculated to be ca. 1800 revertants per µmol. Treatment of acetone solutions of epoxide **2a** with aqueous phosphate buffer prior to incubation of the bacteria revealed decreased mutagenic activity with increasing pretreatment time. Apparently most of the labile benzofuran epoxide **2a** was hydrolyzed in the aqueous solution prior to reaching the DNA target.

Significant in this respect is the potent mutagenicity of the corresponding benzofuran dioxetanes **3a**.[6] Employing the standard procedure of the Ames test[11] (*Salmonella typhimurium* strain TA 100), **3a** induced ca. 117 000 and dioxetane **3b** ca. 370 000 revertants per µmol; these compounds are the first potent mutagens possessing the dioxetane structure; in the strain TA 2638, these dioxetanes were not mutagenic. This suggests that the damage is not due to active oxygen species which are generally involved in the genotoxicity of peroxides.[12] Furthermore, the damage in strain TA 100 could not be photoreactivated; it is, therefore, unlikely that the observed mutagenicity is of photochemical origin, e.g. due to pyrimidine dimerization,[12, 13] despite the fact that the strain TA 100 responds to such DNA damage.

In view of the similarity in the mutagenic action of the benzofuran epoxides **2** and dioxetanes **3**, we propose that the former are the ultimate mutagens of the latter. It is unlikely that the dioxetanes **3** are directly alkylating the DNA, because nucleophilic addition of methanol to the dioxetane **3a** requires acid catalysis and is slow compared to that for the epoxide **2** (Scheme 1). Since the dioxetanes **3** can be efficiently deoxygenated by sulfides to the corresponding epoxides **2**, an attractive chemical pathway is available for in situ generation of such reactive heteroarene oxides from the corresponding dioxetanes. Indeed, a model experiment showed that an aqueous solution of the biologically pertinent sulfide L-methionine effected the deoxygenation of the benzofuran dioxetane **3a** to the epoxide **2a** at $0\,^{\circ}C$, as confirmed by isolation of its hydrolysis product 2,3-dihydro-2,3-dimethylbenzo[*b*]furan-2,3-diol[10] in over 90% yield. Consequently, such deoxygenations of dioxetanes into epoxides by biological sulfides are feasible in cellular systems.

The provocative hypothesis put forth presently, that appropriate dioxetanes such as those derived from benzofurans may serve as precursors of mutagenic epoxides, constitutes an unusual and hitherto unrecognized mode for the induction of mutations. This novel mutagenic mechanism rests on the following key facts: the labile benzofuran epoxides **2** could be isolated for the first time, the benzofuran dioxetanes **3** could be deoxygenated with sulfides to these epoxides **2**, and finally mutagenic activity, similar in quality, could be demonstrated for the epoxides **2** and dioxetanes **3** in *Salmonella typhimurium* strain TA 100. We speculate that this new mutagenicity route may potentially possess wide scope, in that quite generally polycyclic arenes, such as benzo[a]pyrene, or polycyclic heteroarenes, such as furocoumarins, may be oxygenated to epoxides via the corresponding dioxetanes. In fact, in the mutagenic activity of benzo[a]pyrene a dioxetane has been implicated previously[7a, b], but the possibility that the dioxetane might serve also as precursor of its epoxide, analogous to the route **1** → **3** → **2**, has not yet been considered.

Received: October 8, 1990 [Z 4233 IE]
German version: *Angew. Chem. 103* (1991) 187

CAS Registry numbers:
1a, 3782-00-1; **1b**, 1642-79-1; **2a**, 131588-87-9; **2b**, 131588-88-0; **3a**, 33973-15-8; **4a**, 131588-89-1; **4a'**, 131588-90-4; **5a**, 131588-91-5.

[1] B. W. Jennings, J. C. Hurley, S. K. Reeder, A. Holian, P. Lee, C. N. Caughalan, R. D. Larsen, *J. Org. Chem. 41* (1976) 407.
[2] S. W. Baertschi, K. D. Raney, M. P. Stone, T. M. Harris, *J. Am. Chem. Soc. 110* (1988) 7929.
[3] B. L. Oser, R. A. Ford, *Food Technol. 32* (1978) 60.
[4] L. Troisi, L. Cassidei, L. Lopez, R. Mello, R. Curci, *Tetrahedron Lett. 30* (1989) 123.
[5] a) V. Ravindranath, L. T. Burka, M. R. Boyd, *Science (Washington D.C.) 224* (1984) 884; b) L. O. Ruzo, J. E. Casida, I. Holden, *J. Chem. Soc. Chem. Commun. 1985*, 1642; *J. Agric. Food. Chem. 33* (1985) 622; c) K. Manfredi, S. B. Gingerich, P. W. Jennings, *J. Org. Chem. 50* (1985) 535.
[6] W. Adam, A. Beinhauer, T. Mosandl, C. Saha-Möller, F. Vargas, B. Epe, E. Müller, D. Schiffmann, D. Wild, *Environ. Health Perspect. 88* (1990) 89.
[7] a) J. L. Seed, K. G. Specht, T. A. Dahl, W. R. Midden, *Photochem. Photobiol. 50* (1989) 625; b) A. Thompson, J. R. Lever, K. A. Canella, K. Miura, G. H. Posner, H. H. Seliger, *J. Am. Chem. Soc. 108* (1986) 4498; c) K. Yoshikawa, N. Mori, S. Sakakibava, N. Mizuno, P.-S. Song, *Photochem. Photobiol. 29* (1979) 1127.

[8] a) W. Adam, R. Curci, J. O. Edwards, *Acc. Chem. Res. 22* (1989) 205; b) R. W. Murray, *Chem. Rev. 89* (1989) 1187; c) R. Curci in A. L. Baumstark (Ed.): *Advances in Oxygenated Processes*, JAI Press, Greenwich, NC, USA 1990, Vol. 2, Chapter 1.
[9] D. R. Berdahl, H. H. Wasserman, *Isr. J. Chem. 23* (1983) 409.
[10] All the new compounds were fully characterized on the basis of their elemental analyses and spectral data (IR, ^{1}H and ^{13}C NMR, and MS).
[11] D. M. Maron, B. N. Ames, *Mutat. Res. 113* (1983) 173.
[12] W. Adam, A. Beinhauer, B. Epe, R. Fuchs, A. Griesbeck, H. Hauer, P. Mützel, L. Nassi, D. Schiffmann, D. Wild in T. Friedberg, F. Oesch (Eds.): *Primary Changes and Control Factors in Carcinogenesis*, Deutscher Fachschriften-Verlag, Wiesbaden 1986, p. 64.
[13] a) G. Cilento, W. Adam, *Photochem. Photobiol. 48* (1988) 361; b) A. A. Lamola, *Biochem. Biophys. Res. Commun. 43* (1971) 893; c) J. W. Lown, R. R. Koganty, K. R. Kopecky, *Photobiochem. Photobiophys. 12* (1986) 295.

The Diels–Alder Dimer of 6-Hydroxy-2,6-dimethylcyclohexa-2,4-dienone, an Unusual Metabolite in the Bacterial Degradation of 2,6-Xylenol**

By *Helmut Kneifel, Carmen Poszich-Buscher, Susanne Rittich,* and *Eberhard Breitmaier**

The pathways of the microbial degradation of most phenols which occur, e.g., in soils polluted with waste materials from former coke ovens, are well known.[1] Only 2,6-xylenol **1** was for a long time considered as biologically non-degradable; a possible degradation route was first proposed as late as 1987.[2, 3] The special feature of **1** in comparison to other phenols is that its two methyl groups *ortho* to the OH group block *ortho*-hydroxylation of the aromatic ring.

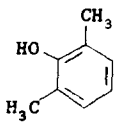

1

A complete degradation of 2,6-xylenol **1** via a hydroxylation in the 3- or 4-position with subsequent ring cleavage was achieved with a mixed culture, which besides containing pseudomonads also contains other still unidentified bacteria. When this mixed culture, however, is allowed to propagate over a long period of time on a mixed substrate of cresol isomers and phenol and **1** is added as further source of carbon and energy at high biomass concentration during the logarithmic growth phase, not only the oxidation products 2,6-dimethylhydroquinone, 2,6-dimethyl-1,4-benzoquinone, and 2-hydroxy-3,5-dimethyl-1,4-benzoquinone but also a new metabolite accumulates in the culture medium. This dead-end metabolite can be extracted with ethyl acetate and purified by preparative reversed-phase HPLC ($k' = 2.8$ upon HPLC on ODS-1 with acetonitrile/0.1% aqueous phosphoric acid 35/65 as eluent). The product absorbs strongly in the UV (λ_{max} = 242, 308 nm, lg ε_{max} = 3.84, 2.38); the GC-MS spectrum of the trimethylsilyl derivative shows peaks at m/z = 210 ($M^{\oplus}$), 195, 180, 167, 75, and 73 (100%).

Elucidation of the structure was accomplished, using 2 mg of substance, by ^{1}H- and ^{13}C-NMR methods. The ^{13}C-NMR spectrum of the metabolite shows 16 signals, yet the mass spectrum of the trimethylsilyl derivative indicates an empirical formula $C_8H_{10}O_2$ for the metabolite. H,H-COSY, C,H-COSY, and C,H-COLOC experiments identified the partial structures **2** and **3** ($\delta(^1H)$ italic figures, $\delta(^{13}C)$ upright figures in the formulas).

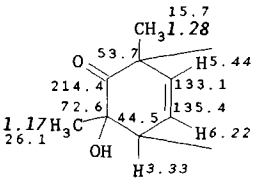

2

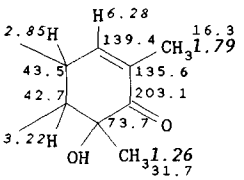

3

The coupling of the fragments **2** and **3** is possible in two ways; realized is the constitution **4**, as follows from the NOE difference spectra, which show a strong NOE between the methyl protons of **2** at δ = 1.28 and the alkene proton of **3** at δ = 6.28 (Scheme 1).

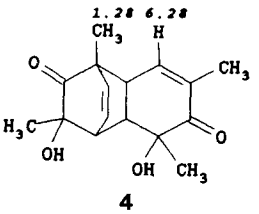

4

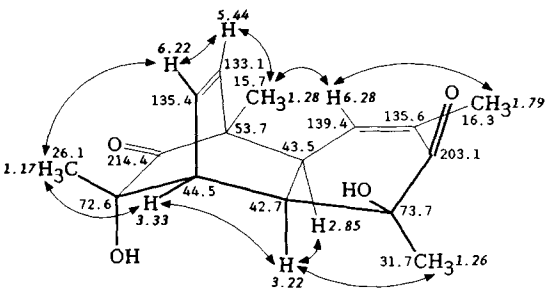

Scheme 1. NMR spectroscopic characterization of the 2,6-xylenol oxidation product **4**. The arrows link the H atoms between which a NOE occurs.

An NOE between the alkene proton of **2** at δ = 6.22 and the methyl protons of **2** at δ = 1.17 establishes the relative configuration of the respective methyl group (*exo*). The *exo* coupling of the six-membered ring follows, in particular, from the NOE between the methyl protons of **3** at δ = 1.26 and the bridgehead proton of **3** at δ = 3.22 as well as the absence of effects between the alkenyl proton pair with δ = 5.44/6.22 (**2**) and the bridgehead proton pair with δ = 2.85/3.22 (**3**). Also the mirror image of the structure shown in Scheme 1 would be possible, since, as a rule, enantiomers are not differentiated by NMR spectroscopy. That no corresponding peak for **4** appears in the mass spectrum can be explained in terms of a retro-Diels-Alder reaction of **4** in the GC-MS apparatus.

[*] Prof. Dr. E. Breitmaier
Institut für Organische Chemie und Biochemie der Universität
Gerhard-Domagk-Strasse 1, W-5300 Bonn 1 (FRG)
Prof. Dr. H. Kneifel, Dipl.-Biol. C. Poszich-Buscher, Dipl.-Biol. S. Rittich
Institut für Biotechnologie 3, Forschungszentrum Jülich
Postfach 1913, W-5170 Jülich (FRG)

[**] This work was supported by the Bundesminister für Forschung und Technologie and by Biodetox, Ahnsen.

The metabolite **4**, which must be formulated as *exo*-3,10-dihydroxy-3,5,8,10-tetramethyltricyclo[6.2.2.$0^{2,7}$]dodeca-5,11-diene-4,9-dione, has already been described in the literature as a product of the oxidation of 2,6-xylenol **1** with sodium periodate.[4] As optically active natural product ($[\alpha]_D^{20} = -39.6°$, $c = 2.6$, $CHCl_3$), in contrast to the synthetic product, it is nevertheless new, as shown by a CAS on-line search. Metabolite and authentic substance prepared by the method described in Ref. [4] have identical HPLC retention times, IR, UV, and NMR spectra.

The metabolite **4** could be formed by Diels-Alder dimerization of the cyclohexadienone **5**, which is formed from **1** by oxidation. The methyl groups prevent a tautomerization of the dienone **5** to a pyrocatechol derivative.

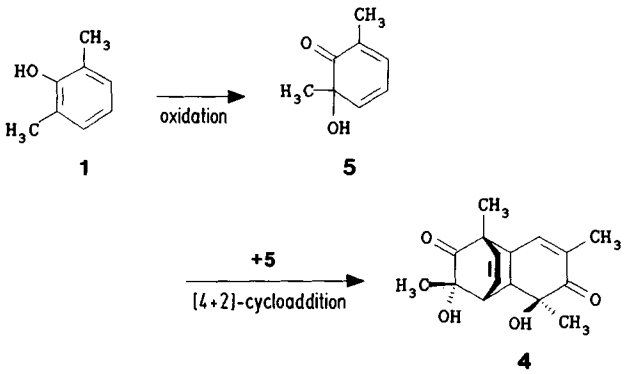

1 **5** **4**

The formation of a 6-hydroxy-2,4-cyclohexadienone such as **6** in biological transformations of phenols has until now never been observed. Since there are numerous naturally occurring phenols with substituents in the 2- and 6-position—in particular methoxy groups are frequent, e.g. in syringic acid—*ortho*-hydroxylations of the type **1** → **5** could be of general importance.

Received: September 17, 1990 [Z 4182 IE]
German version: *Angew. Chem. 103* (1991) 189

CAS Registry number:
4, 35018-89-4.

[1] P. J. Chapman: *Degradation of Synthetic Organic Molecules in the Biosphere*, National Academy of Sciences, Washington, D C, USA, 1972, p. 17; See also H. G. Schlegel, *Allgemeine Mikrobiologie*, Thieme Verlag, Stuttgart, 6th Edit., 1985, p. 423.
[2] J. Evers, *Diplomarbeit*, Wuppertal 1987.
[3] J. Evers, M. A. Rubio, H. J. Knackmuss, D. Freier-Schröder, *Appl. Environ. Microbiol. 55* (1989) 2904.
[4] E. Adler, J. Dahlen, G. Westin, *Acta Chem. Scand. 14* (1960) 1580.

Chelate Complexes with Triisocyanide Ligands**

By *F. Ekkehardt Hahn** and *Matthias Tamm*

Isocyanide ligands form stable complexes of the type $[^{99m}Tc(CNR)_6]^{\oplus}$, which find application in the scintographic myocardium imaging[1] because of excellent radiophysical properties of the metastable isotope ^{99m}Tc.[2] During the search for particularly stable isocyanide complexes we prepared the potentially chelating triisocyanide ligands talc (3,3′,3″-nitrilotripropylisocyanide) and tarc (2,2′,2″-[nitrilotris(trimethyleneoxy)]triphenylisocyanide) (Fig. 1) and studied their coordination chemistry paying particular attention to chelate formation.

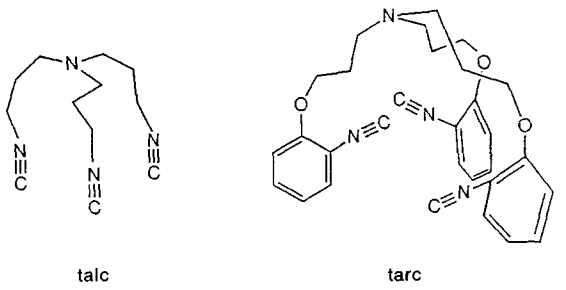

talc tarc

Fig. 1. Structural formulas for the ligands talc and tarc.

Little is known about the coordination chemistry of multidentate isocyanide ligands. The near linearity of the M–C≡N–R unit in metal complexes normally prevents the formation of chelate complexes analogous to those of diphosphanes and diamines. The known bridging di-[3] and triisocyanide ligands[4] do not form chelate complexes where one or more of the isocyanide functions coordinate to the same metal. Triisocyanide ligands which have isocyanide functions linked through longer alkyl chains could, however, act as chelating ligands. Talc and tarc are such examples.

The talc ligand was synthesized according to Scheme 1. We were surprised at the formation of bis(3-aminopropyl)amine

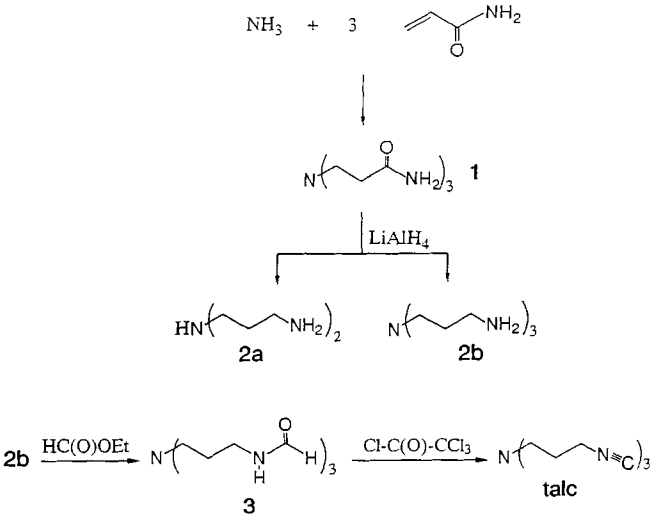

Scheme 1. Synthesis of talc.

(**2a**)[6] besides the desired tris(3-aminopropyl)amine (**2b**)[6] on reduction of **1**.[5] Reaction of **2b** with ethyl formate yields N,N′,N″-[nitrilotris(trimethylene)]triformamide quantitatively. The isocyanide functions of talc were introduced using the method of *Ugi* et al.[7] Talc is a yellow liquid that freezes at −20 °C and is soluble in alcohols, and aromatic and chlorinated hydrocarbons. The ^1H NMR spectrum shows the typical isocyanide[8] ^1H–^{14}N long-range coupling (H_y in Fig. 2);[6] different values for the two ^{13}C–^{14}N coupling constants are observed in the ^{13}C NMR spectrum.[6]

Talc crystallizes from ethanol at −78 °C. The X-ray structure (Fig. 3)[9] shows that talc is monomeric and gives

[*] Priv.-Doz. Dr. F. E. Hahn, Dipl.-Chem. M. Tamm
Institut für Anorganische und
Analytische Chemie der Technischen Universität
Strasse des 17. Juni 135, W-1000 Berlin 12 (FRG)
and
Institut für Diagnostikforschung an der Freien Universität Berlin

[**] Metal Chelates with Medical Implications, Part 4. Part 3: [12]

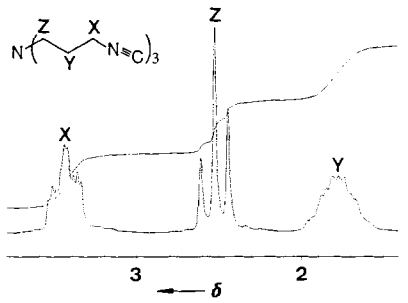

Fig. 2. ^{1}H NMR spectrum of talc.

an accurate N≡C distance for aliphatic isocyanides (1.135(3) Å) which is significantly shorter than the N≡C length determined by electron diffraction for CF_3NC (1.1726(2) Å)[10] or CH_3NC (1.166(1) Å).[11]

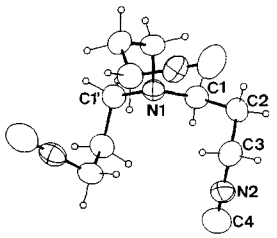

Fig. 3. Structure of talc in the crystal (ORTEP). Selected bond lengths [Å] and bond angles [°]: N2-C3 1.429(3), N2-C4 1.135(3); C3-N2-C4 176.6(2).

The ligand tarc is formed by Williamson etherification of tris(3-chloropropyl)amine[12] with three equivalents of *o*-nitrophenol, reduction of the nitro groups (analogous to reaction **1** → **2b**), formylation of the phenylamine functions with formic acid (analogous to the reaction **2b**→**3**) and the transformation of the thus formed formamide functions into isocyanide functions by the method of *Ugi* et al.[7] The yellow crystalline solid could be completely characterized.[6] Tarc is soluble in THF, CH_2Cl_2 and $CHCl_3$, but only slightly soluble in toluene and benzene.

To test the chelating ability of the new ligands we reacted them with $[(C_7H_8)M(CO)_3]$ (M = Cr, Mo, W) in dichloromethane[13] and examined the products by IR spectroscopy (Table 1) and in part by X-ray crystallography. The IR spectra show that octahedral, facial complexes with C_{3v} symmetry were formed. Whereas no significant shift in frequency for NC and CO absorptions occurs within the series *fac*-[(tarc)M(CO)$_3$], M = Cr, Mo, W, a comparison of the IR spectra of *fac*-[(talc)W(CO)$_3$] and *fac*-[(tarc)W(CO)$_3$] reveals that the aromatic isocyanide, tarc, is a weaker σ donor and a better π acceptor than talc, since the CO stretching frequencies appear at higher and the NC frequencies at lower wavenumbers than for *fac*-[(talc)W(CO)$_3$].

Table 1. IR data of talc, tarc, *fac*-[(talc)W(CO)$_3$], and *fac*-[(tarc)M(CO)$_3$] (M = Cr, Mo, W).

Compound	ν(NC) [cm^{-1}]		ν(CO) [cm^{-1}]	
	A_1	E	A_1	E
talc	2148			
fac-[(talc)W(CO)$_3$]	2160	2115	1932	1854
tarc	2118			
fac-[(tarc)Cr(CO)$_3$]	2140	2078	1940	1885
fac-[(tarc)Mo(CO)$_3$]	2138	2079	1940	1888
fac-[(tarc)W(CO)$_3$]	2137	2068	1933	1878

On crystallization from dichloromethane *fac*-[(tarc)-W(CO)$_3$ · HCl] forms with 2.5 molecules of solvent per formula unit (Fig. 4). The X-ray structure[9] shows that tarc is

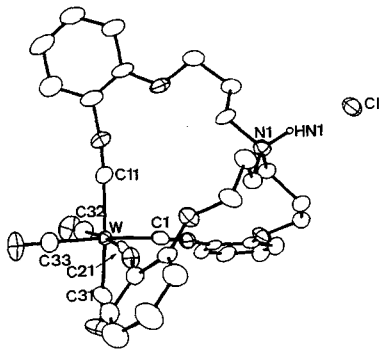

Fig. 4. Structure of *fac*-[(tarc)W(CO)$_3$ · HCl] in the crystal (ORTEP). Selected bond lengths [Å] and bond angles [°]: W-C1 2.109(7), W-C11 2.107(4), W-C21 2.126(7), W-C31 1.988(4), W-C32 1.965(5), W-C33 1.995(7), N1-HN1 0.74(7), HN1 · · · Cl 2.27(7); C1-W-C11 93.6(2), C1-W-C21 98.6(2), C1-W-C31 87.7(2), C1-W-C32 87.6(2), C1-W-C33 174.9(2), C11-W-C21 93.3(2), C11-W-C31 175.4(2), C11-W-C32 88.6(2), C11-W-C33 91.1(2), C21-W-C31 90.8(2), C21-W-C32 173.3(2), C21-W-C33 83.2(2), C31-W-C32 87.1(2), C31-W-C33 87.5(2), C32-W-C33 90.4(2).

indeed a chelating ligand occupying the three facial positions with only slight distortion of the octahedron. Thus the ability of tripodal polyisocyanide ligands to form chelate complexes has been demonstrated unequivocally for the first time.

In *fac*-[(tarc)W(CO)$_3$] the tungsten atoms forms three 18-membered rings with the ligand. These belong among the largest chelate rings known in organometallic compounds. The central nitrogen atom is in the "out" conformation. This is extremely rare for chelating tripodal ligands, as may be seen by comparison with the structures of the tricatechol complexes K_3[V(trencam)][14] and Na_3[Fe(L)] (L = macrocyclic bicapped trencam derivative).[15] The reason for the protonation is unclear. The reaction of the complexed tarc with HCl impurities in solution is improbable, as the free ligand does not form a hydrochloride adduct in dichloromethane. More likely is that the inversion of the central nitrogen atom is hindered by complexation and thus is a strong enough base to react with dichloromethane with concomitant HCl formation.

Structure determinations on aromatic W^0 isocyanides have not yet been undertaken. The W–C bond lengths are, however, in good agreement with values for a W^{II}-*tert*-butylisocyanide.[16]

Received: September 27, 1990 [Z 4215 IE]
German version: *Angew. Chem. 103* (1991) 213

[1] M. J. Clarke, L. Podbielski, *Coord. Chem. Rev. 78* (1987) 253.
[2] H. Münzel in H. K. Kugler, C. Keller (Hrsg.): *Gmelin Handbook of Inorganic Chemistry, Technetium, Supplement Vol. 1*, Springer, Berlin 1982.
[3] K. R. Mann, R. A. Bell, H. B. Gray, *Inorg. Chem. 18* (1979) 2671.
[4] R. A. Michelin, R. J. Angelici, *Inorg. Chem. 19* (1980) 3853.
[5] F. E. Hahn, M. Tamm, *Acta Crystallogr. Sect. C 46* (1990), 1567.
[6] Correct elemental analyses were obtained for all new compounds. Selected physical data: **2a**: M.p. 70 °C/0.05 mbar; ^{1}H NMR (80 MHz, $CDCl_3$): δ = 2.38 (m, 8H; HNCH_2CH_2, CH$_2$CH_2NH$_2$), 1.29 (quint., 4H; CH$_2$CH_2CH$_2$), 0.85 (s, 5H; HNCH$_2$, CH$_2$NH$_2$); ^{13}C NMR (20.15 MHz, $CDCl_3$): δ = 46.9 (HNCH_2CH$_2$), 39.4 (CH$_2$CH_2NH$_2$), 32.8 (CH$_2$CH_2CH$_2$). **2b**: M.p. 110 °C/0.05 mbar; ^{1}H NMR (80 MHz, $CDCl_3$): δ = 2.20 (t, 6H; CH$_2$CH_2NH$_2$), 1.95 (t, 6H; NCH_2CH$_2$), 1.05 (quint., 6H; CH$_2$CH_2CH$_2$), 0.78 (s, 6H; NH$_2$); ^{13}C-NMR (20.15 MHz, $CDCl_3$): δ = 50.7 (NCH$_2$CH$_2$), 39.4 (CH$_2$CH$_2$NH$_2$), 29.9 (CH$_2$CH$_2$CH$_2$). – talc: ^{1}H NMR (400 MHz, $CDCl_3$): δ = 3.48 (tt, ^3J(H,H) = 6.5, ^2J(N,H) = 2 Hz, 6H; CH$_2$CH$_2$NC), 2.54 (t, ^3J(H,H) = 6.5 Hz, 6H; NCH$_2$CH$_2$), 1.76

(m, 6H; $CH_2CH_2CH_2$); ^{13}C NMR (20.15 MHz, $CDCl_3$): δ = 156.54 (t, $^1J(C,N)$ = 5.60 Hz; CH_2NC), 49.75 (NCH_2CH_2), 39.13 (t, $^1J(C,N)$ = 6.35 Hz; CH_2NC), 26.36 ($CH_2CH_2CH_2$). – tarc: ^1H NMR (80 MHz, $CDCl_3$): δ = 7.38–6.32 (m, 12H; H_{aryl}), 3.91 (t, 6H; CH_2CH_2O), 2.69 (t, 6H; NCH_2CH_2), 2.03 quint., 6H; $CH_2CH_2CH_2$); ^{13}C NMR (20.15 MHz, $CDCl_3$): 167.6 (br. s, N≡C), 154.1, 130.2, 127.2, 119.1 (C_{aryl}), 115.9 (br. s, C-NC), 112.1 (C_{aryl}), 65.5 (CH_2CH_2O), 48.4 (NCH_2CH_2), 26.1 ($CH_2CH_2CH_2$).

[7] I. Ugi, R. Meyr, *Chem. Ber. 93* (1960) 239.

[8] I. D. Kuntz, P. von R. Schleyer, A. Allerhand, *J. Chem. Phys. 35* (1961) 1533.

[9] talc: $C_{12}H_{16}N_4$, a = 8.885(2) Å, α = 110.19°, V = 635.5(8) Å^3, Z = 2, ρ_{exp} = 1.093 g cm^{-3}, space group $R\bar{3}$; $Mo_{K\alpha}$ radiation at −105(5) °C, θ-2θ-scans in 2θ range 2° ≦ 2θ ≦ 50°; data reduction with empirical absorption corrections (3 Ψ-Scans), 842 symmetry independent reflections. Solution with direct methods (MULTAN), refinement with least-squares techniques (SDP package); R = 0.044, R_w = 0.054 for 461 structure factors ($I \geq 3\sigma(I)$) and 71 refined parameters. *fac*-[(tarc)W(CO)$_3$ · HCl] · 2.5 CH_2Cl_2: a = 12.491(4), b = 13.414(4), c = 15.365(2) Å, α = 114.73(2), β = 105.39(2), γ = 101.89(2)°, V = 2102(3) Å^3, Z = 2, ρ_{ber} = 1.60, ρ_{exp} = 1.58 g cm^{-3}, space group $P\bar{1}$; $Mo_{K\alpha}$ radiation at −105(5) °C, θ-2θ-scans in 2θ range 2° ≦ 2θ ≦ 45°; data reduction with empirical absorption correction (3 Ψ scans), 5503 symmetry-independent reflections h, ± k, ± l. Solution with Patterson and refinement with least-squares techniques (SDP package); R = 0.0410, R_w = 0.0559 for 5052 structure factors ($I \geq 3\sigma(I)$) and 475 refined parameters. Further details of the crystal structure investigations may be obtained from the Fachinformationszentrum Karlsruhe, Gesellschaft für wissenschaftlich-technische Information mbH, W-7514 Eggenstein-Leopoldshafen 2 (FRG) on quoting the depository number CSD-54942, the names of the authors and the journal citation.

[10] D. Christen, K. Ramme, B. Haas, H. Oberhammer, D. Lentz, *J. Chem. Phys. 80* (1984) 4020.

[11] L. Halonen, I. M. Mills, *J. Mol. Spectrosc. 73* (1978) 494.

[12] F. E. Hahn, S. Rupprecht, *Chem. Ber.*, in press.

[13] [(tarc)W(CO)$_3$] as typical example of the synthesis of the complexes: Two solutions of 0.33 g (0.67 mmol) tarc in 10 mL CH_2Cl_2 and 0.24 g (0.67 mmol) [(C_7H_8)W(CO)$_3$] in 10 mL CH_2Cl_2 were prepared. These solutions were added dropwise under argon, simultaneously and within half an hour, to 10 mL CH_2Cl_2. The deep red [(C_7H_8)W(CO)$_3$] decolorized in the process. The solvent was removed in vacuum and the yellow residue was washed several times with hexane to remove C_7H_8. The yield was 0.35 g (86%) of the analytically pure product. Correct elemental analysis was obtained for the solvent free *fac*-[(tarc)W(CO)$_3$ · HCl].

[14] A. R. Bulls, C. G. Pippin, F. E. Hahn, K. N. Raymond, *J. Am. Chem. Soc. 112* (1990) 2627.

[15] T. J. McMurry, M. W. Hossaini, T. M. Garrett, F. E. Hahn, Z. E. Reyes, K. N. Raymond, *J. Am. Chem. Soc. 109* (1987) 7196.

[16] E. B. Dreyer, C. T. Lam, S. J. Lippard, *Inorg. Chem. 18* (1979) 1904.

syn-Sesqui- and -Sesterbenzobicyclo[2.2.2]octene, Molecules with Stacked Benzene Rings**

By *Wolfram Grimme**, *Heinz Theo Kämmerling*, *Johann Lex*, *Rolf Gleiter**, *Jürgen Heinze** and *Michael Dietrich*

Dedicated to Wolfgang R. Roth on the occasion of his 60th birthday.

Uniform stacking of planar π systems is the basic principle for the construction of conducting organic *crystals*, in which overlap of frontier molecular orbitals forms conducting bands. *Molecules* with stacked π systems are scarce and the number of their layers is limited. In the multidecker cyclophanes,[1] the π systems are twisted relative to one another to reduce strain, which distinguishes them from conducting molecular crystals. Another type of stacking occurs in sesquibenzonorbornene; here a rigid tetracycle holds two benzene rings facing each other but tilts them at an angle of 18.6° from each other.[2] We now report our first attempts at constructing analogous multilayers by stacking benzobicyclo[2.2.2]octene units.

The anhydride **2**, a masked napthalene, reacts as dienophile and was used to synthesize Diels–Alder adducts to the b side of naphthalene.[3] With the isotetralin **1** it forms the *endo* adduct **3**, which is oxidized in two steps to the dibenzotetracycle **4** (Scheme 1). The thermal opening of its

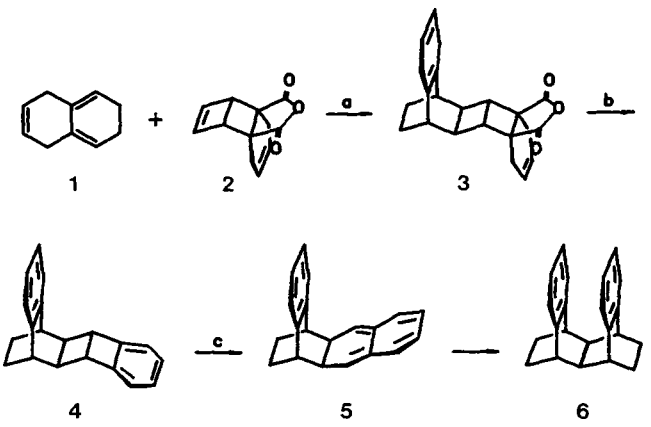

Scheme 1. a: Xylene, 140 °C, 19 h, 60%; b: 1) NEt_3 0.03 M in 90% hydrous pyridine, 20 °C, 3 h, 30 mA cm^{-2}; 2) DDQ in CCl_4, 20 °C, 12 h, 53%; c: 1) CH_2 = CH-COCl 0.8 M in xylene, 120 °C, 4 h; 2) *N*-hydroxy-2-thiapyridone 0.8 M in toluene, 20°, 15 min; 3) *t*BuSH 0.35 M in toluene, reflux 3.5 h, 62%, 0.51 g.

benzobicyclo[2.2.0]hexene unit leads to the 2,3-dihydronaphthalene derivative **5**, which readily adds a dienophile on its convex side. With acrylic acid chloride it forms the *syn*-sesquibenzobicyclo[2.2.2.]octene-5-carbonic acid chloride, which is degraded to the parent compound **6** by the method of *Barton*.

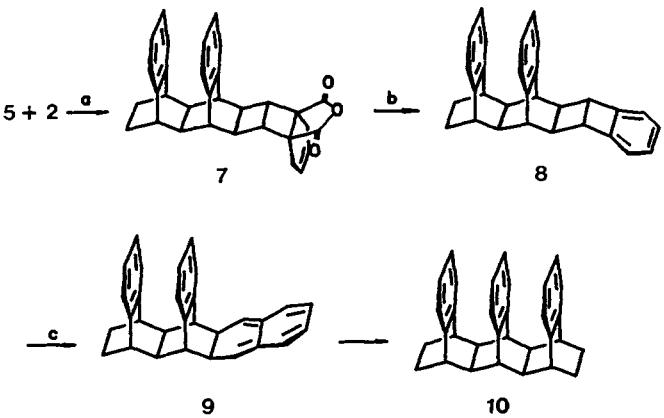

Scheme 2. a: Toluene, reflux, 5 h, 93%; b: 1) NEt_3 0.02 M in 90% hydrous pyridine, 20 °C, 3 h, 20 mA cm^{-2}; 2) DDQ in CCl_4, 20 °C, 12 h, 21%; c: 1) CH_2=CH-COCl 0.3 M in xylene, 120 °C, 3 h; 2) *t*BuOOH 5 M in $CHCl_3$, 20 °C, 2 h; 3) cumene, reflux, 2 h, 43%, 40 mg.

[*] Prof. W. Grimme, Dr. H. T. Kämmerling, Dr. J. Lex
Institut für Organische Chemie der Universität
Greinstrasse 4, W-5000 Köln 41 (FRG)
Prof. R. Gleiter
Organisch-chemisches Institut der Universität
In Neuenheimer Feld 270, W-6900 Heidelberg 1 (FRG)
Prof. J. Heinze, Dipl.-Chem. M. Dietrich
Institut für Physikalische Chemie der Universität
Albertstrasse 21, W-7800 Freiburg (FRG)

[**] This work was supported by the Deutsche Forschungsgemeinschaft within the program for "Noncovalent Interactions".

2,3-Dihydronaphthalene (**5**) also adds the anhydride **2** to its convex side yielding *syn*-sesquibicyclooctene (**7**) (Scheme 2). Electrolysis and subsequent oxidation with 2,3-dichloro-5,6-dicyano-1,4-benzoquinone (DDQ) affords the tribenzohexacycle **8**, which opens thermally to form 2,3-dihydronaphthalene (**9**). Cycloaddition of acrylic acid chloride to the free side of **9** and subsequent decarboxylation via the *tert*-butyl perester yields the all-*syn*-sesterbenzobicyclo[2.2.2]-octene **10**. Important physical data of the new compounds are given in Table 1.

Table 1. Important physical data of **3**, **4**, **6**–**8**, and **10**. ^{1}H NMR spectra were obtained at 90 (**3**, **4**) or 300 MHz, in CCl_4 (**4**) or $CDCl_3$. ^{13}C NMR spectra at 75.5 MHz in $CDCl_3$ with TMS as standard. Satisfactory elemental analyses of **4** and **6** were obtained.

3: M.p. 240 °C (decomp.); ^{1}H NMR: δ = 5.93 (s, 2H), 5.73 (s, 2H), 2.72 (s, 4H), 2.62–2.37 (m, 4H), 2.33 (s, 2H), 2.20 (s, 2H), 1.37 (AA'BB', $\Delta\nu$ = 12 Hz, 4H); MS (70 eV): *m/z* 334 ($M^{\oplus}$, 3%), 132 ($C_{10}H_{10}^{\oplus}$, 57), 91 ($C_7H_7^{\oplus}$, 62), 77 ($C_6H_5^{\oplus}$, 100)

4: M.p. 138 °C; ^{1}H NMR: δ = 7.18 (s, 4H), 7.00 (AA'BB', $\Delta\nu$ = 15 Hz, 4H), 3.10 (m, 2H), 2.90 (s, 2H), 2.50 (m, 2H), 1.55 (AA'BB', $\Delta\nu$ = 18 Hz, 4H)

6: M.p. 125 °C; ^{1}H NMR: δ = 6.59 (AA'XX', $J + J'$ = 8.6 Hz, $\Delta\nu$ = 46 Hz, 8H), 2.79 (s, 4H), 2.36 (s, 2H), 1.45 (AA'XX', $\Delta\nu$ = 184 Hz, 8H); ^{13}C NMR: δ = 140.63, 125.35, 124.73, 43.60, 39.33, 27.87; UV (*n*-hexane): λ_{max}[nm] (ε) = 252(640), 259(910), 273(380); MS (70 eV): *m/z* 286 ($M^{\oplus}$, 23%), 130 ($C_{10}H_{10}^{\oplus}$, 100), 128 ($C_{10}H_8^{\oplus}$, 55)

7: M.p. 275 °C; ^{1}H NMR: δ = 6.60 (AA'XX', $J + J'$ = 8.5 Hz, $\Delta\nu$ = 52 Hz, 4H), 6.59 (AA'XX', $J + J'$ = 8.5 Hz, $\Delta\nu$ = 44 Hz, 4H), 5.94 (m, 2H), 2.81 (s, 4H), 2.78 (s, 2H), 2.44 (AB, ^2J = 17 Hz, $\Delta\nu$ = 72 Hz, 4H), 2.27 (s, 2H), 1.44 (AA'XX', $J + J'$ = 7.1 Hz, $\Delta\nu$ = 176 Hz, 4H), 1.72 (s, 2H); MS (70 eV): *m/z* 460 ($M^{\oplus}$, 10%), 130 ($C_{10}H_{10}^{\oplus}$, 100%)

8: M.p. 148 °C; ^{1}H NMR: δ = 7.04 (AA'XX', $J + J'$ = 8.0 Hz, $\Delta\nu$ = 26 Hz, 4H), 6.67 (AA'XX', $J + J'$ = 8.6 Hz, $\Delta\nu$ = 26 Hz, 4H), 6.53 (AA'XX', $J + J'$ = 8.5 Hz, $\Delta\nu$ = 38 Hz, 4H), 2.99 (s, 2H), 2.83 (s, 2H), 2.65 (s, 2H), 2.54 (m, 2H), 2.19 (s, 2H), 1.43 (AA'XX', $J + J'$ = 7.4 Hz, $\Delta\nu$ = 170 Hz, 4H); MS (70 eV): *m/z* 386 ($M^{\oplus}$, 4%), 130 ($C_{10}H_{10}^{\oplus}$, 100), 128 ($C_{10}H_8^{\oplus}$, 45), 115 ($C_9H_7^{\oplus}$, 15)

10: M.p. 292 °C; ^{1}H NMR: δ = 6.41 (AA'XX', $J + J'$ = 8.6 Hz, $\Delta\nu$ = 59.2 Hz, 8H), 5.98 (AA'XX', $J + J'$ = 8.6 Hz, $\Delta\nu$ = 58.4 Hz, 4H), 2.73 (s, 2H), 2.69 (s, 4H), 2.37 (s, 4H), 1.26 (AA'XX', $\Delta\nu$ = 200 Hz, 4H); ^{13}C NMR: δ = 140.66, 136.60, 126.71, 125.51, 124.92, 124.26, 45.32, 44.68, 38.93, 28.22; UV (*n*-hexane): λ_{max} [nm] (ε) = 250 (840, sh), 258 (980), 264 (750, sh), 272 (540, sh); MS (70 eV): *m/z* 414 ($M^{\oplus}$, 28%), 130 ($C_{10}H_{10}^{\oplus}$, 100), 128 ($C_{10}H_8^{\oplus}$, 70), 115 ($C_9H_7^{\oplus}$, 22)

The X-ray structure shows that **6** closely approximates C_{2v} symmetry (Fig. 1).[4, 5] The benzene rings tilt 21.1° away from each other; at the base their separation is 3.04 and at the upper edge 3.84 Å. This distance is smaller than that of graphite and comparable with that of the partially charged tetrathiafulvalene (TTF) stacks (3.47 Å) in the conducting tetracyanoquinonedimethane (TCNQ)-TTF crystal.[6] MMX force field calculations predict a structure with very similar alignment (18.6°, 3.02 Å) for the benzene rings; we suspect that the strain energy of 41.3 kcal mol^{-1} (merely 1.6 kcal mol^{-1} higher than that of two separate benzobicyclooctene units) is underestimated.

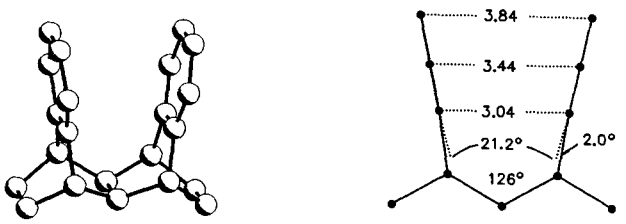

Fig. 1. Structure of **6** in the crystal (hydrogen atoms omitted) as PLUTO drawing and projection in σ_v (dihedral angles [°], distances [Å]).

Compound **10** also has approximate C_{2v} symmetry according to X-ray structure analysis (Fig. 2).[7] The angle between the planes of neighboring benzene rings increases to 21.7° and their distance apart at the base to 3.09 Å. These larger values are surprising at first, because the force field calculations predict 16.9° and 3.01 Å. The wrong trend in the calculated data can be explained by a quantum mechanical effect not considered in the force field: repulsion increases with the number of overlapping, fully occupied orbitals (here HOMOs from benzene).

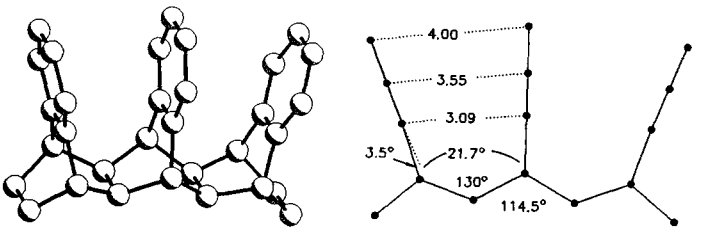

Fig. 2. Structure of **10** in the crystal (hydrogen atoms omitted) as PLUTO drawing and projection in σ_v (dihedral angles [°], distances [Å]).

The photoelectron (PE) spectra of **6** and **10** reveal a large splitting of the orbitals of the stacked benzene rings. The first four (or six for **10**) ionic states (Table 2) arise from the ionization of the π MOs of the two (or three) benzene rings. Each ring contributes two no longer degenerate MOs (e_A, e_S, Scheme 3).

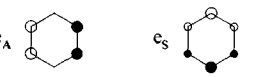

Scheme 3. Benzene π molecular orbitals with e_A and e_S symmetry.

In the case of **6**, the first two PE bands, which are separated by 0.4 eV, may be assigned to the ionization of the bonding and antibonding linear combination of e_A MOs. Bands 3 and 4 result from the corresponding linear combinations of the e_S. The assignment of the PE bands for **10** is similar (Table 2): a strong splitting is observed (0.4 eV) for the e_A molecular orbitals and a weak splitting for e_S.

Table 2. Ionization energies E_v [eV] in the gas phase of **6** and **10** and their assignments.

6: 7.8 ($15b_1$); 8.2 ($17a_1$); 8.8, 8.9 ($11a_2$, $12b_2$)

10: 7.4 ($20b_1$); 7.89 ($26a_1$); 8.2 ($19b_1$); 8.5, 8.8 ($14a_2$, $19b_2$, $13a_2$)

The relatively small ionization energy of **10** suggested that the compound could be oxidized in solution. Indeed, the cyclovoltammogram in CH_2Cl_2/0.1 M Bu_4NPF_6, −20 °C shows the reversible, stepwise formation of the mono- and

dication at $E_1 = 1.280$ V and $E_2 = 1.738$ V (Fig. 3). The unusual occurrence of a stable mono- and dication can be explained by the ionization from energy-rich MOs spread across the whole π system, which delocalizes the positive charges over three benzene rings. The Coulomb repulsion is also thereby decreased. The oxidation of **10** is facilitated by more than 1.2 V compared with the oxidation of benzene ($E^\circ > 2.4$ V).[7] Compound **10** is, to our knowledge, the first reversibly oxidizable hydrocarbon that consists of only benzene π systems.[8]

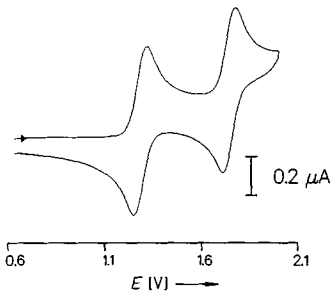

Fig. 3. Cyclovoltammogram of the oxidation of **10** in CH_2Cl_2/0.1 M Bu_4NPF_6. Conditions: $c = 4 \times 10^{-4}$ M, $T = -20$ °C, $V = 100$ mV s^{-1}, E vs. Ag/AgCl.

Further stacking of *syn*-oriented benzobicyclooctenes using the building block **2** is possible, so that the formation of extended MOs from the HOMOs of benzene can be studied in homologues of **6** and **10**.

Received: September, 1990 [Z 4211 IE]
German version: *Angew. Chem. 103* (1991) 215

CAS Registry numbers:
1, 131323-95-0; **2**, 122999-09-1; **3**, 131323-96-1; **4**, 131323-97-2; **5**, 131352-05-1; **6**, 131323-98-3; **7**, 131323-99-4; **8**, 131324-00-0; **9**, 131324-01-1; **10**, 131324-02-2; acrylic chloride, 814-68-6.

[1] T. Otsubo, S. Mizogami, J. Otsubo, Z. Tozuka, A. Sakagami, Y. Sakata, S. Misumi, *Bull. Chem. Soc. Jpn. 46* (1973) 3519.
[2] H. Prinzbach, G. Sedelmeier, C. Krüger, R. Goddard, H.-D. Martin, R. Gleiter, *Angew. Chem. 90* (1978) 297; *Angew. Chem. Int. Ed. Engl. 17* (1978) 271.
[3] W. Grimme, P. Höner, H. T. Kämmerling, R. Waldraff, J. Wirz, *Angew. Chem. 101* (1989) 1390; *Angew. Chem. Int. Ed. Engl. 28* (1989) 1353.
[4] Compound **6** is triclinic with space group $P\bar{1}$, $a = 8.258(1)$ Å, $b = 16.295(3)$, $c = 17.995(3)$, $\alpha = 83.03(2)$, $\beta = 80.86(2)$, $\gamma = 74.76(2)^\circ$, $Z = 6$, $\rho_{ber} = 1.241$ g cm^{-3}, Measurement at room temperature on an Enraf-Nonius CAD 4 diffractometer, $Mo_{K\alpha}$ radiation, $\theta_{max} = 25^\circ$. Of 8109 measured reflections, 3767 with $I \geq 2\sigma(I)$ were used. The C atoms were treated anisotropically in the refinement. Because of the large number of atoms (66 C and 66 H atoms in the asymmetric unit) the H atoms were placed with an H-C distance of 0.95 Å and the isotropic temperature factor of $B = 4$ Å^2 in the final refinement cycle; this leads to $R = 0.062$ and $R_w = 0.068$.
[5] Further details of the crystal structure investigation may be obtained from the Fachinformationszentrum Karlsruhe, Gesellschaft für wissenschaftlich-technische Information mbH, W-7514 Eggenstein-Leopoldshafen 2 (FRG) on quoting the depository number CSD-54967, the names of the authors and the journal citation.
[6] T. J. Kistenmacher, T. E. Phillips, D. O. Cowan, *Acta Crystallogr. Sect. B 30* (1974) 763.
[7] Compound **10** is triclinic with space group $P\bar{1}$, $a = 8.632(1)$, $b = 11.065(3)$, $c = 12.322(3)$ Å, $\alpha = 107.59(2)$, $\beta = 96.89(2)$, $\gamma = 100.19(2)^\circ$, $Z = 2$, $\rho_{ber} = 1.269$ g cm^{-3}. Intensity measurements at room temperature on an Enraf-Nonius CAD 4 diffractometer, $Mo_{K\alpha}$ radiation, $\theta_{max} = 27^\circ$. Of 4717 measured reflections 2090 with $I \geq 2\sigma(I)$ were used in the refinement (C anisotropic. H isotropic), $R = 0.046$, $R_w = 0.045$ [5].
[8] M. Dietrich, J. Mortenson, J. Heinze, *J. Chem. Soc. Chem. Commun. 1986*, 1131.
[9] L. Eberson, J. H. D. Utley in M. M. Baizer, H. Lund (Eds.): *Electrochemistry*, Marcel Dekker, New York 1983, S. 409.

A Cp_2Zr Complex of a Phosphaalkyne Dimer as Educt in the Synthesis of Cyclic Phosphorus Compounds**

By *Paul Binger, Thomas Wettling, Ronald Schneider, Frank Zurmühlen, Uwe Bergsträsser, Jürgen Hoffmann, Gerhard Maas*, and *Manfred Regitz**

Dedicated to Professor Karl Dimroth on the occasion of his 80th birthday

Phosphaalkynes can be cyclooligomerized in the coordination sphere of metal atoms.[1] Thus, for example, the 1,3-diphosphacyclobutadiene complex **1**[2,3] is obtained regiospecifically from the *tert*-butyl-substituted phosphaalkyne **2** and $[CoCp(C_2H_4)_2]$, Cp = η^5-(C_5H_5). However, despite numerous attempts, we have so far been unable to remove the CpCo fragment from the complex **1**.

In contrast, the Cp_2Zr residue in the 1,3-diphosphabicyclo[1.1.0]butane complex **3** can be substituted or eliminated by a series of reaction partners, a finding which we exploited for the synthesis of bi- and tricyclic organophosphorus compounds as well as of 1,3-diphosphetanes and 1,2-dihydro-1,2-diphosphetes. The zirconium complex **3** is readily accessible from Cp_2ZrCl_2/Mg or Cp_2ZrCl_2/BuLi and **2**.[4]

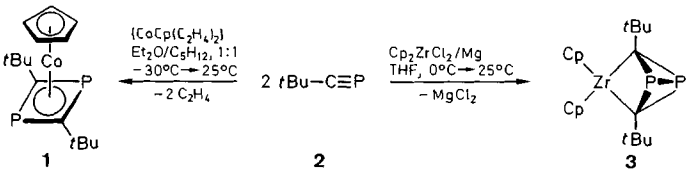

When **3** is heated in the presence of dichloro(phenyl)borane the Cp_2Zr fragment is replaced by the PhB unit with formation of Cp_2ZrCl_2; that is, the tricyclic molecular skeleton remains intact in the product **4** (yield 46%).[5] Germanium tetrachloride reacts in the same way under milder conditions.[6] The boradiphospha-heterocycle **4** has two mirror planes (P–B–P and C–B–C), so that the framework carbon atoms (and also the *t*Bu groups) as well as the two phosphorus atoms are magnetically equivalent (Table 1). The high-field position of the signals in the ^{31}P-NMR spectrum are comparable with those of diphosphabicyclobutanes[7] and those of the educt **3**.[4]

Addition of bromine to the tricycle **4** leads to cleavage of the P–P bond with formation of the boradiphosphabicycle **6** (43%) and **8b** (11%). The NMR spectroscopic non-equivalence of the two phosphorus atoms of the brominated bicycle **6** (Table 1) is consistent with the postulated stereochemistry. In the ^{11}B-NMR spectra, **6** and **4** show similar resonance signals at $\delta = 33.3$ and $\delta = 30.8$, respectively, a confirmation that the environs of the boron change only negligibly during the transition from **4** to **6**. The ^{13}C-NMR spectra are

[*] Prof. Dr. M. Regitz, Dipl.-Chem. T. Wettling, Dipl.-Chem. R. Schneider, Dr. F. Zurmühlen, Dipl.-Chem. U. Bergsträsser, Dipl.-Chem. J. Hoffmann, Prof. Dr. G. Maas
Fachbereich Chemie der Universität
Erwin-Schrödinger-Strasse, W-6750 Kaiserslautern (FRG)
Prof. Dr. P. Binger
Max-Planck-Institut für Kohlenforschung
Kaiser-Wilhelm-Platz 1, W-4330 Mülheim a.d. Ruhr (FRG)

[**] Organophosphorus Compounds, Part 47. This work was supported by the Volkswagen-Stiftung and the Fonds der Chemischen Industrie.—Part 46: T. Wettling, G. Wolmershäuser, P. Binger, M. Regitz, *J. Chem. Soc. Chem. Commun. 1990*, 1541.

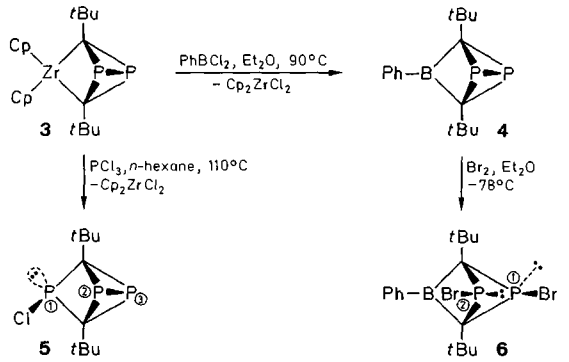

characterized by pseudotriplets, both for the framework carbon atoms as well as for the *t*Bu carbon atoms (Table 1).

Table 1. Some physical data of the cyclic phosphorus compounds **4**–**9** and **11** [a].

4: colorless [b] (after Kugelrohr distillation at 170 °C/10^{-2} torr); ^{1}H NMR: δ = 0.95 (s, 18H, *t*Bu), 7.2–7.6 (m, 5H, aromat. H); ^{13}C NMR: δ = 31.8 (t, ^3J(P,C) = 3.2 Hz, C(CH_3)$_3$), 31.3 (t, ^2J(P,C) = 4.2 Hz, C(CH_3)$_3$), 72.6 (m, br., C-skeleton); ^{31}P NMR: δ = − 341.3; MS (70 eV): *m/z* 288 ($M^{\oplus}$, 82%), 157 ($M^{\oplus}$ − *t*BuCP_2, 86), 131 ($M^{\oplus}$ − PhB*t*Bu, 59), 103 (100).

5: colorless [b] (after Kugelrohr distillation at 130 °C/10^{-2} torr); ^{1}H NMR: δ = 0.84 (s, 18H, *t*Bu); ^{13}C NMR: δ = 29.4 (m, C(CH_3)$_3$, 31.8 (m, C(CH_3)$_3$), 52.6 (m, C-skeleton); ^{31}P NMR: δ = 234.4 (pseudo-t, ^2J(P-1, P-2) = ^2J(P-1, P-3) = 58 Hz, P-1), − 121.4 (dd, ^2J(P-1, P-2) = 58 Hz, ^1J(P-2, P-3) = 146 Hz, P-2), − 306.0 (dd, ^2J(P-1, P-3) = 58 Hz, ^1J(P-2, P-3) = 146 Hz, P-3).

6: colorless [c] (from *n*-pentane/ether at − 20 °C); ^{1}H NMR: δ = 1.19 (s, 18H, *t*Bu), 7.1–8.2 (m, 5H, aromat. H); ^{13}C NMR: δ = 31.5 (t, ^3J(P,C) = 4.0 Hz, C(CH_3)$_3$), 34.8 (t, ^2J(P,C) = 4.2 Hz, C(CH_3)$_3$), 94.7 (t, br., ^1J(P,C) = 57 Hz); ^{31}P NMR: δ = 16.1 (P-2), − 106.9 (P-1); MS(70 eV): *m/z* 448 ($M^{\oplus}$, 96%), 371 ($M^{\oplus}$ − C_6H_5, 74), 368 ($M^{\oplus}$ − Br, 91), 288 ($M^{\oplus}$ − 2 Br, 100).

7a: colorless [b] (after Kugelrohr distillation at 120 °C/10^{-2} mbar); ^{1}H NMR: δ = 1.30 (s, 18H, *t*Bu); ^{13}C NMR: δ = 31.2 (q, ^3J(P,C) = 3.6 Hz, C(CH_3)$_3$), 35.2 (q, ^2J(P,C) = 5.2 Hz, C(CH_3)$_3$), 77.7 (q, ^1J(P,C) = 52.4 Hz, C-skeleton); ^{31}P NMR: δ = 42.9.

7b: yellow [b] (after Kugelrohr distillation at 180 °C/10^{-2} mbar); ^{1}H NMR: δ = 1.23 (s, 18H, *t*Bu); ^{13}C NMR: δ = 30.6 (s, C(CH_3)$_3$), 35.2 (q, ^2J(P,C) = 4.3 Hz, C(CH_3)$_3$), 67.0 (q, ^1J(P,C) = 53.2 Hz, C-skeleton); ^{31}P NMR: δ = 49.7.

7c: yellow [b] (Kugelrohr distillation at 190 °C/10^{-1} mbar); ^{1}H NMR: δ = 1.17 (s, 18H, *t*Bu); ^{13}C NMR: δ = 29.8 (s, C(CH_3)$_3$), 35.4 (q, ^2J(P,C) = 4.4 Hz, C(CH_3)$_3$), 46.5 (q, ^1J(P,C) = 52.6 Hz, C-skeleton); ^{31}P NMR: δ = 77.2.

8a: colorless [b] (Kugelrohr distillation at 120 °C/10^{-2} mbar); ^{1}H NMR: δ = 1.10 (s, 18H, *t*Bu), 3.00 (t, ^2J(P,H) = 12.0 Hz, 2H, CH); ^{13}C NMR: δ = 28.6 (t, ^3J(P,C) = 6.8 Hz, C(CH_3)$_3$), 33.1 (t, ^2J(P,C) = 14.5 Hz, C(CH_3)$_3$), 62.4 (t, ^1J(P,C) = 28.8 Hz, C-skeleton); ^{31}P NMR: δ = 105.5.

8b: colorless [b] (Kugelrohr distillation at 100 °C/10^{-2} mbar); ^{1}H NMR: δ = 1.00 (s, 18H, *t*Bu), 3.55 (t, ^2J(P,H) = 13.5 Hz, 2H, CH); ^{13}C NMR: δ = 28.4 (t, ^3J(P,C) = 7.3 Hz, C(CH_3)$_3$), 33.9 (t, ^2J(P,C) = 13.3 Hz, C(CH_3)$_3$), 57.8 (t, ^1J(P,C) = 29.1 Hz, ^1J(C,H) = 141.2, C-skeleton); ^{31}P NMR: δ = 92.8.

10: colorless crystals m.p. 33 °C (from *n*-pentane at − 20 °C); ^{1}H NMR: δ = 0.90 (s, 18H, *t*Bu), 1.56 (ddd, ^2J(P,H) = 12.5 and 6.2 Hz, ^3J(H,H) = 16.7 Hz, 2H, C*H*-*t*Bu), 2.56 (ddt, ^1J(P1,H) = 171.6 Hz, ^3J(P2,H) = 24.8 Hz, ^3J(H,H) = 16.7 Hz, 1H, PH); ^{13}C NMR: δ = 29.6 (pseudo-t, ^3J(P,C) = 3.2 Hz, C(CH_3)$_3$), 31.8 (d, ^2J(P,C) = 9.7 Hz, C(CH_3)$_3$), 46.4 (dd, ^1J(P,C) = 31.9 and 12.5 Hz, ring-C); ^{31}P NMR: δ = 24.1 (d, ^2J(P,P) = 22.8 Hz, P2), − 133.6 (d, ^2J(P,P) = 22.8 Hz, P1); MS (70 eV): *m/z* 238 ($M^{\oplus}$, 21%), 181 [$M^{\oplus}$ − $(CH_3)_3C$, 43], 70 ($(CH_3)_3CCH^{\oplus}$, 100), 55 ($C_4H_7^{\oplus}$, 18).

11: yellow crystals, m.p. 149 °C (from *n*-pentane at − 20 °C); ^{1}H NMR: δ = 1.30 (s, 18H, *t*Bu); ^{13}C NMR: δ = 30.4 (pseudo-t, X-part of an ABX system, J(P-1, C) + J(P-2,C) = 8.5 Hz, C(CH_3)$_3$), 39.4 (pseudo-t, X-part of an ABX system, J(P-1,C) + J(P-2,C) = 11.2 Hz, C(CH_3)$_3$), 162.5 (pseudo-t, X-part of an ABX system, J(P-1,C) + J(P-2,C) = 22.3 Hz, ring-C); ^{31}P NMR: δ = − 21.5; MS(70 eV): *m/z* 454 ($M^{\oplus}$, 16%), 327 ($M^{\oplus}$ − I, 90), 227 ($M^{\oplus}$ − C_4H_9CP, 38), 169 ($M^{\oplus}$ − PI_2, 58), 57 ($C_4H_9^{\oplus}$, 56).

[a] ^{1}H- (90 or 400 MHz, TMS), ^{13}C- (100.6 MHz, TMS), and ^{31}P-NMR spectra (80.0 MHz, 85% H_3PO_4) in C_6D_6; only **7a** and **c** were measured in $CDCl_3$. [b] The oils obtained on Kugelrohr distillation crystallized from ether or *n*-pentane between − 20 and − 78 °C; the crystals deliquesce between + 10 and + 30 °C. [c] Deliquesce on warming to room temperature.

The reaction of **3** with phosphorus trichloride also proceeds without alteration of the tricyclic framework, smoothly affording **5** in 75% yield. The triphosphatricyclopentane **5** is fully characterized NMR spectroscopically (Table 1). Special attention need only be drawn to the phosphorus atoms, which absorb at very different field strengths (δ = 234.4 P1, − 121.4 P2, − 306.0 P3). As expected, the chlorine can undergo nucleophilic substitution with *tert*-butyllithium in ether at − 78 °C.[8]

In contrast to the reaction of **3** with PCl_3 leading to **5**, the zirconium exchange upon reaction of **3** with phosphorus pentachloride (large excess), phosphorus tribromide (already at room temperature) and phosphorus triiodide under otherwise comparable conditions is accompanied by a halogen cleavage of the P–P bridge. Thus, the final products are the trihalogenotriphosphabicyclo[1.1.1]pentane derivatives **7a** (40%), **7b** (91%)[9] and **7c** (61%), respectively. When the reaction of **3** with PCl_5 is carried out in the molar ratio 1:1, a 1:1 mixture of **5** and **7a** is formed. This means that the tricycle **5** is apparently formed as intermediate in the reaction **3** → **7a**. However, the tricyclic system of **5** is recovered again via a P-P coupling when **7a** is treated with two equivalents of *tert*-butyllithium (ether, − 78 °C); concomitantly, an additional Cl/*t*Bu exchange takes place.

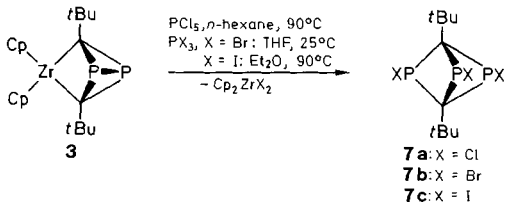

The appearance of only one resonance for the three phosphorus atoms in the ^{31}P-NMR spectra of **7a**–**c** and the quartet splitting of all ^{13}C-NMR signals indicate a highly symmetric structure, which has been confirmed by a crystal structure analysis of **7a**.[10] **7a** has C_3 symmetry both in

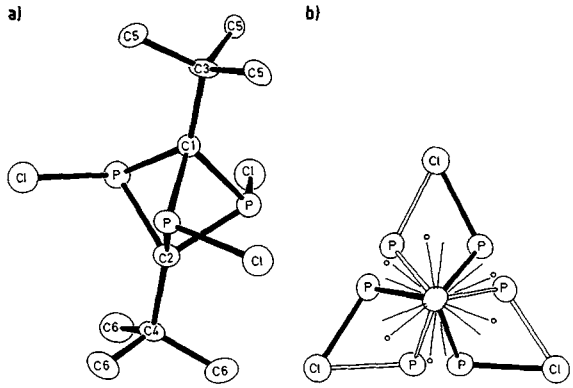

Fig. 1. a) Structure of **7a** in the crystal. Bond lengths [Å]: P-Cl 2.078(2), P-Cl 1.861(5), P-C2 1.860(7), C1-C3 1.558(11), C2-C4 1.539(11), C3-C5 1.561(7), C4-C6 1.536(17). Bond angles [°]: Cl-P-C1 109.6(1), Cl-P-C2 107.0(1), C1-P-C2 74.1(3), P-C1-P′ 87.5(3), P-C1-C3 127.1(3), C1-C3-C5 107.7(4), P-C2-P′ 87.5(3), P-C2-C4 127.0(2), C2-C4-C6 108.2(4). b) Disorder of **7a** in the crystal; view along the C3-C1-C2-C4 axis (3*m* symmetry). The chlorine atoms (shown here isotropically) are fixed on a mirror plane; probably the mirror symmetrically related positions Cl and Cl′ deviate only slightly, however, from this plane (cf. the somewhat too large a value for *d*(P–Cl)). The molecule with the bold printed bonds and with methyl groups shown as open circles O corresponds to that presented in Figure 1 a; assignment of methyl groups on the basis of the smallest *gauche* interactions.

solution (cf. Table 1) and in the crystal (Fig. 1a); in the crystal the molecule is also disordered (Fig. 1b).

When the Cp_2Zr fragment is removed from **3** with mercury(II) chloride or bromine at low temperature, the polycyclic structure of the educt is completely lost: the *P*-halogenated 1,3-diphosphetanes **8a** (14%) and **8b** (73%), respectively, are formed. The incorporated hydrogen can only come from the solvent, indicating a radical reaction. Each of the ^{1}H-NMR spectra of the two compounds shows a triplet with typical ^2J(P,H) coupling. The stereochemistry of **8b** (1,3-substituents always *cis*) follows unequivocally from its crystal structure analysis.[11]

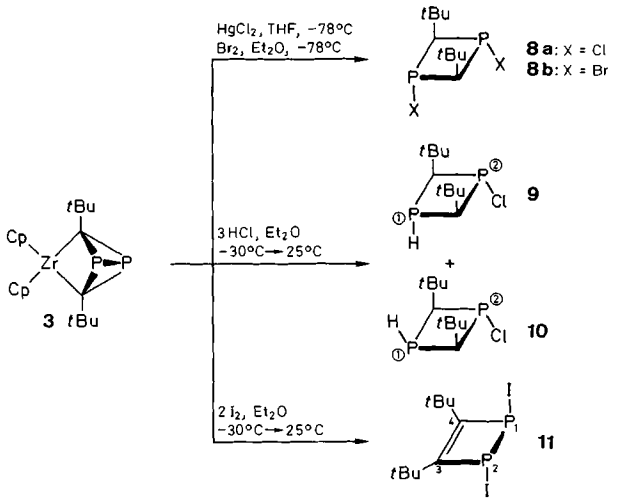

A 1,3-diphosphetane, which has only one P-halogen function, is formed in the reaction of the zirconium complex **3** with hydrogen chloride. It precipitates as a *cis*/*trans* isomeric mixture **9**/**10** (60%), whereby the presumed *trans* isomer **10** apparently dominates in the ratio 2:1 and can be obtained in pure form by fractional crystallization (Table 1). Since both the *t*Bu residues as well as the framework carbons of this isomer each give rise to only one signal in the ^{1}H- and ^{13}C-NMR spectra, both substituents have *cis* arrangement. The 1,3 arrangement of the two P nuclei follows from the comparatively small P,P coupling of 22.8 Hz. P1 is recognizable by the high field position of its NMR signal as well as by the P-H coupling of 171.6 Hz, P2 by the downfield shift of its NMR signal by the chlorine substituents (Table 1).

Reaction of **3** with iodine proceeds differently from that with bromine. Although the Cp_2Zr fragment is likewise cleaved from **3**, in this case the P–P bond remains intact. Both here, and in the case of the reaction of **3** with the interhalogen compounds ClI (70%) and BrI (65%), the 1,2-dihydro-1,2-diphosphete **11** is formed.[12]

In the respective NMR spectra the two ring carbon atoms as well as the two phosphorus atoms are equivalent (Table 1). The crystal structure analysis[10] affords unequivocal proof of the *trans* arrangement of the two iodine atoms as well as of the C_2 symmetry of the molecule (Fig. 2).

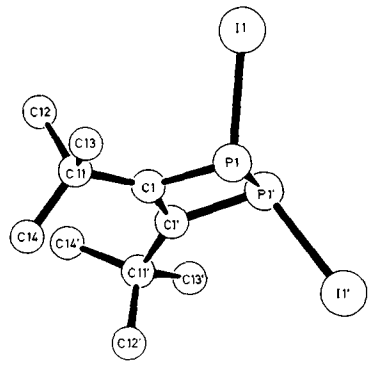

Fig. 2. Structure of **11** in the crystal. Bond lengths [Å]: P1-I1 2.484(2), P1-P1′ = 2.192(4), P1-C1 1.827(6), C1-C1′ 1.334(12) Å. Bond angles [°]:C1-P1-P1′ 75.5(2), C1-P1-I1 106.9(2), P1′-P1-I1 100.5(1), P1-C1-C1′ 102.1(4), C1′-C1-C11 136.4(6)°. Folding angle in the four-membered ring: P1-C1-C1′/P1-P1′-C1′ 12.8°, C1-P1-P1′/C1-C1′-P1′ 20.8°.

Experimental

5: A solution of **3** (0.40 g, 0.95 mmol) in *n*-hexane (10 mL) was heated together with phosphorus trichloride (2 mL, excess) for 2.5 h at 110 °C (Schlenck tube). After cooling, the solution was pipetted from the precipitated Cp_2ZrCl_2, evaporated down at 25 °C/10^{-2} mbar, and the residue distilled at 130 °C/10^{-2} mbar (Kugelrohr). Yield 0.19 g (75%) of a pale yellow oil, which crystallized from *n*-pentane at −78 °C; m.p. ≈ 30 °C.

11: After cooling to −30 °C, the solution of **3** (0.61 g, 1.4 mmol) in ether (30 mL) was treated dropwise with stirring with a 0.5 M ethereal iodine (5.8 mL). The mixture was allowed to warm to room temperature and then evaporated down at 25 °C/2×10^{-2} mbar. The residue was taken up in pentane (20 mL) and filtered free of Cp_2ZrI_2. Evaporation of the filtrate and cooling to −20 °C furnished 0.43 g (65%) of yellow crystals; m.p. 149 °C.

Received: September 4, 1990 [Z 4167 IE]
German version: *Angew. Chem. 103* (1991) 208

CAS Registry numbers:
3, 109613-89-0; **4**, 131298-06-1; **5** (*t*Bu instead of Cl), 131298-16-3; **6**, 131298-08-3; **7a**, 131298-09-4; **7b**, 131298-11-8; **7c**, 131298-14-1; **8a**, 131298-10-7; **8b**, 131298-15-2; **9**, 131350-11-3; **10**, 131298-12-9; **11**, 131298-13-0; $PhBCl_2$, 873-51-8; PCl_3, 7719-12-2; PCl_5, 10026-13-8; PBr_3, 7789-60-8; PI_3, 13455-01-1; $HgCl_2$, 7487-94-7; $HgBr_2$, 7789-47-1; I_2, 7553-56-2.

[1] Reviews: J. F. Nixon, *Chem. Rev. 88* (1988) 1327; M. Regitz, P. Binger, *Angew. Chem. 100* (1988) 1541; *Angew. Chem. Int. Ed. Engl. 27* (1988) 1484; P. Binger in M. Regitz, O. J. Scherer (Eds.): *Multiple Bonds and Low Coordination in Phosphorus Chemistry*, Thieme, Stuttgart 1990, p. 94.

[2] P. Binger, R. Milczarek, R. Mynott, M. Regitz, W. Rösch, *Angew. Chem. 98* (1986) 645; *Angew. Chem. Int. Ed. Engl. 25* (1986) 644; P. Binger, R. Milczarek, R. Mynott, Y.-H. Tsai, E. Raabe, C. Krüger, M. Regitz, *Chem. Ber. 121* (1988) 637.

[3] Analogous Rh complex: P. B. Hitchcock, M. J. Maah, J. F. Nixon, *J. Chem. Soc. Chem. Commun. 1986*, 737.

[4] P. Binger, B. Biedenbach, C. Krüger, M. Regitz, *Angew. Chem. 99* (1987) 798; *Angew. Chem. Int. Ed. Engl. 26* (1987) 764.

[5] Exchange reactions of the same type have recently been described for monocycles: zirconacyclopentadiene system: P. J. Fagan, W. A. Nugent, *J. Am. Chem. Soc. 100* (1988) 2310; zirconacyclopentene system: K. M. Doxsee, G. S. Shen, C. B. Knobler, *ibid. 111* (1989) 9129; zirconacyclobutene system: W. Tumas, J. A. Suziano, R. L. Harlow, *Angew. Chem. 102* (1990) 89; *Angew. Chem. Int. Ed. Engl. 29* (1990) 75.

[6] Ether at 25 °C; 85% colorless crystals; m.p. 129 °C; ^{31}P-NMR(C_6D_6): $\delta = -298.0$.

[7] E. Niecke, H. J. Metternich, R. Streubel, *Chem. Ber. 123* (1990) 67.

[8] **5** (*t*Bu instead of Cl). ^{1}H NMR (C_6D_6): $\delta = 1.54$ (d, ^3J(P,H) = 10.0 Hz, 9H, P-*t*Bu), 1.01 (s, 18H, C-*t*Bu); ^{13}C NMR (C_6D_6): $\delta = 28.8$ (d, ^2J(P,C) = 16.1 Hz, P-C(CH_3)$_3$), 30.2 (s, C-C(CH_3)$_3$), 31.4 (m, C-C(CH_3)$_3$), 35.8 (m, *C*-skeleton), 40.2 (d, ^1J(P,C) = 50.9 Hz, P-C(CH_3)$_3$); ^{31}P NMR (C_6D_6): $\delta = -311.2$ (dd, ^1J(P,P) = 142.4 Hz, ^2J(P,P) = 62.6 Hz, P3), −107.7 (dd, ^1J(P,P) = 144.6 Hz, ^2J(P,P) = 36.4 Hz, P2), 200.1 (dd, ^2J(P,P) = 64.5 and 38.8 Hz, P1).

[9] The bicyclic compound **7b** was obtained independently from PBr_3 and **2**: G. Becker, W. Becker, R. Knebl, H. Schmidt, U. Weber, M. Westerhaus, *Nova Acta Leopold. 59* (1985) 55.

[10] X-ray structure analysis (Enraf-Nonius CAD-4 diffractometer, monochromatated $Mo_{K\alpha}$ radiation, full matrix refinement): **7a** ($C_{10}H_{18}Cl_3P_3$, M = 337.5): trigonal, space group $R\bar{3}m$ (No. 166), $a = b = 10.359(2)$, $c = 25.269(5)$ Å, $\alpha = \beta = 90$, $\gamma = 120°$; $\varrho_{calcd} = 1.43$ g cm^{-3}; $Z = 6$; 2304

reflections measured in a hemisphere, after averaging 554 symmetry independent reflections $2.0 \leq \theta \leq 25.0°$; correction for loss of intensity (max. 14.6%); 379 reflections with $I > 3\sigma(I)$, 73 variables, $R = 0.085$, $R_w = (\Sigma\Delta^2 F/\Sigma F_0^2)^{1/2} = 0.091$; maximum shift/error ratio 1.40; H atoms not localized because of disorder of the molecule.—**11** ($C_{10}H_{18}I_2P_2$, $M = 454.0$): monoclinic, space group $C2/c$ (No. 15), $a = 15.450(3)$, $b = 8.348(1)$, $c = 11.746(4)$ Å, $\beta = 99.17(3)°$; $\varrho_{calcd} = 2.016$ g cm^{-3}, $Z = 4$; 1204 reflections with $I > 2\sigma(I)$ in the range $2.0 \leq \theta \leq 25.0°$, 76 variables, $R = 0.0524$, $R_w = (\Sigma w\Delta^2 F/wF_0^2)^{1/2} = 0.0545$; maximum shift/error ratio 0.15.—Further details of the crystal structure investigations are available on request from the Fachinformationszentrum Karlsruhe, Gesellschaft für wissenschaftlich-technische Information mbH, W-7514 Eggenstein-Leopoldshafen 2 (FRG), on quoting the depository number CSD-54910, the names of the authors, and the journal citation.

[11] R. Boese, Universität Essen, unpublished results 1990.

[12] A further compound of this class of substances was recently synthesized via another route: L. Ricard, N. Maigrot, C. Charrier, F. Mathey, *Angew. Chem. 99* (1987) 590; *Angew. Chem. Int. Ed. Engl. 26* (1987) 548.

$[As^{V}V^{V}_{12}V^{IV}_{2}O_{40}]^{7\ominus}$, a Topologically Interesting, Mixed Valence Cluster as Model for Vanadium Minerals Formed by Weathering **

By *Achim Müller,* Joachim Döring, M. Ishaque Khan,* and *Volker Wittneben*

The geochemistry of basaltophilic vanadium, which occurs in high abundance, for example, in biogenic deposits, is "peculiar and complex",[1a] but also of considerable importance. "Important" vanadium sulfide minerals are relatively rare (patronite VS_4), whereas the number of oxidic species formed by the weathering of magmatic and postmagmatic rocks is very large[1b,c] due to the high affinity of vanadium for oxygen.[2] The easy change of oxidation states, which is characteristic for vanadium (V^{V} to V^{III} in aqueous solution, whereby V^{V} and V^{IV} are stable and can be easily interconverted), has consequences for catalysis (e.g. "V_2O_5" catalyst for the production of sulfuric acid[3]), biochemistry (all the valence states mentioned have been found in V-proteins[4]), and geochemistry[5] owing to the unusual variety of mixed valence minerals (e.g. bluish-green sherwoodite with discrete anion[6]).

We have now been able to synthesize the first cluster which is similar to the anion in sherwoodite. Reduction of V^{V} with $SCN^{\ominus}$ in the presence of As^{V} in acidic aqueous solution leads to formation of bluish-black **1**.

$K_7[As^{V}V^{V}_{12}V^{IV}_{2}O_{40}] \cdot 12H_2O$ **1**

Compound **1** was characterized by elemental analysis (including manganometric determination of the amount of V^{IV} and thermogravimetry (water of crystallization)), IR, Raman (and pre-resonance Raman), UV/VIS/NIR, and ESR spectroscopy, magnetochemical measurements (see *Experimental*), MO calculations, as well as by a single-crystal X-ray structure analysis.[7]

Whereas we have previously found a distinct preference for the formation of V^{IV}/V^{V} clusters with a higher number of V^{IV} centers, we have now also succeeded in preparing species with a lower number of V^{IV} centers by using the weak reducing agent $SCN^{\ominus}$ ($2\,SCN^{\ominus} \rightleftarrows (CNS)_2 + 2e^{\ominus}$) in acidic medium.

The cluster anion in **1** is structurally very interesting (Fig. 1): the $\{AsV_{12}O_{38}\}$ basic unit with O_h symmetry is formed from twelve edge-sharing VO_6 octahedra, which also share faces with a central AsO_6 octahedron. Two additional

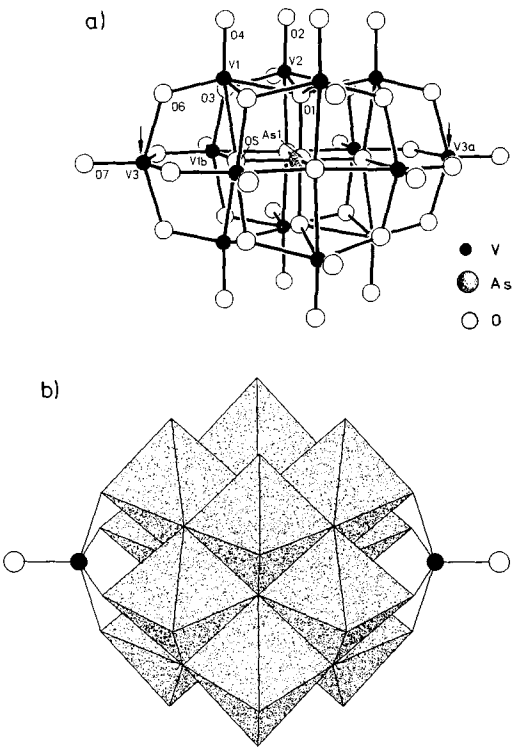

Fig. 1 a) Structure of the anion $[As^{V}V^{V}_{12}V^{IV}_{2}O_{40}]^{7\ominus}$ in crystals of **1**. b) Polyhedral representation of the central $\{AsV_{12}O_{38}\}$ unit with two attached V-O vectors. Distances [pm]: As1-O1 183.9(4), As1-O5 180.4(5), V1-O1 220.2(1), V1-O3 194.7(1), V1-O4 160.6(3), V1-O5 230.9(1), V1-O6 170.4(3), V2-O1 239.2(1), V2-O2 163.1(3), V2-O3 194.5(3), V3-O5 255.7(3) (sherwoodite: 236 (5)), V3-O6 195.9 (3), V3-O7 158.1(6), V1-V1b 322.7(1), V1-V2 318.3(1), V1-V3 317.2(1). V^{IV} centers marked by arrows.

(oppositely disposed) V=O groups are located on the C_4 axis, above the apices of the AsO_6 octahedron, whereby the symmetry is reduced to D_{4h}. The four vanadium atoms (V2) on the *h* mirror plane have two, the remaining ones (V1, V3) only one terminally bound oxygen atom. There are also μ_2-, μ_3-, and μ_5-oxygen atoms, whereby the V–O distances understandably increase with increasing coordination number of the oxygen. The coordination polyhedron of V3 can be described as a square pyramid; the V3–O5 distance (255.7 (3) pm) is too large to count O5 in the polyhedron. The calculated V–O bond valence sums[8] show that the two manganometrically determined V^{IV} centers are located in these two pyramids. The number of $\nu_s(V=O_{term})$ bands (A_{1g}) in the pre-resonance Raman spectrum is, as expected, identical with the number of non-equivalent V atoms (see *Experimental*).

The $\{V_{12}O_{38}\}$-unit in **1** is also topologically remarkable: the V atoms form a cuboctahedron, i.e. one of the 13 Archimedean solids. The unusual octahedral environment of the As atom is enforced by the "hollow" $\{V_{12}O_{38}\}$-aggre-

[*] Prof. Dr. A. Müller, Dipl.-Chem. J. Döring, Doz. Dr. M. I. Khan, Dipl.-Chem. V. Wittneben
Fakultät für Chemie der Universität
Lehrstuhl für Anorganische Chemie I
Postfach 8640, W-4800 Bielefeld 1 (FRG)

[**] This work was supported by the Deutsche Forschungsgemeinschaft, the Fonds der Chemischen Industrie, and the Westfälisch-Lippische Universitätsgesellschaft. We thank Prof. Dr. *K. Wieghardt* for magnetic measurements and Dr. *H. Bögge* for his help with the X-ray structure analysis.

gate. The basic species $[(X)V_{12}O_{38}]^{n\ominus}$, of fundamental importance for the structure of metal-oxygen clusters, has so far not been isolated.

Replacement of a "lower valence" heteroatom center Z such as $Al^{3\oplus}$ or $Fe^{3\oplus}$ (in sherwoodite) by the $As^{5\oplus}$ center remarkably leads to a shortening of the two Z–O5 distances, and thus to a significant lengthening of the V3–O5 distances (cf. caption to Fig. 1). The resulting change in the coordination (possibly) leads to a predominant localization of the two V^{IV}-3d-electrons in **1**. At room temperature, a magnetism corresponding to the spin-only value is measured (see *Experimental*). Since the two V^{IV} centers are intramolecularly 872 pm and intermolecularly 813 pm apart, detailed information on the magnetism can only be obtained by susceptibility measurements at very low temperatures. An SCCC-EH calculation[9] confirms that the two unpaired electrons are localized with more than 50% probability in the d_{xy} orbitals of V3. The 3d functions of these two atoms show a splitting almost undisturbed by the remaining metal atoms, as is expected for isolated, square-pyramidally coordinated vanadyl ions.[10] Also other physical data (e.g. the Raman spectrum with $\lambda_e = 647.1$ nm) are consistent with a mixed valence cluster, which does not belong to class III (delocalized electron ground state; after *Robin* and *Day*[11]).

The E_h(redox potential)–pH diagram, which is of importance for the geochemist,[1c, 1d, 12] demonstrates qualitatively the formation of the mixed valence vanadate minerals from magmatic and post-magmatic primary rocks [Eqs. (a) and (b)]. With the exception of sherwoodite, the vanadium minerals have a three-dimensional network structure.

$$V^{III} \xrightarrow[H_2O]{(O_2)} \{V^{IV}/V^{V}\} \qquad (a)$$

$$V^{III} \xrightarrow[H_2O]{O_2} V^{V} \xrightarrow[H_2O]{\text{weak reducing agent [13]}} \{V^{IV}/V^{V}\} \qquad (b)$$

It appears to be important that mixed valence polyoxovanadates are formed [cf. Eq. (a), (b)], and not, as is fundamentally possible, a mixture of V^{IV} and V^{V} species. In the case of chromium, for example, there are either Cr^{III}- or Cr^{VI}-minerals; mixed valence minerals in a similar abundance as in the case of vanadium are only found with iron.[11] In the formation of the polyoxovanadates, not only the stabilization of V^{IV} centers in a "V^{V}/O matrix" plays a decisive role, but also changes in solubility during the redox processes and easier reduction after a condensation. In the case of molybdenum, often the element most similar to vanadium, the above-mentioned characteristics do not apply, so that besides the primary mineral MoS_2 (in pre-cambrian granites) practically only completely oxidized weathering minerals are found (exception: ilsemannite[1b]).

An understanding of the geochemistry and biogeochemistry of vanadium is important in many respects: 1) In all workable deposits the vanadium concentration is extremely low. 2) Vanadium is frequently associated with uranium (cf. E_h–pH diagram for the U/V mineral system with broad (average) range of existence in the case of the economically interesting carnotite $K_2[(UO_2)_2(V_2O_8)] \cdot 3H_2O$;[1b] extensive exploration in the framework of the Colorado Plateau project[1d, 5]). 3) So far, it is still unclear how the high V-content comes about in fossil fuels in the form of VO-porphyrins (in extreme cases up to 70% V_2O_5 in petroleum ashes),[1e, 14] i.e. whether it is both of biogenic as well as abiogenic origin. The possible origin and importance of these geoporphyrins have been discussed in the literature.[15]

Experimental

Synthesis of **1**: A stirred solution of KVO_3 (1.93 g, 14 mmol), $As_2O_5 \cdot 5/3\,H_2O$ [16] (0.39 g, 1.5 mmol), and KSCN (0.97 g, 10 mmol) in H_2O (50 mL) in a 100 mL Erlenmeyer flask was adjusted to a pH value of ca. 2.0 at 90 °C with 0.5 M H_2SO_4 and the mixture stirred for a further 10 min at this temperature (color change from orange to greenish-brown). The stirred mixture was then adjusted to about pH 4.6 with 10% KOH solution (color change to dark green) and allowed to stand for 16 h (covered with a watch glass) on a hot plate at 70–75 °C. The precipitated dark blue crystals of **1** were filtered off from the hot solution, washed several times with 50% aqueous methanol and pure methanol, and dried on a filter paper. Yield 1 g.

Characterization of **1**: IR (KBr, main absorption bands): $\tilde{\nu}$ [cm^{-1}] = ca. 3400 (vs, ν(OH)), 1624 (s, δ(HOH)), 1010 (m, $\nu(V^{IV}=O_{term})$), 965 (vs, $\nu(V^{V}=O_{term})$), 913 (m, $\nu_{as}(O_{term}=V^{V}=O_{term})$), 774 (s, ν_{as}(V-O-M, M = V, As)), 678 (m), 624 (s), 564 (s). Raman (solid state, main absorption bands of the A_{1g} vibrations. (D_{4h})): 1012 (vw, $\nu(V^{IV}=O_{term})$), 987 (vw, $\nu(V^{V}=O_{term})$), 785 (s, ν_s), 748 (m) (λ_e = 647.1 nm); 1012 (s, $\nu(V^{IV}=O_{term})$), 987 (s, $\nu(V^{V}=O_{term})$), 943 (s, $\nu_s(O_{term}=V^{V}=O_{term})$), 785 (s), 750 (sh), ($\lambda_e$ = 488.0 nm): pre-resonance Raman effect, "active" for ν ($V=O_{term}$) stretching vibrations, since $\pi(O) \rightarrow d(V)$ type charge transfer (CT) involved. UV/VIS/NIR (KBr, in transmission): 14.9, 11.8 (sh) kK (1 kK = 10^3 cm^{-1}; similarity with spectra of $V^{IV}=O(d^1)$ complexes, therefore approximate assignment: d → d transitions in a tetragonal-pyramidal field), 30.8 kK ($\pi(O) \rightarrow d(V)$-CT). ESR (solid state, X band, 9.4351 GHz): g = 1.98 (broad signal with rough indication of structure due to hyperfine interaction (^{51}V: $I = 7/2$) at 10 K). Magnetism: $\mu_{eff} = 1.77\,\mu_B$ (per V^{IV} center, at room temperature). The Curie-Weiss law is only *approximately* fulfilled between room temperature and 80 K.

Received: August 29, 1990 [Z 4160 IE]
German version: *Angew. Chem. 103* (1991) 203

CAS Registry numbers:
1, 131656-27-4; **1** · H_2O, 131656-28-5; KVO_3, 13769-43-2; As_2O_5, 1303-28-2; KSCN, 333-20-0.

[1] a) W. E. Petrascheck, W. Pohl: *Lagerstättenlehre*, Schweizerbart'sche Verlagsgesellschaft, Stuttgart 1982; b) H. J. Rösler: *Lehrbuch der Mineralogie*, 2nd Edit., VEB Deutscher Verlag für Grundstoffindustrie, Leipzig 1981; c) H. T. Evans, Jr., S. Landergren in K. H. Wedepohl (Ed.): "Vanadium", *Handbook of Geochemistry, Vol. II/2*, Springer, Berlin 1978, Chap. 23; d) K. B. Krauskopf: *Introduction to Geochemistry*, 2nd Edit., McGraw-Hill, New York 1979; e) B. Mason, C. B. Moore: *Grundzüge der Geochemie*, F. Enke, Stuttgart 1985.

[2] A. Müller, E. Krickemeyer, M. Penk, H.-J. Walberg, H. Bögge, *Angew. Chem. 99* (1987) 1060; *Angew. Chem. Int. Ed. Engl. 26* (1987) 1045.

[3] E.Bartholomé, E. Biekert, H. Hellmann, H. Ley, W. M. Weigert, E. Weise (Eds.): *Ullmanns Encyklopädie der technischen Chemie, Vol. 13*, 4th Edit., Verlag Chemie, Weinheim 1977, p. 530 ff.

[4] N. D. Chasteen, *Struct. Bonding (Berlin) 53* (1983) 105; K. Kustin, G. C. McLeod, T. R. Gilbert, LeB. R. Briggs, 4th, *ibid. 53* (1983) 139.

[5] Practically no pure vanadium minerals occur in primary magmatic rocks (e.g. magnetite), but only compounds in which Fe^{III} is isomorphically replaced by V^{III}. Weathering processes (also of postmagmatic rocks such as montroseite) lead to formation of an unusually large number of vanadate minerals, e.g. the decavanadates in the minerals pascoite, hummerite and huemulite, but also the yellow, uranium-containing carnotite [1d] and diverse mixed valence species (V^{IV}/V^{V}) [1b, c]. All V-minerals are described in a recent work with numerous figures, including one of sherwoodite: H. T. Evans, Jr., J. S. White, Jr.: "The Colorful Vanadium Minerals", *Mineral. Rec. 18* (1987) 333.

[6] The results of the X-ray structure analysis of sherwoodite (R = 0.22, cf. H. T. Evans, Jr., J. A. Konnert, *Am. Mineral. 63* (1978) 863) are best reconciled with the formula $Ca_{4.5}[AlV_{14}O_{40}] \cdot 28H_2O$, whereby Al is apparently isomorphically replaceable by Fe and Ca by Mg in the minerals [1b]. The structure of the anion can be compared with that of the anion in **1**; it is likewise present in reduced form in the mineral. $K_7[MnV_{13}O_{38}] \cdot 18H_2O$ is a related species with smaller number of V atoms and exclusively oxidation state five (M. T. Pope, *Heteropoly and Isopoly Oxometalates (Inorg. Chem. Concepts 8)*, Springer, Berlin 1983; M. T. Pope, A. Müller, *Angew. Chem. 103* (1991) 56; *Angew. Chem. Int. Ed. Engl. 30* (1991) 34).

[7] *I4/mmm*; a = 1135.7 (2), b = 2002.8 (5) pm, $V = 2583.2 \times 10^6$ pm^3; μ = 3.64 mm^{-1}, $Z = 2$, R = 0.040 for 791 independent reflections ($F_o > 3.92\,\sigma(F_o)$), Siemens R3m/V diffractometer, $Mo_{K\alpha}$ radiation (graphite monochromator). The powder diffractogram calculated from single crystal data agrees with the measured diagram (most intense Bragg reflections: d = 994, 804, 313, 284, 226 pm; Phillips PW1050/70 diffractometer, $Cu_{K\alpha}$ radiation). The reflection profiles in the X-ray structure analysis indicate a weak asymmetry, so that twinning cannot be ruled out. The potassium ions

appear strongly disordered; however, upon long irradiation (>3 days) Bürger precession photographs gave no indication of a "resolvable twinning" or the presence of a superstructure. The R value of 0.04 also indicates that the anion structure, which is lattice determining, was correctly found. Further details of the crystal structure investigation are available on request from the Fachinformationszentrum Karlsruhe, Gesellschaft für wissenschaftlich-technische Information mbH, W-7514 Eggenstein-Leopoldshafen 2 (FRG), on quoting the depository number CSD-54906, the names of the authors, and the journal citation.

[8] The bond valence sums for the V^V centers according to $\sum_i (d(V\text{-}O_i)/179.1\ pm)^{-5.1}$ are 4.98 (V2) and 4.91 (V1) and those for the V^{IV} centers according to $\sum_i (d(V\text{-}O_i)/177.0\ pm)^{-5.2}$ are 4.02 (V3) (after I. D. Brown, K. K. Wu, *Acta Crystallogr. Sect. B32* (1976) 1957). The "primary" V^{IV}/V^V distinction is based on the averaged summation $\sum_i (d(V\text{-}O_i)/178.0\ pm)^{-5.15}$.

[9] For details of the computational method see R. Jostes, A. Müller, *THEOCHEM 164* (1988) 211; the atoms V3 and V3a lie on the z axis.

[10] C. J. Ballhausen, H. B. Gray, *Inorg. Chem. 1* (1962) 111.

[11] D. B. Brown (Ed.): *Mixed-Valence Compounds, Theory and Applications in Chemistry, Physics, Geology and Biology*, Reidel, Dordrecht 1980.

[12] This diagram corresponds to the Pourbaix diagram (D. F. Shriver, P. W. Atkins, G. H. Langford: *Inorganic Chemistry*, Oxford University Press, Oxford 1990).

[13] Cf. also occurrence of organic materials in V-containing sediments [1d,1e].

[14] Consequences are V_2O_5 emissions (toxicity) and the partial poisoning of catalysts such as are used, e.g., for hydrodesulfurization processes (replacement of Co/Ni by V).

[15] R. H. Filby, J. F. Brauthaver (Eds.): *Metal Complexes in Fossil Fuels (Geochemistry, Characterization and Processing) (ACS Symp. Ser. 344* (1987)); E. W. Baker, S. E. Palmer: "Geochemistry of Porphyrins" in D. Dolphin (Ed.): *The Porphyrins. Structure and Synthesis, Part A*, Academic Press, New York 1978.

[16] R. Steudel, P. W. Schenk in G. Brauer (Ed.): "Arsen, Antimon, Wismut", *Handbuch der Präparativen Anorganischen Chemie, Vol. 1*, 3rd Edit., F. Enke, Stuttgart 1975, p. 581.

BOOK REVIEWS

Book Reviews are written by invitation from the editor. Suggestions for books to be reviewed and for book reviewers are welcome. Publishers should send brochures or (better) books to the following address: Redaktion Angewandte Chemie, Postfach 101161, W-6940 Weinheim, Federal Republic of Germany. The editor reserves the right of selecting which books will be reviewed. Uninvited books not chosen for review will not be returned.

Protein Purification. Principles, High Resolution Methods and Applications. Edited by *J.-C. Janson* and *L. Rydén*. VCH Verlagsgesellschaft, Weinheim/VCH Publishers, New York 1989. xi, 502 pp., hardcover, DM 124.00.—ISBN 3-527-26184-2/0-89573-122-3

Genetic engineering has made a wide variety of proteins available for pharmaceutical use. An important aspect of this technology is the maintenance of high standards of quality by efficient methods of purification and analysis. This has given a new impetus to the further development of separation techniques, especially from the standpoint of industrial applications.

This book describes the present state of development of all the most important chromatographic and electrophoretic methods for separating proteins. The aspects covered are well defined by the book's subtitle: it is mainly concerned with high resolution methods of purification, with less emphasis on the early stages of an isolation procedure. The procedures of cell breakdown, extraction, separation from other cell constituents, precipitation methods or ultrafiltration, which can have a crucial effect on the success of the stages that follow, are only briefly summarized in an introductory chapter, as also are the associated analyses by protein determination and enzyme tests. For planning a complete work-up process, other sources of information must be called on; however, the reader is greatly helped in this by well-chosen literature references.

The introduction is followed by ten chapters on chromatography: introduction, gel filtration, ion-exchange chromatography, chromatographic focussing, reversed phase HPLC, hydrophobic interactions, separation on immobilized metal ions, "covalent" chromatography, affinity chromatography, and partition in two-phase systems. Whereas here the emphasis is firmly on the preparative applications, the part dealing with electrophoresis goes beyond the book's title by emphasizing the analytical aspects; this consists of six chapters, on gel electrophoresis, isoelectric focussing, immuno-electrophoresis, protein mapping in 2D gels, recovery of proteins and blotting, and capillary electrophoresis, comprising together a third of the contents.

Each chapter consists of an introduction including theory and a description of the available separating media, followed by a section devoted to methods and lastly a number of examples of applications. The references, whose number varies between 30 and 100, enable the reader to study each method in greater depth if required. With regard to the applications described, differences in quality between the chapters become clearly apparent, ranging from only sparse descriptions (e.g. for RP-HPLC) to detailed accounts of experimental procedures (e.g. for affinity chromatography). As suppliers of separating media usually provide detailed instructions along with their products, the absence of laboratory recipes of this kind from the articles is a problem that can certainly be overcome. In other respects the individual contributions are well matched in style and structure. This consistency and the excellent quality of the text and figures combine to make the book very satisfying to use. The fact that most of the 17 coauthors, as well as the editors themselves, belong to either the research department of Pharmacia LKB or the University of Uppsala was a distinct advantage from the standpoint of editorial efficiency. Although this has no doubt influenced the choice of applications examples, it has not detracted from the value of the rest of the texts of the contributions

from a general use standpoint; these have all benefited from a high level of expertise and the authors' practical experience.

The book offers a wealth of useful information not only for newcomers but also for "insiders", who certainly are not equally familiar with every one of the separation methods, and will find here a valuable overview of the current state of the art (the one exception to this is capillary electrophoresis, which has made a huge step forward in the past year). The book can therefore be recommended for buying not only by libraries but also by everyone working in this field.

Gerhard Seipke [NB 1079 IE]
Pharma Forschung
Hoechst AG, Frankfurt/Main (FRG)

Advanced Practical Organic Chemistry. By *M. Casey, J. Leonard, B. Lygo* and *G. Procter*. Blackie, Glasgow 1990. xii, 264 pp., paperback, £ 14.95.—ISBN 0-216-92796-X

This book is concerned solely with the practical side of preparative organic chemistry. The groups of readers for whom it is intended include not only undergraduates and graduate students of organic chemistry, but also particularly those "non-specialists", such as biologists, biochemists, materials scientists and polymer chemists, for whom, according to the authors, the book can serve as a useful information source.

A general introduction in Chapter 1 is followed by a second chapter which describes in detail how to keep a laboratory notebook (experiment number, date, reaction scheme, references to relevant literature, etc.). Here, as also in other parts of the book, the text seems to be aimed more at the "non-specialists" than at organic chemistry undergraduates and graduate students, who should already have learned these procedures in their elementary practical work.

Chapter 3 describes in detail the fitting out of an individual work-bench station and of the laboratory as a whole. It is of particular interest to anyone who needs to set up a new organic chemistry laboratory. He or she will find here a useful survey of general laboratory equipment (rotary evaporators, balances, vacuum pumps, drying ovens etc.) and a detailed list of all the items required at the laboratory bench (numbers and sizes of flasks, and so forth). There is also a good description of modern vacuum systems which have additional facilities for working under inert gases.

Chapter 4 deals with the purification and drying of solvents, and Chapter 5 with the purification and handling of reagents (e.g. transfering liquids under an inert gas, and the preparation of diazomethane). There then follows a chapter on working with gases and another on the various types of vacuum pumps and their capabilities.

Chapter 8 describes how one carries out an organic reaction. Special attention is devoted to reactions using air-sensitive reagents, and there is a very good account of various techniques for working under inert gases. Some simple methods that the organic chemist can use to monitor the progress of a reaction are also described. The following chapter then deals with the work-up of a reaction mixture, including the various methods available for purifying reaction products. The next two chapters are concerned with special points that arise when carrying out reactions on either a very small or a very large scale.

The chapter on methods of characterization deals with the various spectroscopic techniques (NMR, IR, UV, MS), but unfortunately only very superficially. One must ask whether, instead of this really very scanty treatment of such an important subject, it would not have been more useful to refer the reader to appropriate books on spectroscopic methods where these matters are covered in detail.

Towards the end of the book, in a sequence which seems to make little sense, come chapters on the chemical literature (Chemical Abstracts, Beilstein, computer databases), special techniques (photolysis, ozonolysis, vacuum flash pyrolysis etc.), advice on what to do when a reaction goes wrong, examples of particular reactions (the preparation of *n*-butyllithium, the aldol reaction, Claisen rearrangements etc.), and lastly—incredibly placed at the end of the book—a chapter on safety. Especially in view of the authors' claim, referred to earlier, to have addressed the book in part to a readership less familiar with preparative organic chemistry, the placing of the chapter on safety at the end strikes this reviewer as highly questionable. Paradoxically, this chapter begins by stating that "safety is your primary responsibility".

Despite the criticisms made here concerning a few points, the book as a whole provides a very useful survey of modern preparative techniques used in the organic chemistry laboratory. It can be recommended for advanced students, who should be able to afford it in view of the low price.

Hans-Joachim Knölker [NB 1082 IE]
Institut für Organische Chemie
der Universität Hannover (FRG)

Chemically Modified Carbon Fibers and their Applications. By *I. N. Ermolenko, I. P. Lyubliner* and *N. V. Gulko*. VCH Verlagsgesellschaft, Weinheim/VCH Publishers, New York 1990. x, 304 pp., hardcover, DM 184.00.—ISBN 3-527-26027-4/0-89573-873-2

This monograph summarizes in about 300 pages the considerable amount of knowledge gained during the last two decades on carbon fibers (C-fibers). In 1982 the authors published in book form in the USSR a summary of research on doped C-fibers. The present book is an English translation of a revised and considerably enlarged edition of the earlier work. This review of a specialized field is intended not only for specialists but also for graduate students and scientists who wish to become involved in the area of modern fibers.

The introduction describes the various types of C-fibers and classifies them on the basis of their heat treatment and mechanical properties. Here the authors explain that the emphasis in the chapters that follow is on doped C-fibers, which they call "element-carbon-fibers"; for information on undoped C-fibers the reader is referred to other reviews.

In Chapter 2 the structures of C-fibers are discussed with the help of models and experimental results. The pyrolysis process which is an essential part of the preparation of the fibers can be considerably influenced by elements and compounds introduced as dopants, and this causes variations in the (supermolecular) structure of the resulting fibers and in the distribution and chemical form of the dopants in the matrix. Chapter 3 deals with mechanical, thermal and electrical properties of C-fibers and their chemical stabilities. In particular the relationship between microscopic ordering and mechanical strength is discussed. Two special sections are devoted to the activation of adsorption and desorption and that of ion-exchange processes by chemical modification of the C-fibers.

Chapter 4 deals with the pyrolysis of cellulose fibers as a four-stage process. For each temperature range in the process the characteristic chemical changes undergone by the

cellulose, up to its complete carbonization, are discussed in the light of spectroscopic and chromatographic evidence. However, the number of different variables involved in the pyrolysis process is so great that it is probably not realistic to expect a clear relationship between chemical changes of the fiber matrix and the structural and mechanical properties to emerge here.

Chapter 5 is the longest and the most important as regards detailed information content; it deals with the preparation of doped C-fiber materials, with special attention to the effects of different additives on the pyrolysis process. Although the effects occurring during the different stages of the process are many and varied, the authors succeed very well in deriving a systematic relationship between the chemical properties of the additives and their effects on the pyrolysis process.

Chapter 6 is entitled "Surface Modification of C-Fibers". The main emphasis is on the introduction of ionic groups in relation to ion-exchange applications, and on chemical and thermal methods for increasing the adsorptivity of C-fibers.

Compared with this, the surface modification of C-fibers to improve their adhesion properties in polymer and metal fiber-reinforced composites is treated rather too briefly. Also in the applications described in Chapter 7 the authors limit their account mainly to low-modulus fibers and their typical applications in the areas of adsorption, catalysis and medical science. Uses of C-fibers in composite materials are treated briefly, and for applications of high-modulus fibers the reader is referred to already existing reviews.

Although this monograph does not cover all aspects of the chemical modification of C-fibers, it is a useful survey within this specialized field. The qualities of the book that impress are its high information content and the many literature references, which in some parts raise it to the standard of a handbook. It can be strongly recommended for the readership intended by the authors.

Wolfgang Meyer [NB 1085 IE]
Max-Planck-Institut für Polymerforschung,
Mainz (FRG)

Mycotoxins. Chemical, Biological and Environmental Aspects. (Series: Bioactive Molecules, Vol. 9). By *V. Betina*. Elsevier, Amsterdam 1989. 438 pp., hardcover, HFl 295.00.—ISBN 0-444-98885-8

The book gives an overview of the most important mycotoxins, their occurrence, their structures and physicochemical properties, the fungi that produce them, their biosyntheses and their biological activities.

Chapter 1 covers very briefly, but also in a way understandable even to non-microbiologists, some aspects of the taxonomy and chemotaxonomy of mycotoxin-producing fungi. Mycotoxins and their producers are summarized very clearly in four tables, with indications of the chapters in which they are treated more thoroughly.

Chapter 2 covers general aspects of secondary metabolites, which include mycotoxins. The most important topics and theories are introduced and discussed.

Chapter 3 summarizes the most important biological effects of mycotoxins. In addition to the toxic effects on man and mammals, their effects on insects, plants and other microorganisms are discussed. The relevance of biological screening is also discussed. Chapter 4, on modes of action, describes many different sites of action and metabolic pathways that are affected by mycotoxins. Unfortunately there is not much critical evaluation of published results. A distinction between primary and secondary effects would have been helpful to the non-specialist. Chapter 6 briefly describes some ecological aspects of toxins and the organisms that produce them. With regard to methods of detection, biological tests are described in most detail.

In the second half of the book, covering 12 chapters, the most important mycotoxins are described, and arranged by chemical structure or biological action. The aflatoxins, sterigmatocystins and versicolorins, the ochratoxins and related compounds, citrinin, the tricothecenes, patulin and other small lactones (penicillic acid, mycophenolic acid, butenolide, citreoviridin), zearalenone, the cytochalasans, rubratoxins, anthraquinones, tremorgenic mycotoxins (including penitrems and paspaline) and epipolythiopiperazine-3,6-diones such as gliotoxins and chaetocins, are all comprehensively described.

The chapter "Miscellaneous Toxins" deals very briefly with PR toxin, secalonic acid D, viridicatum toxin, cyclochlorotine, cyclopiazonic acid, moniliformin and fusarin C. For each mycotoxin, information on the organism that produces it, its occurrence, the biosynthesis of the toxin, its isolation and physicochemical characterization, its structure, biological activity, mode of action and ecological aspects is set out very clearly.

The book has several merits; it is easy to follow, well-organized, and contains essential information for all the toxins listed, covering the literature up to 1988 inclusive. The mycotoxin producing organisms are listed separately in the index. It is almost unavoidable for a book of this size to also contain some flaws. The formula of one of the tautomeric forms of mycophenolic acid (p. 244) is incorrect. Beside the formula for moniliformin there is an extra unrelated group.

Overall, this book serves as an up-to-date compilation of the most important mycotoxins. It can be recommended as a reference work, as an introduction to the subject, or as an accompaniment to lectures. Unfortunately the variety of biological effects are often only listed but not evaluated, which reduces the value of the book for the non-biological reader.

Timm Anke [NB 1094 IE]
Lehrbereich Biotechnologie
der Universität Kaiserslautern (FRG)

Biomineralization, Chemical and Biochemical Perspectives. Edited by *S. Mann, J. Webb* and *R. J. P. Williams*. VCH Verlagsgesellschaft, Weinheim/VCH Publishers, New York 1989. xiv, 541 pp., hardcover, DM 274.00.—ISBN 3-527-26750-6/0-89573-672-1

Reports on international conferences about aspects of biomineralization appear at nearly regular intervals of four to five years. A particularly important contribution on this topic was that of the 1981 Dahlem conferences (*Life Science Research Report 23*). Up to then biomineralization had been understood to be a process involving the formation of insoluble calcium compounds. In addition biomineralization had come to be regarded as a biological phenomenon that also includes pathological aspects such as the formation of stones in the body, and demineralization processes (osteoporosis, caries). Since 1983, however, the term biomineralization has started to undergo a change of meaning to include the area of "biological metal accumulation", and appears to be becoming a part of "bioinorganic chemistry". Thus the original meanings of the terms are gradually becoming blurred.

The bood reviewed here is well produced and appears at an opportune time, especially in view of the fact that, in addition to the emergence of the aspects mentioned above,

new developments in techniques now necessitate an updated treatment of the subject. The material is divided into 15 chapters which are written in the style of review papers. The topics covered are as follows: the functional forms of biominerals; crystallographic strategies of biomineralization; the carbonate calcification of algae, matrix-crystal interactions in $CaCO_3$ biomineralization; stereochemical and structural relationships between macromolecules and crystals in biomineralization; in vitro studies of calcium phosphate crystallization; biochemical studies of teeth mineralization in vertebrates, chemical studies of biogenic silicates; function and structure of ferritin and hemosiderin, biomineralization of iron in the teeth of molluscs; mineralization of magnetite in unicellular organisms; structural and analytical studies of metal ion-containing granules; the use of proton beam analysis in studies of mixed biominerals; the significance of studies on biomineralizates for materials technology.

The contents are, without exception, good and the treatment of the subject matter is impeccable. For the specialist the book offers a rich source of ideas and suggestions. However, only three of the articles are concerned with matrix-crystal interactions, which is the central topic of biomineralization. Moreover, two articles on this subject put forward controversial views, giving the impression that the role of the organic matrix is questionable, or at least unimportant (see also the preface). The reader is left alone with this problem, without being given a clear answer. Some time ago *S. Mann*, in his article "Biomineralisation" (*Chem. Unserer Zeit 20* (1986) 69), gave a much better, unambiguous and impressive statement of his position on this question. There he clearly and unequivocally explained the difference between geological minerals and biomineralizates. The fundamentals of techniques and theory are certainly a part of this question. Here an unusually large amount of space is devoted to these aspects and to crystal structure studies. Moreover, of the total of about 500 pages of text, almost 200 are devoted solely to iron, resulting in a serious imbalance. Lengthy discussions about ferritin structures have very little to do with biomineralization. Alongside these chapters the more biologically orientated articles give the impression of having been grafted on. Only one page is given to pathological biomineralization processes. However, apart from these few inconsistencies, the book opens up some useful chemical and biochemical perspectives.

Gottfried Krampitz [NB 1102 IE]
Institut für Anatomie, Physiologie und Hygiene
der Haustiere
der Universität Bonn (FRG)

Reizvolle Moleküle der Organischen Chemie. (Series: Teubner Studienbücher Chemie). By *F. Vögtle*. Teubner, Stuttgart 1989. 402 pp., paperback, DM 39.80.—ISBN 3-519-03503-0

Each volume in the series "Teubner Studienbücher Chemie" deals with fundamental and more advanced aspects of a particular field of chemistry. The books do not aim at the breadth of coverage of a textbook, nor at the depth of treatment of a comprehensive monograph; instead they are intended only to give the student of chemistry an *introduction* to specialized topics that are of current interest, and which are therefore undergoing rapid development.

In the volume "Reizvolle Molecüle der Organischen Chemie" published in 1989 (and also in the following volume "Supramolekulare Chemie – Eine Einführung",[*] which appeared almost simultaneously), *Fritz Vögtle* presents a survey of "attractive molecules" relevant to his field of study. His starting point is a wish to open up to the reader, in a way that is both instructive and entertaining, the great variety of organic chemistry, by taking him or her on a journey of discovery through the field of unusual molecules and all that relates to them (their history, synthesis, chemical and spectroscopic properties, and applications). In the resulting thoroughly readable organic chemistry book, the appeal of the "attractive molecules" referred to in the title is revealed not least through the many lavish stereoscopic illustrations which provide three-dimensional views; *Vögtle*'s artwork studio has already set a high standard of quality with illustrations such as these in numerous publications. They are a delight to the eye! Or, as the author himself puts it on page 23: not least of the aimes was that merely looking at the structures shown here should bring joy to the heart of every chemist!

Among the most notable of the "attractive molecules" that *Vögtle* has in mind in the title of the book are hydrocarbons that are to some degree exotic. Accordingly, the introduction (19 pp.) is followed by detailed excursions into the chemistry of interesting aliphatic hydrocarbons (Chapter 2, 56 pp.), arenes (Chapter 3, 115 pp.), and "araliphatics" (Chapter 4, 65 pp.). It is evident that deciding what to include or leave out must have been a painful choice. Some of the interesting molecules that were filtered out are the following: tetra-*tert*-butyltetrahedrane, cubane, dodecahedrane, adamantane, pagodane, and [1.1.1]propellane (Chapter 2); the triphenylcyclopropenyl cation, azulene, biphenylene, circulene, and [7]helicene (Chapter 3); triptycene, iptycene, 1,8-methanonaphthalene, [2.2.2]cyclophane, and superphane (Chapter 4). As one can see from the restrictions placed on the material included, no attempt has been made in *Vögtle*'s book to cover the *entire* field of exotic hydrocarbons. Instead, rigorously limiting the coverage to just a *few* candidates has made enough space available to allow a satisfying breadth and depth in the treatment of the material.

The meticulous care that *Vögtle* has brought to the task of doing justice to the title of the book is evident from the lengths of the bibliographies to the chapters, which amount to a total of 31 pages! In a literature study of such a high standard as this, it is not surprising to find that only a few years ago it would not have been possible to write this particular book, despite the fact that the topic of exotic hydrocarbons is far from new. Among the recent reactions included are the synthesis of cubene (October 1988), *Prinzbach*'s second-generation syntheses of dodecahedrane (March 1989) and the anionic polymerization of [1.1.1]propellane (May 1989).

Whether one's interest lies mainly in deeper subjects such as a comparison of azulene syntheses, in relationships between structure and color in azulenes, in the regioselectivity of electrophilic substitutions of biphenylenes, of 1,8-methanonaphthalene or of cyclophanes, whether one wishes to become enmeshed in the three-dimensional structural formulas of the helicenes, heterohelicenes or helicenophanes, or goes in search of curiosities such as information about adamantane chemistry being carried out *on a tonnage scale* in Japan with the aim of treating Parkinson's disease, or about evidence for the presence of the cyclopropenylium ion in Halley's comet, *Vögtle*'s book offers something for everyone who enjoys browsing among topics in organic chemistry that

[*] Review: *Angew. Chem. 102* (1990) 112.

are off the well-trodden track of textbooks. Moreover, the reader who has become tired of hydrocarbons will welcome the relief of Chapter 5 on heterocycles and compounds with pharmacological activity, dealing with Tröger's base, acetylsalicylic acid, vitamin B_6 and phthalocyanines. In this reviewer's opinion the chapter might also have very usefully combined the pharmacologically active with the exotic by giving a glimpse into the fascinating chemistry of antitumor antibiotics of the enediyne type (Neocarzinostatin, Esperamycin, Calichemicin), which currently are possibly the "hottest" of all classes of biological substances.

The formula schemes are clear and visually pleasing throughout (some minor exceptions: the undecipherable trishomocubyl moieties on page 65, the nearly invisible C = C bonds in the intermediates **8** and **9** on page 72, and the representation of phthalocyanine on page 332 which seems more like a puzzle. The very small number of errors in the structural formulas include a missing carbonyl oxygen in **8** on page 35, the omission of the second regioisomer of the bis(diazoketone) in the formula on page 72, three missing double bonds in **10** on page 189, and $(CH_2CO)_2O$ instead of $(CH_3CO)_2O$ on page 293. A few of the synthesis schemes (pages 60, 72, 140, 174, 211, 268, 305) could have been made even more informative by inserting the reagents (although these are, of course, referred to in the text).

The text is written in a flowing style, and covers the subject matter with a breadth and depth that are appropriate to the book. The few minor errors are unlikely to lead the reader astray; for example, HCl elimination reactions are described as being base-catalyzed instead of being carried out with stoichiometric quantities of base (pp. 86, 87), "Retro-Alder-Reaktion" appears instead of Retro-Aldol-Reaktion (p. 51), and reference is made to planar conformation instead of configuration (p. 67). On page 61 the Wagner-Meerwein rearrangement does not start out from the adamantyl cation but leads to it. On page 72 the word "Diazotierung" is used to describe the transfer of a diazo group, and on page 122 an azo coupling reaction is wrongly described by the word "Azotierung". "Benzofulvalen" on page 100 should read Benzofulven, on page 264 "*o*-Xylen" appears instead of *o*-Xylylen, on page 266 "Propionsäureester" instead of Propiolsäureester, and on page 269 "Ethyldiazotat" instead of Ethyldiazoacetate. On page 218 it is evident from the structural formula that a "Carbeniat" here means a carbanion. The NMR spectrum described on page 136 is of the AA'BB' type, not A_2B_2. In the chapter on azulenes Figures 7 and 9 show the formulas of intermediates in reactions that are probably better described as concerted processes (an electrocyclic ring-opening and a [2 + 8]-cycloaddition). Occasionally the term mesomerism is used in an unfortunate way which could lead to confusion for beginners in organic chemistry. References such as those to "Einfluß hyperkonjugativer Grenzformen" (effects of hyperconjugated canonical forms, p. 66), or to discontinuance of a "Möglichkeit zur Ausbildung mesomerer Grenzformen" (possibility of formation of mesomeric canonical forms, p. 126), the showing of a mesomerism arrow *between structural isomers* (p. 130), or the analysis of the possible canonical structures for a carbenium *transition state* (p. 137) imply a degree of reality for canonical forms which is of questionable validity.

The preface contains an assurance that *large* portions of the book assume only knowledge of an undergraduate level, but perhaps one should not take this quite literally. In fact, in *many* parts of the book the treatment is of a breadth and depth (as already commended above) such that only very advanced undergraduate or rather graduate students are likely to benefit from reading "Reizvolle Moleküle". However, those at the latter stage of their studies who wish to gain a deeper knowledge of organic chemistry through reading of a less formal kind are assured that, by buying *Vögtle*'s book, they will obtain pleasure from it without undue pain (at a price of only DM 39.80 for 402 pages).

Reinhard Brückner [NB 1091 IE]
Fachbereich Chemie
der Universität Marburg (FRG)

Corrigendum

The address of the authors of the communication "Dynamic HPLC: A Method for Determining Rate Constants, Energy Barriers, and Equilibrium Constants of Molecular Dynamic Processes" (*Angew. Chem. Int. Ed. Engl. 30* (1991) 74) should read:

Dr. J. Veciana, Dipl.-Eng. Chem. M. I. Crespo
Institut de Ciències de Materials – C.I.D., C.S.I.C.
Jordi Girona, 18–26, E-08034 Barcelona (Spain)

Registered names, trademarks, etc. used in this journal, even when not marked as such, are not to be considered unprotected by law.

© VCH Verlagsgesellschaft mbH, W-6940 Weinheim, 1991. – Printed in the Federal Republic of Germany by Konrad Triltsch Druck- und Verlagsanstalt Würzburg.

All rights reserved (including those of translation into foreign languages). No part of this issue may be reproduced in any form — by photoprint, microfilm, or any other means — nor transmitted or translated into a machine language without written permission from the publishers. Only single copies of contributions, or parts thereof, may be made for personal use. This journal was carefully produced in all its parts. Nevertheless, authors, editors and publisher do not warrant the information contained therein to be free of errors. Readers are advised to keep in mind that statements, data, illustrations, procedural details or other items may inadvertently be inaccurate.

Valid for users in the USA: The appearance of the code at the bottom of the first page of an article (serial) indicates the copyright owner's consent that copies of the article may be made for personal or internal use, or for the personal or internal use of specific clients. This consent is given on the condition, however, that the copier pay stated per-copy fee through the Coyright Clearance Center, Inc. (CCC), for copying beyond that permitted by Sections 107 or 108 of the U.S. Copyright Law. This consent does not extend to other kinds of copying, such as copying, for general distribution, for advertising or promotional purposes, for creating new collective works, or for resale. For copying from back volumes of this journal see 'Permissions to Photo-Copy: Publisher's Fee List' of the CCC.

Editorial office: Postfach 10 11 61, W-6490 Weinheim, Federal Republic of Germany, Telephone (06201) 60 23 15, Telex 465 516 vchwh d, Telefax (06201) 602 328, E-Mail Z16@DHDURZ2 in Earn Bitnet.

Editor: *Peter Gölitz*

Associate editors: *D. I. Loewus, K. J. Schneider, A. Stimson.* **Editorial assistant:** *E. Schweikart*

Publishers: VCH Verlagsgesellschaft mbH. (Managing Directors: *Hans Dirk Köhler, Dr. Hardy G. Sehrt.*), Pappelallee 3, W-6940 Weinheim, Federal Republic of Germany.

Advertising office (Advertising Manager *R. J. Roth*): Postfach 10 11 61, W-6940 Weinheim, Federal Republic of Germany, Telephone (06201) 606136, Telex 467155, Telefax (06201) 606156.

ANGEWANDTE CHEMIE

International Edition in English

Volume 30 · Number 3
March 1991
Pages 217–342

Iminophosphanes: Unconventional Compounds of Main Group Elements

By Edgar Niecke* and Dietrich Gudat

Dedicated to Professor Rolf Appel on the occasion of his 70th birthday

The large number of known stable compounds in which phosphorus has a low coordination number makes it clear that such compounds can no longer be regarded as "exotic" in main group chemistry. While the rich chemistry of P–C multiply bonded systems makes clear their affinity to their organic congeners, iminophosphanes in particular are also of increasing importance. The linkage of a phosphinidine fragment with an imine fragment via a multiple bond gives rise to a class of compounds with an unusually wide range of structural types. This in turn leads to a broad spectrum of chemical behavior which makes iminophosphanes extremely useful synthetic building blocks in organoelement chemistry.

1. Introduction

The development of the chemistry of multiply bonded systems involving elements in higher periods is generally regarded as a renaissance of main group chemistry. An extremely important role in this chemistry has been played by phosphorus compounds with low coordination numbers; although the first of these were discovered in the 1960's, either little notice was taken of them because of their low stability ($P{\equiv}CH$[1]) or they were regarded sceptically because of the nature of their bonding (phosphacyanine) cations[2]). The discovery of arenes of the phosphabenzene type[3] led to a more intensive study of compounds with such "exotic" bonding systems. The preparation of acyclic imino-[4] and methylenephosphanes[5] marked the beginning of a rapid phase of development, in the course of which a number of compounds were prepared which are both synthetically useful and also interesting because of their bonding properties.[6] This work culminated in the 1980's in the inclusion of heavier elements of the fourth[7] and fifth main groups[8] and of boron[9] in a stable (p–p)π-bonding system involving phosphorus.

The (3p–2p)π-P–N bonding system occupies a special place among the known compounds with twofold coordinated phosphorus because of the presence of a π-bonded fragment of high electronegativity with a "lone pair". In contrast to the phosphorus atom, the imine nitrogen can vary its bonding state within wide limits by means of formal electron release or acceptance ("isovalent hybridization"[10]); this manifests itself in a series of unconventional structures and gives rise to unusual reactivity patterns. The application of this potential made possible the first successful synthesis of bis(imino)phosphoranes from iminophosphanes; it has also led to the generation of a large number of new heterocycles, so that today the iminophosphanes can be regarded as important synthetic building blocks in organoelement chemistry.

The present account will attempt to provide a critical overview of the chemistry of the P=N double bond, particular attention being paid to structural and bond-theoretical aspects. We have attempted to prepare a comprehensive survey, including more recent work. As experience has shown, systems such as aminophosphenium cations[11] or resonance-stabilized five-membered PN heterocycles of the aza-

[*] Prof. Dr. E. Niecke, Dr. D. Gudat
Institut für Anorganische Chemie, Universität Bonn
Gerhard-Domagk-Strasse 1, W-5300 Bonn 1 (FRG)

phosphole type[12] (in which P–N bonds with (p–p)π-interactions are also present) exhibit a quite different chemical behavior. These classes of compounds will thus not be included in the present discussion, and we refer the reader to relevant reviews.[11, 12] The coordination chemistry of iminophosphanes has also not been included, since it has been covered in detail in a recent survey.[13] We should mention that some aspects of the subject matter covered here have been discussed in earlier reviews.[14, 15]

2. Synthetic Methods

2.1. Elimination Reactions

In analogy to the normal methods for the formation of olefins or heteroolefins (e.g. phosphaalkenes, silaalkenes),

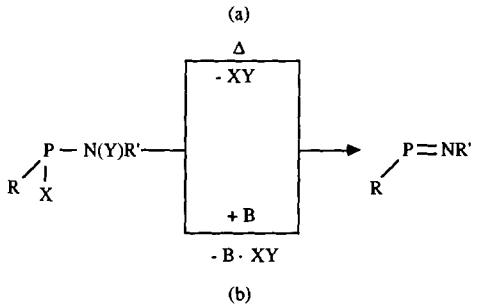

Scheme 1. Formation of the double bond in iminophosphanes by thermally-induced (a) or base-induced elimination (b).

1,2-elimination reactions form by far the most important synthetic route to iminophosphanes. The formation of the double bond by elimination of a molecule XY from aminophosphanes R(X)P–N(Y)R′ can be carried out either thermally or under the influence of a base (Scheme 1). The preparatively most valuable methods involve thermal elimination of organohalogenosilanes (X = F, Cl, Br; $Y = SiMe_3$)[16–40] or lithium halides (X = F, Cl; Y = Li)[24, 36, 41–45] and base-induced dehydrohalogenation reactions (X = Cl, Y = H).[38, 46–47]

The thermal elimination of trimethylchlorosilane from the *N*-silylated diaminohalogenophosphanes **2a–2c**, which were prepared from PX_3 via **1**, provided the first route to an isolable aminoiminophosphane **3** with a P–N-(p–p)π-bonding system[4, 17] (Scheme 2). The synthesis of a variety of

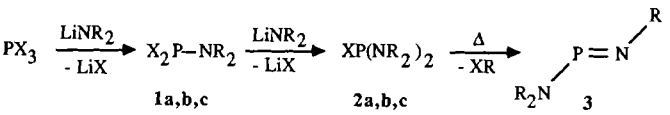

Scheme 2. R = $SiMe_3$; X = F (**a**), Cl (**b**), Br (**c**).

iminophosphanes has been carried out in an analogous manner via thermolysis of suitably substituted precursors; apart from *P*-alkyl or *P*-aryl substituents,[24, 29] these can contain *P*-amino,[16–18, 21–23, 39] *P*-hydrazino,[19, 29, 40] *P*-diorganophosphino[36, 37] or *P*-aryloxy substituents[32] as well as *N*-phosphino[26, 30] or *N*-amino[20, 27, 28] residues. In spite of the versatility of this synthetic principle, it is limited in its generality, as the thermal stability of the precursors requires extremely drastic reaction conditions. The high temperatures required lead to the occurrence of side reactions: for example the thermolysis of diaminofluorophosphanes $R_2N(F)P–N(SiMe_3)tBu$ with sterically undemanding R_2N ligands (**4e–h**) leads to elimination of R_2NSiMe_3 with formation of 1,3-di-*tert*-butyl-2,4-difluoro-1,3,2,4-diazaphosphetidine **6** rather than the expected iminophosphanes **5**[27, 48] (Scheme 3). It is generally necessary to remove the

Edgar Niecke, born 1939 in Berlin, studied chemistry at the University of Göttingen, where he received his doctorate under the supervision of O. Glemser. After his habilitation in 1976 in Göttingen, he took up an appointment as Professor of Inorganic Chemistry at the University of Bielefeld, and in 1986 he was offered and accepted a professorial chair at the University of Bonn. His main fields of interest are the synthesis, structure, and reactivity of compounds of phosphorus with lower coordination numbers (phosphorus-element (p-p)π bond systems), but also phosphorus heterocycles, phosphanediyls and organometallic compounds with novel phosphorus ligands.

Dietrich Gudat, born 1957 in Düsseldorf, studied chemistry at the University of Düsseldorf and then at the University of Bielefeld, where he gained is doctorate under the supervision of E. Niecke. After Postdoc research at the University of Sussex (with J. F. Nixon) and at the Iowa State University (with J. G. Verkade) he accepted a post at the University of Bonn, where he has been working for his habilitation since 1989. His research interests focus on investigations of the coordination chemistry and redox properties of novel podand-like and macrocyclic phosphorus compounds as well as the applications of NMR spectroscopy, particularly for the monitoring of dynamic processes.

iminophosphanes continually from the reaction mixture in order to avoid the occurrence of further reactions, so that this method is only suited for the preparation of volatile compounds which distil without decomposition.

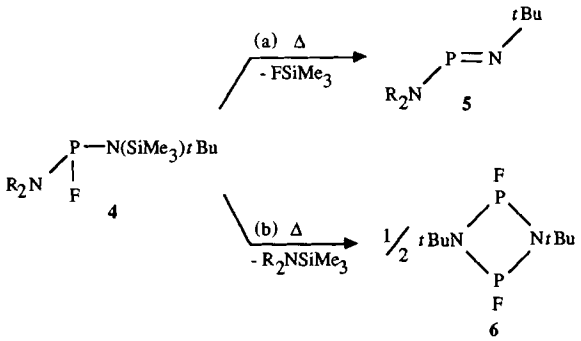

	a	b	c	d	e	f	g	h
R	$SiMe_3$	*t*Bu	*i*Pr	*s*Bu	*n*Bu	*n*Pr	Et	Me
(a)	+	+	+	+	+	+		
(b)					(+)	(+)	+	+

Scheme 3. Product formation in the thermolysis of diaminophosphanes in dependence of residue R.

It is possible to avoid high temperatures in the synthesis of iminophosphanes by using a procedure involving thermal salt elimination, since the decomposition temperature of the *N*-lithiated aminohalogenophosphane precursors is much lower than that of the *N*-silylated derivatives. Thus, the formation of **8** via elimination of LiX from **7a,b** occurs at below 20 °C (X = Cl) or at 60 °C (X = F), while the elimination of Me_3SiCl from *N*-silylated **7c** only occurs at above 150 °C[24] (Scheme 4). The *N*-lithiated aminohalogenophosphanes can readily be prepared from the corresponding NH-substituted derivatives via Li/H exchange. Lithium amides ($LiN(SiMe_3)_2$, $LiN(SiMe_3)$*t*Bu,[41–44] lithium di-*tert*-butylphospide[36,45] or *tert*-butyllithium[24] have been found to be particularly advantageous, as they combine a considerable basicity with a steric demand which suffices to suppress side reactions such as substitution at the phosphorus atom or addition of the organo-H compounds formed to the P=N double bond. In general, as can be seen from the examples **7a,b**, the thermal stability of *N*-lithiated phosphanes decreases on going from fluoro-substituted derivatives (which are in some cases isolable and stable at room temperature) to the chloro- or bromo-substituted derivatives, so that the salt elimination can often be carried out below room temperature.

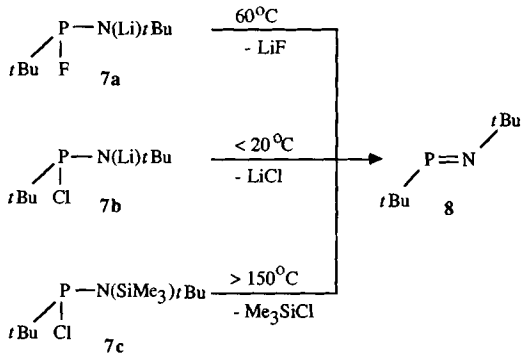

Scheme 4. Variation of reaction conditions by using lithiated aminohalogenphosphanes.

In contrast to the thermal elimination reactions, the amine-induced dehydrohalogenation of NH-substituted aminohalogenophosphanes normally leads to the formation of 1,3,2,4-diazadiphosphetidines (cf.**6**)[49–51] or higher P,N oligomers.[51] It has not yet been demonstrated unequivocally that unsaturated intermediates are formed.[50] Only in a few cases has the formation of isolable P=N double bond systems in such elimination reactions been reported: thus the reaction of the aminochlorophosphanes **9** and **11** with triethylamine and DBU (1,8-diazabicyclo[5.4.0]under-7ene) respectively yields the *P*-functionalized iminophosphanes **10**[46,47] and **12**[38] (Scheme 5), the formation of which is apparently favored by the high steric demand of the substituents at nitrogen.

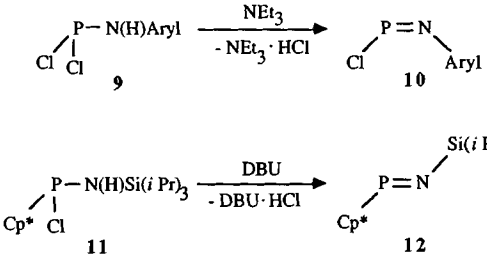

Scheme 5. Aryl = 2,4,6-tri-*tert*-butylphenyl, Cp* = pentamethylcyclopentadienyl.

The synthesis of iminophosphanes is in principle also feasible via 1,1-elimination reactions starting from iminophosphorane precursors, as has been shown for the reductive debromination of the dibromoiminophosphorane **13**[52] and the desulfurization of iminothiophosphoranes such as **14** to **15** (Scheme 6).[50,53] Although this reaction is of theoretical interest, its preparative use has so far been only very limited, as the synthesis of the precursors was carried out starting from iminophosphanes.

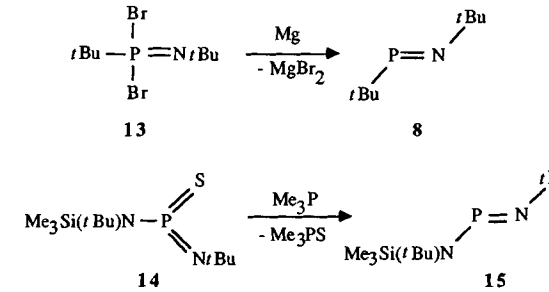

Scheme 6. Synthesis of iminophosphanes by 1,1-elimination.

A recent report[54] has described the preparation of the *N*-aminooxy-substituted iminophosphane **16** via an elimination of water in the course of the reaction between PH_3 and

O-nitroso-*N*,*N*-bis(trifluoromethyl)hydroxylamine.[54] However, the suggested structure **16** involving a P=N double bond does not follow with certainty from the spectroscopic data presented; the IR spectrum in particular supports the isomeric structure **17**.

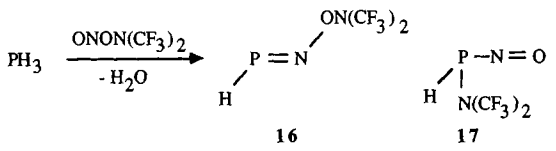

It has in several cases been possible to use the synthetic principles described above for the preparation of homologous molecules with As=N double bonds.[40, 42]

2.2. Substitution Reactions

Iminophosphanes with a nucleofugal leaving group at phosphorus can react with nucleophiles via ligand substitution, the double bond remaining unchanged (Scheme 7). The

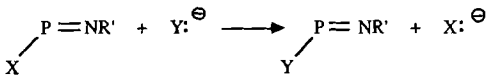

Scheme 7. Synthesis of iminophosphanes by nucleophilic substitution.

first reported preparative applications of this synthetic method involved the transamination of bis(trimethylsilyl)-aminoiminophosphanes with dialkylamides[55] and the preparation of the aryliminophosphane **18** from **3** and 2,4,6-tri-*tert*-butyllithiobenzene[53, 56] (Scheme 8). However, only the

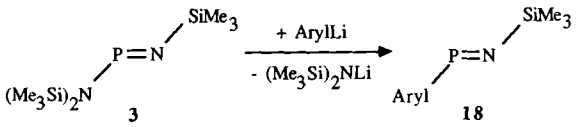

Scheme 8. Aryl = 2,4,6-tri-*tert*-butylphenyl.

recent preparations of stable *P*-chloro[47] and *P*-phenoxy derivatives[32] have permitted such substitution reactions to become of more general importance.[46, 57–61] The chloroiminophosphane **10** in particular has been shown to be a key intermediate in the preparation of a large variety of new *P*-functionalized iminophosphanes[46, 47, 58–60, 62–64] (Scheme 9). Reactions of **10** with *N*-lithiated aminoiminophosphanes should also be mentioned: these afford 1,3,5-triaza-2,4-diphosphapenta-1,4-dienes **20**[61] (Scheme 9), which as heteroanalogues of pentadienyl anions are expected to exhibit interesting coordination properties. While in general *P*-alkyl- or *P*-aryl-substituted iminophosphanes do not undergo ligand substitution reactions, pentamethylcyclopentadienyl-substituted compounds such as **12** are a special case, as the five-membered ring can readily be exchanged in a nucleophilic manner for amino or aryl substituents (e.g. synthesis of **21**, aryl = 2,4,6-tri-*tert*-butylphenyl.[38] An unex-

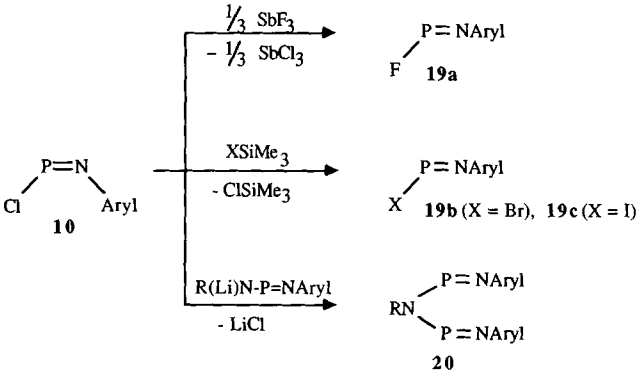

Scheme 9. Aryl = 2,4,6-tri-*tert*-butylphenyl. X can, apart from being F, Br, I also be tBu$_2$As, tBu$_2$P, R'RN, RO, tBuS, R$_2$C=N, Cp*, tBuC≡C, R$_3$P=N. **20a**, R = tBu; **20b**, R = Aryl; **20c**, R = 2,4,6-iPr$_3$C$_6$H$_2$).

pected substitution of the tBu residue (rather than an oxidative addition at phosphorus) was also observed in the reaction of tBuP=NAryl with sterically demanding halogenoamines.[32]

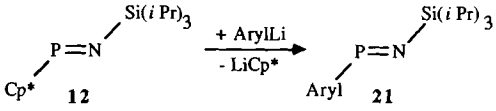

2.3. Rearrangement Reactions

Only a few examples of syntheses of iminophosphanes via rearrangement reactions have so far been described. The formation of a P=N double bond via a [1,3] shift of a silyl group bonded to phosphorus to a doubly bonded oxygen in the α-position, a standard synthetic principle in phosphaalkene chemistry, has only been verified in the preparation of the *N*-silyloxy-substituted iminophosphanes **23**.[65] A

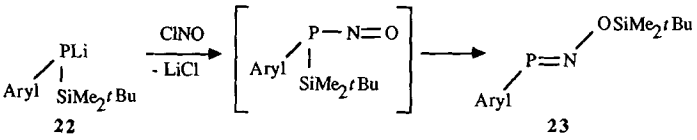

[1,3] silyl shift is also assumed to occur during the reaction of the phosphonium salt **24** with three equivalents of sodium bis(trimethylsilyl)amide, which affords the phosphoranylidenemethyl-substituted iminophosphane **25**.[66] The [1,3]

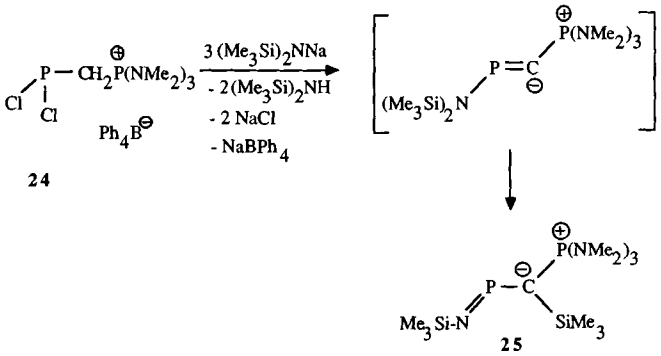

shift of a dialkylamino group has been suggested to occur in the formation of **27** by photolysis of azidobis(diisopropylamino)phosphane in the presence of the iminophosphane **26**[67] (Scheme 10). The reaction of the 2,3-dihydro-1,3,2-

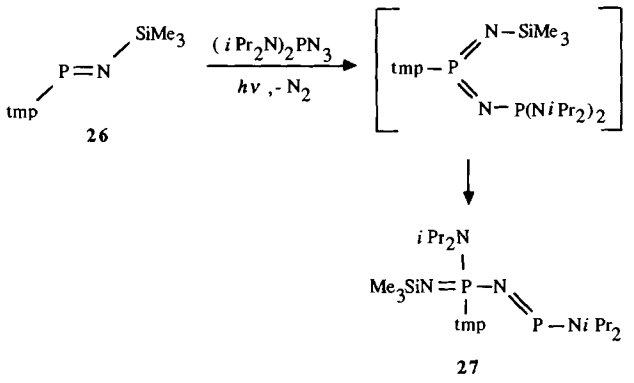

Scheme 10. tmp = 2,2,6,6-tetramethylpiperidyl.

oxazaphosphole **28** with *tert*-butyl(trimethylsilyl)amine leads via elimination of trimethylchlorosilane and [1,5] hydrogen shift to the functionalized aminoiminophosphane **29**.[68]

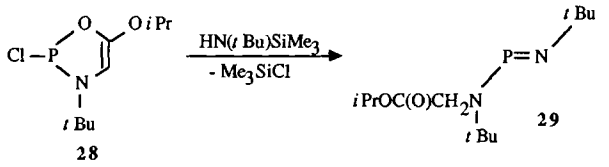

2.4. Cycloreversion Reactions

Because of the reversibility of the [2 + 1] cyclodimerization of iminophosphanes, the λ^3,λ^5-azadiphosphiridines formed in the reverse reaction can in turn be used as precursors for iminophosphanes (Scheme 11). It is thus possible,

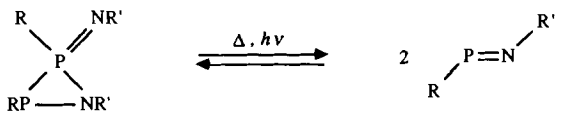

Scheme 11. Azadiphosphiridines as sources of iminophosphanes.

starting from solutions of *P*-alkyl-*N*-alkyl/aryl-substituted $\lambda^3\lambda^5$-azadiphosphiridines to generate the corresponding monomers thermally or photochemically and to characterize them spectroscopically, even though they are not stable in the pure state.[24, 42, 44] The cycloreversion of *N*-silyl-substituted $\lambda^3\lambda^5$-azadiphosphiridines requires considerably higher temperatures; under such conditions the monomers cannot be characterized spectroscopically, but their presence has been detected by means of trapping reactions (see Section 4.3). Thermal [2 + 1] cycloreversion reactions of $\lambda^3\lambda^3$-azadiphosphiridines have been observed in the case of **30**; they lead to the formation of the aminoiminophosphanes **3** and **5** as well as to cyclopolyphosphanes $(RP)_n$[69, 70] (Scheme 12).

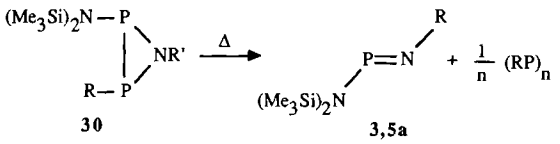

Scheme 12. R = iPr$_2$N, tBu; R' = SiMe$_3$, tBu.

There are very few examples of the formation of iminophosphanes via retroreactions starting from four-membered or larger rings. The diazadiphosphetidine **31** (R = SiMe$_3$) is in equilibrium with the aminoiminophosphane **32** (R = SiMe$_3$),[20] while the formation of iminophosphoranes and alkoxyphosphanes in the course of reactions of the cyclotetramers $(Me_3C_6H_2PNtBu)_4$ with diethylamine and alcohols respectively has been explained as resulting from reactions of the iminophosphane formed from the eight-membered ring by cycloreversion.[51] Electro-

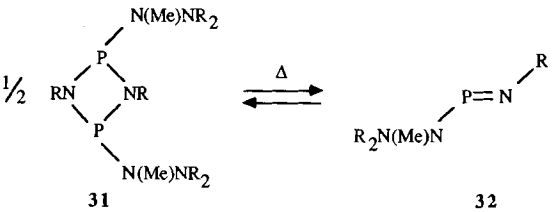

cyclic ring-opening of an intermediate didehydrodiazadiphosphetidine has been postulated to be involved in the formation of the phosphoranyl-substituted iminophosphanes **34** via oxidation of the diazadiphosphetidine **33** with CCl_4[67, 71] (Scheme 13).

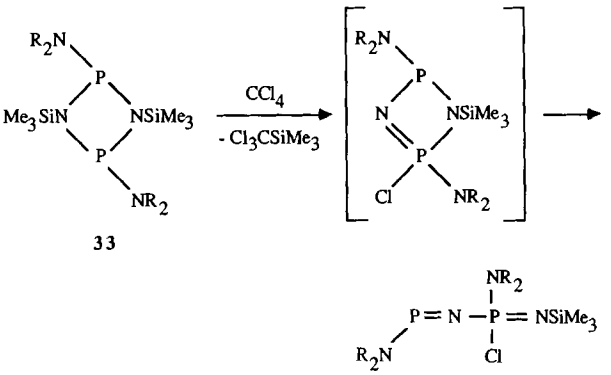

Scheme 13. R = iPr, SiMe$_3$.

3. Structural and Bonding Considerations

3.1. Theoretical Studies

According to ab initio calculations the parent system HP=NH resembles diimine in having a planar bent structure, the (*E*)-conformation being slightly more stable than the (*Z*)-conformation.[72–79] Participation of d orbitals in the double bond system can be neglected.[80] The comparison with structural parameters calculated at the SCF level[76]

(see Fig. 1) shows that the transition from (*E*)- to (*Z*)-HP=NH is accompanied by a shortening of the P–N bond and an increase in the bond angles P and N. The inversion barrier at the nitrogen atom is considerably lower than that in diimine and corresponds to approximately one-third of the activation energy for a rotation about the π bond. According to these calculations, the (*E*)/(*Z*)-isomerization involves a transition state in which the PNH geometry is almost linear[73, 76] (Fig. 1). The low value of the nitrogen inversion barrier can be regarded as the reason why it has so far not been possible to detect the existence of (*E*)/(*Z*) isomer pairs in iminophosphanes.

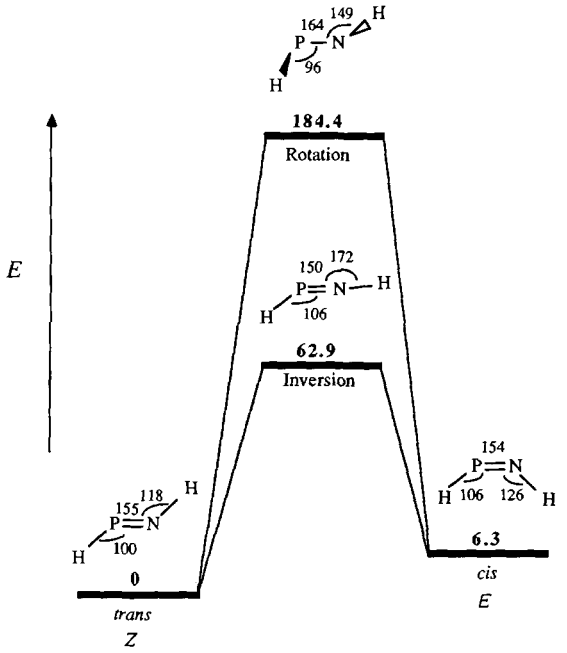

Fig. 1. SCF equilibrium geometries and relative energies for HP=NH (bond lengths in pm, bond angles in degrees, energies in kJ mol^{-1}; after[76]).

Replacement of the hydrogen atom at phosphorus in HP=NH by either more electronegative or more electropositive substituents (π-acceptors/donors) results in the former case in an appreciable strengthening and in the latter in a corresponding weakening of the double bond. At the same time the (*Z*)-configuration becomes more stable with respect to the (*E*)-configuration, while the inversion barrier is decreased.[81] Exactly opposite effects have been forecast for the influence of corresponding substituents at nitrogen,[81] the greatest changes being observed for donor-acceptor ("push-pull")-substituted model compounds.[37, 81] A weakening of the double bond with concomitant formation of a delocalized 4-electron-3-center π-bond system is caused by the introduction of substituents with pronounced π-donor properties (e.g. NH_2) at the phosphorus or nitrogen atoms.[72, 81, 82] The inductive effect of the ligands is either weakened (by *P*-substitution) or strengthened (by *N*-substitution).[81]

An analysis of the frontier orbitals of (*E*)-HP=NH shows that the HOMO is a non-bonding orbital which is mainly localized at phosphorus, while the LUMO is an antibonding π^* orbital. The π(P=N) orbital lies directly below the HOMO in energy.[72, 83–85] The formation of a delocalized π-bonding system in H_2N–P=NH is accompanied by a strong destabilization of the π(P=N) energy level, so that the energy difference between the two highest occupied orbitals is minimal in this case.[72, 82] On the basis of these calculations it was predicted that HP=NH would preferentially undergo [n + 1] addition reactions[86] (oxidative addition at phosphorus, "carbene-analogous reaction behavior"), while in the case of H_2N–P=NH [n + 2] additions to the double bond should be favored[72] (see Section 4.3).

3.2. Electron Spectroscopic and Electrical Measurements

The UV/visible spectra of iminophosphanes show two characteristic absorption bands, which can be identified on the basis of their differing intensities as arising from the expected n–π^* and π–π^* transitions of the P/N chromophore.[87, 88] In the He(I) photoelectron (PE) spectra the double bond system manifests itself in the form of a series of ionization bands at low energies in addition to the undifferentiated bands which result from the ionization of the skeletal MO's.[84, 87, 88] An assignment of these bands to ionization from n(P) or π(P=N) orbitals can be made on the basis of the observed linear correlation (Fig. 2) between the

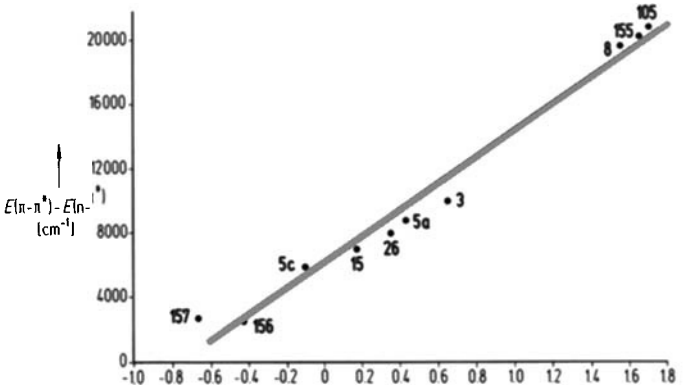

Fig. 2. Correlation between the difference in electron excitation energies $[(\Delta E(\pi\text{-}\pi^*) - \Delta E(\text{n-}\pi^*)]$ and vertical ionization potentials $[I_v(\pi) - I_v(\text{n})]$ for alkyl- and amino-substituted iminophosphanes (after [88], **155**: *t*BuP=$NCEt_3$, **156**: *t*BuP=N–TMP; **157**: *t*Bu-P=N–NMe_2).

ionization energy differences and the corresponding optical excitation energies[27, 87] and is further supported by the comparison with calculated adiabatic ionization potentials.[88] In the case of *P*-alkyl substituted iminophosphanes the first ionization potential corresponds to an ionization from the n orbital, while for *N*-aminoiminophosphanes and *P*-(dialkylamino)iminophosphanes it involves an ionization from the π-orbital. Assuming the validity of *Koopmans'* theorem[89] the bonding situation corresponds in the first case to that of the parent system (*E*)-HP=NH [ε(np) > $\varepsilon(\pi_{P=N})$], while in the second case there is a crossover of the orbital sequence [$\varepsilon(n_P) < \varepsilon(\pi_{P=N})$].

The measurement of dipole moments for iminophosphanes and a comparison with those measured for other P–E multiply bonded systems made possible the determination of

a double bond increment ($p_{P=N} = 2.2 \pm 0.2$ D) and thus demonstrates the high polarity of the double bond.[90] Electrooptical measurements with the help of the Kerr effect made it possible to determine the anisotropy of the polarizability of the P–N bond (3.5–4.0 A^3) as well as to carry out studies on the geometrical orientation of substituents.[91]

3.3. Molecular Structures

A large number of crystallographic investigations on iminophosphanes have been carried out recently (Table 1). While in most cases the double bond was found to have an (*E*)-configuration, a (*Z*)-configuration or even a nearly linear P–N–R geometry was observed in a few cases. Thus, it is now possible to discuss the nature of the P–N bond not only on a theoretical but also on an experimental basis.

Structural studies on iminophosphanes with a C–P=N–C skeleton, which can be considered as homologues of the unknown parent compound (*E*)-HP=NH, have so far been limited to two examples. The experimentally determined double bond distances in **44**[97] and **47**[96] agree well with the results of SCF calculations for (*E*)-HP=NH, while the relative increases in the bond angles at phosphorus and nitrogen are apparently due to the steric bulk of the substituents.

Aminoiminophosphanes have been the subject of intensive study, and in almost all cases an (*E*)-configuration at the double bond was determined. The amine nitrogen generally has a planar coordination geometry, while the R_2N and the PNR′ units are coplanar; this indicates the formation of a delocalized π-electron system. The P–N bond distances lie within the expected ranges: 167 ± 3 pm ($P–N_{amine}$) and 156 ± 2 pm ($P–N_{imine}$). In the azomethine-substituted derivatives **45** and **51** the large values for the bond angles at the azomethine nitrogen (∢ PN′C, **45**: 167.5°, **51**: 165°) and the short $P–N_{azomethine}$ bond distances ($r_{P-N'}$; **45**: 159.5 pm, **51**: 161.4 pm) indicate the existence of a high degree of s-character in this P–N′ bond. The $R_2C=N$- and Aryl N=P- units exhibit an almost orthogonal arrangement (∢ N′PNC/NCR_2, **45**: 87.5°, **51**: 87.9°), also indicating the formation of a 4π-electron system delocalized across the N–P–N sequence rather than of a theoretically possible heterobutadiene system.

Table 1. Selected structural data for compounds R–P=N–R′[a]. Bond lengths [pm], bond angles [°].

Cpd.	R	R′	P=N	R-P=N	P=N-R′	Torsion angle R-P-N-R′	Ref.
35	tBu$_2$P	N(SiMe$_3$)$_2$	161.9(2)	95.8(1)	124.1(2)	176.3(2)	[37]
36	tmp	N(SiMe$_3$)$_2$	159.8(5)	107.7(2)	107.1(3)	175.3	[28]
37	(SiMe$_3$)$_2$N	[tBu$_2$(Me)P]$^{\oplus}$	159.1(2)	107.5(1)	128.3(1)	177.7(1)	[92]
38	tBu$_2$P	Aryl	157.8(2)	105.8(1)	119.9(1)	164.8	[36, 82]
39	(Me$_3$Si)$_2$N	tBu$_2$P(S)	157.5(5)	106.5(2)	120.2(2)	174.2(4)	[93]
40	Aryl (H)N	Aryl	157.3(8)	103.8(5)	126.1(7)	[b]	[43]
41	(Me$_3$Si)$_2$N	Aryl	156.6(2)	109.3(1)	117.6(2)	177.6(2)	[94]
42	Cp*(CO)$_2$Fe	Aryl	156.4(12)	115.4(5)	119.8(9)	180 [c]	[95]
43	(SiMe$_3$)$_3$N$_2$	Aryl	155.8(4)	107.3(2)	115.3(3)	−177.8(3)	[96]
25	(Me$_2$N)$_3$P=C(SiMe$_3$)	SiMe$_3$	155.8(4)	108.4(2)	138.8(3)		[66]
		NiPr$_2$					
27	iPr$_2$N	P=NSiMe$_3$	155.8(3)	107.2(1)	118.2(2)	−174.0(1)	[67]
		tmp					
44	Aryl	tBu	155.6(5)	100.6(3)	122.7(5)	179.0(7)	[97]
45	tBu$_2$C=N	Aryl	155.5(3)	107.3(1)	123.4(2)	−175.6(3)	[59]
46	iPr$_2$N	Aryl	155.5(2)	105.6(1)	129.6(2)	179.9(3)	[98]
50 [d]	tBuS	Aryl	155.4(4)	109.1(2)	131.7(3)	0 [c]	[96]
			154.9(2)	109.0(1)	131.3(2)	1.5(2)	[99]
47	Cp*	Aryl	155.2(6)	105.9(4)	125.9(4)	178.7(7)	[96]
51	Fl=N	Aryl	154.7(3)	114.6(2)	137.2(2)	1.8(4)	[59]
48	tBu$_2$P(SiMe$_3$)N	tBu$_2$P	154.6(9)	106.4(4)	114.0(5)	178.0(8)	[100]
52	tBu(H)N	Aryl	154.5(6)	110.4(3)	128.0(4)	0 [c]	[96]
15	tBu(SiMe$_3$)N	tBu	154.4(4)	104.9(2)	124.4(2)	180 [c]	[101]
3	(SiMe$_3$)$_2$N	SiMe$_3$	154.5(2)	108.4(1)	129.9(1)	179.0	[101]
62	(Ph$_2$C=N)$_2$P(Aryl)N	Aryl	153.9(6)	107.4(3)	135.2(5)	178.6(6)	[102]
53	Me$_2$N	Aryl	153.9(3)	115.9(3)	140.7(4)	−4.9(7)	[98]
49	(Me$_3$Si)$_3$Si(Me)P(Aryl)N	Aryl	153.7(2)	111.2(1)	152.3(3)	−153.7(3)	[96]
54	Me$_3$SiO	Aryl	152.9(3)	115.8(2)	144.4(2)	−1.3(5)	[96]
20a	tBu(ArylN=P)N	Aryl	152.7(5)	106.0(2)	125.,8(3)	177.6(4)	[61]
			152.9(4)	109.4(2)	120.3(3)	−177.8(3)	
56	2,6-tBu$_2$-4-MeC$_6$H$_2$O	Aryl	150.0(1)	110.3(1)	173.7(1)	86.3(8)	[103]
19b	Br	Aryl	149.9(6)	112.6(3)	161.0(6)	0 [c]	[96]
55	2-MeC$_6$H$_4$O	Aryl	149.7(2)	111.8(1)	164.1(1)	−0.5(4)	[104]
10 [d]	Cl	Aryl	149.5(4)	112.4(2)	154.8(4)	0 [c]	[46]
			150.9(2)	111.4(1)	146.5(2)	[b]	[105]
58	tBu$_2$HCO	Aryl	149.1(5)	109.5(2)	179.1(4)	0 [c]	[96]
57	tBu$_3$CO	Aryl	148.6(4)	109.9(2)	175.4(4)	13(5)	[96]
19c	I	Aryl	148.0(3)	118.0(1)	172.5(3)	−140(2)	[96]
12	Cp*	SiiPr$_3$	153.3(3)	–	153.3(2)	–	[38]
59	tBu$_2$PS$_2$	Aryl	148.7(3)	–	169.7(3)	–	[96]
60	tBu$_2$PSe$_2$	Aryl	149.3(1)	–	169.1(11)	–	[106]
61	AlCl$_4$	Aryl	147.5(8)	–	177.0(7)	–	[46]

[a] Abbreviations: Cp* = pentamethylcyclopentadienyl; Fl = fluorenyl; Aryl = 2,4,6-tri-*tert*-butylphenyl; TMP = 2,2,6,6-tetramethylpiperidyl. [b] No literature value available. [c] Due to crystallographic symmetry. [d] Different modification.

A surprisingly short P–N bond distance of 153.7 pm and a torsion of 26° about the double bond have been observed for the sterically hindered derivative **49**. The expected weakening of the π bond caused by the twisting is apparently more than compensated by the considerable increase of the bond angle at the imine nitrogen (152°).[96] The comparatively long $P-N_{amine}$ and short $P-N_{imine}$ distances in the 1,3,5-triaza-2,4-diphosphapenta-1,4 diene **20a**, the P/N skeleton of which is (*S*)-configurated, can be explained in terms of a delocalized 5-center-6-electron π system.[61] The *N,P*-diaminoiminophosphane **36** has two amine ligands in 1,2-position: only the amine residue at nitrogen has the geometry necessary for an effective π conjugation. The $(SiMe_3)_2N$ residue at the imine nitrogen is in contrast orthogonal to the plane of the π system; this leads to a decrease of the angle at the imine nitrogen (107.1°) and an increase in the P–N bond length to 159.8 pm.[28]

An almost planar P–N–NR_2 arrangement, which indicates a conjugation between the double bond and an $(SiMe_3)_2N$ group at nitrogen, has been found for the *N*-amino-*P*-phosphinoiminophosphane **35**. The π-electron delocalization makes itself apparent in the short N–N bond distance (138.1 pm) and the particularly long P–N bond (161.9 pm).[37]

Until now a (*Z*)-configuration of the double bond has only been found for iminophosphanes which bear a tris(*tert*-butyl)phenyl group at nitrogen. The aryl ligand is orthogonal to the plane of the P=N double bond, due no doubt to steric effects. In the pairs of compounds (*E*)-tBu_2C=N-P=N-Aryl (**45**)/(*Z*)-Fl=N-P=N-Aryl (**51**),[59] and (*E*)-iPr_2N-P=N-Aryl (**46**)/(*Z*)-Me_2N-P=N-Aryl (**53**),[98] which contain substituents with comparable steric and electronic properties, a comparison of the bonding parameters confirms the expected larger bond angles and shortening of the P–N bond distances in the (*Z*)-isomers. The observed correlation between the P–N bond length and the valence angle at nitrogen is remarkable: in the halogen-, aryloxy-, or alkoxy-substituted iminophosphanes **10**, **19c**, **56**–**58** in particular it is found that extremely short P–N bond distances (148–151 pm) are accompanied by an almost linear arrangement of the P–N–C_{aryl} fragment (Table 1). The P–O bonds in **54**–**58**, which vary between 159 pm (**54**)[96] and 166 pm (**55**),[104] lie within the range expected for single bonds (164 pm[107]).

Interesting structural effects are shown by the *P*-halogenoiminophosphanes **10** and **19b,c**, the bis(chalcogeno)-phosphinato-substituted derivatives **59** and **60**, and the (C_5Me_5)-substituted derivative **12**. In those modifications of **10** which have been studied there is a significant difference in the valence angle at the imine nitrogen, although the other bonding parameters remain almost unchanged (Table 1). This indicates that the P–N–R unit can very readily undergo deformation, a fact which can be interpreted in terms of the prediction of a low inversion barrier at nitrogen.[81]

The phosphorus–halogen bonds in **10** (r_{P-Cl} = 214.2 pm,[46] 212.7 pm[105]) and **19b** (r_{P-Br} = 233.5 pm[96]) are significantly longer than in the trihalides PX_3 (r_{P-X}[107]: 204 pm (X = Cl); 222 pm (X = Br)); this can be interpreted in terms of an n(N)→σ*(PX) charge transfer.[108] This effect is even more pronounced in the iodo compound **19c** (r_{P-I} = 289.5 pm[96] vs. 252 pm in PI_3[107]). In this case the increasing polarization of the *P*–halogen bond is accompanied by the presence of a short intermolecular P–I contact

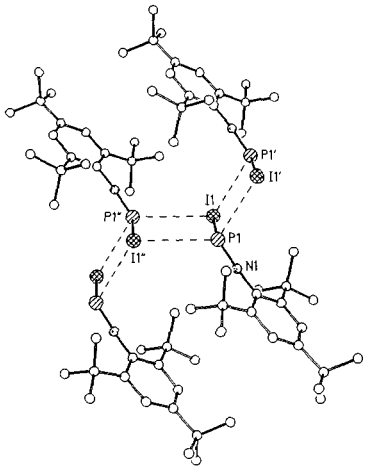

Fig. 3. Crystal structure of **19c**. Bond lengths: P1–I1 289.5(1) pm, P1–I1' 322.4 pm. The additional intermolecular contact P1–I1" (360.5 pm) lies within the range of the sum of the van der Waals' radii and does not correspond to a bonding interaction (after [46]).

(322 pm), so that a transition to a biomolecular donor-acceptor complex is already indicated in the crystal (Fig. 3).

A bonding situation comparable to that in **19c**, in this case in the form of an intramolecular donor-acceptor interaction, can be found in **59**, which has two weak phosphorus–sulfur bonds of different lengths (r_{P-S} 244.2 and 273.9 pm).[96] The two phosphorus–chalcogen bond lengths are less divergent in the selenium derivative **60** (r_{P-Se} 263.6 and 278.8 pm), so that in this case a description of the bonding situation can include the participation of a contact ion pair of the type $[R_2PSe_2]^{\ominus}[PNAryl]^{\oplus}$ as a resonance hybrid.[106] Complete separation into a cation and an anion is realized in the case of **61**, where the extremely short P–N bond distance and the almost linear arrangement of the P–N–C_{Aryl} fragment justify a description in terms of a phosphanetriylammonium ion with partial triple bonding between P and N.[46]

The molecular structure of the iminophosphane **12** can be interpreted as an intramolecular π-complex between $[Me_5C_5]^{\ominus}$ and $[R_3SiNP]^{\oplus}$ (Fig. 4); in contrast to **47** the

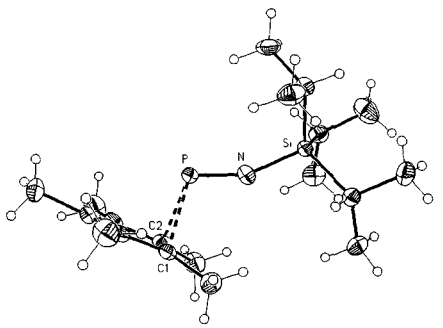

Fig. 4. Crystal structure of **12**. Bond lengths: P–Cl 216.8(4) pm, P–C2 212.2(4) pm, P–N 153.3(3) pm; bond angle P–N–Si 153.3(2)° (after [38]).

cyclopentadienyl ligand is coordinated in a "non-classical" η^2 manner. Important arguments for this description are provided by the almost equal bond distances, the (pseudo)-planar geometry in the five-membered ring, the increase in the length of the P–C bonds (r_{P-C} = 212.2 and 216.8 pm)

and in the valence angle at the imine nitrogen, and the shortening of the P–N bond (see Table 1) in comparison to that in **47**.[38]

3.4. NMR Spectroscopic Investigations

The chemical shift range for the ^{31}P resonance of iminophosphanes covers the wide range between $\delta = 87$ for **19a** and $\delta = 787$ for **42** (see Table 2). The ^{31}P-NMR data

Table 2. ^{31}P-NMR chemical shifts for selected iminophosphanes of the type R–P=N–R' [a, b].

	R	$\delta(^{31}P)$	Ref.		R	$\delta(^{31}P)$	Ref.
R' = Aryl				*R'* = *t*Bu			
42	Cp*(CO)$_2$Fe(*E*)	787	[95]				
63	*t*Bu$_2$As	644	[47]	**8**	*t*Bu	472	[24]
38	*t*Bu$_2$P(*E*)	570	[45]	**5a**	(Me$_3$Si)$_2$N	330	[18]
64	*t*Bu	490	[33, 42]	**67**	tmp	314	[21]
65	Aryl	396	[47]	**68**	Cp*	283	[41]
66	*t*BuSe	315	[47]				
50	*t*BuS(*Z*)	314	[47]	*R'* = SiMe$_3$			
40	ArylNH(*E*)	272	[43]				
46	*i*Pr$_2$N(*E*)	268	[98]	**18**	Aryl	476	[55]
19c	I	218	[46]	**3**	(Me$_3$Si)$_2$N	325	[4]
52	*t*BuNH (*Z*)	210	[47]	**26**	tmp	303	[25]
53	Me$_2$N (*Z*)	203	[34]	**69**	Cp*	140	[36]
47	Cp*(*E*)	194	[47]				
45	*t*Bu$_2$C=N(*E*)	179	[59]	*R'* = N(SiMe$_3$)$_2$			
54	Me$_3$SiO (*Z*)	157	[47]				
19b	Br (*Z*)	153	[46]	**35**	*t*Bu$_2$P(*E*)	428	[37]
10	Cl(*Z*)	135	[46]	**70**	*t*Bu	378	[27]
51	Fl=N (*Z*)	124	[59]	**36**	tmp (*E*)	364	[28]
19a	F	87	[47]	**71**	Cp*	323	[38]

[a] (*E*)/(*Z*): *E* or *Z* double bond geometry in the crystalline state; no data = structure not known. [b] For abbreviations see footnote [a] of Table 1.

published up to mid-1985 have been reviewed.[15] Although a theoretical or empirical treatment of the large chemical shift differences generally observed for compounds in which phosphorus has a coordination number of two is extremely difficult,[109] the shifts in iminophosphanes can be explained to a good approximation in terms of the stereoelectronic effects of the substituents at phosphorus and nitrogen. Thus, for a series of compounds of the type R–P=NAryl there is a linear correlation between $\delta^{31}P$ and the n–π^* electron excitation energy; this indicates that the paramagnetic term makes a dominant contribution to the shielding tensor.[88] According to this postulate, substituents R with strong σ-donor properties ($C_5Me_5(CO)_2Fe$, *t*Bu$_2$As, *t*Bu$_2$P) which cause a red shift of the n-π^* band will lead to deshielding, while ligands with π-donor and/or σ-acceptor properties ($R_2C=N$, R_2N, RO, halogen) will induce a shielding of the phosphorus nucleus. A geometrical effect on the chemical shift, which is well documented for (*E*)/(*Z*) isomer pairs of diphosphenes or phosphaalkenes, is also apparent in the iminophosphane system. Thus, in the pairs **45**/**51**, **40**/**52**, and **46**/**53**, for which the substituents at phosphorus have comparable steric and electronic effects, the (*E*)-configured iminophosphanes **45**, **40** and **46** show a significant deshielding ($\Delta\delta^{31}P$ 60 ± 5 ppm, see Table 2).

Although in the case of phosphaalkenes ^{13}C-NMR spectroscopy acts as an additional probe for studying the nature of the double bond, the unfavorable magnetic properties of the isotopes ^{14}N and ^{15}N are an extreme handicap to such studies on iminophosphanes. $^{14}N/^{15}N$-NMR studies on iminophosphanes have thus so far been carried out in only a few cases,[110] so that it is not at present possible to discuss the data in a systematic manner.

Apart from the interpretation of chemical shifts and coupling constants, NMR can be used for studying dynamic processes and thus provides a further tool for probing the nature of the P=N double bond. Thus in a series of aminoiminophosphanes R'(R)N–P=NR' (R = SiMe$_3$, R' = SiMe$_3$ (**3**), *t*Bu (**15**); R = H, R' = Aryl (**40**)) it has been possible to detect degenerate sigmatropic [1,3] shifts involving either protons or trimethylsilyl groups; these correspond to chemical exchange between the amino and imino positions in the molecule.[4, 17, 43] The 1,3,5-triaza-2,4-diphosphapenta-1,4-diene **20b** undergoes an analogous rearrangement in which the shift of a P=NAryl group and a P–N bond rotation lead to a complete equilibration of all three nitrogen positions[61] (Scheme 14).

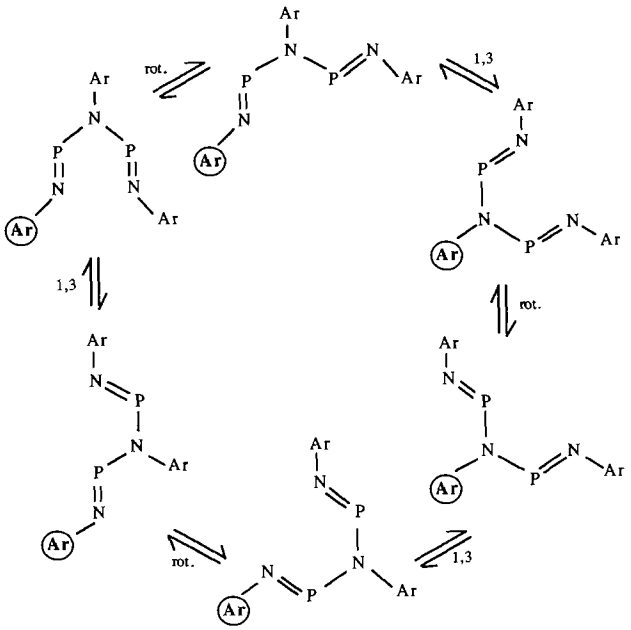

Scheme 14. Schematic representation of the dynamic structure of **20b**; labeled aryl residue passes through all possible positions (after [61]). rot. = rotation about a P–N single bond, 1,3 = [1,3] shift of an arylN=P group. Ar = Aryl.

"Ring whizzing", i.e. a series of very fast [1,5] sigmatropic ring shifts, is observed for *P*-(pentamethylcyclopentadienyl)-substituted iminophosphanes. Since the observed processes are still fast with respect to the NMR time scale even at low temperatures, it can be concluded that the activation energy is considerably lower than in the corresponding $\lambda^3\sigma^3$ phosphorus compounds.[38, 41]

A remarkable temperature dependence is observed in the ^{31}P- and ^{77}Se-NMR spectra of the iminophosphane *t*Bu$_2$P^{A}Se$_2$P^{B}NAryl **60**. While the coupling constants $^2J(P^A, P^B)$ and $^1J(P^B, Se)$ are detectable at −80 °C, they disappear when the temperature is raised, although $^1J(P^A, Se)$ remains almost unchanged. At the same time the signal correspond-

ing to the phosphorus atom of the double bond undergoes a significant low-field shift. An explanation of these results is possible on the basis that the structure in the crystalline state (see Section 3.3), which involves the presence of contact ion pairs $[R_2PSe_2]^{\ominus}[PNAryl]^{\oplus}$, is maintained at low temperatures in solution; the partial disappearance of the couplings when the temperature is increased corresponds to an increasing dissociation into single ions.[47, 106]

4. Reactivity

4.1. Addition Reactions

Product formation in many reactions of iminophosphanes can be understood on the basis of a complex reaction mechanism whose first step is an addition to the P=N double bond. Such an addition can in principle involve either an increase of the coordination number of phosphorus (oxidative 1,1 addition) or a 1,2 addition; the observed regioselectivities indicate a complex dependence on the nature of the substrate. Thus 1,1 additions at phosphorus are preferred in reactions of halogens and halogen derivatives of electronegative elements, while the alkyl and halogen derivatives of electropositive elements undergo 1,2 addition with the formation of a very stable element–nitrogen bond.

Because of the high polarity of the P–N bond we can assume that most addition reactions occur via a two-step mechanism, the initial step of which involves attack of a Lewis acid or base at the double bond. The interaction of iminophosphanes with Lewis acids/bases, which can in this sense be regarded as "incomplete additions", is thus of great importance in understanding the reactivity of these compounds.

4.1.1. Attack by Lewis Acids and Bases

Theoretical treatments of the electron density distribution in the P=N double bond of iminophosphanes lead us to expect that Lewis acids will attack preferably at nitrogen and Lewis bases at phosphorus[74] (Scheme 15). Although such

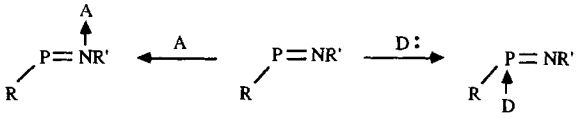

Scheme 15. A = Lewis acid, D = Lewis base.

acid/base adducts are very difficult to study because of their extreme readiness to undergo further reactions, an experimental confirmation of the expected behavior was possible in several cases. Thus the complex **72** was isolated from the reaction of **3** with aluminum trichloride; on raising the temperature this complex decomposed with the formation of the heterocyclic product **73**[111] (Scheme 16). Addition of trifluoroacetic acid to the iminophosphane **68** yielded a product which according to NMR studies is the phosphenium ion **74b** (formed via *N*-protonation of **68**) in dynamic equilibri-

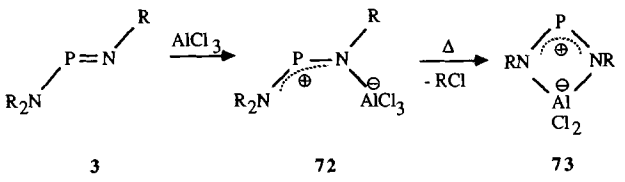

Scheme 16. R = $SiMe_3$.

um with the aminophosphane **74a**[112] (Scheme 17). In an analogous reaction, treatment of the ferrioiminophosphane **42** with Meerwein's salt initially yields an isolable cationic

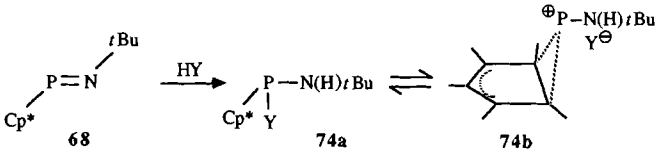

Scheme 17. Y = CF_3SO_3.

phosphinidene complex **75**, which undergoes thermal rearrangement to give the phosphane complex **76** (Scheme 18).[113]

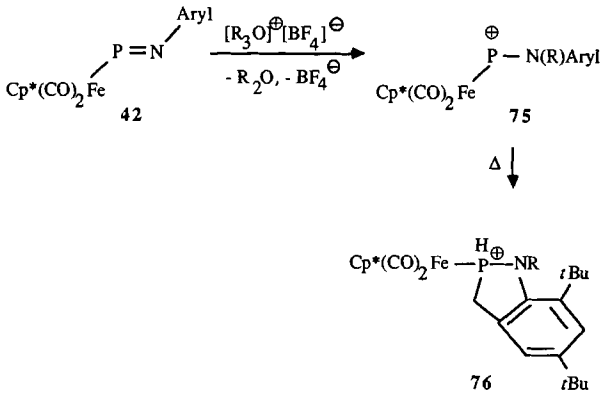

Scheme 18. R = Me, Et; Aryl = 2,4-di-*tert*-butylphenyl.

The intermediate formation of iminophosphoranide anions in the course of the formation of **77** (R = $SiMe_3$) from **3** (R = $SiMe_3$) and $LiAlH_4$ (after hydrolysis) was confirmed

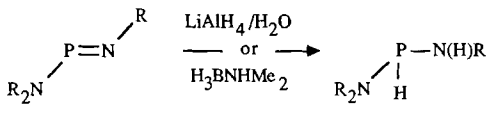

by means of isotopic labeling studies (Schema 19).[114] A similar process has been suggested for the analogous methylation with MeLi/MeI;[114] however, the mechanism of formation of **77** (R = $SiMe_3$) in the reaction of **3** (R = $SiMe_3$) with H_3BNHME_2, which formally involves the transfer of both a hydride ion and a proton, could not be clarified.[115] The dithiophosphinic acid derivative **59**, which was formed

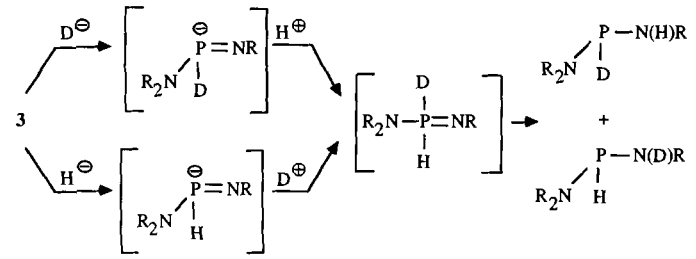

Scheme 19. Isotope labeling experiments for the reduction of **3**. R = $SiMe_3$.

by double sulfurization from **38** via **78**, has the structure of an *intra*molecular iminophosphane/Lewis base complex.[47] Similar *inter*molecular donor-acceptor interactions in the solid state have been detected in the case of the

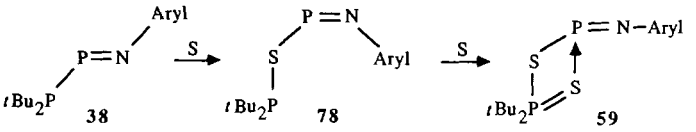

halogenoiminophosphane **19c**.[106] The formation of iminophosphoranyl radicals **79** from **3** and suitable alkyl, alkoxy or acyl radicals can also be considered as an attack of a Lewis base at twofold coordinated phosphorus[116] (Scheme 20).

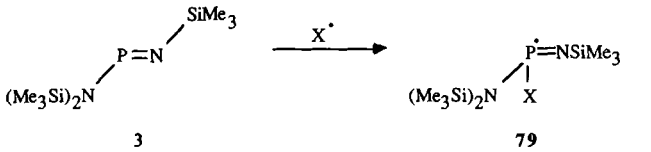

Scheme 20. X = R, RO, RCO.

An alternative mechanism for the interaction of an iminophosphane with a Lewis acid was observed in the reaction of the *P*-chloroiminophosphane **10** with aluminum

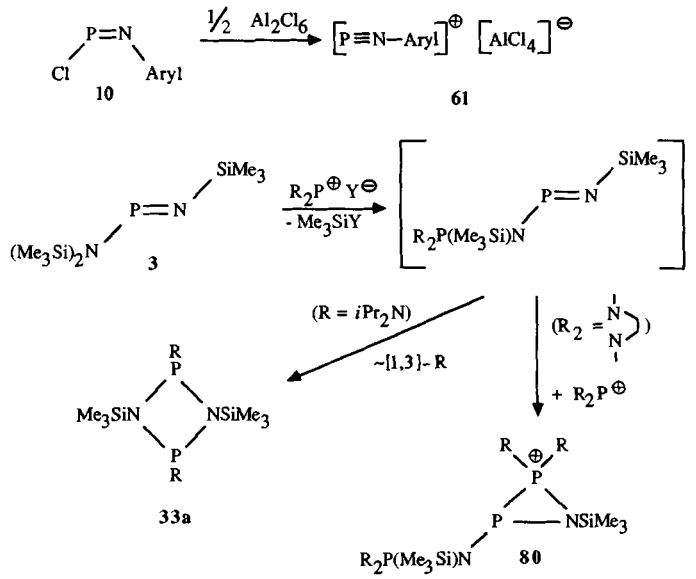

Scheme 21. Y = CF_3SO_3.

trichloride. Attack of the Lewis acid at the chlorine atom, followed by ligand abstraction, led to formation of the first known phosphanetriylammonium ion[46]. In contrast, the reaction of diaminophosphenium ions with **3** occurred in the expected manner; the formation of the final products **33a** and **80** was explained on the basis of an undetectable iminophosphane/Lewis acid complex[117] (Scheme 21). Treatment of the aminoiminophosphane **3** with titanium

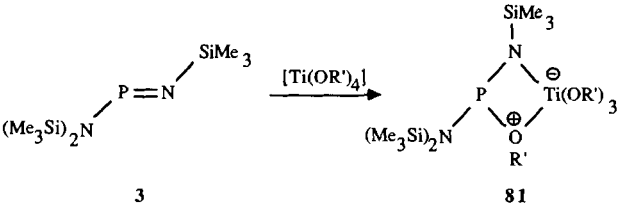

alkoxides led to the occurrence of double Lewis acid/base reactions, giving heterocyclic products which contain two donor–acceptor bonds.[118]

4.1.2. *Addition of Reagents with Acidic Hydrogens*

The relatively polar iminophosphane double bond reacts readily with compounds containing acidic hydrogens to form either correspondingly substituted aminophosphanes (formal 1,2 addition) or the tautomeric iminophosphoranes (formal 1,1 addition) (Scheme 22). Since the tautomeric equi-

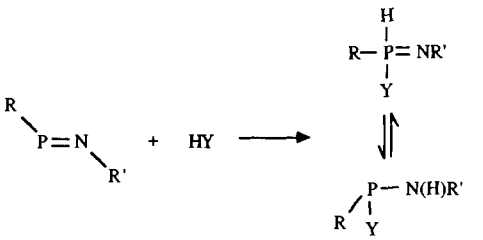

Scheme 22. Reactions of iminophosphanes with H-acidic compounds.

librium reaction must be assumed to be fast,[119] the observed constitution of the reaction products, and not the differing regioselectivities for the two addition reactions, will reflect the relative thermodynamic stabilities of the two forms. The phosphane form is generally found to be of lower energy, so that additions of hydrogen halides[47], alcohols,[30, 31, 120, 121] thiols,[120, 121] amines,[30, 122] phosphanes,[123] and some other compounds with acidic hydrogens[36] to P=N double bond systems lead in most cases to the formation of the corresponding aminophosphanes as the sole products. Stabilization of the hydridophosphorane form requires not only the presence of a trimethylsilyl group at the imino position but also further substituents at phosphorus which increase its basicity. Thus, reactions of $(Me_3Si)_2N$–P=$NSiMe_3$ with sterically less demanding alkyl alcohols and amines lead to the selective formation of the corresponding iminophosphoranes[120–122] while in the reactions with phenol, *tert*-butyl alcohol, and adamantanol the

products are in each case an equilibrium mixture of the two tautomers.[120, 121]

The addition of substrates with acidic hydrogens to iminophosphanes occurs even in the absence of additional bases; however, asymmetric induction was recently observed during the addition of achiral alcohols to iminophosphanes in the presence of chiral tertiary amines, thus indicating a possible base catalysis of the addition reaction.[124]

4.1.3. Halometalation and Organometalation Reactions

The readiness of phosphorus halides and redox-stable halides of more electropositive elements to react with iminophosphanes depends on their Lewis acidity; the initial formation of Lewis acid–iminophosphane adducts (see Section 4.1.1) is followed by a 1,2 shift of a halogen to give aminohalogenophosphanes **82** (Scheme 23). While such

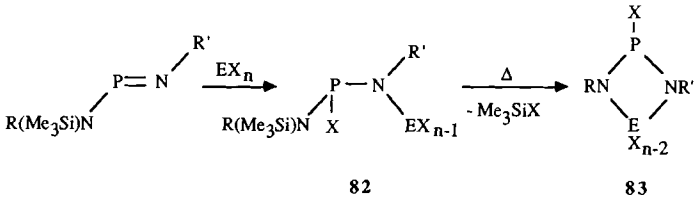

82 83

Scheme 23. E = B, Si, P, As; R, R' = $SiMe_3$, *t*Bu.

products are stable in the case of complete alkyl substitution (R = R^1 = R^2 = alkyl),[23] *N*-silylated derivatives are subject to further reaction steps; the most favored of these is an intramolecular 1,3 elimination of halogenosilanes to give the four-membered heterocycles **83**.[125–129] However, an intermolecular condensation reaction has also been detected in a few cases, for example in the formation of the hexaazadiphosphadiarsatricyclodecane derivative **84** from arsenic trichloride and the iminophosphane $(Me_3Si)_2N$–N(Me)–P=N$SiMe_3$.[130] Multiple addition of an iminophosphane to an element halide was observed in the reaction of **3** with antimony trichloride, which affords the tricyclic compound **85**.[131]

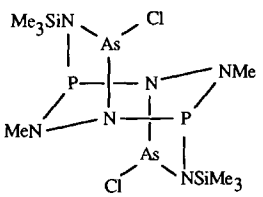

84

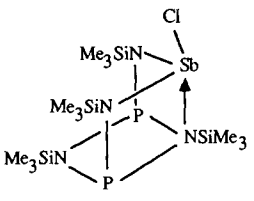

85

In analogy to the halides, alkyl compounds of electropositive elements also add at the P=N double bond. Thus, reaction of **3** with BMe_3 smoothly affords the 1,2-addition product **86**, while the partly alkylated aminoiminophosphane **15** reacts further via a [1,2] trimethylsilyl shift and ring closure to give the heterocycle **87** (Scheme 24). Analogous products are also formed on reaction of **3** or **15** with Al_2Me_6.[132] An unstable organometallic compound which decomposes with

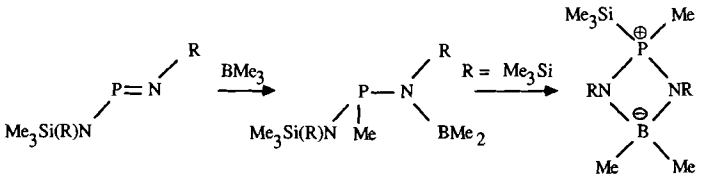

3,15 86 87

Scheme 24. R = $SiMe_3$, *t*Bu.

reductive elimination of mercury can be assumed as intermediate in the formation of diamino(silyl)phosphanes by reaction of aminoiminophosphanes with bis(trimethylsilyl)-mercury.[133] A reaction similar to the hydrozirconation of

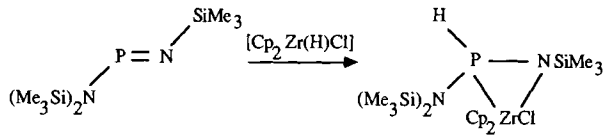

3 88

olefins was observed in the reaction of **3** with $[Cp_2Zr(H)Cl]$, which affords, via 1,2 addition and subsequent intramolecular complexation, the heterocycle **88**.[134]

4.1.4. Oxidative Additions

In contrast to the types of reaction discussed above, iminophosphanes react with alkyl halides and halogen derivatives of electronegative elements such as halogenoamines, alkyl hypohalites, arylchlorosulfanes or with halogens themselves via 1,1 addition to give the corresponding iminophosphoranes[4, 25, 31, 125, 126, 135–141] (Scheme 25). The addition products thus obtained from reactions of

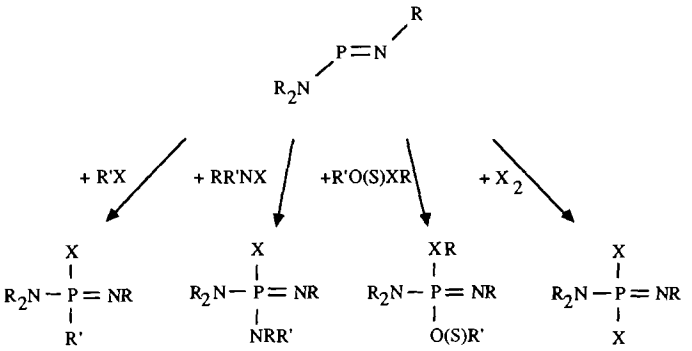

Scheme 25. R = $SiMe_3$; X = Cl, Br.

aminoiminophosphanes with (*N*-trimethylsilyl)halogenoamines are important intermediates in the synthesis of aminobis(imino)phosphoranes (see Section 4.2). A free radical mechanism has been suggested for most of the oxidative addition reactions which have been studied,[126] although an alternative ionic mechanism has been discussed for the addition of CCl_3Br to aminoiminophosphanes.[25] An interesting special case is provided by the reaction of the *N*-phosphi-

noiminophosphane **89** with iodoadamantane; in this case a 1,3 addition of the alkyl halides with concomitant 1,2 shift of the double bond is observed, apparently as the result of steric effects[142] (Scheme 26). Oxidative chlorination with the for

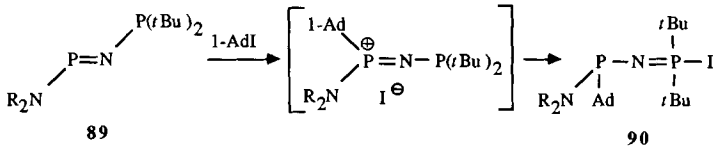

Scheme 26. R = $SiMe_3$; Ad = adamantyl.

mation of a dihalogenophosphorane and an element subhalide was found to occur when tin tetrachloride was allowed to react with **3**.[126]

4.2. Reactions involving the Formation of Diylides R–P(=Z)=NR'

Iminophosphanes play a central role in the preparation of diylidic iminophosphoranes R–P(=Z)=NR' (Z = O, S, Se, "PR"). Systems of this type, in which a trigonal planar coordinated phosphorus(v) atom forms part of a delocalized (p–p)π-bond system, are not only of considerable theoretical interest but also offer interesting synthetic possibilities. Although the formation of these products can formally be regarded as an oxidative addition to iminophosphanes, experimental studies have shown that various reaction mechanisms are in fact involved.

Thus reactions of iminophosphanes with ozone, sulfur or selenium appear to involve a direct oxidative addition; no intermediates could be detected in the formation of either the iminochalcogenophosphoranes (Scheme 27) or the [2 + 2] cyclodimerization products resulting from them.[17, 18, 143–145] Evidence for a formal oxidative trans-

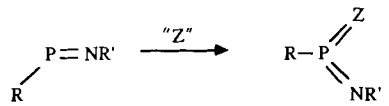

Scheme 27. Z = O, S, Se, "PR".

fer of a phosphanediyl "RP" to an iminophosphane with formation of an imino-λ^3,λ^5-diphosphene was recently presented.[146] Bis(imino)phosphoranes such as **92** can be ob-

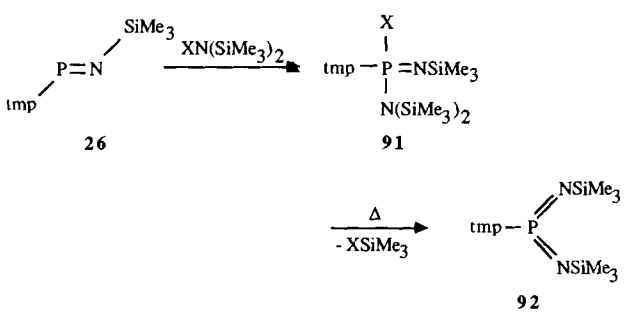

Scheme 28. X = Cl, Br; tmp = 2,2,6,6-tetramethylpiperidyl.

tained in good yields via oxidative addition of chloro(silyl)-amines to iminophosphanes such as **26** to **91** with subsequent chlorosilane elimination[25, 135] (Scheme 28).

In contrast to chalcogenation, alternative reaction mechanisms have been detected in some cases in reactions of iminophosphanes with azides or diazoalkanes, which lead to the formation of iminomethylene- or bis(imino)phosphoranes via a formal oxidative addition of a carbene or a nitrene.[25, 44, 47, 67, 147–154] Thus reaction of the aminoiminophosphane **5c** with alkyl *tert*-butylazide and diazoneopentane led via [2 + 3] cycloaddition to formation of the heterocycles **93**[155] and **96** respectively; these underwent thermal or photolytic elimination of nitrogen to give the corresponding diylides **94** and **97** respectively.[149–151] Un-

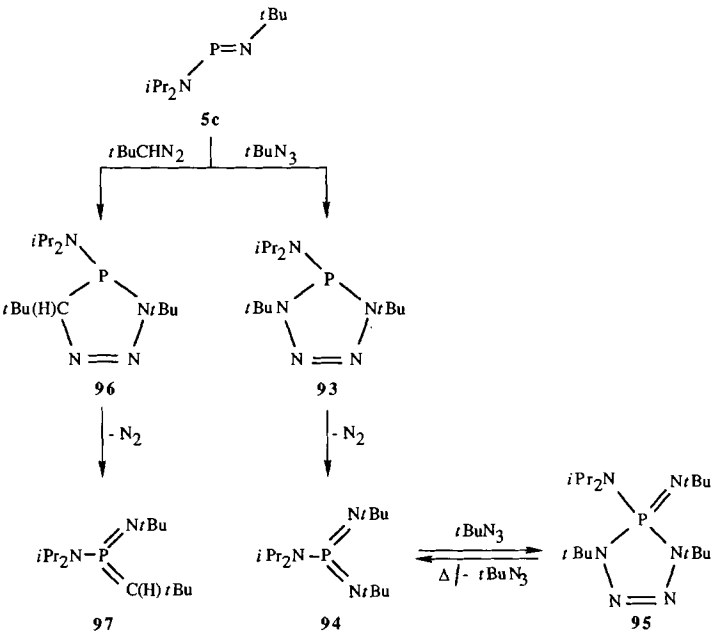

der the reaction conditions the bis(imino)phosphorane **94** can add excess azide to give **95**, from which the diylide can be re-formed by vacuum thermolysis.[151] The chloroiminophosphane **10** reacts in a similar manner via [2 + 3]

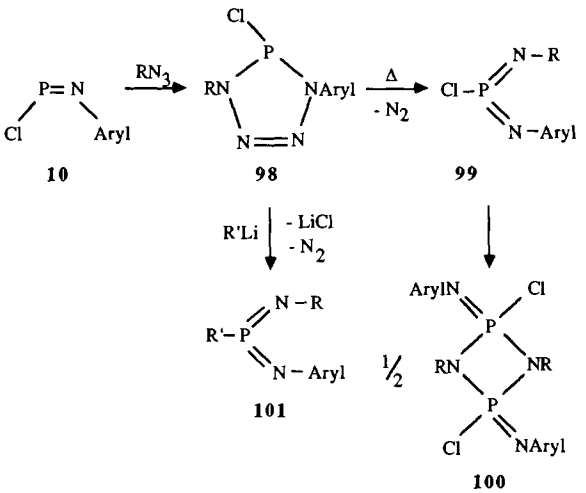

Scheme 29. R = *t*Bu, Et_3C, 1-adamantyl; R' = *n*-Bu, C_5Me_5, Aryl NH, Aryl O, *t*BuS.

cycloaddition to afford the heterocycles **98**; thermolysis of the latter leads to elimination of nitrogen to give the diazadiphosphetidines **100** via the unstable bis(imino)phosphoranes **99**. In the presence of suitable organolithium derivatives, **98** undergoes nucleophilic substitution to give the stable bis(imino)phosphoranes **101** (Scheme 29).[154] A 1,2 addition analogous to the halometalation was observed in the reaction of **3** with trimethylsilyl azide; the unstable azidophosphane **102** thus formed undergoes nitrogen elimination and a Curtius-type rearrangement to afford the bis(imino)phosphorane **103**, which can add reversibly to excess azide to form **104**[149] (Scheme 30).

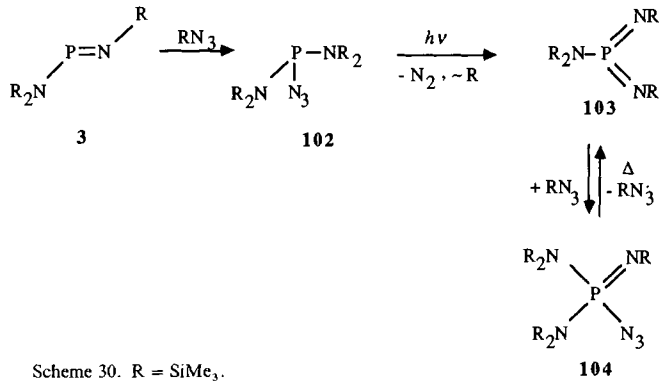

Scheme 30. R = $SiMe_3$.

It was possible to detect an oxidative addition of an azoalkane to the P=N double bond in the reaction of the *P*-alkylated iminophosphane **105** with 2-diazobutane-3,3-dimethyl. In analogy to the Staudinger reaction between tertiary phosphanes and azides, the primary product is the spectroscopically detectable adduct **106**, which undergoes stabilization via a [2 + 2] cycloaddition to give the isolable diazadiphosphetidine **107**.[44] In contrast, the reaction of

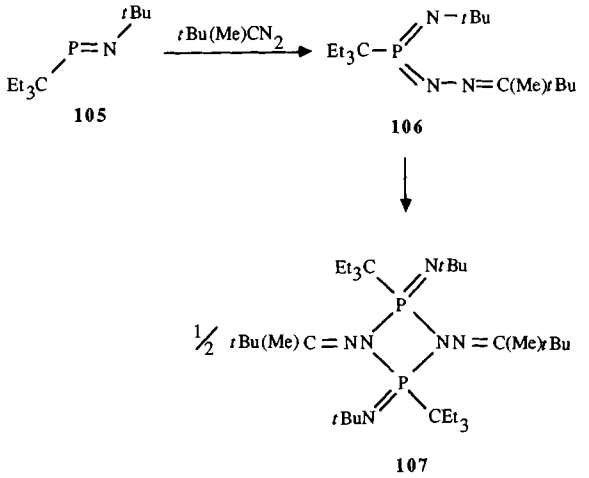

$(Me_3Si)_2N$–P=$NSiMe_3$ **3** with diazomethane occurs spontaneously with the uptake of two methylene groups to give the corresponding λ^5-iminophosphirane; in this case it was not possible to observe the formation of a diylide intermediate.[156]

4.3. Oligomerization Reactions

The low kinetic stability of the double bond in iminophosphanes causes them to undergo cyclodimerization, a reaction typical of other "non-classical" double bond systems. However, in the case of the iminophosphanes a structure-dependent regioselectivity is observed, a phenomenon which is unknown for other heteroolefin systems. Thus *P*-alkyl- and *P*-aryl-substituted iminophosphanes react via a reversible [2 + 1] cycloaddition to give λ^3,λ^5-azaphosphiridines[24, 43–45] (see Scheme 11), while π-donor-substituted aminoiminophosphanes and (*N*-amino)iminophosphanes undergo (with one known exception) irreversible [2 + 2] cyclodimerization with the formation of 1,3,2,4-diazadiphosphetidines **5c** → **108**[20, 23, 38] (for exception see Section 2.3). This observed duality correlates well with theoretical predictions, according to which the reactivity is due to different frontier orbital interactions between the reactants[45, 72, 87] (see Section 3.1).

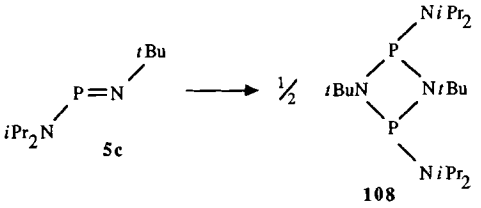

The factors which determine the course of the [2 + 1]-cyclodimerization are the degree of kinetic stability and the temperature. Thus metastable iminophosphanes have a significantly longer lifetime at lower temperatures,[24, 42] while for derivates of the type $Me_{3-n}Et_nC$–P=N*t*Bu (n = 0–3) the dimerization rate decreases with increasing steric demand of the substituent at phosphorus.[33]

Apart from these effects, there is also a remarkable susceptibility of the self-addition to the influence of Lewis acids. For example $(Me_3Si)_2N$–P=$NSiMe_3$, which dimerizes only very slowly in the pure state, undergoes a fast [2 + 2] cyclodimerization in the presence of catalytic amounts of Lewis acid.[157] An apparent change in the regioselectivity was observed in the case of **8**; under the influence of Lewis or Brønsted acids the azadiphosphiridine **109** formed in a reversible [2 + 1] cycloaddition underwent rearrangement to

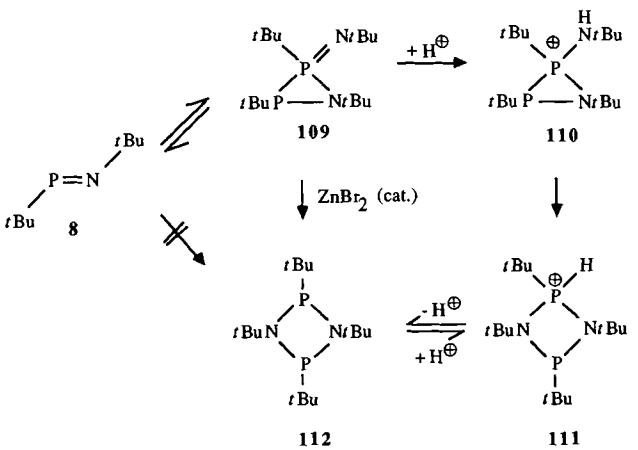

give the diazadiphosphetidine **112**, which is formally the product of a [2 + 2] cycloaddition. The course of the reaction of **109** with trifluoromethanesulfonic acid could be confirmed by isolation of the intermediates **110** and **111**.[52]

An interesting special case of an iminophosphane oligomerization is the thermolysis reaction of the azadiphosphiridine **113**, which affords a mixture of the isomeric azatriphosphetidines **114** and **115**. The reaction has been postulated to involve an oxidative insertion of monomeric iminophosphane, formed in an initial [2 + 1] cycloreversion of **113**, into the P–N single bonds of excess starting material (Scheme 31).[158]

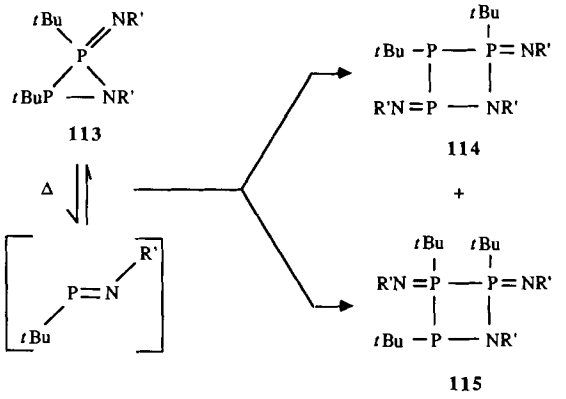

Scheme 31. R′ = $SiMe_3$.

4.4. Cycloaddition Reactions

4.4.1. [2 + 1] Cycloadditions

The *P*-alkylated or arylated iminophosphanes **64** and **105** react readily with activated alkynes or *tert*-butylphosphaalkyne via a [2 + 1] cycloaddition to give the corresponding λ^5-phosphirenes **116** or the λ^3, λ^5-diphosphirenes **118** respectively (Scheme 32); in the presence of Lewis acids (and in the case of **118** also on heating) these undergo a rearrangement similar to the ring expansion reaction of λ^3,λ^5-azadiphosphiridines to form the four-membered heterocycles **117** and **119** respectively.[44, 159, 160] A [2 + 1] cycloaddition leading to an azaphosphaboridine isoelectronic to **116** was postulated as the initial step of the reaction of **8** with the acetylene isostere *tert*-butyl(*tert*-butylimino)borane. However, the product cannot be detected and undergoes a spontaneous disproportionation to give the 1,3,2,4-diazadiphosphaboretidine **120** and the azaphosphaborirene **121**, which in turn reacts via the insertion of a further molecule of **8** to form the final product **122**.[161]

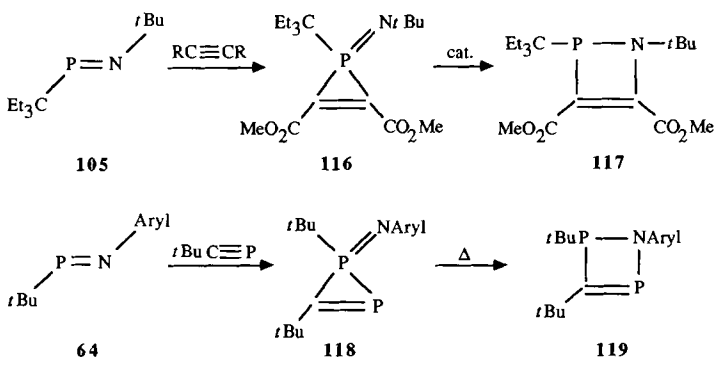

Scheme 32. [2 + 1] Cycloadditionen. R = CO_2Me, Aryl = tri-*tert*-butylphenyl.

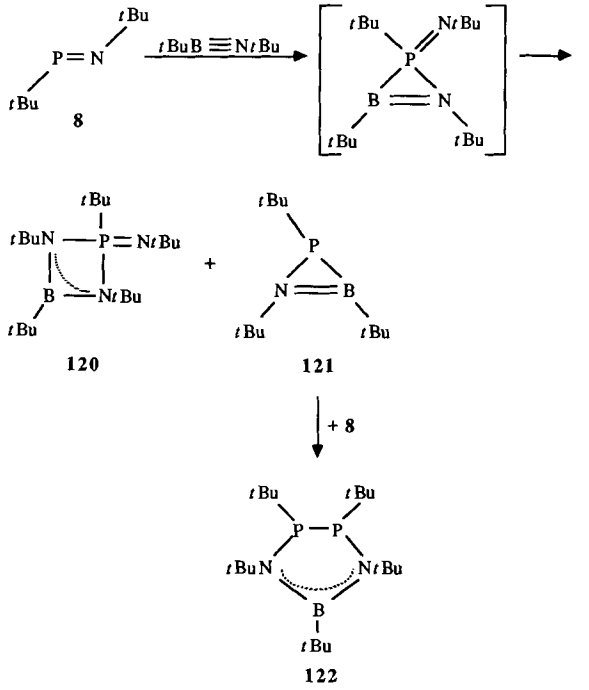

The silyl-substituted aminoiminophosphane **3** reacts very readily with hexafluoroacetone via a [2 + 1] addition to give the 1,2λ^5-oxazaphosphirane **123**.[162] The unusual regioselectivity observed – reactions of aminoiminophosphanes with double-bond systems normally occur via a [2 + 2] cycloaddition (see Section 4.4.2) – can be understood in terms of the frontier orbital model if a crossover between the n(PN) and π(P=N) energy levels is assumed; such a crossover is predicted by quantum-mechanical calculations and confirmed by spectroscopic studies.[72, 87]

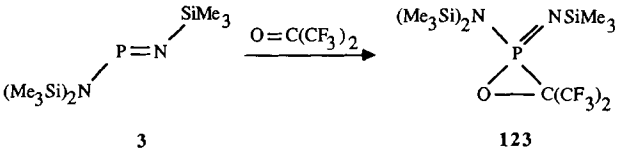

The formation of the λ^5,λ^3-iminodiphosphirane **125** in the thermolysis of from **124**[163] can also be explained on the basis of a [2 + 1] cycloaddition of an iminophosphane to the P=C double bond of excess starting material; the iminophosphane, the existence of which could not be detected, is formed from **124** via a [1,3] silyl shift. The λ^3,λ^3-azadiphosphiridines obtained in the reaction of aminoiminophosphanes with iPr_2NPCl_2 and magnesium can also formally be regarded as products of a [2 + 1] cycloaddition of a phosphanediyl at a P=N double bond; in this case the reaction mechanism is

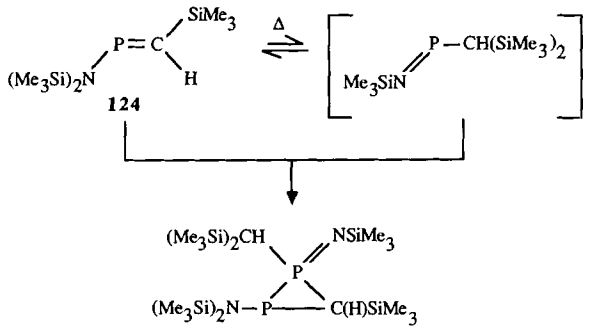

124

125

unknown.[170] The reaction between *t*BuNO and the iminophosphane **105** to give the diazaphosphinidine **126**[164] involves [2 + 1] cycloaddition with subsequent isomerization.

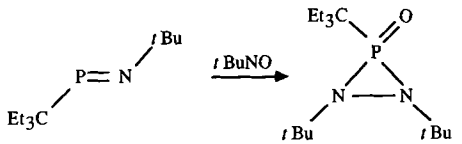

105 126

4.4.2. [2 + 2] Cycloadditions

Theoretical studies (see Section 3.1) have led to the predicition that reactions of aminoiminophosphanes with polar multiple bond systems should occur preferentially via [2 + 2] cycloaddition;[172] they should thus differ from reactions of *P*-alkyl- and *P*-aryl-substituted derivatives. The synthesis of a large number of four-membered heterocycles such as **127–129**, **132**, **133** was indeed possible by reacting **3** or **5a, c** with multiply-bonded systems such as butyl(*tert*-butylimino)borane,[165] phenyl isocyanate,[166] substituted λ^5-azaphospholes[167] or diylides $(Me_3Si)_2N$-P(=Z)=NSiMe$_3$, (Z = NSiMe$_3$, CHMe)[148, 168] (Scheme 33). In analogy, the formation of **130**, **131** and **134** was postulated to involve the trapping of unstable bis(imino)phosphorane, iminothiophosphorane or silandiylamine intermediates via a [2 + 2] cycloaddition with **3**,[169, 170] while [2 + 2] cycloaddition of the iminophosphane and an RBS unit has been suggested to be the key step in the synthesis of **135** from **3** (or **5a, c**) and trithiaborolanes[171] (Scheme 34).

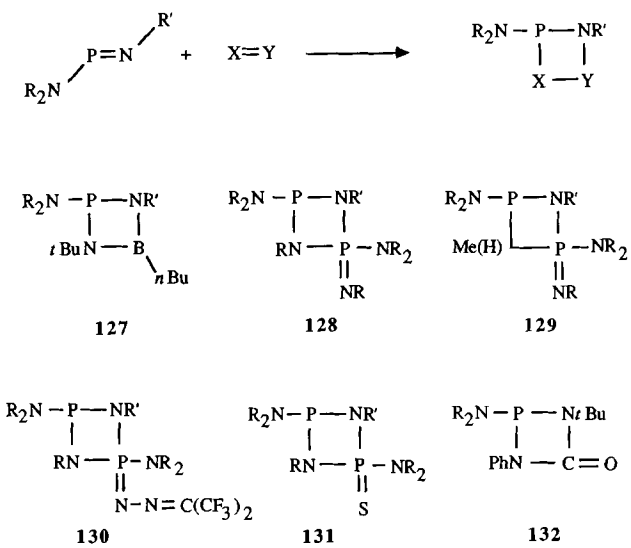

127 128 129

130 131 132

133 134

Scheme 33. R = SiMe$_3$, *i*Pr; R′ = SiMe$_3$, *t*Bu.

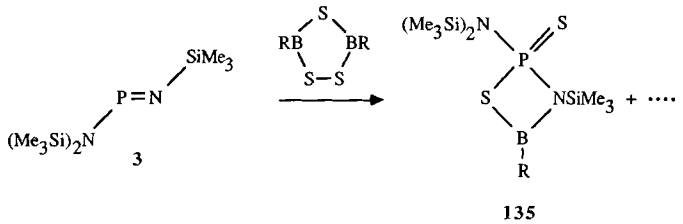

3 135

Scheme 34. R = Me, Et, Bu, Ph, Mes, Me$_2$N, Et$_2$N; the dots denote oligocondensates.

Fast [2 + 2] cycloaddition of the 2-phosphatetrazene **36** to CO_2 or CS_2 afforded the heterocycles **136a, b**, of which **136a** decomposes at room temperature to give the oxaphosphinane **137**.[28] The formation of the latter (and the generation of $(iPr_2NPO)_3$ from **5c** and SO_2[172]) has been suggested to involve a retroreaction of the original cycloadduct with the formation of an unstable oxophosphane, which then trimerizes (Scheme 35).

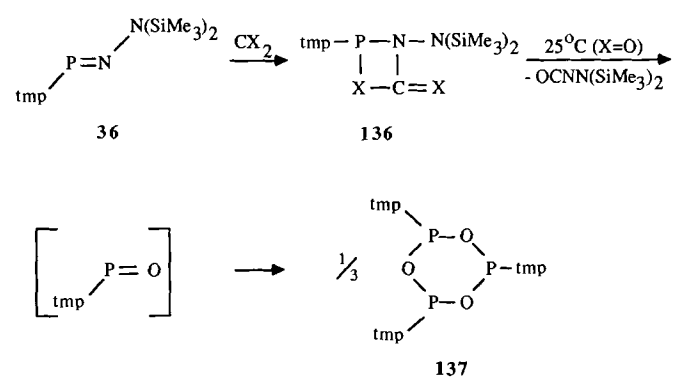

36 136 137

Scheme 35. X = O (**a**), S (**b**).

4.4.3. [2 + 3] Cycloadditions

The importance of this reaction type has already been referred to in the discussion of the reaction between iminophosphanes and alkyl azides or diazoalkanes (see Section 4.3).

4.4.4. [4 + 1] Cycloadditions

Whereas phosphaalkenes react cleanly with butadiene derivatives to give products formed in [4 + 2] cycloadditions

of the Diels-Alder type,[5] *P*-alkyl-*N*-aryl-substituted iminophosphanes react under comparable conditions via oxidative [4 + 1] cycloaddition with formation of dihydro-λ^5-phospholenes such as **138**[159, 173]; they react with 1,2-

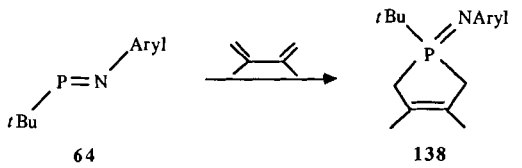

64 **138**

diketones to give analogous dihydro-1,3,2-dioxaphospholes.[44, 162] The dihydrooxadiazaphosphole **139**, which results from the reaction of **105** with diethyl azodicarboxylate, can also formally be regarded as deriving from a [4 + 1]

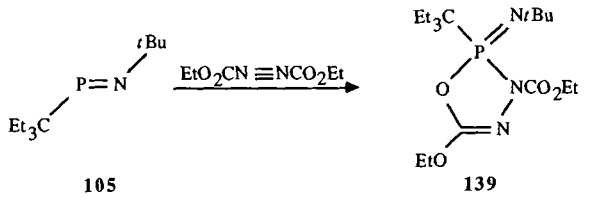

105 **139**

cycloaddition; however, a multistep reaction mechanism cannot be excluded with certainty in this case.[44]

4.5. Rearrangement Reactions

A 1,3 Shift of an α-hydrogen or of a trimethylsilyl group with the formation of a new phosphorus-element double bond was observed in the thermal or base-catalyzed isomerization of the iminophosphanes **140** and **142** to the phosphaalkene **141** and the diphosphene **143** respectively[36, 60].

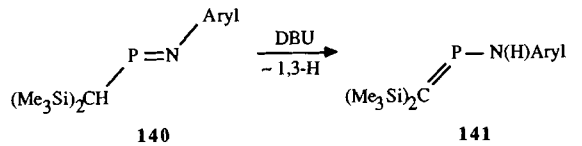

140 **141**

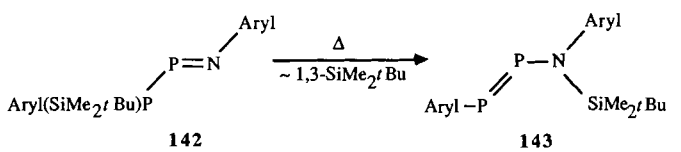

142 **143**

A rearrangement of this type has also been suggested to occur in the synthesis of aminophosphaalkenes and -diphosphenes via the reaction of suitable iminophosphanes with either alkyllithiums[174, 175] or trimethylsilyl-[176] and lithio(tri-*tert*-butylphenyl)phosphane[177] and for the formation of the diphosphane **145** in the thermolysis of **144**;[42] however, it was not possible to detect the corresponding

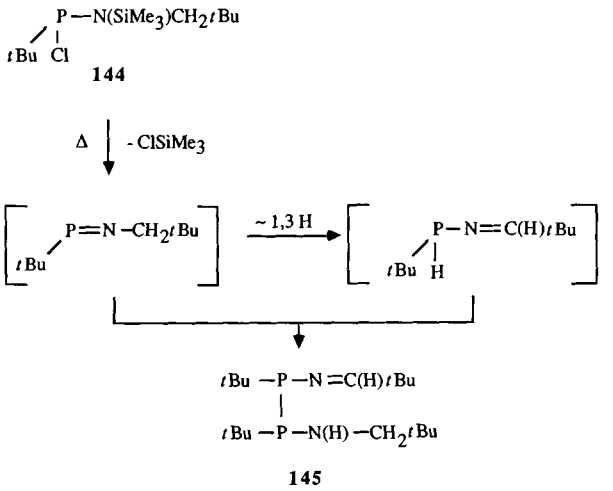

iminophosphane intermediates in these cases. The formation of the terminal phosphinidene complex **147** from **146** via a 1,3 hydrogen shift can be followed spectroscopically.[95]

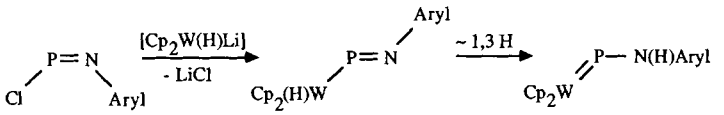

10 **146** **147**

4.6. Reactions at Peripheral Groups

Although a number of iminophosphanes are known which contain further functional groups the extreme reactivity of the latter has so far prevented the discovery of many examples of reactions in which the former underwent transformations while the P=N double bond remained unchanged. Reactions of **89** with chalcogens (**38**, **148**) methyl iodide (**37**) and [$(CO)_5Cr(thf)$] lead to selective derivatization of the

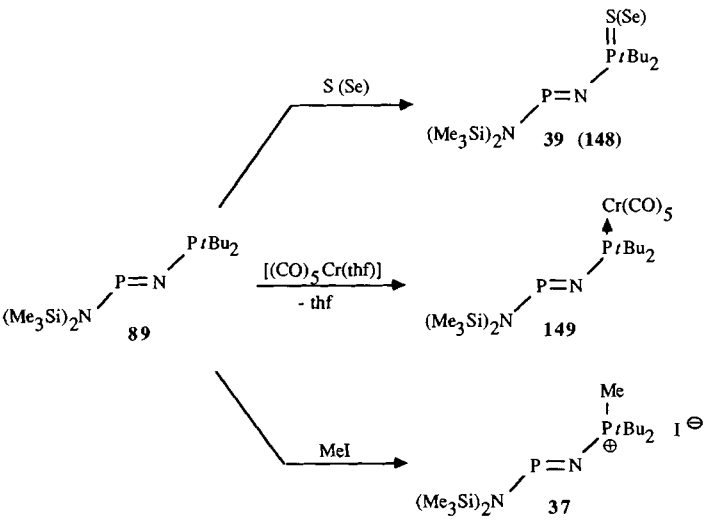

89

threefold coordinated phosphorus with retention of the iminophosphane structure; this indicates that the twofold coordinated phosphorus atom has a relatively low basicity in these cases[26, 142]. The NH-functionalized compound **40**

and Al_2Me_6 do not give the expected organometalation but rather a condensation product in which the low coordination number remains unchanged; the zwitterionic structure of the product **150** results from a nucleophilic attack of the imine nitrogen at aluminum.[178]

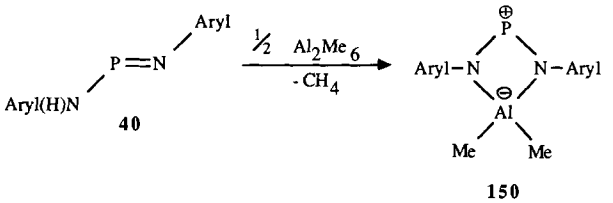

The formation of functionalized iminophosphanes such as **151** via insertion of phenyl isocyanate or tetrafluoropropyl cyanate into an Si–N bond of **3** occurs without formal participation of the double bond.[179, 180] However, a more exact

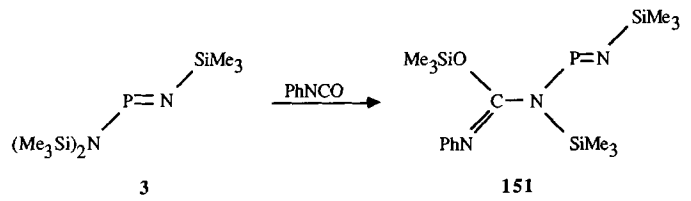

study of the reaction with phenyl isocyanate indicated the presence of a multi-step reaction in which the product is generated via an electrophilic addition of the substrate at the imine nitrogen followed by a 1,5 silyl shift.[166] Participation of the double bond has also been suggested for the selenation of **38**; the formation of the *P*-selenoiminophosphane **152** was explained on the basis of rearrangement of a selenoiminophosphorane intermediate arising from oxidative selenation.[106]

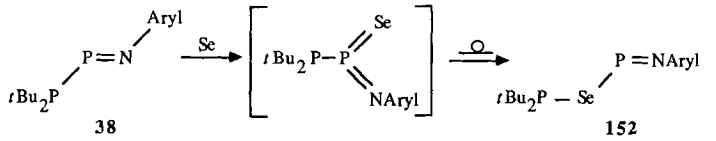

The reactions of **68** with nickel complexes of the type [(olefin)Ni(PR_3)$_2$] to give the metal-substituted derivatives **154** (Scheme 36) are related to nucleophilic substitution reactions. The detection of the intermediates **153a, b**, from which **154** is generated via a 1,2 shift of the cyclopentadienyl residue, also indicates that the double bond system is involved in the reaction. The analogous generation of a metalloiminophosphane and its subsequent [2 + 1] addition to excess starting material was formulated to explain the formation of a spirocyclic $\lambda^3\lambda^5$-azadiphosphiridine from Me_5C_5–P=N*t*Bu and $(MeCN)_3Mo(CO)_3$.[41]

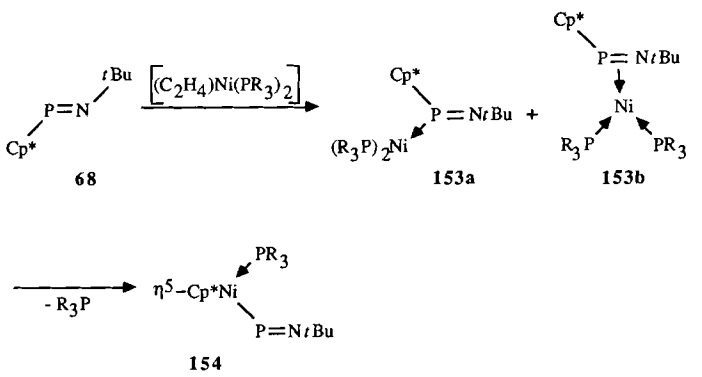

Scheme 36. Bu (**a**), Et (**b**), Ph (**c**).

5. Future Prospects

The present survey shows that the chemistry of the iminophosphanes has undergone a very rapid development in the last few years; the mutual stimulation of theory and experiment has played an important role in making possible such rapid progress. In the initial phase the synthesis of aminoiminophosphanes and their transformation into (from the point of view of bonding theory) "unusual" compounds with $\sigma^3\lambda^5$-phosphorus formed the focus of interest; new applications in catalysis have very recently been reported for the latter.[182] Later studies dealt with "carbene-like" properties of the *P*-alkylated derivatives, which afforded routes to new types of phosphorus heterocycles. The recent synthesis of *P*-halogenated derivatives has made possible the preparation of a broad spectrum of functionalized iminophosphanes, including metalloiminophosphanes and a phosphanetriylammonium ion; the extreme bonding situation in the latter compounds is made clear by their in part extremely unusual crystal structures.

What can we expect in the future? Since the parent system (*E*)–HP=NH has so far resisted all attempts at its detection, one important goal is the generation of further small, highly reactive iminophosphanes and the study of their reactivity in the gas phase or in a matrix. New phospha-analogs of cumulene systems, such as diazo- and azido-compounds, are of both theoretical and synthetic interest. A further aspect which will certainly continue to be of great interest is the study of the coordination chemistry of known or still unknown phosphorus–nitrogen systems; the synthesis of phospha-analogs of pentadiazenes mentioned above (Section 2.2) has certainly provided an initial impulse in this direction. The generation of optically active iminophosphanes and products derived from them, and a study of their chemistry, would certainly be of great promise both from the synthetic point of view and as a tool for carrying out detailed mechanisitic studies.

While until now all attempts have been directed towards the study of monomeric products, the high reaction potential of the double bond of iminophosphanes suggests that the latter are capable of serving as useful precursors in polymer chemistry. In this respect it would be extremely attractive to verify the existence of a phosphandiylimide [RP=N]$^{\ominus}$; such a system could be used in the construction of poly-iminophosphanes $(PN)_xR_y$, and together with the known iminophosphane system RP=NR′ could also serve as a model compound for the study of ionic polymerization and the generation of "living polymers". The possible role of iminophosphanes as precursors for an as yet unknown $(PN)_x$ polymer or corresponding copolymers formed from

iminophosphane and phosphazene units also remains to be studied.

My grateful thanks go to all those co-workers whose enthusiastic collaboration has contributed to the advancement of this area of chemistry, from the initial phase to the present time; many of the most recent results can as yet only be found in doctoral theses, but the names of all involved can be found in the list of references. Thanks are also due to Prof. Dr. W. W. Schoeller (Bielefeld) for many intensive and fruitful discussions, and to Mrs. D. Purschke for her skilful and patient help in the preparation of this manuscript. Much of the work cited here was supported by the Deutsche Forschungsgemeinschaft, the Fonds der Chemischen Industrie and the Minister für Wissenschaft und Forschung des Landes Nordrhein-Westfalen.

Received: March 23, 1990 [A 807 IE]
German version: *Angew. Chem. 103* (1991) 251
Translated by Professor Dr. *I. N. Mitchell*, Dortmund

[1] T. E. Gier, *J. Am. Chem. Soc. 83* (1961) 1769.
[2] K. Dimroth, P. Hoffmann, *Angew. Chem. 76* (1964) 433; *Angew. Chem. Int. Ed. Engl. 3* (1964) 384.
[3] G. Märkl, *Angew. Chem. 78* (1966) 907; *Angew. Chem. Int. Ed. Engl. 5* (1966) 846; K. Dimroth, *Top. Curr. Chem. 38* (1973) 1.
[4] E. Niecke, W. Flick, *Angew. Chem. 85* (1973) 586; *Angew. Chem. Int. Ed. Engl. 12* (1973) 585.
[5] G. Becker, *Z. Anorg. Allg. Chem. 423* (1966) 242; review: R. Appel, F. Knoll, *Adv. Inorg. Chem. 33* (1989) 259.
[6] $\lambda^5\sigma^3$-Phosphoranes: M. Regitz, *Methoden Org. Chem. (Houben-Weyl) 4th Ed. Vol. E2* (1982); $\lambda^3\sigma^1$-phosphaalkynes: M. Regitz, P. Binger, *Angew. Chem. 100* (1988) 1541; *Angew. Chem. Int. Ed. Engl. 27* (1988) 1484; M. Regitz, *Chem. Rev. 90* (1990) 191.
[7] P=Si: C. N. Smit, F. M. Lock, F. Bickelhaupt, *Tetrahedron Lett. 25* (1984) 3011; P=Ge: J. Escudie, C. Couret, J. Satgé, M. Andrianarison, J. D. Andriamizaka, *J. Am. Chem. Soc. 107* (1985) 3378; P=Sn: C. Couret, J. Escudie, J. Satgé, A. Raharinirina, J. D. Andriamizaka, *ibid. 107* (1985) 8280.
[8] P=P: M. Yoshifuji, J. Shima, N. Inamoto, *J. Am. Chem. Soc. 103* (1981) 4587; P=As and P=Sb: A. H. Cowley, J. G. Lash, N. C. Norman, M. Pakulski, B. R. Whittlesey, *J. Chem. Soc. Chem. Commun. 1983*, 881.
[9] R. A. Bartlett, X. Feng, P. P. Power, *J. Am. Chem. Soc. 108* (1986) 6817.
[10] W. Kutzelnigg, *Angew. Chem. 96* (1984) 262; *Angew. Chem. Int. Ed. Engl. 23* (1984) 272.
[11] Review: A. H. Cowley, R. A. Kemp, *Chem. Rev. 85* (1985) 367.
[12] A. Schmidpeter, K. Karaghiosoff, *Nachr. Chem. Tech. Lab. 33* (1985) 793.
[13] O. J. Scherer, *Angew. Chem. 97* (1985) 905; *Angew. Chem. Int. Ed. Engl. 24* (1985) 924.
[14] E. Niecke, O. J. Scherer, *Nachr. Chem. Tech. 23* (1975) 395; E. Fluck, *Top. Curr. Chem. 10* (1980) 193; L. N. Markovskii, V. D. Romanenko, A. V. Ruban, *Sov. Sci. Rev. Sect. B 6* (1984) 269; B. A. Arbusov, E. N. Dianova, *Phosphorus Sulfur 26* (1986) 203; L. N. Markovskii, V. D. Romanenko, A. V. Ruban, *Zh. Obshch, Khim. 57* (1987) 1433; *The Chemistry of Acyclic Twofold Coordinated Phosphorus Compounds*, Naukowa Dumka, Kiew 1988 (in Russian); A. N. Chernega, M. Yu. Antipin, Yu. T. Struchkov, *Zh. Strukt. Khim. 24* (1988) 122.
[15] S. Lochschmidt, A. Schmidpeter, *Phosphorus Sulfur 29* (1986) 73.
[16] O. J. Scherer, N. Kuhn, *Chem. Ber. 107* (1974) 2123.
[17] O. J. Scherer, N. Kuhn, *Angew. Chem. 86* (1974) 899; *Angew. Chem. Int. Ed. Engl. 13* (1974) 811.
[18] O. J. Scherer, N. Kuhn, *J. Organomet. Chem. 82* (1974) C3.
[19] O. J. Scherer, W. Gläßel, *Angew. Chem. 87* (1975) 667; *Angew. Chem. Int. Ed. Engl. 14* (1975) 629.
[20] O. J. Scherer, W. Glässel, *Chem. Ber. 110* (1977) 3874.
[21] L. N. Markovskii, V. D. Romanenko, A. V. Ruban, *Zh. Obshch. Khim. 49* (1979) 1908.
[22] L. N. Markovskii, V. D. Romanenko, V. I. Dzyuba, E. I. Lippmaa, M. A. Alla, *Zh. Obshch. Khim. 50* (1980) 2621.
[23] O. J. Scherer, H. Conrad, *Z. Naturforsch. B 36* (1981) 515.
[24] E. Niecke, R. Rüger, W. W. Schoeller, *Angew. Chem. 93* (1981) 1110; *Angew. Chem. Int. Ed. Engl. 20* (1981) 1034.
[25] V. D. Romanenko, A. V. Ruban, S. V. Iksanova, L. N. Markovskii, *Zh. Obshch. Khim. 54* (1984) 313.
[26] L. N. Markovskii, V. D. Romanenko, E. O. Klebanskii, *Zh. Obshch. Khim. 54* (1984) 1425.
[27] E. Niecke, J. Böske, D. Gudat, M. Lysek, E. Symalla, *Nova Acta Leopold. 264* (1985) 83.
[28] U. Dressler, E. Niecke, S. Pohl, W. Saak, W. W. Schoeller, H.-G. Schäfer, *J. Chem. Soc. Chem. Commun. 1986*, 1086.
[29] V. D. Romanenko, A. B. Drapailo, A. V. Ruban, L. N. Markovskii, *Zh. Obshch. Khim. 56* (1986) 714.
[30] L. N. Markovskii, V. D. Romanenko, E. O. Klebanskii, M. I. Povolotskii, A. N. Chernega, M. Yu. Antipin, Yu. T. Struchkov, *Zh. Obshch. Khim. 56* (1986) 1721.
[31] L. N. Markovskii, V. D. Romanenko, A. B. Drapailo, A. V. Ruban, A. N. Chernega, M. Yu. Antipin, Yu. T. Struchkov, *Zh. Obshch. Khim. 56* (1986) 2231.
[32] V. D. Romanenko, A. V. Ruban, A. B. Drapailo, M. I. Povolotskii, L. N. Markovskii, *Zh. Obshch. Khim. 57* (1987) 235.
[33] V. D. Romanenko, A. B. Drapailo, A. V. Ruban, L. N. Markovskii, *Zh. Obshch. Khim. 56* (1986) 2792.
[34] V. D. Romanenko, A. V. Ruban, A. N. Chernega, M. I. Povolotskii, M. Yu. Antipin, Yu. T. Struchkov, L. N. Markovskii, *Zh. Obshch. Khim. 58* (1988) 948.
[35] L. N. Markovskii, V. D. Romanenko, V. D. Ruban, A. B. Drapailo, A. N. Chernega, M. Yu. Antipin, Yu. T. Struchkov, *Zh. Obshch. Khim. 58* (1988) 291.
[36] M. Lysek, *Dissertation*, Universität Bielefeld 1988.
[37] O. Altmeyer, E. Niecke, M. Nieger, T. Busch, W. W. Schoeller, D. Stalke, *Heteroat. Chem. 1* (1990) 191.
[38] H. Schiffner, M. Nieger, D. Gudat, E. Niecke, unpublished.
[39] J. Neemann, U. Klingebiel, *Chem. Ber. 114* (1981) 527.
[40] S. K. Vasisht, M. Sood, P. K. Verma, T. Kaur, K. Usha, *Phosphorus Sulfur Silicon Relat. Elem. 47* (1990) 349.
[41] D. Gudat, E. Niecke, B. Krebs, M. Dartmann, *Organometallics 5* (1986) 2376.
[42] E. Niecke, M. Lysek, E. Symalla, *Chimia 40* (1986) 202.
[43] P. B. Hitchcock, M. F. Lappert, A. K. Rai, H. D. Williams, *J. Chem. Soc. Chem. Commun. 1986*, 1633.
[44] D. Barion, *Dissertation*, Universität Bonn 1990.
[45] E. Niecke, D. Gudat, M. Leuer, M. Lysek, E. Symalla, *Phosphorus Sulfur 30* (1987) 467.
[46] E. Niecke, M. Nieger, F. Reichert, *Angew. Chem. 100* (1988) 1781; *Angew. Chem. Int. Ed. Engl. 27* (1988) 1715.
[47] F. Reichert, *Dissertation*, Universität Bonn 1990.
[48] R. Keat, D. S. Rycroft, E. Niecke, H. G. Schäfer, H. Zorn, *Z. Naturforsch. B 37* (1982) 1665.
[49] O. J. Scherer, P. Klusmann, *Angew. Chem. 81* (1969) 743; *Angew. Chem. Int. Ed. Engl. 8* (1969) 752.
[50] M. Yoshifuji, K. Shibayama, K. Toyota, N. Inamoto, S. Nagase, *Chem. Lett. 1985*, 237.
[51] C. Lehousse, M. Haddad, J. Barrans, *Tetrahedron Lett. 23* (1982) 4174.
[52] E. Niecke, D. Gudat, E. Symalla, *Angew. Chem. 98* (1986) 817; *Angew. Chem. Int. Ed. Engl. 25* (1986) 834.
[53] O. J. Scherer, N.-T. Kulbach, W. Glaessel, *Z. Naturforsch. B 33* (1978) 652.
[54] H. G. Ang, F. K. Lee, *Polyhedron 8* (1989) 379.
[55] V. D. Romanenko, A. V. Ruban, L. N. Markovskii, *J. Chem. Soc. Chem. Commun. 1983*, 187; L. N. Markovskii, V. D. Romanenko, A. V. Kirsanov, *Phosphorus Sulfur 18* (1983) 31; V. D. Romanenko, A. V. Ruban, L. N. Markovskii, *Zh. Obshch. Khim. 53* (1983) 691.
[56] V. D. Romanenko, A. V. Ruban, L. N. Markovskii, *Zh. Obshch. Khim. 53* (1983) 778.
[57] V. D. Romanenko, A. V. Ruban, A. N. Chernega, L. N. Markovskii, *Zh. Obshch. Khim. 58* (1988) 2802; V. D. Romanenko, A. V. Ruban, A. N. Chernega, M. I. Povolotskii, M. Yu. Antipin, Yu. T. Struchkov, L. N. Markovskii, *ibid. 58* (1988) 948.
[58] E. Niecke, C. Gärtner-Winkhaus, J. Hein, M. Lysek, M. Nieger, F. Reichert, *Euchem Conf.* (Paris-Palaiseau), August 1988.
[59] E. Niecke, M. Nieger, C. Gärtner-Winkhaus, B. Kramer, *Chem. Ber. 123* (1990) 477.
[60] E. Niecke, O. Altmeyer, D. Barion, R. Detsch, C. Gärtner, J. Hein, M. Nieger, F. Reichert, *Phosphorus Sulfur Silicon Relat. Elem. 49/50* (1990) 321.
[61] E. Niecke, R. Detsch, M. Nieger, *Chem. Ber. 123* (1990) 797.
[62] V. D. Romanenko, A. V. Ruban, G. V. Reitel, M. I. Povolotskii, A. N. Chernega, L. N. Markovskii, *Zh. Obshch. Khim. 59* (1989) 2780.
[63] A. M. Caminade, C. Roques, N. Dufour, D. Colombo, F. Gonce, J. P. Majoral, *Tetrahedron Lett. 30* (1989) 6869.
[64] V. D. Romanenko, A. V. Ruban, G. V. Reitel, M. I. Povolotskii, L. N. Markovskii, *Zh. Obshch. Khim. 59* (1989) 2129.
[65] F. Zurmühlen, M. Regitz, *Angew. Chem. 99* (1987) 65; *Angew. Chem. Int. Ed. Engl. 26* (1987) 83; *New J. Chem. 13* (1989) 335.
[66] U. Krüger, H. Pritzkow, H.-J. Grützmacher, *Chem. Ber.*, in press.
[67] J. Böske, E. Niecke, M. Nieger, E. Ocando-Mavarez, J. P. Majoral, G. Bertrand, *Inorg. Chem. 28* (1989) 499.
[68] Y. G. Gololobov, L. I. Nesterova, *Zh. Obshch. Khim. 51* (1981) 2638.

[69] E. Niecke, A. Nickloweit-Lüke, R. Rüger, *Angew. Chem. 93* (1981) 406; *Angew. Chem. Int. Ed. Engl. 20* (1981) 385.
[70] E. Niecke, A. Nickloweit-Lüke, R. Rüger, B. Krebs, H. Grewe, *Z. Naturforsch. B 36* (1981) 1566.
[71] J. Böske, E. Ocando-Mavarez, E. Niecke, J. P. Majoral, G. Bertrand, *J. Am. Chem. Soc. 109* (1987) 2822.
[72] W. W. Schoeller, E. Niecke, *J. Chem. Soc. Chem. Commun. 1982,* 569.
[73] G. Trinquier, *J. Am. Chem. Soc. 104* (1982) 6969.
[74] D. Gonbeau, G. Pfister-Guillouzo, J. Barrans, *Can. J. Chem. 61* (1983) 1371.
[75] T.-K. Ha, M.-T. Nguyen, P. Ruelle, *Chem. Phys. 87* (1984) 23.
[76] M.-T. Nguyen, M. A. McGinn, A. F. Hegarty, *J. Am. Chem. Soc. 107* (1985) 8029.
[77] M. W. Schmidt, M. S. Gordon, *Inorg. Chem. 25* (1986) 248.
[78] K. Ito, S. Nagase, *Chem. Phys. Lett. 126* (1986) 531.
[79] M. W. Schmidt, P. N. Truong, M. S. Gordon, *J. Am. Chem. Soc. 109* (1987) 5217.
[80] W. W. Schoeller, C. Lerch, *Inorg. Chem. 25* (1986) 576.
[81] W. W. Schoeller, T. Busch, E. Niecke, *Chem. Ber. 123* (1990) 1653.
[82] A. N. Chernega, A. A. Korkin, M. Yu. Antipin, Yu. T. Struchkov, A. V. Ruban, V. D. Romanenko, *Zh. Obshch. Khim. 59* (1989) 2243.
[83] V. Galasso, *Chem. Phys. 83* (1984) 407.
[84] S. Elbel, A. Ellis, E. Niecke, H. Egsgaard, L. Carlsen, *J. Chem. Soc. Dalton Trans. 1985,* 879.
[85] D. Gonbeau, J. L. Garcia, G. Pfister-Guillouzo, *Can. J. Chem. 64* (1986) 1530.
[86] W. W. Schoeller, T. Busch, J. Niemann, T. Dabisch, W. D. Stohrer, *Heteroat. Chem.,* in press.
[87] E. Niecke, D. Gudat, W. W. Schoeller, P. Rademacher, *J. Chem. Soc. Chem. Commun. 1985,* 1050.
[88] G. David, T. Busch, P. Rademacher, W. W. Schoeller, E. Niecke, unpublished.
[89] T. Koopmans, *Physica 1* (1934) 104.
[90] Yu. Z. Stepanova, I. I. Patsanovskii, E. A. Ishmaeva, V. D. Romanenko, L. N. Markovskii, *Zh. Obshch. Khim. 57* (1987) 2449.
[91] I. I. Patsanovskii, Yu. Z. Stepanova, E. A. Ishmaeva, V. D. Romanenko, L. N. Markovskii, *Zh. Obshch. Khim. 60* (1990) 502; E. A. Ishmaeva, I. I. Patsanovskii, V. D. Romanenko, L. N. Markovskii, *Phosphorus Sulfur Silicon Relat. Elem. 49/50* (1990) 289.
[92] A. N. Chernega, M. Yu. Antipin, Yu. T. Struchkov, V. D. Romanenko, L. N. Markovskii, *Zh. Obshch. Khim. 58* (1988) 2219.
[93] A. N. Chernega, M. Yu. Antipin, Yu. T. Struchkov, V. D. Romanenko, E. O. Klebanskii, L. N. Markovskii, *Zh. Strukt. Khim. 29* (1988) 121.
[94] A. N. Chernega, M. Yu. Antipin, Yu. T. Struchkov, A. B. Drapailo, A. V. Ruban, V. D. Romanenko, *Izv. Akad. Nauk SSSR Ser. Khim. 1987,* 1304.
[95] E. Niecke, J. Hein, M. Nieger, *Organometallics 8* (1989) 2290.
[96] M. Nieger, *Dissertation,* Universität Bonn 1989.
[97] A. N. Chernega, M. Yu. Antipin, Yu. T. Struchkov, A. V. Ruban, V. D. Romanenko, *Zh. Strukt. Khim. 28* (1987) 105.
[98] A. N. Chernega, M. Yu. Antipin, Yu. T. Struchkov, A. V. Ruban, V. D. Romanenko, *Zh. Strukt. Khim. 31* (1990) 124.
[99] A. N. Chernega, M. Yu. Antipin, Yu. T. Struchkov, A. V. Ruban, V. D. Romanenko, L. N. Markovskii, *Dokl. Akad. Nauk SSSR 307* (1989) 610.
[100] A. N. Chernega, M. Yu. Antipin, Yu. T. Struchkov, I. E. Boldeskul, E. O. Klebanskii, V. D. Romanenko, *Izv. Akad. Nauk SSSR Ser. Khim. 1985,* 2236; A. N. Chernega, A. A. Korkin, M. Yu. Antipin, Yu. T. Struchkov, *Zh. Obshch. Khim. 58* (1988) 2045.
[101] S. Pohl, *Angew. Chem. 88* (1976) 723; *Angew. Chem. Int. Ed. Engl. 15* (1976) 687; *Z. Naturforsch. B 32* (1977) 1344; *Chem. Ber. 112* (1979) 3159.
[102] J. Hein, C. Gärtner-Winkhaus, M. Nieger, E. Niecke, *Heteroat. Chem.,* in press.
[103] A. N. Chernega, M. Yu. Antipin, Yu. T. Struchkov, A. V. Ruban, V. D. Romanenko, *Zh. Strukt. Khim. 30* (1989) 105.
[104] A. N. Chernega, M. Yu. Antipin, Yu. T. Struchkov, A. V. Ruban, V. D. Romanenko, *Zh. Strukt. Khim. 31* (1990) 134.
[105] L. N. Markovskii, A. V. Ruban, A. N. Chernega, M. I. Povolotskii, G. V. Reitel, V. D. Romanenko, *Dokl. Akad. Nauk SSSR 306* (1989) 1137.
[106] E. Niecke, M. Nieger, F. Reichert, W. W. Schoeller, *Angew. Chem. 100* (1988) 1779; *Angew. Chem. Int. Ed. Engl. 27* (1988) 1713.
[107] D. E. C. Corbridge: *The Structural Chemistry of Phosphorus,* Elsevier, Amsterdam 1974.
[108] W. W. Schoeller (Bielefeld), private communication.
[109] E. Fluck, *Methods Stereochem. Anal. 8* (1987) 61.
[110] K. Barlos, G. Hübler, H. Nöth, P. Wanninger, N. Wiberg, B. Wrackmeyer, *J. Magn. Reson. 31* (1978) 363; C. Stader, B. Wrackmeyer, *Z. Naturforsch. B 42* (1987) 1515.
[111] E. Niecke, R. Kröher, *Angew. Chem. 88* (1976) 758; *Angew. Chem. Int. Ed. Engl. 15* (1976) 692; *Z. Naturforsch. B 34* (1979) 837.
[112] D. Gudat, M. Nieger, E. Niecke, *J. Chem. Soc. Dalton Trans. 1989,* 693.
[113] J. Hein, E. Niecke, *J. Chem. Soc. Chem. Commun., 1991,* 48.
[114] A. H. Cowley, R. A. Kemp, *J. Chem. Soc. Chem. Commun. 1982,* 319; *Inorg. Chem. 22* (1983) 547.
[115] E. Niecke, G. Ringel, *Angew. Chem. 89* (1977) 501; *Angew. Chem. Int. Ed. Engl. 16* (1977) 486.
[116] B. P. Roberts, K. Singh, *J. Chem. Soc. Perkin Trans. 2 1981,* 866.
[117] C. Roques, M.-R. Mazieres, J.-P. Majoral, M. Sanchez, *Tetrahedron Lett. 29* (1988) 4547.
[118] A. I. Brusilovets, *Dokl. Akad. Nauk Ukr. SSR Ser. B: Geol. Khim. Biol. Nauki 2* (1990) 39; *Zh. Obshch. Khim. 60* (1990) 216.
[119] H. Binder, R. Fischer, *Chem. Ber. 107* (1974) 205.
[120] W. Flick, *Dissertation,* Universität Göttingen 1975.
[121] V. D. Romanenko, A. V. Ruban, N. N. Kalibabchuk, S. V. Iksanova, L. N. Markovskii, *Zh. Obshch. Khim. 51* (1981) 1726.
[122] L. N. Markovskii, V. D. Romanenko, A. V. Ruban, *Phosphorus Sulfur 9* (1980) 221.
[123] E. Niecke, G. David, S. Pohl, M. Murray, unpublished results.
[124] L. N. Markovskii, V. D. Romanenko, A. V. Ruban, A. B. Drapailo, M. Mikolajczyk, J. Omeljanczuk, V. Perlikovska, *Zh. Obshch. Khim. 58* (1988) 2627; M. Mikolajczyk, J. Omeljanczuk, V. Perlikovska, L. N. Markovskii, V. D. Romanenko, A. V. Ruban, A. B. Drapailo, *Phosphorus Sulfur 36* (1988) 267.
[125] E. Niecke, W. Bitter, *Angew. Chem. 87* (1975) 34; *Angew. Chem. Int. Ed. Engl. 14* (1975) 50.
[126] E. Niecke, W. Bitter, *Chem. Ber. 109* (1976) 415.
[127] U. Klingebiel, P. Werner, A. Meller, *Monatsh. Chem. 107* (1976) 939.
[128] O. J. Scherer, G. Schnabl, *Chem. Ber. 109* (1976) 2996.
[129] O. J. Scherer, G. Schnabl, *Z. Naturforsch. B 31* (1976) 142.
[130] O. J. Scherer, W. Glässel, G. Huttner, A. Frank, P. Friedrich, *Angew. Chem. 88* (1976) 768; *Angew. Chem. Int. Ed. Engl. 15* (1976) 700.
[131] O. J. Scherer, G. Wolmershäuser, H. Conrad, *Angew. Chem. 95* (1983) 427; *Angew. Chem. Int. Ed. Engl. 22* (1983) 404.
[132] A. H. Cowley, J. E. Kilduff, J. C. Wilburn, *J. Am. Chem. Soc. 103* (1981) 1575.
[133] V. D. Romanenko, V. F. Schul'gin, V. V. Skopenko, L. N. Markovskii, *J. Chem. Soc. Chem. Commun. 1983,* 808; *Zh. Obshch. Khim. 55* (1985) 45.
[134] a) J. P. Majoral, N. Dufour, F. Meyer, A. M. Caminade, R. Choukroun, D. Gervais, *J. Chem. Soc. Chem. Commun. 1990,* 507; b) N. Dufour, J. P. Majoral, A. M. Caminade, R. Choukroun, *Organometallics 10* (1991) 45; c) A more exact study has shown the compound HP=NAryl mentioned in Ref. [134a] to be an aminochlorophosphane HP(Cl)–N(H)Aryl.
[135] R. H. Neilson, J. S. Engenito, *Organometallics 1* (1982) 1270.
[136] L. N. Markovskii, V. D. Romanenko, A. V. Ruban, *Synthesis 10* (1979) 811.
[137] L. N. Markovskii, V. D.- Romanenko, V. I. Dzyuba, A. V. Ruban, N. N. Kalibabchuk, S. V. Iksanova, *Zh. Obshch. Khim. 51* (1981) 331.
[138] V. D. Romanenko, A. V. Ruban, S. V. Iksanova, L. N. Markovskii, *Zh. Obshch. Khim. 52* (1982) 581.
[139] A. V. Ruban, A. B. Drapailo, V. D. Romanenko, L. N. Markovskii, *Zh. Obshch. Khim. 56* (1986) 2791.
[140] L. N. Markovski, V. D. Romanenko, A. V. Ruban, A. N. Chernega, N. Yu. Antipin, T. Yu. Struchkov, A. V. Kirsanov, *Dokl. Akad. Nauk SSSR 293* (1987) 1394.
[141] L. N. Markovskii, V. D. Romanenko, A. V. Ruban, *Pure Appl. Chem. 59* (1987) 1047.
[142] L. N. Markovskii, V. D. Romanenko, E. O. Klebanskii, A. N. Chernega, M. Yu. Antipin, Yu. T. Struchkov, I. E. Boldeskul, *Zh. Obshch. Khim. 55* (1985) 219; L. N. Markovskii, V. D. Romanenko, E. O. Klebanskii, M. I. Povolotskii, A. N. Chernega, M. Yu. Antipin, Yu. T. Struchkov, *ibid. 57* (1987) 1020.
[143] O. J. Scherer, N. Kuhn, *J. Organomet. Chem. 78* (1974) C17.
[144] L. N. Markovskii, V. D. Romanenko, A. V. Ruban, A. B. Drapailo, *J. Chem. Soc. Chem. Commun. 1984,* 1692.
[145] E. Niecke, D. Barion, M. Nieger, unpublished results.
[146] R. Streubel, E. Niecke, P. Paetzold, *Chem. Ber.*, in press.
[147] E. Niecke, W. Flick, *Angew. Chem. 86* (1974) 128; *Angew. Chem. Int. Ed. Engl. 13* (1974) 134.
[148] E. Niecke, D.-A. Wildbredt, *Angew. Chem. 90* (1978) 209; *Angew. Chem. Int. Ed. Engl. 17* (1978) 199; *Chem. Ber. 113* (1980) 1549.
[149] H.-G. Schäfer, *Dissertation,* Universität Bielefeld 1981.
[150] E. Niecke, A. Seyer, D.-A. Wildbredt, *Angew. Chem. 93* (1981) 687; *Angew. Chem. Int. Ed. Engl. 20* (1981) 675.
[151] E. Niecke, H.-G. Schäfer, *Chem. Ber. 115* (1982) 185.
[152] L. N. Markovskii, V. D. Romanenko, A. V. Ruban, L. K. Polyachenko, *Zh. Obshch. Khim. 53* (1983) 693.
[153] B.-L. Li, P. Mukherjee, R. H. Neilson, *Inorg. Chem. 28* (1989) 605; Report, TCU/DC/TR-89-02; Order No. AD-A204049, *Gov. Rep. Announce. Index (US) 89* (1989) Abstr. No. 932, 032.
[154] E. Niecke, V. von der Gönna, M. Nieger, *Chem. Ber. 123* (1990) 2329.
[155] S. Pohl, E. Niecke, H.-G. Schäfer, *Angew. Chem. 90* (1978) 135; *Angew. Chem. Int. Ed. Engl. 17* (1978) 136.
[156] E. Niecke, W. Flick, *Angew. Chem. 87* (1975) 355; *Angew. Chem. Int. Ed. Engl. 14* (1975) 363.
[157] E. Niecke, W. Flick, S. Pohl, *Angew. Chem. 88* (1976) 305; *Angew. Chem. Int. Ed. Engl. 15* (1976) 309.

[158] E. Niecke, R. Rüger, B. Krebs, M. Dartmann, *Angew. Chem. 95* (1983) 570; *Angew. Chem. Int. Ed. Engl. 22* (1983) 552.
[159] E. Niecke, M. Lysek, *Tetrahedron Lett. 29* (1988) 605.
[160] E. Niecke, D. Barion, *Tetrahedron Lett. 30* (1989) 459.
[161] D. Gudat, E. Niecke, M. Nieger, P. Paetzold, *Chem. Ber. 121* (1988) 565.
[162] G. V. Röschenthaler, K. Sauerbrey, R. Schmutzler, *Chem. Ber. 111* (1978) 3105.
[163] E. Niecke, R. Streubel, *Chem. Ber. 123* (1990) 1245.
[164] E. Niecke, M. Link, unpublished results.
[165] P. Paetzold, C. von Plotho, E. Niecke, R. Rüger, *Chem. Ber. 116* (1983) 1678.
[166] L. N. Markovskii, V. D. Romanenko, A. V. Ruban, S. V. Iksanova, A. N. Chernega, I. E. Boldeskul, M. Yu. Antipin, A. A. Espenbetov, Yu. T. Struchkov, *Zh. Obshch. Khim. 53* (1983) 525.
[167] A. Schmidpeter, T. von Criegern, *Z. Naturforsch. B 33* (1978) 1330.
[168] R. Appel. M. Halstenberg, *J. Organomet. Chem. 99* (1975) C 25.
[169] E. Niecke, W. Flick, *J. Organomet. Chem. 104* (1976) C 23.
[170] U. Klingebiel, *Chem. Ber. 111* (1978) 2735.
[171] D. Fest, C. D. Habben, A. Meller, *Chem. Ber. 122* (1989) 861.
[172] E. Niecke, H. Zorn, B. Krebs, G. Henkel, *Angew. Chem. 92* (1980) 737; *Angew. Chem. Int. Ed. Engl. 19* (1980) 709.
[173] V. D. Romanenko, A. B. Drapailo, A. V. Ruban, L. N. Markovskii, *Zh. Obshch. Khim. 57* (1987) 1402.
[174] V. D. Romanenko, L. K. Polyachenko, L. N. Markovskii, *Zh. Obshch. Khim. 54* (1984) 965.
[175] V. D. Romanenko, L. K. Polyachenko, L. N. Markovskii, *Phosphorus Sulfur 19* (1984) 189.
[176] E. Niecke, B. Kramer, M. Nieger, *Organometallics 10* (1991) 10.
[177] A. V. Ruban, V. D. Romanenko, G. V. Reitel, L. N. Markovskii, *Zh. Obshch. Khim. 59* (1989) 2781.
[178] P. B. Hitchcock, H. A. Jasim, M. F. Lappert, H. D. Williams, *J. Chem. Soc. Chem. Commun. 1986*, 1634.
[179] L. N. Markovskii, V. D. Romanenko, A. V. Ruban, G. I. Volkov, *Zh. Obshch. Khim. 51* (1981) 1668.
[180] V. D. Romanenko, G. I. Volkov, L. N. Markovskii, *Zh. Obshch. Khim. 52* (1982) 926.
[181] D. Gudat, E. Niecke, *J. Chem. Soc. Chem. Commun. 1987*, 10.
[182] G. Fink, V. Möhring, *Stud. Surf. Sci. Catal. 25* (1986) 231; W. Keim, R. Appel, A. Storeck, C. Krüger, R. Goddard, *Angew. Chem. 93* (1981) 91; *Angew. Chem. Int. Ed. Engl. 20* (1981) 116.

Missing issues?

No problem with a personal subscription to "Angewandte Chemie". Your own copy to read when you want, where you want. Subscribe today!

Just phone or fax

VCH

USA: Tel. (800) 422-8824, Fax (305) 428-8201
Rest of the world: Tel. (06201) 602216, Fax (06201) 602328

3-Amino-2*H*-Azirines. Synthons for α,α-Disubstituted α-Amino Acids in Heterocycle and Peptide Synthesis.

New Synthetic Methods (84)

By Heinz Heimgartner*

The recent upswing in peptide chemistry has been accompanied by an increasing interest in nonproteinogenic amino acids. These include the α,α-disubstituted glycines, the best known of which is Aib (2-aminoisobutyric acid, 2-methylalanine). These α-amino acids occur in natural oligopeptides such as the peptaibols, a class of membrane-active ionophores that has been isolated from fungal cultures. The twofold substitution at the α-C atom of the amino acids severely restricts the conformational freedom of the peptides and causes particular secondary structures to be favored; thus, α,α-disubstituted α-amino acids induce the formation of β turns or helices. 3-Amino-2*H*-azirines are ideal synthons for the construction of oligopeptides, cyclic peptides and depsipeptides (peptolides) containing such α,α-disubstituted α-amino acids. The presence of the ring strain in these molecules means that they can be used in peptide coupling without the need for additional activating reagents. Using 3-amino-2*H*-azirines a large array of heterocycles containing α,α-disubstituted α-amino acids as structural elements within their skeleton can be synthesized. The driving force in these reactions is the release of the strain on the three-membered ring, which usually takes place in a ring-expansion reaction. The mechanistic elucidation of these reactions, which can be quite complex, contains some surprises.

1. Introduction

Molecules with strained, three-membered rings have been arousing the interest of chemists for more than 100 years. At first it was denied that such organic compounds could exist at all,[1] but in 1885 *A. von Baeyer* presented the first theoretical basis for their consideration, with his strain theory.[2] The prediction that three- and four-membered rings would be unstable compounds, and difficult to prepare, proved extremely stimulating for both theoretical and preparative organic chemistry.[3] Today the exclusion of three-membered carbo- and heterocycles from the arsenal of the organic chemist is inconceivable.[4, 5]

One well-studied class of unsaturated, three-membered heterocycles that has found synthetic application comprises the 2*H*-azirines (**1**), whose synthesis and reactivity have been the object of numerous investigations in the past twenty years (cf. [6, 7]). In the course of these studies it has been shown that numerous nitrogen-containing heterocycles can be synthesized using **1**, both by thermal,[8-11] and by photo-

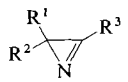

1

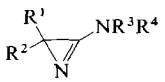

2

chemical[12-16] and metal-catalyzed processes.[17, 18] Remarkably, in different types of reaction, 2*H*-azirines can react by cleavage of the N(1)–C(2), N(1)–C(3), or C(2)–C(3) bonds (for typical examples see [19–21]).

In contrast to the 2*H*-azirines **1**, which are cyclic imines, the 3-amino-2*H*-azirines **2** are cyclic, three-membered amidines with a C–N double bond in an endocyclic position. The first examples of this class of compounds were described by *Rens* and *Ghosez* in 1970.[22] The presence of a nucleophilic amidine group that is at the same time part of the strained azirine structure (with an estimated ring strain of 200 kJ mol^{-1} [23]) is responsible for the varied reactivity of these heterocycles.[25] Since 3-amino-2*H*-azirines are easily accessible via the reactions described below, they are very valuable starting materials for organic synthesis.

2. Synthesis and Structure of 3-Amino-2*H*-Azirines

The most general synthesis is based on the procedure of *Rens* and *Ghosez*[22] already mentioned (Scheme 1). *N,N*-Disubstituted carboxylic amides (**3**) are treated with phosgene, followed by base-catalyzed HCl elimination to yield α-chloroenamines (**4**). These react with sodium azide via

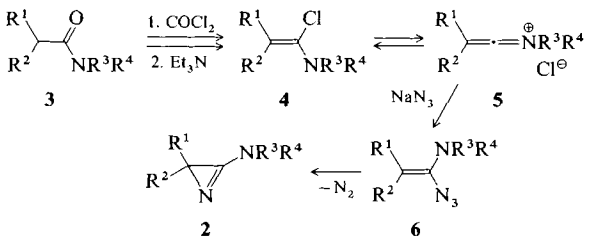

Scheme 1.

keteniminium salts (**5**) to give α-azidoenamines (**6**), which eliminate N_2 in situ to afford **2**.[26] The [1-^{15}N]-labeled azirine **2a*** (R^1–R^4 = Me) used for mechanistic studies was also synthesized in this manner,[27] using sodium [1-^{15}N]azide. In the case of 2,2-dialkyl-3-(dimethylamino)-2*H*-azirines (**2**; R^1, R^2 = alkyl; R^3, R^4 = Me), reaction with phosgene in dichloromethane and with sodium azide in ether

[*] Prof. Dr. H. Heimgartner
Organisch-chemisches Institut der Universität
Winterthurerstrasse 190, CH-8057 Zürich (Switzerland)

or dimethylformamide leads to azirines in yields of ca. 70%. However for slower reacting amides (**3**, R^1 and/or R^3 = aryl), modified conditions are required. For example, if ca. 5% dimethylformamide is added to the reaction with phosgene, the chloroenamine **4** is formed spontaneously.[28,29] A second possibility is provided by a route via the corresponding thioamide,[30,31] where HCl elimination occurs even without addition of base. A slightly modified route has also been used to synthesize C(2)-monosubstituted 3-amino-2*H*-azirines[26,32] (Table 1, **2v–y**). In several cases, reaction of the chloroenamine with sodium azide led to isolable 5-amino-4*H*-1,2,3-triazoles, which could then be transformed into the 3-amino-2*H*-azirines by photochemical N_2 elimination.[33]

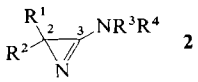

2

Table 1. 3-Amino-2*H*-azirines **2** synthesized via chloroenamines **4**.

2	R^1	R^2	R^3	R^4	Ref.
a	Me	Me	Me	Me	[22,26,29]
aa	Me	Me	Et	Et	[26]
ab	Me	Me	$-(CH_2)_5-$		[26]
ac	Me	Me	$-(CH_2)_2O(CH_2)_2-$		[26]
ad	Me	Me	Me	Ph	[29,30,34]
ae	Me	Me	Me	[a]	[30,34]
af	Me	Me	Me	[b]	[30,34]
ag	Me	Me	Me	$C_6H_4NO_2$ (*p*)	[28]
b	Me	Et	Me	Me	[29]
ba	Me	Et	Me	Ph	[29]
c	Me	*i*Pr	Me	Me	[28,29]
ca	Me	*i*Pr	Me	Ph	[31]
d	Me	*i*Bu	Me	Ph	[35]
e	Me	$PhCH_2$	Me	Me	[29]
ea	Me	$PhCH_2$	Me	Ph	[36]
f	Me	$CH_2=CH$	Me	Me	[26,37]
g	Me	$CH_2=C(CH_3)$	Me	Me	[31]
h	Me	$CH_2=CHCH_2$	Me	Me	[28,38]
i	Me	Ph	Me	Me	[26]
j	Me	MeO_2C	Me	Me	[33]
k	Me	MeS	Me	Me	[39]
l	Me	PhS	Me	Me	[39]
m	Et	Ph	Me	Me	[26]
n	Et	Ph	Me	Ph	[30,34]
o	Pr	Pr	Me	Me	[29]
p	Ph	Ph	Me	Me	[28]
q	Ph	MeO_2C	Me	Me	[33]
r	$-(CH_2)_3-$		Me	Me	[29]
s	$-(CH_2)_4-$		Me	Me	[31]
sa	$-(CH_2)_4-$		Me	Ph	[40]
t	$-(CH_2)_5-$		Me	Me	[26,29]
ta	$-(CH_2)_5-$		Et	Et	[26]
tb	$-(CH_2)_5-$		Me	Ph	[29]
u	$-(CH_2)_6-$		Me	Me	[29]
ua	$-(CH_2)_6-$		Me	Ph	[40]
v	Me	H	Me	Ph	[32]
w	*i*Pr	H	Et	Et	[26]
x	*t*Bu	H	Me	Me	[26]
y	Ph	H	Me	Ph	[32]
z	Ph	N_3	Et	Et	[41]

[a] $C_6H_4OCH_2CH=CH_2$ (*o*). [b] $C_6H_4OCH_2CH=CHCO_2Et$ (*o*).

Other approaches lead to 3-amino-2*H*-azirines **2za–2zd**,[42–45] though these are far less general. The azirines synthesized by these routes contain substituents that are incompatible with the *Ghosez* synthesis.[26] The reaction sequence leading to azirines of type **2zc**[44] is remarkable, because the otherwise short-lived α-azidoenamines are isolable. Compounds **2zd**,[45] which are obtained via a Neber rearrangement, are distinguished by the presence of an unsubstituted amino group on C(3). Hardly any reactions have yet been carried out with azirines **2za–2zd**.

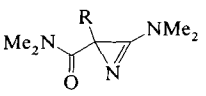

2za (R = H, Et, PhO, Cl[42a])

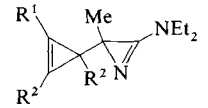

2zb (R^1, R^2 = Aryl[43])

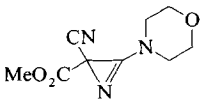

2zc [44]

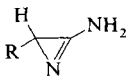

2zd (R = $PhSO_2$, $C_6H_2Cl_3$-NHCO[45])

The 3-amino-2*H*-azirines **2** are generally stable liquids or solids which may be kept for years at 0 °C if moisture and acids are excluded. The vinyl-substituted compounds **2f** and **2g** are exceptions, as they decompose slowly even at 0 °C. Suitable reaction solvents are ether, tetrahydrofuran (THF), dichloromethane, acetonitrile, and dimethylformamide (DMF), i.e. polar aprotic solvents, but also, for example, toluene and 2-propanol.

The structure of the 3-amino-2*H*-azirines has been determined by X-ray crystallography (Table 2). All of them display, besides a relatively short C(2)–C(3) single bond and a long N(1)–C(2) single bond, a lengthened N(1)–C(3) double bond and a shortened C(3)–N(4) single bond. This demonstrates a pronounced delocalization of the N(4) electron pair

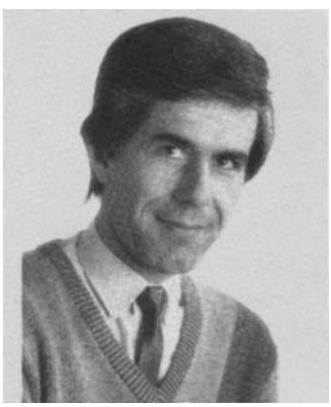

Heinz Heimgartner was born in Münsterlingen, Switzerland in 1941. He completed his doctorate in chemistry at Zürich University in 1972 under Professor Hans Schmid, with distinction for his dissertation on the photochemical and thermal aromatic sigmatropic rearrangements in hydrocarbons. While working on his "habilitation" in the position of chief assistant in 1976, he took over the responsibility for the research groups, "Reaction mechanisms" and "Photochemistry", on the death of Professor Schmid. In 1978 he received the award of the Swiss Chemical Society and the Werner medal for research into the chemistry of the aminoazirines and their application in organic synthesis. Since his habilitation in 1980 he leads his own research group. His particular fields of activity are heterocyclic chemistry, the chemistry of small rings, reaction mechanisms, organic photochemistry and peptide chemistry. In 1987 he become a titular professor.

Table 2. Bond lengths in some 3-amino-2*H*-azirines (in Å).

	R^1	R^2	R^3	R^4	C(2)–C(3)	N(1)–C(2)	N(1)–C(3)	C(3)–N(4)	Ref.
2za'	PhO	$CONMe_2$	Me	Me	1.430	1.490	1.279	1.317	[42b]
2y	Ph	H	Me	Ph	1.440	1.568	1.262	1.345	[46]
2ag	Me	Me	Me	$C_6H_4NO_2$ (*p*)	1.441	1.570	1.270	1.354	[47]
2ze [a]	Me	Me	$-(CH_2)_2-N(R)-(CH_2)_2-$		1.428	1.574	1.254	1.342	[48]

[a] 1,4-bis(2,2-dimethyl-2*H*-azirine-3-yl) piperazine (see structural formula).

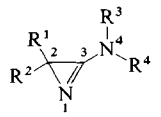

2

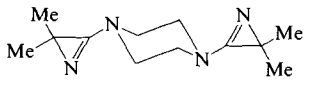

2ze[48]

into the π-system of the C–N double bond[42b, 46–48] (for comparison see [49]). Figure 1 shows the structure of **2ag** in the crystal.

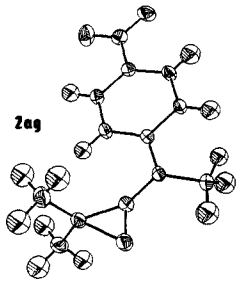

Fig. 1. Structure of 2,2-dimethyl-3-[*N*-methyl-*N*-(4-nitrophenyl)amino]-2*H*-azirin, **2ag**, in the crystal.

As in most amidines, the N(1) atom is the most nucleophilic and presumably also the most basic center in 3-amino-2*H*-azirines (**2**).[50] However, the basicity of **2a** (R^1–R^4 = methyl, $pK_b = 7.1$[54]) is significantly less than that of the comparable *N,N,N'*-trimethylisobutyramidine (pK_b = 3.0[54]).[55] The reduced basicity of 2*H*-azirines compared with noncyclic amidines or imines can be explained by a model with variable hybridization at the N atom. Open-chain (C=N)-containing compounds display sp^2 hybridization and have interorbital angles of ca. 120°, but in the three-membered rings a nonhybridized N atom with interorbital angles of ca. 90° is energetically more favorable. The free pair of electrons is therefore localized in an sp^2 orbital (**7**) in the first case, and in an s orbital (**8**) in the second.

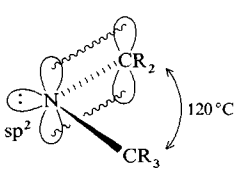

7

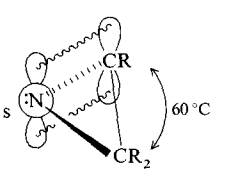

8

The effects of ring strain in 3-amino-2*H*-azirines (**2**) can be seen in the IR, ^{13}C NMR and ^{15}N NMR spectra. The ν(C=N) vibrational absorption in chloroform lies in the 1760–1805 cm^{-1} region; nonstrained amidines absorb at 1590–1680 cm^{-1}.[57] In the ^{13}C NMR spectrum (in $CDCl_3$), the signals for C(2) and C(3) of 3-(dimethylamino)-2,2-dimethyl-2*H*-azirine (**2a**) appear at δ = 39.8 and 168.1, while the corresponding signals in 3,6-bis(dimethylamino)-2,2,5,5-tetramethyl-2,5-dihydropyrazine are found at δ = 54.5 and 162.6, respectively.[58] The ^{15}N NMR spectrum (in $CDCl_3$) of **2a** shows absorptions for N(1) and Me_2N at δ = – 179.7 and – 326.4, respectively ($\delta(CH_3NO_2) = 0$);[27] in comparable amidines without ring strain, the N atoms display shifts of δ ≈ – 155 and ≈ – 312, respectively.[27, 59]

3. Reactions of 3-Amino-2*H*-Azirines

Practically all of the reactions of 3-amino-2*H*-azirines (**2**) known today proceed by opening of the three-membered ring. The only exceptions are reactions with palladium complexes[52] or with transition metal halides,[53] which lead to complexes of the type $(azirine)_2MX_2$ (e.g. **9**, **10**, Fig. 2) and reactions with trimethylsilyltriflate or trityltetrafluoroborate.[51] The latter yield aziridinium salts, which react with nucleophiles to give 2-aminoaziridines or further open-chain products.

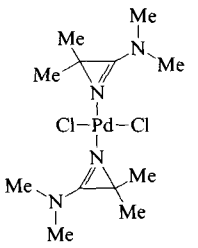

9

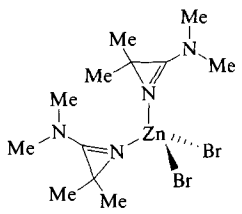

10

It is especially interesting that—as for 3-phenyl-2*H*-azirines—in reactions that proceed via ring opening, each bond of the three-membered ring may be selectively cleaved, depending on the reaction conditions.[25, 60, 61] Reactive intermediates, which may be used in the construction of new *N*-heterocycles, are formed in the process (Scheme 2).

3.1. Reactions with Cleavage of the C(2)–C(3) Bond

Irradiation of 3-(*N*-methyl-*N*-phenylamino)-2*H*-azirines (**2**, R^3 = Me, R^4 = Ph) in dimethoxyethane with UV light (λ = 254 nm), in the presence of dipolarophiles, affords five-membered heterocycles such as **11** (Scheme 3).[30] Here it is clear that the C–C bond of the azirine ring has been broken.

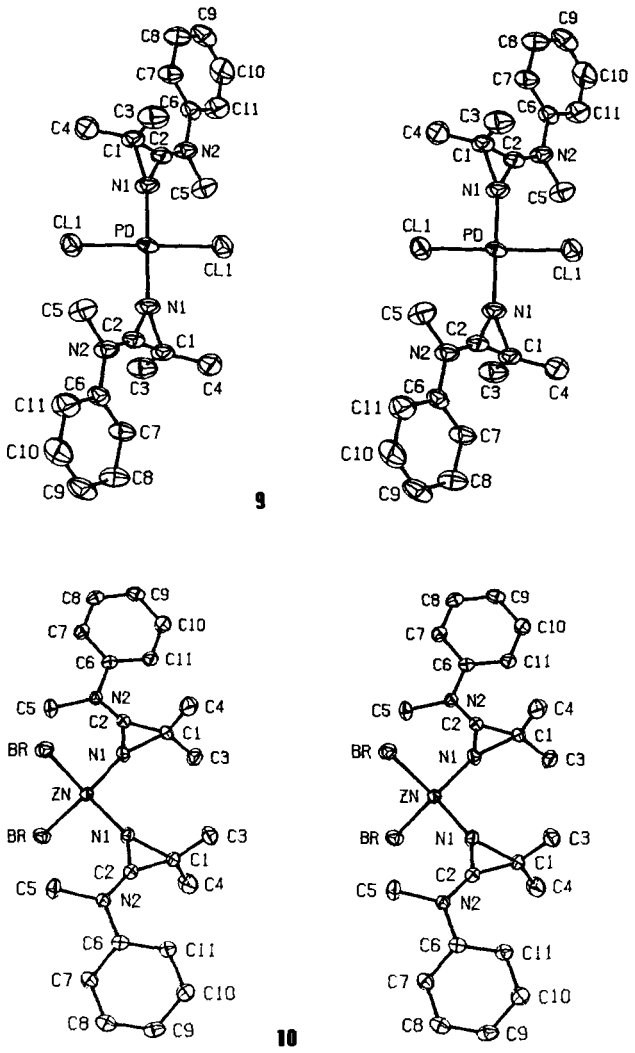

Fig. 2. Stereodrawings of the crystal structures of azirine-metal complexes **9** and **10**.

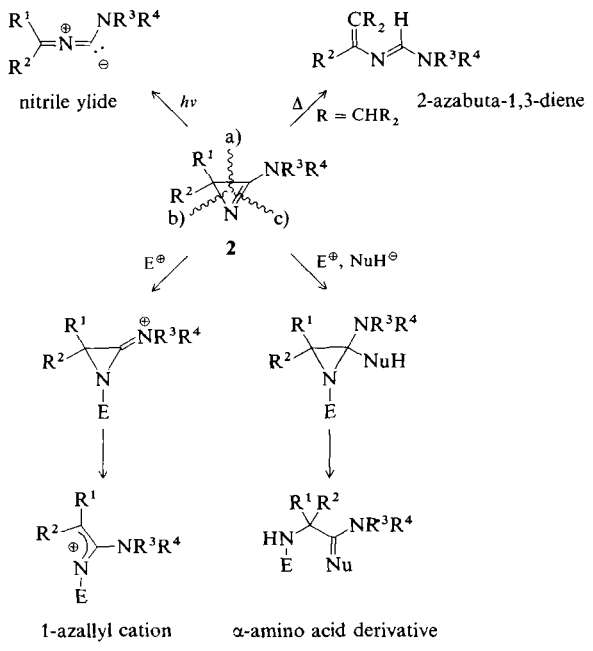

Scheme 2.

This ring-opening mode has been studied in detail for the photolysis of 3-phenyl-2*H*-azirines,[116] and takes place via a 1,3-dipolar intermediate, a nitrile ylide. Since 3-amino-2*H*-azirines (**2**) absorb at shorter wavelengths than the corresponding 3-phenyl-2*H*-azirines, their excitation requires short-wave UV light and their photolysis is therefore of less preparative importance. The photochemical isomerization of azirine **2za** to the 1,3-oxazole **12** also proceeds via cleavage of the C–C bond (Scheme 3).[62a] Analogous thermal oxazole-forming reactions have been described only recently.[62b]

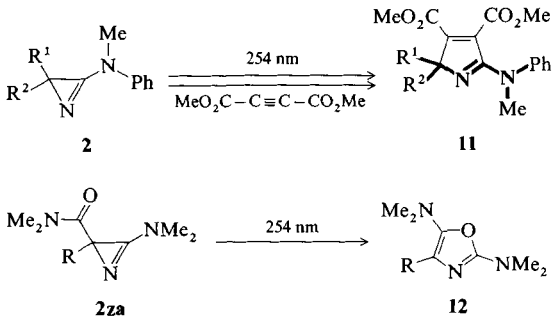

Scheme 3.

The C(2)–C(3) bond of 3-amino-2*H*-azirines can also be cleaved by pyrolysis at 340–400 °C.[30,63] The 2-azabuta-1,3-dienes of type **13** that are formed are useful heterodienes, which can, for instance, be utilized in the synthesis of pyridines (**14**) via *Diels–Alder* reactions (Scheme 4). Ring-expansion of **2f** to pyrrole **16**, observed on thermolysis, also occurs by breakage of the C–C bond.[37] A carbene of type **15** is a likely intermediate, as in the formation of **13**.

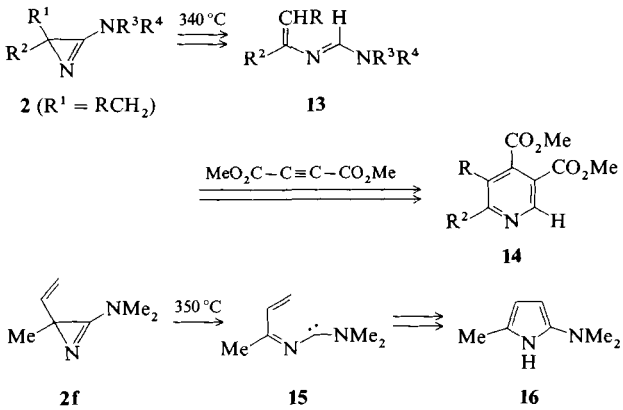

Scheme 4.

3.2. Reactions with Cleavage of the N(1)–C(2) Bond

Once again, analogously to the chemistry of the 3-phenyl- and 3-alkylsubstituted 2*H*-azirines, the 3-amino-2*H*-azirines **2** undergo a ring-opening reaction with very strong protic acids such as $HClO_4$, HCl, RSO_3H, under non-nucleophilic conditions. Here the N–C single bond is broken, and the major products isolated are acrylamidines (**18**) and pi-

perazine-2,5-bis(*N*,*N*-dialkyliminium) salts (**20**) (Scheme 5).[22, 54, 64] An azallyl cation of type **19** probably occurs as an intermediate, by ring-opening of **17**. Reaction of **2** with carboxylic acid chlorides,[65, 66] chloroarenes or chloroquinones[67] also leads to acrylamidines of types **21**, **22** and **23** respectively.

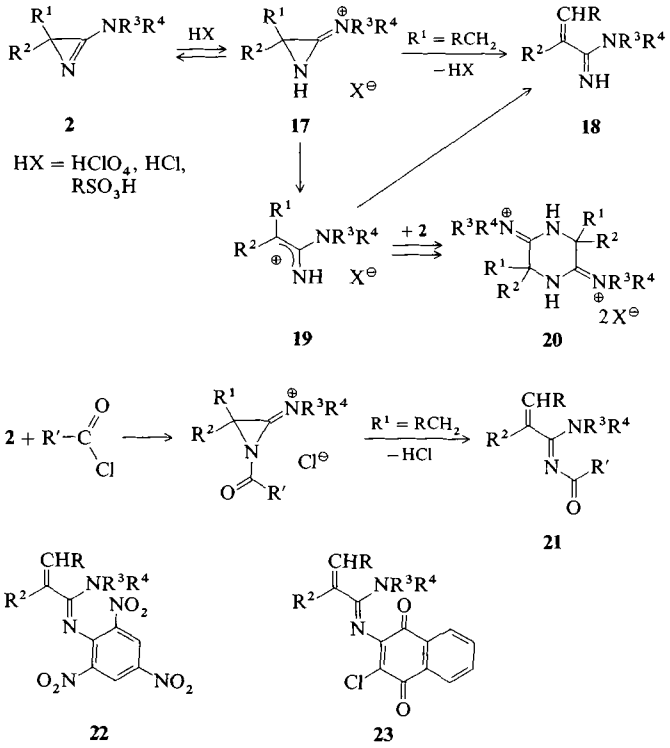

Scheme 5.

The reactions of **2** with electrophiles, leading to new heterocycles, are of special interest. Only two of the known examples will be mentioned here: 2,2-dialkyl-3-(dimethylamino)-2*H*-azirines (**2**; R^1, R^2 = alkyl; R^3, R^4 = Me) react with ketenes to yield 2,5-dihydro-4-(dimethylamino)-2,3-oxazoles **24**,[68, 69] and with cyclopropenones or cyclopropenethiones to afford good yields of the corresponding pyridin-4(3*H*)-one or -thione **25** (Scheme 6).[70]

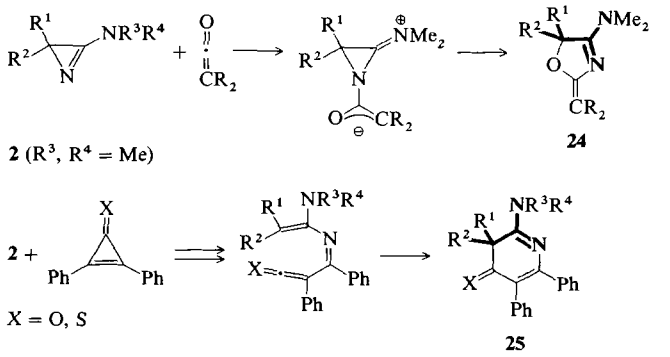

Scheme 6.

3.3. Reactions with Cleavage of the N(1)–C(3) Bond

Cleavage of the N–C double bond of 3-amino-2*H*-azirines (**2**) occurs, for example, on hydrolysis with potassium hydrogen phosphate in water,[54] and leads to an amide of an α,α-disubstituted α-amino acid (e.g. **26**, Scheme 7), as for all examples of this type. Products **27**–**30** are formed on reaction of **2** with activated phenols or thiophenols,[71] with cyclic, enolizable 1,3-diketones,[72] with sulfinic acids,[64] and with carboxylic[72] and thiocarboxylic acids[38, 73] respectively. All of these reactions proceed smoothly, generally even at temperatures around 0 °C.

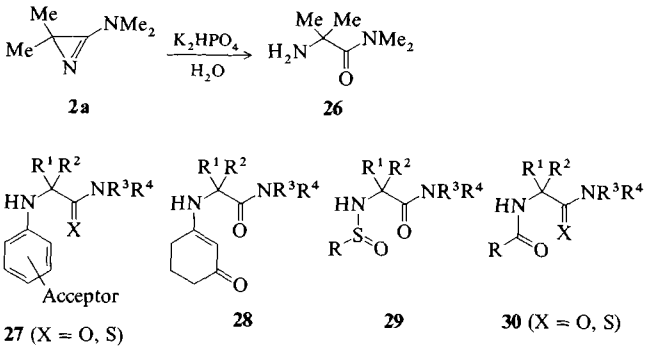

Scheme 7.

Variation of the substrate in reactions with phenols and 1,3-dicarbonyl compounds demonstrated that the initial step in all these reactions is an activation of the 3-amino-2*H*-azirine **2** by protonation, since for substrates with $pK_a > 8$, the reaction no longer occurs. On the other hand, if the reagent is a very strong acid (e.g. HCl, RSO_3H), the N(1)–C(2) bond is cleaved (see Section 3.2). This is explained by the absence of a good nucleophile capable of trapping the iminium aziridine arising from the protonation step before ring-opening takes place.

From these considerations, the following mechanism for the production of diamides **30** in the reaction with carboxylic acids may be proposed (Scheme 8): The aziridine intermediate **31** is formed by protonation of the ring-N atom and nucleophilic carboxylate addition. This then undergoes intramolecular nucleophilic attack by the aziridine-N atom on the carboxyl group, and a ring-expansion to zwitterion **32**. Ring-opening, with concomitant formation of two amide

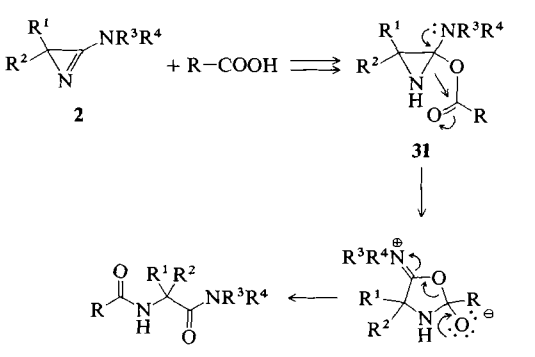

Scheme 8.

groups, leads to the product **30**. The driving force behind the reaction is the ring strain of **2** on the one hand, and the formation of a diamide on the other.

N(1)–C(3) ring openings of **2** are also frequently observed in reactions with NH-acidic compounds[74] and with heterocumulenes such as carbon disulfide,[75–77] isocyanates,[69, 78, 79] isothiocyanates,[78, 80, 81] and ketenimines.[82] Whereas with ketenes the N(1)–C(2) cleavage is the only reaction observed, (as mentioned above), with the other heterocumulenes the mode of ring-opening also depends on the nature of the C(2)-substituent on **2** (e.g., products **33** and **34**, or **35** and **36** are formed with CS_2, depending on the substituent; Scheme 9). A phenyl group at C(2) promotes cleavage of the N(1)–C(2) bond.

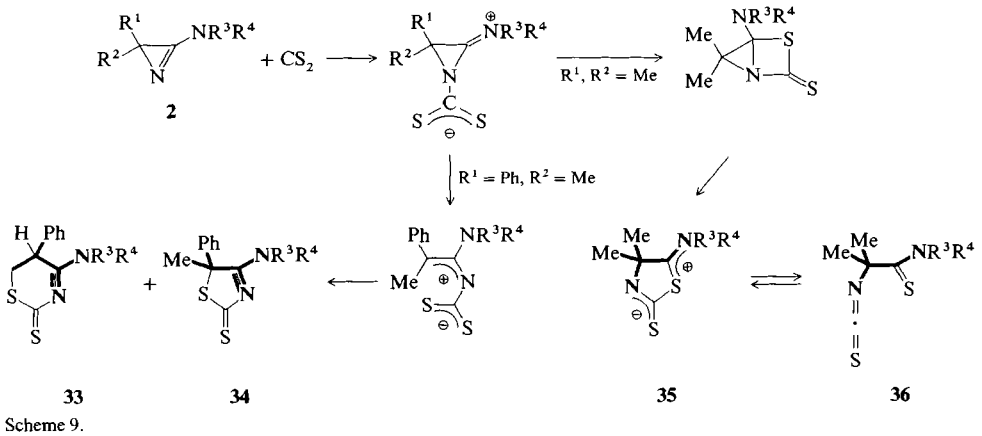

33 **34** **35** **36**

Scheme 9.

In summary, it can be said that on reaction of **2** with moderately strong protic acids ($pK_a \approx 3$–8) and with various heterocumulenes, the C–N double bond is cleaved to afford derivatives of α,α-disubstituted α-amino acids. 3-amino-2*H*-azirines can therefore clearly be regarded as synthetic equivalents of α,α-disubstituted α-amino acids.

4. Occurrence and Importance of α,α-Disubstituted α-Amino Acids

α,α-Disubstituted α-amino acids belong to the group of nonproteinogenic peptide components. As early as 1872, *Urech* synthesized the first member of this class, 2-methylalanine (2-aminoisobutyric acid, Aib), by hydrolysis of 5,5-dimethylhydantoin.[83] Later, *Tiemann* et al. made use of the Strecker synthesis to prepare various α-alkylated α-amino acids, including unsymmetrically-substituted (racemic) examples.[84] The first optically active α,α-disubstituted α-amino acid, (−)-(*R*)-2-ethylalanine (D-isovaline, D-Iva), was obtained by *Ehrlich* and *Wendel* in 1908, by means of microbiological racemate resolution.[85] This method was later replaced by other means of enantiomer separation (mainly by crystallization[86] and chromatographic methods[87]). Today, various enantioselective syntheses of α,α-disubstituted α-amino acids are known, such as the "bislactim ether method" of *Schöllkopf* et al.,[88] the "self-reproduction of the chiral center" of *Seebach* et al.[89] (Scheme 10), enzymatic[90] and other procedures.[91]

The continuing search for new synthetic methods to prepare α,α-disubstituted α-amino acids (see, for example, [92]) demonstrates the current interest in these compounds, due above all to their proven or potential biological activity. In particular, α-methyl α-amino acids and their derivatives can act as inhibitors of enzymes that metabolize the corresponding proteinogenic amino acids.[93] Some well-known examples include 2-methyl-3(3,4-dihydroxyphenyl)alanine (2-methyl dopa; antihypertensive activity by inhibition of dopa-carboxylase[94]), 2-methylaspartic acid (inhibits the corresponding transaminase[95]), and 2-ethylphenylalanine (bacteriostatic activity[96]).

In Nature one finds primarily 2-methylalanine (**39**, Aib)[99] and D-2-ethylalanine (**40**, D-Iva),[100] but various branched serine derivatives such as α-methylserine (**37**, in the antibiotic Amicetin)[97] or 2-amino-2-deoxy-2-hydroxymethyl-D-mannonic acid (**38**, a synthetic intermediate for the

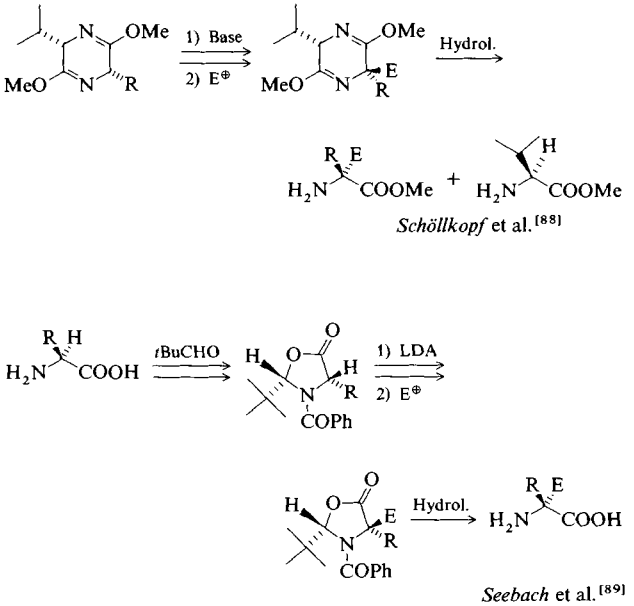

Scheme 10. LDA = lithium diisopropylamide.

antibiotic Thermozymocidin)[98] also occur. Aib and D-Iva make up a high proportion (up to 50%) of natural polypeptide antibiotics and amphiphilic ionophores, the so-called peptaibols.[101, 102]

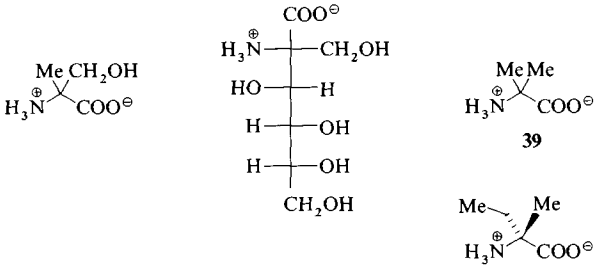

37 38 39 40

Since Aib is not incorporated into proteins, it has been used as a model substance in studies of amino acid transport.[103] However, α-methyl α-amino acids are also employed in modification of peptide hormone sequences, in order to make these more resistant to enzymatic degradation,[104] to stabilize preferred conformations of the peptide backbone,[105–107] or in studies of the factors affecting the biological activity of a peptide (e.g. [116–118]). Because of conformational restrictions, incorporation of α,α-disubstituted α-amino acids into a peptide chain leads to an increase in the helix content,[99b, 119] or the formation of specific β turns,[120–122] and is therefore useful in the synthesis of oligopeptide segments with stable secondary structures.[112] For example, the solubility of hydrophobic peptides in polar solvents can be increased.[99b, 119] As the peptaibols demonstrate, these peptides are also capable of modifying the ion permeability of membranes (see e.g. [102]). In studies of structure-activity relationships, too, the reduced flexibility of the peptide backbone facilitates the search for the "active conformation" recognized by a physiological receptor.[123]

In the equivalent reaction of **2a** with trifluoroacetamide, however, the 4*H*-imidazole **48** is formed even at 0 °C, in 80% yield (Scheme 11, bottom).[124] In this case, intramolecular attack of the aziridine-N atom of **45** on the trifluoroacetamide group obviously takes place, giving rise to zwitterion **46**, which can generate **48** by H_2O elimination. However, the ring-opening analogous to the reactions with carboxylic acids, from **46** to the amide-amidine **47** (cf. Scheme 8), was not observed.

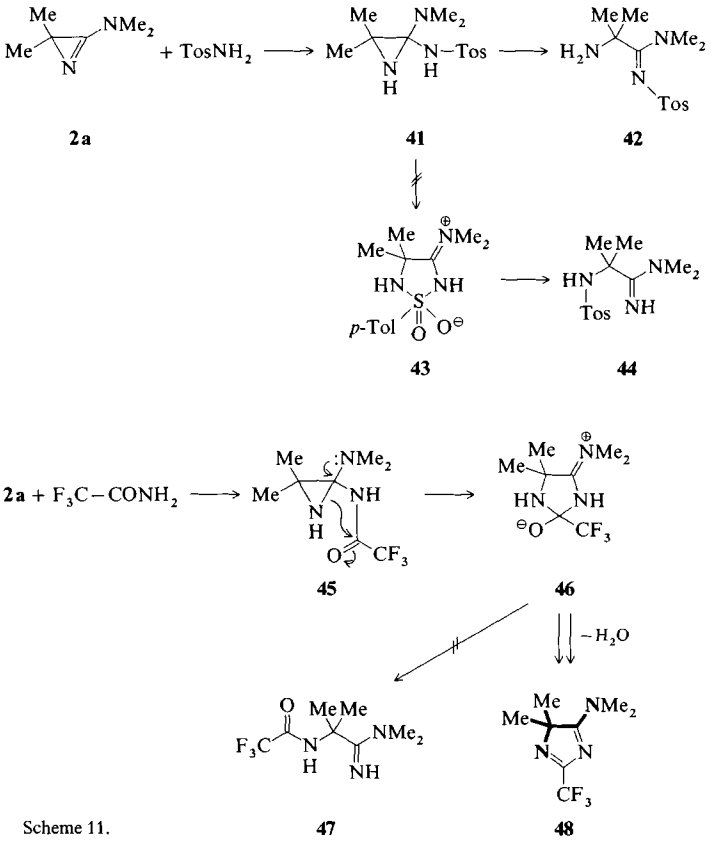

Scheme 11.

5. Synthesis of Heterocycles by Ring-Expansions of 3-Amino-2*H*-Azirines

5.1. Reactions of 3-Amino-2*H*-Azirines with NH-Acidic Heterocycles

As mentioned in Section 3.3, 3-amino-2*H*-azirines react not only with OH-acids, but also with NH-acidic compounds, with cleavage of the N(1)–C(3) bond (see review [74]). For instance, if a 1:1 mixture of 4-toluene-sulfonamide and 3-(dimethylamino)-2,2-dimethyl-2*H*-azirine (**2a**) is heated at reflux in 2-propanol, a single 1:1 adduct **42**[124] is isolated in ca. 60% yield. This adduct is thought to be formed via the aziridine **41** (Scheme 11, top). Remarkably, no products arising from nucleophilic attack on the sulfonamide group are observed.[125] In particular, one does not find **44**, which might be formed in a reaction analogous to that with carboxylic acids, via **43**. Nucleophilic attack on the S atom by the aziridine-N atom of **41** clearly cannot compete with the ring-opening.

5.1.1. Ring Expansions to Seven- to Nine-Membered Heterocycles

The results described above demonstrate that although a sulfonamide reacts with **2** to give aziridines of type **41**, ring-expansion to a zwitterion of type **46** can only occur with neighboring carbonyl groups. The combination of these two groups in the same molecule, e.g. in saccharin, (1,2-benzoisothiazol-3(2*H*)-one-1,1-dioxide, **49**) makes possible an interesting ring-expansion to 4,5-dihydro-1,2,5-benzothiadiazocin-6-one-1,1-dioxide **52** (Scheme 12).[126] The reaction mechanism, via aziridine **50** and ring-expansion to zwitterion **51** and to the product, corresponds to that formulated in Scheme 8 for the reaction with carboxylic acids. The key step in the reaction is the cleavage of the central C–N bond in **51**. Using [1-^{15}N]-labeled **2a*** it has been proved that N(5) of **52** derives from the azirine,[27] and that the latter is therefore built into the ring as an α-amino acid unit.

The same reaction sequence has been realized with a series of isothiazol-3(2*H*)-one- and isothiazolidin-3-one-1,1-diox-

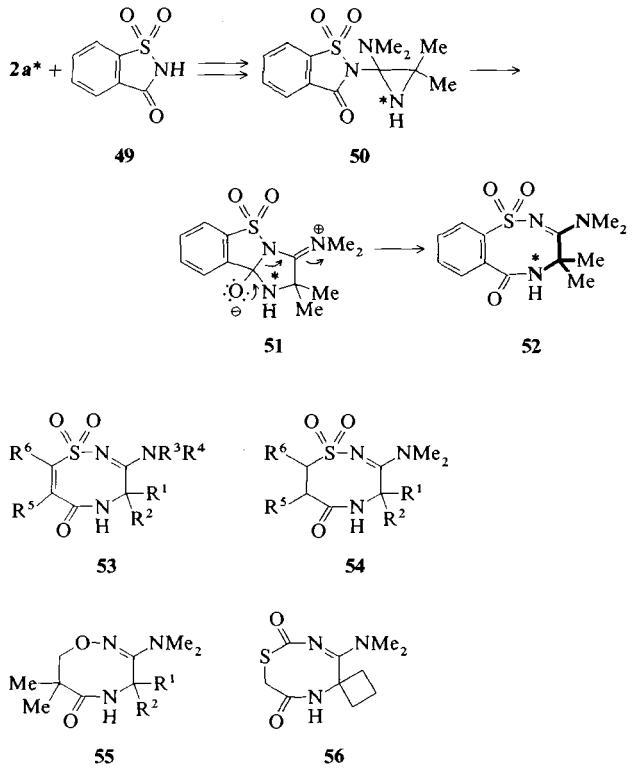

Scheme 12.

ides,[127] with 4,4-dimethylisoxazolidin-3-one,[128] and with 1,3-thiazolidine-2,4-dione,[31, 129] yielding the eight-membered heterocycles **53**–**56** in generally good yields. In selected cases the seven-membered and nine-membered heterocycles are also obtainable. For example, malonimides **57** afford 1,4-diazepine-5,7-dione derivatives **58**[130] and the 2*H*-1,2,4-benzothiadiazin-3(4*H*)-one-1,1-dioxides **59** give 4,5-dihydro-1,2,5,7-benzothiatriazonine-6(7*H*)-1,1-dioxides **60**,[59, 131] as shown in Scheme 13. Except for the seven-

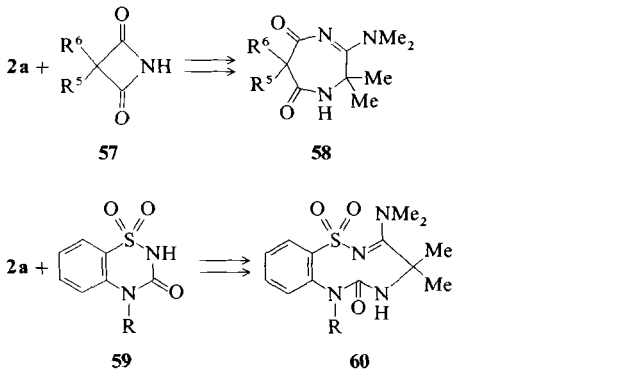

Scheme 13.

membered **58**, the structures of these ring-expansion products are all distinguished by the presence of a *trans*-amide group in the ring.

The reaction of **2a** with **49a** needs special mention. This reaction produces 88% of **53a**, as well as ca. 1% of the isomeric compound **61** (Scheme 14).[127] The crystal structures of this byproduct and **53a** are shown in Figure 3. Compound **61** presumably arises via zwitterion **62**, which is formed by nucleophilic attack of the aziridine-N atom of **50a** on the sulfone group. Ring-expansion to **63**, followed by transannular ring closure, leads to **61**. The occurrence of this

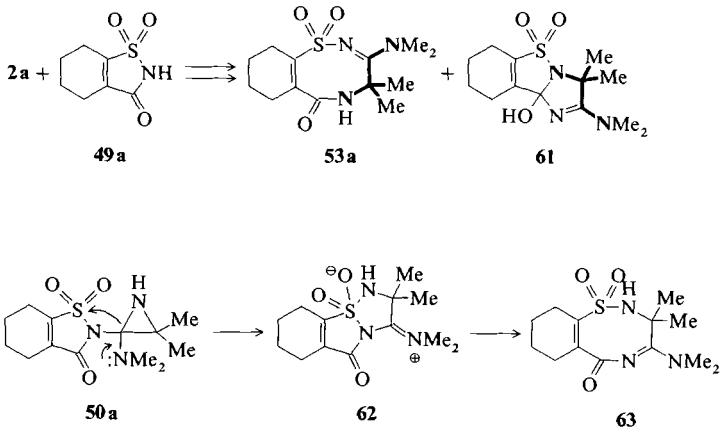

Scheme 14.

byproduct shows that although nucleophilic attack on the SO_2 group is much less efficient than attack on the CO group, it is not impossible. A corresponding nucleophilic attack of azirine **2a** is also observed in the smooth reaction with 4-toluenesulfonic acid chloride, yielding N^1,N^1-dimethyl-N^2-(4-toluenesulfonyl)methacrylamidine,[65] analogously to reactions with carboxylic acid chlorides (Scheme 5).

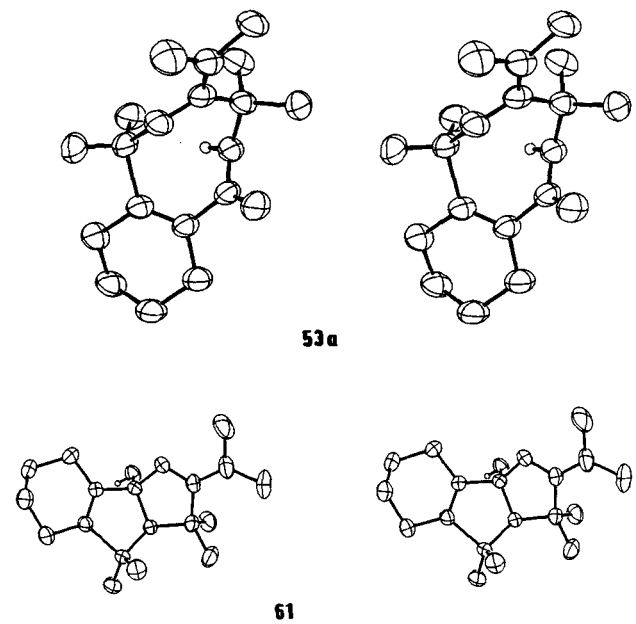

Fig. 3. Stereodrawings of the crystal structures of **53a** (top) and **61** (bottom).

Several reactions of 3-amino-2*H*-azirines (**2**) with NH-acidic heterocycles lead to products which can be explained by a ring-expansion followed by a transannular ring-closure. Thus, for example, a 1:1 adduct is formed from **2a** and

phthalimide in acetonitrile or chloroform at room temperature. On the basis of spectral data, this adduct is assigned the structure 2,3-dihydro-2,5-benzodiazocine-1,6-dione **65** (Scheme 15).[126] Purification of the rather unstable crude product by recrystallization from DMF leads to the tricyclic azacyclol **66**, whose structure has been proven by X-ray crystallography.[132] The same product is obtained directly when the reaction of **2a** and phthalimide is carried out in DMF as solvent.

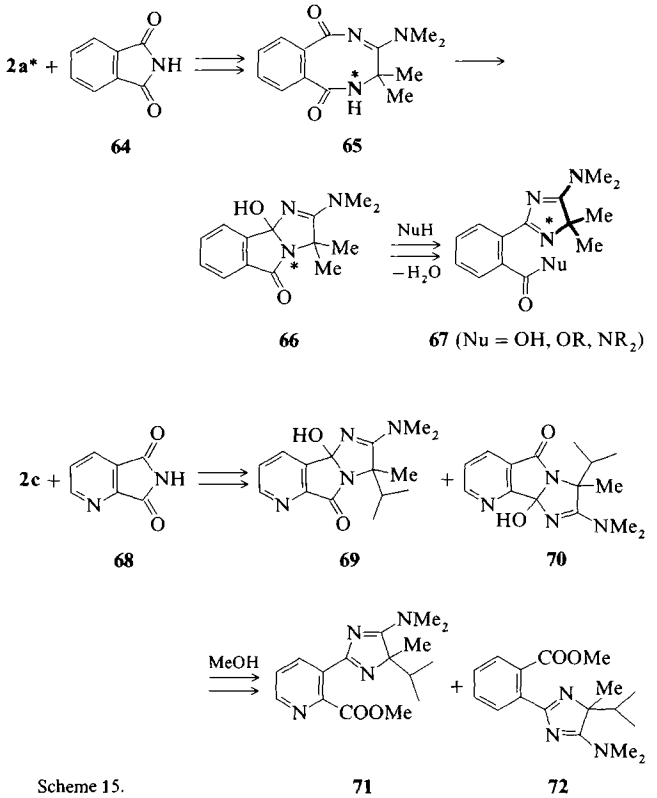

Scheme 15.

This reaction also proceeds via cleavage of the N(1)–C(3) bond of **2**, as is clear from the position of the label after reaction of [1-^{15}N]-labeled **2a***. In azacyclol **66**, only N(4) is labeled (^{15}N NMR).[27] Treatment of **65** or **66** with nucleophilic solvents such as water, alcohols or amines affords 2-(4*H*-imidazol-2-yl)benzoic acid derivatives of type **67**, in good yields. These products are of interest because they are structurally closely related to potent herbicides.[133] The major product isolated from the reaction of 3-(dimethylamino)-2-isopropyl-2-methyl-2*H*-azirine (**2c**) and pyridine-2,3-dicarboxylic acid imide (**68**), after methanolysis, is **72**,[134] which differs from the most biologically active derivative really only in an amidine instead of the corresponding five-membered lactam function. Unfortunately, the hydrolysis to the lactam has not yet been satisfactorily achieved.

Since the synthesis was carried out with racemic **2c**, **71** and **72** were also obtained in their racemic form. It is also worth mentioning that azacyclol formation does not take place regioselectively, but that **69** and **70** are found in approximately equal proportions. Amazingly, both azlactones afford a mixture of **71** and **72** on methanolysis, so that separation of the isomers is only reasonable at this step. A mechanism for this behavior has been formulated.[134]

3-Amino-2*H*-azirines (**2**) react smoothly with 1,3-oxazolidine-2,4-diones **73** in acetonitrile at room temperature to give 3,4-dihydro-2*H*-imidazol-2-ones **74** (Scheme 16).[27, 31, 129] The analogous reaction with 1,3-thiazolidine-2,4-dione is more complex and gives rise not only to the mercapto analogue of **74**, but also to products of further reactions. The result of reaction of **73** with [1-^{15}N]-labeled **2a*** is surprising, since the **74** that is produced is labeled exclusively at the substituted N(3) atom. This finding can be easily explained by the reaction mechanism outlined in Scheme 16, via zwitterion **75**, ring-expansion to the 1,3,6-oxadiazocine derivative **76**, transannular ring-closure to **77**, and a second ring-opening. Further support for this reaction pathway comes from the isolation of **56**, the product analogous to **76** (Scheme 12), from the reaction of **2r** with 1,3-thiazolidine-2,4-dione.

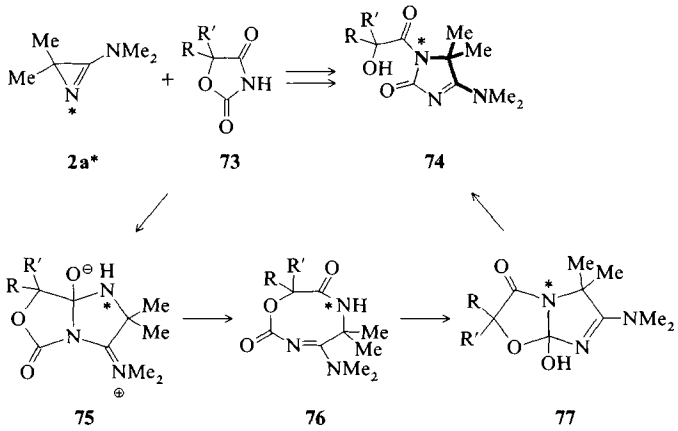

Scheme 16.

The quantitative formation of azacyclol **79** from **2a** and monosubstituted parabanic acids (imidazolidine-2,4,5-triones) **78** in 2-propanol at room temperature also follows a complex reaction mechanism (Scheme 17).[135] If the [3-^{15}N]-labeled N-methyl derivative of **78** is used, in the ^{15}N NMR spectrum of **79** all of the label is found at the amidine-N atom.[59] Zwitterion **81** and the 1,3,6-triazocine-2,4,5-trione **82** are therefore very likely intermediates in the

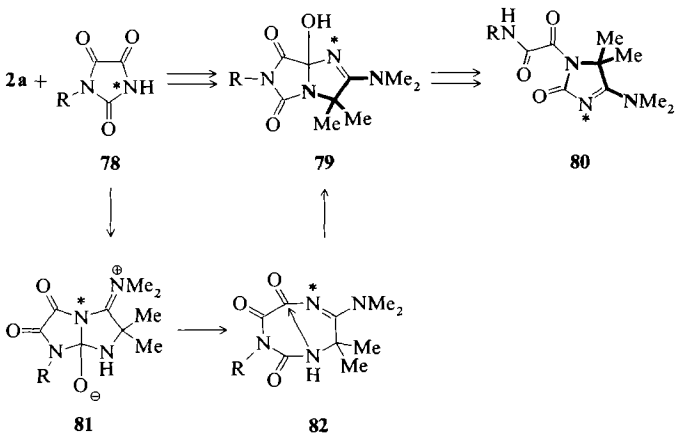

Scheme 17.

reaction. On warming **79** in acetonitrile, a further rearrangement to 3,4-dihydroimidazol-2-one **80** takes place, but the mechanism is not yet clear in all its details.

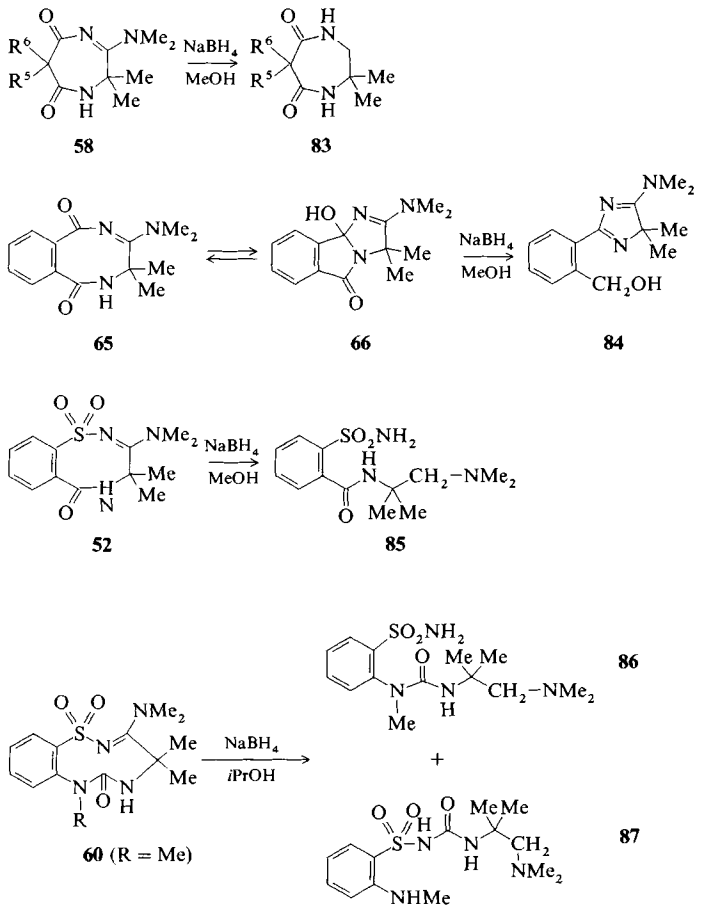

Scheme 18.

The novel seven- to nine-membered heterocycles formed in these reactions show surprising behavior, even in such simple reactions as hydrolysis or reduction. This makes structure determination by classical methods difficult, and in many cases X-ray structures have been determined for key compounds.

To illustrate this, Scheme 18 shows some results of $NaBH_4$ reductions. The diazepine derivative **58** is reduced to **83**, retaining the ring structure,[130] while for **65** ⇄ **66**, the azacyclol is reduced to **84**.[126] In cyclic sulfonamidines **52** and **60**, on the other hand, reduction occurs with ring-opening,[126, 136] whereby in the case of the nine-membered **60**, two isomeric products **86** and **87** are formed. The appearance of the latter requires a transannular ring-closure of **60**.

5.1.2. *Formation of 4H-Imidazoles*

As emerges from the reactions of **2** with NH-acidic compounds described above, there is clearly a great tendency to form imidazole derivatives (Schemes 11 and 15–18). This is confirmed in many further reactions with NH-acidic heterocycles ($pK_a < 8$). Thus, five- and six-membered heterocycles containing the structural element NH–CO–NH–CO (**88**–**92**) are without exception converted by **2** to 4*H*-imidazoles (**93**–**97**, Scheme 19). This reaction is independent of the solvent, though in some cases temperatures of up to 80 °C are required.[59, 137, 138]

Some of the products thus formed readily undergo subsequent reactions. For example, thermolysis of **93** with elimination of HNCO leads to the corresponding 2-alkyl derivative (phenyl groups at C(α) accelerate the fragmentation)[59], and the enamine side chain of derivative **94** is hydrolyzed to the carbonyl compound even on merely standing in air.[138]

The question of reaction mechanism for the formation of 4*H*-imidazoles is an interesting one. These compounds are decarboxylated 1:1 adducts, and clearly, in the course of the reaction, the urea carbonyl group of the NH-acidic heterocycle is eliminated as CO_2. A mechanism that accounts for the findings to date is formulated in Scheme 20. The zwitterion **98**, which arises as usual, has a new reaction pathway open to it, leading via the cyclic urethane **101** and fragmentation to the 4*H*-imidazole **103**. However, an alternative mechanism involving elimination of water from **99** and sub-

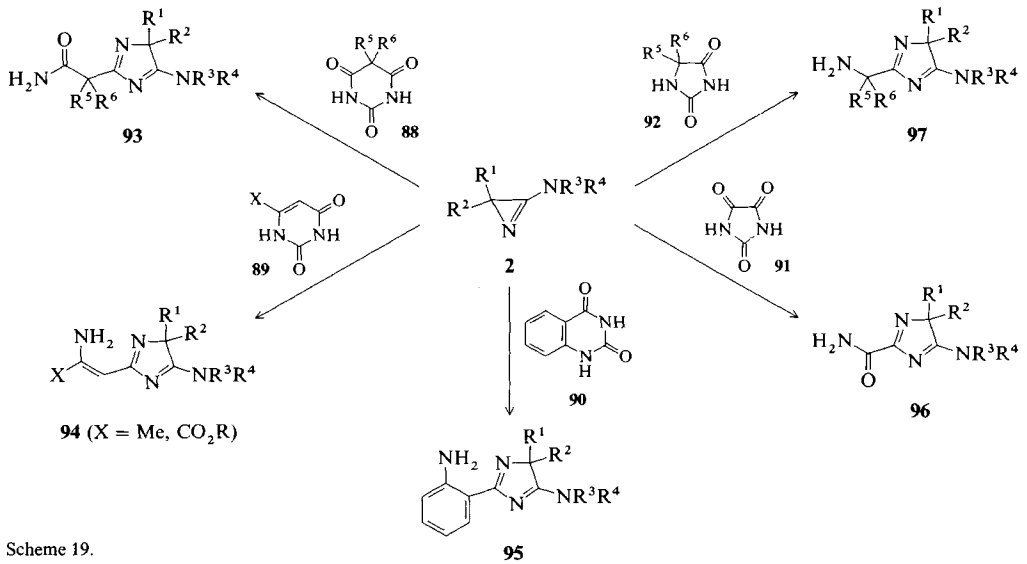

Scheme 19.

sequent hydrolysis of the isocyanate function cannot be ruled out.

Two pieces of evidence that argue for the existence of **99** as an intermediate are the formation of urea derivatives of type **100** in the presence of secondary amines (e.g. morpholine), and the isolation of **102** as a byproduct from the reaction of **2a** and 4,4-dimethylhydantoin (**92**, $R^5 = R^6 = Me$)[59] (see also [74]). In addition, the inhibition of the reaction by the presence of a substituent at N(1) or N(3) of **88**, **90** or **92** supports the proposal in Scheme 20.

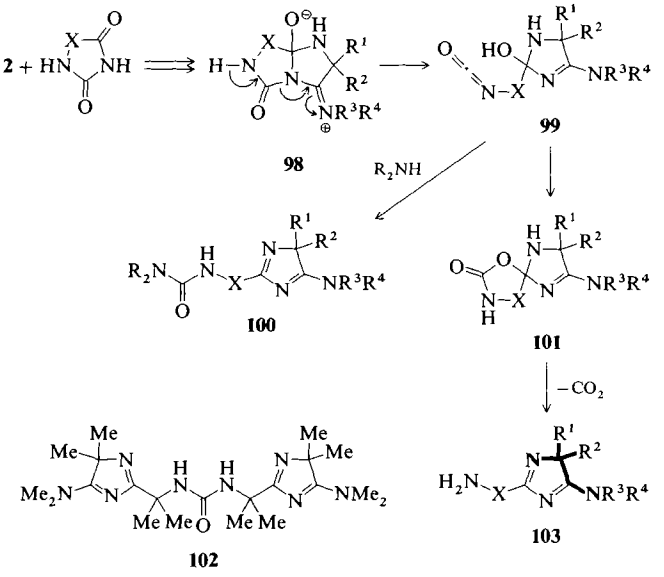

Scheme 20.

Since **2** reacts both with 1,3-benzoxazine-2,4-dione,[27, 139] and with 1,3-oxazolidine-2,4-diones (**73**)[27] and 1,3-thiazolidine-2,4-diones[129] (1-oxa and 1-thia analogues of **90** and **92**), the lack of reaction with the 1-alkyl derivatives of barbituric acids **88**, quinazoline-2,4-dione (**90**) and hydantoins **92** requires an explanation. By introducing an alkyl substituent at N(1), the acidity of the *N*-heterocycle is somewhat reduced (e.g. pK_a of 5,5-diethylbarbituric acid = 7.8, pK_a of 5,5-diethyl-1-methyl-barbituric acid = 8.2–8.4[1401]). Hence, the first step of the reaction, protonation of **2**, probably fails to take place. In accordance with this, the more acidic 1-alkyl parabanic acids **78** (Scheme 17) again react with **2**.

5.1.3. *Synthesis of Polycyclic Compounds*

The reactions of NH-acidic compounds with **2** that lead to polycyclic compounds are largely of mechanistic interest, since they allow conclusions regarding nonisolable intermediates. Phthalic acid hydrazide (2,3-dihydrophthalazine-1,4-dione, **104**) reacts with **2a** in DMF analogously to the corresponding imide **64** (Scheme 15), and yields the dehydrated 1:1 adduct **106**, a direct product of the zwitterion **105** with an intact ring system (Scheme 21).[141] The same reaction also occurs between maleic acid hydrazide (1,2-dihydropyridazine-3,6-dione) and **2a**.

Hydrolysis of **106** with saturated $NaHCO_3$ solution yields a mixture of the tri- and bicyclic compounds **109** and **110** in 35% and 57% yield respectively, while treatment with water/triethylamine affords exclusively **110**. The iminium iodide **108** obtained by methylation of **106** is hydrolyzed by water to **107**, the *O*-methyl derivative of **109**. Reduction of the zwitterion **106** with $NaBH_4$ also leads to two products, **111** and **112** (Scheme 21).

To elucidate the structure of the 6-6-5 ring system **109**, compounds of type **113** (R^5, R^6 = Me, H) have been synthesized for comparison purposes.[142, 143] The monomethyl derivative displays a typical NH signal for an NH-acidic compound in the ^1H NMR spectrum ([D_6]DMSO) at $\delta = 11.2$, and it therefore seemed likely that it would react with **2a**. Indeed, heterocycles of type **113** do react with **2a**, to give a somewhat unstable initial product. After hydrolytic workup, the tetracyclic **114** is obtained (Scheme 22), which contains the intact ring skeleton of the zwitterion postulated as an intermediate.

Reactions of 3-amino-2*H*-azirines **2** with 1,3-thiazolidine- and 1,3-oxazolidine-2-thiones (**115**) also lead to heterobicycles containing α,α-disubstituted α-amino acids, as do reactions with 1,3-benzoxazole-2(3*H*)-thione (**122**). While **115** (X = S) in acetonitrile affords a mixture of the bicyclic **119**

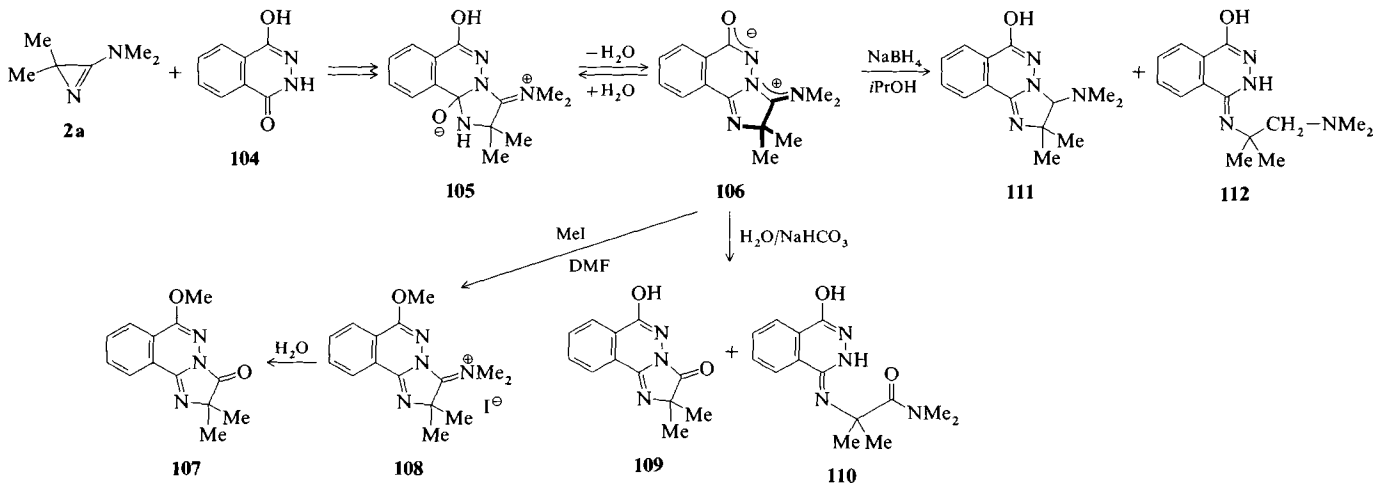

Scheme 21.

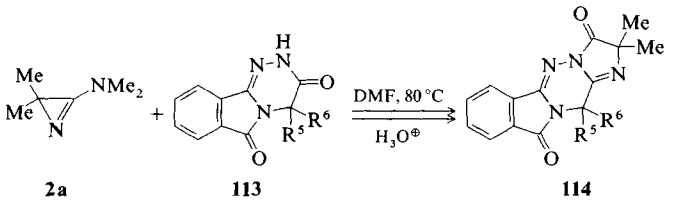

Scheme 22.

and the thiourea **121**, in 2-propanol **121** is formed exclusively (Scheme 23).[144] Control experiments show that the latter is a reaction product from **119**. Under the same conditions, a salt-like, unstable compound is formed in the reaction with **115** (X = O), which on chromatography afforded a small amount of **118**.[145] Compound **118** is obtained in good yields after hydrolytic workup of the crude product. In a few cases direct evaporation of the solvent and recrystallization allowed isolation of **119** (X = O).

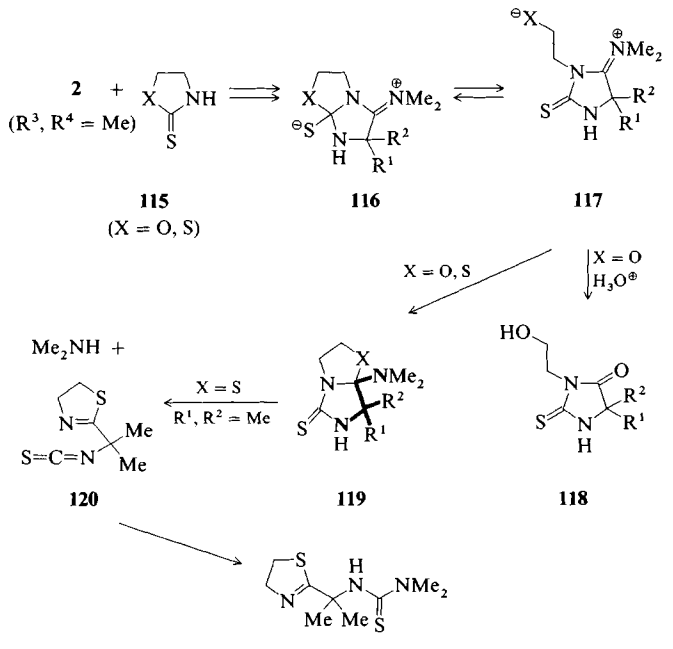

Scheme 23.

These results agree with the reaction mechanism proposed in Scheme 23. In contrast to the ring-expansions described in Section 5.1.1, it is not the central C(2)–N bond of zwitterion **116** that is broken, but the C(2)–X bond. In the thiolate product, **117** (X = S), nucleophilic ring closure occurs to give **119**, whereas for the less nucleophilic alcoholate, **117** (X = O), the reaction largely stops at this stage.

The course of the reaction of **2** with 1,3-benzoxazole-2(3*H*)-thione (**122**) in acetonitrile is as expected; the thiourea **123** and the thiohydantoin **124** are obtained as the major products, each in about 30% yield (Scheme 24).[146] The ring-closure corresponding to **117** → **119** presumably fails to take place because the anion is stabilized as the phenolate.

In the case of spirocyclic **2s**, it was possible to prove that these reactions also proceed via a zwitterion, **125**. Treatment of the reaction mixture with methyl iodide and K_2CO_3, followed by hydrolysis, gives a 38% yield of **126**. The isothiocyanate intermediate postulated for formation of thioureas **121** and **123** can also be trapped in both cases, by addition of morpholine.[144, 146] However, nucleophilic attack of the amine on the C = S group of **119** would also explain the formation of **121**, so that **120** must not necessarily be an intermediate.

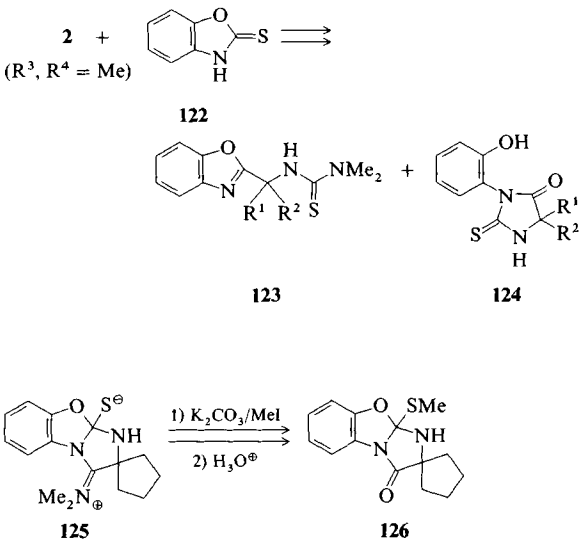

Scheme 24.

Further support for the suggested mechanisms for the reactions of NH-acidic heterocycles with **2** derives from the formation of zwitterionic 1:1 adducts **129**, which correspond to the nonisolable intermediates **117**. 3-Amino-2*H*-azirines (**2**) react at room temperature with 5-substituted 1,3,4-oxadiazol- and 1,3,4-thiadiazol-2(3*H*)-ones (**127**) to yield compounds of type **129** (Scheme 25). These are isolated in very good yields, as astonishingly stable, crystalline substances.[147] The structures of several members of this novel

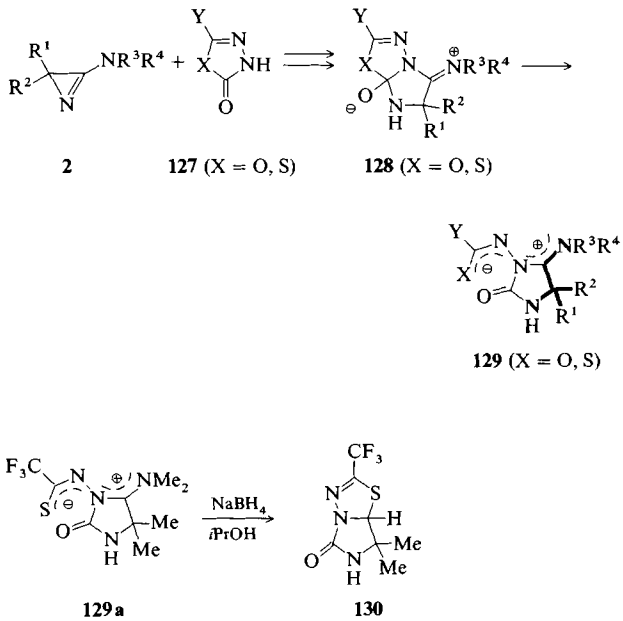

Scheme 25.

class of substances have been determined by X-ray crystallography. In connection with the absence of a ring-closure reaction corresponding to **117** → **119**, it is worth mentioning that the two planes of the delocalized anion and cation lie orthogonal to one another (see **129b** in Fig. 4). In contrast, ring-closure to the bicyclic compound **130** was achieved in the reduction of **129a** by $NaBH_4$.[143]

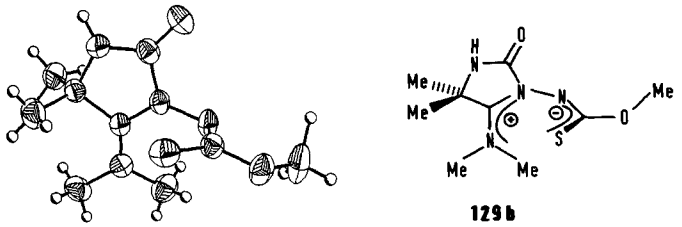

129b

Fig. 4. Structure of the zwitterion **129b** in the crystal.

5.2. Reactions with Phenols

As mentioned in Section 3.3, 3-amino-2*H*-azirines (**2**) react with activated phenols to give *N*-phenylamino acid derivatives (**27**, Scheme 7). With a suitably positioned nucleophilic group, these products ought to provide starting materials for cyclizations. Indeed, reaction of **2** with picramic acid (2-amino-4,6-dinitrophenol, **131**) in boiling acetonitrile yielded the quinazoline derivatives **132** and **133** as the only isolable products, in 10% and 25% yield, respectively (Scheme 26).[67, 74]

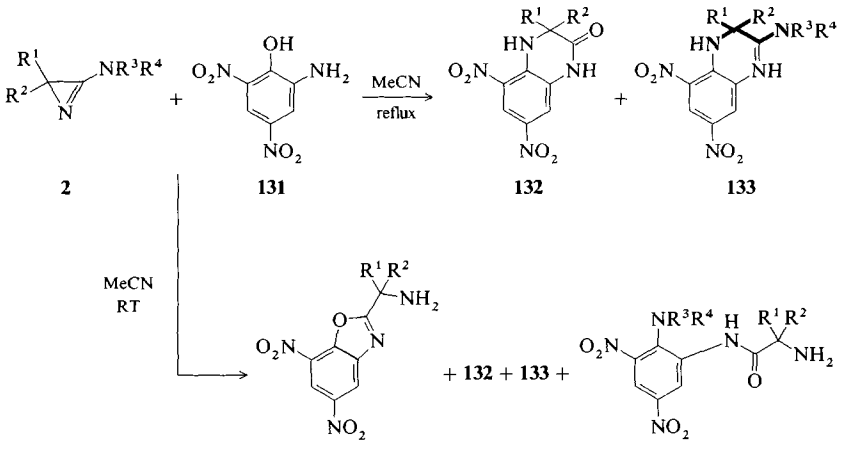

Scheme 26.

The formation of these products is interpreted as occurring via cyclization (transamidation) of an intermediate corresponding to **27**. Attempts to isolate this intermediate at low reaction temperatures (0–25 °C) gave surprising results.[148] The major product, and in some cases (**2**, R^3 = Ph, R^4 = Me) the only one, in yields of up to 83%, was the 1,3-benzoxazole derivative **134**. Byproducts included **135**, and **132** and **133**. The latter two were obtained in high yields on basic hydrolysis of **134**, or on reaction with secondary amines. For these ring-transformations of **134**, a mechanism involving formation of **136** by nucleophilic addition (H_2O, ROH, RNH_2), rearrangement to **137**, and intramolecular, nucleophilic aromatic substitution of the OH group at C(1) by the NH_2 group seems plausible (Scheme 27).

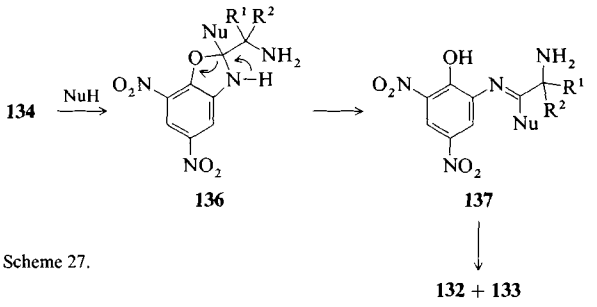

Scheme 27.

Phenolic substrates of the salicylic acid type (**138**) no longer react with **2** by aromatic substitution. Rather, the oxygen atom of the side chain is exchanged by the α,α-disubstituted α-amino acid, similarly to the reaction observed for enolized, cyclic 1,3-diketones[72] and 2-formylcycloalkanones.[64] If R is a nucleophilic group such as NH_2NH or NH_2, the initially formed **141** cyclizes on warming to give 1,2,4-triazine derivatives (**142** and **143**) or imidazole derivatives (**144** and **145**) respectively (Scheme 28). Reaction of **2a** with salicylic acid hydrazide (**138**, R = NH_2NH) in boiling benzene affords a 45% yield of **142** and **143**, in a ratio of ca. 3:2,[74, 149] while in acetonitrile at room temperature the intermediate **141** is obtained in 80% yield. Cyclization to **143** occurs spontaneously in methanolic solution; at 50 °C it proceeds quantitatively with a half time of ca. 45 min. In DMSO, too, the cyclization proceeds quantitatively, but **142** and **143** are produced in a ratio of ca. 1:2.

Salicylamide (**138**, R = NH_2) reacts with **2a** in an analogous manner. Here the products are the 4*H*-imidazole **144** and the 4,5-dihydroimidazol-5-one **145**. However, the ratio of the two is very solvent-dependent (Scheme 28).[74]

Methyl salicylate (**138**, R = OMe) reacts with **2a** to give the iminoester **141** (R = OMe, Scheme 29).[124] Spontaneous cyclization of the product is impossible in this case. Mild

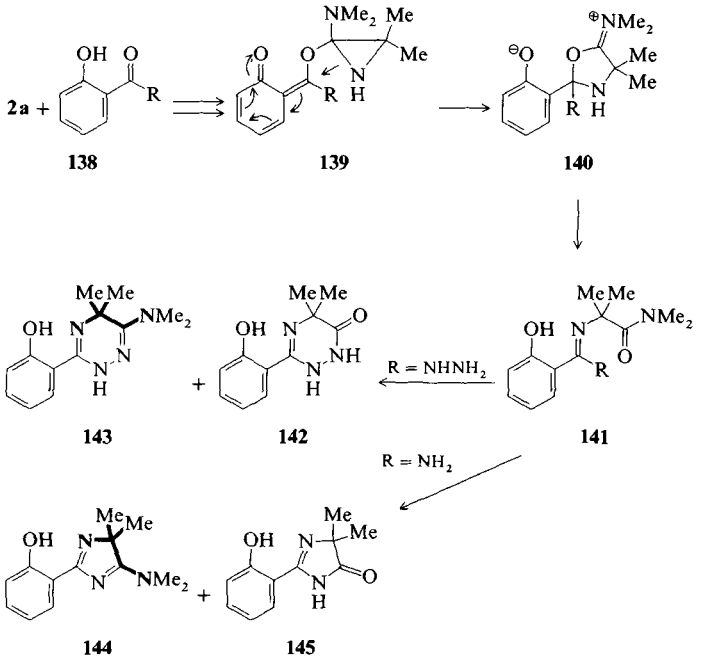

Scheme 28.

hydrolysis gives the diamide **146**, which can be cyclized by heating in toluene in the presence of HCl to give 1,3-oxazol-4(5*H*)-one (**147**, Scheme 29). Products **146** and **147** are also

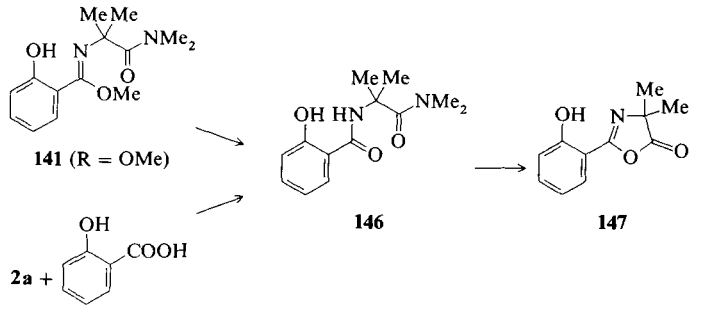

Scheme 29.

obtained from the reaction of **2a** with salicylic acid. This reaction will be discussed in more detail in Sections 5.3 and 6 (see also Scheme 8).

5.3. Reactions with Carboxylic Acids and Carboxylic Acid Derivatives

The diamides **30** (X = O, see Scheme 7) formed from carboxylic acids and the 3-amino-2*H*-azirines **2** are, as already mentioned, suitable substrates for the synthesis of 4,4-disubstituted 1,3-oxazol-5(4*H*)-ones (azlactones, **148** (X = O), Scheme 30). Cyclization with HCl gas in toluene proceeds quantitatively, and the sole byproduct is the hydrochloride of the secondary amine, which can be removed by filtration.[73, 150]

The analogous cyclization of monothioamides (**30**, X = S) does not, however, yield the expected 1,3-oxazole-5(4*H*)-thiones (**148**, X = S), but the isomeric 1,3-thiazol-5(4*H*)-ones (**149**, Scheme 30). Trapping reactions with amines show that the thiazolones **149** arise by a rearrangement of the initially formed, unstable **148** (X = S).[150] Thionation of diamide **30** (X = O) with Lawesson's reagent, for example, constitutes another route to **149**; cyclization of the selectively formed **150** proceeds smoothly under acid catalysis. Thionation of **30** (X = S) to the dithioamides **151** occurs in an analogous manner, and the products then cyclize spontaneously under the reaction conditions to the 1,3-thiazole-5(4*H*)-thiones **152**.[28, 38] These dithio analogous of azlactones have been little known until now and undergo a number of addition reactions.[151] They can also be synthesized by double O/S exchange of **30** (X = O),[152] or directly, by reaction of the 3-amino-2*H*-azirines **2** with dithio acids at − 60 °C.[38]

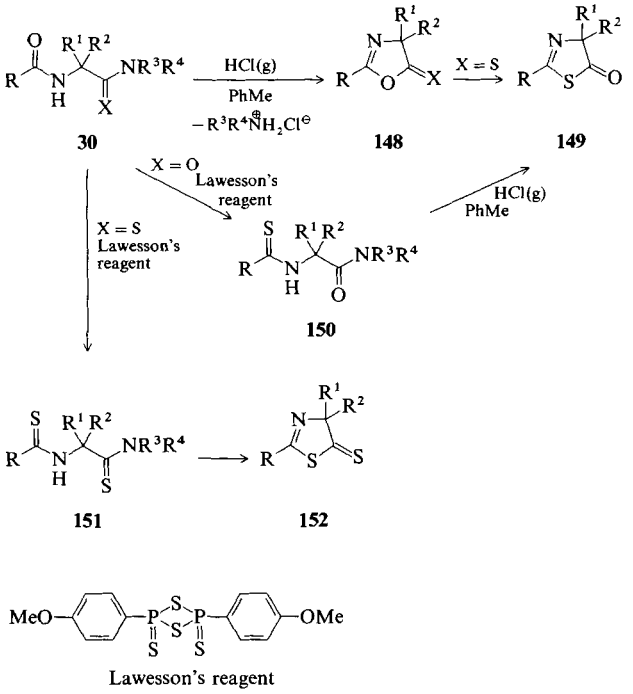

Scheme 30.

Aromatic hydrazides not bearing an OH group in the *ortho* position (cf. Section 5.2) do not react with **2a** at room temperature. However, under more drastic conditions (acetonitrile/reflux; DMF/60 °C), good yields of 1,3,4-oxadiazoles of type **153** (Scheme 31) are obtained.[149, 153] These reactions can proceed either via nucleophilic attack of azirine **2a** on the hydrazide group, or via an initial protonation of **2a**. Both mechanisms are in accord with the finding that acceptor substituents at C(4) accelerate the reaction,

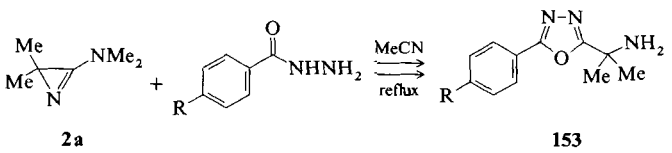

Scheme 31.

while donors retard it ($v_{rel} \approx 7$ (R = NO_2), 1 (R = H), 0.7 (R = MeO)).

1,2,4-Triazine derivatives **156** and **157** (Scheme 32) may be successfully prepared by reaction of **2a** with ethyl hydrazinecarboxylate or oxamic acid hydrazide (**154**, X = EtO or H_2NCO respectively), in 2-propanol at 70 °C[153] (cf. also

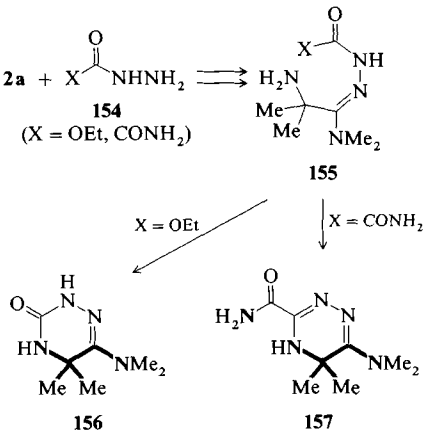

Scheme 32.

[147]). When the reaction with **154** (X = EtO) is performed at room temperature, the open chain intermediate **155** can be isolated as an *E*/*Z* mixture, which cyclizes in the melt or in DMF at 70 °C.

6. Application of the Azirine/Oxazolone Method in Peptide Synthesis

6.1. Construction of Linear Peptides with α,α-Disubstituted α-Amino Acid

Conventional chain elongation techniques either fail completely for peptides containing α,α-disubstituted α-amino acids or suffer from extreme difficulties.[103, 106, 154–157] Apart from low yields, especially in the Merrifield procedure,[158] and cleavage of the acid-labile Aib-peptide bond on removal of the protecting group,[159] problems arise in particular because of racemization (or epimerization) of the carboxyl component, which occurs partly as a result of the necessarily long reaction times.[157, 160] The main reason for the low reactivity of α,α-disubstituted α-amino acids is probably the steric hindrance of the two α-substituents, which is large even for Aib. Various synthetic approaches to larger Aib-containing polypeptides (e.g. alamethicin) failed initially,[161] before they were eventually successful.[157]

Since the difficulties described are attributable to the activation of the carboxyl component in coupling of sterically hindered amino acids, the alternative activation of the amino component should offer great advantages. Donor substituents (alkyl or trialkylsilyl) on the amino group increase the nucleophilicity, but because of the increased steric hindrance they also lower the coupling rate. Use of the *tert*-butyl ester leads to a slight increase in the reactivity of the amino group,[162] but no satisfactory solution for amino group activation has yet been found.[163]

The application of the 3-amino-2*H*-azirines **2** as amino acid synthons in peptide synthesis is thus especially interesting, since it realizes the idea of amino group activation. The formal *N*-activation by the ring strain is so significant that no further activation of the acyl component is required at all; 3-amino-2*H*-azirines are highly reactive synthons for α,α-disubstituted α-amino acids (see reviews [61, 164, 165]).

6.1.1. Principle and Mechanism of Chain Elongation with 3-Amino-2H-Azirines

The principle behind chain elongation with the 3-amino-2*H*-azirines **2** is largely apparent from the transformations described in Sections 3.3 and 5.3. Reaction of carboxylic acids with **2** leads to diamides of type **30** (first coupling step); the acid-catalyzed cyclization to 1,3-oxazol-5(4*H*)-ones **148** (X = O) can be regarded as the activation step for coupling to a further amino component. It should be pointed out that no additional reagents are required under the very mild conditions needed for the coupling with **2**, and no byproducts are observed. This makes workup of the products very simple and also allows the use of bifunctional carboxylic acids (hydroxy, mercapto and amino acids) in unprotected form.[166]

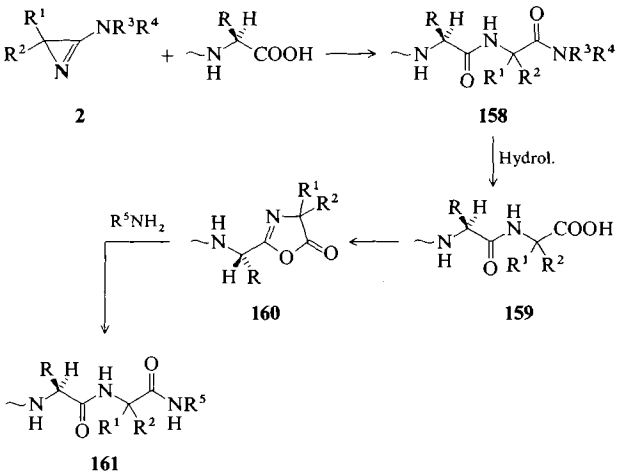

Scheme 33.

The principle of the procedure for incorporation of α,α-disubstituted α-amino acids into peptides by our "azirine/oxazolone method" is described in Scheme 33. In general, reactions of *N*-protected amino acids or peptides with **2** proceed quantitatively at 0–25 °C. The new amide bond is formed in a very rapid, intramolecular rearrangement (**31** → **32** → **30**, Scheme 8), with minimal risk of racemization. An intermediate analogous to **31** is also found in the "four-component condensation" of *Ugi* et al.,[167] where less than 0.01 % racemization is observed. The critical step is the hydrolysis of the peptide amide **158** to the acid **159**. This refunctionalization of the terminal amide group in **158** occurs with a very high selectivity as long as the terminal acid is disubstituted (R^1, $R^2 \neq H$), and an *N*,*N*-disubstituted amide is present (R^3, $R^4 \neq H$), that is, for the products of

coupling to **2**.[29, 150, 166] Treatment of a suspension or solution of **158** (R^3, R^4 = Me) in acetonitrile/water with HCl gas at ca. 60 °C affords **159** in yields higher than 95%. A 1,3-oxazol-5(4*H*)-one occurs as an intermediate in this reaction. This is presumably the reason for the partial epimerization of the penultimate amino acid, which can take place via the intermediate shown in Scheme 34.[168] This epimerization can be completely suppressed if the *N*-methyl anilide **158** (R^3 = Ph, R^4 = Me) is used; this compound can be hydrolyzed under even milder conditions (3 N HCl, THF/H_2O, 25 °C).[168]

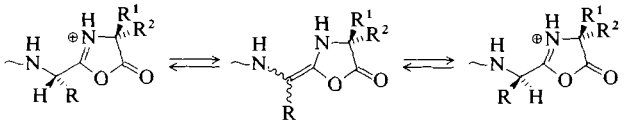

160a **162** **160b**

Scheme 34.

Refunctionalization to esters and thioesters **163** occurs analogously (Scheme 35).[166] Here, **158** is either treated with HCl gas directly in the required alcohol, or in a solution of the phenol or thiophenol in acetonitrile at ca. 70 °C. After evaporation of the solvent, the product is recrystallized or purified by chromatography.

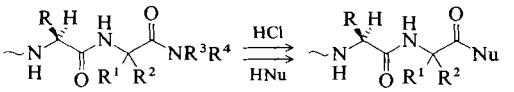

158 **163** (Nu = RO, ArO, PhS)

Scheme 35.

The difficulties that are encountered in the coupling of peptides with *C*-terminal α,α-disubstituted α-amino acids have already been mentioned. Nevertheless, the formation of peptide bonds between Aib and amino components, via 4,4-dimethyl-1,3-oxazol-5(4*H*)-one (**160**, R^1, R^2 = Me), yields encouraging results.[169, 170] However, the high temperatures required greatly restrict the applicability of this method; significant amounts of epimerization are observed,[171] again due to the equilibrium formulated in Scheme 34. Thus, on coupling of Z-Ile-Aib-OH (**164**, R = $CH_3CH_2CH(CH_3)$, R^1 = R^2 = Me) with the slow-reacting amino compound ethyl 4-aminobenzoate by the DCC(dicyclohexylcarbodiimide)/*t*BuOH method,[155] one obtains **165** which is nearly 50% epimerized at the C(2) center of Ile (Scheme 36). Even coupling with isobutyl chloroformate via the mixed anhydride, under Anderson conditions,[172] a method which is recommended for coupling of Aib,[102] gives ca. 5% epimerized **165**. Furthermore, the yield of the reaction is very modest.[171]

The difficulties of epimerization and low yields may be circumvented by catalysis of the coupling reaction. Suitable catalysts have proved to be camphor-10-sulfonic acid (CSA) and zinc chloride. In both cases, **165** forms with DCC even at 0 °C, in yields of 80–95% and without epimerization at

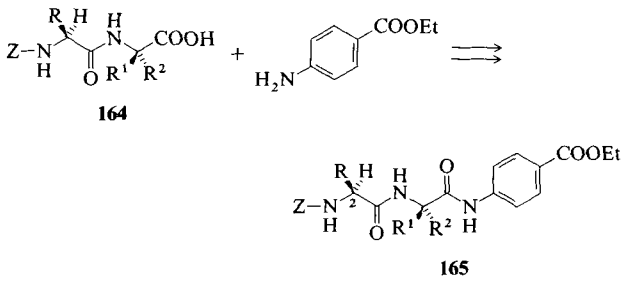

164 **165**

Scheme 36. Z = Benzyloxycarbonyl ($PhCH_2OCO$)

C(2) of Ile.[171] Clearly, both protonation and complexation with the Lewis acid accelerate the ring opening of the 1,3-oxazol-5(4*H*)-one intermediate, and hence reduce the tendency to epimerize.[29] Similar effects have already been reported using $CuCl_2$ as the Lewis acid[173] (see also [174]).

In summary, it can be stated that the reaction of peptides with the 3-amino-2*H*-azirines **2**, together with selective hydrolysis of the terminal amide group and efficient, epimerization-free DCC-coupling via 1,3-oxazol-5(4*H*)-ones, constitutes an attractive method for insertion of α,α-disubstituted α-amino acids into peptides.

6.1.2. Synthesis of Oligopeptides with α,α-Disubstituted α-Amino Acids

To demonstrate the scope of the "azirine/oxazolone" method, several dipeptides,[150, 166] a number of tripeptide analogues of type **165** (Table 3)[175] and tetrapeptides **170** (Scheme 37, Table 4)[122] have been synthesized. These mod-

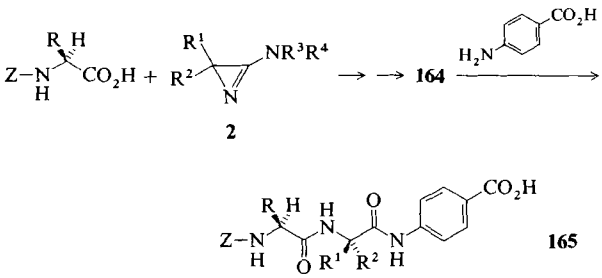

2 **165**

Table 3. Tripeptides **165** synthesized by the azirine/oxazolone method.

R	Azirine	R^1	R^2	Yield [%] [a]	Ref.
Me	**2a**	Me	Me	66	[29, 171]
$PhCH_2$	**2a**	Me	Me	64	[29, 171]
*s*Bu (*S*)	**2a, 2ad**	Me	Me	80, 78	[29, 171]
*s*Bu (*S*)	**2b**	Me	Et	89	[29, 175]
		Et	Me	89	[29, 175]
*s*Bu (*S*)	**2c**	Me	*i*Pr	67	[29, 171]
		*i*Pr	Me	73	[29, 171]
*s*Bu (*S*)	**2e**	Me	$PhCH_2$	90	[29, 175]
		$PhCH_2$	Me	90	[29, 175]
*s*Bu (*S*)	**2o**	Pr	Pr	78	[29, 175]
*s*Bu (*S*)	**2r**	$-(CH_2)_3-$		71	[29, 175]
*s*Bu (*S*)	**2sa**	$-(CH_2)_4-$		81	[29, 171]
*s*Bu (*S*)	**2t, 2ta**	$-(CH_2)_5-$		68, 51	[29, 175]
*s*Bu (*S*)	**2ua**	$-(CH_2)_6-$		89	[29, 175]

[a] Overall yield based on Z-amino acid.

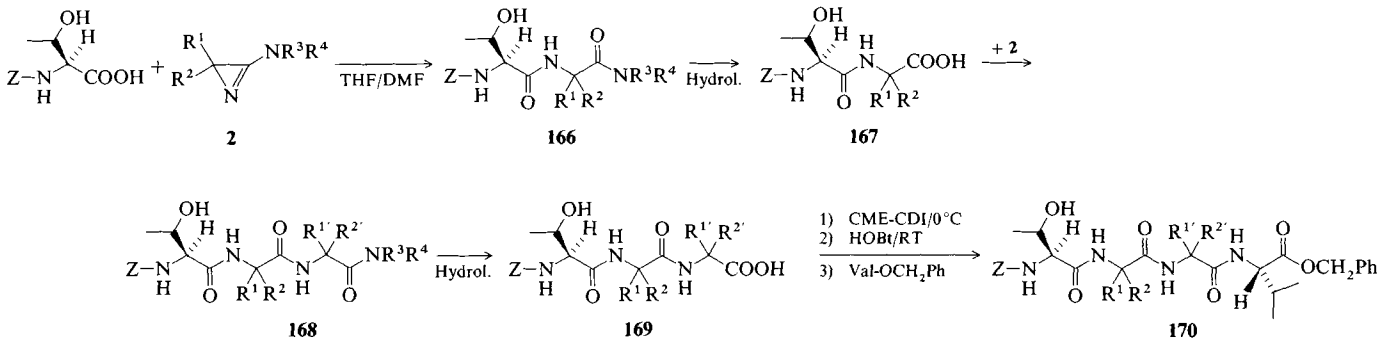

Scheme 37. CME-CDI = *N*-cyclohexyl-*N*-[2-(methylmorpholin-4-ylium)ethyl]carbodiimide-*p*-toluene sulfonate; HOBt = 1-hydroxybenzotriazole.

Table 4. Synthesis of tetrapeptides **170** according to Scheme 37 [40, 122].

Azirine [c]	R^1	R^2	**167** [%] [a]	Azirine	$R^{1'}$	$R^{2'}$	**169** [%] [b]	**170** [%]
2a	Me	Me	**a** 88	**2a**	Me	Me	**aa** 86	**aa** 52
				2o	Pr	Pr	**ab** 79	**ab** 57
2o	Pr	Pr	**b** 96	**2a**	Me	Me	**ba** 83	**ba** 60
				2o	Pr	Pr	**bb** 71	**bb** 57
2r	$-(CH_2)_3-$		**c** 74	**2o**	Pr	Pr	**c** 73	**c** 59
2sa	$-(CH_2)_4-$		**d** 89	**2sa**	$-(CH_2)_4-$		**d** 86	**d** 59
2t	$-(CH_2)_5-$		**e** 84	**2t**	$-(CH_2)_5-$		**e** 63	**e** 72

[a] Overall yield for coupling of **166** to 3-amino-2*H*-azirine (**2**) and hydrolysis to **167**, based on Z-amino acid or Z-dipeptide. [b] Yield for the coupling of **168** to 3-amino-2*H*-azirine (**2**) and hydrolysis to **169**, based on Z-dipeptide **167**. [c] Yield for coupling of **169** with Val-OCH_2Ph.

el peptides were selected as target structures with a view to studying the dependence of their conformations on the nature of the α,α-disubstituted α-amino acids.[121, 122] The tripeptide sequence **165** is also interesting because *Šorm* et al.[176] have shown that peptide derivatives such as ethyl isoleucylalanyl-4-aminobenzoate (Ile-Ala-Benzocain) show structural similarities to certain juvenile hormone analogues (cf. [177, 178]).

Coupling of Z-Ile to the racemic azirines **2b**, **2c** and **2e**, which are asymmetrically substituted at C(2), leads to 1:1 mixtures of diastereomeric dipeptides. These are separated by HPLC before proceeding further. The synthesis of tetrapeptides **170** (Scheme 37) also proceeds in very good yields for the coupling and hydrolysis steps up to tripeptide **169**; the final coupling to Val-OCH_2Ph using a water-soluble carbodiimide still needs improvement (Table 4).

Conformational studies of tripeptides **165**[29, 121] and tetrapeptides **170**[40, 122] demonstrate the pronounced tendency of oligopeptides containing α,α-disubstituted α-amino acids to adopt β turns. That these appear so clearly even in tri- and tetrapeptides is surprising. Another remarkable finding is that α,α-disubstituted α-amino acids with a branched side chain are particularly able to stabilize β turns or helical conformations, while extended forms are increasingly stabilized by longer side chains.

Coupling reactions with **2a** are ideal for the synthesis of poly-Aib peptides, since they can be carried out iteratively; the peptide amide formed with **2a** in each step is hydrolyzed and reacted once more with **2a**. In this way, $PhCH_2CO$-$(Aib)_3$-OMe,[166] PhCH(OH)CO-Aib-OH,[179] H-$(Aib)_4$-OMe[166] and Z-$(Aib)_6$-N(Ph)Me (**171**)[36] (Fig. 5) have been synthesized, amongst others. The selectivity of the hydrolysis step must be specially emphasized; the terminal *N*,*N*-disubstituted amide group is cleaved exclusively.

The Aib-containing peptide Z-$(Aib)_3$-Pro-$(Aib)_3$-N(Ph)-Me has been obtained by coupling the segments Z-$(Aib)_3$-OH and Pro-$(Aib)_3$-N(Ph)Me, using DCC/$ZnCl_2$.[36] The segments themselves were synthesized via the azirine/oxazolone method.

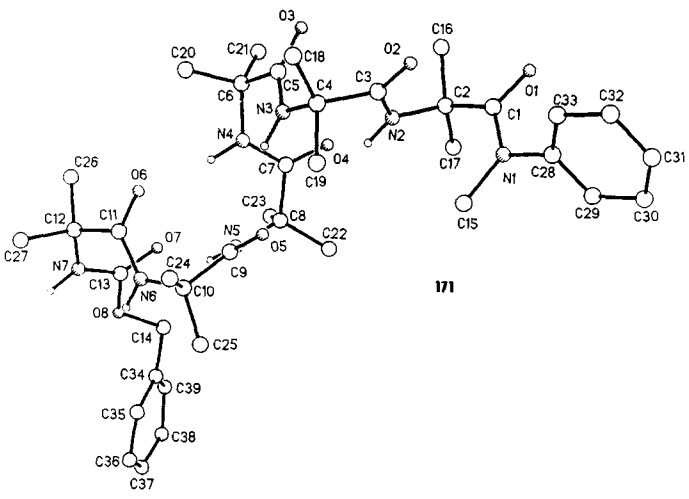

Fig. 5. Structure of Z-$(Aib)_6$-N(Ph)Me (**171**) in the crystal.

6.1.3. *Synthesis of Peptaibol Fragments*

The peptaibols are amphiphilic polypeptide antibiotics and ionophores[180] with a high proportion (up to 50%) of

nonproteinogenic 2-aminoisobutyric acid (Aib) and occasional D-isovaline residues (D-Iva). Further characteristics are an aminoalcohol at the C terminus and an *N*-terminal acetyl group. The peptaibols can be divided into two groups:[181] those with 18–20 amino acids which contain no hydroxyproline (Hyp), and those with 15–16 amino acids, including Hyp (Table 5). Physiologically, the peptaibols are distinguished by their membrane-modifying qualities. They induce a potential-dependent ionic conductance in lipid bilayers, and therefore serve as model systems for studies of the synaptic transfer of nerve impulses.[189–191]

Table 5. Examples of Peptaibols.

Peptaibol	No. of amino acids total	α,α-disubst.	*C*-terminal aminoalcohol	Ref.
Alamethicin F-30	20	8	Pheol	[102,182,183]
Antiamoebin I	16	8	Pheol	[100,184]
Emerimicin IV	15	6	Pheol	[185]
Hypelcin A	20	10	Leuol	[186]
Paracelsin A	20	9	Pheol	[182]
Suzukacillin A	20	9	Pheol	[187]
Trichorzianin A IIIc	19	8	Trpol	[188]
Trichotoxin A-40	18	9	Valol	[100,102,182]
Trichotoxin A-50	18	9	Valol	[182]

It is striking that when the peptaibols are isolated from fungal cultures (e.g. *Trichoderma viride* → Almethicin, Trichotoxin; *Emericellopsis poonensis thirum* → Antiamoebin), each major compound is found along with several sequence isomers, whose preparative separation is most difficult. This microheterogeneity can be traced back to the nonribosomal biosynthesis with low-specificity multienzyme complexes.[192] For some time now, attempts have therefore been made to synthesize chemically homogeneous compounds. Four different syntheses of the best known member of this group, Alamethicin F-30, have been published, in 1981 and 1985.[157, 193]

Ac-Aib-Pro-Aib-Ala-Aib-Ala-Gln-Aib-Val-Aib-Gly-Leu-Aib-Pro-Val-Aib-Aib-Glu-Gln-Pheol.

Alamethicin F-30

The azirine/oxazolone method now constitutes an ideal method for the synthesis of peptaibol fragments. The Z-protected (12–20) nonapeptide Z-Leu-Aib-Pro-Val-Aib-Aib-Glu(OCH_2Ph)-Gln-Pheol, which was also used in the total synthesis reported by *Schmitt* and *Jung*,[157] is obtained by the route outlined in Scheme 38, in 29% yield.[29, 194] A comparison of this yield with that obtained by the classical route (12%) clearly shows the advantages of the new methodology. In particular, the synthesis of the tripeptide segment Z-Val-Aib-Aib-N(Ph)Me, using the 3-amino-2*H*-azirine **2a** as an Aib synthon (95% yield), is vastly superior to previous techniques.

As further attractive target molecules, we selected fragments of Trichotoxin A-50 (G) and of Antiamoebin I.

Ac-Aib-Gly-Aib-Leu-Aib-Gln-Aib-Aib-Aib-Ala-Ala-Aib-Pro-Leu-Aib-D-Iva-Gln-Valol

Trichotoxin A-50 (G)

Ac-Phe-Aib-Aib-Aib-D-Iva-Gly-Leu-Aib-Aib-Hyp-Gln-D-Iva-Hyp-Aib-Pro-Pheol

Antiamoebin I

The synthesis of the (10–13) segment of Trichotoxin A-50 (G), Z-Ala-Ala-Aib-Pro-OMe, proceeds in 60% yield,[165, 195] including a yield of 92% for the coupling of Z-Ala-Ala with **2ad** and subsequent hydrolysis with 3 N HCl (THF/H_2O) to Z-Ala-Ala-Aib-OH. The synthesis of Z-Leu-Aib-Iva-Gln-Valol **174** is outlined in Scheme 39. The tripeptide **173** was obtained as an epimeric mixture (ca. 7:5), since racemic **2ba** was used.[196] Separation of the epimers at the tripeptide amide stage is more difficult than for the dipeptide amides of type **165**. Using HPLC, the (+)-epimer was obtained in pure form, but the (−)-isomer still contained ca. 12% of its epimer.[195]

A further problem appeared while constructing the (6–9) segment. When the peptide amides Z-Gln-$(Aib)_n$-N(Ph)Me are hydrolyzed, even under the mildest conditions, the amide group in the Gln side chain is also partially hydrolyzed (→ Glu). Similar difficulties also appear in the synthesis of

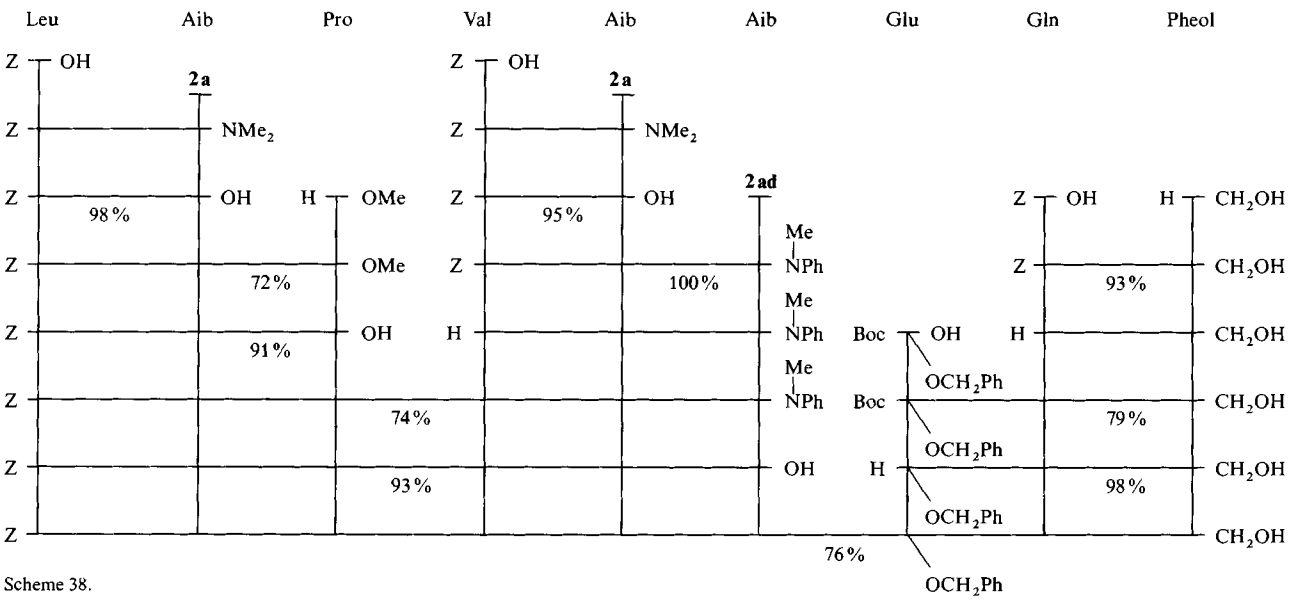

Scheme 38.

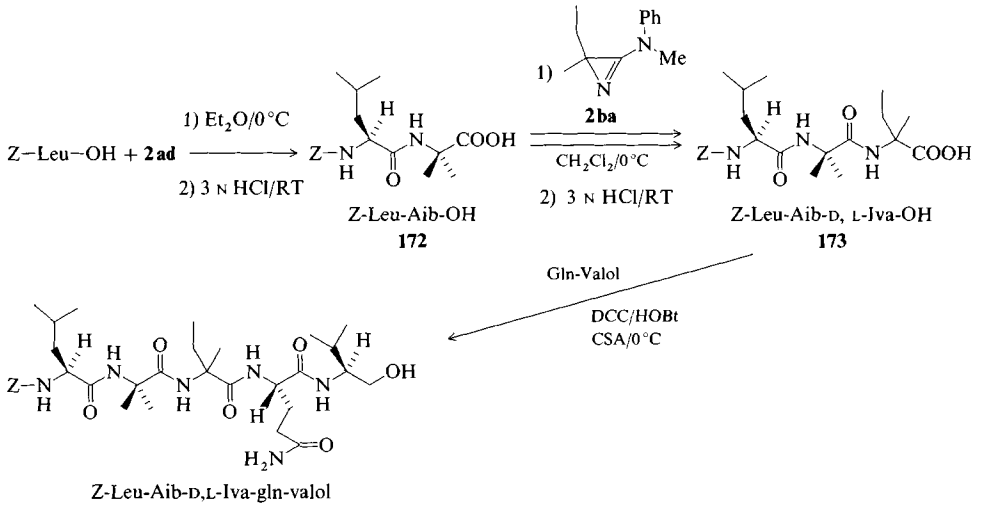

Scheme 39. DCC = dicyclohexylcarbodiimide; CSA = camphor-10-sulfonic acid.

Z-Asn-Aib segments (→Asp). This can only be avoided by introducing a suitable protecting group. The trityl group has proved its worth here; it allows the synthesis of **175**, as shown in Scheme 40, in an overall yield of ca. 60%.[35]

The synthesis of the *N*-terminal nonapeptide of Antiamoebin is presented in Scheme 41. Successive construction of Ac-Phe-Aib-Aib-Aib-D,L-Iva-OH using the 3-amino-2*H*-azirines **2ad** and **2bd** afforded very good yields of an epimer-

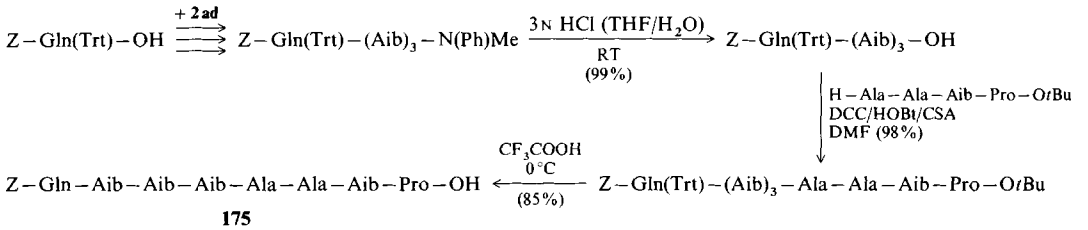

Scheme 40.

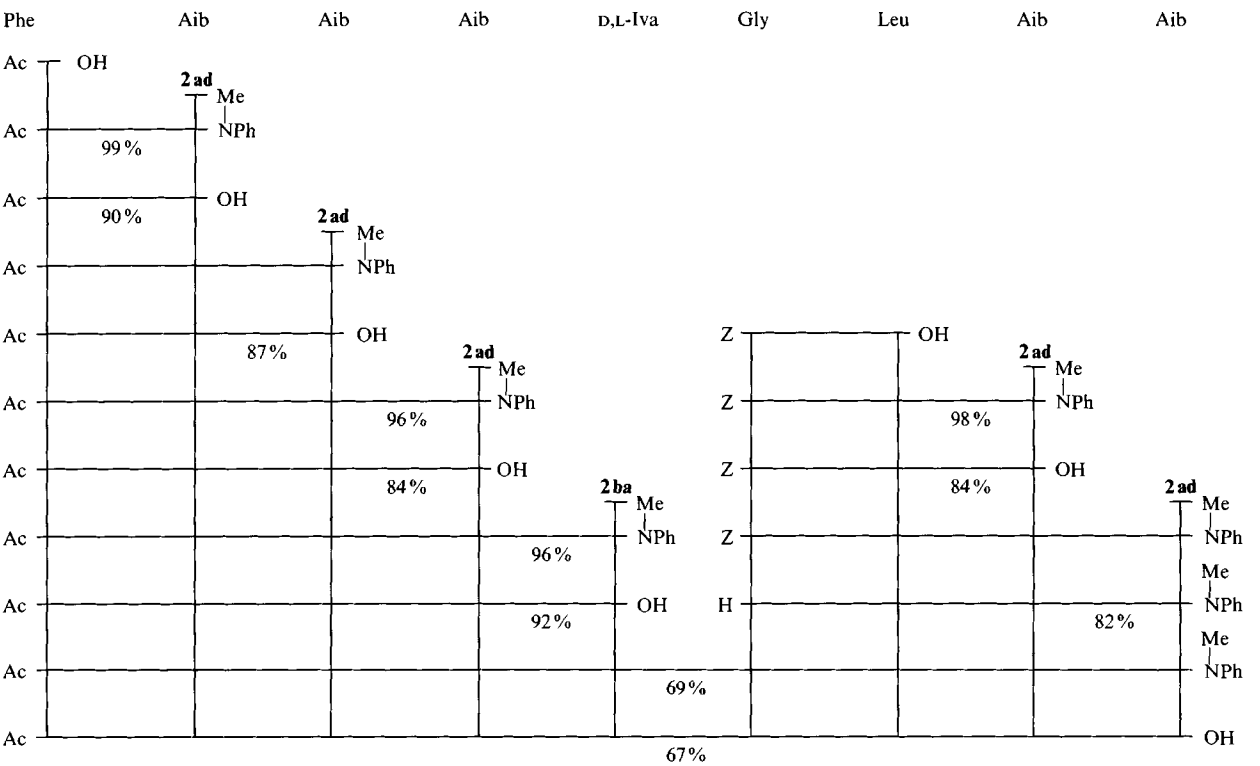

Scheme 41.

ic mixture, which could again be separated by HPLC. Coupling of segments (1–5) and (6–9) has so far only been performed with the epimeric mixture (ca. 4:7), and gives best results via the mixed anhydride with isobutyl chloroformate.[198] The crude yield for the coupling with DCC/CSA via the 1,3-oxazol-5(4*H*)-one is actually higher (92%), but on chromatography to remove the urea produced in the reaction, this falls to ca. 52%.

The X-ray crystal structure of the analogously prepared segment Z-Gly-Leu-Aib-Aib-OH (Fig. 6) shows not only intermolecular hydrogen bonds, but also an intramolecular one between NH(1) and O(4), which stabilizes formation of a β turn.

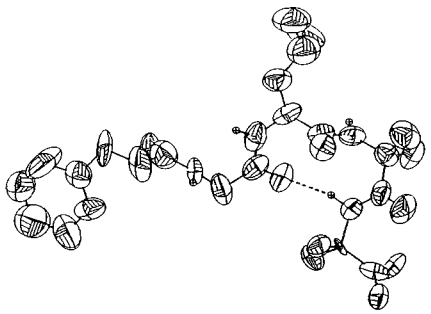

Fig. 6. Structure of Z-Gly-Leu-Aib-Aib-OH in the crystal.

6.2. Direct Amide Cyclization to Cyclic Depsipeptides

As has been discussed in the previous sections, diamides and peptides of type **158** (Scheme 33) are selectively transformed into acids or esters under acidic conditions. The 1,3-oxazol-5(4*H*)-one formed as an intermediate is attacked by a nucleophile in an intermolecular reaction, with ring-opening. In the absence of an external nucleophile, substrates of type **176** undergo an intramolecular reaction with the nucleophilic group they carry, giving rise to cyclic products. Thus, for example, on treatment of a suspension of **176** (Nu = O, R,R′ = Me) in toluene with HCl gas at 100 °C, the morpholine-2,5-dione **178** (Nu = O, R,R′ = Me) is obtained in 87% yield (Scheme 42).[179] However, the success of the cyclization depends greatly on the substituents R and R′. For R,R′ = Ph, for example, the reaction comes to a halt at the level of the 1,3-oxazol-5(4*H*)-one **177**.

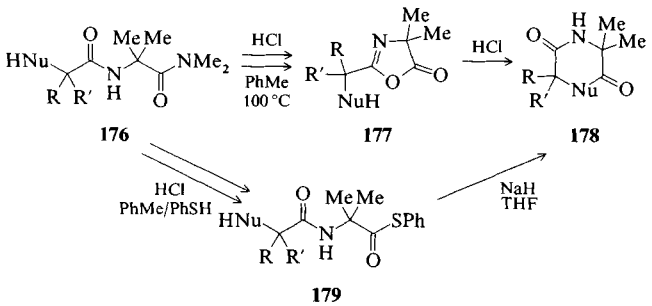

Scheme 42.

One alternative to the "direct amide cyclization" (e.g. **176** → **178**) is the route via the corresponding phenyl thioester **179**. Cyclization is then brought about with sodium hydride in THF. Using this route, the cyclization of **176** (Nu = NH) to piperazine-2,5-diones is also possible; these compounds are only accessible via acid-catalyzed ring closure in exceptional cases.[164]

Base-catalyzed cyclization of phenyl thioesters can also be used to obtain 1,4-diazepine-2,5,7-triones **182** (Scheme 43).[199] The required triamides **180** are usually synthesized by reaction of malonic acid monoamides with the 3-amino-2*H*-azirines **2a** and subsequent acid-catalyzed refunctionalization of the dimethylamide group.

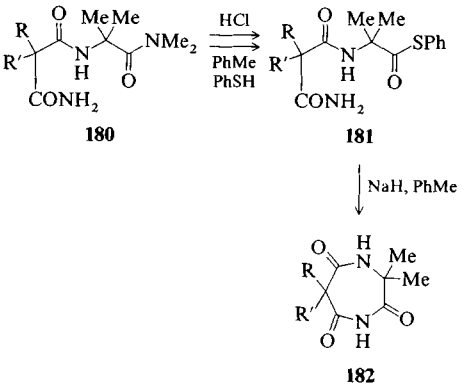

Scheme 43.

"Direct amide cyclization" under acid catalysis is especially well-suited for the synthesis of cyclic depsipeptides (cyclopeptolides) of medium ring size. In Scheme 44 one example of peptide chain extension with aminoazirines and amide cyclization starting from (±)-mandelic acid is presented.[179] Cyclization takes place at ca. 100 °C by bubbling HCl gas through a suspension of the peptide in toluene. During workup the solvent is evaporated, the residue is suspended in THF/ether, and the dimethylamine hydrochloride produced in the reaction is filtered off. This gentle procedure allows the isolation of the 9-, 12- and 15-membered depsipeptides **185**, **188** and **191** in 85%, 90% and 86% yield respectively.[179] The most surprising of these is the easy formation of the nine-membered **185**, since it is known that, with very few exceptions (e.g. cyclotriprolyl[200]), cyclic tripeptides are very difficult to synthesize.[201] Under conventional cyclization conditions, the main products are cyclodimers of *N*-substituted piperazine-2,5-diones. The high ring strain in **185** is obvious in its sensitivity to hydrolysis: while **188** and **191** are stable compounds, **185** is hydrolyzed to the open-chain acid PhCH(OH)CO-Aib-Aib-OH even with only traces of water.

The selectivity of ring closure to the terminal amide group must be specially mentioned. In no case does cyclization occur with cleavage of the peptide chain[179] (cf. [161]). In these model compounds containing only Aib-units within the peptide chains, this selectivity is explained by preferential formation of the 1,3-oxazol-5(4*H*)-one via protonation of the *N*,*N*-dimethylamide group.

The general significance of these new cyclization methods is apparent from the successful syntheses of the 12-mem-

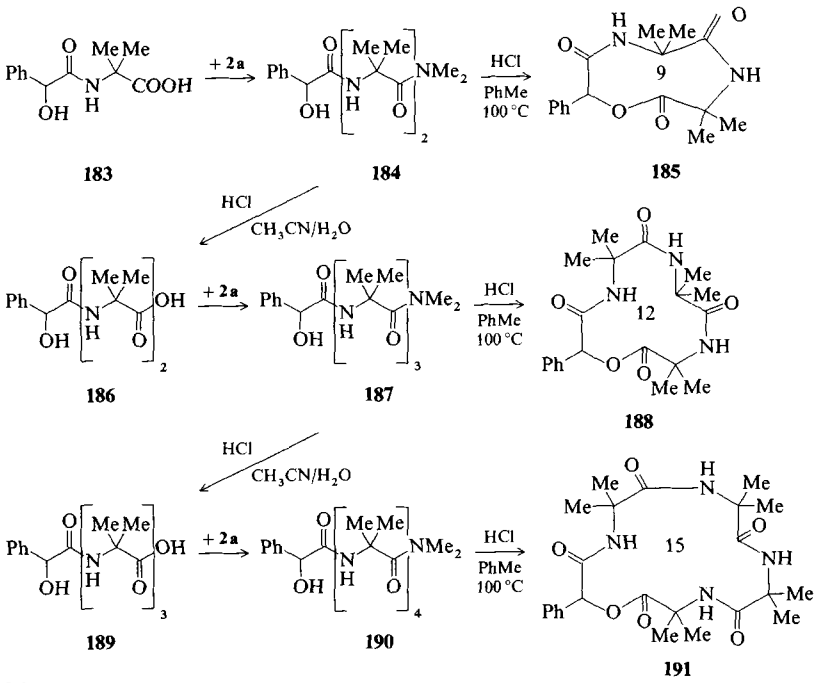

Scheme 44.

bered cyclodepsipeptides **193** (Scheme 45) and **197** (Scheme 46). Cyclo[(*S*)-Pms-(*R*)-Pro-(*S*)-Ala-Aib] (**193**, Pms = phenyl lactic acid) is a lactone analogue of the tetrapeptide cyclo-[(*S*)-Phe-(*R*)-Pro-(*S*)-Ala-Aib] studied by *Rich* et al.,[202] which served as a model compound for optimization of the cyclization to *Chlamydocin*.[203] In the case of the peptide, the ring closure between Phe and Aib proceeded very slowly and in only 2% yield; the corresponding cyclization **192** → **193** took place with a yield of 72% (Scheme 45).[204]

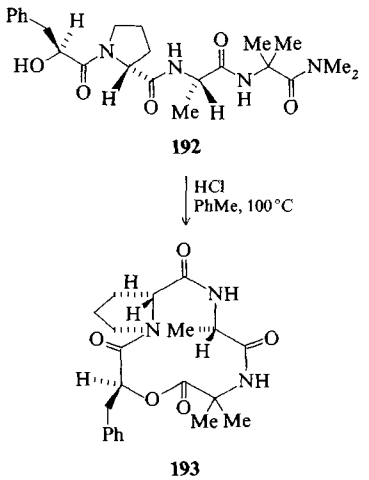

Scheme 45.

Compound **197** displays an alternating sequence of (*R*)-mandelic acid and Aib residues, and therefore serves as a model compound for the cyclization of enniatins.[180, 205, 206] These are natural ionophores containing alternating (*R*)-α-hydroxy- and (*S*)-α-amino acids. In the antibiotic Enniatin B, for example, the 18-membered ring is built up of three identical [(*R*)-2-hydroxy-3-methylbutanoyl-N^{α}-methyl-L-valyl] units. In enniatin syntheses, cyclization is usually carried out by formation of a lactam bond; for model compounds of type **197**, ring closure occurs via amide cyclization and lactone formation.[207]

The linear precursor **196** is easily synthesized by coupling **194**, available from (*R*)-mandelic acid and **2a**, with **195**, in 66% yield. A modified carbonyldiimidazole (CDI) procedure[208] has proved useful for coupling the two fragments, using sodium imidazolide as base. Cyclization with HCl in toluene at 100 °C leads to **197** in 88% yield. No cleavage of the ester group is observed under these conditions.

In summary, acid-catalyzed amide cyclization is ideally suited for lactone ring-closures (cf. also [209]), and hence for the synthesis of cyclic depsipeptides. No dimerization occurs, even when only small solvent volumes are used. Because of the heterogeneous nature of the reaction, the "dilution principle"[210] is probably obeyed nonetheless, since only a small proportion of the reactant is actually present in solution in the toluene. The high yields obtained are also due to the irreversible nature of the activation step (i.e. 1,3-oxazol-5(4*H*)-one formation), to precipitation as its hydrochloride of the dimethylamine produced, and to the gentle workup procedure by filtration and evaporation of the solvent.

6.3. Synthesis of Cyclic Aib-Containing Peptides

The synthesis of cyclic peptides continues to arouse great interest.[211–214] Unfortunately, acid-catalyzed amide cyclization (Section 6.2) cannot be applied to the formation of cyclic peptides. As for the depsipeptide derivatives of type **176** (Nu = NH, Scheme 42), the method fails for longer peptides, since the free amino group is completely protonated under the reaction conditions. Therefore for the synthesis of

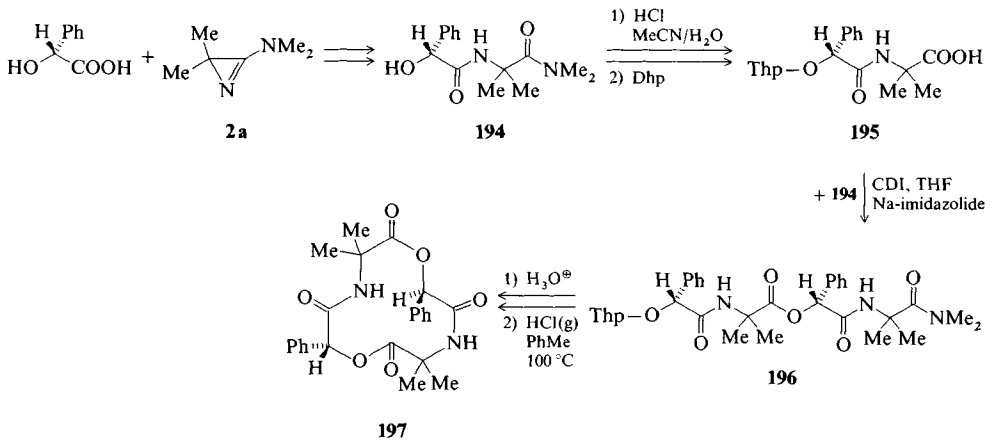

2a 194 195 196 197

Scheme 46. Dhp = dihydropyran, Thp = tetrahydropyranyl, CDI = carbonyldiimidazole.

cyclic, Aib-containing peptides, a combination of the "azirine/oxazolone method" with a conventional cyclization is called for. The pentapeptide **198** was chosen as a model compound and was synthesized from Z-glycine according to the synthetic plan given in Scheme 47, by reactions with 3-amino-2*H*-azirines **2e** and **2ad**, followed by coupling to glycine methyl ester via the 1,3-oxazol-5(4*H*)-one (DCC/$ZnCl_2$). The protecting groups were removed as usual by hydrogenolysis and saponification.[36]

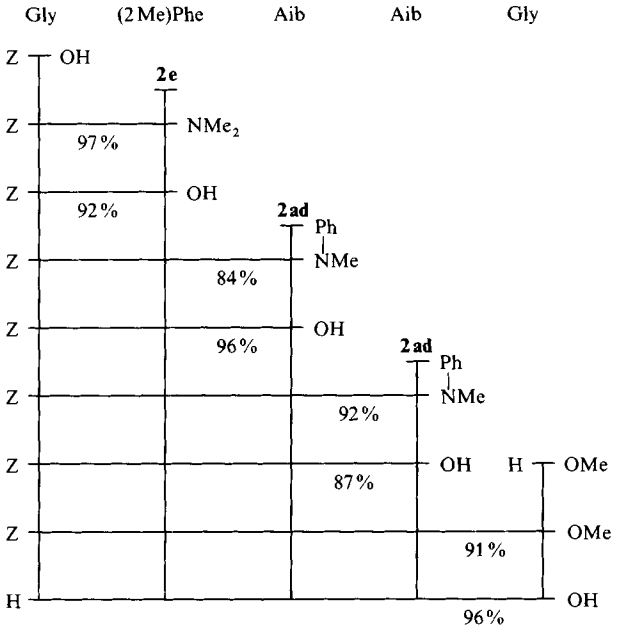

Scheme 47.

Several procedures have been tried out for the cyclization of **198** to the 15-membered **199** (Scheme 48). The pentafluorophenol/DCC method[215] yields **199** in 25% yield. In this procedure, a 10^{-4} M solution of **198** is stirred with 2 equivalents of pentafluorophenol and 1 equivalent of DCC for 30 hr at room temperature, and the cyclized product **199** is purified by HPLC. The highest yield of crystallized product (60%) was obtained by the procedure of *Brady* et al.[216] Compound **198** was stirred in anhydrous DMF (10^{-4} M) with diphenylphosphorylazide (DPPA) and $NaHCO_3$ at 0–4 °C.

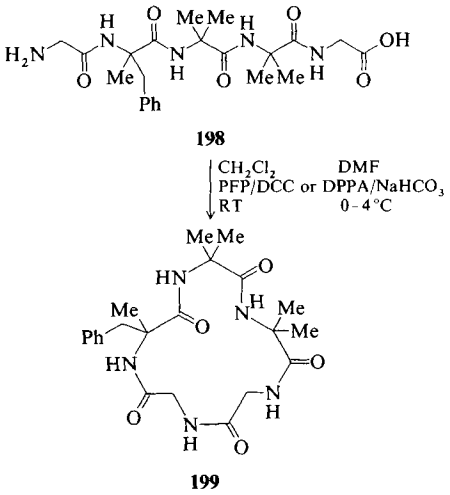

198 199

Scheme 48. PFP = pentafluorophenol, DPPA = diphenylphosphorylazide.

The latter method also allows cyclization of the tetrapeptide H-Gly-(2Me)Phe-Aib-Gly-OH to the 12-membered cyclo[Gly-(2Me)Phe-Aib-Gly]. In this case, however, the yields achieved till now were only 20–25%. The major side reaction is cyclodimerization, which could not be completely suppressed even on dilution to 10^{-5} M.

The structures of the linear and cyclic pentapeptides **198** and **199** have been determined by X-ray crystallography (Fig. 7).[217] The linear compound **198** occurs in the crystalline state as a left-handed 3_{10}-helix, stabilized by two intramolecular hydrogen bonds (N(4)H···O(1) and N(5)H···O(2)).

The relatively rigid conformation of the cyclic compound **199** also shows two intramolecular hydrogen bonds, one of which is comparatively strong (N(1)H···O(3)), while the other appears to be relatively weak (N(3)H···O(3)).

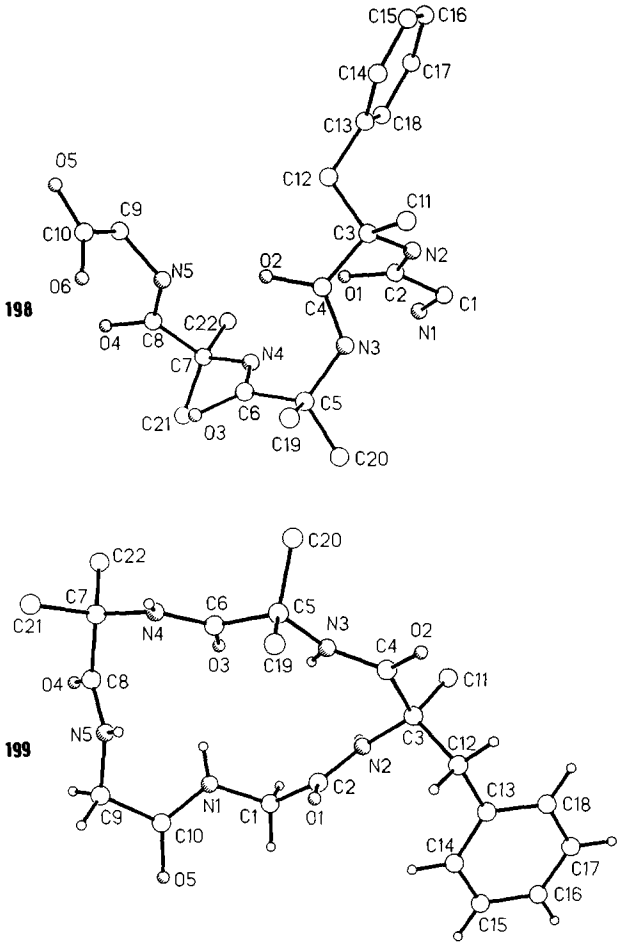

Fig. 7. Structures of the linear pentapeptide **198** (top) and the cyclic pentapeptide **199** (bottom) in the crystal.

6.4. Resolution of Racemic α,α-Disubstituted α-Amino Acids via Diastereomeric Dipeptides

For the dipeptides **200**, the selective amide cleavage (HCl/$MeCN/H_2O$) described in Section 6.1.1 leads to the dipeptide acids **201** if the *C*-terminal amino acid is α,α-disubstituted ($R^{1'}$, $R^{2'} \neq H$; Scheme 49, path a). On the other hand, if

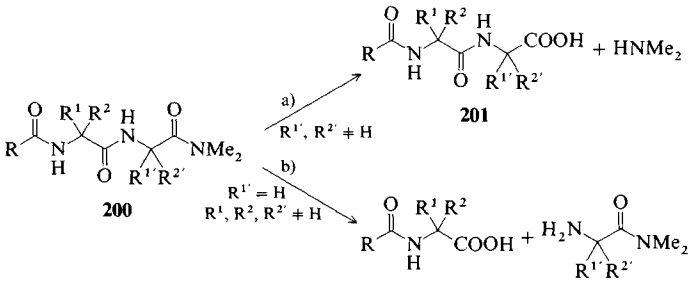

Scheme 49.

the terminal amino acid is monosubstituted and the penultimate one is disubstituted (R^1, R^2, $R^{1'} \neq H$), a selective cleavage of the *C*-terminal amino acid **203** is observed under the same conditions (path b).[73, 150, 166]

On the basis of type b selective cleavage, a resolution of racemic α,α-disubstituted α-amino acids has been developed, following the sequence below:

1. The racemic, *N*-acylated, α,α-disubstituted α-amino acid (in the form of the oxalone **204**) is coupled to the *N*,*N*-dimethylamide of an enantiomerically pure, monosubstituted α-amino acid (e.g. Phe-NMe_2, (*S*)-**205**).
2. The diastereomeric dipeptides thus formed (e.g. (*S*, *S*)- and (*S*, *R*)-**206**) are separated by chromatography.
3. The separated diastereomeric dipeptides are degraded by means of selective amide cleavage into the enantiomerically pure α,α-disubstituted α-amino acids (e.g. (*S*)- and (*R*)-**207**) and the unchanged chiral auxiliary.

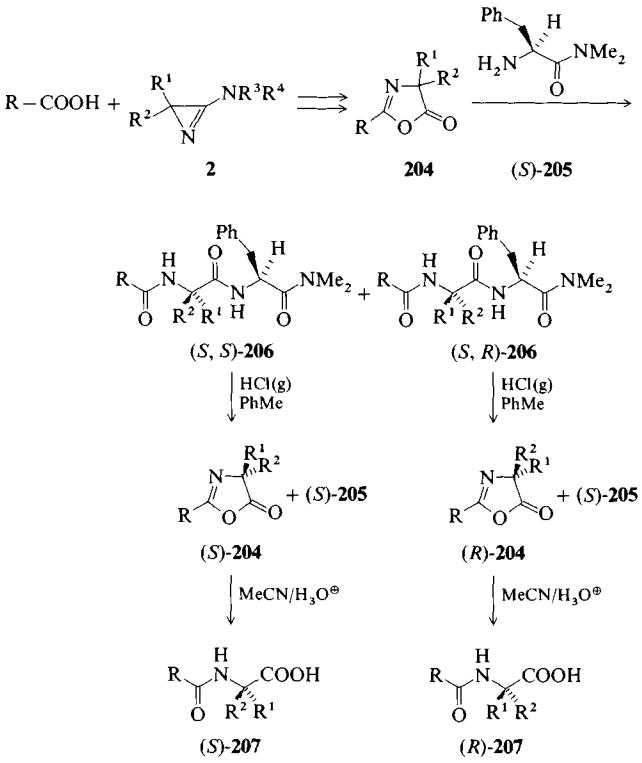

Scheme 50. R^1, R^2 = alkyl; $R^1 > R^2$

This concept has been tested successfully with *N*,*N*-dimethylphenylalanine amide (Phe-NMe_2) and *N*,*N*-dimethyl-N^{α}-phenylalanylphenylalanine amide (Phe-Phe-NMe_2) as chiral auxiliaries, and a series of different α,α-disubstituted α-amino acids (Scheme 50).[218, 219] The 4,4-disubstituted 1,3-oxazol-5(4*H*)-ones **204** used for coupling with the chiral auxiliary were synthesized via the 3-amino-2*H*-azirines **2**, from ketones via hydantoins, or by alkylation of 4-monosubstituted 1,3-oxazol-5(4*H*)-ones. In most cases, separation of diastereomers (*S*, *S*)-**206** and (*S*, *R*)-**206** can be effected by "flash chromatography" on silica gel.[220] Thus, for example, the dipeptides **206** with R^1, R^2 = $PhCH_2$, Me were isolated in 42% and 40% yield, based on **204**. Hydrolysis to the enantiomerically pure *N*-acyl amino acids (*S*)-**207** (R^1 = $PhCH_2$, R^2 = Me; 89%) and (*R*)-**207** (85%) proceeds smoothly at 70 °C, and ca. 80% of the chiral auxiliary can be recovered. The enantiomeric methyl esters, for example, can be obtained in a similar manner if one treats the

separated dipeptides in methanol with HCl gas. With a suspension of (*S*,*S*)- or (*R*, *S*)-**206** in toluene, bubbling HCl gas affords the enantiomeric 4,4-disubstituted 1,3-oxazol-5(4*H*)-ones.

7. Summary and Outlook

The 3-amino-2*H*-azirines **2** have proved themselves to be reactive synthetic intermediates suited for a wide variety of uses. The reactions that they undergo with carboxylic acids, NH-acidic heterocycles and other protic acids proceed with cleavage of the C–N double bond to give α,α-disubstituted α-amino acid derivatives. Nonproteinogenic amino acids of this nature occur in several biologically active heterocycles such as herbicides, and the chemistry of 3-amino-2*H*-azirines offers a convenient pathway for building these amino acid fragments into known and novel heterocycles. However, some of the transformations with the NH-acidic heterocycles studied have led to surprising results. The elucidation of the mechanisms of these reactions, which all proceed via a zwitterion as the key intermediate, has contributed greatly to the understanding of the reactivity of three-membered, cyclic amidines. In certain cases, however, a confident prediction of the course of a reaction is still difficult.

This is not the case, however, for the use of 3-amino-2*H*-azirines as synthons for α,α-disubstituted α-amino acids in the synthesis of peptides and peptidelike compounds. Reactions with amino acids or peptides generally lead to coupling products, that is, to the peptide extended by one α,α-disubstituted α-amino acid. This coupling takes place under very mild conditions, with no additional reagents, and affords high yields. Together with the selective hydrolysis to the peptide acid and Lewis acid catalyzed coupling via 1,3-oxazol-5(4*H*)-ones (also under mild conditions, and without epimerization), this reaction makes a very useful extension to the repertoire of peptide synthesis. This procedure, described by us as the "azirine/oxazolone method", is especially attractive for the synthesis of peptaibols, cyclic depsipeptides (peptolides) and oligopeptides that occur in relatively rigid conformations.

This last aspect is of particular importance, since as well as studies of the relationship between structure, conformation and biological activity, one of the most ambitious aims in peptide chemistry is the construction of artificial proteins with "tailormade" physical and chemical characteristics. One prerequisite for the synthesis of such proteins is the availability of oligopeptide fragments with "stable secondary structure" as building blocks. The α,α-disubstituted α-amino acids strongly induce β turns, and could be suitable for constructing β-turn subunits, which serve as recognition patterns for triggering immunological, endocrine and metabolic reactions. The "azirine/oxazolone method" can play a significant role in constructing such compounds. This synthetic strategy will gain greatly in importance as soon as enantiomerically pure 3-amino-2*H*-azirines become available.

My thanks are due to Zürich University, the Swiss National Science Foundation, F. Hoffmann–La Roche AG, Basel, the Prof.-Hans-E.-Schmid-Stiftung, the Anna-Feddersen-Wagner-Fonds and the Stipendienfonds der Basler Chemischen Industrie for financial support of our research and the doctoral students involved with it. In particular I would like to thank my committed and talented co-workers, whose names appear in the list of references. Their many ideas and their tireless efforts to realize these ideas experimentally, mainly as doctoral and diploma students, have produced the results that are described in this article.

Received: July 2, 1990 [A 806 IE]
German version: *Angew. Chem. 103* (1990) 271
Translated by Dr. Michael Kertesz, Zürich

[1] V. Meyer, *Justus Liebigs Ann. Chem. 180* (1876) 192.
[2] A. von Baeyer, *Ber. Dtsch. Chem. Ges. 18* (1885) 2277.
[3] A. de Meijere, *Chem. Unserer Zeit 16* (1982) 13.
[4] A. Greenberg, J. F. Liebman: *Strained Organic Molecules, Vol. 38* of A. T. Blomquist (Ed.): *Organic Chemistry*, Academic, New York 1978.
[5] A. Hassner (Ed.): *Small Ring Heterocycles, Vol. 1–3*, Wiley, New York 1983.
[6] V. Nair in [5], *Vol. 1*, p. 215.
[7] a) A. Padwa, A. D. Woolhouse in A. R. Katritzky, C. W. Rees (Eds.): *Comprehensive Heterocyclic Chemistry, Vol. 7* (W. Lwowsky, Ed.), Pergamon, Oxford 1984, p. 47; b) J. Y. Vanderhoek, P. A. Cerutti in Houben-Weyl-Müller (Ed.): *Methoden der Organischen Chemie, Band 4/5b*, "Photochemie", Thieme, Stuttgart 1975, p. 1104; c) R. K. Smalley in D. Barton, W. D. Ollis (Eds.): *Comprehensive Organic Chemistry, Vol. 4* (P. G. Sammes, Ed.), Pergamon, Oxford 1979, p. 565; d) A. Hassner in E. F. V. Scriven (Ed.): *Azides and Nitrenes*, Academic, Orlando, FL 1984, p. 35.
[8] F. W. Fowler, *Adv. Heterocy[illegible]hem. 13* (1971) 45.
[9] D. J. Anderson, A. Hassner, [illegible] *hesis 1975*, 483.
[10] V. Nair, K. H. Kim, *Heterocycles 7* (1977) 353.
[11] H. Taniguchi, K. Isomura, T. Tanaka, *Heterocycles 6* (1977) 1563.
[12] A. Padwa, *Acc. Chem. Res. 9* (1976) 371; *Chem. Rev. 77* (1977) 37.
[13] P. Gilgen, H. Heimgartner, H. Schmid, H.-J. Hansen, *Heterocycles 6* (1977) 143.
[14] A. Padwa, P. H. J. Carlsen, N. Kamigata in R. B. Mitra, N. R. Ayyangar, V. N. Gogte, R. M. Acheson, N. Cromwell (Eds.): *New Trends in Heterocyclic Chemistry*, Elsevier, Amsterdam 1979, p. 341.
[15] A. Padwa in P. de Mayo (Ed.): *Rearrangements in Ground and Excited States, Vol. 3*, Academic, New York 1980, p. 501.
[16] H.-J. Hansen, H. Heimgartner in A. Padwa (Ed.): *1,3-Dipolar Cycloaddition Chemistry*, Wiley, New York 1984, p. 177.
[17] H. Alper, *Isr. J. Chem. 21* (1981) 203; H. Alper, C. P. Mahatantila, F. W. B. Einstein, A. C. Willis, *J. Am. Chem. Soc. 106* (1984) 2708.
[18] P. F. dos S. Filho, U. Schuchardt, *Angew. Chem. 89* (1977) 672; *Angew. Chem. Int. Ed. Engl. 16* (1977) 647; U. Schuchardt, P. F. dos S. Filho, *J. Chem. Res. (S) 1983*, 122.
[19] a) A. Padwa, N. Kamigata, *J. Am. Chem. Soc. 99* (1977) 1871; b) H. Bader, H.-J. Hansen, *Helv. Chim. Acta 61* (1978) 286.
[20] a) D. J. Anderson, A. Hassner, *J. Am. Chem. Soc. 93* (1971 4339; *94* (1972) 8255; b) V. Nair, *J. Org. Chem. 37* (1972) 802; c) A. Inanda, H. Heimgartner, *Helv. Chim. Acta 65* (1982) 1489.
[21] a) L. A. Wendling, R. G. Bergman, *J. Am. Chem. Soc. 96* (1974) 308; *J. Org. Chem. 41* (1976) 831; b) A. Padwa, J. Smolanoff, S. I. Wetmore, Jr., *ibid 38* (1973) 1333; c) P. Claus, P. Gilgen, H.-J. Hansen, H. Heimgartner, B. Jackson, H. Schmid, *Helv. Chim. Acta 57* (1974) 2173.
[22] M. Rens, L. Ghosez, *Tetrahedron Lett. 1970*, 3765.
[23] The ring strain of 2*H*-azirines is not known, but it is presumably comparable to that of cyclopropene (224.5 kJ mol^{-1} [24]), since the ring strain of aziridine (115.8 kJ mol^{-1}) is practically identical to that of cyclopropane (115.4 kJ mol^{-1} [24]).
[24] S. W. Benson: *Thermochemical Kinetics*, 2nd Edition, Wiley, New York 1976.
[25] H. Heimgartner: "3-Amino-2*H*-azirine, neue Synthone für heterocyclische Verbindungen", *Habilitationsschrift*, Universität Zürich 1979.
[26] L. Ghosez, J. Marchand-Brynaert in H. Böhme, H. G. Viehe (Eds.): *Iminium Salts in Organic Chemistry, Vol. 9/Part I*, of E. C. Taylor (Ed.): *Advances in Organic Chemistry*, Wiley, New York 1976, p. 421; L. Ghosez in J. Mathieu (Ed.): *Medicinal Chemistry V*, Elsevier, Amsterdam 1977, p. 363.
[27] S. M. Ametamey, R. Hollenstein, H. Heimgartner, *Helv. Chim. Acta 71* (1988) 521.
[28] C. Jenny: „Synthese und Reaktionen von 2-Thiazolin-5-thionen", *Dissertation*, Universität Zürich 1986.
[29] P. Wipf: „Synthese und Konformationsanalyse von Peptiden mit α,α-disubstitiuerten α-Aminosäuren", *Dissertation*, Universtität Zürich 1987.
[30] K. Dietliker, H. Heimgartner, *Helv. Chim. Acta 66* (1983) 262.

[31] S. M. Ametamey: „3-Amino-2*H*-azirine als Aminosäure-Bausteine in der Heterocyclensynthese", *Dissertation*, Universität Zürich 1989.
[32] M. Henriet, M. Houtekie, B. Techy, R. Touillaux, L. Ghosez, *Tetrahedron Lett. 21* (1980) 223.
[33] C. Bernard, L. Ghosez, *J. Chem. Soc. Chem. Commun. 1980*, 940.
[34] K. Dietliker: „I. Photochemie und Übergangsmetallkomplexe von Aminoazirinen; II. Zur photochemisch induzierten Isomerisierung von 4-Aroyl-isoxazolen", *Dissertation*, Universität Zürich 1980.
[35] W. Altherr, H. Heimgartner, unpublished.
[36] I. Dannecker-Doerig, H. Heimgartner, unpublished.
[37] L. Ghosez, A. Demoulin, M. Henriet, E. Sonveaux, M. Van Meerssche, G. Germain, J.-P. Declercq, *Heterocycles 7* (1977) 895.
[38] C. Jenny, H. Heimgartner, *Helv. Chim. Acta 69* (1986) 374.
[39] L. Ghosez, P. Notté, C. Bernard-Henriet, R. Maurin, *Heterocycles 15* (1981) 1179.
[40] M. Sahebi: „Synthese β-Turn bildender Tetrapeptide aus α,α-disubstituierten α-Aminosäuren mittels der Azirin/Oxazolon-Methode", *Diplomarbeit*, Universität Zürich 1987.
[41] T. C. Gallagher, R. C. Storr, *Tetrahedron Lett. 22* (1981) 2905.
[42] a) G. J. de Voghel, T. L. Eggerichs, B. Clamot, H. G. Viehe, *Chimia 30* (1976) 191; b) J. Galloy, J.-P. Putzeys, G. Germain, J.-P. Declercq, M. Van Meerssche, *Acta Crystallogr. Sect. B30* (1974) 2462.
[43] H. Neunhoeffer, H. Ohl, *Chem. Ber. 111* (1978) 299.
[44] R. W. Saalfrank, M. Fischer, U. Wirth, H. Zimmermann, *Angew. Chem. 99* (1987) 1218; *Angew. Chem. Int. Ed. Engl. 26* (1987) 1160; R. W. Saalfrank, E. Ackermann, M. Fischer, U. Wirth, *Chem. Ber. 120* (1987) 2003.
[45] J. A. Hyatt, *J. Org. Chem. 46* (1981) 3953.
[46] C. Gilson, "Contribution à l'Etude Structurale des Azirines", *Mémoire Licencié*, Université Catholique de Louvain 1980.
[47] C. Jenny, R. Prewo, H. Heimgartner, unpublished.
[48] J. Galloy, J.-P. Declercq, M. Van Meerssche, *Cryst. Struct. Commun. 9* (1980) 151.
[49] L. M. Trefonas, R. J. Majeste in R. R. Gupta (Ed.): *Physical Methods in Heterocyclic Chemistry*, Wiley, New York 1984, p. 313.
[50] The nucleophilicity of the N(1) atom is demonstrated by the formation of *N*(1)-silyl and *N*(1)-trityl derivatives from reaction with trimethylsilyl-triflate and trityltetrafluoroborate respectively, [51] and by the existence of azirine-metal complexes coordinated through N(1) [52, 53].
[51] C. Bernard-Henriet, P. Hoet, L. Ghosez, R. Touillaux, *Tetrahedron Lett. 22* (1981) 4717.
[52] a) A. Hassner, C. A. Bunnell, A. Haltiwanger, *J. Org. Chem. 43* (1978) 57; b) P. S. dos S. Filho, L. A. Ortellado Zelada, U. Schuchardt, *Quimica Nova 1983*, 69.
[53] J. H. Bieri, S. Chaloupka, K. Dietliker, H. Heimgartner, unpublished; see also K. Dietliker, U. Schmid, G. Mukherjee-Müller, H. Heimgartner, *Chimia 32* (1978) 164.
[54] P. Hoet, "Etude de la Réactivité des Amino-2 Azirines-1", *Dissertation*, Université Catholique de Louvain 1975.
[55] The same trend is observed when 2,2-dimethyl-3-phenyl-2*H*-azirine (for which a pK_b of ca. 14 can be estimated [56]) is compared with acetophenone-*N*-methylimine ($pK_b = 6$ [54]).
[56] F. W. Fowler, A. Hassner, *J. Am. Chem. Soc. 90* (1968) 2875.
[57] H. Günzler, H. Böck: *IR-Spektroskopie*, Verlag Chemie, Weinheim 1975, p. 218.
[58] J. Lukáč, H. Heimgartner, *Helv. Chim. Acta 62* (1979) 1236.
[59] M. Schläpfer-Dähler: „Umsetzungen von 3-(Dimethylamino)-2,2-dimethyl-2*H*-azirin mit NH-aciden Heterocyclen", *Dissertation*, Universität Zürich 1990.
[60] H. Heimgartner, *Chimia 33* (1979) 111.
[61] H. Heimgartner, *Isr. J. Chem. 27* (1986) 3.
[62] a) K. Dietliker, W. Stegmann, H. Heimgartner, *Heterocycles 14* (1980) 929; b) R. W. Saalfrank, U. Wirth, *Chem. Ber. 122* (1989) 969; R. W. Saalfrank, E. Ackermann, M. Fischer, U. Wirth, H. Zimmermann, *Chem. Ber. 123* (1990) 115.
[63] A. Demoulin, H. Gorissen, A.-M. Hesbain-Frisque, L. Ghosez, *J. Am. Chem. Soc. 97* (1975) 4409.
[64] B. P. Chandrasekhar, U. Schmid, R. Schmid, H. Heimgartner, H. Schmid, *Helv. Chim. Acta 58* (1975) 1191.
[65] E. Schaumann, E. Kausch, W. Walter, *Chem. Ber. 108* (1975) 2500.
[66] U. Widmer, H. Heimgartner, H. Schmid, *Helv. Chim. Acta 61* (1978) 815; R. Prewo, J. H. Bieri, U. Widmer, H. Heimgartner, *ibid. 64* (1981) 1515.
[67] B. P. Chandrasekhar, H. Heimgartner, unpublished.
[68] E. Schaumann, S. Grabley, M. Henriet, L. Ghosez, R. Touillaux, J.-P. Declercq, G. Germain, M. Van Meerssche, *J. Org. Chem. 45* (1980) 2951.
[69] G. Mukherjee-Müller, H. Heimgartner, H. Schmid, *Helv. Chim. Acta 62* (1979) 1429; cf. also [58].
[70] S. Chaloupka, H. Heimgartner, *Chimia 32* (1978) 468; *Helv. Chim. Acta 62* (1979) 86; J. H. Bieri, R. Prewo, H. Heimgartner, *Chimia 36* (1982) 78.
[71] B. P. Chandrasekhar, H. Heimgartner, H. Schmid, *Helv. Chim. Acta 60* (1977) 2270.
[72] P. Vittorelli, H. Heimgartner, H. Schmid, P. Hoet, L. Ghosez, *Tetrahedron 30* (1974) 3737.
[73] D. Obrecht, H. Heimgartner, *Chimia 36* (1982) 78.
[74] H. Heimgartner, *Isr. J. Chem. 21* (1981) 151.
[75] E. Schaumann, E. Kausch, W. Walter, *Chem. Ber. 107* (1974) 3574.
[76] E. Schaumann, S. Grabley, K.-D. Seidel, E. Kausch, *Tetrahedron Lett. 1977* 1351; E. Schaumann, E. Kausch, J.-P. Imbert, K.-H. Klaska, R. Klaska, *J. Chem. Soc. Perkin Trans. 2 1977*, 466; E. Schaumann, E. Kausch, S. Grabley, H. Behr, *Chem. Ber. 111* (1978) 1486.
[77] S. Chaloupka, H. Heimgartner, H. Schmid, H. Link, P. Schönholzer, K. Bernauer, *Helv. Chim. Acta 59* (1976) 2566.
[78] E. Schaumann, S. Grabley, *Justus Liebigs Ann. Chem. 1978*, 1568; I. Handke, E. Schaumann, R. Ketcham, *J. Org. Chem. 53* (1988) 5298.
[79] E. Schaumann, S. Grabley, *Chem. Ber. 113* (1980) 934; E. Schaumann, S. Grabley, G. Adiwidjaja, *Liebigs. Ann. Chem. 1981*, 264.
[80] U. Schmid, H. Heimgartner, H. Schmid, P. Schönholzer, H. Link, K. Bernauer, *Helv. Chim. Acta 58* (1975) 2222; U. Schmid, H. Heimgartner, H. Schmid, W. E. Oberhänsli, *ibid. 59* (1976) 2768; U. Schmid, H. Heimgartner, H. Schmid, *ibid. 62* (1979) 160.
[81] E. Schaumann, E. Kausch, W. Walter, *Chem. Ber. 110* (1977) 820; E. Schaumann, H. Behr, G. Adiwidjaja, *Justus Liebigs Ann. Chem. 1979*, 1322.
[82] E. Schaumann, H. Mrotzek, *Tetrahedron 35* (1979) 1965; E. Schaumann, S. Grabley, *Liebigs Ann. Chem. 1981*, 290.
[83] F. Urech, *Justus Liebigs Ann. Chem. 164* (1872) 255.
[84] F. Tiemann, L. Friedländer, *Ber. Dtsch. Chem. Ges. 14* (1881) 1970; F. Tiemann, K. Köhler, *ibid. 14* (1881) 1976.
[85] F. Ehrlich, A. Wendel, *Biochem. Z. 8* (1908) 438.
[86] a) E. Fischer, R. von Grävenitz, *Justus Liebigs Ann. Chem. 406* (1914) 1; b) E. W. Tristram, J. ten Broeke, D. F. Reinhold, M. Sletzinger, D. E. Williams, *J. Org. Chem. 29* (1964) 2053; c) K. Harada, *Nature (London) 206* (1965) 1354.
[87] a) S. C. Chang, R. Charles, E. Gil-Av, *J. Chromatogr. 238* (1982) 29; b) H. Brückner, *Chromatographia 24* (1987) 725; H. Brückner, M. Langer, A. Esna-Ashari, A. Labudda, Z. J. Kaminski, M. T. Leplawy, R. Jöster in G. Lubec, G. A. Rosenthal (Eds.): *Amino Acids*, Escom, Leiden 1990, p. 159.
[88] a) U. Schöllkopf, *Top. Curr. Chem. 109* (1983) 65; *Pure Appl. Chem. 55* (1983) 1799; U. Schöllkopf, U. Busse, R. Lonsky, R. Hinrichs, *Liebigs Ann. Chem. 1986*, 2150; U. Schöllkopf, R. Hinrichs, R. Lonsky, *Angew. Chem. 99* (1987) 137; *Angew. Chem. Int. Ed. Engl. 26* (1987) 43; U. Schöllkopf, B. Hupfeld, S. Küper, E. Egert, M. Dyrbusch, *ibid. 100* (1988) 438 and *27* (1988) 433; U. Schöllkopf, D. Pettig, E. Schulze, M. Klinge, E. Egert, B. Benecke, M. Noltemeyer, *ibid. 100* (1988) 1238 and 27 (1988) 1194; b) D. Leibfritz, R. M. Brunne, T. Weihrauch, J. Stelten, E. T. K. Haupt, W-D. Stohrer, *Liebigs Ann. Chem. 1989*, 1017.
[89] a) D. Seebach, J. D. Aebi, R. Naef, Th. Weber, *Helv. Chim. Acta 68* (1985) 144; D. Seebach, A. Fadel, *ibid. 68* (1985) 1243; D. Seebach, T. Weber, R. Aeschimann, T. Maetzke, *ibid. 69* (1986) 1365; D. Seebach, J. D. Aebi, M. Gander-Coquoz, R. Naef, *ibid. 70* (1987) 1194; D. Seebach, M. Gander-Coquoz, *ibid. 71* (1988) 224; b) A. Fadel, J. Salaün, *Tetrahedron Lett. 28* (1987) 2243.
[90] a) F. Björkling, J. Boutelje, S. Gatenbeck, K. Hult, T. Norin, *Tetrahedron Lett. 26* (1985) 4975; b) J. Kamphuis, H. F. M. Hermes, J. A. M. van Balken, H. E. Schoemaker, W. H. J. Boesten, E. M. Meijer in G. Lubec, G. A. Rosenthal (Eds.): *Amino Acids*, Escom, Leiden 1990, p. 119.
[91] a) M. Kolb, J. Barth, *Liebigs Ann. Chem. 1983*, 1668; b) J. A. Bajgrowicz, B. Cossec, C. Pigière, R. Jacquier, P. Viallefont, *Tetrahedron Lett. 24* (1983) 3721; c) R. W. Woodard, P. K. Subramaniam, *Synth. Commun. 16* (1986) 337; d) G. I. Georg, X. Guan, J. Kant, *Tetrahedron Lett. 29* (1988) 403; e) J. F. Dellaria, Jr., B. D. Santarsiero, *ibid. 29* (1988) 6079.
[92] a) W. Steglich, H. Wegmann, *Synthesis 1980*, 418; b) G. C. Barrett, *Tetrahedron 36* (1980) 2023; c) R. W. Woodard, D. Kalvin, K. Ramalingam, *Synth. Commun. 15* (1985) 267; d) D. Seebach, R. Häner, *Chimia 39* (1985) 356; e) B. H. Lipshutz, B. Huff, W. Vaccaro, *Tetrahedron Lett. 27* (1986) 4241; f) J. Yaozhong, W. Shengde, Z. Changyou, *Synth. Commun. 16* (1986) 1479; g) G. Chipens, V. Slavinska, Dz. Sile, Dz. Kreile, A. Krikis, A. Strautina, A. Gutmanis, *Latv. P. S. R. Zinat. Akad. Vestis; Kim. Ser. 1986*, 647; h) S. J. B. Tendler, M. D. Threadgill, M. J. Tisdale, *J. Chem. Soc. Perkin Trans. 1 1987*, 2617; i) Y. Jiang, Y. Ma, Z. Chen, G. Li, *Yingyong Huaxue 4* (1987) 44, *Chem. Abstr. 107* (1987) 198 875; j) M. Suzuki, G. F. Orr, C. H. Stammer, *Bioorg. Chem. 15* (1987) 43; k) A. van der Werf, R. M. Kellogg, *Tetrahedron Lett. 29* (1988) 4981.
[93] a) H. R. Almond, D. T. Manning, C. Niemann, *Biochemistry 1* (1962) 243; b) M. Pankaskie, M. Abdel-Monem, *J. Med. Chem. 23* (1980) 121.
[94] J. Neugebauer, J. Morant (Eds.): *Arzneimittel-Kompendium der Schweiz 1985, Band 1*, Documed, Basel 1984, p. 1255.
[95] A. Arnone, P. D. Briley, P. H. Rogers, C. C. Hyde, C. M. Metzler in J. F. Griffin, W. L. Duax (Eds.): *Molecular Structure and Biological Activity*, Elsevier, New York 1981, p. 57.
[96] C. J. Abshire, M. Ostiguy, *J. Med. Chem. 19* (1976) 965.

[97] a) E. H. Flynn, J. W. Hinman, E. L. Caron, D. O. Woolf, Jr., *J. Am. Chem. Soc. 75* (1953) 5867; b) S. Hanessian, T. H. Haskell, *Tetrahedron Lett. 1964*, 2451.
[98] L. Banfi, M. G. Beretta, L. Colombo, C. Gennari, C. Scolastico, *J. Chem. Soc. Perkin Trans. 1 1983*, 1613.
[99] a) C. E. Meyer, F. Reusser, *Experientia 23* (1967) 85; b) R. Bosch, G. Jung, H. Schmitt, G. M. Sheldrick, W. Winter, *Angew. Chem. 96* (1984) 440; *Angew. Chem. Int. Ed. Engl. 23* (1984) 450.
[100] a) I. Wagner, H. Musso, *Angew. Chem. 95* (1983) 827; *Angew. Chem. Int. Ed. Engl. 22* (1983) 816; b) H. Brückner, G. J. Nicholson, G. Jung, K. Kruse, W. A. König, *Chromatographia 13* (1980) 209; R. Bosch, H. Brückner, G. Jung, W. Winter, *Tetrahedron 38* (1982) 3579; c) H. Brückner, M. Przybylski, I. Dietrich, I. Manz, *Biomed. Mass Spectrom. 11* (1984) 569.
[101] C. Toniolo, G. M. Bonora, A. Bavoso, E. Benedetti, B. di Blasio, V. Pavone, C. Pedone *Biopolymers 22* (1983) 205.
[102] a) G. Jung, H. Brückner, H. Schmitt in W. Voelter, G. Weitzel (Eds.): *Structure and Activity of Natural Peptides*, de Gruyter, Berlin 1981, p. 75; b) G. Boheim in A. Maelicke (Ed.): *Molecular Biology of Neuroreceptors and Ion Channels*, Springer, New York 1989, p. 401.
[103] W. Mayr, G. Jung, J. Strähle, *Justus Liebigs Ann. Chem. 1980*, 715.
[104] G. R. Marshall, H. E. Bosshard, N. C. E. Kendrick, J. Turk, T. M. Balasubramanian, S. M. H. Cobb, M. Moore, L. Leduc, P. Needleman in G. Loffet (Ed.): *Peptides 1976, Proc. 14th Eur. Pept. Symp.*, Editions de l'Université de Bruxelles, Brüssel 1976, p. 361.
[105] G. E. Schulz, R. H. Schirmer: *Principles of Protein Structure*, Springer, New York 1979.
[106] H.-D. Jakubke, H. Jeschkeit: *Aminosäuren, Peptide, Proteine*, Verlag Chemie, Weinheim 1982.
[107] The twofold substitution at C(2) severely restricts the conformational freedom of these amino acids and their derivatives [101, 108–113]. While the conformationally allowed areas for Ala in the Ramachandran diagram [114] still make up ~ 15% of the total area, for Aib this value is below 0.5% [115].
[108] Y. Paterson, S. M. Rumsey, E. Benedetti, G. Némethy, H. A. Scheraga, *J. Am. Chem. Soc. 103* (1981) 2947.
[109] E. Benedetti, C. Toniolo, P. Hardy, V. Barone, A. Bavoso, B. di Blasio, P. Grimaldi, F. Lelj, V. Pavone, C. Pedone, G. M. Bonora, I. Lingham, *J. Am. Chem. Soc. 106* (1984) 8146.
[110] a) B. V. V. Prasad, P. Balaram, *CRC Critical Rev. Biochem. 16* (1984) 307; b) R. Bardi, A. M. Piazzesi, C. Toniolo, M. Sukumar, P. Balaram, *Biopolymers 25* (1986) 1635; H. Balaram, M. Sukumar, P. Balaram, *ibid. 25* (1986) 2209.
[111] V. Barone, F. Lelj, A. Bavoso, B. di Blasio, P. Grimaldi, V. Pavone, C. Pedone, *Biopolymers 24* (1985) 1759.
[112] M. Mutter, *Angew. Chem. 97* (1985) 639; *Angew. Chem. Int. Ed. Engl. 24* (1985) 639; M. Mutter, E. Altmann, K.-H. Altmann, R. Hersperger, P. Koziej, K. Nebel, G. Tuchscherer, W. Vuilleumier, H.-U. Gremlich, K. Müller, *Helv. Chim. Acta 71* (1988) 835; M. Mutter, S. Vuilleumier, *Angew. Chem. 101* (1989) 551; *Angew. Chem. Int. Ed. Engl. 28* (1989) 535.
[113] C. Toniolo, *Br. Polym. J. 18* (1986) 221; C. Toniolo, E. Benedetti, *ISI Atlas of Science: Biochemistry 1988*, Institute of Scientific Information, Philadelphia 1988, p. 225.
[114] G. N. Ramachandran, V. Sasiskharan, *Adv. Protein Chem. 23* (1968) 282; C. M. Venkatachalan, G. N. Ramachandran, *Annu. Rev. Biochem. 38* (1969) 45.
[115] A. W. Burgess, S. J. Leach, *Biopolymers 12* (1973) 2599.
[116] a) G. R. Marshall, F. A. Gorin in M. Goodman, J. Meienhofer (Eds.): *Peptides, Proc. 5th Am. Pept. Symp.*, Wiley, New York 1978, p. 84; F. A. Gorin, T. M. Balasubramanian, T. Cicero, J. Schwietzer, G. R. Marshall, *J. Med. Chem. 23* (1980) 113; b) P. M. Hardy, A. Goldsmith, R. Cotton in U. Ragnarsson (Ed.): *Peptides 1984, Proc. 18th Eur. Pept. Symp.*, Almqvist and Wiksell, Stockholm 1984, p. 121; c) P. Cordopatis, D. Gatos, D. Theodoropoulos, J. Mizrahi, D. Regoli, E. Escher, *ibid.*, p. 349; d) Z. Prochazka, M. Lebl, T. Barth, J. Hlavacek, A. Tuka, M. Budesinsky, K. Jost, *Collect. Czech. Commun. 49* (1984) 642.
[117] a) F. R. Pfeiffer, P. A. Chambers, E. E. Hilbert, P. W. Woodward, D. M. Ackerman, *J. Med. Chem. 27* (1984) 325; b) R. Kishore, P. Balaram, *Indian J. Chem. Sect. B 23* (1984) 1137; M. Sukumar, P. A. Raj, P. Balaram, E. L. Becker, *Biochem. Biophys. Res. Commun. 128* (1985) 339.
[118] a) M. L. Moore, G. R. Marshall, F. Stassen, J. Stefankiewicz, L. Sulat, D. Schmidt, L. Kinter, J. McDonald, D. Ashton-Shue in C. M. Deber, V. J. Hruby, K. D. Kopple (Eds.): *Peptides, Structure and Function, Proc. 9th Am. Pept. Symp.*, Pierce, Rockford 1985, p. 607; b) M. Goodman, *Biopolymers 24* (1985) 137.
[119] a) R. Oekonomopulos, G. Jung, *Biopolymers 19* (1980) 203; T. Butters, P. Hütter, G. Jung, N. Pauls, H. Schmitt, G. M. Sheldrick, W. Winter, *Angew. Chem. 93* (1981) 904; *Angew. Chem. Int. Ed. Engl. 20* (1981) 889; R. Bosch, G. Jung, H. Schmitt, W. Winter, *Biopolymers 24* (1985) 961, 979; K. P. Voges, G. Jung, W. H. Sawyer, *Biochim. Biophys. Acta 896* (1987) 64; H. Vogel, L. Nilsson, R. Rigler, K. P. Voges, G. Jung, *Proc. Natl. Acad. Sci. USA 85* (1988) 5067; b) M. Narita, M. Doi, H. Sugasawa, K. Ishikawa, *Bull. Chem. Soc. Jpn. 58* (1985) 1473, 1731; M. Narita, J. Y. Chen, H. Sato, Y. Kim, *ibid. 58* (1985) 2494.
[120] a) R. Bosch, G. Jung, K. P. Voges, W. Winter, *Liebigs Ann. Chem. 1984*, 1117; R.-P. Hummel, C. Toniolo, G. Jung, *Angew. Chem. 99* (1987) 1180; *Angew. Chem. Int. Ed. Engl. 26* (1987) 1150; G. Valle, M. Crisma, C. Toniolo, R. Beisswenger, A. Rieker, G. Jung, *J. Am. Chem. Soc. 111* (1989) 6828; b) J. R. Cann, R. E. London, C. J. Unkefer, R. J. Vavrek, J. M. Stewart, *Int. J. Pept. Protein Res. 29* (1987) 486.
[121] P. Wipf, H. Heimgartner, *Helv. Chim. Acta 71* (1988) 258; P. Wipf, R. W. Kunz, R. Prewo, H. Heimgartner, *ibid. 71* (1988) 268.
[122] M. Sahebi, P. Wipf, H. Heimgartner, *Tetrahedron 45* (1989) 2999.
[123] V. J. Hruby in A. Eberle, R. Geiger, T. Wieland (Eds.): *Perspectives in Peptides Chemistry*, Karger, Basel 1981, p. 207.
[124] S. Chaloupka, H. Heimgartner, unpublished.
[125] However, such an attack on the S atom is observed in the smooth reaction of **2a** with tosyl chloride, which, in analogy to the reactions with carboxylic acid chlorides, affords N^1,N^1,2-trimethyl-N^2-tosylacrylamidine [65].
[126] S. Chaloupka, P. Vittorelli, H. Heimgartner, H. Schmid, H. Link, K. Bernauer, W. E. Oberhänsli, *Helv. Chim. Acta 60* (1977) 2476.
[127] A. Rahm, B. R. Vincent, H. Heimgartner, B. Schulze, M. Mühlstädt, *Helv. Chim. Acta*, in press.
[128] B. Hostettler, J. P. Obrecht, R. Prewo, J. H. Bieri, H. Heimgartner, *Helv. Chim Acta 69* (1986) 298.
[129] S. M. Ametamey, H. Heimgartner, *Helv. Chim. Acta 73* (1990) 1314.
[130] B. Scholl, J. H. Bieri, H. Heimgartner, *Helv. Chim. Acta 61* (1978) 3050.
[131] M. Schläpfer-Dähler, R. Prewo, J. H. Bieri, H. Heimgartner, *Heterocycles 22* (1984) 1667.
[132] M. Schläpfer-Dähler, R. Prewo, J. H. Bieri, G. Germain, H. Heimgartner, *Chimia 42* (1988) 25.
[133] M. Los, *ACS Symp. Ser. 255* (1984) 29; M. Los, Amer. Cyanamid Co., US Pat. 4 188 487 (1980); 4 221 586 (1980); Eur. Pat. 133 309 (1985); *Chem. Abstr. 92* (1980) 180 836; *94* (1981) 1070; *103* (1985) 87 872.
[134] J. P. Obrecht, P. Schönholzer, C. Jenny, R. Prewo, H. Heimgartner, *Helv. Chim. Acta 71* (1988) 1319.
[135] M. Dähler, R. Prewo, J. H. Bieri, H. Heimgartner, *Helv. Chim. Acta 66* (1983) 1456.
[136] M. Schläpfer-Dähler, J. H. Bieri, H. Heimgartner, *Chimia 38* (1984) 316.
[137] G. Mukherjee-Müller, S. Chaloupka, H. Heimgartner, H. Schmid, H. Link, K. Bernauer, P. Schönholzer, J. J. Daly, *Helv. Chim. Acta 62* (1979) 768.
[138] M. Dähler, R. Prewo, J. H. Bieri, H. Heimgartner, *Helv. Chim. Acta 65* (1982) 2302.
[139] B. P. Chandrasekhar, J. H. Bieri, H. Heimgartner, G. Germain, J.-P. Declercq, *Heterocycles 19* (1982) 2079.
[140] D. J. Brown, S. F. Manson: *The Pyrimidines, Vol. 16* of A. Weissberger (Ed.): *The Chemistry of Heterocyclic Compounds*, Wiley, New York 1962, p. 472.
[141] H. Link, K. Bernauer, S. Chaloupka, H. Heimgartner, H. Schmid, *Helv. Chim. Acta 61* (1978) 2116.
[142] S. Chaloupka, J. H. Bieri, H. Heimgartner, *Helv. Chim. Acta 63* (1980) 1797.
[143] F. Stierli, H. Heimgartner, unpublished.
[144] S. M. Ametamey, R. Prewo, J. H. Bieri, H. Heimgartner, J. P. Obrecht, *Helv. Chim. Acta 69* (1986) 2013.
[145] S. M. Ametamey, H. Heimgartner, *Helv. Chim. Acta 73* (1990) 594.
[146] S. M. Ametamey, H. Heimgartner, *Helv. Chim. Acta 73* (1990) 599.
[147] R. Prewo, J. H. Bieri, H. Heimgartner, *Chimia 39* (1985) 354; S. M. Ametamey, B. R. Vincent, H. Heimgartner, *Helv. Chim. Acta 73* (1990) 492.
[148] J. M. Villalgordo, B. R. Vincent, H. Heimgartner, *Helv. Chim. Acta 73* (1990) 959.
[149] S. Chaloupka, H. Heimgartner, *Chimia 32* (1978) 332.
[150] D. Obrecht: „3-Amino-2*H*-azirine als Aminosäure-Äquivalente in der Organischen Synthese", *Dissertation*, Universität Zürich 1983.
[151] H. Heimgartner, *Croat. Chem. Acta 59* (1986) 237; S. Pekcan, H. Heimgartner, *Helv. Chim Acta 71* (1988) 1673; P. Tromm, H. Heimgartner, *ibid. 71* (1988) 2071.
[152] P. Wipf, C. Jenny, H. Heimgartner, *Helv. Chim. Acta 70* (1987) 1001.
[153] H. Link, *Helv. Chim. Acta 61* (1978) 2419.
[154] M. T. Leplawy, D. S. Jones, G. W. Kenner, R. C. Sheppard, *Tetrahedron 11* (1960) 39.
[155] W. König, R. Geiger, *Chem. Ber. 103* (1970) 788.
[156] a) M. Bodansky in E. Gross, J. Meienhofer (Eds.): *The Peptides*, Academic, London 1979, p. 143; b) D. H. Rich, J. Singh, *ibid.* p. 256.
[157] H. Schmitt, G. Jung, *Liebigs Ann. Chem. 1985*, 321, 345.
[158] R. B. Merrifield, *Angew. Chem. 97* (1985) 801; *Angew. Chem. Int. Ed. Engl. 24* (1985) 799.
[159] H. Brückner, W. A. König, M. Greiner, G. Jung, *Angew. Chem. 91* (1979) 508; *Angew. Chem. Int. Ed. Engl. 18* (1979) 476.
[160] E. Katz, H. Schmitt, M. Aydin, W. A. König, G. Jung, *Liebigs Ann. Chem. 1985*, 365.

[161] N. Dubischar, Dissertation, Toledo University 1976; N. C. E. Kendrick, Dissertation, University of Washington, DC 1973.
[162] B. Rzeszotarska, E. Taschner in L. Zervas (Ed.): *Proc. 6th Eur. Pept. Symp. 1963*, Pergamon Press, Oxford 1966, p. 135.
[163] M. Bodansky, *Principles of Peptide Synthesis*, Springer, Berlin 1984.
[164] H. Heimgartner in R. Vlahov (Ed.): *Synthesis of Biologically Active Natural Products, Proc. 5th Int. Conf. on Chem. and Biotechnol. of Biologically Active Natural Products 1989*, Bulgarian Academy of Sciences, Sofia 1989, p. 1.
[165] H. Heimgartner in G. Lubec, G. A. Rosenthal (Eds.): *Amino Acids*, Escom, Leiden 1990, p. 29.
[166] D. Obrecht, H. Heimgartner, *Helv. Chim. Acta 64* (1981) 482; *70* (1987) 102.
[167] I. Ugi in E. Gross, J. Meienhofer (Eds.): *The Peptides*, Vol. 2, Academic, New York 1980, p. 365; R. Urban, D. Marquarding, I. Ugi in E. Gross, J. Meienhofer (Eds.): *Peptides, Structure and Biological Function, Proc. 6th Am. Pept. Symp.*, Pierce, Rockfort 1979, p. 727.
[168] P. Wipf, H. Heimgartner, *Helv. Chim. Acta 70* (1987) 354.
[169] D. S. Jones, G. W. Kenner, J. Preston, R. C. Sheppard, *J. Chem. Soc. 1965*, 6227.
[170] M. Narita, K. Ishikawa, K. Kudo, T. Endo, *Bull. Chem. Soc. Jpn. 58* (1985) 3125.
[171] P. Wipf, H. Heimgartner, *Helv. Chim. Acta 69* (1986) 1153.
[172] G. W. Anderson, J. E. Zimmerman, F. M. Callahan, *J. Am. Chem. Soc. 89* (1967) 5012.
[173] T. Miyazawa, T. Otomatsu, T. Yamada, S. Kuwata in E. Munekata (Ed.): *Peptide Chemistry 1983*, Protein Research Foundation, Osaka 1984, p. 71.
[174] H.-D. Jakubke, C. Klessen, E. Berger, K. Neubert, *Tetrahedron Lett. 1978*, 1497.
[175] P. Wipf, H. Heimgartner, *Helv. Chim. Acta 71* (1988) 140.
[176] K. Poduska, K. Slama, M. Zaoral, F. Šorm, Czech. Pat. 164370 (1976) *Chem. Abstr. 86* (1977) 155989.
[177] a) H. Rembold, *Chimia 39* (1985) 348; b) L. Borowiecki, A. Kazubski, E. Reca, W. Wodzki, *Liebigs Ann. Chem. 1985*, 929; L. Borowiecki, A. Kazubski, E. Reca, *ibid. 1986*, 1428.
[178] The derivative obtained on exchanging the Ile residue in Ile-Ala-benzocain for a chloroisobutyryl group hinders the metamorphosis of insect larvae of the family Pyrrhocoridae(see [106], p. 357).
[179] D. Obrecht, H. Heimgartner, *Helv. Chim. Acta 70* (1987) 329; *Tetrahedron Lett. 24* (1983) 1921.
[180] M. Dobler, *Ionophores and Their Structures*, Wiley, New York 1981.
[181] M. K. Das, S. Raghothama, P. Balaram, *Biochemistry 25* (1986) 7110.
[182] H. Brückner, M. Przybylski, *J. Chromatogr. 296* (1984) 263.
[183] a) B. T. Chait, B. F. Gisin, F. H. Field, *J. Am. Chem. Soc. 104* (1982) 5157; b) R. O. Fox, Jr., F. M. Richards, *Nature (London) 300* (1982) 325; c) D. G. Davis, A. Bax, *J. Am. Chem. Soc. 107* (1985) 2820.
[184] R. C. Pandey, H. Meng, J. C. Cook, K. L. Rinehart, *J. Am. Chem. Soc. 99* (1977) 5203.
[185] R. C. Pandey, J. C. Cook, K. L. Rinehart, *J. Am. Chem. Soc. 99* (1977) 5205.
[186] T. Fujita, Y. Takaishi, K. Matsuura, Y. Takeda, Y. Yoshioka, H. Brückner, *Chem. Pharm. Bull. 32* (1984) 2870.
[187] E. Katz, M. Aydin, N. Lucht, W. A. König, T. Ooka, G. Jung, *Liebigs Ann. Chem. 1985*, 1041.
[188] B. Bodo, S. Rebuffat, M. El Hajji, D. Davoust, *J. Am. Chem. Soc. 107* (1985) 6011.
[189] a) P. Müller, D. O. Rudin, *Nature (London) 217* (1968) 713; b) G. Boheim, G. Irmscher, G. Jung, *Biochem. Biophys. Acta 507* (1978) 485; G. Boheim, W. Hanke, *Biophys. Struct. Mech. 9* (1983) 181; W. Hanke, C. Methfessel, H.-U. Wilmsen, E. Katz, G. Jung, G. Boheim, *Biochem. Biophys. Acta 727* (1983) 108.
[190] M. J. Thirumalacher, *Hind. Antibiot. Bull. 10* (1968) 287.
[191] S. Krishnaswamy, V. Pattabhi, *Indian. J. Biochim. Biophys. 24* (1987) 1.
[192] a) D. Perlman, M. Bodansky, *Annu. Rev. Biochem. 40* (1971) 499; b) H. Kleinkauf, H. Koischwitz, *Prog. Mol. Subcell. Biol. 6* (1978) 59.
[193] a) B. F. Gisin, D. G. Davis, Z. K. Borowska, J. E. Hall, S. Kobayashi, *J. Am. Chem. Soc. 103* (1981) 6373; b) T. M. Balasubramanian, N. C. E. Kendrick, M. Taylor, G. R. Marshall, J. E. Hall, I. Vodyanoy, F. Reusser, *ibid. 103* (1981) 6127; c) R. Nagaraj, P. Balaram, *Tetrahedron 37* (1981) 1263.
[194] P. Wipf, H. Heimgartner, *Helv. Chim. Acta 73* (1990) 13.
[195] W. Altherr: „Verwendung von 3-Amino-2*H*-azirinen in der Peptidsynthese; Synthese von Fragmenten des Antibiotikums Trichotoxin A-50 (G)", *Diplomarbeit*, Universität Zürich, 1988.
[196] Even at low temperatures and with a large excess of a racemic 3-amino-2*H*-azirine **2**, no pronounced diastereoselectivity could be seen in the coupling with Z-amino acids and Z-dipeptides.[197] It has not yet been possible to synthesize enantiomerically pure 3-amino-2*H*-azirines.
[197] B. Grossmann, H. Heimgartner, unpublished.
[198] P. Blaser: „Synthese des (1–9)-Fragments des Antibiotikums Antiamöbin unter Verwendung von 3-Amino-2*H*-azirinen als Synthone für α,α-disubstituierte α-Aminosäuren", *Diplomarbeit*, Universität Zürich 1990.
[199] D. Obrecht, B. Scholl, H. Heimgartner, *Helv. Chim. Acta 68* (1985) 465.
[200] M. Rothe, K. Steffen, I. Rothe, *Angew. Chem. 77* (1965) 347; *Angew. Chem. Int. Ed. Engl. 4* (1965) 356; W. Mästle, M. Rothe in G. Kupryszewski (Ed.): *Peptides 1978*, Wroclaw University Press 1979, p. 179.
[201] M. Rothe, M. Fähnle, S. Wermuth in U. Ragnarsson (Ed.): *Peptides 1984 18th Eur. Pept. Symp.*, Almqvist and Wiksell, Stockholm 1984, p. 573.
[202] J. Pastuszak, J. H. Gardner, J. Singh, D. H. Rich, *J. Org. Chem. 47* (1982) 2982; cf. also U. Schmidt, T. Beuttler, A. Lieberknecht, H. Griesser, *Tetrahedron Lett. 24* (1983) 3573.
[203] A. Closse, R. Huguenin, *Helv. Chim. Acta 57* (1974) 533.
[204] D. Obrecht, H. Heimgartner, *Helv. Chim. Acta 67* (1984) 526.
[205] E. Schröder, K. Lübke, *Experientia 19* (1963) 57.
[206] a) H. A. James in D. H. Hey, D. I. John (Eds.): *MTP Int. Rev. Sci. Org. Chem. Ser. One, Vol. 6*, Butterworths, London 1973, p. 213; b) Yu. A. Ovchinnikov, A. V. T. Ivanov in H. N. Rydon (Ed.): *MTP Int. Rev. Sci. Org. Chem. Ser. Two, Vol. 6*, Butterworths, London 1976, p. 219.
[207] D. Obrecht, H. Heimgartner, *Helv. Chim. Acta 73* (1990) 221.
[208] H. A. Staab, W. Rohr, A. Mannschreck, *Angew. Chem. 73* (1961) 143.
[209] D. Obrecht, H. Heimgartner, *Tetrahedron Lett. 25* (1984) 1717.
[210] P. Ruggli, *Justus Liebigs Ann. Chem. 392* (1912) 92; *399* (1913) 174; *412* (1917) 1; K. Ziegler, H. Eberle, H. Ohringer, *ibid. 504* (1933) 94; K. Ziegler in Houben-Weyl-Müller (Ed.): *Methoden der Organischen Chemie, Band 4/II*, Thieme, Stuttgart 1955, p. 758.
[211] U. Schmidt, *Nachr. Chem. Tech. Lab. 37* (1989) 1034.
[212] M. Kondo, M. Kimura, K. Sato, H. Horimoto, *Bull. Chem. Soc. Jpn. 60* (1987) 1391.
[213] U. Schmidt, D. Weller, A. Holder, A. Lieberknecht, *Tetrahedron Lett. 29* (1988) 3227; D. A. Evans, J. A. Ellman, *J. Am. Chem. Soc. 111* (1989) 1063.
[214] M. Rothe in G. Jung, E. Bayer (Eds.): *Proc. 20th Eur. Pept. Symp., Tübingen 1988*, de Gruyter, Berlin 1988.
[215] J. Kovacs in E. Gross, J. Meienhofer (Eds.): *The Peptides, Vol. 2*, Academic, New York 1980, p. 485; cf. also R. M. Wenger, *Helv. Chim. Acta 67* (1984) 502.
[216] S. F. Brady, R. M. Freidinger, W. J. Paleveda, C. D. Colton, C. F. Homnick, W. L. Whitter, P. Curley, R. F. Nutt, D. F. Veber, *J. Org. Chem. 52* (1987) 764.
[217] I. Dannecker-Doerig, B. R. Vincent, H. Heimgartner, unpublished.
[218] F. Stierli: „I. Anwendung der selektiven Amidspaltung zur Racematspaltung von Aminosäuren; II. Synthese und Reaktionen von 2-Amino-1-azetinen", *Dissertation*, Universität Zürich 1986.
[219] F. Stierli, D. Obrecht, H. Heimgartner, *Chimia 38* (1984) 432; F. Stierli, R. Prewo, J. H. Bieri, H. Heimgartner, *ibid. 38* (1984) 435.
[220] W. C. Still, M. Kahn, A. Mitra, *J. Org. Chem. 43* (1978) 2923.

Pulsed Electron Spin Resonance Spectroscopy: Basic Principles, Techniques, and Examples of Applications

New Analytical Methods (43)

By Arthur Schweiger*

Electron spin resonance (ESR) spectroscopy has recently undergone a major innovative advance, which is described by the magical phrase *pulsed ESR*. To the spectroscopist who rubs this Aladdin's lamp there now opens up the mysterious world of spin acrobatics with its many novel and surprising phenomena. The use of pulse techniques makes it possible to reduce measurement times, increase sensitivity, improve resolution and simplify spectra. This article describes the most important pulse techniques used in ESR spectroscopy. Mathematical descriptions are kept to a minimum, space being devoted instead to examples of applications in various areas of chemical research.

1. Introduction

Today, ESR spectroscopy counts among the most important methods for investigating the structure and dynamics of paramagnetic compounds.[1-4] It is very sensitive and specific and has therefore been used with great success for many years in chemistry, physics, biology, and mineralogy.

Until recently the conventional CW (continuous wave) methods of measurement prevailed in ESR spectroscopy. This contrasts with the situation in applied NMR spectroscopy, where the CW methods have been almost entirely superseded by an impressive variety of elegant pulse methods.[5,6] Although pulse methods were introduced in ESR spectroscopy at about the same time as in NMR, for nearly thirty years this field of work has only been seriously followed by a very small number of research groups.[7,8] This initial reluctance is probably explained by the expensive instrumentation needed and the lack of sufficiently fast digital electronics. However, the situation has changed radically within the last few years. Pulsed ESR spectroscopy is a field of research which has now emerged from its former shadowy existence and is undergoing extraordinarily rapid development.[9-22] One can now build a pulsed ESR spectrometer using components that are mostly commercially available.[10,23-29] A fully developed commercial instrument has recently come onto the market.[30]

There is now scarcely a single topic area of ESR spectroscopy that is not ripe for being permanently affected by the various pulse methods. Techniques of particular importance include time-resolved ESR spectroscopy,[31-33] methods for measuring relaxation times,[9,13,34,35] techniques for studying molecular motions,[9] electron-electron double resonance,[36-41] electron-nuclear double resonance,[42-45] and ESR imaging.[46-49]

This account begins with a short description of CW ESR spectroscopy (Section 2). It aims to remind the reader of the physical basis of electron spin resonance and to provide the background knowledge needed for the sections that follow. The next two sections give a systematic survey of the most important pulsed ESR methods. Section 3 introduces the basic features of pulsed ESR spectroscopy and explains these principles in greater detail with the help of some examples of applications. Section 4 describes a number of pulsed ESR techniques that have been developed only recently, and whose applications potential has not yet been fully exploited. These include both methods that have been adapted from nuclear magnetic resonance and others that specifically take into account the special requirements of ESR.

[*] Priv.-Doz. Dr. A. Schweiger
Laboratorium für Physikalische Chemie
ETH-Zentrum
CH-8092 Zürich (Switzerland)

2. CW Methods in Electron Spin Resonance

2.1. Conventional ESR Spectroscopy

The ESR spectrum of a paramagnetic compound in an external magnetic field B_0 can be described by a Hamiltonian of the form (1).[1-4] The electronic Zeeman operator $\mathcal{H}_{EZ}$

$$\mathcal{H} = \mathcal{H}_{EZ} + \mathcal{H}_F + \mathcal{H}_{HFS} + \mathcal{H}_Q + \mathcal{H}_{NZ} \quad (1)$$

includes the interaction of the electron spin with the external field $\boldsymbol{B}_0$. As the Zeeman energy can also be affected by orbital magnetic moments, the term $\mathcal{H}_{EZ}$ often yields information about excited electronic states and about the symmetry of the environment of a paramagnetic center. The fine structure term $\mathcal{H}_F$ describes the interaction between two or more electron spins, e.g. in triplet states or in compounds containing transition metal ions. The term $\mathcal{H}_{HFS}$ describes the hyperfine interaction between the electron spin and the nuclear spins. Here a distinction is made between the isotropic coupling (Fermi contact term), which arises from the finite probability of the electron being located at the position of the nucleus, and the anisotropic dipolar coupling, which includes the interaction between the magnetic moments of the electron and of the nucleus. The terms $\mathcal{H}_Q$ and $\mathcal{H}_{NZ}$ describe the nuclear quadrupolar energy and the nuclear Zeeman energy respectively. These two quantities are of secondary importance in ESR spectroscopy, since they generally cause only very small shifts in the resonance frequencies.

The static variables specified in Equation (1) contain a wealth of information about the geometrical and electronic structure of a paramagnetic compound.

In the following we consider a simple model system consisting only of one electron spin and one nucleus with spin

$I = 1/2$. The distance between the nucleus and the electron, which is regarded as a point charge, is assumed to be $r = 0.26$ nm, the isotropic coupling is given by $a_{iso}/2\pi = 6$ MHz, and the line joining the electron and the nucleus is assumed to be inclined at an angle θ to the direction of the external field $\boldsymbol{B}_0$ (Fig. 1a). We can further assume, without loss of generality, that the nucleus lies in the xz plane of the laboratory coordinate system. In this article we shall return frequently to this model system in explaining the various techniques.

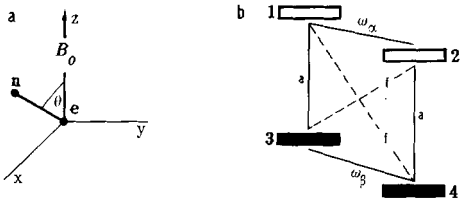

Fig. 1. a) Parameters describing the model system used frequently in this article, consisting of an electron spin (e) and a nucleus with spin $I = 1/2$ (n). x, y, z is the laboratory coordinate system. b) Four-level scheme showing the two allowed ESR transitions (a) and the two forbidden ESR transitions (f), and the NMR (ENDOR) frequencies ω_α and ω_β.

The Hamiltonian for an isotropic g-tensor (expressed in angular frequencies) then has the form (2) in which the elec-

$$\begin{aligned}\mathcal{H} &= \mathcal{H}_{EZ} + \mathcal{H}_{HFS} + \mathcal{H}_{NZ} \\ &= \omega_S S_z + A S_z I_z + B S_z I_x - \omega_I I_z,\end{aligned} \tag{2}$$

tron and nuclear Zeeman frequencies are $\omega_s = g_e\beta_e B_0/\hbar$ and $\omega_I = g_n\beta_n B_0/\hbar$ respectively, and the quantities A and B are defined as in (3).

$$A = A_\parallel \cos^2\theta + A_\perp \sin^2\theta, \quad B = (A_\parallel - A_\perp)\sin\theta\cos\theta \tag{3}$$

The quantities $A_\parallel = A_\parallel^d + a_{iso}$ and $A_\perp = A_\perp^d + a_{iso}$ in (3) describe the principal axis values of the axially symmetric hyperfine tensor with the dipolar components $A_\parallel^d$ and $A_\perp^d$.

In the corresponding energy level scheme (Fig. 1b) four ESR transitions can be distinguished: two "allowed" transitions (ω_{13}, ω_{24}) in which only the magnetic quantum number m_S changes ($\Delta m_S = \pm 1$, $\Delta m_I = 0$), and two "forbidden" transitions (ω_{23}, ω_{14}) for which $\Delta m_S = \pm 1$ and $\Delta m_I = \pm 1$. The corresponding ESR frequencies are collected in (4),[50]

$$\begin{aligned}\omega_{13} &= \omega_S - \omega_-/2 \\ \omega_{24} &= \omega_S + \omega_-/2 \\ \omega_{23} &= \omega_S - \omega_+/2 \\ \omega_{14} &= \omega_S + \omega_+/2\end{aligned} \tag{4}$$

in which $\omega_+ = \omega_\alpha + \omega_\beta$, $\omega_- = \omega_\alpha - \omega_\beta$, the nuclear frequencies ω_α and ω_β being given by:

$$\begin{aligned}\omega_\alpha &= \left[\left(\frac{A}{2} - \omega_I\right)^2 + \left(\frac{B}{2}\right)^2\right]^{1/2} \\ \omega_\beta &= \left[\left(\frac{A}{2} + \omega_I\right)^2 + \left(\frac{B}{2}\right)^2\right]^{1/2}\end{aligned} \tag{5}$$

From the transition probabilities for the allowed (I_a) and forbidden (I_f) ESR transitions, which are given by the expressions in (6) with $\sin\varphi_\alpha = B/\omega_\alpha$ and $\sin\varphi_\beta = B/\omega_\beta$, it follows that the "forbidden" transitions can only take place if the quantity B [see (3)] differs from zero.

$$\begin{aligned}I_a &= \cos^2[(\varphi_\alpha + \varphi_\beta)/2] \\ I_f &= \sin^2[(\varphi_\alpha + \varphi_\beta)/2]\end{aligned} \tag{6}$$

The ESR spectrum of our model system with $\theta = 45°$ is shown in Figure 2a. Here it is assumed, as is usual in ESR spectroscopy, that the field B_0 is varied while the frequency ω_{mw} of the irradiating field, which lies in the microwave (mw) region, is held constant ($\omega_{mw}/2\pi = 9.2$ GHz). The hyperfine splitting[*] $a = \omega_-$ of the two allowed transitions, expressed in frequency units, is 8 MHz for the chosen geometry, whereas the frequency difference between the two forbidden lines is about $2\omega_I/2\pi = 28$ MHz. Owing to the large line widths it is seldom possible to observe forbidden transitions in an ESR spectrum; however, they provide the basis for several important pulsed ESR techniques.

In a disordered system such as a powder or a frozen solution, the ESR spectrum consists of a superposition of the spectra arising from all possible orientations of the electron-

[*] The splitting of ESR signals caused by the hyperfine coupling is customarily referred to as the hyperfine splitting, despite the fact that in the solid phase the quantity a also includes a contribution from the nuclear Zeeman interaction.

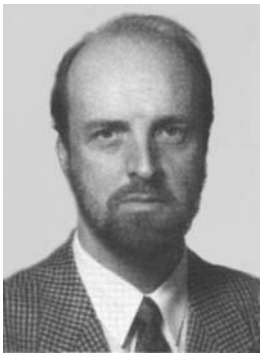

Arthur Schweiger was born in Zürich, Switzerland, in 1946 and studied physics at the Swiss Federal Institute of Technology (ETH) in Zürich. He received his Ph.D. under the guidance of Hans Günthard at the ETH in 1976. From 1976 he was Oberassistent in the Laboratory of Physical Chemistry at ETH, where he habilitated in 1982. In 1985, he was awarded the Werner Prize of the Swiss Chemical Society. His major fields of interest are the development of new methods in ESR spectroscopy and the application of ESR in coordination chemistry.

nucleus axis relative to the field vector B_0. In calculating the powder spectrum shown in Figure 2b an axially symmetric g-tensor was used. The hyperfine coupling is only resolved in the case where B_0 is along the direction of the principal axis $A_{\parallel}$. Furthermore, in Figure 2b the ESR spectrum is shown as the first derivative of the absorption signal, which is the usual convention with the CW method of recording.

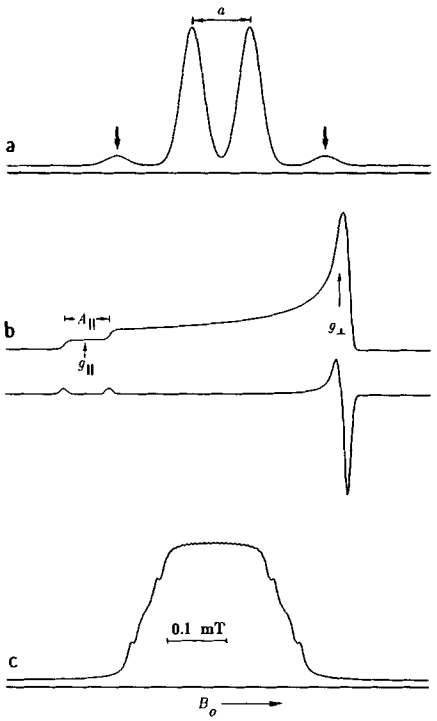

Fig. 2. Typical ESR spectra. a) Single crystal ESR spectrum with two allowed and two forbidden transitions (the two forbidden transitions are indicated by arrows). b) Powder ESR spectrum (absorption spectrum (top) and first derivative (bottom)) of the model system (Fig. 1a) with an axially symmetric g-tensor ($g_{\parallel} = 2.02, g_{\perp} = 2.00$; the g-tensor and the hyperfine tensor are coaxial, the rest of the parameters are as in the model system). c) ESR spectrum of an isotropic system (e.g. in solution), consisting of six nuclei with spin $I = 1/2$ and hyperfine coupling constants $a = 1$, 1.5, 2, 3, 4 and 8 MHz. The 64 signals are not resolved.

Usually the unpaired electron is surrounded by a large number of magnetic nuclei. Since the number of lines increases multiplicatively with the number of magnetic nuclei as a consequence of the ESR selection rules, usually only a small number of hyperfine interactions are resolved in the ESR spectrum. This is illustrated in Figure 2c for the example of a spin system with six nuclei each with $I = 1/2$ (number of lines $= 2^6 = 64$). The spectrum consists of one peak with almost no structure. Inhomogeneously broadened spectra of this sort are, unfortunately, the general rule in solids. This unsatisfactory situation is often made even worse by additional broadening mechanisms, for example the so-called strain effect.[51]

2.2. Electron-Nuclear Double Resonance Spectroscopy

Electron-nuclear double resonance (ENDOR) spectroscopy offers a way around this problem by giving a dramatic increase in resolution.[52-59] The success of the ENDOR method depends on being able to saturate one of the ESR lines with an intense MW field. A second irradiating field in the radiofrequency region induces nuclear spin transitions, thereby altering the populations of the energy levels, and this change is detected by observing changes in the polarization of the saturated ESR transition. Thus, in the ENDOR technique the NMR spectrum in the two m_S states of a paramagnetic compound is measured indirectly via the electron spin. The ENDOR spectrum of our model system with $\theta = 45°$ is shown in Figure 3a. The two resonance lines at ω_{α} and ω_{β} again show a splitting of $a = \omega_{-}$.

As a result of the different selection rules the number of lines now only increases in an additive (linear) way with the number of nuclei. This means that even in complex spin systems with many nuclei the ENDOR spectrum is usually still quite simple. For example, the ENDOR spectrum of the spin system with six nuclei consists of only $2 \times 6 = 12$ lines (Fig. 3b). Moreover, in the solid phase the quadrupolar couplings for nuclei with spin $I \geq 1$, i.e. those described by the operator $\mathcal{H}_Q$, are observed directly as splittings of the lines. It is therefore hardly surprising that ENDOR spectroscopy, with its extensive armory of special techniques,[54-56, 60] has developed into one of the most important methods of electron spin resonance. This method is always used in cases where poor resolution makes it impossible to determine the magnetic parameters from the ESR spectrum.

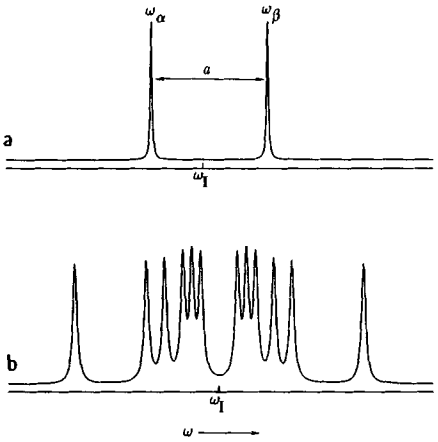

Fig. 3. a) Single crystal ENDOR spectrum of the model system (Fig. 1a). b) ENDOR spectrum of the system defined in Figure 2c. All six hyperfine couplings are resolved.

3. Summary of the Standard Procedures Used in Pulsed ESR Spectroscopy

In this section the standard techniques of pulsed ESR spectroscopy are described with the help of clear and simple vector diagrams. For a more rigorous mathematical description the reader is referred to several review articles and monographs.[5, 7, 9, 12]

3.1. Fourier Transform ESR Spectroscopy

3.1.1. Basic Principles

In an external magnetic field electron spins can assume either a parallel orientation (α state) or an antiparallel orientation (β state). The β state, which is lower in energy, has a larger population than the α state as a consequence of the equilibrium distribution, and this causes a macroscopic magnetization M_z to become established in the direction parallel to B_0. The behavior of this magnetization during a pulsed ESR experiment can be most easily described using a coordinate system which rotates with the frequency ω_{mw}. For this purpose the linearly polarized MW field is decomposed into two circularly polarized components. The component with the same direction of rotation as the coordinate system becomes time-independent as a result of this transformation; in the following discussion we assume that it is parallel to the x-axis of the rotating coordinate system. The effect of the other component which rotates with the frequency $(-2\omega_{mw})$ is in general negligible.

The result of applying a short intense MW pulse is to rotate the magnetization M_z through the flip angle $\beta = \gamma_e B_1 t_p = \omega_1 t_p$ in the plane perpendicular to the x-axis. Here γ_e is the gyromagnetic ratio of the electron spin, B_1 (ω_1) is the field intensity of the MW pulse, and t_p is the pulse duration. In the simplest type of pulsed ESR experiment a single pulse with a flip angle $\beta = 90°$ (called a 90° pulse) transforms the original longitudinal magnetization M_z into a transverse y-magnetization[*] (see also Fig. 4). If the resonance condition $\omega_{mw} = \gamma_e B_0$ is exactly fulfilled, the magnetization stays along the direction of the y-axis after the pulse. However, if the Larmor frequency $\omega = \gamma_e B_0$ does not exactly match the microwave frequency ω_{mw}, the magnetization starts to precess about the z-axis with the frequency $\Omega = \omega - \omega_{mw}$. Since the observer (i.e. the detection system) is aligned in the direction of the y-axis in the rotating coordinate system, the difference frequency Ω is measured directly. The oscillating signal, which decays owing to transverse relaxation or inhomogeneous line broadening, is called the free induction decay (FID). By performing a Fourier transformation (FT) into the frequency domain one obtains the spectrum, consisting of a peak at the frequency Ω.

This FT-ESR method[61-63] becomes of particular interest in a case where magnetic nuclei interact with the electron spin. To understand this we consider our simple model system in the liquid phase, which has a spectrum consisting of two resonance lines with a splitting a_{iso}. Here again a 90° pulse converts M_z into a y-magnetization. Immediately after the pulse the two magnetization vectors begin to precess about the z-axis with their different respective frequencies. Figure 4 shows the behavior of the magnetization in the rotating coordinate system, together with the resulting FID and the FT-ESR spectrum, which is identical to the CW ESR spectrum.

[*] The flip angle is always specified with reference to the on-resonance magnetization. Thus a 90° pulse turns M_z through exactly 90° into the y-direction. Off-resonance magnetization vectors, on the other hand, also contain x- and z-components after the 90° pulse. However, these additional components are irrelevant as regards the basic principles of pulsed ESR spectroscopy.

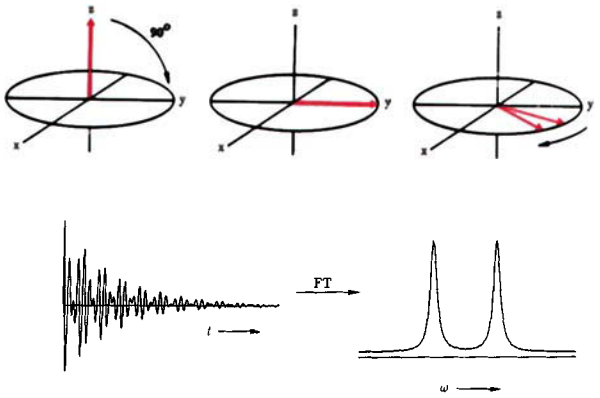

Fig. 4. Top: Evolution of the magnetization during an FT-ESR experiment on a system with $S = 1/2$ and $I = 1/2$. Bottom: FID and corresponding FT-ESR spectrum.

In principle, therefore, the FT-ESR method makes it possible to record the entire ESR spectrum within a few microseconds, whereas in the continuous wave (CW) method the spectrum has to be recorded by slow passage through the resonances.

In nuclear magnetic resonance it is usually possible to achieve complete and simultaneous excitation of the entire spectrum using a single short pulse. In the corresponding ESR experiment, however, this is only possible for a rather limited class of paramagnetic compounds. Problems arise in generating the short MW pulse, and from the limited bandwidth of the detection system and the necessity for very rapid data acquisition. To rotate the magnetization of a sample through 90° about the x-axis the MW field strength must satisfy the condition $B_1 \gg \Omega/\gamma_e$. However, this condition cannot be attained in practice for the majority of spin systems. Often instead only a portion of the spectrum is excited, and even within this partial spectrum there are x- and y-components in the magnetization, and consequently large distortions of intensity and phase. This unsatisfactory situation can be improved to some extent by using quadrature detection.[5,6] In this technique one measures both transverse components of the magnetization, thereby increasing the detector bandwidth by a factor of two. A further problem is that the dead time τ_D of the pulsed ESR spectrometer prevents one from observing the FID during the first 50–100 ns after the 90° pulse. It is therefore not possible to measure broad resonance lines. Consequently it is unlikely in the foreseeable future that FT-ESR could be used to study compounds containing transition metal ions.

The current state of the art in the FT-ESR method is illustrated in Figure 5a by the example of the three-line spectrum of a nitroxide radical in solution at room temperature.[61] The bandwidth of about 200 MHz needed to obtain this spectrum was made possible by using a special probe head known as a bridged loop-gap resonator.[28]

3.1.2. Example of an Application

FT-ESR spectroscopy has now reached a stage of development such as to make it an important research tool for many investigators working in the area of free radical chemistry.

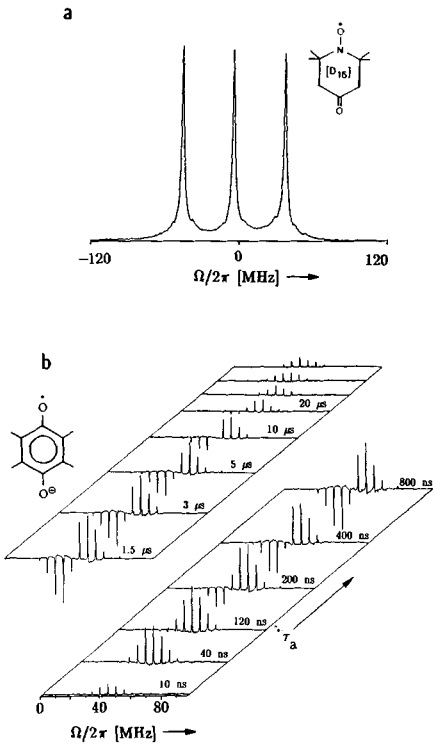

Fig. 5. a) FT-ESR spectrum of perdeuterated tempone in [D_8]toluene (1.5×10^{-4} M) at 22 °C. Duration of the 90° pulse: 6.7 ns; quadrature detection (Ref. [61]). b) FT-ESR spectra of $DQ^{\ominus}$ at 245 K as a function of the interval τ_a between the laser pulse and the 90° MW pulse (upper peaks: absorption; lower peaks: emission) (Ref. [65]).

This applies especially to studies of short-lived paramagnetic species.[64–66] To illustrate this we choose as an example an FT-ESR study of the spin dynamics of the duroquinone radical ion ($DQ^{\ominus}$), which is formed by electron transfer from photoexcited tetraphenylporphyrinatozinc (ZnTPP).[65, 66] Figure 5b shows FT-ESR spectra of $DQ^{\ominus}$ as a function of the time τ_a between a short laser pulse (15 ns), which excites the ZnTPP into the triplet state, and the 90° MW pulse. Up to a τ_a value of about 1 μs the intensities of the peaks continue to increase and the lines on the low-field side become emissive to an increasing extent. Between 1 and 10 μs the signal intensity decreases while the population distribution remains approximately constant, then for greater values of τ_a the emission peaks finally change again into absorption peaks. Detailed information of this kind about the intensity profiles and time variation of the different hyperfine lines makes it possible to seperate the various spin polarization mechanisms, thereby providing a basis for a better understanding of the underlying electron transfer process.

Some alternative FT-ESR spectroscopic techniques, as well as their extension into two dimensions, will be described in Section 4.

3.2. Electron Spin-Echoes

3.2.1. *Basic Principles*

The rapid decay of the FID caused by inhomogeneous broadening can be reversed by performing a spin-echo experiment. This phenomenon, which was first described by *Hahn*[67] for the nuclear spin case, depends on the non-linear behavior of an ensemble of (classical or quantum-mechanical) oscillators with different frequencies. The sequence of events leading to the appearance of an electron spin-echo is shown in Figure 6a. In order to simplify the explanation of the spin-echo phenomenon we assume idealized MW pulses (infinitesimally short and of infinitely high intensity) which give complete and simultaneous excitation of the entire ESR spectrum.

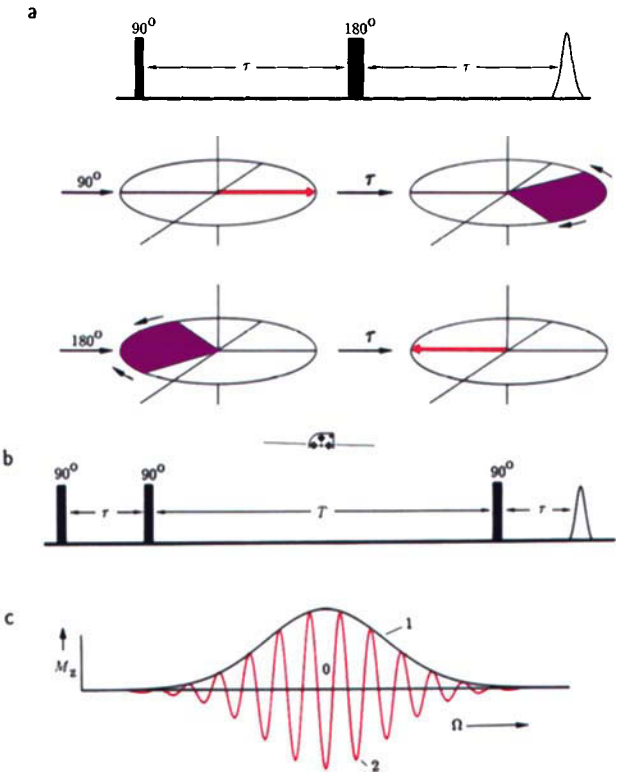

Fig. 6. a) Two-pulse echo sequence and evolution of the magnetization. b) Three-pulse sequence for producing a stimulated echo. c) Inhomogeneous ESR signal; 1: equilibrium condition, 2: z-magnetization pattern after the second 90° pulse.

As before, a magnetization along the y-direction is produced by a 90° pulse. Immediately after this pulse the different transverse magnetization vectors start to precess with their individual frequencies $\Omega_i = \omega_i - \omega_{mw}$, so that the FID decays rapidly, and after a short time there is no detectable signal. After a time interval τ a second MW pulse turns the magnetization vectors through 180° about the x-axis. Since the directions of rotation of the individual components remain unaltered after this refocussing pulse, after a further time interval τ all the vectors are aligned along the $(-y)$-direction. The resulting $(-y)$-magnetization, which builds up and decays again within a short time, is called a spin-echo. The amplitude of this two-pulse echo is a function of the pulse interval τ, and its rate of decay is described by the phase memory time T_M.[*] In solids T_M is usually only a few microseconds, even at low temperatures.

[*] The phase memory time T_M is defined as the time taken for the echo amplitude to decay to $1/e$ of its initial value. In a case where the echo amplitude decays exponentially, T_M corresponds to the transverse relaxation time T_2.

The pulse sequence $90°-\tau-180°-\tau$ is the simplest one that can be used to generate an echo. A second pulse sequence which is often used consists of three 90° pulses (Fig. 6b). In this three-pulse sequence with pulse intervals τ and T a so-called *stimulated* echo is formed after an interval τ following the third pulse. The rather complicated mechanism by which this echo is formed can be best understood if we begin by considering more closely the effects of the first two 90° pulses on the spin system.[68] During the dephasing period which follows the first pulse the transverse magnetization again spreads out in the xy-plane. After the time τ the on-resonance magnetization, and also all the magnetization vectors with off-resonance frequencies $\Omega = 2\pi n/\tau$, are aligned along the y-direction. These are then turned through a further 90° by the second 90° pulse, so that the overall effect on these vectors is an inversion. Magnetization vectors with off-resonance frequencies $\Omega = (2n-1)\pi/\tau$ precess through an angle of $\pm(2n-1)\pi$ during the time τ, and are turned back into the z-direction by the second pulse. Magnetization vectors with $\Omega = (2n-1)\pi/2\tau$ are oriented along the $(\pm x)$-direction after the time τ, and cannot be affected by a second x-pulse. Thus, the sequence $90°-\tau-90°$ generates from the inhomogeneous ESR line an M_Z pattern in the frequency domain which oscillates with the period $2\pi/\tau$ (Fig. 6c). The lifetime of this periodic pattern is determined by the longitudinal relaxation time T_1 of the electron spin, which can be as much as several hundred microseconds at low temperatures. A third 90° pulse applied after a time $T \leq T_1$ generates the FID of this M_Z pattern; it consists of a single peak at a time τ after the pulse and is called a stimulated echo.

The three-pulse sequence also generates several two-pulse echoes, but these can be eliminated by means of a phase cycle.[69] In this procedure the phases of the MW pulses are varied systematically in a succession of experiments and the data from the individual measurements are suitably combined.[5, 6] Just as in nuclear magnetic resonance, such phase cycles are very important in pulsed ESR as a way of suppressing unwanted contributions to the time-domain signal.[70]

Since ESR spectra are often poorly resolved, the FID, and therefore also the spin echo, shows little structure in these cases. For this reason the *amplitude* of the echo is used as the main source of information in spin-echo experiments. This amplitude depends on a number of variables such as the static field strength B_0, the time interval between the MW pulses, or the time between generating a paramagnetic species and applying the pulse sequence. Modulation effects on the amplitudes of the echoes are specifically treated in Section 3.3.

Echo-Detected ESR Spectroscopy

Measuring the intensity of the two-pulse or three-pulse echo as a function of B_0 can be used as an alternative to CW ESR spectroscopy. There are two ways whereby such an echo-detected ESR spectrum can be recorded free from distorting effects. One either measures the maximum echo amplitude using pulses whose duration t_p is larger than the reciprocal resolution $2\pi/\Delta\omega$, or alternatively one measures the integral over the echo (without restriction as to the pulse duration), using an integration window t_i which satisfies the condition $t_i > 2\pi/\Delta\omega$.[30] Figure 7 shows an echo-detected ESR spectrum of a sample of the one-dimensional organic conductor $[(\text{fluoranthene})_2]^{\oplus}PF_6^{\ominus}$ in powder form, recorded at a microwave frequency of 95 GHz (corresponding to a field strength $B_0 = 3.4$ T).[71] The unusually high resonance frequency makes it possible to easily resolve the very small anisotropy of the g-tensor in this compound ($g_\perp/g_\parallel = 1.00018$).[72]

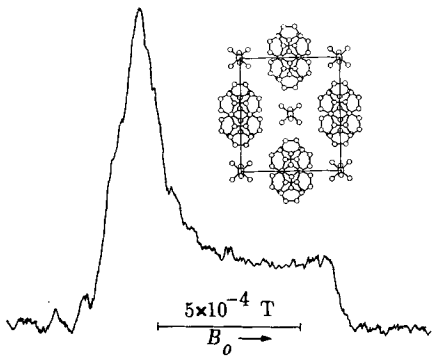

Fig. 7. Echo-detected ESR spectrum of the one-dimensional conductor $[(\text{fluoranthene})_2]^{\oplus}PF_6^{\ominus}$, measured at a microwave frequency of 95 GHz (Ref. [71]).

Echo-detected ESR spectroscopy has some advantages compared with the more usual CW ESR method. This is seen in a particularly impressive way in investigations of short-lived free radicals such as those generated by a laser pulse. The time resolution achieved by this method is determined solely by the interval τ_a between the laser pulse and the first MW pulse. Thus the echo-detected ESR spectrum gives an instantaneous snapshot of the state of a spin system at any instant $t_a \geq 0$.

Measuring the ESR spectrum by means of the echo amplitude is also superior to the usual CW method for stable paramagnetic compounds with very broad ESR lines, such as often occur with polycrystalline samples of compounds containing transition metal ions. This is due to the fact that in the CW method a field modulation is used to generate the first derivative of the absorption spectrum. The available modulation amplitude is often too small compared with the width of the ESR line to measure small changes in the gradient of the absorption spectrum with adequate sensitivity. In contrast to this, the echo method enables one to directly measure the z-magnetization at each point in the spectrum. However, the interaction between the electron spin and the nuclear spins can affect the amplitude of the echo (Section 3.3), and consequently there is a possibility that the line shape may be distorted when measuring powder ESR spectra by the echo-detection method.[73, 74]

Measuring Rates of Chemical Reactions

To obtain data on the kinetics of a short-lived free radical one measures the intensity of an individual ESR line as a function of the time τ_a between the formation of the radical and the first MW pulse. This time profile not only describes the formation and decay of a radical, but also contains information about transient phenomena, for example effects

caused by chemically induced dynamic electron spin polarization (CIDEP).

The Determination of Relaxation Times

The most direct way of measuring relaxation times is that based on echo methods, since in this procedure all the types of interactions that can cause inhomogeneous broadening undergo refocussing. This makes it easy to separate static inhomogeneous contributions to the line width from homogeneous broadening caused by dynamic effects.

The phase memory time T_M is usually determined by measuring the decay of the two-pulse echo as a function of the pulse interval τ. Figure 8a shows the result of such a T_M measurement on a coal sample.[30] If the MW pulse is only capable of exciting a portion of the ESR spectrum, it is possible for some of the transverse magnetization to be lost through spectral diffusion, i.e. as a result of a "leakage" of magnetization into adjacent parts of the spectrum that have not been excited by the MW pulse. This spectral diffusion can be prevented by using a pulse sequence consisting of a 90° pulse followed by a periodic refocussing pulse pattern of the form $(\tau - 180° - \tau)n$; this generates a series of echoes at the times $2m\tau$ ($m = 1,2,\ldots n$).[75] However, with this sequence even small deviations from the optimal setting of the flip angle cause an additional damping of the echo. So as to minimize the cumulative effect of these errors, it is usual to shift the phase of the 180° pulse sequence through 90° relative to that of the 90° pulse.[76] In the case of the coal sample the phase memory time measured using this *Carr-Purcell-Meiboom-Gill* pulse sequence (Fig. 8b) was found to be considerably greater than the value obtained with the simple two-pulse sequence.

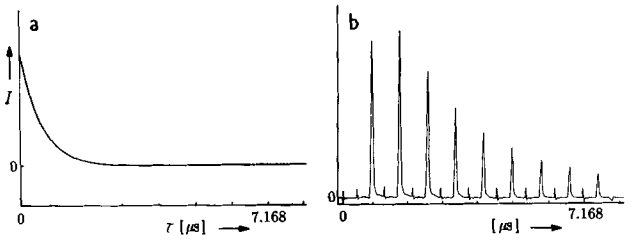

Fig. 8. a) Decay of the two-pulse echo from a coal sample at room temperature as a function of the pulse interval τ. b) Carr-Purcell-Meiboom-Gill multiple echo pattern of the same coal sample (Ref. [30]). I = echo intensity.

For measuring the spin-lattice relaxation time T_1 a number of pulse methods are available. In principle T_1 can be determined from the amplitude of the stimulated echo, as the z-magnetization relaxes towards thermal equilibrium during the variable time T. However, it must be remembered that the first two 90° pulses produce an M_Z pattern (Fig. 6b) with an oscillation frequency which increases with increasing τ. As a result of this, portions of the ESR spectrum with inverted magnetization are immediately adjacent to portions with an unaltered equilibrium magnetization. Consequently the measurement of T_1 is again subject to errors caused by spectral diffusion, since any loss of polarization via non-resonating spins causes the echo amplitude to decay more rapidly.[13]

To avoid spectral diffusion when measuring T_1, the entire ESR spectrum must be saturated ($M_Z = 0$) or inverted ($M_Z = -M_0$), or the width of the excited portion of the ESR spectrum must be greater than the excitation width of the reading pulses that are applied after the time T. Several T_1-measuring pulse sequences whereby spectral diffusion can be partially or completely suppressed are compared in Figure 9. A long pulse or a succession of many short 90° pulses saturates a broad region of the ESR spectrum, as there is then sufficient time for the spectral diffusion to reach adjacent non-resonating parts of the spectrum (Fig. 9a). In the ideal case this results in complete saturation of the ESR signal (saturation recovery method). The measurement of the z-magnetization after the time T is achieved either by a two-pulse echo or by recording the FID, whose duration for broad ESR lines corresponds to the duration of the reading pulse.[77]

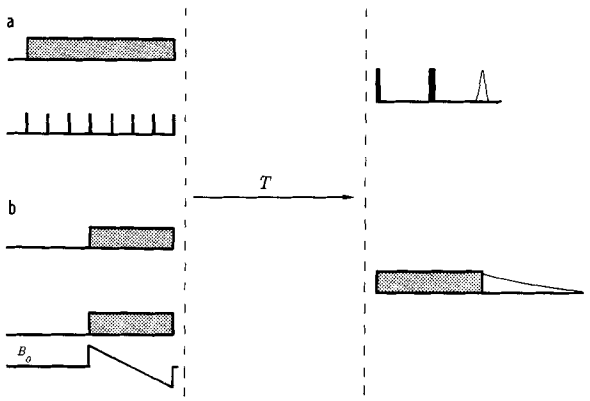

Fig. 9. Pulse sequences for measuring the spin-lattice relaxation time T_1. Left: preparation sequence; right: detection sequence. a) Saturation. b) Inversion.

An alternative method (inversion recovery) uses a 180° excitation pulse. To avoid spectral diffusion in this case one should either use a 180° pulse that is appreciably harder (i.e. of higher intensity and shorter duration) than the reading pulses, or rapidly sweep the field B_0 through a broad spectral range so as to increase the width of the excited region (Fig. 9b).

Other methods in which a weak CW microwave field is used to monitor the recovery from saturation are described in the literature.[78]

3.2.2. *Examples of Applications*

Figure 10 shows an example of the use of electron spin-echoes to observe very rapid processes.[79] The echo-detected ESR spectrum of the benzosemiquinone radical in isopropanol shows a strong emission signal 80 ns after the radical is generated by a laser pulse (Fig. 10a); the appearance of this signal can be attributed to a triplet CIDEP mechanism. Its decay, measured as a function of the time interval τ_a, is mainly caused by spin-lattice relaxation (Fig. 10b).

Relaxation times form an important source of information on the dynamic behavior of a spin system. For example,

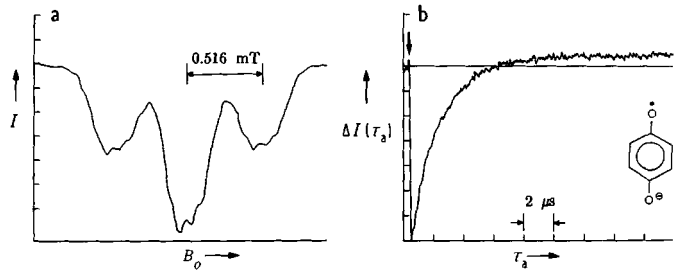

Fig. 10. Photolytically generated benzosemiquinone in 2-propanol. a) Echo-detected ESR spectrum, recorded 80 ns after the laser pulse. b) Decay of the central peak of the ESR spectrum as a function of the interval τ_a between the laser pulse and the first MW pulse; the arrow indicates the position of the laser pulse (Ref. [79]).

they can lead to conclusions about the nature of molecular motions in viscous solutions, characteristic phase transitions in solids, or the distances between paramagnetic centers. The importance of such measurements is illustrated here by three examples.

Crystals of triglycine sulfate (TGS) undergo a ferroelectric phase transition at the Curie temperature $T_C = 47\,^{\circ}C$. To study the dynamics of this transition in greater detail, stable free radicals produced by X-irradiation were used as paramagnetic probes and the relaxation times T_M and T_1 were measured in the region of T_C.[80] Both the longitudinal and transverse relaxation times show critical behavior near the Curie point (Fig. 11). The shortening of T_M can be explained in terms of fluctuations of the order parameter at the ferroelectric phase transition, while the increase of T_1 at the Curie point is due to coupling of the acoustic lattice modes to the ferroelectric relaxational mode.

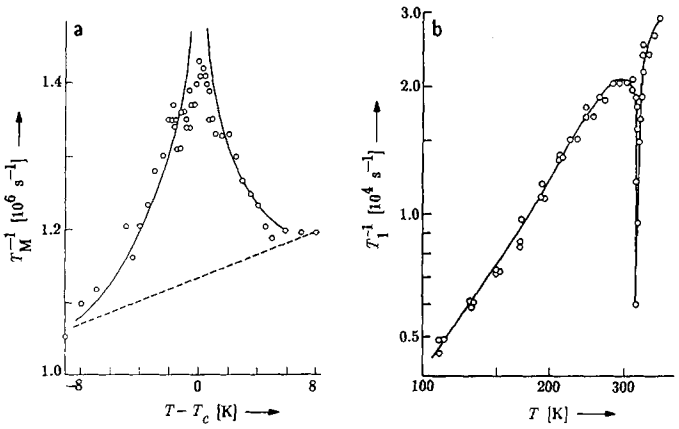

Fig. 11. Temperature anomaly near the Curie temperature T_c in the relaxation times of free radicals in irradiated triglycine sulfate (circles: experimental data, broken line: calculated dependence). a) Phase memory time T_M. b) Spin-lattice relaxation time T_1 (Ref. [80]).

Labeling large molecules with spin probes is a well-established ESR technique for investigating the dynamics of diamagnetic compounds.[81] It has recently been found[82] that the curve of the phase memory time T_M (or of the homogeneous line broadening T_M^{-1}) as a function of B_0 is characteristic of the type of reorientation process occurring.[83-85] The data are easiest to interpret in the form of normalized contour plots in which the shape of the homogeneously broadened line is represented as a function of B_0.

Figure 12 shows two such plots obtained from a model membrane labeled with cholestane as a spin probe.[83] These were produced by measuring the echo-detected two-pulse ESR spectra of the labeled multilayers for two different orientations and 50–60 different τ-values, and applying a Fourier transformation of the data with respect to τ for each field position. A comparison of the experimental data with model calculations shows that the dynamic behavior of this smectic phase can be described in terms of Brownian motion and a high degree of ordering.

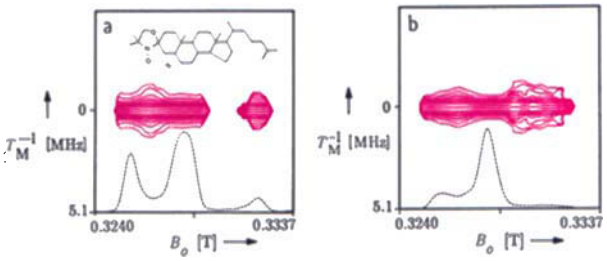

Fig. 12. Experimental contour diagrams of the homogeneous line broadening T_M^{-1} for the spin probe cholestane in orientated dipalmitoylphosphatidylcholine multilayers at $-20\,^{\circ}C$; broken line: spectrum at 0 MHz. Angle between B_0 and the direction of orientation of the multilayers was a) $\theta = 90°$, b) $\theta = 45°$ (Ref. [83]).

If the relaxation times of two paramagnetic centers are sufficiently different, their spectra can be easily separated using the echo-detected ESR method. Figure 13 illustrates this for the example of an undoped *cis/trans*-polyacetylene.[86] With a pulse interval of $\tau = 0.7$ μs the two-pulse ESR spectrum consists of a single structureless line with a width of 1.45 mT (Fig. 13a). For larger values of τ the intensity of this line diminishes rapidly, leaving behind a doublet with a splitting of 2.3 mT (Fig. 13b). The broad

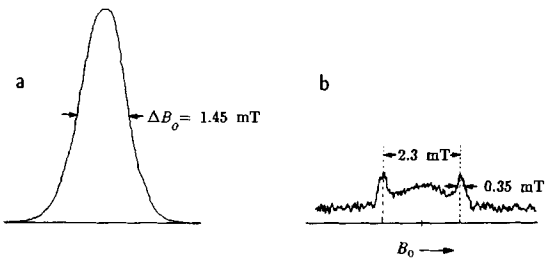

Fig. 13. Separation of overlapping ESR spectra using echo-detected ESR spectroscopy: the example is *cis/trans*-polyacetylene. a) Pulse interval $\tau = 0.7$ μs. b) $\tau = 1.82$ μs (Ref. [86]).

single-line spectrum (relaxation time $T_M = 0.425$ μs) is assigned to trapped solitons whose spin density is distributed over several CH units (Section 3.3.4). On the other hand, the doublet spectrum (with $T_M = 1.6$ μs) arises from a localized defect with a hyperfine coupling characteristic of a proton with sp^2 hybridization.

3.3. The Nuclear Modulation Effect

3.3.1. *Two-Pulse Echo Modulation*

In a two-pulse or three-pulse experiment in which τ or T is varied, the couplings between the electron spin and the nuclear spins can cause a modulation of the echo intensity.[87, 88] As this electron spin echo envelope modulation (ESEEM) can only occur if anisotropic interactions are present, it is only found in the solid phase. For the semiclassical description of the nuclear modulation effect which follows, we return again to our model system (Fig. 1a). The ESR spectrum, with lines corresponding to the two allowed transitions and the two forbidden transitions, is again shown schematically in Figure 14a. By applying sufficiently short MW pulses all four transitions are excited simultaneously, and in particular this includes pairs of transitions that originate from a common energy level.

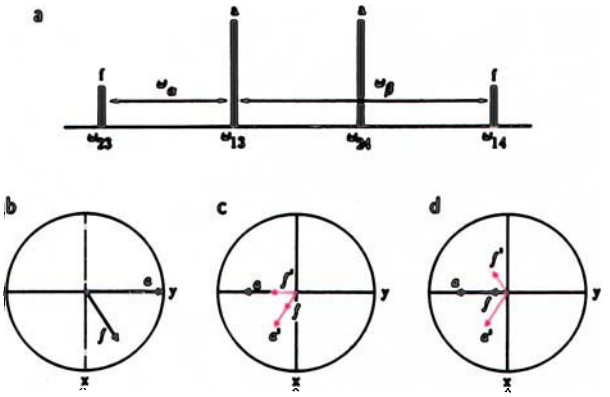

Fig. 14. Diagram illustrating the ESEEM effect. a) Schematic ESR spectrum for a spin system with $S = 1/2$ and $I = 1/2$ showing the two allowed transitions (a) and the two forbidden transitions (f). b) to d) Behavior of the magnetization of an allowed transition (ω_{13}) and of a forbidden transition (ω_{23}) during the two-pulse experiment with $\omega_{mw} = \omega_{13}$.

The way in which the echo modulation arises can easily be shown by means of vector diagrams (Fig. 14b–d).[89] To see this we will follow the behavior of the allowed a-transition ω_{13} and the forbidden f-transition ω_{23}, which both involve a common energy level 3, in a two-pulse experiment. We also assume that the resonance frequency of the allowed transition matches the MW frequency, i.e. $\omega_{13} = \omega_{mw}$. Immediately after the 90° pulse along the x-axis, the magnetization vectors corresponding to these two transitions are parallel to the y-axis. During the first evolution period the orientation of the vector $\boldsymbol{a}$ remains unaltered, whereas the vector $\boldsymbol{f}$ precesses with the frequency $\omega_\alpha = (\omega_{23} - \omega_{13})$ (Fig. 14b). After the time τ the 180° pulse turns the vector $\boldsymbol{a}$ into the $(-y)$-direction, and at the same time gives rise to a new component $\boldsymbol{f}'$. The vector $\boldsymbol{f}$ behaves in an analogous way (Fig. 14c). In the second evolution period the orientation of the vectors $\boldsymbol{a}$ and $\boldsymbol{a}'$ remains unaltered, whereas the two vectors $\boldsymbol{f}$ and $\boldsymbol{f}'$ continue to precess with the frequency ω_α. Thus the vectors $\boldsymbol{a}'$ and $\boldsymbol{f}'$ are no longer orientated along the $(-y)$-direction, and this results in a reduction in the intensity of the echo (Fig. 14d). Since the orientations of these two vectors depend on τ, and their contribution to the echo becomes a maximum when $\omega_\alpha \tau = 2\pi n$, the echo amplitude oscillates in proportion to $\cos(\omega_\alpha \tau)$. This applies for any combination of transitions with a common energy level. The complete modulation formula for the two-pulse experiment is given in (7).

$$E_{mod}(2\tau) = 1 - \frac{k}{4}[2 - 2\cos(\omega_\alpha \tau) - 2\cos(\omega_\beta \tau) + \cos(\omega_+ \tau) + \cos(\omega_- \tau)] \quad (7)$$

This expression, which can be evaluated with the help of the spin density operator formalism,[88] contains not only the two nuclear frequencies but also their sum ω_+ and difference ω_-. The amplitudes of the four modulations with different frequencies are given by the modulation depth parameter $k = 4I_aI_f = (\omega_I B/\omega_\alpha\omega_\beta)^2$. For the case of an isotropic hyperfine interaction a_{iso}, or if $\boldsymbol{B}_0$ is orientated along one of the principal axes of the hyperfine tensor, the echo modulation disappears, since in either of these cases the quantity B in the expression for the modulation depth parameter becomes zero.

Figure 15a shows the modulation pattern for our model compound with $\theta = 45°$. After eliminating the zero frequency component and carrying out a Fourier transformation in the frequency domain, one obtains either the cosine or the magnitude spectrum containing the two nuclear resonance frequencies ω_α and ω_β and their sum and difference frequencies ω_+ and ω_-.

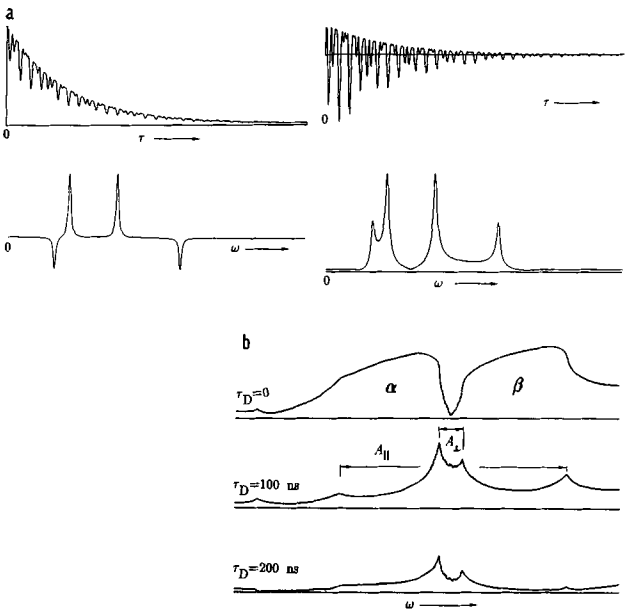

Fig. 15. Two-pulse echo modulation (for parameters see model system). a) upper plots: ESEEM pattern before (left) and after (right) elimination of the constant term; lower plots: cosine spectrum (left) and magnitude spectrum (right) for a particular orientation ($\theta = 45°$). b) Effect of the dead time τ_D on the line shape and intensity in the powder spectrum (sum-frequency peak not shown).

If several nuclear spins are involved in the ESEEM effect, the echo modulation is given by the product rule (8).[88] Thus

$$E^n_{mod}(2\tau) = \prod_i^n E^{(i)}_{mod}(2\tau) \quad (8)$$

the spectrum contains, in addition to the four main frequencies, some combination frequencies. However, as the modulation depth parameters k_i appear as squared or higher order terms in the amplitudes of these modulations, the intensities of the combination peaks are generally small.

Apart from these combination frequencies and the sum and difference frequencies the positions of the lines in the ESEEM spectrum correspond to those in the ENDOR spectrum. The nuclear modulation effect, which arises solely from the interplay of allowed and forbidden transitions without the need for a radiofrequency field, therefore ranks alongside ENDOR spectroscopy as one of the most important tools that can be used for elucidating the structures of paramagnetic compounds.

In studies on disordered systems it is often difficult to determine the magnetic parameters from an ESEEM spectrum, since the broad lines are associated with a rapid decay of the modulation pattern in the time domain, and for short τ-values the observation of the echo modulation is limited by the dead-time of the spectrometer. Despite the use of some clever experimental tricks, this problem cannot be entirely solved.[30, 90, 91]

Figure 15b illustrates how seriously the dead time τ_D can affect a two-pulse ESEEM spectrum. This again uses our model system as an example, by assuming a powder sample which gives averaging over all possible orientations. For the ideal case where $\tau_D = 0$ (which cannot be realized experimentally) one obtains the true spectrum with undistorted line shapes. However, if the dead time is such that data acquisition can only start at $\tau = 100$ ns, the α and β hyperfine lines both split into doublets, due to the fact that steep gradients in the spectrum (corresponding to high frequencies in the frequency domain) are more efficiently detected. The peak maxima of these doublets are directly related to the hyperfine components $A_\perp$ and $A_\parallel$, which means that in simple cases the interpretation of the spectrum can even be made easier by the dead time effect.[92] However, with a dead time $\tau_D = 200$ ns the intensities of the peaks are already reduced by a factor of 10, which often means that they are comparable with the noise level. Often in practice the modulations decay to such an extent during the time τ_D that the weak oscillations still detectable are insufficient to allow reconstruction of the spectrum. Techniques for avoiding this dead-time problem will be discussed in Section 4.

3.3.2. Three-Pulse Echo Modulation

The stimulated echo too shows a nuclear modulation effect. However, whereas in the two-pulse experiment only *electron* spin coherences are produced and mixed, in the three-pulse experiment the second 90° pulse transfers the electron spin coherence into *nuclear* spin coherence.[*] This nuclear spin coherence develops during the evolution time T and decays with the transverse nuclear relaxation time T_{2n} (or T_1 in cases where $T_1 < T_{2n}$), which is usually much longer than the corresponding relaxation time T_M of the electrons. The third 90° pulse transfers the nuclear spin coherence back to observable electron spin coherence. For the stimulated echo of a spin system with $S = 1/2$ and $I = 1/2$, the modulation at the time $\tau + \tau'$ (where $\tau' = \tau + T$) is given by Equation (9).[88]

$$E_{mod}(\tau + \tau') = 1 - \frac{k}{4}\{[1 - \cos(\omega_\alpha \tau)][1 - \cos(\omega_\beta \tau')] + [1 - \cos(\omega_\beta \tau)][1 - \cos(\omega_\alpha \tau')]\} \quad (9)$$

When τ' (T) is varied the echo envelope is modulated only by the two basic frequencies ω_α and ω_β; the sum and difference frequencies do not appear. However, according to Equation (9) the amplitudes at the two frequencies ω_α and ω_β depend on $\omega_\beta \tau$ and $\omega_\alpha \tau$ respectively. Due to this suppression effect individual peaks in the spectrum can disappear completely. These "blind spots" occur for the α peak when $\tau = 2\pi n/\omega_\beta$, with a corresponding condition for the β peak.

For several nuclear spins the product rule (10) applies.[93]

$$E^n_{mod}(\tau + \tau') = \tfrac{1}{2}\left[\prod_i^n E^{(i)}_\alpha(\tau, \tau') + \prod_i^n E^{(i)}_\beta(\tau, \tau')\right] \quad (10)$$

In contrast to the two-pulse experiment, combinations of the nuclear frequencies only occur within the *same* m_S state.

The great advantage of the three-pulse ESEEM experiment lies in the slow decay of the echo modulation, whose duration is no longer limited by a short phase memory time T_M as in the two-pulse experiment. Moreover, there are fewer peaks than in the two-pulse ESEEM spectrum, as the sum and difference frequencies do not appear. The three-pulse method is therefore often preferred in single crystal investigations.

A different situation exists in disordered systems. In powder samples or frozen solutions the modulation pattern usually decays very much faster than the overall amplitude of the echo, owing to destructive interference of the different resonance frequencies. Moreover, the line-shape distortions caused by the suppression effect make the interpretation more difficult. Because of these two effects the two-pulse echo modulation method often gives better results for such systems.

3.3.3. Effect of the Microwave Frequency

The MW frequency can affect the ESEEM pattern in several different ways. According to Equation (7) the modulation depth parameter k depends not only on ω_α and ω_β but also on the Zeeman frequency of the nucleus concerned, and therefore on the field B_0 or the microwave frequency. For small hyperfine couplings the condition $\omega_I \simeq \omega_\alpha \simeq \omega_\beta$ holds, with the result that the modulation depth parameter k is approximately equal to B^2/ω_I^2, and is thus inversely proportional to the square of the nuclear Zeeman frequency. In compounds with small hyperfine couplings a reduction in the microwave frequency therefore causes a considerable increase in the modulation amplitudes. Figure 16a compares the two-pulse ESEEM patterns of vitrinite measured at 3 GHz (S-band) and 9 GHz (X-band).[94] The amplitude of the echo modulation at the lower MW frequency is about ten

[*] A transition between any two arbitrary eigenstates is described as a coherence. This term therefore has a wider meaning than the expression "transverse magnetization", which refers only to allowed transitions. A coherence corresponds to an off-diagonal element in the spin density matrix.

times larger than at the commonly used frequency of 9 GHz, in agreement with the above approximation. However, at low MW frequencies the combination lines also appear more strongly, and for strongly coupled nuclei this can lead to very confused ESEEM spectra.

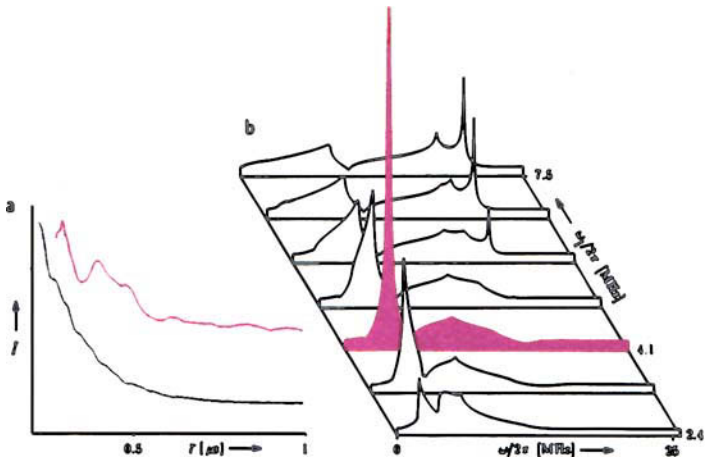

Fig. 16. a) Effect of the microwave frequency on the two-pulse modulation patterns for a vitrinite sample at 298 K. Upper trace: MW frequency = 3 GHz (S-band); lower trace: MW frequency = 9 GHz (X-band) (Ref. [94]). b) Effect of the microwave frequency on the shapes and intensities of the lines in a powder ESEEM spectrum (for parameters see model system, Fig. 1a). At a nuclear Zeeman frequency of $\omega_I/2\pi = 4.1$ MHz the α-transition becomes dispersion-free (spectrum in red).

The microwave frequency affects not only the depth of modulation but other parameters too. For example, in disordered systems the line shape is greatly affected by, among other factors, the choice of MW frequency.[95, 96] As a result it is even possible for individual hyperfine lines to become dispersion-free. For an axially symmetric spin system with $S = 1/2$ and $I = 1/2$ this condition is reached for the α-line at a nuclear resonance frequency given by $\omega_I = A_{||}^d/8 + a_{iso}/2$.[96] The α-line then consists of an intense narrow peak at the frequency $\omega_\alpha = 3A_{||}^d/8$, whereas the β-transitions remain distributed over a wide frequency range, and thus manifest in weak and broad features. It is therefore possible, by varying the MW frequency, to determine the dipolar hyperfine coupling $A_{||}^d$ directly from the ESEEM spectrum. Figure 16b shows a series of powder spectra of our model system for different MW frequencies. In this numerical example the α-peak becomes dispersion-free for $\omega_{mw}/2\pi = 2.7$ GHz ($\omega_I/2\pi = 4.1$ MHz).

A similar narrowing of particular lines can be achieved for quadrupolar nuclei with spin $I = 1$. Especially in the case of weakly coupled ^{14}N nuclei with a nearly isotropic hyperfine tensor, the nuclear Zeeman interaction and the hyperfine interaction cancel each other for $m_S = 1/2$ at a microwave frequency $\omega_{mw} = a_{iso}g_e\beta_e/2g_n\beta_n$.[68, 97, 98] Choosing this particular value for ω_{mw} has the effect of reducing the Hamiltonian for this m_S subsystem to one that contains only the quadrupolar interaction. Since the corresponding transitions are independent of the field B_0, and therefore of the orientation, the ESEEM spectrum consists essentially only of narrow lines which correspond to pure quadrupole frequencies.

3.3.4. *Examples of Applications*

With the limited selection of two-pulse and three-pulse experiments that are discussed in this section, only a rough indication can be given of the wide variety of applications of the nuclear modulation effect. These examples are designed to convince the reader of the usefulness of the method, and at the same time to draw attention to some special aspects of ESEEM spectroscopy.

Surface Complexes

In natural bodies of water the phosphate cycle plays an important role and affects, among other things, the adsorption behavior of heavy metal ions. ESR spectra yield little information about the nature of the bonding between metal ions and hydrated metal oxide surfaces in the presence of phosphates. In particular it is not possible to determine from the spectra whether or not ternary surface complexes are formed, nor whether the bonding of the metal ions at the oxide surfaces involves inner- or outer-sphere coordination. In contrast to CW ESR spectroscopy the ESEEM technique makes it possible to observe the weak interactions between the metal ion and the magnetic nuclei in the immediate environment (ligands, metal oxides). We take as our example Cu^{II} ions, which become adsorbed on δ-Al_2O_3 in the presence of various phosphates.[99]

Figure 17a shows the ESR spectrum of Cu^{II}(pyrophosphate)$_2$ in a frozen aqueous solution, showing very little spectral structure. The only effect of adsorption of the Cu^{II}

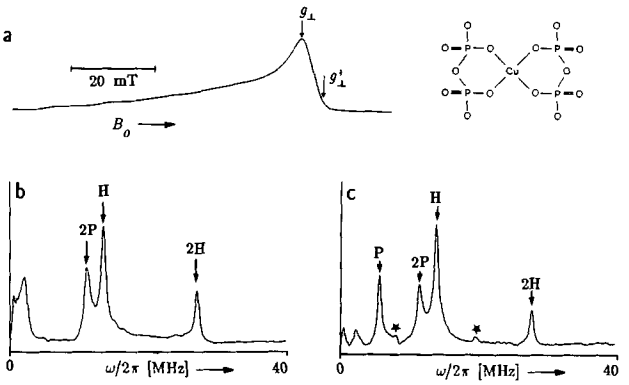

Fig. 17. Two-pulse echo modulation pattern from Cu^{II}(pyrophosphate)$_2$ in frozen aqueous solution. a) CW ESR spectrum (integrated) at 90 K. The arrows indicate the two field positions used for the ESEEM experiment. b) Two-pulse ESEEM magnitude spectrum at 10 K, measured at $g_\perp$. c) Measured under the same conditions at $g'_\perp$; asterisks mark combination signals at $\omega_H \pm \omega_P$ (Ref. [99]).

ions on the δ-Al_2O_3 surface is a further broadening of the ESR lines. Owing to the large anisotropy of the g-tensor and of the copper hyperfine tensor, the ESR spectrum is smeared out over a range of about 80 mT. The high field region of the spectrum is produced by orientations of the magnetic field $\boldsymbol{B}_0$ that lie close to the plane of the complex ($\boldsymbol{B}_0$ parallel to the principal axis direction $g_\perp$). An ESEEM experiment in this field region therefore corresponds to a powder-type averaging over two dimensions. Two such "powder" ESEEM spec-

tra of Cu^{II}(pyrophosphate)$_2$ in frozen solution, for different measuring positions in the neighborhood of $g_\perp$, are shown in Figure 17b,c; both spectra show proton and phosphorus resonances.

As the short MW pulses excite a spectral region corresponding to a field range of about 3 mT, orientations out of the plane of the complex are also observed, and in general this causes a broadening of the lines in the ESEEM spectrum. By shifting the detection window towards the high field end of the spectrum ($g'_\perp$ in Fig. 17a) the orientational selectivity can be considerably improved. This is illustrated by the ESEEM spectrum in Figure 17c, in which additional peaks appear at the Zeeman frequency ω_P of the phosphorus nucleus and at the combination frequencies $\omega_H - \omega_P$ and $\omega_H + \omega_P$.

Figure 18 shows ESEEM spectra of Cu^{II} ions adsorbed on δ-Al_2O_3. The strong aluminum peaks confirm that a surface complex has been formed. Figure 18a shows the spectrum obtained in the presence of orthophosphate, pyrophosphate and tripolyphosphate. The absence of phosphate peaks indicates that in all these frozen solutions the phosphates are no longer coordinated to the copper in the presence of δ-Al_2O_3. This is further confirmed by the doublet structure of the sum peaks of the protons, which results from the binding of water at the remaining free equatorial coordination sites of the copper (Section 4.3).

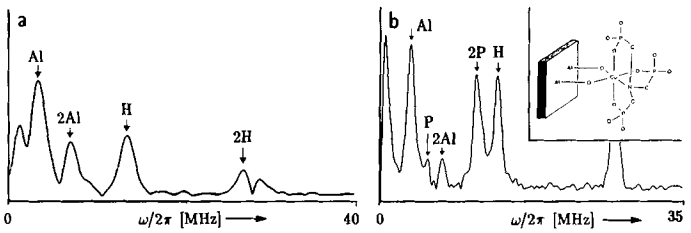

Fig. 18. a) Two-pulse ESEEM magnitude spectrum of Cu^{II} ions adsorbed on the hydrated oxide surface δ-Al_2O_3 at 10 K. b) Two-pulse ESEEM magnitude spectrum of Cu^{II}(NTP) adsorbed on δ-Al_2O_3, measured at 10 K. In both cases the data were apodized before Fourier transformation (Ref. [99]).

In the case of Cu^{II}NTP (NTP = nitrilotrismethylenephosphonate) we find a spectrum which contains not only aluminum peaks but also phosphorus peaks (Fig. 18b). Therefore Cu^{II}NTP is the only one of the phosphates investigated that forms a ternary surface complex when adsorbed on the oxide surface.

Coordination of Water in Metmyoglobin

A number of studies have led to the conclusion that in metmyoglobin (oxidized myoglobin containing $Fe^{3\oplus}$) a water molecule is bonded to the heme iron ion. ESEEM spectroscopy has provided direct evidence for this coordination.[100] For this purpose three-pulse experiments were carried out on metmyoglobin in both H_2O and D_2O and one ESEEM pattern was divided by the other. As a consequence of the product rule, forming this quotient eliminates the oscillations of those nuclei that are present in both samples. However, this suppression is only complete in ordered systems and when using the two pulse sequence [cf. Eqs. (8) and (10)]. Nevertheless, it has been found in practice that even for powder samples and three-pulse sequences the quotient method is very effective in reducing unwanted modulation components due to protons and nitrogen nuclei.

In metmyoglobin the modulation pattern after carrying out the division essentially contains only the frequencies of those deuterium nuclei that belong to exchangeable water molecules. The corresponding ESEEM spectrum is shown in Figure 19a. Positioned symmetrically with respect to the peak (b) of the more distant deuterium nuclei at the nuclear Zeeman frequency ω_D of the deuterons, there appear two further lines (a and c) with a separation of 0.8 MHz. Since

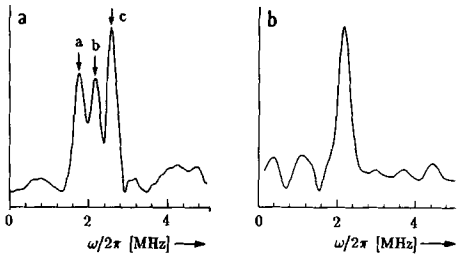

Fig. 19. Deuterium signals in the ESEEM quotient spectra of heme proteins. a) Metmyoglobin, $B_0 = 0.3384$ T. b) Methemoglobin, $B_0 = 0.3330$ T (Ref. [100]).

the only exchangeable protons near the heme group are those of water, the hyperfine splitting observed in the ESEEM spectrum of metmyoglobin proves that a water molecule is coordinated directly to the iron ion. In contrast the spectrum of methemoglobin (Fig. 19b) shows no splitting of this kind, showing that in this protein the bonding of water to the iron ion is much weaker.

Determination of the Structures of the Ligands in a Copper Protein

The ESEEM method ranks with EXAFS (extended X-ray absorption fine structure) as one of the most important tools for determining the structures of active centers in metalloproteins.[18, 68] The ESEEM spectra of these not only contain information about magnetic parameters but often also enable conclusions to be drawn about the number and identities of the ligands. This will be illustrated by the example of the copper protein phenylalanine hydroxylase obtained from *Chromobacterium violaceum*.[101]

Here again it is found that the CW ESR spectrum yields no direct information about the nature of the ligands. Figure 20a shows the three-pulse echo modulation measured at $g_\perp$ and the corresponding ESEEM spectrum of the nitrogen nuclei that are not directly coordinated to the copper ion. As the condition for observing pure quadrupole resonances for the $m_S = 1/2$ state is nearly fulfilled (Section 3.3.3), the ^{14}N spectrum consists of narrow lines at the quadrupolar frequencies $\nu_0 = 0.55$ MHz, $\nu_- = 1$ MHz, and $\nu_+ = 1.55$ MHz ($\nu_0 + \nu_- = \nu_+$). The somewhat broader peak at 4.1 MHz is assigned to the $\Delta m_I = \pm 2$ transition of the $m_S = -1/2$ state, which is also independent of the orientation to a first approx-

imation. A comparison with the data for Cu^{II} complexes with 2-methylimidazole ligands suggests that in the case of phenylalanine hydroxylase the compound histidylimidazole coordinates to the Cu^{II} ion.

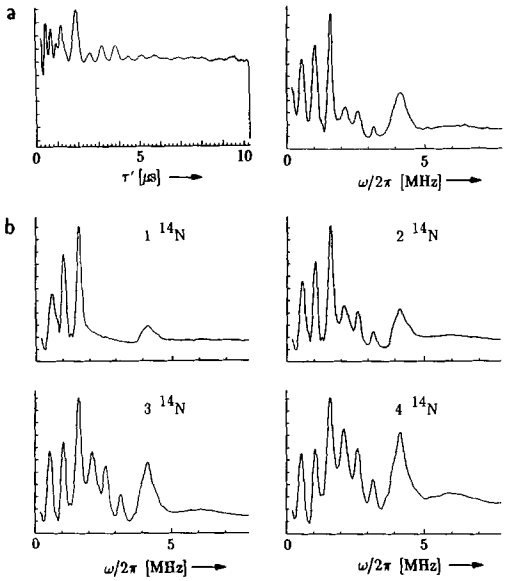

Fig. 20. Determination of the structures of the ligands on the Cu^{II} ion in the protein phenylalanine hydroxylase. a) Three-pulse modulation pattern (left) and ESEEM spectrum (right), measured at $g_\perp$, $\tau = 152$ ns, $T = 4.2$ K. b) Simulated three-pulse ESEEM spectra calculated for one to four nitrogen atoms, using experimental data from Figure 20a as parameters (Ref. [101]).

In the ESEEM spectrum of phenylalanine there are, in addition to the main peaks, three further weak ones. As their positions correspond to the frequencies for combination lines, there must be more than one imidazole ligand coordinated to the copper ion. Figure 20 b shows the corresponding simulated spectra for one to four nitrogen nuclei. These show that the intensities of the combination lines and of the $\Delta m_I = \pm 2$ peaks are strongly dependent on the number of coupled ^{14}N nuclei. Comparing these plots with the experimental spectrum in Figure 20 a leads to the conclusion that the protein studied here must have *two* histidylimidazole groups equatorially coordinated to the Cu^{II} ion.

Magnetic Properties of Triplet States

Magnetic resonance methods such as CW ESR spectroscopy, optically detected magnetic resonance, and ENDOR and ESEEM spectroscopy, have made great contributions to the understanding of triplet states in organic molecules and biological systems. The ESEEM technique in particular is ideally suited for determining small hyperfine couplings in short-lived triplet states.[22, 102–105] For a spin system with $S = 1$ and $I = 1/2$ the two-pulse modulation formula is:

$$E_{mod}(2\tau) = 1 - \frac{k'}{4}[2 - 2\cos(\omega_T\tau) + 2\cos(\omega_I\tau) - \cos(\omega_T + \omega_I)\tau - \cos(\omega_T - \omega_I)\tau] \quad (11)$$

with the modulation depth parameter k' given by the expression (12).

$$k' = [(2B(\omega_T + \omega_I + A))/(B^2 + (\omega_T + \omega_I + A)^2)]^2 \quad (12)$$

In observing the ESR transition $|m_S = 0\rangle \rightarrow |m_S = 1\rangle$ one measures the nuclear frequencies ω_I and

$$\omega_T = \omega_{+1} = [(A - \omega_I)^2 + B^2]^{1/2} \quad (13)$$

whereas for the transition $|m_S = -1\rangle \rightarrow |m_S = 0\rangle$ one measures the frequencies ω_I and

$$\omega_T = \omega_{-1} = [(A + \omega_I)^2 + B^2]^{1/2} \quad (14)$$

As an example of an ESEEM study of a triplet state we may take the determination of the magnetic parameters of anthracene in a single crystal of *p*-terphenyl, which was excited into the triplet state at room temperature by a laser pulse of 40 μs duration.[105] Figure 21 shows the echo modulation patterns of the low field transition with $\boldsymbol{B}_0$ along each of the three principal axes of the fine structure tensor, together with the corresponding ESEEM spectra. With the field along the *x*-axis the spectrum contains four peaks at the two fundamental frequencies $\omega_{-1}/2\pi = 1.73$ MHz and $\omega_I/2\pi = 11.71$ MHz and at the sum and difference frequencies. The peak at 1.73 MHz is assigned to the α-protons (positions 1, 4, 5 and 8). In the spectrum for the *y*-direction the fundamental frequency $\omega_{-1}/2\pi = 7.96$ MHz corresponds to the coupling of the β-protons (2, 3, 6 and 7). From these ESEEM data one can determine the elements of the hyperfine tensor and hence the corresponding spin densities.[105]

Solitons in Polyacetylene

Polyacetylene, $(CH)_x$, exhibits many unusual physical properties. Of particular interest is the behavior of the soli-

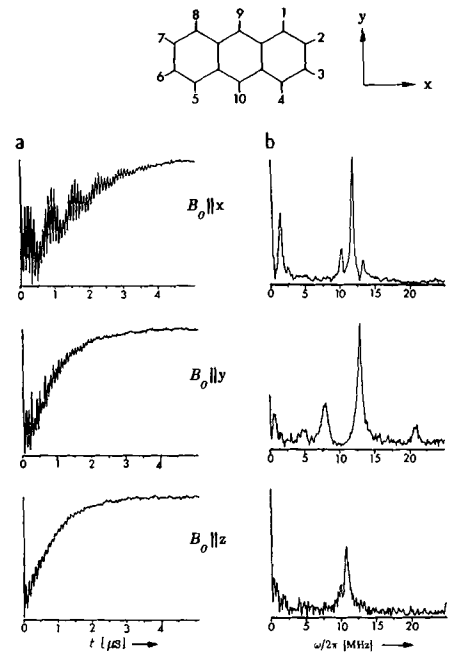

Fig. 21. Two-pulse echo modulation results from photoexcited anthracene in a single crystal of *p*-terphenyl, measured at room temperature. a) Modulation patterns for the low-field transition $|m_S = -1\rangle \rightarrow |m_S = 0\rangle$ with $\boldsymbol{B}_0$ along the *x*, *y* and *z* molecular axes. b) The corresponding ESEEM magnitude spectra (Ref. [105]).

tons which are present in the undoped polymer with a typical concentration of one spin per 2000–3000 carbon atoms. Solitons are neutral π-radicals which arise from defects in the conjugated π-bond system of the polyene chains. Since a delocalization of the electron lowers the energy of the defect, it becomes distributed over about fifty C–C bonds.

The three-pulse ^{13}C-ESEEM spectra of *trans*- and *cis*-polyacetylene (with 99% ^{13}C enrichment) are identical and are independent of temperature between 4 and 300 K.[106] The spectra consist of one peak at the Zeeman frequency ω_C of the ^{13}C nucleus together with a large number of combination lines or multiple-quantum transitions at frequencies $n\omega_C$ (Fig. 22). It is very unusual to find such strong combination

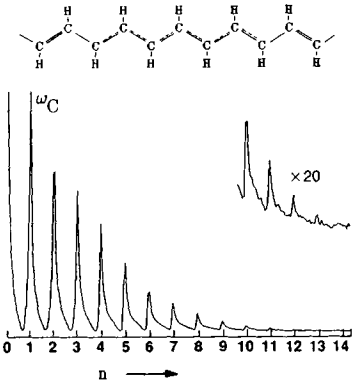

Fig. 22. Solitons in polyacetylene. ^{13}C multiple quantum transitions in *trans*-$(CH)_x$ (three-pulse ESEEM magnitude spectrum, compound 99% ^{13}C enriched) (Ref. [106]).

lines in an ESEEM spectrum measured in the X-band. Since a diffusion of the solitons along the $(CH)_x$ chains would destroy the multi-quantum coherence, it must be concluded from the modulation pattern that the defect structures remain at fixed positions even at room temperature. Attempts have been made to describe the multiple-quantum pattern on the basis of various models. It was found that the experimental results could only be explained by assuming that the delocalized electron interacts with a large number of ^{13}C nuclei in *neighboring* polyacetylene chains.[107]

3.4. Pulsed ENDOR Spectroscopy

3.4.1. Basic Principles

ENDOR spectroscopy is a long-established magnetic resonance technique. The CW ENDOR method, which is still the most commonly used form of ENDOR, has a serious disadvantage in that the signals observed with this technique depend very critically on the balance between the various relaxation times and the MW and RF pumping fields. Moreover, even when the experimental variables are optimized, the signal intensities in ENDOR are only a few percent of those with ESR.

Along with the rapid developments occurring in pulsed ESR spectroscopy, there has recently also been a growing interest in pulsed ENDOR techniques.[42–45] One of the advantages of these methods compared with the CW ENDOR method is that the entire pulse sequence can usually be made short enough to exclude unwanted relaxation effects. This means that the pulsed ENDOR technique can be used at any desired temperature, provided that an electron spin-echo can be detected. The two standard methods used in pulsed ENDOR spectroscopy are described below and illustrated by several examples. Some special pulsed ENDOR techniques are discussed in Section 4.6.

Figure 23 shows the two pulse sequences used, which were introduced a considerable time ago by *Davies*[108] and *Mims*[109] respectively. Both are based on a transfer of spin polarization. The Davies ENDOR experiment (Fig. 23a) starts by inverting the polarization of one of the ESR transitions by means of *selective* 180° MW pulse. As the spin-lattice relaxation time T_1 in the solid phase can be as much as several hundred microseconds, depending on the temperature, this allows enough time to apply a selective 180° RF pulse so as to invert the polarization of a nuclear spin transition in one of the two m_S states. This causes the population difference in the ESR transition that was first excited to disappear (Fig. 23b), and consequently the echo also disappears.

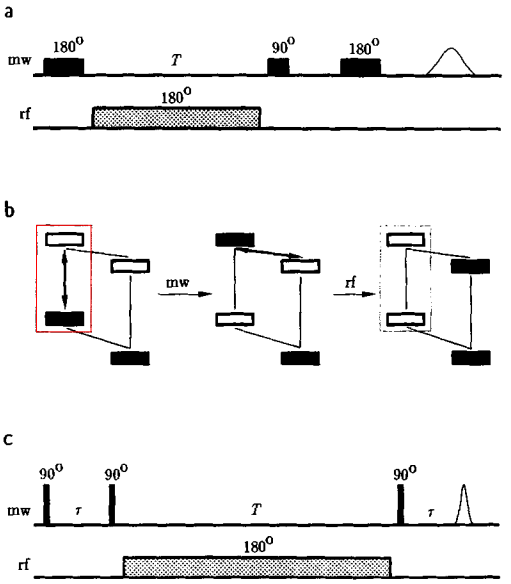

Fig. 23. Standard pulsed ENDOR sequences. a) Davies ENDOR sequence. b) Changes in populations of states in the Davies experiment. c) Mims ENDOR sequence.

Figure 24a shows the Davies ENDOR spectrum of a single crystal of $Mg(NH_4)_2(SO_4)_2 \cdot 6H_2O$ doped with Cu^{II} ions. It consists of proton resonances from water coordinated directly to the copper ion, together with some resonance lines of other nearby protons. A noticeable feature of this spectrum is that the broad matrix line near the nuclear Zeeman frequency of $\omega_H/2\pi = 11.8$ MHz is considerably weaker than the lines of the more strongly coupled protons. This arises from the inadequate selectivity of the first MW pulse, which can therefore excite both ESR transitions in the case of weakly coupled nuclei. This can reduce, or even eliminate altogether, the transfer of polarization by the RF pulse.

Unlike the Davies pulse sequence the pulsed ENDOR technique introduced by *Mims*[109] does not require selective MW pulses. The Mims ENDOR method is based on measuring the stimulated echo as a function of the frequency of a 180° RF pulse applied between the second and third MW pulses (Fig. 23c). The duration of th RF pulse is again limited by the relaxation time T_1. However, the polarization transfer is less transparent than in the Davies experiment, as the first two MW pulses impose a complicated magnetization pattern on the ESR line. As a result of this there are blind spots in the ENDOR spectrum for pulse intervals given by $\tau = 2\,\pi n/a$ ($n = 1,2,\ldots$), similar to those in the three-pulse ESEEM experiment. To avoid the possibility of missing individual lines it is therefore essential to repeat the experiment with different τ-values. For $\tau = 2\pi(2\,n - 1)/a$ the echo intensity is again reduced to zero in the Mims ENDOR experiment (maximum ENDOR effect).

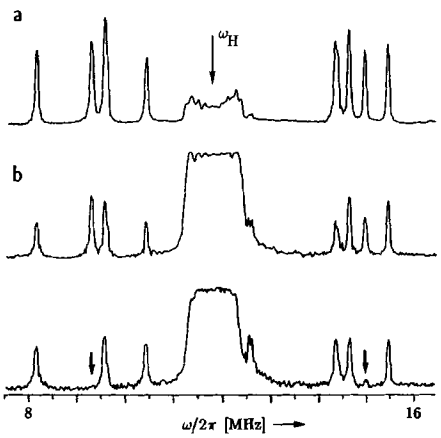

Fig. 24. Pulsed ENDOR single crystal spectra of Cu^{II}-doped $Mg(NH_4)_2(SO_4)_2 \cdot 6H_2O$ at 10 K; ω_H is the nuclear Zeeman frequency of the protons. a) Davies ENDOR spectrum. b) top: Mims ENDOR spectra with $\tau = 430$ ns, bottom: with $\tau = 800$ ns; the arrows mark blind spots in the spectrum.

An important feature of the Mims ENDOR sequence compared with the Davies method is that it gives a greater echo amplitude, since more electron spins are involved in the experiment. Figure 24b shows Mims ENDOR single crystal spectra for two different τ-values. The arrows indicate blind spots.

3.4.2. *Examples of Applications*

An example from the literature will be described here, and the pulsed ENDOR method will be compared with the ESEEM technique.

Pulsed ENDOR Spectroscopy of Free Porphyrin Bases

In order to determine the hyperfine tensor for the two inner protons of the [D_{12}]porphyrin, the compound was incorporated into a single crystal matrix consisting of perdeuterated *n*-octane.[110] The deuteration achieves two objectives: in the first place it increases the sensitivity, as the hyperfine couplings for deuterium are smaller than those for protons and a microwave pulse of a given duration can therefore excite more spins, and secondly it increases the phase memory time T_M. Photoexcitation into the lowest-lying triplet state is achieved at a temperature of 1.4 K by applying a laser pulse 1 μs before the start of the ENDOR pulse sequence. The ENDOR frequencies for the ESR transition $|m_S = 0\rangle \rightarrow |m_S = 1\rangle$, measured in the plane of the porphyrin ring, are shown in Figure 25. As the two inner

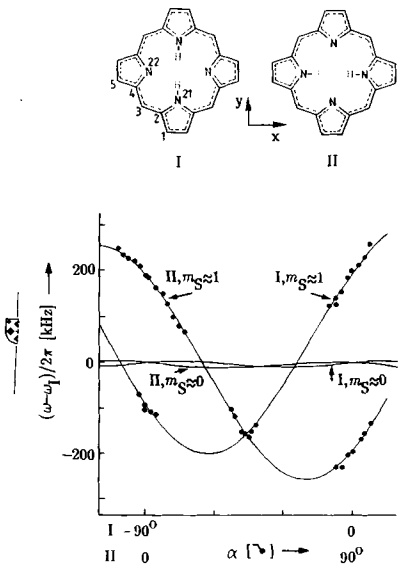

Fig. 25. ENDOR frequencies $(\omega - \omega_I)/2\,\pi$ for the two tautomers I and II in the porphyrin free base, with B_0 in the plane of the porphyrin ring, at 1.4 K (Ref. [110]).

protons can occupy two alternative positions, which can be interchanged by a 90° rotation of the molecule about the *z*-axis, the ENDOR spectra consist of four lines. Although the sample contained only about 10^{13} triplet spins, it was possible by spectrum accumulation to completely determine the hyperfine tensors for the two magnetically equivalent protons from the angular dependence of the nuclear frequencies ω_{+1} [Eq. (13)]. The ENDOR data show that the molecular symmetry departs considerably from D_{2h}. From the values of the tensor components it was also possible to determine the positions of the protons and the spin densities on the porphyrin nitrogen atoms.

ESEEM and Pulsed ENDOR Spectroscopy of ^{14}N nuclei in a Disordered System

Hyperfine couplings of nuclei with small magnetic moments are in general difficult to observe, owing to the fact that the nuclear transition probabilities are small with the ENDOR technique. Furthermore, the electron spin, whose direction of quantization alternates at the radiofrequency, can cause a considerable reduction in the effective RF field at the position of the nucleus (the so-called hyperfine enhancement).[*] An alternative is to use ESEEM spectrosco-

[*] The hyperfine enhancement can cause either an increase or a reduction of the effective RF field experienced by the nuclear spin, depending on the m_S state that is observed. For a spin system with $S = 1/2$ and $I = 1/2$ the RF field strength must be multiplied by the factor $(1 - m_S a_{iso}/\omega_I)$[53].

py, since with this method the relationships that determine the modulation amplitudes, and therefore also the line intensities, are different.

It will now be shown, by taking as an example a copper complex with ^{14}N hyperfine couplings below 4 MHz, that the two methods are often complementary.[111] In Figure 26 two sets of simulated powder spectra are compared, one for ESEEM (a) and the other for ENDOR (b). For a pair of magnetically equivalent nuclei with spin $I = 1$ we expect six transitions altogether, three for each m_S-state ($|-1\rangle \rightarrow |0\rangle$, $|0\rangle \rightarrow |1\rangle$ and $|-1\rangle \rightarrow |1\rangle$), with a corresponding broadening due to powder averaging.

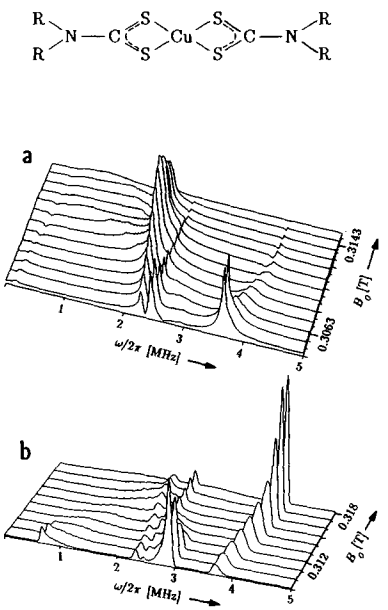

Fig. 26. Comparison of the ESEEM and pulsed ENDOR techniques for the example of ^{14}N powder spectra. The data shown are for $[Cu^{II}(Et_2dtc)_2]$ (Et_2dtc = *N*,*N*-diethyldithiocarbamate). The spectra were calculated for $m_I^{Cu} = 3/2$ with directions of B_0 between $g_{\parallel}$ and $g_{\perp}$. a) ESEEM spectra, τ_D = 800 ns. b) Pulsed ENDOR spectra (Ref. [111]).

The two plots complement each other in a near-ideal fashion. Peaks that are weak or not detectable at all in the ENDOR spectra appear as intense lines in the ESEEM spectra, and vice versa. This example illustrates the fact that in many cases a complete determination of the hyperfine and quadrupolar couplings of nuclei with small magnetic moments is only possible by combining data from ESEEM and pulsed ENDOR.

4. New Techniques in Pulsed ESR Spectroscopy

Following the description of the basic types of experiments of pulsed ESR spectroscopy in Section 3, we now turn to some new developments in techniques.

4.1. Two-Dimensional FT-ESR Spectroscopy

Two-dimensional nuclear magnetic resonance (2D NMR) is now well recognized as one of the most important spectroscopic methods for obtaining detailed information about the structure and dynamics of molecules in solution.[5,6] It is only quite recently that some of the 2D NMR techniques have been successfully carried over into ESR spectroscopy.[61,63,112-114] Two-dimensional ESR methods are essentially subject to the same restrictions as were described for one-dimensional ESR spectroscopy in Section 3.1. As before, the MW pulse must excite the whole of the ESR spectrum, and the line widths must be small enough to ensure that the FID does not die away before the dead time has elapsed.

4.1.1. 2D Correlation Spectroscopy (COSY)

In nuclear magnetic resonance, COSY experiments are used to study the transfer of coherence between coupled nuclear spins.[5,6] Analogous procedures can also be carried out with electron spins. In the simplest form of COSY (Fig. 27a) the preparation stage consists of a 90° pulse.[5,112] The transverse magnetization thus produced is allowed to develop during the evolution period t_1, and thereby becomes labeled according to the precession frequencies present. A second 90° pulse then generates the FID, which is measured during the acquisition period t_2. In the 2D experiment the evolution time t_1 is increased in a stepwise fashion, and a separate FID is recorded for each t_1-value. After shifting the phase of the first pulse by 90° this measurement cycle is then repeated. The two sets of FIDs, whose amplitudes oscillate as functions of t_1, then undergo a two-dimensional complex Fourier transformation, yielding a 2D ESR spectrum in which the variable frequencies are ω_1 and ω_2. In a 2D plot of this kind the diagonal peaks ($\omega_1 = \omega_2$) represent the uncorrelated ESR spectrum, whereas the cross-peaks (off-diagonal peaks) provide evidence of cross-correlations.

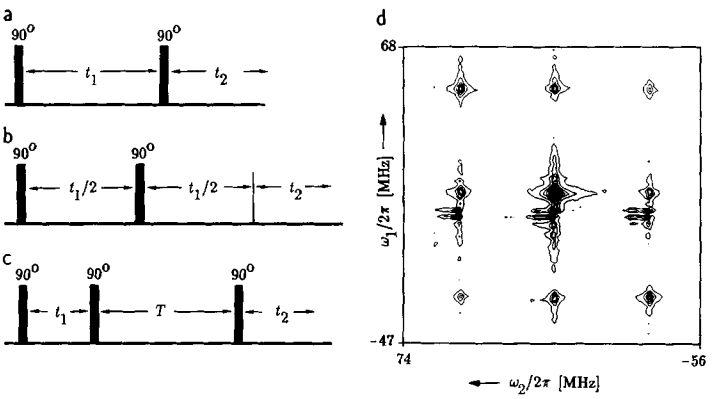

Fig. 27. a) to c) 2D FT-ESR pulse sequences, COSY (a), SECSY (b), EXSY (c). d) EXSY contour line diagram for perdeuterated tempone (for structure see Fig. 5a) in [D_8]toluene (1.17×10^{-3} M), 21 °C, mixing time 310 ns (the doublets at $\omega_1 = 0$ are caused by artefacts) (Ref. [112]).

4.1.2. 2D Spin-Echo Correlation Spectroscopy (SECSY)

In the SECSY experiment (Fig. 27b) the shape of the echo is recorded as a function of the pulse separation $\tau =$

$t_1/2$.[5, 112] The time interval between the first pulse and the echo maximum is equal to the evolution period, whereas the time following the echo maximum corresponds to the detection period. The two-dimensional Fourier transformation gives a SECSY plot with the ESR spectrum along the ω_2-axis and the homogeneous line shape along the ω_1-axis. Provided that the MW pulses are short enough to excite the entire ESR spectrum, one SECSY spectrum contains the same information as a series of echo-detected ESR spectra (Section 3.2.2.). The advantage of SECSY compared with the field sweep method is that the time needed for data acquisition is shortened by an order of magnitude.

4.1.3. 2D Exchange Spectroscopy (EXSY)

EXSY (Fig. 27c) is a 2D technique for monitoring the transfer of magnetization between hyperfine lines.[5, 112] In this the COSY sequence is extended by the addition of a further 90° pulse and a mixing period of constant duration T, during which an exchange of magnetization between individual hyperfine lines can take place. The magnetization of a hyperfine line 'a', which precesses during the evolution period with the frequency $\omega_1 = \omega_a$, acquires a new precession frequency $\omega_2 = \omega_b$ after the transfer of polarization, which corresponds to the frequency of the hyperfine line 'b'.

Figure 27d shows the EXSY spectrum of perdeuterated tempone (contour plot).[112] The transfer of polarization which occurs during the mixing period as a result of Heisenberg spin exchange[*] causes cross-peaks to appear. The Heisenberg exchange rate ω_{HE} can be determined directly from the ratio of the intensities of the diagonal and cross-peaks.

4.2. Special Nuclear Modulation Effects

The nuclear modulation effect is of central importance in pulsed ESR spectroscopy. For this reason a number of techniques have recently been developed for improving resolution and sensitivity, separating overlapping ESEEM spectra, and overcoming various types of instrumental distortions by either eliminating them or taking them into account in the processing of the data.[50, 115]

4.2.1. Eliminating Dead-Time Effects in ESEEM Spectroscopy

It was shown in Section 3.3 that the spectrometer dead time can cause unacceptable distortions of the ESEEM spectrum. A pulse technique which gives results that are completely unaffected by the spectrometer dead time is described below.[116]

The pulse sequence for this is shown in Figure 28a. The first two pulses, separated by the interval τ_i, generate the usual two-pulse echo at a time τ_i after the 180° pulse. However, in contrast to the usual procedure this short-lived transverse magnetization is not recorded, but is instead converted into a longitudinal magnetization by a further 90° pulse, so that it can be "stored" there for a time interval of the order of T_1. After a fixed time delay $\tau_1 < T_1$ the stored z-magnetization can be "read out" by means of a further two-pulse experiment with a pulse interval $\tau_2 > \tau_D$. *Increasing* τ_i in a series of steps gives an ESEEM pattern which corresponds to the usual two-pulse echo modulation, but with the important difference that the dead time after the first two pulses can no longer have any effect on the acquisition of the echo amplitude data.

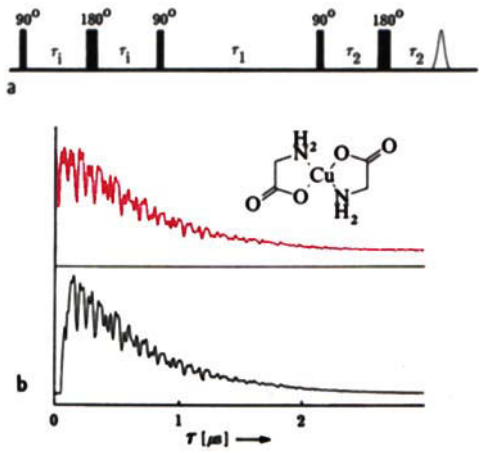

Fig. 28 ESEEM experiment unaffected by the dead time. a) Five-pulse sequence in which the third pulse stores the echo magnetization along the z-direction. b) Comparison of the five-pulse and two-pulse echo modulation patterns from a Cu^{II}-doped single crystal of TGS at 10 K (Ref. [116]).

Introducing these additional storing and reading pulses thus completely eliminates the dead-time problem. However, some sacrifice of signal intensity due to relaxation effects and the finite durations of the pulses is unavoidable. Also the two extra pulses generate further echoes, which can overlap with the echo in which we are interested for certain combinations of τ_i, τ_1 and τ_2. However, unwanted echoes of this kind can in turn be eliminated by suitable phase cycles.[116]

Figure 28b shows a five-pulse and a two-pulse ESEEM pattern from a Cu^{II}-doped single crystal of TGS. The two modulation patterns are practically identical except for the first 120 ns, which is lost in the two-pulse experiment owing to the dead time.

4.2.2. Reconstruction of Broad Hyperfine Lines

It was mentioned in Section 3.3.1 that in three-pulse experiments on powder samples the line shapes can be badly distorted by the suppression effect and by the dead time. However, since the rapid decay of the echo modulation in disordered systems is caused by destructive interference, the original information can be reconstructed by means of a suitable pulse sequence.[117]

The reconstruction method is based on a three-pulse sequence with specially chosen time intervals. According to Equation (9) the intensities at the two modulation frequencies ω_α and ω_β depend on the amplitudes $(1 - \cos(\omega_\beta\tau))$ and

[*] Heisenberg spin exchange is a spin-spin exchange process between pairs of free radicals. This relaxation mechanism is mainly important at high radical concentrations.

$1 - \cos(\omega_a \tau)$) respectively. Consequently, if the time interval τ is several microseconds this causes a rapid modulation of the amplitudes of the hyperfine lines (Fig. 29a). If now the time τ' is varied and the stimulated echo is measured, this amplitude-modulated spectrum corresponds in the time domain to an oscillating pattern consisting of two parts, a signal $f_1(\tau')$ which appears at small values of τ' and rapidly decays, and a signal $f_2(\tau')$ in the region near $\tau' = \tau$ (Fig. 29b).

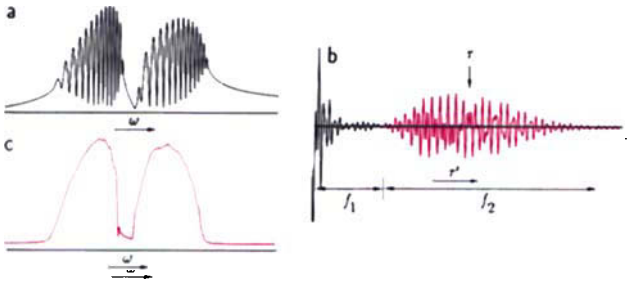

Fig. 29. Reconstruction of broad hyperfine signals in powder samples. a) Magnitude spectrum of the complete modulation pattern with $\tau = 2$ µs. b) Modulation pattern for $\tau = 2$ µs. c) Magnitude spectrum of f_2 (for parameters see model system, Fig. 1a) (Ref. [117]).

The second signal lies well outside the dead time, and is formed by the refocussing of the amplitude modulation; it is therefore called the *echo-modulation echo*. It can be shown that the magnitude spectrum of this echo-modulation echo corresponds to the undistorted hyperfine spectrum (Fig. 29c).[117]

4.2.3. Extended-Time Excitation

In the usual ESEEM methods only the amplitude of the electron spin-echo is measured. To record a modulation pattern one therefore has to increase one of the time intervals in the pulse sequence in a stepwise manner from experiment to experiment, which can be a very time-consuming procedure. However, by using a suitable pulse sequence it is possible to prepare the spin system in such a way that it responds by producing a long transient signal whose variation with time is identical to the echo modulation.[118] It is then possible to measure the complete modulation pattern in a single experiment, similar to the recording of an FID. Extended time excitation can be achieved using coherent microwave radiation of a constant amplitude, or a picket fence consisting of a succession of many short weak pulses, followed in either case by a single hard 180° refocussing pulse (Fig. 30). Stochastic excitation also gives the correct modulation pattern, but only after adding together data from many individual measurements, which is necessary because of the random nature of this form of excitation.

The extended time excitation effect relies on a continuous refocussing of the electron-nuclear interactions due to the special manner of preparation of the spin system. For an infinitely broad inhomogeneous ESR line the duration of the transient signal is exactly equal to that of the excitation pulse.[77] For weak preparation pulses (flip angle $\beta_{tot} \leq 30°$) the modulation phenomenon is easy to understand from a

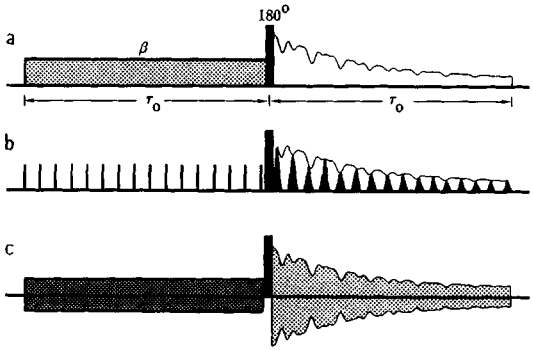

Fig. 30. Pulse sequences for extended time excitation. a) Weak coherent preparation pulse. b) Preparation using a picket fence of short weak pulses. c) Stochastic excitation.

qualitative standpoint, as the behavior of the spin system is then linear. Each brief element of the time interval τ_0 gives rise to a two-pulse echo positioned symmetrically relative to the 180° pulse (Fig. 30b). In the case of a continuous extended time excitation the superposition of all these echoes produces a continuous transient signal, which corresponds to the ESEEM pattern of a two-pulse experiment. In Figure 31a results from the two-pulse echo modulation method and the extended time excitation experiment are compared. In the two-pulse ESEEM experiment (Fig. 31a, top) the individual echoes from a cobalt complex show deep modulations at frequencies below 7 MHz, which are caused by hyperfine and nuclear quadrupolar couplings of the nitrogen-containing ligands (200 echoes recorded by multiple exposure). The same modulation pattern can be obtained by a single experiment using coherent extended time excitation with a duration of $\tau_0 = 2$ µs (Fig. 31a, bottom).

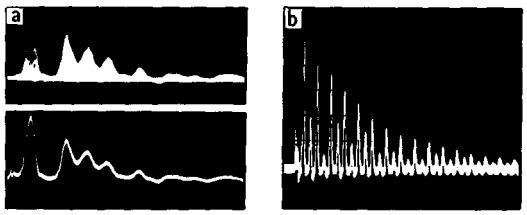

Fig. 31. a) Comparison of transient signals from [Co^{II}(acacen)] (H_2acacen = *N*,*N'*-bis(acetylacetone)ethylenediamine), measured by the standard two-pulse experiment (top) and by extended time excitation with $\tau_0 = 2$ µs (bottom). b) Modulation pattern from [Cu^{II}(bipyam)(dien)] (bipyam = 2,2-bipyridylamine, dien = diethylenetriamine), obtained using a picket fence of 16 weak short pulses. First-order and second-order contributions are separated in time (Refs. [118, 50]).

However, the extended time excitation method only gives a correct echo modulation pattern if the requirements for linear system theory are satisfied. For flip angles $\beta > 30°$ distortions appear in the modulation pattern, and the method can then no longer be used. Nevertheless, since the signal intensities increase with increasing flip angle, variants have been proposed whereby extended time excitation can give correct modulation patterns well into the non-linear region.[50]

A simple example is shown in Figure 31b. The pulse sequence used consists of 16 weak pulses, each with a duration of 10 ns, a flip angle $\beta_b \simeq 7°$, and a pulse interval $\Delta\tau =$

100 ns. The 180° refocussing pulse follows the last of the 16 pulses after an interval $\Delta\tau/2 = 50$ ns. This choice of time intervals results in a time separation of all the unwanted second-order interpulse echoes (stimulated or refocussed echoes formed from two weak pulses and the 180° pulse). In this way the total flip angle $\beta_{tot} = 16\beta_b$ of the extended time excitation period can considerably exceed the linear region without introducing serious distortions into the modulation pattern. In practice this gives an increase of about an order of magnitude in sensitivity.

4.2.4. Soft ESEEM Spectroscopy

A common feature of all the pulse sequences for producing echo modulations that have been described so far is that they make use of at least one intense MW pulse, which is capable of exciting the allowed and forbidden transitions simultaneously. In the technique now to be discussed the allowed and forbidden transitions are excited separately by weak selective pulses.[119] A soft ESEEM experiment of this kind can be achieved in two ways: by using pulses with two different MW frequencies, or by including within the pulse sequence a sudden change of the field strength B_0 (Fig. 32). Since these two procedures are equivalent, only the soft ESEEM technique based on two frequencies will be described.

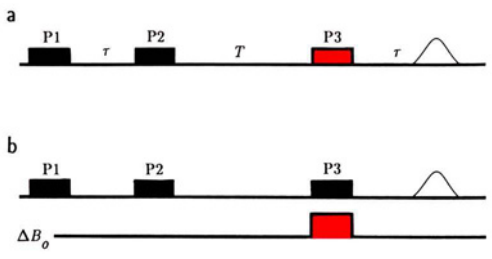

Fig. 32. Soft ESEEM pulse sequences. a) Two-frequency soft ESEEM. b) Two-field soft ESEEM.

The soft ESEEM method consists of a two-pulse echo sequence in which the 180° refocussing pulse is split into two 90° pulses separated by a time interval T. The first pulse of the sequence, with a flip angle of 90° and a frequency $\omega_{mw}^{(1)}$, selectively excites one of the four ESR transitions (allowed or forbidden), thereby producing an electron spin coherence which begins to dephase after the pulse. After a time interval τ the 90° pulse P2 with the same frequency stores a fraction of this coherence in the form of longitudinal magnetization along the $(-z)$-direction. The third pulse P3, with the new frequency $\omega_{mw}^{(2)}$, is applied after a time delay $T > \tau$, so as to avoid distortion by overlapping with the echo generated by the first two pulses. If the frequency of the third pulse is close to an ESR transition which shares a common energy level with the first transition, the stored longitudinal magnetization is converted back into electron spin coherence. During the subsequent evolution period this coherence precesses and produces a stimulated echo after a time τ. In analogy with nuclear magnetic resonance we call this transient signal a *coherence transfer echo*,[120] since it involves dephasing and refocussing processes for different ESR transitions.

Figure 33 (a and b) compares two-pulse and soft ESEEM patterns from a Cu^{II}-doped single TGS crystal. The spectrum of the two-pulse modulation (pulse durations 20 ns and 40 ns) contains essentially three fundamental frequencies and the sum frequency (Fig. 33c). If the durations of both pulses are increased by a factor of ten, while keeping the flip angle unchanged, the modulation almost completely disappears. A similar behavior is observed for the corresponding soft ESEEM pattern using three pulses of the same frequency and $t_{90°} = 300$ ns. However, if the frequency of the pulse P3 differs by an amount $\Delta\omega$ from the frequency of pulses P1 and P2, and if this frequency difference is close to one of the modulation frequencies ω_m, the echo intensity oscillates about the time-axis with the frequency ω_m (Fig. 33b).

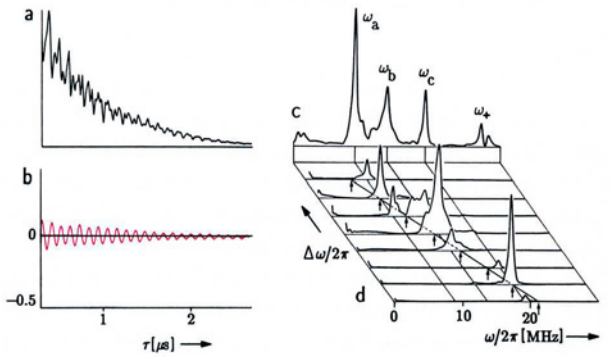

Fig. 33. Two-pulse and soft ESEEM patterns from a Cu^{II}-doped single crystal of TGS at 10 K. a) Two-pulse ESEEM experiment with pulse durations $t_{90°} = 20$ ns and $t_{180°} = 40$ ns. b) Two-frequency soft ESEEM experiment with pulse duration $t_p = 300$ ns and $\Delta\omega/2\pi = 19$ MHz; observed modulation frequency $\omega_m/2\pi = \omega_c/2\pi = 18.9$ MHz. c) Two-pulse ESEEM spectrum. d) Series of soft ESEEM spectra recorded at $\Delta\omega/2\pi$-steps of 2 MHz (Ref. [119]).

As the long excitation pulses cover only a narrow frequency window in the ESEEM spectrum, it is necessary to repeat the experiment with a range of different frequencies $\omega_{mw}^{(2)}$. The spectra obtained by Fourier transformation of a series of soft ESEEM patterns are shown in Figure 33d. To obtain these results the difference frequency $\Delta\omega/2\pi$ was increased from 7 to 21 MHz in 2 MHz steps. From this two-dimensional representation it can be seen that the soft ESEEM method correctly reproduces all the fundamental frequencies in the spectrum. The sum and difference frequencies do not appear, provided that each of the three selective pulses excites only one allowed and one forbidden ESR transition.

The soft ESEEM method has several advantages compared with the standard two-pulse method. The experiment can be performed with a microwave power level two to three orders of magnitude smaller than that for a two-pulse experiment with hard pulses ($P_{mw} \simeq B_2^2$). Also the soft ESEEM method makes it possible to observe modulation frequencies well above 100 MHz.

4.2.5. Increasing the Modulation Amplitude

In a normal three-pulse ESEEM experiment the first two pulses produce nuclear spin coherence, which then evolves during the evolution time T, and is converted by the third

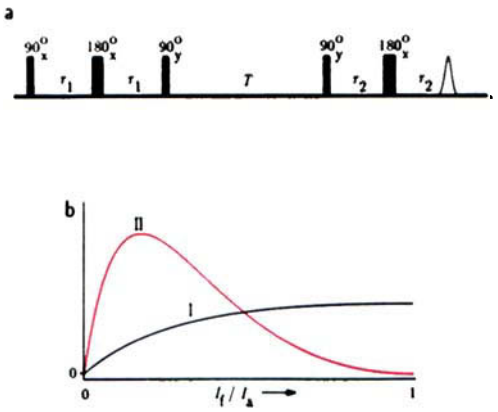

Fig. 34. Five-pulse ESEEM experiment for increasing the modulation amplitude. a) Pulse sequence. b) Amplitude of the echo modulation in the three-pulse (I) and five-pulse experiments (II) as a function of the ratio I_f/I_a of the transition probabilities for forbidden and allowed transitions (Ref. [121]).

pulse into electron spin coherence which can be observed. However, at the same time the three pulses also generate the stimulated echo. Thus, the formation of the echo and the transfer of coherence are closely linked together in the three-pulse experiment, and the experimenter can only influence them by the choice of the time interval τ.

However, by arranging for the formation of the echo and the production of nuclear spin coherence to be separated in time, it becomes possible to control the modulation amplitude over a much wider range.[121] This can be achieved, for example, by a five-pulse sequence (Fig. 34a), in which the first three pulses with a fixed time interval τ_1 are used only to produce the nuclear spin coherence. The nuclear spin coherence is maximized if the phase of the third pulse is shifted by 90° relative to that of the first two pulses. After a variable evolution time T the nuclear spin coherence is measured by a two-pulse echo sequence. To maximize the transfer of nuclear spin coherence back into electron spin coherence the fourth pulse, which comes at the end of the evolution period, should have the same phase as the detector.

With this five-pulse sequence it is theoretically possible, in the case of a small I_f/I_a ratio (or a small modulation depth parameter $k = 4I_aI_f$) to obtain a modulation amplitude up to eight times greater than in the three-pulse experiment, while at the same time keeping the unmodulated component of the echo intensity close to zero. In Figure 34b the modulation amplitudes for the five-pulse and three-pulse experiments are plotted as functions of I_f/I_a, the ratio of the intensities of the forbidden and allowed transitions. In the five-pulse experiment the modulation amplitude reaches a maximum at $I_f/I_a = 0.17$, whereas in the three-pulse experiment the maximum is not reached until $I_f/I_a = 1$, and it is only half that in the five-pulse experiment. Since I_f/I_a is usually small in practice, the increase in modulation obtained by using the five-pulse sequence can be quite considerable.

4.2.6. *Structural Information from the Sum-Frequency Peak*

In two-pulse experiments one observes, for each nucleus with spin $I = 1/2$, not only the fundamental frequencies ω_α and ω_β but also the sum frequency $\omega_+ = \omega_\alpha + \omega_\beta$. Expanding these sum frequencies as power series in A/ω_I and B/ω_I with $A, B < \omega_I$ gives (15).

$$\omega_+ \simeq 2\omega_I + B^2/4\omega_I + (4B^2A^2 - B^4)/64\omega_I^3 \qquad (15)$$

Equation 15 contains only terms of the second and higher orders in A and B. Because of this partial refocussing of the hyperfine interactions, the sum peaks appear as narrow lines in the neighborhood of $2\omega_I$, i.e. twice the nuclear Zeeman frequency.

The sum frequency takes its lower limiting value of exactly $2\omega_I$ when $\boldsymbol{B}_0$ is parallel or perpendicular to the line joining the electron and the nucleus. For all other directions of $\boldsymbol{B}_0$ the sum frequency is greater than $2\omega_I$. When it reaches its maximum value $\omega_{max} = 2\omega_I + \Delta$ the intensity of the sum peak is also at its maximum. Consequently, in a powder sample the sum peak extends over the frequency range from $2\omega_I$ to ω_{max}. As the intensity is reduced in regions where the gradient changes only slightly (i.e. near $2\omega_I$) due to the effect of the dead time, the sum peak spectrum for each nucleus usually appears as only a narrow line at the frequency ω_{max}. The frequency shift Δ is closely related to the dipolar part of the hyperfine coupling, and it contains important information about the positions of the nuclei.[122, 123]

In most cases the widths of the individual sum-frequency peaks are determined by the phase memory time T_M, which is relatively short. To improve the resolution one must therefore use a pulse sequence which allows a nuclear spin coherence to evolve during the variable time interval.[122] However, it is well known that sum frequencies do not appear in the three-pulse ESEEM experiment [Eq. (9)]. On the other hand, if in such a pulse sequence one inserts a 180° pulse at a time $T/2$ after the second 90° pulse (Fig. 35a) and increases T in a stepwise manner, sum frequencies again appear. The appearance of these sum frequencies (and also of the corresponding difference frequencies) is due to a transfer of nuclear spin coherence between the different m_S-states, which is induced by the additional 180° pulse. The slow decay of the echo intensity (determined by T_1) during the evolution time T usually results in a greatly improved resolution of the sum-frequency peaks.

Figure 35b shows such a sum peak spectrum obtained with a powder sample of Cu^{II}-glycine. So as to eliminate the dependence of the individual peak intensities on the value chosen for the time interval τ, several spectra with different τ-values were added together. In addition to the dominant peak at $2\omega_I$, which is caused by the large number of more

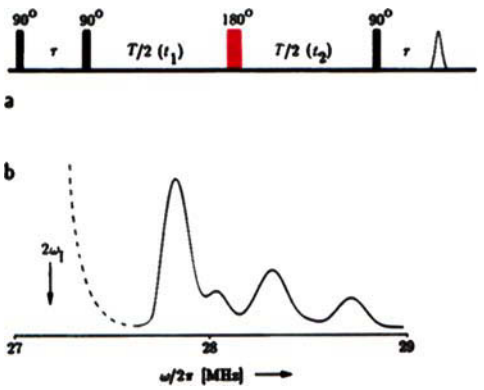

Fig. 35. Four-pulse ESEEM experiment for producing well-resolved sum-peak spectra. a) Pulse sequence. b) Sum-peak spectrum of Cu^{II}-glycine (see Fig. 28b) (cf. Ref. [122]).

distant, and therefore weakly coupled, protons, the sum frequencies of the four protons of the amino and methylene groups of the glycine ligands are clearly resolved. From the dependence of these sum frequencies on the position of the B_0 observing field in the ESR spectrum it is possible to determine the copper-proton distances and the positions of the protons. Thus, it is seen that sum peak spectra can provide valuable additional information about a spin system, especially when the hyperfine lines are broad and show little structure.

4.2.7. *Two-Dimensional ESEEM Techniques*

Two-dimensional echo modulation techniques (2D ESEEM) can often make ESEEM spectra easier to interpret. For example, in overlapping spectra they make it possible to assign the lines to individual paramagnetic centers and to determine the relative signs of the hyperfine couplings.

The 2D Three-Pulse ESEEM Technique

In this experiment both the time intervals $t_1 = \tau$ and $t_2 = \tau'$ in a stimulated echo sequence are independently increased in steps.[124] For a spin system with $S = 1/2$ and $I = 1/2$ the resulting 2D spectrum consists of six lines. Two pairs of axial peaks, one with the frequencies $(\omega_\alpha, 0)$, $(\omega_\beta, 0)$ and the other with the frequencies $(0, \omega_\alpha)$, $(0, \omega_\beta)$, form two identical 1D spectra along the ω_1 and ω_2 axes respectively, while the two cross-peaks at $(\omega_\alpha, \omega_\beta)$ and $(\omega_\beta, \omega_\alpha)$ are positioned symmetrically on either side of the diagonal $\omega_1 = \omega_2$ (Fig. 36a). In the magnitude spectrum all these peaks have the same intensity; blind spots, which caused difficulties in 1D spectra, therefore do not arise in this 2D ESEEM method.

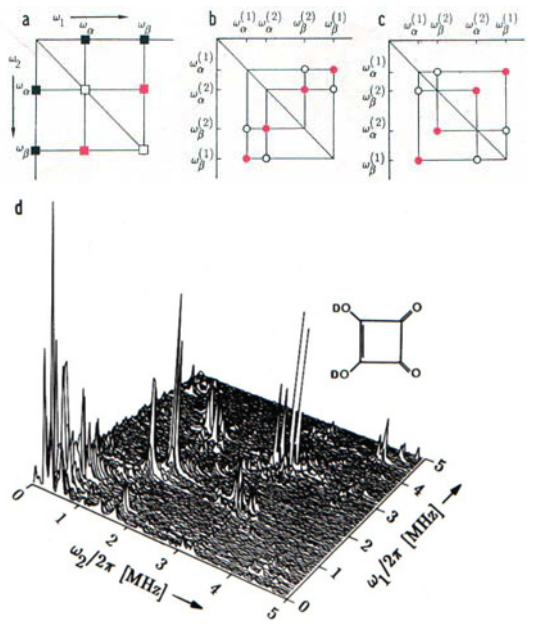

Fig. 36. a) Schematic 2D ESEEM spectrum for a spin system with $S = 1/2$ and $I = 1/2$; ■: peaks observed in both the three-pulse and in the four-pulse spectra, □: diagonal peaks arising from incomplete excitation in the HYSCORE method. b) Schematic 2D ESEEM spectrum for a three-spin system with $S = 1/2$ and $I_1 = I_2 = 1/2$. The two hyperfine coupling constants a_1 and a_2 have the same sign; ○: cross-peaks $(\omega_\alpha^{(i)}, \omega_\beta^{(j)})$ with $i \neq j$, ●: cross-peaks $(\omega_\alpha^{(i)}, \omega_\beta^{(j)})$ with $i = j$ (Ref. [70]). c) Corresponding situation where the hyperfine coupling constants a_1 and a_2 have opposite signs. d) HYSCORE single crystal spectrum at 295 K of deuterated squaric acid irradiated with 2 MeV electrons (Ref. [125]).

In systems with several spins and sufficiently large modulation depth parameters k_i, combination cross-peaks also appear, and these can be used to determine the relative signs of the hyperfine couplings. This is shown in Figure 36 (b and c) for the example of two nuclei with spin $I = 1/2$ and frequencies $\omega_\alpha^{(1)}$, $\omega_\beta^{(1)}$, $\omega_\alpha^{(2)}$ and $\omega_\beta^{(2)}$. In Figure 36b the two hyperfine coupling constants a_1 and a_2 have the same sign, whereas in Figure 36c they have opposite signs.

A disadvantage of the 2D three-pulse ESEEM technique is that the echo intensities decay at different rates along the two time axes, with T_M-relaxation along the t_1-axis and T_1-relaxation along the t_2-axis. As a result the line widths in the two frequency dimensions can differ by orders of magnitude.

The 2D Four-Pulse ESEEM Technique

Undesirable line-width effects of the kind just described do not arise in the HYSCORE (hyperfine sublevel correlation) experiment.[125] The HYSCORE technique is a 2D version of the four-pulse sequence mentioned in Section 4.2.6 (Fig. 35a), with an evolution period t_1, a 180° mixing pulse, and a second evolution period t_2. As nuclear spin coherence evolves during both these evolution periods, the line widths also are determined in both frequency dimensions by T_1 (or T_{2n}). This is illustrated in Figure 36d, which shows the HYSCORE spectrum of an electron-irradiated single crystal of deuterated squaric acid.[125]

When the modulation formulas of the three-pulse and four-pulse 2D ESEEM techniques are compared, it becomes clear that the same six frequencies occur in both experiments. However, in the HYSCORE plot the amplitudes for the different frequencies depend in a complicated way on ω_α, ω_β and τ. In particular, for certain values of these parameters (blind spots) the two cross-peaks can disappear.[70] Moreover, if the MW pulses in a HYSCORE experiment are not sufficiently hard to fully excite the spin system, new peaks appear along the diagonals of the 2D plot at the frequencies $(\omega_\alpha, \omega_\alpha)$ and $(\omega_\beta, \omega_\beta)$ (Fig. 36a). These correspond to the 1D three-pulse ESEEM spectrum, and are produced by components of the magnetization that cannot be completely refocussed by the 180° pulse. As the HYSCORE experiment involves four pulses, up to 13 unwanted echoes can result when the excitation is incomplete; however, all these can be eliminated by suitable phase cycles.[70] In the HYSCORE experiment too the positions of the cross-peaks can be used to determine the relative signs of hyperfine coupling constants (Fig. 36b, c).

4.3. Improving the Resolution of Powder ESR Spectra

Improving resolution is a subject of central importance for the spectroscopist. In ESR the spectra of disordered systems especially are lacking in structure. In this section we consider pulse techniques which suppress parts of the spectrum corresponding to particular orientations, thereby making it possible to greatly improve the resolution of the entire powder ESR spectrum.

The method is based on an echo-detected ESR experiment in which the orientation of the sample relative to the magnetic field vector $\boldsymbol{B}_0$ is altered during the pulse sequence.[126] To understand how this change of orientation affects the powder spectrum we will consider an axially symmetric spin system with $S = 1/2$. The resonance surface has the form of an ellipsoid of rotation B_{res}, the dimensions of the axes being $B_{\parallel} = \hbar\omega_{mw}/\beta g_{\parallel}$ and $B_{\perp} = \hbar\omega_{mw}/\beta g_{\perp}$ where $g_{\parallel}$ and $g_{\perp}$ are the principal values of the g-tensor (Fig. 37). For a given orientation of the magnetic field (defined by the angle θ) the resonance field strength is given by $B_{res}(\theta) = \hbar\omega_{mw}/\beta g(\theta)$, with $g(\theta) = (g_{\parallel}^2 \cos^2\theta + g_{\perp}^2 \sin^2\theta)^{1/2}$. Evidently the directions $B_{\parallel}$ and $B_{\perp}$ correspond to stationary points on the ellipsoid surface (i.e. points at which $dg(\theta)/d(\theta) = 0$), and near these directions the resonance condition remains unchanged when the magnetic field is rotated.

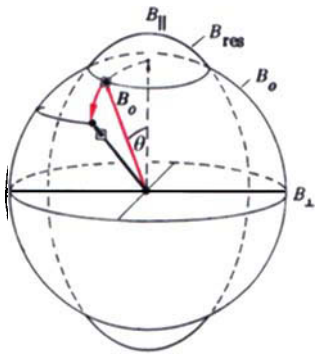

Fig. 37. Diagram to explain the experiment in which the orientation of $\boldsymbol{B}_0$ is changed during the pulse sequence. B_{res}-ELLIPSOID is the ellipsoidal resonance surface for an axially symmetric g-tensor with $g_{\perp} > g_{\parallel}$; B_0-SPHERE is a sphere with radius B_0 (Ref. [126]).

In this experiment the first 90° pulse of a three-pulse sequence excites those centers which satisfy the resonance condition $B_0 = B_{res}(\theta)$. For a given magnetic field strength B_0 this condition is satisfied for all the field vectors $\boldsymbol{B}_0$ that lie along the surface of a cone whose apex angle is 2θ. A change in the orientation of the sample relative to $\boldsymbol{B}_0$ in general alters the angle θ, and therefore also the resonance condition. The two 90° pulses, which are applied following such a reorientation, are unable to generate a stimulated echo because of the change in the resonance condition (Fig. 38a). This applies for all orientations except in the case of those sites for which the principal axes of the g-tensor are parallel or perpendicular to $\boldsymbol{B}_0$ ($\theta = 0$ or 90°), or for which a reorientation does not alter the angle θ (i.e. $\boldsymbol{B}_0$ lies on the same conical surface for both orientations).

Therefore in a powder sample any rotation between the molecular and the laboratory coordinate systems reduces all the contributions for $\theta \neq 0,90°$. If also all the other unwanted components in the spectrum are to be suppressed, the change of orientation during the pulse sequence must occur in two mutually perpendicular directions (Fig. 38b).[126] The spectrum then essentially consists only of contributions from the orientations $\theta = 0$ and $\theta = 90°$. From an experimental standpoint the necessary reorientation can be achieved either by rotating the field vector $\boldsymbol{B}_0$ or by rotating the sample.

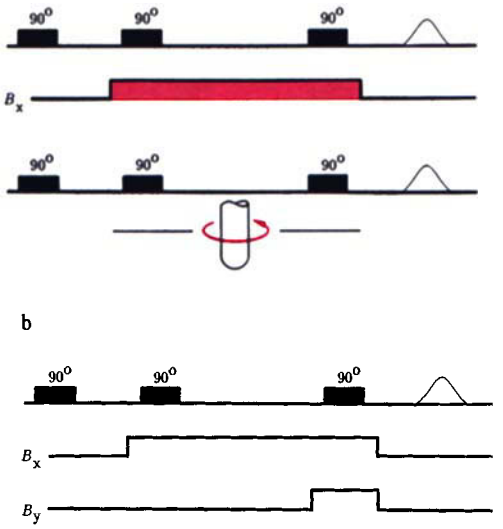

Fig. 38. Three-pulse sequences with orientational changes. a) One reorientation (top: field jump, bottom: sample rotation). b) Two reorientations (two field jumps in mutually perpendicular directions) (Ref. [126]).

Rotation of the Field Vector $\boldsymbol{B}_0$

Deflecting the field vector $\boldsymbol{B}_0$ is most easily achieved by switching on an additional field component perpendicular to the z-axis of the laboratory coordinate system (Fig. 38a, top). By using suitable auxiliary coils close to the resonator a transverse field of up to 10 mT can be established within 300 ns. For a longitudinal field B_0 of 0.3 T this corresponds to a deflection angle δ of about 1°, which is sufficient to give a considerable improvement in resolution for many compounds containing transition metal ions. Figure 39 shows echo-detected powder ESR spectra of a copper complex, measured both with and without a field jump.

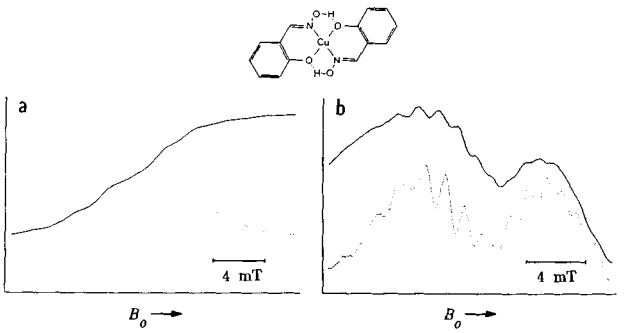

Fig. 39. Improvement in the resolution of powder ESR spectra of [Cu(sal)$_2$] (sal = salicylaldoxime) in [Ni(sal)$_2$] at 10 K using the field jump technique. a) Top: echo-detected three-pulse ESR spectrum, low-field region, bottom: corresponding ESR spectrum with one field jump. b) Top: echo-detected three-pulse ESR spectrum, low-field region, bottom: corresponding ESR spectrum with two field jumps (Ref. [126]).

Rotation of the Sample

Rotating the sample about an axis perpendicular to $\boldsymbol{B}_0$ is exactly equivalent to the experiment in which one of the field directions is altered (Fig. 38a, bottom). So as to be able to

work with low rotation frequencies, it is again preferable to use the three-pulse sequence, in which the decay of the echo intensity is determined by the spin-lattice relaxation time T_1. At sufficiently low temperatures a rotation frequency of a few hundred Hz is usually sufficient to suppress unwanted orientations from the spectrum. For example, with $T = 20\,\mu s$ and a rotation frequency of 200 Hz the sample rotates through an angle of about 1.5° between the second and third MW pulses.

4.4. The Electric Field Effect

The crystal field parameters of a paramagnetic center can be affected by an external electric field. Two mechanisms are mainly responsible for this effect. Firstly the electric field, by shifting the positions of ions, induces electric dipole moments, and secondly the wave functions of the ions become polarized. Since this effect is seen as a shift of the ESR lines which is approximately proportional to the electric field, it is referred to as a "linear" electric field effect (LEFE).[127] However, not all paramagnetic centers show an LEFE. For example, the magnetic parameters of free radicals are insensitive to electric fields. Also metal ions at sites with inversion symmmetry are to a first-order approximation unaffected by an external electric field.

As the local electric fields present are often greater by several orders of magnitude than the highest experimentally attainable fields that can be applied externally, the shifts of the resonance lines are often small, even in compounds without inversion symmetry, and in a CW ESR experiment they are only observable in rare cases. This is especially true of disordered systems. However, the difficulty of measuring small changes in the position of an inhomogeneously broadened line with a width of typically 1 mT or more can be avoided by pulse methods.[128]

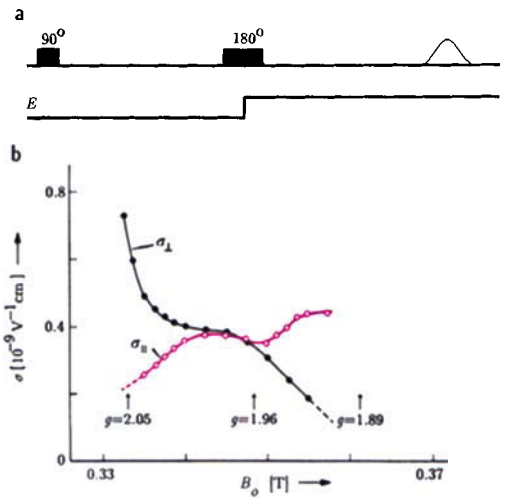

Fig. 40. Linear electric field effect (LEFE). a) Pulse sequence. b) LEFE shift parameters for spinach ferredoxin as a function of the magnetic field B_0 (Ref. [129]). $\sigma_\parallel : E \parallel B_0$, $\sigma_\perp : E \perp B_0$.

The pulsed LEFE experiment is shown in Figure 40a. In a two-pulse sequence an electric field jump is applied at the same time as the 180° pulse. This changes the precession frequency of the magnetization generated by the first pulse by an amount $\Delta\omega$, so that the echo formed at the time 2τ has a phase shift $\Delta\Phi = \tau\Delta\omega$. Since in a disordered system there exists, for every site with a positive $\Delta\Phi$, another site with an equal and opposite negative $\Delta\Phi$, the phase information is lost, and the effect must be detected by measuring a change in the intensity of the echo. For comparison purposes it is usual to define a shift parameter σ,[68] which is the electric field strength for which the echo amplitude is reduced by 50%.

As well as the simple test of whether or not there is inversion symmetry, paramagnetic compounds can also be identified and classified according to the curves of the shift parameters $\sigma_\parallel$ (E parallel to B_0) and $\sigma_\perp$ (E perpendicular to B_0) as functions of B_0.[68] As an example Figure 40b shows the result of an LEFE measurement on spinach ferredoxin, an iron-sulfur protein with two iron atoms.[129] The curves of $\sigma_\parallel$ and $\sigma_\perp$ as functions of B_0 show that the two iron atoms in this complex are non-equivalent.

4.5. Longitudinal Detection

In most pulsed ESR experiments one measures a transverse magnetization during the acquisition period, whether this takes the form of an FID, an echo, or some other transient signal. As well as this normal procedure, however, some other methods of observation can be used. These have been developed for special fields of application, where in many cases they have advantages over the conventional method of observation. One such method is optically detected magnetic resonance, whose most striking feature is its extremely high sensitivity.[130]

The technique that will be described here is a less well-known one, in which one measures the rapid change in the z-magnetization during the short microwave pulses.[73] In the simplest version of such a longitudinal detection (LOD) experiment, a 180° pulse of duration t_p inverts the on-resonance component of an inhomogeneous ESR line. This causes a hole of depth $2\,Mz$ and width $2/t_p$ to appear in the ESR line, and after the pulse this begins to fill up again with the time-constant T_1. The time-derivative $\dot{M}_Z$ of the z-magnetization induces an e.m.f. $U \cong \dot{M}_Z$ in a pick-up coil which has its axis *parallel* to B_0 and is connected to a capacitance C to form a resonant circuit (Fig. 41). This oscillatory circuit, whose resonance frequency $\omega_{res}/2\pi$ is in the range 1–

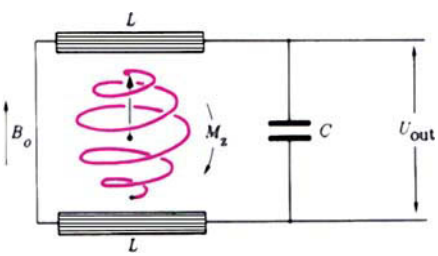

Fig. 41. Schematic arrangement for a pulsed ESR experiment with longitudinal detection (Ref. [73]). L (inductance) indicates the position of the pick-up coils.

100 kHz, acts as a band-pass filter and selects one Fourier component of the signal. Usually the resonance frequency of the oscillatory circuit is chosen to be equal to the repetition rate of the pulse (or of the pulse sequence). The periodic excitation by the pulses builds up an e.m.f. $U_{out}(t) = U \sin(\omega_{res}t + \varphi)$ across the resonant circuit, and after suitable filtering this can be recorded by an RMS voltmeter. As the detection frequency and the microwave frequency differ by many orders of magnitude, the excitation and the detection are completely decoupled from each other. Dead-time effects caused by the microwave pulses do not arise in the LOD method.

Figure 42 shows three alternative LOD sequences, together with the corresponding curves of z-magnetization vs. time. The sequence consisting of a single 180° pulse (Fig. 42a) allows one to measure an ESR spectrum by slowly changing the field B_0. An example of an application for which this

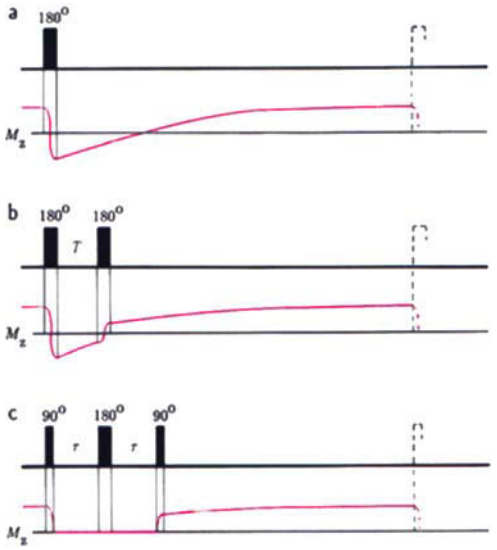

Fig. 42. LOD pulse sequences. a) One-pulse sequence for measuring ESR spectra. b) Two-pulse sequence for measuring T_1. c) Three-pulse sequence for measuring T_M and recording echo modulation patterns (Ref. [73]).

LOD sequence can be used is in detecting short-lived radicals that are produced immediately before the 180° pulse, e.g. by a laser pulse. It is also used for measuring ESR spectra with very broad lines, since the signal intensity is not limited by the amplitude of the modulation as it is in a CW ESR experiment.

The LOD sequence 180°–T–180° (Fig. 42b) is useful for measuring short longitudinal relaxation times. The inverted z-magnetization produced by the first 180° pulse relaxes during the interval T and is measured during the second 180° pulse.

Lastly, in the LOD sequence 90°–τ–180°–τ–90° (Fig. 42c) the third pulse turns the echo magnetization produced by the first two pulses out of the xy-plane. This again constitutes a rapid change of the z-magnetization, which is detected by the pick-up coil. This sequence is suitable for measuring short transverse relaxation times or for recording the rapidly decaying ESEEM patterns of disordered systems, since the data acquisition is then no longer limited by the dead time.

4.6. Special Pulsed ENDOR Techniques

This section describes a number of new pulsed ENDOR methods that have been developed to optimize the ENDOR effect, to determine the number of equivalent nuclei, or to simplify complex ENDOR spectra. All these techniques are based on the transfer and subsequent detection of polarization. Recently also some pulse sequences based on the indirect observation of nuclear spin coherence have been proposed. For double resonance methods in which the ENDOR effect is observed through a change in the electron spin coherence, the reader is referred to the literature.[131, 132]

4.6.1. Optimizing the ENDOR Effect

With the Mims and Davies ENDOR sequences (see Fig. 23) it is possible in the most favorable cases to obtain an ENDOR effect of 50% (disappearance of the echo intensity).[133] If one replaces the RF pulse by a sandwich consisting of a 180° MW pulse flanked by two 180° RF pulses, this increases the ENDOR effect to 100% in both cases (inversion of the echo).[134] The pulse sequence that gives this optimum polarization transfer in the case of the Davies ENDOR experiment is shown in Figure 43a.

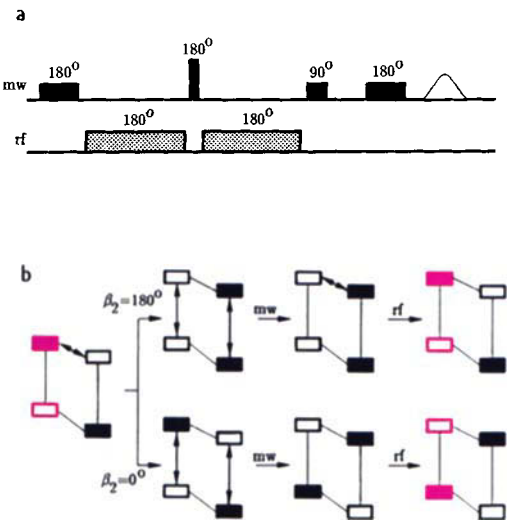

Fig. 43. a) Davies ENDOR with optimized polarization transfer. b) Corresponding changes in populations of states (Ref. [134]).

The transfer of polarization in this extended Davies ENDOR scheme can be followed without difficulty (Fig. 43b). After the first MW pulse, which inverts the polarization of a particular ESR transition, we consider separately the polarization patterns for one on-resonance radiofrequency ($\beta_2 = 180°$) and for one off-resonance radiofrequency ($\beta_2 = 0$). From the diagrams it is evident that for the off-resonance case the polarization of the observed ESR transition at the end of the mixing period has returned to the original equilibrium condition (positive echo amplitude). However, if the frequency of the two RF pulses coincides with that of an ENDOR transition, the polarization remains inverted after the sandwich pulse (negative echo amplitude), which corresponds to an ENDOR effect of 100%.

4.6.2. *Hyperfine-Selective ENDOR Spectroscopy*

Although the double resonance effect usually gives an enormous reduction in the number of lines in an ENDOR spectrum (Section 2.2), it is often difficult in complicated spin systems to assign the transitions to individual nuclei. The pulse sequence used in the hyperfine-selective ENDOR technique (HF-ENDOR) enables one to select from a complex ENDOR spectrum only those lines that belong to a nucleus with a particular hyperfine coupling whose value can be varied at will.[135] Thus an ENDOR spectrum can be decomposed into a number of partial spectra, each of which describes a separate electron-nucleus subsystem.

The HF-ENDOR technique is based on the Davies ENDOR scheme (Section 3.4), but in this case the echo is detected at a position of the magnetic field which is shifted from the preparation stage by an amount equal to the hyperfine coupling (Fig. 44a, b). The change of position in the ESR spectrum is achieved either by a jump in the field strength, B_0[135] or by a change in the MW frequency.[136] Thus the HF-ENDOR technique is an electron-electron-nuclear triple resonance experiment.

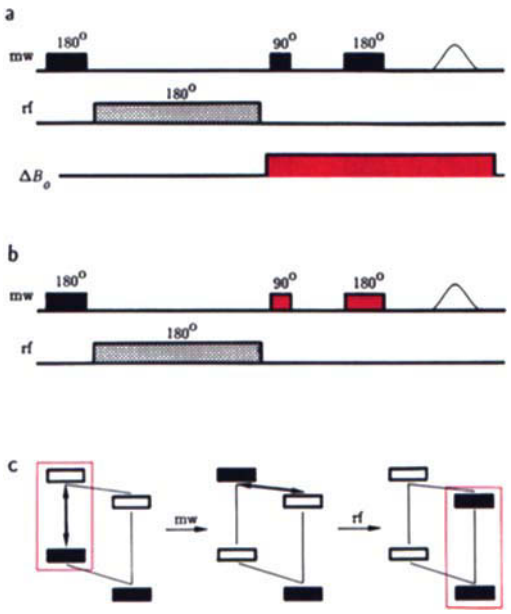

Fig. 44. Hyperfine-selective ENDOR (HF-ENDOR). a) HF-ENDOR with field jump ΔB_0. b) HF-ENDOR with two microwave frequencies. c) Corresponding changes in populations of states (Refs. [135, 136]).

If, in a complicated multilevel system, we consider a subsystem which describes the interaction between the electron spin and one nucleus with spin $I = 1/2$, the selective 180° MW pulse inverts the polarization of one of the two (allowed) ESR transitions of this subsystem (Fig. 44c). It thus "burns a hole" in the ESR line at the existing field position B_0. The selective 180° RF pulse then inverts the polarization of one of the two nuclear spin transitions. This transfers part of the polarization and forms a secondary hole in the ESR line at the position $B_0 + a$, since the two ESR transitions of the subsystem under consideration are at field positions separated by the hyperfine coupling constant a.

In the normal Davies ENDOR experiment the change which the RF pulse induces in the polarization at the field position B_0 is detected by a two-pulse echo sequence. However, since now all the ENDOR transitions can originate from any arbitrary energy level, all the ENDOR lines can be observed by using a variable radiofrequency at the field B_0. But for an observer at the field position $B_0 + \Delta B_0$, the situation appears differently. At this position in the spectrum a transfer of magnetization only occurs if one of the nuclei has a hyperfine coupling constant equal to ΔB_0. Therefore at $B_0 + \Delta B_0$ one observes only the spectrum of this nucleus. This selection principle remains valid for any value of the nuclear spin quantum number I.

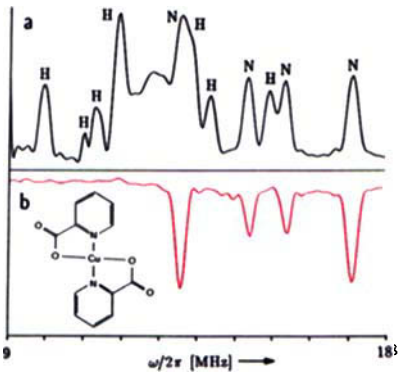

Fig. 45. ENDOR and HF-ENDOR spectra of Cu^{II}-picolinate at 10 K. a) Portion of Davies ENDOR spectrum. b) Hyperfine-selective ENDOR spectrum of the two magnetically equivalent ^{14}N nuclei; the field jump ΔB_0 between excitation and acquisition was 1.1 mT (Ref. [135]).

Figure 45 shows a portion of the ENDOR spectrum of a single crystal of Cu^{II}-picolinate, containing both proton and nitrogen lines, together with an HF-ENDOR spectrum recorded at a field position shifted by an amount equal to the hyperfine coupling constant a_N of the nitrogen nuclei.[135] This selection procedure can be repeated for each set of equivalent nuclei, thereby giving a complete breakdown of the ENDOR spectrum into its components.

4.6.3. *ESR-Detected Nuclear Transient Nutations (Multiple-Quantum ENDOR Spectroscopy)*

An RF pulse can generate nuclear transient nutations[*] within an m_S-state. Various sequences consisting of combinations of MW and RF pulses have been proposed for generating and detecting such nuclear nutations.[44, 137–139] Figure 46a shows two methods, both based on the Davies ENDOR scheme and differing only in their RF pulse sequences. In both cases the first 180° MW pulse serves to generate nuclear spin polarization. The first sequence involves a stepwise increase in the length of the RF pulse, whereas the second method uses a 180° RF pulse which is divided into two 90° pulses and the phase φ of the first 90° pulse is advanced in a

[*] Transient nutations (or Torrey oscillations) are precessions of the on-resonance magnetization in the plane perpendicular to the applied alternating field.

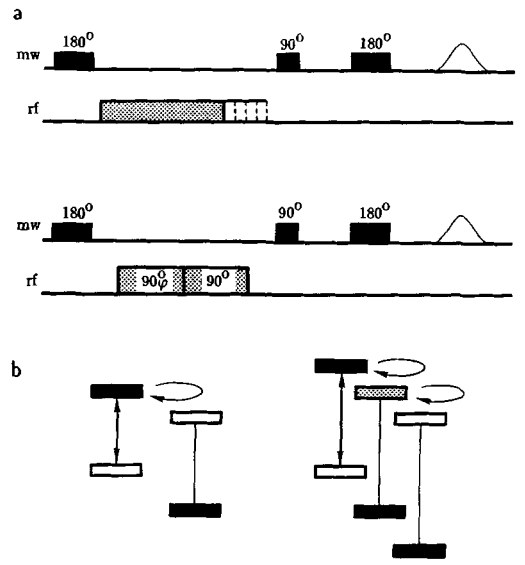

Fig. 46. Indirectly detected nuclear transient nutation. a) Pulse sequence for inducing multiple-quantum nuclear transitions. b) Nuclear nutation within an m_S spin state; left: one $I = 1/2$ nucleus, right: two $I = 1/2$ nuclei (Refs. [137, 138]).

stepwise fashion. For a spin system having a single nucleus with spin $I = 1/2$, this means that the nuclear spin polarization of the observed transition oscillates sinusoidally. These oscillations are then recorded indirectly via the electron spin-echo.

In spin systems with several equivalent nuclei a complicated nutation pattern is produced, as the RF pulse also affects the polarizations of ENDOR transitions whose energy levels have not been involved in the MW preparation pulse. This is shown schematically in Figure 46 b for the case of two nuclei with spin $I = 1/2$. Experimental techniques whereby such transitions become excited are often referred to as multiple-quantum ENDOR spectroscopy (MQ-ENDOR). The Fourier transformation of the nutation pattern yields the MQ-ENDOR spectrum. The particularly interesting feature of such spectra is that the number and intensities of the lines are characteristic of the number of equivalent nuclei in the spin system. This important item of information cannot be obtained from the ENDOR spectrum. Figure 47a shows a series of calculated MQ-ENDOR spectra for one to four equivalent nuclei with spin $I = 1/2$.

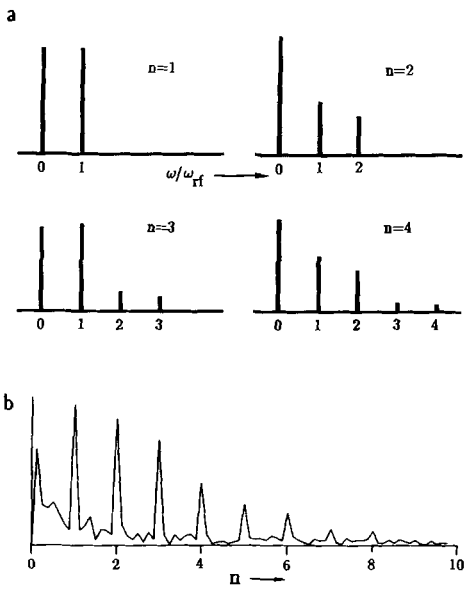

Fig. 47. a) Multiple-quantum patterns for $n = 1$, 2, 3 and 4 equivalent nuclei with spin $I = 1/2$. b) MQ-ENDOR spectrum of the protons of *trans*-polyacetylene with $\omega_{RF} = \omega_H$ (Refs. [137, 138]).

If the field intensity of the RF pulse is greater than the difference between the hyperfine coupling constants, it is also possible to induce MQ-ENDOR transitions of non-equivalent nuclei. The number of MQ transitions observed then provides a measure of the density of the spectral distribution of the hyperfine couplings. An example of such an *n*-quantum spectrum for solitons in *trans*-polyacetylene (Section 3.3.4) is shown in Figure 47b.[138]

4.6.4. *Pulsed ENDOR Spectroscopy in the Time Domain*

In all the ENDOR experiments described above, the RF pulse causes a transfer of nuclear spin *polarization*. However, a disadvantage of these techniques is that if the RF pulses are too short the ENDOR lines can be broadened. This broadening can be avoided by measuring the ENDOR spectrum in the time domain. Two possible pulse sequences for this, based again on the Mims and the Davies ENDOR schemes, are shown in Figure 48 a, b.[140, 141] After generating nuclear spin polarization, an intense 90° RF pulse is used to produce nuclear spin *coherence*. However, the spectral range that can be excited by the RF pulse is only about 1 MHz wide. After a time T the nuclear spin coherence is converted back into electron spin polarization by a further 90° RF pulse, and this is then measured by recording an echo. Measuring the echoes

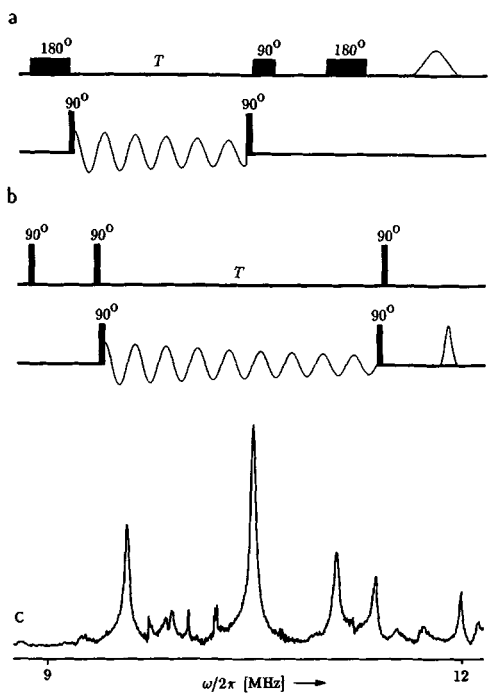

Fig. 48. ENDOR in the time domain. a) and b) Pulse sequences for measuring ENDOR spectra in the time domain. c) ENDOR spectrum of a Cu^{II}-doped single crystal of TGS reconstructed from segments. Magnitude spectra, each 1 MHz in width, with center frequencies 9.2, 9.7, 10.2, 10.7, 11.2, 11.7, and 12.2 MHz (Refs. [139, 140]).

as a function of T and performing a Fourier transformation on the data yields a portion of the ENDOR spectrum with natural line widths determined by the transverse relaxation time T_{2_n} of the nuclei. Thus the FID of the excited nuclear spins is observed indirectly via the electron spin. The entire ENDOR spectrum can be obtained by repeating the experiment with different frequencies of the RF pumping field. Figure 48c shows an ENDOR spectrum obtained by fitting together such spectral segments recorded by the stimulated echo sequence.[141]

5. Summary and Outlook

There can be no doubt that pulsed electron spin resonance techniques open up new and previously undreamed of prospects in ESR spectroscopy. Of the many different pulsed ESR methods that are described in this article, those that appear to be finding the widest application are the ESEEM technique, the FT-ESR method, and the various pulsed ENDOR methods. Since there are in most cases no real alternatives to these methods, i.e. the spectroscopic data of interest cannot be obtained in any other way, the additional cost of the equipment needed can be justified. Furthermore, the pulsed ESR instruments that are now commercially available are remarkably user-friendly, and therefore advanced knowledge of microwave electronics is not required. Moreover, the cost of a pulsed ESR spectrometer is considerably less than that of a modern NMR spectrometer.

Only the future will tell which of the sophisticated pulse techniques described here have the potential for becoming established in the long term. Some methods will undoubtedly soon become part of the everyday repertoire of pulsed ESR spectroscopy, whereas others will perhaps be only of historical interest a few years from now. Whatever the outcome, there are certain to be rapid advances in the development of pulsed ESR techniques. Also new methods will find their way into practical use, filling in gaps in the armory of pulsed ESR spectroscopic techniques.

The theoretical description of these pulsed experiments using the density operator formalism may be unfamiliar to many CW ESR spectroscopists. However, users whose interest is confined to magnetic parameters such as the nuclear resonance frequencies can safely ignore the complications of the spin dynamics on which the experiments are based.

To forecast the future of pulsed ESR spectroscopy is a risky undertaking. It seems unlikely that, as has happened in nuclear magnetic resonance, pulse methods will replace CW spectroscopy or make it obsolete within the foreseeable future. It is much more probable that pulsed ESR spectroscopy will become one of the cornerstones of ESR spectroscopy.

I thank my departmental colleagues for many useful suggestions and discussions during the preparation of this article. Furthermore, I am grateful to Bruker GmbH (Karlsruhe) for their financial support enabling the use of color printing. The support of our research by the Swiss National Science Foundation over a numbers of years is acknowledged.

Received: May 18, 1990 [A 808 IE]
German version: *Angew. Chem. 103* (1991) 223
Translated by Dr. *J. K. Becconsall*, Pwllheli (UK)

[1] A. Abragam, B. B. Bleaney: *Electron Paramagnetic Resonance of Transition Ions*, Clarendon, Oxford 1970.
[2] J. E. Wertz, J. R. Bolton: *Electron Spin Resonance*, McGraw-Hill, New York 1986.
[3] N. M. Atherton: *Electron Spin Resonance*, Ellis Horwood, Chichester 1973.
[4] W. Gordy: *Theory and Applications of Electron Spin Resonance*, Wiley, New York 1980.
[5] R. R. Ernst, G. Bodenhausen, A. Wokaun: *Principles of Nuclear Magnetic Resonance in One and Two Dimensions*, Clarendon, Oxford 1987.
[6] H. Kessler, M. Gehrke, C. Griesinger, *Angew. Chem. 100* (1988) 507; *Angew. Chem. Int. Ed. Engl. 100* (1988) 490.
[7] W. B. Mims in S. Geschwind (Ed.): *Electron Paramagnetic Resonance*, Plenum, New York 1972, p. 263.
[8] K. M. Salikhov, A. G. Semenov, Yu. D. Tsvetkov: *Electron Spin Echoes and their Applications*, Nauka, Novosibirsk 1976.
[9] L. Kevan, R. N. Schwartz (Eds.): *Time Domain Electron Spin Resonance*, Wiley, New York 1979.
[10] C. P. Keijzers, E. J. Reijerse, J. Schmidt (Eds.): *Pulsed EPR*, North Holland, Amsterdam 1989.
[11] A. J. Hoff (Ed.): *Advanced EPR*, Elsevier, Amsterdam 1989.
[12] L. Kevan, M. K. Bowman (Eds.): *Modern Pulsed and Continuous Wave Electron Spin Resonance*, Wiley, New York 1990.
[13] H. Thomann, L. R. Dalton, L. A. Dalton, *Biol. Magn. Reson. 6* (1984) 143.
[14] Yu. D. Tsvetkov, S. A. Dikanov, *Met. Ions Biol. Syst. 22* (1987) 207.
[15] S. A. Dikanov, Yu. D. Tsvetkov, *J. Struct. Chem. 26* (1985) 766.
[16] M. Romanelli, D. Goldfarb, L. Kevan, *Magn. Reson. Rev. 13* (1988) 179.
[17] A. Schweiger, *Chimia 40* (1986) 111.
[18] W. B. Mims, J. Peisach, *Biol. Magn. Reson. 3* (1981) 213.
[19] A. E. Stillman, R. N. Schwartz, *J. Phys. Chem. 85* (1981) 3031.
[20] L. Kevan, *Acc. Chem. Res. 20* (1987) 1.
[21] J. R. Norris, M. C. Thurnauer, M. K. Bowman, *Adv. Biol. Med. Phys. 17* (1980) 365.
[22] T. Lin, *Chem. Rev. 84* (1984) 1.
[23] J.-M. Fauth, *Dissertation*, ETH Zürich, N. 8645, 1988.
[24] M. Huisjen, J. S. Hyde, *Rev. Sci. Instrum. 45* (1974) 669.
[25] R. W. Quine, G. R. Eaton, S. S. Eaton, *Rev. Sci. Instrum. 58* (1987) 1709.
[26] H. Thomann, L. R. Dalton, *Rev. Sci. Instrum. 55* (1984) 389.
[27] C. Mailer, J. D. S. Danielson, B. H. Robinson, *Rev. Sci. Instrum. 56* (1985) 1917.
[28] S. Pfenninger, J. Forrer, A. Schweiger, T. Weiland, *Rev. Sci. Instrum. 59* (1988) 752.
[29] J. Forrer, S. Pfenninger, J. Eisenegger, A. Schweiger, *Rev. Sci. Instrum. 61* (1990) 3384.
[30] K. Holczer, D. Schmalbein, *Bruker-Rep. 1* (1987) 22 (Bruker Analytische Messtechnik, Karlsruhe); K. Holczer, D. Schmalbein, P. Baker, *ibid. 2* (1988) 4; H. Barth, P. Höfer, K. Holczer, *ibid. 2* (1988) 28; K. Holczer, D. Schmalbein, P. Baker, *Bruker application note 113*.
[31] A. D. Trifunac, *Magn. Res. Rev. 7* (1982) 147.
[32] A. D. Trifunac, R. G. Lawler, D. M. Bartels, M. C. Thurnauer, *Prog. React. Kinet. 14* (1986) 43.
[33] K. A. McLauchlan, D. G. Stevens, *Mol. Phys. 57* (1986) 223.
[34] C. Cheng, T. Lin, D. J. Sloop, *J. Magn. Reson. 33* (1979) 71.
[35] D. M. Bartels, R. G. Lawler, A. D. Trifunac, *J. Chem. Phys. 83* (1985) 2686.
[36] A. D. Milov, K. M. Salikhov, M. D. Shchirov, *Sov. Phys. Solid State (Engl. Transl.) 23* (1981) 565.
[37] S. K. Rengan, V. R. Bhagat, V. S. S. Sastry, B. Venkataraman, *J. Magn. Reson. 33* (1979) 227.
[38] S. A. Dzuba, A. G. Maryasov, K. M. Salikhov, Yu. D. Tsvetkov, *J. Magn. Reson. 58* (1984) 95.
[39] J. P. Hornak, J. H. Freed, *Chem. Phys. Lett. 101* (1983) 115.
[40] J. S. Hyde, W. Froncisz, C. Mottley, *Chem. Phys. Lett. 100* (1984) 621.
[41] G. Völkel, S. A. Dzuba, A. Bartl, W. Brunner, J. Fröhner, *Phys. Status Solidi A 85* (1984) 257.
[42] P. Höfer, A. Grupp, M. Mehring in J. A. Weil (Ed.): *Electronic Magnetic Resonance of the Solid State*, The Canadian Society for Chemistry, Ottawa 1987, p. 521.
[43] M. Mehring, P. Höfer, A. Grupp, *Ber. Bunsenges. Phys. Chem. 91* (1987) 1132.
[44] A. Grupp, M. Mehring in [12], p. 195.
[45] K. P. Dinse in [11], p. 615.
[46] D. J. Sloop, H. Yu, T. Lin, *Chem. Phys. Lett. 124* (1986) 456.
[47] A. D. Milov, A. Yu. Pusep, S. A. Dzuba, Yu. D. Tsvetkov, *Chem. Phys. Lett. 119* (1985) 421.
[48] G. G. Maresch, M. Mehring, S. Emid, *Physica B 138* (1986) 261.
[49] S. S. Eaton, G. R. Eaton in [12], p. 405.
[50] A. Schweiger in [12], p. 43.
[51] W. R. Hagen in [11], p. 785.
[52] G. Feher, *Phys. Rev. 103* (1956) 834.

[53] L. Kevan, L. D. Kispert: *Electron Spin Double Resonance Spectroscopy*, Wiley, New York 1976.
[54] M. M. Dorio, J. H. Freed (Eds.): *Multiple Electron Resonance Spectroscopy*, Plenum, New York 1977.
[55] A. Schweiger, *Struct. Bonding (Berlin) 51* (1982).
[56] K. Möbius, M. Plato, W. Lubitz, *Phys. Rep. 87* (1982) 171.
[57] H. Kurreck, B. Kirste, W. Lubitz: *Electron Nuclear Double Resonance Spectroscopy of Radicals in Solution*, VCH, Weinheim 1988.
[58] H. Kurreck, B. Kirste, W. Lubitz, *Angew. Chem. 96* (1984) 171; *Angew. Chem. Int. Ed. Engl. 23* (1984) 173.
[59] J. Stach, R. Böttcher, R. Kirmse, *Z. Chem. 25* (1985) 1.
[60] A. Schweiger in M. C. R. Symons (Ed.): *Electron Spin Reson.* (Specialist Periodical Reports) *10b* (1987) 138.
[61] J. Gorcester, G. L. Millhauser, J. H. Freed in [11], p. 177.
[62] M. K. Bowman in [12], p. 1.
[63] J. Gorcester, G. L. Millhauser, J. H. Freed in [12], p. 119.
[64] A. Angerhofer, M. Toporowicz, M. K. Bowman, J. R. Norris, H. Levanon, *J. Phys. Chem. 92* (1988) 7164.
[65] T. Prisner, O. Dobbert, K. P. Dinse, *J. Am. Chem. Soc. 110* (1988) 1622.
[66] M. Plüschan, A. Zahl, K. P. Dinse, H. van Willigen, *J. Chem. Phys. 90* (1989) 3153.
[67] E. L. Hahn, *Phys. Rev. 80* (1950) 580.
[68] W. B. Mims, J. Peisach in [11], p. 1.
[69] J.-M. Fauth, A. Schweiger, L. Braunschweiler, J. Forrer, R. R. Ernst, *J. Magn. Reson. 66* (1986) 74.
[70] C. Gemperle, G. Aebli, A. Schweiger, R. R. Ernst, *J. Magn. Reson. 88* (1990) 241.
[71] R. T. Weber, J. A. J. M. Disselhorst, L. J. Prevo, J. Schmidt, W. Th. Wenckebach, *J. Magn. Reson. 81* (1989) 129.
[72] E. Dormann, G. Sachs, W. Stöcklein, B. Bail, M. Schwoerer, *Appl. Phys. A 30* (1983) 227.
[73] A. Schweiger, R. R. Ernst, *J. Magn. Reson. 77* (1988) 512.
[74] D. Goldfarb, L. Kevan, *J. Magn. Reson. 76* (1988) 276.
[75] H. Y. Carr, E. M. Purcell, *Phys. Rev. 94* (1954) 630.
[76] D. Gill, S. Meiboom, *Rev. Sci. Instrum. 29* (1958) 688.
[77] A. Schenzle, N. C. Wong, R. G. Brewer, *Phys. Rev. A 22* (1980) 635.
[78] J. S. Hyde in [9], p. 1.
[79] A. D. Trifunac, J. R. Norris, *Chem. Phys. Lett. 59* (1978) 140.
[80] G. Völkel, W. Brunner, W. Windsch, D. Steudel, *Phys. Status Solidi B 95* (1979) 99.
[81] L. J. Berliner, J. Reuben (Eds.), *Biol. Magn. Reson. 8* (1989).
[82] G. L. Millhauser, J. H. Freed, *J. Chem. Phys. 81* (1984) 37.
[83] L. Kar, G. L. Millhauser, J. H. Freed, *J. Phys. Chem. 88* (1984) 3951.
[84] L. Kar, M. E. Johnson, M. K. Bowman, *J. Magn. Reson. 75* (1987) 397.
[85] L. J. Schwartz, G. L. Millhauser, J. H. Freed, *Chem. Phys. Lett. 127* (1986) 60.
[86] M. Mehring, H. Seidel, W. Müller, G. Wegner, *Solid State Commun. 45* (1983) 1075.
[87] L. G. Rowan, E. L. Hahn, W. B. Mims, *Phys. Rev. A 137* (1965) 61.
[88] W. B. Mims, *Phys. Rev. B 5* (1972) 2409.
[89] E. J. Reijerse, Thesis, University Nijmegen 1986.
[90] J. L. Davis, W. B. Mims, *Rev. Sci. Instrum. 52* (1981) 131.
[91] P. A. Narayana, R. J. Massoth, L. Kevan, *Rev. Sci. Instrum. 53* (1982) 624.
[92] A. V. Astashkin, S. A. Dikanov, Yu. D. Tsvetkov, *Chem. Phys. Lett. 136* (1987) 204.
[93] S. A. Dikanov, A. A. Shubin, V. N. Parmon, *J. Magn. Reson. 42* (1981) 474.
[94] R. B. Clarkson, M. D. Timken, D. R. Brown, H. C. Crookham, R. L. Belford, *Chem. Phys. Lett. 163* (1989) 277.
[95] D. J. Singel in [11], p. 119.
[96] A. Lai, H. L. Flanagan, D. J. Singel, *J. Chem. Phys. 89* (1988) 7161.
[97] J. Peisach, W. B. Mims, J. L. Davis, *J. Biol. Chem. 254* (1979) 12379.
[98] H. L. Flanagan, G. J. Gerfen, D. J. Singel, *J. Chem. Phys. 88* (1988) 20.
[99] W. Möhl, A. Schweiger, H. Motschi, *Inorg. Chem. 29* (1990) 1536.
[100] J. Peisach, W. B. Mims, J. L. Davis, *J. Biol. Chem. 259* (1984) 2704.
[101] J. McCracken, S. Pemper, S. J. Benkovic, J. J. Villafranca, R. J. Miller, J. Peisach, *J. Am. Chem. Soc. 110* (1988) 1069.
[102] D. J. Singel, W. A. J. A. van der Poel, J. Schmidt, J. H. van der Waals, R. de Beer, *J. Chem. Phys. 81* (1984) 5453.
[103] H. Seidel, M. Mehring, D. Stehlik, *J. Chem. Phys. 83* (1985) 956.
[104] W. J. Buma, E. J. J. Groenen, J. Schmidt, R. de Beer, *J. Chem. Phys. 91* (1989) 6549.
[105] H. Yu, D. J. Sloop, S. I. Weissman, T. Lin, J. R. Norris, M. K. Bowman, *J. Phys. Chem. 86* (1982) 4287.
[106] H. Thomann, H. Jin, G. L. Baker, *Phys. Rev. Lett. 59* (1987) 509.
[107] E. J. Hustedt, H. Thomann, B. H. Robinson, *J. Chem. Phys. 92* (1990) 978.
[108] E. R. Davies, *Phys. Lett. A 47* (1974) 1.
[109] W. B. Mims, *Proc. R. Soc. A 283* (1965) 452.
[110] W. A. J. A. van der Poel, D. J. Singel, J. Schmidt, J. H. van der Waals, *Mol. Phys. 49* (1983) 1017.
[111] E. J. Reijerse, N. A. J. M. van Aerle, C. P. Keijzers, R. Böttcher, R. Kirmse, J. Stach, *J. Magn. Reson. 67* (1986) 114.
[112] J. Gorcester, J. H. Freed, *J. Chem. Phys. 88* (1988) 4678.
[113] J. Gorcester, S. B. Rananavare, J. H. Freed, *J. Chem. Phys. 90* (1989) 5764.
[114] M. K. Bowman in [10], p. 96.
[115] A. Schweiger in [11], p. 243.
[116] H. Cho, S. Pfenninger, C. Gemperle, A. Schweiger, R. R. Ernst, *Chem. Phys. Lett. 160* (1989) 391.
[117] J.-M. Fauth, A. Schweiger, R. R. Ernst, *J. Magn. Reson. 81* (1989) 262.
[118] A. Schweiger, L. Braunschweiler, J.-M. Fauth, R. R. Ernst, *Phys. Rev. Lett. 54* (1985) 1241.
[119] A. Schweiger, C. Gemperle, R. R. Ernst, *J. Magn. Reson. 86* (1990) 70.
[120] A. A. Maudsley, A. Wokaun, R. R. Ernst, *Chem. Phys. Lett. 55* (1978) 9.
[121] C. Gemperle, A. Schweiger, R. R. Ernst, Chem. Phys. Lett., in press.
[122] G. Aebli, C. Gemperle, A. Schweiger, R. R. Ernst, unpublished.
[123] S. A. Dikanov, A. V. Astashkin in [11], p. 59.
[124] R. P. J. Merks, R. de Beer, *J. Phys. Chem. 83* (1979) 3319.
[125] P. Höfer, A. Grupp, H. Nebenführ, M. Mehring, *Chem. Phys. Lett. 132* (1986) 279.
[126] S. Pfenninger, A. Schweiger, J. Forrer, R. R. Ernst, *Chem. Phys. Lett. 151* (1988) 199.
[127] W. B. Mims: *The Linear Electric Field Effect in Paramagnetic Resonance*, Clarendon, Oxford 1976.
[128] W. B. Mims, *Phys. Rev. 133* (1964) A835.
[129] J. Peisach, N. R. Orme-Johnson, W. B. Mims, W. H. Orme-Johnson, *J. Biol. Chem. 252* (1977) 5643.
[130] A. J. Hoff in [11], p. 633.
[131] I. M. Brown, D. J. Sloop, D. P. Ames, *Phys. Rev. Lett. 22* (1969) 324.
[132] M. Mehring, P. Höfer, A. Grupp, *Phys. Rev. A 33* (1986) 3523.
[133] P. F. Liao, S. R. Hartmann, *Phys. Rev. B 8* (1973) 69.
[134] C. Gemperle, O. W. Sørensen, A. Schweiger, R. R. Ernst, *J. Magn. Reson. 87* (1990) 502.
[135] C. Bühlmann, A. Schweiger, R. R. Ernst, *Chem. Phys. Lett. 154* (1989) 285.
[136] H. Thomann, M. Bernardo, *Chem. Phys. Lett. 169* (1990) 5.
[137] C. Gemperle, A. Schweiger, R. R. Ernst, *Chem. Phys. Lett. 145* (1988) 1.
[138] M. Mehring, P. Höfer, H. Käss, A. Grupp, *Europhys. Lett. 6* (1988) 463.
[139] A. D. Gorlov, A. P. Potapov, Yu. A. Sherstkov, *Sov. Phys. Solid State* (Engl. Transl.) *27* (1985) 1726.
[140] P. Höfer, A. Grupp, M. Mehring, *Phys. Rev. A 33* (1986) 3519.
[141] H. Cho, *J. Chem. Phys.*, in press.

Spontaneous Resolution by Stirred Crystallization**

By *J. Michael McBride** and *Randall L. Carter*

It does not take long for a beginning chemist to develop a naive trust in predictions based on probability. Unlike a physician, who deals with a handful of cases, or an epidemiologist, who deals with hundreds of thousands, a chemist has the luxury of dealing with samples that contain more than 10^{20} molecules. For such large samples, predictions based on probability verge on certainty. Chemists are not disturbed that quantum mechanics precludes strict determinism in the behavior of an individual molecule, because it supplies reliable probabilities, and for macroscopic chemical samples molecular probability amounts to collective determinism. A chemist who has difficulty repeating a literature experiment may attribute the problem to unobserved or unreported differences in procedure or materials, or to error in measurement, but not to sampling error. The precise reproducibility from experiment to experiment that is the hallmark of good chemistry depends on having samples with enormous numbers of molecules.

Because of their training, chemists are particularly intrigued by phenomena that seem improbable. Several such cases involve chirality. A familiar and profound example is the occurrence in nature of only one enantiomer of complex biological molecules. How did living systems become resolved? Does biological handedness result from some weak interaction that provided a tiny evolutionary bias in favor of one set of enantiomers, or from one single molecular event that occurred at random but was destined to become a sort of molecular "Adam" by being multiplied into the whole kingdom of living things?

Crystallization provides a more homely example of curious statistics involving chirality. Although growth of a macroscopic crystal involves a large number of molecular events, formation of the original nucleus occurs but once per crystal. It is not uncommon for a solution to deposit only one crystal. Even if 100 or 1000 crystals grow, the number of nucleation events is small by chemical standards, and they differ from most chemical phenomena in that they can often be counted individually as well as measured collectively. Recently, *Dilip Kondepudi* et al. of Wake Forest University (USA) have reported results from counting chiral crystals that provide new insights into the mechanism of nucleation.[1]

Their interest in the role of competition and autocatalysis in breaking chiral symmetry in the biosphere,[2] led *Kondepudi* et al. to repeat 19th Century work by *Kipping* and *Pope* on the crystallization of $NaClO_3$.[3] This salt is particularly well suited for such experimentation because aqueous solutions of its achiral ions produce beautiful rectangular prisms in the *chiral* cubic space group $P2_13$. Since the individual ions are achiral, they can join either enantiomeric lattice. Thus, in contrast to the situation for a racemic solution of intrinsically chiral molecules, there is no necessity that complete crystallization give equal amounts of the two enantiomeric solids. Furthermore, because of their cubic symmetry crystals of $NaClO_3$ are not birefringent, so that one may easily identify an individual crystal's handedness by its rotation of linearly polarized light ($3.6° \text{ mm}^{-1}$ at 546 nm).

In 1898 *Kipping* and *Pope* measured the handedness of 3137 $NaClO_3$ crystals from 46 separate crystallizations in order to test surprising reports that crystallization of analogous substances had shown strong bias toward formation of one enantiomorphic form. They were pleased to find that among 3137 crystals 1571 (50.08%) were dextrorotatory. This fell well within statistical error of the unbiased 50:50 distribution they anticipated.[4]

Kondepudi et al. confirmed these results by counting 525 dextrorotatory crystals in a sample of 1000. But when they tried stirring the solutions (ca. 100 rpm) to remove the concentration gradients that favor nucleation at the air–liquid interface, they found that each beaker gave a predominance of one enantiomer. There was no systematic bias in favor of one of the enantiomers (dextrorotatory crystals predominated in 18 batches, levorotatory in 14), but the bias within each batch was remarkably strong. Of the 32 batches, 23 formed *only* crystals of one enantiomer, for example one batch consisted of 865 levorotatory crystals and no dextrorotatory crystals. Among 11 829 crystals counted, only 33 had the minority configuration for their respective batch, and 15 of these were formed in one particular crystallization.

In a stirred beaker a single nucleation event apparently gives rise to most or all of the hundreds of crystals formed. The most likely mechanism of this "Adam" effect is that crystals begin nucleating at random, but the first crystal to be struck by the stirrer clones hundreds or thousands of new nuclei. Growth of so many nuclei soon lowers the concentration of the solute below the threshold for spontaneous formation of primary nuclei, so there is no way to begin crystallization of the enantiomer.[5]

We have confirmed this mechanism by video recording a number of stirred crystallizations. Figure 1 presents three stages during crystallization of a supersaturated $NaClO_3$ solution that had been prepared by heating near the boiling point, degassing under vacuum, filtering through glass wool, and reheating to near the boiling point. After about an hour of stirring at room temperature,[6] a single crystal had formed on the bottom of the vial and was growing toward the stirrer at 0.2 mm min^{-1}. Figure 1a shows the first collision of the stirrer with the tip of the crystal. After 20 seconds and 35 collisions stirring was stopped. Within another 30 seconds more than 5000 tiny crystals became visible (Fig. 1b). A minute and a half after the first collision these crystals had grown into beautiful small prisms with dimensions of 0.1 to 0.2 mm (Fig. 1c). The speed with which the new crystals developed leaves no doubt that they grew from

[*] Prof. J. M. McBride, R. L. Carter
Department of Chemistry, Yale University
New Haven, CT 06511 (USA)

[**] This work was supported by the Petroleum Research Fund of the American Chemical Society and by the Office of Naval Research. We thank Professors *Lia Addadi* and *Dilip Kondepudi* for valuable conversations.

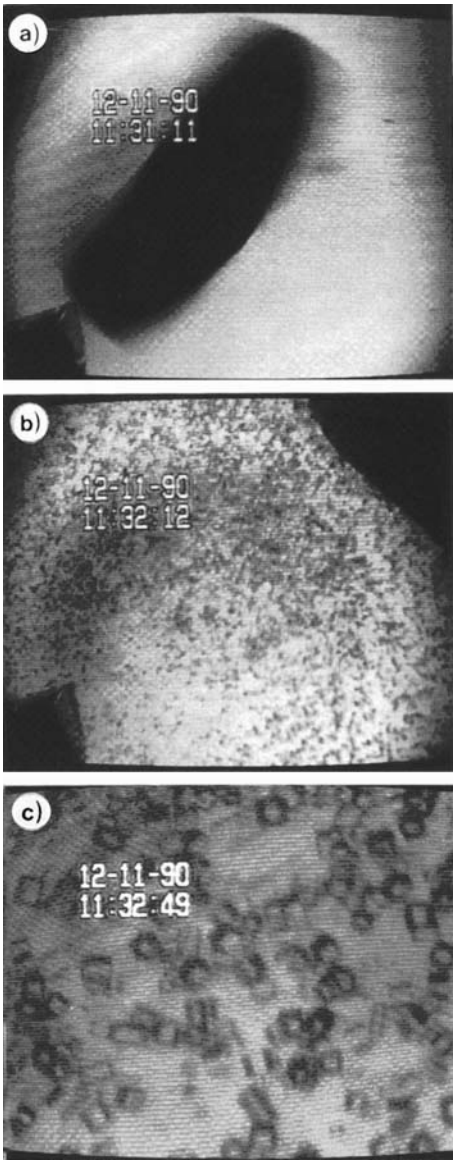

Fig. 1. Figures from a video recording of magnetically stirred crystallization of $NaClO_3$ solution: a) first contact between 10×3 mm stirrer and tip of primary crystal; b) within 1 min stirring has been stopped (stirrer at top right) and solution is filled with new crystals; c) sevenfold increase in magnification shows that new crystals are 0.1 to 0.2 mm prisms. Note in Figure (b) that the tip of the primary crystal was not visibly damaged by spawning thousands of secondary nuclei.

nuclei struck from the tip of the single crystal by these few contacts with the stirrer.[7] Subsequent examination of 48 daughter crystals with a polarizing microscope showed that every one was levorotatory, as was the initial crystal.

Like many other phenomena with such a reasonable explanation, the results of *Kondepudi* et al. may not be surprising, in retrospect. As they point out, the idea of cloning crystals during stirred crystallization is familiar to chemical engineers as secondary nucleation.[8] Their novel contribution has been to study an achiral solute that gives chiral crystals and thus to provide a powerful new tool for demonstrating and studying secondary nucleation. For example, it has been suggested that secondary nuclei arise from an hypothetical layer of adsorbed molecular aggregates that have not yet been incorporated into the crystal lattice,[8] but *Kondepudi's* results show that these nuclei had been incorporated at least enough to acquire the absolute configuration of the bulk crystal.

There have been several previous reports of less dramatic resolutions in *unstirred* solutions. In 1954 *Havinga* gave a clear discussion of "spontaneous asymmetric synthesis" in crystallizing the salt of a slowly racemizing allyl ammonium ion.[9] In 1971 *Pincock* et al. reported spontaneous resolution during crystallization of melted 1,1'-binaphthyl at 150 °C, at which temperature conformational racemization of the molecule in solution is rapid.[10] Like *Havinga*, they measured resolution by optical rotation after dissolving the crystals at room temperature, where molecular racemization is slow. In 1982 *Addadi*, van *Mil*, and *Lahav* reported spontaneous resolution during crystallization of a substituted divinylbenzene from ethanol, but not from other solvents.[11] They measured resolution using optical rotation of the cyclobutane formed by solid-state [2 + 2] photocycloaddition. In seven crystallizations the enantiomeric excess ranged from 46% to "ca. 100%". In 1986 *Evans* et al. reported that solid-state photolysis of chiral crystals of an achiral dibenzobarrelene gave levorotatory product from all eight crystals formed in one batch.[12] In 1990 *Feng* and *McBride* reported that each of the 11 crystals from small-scale crystallization of a diacyl peroxide was of the same chirality.[13]

For achieving practical resolutions *Kondepudi*'s approach of stirring during crystallization has the advantages of reproducibly giving very high enantiomeric excess and of not requiring the growth and separation of large single crystals. Intentional seeding with dust from a single crystal might be equally effective, but cloning nuclei from the first spontaneously nucleated crystal to strike the stirrer automatically introduces a shower of nuclei at an appropriate level of supersaturation. Intentional seeding has the advantage that the chirality of a given batch is predictable. Either technique should work best when applied to a solution of achiral or rapidly racemizing species that form chiral crystals.

Determining resolution by counting individual crystals has an obvious advantage in precision over the previous approach of measuring optical rotations in solution. It would be very difficult by solution rotation to distinguish 99 from 100% purity, but *Kondepudi* had no difficulty in counting ratios of 781:0 or 841:2. Thus his work may form the basis for a new way of studying crystallization; one in which statistical analysis plays an important role. One may now reevaluate previous studies statistically and carry out new studies to look for the contribution of cloning in unstirred systems. It seems clearly to have played a role in *Kipping* and *Pope*'s early work. Their data show that 5 of the 46 batches had distributions that departed from 50:50 by more than 2.3 standard deviations (σ), where only 1 in 50 would be expected to do so. The most dramatic had 24 dextrorotatory crystals and 68 levorotatory crystals, thus deviating from expectation by more that 4σ, an event that should occur only one time in 5000. At the other extreme, where 11 of the batches should have departed from 50:50 by *less* than 0.32σ, in fact only three did so. This suggests that cloning occurred in most, if not all, of their crystallizations.

The role that stirred crystallization may have played in the origin of biological chirality is not clear, but the surprise that many chemists (including the present authors) experienced

on learning of *Kondepudi*'s results shows clearly that mental adjustments are required in order to deal intuitively with "improbable" solid-state phenomena.

German version: *Angew. Chem. 103* (1991) 298

[1] D. K. Kondepudi, R. J. Kaufman, N. Singh, *Science 250* (1990) 975.
[2] R. A. Hegstrom, D. K. Kondepudi, *Sci. Am. 262* (1990) No. 1, p. 108.
[3] W. S. Kipping, W. J. Pope, *J. Chem. Soc. Trans. 73* (1898) 606.
[4] *Kipping* and *Pope* were lucky. Their 50.08% differs from 50% by only 0.09σ, which would be expected to occur once in 14 times of performing their set of experiments.
[5] It is well known that the clusters that precede nuclei are much less stable (and thus more soluble) than larger crystals, because they have such a high fraction of surface molecules.
[6] 10×3 mm magnetic stirrer bar at 185 rpm.
[7] In other runs visible multiple crystallization began within two seconds of striking the primary crystal.
[8] A. D. Randolph, M. A. Larson: *Theory of Particulate Processes*, 2nd Edit. Academic, New York 1988, pp. 122–129.
[9] E. Havinga, *Biochim. Biophys. Acta 13* (1954) 171.
[10] R. E. Pincock, R. R. Perkins, A. S. Ma, K. R. Wilson, *Science 174* (1971) 1018.
[11] L. Addadi, J. van Mil, M. Lahav, *J. Am. Chem. Soc. 104* (1982) 3422.
[12] S. V. Evans, M. Garcia-Garibay, N. Omkaram, J. R. Scheffer, J. Trotter, F. Wireko, *J. Am. Chem. Soc. 108* (1986) 5648.
[13] X. W. Feng, J. M. McBride, *J. Am. Chem. Soc. 112* (1990) 6151.

VCH Index Library

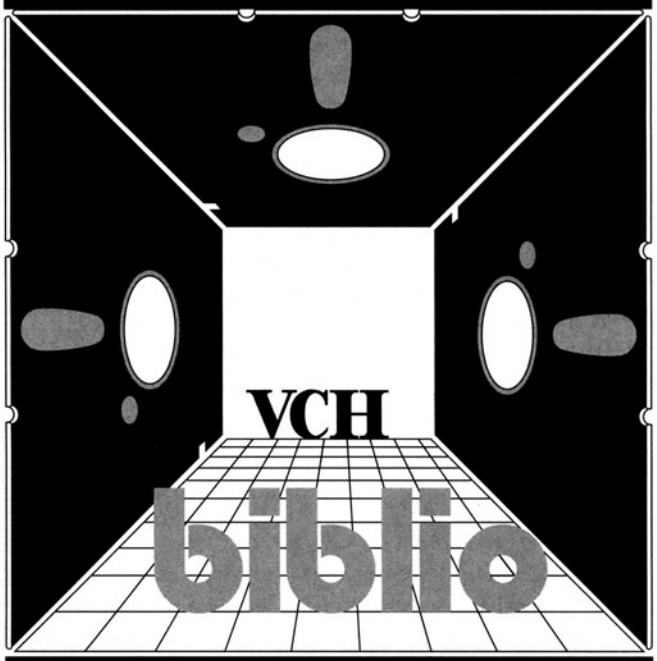

The electronic index comes with the search module of the literature-management program, VCH Biblio. You can use this index on all PCs running with MS-DOS.

ANGEWANDTE CHEMIE
International Edition in English

Soon available

At the press of a button

The annual index of "Angewandte" is soon available on 5 1/4" and 3 1/2" diskettes.

Yearly updates will keep this invaluable electronic library complete. You can search the cumulative contents in mere seconds.

Price: ca. DM 34.00 plus shipping and handling.

Special news! In honor of the 30th anniversary of "Angewandte Chemie I.E." the cumulative index will also be available on diskette.

VCH
Software
P.O. Box 101161
D-6940 Weinheim

VCH

The Rationality of Random Screening— Efficient Methods of Selection of Peptides and Oligonucleotide Ligands

By *Andreas Plückthun** and *Liming Ge*

Words like "random" and "screening" imply ignorance about a system, and, to some, an inefficient, inelegant, and irrational method of research. This article will highlight some examples from the recent literature, where random mutagenesis and screening approaches have been used very elegantly to remove ignorance. Such strategies may, in some cases, contribute to a much faster gain of information than any testing of preconceived theories. They have also been instrumental in gaining insight into evolutionary processes at the molecular level.

To chemists, random screening is entirely familiar. In pharmacological research, "lead"-compounds have traditionally been found by screening natural products from organisms with names often refractory to memorization. The "refinement" of such compounds by the sometimes sarcastically called "methyl-, ethyl-, futile" chemistry is initially a random-walk probing the binding pocket of the affected enzyme or receptor. Quantitative structure–activity relationships can only be derived and applied after enough initial data have been accumulated. Although tremendous progress is being made in various aspects of theoretical chemistry and many facets of molecular modeling (not to be reviewed here), a breakthrough completely obviating empirical approaches is still not in sight.

Much of this reseach ultimately deals with the binding of ligand molecules to proteins: the ligands may be small organic molecules, other proteins, peptides, DNA or RNA. However, the prediction of the magnitude of such binding interactions is in most cases still close to impossible, even if the structures of *both* the proteins *and* the ligand are known. In many cases of interest to the researcher, the structure of the receptor protein will be unknown, and it cannot be predicted from the amino acid sequence. Furthermore, flexible ligands such as peptides have an enormous number of accessible conformations, and it is generally not clear, in which conformation such flexible ligands are bound.

The substances for which very large numbers of variants can be most easily obtained are peptides, proteins and nucleic acids. "Dirty" oligonucleotides can be synthesized by mixing a certain percentage of the "wrong" bases at each position with the correct one, or even with a complete random assortment of bases at predefined positions.[1] Such oligonucleotide mixtures may themselves constitute the ligand mixture, out of which the most efficient binding species can be searched or selected if the ligand or the receptor is DNA (see below). Alternatively, these oligonucleotides may be used to randomize a certain portion of the gene encoding the protein or peptide of interest.

Pioneering work in this area was performed by *J. R. Knowles* et al. Triose phosphate isomerase is an enzyme that may be regarded as having reached its endpoint in evolution.[2] The rate of the reaction it catalyzes is only limited by diffusion of the substrate. This means that the cell producing the enzyme does not gain anything from modifying the enzyme to accelerate the rate of the chemical reaction further, as the turnover will not get any faster. A single mutation in the catalytic base of the enzyme (changing its orientation and distance from the substrate) decreases this rate enough that the reaction is no longer diffusion controlled. Then, there is motivation again for the cell to improve the enzyme. *Knowles* et al. used "dirty" oligonucleotides to create a collection of genes with random mutations and introduced these genes into an *E. coli* strain devoid of its own triose phosphate isomerase. In the presence of appropriate precursors, the cells would grow if and only if a functional isomerase was present. The lower the level of the enzyme present in the cell, the higher the rate of the enzyme-catalyzed reaction had to be to support the growth of the bacterial cell. With this strategy, the research group found enzymes with activities much improved from the starting mutant, but different in amino-acid sequence from the wild-type.[3] This work shows that there are alternative solutions to the design of an efficient catalyst. It is rather unlikely that, with the present low level of understanding of protein structures, these alternative, efficient enzyme variants would have been found by any other way.

The elegance of this approach is its use of a positive in vivo selection. This, however, is also its limitation, as it requires both turnover and a suitable metabolic pathway in the host cell. More general solutions of finding the optimal ligand or the optimal receptor will therefore have to be carried out *outside* of the cell. In the work on triose phosphate isomerase, the underlying question was, which active sites would be most suitable for the catalytic task. In the other examples discussed, the question was which ligand would best fit a certain protein binding site.

Three groups[4–6] devised a rather efficient strategy to investigate which peptide would best fit a given binding site. In this "protein strategy" (Fig. 1) the peptides were, however, not tested as such, but were instead presented on the surface of a protein of bacteriophage M13. The essence of the experiments was to create a collection of phages (a so-called epitope library), retain those on a filter that bind to the given binding protein and amplify them by infecting *E. coli* cells. This example illustrates the basic features that any kind of screening system of binding must have, be it for the ligand or the receptor: a selection step, which separates the functional receptor or ligand molecules from the non-functional ones, and an amplification step. As a very large number of candidates are to be screened, very few molecules of each individual molecular species will be present, making this amplification step necessary for subsequent selection. Also, the manipulation must be facile enough to allow the enrichment to be carried out through various cycles.

Scott and *Smith*[4] inserted the epitopes to be tested into the pIII protein of bacteriophage M13. Apparently, foreign inserts at the chosen position did not prevent the phage from infection. The phage carries a tetracycline resistance gene so

[*] Priv. Doz. Dr. A. Plückthun, Dr. L. Ge
Genzentrum der Universität München
c/o Max-Planck-Institut für Biochemie
Am Klopferspitz, W-8033 Martinsried (FRG)

 © VCH Verlagsgesellschaft mbH, W-6940 Weinheim, 1991 0570-0833/91/0303-0296 $ 3.50+.25/0

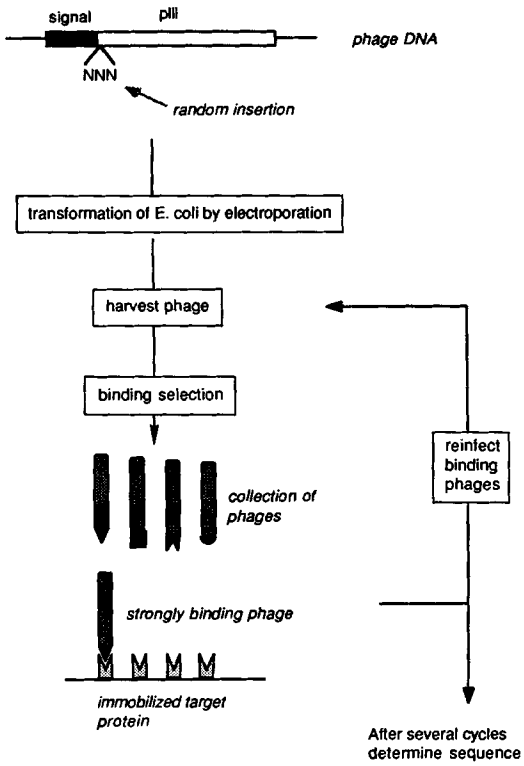

Fig. 1. The protein strategy of random screening.

that only one infection is necessary to propagate the DNA. Phage-carrying bacteria were not recognized as plaques but as colonies on selective medium. Since non-functional frame shift mutants in this protein could be propagated as well, the ability to infect could be used as a selection for epitope inserts which restored the reading frame. The authors tested the system with two monoclonal antibodies specific for a known hexapeptide, an epitope from hemerythrin. The antibodies were biotinylated and mixed with the phage. The antibodies and antibody-phage complexes were then adsorbed to a streptavidin-coated surface—streptavidin forms extremely tight complexes with biotin. Non-adsorbed phages were washed off, while bound phages were eluted with acid and amplified after infection. After several rounds, the DNA of a number of phages encoding the epitopes in protein pIII were sequenced. Reassuringly, sequences very similar to the known epitope were found. A very similar approach was also reported by *Cwirla* et al.[5]

Also using the pIII protein of bacteriophage M13, 15-residue-streches of inserted peptides were randomized by *Devlin* et al.[6] However, mutants that would directly bind to streptavidin were searched. Interestingly, all of the peptides found contained a core consensus sequence. This shows that the approach can be used to detect peptide ligands even for proteins that have no known affinity for any peptides. It will now be necessary to quantify some of the binding constants in order to estimate the minimal affinities that still can be detected.

A related concept has been used to find DNA sequences that bind to a DNA binding protein of unknown specificity. In this case, the random oligonucleotides can either be used directly or be introduced into a larger plasmid ("oligonucleotide strategy") (Fig. 2). In the most general case, the mixture of ligands is incubated with the protein in question and binding species are either physically separated by adsorbing the protein to a solid phase or functionally enriched, e.g. by their ability to function as primer. The polymerase chain reaction

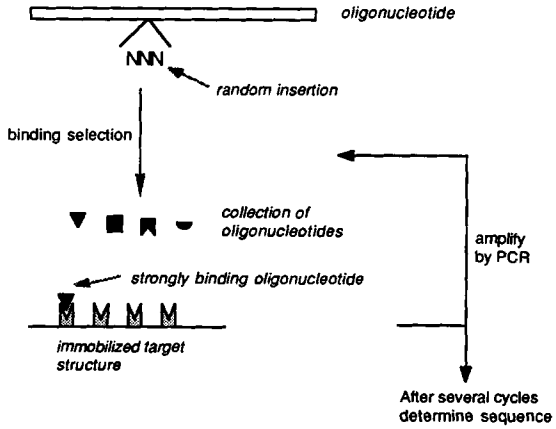

Fig. 2. The oligonucleotide strategy of random screening.

(PCR)[7] is then used to amplify those sequences that are bound by the protein in vitro. The availability of this in vitro exponential amplification method sets DNA and RNA apart from all other ligands.

Thiesen and *Bach*[8] used this strategy to determine the binding sites on DNA recognized by the human transcription factor SP1. The consensus binding site was known from previous work, thus allowing the method to be validated. The template oligonucleotides were designed to contain a defined region of 22 nucleotides on both ends, which served as the hybridization sites for PCR primers of 22 nucleotides in length. The central regions of the double stranded template oligonucleotides were twelve completely random nucleotides. The SP1 protein was incubated with the mixture and protein-DNA complexes were then bound to a nitrocellulose filter. Non-binding DNA was washed off and bound DNA was eluted and amplified by PCR. Further enrichment of binding sequences was achieved by the so-called band-shift electrophoresis: the migration of the functional oligonucleotides in a polyacrylamide gel is retarded by bound proteins. When oligonucleotides from the retarded bands were cloned and sequenced, sequences rather similar to the known consensus sequences of transcription factor SP1 were retrieved.

Tuerk and *Gold*[9] used an in vitro selection and amplification method to determine sequences crucial for the binding of T4 DNA polymerase to the 5′ leader sequences of its own mRNA; they speak of "systematic evolution of ligands by exponential enrichment" (SELEX). The binding of T4 DNA polymerase to a 36-nucleotide (nt) fragment (in which a 5-bp helix with an 8-nt loop is found) of its own mRNA prevents translational initiation. Thus, an autogenous regulation of the gene is achieved. The sequences of these eight crucial nucleotides from bacteriophage T4 and a distantly related bacteriophage RB69 are identical. The question investigated by these authors was whether other sequences besides the one found in T4 and RB69 could give rise to functional interactions. *Tuerk* and *Gold* randomized the sequence of these eight bases in single-stranded DNA templates. They

then transcribed these templates in vitro, and the excess amount of RNA transcripts was mixed with the T4 DNA polymerase. The RNAs retained by the polymerase bound to a nitrocellular filter were used as templates for reverse transcriptase and the resulting cDNAs were amplified by PCR. These template DNAs were again transcribed in vitro and the RNA transcripts were subjected to the next round of competitive binding selection. After the fourth round of selection and amplification, two sequences with equal affinity to the polymerase were predominant. One of them was the wild-type sequence and the other one differed in four bases from the wild-type, giving rise to two new base pairs in the loop. The existence of another sequence with equal binding affinity as the wild-type, but which is not found in nature, strongly suggests that there are other crucial roles played by the wild-type sequence, in addition to the binding of the polymerase.

A similar approach has been used by *Ellington* and *Szostak*[10] to enrich the RNA molecules that bind to dyes resembling a redox cofactor, nicotinamide adenine dinucleotide (NAD), from a random RNA pool. From an initial pool of 10^{13} different sequences, 10^2 to 10^3 were found to bind to the dye, immobilized to a column, after 6 cycles of selection. This implies that there are many different solutions to the binding of a ligand by RNA, and it fuels speculations about wider roles of RNA-based catalysts in prebiotic life.

Also developed in *Szostak*'s laboratory[11] as well as by *Robertson* and *Joyce*,[12] an in vitro method was used to select variants of the *Tetrahymena* self-splicing intron that had ligase activity. The system was designed such that only the active intron variants could be amplified and propagated. The "ribozyme" ligated itself to an RNA oligonucleotide complementary to the internal guide sequence. Both ligated (long) and non-ligated (short) ribozyme molecules were converted to cDNA with reverse transcriptase using a primer complementary to its 3′ end. A second primer then hybridized exclusively with the added sequence resulting from ligation. With these two primers, PCR could be used to selectively amplify those molecules which had undergone the RNA-catalyzed ligation reaction. New RNAs could be transcribed from the DNA templates, and the cycle could then be repeated. Randomization was carried out at several positions in this case. The wild-type was found to be the most active of all.

These examples illustrate the rapid progress being made in the development of new techniques for random screening. It may be useful to summarize again the molecular features and techniques that make these approaches possible: a) the rapid automatic synthesis of oligonucleotides (and to a lesser degree, peptides) can generate an enormous number of variants in a single step; b) the random oligonucleotides may themselves serve as ligands or receptors, or encode peptide ligands or protein receptors; c) the desired molecular species can be multiplied from virtually single molecules either in vivo (by transfection or transformation of bacteria with this DNA) or in vitro by the polymerase chain reaction. It remains to be seen whether analogous strategies can be developed for investigating ligands other than DNA, RNA or proteins. The present strategies will play, however, an increasingly important role in the investigation of molecular interactions of biochemical relevance. For some questions, random screening may be the most rational approach.

German version: *Angew. Chem. 103* (1991) 301

[1] S. A. Goff, S. R. Short-Russell, J. F. Dice, *DNA 6* (1987) 381–388.
[2] W. J. Albery, J. R. Knowles, *Angew. Chem. 89* (1977) 295–304; *Angew. Chem. Int. Ed. Engl. 160* (1977) 285–298.
[3] J. D. Hermes, S. C. Blacklow, J. R. Knowles, *Proc. Natl. Acad. Sci. USA 87* (1990) 696–700.
[4] J. K. Scott, G. P. Smith, *Science 249* (1990) 386–390.
[5] J. J. Devlin, L. C. Panganiban, P. E. Devlin, *Science 249* (1990) 404–406.
[6] S. E. Cwirla, E. A. Peters, R. W. Barrett, W. J. Dower, *Proc. Natl. Acad. Sci. USA 87* (1990) 6378–6382.
[7] N. Arnheim, C. H. Levenson, *Chem. Eng. News 68* (1990) No. 40, p. 36–47.
[8] H. J. Thiesen, C. Bach, *Nucl. Acid. Res 18* (1990) 3203–3209.
[9] C. Tuerk, L. Gold, *Science 249* (1990) 505–510.
[10] A. D. Ellington, J. W. Szostak, *Nature 346* (1990) 818–822.
[11] R. Green, A. D. Ellington, J. W. Szostak, *Nature 347* (1990) 467–468.
[12] D. L. Robertson, G. F. Joyce, *Nature 344* (1990) 467–468.

Communications may be submitted in English *or* in German. Further details regarding the submission of communications can be found in the "Notice to Authors" reproduced in the January issue of the journal. Copies thereof may be obtained from the editorial office upon request.

Novel Strategies for the Construction of Complex Polycyclic Ether Frameworks. Stereocontrolled Synthesis of the FGHIJ Ring System of Brevetoxin A**

By *K. C. Nicolaou,* C. A. Veale, C.-K. Hwang, J. Hutchinson, C. V. C. Prasad* and *W. W. Ogilvie*

Dedicated to Professor Hans Jürgen Bestmann on the occasion of his 65th birthday

Recent reports from these laboratories described new synthetic technologies and strategies for the construction of the ABCD[1] and E[2] ring systems of brevetoxin A (**1**).[3] In this communication we describe an efficient and stereocontrolled synthesis of the FGHIJ ring framework (**2**) of this novel neurotoxin.

An attractive retrosynthetic analysis of brevetoxin A (**1**) with a high degree of convergency is shown in Scheme 1. Thus initial disconnection of the indicated strategic bonds of **1** (dotted lines) leads to the appropriately functionalized intermediate **2** containing the FGHIJ ring framework of the target molecule. Further disconnection of the G ring of the newly generated intermediate **2** as shown leads to compounds **3** and **4** as potential precursors. In order to ensure a high yielding formation of the 8-membered ring system in **3**, an additional ring was temporarily installed in its pregenitor (**5**) (to decrease number of rotations and facilitate ring closure). Finally, disconnection of **6**, **7**, and **4** led to enantiomerically pure precursors of the correct stereogenicity, namely 2-deoxy-D-ribose, tri-*O*-acetyl-D-glucal, and D-mannose, respectively. The successful execution of the designed strategy for reaching **2** is described below.

Syntheses of key intermediates **6** and **7** are briefly summarized in Scheme 2. Thus, 2-deoxy-D-ribose was converted

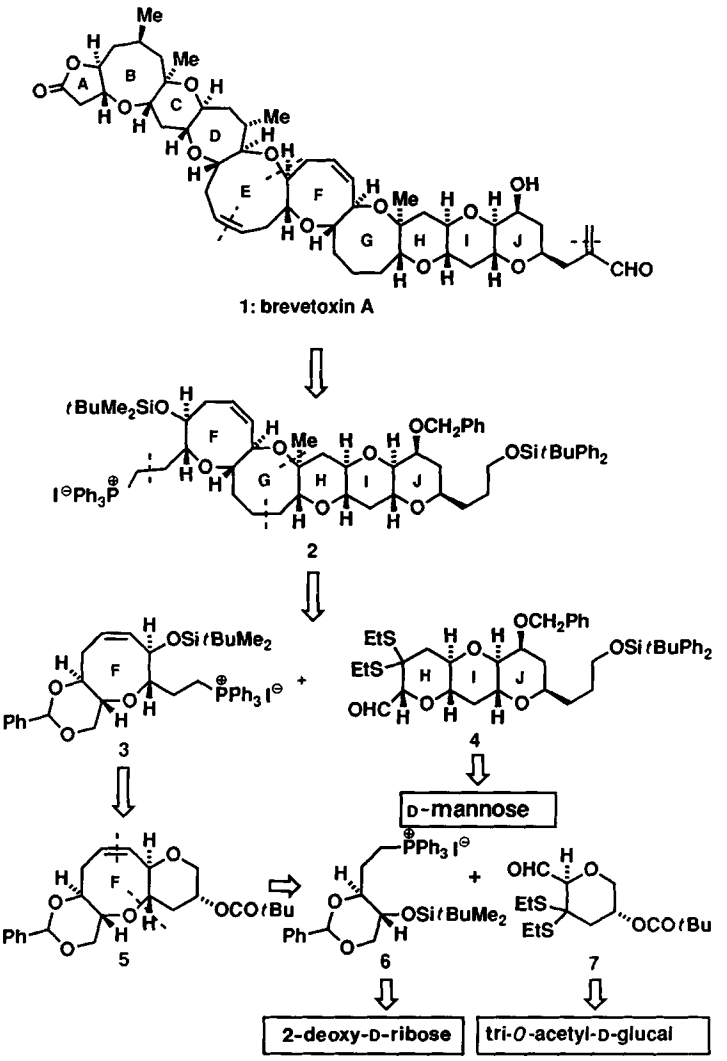

Scheme 1. Retrosynthetic analysis of brevetoxin A (**1**).

into olefin **9** (65% overall yield) by a Wittig reaction followed by sequential and selective protection involving 1,3-benzylidene formation and silylation. Subsequent ozonolysis–reduction led to alcohol **10**, which was then converted into phosphonium salt **6** via iodide **11** by standard chemistry (68% overall yield). For the synthesis of **7**, tri-*O*-acetyl-D-glucal (Scheme 2) was converted into **12** by methods previously described from these laboratories[4] followed by selective monosilylation. Epoxidation with mCPBA gave the α-epoxide **13** as a single product (75%), which was transformed into epoxyketone **14** by PDC treatment (86%). Reductive opening of **14** to **15** (88%) occurred smoothly upon treatment with NaI, whilst transformations **15** → **16** → **17** → **18** → **7**

[*] K. C. Nicolaou, C. A. Veale, C.-K. Hwang, J. Hutchinson, C. V. C. Prasad, W. W. Ogilvie
Department of Chemistry
Research Institute of Scripps Clinic,
10666N. Torrey Pines Road
La Jolla, CA 92037 (USA)
and
Department of Chemistry
University of California San Diego
La Jolla, CA 92093 (USA)

[**] This work was financially supported by the National Institutes of Health (USA), the National Science Foundation (USA), Merck Sharp and Dohme (USA) and Hoffmann LaRoche (USA) and was partially carried out at the University of Pennsylvania. Abbreviations used: mCPBA = *meta*-chloroperbenzoic acid, PDC = pyridinium dichromate, CSA = camphorsulfonic acid, HMPA = hexamethylphosphoric acid triamide, Tf = trifluormethanesulfonate, TBAF = tetrabutylammonium fluoride, DIBAH = diisobutylaluminum hydride, DBU = diazabicyclo[5,4,0]undec-7-ene, py = pyridine, DET = diethyltartrate, 9-BBN = 9-borabicyclo[3,3,1]nonane.

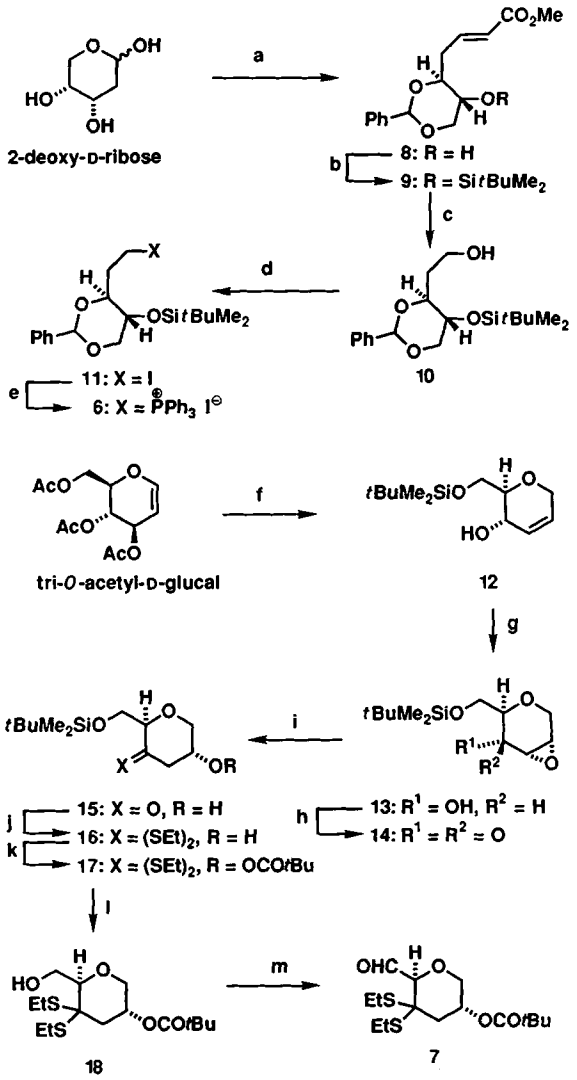

Scheme 2. Preparation of key intermediates **6** and **7**. Reagents and conditions: a) 1: 1.1 equiv of $Ph_3PCHCOOMe$, THF, 80 °C, 4 h, 100%; 2: 1.5 equiv of $PhCH(OMe)_2$, 0.1 equiv of CSA, CH_2Cl_2, 25 °C, 12 h, 65%; b) 1.1 equiv of $tBuMe_2SiOTf$, 1.5 equiv of 2,6-lutidine, CH_2Cl_2, 0 °C, 30 min, 100% c) O_3, CH_2Cl_2, −78 °C, 2 h, then 3.5 equiv of $NaBH_4$, MeOH, 0 °C, 2 h, 90%; d) 1.4 equiv of I_2, 1.4 equiv of PPh_3, 1.4 equiv of imidazole, CH_3CN, 25 °C, 30 min, 84%; e) 1.1 equiv of PPh_3, CH_3CN, 80 °C, 48 h, 90%; f) 1: see ref. [4]; 2: 1.5 equiv of $tBuMe_2SiCl$, 2.0 equiv of imidazole, DMF, 0 °C, 1 h, 94%; g) 1.2 equiv of mCPBA, CH_2Cl_2, 0–25 °C, 12 h, 75%; h) 2.0 equiv of PDC, CH_2Cl_2, 25 °C, 6 h, 86%; i) 5.0 equiv of NaI, 0.5 equiv of NaOAc, 5.0 equiv of HOAc, acetone, 25 °C, 1 h, 88%; j) 4.0 equiv of EtSH, 2.5 equiv of $BF_3{\cdot}OEt_2$, CH_2Cl_2, −40 °C, 1 h, 74%; k) 1.5 equiv of $(CH_3)_3CCOCl$, Et_3N, CH_2Cl_2, 25 °C, 18 h, 84%; l) 1.5 equiv of TBAF, THF, 0 °C, 3 h, 95%; m) 5.0 equiv of $SO_3{\cdot}py$, 5.0 equiv of Et_3N, DMSO, CH_2Cl_2, 0 °C, 1 h, 75%.

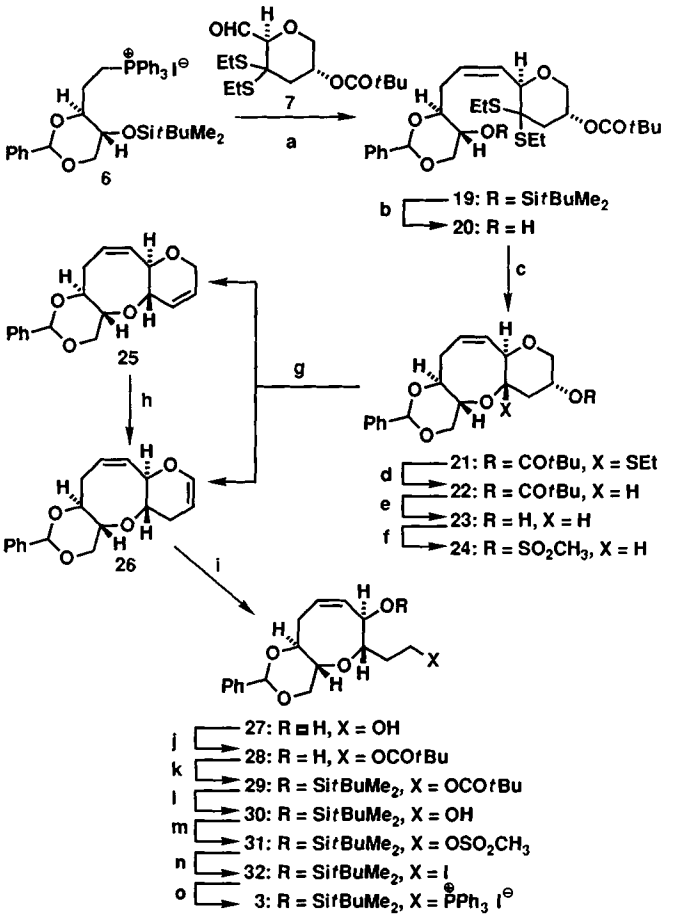

Scheme 3. Synthesis of key intermediate **3**. Reagents and conditions: a) 0.9 equiv of *n*BuLi, THF, −78 °C, 1 h, then 4.0 equiv of HMPA, 1.0 equiv of **7**, −78–25 °C, 18 h, 75%; b) 1.5 equiv of TBAF, THF, 25 °C, 12 h, 98%; c) 4.0 equiv of $AgClO_4$, 5.0 equiv of $NaHCO_3$, 4 Å molecular sieves, silica gel, CH_3NO_2, 25 °C, 4 h, 74%; d) 4.0 equiv of Ph_3SnH, 0.1 equiv of AIBN, toluene, 110 °C, 2 h, 95%; e) 2.5 equiv of DIBAH, CH_2Cl_2. −78 °C, 1 h, 85%; f) 1.5 equiv of CH_3SO_2Cl, 3.0 equiv of Et_3N, CH_2Cl_2. 0 °C, 1 h; g) 5.0 equiv of DBU, DMF, 145 °C, 2 h; 84% from **23** (**25**:**26** = 4.6:1); h) 1.0 equiv of KO*t*Bu, DMSO, THF, 50 °C, 3 h, 60%; i) 1: 1.1 equiv of mCPBA, THF, H_2O, 0–25 °C, 1 h; 2: 10.0 equiv of $NaBH_4$, MeOH, 0 °C, 1 h; 3: excess $NaIO_4$, EtOH, H_2O, 25 °C, 1 h; 4: 3.0 equiv of $NaBH_4$, MeOH, 0 °C, 1 h, 85% from **26**; j) 1.1 equiv of $(CH_3)_3CCOCl$, py, −20–0 °C, 4 h, 82%; k) 1.5 equiv of $tBuMe_2SiCl$, 5.0 equiv of imidazole, DMF, 25 °C, 12 h, 97%; l) 2.7 equiv of DIBAH, CH_2Cl_2, −78 °C, 1 h, 98%; m) 1.4 equiv of CH_3SO_2Cl, 3.0 equiv of Et_3N, CH_2Cl_2, 0 °C, 1 h; n) 10 equiv of NaI, acetone, 56 °C, 2 h, 84% from **30**; o) 1.0 equiv of I_2, 1.0 equiv of PPh_3, CH_3CN, 60 °C, 48 h, 92%.

proceeded uneventfully affording the requisite aldehyde (**7**) in high overall yield.

The coupling of intermediates **6** and **7** and elaboration of the resulting product to compound **3** is summarized in Scheme 3. Generation of the phosphorane from **6** followed by reaction with aldehyde **7** gave selectively the *cis* olefin **19** (75%), which was converted into hydroxydithioketal **20** and then cyclized[5] by the action of $AgClO_4$ to afford oxocene derivative **21** (74%). Desulfurization of **21** (95%) followed by standard manipulations led to methanesulfonate **24** in high overall yield. Base-induced elimination converted **24** into a mixture of **25** and **26** (84%, **25**:**26** ca 4.6:1). The undesired isomer **25** was isomerized to the desired enol ether **26** (60%) under basic conditions. Transformation of **26** to **27** (85% overall yield) required three steps: mCPBA epoxidation of the enol ether in the presence of H_2O leading to a hydroxy lactol, $NaBH_4$ reduction forming a triol, and $NaIO_4$ cleavage of the 1,2-diol system. Compound **27** was converted into phosphonium salt **3** by conventional methods via intermediates **28**–**32** as summarized in Scheme 3 (77% overall yield).

Scheme 4 outlines the construction of the key intermediate **4** from D-mannose. This synthesis was based on synthetic technology for the regio- and stereoselective synthesis of cyclic ethers from hydroxy epoxides previously described from these laboratories[6] and applied[7] to the construction of brevetoxin B intermediates. The highlights of this sequence were the two ring forming reactions **49** → **50** (CSA, 80%) and **59** → **60** (CSA, 80%).

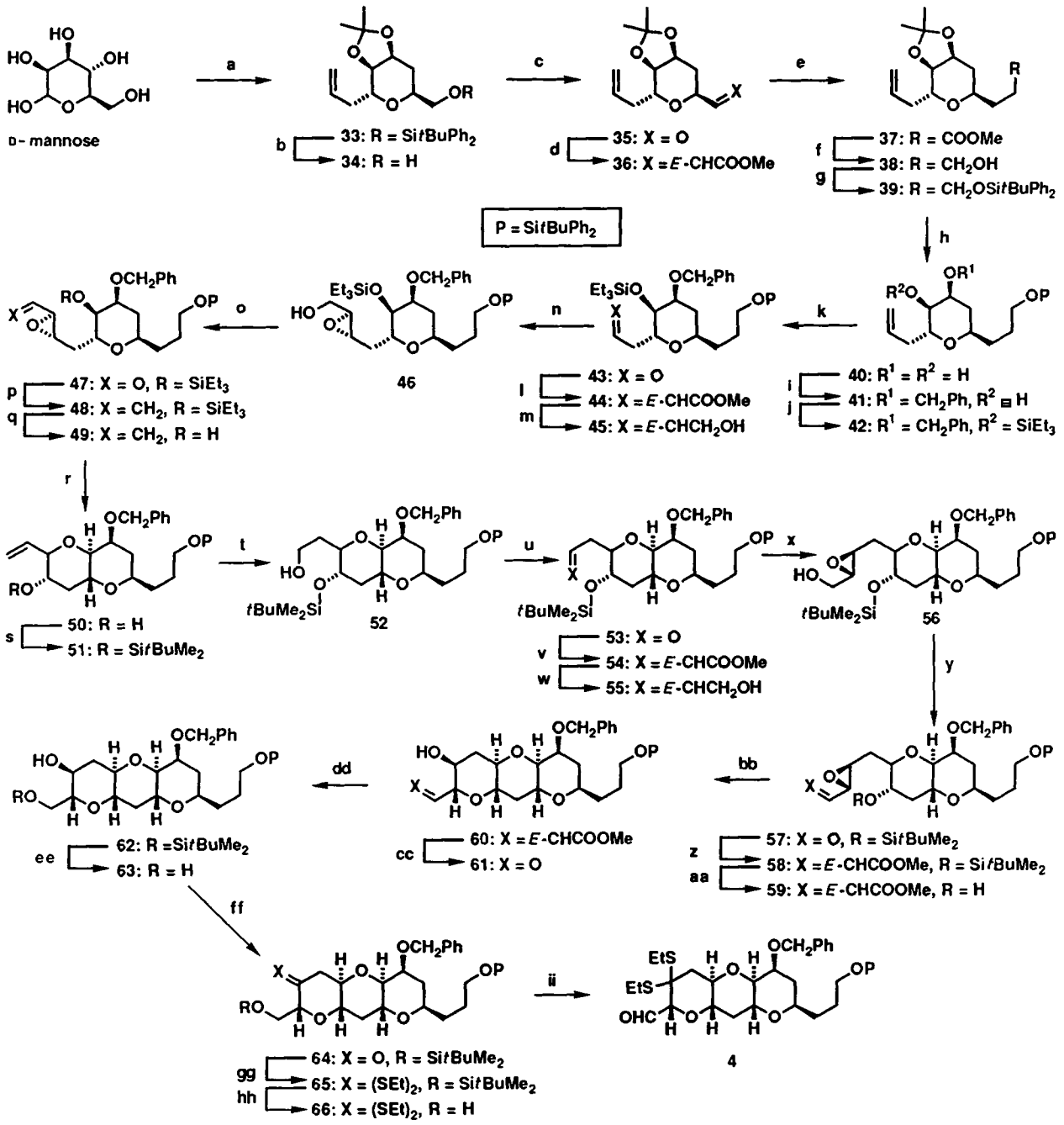

Scheme 4. Reagents and conditions: a) see ref. [7]; b) 1.5 equiv of TBAF, THF, 25 °C, 2 h, 95%; c) 1.5 equiv of $(COCl)_2$, 2.0 equiv of DMSO, 5.0 equiv of Et_3N, CH_2Cl_2, −78 °C, 1 h; d) 1.2 equiv of $Ph_3PCHCOOMe$, CH_2Cl_2, 25 °C, 18 h, 90% from **34**; e) 2.0 equiv of L-selectride, 2.5 equiv of *t*BuOH, THF, −78 °C, 1 h, then 3 equiv of NaOH, 3 equiv of H_2O_2, 0 °C, 1 h; f) 2.5 equiv of DIBAH, CH_2Cl_2, −78 °C, 1 h, 78% from **36**; g) 1.1 equiv of *t*BuPh$_2$SiCl, 3.0 equiv of imidazole, DMF, 0–25 °C, 2 h, 95%; h) 0.1 equiv of CSA, MeOH, 25 °C, 4 h, 90%; i) 1.04 equiv of *n*Bu$_2$SnO, MeOH, 65 °C, 1 h, then 1.2 equiv of CsF, 1.2 eqiv of $PhCH_2Br$, DMF, 25 °C, 18 h, 87%; j) 1.2 equiv of Et_3SiCl, 2.0 equiv of imidazole, DMF, 25 °C, 12 h, 96%; k) excess O_3, CH_2Cl_2, −78 °C, then 1.5 equiv of Ph_3P; l) 1.1 equiv of $Ph_3PCHCOOMe$, benzene, 25 °C, 12 h, 78% from **42**; m) 2.5 equiv of DIBAH, CH_2Cl_2, −78 °C, 1 h, 96%; n) 0.075 equiv of (+)-DET, 0.05 equiv of Ti(*i*OPr)$_4$, 1.3 equiv of *t*BuOOH, 4 Å molecular sieves, CH_2Cl_2, −20 °C, 48 h, 92%; o) 5.0 equiv of SO_3·py, 5.0 equiv of Et_3N, CH_2Cl_2, DMSO, 0 °C, 1 h; p) 1.5 equiv of Ph_3PCH_2Br, 1.4 equiv of NaN(TMS)$_2$, THF, 0 °C, 1 h, 76% from **46**; q) 1.1 equiv of TBAF, THF, −20–0 °C, 3 h, 92%; r) 0.1 equiv of CSA, CH_2Cl_2, 0 °C, 2 h, 80%; s) 1.5 equiv of *t*BuMe$_2$SiCl, 3.0 equiv of imidazole, DMF, 25 °C, 12 h, 99%; t) 2.0 equiv of 9-BBN, THF, 0 °C, 2 h, then excess NaOH, excess H_2O_2, 0 °C, 1 h, 92%; u) 1.5 equiv $(COCl)_2$, 2.0 equiv of DMSO, 5.0 equiv of Et_3N, CH_2Cl_2, −78 °C, 1 h; v) 1.0 equiv of $Ph_3PCHCOOMe$, benzene, 25 °C, 12 h, 86% from **52**, w) 2.5 equiv of DIBAH, CH_2Cl_2, −78 °C, 1 h, 96%; x) 0.075 equiv of (+)-DET, 0.05 equiv of Ti(*i*OPr)$_4$, 1.3 equiv of *t*BuOOH, 4 Å molecular sieves, CH_2Cl_2, −20 °C, 12 h, 92%; y) 5.0 equiv of SO_3·py, 5.0 equiv of Et_3N, DMSO, CH_2Cl_2, 0 °C, 2 h; z) 1.5 equiv of $Ph_3PCHCOOMe$, benzene, 25 °C, 12 h, 78% from **56**; aa) 1.03 equiv of TBAF, THF, 0 °C, 3 h, 87%; bb) 0.2 equiv of CSA, CH_2Cl_2, 0–25 °C, 80%; cc) excess O_3, CH_2Cl_2, −78 °C, then 1.5 equiv of Ph_3P, 25 °C, 3 h; dd) 4.0 equiv of $NaBH_4$, MeOH, 0 °C, 96% from **60**; ee) 1.5 equiv of *t*BuMe$_2$SiCl, 3.0 equiv of imidazole, DMF, 0 °C, 1 h, 93%; ff) 1.5 equiv of $(COCl)_2$, 2.0 equiv of DMSO, 5.0 equiv of Et_3N, CH_2Cl_2, −78 °C, 1 h, 93%; gg) 5.0 equiv of EtSH, 3.0 equiv of $Zn(OTf)_2$, CH_2Cl_2, 25 °C, 5 h; hh) 0.01 equiv of CSA, MeOH, 0 °C, 83% from **64**; ii) 4.0 equiv of SO_3·py, 4.0 equiv of Et_3N, DMSO, CH_2Cl_2, 0 °C, 1 h, 92%.

Scheme 5 outlines the synthesis of the targeted intermediate **2** starting with the coupling of **3** and **4** (*n*BuLi, HMPA) to afford predominantly the *cis* olefin **67**[8] (*cis*:*trans* ca 3:1, 88% total yield).[9] Desilylation of both oxygens in **67** followed by selective monosilylation with *Hanessian*'s[10] more robust and UV-active protecting group gave **69** via diol **68**

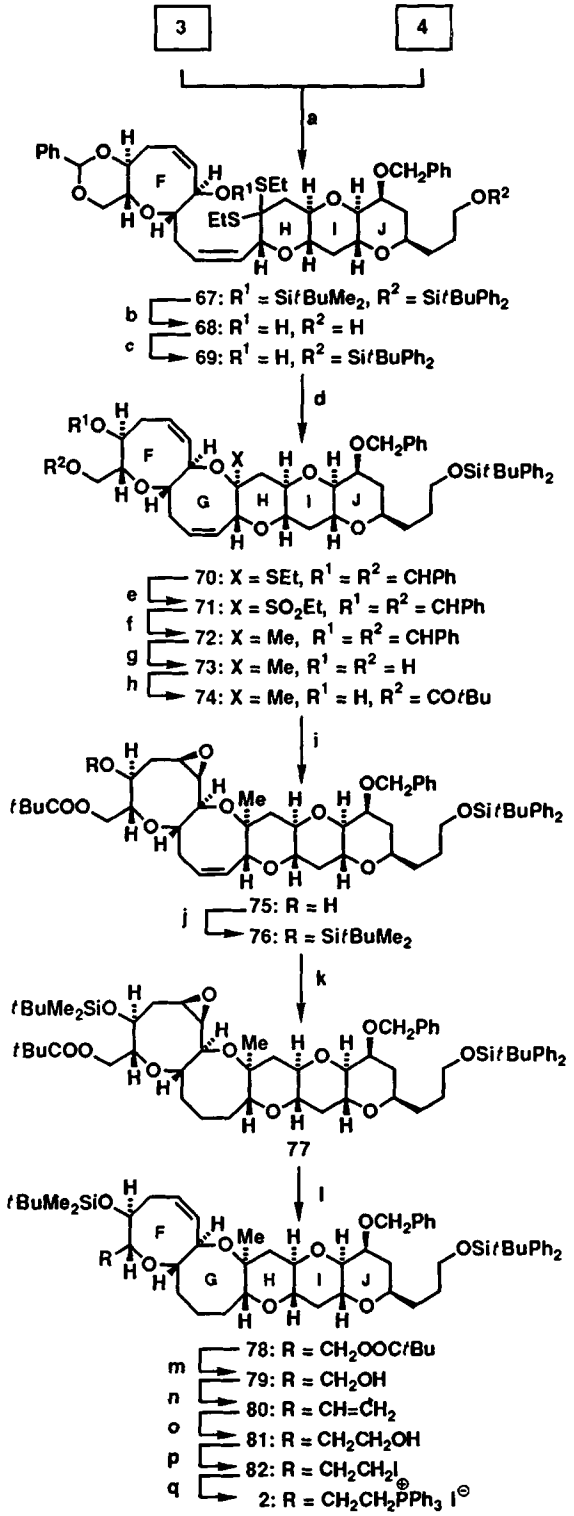

Scheme 5. Synthesis of **2**. Reagents and conditions: a) 0.97 equiv of *n*BuLi, THF, −78–0 °C, 20 min, then 4.0 equiv of HMPA, 0.8 equiv of **4**, −78–25 °C, 3 h, 88%; b) 3.0 equiv of TBAF, THF, 25 °C, 3 h; c) 1.02 equiv of $BuPh_2SiCl$, 3.0 equiv of imidazole, DMF, 0 °C, 3 h, 72% from **67**; d) 8.0 equiv of $AgClO_4$, 10 equiv of $NaHCO_3$, 3 Å molecular sieves, silicagel, CH_3NO_2, 25 °C, 3 h, 87%; e) 2.0 equiv of mCPBA, 3.0 equiv of $NaHCO_3$, CH_2Cl_2, 0 °C; f) 3.0 equiv of $AlMe_3$, CH_2Cl_2, −78 °C, 30 min, 94% from **70**; g) 5.0 equiv of EtSH, 10 equiv of $NaHCO_3$, 3.0 equiv of $Zn(OTf)_2$, CH_2Cl_2, 25 °C, 5 h, 90%; h) 1.05 equiv of $(CH_3)_3CCOCl$, py, 0 °C, 12 h, 86%; i) 1.0 equiv of mCPBA, CH_2Cl_2, 0 °C, 3 h, 75%; j) 1.5 equiv of $tBuMe_2SiOTf$, 3.0 equiv of 2,6-lutidine, CH_2Cl_2, 0 °C, 20 min, 82%; k) 10 equiv of $KO_2CN = NCO_2K$, 20 equiv of HOAc, py, 0 °C, 18 h, 83%; l) 10 equiv of WCl_6, 20 equiv of *n*-BuLi, THF, −78–25 °C, 4 h, 92%; m) 3.0 equiv of DIBAH, CH_2Cl_2, −78 °C, 20 min, 95%; n) 5.0 equiv of SO_3·py, 5.0 equiv of Et_3N, DMSO, CH_2Cl_2, 0 °C, 2 h, then 3.0 equiv of Ph_3PCH_3Br, 2.0 equiv of $NaN(TMS)_2$, THF, 0 °C, 1 h, 83%; o) 1.2 equiv of 9-BBN, THF, 0 °C, 2 h, then excess NaOH, excess H_2O_2, 0 °C, 1 h, 73%; p) 2.0 equiv of CH_3SO_2Cl, 5.0 equiv of Et_3N, CH_2Cl_2, 0 °C, 20 min, then 10 equiv of NaI, acetone, 50 °C, 12 h, 75%; q) 10 equiv of PPh_3, CH_3CN, 60 °C, 24 h, 80%.

(72% overall from **67**). Cyclization[5] of hydroxy dithioketal **69** induced by $AgClO_4$ led to **70** in 87% yield. Application of previously described technology[5] allowed us to replace the ethylthio group in **70** with a methyl group with retention of stereochemistry to give **72** via intermediate **71** (mCPBA oxidation, followed by treatment with $AlMe_3$, 94% overall yield). The benzylidene protecting group was then removed by exposure to $Zn(OTf)_2$·EtSH followed by selective monopivaloate formation to give sequentially **73** (90%) and **74** (86%). At this juncture the double bond in ring G, which assisted in its high-yield formation, was to be hydrogenated to reach the desired goal. To do this it was found necessary to block temporarily and selectively the double bond of the F ring, a task that became possible by utilizing the directing effect of the homoallylic hydroxyl group. Thus, **74** reacted smoothly with stoichiometric amounts of mCPBA to furnish epoxide **75**[11] (75%), which was then protected as the silyl ether **76** (82%). Diimide reduction of **76** proceeded smoothly to afford the saturated system **77** (83%) and deoxygenation by the method of Sharpless[12] (WCl_6-*n*BuLi) led to the desired compound **78** in excellent yield (92%). Finally, the required chain extention and conversion into the phosphonium salt proceeded with standard chemistry and through intermediates **79** (95%), **80** (83%), **81** (73%), and **82** (75%) to afford the targeted FGHIJ ring framework **2** (80% from **82**).

Similar chemistry was carried out with intermediates carrying a one-carbon substituent on ring J. An X-ray crystallographic analysis of the crystalline compound **74a** (Fig. 1), related to **74** (Scheme 2), was performed[13] (see ORTEP drawing, Fig. 1) and confirmed the stereochemical assignments shown in all structures.

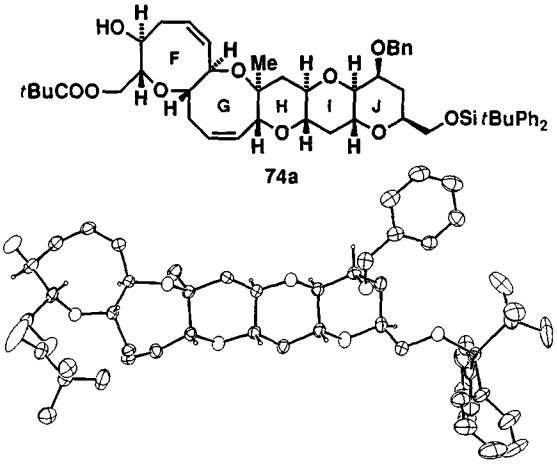

Fig. 1. Structural formula and ORTEP drawing of **74a**.

The described chemistry provides practical and efficient access to the advanced intermediate **2** and related compounds representing the FGHIJ ring assembly of brevetoxin A (**1**). The complexity of the systems and the high yields in which they are obtained demonstrates the power of new synthetic technology and strategies developed in this program for the construction of complex polycyclic frameworks containing medium-size cyclic ethers. Studies towards the total synthesis of brevetoxin A (**1**) are continuing.

Received: October 4, 1990 [Z 4226 IE]
German version: *Angew. Chem.* *103* (1990) 304

[1] K. C. Nicolaou, D. G. McGarry, P. K. Sommers, *J. Am. Chem. Soc. 112* (1990) 3696.
[2] K. C. Nicolaou, C. V. C. Prasad, W. W. Ogilvie, *J. Am. Chem. Soc. 112* (1990) 4998.
[3] Y. Shimizu, H. N. Chou, H. Bando, G. Van Duyne, J. Clardy, *J. Am. Chem. Soc. 108* (1986) 514. See also: M. Pawlak, M. S. Tempesta, J. Golik, M. G. Zagorski, M. S. Lee, K. Nakanishi, T. Iwashita, M. L. Gross, K. B. Tomer, *J. Am. Chem. Soc. 109* (1987) 1144.
[4] K. C. Nicolaou, C.-K. Hwang, B. E. Marron, S. A. DeFrees, E. A. Couladouros, Y. Abe, P. J. Carroll, J. P. Snyder, *J. Am. Chem. Soc. 112* (1990) 3040.
[5] K. C. Nicolaou, M. E. Duggan, C.-K. Hwang, *J. Am. Chem. Soc. 108* (1986) 2468.
[6] K. C. Nicolaou, C. V. C. Prasad, P. K. Somers, C.-K. Hwang, *J. Am. Chem. Soc. 111* (1989) 5330.
[7] K. C. Nicolaou, C.-K. Hwang, M. E. Duggan, *J. Am. Chem. Soc. 111* (1989) 6682.
[8] All new compounds exhibited satisfactory spectral and analytical, and/or exact mass data. Yields refer to spectroscopically and chromatographically homogeneous materials. Selected physical properties of compounds **67**, **72**, and **82**: **67**: oil; $R_f = 0.5$ (20% ether in petroleum ether); IR (neat) $\tilde{\nu}_{max}$ = 3080, 3040, 2980, 2940, 2880, 1480, 1440, 1260, 1100, 840, 710, 680 cm^{-1}; ^1H NMR (500 MHz, $CDCl_3$) δ = 7.7–7.2 (m, 20H, aromatic), 5.7–5.9 (m, 4H, olefinic), 5.39 (s, 1H, benzylic), 4.72 (d, J = 12.5 Hz, 1H, benzylic), 4.58 (d, J = 12.6 Hz, 1H, benzylic), 4.33 (d, J = 8.3 Hz, 1H, CHO), 4.13 (m, 2H, CHO), 3.95–3.6 (m, 8H, CHO), 3.55 (t, J = 10.4 Hz, 1H, CHO), 3.41 (m, 1H, CHO), 3.15 (m, 2H, CHO), 2.88 (dd, J = 6.0, 4.2 Hz, 1H, CH_2), 2.78 (m, 1H, CH_2), 2.67 (m, 4H, CH_2), 2.48 (m, 2H, CH_2), 2.26 (m, 2H, CH_2), 2.01 (m, 1H, CH_2), 1.87 (m, 2H, CH_2), 1.74 (t, J = 12.7 Hz, 1H, CH_2), 1.7 (series of multiplets, 4H, CH_2), 1.31 (t, J = 7.1 Hz, 3H, CH_3), 1.25 (t, J = 7.1 Hz, 3H, CH_3), 1.10 (s, 9H, *t*Bu), 0.89 (s, 9H, *t*Bu), 0.08 (s, 3H, CH_3Si), 0.04 (s, 3H, CH_3Si); MS: *m/z* (intensity) 1135 (24), 1106 (64), 1074 (100), 942 (33), 662 (90); HRMS Calcd for $C_{65}H_{91}O_9S_2Si_2$: $(M + H)^{\oplus}$: 1135.564, found: 1135.560. **72**: oil; R_f = 0.35 (30% ether in petroleum ether); $[\alpha]_D$ + 186° (c = 0.34, $CDCl_3$); IR (neat) $\tilde{\nu}_{max}$ = 3090, 3040, 2950, 2885, 1600, 1460, 1430, 1400, 1105, 1070, 940, 740, 710 cm^{-1}; ^1H NMR (500 MHz, $CDCl_3$) δ = 7.91–7.22 (m, 20H, aromatic), 5.83 (dd, J = 10.0, 6.6 Hz, 1H, olefinic), 5.77 (dd, J = 10.9, 6.2 Hz, 1H, olefinic), 5.69 (m, 2H, olefinic), 5.41 (s, 1H, benzylic), 4.72 (d, J = 12.6 Hz, 1H, benzylic), 4.61 (d, J = 12.6 Hz, 1H, benzylic), 4.36 (t, J = 7.4 Hz, 1H, CHO), 4.17 (dd, J = 9.4, 3.8 Hz, 1H, CHO), 4.00 (d, J = 5.7 Hz, 1H, CHO), 3.90 (m, 1H, CHO), 3.86 (dt, J = 10.6, 4.4 Hz, 1H, CHO), 3.80 (dd, J = 9.3, 4.4 Hz, 1H, CHO), 3.76 (t, J = 8.4 Hz, 1H, CHO), 3.70–3.58 (series of multiplets, 5H, CHO), 3.18 (m, 1H, CHO), 3.15 (dd, J = 9.6, 2.5 Hz, 1H, CHO), 3.06 (m, 1H, CHO), 2.74 (m, 2H, CH_2CH=CH), 2.37 (dd, J = 14.2, 7.0 Hz, 1H, CH_2), 2.25 (m, 3H, CH_2), 2.11 (dd, J = 12.0, 4.3 Hz, 1H, CH_2), 1.88 (bs, 2H, CH_2), 1.71 (t, J = 11.9 Hz, 1H, CH_2), 1.61 (m, 3H, CH_2), 1.44 (dd, J = 11.3, 11.3 Hz, 1H, CH_2), 1.21 (s, 3H, CH_3), 1.04 (s, 9H, *t*Bu); ^{13}C NMR (125 MHz, $CDCl_3$) 139.23, 138.76, 137.66, 135.52, 134.06, 131.83, 129.46, 128.91, 128.91, 128.23, 128.17, 128.09, 127.55, 127.11, 127.06, 126.14, 124.10, 101.61, 85.92, 82.30, 82.14, 81.04, 77.67, 77.58, 76.84, 72.99, 72.33, 72.39, 72.26, 70.30, 69.76, 63.73, 62.65, 44.57, 35.70, 32.98, 32.64, 30.24, 29.85, 28.69, 26.86, 19.20, 16.80; MS *m/z* (intensity) 913 (M + H, 40), 856 (55), 808 (52), 748 (100), 688 (49), 627 (45), 464 (62); HRMS Calcd for $C_{56}H_{69}O_9Si$: $(M + H)^{\oplus}$: 913.471, found: 913.469; Anal. Calcd for $C_{56}H_{68}O_9Si$: C, 73.68; H, 7.45, found: C, 73.88; H, 7.63. **82**: oil; R_f = 0.6 (30% ether in petroleum ether); $[\alpha]_D$ + 108° (c = 0.19, $CHCl_3$); IR (neat) $\tilde{\nu}_{max}$ 3080, 3040, 2940, 2880, 1600, 1440, 1390, 1100, 840, 710 cm^{-1}; ^1H NMR (500 MHz, $CDCl_3$) δ = 7.66–7.22 (m, 15H, aromatic), 5.71 (dd, J = 10.8, 5.4 Hz, 1H, olefinic), 5.62 (m, 1H, olefinic), 4.71 (d, J = 12.6 Hz, 1H, benzylic), 4.61 (d, J = 12.6 Hz, 1H, benzylic, 4.46 (m, 1H, CHO), 3.90 (d, J = 2.7 Hz, 1H, CHO), 3.86 (dt, J = 10.4, 4.7 Hz, 1H, CHO), 3.79 (dd, J = 9.4, 4.1 Hz, 1H, CHO), 3.72 (m, 1H, CHO), 3.68 (t, J = 6.0 Hz, 2H, CH_2OSi), 3.56 (m, 1H, CHO), 3.31 (m, 3H, CHO, CH_2), 3.15 (m, 3H, CHO, CH_2), 3.05 (m, 1H, CHO), 2.68 (m, 1H, CH_2CH=CH), 2.4–1.4 (series of multiplets, 19H, CH_2), 1.21 (s, 3H, CH_3), 1.04 (s, 9H, *t*BuSi), 0.89 (s, 9H, *t*BuSi), 0.09 (s, 3H, CH_3Si), 0.04 (s, 3H, CH_3Si); MS *m/z* (intensity) 1065 (M + H, 5), 809 (7), 199 (100); HRMS Calcd for $C_{56}H_{82}O_8Si_2I$: $(M + H)^{\oplus}$: 1065.459, found 1065.463.
[9] This mixture was taken through the next two steps, at which point the *cis* isomer **69** was separated chromatographically.
[10] a) S. Hanessian, P. Lavallee, *Can. J. Chem. 53* (1975) 2975. b) S. Hanessian, P. Lavallee, *Can. J. Chem. 55* (1977) 562.
[11] The structure of this epoxide was tentatively assigned on the basis of NMR studies.
[12] K. B. Sharpless, M. A. Umbreit, M. T. Nieh, T. C. Flood, *J. Am. Chem. Soc. 94* (1972) 6538.
[13] This X-ray crystallographic analysis was carried out by Dr. *Patrick Carroll* of the University of Pennsylvania. Details are published elsewhere.

Intermediates in Nitrogenase Models: N_2H_3 and N_2H_4 as η^2-Coordinated Ligands**

By *Sabine Vogel, Annette Barth, Gottfried Huttner,* Thomas Klein, Laszlo Zsolnai,* and *Reinhard Kremer*

Dedicated to Professor Dieter Sellmann on the occasion of his 50th brithday

Dinitrogen ligands of the type N_2H_x are important intermediates in all models which attempt to explain the activity of nitrogenase.[1] The hydrazido(1-) ligand, $N_2H_3^{\ominus}$, plays a key role. Only in one case recently was it possible to stabilize this ligand on a organometallic complex fragment.[2] Organoderivatives $R_mN_2H_{(3-m)}$ ($m \geq 1$) of the parent compound N_2H_3, however, have been known as ligands for some time.[3] We report here the synthesis and properties of $[(tripod)Co(\eta^2\text{-}N_2H_3)]^{\oplus}$ (tripod = $CH_3C(CH_2PPh_2)_3$), **1**, the first non-organometallic N_2H_3 complex. The protonation of **1** led to $[(tripod)Co(\eta^2\text{-}N_2H_4)]^{2\oplus}$, **2**. The η^2-coordination of the N_2H_4 ligand, which is as important in the interpretation of nitrogenase activity, could be proven for the first time by the X-ray structure analysis of this complex.

In the presence of tripod, $[Co(BF_4)_2 \cdot 6H_2O]$ reacted with $N_2H_{4\ aq}$ to cation **1** (Fig. 1), which precipitated as the dark green, air-sensitive BPh_4 salt. The analytically pure, crystalline salt **1**-$(BPh_4) \cdot 2THF$ has a magnetic moment of 1.8 μ_B, corresponding to a low spin d^7 configuration at $Co^{2\oplus}$. Figure 1 shows the results of the X-ray structure analysis of this salt.

The coordination geometry of cobalt lies between the two extremes of square pyramid and trigonal bipyramid. The best description of the geometry of **1** is as an ideal tetrahedron around the cobalt atom, where the N_2H_3 unit, as a whole, occupies one tetrahedral site.[4]

The only moderate quality of the crystals[5] did not permit the crystallographic location of the hydrogen atoms attached to nitrogen. The identification of the ligand as an N_2H_3 unit is, however, unambiguous: in the IR spectrum three NH stretching frequencies are observed ($\tilde{\nu}$ = 3290, 3217, 3130 cm^{-1}) as expected for N_2H_3; these bands do not appear when deuterated reagents are used for the synthesis.

The magnetism of **1** mentioned above corresponds to one unpaired electron per cobalt atom. This only allows the formulation of **1** as $[(tripod)Co(N_2H_x)]^{\oplus}$, where $x = 2n + 1$. Furthermore, the structure of **1** points to the existence of the N_2H_3 unit: the N–N distance of 138.4(14) pm lies in the range observed for the N–N bond lengths of η^2-organohydrazido ligands in $R_mN_2H_{(3-m)}$.[3]

Similarly the different Co–N distances (Fig. 1) reflect the familiar pattern[3] of the η^2-coordinated $R_mN_2H_{(3-m)}$ ligands. The shorter metal–N distance agrees with those for the nitrogen atoms which carry only one substituent (H or R).[3] The same pattern is also observed for $[(tripod)Co(\eta^2\text{-}NHNMe_2][BPh_4] \cdot 1.5THF$: $Co\text{–}N_{NMe_2}$ = 205(2), $Co\text{–}N_{NH}$ = 196(2) pm.[7]

[*] Prof. Dr. G. Huttner, Dipl.-Chem. S. Vogel, Dipl.-Chem. A. Barth, Dipl.-Chem. T. Klein, Dr. L. Zsolnai
Anorganisch-chemisches Institut der Universität
Im Neuenheimer Feld 270, W-6900 Heidelberg (FRG)
Dr. R. Kremer [†]
Max-Planck-Institut für Festkörperforschung
Heisenbergstrasse 1, W-7000 Stuttgart 80 (FRG)
[†] Magnetic measurements
[**] This work was supported by the Deutsche Forschungsgemeinschaft and the Fonds der Chemischen Industrie.

Further evidence for the identity of **1** is provided by its protonation to **2**. The dark green BPh_4 salt of **1** is converted into the light green hydrazine complex **2** in THF with 40% $HBF_{4\ aq}$, which is obtained as the analytically pure, crystalline salt $[(tripod)Co(N_2H_4)][(BPh_4)(BF_4)] \cdot THF$.

According to the X-ray analysis, the best description of the coordination geometry around the cobalt atom of **2** is a distorted square pyramid (Fig. 1) in which the phosphorus atoms P1 and P2, and the two nitrogen atoms of the hydrazine ligand form the base of the idealised square pyramid. In agreement with this geometry, the Co-P bond to the apical phosphorus atom P3 is margianally longer than the other Co-P bonds. The magnetism of **2**-$(BPh_4)(BF_4) \cdot THF$ (solid state) of 3.84 μ_B corresponds with the spin-only value for three unpaired electrons.[8] Compound **2** may therefore be described formally as a high spin d^7 $Co^{2\oplus}$ complex.

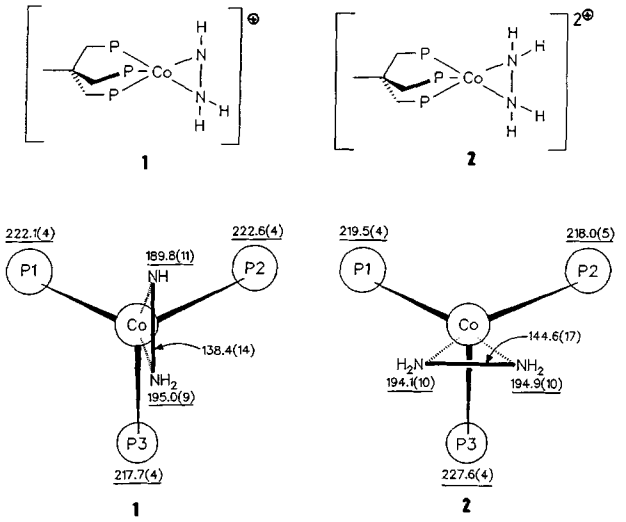

Fig. 1. η^2-Bonding (top) and structure characterization (bottom) of the cations **1** and **2** (phenyl groups of the tripod ligands omitted). Numerical data: distances in pm; underlined values: distances to cobalt; values in parentheses: standard deviations of the last decimal place.

The experimentally determined magnetism of three unpaired electrons confirms the N_2H_x, x = 2n, ligand composition for the dication **2**. The bond lengths suggest a formulation with x = 4: the N–N bond distance of 144.6(17) pm falls into the range found for η^2-coordinated organohydrazines $R_mN_2H_{(4-m)}$ $(m \geq 1)$[9] and precludes the formulation N_2H_2 or N_2[10] as ligand unit for **2**.

The Co–N distances in **2** are equal within experimental error, which confirms that both nitrogen atoms have the same substitution pattern (in contrast to **1**). In the NH stretching region of the IR spectrum, **2**-$(BPh_4)(BF_4) \cdot THF$ shows a broad band at 3229 cm^{-1} with shoulders at 3310 and 3275 cm^{-1}, and a sharp band at 3148 cm^{-1}. These four IR-active NH valence frequencies are expected for a N_2H_4 ligand in **2**.

In nature phosphane ligands do not form part of enzymes, neither does cobalt occur as the active metal center in the known nitrogenases. Nevertheless, the hypothesis that the specific coordination geometry imposed by the tripod ligand stabilizes the elusive N_2H_x intermediates in complexes **1** and **2**, possibly throws some light on the subject.

Experimental Procedure

All work was performed under argon to exclude air and moisture. Before use all glassware was heated with a hot-air blower, evacuated several times on a vacuum line (oil pump) and flushed with inert gas. Solvents were dried under inert gas and freshly distilled. The IR spectra were taken as Nujol mulls.

1: Equimolar amounts of the tripod ligand (624 mg, 1 mmol) in 15 mL THF and carefully dried (over P_2O_5 in a desiccator) $Co(BF_4)_2 \cdot 6H_2O$ [11] (340 mg, 1 mmol) in 15 mL ethanol were mixed at 20 °C. To the orange-red solution was added dropwise 0.5 mL (1 mmol) 64% N_2H_4 (immediate color change to dark green). After addition of 342 mg (1 mmol) sodium tetraphenylborate in 5 mL ethanol, the mixture was stirred for 2 h at 20 °C and then filtered through a G4 frit. Concentration to half the volume (10^{-1} mbar, 20 °C) caused black-green crystals of **1**-$BF_4 \cdot THF$ to separate within 24 h. Decantation, washing of the crystalline product with ethanol till the washings were colorless and then with petroleum ether, and drying under high vacuum gave an analytically pure product. Yield: 435 mg (42%, based on $Co^{2\oplus}$ salt); correct C,H,N,P analyses.

2: To an equimolar mixture of the tripod ligand (624 mg, 1 mmol) in 15 mL THF and $Co(BF_4)_2 \cdot 6H_2O$ [11] (340 mg, 1 mmol) in 15 mL ethanol is added dropwise 0.05 mL (1 mmol) 64% N_2H_4 at 20 °C. The solution is stirred for 1 h (20 °C), after which 4 drops of 40% HBF_4 (ca. 1 mmol) is added to the dark green reaction mixture (no color change); addition of a solution of 684 mg (2 mmol) sodium tetraphenylborate in 10 mL ethanol, 1 h stirring at 20 °C and filtration (G4) gives, after workup as for **1**, dark green crystals of **2**-$(BPh_4)(BF_4) \cdot THF$. Yield: 450 mg (40%, based on $Co^{2\oplus}$ salt); correct elemental analyses (C,H,N,P,Co,F,B).

Received: November 9, 1990 [Z 4271 IE]
German version: *Angew. Chem. 103* (1991) 325

CAS Registry numbers:
1-(BPh_4), 131761-28-9; **1**-$(BPh_4) \cdot 2\,THF$, 131761-29-0; **2**-$(BPh_4)(BF_4) \cdot THF$, 131761-32-5; nitrogenase, 9013-04-1.

[1] D. Sellmann, *Angew. Chem. 86* (1974) 331; *Angew. Chem. Int. Ed. Engl. 13* (1974) 639; J. Chatt, J. R. Dilworth, R. L. Richards, *Chem. Rev. 78* (1978) 589; J. A. McCleverty, *Chem. Soc. Rev. 12* (1983) 331; D. J. Lowe, R. N. Thorneley, B. E. Smith in P. M. Harrison (Ed.): *Metalloproteins, Vol. 1*, VCH, Weinheim 1985, p. 207.

[2] R. R. Schrock, A. H. Lium M. B. O'Regan, W. C. Finch, J. F. Payack, *Inorg. Chem. 27* (1988) 3574.

[3] J. Carroll, A. Sutton, *J. Chem. Soc. Chem. Commun. 1979*, 1058; J. Chatt, J. R. Dilworth, *ibid. 1980*, 786; I. A. Latham, G. J. Leigh, *J. Chem. Soc. Dalton Trans. 1986*, 385.

[4] Note added in proof: *G. Süß-Fink* et al. report a μ_3-η^2-$NHNH_2$ ligand in $HRu_3(CO)_9(N_2H_3)$: T. Jenke, H. Stoeckli-Evans, G. Süß-Fink, *J. Organometal. Chem. 391* (1990) 395.

[5] Crystal structure of **1**-$(BPh_4) \cdot 2\,THF$: $C_{73}H_{78}N_2O_2P_3CoB$, $M = 1178.17$, monoclinic, space group $P2_1/c$ (No. 14), $a = 9.960(2)$, $b = 28.509(7)$, $c = 23.039(5)$ pm, $\beta = 92.33(2)°$, $V = 6253(2) \cdot 10^6$ pm^3, $Z = 4$, $T = 298$ K, θ range $2° < 2\theta < 50°$, scan speed [$°min^{-1}$] $2.3 < \dot{\omega} < 29.3$, 11 072 independent reflections, 6581 observed reflections ($I \geq 2\sigma$), 545 refined parameters, $R_1 = 11.01\%$, $R_g = 9.63\%$. Crystal structure of **2**-$(BPh_4)(BF_4) \cdot THF$: $C_{69}H_{71}N_2OP_3CoB_2F_4$, M 1193.8, triclinic, space group $P\bar{1}$ (No. 2), $a = 12.73(1)$, $b = 13.86(1)$, $c = 19.80(1)$ pm, $\alpha = 71.61(6)$, $\beta = 82.55(6)$, $\gamma = 87.46(7)°$, $V = 3287(5) \cdot 10^6$ pm^3, $Z = 2$, $T = 200$ K, θ range $2° < 2\theta < 47°$, scan speed [$° min^{-1}$ – 1] $2.3 < \dot{\omega} < 29.3$, 9783 independent reflections, 6518 observed reflections ($I \geq 2\sigma$), 596 refined parameters, $R_1 = 12.13\%$, $R_g = 10.84\%$. Measurement on a Siemens (Nicolet-Syntex) R3m/V diffractometer, $Mo_{K\alpha}$ radiation, graphite monochromator, solution and refinement: SHELXTL PLUS [6]. Further details of the crystal structure investigation may be obtained from the Fachinformationszentrum Karlsruhe, Gesellschaft für wissenschaftlich-technische Information mbH, W-7514 Eggenstein-Leopoldshafen 2 (FRG) on quoting the depository number CSD-55033, the names of the authors and the journal citation.

[6] G. M. Sheldrick, *SHELXTL PLUS*, Universität Göttingen 1988.

[7] S. Vogel, *Diplomarbeit*, Universität Heidelberg 1990.

[8] See also: L. Sacconi, *J. Chem. Soc. A 1970*, 248.

[9] N. A. Bailey, P. D. Frisch, J. A. McCleverty, N. W. Walker, J. Williams, *J. Chem. Soc. Chem. Commun. 1975*, 350; J. Bultitude, L. F. Larkworthy, D. C. Povey, G. W. Smith, J. R. Dilworth, G. J. Leigh, *ibid. 1986*, 1748.

[10] R. S. Dickson, J. A. Ibers, *J. Am. Chem. Soc. 94* (1972) 2988; C. Krüger, Y.-H. Tsay, *Angew. Chem. 23* (1973) 1051; *Angew. Chem. Int. Ed. Engl. 12* (1973) 998; K. Jonas, D. J. Brauer, C. Krüger, P. J. Roberts, Y.-H. Tsay, *J. Am. Chem. Soc. 98* (1976) 74.

[11] H. Funk, F. Binder, *Z. Anorg. Allg. Chem. 155* (1926) 327.

Chloride-Induced Conversion of $[Mn_4O_2(OAc)_6(py)_2(dbm)_2]$ to $[Mn_4O_3Cl(OAc)_3(dbm)_3]$: Potential Relevance to Photosynthetic Water Oxidation**

By *Sheyi Wang, Kirsten Folting, William E. Streib, Edward A. Schmitt, James K. McCusker, David N. Hendrickson,** and *George Christou**

We are currently seeking models for the various oxidation levels (S_n states; n = −1 through 4) of the photosynthetic water oxidation center (WOC), to assist in the elucidation of its nature and mode of action.[1] The WOC requires four Mn atoms for activity, and these are oxo-bridged and ligated by O- and perhaps N-based groups, primarily of aspartate and glutamate carboxylates in the protein matrix; recent reports suggest[2] the nitrogen ligation to be minimal, at the level of 1 ± 1 per four Mn centers. The WOC also requires $Cl^{\ominus}$ for activity, and it has been suggested, for example, that the $Cl^{\ominus}$ is a ligand of the Mn atoms, or that it is involved in acid/base chemistry at the polypeptides.[1-3] The $Cl^{\ominus}$ is an essential cofactor for the WOC; in the absence of $Cl^{\ominus}$, an abnormal S_2 state is formed and advancement to S_3 is blocked.[3e, 4] Whatever its precise role, $Cl^{\ominus}$ thus seems to be important at the higher S_n states.

We recently described the preparation of various Mn complexes that were proposed as potential models of certain S_n states.[5, 6] The complexes $[Mn_4O_2(O_2CR)_6(bpy)_2]$ and $[Mn_4O_2(O_2CR)_7(bpy)_2]^{0,\oplus}$ (bpy = 2,2'-bipyridine), whose $[Mn_4O_2]^{Z\oplus}$ core contains a Mn_4 unit that is either planar or nonplanar ("butterfly" structure), were proposed as models for S_{-1}, S_0 and S_1.[5, 7] In addition, the complexes $[Mn_4O_3Cl_6(OAc)_3(HIm)]^{2\ominus}$, (HIm = imidazole) and $[Mn_4O_3Cl_4(OAc)_3(py)_3]$, which contain three Mn^{III} and one Mn^{IV} in a distorted Mn_4O_3Cl cubane core, were proposed as S_2 models.[6, 7] Obviously, the coordination spheres of the Mn_4O_2 and Mn_4O_3Cl complexes are not equivalent. Furthermore, the bpy and terminal $Cl^{\ominus}$ ligands are inconsistent with current WOC data,[8] and we were unable to convert Mn_4O_2- into Mn_4O_3Cl-containing species, which must be possible for potential S_1 and S_2 models. We report herein that all of the above shortcomings have now been redressed and, in addition, that a remarkable influence of $Cl^{\ominus}$ has been observed that may be of significant biological relevance.

Treatment of $[Mn_3O(OAc)_6(py)_3](ClO_4)$ in MeCN with ca. 1.5 equiv. of dibenzoylmethane slowly gives red microcrystals that can be recrystallized from hot MeCN to give red-black crystals in 45–55% overall yield. The product, the Mn_4^{III} complex **1**,[9] has crystallographically imposed C_i symmetry (Fig. 1) with chelating dbm ligands occupying the bpy positions of the previous complexes, and with six bridging $AcO^{\ominus}$ and two terminal py ligands.

$[Mn_4O_2(OAc)_6(py)_2(dbm)_2]$ **1**

Complex **1** displays remarkable reactivity with $Cl^{\ominus}$. If 1 equiv of nBu_4NCl is added to the hot MeCN recrystallization medium, **1** is not recovered; the product on cooling is instead the $Mn_3^{III}Mn^{IV}$ complex **2** in 20–25% nonoptimized yield. Based on the precedence of other systems,[5, 6] we

$[Mn_4O_3Cl(OAc)_3(dbm)_3]$ **2**

believe that **2** is formed from **1** by disproportionation and ligand redistribution. The structure[10] of **2** (Fig. 2) consists of a $[Mn_4O_3Cl]^{6\oplus}$ core with three bridging $AcO^{\ominus}$ and three chelating dbm groups. To emphasize the change that has occurred during the transformation of **1** into **2**, their central

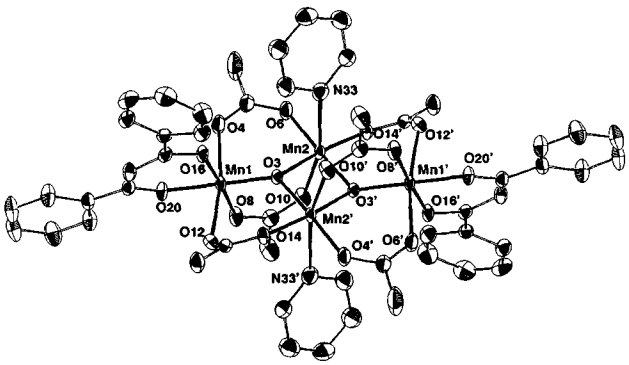

Figure 1. ORTEP representation of complex **1** at the 50% probability level. Selected bond distances (Å) and angles (°): Mn2 ··· Mn2', 2.8749(11); Mn2 ··· Mn1, 3.308(1); Mn2 ··· Mn1', 3.398(1); Mn1-O3, 1.877(2); Mn1-O4, 2.136(2); Mn1-O8, 1.928(2); Mn1-O12, 2.206(2); Mn1-O16, 1.931(2); Mn1-O20, 1.925(2); Mn2-O3, 1.885(2); Mn2-O3, 1.894(2); Mn2-O6, 1.957(2); Mn2-O10, 2.187(2); Mn2-O14, 1.953(2); Mn2-N33, 2.410(3); Mn1-O3-Mn2, 123.17(10); Mn1-O3-Mn2', 128.61(10); Mn2-O3-Mn2', 99.07(9). Primed and unprimed atoms are related by the inversion center.

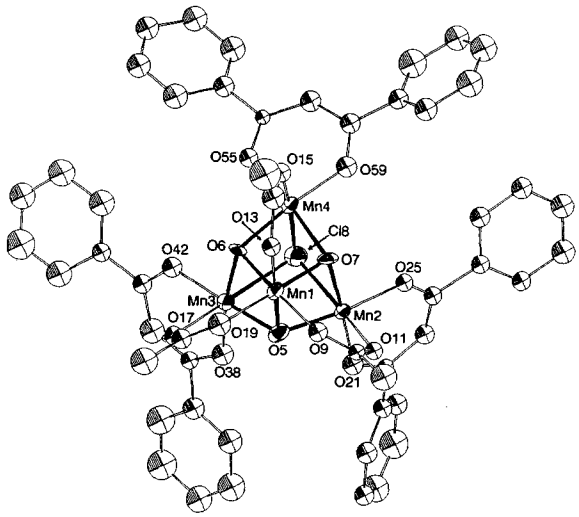

Figure 2. ORTEP representation of complex **2** at the 50% probability level. Selected bond distances (Å) and angles (°): Mn1 ··· Mn2, 2.797(5); Mn1 ··· Mn3, 2.797(4); Mn1 ··· Mn4, 2.792(5); Mn2 ··· Mn3, 3.252(5); Mn3 ··· Mn4, 3.264(5); Mn2 ··· Mn4, 3.237(5); Mn2-Cl8, 2.641(7); Mn-Cl8, 2.656(7); Mn4-Cl8, 2.654(7); O5-Mn(1,2,3), 1.883(15), 1.926(14), 1.922(15), respectively; O6-Mn(1,3,4), 1.867(14), 1.945(13), 1.920(13), respectively; O7-Mn(1,2,4), 1.842(13), 1.945(14), 1.939(14), respectively; Mn2-Cl8-Mn3, 75.74(19); Mn2-Cl8-Mn4, 75.37(19); Mn3-Cl8-Mn4, 75.85(19); Mn1-O5-Mn2, 94.5(7); Mn1-O5-Mn3, 94.6(6); Mn2-O5-Mn3, 115.4(7); Mn1-O6-Mn3, 94.4(6); Mn1-O6-Mn4, 95.0(6); Mn3-O6-Mn4, 115.2(7); Mn1-O7-Mn2, 95.2(6); Mn1-O7-Mn4, 95.2(6); Mn2-O7-Mn4, 112.9(6).

[*] Prof. Dr. G. Christou, Dr. K. Folting, Dr. W. E. Streib, S. Wang
Department of Chemistry and the Molecular Structure Center
Indiana University
Bloomington, IN 47405 (USA)
Professor Dr. D. N. Hendrickson, J. K. McCusker, E. A. Schmitt
Department of Chemistry, D-006
University of California at San Diego,
La Jolla, CA 92093-0506 (USA)

[**] This work was supported by the U.S. National Institutes of Health [GM 39083 and HL 13652]. dbmH = dibenzoylmethane, py = pyridine.

portions are shown below in diagrammatic form. The Mn_4O_3Cl core of **2** is essentially superimposable on those of other Mn_4O_3Cl complexes, showing that the complete exchange of oxygen-ligating ligands (dbm) for the previously present peripheral ligands (py, HIm, $Cl^{\ominus}$) has little structural effect. It does, however, have a small effect on the magnetic exchange interactions within **2**. The effective magnetic moment, μ_{eff}/Mn_4, steadily rises from 8.49 μ_B at 381.5 K to 10.42 μ_B at 10.0 K. Fitting of the data to the theoretical susceptibility equation derived previously[6b] gave J_1 (Mn^{III}–Mn^{IV}) = − 33.4 cm^{-1} and J_2 (Mn^{III}–Mn^{III}) = + 5.1 cm^{-1}; these values are similar to those for $[Mn_4O_3Cl_4(OAc)_3(py)_3]$ for which J_1 = − 26.8 cm^{-1} and J_2 = + 12.1 cm^{-1}.[6b] For complex **1**, the exchange interactions are similar in sign and magnitude to those in $[Mn_4O_2(OAc)_7(bpy)_2]^{\oplus}$, even though the latter has a butterfly rather than a planar disposition of the four Mn ions.[5b]

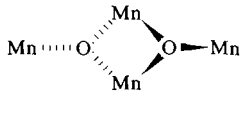

1

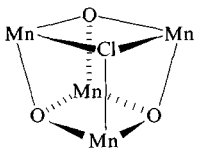

2

The described results represent important progress in our WOC modeling efforts. The predominantly oxygen ligation in **1** is now much more consistent with WOC data,[8] and not only does the S_2 model complex **2** have equivalent ligation, but also an Mn_4O_2 (S_1 model) complex has been directly converted into an Mn_4O_3Cl (S_2 model) complex for the first time, paralleling the native $S_1 \rightarrow S_2$ conversion. In addition, the $Cl^{\ominus}$-dependent nature of the model conversion perhaps sheds light on the $Cl^{\ominus}$-dependence of water oxidation and on why an abnormal S_2 state is formed in the absence of $Cl^{\ominus}$. Finally, we have previously hypothesized,[7] based merely on the structures of Mn_4O_2 and Mn_4O_3Cl materials, that substrate (H_2O) incorporation into the WOC Mn_4 aggregate may occur stepwise as bridging oxides during the $S_1 \rightarrow S_2 \rightarrow S_3$ transitions, and that this may be how H_2O is activated to oxidation to O_2 (eq. a). The conversion of **1** to **2**, while mechanistically unclear, does involve an increase in the number of

$$\underset{S_1}{Mn_4O_2} \xrightarrow[-e^{\ominus},\,-2H^{\oplus}]{+H_2O} \underset{S_2}{Mn_4O_3Cl} \xrightarrow[-e^{\ominus},\,-2H^{\oplus}]{+H_2O} \underset{S_3}{Mn_4O_4} \qquad \text{(a)}$$

oxide bridges, as in eq. (a), emphasizing the feasibility of this suggestion. We are currently investigating whether the Mn_4O_3Cl to Mn_4O_4 conversion can be accomplished. Of course, in the absence of X-ray structural data on the WOC, it is uncertain to what extent these model complexes reproduce the actual structure and transformations of the WOC Mn site. Nevertheless, we believe that the chemistry observed with synthetic complexes may parallel that of the native site and, therefore, at the very least, provide insights into the functioning of the WOC.

Received: August 27, 1990 [Z 4152]
German version: *Angew. Chem. 103* (1991) 314

[1] a) J. Amesz, *Biochim. Biophys. Acta 726* (1983), 1; b) Govindjee, T. Kambara, W. Coleman, *Photochem. Photobiol. 42 (1985), 187*; c) G. C. Dismukes *ibid. 43* (1986) 99; d) G. Renger, *Angew. Chem. 99* (1987) 660; *Angew. Chem. Int. Ed. Engl. 26* (1987) 643; e) G. W. Brudvig, *J. Bioenerg. Biomembr. 19* (1987) 91; f) G. T. Babcock in J. Amesz, (Ed.): *New Comprehensive Biochemistry, Vol. 15*, Elsevier, Dordrecht 1987, pp. 125–158; g) J. B. Vincent, G. Christou, *Adv. Inorg. Chem. 33* (1989) 197.

[2] a) N. Tamura, M. Ikeuchi, Y. Inoue, *Biochim. Biophys. Acta 973* (1989) 281; b) L.-E. Andreasson, *ibid. 973* (1989) 465.

[3] a) C. Critchley, *Biochim. Biophys. Acta 811* (1985) 33; b) C. Preston, R. J. Pace, *ibid. 810* (1985) 388; c) C. Critchley, A. M. Sargeson, *FEBS Lett. 177* (1984) 2; d) W. J. Coleman, Govindjee, H. S. Gutowsky, *Biochim. Biophys. Acta 894* (1987) 43 and 453; e) T. Ono, J.-L. Zimmerman, Y. Inoue, A. W. Rutherford, *ibid. 851* (1986) 193; f) W. J. Coleman, Govindjee *Photosynth. Res. 13* (1987) 199; g) W. F. Beck, G. W. Brudvig, *Chem. Scr. 28* (1988) 93.

[4] a) T. Ono, Y. Inoue, *Biochim. Biophys. Acta 806* (1985) 331; b) P. H. Homann, H. Gleiter, T. Ono, Y. Inoue, *ibid. 850* (1986) 10.

[5] a) G. Christou, *Acc. Chem. Res. 22* (1989) 328; b) J. B. Vincent, C. Christmas, H.-R. Chang, Q. Li, P. D. W. Boyd, J. C. Huffman, D. N. Hendrickson, G. Christou, *J. Am. Chem. Soc. 111* (1989) 2086.

[6] a) J. S. Bashkin, H.-R. Chang, W. E. Streib, J. C. Huffman, D. N. Hendrickson, G. Christou, *J. Am. Chem. Soc. 109* (1987) 6502; b) Q. Li, J. B. Vincent, E. Libby, H.-R. Chang, J. C. Huffman, P. D. W. Boyd, G. Christou, D. N. Hendrickson, *Angew. Chem. 100* (1988) 1799; *Angew. Chem. Int. Ed. Engl. 27* (1988) 1731.

[7] G. Christou, J. B. Vincent, *Biochim. Biophys. Acta 895* (1988) 259.

[8] a) R. D. Guiles, V. K. Yachandra, A. E. McDermott, J. L. Cole, S. L. Dexheimer, R. D. Britt, K. Sauer, M. P. Klein, *Biochemistry 29* (1990) 486, and references cited therein; b) G. N. George, R. C. Prince, S. P. Cramer, *Science (Washington DC) 243* (1989) 789.

[9] The dried solid is hygroscopic; correct elemental analyses (C,H,N,Mn); crystal data: $C_{52}H_{50}N_2O_{18}Mn_4$, triclinic, $P\bar{1}$, T = − 131 °C, a = 10.868(3), b = 13.864(3), c = 10.625(3) Å, α = 108.62(1), β = 118.98(1), γ = 89.34(2)°, V = 1307.24 Å^3, Z = 1, 6° ≤ 2θ ≤ 45°, 3432 unique, 3141 observed reflections, $F > 3.0\sigma(F)$. All non-hydrogen atoms were refined anisotropically; final $R(R_w)$ = 3.24 (3.70)%.

[10] Correct elemental analyses for **2** (C,H,Cl,Mn); crystal data: $C_{51}H_{42}O_{15}ClMn_4$, monoclinic, $P2_1/n$, T = − 155 °C, a = 13.900(3), b = 22.038(5), c = 16.518(5) Å, β = 107.80(1)°, V = 4817.63 Å^3, Z = 4, 6° ≤ 2θ ≤ 45°, 6317 unique, 2267 observed reflections, $F > 2.33\sigma(F)$. Only the Mn_4O_3Cl core atoms were refined anisotropically; final $R(R_w)$ = 7.85 (7.38)%. Further details of the crystal structure investigations are available on request from the Director of the Cambridge Crystallographic Data Centre, University Chemical Laboratory, Lensfield Road, GB-Cambridge CB2 1EW (UK), on quoting the complete journal citation.

1,3-(C → O) Silyl Shift in α-Diazo α-Silyl Ketones: Cycloaddition Reactions and Kinetic Proof for the β-Siloxydiazoalkene Intermediate**

By *Rainer Munschauer* and *Gerhard Maas**

The thermal treatment of α-diazo α-silyl ketones **1** at temperatures up to 80 °C leads by nitrogen elimination to products which are derived from alkylidenecarbenes (**3**).[1] We have suggested that the carbenes **3** are formed from diazoalkenes (**2**) which in turn result from a 1,3-(C → O) silyl migration in **1**. Diazoalkenes have as yet not been isolated. Recently the first low-temperature matrix isolation of a diazoethene derivative was reported;[2] furthermore, there are indications that diazoalkenes are formed in solution as reactive intermediates, which spontaneously eliminate N_2 to yield unsaturated carbenes.[3] In spite of these experimentally documented (and for the parent compound, diazoethene, even calculated[4]) high thermal lability, there are results which can be interpreted as trapping of intermediate diazoalkenes.[5–8]

[*] Prof. Dr. G. Maas, Dipl.-Chem. R. Munschauer
Fachbereich Chemie der Universität
Postfach 3049, W-6750 Kaiserslautern

[**] This work was supported by the Deutsche Forschungsgemeinschaft and the Fonds der Chemischen Industrie. *R. M.* thanks the Fonds der Chemischen Industrie for a study grant. We thank the President of the University of Kaiserslautern for funding to purchase a HPLC system.

In particular, the suggestion of 1,3-dipolar cycloadditions of diazoalkenes[5, 6] prompted us to study the thermolysis of the diazo compound **1** in the presence of dipolarophilic alkenes.

Indeed, **1a** and **1b** react with *N*-phenylmaleimide (NPM) and norbornene already at room temperature, or just above, to give the 1:1 cycloadducts **6a**, **6b** and **7a**, **7b** respectively,[9] which can be interpreted as direct trapping products of the diazoalkenes **2a** and **b**. (For reaction conditions and physical data, see Scheme 1 and Table 1). Silyl enol ethers **7** readily isomerize thermally to *N*-silyl-pyrazolines **8**; with **7b** this reaction takes place in the solid state as well as during the attempt to purify it by column chromatography (silica gel/petroleum ether).

Table 1. Selected physical and spectroscopic data of **6**, **7**, and **8** [a].

6a: colorless solid; m.p. 106 °C; ^{1}H NMR: δ = 1.05 (d, CHMe_2), 1.31 (sept, SiCH), 1.46 (s, *t*Bu), 4.42 (d, ^3J = 8.3, =CCH), 5.66 (d, ^3J = 8.3, NCH); ^{13}C NMR: δ = 14.5 (d, SiCH), 18.1 (q, CHMe_2), 28.4 (q, CMe_3), 39.2 (s, CMe$_3$), 41.6 (d, =CCH), 89.0 (d, NCH), 140.6 (s, O-C=C), 169.3 (s, C=O), 171.6 (s, O-C=C, 174.1 (s, C=O); IR (KBr): $\tilde{\nu}$ = 1592 cm^{-1} (C=C-OSi).

6b: Bright yellow solid; m.p. 100–102 °C; ^{1}H NMR: δ = 1.09 (d, CHMe_2) 1.38 (sept, SiCH), 4.11 (d, ^3J = 7.7, =CCH), 5.72 (d, ^3J = 7.7, NCH); ^{13}C NMR: δ = 13.5 (d, SiCH), 17.9 (q, SiCHMe), 41.9 (d, =CCH), 89.3 (d, NCH), 143.9 (s, O-C=C), 155.5 (s, O-C=C), 168.4 (s, C=O), 173.0 (s, C=O); IR (KBr): $\tilde{\nu}$ = 1618 cm^{-1} (C=C-OSi).

7a: colorless oil; ^{1}H NMR: δ = 0.5–1.5 (m, Si*i*Pr$_3$ und 3 CH$_2$), 1.32 (s, *t*Bu), 2.20 (s, CH), 2.65 (d, ^3J = 7.2, =CCH), 2.80 (s, CH), 4.45 (d, ^3J = 7.2, NCH); ^{13}C NMR: δ = 14.9 (d, SiCH), 18.2 (q, CHMe_2), 26.2(t), 28.0(t), 29.0 (q, CMe_3), 31.8(t), 38.2 (s, CMe$_3$), 39.5(d), 42.9(d), 44.0(d), 93.2 (d, NCH), 146.4 (s, O-C=C), 163.7 (s, O-C=C); IR (Film): $\tilde{\nu}$ = 1608 cm^{-1} (C=COSi).

7b: Reddish oil; ^{1}H NMR: δ = 1.0–1.6 (m, Si*i*Pr$_3$ and 3 CH$_2$), 1.80 (s, CH), 2.77 (d, ^3J = 6.9, =CCH), 2.83 8s, CH), 4.62 (d, ^3J = 6.9, NCH); IR (Film): $\tilde{\nu}$ = 1610 cm^{-1} (C=COSi).

8a: Colorless solid; m.p. 66–67 °C; ^{1}H NMR: δ = 0.8–1.6 (m, Si*i*Pr$_3$ and 3 CH$_2$), 1.30 (s, *t*Bu), 2.40 (s, CH), 2.57 (s, CH), 3.30 (d, ^3J = 10.2, =CCH), 3.85 (d, ^3J = 10.2, NCH); IR (KBr): $\tilde{\nu}$ = 1625 cm^{-1} (vs, C=O).

8b: Yellow crystals; m.p. = 80–81 °C; ^{1}H NMR: δ = 1.0–1.6 (m, Si*i*Pr$_3$ and 3 CH$_2$), 2.48 (s, CH), 2.73 (s, CH), 3.46 (d, ^3J = 10.2, =CCH), 3.98 (d, ^3J = 10.2, NCH); ^{13}C NMR: δ = 12.2 (d, SiCH), 18.2 (q, CHMe_2), 25.1(t), 28.0(t), 33.2(t), 39.8(d), 45.6(d), 52.9(d), 72.2 (d, NCH), 150.7 (s, C=N), 184.9 (s, C=O); IR (KBr): $\tilde{\nu}$ = 1615 cm^{-1} (s, C=O).

[a] NMR spectra in $CDCl_3$, TMS as standard, ^{1}H NMR at 90 and 400 MHz, ^{13}C NMR at 50.3 and 100.6 MHz, *J* in Hz.

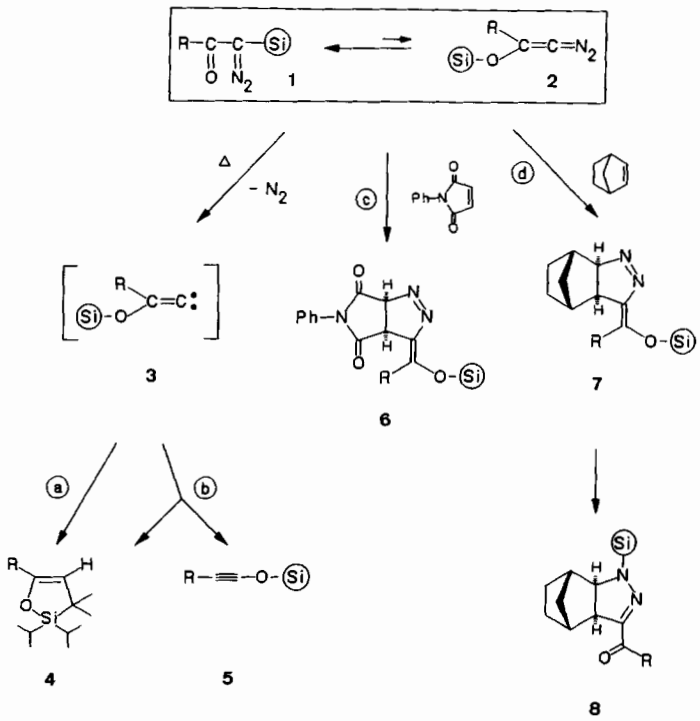

Scheme 1. Ⓢi = Si*i*Pr$_3$, **1a**–**8a**: R = *t*Bu, **1b**–**8b**: R = *p*-NO$_2$C$_6$H$_4$. ⓐ Benzene, 80 °C, 5 h, 57% **4a** [1c]. ⓑ **1b**, benzene, 80 °C, 2 h, 47% **4b**, 34% **5b** ([1a]; the formation of **4b** is not mentioned in this reference). ⓒ *N*-phenylmaleimide (1 equiv), ether, Schlenk pressure tube; for **1a**: 40 °C, 2 h, 79% **6a**; for **1b**: 40 °C, 2 h, 67% **6b**. ⓓ norbornene (20 equiv), ether, Schlenk pressure tube; for **1a**: 60 °C, 19 h, 78% **7a**, 13% **8a**, 5% **4a**; for **1b**: 50 °C, 18 h, 55% **7b** (before column chromatography of the product mixture), 18% **8b**, 16% **4b** + **5b** (or 20 °C, 5 days, 43% **8b** (after column chromatography)).

When the cycloadditions leading to **6** and **7** are carried out at temperatures $\leq$ 40 °C, the thermal decomposition of **1** mentioned in the introduction, which leads via **2** and **3** to **4** and/or **5**, is completely suppressed.

The question remains whether the cycloadducts **6** and **7** are direct trapping products of the diazoalkene **2** or whether they result from a [3 + 2] cycloaddition of the diazoketone **1**, followed by spontaneous silyl ketone to silyl enol ether isomerization (**1** → **9** → **6(7)**, Scheme 2).

Arguments against the route via **9** are first that unimolecular thermal isomerization of simple α-silyl ketones to silyl enol ethers occur typically only above 130 °C.[10, 11] There is no reason why silyl ketones of type **2** should rearrange already between 30 and 60 °C. Further, ethyl diazo(triisopropylsilyl)acetate (**10**) does not form cycloaddition products even under forcing conditions with *N*-phenylmaleimide (36 °C, 10 days) or with norbornene (100 °C, 72 h). Since **10** and also other diazosilylacetates are thermally very stable[12] and show even at 100 °C no tendency to decompose via diazoalkenes as proposed above for the diazosilyl ketones, one may conclude that **6** and **7** are indeed trapping products of the diazoalkenes **2**. Steric influences probably are an important factor causing the diazoalkenes **2** to undergo cycloaddition reactions more readily than the diazo ketones **1**. Similarly, the exclusive formation of (*Z*)-silyl enol ethers, **6** and **7**, is probably due largely to the sterically more favorable arrangement of the space-filling Si*i*Pr$_3$ group.

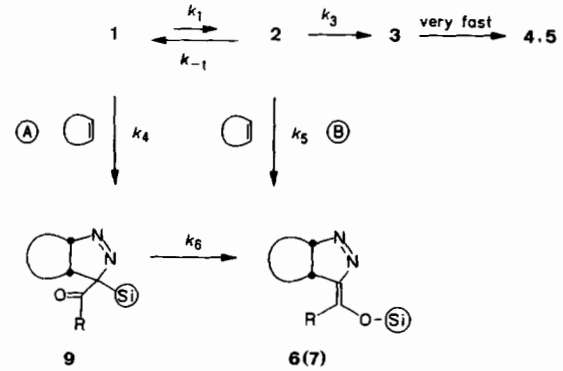

Scheme 2. Possible routes to **6** and **7**.

The diazoalkenes **2** cannot be detected in solution at 30–45 °C by IR or NMR spectroscopy (limit of detection in the ^{1}H NMR spectrum is ca. 1%). A kinetic analysis can, however, distinguish between the formation of cycloadducts **6** and **7** via route Ⓐ or Ⓑ[13] (Scheme 2). In the presence of a large excess of alkene and at temperatures at which the thermal decomposition of **1** is negligible ($k_3 \approx 0$), the decrease in the concentration of **1** is described by a pseudo-first-order

rate law with rate constant k_{obs} (equations (a)–(d)). For route Ⓐ where $k_6 \geq k_4$, equation (a) applies.

$$k_{obs} = k_4[\text{alkene}] \quad (a)$$

For route Ⓑ with d[**2**]/dt = 0, the observed rate constant is described by equation (b),

$$k_{obs} = (k_1 k_5\,[\text{alkene}])/(k_{-1} + k_5[\text{alkene}]), \quad (b)$$

which reduces to equation (c) or (d).

$$k_{obs} = k_1, \text{ when } k_5[\text{alkene}] \gg k_{-1} \quad (c)$$

$$k_{obs} = (k_1 k_5/k_{-1})\,[\text{alkene}], \text{ when } k_5\,[\text{alkene}] \ll k_{-1} \quad (d)$$

We followed the decrease in concentration of **1a** in benzene in the presence of excess NPM by analytical HPLC.[14, 15] The dependence of the k_{obs} values obtained from the function $\ln [\mathbf{1}] = \ln [\mathbf{1}]_0 - k_{obs}\, t$ (correlation coefficient $r \geq 0.999$) on [NPM] at T = 303 K is plotted in Figure 1. Already at relatively low excess of NPM a plateau is reached, that is the condition, k_5[alkene] $\gg k_{-1}$, of Eq. (c) is satisfied. Thus route Ⓑ, via the diazoalkene intermediate **2a**, is confirmed by the kinetic study. From the temperature dependence of the limiting rate constant k_1 for T = 293–303 K, the following activation parameters were calculated: $E_a = 21.6 \pm 0.4$ kcal mol^{-1}, $\Delta H^{\neq} = 21.0 \pm 0.4$ kcal mol^{-1}, $\Delta S^{\neq} = -3.4 \pm 1.2$ cal K^{-1} mol^{-1}. In an analogous study with norbornadiene as trapping agent,[16] a plot of the dependence of rate on concentration of norbornadiene yields a line through the origin. This relationship is described by equations (a) and (d) and no distinction between routes Ⓐ and Ⓑ can be made.

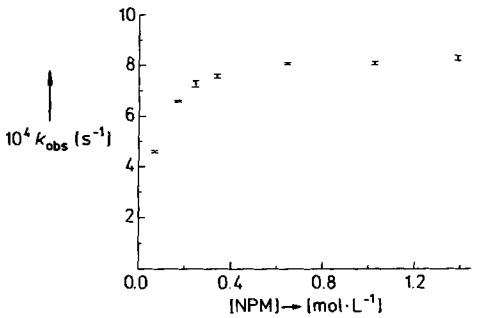

Fig. 1. $k_{obs} = -$ d[**1a**]/dt as a function of [NPM]; see text. Conditions: T = 303 K, solvent benzene, [**1a**] = 0.035 mol L^{-1}, 2.5- to 39.9-fold excess of NPM.

Received: October 12, 1990 [Z 4239 IE]
German version: *Angew. Chem. 103* (1991) 312

CAS Registry numbers:
1a, 106435-62-5; **1b**, 132298-34-1; **2a**, 132298-35-2; **2b**, 132298-36-3; **3a**, 132298-43-2; **3b**, 132298-44-3; **4a**, 106435-70-5; **4b**, 132298-45-4; **5b**, 132298-46-5; **6a**, 132298-37-4; **6b**, 132298-38-5; **7a**, 132298-39-6; **7b**, 132298-40-9; **8a**, 132298-41-0; **8b**, 132298-42-1; NPM, 941 · 69-5; norbornene, 498-66-8.

[1] a) G. Maas, R. Brückmann, *J. Org. Chem. 50* (1985) 2801; b) R. Brückmann, G. Maas, *J. Chem. Soc. Chem. Commun. 1986*, 1782; c) R. Brückmann, G. Maas, *Chem. Ber. 120* (1987) 635.

[2] J. C. Brahms, W. P. Dailey, *J. Am. Chem. Soc. 112* (1990) 4046.

[3] a) P. J. Stang, *Chem. Rev. 78* (1978) 385; b) K. Bott in S. Patai, Z. Rappoport (Eds.): *The Chemistry of Functional Groups, Supplement C*, Wiley, Chichester 1983, Chap. 16; c) J. C. Gilbert, U. Weerasooriya, *J. Org. Chem. 47* (1982) 1837; d) R. W. Saalfrank, E. Ackermann, M. Fischer, B. Weiß, R. Carrié, D. Danion, K. Peters, H. G. von Schnering, *Bull. Soc. Chim. Belg. 94* (1985) 475; further references cited in [1c, 2].

[4] Calculations at the MP2/6-31G* level yield $\Delta H^{\neq} \approx 6.9$ kcal mol^{-1} for the reaction $H_2C{=}C{=}N_2 \rightarrow H_2C{=}C$ M. A. Murcko, S. K. Pollack, P. M. Lahti, *J. Am. Chem. Soc. 110* (1988) 364.

[5] P. M. Lahti, J. A. Berson, *J. Am. Chem. Soc. 103* (1981) 7011.

[6] W. Ando, T. Furuhata, T. Takata, *Tetrahedron Lett. 26* (1985) 4499.

[7] Formation of diazoalkenes during H/D exchange on primary ethene diazonium salts: K. Bott, *Chem. Ber. 120* (1987) 1867.

[8] Diazomethylene phosphoranes, $(i\mathrm{Pr}_2\mathrm{N})_2\mathrm{HalP{=}C{=}N_2}$, have been isolated; they also undergo [3 + 2] cycloadditions: J.-M. Sotiropoulos, A. Baceiredo, G. Bertrand, *J. Am. Chem. Soc. 109* (1987) 4711.

[9] The structures of **6** and **7** (R = *t*Bu), Ⓢⓘ = $SiPh_2t$Bu) were determined by X-ray crystallography, which will be reported elsewhere.

[10] a) A. G. Brook, A. R. Bassindale in P. de Mayo (Hrsg.): *Rearrangements in Ground and Excited States, Vol. 2*, Academic, New York 1980, S. 149; b) I. Matsuda, S. Sato, M. Hattori, Y. Izumi, *Tetrahedron Lett. 26* (1985) 3215.

[11] The contrasting ease of the 1,3-(C → O) silyl shift (**1** → **2**) is probably due to the contribution of a (*Z*)-configured diazonium enolate resonance formula to the bonding in **1**.

[12] a) U. Schöllkopf, D. Hoppe, N. Rieber, V. Jacobi, *Liebigs Ann. Chem. 730* (1969) 1; b) T. Allspach, H. Gümbel, M. Regitz, *J. Organomet. Chem. 290* (1985) 33.

[13] a) R. Huisgen, H. Seidl, *Tetrahedron Lett. 46* (1964) 3381; b) R. Huisgen, F. Mietzsch, *Angew. Chem. 76* (1964) 36; *Angew. Chem. Int. Ed. Engl. 3* (1964) 83. c) R. Huisgen, *ibid. 82* (1970) 783 and *9* (1970) 751; d) F.-G. Klärner, D. Schröer, *Chem. Ber. 122* (1989) 179.

[14] Merck/Hitachi LiChrograph, LiChrospher RP-18 (125 × 4 mm), eluant acetonitrile (1.25 mL min^{-1}); detection at λ = 254 nm, 1,4-diiodobenzene as internal standard; no further absorptions between λ = 254 and 300 nm.

[15] The k_{obs} values were determined for the decrease in the concentration of **1a**, because the calculation of the concentration of **6a** involves larger errors (partial overlapping of peaks, lability of **6a** under HPLC conditions). For comparison one example run under optimal conditions for the detection of **6a** (acetonitrile/water, 95/5 (v/v); 1.25 mL min^{-1}, λ = 290 nm) at 290 K yielded for the decrease in [**1a**] $k_{obs} = (2.692 \pm 0.005) \times 10^{-2}$ min^{-1} (correlation coefficient r = 0.99998), and for the increase in [**6a**], $k_{obs} = (2.77 \pm 0.13) \times 10^{-2}$ min^{-1} (r = 0.9906).

[16] Norbornadiene yields cycloadducts (*endo* and *exo* isomers) with **1a**, which are analogous in structure to **7a**. In contrast to norbornene, norbornadiene is a liquid at room temperature and thus suitable for kinetic studies undiluted.

Diphosphonio Isophosphindoles, Phospholes with a Planar Phosphorus**

By *Alfred Schmidpeter*,* and *Martin Thiele*

Dedicated to Professor Rolf Appel on the occasion of his 70th birthday

Phosphole is an exception among the quartet of heterocycles, pyrrole, phosphole, furan, and thiophene, because it lacks aromaticity:[1, 2] The expected energy gain from cyclic delocalization is too small to meet the energy demand for a planar coordination for the phosphorus atom (inversion barrier for phospholane: 36 kcal mol^{-1}[3]). Thus in all the *P*-substituted phospholes as yet studied, phosphorus is pyramidal; the known phospholes unsubstituted at phosphorus are unstable at room temperature.[1] Their phosphorus atom is also pyramidal, but in one phosphole the inversion barrier is at least reduced to 16 kcal mol^{-1}.[2, 3] A planar environment for phosphorus in the ground state is conceivable when electron-withdrawing substituents occupy 2,5 positions. In fact, this was achieved in the 1,3-bis(triphenylphosphonio)isophosphindoles **6** and **7**.

[*] Prof. Dr. A. Schmidpeter, Dipl.-Chem. M. Thiele
Institut für Anorganische Chemie der Universität
Meiserstraße 1, W-8000 München 2

[**] Four- and five-membered phosphorus heterocycles, Part 76. This work was supported by the Deutsche Forschungsgemeinschaft and the Fonds der Chemischen Industrie. part 75: K.-H. Zirzow, A. Schmidpeter, *Z. Naturforsch. B43* (1988) 1475.

The *o*-xylylenebis(triphenylphosphonium) ion (**1**),[4] which is easily prepared from α,α-dibromo-*o*-xylene and triphenylphosphane, undergoes cyclocondensation with phosphorus trichloride[5] and triethylamine to form the 1,3-bis(triphenylphosphonio)isophosphindole cation (**3**). As intermediate only the PCl_2-substituted ylide cation **2**[6] can be detected spectroscopically and also isolated. Cation **3** is obtained as the bromide; the counterion can be exchanged for $BPh_4^{\ominus}$, $SbCl_6^{\ominus}$, or $HgI_3^{\ominus}$ by precipitating the respective salts from a methanol solution.

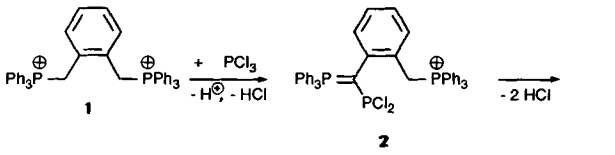

1 **2**

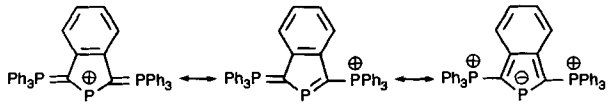

3a **3b** **3c**

The resonance formulas **3a**, **3b**, and **3c** can be written for **3**. Formula **3a** presents the cation as a phosphenium ion stabilized by two methylenephosphorane groups (whose ylide nature is not reflected in the formula), **3b** as a phosphonio-substituted phosphaalkene,[7] and in **3c** a phospholide anion modified by two phosphonio substituents. In fact **3** proves to be more thoroughly "ambiphilic" than other compounds with two-coordinate phosphorus. The ^{31}P NMR shift in **3**, however, ($\delta = 242$) corresponds to a *C*-substituted phosphenium ion (range: $\delta = 168-266$)[8] rather than a phospholide ion ($\delta = 40-103$).[1,9] This suggests that forms **3a** and **3b** predominate.

The Lewis acidity of **3** is small in comparison with other phosphenium ions.[8b] Thus the cyclic chlorophosphane which probably forms en route from **2** to **3** spontaneously loses a chloride ion. Furthermore, cation **3** does not react with water, although it adds the more strongly basic anions $MeO^{\ominus}$ and $HO^{\ominus}$ to form **4** and **5**, respectively.[10]

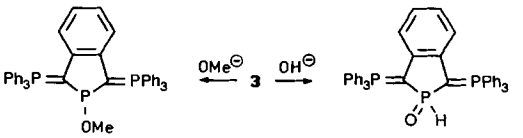

4 **5**

Cation **3**, on the other hand, is more basic than otherwise found for phosphenium ions, which can be neither protonated nor alkylated. Cation **3** is protonated by strong acids like HBF_4 and CF_3SO_3H. Formula **3b** would suggest a protonation at the ylide carbon, **3c** at the two-coordinate phosphorus atom. In fact, the symmetric dication **6** is formed and can be isolated as, for example, the tetrafluoroborate salt. Its formation corresponds to the protonation of phospholide ions to 1*H*-phospholes at low temperature,[11] which are, in contrast to **6**, unstable at room temperature and isomerize to 2*H*-phospholes, which promptly dimerize. Thus **6** is the first stable phosphole not substituted at phosphorus.

The decreasing negative charge on atoms C1 and C3 in the series **4**, **3**, and **6** is reflected in the ^{31}P NMR spectrum by an increase in the deshielding of the onium phosphorus. In particular the P–H coupling of 586 Hz for the isophosphindol **6** is significant: it is extremely high for a three-coordinate phosphorus atom, and far larger than for any other phosphane, in particular, for all known phospholes (217–234 Hz[11]). As the s character of the bond is reflected in the coupling constant, the phosphorus atom in **6** must be sp^2 hybridized and is thus in a planar environment. This bonding, best expressed by formula **6b**, corresponds to that of the bismethylenephosphoranes[11], which have been shown to be planar by X-ray crystallography. Till now for the only existing, but unstable, hydrobismethylenephosphorane $HP[=C(SiMe_3)_2]_2$, $^1J_{PH}$ was found to be 406 Hz.[11b] The distinctly higher value of $^1J_{PH}$ for **6** probably results from the CPC angle, which must be much smaller in the five-membered ring of **6** than in acyclic bismethylenephosphoranes (ca. 130°). With the exception of some azaphosphole transition metal complexes, **6** is the first phosphole or heterophosphole with phosphorus in a planar environment.[12]

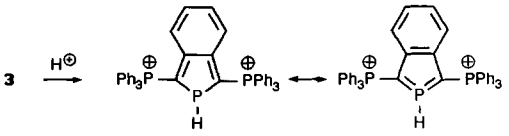

6a **6b**

Cation **3** can be alkylated by Me_3OBF_4 to the methyl derivative of **6**, the dication **7**, which also has a planar phosphorus atom in the ring. The coupling constant between phosphorus and the methyl carbon atom is 14 Hz in trimethyl phosphane, around 19 Hz in 1-methylphospholes,[13] but 98 Hz in **7**. Again this value is far greater than the corresponding coupling in alkylbismethylene phosphoranes (33–44 Hz[14]).

Besides the phosphonio substituents, the condensed benzene ring probably also favors the planar structure of **6**. The planarity of phosphorus in a phosphindole ([2.3]-annelation) demands about 8 kcal mol^{-1} more energy[3] than in a phosphole; it should demand less energy in an isophosphindole. The resonance formula **6b** gains in importance through the [3.4]-annelation.

Earlier attempts to prepare isophosphindoles were unsuccessful and even their oxides proved to be too reactive for isolation.[15]

The arsenic cations analogous to **3** and **6** can also be prepared and other heteroatoms may be stabilized in unusual coordination environments in the same position.

Experimental Procedure

3-Br: 40.2 g (51 mmol) **1**-Br_2 and 7.0 g (51 mmol) PCl_3 were heated under reflux in 100 mL Et_3N and 50 mL CH_2Cl_2 for 48 h. More CH_2Cl_2 was added and the ammonium halides were separated by shaking with water. The organic phase was concentrated and **3**-Br separated on addition of THF. After drying, digestion in THF, and recrystallization from ethanol, the yield of pale yellow crystals was 29.8 g (80%). M.p. 302°C (decomp.); ^{31}P NMR (AB_2 spin system): $\delta(A) = 241.8$, $\delta(B) = 16.8$ ($J(AB) = 91.4$ Hz); $^{13}C\{^1H\}$NMR (ABB'*X* spinsystem): $\delta = 109.0$ ($J(AX) = 56.0$ Hz, $J(BX) = 96.6$ Hz, $J(B'X) = 14.0$ Hz).

6-$(BF_4)_2$: A solution of 1.48 g (2.0 mmol) **3**-Br in 5 mL CH_2Cl_2 was mixed with 0.65 mL of a 6.15 M HBF_4 solution in Et_2O and allowed to stand for 30 min. On addition of 10 mL Et_2O, the product precipitated. Recrystallization from CH_2Cl_2 yielded 0.80 g (48%) colorless, extremely moisture-sensitive crystals. ^{31}P NMR (AB_2 spin system): $\delta(A) = 41.7$, $\delta(B) = 23.1$ ($J(AB) = 12.3$ Hz,

^1J(PH) = 586.2 Hz); $^{13}C\{^1H\}$NMR: δ = 110.1 (dd, ^1J(PC) = 52.7, 38.4 Hz, C1).

7-$(BF_4)_2$: 30 min after the preparation of a solution of 2.50 g (3.4 mmol) **3**-Br and 1.01 g (6.8 mmol) Me_3OBF_4 in 10 mL CH_2Cl_2, the volume was reduced to half. A colorless, very moisture-sensitive powder (1.75 g, 61%) precipitated on addition of 10 mL Et_2O and was recrystallized from CH_2Cl_2/Et_2O. ^{31}P NMR (AB_2 spin system): δ(A) = 69.3, δ(B) = 22.4 (J(AB) = 11.0 Hz, ^2J(PH) = 12.8 Hz; $^{13}C\{^1H\}$NMR: δ = 116.9 (dd, ^1J(PC) = 49.0, 36.4 Hz, C1), 43.0 (d, ^1J(PC) = 97.5 Hz, CH_3).

Received: August 2, 1990 [Z 4112 IE]
German version: *Angew. Chem. 103* (1991) 333

[1] F. Mathey, *Chem. Rev. 88* (1988) 429.
[2] M. H. Palmer, R. H. Findlay, *J. Chem. Soc. Perkin Trans. 2 1975*, 974.
[3] W. Egan, R. Tang, G. Zon, K. Mislow, *J. Am. Chem. Soc. 93* (1971) 6205.
[4] C. E. Griffin, K. R. Martin, B. E. Douglas, *J. Org. Chem. 27* (1962) 1627.
[5] For reactions of phosphonium ylides with chlorophosphances see: K. Issleib, M. Lischewski, *J. Prakt. Chem. 311* (1969) 857; *ibid. 312* (1970) 135; H. Schmidbaur, W. Tronich, *Chem. Ber. 101* (1968) 3545; G. Märkl, W. Bauer, *Angew. Chem. 101* (1989) 1698; *Angew. Chem. Int. Ed. Engl. 28* (1989) 1695; H. Grützmacher, *Z. Naturforsch. B 45* (1990) 170.
[6] ^{31}P NMR (ABC spin system): δ(A) = 170.6 (-PCl_2), δ(B) = δ(C) = 22.6 (-$PPh_3^{\oplus}$), J(AB) = 219.0 Hz.
[7] a) H. H. Karsch, H.-U. Reisacher, G. Müller, *Angew. Chem. 98* (1986) 467; *Angew. Chem. Int. Ed. Engl. 25* (1986) 454; b) H. Grützmacher, H. Pritzkow, *ibid. 101* (1989) 768 and *28* (1989) 740.
[8] a) S. Lochschmidt, A. Schmidpeter, *Phosphorus Sulfur 29* (1986) 73; b) A. H. Cowley, R. A. Kemp, *Chem. Rev. 85* (1985) 367.
[9] K. Karaghiosoff, A. Schmidpeter, *Phosphorus Sulfur 36* (1988) 217.
[10] ^{31}P NMR (AB_2 spin systems): **4** (X = OMe) δ(A) = 83.2, δ(B) = 11.9 (J(AB) = 50.8 Hz); **5**: δ(A) = 27.6, δ(B) = 12.6 (J(AB) = 48.5 Hz, ^1J(PH) = 504.9 Hz).
[11] a) R. Appel in M. Regitz, O. J. Scherer (Eds.): *Multiple Bonds and Low Coordination in Phosphorus Chemistry*, Thieme, Stuttgart, 1990, p. 157; b) A. R. Barron, A. H. Cowley, *J. Chem. Soc. Chem. Commun. 1987*, 1092.
[12] A. Schmidpeter, K. Karaghiosoff in H. W. Roesky (Ed.): *Rings, Clusters and Polymers of Main Group and Transition Elements*, Elsevier, Amsterdam 1989, p. 308.
[13] L. D. Quin, S. G. Borleske, R. C. Stocks, *Org. Magn. Reson. 5* (1973) 161; G. A. Gray, J. H. Nelson, *ibid. 14* (1980) 14.
[14] R. Appel, T. Gaitzsch, F. Knoch, G. Lenz, *Chem. Ber. 119* (1986) 1977; *E. Niecke*, Bonn, personal communication.
[15] L. D. Quin, *The Heterocyclic Chemistry of Phosphorus*, Wiley, New York 1981, p. 90.

Cooligomerization of Phosphaalkynes and Alkynes in the Coordination Sphere of Rhodium Complexes**

By *Paul Binger,* Josef Haas, Albert T. Herrmann, Franz Langhauser*, and *Carl Krüger*

Dedicated to Professor Rolf Appel on the occasion of his 70th birthday

Cyclizations of phosphaalkynes,[1] especially of the kinetically stable, readily accessible *tert*-butylphosphaacetylene (**1a**), in the coordination sphere of transition-metal complexes have attracted increasing interest in recent years. For example, long-sought phosphorus heterocycles such as 1,3-diphosphacyclobutadiene and 1,3,5-triphospha-Dewar-benzene are now accessible via this route.[1] Cooligomerizations between phosphaalkynes and other unsaturated systems (e.g., alkynes), however, are very rare. So far only one monophosphacyclobutadiene complex, formed from 1,2-bis(trimethylsilyl)acetylene and **1a** has been described.[2]

We now report the cooligomerizations of *tert*-butylphosphaacetylene (**1a**)[3] and of *N*-isopropyl-*N*-trimethylsilyl-2-aminophosphaacetylene (**1b**)[4] with tolane or acetylene in the coordination sphere of rhodium(I) complexes. The starting point for the syntheses described here was provided by the rhodium(I) complexes of tolane, **2** and **3**, first synthesized by *H. Werner* et al.,[5] as well as of the vinylidene **6**.[6]

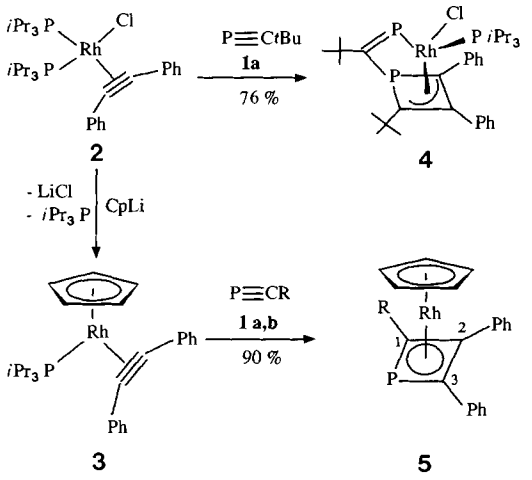

a, R = *t*Bu; **b**, R = N*i*Pr(SiMe$_3$)

The rhodium tolane complex **2** reacts at $-20\,^{\circ}C$ with two equivalents of **1a** to give the cotrimer **4** (yield 76%), in which a monophosphacyclobutenyl group, formed from one molecule of **1a** and the tolane ligand, is bonded as η^3 ligand to rhodium. The second molecule of **1a** is bonded to the P atom of the phosphacyclobutenyl ligand and to the rhodium center in a σ fashion.[7] On the other hand, the rhodium (η^5-cyclopentadienyl)tolane complex **3** reacts with the two phosphaalkynes **1a** and **1b** in refluxing THF to give the two rhodium η^4-monophosphacyclobutadiene complexes **5a** and **5b**, respectively, in 90% yield; that is, complex **3** undergoes codimerization with only one molecule of the phosphaalkyne.

Complex **7**, the first 1-phospha-2-rhodacyclobutene, is formed upon reaction of the rhodium vinylidene complex **6** with **1a** in a [2+2] cycloaddition as yellow needles (79%).[7] The regiochemistry of this cycloaddition indicates that the carbene carbon of **6** has electrophilic character.[8] Replacement of the chloro ligand in **7** by a cyclopentadienyl ligand results in smooth formation of the 1-phospha-2-rhoda-3-methylenecyclobutene **8**.

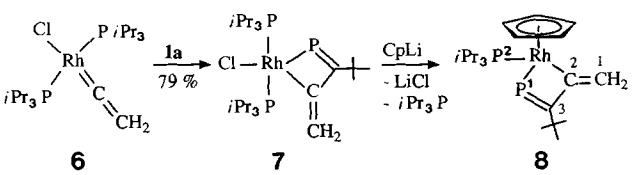

The crystal structure analyses of the rhodium complexes **4** and **7** reveal several structural features.[9] The rhodium atom in **4** is coordinated in a distorted tetrahedral fashion; the corners of the tetrahedron are occupied by Cl, P2, P3, and

[*] Prof. Dr. P. Binger, Dipl.-Chem. J. Haas, Dipl.-Chem. A. T. Herrmann, Dipl.-Chem. F. Langhauser, Prof. Dr. C. Krüger
Max-Planck-Institut für Kohlenforschung,
Kaiser-Wilhelm-Platz 1, D-4330 Mülheim a.d. Ruhr (FRG)

[**] This work was supported by the Volkswagen-Stiftung.

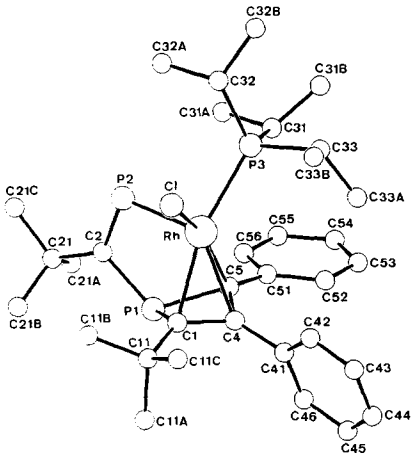

Fig. 1. Molecular structure of **4** (crystallographic numbering). Selected distances [Å] and angles [°]: P1-C1 1.860(3), P1-C5 1.875(2), C1-C4 1.434(4), C4-C5 1.443(4), Rh-P1 2.745(1), Rh-P2 2.226(1), Rh-P3 2.364(1), Rh-C1 2.235(3) Rh-C4 2.276(3), Rh-C5 2.152(3), Rh-Cl 2.409(1), P1-C2 1.813(3), P2-C2 1.657(3); C4-C5-P1 89.0(2), C5-C4-C1 100.7(2), C4-C1-P1 89.8(2), C5-P1-C1 72.8(1), P2-C2-P1 108.4(2).

the η^3-bonded allyl part of the phosphacyclobutenyl ligand (Fig. 1). The phosphacyclobutenyl ring is folded; the angle between the planes C1/P1/C5 and C1/C4/C5 is 29.7°. The η^3-allyl partial structure of this ring is characterized by the nearly equal C1–C4 and C4–C5 distances (1.434(4) and 1.443(4) Å, respectively) and the corresponding Rh–C distances (see caption to Figure 1), which correlate with those of known Rh-η^3-allyl compounds.[10] The P1–C1 and P1–C5 distances (1.860(3) and 1.875(3) Å) are consistent with P–C single bonds, whereas the P1–C2 distance is slightly shortened (1.813(3) Å); there is no bonding interaction between P1 and rhodium (2.745(1) Å). The P2–C2 distance in the phosphaethylene bridge (1.657(3) Å) corresponds to a P–C double bond, and the P2–Rh distance (2.226(1) Å) is typical of a Rh–P single bond.

The rhodium coordination in **7** consists of a slightly distorted tetragonal bipyramid (Fig. 2) with the two triisopropylphosphane ligands in axial positions and P2, C1, and Cl, together with a free coordination site, in equatorial positions. The heterocycle is planar and, along with C31 and the Cl atom, lies in the crystallographic mirror plane of the molecule. The P2–C2 and C1–C11 distances (1.699(9) and 1.32(1) Å, respectively) are in the range of P–C and C–C double bond lengths, respectively; the C1–C2 single bond (1.48(1) Å) is slightly shortened. The Rh–P2 and Rh–C1 distances (2.241(2) and 2.057(9) Å, respectively), as well as the C1–Rh–P2 angle (68.0(2)°), are as expected. The latter agrees with the values found in rhodacyclobutanes.[11]

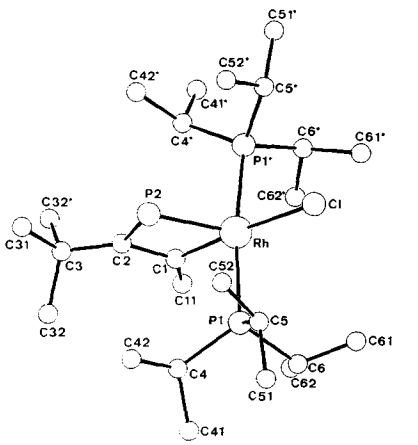

Fig. 2. Molecular structure of **7** (crystallographic numbering). Selected bond distances [Å] and angles [°]: Rh-Cl 2.436(2), Rh-P1 2.399(1), Rh-P2 2.241(2), Rh-C1 2.057(9), P2-C2 1.699(9), C1-C2 1.48(1) C1-C11 1.32(1); P1-Rh-P1* 172.1(1), C1-Rh-Cl 174.7(2), C1-Rh-P2 68.0(2), C2-P2-Rh 89.8(3), C1-C2-P2 98.3(6), C2-C1-Rh 103.9(6).

The structures of the rhodium complexes **5** and **8** were derived from their spectroscopic data (mass spectrum, ^{31}P and ^{13}C NMR spectra). The monophosphacyclobutadiene complexes **5a, b** exhibit the molecular-ion peak as most intense peak; the ^{31}P NMR spectrum contains a doublet at $\delta = -48.75$ ($J_{PRh} = 37.3$ Hz) for **5a** and -26.45 ($J_{PRh} = 36.5$ Hz) for **5b**. In the ^{13}C NMR spectrum, the characteristic signals for the C atoms of the four-membered ring of **5a** lie (see formula for numbering) at $\delta = 85.1$ (C1, $J_{C1P} = 42.3$, $J_{C1Rh} = 13.3$ Hz), 103.9 (C2, $J_{C2P} = 3.9$, $J_{C2Rh} = 9.4$ Hz), and 105.2 (C3, $J_{C3P} = 45.7$, $J_{C3Rh} = 13.5$ Hz). The structure has meanwhile been confirmed by a crystal structure analysis.[12] The values for **5b** are similar to those for **5a**.

In the ^{31}P NMR spectrum of the rhodium complex **8** (see formula for numbering), the signal for the Rh–P single bond ($\delta = 344.71$, $J_{P1Rh} = 35.1$ Hz, $J_{P1P2} = 12.1$ Hz) shows the characteristic low-field shift. The ^{13}C NMR spectrum contains signals at $\delta = 235.1$ (C3, $J_{C3P1} = 55$ Hz) and 124.4 (C2, J_{C2P1} and $J_{C2Rh} = 24.4$, 11.2 Hz) for the C atoms of the four-membered ring; the C atom of the terminal methylene group gives rise to a signal at $\delta = 104.4$ (C1, $J_{CH} = 150.5/160.1$, $J_{C1P1} = 23.7$, $J_{C1Rh} = 1.9$ Hz). Overall, the structure of **8** corresponds to that of known compounds of type **9**.[11]

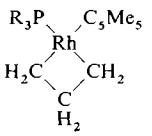

9

We are currently exploring the use of other alkynes and phosphaalkynes in the syntheses describe here and are investigating the properties of the metal-free phosphorus heterocycles released from the complexes.

Experimental Procedure

4: Compound **1a** (2.5 g, 25 mmol) was added to **2** (0.55 g, 0.86 mmol) in 50 mL of diethyl ether at -30 °C. The resulting dark red solution was stirred for 12 h at 20 °C and then concentrated to 10 mL. After cooling for 2 d at -78 °C, the solution afforded **4** as dark red, nearly black crystals; 0.44 g (76%) of **4** was obtained after filtration and drying at 0.5 Torr; m.p. = 155 °C (dec.).

5a: Compound **1a** (0.08 g, 0.8 mmol) was added to a solution of **3** (0.35 g, 0.69 mmol) in 40 mL of THF and the reaction mixture was refluxed for 3 d. The THF was then removed by distillation at 0.5 Torr, the residue was dissolved in 5 mL of pentane, and the resulting solution was cooled to -78 °C. The yellow crystals formed after 3 d were freed of mother liquor and dried at 0.5 Torr; 0.28 g (90%) **5a**, m.p. 95 °C.

7: Compound **6** (0.65 g, 1.3 mmol) was dissolved in 40 mL of THF at 0 °C and **1a** (0.18 g, 1.8 mmol) was then added, resulting in an immediate change in color from yellow to red. The reaction mixture was stirred for 12 h at 20 °C, the volatiles were then removed at 0.5 Torr, and the oily residue was dissolved in 25 mL of diethyl ether; **7** precipitated at -78 °C as a microcrystalline yellow solid. A single recrystallization gave 0.63 g (79%) of yellow needles (m.p. 111 °C).

Received: October 1, 1990 [Z 4219 IE]
German version: *Angew. Chem. 103* (1991) 316
Publication delayed at authors' request

CAS Registry numbers:
1a, 78129-68-7; **1b**, 118375-89-6; **2**, 131564-13-1; **3**, 81423-53-2; **4**, 131458-48-5; **5a**, 131458-49-6; **5b**, 131458-52-1; **6**, 95935-81-2; **7**, 131458-50-9; **7**·$C_4H_{10}O$, 131458-53-2; **8**, 131458-51-0.

[1] Reviews: a) M. Regitz, P. Binger, *Angew. Chem. 100* (1988) 1541; *Angew. Chem. Int. Ed. Engl. 27* (1988) 1484; b) J. F. Nixon, *Chem. Rev. 88* (1988) 1327.

[2] P. Binger, R. Milczarek, R. Mynott, M. Regitz, *J. Organomet. Chem. 323* (1987) C35.

[3] a) G. Becker, G. Grosser, W. Uhl, *Z. Naturforsch. B36* (1981) 16; b) W. Rösch, U. Mees, M. Regitz, *Chem. Ber. 120* (1987) 1645.

[4] R. Appel, M. Poppe, *Angew. Chem. 101* (1989) 70; *Angew. Chem. Int. Ed. Engl. 28* (1989) 53.

[5] H. Werner, J. Wolf, U. Schubert, K. Ackermann, *J. Organomet. Chem. 317* (1986) 327.

[6] H. Werner, F. J. G. Alonso, H. Otto, J. Wolf, *Z. Naturforsch, B43* (1988) 722.

[7] Spectroscopic data for **4** and **7** (for numbering see Figs. 1 and 2): **4**: ^{31}P NMR (81 MHz, [D$_8$]THF, 25 °C, H_3PO_4): $\delta = -142.46$ (P1, J(P1,P2) = 37.3, J(P1,P3) = J(P1,Rh) = 3.4 Hz), 422.75 (P2, J(P2,P3) = 30.6, J(P2,Rh) = 30.6 Hz), 46.7 (P3, J(P3,Rh) = 174.5 Hz). ^{13}C NMR (75.5 MHz, [D$_8$]THF, 30 °C, TMS): $\delta = 195.1$ (C2, J(C2,P2) = 87.5, J(C2,P1) = 72.2 Hz), 157.3 (C1, J(C1,P2) = 24.3, J(C1,P1) = 36.1 Hz), 136.1 (C4, J(C4,P2) = 4.7, J(C4,P1) = 22.0 Hz), 96.7 (C5, J(C5,P1) = J(C5,P2) = 12.6, J(C5,Rh) = 2.0 Hz). **7**: ^{31}P NMR (81 MHz, C_6D_6, 25 °C, H_3PO_4): $\delta = 35.82$ (P1, J(P1,P2) = 18.3, J(P1,Rh) = 114.4 Hz), 379.59 (P2, J(P2,Rh) = 34.3 Hz). ^{13}C NMR (75.5 MHz, [D$_8$]THF, 30 °C, TMS): $\delta = 129.0$ (C1, J(C1,P1) = 8.1, J(C1,P2) = 21.4, J(C1,Rh) = 3.0 Hz), 219.8 (C2, J(C2,P1) = 5.0, J(C2,P2) = 52.5, J(C2,Rh) = 4.9 Hz), 99.1 (C11, J(C,H) = 152/160, J(C11,P2) = 26.5, J(C11,Rh) = 3.1 Hz).

[8] A [2+2] cycloaddition of **1a** to the Ti–C double bond of (vinylcarbene)-titanocenes affords 1-phospha-3-titanocyclobutene derivatives (P. Binger, B. Biedenbach, P. Müller, R. Mynott, unpublished results). The same regioselectivity is observed in the cycloaddition of **1a** to chromium carbene complexes (K. H. Dötz, A. Tiriliomis, K. Harms, M. Regitz, U. Annen, *Angew. Chem. 100* (1988) 725; *Angew. Chem. Int. Ed. Engl. 27* (1988) 713; K. H. Dötz, A. Tiriliomis, K. Harms, *J. Chem. Soc. Chem. Commun. 1989*, 788).

[9] a) Crystal structure analysis of **4** at 20 °C; $C_{33}H_{49}ClP_3Rh$, space group $P2_1/n$, $a = 9.660(1)$, $b = 19.087(2)$, $c = 19.027(2)$ Å, $\beta = 95.75(1)°$, $Z = 4$, $\varrho_{calcd} = 1.29$ g cm^{-3}, $\mu(Mo_{K\alpha}) = 7.13$ cm^{-1}, Enraf-Nonius diffractometer CAD4: 10042 measured reflections, averaged to 9409, 6807 observed ($I > 2\sigma(I)$), $R = 0.042$, $R_w = 0.042$ ($w = 1/\sigma^2(F_0)$) for 343 parameters [9c]; b) crystal structure analysis of **7** at −173 °C: $C_{25}H_{53}ClP_3Rh \cdot C_4H_{10}O$, space group $P2_1/m$, $a = 10.999(4)$, $b = 12.894(3)$, $c = 12.164(2)$ Å, $\beta = 97.99(2)°$, $Z = 2$, $\varrho_{calcd} = 1.28$ g cm^{-3}, $\mu(Mo_{K\alpha}) = 7.28$ cm^{-1}. Enraf-Nonius diffractometer CAD4: 4253 measured reflections, averaged to 4061, 3183 observed ($I > 2\sigma(I)$), $R = 0.065$, $R_w = 0.073$ ($w = 1/\sigma^2(F_0)$) for 172 parameters [9c]; c) Further details of the crystal structure investigations may be obtained from the Fachinformationszentrum Karlsruhe, Gesellschaft für wissenschaftlich-technische Information mbH, D-7514 Eggenstein-Leopoldshafen 2 (FRG), on quoting the depository number CSD-54968, the names of the authors, and the journal citation.

[10] a) M. McPantlein, R. Mason, *Chem. Commun. 1967*, 16; b) H. Pasternack, T. Glowiak, F. Pruchnik, *Inorg. Chim. Acta 19* (1976) 11.

[11] a) R. A. Periana, R. G. Bergmann, *J. Am. Chem. Soc. 106* (1984) 7272; b) L. Andreucci, P. Diverso, G. Ingrosso, A. Lucherini, F. Marchetti, V. Adovasio, M. Nardelli, *J. Chem. Soc. Dalton Trans. 1986*, 477.

[12] C. Krüger, A. T. Herrmann, F. Langhauser, unpublished.

The First Metallobis(methylene)phosphoranes—Unexpected Isomerization to a Phosphaferrocene

By *Hans Jürgen Metternich* and *Edgar Niecke**

Dedicated to Professor Rolf Appel on the occasion of his 70th birthday

The synthesis of bis[bis(trimethylsilyl)methylene]chlorophosphorane (**1**), the first *P*-functionalized $\sigma^3\lambda^5$-phosphorane, by *Appel* et al.[1] led to an intensive investigation of this class of compounds.[2] The focus of this work has been the preparation of compounds with bonds between phosphorus and other main-group elements. However, nothing is known about the relevance of this class of compounds to coordination chemistry and organometallic synthesis. The related bis(imino)phosphoranes,[3] on the other hand, have found applications in catalysis.[4] We report here the synthesis of the first metallobis(methylene)phosphorane as well as the products of its cyclization.

Reaction of the reactive potassium metalate **2**,[5] obtainable from η^3-allyl(tricarbonyl)iodoiron and K/Hg, with the chlorobis(methylene)phosphorane **1** led to substitution of chlorine and formation of **3**, as the main product,[6] together with bis(methylene)propenylphosphorane[7] (**4**), which results from extrusion of the carbonyl fragment.[8]

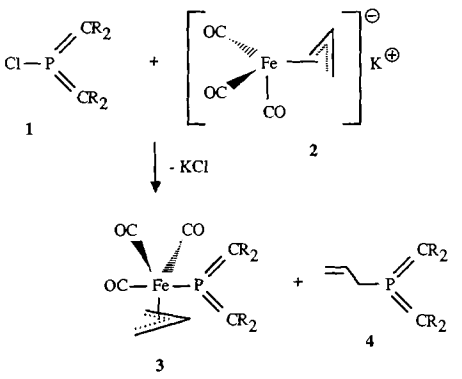

Recently, a transition-metal-substituted bis(methylene)-phosphorane was also assumed to be the product obtained from the reaction of K[(η^5-C_5H_5)Fe(CO)$_2$] (**5**) with **1**.[9] However, the ^{31}P NMR signal ($\delta = -81.6$), which is found at unusually high field for a $\sigma^3\lambda^5$-phosphorus atom, especially compared with the signal for **3** ($\delta = 331.8$), indicates that, instead of the postulated "open" form of a metallobis-(methylene)phosphorane, a cyclic isomer was obtained.

By varying the reaction conditions,[10] we have now succeeded in synthesizing the metallobis(methylene)phosphorane **6** and its rearrangement product, the phosphaferrocene **7**, from **1** and **5**. Both isomers were separated by column chromatography and isolated as pure compounds. The isomerization of **6** and **7** can be regarded as a coupling of the phosphorane fragment with the two carbonyl groups of the Fe fragment. Thus, the rearrangement does not lead to the isomeric metallo- λ^3-phosphirane **8**,[13] as so often observed

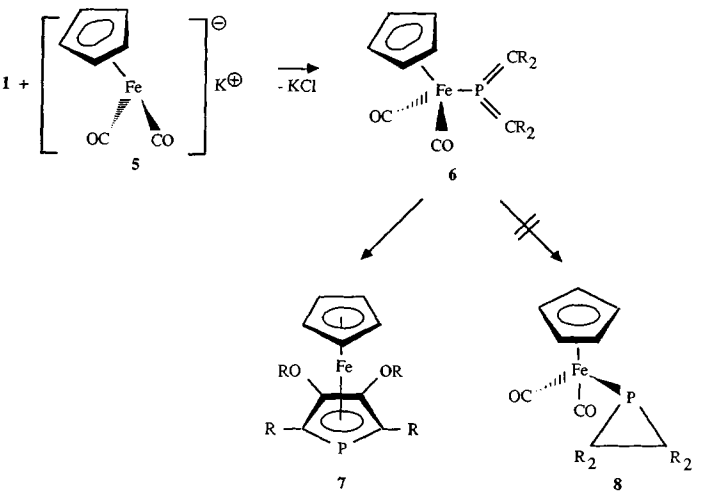

[*] Prof. Dr. E. Niecke, Dipl.-Chem. H. J. Metternich
Anorganisch-chemisches Institut der Universität
Gerhard-Domagk-Strasse 1, W-5300 Bonn (FRG)

[**] This work was supported by the Deutsche Forschungsgemeinschaft and the Fonds der Chemischen Industrie.

with alkyl-substituted bis(methylene)phosphoranes,[12] but results in the formation of a phospholyl ligand in the coordination sphere of the transition metal.

The composition and constitution of compounds **3**, **4**, **6**, and **7** was established by elemental analysis and high-resolution mass spectrometry as well as by IR and NMR spectroscopy.

Like the metallomethylenephosphanes,[14] the metallobis(methylene)phosphoranes **3** and **6** have more strongly deshielded ^{31}P (**6**: $\delta = 347.1$) and ^{13}C nuclei than those of the corresponding organosubstituted compounds.[12] In the phospholyl complex **7**, on the other hand, the ^{31}P nucleus is strongly shielded[15] ($\delta = -83.5$), as expected. The ^{13}C resonances of the ring carbon atoms lie in the usual range.[15] The mass spectrum, which is characteristic for phosphaferrocenes,[15] and the absence of CO vibrational bands in the IR spectrum are additional evidence for a sandwich structure of **7**.[16] Further investigations of the organometallic chemistry of *P*-functionalized phosphoranes with $\sigma^3\lambda^5$-phosphorus are in progress.[17]

Experimental Procedure

3: A freshly prepared solution of $Na[(\eta^3\text{-}C_3H_5)Fe(CO)_3]$ in 40 mL of THF was treated at $-10\,^{\circ}C$ with **1** (1.53 g, 4 mmol) dissolved in 20 mL of toluene. The reaction mixture was allowed to warm to room temperature and then stirred for 3 h. The solvents were removed at 30 °C under vacuum, the residue was dissolved in 60 mL of pentane, and the solution was filtered. Of the reaction products **3**, $Fe_3(CO)_{12}$, **4** [7], and two dihydrophosphole complexes, three were isolated by column chromatography (silica gel, 30×200 mm, pentane, 10 °C). Crystallization of the first, red fraction at 6 °C afforded **3** in 36–49% yield, m.p. 111 °C. ^{31}P NMR (C_6D_6, 25 °C): $\delta = 331.8$ (br). ^{13}C NMR (C_6D_6, 25 °C): $\delta = 220.1$ (s, CO), 219.9 (d, $J = 1.0$ Hz, CO), 137.6 (d, $J = 55.8$ Hz, P = C), 86.4 (d, $J = 3.0$ Hz, C2 (Allyl)), 47.1 (d, $J = 1.9$ Hz, C1,3 (Allyl)), 5.5 (d, $J = 2.6$ Hz, $SiCH_3$), 3.4 (d, $J = 10.2$ Hz, $SiCH_3$), 3.1 (d, $J = 7.0$ Hz, $SiCH_3$). MS (60 eV): $m/z = 528$ (1%) [$M^{\oplus}$], 500 (1) [$M^{\oplus} - CO$], 472 (2) [$M^{\oplus} - 2CO$], 444 (69) [$M^{\oplus} - 3CO$], 429 (2) [$M^{\oplus} - 3CO - Me$], 403 (11) [$M^{\oplus} - 3CO - C_3H_6$], 348 (10) [$M^{\oplus} - Fe(CO)_3C_3H_5$], 73 (100) [$SiMe_3^{\oplus}$], and other fragments. IR (pentane) $\tilde{\nu}$[cm^{-1}] = 2020 w, 1990 vs, 1940 vs (C = O).

4 [8]: Compound **1** (1.15 g, 3 mmol) in diethyl ether (20 mL) was treated at 10 °C with 6 mL of a freshly distilled 0.5 M solution of allylmagnesium iodide in diethyl ether. The reaction mixture was allowed to warm to 22 °C and then stirred for 2 h. The solvent was removed under high vacuum and the orange residue was dissolved in 30 mL of pentane. After filtration of the solution, **4** was crystallized from diethyl ether at $-30\,^{\circ}C$ (yield 93%, m.p. 58 °C). ^{31}P NMR (C_6D_6, 25 °C): $\delta = 177.9$ (dt, $J = 12.9$ Hz and 14.1 Hz. ^{13}C NMR (C_6D_6, 25 °C): $\delta = 132.1$ (d, $J = 8.6$ Hz, $= CH_2$), 119.3 (d, $J = 13.6$ Hz, $-CH =$), 82.6 (d, $J = 41.1$ Hz, P = C), 43.7 (d, $J = 37.9$ Hz, P–CH_2), 4.1 (s, $SiCH_3$), 3.8 (s, $SiCH_3$). MS (60 eV): $m/z = 388$ (16%) [$M^{\oplus}$], 373 (29) [$M^{\oplus} - CH_3$], 347 (46) [$M^{\oplus} - C_3H_5$], 315 (41) [$M^{\oplus} - SiMe_3$], 259 (37) [$M^{\oplus} - SiMe_4 - C_3H_5$], 73 (100) [$SiMe_3^{\oplus}$], and other fragments.

6 and **7**: Compound **1** (1.15 g, 3 mmol), dissolved in 90 mL of toluene, was added dropwise over 4 h to a solution of $K[(\eta^5\text{-}C_5H_5)Fe(CO)_2]$ in 50 mL of THF at 75 °C. After the addition was completed, the reaction mixture was stirred for 1 h and the solvents were then removed under vacuum. The dark brown residue was extracted into 40 mL of pentane and insoluble material was removed. Workup by column chromatography (Florisil, 30×200 mm, pentane, 10 °C) afforded **6** in 39% yield; m.p. 104 °C. ^{31}P NMR (C_6D_6, 25 °C): $\delta = 347.1$ (s). ^{13}C NMR (C_6D_6, 25 °C): $\delta = 221.1$ (s, CO), 219.0 (s, CO), 140.6 (d, $J = 50.1$ Hz, P = C), 81.6 (s, C_5H_5), 6.0 (d, $J = 1.8$ Hz, $SiCH_3$), 4.8 (d, $J = 3.5$ Hz, $SiCH_3$), 3.7 (d, $J = 8.6$ Hz, $SiCH_3$), 3.1 (d, $J = 5.1$ Hz, $SiCH_3$). MS (50 eV): $m/z = 496$ (4%) [$M^{\oplus} - CO$], 468 (69) [$M^{\oplus} - 2CO$], 348 (12) [$(Me_3Si)_2C = P = C(SiMe_3)_2^{\oplus}$], 73 (100) [$SiMe_3^{\oplus}$], and other fragments. IR (pentane) $\tilde{\nu}$[cm^{-1}] = 2021 w, 1938 vs (C = O).

Crystallization of the second fraction at $-80\,^{\circ}C$ afforded bright orange crystals of **7** (in 34–72% yield, depending on the reaction time); m.p. 99–101 °C. ^{31}P NMR (C_6D_6, 25 °C): $\delta = -83.5$ (s). ^{13}C NMR (C_6D_6, 25 °C): $\delta = 126.6$ (d, $J = 28.5$ Hz, P-*C*-COSi), 82.1 (d, $J = 52.9$ Hz, P–C–*C*OSi), 71.9 (d, $J = 2.5$ Hz, C_5H_5), 2.6 (s, $OSiCH_3$), 1.8 (d, $J = 5.9$ Hz, $SiCH_3$). MS (50 eV): $m/z = 524$ (100%) [$M^{\oplus}$], 436 (8) [$M^{\oplus} - SiMe_4$], 73 (36) [$SiMe_3^{\oplus}$].

Received: July 25, 1990 [Z 4091 IE]
Publication delayed at the authors' request
German version: *Angew. Chem. 103* (1991) 336

CAS Registry numbers:
1, 83438-72-6; **3**, 131863-67-7; **4**, 131833-00-6; **6**, 116483-15-9; **7**, 131833-01-7; $Na[(\eta^3\text{-}C_3H_5)Fe(CO)_3]$, 57816-29-2; $K[(\eta^5\text{-}C_5H_5)Fe(CO)_2]$, 60039-75-0.

[1] R. Appel, J. Peters, A. Westerhaus, *Angew. Chem. 94* (1982) 76; *Angew. Chem. Int. Ed. Engl. 21* (1982) 80.
[2] Reviews: a) R. Appel: *"Bis(methylene)phosphoranes"* in M. Regitz, O. J. Scherer (Eds.): *"Multiple Bonding and Low Coordination in Phosphorus Chemistry"* Thieme, 1990, p. 367; b) H. Germa, J. Navech, *Phosphorus Sulfur 26* (1986) 327.
[3] E. Niecke, D. Gudat: *"Bis(imino)phosphoranes"* in [2a], p. 392.
[4] a) W. Keim, R. Appel, A. Storeck, C. Krüger, R. Goddard, *Angew. Chem. 93* (1981) 91; *Angew. Chem. Int. Ed. Engl. 20* (1981) 116; b) G. Fink, V. Möhring, *Stud. Surf. Sci. Catal. 25* (1986) 231.
[5] C. F. Putnik, J. J. Welter, G. D. Stucky, M. J. D'Aniello, B. A. Sosinsky, J. F. Kirner, E. L. Mutterties, *J. Am. Chem. Soc. 100* (1978) 4107.
[6] A side product of the reaction (< 10%) is the phospholene complex. $R_2CH\text{-}\overline{P\text{-}Cr_2\text{-}CH = CH\text{-}CH_2} \cdot Fe(CO)_3$. E. Niecke, H. J. Metternich, unpublished.
[7] Since **4** underwent some decomposition upon column-chromatographic workup, this compound was synthesized alternatively by reaction of allylmagnesium iodide with **1**.
[8] In all experiments, $Fe_3(CO)_{12}$, formed as a side product, was also isolated by column chromatography and identified by IR spectroscopy and high-resolution mass spectrometry.
[9] A. H. Cowley, A. R. Barron, *J. Chem. Soc. Chem. Commun. 1987*, 1272.
[10] For a successful synthesis of **6**, the reaction conditions, such as a sufficient dilution of **1** in toluene, an optimal rate of addition, and the presence of the hot metalate, are crucial. When THF is used as solvent, other undesired side products are obtained, namely, $[(\eta^5\text{-}C_5H_5)Fe(CO)_2]Cl$ and, by dimerization of two phosphorane units, bis[bis(trimethylsilyl)methylene][2,2-dimethyl-3,5,5-tris(trimethylsilyl)-4-phospha-2-sila-3-pentenyl]phosphorane [11].
[11] R. Appel, E. Gaitzsch, K.-H. Dunker, F. Knoch, *Chem. Ber. 119* (1986) 535.
[12] R. Appel, K. H. Dunker, E. Gaitzsch, *Z. Chem. 24* (1984) 384.
[13] E. Niecke, H. Brombach, M. Nieger, *Organometallics*, in press.
[14] K. Karaghiosoff in [2a], p. 463.
[15] F. Mathey, *J. Organomet. Chem. 139* (1977) 77–87.
[16] The preliminary results of an X-ray structure analysis of **8** also confirm the proposed structure.
[17] H. J. Metternich, E. Niecke, J. F. Nixon, P. B. Hitchcock, unpublished.

A Cluster with the Triply Facially Bridging Trimethylenemethane Ligand: Structure and Bonding of $[\{Rh(cod)\}_3(\mu_3\text{-}H)\{\mu_3\text{-}C(CH_2)_3\}]$ **

By *Gerhard E. Herberich,* Ulli Englert, Lars Wesemann,* and *Peter Hofmann**

A great variety of trimethylenemethane (TMM) complexes are known,[1] some of which are important intermediates in organic synthesis.[1, 2] They are almost always mononuclear, as exemplified by $[(\eta^4\text{-tmm})Fe(CO)_3]$.[3] The TMM ligand is seldom bonded in a bridging fashion as in the binuclear complex $[(\mu\text{-}\eta^1\text{:}\eta^3\text{-tmm})Ru_2(CO)(\mu\text{-}CO)Cp_2]$(*Ru–Ru*).[4] Here we report the first example of a facially bridging coordination to a *triangulo* trimetal cluster.

Complexation of $Li_2[TMM] \cdot 2TMEDA$[5] with $[RhCl(cod)]_2$ yields a labile primary product, presumably **1**, which decomposes in solution to form the novel trinuclear complex **2**.

$[\{Rh(cod)\}_2(tmm)]$ **1** $[\{Rh(cod)\}_3(\mu_3\text{-}H)(\mu_3\text{-}tmm)]$ **2**

[*] Prof. Dr. G. E. Herberich, Dr. U. Englert, Dr. L. Wesemann
Institut für Anorganische Chemie der Technischen Hochschule
Professor-Pirlet-Strasse 1, W-5100 Aachen (FRG)
Prof. Dr. P. Hofmann
Anorganisch-chemisches Institut der Technischen Universität München
Lichtenbergstrasse 4, W-8046 Garching (FRG)

[**] This work was supported by the Deutsche Forschungsgemeinschaft and the Fonds der Chemischen Industrie.

Complex **2** (Fig. 1)[6] contains an equilateral Rh_3 triangle ($d_{Rh\text{-}Rh}$ = 298 pm[7]) capped on one side by a nearly planar TMM ligand; CO lies 5.4 pm above the plane C1, C2, C3. A triply bridging hydrido ligand was localized on the other side of the Rh_3 triangle.[8] Owing to coupling with the Rh nuclei, this μ_3-H ligand gives rise to a quartet at $\delta = -13.4$ in the ^1H NMR spectrum. Complex **2** deviates significantly from idealized C_{3v} symmetry. The TMM ligand does not eclipse the Rh_3 triangle but is rotated by 19°. With respect to the Rh_3 plane, the COD rings are tilted by 34° away from the TMM ligand and rotated by 21° around their C_2 axis.

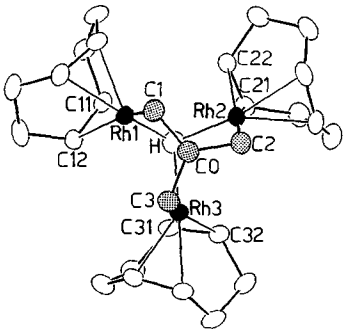

Fig. 1. Molecular structure of **2**. Selected distances [pm] and bond angles [°]: Rh1-Rh2 297.7(1), Rh2-Rh3 298.1(1), Rh3-Rh1 297.7(1), Rh1-H 167(3), Rh2-H 187(3), Rh3-H 196(3), Rh1-C1 213.2(3), Rh2-C2 212.8(2), Rh3-C3 213.8(3), C0-C1 142.2(4), C0-C2 143.2(4), C0-C3 143.0(4); Rh2-Rh1-Rh3 60.08(1), Rh1-Rh2-Rh3 59.96(1), Rh1-Rh3-Rh2 59.96(1), C1-Rh1-H 101(1), C2-Rh2-H 99.5(9), C3-Rh3-H 97.8(9), C1-C0-C2 120.5(2), C1-C0-C3 119.2(2), C2-C0-C3 119.9(2), Rh1-C1-C0 97.7(2), Rh2-C2-C0 98.0(2), Rh3-C3-C0 96.1(2).

Complex **2** is a diamagnetic 44-electron cluster; a 48-electron configuration would have been expected according to the 18-electron rule. In terms of the fragment frontier orbital formalism,[9] **2** can be regarded as a trinuclear metal complex fragment, $[Rh(cod)]_3^{\oplus}$ with a total of 26 d valence electrons, which interacts with both the 6π ligand $TMM^{2\ominus}$ and a μ_3-bridging $H^{\oplus}$.[10] The frontier orbitals of the $[Rh(cod)]_3^{\oplus}$ fragment can be traced back to the characteristic ML_2 orbitals[11] of three [Rh(cod)] units. This is shown for the simplified model $[Rh(C_2H_4)_2]$ (**3**) with C_{2v} symmetry (MO scheme **A** in Fig. 2).

Combination of the MOs of three $[Rh(C_2H_4)_2]$ units (**3**)[12] leads to the MO scheme **B** for $[Rh(C_2H_4)_2]_3^{\oplus}$ (**4**), as derived from extended Hückel (EH) model calculations.[13] Both **4** and the complete model cluster **5** (Fig. 2, MO scheme **C**) adopt C_{3v} symmetry; the $[Rh(C_2H_4)_2]$ fragments, like the

$[\{Rh(C_2H_4)_2\}_3(\mu_3\text{-}H)(\mu_3\text{-}tmm)]$ **5**

[Rh(cod)] units of **2**, are tilted toward the side of the metal triangle opposite to the TMM ligand, but the double bonds are still parallel to the Rh_3 plane. The frontier orbitals b_2 (xz, z) and $3a_1$ (sp hybrid) of the $[Rh(C_2H_4)_2]$ units (**3**) give rise to the valence MOs $1a_1$, 1e, $2a_1$, and 2e of **4**.[12] Owing to their relative energies and symmetry properties, four of these, namely, $1a_1$ (HOMO of **4**) and the empty MOs $1e_s$, $1e_a$, and $2a_1$, are ideally suited for interaction with the occupied π MOs π_1, π_{2s}, and π_{2a} of $TMM^{2\ominus}$ and the empty 1s AO of an $H^{\oplus}$ (**D** in Fig. 2).[14] For **5**, the resulting MO scheme **C** has a HOMO–LUMO separation of more than 1.7 eV and thus reflects the stable, diamagnetic closed-shell electron configuration of **2**, which, for the electron count given, is only made possible by the additional μ_3-H bridging.[15] The three lowest unoccupied orbitals of **5** are linear combinations of 5p AOs of the Rh centers in the Rh_3 plane. At each Rh atom, these orbitals are comparable to the LUMO of mononuclear, square-planar d^8 complexes with usually 16 instead of 18 valence electrons. For clusters **5** and **2**, the appropriate number is already reached at 44 (instead of 48).[16]

The distortion and symmetry reduction to C_3 found in **2**, in contrast to **5**, does not play a crucial role for the electron configuration of this type of TMM cluster. C_{3v} symmetry in **5** (TMM eclipsing the Rh_3 triangle) would have caused too short H–H distances especially between the *endo* H atoms of the C = C units on the hydride side. The same holds for complex **2**. A geometry optimization for **5**, represented by **6** in Scheme 1,[17] results in a ground-state geometry almost identical to that of the real structure. The distortion of the $[\{Rh(cod)\}_3(\mu_3\text{-}H)]$ fragment to C_3 symmetry, in turn, is responsible for the 19° rotation of the planar TMM ligand above the Rh_3 triangle; this rotation restores optimal overlap between the Rh atoms and the C atoms of the TMM ligand. According to the calculation for **5**, a complete rota-

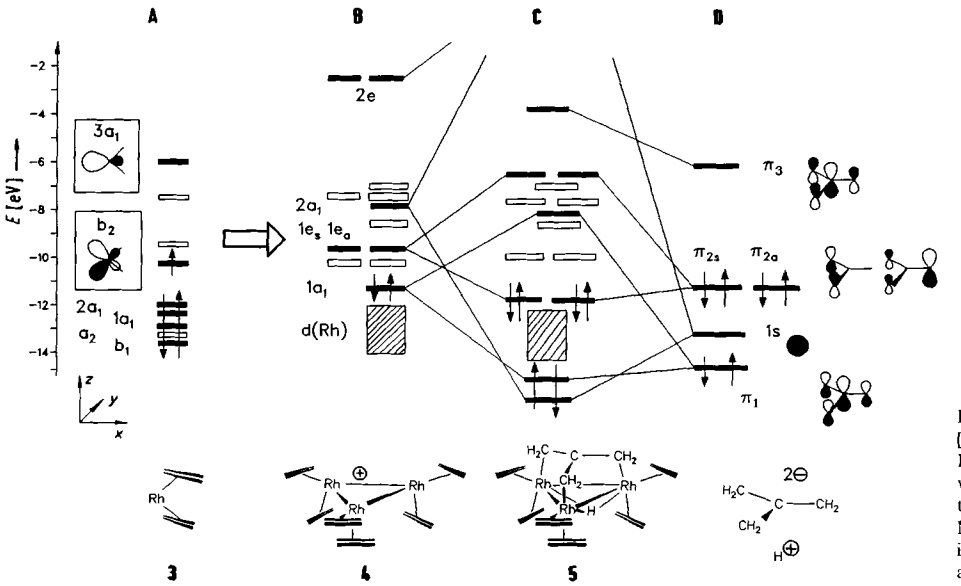

Fig. 2. **A**: Valence orbitals of a bent $[Rh(C_2H_4)_2]$ fragment (**3**) (C_{2v} symmetry, EH calculation); energy levels not drawn with bold lines: [12]. **B**: MO scheme for the trimeric building block **4** (C_{3v} symmetry). **C**: MO scheme for **5** (C_{3v} symmetry) from the interaction of **4** with the MOs of $TMM^{2\ominus}$ and $H^{\oplus}$, shown in the MO scheme **D**.

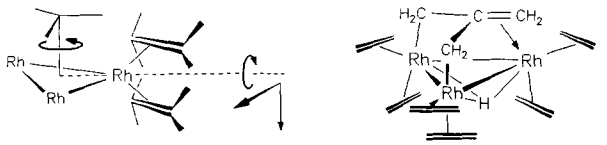

6 **7**

Scheme 1. For explanation, see text and [17].

tion of the TMM ligand would be hampered by a rotation barrier of about 50 kcal mol^{-1}. This high barrier is a consequence of the bonding situation (MO scheme **C** in Fig. 2), which can be represented for **5** by three degenerate ground-state structures of type **7**.

Related *triangulo* clusters (e.g., of heteroanalogues of TMM or complexes containing other ML_2 fragments) can be derived from the electron configuration of **2**. Their synthesis poses an interesting challenge.

Experimental Procedure

1: $Li_2[C(CH_2)_3] \cdot 2TMEDA$ (0.625 g, 3.39 mmol) [5] was allowed to react in THF at −78 °C with $[RhCl(cod)]_2$ (1.67 g, 3.39 mmol). The temperature was allowed to warm to 20 °C and the reaction mixture was stirred for 1 h. The THF was then removed and the residue was dissolved in toluene. Filtration of the solution through a small amount of kieselgur gave a dark red solution of **1**. Complex **1**, which was crystallized at −20 °C from toluene/hexane, is not stable upon storage and decomposes in solution within 10 h at 20 °C (^{1}H NMR). ^{1}H NMR (60 MHz, C_6D_6, TMS int.): δ = 4.6 (s, br, 8HC =), 2.0 (s, br, $8CH_2$), 1.6 (s, TMM).

2: Complex **2** crystallized within 24 h from solutions of **1** in toluene/hexane at 20 °C. The dark red crystals are air-stable. Complex **2** decomposes in solution within 50 h (^{1}H NMR). ^{1}H NMR (80 MHz, [D_8]toluene, int. TMS, not completely assignable owing to low solubility): δ = 4.6 (s, br, 12HC =), 2.1 (s, br, $12CH_2$ from COD), 2.2–0.9 (several signals, TMM not assignable), −13.4 (q, $^1J(^{103}Rh\text{-}^1H)$ = 14 Hz, μ_3-H).

Received: October 19, 1990 [Z 4243 IE]
German version: *Angew. Chem. 103* (1991) 329

CAS Registry numbers:
1, 131833-02-8; **2**, 131863-68-8; **3**, 66454-32-8; **4**, 131833-03-9; **5**, 131863-69-9; $Li_2[C(CH_2)_3] \cdot 2TMEDA$, 107901-60-0; $[RhCl(cod)]_2$, 12092-47-6.

[1] M. D. Jones, R. D. W. Kemmitt, *Adv. Organomet. Chem. 27* (1987) 279.
[2] B. Trost, *Angew. Chem. 98* (1986) 1; *Angew. Chem. Int. Ed. Engl. 25* (1986) 1.
[3] G. F. Emerson, K. Ehrlich, W. P. Giering, P. C. Lauterbur, *J. Am. Chem. Soc. 88* (1966) 3172; A. Almenningen, A. Haaland, K. Wahl, *Acta Chem. Scand. 23* (1969) 1145.
[4] M. J. Fildes, S. A. R. Knox, A. G. Orpen, M. L. Turner, M. I. Yates, *J. Chem. Soc. Chem. Commun. 1989*, 1680.
[5] J. Klein, A. Medlik, *J. Chem. Soc. Chem. Commun. 1973*, 275.
[6] Enraf-Nonius CAD4, $Mo_{K\alpha}$ radiation, measurement at 293 K. **2**: $P\bar{1}$ (No. 2), a = 1213.8(1), b = 1264.5(2), c = 1150.5(2) pm, α = 113.50(2), β = 97.18(1), γ = 112.20(1)°; V = 1.4181(5) nm^3, Z = 2, ϱ_{calcd} = 1.612 g cm^{-3}. Crystal 0.5 × 0.1 × 0.1 mm; empirical absorption correction according to the PSI scan method, 5874 unique reflections, 5484 with $I > 3\sigma(I)$ in the range $6 < \theta < 27°$ used; non-hydrogen atoms refined anisotropically, μ_3-H atom isotropically; with one exception other atoms found, but refined using a riding model; correction for secondary extinction; R = 0.027, R_w = 0.045 (statistical weighting), 285 parameters. Further details of the crystal structure investigation may be obtained from the Fachinformationszentrum Karlsruhe, Gesellschaft für wissenschaftlich-technische Information mbH, W-7514 Eggenstein-Leopoldshafen 2 (FRG), on quoting the depository number CSD-55097, the names of the authors, and the journal citation.
[7] a) 271.5, 273.0 pm (2 ×) for $[(\mu_3\text{-H})(\mu_3\text{-Cp})(RhCp)_3]$: O. S. Mills, E. F. Paulus, *J. Organomet. Chem. 11* (1968) 587; b) 280.2 (4 ×), 297.1 pm (2 ×) for $[(\mu_3\text{-H})Rh(cod)]_4$: M. Kulzick, R. T. Price, E. L. Muetterties, *Organometallics 1* (1982) 1256. c) 261.0 (2 ×), 282.9 pm (4 ×) for $[\{(\mu_3\text{-H})Rh(\eta^5\text{-}C_5Me_5)\}_4][BF_4]_2$: J. S. Ricci, T. F. Koetzle, R. J. Goodfellow, P. Espinet, P. M. Maitlis, *Inorg. Chem. 23* (1984) 1828.
[8] 185–187 pm for $[\{(\mu_3\text{-H})Rh(\eta^5\text{-}C_5Me_5)\}_4][BF_4]_2$, by neutron diffraction: [7c].
[9] R. Hoffmann, *Science (Washington D.C.) 211* (1981) 995; T. A. Albright, *Tetrahedron 38* (1982) 1339; R. Hoffmann, *Angew. Chem. 94* (1982) 725; *Angew. Chem. Int. Ed. Engl. 21* (1982) 711, and references cited therein.
[10] For consideration of hydrido clusters as protonated anionic cluster systems, see R. Hoffmann, B. E. R. Schilling, R. Bau, H. D. Kaesz, D. M. P. Mingos, *J. Am. Chem. Soc. 100* (1978) 6088.
[11] T. A. Albright, J. K. Burdett, M.-H. Whangbo, *"Orbital Interactions in Chemistry"*, Wiley, New York 1985, p. 364 ff.
[12] For **3**, the three MOs (not drawn with bold lines) formed between $1b_1$ and a_2, as well as between b_2 and $3a_1$, possess almost exclusively π and π^* character at the olefin ligands and metal-centered p AO contributions at Rh, respectively. These MOs give rise to corresponding orbitals of the trimeric building block **4**, but they do not play a direct role in the bonding of TMM and H and appear almost unchanged in the composite cluster (Fig. 2, MO scheme **C**). The hatched blocks in **B** and **C** each represent 15 MOs (12 with Rh d character), which result from the five lowest orbitals of **3** (MO scheme **A**).
[13] R. Hoffmann, *J. Chem. Phys. 39* (1963) 1397; R. Hoffmann, W. N. Lipscomb, *ibid. 36* (1962) 2179, 3489; *ibid. 37* (1962) 2872. H_{ij} matrix elements: J. H. Ammeter, H.-B. Bürgi, J. C. Thibeault, R. Hoffmann, *J. Am. Chem. Soc. 100* (1978) 3686. Wave functions and ionization potentials of Rh: A. R. Pinhas, T. A. Albright, P. Hofmann, R. Hoffmann, *Helv. Chim. Acta 63* (1980) 29. Model geometries: adapted from the structure of **2**.
[14] The π_3 and 2e MOs of TMM and **3**, respectively, do not play a dominant role for bonding in **5** and **2**.
[15] Without attachment of μ_3-$H^{\oplus}$, that is, formally without the transfer of two electrons of the cluster framework to the μ_3-H atom (hydridic in **2**), a doubly reduced **4** or an isoelectronic system, even though also isoelectronic to **5**, would have two electrons in twofold degenerate LUMO (MO scheme **B**). This would correspond to an open-shell triplet or to a Jahn–Teller-unstable singlet state.
[16] A stable electron configuration should even result for full occupation of the two LUMO levels in the MO scheme **C** (48 VE) owing to their Rh–Rh bonding character and the large separation from the next-highest MO (Rh–Rh antibonding).
[17] In the model calculations the three $[Rh(C_2H_4)_2]$ units of **5** relax with retention of C_3 symmetry for the complete cluster (corresponding to the arrows in **6**) by (1) tilting toward the hydride and (2) sideways displacement in the same direction and rotation around their local C_2 axes, which causes the rotation of the TMM ligand around the C_3 axis. The geometry-optimized structure of **5** corresponds to the geometry of **2**.

Interaction of Hydrophobically-Modified Poly-*N*-isopropylacrylamides with Model Membranes – or Playing a Molecular Accordion **

By *Helmut Ringsdorf*,* *Joachim Venzmer*, and *Françoise M. Winnik*

One stabilizing element of cell membranes is the cytoskeleton. In the case of the red blood cell this is a two-dimensional protein network which is coupled to the membrane via anchor proteins.[1] Through lateral contractions and expansions the cytoskeleton participates in the cell overall motion and in membrane processes such as protrusions.[2] Simple model membranes such as monolayers[3] and liposomes[4] are lipid assemblies which lack the stabilizing elements present in natural membranes. Approaches to improve the mechanical stability of lipid membranes with the help of polymer science involve either chemical cross-linking of the membrane by use of polymerizable lipids,[5] or fixation onto a lipid bilayer of water-soluble polymers which carry lipid-

[*] Prof. Dr. H. Ringsdorf, Dipl.-Chem. J. Venzmer
Institut für Organische Chemie der Universität
J.-J.-Becherweg 18–20, W-6500 Mainz 1 (FRG)
Dr. F. M. Winnik
Xerox Research Centre of Canada

[**] This work was supported in part by an NSERC (Canada) grant to Professor *M. A. Winnik* and by the "New Energy and Industrial Technology Development Organization of Japan".

compatible anchor groups[6] (Fig. 1). These concepts mostly neglect the dynamical aspect of membranes. If, however, the adsorbed polymer responds by some physical change to an external stimulus, such as a pulse of light or changes in pH, it can be used to modulate the systems properties.[7] This communication describes model membranes which simulate the dynamics of the cytoskeleton by a thermoreversible contraction/expansion of a polymer anchored to a lipid bilayer.

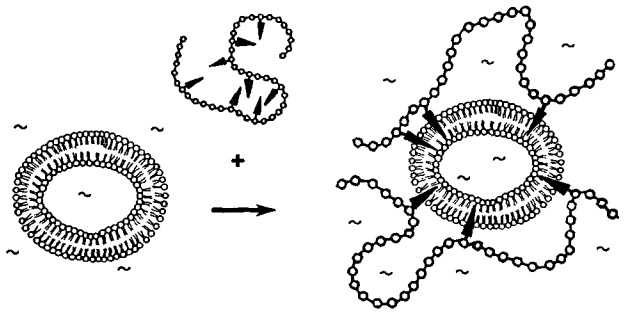

Fig. 1. Schematic drawing of the interaction of a liposome with a water-soluble polymer bearing hydrophobic anchor groups.

To play such a "molecular accordion" the water-soluble polymer must satisfy the following requirements: 1) it must anchor itself tightly onto the lipid bilayer and 2) its dimensions must undergo thermoreversible expansion and contraction. The second feature is characteristic for polymers which form solutions that are clear in cold water, but become turbid upon heating. One example of a polymer exhibiting such a lower critical solution temperature (LCST)[8] is poly-*N*-isopropylacrylamide (PNIPAM).[9] It was selected in this study for the following reasons: 1) its LCST is 32 °C, a temperature convenient for working with membranes; 2) the incorporation of a few anchor groups can easily be achieved by radical copolymerization; 3) investigations of the molecular aspects of the LCST phenomena have confirmed that the hydrodynamic radius of single PNIPAM macromolecules decreases upon precipitation at the LCST.[10] In addition, a suitable detection system is needed to follow the conformational changes of the polymer. Fluorescence spectroscopy of a pyrene-labeled polymer was chosen since pyrene has two distinct emissions: an isolated pyrene exhibits a structured "monomer" emission but if an excited pyrene group comes into close contact with a ground state pyrene, an excimer will form and emit light as a broad featureless band centered at 485 nm.[11] Thus, the changes in the relative intensity of the monomer and excimer emissions constitute a measure of the changes in the number of isolated pyrenes to that of pairs of pyrenes in close proximity.

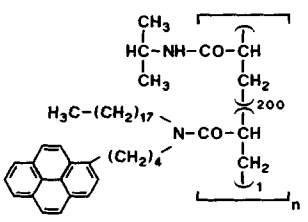

1

The functional labeled polymer **1** used here is a random copolymer of *N*-isopropylacrylamide and *N*-[4-(1′-pyrenyl)-butyl]-*N*-*n*-octadecylacrylamide in a molar ratio of ca. 200/1.[12] In water at 20 °C **1** exhibits an emission due to locally excited pyrene (intensity I_M) and a broad featureless emission centered at 480 nm (intensity I_E) due to pyrene excimer emission (Fig. 2A). The large contribution of excimer

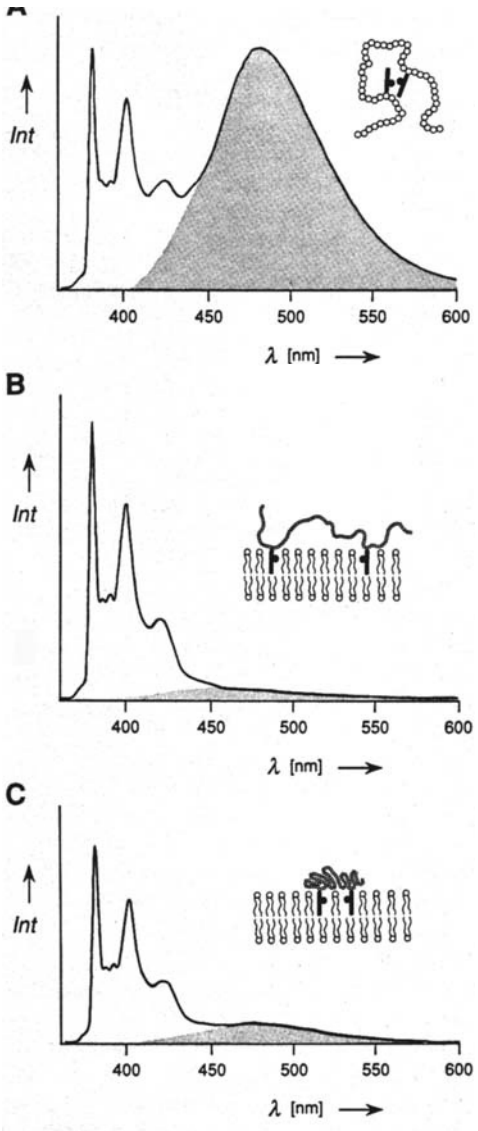

Fig. 2. Fluorescence spectra and schematic representations of the interactions of **1** with liposomes of DMPC (λ_{exc} = 347 nm): (**A**) polymer without liposomes (I_E/I_M = 1.10); (**B**) polymer with DMPC liposomes at 26 °C (I_E/I_M = 0.04); (**C**) same system at 34 °C (I_E/I_M = 0.12).

emission to the total fluorescence of **1** (I_E/I_M = 1.10) is indicative of the existence in the solution of microdomains with high local pyrene concentration. These have been identified as the inner core of unimolecular polymeric micelles, consisting of a hydrophobic domain formed by the octadecyl chains and the pyrene groups, surrounded by the more polar PNIPAM backbone, which lends to the polymer its solubility in water.[12] Solutions of **1** heated above their LCST present a much altered emission. Most notable is the large increase of the monomer emission at the expense of the excimer emission (I_E/I_M = 0.45), signaling heat-induced disruption of the hydrophobic microdomains. Above the LCST the pyrene groups are solubilized largely as isolated species in the separated polymer-rich phase.

Addition of small unilamellar liposomes of dimyristoyllecithin (DMPC, 1 gL^{-1}) to a solution of **1** (20 ppm) at 26 °C has a dramatic effect on the structure of this polymer in water, as evidenced by a remarkable decrease in the pyrene excimer emission ($I_E/I_M = 0.04$, Fig. 2B). This decrease indicates that the octadecyl/pyrene-anchor groups are inserted into the lipid bilayer. Among the lipidic alkyl chains they experience a hydrophobic environment such that the driving force for micellar aggregation is lost. The pyrene groups are separated from each other among the lipidic chains and excimer formation is almost entirely precluded.[13] This effect depends on the relative concentrations of liposomes and **1**. When increasing amounts of polymer are added to a liposome solution, a polymer concentration is reached at which I_E/I_M increases again. This signals the point at which the surface of the liposomes is covered entirely with polymer (35 macromolecules per liposome or 1 pyrene per 110 lipids). The excess polymer adopts a micellar structure identical to that of pure **1** in water, characterized by a strong excimer emission.

When the temperature of a solution of functionalized liposomes is raised to 34 °C, i.e. above the LCST of PNIPAM, there results a small, but significant increase in the excimer emission ($I_E/I_M = 0.12$, Fig. 2C). This effect is reversible: upon cooling the solution I_E/I_M fell to its original value (0.04). The increase in excimer emission upon application of heat can be explained by the following sequence of events. At the LCST the PNIPAM loops in the aqueous environment collapse. The anchor groups attached to the polymer are forced to move closer together by lateral diffusion within the membrane. The number of pyrene pairs close enough to form excimers increases, resulting in an enhanced excimer emission. Upon cooling the polymer loops in water expand forcing the anchor groups to move apart from each other. Hence the excimer emission all but vanishes. There is however another scenario to account for the heat-induced increase in excimer emission: a small number of anchor groups might be pulled out of the membrane. Thus, free polymer would exist in solution and adopt a conformation typical of pure **1** solution above its LCST. This mechanism too would account for the observed increase in I_E/I_M. A control experiment is needed to distinguish between these two mechanisms. This experiment, carried out with liposomes made with a lipid of a higher phase transition, provided the proof that the "molecular accordion" was indeed playing our tune.

Structure and fluidity of liposomes are temperature dependent.[14] Above a characteristic transition temperature liposomes exist in the liquid-analogous phase, in which the lipid alkyl chains are molten. In this phase lateral diffusion within the plane of the membrane is permitted. Below the phase transition temperature liposomes exist in the solid-analogous phase, in which the alkyl chains of the lipids are crystallized in all-*trans* configuration. There is practically no lateral diffusion within the membrane in this phase. In the experiment described above, the DMPC liposomes (phase transition temperature 23 °C)[15] were in the liquid-analogous phase in the entire temperature range probed. The next set of experiments was carried out with liposomes made from distearoyllecithin (DSPC). Their phase transition temperature is 54 °C,[15] a temperature well above the LCST of PNIPAM. Therefore, by scanning temperatures from 26 °C to 56 °C one can observe separately the events occurring at the LCST of PNIPAM and at the liposome phase transition temperature. Figure 3 illustrates the results of a temperature scan performed with DSPC liposomes (1 gL^{-1}) and **1** (20 ppm). Fluorescence of this solution at 26 °C (Fig. 3A) consists almost entirely of pyrene monomer emission

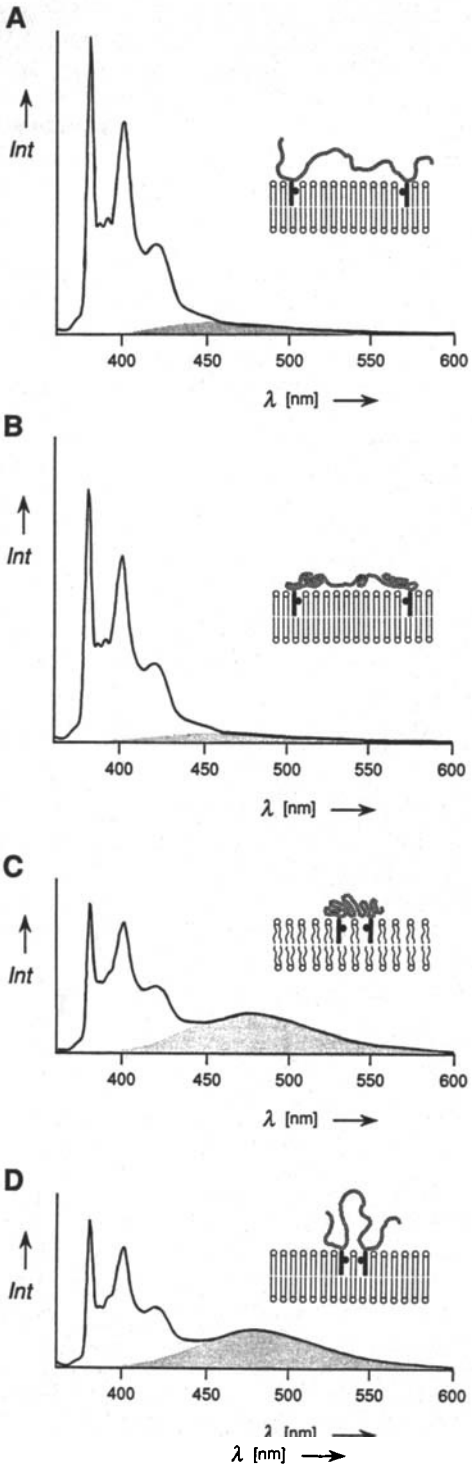

Fig. 3. Fluorescence spectra and schematic representations of the interactions of **1** with liposomes of DSPC (λ_{exc} = 347 nm): (**A**) polymer with DSPC liposomes at 26 °C ($I_E/I_M = 0.03$); (**B**) same system at 34 °C ($I_E/I_M = 0.03$); (**C**) same system at 56 °C ($I_E/I_M = 0.28$); (**D**) same system cooled to 26 °C ($I_E/I_M = 0.28$).

($I_E/I_M = 0.03$), indicating that the polymer anchor groups are inserted in the liposomes in their solid-analogous phase, as they were in the liquid-analogous phase of DMPC liposomes. At 34 °C, a temperature higher than the LCST of PNIPAM but lower than the liposome phase transition, the pyrene emission still originates almost entirely from isolated chromophores ($I_E/I_M = 0.03$, Fig. 3B). Therefore, even though the PNIPAM loops are collapsed, the pyrene groups are still unable to get in close proximity. This observation is consistent with the fact that in the solid-analogous phase

 © VCH Verlagsgesellschaft mbH, W-6940 Weinheim, 1991 0570-0833/91/0303-0317 $ 3.50+.25/0

lateral diffusion within the membrane is precluded. Finally at 56 °C, a temperature above the DSPC phase transition, pyrene excimer emission accounts for a significant part of the total emission ($I_E/I_M = 0.28$, Fig. 3C). At this temperature the anchor groups are free to diffuse within the membrane. They move closer together, presumably to relieve some of the strain caused by the collapse of the PNIPAM loops.

Next, the system was cooled to 26 °C. No change occurred in the fluorescence of the system: the ratio I_E/I_M retained its large value of 0.28 (Fig. 3D). Again the membrane has lost its fluidity and, even though the polymer dimensions are expanded, the anchor groups unable to move within the membrane cannot be pulled apart from each other. Therefore this heating/cooling cycle has left the DSPC liposome/**1** system in a state different from the original one. While initially the anchor groups were separated from each other within the membrane, at the end of the experiment they are locked in the configuration reached in the liquid-analogous phase of the liposome. This observation constitutes the ultimate proof that the "molecular accordion" is playing its tune: if the anchor groups had been pulled out of the membrane at any stage of the cycle, their re-insertion within the membrane below the LCST of PNIPAM would lead to the configuration depicted in Figure 3A, with separated anchor groups and hence drastically reduced pyrene excimer emission.

One may wonder whether the contractions of the anchored PNIPAM described here lead to a change in the shape of the liposomes, thus simulating the effects of the cytoskeleton contractions in the case of erythrocytes. This seems unlikely for two reasons. First, small unilamellar liposomes are not form-flexible. For a given surface to volume ratio the sphere is the only shape possible. Second, an anchored linear macromolecule capable of lateral diffusion cannot be expected to cause protrusions. Such changes in shape may possibly be achievable with a cross-linked polymeric network. This may be the next step towards a more advanced simulation of the natural process.

Experimental

The synthesis and characterization of **1** (LCST = 30.6 °C, M_V = 360 000, on average 16 octadecyl/pyrene groups per macromolecule) have been described in detail elsewhere [12]. The liposomes ($d \approx 100$ nm, BI 90 Particle Sizer, Brookhaven Instrument Corp.) were prepared by sonication of the lipids in deionized water (1 gL^{-1}, 40 W, Ultrasonic Homogenizer, Series 4710, Cole and Parmer Instrument Corp.) above the phase transition temperature of the lipid. Solutions for fluorescence measurements were prepared by addition of a polymer stock solution (50 µL, 1 gL^{-1}) to a liposome solution (2.5 mL). Fluorescence spectra were recorded with a SPEX spectrometer as described previously [12]. The excimer to monomer ratios (I_E/I_M) were calculated by taking the ratio of the emission intensity at 480 nm to the mean of the emission intensities at 379 nm and 399 nm. For measurements at different temperatures the samples were heated at a rate of 0.2 K min^{-1}.

Received: September 20, 1990 [Z 4193 IE]
German version: *Angew. Chem. 103* (1991) 323

[1] B. Alberts, D. Bray, J. Lewis, M. Raff, K. Roberts, J. D. Watson: *Molecular Biology of the Cell*, Garland Publishing, New York 1983, p. 268.
[2] E. Sackmann, H. P. Duwe, K. Zeman, A. Zilker in E. Clementi, S. Chin (Eds.): *Structure and Dynamics of Nucleic Acids, Proteins and Membranes*, Plenum, New York 1986, p. 251.
[3] G. L. Gaines: *Insoluble Monolayers at Liquid-Gas Interfaces*, Wiley Intersciences, New York 1966.
[4] a) M. J. Ostro (Ed.): *Liposomes*, Dekker, New York 1983; b) *Liposomes: From Biophysics to Therapeutics*, Dekker, New York 1987; c) G. Gregoriadis (Ed.): *Liposome Technology, Vol. I–III*, CRC Press, Boca Raton 1984.
[5] a) H. Bader, K. Dorn, B. Hupfer, H. Ringsdorf, *Adv. Polym. Sci. 64* (1985) 1; b) S. L. Regen in [4b], p. 73.
[6] M. Takada, T. Yuzuriha, K. Katayama, K. Iwamoto, J. Sunamoto, *Biochim. Biophys. Acta 802* (1984) 237; b) G. Decher, E. Kuchinka, H. Ringsdorf, J. Venzmer, D. Bitter-Suermann, C. Weisgerber, *Angew. Makromol. Chem. 166/167* (1989) 71; c) for a review see: H. Ringsdorf, B. Schlarb, J. Venzmer, *Angew. Chem. 100* (1988) 117, *Angew. Chem. Int. Ed. Engl. 27* (1988) 113.
[7] D. A. Tirrell, *J. Controlled Release 6* (1987) 15.
[8] L. D. Taylor, L. D. Cerankowsky, *J. Polym. Sci., Polym. Chem. Ed. 13* (1975) 2251.
[9] M. Heskins, J. E. Guillet, *J. Macromol. Sci. Chem. A2(8)* (1968) 1441.
[10] a) I. Yamamoto, K. Iwasaki, S. Hirotsu, *J. Phys. Soc. Jpn 58* (1989) 210; b) F. M. Winnik, *Polymer 31* (1990) 2125.
[11] J. B. Birks: *Photophysics of Aromatic Molecules*, Wiley Intersciences, London 1970, Chapter 7.
[12] a) H. Ringsdorf, J. Venzmer, F. M. Winnik, *Polym. Prepr. Am. Chem. Soc. Div. Polym. Chem. 31/1* (1990) 568; b) H. Ringsdorf, J. Venzmer, F. M. Winnik, *Macromolecules 24* (1991), in press.
[13] Addition of **1** to liposomes did not lead to a complete vanishing of the excimer emission with all liposomes tested. For example with liposomes composed of lecithin from egg yolk (high degree of unsaturation in the lipid chains) the system reached an equilibrium state at 26 °C where $I_E/I_M = 0.43$. Compatibility of the anchor groups with the lipid chains plays an important role in controlling the distribution of the anchor groups within the membrane.
[14] E. Sackmann in W. Hoppe, W. Lohmann, H. Markl, H. Ziegler (Eds.): *Biophysik*, Springer, Berlin 1982, p. 439.
[15] S. Mabrey, J. M. Sturtevant, *Proc. Natl. Acad. Sci. USA 73* (1976) 3862.

RS-P=S in the Gas Phase—First Generation of (Organothio)thioxophosphanes **

By *Helmut Keck, Wilhelm Kuchen,* Heike Renneberg, Johan K. Terlouw*, and *Herman C. Visser*

Dedicated to Professor Rolf Appel on the occasion of his 70th birthday

Organodithioxophosphoranes $RP(=S)_2$ **1** are formed upon heating their dimers, the dithiadiphosphetane disulfides $[RP(S)S]_2$ **2**, in a vacuum.[1] They can be stabilized as ligands in complexes;[2] with R = 2,4,6-tBu$_3$C$_6$H$_2$ (supermesityl), monomeric **1** can be kinetically stabilized and isolated in substance.[3] Furthermore, compounds of type **1** are discussed as intermediates in syntheses with Lawesson's reagent (**2**: R = p-$CH_3OC_6H_4$).[4] The generation of a structurally

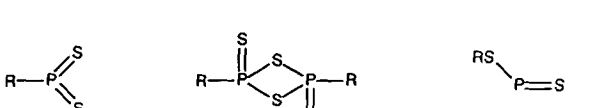

1 **2** **3**

1 a b: R = CH_3, C_6H_5

2 a b c: R = CH_3, C_6H_5, CH_3S

3 a b: R = CH_3, C_6H_5

comparable dithiophosphorus(v) chloride $ClP(=S)_2$ in a vacuum and its characterization by means of photoelectron spectroscopy have been reported recently.[1]

[*] Prof. Dr. W. Kuchen, Dr. H. Keck, Dipl.-Chem. H. Renneberg
Institut für Anorganische Chemie und Strukturchemie I der Universität
Universitätsstr. 1, W-4000 Düsseldorf 1 (FRG)
Prof. Dr. J. K. Terlouw
McMaster University, Department of Chemistry
1280 Main Street West, Hamilton, Ontario L8S 4M1 (Canada)
H. C. Visser
Analytical Chemistry Laboratory, University of Utrecht (Netherlands)
[**] This work was supported by the Fonds der Chemischen Industrie.

To our knowledge nothing has so far been reported in the literature about the existence of the (organothio)thioxophosphanes **3** isomeric with **1** and containing trivalent phosphorus of coordination number two. We have now been able to show that stable (organothio)thioxophosphanes RS–P=S **3a** and **3b** can be generated under unimolecular conditions by neutralization-reionization mass spectrometry (NRMS).[5]

Radical cations of the composition "$[RPS_2]^{\cdot\oplus}$" are formed upon mass spectrometric decomposition [electron impact ionization (EI): 70 eV] of the molecular ions of the dithiadiphosphetane disulfides **2a**–**2c**.[6]

Intense signals are observed for ions of the composition $[CH_3PS_2]^{\cdot\oplus}$ (m/z = 110) in both the EI mass spectrum of **2c** and of **2a**. These radical cations are formed from **[2c]**$^{\cdot\oplus}$ by ring cleavage, loss of CH_3SPS_2, and subsequent elimination of sulfur [Eq. (a)], and from **[2a]**$^{\cdot\oplus}$ by loss of CH_3PS_2 after ring opening [Eq. (b)]. It can be assumed that, depending on

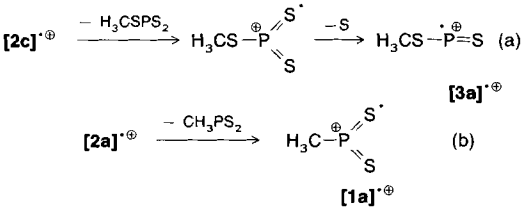

their origin, ions of composition $[CH_3PS_2]^{\cdot\oplus}$ (m/z = 110) have a different structure, which can be derived either from a (methylthio)thioxophosphane **[3a]**$^{\cdot\oplus}$ or from a dithioxophosphorane **[1a]**$^{\cdot\oplus}$. To check this, the ions with m/z = 110 were mass selected and collisional activation (CA) mass spectra recorded;[7, 8] these differ from one another depending on the origin of the ions: in the case of the ions generated from **2c**, intense signals are observed for $PS^{\oplus}$ (m/z = 63) and $[CH_3S]^{\oplus}$ (m/z = 47) (Fig. 1a). Loss of an intact methyl group confirms that no isomerization reaction with participation of the methyl group, such as H-migration from C to S, has taken place. It can therefore be concluded that, in this case, the ions with m/z = 110 indeed have the structure **[3a]**$^{\cdot\oplus}$ containing a C–S bond. The NR mass spectrum (neutralization with Xe; reionization with O_2)[8] (Fig. 1b) shows

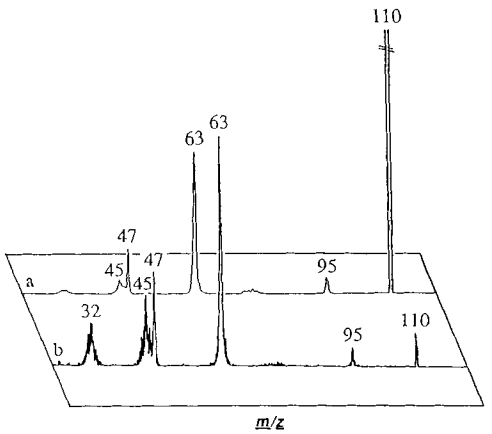

Fig. 1. CA- (a) and NR-mass spectrum (b) of "$[CH_3PS_2]^{\cdot\oplus}$" (m/z 110) (generated from **2c**).

that the neutral (methylthio)thioxophosphane **3a** (C_s) is really able to exist: for not only a "survivor signal" m/z = 110 is observed, but also the characteristics of the CA and NR mass spectra correlate well.

On the other hand, the CA mass spectrum (Fig. 2a) of the ions with m/z = 110 generated from **2a** according to Equation (b) differs from that of the ions that have been generated from **2c** according to Equation (a) (Fig. 1a). The most striking difference is the high intensity of the signal for $[PS_2]^{\oplus}$ (m/z = 95; base peak). Most likely the latter is formed by cleavage of a methyl group from **[1a]**$^{\cdot\oplus}$. Signals also appear, however, for $[CH_3S]^{\oplus}$ (m/z = 47), and these can only arise from **[3a]**$^{\cdot\oplus}$.

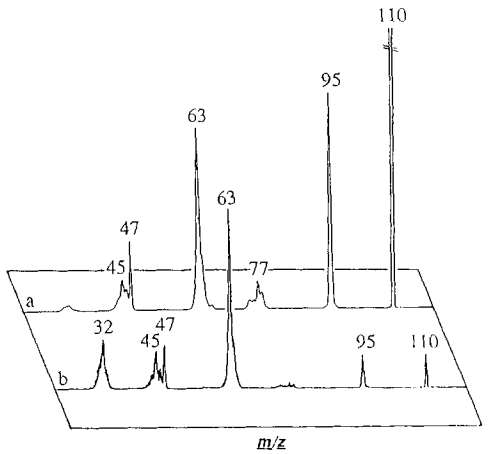

Fig. 2. CA- (a) and NR-mass spectrum (b) of "$[CH_3PS_2]^{\cdot\oplus}$" (m/z = 110) (generated from **2a**).

Apparently the methyl group in **[1a]**$^{\cdot\oplus}$ undergoes a [1, 2]-shift from P to S with formation of **[3a]**$^{\cdot\oplus}$ and lowering of the coordination number of the P from three to two [Eq. (c)].

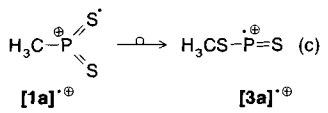

In this case the ions with m/z = 110 should be coextisting in the structures **[3a]**$^{\cdot\oplus}$ and **[1a]**$^{\cdot\oplus}$. The respective NR mass spectrum (Fig. 2b) is consistent with that of **[3a]**$^{\cdot\oplus}$ (Fig. 1b), so that there is no evidence for decomposition of **1a**. It can be assumed that only neutral molecules of the structure **3a** are formed in the neutralization, since the **1a** formed in a highly excited state immediately before the reionization completely isomerizes to **3a** in the second collision cell.

Semiempirical MO calculations (MNDO)[9] confirm the experimental findings. It should be noted that according to such calculations the ionized (methylthio)thioxophosphane **[3a]**$^{\cdot\oplus}$ (ΔH_f^0 = 219 kcal mol^{-1}) is thermodynamically more stable than the ionized isomeric methyldithioxophosphorane **[1a]**$^{\cdot\oplus}$ (ΔH_f^0 = 242 kcal mol^{-1}). A standard enthalpy of formation of $\Delta H_f^0 = -9$ kcal mol^{-1} was found for **3a** and of ΔH_f^0 = 21 kcal mol^{-1} for **1a**.

In the EI mass spectrum of the 2,4-diphenyl-1,3,2,4-dithiadiphosphetane 2,4-disulfide **2b**, an intense signal is observed for ions of the composition "$[C_6H_5PS_2]^{\cdot\oplus}$" ($m/z$ = 172), which are formed directly from the molecular ions

 © VCH Verlagsgesellschaft mbH, W-6940 Weinheim, 1991 0570-0833/91/0303-0319 $ 3.50+.25/0

$[2b]^{\bullet\oplus}$, and for which likewise the structure of a phenyldithioxophosphorane $[1b]^{\bullet\oplus}$ or of a (phenylthio)thioxophosphane $[3b]^{\bullet\oplus}$ is open to discussion.

Signals at $m/z = 77$ ($[C_6H_5]^{\oplus}$) and $m/z = 51$ ($[C_4H_3]^{\oplus}$) in the CA mass spectrum (Fig. 3a) of "$[C_6H_5PS_2]^{\bullet\oplus}$" confirm that it contains an intact phenyl group. Consecutive elimination of S to $m/z = 140$ and $m/z = 108$ is an indication of the presence of the structure $[1b]^{\bullet\oplus}$. The ions $[C_6H_5S]^{\oplus}$ ($m/z = 109$), which can only be formed from $[3b]^{\bullet\oplus}$, and $[C_6H_5P]^{\bullet\oplus}$ ($m/z = 108$), which can only come from $[1b]^{\bullet\oplus}$ lead to the conclusion that radical cations "$[C_6H_5PS_2]^{\bullet\oplus}$" in the form of $[1b]^{\bullet\oplus}$ and $[3b]^{\bullet\oplus}$ exist alongside each other. Analogously to the ions that stem from **2a**, here also it follows from the NR mass spectrum that only neutral **3b** (C_s) is formed from both components of the ionic mixture. That is, neutral **1b** must have rearranged into the (phenylthio)-thioxophosphane **3b**. Figure 3b shows namely a "survivor

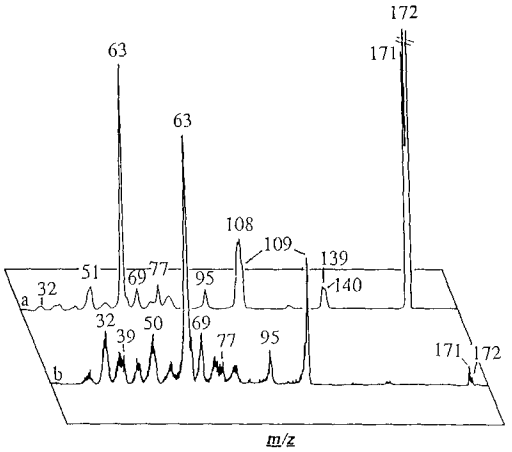

Fig. 3. CA- (a) and NR-mass spectrum (b) of "$[C_6H_5PS_2]^{\bullet\oplus}$" ($m/z$ 172) (generated from **2b**).

signal" at $m/z = 172$, which is only of small intensity. The spectral characteristic of the NR mass spectrum, however, differs from that of the CA mass spectrum. In the former, only an intense signal for $[C_6H_5S]^{\bullet\oplus}$ ($m/z = 109$) is still observed, which can be reconciled only with the thioxophosphane structure $[3b]^{\bullet\oplus}$, whereas the signal for $[C_6H_5P]^{\bullet\oplus}$ ($m/z = 108$) in the CA mass spectrum, which can be regarded as characteristic for the presence of $[1b]^{\bullet\oplus}$, is no longer present.

The results show that both the neutral molecules $RP(=S)_2$ **1a** and **1b** as well as their singly positively charged ions isomerize to (organothio)thioxophosphanes RS–P=S **3a** and **3b** and to the corresponding ions, respectively. Thus, NRMS[10] proves once again to be an effective method for the generation of highly reactive phosphorus compounds of low coordination number, for which there is so far no other synthetic route.

Received: March 13, 1990 [Z 3854 IE]
German version: *Angew. Chem. 103* (1991) 331
Publication delayed at authors' request

[1] M. Meisel, H. Bock, B. Solouki, M. Kremer, *Angew. Chem. 101* (1989) 1378; *Angew. Chem. Int. Ed. Engl. 28* (1989) 1373.

[2] a) G. J. Kruger, S. Lotz, L. Linford, M. van Dyk, H. G. Raubenheimer, *J. Organomet. Chem. 280* (1985) 241; b) E. Lindner, K. Auch, G. A. Weiß, W. Hiller, R. Fawzi, *Chem. Ber. 119* (1986) 3076.

[3] a) R. Appel, F. Knoch, H. Kunze, *Angew. Chem. 95* (1983) 1008; *Angew. Chem. Int. Ed. Engl. 22* (1983) 1004; b) J. Navech, J. P. Majoral, R. Kraemer, *Tetrahedron Lett. 24* (1983) 5885; c) M. Yoshifuji, K. Toyota, K. Ando, N. Inamoto, *Chem. Lett. 1984*, 317.

[4] H. Z. Lecher, R. A. Greenwood, K. C. Whitehouse, T. H. Chao, *J. Am. Chem. Soc. 78* (1956) 5018.

[5] Reviews: a) C. Wesdemiotis, F. W. McLafferty, *Chem. Rev. 87* (1987) 485; b) J. K. Terlouw, H. Schwarz, *Angew. Chem. 99* (1987) 829; *Angew. Chem. Int. Ed. Engl. 26* (1987) 805; c) H. Schwarz, *Pure Appl. Chem. 61* (1989) 685; d) J. L. Holmes, *Mass Spectrom. Rev. 8* (1989) 513; e) F. W. McLafferty, *Science (Washington D.C.) 247* (1990) 925.

[6] a) EI-MS of **2a** and **2b**: H. Keck, W. Kuchen, *Phosphorus Sulfur 4* (1978) 173; b) EI-MS of **2c**: m/z 284 $[M]^{\bullet\oplus}$ (15%), 205(9), 157(12), 142(96), 110(10), 95(15), 79(7), 63(100), 47(23), 45(18).

[7] Reviews of CA mass spectrometry: a) K. Levsen, H. Schwarz, *Angew. Chem. 88* (1976) 589; *Angew. Chem. Int. Ed. Engl. 15* (1976) 509; b) K. Levsen, H. Schwarz, *Mass Spectrom. Rev. 2* (1983) 77; c) J. L. Holmes, *Org. Mass Spectrom. 20* (1985) 169.

[8] The CA mass spectra were recorded with a Varian MAT 311A (Düsseldorf) and a VG ZAB-2F (Utrecht). The NR mass spectra were also recorded with the latter apparatus.

[9] J. J. Stewart, *A General Molecular Orbital Package* (MOPAC), QCPE Program 464 (Siemens 7.580-S); energy optimization by the DFP (Davidon-Fletcher-Powell) method. For want of space, only a few of the structural details and charge distributions are given here. Further data are available on request from the authors.

[10] a) H. Keck, W. Kuchen, H. Renneberg, J. K. Terlouw, *Phosphorus Sulfur 40* (1988) 227; b) H. Keck, W. Kuchen, H. Renneberg, J. K. Terlouw, H. C. Visser, *Chem. Ber. 122* (1989) 2265; c) *Z. Anorg. Allg. Chem. 580* (1990) 181.

Enantioselective Metabolism of (±)-α-1,2,3,4,5,6-Hexachlorocyclohexane in Organs of the Eider Duck **

By *Roland Kallenborn, Heinrich Hühnerfuss,** and *Wilfried A. König*

Many investigations are being carried out on the fate of organic pollutants in marine and terrestrial ecosystems. Of primary interest are the questions of stability, degradation, and enrichment of anthropogenic organic compounds in the food chain. A problem has long been the differentiation between enzymatic and nonenzymatic degradation processes. Only the recently developed cyclodextrin phases,[1] which very quickly found application as chiral stationary phases in gas chromatography, made it possible to distinguish between the two degradation processes for very small concentrations of pollutants. Applying this new method to environmental analysis, *Faller* et al.[2] were able to study the microbial degradation of α-1,2,3,4,5,6-hexachlorocyclohexane (HCH), the only chiral isomer of the eight conceivable HCH isomers (Fig. 1), in the North Sea, where it is present at concentrations of several nanograms per dm^3 of seawater. For this low trophic stage of the marine ecosystem, the enantiomeric ratio (+)-α-HCH/(−)-α-HCH, which is 1 for technical α-HCH, was found to vary from 0.85 in the eastern North Sea to about 1.15 in the western North Sea. Using liver, kidney, and muscle tissue of the eider duck (*Somateria mollissima L.*), we have now examined whether comparable enantiomeric ratios are found for a considerably higher

[*] Dr. H. Hühnerfuss, R. Kallenborn, Prof. Dr. W. A. König
Institut für Organische Chemie der Universität
Martin-Luther-King-Platz 6, W-2000 Hamburg 13 (FRG)

[**] Gas-Chromatographic Separation of the Enantiomers of Organic Marine Pollutants, Part 2. This work was supported by the Bundesministerium für Forschung und Technologie (MFU 0620). Part 1: [2].

trophic stage in the marine ecosystem or whether enantioselective degradation processes lead to even more pronounced shifts. The eider duck was chosen because it largely favors mussels (*Mytilus edulis*) in its diet. Mussels, in turn, are capable of strongly enriching pollutants and thus serve as "indicator organisms" to provide insight into the state of an aquatic environment.

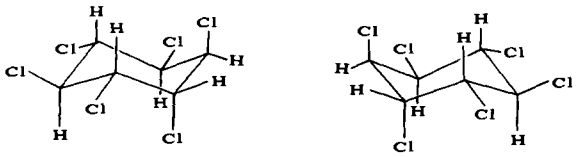

Fig. 1. The two enantiomers of α-HCH. The absolute configuration of the (+) and (−) enantiomers have not yet been determined.

Typical chromatograms of liver, kidney, and muscle extracts are shown in Figure 2. In all three extracts, (+)-α-HCH is clearly enriched; almost enantiomerically pure (+)-α-HCH is present in liver extracts. The enantiomeric purity of (+)-α-HCH isolated from liver extract is so high that, after purification by HPLC, it can be used directly in model experiments. By contrast, the enantiomeric ratio (+)-α-HCH/(−)-α-HCH was about 7.0 in muscle samples and about 1.6 in kidney extracts, whereby the values for these organs are slightly larger or smaller for different eider ducks.

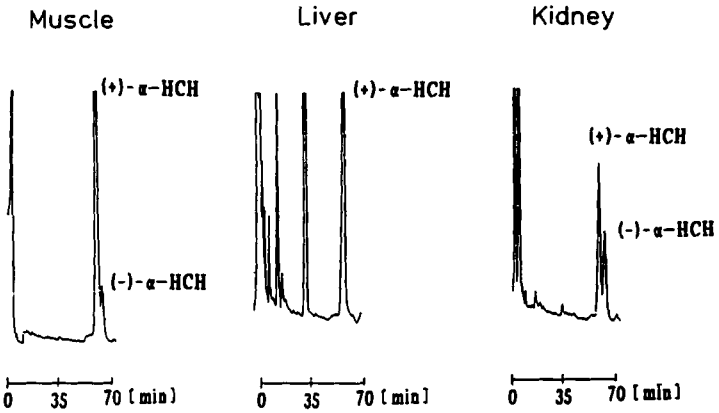

Fig. 2. Comparison of the chromatograms of extracts from the muscle, liver, and kidney of eider ducks (60-m glass capillary with heptakis(3-*O*-butyryl-2,6-di-*O*-pentyl)-β-cyclodextrin as chiral stationary phase, columns temperature 423 K (isothermal); carrier gas, 100 kPa helium, on-column injection, electrochemical detection).

An exact explanation for the appearance of different enantiomeric ratios of α-HCH in the organs of eider ducks cannot be given at the present time. It may be assumed, however, that the reason lies in the different physiological functions of the organs. For muscle and kidney, whose main functions are locomotion and excretion, respectively, the content of extractable lipids is about 2%; these organs can therefore store lipophilic pollutants. Liver, which contains about 2.5% of extractable matrix, serves as a "detoxification organ" and therefore is not only capable of storing toxic compounds but can also metabolize them to substances that the body can tolerate or excrete. Since the (+)-α-HCH found in the liver of eider duck is almost enantiomerically pure, (−)-α-HCH is presumably more readily degraded enzymatically than the (+) isomer in the liver. Although such a nearly enantioselective degradation has already been observed for biogenic organic compounds, this study represents the first demonstration for synthetic substances.

Experimental Procedure

Animals from the Oehe/Schleimünde wildlife refuge on the Baltic coast of Germany were investigated. Organ samples were taken only from healthy animals that, upon diving, had become trapped in the fishing nets of local fishermen and were thereby drowned. The tissue samples were homogenized with a threefold amount of anhydrous sodium sulfate; 60 g of the resulting powder was treated with 80 ng of the internal standard ε-HCH and then extracted in a Soxhlet apparatus for 8 h with 100 mL of ultrapure *n*-hexane. The extract was concentrated to 5 mL at 360 mbar and 313.2 K and then placed on a colums of partially deactivated alumina (5% water). The column was eluted with 70 mL of ultrapure *n*-hexane and the eluate was concentrated to 0.4 mL. Of this solution, 0.2 mL was separated on a LiChrosorb 100 Si column (Merck) by HPLC and the α-HCH fraction was measured by gas chromatography (Carlo Erba Vega gas chromatograph, 60-m glass capillary column with heptakis-(3-*O*-butyryl-2,6-di-*O*-pentyl)-β-cyclodextrin as chiral stationary phase, oven temperature 423 K (isothermal); carrier gas, 100 kPa helium, "on-column" injection, electrochemical detection). The organs from a total of six eider ducks were investigated, so that these results can be considered sufficiently reliable.

Received: September 19, 1990 [Z 4188 IE]
German version: *Angew. Chem. 103* (1991) 328

CAS Registry numbers:
α-HCH, 319-84-6; (±)-α-HCH, 60291-32-9; (+)-α-HCH, 119911-69-2; (−)-α-HCH, 119911-70-5.

[1] W. A. König, R. Krebber, P. Mischnick, *J. High Res. Chromatogr. 12* (1989) 732; W. A. König, *Nachr. Chem. Tech. Lab. 37* (1989) 471, and references cited therein.
[2] J. Faller, H. Hühnerfuss, W. A. König, P. Ludwig, *Mar. Pollut. Bull.* (1990), in press.

η^1-(1*S*, 2*E*)-1-(*N*,*N*-diisopropylcarbamoyloxy)-3-trimethylsilylallyllithium·(−)-Sparteine: Structure of a Chiral, Carbamoyloxy-substituted Allyllithium Compound**

By *Michael Marsch, Klaus Harms, Oliver Zschage, Dieter Hoppe* and *Gernot Boche**

Organolithium compounds bearing an oxygen substituent in the α position play an important role in organic synthesis.[1-3] Especially important is the discovery by *Still* et al. that the aliphatic derivatives are configurationally stable.[2] *Hoppe* et al. found that the carbamoyloxy-substituted allyllithium compounds **1** are useful reagents for the stereoselective synthesis of homoallyl alcohols.[3] (*S*)-**1a**, obtainable by deprotonation with retention of configuration, is configurationally stable at −70 °C on a preparative scale. Use of a chiral diamine allows (*R*)-**1b** to be isolated: in the presence of (−)-sparteine (**2**),[4] only (*R*)-**1b** crystallizes from the racemic mixture of the corresponding allyllithium compounds and is thus likewise accessible for enantioselective reactions.[3b] In a similar way we obtained (*S*)-**1c**[5] and

[*] Prof. Dr. G. Boche, M. Marsch, Dr. K. Harms
Fachbereich Chemie der Universität
Hans-Meerwein-Strasse, W-3550 Marburg (FRG)
Dipl.-Chem. O. Zschage, Prof. Dr. D. Hoppe
Institut für Organische Chemie der Universität
Olshausenstrasse 40, W-2300 Kiel (FRG)

[**] This work was supported by the Fonds der Chemischen Industrie and the Deutsche Forschungsgemeinschaft (SFB 260).

determined its crystal structure, the first of an organolithium compound bearing an oxygen substituent in α position (Fig. 1).

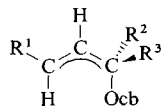

1, Cb = C(O)N*i*Pr$_2$

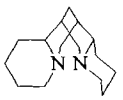

2

(*S*)-**1a**, $R^1 = R^2 = CH_3$, R^3 = Li · TMEDA
(*R*)-**1b**, $R^1 = CH_3$, R^2 = H, R^3 = Li · **2**
(*S*)-**1c**, $R^1 = SiMe_3$, R^2 = Li · **2**, R^3 = H

As revealed in Figure 1, sparteine-coordinated Li1 is bonded only to C1 (Li1-C1 220.7(8) pm) of the anionic allyl unit: the Li1–C2 distance is 293.2(8) pm. This structural feature is due to intramolecular chelate formation with the O atom of the carbamoyl group (Li1-O2 189.7(8) pm) to form a stable five-membered ring and is favored over η^3 coordination of the Li atom to the allyl unit.[10] The C1–C2–C3

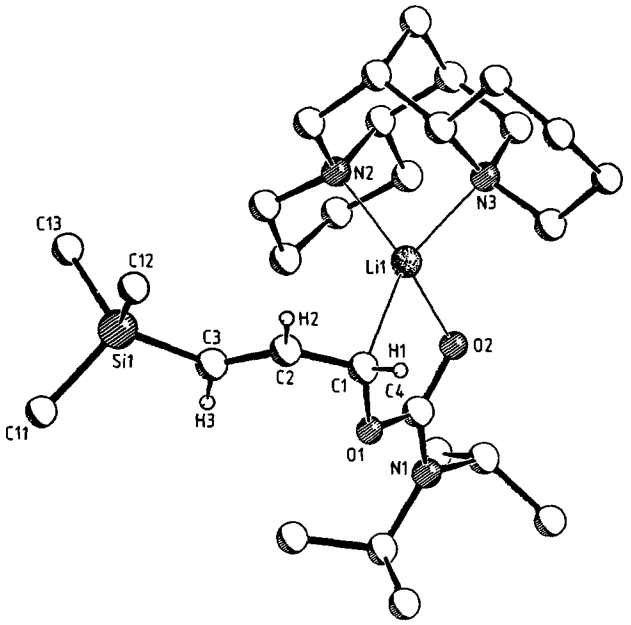

Fig. 1. Molecular structure of (*S*)-**1c**. [6] Important bond lengths [pm] as well as bond and torsional angles [°]: C1-C2 139.2(6), C2-C3 136.2(6), C3-Si1 182.0(5), C13-Si1 187.3(6), Li1-C1 220.7(9), Li1-O2 189.8(8), Li1-O1 284.0(8), Li1-N2 207.5(8), Li1-N3 201.7(8), C1-O1 147.6(6), C4-O1 133.8(6), C4-O2 123.9(5); C1-C2-C3 133.4(4); Li1-C1-C2-C3 91.7(6), Li1-C1-C2-H2 – 88(2), O1-C1-C2-C3 – 17.1(8); O1-C1-C2-H2 163(2), H1-C1-C2-C3 – 157(3), H1-C1-C2-H2 23(3).

angle is very strongly increased (133.4(4)°). Whereas the bonding geometry at C3 and C2 is nearly planar (sum of angles 359.7 and 360.4°, respectively), that at C1 is pyramidal. Thus, the sum of the angles at C1 is decreased to 347°, and the C1–H1 and C1–O1 bonds point away from Li1 and form angles of 23 and 17°, respectively, with the plane of the substituents at C2. The Li1–C1 bond is nearly perpendicular (Li1-C1-C2-C3 91.7°) to this plane. The preferential silylation at C1 and the stereoselective reaction with aldehydes at C3 (after complexation of the O atom of the aldehyde group by Li1[3]) are in agreement with the solid-state structure of (*S*)-**1c**.

It is remarkable that the structures of a *tert*-butylthio-[10b] and an (*S*)-2-(methoxymethyl)pyrrolidine-substituted[11] homoenolate equivalent are so clearly different from that of (*S*)-**1c**. In dimeric, intramolecularly chelated (3*S*)-3-lithio-1-[(*S*)-2-(methoxymethyl)pyrrolidino]-1,3-diphenylpropene,[11] each of the two Li atoms is bonded to the C3 atoms of both anionic allyl units as well as to the N and O atoms of a methoxymethylpyrrolidine substituent; the C1–C2 and C2–C3 bonds are 136(1) and 140(1) pm long, respectively. This is indicative of a strongly delocalized 3-metalated enamine system, which corresponds to the high C3 regioselectivity in reactions with electrophiles. In *tert*-butylthiobutenyllithium[10b] the Li atom is coordinated in an η^3 fashion to the anionic allyl unit (C1-Li 218, C3-Li 238 pm), whereby the C1–C2 distance (147 pm) is considerably longer than the C2–C3 distance (134 pm). In agreement with experimental observations, a metal-controlled regioselectivity of electrophilic attack is more difficult to establish here.[10b]

What can be said about the C1–O1 distance in (*S*)-**1c**? A search of the Cambridge Structural Database, as well as of published structures of carbamoyloxy-substituted compounds,[12] revealed the following average values: C_{sp2}–OCb = 139.9 pm (six values) and C_{sp3}–OCb = 143.6 pm (eleven values). Since the hybridization of C1 lies between sp^2 and sp^3 owing to pyramidalization, the C1–O1 distance found (147.6 pm) is markedly longer than the distance expected at least for a neutral molecule. A Li1–O1 interaction is not observed for (*S*)-**1c** (Li1-O1 284.0(8) pm). In ab initio studies on the structure of α-lithiomethanol, four different minima were found; the structure of (*S*)-**1c** corresponds to the "classical" structure in which the C–O bond is also lengthened compared with that in methanol.[13] The situation is exactly the opposite in α-lithiated thioethers owing to the different stabilization of a negative charge by an RS substituent (polarization and negative hyperconjugation versus induction by oxygen): the C_α–S bond is consistently shorter than that in the corresponding thioethers.[14]

The C4–O1 distance in (*S*)-**1c** (133.8(6) pm) is shorter than the mean value of the corresponding distances in neutral carbamoyloxy-substituted compounds (136.0 pm[12]), whereas C4–O2 (123.9(5) pm) is longer (mean value 120.5 pm[12]). This can be visualized as "dipole-stabilization" of the negative charge at C1.[15]

Received: November 7, 1990 [Z 4269 IE]
German version: *Angew. Chem. 103* (1991) 338

CAS Registry numbers:
(*S*)-**1c**, 131863-66-6.

[1] a) W. C. Still, *J. Am. Chem. Soc. 100* (1978) 1481; b) P. Beak, L. G. Carter, *J. Org. Chem. 46* (1981) 2363; c) N. Meyer, D. Seebach, *Chem. Ber. 113* (1980) 1290; d) P. Magnus, G. Roy, *J. Chem. Soc. Chem. Commun. 1979*, 822; e) E. J. Corey, T. M. Eckrich, *Tetrahedron Lett. 24* (1983) 3163, 3165; f) F. Lehmann, M. Schlosser, *ibid. 25* (1984) 745; g) D. Hoppe, R. Hanko, A. Brönnecke, *Angew. Chem. 92* (1980) 637; *Angew. Chem. Int. Ed. Engl. 19* (1980) 625; h) T. Cohen, M. Bupathy, *Acc. Chem. Res. 22* (1989) 153; i) J. S. Sawyer, A. Kucerovy, T. L. Macdonald, G. J. Mc Garvey, *J. Am. Chem. Soc. 110* (1988) 842; j) J. Eisch, J. E. Galle, *J. Org. Chem. 55* (1990) 4835; k) C. S. Shiner, T. Tsunoda, B. A. Goodman, S. Ingham, S. Lee, P. E. Vorndam, *J. Am. Chem. Soc. 111* (1989) 1381; l) G. A. Molander, K. Mautner, *J. Org. Chem. 54* (1989) 4042.

[2] For the configurational stability of lithium α-oxyalkanides, see: a) W. C. Still, C. Sreekumar, *J. Am. Chem. Soc. 102* (1980) 1201; b) A. Fernandez-Mayoralas, A. Marra, M. Trumtel, A. Veyrières, P. Sinaÿ, *Tetrahedron Lett. 30* (1989) 2437; c) J. A. Marshall, E. D. Robinson, *ibid. 30* (1989) 1055; d) J. M. Chong, E. K. Mar, *ibid. 31* (1990) 1981; e) S. D. Rychnovsky, D. E. Mickus, *ibid. 30* (1989) 3011; f) D. S. Matteson, P. B. Tripathy, A. Sarkar, K. M. Sadhu, *J. Am. Chem. Soc. 111* (1989) 4399; g) R. J. Linderman, A. Ghannam, *ibid. 112* (1990) 2392; h) D. Hoppe, F. Hintze, P. Tebben, *Angew. Chem. 102* (1990) 1457; *Angew. Chem. Int. Ed. Engl. 29* (1990) 1422; i) D. Hoppe, A. Carstens, T. Krämer, *ibid. 102* (1990) 1455 and *29* (1990) 1424.

[3] a) Reviews: D. Hoppe, T. Krämer, J.-R. Schwark, O. Zschage, *Pure Appl. Chem. 62* (1990) 1999; b) D. Hoppe, O. Zschage, *Angew. Chem. 101* (1989)

67; *Angew. Chem. Int. Ed. Engl. 28* (1989) 65; c) O. Zschage, J.-R. Schwark, D. Hoppe, *ibid. 102* (1990) 336 and *29* (1990) 296.
[4] Crystal structures with sparteine as complex ligand: a) L. T. Byrne, L. M. Engelhardt, G. E. Jacobsen, W.-P. Leung, R. I. Papasergio, C. L. Raston, B. W. Skelton, A. H. White, *J. Chem. Soc., Dalton Trans. 1989*, 105; b) A. Togni, G. Rihs, P. S. Pregosin, C. Ammann, *Helv. Chim. Acta 73* (1990) 723.
[5] For the torsional isomerization and synthetic use of *rac*-**1c** with TMEDA instead of sparteine, see: E. van Hülsen, D. Hoppe, *Tetrahedron Lett. 26* (1985) 411.
[6] Crystal structure data for (*S*)-**1c**: $C_{28}H_{51}N_3O_2Si_1Li_1$, $M = 496.75$, orthorhombic crystals, space group $P2_12_12_1$, $a = 11.886(1)$, $b = 13.827(2)$, $c = 18.591(3)$ Å, $Z = 4$, $\rho_{calcd} = 1.080\ g\,cm^{-3}$. Of 7970 reflections measured on an Enraf-Nonius diffractometer ($Cu_{K\alpha}$ radiation, graphite monochromator, $T = -80°C$), 2205 were unique ($R_{int} = 0.1466$) and 1955 with $F_0 > 4\sigma(F_0)$ were considered as observed. Solutions by direct methods (SHELXTL-Plus), refinement (SHELXTL-Plus) to $R = 0.063$, $R_w = 0.044$, $w = 1/\sigma^2(F_0)$. Non-hydrogen atoms anisotropic, H atoms at calculated positions with fixed isotropic temperature factors. The H atoms H1, H2, and H3 were localized and refined with a common temperature factor. All calculations were performed on a Micro-Vax II [7–9].
[7] A. L. Spek, *Platon 88, Program for Geometrical Analysis of Crystal Structures*, Utrecht 1988.
[8] E. Keller, *SCHAKAL 88B, A Fortran Program for the Graphic Representation of Molecular and Crystallographic Models*, Freiburg 1988.
[9] Further details of the crystal structure investigation may be obtained from the Fachinformationszentrum Karlsruhe, Gesellschaft für wissenschaftlich-technische Information mbH, W-7514 Eggenstein-Leopoldshafen 2 (FRG), on quoting the depository number CSD-320191, the names of the authors, and the journal citation.
[10] G. Boche, H. Etzrodt, M. Marsch, W. Massa, G. Baum, H. Dietrich, W. Mahdi, *Angew. Chem. 98* (1986) 84; *Angew. Chem. Int. Ed. Engl. 25* (1986) 104; b) D. Seebach, T. Maetzke, R. K. Haynes, M. N. Paddon-Row, S. S. Wong, *Helv. Chim. Acta 71* (1988) 299.
[11] H. Ahlbrecht, G. Boche, K. Harms, M. Marsch, H. Sommer, *Chem. Ber. 123* (1990) 1853.
[12] *D. Hoppe*, personal communication. Note added on December 6, 1990: In the meantime, the crystal structure of a second organolithium compound bearing an oxygen substituent in α position has been performed: diphenyl(trimethylsiloxy)methyllithium · 3 THF. In this compound, the distance of the anionic C atom from the O atom is 148.8(8) pm. This distance is thus clearly longer than the C_{sp3}–$OSiMe_3$ distances found in the Cambridge Structural Database (135 values, mean value 140.2 pm, maximum value 146.1 pm) as well as the C_{sp2}–$OSiMe_3$ distances (24 values, mean value 137.5 pm, maximum value 142.8 pm). The long C1–O1 distance found for (*S*)-**1c** is thus confirmed: A. Opel, M. Marsch, K. Harms, G. Boche, unpublished.
[13] a) T. Clark, P. von R. Schleyer, K. N. Houk, N. G. Rondan, *J. Chem. Soc. Chem. Commun. 1981*, 579; b) P. von R. Schleyer, T. Clark, A. J. Kos, G. W. Spitznagel, C. Rohde, D. Arad, K. N. Houk, N. G. Rondan, *J. Am. Chem. Soc. 106* (1984) 6467.
[14] a) Reviews: G. Boche, *Angew. Chem. 101* (1989) 286; *Angew. Chem. Int. Ed. Engl. 28* (1989) 277; experimental details: b) R. Amstutz, T. Laube, W. B. Schweizer, D. Seebach, J. D. Dunitz, *Helv. Chim. Acta 67* (1984) 224; c) W. Zarges, M. Marsch, K. Harms, W. Koch, G. Frenking, G. Boche, *Chem. Ber.*, in press; calculations d) S. Wolfe, *Stud. Org. Chem. (Amsterdam) 19* (1985) 133; e) [13b].
[15] See, e.g., P. Beak, W. J. Zaidel, *J. Am. Chem. Soc. 106* (1984) 1010, and references cited therein. It is remarkable that D. Seebach, J. Hansen, P. Seiter, J. M. Gromek, *J. Organomet. Chem. 285* (1985) 1, did not find a comparable bonding situation in the solid state structure of 1-magnesio-2-pivaloyl-1,2,3,4-tetrahydroisoquinoline.

The Structure of $IF_6^{\ominus}$ **

By *Ali Reza Mahjoub* and *Konrad Seppelt**

The $BrF_6^{\ominus}$ ion has an octahedral structure in solution[1] and in the crystal.[2] This finding contradicts the electron-pair repulsion model as well as the often discussed fact that the structure of xenon hexafluoride in the gas phase,[3] in solution,[4] and in the crystal[5] deviates strongly from octahedral symmetry. The recently proposed octahedral symmetry of the very unstable species $ClF_6^{\ominus}$ in solution[6] thus makes the unknown structure of the $IF_6^{\ominus}$ ion especially interesting.

The structural information so far reported for the $IF_6^{\ominus}$ ion is dubious, since it was established in 1971 that $I_3F_{16}^{\ominus}$ is the initial product of the reaction of $F^{\ominus}$ with IF_5. Pure $IF_6^{\ominus}$ is only formed when $I_3F_{16}^{\ominus}$, whose structure is now known,[2] is subjected to vacuum pumping over a long period.[7] Earlier investigations (e.g., vibrational[8] or ^{129}I-Mössbauer spectroscopy[9]) were possibly carried out with samples of unclear composition. Moreover, the vibrational spectra and X-ray powder data of pure $IF_6^{\ominus}$ salts do not lead to unequivocal conclusions about the structure.[7]

Attempts to grow single crytals of pure $Cs^{\oplus}IF_6^{\ominus}$ from, for example, BrF_5 or CH_3CN solutions failed. Either the solvent still contains some HF, which leads to interesting cocrystallizations (e.g., $IF_5 \cdot HF_2^{\ominus}$, $2IF_5 \cdot HF_2^{\ominus}$, and $3IF_5 \cdot H_3F_4^{\ominus}$,[10] or it causes solvolysis [Eq. (a)].

$$3IF_6^{\ominus} + 2BrF_5 \longrightarrow I_3F_{16}^{\ominus} + 2BrF_6^{\ominus} \qquad (a)$$

On the other hand, the preparation of $(CH_3)_4N^{\oplus}IF_6^{\ominus}$ and its recrystallization from CH_3CN gave crystals of an $IF_6^{\ominus}$ salt which were suitable for structure analysis.

At room temperature, the crystals appear to be monoclinic. However, a structure analysis could only be performed by assuming a disorder or a merohedral twin and, even then, the positions of the fluorine atoms were very inexact. At lower temperatures, the crystals become triclinic and are always twinned ($a' = -a$, $b' = -c$, $c' = -b$). Extrapolation of the reflection splitting versus temperature gave a value of about 60 °C where $b = c$ and $\beta = \gamma$. Differential thermal analysis (DTA) revealed a first-order phase transition at 51.2 °C. The X-ray data were collected at the lowest temperature possible (−163 °C), since overlap of the reflections is thereby minimized. The structure of the $IF_6^{\ominus}$ ion can be described as a distorted octahedron of near C_{3v} symmetry (Fig. 1). Three

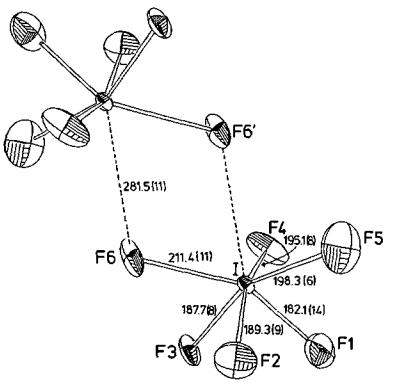

Fig. 1. The structure of the $IF_6^{\ominus}$ ion in crystals of $(CH_3)_4N^{\oplus}IF_6^{\ominus}$ (ORTEP, 50% thermal ellipsoids at −163 °C). Angles [°]: F1-I-F2 81.0(4), F1-I-F3 80.6(5), F2-I-F3 85.0(3), F4-I-F5 99.6(4), F4-I-F6 111.1(4),F5-I-F6 123.8(5), F1-I-F6 152.0(3), F2-I-F5 156.6(5), F3-I-F4 158.9(6).

fluorine atoms (F1, F2, F3) have shorter bonds that form angles of $< 90°$ with each other. There are three longer bonds with angles of $> 90°$. The bonds to fluorine atoms lying on opposite sides of the molecule have angles of about

[*] Prof. Dr. K. Seppelt, Dipl.-Chem. A. R. Mahjoub
Institut für Anorganische und Analytische Chemie der Freien Universität Fabeckstrasse 34–36, W-1000 Berlin 33 (FRG)

[**] This work was supported by the Deutsche Forschungsgemeinschaft and the Fonds der Chemischen Industrie.

150–160°. Current knowledge suggests that the sterically active electron pair occupies the cone between fluorine atoms F4, F5, and F6. This finding confirms the most recent theoretical prediction for the "free" $IF_6^\ominus$ ion, according to which C_{3v} symmetry is favored by 23 kcal mol^{-1} over O_h symmetry.[11]

Fluorine atom F6′, which occupies a seventh coordination site, is 281.5 pm from bromine in the direction of the nonbonding electron pair. A weakly bonded dimer with a center of symmetry is thereby formed. Thus, the $IF_6^\ominus$ ion may also be described as an adduct consisting of two IF_5 units and two $F^\ominus$ ions, the latter of which roughly lie opposite the apical positions of the $IF_5^\ominus$ square pyramids.

The intergrowth of the twins to form merohedral twins or a disordered single crystal when the temperature is increased corresponds to the pairwise exchange of F6 and F6′ between the two iodine atoms of the dimer, whereby the positions of these fluorine atoms change by only 110 pm. The other fluorine atoms follow this motion. In the crystal structure measured at room temperature (pseudo-monoclinic symmetry), therefore, the fluorine atoms have extremely large vibrational amplitudes. However, the cations are not measurably involved in this motion. In solution, on the other hand, rapid exchange of all of the fluorine atoms occurs (^{19}F NMR (0 °C, CH_3CN, $CFCl_3$ ext.): singlet at $\delta = -19$).

The analogy of the $IF_6^\ominus$ partial structure to the crystal structure of XeF_6 is even more apparent when a salt with a smaller counterion is investigated: in contrast to $(CH_3)_4N^\oplus IF_6^\ominus$, $NO^\oplus IF_6^\ominus$ crystallizes as a tetramer (Fig. 2) whose structure is qualitatively the same as that of the tetrameric unit $(XeF_5^\oplus F^\ominus)_4$ in crystalline XeF_6.[5] The small

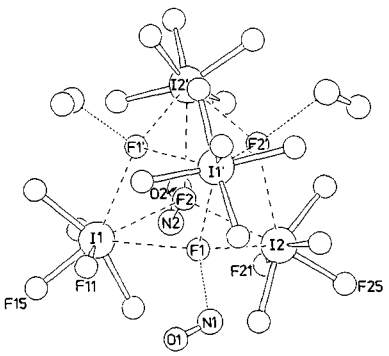

Fig. 2. The tetrameric structural unit in crystalline $NO^\oplus IF_6^\ominus$. A nearly regular $(IF_5)_4$ tetrahedron is held together by triply bridging fluoride ions, so that a cubane structure results. The bridging fluorine atoms originate from NOF (synthesis of the salt from NOF and IF_5): N(1) ··· F(1) = 197.2(9), N(2) ··· F(2) = 208.3(8) pm. The distances and angles of the IF_5 units are similar to those in free IF_5 [12]. The F–I distances in the cubane framework lie between 260.9(4) and 276.9(6) pm.

difference is only the highly symmetric bridging by the fluorine atoms F1 and F2 in the iodine tetramer. The three contacts of these atoms to the iodine atom are almost equal (260.9, 267.9, 274.9, and 262.3, 265.1, 276.9(4) pm), whereas one shorter and two longer contacts (223, 260, 283(3) pm) are present in $(XeF_5^\oplus F^\ominus)_4$.

XeF_6 and $IF_6^\ominus$ are not yet fully analogous, since the iodine system lacks an octahedral hexamer such as $(XeF_5^\oplus F^\ominus)_6$ in the crystalline state[5] as well as a nonrigid analogue to Xe_4F_{24} in solution.[4]

Experimental Procedure

$(CH_3)_4N^\oplus IF_6^\ominus$: IF_5 and $(CH_3)_4N^\oplus F^\ominus$ were combined in an FEP tube equipped with a valve (FEP = tetrafluoroethylene-hexafluoropropylene copolymer) under moisture-free conditions [13]. After completion of the reaction, the mixture was subjected to vacuum pumping. CH_3CN was then condensed into the tube to dissolve the product. Cooling to 0 °C resulted in formation of large, colorless crystals. The X-ray structure analysis at room temperature gave the following structural data: $a = 1126.6(5)$, $b = 1359.7(7)$, $c = 649.0(3)$ pm, $\beta = 93.73(3)°$, $C2/m$ (No. 12). The primitive unit cell has the parameters $a = 649.0$, $b = c = 883.0$ pm, $\alpha = 100.72$, $\beta = \gamma = 92.380$; cooling results in formation of a triclinic twin with ($T = -163$ °C): $a = 656.2(1)$, $b = 838.9(1)$, $c = 873.5(1)$ pm, $\alpha = 100.1(1)$, $\beta = 93.5(1)$, $\gamma = 91.8(1)°$, twinned according to $(-1\,0\,0)$, $(0\,0\,-1)$, $(0\,-1\,0)$, $P\bar{1}$. The Gemini program [14] was used to show that 1468 of 2882 measured reflections are nonoverlapping. Of these, 1384 are unique and 1273 have $I \geq 3\sigma(I)$ at $2° \leq \theta \leq 30°$, $\omega - 2\theta$ scan. Enraf–Nonius CAD4 diffractometer, $Mo_{K\alpha}$ radiation, $\mu = 34.28$ cm^{-1}, full matrix, SHELXTL plus, $R = 0.066$, $R_w = 0.056$. $NO^\oplus IF_6^\ominus$: Equimolar amounts of IF_5 and NOF were condensed into an FEP tube connected to a metal vacuum line and the tube was sealed under vacuum. At −20 °C, millimeter-size, colorless crystals formed spontaneously by sublimation. Great care must be taken to avoid the presence of HF, which leads to the formation of $NO^\oplus HF_2^\ominus \cdot IF_5$ (known crystal structure [10]). X-ray structure analysis at −157 °C gave the following structural data: $a = 1752.9(6)$, $b = 814.6(2)$, $c = 1588.1(6)$ pm, $\beta = 116.83(3)°$, $C2/c$, (No. 15), $Z = 8$. $R = 0.045$, $R_w = 0.041$. Further details of the crystal structure investigations may be obtained from the Fachinformationszentrum Karlsruhe, Gesellschaft für wissenschaftlich-technische Information mbH, W-7514 Eggenstein-Leopoldshafen 2 (FRG), on quoting the depository number CSD-55031, the names of the authors, and the journal citation.

Received: August 13, 1990;
supplemented: October 22, 1990 [Z 4130 IE]
German version: *Angew. Chem. 103* (1991) 309

CAS Registry numbers:
$(CH_3)_4N^\oplus IF_6^\ominus$, 20916-99-8; IF_5, 7783-66-6; NOF, 7789-25-5; $(CH_3)_4N^\oplus F^\ominus$, 373-68-2; $NO^\oplus IF_6^\ominus$, 65449-73-2.

[1] K. O. Christe, W. W. Wilson, *Inorg. Chem. 28* (1989) 3275; W. W. Wilson, K. O. Christe, *ibid. 28* (1989) 4172.
[2] A. R. Mahjoub, A. Hoser, J. Fuchs, K. Seppelt, *Angew. Chem. 101* (1989) 1528; *Angew. Chem. Int. Ed. Engl. 28* (1989) 1526.
[3] R. M. Gavin, L. S. Bartell, *J. Chem. Phys. 48* (1968) 2460; L. S. Bartell, R. M. Gavin, *ibid. 48* (1968) 2466.
[4] H. H. Rupp, K. Seppelt, *Angew. Chem. 86* (1974) 669; *Angew. Chem. Int. Ed. Engl. 13* (1974) 612; K. Seppelt, H. H. Rupp, *Z. Anorg. Allg. Chem. 409* (1974) 331; G. J. Schrobilgen, J. H. Holloway, P. Granger, C. Brevard, *Inorg. Chem. 17* (1978) 980.
[5] R. D. Burbank, G. R. Jones, *J. Am. Chem. Soc. 96* (1974) 43.
[6] K. O. Christe, R. V. Chirakal, J. C. P. Sanders, G. J. Schrobilgen, W. W. Wilson, *Inorg. Chem. 29* (1990) 3506.
[7] K. O. Christe, *Inorg. Chem. 11* (1972) 1215.
[8] S. P. Beaton, D. W. A. Sharp, A. J. Perkins, I. Sheft, H. H. Hyman, K. O. Christe, *Inorg. Chem. 7* (1968) 2174; K. O. Christe, J. P. Guertin, W. Sawodny, *ibid. 7* (1968) 626; H. Klamm, H. Meinert, P. Reich, K. Wittke, *Z. Chem. 8* (1968) 393, 469.
[9] S. Bukshpan, J. Soriano, J. Shamir, *Chem. Phys. Lett. 4* (1969) 241.
[10] A. R. Mahjoub, D. Leopold, K. Seppelt, *Europ. J. Solid State Inorg. Chem.*, in press.
[11] M. Klobukowski, S. Huzinaga, L. Seijo, Z. Barandiaran, *Theor. Chim. Acta 71* (1987) 237.
[12] A. G. Robiette, R. H. Bradley, P. N. Brier, *Chem. Commun. 1971*, 1567.
[13] The method of preparation is simpler than an older method based on the reaction of $AgIF_6$ and $(CH_3)_4N^\oplus Cl^\ominus$: H. Meinert, H. Klamm, *Z. Chem. 8* (1986) 195.
[14] A. Parlow (Freie Universität Berlin), personal communication 1988.

Solvent-free Tris(trimethylsilyl)methyllithium**

By *Wolfgang Hiller, Marcus Layh,* and *Werner Uhl**

Bulky substituents stabilize compounds with unusual structural elements and properties. Recently we used this

[*] Dr. W. Uhl, M. Layh
Institut für Anorganische Chemie der Universität
Pfaffenwaldring 55, W-7000 Stuttgart 80 (FRG)
Dr. W. Hiller
Institut für Anorganische Chemie der Universität Tübingen

[**] This work was supported by the Deutsche Forschungsgemeinschaft and the Fonds der Chemischen Industrie.

principle to synthesize a dialane(**4**) with aluminum-aluminum bond,[1] which was protected from disproportionation by the very large bis(trimethylsilyl)methyl substituent. Tris(trimethylsilyl)methyl analogues could not be prepared before, because the starting compound, tris(trimethylsilyl)-methyllithium,[2] was hitherto described as an ether or amine adduct, which in the presence of aluminum halides gave decomposition products formed by ether fission.[3] The boron halides behave similarly; however, these difficulties are overcome by using trimethoxyborane instead of halide.[4] The application of this variation to aluminum compounds was not successful. We hoped to find a route to the desired organoaluminum compounds through solvent-free tris(trimethylsilyl)methyllithium **1**.

Usually solvent-free lithium compounds are obtained by the reaction of the corresponding organomercury compounds with elemental lithium. Because of the high steric shielding in bis[tris(trimethylsilyl)methyl]mercury,[5] the compound reacted only on treatment with ultrasound and UV radiation: the attack of the very stable tris(trimethylsilyl)methyl radical[6] on the solvent, *n*-hexane, yielded quantitatively tris(trimethylsilyl)methane [eq. (a)]. Bromotris(trimethylsilyl)methylmercury (**2**), readily available from equivalent amounts of mercury dibromide and alkyllithium, reacted with lithium without further activation at room temperature [eq. (b)]; again only the formation of trisilylmethane and an equal quantity of the dialkylmercury derivative was observed [Eq. (c)].

$$Hg[C(SiMe_3)_3]_2 + Li \xrightarrow[2.\ h\nu]{1.\ \text{ultrasound}} Li/Hg + 2\,HC(SiMe_3)_3 \quad (a)$$

$$HgBr_2 + LiC(SiMe_3)_3 \cdot 2\,THF \xrightarrow[-THF]{} \underset{\mathbf{2}}{Br{-}Hg{-}C(SiMe_3)_3} + LiBr \quad (b)$$

$$\underset{\mathbf{2}}{Br{-}Hg{-}C(SiMe_3)_3} + Li \longrightarrow LiBr + HC(SiMe_3)_3 + Hg[C(SiMe_3)_3]_2 \quad (c)$$

Finally a method described by *Bickelhaupt* et al. for the synthesis of 1,3-dilithiopropanes[7] from 1,3-HgBr derivatives and *tert*-butyllithium was successful. Probably for steric reasons the reaction of this organolithium compound with **2** stopped at *tert*-butyltris(trimethylsilyl)methylmercury, so we had to use the less voluminous *n*-butyllithium. Equation (d) shows the reaction steps for the synthesis of **1**; the isolable intermediate with mixed substituents, a dialkylmercury compound, reacted with excess *n*-butyllithium at 65–70 °C in the melt over a period of 15 h to afford the desired product, which was easily separated from the organomercury compound by recrystallization from *n*-pentane.

$$\underset{\mathbf{2}}{Br{-}Hg{-}C(SiMe_3)_3} + n\text{BuLi} \longrightarrow n\text{Bu}{-}Hg{-}C(SiMe_3)_3 + LiBr$$

$$n\text{Bu}{-}Hg{-}C(SiMe_3)_3 + n\text{BuLi} \xrightarrow{65-70\,^\circ C} \underset{\mathbf{1}}{LiC(SiMe_3)_3} + n\text{Bu}_2Hg \quad (d)$$

Compound **1** ignites spontaneously in air and with traces of oxygen characteristic red intermediates are formed. It may be kept under argon at room temperature, however, and is thermally very stable. Although cryoscopic molecular mass determination shows that **1** is monomeric in benzene, a low-intensity dimer peak is detected in the mass spectrum but only at low vaporization temperature and ionization energy (340 K, 20 eV). The monomer is not observed and appears only under more drastic conditions (380 K, 70 eV).

Crystals of **1** suitable for a single crystal X-ray structure determination were obtained by recrystallization from cyclopentane. Compound **1** crystallizes in the centrosymmetric space group $P\bar{1}$ with a Li_2C_2 dimer in the unit cell.[8] The Li_2C_2 four-membered ring includes a crystallographic inversion center (Fig. 1). The Li–C distances (average 230 pm) are almost identical and over 10 pm longer than in the THF adduct of **1**, which has linear C–Li–C bridges,[2] but lie well within the range expected for Li–C bonds.[9–11] The angles within the heterocycle are very different and the Li–C–Li angle of 61.6° is what is expected for a three-center geometry.[12] Interestingly the Si–C bonds to the anionic C atom (on average 185.8 pm) are significantly shorter than the bonds to the methyl groups (on average 188.0 pm); this is possibly caused by an interaction between the anionic C atoms and the silicon atoms.

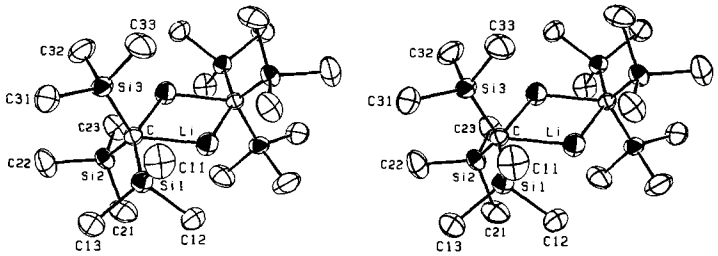

Fig. 1. Stereoview of **1** in the crystal (ORTEP, ellipses with 40% probability, hydrogen atoms omitted for clarity). Important distances [pm] and angles [°]: Li-C 229.1(6), Li'-C 230.3(6), C···C 394.6(5), Li···Li 235.3(9), C-Si1 185.7(3), C-Si2 184.4(3), C1-Si3 186.4(3), Si-C_{Me} 187.2(3)–189.4(4), C-Li-C 118.4(3), Li-C-Li 61.6(2).

In addition to the two bonds to the inner carbon atoms, every lithium atom shows close interaction with two C–H σ bonds (agostic interactions[13]), so that it is surrounded by four ligands in a distorted tetrahedral environment (Fig. 2).

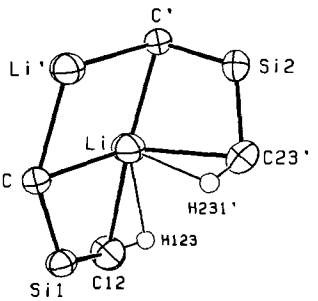

Fig. 2. Environment of the lithium atom. The primed atoms were found by reflection across the crystallographic symmetry center. Important distances [pm] and angles [°] not given in Fig. 1: C12-Li 254.1(7), H123-Li 224(4), C23'-Li 246.6(6), H231'-Li 219(4), C'···C-Si1 114.8(1), C'···C-Si2 98.5(1), C'···C-Si3 111.3(1).

Similar structural elements have been found in many organolithium compounds,[9, 10] including for example, the adduct of *n*-butyllithium and lithium-*tert*-butanolate,[14] lithium tetramethylboranate,[15] and lithium(μ-hydrido)tri(*tert*-butyl)alanate.[16]

Thus, besides the tetrameric structure for methyl- and ethyllithium,[9] the hexameric for (trimethylsilyl)methyl- and

cyclohexyllithium,[10] and the polymeric for bis(trimethylsilyl)methyllithium,[11] in dimeric tris(trimethylsilyl)methyllithium (**1**) a fourth structural type for alkyllithium derivatives occurs. Hitherto only in the presence of donor atoms could dimeric organolithium compounds be detected.[17]

The reaction of **1** with aluminum halides leads to crystalline products which are at present under investigation.

Experimental Procedure

2: 7.53 g (0.0209 mol) $HgBr_2$ was suspended in 125 mL diethyl ether and allowed to react slowly at 0 °C with a solution of 7.57 g (0.0198 mol) tris(trimethylsilyl)methyllithium · 2THF in 55 mL diethyl ether, which was added in two equal portions separated by 30 min of stirring. The reaction mixture was stirred for 3 h at room temperature; then the solvent was removed under vacuum, the residue taken up in 30 mL *n*-pentane and separated from LiBr by filtration. Colorless crystals of **2** precipitated from the filtrate at − 60 °C. Yield: 7.4 g (73%); m.p. (under Ar) 229 °C; molecular mass (cryoscopic, in benzene) found: 514, calc. 512.1 g mol^{-1}. ^1H NMR (60 MHz, C_6D_6): $\delta = 0.07$; IR (Nujol, CsBr plates): $\nu[cm^{-1}] = 1295$ w, 1265 s, 1255 s (δCH_3); 845 vs, 840 sh, 780 m (ϱCH_3); 675 s, 660 m, 615 m (νSiC); 460 vw, 360 vw, 310 (δSiC).

1: 11.82 g (0.0231 mol) **2** dissolved in 50 mL *n*-pentane was mixed at 0 °C with 18.5 mL (2.5M, 0.0462 mol) *n*-butyllithium in *n*-hexane, diluted with 50 mL *n*-pentane. The mixture was warmed to room temperature and stirred for 15 min, before the solvent was distilled off under vacuum and the highly viscous residue allowed to stand with stirring for 15 h at 65–70 °C. On cooling, the mixture crystallized. It was treated with 180 mL *n*-pentane and LiBr was filtered off. Colorless crystals of **1** precipitated from the filtrate at − 60 °C. Yield 4.43 g (81%); m.p. (under Ar) 214–215 °C (decomp.); mol. mass (cryoscopic, in benzene) found 242, calc. 238.2 g mol^{-1}; mass spectrum (340 K, 20 eV): 476.2 (1.6%) [$M^{\oplus}$], 245.2 (2.8) [$Li_2C(SiMe_3)_3$]; (385 K, 70 eV): 245.2 (1.7%) [$Li_2C(SiMe_3)_3$], 238.2 (12.4) 1/2 [$M^{\oplus}$]. ^1H-NMR (60 MHz, C_6D_6): $\delta = 0.22$; ^{13}C-NMR (62.896 MHz, C_6D_6): $\delta = 7.7$ ($SiMe_3$), central C atom not observed. IR (Nujol, CsBr plates): $\tilde{\nu}[cm^{-1}] = 1250$ vs (δCH_3), 1105 vw, 1000 w; 875 vs, 845 vs, 825 vs, 760 m (ϱCH_3); 715 w, 655 sh, 650 m, 600 m (νSiC); 522 m,br. (νLiC); 365 w,br., 320 w,br., 310 sh (δSiC + δLiC).

Received: October 24, 1990 [Z 4249 IE]
German version: *Angew. Chem. 103* (1991) 339

CAS Registry numbers:
1, 131704-10-4; **2**, 71248-01-6; $LiC(SiMe_3)_3 \cdot 2THF$, 131684-05-4.

[1] W. Uhl, *Z. Naturforsch. B43* (1988) 1113.
[2] Z. H. Aiube, C. Eaborn, *J. Organomet. Chem. 269* (1984) 217; C. Eaborn, P. B. Hitchcock, J. D. Smith, A. C. Sullivan, *J. Chem. Soc. Chem. Commun. 1983*, 827; N. H. Buttrus, C. Eaborn, P. B. Hitchcock, J. D. Smith, J. G. Stamper, A. C. Sullivan, *ibid. 1986*, 969.
[3] $Cl_2AlC(SiMe_3)_3$ has been reported; it was not detected during our investigations. C. Eaborn, M. N. El-Kheli, N. Retta, J. D. Smith, *J. Organomet. Chem. 249* (1983) 23.
[4] S. S. Al-Juaid, C. Eaborn, M. N. A. El-Kheli, P. B. Hitchcock, P. D. Lickiss, M. E. Molla, J. D. Smith, J. A. Zora, *J. Chem. Soc. Dalton Trans. 1989*, 447; R. Boese, P. Paetzold, A. Tapper, R. Ziembinski, *Chem. Ber. 122* (1989) 1057.
[5] F. Glockling, N. S. Hasmane, V. B. Mahale, J. J. Swindall, *J. Chem. Res. Miniprint 1977*, 1201.
[6] A. R. Bassindale, A. J. Bowles, M. A. Cook, C. Eaborn, A. Hudson, R. A. Jackson, A. E. Jukes, *J. Chem. Soc. Chem. Commun. 1970*, 559.
[7] J. W. F. L. Seetz, G. Schat, O. S. Akkerman, F. Bickelhaupt, *J. Am. Chem. Soc. 104* (1982) 6848.
[8] Crystal structure of **1**: Diffractometer CAD-4; $Mo_{K\alpha}$ radiation; room temperature; Programs VAXSDP and MOLEN; triclinic, $P\bar{1}$; $a = 888.30(7)$, $b = 900.38(4)$, $c = 1119.01(6)$ pm; $\alpha = 101.863(4)$, $\beta = 102.179(6)$, $\gamma = 109.576(5)°$; $V = 786.3$ Å^3; $Z = 1$; $\mu = 2.67$ cm^{-1}; crystal dimensions $0.2 \times 0.2 \times 0.4$ mm; $\theta/2\theta$-Scan; 2412 reflections $> 3\sigma(I)$; 236 parameters; atoms other than H anisotropically, H isotropically refined; $R = R_w = 0.043$. Further details of the crystal structure investigation may be obtained from the Fachinformationszentrum Karlsruhe, Gesellschaft für wissenschaftlich-technische Information mbH, W-7514 Eggenstein-Leopoldshafen 2 (FRG) on quoting the depository number CSD-54744, the names of the authors, and the journal citation.
[9] E. Weiss, T. Lambertsen, B. Schubert, J. K. Cockcroft, A. Wiedenmann, *Chem. Ber. 123* (1990) 79; H. Dietrich, *J. Organomet. Chem. 205* (1981) 291.
[10] B. Tecle, A. F. M. M. Rahman, J. P. Oliver, *J. Organomet. Chem. 317* (1986) 267; R. Zerger, W. Rhine, G. Stucky, *J. Am. Chem. Soc. 96* (1974) 6048.
[11] J. L. Atwood, T. Fjeldberg, M. F. Lappert, N. T. Luong-Thi, R. Shakir, A. J. Thorne, *J. Chem. Soc. Chem. Commun. 1984*, 1163.
[12] J. C. Huffman, W. E. Streib, *J. Chem. Soc. Chem. Commun. 1971*, 911; J. Malone, W. S. McDonald, *J. Chem. Soc. Dalton Trans. 1972*, 2646 and 2649.
[13] M. Brookhart, M. L. H. Green, L.-L. Wong, *Prog. Inorg. Chem. 36* (1988) 1.
[14] M. Marsch, K. Harms, L. Lochmann, G. Boche, *Angew. Chem. 102* (1990) 334; *Angew. Chem. Int. Ed. Engl. 29* (1990) 308.
[15] W. E. Rhine, G. Stucky, S. W. Peterson, *J. Am. Chem. Soc. 97* (1975) 6401.
[16] W. Uhl, *Z. Anorg. Allg. Chem. 570* (1989) 37.
[17] W. Bauer, G. Müller, R. Pi, P. von R. Schleyer, *Angew. Chem. 98* (1986) 1130; *Angew. Chem. Int. Ed. Engl. 25* (1986) 1103; D. Stalke, K. H. Whitmire, *J. Chem. Soc. Chem. Commun. 1990*, 833; W. Moene, M. Vos, F. J. J. de Kanter, G. W. Klumpp, A. L. Spek, *J. Am. Chem. Soc. 111* (1989) 3463.

$[InAs_3]^{6\ominus}$ and $[AlSb_3]^{6\ominus}$, Trigonal Planar Anions in Cs_6InAs_3 and Cs_6AlSb_3**

By *Wolfgang Blase, Gerhard Cordier, Karl Peters, Mehmet Somer*, and *Hans Georg von Schnering**

In the series of oxoanions of the earth metals, anions with trigonal-planar coordination are so far known only in the case of borates. If the $O^{2\ominus}$ ligands are replaced by isoelectronic $As^{3\ominus}$ or $Sb^{3\ominus}$ ligands also the homologues of boron can be trigonal-planar coordinated. Hitherto, only compounds were known in which such AX_3 units are condensed to form large anionic assemblies. Thus, in the crystal structures of K_2GaSb_2 or Cs_2GaSb_2,[1] $GaSb_3$ units are coupled via common antimony atoms and antimony-antimony bonds into chains, which are isostructural with BS_2.[2]

The crystal structures of $K_{20}Ga_6Sb_{12.66}$ and $K_{20}Ga_6As_{12.66}$[3] contain the corner-sharing trinuclear anions $[Ga_3Sb_6]^{9\ominus}$ and $[Ga_3As_6]^{9\ominus}$, respectively, and those of Cs_3AlP_2 and Cs_3GaP_2 the dinuclear edge-sharing moieties $[Al_2P_4]^{6\ominus}$ and $[Ga_2P_4]^{6\ominus}$.[4]

With the synthesis of Cs_6InAs_3 and Cs_6AlSb_3 we have now also succeeded in characterizing for the first time compounds containing the units $[InAs_3]^{6\ominus}$ and $[AlSb_3]^{6\ominus}$, respectively. Both compounds are formed as shiny metallic crystals from the elements at 950 K.[5] In the planar anions[6] (Fig. 1) the deviation from D_{3h} symmetry is only slight ($119.0 < \beta < 121.8°$). The bond lengths $d_{Al-Sb} = 261.8(3)$, 262.3(3) and 267.0(4) pm and $d_{In-As} = 258.6(3)$, 261.4(3) and 264.5(3) pm, respectively, lie, according to the *Pauling*[7] bond order, in the range of single bond lengths.

In the crystal the Cs atoms form chains of elongated trigonal prisms, condensed in bundles of four along [010]. The atoms of the trigonal-planar anions $[InAs_3]^{6\ominus}$ and $[AlSb_3]^{6\ominus}$ align the bundles of four Cs_6-prisms centrally to give the polymeric structure $^1_\infty\{Cs_{12/2}[MX_3]\}$. The packing of these bundles essentially corresponds to a unidimensional hexagonal rod packing. The periphery of the bundles consists of six elongated rectangular faces. The space between the rods consists of empty half-cubes (partition along the (110) face of

[*] Prof. Dr. H. G. von Schnering, Dr. K. Peters, Dr. M. Somer
Max-Planck-Institut für Festkörperforschung
Heisenbergstrasse 1, W-7000 Stuttgart 80 (FRG)
Dipl.-Ing. W. Blase, Dr. G. Cordier
Eduard-Zintl-Institut der Technischen Hochschule
Hochschulstrasse 10, W-6100 Darmstadt (FRG)

[**] We thank *W. König*, Stuttgart, for recording the IR spectra. This work was supported by the Deutsche Forschungsgemeinschaft, the Fonds der Chemischen Industrie, and the Vereinigung von Freunden der Technischen Hochschule Darmstadt.

the cube), and empty doubly capped trigonal prisms. The half-cubes are each bounded by two prism bundels, while the capped prisms are each bounded by four prism bundles. The stacking of the trigonal prisms extends the coordination between Cs and As(Sb) atoms.

The X atoms are each bound to an M atom and are coordinated by seven Cs atoms (d_{Sb-Cs} = 380.4–443.7, d_{As-Cs} = 358.7–427.6 pm). The Cs atoms exhibit 5- and 6-coordination towards X.

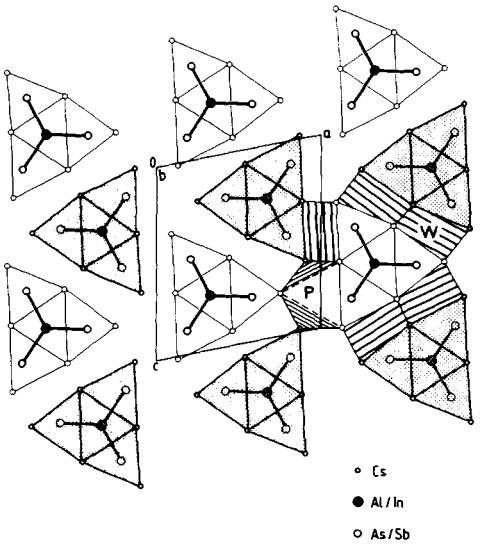

Fig. 1. Projection of the crystal structure of the compounds Cs_6InAs_3 and Cs_6AlSb_3 on (010). Lines of different thickness mark the positions of the atoms with $y = 0$ and $y = 1/2$; the upper prism bundles are shaded. The empty halves of cubes W and the empty capped prisms P on the right-hand side are emphasized by hatching.

The anions $[AlSb_3]^{6\ominus}$ and $[InAs_3]^{6\ominus}$ are members of an isosteric series with 24 valence electrons, which extends via $[SiP_3]^{5\ominus}$ in Cs_5SiP_3 or $[SiAs_3]^{5\ominus}$ in Cs_5SiAs_3[8] through to the oxoanions $[BO_3]^{3\ominus}$, $[CO_3]^{2\ominus}$ and $[NO_3]^{\ominus}$. Starting with the D_{3h} symmetry of an isolated $[MX_3]^{6\ominus}$ unit, the vibration analysis yields $\Gamma_{vib} = A_1' + A_2'' + 2E'$, whereby A_1' is only Raman active and A_2'' only IR-active. Vibrations of type E′ are both IR-active and Raman-active.

In the crystal (factor group C_{2h}, point group Cs) the symmetry of the planar $[MX_3]^{6\ominus}$-group is perturbed. This leads to splitting of the degenerated vibrations of type E′ and partial removal of the inactivity of the A_1' and A_2'' vibrations in the Raman or IR spectrum. The effects are, however, small, but allow interpretation in terms of an only slightly distorted D_{3h} symmetry.

In accord with the reduction in symmetry four bands are observed above 100 cm^{-1} in the IR spectra[9]; these can be assigned to the three fundamental vibrations $A_1' + A_2'' + E'$ (Fig. 2). The antisymmetric valence vibration ν_3 (E′) splits, and in each case two separate, very strong bands are observed at 318 and 293 ($[AlSb_3]^{6\ominus}$) and 215 and 197 cm^{-1} ($[InAs_3]^{6\ominus}$), respectively. The moderately strong bands at 181 cm^{-1} ($[AlSb_3]^{6\ominus}$) and 99 cm^{-1} ($[InAs_3]^{6\ominus}$) are assigned to the non-planar vibration A_2''. The IR inactive vibration $\nu_1(A')$ observed in the case of D_{3h} symmetry appears, as expected, in each case as weak intensity band at 132 cm^{-1} ($[AlSb_3]^{6\ominus}$) and 171 cm^{-1} ($[InAs_3]^{6\ominus}$), respectively. The observed wave numbers are comparable with the corresponding valence vibrations ν_1 of the isosteric molecules AlI_3 ($\tilde{\nu}$ = 156 cm^{-1})[10] and $InBr_3$ ($\tilde{\nu}$ = 212 cm^{-1}).[11] The weak intensity deformation vibration ν_4 (E′) could not be localized because of complete superposition with lattice vibrations. From the frequencies[12] one obtains, after using an approximation procedure,[13] values of 0.99 and 1.07 N cm^{-1} for the valence force constants f, 0.13 and 0.15 N cm^{-1} for the interaction constants f', and 0.16 and 0.15 N cm^{-1} for the force constants of the non-planar vibration f_γ' of $[AlSb_3]^{6\ominus}$ and $[InAs_3]^{6\ominus}$, respectively. Interesting is a comparison of

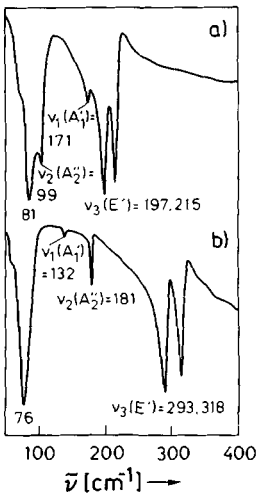

Fig. 2. FIR spectra of Cs_6InAs_3 (a) and Cs_6AlSb_3 (b).

these values with the f values 1.74 and 1.91 N cm^{-1} of the isosteric molecules AlI_3[10] and $InBr_3$.[14] The marked decrease in the valence force constants (ca. 45%) for the anions is consistent with previous observations, according to which an increase in formal ionic charge weakens the bonds and thus reduces the frequencies and force constants. Raman spectra could not be obtained because of ready decomposition in laser light.

Received: October 27, 1990 [Z 4250 IE]
German version: *Angew. Chem. 103* (1991) 335

CAS Registry numbers:
Cs_6InAs_3, 131863-59-7; Cs_6AlSb_3, 131863-60-0; Cs, 7440-46-2; In, 7440-74-6; Al, 7429-90-5; Sb, 7440-36-0; As, 7440-38-2.

[1] G. Cordier, H. Ochmann, H. Schäfer, *J. Less-Common Met. 119* (1986) 291; *III. European Conf. Solid State Chem.*, Regensburg 1986.
[2] B. Krebs, H. U. Hürter, *Acta Crystallogr. Sect. A 37* (1981) 163; B. Krebs, *Angew. Chem. 95* (1983) 113; *Angew. Chem. Int. Ed. Engl. 22* (1983) 113.
[3] G. Cordier, H. Ochmann, *Z. Naturforsch. B 45* (1990) 277.
[4] M. Somer, M. Hartweg, L. Walz, D. Thiery, T. Popp, H. G. von Schnering, *Z. Kristallogr.*, in press.
[5] Weighing was carried out in welded Nb ampoules with a Cs excess of 30% compared to the stoichiometric ratio. The samples were heated to 950 K within 4 h and then allowed to cool to 298 K in 40 h. The excess Cs was removed by distillation at 475 K in a high vacuum. Both compounds form shiny metallic prisms, which react on exposure to air giving products whose composition is still unknown.
[6] Crystal structure data for Cs_6AlSb_3: Measurement: Nicolet R3m/V four-circle diffractometer, graphite monochromator, scintillation counter, $3.5° \leqq 2\theta \leqq 55°$, Wyckoff scan, $Mo_{K\alpha}$ radiation. Evaluation: Nicolet SHELXTL PLUS-76, direct methods, least squares errors, full matrix, 62 free variables. a = 1084.5(2), b = 650.7(2), c = 1270.7(4) pm, β = 100.95(2)°; space group $P2_1/m$; Z = 2; R_{aniso} = 0.031 for $N(hkl)$ = 1939.

Crystal structure data for Cs_6InAs_3: Measurement: PW1100 four-circle diffractometer, graphite monochromator, scintillation counter, $5° \leq 2\theta \leq 50°$, $\theta/2\theta$ scan, $Mo_{K\alpha}$ radiation: SHELXS-86, SHEL-76, direct methods, least squares errors, full matrix, 61 free variables. $a = 1046.9(3)$, $b = 635.6(1)$, $c = 1220.8(2)$ pm, $\beta = 101.3(1)°$; space group $P2_1/m$; $Z = 2$; $R_{aniso} = 0.057$ for $N(hkl) = 1379$; for further details see *Z. Kristallogr.*, in press.

[7] L. Pauling: *Die Natur der chemischen Bindung*, Verlag Chemie, Weinheim 1962, p. 210–227; *The Nature of Chemical Bond*, Cornell University Press, Ithaca, NY, USA 1960.

[8] B. Eisenmann, J. Klein, M. Somer, *Angew. Chem. 102* (1990) 92; *Angew. Chem. Int. Ed. Engl. 29* (1990) 87.

[9] The IR pellet was embedded in polyethylene.

[10] C. E. Sjogren, P. Klaeboe, E. Rytter, *Spectrochim. Acta Part A 40* (1984) 457.

[11] I. R. Beattie, J. R. Horder, *J. Chem. Soc. A 1969*, 2655.

[12] In each case the frequencies of the ν_3 vibrations were determined from the respective band pairs.

[13] I. R. Beattie, H. E. Blayden, S. M. Hall, S. N. Jenny, J. S. Ogden, *J. Chem. Soc. Dalton Trans. 1976*, 666.

[14] S. J. Cyvin, A. Phongsatha, *Spectrosc. Lett. 8* (1975) 71.

Synthesis and Crystal Structure of $Br_5^{\oplus}MF_6^{\ominus}$ (M = As, Sb)**

By *Hans Hartl,** *Joachim Nowicki,* and *Rolf Minkwitz*

Homonuclear iodine cations $I_n^{\oplus}$ (n = 2,3,5,7)[1] have already been the subject of numerous investigations; in contrast little is known about the analogous bromine ions. Only the crystal structure of $Br_2^{\oplus}Sb_3F_{16}^{\ominus}$[2] and the syntheses of $Br_3^{\oplus}X^{\ominus}$ ($X^{\ominus} = AsF_6^{\ominus}$,[3] $SO_3F^{\ominus}$,[4] $[Au(SO_3F)_4]^{\ominus}$)[5] and $Br_5^{\oplus}[Au(SO_3F)_4]^{\ominus}$[5] have been reported.

Liquid bromine reacts with the extremely mild and selective fluorinating reagent $XeF^{\oplus}MF_6^{\ominus}$ (M = As, Sb) at room temperature in a complex reaction sequence to give $Br_5^{\oplus}MF_6^{\ominus}$ [Eq. (a)].

$$3\,XeF^{\oplus}MF_6^{\ominus} + 8\,Br_2 \xrightarrow{\text{room temperature}} 3\,Br_5^{\oplus}MF_6^{\ominus} + 3\,Xe + BrF_3 \quad (a)$$

In this reaction $Br_3^{\oplus}$ can be detected as intermediate by vibration spectroscopy[6] and BrF_3 as by-product by ^{19}F-NMR spectroscopy.[7] Only three lines (272, 220, 170 cm^{-1}) are observed in the Raman spectrum of $Br_5^{\oplus}AsF_6^{\ominus}$, consistent with the C_{2h} symmetry of the $BR_5^{\oplus}$ ion, and in the IR spectrum only three (290, 275, 185 cm^{-1}) of the expected six bands are unequivocally assignable.

In the pentahalides $I_5^{\ominus}$, $[I_3Cl_2]^{\ominus}$ and $[I_3Br_2]^{\ominus}$[8] the halogen atoms form V-shaped anions, whereas the centrosymmetric pentabromonium ion $Br_5^{\oplus}$ has a Z-shaped structure analogous to the cations $I_5^{\oplus}$, $[I_3Cl_2]^{\oplus}$ and $[I_3Br_2]^{\oplus}$[1a, 9] (Fig. 1). In all ions there are two short bonds between the external halogen atoms and two longer bonds to the central halogen atom. Thus, the array of halogen atoms can formally be described as an adduct of two halogen or interhalogen molecules with a central halide or halonium ion. In accord with the electron pair repulsion model (VSEPR)[10] the central halogen atom in the pentahalide(− 1) has an AX_2E_2 coordination with bent structure, whereas that in the pentahalogen(+ 1) ion shows an AX_2E_3 coordination with formation of a linear 3c,4e bond. The Br2–Br3 bond lengths (2.275(1) Å in $Br_5^{\oplus}AsF_6^{\ominus}$ and 2.268(2) Å in $Br_5^{\oplus}SbF_6^{\ominus}$) are somewhat shorter than in crystalline bromine (2.289(3) Å at − 100 °C[11]). The bond lengths to the central Br1 on the other hand (2.514(1) and 2.512(1) Å) are larger, and are comparable with those in linear anionic $Br_3^{\ominus}$ with 3c,4e bonding (e.g. $[Cs(AuBr_4)_2]Br_3$ (2.540(2) and 2.562(1) Å[12]).

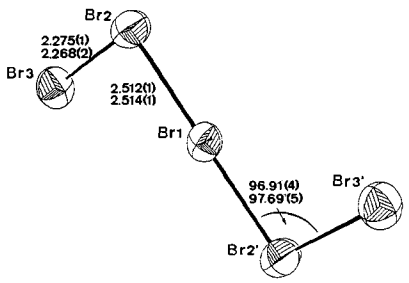

Fig. 1. ORTEP plot of the $Br_5^{\oplus}$ ion [13]. Bond lengths [Å] and bond angles [°]: top row of figures refer to $Br_5^{\oplus}AsF_6^{\ominus}$, bottom row of figures to $Br_5^{\oplus}SbF_6^{\ominus}$.

The most stable geometry for $X_5^{\oplus}$ cations seems to be the planar *trans*-configuration as found in $I_5^{\oplus}$ and $Br_5^{\oplus}$. This is consistent with STO-3G calculations, which show that all other rotamers are energetically unfavorable.[1a] In analogy to $[I_3Cl_2]^{\oplus}$, however, the energy differences are so small that

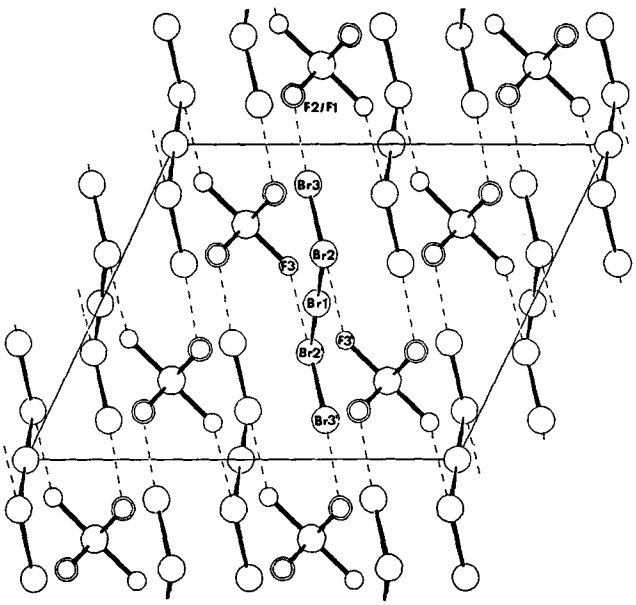

Fig. 2. Structure of $Br_5^{\oplus}MF_6^{\ominus}$ (M = As, Sb) in the crystal (projection in the [010] direction). The fluorine atoms F1 and F2 of the $MF_6^{\ominus}$ octahedron are superposed in this projection; bond lengths [Å], bond angles [°]: As-F1 = 1.727(7), As-F2 = 1.699(8), As-F3 = 1.730(5), Br2-F3 = 2.847(6), Br3-F1 = 2.782; F-As-F = 88.85–91.00° and 177.5–179.2, Br2-Br3-F1 = 173.5(2), Br3-Br2-F3 = 178.0(2); Sb-F1 = 1.879(8), Sb-F2 = 1.857(9), Sb-F3 = 1.874(6), Br2-F3 = 2.768(7), Br3-F1 = 2.767(7); Br2-Br3-F1 = 174.5(2), Br3-Br2-F3 = 178.1(2).

[*] Prof. Dr. H. Hartl
Institut für Anorganische und Analytische Chemie der Freien Universität Fabeckstrasse 34–36, W-1000 Berlin 33 (FRG)
Dipl.-Chem. J. Nowicki, Prof. Dr. R. Minkwitz
Institut für Anorganische Chemie der Universität Dortmund (FRG)

[**] This work was supported by the Minister für Wissenschaft und Forschung des Landes Nordrhein-Westfalen and the Fonds der Chemischen Industrie.

in the presence of a suitable counterion,[9] deviations from the planar arrangement are expected.

In $Br_5^{\oplus}AsF_6^{\ominus}$ and $Br_5^{\oplus}SbF_6^{\ominus}$ the anions and cations are, in each case, coupled by four fluorine atoms of the $MF_6^{\ominus}$ octahedron to form layers (Fig. 2). The Br–Br···F moieties are approximately linear, the fluorine atoms participating in the anion–cation contacts have As–F and Sb–F distances ca. 0.03 Å longer than those not participating in the contacts. Comparable interionic contacts also occur in other polyhalogen cations.[1a, 1c, 2b]

Experimental

Br_2 (ca. 5 mL) was distilled under an inert gas onto $XeF^{\oplus}MF_6^{\ominus}$ (M = As, Sb) in a two-limbed ampule. After ca. 3–4 hours at room temperature a brown solid of $Br_3^{\oplus}MF_6^{\ominus}$ separated, which, within two days, formed rectangular dark brown crystals. After decanting off the liquid Br_2, the solid was pumped dry.

Received: September 14, 1990 [Z 4181 IE]
German version: *Angew. Chem. 103* (1991) 311

CAS Registry numbers:
$XeF^{\oplus}AsF_6^{\ominus}$, 26024-71-5; $XeF^{\oplus}SbF_6^{\ominus}$, 36539-18-1; Br_2, 7726-95-6; $Br_5^{\oplus}AsF_6^{\ominus}$, 131906-72-4; $Br_5^{\oplus}SbF_6^{\ominus}$, 131906-73-5; $Br_3^{\oplus}AsF_6^{\ominus}$, 12429-01-5; $Br_3^{\oplus}SbF_6^{\ominus}$, 131906-74-6.

[1] a) A. Apblett, F. Grein, J. P. Johnson, J. Passmore, P. S. White, *Inorg. Chem. 25* (1986) 422; b) C. G. Davies, R. J. Gillespie, P. R. Ireland, J. M. Sowa, *Can. J. Chem. 52* (1974) 2048; c(J. Passmore, G. Sutherland, P. S. White, *Inorg. Chem. 20* (1981) 2169; d) J. Passmore, P. Taylor, T. Whidden, P. S. White, *Can. J. Chem. 57* (1979) 968; e) R. J. Gillespie, R. Kappor, R. Faggiani, C. J. L. Lock, M. Murchie, J. Passmore, *J. Chem. Soc. Chem. Commun. 1973*, 8.

[2] a) A. J. Edwards, G. R. Jones, *J. Chem. Soc. A 1971*, 2318; b) A. J. Edwards, G. R. Jones, R. J. C. Sills, *Chem. Commun. 1968*, 527.

[3] O. Glemser, A. Šmalc, *Angew. Chem. 81* (1969) 531; *Angew. Chem. Int. Ed. Engl. 8* (1969) 517.

[4] a) W. W. Wilson, J. M. Winfield, F. Aubke, *J. Fluorine Chem. 7* (1976) 245; b) R. J. Gillespie, M. J. Morton, *Chem. Commun. 1968*, 1565; c) *Inorg. Chem. 11* (1972) 586.

[5] K. C. Lee, F. Aubke, *Inorg. Chem. 19* (1980) 119.

[6] R. Minkwitz, J. Nowicki, W. Sawodny, H. Härtner, unpublished results.

[7] $\delta(BrF_3) = -24.03$, measurement in liquid Br_2 at room temperature, 4 mm-polytetrafluoroethylene tube, standard $CFCl_3$.

[8] a) I. Broekema, E. E. Havinga, E. H. Wiebenga, *Acta Crystallogr. 10* (1957) 596; b) A. Parlow, H. Hartl, *Acta Crystallogr. Sect B 35* (1979) 1930; c) *Z. Naturforsch. B 40* (1985) 45.

[9] S. Pohl, W. Saak, *Z. Naturforsch. B 36* (1981) 283.

[10] a) R. J. Gillespie: *Molecular Geometry*, Van Nostrand-Reinhold, London 1972; b) T. Birchall, R. D. Myers, *Inorg. Chem. 21* (1982) 213.

[11] B. M. Powell, K. M. Heal, B. H. Torrie, *Mol. Phys. 53* (1984) 929.

[12] B. Lehnis, J. Strähle, *Z. Naturforsch. B36* (1981) 1504.

[13] X-ray structure analysis of $Br_5^{\oplus}AsF_6^{\ominus}$ and $Br_5^{\oplus}SbF_6^{\ominus}$ at −150 °C, Enraf-Nonius CAD4 single-crystal diffractometer, $Mo_{K\alpha}$ radiation, graphite monochromator, $\omega/2\theta$ scan, $2\theta \leq 60°$. Refinement of structures with scattering factors for neutral atoms, absorption correction by DIFABS [14], isotropic extinction factors[15] and weighting of the reflections with $w = [\sigma^2(F_0)]^{-1}$.
$Br_5^{\oplus}AsF_6^{\ominus}$: $M = 588.46$, monoclinic, $C2/c$, $a = 12.687(3)$, $b = 8.693(3)$, $c = 10.170(5)$ Å, $\beta = 115.82(4)°$, $V = 1009.7$ Å^3, $Z = 4$, $\rho_{calcd} = 3.871$ g cm^{-2}, $\mu(Mo_{K\alpha}) = 24.55$ mm^{-1}, $F(000) = 262$. 2446 measured reflections, 1475 independent and 1159 observed ($F_0 > 3\sigma$); isotropic extinction factor = 0.221; $R = 0.039$, $R_w = 0.047$.
$Br_5^{\oplus}SbF_6^{\ominus}$: $M = 635.29$, monoclinic, $C2/c$, $a = 12.821(3)$, $b = 8.884(3)$, $c = 10.136(2)$ Å, $\beta = 115.00(5)°$, $V = 1046.3$ Å^3, $Z = 4$, $\rho_{calcd} = 4.033$ g cm^{-3}, $\mu(Mo_{K\alpha}) = 24.75$ mm^{-1}, $F(000) = 280$. 3987 measured reflections, 1527 independent and 1297 observed ($F_0 > 3\sigma$); isotropic extinction factor 0.235; $R = 0.048$, $R_w = 0.055$.
Further details of the crystal structure investigations are available on request from the Fachinformationszentrum Karlsruhe, Gesellschaft für wissenschaftlich-technische Information mbH, W-7514 Eggenstein-Leopoldshafen 2 (FRG), on quoting the depository number CSD-55092, the names of the authors, and the journal citation.

[14] N. Walker, D. Stuart, *Acta Crystallogr. Sect. A 39* (1983) 158.

[15] W. H. Zachariasen, *Acta Crystallogr. 23* (1967) 558.

$(I_3O_6)^{\oplus}$, a Novel Polyoxo Cation of Iodine**

By *Anette Rehr* and *Martin Jansen**

Dedicated to Professor Rolf Appel on the occasion of his 70th birthday

More on the basis of speculation than on unequivocal structural and analytical data, I_4O_9 and I_2O_4 are usually described as $I(IO_3)_3$[1] and $(IO)IO_3$.[1a, b, 2] Equally vague is the situation regarding the ternary derivatives of these pseudobinary oxides, which are sometimes formulated as adducts, e.g. $I_2O_4 \cdot 3SO_3$,[3] and sometimes as salts, like $(IO_2)_2(S_2O_7)$.[4] So far only the existence and structure of the polymeric iodosyl cation $(IO)_n^{n\oplus}$[5] have been established. In all other cases it was at best possible to deduce the common structural units for the first time from vibration spectra.[2, 4a, 6] In connection with our studies on halogen-oxygen compounds[7] we have now also directed our attention to the frequently mixed valence, iodine compounds. Because of the complex phase relationships and structures it was essential to prepare the compounds in the crystalline state and as pure phases.

By thermal decomposition of H_5IO_6 in conc. phosphoric acid and subsequent addition of pure sulfuric acid we not only succeeded in growing single crystals, but also in synthesizing preparative amounts of the previously unknown $(I_3O_6)(HSO_4)$. Not unexpectedly, with the numerous neighboring phases in the system investigated, a precise control of the reaction conditions (temperature, atmosphere, time) is absolutely necessary for reproducibility of the experiments. We achieved the best results using a metal bath as source of heat.[8]

The crystal structure[9] consists of two clearly separable moieties, a cationic one of the composition $(I_3O_6)_n^{n\oplus}$ and an anionic one ($HSO_4^{\ominus}$), between which there exist predominantly electrostatic interactions; the novel isopolycation $(I_3O_6)_n^{n\oplus}$ contains mixed-valence iodine. The pyramidal (pseudotetrahedral) environment of the crystallographically independent iodine atoms I1–I4 with distances and angles as found in numerous other iodates(v),[10] clearly points to I^V, while the square planar (double pseudooctahedral) coordination of I5 and I6 by oxygen characterizes these iodine atoms as I^{III}. Since this is, to our knowledge, the first reported planar IO_4 structure group, and since no structural data for other analogous species such as $IF_4^{\ominus}$ in KIF_4 are available, a categorizing of the distances found is not possible. Although the O–I–O bond angles in particular deviate considerably from the ideal geometry, the IO_4 unit deviates at a maximum of only 4 pm in each case from the best plane through the five atoms. The structural groups described here are coupled via all four corners of the polyhedron around I^{III} and two of the three oxygen atoms around I^V to give a $^1_\infty$ ribbon (Fig. 1). The structural groups in this network, which are identifiable as typical for tri- and pentavalent iodine respectively, could mislead one to formulate the cationic moiety of the structure as $[I^{3\oplus}(IO_3^{\ominus})_2]^{\oplus}$ or $[(IO^{3\oplus})_2IO_4^{5\ominus}]^{\oplus}$. This would indeed furnish a perfectly clear interpretation of the make-up of the cation, but would not account for the bonding properly. The I–O bond lengths and the pronounced steric effect of the free electron pair point to a dominant covalent bonding in the I–O structural moiety.

[*] Prof. Dr. Martin Jansen, Dipl.-Chem. Anette Rehr
Institut für Anorganische Chemie der Universität
Gerhard-Domagk-Strasse 1, W-5300 Bonn 1 (FRG)

[**] This work was supported by the Fonds der Chemischen Industrie.

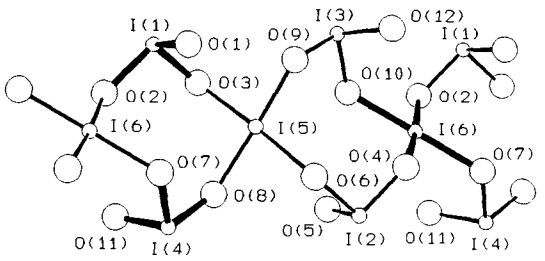

Fig. 1. Crystal structure of the isopolycation $(I_3O_6)_n^{n\oplus}$. Bond lengths [pm] around I^V: I1-O1 179.3, I1-O2 186.7, I1-O3 182.4, I2-O4 182.4, I2-O5 176.8, I2-O6 186.9, I3-O9 185.0, I3-O10 184.1, I3-O12 177.0, I4-O7 182.3, I4-O8 182.5, I4-O11 177.2; about I^{III}: I5-O3 211.2, I5-O6 217.8, I5-O8 215.6, I5-O9 209.7, I6-O2 212.8, I6-O4 213.2, I6-O7 212.1, I6-O10 214.1; angles [°] about I^V 94.0–105.0, mean value 98.5; about I^{III} 83.9–97.5, mean value 90.0 and 175.1–179.3, mean value 176.9; about I^{III}-O-I^V 122.8–133.2, mean value 126.2.

Although, as expected, the positions of the hydrogen atoms next to the strongly scattering iodine atoms could not be determined, the oxygen atoms which participate in H-bridge bonding can be identified on the basis of crystallochemical considerations: from the S–O and "intermolecular" O–O distances it follows that H-bridge bonding only occurs between the sulfate anions, never in (or to) the $(I_3O_6)^{\oplus}$ polycation. The SO_4 anions are in each case coupled by H-bridges one-dimensionally along [100]. The cationic and anionic structural moieties are arranged in layers parallel to (010) (Fig. 2).

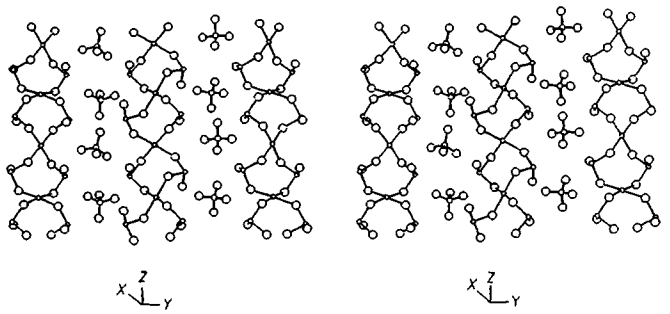

Fig. 2. Stereodiagram of $(I_3O_6)(HSO_4)$ in the crystal.

The possible existence of an iodyl cation $(IO_2)^{\oplus}$ has been discussed by several authors,[1a, 4a, 6a, 11] but in no case has it been confirmed. The X-ray powder data and vibration spectra reported in previous cases give no indication that the compound described here is identical with any of those investigated earlier.

The structure and existence of $(I_3O_6)HSO_4 \triangleq I(IO_3)_2HSO_4$ can be regarded as supporting evidence for the constitution postulated for $I_4O_9 \triangleq I(IO_3)_3$.

Received: September 19, 1990 [Z 4191 IE]
German version: *Angew. Chem. 103* (1991) 327

CAS Registry numbers:
H_5IO_6, 10450-60-9; H_3PO_4, 7664-38-2; H_2SO_4, 7664-93-9; $(I_3O_6)(HSO_4)$, 131589-69-0.

[1] a) M. Schmeisser, K. Brändle, *Adv. Inorg. Chem. Radiochem. 5* (1963) 41–89; b) M. Dratovsky, L. Pacesova, *Russ. Chem. Rev. (Engl. Transl.) 37* (1968) 243–254; H. Kappeler, *Ber. Dtsch. Chem. Ges. 44* (1911) 3496–3501; c) F. Fichter, H. Kappeler, *Z. Anorg. Chem. 91* (1915) 134–144.
[2] J. H. Wise, H. H. Hannan, *J. Inorg. Nucl. Chem. 23* (1961) 31–32.
[3] M. M. P. Muir, *J. Chem. Soc. 1909*, 656–662.
[4] a) H. Siebert, U. Woerner, *Z. Anorg. Allg. Chem. 429* (1977) 39–46; b) H.-A. Lehmann, H. Hesselbarth, *ibid. 299* (1959) 51–57.
[5] S. Furuseth, K. Selte, H. Hope, A. Kjekshus, B. Klewe, *Acta Chem. Scand. Ser. A 28* (1974) 71–76.
[6] a) H. Siebert, M. Handrich, *Z. Anorg. Allg. Chem. 426* (1976) 173–183; b) W. E. Dasent, T. C. Waddington, *J. Chem. Soc. 1960*, 3350–3356 und *J. Inorg. Nucl. Chem. 25* (1963) 132–133; c) O. H. Ellestad, T. Woldbaek, A. Kjekshus, P. Klaeboe, K. Selte, *Acta Chem. Scand. Ser. A 35* (1981) 155–164.
[7] K. M. Tobias, M. Jansen, *Z. Anorg. Allg. Chem. 550* (1987) 16–26; K. M. Tobias, M. Jansen, *Angew. Chem. 98* (1986) 994–995; M. Jansen, K. M. Tobias, H. Willner, *Naturwissenschaften 73* (1986) 734–735; M. Jansen, G. Schatte, K. M. Tobias, H. Willner, *Inorg. Chem. 27* (1988) 1703–1706.
[8] 10 mL of conc. phosphoric acid contained in a glass beaker was dehydrated for 1/2 h in a metal bath at 270–280 °C. After cooling, 3 g of pulverized H_5IO_6 were admixed and heating continued at 310–330 °C until the first appearance of iodine vapor (duration about 10 min). The mixture was then cooled under vacuum in a desiccator and was allowed to stand for a few hours. Subsequently, the mixture was treated with 50 mL of pure H_2SO_4, stirred, transferred to an ampoule, and the ampoule and contents tempered for a week at 60 °C in a resistance furnace. After pouring off the supernatant acid mixture, the residue was dried on a porous plate over conc. H_2SO_4 in a desiccator. The crystals are hygrosyopic; they were sealed under argon in a capillary for the X-ray structure investigations.
[9] Crystal structure: *Pna* 2_1; $a = 888.6(6)$, $b = 2043.9(12)$, $c = 979.2(8)$ pm, $Z = 8$, four-circle diffractometer Enraf-Nonius; $Mo_{K\alpha}$; data collection at room temperature, 5052 independent reflections, 4354 with $F > 2\sigma(F)$; $R = 0.087$, $R_w = 0.056$. Further details of the crystal structure investigation are available on request from the Fachinformationszentrum Karlsruhe, Gesellschaft für wissenschaftlich-technische Information mbH, W-7514 Eggenstein-Leopoldshafen 2 (FRG), on quoting the depository number CSD-54907, the names of the authors, and the journal citation.
[10] Typically: 3 × 181 pm, 3 × 98°, I. D. Brown, *J. Solid State Chem. 11* (1974) 214–233.
[11] M. Schmeisser, K. Lang, *Angew. Chem. 67* (1955) 156; M. Schmeisser, D. Naumann, R. Renk, *Z. Anorg. Allg. Chem. 470* (1980) 84–88; G. Kempe, D. Robus, *Z. Chem. 5* (1965) 394–395; J. J. Pitts, S. Kongpricha, A. W. Jache, *Inorg. Chem. 4* (1965) 257–259; F. Aubke, G. H. Cady, C. H. L. Kennard, *ibid. 3* (1964) 1799–1800; J. R. Dalziel, H. A. Carter, F. Aubke, *ibid. 15* (1976) 1247–1251; E. E. Aynsley, R. Nichols, P. L. Robinson, *J. Chem. Soc. 1953*, 623–626; R. J. Gillespie, J. B. Senior, *Inorg. Chem. 3* (1964) 972–977 und 440–444; J. Arotsky, H. C. Mishra, M. C. R. Symons, *J. Chem. Soc. 1962*, 2582–2591; E. E. Aynsley, S. Sampath, *ibid. 1959*, 3099.

The Neutral Transition Metal Thiolates $[M(SAr)_2]_2$ (M = Mn, Fe or Co, Ar = 2,4,6-*t*-$Bu_3C_6H_2$)**

By *Philip P. Power** and *Steven C. Shoner*

The chemistry of transition metal thiolate complexes constitutes a large and rapidly expanding area of chemistry.[1, 2] The relevance of such complexes to the structure, bonding and function of biologically active reaction centers in metalloproteins such as ferredoxins, nitrogenases, blue copper proteins and metallothioneins has provided a significant portion of the impetus for their study.[3] A characteristic feature of the vast majority of well-characterized homoleptic transition metal thiolates is that they are ionic.[1–3] Most typically, the transition metal is surrounded by four thiolate ligands, and it has approximately tetrahedral coordination. This unit may be a mononuclear complex or form part of a multinuclear aggregate. The anionic nature of the complexes is of fundamental importance since it plays an important role in the prevention of polymer formation. In contrast, neutral

[*] Prof. P. P. Power, S. C. Shoner
Department of Chemistry
University of California
Davis, CA 95616 (USA)

[**] This work was supported by the donors of the Petroleum Research Fund administered by the American Chemical Society.

homoleptic transition metal thiolates are normally found as insoluble polymers which are not well characterized. Exceptions to this involve the structures of a small number of neutral, open-shell transition metal thiolate complexes. Some examples are $[Mo(SR)_4]$ or $[Mo_2(SR)_6]$ (R = *t*Bu,[4] 2,4,6-$Me_3C_6H_2$,[5] 2,4,6-*i*$Pr_3C_6H_2$),[4,5] $[Ni_4(SR)_8]$ (R = C_5H_9NMe,[6] C_6H_{11},[7] C_3H_7[8], $[Ni_5(SEt)_{10}]$,[9] $[Ni_5(SCH_2SiMe_3)_{10}]$,[9] $[Ni_6(SR)_{12}]$ (R = Et,[9] C_2H_4OH[10]) or $[Ni_8(SCH_2COO\text{-}Et)_{16}]$[11] and $[Pd_6(SR)_{12}]$ (R = *i*Pr, CH_2CH_2OH)[10] or $[Pd_8\{S(nPr)\}_{16}]$.[12] All of these complexes involve four-coordinate metals and the aggregated structures of the nickel and palladium species illustrate the tendency of these complexes to associate. No open-shell transition metal thiolate complexes with low (3 or less) coordination numbers have been reported.[14] In this paper the syntheses and structures of the first well-characterized neutral thiolate complexes of Mn, Fe, and Co are now described.

The title compounds $[\{M(SAr)_2\}_2]$ (M = Mn, **1**; Fe, **2**; Co, **3**; Ar = 2,4,6-*t*$Bu_3C_6H_2$) were synthesized as described below by the treatment of $[M\{N(SiMe_3)_2\}_2]$ (M = Mn,[15] Fe,[16] or Co[17]) with two equivalents of HSAr.[18] The X-ray crystal structures[19] of **1**–**3** may be illustrated by the iron complex **2** in Figure 1. Important structural features are

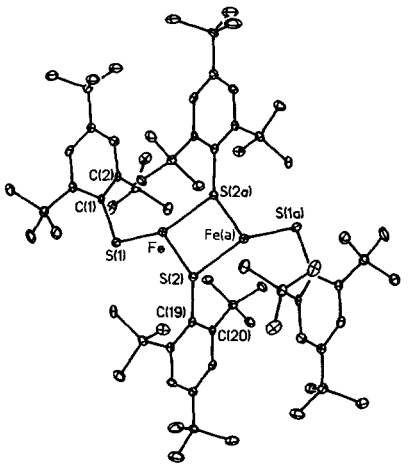

Fig. 1. Computer generated thermal ellipsoidal plot (H atoms omitted) of $[\{Fe(SAr)_2\}_2]$ **2**. The structures of **1** and **3** in the crystal are similar, bond distances and angles for **1**, **2** and **3** are listed in Table 1.

listed in Table 1. The complexes, which are isomorphous, consist of well-separated dimers that have a crystallographically imposed center of inversion. The $[M_2S_2]$ cores are therefore planar as required by symmetry. The metal centers have either planar or nearly planar coordination. The sulfur atoms of the thiolato bridges are all pyramidally coordinated with the pyramidicity increasing in the sequence **3** > **2** > **1**. Although the coordination of each metal atom is roughly trigonal planar, the angles at the metal center are very irregular (Table 1). The degree of angular irregularity decreases in the sequence Mn > Fe > Co. The M–S bridging distances are, as expected, longer than the M–S terminal bond lengths but the difference becomes progressively less on going from Mn to Co and in complex **3** the difference is only 0.04 Å. The M–S bond lengths in **1**–**3** appear to be about 0.03 Å–0.09 Å shorter than the distances found in four-coordinate complexes. This is in keeping with the lower coordination number of these metals. The M ··· M distance decreases steadily on going from Mn to Co until in **3** it is only 2.818 Å.

Table 1. Important bond distances [Å] and angles [°] for **1**–**3**.

	1 $[Mn(SAr)_2]_2$	**2** $[Fe(SAr)_2]_2$	**3** $[Co(SAr)_2]_2$
M–S(1)	2.317(3)	2.256(3)	2.222(2)
M–S(2)	2.446(3)	2.365(3)	2.265(2)
M–S(2a)	2.440(3)	2.366(3)	2.269(2)
S(1)–M–S(2)	123.5(1)	123.6(1)	121.9(1)
S(1)–M–S(2a)	147.8(1)	138.2(1)	134.9(1)
S(2)–M–S(2a)	86.7(1)	92.8(1)	103.2(1)
M–S(1)–C(1)	93.1(3)	96.7(2)	107.2(2)
M–S(2)–M(a)	93.3(1)	87.2(1)	76.8(1)
M–S(2)–C(19)	120.2(3)	118.4(2)	114.1(2)
M(a)–S(2)–C(19)	126.9(3)	125.2(2)	122.3(2)
Σ°M	358.0	354.6	360.0
Σ°S (bridging)	340°	330.8°	313.2°
M ··· M	3.554	3.262	2.818

The compounds **1**–**3** are the first well-characterized, neutral, homoleptic thiolates of Mn, Fe and Co. In addition, they are the first three-coordinate open-shell transition metal thiolate complexes to be structurally characterized.[14] The low-coordination of the metal atoms and the low degree of aggregation of the $[M(SAr)_2]$ moieties are due to steric crowding by the bulky aryl groups. The utility of the 2,4,6-*t*$Bu_3C_6H_2S$ ligand in preventing association has been demonstrated in the main group elements[20,21] and, most recently, in the case of a cadmium complex.[22] The dimeric bridged structures of **1**–**3** bear a resemblance to that of the cadmium complex and to those of the amides $[M\{N(SiMe_3)_2\}_2]$ (M = Mn,[23,24] Fe[26] or Co[24]). Unlike the latter, the complexes **1**–**3** do not apparently dissociate to monomers in solution. Presumably, the amido complexes dissociate more readily because they are more crowded owing to the shorter M–N distance and the presence of two substituents on nitrogen. Preliminary magnetic data on **1**–**3** indicate magnetic moments that are marginally higher than those of the complex $[M\{N(SiMe_3)_2\}_2]$,[16] which indicates the presence of two high-spin, antiferomagnetically coupled metal centers. This is in harmony with the low coordination number and consequently low overall ligand field strength of the coordinating ligands. All complexes decompose above 140 °C and a white crystalline substance (thought to be SAr_2) is formed.[26] Presumably, the other product of this decomposition is the metal sulfide.

Experimental

Synthesis of $[Fe\{(2,4,6\text{-}tBu_3C_6H_2)S\}_2]_2$ **2**: 1.11 g (4 mmol) of 2,4,6-*t*$Bu_3C_6H_2SH$ [18] was dissolved in ca. 20 mL of pentane. To this was added 0.753 g (2 mmol) of $[Fe\{N(SiMe_3)_2\}_2]$ [16] via a solid addition funnel. The solution immediately turned dark red with the formation of an orange microcrystalline precipitate. After the addition was completed, the solution was stirred for an additional hour, and filtered to give a quantitative yield of **2**. To obtain crystals suitable enough for an X-ray structure analysis the reactions were carried out in 80 mL of toluene (Mn,Fe) or diethylether (Co), heated until the precipitate dissolved, and allowed to cool slowly to room temperature to give almost colorless (Mn), dark red (Fe) or metallic green (Co) crystals of the title compounds in moderate yield (40–50%). The compounds display very low solubility in hydrocarbons such as hexane, benzene or toluene. Greater solubility was observed in donor solvents but it is not clear, at present, if this is due to solvation of the low-coordinate metals.

Received: September 6, 1990 [Z 4170 IE]
German version: *Angew. Chem. 103* (1990) 308

CAS Registry numbers:
1, 131794-02-0; **2**, 131794-03-1; **3**, 131794-04-2; $Mn[N(SiMe_3)_2]_2$, 926-76-1; $Fe[N(SiMe_3)_2]_2$, 14760-22-6; $Co[N(SiMe_3)_2]_2$, 14760-23-7.

[1] I. G. Dance, *Polyhedron 5* (1986) 1037.
[2] P. J. Blower, J. R. Dilworth, *Coord. Chem. Rev. 76* (1987) 121.
[3] B. Krebs, G. Henkel in H. Roesky (Ed.): *Rings. Clusters and Polymers of Main Group Transition Elements*, Elsevier, Amsterdam 1989, p. 439.
[4] S. Otsuka, M. Kamata, K. Hirotsu, T. Higuchi, *J. Am. Chem. Soc. 103* (1981) 3011; E. Roland, E. C. Walborsky, J. C. Dervan, R. R. Schrock, *ibid.* (1985) 5795.
[5] P. J. Blower, J. R. Dilworth, J. P. Hutchinson, J. Zubieta, *Trans. Met. Chem. Weinheim Ger. 7* (1982) 353. M. H. Chisholm, J. F. Corning, J. C. Huffman, *J. Am. Chem. Soc. 105* (1983) 5924.
[6] W. Gaete, J. Ros, X. Solans, M. Font-Altaba, J. L. Brianso, *Inorg. Chem. 23* (1984) 39.
[7] M. Kriege, G. Henkel, *Z. Naturforsch. B. Chem. Sci. 42* (1987) 1121.
[8] T. Krüger, B. Krebs, G. Henkel, *Angew. Chem. 101* (1989) 54; *Angew. Chem. Int. Ed. Engl. 28* (1989) 61.
[9] P. Woodward, L. F. Dahl, E. W. Abel, B. C. Cross, *J. Am. Chem. Soc. 87* (1965) 5251. H. Miyamae, T. Yamamura, *Acta Crystallogr. Sect. C 44* (1988) 606; T.Yamamura, *Bull. Chem. Soc. Jpn. 61* (1988) 1975; B. K. Koo, E. Block, H. Kang, S. Liu, J. Zubieta, *Polyhedron 7* (1988) 1397.
[10] R. O. Gould, M. M. Harding, *J. Chem. Soc.A* (1970) 875.
[11] I. G. Dance, M. L. Scudder, R. Secomb, *Inorg. Chem. 24* (1985) 1201.
[12] R. G. Mayter, F. S. Humiec, *J. Inorg. Nucl. Chem. 26* (1964) 807; N. Kunchur, *Acta Crystallogr. Sect. B24* (1968) 1623.
[13] J. D. Higgins, J. W. Suggins, *Inorg. Chim. Acta 145* (1988) 247.
[14] Three-coordinate anionic thiolate complexes of the Zn group and of Cu^{I} have been reported. However, they all involve a d^{10} configuration at the metal; E. S. Gruff, S. A. Koch, *J. Am. Chem. Soc. 11* (1989) 8762; D. Coucouvanis, C. N. Murphy, S. K. Kanodia, *Inorg. Chem. 19* (1980) 2993. For a two-coordinate thiolatocuprate see: S. A. Koch, R. Fikar, M. Millar, T. O'Sullivan, *Inorg. chem. 23* (1984) 122.
[15] H. Bürger, U. Wannagat, *Monatsh. Chem. 94* (1963) 1007.
[16] R. A. Andersen, K. Faegri, J. C. Green, A. Haaland, M. F. Lappert, W.-P. Leung, K. Rypdal, *Inorg. Chem. 27* (1988) 1782.
[17] H. Bürger, U. Wannagat, *Monatsh. Chem. 95* (1964) 1097.
[18] W. Rundel, *Chem. Ber. 101* (1968) 2956.
[19] Crystal data at 130 K with $Mo_{K\alpha}$ ($\lambda = 0.71069$ Å); **1**, $a = 9.844(3)$ Å, $b = 19.422(5)$ Å, $c = 17.905(8)$ Å, $\beta = 91.32(3)°$, monoclinic, $P2_1/n$, $Z = 2$, 2663 unique observed ($I > 2\sigma I$) data, $R = 0.077$; **2**, $a = 9.816(5)$ Å, $b = 19.447(6)$ Å, $c = 17.901(15)$ Å, $\beta = 91.22(6)°$, monoclinic, $P2_1/n$, $Z = 2$, 3136 unique observed ($I > 2\sigma I$) data, $R = 0.063$; **3**, $a = 10.264(4)$ Å, $b = 19.400(3)$ Å, $c = 17.498(7)$ Å, $\beta = 91.25(3)°$, monoclinic $P2_1/n$, $Z = 2$, 3593 unique observed ($I > 2\sigma I$) data, R = 0.077. Further details of the crystal structure investigation may be obtained from the Fachinformationszentrum Karlsruhe, Gesellschaft für wissenschaftlich-technische Information mbH, W-7514. Eggenstein Leopoldshafen 2 (FRG), on quoting the depository number CSD-55059, the names of the authors, and the journal citation.
[20] P. B. Hitchcock, M. F. Lappert, B. J. Samways, E. Weinberg, *J. Chem. Soc. Chem. Commun.* (1983) 1492.
[21] G. A. Sigel, P. P. Power, *Inorg. Chem. 26* (1987) 2819.
[22] M. Bochmann, K. Webb, M. Harman, M. B. Hursthouse, *Angew. Chem. 102* (1990) 703; *Angew. Chem. Int. Ed. Engl. 29* (1990) 638.
[23] D. C. Bradley, M. B. Hursthouse, K. M. A. Malik, R. Moseler, *Transition Met. Chem. Weinheim Ger. 3* (1978) 253.
[24] B. D. Murray, P. P. Power, *Inorg. Chem. 23* (1984) 4584.
[25] P. P. Power, *Comments Inorg. Chem. 8* (1989) 177.
[26] This decomposition also occurs in the case of the Cd complex to give CdS and SAr_2 [22] and also in the case of the zinc complex $Zn(SAr)_2 \cdot Et_2O$ to give SAr_2 and ZnS; S. C. Shoner, P. P. Power, *Angew. Chem. 102* (1990) 1484; *Angew. Chem. Int. Ed. Engl. 29* (1990) 1403.

1,3,5,7-Tetrakis(diethylamino)-*s*-indacenediylium-bis(tetrafluoroborate)—a Stable *s*-Indacene Dication**

By *Rudolf Gompper,* Kurt Polborn, Christian Seifert,* and *Hans-Ulrich Wagner*

As a 12π-electron system *s*-indacene should formally be classed with the antiaromatic compounds. According to the largest eigenvalue of the bond–bond polarizability matrix "λ_{max}" = 1.57 ($\lambda_{crit} \approx 1.7$)[1] and the resonance energy per electron (REPE = 0.0092 β),[2] *s*-indacene lies in the transition region between aromatic and antiaromatic compounds. The parent compound was isolated as an unstable air-sensitive oil;[3,4] 1,3,5,7-tetra-*tert*-butyl-*s*-indacene[5] ("λ_{max}" = 1.38[11]) and 4,8-bis(dimethylamino)-*s*-indacene[6] ("λ_{max}" = 1.03[11]), on the other hand, are stable. The frontier orbitals indicate that *s*-indacene should be stabilized by donor moieties in the 4,8 position and acceptor moieties in the 2,6 position. Compounds with this substitution pattern include 4,8-bis(dimethylamino)-*s*-indacene,[6] hexamethyl 4,8-dihydroxy-*s*-indacene-1,2,3,5,6,7-hexacarboxylate,[7] and 1,3,5,7-tetrakis(diethylamino)-2,6-diaza-*s*-indacene[8] **1b**, which, with "λ_{max}" = 1.22, has a delocalized π-electron system and accordingly must be described as an aromatic (4n)π-system.[9]

With "λ_{max}" = 1.18, a 1,3,5,7-tetraamino-*s*-indacene, e.g. **1a**, should also still show double bond delocalization, but, owing to its wealth of electrons should be more difficult to handle than **1b**. Analogously to the preparation of **1b** from **2b**, **1a** ought to be accessible by reduction of **2a**. Compound

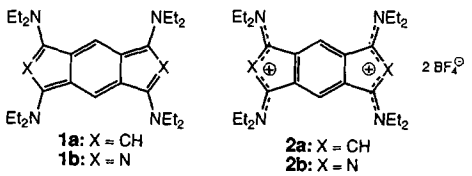

2a is a derivative of the *s*-indacene dication, which, although a 10π-electron system, has thus far never been reported. On the basis of calculated bond orders,[10] *s*-indacene dications should be composed of an aromatic sextet and two annelated alkyl cation units (in contrast, according to calculated bond orders and the measured ^{1}H-NMR spectra, *s*-indacene dianions possess a delocalized 14π-electron system[10–12]). The only derivative of an *s*-indacene dication reported so far[13] carries a partial positive charge on C-2,6 and is therefore not comparable with **2a**. We have now synthesized **2a**, investigated its properties, and shown that it can be reduced to **1a**.

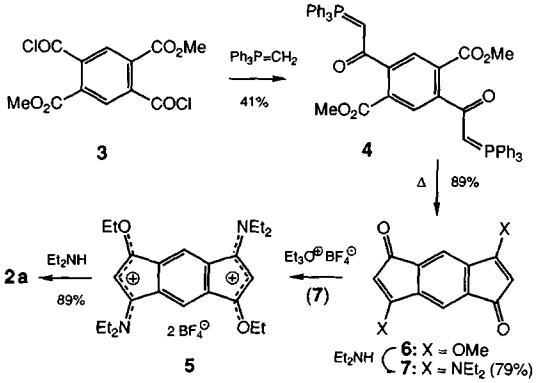

Transylidation[15–17] of dimethyl 2,5-bis(chlorocarbonyl)terephthalate[14] **3** with methylenetriphenylphosphorane affords the ylide **4**, which can be cyclized by double intramolecular Wittig reaction at the ester groups (cf. Refs. [18–20]) to give **6**. Reaction of **7**, obtained from **6** and diethylamine, with triethyloxonium tetrafluoroborate leads to

[*] Prof. Dr. R. Gompper, Dr. K. Polborn, Dipl.-Chem. C. Seifert, Dr. H.-U. Wagner
Institut für Organische Chemie der Universität
Karlstrasse 23, W-8000 München 2 (FRG)

[**] This work was supported by the Deutsche Forschungsgemeinschaft and the Fonds der Chemischen Industrie.

the dicationic salt **5**, which can be converted directly, i.e. without prior isolation, into **2a** by reaction with diethylamine (cf. Table 1).

Table 1. Yields, physical and spectroscopic data of compounds **2a**, **2a'**, **2b**, **4**, **6**, **7**, **8a**, **8b**, and of 3-dimethylamino-*N*,*N*-dimethylpropeniminium tetrafluoroborate [a].

2a: Yield 89%; blue cyrystals, m.p. > 300 °C (from CH_3CN/ether), UV/VIS (CH_3CN): λ_{max} [nm] (ε) = 303 (sh), 312 (74100), 340 (sh), 597 (5890), 630 (5880), 710 (sh); ^1H NMR (80 MHz, CD_3CN): δ = 5.40 (s, 2H, $C^{2,6}H$), 7.70 (s, 2H, $C^{4,8}$-H); ^{13}C NMR (100 MHz, CH_3CN): δ = 92.5 (s, $C^{2,6}$), 121.6 (s, $C^{4,8}$), 139.0 ($C^{3a,4a,7a,8a}$), 164.8 (s, $C^{1,3,5,7}$).

2a': Yield 81%; deep-violet rectangles, m.p. 202–203 °C (from CH_3CN/ethyl acetate), UV/VIS ($CHCl_3$): λ_{max} [nm] (ε) = 593 nm (4786), 630 (4266)

2b: UV/VIS ($CHCl_3$): λ_{max} [nm] (ε) = 440 (9770))[8]

4: Yield 41%; colorless crystals, m.p. > 180 °C (decomp.) (from $CHCl_3$/ether)

6 (Yield 89%; red leaflets, m.p. > 300 °C (from DMF), UV (DMSO): λ_{max} [nm] (ε) = 465 (540)

7: Yield 79%; shiny metallic needles, m.p. 246–247 °C (from ethyl acetate), UV/VIS ($CHCl_3$): λ_{max} [nm] (ε) = 545 (2800)

8a[21]: UV/VIS (CH_2Cl_2): λ_{max} [nm] (ε) = 476 (7080); ^1H NMR (CD_3CN): δ = 5.28 (s, C^2H); ^{13}C NMR (CH_3CN): δ = 89.9 (s, C^2), 165.6 (s, C^1/C^2)

8b[22]: UV/VIS (CH_2Cl_2): λ_{max} [nm] (ε) = 375 (6920)
3-dimethylamino-*N*,*N*-diemethylpropeniminium tetrafluoroborat[24]: ^1H NMR ([D_6]DMSO): δ = 5.37 (s, C^2H); ^{13}C NMR (DMSO): δ = 90.8 (s, C^2), 163.7 (s, C^1/C^2)

[a] $[(CH_3)_2N{=}CH{-}CH{=}CH{-}N(CH_3)_2](BF_4)$

Especially striking is the blue color of **2a** (**2b**[8] is only yellow). The great difference in color ($\Delta\lambda_{2a/2b}$ = 190 nm, $\Delta\nu_{2a/2b}$ = 6854 cm^{-1}) can be explained qualitatively on the basis of the frontier orbitals (Fig. 1). PPP-π-SCF calculations show that the longest wavelength band of **2a** corresponds to the extent of 85% to a HOMO-LUMO transition; the calculated spectrum is in good agreement with the measured spectrum. In positions 2 and 6 the HOMO has very large coefficients, whereas the LUMO shows nodes in these positions. It follows, therefore, that the HUMO-LUMO gap is very much greater in the case of **2b** (0.684 β) than in the case of **2a** (0.256 β). The same substituent effect is observed with the indenylium salts **8a**[21] ($\Delta E_{HOMO-LUMO}$ = 0.697 β) and **8b**[22] ($\Delta E_{HOMO-LUMO}$ = 0.921 β) but is less pronounced ($\Delta\lambda_{max\ 8a/8b}$ = 101 nm, $\Delta\nu_{max\ 8a/8b}$ = 5658 cm^{-1}). Remarkably, the difference in color between **2a** and **8a** ($\Delta\lambda_{max}$ = 154 nm, $\Delta\nu_{max}$ = 5135 cm^{-1}) is substantially greater than that between **2b** and **8b** ($\Delta\lambda$ = 65 nm, $\Delta\nu$ = 3939 cm^{-1}). Also interesting is that 1,5-bis(1-methyl-4-pyridino)-3,7-bis(1-methyl-4-pyridylene)-3,7-dihydro-*s*-indacene diiodide (UV/VIS (CH_3OH): λ_{max} [nm] = 586;[13] $\Delta E_{HOMO/LUMO}$ = 0.642 β [calculated without Cl]), in contrast to **2**, absorbs at shorter wavelength than corresponding indene derivatives (UV/VIS (CH_3OH): λ_{max} [nm] = 584/607/601;[13] $\Delta E_{HOMO/LUNO}$ = 0.843 β [calculated without Cl]).

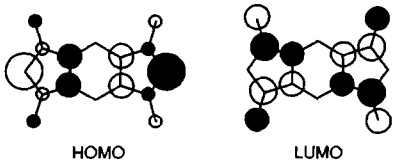

Fig. 1. Frontier orbitals of **2a**.

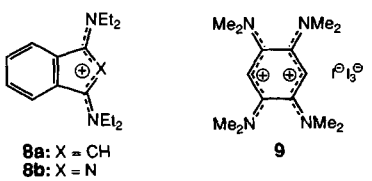

From the calculated π-bond orders of the ground state (p_{3a-8a} = 0.597, p_{1-8a} = 0.313) and the first excited state (p_{3a-8a} = 0.429, p_{1-8a} = 0.447) of **2a** it can be deduced that the excited state approximates a delocalized 10π-electron system.

The crystal structure analysis of **2a'** ($[(NC)_2C{=}CH{-}C(CN)_2]^{\ominus}$ instead of $BF_4^{\ominus}$ in **2a**, prepared by reaction of **2a** with $K[(NC)_2C = CH{-}C(CN)_2]$ in H_2O) shows (Fig. 2) that the dication of **2a'** (and **2a**) can, in accordance with theoretical predictions, be best described as a benzene ring with two annelated trimethinecyanine units. This is further supported

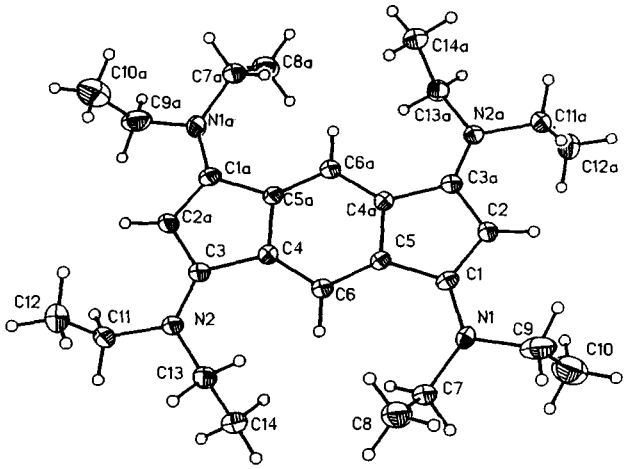

Fig. 2. Structure of **2** in the crystal (ORTEP)[23]: selected bond lengths [pm] and angles [°]:C1-C2 138.4(4), C2-C3a 139.1(4), C5-C4a 139.5(4), C5-C6 137.7(4), C4-C6 139.0(4), C1-N1 132.0(4); C2-C1-C5 108.2(2), C1-C2-C3a 110.1(2), C1-C4-C5a 106.9(2), C1-C5-C6 132.1(3), C6-C5C4a 120.8(2), N1-C1-C5 125.4(2), N2-C3-C2a 125.7(2), C1-N1-C7 125.5(2), C1-N1-C9 119.3(2).

by a comparison of the ^1H- and ^{13}C-NMR data of **2a** with those of **8a** and 3-dimethylamino-*N*,*N*-dimethylpropeniminium tetrafluoroborate.[24] Also informative is a comparison of **2a** with **9**.[25] An X-ray structure analysis has confirmed that **9** contains two vinamidinium units which are coupled by single bonds. That is, **2a** can be regarded as a phenylogous derivative of **9**; in contrast to **9**, however, **2a** is completely planar. The ring-proton signals of **9** (^1H NMR ($CDCl_3$): δ = 5.85) are shifted downfield compared to the corresponding C^2H-proton signals of **2a** and **8a**, probably as a result of the acceptor effect of the second vinamidinium unit. The large dication–dication distance in the crystal of **2a'** (890 pm) rules out an interaction of the indacene dication moieties.

The cyclic voltammogram of **2a** ($CH_3CN/Bu_4N^{\oplus}BF_6^{\ominus}$, Pt-electrode versus $Ag/Ag^{\oplus}$) shows two reversible reduction steps at -0.38 V (formation of the radical cation) and -0.81 V (formation of the *s*-indacene **1a**). **2b** is reduced reversibly to the radical cation (-0.11 V) and to **1b** (-0.56 V) more readily than **2a**.

Received: August 7, 1990 [Z 4121 IE]
German version: *Angew. Chem. 103* (1991) 318

CAS Registry numbers:
2a, 131636-72-1; **2a'**, 131636-73-2; **3**, 19014-14-3; **4**, 131636-14-3; **6**, 131636-75-4; **7**, 131636-76-5; $Ph_3P{=}CH_2$, 3487-44-3; Et_2NH, 109-89-7.

[1] E. Heilbronner, Z-z. Yang, *Angew. Chem. 99* (1987) 369; *Angew. Chem. Int. Ed. Engl. 26* (1987) 360.
[2] L. J. Schaad, B. A. Hess, Jr., *J. Am. Chem. Soc. 94* (1972) 3068.
[3] K. Hafner, K. H. Häfner, C. König, M. Kreuder, G. Ploss, G. Schulz, E. Sturm, K. H. Vöpel, *Angew. Chem. 75* (1963) 35; *Angew. Chem. Int. Ed. Engl. 2* (1963) 123.
[4] K. Hafner, *Angew. Chem. 75* (1963) 1041; *Angew. Chem. Int. Ed. Engl. 3* (1964) 165.
[5] K. Hafner, B. Stowasser, H. P. Krimmer, S. Fischer, M. C. Böhm, H. J. Lindner, *Angew. Chem. 98* (1986) 646; *Angew. Chem. Int. Ed. Engl. 25* (1986) 630.
[6] K. Hafner, H. P. Krimmer, *Angew. Chem. 92* (1980) 202; *Angew. Chem. Int. Ed. Engl. 19* (1980) 199.
[7] E. LeGoff, R. B. LaCount, *Tetrahedron Lett. 1964*, 1160.
[8] F. Closs, R. Gompper, U. Nagel, H.-U. Wagner, *Angew. Chem. 99* (1987) 1068; *Angew. Chem. Int. Ed. Engl. 26* (1987) 1037.
[9] R. Gompper, H.-U. Wagner, *Angew. Chem. 100* (1988) 1492; *Angew. Chem. Int. Ed. Engl. 27* (1988) 1437.
[10] C. Glidewell, D. Lloyd, *Tetrahedron 40* (1984) 4455; *J. Chem. Educ. 63* (1986) 306.
[11] U. Edlund, B. Eliasson, J. Kowaleski, L. Trogen, *J. Chem. Soc. Perkin Trans. 2 1981*, 1260.
[12] G. Gandillon, B. Bianco, U. Burger, *Tetrahedron Lett. 22* (1981) 51.
[13] A. R. Katritzky, W.-Q. Fan, Q.-L. Li, *J. Heterocycl. Chem. 25* (1988) 1311.
[14] M. Ueda, T. Takahashi, Y. Imai, *J. Polym. Sci. Polym. Chem. Ed 6* (1978) 1735.
[15] H. J. Bestmann, B. Arnason, *Chem. Ber. 95* (1962) 1513.
[16] H. J. Bestmann, *Angew. Chem. 77* (1965) 651; *Angew. Chem. Int. Ed. Engl. 4* (1965) 645.
[17] G. Märkl, *Chem. Ber. 94* (1961) 3005.
[18] H. J. Bestmann, G. Schade, H. Lütke, T. Mönius, *Chem. Ber. 118* (1985) 2640.
[19] P. Babin, J. Donogues, *Tetrahedron Lett. 24* (1983) 3071.
[20] H. J. Bestmann, G. Schade, G. Schmid, *Angew. Chem. 92* (1980) 856; *Angew. Chem. Int. Ed. Engl. 19* (1980) 822.
[21] R. Mertz, *Dissertation*, Universität München 1983.
[22] K. P. Bichlmayer, *Dissertation*, Universität München 1979.
[23] Crystal structure analysis of **2a'**: Enraf-Nonius CAD-4 diffractometer $Mo_{K\alpha}$ radiation, $\lambda = 71.069$ pm, single crystal $0.27 \times 0.54 \times 0.54$ mm^3, $T = 294$ K. Crystal data: $M_r = 718.92$, $\rho_{calcd} = 1.192$ g cm^{-3}, monoclinic, space group $P2_1/n$, $a = 895.5(2)$, $b = 1771.6(3)$, $c = 1310.0(3)$ pm, $\beta = 105.45(2)°$, $V = 2.00325$ nm^3, $Z = 2$. ω-Scan: $2\theta = 4°$–$46°$; maximum measuring time 30 s. 3038 measured ($\pm h, +k, +l$), 2918 symmetry independent reflections, 2293 classed as observed $I \geq \sigma(I)$ Refined parameters: 244. Solution of structure: SHELXS 86, refinement SHELXTL. Non-hydrogen atoms anisotropic, hydrogen atoms as "riding" atoms in calculated positions and isotropic. $R = 0.0645$, $R_w = 0.0533$; largest residual electron density $\rho = +0.31$ e pm^{-3} 10^6.—Further details of the crystal structure investigation are available on request from the Fachinformationszentrum Karlsruhe, Gesellschaft für Wissenschaftlich-technische Information, W-7514 Eggenstein-Leopoldshafen 2 (FRG), on quoting the depository number CSD-54998, the names of the authors, and the journal citation.
[24] H. G. Viehe in H. Böhme, H. G. Viehe (Eds.): *Iminium Salts in Organic Chemistry*, Wiley, New York 1976, p. 48, 65.
[25] K. Elbl, C. Krieger, H. A. Staab, *Angew. Chem. 98* (1986) 1024; *Angew. Chem. Int. Ed. Engl. 25* (1986) 1023.

2,3a,5,6a-Tetrapentalene Dications and Tetraamino-1,3,5,7-tetrazocine **

By *Stefan Ehrenberg, Rudolf Gompper,* Kurt Polborn,* and *Hans-Ulrich Wagner*

Pentalene can be stabilized sterically and electronically;[1] using 1,3,4,6-tetrakis(dimethylamino)-2,5-diazapentalene **1**, R = Me, as example we have been able to show[2] that donor-acceptor-substituted pentalenes exhibit double-bond delocalization and accordingly are to be classed as "aromatic (4n)π-electron systems".[1] The question arises, however, whether also the pentalene derivatives **3**, which have N atoms in positions 3a and 6a, and thus are doubly positively charged (3a,6a-diazapentalene dications), show such a double bond delocalization corresponding to **3'** or whether they are valence tautomeric systems. As 8π-electron systems the dications **3** are related with bimanes[3] (partly planar, partly non-planar):[3–5] anhydro-1-hydroxy-3-oxo-pyrazalo[1,2-*a*]-pyrazolium hydroxides[6, 7] (planar), 1,3,5,7-tetraaza-2,4,6,8-tetraborabicyclo[3.3.0]octanes[8] and 3,7-dithia-1,5-diaza-2,4,6,8-tetraborabicyclo[3.3.0]octanes[9] (non-planar). In contrast to these compounds, however, the dications **3** can exist not only as planar, but, moreover, also as delocalized "aromatic" 8π-electron ring systems **3'** (cf. Gimarcs rule of "topological charge stabilization"[10]). And, as further partially localized planar structures **3''** and the folded structures **3'''** must be taken into consideration (compound **2**, which was obtained by protonation of **1**, can serve as model for **3'''**[2]).

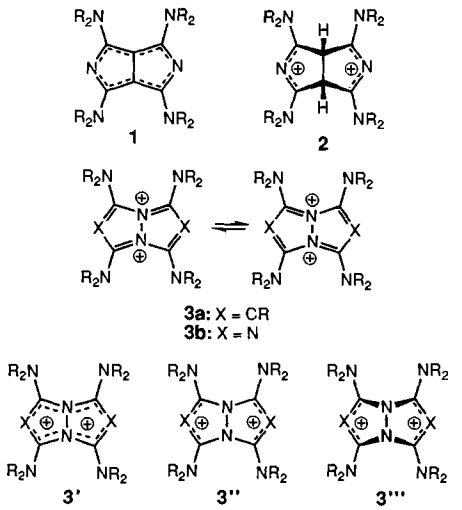

An indication of whether **3** or **3'** is likely to be present is provided by Hückel molecular orbital (MO) calculations (see Table 1). Nitrogen atoms in the positions 3a and 6a give rise to a greater decrease in the energy of the HOMO than N-

Table 1. Effect of substituents on the double-bond delocalization in pentalenes (ring N-atoms are counted as substituents here). HMO frontier orbital energies (β) and largest eigenvalues of the bond–bond polarizability matrix ("λ_{max}"[11, 12]) [$\alpha_X = \alpha_C + h_X\beta_{CC}$; $h_{NR}2 = 1.5$; $h_N = 0.5$].

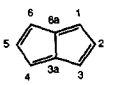

Substituents	HOMO	LUMO	"λ_{max}"
none	0.471	0.000	2.375[11]
2,5-diaza	0.738	0.000	1.677[2]
1,3,4,6-tetraamino	0.418	−0.500	1.153[2]
1,3,4,6-tetraamino-2,5-diaza (≙ **1**)	0.442	−0.500	0.967[2]
3a,6a-diazonia	0.917	0.000	1.203
2,5-diaza-3a,6a-diazonia	1.219	0.000	1.048
1,3,4,6-tetraamino-3a, 6a-diazonia (≙ **3a**)	0.672	−0.500	0.939
1,3,4,6-tetraamino-2,5-diaza-3a,6a-diazonia (≙ **3b**)	0.976	−0.500	0.801

[*] Prof. Dr. R. Gompper, Dipl.-Chem. S. Ehrenberg, Dr. K. Polborn
Dr. H.-U. Wagner
Institut für Organische Chemie der Universität
Karlstraße 23, W-8000 München 2 (FRG)

[**] This work was supported by the Deutsche Forschungsgemeinschaft and the Fonds der Chemischen Industrie.

atoms in the 2- and 5-position. **3a** and **3b** have large HOMO-LUMO gaps and the smallest "λ_{max}" values and therefore the greatest tendency to exhibit double-bond delocalization.

Triazolo[1,2-*a*]triazolediylium salts **6** (cf. Table 2) of the type **3b** are accessible by reaction of 3,5-diaminotriazoles **4a** and **4b**[14] with 1,3-dichloro-2-azapropeniminium tetrafluoroborates **5** in the presence of triethylamine in chloroform (in

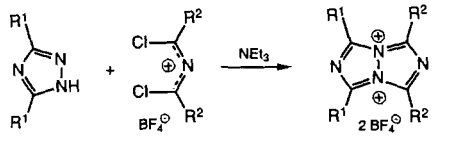

4 **5** **6**

a: $R^1 = NMe_2$ **a**: $R^1 = NMe_2$ **a**: $R^1, R^2 = NMe_2$
b: R^1 = Morph **b**: R^2 = Morph **b**: $R^1 = NMe_2$, R^2 = Morph
c: R^1, R^2 = Morph

the case of **6a**) or dichloromethane (in the case of **6b, c**); **4a**, which is reported here without giving any detailed data,[13] was prepared analogously to **7** using the procedure described in Ref. [15]).

Table 2. Yields and physical and spectroscopic data of the compounds **6**, **9**, **10**, and 1,2-dimethyl-3,5-dimorpholino-1,2,4-triazolium tetrafluoroborate.

6a: Yield 18%; m.p. 235–240°; UV/VIS (CH_3CN): λ_{max} [nm] (ε) = 283 (28200), 310 (sh); ^1H NMR (80 MHz, CD_3CN): δ = 3.25 (s, NCH_3); ^{13}C NMR (100 MHz, CD_3CN): δ = 154.9 (C-1,3,5,7), 42.1 (NCH_3); IR (KBr): $\tilde{\nu}$[cm^{-1}] = 1648, 1452, 1347, 1083.

6b: Yield 25%; m.p. 250° C; UV/VIS (CH_3CN): λ_{max} [nm] (ε) = 296 (31600), 320 (sh); ^1H NMR (CD_3CN): δ = 3.77 (s, 4H, NC_2H_4O), 3.26 (s, 3H, NCH_3); ^{13}C NMR (CD_3CN): δ = 153.7, 152.69 (C-1,3,5,7), 66.9 (OCH_2), 51.7 (NCH_2), 42.1 (NCH_3); IR (KBr): $\tilde{\nu}$[cm^{-1}] = 1644, 1611, 1385, 1084.

6c: Yield 80%; m.p. 240–246°C; UV/VIS (CH_3CN): λ_{max} [nm] (ε) = 312 (34700); ^1H NMR (CF_3CO_2H): δ = 4.18 (s, NC_2H_4O); IR (KBr): $\tilde{\nu}$[cm^{-1}] = 2862, 1626, 1414, 1354, 1084.

6a': Yield 75%, colorless needles m.p. 130–132°C (from CH_3CN/Et_2O). 1,2-dimethyl-3,5-dimorpholino-1,2,4-triazoliumtetrafluoroborate: m.p. 156°C; UV/VIS (CH_3CN): λ_{max} [nm] (ε) = 242 (28800); ^1H NMR (80 MHz, CD_3CN): δ = 3.65 (AA'BB', 8H, NCH_2CH_2O), 3.35 (s, 3H, NCH_3); ^{13}C NMR (100 MHz, CD_3CN): δ = 165.4 (C-3, C-5), 66.7 (OCH_2), 49.2 (NCH_2), 38.6 (NCH_2); IR (KBr): $\tilde{\nu}$[cm^{-1}] = 2970, 2917, 2863, 1653, 1117, 1053.

9a: m.p. 227–230°C; UV/VIS (CH_3CN): λ_{max} [nm] (ε) = 209 (23400). 235 (sh), 317 (20400), 340 (sh), 396 (9770); ^1H NMR (80 MHz, CD_3CN): δ = 2.81 (s, 12H, NCH_3), 3.30 (s, 12H, NCH_3), 7.45 (m, 5H, phenyl-H); ^{13}C NMR (100 MHz, CD_3CN): δ = 41.8, 43.6 (NCH_3), 105.4 (C-6), 128.4 (Ph-*ipso*), 129.7 (Ph-*m*), 131.2 (Ph-*p*), 133.7 (Ph-*o*), 154.6, 155.3, (C-1,3,5,7); IR (KBr): $\tilde{\nu}$[cm^{-1}] = 1700, 1639, 1583, 1381, 1058.

9b: m.p. 275–280°C; UV/VIS (CH_3CN): λ_{max} [nm] (ε) = 240 (16200), 366 (33900, 453 (sh); ^1H NMR (80 MHz, CD_3CN): δ = 2.79 (s, 12H, NCH_3), 7.25 (m, 5H, phenyl-H); ^{13}C NMR (100 MHz, CD_3CN): δ = 43.1 (NCH_3), 107.7 (C-2,6), 128.4 (Ph-*ipso*), 130.1 (Ph-*m*), 131.2 (Ph-*p*), 133.7 (Ph-*o*), 154.4 (C-1,3,5,7); IR (KBr): $\tilde{\nu}$[cm^{-1}] = 1594, 1510, 1422, 1332, 1061.

10a: Yield 8%; m.p. 96°C; ^1H NMR (80 MHz, $CDCl_3$): δ = 2.94 (s, 6H, NCH_3), 3.55 (AA'BB', 8H, NC_2H_4O); ^{13}C NMR (100 MHz, CD_3CN): δ = 37.3 (NCH_3), 45.1 (NCH_2), 66.7 (OCH_2), 162.0, 162.4 (C-2,4,6,8); IR (KBr): $\tilde{\nu}$[cm^{-1}] = 2855, 1578, 1399, 1378.

10b: Yield 28%; m.p. 197–199°C; UV/VIS (CH_2Cl_2): λ_{max} [nm] (ε) = 233 (27500), 248 (sh); ^1H NMR (80 MHz, $CDCl_3$): δ = 3.57 (AA'BB'); ^{13}C NMR (100 MHz, $CDCl_3$): δ = 45.0 (NCH_2), 66.5 (OCH_2), 162.1 (C-2,4,6,8); IR (KBr): $\tilde{\nu}$[cm^{-1}] = 2965, 2899, 2851, 1578, 1310.

The crystal structure analysis (Fig. 1) of **6a'**, $[(NC)_2C{=}CH\text{-}C(CN)_2]^{\ominus}$ instead of $BF_4^{\ominus}$ in **6a** (prepared by reaction of **6a** with $K[(NC)_2C{=}CH\text{-}C(CN)_2]$ in water) revealed a slightly bent ring system; the angle between the N1–N2–N3 and N1–N2–N4 planes is 159.2° (in the case of urazourazole 156°[16]; 1,5-diazabicyclo[3.3.0]octane-2,4,6,8-tetrone is planar[17]). In addition, **6a'** (torsional angles C2–N1–N2–C1 and C3–N1–N2–C4 17.8(3)° and 18.5(3)° respectively), as also 2,4,6,8-tetramethyl-3,7-dithia-1,5-diaza-2,4,6,8-tetraborabicyclo[3.3.0]octane[9] (torsion angle 18°), is twisted.

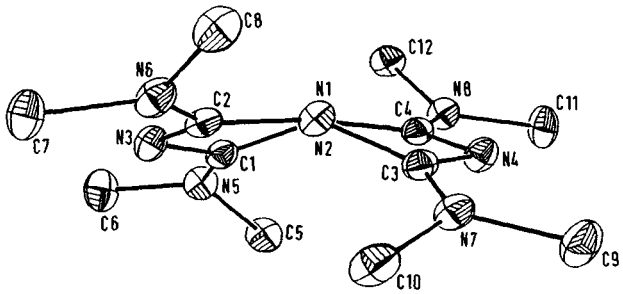

Fig. 1. Structure of **6a'** in the crystal (ORTEP)[18]: selected bond lengths [pm] and angles [°]: N1-N2 141.8(4), C1-N3 133.3(5), C1-N2 139.4(5), C2-N3 132.3(5), C2-N1 141.3(5), C3-N1 140.6(5), C3-N4 134.4(4), C4-N4 132.1(5), C4-N2 140.4(5), C1-N5 130.6(5), C2-N6 131.3(5); C1-N3-C2 106.6(3), N3-C1-N2 110.3(3), C1-N2-N1 104.7(3), C2-N1-N2 102.9(3), N3-C1-N5 123.4(4), C1-N2-C4 141.7(3), C2-N1-C3 142.5(3).

The sums of the angles at N1 and N2 (349.2 and 350.1°, respectively, hydrazine 324°[19]) are consistent with a marked sp^2 hybridization corresponding to the formulas **3b** and **3b'** (in the case of **6b** the sums of the angles at N1 and N2 are even 358.1° and 358.5 respectively). The N1–N2 bond (141.8 pm) is only slightly shorter than the N–N bonds in hydrazine[19] and in the dimethylhydrazines,[20] and comes close to that in 2,4,6,8-tetramethyl-3,7-dithia-1,5-diaza-2,4,6,8-tetraborabicyclo[3.3.0]octane[9] (144.9 pm); *in* contrast, the N–N bond in anhydro-1-hydroxy-3-oxopyrazolo[1,2-*a*]pyrazolium hydroxide[6] (134 pm) is distinctly shorter.

The C1–N3 bond (133.3 pm) and C1–N5 bond (130.6 pm) have ca. 50% double bond character,[21] indicating a larger share of structure **3b''** in the ground state. However, the C1–N2 bond (139.4 pm) is likewise significantly shorter than a $C(sp^2)$–$N(sp^2)$ bond (147 pm, 0% double bond character[21]), so that **3b** and **3b'** must also participate in the ground state. A certain delocalization of **6b, c** in keeping with **3b** and **3b'** also follows from the electron spectra of **6b, c** and 1,2-dimethyl-3,5-dimorpholino-1,2,4-triazolium tetrafluoroborate (prepared by reaction of **5b** with 1,2-dimethylhydrazine); the compounds **6b, c** absorb at significantly longer wavelength.

An MNDO calculation for **6a**, NH_2 instead of NMe_2, indicated a very flat double minimum between the dihedral angles (N1–N2–N3 and N1–N2–N4 planes) 148° and −148°. The energy barrier of ca. 1 kcal mol^{-1} lies within the limits of error of the method, so that a distortion of the molecule could be primarily caused by the spatial interactions of the large dimethylamino groups. The calculated bond lengths correlate well with the measured bond lengths.

Indeed, 3,5-bis(dimethylamino)-4-phenylpyrazole[22] **7** can be converted by reaction with **5a** and **8** into the triazapentalenediylium salt pyrazolo[1,2-*a*]triazoldiylium salt) **9a** and

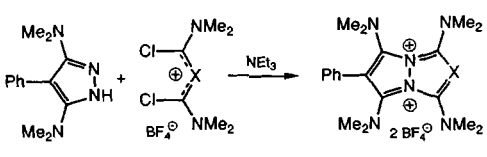

7 **5a**: X = N **9a**: X = N
8: X = C-Ph **9b**: X = C-Ph

diazapentalenediylium salt (pyrazolo[1,2-*a*]pyrazoldiylium salt) **9b**, respectively.

The dication salts **6b, c** can be reduced with zinc in acetonitrile to give the tetraaminotetrazocines **10**, i.e. the first fourfold donor-substituted 1,3,5,7-tetrazocines. On the basis of the donor-acceptor pattern one could expect an almost planar structure for **10**. However, as the crystal structure analysis of **10b** (Fig. 2) shows, it has a boat-shaped configu-

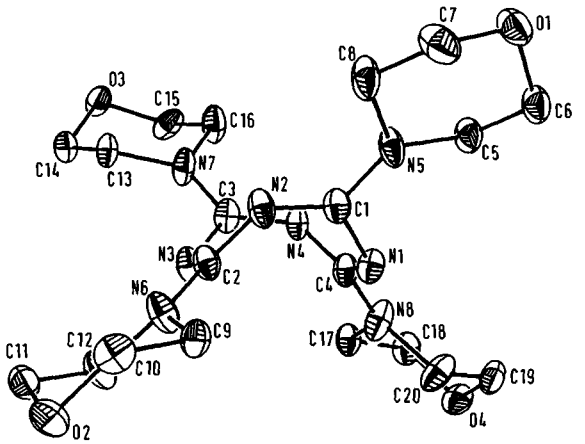

Fig. 2. Structure of **10b** in the crystal (ORTEP)[18]: selected bond lengths [pm] and angles [°]: N1-C1 139.6(10), N2-C1 130.1(9), N2-C2 136.9(10), N3-C2 130.2(9), N3-C3 138.7(10), N4-C3 132.0(9), N4-C4 135.0(10), N1-C4 130.9(9), C1-N5 135.2(10); C1-N1-C4 116.6(6), C2-N3-C3 118.8(6), N1-C1-N2 124.5(7), N3-C3-N4 124.4(7), C1-N2-C2 119.7(7), C3-N4-C4 119.2(6), N2-C2-N3 126.0(7), N1-C4-N4 127.2(7), N1-C1-N5 114.5(6), N2-C1-N5 119.9(7).

ration, like 2,6-diethoxy-4,8-diphenyl-1,3,5,7-tetrazocine.[23] Similarly to octamethylcyclooctatetraene,[24] however, **10b** is somewhat more planar than cyclooctatetraene. The mean of the internal bond angles is 121.6° and that of the torsion

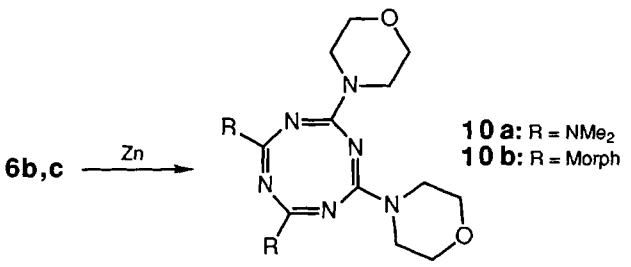

angles 66.7° (in the case of octamethylcyclooctatetraene[24] the corresponding values are 122.2° and 66.6°, respectively, in the case of cyclooctatetraene (cf. Ref. [24]) 126.8° and 55.7°, respectively).

Received: August 7, 1990 [Z 4122 IE]
German version: *Angew. Chem. 103* (1991) 320

CAS Registry numbers:
1 (R_2 = H), 123062-07-7; **2** (R_2 = H), 131833-30-2; **3b** (R_2 = H), 131833-31-3; **4a**, 18377-94-1; **4b**, 18377-91-8; **5a**, 131833-33-5; **5b**, 131833-35-7; **6a**, 131833-73-5; **6b**, 131833-37-9; **6c**, 131833-39-1; **7**, 98635-15-5; **8**, 131833-40-4; **9a**, 131833-42-6; **9b**, 131833-44-8; **10a**, 131833-45-9; **10b**, 131833-46-0.

[1] R. Gompper, H.-U. Wagner, *Angew. Chem. 100* (1988) 1492; *Angew. Chem. Int. Ed. Engl. 27* (1988) 1437.
[2] F. Closs, R. Gompper, H. Nöth, H.-U. Wagner, *Angew. Chem. 100* (1988) 875; *Angew. Chem. Int. Ed. Engl. 27* (1988) 842.
[3] E. M. Kosower, B. Pazhenchevsky, E. Hershkowitz, *J. Am. Chem. Soc. 100* (1978) 6516; E. M. Kosower, J. Bernstein, I. Goldberg, B. Pazhenchevsky, E. Goldstein, *ibid. 101* (1979) 1620.
[4] J. Bernstein, E. Goldstein, I. Goldberg, *Cryst. Struct. Commun. 9* (1980) 295.
[5] I. Goldberg, *Cryst. Struct. Commun. 9* (1980) 329.
[6] K. T. Potts, P. M. Murphy, W. R. Kuehnling, *J. Org. Chem. 53* (1988) 2889; K. T. Potts, P. M. Murphy, M. R. DeLuca, W. R. Kuehnling, *ibid. 53* (1988) 2898.
[7] G. Zvilichovsky, M. David, *J. Org. Chem. 47* (1982) 295.
[8] D. Nölle, H. Nöth, *Z. Naturforsch.-B 27* (1972) 1425.
[9] H. Nöth, R. Ullmann, *Chem. Ber. 108* (1975) 3125.
[10] B. M. Gimarc, *J. Am. Chem. Soc. 105* (1983) 1979.
[11] G. Binsch, E. Heilbronner, *Tetrahedron 24* (1968) 1215.
[12] E. Heilbronner, Z-z. Yang, *Angew. Chem. 99* (1987) 369; *Angew. Chem. Int. Ed. Engl. 26* (1987) 360.
[13] C. Jutz in H. G. Viehe, H. Böhme (Eds.): *Iminium Salts in Organic Chemistry, Part 1*, Wiley, New York 1979, p. 401.
[14] H. G. O. Becker, V. Eisenschmidt, *Z. Chem. 8* (1968) 105.
[15] J. E. Oliver, S. C. Chang, R. T. Brown, J. B. Stokes, A. B. Borkovec, *J. Med. Chem. 15* (1972) 315.
[16] E. Nachbaur, G. Faleschini, F. Belaj, R. Janoschek, *Angew. Chem. 100* (1988) 703; *Angew. Chem. Int. Ed. Engl. 27* (1988) 701.
[17] G. Fritsch, G. Zinner, D. Mootz, M. Scherf, H. Wunderlich, *Arch. Pharm. (Weinheim. Ger.) 319* (1986) 646.
[18] Crystal structure analysis of **6a'**: Enraf-Nonius CAD4 diffractometer, $Mo_{K\alpha}$ radiation, single crystal $0.27 \times 0.33 \times 0.6$ mm^3, $T = 294$ K. Crystal data: $M_r = 562.599$, $\rho_{calcd} = 1.270$ g cm^{-3}, monoclinic, space group $C2/c$, $a = 2521.7(5)$, $b = 932.0(3)$, $c = 2507.2(6)$ pm, $\beta = 93.19(2)$, $V = 5.8831$ nm^3, $Z = 8$. scan: $2\theta = 4°$–$44°$; maximum measuring time 120 s. 3963 measured ($\pm h$, $+k$, $+l$), 3228 symmetry independent reflections, 2672 as observed [$I > 2\sigma(I)$]. Refinement parameters: 379. Solution of structure: MULTAN. Refinement with SHELXTL-Plus. $R = 0.0486$, $R_w = 0.0391$; largest residual electron density $= +0.24/-0.22$ e pm^{-3} 10^{-6}. Weighting $w = 1/\sigma^2(F_0)$.—Crystal structure analysis of **10b**: Enraf-Nonius CAD4 diffractometer, $Mo_{K\alpha}$ radiation, single crystal $0.2 \times 0.47 \times 0.53$ mm^{-3}, $T = 294$ K. Crystal data: $M_r = 448.53$, monoclinic space group $P2/c$, $a = 1673.7(4)$, $b = 786.7(2)$, $c = 3528.6(7)$ pm, $\beta = 90.4$, $V = 4.64989$ nm^3, $Z = 8$, $\rho_{calcd} = 1.282$ g cm^{-3}. Data collection: $2\theta = 4$–$46°$; maximum measuring time 120 s. 7139 measured ($\pm h$, $+k$, $+l$) reflections, 4800 as observed [$I > 2\sigma(I)$]. Refined parameters: 577. Solution of structure by MULTAN. Refinement with SHELXTL-Plus. $R = 0.0910$. Largest residual electron density $\rho = +0.43/-0.39$ e pm^{-3} 10^{-6}. There are three independent molecules. One molecule at general positions but with almost exactly twofold axis. Two molecules lie on twofold axes. (2f and 2c, resp.).—Further details of the crystal structure investigation are available on request from the Fachinformationszentrum Karlsruhe, Gesellschaft für wissenschaftlich-technische Information mbH, W-7514 Eggenstein-Leopoldshafen 2 (FRG), on quoting the depository number CSD-54997, the names of the authors, and the journal citation.
[19] P. A. Giguère, V. Schomaker, *J. Am. Chem. Soc. 65* (1943) 2025.
[20] W. H. Beamer, *J. Am. Chem. Soc. 70* (1948) 2979.
[21] H. L. Ammon, *Acta Crystallogr. Sect. B 30* (1974) 1731.
[22] R. Gompper, R. Guggenberger, R. Zentgraf, *Angew. Chem. 97* (1985) 998; *Angew. Chem. Int. Ed. Engl. 24* (1985) 984.
[23] R. Gompper, M. L. Schwarzensteiner, *Angew. Chem. 95* (1983) 553; *Angew. Chem. Int. Ed. Engl. 22* (1983) 543.
[24] J. Bordner, R. G. Parker, R. H. Stanford, Jr., *Acta Crystallogr. Sect. B 28* (1972) 1069.

Book Reviews are written by invitation from the editor. Suggestions for books to be reviewed and for book reviewers are welcome. Publishers should send brochures or (better) books to the following address: Redaktion Angewandte Chemie, Postfach 101161, D-6940 Weinheim, Federal Republic of Germany. The editor reserves the right of selecting which books will be reviewed. Uninvited books not chosen for review will not be returned.

Electrophilic Aromatic Substitution. By *R. Taylor*. Wiley, Chichester 1990. xvi, 513 pp., hardcover £ 85.00. – ISBN 0-471-92482-2

Twenty-five years ago this same author (in collaboration with *R. O. C. Norman*) wrote the highly regarded monograph "Electrophilic Substitution in Benzenoid Compounds". The present state of knowledge on electrophilic substitution in arenes has now been systematically and comprehensively covered in an almost completely rewritten book of eleven chapters. Heteroarenes are not included here, but benzenoid compounds such as annulenes, metallocenes and carboranes are. (Electrophilic substitutions in heteroarenes are soon to be treated by this author in collaboration with *A. R. Katritzky* in Volume 47 of the series *Advances in Heterocyclic Chemistry*.)

Electrophilic substitutions in arenes are among the classical reactions of organic chemistry that students have always been introduced to early in their courses. The book's preface tells us that about one third of world chemical production consists of arenes and substituted arenes. So, one might ask, in a field that has been so widely studied and worked over, is there much that is new to be reported? Indeed there is, as this book proves.

The first two chapters ("Introduction" and "The Mechanism of Electrophilic Aromatic Substitution") give a brief but adequate account of the theoretical and mechanistic basis needed to understand the chapters that follow (the theory of aromaticity; inductive, mesomeric and steric effects of substituents; possible mechanisms of S_EAr reactions, such as S_E1, B-S_E1, S_E3, S_E2 and A-S_E2). Chapter 3 ("Hydrogen Exchange") deals with the simplest types of electrophilic aromatic substitutions: deuteriodeprotonation (H/D exchange), tritiodeprotonation (H/T exchange), protiodedeuteriation (D/H exchange), protiodetritiation (T/H exchange) and deuteriodetritiation (T/D exchange) – all of which are reactions of special interest from a mechanistic standpoint. Chapter 4 ("The Replacement of a Substituent by Hydrogen") discusses fourteen reactions in which a substituent already present in the arene ring undergoes electrophilic replacement by a proton, ranging from protiodeauration through protiodealkylation to protiodesilylation. Also included in this group of reactions from a mechanistic standpoint is the hydrolysis of arylmagnesium halide Grignard reagents (protiodemagnesiation). Chapter 5 ("Metallation") deals with the replacement of hydrogen atoms in arenes by metals (Li, Au, Hg, B, Tl, Si, Pb, Sb, Te, Rh, Pd); however, the only one of these that has so far been categorized unequivocally as an electrophilic aromatic substitution is mercuration. Nevertheless, the author describes all the known arene metallation reactions, and invites further experimental investigations to remedy this gap in mechanistic knowledge. In Chapters 6 to 9 we find descriptions of electrophilic aromatic substitution reactions that are more familiar to the average chemist, with the various electrophiles arranged according to the periodic system. Thus Chapter 6 describes reactions using carbon electrophiles (e.g. Friedel-Crafts alkylations and acylations), Chapter 7 describes reactions using nitrogen electrophiles (e.g. azo couplings and nitrations), Chapter 8 deals with reactions involving oxygen, sulfur and selenium electrophiles (e.g. sulfonations), and Chapter 9 covers electrophilic halogenations. Chapter 10 ("The Replacement of a Substituent X by a Substituent Y") deals with 63 known *ipso*-substitution reactions, ranging from silyldelithiation through sulfodealkylation to halogen exchange. Lastly, in Chapter 11 ("Quantitative Evaluation of Electronic and Steric Effects in Electrophilic Aromatic Substitution") we learn something about quantitative relationships between structure and reactivity in electrophilic substitutions of arenes, about suitably modified Hammett equations with detailed tables of substituent constants and reaction constants, and about the factors that determine the *ortho/para* ratio in the product. A subject index completes this comprehensive work; however, there is no index of authors.

There is scarcely any aspect of electrophilic substitution of arenes that is not covered in this book, as can be judged from the inclusion of about 2700 literature references and 127 tables. The clear and attractive typography and lucid formula schemes make the book easy to read, and one quickly becomes absorbed. In doing so one comes across unexpected recent results, even concerning named reactions that have long been familiar. Anyone who seeks comprehensive and reliable information about electrophilic substitution in arenes would be well advised to borrow this book from the nearest library, which certainly ought to have it in its collection. However, the comparatively high price means that not many readers are likely to have their own copy for reference.

Christian Reichardt [NB 1093 IE]
Fachbereich Chemie
der Universität Marburg (FRG)

The Chemistry of Metal Cluster Complexes. Edited by *D. F. Shriver, H. D. Kaesz* and *R. D. Adams*. VCH Verlagsgesellschaft, Weinheim 1990. 439 pp., hardcover DM 164.00. – ISBN 3-527-28047-2

Not surprisingly for such a rapidly expanding field of research, another monograph on the chemistry of metal clusters has now appeared; it is certainly the most up-to-date and well presented. This is not least because of the publishers' attractive production of the book. Like its predecessors (B. F. G. Johnson (Ed.): *Transition Metal Clusters*, Wiley, Chichester 1980; M. Moskovits (Ed.): *Metal Clusters*, Wiley, New York 1986; B. C. Gates, L. Guczi, H. Knözinger (Eds.): *Metal Clusters in Catalysis*, Elsevier, Amsterdam 1986) this monograph edited by acknowledged experts is a collection of individual contributions by well-known authors, some of whom have published similar articles elsewhere. This naturally means that the book does not have the character of a unified whole. Despite the evident efforts by the editors to achieve some unity, it remains true that the chapters of this book are independent articles; in this situa-

tion instances of overlapping and conflicting descriptions are unavoidable. The reader should therefore not expect to be given an overall view of cluster chemistry; instead he or she is presented with a collection of independent progress reports on different aspects of cluster chemistry, all of which are of a high standard.

A brief introduction by *H. D. Kaesz* and *D. F. Shriver* explaining the layout of the subject matter is followed by a detailed chapter on structures and bonding theories which is very useful for the reader who seeks a systematic treatment; what is especially impressive is the strict separation of facts from interpretations. The types of structures that are observed, the rules regarding numbers of electrons and their theoretical basis are kept clearly separate. In the following chapter *R. D. Adams* sets out to bring some systematic order into the synthesis of metal clusters, a very difficult task in view of the many facets of their chemistry and the random nature of the preparative methods used. More amenable to classification are ligand substitution reactions and ligand transformations in metal clusters, which are treated in two chapters by *D. J. Darensbourg* and *G. Lavigne* respectively, though with some overlapping. Despite the very compressed style, the article by *Lavigne* is undoubtedly of great importance for the synthetic chemist. The chapter by *B. F. G. Johnson* and *A. Rodgers* on polyhedral rearrangements and fragmentations of metal clusters, unlike the rest of the chapters in the book, does not aim to systematically treat a large amount of information; instead it consists of a fundamental discussion of the energetic aspects of metal clusters. In the chapter on metal clusters as homogeneous catalysts and catalyst precursors *W. L. Gladfelter* and *K. J. Roesselet* give an up-to-date though not exhaustive review of the state of knowledge in this area. The book ends with a very useful literature survey by *M. I. Bruce* listing review articles on cluster chemistry, covering the period from 1965 to 1988.

Among the faults noted are a number of inconsistencies in formulas which are rather more serious than isolated printing errors. There are arbitrary differences in the sequence of the ligands in the formulas of analogous complexes, as in $[HRu_3(CO)_{11}]^{\ominus}$ (p. 230) and $[Fe_3(\mu\text{-}H)(CO)_{11}]^{\ominus}$ (p. 239). Ionic complexes mentioned in the same context are written in one case with square brackets and in another case without: $Co_6(CO)_{15}^{2\ominus}$ (p. 310) and $[H_3Os_4(CO)_{12}]^{\oplus}$ (p. 311). Then neutral clusters too are shown in square brackets, though again not in all cases: $[Au_{11}(PPh_3)_7(SCN)_3]$ (p. 65) in contrast to $Au_{11}(PPh_3)_7(SCN)_3$ (p. 67). The representation of ionic complexes generally is very confused: thus on page 222 the cation $[Co_3Cp_3(\mu\text{-}H)(\mu_3\text{-}\eta^2\text{-}CH_2]^{\oplus}$ is identified as **[75]**, whereas in the figure on the same page the formula shows no charge but has the symbol **[75]**$^{\oplus}$. Furthermore, the coordination number assigned to a complex in the ionic complexes relates in one case to the cluster ion alone but in another to the salt as a whole, **[83b]** (p. 223). Also the coordination numbers are written, apparently arbitrarily, in one case in square brackets and in another case in curved brackets: **[179]** and **(179)** on page 250. In the reaction schemes the formulas are occasionally printed without the subscript or superscript forms of the numbers: e.g. PR3 and BuCHN2 (p. 210). Naturally all these errors in the formulas cause difficulties in reading the book.

Lastly there is the question of the choice of material. It is unpardonable that the superclusters discovered recently by *G. Schmid* and the concept of the "magic numbers" are nowhere mentioned. This very important discovery, which fills the much discussed gap between "molecular" and "metallic" metal clusters, should certainly be included in an up-to-date monograph on metal clusters. There is also no mention (even in the bibliography) of one of the best introductory review articles on metal cluster compounds, the three-part review by *B. Walther* in *Zeitschrift für Chemie (Leipzig)*; the first two parts of this appeared in 1986 and 1988. These two examples show once again that even important publications in German journals become known to only a limited extent, or very late, in the English language science world.

Summary: A book which is indispensable to the cluster chemist, and is very useful despite its shortcomings.

Georg Süss-Fink [NB 1106 IE]
Institut de Chimie
Université de Neuchâtel (Switzerland)

Lectins. By *N. Sharon* and *H. Lis*. Chapman and Hall, London 1989. vii, 127 pp., hardcover £ 19.50. – ISBN 0-412-27380-2

Anyone who looks up the keyword "Lectin" in a textbook of biochemistry will find little space devoted to this topic. Although one can certainly justify an individual treatment of a special field of study, the question arises as to whether such a book is likely to find a readership beyond the narrow confines of the specialist discipline. To assess how useful reading this book is likely to prove, the main factors to be considered are the degree of importance of the research topic in relation to other areas, and the didactic quality of the presentation.

The coining of expressions such as glycobiology or tumor lectinology, and the considerable increase in the last few years in the number of papers on lectins that appear in journals dealing with remarkably varied fields of work, are evidence of a growing interest in this topic, and especially in the function of the interaction between the sugar part of the cellular glycoconjugate and the specific binding proteins. Proteins that have the capacity to recognize sugar structures of this type therefore constitute an essential link in this form of biological information transfer; our present state of knowledge concerning these is merely the tip of the iceberg. This class of sugar receptors, which according to their definition are distinct from enzymes and antibodies, includes the lectins. To isolate them, to determine their sugar specificity, and to localize them, one requires sugar structures that are coupled to suitable carriers. To produce these represents a challenge for organic chemists and biochemists. The fact that lectins can be localized using suitable sugar ligands, and the availability of the lectins as sugar-specific laboratory agents, leads to uses in cell biology, immunology and histochemistry. Our present understanding of the way in which they function, which is still only in its infancy, indicates a great potential for clinical applications, the exploitation of which can indicate ways of overcoming infections, of achieving therapeutically advantageous immune modulation, and of extending the armory of agents for labeling tumors.

N. Sharon and *H. Lis* are therefore to be commended on having emphasized in their book on lectins the inherently interdisciplinary nature of the subject, in a presentation that is consistently lucid and comprehensible. For this reason interested students can benefit from using the book as an extension to textbooks, by working through seminar topics with the help of relevant individual chapters. In a clearly arranged sequence the authors describe the occurrence of lectins, their biological activities and functions insofar as these have been measured up to now, their sugar specificities, structural and biosynthetic aspects, and the many different ways in which they are used as a laboratory tool.

The book includes an excellent and entertaining outline of the history of the scientific study of lectins, which goes back more than a hundred years. Every chapter makes it clear, even to the non-specialist reader, that this history will be enriched by further additions as a result of studies that are now in progress or will be carried out in the future. This gives one an extra incentive to absorb the information presented here, so as to provide a basis for following and understanding such future developments as they occur. Therefore it is to be hoped that the book will be widely read, and that it will not be too long before a new updated edition appears. However, the reader interested in this topic is not advised to wait for such a new edition. It is to be hoped, and is indeed likely in view of the quality and presentation of the material in this well set out and easily digestible survey, that readers—especially those who are not lectins specialists—will be motivated to keep informed about progress in relevant sectors of the field of lectins. Finally, it can be assumed that some of the information that this book contains, such as the role of lectins in viral and bacterial infections or in transport of glycoproteins, will also in due course find its way into the standard textbooks.

Hans-Joachim Gabius [NB 1097 IE]
Max-Planck-Institut für experimentelle Medezin,
Göttingen (FRG)

A Random Walk Through Fractal Dimensions. By *B. H. Kaye*. VCH Verlagsgesellschaft, Weinheim/VCH Publishers, New York 1989. xxv, 421 pp., hardcover DM 138.00 (paperback DM 64.00).—ISBN 3-527-26468-X/0-89573-496-6

The concept of fractals, invented by *Benoît B. Mandelbrot*, has by its vivid imagery altered ways of scientific thought to an extent that is perhaps greater than that caused by the second law of thermodynamics. It is doubtless also because of this graphic quality that a large number of scientists have already become involved with this new tool. Publications reviewing this subject are therefore to be welcomed. The book by *B. H. Kaye* is neither a handbook nor a work of reference; instead it contains exactly what its title promises: a random walk through fractal dimensions, confined to the scientific and mathematical aspects. The mathematical procedure of fractals is likewise a random one, but it certainly does not lack a plan. Its basic operations are governed by strict rules, but these are then applied to random numbers. Although fractals are ultimately a mathematical device, formulas are avoided in the book. Regrettably, this is taken so far that one is not even given a mathematical definition of the term "fractal". An extreme case is the chapter entitled "Mathematical Description of Fractal Clusters", which contains only two quite unimportant formulas. The vague references in the text to "famous" names in the field are rather annoying; for more detailed information one has to refer to the bibliography.

The value of the book lies in its plentiful illustrations and the directness of its style, together with the fact that, due to the absence of mathematical detail, it is very easy to read. It is therefore very suitable as a first introduction to the topic. It can be used as a supplement to basic treatments of the subject, in particular to those by *Mandelbrot* or to those that deal with special aspects. It offers a wealth of new examples drawn from mathematics, scientific statistics and various fields of science. The main emphasis of the application examples is in the author's special field of dispersed phases. The book also serves as a stimulus for further research.

Erich Robens [NB 1115 IE]
Institut für Anorganische und Analytische Chemie
der Universität Mainz (FRG)

Structure and Reactivity in Reverse Micelles. (Series: Studies in Physical and Theoretical Chemistry, Vol. 65). Edited by *M. P. Pileni*. Elsevier, Amsterdam 1989. xviii, 379 pp., hardcover, HFl 285.00.—ISBN 0-444-88166-2

This book, which is published as Volume 65 in the series "Studies in Physical and Theoretical Chemistry", is concerened with topical problems in the field of reverse micelles. It consists of 21 individual contributions by different authors, most of whom do not confine themselves to a narrow definition of reverse micelles but also include microemulsions in this class. The aspects emphasized in the articles fall under three headings: the applications of various analytical techniques, solubilization, and chemical reactions in reverse micelles and microemulsions. The treatment of structural problems which is promised in the book's title is limited to that arising in the chapters on analytical techniques and solubilization, and is mainly restricted to "classical" reverse micelles.

The analytical techniques that are described include methods of investigating structure, such as light-, X-ray- and neutron-scattering measurements, as well as electron microscopy and various spectroscopic methods. First the applicability of each individual technique to the study of structure and reactions in reverse micelles is discussed, then particular types of reverse micelles are used as examples to illustrate the capabilities and limitations of the various analytical methods.

In the articles on solubilization in reverse micelles and microemulsions the main emphasis is on discussions concerning the site of the preferential solubilization and the associated structural changes. Also the various solubilization techniques and their advantages and disadvantages are discussed in detail.

The reactions that can be carried out in reverse micelles and microemulsions include such widely different processes as pulse radiolysis, electron transfer, photoreactions, the preparation of clusters of metallic and semiconducting elements, polymerizations and enzymic catalysis. Although here too the reactions are in some cases used to gain more detailed knowledge about the structures of reverse micelles, the dominant theme is the idea of using reverse micelles as variable microreactors.

The form of the book, consisting of separate individual contributions, has made it possible to present a very wide range of topics within the overall theme of reverse micelles. The articles provide the reader with numerous up-to-date references to original papers on each of the topics treated. Representatives of widely differing schools of thought such as *P. L. Luisi* and *K. Martinek* have an opportunity to put their views; this area of research is thereby presented, with its attendant controversies, as one that is active and exciting, and in which one can still expect many interesting developments.

Although good use has been made of the opportunities presented by a book made up of separate contributions, one is left with the usual problems of this format: the following of a central theme is sacrificed in favor of breadth of subject matter. The attempt by *P. L. Luisi* to provide an aid to orientation alongside the contributions dealing with their

special topics is a very good idea, even though it is not ideally placed in the book. In their efforts to convey their special interests the authors of the individual articles have tended to neglect the treatment of the fundamentals, and they often assume that the reader has an extensive knowledge of colloid chemistry. In many cases it is difficult to relate the individual contributions to each other, especially as their subject matter is not always well harmonized: many points are explained several times, others not at all, so that parts of the book are quite laborious to read. Also some expressions are used with different meanings in different chapters, and no consistent notation is used for the mathematical equations.

One has a general impression that the proofreading has been rather perfunctory. Often one comes across errors that might be excused as mere blemishes in the main text, but which cause problems when they occur in keywords (e.g. "Stibene" frequently instead of "Stilbene") or in literature references. There are other minor errors which cause annoyance, such as missing chapter numbers (which frustrate the laudable attempts of some of the authors to refer to "Chapter X" by one of the others), or gaps in the subject index: for example, one searches in vain for "NMR" under the letter N – instead it appears under R with just one entry (!) as "Reversed micelle, NMR in".

Despite its shortcomings the book can definitely be recommended as a source of more advanced information on the field of reverse micelles, not least because of its references to recent literature for further reading. However, as a first introduction to this field the book is of only limited suitability. Some of the many review articles that are available on this subject offer better introductions.

André Laschewsky [NB 1090 IE]
Institut für Organische Chemie
der Universität Mainz (FRG)

Organic Chemistry in Action. The Design of Organic Synthesis. (Series: Studies in Organic Chemistry 41). By *F. Serratosa*. Elsevier, Amsterdam 1990. xxi, 395 pp., hardcover HFl. 290.00.—ISBN 0-444-88345-2

Synthesis is still the main occupation of many organic chemists. The systematic development of retrosynthesis by *Corey* has contributed to the "renaissance" of synthetic chemistry as a whole. The large number of recently published natural products syntheses are a lively proof of this fact. In spite of the large efforts in synthesis relatively few books are available to introduce synthesis and synthesis planning to students. The book "Organic Chemistry in Action" by *F. Serratosa* together with a copy of the program CHAOS aims to provide such an introduction to organic synthesis. The combination of a book with a computer program is new and should hopefully facilitate the learning process for beginners.

Serratosa's book can be divided into four parts. Chapters 1 to 4 present the basic concepts of synthesis planning. After a short introduction to the history of synthesis the criteria for evaluating synthetic schemes are introduced. The next chapter treats the systematic analysis of reactivity according to *Evans*. A short introduction to retrosynthesis follows. In the second part specific synthetic problems are treated. The first problem is the synthesis of "dissonant" systems or, according to *Seebach*'s more familiar nomenclature, the application of the "Umpolung" concept. Next a series of synthetic methods for synthesizing rings are presented. Strategies for synthesizing structures with quaternary carbon atoms and bridged systems are described in Chapter 7. *Corey*'s rules for finding strategic bonds are nicely introduced using patchouli alcohol as an example. This part concludes with a discussion of how to achieve stereochemical control in ring and acyclic systems. In Chapter 9 on diastereoselectivity in reactions of acyclic compounds, several variations of the aldol reaction are treated followed by a short overview on Sharpless epoxidation. A recapitulation of the heuristic rules and their application, illustrated by a series of examples taken from the literature, forms the third part, which concludes the main text. The last part is unfortunately arranged in a rather fragmented way, consisting of Chapter 11, Appendices 2 to 4, and the diskette containing a copy of the program CHAOS (Computerisation and Heuristics Applied to Organic Synthesis). Appendix 2 is a tutorial for the use of CHAOS. In addition there is a list of the retrosynthetic steps used by CHAOS and some suggestions for exercises. Chapter 11, which is a description of CHAOS, fits uneasily into the book's text.

To try to combine a textbook on organic synthesis and planning with a computer program is certainly a good idea. Unfortunately the present publication cannot be considered to be a good combination of the two media. The program is not polished enough to be a valuable help in the learning process. CHAOS certainly cannot be used as an alternative to other synthesis programs or reaction data bases. Looking at the price the purchase of this book can only be recommended for libraries or for lecturers preparing courses on organic synthesis. It only can be hoped that a much cheaper version without the diskette will appear soon, thus enabling students to profit from the nicely chosen examples; at the same time the numerous printing mistakes could be eliminated.

Reinhard Neier [NB 1127 IE]
Institut für Organische Chemie
der Universität Fribourg (Switzerland)

EPR of Exchange Coupled Systems. By *A. Bencini* and *D. Gatteschi*. Springer, Berlin 1990. x, 287 pp., hardcover DM 178.00.—ISBN 3-540-50944-6

This book is concerned with the theory of electron paramagnetic resonance spectroscopy (EPR) and magnetic properties for systems containing two or more magnetically coupled paramagnetic centers (transition metal ions and/or free radicals). A knowledge of the basic theory of EPR spectra of isolated centers is an essential prerequisite for understanding this monograph.

After discussing the exchange and superexchange interaction mechanisms, including an explanation of the empirical rules established by *Goodenough* and *Kanamori* for the occurrence of ferromagnetic and antiferromagnetic exchange in magnetically coupled systems, the authors discuss in detail the spin Hamiltonian operator for such systems. Chapter 3 then deals with the spin levels and EPR spectra of magnetically coupled pairs and their dependence on the exchange interaction. The spin Hamiltonian operators of the isolated centers and the interaction operator are then used as the basis for deviving the spin Hamiltonian operator for the coupled system, by using irreducible tensor operators. From this one obtains the relationship between the parameters in the spin Hamiltonian for the individual centers (g-tensor, fine structure tensor D and hyperfine structure tensor A) and those for the coupled system. Following this, the spin Hamiltonian operators and EPR spectra of clusters of paramagnetic species are analyzed, with the emphasis on treating systems with strong exchange interactions (triads and tetrads). For

these systems too the relationships between the spin Hamiltonian parameters for the individual centers and those for the coupled system are derived; the matrix elements needed for this derivation are set out in the form of clear tables. Chapter 5 deals with spin-lattice relaxation processes in magnetically coupled spin systems; the authors limit their discussion almost exclusively to the relaxation behavior of paramagnetic ion pairs (dimers of Ir^{4+}, Fe^{3+} and Cu^{2+}).

The chapters that follow provide a good review of experimental EPR studies on model systems with magnetically coupled centers that are of importance in physics, chemistry and biology. Chapter 7 discusses EPR spectra of paramagnetic ion pairs and of diradicals, and Chapter 8 deals with spectra of systems in which paramagnetic ions and free radicals are magnetically coupled. The application of EPR spectroscopy to studies of magnetically coupled species in biological materials is currently a topic of great importance, and Chapter 9 therefore deals with EPR spectra and the structural information that they yield for copper and iron proteins and for exchange coupled species in complexes that are important for photosynthesis. Chapter 10 describes the magnetic properties and EPR spectra of low-dimensional spin systems consisting of a large number of magnetically coupled paramagnetic ions. One- and two-dimensional structures are considered in detail. The final chapter describes the application of EPR spectroscopy to studies of excitons and their motions in diamagnetic solids.

The book is intended for advanced students and for scientists (physicists, chemists and biologists) involved in work in the area of EPR spectroscopy or on the magnetic properties of materials. For these readers the monograph provides a speedy and thorough introduction to studies of the magnetic properties and EPR spectroscopy of magnetically coupled systems, without having to read the widely scattered original publications. However, in order to understand the theories treated in the book one must have a knowledge of certain aspects of quantum mechanics (second-order quantization, properties of angular momentum operators, irreducible tensor operators). The book concludes with an appendix on second-order quantization and the properties of the angular momentum and irreducible tensor operators.

Rolf Böttcher [NB 1110]
Sektion Physik
der Universität Leipzig (FRG)

Chemical Reactions of Natural and Synthetic Polymers. (Ellis Horwood Series in Polymer Science and Technology). By *M. Lazár, T. Bleha* and *J. Rychlý*. Ellis Horwood, Chichester 1989. 250 pp., hardcover, £ 35.00.—ISBN 0-7458-0193-5

Previous titles in the "Polymer Science and Technology" series have included "Chromatography of Synthetic and Biological Polymers", "Polymers and their Properties", "Cellulose and its Derivatives", "Wood and Cellulosics", "Chemical Reactions of Natural and Synthetic Polymers", "Cellulose Chemistry and its Applications", "Polymers as Materials for Packaging" and "Styrene-Based Plastics and their Modifications". The declared aim of this series is to cover the field of natural and synthetic polymers, including the latest developments in basic research and in industry. It is against this claim that the quality of the present book must be evaluated. A further question that seems important to me is whether there is a need for monographs of this kind, which have recently been published in increasing numbers. In principle I welcome books of this type, in which experts provide the reader with an introduction to a specialized field. There is hardly a better way of familiarizing oneself with a specialist topic.

The monograph consists of ten chapters. Chapter 1 discusses the most important aspects of chemical reactions of polymers, such as the effects of neighboring groups, the influence of the medium, and intra- and intermolecular reactions. These effects are treated in textbook style with well-chosen examples. It is annoying to find it stated (pp. 14, 27) that the functional groups in a polymer react at rates equal to those for the same groups in small molecules. If that were so one would have no need for this monograph. A few lines later the authors contradict the statement by pointing out that it is only *very rarely* the case. The authors' arguments are in most cases easy to follow. However, the generalization that in carrying out reactions on polymers one should choose a solvent such that the product is precipitated (p. 21) seems ill-conceived; in many cases the opposite course is more sensible. Apart from these points the chapter is clearly presented, leaving aside the microdiagrams and especially the microcaptions.

The next chapter describes ways of modifying structural units that are also used in technological applications. These include fluorinations and chlorinations of hydrocarbon polymers, reactions at double bonds and cyclizations. In each case there is a very detailed discussion of mechanisms. The doping of polymers to increase the electrical conductivity is also described. Three pages are devoted to the many different reactions of polymers containing aromatic structural units. This section is rather too short in view of importance of such reactions, e.g. for synthesizing ion-exchange media. In this chapter, of course, one should not omit to describe such technologically important reactions as the hydrolysis of polyvinylacetates or the modification of natural polymers, e.g. in the xanthane reaction of cellulose. The rearrangement reaction described on pages 71–72 is due to *A. W. von Hofmann*, not to a man named *Hoffman*.

Chapter 3 deals with branched polymers, and especially with grafting. Regrettably, the section on "Macromolecular Initiators" deals only with peroxides and redox systems; there is no mention of the more than twenty publications on polymeric azo initiators that have come from the *Kerber* and *Heitz* groups.

Another polymer modification reaction that is certainly of great importance is crosslinking. Chapter 4 describes the main methods used for synthesizing network structures. These are presented very clearly, including modern approaches such as ionomers and the principle of physical crosslinking. A description of the general principles is followed by detailed accounts of particular systems and the crosslinking methods that can be used in each case. Interpenetrating networks are also briefly touched on. The very short Chapter 5 deals with polymer-polymer exchange reactions. Unfortunately the important "urethane exchange" class of reactions is not mentioned here. However, this chapter does to some extent live up to the book's title, as it deals with the interactions between dissimilar DNA molecules which can be used, for example, to study genetic defects.

The next chapter, on polymer degradation, is much more comprehensive; this deals with photooxidative degradation, thermolysis, thermooxidative degradation, and also the burning of polymers. Further sections on mechanochemical degradation, ozonolysis, and radiolytic, ionic and biological degradation complete this chapter.

The protection of polymers from degradation is an important prerequisite to allow their use as constructional materials. Chapter 7 deals with additives that confer this protec-

tion. These include UV stabilizers, antioxidants, quenching agents and fire-retardants. These are all substances designed to prevent or hinder reactions of the polymer. In my view, therefore, this chapter does not quite fit into the overall theme of the book. Moreover, there exists a considerable number of fundamental monographs and review articles on the subject which are not mentioned in the bibliography of this chapter.

One of the most important aims of polymer modification is to obtain materials with new combinations of properties, and to synthesize structures that cannot be obtained in other ways. This topic is covered in Chapter 8. Methods are described that can be used to alter the crystallinity, solubility, permeability, and also the mechanical and electrical properties.

The next chapter is concerned with present and future applications of materials produced by modifying polymers. Included here are, of course, the cellulose derivatives, crosslinked polyethylene, crosslinked casein, polyisobutylene copolymers, and various other types of elastomers such as modified PVC. The principles of manufacturing and using semipermeable membranes, functionalized polymers, polymeric reagents and polymeric catalysts are also described.

The final chapter describes recent developments such as the measurement of molecular motions in polymers by introducing fluorescence probes. Theoretical models for energy conversion processes such as thermal to mechanical, chemical to mechanical and light to chemical energy are at least briefly mentioned.

This book offers interesting reading both for experts and for those wishing to begin work in this area. Despite the weaknesses mentioned, the different aspects of the subject are covered in a way which gives an impression of uniformity. The book is fluently written and deals with all the important aspects of this highly complex area of polymer research. In view of the increasing level of activity in the area of polymer modification I consider this to be a useful book.

Oskar Nuyken [NB 1120 IE]
Lehrstuhl für Makromolekulare Chemie I
der Universität Bayreuth (FRG)

Registered names, trademarks, etc. used in this journal, even when not marked as such, are not to be considered unprotected by law.

© VCH Verlagsgesellschaft mbH, W-6940 Weinheim, 1991. – Printed in the Federal Republic of Germany by Konrad Triltsch Druck- und Verlagsanstalt Würzburg.

All rights reserved (including those of translation into foreign languages). No part of this issue may be reproduced in any form — by photoprint, microfilm, or any other means — nor transmitted or translated into a machine language without written permission from the publishers. Only single copies of contributions, or parts thereof, may be made for personal use. This journal was carefully produced in all its parts. Nevertheless, authors, editors and publisher do not warrant the information contained therein to be free of errors. Readers are advised to keep in mind that statements, data, illustrations, procedural details or other items may inadvertently be inaccurate.

Valid for users in the USA: The appearance of the code at the bottom of the first page of an article (serial) indicates the copyright owner's consent that copies of the article may be made for personal or internal use, or for the personal or internal use of specific clients. This consent is given on the condition, however, that the copier pay stated per-copy fee through the Coypright Clearance Center, Inc. (CCC), for copying beyond that permitted by Sections 107 or 108 of the U.S. Copyright Law. This consent does not extend to other kinds of copying, such as copying, for general distribution, for advertising or promotional purposes, for creating new collective works, or for resale. For copying from back volumes of this journal see 'Permissions to Photo-Copy: Publisher's Fee List' of the CCC.

Editorial office: Postfach 10 11 61, W-6490 Weinheim, Federal Republic of Germany, Telephone (06201) 60 23 15, Telex 465 516 vchwh d, Telefax (06201) 602 328, E-Mail Z16@DHDURZ2 in Earn Bitnet.

Editor: *Peter Gölitz*

Associate editors: *D. I. Loewus, K. J. Schneider, A. Stimson.* **Editorial assistant:** *E. Schweikart*

Publishers: VCH Verlagsgesellschaft mbH. (Managing Directors: *Hans Dirk Köhler, Dr. Hardy G. Sehrt.*), Pappelallee 3, W-6940 Weinheim, Federal Republic of Germany.

Advertising office (Advertising Manager *R. J. Roth*): Postfach 10 11 61, W-6940 Weinheim, Federal Republic of Germany, Telephone (0 62 01) 60 61 36, Telex 467 155, Telefax (0 62 01) 606 156.

ANGEWANDTE CHEMIE
International Edition in English
Volume 30 · Number 4
April 1991
Pages 343–454

Ribonuclease T1: Structure, Function, and Stability**

By C. Nick Pace, Udo Heinemann, Ulrich Hahn, and Wolfram Saenger*

Proteins carry out the most important and difficult tasks in all living organisms. To do so, they must often interact specifically with other small and large molecules. This requires that they fold to a globular conformation with a unique active site that is used for the specific interaction. Consequently, protein folding can be regarded as the "secret of life". Biochemists and chemists have a great interest in elucidating the mechanism by which proteins fold and in predicting the folded conformation and its stability given just the amino acid sequence. This challenge is sometimes called the "protein folding problem". The ability to construct proteins differing in sequence by one or more amino acids and to analyze their three-dimensional structures by X-ray crystallography and NMR spectroscopy is a powerful tool for investigating the conformational stability and folding of proteins. Several proteins are now under intensive study by this approach. One of these is ribonuclease T1.

1. Introduction

Studies of the ribonucleases have made a major contribution to our understanding of the structure, function, and stability of enzymes.[1–5] Ribonuclease A (RNase A), the best-studied mammalian enzyme, and ribonuclease T1 (RNase T1), the best-studied microbial enzyme, resemble each other in function and small size, but are not homologous in amino acid sequence or three-dimensional structure.[1, 4] Detailed crystallographic studies of RNase A and its derivatives and complexes have been published by over 12 laboratories,[2] and 9 crystal structures have been determined for RNase T1. This wealth of structural information and the small size of these enzymes ensure that future studies of the ribonucleases will continue to improve our understanding of enzymes.

The active center of the ribonucleases is clearly divided into a substrate recognition site, which is specific for certain nucleic acid bases, and a catalytic site, where cleavage of the phosphodiester bond takes place.[2, 5] RNase A recognizes the pyrimidine bases uracil and cytidine, whereas the microbial RNases are specific for guanine or for guanine and adenine, or they are nonspecific. Due to its high specificity for guanine in single-stranded RNA, RNase T1 has found wide application as a tool in RNA sequencing and mapping studies.[6–8] RNase A and the microbial RNases act on RNA in a similar acid/base-catalyzed two-step mechanism, which first involves a transesterification to produce a 2′,3′-cyclic phosphate and then hydrolysis to the 3′-phosphate.

Originally, RNase T1 was isolated from Takadiastase, a commercial preparation of the culture medium of the mold fungus *Aspergillus oryzae*, in two isoforms with either Gln or Lys at position 25 (Gln25-RNase T1 or Lys25-RNase T1,

[*] Prof. Dr. W. Saenger, Priv.-Doz. Dr. U. Heinemann, Priv.-Doz. Dr. U. Hahn
Institut für Kristallographie der Freien Universität
Takustrasse 6, W-1000 Berlin 33 (FRG)
Prof. C. N. Pace
Biochemistry Department, Texas A & M University
College Station, TX 77843 (USA)

[**] The authors' work was supported by the National Institutes of Health (NIH), the Robert A. Welch Foundation, the Texas Agricultural Experiment Station, and the Deutsche Forschungsgemeinschaft.

 © VCH Verlagsgesellschaft mbH, W-6940 Weinheim, 1991 0570-0833/91/0404-0343 $ 3.50+.25/0

Fig. 1).[5, 9] More recently, the gene for RNase T1 was cloned in *Escherichia coli* by genetic engineering methods using three strategies.[10–13] In one, RNase T1 was expressed as a fusion protein and cleaved by cyanogen bromide to produce RNase T1 in modest quantities;[10] in the other two, the gene was cloned downstream from a gene for a transmembrane signal peptide and active RNase T1 was excreted into the periplasm, from which it could be isolated in quantities of up to 50 mg per liter of culture medium.[11–13] This work has provided access to RNase T1 molecules specifically altered at any desired amino acid residue by site-directed mutagenesis. In the discussion that follows, mutant ribonucleases will be designated XnY to show that amino acid X at position n has been replaced by amino acid Y.

In this review, we first describe the structure of RNase T1 bound to various ligands and inhibitors, next we summarize a series of experimental studies of the conformational stability of RNase T1, and, finally, we consider the conformational stability of RNase T1 in terms of the three-dimensional structure. These studies are helping us gain a better understanding of the forces that stabilize the folded, biologically active conformations of proteins and should eventually contribute to a solution of the protein folding problem.

2. Three-Dimensional Structure of RNase T1 Complexed with Different Ligands

Several crystal structures of RNase T1 have been determined at medium to high resolution (Table 1). They often contain derivatives of guanosine bound to the enzyme recognition site, but crystal structures of wild-type and mutant

C. Nick Pace was born in 1940 in Delta, Utah (USA). He studied chemistry at the University of Utah (B.S., 1962) and biochemistry at Duke University (Ph.D., 1966). After working as a postdoctoral fellow in the chemistry department at Cornell University, he became Professor in the Biochemistry Department at Texas A & M University in 1968. His main research interest is the conformational stability and mechanism of folding of globular proteins.

Udo Heinemann was born in 1953 in Bebra-Iba, Hessen (FRG) and studied chemistry at the Universität Göttingen, where he received his Ph.D. in 1982 for work done at the Max-Planck-Institut für experimentelle Medizin in Göttingen. He then worked as a postdoctoral fellow at the Molecular Biology Institute, University of California at Los Angeles. From 1985 to 1991, he was an "Assistent" at the Institut für Kristallographie der Freien Universität Berlin, where he became a Privatdozent in 1989 and a Heisenberg fellow of the Deutsche Forschungsgemeinschaft in 1991. Crystallographic and biochemical studies of nucleic acid and protein structure are his major fields of interest.

Ulrich Hahn was born in 1950 in Kassel (FRG). He studied agricultural sciences and biology at the Universität Göttingen, where he received his Ph.D. in 1980 for work done at the Max-Planck-Institut für experimentelle Medizin in Göttingen. After working as a postdoctoral fellow at this institute, he moved to the Institut für Kristallographie der Freien Universität Berlin in 1982 as a staff scientist (Akademischer Rat). Since 1989, he has been a Privatdozent. Gene technology and protein engineering of nucleic acid binding proteins are his fields of interest.

Wolfram Saenger was born in 1939 in Höchst/Main (FRG). He studied chemistry in Darmstadt and Heidelberg and received his Ph.D. in 1965 at the Technische Hochschule Darmstadt for work done at the Max-Planck-Institut für experimentelle Medizin in Göttingen. After working as a postdoctoral fellow at Harvard University, he served as head of the X-ray crystallography group at the Max-Planck-Institut für experimentelle Medizin from 1967 to 1981. He was also a Privatdozent (1971–77) and Professor (1977–81) at the Universität Göttingen. Since 1981, he has been a full professor at the Institut für Kristallographie der Freien Universität Berlin. In 1987 he received the Leibniz award of the Deutsche Forschungsgemeinschaft and in 1988 the Humboldt award. His interests focus on structural chemistry and structure–function relationships of biological macromolecules.

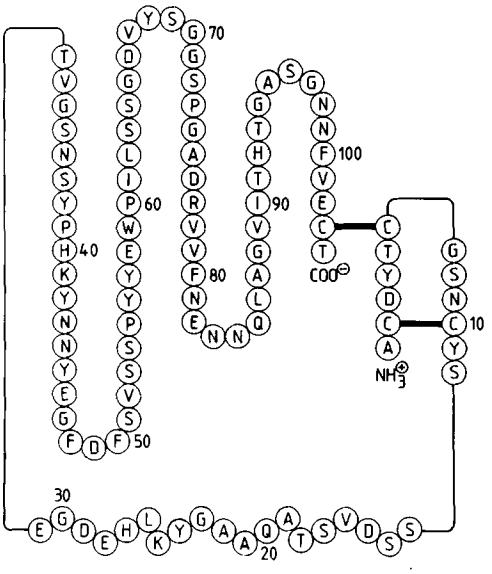

Fig. 1. Amino acid sequence of RNase T1 [5, 9] drawn in a way that emphasizes the secondary structure of the protein. Standard one-letter code has been used to denote amino acid residues.

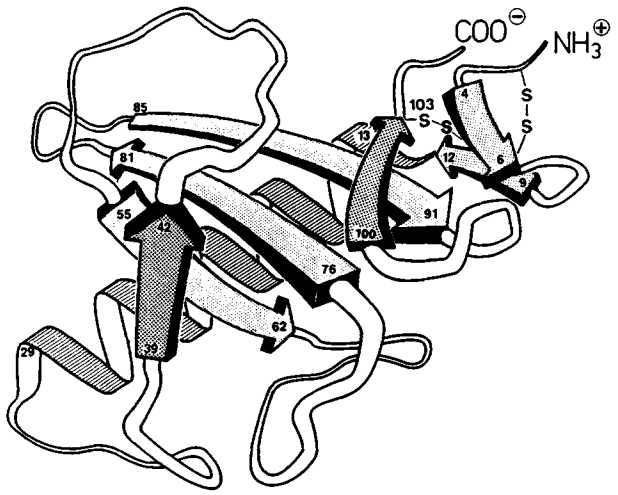

Fig. 2. Three-dimensional structure of RNase T1. The α-helix is shown as a wound ribbon; arrows mark the strands of the pleated sheets. Numbers indicate beginning and end of secondary structure elements, and the disulfide bonds are shown.

RNase T1 where this site is free have also been described. In all the crystal structures, RNase T1 adopts essentially the same three-dimensional polypeptide folding as displayed in Figure 2.

The polypeptide chain is cross-linked by two disulfide bonds from Cys 2 and Cys 10 and from Cys 6 to Cys 103. The

Table 1. Crystal structures of ribonuclease T1.

Enzyme [a]	Bound inhibitor [b]	Space group	Lattice constants	d_{min} [c] [Å]	R [d]	Ref.	Protein data bank entry [e]
Lys25-RNase T1	2′-GMP	$P2_12_12_1$	$a = 46.81$ Å $b = 50.11$ Å $c = 40.44$ Å	1.9	0.180	[14–16]	1RNT
Gln25-RNase T1	2′-GMP	$P2_12_12_1$	$a = 46.65$ Å $b = 50.26$ Å $c = 40.60$ Å	1.9	0.203	[17,18]	–
Gln25-RNase T1	3′-GMP	$P2_12_12_1$	$a = 47.58$ Å $b = 50.92$ Å $c = 40.32$ Å	2.6	0.274	[19]	–
Lys25-RNase T1	2′,5′-GpG	$P2_12_12_1$	$a = 47.44$ Å $b = 50.90$ Å $c = 40.43$ Å	1.8	0.149	[20]	2RNT
Lys25-RNase T1	vanadate	$P2_12_12_1$	$a = 48.82$ Å $b = 46.83$ Å $c = 41.20$ Å	1.8	0.137	[21]	3RNT
Lys25-RNase T1	guanosine	$P2_12_12_1$	$a = 47.65$ Å $b = 51.00$ Å $c = 40.46$ Å	1.8	0.132	[22]	[f]
Lys25-RNase T1	3′,5′-GDP	$I23$	$a = 86.47$ Å	3.2	0.158	[22]	[f]
Lys25-RNase T1 (His92Ala)	–	$P2_12_12_1$	$a = 31.04$ Å $b = 62.31$ Å $c = 43.70$ Å	2.2	0.152	[23]	[f]
Lys25-RNase T1 (His40Lys)	2′-GMP	$P2_1$	$a = 49.17$ Å $b = 47.99$ Å $c = 40.11$ Å $\beta = 90.26°$	2.0	0.149	[24]	[f]

[a] Lys 25-RNase T1 and Gln 25-RNase T1 are the two isoforms of the protein; mutations are given in parentheses when appropriate. The crystal structures of the 2′-GMP complexes of both Lys 25-RNase T1 and Gln 25-RNase T1 were solved by multiple isomorphous replacement [14, 17]; all other crystal structures were either isomorphous with known structures of RNase T1 or solved by molecular replacement [25] using a known three-dimensional structure as start. All crystal structures were refined using stereochemical restraints [26] and routinely checked by computer graphics [27]. [b] 2′-GMP, 2′-guanylic acid; 3′-GMP, 3′-guanylic acid; 2′,5′-GpG, guanylyl-2′,5′-guanosine; vanadate, $[H_2VO_4]^{\ominus}$; 3′,5′-GDP, guanosine-3′,5′-diphosphate. [c] d_{min} is the maximum resolution of the diffraction data used. [d] The crystallographic residual is $R = \sum_h (F_o - F_c)/\sum_h F_o$, where F_o and F_c are observed and calculated structure amplitudes, respectively, and the summation is over all h reflections. [e] For structures that have an identifier, coordinates are available from the Brookhaven Protein Data Bank upon request. [f] In preparation.

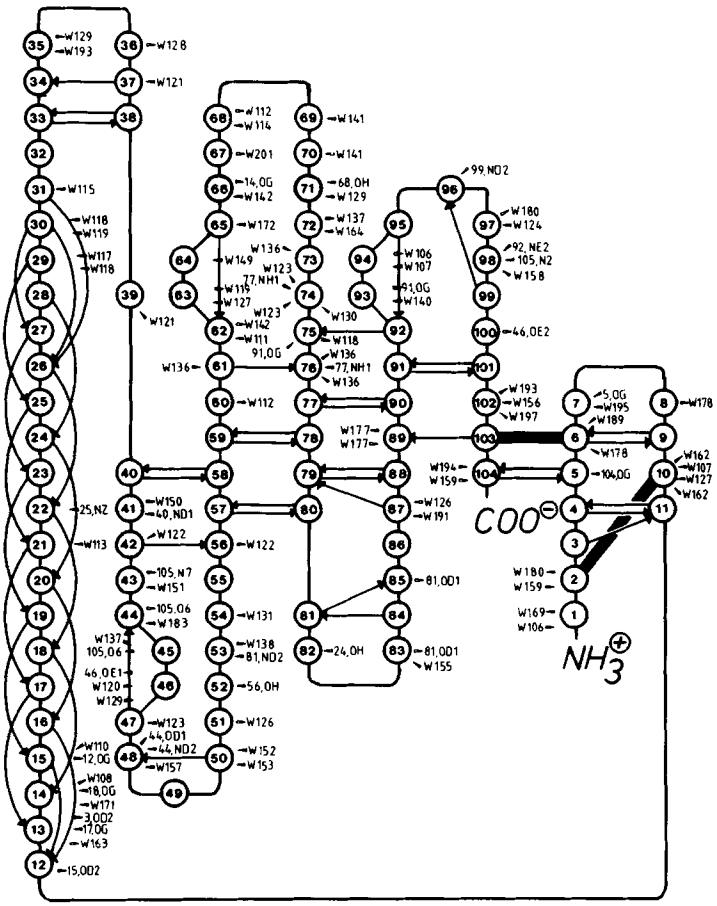

Fig. 3. Main-chain hydrogen bonding of RNase T1. Solvent sites are given the letter W and numbered (e.g., W129), and protein side chain atoms are indicated with sequence number and atom name (e.g., 77NH1). Arrows and arrowheads indicate the hydrogen bonds. The bold lines connecting residues 2 and 10 and residues 6 and 103 represent disulfide bonds. All hydrogen bonds discussed in this article are assigned according to the geometric criteria of *Baker* and *Hubbard* [28].

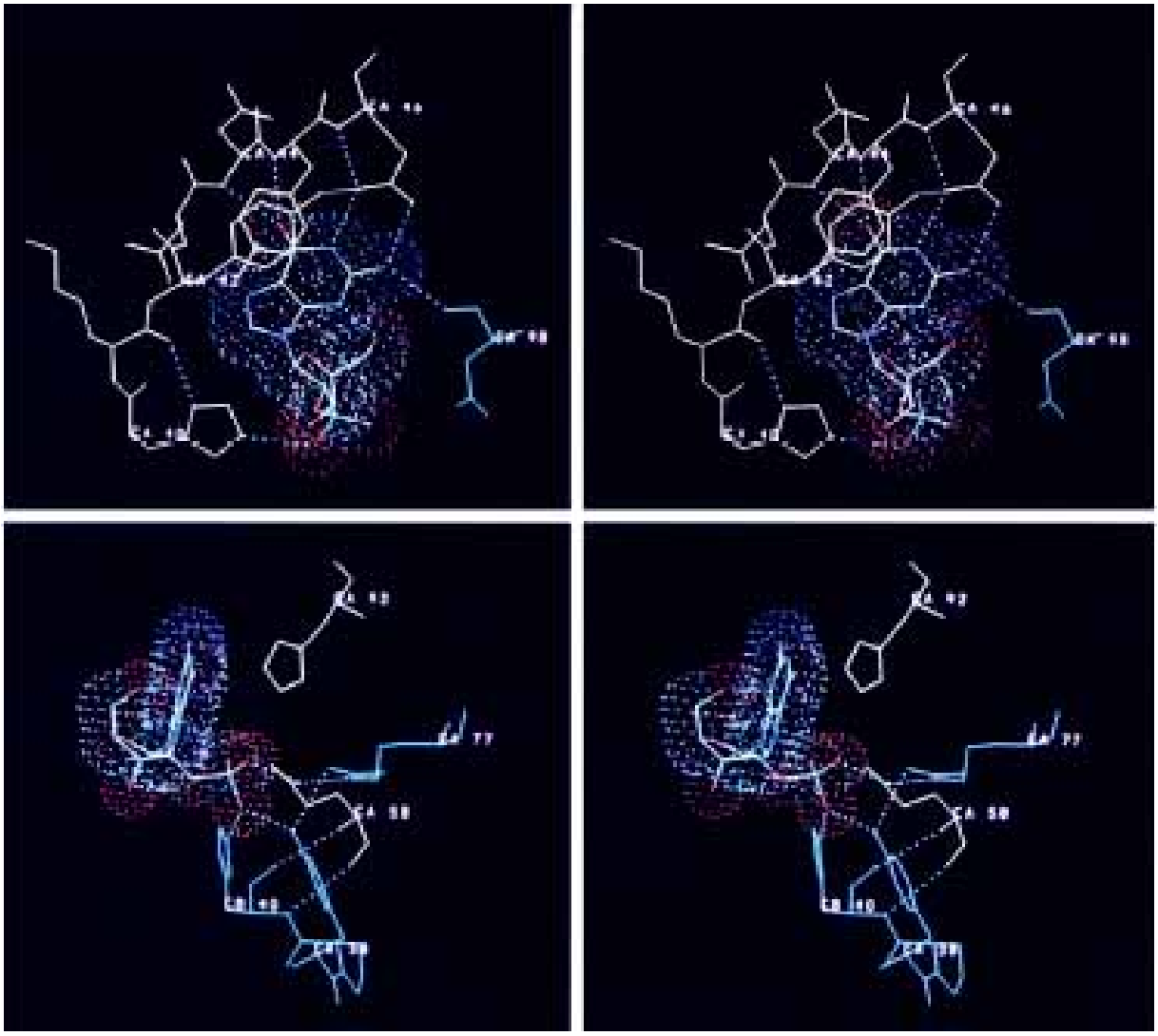

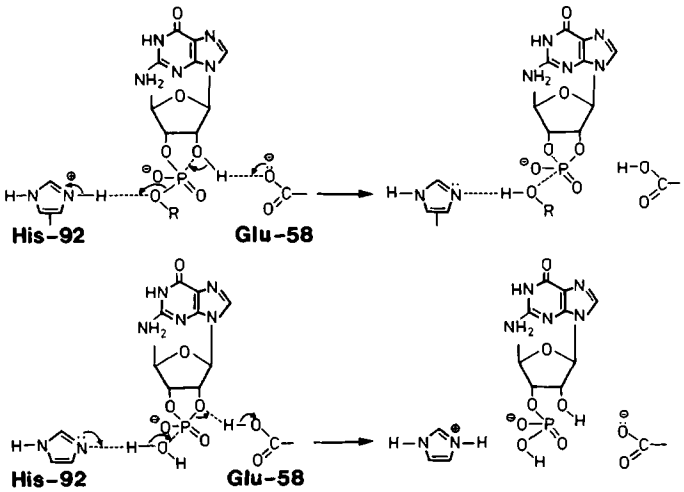

Fig. 4. Top and middle: Stereoview of the active site of RNase T1. The bound inhibitor, 2′-guanylic acid, is drawn with its van der Waals surface: white, carbon; blue, nitrogen; red, oxygen; light blue, phosphorus. The protein atoms are light blue and yellow; α-carbon positions are labeled, and hydrogen bonds are shown as dashed lines. Top: Base recognition site: the polypeptide stretch His40 to Glu46 is shown in yellow; Asn98 is blue. Middle: Catalytic site: Glu58 and His92, which are implicated in catalysis by RNase T1, are drawn in yellow; the other amino acids interacting with the phosphate group are blue. Bottom: In the reaction scheme the most probable mechanism for phosphodiester bond hydrolysis by RNase T1 [31] is outlined.

secondary structure is stabilized by 51 N–H···O=C hydrogen bonds (Fig. 3). It consists of a short two-stranded antiparallel β-sheet followed by a 4.5-turn α-helix and a second antiparallel β-sheet composed of five strands. The connections between the secondary-structure elements are more or less extended loops incorporating several β-turns. The five-stranded sheet is strongly twisted to form a barrel-like structure. If an enzyme–substrate complex is formed, the bound RNA single strand represents the missing sixth strand to complete the barrel.

The tertiary structure is stabilized by burying about 80% of the nonpolar side chains in a hydrophobic core and thereby removing them from contact with water. In addition to the hydrogen bonds in the α-helix and β-sheets, 31 hydrogen bonds between the main chain and the side chains and 14 hydrogen bonds between the side chains[16] help to stabilize the folded conformation of RNase T1.

2.1. The Guanine-Binding Site of RNase T1

Specific binding of guanine occurs through the polypeptide segment Tyr42 to Glu46 and the peptide C=O group of Asn98 (Fig. 4). Guanine N(7) and O(6) accept hydrogen

bonds from the peptide N-H groups of Asn43, Asn44, and Tyr45; guanine N(1)-H, and N(2)-H donate hydrogen bonds to the side chain of Glu46, and the second N(2)-H hydrogen bonds to the carbonyl oxygen of Asn98. Moreover, the carbonyl group at the 6-position of the guanine moiety is sandwiched between the phenolic side chains of Tyr42 and Tyr45, so that the hydrogen bonds are shielded from competition with bulk water and consequently stabilized.

In the crystal structures of RNase T1 with guanosine 2′-phosphate and guanosine,[14-18, 20, 22] the guanosine moiety is in the *syn* conformation, which permits an intranucleoside O(5′)-H ··· N(3) hydrogen bond to be formed. X-ray crystallography has revealed no hydrogen-bonding interaction between the ribose and the enzyme in any complex between RNase T1 and a substrate analogue. The phosphate group of guanosine 2′-phosphate is hydrogen-bonded to the side chains of Tyr38 (O_η), His40 (N_ε), and Glu58 (O_ε) (see Fig. 4), but not to the side chain of Arg77. Comparable interactions were also found with the phosphate group in guanylyl-2′,5′-guanosine, for which the phosphate group and the 3′-terminal guanosine are seen in twofold disordered positions.[20] The reason is that there are only a few interactions between RNase T1 and the 3′-terminal guanosine and there are some additional contacts to a symmetry-related RNase T1 molecule.

In the adduct between RNase T1 and vanadate, the anion $[H_2VO_4]^\ominus$ binds to the site where the phosphate group is bound in the complex with guanosine 2′-phosphate.[21] In the base recognition site, there is a water molecule close to the position where O(6) of guanine would be. The Glu46 side chain is rotated away from the guanine binding site, the side chain of Tyr45 is in a different position, and the Asn43–Asn44 peptide link is flipped by nearly 180° with respect to the other crystal structures which contain a bound guanine. This suggests that the guanine binding site is to a certain extent flexible to facilitate the binding of the substrate and the expulsion of the product.

The specificity of RNase T1 for guanosine has been investigated in a free-energy perturbation study,[29] which arrived at approximately the same difference between the free energies of binding of guanosine and adenosine as experimental studies. The simulation suggested that removal of the Glu46 carboxylate group should render RNase T1 an adenosine-specific ribonuclease. This conclusion, however, is not supported by biochemical studies of the RNase T1 Glu46Ala mutant.[30]

2.2. The Catalytic Site of RNase T1

The catalytic site of RNase T1 is defined by the environment of the phosphate group in the complexes with guanosine 2′-phosphate and guanylyl-2′,5′-guanosine (Fig. 4). Since the ligands contain phosphate in the 2′ position so that the phosphodiester link cannot be hydrolyzed, model building studies have been performed to construct the corresponding 3′-phosphate.[31] These suggest that the hydrogen-bonding scheme is different, as it is now possible to form a hydrogen bond between one of the phosphate oxygens and the imidazole of His92 and between the ribose O(2′)-H and the carboxylate of Glu58. The imidazole group of His40 is nearby, but probably not involved in hydrogen bonding to the ribose.

Based on this geometry and on the information known from numerous biochemical studies,[4, 32, 33] a reaction mechanism of RNase T1 (Fig. 4, bottom) was proposed where Glu58, possibly activated by His40, acts as a base and abstracts the proton from O(2′)-H; the $O(2')^\ominus$ then attacks the phosphodiester bond and O(5′) of the next nucleotide receives a proton from the protonated His92. The newly formed terminal guanylyl-2′,3′-cyclic phosphate is hydrolyzed by a water molecule activated by His92, to which it donates a proton, the leaving O(2′) receives a proton from Glu58, and the terminal guanosine 3′-phosphate product is formed.[14, 31]

Whereas the stereochemistry of this reaction[33] and the proposed role of His92 in catalysis are nearly universally accepted, site-directed mutagenesis of active-site residues has fueled a dispute about the function of Glu58 and His40. Removal of either residue preserves significant residual ribonuclease activity.[34-36] Support for the proposed action of Glu58 (and not His40) on guanosine O(2′)-H comes mainly from an analysis of the pH profiles of dinucleotide hydrolysis for wild-type RNase T1 and several single-site mutants by *Steyaert* et al.[36] Mutants lacking His40 display the same pH profiles as the wild type, while replacement of Glu58 leads to a change in pH dependence.

To date, two mutants of RNase T1 have been studied by crystallographic methods, His92Ala and His40Lys.[23, 24] The former is inactive because the catalytically important His92 is replaced by Ala,[34, 35] but the latter is still 13% active relative to the wild-type enzyme.[13, 36] In His92Ala, the replacement of the imidazole group by a hydrogen atom results in some major structural changes, because a hydrogen bond between the histidine side chain and the main-chain Asn99 C = O group is no longer possible and the loop formed by segment Ile90 to Asn99 thereby is destabilized. Similarly, the His40Lys mutant displays some local structural changes in this loop region; however, these changes are not as severe as in case of the His92Ala mutant.

2.3. The Distribution of Thermal Parameters Suggests Segmental Flexibility

In the course of refinement of an X-ray crystal structure, the atomic thermal parameters are refined as well as the atomic coordinates. They are indicative of the vibrations of the atoms in the crystal lattice. The thermal parameters of the main-chain and side-chain atoms are shown as a function of sequence number in Figure 5. Amino acids incorporated into β-sheets are more "rigid" than those in the α-helix; those in the loop structures vibrate the most. This is in line with our understanding of the stabilization of secondary structure by N–H ··· O=C hydrogen bonds between main-chain peptide groups; this hydrogen bonding also affects the thermal vibration of the associated side chains. Molecular dynamics studies based on the X-ray crystal structure atomic coordinates[37] also show the same tendency in the positional fluctuations of the main-chain and side-chain atoms illustrated in Figure 5.

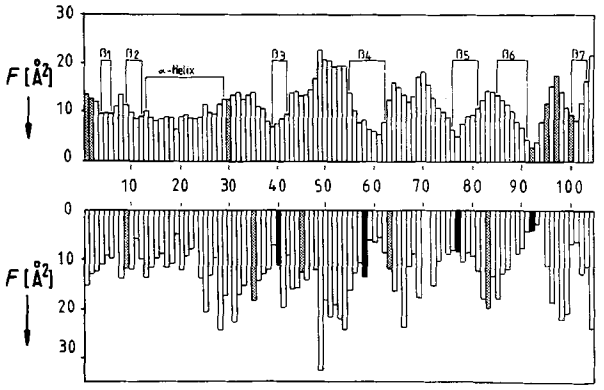

Fig. 5. Local mobility within the RNase T1 molecule represented by the mean crystallographic temperature factors of backbone (top) and side-chain atoms (bottom). Solid histogram bars mark the catalytically important residues His40, Glu58, Arg77, and His92, which are located near mobility minima. Amino acid side chains and main-chain portions involved in crystal lattice contacts have stippled bars.

The solution structure of RNase T1 has been investigated by 2D NMR techniques in the laboratory of *H. Rüterjans*.[38] There is no significant difference between the solid-state and solution-state structures of the wild-type enzyme, and the NMR data are also consistent with the X-ray structure for the His92 Ala mutant. In the low-resolution tertiary structure derived from NMR spectroscopy, especially the secondary structure of RNase T1 agrees well with that determined in the crystalline state. In addition, since the interpretation of the NMR data relies strongly on molecular dynamics methods, the distribution of thermally more rigid and more flexible sections of the RNase T1 structure in solution is also consistent with Figure 5.

2.4. Conserved Water Molecules and a Bound Metal Ion Are Integral Parts of the RNase T1 Structure

In the complex between RNase T1 and 2′-GMP, about 90 water molecules were located in the asymmetric unit and, after generation of symmetry-related water molecules, about 150 water molecules surround each RNase T1 molecule.[16] Comparison of hydrated RNase T1 molecules observed in four different crystal structures showed that about 30 water molecules are in the "same" position, that is, within 0.5 Å of the mean position. These water molecules are considered as conserved and integral parts of the RNase T1 molecular structure.[39]

Some of the conserved water molecules cross-link different parts of the RNase T1 polypeptide chain and help to stabilize its three-dimensional folding. One water molecule is simultaneously hydrogen-bonded to Tyr68 (O_η) and the peptide N–H groups of Ser35 and Asn36; one is in a strategic position and coordinates Cys6 (O), Ser8 (N), Asn9 (N_δ), Asp76 (O_δ), and Thr93 (O_γ); one connects the C-terminal carboxylate of Thr104 with the N-terminal Cys2 (O); three water molecules stabilize the loop structure at the C-terminus of the α-helix. Most notable is a chain of ten hydrogen-bonded water molecules. Waters 1 to 5 of this chain are anchored at the indole N atom of Trp59 and stitch together the narrow loop, residues 60 to 68 (Fig. 2); they are buried between this loop and the α-helix and inaccessible to solvent. Waters 5 to 8 of the chain coordinate to the metal ion ($Ca^{2\oplus}$ in the investigated structures), and waters 9 and 10 are hydrogen-bonded to side chains at the N-terminus of the α-helix.

The $Ca^{2\oplus}$ ion is eightfold coordinated in the form of a dodecahedron with trigonal faces[20,21] (Fig. 6). Its ligands

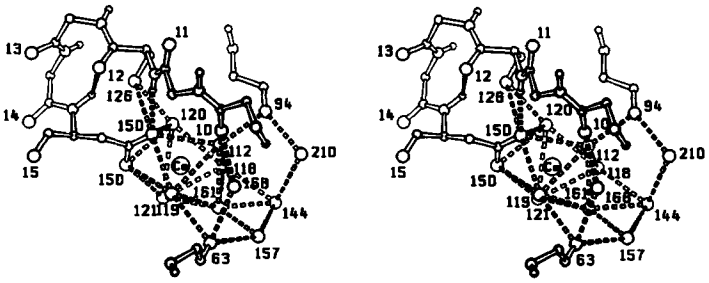

Fig. 6. Stereoview of the calcium binding site of RNase T1.

are the two carboxylate oxygens of Asp15 and six water molecules, four of which belong to the ten-water chain. The water molecules of the dodecahedron are additonally hydrogen-bonded to the main-chain C=O groups of residues 10, 12, and 63. The spatial arrangement of these carbonyl oxygen atoms and of the ten-water chain appears to be suitable to support the formation of a cation coordination site since, besides $Ca^{2\oplus}$, other cations bind to and structurally stabilize the RNase T1 molecule (see Section 3.5).

3. Experimental Studies of the Conformational Stability

The conformational stability of a globular protein, $\Delta G(H_2O)$, is defined as the difference in free energy between the folded and unfolded conformations under physiological conditions. In Section 3.1 we briefly describe how the conformational stability is measured,[40,41] and in the following sections we discuss experimental studies of the conformational stability of RNase T1 as a function of the variables of most interest to biochemists: temperature, pH, salt concentration, disulfide bond content, and amino acid sequence. The results provide insight into the structural features and forces that stabilize this small globular protein.

3.1. Measuring the Conformational Stability

When a protein unfolds, the unique three-dimensional structure, such as that shown in Figure 2, is disrupted and the protein approaches a randomly coiled conformation (see Section 3.6).[41–45] This is such a dramatic conformational change that it can be followed by almost any physical technique. For example, the near-UV absorption spectra of folded and unfolded RNase T1 are shown in Figure 7 (top). RNase T1 contains a single tryptophan residue that is completely buried and nine tyrosine residues that are, on the average, 82% buried in the interior of the folded protein.

The exposure of these residues to solvent on unfolding is the major factor that contributes to the observed blueshift in the absorption spectrum.[46] The intrinsic fluorescence spectra of folded and unfolded RNase T1 are shown in Figure 7 (bottom). The decrease in the fluorescence intensity arises because the buried Trp side chain is transferred from a nonpolar to a polar environment by unfolding and also because energy transfer from the nine Tyr residues to the Trp residue is less efficient after unfolding.[47]

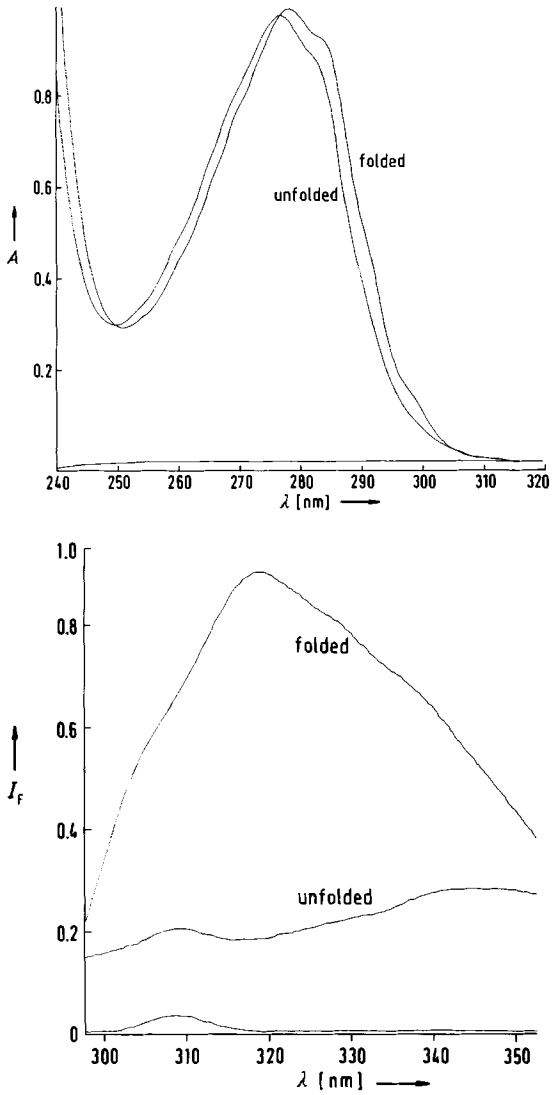

Fig. 7. Top: Absorption spectra of folded and unfolded (8 M urea) RNaseT1 (0.52 mg mL^{-1}) [41]. Bottom: Fluorescence emission spectra for folded and unfolded (8 M urea) RNase T1 (278-nm excitation wavelength, 0.01 mg mL^{-1} RNase T1) [40].

Two typical urea unfolding curves determined using fluorescence measurements are shown in Figure 8 (top), and two typical thermal unfolding curves determined using UV absorption measurements are shown in Figure 8 (bottom). Note that unfolding occurs as a steep, single step reflecting the cooperativity of this process. To analyze these curves, we assume a two-state folding mechanism [Eq. (a)], where only

folded (native) $\rightleftharpoons$ unfolded (denatured) (a)

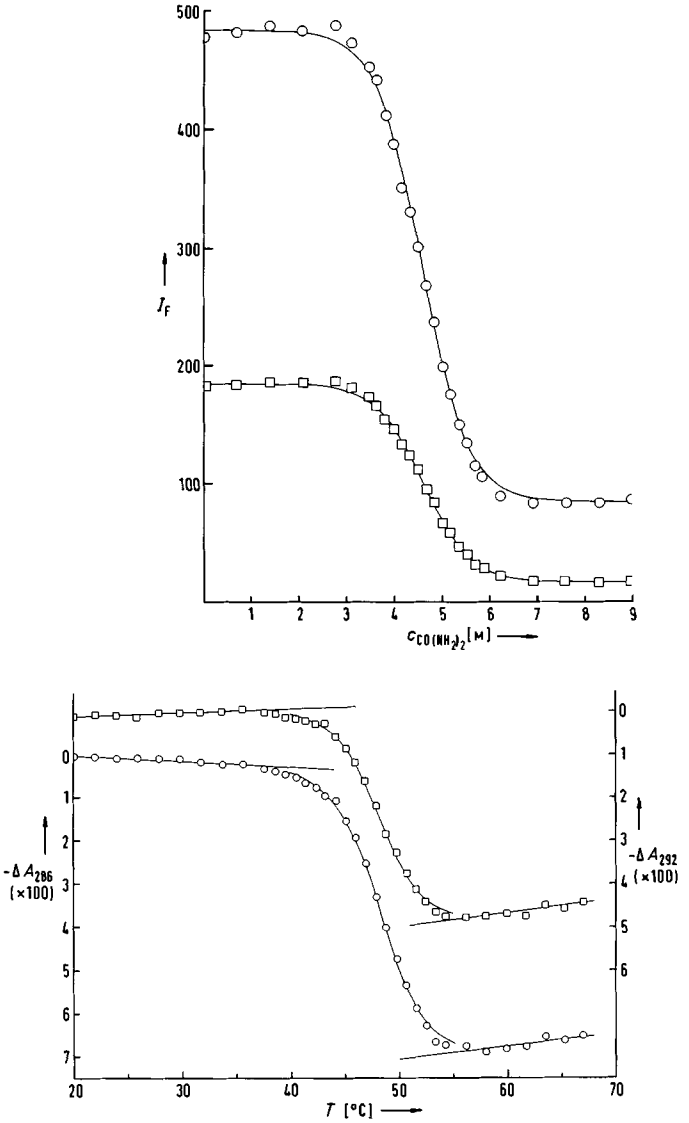

Fig. 8. Top: Urea unfolding curves for RNase T1 as a function of urea concentration $c_{CO(NH_2)_2}$ at 25 °C and pH 7 in 30 mM MOPS buffer (MOPS = 3-*N*-morpholinopropanesulfonic acid, sodium salt), monitored by measuring the fluorescence intensity at 320 nm after excitation at 278 nm (○) or 295 nm (□). Bottom: Thermal unfolding curves for RNase T1 as a function of temperature at pH 7 in 30 mM MOPS buffer, monitored by measuring the absorbance difference at 286 nm (○) or 292 nm (□) [41].

the folded and unfolded conformations are present at significant concentrations at equilibrium. This allows us to calculate the fraction of unfolded molecules, F_u, in the transition region with Equation (b), where y is the parameter used to follow unfolding, and y_f and y_u are the values of y characteristic of the folded and unfolded conformations. The values y_f

$$F_u = (y_f - y)/(y_f - y_u) \quad \text{(b)}$$

and y_u are obtained by extrapolating the pre- und post-transition baselines into the transition region. Figure 9 shows F_u values as a function of urea concentration derived from measurements made by four experimental techniques. The agreement of these measurements indicates that the concentration of partially folded intermediates present at equilibrium is low. This and other evidence supports the analysis of equilibrium data with a two-state folding mechanism.[41, 48]

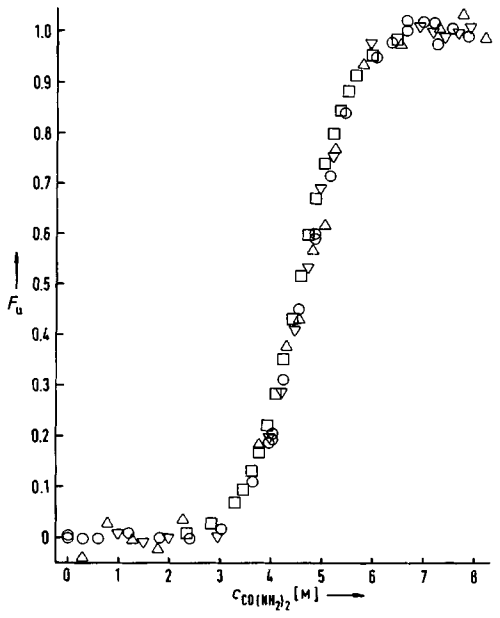

Fig. 9. Fraction unfolded RNase T1 as a function of urea concentration calculated with Equation (b). The following techniques were used to follow unfolding [41]: △, circular dichroism (CD) at 238 nm; ▽, UV absorption at 287 nm; ○, optical rotary dispersion (ORD) at 295 nm; □, fluorescence intensity at 320 nm.

Using kinetic methods, *Schmid*'s group has shown, in contrast, that partially folded intermediates can be detected during the transient phase of refolding.[48] (The unfolding of RNase T1 by urea or guanidine hydrochloride is a completely reversible reaction.) The intermediates formed very early during folding have extensive secondary structure, and there is great interest in characterizing these intermediates since this will give us a better understanding of the mechanism of protein folding.[49] RNase T1 refolds in three major phases: a fast phase that is completed in less than a second, and two slow phases that require minutes to hours.[48] As with many other proteins, the slow phases can be explained by the proline model:[50] the configuration of the Tyr 38–Pro 39 and Ser 54–Pro 55 peptide bonds is *cis* in folded RNase T1, but will be predominantly *trans* in the unfolded state; the *trans*/*cis* isomerization of these bonds gives rise to the slow folding phases. This was confirmed by replacing Ser 54–Pro 55 with Gly 54–Asn 55.[51] The conformational stability of this mutant is only about 0.9 kcal mol^{-1} less than that of wild-type RNase T1, but one of the two slow phases of folding is now absent, and the mechanism of folding is much simpler since there is now only one slow folding species rather than three.[51]

Equation (c) can be used to calculate the free energy of unfolding, ΔG, as a function of urea concentration or temperature from results such as those shown in Figure 8; R is the gas constant and T is the absolute temperature. ΔG is

$$\Delta G = -RT\ln[F_u/(1-F_u)] = -RT\ln[(y_f - y)/(y - y_u)] \quad (c)$$

found to vary linearly with urea concentration (Fig. 10), and $\Delta G(H_2O)$ is obtained by extrapolating to zero concentration of urea.[40] Recent theoretical[52] and experimental studies[53, 54] support the use of a linear extrapolation, but other means of extrapolation have been used in the past.[40, 44, 55]

Estimates of ΔG at 25 °C can also be obtained from thermal unfolding curves (see Section 3.3) or from calorimetric data.[45]

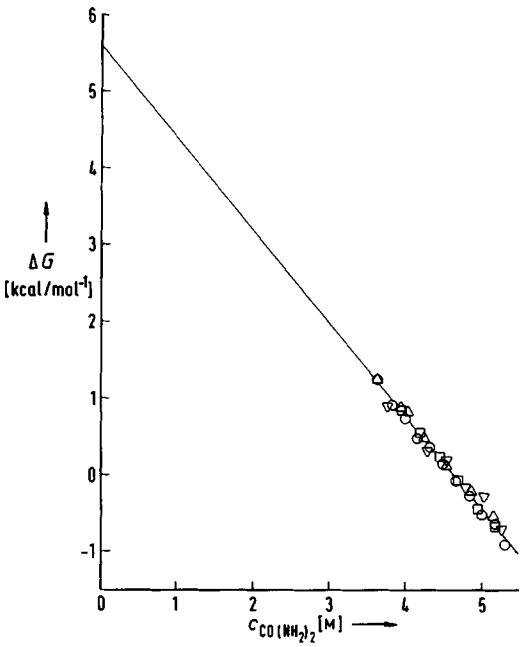

Fig. 10. ΔG as a function of urea concentration. The ΔG values were calculated with Equation (c) using data obtained by the techniques shown in Figure 9. The solid line was calculated with the following equation [41]: $\Delta G = \Delta G(H_2O) - m(CO(NH_2)_2)$, where $m = 1.21$ kcal mol^{-1} M^{-1} and $\Delta G(H_2O) = 5.6$ kcal mol^{-1}.

3.2. The Conformational Stability of Globular Proteins Is Surprisingly Low

"The tendency to assume a unique stable conformation in a 'physiological' medium is characteristic of the globular proteins . . . it is probably not a property of polypeptide chains in general. The natural proteins, numerous as they are, represent only a tiny fraction of the vast number of possible combinations of amino acid residues. The great majority of these possible sequences may have no tendency, in any solvent medium whatever, to assume a unique conformation."

J. T. Edsall[56]

"The stability must be great enough for the protein to find and maintain its native conformation relative to other conformations, but not so great that conformational changes or adjustments, considered an integral part of many protein functions, are precluded."

W. J. Becktel, J. A. Schellman[57]

Estimates of the conformational stability, $\Delta G(H_2O)$, as well as some pertinent structural information for RNase T1 and a number of other proteins, are given in Table 2. The conformational stability of almost all naturally occurring globular proteins lies between 5 and 15 kcal mol^{-1}. It appears to be advantageous to living organisms to have proteins in which the folded, biologically active conformation is only marginally more stable than an unfolded, inac-

Table 2. Structural information and measured conformational stabilities for nine globular proteins.

Protein[a]	R[b]	-SS-[c]	R type [%][d] c	p	np	np(bur) [%][e]	H bonds [f]	$\Delta G(H_2O)$[a] [kcal mol^{-1}]
PPT	36	0	22	36	42	62	21	1.4
BPTI	58	3	24	21	55	65	32	14.3
RNase T1	104	2	14	43	43	79	96	8.9
RNase A	124	4	19	42	39	79	116	9.0
Lysozyme	129	4	21	29	50	85	111	8.8
Nuclease	149	0	32	26	43	80	104	6.1
DHFR	159	0	25	21	54	79	123	5.9
T4 Lyso	164	0	27	25	48	83	109	7.6
α-CT	241	5	13	32	55	86	156	14.0

[a] PPT = pancreatic polypeptide (1 PPT) [58]; BPTI = bovine pancreatic trypsin inhibitor (4 PTI) [59]; RNase T1 = ribonuclease T1 (1 RNT) [60]; RNase A = ribonuclease A (1 RN 3) [60]; lysozyme (5 LYZ) [61]; Nuclease = staphylococcal nuclease (2 SNS) [62]; DHFR = dihydrofolate reductase (4 DFR) [63]; T4 Lyso = bacteriophage T4 lysozyme (1 LZM) [64]; α-CT = α-chymotrypsin (4 CHA) [65]. For each protein, the identification code of the atomic coordinate set from the Protein Data Bank at Brookhaven National Laboratories is given in parentheses, followed by the reference for the estimate of $\Delta G(H_2O)$. [b] Number of amino acid residues. [c] Number of disulfide bonds. [d] Percentage content of different classes of amino acid side chains: c = charged side chains (Asp, Glu, Lys, Arg); p = polar side chains (Tyr, Ser, Thr, Asn, Gln, His); np = nonpolar side chains (Gly, Ala, Pro, Val, Ile, Leu, Cys, Met, Phe, Trp). [e] The percentage of the nonpolar side chains which are buried. For each side chain the accessibility was determined according to the program developed by *Lee* and *Richards* [66]. [f] The number of intramolecular hydrogen bonds for each protein was estimated as described by *Presta* and *Rose* [67].

tive conformation. The reasons for this are not clear. It may be important to the function of a protein as *Becktel* and *Schellman* suggest,[57] or it may play a role in metabolic regulation by influencing the levels of key enzymes through protein turnover.[68] Extending *Edsall*'s thoughts,[56] it might be argued that it is not possible to make the globular conformation of a protein significantly more stable through changes in the amino acid sequence. However, a protein based on a four-helix bundle has been constructed with a conformational stability of 22.5 kcal mol^{-1},[69] and single amino acid substitutions have been found that increase the conformational stability of globular proteins by 4.2,[70] 4.8,[71] and 9.7[72] kcal mol^{-1} (see Section 3.7). Thus, it seems likely that evolution could have generated more stable proteins if they were desired.

3.3. RNase T1 Can Be Unfolded by Heating or Cooling

At pH 7, RNase T1 is most stable at $-5\,^{\circ}C$ (≈ 8 kcal mol^{-1}); the stability decreases at both higher and lower temperatures, as indicated by the protein stability curve (Fig. 11)[57]. The interesting temperature dependence is described by a form of the Gibbs–Helmholtz equation [Eq. (d)], where $\Delta G(T)$ is ΔG at temperature T, T_m is the midpoint

$$\Delta G(T) = \Delta H_m(1 - T/T_m) - \Delta C_p[(T_m - T) + T\ln(T/T_m)] \quad (d)$$

of the thermal unfolding curve, ΔH_m is the enthalpy change for unfolding measured at T_m, and ΔC_p is the difference in heat capacity between the unfolded and folded conformations.[57] All of these parameters can be determined from either thermal unfolding curves[40] or from data obtained with a differential scanning calorimeter (DSC).[73] In Figure 11, the ΔG values below 40 °C are $\Delta G(H_2O)$ values from urea unfolding curves and they were used to estimate ΔC_p.[53] The ΔG values above 40 °C were obtained from thermal unfolding curves. The temperature of maximum stability, T_s,

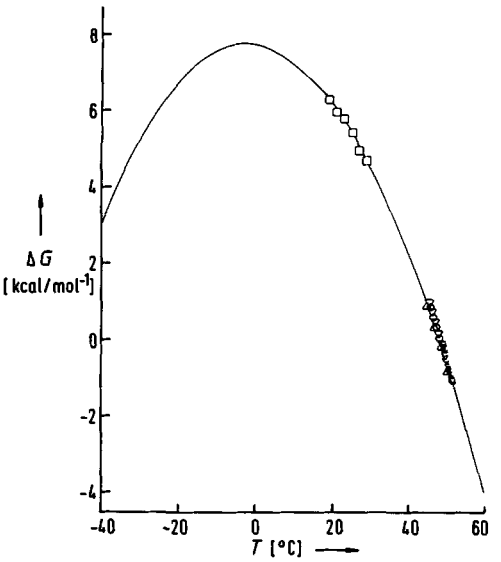

Fig. 11. ΔG as a function of temperature for the unfolding of RNase T1 at pH 7. The data points below 30 °C are from urea unfolding curves, and those above 40 °C are from thermal unfolding curves. The solid line was calculated with Equation (d) using the following thermodynamic parameters [53]: T_m = 48.1 °C, ΔH_m = 97.1 kcal mol^{-1}, ΔC_p = 1.65 kcal mol^{-1} K^{-1}, $\Delta G(25\,^{\circ}C)$ = 5.6 kcal mol^{-1}.

occurs at the temperature where $\Delta S = 0$ and is given by Equation (e). T_s is $-5\,^{\circ}C$ for RNase T1 and lies between

$$T_s = T_m \exp(-\Delta H_m/(T_m \Delta C_p)) \quad (e)$$

-10 and 35 °C for the proteins that have been studied to date. *Brandts* was the first to recognize the importance of ΔC_p in the thermodynamics of proteins folding,[74] and cold denaturation was first observed directly by *Pace* and *Tanford*[75] with β-lactoglobulin. Recent studies of T4 lysozyme,[64] myoglobin,[76] and staphylococcal nuclease[77] have shown that, for these proteins, T_s occurs above 0 °C, so that both low- and high-temperature unfolding can be observed directly.

The large positive value of ΔC_p for protein unfolding gives rise to a strong temperature dependence for ΔH and ΔS. In this case, Kirchhoff's law is given by Equation (f), where

$$\Delta C_p = C_p(u) - C_p(f) = d(\Delta H)/d(T) \quad (f)$$

$C_p(u)$ and $C_p(f)$ are the heat capacities of the unfolded and folded conformations, respectively. Thus at pH 7, ΔH increases from ≈ 18 kcal mol^{-1} at 0 °C to 97 kcal mol^{-1} at T_m (48.1 °C) for the unfolding of RNase T1. This thermodynamic behavior is observed for any reaction in which hydrophobic interactions are important. When a protein unfolds, the buried nonpolar side chains are brought into contact with water. (As shown in Table 2, 80–85% of the nonpolar side chains are buried in the folded conformation of all but the smallest globular proteins.) In the unfolded state these side

chains are clathrated by water molecules. The heat capacity of the unfolded protein is greater than that of the folded protein, because now these clathrates must melt in order to raise the temperature. Thus, the same effect that gives rise to hydrophobic interactions also gives rise to the large ΔC_p value that dominates the thermodynamics of protein folding.[73, 78–80]

3.4. RNase T1 Is Most Stable Near the Isoelectric Point

At 25 °C, RNase T1 is most stable ($\Delta G(H_2O) \approx 8.9$ kcal mol^{-1}) near pH 4.5, where the net charge is close to zero (Fig. 12). The pH dependence of the conformational stability of a globular protein will depend mainly on two related factors: (1) electrostatic interactions due to the charged groups and (2) differences between the pK values of the ionizable groups in the folded and unfolded conformations.[43, 81–84] The locations of the charged groups on the surface of RNase T1 at pH 7 are shown in Figure 13. At zero net charge, RNase T1 has seven positive charges (3 His, 2 Lys, 1 Arg, and 1 α-amino) and a total of seven negative charges from the 13 carboxylate groups (6 Asp, 6 Glu, and 1 α-carboxyl).

The charges on the surface of globular proteins are generally arranged so that a preponderance of favorable over unfavorable electrostatic interactions among the charged groups contributes favorably to the conformational stability.[85] When the protein unfolds, the charges will be further apart and the effective dielectric constant increased; consequently, electrostatic interactions will be substantially reduced, especially at moderate salt concentrations. There has been considerable interest recently in theoretical calculations of electrostatic effects in proteins.[86] These calculations are fraught with problems. For example, it is very difficult to represent the effective dielectric constant[87, 88] and to take into account solvation.[89] In addition, reliable experimental data with proteins to test the models are scarce. Calculations of the electrostatic interactions for RNase T1 by *Wodak*'s group[88] are discussed in Section 4.4.

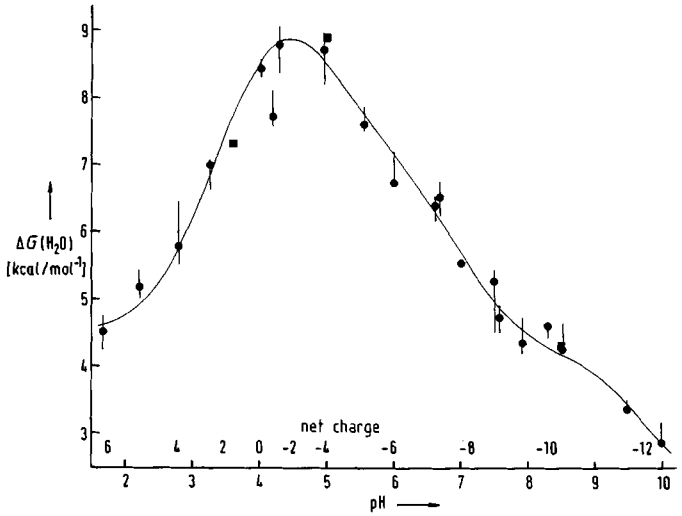

Fig. 12. $\Delta G(H_2O)$ as a function of pH for the unfolding of RNase T1 at 25 °C. The approximate net charge given is based on the titration curve for RNase T1 [84]. The solid curve was calculated using the following pK values for the folded conformation, pK_f, and unfolded conformations, pK_u: 3 Asp, pK_f = 2.7, pK_u = 4.1; 2 Glu, pK_f = 5.5 and 5.7, pK_u = 4.5; 2 His, pK_f = 7.2 and 7.8, pK_u = 6.4; 5 Tyr, pK_f = 9.9, pK_u = 9.6 [60].

The results in Figure 12 do allow one conclusion that also applies to RNase A.[60] The conformational stability of RNase T1 is reduced by about 6 kcal mol^{-1} at pH 10, where the net charge on the molecule is about −12 and repulsive electrostatic interactions should predominate. This suggests that electrostatic interactions involving the charges on globular proteins make a relatively small contribution to their conformational stability, probably much less than hydrogen bonding and hydrophobic interactions (see Sections 4.2 and 4.3).

Another important contribution to the pH dependence of $\Delta G(H_2O)$ results from differences between the pK's of groups in the folded and unfolded conformations.[43, 90] For RNase T1, the 6-kcal mol^{-1} increase in $\Delta G(H_2O)$ on going from pH 10 to 5 results mainly from the presence of groups that bind protons more tightly (higher pK's) in the folded

Fig. 13. Stereoview of RNase T1 showing the location of the basic side chains in blue and the acidic side chains in red.

than in the unfolded conformations and thereby shift the equilibrium toward the folded conformation and increase the stability. NMR titrations have shown that the pK's of the His residues are 7.9 (His92), 7.8 (His40), and 7.3 (His27) in folded RNase T1,[91] and a pK of about 6.6 would be expected for the His residues in the unfolded conformations. This alone would account for a change of over 4 kcal mol^{-1} in $\Delta G(H_2O)$ with pH.[60] Higher pK's are expected when the net charge on the molecule is negative, and lower pK's are expected when the net charge is positive. Thus, the entire decrease in $\Delta G(H_2O)$ at low pH can be explained by the presence of three Asp residues with pK's of 2.7 in the folded and 4.1 in the unfolded conformations. A set of pK's that gives the pH dependence shown by the solid line in Figure 12 is given in the figure legend. This set of pK's has been chosen arbitrarily to fit the observed data and is obviously not the only possible combination of pK differences that would account for the observed dependence of $\Delta G(H_2O)$ on pH.

Thus, both pK differences and electrostatic interactions among the charged groups will tend to favor the maximum conformational stability of ribonuclease T1 near the isoelectric pH, as is generally observed with globular proteins.

3.5. Specific Binding to the Folded Conformation Stabilizes RNase T1

The conformational stability of RNase T1 is increased by salts and can be almost doubled by adding 0.2 M Na_2HPO_4 (Fig. 14). This remarkable increase in the conformational

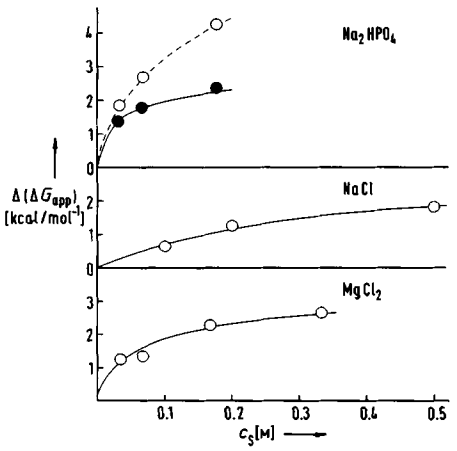

Fig. 14. Change in ΔG, $\Delta(\Delta G)$, for the unfolding of RNase T1 as a function of salt concentration. For Na_2HPO_4, the contribution of the $Na^{\oplus}$ ions was substracted from the $\Delta(\Delta G)$ values for Na_2HPO_4 to give the contribution of $[HPO_4]^{2\ominus}$ to $\Delta(\Delta G)$ (●). The solid lines were calculated with Equation (g) using the following binding constants: 155 M^{-1} for $MgCl_2$, 6.2 M^{-1} for NaCl, and 282 M^{-1} for Na_2HPO_4 [92].

stability results primarily from the preferential binding to folded RNase T1 of one divalent cation or two monovalent cations at a cation binding site involving Asp 15, or the binding of one $[HPO_4]^{2\ominus}$ ion at an anion binding site (the active site)[92] (see Figs. 4 (middle) and 6). The relationship between the increase in the conformational stability, $\Delta(\Delta G)$, the free concentration of the compound bound, [L], and the binding constant, K, is given by Equation (g).[43, 93, 94] Only

$$\Delta(\Delta G) = \Delta G(L) - \Delta G(L = 0) = RT \ln(1 + K[L]) \qquad (g)$$

modest binding constants, 6.2 ($Na^{\oplus}$), 155 ($Mg^{2\oplus}$), and 282 M^{-1} ($[HPO_4]^{2\ominus}$), are required to account for the enhanced stability.[92] One important goal of the modification of proteins through genetic engineering is to increase their stability. Our results suggest that the creation of specific cation and anion binding sites on the surface of a protein through amino acid substitutions might be a generally useful way of increasing their conformational stability. The design of these sites will be aided by the recent availability of detailed structural information on cation and anion binding sites in proteins.[20, 21, 95]

The use of specific ligand binding to stabilize a protein is not a new idea. In 1890, *O'Sullivan* and *Thomson* reported:[96] ". . . we have shown that invertase when in the presence of cane sugar will stand without injury a temperature fully 25 °C higher than in its absence. This is a striking fact, and as far as we can see, there is only one explanation of it, namely, the invertase enters into combination with the sugar." Since then, many aspects of the stabilization of enzymes by substrates and inhibitors have been studied.[97] For example, we have measured the stabilization of lysozyme by tri-*N*-acetylglucosamine[94] and the stabilization of RNase T1 by the inhibitor 2'-GMP. The presence of just 80 μM 2'-GMP increases the conformational stability of RNase T1 by over 0.5 kcal mol^{-1}. An obvious advantage of using ion binding for stabilization, rather than an inhibitor, is that it need not interfere with the functioning of the active site of the enzyme.

3.6. Disulfide Bonds Stabilize RNase T1 by Raising the Free Energy of the Unfolded Conformations

The 2–10 disulfide bond in RNase T1 is about 90% accessible to solvent, but the 6–103 disulfide bond is completely buried (Fig. 2). Thus, it is not surprising that the 2–10 disulfide bond is reduced more rapidly than the 6–103 disulfide bond, so that a derivative can be prepared with just the 2–10 disulfide bond broken.[98] To investigate the contribution of the disulfide bonds to the conformational stability of RNase T1, derivatives with one or both disulfide bonds broken have been prepared.[99] The activity, melting temperature, and conformational stability of these derivatives are listed in Table 3. Breaking the 2–10 disulfide bond lowers the conformational stability by over 3 kcal mol^{-1}, and breaking both disulfide bonds lowers the stability by 7–9 kcal mol^{-1} depending on the blocking group. Thus, disulfide bonds make a significant contribution to the stability of RNase T1. This is particularly interesting because barnase, a homologous ribonuclease with a similar folded conformation,[100, 101] is more stable than RNase T1, yet it contains no disulfide bonds.[71, 102]

The five proteins in Table 2 that contain disulfide bonds all unfold when the disulfide bonds are broken. Only RNase T1 refolds and functions with both disulfide bonds broken and the cysteine residues carboxymethylated. The results with RNase T1 are not unique. For both RNase A[103] and

lysozyme,[104] enzymatically active derivatives have been prepared in which two of the four disulfide bonds that are largely buried are broken and the cysteine residues blocked. These studies indicate that the folded conformations of proteins are to some extent flexible,[105] as also suggested by H–D exchange experiments in the crystalline state.[106]

Table 3. Activity, melting temperature, and conformational stability of RNase T1 and derivatives with one or both disulfide bonds broken [a] [99].

Protein	Activity [b] [%]	T_m [c] [°C]	$\Delta G(H_2O)$ [d] [kcal mol^{-1}]	$\Delta(\Delta G)$ [kcal mol^{-1}]
RNase T1	100	59.3	10.2	
(2–10)-RCM-T1	86	53.5	6.8	3.4
R-T1	53	27.2	3.0	7.2
RCAM-T1	43	21.2	1.5	8.7
RCM-T1	35	16.6	0.9	9.3

[a] (2–10)-RCM-T1 = RNase T1 with the 2–10 disulfide bond broken and the cysteine residues carboxymethylated; R-T1 = reduced RNase T1; RCAM-T1 = reduced carboxamidomethylated RNase T1; RCM-T1 = reduced carboxymethylated RNase T1. All of the experiments were done in 0.1 M sodium formate buffer, pH 5.0, containing 0.25 M NaCl. [b] RNA hydrolysis at 5 °C. [c] Midpoint of the thermal unfolding curve. [d] Conformational stability at 12.5 °C.

The notion that proteins with their disulfide bonds broken approach a randomly coiled conformation in 6 M guanidine hydrochloride (GdnHCl) or 8 M urea[42] may be incorrect. Recent studies on wild-type and mutant staphylococcal nuclease[107] and on several other proteins without disulfide bonds whose unfolded states differ significantly in their interaction with denaturants[60] suggest that the conformations assumed by unfolded proteins are not "random" and depend to at least some extent on the amino acid sequence of the protein. This suggests that the unfolded states of proteins may have a larger effect on the conformational stability of globular proteins than had been generally thought.[107] Since RCM- and RCAM-RNase T1 (Table 3) have melting temperatures below 25 °C, the unfolded states existing under physiological conditions can be compared with the unfolded states existing at higher temperatures and in the presence of GdnHCl or urea. Thus, RNase T1 provides a good model for reaching a better understanding of the unfolded states of proteins.

Disulfide bonds increase the conformational stability mainly by constraining the unfolded conformations of the protein and thereby decreasing their conformational entropy. Based on our results and other experimental evidence, we have proposed Equation (h) for predicting the effect of a cross-link on the conformational entropy of a protein, where n is the number of residues in the loop forming the cross-link.[99] Equation (h) predicts that the conformational stability of a protein will be raised by 3, 4, and 5 kcal mol^{-1} by adding loops of 15, 45, and 135 residues, respectively. In globular proteins, 49% of the disulfide bonds are separated by less than 24 residues and the average separation is 15 residues.[108]

$$\Delta S_{conf} = -2.1 - (3/2)R \ln n \qquad \text{(h)}$$

These results suggest that adding disulfide bonds would be a good means of making proteins more stable, but the first results have been discouraging. Seven different disulfide bonds were added to subtilisin, and none of the resulting proteins was more stable than wild type.[109] This indicates that it is difficult to add a disulfide bond to a protein without introducing some strain in the folded conformation and thereby destabilizing the protein. Recent results with T4 lysozyme were more encouraging.[110] Three different disulfides have been added and they raise the T_m's of the resulting proteins by 5, 6, and 11 °C. When all of the disulfides were incorporated in the same protein, T_m was increased by 23 °C.

3.7. RNase T1 Can Be Stabilized or Destabilized by Amino Acid Substitutions

We are using mutants prepared by site-directed mutagenesis to learn more about the forces that contribute to the conformational stability of RNase T1.[5, 111] Some of our first results with a mutant of RNase T1 that increases the conformational stability by about 0.9 kcal mol^{-1} and one that decreases the stability by about 0.8 kcal mol^{-1} are presented in Table 4. In the double mutant, these two contributions cancel and the stability does not differ significantly from that of wild-type RNase T1.

Table 4. Parameters characterizing the "urea and thermal unfolding" of RNase T1 and three mutants at pH 7.0 in 30 mM MOPS buffer [111].

	Urea unfolding			
Protein [a]	$\Delta G(H_2O)$ [b] [kcal mol^{-1}]	m [b] [cal mol^{-1} M^{-1}]	$[urea]_{1/2}$ [b] [M]	$\Delta(\Delta G)$ [c] [kcal mol^{-1}]
Wild type (*A. oryzae*)	5.62	1240	4.53	
Wild type (clone)	5.61	1235	4.54	
Gln25 → Lys	6.39	1210	5.30	0.94
Glu58 → Ala	4.72	1200	3.92	−0.77
Double mutant	6.29	1360	4.58	0.05

	Thermal unfolding				
Protein [a]	ΔS_m [d] [cal mol^{-1} K^{-1}]	ΔH_m [d] [kcal mol^{-1}]	T_m [d] [°C]	$\Delta G(25)$ [e] [kcal mol^{-1}]	$\Delta(\Delta G)$ [f] [kcal mol^{-1}]
Wild type (*A. oryzae*)	298	96	48.3	5.5	
Wild type (clone)	288	93	49.3	5.5	
Gln25 → Lys	330	107	51.7	6.9	0.93
Glu58 → Ala	270	86	46.0	4.5	−0.78
Double mutant	299	93	48.8	5.4	0.06

[a] The naturally occurring RNase T1 isoform Lys25-RNase T1 is here referred to as mutant Gln25 → Lys. [b] A least-squares analysis was used to fit plots of ΔG vs. urea molarity to the following equation: $\Delta G = \Delta G(H_2O) - m(\text{urea})$. $[urea]_{1/2}$ = midpoint of the urea unfolding curve. [c] $\Delta(\Delta G) = \Delta([urea]_{1/2}) \times m(\text{wild type})$. This equation gives $\Delta(\Delta G)$ at a urea concentration between the respective $[urea]_{1/2}$ values. [d] T_m = midpoint of the thermal unfolding curve; ΔS_m and ΔH_m are the entropy and enthalpy change at T_m. [e] ΔG at 25 °C, $\Delta G(25)$, was calculated using Equation (d) with ΔC_p = 1650 cal mol^{-1} K^{-1} [53]. [f] $\Delta(\Delta G) = \Delta(T_m) \times \Delta S_m(\text{wild type})$. This equation gives $\Delta(G)$ at a temperature between the respective T_m values.

The Gln25Lys mutation occurs in the α-helix of RNase T1 at a site that is largely exposed to solvent (Fig. 2). It is encouraging that this substitution increases the conformational stability by almost 1 kcal mol^{-1} without changing the activity. The Glu58Ala mutant was of interest because Glu58 is a central residue at the active site of RNase T1 (Fig. 4, middle) and has a unique chemical reactivity.[4] More recent studies of this mutant have shown an interesting pH dependence: wild-type RNase T1 is more stable than the

mutant below pH 7.5 and less stable above pH 7.5.[60b] This results because the average pK of the His residues is reduced from 7.6 in wild-type RNase T1 (see Section 3.4) to 7.1 in the mutant. The major effect is on His 40, whose pK is reduced from 7.9 in wild-type RNase T1 to 7.1 in the mutant. This confirms a suggestion by *Rüterjans* and *Pongs*[39c] made long before the structure of RNase T1 was known that the high pK results because His 40 ". . . is interacting with a carboxylate anion of an acidic amino acid residue . . ." Both of these mutations are complex, and changes in conformational entropy, hydrogen bonding, electrostatic interactions, and hydrophobic bonding probably all contribute to the observed differences in conformational stability.

Genetically engineered or natural mutations generally decrease the stability of a protein, but some single amino acid substitutions have been found to give large increases in the conformational stability. This is of great interest in biotechnological applications where the goal is often to make a protein as stable as possible.[112–115] In barnase, T_m is increased by 12 °C and $\Delta G(H_2O)$ by 4.8 kcal mol^{-1} in the Ala 14 Leu mutant,[71] and in cytochrome c, T_m is increased by 17 °C and $\Delta G(H_2O)$ by 4.8 kcal mol^{-1} in the Asn 57 Ile mutant.[70] The conformational stability of tryptophan synthase has been measured with every amino acid except Arg at position 49, where Glu is present in the wild-type enzyme.[72] For the Glu 49 Ile mutant, $\Delta G(H_2O)$ is increased by 9.7 kcal mol^{-1}. This is the largest increase in conformational stability reported for a single change in amino acid sequence. Several studies have shown that the effects of amino acid substitution are often localized, so that their effects on stability are additive. For example, six amino acid substitutions that each increase the stability by from 0.3 to 1.3 kcal mol^{-1} have been made in subtilisin; when they are all incorporated in the same molecule, the stability is increased by 3.8 kcal mol^{-1}.[115] So far, nature and random mutagenesis have proven better at finding stable mutants than biochemists working from the three-dimensional structures of folded proteins.

4. Theoretical Studies of the Conformational Stability

In this section, we will use the information available at present about conformational entropy, hydrophobic interactions, and hydrogen bonding and other electrostatic interactions to estimate the contribution of the most important forces to the conformational stability of RNase T1. These should be regarded as order of magnitude estimates, but they serve to point out that the fragile conformational stability of RNase T1 is the result of opposing forces of much larger magnitude.

4.1. Conformational Entropy

The conformation of the backbone of a folded protein can be specified by giving the angle of rotation at each N–C_α bond, φ, and each C_α–C_{CO} bond, ψ.[116] The fact that the conformation of the backbone and most of the side chains can be determined by X-ray diffraction studies indicates that rotation around these bonds is limited in the folded protein. When the protein unfolds, rotation about these bonds will be less restricted and many more conformations will be accessible to the polypeptide chain. As a consequence, the unfolded states will have a much greater conformational entropy than the folded states, and this is the major force that favors unfolding.

In 1954, *Kauzmann*[117] suggested that a randomly coiled polypeptide chain would be able to assume z^x conformations, where x is the number of bonds about which rotation can occur and z is the number of rotational states of equal energy per bond. As a first approximation, he assumed $x = 3.33$ and $z = 2$ for each amino acid residue in a polypeptide chain. If the folded protein had only one allowed conformation, the conformational entropy, ΔS_{conf}, [Eq. (i)], would

$$\Delta S_{conf} = R \ln z^x \qquad \text{(i)}$$

favor the unfolded conformations by 4.1 cal mol^{-1} K^{-1}, or 1.2 kcal mol^{-1} per amino acid at 25 °C. This question has been considered from a different point of view by *Dill*.[118]

Privalov[45] showed that for several small compact globular proteins, the specific enthalpy of unfolding converges to a value of about 13 cal g^{-1} near 110 °C. He argued that ". . . at 110 °C, the contribution of water to the entropy of unfolding is small, and the observed effects can be attributed to the increase in configurational freedom of polypeptides on unfolding." The average value observed was 4.2 cal mol^{-1} K^{-1} for each amino acid, a value remarkably close to that *Kauzmann* proposed.

Since the folded conformations of globular proteins are not rigid structures,[105] it is surely not reasonable to assume that they can be represented by a single conformation. On the basis of theoretical calculations, *Karplus* et al.[119] suggested that the conformational entropy of a folded protein is large ($\approx$ 35 cal mol^{-1} K^{-1} per residue), but about the same as it would be for a given unfolded conformer of the same protein. Thus, perhaps just counting the number of unfolded conformations by the simple approach suggested more than thirty years ago by *Kauzmann* does provide at least a rough estimate for ΔS_{conf}, and we have used this in Table 5 to estimate the contribution of conformational entropy to the stability of RNase T1.

Disulfide bonds will limit the conformations accessible to a randomly coiled polypeptide chain and thereby reduce the conformational entropy. *Schellman*[120] and *Flory*[121] and, more recently, *Chan* and *Dill*[122] derived equations based on polymer theory[123] to estimate the magnitude of this effect in proteins. We have used Equation (h) (Section 3.6) to correct ΔS_{conf} for the restraints imposed on the unfolded conformations by the two disulfide bonds in RNase T1. This seems reasonable since Equation (h) is an empirical equation based on experimental results including those for RNase T1.[99]

4.2. Hydrophobic Interactions

In order to estimate the contribution of hydrophobic interactions to the stability of globular proteins, two pieces of information are needed. First, we need to know which nonpolar groups are removed from contact with solvent when

Table 5. Estimating the contributions of conformational entropy, hydrophobic interactions, and hydrogen bonding to the conformational stability of RNase T1.

A. *Conformational entropy*

Rotation about φ, ψ, and χ:
104 residues × − 1.2 kcal per residue [a] = − 124 kcal mol^{-1}.

Disulfide bond restraints:
$T\Delta S(-\text{SS}-) = T(2.1 - (3/2)R\ln n)$, where n is the number of amino acid residues in the loop formed by the disulfide bond [b].

RNase T1 disulfides: 2 to 10 ($n = 9$) and 6 to 103 ($n = 98$).

$T\Delta S(-\text{SS}-) = 2.6 + 4.7 \approx 7.3$ kcal mol^{-1}.

Net: $T\Delta S_{conf} = -124 + 7 = -117$ kcal mol^{-1}.

B. *Hydrophobic interactions*:

Side chain	Number present	Number buried [c]	ΔG_{tr} [d]	Number buried [c] × ΔG_{tr}
Trp	1	1.0	3.1	3.1
Phe	4	3.7	2.4	8.9
Ile + Leu	5	4.4	2.4	10.6
Val	8	6.7	1.7	11.4
Tyr	9	8.9	1.3	11.6
Cys	4	3.3	1.3	4.3
Pro	4	3.4	1.0	3.4
Thr	6	3.3	0.4	1.3
Ala	7	4.7	0.4	1.9
His	3	2.3	0.2	0.5
Ser	15	3.5	0.0	0.0
Gln	3	2.4	−0.3	−0.7
Asn	9	5.0	−0.8	−4.1
-CH_2- [e]	23	16.6	0.7	11.6

Net: Hydrophobic interactions = 64 kcal mol^{-1}.

C. *Hydrogen bonding*
Folded RNase T1 contains 96 marginal to good hydrogen bonds [f].
96 H bonds × 0.76 kcal per H bond [g] = 73 kcal mol^{-1}.

Folded RNase T1 has four peptide NH and two peptide C=O groups that are not hydrogen-bonded and are completely buried [h]. All side-chain oxygen atoms are hydrogen-bonded.

4 × 1.4 kcal per NH H bond [h] + 2 × 2.8 kcal per C=O H bond [h] = − 11 kcal mol^{-1}.

Net: H bonding = 73 − 11 = 62 kcal mol^{-1}.

D. *Sum*
$\Delta G(H_2O) = T\Delta S_{conf}$ + hydrophobic interactions + H bonds
$\Delta G(H_2O) = -117 + 64 + 62 = 9$ kcal mol^{-1}.

[a] Based on a theoretical guess of 4.1 cal mol^{-1} K^{-1} per residue by *Kauzmann* [117] and an experimental guess of 4.2 cal mol^{-1} K^{-1} per residue by *Privalov* [45]. [b] See [99]. [c] See [66]. [d] ΔG_{tr} is the free energy change for transfer of amino acid side chains from a nonpolar medium (*n*-octanol) to water [126]. [e] The CH_2 groups in the side chains of Asp, Glu, Arg, and Lys. [f] See [16]. [g] *Fersht* [125] suggests 0.5 to 1.8 kcal mol^{-1}. 0.76 kcal mol^{-1} was chosen so that $\Delta G(H_2O)$ (experimental) = $\Delta G(H_2O)$ (theoretical). [h] *N. Pace, R. Erickson*, unpublished observations.

the protein folds, and second, we need to know the free energy change for the transfer of a given nonpolar group from water to the interior of a globular protein.

The accessibility to water of the amino acid residues in 37 monomeric globular proteins whose crystal structures have been determined at high resolution has been analyzed recently.[124] The amino acid side chains can be subdivided on the basis of their properties into charged, polar, and nonpolar side chains (Table 2). According to this classification, the solvent-accessible portion of an average globular protein contains comparable amounts of the three classes of side chains, but the buried portion contains mainly nonpolar side chains and very few charged side chains. Note that the content of nonpolar residues varies from 42 to 55% for the proteins in Table 2 and that the percentage of buried nonpolar residues increases with increasing size, as expected, reaching 86% for α-chymotrypsin.

For RNase T1, 70% of the peptide groups and 79% of the nonpolar side chains are inaccessible to water in the folded protein. Figure 15 shows which of the peptide groups and which of the side chains are at least 50% buried in folded RNase T1. The accessibility of each type of polar and nonpolar side chain is given in Table 5. For the calculations, we assume that all of these buried side chains will become fully accessible when the protein unfolds. This is probably not the case (see Section 3.6), but we have no other choice at present because our understanding of the solvent accessibility of unfolded proteins is still limited. Consequently, our estimate of the contribution of hydrophobic interactions to the stability of RNase T1 should be regarded as an upper limit.

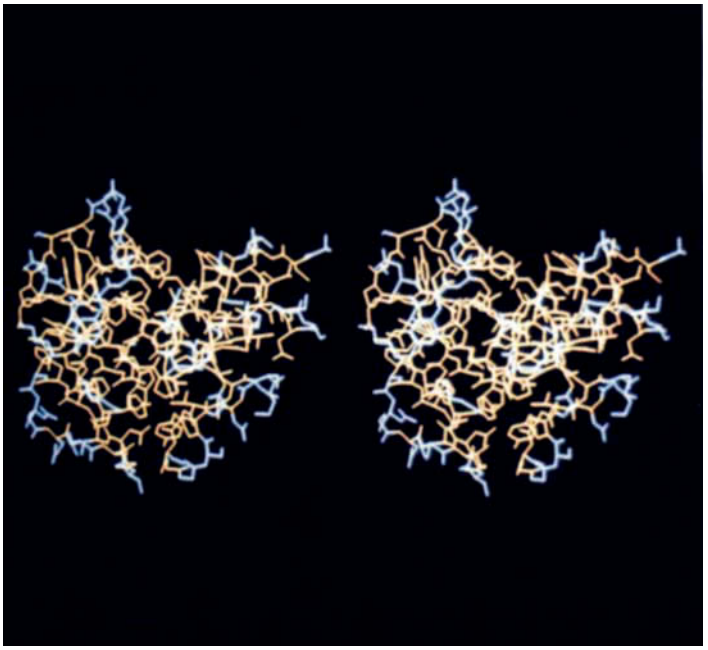

Fig. 15. Stereoview showing the buried and accessible peptide groups and side chains of RNase T1. All groups that are 50% or more accessible are shown in light blue; the remaining groups are yellow.

The free energy change for the transfer of the amino acid side chains from nonpolar environments such as *n*-octanol, hexane, or *N*-methylacetamide to water, ΔG_{tr}, has been determined experimentally in a series of studies since 1962.[126–132] No single solvent system can represent the heterogeneous interior of a globular protein, but *n*-octanol is probably a better model than more nonpolar solvents such as cyclohexane. In Table 5, we have therefore used ΔG_{tr} values for *n*-octanol for estimating the contribution of hydrophobic interactions to the stability of RNase T1.

The contribution of the hydrophobic interactions of a Val side chain to the conformational stability of a protein is illustrated in Table 6. The stability of the folded conformation is increased by 1.7 kcal mol^{-1} for each Val side chain that is buried on folding. This approach is used in Table 5 to estimate the contribution of all the polar and nonpolar side chains plus the CH_2 groups from the charged side chains to the conformational stability of RNase T1. It suggests that hydrophobic interactions restore over half of the free energy lost to conformational entropy. Some of the drawbacks of

Table 6. Contributions of hydrogen bonding and hydrophobic interactions to the conformational stability.

Interaction	ΔG [kcal mol^{-1}]
Hydrophobic interactions	
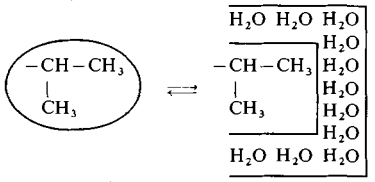	1.7 [a]
Hydrogen bonding	
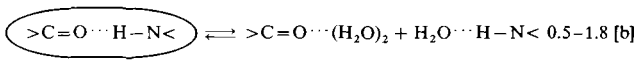	0.5–1.8 [b]
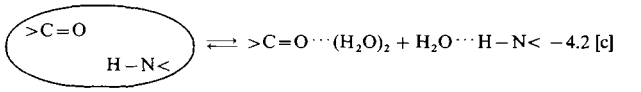	−4.2 [c]
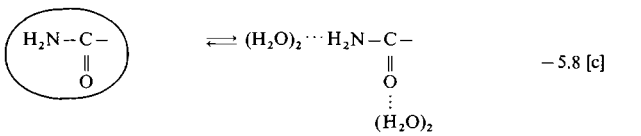	−5.8 [c]
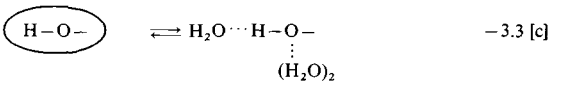	−3.3 [c]

[a] See [126]. ΔG_{tr} (*n*-octanol to water) values for the other side chains are given in Table 5. [b] See [125]. [c] *N. Pace*, unpublished results. The ΔG value for the OH of Tyr is 2.2 kcal mol^{-1}.

this general approach have been discussed,[71, 133–135] and a related approach that uses different model compound data has been described.[80]

4.3. Hydrogen Bonding

In an unfolded protein, the groups capable of hydrogen bonding will generally be completely hydrogen-bonded to water molecules. When a protein folds, about half of the groups form intramolecular hydrogen bonds,[136, 137] most of the rest will remain hydrogen-bonded to water, and only a few or none will be left with unsaturated hydrogen-bond donors or acceptors.[28, 136–138] The groups that are hydrogen-bonded to water in both states will not contribute significantly to the conformational stability. However, for the groups that form intramolecular hydrogen bonds and those that form no hydrogen bonds, we need to know the energetics for the hydrogen-bonding reactions and we need to know the number of groups in each category.

On the basis of experimental studies, *Fersht*[125] has suggested that intramolecular hydrogen bonds between uncharged groups will be favored over hydrogen bonds to water by from 0.5 to 1.8 kcal mol^{-1}. In a folded protein there will surely be a range of values for the contribution of individual hydrogen bonds because of differences in geometry and environment. It is reassuring that experimental studies by *Turner*'s group[139] have suggested that the net gain in stability per hydrogen bond in DNA double helices is very similar (0.5 to 2.0 kcal mol^{-1}).

The groups that do not form hydrogen bonds on folding will favor the unfolded state, where they will be able to hydrogen-bond to water. Estimates of ΔG for this process are given in Table 6. Note that the gain in stability from the formation of an intramolecular hydrogen bond between the groups in a peptide bond, 0.5 to 1.8 kcal mol^{-1}, is considerably less than the loss in stability, −4.2 kcal mol^{-1}, when the same groups fail to form a hydrogen bond when a protein folds. This is surely why the extent of hydrogen bonding in globular proteins is so high and why they have such a high content of secondary structures like α-helices and β-sheets in which the peptide N–H and C=O groups are completely hydrogen-bonded.

RNase T1 contains 293 nitrogen and oxygen atoms capable of accepting or donating hydrogen bonds, 205 backbone and 88 side-chain atoms. These atoms can form a total of 503 hydrogen bonds, 312 by the backbone and 191 by the side chains,[140] according to the hydrogen-bonding capabilities given by *Baker* and *Hubbard*.[28] Using the geometrical criteria suggested by these authors, we find that RNase T1 contains 96 marginal to good hydrogen bonds with an average N···O length of 2.98 Å.[16] Fifty-one of these hydrogen bonds are between the peptide groups in the polypeptide backbone, most of which occur in the secondary structure of RNase T1, as shown in Figure 3.

A sample of ten well-refined protein structures gave the following percentages of non-hydrogen-bonded groups: for peptide groups, 11.2% >C=O and 12.4% >N–H; for the uncharged, polar side chains, 22% Tyr, 18% Ser, 16% Thr, 17% Gln, 17% Asn; for the charged side chains, 3% Asp, 5% Glu, 2% His, 11% Arg, and 24% Lys (the value for Lys is high because this side chain wiggles more than the others and makes it difficult to assess the hydrogen bonding).[28] These percentages should be regarded as upper limits for the content of non-hydrogen-bonded groups: less tightly bound water molecules will not be seen so that some of these groups are sure to be partially hydrogen-bonded to water.

For RNase T1, we have counted the groups that are both not hydrogen-bonded and completely buried in the folded protein. No side-chain hydrogen-bonding groups meet these criteria, but four N–H groups and two C=O groups from peptide bonds do. These are the groups we have included in Table 5 to calculate the unfavorable contribution of unsaturated hydrogen-bond donors and acceptors to the conformational stability of RNase T1.

In order to estimate the contribution of hydrogen bonding to the conformational stability of RNase T1 in Table 5, we need to choose an average value for the contribution of each intramolecular hydrogen bond. We have chosen a value of 0.76 kcal mol^{-1} simply because this leads to agreement between the experimentally determined value of $\Delta G(H_2O)$ and the estimate from the analysis given Table 5. This is in the range of 0.5 to 1.8 kcal mol^{-1} suggested by *Fersht*.[125] Thus, the analysis in Table 5 suggests that the net contribution of hydrogen bonding to $\Delta G(H_2O)$ for RNase T1 is similar in magnitude to the contribution from hydrophobic interactions.

4.4. Electrostatic Interactions

"The general electrostatic interaction between the charged groups on the surface of these proteins appears not to be

energetically important for stability of the folded conformations. All of the 11 amino groups of ribonuclease A, 18 of the 19 of cytochrome c, and up to 10 of β-lactoglobulin were converted to acidic residues with only marginal changes in net stability."

Hollecker and *Creighton*[141]

The results presented in Section 3.4 suggest that electrostatic interactions among the charged groups contribute less than 6 kcal mol^{-1} to the conformational stability of RNase T1 and consequently are not a major factor. It is considerably more difficult to experimentally probe the contributions of permanent dipoles and induced dipoles to the conformational stability. Theoretical calculations by *Wodak*'s group[88] suggest that electrostatic interactions involving both the charged groups and all of the permanent dipoles destabilize the folded conformation of RNase T1. However, this may be more than offset by the favorable contribution of interactions involving induced dipoles, so that the net contribution of all of the electrostatic interactions to the conformational stability is favorable. The model of *Wodak* and colleagues attempts to take into account dielectric effects due to the protein matrix, but effects from the surrounding solvent have not yet been included.

The approach we have taken above in estimating the contribution of hydrogen bonding will take into account some, but certainly not all, of the electrostatic interactions between the permanent dipoles. Likewise, the approach used to estimate the contribution of hydrophobic interactions will account for some, but certainly not all, of the contributions of induced dipoles (London dispersion forces) to the conformational stability. The availability of experimental results on proteins in which local changes in the electrostatic interactions have been made by point mutations will allow refinement of the theoretical models so that we can reach a better understanding of the contribution of electrostatic interactions to the stability of globular proteins.

5. Summary and Outlook

RNase T1 is surely one of the most suitable proteins available for investigating the relationship between the structure of a protein and its chemical, physical, and functional properties. In this article we have summarized what is known about the structure of RNase T1 based on several high-resolution structure analyses by X-ray crystallography. We have also summarized results from a series of experimental studies of the conformational stability of RNase T1. In the final section of the article we have used the structural information and model compound data to guess at the contribution of hydrogen bonding, hydrophobic interactions, and conformational entropy to the conformational stability of RNase T1. We have discussed some of our initial results with site-directed mutants of RNase T1 that illustrate the enormous power of this technology for improving our understanding of all aspects of proteins and their function. Similar results with other proteins have been summarized in several recent reviews.[142]

The combination of structural studies in both the crystal and solution states with biophysical investigations of RNase T1 and selected mutant molecules is expected to yield insight to the structure and function of proteins in general. A very high resolution crystal structure analysis is under way and will provide the still missing fine details concerning side-chain orientations, solvation, and intramolecular hydrogen bonding. Along with kinetic studies of mutants, these structural data will help to clarify the still controversial mechanism of RNA hydrolysis by RNase T1. Similar studies of related microbial ribonucleases are in progress.[143] Further theoretical studies of RNase T1 structure, stability, dynamics, and ligand binding should be designed such that direct experimental testing of the results is possible. Very encouraging in this respect are recently developed spectroscopic methods that yield information about protein motions on a time scale accessible to molecular dynamics simulations.[144] It may be possible to identify intermediates on the folding pathway of RNase T1, as has recently been achieved for the related bacterial ribonuclease barnase.[145] Finally, it is hoped that the biology of the microbial ribonucleases will be investigated to answer obvious but entirely open questions regarding their role in nucleic acid metabolism and the origin of base specificity in these enzymes.

Received: April 6, 1990;
revised: September 3, 1990 [A 809 IE]
German version: *Angew. Chem. 103* (1991) 351

[1] a) P. Blackburn, S. Moore, *Enzymes, 3rd Ed. 15* (1982) 317; b) L. X.-Q. Chen, J. W. Longworth, G. R. Fleming, *Biophys. J. 51* (1987) 865.
[2] a) A. Wlodawer in F. A. Jurnak,A. McPherson (Eds.): *Biological Macromolecules & Assemblies, Vol. 2, Nucleic Acids and Interactive Proteins*, Wiley, New York 1985, p. 393; b) A. Wlodawer, L. A. Svensson, L. Sjölin, G. L. Gilliland, *Biochemistry 27* (1988) 2705.
[3] F. Egami, T. Oshima, T. Uchida, *Mol. Biol. Biochem. Biophys. 32* (1980) 250.
[4] K. Takahashi, S. Moore, *Enzymes 3rd Ed. 15* (1982) 435.
[5] U. Heinemann, U. Hahn in W. Saenger, U. Heinemann (Eds.): *Protein-Nucleic Acid Interaction*, MacMillan, London 1989, p. 111.
[6] H. Donis-Keller, A. M. Maxam, W. Gilbert, *Nucleic Acids Res. 4* (1977) 25.
[7] A. Simoncsits, G. G. Brownlee, R. S. Brown, J. R. Rubin, H. Guilley, *Nature 269* (1977) 833.
[8] M. Silberklang, A. M. Gillum, U. L. RajBhandary, *Methods Enzymol. 59* (1979) 58.
[9] K. Takahashi, *J. Biochem. 70* (1971) 617; *ibid. 98* (1985) 815.
[10] M. Ikehara, E. Ohtsuka, T. Tokunaga, S. Nishikawa, S. Uesugi, T. Tanaka, Y. Aoyama, S. Kikyodani, K. Fujimoto, K. Yanase, K. Fuchimura, H. Morioka, *Proc. Natl. Acad. Sci. USA 83* (1986) 4695.
[11] R. Quaas, Y. McKeown, P. Stanssens, R. Frank, H. Blöcker, U. Hahn, *Eur. J. Biochem. 173* (1988) 617.
[12] R. Quaas, H.-P. Grunert, M. Kimura, U. Hahn, *Nucleosides Nucleotides 7* (1988) 619.
[13] J. Steyaert, C. Thoen, P. Stanssens in A. Pavlovsky, K. Polyakov (Eds.): *Structure and Chemistry of Ribonucleases*, Academy of Sciences of the USSR, Moscow 1989, p. 216.
[14] U. Heinemann, W. Saenger, *Nature 299* (1982) 27.
[15] R. Arni, U. Heinemann, M. Maslowska, R. Tokuoka, W. Saenger, *Acta Crystallogr. Sect. B43* (1987) 548.
[16] R. Arni, U. Heinemann, R. Tokuoka, W. Saenger, *J. Biol. Chem. 263* (1988) 15358.
[17] S. Sugio, T. Amisaki, H. Ohishi, K.-I. Tomita, U. Heinemann, W. Saenger, *FEBS Lett. 181* (1985) 129.
[18] S. Sugio, T. Amisaki, H. Ohishi, K.-I. Tomita, *J. Biochem. 103* (1988) 354.
[19] S. Sugio, K.-I. Oka, H. Ohishi, K.-I. Tomita, W. Saenger, *FEBS Lett. 183* (1985) 115.
[20] J. Koepke, M. Maslowska, U. Heinemann, W. Saenger, *J. Mol. Biol. 206* (1989) 475.
[21] D. Kostrewa, H.-W. Choe, U. Heinemann, W. Saenger, *Biochemistry 28* (1989) 7592.
[22] a) A. Lenz, F. Cordes, U. Heinemann, W. Saenger, *J. Biol. Chem.*, in press; b) A. Lenz, U. Heinemann, W. Saenger, *Acta Crystallogr. Sect. B*, in press.
[23] G. Koellner, H.-W. Choe, U. Heinemann, U. Hahn, H.-P. Grunert, W. Saenger, unpublished.

[24] P. Verhelst, I. Zegers, U. Heinemann, W. Saenger, L. Wyns, unpublished.
[25] P. M. D. Fitzgerald, *J. Appl. Crystallogr. 21* (1988) 273.
[26] a) W. A. Hendrickson, J. H. Konnert in R. Diamond, S. Ramaseshan, K. Venkatesan (Eds.): *Computing in Crystallography*, Indian Academy of Sciences, Bangalore 1981, Chaper 13.01; b) W. A. Hendrickson, *Methods Enzymol. 115* (1985) 252; c) B. C. Finzel, *J. Appl. Crystallogr. 20* (1987) 58; d) S. Sheriff, *ibid. 20* (1987) 55.
[27] T. A. Jones, *J. Appl. Crystallogr. 11* (1987) 268; *Methods Enzymol. 115* (1985) 157.
[28] E. N. Baker, R. E. Hubbard, *Prog. Biophys. Mol. Biol. 44* (1984) 97.
[29] S. Hirono, P. M. Kollman, *J. Mol. Biol. 212* (1990) 197.
[30] S. Nishikawa, T. Kimura, H. Morioka, S. Uesugi, T. Hakoshima, K. Tomita, E. Ohtsuka, M. Ikehara, *Biochem. Biophys. Res. Commun. 150* (1988) 68.
[31] U. Heinemann, W. Saenger, *J. Biomol. Struct. Dyn. 1* (1983) 523.
[32] K. Takahashi, *J. Biochem. 67* (1970) 833.
[33] F. Eckstein, H. H. Schulz, H. Rüterjans, W. Haar, W. Maurer, *Biochemistry 11* (1972) 3507.
[34] a) M. Ikehara, E. Ohtsuka, T. Tokunaga, S. Nishikawa, S. Uesugi, T. Tanaka, Y. Aoyama, S. Kikyodani, K. Fujimoto, K. Yanase, K. Fuchimura, H. Kim, Y. Ueda, T. Kimura, H. Morioka in K. S. Bruzik, W. J. Stec (Eds.): *Biophosphates and Their Analogues—Synthesis, Structure, Metabolism and Activity*, Elsevier, Amsterdam 1987, p. 335; b) S. Nishikawa, H. Morioka, H. J. Kim, K. Fuchimura, T. Tanaka, S. Uesugi, T. Hakoshima, K.-I. Tomita, E. Ohtsuka, M. Ikehara, *Biochemistry 26* (1987) 8620.
[35] H.-P. Grunert, A. Zouni, M. Beineke, R. Quaas, Y. Georgalis, W. Saenger, U. Hahn, *Eur. J. Biochem.*, in press.
[36] a) P. Verhelst, U. Heinemann, W. Saenger, P. Stanssens, J. Steyaert, L. Wyns in A. Pavlovsky, K. Polyakov (Eds.): *Structure and Chemistry of Ribonucleases*, Academy of Sciences of the USSR, Moscow 1989, p. 202; b) J. Steyaert, K. Hallenga, L. Wyns, P. Stanssens, *Biochemistry 29* (1990) 9064.
[37] a) A. D. MacKerell, Jr., R. Rigler, L. Nilsson, U. Heinemann, W. Saenger, *Eur. Biophys. J. 16* (1988) 287; b) A. D. MacKerell, Jr., L. Nilsson, R. Rigler, W. Saenger, *Biochemistry 27* (1988) 4547; c) A. D. MacKerell, Jr., L. Nilsson, R. Rigler, U. Heinemann, W. Saenger, *Proteins: Struct. Funct. Genet. 6* (1989) 20.
[38] a) H. Rüterjans, E. Hoffmann, J. Schmidt, J. Simon in J. Zelinka, J. Balan (Eds.): *Metabolism and Enzymology of Nucleic Acids Including Gene Manipulations, Vol. 6*, Slovak Academy of Sciences, Bratislava 1987, p. 81; b) E. Hoffmann, H. Rüterjans, *Eur. J. Biochem. 177* (1988) 539; c) E. Hoffmann, J. Schmidt, J. Simon, H. Rüterjans, *Nucleosides Nucleotides 7* (1988) 757; d) H. Rüterjans, O. Pongs, *Eur. J. Biochem. 18* (1971) 313.
[39] R. Malin, P. Zielenkiewicz, W. Saenger, *J. Biol. Chem.*, in press.
[40] a) C. N. Pace, *Methods Enzymol. 131* (1986) 266; b) C. N. Pace, B. A. Shirley, J. A. Thomson in T. E. Creighton (Ed.): *Protein Structure: A Practical Approach*, IRL Press, Oxford 1988, p. 311.
[41] J. A. Thomson, B. A. Shirley, G. R. Grimsley, C. N. Pace, *J. Biol. Chem. 264* (1989) 5315.
[42] C. Tanford, *Adv. Protein Chem. 23* (1968) 121.
[43] C. Tanford, *Adv. Protein Chem. 24* (1970) 1.
[44] C. N. Pace, *Crit. Rev. Biochem. 3* (1975) 1.
[45] P. Privalov, *Adv. Protein Chem. 33* (1979) 167.
[46] J. W. Donovan in S. J. Leach (Ed.): *Physical Principles and Techniques of Protein Chemistry, Vol. 5*, Academic Press, Orlando, FL, USA 1969, p. 101.
[47] J. W. Longworth, *Photochem. Photobiol. 8* (1968) 589.
[48] T. Kiefhaber, R. Quaas, U. Hahn, F. X. Schmid, *Biochemistry 29* (1990) 3053, 3061.
[49] a) P. S. Kim, R. L. Baldwin, *Annu. Rev. Biochem. 59* (1990) 631; b) R. L. Baldwin, *Trends Biochem. Sci. 14* (1989) 276; c) K. Kuwajima, *Proteins: Struct. Funct. Gen. 6* (1989) 87; d) R. Jaenicke, *Angew. Chem. 96* (1984) 385; *Angew. Chem. Int. Ed. Engl. 23* (1984) 395.
[50] J. F. Brandts, H. R. Halvorson, M. Brennan, *Biochemistry 14* (1975) 4953.
[51] T. Kiefhaber, H.-P. Grunert, U. Hahn, F. X. Schmid, *Biochemistry 29* (1990) 6475.
[52] a) J. A. Schellman, *Biopolymers 17* (1978) 1305; b) *ibid. 26* (1987) 549; c) K. A. Dill, *Biochemistry 24* (1985) 1501.
[53] C. N. Pace, D. V. Laurents, *Biochemistry 28* (1989) 2520.
[54] M. M. Santoro, D. W. Bolen, *Biochemistry 27* (1988) 8063.
[55] a) K. A. Aune, C. Tanford, *Biochemistry 8* (1969) 4568; b) C. N. Pace, K. E. Vanderburg, *ibid. 18* (1979) 288.
[56] J. T. Edsall in A. Rich, N. Davidson (Eds.): *Structural Chemistry and Molecular Biology*, Freeman, San Francisco 1968, p. 88.
[57] W. J. Becktel, J. A. Schellman, *Biopolymers 26* (1987) 1859.
[58] I. Kanazawa, H. Hamaguchi, *J. Biochem. 100* (1986) 207.
[59] H. Schwarz, H.-J. Hinz, A. Mehlich, H. Tschesche, H. R. Wenzel, *Biochemistry 26* (1987) 3544.
[60] a) C. N. Pace, D. V. Laurents, J. A. Thomson, *Biochemistry 29* (1990) 2565; b) M. McNutt, L. S. Mullins, F. M. Rauschel, C. N. Pace, *ibid. 29* (1990) 7572.
[61] F. Ahmad, C. C. Bigelow, *J. Biol. Chem. 257* (1982) 12935.
[62] D. Shortle, A. K. Meeker, *Proteins: Struct. Funct. Gen 1* (1986) 81.
[63] E. P. Garvey, C. R. Matthews, *Biochemistry 28* (1989) 2083.
[64] B. Chen, J. A. Schellman, *Biochemistry 28* (1989) 685.
[65] R. Lumrey, R. Biltonen in S. N. Timasheff, G. D. Fasman (Eds.): *Structure and Stability of Biological Macromolecules*, Marcel Dekker, New York 1969, p. 65.
[66] a) F. M. Richards, *Annu. Rev. Biophys. Bioeng. 6* (1977) 151; b) B. Lee, F. M. Richards, *J. Mol. Biol. 55* (1971) 379.
[67] L. G. Presta, G. D. Rose, *Science 240* (1988) 1632.
[68] a) R. A. Bradshaw, *Trends Biochem. Sci. 14* (1989) 276; b) S. M. Arfin, R. A. Bradshaw, *Biochemistry 27* (1988) 7979; c) A. L. Goldberg, A. C. St. John, *Annu. Rev. Biochem. 45* (1976) 747; d) C. N. Pace, A. J. Barrett, *Biochem. J. 219* (1984) 411; e) C. N. Pace, L. M. Fisher, J. F. Cupo, *Acta Biol. Med. Ger. 40* (1981) 385; f) E. R. Stadtman, *Biochemistry 29* (1990) 6323.
[69] a) S. P. Ho, W. F. Degrado, *J. Am. Chem. Soc. 109* (1987) 6751; b) L. Regan, W. F. Degrado, *Science 241* (1988) 976.
[70] G. Das, D. R. Hickey, G. McLendon, F. Sherman, *Proc. Natl. Acad. Sci. USA 86* (1989) 496.
[71] J. T. Kellis, K. Nyberg, A. R. Fersht, *Biochemistry 28* (1989) 4914.
[72] K. Yutani, K. Ogasahara, T. Tsujita, Y. Sugino, *Proc. Natl. Acad. Sci. USA 84* (1987) 4441.
[73] a) P. L. Privalov, S. J. Gill, *Adv. Protein Chem. 39* (1988) 191; b) J. M. Sturtevant, *Annu. Rev. Phys. Chem. 38* (1987) 463.
[74] a) J. F. Brandts, L. Hunt, *J. Am. Chem. Soc. 89* (1967) 4826; b) J. F.-Brandts, *ibid. 86* (1964) 4291, 4302.
[75] C. N. Pace, C. Tanford, *Biochemistry 7* (1968) 198.
[76] P. L. Privalov, Y. V. Griko, S. Y. Venyaminov, V. P. Kutyshenko, *J. Mol. Biol. 190* (1986) 487.
[77] Y. V. Griko, P. L. Privalov, J. M. Sturtevant, S. Y. Venyaminov, *Proc. Natl. Acad. Sci. USA 85* (1988) 343.
[78] B. Lee, *Biopolymers 24* (1985) 813.
[79] R. L. Baldwin, *Proc. Natl. Acad. Sci. USA 83* (1986) 8096.
[80] R. S. Spolar, J.-H. Ha, M. T. Record, Jr., *Proc. Natl.Acad. Sci. USA 86* (1989) 8382.
[81] C. Tanford: *Physical Chemistry of Macromolecules*, Wiley, New York 1961.
[82] T. Imoto, *Biophys. J. 44.* (1983) 293.
[83] R. L. Baldwin, D. Eisenberg in D. L. Oxender, C. F. Fox (Eds.): *Protein Engineering*, Alan R. Liss, New York 1987, p. 127.
[84] S. Iida, T. Ooi, *Biochemistry 8* (1969) 3897.
[85] a) A. Wada, H. Nakamura, *Nature 293* (1981) 757; b) D. J. Barlow, J. M. Thornton, *Biopolymers 25* (1986) 1717.
[86] a) S. C. Harvey, *Proteins: Struct. Funct. Genet. 5* (1989) 78; b) M. K. Gilson, B. H. Honig, *ibid. 3* (1988) 32; c) M. Delepierre, C. M. Dobson, M. Karplus, F. M. Poulsen, D. J. States, R. E. Wedin, *J. Mol. Biol. 197* (1987) 111; d) M. J. E. Sternberg, F. R. F. Hayes, A. J. Russell, P. G. Thomas, A. R. Fersht, *Nature 330* (1987) 86; e) A. Warshel, *ibid. 330* (1987) 15.
[87] A. R. Fersht, M. J. E. Sternberg, *Protein Eng. 2* (1989) 527.
[88] D. Van Belle, I. Couplet, M. Prevost, S. J. Wodak, *J. Mol. Biol. 198* (1987) 721.
[89] M. K. Gilson, B. Honig, *Proteins: Struct. Funct. Genet. 4* (1988) 7.
[90] a) J. J. Hermans, H. A. Scheraga, *J. Am. Chem. Soc. 83* (1961) 3283; b) K. A. Aune, C. Tanford, *Biochemistry 8* (1969) 4582.
[91] F. Inagaki, Y. Kawano, I. Shimada, K. Takahashi, T. Miyazawa, *J. Biochem. 89* (1981) 1185.
[92] C. N. Pace, G. R. Grimsley, *Biochemistry 27* (1988) 3242.
[93] J. A. Schellman, *Biopolymers 14* (1975) 999.
[94] C. N. Pace, T. McGrath, *J. Biol. Chem. 255* (1980) 3862.
[95] a) M. Fujinaga, T. J. Delbare, G. D. Brayer, M. N. G. James, *J. Mol. Biol. 183* (1985) 479; b) O. Herzberg, M. N. G. James, *Biochemistry 24* (1985) 5298; c) J. W. Pflugrath, F. A. Quiocho, *Nature 314* (1985) 257; d) D. I. Stuart, K. R. Acharya, N. P. C. Walker, S. G. Smith, M. Lewis, D. C. Phillips, *ibid. 324* (1986) 84; e) N. K. Vyas, M. N. Vyas, F. A. Quiocho, *ibid. 327* (1987) 635.
[96] C. O'Sullivan, F. W. Thomson, *J. Chem. Soc. 57* (1890) 834.
[97] a) N. Citri, *Adv. Enzymol. 37* (1973) 397; b) S. Grisolia, *Physiol. Rev. 44* (1964) 657.
[98] C. N. Pace, T. E. Creighton, *J. Mol. Biol. 188* (1986) 477.
[99] C. N. Pace, G. R. Grimsley, J. A. Thomson, B. J. Barnett, *J. Biol. Chem. 263* (1988) 11820.
[100] C. Hill, G. Dodson, U. Heinemann, W. Saenger, Y. Mitsui, K. Nakamura, S. Borisov, G. Tischenko, K. Polyakov, S. Pavlovsky, *Trends Biochem. Sci. 8* (1983) 364.
[101] R. W. Hartley, *Trends Biochem. Sci. 14* (1989) 450.
[102] R. W. Hartley, *Biochemistry 8* (1969) 2929.
[103] H. Neumann, I. Z. Steinberg, J. R. Brown, R. F. Goldberger, M. Sela, *Eur. J. Biochem. 3* (1967) 171.
[104] A. S. Acharya, H. Taniuchi, *Int. J. Pept. Protein Res. 15* (1980) 503.
[105] a) F. R. N. Gurd, T. M. Rothberg, *Adv. Protein Chem. 33* (1981) 1; b) G. Wagner, K. Wüthrich, *Naturwissenschaften 70* (1983) 105.

[106] A. A. Kossiakoff, *Nature 296* (1982) 713.
[107] D. Shortle, *J. Biol. Chem. 264* (1989) 5315.
[108] J. M. Thornton, *J. Mol. Biol. 151* (1981) 261.
[109] C. Mitchinson, J. A. Wells, *Biochemistry 28* (1989) 4897.
[110] a) M. Matsumura, G. Signor, B. W. Matthews, *Nature 342* (1989) 291; b) M. Matsumura, W. J. Becktell, M. Levitt, B. W. Matthews, *Proc. Natl. Acad. Sci. USA 86* (1989) 6562.
[111] B. A. Shirley, P. Stanssens, J. Steyaert, C. N. Pace, *J. Biol. Chem. 264* (1989) 11 621.
[112] M. Mutter, S. Vuilleumier, *Angew. Chem. 101* (1989) 551; *Angew. Chem. Int. Ed. Engl. 28* (1989) 535.
[113] W. F. DeGrado, *Adv. Protein Chem. 39* (1988) 51.
[114] J. S. Richardson, D. C. Richardson, *Trends Biochem. Sci. 14* (1989) 304.
[115] M. W. Pantoliano, M. Whitlow, J. F. Wood, S. W. Dodd, K. D. Hardman, M. L. Rollence, P. N. Bryan, *Biochemistry 28* (1989) 7205.
[116] G. E. Schulz, R. H. Schirmer: *Principles of Protein Structure*, Springer, New York 1979.
[117] W. Kauzmann in W. D. McElroy, B. Glass (Eds.): *The Mechanism of Enzyme Action*, Johns Hopkins Press, Baltimore 1954.
[118] K. A. Dill, *Biochemistry 24* (1985) 1501.
[119] M. Karplus, T. Ichiye, B. M. Pettitt, *Biophys. J. 52* (1987) 1083.
[120] J. A. Schellman, *C. R. Trav. Lab Carlsberg Ser. Chim. 29* (1955) 230.
[121] P. J. Flory, *J. Am. Chem. Soc. 78* (1956) 5222.
[122] H. S. Chan, K. A. Dill, *J. Chem. Phys. 90* (1989) 492.
[123] H. Jacobson, W. H. Stockmayer, *J. Chem. Phys. 18* (1950) 1600.
[124] S. Miller, J. Janin, A. M. Lesk, C. Chothia, *J. Mol. Biol. 196* (1987) 641.
[125] A. R. Fersht, *Trends Biochem. Sci. 12* (1987) 301.
[126] J.-L. Fauchere, V. Pliska, *Eur. J. Med. Chem.-Chim. Ther. 18* (1983) 369.
[127] Y. Nozaki, C. Tanford, *J. Biol. Chem. 246* (1971) 2211.
[128] D. J. Abraham, A. J. Leo, *Proteins Struct. Funct. Genet. 2* (1987) 130.
[129] J. H. Fendler, F. Nome, J. Nagyvary, *J. Mol. Evol. 6* (1975) 215.
[130] S. Damodaran, K. B. Song, *J. Biol. Chem. 261* (1986) 7220.
[131] E. J. Cohn, J. T. Edsall: *Proteins, Amino Acids and Peptides*, Hafner Publishing, New York 1965, p. 212.
[132] A. Radzicka, R. Wolfenden, *Biochemistry 27* (1988) 1664.
[133] J. Bello, *Int. J. Pept. Protein Res. 12* (1978) 38.
[134] J. Bello, *J. Theor. Biol. 67* (1977) 335.
[135] T. E. Creighton, *J. Phys. Chem. 89* (1985) 2452.
[136] C. Chothia, *Nature 245* (1975) 304.
[137] J. L. Finney, B. J. Gellatly, I. C. Golton, J. Goodfellow, *Biophys. J. 10* (1980) 17.
[138] J. J. Birktoft, D. M. Blow, *J. Mol. Biol. 68* (1972) 187.
[139] a) D. H. Turner, N. Sugimoto, R. Kierzek, S. D. Dreiker, *J. Am. Chem. Soc. 109* (1987) 3783; b) S. M. Freier, N. Sugimoto, A. Sinclair, D. Alkema, T. Neilson, R. Kierzek, M. H. Caruthers, D. H. Turner, *Biochemistry 25* (1986) 3214.
[140] The 103 peptide groups of RNase T1 can each engage in three hydrogen bonds, two accepted by the carbonyl oxygen and one donated by the N–H group, except for the four X–Pro peptide bonds which have no peptide N–H and thus lack one hydrogen bond each. Adding to the resultant 305 potential hydrogen bonds three from the terminal amino group and four from the terminal carboxylate yields 312 potential backbone hydrogen bonds. The side chain bonds in RNase T1 come from the 15 Ser (3), 6 Thr (3), 6 Glu (4), 6 Asp (4), 2 Gln (4), 9 Asn (4), 2 Lys (3), 1 Arg (5), 3 His (2), 9 Tyr (2), and 1 Trp (1) residues, where the numbers of potential hydrogen bonds are given in parentheses for each side chain type.
[141] M. Hollecker, T. E. Creighton, *Biochim. Biophys. Acta 701* (1982) 395.
[142] a) B. W. Matthews, *Biochemistry 26* (1987) 6885; b) D. P. Goldenberg, *Annu. Rev. Biophys. Biophys. Chem. 17* (1988) 481; c) T. Alber, *Annu. Rev. Biochem. 58* (1989) 765.
[143] a) D. E. Mossakowska, K. Nyberg, A. R. Fersht, *Biochemistry 28* (1989) 3843; b) J. Sevcik, R. G. Sanishvili, A. G. Pavlovsky, K. M. Polyakov, *Trends Biochem. Sci. 15* (1990) 158.
[144] a) A. D. MacKerell, Jr., R. Rigler, L. Nilsson, U. Hahn, W. Saenger, *Biophys. Chem. 27* (1987) 4547; b) P. H. Axelsen, F. G. Prendergast, *Biophys. J. 56* (1989) 43.
[145] a) A. Matouschek, J. T. Kellis, Jr., L. Serrano, M. Bycroft, A. R. Fersht, *Nature 346* (1990) 440; b) M. Bycroft, A. Matouschek, J. T. Kellis, Jr., L. Serrano, A. R. Fersht, *ibid. 346* (1990) 488.

Fluorine-Stabilized Sulfur–Carbon Multiple Bonds

By Konrad Seppelt*

Alkylidene and alkylidyne sulfur fluorides contain sulfur–carbon multiple bonds. In contrast to the sulfur ylides, alkylidene sulfur fluorides fulfill all the criteria for double bonds, i.e. they have short bond lengths, strong anisotropic distribution of electron density, and rotation about the C–S bond is restricted. Alkylidyne sulfur fluorides have especially short bond distances and, due to a high amplitude bending motion, appear to be more or less linear, depending on the physical state. The advantage of the C–S multiple bond systems in contrast with numerous others, e.g. those of phosphorus and silicon, is that they exist without steric stabilization. Moreover, the limits of the triple-bond principle are outlined: the prognosis for triple bonds between two elements of higher periods is poor, because carbene-like or fully bridged structures win in terms of stability.

1. Introduction

In the last decade there has been a rapid development in the preparation of double bond systems with heavy main group elements which contradict the predictions of the Double Bond Rule. This development followed the investigations of compounds with metal–metal and metal–carbon multiple bonds. Among the main group elements, silicon and phosphorus have attracted most attention. The number of review articles on multiple bond systems of these elements is considerable.[1–10] Meanwhile, interest in the heavier homologues of the fourth and fifth main groups has also been aroused.[4, 5]

Independently of these developments, there has concomitantly been increased activity in the area of sulfur–carbon multiple bonds in the last few years, particularly regarding the compounds to be discussed herein with sulfur in higher oxidation states. On the one hand, the element sulfur has, until now, stood somewhat in the shadow of the elements phosphorus and silicon, not only because one always conceded that sulfur readily forms double bonds (SO_2, CS_2, and others), but also because the synthetic methods are more limited and often much more specific. On the other hand, the peculiarity of sulfur to have available three easily accessible oxidation states (II, IV, VI) can stimulate the imagination of the preparative chemist.

No compound is so unique that parallels or comparisons with other compounds or classes of compounds cannot be drawn. A new substance, which alone through its existence or its structure first causes great astonishment, after some time falls into the general picture of chemistry. Double bond systems of the type $R_2C{=}SF_4$, $R_2C{=}SF_2$, $R_2C{=}SF_2{=}O$, $R_2C{=}S{=}O$, and $R_2C{=}SO_2$ will be discussed herein and compared with the sulfur ylides $R_2\overset{\ominus}{C}{-}\overset{\oplus}{S}R'_2$ and oxosulfur ylides $R_2\overset{\ominus}{C}{-}\overset{\oplus}{S}OR'_2$. As a result, a discussion of the double bond becomes of central importance. Criteria which are measurable, or at least in principle measurable, will be drawn into the discussion: atomic spacings, electron densities, charge distribution, potentials such as vibrational energies and particularly torsional energies. MO models or their simplifications serve only occasionally to make the results plausible.

[*] Prof. Dr. K. Seppelt
Institut für Anorganische und Analytische Chemie der Freien Universität
Fabeckstrasse 34–36, W-1000 Berlin 33 (FRG)

In spite of all of the remarkable success with the synthesis of such compounds, the fact remains that these double bonds still form, in the final analysis, more unfavorable bonding systems than those of elements of the second period. There is no lack of possible explanations.[11–13] A constantly repeated, simplified argument in the discussion is the increasing size of the elements, and the resulting "poor π-overlap". One can subdivide the bond energy of a double bond into a σ- and a π-increment, provided that the thermodynamic data of a large number of comparable compounds are known. Thus, one comes to the conclusion that the π increment in N=N and O=O double bonds is greater than the σ increment; in C=C double bonds both are about the same, and in all other multiple bonds the π increment is smaller.

Compounds with sulfur–carbon triple bonds of the type $R{-}C{\equiv}SF_3$ will be compared, for want of a better possibility, with the few known triple bond systems in which an element of the third or higher period takes part in the triple bond. This class of compound (R–C≡P, R–C≡As, R–N≡Si, $R_2P{\equiv}N$, $R{-}N{\equiv}P^{\oplus}$, $R_2P{\equiv}C{-}R$, $F_3S{\equiv}N$, $FS{\equiv}N$) is very heterogenous. Generally speaking triple bonds of this type are always a novelty. Naturally, the steric protection of the linear grouping of atoms of triple bond systems is much less possible than in the case of double bond systems so that the syntheses are very problematical. There are also indications that the range of existence for such triple bond systems is in principle limited. It will be shown that compound **1**

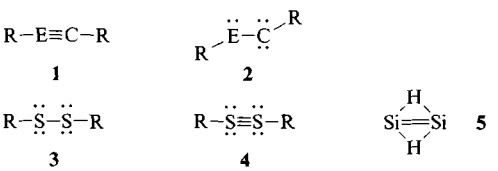

1 **2** **3** **4** **5**

offers little resistance to a sharp bending to give **2**. If one binds together two elements of the third period with a triple bond, then in these systems the "dicarbene structure" **3** will be more stable than **4**.

Even a doubly bridged structure **5** is theoretically predicted for disilaethyne.[14–19] The limitations of a bonding principle can be probed here, a particularly attractive challenge for the synthetic chemist.

2. Sulfur–Carbon Double Bonds

Sulfur–carbon double bonds have been known for some time in the form of carbon disulfide and its homologues O=C=S and S=C=Se. Subsequent findings prompted the question of why these compounds are so stable towards polymerization. The same applies here as with the outstanding stability of CO_2: The average C–O bond energy of CO_2 is clearly greater than the bond increment C–O in ketones. This is a result of the symmetry of the CO_2 molecule, in which according to a simple HMO model, each C–O bond has a bond order of 2.4.[20] CS_2 is an analogus special case.

The simplest conceivable molecule with a C–S double bond $H_2C{=}S$, on the other hand, behaves "normally". This can be prepared by the elimination of HCl from $H_3C{-}S{-}Cl$, but is stable against polymerization only under reduced pressure.[21–24] Thus, thioformaldehyde was also discovered as a component of interstellar matter by means of its microwave spectrum.[25] The polymerization can be hindered by substitution at carbon, $(C_6H_5)_2C{=}S$ is already stable. Thioketones react preferably at the sulfur atom, which means indirectly that the double bond character of the C–S bond is less than in ketones. The color can also be interpreted in this way.

Sulfur ylides are also often stable in the conventional sense,[27] and even the simplest compounds $H_2\overset{\ominus}{C}{-}\overset{\oplus}{S}(CH_3)_2$ and $H_2\overset{\ominus}{C}{-}\overset{\oplus}{S}O(CH_3)_2$ are easily prepared.[28] The ylidic bond in the sulfur ylides (171–174 pm)[29] is indeed somewhat shorter than a C–S single bond ($\simeq$ 180 pm), but up to now there is no indication of a hindered rotation about the C–S bond.[30] Therefore, the conventional description as a single bond with zwitterionic bond strengthening is justifiable here.[31]

In order to strengthen the double bond character of the C–S bond, it was necessary to increase the electronegativity of the sulfur atom. This can best be achieved by means of the highest possible fluorine substitution at sulfur. Hence the preparation of $H_2C{=}SF_4$ **11** was considered possible, and in fact was achieved. Carbon bound fluorine has a similar influence on C–S double bonds. For the sake of simplicity, only α- and β-fluorinated molecules will be considered here.

Fluorine substitution in the α-position weakens the double bond. This can go so far that even no bond exists any more. Thus according to calculations the molecule $F_2\overset{\ominus}{C}{-}\overset{\oplus}{P}H_3$ does not exist, except possibly as a van der Waals adduct (354 ppm) between F_2C and PH_3.[32] Yet according to corresponding calculations, $HF\overset{\ominus}{C}{-}\overset{\oplus}{P}H_3$ is a chemically bound state with a P–C distance of 172.3 pm (for comparison $H_2\overset{\ominus}{C}{-}\overset{\oplus}{P}H_3$ calcd. 167.5 pm). This destabilization by an α fluorine obviously has several reasons: the carbene fragmentation is favored by the stability of the fluorinated carbene, and the strong interaction of the carbon's p-orbitals with the neighboring fluorine substituents weakens π bonds in general (fluoro effect in olefins). However, α-fluoro and α-difluoro phosphorus ylides have been successfully detected by trapping reactions.[33–39] Among sulfur compounds there is with few exceptions ($CF_3{-}CF{=}S{=}O$, $F_2C{=}S{=}O$, $F_2C{=}SF_2$) only sparse information available (see Section 5 and 7, compounds **27**, **35** and **39**).

According to all previous findings, the role of a β-fluorine substituent is stabilizing. Examples in the series of phosphorus ylides are **6**,[40] **7**,[41] **8**,[42] and **9** (with crystal structure

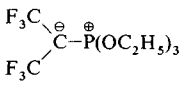

6

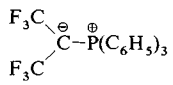

7

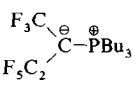

8

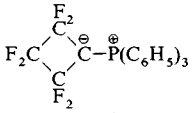

9

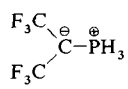

10

analysis[43]), and calculations on **10**.[32] With the sulfur compounds to be discussed herein, this stabilization by β-fluorine substitution can be decisive in actually obtaining a desired compound, for example $F_3C{-}C{\equiv}SF_3$, Firstly, a CF_3 group already exerts a certain steric protection, but also the acceptance of partial charge from the multiple bonded carbon atom can occur in the sense of a negative hyperconjugation.

The carbene-metal complexes, which were first prepared approximately fifteen years earlier,[44,45] were one other model for the synthesis of $R_2C{=}SF_4$. Without pushing the analogy too far, these classes of substances are similar in the coordinative saturation of the heavy atom (metal or sulfur), in the significance of the substituents on the carbon for stability, in certain structural principles, and in molecular dynamics (see Section 3).

One sees with the molecule $H_2C{=}SF_4$ that here the double bond problem can be genuinely studied free of steric effects. The amazing success in the synthesis of Si=Si, P=P, and other double bonds rests ultimately on the success of the steric shielding of the unstable part of the molecule against

Konrad Seppelt, born in Leipzig in 1944, studied chemistry in Hamburg and Heidelberg, where he gained his doctorate in 1970 under the supervision of Professor W. Sundermeyer. After his habilitation in Heidelberg with work on selenium-fluorine compounds he joined Professor N. Bartlett at the University of California at Berkeley for one year. Following his appointment as Heisenberg Professor at the University of Heidelberg he accepted a post as professor at the Freie Universität Berlin. His research activities center on the chemistry of electronegative elements. He was awarded a Karl-Winnacker fellowship and the Chemistry Prize of the Akademie der Wissenschaften zu Göttingen.

polymerization and/or oxidation. This steric shielding will influence the structure. Thereby the length of the double bond might be afflicted least, but the angle deformations (twist angle, pyramidalization) to a great extent.[3]

3. Alkylidene Sulfur Tetrafluoride

As long ago as 1972 *J. I. Musher* predicted the possible existence of compounds of the type $R_2C{=}SR'_4$ and had designated them as persulfuronium ylides,[46] however, they have so far never been synthesized. It is also questionable whether these compounds would be stable against ligand elimination (R'–R) with the simultaneous formation of normal sulfur ylides $R_2\overset{\ominus}{C}{-}\overset{\oplus}{S}R'_2$. The corresponding decomposition reaction is not expected for R'=F. So the first alkylidene sulfur tetrafluoride, $H_2C{=}SF_4$, was prepared by *G. Kleemann* and *K. Seppelt* in 1978 by a tedious synthetic route.[47, 48]

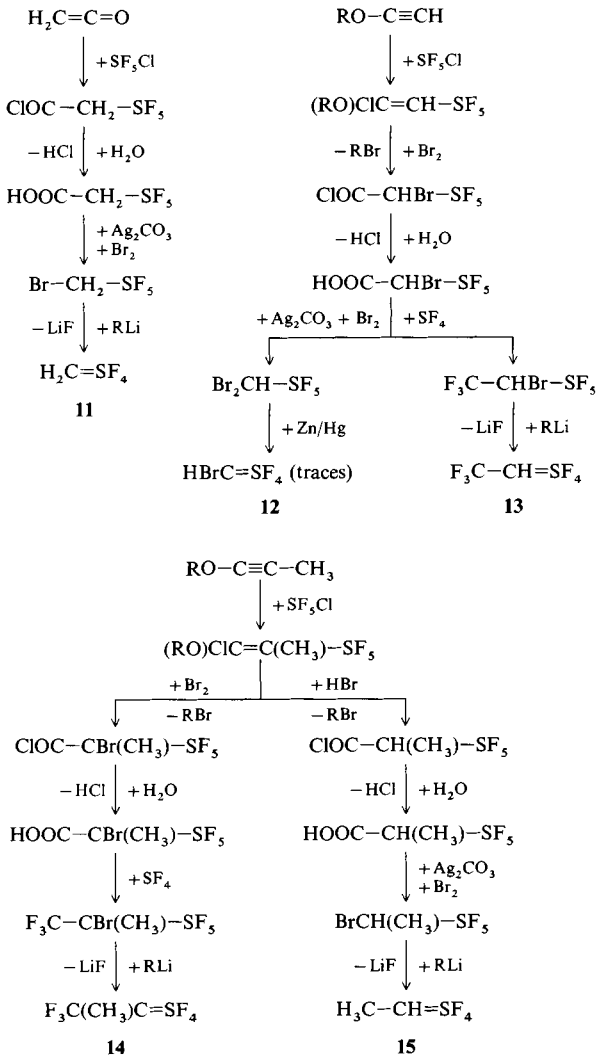

The substituted alkylidene sulfur tetrafluorides **12**,[51] **13**, **14**,[50] and **15**[49] could be prepared in a similar way. The long reaction route resulted in these compounds always being available in only small amounts. **13** and **14** had in addition to be separated from isomers. This difficult situation changed when **13**[52] and **16**[53] became easily accessible [Eq. (a) and (b)] with the accidental discovery of rearrangement reactions. An elegant method for small amounts of **11** is the decarbonylation by means of $Na[Mn(CO)_5]$[54] [Eq. (c)]. An HF elimination succeeds especially easily if the proton is a strongly acidic, as in the sultone **17**[55] [Eq. (d)].

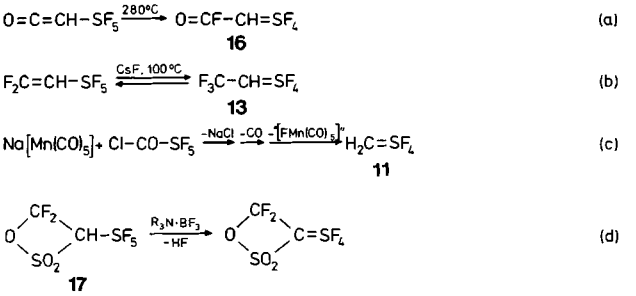

All alkylidene sulfur tetrafluorides are colorless liquids or gases with — in part — remarkable stability. Thus, **13** can be stored at room temperature for months without decomposition; **14** does not react with water. **11**,[56] **14**,[57] and **16**[53] have been characterized by X-ray structural analyses, **11** also by electron diffraction,[58] a normal coordinate analysis,[59] and an ab initio calculation[58] (Table 1).

Table 1. Bond lengths [pm] and bond angles [°] of alkylidene sulfur tetrafluorides in the crystal (low-temperature measurements) in comparison with structurally related compounds.

	C–S	F_{ax}-S-F_{ax}	F_{eq}-S-F_{eq}	Ref.
$H_2C{=}SF_4$ **11**	155.3	170.44	96.44	[56]
F_3C-C(CH_3)=SF_4 **14**	159.9(3)	170.40(5)	98.4(2)	[57]
O=CF-CH=SF_4 **16**	160.2(2)	172.19(9)	101.72(7)	[53]
$O{=}SF_4$		164.4(6)	114.9(34)	[60–63]
SF_4		173.1(5)	101.6(5)	[62, 64]
$H_2C{=}S$	161.1(2)			[22]
S=C=S	155.3			[65, 66]
R_2C-SR'_2	170–175			[67, 70]

Typical structural features, which are found in all alkylidene sulfur tetrafluorides include: the planarity of the $C_2C{=}SD_2^{ax}$ framework, the short C–S bond length, typical sp^2 bond angles at carbon, almost linear arrangement of the axial fluorine atoms, but a relatively small angle between the equatorial fluorine atoms (Table 1 and Fig. 1). The most exact structure is doubtlessly that of **14**, because no inaccurately determined hydrogen atoms exist on the double bonded carbon as in **11** (here, even hydrogen–fluorine bridges could exist, but evidently do not), and because the crystal structure is not predestined by the lattice symmetry on account of the low molecular symmetry (as is the case in **16**,[53] where eight of the ten atoms lie in a mirror plane). Not one of the six skeletal atoms in **14** is removed more than 3.5 pm from the principle plane. The C–S bond length (159.9(4) pm) is very much shorter than in the sulfur ylides (170–175 pm).[67–70] The slight bending from ideal angles of the axial fluorine atoms [F_{ax}–S–F_{ax} = 170.40(5)°] is far less than that of the equatorial fluorine atoms [F_{eq}–S–F_{eq} = 98.4(2)°].

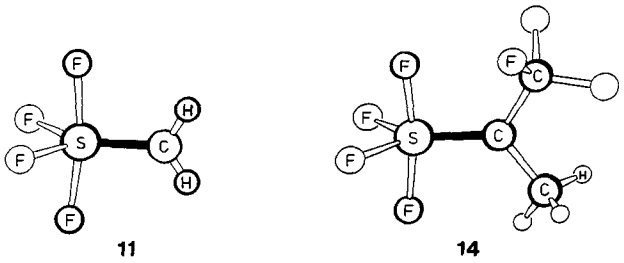

11 14

Fig. 1. Structures of **11** and **14** from low-temperature X-ray measurements and electron diffraction. Double bonds are drawn darkened in. The carbon substituents as well as the carbon, sulfur, and axial fluorine atoms always lie in a plane which is symbolized by boldface type. In the case of the very accurately determined structure of **14**, the planes $F_2^{ax}S=C$ and $S=CC_2$ have a torsion angle of 2–3°, presumably caused by repulsion between the (C)-F and (S)-F^{ax} atoms. The slightly distorted trigonal bipyramidal geometry around sulfur is typical [56, 57].

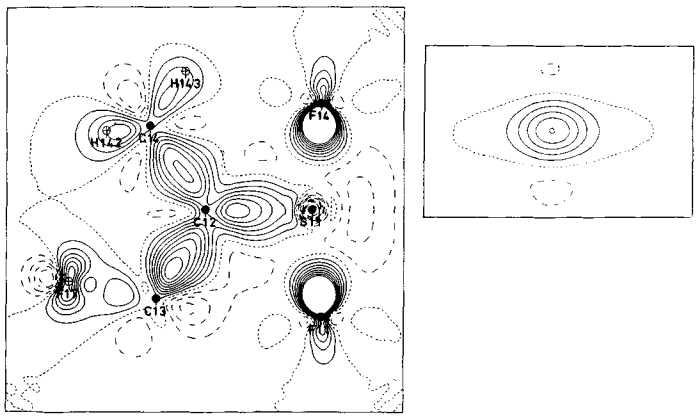

Fig. 3. X-X-Electron density contour lines of **14**. Left: All measurable details of our bonding concepts are reproduced in this diagram: largely nonpolar C–CH_3 and C–H bonds, semipolar C–S and C–CF_3 bonds, and strongly polar C–F and S–F bonds. Right: Cross-section perpendicular to the double bond, in the middle between C and S. The greater extension in the equatorial plane, typical for a double bond, is easily recognized. For the specific experimental and mathematical details of such high quality electron density analyses see Ref. [57]. Reproduced by kind permission of the American Chemical Society.

There are conceptional models which make these characteristic structures plausible. Use of the electron pair repulsion model yields a trigonal bipyramidal molecular shape at the sulfur with carbon as an equatorial ligand and preferably an equatorial position for the electron density of the double bond. Simpler yet is the representation of the molecule through connecting the edges of an octahedron (SF_6) with a tetrahedron (CH_4) (Fig. 2). Calculated π-electron density is

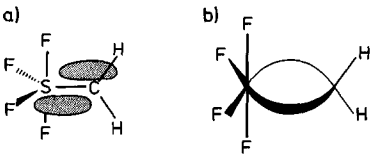

Fig. 2. Molecular models for alkylidene sulfur tetrafluorides with **11** as example. a) Electron pair replusion model; b) bent-bond model. In the final analysis, both models are identical, but they both depend on the existence of a double bond.

found predominately in the equatorial plane.[71] The experimental determination of the electron density distribution of the C=S double bond in **14** shows the typical anisotropy for double bonds, that is, the greater expansion of the electron density is found in the equatorial plane (Fig. 3).[57]

This structure is also in accord with the findings from vibrational spectroscopy.[59] The photoelectron (PE) spectrum of **11** is strikingly similar to that of SF_4.[58] However the lowest band doubtlessly corresponds to the π_{CS} ionization, which at 10.7 eV lies almost 4 eV higher than the comparable ionization in phosphorus ylides,[72] whereby the chemical difference becomes very clear: the π_{CS} electrons are found in a strongly bonding orbital. **16** is a special case in that the C=S double bond is evidently conjugated with the C=O double bond, and thereby somewhat lengthened[53] (see Figure 4).

The C=S double bond also has the most typical property of double bonds, namely to be rigid against torsion. This is easy to discern from the ^{19}F-NMR resonances, in that even at the highest experimentally obtainable temperatures the different fluorine atoms do not coalesce. Since an axial-equatorial fluorine exchange by the Berry mechanism[73] must be coupled to a 90° rotation of the double bond, the torsional barrier can be estimated to be at least 103 kJ mol^{-1}. From mass spectrometric and thermodynamic data, one comes to similar values for the double bond portion.[52] This torsional barrier of the methylene group is therefore high, but by no means as high as in ethene (267 kJ mol^{-1}).

The structures of the alkylidene sulfur tetrafluorides are comparable with those of similar classes of compounds. The cylindrically symmetrical S–O bond in $O=SF_4$ does not define a plane, thus the F_{ax}-F_{eq} exchange processes are very fast. It also happens that the bond angles and distances of the axial and equatorial fluorine atom are much more similar than in comparable molecules.[61–64] The *N*-alkyl sulfur

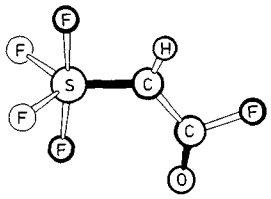

Fig. 4. Structure of **16** in the crystal (low-temperature measurements) [53]. The molecule is completely planar (bold-face type) except for the equatorial fluorine atoms. The conjugation of both double bonds (darkened in) as far as a lengthening of the C=S and a shortening of the C–C bond lengths is also discernible. The preference of the *cis*- over the *trans*-conjugation probably has only steric grounds.

imide tetrafluorides R–N=SF_4 are already much more similar to the alkylidene sulfur tetrafluorides. According to structural investigations the alkyl ligand is also found in the axial plane,[74] the π-electron density mostly in the equatorial plane, but not so pronounced as in the alkylidene sulfur tetrafluorides.[71] *N*-alkyl sulfur imide tetrafluorides are, depending on the residue R (R = CF_3,[75] CH_3,[76] and F[77, 78]) and temperature, no longer rigid. Aminophosphorus tetrafluorides R_2N–PF_4 are isoelectronic with $R_2C=SF_4$ and evidently have the same molecular geometry. The double bond character of the strongly polar N–P bond is never-

theless decreased so much that rotation, and therewith the axial–equatorial equilibrium of the fluorine atoms, is observed at about room temperature (depending on R).[75, 79, 80]

The carbene complexes **18**[81, 82]–**20**[81] and the corresponding ruthenium complexes[83] (Scheme 1) all have a comparable trigonal bipyramidal structure with the phos-

$[(PPh_3)_2Cl(NO)Os{=}CHR]$ **18**

$[(PPh_3)_2Cl(NO)Os{=}CF_2]$ **19**

$[(PPh_3)_3(CO)_2Os{=}CF_2]$ **20**

Scheme 1. Carbene complexes **18**–**20**. Compound **18**: R = H,CH_3, C_6H_5, C_2H_5COO.

phorus ligands in the axial positions and the carbon substituents in the equatorial plane. Complexes of the type $L_4(\eta^2$-alkene)M are the best analyzed examples for the coupling of axial-equatorial ligand exchange (Berry mechanism) with the torsion of the alkene (Fig. 5). Always, as also in the

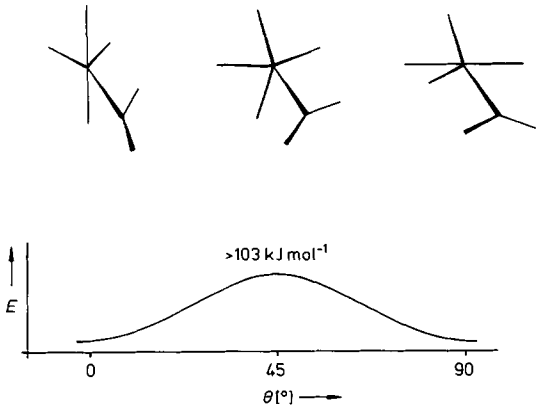

Fig. 5. Coupling of the torsion of the substituents with the axial-equatorial ligand exchange in **11**. This coupling makes it possible to reach the ground state again after a torsion of 90°. The same mechanism holds for the rotation of the ethylene ligand in $(CO)_4(\eta^2$-$C_2H_4)Fe$ though the barrier is much smaller here.

simplest case $[(CO)_4(\eta^2$-$C_2H_4)Fe]$, the ethylene ligand occupies an equatorial position of a trigonal bipyramid and is aligned in the equatorial plane.[84] According to calculations, rotation of the ethylene ligand through 90° requires 134 kJ mol^{-1}.[85] The torsional barrier of the ethylene rotation is in reality, however, less than 40 kJ mol^{-1} and thereby not freezable because it is coupled to the Berry mechanism of the carbonyl groups.[86] If the complex is modified by alkyl ligands,[87] carbonyl ligands,[88] and/or central atom (Ru,[89] Os[90]), this mechanism becomes freezable and therefore observable NMR spectroscopically.

4. Chemistry of the Alkylidene Sulfur Tetrafluorides

The stability of the alkylidene sulfur tetrafluorides varies strongly with the nature of substituents on the carbon (Scheme 2).

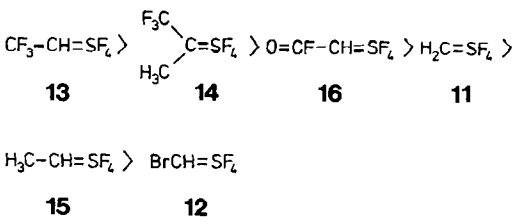

Scheme 2. Stability of the alkylidene sulfur tetrafluorides **11**–**16**.

13 is storable at room temperature in a sealed capillary tube for months without decomposition, while **12** is completely decomposed after a few hours. As decomposition products SF_4 is observed, in the pyrolysis of **11** in vacuum also ethylene, and in the thermal decomposition of **15**, inter alia 1,1-difluoroethane. These results indicate a carbene decomposition according to Equation (e), whereby the stabi-

$$R_2C{=}SF_4 \longrightarrow R_2C{:} + SF_4 \qquad (e)$$

lized carbene is formed easier than the electron-poor carbene. The prognosis for $F_2C{=}SF_4$ and $O{=}C{=}SF_4$ is poor in this respect, since the fragments CF_2 and $C{\equiv}O$ are especially stable. This prediction is in unison with the aforementioned calculations on the ylides $H_3\overset{\oplus}{P}{-}\overset{\ominus}{C}PR$ (R = R′: H,F,CF_3; R = H, R′ = F). It was calculated that the difluorinated ylide is not a bound state and that the trifluoromethyl-substituted ylide should be especially stable against carbene decomposition.[32]

The preparative use of alkylidene sulfur tetrafluorides as carbene sources is thwarted by the simultaneous formation of reactive SF_4. Addition reactions at the double bond are more clear.[48] Polar agents (HF, HCl, HBr, ICl, $BrOSeF_5$, HgF_2, AsF_5) add quickly. SO_3 adds with ring formation (Scheme 3).[91] The direction of the reaction is uniform so

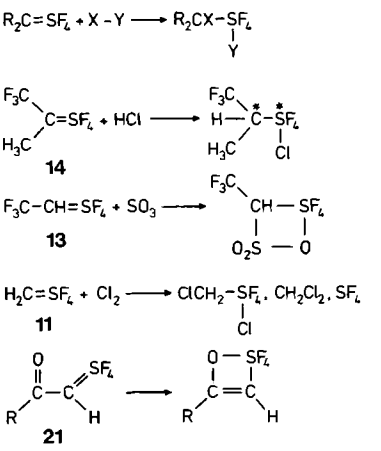

Scheme 3. Addition reactions of alkylidene sulfur tetrafluorides.

that the partial positive part of the reactant approaches the carbon. This reveals the polarity of the C=S double bond in the sense of the ylidic formula. The addition yields always and exclusively *cis*-products concerning the substitution on the sulfur atom.

cis-Addition products are immediately recognizable by the characteristic AB_2C spectra of the fluorine atoms at sulfur.

A four-membered ring addition mechanism can be inferred from the uniformity of the direction of the addition (> 99%) and the rapidity (see at −78 °C). If one adds to a prochiral alkylidene sulfur tetrafluoride, then the chirality of the product becomes immediately recognizable from the ABCD spectrum (instead of AB_2C) of the fluorine atoms on the sulfur. Unpolar reagents yield larger amounts of side products, which often point to a carbene intermediate. Besides the expected addition product, CH_2Cl_2 is formed in the reaction of **11** with chlorine (Scheme 3). Thus far the alkylidene sulfur tetrafluorides show no reactivity as dienophiles in Diels-Alder reactions or as olefin-ligands in metal complexes. The oxidation or fluorination potential is too great for the latter.[92] Also, the reaction with carbonyl compounds does not yield products corresponding to the Wittig reaction. Fluorination of the carbonyl is observed, which could also be traced back to SF_4 which is formed as an intermediate.[48] Carbonyl-substituted alkylidene sulfur tetrafluorides such as **21** with R = C_6H_5 are subject to an irreversible isomerization to oxathietanes,[93] with R = F, on the other hand, the compound is stable. In contrast to the simple addition reactions, this cyclization requires a breaking up of the special molecular geometry for the transition state. A dimerization of an alkylidene sulfur tetrafluoride to an octa-*S*-fluorodithietane $F_4S(\mu\text{-}CR_2)_2SF_4$ in the sense of a [2 + 2] cycloaddition has as yet never been observed.

5. Alkylidene Sulfur Difluorides $R_2C{=}SF_2$

If one compares the alkylidene sulfur difluorides, $R_2C{=}SF_2$, with well-known analogues such as sulfur ylides $R_2\overset{\ominus}{C}\text{–}\overset{\oplus}{S}R'_2$, thionyl fluoride $O{=}SF_2$, or sulfur difluoride imides $R\text{–}N{=}SF_2$, it is certainly a wonder that this class of compounds was first discovered only in 1989. By chance an addition-elimination reaction was observed with the highly fluorinated olefin **22** which could thereafter be carried out with **23**[94] [Eq. (f) and (g)]. The method fails to work with all

$$\underset{\mathbf{22}}{F_5S\text{–}CH{=}CF_2} + SF_4 \xrightarrow[-HF]{CsF} \underset{\mathbf{24}}{F_5S(F_3C)C{=}SF_2} \quad (E \text{ and } Z) \qquad \text{(f)}$$

$$\underset{\mathbf{23}}{F_3C\text{–}CH{=}CF_2} + SF_4 \xrightarrow[-HF]{CsF} \underset{\mathbf{25}}{(F_3C)_2C{=}SF_2} \qquad \text{(g)}$$

other olefins which were tested. In some cases no reaction takes place or the intermediate alkylidene sulfur difluoride rapidly reacts further.

The geometry of the alkylidene sulfur difluorides arises immediately from the fact that **24** appears as two isomers and the CF_3 groups in **25** are not equivalent. The plane formed by the carbon substituents bisects the SF_2 angle (Fig. 6). This was not absolutely predictable, even though sulfur imide fluorides such as $Cl\text{–}N{=}SF_2$ and others show a comparable structure.[95] The C=S double bond is so torsionally stable that no interconversion of the isomers occurs up to 100 °C. The experimentally determined structure was confirmed by ab initio calculations.[94] However, these calculations gave a second structure for **25** with somewhat higher energy, which has a completely planar molecular framework as well as an almost linear SF_2 geometry (Fig. 6). This particular molecular geometry turns out to be the more stable one for the hypothetical compound **27**, so that here the realization of a non-Gillespie configuration, one which grossly violates the electron pair repulsion model, could succeed.

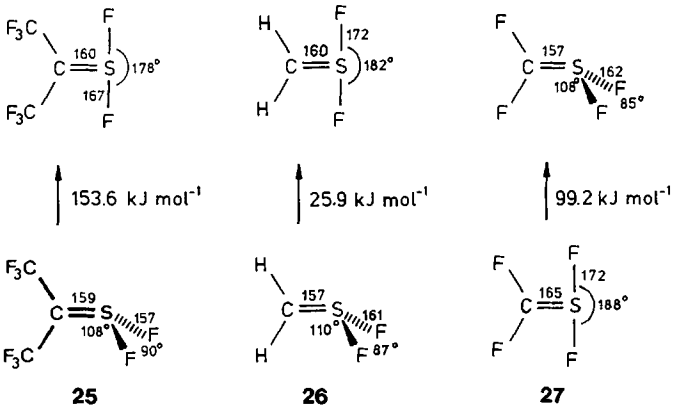

Fig. 6. Calculated structures of alkylidene sulfur difluorides [94]; bold-faced: known **25**. **26** and **27** have a completely different ground state structure. The pyramidal structures of **25** and **26** are as expected. In the case of **24**, the pyramidal structure gives rise to the appearance of two isomers. The planar T-shaped ground state structure of **27** has not yet been confirmed experimentally.

At this point a comparison with the structures of 1,6,4a-λ^4-trithiapentalene and 1,6-dioxa-6a-λ^4-thiapentalene **28** should be possible. These compounds have a planar T-shaped coordination at the sulfur. The question of whether "hypervalency" or "bond tautomerism" is involved has already been discussed in detail.[96, 97] The majority of the facts speak in favor of the symmetrical structure,[98–108] but probably with a decidedly flat potential for the back and forth motion of the central sulfur atom. Here the geometry might be enforced through the chelating ring, but in the theoretically postulated $F_2C{=}SF_2$ it is the ground state. Afterall, the same phenomenon was also found in the chemistry of phosphorus[109] with a larger group of calculated "non-Gillespie" structures. This T-shaped geometry can be important as a transition state for intramolecular ligand exchange in pyramidal molecules.[110–112] (This transition state corresponds to a planar transition state for a tetrahedral molecule.)

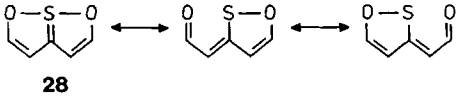

28

The investigation of the alkylidene sulfur difluorides showed that they rearrange easily. Thus, it is understandable why only decomposition products were observed earlier.[113] This instability corresponds to a [1,2]-fluoride migration with formation of the rare sulfenyl fluorides[114–116] [Eq. (h)].

The direction of this isomerization is opposite to that of the $F_2S{=}S/F\text{–}S\text{–}S\text{–}F$ isomers [Eq. (i)] and is largely caused by the energy gain of a C–F bond versus the energy cost of

a S–F bond. These experimental results are also supported by calculations.[94, 117]

The 1,2 fluoride migration in **24** is strongly accelerated by Lewis acids (BF_3, AsF_5). However, with BI_3 a dehalogena-

$$R_2C{=}SF_2 \xrightarrow{(BF_3)} R_2FC{-}S{-}F \qquad (h)$$

$$F_2S{=}S \longleftarrow F{-}S{-}S{-}F \qquad (i)$$

$$\underset{\mathbf{24}}{F_5S(F_3C)C{=}SF_2} \xrightarrow[-BF_3,-I_2]{+BI_3} \underset{\mathbf{29}}{F_5S(F_3C)C{=}S} \qquad (j)$$

tion occurs with formation of **29** as a stable, deep violet liquid[118] [Eq. (j)].

6. Alkylidene Sulfur Difluoride Oxides $R_2C{=}SF_2{=}O$

The first preparation of an alkylidene sulfur difluoride oxide was reported in 1988.[30] This is again remarkable because analogues such as sulfuryl halides, sulfur difluoride imide oxides $R{-}N{=}SF_2{=}O$, and oxosulfur ylides have been known for a long time. After the discovery of the alkylidene sulfur tetrafluorides, the discovery of the alkylidene sulfur difluoride oxides could essentially be reckoned with at any time, because it required only a simple hydrolysis. It is true though, that up to now, the desired reaction has succeeded in only one case[30] [Eq. (k)].

$$\underset{\mathbf{16}}{O{=}CF{-}CH{=}SF_4} \xrightarrow[-2HF]{H_2O} \underset{\mathbf{30}}{O{=}CF{-}CH{=}SF_2{=}O} \qquad (k)$$

$$\xrightarrow[-HF]{HgF_2} \underset{\mathbf{31}}{Hg[C(COF){=}SF_2{=}O]_2} \qquad (l)$$

Structurally, alkylidene sulfur difluoride oxides should not display any peculiarities, for they are derived from such well-known compounds as sulfones, etc. Nevertheless, the presently known species **30** shows a complicated dynamic behavior that can only be satisfactorily explained with the help of several assumptions. The environment of the sulfur atom is assumed to be quasi-tetrahedral. The temperature-dependent NMR spectra show three different isomers, all of which have equivalent fluorine atoms on the sulfur. It is clear therefore that the plane of the substituents on carbon bisects the SF_2 angle, as in the alkylidene sulfur difluorides. The two isomers observed at $-70\,^{\circ}C$ were interpreted as *E,Z* isomers. The third isomer results from the freezing of the conjugation. The still to be expected fourth isomer is not observed, perhaps for lack of intensity[30] (Fig. 7). Ab initio calculations yielded slightly different energies for these four isomers, so that one can tentatively assign the NMR resonances.[119] The question remains open why here for the first time the torsion of the C=S double bond freezes only at $-70\,^{\circ}C$, quite unlike all other C=S double bond systems discussed herein. A possible explanation could be: The approximate "three-fold" symmetry of the $\approx SOF_2$ group places less resistance on the torsion of the C=S double bond in contrast to the two-fold symmetry of the SF_4, SF_2, and S=O groups. In

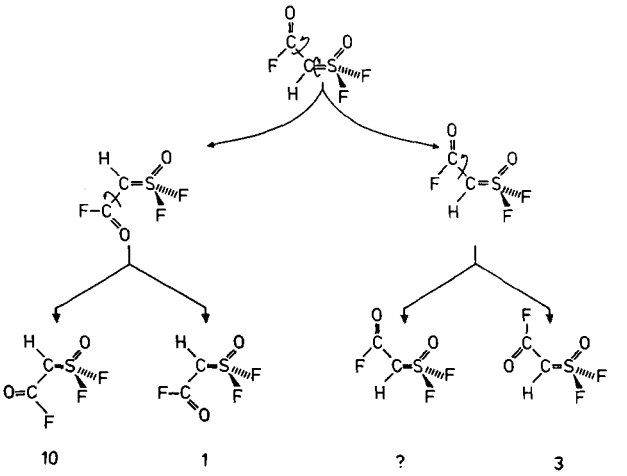

Fig. 7. Structural dynamics of **30**. The C=S double bond is freely rotating above room temperature, the C–C single bond above $-70\,^{\circ}C$. Three of the four possible isomers are observed at $-136\,^{\circ}C$ [30]. The numerical values indicate the quantitative relationship. The slight energy differences and thereby the concentrations of the isomers depend possibly on the number of weak intramolecular hydrogen-oxygen contacts.

this respect **30** resembles the sulfur and phosphorus ylides. In these, the ylidic bond is (with one exception, which can have steric reasons[121]) always freely rotating. This is also confirmed by calculations.[122, 123] The torsion angle of the ylidic P–C bond takes on entirely different values in crystal structures.[43, 124, 125] In the four published cases of crystal structures of sulfur ylides, the plane of the carbon substituents is found in the vicinity of the bisector of the SF_2 angle (variations up to 9.8°).[67–70] The appearance of isomers has not been observed up to now.[126] Accurate structural investigations of oxosulfur ylides, which are related the closest to **30**, are not known. But there is a parallel to the hindered rotation of the conjugated system: $H_2C{=}CH{-}CF{=}O$ appears as two isomers at $-140\,^{\circ}C$.[127]

30 can be derivatized to give the mercury compound **31** [Eq. (l)] which exists in solution as only one isomer. In the crystal structure of **31** the central mercury atom clearly fixes the C=S double bond in a definite way through oxygen-mercury contacts (Fig. 8). It is probably no coincidence that the

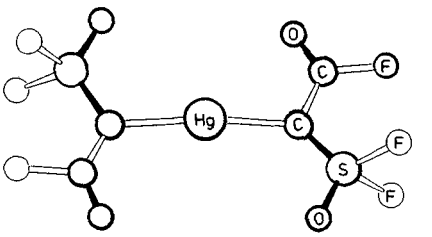

Fig. 8. Crystal structure of **31**. The molecule is largely planar except for the fluorine atoms (bold-face type, double bonds darkened in). Hg···O contacts fix the ligands in this configuration [120].

lowest energy form for **30** is calculated in the corresponding configuration: maximalization of hydrogen-oxygen contacts.[119] The C–S bond length (155(3) pm) is very short, as in the alkylidene sulfur tetrafluorides. In any case, the easy rotation of the double bond cannot be interpreted as weak bonding.

At this point it becomes recognizable that the behavior of a class of compounds is difficult to study from one or two cases. The synthesis, especially of nonfunctional and nonconjugated alkylidene sulfur difluoride oxides, would be desirable before generally valid conclusions can be drawn. A complex synthesis of $FSO_2(COF)C{=}SF_2{=}O$ was reported quite recently,[128] but no structural dynamics were observed.

7. Fluorine-Substituted Sulfines, R–CX=S=O

Interestingly enough the first sulfine resulted from an attempt to prepare a sulfene.[129] Its identity was first clarified in 1963. It has been known since the middle of the sixties, that sulfines occur in stable *E* and *Z* isomers as a consequence of the nonlinearity of the C–S–O system ($\sphericalangle$ CSO $\approx$ 114°). Besides several special cases, their production results from the oxidation of thioketones by means of *meta*-chloroperbenzoic acid or through a variant of the Peterson olefination (Scheme 4).

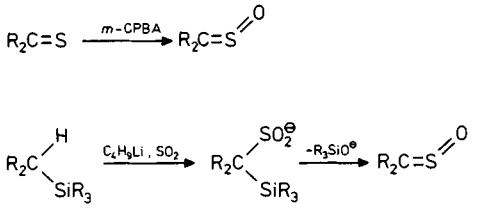

Scheme 4. General reactions for the preparation of sulfines.

The parent substance **33** could be prepared through the pyrolytic elimination of HCl from **32** and was identified spectroscopically as an unstable particle (Scheme 5).[131, 132] The first perfluorinated sulfine **35** resulted from dechlorination of **34** or better of late through thermal decomposition of the *S,S'*-dioxodithietane.[133, 134]

Thus far it is not clear which of the two possible isomers is formed here. The thermal decomposition of *S,S'*-dioxodithietanes has proven to be a productive synthetic method for fluorinated (and other) sulfines.[135–139] **39** could be obtained by this and by another route, and it turns out to be unstable above $-100\,^{\circ}C$.[140–142] However, it could be unequivocally identified both spectroscopically and through trapping reactions.

The only other α-fluorinated sulfine is **42**, which was also obtained through the cleavage of a four-membered ring or from the pyrolysis of **41**. It is only slightly more stable than **39**, so that again it could only be identified spectroscopically and through trapping reactions. But at least *E* and *Z* isomers could be assigned here.[141–143] Only $X_2C{=}S{=}O$[142–145] (X = Cl,Br) show moderate thermal stability at room temperature.

As expected β-fluorination shows a drastic effect: $(CF_3)_2C{=}S{=}O$ is a stable liquid capable of being produced by different methods of four-membered ring cleavage. The structure, though still not investigated in detail, results easily from the fact that the CF_3 groups are different according to NMR spectroscopy. Because of the stability of this special

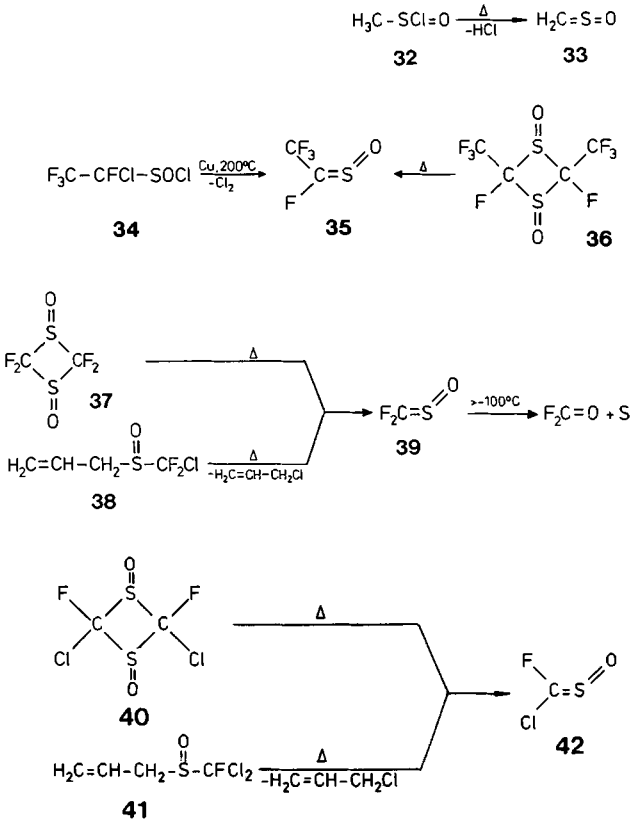

Scheme 5. Preparation of fluorine-substituted sulfines.

sulfine, it could be subjected to numerous chemical reactions. Particularly important are the addition reactions to the C=S double bonds which, in the case of the Diels-Alder reaction with anthracene, is reversible.[135–137]

8. Fluorine-Substituted Sulfenes $R_2C{=}SO_2$

Our knowledge of sulfenes is by far worse than our knowledge of sulfines.[146] Sulfenes are prepared by elimination upon sulfonic acid compounds. They can be identified through trapping reactions or stabilized through reaction with bases in the "normal" ($R_3N^{\oplus}$–$SO_2{=}\overset{\ominus}{C}R'_2$) or the "reversed"[147, 148] ($R_3N^{\oplus}$–CR'_2-$SO_2^{\ominus}$) way. Reports about free sulfenes are incomplete. **46** could be identified spectroscopi-

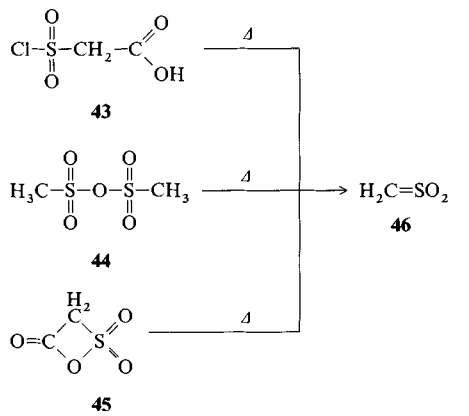

cally (IR) among many other products from the thermolysis of **43**–**45**.[149–151] In this way a C–S double bond energy of 150 ± 20 kJ mol^{-1} was estimated.[152] It is predicted on the basis of calculations that electron-donating groups on carbon will stabilize sulfenes.[153] Diaminosulfenes (thiourea *S*,*S*-dioxides) actually exist in the sulfene form, but with strong hydrogen bridges.[154–157] The framework N_2C–SO_2 is not planar, but twisted through 68°, whereas planarity is predicted for $H_2C{=}SO_2$.[153]

The perfluorinated sulfene **48** has up to now only been detected as an unstable intermediate. It is formed in solution from $[(CH_3)_2N]_3S^{\oplus}(CF_3)_2C{-}SO_2F^{\ominus}$ by reaction with BF_3, BF_3-etherate or SiF_4.[158] If it is not trapped, it rearranges to $F_2C{=}C(CF_3){-}SO_2F$. An alternative method of preparation is again four-membered ring cleavage (cf. Section 7).

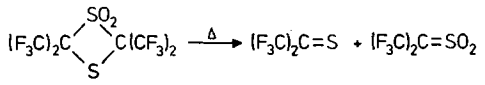

47 **48**

1,1-Dioxo-2,2,4,4-tetrakis(trifluoromethyl)1,3-dithietane **47** can be cleaved with quinuclidine, and isolation as the "normal" base adduct **48** was thus successful.[159]

This sulfene adds to moderately electron-rich olefins. The reactions are to some extent regio- and stereospecific. Diels-Alder reactions succeed in the same way. There are also hints of an electron transfer mechanism prior to the loss of SO_2.[158]

There are few materials comparable with sulfenes. Other derivatives with hexavalent sulfur in trigonal planar geometries are the sulfur triimides $(RN{=})_3S$[160–164] and sulfur diimide oxides $(RN{=})_2S{=}O$.[165] These have a completely planar molecular framework including the nitrogen ligands, which still requires a satisfactory theoretical explanation. Altogether our knowledge of this class of molecules is still seen as very incomplete.

9. Sulfur–Carbon Triple Bonds

The two known compounds with sulfur–carbon triple bonds, $F_3C{-}C{\equiv}SF_3$ (**49**) and $F_5S{-}C{\equiv}SF_3$ (**51**), are special cases in which the triple bond is formed between an element of the second and one of a higher period. The total number of these compounds is still easily surveyable. Long ago this class of substances aroused interest when *Glemser* et al. discovered N≡SR compounds (R = F_3,F,Cl).[166–168] In the meantime, a few derivatives and their organic and organometallic chemistry have been reported.[169] Since then phosphaalkynes R–C≡P (R = H[170]; F[171,172], CH_3[173,174], CN[175]) have been detected as unstable molecules against polymerization. In 1981 *Becker*, *Gresser*, and *Uhl* succeeded in synthesizing phosphaalkynes with R = $(CH_3)_3C$ as a stable, colorless liquid.[176] Since then, numerous additional phosphaalkynes have been prepared with R = C_6H_5,[177] $(CH_3)_3Si$[178], 2,4,6-$(C_4H_9)_3C_6H_2$,[178,179] tripticyl,[180] adamantyl,[181] and others.[182] Predominately $(H_3C)_3C$–C≡P has become a versatile reaction partner in cycloaddition reactions as well as in organometallic syntheses.[182] Recently, the phosphadiazonium cation 2,4,6-(t-$C_4H_9)_3C_6H_2$–$N{\equiv}P)^{\oplus}$ was reported.[183] In 1986 *G. Märkl* and *H. Sepjpka* succeeded in synthesizing 2,4,6-(t-$C_4H_9)_3C_6H_2$–C≡As as a pale yellow, crystalline solid.[184]

Known compounds which contain λ^5-phosphorus are: $(C_6H_5)_2P{\equiv}C{-}Si(CH_3)_3$,[185] and $[(i\text{-}C_3H_7)_2N]_2P{\equiv}E$ (E=N,[186] C–$Si(CH_3)_3$[187]). The latter result from photolysis or thermolysis of azide- or diazo-precursors. Ab initio calculations show that in the phosphinonitrene H_2P–N the bond length (152 pm) is so shortened that it can be formulated as $H_2P{\equiv}N$[188] or $H_2\overset{\oplus}{P}{=}\overset{\ominus}{N}$.[189] Compounds with triply bonded silicon are thus far unstable. H–N≡Si has been isolated in a matrix from the decomposition of H_3Si–N_3, and C_6H_5–N≡Si was detected by photoelectron spectroscopy in the pyrolytic decomposition of $C_6H_5Si(N_3)_3$.[190,191]

It is conspicuous that the heavier element prefers the terminal position (coordination number 1) in R–C≡P, R–N≡Si and R–$N{\equiv}P^{\oplus}$. It emerges from calculations that H–N≡Si is approximately 372 kJ mol^{-1} more stable than the isomer H–Si≡N[192] with only a small activation barrier of 55 kJ mol^{-1}.[193] An electrostatic consideration presents itself as a simple explanation. The proton (or the organic substituent) will bond to the hypothetical dipole $N{\equiv}Si^{\ominus}$ at the negative position. If such a simple consideration is reasonable, then F–Si≡N should be more stable than F–N≡Si. Similar comparisons are applicable for example to F–N=O and F–S≡N.

The success with the preparation of stable alkylidene sulfur tetrafluorides gave rise to the hope that compounds of the type R–$C{\equiv}SF_3$ should be capable of being synthesized too. This was first successful in 1984 when **49** and later **51** were prepared from **13** and **50** respectively.[194,195] The critical reactions are HF eliminations under basic conditions.

11 can also be forced to eliminate HF, but the intermediate **52** is not isolable, and **53**, formed through fluoride rearrangement, is obtained. **49** and **51** occupy a middle position with regard to their stability. They neither remain unchanged at room temperature (like some phosphalkynes with large R), nor are they very short-lived molecules (as C_6H_5–N≡Si, for example). They have half-lives of minutes at room temperature, and are almost indefinitely stable at −78 °C.

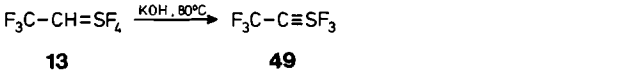

13 **49**

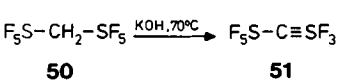

50 **51**

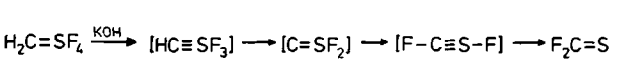

11 **52** **53**

In the following, this C≡S triple bond should be measured against the standard criteria, such as short bond length, linearity of the molecular framework, and strong electron density (so far as measurable) between the atoms bound by the triple bond. In all cases enumerated here, the triple-bond length is found to be very short (Table 2 and Fig. 9). Table 2

contains only experimentally determined values. Numerous calculated values exist for comparable systems.

These triple bonds are ca. 9% shorter than a comparable double bond and ca. 20% shorter than a comparable single bond. Consequently, the distance criterion is met. Bond contractions in C–C double and triple bonds amount to 13 and 22%, respectively.

Table 2. Triple bond lengths [d] of R–C≡SF_3 and comparable heteroalkynes.

Compound	d [pm]	Method [a]	Ref.
F_3C-C≡SF_3 **49**	142.0	XR, ED	[196, 197]
F_5S-C≡SF_3 **51**	139.2(4)	XR, ED	[195, 198]
N≡$S^{\oplus}SB_2F_{11}^{\ominus}$	142.8(10)	XR	[199]
N≡SF	144.8(2)	MW	[200]
N≡SCl	145.0(3)	MW, ED	[210, 202]
N≡SF_3	141.6(3)	MW	[203]
$(H_3C)_3$C-C≡P	153.6(2)	ED, MW	[204]
2,4,6(t-C_4H_9)$_3C_6H_2$-C≡P	151.6(13)	XR	[179]
H-C≡P	154.21(5)	MW	[205]
CH_3C≡P	154.38(4)	MW	[174]
2,4,6(t-C_4H_9)$_3C_6H_2$-N≡$P^{\oplus}AlCl_4^{\ominus}$	147.5(8)	XR	[183]

[a] MW = microwave spectroscopy, XR = X-ray structure analysis, ED = electron diffraction

Information about the electron density is at present only very limited. Only the X-ray structure analysis of **51** has such quality that a preliminary statement about the electron density can be made. Here a maximum of electron density in the shape of a little disk can be made out. It stands perpendicular to the bond axis between C and S, somewhat closer to C than to S (Fig. 9). The clover-leaf contour of this electron density

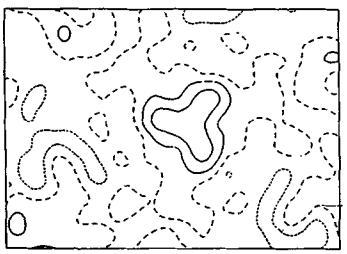

Fig. 9. Electron density perpendicular to the C≡S triple bond in **51**, approximately 60% of the bond length away from sulfur. The little disk-shaped area of electron density is typical for triple bonds. The clover-leaf form is enforced by the three-fold symmetry of the ≡SF_3 group and the crystal symmetry. Normally, a cylindrically symmetrical distribution of electron density is found in alkynes. That this measurement is much less informative in comparison to Figure 3 is due to poorer crystal quality, the disorder of the molecule, and insufficient measurement time.

is a result of a three-fold axis of rotation of the cubic crystal system, which coincides with the three-fold axis of the SF_3 part of the molecule. Whether this, in fact, indicates a deviation from the typical cylindrically symmetrical electron density in alkynes can at present not yet be stated with certainty. But such a trefoil distribution of electron density is essentially expected for R–C≡SF_3, since generally the atomic symmetry dominates the electronic symmetry, and in **51** no cylindrical symmetry exists as in acetylene. A cylindrically symmetrical distribution of electron density is in fact found experimentally in acetylene itself.[206]

The question of linearity of the bonding system is more complex. This question did not present itself for F_3S≡N and FS≡N since the terminal nitrogen cannot coordinate an additional atom. The phosphaalkynes R–C≡P in Table 2 are linear, 2,4,6-(t-C_4H_9)$_3C_6H_2$–C≡P[179] and 2,4,6-(t-C_4H_9)$_3C_6H_2$–N≡$P^{\oplus}$[183] deviate (177°) only slightly from the linear arrangement.

But **49** is already distinctly bent in the cystalline state: 171.5° (2.0).[196] In the gaseous state this deviation is very much larger: 155°(3).[197] These conflicting results first led to

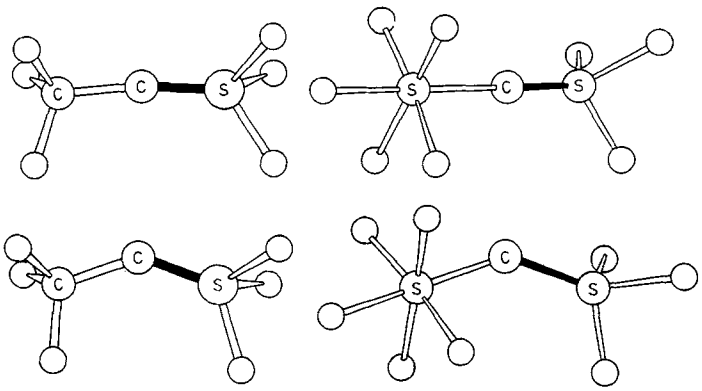

Fig. 10. Crystal structures of **49** and **51** (above) in comparison to the gas structures (below). The C≡S triple bond is darkened. In both cases one observes a strong bending of the molecule in the gas phase.

considerable confusion, especially since ab initio calculations initially predicted linearity, then perhaps a slight deviation from linearity, and finally a value of even 130°.[32, 197, 207] But these calculations are qualitatively in agreement that the bending requires only minimal energy (Fig. 11).

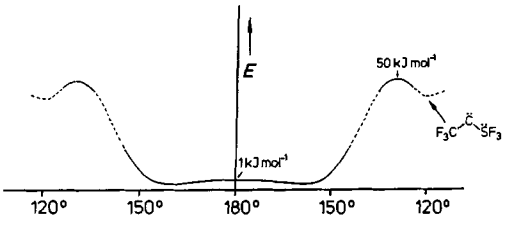

Fig. 11. Dependence of the energy from the C–C–S angle in **49**. The flatness of the potential, even at considerable bending angles, is remarkable. At still stronger bending angles the molecule transforms into the carbene state, F_3C-C̈-S̈F_3. Solid lines represent measured or calculated states, dashed lines denote interpolation and extrapolation. In particular, the energy level of the carbene F_3C-C̈-S̈F_3 with respect to the ground state is unknown. The energetic proximity of the strongly angled carbene state gives rise to the flatness of the potential.

The most sophisticated calculation at present is the geometry optimization by means of the 3-21G* basis set with stepwise bending of the angle by 0, 5, 10, 15, 20, 30, 40, 50, and 60° and the respective energy calculation with inclusion of electron correlation (MP4SDQ).[197] A bond angle of 130° emerges from this with a still small energy difference of 0.92 kJ mol^{-1} when compared with linearity (exp. > 2.0 kJ mol^{-1}).

This structural discrepancy is even more serious for the second compound of this class of substances, namely **51**. The solid structure shows a linear S–C–S framework prescribed by the cubic crystal symmetry. Even under the most optimistic assumptions (disorder!), the deviation from linearity cannot be greater than 4°.[195] But this molecule is also bent in the gas phase (*159*(3)°).[198]

In addition to the above-mentioned crystal structure analysis, electron diffraction, and ab initio calculations, the nonlinearity of **49** is based upon the interpretation of band broadening in the matrix IR spectrum and upon the broad band microwave spectrum and can thus be considered as certain.[197] In any case the small energy barrier for a bending motion made the development of a static model impossible here. The bending motion is much more a two-dimensional large amplitude motion. The linear case lies at a (quite weak) energy maximum, and the crystal lattice forces can vary the angle within certain limits. This accounts for the paradox that lattice forces have had to serve first of all as the explanation for a deviation from linearity and later as the explanation for not large enough a deviation from linearity.[208] These structural circumstances are thus far unprecedented for a triply-bonded carbon atom. But there are parallels among the cumulenes. For example, propadienone $H_2C{=}C{=}C{=}O$ and $(C_6H_5)_3P{=}C{=}P(C_6H_5)_3$ are both distinctly bent at the central carbon atom.[209, 210] Instructive is the case of $H_2C{=}C{=}C{=}O$, in which only the consideration of electron correlation in the ab initio calculation confirmed the previous experimentally determined nonlinearity.[211, 212]

The comparison of alkylidyne sulfur trifluorides with carbyne complexes is interesting. The metal–C triple-bond lengths are short (165–175 pm), as expected for metals of the first row of transition metals and 175–190 pm for the heavier homologues. Historically, it is noteworthy that the first carbyne complex $[(CO)_4IW{\equiv}C{-}C_6H_5]$ was also distinctly nonlinear (162).[214] However, after the crystal structures of many more compounds became known, linearity at the carbyne carbon dominated more and more.[215] Larger deviations can likewise be brought about by lattice forces when one assumes that the bending motion has a very flat potential as in **49**. Seen altogether, these considerations have, nevertheless, played no great role in the chemistry of the carbyne-metal complexes.

How can this nonlinearity of the $R{-}C{\equiv}SF_3$ molecules be plausibly explained? The bond is certainly polar. This emerges not only from the calculated charge distribution of the bond according to $F_3C{-}C{\equiv}SF_3 \leftrightarrow CF_3{-}\overset{\ominus}{C}{=}\overset{\oplus}{S}F_3$, $(C^{-0.7}\,S^{+1.6})$ and the surprisingly high ^{13}C-NMR resonance[196] (almost identical to $F_3C{-}CH_2{-}SF_5$), but also from the fact that in **51** the maximum of the electron density is clearly shifted towards the carbon.[195] On the other hand, the substituents F_3C or F_5S are not large enough to enforce linearity through the repulsive forces. If this qualitative consideration is supposed to hold true, it remains incomprehensible why the criteria for a double bond are fully preserved with the alkylidene sulfur tetrafluorides $R_2C{=}SF_4$ ($\leftrightarrow R_2\overset{\ominus}{C}{-}\overset{\oplus}{S}F_4$).

Trinquier and *Malrieu* have theoretically investigated such nonclassical distortions at multiple bonds more carefully, and thereby developed a semi-quantitative relationship[217] based upon earlier recommendations.[216] A (hetero)ethene will be planar only if the energy sum of the singlet–triplet separations of the carbene fragments R_2X: and R_2Y: does not exceed a certain value. Otherwise the molecular geometry will become distorted, for example pyramidal. Since the singlet–triplet separation for $:CH_2$ is quite negative, C=C double bonds are planar. This is the reason for there being so-called nonclassical distortions with groupings such as $:GeR_2$, $:SiF_2$, and others. Likewise, the bending in cumulenes such as $H_2C{=}C{=}C{=}O$ and $O{=}C{=}C{=}C{=}O$ is semi-quantitatively predictable with this method.[217] The extension of this model to triple bonds requires that the energy sum of the doublet-quartet separations of the carbyne fragments R–X and Y–R′ of the (hetero)acetylene $R{-}X{\equiv}Y{-}R'$ not be permitted to be too large. CH is a doublet in the ground state, but the quartet lies only 70 kJ mol^{-1} higher. The SF_3 radical also has a doublet ground state,[218] but nothing is known about the energy level of the quartet state. However, since paired electronic states of heavy elements are generally stabilized, and even more so through fluorine substitution, the case of a nonclassical distortion is already predictable for **52**. The prognosis is similar for $H_3C{-}C{\equiv}SF_3$ and **49**. The unknown $F{-}C{\equiv}SF_3$ is certainly very strongly bent.[219] This is consistant with the SCF-MP4 ab initio calculation, which predicts a very low energy minimum of 55 kJ mol^{-1} with an angle of only ca. 113°.[197] The calculated geometry at the sulfur atom can also be described only with the formula $F{-}\ddot{C}{-}\ddot{S}F_3$. Also the very unstable difluoroacetylene[220] could be subject to a nonclassical distortion, and the hypothetical $F{-}C{\equiv}Si{-}F$ by all means.[221]

Even if the ground state is linear as in acetylene, the *trans*-bent form occurs in the excited state.[222, 223] But the energy difference might be considerable. Qualitatively, in the case of **49** the situation is the same, except that the excited state $F_3C{-}\ddot{C}{-}\ddot{S}F_3$ is separated from the ground state by a barrier of only ca. 50 kJ mol^{-1}, (Fig. 11). In short, it is the energetically close lying, certainly strongly bent dicarbene state which causes the weak bending potential.

The conclusion may be drawn from this result that real triple bonds between two elements of the third or higher periods should be observed only in exceptional cases, because the carbene state should definitely be more stable. Thus one limitation of a bond principle emerges for which nature is responsible, and which cannot be overcome no matter how refined the experimental technique might be.

Interesting transitions are possible: F–S–S–F should possess a normal S–S single bond like H–S–S–H. However the S–S bond length corresponds to that of a double bond (188.8(15) pm),[224] as is found, for example, in the isomer $F_2S{=}S$ with 186.0(20) pm[224, 225] or in the S_2 molecule with 188.9 pm.[226] If one extrapolates the bond characteristics in the series $N{\equiv}N$, $N{\equiv}S{-}F$ to $F{-}S{\equiv}S{-}F$, then one could have quite naively expected a triple bond. In any case, one must assume that the so-called free electron pairs on the sulfur in F–S–S–F have partial bonding character as is symbolized, but not explained, by the manner of writing $F{-}S{-}S{-}F \leftrightarrow {}^{-}F{-}S{=}S^{\oplus}{-}F \leftrightarrow F{-}{}^{\oplus}S{=}S{-}F^{\ominus}$ (cf. structure of O_2F_2).

Similarities hold for $F_3S{-}SF$: the molecule has a structure in which the nonbonding electron pairs on both sulfur atoms are in the eclipsed position, and at the same time the torsion

about the S–S bond is hindered.[227] Calculations show that the S–S bond has 20% π-character.

Also with the double bond principle there seems to be a limit lower in the Periodic Table. It has already been pointed out that the bond lengths in C=C, Si=Si, Ge=Ge and Sn=Sn containing compounds approach more and more the single bond lengths (a bond contraction of only 2% is observed for the Sn=Sn double bond[5]). This has been symbolized by the formulas $R_2Sn{=}SnR_2 \leftrightarrow R_2\overset{\oplus}{S}n{-}\overset{\ominus}{S}nR_2$, and with this also the nonplanarity at the Sn atoms has been "explained". Naturally, the description of a nonpolar bond with two polar boundary structures is not elegant, but this is the weakness of the method. The MO model is more elegant here: in the transition from C=C to Sn=Sn double bonds, the bonding π electron pair becomes increasingly a nonbonding electron pair localized on both Sn atoms.

10. Reactions of $F_3C{-}C{\equiv}SF_3$

The facts that **49** cannot be readily prepared in amounts greater than 1 g and that it is not stable at room temperature have thus far largely restricted chemical investigations. No chemical reactivity whatever has yet been described for **51**. The addition of HF to the triple bond in two steps is the most predictable reaction, but also the only one thus far in which the compound reacts as a triple bond.

In numerous attempts, the triple bond failed in every case to coordinate to metal complexes because **49** is too strong an oxidation and fluorination reagent. Likewise all attempts to carry out cycloaddition reactions have thus far met without success. These negative results are in complete contrast to the extensive complex chemisty of $t\text{-}C_4H_9{-}C{\equiv}P$[182] and $N{\equiv}SF$[169] and to some results of Diels-Alder reactions which these undergo.

The mechanism for the reaction of **49** with amidines to give thiadiazolines remains unclear.[92]

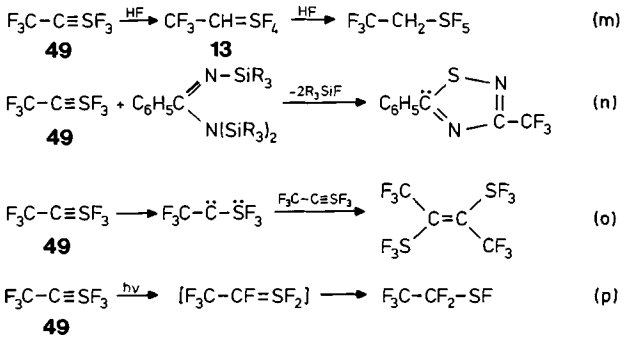

In all reactions, spontaneous dimerization is always observed, a remarkable reaction for a triple bond. The thermal tetramerization of $(H_3C)_3C{-}C{\equiv}P$, however, leads to a cubane.[230] Corresponding to the crystal structure analysis,[196] the geometry of the sulfur environment in the dimer indicates an oxidation state 4 for the sulfur atoms. From kinetic measurements it emerges that a first order reaction with $\Delta H^{*} = 50\ kJ\ mol^{-1}$ is the rate determining step of the dimerization reaction, which is attributed to the transformation of $F_3C{-}C{\equiv}SF_3$ into the carbene-like intermediate. A more rigorous proof for the intermediate existence of the carbene state would be a carbene trapping reaction, which nevertheless has failed thus far. The recently discovered $[(iC_3H_7)_2N]_2P{\equiv}C{-}Si(CH_3)_3$, which according to NMR data likewise contains a triple bond reacts as a heteroalkyne and also as a dicarbene.[231]

Upon irradiation in a matrix **49** is converted into $CF_3CF_2{-}SF$.[232] It must be assumed that the intermediate stage of an alkylidene sulfur difluoride is passed through (see Section 5).

11. Outlook

Often only a few examples are known of the novel bonding systems described herein, of the alkylidene sulfur difluorides and the alkylidyne sulfur trifluorides only two of each, of the alkylidene sulfur difluoride oxides only three. So it happens that the answers to the questions with regard to structure and bonding must be tentative, and particular so because the current representations serving as models cannot be applied completely unconstrained.

However, such simple new compounds are interesting for they often illustratively elucidate theoretical problems of bonding.

I would like to thank my co-workers Dr. J. Bittner, Dr. R. Damerius, R. Gerhardt, T. Grelbig, T. Henkel, Dr. G. Kleemann, Dr. T. Krügerke, R. Kuschel, and Dr. B. Pötter for their commitment to this area of research. Only through world wide cooperation, e.g. with H. Bock, J. Boggs, D. Dixon, H. Oberhammer, C. Marsden, A. Simon, J. Thrasher, have we been able to make any advance in this difficult field. Thanks are also due to the Deutsche Forschungsgemeinschaft and the Fonds der Chemischen Industrie for the continuous financial support.

Received: October 27, 1989 [A 812 IE]
German version: *Angew. Chem. 103* (1991) 399
Translated by Professor Dr. Joseph S. Thrasher, Alabama (USA)

[1] T. Tsumuraya, S. A. Batcheller, S. Masamune, *Angew. Chem. 103* (1991); *Angew. Chem. Int. Ed. Engl. 30* (1991), in press.
[2] R. Appel, F. Knoll, I. Ruppert, *Angew. Chem. 93* (1981) 771; *Angew. Chem. Int. Ed. Engl. 20* (1981) 731.
[3] R. West, *Angew. Chem. 99* (1987) 1231; *Angew. Chem. Int. Ed. Engl. 26* (1987) 1201.
[4] P. Jutzi, *Angew. Chem. 8* (1975) 269; *Angew. Chem. Int. Ed. Engl. 14* (1975) 232.
[5] M. Regitz, P. Binger, *Angew. Chem. 100* (1988) 1541; *Angew. Chem. Int. Ed. Engl. 27* (1988) 1484; M. Regitz, *Chem. Rev. 90* (1990) 191.
[6] A. H. Cowley, *Polyhedron 3* (1984) 389.
[7] G. Raabe, J. Michl, *Chem. Rev. 85* (1985) 419.
[8] N. Wiberg, *J. Organomet. Chem. 273* (1984) 141.
[9] L. E. Guselnikov, N. S. Namethkin, *Chem. Rev. 79* (1979) 529.
[10] E. W. Abel, S. A. Muehlejohn, *Phosphorus Sulfur 9* (1981) 235.
[11] H. F. Schaefer III, *Acc. Chem. Res. 15* (1982) 283.
[12] M. W. Schmidt, P. N. Truong, M. S. Gordon, *J. Am. Chem. Soc. 109* (1987) 5217.
[13] W. Kutzelnigg, *Angew. Chem. 96* (1984) 262; *Angew. Chem. Int. Ed. Engl. 23* (1984) 272.
[14] J. S. Binkley, *J. Am. Chem. Soc. 106* (1984) 603.
[15] H. Lischka, H. J. Köhler, *J. Am. Chem. Soc. 105* (1983) 6646.
[16] F. Kawai, T. Noro, A. Murakama, K. Ohno, *Chem. Phys. Lett. 29* (1982) 429.
[17] J. Kalcher, A. Sax, G. Olbrich, *Int. J. Quantun Chem. 25* (1984) 543.
[18] N. Baird, *Can. J. Chem. 63* (1985) 71.
[19] B. T. Luke, J. A. Pople, M.-B. Krogh-Jesperson, Y. Apeloig, M. Karni, J. Chandrasekhar, P. von R. Schleyer, *J. Am. Chem. Soc. 108* (1986) 270.
[20] W. Kutzelnigg: *Einführung in die Theoretische Chemie, Vol. 2*, Verlag Chemie, Weinheim, 1978, p. 334.
[21] B. Solouki, P. Rosmus, H. Bock, *J. Am. Chem. Soc. 98* (1976) 6054.

[22] D. R. Johnson, F. X. Powell, W. H. Kirchhoff, *J. Mol. Spectrosc. 39* (1971) 136.
[23] H. W. Kroto, R. J. Suffolk, *Chem. Phys. Lett. 15* (1972) 545.
[24] M. E. Jacox, D. E. Milligan, *J. Mol. Spectrosc. 58* (1975) 142.
[25] M. W. Sinclair, J. C. Ribes, N. Fourikis, R. D. Brown, P. D. Godfrey, *Int. Astron. Union Colloq.* (1971) No. 2362.
[26] Eine Übersicht über die Chemie der Thioketone: F. Duus: *Theocarbonyl Compounds, Compr. Org. Chem. 3* (1979) 373.
[27] For a review of sulfur ylides see: P. K. Claus, Methoden Org. Chem. (Houben-Weyl) 4th Ed. Vol. E11 (1985) 1344.
[28] E. J. Corey, M. Chaykowsky, *J. Am. Chem. Soc. 87* (1965) 1353.
[29] B. U. Frost, L. S. Malvin, Jr., *Sulfur Ylids (Organic Chemistry (NY) 31* (1975)).
[30] T. Krügerke, K. Seppelt, *Chem. Ber. 121* (1988) 1977.
[31] The zwitterionic notation for organic ylides, which has largely been accepted, is used in this article.
[32] D. A. Dixon, B. E. Smart, *J. Am. Chem. Soc. 108* (1986) 7172.
[33] D. G. Naae, D. J. Burton, *J. Fluorine Chem. 1* (1971/72) 123.
[34] D. J. Burton, H. C. Krutzsch, *J. Org. Chem. 35* (1970) 2125.
[35] F. E. Herkes, D. J. Burton, *J. Org. Chem. 32* (1967) 1311.
[36] D. J. Burton, H. S. Kesling, D. G. Naae, *J. Fluorine Chem. 18* (1981) 293.
[37] D. J. Burton, R. Takei, S. Shin-Ya, *J. Fluorine Chem. 18* (1981) 197.
[38] D. J. Burton, P. E. Greenlimb, *J. Org. Chem. 40* (1975) 2796.
[39] R. W. Vanderhar, D. J. Burton, D. G. Naae, *J. Fluorine Chem. 1* (1971/72) 381.
[40] W. J. Middleton, W. H. Sharkey, *J. Org. Chem. 30* (1965) 1384.
[41] D. J. Burton, Y. Inouye, *Tetrahedron Lett. 1979,* 3397.
[42] D. J. Burton, S. Shinya, R. D. Howells, *J. Am. Chem. Soc. 101* (1979) 3689.
[43] M. A. Howells, R. D. Howells, N. C. Baenziger, D. J. Burton, *J. Am. Chem. Soc. 95* (1973) 5366.
[44] E. O. Fischer, A. Maasböl, *Angew. Chem. 76* (1964) 645; *Angew. Chem. Int. Ed. Engl. 3* (1964) 580.
[45] U. Schubert, H. Fischer, P. Hoffmann, K. Weiss, K. H. Dötz, F. R. Kreissl: *Transition Metal Carbene Complexes,* Verlag Chemie, Weinheim, 1983.
[46] J. I. Musher, *Adv. Chem. Ser. 110* (1972) 44.
[47] G. Kleemann, K. Seppelt, *Angew. Chem. 90* (1978) 547; *Angew. Chem. Int. Ed. Engl. 17* (1978) 516.
[48] G. Kleemann, K. Seppelt, *Chem. Ber. 116* (1983) 645.
[49] B. Pötter, K. Seppelt, *Inorg. Chem. 21* (1982) 3147.
[50] B. Pötter, G. Kleemann, K. Seppelt, *Chem. Ber. 117* (1984) 3255.
[51] G. Kleemann, K. Seppelt, unpublished results.
[52] T. Grelbig, B. Pötter, K. Seppelt, *Chem. Ber. 120* (1987) 815.
[53] T. Krügerke, J. Buschmann, G. Kleemann, P. Luger, K. Seppelt, *Angew. Chem. 99* (1987) 808; *Angew. Chem. Int. Ed. Engl. 26* (1987) 799.
[54] R. Damerius, D. Leopold, W. Schulze, K. Seppelt, *Z. Anorg. Allg. Chem. 578* (1989) 110.
[55] R. Winter, D. H. Peyton, G. L. Gard, *Inorg. Chem. 28* (1989) 3766.
[56] A. Simon, E. M. Peters, D. Lentz, K. Seppelt, *Z. Anorg. Allg. Chem. 468* (1980) 7.
[57] J. Buschmann, R. Kuschel, T. Koristsanszky, P. Luger, K. Seppelt, *J. Am. Chem. Soc. 113* (1991) 233.
[58] H. Bock, J. E. Boggs, G. Kleemann, D. Lentz, H. Oberhammer, E. M. Peters, K. Seppelt, A. Simon, B. Soulouki, *Angew. Chem. 91* (1979) 1008; *Angew. Chem. Int. Ed. Engl. 18* (1979) 944.
[59] S. Sunder, H. H. Eysel, G. Kleemann, K. Seppelt, *Inorg. Chem. 18* (1979) 3208.
[60] G. Gundersen, K. Hedberg, *J. Chem. Phys. 51* (1969) 2500.
[61] K. S. R. Murty, A. K. Mohanty, *Indian J. Phys. 45* (1971) 535.
[62] K. Kimura, S. H. Bauer, *J. Chem. Phys. 39* (1963) 3172.
[63] J. L. Hencher, D. W. L. Cruickshank, S. H. Bauer, *J. Chem. Phys. 48* (1968) 518.
[64] W. M. Tolles, W. D. Gwinn, *J. Chem. Phys. 36* (1962) 1119.
[65] G. Blanquet, J. Walrand, C. P. Courtoy, *Ann. Soc. Sci. Bruxelles 88 Ser. 2* (1974) 87.
[66] Y. Morino, T. Iijima, *Bull. Chem. Soc. Jpn. 35* (1962) 1661.
[67] A. T. Christensen, W. G. Witmore, *Acta Crystallogr. Sect. B 25* (1969) 73.
[68] V. G. Adrianov, Y. T. Struchkov, *Izv. Akad. Nauk SSSR 26* (1977) 687; *Bull. Acad. Sci. USSR Div. Chem. Sci. (Engl. Transl.) 26* (1977) 624.
[69] A. T. Christensen, E. Thom, *Acta Crystallogr. Sect. B 27* (1971) 581.
[70] J. L. Atwood, H. T. Mayfield, *Cryst. Struct. Commun. 7* (1978) 739.
[71] M. Clark, *Dissertation,* University of Alabama, USA 1987.
[72] K. A. Ostoja Starzewski, H. Bock, *J. Am. Chem. Soc. 98* (1976) 8486.
[73] R. S. Berry, *J. Chem. Phys. 32* (1960) 933.
[74] H. Günther, H. Oberhammer, R. Mews, I. Stahl, *Inorg. Chem. 21* (1982) 1872.
[75] E. L. Muetterties, W. Mahler, K. J. Packer, R. Schmutzler, *Inorg. Chem. 3* (1964) 1298.
[76] R. Mews, *Angew. Chem. 90* (1978) 561; *Angew. Chem. Int. Ed. Engl. 17* (1978) 530.
[77] D. D. DesMarteau, K. Seppelt, *Angew. Chem. 92* (1980) 659; *Angew. Chem. Int. Ed. Engl. 19* (1980) 43.
[78] D. D. DesMarteau, H. H. Eysel, H. Oberhammer, H. Günther, *Inorg. Chem. 21* (1982) 1607.
[79] A. H. Cowley, J. R. Schweiger, *J. Chem. Soc. Chem. Commun. 1972,* 560.
[80] G. M. Whitesides, H. L. Mitchell, *J. Am. Chem. Soc. 91* (1969) 5384.
[81] W. R. Roper, *J. Organomet. Chem. 300* (1986) 167.
[82] A. F. Hill, W. R. Roper, J. M. Waters, A. H. Wright, *J. Am. Chem. Soc. 105* (1983) 5939.
[83] G. R. Clark, S. V. Hoskins, T. C. Jones, W. R. Roper, *J. Chem. Soc. Chem. Commun. 1983,* 719.
[84] M. I. Davis, C. S. Speed, *J. Organomet. Chem. 21* (1970) 401.
[85] T. A. Albright, R. Hoffmann, J. C. Thibeault, D. L. Thorn, *J. Am. Chem. Soc. 101* (1979) 3801.
[86] J. W. Faller, *Adv. Organomet. Chem. 16* (1977) 211.
[87] S. T. Wilson, M. J. Coville, J. R. Shapely, J. A. Osborne, *J. Am. Chem. Soc. 96* (1974) 4038.
[88] C. A. Tolman, S. D. Ittel, A. D. English, J. P. Jesson, *J. Am. Chem. Soc. 100* (1978) 4080.
[89] L. Kruczynski, J. L. Martin, J. Takats, *J. Organomet. Chem. 80* (1974) C9.
[90] J. A. Segal, B. F. J. Johnson, *J. Chem. Soc. Dalton Trans. 1975,* 677.
[91] R. Gerhardt, R. Kuschel, K. Seppelt, unpublished results.
[92] R. Boeré, K. Seppelt, *Angew. Chem. 102* (1990) 1171; *Angew. Chem. Int. Ed. Engl. 29* (1990) 1128.
[93] T. Henkel, T. Krügerke, K. Seppelt, unpublished results.
[94] R. Damerius, K. Seppelt, J. Thrasher, *Angew. Chem. 101* (1989) 783; *Angew. Chem. Int. Ed. Engl. 28* (1989) 769.
[95] J. Haase, H. Oberhammer, W. Zeil, O. Glemser, R. Mews, *Z. Naturforsch. A 25* (1970) 153.
[96] N. Lozac'h, *Adv. Heterocyc. Chem. 13* (1971) 161.
[97] R. Gleiter, R. Gygax, *Top. Curr. Chem. 63* (1976) 49.
[98] J. P. Jacobsen, J. Hansen, C. T. Pedersen, *J. Chem. Soc. Perkin Trans. 2 1979,* 1521.
[99] L. K. Hansen, A. Hordvik, *Acta Chem. Scand. 27* (1973) 411.
[100] A. Hordvik, J. Saethre, *Isr. J. Chem. 10* (1972) 239.
[101] Q. Shen, K. Hedberg, *J. Am. Chem. Soc. 96* (1974) 289.
[102] L. J. Saethre, S. Svensson, N. Martensson, U. Gelius, P. A. Malmquist, E. Bassilier, K. Siegbahn, *Chem. Phys. 20* (1977) 431.
[103] D. T. Clark, *Int. J. Sulfur Chem. Part C 7* (1972) 11.
[104] R. D. Lapper, A. J. Poole, *Tetrahedron Lett. 1974,* 2783.
[105] C. T. Pedersen, K. Schaumburg, *Org. Magn. Reson. 6* (1975) 5861.
[106] C. T. Pedersen, E. G. Frandsen, K. Schaumburg, *Org. Magn. Reson. 9* (1977) 546.
[107] E. G. Frandsen, J. P. Jacobsen, *Org. Magn. Reson. 10* (1977) 43.
[108] T. Pedersen, S. V. Skaarup, C. T. Pedersen, *Acta Chem. Scand. B 31* (1977) 711.
[109] A. J. Arduengo III, C. A. Steward, F. Davidson, D. A. Dixon, J. Y. Baker, S. A. Culley, M. B. Mizen, *J. Am. Chem. Soc. 109* (1987) 627.
[110] D. A. Dixon, A. J. Arduengo III, T. Fukunaga, *J. Am. Chem. Soc. 108* (1986) 2461.
[111] A. J. Arduengo III, D. A. Dixon, D. C. Roe, *J. Am. Chem. Soc. 108* (1986) 6821.
[112] D. A. Dixon, A. J. Arduengo III, *J. Chem. Soc. Chem. Commun. 1987,* 498; *J. Am. Chem. Soc. 109* (1987) 338; *J. Phys. Chem. 91* (1987) 3195.
[113] R. M. Rosenberg, E. L. Muetterties, *Inorg. Chem. 1* (1962) 756.
[114] F. Seel, *Adv. Inorg. Chem. Radiochem. 16* (1974) 297.
[115] A. Haas, *Adv. Inorg. Chem. Radiochem. 18* (1976) 143.
[116] W. Gombler, *Z. Anorg. Allg. Chem. 439* (1978) 193.
[117] B. Solouki, H. Bock, *Inorg. Chem. 16* (1977) 665.
[118] R. Kuschel, K. Seppelt, unpublished results.
[119] J. Thrasher, unpublished results.
[120] J. Bittner, K. Seppelt, *Chem. Ber. 122* (1991), in press.
[121] B. Neumüller, E. Fluck, *Phosphorus Sulfur 29* (1986) 23.
[122] I. Absar, J. R. Van Wazer, *J. Am. Chem. Soc. 94* (1972) 2382.
[123] H. Lischka, *J. Am. Chem. Soc. 99* (1977) 353.
[124] H. Schmidbaur, A. Schier, D. Neugebauer, *Chem. Ber. 116,* (1983) 2173.
[125] E. F. Perozzi, I. C. Paul in C. J. M. Stirling (Ed.): *The Chemistry of the Sulfonium Group,* Wiley, Chichester 1981, p. 15.
[126] Due to mesemerism conjugated ylides such as $R_3P\text{-}CR'\text{-}CR''=O$ and $R_2S\text{-}Cr'\text{-}CR=O$ show restricted rotation at about the C-C bond at low temperatures. ($R_3P\text{-}CR'=CR''\text{-}O$). This is not to be confused with the torsion about the ylidic bond.
[127] F. S. Lin, K. L. Sekris, *J. Am. Chem. Soc. 94* (1972) 5794.
[128] R. Winter, G. L. Gard, *Inorg. Chem. 29* (1990) 2386.
[129] E. Wedekind, D. Schenk, R. Stüsser, *Ber. Dtsch. Chem. Ges. 56* (1923) 633.
[130] Reviews of sulfines: a) J. F. King, T. Durst, *Tetrahedron Lett.* (1963) 585; b) G. Opitz, *Angew. Chem. 79* (1967) 161; *Angew. Chem. Int. Ed. Engl. 6* (1967) 107; c) J. C. J. Bart, *Angew. Chem. 80* (1968) 697; *Angew. Chem. Int. Ed. Engl. 7* (1968) 730; d) B. Zwanenburg in S. Oal (Ed.): *Reviews on Heteroatom Chemistry,* Myo, Tokyo 1988, p. 218; e) B. Zwanenburg, B. G. Lenz, *Methoden Org. Chem. (Houben-Weyl) 4th Ed. Vol. E11,* (1985) 911.
[131] E. Block, R. E. Penn, R. J. Olsen, P. F. Sherwin, *J. Am. Chem. Soc. 98* (1976) 1264.

[132] E. Block, H. Bock, S. Mohmand, P. Rosums, B. Solouki, *Angew. Chem. 88* (1976) 380; *Angew. Chem. Int. Ed. Engl. 15* (1976) 383.
[133] S. Samejima, *Asahi Garasu Kenkyn Hokoku 33* (1983) 45.
[134] H. Fritz, W. Sundermeyer, unpublished results.
[135] A. Elsässer, W. Sundermeyer, *Tetrahedron Lett. 24* (1983) 2141.
[136] A. Elsässer, W. Sundermeyer, D. S. Stephenson, *Chem. Ber. 118* (1985) 116.
[137] A. Elsässer, W. Sundermeyer, *Chem. Ber. 118* (1985) 4553.
[138] M. Schwab, W. Sundermeyer, *Chem. Ber. 119* (1986) 2458.
[139] M. Schwab, W. Sundermeyer, *Chem. Ber. 121* (1988) 75.
[140] M. Eschwey, W. Sundermeyer, D. S. Stephenson, *Chem. Ber. 116* (1983) 1623.
[141] W. Sander, R. Henn, W. Sundermeyer, *Spectrochim. Acta Part A 42* (1986) 1281.
[142] J. Holoch, W. Sundermeyer, *Chem. Ber. 119* (1986) 269.
[143] B. Zwanenburg, L. Thijs, J. Strating, *Tetrahedron Lett. 1969,* 4461.
[144] R. Schork, W. Sundermeyer, *Chem. Ber. 118* (1985) 1415.
[145] J. Silhanek, M. Zbirovsky, *J. Chem. Soc. Chem. Commun. 1969,* 878.
[146] Übersichten zu Sulfenen a) B. G. Lenz, B. Zwanenburg, *Methoden Org. Chem. (Houben-Weyl) 4th Ed. Vol. E11* (1985) 1344; b) G. Opitz, *Angew. Chem. 79* (1967) 161; *Angew. Chem. Int. Ed. Engl. 6* (1967) 107; c) J. F. King, *Acc. Chem. Res. 8* (1975) 10.
[147] R. Allmann, W. Hanefeld, M. Krestel, B. Spangenberg, *Angew. Chem. 99* (1987) 1175; *Angew. Chem. Int. Ed. Engl. 26* (1987) 1133.
[148] U. Rheude, W. Sundermeyer, *Chem. Ber. 118* (1985) 2208.
[149] J. F. King, P. de Mayo, D. L. Verdun, *Can. J. Chem. 47* (1969) 4509.
[150] J. F. King, R. A. Marty, P. de Mayo, D. L. Verdun, *J. Am. Chem. Soc. 93* (1971) 6304.
[151] R. Langendries, F. C. De Schryver, P. de Mayo, R. A. Marty, J. Schutyser, *J. Am. Chem. Soc. 96* (1974) 2964.
[152] J. F. King, E. G. Lewars, *Can. J. Chem. 51* (1973) 3044; *J. Chem. Soc. Chem. Commun. 1972,* 700.
[153] J. P. Snyder, *J. Org. Chem. 38* (1973) 3965.
[154] E. de Barry Barnett, *J. Chem. Soc. 97* (1910) 63.
[155] R. Kitamura, S. Suzuki, *Yakugaku Zasshi 58* (1938) 818.
[156] J. Böseken, *Recl. Trav. Chim. Pays-Bas 67* (1948) 603.
[157] R. A. L. Sullivan, A. Hargreaves, *Acta Crystallogr. 15* (1962) 675.
[158] B. E. Smart, W. J. Middleton, *J. Am. Chem. Soc. 109* (1987) 4982.
[159] U. Hartwig, H. Pritzkow, K. Rall, W. Sundermeyer, *Angew. Chem. 101* (1989) 224; *Angew. Chem. Int. Ed. Engl. 18* (1989) 221.
[160] O. Glemser, A. Wegener, *Angew. Chem. 82* (1970) 324; *Angew. Chem. Int. Ed. Engl. 9* (1970) 309.
[161] O. Glemser, S. Pohl, F. M. Tesky, R. Mews, *Angew. Chem. 89* (1977) 829; *Angew. Chem. Int. Ed. Engl.* (1977) 789.
[162] F. M. Tesky, R. Mews, O. Glemser, *Z. Anorg. Allg. Chem. 452* (1979) 103.
[163] F. M. Tesky, R. Mews, B. Krebs, M. R. Upta, *Angew. Chem. 90* (1078) 722; *Angew. Chem. Int. Ed. Engl. 17* (1978) 677.
[164] F. M. Tesky, R. Mews, *Chem. Ber. 113* (1980) 2183.
[165] O. Glemser, M. F. Feser, S. P. von Halasz, *Inorg. Nucl. Chem. Lett. 8* (1972) 321.
[166] O. Glemser, H. Schröder, H. Haeseler, *Naturwissenschaften 42* (1955) 44; *Z. Anorg. Allg. Chem. 279* (1955) 28.
[167] O. Glemser, H. Schröder, *Z. Anorg. Allg. Chem. 284* (1956) 97.
[168] O. Glemser, H. Richert, *Spectrochim. Acta Part A 23* (1967) 2683.
[169] O. Glemser, R. Mews, *Angew. Chem. 92* (1980) 904; *Angew. Chem. Int. Ed. Engl. 19* (1980) 883.
[170] T. E. Gier, *J. Am. Chem. Soc. 83* (1961) 1769.
[171] H. W. Kroto, J. F. Nixon, N. P. C. Simmons, N. P. C. Westwood, *J. Am. Chem. Soc. 100* (1978) 446.
[172] H. E. Hosseini, H. W. Kroto, J. F. Nixon, S. Brownstein, J. R. Morton, K. F. Preston, *J. Chem. Soc. Chem. Commun. 1979,* 653.
[173] M. J. Hopkinson, H. W. Kroto, J. F. Nixon, N. P. C. Simmons, *Chem. Phys. Lett. 42* (1976) 460.
[174] H. W. Kroto, J. F. Nixon, N. P. C. Simmons, *J. Mol. Spectrosc. 77* (1979) 270.
[175] T. A. Cooper, H. W. Kroto, J. F. Nixon, O. Ohashi, *J. Chem. Soc. Chem. Commun. 1980,* 333.
[176] G. Becker, G. Gresser, W. Uhl, *Z. Naturforsch. B 36* (1981) 16.
[177] R. Appel, A. Westerhaus, *Tetrahedron Lett. 22* (1981) 2159.
[178] G. Märkl, H. Sejpka, *Tetrahedron Lett. 27* (1986) 171.
[179] A. M. Arif, A. R. Barron, A. H. Cowley, S. W. Hall, *J. Chem. Soc. Chem. Commun. 1988,* 171.
[180] G. Märkl, H. Sejpka, *Tetrahedron Lett. 26* (1985) 5507.
[181] T. Allspach, M. Regitz, G. Becker, W. Becker, *Synthesis 1985,* 31.
[182] For a summary of the phosphaalkynes known prior to 1988 see Ref. [5].
[183] E. Niecke, M. Nieger, F. Reichert, *Angew. Chem. 100* (1988) 1781; *Angew. Chem. Int. Ed. Engl. 27* (1988) 715.
[184] G. Märkl, H. Sejpka, *Angew. Chem. 98* (1986) 286; *Angew. Chem. Int. Ed. Engl. 25* (1986) 264.
[185] R. Appel, J. Peters, R. Schmitz, *Z. Anorg. Allg. Chem. 475* (1981) 18.
[186] G. Sicard, A. Baceiredo, G. Bertrand, J.-P. Majoral, *Angew. Chem. 96* (1984) 450; *Angew. Chem. Int. Ed. Engl. 23* (1984) 459.
[187] A. Igau, H. Grützmacher, A. Baceiredo, G. Bertrand, *J. Am. Chem. Soc. 110* (1988) 6463.
[188] G. Trinquier, *J. Am. Chem. Soc. 104* (1982) 6969.
[189] R. Ahlrichs, H. Schiffer, *J. Am. Chem. Soc. 107* (1985) 6494.
[190] J. F. Ogilvie, S. Cradock, *J. Chem. Soc. Chem. Commun. 1966,* 364.
[191] H. Bock, R. Dammel, *Angew. Chem. 97* (1985) 128; *Angew. Chem. Int. Ed. Engl. 24* (1985) 111.
[192] H. W. Kroto, J. N. Murell, A. Al-Derzi, M. F. Guest, *Astrophys. J. 219* (1978) 886.
[193] R. Preuss, R. J. Buenker, S. D. Peyerimhoff, *J. Mol. Struct. 49* (1978) 171.
[194] B. Pötter, K. Seppelt, *Angew. Chem. 96* (1984) 138; *Angew. Chem. Int. Ed. Engl. 23* (1984) 150.
[195] R. Gerhardt, T. Grelbig, J. Buschmann, P. Luger, K. Seppelt, *Angew. Chem. 100* (1988) 1592; *Angew. Chem. Int. Ed. Engl. 27* (1988) 1534.
[196] B. Pötter, K. Seppelt, A. Simon, E.-M. Peters, B. Hettich, *J. Am. Chem. Soc. 107* (1985) 980.
[197] D. Christen, H.-G. Mack, C. J. Marsden, H. Oberhammer, G. Schatte, K. Seppelt, H. Willner, *J. Am. Chem. Soc. 109* (1987) 4009.
[198] J. Weiss, H. Oberhammer, R. Gerhardt, K. Seppelt, *J. Am. Chem. Soc. 112* (1990) 6839.
[199] W. Clegg, O. Glemser, K. Harms, G. Hartmann, R. Mews, M. Noltemeyer, G. M. Sheldrick, *Acta Crystallogr. Sect. B 37* (1981) 548.
[200] R. L. Cook, W. H. Kirchhoff, *J. Chem. Phys. 47* (1967) 4521.
[201] T. Beppu, E. Hirota, Y. Morino, *J. Mol. Spectrosc. 36* (1970) 386.
[202] W. C. Emken, K. Hedberg, *J. Chem. Phys. 58* (1973) 2195.
[203] W. H. Kirchhoff, E. B. Wilson, *J. Am. Chem. Soc. 84* (1962) 334.
[204] H. Oberhammer, G. Becker, G. Gresser, *J. Mol. Struct. 75* (1981) 283.
[205] J. K. Tyler, *J. Chem. Phys. 40* (1964) 1170.
[206] G. J. H. von Nes *Dissertation* (Single-Crystal Structures, Electron Density Distributions of Ethane, Ethylene, Acetylene) Rijks Universiteit Groningen, 1978.
[207] J. E. Boggs, *Inorg. Chem. 23* (1984) 3577.
[208] A. Simon, *Angew. Chem. 100* (1988) 163; *Angew. Chem. Int. Ed. Engl. 27* (1988) 159.
[209] A. T. Vincent, P. J. Wheatley, *J. Chem. Soc. Dalton Trans. 1972,* 617.
[210] R. D. Brown, P. D. Godfrey, P. S. Elmes, M. Rodler, L. M. Tack, *J. Am. Chem. Soc. 107* (1985) 4112.
[211] L. Farrell, L. Radom, *Chem. Phys. Lett. 91* (1982) 373.
[212] R. D. Brown, R. D. Dittmann, *Chem. Phys. 83* (1984) 77.
[213] H. Fischer, P. Hofmann, F. R. Kreissl: *Carbyne Complexes,* VCH, Weinheim 1988.
[214] E. O. Fischer, G. Kreis, C. G. Kreiter, J. Müller, G. Huttner, H. Lorenz, *Angew. Chem. 85* (1973) 618; *Angew. Chem. Int. Ed. Engl. 12* (1973) 564.
[215] G. Huttner, H. Lorenz, W. Gartzke, *Angew. Chem. 86* (1974) 667; *Angew. Chem. Int. Ed. Engl. 13* (1974) 609.
[216] E. A. Carter, W. A. Goddard, *J. Phys. Chem. 90* (1986) 998.
[217] G. Trinquier, J.-P. Malrieu, *J. Am. Chem. Soc. 109* (1987) 5303.
[218] A. J. Colussi, J. R. Morton, K. F. Preston, R. W. Fessenden, *J. Chem. Phys. 61* (1974) 1247.
[219] Singlet-triplet splitting in CH_2 − 41, CF_2 + 50, $C(CF_3)_2$ − 62 kJ mol^{-1}, doublet-quartet splitting in CH +70, CF + 260 kJ mol^{-1} (P. K. Huber, G. Hertzberg; *Constants of Diatomic Molecules,* Van Nostrand Reinhold, New York 1979).
[220] W. J. Middleton, US-A 2831835 (1958), *Chem. Abstr. 52* (1958) 14658f; J. C. Brahms, W. P. Dailey, *J. Am. Chem. Soc. 111* (1989) 8940. *Note added in proof:* F–C≡C–F is linear. Its extreme instability may be due to a very non-rigid molecular skeleton: H. Bürger.
[221] A. C. Hopkinson, M. H. Lien, I. G. Csizmadia, *Chem. Phys. Lett. 109* (1984) 246.
[222] C. K. Ingold, *J. Chem. Soc. 1953,* 2707.
[223] K. K. Innes, *J. Chem. Phys. 22* (1954) 863.
[224] R. L. Kuczkowsky, *J. Am. Chem. Soc. 86* (1964) 3617.
[225] R. L. Kuczkowsky, *J. Am. Chem. Soc. 85* (1963) 3047.
[226] B. Rozen: *International Tables of Selected Values, Spectroscopic Data of Diatomic Molecules,* Pergamon Press, New York 1970.
[227] M. V. Carlowitz, H. Oberhammer, H. Willner, J. E. Boggs, *J. Mol. Struct. 100* (1983) 161.
[228] P. J. Davidson, D. H. Harris, M. F. Lappert, *J. Chem. Soc. Dalton Trans 1976,* 2268.
[229] L. Pauling, *Proc. Natl. Acad. Sci. USA 80* (1983) 3871.
[230] T. Wettling, J. Schneider, O. Wagner, C. G. Kreiter, M. Regitz, *Angew. Chem. 101* (1989) 1035; *Angew. Chem. Int. Ed. Engl. 28* (1989) 1013.
[231] A. Igau, A. Baceiredo, G. Trinquier, G. Bertrand, *Angew. Chem. 101* (1989) 617; *Angew. Chem. Int. Ed. Engl. 28* (1989) 621.
[232] H. Willner (Hannover), private communication.

Metallomesogens: Metal Complexes in Organized Fluid Phases

By Anne-Marie Giroud-Godquin and Peter M. Maitlis*

Metallomesogens, metal complexes of organic ligands which exhibit liquid crystalline (mesomorphic) character, combine the variety and range of metal-based coordination chemistry with the extraordinary physical properties exhibited by liquid crystals. Thermotropic metallomesogens have been made incorporating many metals, including representatives of s-, p-, d- and even f-block elements. Both rodlike (calamitic) and disklike (discotic) thermotropic metallomesogens are known, and examples of all the main mesophase types are found. Many different varieties of ligand can be used: monodentate (4-substituted pyridines), bidentate (β-diketonates, dithiolenes, carboxylates, cyclometalated aromatic amines), or polydentate (phthalocyanines, porphyrins). As with organic mesogens, molecular shape and intermolecular forces play an important role, i.e. the ligands are important in determining mesophase character. The chief requirement for a metallomesogen is a rigid core, usually unsaturated and either rod- or disklike in shape, bearing several long hydrocarbon tails. The metal atom is usually at or near the center of gravity of the molecule. In some cases the ligands are themselves mesogenic, but this is not a requirement. The presence of one or more metals opens many exciting possibilities: new shapes, not easily generated by organic compounds, and hence new properties are then accessible. The incorporation of d-block metals brings with it features such as color and paramagnetism. Profound effects arise from the large and polarizable concentration of electron density that every metal atom possesses, since the molecular polarizability is a key factor in determining whether a molecule will form liquid crystals. Enhanced physical properties (e.g. high birefringencies), as well as new and unexpected ones, will result. A major requirement for metallomesogens to find applications in new device technology is that the metal–ligand bonds are strong and inert and the complexes stable; this can be accomplished with, for example, chelating ligands and the 5d metals.

1. Introduction

Scientific advances frequently take place at the interfaces between disciplines. *Metallomesogens* introduce to metal-based coordination chemistry the unusual physical properties exhibited by liquid crystals, so useful in electronic devices and elsewhere. Although metallomesogens have been known for some eighty years, only now is this area, which we have had the pleasure of helping to develop, springing into prominence.

Most work has concentrated on organic materials, but recent developments have highlighted the many new possibilities which can result from the introduction of one or more metal atoms into a liquid crystal; there are, after all, some sixty metals which can in principle be coordinated.

Reasons for putting a metal into a liquid crystal range from satisfying intellectual curiosity (it's an intriguing combination: what will the properties be?) through to the severely practical (novel substances for molecular electronics, new electrical or magnetic switches, conductors, new optical devices). Geometries and hence shapes not easily found in organic chemistry can result from coordinating a metal; metals show square planar, square pyramidal, trigonal bipyramidal, octahedral, and a remarkable variety of geometries for coordination numbers ≥ 7.

Many of the d- and f-block transition metal complexes are in oxidation states which give colored compounds, and many of them have unpaired electrons and exhibit paramagnetism, further extending the range of potentially useful physical properties.

But perhaps the most important effects arise from the large and polarizable electron density which is a feature of every metal atom. Polarizability is one of the most important attributes of molecules which form liquid crystals and any increase will have very profound effects on the physical characteristics, with the possibility of a useful but unexpected macroscopic property resulting.

1.1. What are Liquid Crystals?

Liquid crystals form a state of matter intermediate between the solid and the liquid. The terms *mesomorph* (Greek, *mesos morphe*, between two states, forms) and *mesophase* are also used; a *mesogen* is the molecule which gives rise to a mesophase. Organic liquid crystals have been known for over a century.[1] They can be divided into two broad families, the *thermotropics*[2] and the *lyotropics*.[3] Thermotropic liquid crystals change phase on heating or cooling; the crystal phase melts to the mesophase, which then clears to the isotropic liquid at a higher temperature. Some exhibit poly-

[*] Prof. P. M. Maitlis FRS
Department of Chemistry, The University
Sheffield S 3 7HF (UK)
Dr. A. M. Giroud-Godquin
Laboratoire de Chimie, Chimie de Coordination
Departement de Recherche Fondamentale
Centre d'Etudes Nucleaires de Grenoble
38041 Grenoble Cedex (France)

[*] The terms "dithiolenes" and "dithiolene complexes" introduced here are treated as trivial names. Strictly speaking these compounds should be called "enedithiols" and "enedithiolate complexes", respectively.

morphism: they show several mesophases. Lyotropic phases are formed by molecules in a solvent (generally water) and the appearance of the mesophase is controlled by the concentration.

A crystal (denoted by K or C) has defined shape, and most of its physical properties are anisotropic because the constituent molecules or ions are ordered in position and orientation. By contrast, the component molecules (or ions) of a fluid lack positional and orientational ordering; hence the physical properties are isotropic (I) and a fluid takes up the shape of the container. In a thermotropic mesophase the positional order is largely absent, giving a fluidity, while some orientational order is retained, giving the anisotropy. The transition from the crystal to the mesophase is often termed the *melting point*, and that from the highest mesophase to the isotropic, the *clearing point*, reflecting the fact that mesophases often appear turbid while the isotropic liquid is clear.

One consequence of this anisotropy is that mesophases can have two (or even three) different refractive indices, magnetic susceptibilities, and electric permittivities. As a result, some thermotropic molecules can be oriented by applied electric fields.

Thermotropics can be further sub-divided into *calamitic* (reed- or rodlike) and *discotic* (disklike, denoted by D);[4] *polymeric*[5] liquid crystals are also known. Rodlike thermotropics form two broad classes [*nematics* (N) and *smectics* (S)] and several subgroups of discotics are also known.

In the least ordered phase, the nematic, the rodlike molecules line up approximately parallel to each other (Fig. 1); this direction is known as the *director*. The transition from the crystalline to the nematic phase (K → N) is usually associated with an enthalpy change about ten times higher than the nematic to isotropic (N → I) transition.

A very useful characteristic of nematic mesophases is the ease with which they are reoriented by a magnetic or electric field. This has found practical application in electronic display devices. Nematic molecules are achiral (or racemic); the introduction of a chiral center into such a molecule gives rise to cholesteric behavior, where the director is now helical.

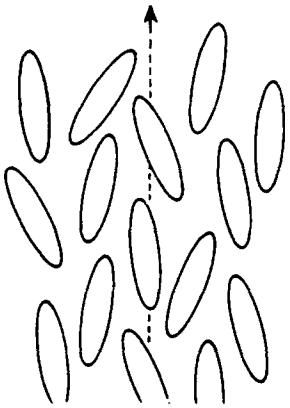

Fig. 1. Schematic representation of a calamitic nematic phase.

Smectic liquid crystals form a variety of layered phases, which offer additional order over that found for nematics; some have phases with the molecules perpendicular to the layers (e.g. S_A; Fig. 2, top), in others they are inclined to them (e.g. S_C; Fig. 2, bottom).

Discotic liquid crystalline phases are obtained with disklike molecules where the director is perpendicular to the molecular plane; columnar and nematic (Fig. 3) as well as

Peter Maitlis is Professor of Inorganic Chemistry at Sheffield University. He was educated in England (PhD with Professor M. J. S. Dewar in London, in 1956), and then spent twelve years in North America where he was Professor at McMaster University in Canada before returning to England and taking up the Chair in Sheffield in 1972. His research interests include organotransition metal chemistry and homogeneous catalysis. During the last five years he has become increasingly involved in the design of coordination complexes as Advanced Materials, in particular as liquid crystals, where he has developed the study of metallomesogens with his group. In 1984 he was elected to the Royal Society, and in 1986 he received the Sir Edward Frankland Prize Lectureship of the RSC for his work in organometallic chemistry. He has also been President of the Dalton Division of the RSC and was Chairman of the Chemistry Committee of the Science and Engineering Research Council.

Anne-Marie Giroud-Godquin was born in Casablanca (Morocco). After secondary school (Lycée de Casablanca) she completed her undergraduate studies in physics and chemistry at La Sorbonne (University of Paris). She discovered the excitement of chemical research with Dr. J. Jacques at the Collège de France during her Thèse troisième cyle in 1961. She then entered the Centre National de la Recherche Scientifique, where she gained her PhD (in steroid chemistry) from the University of Grenoble with Professor A. Rassat. After postdoctoral work with Professor G. Luckhurst at the University of Southampton, she returned to Grenoble to develop her original research on metal-containing liquid crystals. Later she spent some months at IBM in California with Professor U. Müller-Westerhoff. She is now Directeur de Recherche at the CNRS Chemistry Laboratory of the Centre d'Etudes Nucléaires at Grenoble, where she pursues her researches on metallomesogens.

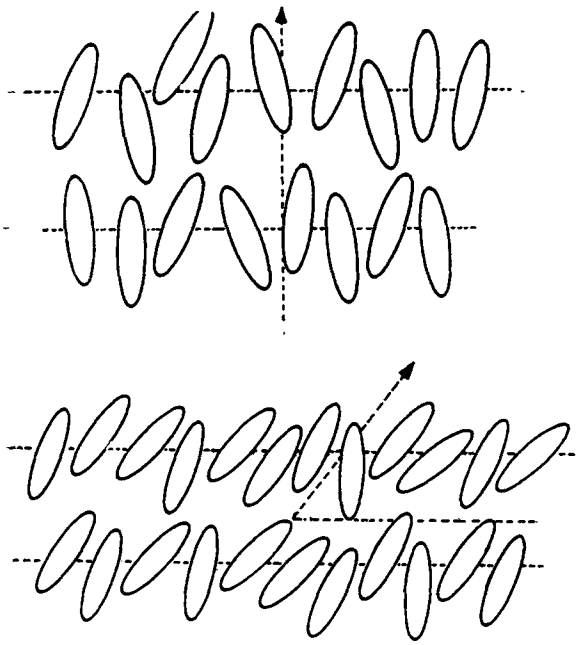

Fig. 2. Schematic representations of calamitic smectic phases. Top: S_A phase; bottom: S_C phase.

other types are known. Typical organic discotics are benzene derivatives with six long *n*-alkyloxy tails, **1**; many metallo-

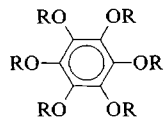

1

mesogens (such as those based on phthalocyanine, porphyrin, or even β-diketonate ligands) also form discotic phases. The two-dimensional network of such a columnar

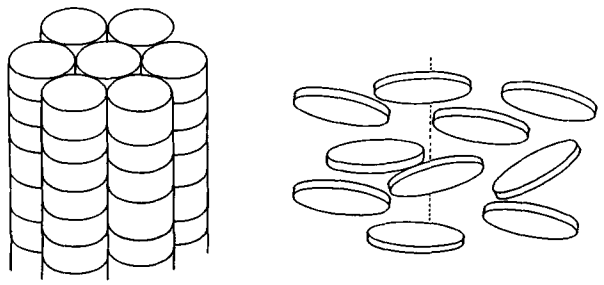

Fig. 3. Schematic representations of columnar-discotic (left) and nematic-discotic phases (right).

mesophase can be hexagonal, rectangular, or oblique, and the molecules can be either ordered or disordered along the long axes of the columns (Fig. 4).

Thermotropics are held together by weak dipole-dipole and dispersion forces. Their magnitude is critical: when they are too weak or when they are too strong, the liquid crys-

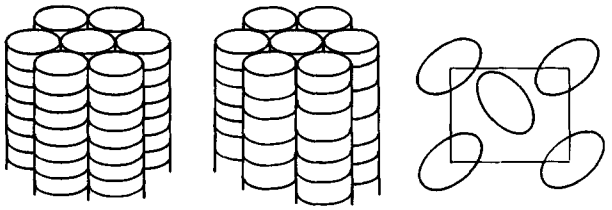

Fig. 4. Schematic representations of columnar-discotic phases. Left: ordered hexagonal, D_{ho}; center: disordered hexagonal D_{hd}; right: rectangular, D_r.

talline character is lost. Hence the molecular features which optimize thermotropic behavior are very important.

To exhibit liquid crystalline properties organic compounds require strongly polarizable groups, such as aromatic rings (A, B in Fig. 5), esters, or other oxy- (X, Y) or nitrile-functions. Rodlike thermotropic mesogens also require a long rigid group (often phenyl rings which form a core), while a rigid conjugated platelike grouping is usually associated with the core of a discotic mesogen. Both types need several long flexible *n*-alkyl- (or *n*-alkyloxy-) tails (R). The rod- or disklike shapes, together with the polarizable groups, increase the molecular anisotropy and facilitate formation of liquid crystal phases.

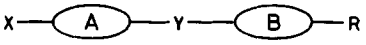

Fig. 5. Schematic representation of a rodlike, thermotropic, organic mesogen.

It is important to note that none of the mesophase structures illustrated is static; each representation is a snapshot; for example, smectic layers can be described by one-dimensional density waves.

The characterization of thermotropic mesophases relies first, on optical microscopy, where the different phases show characteristic textures when viewed between crossed polarizers, as the temperature is changed. Mixing with a known mesophase is widely used to confirm the observations, since two identical mesophases are frequently miscible. These optical methods are complemented by Differential Scanning Calorimetry (DSC), and by low angle X-ray scattering in the mesophase.

1.2. Early Work on Metallomesogens

The first thermotropic metal-containing liquid crystals were reported by *Vorländer* in 1910.[6] He discovered that the alkali-metal carboxylates, $R(CH_2)_nCOONa$, formed classical lamellar phases characteristic of soaps. In 1923 *Vorländer* also found that the diarylmercurials **2** form smectic phases.[7]

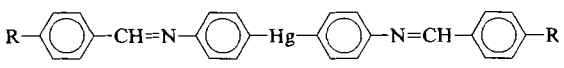

2

Between 1959 and 1961 *Skoulios* et al. characterized alkali and alkaline earth salts of carboxylic acids and showed them

to possess a large variety of organizational types: lamellar, ribbonlike, and cylindrical.[8] The smectic ferrocenyl Schiff bases **3**, the first well-characterized organotransition metallomesogens, were synthesized by *Malthête* and *Billard* in 1976.[9]

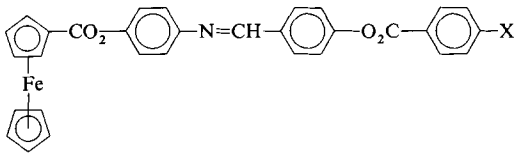

3, X = C_nH_{2n+1} (n = 5, 6, 8); OC_nH_{2n+1}(n = 8, 10)

The first to seek advanced materials in this area were *Giroud* and *Müller-Westerhoff*, who in 1977 reported the mesogenic nickel and platinum dithiolenes.[10] This work laid the foundations for the study of mesogens containing d-block elements and marked the practical beginnings of interest in the subject. Since then many researchers have entered the field, and many new types of metallomesogen have been synthesized.

This article reviews progress, developments, and problems in the field up to early 1990, and offers indicators to the principles by which new representatives may be constructed, and to the relations between mesomorphism and structure at the molecular level, as they appear at the moment.

Because mesophase formation depends on intermolecular forces and because much of the space around the metal is occupied by the ligand, the properties of metallomesogens are, to a first approximation, dominated by the ligands and their arrangement, in other words by the overall shape of the molecule. Thus, for example, long monodentate ligands will tend to give rodlike nematics and smectics, while flat, disklike polydentate ligands (for example, macrocycles) will give discotics. For this reason the material in this review is arranged by ligand type.

This organization also brings out the exceptions—for example molecules which one might expect to show discotic phases but which have been reported as smectics—and shows how critical the substituents on the *perimeter* of the ligand to the type of mesophase behavior are. Where X-ray data are available on the single crystals, it also becomes clear that many metallomesogens have interactions which enable the metal to interact axially (though weakly) with a donor atom on a neighboring molecule. Examples of this are found in the dimetal tetracarboxylates, in copper β-diketonates, in zinc, mercury, and palladium dithiocarboxylates, in salicylaldimines and, in a modified sense, in the metallophthalocyanines. This feature appears to have an important, if as yet unquantified, bearing on mesophase formation.

The metallomesogens have therefore been arranged by ligand, starting with the simplest, monodentate, and progressing to more complex bidentate and polydentate types: carboxylates, β-diketonates, dithiolenes, and dithiocarboxylates, polyamines (phthalocyanines, etc), salicylaldimines (Schiff bases with *N-O* chelate formation), and cyclometalated mesogens.

2. Metallomesogens with Monodentate Ligands

2.1. Nitrile Complexes

Nitriles bind readily to a variety of metals. The commercially available thermotropic CN-substituted biphenyls **4** and **5** and the bicyclohexyl derivative **6** analogous to **4** (**4** = n-CB, **5** n-OCB, **6** = n-CCH; n is the C number of the alkyl or alkoxy substituents) were first used by *Maitlis* and the Sheffield Liquid Crystal group for the synthesis of metallomesogens with a linear geometry. The (D_{2h}) *trans*-bis (neutral) ligand complexes **7**, **8** (L = n-CB and n-OCB), as well as

4 (n-CB)

5 (n-OCB)

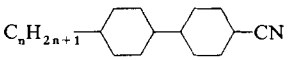

6 (n-CCH)

the monoligand complexes, **9** (L = n-OCB), were synthesized.[11] Synthetic routes were by displacement of one nitrile by another for **7** [Eq. (a)], by direct reaction, for **8** [Eq. (b)] or by bridge-splitting, for **9** [Eq. (c)].

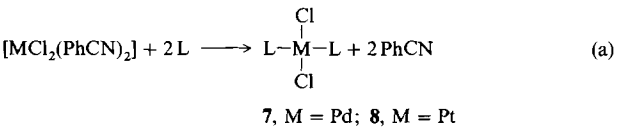

(a)

7, M = Pd; **8**, M = Pt

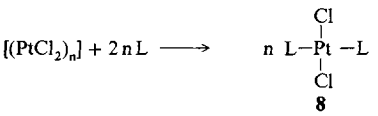

(b)

8

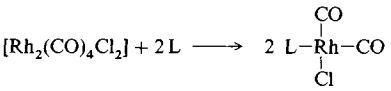

(c)

9

The palladium *alkyl* complexes **7** (L = n-CB) showed nematic *monotropic* behavior (thermodynamically unstable mesophases, which appear only on cooling). Lower homologues of the *alkyloxy* ligand complexes **7** (L = n-OCB, n = 4–7) showed nematic phases while the higher ones (n = 9) showed *enantiotropic* (thermodynamically stable) S_A and S_C phases.[12, 13] By contrast, platinum complexes, with both n-OCB and n-CB, showed enantiotropic phases.

Detailed comparisons are instructive (Table 1). Thus, while the ligand **4** (n = 5) has a nematic phase (24–35 °C) before clearing, and its $PtCl_2$ complex **8** behaves similarly, but at much higher temperature (K → N 189 °C, N → I 208 °C), the $PdCl_2$ complex shows only a monotropic nematic (I → N 92 °C). The ligand **5** (n = 9) shows an S_A phase (64–77 °C) and a nematic phase (77–80 °C) before clearing. The $PtCl_2$ complex shows an N and an S_C phase, but at higher temperatures (K → S_C 172 °C; S_C → N 183 °C; N → I

Table 1. Transition temperatures [°C] for mesomorphic alkyl- and alkyloxycyanobiphenyl complexes of palladium(II) and platinum(II) [13].

Complex	Mesophases			
trans-[PdL_2Cl_2] **7**	S_C	S_A	N	I
L = 5-CB		–	(92) [a]	125
L = 8-CB		–	(89) [a]	120
L = 9-CB		–	(98) [a]	110
L = 9-OCB	119	122	–	146
L = 3-CCH		–	(178.3) [a]	181.4
L = 5-CCH		–	(161.8) [a]	164.4
trans-[PtL_2Cl_2] **8**				
L = 3-CB			–	221
L = 4-CB			178	205
L = 5-CB			189	208
L = 6-CB			192	199
L = 7-CB			181	198
L = 8-CB			170	190
L = 9-CB	168		170.5	190
L = 10-CB	157	173	179	190
L = 1-OCB			245	248
L = 2-OCB			235	246
L = 3-OCB			196	235
L = 4-OCB			197	229
L = 5-OCB			167	219
L = 6-OCB			161	216 [b]
L = 7-OCB			174	211 [b]
L = 8-OCB			179	209 [b]
L = 9-OCB	172		183	206 [b]
L = 10-OCB	159	–	194	204

[a] Monotropic (thermodynamically unstable) mesophase, observed only on cooling. [b] Clears with (some) decomposition.

206 °C), whereas the $PdCl_2$ complex just shows smectic phases (K → S_C 119; S_C → S_A 122; S_A → I 146 °C).[12, 13] In some cases the complexes decompose close to the (rather high) clearing temperatures.

The structures of the Pd^{II} complex **7** (L = 5-CB) and the Pt^{II} complexes **8** (L = 5-CB and 8-CB) were confirmed by single crystal X-ray determinations (Fig. 6).[13] Since Pd and Pt are nearly equal in size, the 5-CB complexes are virtually identical, even with similar inter- as well as intramolecular dimensions. The ground state structures offer no immediate explanation for the differences in mesophase behavior, which may therefore be due to the generally higher lability of Pd^{II} complexes compared to their Pt^{II} analogs.

Although the bicyclohexylcyanopalladium complex **7** (L = 5-CCH), in contrast to the non-mesomorphic 3-CCH analogue, forms monotropic nematic phases (shown in Color figure 1 for L = 7-CCH), enantiotropic materials with a nematic range of ca. 5 °C can be prepared if the two complexes are mixed in a 1:1 ratio (Fig. 7).[12] This illustrates an important aspect of mesogens: even when the correct molecular shape does not produce the desired properties directly, they can often be induced by judicious mixing.

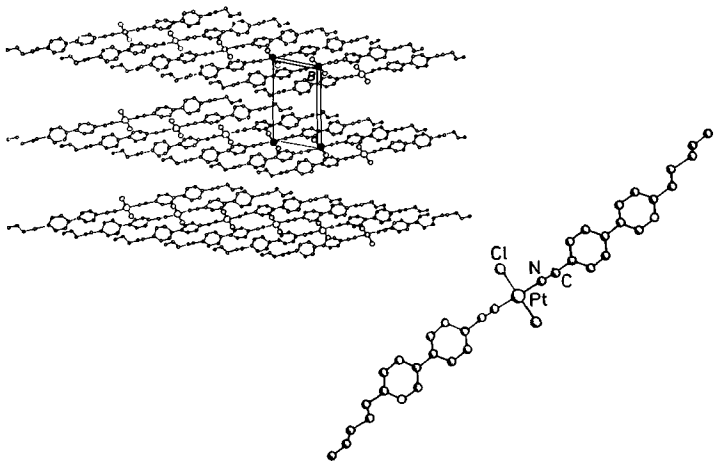

Fig. 6. Crystal structure of **8** (L = 5-CB) (after Ref. [13]).

Color figure 1. Polarization microscopic photograph of the nematic phase of **7** (L = 7-CCH) at 158 °C obtained by cooling of the isotropic liquid phase.

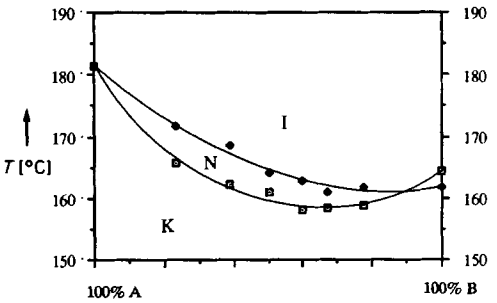

Fig. 7. Formation of a stable nematic phase by mixing non-mesogenic components [$PdCl_2$(3-CCH)$_2$] (A) with the monotropic complex [$PdCl_2$(5-CCH)$_2$] (B), □ K → N, ◆ N → I, □ K → I (after Ref. [12]).

An unanticipated benefit of complexing to a metal is the sharp increase in the birefringence, Δn, the difference between the parallel and the perpendicular refractive indices. Thus, while Δn for the ligands **4**–**6** is around 0.18, a mixture of $PdCl_2$ complexes of 2-OCB, 4-OCB and 6-OCB ligands gave a birefringence, $\Delta n \approx 0.45$ (at room temperature, by extrapolation).[14]

Mesogenic rhodium complexes with one cyanobiphenyl ligand, e.g. **9**, (L = 9-OCB) have also been made, but show very short nematic ranges and decompose close to their clearing temperatures.[13]

2.2. *n*-Alkyloxystilbazole Ligands

The 4′-alkyloxy-4-stilbazoles **10** (n-OST) are 4-substituted pyridines with extra polarizable functions (conjugation) and

a flexible tail. Since pyridines complex well to a large number of transition metals, the stilbazoles have been widely used by the Sheffield group as ligands for metallomesogen formation.

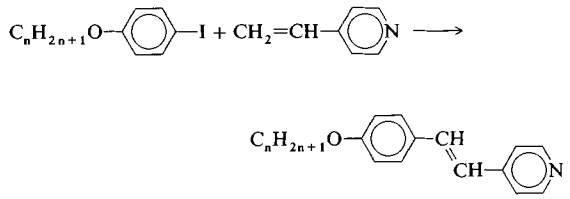

(d)

10 (n-OST)

The stilbazoles are made by a Heck reaction (palladium acetate and triethylamine in acetonitrile) between the 4-(alkyloxy)iodobenzene and 4-vinylpyridine [Eq. (d)]. The C=C double bond is *trans* in the ligand and in all the complexes examined. The ligands themselves show monotropic S_E and S_B phases for 3- and 4-OST, and enantiotropic S_E and S_B phases for $n > 5$, with clearing points around 85–90 °C.[15]

2.2.1. *Distilbazole Complexes*

Reaction of the stilbazoles with silver salts, AgY, led to a quite unexpected series of mesogenic materials, the ionic bis-ligand silver salts, $[Ag(n\text{-}OST)_2]Y$ **11** (**11a**: $Y = BF_4^{\ominus}$, **11b**: $Y = NO_3^{\ominus}$, **11c**: $Y = C_{12}H_{25}SO_4^{\ominus}$, **11d**: $Y = CF_3SO_3^{\ominus}$). The tetrafluoroborates **11a** were very sensitive to light, hygroscopic, and showed high transition temperatures.[16]

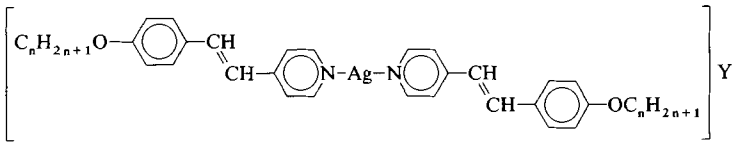

11

However, the dodecyl sulfate salts **11c** formed mesophases at lower temperatures and showed quite unusual behavior; for example, **11c** (n = 3) gave a *nematic* phase 146–159 °C before clearing.[17] Salts with longer alkyloxy chains exhibited complex behavior; for example, **11c** (n = 12) showed a lamellar (S_C) phase (108–132 °C), as well as a cubic (M_I) and an S_A phase before clearing at 178 °C to the isotropic liquid.[17, 18] Figure 8 shows a typical phase diagram relating transition temperatures to alkyl chain length. Phase identification was assisted by simultaneous X-ray diffraction and differential scanning calorimetry (XDDSC). The nitrate and triflate salts **11b** and **11d** are broadly similar to the dodecyl sulfates, but do not show such a variety of mesophases.

The existence of ionic nematics among the salts with shorter alkyloxy tails is quite unexpected, given the conflicting presence of both strong isotropic ionic forces and weak, anisotropic dispersion forces which stabilize the liquid crystal phases. The rich and varied polymorphism in these ionic systems may have some electrochemical applications.

A gold complex, [AuCl(8-OST)], which showed a mesophase between 120 and 200 °C,[12] and some very high melting palladium and platinum complexes, $[MCl_2$-

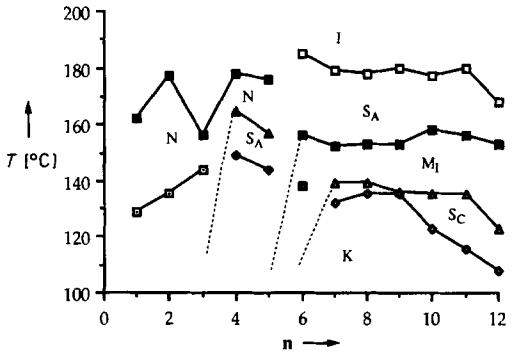

Fig. 8. Phase diagrams of $[Ag(n\text{-}OST)_2]C_{12}H_{25}OSO_3$ showing the extensive polymorphism of this system. ⊡ K → N, ◆ K → S_A, □ K → M_I, ◇ K → S_C, ■ N → I, □ S_A → I, ▲ S_A → N, △ S → M_I, ■ M_I → S_A (after Ref. [18]).

$(n\text{-}OST)_2]$ have also been prepared. Only $[PdCl_2(12\text{-}OST)_2]$ showed any mesophases (K → S 280 °C; S → N 290 °C; N → I 315 °C).

However, the related carboxylato complexes, prepared by reaction of $[Pd_2(O_2CR)_4]$ with the n-OST ligand, formed mesophases at much lower temperatures, for example $[Pd(O_2CC_9H_{19})_2(12\text{-}OST)_2]$, K → N 144 °C; N → I 151 °C.[19, 20] *Maitlis* et al. have found that the replacement of "hard" anions or ligands by softer organic amphiphilic anions or ligands is a generally useful strategy for lowering transition temperatures.

2.2.2. Monostilbazole Complexes

Another way to achieve lower transition temperatures is to incorporate some asymmetry. Since such complexes tend to disproportionate, this may not always be straightforward, but their synthesis has been accomplished in the case of the platinum complexes **12** which have one stilbazole and one η^2-olefin ("π-bonded") in the *trans* position. The complexes were prepared from Zeise's salt, $K[PtCl_3(C_2H_4)]$ by reaction with n-OST; the ethene can be readily displaced by other α-olefins [Eq. (e)].[20]

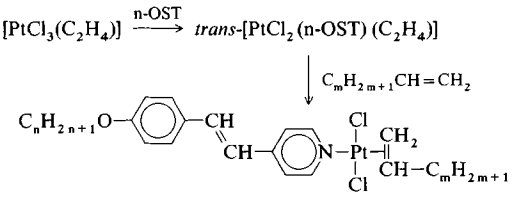

(e)

12

The chain lengths n and m were systematically varied (n = 3–12; m = 0–8) and it was found that mesophase behavior (all S_A) occurred for those with longer chains (Fig. 9). Complexes with $m + n \approx 8$–11 showed monotropic behavior (S_A); those with $m + n \gtrsim 11$–13 showed enantiotropic S_A phases (Color figure 2), while those with $m + n \lesssim 8$ were non-mesomorphic.[20]

The mesogenic complexes **12** had transition temperatures below 100 °C; these were further reduced on mixing. Thus, a 70:30 mixture of the pentene complex **12** (n = 12, m = 3)

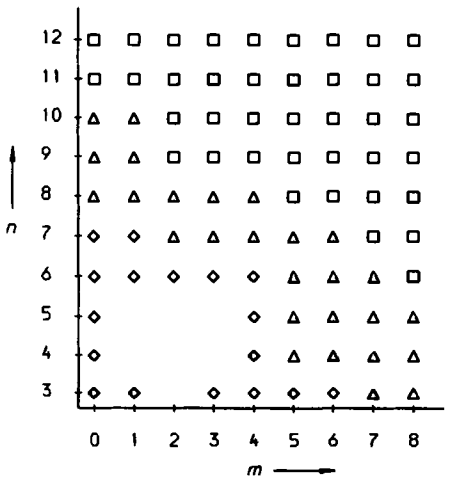

Fig. 9. The properties of the mesophases of *trans*-[$PtCl_2$(n-OST)-(CH_2=CHC_mH_{2m+1})] 12 as a function of n and m. ◇ non-mesogenic, △ monotropic, ◻ enantiotropic (after Ref. [20]).

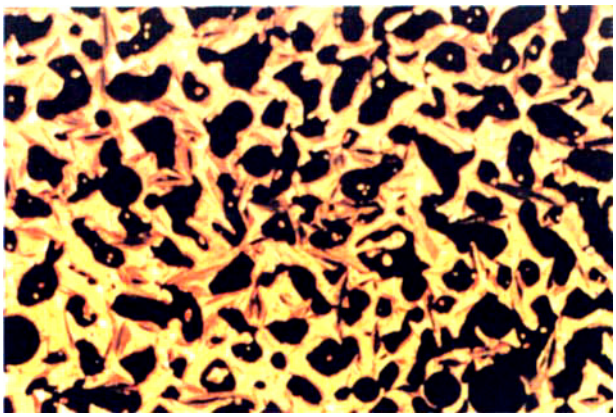

Color figure 2. Polarization microscopic photograph of the octene complex **12** during the transition from the isotropic liquid phase into the S_A mesophase.

and the related octene complex **12** (n = 12, m = 6) showed a much lower melting temperature (45 °C) than either component, while the clearing temperature (91 °C) remained unaffected (Fig. 10).

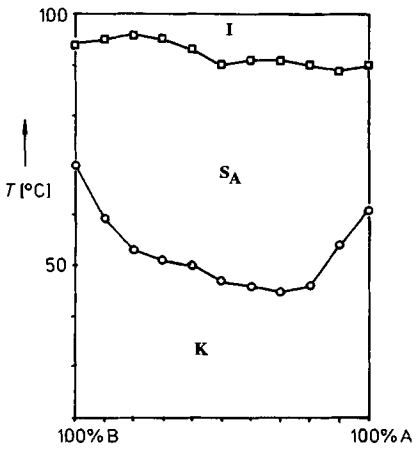

Fig. 10. Phase behavior of a mixture of the complex A (**12**; n = 12, m = 3) and B (**12**; n = 12, m = 6) (after Ref. [20]).

A series of unsymmetric stilbazole rhodium and iridium complexes **13** and **14** were prepared by the route shown in Equation (f). The burgundy iridium complexes **14** became yellow, both in solution and on melting, and showed nematic phases for n = 5–8, and S_A phases for n = 7–12, in the temperature range 80–130 °C (Table 2).[21] The rhodium com-

Table 2. Transition temperatures [°C] for mesomorphic alkoxystilbazole-rhodium(I) and -iridium(I) complexes[21].

Complex	Mesophases		
cis-[Rh(n-OST)$(CO)_2$Cl] **13**	S_A	N	I
n = 5	–	110	121 [b]
n = 6	–	106	124 [b]
n = 7	87	117	130 [b]
n = 8	85	123	130 [b]
n = 9	85	–	133 [b]
n = 10	82	–	137 [b]
n = 11	85	–	139 [b]
n = 12	82	–	143 [b]
cis-[Ir(n-OST)$(CO)_2$Cl] **14**	S_A	N	I
n = 5	–	(93) [a]	108
n = 6	–	106	110
n = 7	(87) [a]	92	113
n = 8	92	104.5	113
n = 9	87	–	121
n = 10	87	–	131
n = 11	88	–	133
n = 12	85	–	137

[a] Monotropic mesophase. [b] Clears with (some) decomposition.

plexes **13** behaved similarly but those with shorter alkoxy chains had lower melting and lower clearing temperatures. However for n = 12 the mesophase transitions were identical for the two metals.

$$[\{MCl(C_8H_{12})\}_2] + 2\,\text{n-OST} \xrightarrow{CO} \quad (f)$$

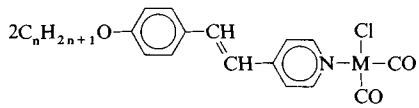

13, M = Rh; **14**, M = Ir

The mean electronic polarizabilities of the iridium complexes **14** (n = 5–12) were very substantially enhanced by comparison with those of the free ligands **10**.[22]

2.3. Complexes with Other Pyridine Ligands

Serrano et al. in Zaragoza have used other substituted pyridines as ligands for metallomesogen formation. Thus the *cis*-iridium complexes **16** containing the short-chain, non-

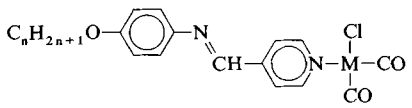

15, M = Rh; **16**, M = Ir

mesomorphic iminopyridine ligand (n-OIP, 4-alkoxy-*N*-(4-methylpyridine)aniline) formed nematic phases (mostly monotropic), while those with longer chains ($n \geq 9$) formed S_A phases.[23] These again had low transition temperatures, e.g. **16**, (n = 10, K→S_A 63 °C; S_A→I 85 °C) (Table 3). The related rhodium complexes **16** ($n \geq 8$) are also mesogenic;[24] e.g. **15**, (n = 9, K → S_A 76 °C; S_A→I 83 °C). It is quite remarkable that mesogenic complexes are formed here with a single organic ligand which is itself non-mesogenic. Further, and quite surprisingly, the *trans*-[Rh(n-OIP)$_2$(CO)Cl] complexes (n = 4, 8) were very high melting and showed no mesogenic character.[24]

Table 3. Transition temperatures [°C] for mesomorphic alkyloxyiminopyridineiridium(I) complexes[23].

Complex	Mesophases		
cis-[Ir(n-OIP)(CO)$_2$Cl] **16**	S_A	N	I
n = 5	–	–	72.1
n = 6	–	(56.9) [a]	88.2
n = 7	(35.3) [a]	(63.1) [a]	85.0
n = 8	(66.2) [a]	68.1	76.2
n = 9	63.8	–	75.2
n = 10	62.8	–	84.8
n = 12	70.1	–	92.1
n = 14	79.6	–	99.4
n = 16	84.4	–	104.1

[a] Monotropic mesophase.

The silver(I) complexes with n-OIP, [Ag(n-OIP)$_2$]Y **17** (Y = $BF_4^\ominus$, $CF_3SO_3^\ominus$, $NO_3^\ominus$, and $PF_6^\ominus$) and with the pyridine carboxylate ligand n-OCP [Ag(n-OCP)$_2$]Y **18**, also showed mesogenic behavior.[25] Only one salt, **17** (Y = $BF_4^\ominus$, n = 2), was nematic (194.9–223.8 °C); all the others showed S_A or S_C phases (for example, **17**, Y = $BF_4^\ominus$, n = 12, K→S 104 °C; S→N 195 °C; N→I 211 °C, with decomposition).

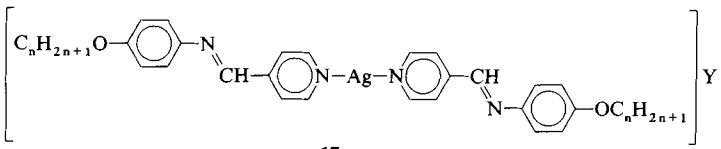

17

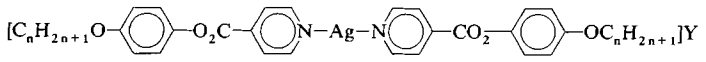

18

The ester salts **18** showed somewhat wider mesophase ranges and greater smectic polymorphism than the imino salts **17**, and smaller anions gave wider mesophases and lower melting points. Low angle X-ray data for four complexes with n = 10 showed the layer thickness in the mesophase to be 41–42 Å, i.e. shorter than the fully stretched linear cations (48 Å in **17**, 53 Å in **18**).[25]

2.4. Organometallic Complexes with $\eta^1(\sigma)$-Bonded Ligands

The first thermotropic metallomesogens were the smectic organomercury compounds **2**, described by *Vorländer* in 1923;[7] they were prepared by the condensation of bis(4-aminophenyl)mercury with aromatic aldehydes, RCHO, R = PhCH=CH, *p*-tolyl, or *p*-alkyloxyphenyl. All the compounds gave mesophases, and even those from benzaldehyde, R = Ph (mesophase 180–184 °C), as well as *p*-$MeOC_6H_4CH{=}NC_6H_4HgX$ (X = OAc, Cl) showed small mesogenic ranges. Unfortunately all these organomercury compounds are thermally unstable.

The very unusual organometallic liquid crystals **19** and **20** (M,M′ = Pd, Pt or Ni; M = M′ or M ≠ M′) have been made by *Takahashi* et al,[26] by a copper chloride–triethylamine coupling of the appropriate metal halide with an alkyne [Eq. (g)]. A wide variety of such compounds have been

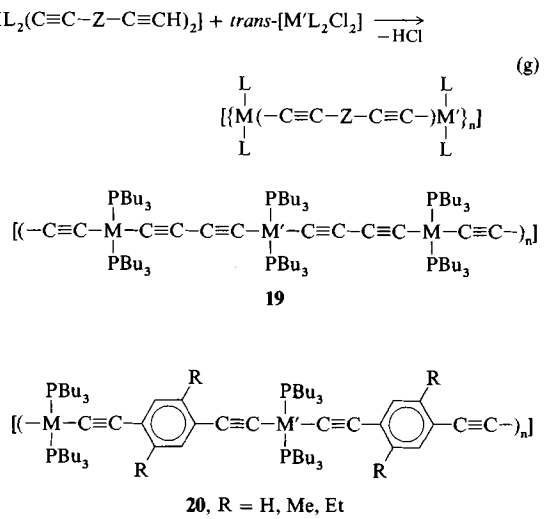

19

20, R = H, Me, Et

made. These materials are very high melting and do not show thermotropic properties; however, they are *lyotropic nematic* in trichloroethylene solution, and can be aligned in a magnetic field. Whether the particular polymer aligns perpendicular to the magnetic field or parallel to it is determined by its diamagnetic anisotropy $\Delta\chi'$, which in turn is dependent on the $\Delta\chi$'s of the components of the polymer. Thus, for example, $\Delta\chi$ for acetylene is negative, while it is positive for benzene and *p*-xylene.

2.5. Ferrocenes

A series of mesogenic ferrocenes **3** (which have an overall shape not too dissimilar to the mercury compounds **2**) were made by *Malthête* and *Billard* in 1976,[9] by condensation of the appropriate benzaldehyde derivative with 4-aminophenyl ferrocene carboxylate. Recently, it was shown with the ferrocene carboxylic acid building block that the bis-substituted ferrocene [Fe(C_5H_4–COO–C_6H_4–C_6H_4–X)$_2$] gave monotropic S_C phases for X = $C_5H_{11}O$, and C_6H_{13}, whereas the monosubstituted [Fe(C_5H_5)(C_5H_4–COO–C_6H_4–C_6H_4–X)] was non-mesogenic.[27]

3. Metallomesogens with Carboxylato ligands

Metal soaps have long been known to have mesogenic properties. Thus, in 1910 *Vorländer* reported the existence of

lamellar phases in the anhydrous salts of alkali carboxylates,[6] and in 1938 *Lawrence* noted that copper stearate, for example, melted from a hard crystalline solid to a plastic fluid, which then transformed into a clear liquid.[28]

3.1. Alkali and Alkaline Earth Carboxylates

Structural data, indicating the existence of columnar and even disklike mesophases for the anhydrous alkali, alkaline earth, and cadmium salts of long-chain fatty acids ($C_nH_{2n+1}COOH$, n = 9, 11, 13, 15, 17, 19), were first reported by *Skoulios* et al.[29] The transition temperatures increased with increasing chain length, and several types of structure were found, depending on the metal (Fig. 11).

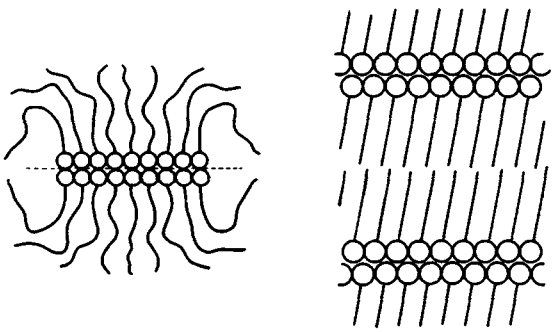

Fig. 11. Structures found in the mesophases of anhydrous alkali-metal carboxylates (after Ref. [29]).

Thus, the potassium salts can be: 1) lamellar, with ordered polar groups and alkyl chains; 2) lamellar with disordered polar groups and alkyl chains; 3) ribbonlike; or 4) disklike in a three-dimensional lattice. In the latter two, the polar groups are ordered while the alkyl chains are disordered.[30] As well as exhibiting thermotropic properties the alkali metal soaps also show lyotropic behavior with solvents.

The calcium carboxylates, for example, showed a lamellar phase below 110 °C with the paraffin chains perpendicular to the lamellae; between 120 and 180 °C the structure becomes disklike, while above 180 °C it consists of cylinders in a two-dimensional hexagonal array (Fig. 12). This last mesophase is also found for the cadmium soaps.

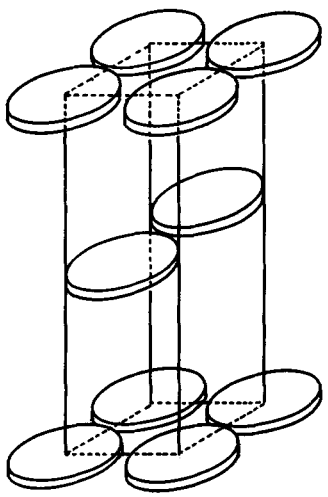

Fig. 12. Disklike structure adopted by anhydrous calcium carboxylate (after Ref. [30]).

3.2. Lead, Mercury and Thallium Carboxylates

S_C phases have been reported for the lead(II) carboxylates, $[Pb(C_nH_{2n+1}COO)_2]$ where n = 5, 7, 9 and 11.[31] The compounds (with n = 7, 9, 11, 13, 15, and 17) investigated further by DSC, optical microscopy, X-ray diffraction and various spectroscopic techniques, were found to transform from a lamellar crystalline to another lamellar highly ordered phase (between 80–100 °C, depending on chain length) and then to melt (at ca. 100 °C) to S_A phases (for n = 7, 9, 11). The alkyl chains melt in more than one step and, on recooling, a crystalline phase different from the original results.[32] The mercury carboxylates, $[Hg(O_2CC_nH_{2n+1})_2]$ (n = 7–17), are not mesogenic, but $[Tl(O_2CR)]$ with branched alkyls R, gave stable lamellar phases.[33]

3.3. Discotic Dinuclear Copper Carboxylates

The liquid crystalline phase obtained on heating copper stearate $[Cu_2(\mu\text{-}O_2CC_{17}H_{35})_4]$ was reinvestigated in 1964;[34] but it was not until considerably later that it was definitively characterized.[35] *Giroud-Godquin* et al.[36] identified the mesophase of copper laurate as hexagonal columnar (Fig. 13) by DSC, optical microscopy, and X-ray diffraction. This was the first example of a thermotropic hexagonal

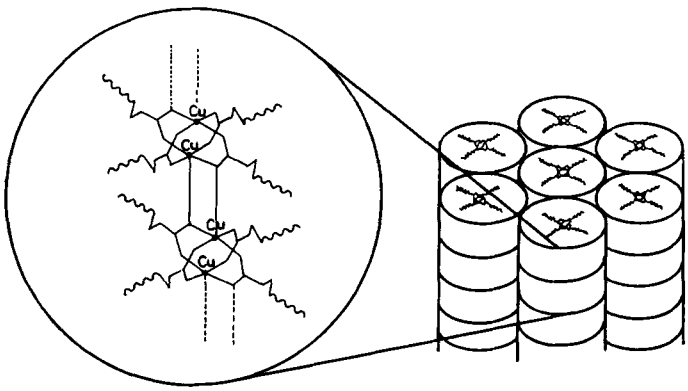

Fig. 13. Schematic view of the columnar mesophase of a copper(II) soap. Each column is made of stacked dicopper tetracarboxylate units. The polar "inorganic" cores are surrounded by disordered alkyl chains. The column axes define a two-dimensional hexagonal lattice (after Ref. [41]).

discotic mesophase bearing only four alkyl chains. The other carboxylates, $[Cu_2(\mu\text{-}O_2CC_nH_{2n+1})_4]$ (n = 4–24), showed the same structures. The X-ray studies showed that the complexes crystallize in lamellar structures, in which planes of polar copper carboxylate groups are separated by a double layer of aliphatic chains, slightly tilted with respect to the perpendicular of the plane. The lamellar spacing is a function of chain length. Above 120 °C there exists a columnar two-dimensional hexagonal structure in which columns of polar groups are surrounded by disordered alkyl chains. The dinuclear

$[Cu_2(\mu\text{-}O_2CC_nH_{2n+1})_4]$ unit is repeated along the column, with a stacking period of 4.7 Å independent of chain length, n; the columns are 15–25 Å apart, depending on n. A sharp increase in the molar volume at the transition temperature, consistent with a first order phase transition, was observed in dilatometric studies of $[Cu_2(\mu\text{-}O_2CC_nH_{2n+1})_4]$ (n = 18, 22, 24).[37]

X-ray single crystal data of copper carboxylates show them to be dinuclear (Fig. 14) with each copper surrounded by five oxygen atoms at a mean distance of 2.01 Å, one copper atom at a distance of 2.59 Å (its neighbor within a dimer), and another copper atom at 3.19 Å, belonging to the closest neighboring dimer.[38] The Cu-K edge EXAFS (*E*xtended *X*-ray *A*bsorbtion *F*ine *S*tructure) data on $[Cu_2(\mu\text{-}O_2CC_nH_{2n+1})_4]$ (n = 6, 7, 12, 18 and 22) confirmed this and also showed that the bond lengths of the dinuclear core remained the same at 20, 70, and 120 °C; i.e., no change was detectable on going from the solid to the mesophase.[39] Magnetic susceptibility measurements showed a small but sharp decrease in the magnetic moment of the dicopper unit at the transition temperature ($\Delta\mu_{eff} \approx -0.04\ \mu_B$). This was ascribed to a structural deformation of the dinuclear core, as a consequence of which the singlet–triplet gap is higher in the columnar mesophase ($-2J = 310-330\ cm^{-1}$) than in the crystal ($290-300\ cm^{-1}$).[40] Since the EXAFS data indicate no change in bond lengths, the phase change probably affects only the bond angles.[41]

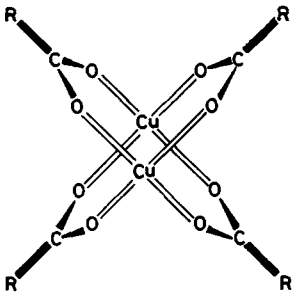

Fig. 14. Crystal structure of a dinuclear copper carboxylate.

Isotopic labeling has facilitated band assignments in the IR spectra of these complexes, allowing the detection of structural variants from changes in the methylene stretching frequency.[42] The dynamic behavior of the alkyl chains in copper carboxylates has been studied by incoherent quasielastic neutron scattering.[43]

Copper laurate has also been melt spun into fibers in its mesophase by the Grenoble group;[44] electron microscopy and X-ray diffraction measurements indicate that the fibers have high degrees of orientation both in the crystalline and the columnar phases.

3.4 Discotic Dinuclear Rhodium, Ruthenium, and Molybdenum Carboxylates

The rhodium(II) carboxylates, $[Rh_2(\mu\text{-}O_2CC_nH_{2n+1})_4]$, behave very similarly to the copper complexes,[45] and form columnar thermotropic mesophases of the same structures. Rh K-edge EXAFS measurements of $[Rh_2(\mu\text{-}O_2CC_7H_{15})_4]$ again show negligible differences between the dimensions in the crystal and in the mesophase [intramolecular, metal–metal bonded, Rh–Rh 2.38 (20 °C), 2.37 Å (120 °C); intermolecular Rh···Rh 3.16 Å (20 and 120 °C)]. A band at 350 cm^{-1} has been assigned to ν(Rh–Rh) in the Raman spectrum; these are the first metal–metal bonded compounds which show a two-dimensional hexagonal columnar lattice.[41]

The Grenoble group has also shown that the air-sensitive dinuclear Ru^{II} and the mixed valence Ru^{II}–Ru^{III} carboxylates, $[Ru_2(\mu\text{-}O_2CC_nH_{2n+1})_m]$ (m = 4 or 5), form thermotropic columnar mesophases.[41, 46] They are prepared by Cr^{II} reduction of the mixed valence (and non-mesogenic) $[Ru_2Cl(O_2CC_3H_7)_4]$, followed by carboxylate exchange. The magnetic moment of $[Ru_2(\mu\text{-}O_2CC_{15}H_{31})_4]$ increased sharply at ca. 100 °C, and a change, corresponding to the transition to the columnar mesophase, was also detected by DSC and X-ray diffraction. The quadruply bonded Mo≡Mo carboxylates $[Mo_2(O_2CC_nH_{2n+1})_4]$ form analogous discotic mesophases.[46b]

4. Mesogenic β-Diketonato Complexes

β-Diketonates form flat bis-ligand complexes with a variety of metals that can take up square planar geometries (including Ni, Pd, and Cu). When appropriate substituents are present, copper(II) diketonate complexes can give rise to discotic mesophases; nematic and occasionally lamellar mesophases have also been found. Mesogenic behavior seems to be optimized when the molecules have two pairs of *p*-substituted phenyls, situated 1,3 on each diketone. Some other variations are also tolerated. The complexes are easily made by reaction of the β-diketone with the appropriate copper salt.[47] Mesogenic β-diketones of other metals appear, so far, to have largely eluded workers in the field, though the synthesis of a discotic vanadyl β-diketonate analogous to **26** has recently been accomplished.[47b]

The first β-diketonate to be examined for mesophase behavior was the palladium(II) complex, **21**. *Bulkin* et al.[48] reported that DSC data for this complex indicated potential mesomorphism, but were unable to confirm this optically because the complex darkened on heating.

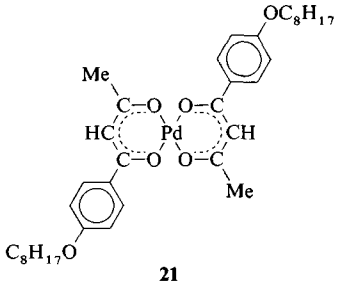

21

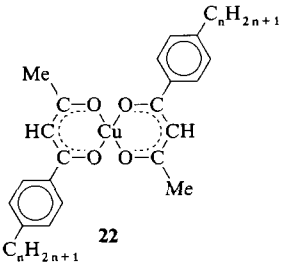

22

No liquid crystal properties were found for the copper(II) complexes **22** either.[49, 50] Only crystal-crystal transitions were observed; the polymorphism in the solid depended on chain length and showed an odd–even effect, but involved no change in coordination geometry.[51]

4.1. Copper Complexes of 1,3-Bis(*p*-substituted-phenyl)-*β*-diketones

The 1,3-bis(*p*-substituted-phenyl)-*β*-diketones **23** and **24** are prepared by a standard condensation of the *p*-substituted acetophenone with the corresponding *p*-substituted methyl benzoate [Eq. (h)].[52] Ligands **23** with $m + n \geq 18$ exhibit smectic E phases, and show the unusual feature that the enthalpy changes observed on clearing are larger than those found on melting.[53] This situation is frequently observed for discotics but is exceptional for rodlike mesogens.[54]

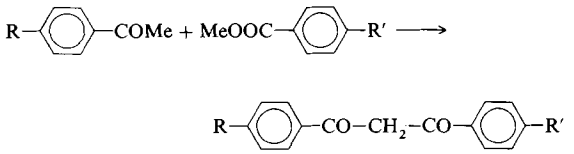

(h)

23, $R = C_mH_{2m+1}$, $R' = C_nH_{2n+1}$
24, $R = C_mH_{2m+1}O$, $R' = C_nH_{2n+1}O$

The mesogenic copper(II) *β*-diketonates **25**, first described by *Giroud-Godquin* et al.[53, 55] in 1981, have a square planar geometry about the metal[56] and a d^9 configuration (one unpaired electron).[47] Both the symmetrically and the unsymmetrically substituted complexes **25** ($m = n$ or $m \neq n$) exhibit very organized discotic mesophases. The more symmetric have the higher melting and clearing temperatures and the larger molar enthalpy changes, for example **25** ($m = 7$ and $n = 13$; 71–122 °C) and **25** ($m = n = 10$; 85.5–128.5 °C).[53] Later work on these complexes, particularly NMR investigations of the spin-lattice relaxation time T_1,[57]

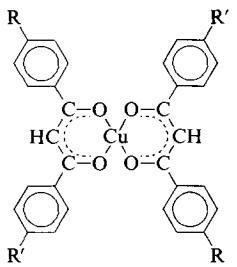

25, $R = C_mH_{2m+1}$, $R' = C_nH_{2n+1}$
26, $R = C_mH_{2m+1}O$, $R' = C_nH_{2n+1}O$
27, $R = C_mH_{2m+1}$, $R' = C_nH_{2n+1}O$

suggested that a lamellar phase is present, where the disklike molecules are organized in columns as shown in Figure 15. The complexes **25** ($m = n = 7-12$) and **26** ($m = n = 8$) also showed discotic mesophases;[53, 58, 59] the mesophase range for the alkyloxy ligand **24** with $m = n = 8$ was narrower than that for the alkyl ligand **23** with $m = n = 8$, but the opposite was true for the copper complexes **25** and **26** derived from them. Nickel analogs of **25** showed no mesogenic character.[53]

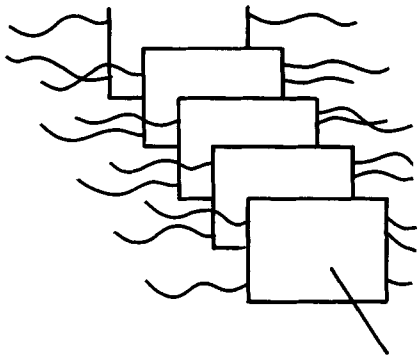

Fig. 15. Schematic representation of the tilted discotic lamellar phase of **25** ($n = 12$) (after Ref. [53]).

Eastman et al.[60] have found that the ESR spectra of single crystals of the symmetrical copper complex **25**, ($m = n = 8$) show features at 298 K associated with a one-dimensional Heisenberg antiferromagnet, while those of complex **26** do not. These workers also followed the phase changes by ESR spectroscopy, and in both cases detected a crystalline to discotic transition. The ESR spectra of complex **25** have been interpreted as showing that exchange interactions are significant and that a degree of long range order is maintained in the discotic phase.

The ligand *β*-diketones **24**, ($m = n$) showed triple melting behavior for $n = 1$, double melting for $n = 2-7$, and were mesogenic (smectic) only for $n = 8-12$,[61] but each of the copper complexes **26** derived from them ($m = n = 3-12$) had only one discotic mesophase. X-ray diffraction established that the mesophase in complex **25** ($n = 12$) is discotic lamellar, characterized by a tilt of the molecule to the layer and by a random positioning of the molecules within the layer (Fig. 16); there was no columnar structure.[62]

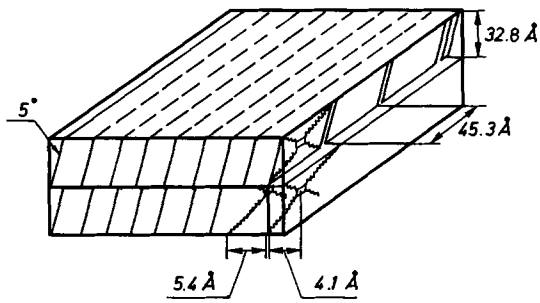

Fig. 16: Schematic representation of the structure of the discotic lamellar phase (D_L) of **25** ($n = 12$) (after Ref. [53]).

A reinvestigation of the mesophase originally identified for the unsymmetrical complexes **27** has shown that it is lamellar when $m = n = 5-12$).[63]

A very interesting discovery, by *Chandrasekhar* et al.[64, 65] is that the mesophases of the copper(II) complexes of the

dialkyl- and of the alkyl,alkyloxy-substituted β-diketonates **28** (R′ = Me, Et, OMe, OEt, and OPr) are monotropic nematic, and are miscible with a nematic organic compound, 4″-*n*-pentyl-4-cyano-*p*-terphenyl (5-CT). These complexes incorporate features of both rodlike and disklike molecules,

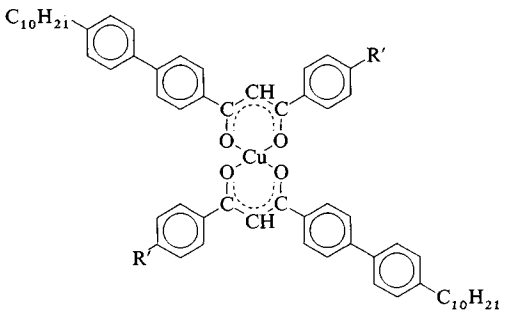

28

and are claimed to be the first examples of biaxial nematic metallomesogens.[66, 67] On addition of small quantities of the uniaxial nematic 5-CT, the sequence of transitions, isotropic → $N_{uniaxial}$ → $N_{biaxial}$, was observed on cooling. Magnetic, dielectric, and ESR measurements indicated the existence of antiparallel correlations in the nematic phase.

The biphenylylphenyl-substituted 1,3-propanediones **29**, the parent diketones of this series, also showed mesomorphic character.[68] Those with n = 4–7 showed both S_A and N phases, the higher ones only S_A phases.

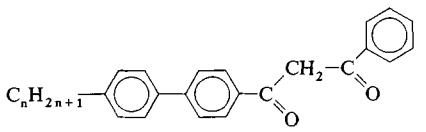

29

X-ray studies of the 4″-alkylcyclohexylphenylalkyl analogs **30** of the Chandrasekhar complexes **28** by *Mühlberger* and *Haase*[69] showed that the β-diketonate ring was planar and that identical substitutents were *trans* to each

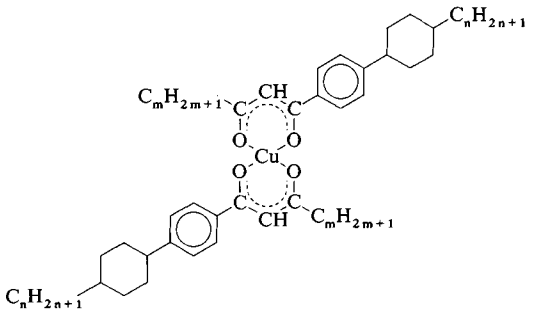

30

other (Fig. 17). These complexes only gave monotropic nematic phases, but an enantiotropic nematic phase was obtained by mixing **30** (n = 3, m = 8) and the organic nematic 5-CT.

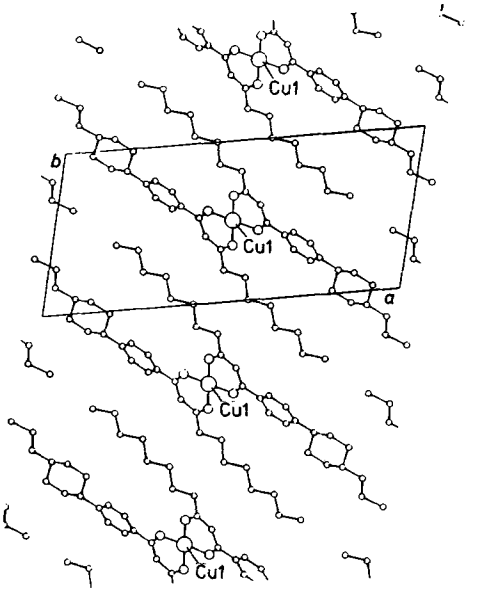

Fig. 17. Crystal structure of **30** (n = 3, m = 8). Projection along the lattice plane (001) (after Ref. [69]).

4.2. Copper Complexes of 1,3-Bis(3,4-disubstituted-phenyl)-β-diketones

Early studies had indicated that at least six *n*-alkyl tails were needed on a disklike core in order to obtain a columnar mesophase.[70] *Giroud-Godquin* et al.[71, 72] reported four columnar copper β-diketonate complexes **31**; the phenyls at the ends of the β-diketonate were each substituted (3,4) by two alkyloxy substituents, giving a total of eight tails. These complexes were shown to have a hexagonal columnar (D_h) mesophase by miscibility studies with the triphenylene

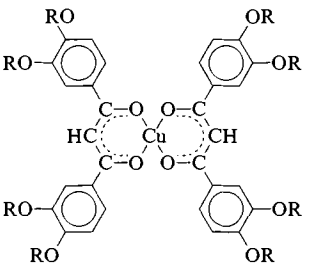

31

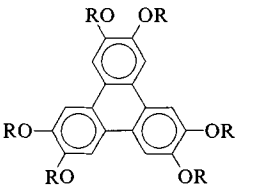

32

hexadecylalkanoate **32** (R = $C_{15}H_{31}CO$), an organic disklike molecule.[73] X-ray diffraction of the complex **31**, (R = C_9H_{19}) showed neighboring columns to be 29 Å apart in the mesophase; this value is substantially smaller than the molecular diameter with stretched conformation of the aliphatic chains (42 Å).[71]

The nickel complex corresponding to **31** showed no mesophase, neither did the copper complexes in which the phenyl was substituted in the 3,5 rather than 3,4 positions. The copper complex of the asymmetric β-diketonato ligand **29′** with R^1 = C_9H_{19} also showed a D_h mesophase, but those with R^1 = C_3H_7 or C_7H_{15} were not mesogenic.[72] Similar complexes were studied by *Ohta*[74] who found (by optical and DSC measurements) that the β-diketonates with four

pairs of OC_8H_{17} substituents in the 3,4 positions of the phenyl rings showed discotic mesophases. However the corresponding complex with four pairs of n-C_8H_{17} tails was not discotic.

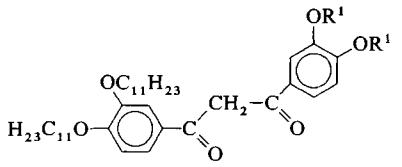

29'

Preliminary measurements suggested that the presence of a transition metal in a discotic mesogen such as **31**, (R = C_9H_{19}) may enhance the electrical conductivity in the uniaxial columnar (D_h) mesophase; the complex also gels in cyclohexane.[71]

4.3. Other Metal β-Diketonates

The octahedral iron(III) tris-β-diketonate Fe(RCOCHCOR)$_3$ **33** (R = $C_{10}H_{21}C_6H_4$) shows endothermic transitions at −10.5 °C (ΔH = 13.7 kJ mol^{-1}) and 37 °C (ΔH = 40.0 kJ mol^{-1}), and a birefringent structure within this range.[75] If confirmed, this would be the first octahedral metallomesogen.

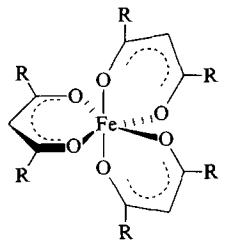

33

5. Metallomesogens with Sulfur-containing Ligands

5.1. Dithiolene Complexes

The first systematic study of d-block metallomesogens was carried out by *Giroud* and *Müller-Westerhoff* on dithiolene complexes of Ni^{II}, Pd^{II}, and Pt^{II} (d^8 electron configuration).

The main series investigated, complexes **34** with two *p*-alkylphenyl substituents, were synthesized by the route outlined in Scheme 1.[10, 76–78] A single crystal X-ray diffraction of the nickel complex **34**, (M = Ni, n = 8) showed the expected M^{II} square planar geometry, with the substituents in a *trans*-conformation. The molecules are arranged zig-zag in layers in the unit cell (Fig. 18); this is the arrangement which would be anticipated as the precursor to a smectic C phase.[79]

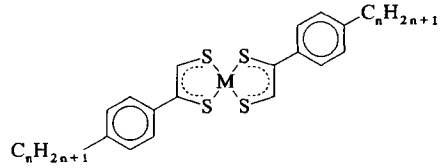

34, M = Ni, Pd, Pt

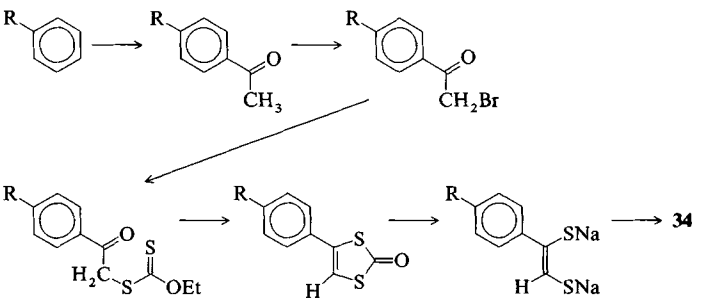

Scheme 1. Synthetic route for the bis(alkylphenyl)dithiolene metal complexes **34**.

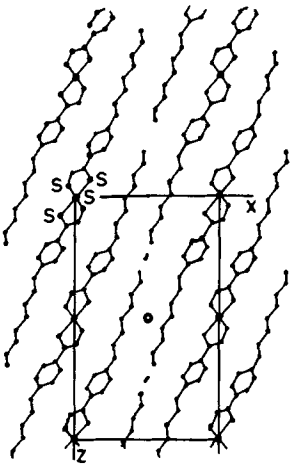

Fig. 18. The packing of a complex **34** (n = 8) in the unit cell (after Ref. [79]).

The Ni and Pt complexes **34** (M = Ni, Pt; n > 6) formed nematic and smectic mesophases (Table 4); those with n = 4,5 showed nematic and those with n > 6 showed only

Table 4. Transition temperatures [°C] for mesomorphic bis(alkylphenyl)dithiolene nickel and platinum complexes [78].

Complex	Mesophases		
trans-[Ni($C_nH_{2n+1}C_6H_4C_2HS_2$)$_2$] **34**	S_A	N	I
n = 4		117	175 [a]
n = 5		133	185 [a]
n = 6	139	169	181 [a]
n = 7	130	–	185 [a]
n = 8	121	–	191 [a]
n = 9	108	–	191 [a]
n = 10	103	–	189 [a]
trans-[Pt($C_nH_{2n+1}C_6H_4C_2HS_2$)$_2$] **34**	S_A	N	I
n = 4		158	202
n = 5		167	202
n = 6		175	200
n = 7	169	–	199
n = 8	150	–	209
n = 9	146	–	205
n = 10	140	–	202

[a] Clears with (some) decomposition.

smectic phases. The platinum complexes had significantly higher melting and clearing temperatures than the nickel analogs, but the clearing temperatures became more similar with larger n. The reason why the palladium analogs do not possess any mesomorphic properties is not clear.

The overall molecular structure of **34** is reminiscent of the organic 4,4″-dialkylterphenyls **35**, which form smectic mesophases when n = 3–18.[80] The melting points and the mesophase ranges of **35** are higher than those of the corresponding complex; for example, the smectic range is 161–181 °C for **35**, (n = 10), 103–189 °C for the nickel complex **34**, (M = Ni, n = 10), and 140–202 °C for the platinum complex **34**, (M = Pt, n = 10).

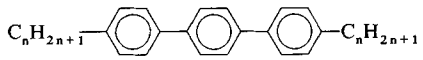

35

The dithiolenes have interesting electron acceptor properties and unusual electronic structures, with strong absorption bands ($\lambda_{max} > 750$ nm, $\varepsilon > 25\,000$). Smectic and nematic derivatives of the nickel dithiolenes **34** with a strong electron donor, tetrathiafulvalenes **36**, were synthesized, but no charge transfer complex resulted.[81]

The complex **34** (M = Ni, n = 4), dissolved in the cyanobiphenyl **4** (n = 5), has been shown to be useful as a near-infrared dichroic dye in active and passive devices for lasers operating near 800 nm. The solubility and blocking

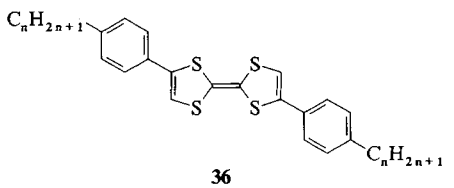

36

extinction of this complex were considerably superior to the structurally similar but non-mesogenic laser dye, [Ni-(3-$Me_2NC_6H_3CSCSC_6H_5)_2$].[82]

Analogous di- and tetrasubstituted nickel dithiolenes **37** (R = *p*-$C_{12}H_{25}OC_6H_4$; R′ = H or R′) prepared by *Strzelecka* et al.[83] were originally tentatively described as discotic mesogens. However, recent X-ray data for **37** (R = R′ = *p*-$C_nH_{2n+1}OC_6H_4$, n = 9, 11, and 13) showed that the phase changes were between different crystal forms

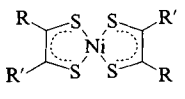

37

(K → K′) and that these compounds were not mesogenic.[84] In 1986 *Ohta* et al. reported that the tetraalkoxyphenyl compounds **37** (R = R′ = *p*-$C_9H_{19}OC_6H_4$, and R = R′ *p*-$C_{11}H_{23}OC_6H_4$) also formed discotic mesophases; this report was based on the miscibility of the two compounds giving a eutectic, and other optical observations.[85] No X-ray data are yet available to confirm the claim. However, the related nickel dithiolene **38** with four 3,4-bis(dodecyloxy)phenyl substituents was shown by X-ray diffraction to give rise to a hexagonal disordered columnar (discotic) mesophase (D_{hd}).[86]

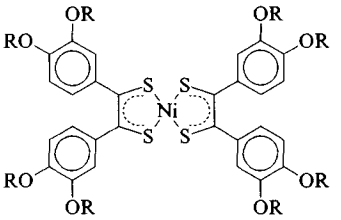

38, R = $C_{12}H_{25}$

5.2. Dithiocarboxylates

Dithiocarboxylates ($RCS_2^{\ominus}$) and xanthates ($ROCS_2^{\ominus}$), which react with metals to give MS_2C four-membered rings, are related to the dithiolenes, which form five-membered MS_2C_2 rings.

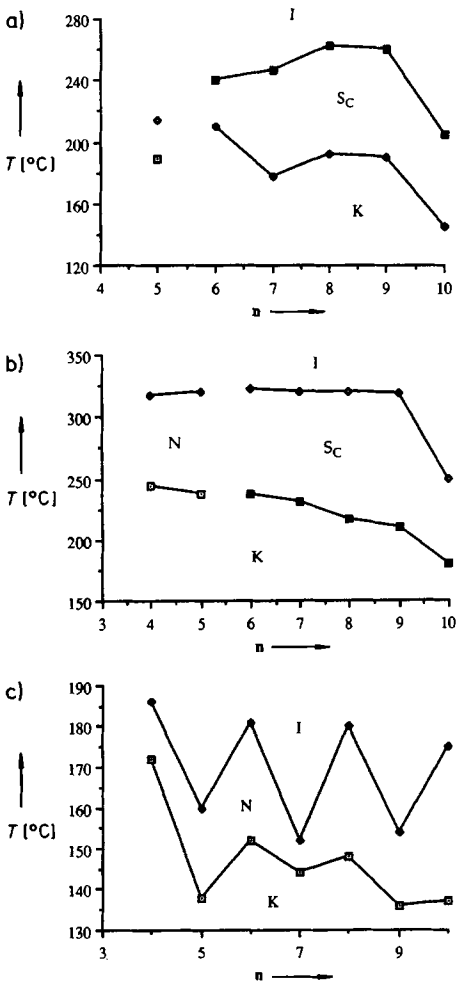

Fig. 19. Phase diagrams of complexes of the type **39**. a) M = Ni; □ K → N, ● K → S_C, ■ S_C → I, ◇ N → I. b) M = Pd; □ K → N, ◆ N → I, □ K → S_C, ◇ S_C → I. c) M = Zn; ⊡ K → N, ◆ N → I. Various mesophases occur depending on the metal (after Ref. [87]).

Studies by the Sheffield group on the bis(4-alkyloxydithiobenzoato) complexes showed that the Ni^{II} and Pd^{II} complexes **39** (M = Ni, Pd) were mesogenic (Fig. 19a, 19b).[87, 88] Optical microscopy, combined with an X-ray diffraction and DSC (XDDSC) study, confirmed the occurrence of S_C mesophases for palladium complexes **39** with longer-chain ligands (e.g. n = 8; 214–320 °C) and of N phases in the case of shorter-chain ligands (n = 4,5).[118] Similar results were obtained for the nickel complexes, **39**, (M = Ni).

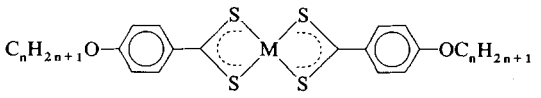

39

The single crystal X-ray structure analysis of the palladium complex **39** (M = Pd, n = 8; Fig. 20) showed it to be composed of monomeric species, with square-planar coordinated Pd centers (four Pd–S bonds with bond lengths of 2.29–2.35 Å), loosely associated into dimers via long intermolecular Pd···S contacts (≥ 3.38 Å).[88]

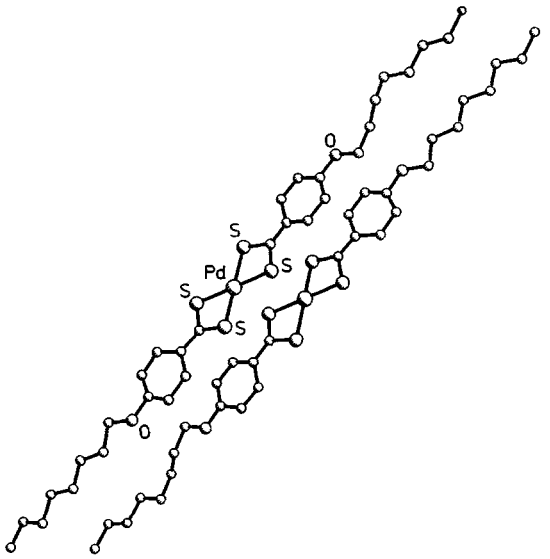

Fig. 20. Crystal structure of a complex **39** (M = Pd, n = 8) (after Ref. [88]).

The molecular structure of the unsubstituted bis (dithiobenzoato) zinc complex (Fig. 21)[89] suggested that even a tetrahedrally coordinated metal center would induce such compounds to form rodlike mesogens. Mesophases were indeed observed for the dialkyloxy-substituted zinc complexes **39** (Fig. 19c). However, although monomeric in solution, single crystal X-ray diffraction studies showed that in the solid the molecules are dinuclear with an eight-membered $Zn_2S_4C_2$ ring, making each zinc effectively five-coordinate (Zn–S 2.22–2.77 Å, Fig. 22).[87, 88]

Recent single crystal X-ray data on the related bis(4-alkyloxydithiobenzoato)mercury complexes $Hg(S_2CC_6H_4OR)_2$ (R = C_4H_9 and C_8H_{17}; nematic phases at 178–192 °C and 137–200 °C, respectively), indicate that these too have a

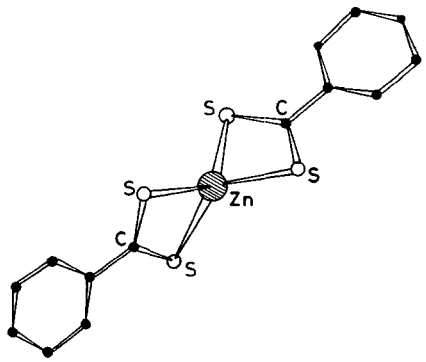

Fig. 21. Structure of $[Zn(S_2CPh)_2]$ (after Ref. [89]).

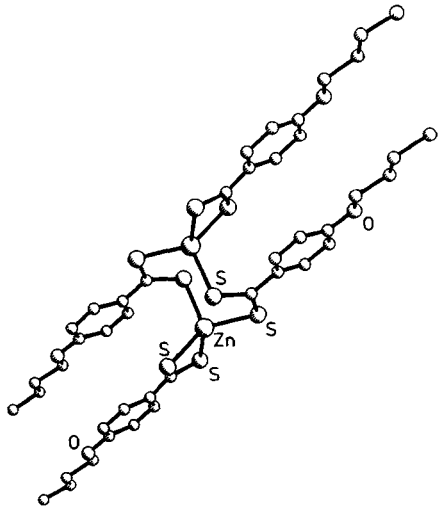

Fig. 22. Crystal structure of a complex **39** (M = Zn, n = 4) (after Ref. [88]).

more complex coordination geometry than might be expected: two shorter *trans* Hg–S bonds (2.41 Å) and two longer *trans* Hg–S bonds (2.96 Å) in the same plane, with two additional axial intermolecular Hg···S contacts (3.36 Å, Fig. 23).[90]

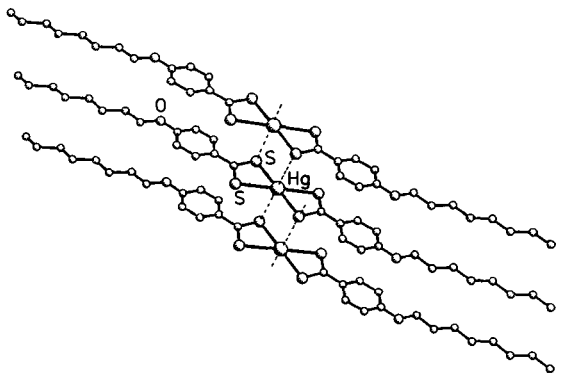

Fig. 23. Crystal structure of a complex **39** (M = Hg, n = 8).

Again, the metal center, as in the Pd complex (Fig. 20), is planar and not tetrahedrally coordinated. An effect of the alkyloxy chains, which confer mesomorphism, also appears to be to reduce the tendency towards tetrahedral geometry at the metal center.

The use of **39** (M = Ni, Pd) in display and thermal recording materials has in the meantime been patented.[91]

The dimeric tetrakis(*n*-alkyldithiocarboxylato)dinickel complexes **40** (R = C_5H_{11} to $C_{12}H_{25}$) have been described; they show monotropic lamellar mesophases with broken fan textures. Identification of the phases has been checked by

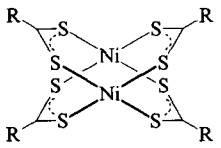

40

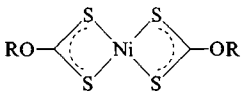

41

X-ray measurements. The corresponding monomeric xanthates, [Ni($ROCS_2$)$_2$] **41** (R = CH_3 to $C_{12}H_{25}$) exhibit complex double- and triple-melting behavior.[92]

6. N_4-Macrocycles and Other Polyamine ligands

In view of the range of polyamine ligands, it is not surprising that they also occur as components of metallomesogens. The discotic metallophthalocyanines, first studied by *Simon* et al. in Paris,[93] are especially interesting.

6.1. Phthalocyanine Complexes

6.1.1. Copper Complexes

Discotic metallophthalocyanines **42** (M often Cu) were originally envisaged as one-dimensional conductors, but also have other potential applications.[93] A typical synthetic path to such compounds is presented in Scheme 2. The copper phthalocyanine **42** with eight dodecyloxymethylene substituents (R = $CH_2OC_{12}H_{25}$) gave a stable mesophase be-

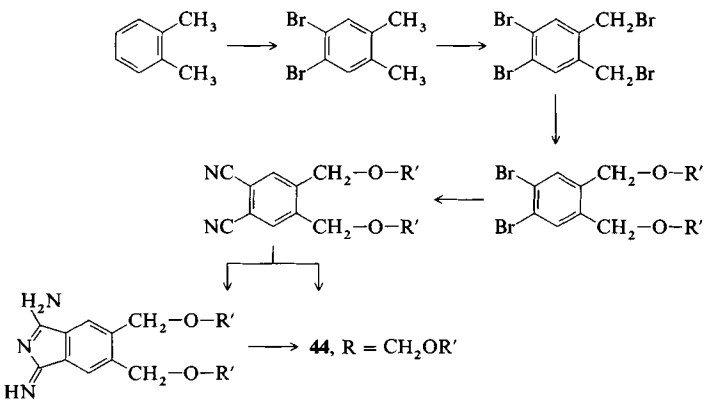

Scheme 2. Synthetic route for octakis(alkoxymethylene)phthalocyanine (after Ref. [100]).

tween 53 and ca. 300 °C; X-ray data indicated that the macrocycles are stacked at a distance of 4.5 Å in columns, with the columns ca. 31 Å apart (Fig. 24).[93]

Discotic columnar mesophases (D_{ho}) were also found in the case of complexes **42** (R = $CH_2OC_nH_{2n+1}$, and

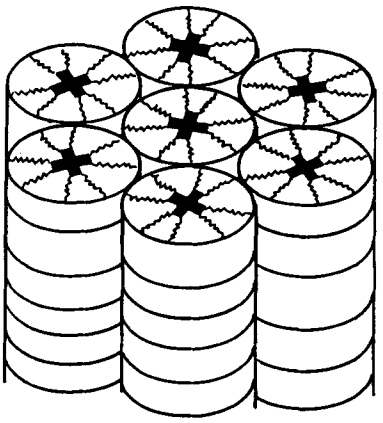

Fig. 24. Structure of the discotic mesophase of **42** (R = $CH_2OC_{12}H_{25}$). The zig zag tails from the central unit symbolize the substituents on the phthalocyanine ring.

OC_nH_{2n+1}, n = 6–11) by *van der Pol* et al.[94] The transition temperatures (as well as the related enthalpies and entropies) are only slightly different from those of the corresponding metal-free molecules. X-ray data showed inter-disk distances

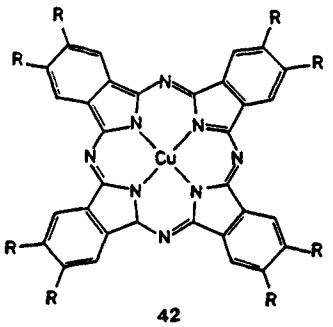

42

within one stack of 3.4 Å. Copper phthalocyanines **43** bearing four benzo[15]crown-5 substituents have also been made; they stack to give channels through which ions may be transported.[95]

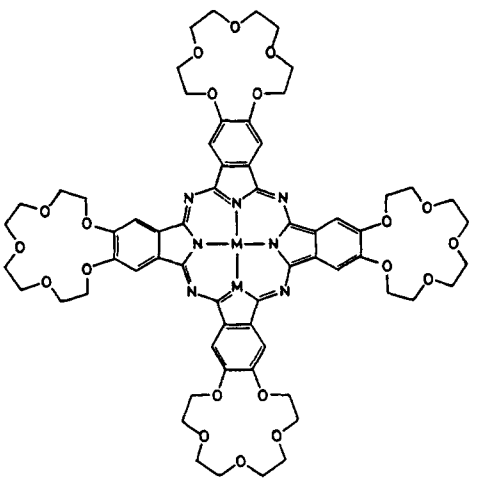

43

Although ESR spectra indicated good electron mobility in **42** (R = $CH_2OC_{12}H_{25}$),[93] the complexes are semiconductors with mesophase conductivities very similar to that of the unsubstituted and non-mesogenic copper phthalocyanine itself ($\sigma = 6 \times 10^{-8}\,S\,m^{-1}$ at 175 °C);[94] a slight decrease in conductivity was found on going from the solid to the mesophase. As is very often found with insulating or semiconducting materials, the conductivity increased by several orders of magnitude on doping with I_2.[94, 96]

Van der Pol et al. examined the luminescence properties of **42** (R = $CH_2OC_{12}H_{25}$) as a function of temperature, and found a sharp drop in intensity at the melting point.[97]

Interestingly, many of the metal-free phthalocyanines themselves are discotic, for example **44** (R = $CH_2OC_{12}H_{25}$) has a structure very similar to that of its copper complex.

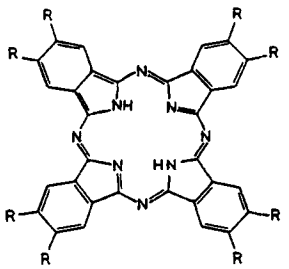

44

The stacking distance here is 4.5 Å and the columns form a hexagonal lattice with the columns 31.2 Å apart; X-ray diffraction measurements on the phthalocyanine **44** (R = 2-$EtC_6H_{12}OCH_2$) show a nematic phase.[93] Many other discotic metal-free phthalocyanines have also been made.[98]

A cholesteric columnar copper complex **42** (R = $C_{12}H_{25}OC^*H(Me)CH_2OCH_2CH_2$), with eight optically active substituents on the phthalocyanine ring, has been reported.[99] Differences in mesophase behavior between the chiral material and its achiral analog (with racemic $C_{12}H_{25}OCH(Me)CH_2OCH_2CH_2$ substituents) were found; the chiral material showed polymorphism, while the achiral analog showed only one mesophase.

6.1.2. *Mn, Co, Ni, and Zn Phthalocyanines*

Complexes of Co, Ni, and Pb with the phthalocyanine **44** (R = $CH_2OC_8H_{17}$) exhibit mesophases below 100 °C;[100] the cobalt compound reacts with NaCN to give a polymeric material, thought to be **45**. Discotic zinc and manganese complexes of **44** (R = $CH_2OC_{12}H_{25}$) have also been reported.[101]

The use of liquid crystalline host materials containing colored compounds, which absorb laser light and cause local heating, has been considered for laser addressed devices.[102] The brightly colored phthalocyanines, their benzo-homologues (the naphthalocynines), and eight complexes with Cu, and one each with Ni and Zn, have been investigated for this purpose. Major changes in spectra are achieved by introduction of nuclear alkyloxy substituents; changing the metals offers the opportunity for further spectral fine tuning. Moreover, the parent compounds and the metal complexes with

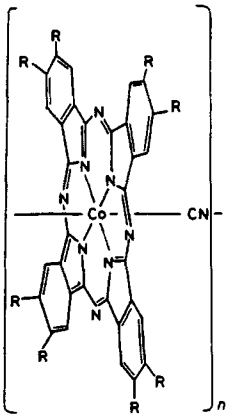

45

long chain alkyls dissolve in nematic liquid crystals, which is also useful. A variety of mesophases was found, again below 100 °C for longer chain substituents. The textures of one mesophase are consistent with hexagonal columnar, and those of another, with a rectangular columnar discotic phase.

6.1.3. *Lutetium Phthalocyanines*

Simon et al. found that bis(phthalocyanine)lutetium is a molecular semiconductor. Discotic mesophases were found for the complexes of the subtstituted phthalocyanines [Lu{$(ROCH_2)_8C_{32}H_8N_8$}$_2$] **46** (R = $C_{12}H_{25}$).[103] Both the

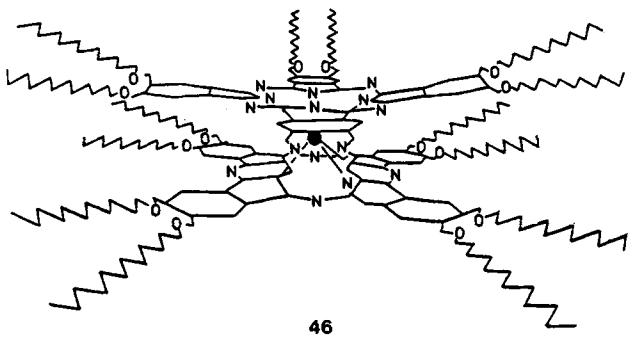

46

green neutral form and the red oxidized form, as the $SbCl_6^{\ominus}$ salts, were prepared. The ionic compounds formed the more stable mesophases. X-ray data for the mesophase of **46** (R = $C_{18}H_{37}$) indicated an intercolumnar distance of 37 Å and a repeating unit of 7.3 Å, twice the thickness of the phthalocyanine ring, as expected (Fig. 25). The X-ray pat-

Fig. 25. Schematic representation of the repeat units of the bis(phthalocyaninato)lutetium derivatives **46**.

tern remains unchanged on going from ambient temperature to the temperature where the isotropic phase appears, indicating that the mesophase and the solid have similar structures. The ESR spectrum of the neutral species shows broadening in the mesophase; there is some uncertainty about the magnetic state of the oxidized form. The electrical properties of the neutral form of **46** (R = $C_{18}H_{37}$) are also very similar in the solid and in the mesophase (conductivity $1.8 \times 10^{-9}\,\Omega^{-1}\,cm^{-1}$ at 10^4 Hz), but the conductivity increases on oxidation. It was estimated that the hopping probability of an electron is 10^7 greater within a column than between columns for the same activation energy.

6.1.4. Si, Sn and Pb Phthalocyanines

Columnar phthalocyanines linked by O–Si–O[104] or O–Sn–O[105] spacers have also been described. The tin complex **47** shows a columnar mesophase between 59 and 114 °C,

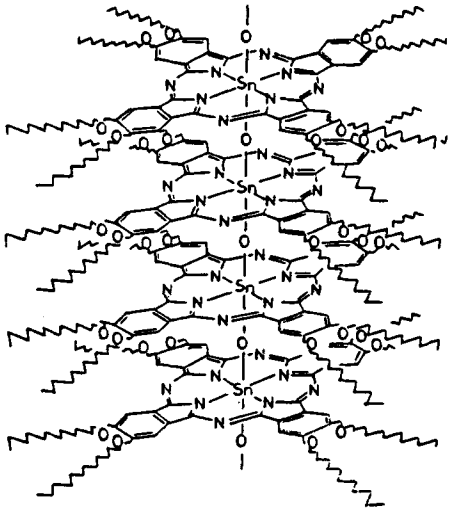

47

characterized by X-ray diffraction measurements as a rectangular packing of columns (column separation 25.2 and 30.7 Å), and with a probable intermetallic spacing of 3.85 Å.[105] The fluid isotropic phase is slowly transformed into a highly viscous anisotropic material, which has a polymeric {–O–Sn–}$_n$ backbone; this in turn becomes isotropic at 290 °C.

The silicon-containing phthalocyanine **48** showed hexagonal-columnar mesophases (D_{hd}) between ambient and 300 °C

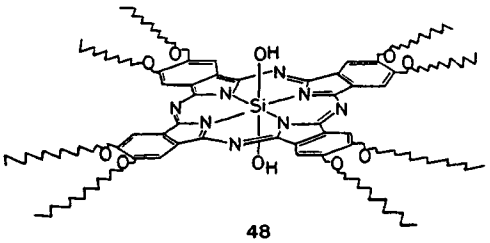

48

for n ≥ 4. On heating in air at 180 °C loss of water occurred, accompanied by oligomerization to dimers, trimers, and some higher oligomers, e.g. **49**.[104]

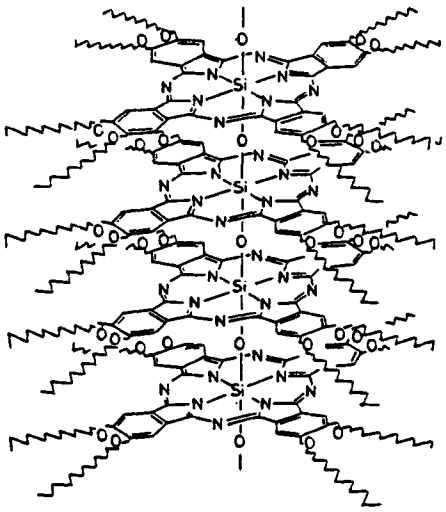

49

Also Sn^{II} and Pb^{II}, form a series of complexes of the type just outlined.[106] The Sn^{II} complex is readily oxidized to the Sn^{IV} complex **47**. The lead complex forms columnar discotic liquid crystals, with intercolumnar spacings of 26.9, 31 and 36 Å for the $C_8H_{17}OCH_2$, $C_{12}H_{25}OCH_2$, and $C_{18}H_{37}OCH_2$ chains respectively. The mesophase was stable down to

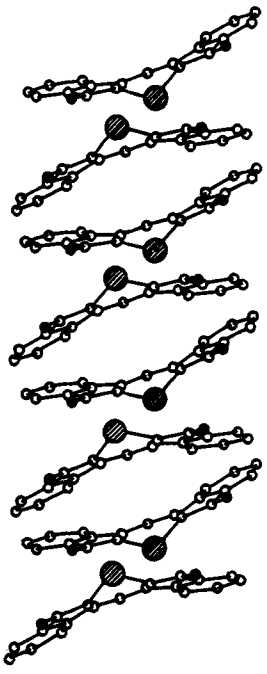

Fig. 26. Side-view of the proposed structure of Pb (phthalocyanine) illustrating the antiferroelectric coupling of the Pb atoms (⊘) (after Ref. [107]).

– 45 °C; the X-ray data have been interpreted in terms of dimers (Fig. 26) which exhibit antiferroelectric coupling.[107]

6.2. Other N_4 Macrocycles

Mesogenic metal-containing prophyrin complexes **50** (R = CH_2OH, M = Cu, Cd, Zn, and Pd) have been reported, as well as some which are not mesogenic but which, on

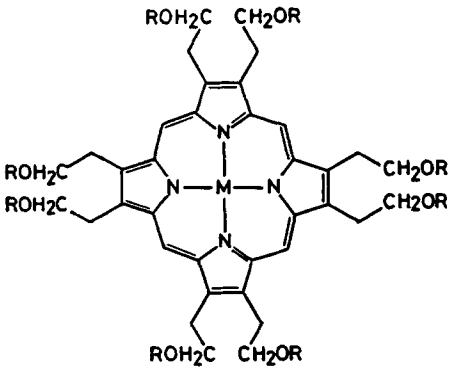

50

mixing with long-chain alkanes or *n*-alkyl halides, form monotropic mesophases.[108]

The disklike octadodecyltetrapyrazinoporphyrazine **51** (R = $C_{12}H_{25}$) and its copper complex show discotic mesophases (by X-ray).[109] Although the structure of this

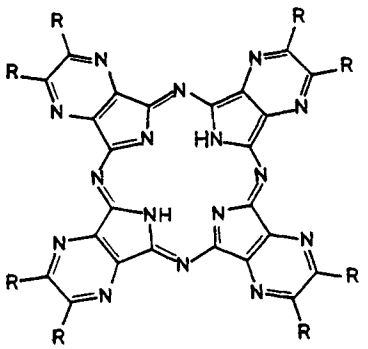

51

ligand differs little from that of its copper complex, there is still a change of mesomorphic character. The former shows a hexagonal disordered columnar mesophase (D_{hd}) between 118 and 238 °C, the decomposition temperature, while the copper complex has a rectangular disordered columnar mesophase (D_{rd}) between 114 °C and the decomposition temperature 288 °C.

Discotic phases have been reported in a patent for a series of substituted dibenzotetraza[14]annulenes **52** containing divalent Ni, Pd, Pt, Co, or Cu. The complexes have been considered for use in electro- or thermooptical displays.[110]

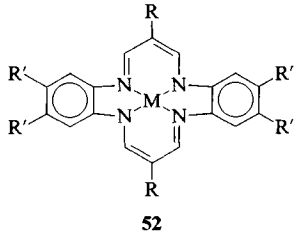

52

6.3. Other Amine Complexes

The "annelides" $C_{16}H_{33}CH\{CH_2NHCH_2CH_2NH(CH_2CH_2O)_6Me\}_2$ form mesogenic copper complexes such as **53**.[111] Between 77 and 95 °C, both the hydrophilic and the hydrocarbon chains are in a quasi-liquid state, whereas the polar head groups remain in a two-dimensional crystalline array. These lamellar phases, intermediate between

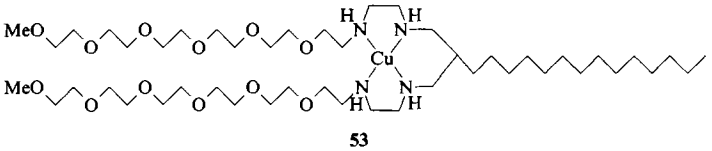

53

crystalline solids and liquid crystals, have been termed tegma crystals. The ESR spectra of the complex in the mesophase, in the solid, and in solution point in each case to a weak magnetic coupling between the copper atoms.[112]

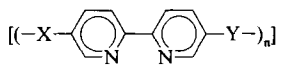

54, X, Y, = CO, CO_2CH_2, $CO_2(CH_2)_{10}O$

The 5,5′-linked 2,2′-bipyridyls **54** constitute an unusual series of thermotropic polymers; they complex metals such as Fe^{II}, Cu^{I} or Cu^{II} to give metallomesogenic materials.[113]

7. Salicylaldimine Complexes

Schiff bases derived from substituted salicylaldehydes are very versatile ligands which form (*N–O*) chelates with many metals. Ligands for thermotropic liquid crystals are usually made by condensing the appropriate 4-substituted ether of 2,4-hydroxybenzaldehyde with a 4-substituted aniline or other primary amine [Eq. (i)]; many of these ligands are

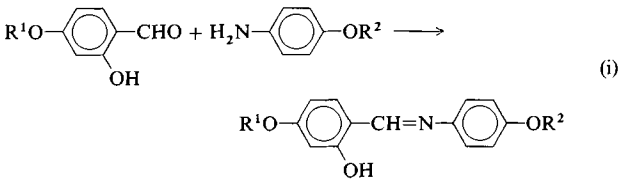

(i)

themselves mesogenic (nematic). Metal complexes can be prepared in good yield when the salicylaldimine is refluxed in ethanol in the presence of (for example) copper(II) acetate.

7.1. Copper, Nickel, and Palladium [$M(N_1O_1)_2$] and [$M(N_2O_2)$] Complexes

Most of the paramagnetic salicylaldimine copper(II) complexes **55** [n = 1, 3, 5–8; R = C_mH_{2m+1} (m = 2, 8, 12), F, $O_2CC_6H_4OC_{12}H_{25}$], first reported by *Ovchinnikov* et al. in 1984, showed smectic mesophases.[114, 115] However, nematic behavior was observed by *Galyametdinov* et al. for **55** (n = 7; R = $O_2CC_6H_4OC_{12}H_{25}$).[116]

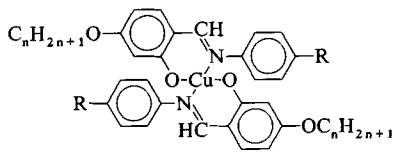

55

Calorimetric and microscopic investigations revealed that the complex **56** forms S_A (142–157 °C) and S_C (157–165 °C) mesophases. ESR spectra showed that it was a slightly distorted square planar complex with *trans* conformation, both in dilute toluene solution and in the isotropic liquid phase,[117] but that some of the planar molecules had undergone tetrahedral distortion in the mesophase. The data were interpreted as indicating that the planar molecules formed the smectic phase while the tetrahedral ones were concentrated in microscopic isotropic droplets, i.e. that the mesophase was heterogeneous.

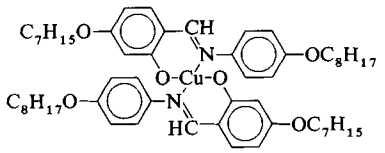

56

The X-ray single crystal structure of mesogenic **57** (n = 4, R = *p*-$C_6H_4C_6H_{13}$) showed that, owing to a twist of the *N*-phenyl and the benzoyl moieties relative to each other, the molecule adopts a lathlike rather than a disklike structure (Fig. 27).[118] The coordination about copper is distorted square-pyramidally, with a torsion angle of 22° between the two Cu–N–O chelate planes, and a weak axial interaction with the ester carbonyl group of the adjacent molecule

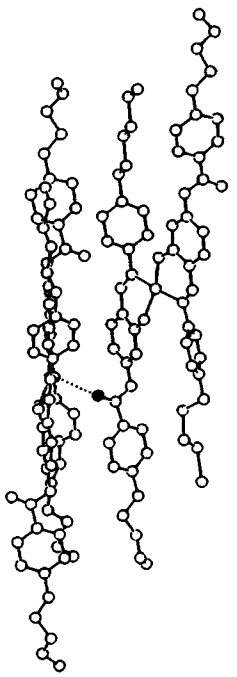

Fig. 27. Crystal structure of a complex **57** (n = 4, R = *p*-$C_6H_4C_6H_{13}$) showing weak axial coordination (dotted line) of the carbonyl O-atom (black) to the neighboring copper center (after Ref. [118]).

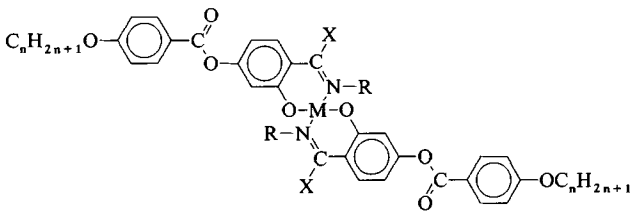

57, M = Cu, X = H
58, M = Ni, X = Me
59, M = Cu, X = Me

(Cu···O 3.04 Å). This compound shows a nematic phase above 223 °C and is also a model for a series of complexes of the type **57** (R = 4-C_6H_4OEt), which show S_C and N phases (Table 5). Again, in this series, complexes with smaller n (6–10) form nematic, those with n = 11, 12, 14 form both nematic and S_C phases, while those with n = 16, 18 form only S_C phases.

Table 5. Transition temperatures [°C] of the mesomorphic copper(II) complex **57** (R = 4'-$EtOC_6H_4$)[118].

Complex	Mesophases		
trans-[Cu{$C_nH_{2n+1}C_6H_3(O)CH=NR$}$_2$] **57**	S_C	N	I
n = 6		222	274 [a]
n = 7		211	272 [a]
n = 8	–	201	275 [a]
n = 9	–	192	262 [a]
n = 10	–	189	271 [a]
n = 11	181	185	268 [a]
n = 12	178	204	264 [a]
n = 14	170	230	260 [a]
n = 16	162	–	256
n = 18	156	–	251

[a] Clears with (some) decomposition.

Both copper(II) and nickel(II) complexes **57** and **58** (R = 4-$C_6H_4OC_nH_{2n+1}$; n = 1–6; 8, 10, 14, and R = C_mH_{2m+1}; m = 1–10) derived from the *n*-alkylamines ($C_mH_{2m+1}NH_2$) show mainly nematic mesophases, while those derived from arylamines show largely smectic mesophases.[119, 120] The nickel complexes were more stable thermally but the copper complexes had lower melting points. The nickel complexes were diamagnetic, and hence square planar.

All the copper complexes **57** (X = H, Me; R' = Me, *n*-$C_{10}H_{21}$, *p*-$C_6H_4OC_{10}H_{21}$) derived from 2,4-dihydroxybenzaldehyde showed nematic or S_C phases, whereas those from 2,5-dihydroxybenzaldehyde were only mesogenic when the imine (R'N=) was derived from methylamine.[121] The stability of the nematic phase of **57** (R = Me) was found to decrease with increasing n, until, for n = 14, only an S_C phase is observed.[122] Nematic mesophases have also been reported for complexes of type **57'**.[123]

X-ray studies on the mesophase have been carried out for **55** (R = C_4H_9, *n* = 7, 12); the complexes show smectic phases, whereas the free ligands form only nematic phases.[124] There is also evidence favoring the presence of interdigitated layers of partially melted chains, and a pos-

sible coupling of copper atoms in pairs inside the smectic layers. X-ray studies of the nematic and smectic phases of **57** (R = Me, $C_{10}H_{21}$, and $C_{10}H_{21}OC_6H_4$) have also been carried out.[125]

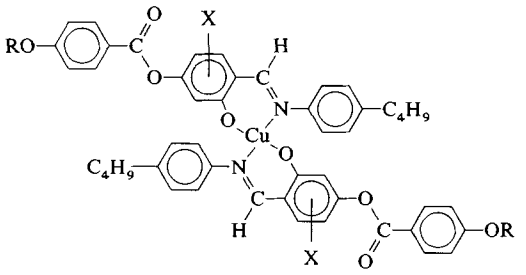

57'

Other salicylaldimines have also been used for the synthesis of mesogenic copper and nickel complexes. Thus, the bis(salicylidene)ethylenediamine (H_2salen) ligands (derived from 5-alkoxy-2-hydroxybenzaldehydes), form complexes **60** (M = Cu, Ni, n = 4–8), all of which show highmelting S_A phases.[126] By contrast, related complexes with the *N*-methylalkyloxysalicylaldimine ligands, $[M\{ROC_6H_3(O)CH{=}NMe\}_2]$ were not mesogenic.

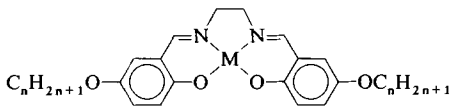

60

The copper and palladium complexes **61** have also been shown to exhibit smectic mesomorphism, forming mainly S_C phases.[127] The palladium complexes have much higher melting and clearing temperatures than the corresponding copper complexes. The crystal structures of representatives

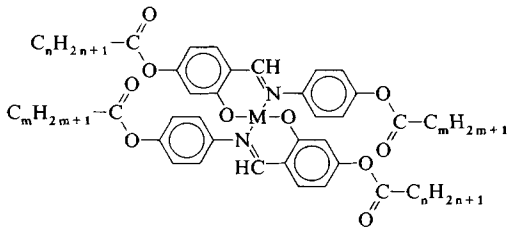

61

of each series have been determined; both in the case of Pd^{II} as well as in the case of Cu^{II}, the coordination is square planar (Fig. 28).[128] The prosmectic packing of the copper complexes in the crystal (in layers with their major axes inclined at ca. 60° to the layer plane) explains why these complexes do not show discotic behavior. Copper, nickel, and palladium complexes **57** and **58** have been compared. None of the nickel complexes show mesomorphic behavior, whereas the corresponding copper complexes show nematic (and some smectic) phases, and the two palladium complexes synthesized show both smectic and nematic phases.[127]

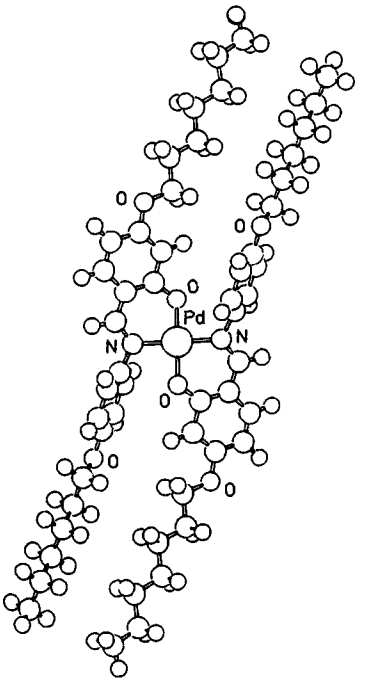

Fig. 28. Molecular structure of the palladium salicylaldimine complex **61** (m = 6, n = 7) (according to [128]).

7.2. Vanadyl and Iron $[M(N_1O_1)_2]$ Complexes

Of the complexes of type **61** with esterified salicylaldiminatoligands (M = Zn, Co, Ni, Cu, VO, and Pd)[129] the zinc, the cobalt, and the nickel complexes showed no mesomorphic behavior, but the copper, the vanadyl, and the palladium complexes (m = 8, n = 7) all showed smectic mesophases: S_C phases (Cu: 142–156; VO: 151.8–170; Pd: 164.5–198 °C) and S_A phases (Cu: 156–165; VO: 170–179.8; and Pd: 198–209 °C). The absence of mesophases for the nickel and the cobalt complexes was ascribed to the tetrahedral geometry about the metal, as shown by ESR and electronic spectroscopy; the copper and the palladium centers are square planar, while the vanadyl unit is square pyramidal.[130]

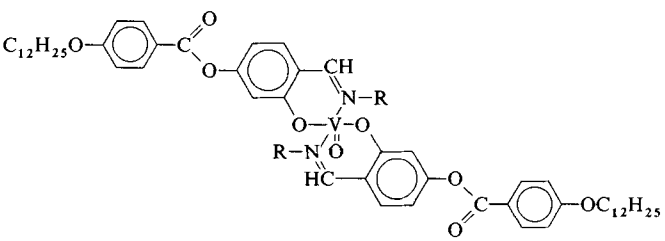

62

The first mesogenic Schiff base-vanadyl complex was reported in 1984.[130] The complexes **62** (R = Me, *n*-C_5H_{11}, $C_{10}H_{21}$, and *p*-alkylOC_6H_4), form nematic (e.g. for R = *n*-C_5H_{11} 109–131 °C) as well as smectic mesophases.[131] The low viscosity of the mesophases allowed easy orientation of the molecules by a magnetic field; the orientation remained unaltered in the solid state.

The mesogenic iron(III) complex **63**, recently reported by *Galyametdinov* et al.[132] is paramagnetic (ESR parameters, $g_1 = 2.096$, $g_2 = 4.30$), and forms an S_A phase (85–151 °C).

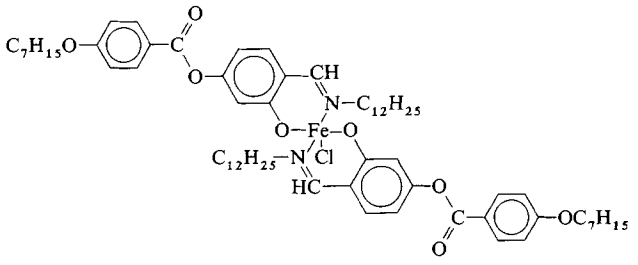

63

Although the available data are still patchy, it appears that mesophases are formed when the molecular geometry of the salicylaldimine moiety of the ligand about the metal atom is planar or planar with an axial interaction (square pyramidal), but not for tetrahedral geometries. Within the series most closely examined, those of Cu^{II}, nematic phases tend to be favored with short alkyloxy chains, and smectic phases with longer ones.

7.3. Polymeric Liquid Crystals Based on Salicylaldimine Ligands

Carfagna et al.[133] reported the synthesis and properties of mixed ethylene oxide-dodecanediol-Schiff base polymers of the type **64**, as well as of the monomeric complex **65**. Complex **65** forms a clear S_A phase, the polymers, on the other hand, are monotropic, and presumably show S_A phases. However, in solution there is some evidence for de-

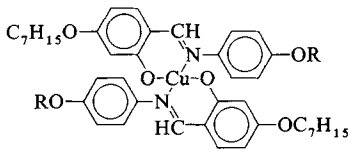

64, R = $[\{(CH_2)_{12}O\}_x\{(CH_2CH_2O)_3\}_{110-x})_2]_n$
65, R = C_6H_{13}

polymerization. Related polymeric copper complexes based on salen-type units have also been found to be mesogenic.[134]

8. Cyclometalated Mesogens

Up to now, only palladium-containing cyclometalated mesogens have been reported. However, since many other metals form stable cyclometalates this is likely to be a fruitful area for future development.

8.1. Complexes Derived from Azobenzenes

Ghedini et al. in Calabria prepared the first cyclopalladated liquid crystals **66**; (R = EtO or Et; R′ = C_4H_9, C_5H_{11}, C_6H_{13}, and $(CH_2)_8CH = CH_2$), by cyclopalladation of the appropriate 4,4′-substituted azobenzene derivative with K_2PdCl_4 in aqueous dioxane (25 °C, one week) [Eq. (j)].[135] These dinuclear chloro-bridged complexes formed nematic phases on melting, typically at ca. 200 °C, i.e. at much higher

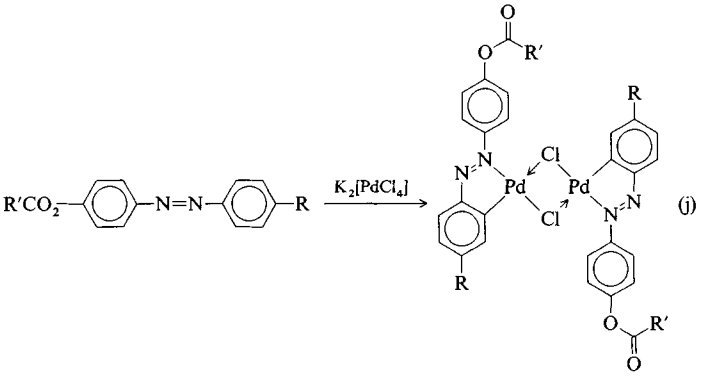

66

temperature and in a narrower range than the free ligands; for example, while the nematic range for the ligand $EtOC_6H_4N = NC_6H_4O_2CC_6H_{13}$ was 59–112 °C, that for the complex derived from it was 190–205 °C. The monomeric complexes **67** (L = PPh_3) obtained by cleaving **66** with PPh_3 are not esogenic; however, the amine adducts **67** (L = pyridine, or quinoline) form smectic and nematic

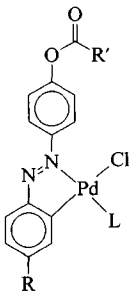

67

mesophases.[136] The adduct with the planar quinoline showed an S_A phase already at 136–151 °C, and a nematic phase from 151–180 °C; the importance of the geometry of the added ligand L was reinforced by the observation that the aniline adduct is not mesogenic and simply decomposes

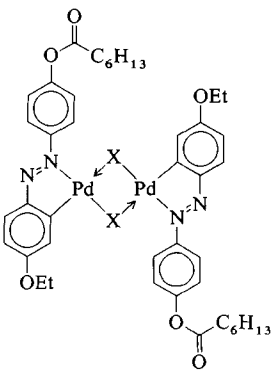

68

at 173–175 °C. The dimeric complexes **66** show a high birefringence in the mesophase.[135]

All three μ-halogeno-complexes **68** show similar nematic phases, but the melting temperatures decrease in the sequence X = I > Br > Cl.[136] The chloride showed only a nematic phase (190–205 °C), while the bromide showed enantiotropic S_A (210–215 °C) and N (215–250 °C) phases as well as a monotropic S_B phase, and the iodide showed enantiotropic S_A (220–225 °C) and nematic (225–230 °C) phases.

The Calabria group also found that mesogenic azobenzene ligands were not essential for the synthesis of mesogenic complexes; however, in this case only monotropic materials are formed.[137] Thus, the complex derived from $C_{12}H_{25}OC_6H_4N = NC_6H_5$ showed a smectic phase (150–136 °C) on cooling the isotropic liquid.

Other nematogenic cyclopalladated 4,4′-azobenzenes have been reported;[138] and a non-mesogenic complex derived from 4,4′-dimethoxyazobenzene has been characterized by a single-crystal X-ray structure determination (Fig. 29).[139]

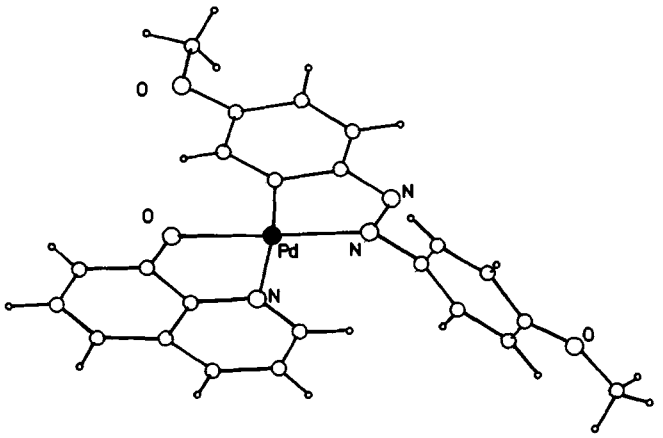

Fig. 29. Structure of the non-mesomorphic, cyclopalladated complex formed from the PdCl adduct of 4,4′-dimethoxyazobenzene and 8-hydroxyquinoline (after Ref. [139]).

8.2. Complexes Derived from Arylimines

Espinet et al. in Spain have prepared the mesogenic complexes **69** and **70** from the corresponding Schiff bases and $Pd_3(OAc)_6$ (Z = H, R = $C_{10}H_{21}$ or $C_{10}H_{21}O$; Z = Me, R = $C_{10}H_{21}$ for **69**, and X = H, halide, OCOR, CN, NO_2, CF_3, etc for **70**)[140]

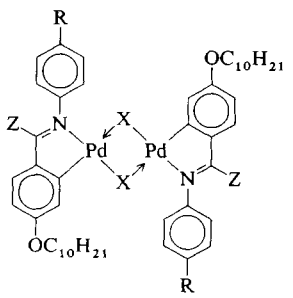

69

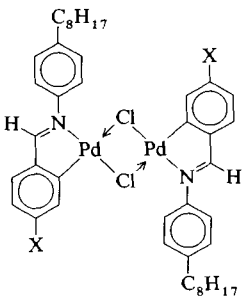

70

The complexes **69** showed smectic phases (usually S_A) when X = Cl, Br, and SCN, (Table 6) but the acetato-bridged complexes were generally non-mesogenic. It was suggested that this was due to the nonplanarity usually found for complexes with di-μ-acetato bridges in contrast to the planar arrangements with other bridging ligands. Again for this series, the

Table 6. Transition temperatures [°C] for mesomorphic *ortho*palladated iminoarenes **69** (R = $C_{10}H_{21}$, Z = Me)[140].

Komplex	Mesophases		
69	S_C	S_A	I
X = Cl	112.4	135.0	237.6 [b]
X = Br	–	102.6	241.2
X = SCN	–	166.6	219.6
X = OAc		(160.0) [a]	169.9

[a] Monotropic mesophase. [b] Clears with (some) decomposition.

melting and especially the clearing temperatures of the complexes are very significantly higher than those of the free ligands; e.g. in the case of $C_{10}H_{21}OC_6H_3CH = NC_6H_4C_{10}H_{21}$ the phase changes occur at 53.3 (K→S_F), 84.4 (S_F→S_A), and 89.1 °C (S_A→I), while the corresponding di-μ-chloro complex showed phase changes at 112.4 (K′→S_C), 135.0 (S_C→S_A), and 237.6 °C (S_A→I, decomposition; Table 6). The chloro complexes **70** showed similar behavior; again the acetates were non-mesogenic.

8.3. Complexes Derived from Diarylazines

In contrast to the above-mentioned compounds the di-μ-acetato complexes **71** (X = $MeCO_2$) derived from the symmetrical 4,4′-bis(alkyloxybenzylidene)azines $C_nH_{2n+1}OC_6H_4CH = N–N = CHC_6H_4OC_nH_{2n+1}$ (n = 7–10, 12, 14) showed S_C (and in two cases, also N) mesophases. The μ-acetato ligands constrain the complexes to be nonplanar, and a novel type of structure based upon "open-book"-shaped molecules (Fig. 30) has been proposed.[141]

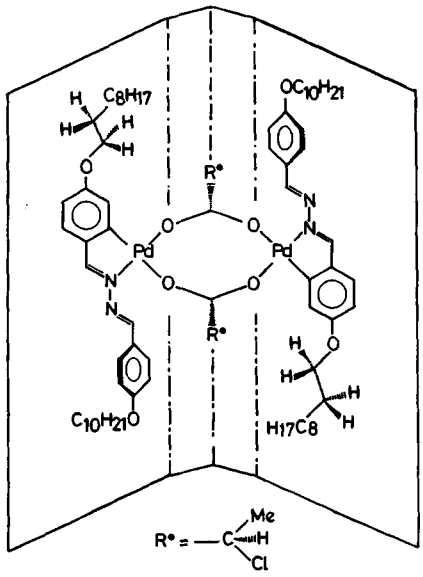

Fig. 30. The proposed structure of the optically active complex **71** reminiscent of an "open book". The complex exhibits a ferroelectric phase (after Ref. [142]).

Reaction of **71**, (n = 10, X = Cl) with (R)-MeCH-$ClCO_2Na$ furnished the optically active complex **71** (n = 10, R = C*Me(H)Cl), which was shown by NMR spectroscopy to contain a mixture of the *trans-ΔR,R*, *trans-ΔR,R* and *cis-R,R* isomers.[142] The complex showed an enantiotropic S_C phase (102–119 °C), making it the first organometallic ferroelectric. However, the electrooptic response is substantially slower than for organic calamitic S_C^* phases, due to the high viscosity of the material. The high viscosity may be due to the bulkiness of the open-book molecular shape.

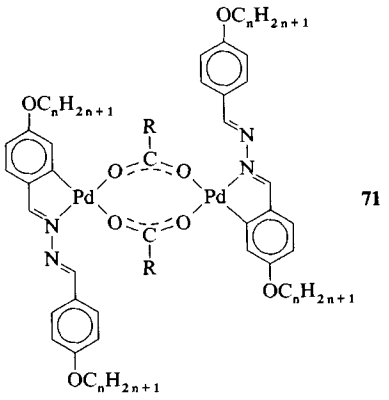

71

Further μ-carboxylato-complexes of the type **71**, (n = 10, $R = C_mH_{2m+1}$) have been studied.[143] It was found that short chains (m = 1–3) gave rise to S_C (and N) mesophases, while for m = 4–6 enantiotropic N and for m = 7–9 monotropic N mesophases are observed. A more complex behavior was found with m ≥ 10: monotropic S_C and N as well as enantiotropic N mesophases were formed. It is argued that these effects arise from a perturbation of the molecular packing, a point which is reinforced by X-ray data.

9. Structure–Property Relationships

The study of metallomesogens is very much in its infancy and considerable information must still be accumulated before relationships similar to those now available for organic mesogens can be drawn. Many metallomesogens are colored and this, together with their somewhat high melting temperatures, can make optical phase identification difficult. Owing to their high viscosity, smectic, discotic, and disordered crystal phases can sometimes be confused; this makes the use of additional techniques for mesophase identification imperative. Phase behavior needs to be definitively established, and this will require more low angle X-ray determinations in the mesophases.

Further, the detailed molecular geometries of many quite simple metal complexes are not yet known, and single crystal X-ray structures are also necessary. The assignment of structures by spectroscopy, extrapolation and analogy, so widely used in both organic and inorganic chemistry, may not always be reliable for metallomesogens.

The information gathered in this review allows the following generalizations to be made.

Both disk- and rodlike metallomesogens of many different types are known. Most of the mononuclear systems have the metal at or near the center of gravity of the molecule; this is true of the discotic mesogens (e.g. phthalocyanines, β-diketonates, and of the dinuclear carboxylates) as well as for the nematic and smectic calamitic mesogens.

The basic requirements for a metal complex to show mesomorphism are not dissimilar to those for many organics. Thus, a calamitic mesogen will typically have a long rigid group, which, frequently, but not essentially, corresponds to the core of the molecule containing the metal atom and two *trans*-ligands containing aromatic rings, carrying *n*-alkyl (or *n*-alkyloxy) tails in the *p*-positions. Shorter tails tend to give rise to nematic mesogens, longer ones to smectic mesogens, while the stretched S-shape with the "outboard dipoles" characteristic of many organic compounds forming S_C phases (Fig. 31) is also found in many S_C metallomesogens with *n*-alkyloxyphenyl tails. In some cases it is possible to construct calamitic mesogens with only one long organic ligand; these often show S_A phases (e.g. **12**–**16**).

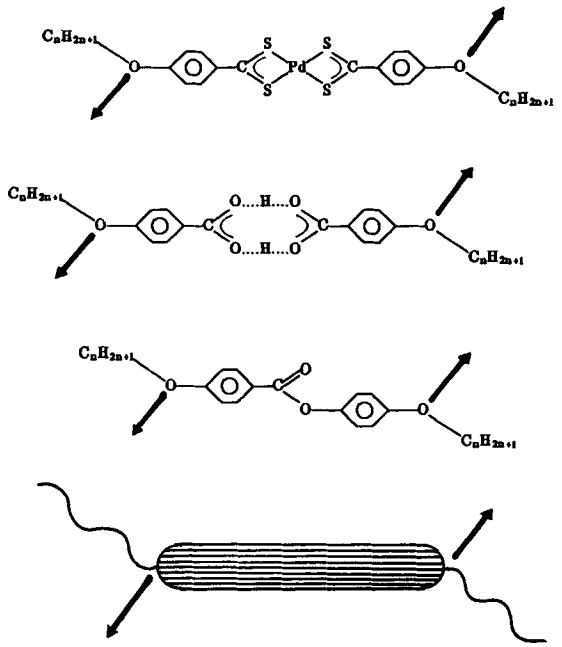

Fig. 31. Molecules forming S_C phases with S shape.

A discotic molecule will usually have a flattish platelike form with the metal in the center surrounded by a highly unsaturated organic ligand bearing at least four and preferably six or eight *n*-alkyl (or *n*-alkyloxy) substituents. A great many of the metallomesogens known to date are of the columnar discotic type, including carboxylates, β-diketonates, and phthalocyanines (cf. Sections 3.3, 4 and 6.1). By contrast, the complexes of salicylaldiminato ligands (Section 7), especially those with longer hydrocarbon tails, tend to give smectic phases. Both for calmitic compounds as well as for discotic compounds, the tails usually need to be at least five atoms long to show mesomorphism; and the presence of an extra phenyl in the tail is often advantageous.

Many metallomesogens are composed of ligands which are *not* mesomorphic. When the free ligands *are* themselves

mesomorphic, the derived metallomesogens show similar phase behavior when incorporation of the metal changes the molecular shape to only a small extent, for example in the phthalocyanines (Section 6.1). In other cases, the considerable difference in structure which the organization of ligands by the metal makes to the overall molecular shape ensures quite different mesophase behavior, for example in the copper β-diketonates.

Thermotropic metallomesogens have been made which incorporate alkali metals, alkaline earths, many 3d metals (V, Mn, Fe, Co, Ni, Cu), some 4d and 5d metals (Mo, Rh, Pd, Ag, Ir, Pt, Au), several p-block metals (Zn, Cd, Hg, Pb, Tl), and the lanthanide Lu.

Linear, square planar, and 5-coordinate (usually distorted square pyramidal) geometries have so far been found for the metals in mesogenic complexes. It seems that most metallomesogens need at least one "vacant" coordination site on the metal, which, in the crystal, loosely associates with a donor atom in a neighboring molecule. Thus, for example, the X-ray single crystal data of mesogenic square planar complexes show such axial interactions between the metal (M) and a liganding atom (X) on a neighboring molecule (cf. e.g., the structures in Figures 13, 20, 22, 23, 24, 27 and in Section 6.1). No complexes having an unequivocal tetrahedral geometry about the central metal have yet been found to be mesomorphic. This *may* be because intermolecular M···X interactions are not compatible with a tetrahedral geometry, but that they are needed to confer mesomorphism. Furthermore, for dithiobenzoate or salicylaldimine mesogens (Sections 5.2 and 7.1) it appears that attempts to impose a tetrahedral geometry lead to distortion.

The tails needed to confer mesomorphism on a complex may even be able to change the structure subtly, at least in the solid-state. For example, in the bis(dithiobenzoato) zinc complex (Section 5.2): while the unsubstituted complex shows a clear tetrahedral geometry about the zinc, the 4-octyloxy and the 4-butyloxy complexes have a loose dinuclear structure with a 5-coordinated metal.

Only one possible molecular metallomesogen with a presumed octahedral arrangement of six oxygen ligand atoms about the metal has so far been reported (see **33**). It is important to confirm this and to make other similar molecules.

These generalizations all depend on the assumption that the structure in the crystal is closely related to that in the mesophase, but this may not always be valid. In a few cases it has been checked: thus, in the columnar discotic dicopper and dirhodium tetracarboxylates there is no detectable change in bond lengths (by EXAFS) on going from the crystal to the mesophase (Section 3.3).

It is found that ligands with *n*-alk*oxy* tails often have beneficial effects in stabilizing mesophases; for example while the palladium alkoxy-CB complexes **7** show thermodynamically stable (enantiotropic) phases, the closely related alkyl-CB complexes at best only form the unstable (monotropic) phases (Section 2.1). Similarly, whereas the copper β-diketonates with 1,3-phenyls bearing p-$C_8H_{17}O$ substituents gave discotic mesophases, those where the phenyls had p-C_8H_{17} substituents did not (Section 4.2).

The introduction of a metal can lead to rather high-melting mesophases, perhaps due to strong axial (M···X) intermolecular interactions. This can be counteracted i) by introducing asymmetry into the molecule (Sections 2.2.2 and 2.3), which makes the molecular packing more difficult; ii) by introducing more amphiphilic coligands (e.g. carboxylate in place of halide, Section 2.2.1); or iii) by mixing two or more related complexes (this lowers the melting point without seriously affecting the clearing temperature, Figs. 7 and 10). These methods have been used to bring transition temperatures close to ambient, and further decreases are certainly possible.

In order to be useful as *advanced materials*, metallomesogens must be reasonably *inert* and quite thermally robust. Since complexes often have the metal as center of reactivity, for example towards air or moisture, inertness and stability must be added. This can be done by using very strongly binding ligands or by incorporating the heavier 5d metals, or both. Suitable ligands are those with donor atoms having large stability constants (e.g. S or P in compounds of the heavy Group VIII metals) and especially chelates.

Apart from those needed to characterize the materials, rather few serious physical measurements have yet been undertaken on metallomesogens. However, considerable increases in polarizability have been found (as expected),[22] as well as (unanticipated) high birefringences.[14, 135] This latter observation parallels the use of heavy metal oxides in high refractive index glasses.

Currently available metallomesogens may have long electrooptic response times (see Ref. [142]), which could be a disadvantage for some electronic displays. However, there are many other potential applications and their uses as passive NIR blockers[82] in laser addressable or thermal recording materials[91, 110] have already been proposed. New and interesting is the suggestion that, since the incorporation of alkali-metal cations into cholesteric crown ethers causes a change in the helical pitch, this can be made the basis of an alkali-metal sensor.[144] Another is the observation by scientists at the 3M-Company in the USA that salts such as the fluorescent pink compounds $[Pt(RNC)_4][Pd(CN)_4]$ (RNC, e.g., decylphenyl isocyanide), turn blue when exposed to the vapors of many hydro- or fluorocarbons.[145] Although not specifically identified as liquid crystals, such materials must at least be closely related to metallomesogens.

10. Outlook

Metallomesogens now form a viable and challenging interdisciplinary topic which offers much scope to the imagination of both the synthetic chemist, for the design of new ligands and their metal complexes, and the materials scientist and engineer for new uses for these advanced materials. The knowledge is now at hand to design complexes offering rod-like nematic or smectic mesophases or, by suitably modifying the ligands, a variety of discotic phases. Colors can be incorporated by the use of suitable metals and ligands, as can magnetic, ferroelectric, and many more exotic properties The organized stacks of some of the metallomesogens, for example the dimetal tetracarboxylates, suggest that, with suitable manipulation, electrically conducting materials may result.[71, 94, 103]

Although a substantial number of metals have already been incorporated into metallomesogens, many still remain to be explored. The design of ligands for metallomesogen character is also in its infancy and new applications will require new types of complexes. This is one challenge to workers in the field.

Possible device applications for metallomesogens, which may presently be anticipated, are as new thermal or nonlinear optical materials, and in electrochemistry and sensors.

The effects of organic mesogens on organic reactions are just beginning to be explored.[146] Metal-promoted reactions are in general more sensitive to steric factors than organic ones, thus there appears considerable scope for using mesophases and metallomesogens to promote stereoselectivity both in stoichiometric organometallic reactions and in metal catalyzed processes. However, great care will be needed in the design of properly controlled experiments and their careful execution to avoid spurious results.

Thus far one can speculate, but we suspect the best application has not yet been thought of. What a challenge for the future!

We thank all our many colleagues and co-workers who have contributed to metallomesogens and who made this review possible. We are especially grateful to Dr. N. A. Bailey, Dr. D. W. Bruce and Dr. D. A. Dunmur (Sheffield), Professor P. Espinet (Valladolid), Dr. D. Guillon (Strasbourg), Dr. J. C. Marchon, and Dr. P. Maldivi (Grenoble), and Professor J. L. Serrano (Zaragoza) for most fruitful collaborations. We also thank the SERC, the Royal Society, the EC Science Progamme (Grant ST2J-0387-C), CNRS, CEA, and BDH Chemicals plc for their strong support, and M Aubert for assistance with the drawings.

Received: June 25, 1990 [A 811 IE]
German version: *Angew. Chem. 103* (1991) 370

[1] F. Reinitzer, *Monatsh. Chem. 9* (1888) 421.
[2] Useful reviews on various aspects of thermotropic organics mesophases include: G. W. Gray, *Advances in Liquid Crystals, Vol. 2*, Academic, London 1976; *Proc. R. Soc. Ser. A 402* (1985) 1; *Philos. Trans. R. Soc. London A 330* (1990) 73; G. Vertogen, W. H. de Jeu, *Thermotropic Liquid Crystals, Fundamentals*, Springer, Berlin 1988; D. Demus, *Liq. Cryst. 5* (1989) 75; R. Eidenschink, *Angew. Chem. Adv. Mater. 101* (1989) 1454; *Angew. Chem. Int. Ed. Engl. Adv. Mater. 28* (1989) 1424; *Adv. Mater. 1989*, 338.
[3] G. J. D. Tiddy, *Phys. Rev. 57 C* (1980) 1.
[4] S. Chandrasekhar, G. S. Ranganath, *Rep. Prog. Phys. 53* (1990) 57; J. Billard, *C.R. Acad. Sci. Ser. 2 299* (1984) 905.
[5] H. Ringsdorf, B. Schlarb, J. Venzmer, *Angew. Chem. 100* (1988) 117; *Angew. Chem. Int. Ed. Engl. 27* (1988) 113; H. Ringsdorf, R. Wuestefeld, *Philos. Trans. R. Soc. London Ser. A 330* (1990) 95; H.-W. Schmidt, *Angew. Chem. Adv. Mater. 101* (1989) 964; *Angew. Chem. Int. Ed. Engl. Adv. Mater. 28* (1989) 940; *Adv. Mater. 1989*, 218; R. Zentel, *ibid. 101* (1989) 1437 and *28* (1989) and 321.
[6] D. Vorländer, *Ber. Dtsch. Chem. Ges. 43* (1910) 3120.
[7] D. Vorländer, *Z. Phys. Chem. Stoechiom. Verwandschaftsl. 105* (1923) 211.
[8] A. Skoulios, *Ann. Phys. (Paris) 3* (1978) 421.
[9] J. Malthête, J. Billard, *Mol. Cryst. Liq. Cryst. 34* (1976) 117. A liquid crystal phase claimed for ferrocenecarboxaidehyde [P. J. Graham, R. V. Lindsay, G. W. Parshall, M. L. Peterson, G. M. Whitman, *J. Am. Chem. Soc. 79* (1957) 3416] is probably a plastic crystal phase] L. Verbit, T. R. Halbert, *Mol. Cryst. Liq. Cryst. 30* (1975) 209.
[10] A.-M. Giroud, U. T. Müller-Westerhoff, *Mol. Cryst. Liq. Cryst. 41* (1977) 11; A.-M. Giroud, FR-B. 771667 (1977).
[11] D. W. Bruce, E. Lalinde, P. Styring, D. A. Dunmur, P. M. Maitlis, *J. Chem. Soc. Chem. Commun. 1986*, 581; P. M. Maitlis, D. W. Bruce, D. A. Dunmur, Int. Pat. WO 87/02693; *Chem. Abstr. 107* (1987) 145374n.
[12] P. Styring, *PhD Thesis*, Sheffield Universtiy 1988.
[13] H. Adams, N. A. Bailey, D. W. Bruce, D. A. Dunmur, E. Lalinde, M. Marcos, C. Ridgway, A. J. Smith, P. Styring, P. M. Maitlis, *Liq. Cryst. 2* (1987) 381.
[14] D. W. Bruce, D. A. Dunmur, M. R. Manterfield, P. M. Maitlis, and R. Orr, *J. Mater. Chem. 1* (1991), in press.
[15] D. W. Bruce, D. A. Dunmur, E. Lalinde, P. M. Maitlis, P. Styring, *Liq. Cryst. 3* (1988) 385.
[16] D. W. Bruce, D. A. Dunmur, E. Lalinde, P. M. Maitlis, P. Styring, *Nature (London) 323* (1986) 791.
[17] D. W. Bruce, D. A. Dunmur, P. M. Maitlis, P. Styring, M. A. Esteruelas, L. A. Oro, M. B. Ros, J. L. Serrano, E. Sola, *Chem. Mater. 1* (1989) 479.
[18] D. W. Bruce, D. A. Dunmur, S. A. Hudson, E. Lalinde, P. M. Maitlis, M. P. McDonald, R. Orr, P. Styring, A. S. Cherodian, R. M. Richardson, J. L. Feijoo, G. Ungar, *Mol. Cryst. Liq. Cryst.* (1991), in press.
[19] N. J. S. Salt, *PhD Thesis*, Sheffield University 1989.
[20] J. P. Rourke, F. P. Fanizzi, N. J. S. Salt, D. W. Bruce, D. A. Dunmur, P. M. Maitlis, *J. Chem. Soc. Chem. Commun. 1990*, 229; J. P. Rourke, *PhD Thesis*, Sheffield University 1989.
[21] D. W. Bruce, D. A. Dunmur, S. E. Hunt, R. LeLagadec, P. M. Maitlis, J. R. Marsden, J. M. Stacey, M. A. Esteruelas, E. Sola, *J. Mater. Chem. 1* (1991), in press.
[22] C. Bertram, D. W. Bruce, D. A. Dunmur, S. E. Hunt, P. M. Maitlis, M. McCann, *J. Chem. Soc. Chem. Commun. 1991*, 69; S. E. Hunt, *PhD Thesis*, Sheffield University 1990.
[23] M. A. Esteruelas, L. A. Oro, E. Sola, M. B. Ros, J. L. Serrano, *J. Chem. Soc. Chem. Commun. 1989*, 55.
[24] M. A. Esteruelas, E. Sola, L. A. Oro, M. B. Ros, M. Marcos, J. L. Serrano, *J. Organomet. Chem. 387* (1990) 103.
[25] M. Marcos, M. B. Ros, J. L. Serrano, M. A. Esteruelas, E. Sola, L. A. Oro, J. Barbera, *Chem. Mater. 2* (1990) 748.
[26] N. Hagihara, K. Sonogashira, S. Takahashi, *Adv. Polym. Sci. 41* (1980) 149; S. Takahashi, Y. Takai, H. Morimoto, K. Sonogashira, N. Hagihara, *Mol. Cryst. Liq. Cryst. 82* (1982) 139; S. Takahashi, H. Morimoto, E. Murata, M. Kariya, K. Sonogashira, N. Hagihara, *J. Polym. Sci. 20* (1982) 565; S. Takahashi, Y. Takai, H. Morimoto, K. Sonogashira, *J. Chem. Soc. Chem. Commun. 1984*, 3; see also T. Kaharu, H. Matsubara, S. Takahashi, *J. Mater. Chem. 1* (1991) 1.
[27] J. Bhatt, B. M. Fung, K. M. Nicholas, C. D. Poon, *J. Chem. Soc. Chem. Commun. 1988*, 1439.
[28] A. S. C. Lawrence, *Trans. Faraday Soc. 34* (1938) 660.
[29] A. Skoulios, V. Luzzati, *Nature (London) 183* (1959) 1310; A. Skoulios, V. Luzzati, *Acta Crystallogr. 14* (1961) 278; B. Gallot, *ibid. 15* (1962) 826; B. Gallot, A. Skoulios, *ibid. 14* (1961) 419; P. Spegt, A. Skoulios, *ibid. 16* (1963) 301; P. Spegt, A. Skoulios, *ibid. 17* (1964) 198.
[30] B. Gallot, A. Skoulios, *Kolloid Z. Z. Polym. 209* (1966) 164; *ibid. 210* (1966) 143; *ibid. 213* (1966) 143; *ibid. 222* (1986) 51.
[31] H. A. Ellis, *Mol. Cryst. Liq. Cryst. 139* (1986) 281.
[32] C. G. Bazuin, D. Guillon, A. Skoulios, A. M. Amorim da Costa, H. D. Burrows, C. F. G. C. Geraldes, J. J. C. Texeira-Dias, E. Blackmore, G. J. T. Tiddy, *Liq. Cryst. 3* (1988) 1655; H. A. Ellis, *Mol. Cryst. Liq. Cryst. 138* (1986) 321; A. M. Amorim da Costa, H. D. Burrows, C. G. C. Geraldes, J. J. C. Texeira-Dias, C. G. Bazuin, D. Guillon, A. Skoulios, E. Blackmore, G. J. T. Tiddy, D. L. Turner, *Liq. Cryst. 1* (1986) 215.
[33] J. Lindau, W. Hillman, H. D. Doerfler, H. Sachmann, *Mol. Cryst. Liq. Cryst. 133* (1986) 259.
[34] R. F. Grant, *Can. J. Chem. 42* (1964) 951.
[35] H. Abied, D. Guillon, A. Skoulios, P. Weber, A.-M. Giroud-Godquin, J. C. Marchon, *Liq. Cryst. 2* (1987) 269; see also M. Takeoshi, N. Watanabe, B. Tamamushi, *Colloid Polym. Sci. 256* (1978) 588.
[36] A.-M. Godquin-Giroud, J. C. Marchon, D. Guillon, A. Skoulios, *J. Phys. Lett. (Orsay, Fr.) 45* (1984) L681.
[37] H. Abied, D. Guillon, A. Skoulios, A.-M. Giroud-Godquin, P. Maldivi, J. C. Marchon, *Colloid Polym. Sci. 266* (1988) 579.
[37] H. Abied, D. Guillon, A. Skoulios, A.-M. Giroud-Godquin, P. Maldivi, J. C. Marchon, *Colloid Polym. Sci. 266* (1988) 579.
[38] J. R. Lomer, K. Perrera, *Acta Crystallogr. Sect. B 30* (1974) 2912.
[39] P. Maldivi, D. Guillon, A.-M. Giroud-Godquin, J. C. Marchon, H. Abied, H. Dexpert, A. Skoulios, *J. Chim. Phys. 86* (1989) 1651; H. Abied, D. Guillon, A. Skoulios, H. Dexpert, A.-M. Giroud-Godquin, J. C. Marchon, *J. Phys. (Orsay, Fr.) 49* (1988) 345.
[40] A.-M. Giroud-Godquin, J. M. Latour, J. C. Marchon, *Inorg. Chem. 24* (1985) 4452.
[41] J. C. Marchon, P. Maldivi, A.-M. Giroud-Godquin, D. Guillon, A. Skoulios, D. P. Strommen, *Philos. Trans. R. Soc. London A330* (1990) 109; O. Poizat, D. P. Strommen, P. Maldivi, A.-M. Giroud-Godquin, J.-C. Marchon, *Inorg. Chem. 29* (1990) 4853.
[42] D. P. Strommen, A. M. Giroud-Godquin, P. Maldivi, J. C. Marchon, B. Marchon, *Liq. Cryst. 2* (1987) 689.
[43] A.-M. Giroud-Godquin, P. Maldivi, J. C. Marchon, M. Bee. L. Carpentier, *Mol. Phys. 68* (1989) 1353; L. Carpentier, M. Bee, A.-M. Giroud-Godquin, P. Maldivi, J. C. Marchon, *ibid. 68* ((1989) 1367.
[44] A.-M. Giroud-Godquin, P. Maldivi, J. C. Marchon, P. Aldebert, A. Peguy, D. Guillon, A. Skoulios, *J. Phys. (Orsay, Fr.) 50* (1989) 513.

[45] A.-M. Giroud-Godquin, J. C. Marchon, D. Guillon, A. Skoulios, *J. Phys. Chem. 90* (1986) 5502.

[46] a) P. Maldivi, A.-M. Giroud-Godquin, J. C. Marchon, D. Guillon, A. Skoulios, *Chem. Phys. Lett. 157* (1989) 552; F. Cukiernik, P. Maldivi, A.-M. Giroud-Godquin, J. C. Marchon, M. Ibn-Elhat, D. Guillon, A. Skoulios, *Liq. Cryst.*, in press; b) R. H. Cayton, M. H. Chisholm, F. D. Darrington, *Angew. Chem. 102* (1990) 1490; *Angew. Chem. Int. Ed. Engl. 29* (1990) 1481.

[47] a) R. C. Mehrotra, R. Bohra, D. P. Gaur, *Metal β-Diketonates and Allied Derivatives*, Academic, London 1978; b) F. P. Fanizzi, A. Servante, D. W. Bruce, P. M. Maitlis, unpublished.

[48] B. J. Bulkin, R. K. Rose, A. Santoro, *Mol. Cryst. Liq. Cryst. 43* (1977) 53.

[49] K. Ohta, M. Yokoyama, S. Kusabayashi, H. Mikawa, *J. Chem. Soc. Chem. Commun. 1980*, 392; K. Ohta, M. Yokoyama, S. Kusabayashi, H. Mikawa, *Mol. Cryst. Liq. Cryst. 69* (1981) 131.

[50] K. Ohta, G. J. Jiang, M. Yokoyama, S. Kusabayashi, H. Mikawa, *Mol. Cryst. Liq. Cryst. 66* (1981) 283.

[51] K. Ohta, M. Yokoyama, H. Mikawa, *Mol. Cryst. Liq. Cryst. 73* (1981) 205.

[52] J. G. Burr, W. F. Holton, G. N. Webb, *J. Am. Chem. Soc. 72* (1950) 4903.

[53] A.-M. Giroud-Godquin, J. Billard, *Mol. Cryst. Liq. Cryst. 97* (1983) 287.

[54] R. Fugnitto, H. Strzelecka, A. Zann, J. C. Dubois, J. Billard, *J. Chem. Soc. Chem. Commun. 1980*, 271.

[55] A.-M. Giroud-Godquin, J. Billard, *Mol. Cryst. Liq. Cryst. 66* (1981) 147; A.-M. Giroud-Godquin, FR-B. 8016032 (1980).

[56] K. Usha, K. Vijayan, *Mol. Cryst. Liq. Cryst. 174* (1989) 39; see also A. N. Knyazeva, E. A. Shugam, L. M. Shkol'nikova, *Zh. Strukt. Khim. 10* (1969) 83.

[57] A. C. Ribeiro, A. F. Martins, A.-M. Giroud-Godquin, *Mol. Cryst. Liq. Cryst. Lett. Sect. 5* (1988) 133.

[58] K. Ohta, A. Ishii, I. Yamamoto, K. Matsuzaki, *J. Chem. Soc. Chem. Commun. 1984*, 1099; K. Ohta, A. Ishii, H. Muroki, I. Yamamoto, K. Matsuzaki, *Mol. Cryst. Liq. Cryst. 116* (1985) 299.

[59] K. Ohta, H. Muroki, A. Takagi, I. Yamamoto, K. Matsuzaki, *Mol. Cryst. Liq. Cryst. 135* (1986) 247.

[60] M. P. Eastman, M. L. Horng, B. Freiha, K. W. Sheu, *Liq. Cryst. 2* (1987) 223.

[61] K. Ohta, H. Muroki, K.-I. Hatada, A. Takagi, H. Ema, I. Yamamoto, K. Matsuzaki, *Mol. Cryst. Liq. Cryst. 140* (1986) 163; K. Ohta, H. Muroki, A. Takagi, K. I. Hatada, H. Ema, I. Yamamoto, K. Matsuzaki, *ibid. 140* (1986) 131; see also K. Ohta, H. Muroki, H.-I. Hatada, I. Yamamoto, K. Matsuzaki, *ibid. 130* (1985) 249.

[62] H. Sakashita, A. Nishitani, Y. Sumiya, H. Terauchi, K. Ohta, I. Yamamoto, *Mol. Cryst. Liq. Cryst. 163* (1988) 211.

[63] B. K. Sadashiva, S. Ramesha, *Mol. Cryst. Liq. Cryst. 141* (1986) 19; V. Prasad, B. K. Sadashiva, *ibid.*, in press.

[64] S. Chandrasekhar, B. K. Sadashiva, S. Ramesha, B. S. Srikanta, *Pramana 27* (1986) L 713.

[65] S. Chandrasekhar, B. K. Sadashiva, B. S. Srikanta, *Mol. Cryst. Liq. Cryst. 151* (1987) 93; see also *ibid. 166* (1989) 231.

[66] S. Chandrasekhar, B. R. Ratna, B. K. Sadashiva, V. N. Raja, *Mol. Cryst. Liq. Cryst. 165* (1988) 123.

[67] S. Chandrasekhar, B. K. Sadashiva, B. R. Ratna, V. N. Raja, *Pramana 30* (1988) L 491.

[68] B. K. Sadashiva, P. R. Rao, B. S. Srikanta, *Mol. Cryst. Liq. Cryst. 168* (1989) 103.

[69] B. Mühlberger, W. Haase, *Liq. Cryst. 5* (1989) 251.

[70] C. Destrade, H. Gasparoux, P. Foucher, N. Huu Tinh, J. Malthete, J. Jacques, *J. Chim. Phys. Phys. Chim. Biol. 80* (1983) 137.

[71] A.-M. Giroud-Godquin, G. Sigaud, M. F. Achard, F. Hardouin, *J. Phys. Lett. (Orsay, Fr.) 45* (1984) L 387; A.-M. Giroud-Godquin, FR-B. 8 319 072 (1983); P. Terech, C. Chachaty, J. Gaillard, A.-M. Giroud-Godquin, *J. Phys. (Orsay, Fr.) 48* (1987) 663.

[72] A.-M. Giroud-Godquin, M. M. Gauthier, G. Sigaud, F. Hardouin, M. F. Achard, *Mol. Cryst. Liq. Cryst. 132* (1986) 35.

[73] C. Destrade, M. C. Mondon, J. Malthete, *J. Phys. Collog. (Orsay, Fr.) 40* (1979) C3.

[74] K. Ohta, H. Ema, H. Muroki, I. Yamamoto, K. Matsuzaki, *Mol. Cryst. Liq. Cryst. 147* (1987) 61.

[75] A.-M. Giroud-Godquin, A. Rassat, *C.R. Seances Acad. Sci. Ser. 2 294* (1982) 241.

[76] A.-M. Giroud, *Ann. Phys. (Paris) 3* (1978) 147.

[77] A.-M. Giroud, A. Nazzal, U. T. Müller-Westerhoff, *Mol. Cryst. Liq. Cryst. 56* (1980) 225.

[78] U. T. Müller-Westerhoff, A. Nazzal, R. J. Cox, A.-M. Giroud, *Mol. Cryst. Liq. Cryst. 56* (1980) 249.

[79] M. Cortrait, J. Gaultier, C. Polycarpe, A.-M. Giroud, U. T. Mueller-Westerhoff, *Acta Crystallogr. Sect. C39* (1983) 833.

[80] H. Schubert, H. J. Lorenz, R. Hoffmann, F. Franke, *Z. Chem. 6* (1955) 337.

[81] U. T. Müller-Westerhoff, A. Nazzal, R. J. Cox, A.-M. Giroud, *J. Chem. Soc. Chem. Commun. 1980*, 497.

[82] K. L. Marshall, S. D. Jacobs, *Mol. Cryst. Liq. Cryst. 159* (1988) 181.

[83] M. Veber, R. Fugnitto, H. Strzelecka, *Mol. Cryst. Liq. Cryst. 96* (1983) 221.

[84] M. Veber, P. Davidson, C. Jallabert, A. M. Levelut, H. Strzelecka, *Mol. Cryst. Liq. Cryst. Sect. 5* (1987) 1.

[85] K. Ohta, A. Takagi, H. Muroki, I. Yamamoto, K. Matsuzaki, T. Inabe, Y. Maruyama, *J. Chem. Soc. Chem. Commun. 1986*, 883; K. Ohta, A. Takagi, H. Muroki, I. Yamamoto, K. Matsuzaki, *Mol. Cryst. Liq. Cryst. 147* (1987) 15.

[86] K. Ohta, H. Hasebe, H. Ema, T. Fujimoto, I. Yamamoto, *J. Chem. Soc. Chem. Commun. 1989*, 1610.

[87] R. Dhillon, *MSc-Thesis*, Sheffield University 1987.

[88] H. Adams, N. A. Bailey, D. W. Bruce, R. Dhillon, D. A. Dunmur, S. E. Hunt, E. Lalinde, A. A. Maggs, R. Orr, P. Styring, M. S. Wragg, P. M. Maitlis, *Polyhedron 7* (1988) 1861.

[89] M. Bonamico, G. Dessy, V. Fares, L. Scaramuzza, *J. Chem. Soc. Dalton Trans. 1972*, 2515.

[90] H. Adams, N. A. Bailey, D. W. Bruce, R. Dhillon, D. A. Dunmur, P. Espinet, P. M. Maitlis, unpublished data.

[91] I. Yamamato, K. Ota, H. Takatsu, Jpn. Kokai Tokkyo Koho JP 01 242 566 [89 242 566], *Chem. Abstr. 112* (1990) 149 141k.

[92] K. Ohta, H. Ema, I. Yamamoto, K. Matsuzaki, *Liq. Cryst. 3* (1988) 1671.

[93] C. Piechocki, J. Simon, A. Skoulios, D. Guillon, P. Weber, *J. Am. Chem. Soc. 104* (1982) 5245; see also D. Guillon, A. Skoulios, C. Piechocki, J. Simon, P. Weber, *Mol. Cryst. Liq. Cryst. 100* (1983) 275; J. J. Andre, M. Bernard, C. Piechocki, J. Simon, *J. Phys. Chem. 90* (1986) 1327; C. Piechocki, J. Simon, *Nouv. J. Chim. 9* (1985) 159; D. Lelievre, M. A. Petit, J. Simon, *Liq- Cryst. 4* (1989) 707; J. Simon, C. Sirlin, *Pure Appl. Chem. 61* (1989) 1625.

[94] J. F. van der Pol, E. Neeleman, J. W. Zwikker, R. J. M. Nolte, W. Drenth, J. Aerts, R. Visser, S. J. Picken, *Liq. Cryst. 6* (1989) 577; J. F. van der Pol, E. Neeleman, J. W. Zwikker, R. J. M. Nolte, W. Drenth, *Recl. Trav. Chim. Pays-Bas 107* (1988) 615.

[95] C. Sirlin, L. Bosio, J. Simon, V. Ahsen, E. Yilmazer, O. Bekaroglu, *Chem. Phys. Lett. 139* (1987) 362.

[96] N. Boden, R. J. Bushby, J. Clements, M. V. Jesudason, P. F. Knowles, G. Williams, *Chem. Phys. Lett. 152* (1988) 94; *ibid. 154* (1988) 613.

[97] G. Blasse, G. J. Dirksen, A. Meijerink, J. F. van der Pol, E. Neeleman, W. Drenth, *Chem. Phys. Lett. 154* (1989) 420.

[98] I. Cho, Y. Lim, *Mol. Cryst. Liq. Cryst. 154* (1988) 9.

[99] I. Cho, Y. Lim, *Chem. Lett. 1987*, 2107; *Bull. Korean Chem. Soc. 9* (1988) 98.

[100] M. Hanack, A. Beck, H. Lehmann, *Synthesis 1987*, 703.

[101] D. Guillon, P. Weber, A. Skoulios, C. Piechoki, J. Simon, *Mol. Cryst. Liq. Cryst. 130* (1985) 223.

[102] M. J. Cook, M. F. Daniel, K. J. Harrison, N. B. McKeown, A. J. Thomson, *J. Chem. Soc. Chem. Commun. 1987*, 1086; M. J. Cook, A. J. Dunn, S. D. Howe, A. J. Thomson, K. J. Harrison, *J. Chem. Soc. Perkin Trans. 1 1988*, 2453; see also D. Markovitsi, T. H. Tran-Thi, V. Briois, *J. Am. Chem. Soc. 110* (1988) 2001.

[103] C. Piechocki, J. Simon, J. J. Andre, D. Guillon, P. Petit, A. Skoulios, P. Weber, *Chem. Phys. Lett. 122* (1985) 124; F. Castaneda, C. Piechocki, V. Plichon, J. Simon, J. Vaxiviere, *Electrochim. Acta 31* (1986) 131; S. Besbes, V. Plichon, J. Simon, J. Vaxviere, *J. Electroanal. Chem. Interfacial Electrochem. 237* (1987) 61 Z. Belarbi, M. Maitrot, K. Ohta, J. Simon, J. J. Andre, P. Petit, *Chem. Phys. Lett. 143* (1988) 400; Z. Belarbi, C. Sirlin, J. Simon, J. J. Andre, *J. Phys. Chem. 93* (1989) 8105.

[104] C. Sirlin, L. Bosio, J. Simon, *J. Chem. Soc. Chem. Commun. 1988*, 236; *Mol. Cryst. Liq. Cryst. 155* (1988) 231; see also T. Sauer, G. Wegner, *Mol. Cryst. Liq. Cryst. 162* (1988) 97.

[105] C. Sirlin, L. Bosio, J. Simon, *J. Chem. Soc. Chem. Commun. 1987*, 379.

[106] C. Piechocki, J. C. Boulou, J. Simon, *Mol. Cryst. Liq. Cryst. 149* (1987) 115.

[107] P. Weber, D. Guillon, A. Skoulios, *J. Phys. Chem. 91* (1987) 2242.

[108] B. A. Gregg, M. A. Fox, A. J. Bard, *J. Am. Chem. Soc. 111* (1989) 3024; S. Gaspard, P. Maillard, J. Billard, *Mol. Cryst. Liq. Cryst. 123* (1985) 369.

[109] K. Ohta, T. Watanabe, T. Fujimoto, I. Yamamoto, *J. Chem. Soc. Chem. Commun. 1989*, 1611.

[110] M. Hunziker, EP-B 0162804; *Chem. Abstr. 106* (1987) 41716p.

[111] D. Markovitsi, J. J. Andre, A. Mathis, J. Simon, P. Spegt, G. Weill, M. Ziliox, *Chem. Phys. Lett. 104* (1984) 46.

[112] D. Markovitsi, M. Bernard, J.-J. Andre, J. Simon, *J. Phys. Chem. 90* (1986) 1323.

[113] K. Hanabusa, J.-I. Higashi, T. Koyama, H. Shirai, N. Hojo, A. Kurose, *Makromol. Chem. 190* (1989) 1.

[114] I. V. Ovchinnikov, Yu. G. Galyametdinov, G. I. Ivanova, L. M. Yagfarova, *Dokl. Akad. Nauk SSR 276* (1984) 126; Yu. G. Galyametdinov, G. I. Ivanova, I. V. Ovchinnikov, SU-B 1 085 979; *Chem. Abstr. 101* (1984) 102799p; I. V. Ovchinnikov, Yu. G. Galyametdinov, I. G. Bikchantaev, *Izv. Akad. Nauk SSSR Ser. Fiz. 53* (1989) 1870.

[115] Yu. G. Galyametdinov, I. V. Ovchinnikov, B. M. Bolotin, N. B. Etingen, G. I. Ivanova, L. M. Yagfarova, *Izv. Akad. Nauk SSSR, Ser. Khim. 1984*, 2379; R. M. Galimov, I. G. Bikchantaev, I. V. Ovchinnikov, *Zh. Strukt. Khim. 30* (1989) 65.

[116] Yu. G. Galyametdinov, D. Z. Zakieva, I. V. Ovchinnikov, *Izv. Akad. Nauk SSSR Ser. Khim. 1986*, 491.
[117] I. G. Bikchantaev, R. M. Galimov, I. V. Ovchinnikov, *Teor. Eksp. Khim. 24* (1988) 370.
[118] N. Hoshino, H. Murakami, Y. Matsunaga, T. Inabe, Y. Maruyama, *Inorg. Chem. 29* (1990) 1177.
[119] M. Marcos, P. Romero, J. L. Serrano, C. Bueno, J. A. Cabeza, L. A. Oro, *Mol. Cryst. Liq. Cryst. 167* (1989) 123.
[120] M. Marcos, P. Romero, J. L. Serrano, *J. Chem. Soc. Chem. Commun. 1989*, 1641.
[121] M. Marcos, P. Romero, J. L. Serrano, *Chem. Mater. 2* (1990) 495.
[122] U. Caruso, A. Roviello, A. Sirigu, *Liq. Cryst. 7* (1990) 421, 431.
[123] E. Bui, J. P. Bayle, F. Perez, L. Liebert, J. Courtieu, *Liq. Cryst. 8* (1990) 513.
[124] M. Ghedini, S. Armentano, R. Bartolino, G. Torquati, F. Rustichelli, *Solid State Commun. 64* (1987) 1191; M. Ghedini, S. Armentano, R. Bartolino, N. Kirov, M. Petrov, S. Nenova, *J. Mol. Liq. 38* (1988) 207; A. M. Levelut, M. Ghedini, R. Bartolino, F. P. Nicoletta, F. Rustichelli, *J. Phys. (Orsay, Fr.) 50* (1989) 113.
[125] M. Marcos, P. Romero, J. L. Serrano, J. Barbera, A.-M. Levelut, *Liq. Cryst. 7* (1990) 251.
[126] R. Paschke, H. Zaschke, A. Madicke, J. R. Chipperfield, A. B. Blake, P. G. Nelson, G. W. Gray, *Mol. Cryst. Liq. Cryst. Lett. Sect. 6* (1988) 81; T. D. Shaffer, K. A. Sheth, *Mol. Cryst. Liq. Cryst. 172* (1989) 27.
[127] U. Caruso, A. Roviello, A. Sirigu, *Liq. Cryst. 3* (1988) 1515; see also J. P. Bayle, E. Bui, F. Perez, J. Courtieu, *Bull. Soc. Chim. Fr. 1989*, 532.
[128] A. Roviello, A. Sirigu, P. Iannelli, A. Immirzi, *Liq. Cryst. 3* (1988) 115; P. Iannelli, A. Immirzi, U. Caruso, A. Roviello, A. Sirigu, *Acta Crystallogr. Sect. C45* (1989) 879.
[129] Yu. G. Galyametdinov, I. G. Bikchantaev, I. V. Ovchinnikov, *Zh. Obshch. Khim. 58* (1988) 1326.
[130] Yu. G. Galyametdinov, G. I. Ivanova, I. V. Ovchinnikov, *Zh. Obshch. Khim. 54* (1984) 2796.
[131] J. L. Serrano, P. Romero, M. Marcos, P. J. Alonso, *J. Chem. Soc. Chem. Commun. 1990*, 859.
[132] Yu. G. Galyametdinov, G. I. Ivanova, I. V. Ovchinnikov, *Izv. Akad. Nauk SSSR Ser. Khim. 1989*, 1931.
[133] C. Carfagna, U. Caruso, A. Roviello, A. Sirigu, *Makromol. Chem. Rapid Commun. 8* (1987) 345.
[134] J. S. Moore, S. I. Stupp, *Polymer Bull. (Berlin) 19* (1988) 251.
[135] M Ghedini, M. Longeri, R. Bartolino, *Mol. Cryst. Liq. Cryst. 84* (1982) 207.
[136] M. Ghedini, S. Licoccia, S. Armentano, R. Bartolino, *Mol. Cryst. Liq. Cryst. 108* (1984) 269; see also M. Ghedini, S. Armentano, R. Bartolino, F. Rustichelli, G. Torquati, N. Kirov, M. Petrov, *ibid. 151* (1987) 75.
[137] M. Ghedini, S. Armentano, F. Neve, S. Licoccia, *J. Chem. Soc. Dalton Trans. 1988*, 1565.
[138] M. Ghedini, S. Armentano, F. Neve, *Inorg. Chim. Acta 134* (1987) 23.
[139] A. M. M. Lanfredi, F. Ugozzoli, M. Ghedini, S. Licoccia, *Inorg. Chim. Acta 86* (1984) 165; M. Ghedini, C. Pellegrino, S. Armentano, G. de Munno, G. Bruno, *ibid. 122* (1986) 193.
[140] J. Barbera, P. Espinet, E. Lalinde, M. Marcos, J. L. Serrano, *Liq. Cryst.* 2 (1987) 833; see also M. A. Ciriano, P. Espinet, E. Lalinde, M. B. Ros, J. L. Serrano, *J. Mol. Struct. 196* (1989) 327; M. Marcos, M. B. Ros, J. L. Serrano, *Liq. Cryst. 8* (1988) 1129; M. B. Ros, N. Ruiz, J. L. Serrano, P. Espinet, *Liq. Cryst. 9* (1991) 77.
[141] P. Espinet, E. Lalinde, M. Marcos, J. Perez, J. L. Serrano, *Organometallics 9* (1990) 555.
[142] P. Espinet, J. Extebarria, M. Marcos, J. Perez, A. Remon, J. L. Serrano, *Angew. Chem. 101* (1989) 1076; *Angew. Chem. Int. Ed. Engl. 28* (1989) 1065.
[143] P. Espinet, J. Perez, M. Marcos, M. B. Ros, J. L. Serrano, J. Barbera, A. M. Levelut, *Organometallics 9* (1990) 2028.
[144] S. Shinkai, T. Nishi, A. Ikeda, T. Matsuda, K. Shimamoto, O. Manabe, *J. Chem. Soc. Chem. Commun. 1990*, 303.
[145] *Chem. Eng. News 1990*, No. 38, p. 36.
[146] R. G. Weiss, *Tetrahedron 44* (1988) 3413.

Catalytic Enantioselective Epoxidations of Simple Olefins

By *Carsten Bolm**

Asymmetric oxidation is of general importance for the synthesis of optically active organic compounds. With the enantioselective epoxidation of allyl alcohols, *Sharpless* and *Katzuki* introduced in 1980 an extremely efficient transition metal-catalyzed oxygen transfer, by means of which 2,3-epoxyalcohols can be synthesized in good yields and with very high enantiomeric excesses [Eq. (a), X = OH].[1] The titanium tartrate catalyst employed tolerates a high degree of structural variation in the prochiral substrate. By covalent bonding of the allyl alcohol to the chirally modified metal center, conformational freedom is restricted and generally enantioselectivities of over 90% are achieved.

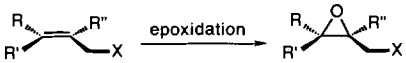

(a)

Also other catalytic systems, such as the ruthenium-BINAP complex developed by *Noyori* et al. for the homogeneous enantioselective hydrogenation of ketones and olefins,[2] require directing groups which temporarily bind the substrate tightly to the metal center. This binding and any subsequent reaction are influenced by the interactions between substrate and optically active ligand, whereby the stereochemical course of the reaction is determined.

An especially interesting challenge in this connection was the development of catalysts for enantioselective oxidations of *unfunctionalized* olefins [Eq. (a), X = H, alkyl, etc.]. These alkenes cannot form conformationally restricting chelate complexes, and consequently differentiation of the enantiotropic sides of the substrate is rendered considerably difficult. The catalytic asymmetric dehydroxylation of unfunctionalized *trans*-alkenes with osmium tetroxide–alkaloid complexes first described by *Sharpless* et al.,[3] stimulated the development of enantioselective catalysts for the epoxidation of these substrates too, and numerous relevant studies have since been reported.

With the cationic (salen)manganese(III) complex **1**, *Jacobsen* et al. were able to epoxidize mono-, di, and trisubstituted olefins with good asymmetric induction (20–93% *ee*) (Fig. 1).[4] 1–8 mol-% of the complex catalyzes the transfer of oxygen from oxidants such as iodosylmesitylene or sodium hypochlorite to the prochiral substrate. The course of the enantioselection is interpreted in terms of a side-on approach of the substrate to the active oxomanganese(V) intermediate. To achieve higher enantioselectivities, sterically demanding *tert*-butyl groups have proven essential. Their interactions with the more hindered side of an unsymmetrical olefin determine the orientation of the substrate during its approach to the metal-oxo bond, and thus the enantiofacial selectivity of the oxygen transfer. In accord with this model, *cis*-disubstituted olefins are as a rule epoxidized with higher asymmetric induction than are comparable *trans*-alkenes (Fig. 1). Replacement of the *tert*-butyl groups by optically active substituents and addition of 2-methylimidazole can, in individual cases, lead to a slight increase in asymmetric induction.[5] These studies by *Katzuki* et al. also indicate possible radical intermediates, as were previously discussed in fundamental investigations by *Kochi* et al.[6]

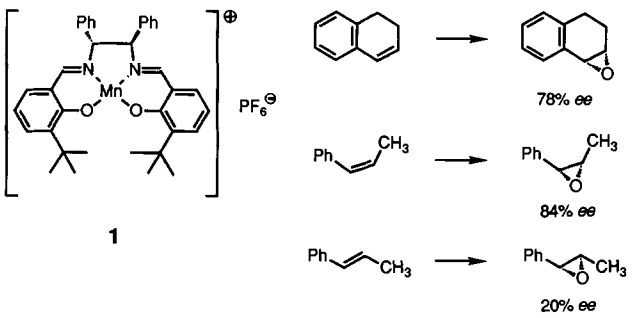

Fig. 1. Examples of enantioselective epoxidations of simple olefins with the (salen)manganese(III) complex **1** according to the method of *Jacobsen* et al. [4].

The development of chirally modified metalloporphyrins by the groups of *Groves, Mansuy*, and *Kodadek* provided a further transition metal-catalyzed entry to optically active epoxides.[7] Simple prochiral olefins such as β-methylstyrene can be epoxidized with enantiomeric excesses of up to 72%, both with bridged (basket handle) and with peripherally highly-substituted (picket) metalloporphyrins **2** and **3**, respectively. The chiral binaphthyl bridges in **2** generate a conformationally rigid, chiral environment at the metal center, which effectuates molecular recognition of the substrate. The inherent sensitivity of the porphyrins to oxidation can be reduced by skillful substitution of the *meso* phenyl groups, making higher turnover numbers in catalytic processes possible. Here again, hypochlorite or iodosylarenes are used as oxidizing agent.

The catalytic activity of the metalloporphyrins in oxidations is not limited to only epoxidations. *Groves* and *Viski* have also succeeded in carrying out the asymmetric hydroxylation of benzylic methylene groups and the enantioselec-

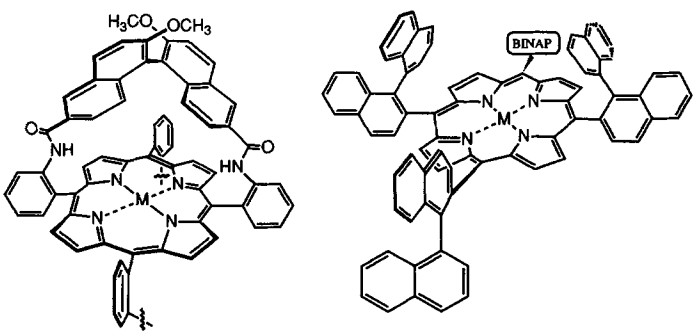

2, M = Mn, Fe **3**, M = Mn

Fig. 2. Metalloporphyrins for catalytic asymmetric epoxidation according to the methods of *Groves* et al. [7a] and *Kodadek* et al. [7d].

[*] Dr. C. Bolm
Institut für Organische Chemie der Universität
St.-Johanns-Ring 19, CH-4056 Basel (Switzerland)

tive sulfoxidation of prochiral alkyl sulfides with the metalloporphyrins **2**.[7a] With iron- and manganese-complexes they achieved enantiomeric excesses of up to 72%. Metalloporphyrins are thus not only important model compounds for oxygen transfer in cytochrome P-450, but they can also be used as effective catalysts for interesting asymmetric oxidations.

As long as ten years ago *Juliá* et al. described the efficient epoxidation of chalcones in the three-phase system toluene–water–polyamino acid.[8] The optically active epoxychalcones are obtained in good chemical and high optical yields (up to 96% *ee*) by oxidation with H_2O_2/NaOH at room temperature. Poly-α-amino acids can be synthesized via polymerization of the corresponding *N*-carboxyanhydrides with various chain lengths and different end groups. They are formed both in a stretched as well as in a helical conformation. To achieve higher enantioselectivities in the epoxidation of chalcones a polymer chain length of least ten amino acid units is necessary. Very good results were achieved with poly-L-leucine and poly-L-isoleucine, poly-L-valine on the other hand proved to be less efficient with respect to chemical yield and enantioselectivity.

Flisak et al. have recently described a further potential application of this reaction.[9] Using a commercially available poly-L-leucine they were able to epoxidize substituted chalcones with high enantioselection (up to 92% *ee*) by the Juliá method. The polymer can be recovered without loss of activity and used for further epoxidations. By regioselective Baeyer-Villiger oxidation of the epoxychalcones with *meta*-chloroperbenzoic acid (MCPBA) in boiling dichlormethane the synthetically valuable glycidic esters can be synthesized. The enantiomeric excess is increased by recrystallization, so the products are obtained almost enantiomerically pure (> 99% *ee*) [Eq. (b)]. This two-step oxidation sequence—enantioselective epoxidation with poly-L-leucine and regioselective Baeyer-Villiger oxidation—thus enables an efficient entry to important optically active intermediates for organic synthesis.

Asymmetric epoxidation with catalytic amounts of polyamino acids has thus far been restricted to only chalcones. Other electron-deficient olefins, such as nitroalkenes or cycloalk-2-enones, could be oxidized in this way only with slight asymmetric induction.[10] The development of new polymer-supported polyamino acids could fulfill far-reaching hopes in this area.[11]

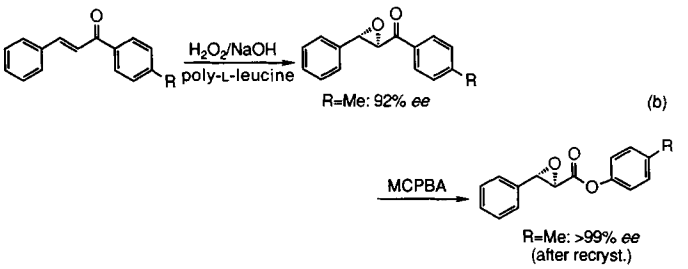

German version: *Angew. Chem. 103* (1991) 414

[1] a) T. Katsuki, K. B. Sharpless, *J. Am. Chem. Soc. 102* (1980) 5974; b) Y. Gao, R. M. Hanson, J. M. Klunder, S. Y. Ko, H. Masamune, K. B. Sharpless, *ibid. 109* (1987) 5765.
[2] R. Noyori, *Science 248* (1990) 1194.
[3] E. N. Jacobsen, I. E. Markó, W. S. Mungall, G. W. Schröder, K. B. Sharpless, *J. Am. Chem. Soc. 110* (1988) 1968.
[4] W. Zhang, J. L. Loebach, S. R. Wilson, E. N. Jacobsen, *J. Am. Chem. Soc. 112* (1990) 2801.
[5] R. Irie, K. Noda, Y. Ito, N. Matsumoto, T. Katsuki, *Tetrahedron Lett. 31* (1990) 7345.
[6] K. Srinivasan, P. Michaud, J. K. Kochi, *J. Am. Chem. Soc. 108* (1986) 2309.
[7] a) J. T. Groves, P. Viski, *J. Org. Chem. 55* (1990) 3628; b) J. T. Groves, R. S. Myers, *J. Am. Chem. Soc. 105* (1983) 5791; c) D. Mansuy, P. Battioni, J.-P. Renaud, P. Guerin, *J. Chem. Soc. Chem. Commun. 1985*, 155; d) S. O'Malley, T. Kodadek, *J. Am. Chem. Soc. 111* (1989) 9116.
[8] a) S. Juliá, J. Masana, J. C. Vega, *Angew. Chem. 92* (1980) 968; *Angew. Chem. Int. Ed. Engl. 19* (1980) 929; b) S. Colonna, H. Molinari, S. Banfi, S. Juliá, J. Masana, A. Alvarez, *Tetrahedron 39* (1983) 1635; c) S. Juliá, J. Guixer, J. Masana, J. Rocas, S. Colonna, R. Annuziata, H. Molinari, *J. Chem. Soc. Perkin Trans. 1, 1982*, 1317.
[9] P. W. Baures, D. S. Eggleston, J. R. Flisak, K. Gombatz, I. Lantos, W. Mendelson, J. J. Remich, *Tetrahedron Lett. 31* (1990) 6501.
[10] For the use of alkaloids as phase transfer catalysts in asymmetric epoxidation see: H. Wynberg, *Top. Stereochem. 16* (1986) 87, and references cited therein.
[11] S. Itsuno, M. Sakakura, K. Ito, *J. Org. Chem. 55* (1990) 6047.

 © VCH Verlagsgesellschaft mbH, W-6940 Weinheim, 1991 0570-0833/91/0404-0404 $ 3.50+.25/0

Piezoelectric Liquid-Crystalline Elastomers

By *J. H. Wendorff**

In 1880 *Paul Jacques* and *Pierre Curie*[1] made the discovery that certain materials form electric charges on their surface if subjected to a mechanical stress. They called this effect *piezoelectricity*. This term denotes also the inverse effect: the induction of mechanical deformations due to the application of an electric field. Quarz is a typical example of a material displaying piezoelectricity and certain ceramics were later found to display huge piezoelectric effects.[2] They are used today in a large variety of applications: sensors, electromechanical or electroacoustic transducers, positioning elements (for instance in the scanning tunnel electron microscope) are some examples. Piezoelectric ceramics possess, however, disadvantages like brittleness (which makes handling and shaping difficult) and high dielectric constants and densities.

The report in 1969 of *Kawai*[3] that piezoelectric effects for the partially crystalline polymer poly(vinylidene fluoride) (PVDF) were orders of magnitude larger than usually observed for polymers and well within a range suitable for applications repesented important progress. This observation has stimulated much experimental and theoretical work on the nature of this effect and on the development of other polymers with similar or even higher piezoelectric responses.

Major advantages of piezoelectric polymers are, of course, the ease of manufacturing piezoelectric elements in any shape (including film elements as thin as 1 μm), the good mechanical properties of the polymers, their resistence to moisture and many organic solvents, and their low dielectric constant and density. PVDF and copolymers derived from it are currently used with great advantage in electroacoustic and electromechanical transducers because of their low impedance, their broad band modulation characteristics, and the low mass of active elements made form them.[2] Microphones, loudspeakers, positioning elements for robots, sensors used in medicine and biology, information storage—the number of applications of piezoelectric polymers is indeed very large today.

It could be much larger if we had piezoelectric polymers with a broad range of mechanical responses, dielectric properties, optical properties etc. *Kawai*'s discovery and the subsequent investigations, however, have not opened up promising routes to novel polymers with strong piezoelectric responses. The reason is simple: a fundamental requirement for the occurrence of piezoelectric properties is the absence of an inversion center. Even today when we can take advantage of computer-aided molecular modeling, it is almost impossible to design polymers so that their crystal structures have no inversion center.

It seems, however, that we are currently experiencing a major breakthrough in this area[4–8] as a result of the efforts of theoreticians and of experimentalists alike. The approach is based on a suitable combination of network properties and properties characteristic of certain liquid-crystalline phases.

As pointed out above, the absence of an inversion symmetry is essential for the occurrence of piezoelectricity. The cholesteric phase which displays locally a nematic structure (director $\vec{n}$) and a helical arrangement of this director in space (Fig. 1 a) does not have this symmetry. The same holds for the chiral smectic C* phase, where the molecules in the smectic layers (Fig. 1 b) are tilted in a regular fashion. Symmetry arguments suggest that such phases should display piezoelectric effects, but low molar mass liquid crystals displaying these phases are hardly suitable for technical applications.

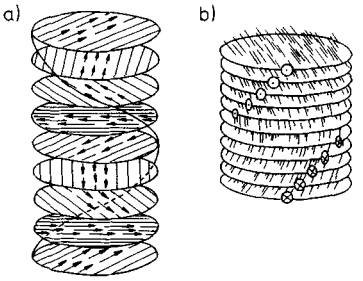

Fig. 1. Schematic representation of the structure of the cholesteric phase (a) and the chiral smectic C* phase (b).

A solution to this problem is on the horizon. The first step was made when *H. Finkelmann*[9] showed in 1981 that liquid-crystalline structures can be obtained in a lightly cross-linked polymeric network. A whole series of liquid-crystalline elastomers were synthesized and characterized by him and later by other groups,[8] among them cholesteric and chiral smectic C* elastomers. These polymers display mechanical properties similar to non-liquid-crystalline elastomers such as ductility of up to several 100%.

The second stop towards novel piezoelectric materials was made very recently when *H. Brand* et al.[4, 5] used a phenomenological approach—a Landau–Ginzburg type of expansion of the free energy of the elastomers for coupling to mechanical and electric fields—and came to the conclusion that such cholesteric and chiral smectic C* elastomers should display interesting electromechanical properties including special piezoelectric properties. Such properties result, according to this analysis, from the combination of network properties and the intrinsic properties of chiral liquid-crystalline phases. Predictions were that an electric polarization is caused by the deformation (compression) of the helix, as in the case of low molar mass liquid crystals. In addition, piezoelectric effects should arise from the coupling of the electric field and the network. Thus mechanical distortions cause an electric polarization and vice versa. Furthermore, the theoretical analysis suggests that various modes of distortion (shear, compression) give rise to piezoelectric effects.

The last months have seen the third step towards novel classes of piezoelectric materials. It was shown experimentally by *H. Finkelmann* et al.[6] and *S. U. Vallerian* et al.[7] that, qualitatively at least, these predictions are correct. Figure 2 shows the chemical structure of a typical cholesteric elastomer and Figure 2 b experimental proof of its piezoelectric properties.

[*] Dr. J. H. Wendorff
Deutsches Kunststoff-Institut
Schlossgartenstrasse 6, W-6100 Darmstadt (FRG)

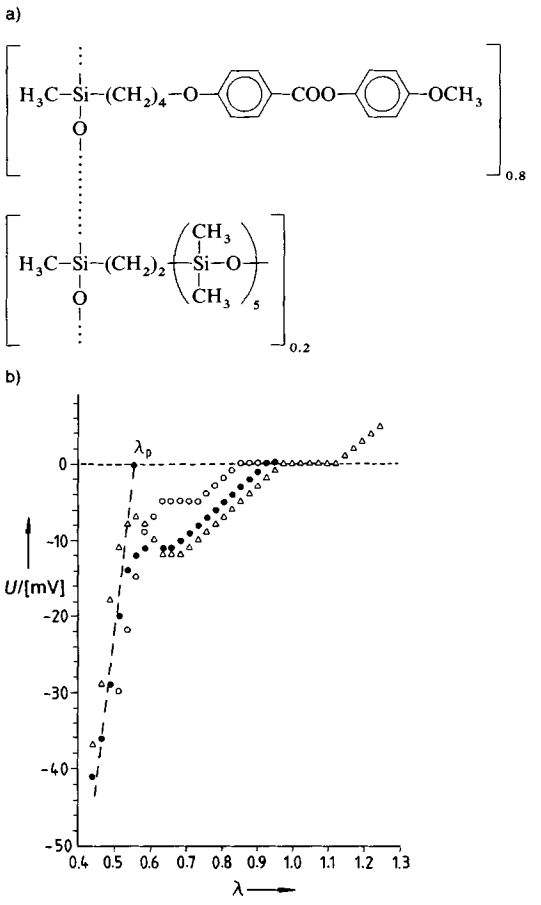

Fig. 2. a) Chemical structure of an elastomer displaying piezoelectric properties [6]. b) Dependence of the mechanically induced voltage U on the deformation (λ) for different reduced temperatures $T_{red} = T/T_i$ where T_i is the clearing temperature of the liquid-crystal elastomer. Δ: $T_{red} = 0.965$; ●: $T_{red} = 0.993$; ○: $T_{red} = 0.997$. The dashed line indicates extrapolation to a threshold deformation.

What are the advantages of this new class of piezoelectric polymers? First we know well-defined routes—drawn from the study of low molar mass and polymeric liquid crystals—to cholesteric or chiral smectic structures in elastomers. Second, we know from studies on non-liquid-crystalline networks how to modify the mechanical properties of the elastomers, varying for instance the cross-link density or the functionality of the cross-links. So we have most of the knowledge at hand to optimize the piezoelectric properties and other properties (mechanical, dielectric) relevant to piezoelectric applications and the manufacture of such materials.

The unique superposition of the piezoelectric responses of the intrinsic LC structure on one hand and the network on the other may even lead to surprising new modes of behavior and thus to new applications. Finally, based on the theoretical analysis,[5] we can expect these elastomers to display pyroelectric effects (charges induced on the surface as the temperature is changed), flexoelectric effects (electric response due to director field distortions), and electrostriction. Such effects may eventually be exploited in suitable applications.

After so much enthusiasm a word of caution should be sounded. Actual applications require, as pointed out above, a whole set of optimized properties: low impedance, broad band modulation characteristics, and optimized electromechanical coupling properties are just some of them. A minimum is known about these today. Many other properties come to mind, which have to be quantified, such as the actual strength of the coupling of the electric field to the network. A phenomenological treatment is, of course, not able to make predictions on the magnitude of effects. We do not know what will happen as we extend the elastomers up to large deformations, although this problem was briefly considered by *H. Brand*.[5] Now a major task, for which the theoretical predictions may serve as a guideline, is to investigate in detail the piezoelectric properties, but also other properties relevant to applications.

German version: *Angew. Chem. 103* (1990) 416

[1] J. Curie, P. Curie, *Hebd. Seances Acad. Sci. 91* (1890) 294.
[2] G. M. Sessler (ed.): *Electrets (Top. in Appl. Phys. 33* (1987)).
[3] H. Kawai, *Jpn. J. Appl. Phys. 8* (1969) 975.
[4] H. R. Brand, *Makromol. Chem. Rapid Commun. 10* (1989) 441.
[5] H. R. Brand, H. Pleiner, *Makromol. Chem. Rapid Commun. 11* (1990) 607.
[6] W. Meier, H. Finkelmann, *Makromol. Chem. Rapid Commun. 11* (1990) 599.
[7] S. U. Vallerien, F. Kremer, E. W. Fischer, H. Kapitza, R. Zentel, H. Poths, *Makromol. Chem. Rapid Commun. 11* (1990) 593.
[8] R. Zentel, *Angew. Chem. Adv. Mat. 101* (1989) 1437 (1797); *Angew. Chem. Int. Ed. Engl. Adv. Mat. 28* (1989) 1407 (1757); *Adv. Mat. 1989*, 321 (455).
[9] H. Finkelmann, H. J. Kock, G. Rehage, *Makromol. Chem. Rapid Commun. 2* (1981) 317.

Sandwiches Bring a New Element to Molecular Recognition

By *Edwin C. Constable**

Contemporary chemistry is characterized by the number and variety of topics which cut across the traditional divides, both between organic, inorganic, physical, and theoretical chemistry and between chemistry and the biological sciences. Recently the term "molecular recognition" has been widely employed to describe the investigation of molecular systems which show specific and designed interactions with particular molecules or ions. This area of study is clearly at the interface of organic and biological chemistry. However, it is now apparent that the unique properties of metal ions may also be exploited. Recent examples have included the use of metal ions in the self-assembly of large molecular aggregates and novel topological arrays, and in the design of novel receptor systems. Transition metal complexes are also frequently characterized by their ability to undergo metal-centered redox processes to generate oxidized or reduced compounds with differing properties. In two recent papers, *Gokel* and his co-workers have described some unusual and imaginative applications of organometallic compounds to problems which are more commonly regarded as organic.[1, 2]

Ferrocene (**1**, $X^1 = X^2 = H$) is a simple and remarkably robust organometallic complex which may be formally considered in terms of two coplanar cyclopentadienyl rings lying above and below an iron center. *Gokel* et al. have considered the consequences of this unit in highly derivatized systems. In the first paper,[1] the consequences of the oxidation of the iron(II) center of a ferrocene are considered. A range of derivatives of **1** incorporating long-chain fatty acid or cholesterol residues were prepared by esterification or amidation reactions (**1**, $X^1 = X^2 = COCl \rightarrow$ **1**, $X^1 = X^2 = CO_2R$, CONHR, or $CONR_2$), or sequential Menschutkin and alcoholysis reactions (**1**, $X^1 = H$, $X^2 = CH_2NMe_2 \rightarrow$ **1**, $X^1 = H$, $X^2 = CH_2OR$). Although some of these compounds showed evidence for the formation of aggregates, the most interesting behavior was noted with the dihydrocholesteryl ester **2**. The neutral molecule **2** exhibited no aggregation phenomena in solution, but electron micrographs show that upon electrochemical or chemical oxidation to the cation, $\mathbf{2}^{\oplus}$, approximately spherical vesicles with membranes of ca. 45 Å thickness were formed and could be obtained in aqueous dispersion after ultrasonic treatment.

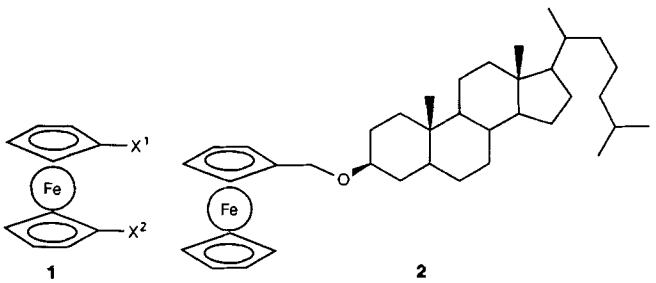

1 **2**

The most important observation that *Gokel* and *Echegoyen* have made is that the formation of the vesicles is genuinely redox-triggered: compound **2** does not aggregate in solution but upon oxidation the vesicles are formed; chemical reduction of these vesicles with dithionite results in their destruction. This use of a redox-active metal center as a molecular switch to control the formation of macromolecular assemblies is remarkable and suggests an entirely new methodology for the formation of membranes, micellar, and other supramolecular assemblies.

In the following paper,[2] entitled "A molecular receptor based on the ferrocene system: selective complexation using atomic ball bearings", *Gokel* et al. utilise some of the other properties of the ferrocene moiety in the design of diamine binders. The title refers to the fact that the two coplanar cyclopentadienyl rings of a ferrocene may rotate with respect to each other about the iron center as if the metal were a ball-bearing between two plane surfaces. Thus in the case of functionalized ferrocenes, a wide range of relative orientations of the substituents may be achieved. Since rotational barriers in substituted ferrocenes are low (similar to those in substituted ethanes), it is now possible to design a system which has all of the correct functionality for binding of a particular molecule, but which does not have this functionality in the correct spatial positions. The correct spatial arrangement is induced by the substrate, which organizes the functional groups of the receptor in an optimal manner by selective rotation of the cyclopentadienyl rings (Fig. 1). Only the correct substrate can selectively organize the receptor to the correct conformation, which provides an additional element of recognition.

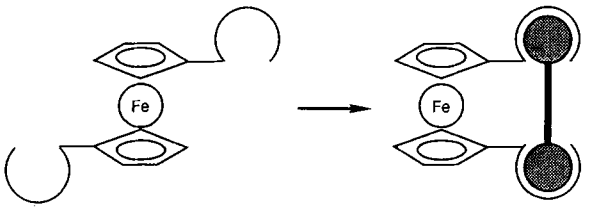

Fig. 1. The principle of binding of difunctional molecules to a ferrocene receptor. The active conformation of the receptor is induced by the presence of the substrate.

Gokel et al. have used the readily available substituted ferrocene **1**($X^1 = X^2 = CO_2H$) to prepare a series of bisferrocenes (**3a–d**) containing a potential bonding cavity designed for diamines. The primary receptor-substrate interaction is between the carboxylic acid residues and the amino groups, but a number of other features increase the specificity. The correct spatial arrangement of the carboxylic acids may be achieved by the "ball bearing" motion of the two cyclopentadienyl rings of an individual ferrocene unit (and also by the rotation of the two ferrocenyl units about the spacer group when appropriate). The use of aromatic spacer groups between the ferrocenes allows π-stacking interactions between the substrate and the receptor as an additional form of recognition.

Models suggested that the cavity size between the carboxylic acids in the correct conformation was 7–8 Å, and

[*] Dr. E. C. Constable
University Chemical Laboratory
Lensfield Road, GB-Cambridge, CB2 1EW (UK)

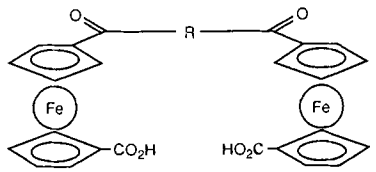

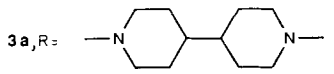

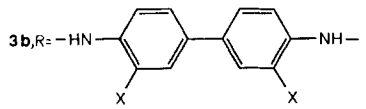

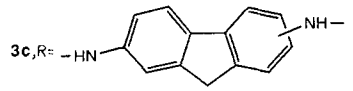

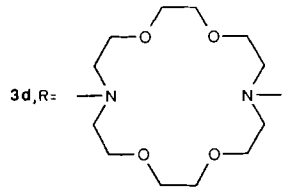

the binding of substrates such as **4a–e** was investigated. ^{1}H NMR chemical shift methods detected significant substrate-receptor binding interactions with compounds **4b** and **4c** ($K \approx 10^3\ M^{-1}$). These are the first members of a new non-macrocyclic receptor for organic substrates; future developments are likely to include the introduction of different functionality designed to bind other substrates.

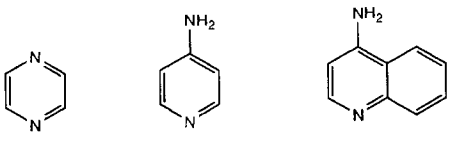

The elegant fusion of organic and inorganic chemistry and the application to current problems presented in these two papers is most impressive. However, other workers have also recognised the potential of substituted ferrocenes as molecular switches or receptors.[3, 4, 5] In particular, the group of *Beer* has been especially interested in the design of molecular systems in which a ferrocene bears a metal binding substituent such as a crown ether. Coordination of an alkali metal ion to the crown ether results in steric and electronic changes to which the iron center is sensitive, and which may be monitored by electrochemical studies. In principle, this approach leads to the design of molecular switches or sensors in which a change in the redox potential of the ferrocene unit is triggered by alkali metal ion binding, a phenomenon of obvious biological relevance.

The concept of utilizing conformational changes upon substrate binding to optimize that binding are inherent in many descriptions of biological interactions and have been successfully applied to other chemical systems. Of particular note in this context is the work of *Rebek* who termed such phenomena "allosteric effects".[6] In a series of seminal papers, *Rebek* demonstrated that co-operative metal binding could be associated with conformational changes in 3,3′-di-substituted-2,2′-bipyridines.

The design of receptors for small organic molecules has been a recurrent theme in contemporary organic chemistry, and the work of *Lehn* and his group must be highlighted in this context.[7] Although the interactions of metal ions with amines have been known for several centuries, and played a pivotal role in the development of coordination chemistry, it is only relatively recently that the potential of inorganic systems for the selective, reversible binding of such species has been exploited. A very elegant example of this has been demonstrated recently by *Sanders* et al.[8] They have shown that cyclo-oligomers containing zinc porphyrins may be prepared in high yields by copper-mediated acetylenic coupling reactions. The relevance to the work of *Gokel* is that the reactions are performed in the presence of polyamines such as 4,4′-bipyridine or 2,4,6-tri(2-pyridyl)-1,3,5-triazine which assemble the precursors about them in the correct conformation by direct interactions between the heterocyclic nitrogen atoms and the zinc centers. Here we see the recognition extending one step further back; the substrate does not simply trigger a conformational change in the receptor, it also controls the synthesis of the correct receptor site. Such template reactions are well-known to inorganic chemists.

These papers illustrate the current trend of applying methodology and concepts from one discipline to another. In particular, they emphasize once again that the inorganic chemist, with an arsenal of 100 or so elements at his command, may be able to introduce novel and subtle elements of control into organic systems. These ideas are excellently summarized in *Seebach*'s recent review article entitled "Organic synthesis—where next".[9] The concepts of metal-directed reactivity are discussed in a recent book.[10]

German version: *Angew. Chem. 103* (1991) 418

[1] J. C. Medina, I. Gay, Z. Chen, L. Echegoyen, G. W. Gokel, *J. Am. Chem. Soc. 113* (1991) 365.
[2] J. C. Medina, C. Li, S. G. Bott, J. L. Atwood, G. W. Gokel, *J. Am. Chem. Soc. 113* (1991) 366.
[3] C. D. Hall, N. W. Sharpe, I. P. Danks, Y. P. Sang, *J. Chem. Soc. Chem. Commun. 1989*, 417.
[4] P. D. Beer, C. D. Bush, T. A. Hamor, *J. Organomet. Chem. 339* (1988) 133; P. D. Beer, H. Sikanyika, C. Blackburn, J. F. McAleer, *ibid. 350* (1988) C15; P. D. Beer, C. Blackburn, J. F. McAleer, H. Sikanyika, *Inorg. Chem. 29* (1990) 378; P. D. Beer, *Chem. Soc. Rev. 18* (1989) 409; P. D. Beer, H. Sikanyika, *Polyhedron 9* (1990) 1091.
[5] T. Saji, I. Kinoshita, *J. Chem. Soc. Chem. Commun. 1986*, 716.
[6] J. Rebek, Jr., *Acc. Chem. Res. 17* (1984) 258.
[7] J.-M. Lehn, A. Rigault, *Angew. Chem. 100* (1988) 1121; *Angew. Chem. Int. Ed. Engl. 27* (1988) 1095; J.-M. Lehn, *ibid. 100* (1988) 91 and *27* (1988) 89; *ibid. 102* (1990) 1347 and *29* (1990) 1304.
[8] H. L. Anderson, J. K. M. Sanders, *Angew. Chem. 102* (1990) 1478; *Angew. Chem. Int. Ed. Engl. 29* (1990) 1400.
[9] D. Seebach, *Angew. Chem. 102* (1990) 1363; *Angew. Chem. Int. Ed. Engl. 29* (1990) 1320.
[10] E. C. Constable: *Metals and Ligand Reactivity*, Ellis Horwood, Chichester, England 1990.

Communications may be submitted in English *or* in German. Further details regarding the submission of communications can be found in the "Notice to Authors" reproduced in the January issue of the journal. Copies thereof may be obtained from the editorial office upon request.

A New Look at Electron Localization**

By *A. Savin,* A. D. Becke, J. Flad, R. Nesper, H. Preuss* and *H. G. von Schnering*

Ubiquitous chemical terms such as "the electron pair" and "the chemical bond" do not correspond unambiguously to directly measurable physical quantities. Because of their undeniable conceptual utility, however, clear and rigorous physical definitions are essential. The chemical bond is often described by localized molecular orbitals (see for example ref. [1]), but localized orbital sets are not unique. For example, two possibilities for bond localization of the π orbitals in benzene are shown in **1** and **2**, yet other, indeed infinitely many, mathematically equivalent schemes are also possible.[2] The localized molecular orbital description of chemical bonding is physically and mathematically arbitrary.

1 **2**

In this work it will be demonstrated, through a series of examples, that a new quantity, the Electron Localization Function (ELF),[3] is especially well suited to describe chemical bonds and electron pairs. ELF is based on measurable quantities and, moreover, the problem of nonuniqueness of localized molecular orbitals is not shared by ELF, at least in closed-shell systems.

In 1952 *Lennard-Jones* had already shown how, with the help of quantum mechanics, regions of space could be related to bonds and lone electron pairs.[4] He employed the two-particle density for electrons of parallel spin, a function of two electrons' coordinates (x, y, z and x', y', z') which gives the joint probability of finding one electron at position x, y, z and another electron of the same spin at position x', y', z'. The analysis showed that electrons of parallel spin restrict themselves to separate regions of space, and hence follows the notion of localized electron pairs. A well-known application of these concepts are the *Gillespie* and *Nyholm* rules.[5]

Becke and *Edgecombe* investigated another way of defining such regions of electron localization. They likewise made use of the two-electron density, exploiting its behavior at small interelectronic distances.[3] They showed that the probability of finding two electrons of the same spin close to one another is highly position dependent, leading to regions of both particularly high and particularly low pair probability. In the latter case, the electrons are "well localized". As a measure of this, *Becke* and *Edgecombe* introduced the Electron Localization Function (ELF), defined so as to have the convenient range of values $0 \leq \mathrm{ELF} \leq 1$. Regions in which the value of ELF is close to 1 correspond to well-localized electrons, and may be identified with atomic shells, chemical bonds and lone electron pairs. It is remarkable that the behavior of only the parallel-spin electrons so clearly discerns these details. The nature of electron pair correlation for opposite spins will not be considered here.

Technical details: Let us consider two electrons with parallel spins at positions x, y, z and x', y', z' (with separation r_{12}). The two-particle density is a function of both x, y, z and x', y', z'. Upon averaging over a sphere centered on x, y, z, one obtains a function of x, y, z and r_{12}, whose power series in r_{12} has the leading term $D(x,y,z)r_{12}^2$. The definition of ELF is then given by equation (a), where $D_h(x,y,z)$ is the value of D for a homogeneous electron gas with

$$\mathrm{ELF} = \frac{1}{1 + [D(x,y,z)/D_h(x,y,z)]^2} \qquad \text{(a)}$$

density $\varrho(x,y,z)$. In the Hartree–Fock approximation (closed shell) one obtains the explicit expression given in equation (b), where φ_i are the occupied orbitals

$$D/D_h = 0.3483\,\varrho^{-5/3}\left[\sum_i |\nabla\varphi_i|^2 - \frac{1}{8}|\nabla\varrho|^2/\varrho\right] \qquad \text{(b)}$$

and all quantities are expressed in atomic units. In this work, ELF has been calculated at the Hartree–Fock level [6], with pseudopotentials used for the tin compounds [7].

It is, in principle, possible to determine ELF from measured data. Knowledge of only the single-particle density matrix $\sum_i \varphi_i(\boldsymbol{r})\varphi_i(\boldsymbol{r}')$ is required at the Hartree–Fock level and methods to determine this from experimental data have been proposed long ago [8]. In many cases the experimental electron density was used to determine the density matrix. Knowledge of the density should be supplemented, however, by additional information from sources such as Compton spectroscopy [9, 10].

Here we present, using a newly developed computer graphics program,[11] the first extensive study of the utility of the Electron Localization Function. In the graphical representations of Figure 1, we see how well ELF reflects various intuitive concepts of atomic and molecular structure. The program calculates both the electron density and ELF for selected molecular planes, which generally contain atomic nuclei, and portrays them simultaneously. Electron density is represented by point density (i.e., electron clouds) as, for

[*] Dr. A. Savin, Prof. Dr. R. Nesper[†], Prof. Dr. H. G. von Schnering
Max-Planck-Institut für Festkörperforschung
Heisenbergstrasse 1, W-7000 Stuttgart 80 (FRG)
Dr. J. Flad, Prof. Dr. H. Preuss
Institut für Theoretische Chemie, Universität Stuttgart
Pfaffenwaldring 55, W-7000 Stuttgart 80 (FRG)
Prof. Dr. A. D. Becke
Department of Chemistry, Queen's University
Kingston, Ontario K7L 3N6 (Canada)

[**] This work was supported by the Fonds der Chemischen Industrie, the Deutsche Forschungsgemeinschaft, the Höchst AG (Frankfurt), the Bundesministerium für Forschung und Technologie and the Natural Sciences and Engineering Research Council of Canada. We thank *F.-X. Fraschio, M. Kohout* and *B. Miehlich* (Universität Stuttgart) for the assistance with the computer graphics. We are indebted to Prof. *P. Fulde* (Stuttgart) and Prof. *W. H. E. Schwarz* (Siegen) for valuable suggestions.

[†] New address: Laboratorium für Anorganische Chemie der Eidgenössischen Technischen Hochschule, Zürich

example, in Frame 1 for the electron density of the NH_3 molecule, **3**. With white points on a black background, one

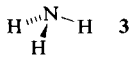

immediately recognizes the high-density maxima at the positions of the N nucleus and the H nucleus. Representations of this kind were introduced in 1931.[12]

In addition our points are assigned colors depending on the local value of ELF and inspired by geographical maps: the blue color of the sea corresponds to low ELF and the white of the mountains to high ELF, with green and brown in between. The color scale is given on the left in Frame 2. Thus our backgrounds remain black, and white points now indicate very highly localized electrons. This representation of ELF conveys considerable additional information. One now identifies in **3**, for instance (compare Frames 1 and 2), three regions of higher localization: one around the N nucleus, one containing the N and H atoms (lower right) and one on the free side of the N atom (top). These regions can be attributed to the core, the N–H bond and the lone pair.

At this stage it should be pointed out that the Electron Localization Function, like the electron density, always possesses the full symmetry of the molecule, and therefore all symmetry-equivalent planes will give the same ELF. For NH_3 (**3**) all planes containing the C_3 axis and one of the N–H bonds will yield the same picture. Furthermore for linear molecules both the electron densities and ELF have axial symmetry. In the case of the Ne atom, ELF yields two spherical regions of higher localization which correspond to the core and valence shells (Frame 3). The same sharp separation between core and valence shells is also visible in molecules such as Li_2 (Frame 4).

In the C_2 molecule ($^1\Sigma_g^+$ state) the π-orbital bonding is discernible (Frame 5). In the N_2 molecule there exists within the valence shell a clear separation between the bonding region and the lone pair electrons, not as distinct, however, as the separation between core and valence regions (Frame 6). The F_2 molecule (Frame 7) shows a weak bond, whereas two Ne atoms at the same interatomic distance merely show a distortion of their valence shells (Frame 8).

Even with simple hydrides we find a large variety of bonding forms. The LiH molecule consists of a $Li^{\oplus}$ core (Frame 9, left) and a polarized $H^{\ominus}$ ion (right, white). In the BH molecule (Frame 10, B middle, H right) there exists along with the B–H bond an additional electron lone pair (left). In the HF molecule (Frame 11) the region of space to which one would assign the H–F bond is smaller and more difficult to discern from the region of the free electrons than in, for example, the BH molecule. We see already an indication of the tendency to form $H^{\oplus}F^{\ominus}$. In the LiF molecule we have essentially an ionic bond (Frame 12; compare with LiH,

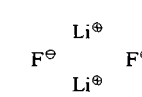

4

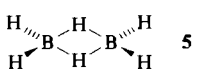

5

Frame 9), as implied by the nearly spherical structure of the ELF around each nucleus and the appearance of an intervening region with very low ELF values. This ionic character also appears, of course, in the dimer Li_2F_2 (**4**, Frame 13). In contrast, a polarized bond is found in the ClF molecule (Frame 14).

The more complicated case of three-center bonding appears in diborane (**5**, Frame 15). Here also, the agreement with classical concepts is very clearly illustrated by the electron density and ELF. In planar Li_4 and Li_6 clusters, calculated to be stable, the three-center bonds likewise appear.[6] In these cases, however, one might also expect bonds involving more than three centers. According to ELF (Frames 16 and 17), these clusters are held together almost exclusively by peripheral three-center bonds.

When H bridges two strongly electronegative partners the bonds show distinct ionic character, as indicated by the formic acid molecule **6** (Frame 18) and its dimer **7** (Frame 19). What happens, though, if the H atom lies symmetrically

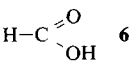

6

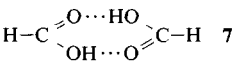

7

between two equally electronegative atoms as in the FHF anion (Frame 20)? Here one notices a region of high ELF around the proton clearly separated from those of the neighboring atoms. A similar picture results if, in **7**, one imagines the transition state for the transfer of a proton from one O atom to another. In the change from an asymmetric to a symmetric H bridge the ionic nature of the bond is largely lost.

With the Electron Localization Function weaker effects, such as change in delocalization, can also be recognized. Let

Fig. 1. Electron density ρ as "cloud" and the color pattern of the Electron Localization Function, ELF (scale in Frame 2: small values of the ELF are represented as blue, large values as white; scale for remaining frames: blue, green, brown, white; background: black). Frame 1: ρ(**3**) as white cloud. The selected plane contains the N nucleus (middle), a H nucleus (bottom right) and the center point between two other H nuclei. Frame 2: ρ(**3**) and the ELF. The white regions correspond to the core, the lone electron pair and the N–H bond. Frame 3: Core and valence shells of the Ne atom. Frame 4: Core and bonding regions (white) in the Li_2 molecule. Frame 5: Core and π bond (white periphery) in the C2 molecule. Frame 6: Core, bond and lone electron pair (white) in the N_2 molecule. Frame 7: Core, cylindrical symmetric regions of the lone electron pair (white) and weak covalent bond (yellow-brown) in the F_2 molecule. Frame 8: Deformation of the electron density in the Ne_2 molecule (compare Frame 3). Frame 9: LiH molecule with $Li^{\oplus}$ core (left) and $H^{\ominus}$ ion (right). Frame 10: BH molecule with the lone electron pair, the B core and the B–H bond as white regions from left to right. Frame 11: HF molecule with the cylindrical symmetric regions of the lone electron pair, the F core and the F–H bond. Frame 12: LiF molecule with $Li^{\oplus}$ (left) and $F^{\ominus}$ (right). Model for an ion pair with separated region (small ELF values: blue). Frame 13: **4** with $Li^{\oplus}$ cations (top and bottom) and $F^{\ominus}$ anions (left and right). Frame 14: ClF molecule with Cl (left) and F (right); core and lone electron pair regions (large white regions); weak, polarized bond (brown-yellow region). Frame 15: **5** (plane of the B_2H_2 ring with the B atoms left and right) with core and two three-center bonds (large white regions around the H atoms). Frame 16: Planar Li_4 cluster with core and two three-center bonds. Frame 17: Planar Li_6 cluster with core and three peripheral three-center bonds; one notices that a central three-center bond is absent. Frame 18: **6** with cores, bonds and lone electron pairs (ketone oxygen at top right). Frame 19: **7** (compare Frame 18) shows the ionic character of the hydrogen bonds (blue regions between the monomers). Frame 20: $FHF^{\ominus}$ ion with a small area of high ELF values around the H nucleus. Frame 21: **8** (selected plane is 1 Bohr above the nuclear plane) with the C–H and C–C bonds (white regions). Frame 22: **9** (plane same as in Frame 21) shows a larger π region at the central C–C bond than **8**. Frame 23: ClF_3 molecule emphasizing the difference between the axial and equatorial Cl–F bonds. Frame 24: SnO molecule with Sn (left) and O (right) and the lone electron pair on the Sn (large white region). Frame 25: Sn_2O_2 molecule with the Sn atoms lying horizontally. Frame 26: **12** (plane through the Sn nuclei splits the H-Sn-H angle; the H nuclei are located top right and bottom left above and below the plane), see text for discussion. Frame 27: Sn_2H_2 molecule with hypothetical planar structure (Sn atoms sit right and left from the center point of the picture: all H atoms are located in a plane perpendicular to the represented plane. Frame 28: Cu_4Sn_4 molecule with heterocubane structure (Sn atoms top, Cu atoms bottom), for discussion see text.

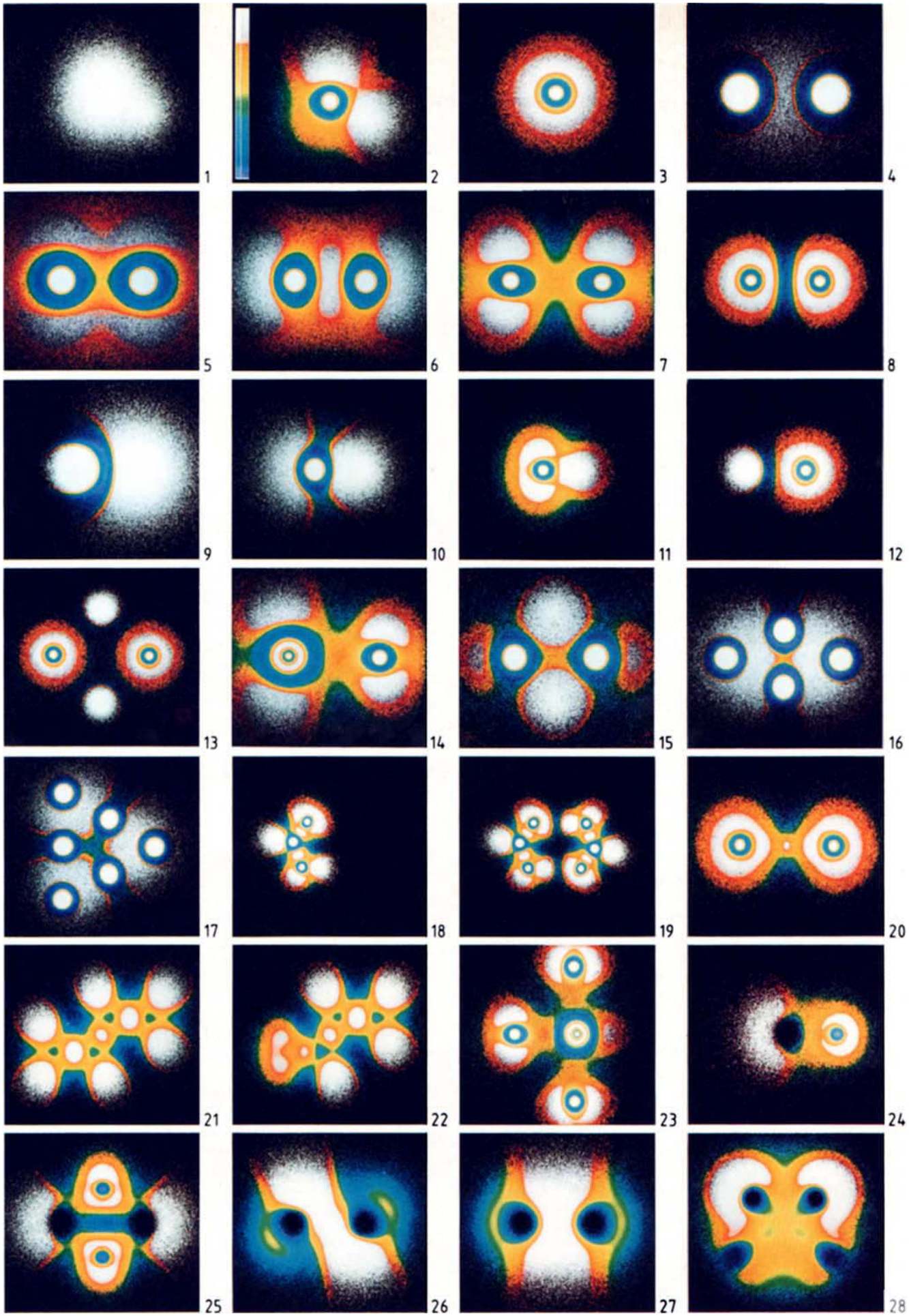

 © VCH Verlagsgesellschaft mbH, W-6940 Weinheim, 1991 0570-0833/91/0404-0411 $ 3.50+.25/0

us compare the C–C bonds in butadiene (**8**, Frame 21), and acrolein (**9**, Frame 22). The illustrations present ELF values in a plane lying 1 Bohr above the plane of the nuclei and intersecting the π-bonding region, and show that the π component of the C–C bond is larger in **9** than it is in **8**.

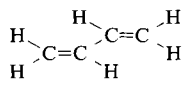

8

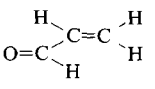

9

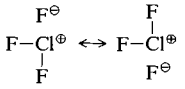

10 **11**

That ELF also represents three-center–four-electron bonds is shown by the example of ClF_3 (Frame 23). The two axial Cl–F bonds clearly have a weaker covalent character than the equatorial bond, corresponding well to the canonical forms **10** and **11**.[13]

The core electron densities vanish if one uses a pseudopotential method rather than performing all-electron calculations. We have done this in the case of Sn compounds, and therefore our representations of the Sn compounds exhibit no high electron densities around the nuclei but only the black background. The lone-pair electrons in Sn^{II} compounds are nicely illustrated by ELF. The spatial distribution of the lone pair in the SnO molecule (Frame 24) is clearly deformed and remarkably large. The Sn_2O_2 dimer (Frame 25) shows a similarly expanded spatial distribution of these electron pairs and is an impressive indication of its stereochemical activity. Unlike their carbon analogues, Sn_2R_4 molecules are not planar. The explanation involves the influence of the electron lone pairs.[14] For the bent Sn_2H_4 molecule **12**, ELF actually shows a strong deformation (Frame 26), and the influence of the lone pairs is especially clear in comparison with the hypothetical planar structure of Frame 27. The large white region is intermediate between the case of two isolated lone pairs (as in Frame 25) and the case of a pure double bond (as in Frame 27).

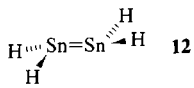

12

The heterocubane cluster Cu_4Sn_4 possesses an Sn_4 tetrahedron. Here one finds multicenter bonding with participation of the Cu atoms. The plane depicted in Frame 28 contains an edge of the Sn_4 tetrahedron (Frame 28 top, connecting the dark nuclear positions) and the middle of the opposite edge (Frame 28 bottom, middle of the yellow region). Two Cu atoms also lie in this plane (Frame 28 bottom, outer nuclear positions). Here again, the distribution of the Sn lone pairs is deformed.

In this first survey of the potential applications of the Electron Localization Function, ELF, we have demonstrated that notions such as atomic shells, chemical bonds, and lone electron pairs are readily manifested by a function that is based, in principle, on measurable physical quantities. Empirical findings, such as those expressed in the Gillespie–Nyholm rules, may be easily visualized thereby. Perhaps further investigations with the Electron Localization Function will prove beneficial in cases where classical concepts and chemical intuition fail.

Received: June 19, 1990
Revised: October 24, 1990 [Z 4023 IE]
German version: *Angew. Chem. 103* (1991) 421

[1] W. England, L. S. Salmon, K. Ruedenberg, *Top. Curr. Chem. 23* (1971) 31.
[2] W. England, *Int. J. Quantum Chem. 5* (1971) 683.
[3] A. D. Becke, K. E. Edgecombe, *J. Chem. Phys. 92* (1990) 5397.
[4] J. E. Lennard-Jones, *J. Chem. Phys. 20* (1952) 1024.
[5] R. J. Gillespie, R. S. Nyholm, *Q. Rev. 11* (1957) 339.
[6] Details of the calculations: a) Basis sets: W. J. Hehre, R. Ditchfield, J. A. Pople, *J. Chem. Phys. 56* (1972) 2257; P. C. Hariharan, J. A. Pople, *Theor. Chim. Acta 28* (1973) 213; M. F. Frankl, W. J. Pietro, W. J. Hehre, J. S. Binkley, M. S. Gordon, D. J. Defrees, J. A. Pople, *J. Chem. Phys. 77* (1982) 3654 (for **6**–**11**, ClF), G. Igel-Mann, C. Feller, H.-J. Flad, A. Savin, H. Stoll, H. Preuss, *Mol. Phys. 68* (1989) 209 (for the Sn compounds); F. B. van Duijneveldt, *IBM Res. Rep. 945* (1991) (contracted after G. C. Lie, E. Clementi, *J. Chem. Phys. 60* (1974) 1275) (for all other compounds); b) Molecular Structures: K. P. Huber, G. Herzberg: *Molecular Spectra and Molecular Structures, Vol. 4*, Van Nostrand, New York 1979 (diatomic molecules); L. E. Sutton (ed.): *Tables of Interatomic Distances and Configurations in Molecules and* Ions, The Chemical Society, London 1958 (**5**–**9** and $FHF^{\ominus}$); I. Boustani, W. Pewestorf, P. Fantucci, V. Bonačić-Koutecký, J. Koutecký, *Phys. Rev. B25* (1987) 9437 (Li cluster); G. Igel-Mann, C. Feller, H.-J. Flad, A. Savin, H. Stoll, H. Preuss, *Mol. Phys. 68* (1989) 209 (SnO); G. Igel-Mann, H.-J. Flad, C. Feller, H. Preuss, *J. Mol. Struct. (THEOCHEM) 209* (1990) 313 (Sn_2O_2); G. Trinquier, J. P. Malrieu, P. Riviere, *J. Am. Chem. Soc. 104* (1982) 4529 (18); W. Plass, A. Savin, H. Stoll, H. Preuss, R. Nesper, H. G. von Schnering, *Inorg. Chem. 29* (1990) 260 (Cu_4Sn_4); c) SCF program: L. E. McMurchie, S. T. Elbert, S. R. Langhoff, E. R. Davidson: *Program MELD*, NRCC program QC04 (graciously supplied by Prof. Dr. *E. R. Davidson*); W. Meyer, P. Pulay, E. A. Reinsch, H. J. Werner: *Program MOLPRO* (graciously supplied by Prof. *H. J. Werner*); both programs were installed on the Cray-2 of the Computer Center of the Universität Stuttgart by Prof. *H. Stoll*, Dr. *U. Wndig* and *B. Miehlich*.
[7] G. Igel-Mann, H. Stoll, H. Preuss, *Mol. Phys. 65* (1988) 1321.
[8] W. C. Clinton, J. Nakhleh, F. Wunderlich, *Phys. Rev. 177* (1969) 1; W. C. Clinton, A. J. Galli, L. J. Massa, *ibid. 177* (1969) 7; W. C. Clinton, G. A. Henderson, J. V. Prestia, *ibid. 177* (1969) 13; W. C. Clinton, G. B. Lamers, *ibid. 177* (1969) 19; W. C. Clinton, A. J. Galli, G. A. Henderson, G. B. Lamers, L. J. Massa, J. Zarur, *ibid. 177* (1969) 27; W. C. Clinton, L. J. Massa, *Phys. Rev. Lett. 29* (1972) 1363; R. F. Stewart, *J. Chem. Phys. 51* (1969) 4569.
[9] P. Coppens, T. V. Willoughby, L. N. Gonka, *Acta Crystallogr. Sect. A 27* (1971) 248; W. H. E. Schwarz, B. Müller, *Chem. Phys. Lett. 166* (1990) 621.
[10] H. Schmider, V. H. Smith, Jr., W. Weyrich, *Trans. Am. Crystallogr. Assoc. 26* (1991), in press.
[11] J. Flad, F.-X. Fraschio, B. Miehlich: *Program GRAPA*, Institut für Theoretische Chemie der Universität Stuttgart, 1989.
[12] H. E. White, *Phys. Rev. 37* (1931) 1416.
[13] W. Kutzelnigg: *Einführung in der Theoretische Chemie, Vol. 2*, Verlag Chemie, Weinheim, 375.
[14] Compare D. E. Goldberg, P. B. Hitchock, M. F. Lappert, K. M. Thomas, A. J. Thomas, T. Fjeldberg, A. Haaland, B. E. R. Schilling, *J. Chem. Soc. Dalton Trans. 1986, 2387*.

Synthesis of a Biologically Active Taxol Analogue **

By *Siegfried Blechert** and *Andrea Kleine-Klausing*

The taxanes from the plant family Taxaceae form a group of very unusual tricyclic diterpenes.[1] An eight-membered ring with two geminal methyl groups, an annulated six-membered ring, and a C3-bridge results in a strained half-spherical ring system, that has many oxygen functionalities. One of the most interesting members is taxol **1**,[2] which at present is being intensively studied as a promising chemotherapy agent for several types of tumors.[3] Till now it has remained the only known naturally occurring compound that accelerates the polymerization of tubulin and blocks its depolymer-

[*] Prof. Dr. S. Blechert, A. Kleine-Klausing
Institut für Organische Chemie der Technischen Universität
Strasse des 17. Juni 135, W-1000 Berlin 12 (FRG)

[**] This work was supported by the Deutsche Forschungsgemeinschaft and the Fonds der Chemischen Industrie.

ization. Because of this novel mode of action, it has also become an important agent in cell research.

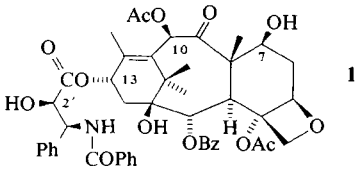

1

The limited accessibility of this natural compound (Taxaceae belong to the slowest-growing trees and the taxol content of the bark is very low), its insolubility, and its complex composition create an immense motivation to synthesize this class of substance. Till now, however, only very few groups have succeeded in preparing the functionalized taxane framework,[4] from which the analogues of **1** could be synthesized. We report herein on the first synthesis of a less highly functionalized taxol analogue that also restricts the depolymerization of tubulin.

Biological tests on taxol and its derivatives have shown the significance of the C-13 ester side chain and here in particular the C-2′ hydroxyl group.[5] We therefore planned the synthesis of a tricyclic C-13 hydroxylated taxane framework, that should have the spatial features of the natural product. The C-8 α-ring-formation required for the half-spherical construction of the tricycle was achieved through a stereoselective de Mayo reaction of cyclohexene with a suitable functionalized 1,3-diketone. The β-*exo*-attack directed by the ketal afforded photoadduct **2**. The Pd^0-catalyzed removal of the protecting group, retroaldol reaction, stereoselective reduction of the C-10 carbonyl group, base-catalyzed epimerization at C-3 and transformation of the ketal into the C-13 α-alcohol lead to the desired tricycle **3**.[6] The planned regioselective esterification at C-13 could not be achieved and the detour via a protected C-10 alcohol proved to be inefficient. A solution for the problem was found in the reaction sequence of Scheme 1.

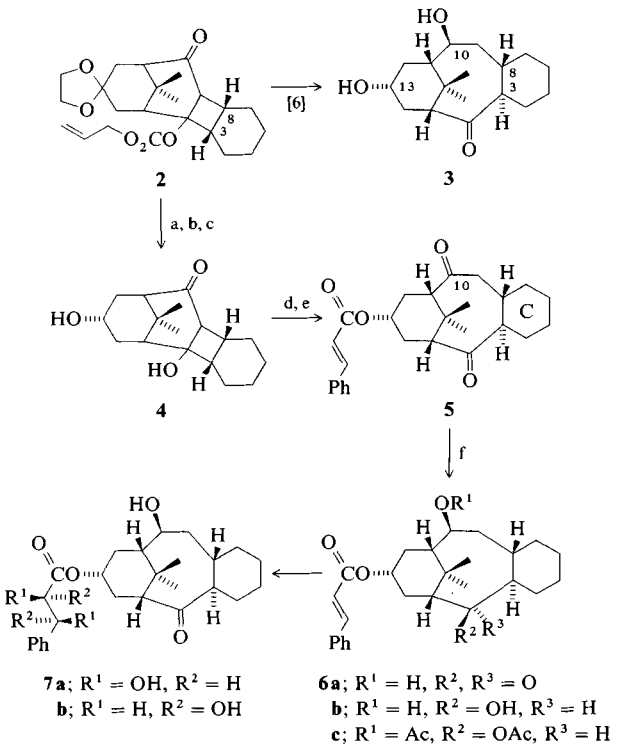

7a; R^1 = OH, R^2 = H
b; R^1 = H, R^2 = OH

6a; R^1 = H, R^2, R^3 = O
b; R^1 = H, R^2 = OH, R^3 = H
c; R^1 = Ac, R^2 = OAc, R^3 = H

Scheme 1. a) Cat. $Pd(PPh_3)_4$, THF, morpholine (98%). b) THF, 2 N HCl(1:1). c) THF, lithium selectride, −70 °C (78%). d) *t*BuOH, KO*t*Bu, 70 °C, 2 h, (86%). e) Cinnamic acid, dicyclohexylcarbodiimide, 4-dimethylaminopyridine, toluene, 80 °C (70%). f) $NaBH_4$, citric acid, CH_3OH, 3 min (72%); **6b**: 30 min reaction time. **6c**: acetic anhydride, pyridine, 4-dimethylaminopyridine. g) OsO_4, *N*-methylmorpholine-*N*-oxide, pyridine, 1 h, (70%). For spectroscopic and physical data of compounds **6a**, **6c**, and **7**, see Table 1.

After liberating the aldol and deketalizing with aqueous acid, a diketone is obtained that can be reduced stereoselectively, still as crude product in THF, with lithium selectride to diol **4** at −70 °C at the sterically more accessible carbonyl group. The retroaldol reaction affords an eight-membered ring, whereby the complete isomerization to the thermodynamically favored *trans* orientation of ring **C** under the basic reaction conditions is achieved. The easy C-3 epimerization in this reaction step deserves special mention. Comparable retroaldol reactions with C-13 ketals in CD_3OD can be shown by H/D exchange to have an almost rigid conformation which is unfavorable for enolate formation, and no deprotonation at C-13 takes place. Only on reduction of the C-10 carbonyl group or through formation of the C-13 alcohol does the conformational flexibility of the eight-membered ring increase to allow the isomerization via enolate formation. The C-13 alcohol may be transformed without difficulty into the cinnamic acid ester **5**. The regio- and stereoselective reduction of the sterically more accessible C-10 ketone (over the C-2 ketone) is achieved with sodium borohydride/citric acid, whereby short reaction times lead exclusively to the desired α-alcohol **6a**. Over longer reaction times the diol **6b** is also formed, and its stereochemical assignment by NMR experiments at the diacetate stage (**6b**) is unambiguous. The chemical shift of all relevant protons could be assigned without doubt through $^1H,^1H$-correlated 2D NMR spectra. The nuclear Overhauser enhancement (NOE) difference spectra confirm the spatial proximity of H-3 and H-10, H-13 and C-15-methyl, H-2 and H-4, as well as H-2 and H-14. The coupling constants of H-2, H-3, H-10, and H-13 correspond to those calculated from the dihedral

Table 1. Selected data for **6a**, **6c** and **7**.

6a: ^1H NMR (400 MHz, $CDCl_3$): δ = 1.13 (s, CH_3), 1.23 (s, CH_3), 1.34 (m, 1H), 1.49 (m, 1H), 1.59 (m, 9-H, 2H), 1.71 (m, 5H), 1.86 (m, 11-H, 12-Hα, 2H), 1.98 (ddd, J = 16.5, J = 4.0, J = 2.0 Hz, 14-H, 1H), 2.32 (d, broad, J = 9.0 Hz, 1-H, 1H), 2.42 (ddd, J = 11.0, J = 11.0, J = 5.5 Hz, 9-H, 1H), 2.45 (dt, J = 16.5, J = 8.5 Hz, 14-H, 1H), 2.62 (ddd, J = 16.5, J = 10.0, J = 8.0 Hz, 12-Hβ, 1H), 3.16 (td, J = 11.0, J = 3.5 Hz, 3-H, 1H), 4.11 (ddd, J = 10.5, J = 4.0, J = 2.0 Hz, 10-H, 1H), 5.51 (m, 13-H, 1H), 6.45 (d, J = 16.0 Hz, 1H), 7.39 (m, 3H), 7.51 (m, 2H), 7.71 (d, J = 16.0 Hz, 1H); ^{13}C NMR (100 MHz, $CDCl_3$): δ = 25.4 (CH_2), 26.4 (CH_2), 27.1 (CH_2), 28.0 (CH_3), 30.1 (CH_2), 32.0 (CH_2), 34.8 (C), 35.4 (CH_3), 38.5 (CH), 40.3 (CH_2), 48.7 (CH), 49.1 (CH), 57.6 (CH), 66.9 (CH), 74.3 (CH), 118.2 (CH), 128.1 (CH), 129.0 (CH), 130.6 (CH), 134.2 (C), 145.3 (CH), 166.2 (C), 218.4 (C).

6c: M.p. = 150–152 °C; ^1H NMR (400 MHz, $CDCl_3$): δ = 1.06 (s, CH_3), 1.07–1.22 (m, 3H), 1.35 (m, H-9α, 1H), 1.40 (s, CH_3), 1.45–1.60 (m, 5H), 1.61–1.71 (m, H-12α, H-14α, H-8, H-11, 4H), 2.02 (m, H-1, 1H), 2.04 (s, $COCH_3$), 2.05 (s, $COCH_3$), 2.22 (t, broad, J = 9.6 Hz, H-3, 1H), 2.33 (dt, J = 16.0, J = 6.8 Hz, H-12β, 1H), 2.45 (ddd, J = 16.0, J = 9.6, J = 7.2 Hz, H-14β, 1H), 2.80 (broad, H-9β, 1H), 4.80 (d, J = 5.0 Hz, H-2, 1H), 5.30 (m, H-13, 1H), 5.43 (dd, broad, J = 9.6, J = 6.4 Hz, H-10, 1H), 6.44 (d, J = 16.0 Hz, 1H), 7.38 (m, 3H), 7.59 (m, 2H), 7.85 (d, J = 16.0 Hz, 1H). The stereochemical assignment is by NOE experiments.

7 (biologically active): ^1H NMR (400 MHz, $CDCl_3$): δ = 1.07 (s, CH_3), 1.12 (m, 1H), 1.18 (s, CH_3), 1.25–1.80 (m, 11H), 1.91 (d, broad, J = 16.0 Hz, H-14, 1H), 2.31 (d, J = 9.0 Hz, H-1, 1H), 2.36–2.47 (m, H-9, H-14, H-12β, 3H), 2.63 (broad, OH, 3H), 2.97 (td, J = 11.0, J = 4.0 Hz, H-3, 1H), 3.98 (ddd, J = 10.5, J = 4.0, J = 2.0 Hz, H-10, 1H), 4.38 (d, J = 3.6 Hz, 1H), 5.04 (d, J = 3.6 Hz, 1H), 5.51 (m, H-13, 1H), 7.35 (m, 5H); IR ($CHCl_3$): ν[cm^{-1}] = 3500 (broad, OH), 1725 (C=O), 1680 (C=O).

angles according to the Karplus equation. The isolated compound **6a** is, however, not able to be transformed into the diol under the same reaction conditions. This may be explained by a transannular reduction of the C-2 ketone by a C-10 alkoxy borohydride. The *cis* hydroxylation of **6a** with osmium tetroxide yields a 1:1 mixture of two easily separable diastereomers (**7**). The relative orientation of the stereocenters between the ester side chain and the tricycle cannot be determined; a crystal structure analysis has as yet not been possible. Both diastereomers **7** were subjected to an in vitro tubulin test.[7] The diastereomer which is less polar in an eluant system of dichloromethane/methanol on silica gel inhibits the depolymerization of tubulin and is thus the first synthesis product with a taxol-analogous action. This result confirms that less functionalized taxol derivatives also can be of interest. We are at present studying a further simplification of the structure and its influence on the activity.

Received: October 30, 1990 [Z 4260 IE]
German version: *Angew. Chem. 103* (1991) 428

CAS Registry numbers:
1, 33069-62-4; **2**, 132203-65-7; **2** (OH instead of O–CO–O–CH_2–CH=CH_2), 92695-03-9; **4**, 132157-41-6; **4** (carbonyl instead of hydroxy), 132178-08-6; **5**, 132157-42-7; **5** (OH instead of Ph–CH=CH–CO–O), 123483-62-5; **6a**, 132157-43-8; **6b**, 132157-45-0; **6c**, 132157-46-1; **7a**, 132157-44-9; **7b**, 132203-66-8.

[1] a) B. Lythgoe, *The Alkaloids (Academic Press) 12* (1968) 597; b) R. W. Miller, *J. Nat. Prod. 43* (1980) 425; c) S. Blechert, D. Guénard in A. Brossi (Hrsg.): *The Alkaloids, Vol. 39*, Academic Press, New York 1990, in press.
[2] M. C. Wani, H. L. Taylor, M. E. Wall, P. Coggon, A. T. McPhail, *J. Am. Chem. Soc. 93* (1971) 2325.
[3] M. Suffness, G. A. Cordell in A. Brossi (Ed.): *The Alkaloids, Chemistry and Pharmacology, Vol. 25*, Academic Press, Orlando 1985, p. 6.
[4] Syntheses of tricyclic taxane frameworks with oxygen at C-13: C. S. Swindell, B. P. Patel, *J. Org. Chem. 55* (1990) 3; R. A. Holton, R. R. Juo, H. B. Kim, A. D. Williams, S. Harusawa, R. E. Lowenthal, S. Yogai, *J. Am. Chem. Soc. 110* (1988) 6558; A. S. Kende, S. Johnson, P. Sanfilippo, J. C. Hodges, L. N. Jungheim, *ibid. 108* (1986) 3513.
[5] a) V. Senilh, F. Gueritte, D. Guénard, M. Colin, P. Potier, *C. R. Acad. Sci. Ser. 2 299* (1984) 1039; b) D. G. I. Kingston, D. R. Hawkins, L. Ovington, *J. Nat. Prod. 45* (1982) 466.
[6] H. Neh, A. Kühling, S. Blechert, *Helv. Chim. Acta 72* (1989) 101.
[7] Test according to F. Gaskin, C. R. Cantor, M. J. Shelanski, *J. Mol. Biol. 89* (1974) 73; we thank Dr. *D. Guénard*, Institut de Chimie des Substances Naturelles, Gif-Sur-Yvette, France, for its execution.

Intramolecular Diels–Alder Reactions: Diastereofacial Selectivity and Coupling with an Aliphatic Claisen Rearrangement**

By *Johann Mulzer*, Harald Bock, Wolfgang Eck, Jürgen Buschmann*, and *Peter Luger*

Intramolecular Diels–Alder reactions (IMDA reactions) are often studied because of their high regio- and stereoselectivity.[1] We were interested in two aspects of these reactions: 1) How can they be used for the rapid construction of acyclic chiral compounds? 2) Do they, like other pericyclic six-electron processes (Cope[2] or ene reactions[3]), allow coupling with the aliphatic Claisen rearrangement in a tandem reaction?

Allylic hydroxyl functions can be used in different ways for stereocontrolled C-C bond formation, as shown by the examples in equation (a) (1,3-chirality transfer[4]) and (b)

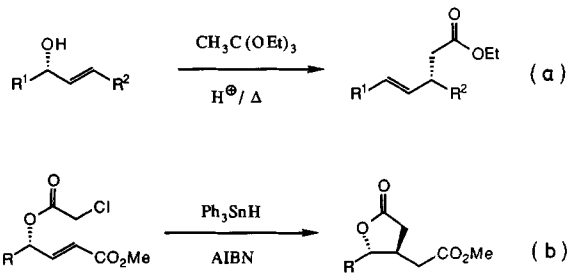

(1,2 induction through radical cyclization[5]). In this way a maximum of two (a) and three (b) stereocenters can be created; with the Diels–Alder reaction, however, up to four stereocenters per step are created. Thus we esterified the hydroxyester **1**, obtained in two steps from *O*-tetrahydropyranyl(THP)lactaldehyde, with sorbic acid to obtain triene **2**, which yields on heating (xylene, 160 °C, 3 days) the bicycle **4** (81 %) as well as two further diastereomers (5 and 9 % by HPLC analysis) (Scheme 1). According to an X-ray crystal

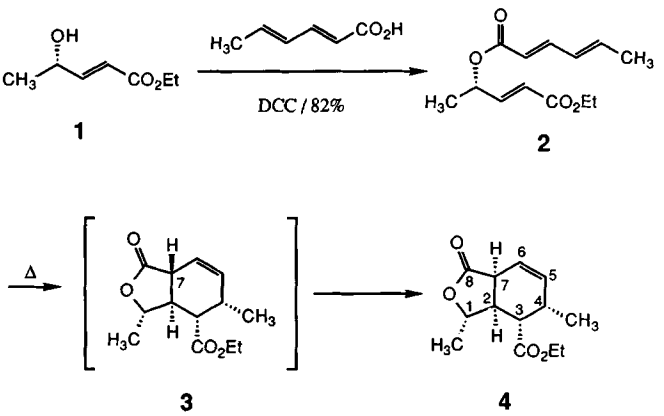

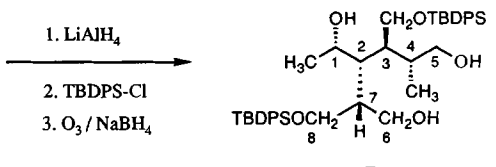

Scheme 1. DCC = Dicyclohexylcarbodiimide, TBDPS = *tert*-butyldiphenylsilyl.

structure analysis on **4**,[6] H-2 and H-7 are in *cis* orientation, in contrast to the (*E*,*E*) configuration in diene system **2**. Probably the primary adduct **3** epimerizes in situ at the CH-acidic 7-position.

The relative configuration at the four new chirality centers of **3** indicates that **2** reacts via conformation **6**, in which the methyl group shields one diastereoface of the dienophile. The Newman projection of **6** (**7**) shows that the attack on the dienophile conforms to the *Houk* model.[7]

[*] Prof. Dr. J. Mulzer, Dipl.-Chem. H. Bock, Dipl.-Chem. W. Eck
Institut für Organische Chemie der Freien Universität
Takusstrasse 3, W-1000 Berlin 33 (FRG)
Dr. J Buschmann, Prof. Dr. P. Luger
Institut für Kristallographie der Freien Universität Berlin

[**] This work was supported by the Graduiertenkolleg "Structure determination and synthesis of small molecular compounds", the Fonds der Chemischen Industrie, and Schering AG, Berlin-Bergkamen.

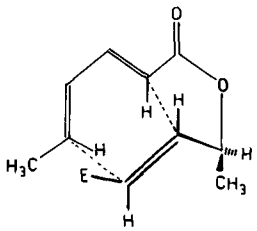

6 (E=CO_2Et)

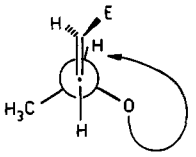

7

The opening of **4** to further acyclic products can occur in several ways; for example, to **5**, which has a total of five distinguishable hydroxyl functions. The chiral information of **1** is thus transferred with high selectivity to the centers C-2, 3, 4, and 7 of the open chain compound **5** (numbering arbitrary).

The coupling of two reactions is often considered a tandem reaction when they proceed one after the other without change in reaction conditions or buildup of intermediates.[8] In Scheme 2 we describe the first example of the coupling of an aliphatic Claisen rearrangement with an IMDA reaction.[9]

following conclusions: a) The relative amounts of products formed via route **A** or **B** is controlled by the degree of substitution of the internal double bond.[12] If it is trisubstituted (**8a**), route **A** dominates and chiefly the cyclization product

Table 1. Analysis of the tandem reactions of **8**; see also Scheme 2.

Compound	Diels–Alder reaction to **10** (route A)	**12** (route B)	expected	Product found (yield [%], ratio)
8a (n = 3)	favored: [6.6]-bicycle	unfavored: [7.6]-bicycle	**10, 11**	**10a/11a** (75, 10:1)
8b (n = 1)	unfavored: [4.6]-bicycle	favored: [5.6]-bicycle	**9, 12**	**9b/12b** (72, 1.3:1)

10a forms via intermediate **9a**. In the case of disubstitution (**8b**) on the other hand, the routes **A** and **B** are equally favored so that **9b** and **11b** form in approximately equal amounts. b) Diels–Alder reactions leading to rings of unfavorable size are avoided (**9a** → **10b** and **11a** → **12b**). Thus the reaction of **8b** leads to the formation of **9b** and **12b** in

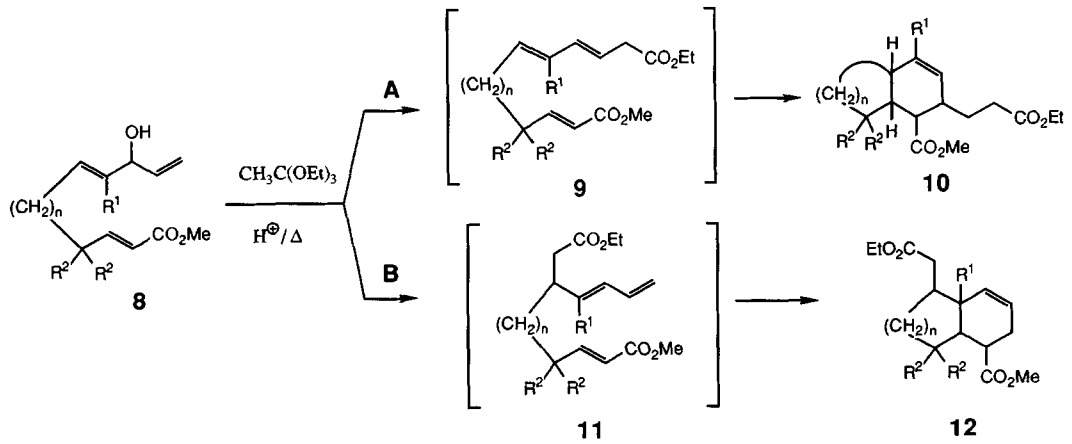

Scheme 2. **8a**–**12a**: n = 3, R^1 = Me, R^2 = H; **8b**–**12b**: n = 1, R^1 = H, R^2 = Me.

The trienols **8a** and **8b** are prepared from the known precursors **13**[10] and **14**[11] according to Scheme 3 and on heating with ethyl orthoacetate in diglyme (2 mol% propionic acid, 160 °C, 48 h) undergo a Claisen rearrangement (route **A** and **B**), followed by the spontaneous Diels-Alder reaction to **10** or **12**. The analysis of the reaction (Table 1) leads to the almost equal proportions, whereas **8a** yields **10a** as dominant product.

Stereochemically cyclization **9a** → **10a** differs from **11b** → **12b**. Compound **12b** is generated as a 43:35:14:4 mixture of the four diastereomers, whereas **10a** yields an isomer distribution of 91:9 (HPLC analysis). The relative configuration

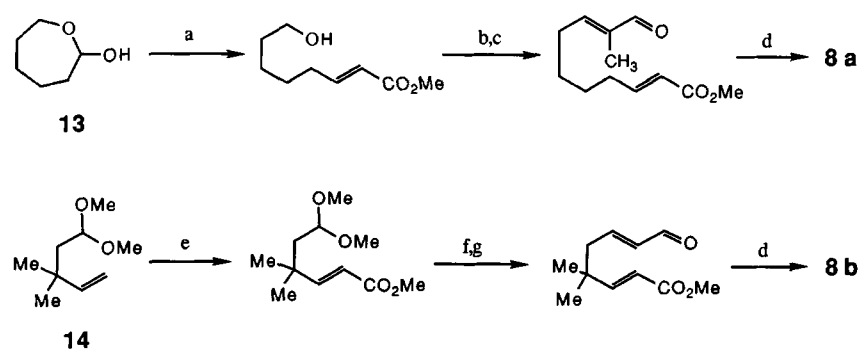

Scheme 3. a) Ph_3PCHCO_2Me, $CHCl_3$, Δ (61%, *E*/*Z* = 10:1); b) Dimethylsulphoxide, CH_2Cl_2, $(CO)_2Cl_2$, −60 °C, (quant.); c) $Ph_3PC(CH_3)CHO$, $CHCl_3$, Δ (73%); d) $(CH_2{=}CH)MgCl$, Et_2O, −15 °C, (70–80%); e) $OsO_4/NaIO_4$ (80%); pyridine, H_2O; Ph_3PCHCO_2Me, $CHCl_3$, Δ (70%); f) SiO_2/CH_2Cl_2/*p*-TsOH (95%); g) $Ph_3PCHCHO$, $CHCl_3$, Δ (71%).

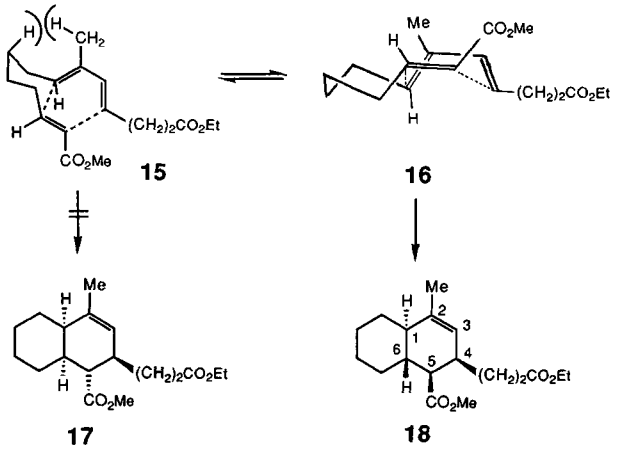

of the main diastereomer (**18**) of **10a** was determined by nuclear Overhauser enhancement (NOE) difference spectroscopy.[13] The cyclization **9a** → **10a** may be explained by considering the reactive intermediates **15** and **16**: intermediate **15** appears to be less favorable than **16** as a result of transannular H-methyl repulsion, and the cyclization product **17** is formed in only small amounts. Table 2 lists analytical data of the key compounds **4**, **12b** (major diastereomer) and **18**.

Table 2. Analytical data for the compounds **4**, **12b** (major diastereomer) and **18**. ^{1}H NMR: 270 MHz, $CDCl_3$, TMS as internal standard; ^{13}C NMR: 67.5 MHz, $CDCl_3$, TMS.

4: $[\alpha]_D^{20} = +32.5$ ($c = 2$, $CHCl_3$); ^{1}H NMR: $\delta = 0.90$ (d, $J = 7$ Hz, 3H; CH_3), 1.29 (t, $J = 7$ Hz, 3H; CH_3), 1.48 (d, $J = 7$ Hz, 3H; CH_3), 2.68 (m, 3H), 3.35 (ddd, $J = 2.5$, 4.5, 8 Hz, 1H), 4.19 (q, $J = 7$ Hz, 1H), 4.21 (q, $J = 7$ Hz, 1H). 4.34 (dq, $J = 1$, 7 Hz, 1H), 5.84 (dd, $J = 4.5$, 10 Hz, 1H), 5.97 (ddd, $J = 2.5$, 6, 10 Hz, 1H); ^{13}C NMR: $\delta = 14.03$, 15.436, 20.38, 30.248, 36.797, 38.417, 44.860, 60.612, 79.917, 119.503, 133.691, 172.877, 175.630; IR (Film): $\tilde{\nu} = 2980$, 1800–1700, 1380, 1280, 1250, 1230, 1175, 1110, 1035, 1020, 970 cm^{-1}; C,H elemental analyis.

12b: ^{1}H NMR: $\delta = 0.86$, 1.01 (2 × s, each CH_3), 1.19 (t, $J = 6$ Hz, CH_3), 1.63–1.77 (m, 2H), 1.92–2.11 (m, 2H), 2.13–2.29 (m, 4H), 2.31–2.42 (m, 1H), 2.49 (dd, $J = 5$, 15 Hz, 1H), 3.60 (s, OCH_3), 4.07 (q, $J = 6$ Hz, 2H), 5.58–5.75 (m, 2H); IR (Film): $\tilde{\nu} = 2950$, 1735, 1160, 1030 cm^{-1}; MS (EI, 80 eV, 100 °C): *m/z* 294 ($M^{\oplus}$), 279, 262, 249, 234, 219, 206, 191, 147, 131, 119, 105, 91, 79; HRMS: 279.1594 (calcd. for $M^{\oplus} - CH_3$: 279.1596)

18: ^{1}H NMR: (assignment by ^{1}H-^{1}H COSY): $\delta = 0.77$–0.97 (m, 1H), 0.86–1.06 (m, 1H), 1.23 (t, $J = 7$ Hz, CH_3), 1.22–1.38 (m, 1H), 1.26–1.43 (m, 1H), 1.44–1.61 (m, 1H; 6-H), 1.50–1.79 (m, 2H), 1.56–1.74 (m, 1H; 1-H), 1.62 (s, 3H; 2-CH_3), 1.69–1.80 (m, 1H), 1.76–1.88 (m, 1H), 1.89–2.00 (br. d, 1H), 1.99–2.11 (br.d, 1H), 2.18–2.50 (m, 2H), 2.28–2.45 (m, 1H; 4-H), 2.54 (dd, $J = 5.5$, 10.5 Hz, 1H; 5-H), 3.65 (s, OCH_3), 5.10 (q, $J = 7$ Hz, 2H), 5.36 (dq, $J = 1.5$, 3 Hz, 1H, 3-H); ^{13}C NMR: $\delta = 14.08$, 20.73, 26.24, 26.87, 27.80, 29.64, 30.49, 32.01, 35.78, 37.39, 45.45, 49.56, 50.86, 60.01, 123.05, 136.95, 173.37, 174.03; MS (EI, 80 eV, 40 °C): *m/z* = 308 ($M^{\oplus}$), 276, 263, 248, 220, 202, 174, 161, 147, 119, 105, 91, 79; IR (film): $\tilde{\nu} = 2930$, 1735, 1160 cm^{-1}; HRMS: 308.1987 (calcd. for $M^{\oplus}$ 308.1987), 276.1726 (calcd. for $M^{\oplus} - CH_3OH$: 276.1725.)

Received: November 22, 1990 [Z4289 IE]
German version: *Angew. Chem.* *103* (1991) 450

CAS Registry numbers:
1, 132341-85-6; **2**, 132298-17-0; **3**, 132298-18-1; **4**, 132298-19-2; **5**, 132298-20-5; **8a**, 132298-22-7; **8b**, 132298-21-6; **9b**, 132298-23-8; **10a**, 132298-24-9; **11a**, 132298-25-0; **12b**, 132298-26-1; **13**, 93545-84-7; **14**, 79898-62-7; **16**, 132298-27-2; **18**, 132298-29-4; (*E*)-$HO(CH_2)_5CH{=}CHCO_2Me$, 68750-31-2; (*E*)-$HO(CH_2)_5CH{=}CHCO_2Me$, 132298-28-3; $OHCCH{=}CH(Me)(CH_2)_4CH{=}CHCO_2Me$, 132298-30-7; $(MeO)_2CHCH_2C(Me)_2CH{=}CHCO_2Me$, 132298-31-8; (*E*)-$OHCCH_2C(Me)_2CH{=}CHCO_2Me$, 132298-32-9; $OHCCH{=}CHCH_2C(Me)_2CH{=}CHCO_2Me$, 132298-33-0.

[1] Reviews: G. Brieger, J. N. Bennett, *Chem. Rev. 80* (1980) 63; E. Ciganek, *Org. React. 32* (1984) 1; A. G. Fallis, *Can. J. Chem. 62* (1984) 183; particular examples: R. K. Boekman, Jr., D. M. Demko, *J. Org. Chem. 47* (1982) 1789; G. Stork, E. Nakamuru, *J. Am. Chem. Soc. 105* (1983) 5510; H. Dyke, P. G. Steel, E. J. Thomos, *J. Chem. Soc. Perkin Trans. 1 1989*, 525; J. W. Coe, W. R. Roush, *J. Org. Chem. 54* (1989) 915; K. Takeda, Y. Igarishi, K. Okazai, E. Yoshii, K. Yamaguchi, *ibid. 55* (1990) 3431, and references quoted therein.
[2] A. F. Thomas, *J. Am. Chem. Soc. 91* (1969) 3281; F. E. Ziegler, J. J. Piwinski, *ibid. 101* (1979) 1611.
[3] T. Mandai, S. Matsumoto, M. Kohama, M. Kawada, J. Tsuji, S. Saito, T. Moriwake, *J. Org. Chem. 55* (1990) 5671, and references quoted therein.
[4] Review: R. K. Hill in J. D. Morrison (Eds.): *Asymmetric Synthesis, Vol. 3*, Academic Press, Orlando, FL, USA 1984, p. 503ff.
[5] S. Hanessian, R. DiFabio, J.-F. Marcoux, M. Prud'homme, *J. Org. Chem. 55* (1990) 3436; G. Stork, M. Kahn, *J. Am. Chem. Soc. 107* (1985) 500.
[6] The X-ray crystal structure analysis was undertaken on racemic **4** (m.p. < 20 °C). Details of the crystal structure investigation may be obtained from the Fachinformationszentrum Karlsruhe, Gesellschaft für wissenschaftlich-technische Information mbH, W-7514 Eggenstein-Leopoldshafen 2 (FRG) on quoting the depository number CSD-55094, the names of the authors and the journal citation. The starting compound for the synthesis of the enantiomerically pure **4** was (*S*)-**1**. For physical and spectroscopic data of **4** data see Table 2.
[7] P. Caramella, N. G. Rondan, M. N. Paddon-Row, K. N. Houk, *J. Am. Chem. Soc. 103* (1981) 2438; K. N. Houk, M. N. Paddon-Row, N. G. Rondan, Y. D. Wu, K. F. Brown, D. C. Spellmeyer, J. T. Metz, Y. Li, R. J. Loncharich, *Science 231* (1986) 1108.
[8] Therein lies the difference from sequential reactions, which can be carried out separately. See also F. E. Ziegler, *Chem. Rev. 88* (1988) 1423; T. Nakai, K. Mikami, *ibid. 86* (1986) 885.
[9] Aromatic series: G. A. Kraus, B. S. Fulton, *J. Org. Chem. 50* (1985) 1782; G. A. Kraus, S. H. Woo, *ibid. 52* (1987) 4841.
[10] J. F. Carvalho, G. D. Prestwich, *J. Org. Chem. 49* (1984) 1251.
[11] R. K. Boekman, Jr., S. S. Ko, *J. Am. Chem. Soc. 104* (1982) 1033.
[12] K. A. Parker, J. G. Farmar, *Tetrahedron Lett. 25* (1985) 3655; S. Bancel, P. Cresson, *C.R. Acad. Sci. Ser C 268* (1989) 1535, and references cited therein.
[13] Strong interactions are observed between H-1 and H-5 as well as between H-4 and H-5, whereas H-1 and H-6 do not influence each other.

Enantioselective Protonation of a Simple Enol: Aminoalcohol-Catalyzed Ketonization of a Photochemically Produced 2-Methylinden-3-ol**

By *Françoise Henin,** *Jacques Muzart,** *Jean-Pierre Pete, Anastase M'boungou-M'passi*, and *Hermann Rau*

During the past few years, we have been concerned with asymmetric protonations of dienols produced by a Norrish type II photorearrangement of α,β-unsaturated carbonyl compounds.[1] The mechanistic model that we have proposed to rationalize the stereochemistry of the discrimination step involves principally the enol part of the dienol[2] and should apply equally well to enantioselective protonation of simple enols. As simpler enols could be generated from a Norrish type II photoelimination,[3] we examined the behavior of such prochiral enols under analogous conditions. Intensive research work has been devoted to the syn-

[*] Dr. F. Henin, Dr. J. Muzart, Prof. Dr. J. P. Pete, A. M'boungou-M'passi
Unité des Rearrangements Thermiques et Photochimiques Associée au C.N.R.S.
Université de Reims Champagne-Ardenne
F-51062 Reims (France)
Prof. Dr. H. Rau
Fachgebiet Physikalische Chemie
Institut für Chemie der Universität Hohenheim
W-7000 Stuttgart 70 (FRG)
[**] This work was supported by the Direction des Relations et la Coopération Internationales (D.R.C.I.) (travel grants to F. H. and J. M.); We gratefully acknowledge *A. Woll* and *B. Vogler* for their efficient assistance.

thesis and reactivity of stable enols[4] and to the asymmetric protonation of enolates,[5, 6] but to the best of our knowledge, the asymmetric protonation of a simple enol has never been reported.[7] We report here the results of such a study on 2-methylinden-3-ol **1** which is constrained to a single, rigid geometry and which was obtained photochemically from 2-methyl-2-isobutylindan-1-one **2**.

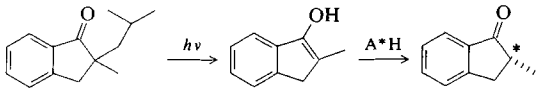

2 **1** **3**

Irradiations of deoxygenated acetonitrile solutions of **2** ($c = 3 \times 10^{-3}$ M) were first carried out in circular dichroism (CD) cells ($l = 1$ cm) with a nitrogen laser ($\lambda = 337$ nm) for 3–4 min. When an excess of (−)-ephedrine was added to the reaction mixture in the dark after irradiation, CD signals were observed at $\lambda > 300$ nm (Fig. 1, solid curve). These signals did not appear if a few drops of an aqueous NaOH solution were added before the ephedrine or when CH_2Cl_2 or MeOH was used as solvent in place of MeCN. Such CD signals could be attributed to chiral 2-methylindan-1-one **3**. Irradiations were also carried out with methylene chloride, dioxane, benzene, or acetonitrile solutions of **2** containing an excess of (−)-ephedrine. Similar signals appeared in the CD spectrum recorded after a few minutes of irradiation (Fig. 1, dotted curve). These CD signals disappeared in the presence

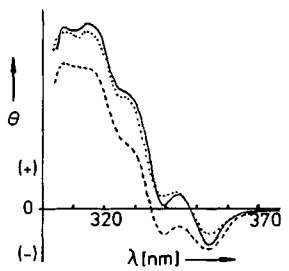

Fig. 1. CD spectra of irradiated mixtures of **2** and (−)-ephedrine (— and ···) and of pure **3** (---, in CH_2Cl_2). For details see text.

of an aqueous NaOH solution. These results suggest that **1** is formed and has a lifetime long enough to be protonated by (−)-ephedrine to form **3**. Similar CD signals were also observed when cinchonine was used instead of (−)-ephedrine. By contrast, such signals were not observed when (*S*)-α-methylbenzylamine, (*S*)-octan-2-ol or (−)-mandelic acid was the added chiral protonating species or when hexane was used as the solvent.

To support our interpretation, irradiation of a CD_3CN solution of **2** was carried out at 0 °C in an NMR tube. The 250 MHz ^1H NMR spectrum registered immediately after laser irradiation indicated a partial transformation of the starting material (40–50%) and showed the presence of singlet signals at $\delta = 1.96$, 3.16, and 6.38, which could be attributed respectively to the CH_3, CH_2, and OH groups of **1**. Addition of (−)-ephedrine induced the disappearance of these three signals with concomittent appearance of signals at $\delta = 1.24$(d), 2.7(m), 2.71(dd), and 3.41(dd), identical to the CH_3, CH, and CH_2 signals exhibited by the NMR spectrum of an authentic sample of **3**. From NMR integration, the yield was found to be essentially quantitative for this transformation. When this irradiated solution was transferred to a CD cell, we again observed the CD signals attributed to chiral **3**.

As the asymmetric formation of **3** had now been clearly established, we carried out semipreparative experiments. Chemical and optical yields are shown in Table 1 while the CD spectrum of purified **3** is shown in Figure 1, dashed curve. From these experiments, it appears that catalytic amounts of (−)-ephedrine are sufficient to induce an important enantioselectivity to the protonation of the enol. Furthermore, the best optical yields were reached with smaller amounts of added chiral species, and the major enantiomer of **3** isolated has the (*R*)-configuration,[8] as anticipated from the mechanistic scheme previously proposed for asymmetric protonation of dienols.[2]

Table 1. Asymmetric synthesis of 2-methylindan-1-one **3** from photolysis of **2**.

Solvent	(−)-ephedrine [equiv]	Conversion of **2** [%]	Yield of **3** [%] [a]	$[\alpha]_D^{22}$ (*c*, dioxane)	*ee* [%] config. [b]
CH_2Cl_2	0.68	90	42	−9 (0.19)	21 ± 3, (*R*)
CH_3CN	0.74	98	48	−12 (0.18)	28 ± 3, (*R*)
CH_3CN	0.10	98	59	−20 (0.26)	47 ± 3, (*R*)
CH_3CN	0.01	86	41	−19 (0.18)	45 ± 2, (*R*)

[a] Yield calculated on the amount of **2** introduced. [b] Determined on isolated **3** by comparison with literature data [8]; pure (*R*)-**3**: $[\alpha]_D^{22} = -42$ in dioxane.

Thus an enantioselective protonation of a simple enol was achieved.[9] Further developments of this photochemical approach towards chiral reactions are under way.

Experimental Procedure

Stirred deoxygenated solutions (15 mL) of **2** (10^{-2} M) and (−)-ephedrine (for concentrations see Table 1) in a round cell ($l = 5$ cm) were irradiated at 0 ± 3 °C with a nitrogen laser for 1.5 h. The irradiated mixture was then stirred overnight while the temperature of the cooling bath increased slowly to room temperature. After evaporation of solvent, **3** was isolated by preparative TLC (eluant EtOAc/petroleum ether, 5:95) followed by filtration on silica gel (same eluant). During the purification, precautions were taken to preclude enantiomer-differentiation of **3** [10].

Received: October 29, 1990 [Z 4256]
German version: *Angew. Chem. 103* (1990) 460

CAS Registry numbers:
2, 132540-64-8; **3**, 57128-12-8; (−)-ephedrine, 299-42-3.

[1] F. Henin, R. Mortezaei, J. Muzart, J. P. Pete, *Tetrahedron Lett. 26* (1985) 4945–4948; J. P. Pete, F. Henin, R. Mortezaei, J. Muzart, O. Piva, *Pure Appl. Chem. 58* (1986) 1257–1262; F. Henin, R. Mortezaei, J. Muzart, J. P. Pete, O. Piva, *Tetrahedron 45* (1989) 6171–6196; O. Piva, J. P. Pete, *Tetrahedron Lett. 31* (1990) 5157–5160.

[2] R. Mortezaei, O. Piva, F. Henin, J. Muzart, J. P. Pete, *Tetrahedron Lett. 27* (1986) 2997–3000; O. Piva, R. Mortezaei, F. Henin, J. Muzart, J. P. Pete, *J. Am. Chem. Soc. 112* (1990) 9263–9272.

[3] G. R. Mc Millan, J. G. Calvert, J. N. Pitts, *J. Am. Chem. Soc. 86* (1964) 3602–3605; P. J. Wagner, *Acc. Chem. Res. 4* (1971) 168–177; A. Henne, H. Fischer, *Angew. Chem. 88* (1976) 445; *Angew. Chem. Int. Ed. Engl. 15* (1976) 435.

[4] Reviews: H. Hart, *Chem. Rev. 79* (1979) 515–528; A. J. Kresge, *Actual. Chim. 1988*, 233–240; Z. Rappoport, S. E. Biali, *Acc. Chem. Res. 21* (1988) 442–449; B. Capon, B. Z. Guo, F. C. Kwok, A. K. Siddhanta, C. Zucco, *ibid. 21* (1988) 135–140; A. J. Kresge, *ibid. 23* (1990) 43–48; recent examples: Y. Chiang, A. J. Kresge, N. P. Schepp, *J. Am. Chem. Soc. 111* (1989) 3977–3980; N. Shimizu, T. Miyahara, M. Mishima, Y. Tsuno, *Bull. Chem. Soc. Jpn. 62* (1989) 2032–2039; G. D. Dzingeleski, G. Blotny, R. M. Pollack, *J. Org. Chem. 55* (1990) 1019–1023; E. B. Nadler, Z. Rappoport, *ibid. 55* (1990) 2673–2682; J. R. Keeffe, A. J. Kresge, N. P. Schepp, *J. Am.*

Chem. Soc. 112 (1990) 4862–4868; M. Schmittel, U. Baumann, *Angew. Chem. 102* (1990) 571–572; *Angew. Chem. Int. Ed. Engl. 29* (1990) 541–543; B. Urwyler, J. Wirz, *ibid. 102* (1990) 807–809 and 29 (1990) 790–792; Y. Chiang, A. J. Kresge, P. Pruszynski, N. P. Schepp, J. Wirz, *ibid. 102* (1990) 810–812 and *29* (1990) 792–794.

[5] For a review, see: L. Duhamel, P. Duhamel, J. C. Launay, J. C. Plaquevent, *Bull. Soc. Chim. Fr. II. 1984*, 421–430.

[6] a) H. Pracejus, R. Rennau, *React. Kinet. Catal. Lett. 15* (1980) 203–207; b) H. Hogeven, L. Zwart, *Tetrahedron Lett. 23* (1982) 105–108; c) L. Duhamel, J. C. Launay, *ibid. 24* (1983) 4209–4212; d) S. Takano, J. Kudo, M. Takahashi, K. Ogasawara, *ibid. 27* (1986) 2405–2408; e) L. Duhamel, S. Fouquay, J. C. Plaquevent, *ibid. 27* (1986) 4975–4978; f) L. Duhamel, P. Duhamel, S. Fouquay, J. J. Eddine, O. Peschard, J. C. Plaquevent, A. Ravard, R. Solliard, J. Y. Valnot, H. Vincens, *Tetrahedron 44* (1988) 5495–5506; g) U. Gerlach, S. Hünig, *Angew. Chem. 99* (1987) 1323–1325; *Angew. Chem. Int. Ed. Engl. 26* (1987) 1283–1285; h) C. Fehr, J. Galindo, *J. Am. Chem. Soc. 110* (1988) 6909–6911; i) D. Potin, K. Williams, J. Rebek, Jr., *Angew. Chem. 102* (1990) 1485–1486; *Angew. Chem. Int. Ed. Engl. 29* (1990) 1420-1422.

[7] An enediol was postulated as an intermediate in the asymmetric protonation of the potassium enediolate of (±) benzoin, see [6c].

[8] G. Jaouen, A. Meyer, *J. Am. Chem. Soc. 97* (1975) 4667–4672.

[9] From preliminary experiments, it appears that the protonation of the enolate of **1** in the presence of (−)-ephedrine leads to **3** with very low *ee*.

[10] W. Tsai, K. Hermann, E. Hug, B. Rohde, A. S. Dreiding, *Helv. Chim. Acta 68* (1985) 2238–2243; R. Matusch, C. Coors, *Angew. Chem. 101* (1989) 624; *Angew. Chem. Int. Ed. Engl. 28* (1989) 626–627.

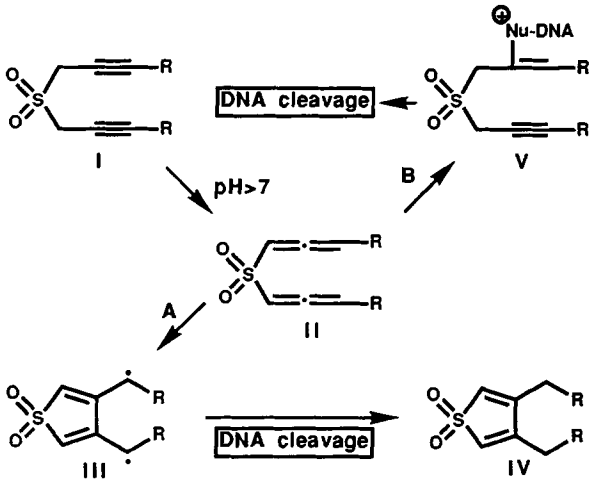

Scheme 1. Mechanistic rationale for propargylic sulfones.

Selectivity and Mechanism of Action of Novel DNA-Cleaving Sulfones**

By *K. C. Nicolaou,* S. Wendeborn, P. Maligres, K. Isshiki, N. Zein* and *G. Ellestad*

DNA is the target of several anticancer agents and antibiotics.[1] In recent years considerable effort has been directed towards the synthesis of DNA-cleaving molecules,[2] and site-specificity receives particular emphasis.[3] Recently we described[4] a simple class of propargylic sulfones that cleave DNA in a pH-dependent fashion. In this communication we report a) site-selective cleavage of double-stranded DNA by sulfone **1**, b) enhancement of the potency of these compounds by incorporating simple intercalators (compounds **2** and **3**), and c) studies elucidating the mechanism of action of this class of compounds.

Scheme 1 summarizes the two alternative modes of action of bis(propargylic) sulfones as originally proposed:[4] A Garratt–Braverman pathway[5, 6] proceeding via bis(allenes) **II** and diradicals **III** (path A), and an alkylation mechanism proceeding via intermediates **II** and **V** (path B). Compound **1** caused single- and double-strand breaks in covalently closed circular DNA. In order to probe mechanistic and reactivity questions, compounds **2**–**4**[7] were synthesized and tested.[8] Figure 1 shows the cleavage results with supercoiled ΦX174 DNA at pH 8.5 and 37 °C. Both compounds **2** (lane 3) and **3** (lane 4) exhibited much higher potencies (500–1000 times) than **1** (lane 2) as DNA-cleaving agents, whereas the saturated compound **4** was devoid of any activity (lane 5) as expected. Ethidium bromide, a known DNA intercalator,

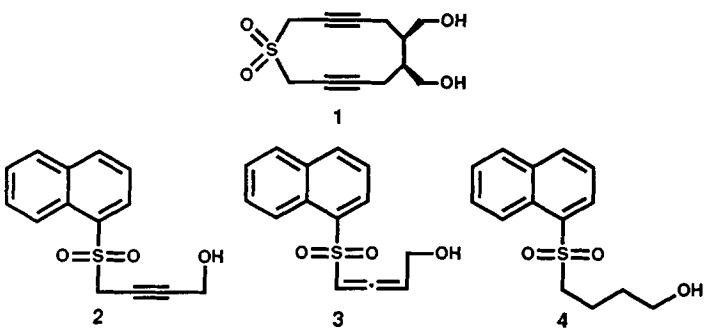

inhibited the action of **2** (lane 8) and **3** (lane 9), but had no effect on the DNA-cleaving action of **1**. It was further observed that compound **4** also served as a weak inhibitor of the action of **2** and **3** on DNA (lanes 11 and 12 respectively), but again had no effect on the action of **1**. Neither catalase nor superoxide dismutase[9] showed any effect on the cleavage by these compounds, but the reaction was heavily dependent on the pH (best results pH 7.4–9.0). These results

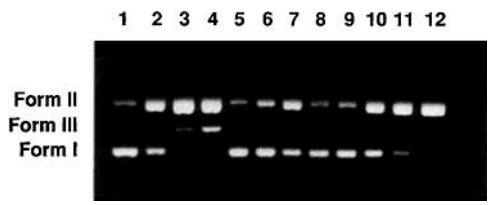

Fig. 1. ΦX174 form I DNA was incubated for 24 h at 37 °C with compounds **1**–**3** in buffer (50 mM Tris-Hcl, pH 8.5) and analyzed by electrophoresis (1% agarose gel, ethidium bromide stain). Lane 1: DNA control; lane 2: **1** [100 μM]; lane 3: **2** [5 μM]; lane 4: **3** [5 μM]; lane 5: **4** [10 mM]; lane 6: ethidium bromide [100 μM]; lane 7: **1** [100 μM] + ethidium bromide [100 μM]; lane 8: **2** [5 μM] + ethidium bromide [5 μM]; lane 9: **3** [5 μM] + ethidium bromide [5 μM]; lane 10: **1**[100 μM] + **4** [10 mM]; lane 11: **2** [5 μM] + **4** [10 mM]; lane 12: **3** [5 μM] + **4** [10 mM].

[*] Prof. Dr. K. C. Nicolaou, S. Wendeborn, P. Maligres, Dr. K. Isshiki, Department of Chemistry Research Insitute of Scripps Clinic, 10666 N. Torrey Pines Road, La Jolla, CA 92037 (USA)
and
Department of Chemistry, University of California, San Diego La Jolla, CA 92093
Dr. N. Zein, Dr. G. Ellestad
American Cyanamid Co. Lederle Research Division
Lederle Laboratories, Pearl River, NY 10965 (USA)

[**] This work was supported by the National Institutes of Health. *S. W.* thanks the Fonds der Chemischen Industrie for a Doctoral Fellowship (1989–1990); K. I. is a visiting scientist from Mercian Co., Japan.

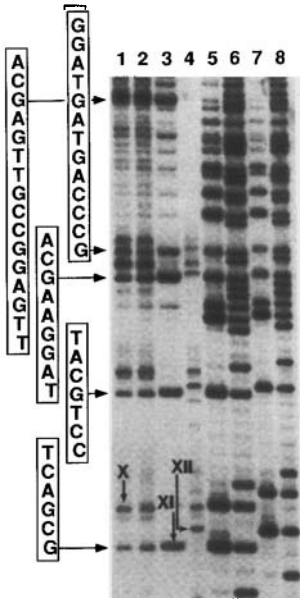

Fig. 2. High-resolution denaturing gel autoradiogram of cleavage of 5'-end ^{32}P-labeled Sal I/BamH I 275 bp restriction fragment of pBR 322 induced by sulfone **1** (bases 18–68 are shown). All incubations were carried out with 5 mM concentrations of **1** at 37 °C for 16 h. Lane 1: no further treatment; lane 2: 90 °C, 0.5 h; lane 3: piperidine (1 M), 90 °C, 0.5 h; lane 4: T4 polynucleotide kinase, 37 °C, 0.5 h; lanes 5 and 6: Maxam–Gilbert G and AG reactions respectively; lanes 7 and 8: Maxam–Gilbert G and AG reactions respectively, followed by T4 polynucleotide kinase, 37 °C, 0.5 h.

strongly suggested that a) the alkylation mechanism B rather than the radical mechanism A (Scheme 1) is the predominant (or exclusive) mode of action of compounds **1**–**3** and b) intercalation of the naphthalene nucleus of compounds **2** and **3** occurs prior to alkylation.[10]

To further examine and confirm the alkylation mechanism, 5'-end as well as 3'-end labeled restriction fragments from pBR 322 were reacted with compounds **1**–**3**. Figure 2 shows the cleavage results with compound **1** and 5'-end labeled DNA. Comparisons of the cleavage products (lane 3) with the chemically produced Maxam–Gilbert markers[11] (lanes 5–8) indicated preferential attack at guanine and, significantly, high selectivity for sequences 5-GCA, 5-GCG and 5-GCC (see horizontal arrows in Fig. 2). Several guanine residues present at various other sites remained unaffected or only slightly affected. Two products, **X** and **XI** (lanes 1–3), were observed on the gel autoradiogram. Whereas heating to 90 °C after incubation did not cause any significant changes (lane 2), piperidine treatment converted band **X** to band **XI** (lane 3). Band **XI** comigrates with the 3'-phosphorylated Maxam–Gilbert markers (lanes 5 and 6), and both had identical mobilities upon treatment with T_4 polynucleotide kinase[12] (**XII**, lane 4 and lanes 7 and 8). These observations are in accord with the mechanism of action depicted in Scheme 2.

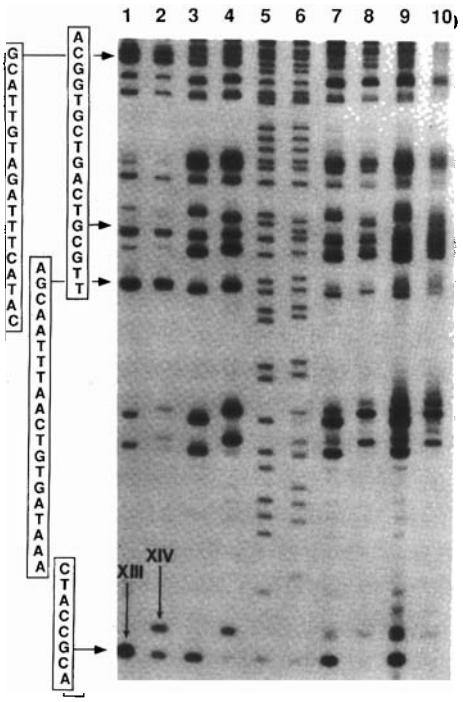

Fig. 3. High-resolution denaturing gel autoradiogram showing cleavage of 3'-end ^{32}P-labeled Cla I/BamH I 351 bp restriction fragment of pBR 322 induced by compounds **1**–**3** (bases 12–76 are shown). Lane 1: **1** [5 mM], 37 °C, 16 h; lane 2: **1** [5 mM]; 37 °C, 16 h, then calf intestine alkaline phosphatase (CIAP), 37 °C, 1 h; lane 3: Maxam–Gilbert G reaction; lane 4: Maxam–Gilbert G reaction followed by CIAP, 37 °C, 1 h; lane 5: Maxam–Gilbert AG reaction; lane 6: Maxam–Gilbert AG reaction followed by CIAP, 37 °C, 1 h; lane 7: **2** [100 μM], 37 °C, 16 h; lane 8: **2** [100 μM], 37 °C, 16 h, then CIAP, 37 °C, 1 h; lane 9: **3** [100 mM], 37 °C, 16 h; lane 10: **3** [10 μM], 37 °C, 16 h, then CIAP, 37 °C, 1 h.

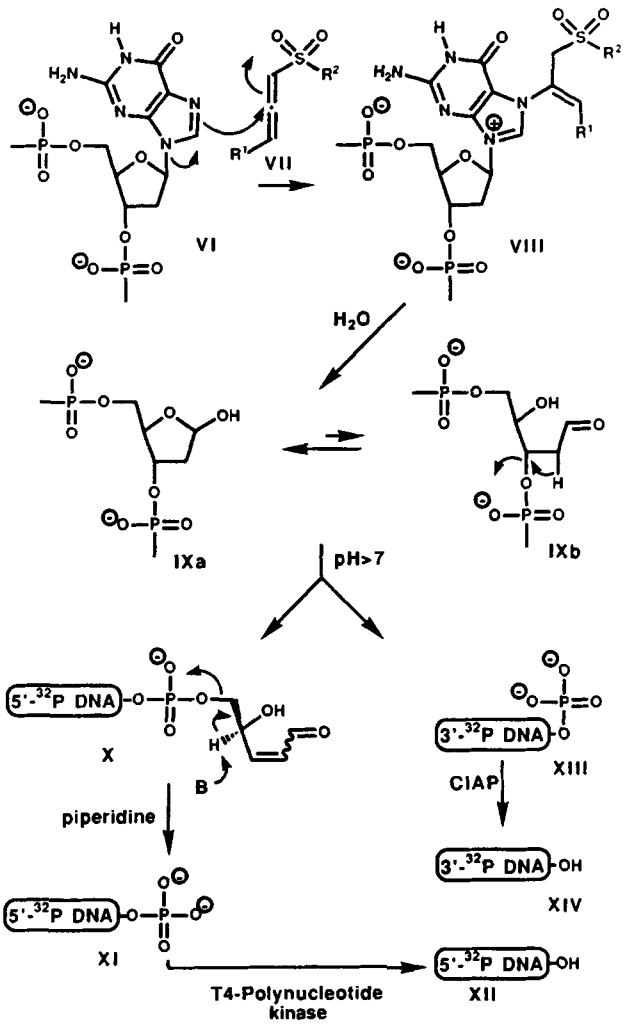

Scheme 2. Mechanism of action of 1–3 on DNA.

Similar experiments with 3'-end labeled DNA and compounds **1**–**3** (Fig. 3) provided further support for these intermediates and the overall alkylation mechanism presented in Scheme 2. Thus intermediates **XIII** and **XIV** were detected for compound **1** (Fig. 3, lanes 2 and 3, respectively). Com-

pounds **2** and **3** also exhibited identical cleavage profiles (Fig. 3, lanes 7 and 9), but different from that of **1** (Fig. 3, lane 1). The susceptibility of conjugated sulfones to nucleophilic attack is also in line with the proposed mechanism.[13]

The selectivity of compounds **1**–**3** in recognizing DNA regions may reflect not only their reactivity towards individual bases, but also local DNA shapes. This selectivity may be amplified synergistically by attaching these new DNA-cleaving moieties onto sequence-specific delivery systems.

Received: October 9, 1990 [Z 4236]
German version: *Angew. Chem. 103* (1990) 462

[1] W. A. Remers (Ed.): *Antineoplastic Agents*, Wiley, New York 1984; S. Neidle, M. J. Waring (Eds.): *Molecular Aspects of Anticancer Drug Action*, Verlag Chemie, Weinheim, FRG 1983; C. Chagas, B. Pullman (Eds.): *Molecular Mechanism of Carcinogenic and Antitumor Activity*, Adenine Press, Schenectady, NY, USA 1987.

[2] For some selected examples, see: a) R. P. Hertzberg, P. B. Dervan, *J. Am. Chem. Soc. 104* (1982) 313; b) H. E. Moser, P. B. Dervan, *Science (Washington DC) 238* (1987) 645; c) K. C. Nicolaou, Y. Ogawa, G. Zuccarello, H. Kataoka, *J. Am. Chem. Soc. 110* (1988) 7247; d) T. J. Posvic, P. B. Dervan, *ibid. 111*, (1989) 3059; e) D. R. Corey, P. G. Schulz, *ibid. 111* (1989) 8523; f) A. M. Pyle, E. C. Long, J. K. Barton, *ibid. 111*, (1989) 4520; g) D. S. Sigman, *ibid. 111* (1989) 4941; h) N. B. Mantlo, S. J. Danishefsky, *J. Org. Chem. 54* (1989) 2781; i) M. Ohno, M. Otsuka, *ibid. 112* (1990) 838; k) D. Natans, H. O. Smith, *Annu. Rev. Biochem. 44* (1975) 273; l) K. C. Nicolaou, G. Skokotas, S. Fuyura, H. Suemune, D. C. Nicolaou, *Angew. Chem. 102* (1990) 1066; *Angew. Chem. Int. Ed. Engl. 29* (1990) 1064.

[3] B. F. Baker, P. B. Dervan, *J. Am. Chem. Soc. 111* (1989) 2700; D. P. Mack, P. B. Dervan, *ibid. 112* (1990) 4604; D. Pei, P. G. Schultz, *ibid. 112* (1990) 4579; S. A. Strobel, P. B. Dervan; *Science (Washington, DC) 249* (1990) 73, and references cited therein.

[4] K. C. Nicolaou, G. Skokotas, P. Maligres, G. Zuccarello, E. J. Schweiger, K. Toshima, S. Wendeborn, *Angew. Chem. 101* (1989) 1255; *Angew. Chem. Int. Ed. Engl. 28* (1989) 1272.

[5] P. J. Garratt, S. B. Neoh, *J. Org. Chem. 44* (1979) 2667; Y. S. P. Cheng, P. J. Garratt, S. B. Neoh, V. H. Rumjanek, *Isr. J. Chem. 26* (1985) 101.

[6] S. Braverman, D. Segev, *J. Am. Chem. Soc. 96* (1974) 1245; S. Braverman, Y. Duar, D. Segev, *Tetrahedron Lett. 1976*, 3181.

[7] Selected physical data of compounds **2**–**4**. **2**: ^{1}H NMR (500 MHz, $CDCl_3$): δ = 8.78 (d, J = 8.5 Hz, 1H, naphthyl), 8.35 (dd, J = 7.5, 1 Hz, 1H, naphthyl), 8.16 (d, J = 8.0 Hz, 1H, naphthyl), 7.98 (d, J = 8.5 Hz, 1H, naphthyl), 7.71 (ddd, J = 8.5, 7.0, 1.0 Hz, 1H, naphthyl), 7.45 (m, 2H, naphthyl), 4.19 (m, 2H, CH_2SO_2), 4.12 (m, 2H, CH_2OH); IR($CHCl_3$): $\tilde{\nu}_{max}$ [cm^{-1}] = 3602, 3080, 2950, 1346, 1169, 1124; HRMS (CI): m/z Calcd for $C_{14}H_{12}O_3S$ ($M^{\oplus}$): 260.050, found: 260.048; **3**: ^{1}H NMR (500 MHz, $CDCl_3$): δ = 8.66 (d, J = 9 Hz, 1H, naphthyl), 8.34 (d, J = 7.0 Hz, 1H, naphthyl), 8.12 (d, J = 8.0 Hz, 1H, naphthyl), 7.96 (d, J = 8.0 Hz, 1H, naphthyl), 7.61 (m, 2H, naphthyl), 6.42 (ddd, J = 6.0, 3.0, 3.0 Hz, 1H, $CHSO_2$), 6.02 (ddd, J = 6.0, 6.0, 6.0 Hz, $CHCH_2$), 4.19 (m, 2H, CH_2OH); IR($CHCl_3$): $\tilde{\nu}_{max}$ [cm^{-1}] = 3608, 3080, 2950, 1959, 1318, 1156, 1127; HRMS (CI): m/z Calcd for $C_{14}H_{12}O_3S$ ($M^{\oplus}$): 260.050, found: 260.051; **4**: ^{1}H NMR (250 MHz, $CDCl_3$): δ = 8.73 (d, J = 8.45 Hz, 1H, naphthyl), 8.31 (dd, J = 8.6, 1.2 Hz, 1H, naphthyl), 8.14 (d, J = 8.1 Hz, 1H, naphthyl), 7.99 (d, J = 8.0 Hz, 1H, naphthyl), 7.66 (m, 3H, naphthyl), 3.61 (t, J = 6.5 Hz, 2H, CH_2OH), 3.36 (t, J = 7.64 Hz, 2H, CH_2SO_2), 1.83 (m, 2H, CH_2), 1.64 (m, 2H, CH_2); IR($CHCl_3$): $\tilde{\nu}_{max}$ [cm^{-1}] = 3627, 3550, 3080, 2945, 1346, 1156, 1125; HRMS (CI): m/z Calcd for $C_{14}H_{16}O_3S$ ($M^{\oplus}$): 264.082, found: 264.082.

[8] Compound **2** was synthesized from naphthalene-1-thiol via reaction with $BrCH_2C{\equiv}CCH_2OSitBuMe_2$ under basic conditions followed by *meta*-chloroperbenzoic acid oxidation and fluoride-induced desilylation. Compound **3** was prepared from **2** by exposure to triethylamine. Compound **4** was prepared in a similar manner to compound **1** by using $I(CH_2)_4OSitBuMe_2$.

[9] J. M. McCord, I. Fridorich, *J. Biol. Chem. 244* (1969) 6049.

[10] The DNA-cleaving properties of compounds **1**–**3** were not affected by EDTA. Participation of EDTA-binding metals in the cleavage reaction mechanism can thus be excluded.

[11] A. M. Maxam, W. Gilbert, *Methods Enzym. 65* (1980) 499; A. M. Maxam, W. Gilbert, *Proc. Natl. Acad. Sci. USA 74* (1977) 560.

[12] V. Cameron, O.C. Uhlenbeck, *Biochemistry 16* (1977) 5120.

[13] Compound **3** reacted with adenine, guanine and benzylamine giving rather labile adducts which hydrolysed to the expected 2-keto compound. For some previous reports of additions of nucleophiles to propargylic and allenic sulfones, see: L. Skattebol, B. Boulette, S. Solomon, *J. Org. Chem. 33* (1968) 548; C. J. M. Stirling, *J. Chem. Soc. 1964*, 5856, 5863, 5875; H. F. Schuster, G. M. Coppola: *Allenes in Organic Synthesis*, Wiley, New York 1984, pp. 235–239 and references cited therein.

Stereospecific γ-Ray-Induced Trimerization of Crystalline Sodium *trans*-2-Butenoate **

By *Graciela C. Diaz de Delgado, Kraig A. Wheeler, Barry B. Snider*, and *Bruce M. Foxman**

Solid state reactions offer both an exceptional opportunity and a distinct challenge. In optimal cases, irradiation or thermolysis of crystals can lead to unusual stereospecific intermolecular reactions that cannot be accomplished in solution. The challenge lies in discovering new classes of materials capable of solid state reactivity, and in determining the principles which govern their behavior.[1]

For several years, we have been exploring the solid state reactivity of transition and nontransition metal salts of unsaturated carboxylic acids.[2] We were therefore fascinated by the unusual thermal reactivity reported[3] for sodium *trans*-2-butenoate (**1**). Heating **1** for four hours at 320 °C converts it stereospecifically, in high yield, to the dicarboxylate **2** by a unique ene reaction.[3] The unprecedented high thermal reactivity of crystalline **1** suggests the presence of short C=C···C=C interactions in its crystal structure.[4] We therefore anticipated interesting solid state chemistry during γ-irradiation of crystalline **1**.

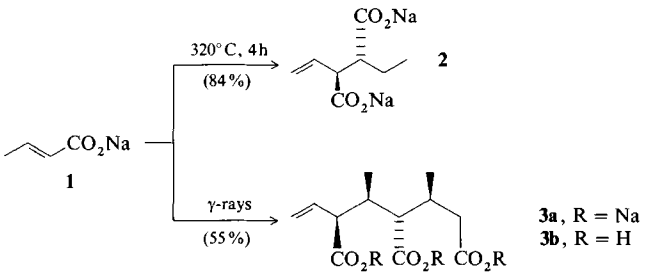

Irradiation of crystalline **1** with ^{60}Co γ-rays (15–20 Mrad radiation dose) leads to a mixture containing 75–80% of *one of eight* possible diastereoisomers of the trisodium salt of 2,4-dimethyl-6-heptene-1,3,5-tricarboxylic acid (**3a**) in 70–80% conversion. GC analysis of the methyl esters of the crude reaction mixture showed the major products to be trimer **3a**, a head-to-tail dimer,[5] and two other trimers in a 12:2:1:1 ratio; the head-to-head dimer **2** was not formed upon γ-irradiation of sodium *trans*-2-butenoate. Dissolution of the irradiated solid in water followed by neutralization with hydrochloric acid precipitates triacid **3b** in 50–55% yield. The connectivity of **3b** was determined by analysis of the ^{1}H and ^{13}C NMR spectra of the crude triacid, which showed (along with GC analysis of the methyl esters) that the precipitated **3b** was greater than 90% pure. An X-ray structure determination[6] of **3b** recrystallized from 1:1 THF/H_2O confirmed the connectivity and allowed assignment of the four chiral centers (2*R**,3*R**,4*S**,5*R**; Fig. 1).

A number of unusual features characterize this process. The selective formation of a trimer is unprecedented. Solid state reactions of olefinic monomers usually result in either polymerization,[7–10] or dimerization as in the thermal reaction[3] of **1** and the classic ultraviolet irradiation of cinnamic acid derivatives.[4a] This work presents the first (to our

[*] Prof. B. M. Foxman, G. C. D. de Delgado, K. A. Wheeler, Prof. B. B. Snider
Department of Chemistry, Brandeis University
P.O. Box 9110, Waltham, MA 02254-9110 (USA)

[**] This work was supported by the National Science Foundation (DMR-8812427)

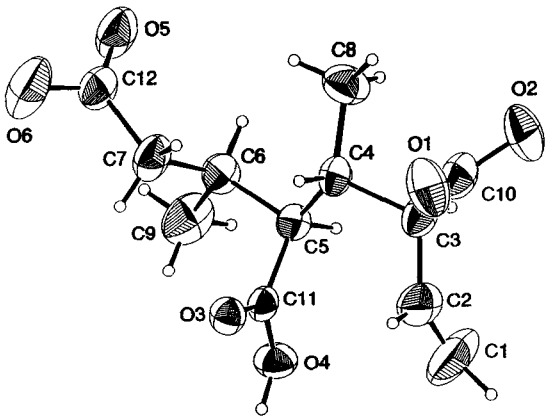

Fig. 1. Molecular structure of **3b**, showing 50% probability ellipsoids for atoms refined using anisotropic thermal parameters (H atoms have been reduced in size to improve clarity).

knowledge) efficient solid state synthesis of a small molecule using ionizing radiation.[11] The reaction is all the more remarkable since it is stereospecific, and the product cannot be prepared at all in solution[5, 12–14] by thermolysis, or by ultraviolet irradiation of crystalline **1**. Gamma ray irradiation of olefinic monomers, in either the solid state or in solution, produces polymers or oligomers with little, or at best incomplete stereochemical control.[7, 15] Stereoregular triads have been observed in the solid state polymerization of barium methacrylate[7a] and methacrylic acid,[7b] and thus the present reaction may be an excellent model for the early stages of oligomer formation in a solid state polymerization reaction.

X-ray powder patterns show that the present process minimally involves a crystal-to-polycrystal transformation, while the polymerization of related materials[7–10] produces amorphous products. Knowledge of the crystal structure of **1** would greatly aid our understanding of the course of the thermal[3] and radiation-induced solid state reactions. However, in spite of efforts by ourselves and others,[16] it has not been possible to grow crystals suitable for X-ray structure determination. We have recently obtained highly mosaic crystals of **1** from DMSO/H_2O solution (DMSO = dimethylsulfoxide). Interpretation of Weissenberg photographs of very thin, fragile crystals suggests the monoclinic crystal system, space group $P2_1$ or $P2_1/m$, with $a = 28.35$, $b = 5.28$, $c = 3.47$ Å; $\beta = 93.0°$. The unusually short c axis formally requires C=C···C=C distances ≤ 3.47 Å, and these must provide a pivotal influence on the reactivity of **1**.

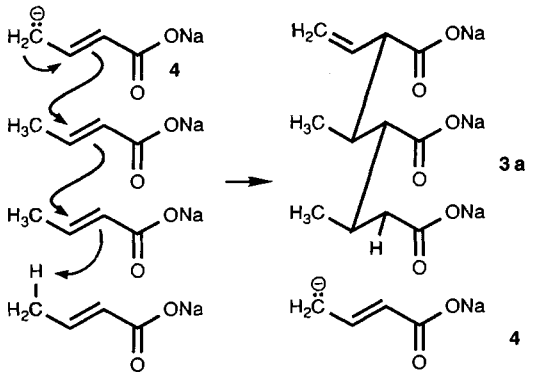

Fig. 2. Possible mechanism for the solid state formation of **3a**.

A possible mechanism consistent with the formation of the head-to-tail trimer is a γ-ray-induced anionic chain reaction (Fig. 2). Gamma-irradiation could result in the loss of an allylic proton to give anion **4**, which adds to the double bond of a neighboring molecule of **1**. A further addition step leads to the formation of a second carbon-carbon bond. The constraints of a reaction in a crystal and distortions caused by the formation of two carbon-carbon bonds could then favor abstraction of an allylic proton (rather than further C-C bond formation) to form **3a**; this would generate a second monomeric anion **4**, which would repeat the process. The reaction might, however, occur by a related free-radical mechanism with hydrogen atom (rather than proton) transfer, and radical addition to the double bonds. A full understanding of the mechanistic aspects of this reaction is precluded by the lack of a crystal structure analysis of **1** and the limited knowledge of interaction of γ-rays with organic molecules in crystals.[17]

In conclusion, a remarkable γ-ray-induced solid state reaction has been discovered that leads to *one of eight possible* diastereoisomers of a unique carboxylic acid.

Experimental Procedure

3b: **1** (3.24 g, 29.9 mmol) was irradiated (15.6 Mrad) in a Gammacell 220 Irradiation Chamber (Atomic Energy of Canada, Ltd.), equipped with a ^{60}Co source (nominal activity as of June 1990, 0.049 Mrad h^{-1}). The resulting colorless powder was dissolved in H_2O (20 mL) to give a homogeneous solution which was acidified with conc. HCl (3.5 mL). The colorless precipitate that formed was isolated by filtration and dried in vacuo (0.25 Torr) over anhydrous $CaSO_4$ to give **3b** (colorless powder, 1.40 g, 5.43 mmol, 55%). A small single crystal of **3b** was grown for X-ray crystal analysis by slow evaporation of a 1:1 THF/H_2O solution. Mp 203–205 °C; IR (KBr): $\tilde{\nu}$[cm^{-1}] = 2973 (C–H); 1721, 1706 (C=O); 990, 906 (C=C). ^1H NMR (300 MHz, [D_6]DMSO, 21 °C, TMS): δ = 12.2 (s, 3H; CO_2H), 5.85 (ddd, ^3J(H,H) = 16.5, 10.9, 8.6 Hz, 1H; CH), 5.11 (br d, ^3J(H,H) = 10.9, 1H; CH), 5.10 (dd, ^3J(H,H) = 16.5, 2.9, 1H; CH), 2.89 (dd, ^3J(H,H) = 8.6, 6.4, 1H; CH), 2.37–2.29 (m, 3H; CH), 2.10 (ddq, ^3J(H,H) ≈ 7.1, 7.1, 7.1, 1H; CH), 1.88 (dd, ^3J(H,H) = 15.3, 10.5, 1H; CH), 0.95 (d, ^3J(H,H) = 6.7, 3H; CH_3), 0.93 (d, ^3J(H,H) = 6.7, 3H; CH_3); irradiation at δ = 2.89 collapsed the peaks at 5.85 (dd, ^3J(H,H) = 16.5, 10.9, 1H; CH) and at 2.10 (dq, ^3J(H,H) ≈ 7.1, 7.1, 1H; CH); irradiation at 2.10 collapsed the peaks at 2.89 (d, ^3J(H,H) = 8.6, 1H; CH), 0.93 (s, 3H; CH_3) and 2.33 (sharper multiplet). ^{13}C NMR (300 MHz, [D_6]DMSO, 21 °C): δ = 174.8(C), 173.8(C), 173.4(C), 136.0(CH), 117.5 (CH_2), 53.9 (CH), 52.2 (CH), 36.6 (CH_2), 35.4 (CH), 28.3 (CH), 19.1 (CH_3), 13.3 (CH_3). Correct C,H analysis.

Methyl esters were prepared by diazomethane treatment of either a) an ethereal solution prepared by extraction of an acidified solution of the irradiated solid, or b) an ethereal solution of precipitated **3b**. Capillary GC analysis of the crude ester (poly(dimethylsiloxane), 30 m × 0.25 mm, 60→150 °C, 10° min^{-1}; 150→190 °C, 20° min^{-1}) indicated the presence of four components in a 2:1:12:1 ratio at 5.2, 11.9, 12.6, and 12.8 min. The methyl ester of the head-to-head dimer **2** (4.5 min) was not present. The peak at 5.2 min co-elutes with an authentic sample of the head-to-tail dimer. [5]

Received: August 29, 1990 [Z 4161 IE]
German version: *Angew. Chem. 103* (1990) 438

CAS Registry numbers:
1, 21988-86-3; **3a**, 132340-36-4; **3b**, 132259-71-3.

[1] a) G. R. Desiraju (Ed.): *Organic Solid State Chemistry*, Elsevier, Amsterdam 1987 (photochemical examples); b) G. Wegner, *Adv. Polym. Sci. 63* (1984) v, and references therein (poly(diacetylenes)).

[2] a) B. M. Foxman, J. D. Jaufmann, *Mol. Cryst. Liq. Cryst. 106* (1984) 187; b) C. A. Booth, B. M. Foxman, J. D. Jaufmann, in D. J. Sandman (Ed.): *Crystallographically Ordered Polymers (ACS Symp. Ser. 337* (1987) pp. 95–105).

[3] K. Naruchi, S. Tanaka, M. Yamamoto, K. Yamada, *Nippon Kagaku Kaishi 1983*, 1291; *Chem. Abstr. 99* (1983) 195488q; K. Naruchi, M. Miura, *J. Chem. Soc. Perkin Trans. 2, 1987*, 113.

[4] a) M. D. Cohen, G. M. J. Schmidt in J. H. de Boer (Ed.): *Reactivity of Solids*, Elsevier, Amsterdam 1961, p. 556; b) M. D. Cohen, G. M. J. Schmidt, *J. Chem. Soc. 1964*, 1996; c) F. L. Hirshfeld, G. M. J. Schmidt, *J. Polym. Sci. Part A 2* (1964) 2181.

[5] S. G. Alcock, J. E. Baldwin, R. Bohlmann, L. M. Harwood, J. I. Seeman, *J. Org. Chem. 50* (1985) 3526.

[6] Crystals of **3b** are orthorhombic, space group *Pbca*, $a = 18.944(6)$, $b = 19.061(6)$, $c = 7.219(3)$ Å; $Z = 8$; $\rho_{obs} = 1.31(1)$, $\rho_{calc} = 1.290$ g cm^{-3}. Data were collected to a maximum $2\theta(\lambda_{Mo\text{-}K\alpha}) = 48°$. Full matrix least-squares refinement of positional and anisotropic thermal parameters for all atoms (fixed H atoms, except for H attached to O5, total parameters = 167); $R = 0.072$ and $R_w = 0.075$, 1354 data for which $I > 1.96\,\sigma(I)$. Further details of the crystal structure investigation are available on request from the Director of the Cambridge Crystallographic Data Centre, University Chemical Laboratory, Lensfield Road, GB-Cambridge CB21 1EW (UK) on quoting the full journal citation.

[7] a) J. B. Lando, H. Morawetz, *J. Polym. Sci. Part C 4* (1964) 789; b) J. B. Lando, J. Semen, *J. Polym. Sci. Polym. Chem. Ed. 10* (1972) 3003; c) Y. V. Kissin in J. I. Kroschwitz (Ed.): *Concise Encyclopedia of Polymer Science*, Wiley, New York 1990, pp. 1087–1107.

[8] H. Morawetz, I. D. Rubin, *J. Polym. Sci. 57* (1962) 669.

[9] F. M. Costachuk, D. F. R. Gilson, L. E. St. Pierre, *Macromolecules 3* (1970) 393; *ibid. 4* (1971) 16; b) J. H. O'Donnell, R. D. Sothman, *J. Macromol. Sci. Chem. A 14* (1980) 879.

[10] G. Adler, *Trans. Am. Crystallogr. Assoc. 7* (1971) 55, and references therein.

[11] For solid acenaphthylene, a dose of 100 Mrad γ-radiation yields 2.1% of *trans*-cyclodimer: A Chapiro, G. Lozach, *Int. J. Radiat. Phys. Chem. 4* (1972) 285.

[12] Polymerization behavior: a) M. L. Miller, J. Skogman, *J. Polym. Sci. Part A 2* (1964) 4551; b) T. Kitano, T. Fujimoto, M. Nagasawa, *Macromolecules 7* (1974) 719; c) Y. Muroga, M. Nagasawa, *Polym. J. 18* (1986) 15.

[13] Dimerization: a) O. C. Bockman, C. Schuerch, *J. Polym. Sci. Part B 1* (1963) 145; b) H. V. Pechmann, *Ber. Dtsch. Chem. Ges. 33* (1900) 3323; c) M. Ikeda, T. Hirano, T. Tsuruta, *Tetrahedron 30* (1974) 2217; d) T. Saegusa, Y. Ito, S. Kobayashi, S. Tomita, *J. Chem. Soc. Chem. Commun. 1968*, 273; e) T. Saegusa, Y. Ito, S. Tomita, H. Kinoshita, *J. Org. Chem. 35* (1970) 670.

[14] Under conditions of high temperature and pressure, solution trimerization of methyl acrylate has been observed in 17% yield: J. O. Metzger, P. Köll, *Makromol. Chem. 184* (1983) 63.

[15] Certain butadiene derivatives are a notable exception: B. Tieke, G. Chapuis, *Mol. Cryst. Liq. Cryst. 137* (1986) 101.

[16] K. Naruchi, Chiba University, personal communication.

[17] J. E. Willard in Farhataziz, M. A. J. Rogers (Eds.): *Radiation Chemistry, Principles and Applications*, VCH, Weinheim 1987, pp. 395–434.

An Unusual Polyoxovanadium Organophosphonate Anion, $[H_6(VO_2)_{16}(CH_3PO_3)_8]^{8\ominus}$ **

By *Guohe Huan*,* *Allan J. Jacobson*, and *Victor W. Day*

Although the chemistry of polyoxovanadates is very diverse, a few structural motifs are commonly observed.[1] Vanadium atoms are usually square pyramidally coordinated by oxygen atoms. The VO_5 square pyramids are then condensed by sharing edges to form dimers as observed in $VOSO_4 \cdot 3H_2O$[2] or larger units, for example, the ring of eight edge-shared square pyramids $[V_8O_{24}]$ found in the anions $[V_8O_8(OCH_3)_{16}(C_2O_4)]^{2\ominus}$[3a] and $[V_{12}O_{32}]^{4\ominus}$.[3b] The basketlike shape of the $[V_{12}O_{32}]^{4\ominus}$ anion is completed by condensation with four additional VO_5 square pyramids through formation of μ_3-O connections. In the *closo* anion $[V_{15}O_{36}]^{5\ominus}$,[4] the shared oxygen atoms are either μ_2 or μ_3 connected, whereas in the $[V_{18}O_{42}(X)]^{n\ominus}$ (X = H_2O, VO_4, SO_4, Br, and I)[5–7] anions they are all of the μ_3 type. Other molecular units may also be used to complete the connectivity in polyoxovanadates, for example, the oxalate ion in $[V_8O_8(OCH_3)_{16}(C_2O_4)]^{2\ominus}$[2] and the $C_6H_5CO_2^{\ominus}$ group in the $[V_6O_6(\mu\text{-}O)_4(\mu\text{-}O_2CC_6H_5)]^{6\ominus}$[8] anion. Here we describe the synthesis and structure of **1**, a new heteropolyoxovanadate based on VO_5 square pyramids and R-PO_3 tetrahedra with μ_2 and μ_3 connections.

$$[N(CH_3)_4]_8[H_6(VO_2)_{16}(CH_3PO_3)_8] \cdot 11\,H_2O \qquad \mathbf{1}$$

X-ray structrual analysis[9] of **1** revealed the presence of discrete $Me_4N^{\oplus}$ ions and water of crystallization in the lattice, as well as $[H_6(VO_2)_{16}(CH_3PO_3)_8]^{8\ominus}$ anions (Figure 1) which each contain a single $Me_4N^{\oplus}$ cation at their center. The formulation of the anion is based on the results of the redox titration[10] which indicates that two of the total of sixteen vanadium atoms are V^V and fourteen are V^{IV}. The

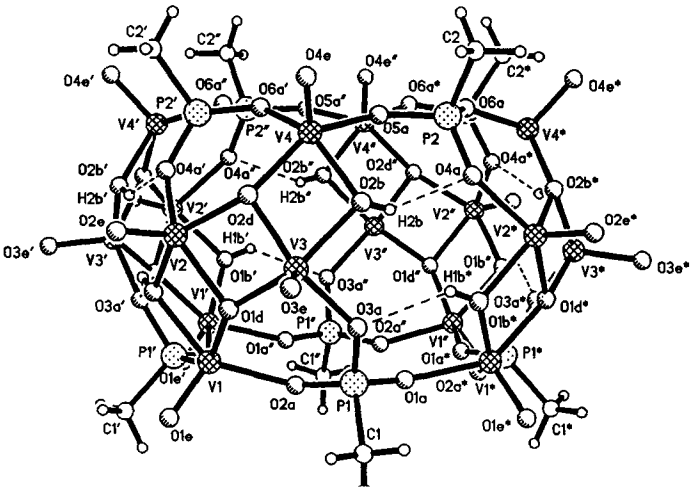

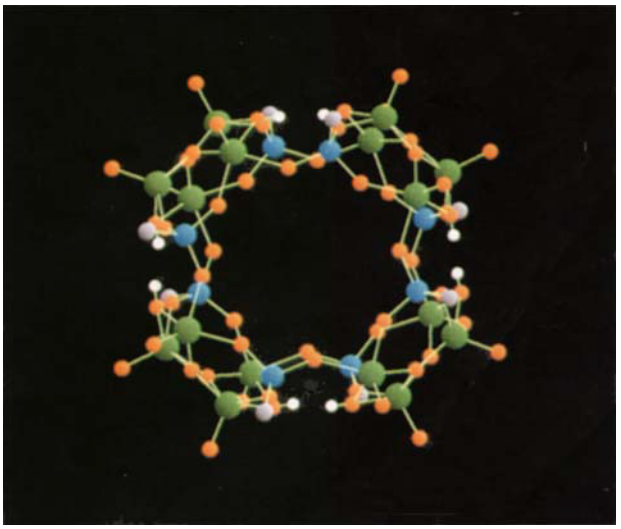

Figure 1. Perspective plots of anion **1** in the crystal structure. Top: View perpendicular to the crystallographic C_4-axis at 1/4,1/4, *z* in the unit cell; hydrogen bonds are indicated by dashed lines. Atoms labeled ′, ″, or * are related to atoms without one of those labels by the symmetry operations *y*, 1/2−x, *z*; 1/2−*x*, 1/2−*y*, *z*; and 1/2−*y*, *x*, *z*, respectively. Below: View down the C_4-axis; V, green, P blue, O red, C gray, H white. Bond distances [Å] and angles [°] of interest: V-O_{term} 1.580(4)–1.607(4), V-(μ_3-O) 1.925(4)–1.938(4), V-(μ_2-O(H)) 1.966(4)–1.990(4), V-(μ_2-O) 1.964(4)–1.979(4), V_{waist}-V_{waist} = 2.932(1), V_{waist}-V_{ring} 3.060(1)–3.066(1), O-(μ_2-O(H)) 2.76(1)–2.82(1); O_{term}-V-(μ_3-O) 107.8 (2)–112.6(2), O_{term}-V-(μ_2-O(H)) 105.9(2)–108.0(2), O_{term}-V-(μ_2-O) 106.5(2)–109.8(2), (μ_3-O)-V-(μ_3-O) 80.9(2)–81.3(2), (μ_3-O)-V-(μ_2-O(H)) 76.3(2)–77.1(2), (μ_3-O)-V-(μ_2-O) 88.3(2)–91.4(2), (μ_2-O)-V-(μ_2-O(H)) 87.3(2)–87.9(2), (μ_2-O)-V-(μ_2-O) 84.3(2)–85.2(2); V_{waist}-(μ_3-O)-V_{waist} 98.3(2)–98.5(2), V_{waist}-(μ_3-O)-V_{ring} 104.4(2)–105.2(2), V_{waist}-(μ_3-O)-V_{ring} 144.7(2)–146.1(2) ("Waist" designates atoms between the rims of the tire, "ring" the atoms in the outer rings).

[*] Dr. G. Huan, Dr. A. J. Jacobson
Exxon Research & Engineering Company
Annandale, NJ 08801 (USA)
Dr. V. W. Day
Crystalytics Company
Lincoln, NB 68501 (USA)

[**] We thank *D. P. Goshorn* for magnetic measurements and *M. A. Greaney* for help with the cyclic voltammetry.

anion possesses rigorous crystallographic C_4 symmetry and resembles a set of chains on a tire (recognized best when Fig. 1 (top) is turned through 90°). It consists of four condensed $(VO_2)_4$ tetramers, which span the "tread" and are covalently linked together along each "rim" by four PO_3C tetrahedra through corner-sharing oxygen atoms. The $H_{1.5}V_4O_8$ unit arises when distorted VO_5 square pyramids share an edge to form dimers which in turn share half of a long dimer edge to form step-shaped tetramers (see Fig. 2).

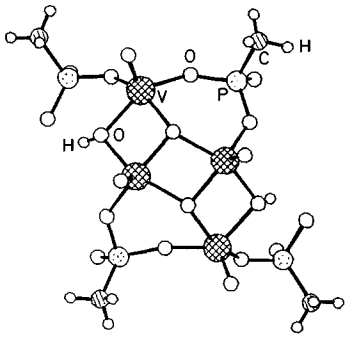

Figure 2. A projection of the tetramer and its covalently bonded $CH_3PO_3^{2\ominus}$ groups viewed as in Figure 1 top.

Each organophosphonate group shares two of its oxygens with one tetramer and its third oxygen with the adjacent tetramer. This results in the formation of sixteen-membered $(-O-V-O-P)_4$ rings (whose atoms are coplanar within 0.20 Å) along each "rim of the tire".

The six hydrogen atoms are disordered over eight sites in the anion and are covalently bonded to a $V-O_b-V$ oxygen atom. They form hydrogen bonds along the "tread" from the covalently bonded O_b oxygens in one tetramer to "non-rim" $P-O_a-V$ oxygen (O_{3a} or O_{4a}) atoms in an adjacent tetramer. A total of six such hydrogen bonds are used to stabilize each $[H_6(VO_2)_{16}(CH_3PO_3)_8]^{8\ominus}$ anion. The average oxygen-to-oxygen distance across the 16-membered rings at each "rim" is 6.68 Å and between the rings is 5.86 Å. If the oxygen ionic radius is assumed to be 1.40 Å, the free diameter of each 16-membered ring is estimated to be ~ 4 Å. The eight-membered silicon (aluminum) oxygen atom ring in zeolite A has similar dimensions. The free diameter across the "tire" midway between the two "rims" is much bigger (10.13 Å average oxygen-to-oxygen distance, free diameter ~7.5 Å). The $Me_4N^{\oplus}$ ion at the center of each "tire" is disordered about the crystallographic C_4 axis which contains the nitrogen and one methyl carbon atom.

1 is soluble in water and in a mixture of CH_3OH/CH_3CN. In the presence of oxygen, aqueous solutions gradually change color from dark to yellow indicating oxidation of V^{IV} to V^{V}. Cyclic voltammetry measurements under anerobic conditions in degassed water did not show reversible redox behavior. When exposed to air, the crystals of **1** slowly degrade by losing the water of crystallization.

The ethyl and phenyl analogues have also been prepared in similar hydrothermal syntheses from the corresponding phosphonic acids. The ethyl compound precipitates as deep blue prismatic crystals isostructural with **1** and contains the anion $[H_8(VO_2)_{16}(C_2H_5PO_3)_8]^{8\ominus}$. The phenyl analogue forms black hexagonal prismatic crystals with space group $C2/c$ but contains a structurally similar anion $[H_4(VO_2)_{16}(C_6H_5PO_3)_8]^{9\ominus}$. Preliminary results indicate that the solubility in water increases as the size of the organic group decreases and that the vanadium oxidation state can be controlled by varying reaction conditions.

Experimental Procedure

To 1.152 g (12 mmol) $CH_3PO_3H_2$ (Alfa), 0.300 g (2 mmol) V_2O_3 (Alfa), and 0.364 g (2 mmol) V_2O_5 (Alfa) in a Teflon lined autoclave was added ~ 2 mL of distilled water followed by 6.4 g Me_4NOH (25% in water, Aldrich). The autoclave was filled to 80% with distilled water and heated at 200 °C for 2 days. The autoclave was then cooled to room temperature. The black, prismatic crystals of the reaction product **1** (yield 0.60 g, ~ 42% based on vanadium) were suction-filtered, washed several times with distilled water, and air-dried. Satisfactory elemental analysis for $C_{40}H_{148}N_8V_{16}P_8O_{67}$. Main absorption bands in the IR spectrum (KBr pellet): $\tilde{\nu}[cm^{-1}]$ = 3399 (s), 3010 (m), 1625 (m), 1480 (s), 1410 (m), 1300 (s), 1110 (s), 1050 (s), 1000 (vs), 970 (vs), 935 (vs), 770 (m), 720 (s), 700 (s), 615 (s), 570 (s), 530 (s), 485 (s), 435 (m).

Received: August 20, 1990
Revised: January 2, 1991 [Z 4141 IE]
German version: *Angew. Chem. 103* (1991) 426

CAS Registry numbers:
1, 132698-13-6; **1** (without 11 H_2O), 132672-13-0; $[H_8(VO_2)_{16}(C_2H_5PO_3)_8](Me_4N)_8$, 132672-15-2; $[H_4(VO_2)_{16}(C_6H_5PO_3)_8](Me_4N)_9$, 132644-34-9; V_2O_3, 1314-34-7; V_2O_5, 1314-62-1; $CH_3PO_3H_2$, 993-13-5; $C_2H_5PO_3H_2$, 6779-09-5; $C_6H_5PO_3H_2$, 1571-33-1.

[1] M. T. Pope, A. Müller, *Angew. Chem. 103* (1991) 56; *Angew. Chem. Int. Ed. Engl. 30* (1991) 49.
[2] M. Tachez, F. Theobald, *Acta Crystallogr. Sect. B 36* (1980) 2873.
[3] a) Q. Chen, S. Liu, J. Zubieta, *Inorg. Chem. 28* (1989) 4433; b) V. W. Day, W. G. Klemperer, O. M. Yaghi, *J. Am. Chem. Soc. 111* (1989) 5959.
[4] A. Müller, E. Krickemeyer, H. Penk, H.-J. Walberg, M. Bögge, *Angew. Chem. 99* (1987) 1060; *Angew. Chem. Int. Ed. Engl. 26* (1987) 1045.
[5] G. K. Johnson, E. O. Schlemper, *J. Am. Chem. Soc. 100* (1978) 3645.
[6] A. Müller, J. Döring, H. Bögge, E. Krickemeyer, *Chimia 42* (1988) 300.
[7] A. Müller, M. Penk, R. Rohfling, E. Krickemeyer, J. Döring, *Angew. Chem. 102* (1990) 927; *Angew. Chem. Int. Ed. Engl. 29* (1990) 926.
[8] D. Rehder, W. Priebsch, M. von Oeynhausen, *Angew. Chem. 101* (1989) 1295; *Angew. Chem. Int. Ed. Engl. 28* (1989) 1221.
[9] **1**: Tetragonal, space group $P4/ncc$ (No. 130) with $a = 23.660(3)$, $c = 22.708(3)$ Å, $V = 12.711(3)$ Å^3, and $Z = 4$ ($\rho_{calcd} = 1.399$ g cm^{-3}; $\mu_a(Mo_{K\alpha}) = 1.25$ mm^{-1}), $R = 0.041$ for 3130 independent reflections having $2\theta < 48.3°$ and $I > 3\sigma(I)$; Nicolet P1 auto-diffractometer, graphite-monochromated $Mo_{K\alpha}$ radiation. The structure was solved at Crystalytics Company using "Direct Method" techniques with the Siemens Nicolet SHELXTL-Plus software package. Further details of the crystal structure investigation may be obtained from the Fachinformationszentrum Karlsruhe, Gesellschaft für wissenschaftlich-technische Information mbH, W-7514 Eggenstein-Leopoldshafen 2 (FRG), on quoting the depository number CSD-54969, the names of the authors, and the journal citation.
[10] The vanadium oxidation states in **1** were determined by redox titration. Samples were dissolved in 1 M sulfuric acid. A known excess of cerium(IV) ammonium nitrate was added to the vanadium solutions to oxidize all the vanadium ions to the pentavalent state. The total vanadium content and the average vanadium oxidation state were determined by potentiometric titration using a standard solution of ferrous ammonium sulfate. Redox titrations of **1** gave an average vanadium oxidation state of 4.10 ± 0.02.

Parabolic Growth of a Self-Replicating Hexadeoxynucleotide Bearing a 3′-5′-Phosphoamidate Linkage **

By *Günter von Kiedrowski,* Britta Wlotzka, Jörg Helbing, Matthias Matzen*, and *Stephan Jordan*

The search for minimal models of self-replicating systems based on oligonucleotide constituents or related molecules is of considerable interest within the context of early biochemical evolution ("RNA-world").[1] In 1986 we showed that the

[*] Dr. G. von Kiedrowski, Dipl.-Chem. B. Wlotzka, Dr. J. Helbing, Dipl.-Chem. M. Matzen, Dipl.-Chem. S. Jordan
Institute for Organic Chemistry of the University
Tammannstrasse 2, W-3400 Goettingen (FRG)

[**] This work was supported by the Deutsche Forschungsgemeinschaft and the Fonds der Chemischen Industrie. The results were presented at the symposium on "Molecular Biology and the Origin of Life" held in Berkeley, USA, July 15–21, 1990.

formation of the hexadeoxynucleotide template $\mathbf{T}^1$ from two trideoxynucleotides $\mathbf{A}^1$ and $\mathbf{B}^1$ in the presence of the carbodiimide EDC (EDC: $CH_3CH_2N{=}C{=}N(CH_2)_3N(CH_3)_2$) proceeds to a small but well-defined extent via an autocatalytic reaction channel. Here was evidence for self-replication in a nonenzymatic reaction system for the first time.[2] Initial rate kinetics resulted in a square-root law of template catalysis,[3] which has been corroborated for the condensation of $\mathbf{A}^2$ and $\mathbf{B}^2$,[4] as well as for the formation of a tetrameric template reported by *Zielinsky* and *Orgel*.[5] The same type of autocatalysis underlies the kinetic data of the self-replicating system recently described by *Rebek* et al.,[6] although this is not explicitely stated by the authors.

autocatalytic effect of the 3′5′-phosphoamidate template $\mathbf{T}^3$. The "sigmoidicity" (S-shape) of curve b is not a consequence of the preceeding activation, since it is less pronounced upon addition of template $\mathbf{T}^1$ (curves c–e). Furthermore, ^{31}P and ^1H NMR kinetic studies of the hydrolysis of EDC in the presence of various mononucleotides have revealed that the formation of EDC adducts is a quasireversible process[8] and that the maximum degree of activation (typically 5–10% at an EDC concentration of $c_{EDC} = 0.2$ M) is reached within a few minutes,[8] whereas the inflection of curve b occurs considerably later.

A computer program for the evaluation of self-replication experiments has been written to fit the complete set of exper-

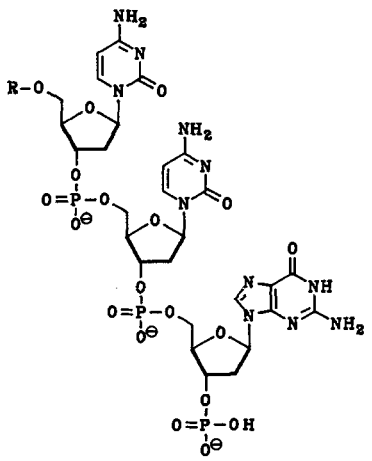

$\mathbf{A}^1$: R = CH_3
$\mathbf{A}^2$: R = CH_2SCH_3

EDC:
$CH_3CH_2{-}N{=}C{=}N{-}CH_2CH_2CH_2N(CH_3)_2$

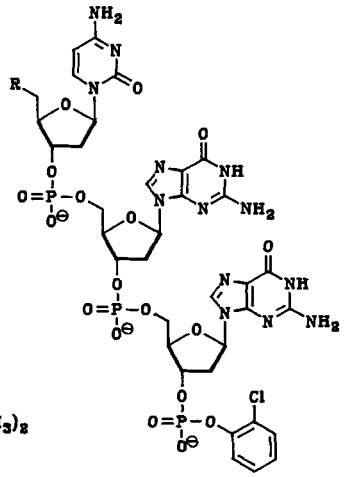

$\mathbf{B}^1$: R = HO
$\mathbf{B}^2$: R = $HO_3PO^{\ominus}$
$\mathbf{B}^3$: R = H_2N

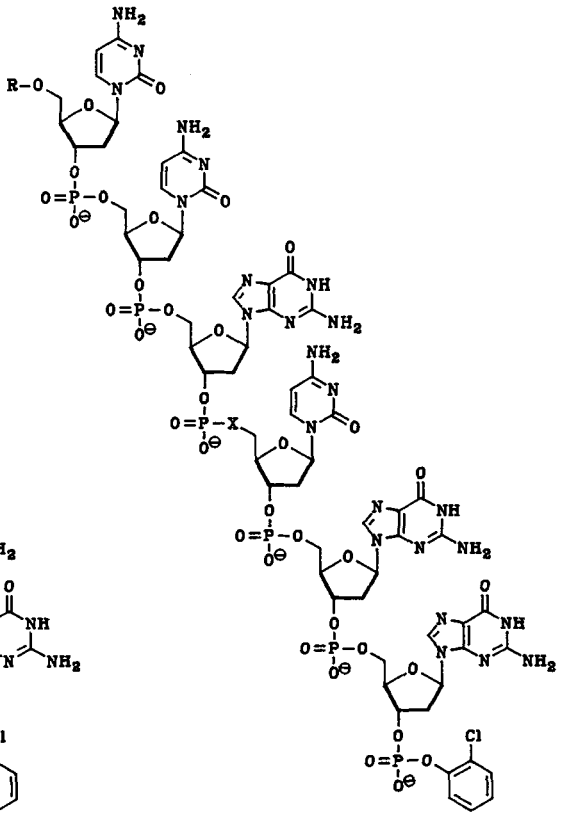

$\mathbf{T}^1$: R = CH_3, X = O
$\mathbf{T}^2$: R = CH_2SCH_3, X = $PO_4^{\ominus}$
$\mathbf{T}^3$: R = CH_2SCH_3, X = NH
$\mathbf{T}^4$: R = H, X = NH

We now report on the first recognition of sigmoidal (S-shaped) growth of template molecules in a remarkably efficient, nonenzymatic template-directed reaction. The synthesis of the oligonucleotides is described elsewhere.[7] In the presence of the carbodiimide EDC, the trideoxynucleotide 3′-phosphate $\mathbf{A}^2$ reacts with the 5′-aminotrimer $\mathbf{B}^3$ to give the self-complementary hexameric 3′-5′-phosphoamidate $\mathbf{T}^3$ as exclusive product. The reaction was performed on a nanomolar scale using the capillary technique as previously described.[2, 4] The time course for product formation was monitored by HPLC[4] (Fig. 1, curve b). The synthesis of $\mathbf{T}^3$ proceeds substantially faster in the presence of the phosphodiester template $\mathbf{T}^1$ (curves c–e), whose catalytic effect is comparable to that produced by the 3′-5′-phosphoamidate template $\mathbf{T}^4$ and therefore gives an indirect measure of the

imental time courses (b–e) to the integrated form of equation (a) by means of nonlinear regression. Equation (a) is derived from the original square-root law of template catalysis[2–4] with further consideration of the mass balance between $\mathbf{A}^2$, $\mathbf{B}^3$, and $\mathbf{T}^3$; c_A, c_B, and c_T are the initial concentrations of $\mathbf{A}^2$,

$$dc/dt = (c_A - c)(c_B - c)[k_a(c + c_T)^{1/2} + k_b] \exp(-k_c t) \quad (a)$$

$\mathbf{B}^3$, and $\mathbf{T}^1$, c is the concentration of the product $\mathbf{T}^3$, k_a and k_b apparent rate constants for the autocatalytic and the nonautocatalytic reaction channel, respectively, and k_c the apparent rate constant of the carbodiimide hydrolysis, which can be described as a pseudo-first-order process for low degrees of activation and low conversions of the phosphate constituent. The resulting rate constants are given in Table 1.

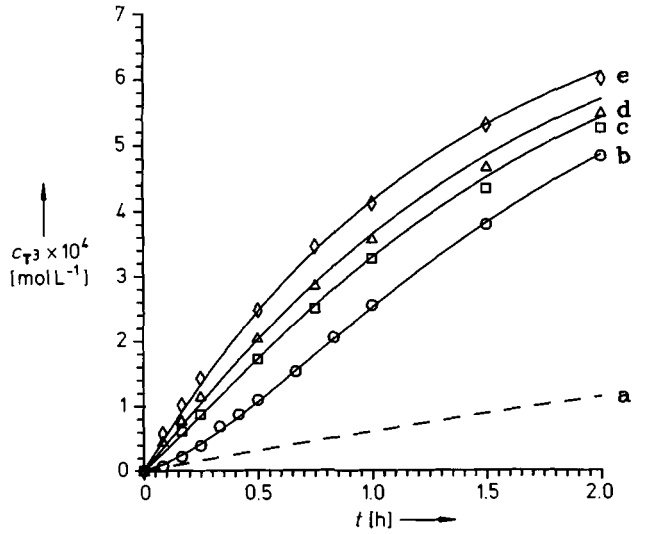

Fig. 1. Time course for the formation of the hexameric 3′-5′-phosphoamidate $\mathbf{T^3}$ in the absence (curve b) and in the presence of template $\mathbf{T^1}$ (curves c–e) as measured by HPLC. The data points shown are averages from the experimental time courses of $\mathbf{A^2}$, $\mathbf{B^3}$, $\mathbf{T^3}$. The set of theoretical curves b–e represents the solution of differential equation (a) for the parameters given in Table 1 and the experimental set of initial concentrations shown below. The yield of $\mathbf{T^3}$ is 50% after 2 h (curve b). Curve a represents the theoretical time course if no autocatalysis occurs. Initial concentrations and reaction conditions: $c_A = c_B =$ 1 mM, [EDC] = 0.2 M, [HEPES] = 0.1 M, pH = 7.5, T = 30 °C, c_{T^1} = 0(b), 0.08(c), 0.16(d), 0.32 mM (e), HEPES = 2-[4-(2-hydroxyethyl)-1-piperazino]-ethanesulfonic acid/sodium salt.

The exponential factor in equation (a) has been omitted for the system presented here, since the hydrolysis of EDC is negligible within the first two hours under the reaction conditions. As a consequence a three-parameter fit would produce a less reliable k_c. To show the general applicability of our method and for the sake of comparison, we have also evaluated by equation (a) the set of experimental time courses for the systems reported by *Orgel* et al.[5] and *Rebek* et al.[6] (exp $(-k_c t)$ omitted).[9]

Table 1. Apparent rate constants for the autocatalytic and the nonautocatalytic template production (k_a and k_b) and for the hydrolysis of the activated species (k_c). The experimental time courses of the systems reported by *Orgel* et al. and *Rebek* et al. have been taken from the literature.

System	k_a[M$^{-3/2}$ s^{-1}]	k_b[M^{-1} s^{-1}]	k_c[s^{-1}]
$\mathbf{A^2}$, $\mathbf{B^3}$, $\mathbf{T^3}$, $\mathbf{T^1}$	(7.43 ± 0.12) [a]	$(1.77 \pm 0.15) \times 10^{-2}$ [a]	
Orgel [5]	$(5.71 \pm 0.23) \times 10^{-2}$	$(1.66 \pm 0.19) \times 10^{-4}$	$(1.92 \pm 0.46) \times 10^{-6}$
Rebek [6]	$(9.87 \pm 0.17) \times 10^{-2}$	$(1.24 \pm 0.04) \times 10^{-3}$	

[a] The computation is conservative in the sense that k_b is slightly overestimated at the cost of k_a. This is because our method of calibration reflects a concentration dependant-recovery of single-component HPLC peaks, assuming that the recovery of the respective component is not influenced by other components. A multicomponent calibration method is in the development stages. However, the present method of calibration is more reliable than methods which assume direct proportionality between HPLC peak areas and concentrations.

An efficient self-replicating system should exhibit a high apparent rate constant k_a and a low constant k_b. The first criterion is especially important if the self-replicating template is formed via a condensation reaction in water, since template formation has to compete with hydrolysis of the activated species, i.e., the EDC adducts. If all three systems were measured under optimal conditions (especially with respect to the temperature), the above system is roughly 130 and 75 times more efficient than Orgel's and Rebek's system, respectively, in terms of k_a. A low k_b is necessary to achieve sigmoidal growth. Thus, the quotient k_a/k_b, which defines the factor by which the autocatalytic synthesis exceeds the noninstructed process at a template concentration of 1 M, must be large enough to observe sigmoidicity. With respect to the autocatalytic excess factor ε, as this quotient is termed hereafter, the above system ($\varepsilon = 420$) is comparable to Orgel's system ($\varepsilon = 340$) but exceeds Rebek's system ($\varepsilon = 80$). The type of growth observed in curve b is, however, an experimental novelty. We term it parabolic since the growth of an autocatalyst with a reaction order of 1/2 in the rate equation of its synthesis can be expressed as a second order polynomial of time for early reaction times.

The reasoning behind the mechanism proposed for the autocatalytic template production is the same as for the original system.[2] It is generalized in Figure 2 to account for

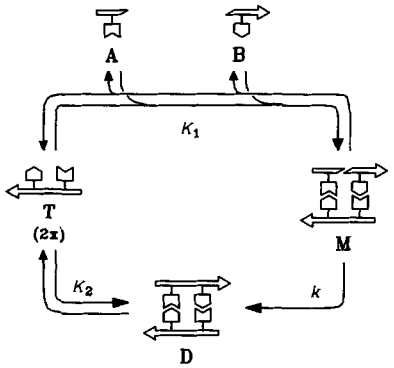

Fig. 2. General mechanism for a minimal self-replicating system. Constituent A represents the activated form of trimer A^2 here. Large arrowheads at the reaction arrows for the reversible reactions indicate the favored site of the equilibrium.

similarities between the systems known so far. The following should be noted:

1) The rate determining step is the irreversible formation of a 3′-5′-phosphoamidate linkage leading from the ternary complex **M** to the self-complementary duplex **D** which is expressed by: $d[\mathbf{D}]/dt = k[\mathbf{M}]$.
2) The system is in dynamic equilibrium with respect to all single- and double-stranded oligonucleotide constituents. With $K_1 = [\mathbf{M}]\,[\mathbf{A}]^{-1}\,[\mathbf{B}]^{-1}\,[\mathbf{T}]^{-1}$ and $K_2 = [\mathbf{D}]\,[\mathbf{T}]^{-2}$ it follows for the formation of duplex molecules that $d[\mathbf{D}]/dt = kK_1K_2^{-1/2}\,[\mathbf{A}]\,[\mathbf{B}]\,[\mathbf{D}]^{1/2}$.
3) Under parabolic growth conditions ($K_2 \gg K_1 \gg 1$), and for the special case of complete activation, the apparent rate constant k_a can be rationalized in terms of the elementary rate and equilibrium constants: $k_a = 2^{1/2}\,kK_1K_2^{-1/2}$.

According to *Eigen* and *Schuster*[10] parabolic growth should lead to Darwinian selection under conditions which allow self-replicating templates to compete for their constituents when the total concentration of templates is kept constant (i.e. in a chemostat). This statement has been refuted recently by *Szathmary* who proposes, with reference to experimental results,[2, 5] that parabolic growth invariably leads to coexistence of self-replicating templates,[11] (i.e., the most efficient template is not able to supersede its less efficient competitors completely). We agree with *Szathmary* on the point that this type of growth must have preceeded exponential growth in an RNA world, since it allows autocatalyt-

ic amplification while at the same time keeping a variety of "sequence modules", which seems necessary to assemble complex, functional molecules (i.e. ribozymes). Now that the proper chemistry is known, minimal models of coexistence and/or selection based on self-replicating oligonucleotide derivatives are visible on the horizon of bio-organic chemistry.

Received: October 10, 1990 [Z 4237]
German version: *Angew. Chem. 103* (1990) 456

CAS Registry numbers:
A[2], 122238-13-5; **B**[3], 132491-61-3; **T**[1], 104599-59-9; **T**[3], 132491-62-4.

[1] Reviews: a) L. E. Orgel, *Cold Spring Harbor Symp. Quant. Biol. 7* (1987) 9–16; b) G. F. Joyce, *ibid. 7* (1987) 41–51; c) G. F. Joyce, *Nature (London) 338* (1989) 217–224; d) G. von Kiedrowski in Verband der Chemischen Industrie (Ed.): *40 Jahre Fonds der Chemischen Industrie*, published by VCI, Frankfurt am Main 1990, pp. 197–218.

[2] G. von Kiedrowski, *Angew. Chem. 98* (1986) 932–934; *Angew. Chem. Int. Ed. Engl. 25* (1986) 932–935.

[3] The equation $dc_T/dt = a\ c_T^{1/2} + b$ (square-root law) describes the initial rate of template production as the sum of an autocatalytic ($a\ c_T^{1/2}$) and a nonautocatalytic rate contribution (b). From the linear plot of the initial rates vs. the square root of the initial template concentrations, the parameters a and b are obtained from the slope and the intercept. These parameters have been named K_a and K_b in [1b], k_a and k_b in [2] and α and β in [5]. They should not confused with the apparent rate constants k_a and k_b of equation (a) although they correspond to these quantities in the special case of complete phosphate activation as follow: $a = k_a c_A c_B$, $b = k_b c_A c_B$.

[4] G. von Kiedrowski, B. Wlotzka, J. Helbing, *Angew. Chem. 101* (1989) 1259–1261; *Angew. Chem. Int. Ed. Engl. 28* (1989) 1235–1237.

[5] W. S. Zielinski, L. E. Orgel, *Nature (London) 327* (1987) 346–347.

[6] T. Tjivikua, P. Ballister, J. Rebek, Jr., *J. Am. Chem. Soc. 112* (1990) 1249–1250.

[7] J. Helbing, Dissertation, University of Goettingen 1990.

[8] M. Matzen, G. von Kiedrowski, unpublished.

[9] Results from NMR titration studies [6] suggest that in the Rebek system the complex **M** is more stable than the corresponding duplex **D** (see Fig. 2): $K_2 = 630\ M^{-1}$, $K_1 = 3600\ M^{-2}$ (the latter quantity is not directly measurable and was estimated by the authors). [6] In this case the square-root model is no longer applicable and the Rebek system should more closely resemble an exponential replicator (reaction order of autocatalyst closer to 1 than to 1/2). If one substitutes the exponent 1/2 in equation (a) for 1, nonlinear regression yields a *substantially* poorer fit resulting in distances between the theoretical curves which do not correspond those found experimentally. The exponential model ($\exp(-k_c t)$ omitted) yields the regression coefficients $k_a = 2.02 \pm 0.08\ M^{-2}\ s^{-1}$ and $k_b = (2.22 \pm 0.07) \times 10^{-3}\ M^{-1}\ s^{-1}$; the sum of least squares of $S = 1.73 \times 19^{-8}\ M^2$ exceeds that of the square-root model by a factor of 6.6.

[10] M. Eigen, P. Schuster: *The Hypercycle. A Principle of Natural Self-Organization*, Springer, Berlin 1979, p. 12.

[11] E. Szathmary, *J. Theor. Biol. 138* (1989) 55–58.

Characterization of Intermediate Steps in the Polymerizations with Ziegler Catalysts on MgH_2 by CP/MAS NMR Spectroscopy**

By *Reinhard Benn** and *Wolfram Hermann*

A significant number of the numerous investigations on heterogeneous catalysis[1] deal with the polymerization of α-olefins using third-generation Ziegler catalysts.[2] Although there are many proposals regarding the mechanism,[3] direct spectroscopic evidence of the intermediates has hitherto been found only in particular cases.[4, 5] With MgH_2 as support,[6] and zirconocene and ethylaluminum complexes as cocatalysts, we can now characterize components and intermediates fixed on the support by CP/MAS ^{13}C NMR spectroscopy (CP = Cross Polarization, MAS = Magic Angle Spinning)[7] during the polymerization of ethylene.

In toluene, dissolved $[Cp_2ZrMe_2]$ (**1**) evolves methane on reaction with MgH_2;[8] after evaporation of the solvent, the residue is characterized by CP/MAS ^{13}C NMR spectroscopy. Besides the signals assigned to **1** at $\delta = 111$ and 31, two new signals appear in the ^{13}C NMR spectrum at $\delta = 107$ and 17 (Fig. 1). Experiments with ^{13}C-labeled methyl groups in

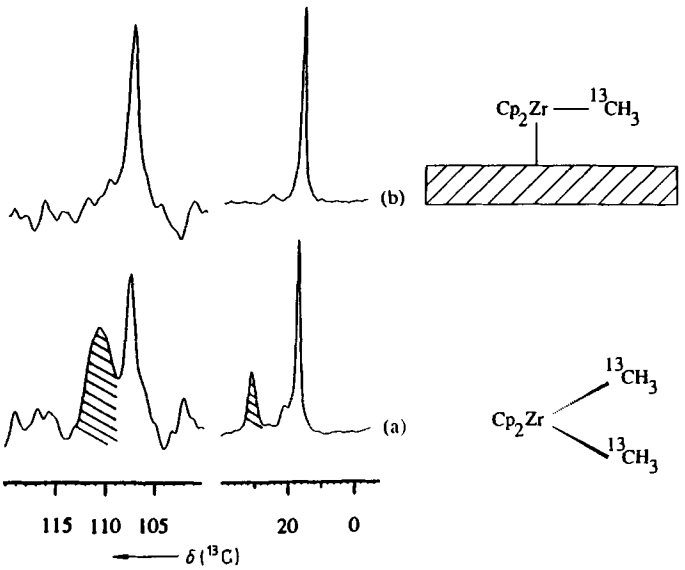

Fig. 1. CP/MAS ^{13}C NMR spectra (75.5 MHz) (a) after loading the support MgH_2 with $[Cp_2ZrMe_2]$ (**1**, hatched signals) and (b) after appearance of the complex $[Cp_2ZrMe]$ (**2**), chemically bound to the support, and removal of the starting material by washing with toluene. The methyl groups are labeled with ^{13}C (99%). ($T = 300$ K, rotation frequency (a) 3314 Hz and (b) 2968 Hz, contact time 1 ms, 90° (^1H) = 4.4 μs).

1 confirm that the new signals belong to one species. On the basis of the chemical shifts and experiments with interrupted proton decoupling,[9] these signals were assigned to Cp and methyl groups of a zirconocene complex. The ratio of intensities (samples with natural isotope abundance) of the signals 107:17 is 10:1. The support can be loaded to 5% capacity and washing with toluene can elute only **1** completely. From all these facts we conclude that the signals at $\delta = 107$ and 17 belong to a $[Cp_2ZrMe]$ species (**2**), which is chemically bound to the support through Zr. The NMR data of **2** resemble those of the complex $[\{Cp_2ZrMe\}_2O]$, whereas the signal for the methyl group of cationic $[Cp_2Zr(thf)Me]$ is found down-field at $\delta = 38.9$.[10, 11] The catalyst **2** requires a cocatalyst like $(Et_2AlCl)_2$ to polymerize ethylene, while the ionic complex mentioned above does not.

Addition of $(Et_2AlCl)_2$ to **2** changes the CP/MAS ^{13}C NMR spectrum as follows: the Cp signal is shifted to $\delta \approx 105$ and broadens ($W_{1/2} \approx 400$ Hz). Experiments with ^{13}C-labeled **2** show that the intensity of the signals for the methyl groups at the zirconium atom ($\delta = 17$) decreases and a broad signal appears at $\delta \approx -10$ ($W_{1/2} \approx 350$ Hz). This signal is attributed to a terminal methyl group bonded to aluminum.[12] In addition, two new signals appear at $\delta = 9.3$ and 10.3, whose intensities are not changed when the methyl-C

[*] Prof. Dr. R. Benn, Dipl.-Chem. W. Herrmann
Max-Planck-Institut für Kohlenforschung
Kaiser-Wilhelm Platz 1
W-4330 Mülheim a. d. Ruhr

[**] We thank Prof. Dr. *Bogdanovic* for a gift of MgH_2 and Ms *P. Philipps* for the preparation of **1**.

atom of **1** is isotopically labeled. These signals must therefore arise from the cocatalyst components. Experiments with interrupted proton decoupling[9] show that they belong to methyl groups. The signal at 9.3 is not resolved; the smaller section of the area under the peak is assigned to the methyl carbon of a terminal ethyl group of $(Et_2AlCl)_2$, on the grounds of MAS experiments without cross-polarization (in these experiments more mobile groups have more intense signals)[13] (Fig. 2). The major portion of the area is assigned to the terminal ethyl group of an AlMeEt residue, which is bound through a μ-Cl and a μ-CH_2Me bridge to a $[Cp_2Zr]$ fragment attached to the support. The signal at 10.3 is assigned to the methyl groups of this bridging μ-CH_2Me group of the binuclear complex $[\{Cp_2Zr\}(\mu\text{-}Cl)(\mu\text{-}CH_2Me)\{AlMeEt\}]$, **3**. In control experiments without zirconium components, this signal is absent, and again no polymerization of ethylene takes place. Binuclear complexes with $[Cp_2Zr]$ and (AlR_2) units bridged via Cl and alkyl groups have been discussed previously as intermediates for polymerizations in the homogeneous phase.[14]

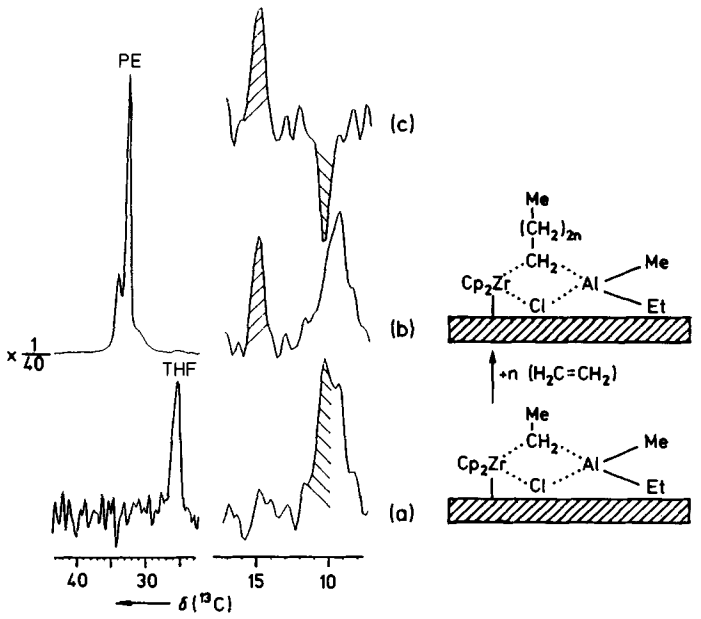

Fig. 2. CP/MAS ^{13}C NMR spectra (75.5 MHz, THF adsorbed on MgH_2 as reference) of $[Cp_2ZrMe]$ (**2**), attached to the support (a) after adding the cocatalyst $(Et_2AlCl)_2$ and (b) after adding ethylene. (c) The difference spectrum [(b)–(a)]. The signal of the methyl groups at $\delta = 10.3$ is shifted to 14.8. The intensity scale for the polyethylene peak in (b) is multiplied by a factor $^1/_{40}$.

Samples of **3** were subjected to dosed quantities of ethylene at 77 K and then slowly warmed to 300 K.[15] CP/MAS ^{13}C NMR spectra taken during the course of this reaction show that polyethylene is formed, and the signal at $\delta = 10.3$ decreases in favor of a new signal at 14.8. This new signal is assigned to the terminal methyl groups of linear polyethylene. Depending on the orthorhombic or monoclinic modifications of polyethylene,[16] the methylene signals appear at $\delta = 34.1$ and 32.7. The formation of polyethylene can be understood as the insertion of ethylene molecules into the zirconium-μ-CH_2Me bond.[17] The activity of the investigated systems at 310 K is ca. 50 kg polyethylene/(mol_{Zr} h bar) and is thus the same order of magnitude as related homogeneous systems.[18]

Experiments in which $[Cp_2ZrCl_2]$ (**1a**) is used as the zirconium complex, agree with this interpretation. Compound **1a** reacts with MgH_2 to give a species bound to the support, which gives a signal at $\delta = 103$ (probably $[Cp_2ZrCl]$). Addition of $(Et_2AlCl)_2$ produces no signal at $\delta = 10.3$ and the amount of polymerization of ethylene is negligible. If, on the other hand, $(Et_3Al)_2$ is used as cocatalyst, a Cp signal is observed, as with **3**, at $\delta = 105$ and a methyl signal at $\delta = 10.3$. This is again an active polymerization system.

Compound **3** also polymerizes propene, but only atactic oligomers are detected in the CP/MAS ^{13}C NMR spectrum. In the case of alkyl-substituted zirconium complexes a chirality center is generated directly at the zirconium atom.[19] Because the rotation barrier for Cp is significantly higher in the solid than in solution,[20] these systems could be interesting from the aspect of heterogeneous, stereospecific polymerization of α-olefins.[21]

Received: October 20, 1990 [Z 4244 IE]
German version: *Angew. Chem. 103* (1991) 436

[1] Y. Iwasawa, B. C. Gates, *CHEMTECH. 19* (1989) 173–181; J. M. Basset (Ed.): *Surface Organometallic Chemistry: Molecular Approaches to Surface Catalysis*, Kluwer, Dordrecht 1988; F. R. Hartley: *Supported Metal Complexes: A New Generation of Catalysts*, Reidel, Boston 1985.

[2] T. Keii, K. Soga (Eds.): *Catalytic Polymerization of Olefins*, Elsevier, Amsterdam 1986; D. L. Myers, J. H. Lundsford, *J. Catal. 99* (1986) 140.

[3] P. Cossee, *J. Catal. 3* (1964) 80; E. J. Arlman, *ibid.* (1964) 89; M. L. H. Green, *Pure Appl. Chem. 50* (1978) 27; M. Brookhart, M. L. H. Green, *J. Organomet. Chem. 250* (1983) 395.

[4] D. Hedden, T. J. Marks, *J. Am. Chem. Soc. 110* (1988) 1647; W. C. Finch, R. D. Gillespie, D. Hedden, T. J. Marks, *J. Am. Chem. Soc. 112* (1990) 6221 and references cited therein.

[5] J. J. Eisch, A. M. Piotrowski, S. K. Brownstein, E. J. Gabe, F. L. Lee, *J. Am. Chem. Soc. 107* (1985) 7219.

[6] E. Kinkelin, G. Fink, B. Bodganović, *Makromol. Chem. Rapid Commun. 7* (1986) 85.

[7] C. A. Fyfe: *Solid State NMR for Chemists*, C. F. C. Press, Guelph, Ontario, Canada 1983; B. C. Gerstein, C. R. Dybrowski: *Transient Techniques in NMR of Solids*, Academic Press, Orlando, FL, USA 1985.

[8] Compound **1** also reacts with MgH_2 under CP/MAS ^{13}C NMR conditions in the rotor to yield **2** and methane quantitatively ($\delta = -11.1$, $W_{1/2} = 18$ Hz, $^1J(CH) = 122$ Hz. $\delta(CH_4)_{gas} = -11.53$, see D. Denney, V. M. Mastikhin, S. Namba, J. Turkevich, *J. Phys. Chem. 82* (1978) 1752.

[9] S. J. Opella, M. H. Frey, *J. Am. Chem. Soc. 101* (1979) 5854.

[10] $[\{Cp_2ZrMe\}_2O]$ cf. W. E. Hunter, D. C. Hrncir, R. V. Bynum, R. A. Penttila, J. L. Atwood, *Organometallics 2* (1983) 750; $[Cp_2Zr^{\oplus}(thf)Me]$ cf. R. F. Jordan, W. E. Dasher, S. F. Echols, *J. Am. Chem. Soc. 108* (1986) 1718; R. F. Jordan, C. S. Bajgur, R. Willett, B. Scott, *J. Am. Chem. Soc. 108* (1986) 7410; R. F. Jordan, C: S. Bajgur, W. E. Dasher, A. L. Rheingold, *Organometallics 6* (1987) 1041; G. G. Hlatky, H. W. Turner, R. R. Eckman, *J. Am. Chem. Soc. 111* (1989) 2728; K. H. Dahmen, D. Hedden, R. L. Burwell, T. J. Marks, *Langmuir 4* (1988) 1212; M. Bochmann, A. J. Jaggar, J. C. Nicholls, *Angew. Chem. 102* (1990) 830; *Angew. Chem. Int. Ed. Engl. 29* (1990) 780; R. F. Jordan, P. K. Bradley, N. C. Baenziger, R. E. La Pointe, *J. Am. Chem. Soc. 112* (1990) 1289 and references cited therein.

[11] The nature of the bond between $[Cp_2ZrMe]$ and the support is not clear. Experiments with $Mg(OH)_2$, MgH_2 prepared from the elements, and dissolved MgH_2 discount a Zr-O-Mg species, so that **2** may be bonded to the support via μ-H bridges or via a Zr-Mg bond similar to $[Cp(\eta^3\text{-}C_3H_5)Co\text{-}MgBr(thf)_2]$ (cf. K. Jonas, G. Koepe, C. Krüger, *Angew. Chem. 98* (1986) 901; *Angew. Chem. Int. Ed. Engl. 25* (1986) 923).

[12] An Al-Me fragment is distinguished from an Mg-Me fragment more characteristically by the quadrupole broadening than by the chemically shifts; see P. J. Toscano, T. J. Marks, *J. Am. Chem. Soc. 107* (1985) 653.

[13] G. E. Maciel, J. F. Haw, I. Chuang, B. L. Hawkins, T. A. Early, D. R. McKay, L. Petrakis, *J. Am. Chem. Soc. 105* (1983) 5529.

[14] F. Patat, H. Sinn, *Angew. Chem. 70* (1958) 496. Related species that have been examined by X-ray crystallography: $[Cp_2Zr(\mu\text{-}Cl)(\mu\text{-}CH_2CHR)AlEt_2]$ W. Kaminsky, J. Kopf, H. Sinn, H. J. Vollmer, *Angew. Chem. 88* (1976) 688; *Angew. Chem. Int. Ed. Engl. 15* (1976) 629; $[Cp_2M(\mu\text{-}Me)_2AlMe_2]$ J. Holton, M. F. Lappert, G. R. Scollary, *J. Chem. Soc. Chem. Commun. 1976*, 425. For five-coordinate zirconocenes see S. B. Jones, J. L. Petersen, *Inorg. Chem. 20* (1981) 2889; W. K. Kot, N. M. Edelstein, A. Zalkin, *Inorg. Chem. 26* (1987) 1339.

[15] Only the heterogeneous three-component system $MgH_2/[Cp_2ZrMe_2]/(AlEt_2Cl)$ catalyzes polymerization. Its filtrate is active only after renewed addition of MgH_2.
[16] D. L. Van der Hart, F. Khoury, *Polymer 25* (1984) 1589; I. Ando, T. Sorita, T. Yamanobe, T. Komoto, H. Sato, K. Deguchi, M. Imanari, *Polymer 26* (1985) 1865.
[17] C. A. Jolly, D. S. Marynick, *J. Am. Chem. Soc. 111* (1989) 7968.
[18] H. J. Sinn, W. Kaminsky, *Adv. Organomet. Chem. 18* (1980) 99.
[19] G. Erker, T. Mühlenbernd, A. Rufinska, R. Benn, *Chem. Ber. 120* (1987) 507.
[20] R. Benn, H. Grondey, R. Nolte, G. Erker, *Organometallics 7* (1988) 777; R. Benn, H. Grodney, G. Erker, R. Ault, R. Nolte, *Organometallics 9* (1990) 2493.
[21] J. A. Ewen, *J. Am. Chem. Soc. 106* (1984) 6355; W. Kaminsky, K. Külper, H. H. Brintzinger, F. R. W. P. Wild, *Angew. Chem. 97* (1985) 507; *Angew. Chem. Int. Ed. Engl. 24* (1985) 507; P. Pino, P. Cioni, J. Wei, *J. Am. Chem. Soc. 109* (1987) 6189; G. Erker, R. Nolte, Y.-H. Tsay, C. Krüger, *Angew. Chem. 101* (1989) 642; *Angew. Chem. Int. Ed. Engl. 28* (1989) 628; W. Kaminsky, R. Spiehl, *Markomol. Chem. 190* (1989) 515.

Alkaline Earth Metal Complexes Containing Deprotonated Organic Acids and Water: Preparation, Structures and a New Synthetic Strategy**

By *Patrizia Mikulcik, Paul R. Raithby, Ronald Snaith,* and *Dominic S. Wright**

We reported recently the first lithiated organic compound containing water as a ligand, monomeric OxLi · TMEDA · H_2O (OxH = $\overline{C_6H_4O(C{=}S)\text{-}NH}$, TMEDA = *N,N,N',N'*-tetramethylethylenediamine).[1] This was prepared simply by adding H_2O to a solution of $(OxLi \cdot TMEDA)_n$ obtained by lithiating OxH in toluene containing TMEDA. The co-existence of H_2O within a lithiated organic ($R^{\ominus}Li^{\oplus}$, where $R^{\ominus}$ is an organic anion derived from an alkane or arene, an amine, an alcohol, etc) was startling. Usually the products of equation (a) dominate, i.e., such species are exceedingly moisture-sensitive.

In this case, however, the adduct of equation (b) is favored.

$$R^{\ominus}Li^{\oplus} + H_2O \rightleftarrows RH + LiOH \quad (a)$$
$$R^{\ominus}Li^{\oplus} + H_2O \rightleftarrows R^{\ominus}Li^{\oplus} \cdot H_2O \quad (b)$$

The reasons for this behaviour are: 1) the p*K*a of OxH is slightly less than that of H_2O and 2) after the H_2O displaces the S atom of the $(\overline{NCS})Li$ chelate in $(OxLi \cdot TMEDA)_n$ it is stabilized by intramolecular hydrogen bonding ($-S \cdots H_2O$). Related complexes containing hexamethylphosphoric acid triamide (HMPA) have since been prepared: $(OxLi \cdot HMPA \cdot H_2O)_2$ by addition of H_2O to $(OxLi \cdot HMPA)_n$, and $(OxLi \cdot HMPA)_2 \cdot H_2O$ by mixing the fully hydrated $(OxLi \cdot HMPA \cdot H_2O)_2$ and the anhydrous species.[2] Here we extend these findings to alkaline-earth metal complexes, revealing a new synthetic strategy, based on tested chemical procedures but with a key modification. The standard method of dissolving an organic acid, RH, is to treat it with aqueous alkali (equation (c); M = alkali metal). An ion-separated species (not a complex) results.

However, why not do the reaction using *solid* MOH (or $M(OH)_2$ etc.) in a *hydrocarbon* medium containing an additional Lewis base, L [Equation (d)]?

$$RH + MOH_{aq} \xrightarrow{H_2O} R^{\ominus} + M^{\oplus}{}_{aq} \quad (c)$$
$$RH + MOH_{(s)} + xL \xrightarrow{\text{hydrocarbon}} R^{\ominus}M^{\oplus} \cdot xL \cdot H_2O \quad (d)$$

This "assembles" H_2O in the stoichiometric amount required for ligation, the metal cation is not swamped, and a true complex (a contact-ion species) should result. The aqua complex produced thus could then be dehydrated, giving the anhydrous species. Here we illustrate two procedures: we describe the synthesis (using Ba metal) of $Ox_2Ba \cdot 3HMPA$, **1**, its crystal structure, and the addition of H_2O to **1** to give $Ox_2Ba \cdot 3H_2O$, **2**, as well as the *direct* synthesis [according to eq. (d)] of $Ox_2Ca \cdot 2HMPA \cdot 2H_2O$, **3**, by reaction of OxH with solid $Ca(OH)_2$ in toluene containing HMPA, its crystal structure, and its dehydration to give $Ox_2Ca \cdot 2HMPA$, **4**.

$[\overline{C_6H_4O(C{=}S)N}]_2Ba \cdot 3HMPA$ **1** $[\overline{C_6H_4O(C{=}S)N}]_2Ba \cdot 3H_2O$ **2**

$[\overline{C_6H_4O(C{=}S)N}]_2Ca \cdot 2HMPA \cdot 2H_2O$ **3** $[\overline{C_6H_4O(C{=}S)N}]_2Ca \cdot 2HMPA$ **4**

The anhydrous complex **1** was obtained in moderate yield by reacting Ba metal with OxH (molar ratio 1:1) in toluene containing HMPA (2 equiv). Treatment of a toluene solution of **1** with H_2O produces a white precipitate, which dissolves in excess of hot toluene. Cooling of the solution gives microcrystalline **2**. This route thus affords an aqua complex of Ox_2Ba, although the HMPA ligands of **1** are thereby displaced (TMEDA and HMPA remain coordinated in the OxLi complexes). Furthermore, the yield of **2** is poor; refrigeration of the mother liquor affords only the starting material **1**. The identities of **1** and **2** were confirmed by elemental analyses, by IR spectroscopy (ν(N-H) bands absent; ν(O-H) of H_2O present for **2** but not for **1**), and by ^1H NMR spectroscopy. X-ray crystallography (Fig. 1)[3] shows that the

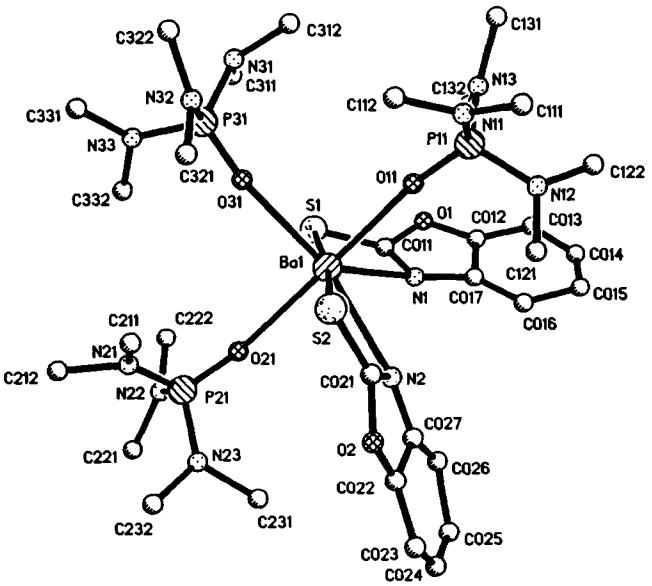

Fig. 1. Molecular structure of **1** [3].

[*] Dr. D. S. Wright, Dr. P. R. Raithby, Dr. R. Snaith
University Chemical Laboratory
Lensfield Road, Cambridge CB2 1EW (UK)
Patrizia Mikulcik
Institut für Anorganische Chemie der Technischen Universität München
Lichtenbergstrasse 4, W-8046 Garching (FRG)

[**] This work was supported by Gonville and Caius College, Cambridge (Fellowship for D. S. W.), the Associated Octel Co. Ltd. (R. S.), and the Deutscher Akademischer Austauschdienst (fellowship for P. M.). The reactions and products described are being patented by the Associated Octel Co. Ltd. (U.K.)

solid-state structure of **1** is monomeric and, as anticipated from structures of analogous lithium species, both $Ox^{\ominus}$ ligands chelate the $Ba^{2\oplus}$ center (mean Ba–N and Ba–S distances, 2.91(2) and 3.31(1) Å respectively). The $Ba^{2\oplus}$ cation is also ligated by three HMPA molecules (mean Ba–O distance 2.60(3) Å), making it seven-coordinate (low for a cation such as $Ba^{2\oplus}$[4]).

For the synthesis of **3**, solid $Ca(OH)_2$ (1 equiv) was stirred in a toluene solution of OxH and HMPA (2 and 4 equiv respectively) and soon dissolved. Further brief stirring causes precipitation of another solid which dissolves on heating. Cooling affords crystals of **3** in high yield. This aqua complex can be dehydrated easily by heating at 130 °C under vacuum. Crystallization of the resulting white powder from toluene solution gives the anhydrous complex **4**. The complexes **3** and **4** were identified as detailed for **1** and **2**. Complex **3** is monomeric in the solid state (Fig. 2).[5] The $Ca^{2\oplus}$

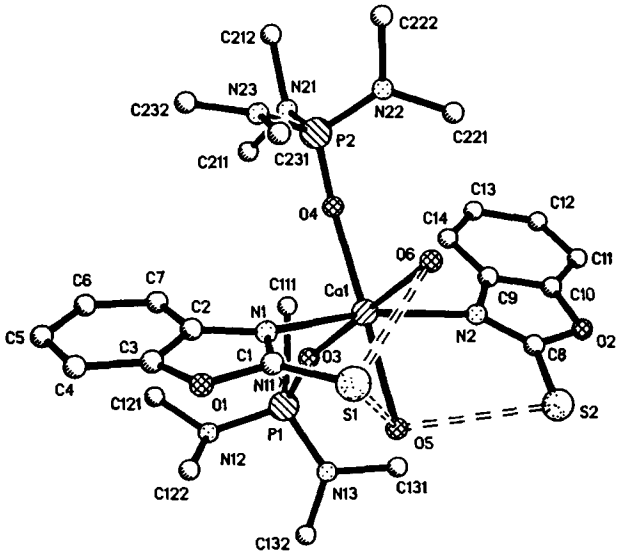

Fig. 2. Molecular structure of **3** [5].

cation is complexed octahedrally: by two *cis* H_2O molecules (mean Ca–O distance 2.390(5) Å), by two *cis* HMPA ligands (mean Ca–O distance 2.267(4) Å), and by two *trans* *N*-attached $Ox^{\ominus}$ anions (mean Ca–N distance 2.545(6) Å). The S atoms of these anions are not attached to $Ca^{2\oplus}$, but hydrogen bond with H_2O molecules (intramolecular: S(1)···O(5), 3.20; S(2)···O(5), 3.14; S(1)···O(6), 3.25 Å; intermolecular: S(2)···O(6'), 3.30 Å].[6] On dehydration to give **4**, the $Ca^{2\oplus}$ center will probably remain six-coordinate; the $S^{\delta\ominus}$ centers, displaced in **3**, will simply re-engage the metal (cf. structure of **1**, Fig. 1).

These results herald some major synthetic advances. Firstly, organic acid precursors of type Y-R'-XH(R' is, for example, CH in a ring, $(CH_2)_n$ in a chain) with p*K*a close to that of H_2O and with two electronegative centers X and Y (N, O, or S) can be metalated at one center (X), while the other (Y) hydrogen bonds to H_2O ligands. For example, the lithiated derivatives[7] of **5**–**8** will all complex H_2O. Secondly, the

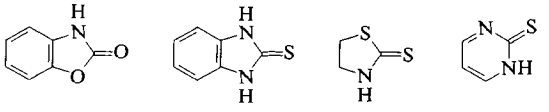

5 **6** **7** **8**

direct synthesis of aqua complexes by assembling H_2O ligands via solid metal hydroxides is very flexible: in the system nRH (organic acid) + xL (other ligand) + $M(OH)_{n(s)}$, R, L and/or x, and M (thus n) can be varied. LiOH also reacts with OxH and HMPA to give $(OxLi \cdot HMPA \cdot H_2O)_2$, and $Ba(OH)_2$ with OxH (2 equiv) and HMPA to give $Ox_2Ba \cdot 2HMPA \cdot 2H_2O$ (cf. **1** and **2**).[8] The use of metal oxides rather than hydroxides promises further variations: for example, solid CaO reacts with OxH (2 equiv) and HMPA to give $Ox_2Ca \cdot 2HMPA \cdot H_2O$ (cf. **3**).[8] Thirdly, other small complexants can be assembled by this direct method, e.g., Li_2S reacts with OxH (2 equiv) and HMPA to provide $(OxLi \cdot 2HMPA)_2 \cdot H_2S$.[8] Finally, all such assembled ligands (H_2O, H_2S; also NH_3) will be activated (as shown by ab initio MO calculations[2]), both by complexation and by hydrogen bonding to $Y^{\delta\ominus}$ centers of the anionic ligands. Thus, their metalation (by M' or M) will be enhanced, providing volatile homo- and heteronuclear metal hydroxides, oxides, sulphides, etc. For example, OxLi · TMEDA · H_2O,[1] provides OxLi · TMEDA · LiOH on treatment with *n*BuLi.[8]

Experimental Procedure

1: 2-Mercaptobenzoxazole (1.16 g, 7.7 mmol) and barium metal (1.06 g, 7.7 mmol) were taken in chilled toluene (10 mL) containing HMPA (2.76 g, 15.4 mmol). A reaction began at room temperature and continued, with gas evolution, for two days. The resulting orange-yellow precipitate was dissolved by heating, and the mixture filtered to remove excess metal. Cooling at 0 °C produced pale yellow cubic crystals of **1**. First batch yield 1.64 g (44%); m.p. 142–145 °C; correct C,H,N,P analysis; ^{1}H NMR (C_6D_6, 250 MHz, 25 °C): δ = 7.68 (m, 1H), 7.24 (m, 1H), 7.10 (m, 1H), 6.88 (m, 1H), 2.32 (d, J = 9.5 Hz, 27H of HMPA).

2: Complex **1** (4.87 g, 5.0 mmol) was dissolved in toluene (10 mL) and distilled water (0.18 mL, ca. 10 mmol) added. A white precipitate formed at once. Addition of more toluene (30 mL) and heating, caused the white solid to dissolve. Cooling of the resulting solution gave microcrystalline **2**. Yield 0.30 g (18%); m.p. (dec) 200 °C; correct C,H,N analysis; IR (Nujol mull): ν(O-H) of H_2O at 3315 (vs) cm^{-1}; ^{1}H NMR (C_6D_6SO, 250 MHz, 25 °C) δ = 7.08 (m, 2H), 6.94 (m, 1H), 6.83 (m, 1H), 3.37 (s, 3H of H_2O).

3: Solid calcium hydroxide (99%, anhydrous; 0.37 g, 5 mmol) was added to a solution of 2-mercaptobenzoxazole (1.51 g, 10 mmol) and HMPA (3.58 g, 20 mmol) in toluene (20 mL). After stirring for 5 min, most of the $Ca(OH)_2$ had dissolved. On further stirring (15 min), an off-white precipitate formed. This dissolved on heating, and overnight cooling of the solution then gave colorless crystals of **3**. Yield 3.31 g (90%); m.p. 104–106 °C; correct C,H,N,P, analysis; IR (Nujol mull): ν(O–H) of H_2O at 3388 (s), 3260 (w), 3150 (s) cm^{-1}; ^{1}H NMR (C_6D_6, 250 MHz, 25 °C) δ = 7.51 (m, 1H), 7.13 (m, 1H), 6.96 (m, 1H), 6.84 (m, 1H), 4.68 (s, 2H of H_2O), 2.21 (d, J = 9.6 Hz, 18H of HMPA).

4: Complex **3** (1.13 g, 1.54 mmol) was heated at 130 °C under reduced pressure (4 mbar) for 3 h. The initial semi-solid was thereby converted into a dry white powder, which was dissolved in hot toluene (10 mL). Cooling of the solution afforded colorless crystals of **4**. Yield 0.83 g (77%); m.p. 158–161 °C; correct C,H,N,P analysis; IR (Nujol mull): no ν(O–H) of H_2O, though brief exposure to air produces a spectrum identical to that of **3**; ^{1}H NMR (C_6D_6, 250 MHz, 25 °C) δ = 7.40 (m, 1H), 7.11 (m, 1H), 6.91 (m, 1H), 6.76 (m, 1H), 2.23 (d, J = 9.4 Hz, 18H of HMPA).

Received: November 27, 1990 [Z 4297 IE]
German version: *Angew. Chem. 103* (1991) 452

CAS Registry numbers:
1, 132438-87-0; **2**, 132438-88-1; **3**, 132438-89-2; **4**, 132461-58-6; Ba, 7440-39-3.

[1] D. Barr, P. R. Raithby, P. von R. Schleyer, R. Snaith, D. S. Wright, *J. Chem. Soc. Chem. Commun. 1990*, 643.

[2] D. R. Armstrong, D. Barr, P. R. Raithby, P. von R. Schleyer, R. Snaith, D. S. Wright, *Inorg. Chim. Acta*, in press.

[3] **1**: $C_{32}H_{62}BaN_{11}O_5P_3S_2$, M_r = 975.3, monoclinic, space group $P2_1/n$, a = 10.554(3), b = 43.948(10), c = 11.022(4) Å, β = 107.71(3)°, V = 4870(3) Å^3, Z = 4, ρ_{calc} = 1.330 g cm^{-3}, F(000) = 2016, $Mo_{K\alpha}$ radiation, λ = 0.71069 Å, μ = 1.04 mm^{-1}. The structure was determined by Patterson techniques and subsequent Fourier difference methods, and refined from 2643 unique observed reflections measured at room temperature with a

Nicolet R3mV diffractometer ($2\theta_{max} = 45.0°$), with anisotropic thermal parameters for Ba, S, P, O, and some N atoms; the HMPA ligands showed severe positional disorder; H atoms were not included in refinement; $R = 0.122$, $R_w = 0.128$ for 320 parameters [9].

[4] N. S. Poonia, A. V. Bajaj, *Chem. Rev. 87* (1988) 55, a review concerning the structures of Group 2 (especially the heavier metals, Ca, Sr, Ba) complexes with macrocycles and with small donor molecules.

[5] **3**: $C_{26}H_{48}CaN_8O_6P_2S_2$, $M_r = 734.86$, monoclinic, space group $P2_1/n$, $a = 11.412(1)$, $b = 22.423(2)$, $c = 15.537(2)$ Å, $\beta = 104.28(1)°$, $V = 3852.9$ Å^3, $Z = 4$, $\rho_{calc} = 1.266$ g cm^{-3}, $F(000) = 1560$, $Mo_{K\alpha}$ radiation, $\lambda = 0.71069$ Å, $\mu = 0.34$ mm^{-1}. The structure was determined by direct methods and Fourier difference techniques, and refined from 3701 unique observed reflections measured at room temperature with a Stoe-Siemens diffractometer ($2\theta_{max} = 45.0°$), with anisotropic thermal parameters for Ca, S, P, N, O, and C atoms of the Ox ligand, and with isotropic H atoms in calculated positions; $R = 0.073$, $R_w = 0.079$ for 382 parameters.

[6] W. C. Hamilton, J. A. Ibers: *Hydrogen Bonding in Solids*, Benjamin, New York 1968, pp. 14–16.

[7] D. R. Armstrong, R. E. Mulvey, D. Barr, R. W. Porter, P. R. Raithby, T. R. E. Simpson, R. Snaith, D. S. Wright, K. Gregory, P. Mikulcik, *J. Chem. Soc. Dalton Trans.*, in press.

[8] M. G. Davidson, R. Snaith, D. S. Wright, unpublished observations.

[9] Further details of the crystal structure investigation are available on request from the Director of the Cambridge Crystallographic Data Centre, University Chemical Laboratory, Lensfield Road, Cambridge CB2 1EW (U.K.), on quoting the full journal citation.

Reactions of Substituted Alkynes at a Conformationally Rigid (Olefin)cobalt Fragment**

By *Jun Okuda,** *Karl Heinz Zimmermann,* and *Eberhardt Herdtweck*

Two alkynes can be coupled with an olefin in the coordination sphere of the 14-electron fragment (η^5-cyclopentadienyl)cobalt (CpCo) in a [2 + 2 + 2] cycloaddition to form cyclohexadiene derivatives.[1] In this way *Vollhardt* et al. have successfully applied the *intra*molecular cyclization of enediynes with $[CpCo(CO)_2]$ to construct steroid frameworks.[2] The *inter*molecular coupling of two alkynes with an olefin[3] promises to be useful synthetically, when the aim of suppressing the cobalt-induced di- and trimerization of the alkynes and of elucidating the stereochemical course of the reaction is achieved. In this process, metallacycle **A** (Scheme 1[1,4]) plays a key role as reactive intermediate. Molecular mechanical considerations led us to fix the olefin within the coordination sphere of the cobalt center using a 3-butenyl substituent on the cyclopentadienyl ligand. The reaction of alkynes at the resulting (η^2-alkene)cobalt fragment **B** yielded, depending on the alkyne substituents, cyclohexadiene complexes as well as for the first time an (η^2-alkene)(η^2-alkyne)cobalt and an (η^2-alkene)cobaltacyclopentadiene complex.

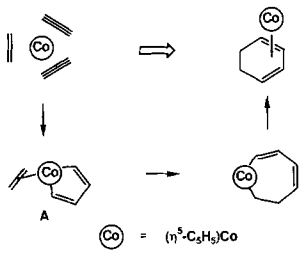

Scheme 1.

The coordinatively unsaturated 16-electron fragment **B** is formed in the reduction of the diiodide $[(\eta^5\text{-}C_5Me_4CH_2CH_2CH{=}CH_2)CoI_2]_2$ with sodium amalgam in THF and can be trapped with two-electron donor ligands L like PR_3 and CO.[5,6] The ethene complex **1** ($L = C_2H_4$) loses ethene in boiling hexane and is thus also suitable as a source of **B** (Scheme 2).[6b] If **B** is generated in the presence of bis(trimethylsilyl)acetylene, the alkyne complex **2** is obtained quantitatively under various reaction conditions and irrespective of the stoichiometry applied. Compound **2** forms red crystals, which melt at 27 °C (Scheme 3). Its chiral structure, which is also rigid in solution on the NMR time scale, is confirmed by spectroscopic data[7] and X-ray crystallographic analysis.[8] Each enantiomer in the racemate **2** bears an alkyne and an alkene ligand,[9] which lie parallel to each other, and together with the almost planar, η^5-coordinated Cp ligand determine the trigonal planar geometry around the cobalt(I) center (Fig. 1).

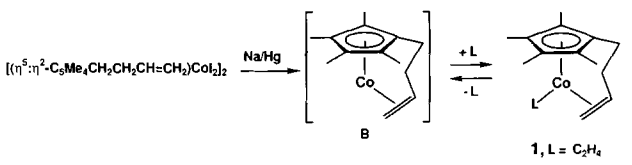

Scheme 2.

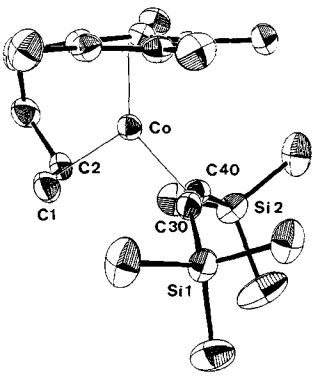

Fig. 1. Structure of an enantiomer of **2** in the crystal (ORTEP), 50% probability ellipsoids, without H atoms). Selected bond distances [Å] and bond angles [°]: C1-C2 1.409(3), Co-C1 2.023(2), Co-C2 2.036(2), C30-C40 1.249(3), Co-C30 2.010(2), Co-C40 2.007(2), Co-Cp (center of five-membered ring) 1.692, Si1-C30-C40 151.4(2), Si2-C40-C30 151.3(2), C1-C2-C3 122.5(3), C2-C3-C21 111.5(2).

On the other hand, 1,7-octadiyne reacts with **1** to give, in 90% yield, cobaltacyclopentadiene **3**, a red-brown oil that is shown by ^1H, ^{13}C NMR and IR spectroscopy to contain a five-membered metallacycle and the intact fragment **B** (Scheme 3).[7] Analogous to spectra of chelate complexes of type **1** ($L = CO, PR_3$), the signals of the two olefinic carbon atoms occur at $\delta = 48.56$ as triplet ($^1J = 153$ Hz) and at 68.49 as doublet ($^1J = 151$ Hz). In contrast to the cobaltacyclopentadienes thoroughly studied by *Yamazaki* et al.,[10] **3**

[*] Dr. J. Okuda, Dipl.-Chem. K. H. Zimmermann, Dr. E. Herdtweck
Anorganisch-chemisches Institut der Technischen Universität München
Lichtenbergstrasse 4, W-8046 Garching (FRG)

[**] Functionalized Cyclopentadienyl Ligands, Part 5. This work was supported by the Volkswagen-Stiftung, the Bund der Freunde der TU München, the Leonhard-Lorenz-Stiftung and the Fonds der Chemischen Industrie. We thank Prof. *W. A. Herrmann* for his support. Part 4: J. Okuda, *Chem. Ber. 123* (1990) 1649.

is unusually inert and does not cyclize, even at higher temperatures (80 °C, 24 h), to the corresponding cyclohexadiene complex. To our knowledge, **3** is the first isolable cobaltacyclopentadiene complex with a π-coordinated ligand such as alkene or alkyne.[11]

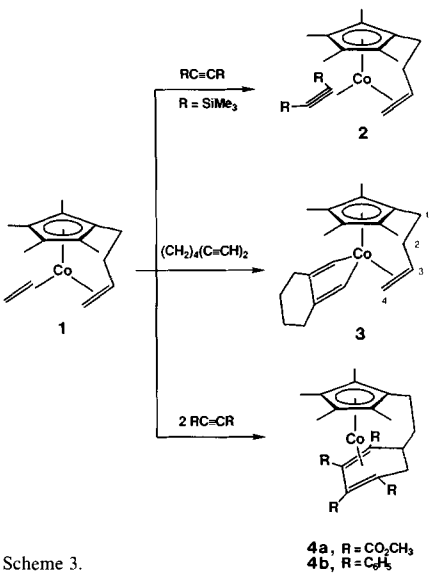

Scheme 3.

The cobalt-centered [2 + 2 + 2] cycloaddition with **B** is observed with activated alkynes such as dimethyl acetylenedicarboxylate (DMAD) or tolane. Thus the reaction of **1** with DMAD leads quantitatively to the brown crystalline η^4-cyclohexadiene complex **4a** with a bridged ligand system. Spectroscopic data show unambiguously that the cyclization involves the C–C double bond of the 3-butenyl chain.[7] The proof lies in the ^{13}C NMR resonance signals of the original olefinic carbon atoms of the 3-butenyl chain, which occur in **4a** at $\delta = 35.32$ as doublet and 42.55 as triplet, each with $^1J_{CH} = 126$ Hz. An X-ray structure analysis on the analogous complex derived from tolane (**4b**) confirms the presence of a cyclohexadiene ring that is distorted as a result of the Cp–cyclohexadiene ethylene "handle".

The rigidity of the C–C double bond of the cobalt fragment **B** is apparently responsible for high activation barriers for the individual steps of the cycloaddition reaction, depending upon the nature of the alkyne substituents. Thus no catalytic alkyne trimerization is observed at the cobalt fragment **B**. Instead, **2**, **3**, and **4** are formed chemoselectively. Furthermore the fact that **3** is isolable, and in particular the unexpected inertness[12] of **3**, can be interpreted as another indication that the cobalt-induced cyclohexadiene formation

C

occurs via an (η^2-alkyne)cobaltacyclopentene complex **C** as reactive intermediate.

Received: December 21, 1990 [Z 4282 IE]
German version: *Angew. Chem. 103* (1991) 446

CAS Registry numbers:
1, 132157-56-3; **2**, 132157-57-4; **3**, 132157-58-5; **4a**, 132157-59-6; **4b**, 132157-60-9; $Me_3SiC{\equiv}CSiMe_3$, 14630-40-1; $(CH_2)_4(C{\equiv}CH)_2$, 871-84-1; $H_3CO_2C{\equiv}CCO_2CH_3$, 762-42-5; $H_5C_6C{\equiv}CC_6H_5$, 501-65-5.

[1] C.-A. Chang, C. G. Francisco, T. R. Gadek, J. A. King, Jr., E. D. Sternberg, K. P. C. Vollhardt in B. M. Trost, C. R. Hutchinson (Eds.): *Organic Synthesis Today and Tomorrow*, Pergamon, Oxford 1981, p. 81; K. P. C. Vollhardt, *Angew. Chem. 96* (1984) 525; *Angew. Chem. Int. Ed. Engl. 23* (1984) 539.

[2] E. D. Sternberg, K. P. C. Vollhardt, *J. Org. Chem. 49* (1984) 1574.

[3] D. W. Macomber, A. G. Verma, *Organometallics 7* (1988) 1241.

[4] Y. Wakatsuki, H. Yamazaki, *J. Organomet. Chem. 139* (1977) 169; U. Kölle, B. Fuss, *Chem. Ber. 119* (1986) 116; Rhodium: P. Caddy, M. Green, E. O'Brien, L. E. Smart, P. Woodward, *J. Chem. Soc. Dalton Trans. 1980*, 962.

[5] The ligand concept took into account both preparative aspects (peralkylation of the cyclopentadienyl ring) and the fact that only a specific chain length would yield a cobalt fragment with as rigid as possible a chelate framework. The total energy of the model fragment [CpCo(η^2-C_2H_4)] obtained from an EHMO calculation hardly depends on the Cp-Co-C_2H_4 angle: P. Hofmann, Technische Universität München, unpublished. Details of the electronic structure of the fragment CpCoL: P. Hofmann, M. Padmanabhan, *Organometallics 2* (1983) 1273.

[6] a) J. Okuda, K. H. Zimmermann, *Chem. Ber. 122* (1989) 1645; *ibid. 123* (1990) 1641. b) K. H. Zimmermann, *Dissertation*, Technische Universität München 1990; J. Okuda, E. Herdtweck, K. H. Zimmermann in K. H. Dötz, R. W. Hoffmann (Eds.): *Organic Synthesis via Organometallics*, Vieweg, Braunschweig 1991, p. 207.

[7] Consistent spectroscopic data and correct elemental analyses have been obtained for **2**, **3**, **4a** and **4b**. **2**: ^{13}C NMR (100 MHz, C_6D_6, 25 °C): $\delta = 2.07$, 2.37 (q, $^1J(CH) = 119$ Hz, $SiCH_3$), 8.80, 10.42, 12.48 (q, $^1J(CH) = 126$ Hz, CCH_3), 19.63 (t, $^1J(CH) = 125$ Hz, C-1), 38.84 (t, $^1J(CH) = 126$ Hz, C-2), 44.40 (t, $^1J(CH) = 153$ Hz, C-4), 62.13 (d, $^1J(CH) = 153$ Hz, C-3), 93.21, 94.01, 94.07, 95.17, 98.26 (s, five-membered ring-C), 109.80, 111.58 (s, C≡C). No coalescence of resonance signals of diastereotopic carbon atoms to + 80 °C. **3**: ^{13}C NMR (100 MHz, C_6D_6, 25 °C): $\delta = 9.38$, 9.58, 10.31, 11.62 (q, $^1J(CH) = 126$ Hz, CCH_3), 19.58 (t, $^1J(CH) = 127$ Hz, C-1), 28.08 (t, $^1J(CH) = 127$ Hz, C-2), 30.08, 32.15, 39.42, 40.37 (t, $^1J(CH) = 126$ Hz, CH_2CH_2), 48.56 (t, $^1J(CH) = 153$ Hz, C-4), 68.49 (d, $^1J(CH) = 151$ Hz, C-3), 76.42 (d, $^1J(CH) = 153$ Hz, CoCH), 81.10 (s, CoCH=*C*), 92.31, 93.51, 93.69, 96.57, 102.71 (s, five-membered ring-C), 126.03 (d, $^1J(CH) = 153$ Hz, CoCH, 151.44 (s, CoCH=*C*). **4a**: ^{13}C NMR (100 MHz, C_6D_6, 25 °C): $\delta = 8.36$, 8.73, 8.82, 9.30 (q, $^1J(CH) = 128$ Hz, CCH_3), 18.97 (t, $^1J(CH) = 128$ Hz, C-1), 27.27 (t, $^1J(CH) = 133$ Hz, C-2), 35.32 (d, $^1J(CH) = 126$ Hz, C-3), 42.55 (t, $^1J(CH) = 126$ Hz, C-4), 50.90, 51.02, 52.09, 52.17 (q, $^1J(CH) = 146$ Hz, OCH_3), 53.94, 59.88, 93.34, 98.44 (s, six-membered ring C), 85.36, 90.89, 91.65, 97.30, 99.84 (s, five-membered ring C), 168.88, 168.90, 173.37, 173.60 (s, CO).

[8] X-ray structure analysis of **2**: red rectangular crystals 0.75 × 0.5 × 0.5 mm; space group *Pbca* (No. 61); $a = 14.251(1)$, $b = 17.414(1)$, $c = 18.234(2)$ Å; $V = 4525$ Å^3; $C_{21}H_{37}CoSi_2$; $M_r = 404.6$; $Z = 8$; $F(000) = 1740$; $\rho_{calc} = 1.188$ g cm^{-3}. Enraf-Nonius CAD-4, $Mo_{K\alpha}$ radiation ($\lambda = 0.70930$ Å), graphite monochromator; $T = -100 \pm 5$ °C; $1.0 < \theta < 25.0°$; ω-scan; scan width: $(1.50 + 0.30\ \mathrm{tg}\theta) \pm 25\%$ before and after each reflection for background determination; t(max): 90 s. 4462 reflections, 3187 independent reflections with $I > 1.0(I)$; 217 parameters, full-matrix least-squares refinement; direct methods, difference Fourier technique; LP correction; numerical absorption correction; correction for decay, extinction corrected; H atom positions found in some cases and refined with isotropic temperature factors. Anomalous dispersion taken into account. Shift/Err.: < 0.001 in the last refinement cycle; residual electron density: 0.049/ − 0.46 e_o/Å^3. $R = 0.054$, $R_w = 0.040$. Further details of the crystal structure investigation may be obtained from the Fachinformationszentrum Karlsruhe, Gesellschaft für wissenschaftlich-technische Information mbH, W-7514 Eggenstein-Leopoldshafen 2 (FRG) on quoting the depository number CSD-55144, the names of the authors and the journal citation.

[9] M. E. Howden, R. D. W. Kemmitt, M. D. Schilling, *J. Chem. Soc. Dalton Trans. 1980*, 1716; M. Green, K. R. Nagle, C. M. Woolhouse, D. J. Williams, *J. Chem. Soc. Chem. Commun. 1987*, 1793.

[10] Y. Wakatsuki, O. Nomura, K. Kitaura, K. Morokuma, H. Yamazaki, *J. Am. Chem. Soc. 105* (1983) 1907.

[11] K. Pörschke, *Angew. Chem. 99* (1987) 1321; *Angew. Chem. Int. Ed. Engl. 26* (1987) 1288.

[12] Attempts at the intermolecular [2 + 2 + 2] cycloaddition of DMAD with **3** led to the formation of **4a** in small amounts, but not to detectable amounts of dimethyl 5,6,7,8-tetrahydronaphthalene-2,3-dicarboxylate. The large difference in the ^{13}C NMR chemical shifts for the metallacyclic carbon atoms of **3** [7] suggests a special bonding relationship.

[13] Y. Wakatsuki, K. Aoki, H. Yamazaki, *J. Am. Chem. Soc. 101* (1979) 1123; M. Scozzafava, A. M. Stolzenberg, *Organometallics 7* (1988) 1073; M. E. Howden, R. D. W. Kemmitt, M. D. Schilling, *J. Chem. Soc. Dalton Trans. 1983*, 2459.

An Exception to the Bredt Rule in the Photoenolization of 4-Benzoyl[2.2]paracyclophane **

By *Henning Hopf*,* Thomas Laue*, and *Maximilian Zander**

Dedicated to Professor Siegfried Hünig on the occasion of his 70th birthday

The photoenolization of *ortho*-alkylated benzophenones **1** to *ortho*-quinodimethane derivatives **2** has been known since the work of *Yang* et al. in the early sixties[1] and has been studied by several authors.[2, 3]

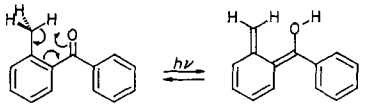

1 **2**

We posed the question whether this photoreaction can be applied to 4-benzoyl-[2.2]paracyclophane (**3a**),[4] which is easily prepared by Friedel-Crafts benzoylation of [2.2]paracyclophane. The resulting *ortho*-quinoid system **4** is a possible intermediate for the construction of [1.2]phanes by Diels–Alder addition. The [1.2]phanes form an unknown group of phanes with extremely short bridges. According to molecular models the C2-C3 double bond, which violates Bredt's rule, is extremely twisted. Nevertheless we could not exclude the formation of this bridgehead olefin during the irradiation of **3a** by a 1,5-migration of the *endo* hydrogen atom R^1 to the keto function, first because we had already observed that the ethano bridges in [2.2]paracyclophanes tolerate drastic deformations (for example, the formation of a triple bond[5]), and second because intramolecular charge-transfer stabilization in **4** by the benzene ring situated opposite was to be expected.

On irradiation of ethanolic solutions of **3a** at 88 K (with light of wavelength 320 nm or with the unfiltered light of a mercury lamp), we observed a pronounced yellow coloration, which was characterized in the low-temperature UV spectrum by a new broad band at 430 nm (half-height width: 5200 cm^{-1}). On slow warming of the irradiated, yellow solid reaction mixture, the color disappeared again and the absorption spectrum of the ketone **3a** was observed. The processes were completely reversible and could be repeated several times on the same solution. To test for the enol **4**, the photoenolization was repeated at $-30\,^{\circ}C$ in [D_4]methanol to which a catalytic amount of [D_3]sodium methanolate had been added. Already after a few seconds the photolysis mixture had assumed its characteristic yellow color, which again paled slowly on melting. An analytically pure sample of the ketone (84%) was recovered from the photolyzed solution by chromatography on silica gel. According to the mass spectrum, this ketone was 36% mono- and 8.5% dideuterated. The sites of deuteration were determined by 400-MHz ^1H NMR spectroscopy. The signals of the protons R^1 (multiplet shifted to lower field, $\delta = 3.33$) and R^2 (multiplet shifted to higher field, $\delta = 2.85$) lie apart from all other signals of the bridge protons (which appear between $\delta = 2.90$ and 3.28). The degree of deuteration was calculated from the reduced signal intensities: ca. 36% for the position R^1 and 24% for R^2. These results may be understood if two H/D exchange mechanisms are postulated, both of which begin with the loss of the hydroxyl proton of **4**. The resulting enolate **6** can then react further with the large excess of deuterated solvent to yield **5**, which equilibrates with the *endo*-deuterated ketone **3b** (stereospecific exchange of R^1 = H with deuterium). Alternatively, **6** can be deuterated at C2 by the solvent. For steric reasons this occurs from the side opposite to the substituents and yields the *exo*-monodeuterated product **8**. Through both exchange processes, which occur with approximately equal probability as the NMR data show, the 2-position is completely deuterated and the product is **7**. In the absence of light no H/D exchange in **3a** takes place even at $60\,^{\circ}C$ and in dimethylsulfoxide, a solvent known to favor this type of exchange.[3]

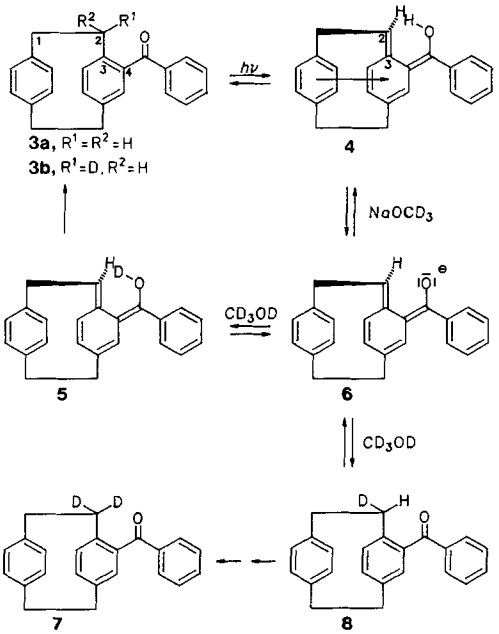

Bridged benzophenones like **3a** are not only of interest because of their reactivity, but may also be used as chiral sensitizers for photoreactions. We have therefore also characterized **3a** by luminescence spectroscopy. The intensity maximum of the broad phosphorescence band (ethanol, 77 K) lies at 19 880 cm^{-1}. Even when the (0,0) transition is taken into account, it should lie $< 22\,200$ cm^{-1} ((0,0) phosphorescence transition of benzophenone: 24 040 cm^{-1}). The average phosphorescence lifetime of **3a** is 128 ms (benzophenone: 5 ms). From this relatively long lifetime, we conclude that the lowest triplet level of **3a** is a $^3\pi,\pi^*$ state. The phosphorescence emission spectrum of **3a** corresponds to the UV absorption spectrum. Compound **3a** does not fluoresce. The most likely explanation is that the $^1n,\pi^*$ and $^3n,\pi^*$ levels, or just the $^3n,\pi^*$ level, lie between the lowest singlet π,π^* and the lowest triplet n,π^* state.[6] Characteristic of compounds with such term diagrams are high quantum yields when the lowest triplet state is occupied. It follows that the application

[*] Prof. Dr. H. Hopf, Dipl.-Chem. T. Laue
Institut für Organische Chemie der Universität
Hagenring 30, W-3300 Braunschweig (FRG)
Prof. Dr. M. Zander
Rütgerswerke AG
Kekuléstrasse 30, W-4620 Castrop-Rauxel (FRG)

[**] Cyclophanes, Part 36. This work was supported by the Fonds der Chemischen Industrie. We thank Mr. *K. Bullik*, Rutgerswerke AG, for the spectroscopic measurements. Part 35: G. J. Bodwell, L. Ernst, H. Hopf, P. G. Jones, J. P. McNally, D. Schomburg, *Chem. Ber. 123* (1990) 2381.

of **3a** as triplet sensitizer in suitable photochemical systems is theoretically possible.[7]

Received: November 15, 1990 [Z 4285 IE]
Publication delayed at author's request.
German version: *Angew. Chem. 103* (1991) 441

CAS Registry numbers:
3a, 10028-97-4; **4**, 132259-72-4.

[1] N. C. Yang, C. Rivas, *J. Amer. Chem. Soc. 83* (1961) 2213.
[2] For a review see D. C. Neckers, *Mechanistic Organic Photochemistry*, Van Nostrand-Reinhold, New York 1967, p. 174ff.
[3] R. Haag, J. Wirz, P. J. Wagner, *Helv. Chim. Acta 60* (1977) 2595.
[4] A. Izuoka, S. Murata, T. Sugawara, H. Iwamura, *J. Am. Chem. Soc. 109* (1987) 2631.
[5] H. Hopf, M. Psiorz, *Angew. Chem. 94* (1982) 639; *Angew. Chem. Int. Ed. Engl. 21* (1982) 623.
[6] For a review see M. Zander, *Fluorimetrie*, Springer, Heidelberg 1981, p. 28ff.
[7] N. J. Turro, *Modern Molecular Photochemistry*, Benjamin/Cummings, Menlo Park 1978, p. 351ff.

Triaurated Phosphonium Cations $[RP(AuPPh)_3]^{\oplus}$ and the Electron-deficient, Hypercoordinated Phosphonium Dication $[P(AuPPh_3)_5]^{2\oplus}$ **

By *Hubert Schmidbaur,* Gabriele Weidenhiller,* and *Oliver Steigelmann*

Complex compounds of monovalent gold tend to display *intra-* and *inter*molecular Au···Au interactions.[1] This is especially noticeable in the aggregation of gold atoms around heteroatoms to give novel centered gold clusters. Thus, not only could species of the type $[RC(AuL)_3]$,[2] $[RN(AuL)_3]^{\oplus}$,[3,4] and $[N(AuL)_4]^{\oplus}$[5] with classical four-coordination of carbon or oxygen (L = tertiary phosphane) be synthesized, but also the hypercoordinated cations $[RC(AuL)_4]^{\oplus}$,[6] $[C(AuL)_5]^{\oplus}$[7] and $[C(AuL)_6]^{2\oplus}$,[8] and $[N(AuL)_5]^{2\oplus}$,[9] but not $[N(AuL)_6]^{3\oplus}$.[10] The results allowed to correct literature inconsistencies[11], confirmed predictions based on MO considerations,[12] and could be placed on a sounder theoretical footing by new calculations taking into account relativistic effects.[13,14] Our studies were now also extended to *phosphorus*-centered gold clusters. After preliminary investigations on mono- and dinuclear gold complexes of tertiary,[11] secondary[15] and finally primary phosphanes,[16] the latter were now also triply aurated. Similarly as in the case of primary amines, this was achieved especially easily by reaction with tris(triphenyl phosphanegold(I))oxonium tetrafluoroborate **1**[17] at room temperature in tetrahydrofuran. The best results were obtained with arylphosphanes, but even there the yields were only moderate.

$$\underset{\mathbf{1}}{RPH_2} + [(Ph_3PAu)_3O]\,BF_4 \longrightarrow \underset{\mathbf{2}}{[RP(AuPPh_3)_3]\,BF_4} + H_2O$$

The complex **2a** (R = *o*-tolyl), obtained in 29% yield from *ortho*-tolylphosphane, crystallizes in the form of colorless needles (m.p. 183–186 °C, decomp) from a mixture of tetrahydrofuran, diethyl ether, and dichloromethane, and is readily identifiable by analytical data and NMR spectra.[18] In the case of the analogue **2b** (R = Ph) the yield and thermal stability are significantly lower. The very similar spectroscopic data, however, reveal a close structural relationship.

The ^{31}P-NMR spectra of **2a** at −70 °C show the expected doublet/quartet multiplicity of the signals (δ = 46.0(d), −19.0 (q, J_{PP} = 249 Hz)); at higher temperature, signal broadening with disappearance of coupling occurs. This is attributed to exchange processes in which presumably $LAu^{\oplus}$ and not L units are involved.

The X-ray structure analysis of **2a**[18] confirms the presence of organo(triaurio)phosphonium cations and tetrafluoroborate anions. The triclinic unit cell (space group $P\bar{1}$) contains two formular units, which are related to each other via a center of symmetry. The most important features are the small deviation of the Au-P-Au angle (average 106°) from ideal tetrahedral geometry and the associated long Au···Au contacts of ca. 3.7 Å (Fig. 1), i.e. the dimensions of the

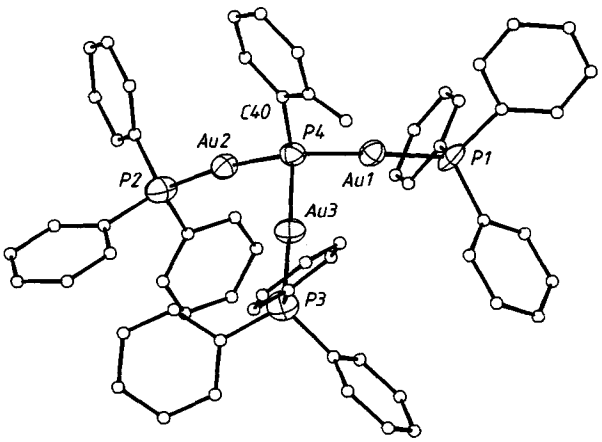

Fig. 1. Structure of the cation in **2a** in the crystal (ORTEP, thermal ellipsoids at the 50% probabiity level; C atoms with arbitrary radii, H atoms omitted; of the two possible positions of the methyl group of the disorded *o*-tolyl moiety only one is shown.)—Selected bond lengths [Å] and angles [°]: Au1-P1 2.315(8), Au2-P2 2.288(8), Au3-P3 2.280(9), Au1-P4 2.277(7), Au2-P4 2.317(8), Au3-P4 2.321(8); Au1-Au2 3.709, Au1-Au3 3.696, Au2-Au3 3.639; P1-Au1-P4 176.4(3), P2-Au2-P4 172.3(3), P3-Au3-P4 176.4(3); Au1-P4-Au2 107.7(3), Au1-P4-Au3 107.0(3), Au2-P4-Au3 103.3(3), Au1-P4-C40 114.7(7), Au1-P4-C40 113.7(9), Au3-P4-C40 109.6(9).

cations $[RP(AuL)_3]^{\oplus}$ differ significantly from those of the cations $[RN(AuL)_3]^{\oplus}$, where markedly smaller Au-N-Au angles (ca. 102°) and correspondingly short Au···Au contacts (ca. 3.1 Å) are found.[3,4] Apparently, the peripheral gold–gold distances are so large, due to the much larger radius of the phosphorus atom compared to that of nitrogen, that no noteworthy energy contributions to the stabilization of the cluster can result from direct metal–metal interactions. At least they do not suffice to induce a drastic distortion of the tetrahedral framework. The same also holds true in the case of diauriophosphonium salts.[19] Only an increase in the number of the polyhedral corners, e.g. from four to five, could lead to a convergence of the metal atoms.

All earlier attempts[20] to carry out tri- or tetraauration of PH_3 or its trimethylsilyl derivative $P(SiMe_3)_3$[21] failed at

[*] Prof. Dr. H. Schmidbaur, Dipl.-Chem. G. Weidenhiller, Dipl.-Chem. O. Steigelmann[+]
Anorganisch-chemisches Institut der Technischen Universität München
Lichtenbergstrasse 4, W-8046 Garching (FRG)

[+] X-ray structure analysis.

[**] This work was supported by the Deutsche Forschungsgemeinschaft (Leibniz Program), the Fonds der Chemischen Industrie, Hoechst AG, Degussa AG, and Heraeus GmbH. The authors thank *J. Riede* and *H. Beruda* for assistance with the structure determination and Dr. *Kreissl* for the mass spectra.

first. With stoichiometric amounts of reaction partners decomposition always took place. The poor stability of triauriophosphanes $P(AuL)_3$ and tetraauriophosphonium cations $(P(AuL)_4^{\oplus}$ is remarkable and has a parallel in the non-existence of the tetraauriomethanes and triauricamines,[1] but not of the tetraaurioammonium salts.[5]

With sufficient supply of **1**, however, the $P(AuPPh_3)_4^{\oplus}$ cation can be stabilized by formation of the novel dication in **3** with a *five*-coordinate, electron-deficient central phosphorus atom.

$$\underset{\mathbf{1}}{[(Ph_3PAu)_3O]BF_4} \xrightarrow[-(Me_3Si)_2O]{P(SiMe_3)_3} \underset{\mathbf{3}}{[(Ph_3PAu)_5P](BF_4)_2}$$

3 can be precipitated from the yellow reaction mixture with diethyl ether and isolated from dichloromethane/pentane in the form of light-brown, air-stable crystals. The yields are below 10%, so that a commitment to a stoichiometry of an equation is not really justified. The by-product hexamethyldisiloxane is, however, unequivocally detectable in the reaction mixture by GC/MS analysis.

A first indication of the composition of **3** was provided by field desorption mass spectrometry: the (half) mass of the intact dication is observed at $m/z = 2327.4/2 = 1163.7$ (100%). Further high-intensity peaks at $m/z = 721.0$ (83%) and 262.1 (71%, from CH_2Cl_2) are assignable to $[(Ph_3P)_2Au]^{\oplus}$ and $[PPh_3]^{\oplus}$, respectively. Since no crystals suitable for an X-ray diffraction analysis could be obtained, low-temperature $^{31}P\{^1H\}$-NMR spectroscopy played the key role in the elucidation of the structure: at $-75\,^{\circ}C$, solutions of **3** in CD_2Cl_2 show a doublet ($\delta = 39.6$) and a sextet ($\delta = 122$, $^2J_{PP} = 186$ Hz) in the area ratio 5:1, thus demonstrating that a highly coordinated central phosphorus atom (recognizable by a marked upfield shift) is surrounded by five equivalent $AuPPh_3$ groups. The coupling constant is reduced significantly compared to that in **2a** ($^2J_{PP} = 249$ Hz), and thus is consistent with the diminished *s*-character of the orbitals of the central atom (sp^3 vs. sp^3d). On the basis of the structurally characterized C- and N-analogues a trigonal-bipyramidal structure, which apparently is fluctional in solution, is proposed for the dication (Fig. 2). The exchange processes are intramolecular, as recognizable by the persistence of the $^2J_{PP}$ coupling. The bonding situation can be described in terms of an MO scheme in which, under the point group D_{3h}, four strongly bonding states can be occupied by the available eight valence electrons to give a diamagnetic ground state.[7, 12] More recent relativistic calculations also indicate a dominance of these radial bonds if the radius of the central atom is larger.[13, 14] The bond order for each of the five central Au–P bonds is 4/5.

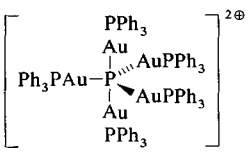

Fig. 2. Structure proposed for the dication in **3**.

Finally, it should be mentioned that electron-deficient, pentacoordinated phosphorus atoms have recently also been found in copper- and gold/platinum-clusters, so that this type of bonding is more common than was hitherto assumed.[22]

Experimental

2a: A suspension of **1** (0.90 g, 0.61 mmol) in tetrahydrofuran was treated dropwise with stirring with a solution of *o*-tolylphosphane (0.08 g, 0.61 mmol) in THF (10 mL). The color of the mixture changed to yellow and then to brown. After 20 min, the mixture was filtered and the residue recrystallized, first from CH_2Cl_2/Et_2O and then, for the isolation of single crystals, from CH_2Cl_2/THF/Et_2O. Yield 0.28 g (29%), m.p. 183–186 °C (decomp.), correct elemental analysis. ^1H NMR (CD_2Cl_2): $\delta = 2.91$ (s, 3H, CH_3), 7.11–7.25 and 8.23–8.30 (m, 4H, C_6H_4), 7.37–7.56 (m, 45H, C_6H_5); $^{31}P\{^1H\}$NMR (CD_2Cl_2, −70 °C): $\delta = 45.4$ (d, $^2J(PP) = 249$ Hz, PPh_3), −19.0 (q, PAu_3); at room temperature: $\delta = 46.0$ (br), −19.1 (br). − **2b** was prepared analogously. $^{31}P\{^1H\}$NMR (CD_2Cl_2, −70 °C): $\delta = 46.1$ (PPh_3), −4.6 (br, $^2J(PP) = 260$ Hz, PAu_3).

3: A suspension of **1** (1.10 g, 0.74 mmol) in THF (25 mL) was treated dropwise with stirring at −50 °C with a solution of $P(SiMe_3)_3$ (0.11 g, 0.57 mmol) in THF (20 mL). A yellow solution formed, from which a yellow precipitate of unknown composition was obtained 90 min after addition of 100 mL of Et_2O. Upon addition of a further 80 mL of Et_2O to the orange filtrate at −30 °C a light-brown precipitate was formed; this was recrystallized from CH_2Cl_2/pentane (1:1); yield 5–10%; air-stable, slow decomposition upon heating.

Received: November 9, 1990 [Z 4272 IE]
German version: *Angew. Chem. 103* (1991) 442

CAS Registry numbers:
1, 53317-87-6; **2a**, 132157-62-1; **2b**, 132157-66-5; **3**, 132157-64-3; *o*-TolPH$_2$, 53772-59-1; $PhPH_2$, 638-21-1; $P(SiMe_3)_3$, 15573-38-3.

[1] H. Schmidbaur, *Gold Bull. 23* (1990) 11; P. G. Jones, *ibid. 14* (1981) 102, 159; *ibid. 16* (1983) 114; *ibid. 19* (1986) 46.
[2] H. Schmidbaur, F. Scherbaum, B. Huber, G. Müller, *Angew. Chem. 100* (1988) 441; *Angew. Chem. Int. Ed. Engl. 27* (1988) 419.
[3] V. Ramamoorthy, P. R. Sharp, *Inorg. Chem. 29* (1990) 3336.
[4] A. Grohmann, J. Riede, H. Schmidbaur, *J. Chem. Soc. Dalton Trans.*, in press.
[5] Y. L. Slovokhotov, Y. T. Struchkov, *J. Organomet. Chem. 277* (1984) 143. See also A. Kolb, *Diplomarbeit*, Technische Universität München 1990, P. Bissinger, *Diplomarbeit*, TU München 1990 sowie A. Brodbeck, *Dissertation*, Universität Tübingen 1990.
[6] F. Scherbaum, B. Huber, G. Müller, H. Schmidbaur, *Angew. Chem. 100* (1988) 1600; *Angew. Chem. Int. Ed. Engl. 27* (1988) 1542.
[7] F. Scherbaum, A. Grohmann, G. Müller, H. Schmidbaur, *Angew. Chem. 101* (1989) 464; *Angew. Chem. Int. Ed. Engl. 28* (1989) 463.
[8] F. Scherbaum, A. Grohmann, B. Huber, C. Krüger, H. Schmidbaur, *Angew. Chem. 100* (1988) 1602; *Angew. Chem. Int. Ed. Engl. 27* (1988) 1544.
[9] A. Grohmann, J. Riede, H. Schmidbaur, *Nature (London) 345* (1990) 140.
[10] Relevant reports (A. Brodbeck, *Dissertation*, Universität Tübingen 1990; A. Brodbeck, J. Strähle, *Acta Crystallogr. Sect. A Found. Crystallogr. A 46* (1990) C-232) do not seem to be confirmatory: checking of the X-ray crystallographic data showed us that presumably the C-centered cluster has been the subject of these studies too.
[11] P. L. Bellon, F. Cariati, M. Manaserro, L. Naldini, M. Sansoni, *Chem. Commun. 1971*, 1423; P. L. Bellon, M. Manaserro, M. Sansoni, *J. Chem. Soc. Chem. Commun. 1972*, 1035.
[12] D. M. P. Mingos, *J. Chem. Soc. Dalton Trans. 1976*, 1163; *Gold Bull. 17* (1984) 5; K. P. Hall, D. M. P. Mingos, *Prog. Inorg. Chem. 32* (1984) 237; D. G. Evans, D. M. P. Mingos, *J. Organomet. Chem. 232* (1982) 171.
[13] N. Rösch, A. Görling, D. E. Ellis, H. Schmidbaur, *Angew. Chem. 101* (1989) 1410; *Angew. Chem. Int. Ed. Engl. 28* (1989) 1357.
[14] P. Pyykkö, *Chem. Rev. 88* (1988) 563; P. Pyykkö, Y. Zhao, *Chem. Phys. Lett. 177* (1991) 103.
[15] D. B. Dyson, R. V. Parish, C. A. McAuliffe, R. G. Pritchard, R. Fields, B. Beagley, *J. Chem. Soc. Dalton Trans. 1989*, 907; H. Schmidbaur, G. Weidenhiller, A. A. M. Aly, O. Steigelmann, *Z. Naturforsch. B 44* (1989) 1503.
[16] H. Schmidbaur, G. Weidenhiller, O. Steigelmann, G. Müller, *Chem. Ber. 123* (1990) 285; *Z. Naturforsch. B 45* (1990) 747.
[17] A. N. Nesmeyanov, E. G. Perevalova, Yu. T. Struchkov, M. Yu. Antipin, K. I. Grandberg, V. P. Dyadchenko, *J. Organomet. Chem. 201* (1980) 343.
[18] **2a**: $C_{61}H_{52}Au_3BF_4P_4$, $M_r = 1586.7$, triclinic, space group $P\bar{1}$, $a = 13.341(3)$, $b = 15.363(3)$, $c = 16.369(3)$ Å, $\alpha = 107.88(2)$, $\beta = 98.17(2)$, $\gamma = 103.02(2)^{\circ}$, $V = 3027.8$ Å^3, $Z = 2$, $\delta_{calcd} = 1.740$ g cm^{-3}, Syntex $P2_1$ diffractometer, $Mo_{K\alpha}$ radiation, $\lambda = 0.71069$ Å, $\mu(Mo_{K\alpha}) = 73.8$ cm^{-1}, $T = 24\,^{\circ}C$, 9431 independent reflections, 5407 "observed" with $F_o \geq$

$4\sigma(F_o)$, empirical absorption correction ($T = 0.33-1.00$). Solution by direct methods (SHELXS-86), $R(R_w) = 0.091(0.083)$ for 212 refined parameters (Au, P anisotropic, Ph in idealized geometry isotropic, Me–C as split model (SOF 0.5:0.5) for both *ortho* positions, $BF_4^{\ominus}$ refined as idealized tetrahedron in the region of highest electron density, $\Delta\varrho_{fin}$ (max/min) = + 3.07/−2.93 Å^3). Further details of the crystal structure investigation are available on request from the Fachinformationszentrum Karlsruhe, W-7514 Eggenstein-Leopoldshafen 2 (FRG), on quoting the depository number CSD-55096, the names of the authors, and the journal citation.

[19] R. G. Pritchard, D. B. Dyson, R. V. Parish, C. A. McAuliffe, B. Beagley, *J. Chem. Soc. Chem. Commun. 1987*, 371.

[20] W. Kress, *Dissertation*, Universität Erlangen-Nürnberg 1983; K.-D. Schröter, *Dissertation*, Universität Erlangen-Nürnberg 1976.

[21] H. Schumann, L. Rösch, *Chem. Ber. 107* (1974) 854.

[22] G. Hessler, P. C. Knüppel, O. Stelzer, W. S. Sheldrick, *Chem. Ber. 123* (1990) 653 and references cited therein; R. Bender, P. Braunstein, A. Dedieu, Y. Dusansoy, *Angew. Chem. 101* (1989) 931; *Angew. Chem. Int. Ed. Engl. 27* (1989) 923, and references cited therein.

$[Cp_2^*La(thf)(\mu\text{-}\eta^1,\eta^3\text{-}C_4H_6)LaCp_2^*]$: Synthesis and Structure of a Butadiene-Lanthanoid Complex**

By *Annett Scholz, Astrid Smola, Joachim Scholz, Jörg Loebel, Herbert Schumann,* and *Karl-Heinz Thiele**

One reason for the increased interest in organolanthanoid compounds is that they frequently show high activity in the polymerization and hydrogenation of olefins.[1] The structural characterization of some olefin[2] and hydride complexes[3] of the lanthanoids and investigations related to the suitability of organolanthanoid compounds in the activation of C–H bonds[4] help to interpret important elementary steps of the complex reactions of homogeneously catalyzed olefin polymerization and olefin hydrogenation.[5] In this connection dienelanthanoid complexes are also of interest as model compounds; however, their synthesis was hitherto limited merely to the co-condensation of diene molecules and lanthanoid atoms in a metal-vapor reactor[6a] or to the reaction of lanthanoids with dienes in the presence of iodine or 1,2-diiodoethane.[6, bc] By using "magnesium(butadiene)"[7] as diene source we have now succeeded in preparing a dinuclear lanthanumbutadiene complex, whose X-ray structure analysis shows a novel type of bonding of a diene molecule to two metal atoms. To our knowledge this is the first structurally characterized butadienelanthanoid complex.

$[Cp_2^*La(\mu\text{-}Cl)_2K(dme)_2]$ **1**[8] (dme = 1,2-dimethoxyethane), dissolved in THF, reacts according to Equation (a) with "magnesiumbutadiene" in strict absence of air and moisture to give the dinuclear complex **2**, which, after recrystallization from pentane, precipitates as brilliant red crystals in ca. 10% yield.

$$2[Cp_2^*La(\mu\text{-}Cl)_2K(dme)_2] + [Mg(C_4H_6)(thf)_2] \xrightarrow[-MgCl_2,\ -2KCl]{} [Cp_2^*La(\mu\text{-}\eta^1,\eta^3\text{-}C_4H_6)LaCp_2^*(thf)] \quad (a)$$

1 → **2**

[*] Prof. Dr. K.-H. Thiele, Dipl.-Chem. A. Scholz, Dr. A. Smola, Dr. J. Scholz
Technische Hochschule, Sektion Chemie
Otto-Nuschke-Strasse, O-4200 Merseburg (FRG)
Prof. Dr. H. Schumann, Dipl.-Chem. J. Loebel
Institut für Anorganische und Analytische Chemie
der Technischen Universität
Strasse des 17. Juni 135, W-1000 Berlin 12 (FRG)

[**] This work was supported by the Fonds der Chemischen Industrie.
$Cp^* = \eta^5\text{-}C_5Me_5$.

2 is readily soluble in the usual aromatic and aliphatic hydrocarbons and ethers, and, with a decomposition temperature of ca. 200 °C, is markedly stable towards heat. Upon exposure to air, butadiene is immediately liberated. Protolytically active agents lead to formation of 1-butene as well as *cis*- and *trans*-2-butene.

The observation of four signals in the ^{13}C-NMR spectrum[9] suggests an unsymmetrical charge distribution in the diene, i.e. a different participation in the bonding to the two La atoms is to be expected for each of the carbon atoms. A bond behavior as is characteristic, for example, for diene complexes of electron-deficient transition metals[10] may therefore be ruled out.

An X-ray structure analysis of **2** (Fig. 1)[11] confirmed this assumption. One La atom is located at the midpoint of each of the two different coordination polyhedra. The two metal centers are bridged by a *cis*-configurated butadiene unit: C42, C43 and C44 are η^3-coordinated to La1 with formation of an allyl system, while the terminal C41 is σ-bonded to the second Cp_2^*La unit. The bond parameters of the allyl system

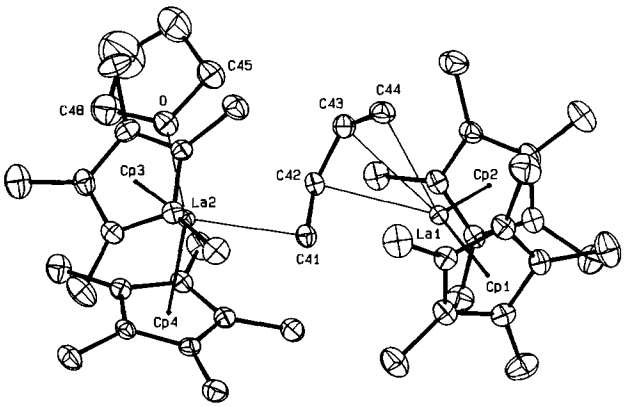

Fig. 1. Structure of **2** in the crystal: Selected bond lengths [pm] and angles [°]: La1-C41 289.4(4), La1-C42 273.4(4), La1-C43 275.9(4), La1-C44 268.8(4), La2-C41 263.3(4), La2-C42 284.2(4), La2-O 263.7(3), La1-Cp*1 258.6(1), La1-Cp*2 261.1(2), La2-Cp*3 255.7(2), La2-Cp*4 257.0(2), C41-C42 146.3(5), C42-C43 139.2(6), C43-C44 140.6(6); Cp*1-La1-Cp*2 129.56(5), Cp*3-La2-Cp*4 134.25(5), C41-C42-C43 126.2(4), C42-C43-C44 126.8(4), C41-C42-C43-C44 15.3(7), (Cp*1-La1-Cp*2)(Cp*3-La2-Cp*4) 88.00(4). Cp*1(C1-C5), Cp*2(C11-C15), Cp*3(C21-C25), and Cp*4(C31-C35) are the positions of the centroid of the carbon atoms given in the brackets.

C42–C43–C44, which formally require two coordination sites of La1, are comparable with those of other π-allyl complexes;[12] the La2–C41 distance is 263.3(4) pm and thus corresponds to a "normal" La–C σ-bond (e.g. Cp*La-$[CH(SiMe_3)_2]_2$: La–C 265.1(8) pm and 262.7(10) pm[13]). It seems remarkable that, despite this bond differentiation, the four C atoms deviate only slightly from the plane (torsional angle C41–C42–C43–C44: 15.3(7)°).

La2 is coordinatively saturated by a THF molecule. Nevertheless, the steric crowding of La1 by the allyl system is greater, as manifested in the small Cp*1-La1-Cp_2^* angle of 129.55(5)° (Cp*3-La2-Cp*4: 134.25(5)°) and large Cp*–La1 distances of 258.6(1) and 261.1(1) pm (La2–Cp*: 255.7(2) and 257.0(2) pm). Also worth mentioning is the sterically enforced staggering of the two Cp_2^*La units—the metallocene planes are oriented at almost 90° to each other (Cp*1, La1, Cp*2)(Cp*3, La2, Cp*4) = 88.00(4)°.

Surprisingly, the NMR spectra of **2** at room temperature do not reflect the different coordination of La1 and La2. The

methyl groups of all four Cp* ligands give rise to one sharp signal in the ^{1}H-NMR spectrum ([D]$_8$THF) at 25 °C.[9] However, it was possible to slow down the dynamic exchange process, which simulates the equivalence of the Cp* ligands, to such an extent that this signal splits into three singlets at $\delta = 1.95$, 1.91, and 1.85 at -80 °C.

The mode of coordination of the butadiene remains unaltered in solution and gives rise to a characteristic signal pattern for the allyl system C42–C43–C44 in the ^{1}H-NMR spectrum.[9]

For a $Cp^*_2La^{III}$ complex, the intense red color of **2** is unusual. Possibly, this points to a partial ionic character of the bonds, as is typical of organolanthanoid complexes.[14]

Experimental Procedure

$LaCl_3$ (2.83 g, 11.0 mmol) was added portionwise to a suspension of 6.10 (23.00 mmol) of [C_5Me_5K(dme)] in 150 mL of THF at room temperature. The reaction mixture was then stirred for 6 d, and, after cooling to -78 °C, treated with 1.28 g (5.0 mmol) of "butadienemagnesium". The resulting brilliant red reaction solution was warmed to room temperature and stirred for several hours before removing the solvent in a vacuum. The residue was extracted with 100 mL of pentane. Upon cooling the extract to -30 °C, 1.30 g (11%) of brilliant red crystals of **2** could be isolated. Corect C,H,La analysis, m.p. 215 °C (decomp.).

Received: September 11, 1990 [Z 4176 IE]
German version: *Angew. Chem. 103* (1991) 444

CAS Registry numbers:
1, 101933-10-2; **2**, 132409-18-8; $Mg(C_4H_6)(thf)_2$, 83995-88-4; C_5Me_5K·DME, 132409-19-9; $LaCl_3$, 10099-58-8; *cis*-2-Butene, 590-18-1; *trans*-2-Butene, 624-64-6.

[1] a) H. Mauermann, P. N. Swepston, T. J. Marks, *Organometallics 4* (1985) 200; b) G. Jeske, H. Lauke, H. Mauermann, P. N. Swepston, H. Schumann, T. J. Marks, *J. Am. Chem. Soc. 107* (1985) 8091; c) G. Jeske, L. E. Schock, P. N. Swepston, H. Schumann, T. J. Marks, *ibid. 107* (1985) 8103; d) G. Jeske, H. Lauke, H. Mauermann, H. Schumann, T. J. Marks, *ibid. 107* (1985) 8111.

[2] a) W. J. Evans, T. A. Ulibarri, J. W. Ziller, *J. Am. Chem. Soc. 112* (1990) 219; b) C. J. Burns, R. A. Andersen, *ibid. 109* (1987) 915.

[3] a) W. J. Evans, J. H. Meadows, A. L. Wayda, W. E. Hunter, J. L. Atwood, *J. Am. Chem. Soc. 104* (1982) 2008; b) W. J. Evans, I. Bloom, W. E. Hunter, J. L. Atwood, *ibid. 105* (1983) 1401; c) W. J. Evans, D. K. Drummond, T. P. Hanusa, R. J. Doedeus, *Organometallics 6* (1987) 2279.

[4] a) W. J. Evans, L. R. Chamberlain, T. A. Ulibarri, J. W. Ziller, *J. Am. Chem. Soc. 110* (1988) 6423; b) P. L. Watson, *ibid. 105* (1983) 6491; c) P. L. Watson, *J. Chem. Soc. Chem. Commun. 1983*, 276.

[5] a) P. L. Watson, *J. Am. Chem. Soc. 104* (1982) 337; b) P. L. Watson, G. W. Parshall, *Acc. Chem. Res. 18* (1985) 51.

[6] a) W. J. Evans, S. S. Engerer, A. C. Neville, *J. Am. Chem. Soc. 100* (1978) 331; b) L. Saussine, H. Olivier, D. Commereuc, Y. Chauvin, *New J. Chem. 12* (1988) 13; c) K. Mashima, H. Takaya, *Tetrahedron Lett. 30* (1989) 3697.

[7] K. Fujita, Y. Ohnuma, H. Yasuda, H. Tani, *J. Organomet. Chem. 113* (1976) 201.

[8] H. Schumann, I. Albrecht, J. Loebel, E. Hahn, M. Bilayet Hossain, D. van der Helm, *Organometallics 5* (1986) 1296.

[9] ^{1}H NMR (200 MHz, [D_8] THF, 25 °C, TMS, J in Hz): $\delta = 5.71$ (m, ^3JH$_m$-H$'_{s,s'}$ = 11.1, ^3JH$_m$-H$_a$ = 14.8, H 43$_{meso}$), 3.87 (m, ^3JH$_{s'}$-H$_{CH2}$ = 6.8, ^3JH$_{s'}$-H$'_{CH2}$ = 15.4, H 42$_{syn}$), 2.96 (m, ^2JH$_a$-H$_s$ = 5.5, H 44$_{anti}$), 1.48 (dd, H 41), 0.82 (dd, H 41), H 44$_{syn}$-signal superimposed by C_5Me_5 signal, 1.91 (s, C_5Me_5), 3.57 (OCH_2, THF), 1.71 (OCH$_2$CH_2), THF); ^{13}C NMR (50.3 MHz, [D_8] THF, 25 °C, TMS): $\delta = 146.23$ (C 43), 117.36 (C_5Me$_5$), 86.93 (C 42), 72.74 (C 44), 68.22 (OCH$_2$, THF), 52.68 (C 41), 26.36 (OCH$_2$CH$_2$, THF), 11.87 (C_5Me_5) Labeling of H and C atoms same as in the X-ray structure analysis.

[10] a) G. Erker, C. Krüger, G. Müller, *Adv. Organomet. Chem. 24* (1985) 1; b) H. Yasuda, A. Nakamura, *Angew. Chem. 99* (1987) 745; *Angew. Chem. Int. Ed. Engl. 26* (1987) 723.

[11] Crystal structure analysis: Enraf-Nonius CAD4 diffractometer. Mo$_{K\alpha}$ radiation, graphite monochromator, $T = 138(5)$ K, monoclinic: $a = 1066.2(6)$, $b = 2119.6(5)$, $c = 2050.7(9)$ pm, $\beta = 103.74(5)°$, $V = 4502 \times 10^{-30}$ m^3, $Z = 4$, $\varrho_{calcd} = 1.394$ cm^{-3}, μ (Mo$_{K\alpha}$) = 19.1 cm^{-1}, crystal dimensions $0.30 \times 0.24 \times 0.19$ mm^3, ω/θ scan, $2\theta_{max} = 50°$, 7394 independent reflections, $R(R_w) = 0.0285$ (0.0351) for 6643 reflections with $F_o \geq 4\sigma(F_o)$, empirical absorption correction, SHELX 76 computer program, Patterson Methods, all non-hydrogen atoms refined with anisotropic temperature factors. H atoms of the butadienediyl group refined isotropically, other H positions calculated.—Further details of the crystal structure investigation are available on request from the Fachinformationszentrum Karlsruhe, Gesellschaft für wissenschaftlich-technische Information mbH, W-7514 Eggenstein-Leopoldshafen 2 (FRG), on quoting the depository number CSD-54908, the names of the authors, and the journal citation.

[12] a) W. J. Evans, T. A. Ulibarri, J. W. Ziller, *J. Am. Chem. Soc. 112* (1990) 2314; b) G. Wilkinson, F. G. A. Stone, E. W. Abel (Eds.): *Comprehensive Organometallic Chemistry*, Pergamon, Oxford 1982, Chap. 37–39.

[13] H. van der Heijden, C. J. Schaverien, A. G. Orpen, *Organometallics 8* (1989) 255.

[14] K. N. Raymond, C. W. Eigenbrodt, Jr., *Acc. Chem. Res. 13* (1980) 276.

Hexaspiro[3.0.3.0.3.0.3.0.3.0.3.0]tetracosane ([6.4]Rotane)**

By *Lutz Fitjer,* Karl Justus, Peter Puder, Martin Dittmer, Carla Hassler,* and *Mathias Noltemeyer**

Fully substituted cyclohexanes are characterized by a frequent occurrence of anomalies in structure, conformation and dynamics.[1] Examples are the hexaspiranes **1**,[1a] **2**,[1c] and **3**[1e] in which a stepwise reduction of alternations, which are determined by different ring sizes, leads to a change from a chair/twist boat equilibrium in the case of **1** to a chair conformation in the case of **2** and **3** and to a precipitous rise in the inversion barriers (chair-chair) (**1**: $\Delta G^{\ddagger}_{298(c/c)} = 92.0$ kJmol^{-1},[1a] **2**: $\Delta G^{\ddagger}_{333(c/c)} = 112.1$ kJmol^{-1},[1e] **3**: $\Delta G^{\ddagger}_{423(c/c)} = 136.0$ kJmol^{-1}[1e]). It was therefore to be expected that the [6.4]rotane **4**, which is free from alternations, exists in a chair conformation and has the highest inversion barrier of all cyclohexanes known so far.[2]

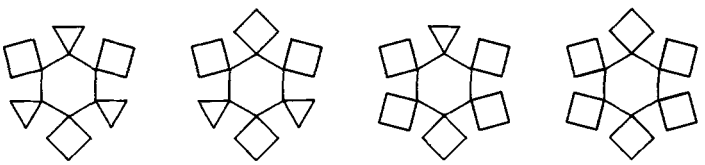

1 **2** **3** **4**

In a model attempt to synthesize **4** the tetraspiroketone **5**[3] was converted, via a cyclopropylcarbene–cyclobutene rearrangement[4] as key step (**10** → **11**), into [5.4]rotane **12**. The spiroketone **5** was then homolyzed to **13**, which was subjected to the same reaction sequence as was used for the preparation of **12**.[5]

For the experimental realization **5** and **13** were methylenated (5 and 10 molar equivalents, 20 and 60 h respectively, at 130 °C) and the products **6** (liq)[6] and **14**[1e] (Scheme 1) converted by copper-catalyzed decomposition of methyl diazo-

[*] Prof. Dr. L. Fitjer, Dipl.-Chem. K. Justus, Dipl.-Chem. P. Puder, Dr. M. Dittmer, Dipl.-Chem. C. Hassler
Institut für Organische Chemie der Universität
Tammannstrasse 2, W-3400 Göttingen (FRG)
Dr. M. Noltemeyer
Institut für Anorganische Chemie der Universität
Tammannstrasse 4, W-3400 Göttingen (FRG)

[**] Polyspiranes, Part 20. This work was supported by the Deutsche Forschungsgemeinschaft and the Fonds der Chemischen Industrie. Part 19: L. Fitjer, A. Kanschik, M. Majewski, *NATO Adv. Study Inst. Ser. C 273* (1989) 431.

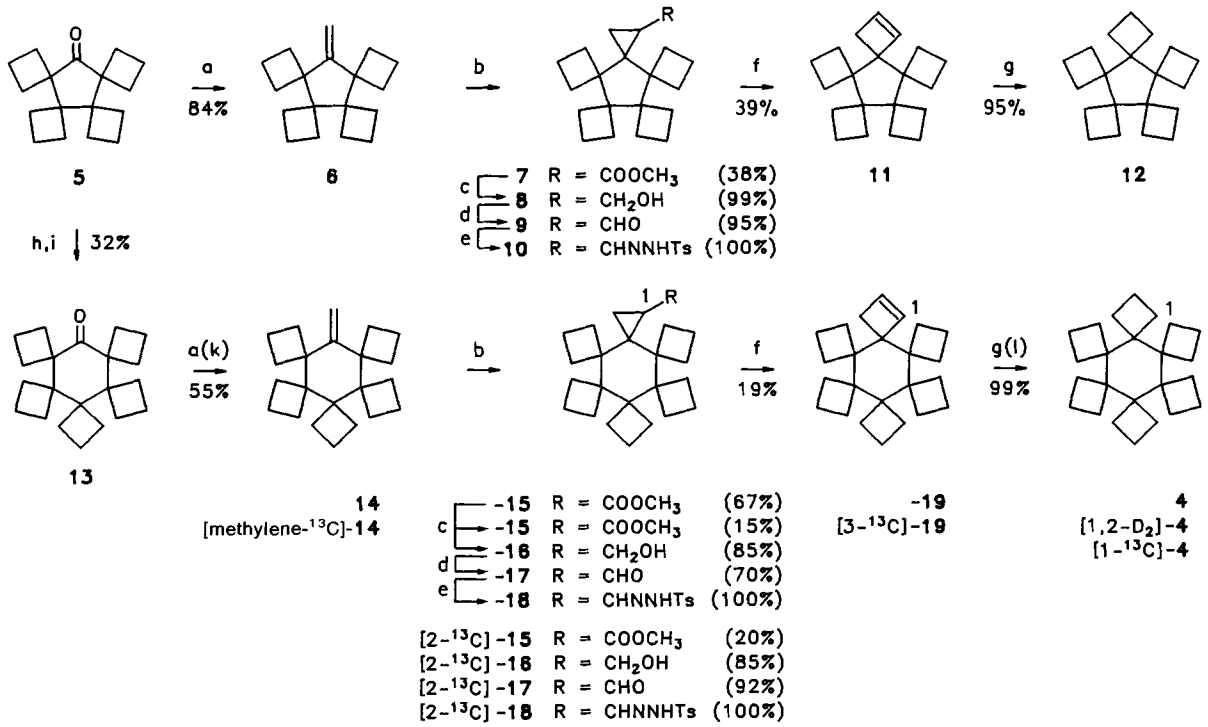

Scheme 1. (a) $Ph_3P{=}CH_2$, (b) $N_2CHCOOCH_3$/Cu, (c) $LiAlH_4$, (d) $(COCl)_2$/DMSO/NEt_3, (e) $TsNHNH_2$/NEt_3, (f) CH_3ONa, (g) H_2/Pd/C, (h) c-C_4H_6(Li)$SeCH_3$, (i) $AgBF_4/Al_2O3$, (k) $Ph_3P = [^{13}C]H_2$, (l) D_2/Pd/C. Formulas designated with primed numbers have C1 in the axial position referred to the central six-membered ring, in the case of those without a prime C1 is equatorial.

acetate (4 and 10 molar equivalents respectively at 110 °C) into the cyclopropanecarboxylates. This resulted in the formation of the pentaspirane **7** (m.p. 65 °C)[6] and the conformationally isomeric hexaspiranes **15** (m.p. 130–134 °C)[6, 7] and **15′** (m.p. 147–151 °C),[6, 7] of which, after chromatographic separation, only the excess conformer was used for further reaction. Reduction with lithium aluminum hydride afforded the alcohols **8** (m.p. 49 °C)[6] and **16** (m.p. 135–185 °C),[6] respectively, while oxidation with dimethyl sulfoxide/oxalyl chloride/triethylamine[8] furnished the aldehydes **9** (oil)[6] and **17** (oil),[6] respectively. Reaction with tosyl hydrazide in dichloromethane/triethylamine[9] and heating of the crude hydrazones **10** and **18** for a short time with sodium methoxide in diethylene glycol dimethyl ether (5 min at 135 °C) led to the cyclobutenes **11** (m.p. 105 °C)[6] and **19** (m.p. 175–188 °C),[6] respectively. Hydrogenation over palladium/carbon in pentane afforded the desired compounds [5,4]rotane **12** (m.p. 70–110 °C)[6] and [6.4]rotane **4** (m.p. 274 °C),[6] respectively; deuteration of **19** yielded [1,2-D_2]-**4**.[10]

The structures of the new rotanes follow from their ^{13}C-NMR spectra. **12** (δ = 16.78, 27.40, 55.30) shows three resonances for a planar species or a species rapidly inverting at room temperature (effective symmetry D_{5h}); in contrast, **4** shows four resonances for a fixed chair conformation (D_{3d} symmetry) at room temperature. **4** is present in the chair conformation, even in the crystal,[11] and has an inversion center. The cyclobutane rings show interesting anomalies: they are staggered almost ideally (dihedral angles 48.1–49.9°), are approximately planar (dihedral angles 0.6–2.5 °C), and are distorted in the shape of a kite with the smallest bond angle at the spirocenters (87.2–87.5°). Hereby, 1,3-diaxial interactions are apparently more effectively removed than by a more obvious flattening of the central ring ($\sum\omega = 306°$), for this would have led to stronger 1,2-diequatorial interactions.

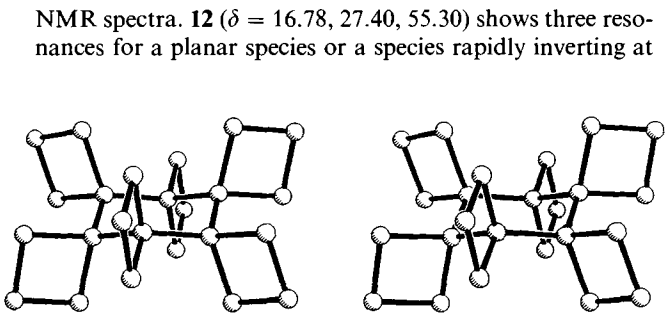

Fig. 1. Stereoscopic side-view of the structure of **4** (without hydrogen atoms) in the crystal. Bond lengths [pm] and angles [°]; cyclohexane ring: C–C 154.4–154.6, C-C-C 112.6–112.9; cyclobutane ring: C-C_{spiro} 157.0–157.6, C-$C_{peripher}$ 152.8–153.5, C-C_{spiro}-C 87.2–87.5, remaining C-C-C 90.2–91.3.

[6.4]Rotane **4** is very sparingly soluble. Attempts to determine its inversion barrier ^{2}H-NMR spectroscopically via a high-temperature equilibrium of [1,2-D_2]-**4** failed because of the large line widths and the poor solubility. To increase the sensitivity, stereospecifically ^{13}C-labeled material had to be prepared. To do this **13** was methylenated with ([^{13}C]methylene)triphenylphosphorane and subsequently converted as described for unlabeled **4** into [1-^{13}C]-**4′** (**13** → [methylene-^{13}C]-**14** → [2-^{13}C]-**15** → [2-^{13}C]-**16** → [2-^{13}C]-**17** → [2-^{13}C]-**18** → [3-^{13}C]-**19′** → [1-^{13}C]-**4′**).[12] For the determination of the barrier, [1-^{13}C]-**4′** was dissolved in 1,3-di-([D_3]methoxy)-benzene and the equilibration with [1-^{13}C]-**4** at + 214 ± 3 °C monitored by integration of the relevant ^{13}C-resonances.[13] This revealed a rate constant for the equilibriation at + 214 ± 3 °C of $k = (1.547 + 0.019) \times 10^{-4} s^{-1}$ and thus a free activation enthalpy for the chair/chair inversion of $\Delta G^{\neq}_{487(c/c)} = 156.8 \pm 1.1$ kJmol^{-4}. This is by far the highest inversion barrier reported so far for a cyclohexane.[2] Force field calculations are currently being carried out for an interpretation of this result.

Received: October 29, 1990 [Z 4257 IE]
German version: *Angew. Chem.* *103* (1991) 431

CAS Registry numbers:
4, 117593-17-6; [1,2-D_2]-**4**, 132235-13-3; [1-^{13}C]-**4**, 132235-14-4; **5**, 108451-21-4; **6**, 132235-15-5; **7**, 132235-16-6; **8**, 132235-17-7; **9**, 132235-18-8; **10**, 132235-19-9; **11**, 132235-20-2; **12**, 132235-21-3; **13**, 89546-45-2; **14**, 118162-34-8; [methylene-^{13}C]-**14**, 132235-12-2; **15**, 132235-22-4; **15'**, 132339-27-6; [2-^{13}C]-**15**, 132235-30-4; **16**, 132235-23-5; [2-^{13}C]-**16**, 132235-31-5; **17**, 132235-24-6; [2-^{13}C]-**17**, 132235-32-6; **18**, 132235-25-7; [2-^{13}C]-**18**, 132235-33-7; **19**, 132235-26-8; [3-^{13}C]-**19**, 132235-29-1; **20**, 132339-25-4; **21**, 132235-27-9; **22**, 132339-26-5; **23**, 132235-28-0; C–C_4H_6(Li)$SeCH_3$, 78814-62-7.

[1] a) L. Fitjer, U. Klages, W. Kühn, D. S. Stephenson, G. Binsch, M. Noltemeyer, E. Egert, G. M. Sheldrick, *Tetrahedron 40* (1984) 4337; b) L. Fitjer, H.-J. Scheuermann, U. Klages, D. Wehle, D. S. Stephenson, G. Binsch, *Chem. Ber. 119* (1986) 1144; c) D. Wehle, H.-J. Scheuermann, L. Fitjer, *ibid. 119* (1986) 3127; d) D. Wehle, L. Fitjer, *Tetrahedron Lett. 27* (1986) 5843; e) L. Fitjer, M. Giersig, D. Wehle, M. Dittmer, G.-W. Koltermann, N. Schormann, E. Egert, *Tetrahedron 44* (1988) 393; f) L. Fitjer, U. Klages, D. Wehle, M. Giersig, N. Schormann, W. Clegg, D. S. Stephenson, G. Binsch, *ibid. 44* (1988) 405; g) D. Wehle, N. Schormann, L. Fitjer, *Chem. Ber. 121* (1988) 2171.

[2] The previously highest inversion barriers were those of **20a** ($\Delta G^{\ddagger}_{413}$ = 134.9 kJ mol^{-1} [1 d], **20b** ($\Delta G^{\ddagger}_{413}$ = 136.9 kJ mol^{-1}) [1 d] and **3** ($\Delta G^{\ddagger}_{423}$ = 136.0 kJ mol^{-1}) [1 e].

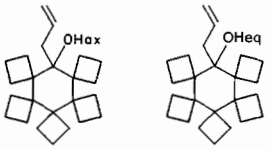

20a **20b**

[3] L. Fitjer, U. Quabeck, *Angew. Chem. 99* (1987) 1054; *Angew. Chem. Int. Ed. Engl. 26* (1987) 1023.

[4] R. H. Shapiro, *Org. React. (N.Y.) 23* (1976) 405.

[5] M. Giersig, D. Wehle, L. Fitjer, N. Schormann, W. Clegg, *Chem. Ber. 121* (1988) 525.

[6] All the new compounds (**4**, **6–9**, **11**, **12**, **15**, **15'**, **16**, **19**, **21–23**) gave correct C,H analyses and/or correct values in the highly resolved mass spectrum. The IR, ^{1}H-NMR and mass spectrometric data are consistent with the given structures. ^{13}C-NMR data (so far as not mentioned in the text): **6** (126 MHz, $CDCl_3$): δ = 15.46, 15.92, 23.55, 31.56 (C_{sec}), 53.53, 53.60 (C_{quart}), 101.76 (C_{sec}), 171.60 (C_{quart}); **7** (50.3 MHz, $CDCl_3$): δ = 15.92, 15.94, 16.05, 16.53, 16.84 (C_{sec}), 23.61 (C_{tert}), 24.53, 24.96, 25.07, 25.16, 27.48, 28.57, 29.15, 29.42 (C_{sec}), 48.27, 51.62 (C_{quart}), 51.78 (C_{prim}), 53.87, 54.40, 55.39, 173.68 (C_{quart}); **8** (20 MHz, $CDCl_3$): δ = 14.01, 15.40, 15.64, 16.08, 16.47, 24.15, 24.32, 24.95, 25.29, 25.51, 27.95, 28.24, 29.22, 29.65, 41.73, 51.95, 53.12, 54.55, 55.58, 63.22; **9** (20 MHz, $CDCl_3$): δ = 14.87, 15.54, 15.76, 16.29, 18.84, 24.37, 24.63, 24.86, 24.97, 27.19, 28.66, 28.71, 32.07, (C_{sec}), 35.03 (C_{tert}), 51.33, 51.75, 53.67, 54.23, 54.99 (C_{quart}), 200.68 (C_{tert}); **11** (50.3 MHz, $DCDl_3$): δ = 16.36, 16.83, 26.62, 26.72, 27.57, 28.27, 36.40 (C_{sec}), 53.47, 54.74, 64.74 (C_{quart}), 136.30, 141.50 (C_{tert}); **15** (20 MHz, $CDCl_3$): δ = 11.90, 15.65, 16.25, 16.43, 16.51, 16.75, 18.80, 25.27, 25,34, 25.38, 25.88, 26.34, 26.56, 27.89, 28.61, (coincidence of two lines), 28.77, 34.06, 47.95, 49.16, 49.78, 50.72, 51.16, 51.90, 173.39; **15'** (20 MHz, $CDCl_3$): δ = 9.16, 16.18, 16.30, 16.49, 16.77, 16.80, 25.11, 25.33 (coincidence of two lines), 26.00, 26.15, 26.34, 27.20 (coincidence of two lines), 28.75 (coincidence of two lines), 31.27, 36.68, 49.41, 50.02, 50.23, 50.39, 50.59, 51.55, 174.14; **16** (20 MHz, $CDCl_3$): δ = 11.15, 15.29, 16.54 (coincidence of three lines), 16.83 (C_{sec}), 18.53 (C_{tert}), 25.22, 25.47, 25.62, 25.67, 26.50, 28.00, 28.27, 28.76, 28.92, 29.00, 29.62 (C_{sec}), 47.47, 49.17, 49.77, 50.61, 51.28, 61.37 (C_{quart}); **17** (20 MHz, $CDCl_3$): δ = 14.52, 15.41, 16.10, 16.43 (coincidence of two lines), 16.57, 25.09, 25.31 (coincidence of two lines), 26.01, 27.00, 27.87, 28.66, 29.01 (coincidence of two lines), 29.16 (C_{sec}), 29.52 (C_{tert}), 40.62, 48.13, 48.93, 50.29, 50.79, 51.20 (C_{quart}), 201.59 (C_{tert}); **19** (20 MHz, $CDCl_3$): δ = 16.10, 16.46, 16.57, 24.91, 25.16, 26.96, 27.15, 27.88, 28.03, 35.22, 47.99, 49.25, 49.69, 57.45, 135.39, 140.91; **21** (**22**, 20 MHz, $CDCl_3$): δ = 9.80, 18.86, 23.92, 25.23, 28.07, 31.31, 33.32, 33.92, 34.39, 35.55, 35.87, 37.36, 37.59, 37.99, 54.30, 58.01, 59.44, 63.75, 64.14, 200.85; **22** (**21**, 20 MHz, $CDCl_3$): δ = 18.74, 19.28, 25.57, 27.00, 27.87, 30.61 (C_{sec}), 30.95 (C_{tert}), 33.37, 33.92, 34.24, 34.41, 35.90, 37.40, 37.78 (C_{sec}), 51.00, 56.37, 58.86, 62.98, 65.09 (C_{quart}), 200.81 (C_{tert}); **23** (50.3 MHz, $CDCl_3$): δ = 9.07, 19.00 (C_{sec}), 21.54 (C_{prim}), 23.73, 25.40 (C_{sec}), 26.87 (C_{tert}), 28.22, 31.28, 33.26, 33.88, 33.93, 34.18, 36.02, 37.18, 38.07 (C_{sec}), 48.45, 57.61, 58.96, 63.51, 64.28 (C_{quart}), 127.98, 129.55 (C_{tert}), 135.22, 143.89 (C_{quart}), 154.10 (C_{tert}).

[7] We have already observed conformational isomers on several occasions in the case of comparable structures. The stereochemical assignment is tentative and assumes that methoxycarbonylcarbene is preferentially transferred equatorially. A direct domonstration in the form of a crystal structure analysis of **15'**, **15** or one of its secondary products (**16**, **17**) is still lacking [14].

[8] A. J. Mancuso, D. Swen, *Synthesis 1981*, 165. **9** and **17** were used as crude products and contained small amounts or triethylamine. Upon attempting a chromatographic purification on silica gel in dichloromethane **9** rearranged to a mixture of the aldehydes **21** (**22**) m.p. 202–212 °C, 55% [6] and **22** (**21**) m.p. 188–198 °C, 29% [6].

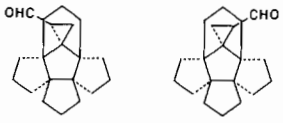

21(22) **22(21)**

[9] The successful conversion of cyclopropanecarboxaldehyde with tosyl hydrazide in aqueous methanol [K. B. Wiberg, J. M. Lavanish, *J. Am. Chem. Soc. 88* (1966) 5272] led in the case of **9** to a tosyl hydrazone **23** (m.p. 40–50 °C, 87%) derived from **21** or **22** [6].

[10] ^{2}H NMR (30.7 HMz, $CDCl_3$): δ = 1.70 (s, br, 1D), 2.52 (s, br, 1D).

[11] Crystal structure analysis of **4** ($C_{24}H_{36}$): space group $P\bar{1}$, a = 775.5(2), b = 807.0(2), c = 827.8(2) pm, α = 69.030(10), β = 74.14(3), γ = 76.130(10)°, V = 0.4595(2) nm^3, Z = 1, ρ_{calcd} = 1.173 g cm^{-3}, $\mu(Mo_{K\alpha})$ = 0.061 mm^{-1}. Of 1201 independently measured reflections 999 with $|F| > 3\sigma(F)$ were taken into account for the structure solution and refinement. The anisotropic refinement with inclusion of the hydrogen atoms converged with R = 0.036. Further details of the crystal structure investigation are available on request from the Fachinformationszentrum Karlsruhe, Gesellschaft für wissenschaftlich-technische Information, W-7514 Eggenstein-Leopoldshafen 2 (FRG), on quoting the depository number CSD-54863, the names of the authors and the journal citation.

[12] The ^{1}H- and ^{13}C-NMR spectra of all ^{13}C-labeled compounds are consistent with the given structures. The degree of labeling is in each case 99% and follows from the degree of labeling of the ([^{13}C]methyl)triphenylphosphonium iodide (99%, ^{13}C) used for the methylenation of **14**.

[13] ^{13}C NMR (126 MHz, 1,3-di-([D_3]methoxy)benzene, 1,3-di-([D_3]methoxy)-benzene int.) [1-^{13}C]-**4'**: δ = 26.01; [1-^{13}C]-**4**: δ = 28.82. As reference we used the heptet of the methoxy groups of 1,3-di-([D_3]methoxy)benzene [$\delta_C(CDCl_3)$ = 54.05].

[14] *Note added in proof (February 18, 1991):* According to a crystal structure analysis of **15'** the stereochemical assignment is correct.

Synthesis and Structure of a *rac*-Tris(divinyldisiloxane)diplatinum(0) Complex and its Reaction with Maleic Anhydride**

By *Peter B. Hitchcock, Michael F. Lappert,** and *Nicholas J. W. Warhurst*

Speier's catalyst (hexachlorplatinic acid) is widely used in the commercially important hydrosilylation of unsaturated substrates such as alkenes.[1] A useful form of $H_2[PtCl_6].xH_2O$, Karstedt's solution, is obtained by treating it with a vinylsiloxane.[2] The catalytic hydrosilylation cycle was generally assumed to be initiated by a platinum(0) species. This was originally believed to have been formed by an $HSiX_3$-induced reduction of hexachloroplatinic acid.[1] Recently, however, it was shown that $H_2[PtCl_6].xH_2O$ and an excess of *sym*-tetramethyldivinyldisiloxane, $(H_2C{=}CHSiMe_2)_2O$, afforded a catalytically active solution, solution A, which, largely on the basis of its reaction with $PtBu_3$ to form the X-ray characterized com-

[*] Prof. M. F. Lappert, Dr. P. B. Hitchcock, and Dr. N. J. W. Warhurst School of Chemistry and Molecular Sciences, University of Sussex Brighton BN1 9QJ (UK)

[**] We thank Johnson Matthey PLC for a loan of Pt, S: E. R. C. and Dow Corning PLC (Barry) for a C. A. S. E. award to *N. J. W. W.*, Dr. *P. Y. Lo* and Dr. *R. G. Taylor* for useful discussions, and Dr. *A. G. Avent* for NMR data.

plex $[Pt\{(\eta\text{-}H_2C=CHSiMe_2)_2O\}(PtBu_3)]$, was thought to be a platinum(0) complex.[3] Furthermore, solution A in C_6D_6 showed NMR features similar to those found for the product obtained from the reaction of $[Pt(cod)_2]$ with $(H_2C=CHSiMe_2)_2O$ (cod = cycloocta-1,5-diene) in toluene. It was concluded that solution A contained preponderantly compounds of the type **A**.

$[Pt\{\eta\text{-}H_2C=CHSiMe_2O(SiMe_2O)_x(SiMe_2CH=CH_2\eta)\}_y]$ **A**

$x = 0-14$ (usually = 0), $y = 2-4$ (usually 2)

We now report that reaction of $[Pt(cod)_2]$ with 3/2 tetramethyldivinyldisiloxane in diethyl ether affords colorless crystals of the complex *rac*-**1**, whose structure was established ultimately by X-ray crystallography (Fig. 1). Detailed multinuclear NMR spectroscopic studies of complex **1** showed that in [D$_8$]toluene it was converted into a mixture of isomers, probably principally the *rac*- and *meso*-form (vide infra) of **1**; thus, at ambient temperature there were two somewhat broad $^{195}Pt\{^1H\}$ signals separated by ca. 20 Hz centered at $\delta = -6151$ (rel. to $K_2[PtCl_6]$) of roughly similar intensity, and four $^{29}Si\{^1H\}$ signals at $\delta = 3.45$ and 2.63 (chelating ligand) and $\delta = 0.18$ and 0.17 (bridging ligand) (rel. to TMS).[4] (At lower temperatures, there is NMR evidence for the existence of fluxional processes.) Furthermore, this [D$_8$]toluene solution of **1** was essentially identical to that of solution A in C_6D_6; and similar products were obtained as with $[Pt(cod)_2]$ upon reaction of $(H_2C=CHSiMe_2)_2O$ with the platinum complexes **5**–**7** (Scheme 1) and most conveniently from **7**.

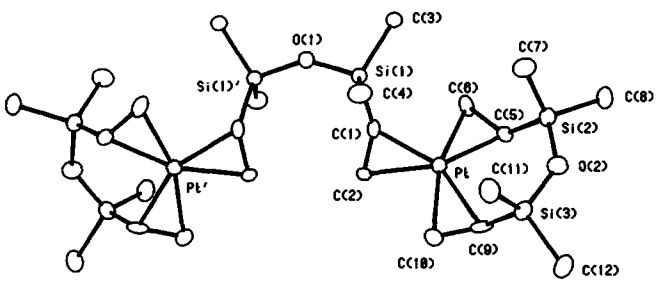

Fig. 1. Crystal structure of *rac*-**1**. Selected bond lengths [Å] and angles [°]: Pt-C(1) 2.19(2), Pt-C(2) 2.18(2), Pt-C(5) 2.19(2), Pt-C(6) 2.16(2), Pt-C(9) 2.21(2), Pt-C(10) 2.19(2), C(1)-C(2) 1.36(2), C(5)-C(6) 1.43(2), C(9)-C(10) 1.39(3), Si(1)-O(1) 1.645(7), Si(2)-O(2) 1.607(11), Si(3)-O(2) 1.631(13); C(1)-Pt-C(2) 36.4(6), C(5)-Pt-C(6) 38.3(6), C(9)-Pt-C(10) 37.0(7), Si(1)-O(1)-Si(1)' 146(1), Si(2)-O(2)-Si(3) 134.7(8).

In the crystalline state complex **1** is relatively air-stable at ambient temperature, but in solution or as an oil it is somewhat thermally, photochemically, and aerobically sensitive, tending then to deposit platinum.

The siloxane by-products obtained by reaction of $(H_2C=CHSiMe_2)_2O$ with either $H_2[PtCl_6].xH_2O$[3] or **7** and subsequent aqueous washing were identical (GC/MS) and comprised the oligosiloxanes **3** (Scheme 1). Evidently a similar mechanism operates in the reduction of both a Pt^{IV}- and a Pt^{II}-chloride precursor to the Pt^0 complex **1**; this aspect is under further investigation, as are variable temperature NMR studies of **1** in [D$_8$]toluene.

The structure of *rac*-**1** (Fig. 1[5]) in the crystal revealed that the divinyldisiloxane ligand is present in both a bridging and chelating mode (cf. the cod ligand in $[Pt(cod)_2]$.[6] The term *rac* describes the relative configuration of the α-carbon atoms C(1) and C(1)′ of the bridging divinyldisiloxane ligand. **1** has a C_2 axis through the oxygen atom on the bridging divinyldisiloxane and the midpoint between the two platinum centers. The three vinyl groups are in a trigonal planar geometry about each Pt, with a deviation of less than 0.120(5) Å from the plane. Such an arrangement is similar to that observed for the tris(alkene)platinum(0) complexes $[Pt(\eta\text{-}H_2C=CH_2)_3]$[7] and $[Pt(\eta\text{-}C_7H_{10})_3]$ (C_7H_{10} = bicyclo-(2.2.1)heptene).[8] The mean C=C bond distances [1.39(3) Å] and Pt-C [2.19(2) Å] are unexceptional (cf.[7] $[Pt(\eta\text{-}H_2C=CH_2)_3]$ has C=C 1.402(7) Å and Pt–C 2.176(2) Å). The Si–O–Si angle of the chelating divinyldisiloxane [134.7(8)°] in complex **1** is smaller than that of the bridging ligand [146(1)°], and the chelating ligand is in a chair conformation around the platinum center.

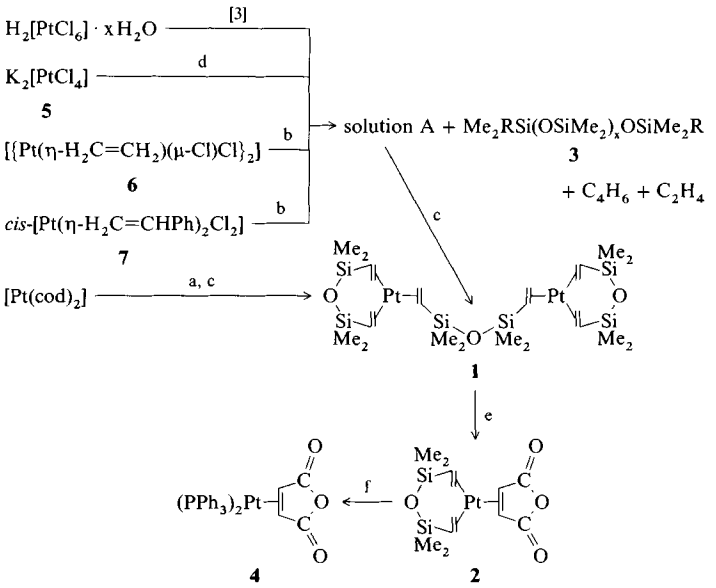

Schema 1. Synthesis of *rac*-**1** and its conversion with maleic anhydride into complexes **2** and **4**, and routes to the catalytically active solution A. In the case of **3**: $x = 0-8$ (usually 0), mostly R = H_2C = CH, sometimes R = Et, seldom R = CH_2CH_2Cl[3]. Reagents and conditions: a) 3/2 $(H_2C=CHSiMe_2)_2O$, Et_2O, 25 °C, 2 h; b) 5 $(H_2C=CHSiMe_2)_2O$, toluene, 50 °C, 4 h; c) removal of excess $(H_2C=CHSiMe_2)_2O$, crystallization from EtOH/Et_2O at 30 °C; d) 5 (H_2C = $CHSiMe_2)_2O$ (560 mg), H_2O (1 mL), toluene (10 mL), 50 °C; e) maleic anhydride, toluene, 50 °C, 4 min; f) 2 PPh_3, tetrahydrofuran, 25 °C, 30 min.

If we assume that in solution the chelated disiloxane always has the "chair" conformation as in the crystal, then atoms C(5) and C(9) must have the opposite configuration, i.e. (*R*,*S*) or (*S*,*R*). If we further assume that there is free rotation about the Pt to C(1)–C(2) vinyl bond, which is rapid on the NMR time scale, then the two atoms C(5) and C(9) become equivalent and there is only one isomeric form of the coordinated chelating disiloxane. One is then left with the question of the configuration at C(1) and C(1)′, each of which can be either (*R*) or (*S*), giving rise to two possible isomers (*R*,*R*)/(*S*,S) (*rac*) or (*R*,*S*) (*meso*).

Reaction of complex 1 with maleic anhydride yielded **2**.[9] Treatment of complex **2** with PPh_3 led to displacement of the divinyldisiloxane, in preference to the maleic anhydride ligand, to form the known complex **4**[10] (Scheme 1).

Experimental Procedure

1: $[Pt(cod)_2]$ (400 mg, 0.97 mmol) was added slowly (50 mg portions) to a rapidly stirred solution of $(H_2C=CHSiMe_2)_2O$ (0.30 mL, 270 mg, 1.46 mmol) in diethyl ether (10 mL) at 25 °C. After ca. 2 h the volatile components were removed in vacuo to leave a colorless oil, which was dissolved in diethyl ether (5 mL) and transferred via a cannula onto a small Florisil column (1.5 × 2.5 cm) and washed with diethyl ether (2 × 10 mL). The solvent was removed from the eluant in vacuo to leave a pale white oil, from which the white solid **1** (380 mg, 0.40 mmol, 84 %) was obtained after ca. 50 h at 25 °C. Crystals suitable enough

for an X-ray structure analysis were obtained by dissolving the white solid in a mixture of ethanol/diethyl ether and cooling the solution to −30 °C for ca. 24 h.

Received: November 23, 1990 [Z 4292 IE]
German version: *Angew. Chem. 103* (1991) 439

CAS Registry numbers:
1, 132513-41-8; **2**, 132513-42-9; **4**, 24508-00-7; $Pt(cod)_2$, 12130-66-4; $(H_2C{=}CHSiMe_2)_2O$, 2627-95-4; maleic anhydride, 108-31-6.

[1] For reviews, see C. S. Cundy, B. M. Kingston, M. F. Lappert, *Adv. Organomet Chem. 11* (1973) 330; J. L. Speier, *ibid. 17* (1979) 407; F. O. Stark, J. R. Falkender, A. P. Wright in G. Wilkinson, F. G. A. Stone, E. W. Abel (Eds.): *Comprehensive Organometallic Chemistry, Vol. 2*, Pergamon, Oxford, 1982, p. 305.

[2] (a) D. N. Willing, US-A 3419593 (1968); (b) B. D. Karstedt, US-A 3775452 (1973).

[3] G. Chandra, P. B. Hitchcock, M. F. Lappert, P. Y. Lo, *Organometallics 6* (1987) 191.

[4] Complex **1** in [D$_8$]toluene (or + 10% toluene for ^{195}Pt-NMR spectrum) solution was characterized by $^{195}Pt\{^1H\}$, $^{29}Si\{^1H\}$, $^{13}C\{^1H\}$, ^1H, and 2D ^1H-^1H COSY NMR spectroscopy [this enabled a correlation to be made of the coupling between the adjacent protons on each of the vinyl groups; there are three distinct vinyl groups coordinated to each Pt center, $^2J(^1H$-$^{195}Pt)$ ca. 55 Hz] [11]. The $^{13}C\{^1H\}$-NMR data showed (DEPT) the presence of three methine (δ = 58.1, 56.4, 57.3) and three methylene (δ = 57.0, 57.2, 56.4) vinylic carbon atoms, each with coupling constants $^1J(^{13}C$-$^{195}Pt)$ of ca. 110 Hz. The assignment of the bridging/chelating vinylic protons was established by a sequence of decoupling and NOE experiments[11].

[5] Crystal data of **1**: $C_{24}H_{54}O_3Pt_2Si_6$, M = 949.4, monoclinic, space group $C2/c$, a = 29.810(5), b = 10.180(3), c = 12.527(2) Å, β = 107.64°, V = 3622.8 Å^3. Z = 4, ρ_{calcd} = 1.74 g cm^{-3}. The crystal data were collected on a CAD-4 diffractometer [$\mu(Mo_{K\alpha})$ = 80.1 cm^{-1}]. A total of 3330 unique reflections was measured for $2 < \theta < 25°$ and $+h + k \pm l$, and 1775 reflections with $|F^2| > 1.5\ \sigma(F^2)$ were used in the refinement where $\sigma(F^2) = \{\sigma^2(I) + 0.04(I)^2\}^{1/2}/L_p$. The structure was solved by routine heavy atom methods and refined by full matrix least squares. Hydrogen atoms were at fixed calculated positions with a common B_{iso} of 6.0 Å^2. The final residuals were R = 0.046, R' = 0.070. Further details of the crystal structure investigation are available on request from the Director of the Cambridge Crystallographic Data Centre, University Chemical Laboratory, Lensfield Road, Cambridge CB2 1EW on quoting the full journal citation.

[6] J. A. K. Howard, *Acta Crystallogr. Sect. B(38)* (1982) 2896.

[7] J. A. K. Howard, S. A. Mason, J. L. Spencer, *Proc. Roy. Soc. London A 386* (1983) 145.

[8] M. Green, J. A. K. Howard, J. L. Spencer, F. G. A. Stone, *J. Chem. Soc. Dalton Trans. 1977*, 271.

[9] The $^{195}Pt\{^1H\}$-NMR spectrum of complex **2** showed a sharp singlet at δ = −5987 rel. to external $K_2[PtCl_6]$ (recorded in 10% [D$_8$]toluene/toluene, 303 K, 17.2 MHz). The coordinated maleic anhydride protons were observed as a singlet at δ = 4.98. [$^2J(^1H$-$^{195}Pt)$ = 63 Hz] (recorded in [D$_6$]acetone, 303 K, 360.1 MHz).

[10] M. T. Chicote, M. Green, J. L. Spencer, F. G. A. Stone, J. Vicente, *J. Organomet. Chem. 137* (1977) C8.

[11] N. J. W. Warhurst, D. Phil. thesis, University of Sussex 1990.

Bolaamphiphilic Polyols, a Novel Class of Amphotropic Liquid Crystals

By *Frank Hentrich, Carsten Tschierske,** and *Horst Zaschke*

Amphiphilic molecules can aggregate to supramolecular systems. An important form of this molecular self-organization is the formation of liquid crystalline phases.[1] Thus, amphiphilic *n*-alkane-1,2-diols **1**, with a chain length of n ≧ 5, exhibit monotropic mesophases which are stabilizable by addition of water.[2] These compounds are structurally related with liquid crystalline carbohydrate derivatives[3] and can be regarded as the simplest members of this large

[*] Dr. C. Tschierske, Dipl.-Chem. F. Hentrich, Prof. Dr. H. Zaschke
Sektion Chemie, WB Organische Chemie der Universität Halle-Wittenberg
Weinbergweg 16, O-4050 Halle (FRG)

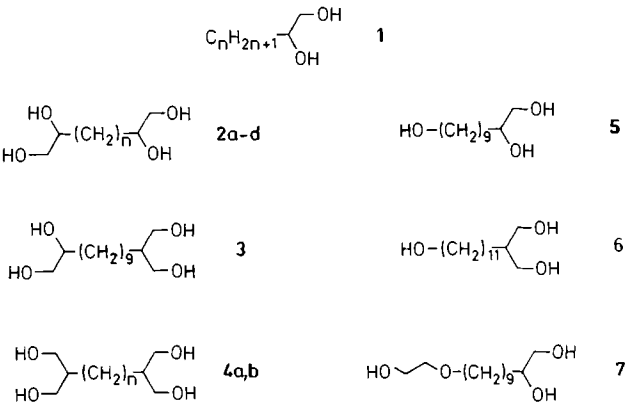

Scheme 1. n = 18 (**2a** [4]), 12 (**4b**), 9 (**2b**, **4a**), 5 (**2c**), 4 (**2d**).

class of amphiphilic mesogens. As recently reported, liquid crystalline phases are drastically stabilized by the coupling of two amphiphilic diols **1** (n = 9) via their hydrophobic molecular terminals to give the biamphiphilic (bolaamphiphilic) tetrol **2a**.[4]

We have now synthesized further bolaamphiphilic polyols with substantially shorter polymethylene chains and structurally different hydrophilic head groups,[5] in order to generalize this structural principle.[6] The liquid crystalline properties of the new substances **2**–**7** determined by polarization microscopic and differential scanning calorimetric (DSC) investigations are listed in Table 1. Surprisingly, even compound **2c**, with the very short pentamethylene spacer between ethane-1,2-diol groups, still has thermotropic liquid crystalline properties, although its hypothetical molecular halves (compound **1** with n = 2 and 3) do not display mesophases. Therefore, bolaamphiphilic polyols should not only be considered as simple, dimeric amphiphilic diols, but as an independent class of amphotropic mesogens.[13] The general validity of this structural concept is further supported by the variety of hydrophilic groups. Only in the case of compound **2d** and the symmetrical propane-1,3-diol derivatives were no mesophases detectable. The isotropic melts of compounds **4** are only very slightly supercoolable, and possible metastable mesophases are not recognizable. All other compounds show only a slight tendency to crystallize (often only after several days), so that their monotropic mesophases are easily observable. As a comparison of compounds **2a**–**2d** shows, the clearing points increase drastically with increasing length of the polymethylene chain. Compound **2b** and the bolaamphiphilic triol **5** are liquid crystalline above the melting point. The unsymmetrical tetrol **3** has the greatest mesophase diversity. On cooling the isotropic melts the appearance of a birefringence is observed under the polarizing microscope at 84 °C with a fan-like texture typical for lamellar α-phases, which can be oriented homeotropically very easily by shearing. This points to a layer structure, whereby the individual molecules in the layers do not exhibit long-range order. The hydroxy groups should, like those of amphiphilic diols, be coupled via a dynamic network of cooperative hydrogen bridges to give tile-shaped aggregates, which are both separated as well as bound by the conformationally mobile (molten) polymethylene chains (L_α phase). On further cooling to 75 °C the texture changes and the viscosity increases considerably. Probably the transition to a more highly ordered mesophase with rigid parallel polymethylene chains (L_β) occurs at this point.[7, 8] Both phase transformations have unusually high phase-transition enthalpies. At 43 °C, a further phase transition of small enthalpy takes

place, which, however, cannot be observed in more detail as a result of the onsetting crystallization.

The liquid crystalline phases of bolaamphiphilic polyols can be modified by addition of water, whereby the mesophases of compounds with long polymethylene spacers (e.g. **2a** and **6**) are stabilized and those with shorter polymethylene chains are destabilized (Table 1). The mesophase destabilization is more pronounced the greater the ratio between hydrophilic and hydrophobic structural units (hydrophilic–hydrophobic balance). This can be interpreted as resulting from the effect of two counteracting influences: the incorporation of water molecules in the region of the head groups leads to a strengthening of the hydrogen bonding between the hydrophilic groups and stabilizes the mesophases. The hydration of the head groups, however, also forces the polymethylene chains apart. The resulting free space between the molecules can, only in the case of sufficiently long polymethylene chains, be filled through their additional motions. As a result, one observes in the case of water-saturated samples, the appearance of the L_α phase, and, in the case of short-chain compounds, a destabilization or complete suppression of liquid crystalline phases. Figure 1 illustrates the stepwise transition from the amphiphilic diol to the bolaamphiphilic polyol. On introduction of increasingly polar terminal substituents into the hydrophobic moiety of the molecule of amphiphilic diols,[9] the distinct orientation of the molecules in the double layers is lost, since these polar groups can be incorporated into the network of the intermolecular hydrogen bridges in ever increasing amount with increasing ability to participate in hydrogen bonding. If these terminal substituents function only as proton acceptors, then they break the hydrogen bridge network and thereby destabilize the associates. However, if this terminal group is both proton acceptor as well as proton donor, then it can be incorporated concurrently in the hydrogen-bridge network of the head groups and additionally stabilize the mesophase.

Table 1. Phase transition temperatures [a] T [°C] of the bolaamphiphilic polyols 2–7 [b]. The values in brackets refer to the enthalpies ΔH kJmol^{-1} [c].

Cpd.	n [d]	Water-free samples	Water-saturated samples
2a [e]	18	k 87 L_β 142 L_α 145 i	L_α 166 i
2b	9	k 110 L_β 115 i (42.4) (17.2)	L_α 59 i
2c	5	k 77 L_β 36 i (37.8) (7.2)	–
2d	4	k 83 i	–
3	9	k 95 ($L_{\beta'}$ 43 L_β 75 L_α 84) i (58.9) (0.9) (6.2) (7.0)	L_α 41.5 i
4a	9	k 103 i	– [f]
4b	12	k 135 i	– [f]
5 [g]	9	k 48 ($L_{\beta'}$ 45) L_β 70.5 i (18.2) (0.9) (11.1)	L_α 56 i
6 [h]	11	k 89.5 (L_β 61.5 L_α 62) i (59.9) (13.2) [i]	L_α 77 i
7	9	k 69 ($L_{\beta'}$ 35 L_β 48) i (53.2) (2.6) (18.3)	L_α 21 i

[a] Abbreviations: c = crystalline (the compounds have different melting temperatures and exhibit further solid–solid transitions depending on their previous history. In each case, the highest melting temperatures are quoted); L_α, L_β = lamellar mesophases; i = isotropic phase; [b] correct C, H analyses, ^{1}H-NMR and ^{13}C-NMR spectra have been recorded; [c] see [10]; [d] length of the polymethylene chain between the head groups; [e] see [4]; [f] crystallizes out; [g] see [11]; [h] see [12]; [i] peaks not separated.

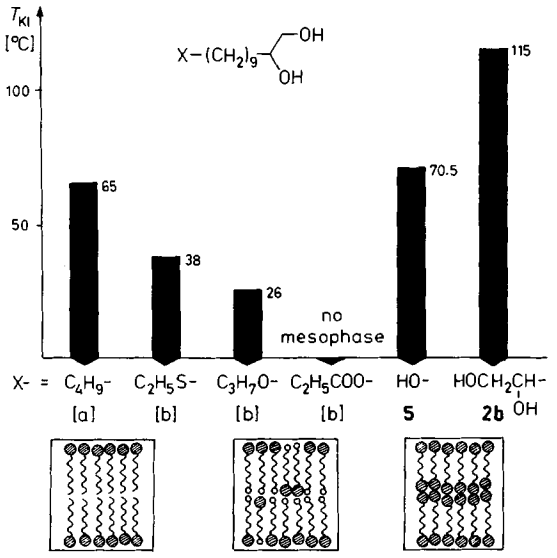

Fig. 1. Influence of polar substituents X on the clearing temperatures T_{cl} [°C] of amphiphilic diols and the stepwise transition of amphiphilic diols to bolaamphiphilic polyols. [a] See [2a], [b] see [9].

Received: October 31, 1990 [Z 4262 IE]
German version: *Angew. Chem. 103* (1991) 429

[1] H. Kelker, R. Hatz: *Handbook of Liquid Crystals*, Verlag Chemie, Weinheim 1980.
[2] a) C. Tschierske, G. Brezesinski, F. Kuschel, H. Zaschke, *Mol. Cryst. Liq. Cryst. Lett. Sect. 6* (1989) 139; b) H. van Doren, *Dissertation*, Groningen 1989.
[3] G. A. Jeffrey, *Acc. Chem. Res. 19* (1986) 168; J. W. Goodby, M. A. Marcus, E. Chin, P. L. Finn, B. Pfannemüller, *Liq. Cryst. 3* (1988) 1569; V. Vill, T. Böcker, J. Thiem, F. Fischer, *ibid. 6* (1989) 349; H. van Doren, R. van der Geest, C. F. De Ruijter, R. M. Kellogg, H. Wynberg, *ibid. 8* (1990) 109; K. Praefcke, B. Kohne, A. Eckert, J. Hempel, *Z. Naturforsch. B 45* (1990) 1084; W. V. Dahlhoff, *ibid. B 42* (1987) 661; D. Baeyens-Volant, R. Fornasier, E. Szalai, C. David, *Mol. Cryst. Liq. Cryst. 135* (1986) 93 and references cited therein.
[4] C. Tschierske, H. Zaschke, *J. Chem. Soc. Chem. Commun. 1990*, 1013.
[5] The compounds **2b**–**2d**, **3**, **5**, and 7 were obtained by OsO_4-catalyzed dihydroxylation of the corresponding olefins according to the method described by V. van Rheenen, R. C. Kelley, D. F. Cha, *Tetrahedron Lett. 1976*, 1973; 1,(ω−1)-alkanedienes → **2b**–**2d**; 2-hydroxymethyltridec-12-en-1-ol [12] → **3**; undec-10-en-1-ol → **5**; 3-oxatetradec-13-en-1-ol (prepared by reaction of 1-bromoundec-10-ene with ethylene glycol/NaOMe/MeOH) → 7. The synthesis of the compounds **4a** and **4b** was achieved by reduction of tetraethyl undecane-1,1,11,11-tetracarboxylate and tetraethyl tridecane-1,1,13,13-tetracarboxylate, respectively, with $LiAlH_4$ in THF. The synthesis of compound **6** is described in Ref. [12]. The polyols were purified by column chromatography ($CHCl_3$/MeOH 95:5) and finally recrystallized from hexane/ethyl acetate or $CHCl_3$.
[6] Bolaamphiphilic carbohydrates and bolaamphiphilic polyols with two hydrocarbon chains; W. V. Dahlhoff, *Z. Naturforsch. B 43* (1988) 1367; J.-H. Fuhrhop, D. Fritsch, *Acc. Chem. Res. 19* (1986) 130; A. Gulik, V. Luzzati, M. De Rosa, A. Gambacorta, *J. Mol. Biol. 182* (1985) 13.
[7] Preliminary X-ray diffraction investigations by Dr. *S. Diele* (Universität Halle-Wittenberg) confirm the proposed structure of the mesophases.
[8] A birefringence also occurs in the homeotropically oriented regions; it can be greatly increased by shearing the sample. A non-orthogonal orientation of the polymethylene chains with respect to the layer planes can therefore not be ruled out as yet.
[9] C. Tschierske, H. Zaschke, S. Wolgast, G. Brezesinski, F. Kuschel, *Mol. Cryst. Liq. Cryst. Lett. Sect. 7* (1990) 131.
[10] We thank Herr *D. Lötsch* and Prof. *Dr. G. Heppke* (Technische Universität Berlin) for kind permission to carry out the measurements with their facilities.
[11] K. Shishido, M. Kawanishi, K. Kondo, T. Morimoto, A. Saito, N. Fukue, *J. Org. Chem. 27* (1962) 4073.
[12] N. Pietschmann, G. Brezesinski, C. Tschierske, H. Zaschke, F. Kuschel, *Liq. Cryst. 5* (1989) 1697.
[13] Amphotropic mesogens form thermotropic and, after addition of solvent, also lyotropic, liquid crystalline phases. H. Ringsdorf, B. Schlarb, J. Venzmer, *Angew. Chem. 100* (1988) 117; *Angew. Chem. Int. Ed. Engl. 27* (1988) 113.

Molecular Recognition and Transport of Nucleobases — Superiority of Macrobicyclic Host Molecules**

By *Christian Seel* and *Fritz Vögtle**

Dedicated to Professor Heinz A. Staab on the occasion of his 65th birthday

A few years ago we reported on large cavity molecules, cage-like tris(catechol)[1] and tris(bipyridine) ligands,[2] which, through optimal preorganization of the binding centers, complex metal cations such as $Fe^{3\oplus}$[3] and $Ru^{2\oplus}$[4] extremely strongly. By means of a modular donor spacer strategy[5] we were able to obtain tris(bipyridine) host compounds with successively larger cavities which bind trihydrobenzenes selectively in organic solution.[6] Using the same strategy it was also possible to synthesize larger tris(catechol) hosts; due to their sparing solubility, however, so far all attempts to encapsulate organic molecules failed.[7] By increasing the lipophilicity with six *N*-benzyl groups we have now been able, with new cavity sizes, to selectively complex biological relevant guest compounds.

Reaction of the tricarboxylic acid chloride **3a** with the triamine **2** in chlorobenzene under dilution conditions[8] (cyclization yield 61%) and subsequent sixfold cleavage of the methoxy groups ($BBr_3 \cdot CH_2Cl_2$, 86% yield) yielded the macrobicyclic **1** in preparative amounts (2–3 g per run). **4** with all-*para*-substituted triphenylbenzene units was prepared analogously (yield 19% for the cyclization, 65% for the ether cleavage).[9]

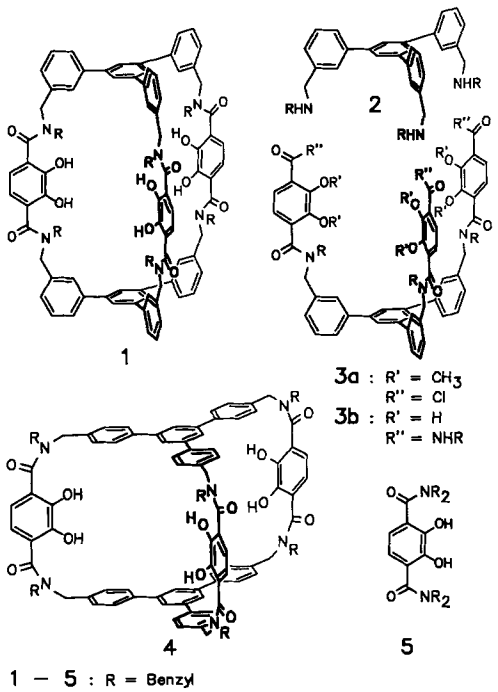

In contrast to the above-mentioned tris(bipyridine) compounds (basic endoreceptors) the new macrobicycles, with their six phenolic hydroxy groups have pronounced proton-donor character (acidic endoreceptors); topologically complementary guest molecules with hydrogen bridge acceptor functionalities should therefore be readily bound. Whereas **4** dissolves in chloroform and dichloromethane only on addition of at least 10% methanol, **1** itself is sufficiently soluble to permit host–guest experiments even on addition of 25% *n*-hexane. This is remarkable when one considers that **1** is a hexahydroxy-hexaamide. Preliminary complexation experiments with strongly basic C_3-symmetrical compounds such as 1,3,5-tris(aminomethyl)benzene **6** led to saltlike solids of unknown composition. The non-benzylated macrocycles, with their symmetrical molecular frameworks, afforded well resolved and easily interpretable ^{1}H-NMR spectra with few signals, while the conformationally flexible benzyl groups on the amide nitrogen atoms of **1** and **4** led to strongly broadened, unclear multiplets. Consequently, the changes in the spectra observed in complexation experiments could not be interpreted precisely.[10]

When investigating the encapsulation of pyrimidine and purine bases and similar guest compounds[11] (less basic than **6**) we made use of the fact that they dissolve in acidic aqueous phases, whereas the lipophilic host **1**, however, just as sparingly so as the podand **3b** and the simple catechol derivative **5** used for comparison do not.[9] By extraction of the organic host-guest solutions with 1N hydrochloric acid, the complexation can be readily monitored UV spectroscopically. The sparing solubility of the guests in CH_2Cl_2 (mostly

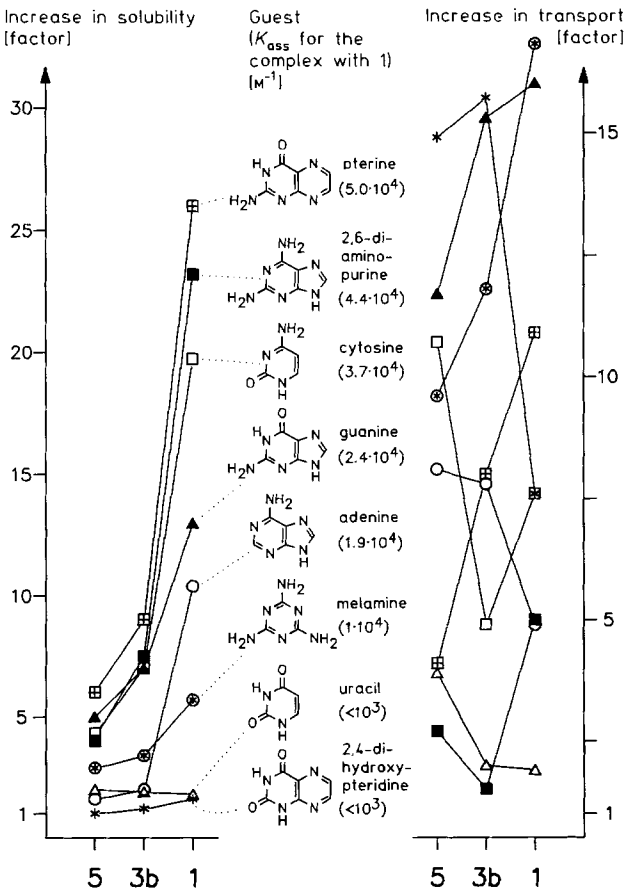

Fig. 1. Left: Enhancement factors of the solubility of the guests in CH_2Cl_2 at host concentrations of 5×10^{-4} M (in the case of **1** and **3b**) and 1.5×10^{-3} M (in the case of **5**). The data obtained were used for the calculation of the association constants of the complexes **1**. Right: Enhancement factors of the transport of the guests (solid) through CH_2Cl_2/*n*-hexane (3:1) in a 1N hydrochloric acid solution at host concentrations of 1×10^{-4} M (in the case of **1** and **3b**) and 3×10^{-4} M (in the case of **5**).

[*] Prof. Dr. F. Vögtle, Dipl.-Chem. C. Seel
Institut für Organische Chemie und Biochemie der Universität
Gerhard-Domagk-Strasse 1, W-5300 Bonn 1 (FRG)

[**] This work was supported by the Deutsche Forschungsgemeinschaft.

$< 10^{-5}$ M) is as a rule increased in the presence of the chatechol ligands but to very different extents.

Figure 1 (left) illustrates the superiority of the macrobicyclic host **1**, which in almost all cases affords by far the highest values.[12] The complexability of the podand **3b**, as anticipated, is nearer to that of **5** than that of **1**. This means that the number of binding centers alone is not crucial, but that the comparably rigid molecular structure has a decisive involvement (macrobicyclic effect). The linear dependence of the solubility of the guest compounds on the concentration of the host indicates a 1:1 stoichiometry in the case of complexes of **1**.[13] With other catechol compounds this is not so, therefore no complex constants can be quoted for these.

2,6-Diaminopurine is bound tighter than adenine. Apart from the stronger basicity the additional amino group seems to increase the degree of complementarity of host and guest. The association constants determined on the basis of the increase in solubility were $K_{ass} = 4.4 \times 10^{-4}$ and 1.9×10^{4} M^{-1}, respectively for the complexes of **1** with these two guests.[13] Also remarkable is the selectivity in the case of the cytosine/uracil and pterine/2,4-dihydroxypteridine pairs. They differ structurally only in that in each of the first (strongly bound) the amino group is replaced in the others by a hydroxy group. The correct harmonization of the pK_a and pK_b values respectively, of host and guest could be the decisive factor here for discrimination. The NH_2 groups are undoubtedly the better acceptors for the donor centers of the hosts.[14] In the case of the macrobicycle **1**, the strongly pronounced solution effects, the 1:1 stoichiometry, and the magnitude of the association constants justify the assumption that a guest molecule is encapsulated in the cavity and bound by multiple hydrogen bridges.

Particularly impressive are the extraction experiments with the phenothiazine dye thionine acetate **7a**, since they can be followed with the naked eye. A saturated dichloromethane solution is only weakly pink (λ_{max} = 581 nm), at a

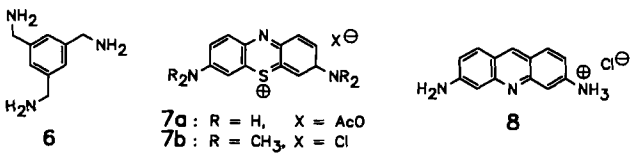

concentration of **1** of 5×10^{-4} M, however, deep blue (λ_{max} = 614 nm, in methanol: λ_{max} = 599 nm; Table 1). The strong bathochromic shift of the absorption maximum likewise suggests an encapsulation of the ionic dyes **7a** and **8**. Their complexation is comparable with the solubilization of metal salts such as potassium permanganate by crown ethers in organic solvents.

Table 1. Some results of the complexation experiments with dye-guests (conditions as in Fig. 1).

Guest	Absorption maximum [nm] CH_2Cl_2	5[a]	1[b]	MeOH	HCL	K_{ass} [Guest · 1]
7a	581	589	614	599	601	61 000
8	442	442	456	456	450	17 000
	Increase in solubility by			Increase in transport by		
	5	**3b**	**1**	**5**	**3b**	**1**
7a	2.7	5.5	31.3	6.9	5.2	15.5
8	1.4	3.1	8.5	1.5	3.3	8.7

[a] 3×10^{-3} M solution of **5** in CH_2Cl_2, saturated with guest. [b] 1×10^{-3} M solution of **1** in CH_2Cl_2, saturated with guest.

The novel catechol compounds **1**, **3b** and **5** can also be used for the transport of the same guests through lipophilic phases. Owing to the low solubility of most purine and pyrimidine bases in water (pH 7) the well-proven liquid-liquid extraction (U-tube or coaxial tube) technique[5a, 13b, 15] could not be resorted to in this case. We therefore designed a simple apparatus, with which solid–liquid–liquid extractions can easily be carried out (Fig. 2). It consists of a dismountable glass tube; the guest is suspended as solid below an incorporated frit, which separates the organic phase (either pure solvent or a solution of one of the hosts). The frit prevents solid particles reaching the interface to the uppermost aqueous-acidic phase and thus to go into solution during the stirring. The host complexes the guest and transports it through the organic to the aqueous phase. The phase transfer of the complexed guest takes place there with dissociation of the supramolecular aggregates. Samples of the aqueous phase are taken at certain intervals of time and the change in guest concentration is monitored.

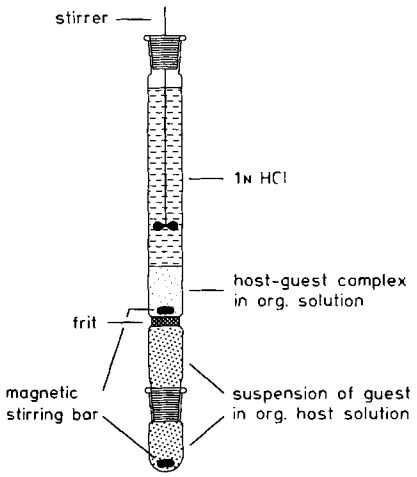

Fig. 2. Apparatus for the investigation of the transport of sparingly soluble guests through CH_2Cl_2/*n*-hexane (3:1) into an aqueous phase accelerated by the hosts.

Since relatively high transport rates can already be achieved in pure dichloromethane, we chose dichloromethane/*n*-hexane (3:1) as solvent. Even in this less polar solvent, purine and methylene blue **7b** are so readily soluble that the host has no noticeable influence on them.[16] In all other cases, significant, in part drastic, effects are recorded (Fig. 1, right). Thereby it must be remembered that, not only the thermodynamics and kinetics of the solution process play a role but also complexation and decomplexation; high complex stability and large increase in solubility do not necessarily mean therefore also rapid transport. Accordingly, the results also show no simple trend. For example, even the transport of such guests whose solubility is not substantially increased (e.g. 2,4-dihydroxypteridine) is accelerated by the hosts. This could be attributed to more rapid complexation/decomplexation. In some cases the macrocycle **1** affords, contrary to expectation,[17] the highest values; in this case the large increase in solubility seems to overcompensate the obvious slower decomplexation. The superior complexation of the cage host **1** justifies the higher synthetic effort compared to the acyclic compounds **3b** and **5**. The results of this work pose the question of whether the siderphores[18] containing catechol or hydroxamate units, which are important for the

transport of iron, play a role in the transport of purine and pyrimidine bases or nucleotides.

Received: December 11, 1990 [Z 4316 IE]
German version: *Angew. Chem. 103* (1991) 433

[1] W. Kiggen, F. Vögtle, *Angew. Chem. 96* (1984) 712; *Angew. Chem. Int. Ed. Engl. 23* (1984) 714.
[2] a) S. Grammenudi, F. Vögtle, *Angew. Chem. 98* (1986) 1119; *Angew. Chem. Int. Ed. Engl. 25* (1986) 1119; b) S. Grammenudi, M. Franke, F. Vögtle, E. Steckhan, *J. Incl. Phenom. 5* (1987) 695.
[3] a) W. Kiggen, F. Vögtle, S. Franken, H. Puff, *Tetrahedron 42* (1986) 1859; b) for complexes with $Pb^{2\oplus}$ and $Bi^{3\oplus}$ see: M. Magerstädt, O. A. Gansow, L. K. Pannell, F. Vögtle, W. Kiggen, *Nucl. Med. Biol. 17* (1990) 409; c) for complexes with alkali-metals see: J. Peter-Katalinić, F. Ebmeyer, C. Seel, F. Vögtle, *Chem. Ber. 122* (1989) 2391. d) For comparable siderands see: T. J. McMurry, M. W. Hosseini, T. M. Garret, F. E. Hahn, Z. E. Reyes, K. N. Raymond, *J. Am. Chem. Soc. 109* (1987) 7196.
[4] a) L. De Cola, F. Barigelletti, V. Balzani, P. Belser, A. von Zelewsky, F. Vögtle, F. Ebmeyer, S. Grammenudi, *J. Am. Chem. Soc. 110* (1988) 7210; b) F. Barigelletti, L. De Cola, V. Balzani, P. Belser, A. v. Zelewsky, F. Vögtle, F. Ebmeyer, S. Grammenudi, *ibid. 111* (1989) 4662; c) P. Belser, *Chimia 44* (1990) 226; d) F. Ebmeyer, F. Vögtle, *Chem. Ber. 122* (1989) 1725.
[5] a) F. Vögtle, W. M. Müller, U. Werner, H.-W. Losensky, *Angew. Chem. 99* (1987) 930; *Angew. Chem. Int. Ed. Engl. 26* (1987) 901; b) A. Wallon, J. Peter-Katalinić, U. Werner, W. M. Müller, F. Vögtle; *Chem. Ber. 123* (1990) 375; c) A. Wallon, U. Werner, W. M. Müller, M. Nieger, F. Vögtle, *ibid. 123* (1990) 859; d) F. Vögtle, A. Wallon, W. M. Müller, U. Werner, M. Nieger, *J. Chem. Soc. Chem. Commun. 1990*, 158.
[6] F. Ebmeyer, F. Vögtle, *Angew. Chem. 101* (1989) 95; *Angew. Chem. Int. Ed. Engl. 28* (1989) 79.
[7] P. Stutte, W. Kiggen, F. Vögtle, *Tetrahedron 43* (1987) 2065.
[8] 1.5 L, 50 °C, catalytic amounts of 4-*N*,*N*-dimethylaminopyridine, duration of addition 12 h, column chromatography (see Ref. [9]).
[9] The spectroscopic data (^1H and ^{13}C NMR, MS) of the new compounds are consistent with the structures. For details of the procedures see Refs. [7] and [3c]. MS (FAB, *m*-nitrobenzyl alcohol) of **1**: *m/z* 1814 ($M^{\oplus}$ + H, 89%), 1815 ($M^{\oplus}$ + 2, 100%); of **3b**: *m/z* 1471 ($M^{\oplus}$ + H, 88%), 1472 ($M^{\oplus}$ + 2, 100%); of **4**: *m/z* 1814 ($M^{\oplus}$ + H, 86%), 1815 ($M^{\oplus}$ + 2, 100%). MS (70 eV) of **5**: 556 ($M^{\oplus}$, 8%), 465 ($M^{\oplus}-C_7H_7$, 24%). R_f values (SiO_2, CH_2Cl_2/ethanol 20:1) of the methyl ether precursors of **1**: 0.24, of **3b**: 0.32, of **4**: 0.22, of **5**: 0.41.
[10] Due to hydrogen bridge bonds, the phenolic protons show, inter alia, smaller intensities, are shifted or disappear completely. With an empirical formula of $C_{120}H_{96}N_6O_{12}$ for **1** and **4**, the host signals clearly predominate compared to the guest signals.
[11] Adenine hosts: a) K. Williams, B. Askew, P. Ballester, C. Buhr, K. S. Jeong, S. Jones, J. Rebek, Jr., *J. Am. Chem. Soc. 111* (1989) 1090; b) S. Goswami, A. D. Hamilton, D. VanEngen, *ibid. 111* (1989) 3425; c) S. C. Zimmerman, W. Wu, *ibid. 111* (1989) 8054; d) J. C. Adrian, C. S. Wilcox, *ibid. 111* (1989) 8055; Guanine hosts: e) A. D. Hamilton, N. Pant. *J. Chem. Soc. Chem. Commun. 1988*, 765; f) J. Rebek, Jr., *Chemtracts: Org. Chem. 2* (1989) 337; uracil and thymine hosts: g) A. D. Hamilton, D. VanEngen, *J. Am. Chem. Soc. 109* (1987) 5035; h) A. V. Muehldorf, D. VanEngen, J. C. Warner, A. D. Hamilton, *ibid. Chem. Soc. 110* (1988) 6561; cytosine hosts: J. Rebek, Jr., K. S. Jeong, *ibid. 110* (1988) 3327.
[12] Procedure as in Ref. [13b] (ultrasound, centrifugation). Guanine and pterine are so sparingly soluble in pure dichloromethane—other than on addition of the hosts—that the values lie below the error limit. The data quoted for these two guests are estimated lowest values.
[13] a) K. A. Connors: *Binding Constants. The Measurement of Molecular Complex Stability*, Wiley, New York 1987; b) F. Diederich, K. Dick, *J. Am. Chem. Soc. 106* (1984) 8024.
[14] It must be remembered here that the more strongly bound guests are, at the same time, also very sparingly soluble. That is in these cases the solvent also competes less strongly with the hosts.
[15] a) W. H. Mandeville, G. M. Whitesides, *J. Org. Chem. 51* (1986) 3257; b) A. Harada, S. Takahashi, *J. Chem. Soc. Chem. Commun. 1987*, 527; c) M. Bühner, W. Geuder, W. K. Gries, S. Hünig, M. Koch, T. Poll, *Angew. Chem. 100* (1988) 1611; *Angew. Chem. Int. Ed. Engl. 27* (1988) 1553; d) V. Prelog, M. Dumić, *Helv. Chim. Acta 69* (1986) 5.
[16] The transport starts more quickly here but with time the rates equal the blank values.
[17] a) M. Kirch, J.-M. Lehn, *Angew. Chem. 87* (1975) 542; *Angew. Chem. Int. Ed. Engl. 14* (1975) 555; b) J.-M. Lehn, *Pure Appl. Chem. 51* (1979) 979; c) J. D. Lamb, R. M. Izatt, J. J. Christensen, *Prog. Macrocyclic Chem. 2* (1981) 41.
[18] a) K. N. Raymond, G. Müller, B. F. Matzanke, *Top. Curr. Chem. 123* (1984) 49; b) R. C. Hider, *Struct. Bonding (Berlin) 58* (1984) 25; c) G. Winkelmann, D. van der Helm, J. B. Neilands (Eds.): *Iron Transport in Microbes, Plants and Animals*, VCH, Weinheim 1987.

Novel Naphthalene- and Cyclohexa-1,3-diene–Silene Cycloadducts**

By *Norbert Auner,** *Claudia Seidenschwarz, Eberhardt Herdtweck,* and *Norbert Sewald*

Since the formulation of the Woodward-Hoffmann rules,[1] investigation of the mechanisms of cycloaddition reactions has constituted the central activity of numerous research groups.[2] This area of research has gained enormous impetus through the employment of more reactive heterodienophiles,[3] including recently Si=C-systems[4] and Si=Si-systems[4, 5]. Alongside the dimethylneopentylsilene $Me_2Si{=}CHCH_2tBu$ investigated by *Jones*[6] we now present a dichlorinated analog $Cl_2Si{=}CHCH_2tBu$ **1**, which exhibits a markedly different cycloaddition behavior; this can be attributed to the influence of the chlorine atoms on the position of the frontier orbitals and the magnitude of the orbital coefficients. The characteristic combination of higher dienophilicity and strongly dipolar Si=C character in the case of **1**[7] manifests itself in its different behavior towards naphthalene **2**, which has only slight diene qualities,[8] and cyclohexa-1,3-diene **6**, which finds frequent use as a [4 + 2]-trapping reagent for heterodienophiles.[9]

Reaction of $Cl_3SiCH{=}CH_2$ with an equimolar amount of Li*t*Bu and excess **2** at 0 °C leads (even in the dark) to formation of the thermally stable *endo* [4 + 2]-cycloadduct **3** in about 75% yield (GC integration of the product mixture), and can be isolated by sublimation at 10^{-2} mbar in ca. 40% yield. After recrystallization from *n*-pentane **3** precipitates in the form of colorless needles, which have been characterized analytically and NMR spectroscopically.[10]

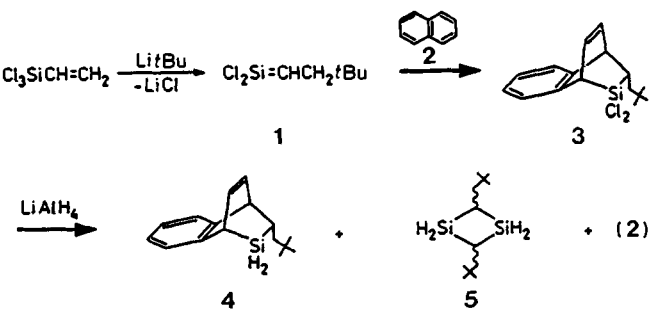

Reduction of **3** with $LiAlH_4$ under mild conditions furnishes crystalline *endo*-**4**;[10] (*E*)/(*Z*)-isomeric 2,4-dineopentyl-1,3-disilacyclobutane **5**[11] and **2** are also formed. The colorless, slightly air-sensitive crystals of **4** are readily soluble in nonpolar solvents and were subjected to an X-ray structure analysis.[12] Thus, for the first time, it was possible to determine the structure of a [4 + 2]-cycloadduct of a silene with naphthalene. Characteristically, the molecule shows hardly any structural peculiarities compared to the [4 + 2]-cycloadduct of **1** and anthracene;[7] only the C3–C4 bond length (157.2(1) pm) is significantly longer than the mean value ($\bar{d}$ = 152.1 pm) of the other C–C single bonds. Due to the larger atomic radius of the Si atom the 2-silabicy-

[*] Prof. Dr. N. Auner, Dipl.-Chem. C. Seidenschwarz, Dr. E. Herdtweck, Dipl.-Chem. N. Sewald
Anorganisch-chemisches Institut der Technischen Universität München
Lichtenbergstrasse 4, W-8046 Garching (FRG)

[**] Silaheterocycles, Part 10. This work was supported by the Volkswagen-Stiftung, the Deutsche Forschungsgemeinschaft, and the Fonds der Chemischen Industrie.—Part 9: [11].

clo[2.2.2]octadiene parent compound is slightly distorted in comparison to the analogous carbon-compound.[13] The *endo* position of the neopentyl group to the ring skeleton in **4**[14] follows from the torsional angles C1-Si-C3-C13 [− 125.7(1)°] and C8-C4-C3-C13 [− 173.7(1)°].

Consistent with theoretical considerations,[15] the diene quality towards **1** increases in the series benzene → naphthalene → anthracene.[6, 14, 16] Formation of the thermodynamically unfavorable *endo*-product **3** suggests a concerted cycloaddition, especially since we could not trap any dipolar intermediates during the course of the reaction.

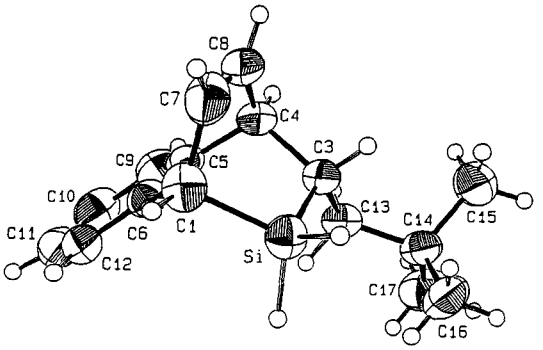

Fig. 1. Structure of **4** in the crystal (ORTEP at the 50% probability level, the hydrogens were given an arbitrary radius). Important bond lengths [pm] and angles [°]: Si–Cl 189.7(1), Si-C3 189.3(1), Si-H1 145.0(8), Si-H2 141.6(8), C3-C13 154.0(1), C13-C14 153.0(1), C3-C4 157.2(1), C4-C5 151.3(1), C5-C6 139.1(1), C1-C6 150.4(1), C1-C7 150.8(1), C7-C8 131.4(1), C4-C8 150.6(1); C1-Si-C3 100.29(4), Si-C3-C13 116.45(6), Si-C3-C4 105.87(6), Si-C1-C6 102.69(5), C6-C1-C7 109.84(8), C3-C4-C5 108.91(7), C3-C4-C8 107.70(8); C13-Si-C3-C1 − 125.7(1), C13-C3-C4-C8 − 173.7(1).

Even though **6** reacts mainly as a [4 + 2]-trapping reagent,[9] the [2 + 2]-addition is preferred in the cycloaddition of **1** with **6**. Thus, electrophilic attack of the silene at the diene leads mainly to regioselective formation of the stereoisomeric (*E*)/(*Z*)-silacyclobutane derivative **7**. Upon reaction of the product mixture (**7**/**8**) with phenyl-Grignard reagent only the Si atom in **7** is phenylated, probably on steric grounds. The cycloadducts **8** and **9** can therefore be separated from each other and be characterized by NMR spectroscopy (NMR data of **7** determined by difference spectrum).[10] **7** is obtained in 74% yield (isomeric ratio **7a**/**7b** 62/38) and **8** in 26% yield (**8a**/**8b** 63/37). Surprisingly, during storage (daylight, room temperature) the [2 + 2]-cycloadducts **7** transform completely within eight weeks into the thermodynamically more stable bicyclic 2-silaoctenes **8**, whose isomeric ratio remains unaltered; the silacyclobutanes **9**, on the other hand, are stable. Comparative studies on the [2 + 2]-cycloadducts **7** and **9** and on the reactivity of the diphenylneopentylsilene confirm that the unusual [2 + 2]-cycloaddition of **1** with **6** and the isomerization behavior of **7** are caused by the influence of the chlorine substituents. Dialkyl- and diaryl-substituted neopentylsilenes exhibit a markedly different cycloaddition behavior towards **6**.

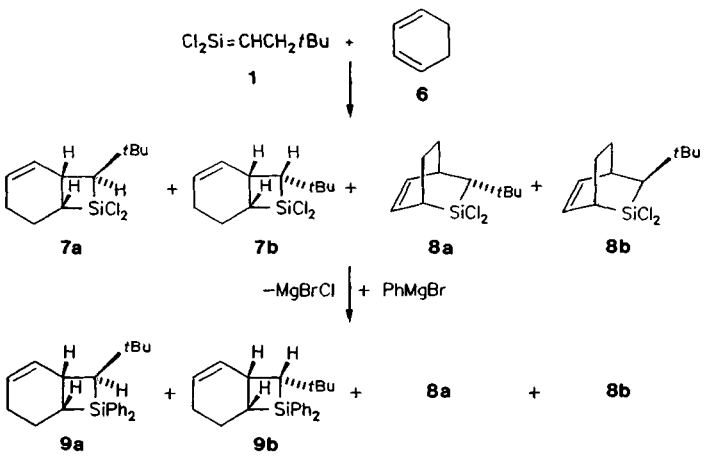

Experimental procedure

3: A stirred mixture of 19 g (148 mmol) of **2** and 4.7 g (30 mmol) of H_2C=$CHSiCl_3$ in 600 mL of anhydrous benzene was treated slowly at 0 °C with 21.5 mL (30 mmol) of Li*t*Bu; this resulted in elimination of LiCl. After filtration and removal of the solvent by distillation, the oily solid residue was freed of excess **2** by sublimation (40 °C/10^{-2} mbar), whereby considerable amounts of **3** were lost. **3** was initially isolated as a highly viscous, colorless liquid (b.p. 65–70 °C/10^{-2} mbar); it subsequently crystallized in the receiver (m.p. 70 °C). Yield: 3.72 g, 12 mmol, 40%.

4: A suspension of $LiAlH_4$ (0.57 g, 15 mmol) in anhydrous Et_2O (40 mL) was treated dropwise at 0 °C with a solution of **3** (2.0 g, 6.5 mmol) in Et_2O (15 mL). After warming to room temperature the reaction mixture was filtered. Distillation of the solution yielded **4** and **5** at 50 °C/10^{-2} mbar, while **2** sublimed. After storage for 3 months at 20 °C, **4** crystallized (m.p. 60 °C) and was separated from **5**. Yields: **4**: 1.04 g (4.29 mmol), 66%; **5**: 0.25 g (1.1 mmol), 34%.

7: A mixture of 7.2 g (90 mmol) of **6** and 4.7 g (30 mmol) of H_2C=$CHSiCl_2$ in 500 mL of *n*-pentane was treated at −78 °C with 21.5 mL Li*t*Bu (30 mmol; 1.4 mmol/mL *n*-pentane). The stirred mixture was warmed to room temperature (LiCl precipitation at ca. − 5 °C), filtered, and the filtrate worked-up by distillation. **7** and **8** were isolated as colorless, viscous liquids (b.p. 60 °C/10^{-2} mbar). Yield 7.82 g, 29.8 mmol, 99.5%.

Received: November 23, 1990 [Z 4290 IE]
German version: *Angew. Chem. 103* (1991) 425

CAS Registry numbers:
2, 91-20-3; **3**, 132438-94-9; **4**, 132438-95-0; (*E*)-**5**, 130992-05-1; (*Z*)-**5**, 130992-17-5; **6**, 592-57-4; **7a**, 132438-96-1; **7b**, 132489-62-4; **8a**, 132438-97-2; **8b**, 132489-63-5; **9a**, 132438-98-3; **9b**, 132489-64-6; Cl_3SiCH=CH_2, 75-94-5; Ph_2Si=$CHCH_2t$Bu, 132439-00-0; *endo*-2,2-diphenyl-3-(2',2'-dimethylpropyl)-2-silabicyclo[2.2.2]oct-5-ene, 132489-65-7; *exo*-2,2-diphenyl-3-(2',2'-dimethylpropyl)-2-silabicyclo[2.2.2]oct-5-ene, 132438-99-4.

[1] R. B. Woodward, R. Hoffmann: *The Conservation of Orbital Symmetry*, Verlag Chemie, Weinheim 1970; *Angew. Chem. 81* (1969) 797; *Angew. Chem. Int. Ed. Engl. 8* (1969) 781.
[2] J. Sauer, R. Sustmann, *Angew. Chem. 92* (1980) 773; *Angew. Chem. Int. Ed. Engl. 19* (1980) 779.
[3] D. L. Boger, S. N. Weinreb: *Hetero Diels-Alder Methodology in Organic Synthesis*, Academic Press, London 1987.
[4] For reviews see: N. Wiberg, *J. Organomet. Chem. 273* (1984) 141; G. Raabe, J. Michl, *Chem. Rev. 85* (1985) 419.
[5] Review: R. West, *Angew. Chem. 99* (1987); 1231; *Angew. Chem. Int. Ed. Engl. 25* (1987) 1201.
[6] P. R. Jones, T. F. O. Lim, *J. Am. Chem. Soc. 99* (1977) 8447; P. R. Jones, T. F. O. Lim, R. A. Pierce, *ibid. 102* (1980) 4970.
[7] N. Auner, *Habilitationsschrift*, Münster, 1987; *Z. Anorg. Allg. Chem. 558* (1988) 55; *J. Organomet. Chem. 353* (1988) 275.
[8] Review: J. Sauer, *Angew. Chem. 78* (1966) 233; *Angew. Chem. Int. Ed. Engl. 5* (1966) 211.
[9] U. Annen, M. Regitz, *Tetrahedron Lett. 1988*, 1681; J. Grobe, J. Szameitat, *Z. Naturforsch. B 43* (1988) 427; C. Larson, D. N. Hopp, *J. Org. Chem. 45* (1980) 3713; E. Kessler, *J. Heterocycl. Chem. 17* (1980) 1113; K. Friedrich, H.-J. Gallmeier, *Tetrahedron Lett. 1981*, 2971; reaction of tBu$_2$Si=Si*t*Bu$_2$ with **6**, however, leads to the [2 + 2]-adduct: M. Weidenbruch, A. Schäfer, K.-L. Thom, *Z. Naturforsch. B 38* (1983) 1695.
[10] The compounds **3**–**5** and **7**–**9** were characterized by elemental analysis (C,H,Si) and mass spectroscopically (70 eV). Their ^{1}H- and ^{13}C-NMR parameters were determined by H,H-, C,H-COSY and -NOESY investigations. In addition to the ^{29}Si-NMR values the data sets for **4** and **7a** are given. **4**: ^{1}H NMR (360 MHz, $CDCl_3$, 25 °C, TMS, J(H,H) in Hz): δ = 7.22–7.12 (m, 4 H aromat.), 6.38 (ddd, ^3J = 7.9, 6.6, ^4J = 1.2, 1 H olefin.), 6.32 (dddd, ^3J = 7.9, 6.3, ^4J = 1.2, 0.8, 1 H olefin.), 3.83 (m, 1 H, H4), 3.81 (m, 1 H, SiH_2), 3.80 (m, 1 H, H1), 3.27 (dd, broad, ^2J = 14.0, ^3J = 1.5, 1 H, SiH_2), 1.30–0.85 (m, 3 H, H3, H9), 0.87 (s, 9 H, *t*Bu); ^{13}C NMR (90.6 MHz, $CDCl_3$, TMS, DEPT, C,H-COSY [with f_1-decoupling: 200 × 2 K FIDs, zero filling to 512 × 2 K, apodized (improvement of resolution) with sinus function]): δ = 140.10, 139.64 (C aromat.); 132.39, 130.66 (CH olefin.); 125.93, 125.77, 124.52, 123.73 (CH aromat.); 48.24 (C4), 46.79

(C9), 31.78 (C1), 31.41 ($C(CH_3)_3$), 29.79 ($C(CH_3)_3$), 19.49 (C3); ^{29}Si-NMR (79.4 MHz, $CDCl_3$, TMS): $\delta = -30.4$ (t), $^1J(^{29}Si^1H) = 204$ Hz; IR: ν[cm^{-1}] = 2145 (SiH); UV: λ_{max}[nm] = 268.2, 274.2. **7a**: ^{1}H NMR: $\delta = 2.49$ (m, 1H, H1), 5.91 (m, 1H, H2), 5.74 (m, 1H, H3), 1.94 (m, 1H, H_a4), 2.05 (m, 1H, H_b4), 1.78 (m, 1H, H_a5), 1.96 (m, 1H, H_b5), 2.21 (m, 1H, H6), 2.01 (m, 1H, H8), 1.49, 1.71 (m, 2H, H9), 0.77 (s, 9H, *t*Bu); ^{13}C NMR: $\delta = 38.42$ (C1), 130.27 (C2), 126.00 (C3), 23.84 (C4), 20.01 (C5), 35.52 (C6), 44.58 (C8), 43.14 (C9), 31.08 ($C(CH_3)_3$), 29.55 ($C(CH_3)_3$). ^{29}Si NMR: $\delta = 15.8$ (**3**), 19.7 (**7a**), 14.2 (**7b**), 25.6 (**8a**), 26.5 (**8b**).

[11] N. Auner, R. Gleixner, *J. Organomet. Chem. 393* (1990) 33.

[12] P. Kiprof, E. Herdtweck, R. E. Schmidt, M. Birkhan, W. Massa: STRUX-III (Programmsystem zur Verarbeitung von Röntgendaten, Technische Universität München/Universität Marburg, 1989/1985). Compound **4** crystallizes from *n*-pentane as colorless rods, monoclinic space group $P2_1/c$. $a = 1502.9(1)$, $b = 860.4(1)$, $c = 1182.7(1)$ pm, $\beta = 106.80(2)°$, $V = 1464 \times 10^6$ pm^3, $C_{16}H_{22}Si$, $M = 242.4$, $Z = 4$, $F_{(000)} = 528$, $\varrho_{calcd} = 1.100$ g cm^{-3}; apparatus: Enraf-Nonius CAD-4, $Cu_{K\alpha}$ radiation ($\lambda = 154.184$ pm), graphite monochromator, $T = 21 \pm 1$ °C; range of measurement: $1.0° \leq \theta \leq 65.0$, $\theta/2\theta$ scan. 5604 measure reflections ($\pm h,k,l$, each at $\psi = 0°$ and 3°) were determined after LP correction and correction for a slight distortion (376 cancelled reflections and 278 with $I < 0$ were considered as unobserved). No absorption correction ($\mu = 12.0$ cm^{-1}). All 2425 independent reflections ($I > 0$) were refined with 243 parameters using full matrix least squares. $R = 0.043$, $R_w = 0.038$, GOF = 3.732 ($p = 0.00$) with $\omega = 1/\sigma^2(F_o)$. Solution of structure by direct methods and difference Fourier technique. Extinction effects ($\varepsilon = 0.1995 \times 10^{-5}$) were corrected. All hydrogen atom positions are successively taken from difference Fourier syntheses and refined with isotropic temperature factors. Anomalous dispersion is taken into account. After the last refinement cycle (shift/error < 0.00) the maximal/minimal residual electron density contributed + 0.19/− 0.29 e_o-/Å^3. Further details of the crystal structure investigation are available on request from the Fachinformationszentrum Karlsruhe, Gesellschaft für wissenschaftlich-technische Information mbH, W-7514 Eggenstein-Leopoldshafen 2 (FRG), on quoting the depository number CSD-54651, the names of the authors, and the journal citation.

[13] To our knowledge no solid-state structure has been published for the parent compound bicyclo[2.2.2]octadiene. For a structural comparison see D. Döpp, C. Krüger, H. R. Memarian, Y.-H. Tsay, *Angew. Chem. 97* (1985) 1059; *Angew. Chem. Int. Ed. Engl. 24* (1985) 1048; B. Karlsson, A.-M. Pilotti, A.-C. Söderholm, *Acta Chem. Scand. Ser. B 31* (1977) 619; P. Argos, R. Clayton, *Acta Crystallogr. Sect. B 29* (1973) 910; S. Hechtfischer, W. Steigemann, W. Hoppe, *Acta Crystallogr. Sect. B 26* (1970) 1713.

[14] In the meantime *endo/exo*-[2,2-diphenyl-3-(2',2'-dimethylpropyl)-2-silabicyclo[2.2.2]oct-5-ene] has been synthesized by [4 + 2]-cycloaddition from $Ph_2Si{=}CHCH_2tBu$ and **6** and was characterized analytically and mass spectroscopically by us. The isomeric ratio of 70/30 was demonstrated by GC and NMR studies in solution and by X-ray structure analysis in the crystalline state: N. Auner, W. Ziche, E. Herdtweck, unpublished results.

[15] A. Streitwieser: *Molecular Orbital Theory for Organic Chemists*, Wiley, New York 1961, p. 432.

[16] N. Auner, *J. Organomet. Chem. 377* (1989) 175.

Tercalicene and Quatercalicene

By *Toyonari Sugimoto,* Mitsuhiro Shibata, Akihiko Sakai, Hiroshi Ando, Yoshihisa Arai, Masashi Sakaguchi, Zen-ichi Yoshida,* Yasushi Kai,* Nobuko Kanehisa,* and *Nobutami Kasai**

In contrast to calicene,[1] which still remains a synthetic challenge, bicalicene **1a**, which is composed of two calicene units in a head-to-tail orientation, was already prepared by us a few years ago.[2] An X-ray structural analysis, ^{1}H- and ^{13}C-NMR spectra and theoretical calculations indicated that 2π (three-membered ring) and 6π (five-membered ring) electron conjugations, due to polarization of each calicene unit, significantly contribute to the electronic structure in the ground state.[3] This polarization could also be favored by the avoidance of an antiaromatic 16π electron conjugation in the periphery. In the next higher homologue, tercalicene **2a**, however, an aromatic 22 π electron conjugation could be present, whereas quatercalicene **3a** adopts a similar π electron conjugation mode to that of **1a** because of the presence of 28 π electrons in the periphery. We report here on the synthesis of **2a** and the 3, 10- and 3,17-bis(*tert*-butylthio) derivatives **2b** and **3b**, respectively, and discuss the possible electronic structures of **2a** and **3a** based on the molecular structure of **2b**, and the ^{1}H- and ^{13}C-NMR spectral data for **2a**, **2b** and **3b**.

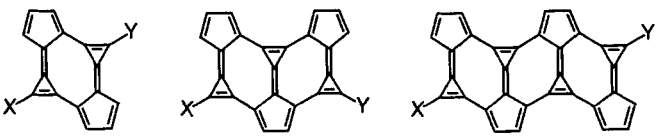

1a: X=Y=H
1b: X=Y=S*t*Bu

2a: X=Y=H
2b: X=Y=S*t*Bu
2c: X=Y=Sn*n*Bu

3a: X=Y=H
3b: X=Y=S*t*Bu
3c: X=Y=Sn*n*Bu

2b and **3b** were synthesized from **1b** as shown in Scheme 1, and converted in a two-step process—distannylation and acid- or base-catalyzed hydrolysis—into **2a** and **3a**.

Thus, the 3,11-bis(*tert*-butylthio)derivative **1b**[2b] was allowed to react with lithium cyclopentadienide (20 equiv.) in THF at 0 °C to give the central intermediate **4** (yield 82%, Table 1). By successive reaction of **4** with lithium diisopropylamide (LDA) (2 equiv.) and 1,2-bis(*tert*-butylthio)-3,3-

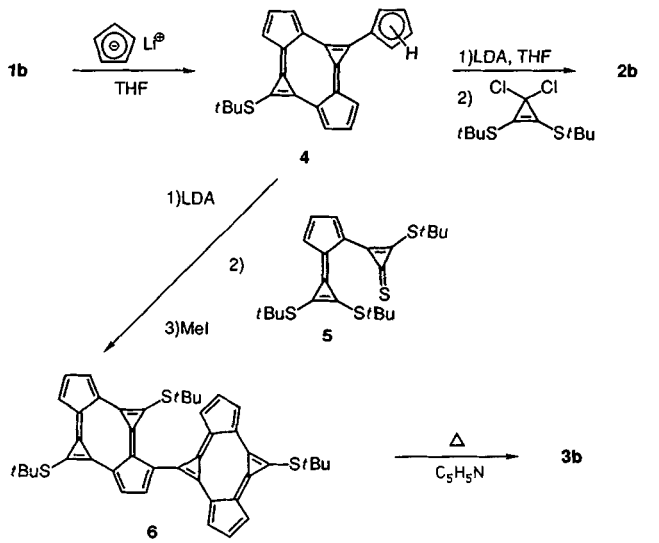

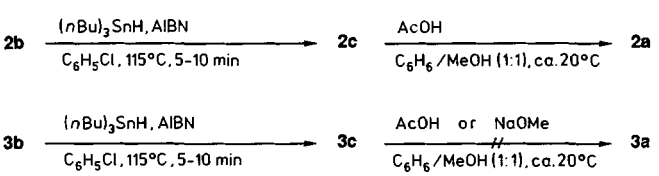

Scheme 1.

[*] Prof. Dr. T. Sugimoto, Prof. Dr. Z. Yoshida, Dr. M. Shibata, A. Sakai, H. Ando, Y. Arai, M. Sakaguchi
Department of Synthetic Chemistry
Kyoto University
Yoshida, Kyoto 606 (Japan)
Prof. Dr. Y. Kai, Prof. Dr. N. Kasai, N. Kanehisa
Department of Applied Chemistry
Osaka University,
Yamadaoka, Osaka 565 (Japan)

dichlorocyclopropene[4] (1 equiv.) in THF at −78 °C, **2b** was obtained (11%). On the other hand, when **4** was treated successively with LDA (2 equiv.), the calicene derivative **5**[4] (1 equiv.) at −78 °C, and then with CH_3I (2 equiv.) at room temperature, the bis(bicalicene) **6** was formed (20%), which was converted into **3b** (48%) by refluxing in dry pyridine for 1 h. By reaction of **2b** and **3b** with tri-*n*-butyltin hydride (10 equiv.) and azobisisobutyronitrile (AIBN) (3 equiv.) in chlorobenzene,[5] the stannyl derivatives **2c** and **3c** were obtained (8 and 10%, respectively). Treatment of **2c** with an excess of acetic acid in methanol-benzene (1:1 v/v)[5] afforded **2a** (59%). Attempts to prepare **3a**, however, failed even though **3c** was allowed to react with acetic acid and sodium methoxide[8] under various conditions. Presumably, **3a** is extremely sensitive to both acids and bases.

An X-ray structure analysis of **2b**,[6, 7] showed that the crystal lattice contains two crystallographically independent molecules, which are characterized by the *syn* and *anti* positions of the two *tert*-butylthio substituents, (Fig. 1 shows *syn*-**2b**). Just as high planarity is observed in the skeletons of

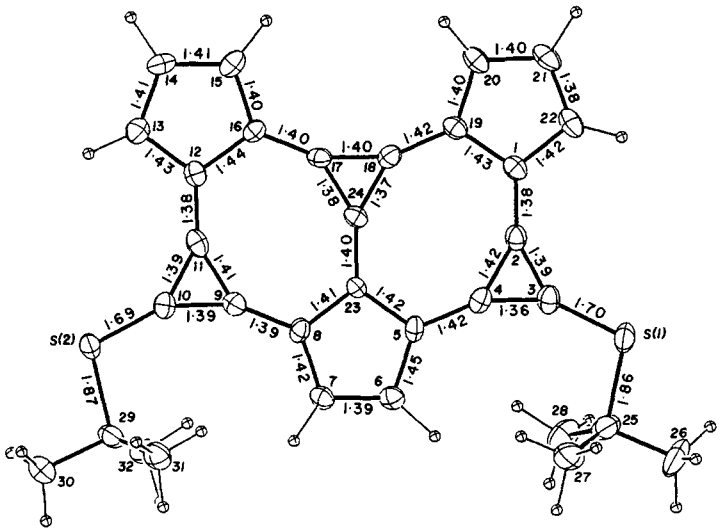

Fig. 1. Crystal structure of *syn*-**2b** with interatomic bond distances. Thermal ellipsoids for the non-hydrogen atoms are drawn at the 20% probability level while the hydrogen atoms are given by spheres with a temperature factor of 1.0 Å^2. The ESD values for bond distances are in the range of 0.009 and 0.019 Å.

1a and **1b**,[2, 3] the tercalicene skeleton in **2b** is also almost completely planar. With regard to the bond lengths, the following points are noteworthy: 1) the bridge bond of the inner calicene (C23–C24) is longer than those of the outer ones; 2) the C1–C19 and C12–C16 bonds are the longest in the five-membered rings of the outer calicenes; 3) the C2–C4 and C9–C11 bonds are equal to or longer than the other bonds in the three-membered rings of the outer calicenes; 4) the C6–C7 bond is the shortest in the five-membered ring of the inner calicene; and 5) the C17–C18 bond is longer than the other bonds in the three-membered ring of the inner calicene. The outer calicenes of **2b** have a very similar molecular structure as that of **1b**, while the inner calicene is markedly different.

The ^{1}H-NMR spectral data of **2a**, **2b** and **3b** are summarized (Table 1).[8] The chemical shifts (δ = 7.94, 7.06, 6.96, 6.39) of the protons of the outer calicene of **2a** resemble those (7.91, 7.11, 6.58) of **1a**. For the protons of the five-membered ring of the inner calicene the chemical shift (6.80) is intermediate between those of the down- and upfield shifted protons of the outer five-membered rings. The situation is similar upon comparing the chemical shifts of **1b**, **2b**, and **3b**. These results provide no significant evidence for diamagnetic and paramagnetic ring currents in the 22 π electron system **2a**[9] and in the 28 π electron system **3a**, just as there was no paramagnetic ring current induced in the peripheral 16 π electron system **1a**. The ^{13}C-NMR spectra of **2a** and **2b**[10] show the expected 13 signals. According to the chemical shifts of **1a** and **1b**,[11] there is no difference between **1** and the outer calicene **2**. The three carbons of the three-membered ring of the inner calicene have almost the same chemical shifts. In contrast, three carbons (C5, C8, and C23) are shifted upfield by 5–12 ppm compared with those of the remaining carbons. This result suggests preferential delocalization of a positive charge on the three-membered ring and preferential localization of a negative charge at the C5, C8 and C23 carbons of the five-membered ring.

Summarizing: as in **1a** the polarization of each calicene makes an important contribution to the electronic structures of **2a** and **3a**.[12] Furthermore, the degree of polarization is almost the same (ca. 50%) irrespective of the kind of calicene in **1a**, **2a** and **3a**, although the inner calicene in **2a** assumes a markedly different polarization structure from that of the outer one. The contribution of the mesomeric limiting structures shown in the formulas is also significant. Since the bridging bond of the inner calicene **2b** is longest a 16 π electron conjugation (as in **1a**) might describe **2b** better than a peripheral 22 π electron conjugation. This could also be val-

Table 1. Selected physical data of the compounds **2a**, **2b**, **2c**, **3b**, **3c**, **4**, and **6**[a].

2a: Dark brown crystals, m.p. 110–115 °C (dec.); IR: $\tilde{\nu}$[cm^{-1}] 2930, 1770, 1740, 1573, 1535, 1260, 1100, 1025, 800; UV: λ_{max} [nm] (log ε) = 251 (4.63), 290 (4.34), 345 (4.29), 382 (4.36), 435 (4.65), 522 (3.31), 574 (3.20), 662 (2.87), 730 (2.76); ^{1}H NMR: δ = 7.94 (s, 2H), 7.01 (dd, J = 3.5, 1.5 Hz, 2H), 6.96 (dd, J = 4.0, 1.5 Hz, 2H), 6.80 (s, 2H), 6.39 (dd, J = 4.0, 3.5 Hz, 2H); ^{13}C NMR: δ = 141.5, 131.9, 131.6, 126.0, 124.3, 120.4, 118.0, 114.5, 112.4, 109.3; FD-MS: m/z 298 ($M^{\oplus}$).

2b: Dark green crystals, m.p. 110–115 °C (dec); IR: $\tilde{\nu}$[cm^{-1}] 2970, 2940, 1565, 1535, 1265, 1100, 1020, 805; UV: λ_{max} [nm] (log ε) = 268 (4.57), 322 (4.42), 352 (4.36), 403 (4.42), 425 (4.47), 454 (4.68), 547 (3.30), 610 (3.47), ca. 760 (2.52); ^{1}H NMR: δ = 6.99 (dd, J = 3.4, 1.5 Hz, 2H), 6.90 (dd, J = 4.0, 1.5 Hz, 2H), 6.73 (s, 2H), 6.41 (dd, J = 4.0, 3.4 Hz, 2H), 1.72 (s, 18H); ^{13}C NMR: δ = 137.5, 134.8, 131.4, 131.3, 130.0, 129.5, 126.8, 124.4, 123.1, 119.0, 114.4, 111.2, 108.7, 48.4, 31.4; FD-MS: m/z 386 ($M^{\oplus}$).

2c: Dark brown semisolid; IR: $\tilde{\nu}$ [cm^{-1}] 2930, 1775, 1530, 1405, 1260, 1100; UV: λ_{max} [nm] (log ε) = 700 (2.94), 628 (3.06), 560 (3.38), 437 (4.72), 384 (4.49), 342 (4.48), 311 (4.43); ^{1}H NMR: δ = 7.10–6.96 (m, 4H), 6.83 (s, 2H), 6.50 (t, J = 3.6 Hz, 2H), 1.55–0.77 (m, 5H); FD-MS: m/z 878 ($M^{\oplus}$).

3b: Brown solid, m.p. 186–200 °C (dec); IR: $\tilde{\nu}$[cm^{-1}] 2900, 1795, 1510, 1450, 1385, 1365, 1265, 735; UV: λ_{max} [nm] (log ε) = 250 (4.58), 268 (4.55), 307 (4.40), 340 (sh, 4.43), 373 (4.46), 414 (4.36) 466 (4.44), 498 (4.78), 560 (sh, 3.88), 660 (3.67), 740 (sh, 3.18); ^{1}H NMR: δ = 6.97 (dd, J = 3.7, 1.2 Hz, 2H), 6.94 (dd, J = 3.7, 1.2 Hz, 2H), 6.81 (d, J = 4.0 Hz, 2H), 6.79 (d, J = 4.0 Hz, 2H), 6.46 (t, J = 3.7 Hz, 2H), 1.75 (s, 18H); MS: m/z 572 ($M^{\oplus}$).

3c: Dark brown semisolid; IR: $\tilde{\nu}$[cm^{-1}] 2958, 2925, 2852, 1770, 1716, 1552, 1516, 1468, 1402, 1365, 1329, 1261, 1088, 798, 742; ^{1}H NMR: δ = 7.15 (dd, J = 3.8, 1.5 Hz, 2H), 7.11 (dd, J = 3.8, 1.5 Hz, 2H), 6.97 (d, J = 4.1 Hz, 2H), 6.90 (d, J = 4.1 Hz, 2H), 6.61 (t, J = 3.8 Hz, 2H), 1.66–0.81 (m, 54H); FD-MS: m/z 976 ($M^{\oplus}$).

4: Reddish orange crystals, m.p. 197–199 °C; IR: $\tilde{\nu}$[cm^{-1}] 2900, 1820, 1557, 1340, 1068; UV: λ_{max} [nm] (log ε) = 252 (4.26), 338 (4.20), 403 (4.23), 520 (3.72); ^{1}H NMR: δ = 7.45 (m, 1H), 6.90 (d, 4H), 6.80 (m, 2H), 6.45 (t, 2H), 3.55 (br. s, 2H), 1.75 (s, 9H); MS: m/z 474 ($M^{\oplus}$).

5: Reddish purple crystals, m.p. 175-190 °C (dec); IR: $\tilde{\nu}$ = [cm^{-1}] 2940, 1805, 1545, 1340, 1255, 1090, 1065, 1020, 800; UV: λ_{max} [nm] (log ε) = 267 (4.49), 344 (4.46), 386 (4.31), 416 (sh, 4.20), 530 (4.05); ^{1}H NMR: δ = 7.05 (dd, 1H), 6.92 (m, 5H), 6.88 (d, 1H), 6.87 (d, 1H), 6.40 (t, 1H), 6.39 (t, 2H), 1.76 (s, 18H), 1.60 (s, 9H); MS: m/z 662 ($M^{\oplus}$).

[a] ^{1}H- and ^{13}C-NMR spectra at 400 and 100.6 MHz, respectively; solvent, $CDCl_3$. IR spectra: in KBr pellet. UV spectra: solvent, CH_2Cl_2.

id for the π electron conjugation mode of the covalent structure of **3a**.

Received: November 6, 1990 [Z 4268 IE]
German version: *Angew. Chem. 103* (1991) 454

[1] H. Prinzbach, H. Knöfel, E. Woischnik in E. D. Bergman, B. Pullman (Eds.): *Aromaticity, Pseudo-Aromaticity, Anti-Aromaticity*, Academic New York 1971.
[2] (a) Z. Yoshida, *Pure Appl. Chem. 54* (1982) 1115. (b) S. Yoneda, M. Shibata, S. Kida, Z. Yoshida, Y. Kai, K. Miki, N. Kasai, *Angew. Chem. 96* (1984) 95; *Angew. Chem. Int. Ed. Engl. 23* (1984) 63.
[3] T. Sugimoto, M. Shibata, S. Yoneda, Z. Yoshida, Y. Kai, K. Miki, N. Kasai, T. Kobayashi, *J. Am. Chem. Soc. 108* (1986) 7032.
[4] Z. Yoshida, M. Shibata, S. Kida, S. Miki, T. Sugimoto, S. Yoneda, *Tetrahedron Lett. 25* (1984) 345.
[5] T. Sugimoto, M. Sakaguchi, H. Ando, T. Tanaka, Z. Yoshida, J. Yamauchi, A. A. Bothner-By, M. Lisicki, *J. Am. Chem. Soc. 104* (1991), in press.
[6] Single crystals of **2a** and **3b** have not been successfully prepared.
[7] Crystal data of **2b**: orthorhombic, space group *Pbca*, $a = 25.723(2)$, $b = 21.979(3)$, $c = 18.384(1)$ Å, $V = 10393.9(16)$ Å^3, $Z = 16$, $\rho_{calcd} = 1.213$ g cm^{-3}, $F(000) = 4000$, $\mu(Mo_{K\alpha}) = 19.4$ cm^{-1}. X-Ray diffraction data were measured on a Rigaku four-circle diffractometer using nickel-filtered $Cu_{K\alpha}$ radiation. A total of 6529 independent reflections were collected up to $2\theta = 110°$ by the $\theta - 2\theta$ scan technique. The intensity data were corrected for the usual Lorentz and polarization effects, but an absorption correction was not carried out. The structure was solved by direct methods (SHELXS-86) and refined by full-matrix least-squares using the 3477 observed reflections [$|F_o| > 3\sigma(F_o)$] to an R value of 0.084 and R_w value of 0.099 including non-hydrogen atoms with anisotropic thermal parameters and hydrogen atoms with isotropic ones, where $R = \Sigma(|F_o| - |F_c|)/\Sigma|F_o|$, $R_w = [\Sigma w(|F_o| - |F_c|)^2/\Sigma w|F_o|^2]^{1/2}$, and the weighting scheme used was $w = [\sigma^2(F_o) + 0.003\,(F_o)^2]^{-1}$. The limited accuracy of the molecular structure may result from the rather weak diffraction intensity of the high angle reflections. Further details of the crystal structure investigation are available on request from the Director of the Cambridge Crystallographic Data Centre, University Chemical Laboratory, Lensfield Road, GB-Cambridge, CB2 1EW (UK), on quoting the full journal citation.
[8] Measured in $CDCl_3$. **1a**: $\delta = 7.91$ (s, 2H), 7.11 (d, $J = 3.7$ Hz, 4H), 6.58 (t, $J = 3.7$ Hz, 2H); **1b**: $\delta = 6.87$ (d, $J = 3.8$ Hz, 4H), 6.40 (t, $J = 3.8$ Hz, 2H), 1.75 (s, 18H).
[9] For the outer protons of [22]annulene the signals appear at $\delta = 9.70$–8.50 (R. M. McQuilkin, B. W. Metcalf, F. Sondheimer, *Chem. Commun. 1971*, 338).
[10] Due to the poor solubility of **3b** a ^{13}C-NMR spectrum could not be measured.
[11] Measured in $CDCl_3$. **1a**: $\delta = 140.9$, 130.5, 124.7, 117.8, 110.2; **1b**: $\delta =$ 135.9, 128.2, 127.5, 123.0, 109.0, 48.0.
[12] This suggestion was supported by theoretical calculations (J. Aihara, *J. Am. Chem. Soc. 101* (1979) 5913; J. Aihara, T. Horikawa, *Bull. Chem. Soc. Jpn. 56* (1983) 1853). Of all the possible constituent rings, both inner and outer three- and five-membered rings have large resonance energies, while the values of peripheral 22- and 28-membered rings are negligibly small. The calculations also indicate that the percent resonance energies, representing a measure of stabilization of π electron systems, are still large (0.63 for **2a** and 0.57 for **3a**) in spite of being smaller than that of **1a** (0.87).

[{$Re_2Cl_4(dppm)_2$}$_2$(μ-TCNQ)], a Novel Charge Transfer Complex Derived from a Donor with a Metal-Metal Multiple Bond**

By *Stuart L. Bartley* and *Kim R. Dunbar**

The design of synthetic metals is a fertile area of research that continues to grow as new molecular-based materials are discovered. Many low-dimensional materials exhibit interesting optical and magnetic properties in addition to electrical conductivity.[1] The field of organic charge-transfer (CT) chemistry has been particularly well-investigated due to the discovery of highly conducting salts of tetrathiafulvalene (TTF) and tetramethyltetraselenafulvalene (TMTSF) with TCNQ.[2] Our interest focuses on the synthesis of new inorganic/organic charge-transfer solids comprised of multiply-bonded binuclear transition-metal complexes and organic donors or acceptors. There exists a wide variety of redox-active metal–metal bonded binuclear compounds whose properties may be easily tailored by subtle changes in the supporting ligand set.[3] To our knowledge, however, the reaction between the quadruply bonded [$Mo_2(C_{22}H_{22}N_4)_2$] (*Mo*≡*Mo*) and TCNE (tetracyanoethylene) represents the only example of the use of multiply-bonded systems in charge-transfer chemistry.[4] Herein we report the preparation, structure and properties of the novel paramagnetic donor-acceptor complex [{$Re_2Cl_4(dppm)_2$}$_2$ (μ-TCNQ)], **1** prepared from an electron-rich triply bonded metal complex.

The title compound was prepared by reaction of two equivalents of $Re_2Cl_4(dppm)_2$ ($E_{1/2(ox)} = +0.35$ volts vs Ag/AgCl) and one equivalent of TCNQ ($E_{1/2(red)} = +0.24$ V) under N_2 in THF or CH_2Cl_2. Black crystals of **1** were grown by slow diffusion of THF solutions of the starting materials at 0 °C. Bulk reactions carried out at room temperature proceeded through a kinetic intermediate before a stable product was obtained. Immediately upon mixing, the reaction solution turned an intense blue color which slowly converted to olive-green within 24 h.[5] An opaque green-brown solution formed within 48 h. Figure 1 shows the electronic spectrum of the reaction solution at various intervals in a 14 h period. The intense features in the near-infrared region of the spectrum are assigned to a metal→TCNQ charge-transfer band and a mixed-valence transition. The absorption in the high energy visible region ($\lambda_{max} = 420$ nm) is in accord with the $\pi \rightarrow \pi^*$ transition of a reduced TCNQ.[6]

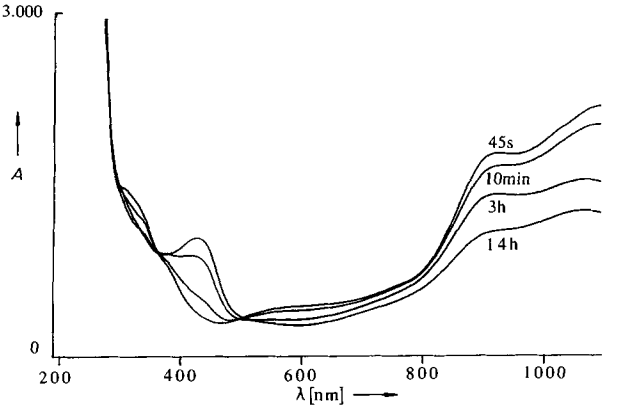

Fig. 1. Electronic spectrum of a 2:1 mixture of [$Re_2Cl_4(dppm)_2$] and TCNQ in CH_2Cl_2. A = absorption.

Infrared spectra were collected on dichloromethane solutions at various intervals starting with 1.5 min after mixing the reactants. The initial blue solution exhibits a sharp $\nu(C\equiv N)$ stretching vibration at 2195 cm^{-1} and an intense broad absorption at 2118 cm^{-1}. The position and number of $\nu(C\equiv N)$ bands indicates that the blue phase contains partially reduced TCNQ as well as TCNQ that is coordinated through at least one cyano group. The higher energy band is assigned to a free cyano moiety whereas the broad absorp-

[*] Prof. K. R. Dunbar, S. L. Bartley
The Center For Fundamental Materials Research and
Department of Chemistry Michigan State University
East Lansing, MI 48824 (USA)

[**] This work was supported by The Center for Fundamental Materials Research at Michigan State University. The X-ray equipment was supported by a grant from the National Science Foundation (Grant CHE-8403823). The authors gratefully thank Dr. *L. R. Falvello* for help with the crystallographic refinement.

tion at 2118 cm^{-1} is attributed to a nitrile interaction. As points of reference, neutral TCNQ exhibits a single nitrile absorption located at 2221 cm^{-1} while the C≡N stretching vibration for $TCNQ^{\ominus}$ occurs at 2183 cm^{-1}.[7] During the next several hours of the reaction, the bands due to the blue species disappeared and two absorptions grew in which correspond to the final product. A Nujol mull sample of crystalline **1** shows a medium strong band at 2190 cm^{-1} and an intense band at 2109 cm^{-1}. Since the ν(C≡N) stretching frequency for the free CN group of **1** occurs at a value close to that found for fully reduced TCNQ (vide supra), we favor this assignment of the oxidation state for the *N*-bound TCNQ unit. The shifts of the metal-bound nitrile stretching vibrations to lower frequency relative to metal-free TCNQ are consistent with back-donation from the dirhenium molecules to *N*-bound TCNQ. These results suggest that an initial partial charge-transfer occurs to produce most likely a 1:1 kinetic product which undergoes further charge transfer and a structural change to form the 2:1 compound **1**. The olive-green "phase" is a physical mixture of the initial blue species and the final green-brown product.

The CT complex **1** exhibits a strong electronic transition centered at ca. 3000 cm^{-1} which extends well into the mid-infrared region. This feature is characteristic of CT phenomena and has been observed in many such complexes.[8] ESR spectra of **1** at − 160 °C (Fig. 2) indicate the presence of

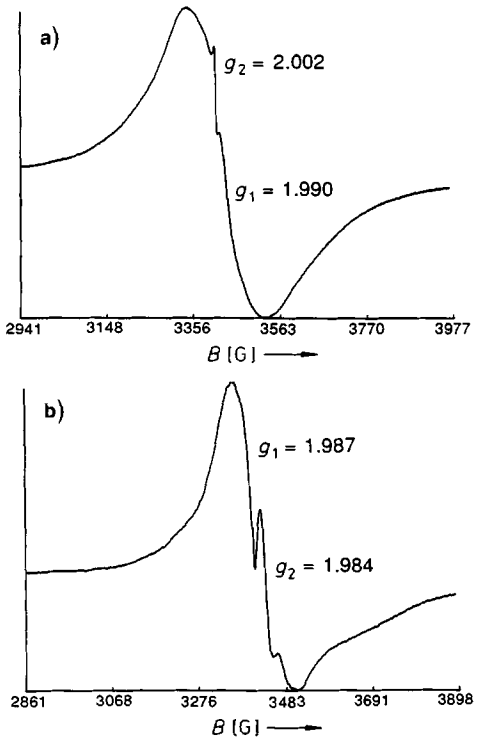

Fig. 2. ESR spectra of **1** at − 160 °C; (a) in the solid state and (b) in CH_2Cl_2 solution.

localized non-interacting spins on the Re_2 and TCNQ units. The solid sample exhibits a broad isotropic signal at $g_1 = 1.990$ and a sharp signal at $g_2 = 2.002$ whereas a CH_2Cl_2 solution shows the same features at $g_1 = 1.987$ and $g_2 = 1.984$.

A single crystal X-ray study of **1** confirmed its 2:1 formulation, and revealed the presence of a novel bridging bidentate mode for TCNQ.[9] The molecular structure of **1**, depicted in Figure 3, consists of two Re_2 units which are covalently linked through the *trans* cyanide groups of a bridging TCNQ molecule. The molecule is centrosymmetric, with the midpoint of the TCNQ moiety being situated on an inversion center. The coordination geometry of the two Re atoms within each dimer unit is different, with the nitrile-substituted metal center, Re(1), adopting an octahedral arrangement consisting of a terminal chloride, Cl(2), as well as an equatorial chloride, Cl(1), and a nitrogen ligand. Re(2) exhibits a trigonal bipyramidal structure similar to the parent complex $Re_2Cl_4(dppm)_2$. This structural type has been noted previously in a nitrile complex by *Walton* et al. who isolated the M_2L_9 cation complex $[Re_2Cl_3(dppm)_2(NCC_2H_5)_2](PF_6)$, in which a chloride ligand occupies an axial site.[10]

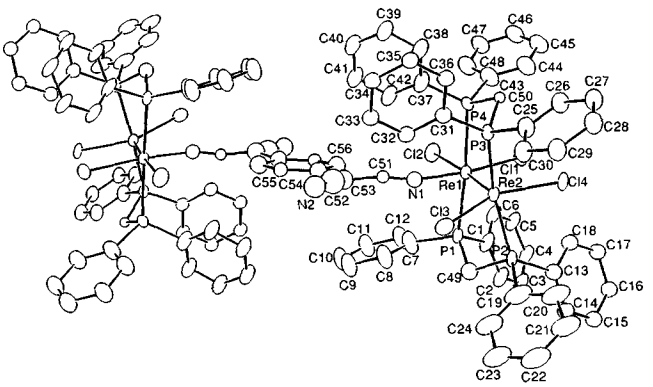

Fig. 3. ORTEP diagram of a molecule of $[Re_2Cl_4(dppm)_2]_2(\mu$-TCNQ) with 50% probability ellipsoids. Selected distances [Å] and angles [°]: Re1-Re2, 2.271(4); Re1-Cl1, 2.40(1); Re1-Cl2, 2.64(2); Re1-P1, 2.51(1); Re1-N1, 1.96(4); Re2-Cl3, 2.33(1); Re2-Cl4, 2.36(1); N1-C51, 1.11(6); N2-C52, 1.16(1); Re2-Re1-Cl1, 98.1(4); Re2-Re1-Cl2, 176.0(4); Re2-Re1-N1, 91(1); Cl1-Re1-N1, 169(1).

Distances and angles within the dirhenium unit are within the usual observed ranges for derivatives of $Re_2Cl_4(dppm)_2$.[11] A selection of important distances and angles in **1** is listed in the caption for Figure 3. Of special note is the Re–Re separation of 2.271(4) Å, which is longer than the distance of 2.234(3) Å found in the parent triply-bonded complex. In the absence of other considerations, one would predict a shorter metal–metal bond resulting from depopulation of an antibonding orbital upon oxidation (i.e. $\sigma^2\pi^4\delta^2\delta^{*2} \rightarrow \sigma^2\pi^4\delta^2\delta^{*1}$), but in the present system the application of an M_2L_8 bonding scheme is an oversimplification. The combined affect of structural changes and π-delocalization on the extent of Re–Re bonding must be taken into consideration. It is reasonable to argue, however, that a strong axial chloride interaction serves to weaken the σ-component of the metal–metal bond thus resulting in an overall lengthening of the Re–Re distance.

The structural characterization of a μ-TCNQ bonding mode is unprecedented to our knowledge. We found only two crystallographically determined examples of monodentate σ-bonded TCNQ or TCNE in the literature.[6] The existence of an η^4-TCNQ bonding mode was detected spectroscopically for TCNQ complexes of the unstable $[CpMn(CO)_2]$ fragment, but no solid-state structure was reported.[12] *Hünig* et al. have recently shown that *N,N'*-dicyanoquinonediimines (DCNQI's) interact with metal ions and organic donors through the nitrogen atoms of the CN groups.[13] Their results show great promise for the synthesis of highly conducting radical anion salts. As in the purely

organic systems, the conduction pathway is along the stacks of π-rings. An examination of the packing diagrams for the title compound revealed that our structure does not exhibit TCNQ–TCNQ interactions, since the separation of ca. 10 Å between the planar faces of TCNQ in adjacent molecules is far too large (Fig. 4).

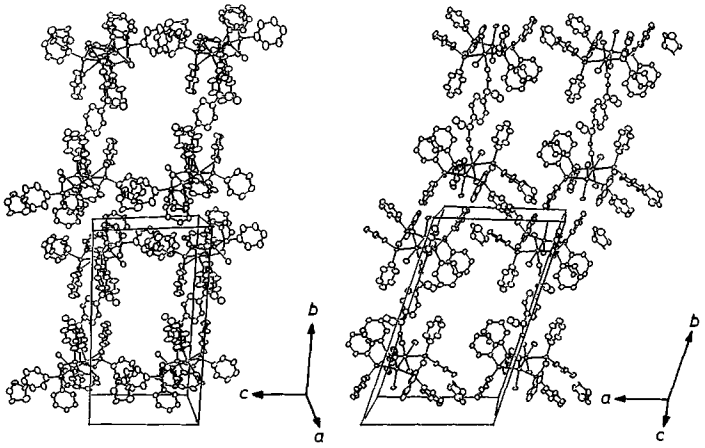

Fig. 4. Unit cell packing diagram of **1** viewed along the *c* and *a* axes.

According to preliminary magnetic measurements obtained between 2 and 300 K on a microcrystalline sample of **1**, the compound shows non-Curie-Weiss behavior with a constant increase in μ_{eff} up to ca. 5.0 B.M. at 300°K. This is surprising, as we would expect two unpaired spins based on the ESR spectra (vide supra); further studies to explain the magnetism are planned. Four-probe conductivity measurements performed on pressed pellets of both the initial blue product and the title compound, **1**, resulted in band gaps of 0.50 and 0.43 eV and room temperature conductivities of 3×10^{-7} and 1×10^{-5} S cm^{-1} respectively.

A final and interesting result in this work emerged from our studies of the reaction of $Re_2Cl_4(dppm)_2$ with TCNQ in the ratio 1:1. This ratio of donor:acceptor may lead to a polymeric phase with higher conductivity. Dichloromethane solutions of the 1:1 Re_2 complex/TCNQ reaction mixture produced a blue phase which turned black and deposited a highly reflective film upon evaporation. The physical properties of the film suggest that a polymerization reaction occurred to form an amorphous material. The electrical and magnetic properties of this film, as well as attempts to further elucidate the chemistry of various stoichiometries of $Re_2Cl_4(dppm)_2$ and TCNQ, are under further investigation.

Experimental Procedures

In a typical bulk reaction, 0.100 g of $Re_2Cl_4(dppm)_2$ (0.078 mmol) was stirred in 15 ml of THF together with 0.0080 g of TCNQ (0.039 mmol) at room temperature. The reaction solution immediately turned blue and within 4 h the color noticeably darkened in hue. The solution was stirred for 2 days, after which time the insoluble green-brown solid was collected, washed with THF, and dried in vacuo [yield 0.085 g, 77%]. A crystalline form of the product was obtained by slow diffusion of THF solutions of $Re_2Cl_4(dppm)_2$ and TCNQ. C,H,Cl analysis. The rod-like crystal contain two interstitial THF molecules which are easily removed by drying the crystals.

Received: July 11, 1990;
revised: January 14, 1991 [Z 4062 IE]
German version: *Angew. Chem. 103* (1991) 447

[1] See for example: a) J. S. Miller: *Extended Linear Chain Compounds*, Vol. 1–3, Plenum, New York 1982, 1983; b) J. R. Ferraro, J. M. Williams: *Introduction to Synthetic Electrical Conductors*, Academic, San Diego, 1987; c) T. J. Marks, *Science 227* (1984) 881; d) J. S. Miller, A. J. Epstein, W. M. Reiff, *Chem. Rev. 88* (1988) 201.

[2] a) Proceedings of the International Conference on Science and Technology of Synthetic Metals (ICSM 88) Santa Fe, NM, USA (*Synth. Met. 27* (1988) B1-B656); b) J. Ferrarls, D. O. Cowan, V. Walatka, J. H. Perlstein, *J. Am. Chem. Soc. 95* (1973) 948; c) M. D. Ward *Electroanal. Chem. 16* (1988) 181.

[3] F. A. Cotton, R. A. Walton: *Multiple Bonds Between Metal Atoms*, Wiley, New York 1982; and references cited therein.

[4] J.-M. Giraudon, J.-E. Guerchais, J. Sala-Pala, L. Toupet, *J. Chem. Soc. Chem. Commun.* (1988) 921.

[5] The blue phase persists indefinitely if the temperature of the reaction is maintained at −78°C.

[6] B. Olbrich-Deussner, W. Kaim, G. Gross-Lannert, *Inorg. Chem. 28* (1989) 3113; and references cited therein.

[7] J. S. Chappel, A. N. Bloch, W. A. Bryden, M. Maxfield, T. O. Peolhler, D. O. Cowan, *J. Am. Chem. Soc. 103* (1981) 2442.

[8] J. B. Torrance, B. A. Scott, F. B. Kaufman, *Solid State Commun. 17* (1975) 1369.

[9] Crystal data for **1** · 2THF at −100°C. $Re_4Cl_8P_8O_2N_4C_{120}H_{108}$, M_r = 2914.44, triclinic, space group $P\bar{1}$, a = 14.311(4), b = 23.25(7), c = 12.205(3) Å, α = 97.35(2), β = 103.75(2), γ = 72.73(2)°, V = 3761(2) Å^3, Z = 1, ϱ_{calcd} = 2.573 g cm^{-3}. Crystal dimensions 0.30 × 0.10 × 0.05 mm^3. The metal atoms were located by a Patterson Fourier synthesis. All remaining non-hydrogen atoms were obtained by the application of alternating least squares and difference Fourier syntheses. The crystal diffracted weakly, thus data were collected between 4 and 35° in 2θ. On the basis of the available data, the SHELEX program was used to refine phenyl groups as C_6H_5 rigid bodies with group anisotropic thermal parameters for the six carbon atoms and one parameter for the hydrogens. The P–C distances were fixed as were the distances in the TCNQ ring. The TCNQ atoms were refined isotropically. After this, the data-to-parameters ratio was 0.076. The structure converged with R and R_w values of 0.0715 and 0.0749 for 2073 observed reflections with $I > 3\sigma(I)$. Further details of the crystal structure investigation are available on request from the Director of the Cambridge Crystallographic Centre, University Chemical Laboratory, Lensfield Road, GB-Cambridge CB21EW(UK), on quoting the full journal citation.

[10] T. J. Barder, F. A. Cotton, L. R. Falvello, R. A. Walton, *Inorg. Chem. 24* (1985) 1258.

[11] a) Part 5: P. E. Fanwick, A. C. Price, R. A. Walton, *Inorg. Chem. 27* (1988) 2601; b) A. C. Price, R. A. Walton *Polyhedron 6* (1987) 729. See also references cited therein.

[12] R. Gross, W. Kaim, *Angew. Chem. 99* (1987) 257; *Angew. Chem. Int. Ed. Engl. 26* (1987) 251.

[13] a) A. Aumüller, S. Hünig, *Angew. Chem. 96* (1984) 437; *Angew. Chem. Int. Ed. Engl. 23* (1984) 447; b) *Liebigs Ann. Chem. 1986*, 142, 165; c) A. Aumüller, E. Hadicke, S. Hünig, A. Schatzle, J.-U. von Schütz *Angew. Chem. 96* (1984) 439; *Angew. Chem. Int. Ed. Engl. 23* (1984) 449. d) A. Aumüller, P. Erk, G. Klebe, S. Hünig, J.-U. von Schütz, H.-P. Werner, *ibid. 98* (1986) 759 and *25* (1986) 740; e) A. Aumüller, P. Erk, S. Hünig, H. Meixner, J.-U. von Schütz, *Liebigs Ann. Chem. 1987* 997; f) P. Erk, H.-J. Gross, S. Hünig, U. Langohr, H. Meixner, H.-P. Werner, J.-U. von Schütz, H. C. Wolf, *Angew. Chem. 101* (1989) 1297; *Angew. Chem. Int. Ed. Engl. 28* (1989) 1245.

Synthesis and Characterization of Radical-Substituted Diacetylene Derivatives**

By *Douglas W. Wiley,* Joseph C. Calabrese, Richard L. Harlow*, and *Joel S. Miller*

A few diradical di-*N*-oxide diacetylenes have been synthesized for the purpose of preparing a polymeric ferromag-

[*] Dr. D. W. Wiley, Dr. J. C. Calabrese, Dr. R. L. Harlow, Dr. J. S. Miller
Central Research & Development
Experimental Station E328
Du Pont
P.O. Box 80328 Wilmington, DE 19880-0328 (USA)

[**] Publication no. 5674. We thank *F. W. Barney, A. P. Berry, W. J. Marshall, R. S. McLean*, and *H. Williams* for assistance in these studies.

net, because prototype diacetylenes crystallize in a manner that enables topochemical polymerization.[1] Although several polymorphs have been identified, these diacetylenes did not crystallize with the -C≡C-C≡C-fragments parallel and close enough to each other to support the single crystal topochemical polymerization.[2] As part of our interest in molecular based ferromagnetic materials,[3] we have prepared 3-(6-hydroxyhexa-2,4-diynyloxycarbonyl)-2,2,5,5-tetramethyl-2,5-dihydropyrrolyl-1-oxide **1a** and 4-(5-hydroxypenta-1,3-diynyl)-2,2,6,6-tetramethyl-1,2,5,6-tetrahydropyridyl-1-oxide **2a** and their *p*-toluenesulphonates **1b** and **2b**, *p*-methoxybenzenesulphonates **1c** and **2c**, and *n*-butoxycarbonylmethylcarbamoyl derivatives **1d** and **2d**. In symmetrical diacetylenes with these substituents, as well as in the unsubstituted alcohols, topochemical polymerization readily occurs,[1] and it was hoped that the unsymmetrical derivatives of **1** and **2** would have the desired crystal packings. Unfortunately only the two alcohols crystallized. **1a–c** were obtained as pure oils; **2a–c** were unstable at room temperature resulting in poor analytical results.

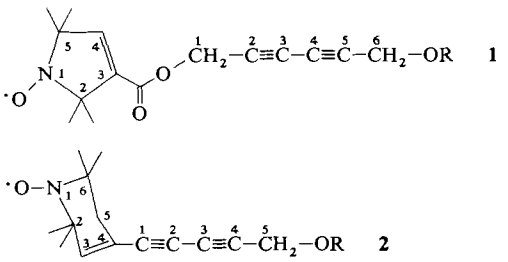

1

2

a, R = H; **b**, R = OSO_2-*p*-$C_6H_4CH_3$; **c**, R = OSO_2-*p*-$C_6H_4OCH_3$; **d**, R = $CONHCH_2CO_2n$Bu

1a was synthesized by the condensation of 2,4-hexadiyne-1,6-diol with 3-carboxy-2,2,5,5-tetramethyl-2,5-dihydropyrrolyl-1-oxide[4a] and **2a** was prepared by the oxidative coupling of 4-ethynyl-2,2,6,6-tetramethyl-1,2,5,6-tetrahydropyridyl-1-oxide and propargyl alcohol.[4b] The derivatives were prepared by reacting **1a** and **2a** with the corresponding sulfonyl chlorides or with *n*-butyl isocyanatoacetate.

The structures of **1a**[5] and **2a**[6] were determined by X-ray diffraction. All bond distances are normal; the C≡C and CC-CC distances are 1.183 and 1.382 Å for **1a** and 1.191 and 1.396 Å for **2a**. In the solid **1a** packs as hydrogen bonded head-to-tail dimers with an NO ··· HO distance of 1.84(5) Å. These hydrogen bonds link the molecules into chains with aligned hexadiyne groups. However, the distance between the tails is relatively long and in the best case there are pairs where the distance is ca. 4.27 Å, so that topographical polymerization is not likely. The crystal structure of **2a** likewise shows strong head-to-tail hydrogen bonding [NO ··· O = 2.726(2) Å and NO ··· HO = 1.862(35) Å] which aligns the molecules in parallel sheets. The sheets are stacked with the tetrahydropyridyl rings shifted relative to adjacent sheets so that the center-to-center vector of the closest diacetylenic groups is 5.8 Å. The angle that each diacetylenic rod makes with this vector is 41.9°. *Baughman* and *Chance*[8] described as favorable conditions for topographical polymerization a vector length of between 4.4 and 5.4 Å and a diacetylenic rod–vector angle between 39 and 58°. Thus, even though the closest distance between end carbons of the two rods is only 3.90 Å, close enough for bond formation, the resulting displacements within the crystal packing would result in excessive lattice energy changes and preclude easy polymerization. In an attempt to induce topochemical polymerization,

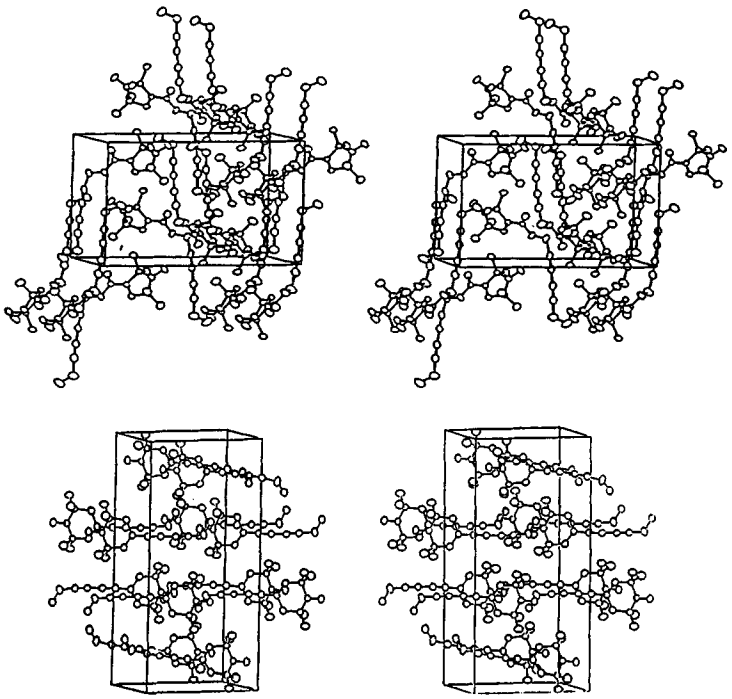

Fig.1. Top: stereoview of the unit cell of **1a**. Bottom: stereoview of the unit cell of **2a**.

both **1a** and **2a** were subjected to electron beam irradiation. As expected, no change in appearance or in the magnetic moment was noted for either compound.

The magnetic susceptibilities of **1a**, **1b**, **1c**, **1d**, and **2a** obey the Curie–Weiss expression, $\chi_M = C/(T-\theta)$, between 3 and 300 K with effective magnetic moments μ_{eff} ranging between 1.72 and 1.77 μ_B and θ between -0.26 and -5.77 K, consistent with one unpaired electron ($S = 1/2$) per molecule. **2b–d** slowly decomposed at room temperature resulting in poor elemental analyses and lower magnetic moments. The EPR spectra at 294 K of the solids **1a** and **2a** each consisted of a single line (at 2.011 with $\Delta H_{pp} = 15$ G and at 2.069 G with $\Delta H_{pp} = 32$ G, respectively). In deoxygenated toluene all compounds **1** and **2** exhibited the expected splitting to three lines centered at 2.011 G with $\Delta H = 14.5 \pm 1$ G.

Experimental Procedure

1: A solution of 3-carboxy-2,2,5,5-tetramethyl-2,5-dihydropyrrolyl-1-oxide and 2,4-hexadiyne-1,6-diol in THF was treated with dicyclohexylcarbodiimide in the presence of 4-dimethylaminopyridine as catalyst and stirred for ca. 15 h at 22 °C. The insoluble dicyclohexylurea was filtered off and the THF removed by distillation. The resulting mixture of the monoester **1a** and the corresponding diester was separated by chromatography on silica gel. Flash chromatography on silica (eluant petroleum ether/EtOAc, 3:2) gave pure **1a** (44%); hexane/EtOAc (4:1) was used for recrystallization.

2a: 4-Ethynyl-2,2,6,6-tetramethyl-1,2,5,6-tetrahydropyridyl-1-oxide and propargyl alcohol (1:4) was stirred in a methanol/pyridine solution (1:1) of cupric acetate for 3 hr at 22 °C. Dilution with water gave an insoluble coupling product from two moles of the tetrahydropyridyloxide. Extraction with ether, concentration, and removal of the pyridine by addition of 2 N NCl afforded crude product. Flash chromatography on silica gel (eluant, $CHCl_3$/EtOAc, 9:1) was used to separate more dimeric product and other impurities from **2a**. Recrystallization from hexane/EtOAc (4:1) gave pure **2a** (yield 35%).

The sulphonates of **1a** and **2a** were prepared by the slow addition of aqueous KOH to cold THF solutions of alcohol and sulphonyl chloride. The urethane

acetates of **1a** and **2a** were obtained by treatment with *n*-butyl isocyanatoacetate in THF for 24 hr at 0 °C with triethylamine catalyst. the reactions were worked up by diluting with water and extracting with ether. Purification was achieved by flash chromotography.

Received: September 15, 1990 [Z 4245 IE]
German version: *Angew. Chem. 103* (1990) 459

CAS Registry numbers:
1a, 132540-65-9; **2a**, 128141-84-4; 3-carboxy-2,2,5,5-tetramethyl-2,5-dihydropyrrolyl-1-oxide, 2154-67-8; 2,4-hexadiyne-1,6-diol, 3031-68-3; 4-ethynyl-2,2,b,b-tetramethyl-1,2,5,6-tetrahydropyridyl-1-oxide, 69116-02-5; propargyl alcohol, 107-19-7.

[1] D. Bloor, R. R. Chance, *NATO ASI Ser. E 102* (1985) (Polydiacetylenes).
[2] a) Yu. V. Korshak, T. V. Medvedeva, A. A. Ovchinnikov, V. N. Spector, *Nature 326* (1987) 370; A. L. Buchachenko, R. P. Shibaeva, L. P. Rozenberg, A. A. Ovchinnikov *Kim. Fiz. 6* (1987) 773; D. J. Sandman, G. P. Hamill, M. Levinson, P. G. Rossoni, E. A. Yost, G. C. Papaefthymiou *MRS Symp. Proc. 173* (1990) 567; J. S. Miller, D. T. Glatzhofer, R. Laversanne, S. Chittipeddi, P. Vaca, T. B. Brill, M. D. Timken, C. J. O'Connor, J. H. Zhang, J. C. Calabrese, A. J. Epstein *Chem. Mater. 2* (1990) 60; b) Y. Cao, P. Wang, Z. Hu, S. Ki, L. Zhang, J. Zhao *Solid State Commun. 68* (1988) 817; *Synth. Met. 27* (1988) B625; c) D. W. Wiley, J. C. Calabrese, J. S. Miller, *J. Chem. Soc. Chem. Commun. 1989*, 1523.
[3] J. S. Miller, A. J. Epstein, *J. Am. Chem. Soc. 109* (1987) 3850; J. S. Miller, A. J. Epstein, W. M. Reiff, *Chem. Rev. 88* (1988) 201.
[4] a) **1a**: m.p. 105.5–106.5 °C. Correct elemental analysis (C,H,N); $MW_{calc.} = 276.31$; mass spectroscopy yielded a parent at *m/e* 276 ($M^{\oplus}$) and major peaks at 246 ($M^{\oplus} - CH_2O$) and 153. Thermal gravimetric analysis (TGA) and differential scanning calorimetry (DSC) (10° min^{-1}) showed no change until the 107 °C m.p., after which a mild exotherm preceded an endothermic weight loss of 8–9% over the range 160–190 °C. At 250–280 °C, more rapid decomposition started with a total weight loss of 50% by 350 °C. b) **2a**: mp 119.3–120.1 °C. **2a** is completely stable in the solid state, but darkens slowly and loses its free radical characteristics when dissolved in organic solvents. Correct elemental analysis (C,H,N); $MW_{calc.} = 232.30$; mass spectroscopy yielded a parent at *m/e* 232 ($M^{\oplus}$) and 202 ($M^{\oplus} - CH_2O$). TGA and DSC (10° min^{-1}) showed no change until the 117–121 °C mp, after which a sharp exotherm occurred. Small samples showed a slow weight loss of 3–5% up to 170 °C, where larger samples lost up to 60% of their weight already at 140 °C. This behavior reflects a weight loss owing to a sputtering of material out of the measuring cup.
[5] A $0.25 \times 0.15 \times 0.36$ mm crystal was grown from $MeOH/H_2O$: orthorhombic $P2_12_12_1$(No. 19) space group; $a = 8.217(2)$, $b = 10.465(2)$, $c = 17.119(2)$ Å; $V = 1472.1$ Å^3; $Z = 4$; $\rho_{calc.} = 1.247$ g/cm^3; μ_{Mo}, 0.85 cm^{-1} at −60 °C. Enraf-Nonius CAD4 diffractometer; graphite-monochromated $Mo_{K\alpha}$ radiation; 3923 reflections. Refinement: 1285 reflections for which $I > 2\sigma(I)$ to convergence of $R = 0.047$ and $R_w = 0.039$. See also [7].
[6] A $0.35 \times 0.21 \times 0.43$ mm crystal was grown from warm 40% aqueous MeOH: monoclinic $P2_1/n$ (No. 14) space group; $a = 5.784(2)$, $b = 22.158(3)$, $c = 10.541(3)$ Å; $\beta = 104.05(1)°$; $V = 1310.5$ Å^3; $Z = 4$; $\rho_{calc.} = 1.177$ g cm^{-3}; μ_{Mo}, 0.73 cm^{-1} at −70 °C. Enraf-Nonius CAD4 diffractometer; graphite-monochromated $Mo_{K\alpha}$ radiation; 3249 reflections. Refinement which 1513 reflections for which $I > 3\sigma(I)$ to convergence of $R = 0.051$ and $R_w = 0.051$. See also [7].
[7] Further details of the crystal structure investigation are available upon request from the Director of the Cambridge Crystallographic Data Centre, University Chemical Laboratory, Lensfield Road, GB-Cambridge CB2 1EW (UK), on quoting the full journal citation.
[8] R. Baughman, R. R. Chance, *Ann. N.Y. Acad. Sci. 313* (1985) 705.

BOOK REVIEWS

Book Reviews are written by invitation from the editor. Suggestions for books to be reviewed and for book reviewers are welcome. Publishers should send brochures or (better) books to the following address: Redaktion Angewandte Chemie, Postfach 101161, D-6940 Weinheim, Federal Republic of Germany. The editor reserves the right of selecting which books will be reviewed. Uninvited books not chosen for review will not be returned.

Reviews in Computational Chemistry. Edited by *K. B. Lipkowitz* and *D. B. Boyd*. VCH Publishers, New York/VCH Verlagsgesellschaft, Weinheim 1990. xix, 419 pp., hardcover, DM 176.00.—ISBN 0-89573-754-X/3-527-27845-1

In the introduction to this book the editors try to arrive at a definition of "computational chemistry". According to the broadest of the definitions offered here, it includes all those areas of chemical research in which computers are used either to obtain results more quickly or to make the work possible at all. On this criterion there is nowadays scarcely a single area of chemical research that does not overlap with computational chemistry. The present volume is intended as the first of a series that will follow, by means of review articles, the development of every aspect of computational chemistry, including molecular modeling. It can be stated at the outset that the editors have succeeded here in presenting some excellent articles on topics of current interest in the field of computer applications in chemistry.

The first and last chapters in the book are both concerned with ab initio quantum chemistry. In the first of these, on "Basis Sets for Ab Initio Molecular Orbital Calculations and Intermolecular Interactions", *D. Feller* and *E. R. Davidson* describe basic principles and recent developments in this area; they include a section entitled "In-Depth Discussion", which well deserves this description. There is a useful table listing the polarization functions in common use, information which would be hard to find elsewhere.

In the second chapter *J. J. P. Stewart* discusses semiempirical methods. The rather bewildering array of methods originating from the *Dewar* school that have been developed in the last few years (MNDO, MNDOC, AM1, PM3, etc.) are described in chronological order. The theoretical fundamentals are only treated very briefly. The author justifies this by

referring to a recent review article on this topic by *W. Thiel*, commenting that to attempt to cover the same ground here would merely result in repetition—an admirable example of self-restraint! Although the account of the areas of application of the methods contains some slight inaccuracies—for example, it is wrongly stated on page 62 that for MINDO/3 no parameters for the P–O bond are available—these do not detract from the value of this fluently written article. The detailed survey, in the form of a table, of the average errors with the three main methods (MNDO, AM1 and PM3) for several classes of compounds is a very useful guide for the potential user.

In the third chapter ("Properties of Molecules by Direct Calculation") *C. E. Dykstra, J. D. Augspurger, B. Kirtman* and *D. J. Malik* address the question of which are the most suitable theoretical methods for directly calculating properties from the wave functions. They limit their discussion to the calculation of electrical, magnetic and optical properties, force constants and transition probabilities. The article is worth reading as an introduction and a concise account of the basic mathematics, but the discussion of the results, consisting of a mere nine pages, is too brief for such an extensive topic.

Four chapters are devoted to the subjects of molecular modeling and quantitative structure-activity relationships. This is appropriate and welcome in view of the rapid developments taking place in this area and the shortage of review articles. For this strongly applications-orientated area of computational chemistry it is also fitting that three of the four articles have been written by authors from industry. *D. B. Boyd* introduces this topic in Chapter 9 ("Aspects of Molecular Modeling"), where he discusses the usefulness of the different theoretical approaches from the viewpoint of the industrial chemist dealing with large molecules. The fact that molecular modeling is very far from being an "amateurish, watered-down, or incidental computational chemistry" (p. 321) is made clear by *E. L. Plummer* in Chapter 4 ("The Application of Quantitative Design Strategies in Pesticide Discovery"). This detailed article (49 pages) describes the application of theoretical aids, especially statistical methods, to synthetic and analytical strategies in the search for new pesticides compatible with present-day restrictions (ecological requirements). It has been known for some time that in order to realistically model the properties of large molecules one must take into account their dynamic behavior. The development of the three main approaches, namely Monte Carlo methods, molecular dynamics calculations, and the calculation of the free energy using perturbation theory, is sketched rather briefly (in 25 pages) by *T. P. Lybrand* in Chapter 8. The practical usefulness of computational chemistry is illustrated by *D. B. Boyd* in Chapter 9 by taking as examples four commercial compounds whose development depended crucially on computer-aided methods.

The importance to analytical chemistry of computers and of the multivariate analysis methods that are thereby possible is described in Chapter 5 ("Chemometrics and Multivariate Analysis in Analytical Chemistry", 43 pp.) by *P. C. Jurs*. This chapter too can be regarded as belonging to the area of molecular modeling in the wider sense, since the main emphasis is on applications concerning structure-activity relationships for biologically active substances.

The development of computer graphics, which allows one to quickly and conveniently display three-dimensional structures on the VDU screen, is of enormous significance for chemistry. The influence that this is having on the development of modern data banks, which allow one to rapidly test ideas about molecular structures using stored three-dimensional information, is described in Chapter 6 ("Searching Databases of Three-Dimensional Structures", 51 pp.) by *Y. C. Martin, M. G. Bures* and *P. Willet*. Whereas older data banks such as the Cambridge Structural Database are used essentially for storing data on atomic coordinates, the newer types of programs allow one to search for information about specific partial structures. References to available programs and information sources are included in this detailed report.

Advances in computer graphics have also contributed significantly to the development of concepts in which one is mainly interested in the molecular surface. In Chapter 7 ("Molecular Surfaces", 30 pp.) *P. G. Mezey* reviews theoretical models in which molecular properties are correlated with the shape of the surface. One such model is that developed by *M. L. Connolly* to describe the surface accessible to a solvent; this has contributed to a better understanding of solvent effects on proteins. It becomes clear from the article that this new concept would scarcely have been possible without the development of computer graphics.

The final chapter ("Perspectives on Ab Initio Calculations" by *E. R. Davidson*) is not concerned with the practical details of the development of ab initio methods but with the question of what can be learned, and has already been learned, by using ab initio programs. The author's personal views, supported by historical examples, are briefly set out under five headings; everyone will undoubtedly agree with the last of these headings, which asserts that "Computers do not Solve Problems, People do".

The book contains as an appendix a survey by *D. B. Boyd* of hardware and software relevant to molecular modeling (together with details of suppliers); this is prefaced by a useful and amusing checklist of points about which one needs to be clear *before* buying a computer or software.

The standard of production of the book is excellent, there are few printing errors, and the price seems reasonable in relation to the levels that are now typical. It can be recommended for everyone who wants to learn about the present state of development in computational chemistry, and is willing to look beyond the boundaries of his or her particular field of study. Specialists will need to decide for themselves whether the chapters of particular interest to them offer something new. Libraries of chemistry departments are strongly recommended to buy the book. The choice of topics is certainly subjective, but is sensible and relevant to current developments in computational chemistry. It is to be hoped that further volumes of the series will appear at intervals of, say, two years. The editors can be congratulated on this first volume.

Gernot Frenking [NB 1113 IE]
Fachbereich Chemie
der Universität Marburg (FRG)

Chemistry of Plant Protection. Vol. 4: Synthetic Pyrethroid Insecticides. By *K. Naumann*. Springer, Berlin 1990. xvi, 241 pp., hardcover, DM 224.00.—ISBN 3-540-51313-2

The series "Chemistry of Plant Protection" is the successor to the well-known handbook "Chemie der Pflanzenschutz- und Schädlingsbekämpfungsmittel" by *R. Wegler*. It is not only the language that has altered, there has also been a change in the editorial policy. Whereas the *Wegler* handbook follows a conventional division of subject matter, dealing in turn with herbicides, fungicides and insecticides, the volumes of this series will deal with individual topics of current importance. Thus Volume 1 is devoted to the inhibition of sterol biosynthesis, Volume 2 to the biological breakdown

of pesticides, the defoliation and dessication of green plants, and methods of influencing acetylcholine receptors, and Volume 3 to the detection of pyrethroid residues and the measurement of active substances of low molecular mass by immunoassay. With Volumes 4 and 5, which take pyrethroids as their common central theme, the editors now face the risk of breaking down the subject into too many individual topics. Volume 4 deals with the structures and biological activities of the most important pyrethroids, while Volume 5 (in preparation) will describe their synthesis and chemical properties.

Volume 4 begins with a brief historical account of the development of the synthetic pyrethroids based on the natural pyrethrins; the latter still play an important role in human hygiene (lice etc.), although they are unsuitable for plant protection uses because of their photolability. Many modern pyrethroids bear only a marginal resemblance to the natural pyrethrins; in some cases the only indispensable structural element that is retained is the geminal carbon branching, which acts as a lipophilic anchor. The author identifies the structural characteristics that need to be present in a "good" pyrethroid, and includes extensive tables describing the structure–activity relationships. It is interesting that the (1*R*) enantiomers are found to have the highest activities. With regard to the *cis*/*trans*-1,2-substitution of the cyclopropane ring or at the double bond the diastereomers show characteristic differences in their activities; which of the stereoisomers has the highest activity depends very markedly on the substitution pattern and the insect target group. However, the alcohol component of the cyclopropanecarboxylic acid ester also has a crucial effect; a phenoxyether has the effect of causing the molecule to adopt the important "horseshoe" conformation (pp. 76f).

About 80 pages are devoted to the biological effects of pyrethroids on insects and other forms of life. Nearly all insect species suffer physiological effects from pyrethroids. After absorption through the cuticulum (contact toxicity!) the substance produces the immediate "knock-down" effect, which may or may not be followed by death. In this respect it is possible to obtain some discrimination between harmful insects and those that are useful; useful insects such as bees can recover from the initial "knock-down", whereas harmful insects are killed. However, a serious drawback of nearly all pyrethroids is their high level of toxicity towards marine life (fishes, leeches etc.), which prevents their use in rice-fields. Pyrethroids are essentially harmless to warm-blooded species, although they cause unpleasant skin irritations in humans, which nevertheless quickly clear up. In insects, in contrast to warm-blooded species, pyrethroids rapidly penetrate into the nerve fibers, where they open up presynaptic sodium channels and thereby disrupt the entire nervous system. In warm-blooded species the pyrethroid molecules first undergo ester hydrolysis and hydroxylation which destroys the activity.

The final chapter discusses the market share enjoyed by pyrethroids (currently about 20%) and the areas of use. In addition there is a comprehensive list of the various derivatives, including not only the usual commercial products but also those still at the development or experimental stage, together with manufacturers and licensees.

On the whole this is an excellent book. No important aspect of the subject appears to have been overlooked; the factual information is supplemented by extensive numerical tables that have been carefully prepared. A possible criticism is that the environmental acceptability of the pyrethroids is only briefly discussed. For example, there is very little information (six lines on p. 124) about the biological degradation of the insecticides on cultivated land, and the avoidance of harm to useful insects is undoubtedly a serious problem. A minor detail that can be criticized is the frequent use of trivial names (deltamethrin, permethrin etc.) without giving the reader quick access to the structural formulas. It is only when one reaches page 192 that one finds, without an earlier reference to it, a table giving such information, and even here the compounds are not arranged alphabetically. However, these relatively minor criticisms scarcely detract from the favorable overall impression. The book is undoubtedly a must for everyone working in the area of pyrethroids, whether as a chemist, biologist, pharmacologist or toxicologist.

Johann Mulzer [NB 1126 IE]
Institut für Organische Chemie
der Freien Universität Berlin (FRG)

Registered names, trademarks, etc. used in this journal, even when not marked as such, are not to be considered unprotected by law.

© VCH Verlagsgesellschaft mbH, W-6940 Weinheim, 1991. – Printed in the Federal Republic of Germany by Konrad Triltsch Druck- und Verlagsanstalt Würzburg.

All rights reserved (including those of translation into foreign languages). No part of this issue may be reproduced in any form — by photoprint, microfilm, or any other means — nor transmitted or translated into a machine language without written permission from the publishers. Only single copies of contributions, or parts thereof, may be made for personal use. This journal was carefully produced in all its parts. Nevertheless, authors, editors and publisher do not warrant the information contained therein to be free of errors. Readers are advised to keep in mind that statements, data, illustrations, procedural details or other items may inadvertently be inaccurate.

Valid for users in the USA: The appearance of the code at the bottom of the first page of an article (serial) indicates the copyright owner's consent that copies of the article may be made for personal or internal use, or for the personal or internal use of specific clients. This consent is given on the condition, however, that the copier pay stated per-copy fee through the Coyright Clearance Center, Inc. (CCC), for copying beyond that permitted by Sections 107 or 108 of the U.S. Copyright Law. This consent does not extend to other kinds of copying, such as copying, for general distribution, for advertising or promotional purposes, for creating new collective works, or for resale. For copying from back volumes of this journal see 'Permissions to Photo-Copy: Publisher's Fee List' of the CCC.

Editorial office: Postfach 10 11 61, W-6490 Weinheim, Federal Republic of Germany, Telephone (06201) 60 23 15, Telex 465 516 vchwh d, Telefax (06201) 602 328, E-Mail Z16@DHDURZ2 in Earn Bitnet.

Editor: *Peter Gölitz*

Associate editors: *D. I. Loewus, K. J. Schneider, A. Stimson.* **Editorial assistant:** *E. Schweikart*

Publishers: VCH Verlagsgesellschaft mbH. (Managing Directors: *Hans Dirk Köhler, Dr. Hardy G. Sehrt.*), Pappelallee 3, W-6940 Weinheim, Federal Republic of Germany.

Advertising office (Advertising Manager *R. J. Roth*): Postfach 10 11 61, W-6940 Weinheim, Federal Republic of Germany, Telephone (0 62 01) 606 1 36, Telex 4 67 155, Telefax (0 62 01) 606 156.

ANGEWANDTE CHEMIE
International Edition in English
Volume 30 · Number 5
May 1991
Pages 455–612

The Logic of Chemical Synthesis: Multistep Synthesis of Complex Carbogenic Molecules (Nobel Lecture)**

By Elias James Corey*

Carbogens, members of the family of carbon-containing compounds, can exist in an infinite variety of compositions, forms and sizes. The naturally occurring carbogens, or organic substances as they are known more traditionally, constitute the matter of all life on earth, and their science at the molecular level defines a fundamental language of that life. The chemical synthesis of these naturally occurring carbogens and many millions of unnatural carbogenic substances has been one of the major enterprises of science in this century. That fact is affirmed by the award of the Nobel Prize in Chemistry for 1990 for the "development of the theory and methodology of organic synthesis." Chemical synthesis is uniquely positioned at the heart of chemistry, the central science, and its impact on our lives and society is all pervasive. For instance, many of today's medicines are synthetic and many of tomorrow's will be conceived and produced by synthetic chemists. To the field of synthetic chemistry belongs an array of responsibilities which are crucial for the future of mankind, not only with regard to the health, material and economic needs of our society, but also for the attainment of an understanding of matter, chemical change and life at the highest level of which the human mind is capable.

The post World War II period encompassed remarkable achievement in chemical synthesis. In the first two decades of this period chemical syntheses were developed which could not have been anticipated in the earlier part of this century. For the first time, several very complex molecules were assembled by elaborately conceived multistep processes, for example vitamin A (*O. Isler*, 1949), cortisone (*R. B. Woodward, R. Robinson*, 1951), morphine (*M. Gates*, 1956), penicillin V (*J. C. Sheehan*, 1957), and chlorophyll (*R. B. Woodward*, 1960).[1] This striking leap forward, which was recognized by the award of the Nobel Prize in Chemistry to *R. B. Woodward* in 1965,[2] was followed by an equally dramatic scientific advance during the past three decades, in which chemical synthesis has been raised to a qualitatively higher level of sophistication. Today, in many laboratories around the world, chemists are synthesizing at an astonishing rate complex carbogenic structures which could not have been made effectively in the 1950's or early 1960's. This advance has been propelled by the availability of more powerful conceptual processes for the planning of chemical syntheses, the use of new chemical methods, in the form of reactions and reagents, and the advent of improved methods for analysis, separation and determination of structure. Many talented investigators all over the world have contributed to the latest surge of chemical synthesis. Their efforts constitute a collective undertaking of vast dimensions, even though made independently, and their ideas and discoveries interact synergistically to the benefit of all. I am happy to have been selected by the Nobel Committee for contributions to the science of chemical synthesis, but I am even more pleased that this important field of science has again received high recognition.

Genesis

In the fall of 1947, as an undergraduate at the Massachusetts Institute of Technology, I took a course in Advanced Synthetic Organic Chemistry, taught by the distinguished chemist *A. C. Cope*, in which the major reactions of synthesis were surveyed. It was explained that very few new synthetic methods remained to be found, since only five important

[*] Prof. E. J. Corey
Department of Chemistry, Harvard University
Cambridge, MA 02138 (USA)
[**] Copyright © The Nobel Foundation, 1991. We thank the Nobel Foundation, Stockholm, for permission to print this lecture.

reactions had been discovered in the preceding fifty years; and we students were advised to learn how to devise chemical syntheses using the available portfolio of known constructions. We were given numerous molecular structures as synthetic problems. After doing a few of the problem sets, I had developed sufficient skill and experience to handle all of the remaining assignments with ease, much as I had learned to use the English language, to prove mathematical theorems, or to play chess. My new found competence in chemical problem solving seemed to result from an automatic "know how" rather than from the conscious application of well-defined procedures. Nonetheless, even though I had mastered the classical reactions, designing syntheses of molecules beyond the modest level of complexity of these instructional problems still eluded me. Molecules such as morphine, cholesterol, penicillin, or sucrose were so forbidding that they defined the frontiers of 1947; each seemed to be unique and to require a very high level of creativity and invention. Much of my research over the years has been devoted to probing those frontiers and advancing the level of synthetic science by an approach consisting of three integral components: the development of more general and powerful ways of thinking about synthetic problems, the invention of new general reactions and reagents for synthesis, and the design and execution of efficient multistep syntheses of complex molecules at the limits of contemporary synthetic science.

Retrosynthetic Analysis

During the first half of this century most syntheses were developed by selecting an appropriate starting material, after a trial and error search for commercially available compounds having a structural resemblance to the target of synthesis. Suitable reactions were then sought for elaboration of the chosen starting material to the desired product. Synthetic planning in most instances was strongly dependent on an assumed starting point. In the fall of 1957 I came upon a simple idea which led to an entirely different way of designing a chemical synthesis. In this approach the target structure is subjected to a deconstruction process which corresponds to the reverse of a synthetic reaction, *so as to convert that target structure to simpler precursor structures, without any assumptions with regard to starting materials.* Each of the precursors so generated is then examined in the same way, and the process is repeated until simple or commercially available structures are arrived at. This "retrosynthetic" or "antithetic" procedure constitutes the basis of a general logic of synthetic planning which was developed and demonstrated in practice over the ensuing decade.[3, 4, 5] In an early example, retrosynthetic planning for the tricyclic sesquiterpene longifolene **1** (Scheme 1 at end of this section) produced several attractive pathways for synthesis, one of which was selected and validated by experimental execution.[6] The basic ideas of retrosynthetic analysis were used to design many other syntheses and to develop a computer program for generating possible synthetic routes to a complex target structure without any input of potential starting materials or intermediates for the synthesis.[4, 5] The principles of retrosynthetic analysis have been summarized most recently in the textbook, "The Logic of Chemical Synthesis"[7] which was written for advanced undergraduate and graduate students of chemistry. The retrosynthetic way of thinking about chemical synthesis also provided a logical and efficient way to teach synthetic planning to intermediate and advanced students, a good example of the intimate link between teaching and research in an academic setting. A brief synopsis of the retrosynthetic planning of syntheses will now be given.

Retrosynthetic[8] (or *antithetic*) analysis is a problem-solving technique for transforming the structure of a *synthetic target* (TGT) molecule to a sequence of progressively simpler structures along a pathway which ultimately leads to simple or commercially available starting materials for a chemical synthesis. The transformation of a molecule to a synthetic precursor is accomplished by the application of a *transform*, the exact reverse of a *synthetic reaction*, to a target structure. Each structure derived antithetically from a TGT then itself becomes a TGT for further analysis. Repetition of this process eventually produces a tree of intermediates having chemical structures as nodes and pathways from bottom to top corresponding to possible synthetic routes to the TGT. Such trees, called EXTGT trees since they grow out from the TGT, can be quite complex since a high degree of branching is possible at each node and since the vertical pathways can include many steps. This central fact implies the need for strategies which control or guide the generation of EXTGT trees so as to avoid explosive branching and the proliferation of useless pathways.

Each retrosynthetic step requires the presence of a target structure of a keying structural subunit or *retron* which allows the application of a particular transform. For example,

Elias J. Corey, born in 1928 in Methuen, 30 miles north of Boston, studied chemistry from 1945–1950 at the Massachusetts Institute of Technology, where he gained his doctorate for work on synthetic penicillins under the supervision of John C. Sheehan. At the early age of twenty-two he joined the University of Illinois at Urbana-Champaign as an Instructor in Chemistry under the distinguished chemists Roger Adams and Carl S. Marvel, and as a result of the success of his research, he was appointed in 1956, at age twenty-seven, as Professor of Chemistry. His areas of research at that time ranged from enantioselective syntheses to enzymology. In 1959 he received and accepted an offer of a Professorship at Harvard University which he still holds. His scientific successes, like the honors conferred him, are numerous and, culminated last year in the Nobel prize for chemistry.

the retron for the aldol transform consists of the subunit HO–C–C–C=O, and it is the presence of that subunit which permits transform function, e.g. as follows:

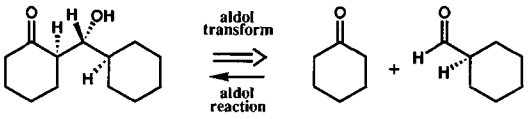

Transforms vary in terms of their power to simplify a target structure. The most powerful of simplifying transforms, which reduce molecular complexity in the retrosynthetic direction, occupy a special position in the hierarchy of all transforms. Their application, even when the appropriate retron is absent, may justify the use of a number of non-simplifying transforms to generate that retron. In general, simplifying transforms function to modify structural elements which contribute to molecular complexity: molecular size, cyclic connectivity (topology), stereocenter content, element and functional group content, chemical reactivity, structural instability, density of complicating elements.

Molecular complexity is important to strategy selection. For each type of molecular complexity there is a collection of general strategies for dealing with that complexity. For instance, in the case of a complex polycyclic structure, strategies for the simplification of the molecular network, i.e. topological strategies, must play an important part in transform selection. However, the most efficient mode of retrosynthetic analysis lies not in the separate application of individual strategies, but in the concurrent application of as many different independent strategies as possible.

The major types of strategies[7] which are of value in retrosynthetic analysis may be summarized briefly as follows.[8]

1. Transform-based strategies—long range search or look-ahead to apply a powerfully simplifying transform (or a tactical combination of simplifying transforms) to a TGT with certain appropriate keying features. The retron required for application of a powerful transform may not be present in a complex TGT and a number of antithetic steps (subgoals) may be needed to establish it.

2. Structure-goal strategies—directed at the structure of a potential intermediate or potential starting material. Such a goal greatly narrows a retrosynthetic search and allows the application of bidirectional search techniques.

3. Topological strategies—the identification of one or more individual bond disconnections or correlated bond-pair disconnections as strategic. Topological strategies may also lead to the recognition of a key substructure for disassembly or to the use of rearrangement transforms.

4. Stereochemical strategies—general strategies which clear, i.e. remove, stereocenters and stereorelationships under stereocontrol. Such stereocontrol can arise from transform-mechanism control or substrate-structure control. In the case of the former the retron for a particular transform contains critical stereochemical information (absolute or relative) on one or more stereocenters. Stereochemical strategies may also dictate the retention of certain stereocenter(s) during retrosynthetic processing or the joining of atoms in three-dimensional proximity. A major function of stereochemical strategies is the achievement of an experimentally valid clearance of stereocenters, including clearance of molecular chirality.

5. Functional group-based strategies. The retrosynthetic reduction of molecular complexity involving functional groups (FG's) takes various forms. Single FG's or pairs of FG's (and the interconnecting atom path) can key directly the disconnection of a TGT skeleton to form simpler molecules or signal the application of transforms which replace functional groups by hydrogen. Functional group interchange (FGI) is a commonly used tactic for generating the retrons of simplifying transforms from a TGT. FG's may key transforms which stereoselectively remove stereocenters, break topologically strategic bonds or join proximate atoms to form rings.

6. "Other" types of strategies. The recognition of substructural units within a TGT which represent major obstacles to synthesis often provides major strategic input. Certain other strategies result from the requirements of a particular problem, for example a requirement that several related target structures be synthesized from a common intermediate. A TGT which resists retrosynthetic simplification may require the invention of new chemical methodology. The recognition of obstacles to synthesis provides a stimulus for the discovery of such novel processes. The application of a chain of hypotheses to guide the search for an effective line of retrosynthetic analysis is important.

Other strategies deal with optimization of a synthetic design *after* a set of pathways has been generated antithetically, specifically for the ordering of synthetic steps, the use of protection or activation steps, or the determination of alternate paths.

Systematic and rigorous retrosynthetic analysis is the *broad principle* of synthetic problem solving under which the individual strategies take their place. Another overarching idea is the use *concurrently* of as many independent strategies as possible to guide the search for retrosynthetic pathways. *The greater the number of strategies which are used in parallel to develop a line of analysis, the easier the analysis and the simpler the emerging synthetic plan is likely to be.*[10]

An abbreviated form of the 1957 retrosynthetic plan for the synthesis of longifolene (**1**) is shown in Scheme 1. Changes in the retrosynthetic direction are indicated by a double arrow (⇒) to distinguish them from the synthetic direction of chemical reactions (→) and the number below indicates the number of transforms required for the retrosyn-

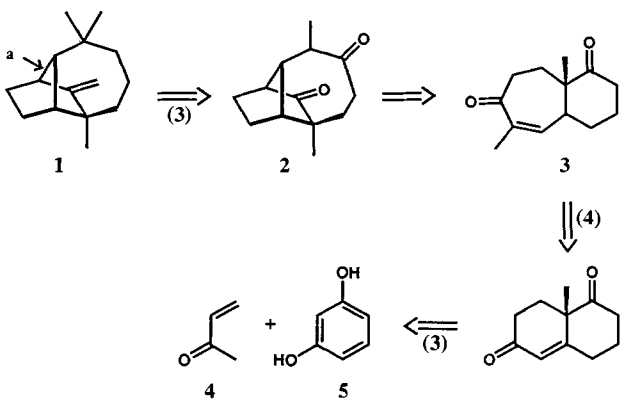

Scheme 1. Retrosynthetic analysis for longifolene **1** (1957) (see text).

thetic change if greater than one. The selection of transforms was initially guided by a topological strategy (disconnection of bond *a* in **1**). The Michael transform, which simplifies structure **2** to precursor **3**, can be found by general transform selection procedures.[5, 9] The starting materials for the synthesis which emerge from retrosynthetic analysis, **4** and **5**, have little resemblance to the target structure **1**.

A detailed explanation of this example of retrosynthetic analysis has been given.[6b, 10] During the past 20 years systematic retrosynthetic thinking has permeated all areas of carbogenic synthesis. It is no longer possible to teach the subject of carbogenic synthesis effectively without the extensive use of retrosynthetic concepts and thinking.

Computer-Assisted Retrosynthetic Analysis

The use of computers to generate possible pathways for chemical synthesis, which was first demonstrated in the 1960's,[4, 5, 9, 11] was made possible by the development of the retrosynthetic methods outlined above and the required computer methodology. Graphical input of structures by hand drawing using an electrostatic tablet and stylus, in the natural manner of a chemist, and output to a video terminal[4, 12] provided an extraordinarily simple and effective interface between chemist and machine. Chemical structures were represented in the machine by means of atom and bond tables, and manipulated by appropriate instructions. Algorithms were devised for perception by machine of structural features, patterns, and subunits which are needed for synthetic analysis. Techniques were developed for storage and retrieval of information on chemical transforms (including retron recognition and keying) using a higher level "chemical English" language. The program (LHASA) was designed to be interactive, with any level of control or input desired by the user, and to emulate the problem-solving approaches of synthetic chemists. The chemical knowledge base, written so as to be intelligible to a practicing chemist, contains all the types of information required for generation and evaluation of retrosynthetic changes, for example, data on individual transforms and their mechanisms, scope, and limitations.

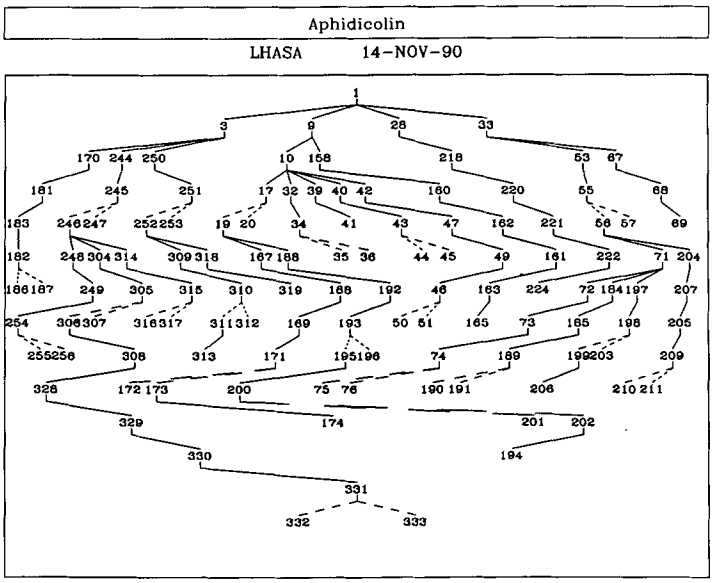

Scheme 2. A retrosynthetic analysis of aphidicolin carried out with the computer program LHASA.

The performance of the program is below that which should eventually be possible because of the immensity of the task and the modest size of our research effort. However, despite present limitations, including an incomplete knowledge base of about 2000 transforms, LHASA is capable of providing interesting suggestions of synthetic pathways for challenging targets. The present level of capability of LHASA can best be appreciated by its performance on specific problems. Shown in Scheme 2 is the EXTGT tree generated by LHASA for the antiviral agent aphidicolin, using just one particular line of analysis. The pathway in this tree from intermediates **332** and **333** to aphidicolin consists of the structures shown in Scheme 3.[13] The suggestion by LHASA of such non-obvious pathways is both stimulating and valuable to a chemist.

The field of computer assisted synthetic analysis is fascinating in its own right, and surely one of the most interesting problems in the area of machine intelligence. Because of the enormous memory and speed of modern machines and the

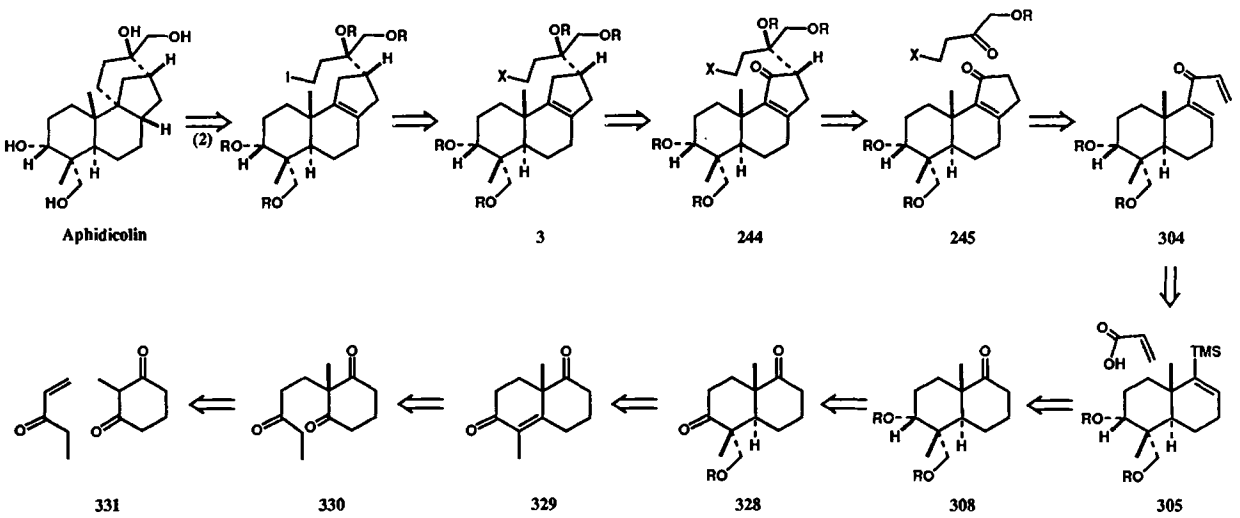

Scheme 3. A retrosynthetic path from Scheme 2 which leads from the structure **321** to aphidicolin.

probability of continuing advances, it seems clear that computers can play an important role in synthetic design. However, before that potential can be realized many difficult computing problems must be solved. Multistep retrosynthetic look-ahead, even under strategic guidance, requires complex and powerful software. Vast amounts of information—structural, stereochemical, and chemical—must be generated and analyzed using all available chemical knowledge. A massive undertaking will be required.

New Synthetic Methodology and Multistep Synthesis of Complex Molecules

The invention of new reactions and reagents has revolutionized the field of carbogenic synthesis, literally placing an extraordinarily powerful new chemistry alongside the classical reactions of the pre-1950 period. Without this methodology, the achievements of modern chemical synthesis would not have been possible. Two early landmarks in this advance, the discovery of the Wittig synthesis of olefins and the hydroboration of olefins, were highlighted by the award of the Nobel Prize in Chemistry for 1979 to *G. Wittig* and *H. C. Brown*. More recent developments have provided many methods which are noteworthy for their great chemical selectivity and stereochemical control and for their suitability in the construction of complex molecules. Indeed, many new synthetic processes have been discovered as a result of a perceived need in connection with specific problems involving novel or complicated structures and a deliberate search for suitable methodology. The rational design of such methods depends on the use of mechanistic reaction theory, stereochemical principles, and a wide range of chemistry involving many elements and ephemeral reactive intermediates.

A key to the success of many of the multistep chemical syntheses which have been demonstrated in our laboratories over the years has been the invention of new methodology. Since more than fifty such methods have been developed in our laboratory, it is impossible to summarize this aspect of synthetic research in a brief article. However, a few examples may serve to illustrate the effectiveness of these new methods in providing access to rare and valuable carbogenic compounds and their impact on the whole field of chemical synthesis.

The discovery and identification of the insect juvenile hormone of *Cecropia* (**6**, now known as JH-I)[14] in 1967 generated immense interest because of the potential of such nontoxic compounds for insect control.[15] Chemical synthesis was essential because of the extreme paucity of material from natural sources. Despite the apparent simplicity of structure **6**, a stereospecific route for the synthesis was not obvious, because no general methods existed in 1967 for the stereocontrolled generation of the trisubstituted olefinic units which it contains. The first stereospecific synthesis of **6**[16] was possible using new methodology which was specifically devised for this application. An abbreviated version of the synthesis is shown in Scheme 4. The first olefinic intermediate (**7**) was synthesized from *p*-methoxytoluene in a way which guarantees the *Z*-configuration of the stereocenter. Reaction of **8** with $LiAlH_4$ (*trans* hydroalumination) followed by iodine (replacement of Al by I) produced **9** stereospecifically by a novel sequence.[16] The replacement of iodine in **9** by ethyl was effected by another new process, cross coupling of a vinylic iodide with an organocopper reagent, which provided **10** stereospecifically. A completely analogous series of reactions converted **10** to triene **11**, from which JH-I (**6**) was obtained by a novel selective oxidation sequence. Thus the synthesis outlined in Scheme 4 depended on no less than four new synthetic methods. Three of these methods have come into very general use. The coupling of carbon groups using organocopper chemistry is now a major method of chemical synthesis.[17] The related carbometalation of acetylenes, also developed in connection with the synthesis of **6**,[16b, 18] has been extended in many directions, and this approach has become commonplace for the stereospecific construction of trisubstituted double bonds, a frequently occurring type of structural unit in biologically active natural substances.

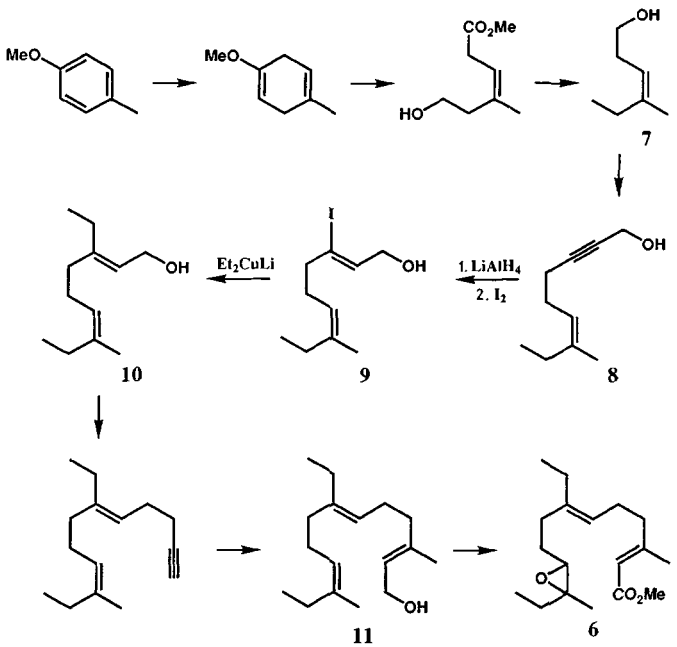

Scheme 4. Synthesis of the insect juvenile hormone JH-I **6**.

The ready availability of the insect juvenile hormone **6** permitted a wide range of biological studies and an understanding of the best ways of using such "third generation" agents for insect control. Inexpensive synthetic mimics of insect juvenile hormone are now produced commercially as environmentally safe insect control products.

Numerous naturally occurring microbial substances, especially antibiotics, are members of the "macrolide" structural family and contain a lactone functional group as part of a many membered ring. The key to the successful synthesis of complex macrolides such as erythronolide B (**12**), the precursor of the erythromycin antibiotics, was the development of new methodology for macrolactone ring formation (Scheme 5). Our group developed a very mild, effective and general method for this synthetic operation, the double-activation method,[19] which subsequently has been widely used. Thio ester **13**, produced by total synthesis,[20] was converted into macrolactone **15** simply by heating in toluene solution.

Internal proton transfer in **13** generates the internal ion pair **14**, which is doubly activated for the internal carbonyl addition required for ring closure to **15**. Erythronolide B was obtained from **15** by a simple reaction sequence.[20] The double-activation method has been used effectively for the synthesis of a number of other remarkable natural macrocyclic lactones (Scheme 5) including brefeldin A (**16**), an inhibitor of protein transport and processing in mammalian cells,[21] the microbial iron transporter enterobactin (**17**),[22] and the marine eicosanoid, hybridalactone (**18**).[23]

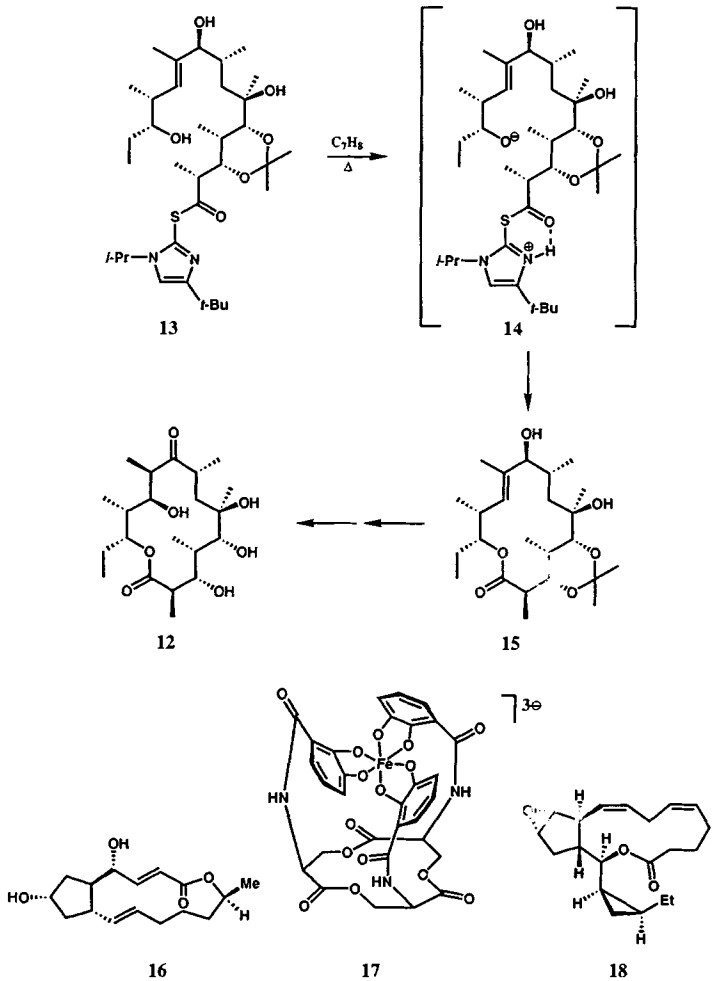

Scheme 5. Synthesis of macrocyclic lactones.

Bilobalide (**19**) is a complex and unusual molecule produced by the ginkgo tree, *Ginkgo biloba*. An effective synthesis of **19** was made possible by the development of a remarkable reaction for the formation of five-membered rings (Scheme 6).[24] The readily available chiral diester **20** was converted by Claisen acylation to the acetylenic keto diester **21**. Treatment of **21** with base effected a novel ring closure to give the bicyclic ketone **22**, which was then transformed into bilobalide (**19**) by a multistep sequence. There are several variants of this cyclization methodology which demonstrate considerable scope.[25]

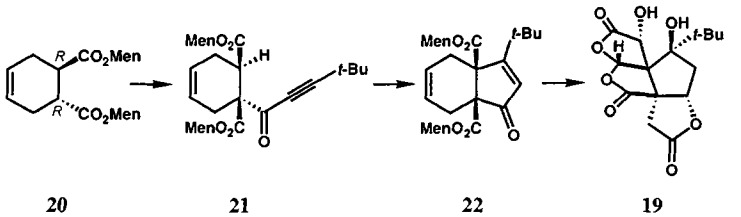

Scheme 6. Synthesis of bilobalide.

A wide range of reagents and reactants have played a role in the new methodology developed in our group: transition metals; metal-ion complexes; and silico, sulfo, boro, alumino, phospho, and stanno carbogens. The new general methods which have resulted include processes for ring formation, chain extension, oxidation, reduction, functional group transformation, activation, protection, and stereochemical control.

Multistep Synthesis—General

To a synthetic chemist, the complex molecules of nature are as beautiful as any of her other creations. The perception of that beauty depends on the understanding of chemical structures and their transformations, and, as with a treasured work of art, deepens as the subject is studied, perhaps even to a level approaching romance. It is no wonder that the synthetic chemist of today is filled with joy by the discovery of a new naturally occurring structure and the appearance of yet another challenge to synthesis. It makes no difference that the realization of a difficult synthesis entails long hours of study, thought and physical effort, since a complex chemical synthesis is an exciting adventure which leads to a beautiful creation. I believe that the case for molecular synthesis, as a high intellectual endeavor and as a scientific art form, can stand on these merits. The chemist who designs and completes an original and aesthetically pleasing multistep synthesis is like the composer, artist or poet who, with great individuality, fashions new forms of beauty from the interplay of mind and spirit.

It is fortunate that molecular synthesis also serves the utilitarian function of producing quantities of rare or novel substances which satisfy human needs, especially with regard to health, and the scientific function of stimulating research and education throughout the whole discipline of chemistry.

Our research group has been responsible for the creation of more than one hundred new multistep syntheses of interesting molecules, our sonatas and string quartets. The step-by-step construction of most of these targets of synthesis is outlined in the *"Logic of Chemical Synthesis"*[7] and is discussed in detail in the original research papers referred to therein. The structures of a small, and somewhat random, selection of these synthetic targets are shown in Scheme 7. A few comments will be given here on the syntheses of each of these to provide an overview of this aspect of our research.

Maytansine[26a] and aplasmomycin,[26b] each scarce and therapeutically interesting, were synthesized enantioselectively and with control of stereochemistry using novel methodology for assembling the molecular skeleton and for forming the macrocyclic unit. These syntheses and that of erythronolide B[19, 26c] provided early demonstrations that such complex, macrocyclic molecules can be made efficiently by multistep total synthesis.

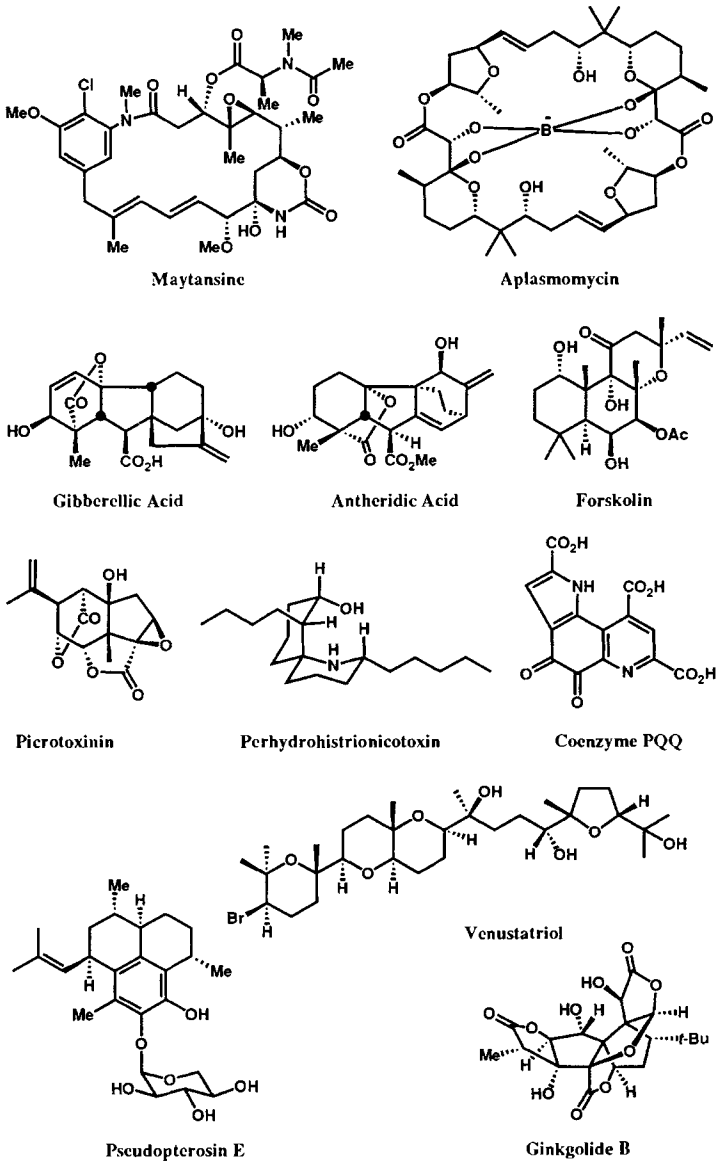

Scheme 7: Structures of some complex natural products whose total syntheses have been arried out in our laboratories.

Gibberellic acid resisted total synthesis, despite studies in several leading laboratories, for more than two decades because of an unusually forbidding arrangement of structural subunits. The first successful synthesis, and subsequent improved versions,[26d] required a deep and complex retrosynthetic analysis[26e] and a number of new concepts and methods. An entirely different strategic approach was utilized for the first synthesis of the biosynthetically related plant regulator antheridic acid[26f] which confirmed the proposed gross structure and clarified the stereochemistry. The availability of synthetic antheridic acid is essential to the further study of this rare and potent plant hormone.

Forskolin, the first known activator of the enzyme adenylate cyclase, is a promising therapeutic agent which is available only in limited quantity from plant sources. An efficient multistep synthesis of forskolin, which is both enantio- and stereocontrolled, has been developed[26g] based on several new synthetic methods. The synthesis of picrotoxinin, known since 1811 and a potent inhibitor of the neurotransmitter γ-aminobutyric acid (GABA) would not have been possible without retrosynthetic analysis and new methodology.[26h] Perhydrohistrionicotoxin, a rare and highly bioactive alkaloid from poisonous frogs, is a useful tool in neuroscience which was easily produced by total synthesis.[26i]

Pseudopterosin E,[26j] a powerful antiinflammatory agent, and venustatriol,[26k] an antiviral agent, are biosynthesized by marine organisms in only trace amounts. Both are available in chiral form by efficient enantiocontrolled multistep syntheses.

Last, but no means least, in this brief summary of our studies on the total synthesis of complex molecules, is the case of ginkgolide B, an unusual substance for several reasons. Ginkgolide B is biosynthesized in the roots of the unique and ancient ginkgo tree, *Ginkgo biloba*, by an extraordinarily complex biosynthetic process, for reasons that are unknown. It is an active ingredient in the medicinal extract of ginkgo which is now widely used in oriental and western medicine. The total synthesis of ginkgolide B posed a challenge for synthesis in the 1980's which was comparable to the most difficult problems of earlier eras, for example, steroids in the 1950's or vitamin B-12 and gibberellic acid in the 1970's. That challenge was met in just three years of research, thanks again to the power of modern retrosynthetic planning and to the invention of new tools for this particular synthesis.[26i, 27]

Multistep Synthesis Exemplified—The Prostaglandins

The prostaglandins, the first of the known eicosanoids, were detected as bioactive substances more than fifty years ago. However, it was not until the pioneering work of *K. Sune Bergström* and his group in Sweden in the 1950's and 1960's that the structures of the various members of the prostaglandin family were determined.[28] For that research *Bergström* and *Bengt Samuelsson* received (together with *John Vane*) the Nobel Prize in Medicine and Physiology for 1982, and deservedly so since, as has been written of the prostaglandins: "Their actions and the pharmacologic agents that influence their formation affect almost every aspect of medical practice."[29] The occurrence of only trace amounts of prostaglandins (PG's) in mammalian sources and the potent effect of these C_{20} carboxylic compounds on muscle and blood vessels indicated the need for an effective synthesis that would make available all of the PG's in ample amounts for the study of their physiologic effects and therapeutic uses. The problem of chemical synthesis was complicated by uncertainties regarding the stability and chemistry of PG's, and the existence of three different families (PG_1's, PG_2's and PG_3's) each consisting of several members. The first total synthesis of the principal PG's, demonstrated by 1967,[30, 31] made available the important members of the first family (PGA_1, PGE_1 and $PGF_{1\alpha}$) and allowed an evaluation of their chemical properties which facilitated the design of a general synthetic route to all of the prostaglandins. This general synthesis of prostaglandins provided access to all PG's from a single intermediate, commonly known as the Corey lactone aldehyde.[32, 33] In various forms this flexible synthesis has been used by laboratories all over the world to

prepare not only naturally occurring PG's but also countless structural analogs on any scale.[34]

The original version of the 1969 general synthesis of PG's is summarized briefly in Scheme 8. The bicycloheptenone **23** was synthesized stereospecifically by a novel Cu^{II}-catalyzed Diels-Alder reaction followed by alkaline hydrolysis of the resulting adduct. Alkaline peroxide converted **23** into the hydroxy acid **24** which was readily resolved using (+)-ephedrine. Lactonization and functional group interchange operations transformed **24** into the Corey lactone aldehyde **25**, a versatile precursor of all of the PG's and analogs thereof. Enone **26**, produced stereospecifically from **25** by Horner-Emmons coupling, upon reduction with zinc borohydride generated the required (15*S*)-alcohol along with the (15*R*)-diastereomer which was separated and recycled via **26** to the (15*S*)-alcohol. Protection of the hydroxyl groups at C11 and C15 afforded the corresponding bistetrahydropyranyl (bis THP) ether, **27**. Reduction of the lactone function of **27** to lactol (R_2AlH) and Wittig coupling produced **28** stereospecifically. Acidic hydrolysis of **28** afforded $PGF_{2\alpha}$ (**30**), whereas oxidation of **28** followed by hydrolysis gave PGE_2 (**29**). Hydrogenation of the 5,6-double bond in **28** followed by these same final steps produced $PGF_{1\alpha}$ and PGE_1. A parallel series of transformations was used to convert **25** into $PGE_{3\alpha}$ and PGE_3.

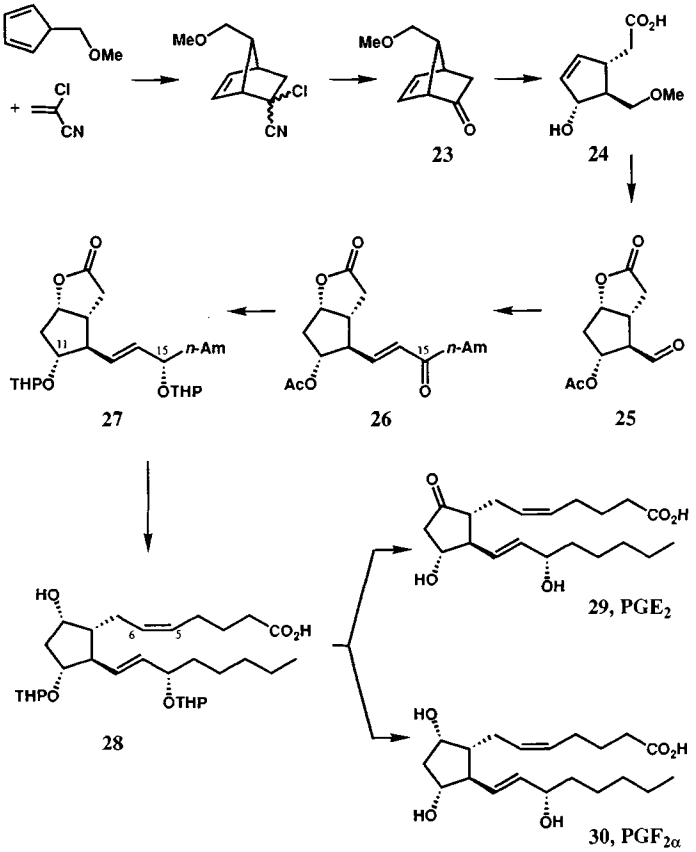

Scheme 8. General synthesis of prostaglandin. Am = C_5H_{11}, THP = tetrahydropyranyl.

Although the 1969 bicycloheptenone route to PG's was highly effective for the synthesis on a large scale, it was not the ultimate. The Diels-Alder route to **23** produced racemic material which in turn necessitated the resolution of hydroxy acid **24**. Another problem was the lack of stereospecificity in the reduction of the C15 keto group of **26**. Both of these limitations were overcome by the invention of novel methodology which has simultaneously opened up large new areas of synthetic endeavor.

The problem of controlling the stereochemistry of reduction of the 15-keto group in **26** was solved in a number of different ways (Scheme 9). First, the use of a bulky trialkyl-

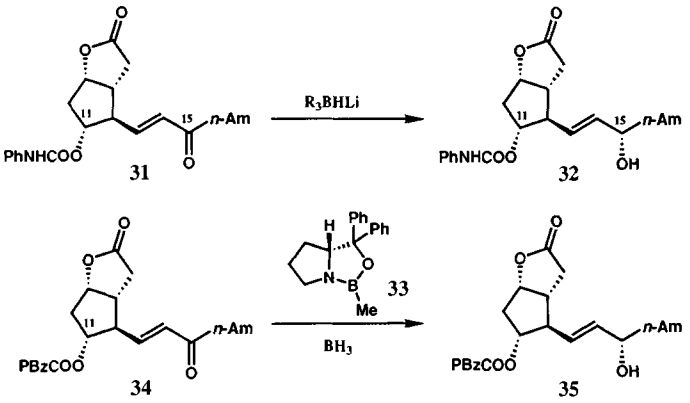

Scheme 9. Two routes of the highly heteroselective reduction of the C15 keto group in prostaglandin synthesis.

borohydride reagent with a suitably chosen "controller" group at the C11 oxygen, for example phenylcarbamoyl, resulted in reduction of C15 to give the required (15*S*) product with greater than 10:1 diastereoselectivity.[33, 35] Further, the small amount of (15*R*) by-product was easily separated for recycling. Second, using the chiral catalyst **33** (10 mole %) and borane (0.6 mole equivalent) in tetrahydrofuran as solvent at ambient temperature, the 15-ketone **34** was reduced to the (15*S*) alcohol **35** with 9:1 diastereoselectivity.[33, 36]

Oxazaborolidine **33** is a remarkable catalytic reagent. It controls the absolute stereochemistry of reduction of a large variety of ketones in addition to accelerating the rate of reduction by borane. The absolute stereochemistry of the reduction product of an achiral ketone R_SCOR_L, where R_S is smaller than R_L, is predictable.[37, 38] The observed catalysis and enantioselectivity are in accord with the mechanism outlined in Scheme 10. The catalyst **33** has been shown to complex with borane stereospecifically to give a species which is activated for binding to the ketonic substrate. Complexation at the sterically more available lone pair of the carbonyl oxygen and internal hydride transfer then leads to the observed enantiomeric secondary alcohol. In this mechanism the reagent **33** literally acts like a *molecular robot*: It first picks up and holds one of the reactants, BH_3, and becomes activated toward the other. It attaches to the ketone in a precise three-dimensional assembly that facilitates a transfer of hydrogen between the two reactants to form a *specific* enantiomer of the reduction product. The molecular robot finally discharges these products and repeats the reaction cycle. Such action by the small molecule **33** resembles catalysis by enzymes, which can also be regarded as molecular robots. Of course, **33** lacks the substrate-shape

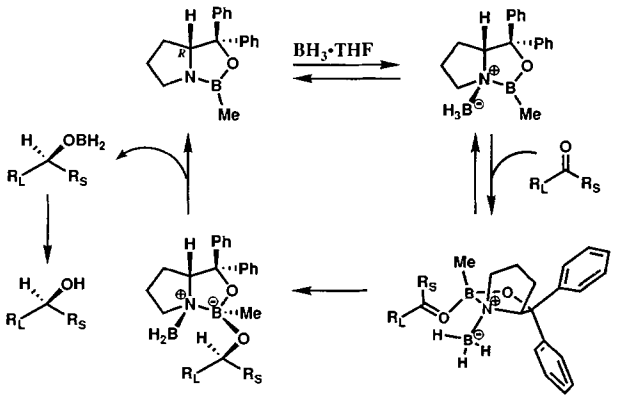

Scheme 10. Mechanism of the catalytic enantioselective reduction of ketones with the reagent 33/BH_3.

and size discrimination of enzymes because it is too small to possess a binding pocket or distal multicontact recognition sites.

The action of the molecular robot **33** represents a new direction for chemical synthesis. In the past, most synthetic constructions have depended on pairwise collisions between reactants without the help of a robot-like assembler. It is likely that synthetic chemistry will produce many new molecular robots in the future as a part of its advance to greater heights.

Two solutions were developed for the enantioselective synthesis of bicycloheptenone **23** (Scheme 8), of the correct chirality for the production of natural prostaglandins. In the first of these, a stereocontrolled aluminum chloride-catalyzed Diels-Alder reaction between benzyloxymethylcyclopentadiene (**37**) (Scheme 11) and the acrylate ester of 8-phenylmenthol (**36**) was used with the result that the required adduct **38** was formed with very high (32:1) enantioselectivity.[39] Adduct **38** was converted via ketone **23** into iodolactone **39** which was obtained in enantiomerically pure form in high yield by a single recrystallization and converted into the standard PG intermediate **40**. In addition, 8-phenylmenthol was recovered efficiently. The enantioselective formation of **38** can be understood from the geometry shown for the complex **36** · $AlCl_3$ and the steric screening by phenyl of the *si* (rear) face of the acrylate α,β-double bond. The efficiency of the 8-phenylmenthol controller stimulated the development of other controllers (chiral auxiliaries) for use in enantioselective synthesis.[40]

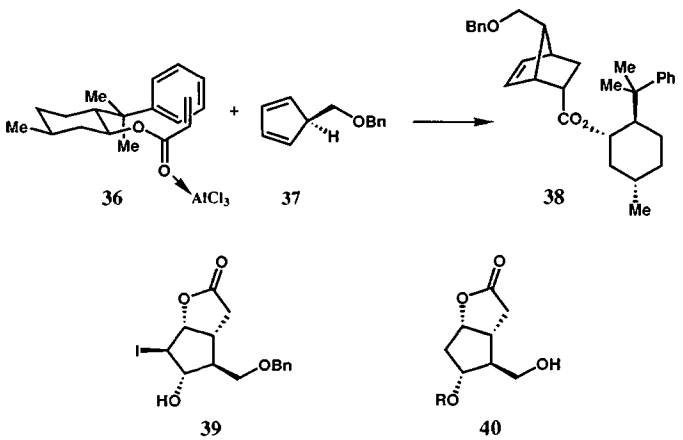

Scheme 11. Enantioselective Diels-Alder reaction for the synthesis of the bicycloheptenone **23** (see Scheme 8).

More recently, this achievement has been surpassed by the development of a *molecular robot* which assembles the achiral components, as shown in Scheme 12, to give the required Diels-Alder adduct in 94% yield and almost 50:1 enantioselectivity.[38,41] Conversion to enantiomerically pure iodolactone **39** was accomplished using standard procedures.[42]

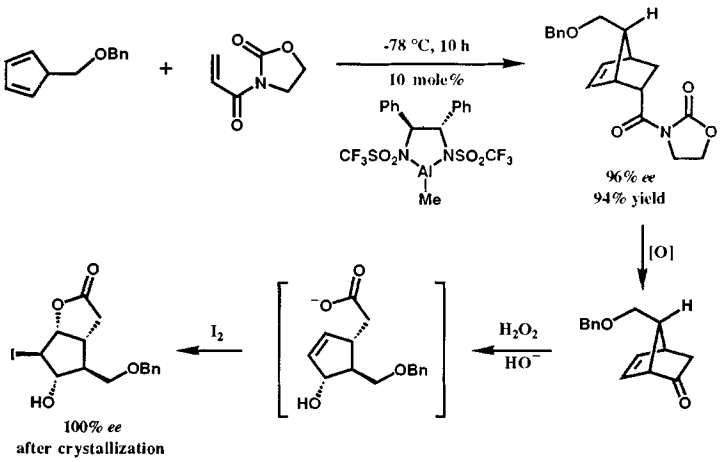

Scheme 12. Enantioselective, catalytic Diels-Alder reaction for the Synthesis of the bicycloheptenone **23**.

The general synthesis of prostaglandins by the 1969 pathway can now be carried out efficiently and with total stereochemical control, in a way that could not have been foreseen twenty years ago. Such progress augurs well for the future of chemical synthesis. It is not unlikely that today's chemical synthesis, magnificent as it may now appear, will prove to be rudimentary as compared to that of the next century.

The trail of research which originated with the synthesis of prostaglandins was followed for more than two decades, eventually including the synthesis of many other members of the eicosanoid (twenty-carbon) class of mammalian cell regulators. A few of the highlights of this program deserve mention. The biosynthesis of prostaglandins occurs by the oxidative conversion of the C_{20} unsaturated acid arachidonic acid to the bicyclic endoperoxide PGH_2, which serves as a precursor not only of PGE_2 and $PGF_{2\alpha}$, but also of PGI_2 and thromboxane A_2.[43] We were able to synthesize a stable, active azo analog (**41**) of the unstable PGH_2[44] (Scheme 13) and stable, active analogs (e.g. **42**) of the unstable thromboxane A_2[45] as well as PGI_2 itself (**43**).[46] In 1977 we suggested the structure of the unstable eicosanoid which is now known as leukotriene A_4 (LTA_4) (**44**) and, by early 1979, had synthesized that structure in advance of isolation from natural sources.[47] Collaborative research between our group and the Karolinska team headed by *Bengt Samuelsson* established that LTA_4 combines with glutathione to form the pri-

mary "slow reacting substance," now known as LTC_4 (**45**).[47] The detailed stereochemistry of the chemotactic leukotriene LTB_4 (**46**) was first established by synthesis.[47, 48] The chemical syntheses of these leukotrienes made these compounds available in quantity for the many hundreds of biological studies which ensued. Useful new compounds which are active as antagonists of $PGF_{2\alpha}$,[49] thromboxane A_2,[50] and LTB_4,[51] and as inhibitors of leukotriene biosynthesis[52] have also emerged from our synthetic program.

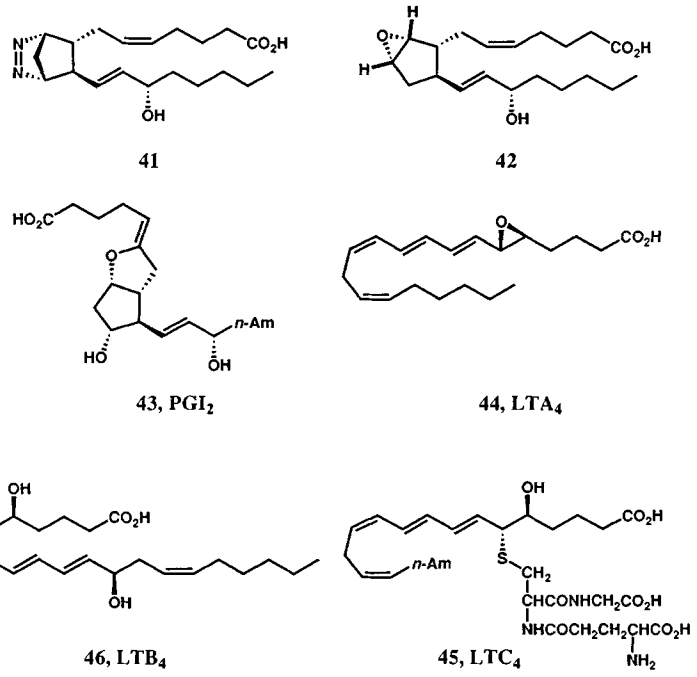

Scheme 13. Some unsaturated C_{20} compounds.

It is my hope that our studies in the eicosanoid field[34] will prove to be a harbinger of future programs in academic synthetic research, since there is an unparalleled opportunity for the application of chemical synthesis to biological and medical problems at a fundamental level.

Acknowledgement

It gives me great pleasure to express my indebtedness to many individuals who deserve credit for the accomplishments summarized herein: my teachers at the Lawrence High School and the Massachusetts Institute of Technology, my colleagues at the University of Illinois and Harvard University, my wonderful collaborators in research, and my very dear family. Research grants from the National Science Foundation, the National Institutes of Health, Pfizer Inc. and numerous other donors have provided the necessary financial support.

Received: January 11, 1991 [A 815 IE]
German version: *Angew. Chem. 103* (1991) 469

[1] N. Anand, J. S. Bindra, S. Ranganathan: *Art in Organic Synthesis*, (Holden-Day, San Francisco, 1st Edit. 1970, This book contains a summary of these and other noteworthy syntheses of the period 1940–1970..
[2] R. B. Woodward in: *Les Prix Nobel en 1965*, Almquist & Wiksell, Stockholm 1966 p. 192; *Angew. Chem. 78* (1966) 557.
[3] E. J. Corey, *Pure Appl. Chem. 14* (1967) 19.
[4] E. J. Corey, W. T. Wipke, *Science 166* (1969) 178.
[5] E. J. Corey, *Q. Rev. Chem. Soc. 25* (1971) 455.
[6] a) E. J. Corey, M. Ohno, P. A. Vatakencherry, R. B. Mitra, *J. Am. Chem. Soc. 83* (1961) 1251; b) *ibid. 86* (1964) 478.
[7] E. J. Corey, X.-M. Cheng: *The Logic of Chemical Synthesis*, Wiley, New York 1989.
[8] This section is essentially taken from Ref. [7].
[9] E. J. Corey, R. D. Cramer III, W. J. Howe, *J. Am. Chem. Soc. 94* (1972) 440.
[10] See Ref. [7], Chapter 6.
[11] E. J. Corey, A. K. Long, S. D. Rubenstein, *Science 228* (1985) 408.
[12] E. J. Corey, W. T. Wipke, R. D. Cramer III, W. J. Howe, *J. Am. Chem. Soc. 94* (1972) 421.
[13] This computer analysis was performed by Mr. *John Kappos* of our LHASA group.
[14] H. Röller, K.-H. Dahm, C. C. Sweeley, B. M. Trost, *Angew. Chem. 79* (1967) 190; *Angew. Chem. Int. Ed. Engl. 6* (1967) 179.
[15] S. S. Tobe, B. Stay, *Adv. Insect Physiol. 18* (1985) 305.
[16] a) E. J. Corey, J. A. Katzenellenbogen, N. W. Gilman, S. A. Roman, B. W. Erickson, *J. Am. Chem. Soc. 90* (1968) 5618; b) E. J. Corey, *Mitt. Schweiz. Entomol. Ges. 44* (1971) *87*; c) Ref. [7], p. 146; d) E. J. Corey, G. H. Posner, *J. Am. Chem. Soc. 89* (1967) 3911.
[17] G. H. Posner: *An Introduction to Organic Synthesis Using Organocopper Reagents*, Wiley, New York 1980.
[18] E. J. Corey, J. A. Katzenellenbogen, *J. Am. Chem. Soc. 91* (1969) 1851.
[19] a) E. J. Corey, K. C. Nicolaou, *J. Am. Chem. Soc. 96* (1974) 5614; b) E. J. Corey, K. C. Nicolaou, L. S. Melvin, Jr., *ibid. 97* (1975) 654; c) E. J. Corey, D. J. Brunelle, P. J. Stork, *Tetrahedron Lett. 1976* 3405; d) E. J. Corey, D. J. Brunelle, *ibid. 1976*, 3409.
[20] E. J. Corey, S. Kim, S.-e. Yoo, K. C. Nicolaou, L. S. Melvin, Jr., D. J. Brunelle, J. R. Falck, E. J. Trybulski, R. Lett, P. W. Sheldrake, *J. Am. Chem. Soc. 100* (1978) 4620.
[21] a) E. J. Corey, R. H. Wollenberg, *Tetrahedron Lett. (1976)* 4705; b) E. J. Corey, R. H. Wollenberg, D. R. Williams, *ibid. 1977*, 2243; E. J. Corey, P. Carpino, *ibid. 31* (1990) 7555.
[22] E. J. Corey, S. Bhattacharyya, *Tetrahedron Lett. 1977*, 3919.
[23] E. J. Corey, B. De, *J. Am. Chem. Soc. 106* (1984) 2735.
[24] a) E. J. Corey, W.-g. Su, *J. Am. Chem. Soc. 109* (1987) 7534; b) E. J. Corey, W.-g. Su, *Tetrahedron Lett. 29* (1988) 3423.
[25] a) E. J. Corey, W.-g. Su, I. N. Houpis, *Tetrahedron Lett. 27* (1986) 5951; b) E. J. Corey, W.-g. Su, *ibid. 28* (1987) 5241.
[26] a) Ref. [7], pp. 116–123; b) Ref. [7], pp. 128–133; c) Ref. [7], pp. 104–107; d) Ref. [7], pp. 205–211; e) Ref. [7], pp. 84–85; f) Ref. [7], pp. 212–214; g) Ref. [7], pp. 230–233; h) Ref. [7], pp. 86–87, 178–179; i) Ref. [7], pp. 83–84, 136–137; j) Ref. [7], pp. 237–238; k) Ref. [7], pp. 234–236; l) Ref. [7], pp. 89–91; 221–226.
[27] E. J. Corey, *Chem. Soc. Rev. 17* (1988) 111.
[28] S. Bergström, *Science 157* (1967) 382.
[29] J. A. Oats, G. A. Fitzgerald, R. A. Branch, E. K. Jackson, H. R. Knapp, L. J. Roberts, II, *New Eng. J. Med. 319* (1988) 689.
[30] a) E. J. Corey, N. H. Andersen, R. M. Carlson, J. Paust, E. Vedejs, I. Vlattas, R. E. K. Winter, *J. Am. Chem. Soc. 90* (1968) 3245; b) E. J. Corey, I. Vlattas, N. H. Andersen, K. Harding, *ibid. 90* (1968) 3247; c) E. J. Corey, I. Vlattas, K. Harding, *ibid. 91* (1969) 235; d) E. J. Corey, *Ann. N.Y. Acad. Sci. 180* (1971) 24.
[31] Ref. [7], pp. 250–254.
[32] a) E. J. Corey, N. M. Weinshenker, T. K. Schaaf, W. Huber, *J. Am. Chem. Soc. 91* (1969) 5675; b) E. J. Corey, T. K. Schaaf, W. Huber, U. Koelliker, N. M. Weinshenker, *ibid. 92* (1970) 397; c) E. J. Corey, R. Noyori, T. K. Schaaf, *ibid. 92* (1970) 2586.
[33] Ref. [7], pp. 255–296.
[34] For another general account of this project and subsequent studies on eicosanoids, see E. J. Corey, *Japan Prize in Science for 1989 (Annu. Rep. Sci. Tech. Found. Jpn., pp. 95–109, 1989).*
[35] E. J. Corey, S. M. Albonico, U. Koelliker, T. K. Schaaf, R. K. Varma, *J. Am. Chem. Soc. 93* (1971) 1491.
[36] E. J. Corey, R. K. Bakshi, S. Shibata, C.-P. Chen, V. K. Singh, *J. Am. Chem. Soc. 109* (1987) 7925.
[37] E. J. Corey, R. K. Bakshi, S. Shibata, *J. Am. Chem. Soc. 109* (1987) 555.
[38] E. J. Corey, *Pure Appl. Chem. 62* (1990) 1209.
[39] E. J. Corey, H. E. Ensley, *J. Am. Chem. Soc. 97* (1975) 6908.
[40] a) W. Oppolzer, *Angew. Chem. 96* (1984) 840; *Angew. Chem. Int. Ed. Engl. 23* (1984) 876; b) G. Helmchen, R. Karge, J. Weetman, *Mod. Synth. Methods 4* (1986) 261.
[41] E. J. Corey, R. Imwinkelried, S. Pikul, Y. B. Xiang, *J. Am. Chem. Soc. 111* (1989) 5493.
[42] E. J. Corey, N. Imai, Tetrahedron Lett., in press (1991).

[43] N. A. Nelson, R. C. Kelly, R. A. Johnson, *Chem. Eng. News 60* (1982), p. 30.
[44] a) E. J. Corey, K. C. Nicolaou, Y. Machida, C. L. Malmsten, B. Samuelsson, *Proc. Natl. Acad. Sci. USA 72* (1975) 3355; b) E. J. Corey, K. Narasaka, M. Shibasaki, *J. Am. Chem. Soc. 98* (1976) 6417.
[45] a) T. K. Schaaf, D. L. Bussolotti, M. J. Parry, E. J. Corey, *J. Am. Chem. Soc. 103* (1981) 6502; b) E. J. Corey, W.-g. Su, *Tetrahedron Lett. 31* (1990) 2677.
[46] a) E. J. Corey, G. E. Keck, I. Székely, *J. Am. Chem. Soc. 99* (1977) 2006; b) E. J. Corey, H. L. Pearce, I. Székely, M. Ishiguro, *Tetrahedron Lett. 1978*, 1023.
[47] a) E. J. Corey, *Experientia 38* (1982) 1259; b) Ref. [7], pp. 312–317; c) E. J. Corey, Y. Arai, C. Mioskowski, *J. Am. Chem. Soc. 101* (1979) 6748; d) E. J. Corey, D. A. Clark, G. Goto, A. Marfat, C. Mioskowski, B. Samuelsson, S. Hammarström, *ibid. 102* (1980) 1436, 3663.
[48] a) E. J. Corey, A. Marfat, G. Goto, F. Brion, *J. Am. Chem. Soc. 102* (1980) 7984; b) E. J. Corey, A. Marfat, J. E. Munroe, K. S. Kim, P. B. Hopkins, F. Brion, *Tetrahedron Lett. 22* (1981) 1077.
[49] R. B. Stinger, T. M. Fitzpatrick, E. J. Corey, P. W. Ramwell, J. C. Rose, P. A. Kot, *J. Pharmacol. Exp. Ther. 220* (1982) 521.
[50] E. J. Corey, W.-g. Su, *Tetrahedron Lett. 31* (1990) 3833.
[51] H. J. Showell, I. G. Otterness, A. Marfat, E. J. Corey, *Biochem. Biophys. Res. Commun. 106* (1982) 741.
[52] See Ref. [7], pp. 345–352.

Chemical Characterization of Aerosols: On-Line and In Situ

By Reinhard Nießner*

Whereas aerosols were formerly considered to be important in meteorological processes but in little else, today they play a significant role not only in environmental protection but also in "new technologies" such as the formation of high performance ceramics, sinter metals, optical waveguides, and superconductors. Analytical procedures which are capable of a continuous qualitative and quantitative description of processes in which aerosols are formed are, however, still almost unknown. The present review will discuss initial developments (which will often appear exotic in nature) such as the use of the condensation properties of ultrafine particles or time-resolved laser-induced aerosol fluorescence spectroscopy. The progress of analytical chemistry in the last few years makes it clear that advances in miniaturization, data processing, and optronics will probably be capable of solving many problems which are presently regarded as unsolvable.

1. Introduction

1.1. Aerosols

Aerosols are colloidally disperse systems consisting of ultrafine or finely divided material (particle diameter between ca. 2 nm and a few μm) in a carrier gas. No distinction is made between liquids and solids in the suspension.

Aerosols play an important role in the atmosphere: they are responsible for atmospheric turbidity and thus for the limitation of visibility, they act as a source or sink for gaseous emissions (e.g. SO_x, NO_x, R_2S), and in addition they provide the condensation nuclei which are of prime importance in the life-giving water cycle. Aerosols are, however, also of increasing importance in technological processes. New technologies involve a large number of process stages in which substances are used or produced in a finely disperse form as aerosols: a) preparation of ultrapure, monodisperse and chemically homogeneous dusts as precursors for high-performance ceramics or for ceramic and metallic coatings,[1-7] b) solvent-free lacquer technologies (electrostatic coating),[8] c) production of optical waveguides,[9] d) microencapsulation of reactive substances,[10,11] e) manufacture of catalysts,[12,13] f) preparation of single crystals,[14,15] g) preparation of superconducting materials,[16,17] h) production of magnetically anisometric pigments,[18] and i) increasing the rate of slow reactions (e.g. aerosol fluorination of hydrocarbons[19,20]).

More exotic applications, which document the potential of aerosols in technical processes, are firstly their use in fusion experiments (neutron production during the formation of deuterated polyethylene aerosols from an exploding polyethylene fiber[21]), the development of "chemical lasers" (production of high concentrations of singlet oxygen for energy storage[22]), or the rapid and selective distribution of fertilizing and neutralizing mineral aerosols for the rehabilitation of woodland which has suffered damage from "acid" conditions.[23]

Aerosols also cause problems in everyday life. When certain types of emission are involved they are considered a toxicological risk for humans. The main subjects of discussion in this case are aerosols formed in combustion processes or at the workplace during production processes. Aerosol emissions result from incomplete combustion of polycyclic aromatic hydrocarbons (PAHs), polychlorinated biphenyls (PCBs), dioxins, and dibenzofurans. Sources include automobiles, refuse incineration, domestic fuel, cigarette smoke, and coal-fired power stations. These substances are generally also found at the workplace since pyrolysis processes or direct contact with toxicologically relevant aerosols are often involved in work processes. A further important toxic class comprises the heavy metal aerosols formed in grinding, welding, and casting processes.

Particle size plays a particularly important role. Present knowledge lists aerosols with aerodynamic particle sizes below 3 μm diameter as particularly dangerous, because they represent the fraction which can penetrate the lung. However, conflicting reports exist on the metabolism of particles deposited in the lung and on synergistic effects (for example how irritant gases and solid aerosol particles act in combination to determine the risk potential), as demonstrated by the continuing discussion on the risk potential of diesel exhausts and tobacco smoke aerosols.

1.2. Problems of Measurement in Aerosol Characterization

The problem areas mentioned in Section 1.1 make it clear that a powerful measurement technique would be of great interest; the following properties of such a technique must be considered:

- *limits of detection*: Many substances, including PAHs and dioxins, are emitted in sub-ppb concentrations.
- *selectivity*: High selectivity is not necessarily required in control and regulation procedures, or when screening is to be carried out as a rapid initial measure. In particular for process technologies or in warning systems at the work place, the matrix composition of the environment is well-defined. A final analysis, however, requires the highest selectivity.

[*] Prof. Dr. R. Nießner
Institut für Wasserchemie der Technischen Universität
Marchioninistrasse 17, W-8000 München 70 (FRG)

- *on-line signal emission*: A continuous determination of the aerosol composition is required for devices which give a warning of toxic emissions or immission. Aerosol measurement techniques which form chemically sensitive elements in a measurement and regulation procedure can also dictate the time constant: thus the response time should be as short as possible so that signal generation is as close to continuous as possible.
- *in situ concentration determination*: The thermodynamic and kinetic stabilities of many substances are particularly low when they are present in the form of aerosols. Well-documented examples are ammonium salt aerosols and tri- and tetranuclear PAHs produced in combustion processes. If an enrichment step such as filtration collection on membrane filters is necessary prior to the actual analysis, a substantial amount of the substance will be transferred from the solid to the gas phase. As a consequence the analysis will give a reading which is much too low unless the sampling method takes account of both solid aerosol particles from the filter and gaseous components which pass through the filter. Other possibilities for falsification are provided by interactions between neighboring particles at the surface of the collection medium (filter, impactor) or by an irreversible reaction of the aerosol with the collector medium itself. It is also necessary to take into account reactions between the deposited material and reactive trace gases (e. g., HNO_3/NO_2 + pyrene → 1-nitropyrene). It is thus desirable to devise a technique for direct determination of the relevant substance in its state of suspension (i.e., in situ). The technique should subject the aerosol to as little disturbance as possible.

A complete characterization of an aerosol (see Fig. 1) can be divided into a chemical and a physical stage. The physical stage consists of the determination of particle concentration, particle size distribution, form and structure of single particles, electrical properties of the suspended particles, as well as of pressure, temperature, and relative humidity. That this area of aerosol characterization can in general be considered as already fully developed[24-26] is documented by the large number of commercially available devices.

The chemical part of a comprehensive aerosol characterization should take into account the composition of both the gas phase and the dispersed material, because they are dependent on each other. A simple example in the area of

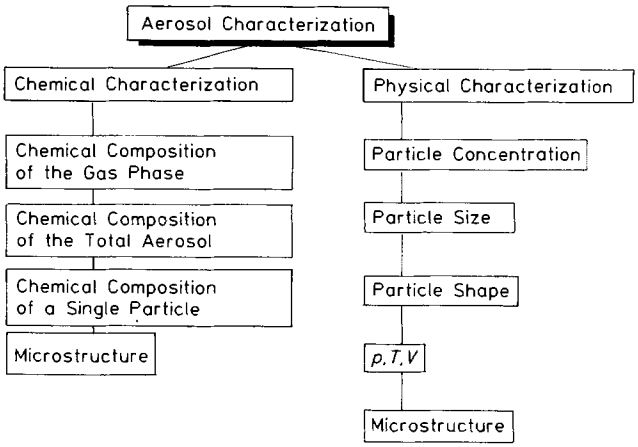

Fig. 1. Parameters of a complete aerosol characterization.

atmospheric aerosols is provided by the NH_4NO_3 aerosol [Eq. (a)].

$$NH_4NO_3(s) \underset{\text{cooling}}{\overset{\text{heating}}{\rightleftharpoons}} NH_3(g) + HNO_3(g) \qquad \text{(a)}$$

Even small variations in temperature cause as significant a change in the amount of solid NH_4NO_3 in the gas phase as a variation in the concentrations of the gases NH_3 and HNO_3. Similar effects have been observed in organic aerosol systems such as fluoranthene.

A further peculiarity of aerosol systems, namely the microstructure of aerosol particles, which is becoming increasingly important, makes their characterization more difficult.

The substance distribution across the total particle cross-section is not homogeneous (Fig. 2). A typical example of this behavior is the structure of fly ash particles: as a result of the stages in the cooling of a combustion gas (see Fig. 3), the toxicologically relevant substances become attached successively at the particle surface, either by adsorption or by condensation. In addition, because of the high particle concentration near the combustion center ($N > 10^{10}$ cm^{-3}), agglomerated submicron particles are found on the surface of the fly ash, which in turn can be microstructured. Another model for a microstructured particle, for example, a fog or cloud droplet, consists of an insoluble particle nucleus which as the result of a condensation process is covered by a liquid

Reinhard Nießner was born in Tuttlingen (FRG) in 1951 and started his studies in chemistry in Freiburg in 1972. He obtained his Diplom there in 1976 in analytical chemistry and his doctorate at Dortmund under Prof. D. Klockow in 1981, where he continued research for his habilitation till 1986. He was appointed full professor for Hydrogeology, Hydrochemistry and Environmental Analysis and head of the Institute for Aqueous Chemistry and Chemical Balneology at the Technische Universität München in 1989. Prof. Nießner was awarded the prize of the "Fachgruppe Analytische Chemie" in 1988 and the Heinrich-Emanuel-Merck Prize in 1990. His research interests lie in the classical analytical chemistry of water, the supervision of disposal sites, the chemical interaction of Xenobiotics with soil, the development of highly sensitive and selective immunoassays to detect harmful substances in the environment, analysis of aerosols, and in particular, the applications of laser spectroscopic techniques.

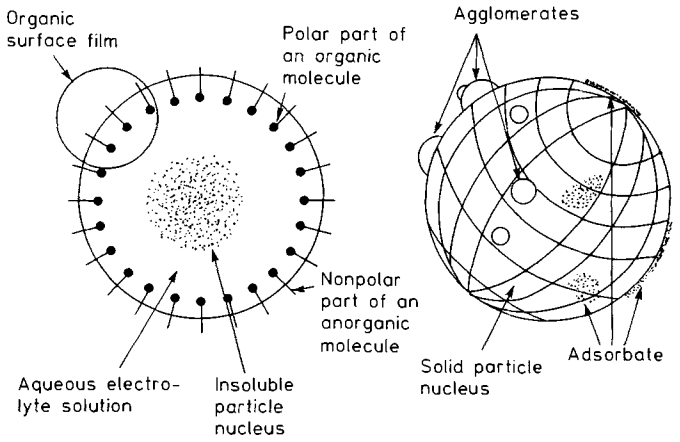

Fig. 2. Examples of microstructured aerosol particles.

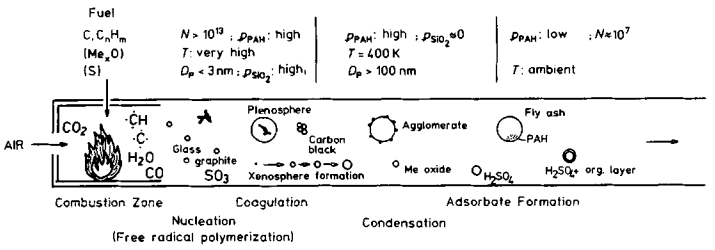

Fig. 3. A model of aerosol formation during cooling of combustion exhaust gases.

electrolyte layer. Because of the many subsequent evaporation and condensation processes occurring during the "lifetime" of these particles they can also be covered by a film of volatile organic substances such as terpenes, alkanes, alcohols, and carboxylic acids. This leads to an inverse micelle microstructure (see Fig. 2). Laboratory studies of artificially microstructured aerosols of this type have shown that such films can have a great influence on the phase transition of gaseous substances into the dissolved liquid phase (e.g., $NH_3(g)$ into $H^{\oplus}/H_2O$).[27, 28]

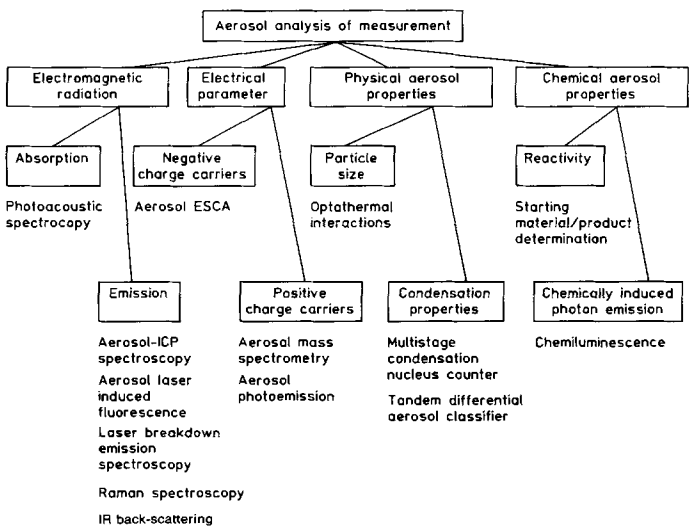

Fig. 4. In-situ and on-line aerosol determination procedures which are either already in use or potentially useful.

In the following discussion an attempt will be made to give a systematic overview of in situ and on-line aerosol characterization methods which either appear feasible or have already been realized. The special features and characteristics of these procedures will be discussed. A schematic summary is given in Figure 4.

2. Aerosol Characterization Based on Interactions with Electromagnetic Radiation

A large number of old and new techniques for on-line measurements based on the interaction of aerosols with electromagnetic radiation is now available. Well-known principles, such as emission, absorption, and scattering, covering the complete electromagnetic spectrum, can be used. Difficulties are, however, often encountered because of the small dimensions of the aerosol under study or because of the influence of the carrier gas, such as for example the production of unwanted new particles during photolysis. On the other hand, the observation of optical properties is the direct route to an in situ and on-line analysis.

2.1. Characterization on the Basis of the Light Extinction by Particles

The majority of procedures used in analytical chemistry are based on extinction measurements. For aerosols such a measurement is no longer trivial. Light incident on a particle can be either absorbed or scattered. Natural aerosols contain particles whose sizes lie between ca. 2 nm and 20 μm, while particle concentrations lie between less than 1 per cm^3 (e.g. in clean rooms) and greater than 10^9 per cm^3 (in combustion processes). Thus the extremely low effective interaction cross-section for the extinction measurement can readily be calculated. At present no simple procedure based on an extinction measurement is known which permits analysis at such low limits of detection. Improvements could perhaps be realized in applications involving synchrotron radiation and by the use of laser radiation within a laser resonator.

Luckily photoacoustic spectroscopy[29] is an indirect way of determining the absorption coefficient of an aerosol. The optoacoustic interaction is based on the conversion of vibration energy of excited vibration modes of molecular species into heat. This process causes the formation of a pressure wave in the surrounding gas. When the exciting energy source (typically a CW–IR laser) is modulated, the acoustic signal is subject to a similar modulation and can therefore be detected above the background noise by a sensitive microphone acting as a pressure sensor.

The absorbed photons thus cause a pressure increase as a result of the absorbing aerosol particles. If a resonant cell is used to create a standing wave, the acoustic signal is amplified, and the pressure p within the cell induced by irradiation with a sinusoidally modulated laser beam of frequency ω is described by Equations (b) and (c).[32]

Equations (b) and (c) represent the relation between the observed pressure in the resonant cell and the absorption coefficients β of the irradiated aerosol particles. The integral

$$p(\omega) = \sum A_j p_j \quad \text{(b)}$$

$$A_j = \frac{-i\omega(\gamma - 1)\beta(V_c)^{-1} \int p_j I dV}{\omega^2[1 - (\omega/\omega_j)^2 - i(\omega/\omega_j Q_j)]} \quad \text{(c)}$$

ω = frequency of the chopped laser source,
ω_j = frequency of the jth mode,
γ = ratio of the specific heats C_p/C_v at constant pressure and temperature,
β = absorption coefficient,
I = spatial variation of the light intensity,
Q_j = amplification factor of a mode j at resonance,
p_j = vibrational modes,
V_c = cell volume

$V_c^{-1} \int p_j I dV$ represents the coupling between the spatial profile of the irradiation intensity and the pressure waves p_j. The final result is that, within certain limits, the induced pressure p (the signal which is detected!) is a function of the applied irradiation intensity I.

Several groups are at present working on the development of photoacoustic aerosol sensors, in particular for the monitoring of diesel aerosols. Unsolved problems include the background signals caused by absorption of the incident light at cell walls or windows. The wide linear measurement range is a general advantage of this procedure. The application of photoacoustic spectroscopy to sulfate determination, initially demonstrated by *Röhl* et al.[31] for aerosol filter samples, is promising.

Adams et al.[32, 33] have recently published details of an aerosol spectrophotometer (Fig. 5). The photoacoustic cell

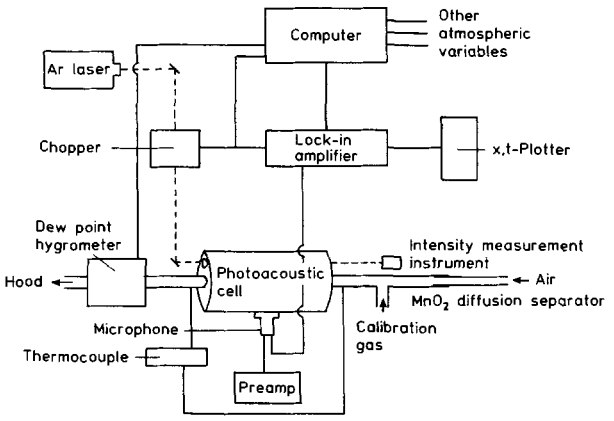

Fig. 5. Construction principle of a photoacoustic aerosol spectrometer. Preamp = preamplifier, Ar = argon.

consists of a brass cylinder which is constructed in the form of a resonant cell. The light source is an argon ion laser. The aerosol is drawn through the cell by a pump at the rate of 0.45 L min^{-1}. The aerosol is first passed through a MnO_2 diffusion separator to remove NO_2, which interferes in the measurement; the aerosol fraction is not reduced thereby. *Adams* et al. report a detection limit of 300 ng carbon per m^3.

A further improvement can be expected when cells are constructed within a laser resonator, in analogy with an application as a photoacoustic gas chromatographic detector as published by *Fung* and *Gaffney*.[34]

2.2. Analysis Based on Light Emission from the Particles

Another useful detection principle for quantitative or qualitative analysis of aerosols is photon emission from selectively stimulated molecules or particles. Relatively inexpensive techniques for the registration of single photons in the visible region already exist. There are thus a number of attractive possibilities for on-line and in situ detection of aerosols, such as laser-induced aerosol fluorescence (LIF), laser-induced breakdown spectrometry at aerosols (LIBS), laser-induced Raman spectroscopy at aerosols, IR backscattering at aerosols, and inductively coupled plasma (ICP) spectrometry.

2.2.1. *Analysis by Laser-Induced Fluorescence (LIF)*

Laser-induced fluorescence has been known for many years as an unwanted side effect of Raman spectroscopic studies in flame experiments.[35, 36] The first selective experiments designed to use these effects for the characterization of aerosols were reported by *Omenetto* and *Allegrini*,[37, 38] who generated pure polydisperse anthracene and fluoranthene aerosols.

Fluorescence occurs as a result of excitation of molecular or atomic systems by the absorption of one or more photons. Apart from fluorescence, other possibilities for a return to the ground state are available; their importance depends on structural considerations and on the nature of the excited state. Competing processes are quenching, internal relaxation (which leads to warming), and intersystem crossing (which leads to phosphorescence).

When fluorescence is compared as a detection principle with other optical principles, the high sensitivity and the possibility of achieving a high selectivity are immediately obvious. In contrast to photometry, where the sole available selectivity parameter is the absorption wavelength, two additional parameters can be used in fluorimetry: the fluorescence emission wavelength and the characteristic decay time for the fluorescence process. These three fluorimetric parameters should help either to identify and to quantify the various components in a mixture in the ideal case or at least to characterize of a group of similar substances.

A typical setup of an in situ and on line analysis of aerosols by time-resolved fluorimetry is shown in Figure 6.[39] It consists of three main components: the tuned laser system (207 nm–860 nm), the sensor unit (which is connected to the laser system by fiber optical cable), and the data accumulation and processing module.

The laser light (pulse length ca. 20 nsec, repetition rate up to 100 Hz) is transmitted via a fiber coupler to the optical wave-guide fiber and from thence to the sensor unit. Here the laser light is parallelized and subsequently crosses the aerosol flow. Within the light interaction volume the aerosol flow is conducted as a free-flowing current in a sheath air arrangement. The fluorescent light from the interaction volume is led perpendicular to both laser light and aerosol-flow axes through parallelization optics, an interference filter as a wavelength selector, and a second set of parallelization optics, and allowed to impede on the window of a fast-response photomultiplier.

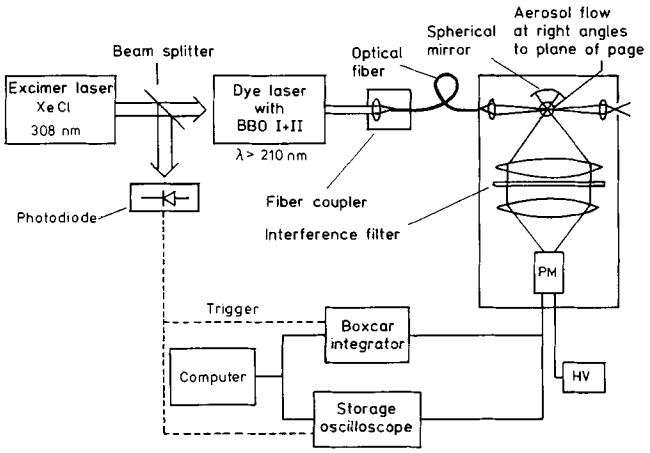

Fig. 6. Apparatus for the determination of polycyclic aromatic hydrocarbons on submicron aerosols by means of laser-induced time-resolved fluorescence. PM = photomultiplier, HV = high voltage, BBO = barium-β-borate crystal.

The data registration is performed by a 400 MHz storage oscilloscope. Triggering is accomplished by allowing a fraction of the exciting laser light to shine on a fast-response photodiode. The oscilloscope can now record a time-dependent study of the fluorescence process occurring after a laser discharge. The monitor image is processed by a CCD camera and transferred to the computer, where all subsequent processing is carried out.

The analytical possibilities are at present being studied on test aerosols. Initial results on monodisperse NaCl carrier aerosols with adsorbed polycyclic aromatic hydrocarbons (PAHs) gave decay times between 18 and 114 nsec. The absolute limit of detection lies in the femtogram range and is proportional to the amount of PAH adsorbed (Fig. 7).

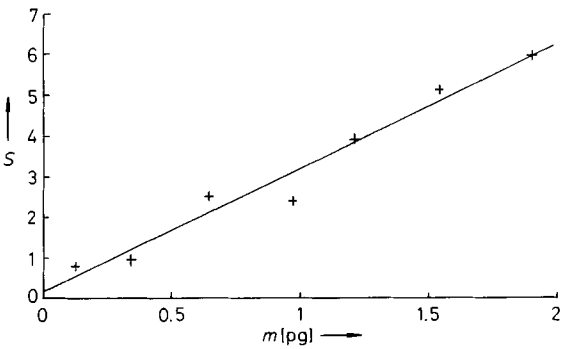

Fig. 7. Laser-induced fluorescence of a benzo[*a*]pyrene (BaP) coated aerosol. The fluorescence signal S (laser pulse energy normalized) is represented as a function of the amount of BaP [pg]. d_p = 80 nm (constant), T = 90–120 °C.

Fluorescence spectra of, for example, NaCl aerosols coated with benzo[a]pyrene or of particles consisting of pure BaP differ considerably from those of dissolved PAHs. Depending on the degree of surface coverage of the particles, a fraction of the fluorescence is red-shifted (see Fig. 8), due to the formation of PAH dimers on the particle surface at higher vapor pressures (i.e., higher PAH source temperatures).

Since the complete system (laser/photomultiplier/interference filter) can be connected via fiber optics, the procedure in principle enables remote sensing of toxic aerosols by fiber optics.

Work is presently in progress on deconvolution algorithms for the interpretation of superimposed fluorescence decay processes. One of the more severe problems in this type of measurement involves contributions from fluorescing substances in the air and from quench processes. On the other

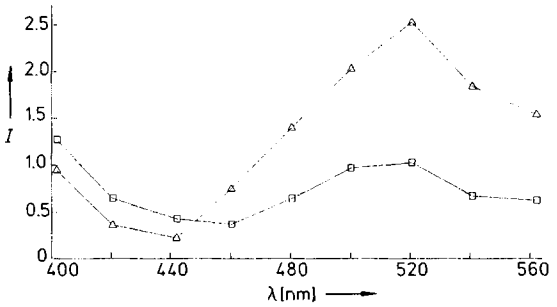

Fig. 8. Laser-induced aerosol fluorescence as a function of the observed fluorescence emission and the degree of coating (BaP on NaCl aerosol). Fluorescence intensity I [relative units], fluorescence wavelength λ [nm], □ at 95 °C, △ at 110 °C.

hand, the availability of further small lasers (e.g., the 337 nm N_2 laser or frequency-doubled semiconductor lasers) makes it possible to develop mobile measurement systems.

2.2.2. *Analysis by Laser-Induced Breakdown Spectroscopy (LIBS)*

The LIBS technique and its application to aerosols have been reviewed recently.[40–42] The procedure is based on a series of single processes: if a laser beam is focussed on solid material or on material particles, an aerosol cloud containing evaporated material is formed. If the laser pulse is of high energy (E > 100 mJ per pulse, pulse length ca. 10 nsec), the aerosol cloud forms a microplasma consisting of evaporated atoms, ions, electrons, and molecular fragments. All the molecules and particles within the plasma contribute to the light emission and can thus be determined both qualitatively and quantitatively. For example, detection limits of ca. 200 μg metal per m^3 were observed for aerosols containing cadmium, lead, and zinc.

2.2.3. *Analysis by ICP–Atomic Emission Spectroscopy*

The process of inductively coupled atomic emission has been applied to ceramic powder aerosols during studies involving materials science problems.[43] In ceramics technology, where the highest purity of trace elements is of prime importance, there would seem to be potential for further development. The generation of dry ceramic powder aerosols affords advantages over the previously used wet aerosols derived from slurries,[44] since a quench effect due to large amounts of water in the plasma can no longer occur.

Broekart et al.[45] have carried out a detailed study of the use of this technique in direct trace analysis of Al_2O_3 ceramic

powder aerosols. Problems exist in the case of larger particles (> 5 μm particle diameter), since when these are present the material is not completely evaporated.

2.2.4. *Analysis by Raman Spectroscopy*

Raman spectroscopy provides an extremely interesting tool for the characterization of suspended material. The phenomenon of Raman scatttering is caused by interaction between electromagnetic radiation and molecules or atoms in all aggregate states. Apart from the absorption or emission of photons, which is irrelevant in Raman spectroscopy, light scattering is observed within a very short time (ca. 10^{-14} sec). The energy of the incident photon can remain unchanged (Rayleigh scattering) or change (Raman scattering). The electric field of an electromagnetic wave induces a dipole moment proportional to the electric field strength. If vibrations are excited, the molecule's polarizability changes, and the prerequisite for observing a Raman spectrum is fulfilled. The identification of functional groups is possible, as in infrared spectroscopy.

The first Raman spectra of aerosol particles floating freely in an electrostatic suspension chamber were recorded by *Fung* and *Tang*,[46,47] who used an argon ion laser (488 nm) as the excitation source. The scattered light is focussed by a lens on the entrance slit of a double monochromator. Photon counting is carried out by means of a cooled photomultiplier and the necessary counting electronics. When this technique was applied to ammonium sulfate particles in the micrometer range, the resolution was excellent. However, no applications to freely flowing aerosols have so far been reported.

The use of resonance Raman spectroscopy in the ultraviolet range can be expected to bring a considerable amplification of the Raman intensity. *Asher*[48] applied this technique to deposited PAHs and achieved a remarkable selectivity and sensitivity.

2.2.5. *Analysis by IR Laser Back-scattering*

A laser beam which is allowed to pass through an aerosol cloud produces both absorption and scattering effects. This can be used as the basis for a remote investigation process for the physical and chemical description of an aerosol, the DISC process (differential scatter LIDAR system). *Wright* et al.[49] and *Mudd* et al.[50] were the first to study sulfuric acid and ammonium sulfate aerosols by this technique. DISC uses characteristic differences in the back-scattered IR radiation for quantification and differentiation purposes.

The LIDAR answer signal for a "laser shot" is given by Equation (d).[50] The qualitative information is obtained from β.

$$V(r) = \frac{KE_0\beta(r)\,T^2(r)}{r^2} \qquad \text{(d)}$$

$V(r)$ = direct back-scattered signal at a distance r
E_0 = transmitted laser pulse energy
$\beta(r)$ = back-scattering coefficient at a distance r
$T(r)$ = simple transmission of the mass of air from r to the detector
K = calibration constant.

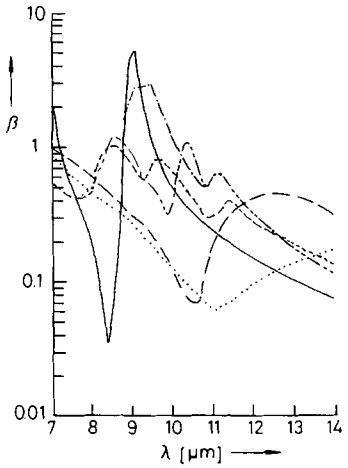

Fig. 9. Relative back-scattering of some environmental aerosols[50]. -·-· Basalt, ———— H_2SO_4 (95%), – – – H_2SO_4 (50%), — $(NH_4)_2SO_4$, ··· H_2O, and — — ice. β = relative volume back-scattering coefficient, λ = wavelength.

The relative back-scattering of various atmospheric aerosols as a function of the applied wavelength is shown in Figure 9. The limit of detection which can be achieved lies at best in the lower mg per m^3 range.

3. Aerosol Analysis by Measurement of Electrons, Ions, or Ionized Particles

Various techniques in analytical chemistry use electrons or ions as a measure of the amount of the species to be determined. These techniques include X-ray photoelectron spectroscopy (ESCA, UPS, XPS), photoemission, and mass spectrometry.

3.1. Analysis by Determination of the Kinetic Energy of the Electrons Released

The classical technique for the determination of the kinetic energy of emitted electrons is photoelectron spectroscopy or ESCA, which can in principle be used for all the elements of the periodic table (with the exception of hydrogen) in a quantitative manner. From the kinetic energy of the emitted photoelectrons and the energy of the exciting irradiation, the bonding energy E_b can be calculated. Detailed measurements of the bonding energy (chemical shift) provide information on the bonding states of the various elements.

It is a feature of ESCA that the observed photoelectrons arise mainly from the surface atom layers (the outer 5 nm or less, dependent on E_b, the material, and the exciting wavelength). ESCA can thus also be regarded as a very promising tool in the area of aerosol analysis.

One important drawback is that ESCA measurements on aerosol samples are normally carried out off-line.[51-53] The samples (e.g. from an aerosol-generating system) must be transferred as rapidly as possible from atmospheric pressure to the high-vacuum conditions of the spectrometer (up to 10^{-10} Torr) in order to avoid contamination by the pump oil or similar materials. On the other hand, many studies show that labile material such as organic substances and volatile

inorganic materials (e.g. ammonium salts) only survive for minutes or even seconds under these conditions.[54, 55] An on-line version of an ESCA spectrometer with a direct coupling between the aerosol and the high-vacuum compartment would thus be extremely useful.

Goldmann[56] was the first to develop such an instrument. As can be seen from the schematic diagram in Figure 10, expansion of the aerosol under vacuum forms an aerosol beam comparable with a molecular beam. This aerosol beam is irradiated by X-rays ($Al_{K\alpha}$ or $Mg_{K\alpha}$). Particle transfer through the two nozzles is particularly critical; transfer efficiencies have so far not been determined. The relatively complex pump system consists of Roots and turbomolecular pumps, which continuously pump off the incursing air.

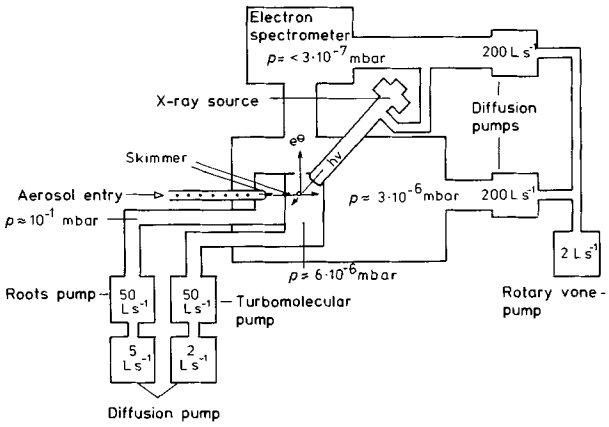

Fig. 10. Schematic diagram of an on-line aerosol ESCA apparatus as proposed by *Goldmann*[56].

The application of photoelectron spectroscopy as a quantitative analysis technique is limited in the case of aerosols by a marked dependence on particle size.[57] This is shown clearly in Figure 11 for a deposited sulfate aerosol. If the particles are perfectly spherical, the ESCA signal is expected to be proportional to the square of the particle radius. Since we are, however, generally interested in obtaining information on particle mass, the expected relationship is proportional to $1/r$. In Figure 11 the area of the S atom's 2p orbital, normalized with respect to carbon (the filter matrix) and the mass of sulfate, is plotted against particle size. The predicted $1/r$ dependence is reproduced very well.

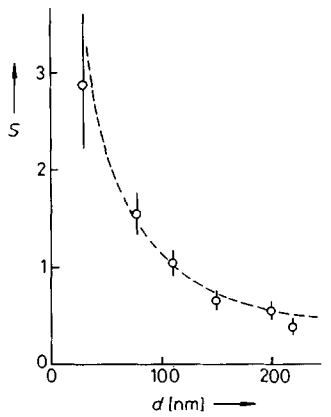

Fig. 11. ESCA signal S (in relative units) of the S atom's 2p orbital (normalized with respect to C 1s signal of the filter matrix and the mass of deposited sulfate) of monodispersed Na_2SO_4 aerosol as a function of the particle size (d = particle diameter). Dashed line: expected $1/r$ dependence.

Photoelectron spectroscopy can therefore only be used for mass determination of aerosols when an additional particle size determination is carried out; the surface-to-mass conversion assumes a homogeneous particle composition.

3.2. Analysis by Mass Spectrometry

The first analysis of airborne particles by mass spectrometry was reported by *Davis*.[58] His method involved focussing a particle beam from the surrounding air onto the ion source. Just as for the technique discussed in Section 3.1, the construction of an aerosol–vacuum interface is accompanied by substantial transmission losses. After a detailed study, *Stoffels*[59] suggested a solution in which the particle stream was passed through a capillary via a skimmer and a collimator and impacted directly onto a heated rhenium filament. This leads to surface ionization of the particles, giving charged fragments. A problem with this technique is the necessity for continuous pumping, which leads to the danger of contamination by back-diffusion of the pump oil.

The best solution at present is that proposed by *Sinha*.[60] Single particles are allowed to enter the ion source of a Mattauch–Herzog mass spectrometer in a sequential manner, where they are completely vaporized and ionized. The mass fragments are separated in space along a focusing plane of the magnetic sector. The electro-optical ion detector, which allows the simultaneous detection of all ions across the focusing plane, makes this apparatus unique. The ions impact on the active surfaces of a two-dimensional electron multiplier array. The electrons from the array are in turn accelerated and strike the end of the fiber optics, which is coated with a luminous material. The procedure generates "light pulse images" for the corresponding ion masses. The intensity of the bright spots is proportional to the total number of ions of a particular mass. The position and intensity of the ion images are registered by a CCD array. The detection limit of this mass spectrometer, determined using a dibromodiphenyl aerosol (particle size 1.8 μm), is ca. 10^{-13} g, and the simple relative standard deviation is 10–19%.

These results indicate areas of potential development for the mass spectrometric technique.

3.3. Characterization by Aerosol Photoemission

The principle of aerosol photoemission (APE) is the detection of positively charged aerosol particles.[61–63] In contrast to photoelectron spectroscopy, where the actual signal represents the kinetic energy of the emitted photoelectrons, APE makes use of the positive particles (their determination at atmospheric pressure by an aerosol electrometer is relatively easy) as a measure of the photoemitting material at the surface of the particles [Eq. (e)].

Nießner et al.[64] were able to show that $N^{\oplus}$ is directly proportional to the total photoelectrically active surface

$$dN^{\oplus}/dt = f\left\{\frac{\pi}{2} d^2 F,\ Y(h\nu),\ \Phi_{UV},\ N\right\} \quad \text{(e)}$$

$N^{\oplus}$ = number of positively charged particles
N = total number of all photoemitting particles
F = degree of surface coverage by photoemitting material
t = time
d^2 = irradiated particle cross-section
$Y(h\nu)$ = photoelectrical quantum yield at a photon energy $h\nu$ (dependent on the material and the light wavelength used)
Φ_{UV} = photon flux

area, which in turn comprises the surface areas of the various particles and the frequency of their occurrence in a polydisperse aerosol [Eq. (f)].

$$N^{\oplus} \sim S_{total}\left\{\frac{\pi}{2} d_i^2,\ N_i\right\} \quad \text{(f)}$$

S_{total} = total photoelectrically active surface of all particles
d_i = particle diameter of the component i
N_i = number of the particles of diameter d_i

The various components of a mixture of different photoelectrically active substances can be individually determined when their characteristic quantum yields are known from prior calibration experiments.[64] In analogy to photoelectron spectroscopy the height of the signal is proportional to the surface area; a mass determination thus shows a $1/r$ relationship between the signal's height and the aerosol mass. Photoemitting materials which can be studied include metal dust, some heavy metal oxide aerosols, and polycyclic aromatic hydrocarbons. The technique is at present applied in the control of diesel exhaust gases,[65] the control of waste incineration,[66] cigarette smoke analysis,[67, 68] and workplace monitoring.[64]

Figure 12 shows, as an example, the aerosol photoemission signals at an irradiation wavelength of 185 nm as a function of the PAH concentration in the smoke generated by six different brands of cigarette. There is a good linear correlation between the photoemission signal and the PAH concentrations in the aerosol as determined by HPLC analysis. It could be concluded that the PAH profile in the cigarette smoke varies only in the concentration but not in the relative ratios of the PAHs. The detection limit of the photoemission technique is in general in the lower ng m^{-3} range.[69, 70] The reproducibility of this technique is determined solely by the electronics and the stability of the UV lamp.

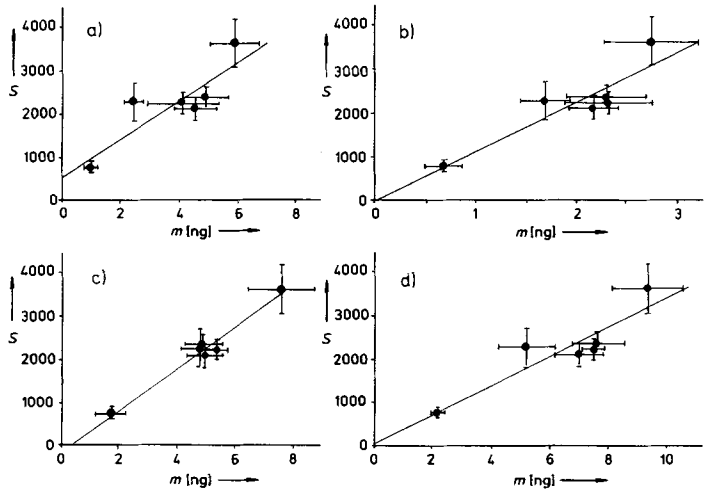

Fig. 12. Correlation between the photoelectric signal S and the content determined by wet chemical methods (m per cigarette) of a) benzo[*a*]pyrene, b) dibenzo[*a*,*h*]anthracene, c) benzo[*b*]fluorene, and d) benzo[*b*]fluoranthene. Each point represents the average of 5 analyses (with simple standard deviations) of one of 6 types of cigarettes.

4. Aerosol Analysis by Measurement of Physical Properties

4.1. Analysis by Observation of Hygroscopic Properties

Several techniques for aerosol characterization depend on the observation of the particle size after treatment with moisture or heat.

A good example is provided by the sulfuric acid aerosol detector proposed by *Liu* et al.[71] The process has also been described as an aerosol mobility chromatograph, since it depends on a continuous selection of particles which have different mobilities in an electric field. H_2SO_4 particles are mixed with air of a well-defined relative humidity, and as a result they swell. In combination with a differential electrostatic classifier (DMA) it is possible to perform extremely precise measurements of the particle diameter.

The construction of such an instrument is shown schematically in Figure 13. The aerosol to be analyzed is first passed

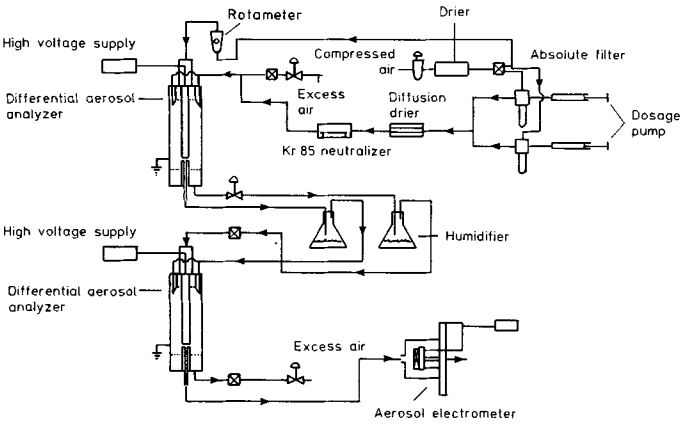

Fig. 13. Block diagram of the continuously operating aerosol mobility chromatograph [71].

through a krypton-85 neutralizer in which the particles are electrically charged according to a Boltzmann distribution. The charged particles are then allowed to pass into the first DMA. Particles of a certain polarity and electrical mobility are continually removed, humidified to a defined extent and fed into a second identically constructed and operated DMA. If water absorption and subsequent swelling has caused the particle diameter to increase and thus changed the electrical mobility, the "swollen" aerosol fraction will be able to pass through the apparatus (as a band pass) at a different collector voltage. The new particle diameter can be determined exactly from the voltage difference (see Fig. 14). At 53% relative humidity sulfuric acid particles swell, while

chloride, sulfate etc. remain unchanged. Aerosol electrometers or condensation nucleus counters are used as the on-line particle detector. The detection limit of this technique is ca. 10 ng H_2SO_4 per m^3 with an aerosol electrometer as detector and ca. 1 ng H_2SO_4 per m^3 with a condensation nucleus counter.

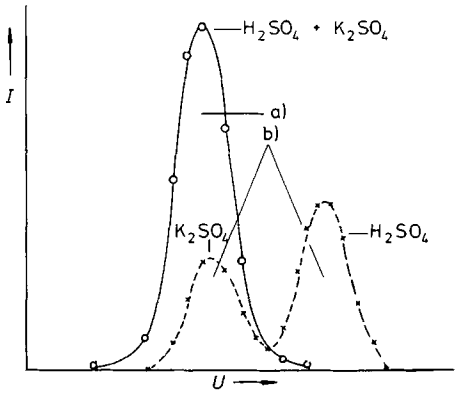

Fig. 14. Current/voltage curve for aerosol mobility chromatography of humidified and dry H_2SO_4/K_2SO_4 mixtures[71]. I = electrometer current, in relative units; u = voltage at central electrode, in relative units; a) without humidification: relative humidity 8.4%; b) with humidification: relative humidity 53%.

The same principle has been applied by *Charlson* et al.[72] who used a nephelometer to detect particle size changes. The resolution is, however, much lower than with a DMA, so that the detection limit lies in the µg range.

4.2. Characterization by Observation of the Particle Size after IR Absorption

An optothermal procedure in which submicron particles are irradiated by modulated CO_2 laser light has been combined with the observation of the particle size-dependent Mie scattering.[73-78] Under certain conditions when modulated IR radiation is used, the observed light scattering amplitude is proportional to the IR photon absorption. It is thus possible to record optothermally induced absorption spectra when a tunable IR laser is used.

The principle of the method is shown in Figure 15. A chopped IR source irradiates the aerosol particles. When light is absorbed, the particle radius of liquid aerosols varies according to the rhythm of the modulation. Photons from a second laser (in the visible range) are subjected to continuous elastic scattering at the aerosol particles. The resulting Mie scattering thus contains a component dependent on the modulation frequency and one dependent on the absorption cross-section of the particles. The first applications involved flowing ammonium sulfate aerosols (IR absorption band at 1110 cm^{-1}).

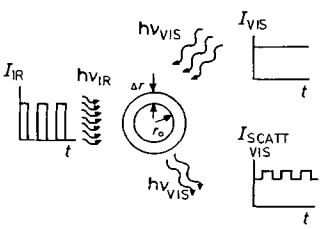

Fig. 15. The principle of optothermal absorption spectroscopy (after *Campillo* et al. [73]). For further details, see text.

4.3. Characterization Based on the Condensation Properties of Monodisperse Particles

The ability of ultrafine particles to act as condensation nuclei can be used for the characterization of the surface properties of such particles.[28, 79] Monodisperse particles with differing surface compositions can thus be characterized by observing the point at which water condensation occurs. The particles for study are selected by an electrostatic classifier. Droplet growth is then registered by a multistage condensation nucleus counter (Fig. 16). Hydrophobic organic layers deposited on hygroscopic nuclei can be studied especially well.

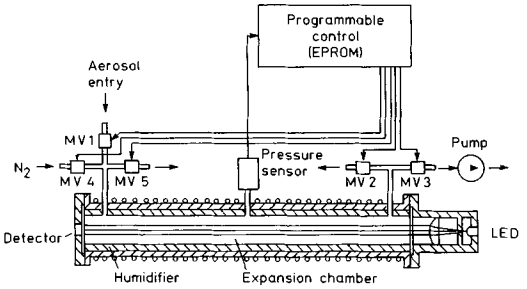

Fig. 16. Block diagram of a multistage condensation nucleus counter for the detection of the condensation properties of a monodisperse aerosol[79]. MV = magnetic valve; LED = light emitting diode.

Exemplary results, which were obtained by applying various degrees of water vapor supersaturation to monodisperse aerosols (Fig. 17), clearly show the effect of a small number

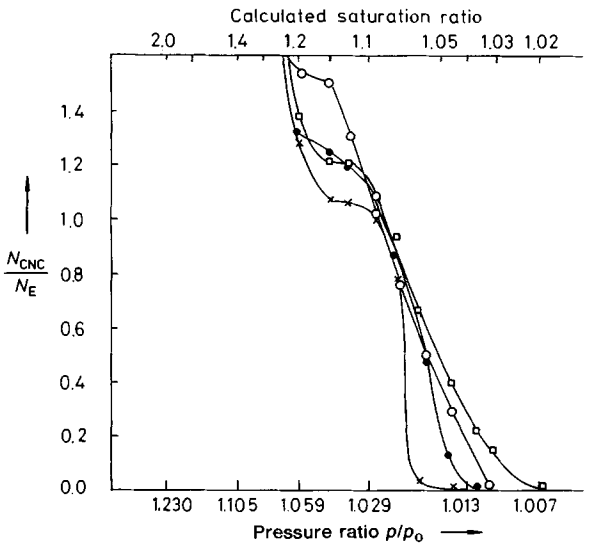

Fig. 17. Condensation spectra of monodisperse H_2SO_4 aerosol at constant total diameter as a function of water supersaturation. $d_p = 20$ nm; $p_o = 760$ Torr; □ H_2SO_4, $r = 10$ nm; organic coating ($r_{H_2SO_4} = 5$ nm, $\Delta r = 5$ nm): ○ 1-(hydroxymethyl)adamantine; ● n-hexadecane, × n-hexadecanol. N_{CNC}/N_E = droplet formation parameter.

of monolayers of a hydrophobic material on sulfuric acid droplets in a condensation process. The molecular structure of the coating material apparently causes an incomplete shielding of the nucleus in some cases. Thus a particle which is coated with *n*-hexadecanol is apparently wetted only with difficulty, while an H_2SO_4 droplet coated with 1-hydroxyadamantane can be activated even at low degrees of supersaturation.

5. Aerosol Characterization Based on Chemical Properties

The natural way for a chemist to carry out an aerosol determination is by chemical identification. Many such detection reactions are now available. Suitable identification reactions must be well-defined and reproducible, and must lead to a readily observable and easily quantifiable "signal".

5.1. Characterization by Means of a Selective Stoichiometric Reaction and Observation of the Products

A good example of an in situ and on-line process is the determination of aerosol sulfuric acid by a diffusion separator technique using radioactively labeled $Na^{36}Cl$.[80] A tube coated with $Na^{36}Cl$ is heated to 140 °C; though it is used as a sampler for H_2SO_4 aerosols, it also acts as an analyzer. The $H^{36}Cl$, which is formed in the stoichiometric reaction [Eq. (g)] can readily be bound on a filter impregnated with alkali or in an absorber solution and quantified by means of radiometric techniques.

$$H_2SO_4 + Na^{36}Cl \longrightarrow NaHSO_4 + H^{36}Cl\uparrow \qquad (g)$$

Figure 18 shows an automatic system for a quasicontinuous determination of sulfuric acid and ammonium sulfate in an atmospheric aerosol.[81] The air is first freed from gaseous inorganic and organic sulfur compounds (without any particle loss) by passing it through K_2CO_3 and activated charcoal diffusion tubes. The aerosol to be analyzed then passes through a Cu/CuO diffusion tube system heated to 120 °C or 220 °C. At 120 °C only the sulfuric acid is vaporized, while

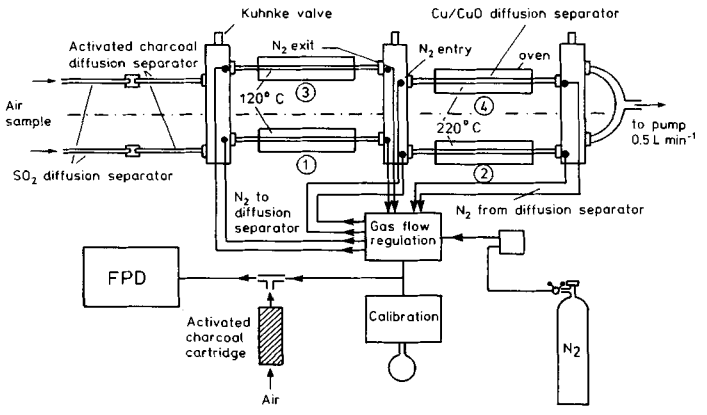

Fig. 18. Block diagram of a microprocessor-controlled H_2SO_4/ammonium sulfate aerosol analyzer. FPD = flame photometric detector.

the ammonium sulfate is decomposed at 220 °C. The fragments (molecular H_2SO_4) diffuse to the sink at the wall of the tube, where they are irreversibly sorbed. Thermostable aerosols pass through the various diffusion tubes without loss. After a predetermined sampling time the system is purged with ultrapure gas regulated by computer-controlled magnetic valves. Each sample tube is separately subjected to a short heating pulse, during which the sorbed acid is desorbed and converted at the Cu/CuO surface to SO_2, and each reproducible SO_2 pulse is registered on-line by a flame photometric detector. During SO_2 detection, sampling continues in a second system driven in parallel. The detection limit is ca. 0.1 μg H_2SO_4 per m^3 with a sampling time of ca. 5 min.

A similar apparatus has been developed for the determination of nitric acid and ammonium nitrate aerosols.[82] In this case thermolysis gives NO, which is detected via a chemiluminescence reaction with ozone.

5.2. Characterization by Chemiluminescence

Stauff and *Stark* et al.[83–86] were the first to make use of chemiluminescence in aerosols during combustion processes to characterize aerosols. A particularly promising improvement of this technique involves the use of CCD arrays for the simultaneous observation of luminescence across a wide wavelength range.

6. Summary and Future Prospects

This review makes it clear that a large number of classical optical techniques can be applied to aerosol systems. The procedures presented include not only typical surface-sensitive techniques such as ESCA and photoemission, but also mass-proportional methods such as LIF, LIBS, and aerosol mass spectrometry.

In the near future it will be of prime importance to have available chemometric evaluation methods coupled with broad-band detection techniques. A great deal of effort will also have to go into the miniaturization of the methods presently available. In this respect integrated optical circuits in combination with frequency-doubled laser diodes as UV source and CCD arrays as receiver optics have a great future. Aerosols in the form of selectively prepared substances with a high specific surface area, a particle size distribution which is as narrow as possible, and whose formation is continuously controlled will surely take up a permanent place in further technologies in the future.

The author wishes to thank all those who were responsible for stimulating, encouraging, and sustaining his interest in the analytical chemistry of finely dispersed systems.

Received: February 2, 1990 [A 814 IE]
German version: *Angew. Chem. 103* (1991) 542
Translated by Dr. T. N. Mitchell, Dortmund.

[1] S. Prochazka, C. Greskovich, *Am. Ceram. Soc. Bull. 57* (1978) 579–586.
[2] W. Cannon, S. Danforth, J. Flint, J. Haggerty, R. Marra, *J. Am. Ceram. Soc. 65* (1982) 324–330.

[3] W. Cannon, S. Danforth, J. Haggerty, R. Marra, *J. Am. Ceram. Soc. 65* (1982) 330–335.
[4] M. Khvorov, Y. Khimchenko, A. Chirkov, A. Dudchenko, *Kolloidn. Zh. 48* (1986) 597–600.
[5] F. Mayville, R. Partch, E. Matijevic, *J. Colloid Interface Sci. 120* (1987) 135–139.
[6] J. Wu, H. Nguyen, R. Flagan, *Langmuir 3* (1987) 266–271.
[7] A. Garg, E. Matijevic, *J. Colloid Interface Sci. 126* (1988) 243–250.
[8] S. Harris (Ed.): *The Technology of Powder Coatings,* Portcullis Press, London 1976.
[9] S. Pratsinis, P. Biswas in *Aerosols: Formation and Reactivity* (2nd Int. Aerosol Conf. Berlin 1986), Pergamon, Oxford 1986, p. 931–934.
[10] P. Guiot, P. Couvreur (Eds.): *Polymeric Nanoparticles and Microspheres,* CRC Press, Boca Raton, FL, USA 1986.
[11] M. Gutcho (Ed.): *Capsule Technology and Microencapsulation,* Noyes Data Corporation, Park Ridge, NJ, USA 1972.
[12] H. Krauss, H. Schmidt, *Z. Anorg. Allg. Chem. 392* (1970) 258–270.
[13] J. Otterstedt, H. Carlö, A. Askengren, P. Ahlquist, patent application: PCT-Anmeldung WO 85/03239 Klasse B 01 J 35/00, 1985.
[14] W. Seifert, DE-A 27 42182, Klasse B 01 J 17/24, 1977.
[15] T. Kodas, A. Datye, V. Lee, E. Engler, *J. Appl. Phys. 65* (1989) 2149–2151.
[16] T. Kodas, E. Engler, V. Lee, R. Jacowitz, T. Baum, K. Roche, S. Parkin, W. Young, S. Hughe, J. Kleder, W. Auser, *Appl. Phys. Lett. 52* (1988) 1622–1624.
[17] T. Kodas, E. Engler, V. Lee, *Appl. Phys. Lett. 54* (1989) 1923–1925.
[18] P. Ravindranathan, G. Mahesh, K. Patil, *J. Solid State Chem. 66* (1987) 20–25.
[19] J. Adcock, K. Horita, E. Renk, *J. Am. Chem. Soc. 103* (1981) 6937–6947.
[20] J. Adcock, W. Evans, L. Heller-Großman, *J. Org. Chem. 48* (1983) 4053–4957.
[21] F. Young, S. Stephanakis, D. Mosher, *J. Appl. Phys. 48* (1977) 3642–3650.
[22] J. Blauer, S. Munjee, K. Truesdell, E. Curtis, J. Sullivan, *J. Appl. Phys. 62* (1987) 2508–2517.
[23] U. Krone, W. Kühn, B. Georgi, A. Hüttermann, *Proc. Int. Pyrotech. Semin. 9th 1984.*
[24] W. Holländer, *VDI-Ber. 429* (1982) 35–57.
[25] K. Leschonski, *Ber. Bunsen-Ges. Phys. Chem. 88* (1984) 1112-1123.
[26] D. Pui, B. Liu, *Phys. Scr. 37* (1988) 252–269.
[27] B. Däumer, R. Nießner, D. Klockow in W. Asman, H. Diederen (Eds.): *Ammonia and Acidification,* EURASAP, Bilthoven, The Netherlands 1987, p. 86–96.
[28] R. Nießner, B. Däumer, D. Klockow in P. Wagner, G. Vali (Eds.): *Atmospheric Aerosols and Nucleation,* Springer, Berlin 1988, p. 538–541.
[29] P. Hess, *Top. Curr. Chem. 111* (1983) 1–32.
[30] C. Patel, A. Tam, *Rev. Mod. Phys. 53* (1981) 517–550.
[31] R. Röhl, Z. Childen, M. Palmer, *Appl. Spectrosc. 39* (1985) 668–672.
[32] K. Adams, *Appl. Opt. 27* (1988) 4052–4056.
[33] K. Adams, C. Davis, S. Japar, W. Pierson, *Atmos. Environ. 23* (1989) 693–700.
[34] K. Fung, J. Gaffney, *J. Chromatogr. 363* (1986) 207–215.
[35] A. Eckbreth, P. Bonczyk, J. Verdieck, *Prog. Energy Combust. Sci. 5* (1979) 253–322.
[36] D. Aeschliman, R. Setchell, *Appl. Spectrosc. 29* (1975) 426-429.
[37] N. Omenetto in P. Camagni, S. Sandroni (Eds.): *Optical Remote Sensing of Air Pollution,* Elsevier, Amsterdam 1983, p. 329–350.
[38] I. Allegrini, N. Omenetto, *Environ. Sci. Technol. 13* (1979) 349–350.
[39] R. Nießner, W. Robers, A. Krupp, *Proc. SPIE 1989 Boston Symp. OE/Fibers 1989,* 1172 (1990) 145–156.
[40] A. Biswas, H. Latifi, P. Shah, L. Radziemski, R. Armstrong, *Opt. Lett. 12* (1987) 313-315.
[41] M. Essien, L. Radziemski, J. Sneddon, *J. Anal. At. Spectrom. 3* (1988) 985-988.
[42] M. Pötschke, H.-P. Sattler, K. Hohla, T. Loree, DE-A 371 8672 A1 (1988).
[43] B. Raeymakers, T. Graule, J. Broekart, F. Adams, P. Tschöpel, *Spectrochim. Acta Part B 43* (1988) 923–940.
[44] L. Ebdon, J. Wilkinson, *J. Anal. At. Spectrom. 2* (1987) 39–44.
[45] J. Broekart, F. Leis, B. Raeymakers, G. Zaray, *Spectrochim. Acta Part B 43* (1988) 339–353.
[46] K. Fung, I. Tang, *Chem. Phys. Lett. 147* (1988) 509–513.
[47] K. Fung, I. Tang, *Appl. Opt. 27* (1988) 206–208.
[48] S. Asher, *Anal. Chem. 56* (1984) 720–724.
[49] M. Wright, J. Pollack, D. Colburn, *NBS Spec. Publ. (US) 464* (1977) 301–303.
[50] H. Mudd, C. Kruger, E. Murray, *Appl. Opt. 21* (1982) 1146–1154.
[51] R. Schlögl, G. Indlekofer, P. Oelhafen, *Angew. Chem. 99* (1987) 312–322; *Angew. Chem. Int. Ed. Engl. 26* (1987) 309–319.
[52] R. Tandon, R. Payling, B. Chenhall, P. Crisp, J. Ellis, R. Baker, *Appl. Surf. Sci. 20* (1985) 527–537.
[53] J. Campbell, R. Smith, L. Davis, K. Smith, *Sci. Total Environ. 12* (1979) 75–85.
[54] D. Natusch, E. Denoyer, T. Keyser, S. Kirton, D. Taylor, M. Zeller, *AIChE Symp. Ser. 201* (1980) 127–133.
[55] B. Barbaray, J.-P. Contour, G. Mouvier, *Environ. Sci. Technol. 12* (1978) 1294–1296.
[56] A. Goldmann in *Stoff- und Energietransport in Aerosolen, Arbeits- und Ergebnisbericht des SFB 209, 1986–1988,* Universität Duisburg 1988, p. 197–207.
[57] F. Müller, K. Kleinherbers, A. Goldmann, R. Nießner, *Aerosol Sci. Technol. 7* (1987) 109–111.
[58] W. Davis, *Environ. Sci. Technol. 10* (1973) 278.
[59] J. Stoffels, *Int. J. Mass Spectrom. Ion Phys. 40* (1981) 217–222, 223–234.
[60] M. Sinha in *Aerosols: Formation and Reactivity* (2nd Int. Aerosol Conf. Berlin 1986), Pergamon, Oxford 1986, p. 875–878.
[61] H. Burtscher, L. Scherrer, H. Siegmann, A. Schmidt-Ott, B. Federer, *J. Appl. Phys. 53* (1982) 3787–3791.
[62] R. Nießner, *J. Aerosol Sci. 17* (1986) 705–714.
[63] R. Nießner, *Fresenius Z. Anal. Chem. 329* (1987) 406–409.
[64] R. Nießner, B. Hemmerich, U. Panne, *Fresenius Z. Anal. Chem. 35* (1989) 728–737.
[65] N. Pelz, M. Bäcker, Daimler-Benz AG (1990) personal communication.
[66] A. Zajc, E. Uhlig, H. Hackfort, R. Nießner, *J. Aerosol Sci. 20* (1989) 1465–1468.
[67] R. Nießner, G. Walendzik, *Fresenius Z. Anal. Chem. 333* (1989) 129–133.
[68] R. Nießner, F. Lutz, *Polycyclic Aromat. Cmpd.,* in press.
[69] R. Nießner, W. Robers, P. Wilbring, *Anal. Chem. 61* (1989) 320–325.
[70] R. Nießner, P. Wilbring, *Anal. Chem. 61* (1989) 708–714.
[71] B. Liu, D. Pui, K. Whitby, D. Kittelson, Y. Kousaka, R. McKenzie, *Atmos. Environ. 12* (1978) 99–104.
[72] R. Charlson, A. Vanderpol, D. Covert, A. Waggoner, N. Ahlquist, *Atmos. Environ. 8* (1974) 1257–1267.
[73] A. Campillo, C. Dodge, H.-B. Lin, *Appl. Opt. 20* (1981) 3100–3103.
[74] A. Campillo, S. Petuchowski, S. Davis, H.-B. Lin, *Appl. Phys. Lett. 41* (1982) 327–329.
[75] S. Arnold, *Aerosol Sci. Technol. 2* (1983) 194.
[76] H.-B. Lin, A. Campillo, *Appl. Opt. 24* (1985) 422–433.
[77] D. Fluckiger, H.-B. Lin, W. Marlow, *Appl. Opt. 24* (1985) 1668–1681.
[78] S. Arnold, E. Murphy, G. Sageev, *Appl. Opt. 24* (1985) 1048–1053.
[79] R. Nießner, B. Däumer, D. Klockow *Aerosol Sci. Technol.* 12 (1990) 953–963.
[80] R. Nießner, D. Klockow, *Int. J. Environ. Anal. Chem. 8* (1980) 163–175.
[81] J. Slanina, C. Schoonebeek, D. Klockow, R. Nießner, *Anal. Chem. 57* (1985) 1955–1960.
[82] D. Klockow, R. Nießner, M. Malejczyk, H. Kiendl, B. vom Berg, M. Keuken, A. Wayers-Ypelaan, J. Slanina, *Atmos. Environ. 23* (1989) 1131–1138.
[83] J. Stauff, H. Fuhr, *Angew. Chem. 87* (1975) 132; *Angew. Chem. Int. Ed. Engl. 14* (1975) 105.
[84] J. Stauff, H. Fuhr, *Staub Reinhalt. Luft 35* (1975) 372–373.
[85] G. Stärk, D. Überschär, J. Stauff, *Erdöl Kohle Erdgas Petrochem. 39* (1986) 78–81.
[86] J. Stauff, G. Stärk, *Z. Naturforsch. B41* (1986) 113–121.

The Isoinversion Principle— a General Model of Chemical Selectivity

By Helmut Buschmann, Hans-Dieter Scharf,* Norbert Hoffmann, and Peter Esser

Dedicated to Vladimir Prelog and to the memory of Horst Pracejus

A large number of successful methods for chirality transfer, using either stoichiometric or catalytic chiral auxiliaries, are in use today. However, there is a lack of practical and dynamic selectivity models, i.e. models which take into account the entire reaction sequence, and which allow simple and reliable assessment, optimization and prediction of selectivity in asymmetric syntheses. The models that are available are either too strongly biased to the steric requirement of the particular molecules reacting, but do not go beyond classical considerations of static facial differentiation, or they take a demanding, theoretical approach, which because of its inherent limitations and the great theoretical effort required has not yet found its way into the practical world of the synthetic chemist. The "Isoinversion Principle", developed on the basis of Eyring's theory, closes this gap. With its aid, the synthetic chemist can determine the characteristic isoinversion temperature T_i for the reaction type of interest from a few temperature-dependent measurements of selectivity parameters. T_i then affords information on interesting questions such as optimization etc. The advantage of this method is that it is useful not only for stereoselectivity, but for any kind of process where selectivity in general (regio-, chemo-, etc) is generated at two or more stages of a reaction sequence, regardless of whether these reactions involve the ground state or a diabatic photoprocess. The present review will demonstrate that this generation of selectivity at two or more stages of a reaction sequence occurs more commonly than is generally thought.

1. Introduction

Since the discovery of the phenomenon of molecular chirality last century,[1-3] chemists have been more and more interested in devising methods and conditions which would enable them not merely to resolve racemates in the classical manner, but to direct chemical reactions asymmetrically.[4, 5] The chemist's aim is to produce only one of the two enantiomers of a compound, either selectively or specifically.

The last twenty years have seen a storm of developments in this field,[6-8, 46] spurred on by the aims of exploiting the increasing knowledge of enzyme reactions, of understanding and imitating their mechanisms, and by the discovery that enantiomers can have different physiological effects.[46b]

Today, good empirical knowledge, and the model-like ideas of ground-state chirality transfer that arise from it, are part of the everyday experience of the synthetic chemist.[6-8] Based on the classical work of *Cram* et al.[6-9] and *Prelog* et al.,[6-8, 10-15] *Helmchen* and *Schmierer*[16] have recently proposed a qualitative working model in their "concave-convex model" (Fig. 1). This model is based on the conformational effects of reactant molecules, and is now used all over the world as an aid in assessing asymmetric syntheses. It has led to numerous successes in the preparation of enantiomerically pure synthons for natural and synthetic products.[17, 18]

In so-called stoichiometric asymmetric synthesis, this has led to the successful application of a series of "concave" secondary alcohols as chiral auxiliaries. A selection of the most commonly used members of this group, with no guarantee of completeness, is shown in Figure 1.

The predictions of this model are quite general, and are limited to the reactant molecule. To achieve high diastereomeric excesses they require firstly chiral auxiliaries as bulky as possible, and secondly reaction temperatures as low

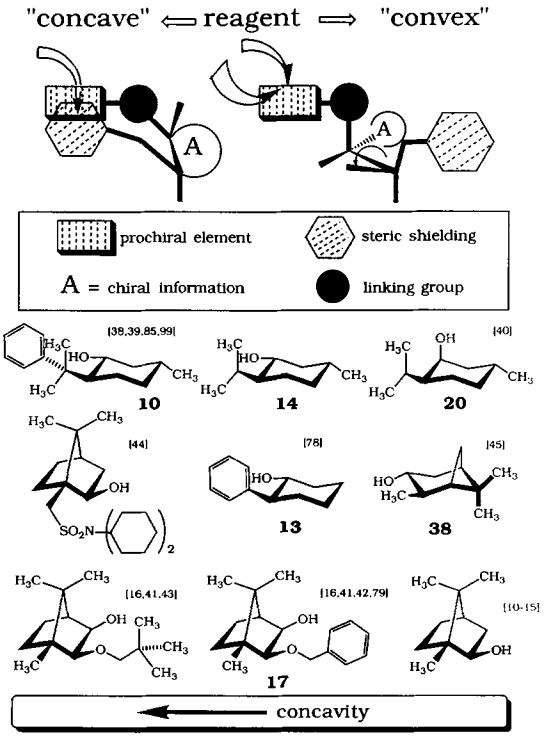

Fig. 1. Schematic diagram of concave and convex reagents, after *Helmchen* and *Schmierer* [16]. The figure shows a selection of the most important concave, secondary alcohols which have found use as chiral auxiliaries in stoichiometric asymmetric synthesis.

[*] Prof. Dr. H.-D. Scharf, H. Buschmann, N. Hoffmann, P. Esser
Institut für Organische Chemie der Technischen Hochschule
Prof.-Pirlet-Strasse 1, W-5100 Aachen (FRG)

as possible, in order to freeze the concave conformation (usually the more energy-rich) and achieve complete facial differentiation.

Attempts to construct quantitative models for stereodifferentiation have so far proved less productive for the practical chemist. Possible solutions in this direction have been provided by *Izumi* et al.[8, 9] and *Salem*[8, 264a, 268] and by approaches on the basis of free reaction enthalpy by *Ugi* and *Ruch*,[8, 20–24] and *Fukui*.[25]

Reports of successful diastereoselectivity in photochemical reactions appeared only after a long delay.[26–33] They extended the spectrum of synthetic possibilities in many ways. Detailed studies of the temperature dependence of the Paternò-Büchi reaction,[34–36] especially, led to the discovery of the Isoinversion Principle.[37] The Principle of Isoinversion includes the Helmchen-Schmierer model as a boundary case. It is a dynamic model, which takes into account *all* the reaction components in the planning and optimization of selective steps. It judges both the usefulness of auxiliaries or catalysts and the suitability of substrates, and, in addition, can be used to test mechanisms. It can be applied wherever selectivity is generated on two or more reaction levels. This article will show that this is clearly the case for a wide variety of selective reactions.

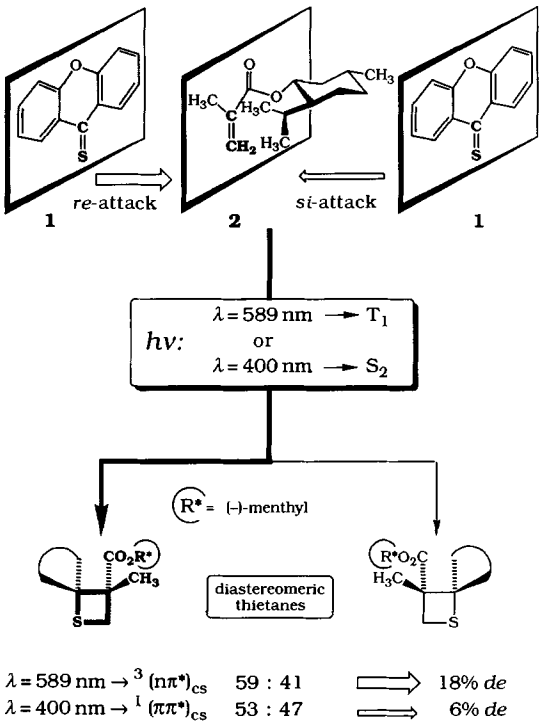

Fig. 2. Photochemically-induced, diastereoselective thietane formation, after *Gotthard* and *Lenz* [32b].

2. Asymmetric Induction in the Paternò-Büchi Reaction

Asymmetric induction in [2 + 2]-cycloadditions has been reported several times in the literature.[31, 47] The first example of a photochemical, diastereoselective hetero-[2 + 2]-cycloaddition appeared in 1979, in an article by *Gotthardt* and *Lenz*,[32b] who prepared thietanes by this method. The authors made use of the known fact that for their starting molecule, xanthione **1**, either the singlet or the triplet state can be specifically excited, in a wavelength-dependent manner. The chiral information is present here in the form of a menthyl residue in the methacrylate ester **2**, which functions as the olefinic partner (Fig. 2).

Although the *de* values achieved were low on an absolute basis, the most remarkable outcome of the experiment was that the singlet and triplet reactions afforded different diasteromeric excesses, with the triplet value higher than that for the singlet. If anything, the opposite result was expected, since the triplet pathway passes through a conformationally less rigid biradical intermediate.

In the same year, the authors also reported an "unusually high asymmetric induction" in the analogous photochemical

Hans-Dieter Scharf, born 1930 in Leipzig, studied chemistry from 1949 to 1950 at the University of Leipzig and from 1954 to 1960 at the University of Bonn. After receiving his doctorate in 1960 for work on the Ipatiev reaction under the supervision of F. Korte he joined the staff of the Shell-Grundlagenforschungs GmbH in Birlinghoven near Bonn, where he carried out fundamental research, first as research chemist, later as section leader. From 1966 to 1968 he completed his habilitation at the University of Bonn on the theme "Photochemical [2 + 2] Cycloadditions", and shortly thereafter he accepted an appointment as Wissenschaftlicher Rat and as Professor of Organic Chemistry at the Technische Hochschule Aachen. After rejecting several calls from other places, in 1972 he was appointed Full Professor and Director of the Institute for Organic Chemistry. His areas of research include photochemistry, chiral induction in photochemical and ground-state reactions, applicaton of solar photons in photochemistry and energy storage, the synthesis of bicyclic acetal pheromones of pests and of deoxy sugars and their employment in the partial synthesis of antibiotics.

Helmut Buschmann, born 1960 in Kaldenkirchen, studied chemistry from 1980 to 1987 at the Technische Hochschule Aachen, where he is now finishing his doctorate.

Peter Esser, born 1963 in Jülich, completed his graduate studies in chemistry in 1989 at the Technische Hochschule Aachen, where he is now working for his doctorate.

Norbert Hoffmann, born 1960 in Kesfeld, studied chemistry at the Technische Hochschule Aachen from 1979 to 1986, and is now also finishing his doctorate.

oxetane formation. They treated menthyl phenylglyoxylate **35** with tetramethylethylene **3** or ketene acetal **4**, and obtained diastereomeric excesses of 37% and 53% respectively.[32b]

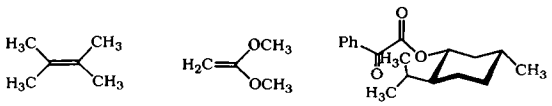

3 **4** **35**

In 1982, *Jarosz* and *Zamojski*[48,49] reported a further example of diastereoselectivity in oxetane formation in the sense of the Paternò-Büchi reaction, on treatment of glyoxylic acid derivatives esterified to chiral alcohols with furan **5**.[30] However, the diastereomeric excesses obtained lay only in the region 2–7%.[30]

We were able to show, in 1983, that on reaction of optically active phenylglyoxylates with electron-rich cyclic olefins such as 2,2-dimethyldioxol **6** or furan **5**, using 8-phenylmenthol as a chiral auxiliary, complete induction in photochemical oxetane formation can be achieved.[50,51] Since then, a series of successful examples of photochemical [2 + 2]-cycloadditions have been described, with average to very good diastereomeric excesses obtained by chiral induction.[52–55,282]

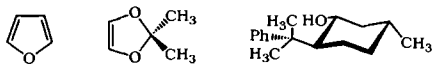

5 **6** **10**

2.1. Studies on the Mechanism of Stereoselectivity

Systematic studies on the mechanism of stereoselectivity in the diastereoselective Paternò-Büchi reaction showed the *de* value of the oxetane product mixture to be a sensitive mechanistic probe, which responds even to minor structural changes in the reactants and to the slightest perturbations of experimental conditions.[34–37,56–58] The addition of $^3(n\pi)^*$-excited chiral α-keto esters of type **7** to electron-rich olefins, as shown in Equation (1), leads to the diastereomeric oxetanes **8** and **8'** in high yield.[48–50]

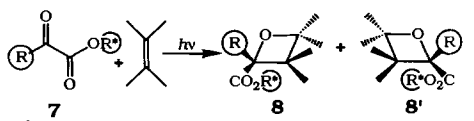

7 **8** **8'**

Ⓡ* = chirale auxiliary

(1)

This reaction was discovered in 1909 by *Paternò* and *Chieffi*,[59] and was later studied in detail by *Büchi*,[60] *Caldwell* et al.,[61] *Turro* et al.[62,63] and *Wagner*,[64] and more recently by *Peters* and *Freilich*.[65,66] Its mechanism is one of the best known for photoreactions, and it is also of great preparative importance.[67–69] The scheme given in Figure 3 was proposed by *Peters* et al.[66] and contains a resumé of the

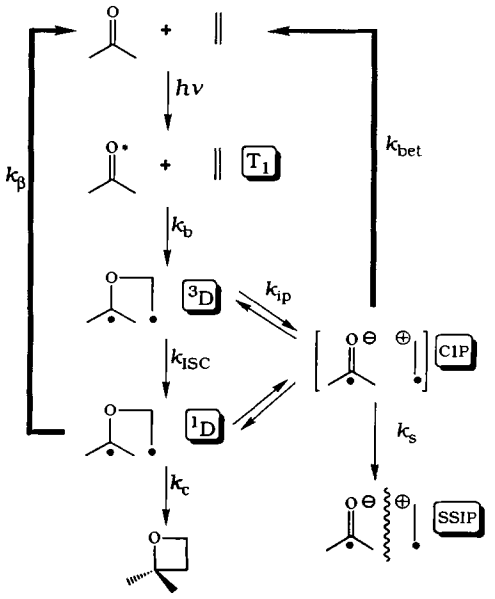

Fig. 3. Mechanism of photochemically-induced oxetane formation, from *Freilich* and *Peters* [66]. After photoexcitation of the ketone to the first excited singlet state, there follows a rapid intersystem crossing step into the lowest energy triplet state (T_1). The excited ketone attacks the olefin with its electrophilic oxygen atom, forming the 1,4-biradical triplet (^3D) (k_b). The possibility of a charge-transfer complex with subsequent exciplex formation is disregarded. Before ring closure to the oxetane (k_c), or retrocleavage to the ground state ketone and olefin with loss of the excitation energy (k_β) can occur, the 1,4-biradical species (^3D) must be converted into a singlet state (^1D) by intersystem crossing (k_{ISC}). Starting from the triplet biradical, however, an initial heterolytic cleavage (k_{ip}) to a contact ion pair (CIP) can also take place, before the triplet biradical is formed. Alternatively, the contact ion pair may be transformed (k_s) by the solvent into a solvent separated ion pair (SSIP), or may decompose to the ground state ketone and olefin by a second, reverse charge transfer (k_{bet}).

mechanism for photochemical oxetane formation widely accepted today. The individual weighting of each postulated intermediate is largely determined by the electronic and steric nature of the substrates concerned.

In the literature, the formation of an exciplex from the olefin and the T_1-excited carbonyl compound is often postulated.[67] Indirect evidence for the existence of an exciplex does exist,[62–67] but to date there is no direct proof of its existence.[70,100] After dissipation of a large part of the excitation energy, a 1,4-biradical intermediate is formed,[86] which has been detected by trapping reactions[71] and transient analysis.[65,66] This 1,4-biradical intermediate now has two possible paths for further reaction: either bond formation occurs to give the oxetane, or the 1,4-biradical undergoes bond cleavage to re-form the starting material (retrocleavage). In the model reaction (1) studied, high chemical yields are obtained, and side-products are not observed. Stereoselectivity in this reaction is determined by the chiral auxiliary Ⓡ*,[34,56,57,72–74] the nature of the olefinic reaction partner,[50,72,74] the nature of the Ⓡ substituent of the α-keto ester,[36,50] and the reaction conditions (temperature,[34–37,54,56] solvent, metal ions[75]).

When cyclic, electron-rich olefins of type **9** react with chiral α-ketoesters as in (1), the diastereomeric, bicyclic oxe-

9

tanes **31** and **31'** are generally formed *endo*-selectively relative to the Ⓡ substituent of the α-keto ester[51, 74] (Fig. 4).

The period of illumination and the rate of conversion have no effect on the diastereomeric product ratio. Light-induced secondary products, isomerizations or photolytic cleavage of the products are not observed under the reaction conditions given.[74] The concentration of the carbonyl and olefin components could be varied widely without any change in the *de* value, under otherwise identical conditions.[74] The effect of the spin multiplicity of the excited carbonyl component could not be studied with reaction (1), since oxetane formation in this case proceeds entirely from the carbonyl triplet state, passing through 1,4-biradical intermediates.[62]

2.1.1. The Influence of the Auxiliary

Table 1 shows some examples of the influence of the chiral auxiliary on diastereoselectivity. Chiral phenylglyoxylates **7** were transformed with **6** as olefinic partner at room temperature, and the diastereomeric excess obtained for the various chiral auxiliaries was measured by ^{13}C-NMR spectroscopy.[76]

Table 1. The influence of the chiral auxiliary on the *de* value in the photochemical formation of oxetanes from **7** and **6**. The *de* values were determined from the ^{13}C-NMR spectra [76].

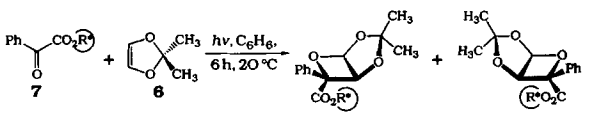

No.	R*–OH		R	de[%]	Ref.
1	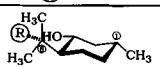		H (14)	58	[51]
2			CH_3	90	[74]
3			*n*Bu	92	[74]
4			C_6H_5 (10)	> 96	[51, 74]
5	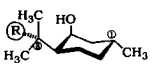		H (20)	26	[74]
6			C_6H_5 (21)	86	[74]
7	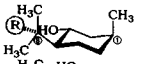		H (18)	22	[74]
8	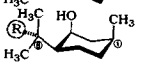		H	20	[74]
9			CH_3 (16)	42	[74]
10			*n*Pr	44	[74]
11			*i*Pr (19)	58	[74]
12	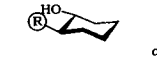		*t*Bu (12)	92	[74]
13			C_6H_5 (13)	56	[74]
14			*cyclo*-C_6H_{11}	49	[74]
15			C_6H_5-CH_2 (39)	48	[74]
16			C_6H_5-C_6H_4 (15)	42	[74]
17	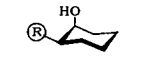		CH_3	26	[74]
18			*t*Bu	91	[74]
19			H (37)	60	[74]
20			*t*Bu	67	[74]
21	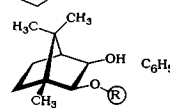		C_6H_5-CH_2 (17)	16	[74]

When **10** was used, complete induction was observed.[51] With the methyl derivative **11** the extent of induction is reduced only slightly.[74] Electronic interactions between the phenyl ring and the ester carbonyl function (π–π interaction[77]), which have been suggested to be important for certain ground state reactions, are hence unimportant in the course of the diastereoselective reaction. Removal of the methyl group in the 1-position in **11** gives **12**, without decreasing the induction potential of the reaction.[74] With *trans*-2-phenylcyclohexanol **13** (a strictly concave substitute for **10** which has been used successfully in a number of ground state reactions[78]), a diastereomeric excess of only 56% was obtained, comparable with the induction potential of menthol **14**.[74] If the sterically shielding group is enlarged by introducing a second phenyl ring, as in *trans*-2-(*p*-biphenyl)cyclohexanol **15**, the *de* value even falls significantly to 42%. This value, on the other hand, can be achieved even with simple *trans*-2-methylcyclohexanol **16**, from which one expects no facial selectivity in the sense of the static "concave/convex model" (Fig. 1).

Auxiliaries of the bornane type, like *exo*-2-benzyloxy-*exo*-3-bornanol **17**,[16, 41, 42, 79] an auxiliary usually regarded as highly concave, have proved highly effective inducers in many ground state reactions. In the Paternò-Büchi reaction, however, they yielded diastereomeric excesses which can only be placed in the lower third of the *de* value scale.

Configurational isomers of the menthol type (Systems 1, 5, 7, 8 in Table 1) reveal the considerable influence of the configuration of the methyl group in the 1-position on stereoselectivity.

In isomenthol **18** (No. 7), the methyl group is in the axial position and the inductive potential is decidedly reduced, although according to the simple shielding model this methyl group ought not to have any influence on facial differentiation.[74] The methyl group in the equatorial position, however, shows no significant effect on stereoselectivity, as a comparison of the *de* values for menthol **14** (No. 1) and *trans*-2-isopropylcyclohexanol **19**, or for 8-methylmenthol **11** and *trans*-2-*tert*-butylcyclohexanol **12** shows. Auxiliaries of the neomenthol type **20** (No. 5) also give reduced stereoselectivity in comparison with alcohols with the substitution pattern of menthol **14**, but the effect is not as great as for the axial methyl group in the 1-position. In addition, with neomenthyl type **20** auxiliaries the opposite chiral information to the corresponding menthol derivative is induced, so that the easily accessible (+)-8-phenylneomenthol[80] **21** has been discussed in the literature as a substitute for the less available (+)-8-phenylmenthol *ent*-**10**.[85]

From these few examples it can be seen that the predictive power of the static concave/convex model (Fig. 1), which only accounts for steric effects, is most uncertain in the cases shown, and explains the observed effects either poorly or not at all.

2.1.2. The Influence of the Olefinic Component

Table 2 shows the *de* values obtained for reaction of the phenylglyoxylates of menthol **35** or 8-phenylmenthol **22** with a variety of olefins.

Extremely high diastereomeric excesses are observed for the ester **22** in all cases. Use of menthol **14** as chiral auxiliary, however, gave a considerable spread of *de* values, depending on the structure of the olefin used under otherwise identical conditions.[98]

Table 2. The influence of the olefinic component on the *de* value in the photochemical formation of oxetanes from the phenylglyoxylates **22** and **35**. The chiral auxiliaries used were **14** and **10**. The major oxetane obtained is printed in bold face.

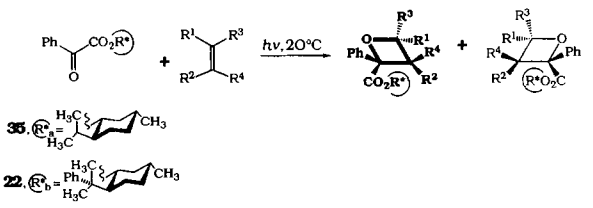

No.	Olefin	Oxetane	*de*[%] R^*_a	*de*[%] R^*_b	Ref.
1	**23**, R = H		48	90	[74]
2	**6**, R = CH_3		58	> 96	[51]
3	**25**, R = *i*Pr		29	90	[73,75]
4	**24**, R = C_6H_5		51	90	[74]
5	**5**		58	> 96	[50]
6	**36**		59	> 96	[74]
7a	**32**		50	1 : 96	[50]
7b			33	2 : 96	[50]
8	**33**	**34**	34	96	[50]
9			42	92	[50]
10	**3**		54	90	[50]
11a	**4**		41	5 : 90	[34,50]
11b			28	1 : 76	[34,50]
12	**29**		25	83	[34,50]
13a			68	1 : 1 : > 95	[58]
13b			46	2 : 1.3 : > 95	[58]
14a	**26**		30	8 : 10	72 [81]
14b		**27**	-	1 : 1	- [81]

The influence of the R substituent in the 2-position of the dioxols on selectivity is remarkable, for instance. This cannot be explained by purely steric effects. The dimethyl derivative **6** always yields the highest diastereomeric excesses, regardless of the auxiliary used. Dioxols with R = H (**23**) or R = Ph (**24**) bring about a moderate fall in the *de* value, while in the case of the menthol auxiliary **14** the 2,2-diisopropyl-1,3-dioxol **25** gives rise to a drastic decrease. With cyclic olefins, photooxetane formation generally proceeds in a strictly *endo*-phenyl-selective manner. Only when the imidazole derivative[284] **26** was used could a small amount of the corresponding *exo*-product **27** be detected.[81]

Ketene acetal **4** is a noncyclic, C_{2v}-symmetric olefin with the C_2 axis lying parallel to the double bond. When the 1,4-biradical intermediate (**28** and **28'**) is formed, no new chiral center is created (Fig. 4). Here, diastereoselective oxetane formation leads to an additional regioisomerism,[82, 94] which is eliminated when symmetrical, tetrasubstituted olefins such as tetraethoxyethylene **29** or tetramethylethylene **3** are used.

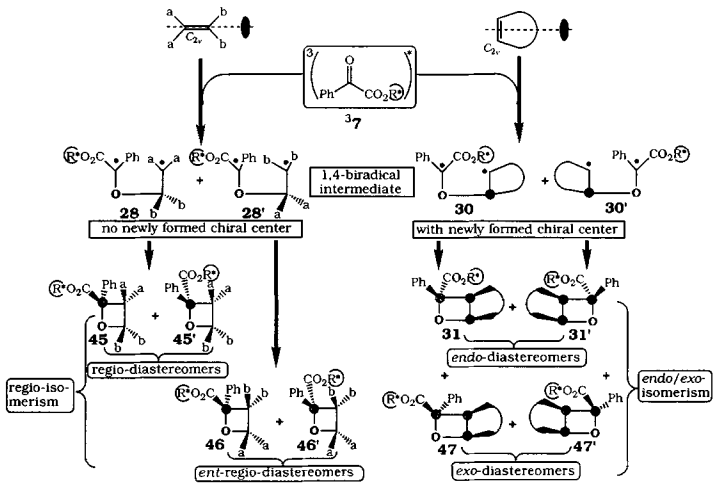

Fig. 4. The formation of diastereomeric, regioisomeric and *exo*/*endo* isomeric oxetanes by reaction of chiral phenylglyoxylates **7** with C_2-symmetric olefins that possess a C_2-axis parallel or perpendicular to the double bond. (• denotes a newly formed chiral center).

Cyclic C_{2v}-symmetric olefins with the double bond perpendicular to the C_2 axis already form a new chiral center in the 1,4-biradical intermediate (**30** and **30'** in Fig. 4). This chiral center then determines all the other chiral centers, due to the *endo*-phenyl selectivity of the oxetane formation reaction (1). One exception—already mentioned—is olefin **26**, which also leads to oxetanes with an *exo*-directed phenyl group (**27** and **27'**).

Figure 4 shows schematically the possibilities for *endo*/*exo*, regio-, and diastereomeric products[82] in Reaction (1), when symmetrically-substituted olefins with a C_2 axis parallel or perpendicular to the double bond are used.

Furan **5** is a cyclic olefin with a C_2 axis external to the double bond. In the biradical intermediate a new chiral center is also generated, but cycloaddition to phenylglyoxylates of hindered alcohols leads regioselectively to the diastereomeric bicyclic oxetanes **31** and **31'**.[48–50, 69]

2-Methylfuran **32** is a cyclic olefin without a C_2-symmetry element, and yields regiomeric oxetanes. In the structural analogue 1-methylcyclopentadiene **33**, only one regiomeric pair of diastereomers with structure **34** is observed.[50]

2.1.3. The Influence of the Glyoxylic Acid Residue (R)

In order to investigate the influence of the residue (R) on diastereoselectivity we treated variously substituted α-keto esters of **14** and **10** with **5**. Table 3 shows that the diastereoselectivity is directed considerably by the substituent (R).[36]

Table 3. The influence of the (R) substituent in the α-keto ester component on the *de* value in the photochemical formation of oxetane according to Equation (1). The menthyl and phenylmenthyl phenylglyoxylates were treated with furan **5** at 20 °C or − 23 °C. The major oxetane obtained is printed in bold face.

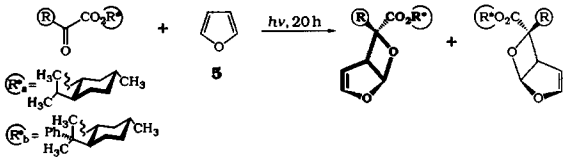

No.	(R)	de[%] (R*a)	de[%] (R*b)	T[°C]	Ref.
1	H	7	12	20	[73]
2	CH_3	8	21	20	[50]
3	*i*Bu	36	60	20	[36,50]
4	*t*Bu	58	96	20	[36,50]
5	*cyclo*-C_6H_{11}	48	-	- 23	[36]
6	*cyclo*-C_5H_9	47	-	- 23	[36]
7		64	94	20	[36]
8	C_6H_5	58	> 96	20	[51]
9	C_6H_5	60.2	-	- 23	[36]
10	*p*-H_3CO-C_6H_4	61.9	-	- 23	[36]
11	*p*-C_6H_4F	58.2	-	- 23	[36]
12	*p*-C_6H_4Cl	57.4	-	- 23	[36]
13	*p*-NO_2-C_6H_4	47.9	-	- 23	[36]
14	*p*-*t*Bu-C_6H_4	62.3	-	- 23	[36]
15	(H_3Cl_2N-C_6H_4	no reaction		20	[36]
16	C_6H_5-CH=CH	no reaction [a]		20	[73]

[a] With 2,2-diisopropyl-1,3-dioxol **25** as olefin, however, oxetanes were obtained in 95% yield [73].

The diastereomeric excesses that could be obtained varied from 7% to 60% in the case of menthol **14**, and between 12% and complete induction for 8-phenylmenthol **10**.

The Paternò-Büchi reaction is a diabatic photoreaction, i.e., after excitation of the carbonyl component to form the 1,4-biradical intermediate, a large part of the absorbed photon energy has to be dissipated. The substituent (R) exerts a decisive influence here on the extent of energy dissipation. Along with the phenyl (No. 8) and 2-thienyl groups (No. 7) the *tert*-butyl group (No. 4) proved especially effective in this sense; in all these cases, complete induction was observed with **10**, while reactions of glyoxylates ((R) = H, No. 1) afforded only low levels of induction.[36, 50]

To obtain information on how far the action of substituent (R) in the selectivity process can be traced to electronic and/or steric effects, we treated various *para*-substituted phenylglyoxylates with furan **5** in the Paternò-Büchi reaction, and correlated the *de* values obtained with the σ_p-values of the substituents in the Hammett Equation (2).[83]

$$\lg(k/k_0) = \sigma\rho \qquad (2)$$

From the linear dependence observed ($\rho = -0.176 \pm 0.051$, correlation coefficient = 0.99, $T = -23$ °C),[84] it can be concluded that the influence of substituent (R) is clearly mainly of an electronic nature,[83b] and that a uniform mechanism exists. No correlation was found to the values for direct conjugation, σ^+ and σ^-, which indicates that purely ionic intermediates are probably not important, although a certain dependence of the *de* value on the polarity of the solvent can be seen.[75] Hence, the initial assumptions, according to which substituent (R) plays a purely steric role in diasteroselectivity,[50] are not confirmed. The *de* values obtained for alkyl-substituted α-keto acid derivatives (Table 3, No. 2–6) also display a dependence on the ionization potential of these residues. This can be seen as a further indication of the importance of electronic effects in stereoselectivity by (R). This argues that the selectivity process in the Paternó-Büchi reaction takes place close to the ground state.

2.1.4. The Influence of Reaction Temperature

The influence of reaction temperature on the selectivity of photochemical processes has, until now, been studied for only a few cases.[54, 87] We made the first observations of temperature-dependent diastereoselectivity in the reaction of menthyl phenylglyoxylates **35** with tetramethylethylene **3** and ketene acetal **4** (Table 2), i.e., with C_{2v}-symmetric olefins having a C_2 axis parallel to the double bond.[34] Following the modified Eyring approach[88] of Equation (3a), a linear dependence of the ln(P) value on the reciprocal temperature was found. P is defined by Equation (3b), where k and k' are the overall rate constants for the formation of diastereomeric or regioisomeric oxetanes according to Equation (1) and I and I' are the intensities of the selected signals in the ^{13}C-spectrum of the diastereomeric or regioisomeric product mixture.[76]

$$\ln(P) = -\frac{\Delta\Delta H^{\ddagger}}{R}\frac{1}{T} + \frac{\Delta\Delta S^{\ddagger}}{R} \qquad (3a)$$

$$P = \frac{k(\text{excess oxetane})}{k'(\text{oxetane deficit})} = \frac{I(\text{excess oxetane})}{I'(\text{oxetane deficit})} \qquad (3b)$$

Figure 5 shows the temperature dependence of diastereoselectivity in the form of an Eyring diagram.[36]

Even in these early studies it was found[50] that the reaction temperature does not exert a uniform influence on the diastereoselectivity of photooxetane formation (1). As the temperature falls, an increase in the *de* value is not the only effect observed. In contrast to current opinion the diastereomeric excess may also fall or remain constant.

In addition, an isoselectivity relationship was observed, as has been reported by *Pracejus*[91] and later by *Giese* et al.,[92] who studied temperature-dependent selectivity in carbene and simple radical reactions. These reports are based on the observations of isokinetic phenomena,[269] described in the fifties and sixties by *Exner*[89] and *Leffler*.[90]

In further studies of temperature dependence in the diastereoselectivity of photooxetane formation, we treated C_{2v}-symmetric, cyclic olefins of type **9** with a series of chiral,

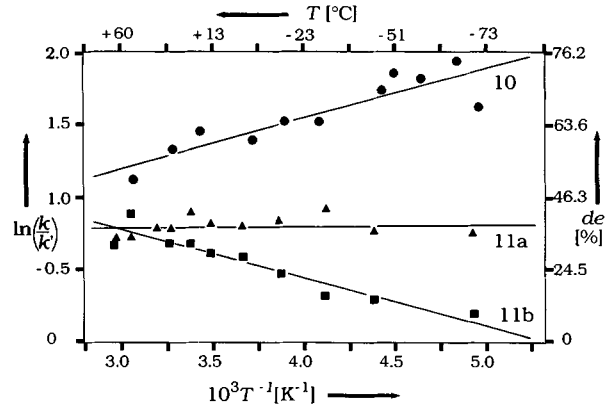

Fig. 5. Temperature-dependence of diasteroselectivity in the reaction of menthyl phenylglyoxylate with tetramethylethylene **3** and ketene acetal **4** (Systems 10, 11a, 11b in Table 2).

unsubstituted and *p*-phenyl-substituted glyoxylates. Table 4 presents a summary of all reactions studied so far.

As chiral information bearers we used a number of substituted cyclohexanols, since these afford average diastereomeric excesses (*de* values in the region 20–70%). In this region the activation parameters $\Delta\Delta H^{\neq}$ and $\Delta\Delta S^{\neq}$ are particularly easy to determine experimentally.

In reactions with the cyclic olefins **6**, **23**, **25** and **36**, toluene was used as solvent. In the case of furan **5**, the olefin itself acts as a solvent, because of the greatly decreased reactivity of the furan to photochemical oxetane formation. The temperature region studied reached from + 50 to − 90 °C. In our case,[37] the period of illumination was 6 h for **6**, **23**, **25**, and 15 h for **5** and **36**.

Surprisingly, for all the systems in Table 4 that were studied, we found two linear regions in the Eyring-diagram, with a characteristic inversion point. Some typical results of temperature measurements on the systems in Table 4 are given in Figures 6 and 7, in the form of Eyring diagrams. Figure 6 shows diagrams for oxetane formation from *trans*-2-phenylcyclohexyl phenylglyoxylate **40** with the olefins **5**, **6**, **23**, **25** and **36** (Table 4, Nos. 1–5), while for the Eyring diagram of Figure 7 the phenylglyoxylates of **39** (**41**), **37** (**42**), **14** (**35**), **18** (**44**) and **12** (**43**) were treated with the unsubstituted dioxol **23** (Table 4, Nos. 6, 11, 16, 21, 26).

Table 4. Overview of the systems in which the influence of temperature on the *de* values have already been investigated. the phenylglyoxylates of **13**, **37**, **39** and **12** were used in racemic form. Control experiments with the enantiomerically pure phenylglyoxylates gave the same product distribution of diastereomeric oxetanes [264, 265].

No.	R	R*	9	Ref.	No.	R	R*	9	Ref.
1	C_6H_5	**13**	**23**	[37, 74]	17	C_6H_5	**14**	**6**	[37, 74]
2	C_6H_5	**13**	**6**	[37, 74]	18	C_6H_5	**14**	**25**	[37, 74]
3	C_6H_5	**13**	**25**	[37, 74]	19	C_6H_5	**14**	**36**	[74]
4	C_6H_5	**13**	**36**	[74]	20	C_6H_5	**14**	**5**	[37, 74]
5	C_6H_5	**13**	**5**	[37, 74]	21	C_6H_5	**18**	**23**	[74]
6	C_6H_5	**39**	**23**	[37, 74]	22	C_6H_5	**18**	**6**	[74]
7	C_6H_5	**39**	**6**	[37, 74]	23	C_6H_5	**18**	**25**	[74]
8	C_6H_5	**39**	**25**	[37, 74]	24	C_6H_5	**18**	**36**	[74]
9	C_6H_5	**39**	**36**	[74]	25	C_6H_5	**18**	**5**	[74]
10	C_6H_5	**39**	**5**	[37, 74]	26	C_6H_5	**12**	**23**	[74]
11	C_6H_5	**37**	**23**	[74]	27	C_6H_5	**12**	**6**	[74]
12	C_6H_5	**37**	**6**	[74]	28	C_6H_5	**12**	**25**	[74]
13	C_6H_5	**37**	**25**	[74]	29	C_6H_5	**38**	**5**	[74]
14	C_6H_5	**37**	**36**	[74]	30	p-H_3CO-C_6H_4	*ent*-**14**	**5**	[36]
15	C_6H_5	**37**	**5**	[74]	31	p-tBu-C_6H_4	*ent*-**14**	**5**	[36]
16	C_6H_5	**14**	**23**	[37, 74]					

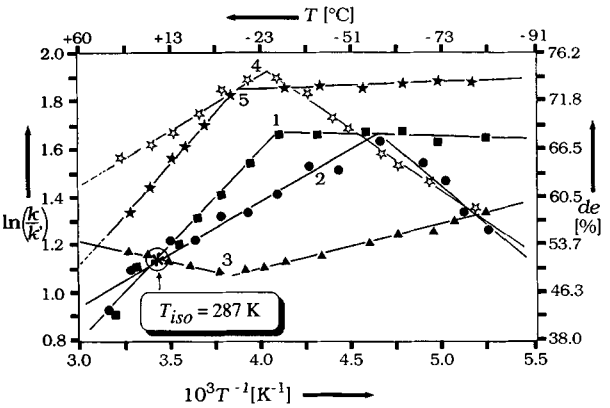

Fig. 6. Temperature-dependence of stereoselectivity in the reaction of *trans*-2-phenylcyclohexyl phenylglyoxylate **40** with olefins **5**, **6**, **23**, **25**, and **36**, presented as an Eyring diagram (Systems 1–5 in Table 4). Systems 1–3 yield an isoselective point in the high-temperature region ($T > T_{inv}$), with isoselective temperature T_{iso} = 287 K.

We describe the temperature at the isoinversion point as the inversion temperature T_{inv} of the system,[*] because at this temperature it is clear that a change occurs in the dominance of enthalpy and entropy in the partial selectivity steps. The inversion temperature found varies between − 61 °C and − 8 °C. In contrast to general opinion—the lower the reaction temperature, the higher the stereoselectivity—this result teaches us that the opposite relation can also be true. Even if an increase in selectivity is found on decreasing the temperature, this relationship need only hold for a particular temperature region. For the systems studied in Table 4, two temperature regions can be identified, with different linear

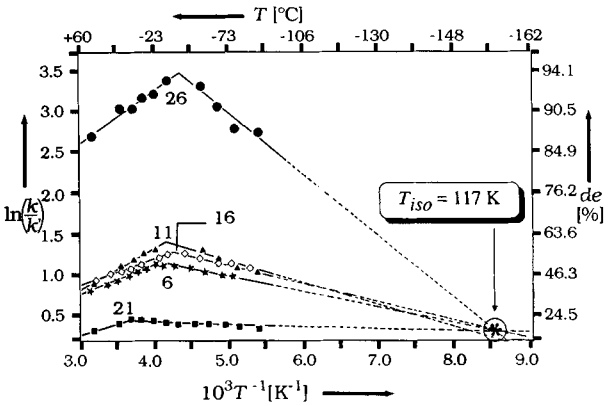

Fig. 7. Temperature-dependence of diastereoselection in the reaction of 1,3-dioxol **23** with chiral phenylglyoxylates, presented as an Eyring diagram (Systems 6, 11, 16, 21 and 26 in Table 4). Other than in Figure 6 an isoselective point occurs in the low-temperature region ($T < T_{inv}$) with T_{iso} = 117 K.

[*] We define a system as an ensemble of reactants, which react in a certain ratio of concentration under well-defined reaction conditions (e.g. solvent, catalytic additives). Temperature and/or pressure are the variable parameters of the system.

temperature dependence of the diastereoselectivity. In the case of Systems 1, 2, 4 and 5 of Table 4, the *de* value first increases as the temperature falls to the inversion point, and then decreases. With 2,2-diisopropyl-1,3-dioxol **25** (System No. 3) the inverse course is observed in the high- and low-temperature regions. This is a result of the Price-Hammett principle,[93] which states that as the degrees of freedom of the substituents at the 2-position of the dioxol increase, the influence of entropy in the high-temperature region will overcompensate for the enthalpy effect in comparison to dioxols **6** and **23**, under otherwise identical conditions. The corresponding line in the high-temperature region of the Eyring diagram constitutes an isoselectivity relationship with the corresponding lines for dioxols **6** and **23**.[92]

2.2. The Isoinversion Principle for the Paternò-Büchi Reaction

Because of the appearance of inversion temperatures T_{inv}, i.e. of two linear regions in the Eyring-diagram, two sets of activation parameters ($\Delta\Delta H_1^{\ddagger}$, $\Delta\Delta S_1^{\ddagger}$ ($T > T_{inv}$) and $\Delta\Delta H_2^{\ddagger}$, $\Delta\Delta S_2^{\ddagger}$ ($T < T_{inv}$) are available which correspond to enthalpy and entropy in each of the partial selectivity steps. By simple subtraction of the activation parameters for the high- and low-temperature regions ($T > T_{inv}$ and $T < T_{inv}$), one obtains the new parameters $\delta\Delta\Delta H^{\ddagger}$ and $\delta\Delta\Delta S^{\ddagger}$ [Eqs. (4) and (5)]. These represent the change in dominance of enthalpy and entropy in the partial selectivity steps within one system.

$$\delta\Delta\Delta H^{\ddagger} = \Delta\Delta H_2^{\ddagger} - \Delta\Delta H_1^{\ddagger} \quad (4)$$

$$\delta\Delta\Delta S^{\ddagger} = \Delta\Delta S_2^{\ddagger} - \Delta\Delta S_1^{\ddagger} \quad (5)$$

If these new parameters $\delta\Delta\Delta H^{\ddagger}$ and $\delta\Delta\Delta S^{\ddagger}$ for all the systems in Table 4 are plotted on an enthalpy/entropy diagram, a strictly linear correlation (correlation coefficient > 0.99, passing through the origin) is observed for all systems studied for this reaction.

Clearly there exists a common relationship for the change in dominance of the activation parameters in the partial selectivity steps, for all the systems studied. This relationship is independent of the actual *de* values measured, and hence also of the factors that influence the *de* value (e.g. the chiral auxiliary, the partner olefin, the Ⓡ residue of the α-keto acid fragment, the solvent and the concentration).

We have called this linear correlation in the $\delta\Delta\Delta H^{\ddagger}/\delta\Delta\Delta S^{\ddagger}$ diagram the *Isoinversion Relationship*.[37]

The gradient of the line in the isoinversion diagram has the dimensions of a temperature, which is defined as the Isoinversion Temperature T_i [Eq. (6)].[37] (For the case of the diastereoselective Paternò-Büchi reaction, it has the value 231 K.)

$$T_i = \frac{\partial(\delta\Delta\Delta H^{\ddagger})}{\partial(\delta\Delta\Delta S^{\ddagger})}. \quad (6)$$

This temperature is a characteristic constant for the selectivity of the reaction studied. The practical significance of this T_i is that at this temperature the optimal value of a selectivity parameter (here, for instance, the *de* value) is to be expected. If, for example, one plots the *de* values obtained for the systems in Table 4 at the inversion temperature T_{inv} against the inversion temperatures T_{inv}, one obtains the diagram shown in Figure 9.

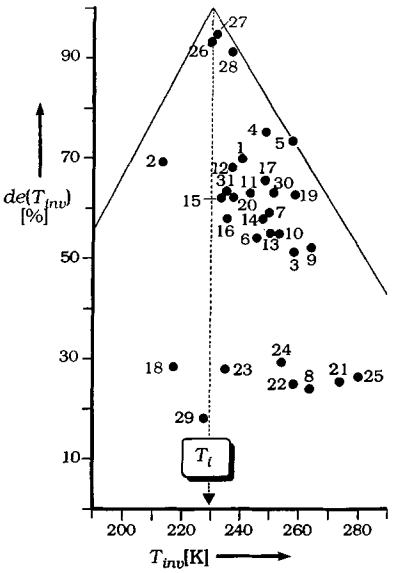

Fig. 9. $de(T_{inv})/T_{inv}$ diagram for the systems from Table 4.

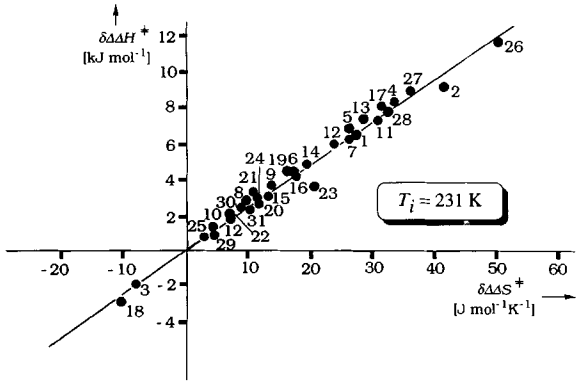

Fig. 8. $\delta\Delta\Delta H^{\ddagger}/\delta\Delta\Delta S^{\ddagger}$ diagram (isoinversion relationship) for diastereoselective photooxetane formation from chiral *p*-substituted and unsubstituted phenylglyoxylates with cyclic olefins of type **9** (correlation coefficient > 0.99). The numbers correspond to those in Table 4.

In systems which produce high diastereoselectivity, the inversion temperature T_{inv} lies close to the isoinversion temperature T_i (Systems 26–28 from Table 4) while for systems with lesser selectivity a broad spread of inversion temperatures is found. If, then, one takes any one example of the reaction under study, measures the *de* value at temperature T_i, and finds a low selectivity, one may be sure that no notable improvement can be achieved by varying the temperature. A "bad" system will remain a "bad" system, and this cannot be changed by even the most bulky substituents (Price-Hammett principle). In addition, from the charge and size of the $\delta\Delta\Delta H^{\ddagger}$ and $\delta\Delta\Delta S^{\ddagger}$ parameters, some insight can be obtained into what structural variations in the system could lead to an increase in selectivity.

2.2.1. *Mechanistic Conditions for the Occurrence of Inversion Points*

The question of why certain systems display inversion points in selectivity in the Eyring-diagram while others do not, can be answered by explaining the mechanism of stereoselectivity in the Paternò-Büchi reaction. If one extends the mechanistic knowledge of achiral, photochemical oxetane formation (Fig. 2) to the reaction of chiral α-keto esters with cyclic, electron-rich olefins of type **9**, then the mechanism of diastereoselectivity in oxetane formation can be understood by the simplified, kinetic model of Figure 10.

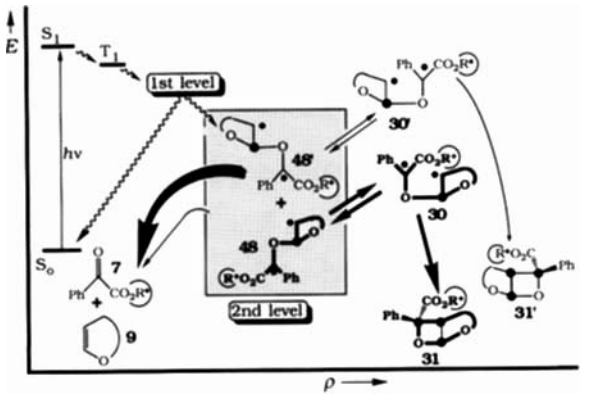

Fig. 10. A simplified kinetic model for the diastereoselective Paternò-Büchi reaction with cyclic olefins of type **9**. The *trans*-1,4-biradical intermediates **48** and **48'** are very probably formed first, and must then be converted into the *cis*-configurations **30** and **30'** for ring closure to occur. The intermediate formed preferentially, **48**, gives rise to the major oxetane **31**, while the minor 1,4-biradical intermediate **48'** undergoes preferential retrocleavage.

According to this model, the selectivity of the reaction occurs at two different levels. After photochemical excitation of the keto carbonyl group, and subsequent dissipation processes, the biradical intermediates **48** and **48'** are formed. In the case of cyclic olefins of type **9**, these two intermediates are diastereomeric, since a chiral center is formed with the first bond (first level of selectivity). The formation of this chiral center in the biradical intermediate determines all further, newly generated chiral centers in the oxetane, providing oxetane formation proceeds *endo*-phenyl selectively. For the biradical intermediates (one of them is generated preferentially), however, two reaction pathways are possible (second level of selectivity). They may undergo ring closure to give oxetanes, or they may decompose to the starting materials, losing all their excitation energy (retrocleavage). The system will then be excited once more, and may pass through the reaction cycle again. After the intermediate has formed, a further increase in diastereoselectivity is only possible by retrocleavage, whereby one diastereomeric intermediate is preferentially cleaved to the starting materials and the other preferentially transformed into oxetane. Retrocleavage therefore gives a second level of selectivity. The entire system may be described as a photon-driven selectivity amplifier, which continues to function until a significant proportion of the starting material has accumulated as the major diastereomer. This requires that apart from bond formation and retrocleavage, no side reactions take place. Further indications that retrocleavage functions as a selectivity step also

Table 5. Selected quantum yields for diastereoselective photochemical formation of oxetane according to Equation (1).

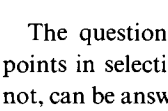	Olefin	Quantum yield ϕ		de[%] (T=20 °C, C_6H_6)	Ref.
C_6H_5	**10**	**3**	0.22	for the formation of the major oxetane diastereomer	90	[34]
C_6H_5	**10**	**3**	0.06	for the formation of the minor oxetane diastereomer	90	[34]
C_6H_5	**10**	**3**	0.34	for the substrate consumption	90	[34]
C_6H_5-CH=CH	**10**	**25**	0.78	for the substrate consumption	28	[73]

derive from measured quantum yields, a few of which are summarized in Table 5.

It turns out that there is a corresponding difference in the quantum yields for consumption of starting material and those for product formation, in the absence of any side reactions. Systems that generate high diastereoselectivity yield smaller quantum yields than those with lower selectivity. The fact that on irradiation in the absence of the olefinic component α-keto esters rapidly decompose by photofragmentation[50] is a further indication for retrocleavage. In the presence of the olefin, the biradical intermediate is formed very rapidly (first level), but oxetane formation is very slow, because of retrocleavage (second level). The existence of inversion temperatures T_{inv} suggests that the selectivity levels described are weighted differently according to temperature. In the high temperature region ($T > T_{inv}$) we observe enthalpy-determined selectivity[37] in the vast majority of systems. According to *Skell* et al.[95] and *Giese*,[92a] this behavior is found for transition states close to the starting materials in the fragmentation of energy-rich compounds (the 1,4-biradical intermediate must be seen as the starting material here). Hence, retrocleavage, the second level of selectivity, is dominant in the high-temperature region for enthalpy reasons. In contrast, in the low-temperature region ($T < T_{inv}$), we find entropy-determined selectivity, with the formation of the biradical intermediate from as an energy-rich precursor.[37] This is a bond formation step (approach of the olefin to the prochiral triplet carbonyl) with a transition state like the starting material; here, the triplet carbonyl may be regarded as the starting compound.

By a kinetic description of the selectivity process we have also shown[37] that for the first selectivity step, where the diastereomeric 1,4-biradical intermediates are formed, the nature of the auxiliary has a dominant influence on the selectivity process. In the second step, the nature of the olefin gains importance.

The good correlation for the isoinversion line shows that the activation entropy difference for the selectivity steps gains in importance as a determinant energy parameter at the same rate as the activation enthalpy loses it, and vice versa (compensation[96] of enthalpy and entropy on the $\delta\Delta\Delta H^{\neq}$ and $\delta\Delta\Delta S^{\neq}$ levels). If substrates are used where no new chiral center is formed in the biradical intermediate, then the production of diastereoselectivity is the result of only one selectivity level, so that inversion points (T_{inv}) are not expected in the Eyring diagram.

Indeed, the reactions of menthyl phenylglyoxylate **35** with tetramethylethylene **3** and ketene acetal **4** show only one linear region with respect to temperature.[34] In the case of ketene acetal **4**, two regioisomeric intermediates **28** and **28'** are formed, which yield two regioisomeric pairs of two diastereomeric oxetanes, **45** and **45'**, and **46** and **46'** (Fig. 4). The temperature-dependence of the regioisoselectivity R[97] then gives an inversion point in the Eyring diagram (Fig. 11),

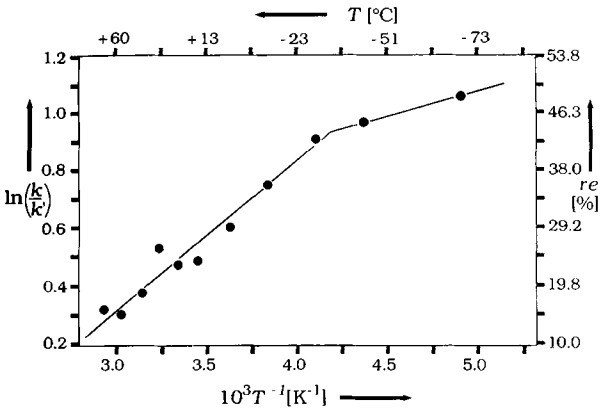

Fig. 11. Eyring diagram for the temperature dependence of the regioselectivity R in the reaction of **35** with **4** (Systems 11a and 11b in Table 2). This reaction leads to two regioisomeric pairs of two diastereomeric oxetanes **45** and **45'** or **46** and **46'** respectively. The *re* value (regioisomeric excess) is defined analogously to the *de* value.

since selectivity (in this case regioselectivity) plays a role in the formation of the intermediate. R is here defined in terms of Equation (7) with n as amount of oxetanes in the product mixture and k, k' ($k > k'$) as overall rate constants of the reactions leading to oxetanes of type **45**/**45'** and **46**/**46'** respectively.

$$R = \frac{n(45) + n(45')}{n(46) + n(46')} = \frac{k}{k'} \tag{7}$$

The parameters $\delta\Delta\Delta H^{\neq}$ and $\delta\Delta\Delta S^{\neq}$ for the regioselectivity give a pair of values which obey the isoinversion relationship in Figure 8 exactly. Here again, we see the general importance of the isoinversion temperature T_i for all types of selectivity processes, regardless of the nature of the selectivity, as long as they are generated on different levels. Accordingly, the temperature dependence of the ratio of *endo* isomers **31**, **31'** to *exo* isomers **47**, **47'** (see Fig. 4) in the Paternò-Büchi reaction should also follow the isoinversion relationship. Indeed, this has been confirmed by the latest experimental results.[81]

The assignment of the activation parameters $\Delta\Delta H^{\neq}_{1,2}$ and $\Delta\Delta S^{\neq}_{1,2}$ to the selectivity levels is supported by the nature of the isoselectivities found.[92] In the high-temperature region ($T > T_{inv}$), there exist several isoselective points with respect to variation of the olefin with constant auxiliary, whereas in the low-temperature region ($T < T_{inv}$) the isoselective points observed are for variation of the auxiliary with the same olefin.

All of the isoselective points for the high- and low-temperature regions are shown in Figure 12 as an Eyring diagram.

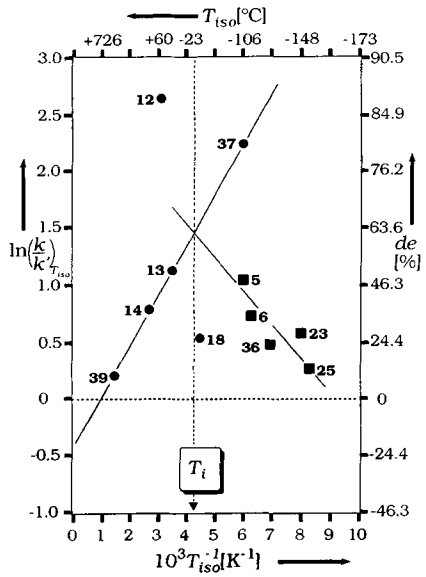

Fig. 12. The isoselective points for all of the Systems 1–28 in Table 4, for the high- and the low-temperature regions ($T > T_{inv}$ and $T < T_{inv}$, respectively) in an Eyring diagram. For the high-temperature region the isoselective points shown are those obtained by variation of the dioxols **6**, **23** and **25** (see Table 2) with a constant phenylglyoxylate of **12**–**14**, **18**, **37** and **39** (see Table 1), for the low-temperature region, those obtained by variation of the same phenylglyoxylates with a constant olefin **5** (furan), **6**, **23**, **25**, and **36**. The T_{iso} values were determined in each case from a $\Delta\Delta H_i^{\neq}/\Delta\Delta S_i^{\neq}$ diagram (i = 1, 2) accroding to *Giese* et al. [92].

The position of the isoselective points in the high-temperature region represents a measure of the induction potential of an auxiliary independent of the partner olefin. The closer the isoselective temperature T_{iso} comes to the isoinversion temperature T_i, and the higher the *de* value which can theoretically be obtained at T_{iso}, then the higher the selectivity that can be expected from the auxiliary. The position of isoselective points in the low-temperature region can be seen as a measure of the importance of the olefin in the selectivity process, independent of the auxiliary. Here, too, the closer T_{iso} lies to T_i, and the higher the *de* values obtainable at T_{iso}, then the greater the effect of the olefinic component on selectivity.

2.2.2. *A General Kinetic Scheme for all Types of Selectivity Process*

These results were first obtained from a study of the diastereoselective Paternò-Büchi reaction (see Section 2.2), but they can be couched in a universal kinetic scheme, as shown in Figure 13.

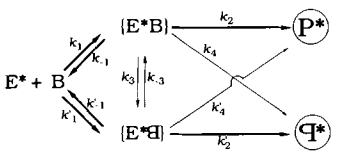

Fig. 13. Generalized kinetic scheme for the isoinversion relationship for any desired selectivity process. As stated by the isoinversion principle, the selectivity is generated at two distinct levels: 1) formation of isomeric intermediates, and 2) the possibility of retrocleavage of the intermediates, or their mutual interconvertibility. The overall rate constants k_1 and k'_1 are decisive for the first selectivity level, while the rate constant ratios k_2/k_{-1} and k'_2/k'_{-1} (or alternatively k_2/k_3 and k'_2/k'_3) represent the second level of selectivity.

Starting material B, containing a prochiral element, reacts with a chiral substrate or chiral catalyst E* to afford the two diastereomeric intermediates [E*B] and [E*Ɓ]. These can be formed in different proportions and are in equilibrium with each other. Formation of this diastereomeric intermediate represents the first level of the selectivity process. The intermediates can either react further, yielding the diastereomeric products P* and Ƥ*, where one of the two products is generally greatly favored, or retrocleavage of the intermediate to the starting materials may occur. These can then be fed back into the reaction cycle.

As an alternative to retrocleavage, the conversion of one diastereomeric intermediate into the other is conceivable. Hence, the second selectivity level is made up of the possibility of retrocleavage and that of interconvertibility of the intermediates.

Whenever selectivity is generated on two or more different levels, in any kind of selectivity process, inversion points are expected in the Eyring diagram for temperature-dependent measurement of a selectivity parameter. We understand the kinetic model in Figure 13 as a general principle, with which Nature produces most cases of selectivity. Each particular case of selectivity can hence be reduced to the temperature-dependent interaction of all relevant rate constants, which themselves are determined by the temperature-dependent dominance of activation entropy or enthalpy. This makes it possible for Nature to optimize the selectivity of a system either by choice of temperature or by structural changes to the system for a prescribed temperature. In the sense of the isoinversion principle, enzymes are species structurally adapted for $T_i = 37\,^{\circ}C$, for optimal stereoselectivity in biochemical reactions. The importance of each of the rate constants shown in Figure 13 for selectivity depends in any given case on the reaction concerned. For the diastereoselective Paternò-Büchi reaction, in the sense of Equation (1), the isoinversion principle from Figure 13 may, for example, be reduced to the reaction step shown in Scheme 1.

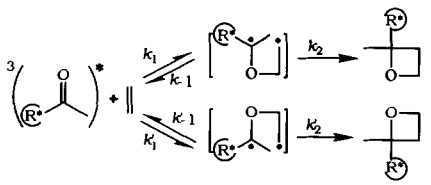

Scheme 1. Reduction of the kinetic scheme of Figure 13 for the case of the diastereomeric Paternò-Büchi reaction.

The rate constants shown have achieved the quality of overall rate constants, implicitly containing all the partial steps that are not relevant to the selectivity process. In this case the 1,4-biradical intermediates are not interconvertible. By formation of a new element of chirality in the intermediate the entire stereoselectivity of the oxetane is fixed, so that once an intermediate is formed it can give rise to *only one* diastereomeric product, provided no retrocleavage takes place.

For the weighting of the rate constants k_1 and k_1' on the one hand, and k_2/k_{-1} or k_2'/k_{-1}' on the other, two boundary cases can be discussed in the simplified kinetic inversion model of Scheme 1:

1. The intermediate formed preferentially can also react preferentially to give the product (Fig. 14).

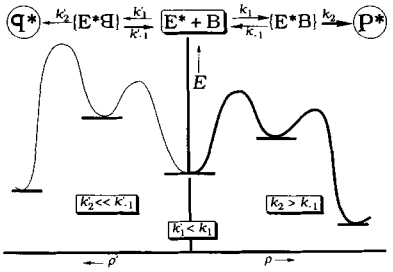

Fig. 14. Schematic diagram for the simplified isoinversion relationship of Scheme 1. The intermediate formed in excess {E*B} also gives rise to the major diastereomer P*.

2. The minor intermediate may be responsible for the major diastereomeric product, because of greater reactivity (Fig. 15).

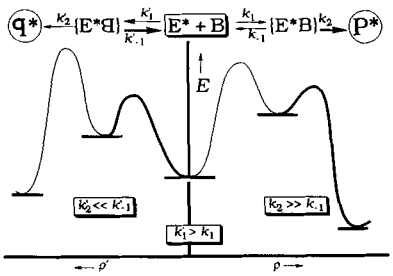

Fig. 15. Schematic diagram for the simplified isoinversion relationship of Scheme 1. Because of its greater reactivity, the minor intermediate {E*B} is responsible for the major diastereomer P*.

While the latter behavior has been considered for generation of chirality in catalytic, homogeneous processes, in the diastereoselective Paternò-Büchi reaction the former is relevant, i.e., the major diastereomer arises from the preferentially formed intermediate, while the minor intermediate undergoes preferential retrocleavage. Therefore, no inversion of the stereochemistry of the major oxetane by temperature effects is observed, as might be expected for an otherwise weighted selectivity mechanism.

In the following, it will be shown that from knowledge of a particular reaction—the diastereoselective Paternò-Büchi reaction—it is possible to develop a universal selectivity model, which is also applicable to selectivity processes in ground state reactions as shown below. The temperature dependence proves to be the most important instrument for understanding the selectivity process here.

In their monograph on asymmetric synthesis, *Morrison* and *Mosher* confine themselves to the remark: "Obviously, temperature-dependence measurements of asymmetric synthetic reactions should be made whenever possible."[101]

With this in mind, we have worked through the literature on stereoselective reactions from recent years, initially seeking temperature-dependent measurements of optical yield.

We found a series of examples of widely varying reaction types, all of which fitted readily into the kinetic scheme of Figure 13. For each reaction type it was possible to draw an isoinversion line from the literature data, regardless of whether the reactions were stoichiometric or catalytic, and of whether they were photochemically induced or in the ground state. Finally, we could show that the isoinversion principle is applicable not only to asymmetric reactions, but can be extended to any selectivity process, as long as the temperature dependence of a selectivity parameter has been conscientiously determined. Even pressure-dependent selective processes may be characterized with the aid of the isoinversion principle.

3. Asymmetric Ester Synthesis

3.1. Enantioselective Amine-Catalyzed Additions of Alcohols to Ketenes in Homogeneous Phases

In the early sixties, *Pracejus*[91] carried out extensive studies of the addition of achiral alcohols to unsymmetrical, disubstituted ketenes, catalyzed by chiral tertiary amines [Eq. (8)].[102-104]

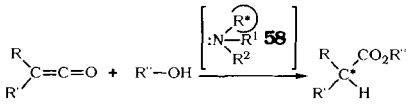

(8)

Remarkably, the author even at that time performed an extended test of the temperature dependence of stereoselectivity at the start of his systematic studies.

The ester synthesis (8) proved especially suitable for a study of temperature dependence, as it proceeds at a sufficiently high rate in a homogeneous phase throughout the temperature range +75 °C to below −100 °C. Addition of the amines causes a sharp acceleration in rate. In addition, the reaction is irreversible in the selectivity determining step, so that the basic catalyst causes no racemization of the product ester. In the temperature range studied, no side reactions were observed.

The *ee* values obtained in reaction (8) could be influenced by the following parameters;[91, 103, 104] the ketene component, the alcohol component, the structure of the catalyst, the reaction conditions (concentration of the reactants, solvent, temperature).

3.1.1. The Influence of Ketene and Alcohol Components and of Catalyst Structure

The ketene components used were methylphenylketene **49** and 1-carbonyltetrahydronaphthalene **50**.[105] Methanol and ethanol served as the alcohol component. Numerous

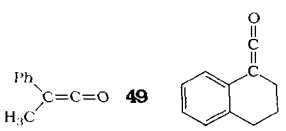

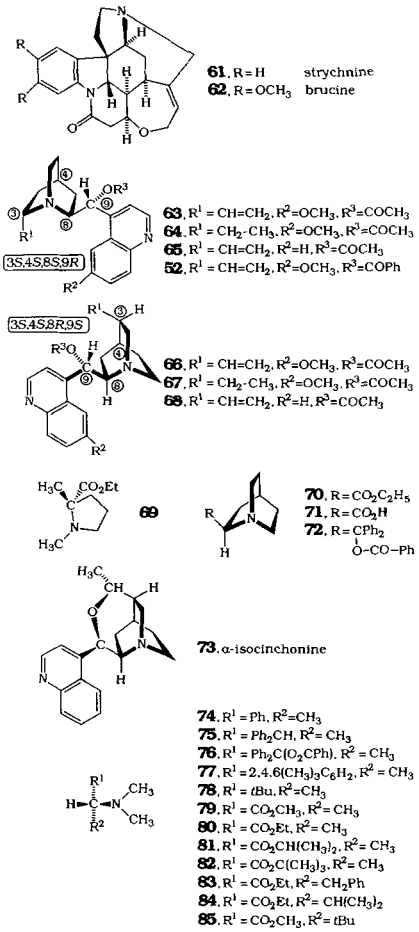

Fig. 16. Overview of the tertiary, chiral amines of general structure **58** that were used by *Pracejus* et al. [91, 102, 103] as catalysts in asymmetric ester synthesis (8).

derivatives of strychnine and quinine bases were studied as catalysts, as well as a series of chiral tertiary amines with an acyclic C–N bond. Figure 16 gives an overview of the structural diversity of the chiral catalysts **61**–**85** used by *Pracejus*.

Cinchona alkaloids have been studied in catalytic asymmetric synthesis since the discovery of their catalytic action in asymmetric cyanohydrin synthesis, by *Bredig* and *Fiske* in 1912,[106] to the present day.[107] Thus, for example, quinine **51** has been used as a chiral catalyst in Michael reactions,[110] epoxidations,[111] thiol additions,[112] and even in [2 + 2]-cycloadditions.[113] The catalytic effect of **51** in autoinduction processes is especially remarkable.[115]

The *ee* values obtainable in the asymmetric ester synthesis (8) described proved to be a sensitive probe of structural variations in the substrate and particularly of the structure of the chiral catalyst.

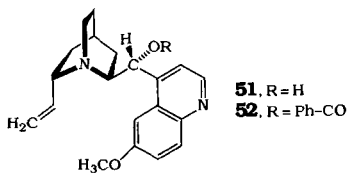

As well as displaying remarkable enantiomeric excesses (e.g. methylphenylketene **49** reacts with methanol in the pres-

ence of benzoylquinine **52** at $-110\,^{\circ}C$ according to Equation (8) to give methyl (*R*)-(−)-α-phenylpropionate **53** in an enantiomeric excess of 76%), even the minor steric differences between CMe_2 and CD_2, which generate the chirality of nitrogen base **54**, can be observed in an asymmetric reaction.[114]

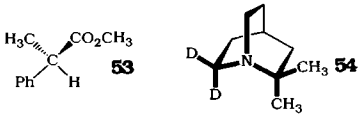

3.1.2. *The Influence of Temperature*

Table 6 lists the systems for which the temperature dependence of stereoselectivity has been studied. We have transferred the published results of temperature-dependence measurements to an Eyring diagram. In doing so it becomes clear that the temperature dependencies of all the systems listed in Table 6 are characterized by two linear regions, and the appearance of an inversion point. In several cases, indeed, an inversion of stereoselectivity could only be achieved by variation of the temperature.

Table 6. An overview of the systems whose stereoselectivity in the reaction (8) has been measured with respect to temperature [91, 102, 103]. Ketene (0.1 mol) was treated with alcohol (0.11 mol) under standard conditions, using 10^{-3} mol of the catalyst. Deviations from these standard conditions are indicated. Toluene served as solvent; at temperatures below 173 K a 1:1 mixture of toluene and pentane was used. Enantiomeric excesses were determined from the optical rotation, by setting the optical yield equal to the *ee* value.

No.	R,R'C=C=O	R"-OH	:N(R*)(R1)(R2)	Ref.	No.	R,R'C=C=O	R"-OH	:N(R*)(R1)(R2)	Ref.
1	**49**	MeOH	**62**	[91]	20	**49**	MeOH	**79**	[103]
2	**49**	MeOH	**63**	[91]	21	**49**	MeOH	**80**	[103]
3	**49**	MeOH	**63** [c]	[91]	22	**49**	MeOH	**81**	[103]
4	**49**	MeOH [a]	**63**	[91]	23	**49**	MeOH	**82**	[103]
5	**49**	MeOH [a]	**63** [c]	[91]	24	**49**	MeOH	**83**	[103]
6	**49**	MeOH [b]	**63**	[91]	25	**49**	MeOH	**84**	[103]
7	**49**	MeOH [b]	**63** [d]	[91]	26	**49**	MeOH	**85**	[103]
8	**49**	MeOH	**66**	[91]	27	**49**	MeOH	**70**	[103]
9	**49**	MeOH	**61** [e]	[102]	28	**49**	MeOH	**71**	[103]
10	**49**	MeOH	**52**	[102]	29	**49**	MeOH	**72**	[103]
11	**49**	MeOH	**64**	[102]	30	**49**	MeOH	**73**	[103]
12	**49**	MeOH	**65**	[102]	31	**49**	EtOH	**63**	[91]
13	**49**	MeOH	**68**	[102]	32	**49**	EtOH	**66**	[91]
14	**49**	MeOH	**67**	[102]	33	**49**	EtOH	**62**	[91]
15	**49**	MeOH	**74**	[102]	34	**50**	MeOH	**61** [e]	[102]
16	**49**	MeOH	**75**	[103]	35	**50**	MeOH	**62**	[102]
17	**49**	MeOH	**76**	[103]	36	**50**	MeOH	**63**	[102]
18	**49**	MeOH	**77**	[103]	37	**50**	MeOH	**66**	[102]
19	**49**	MeOH	**78**	[103]	38	**50**	MeOH	**68**	[102]

[a] 0.3 mol. [b] 1.0 mol. [c] 0.003 mol. [d] 0.0001 mol. [e] 0.0002 mol.

A selection of typical results from the diverse data published is presented in Figure 17.

On the basis of the temperature dependence of stereoselectivity, *Pracejus* developed his "model for the preferred conformations of transition states".[116] This mechanism, which has been confirmed by kinetic studies,[108] is depicted in Figure 18.

The rate-determining step is the nucleophilic attack of an intermediate catalyst–alcohol associate **55** on the ketene. The next step is seen as a rapid proton transfer within the

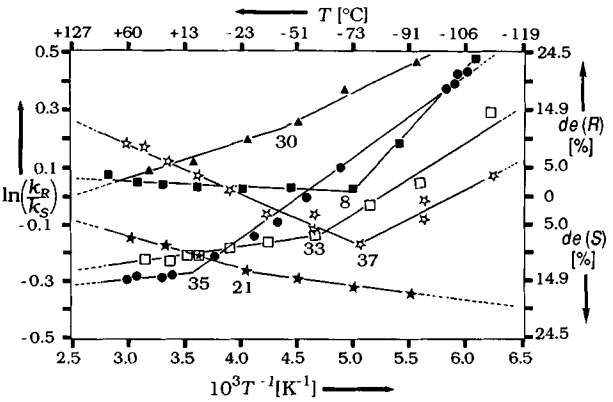

Fig. 17. Representation of the temperature-dependent *ee*-values in asymmetric ester synthesis (8), in the form of an Eyring diagram. Systems 8, 21, 30, 35 and 37 in Table 6 are shown as examples.

ammonium ester–enolate ion pair **56** thus formed. The chiral information is transferred in this step.[271] Early work by *Prelog* and *Wilhelm* has shown that the chiral nitrogen catalysts transfer chiral information to the substrate not as the free bases but in their protonated form.[109]

In the transition state for the "specificity-determining proton transfer", *Pracejus*[116] assumes a linear $^{\delta\oplus}N\cdots H\cdots C^{\delta\ominus}$ conformation, oriented perpendicular to the bond framework of the anionic partner. If one imagines the $^{\delta\oplus}N\cdots H\cdots C^{\delta\ominus}$ grouping as a pseudo-bond of the ethane type, then the conformation may be drawn as a Newman projection (**57a** and **57b** in Fig. 18; in **57b** the anionic C-atom of **57a** conceals the proton and the N atom behind it).

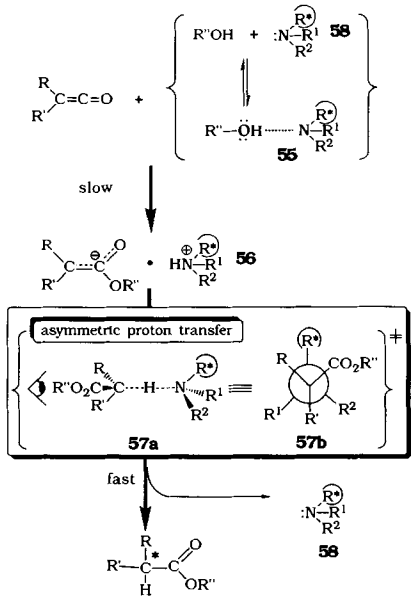

Fig. 18. Mechanism of nucleophilic addition of achiral alcohols to unsymmetrically substituted ketenes, catalyzed by chiral, tertiary amines **58** [Eq. (8)] [108].

The extent of chiral induction in the selectivity-determining step with ionic pair **56** ($N^{\oplus} \rightarrow C^{\ominus}$ proton transfer) is determined by a series of competing transition states, which show varying degrees of steric hindrance and are in equilibrium with each other. For catalysts of the general type **58**, the

situation is explained in Figure 19. (Here, Ⓛ, Ⓜ, and Ⓢ symbolize large, medium and small residues on the asymmetric C-atom in **58**, in the Cram sense.)

The protonated bases **58** are depicted by the authors in three staggered conformations **59a–c**, which are interconvertible by rotation around the C–N bond. Of the conformations shown, **59a** is regarded as the most stable, and **59c** as the least hindered for proton transfer. On addition of the ester enolate, each of these conformations leads to two diastereomeric transition states, for each of which three new, staggered conformations may be drawn. Of all the possible transition states, Figure 19 shows only those presumed lowest in energy, formulas **60a–c**.

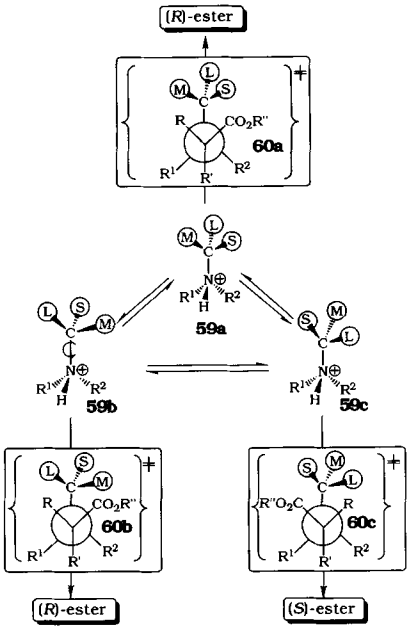

Fig. 19. Conformations **59a–c** of the ion pair formed as an intermediate are in equilibrium with each other. In the asymmetric reaction step they pass through diastereomeric reaction channels. Here, only the lowest energy tansition states **60a–c** are depicted. In our opinion, the data available do not allow us to order the conformations clearly with respect to enthalpy or entropy content.

The temperature dependence of the stereoselectivity of this reaction is currently understood as the interplay of these competing, mutually interconvertible conformations of the species and transition states involved in the selectivity-determining step. *Pracejus* et al. describe the situation thus:[103] "The causes are not to be sought in a temperature-determined alteration of reaction mechanism, but in the antagonism of enthalpy and entropy effects on the stability of the diastereomeric transition states."

3.1.3. *The Isoinversion Relationship for Asymmetric Ester Synthesis*

If one analyzes the published data in the sense of the isoinversion relationship, i.e., if the activation enthalpy and entropy differences for the high- and low-temperature regions of the relevant Eyring diagram are converted into the $\delta\Delta\Delta H^{\neq}$ and $\delta\Delta\Delta S^{\neq}$ values, one obtains the isoinversion relationship shown in Figure 20, with isoinversion temperature $T_i = 210$ K. The correlation coefficient for the isoinversion line is > 0.99.

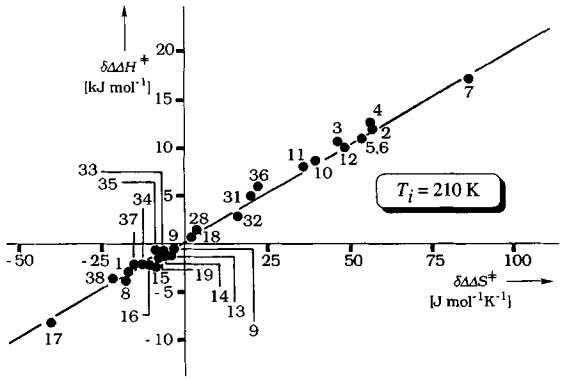

Fig. 20. The isoinversion line for homogeneous-phase, asymmetric ester synthesis (8), catalyzed by chiral bases (the numbers correspond to those in Table 6). The $\delta\Delta\Delta H^{\neq}$ and $\delta\Delta\Delta S^{\neq}$ values were determined from Equations (4) and (5), respectively. In order to calculate the fundamental $\Delta\Delta H^{\neq}_{i,2}$ and $\Delta\Delta S^{\neq}_{i,2}$ values, the (*R*)-ester was assumed to be uniformly the major enantiomer, even though in a few cases the (*S*)-enantiomer was present in excess. The corresponding $\delta\Delta\Delta H^{\neq}$ and $\delta\Delta\Delta S^{\neq}$ values do not differ from each other in magnitude in these cases, but carry the opposite sign. The $\delta\Delta\Delta H^{\neq}$ and $\delta\Delta\Delta S^{\neq}$ values for Systems 20–27 and 29, 30 (Table 6) all lie in the range -0.4 to -1.5 kJ mol^{-1}, or -1.4 to -4.1 J mol^{-1} K^{-1} respectively, and are not plotted because of the density of data points in this region.

The mechanistic evidence (Figs. 18, 19) can now be readily represented by the simple kinetic scheme of Figure 13: In the nucleophilic addition of a chiral particle to a prochiral substrate, chiral intermediates are generated, which may exist in several different diastereomeric conformations in equilibrium with one another.

This is an alternative selectivity level to retrocleavage. For a given temperature region, one conformation will develop preferentially, determined by enthalpy or entropy. This conformation will then be channeled—influenced again by enthalpy or entropy differences—through diastereomeric reaction pathways to give differing amounts of enantiomeric products. The temperature dependence of stereoselectivity gives insight into the interplay of enthalpy and entropy.

At this point it should be emphasized that as early as 1960 *Pracejus* recognized the great importance of the temperature dependence of asymmetric reactions for efficient practical application.[116] However, the consequences of this were not sufficiently appreciated by his colleagues: "Vergleicht man die wenigen bisher vorliegenden Beobachtungen über die Temperaturabhängigkeit der Stereospezifität asymmetrischer Synthesen miteinander, so gewinnt man den überraschenden Eindruck, daß in der Regel Aktivierungsenthalpie und Aktivierungsentropie-Differenzen einander entgegenwirken und daß es von der Reaktionstemperatur abhängt, welcher von beiden Faktoren überwiegt und das Vorzeichen der Spezifität bestimmt. Es bleibt abzuwarten, ob sich diese "Regel" für eine größere Zahl von Reaktionstypen bewährt; im positiven Falle hätte das wichtige Konsequenzen für die Interpretation des sterischen Verlaufs asymmetrischer Synthesen. Das heute allgemein übliche Verfahren, aus dem Vorzeichen der Stereospezifität bei einer willkürlich gewählten Reaktionstemperatur Schlüsse auf Konformation und Konfiguration der Reaktanten zu ziehen, würde damit in Frage gestellt oder in seiner Anwendbarkeit eingeengt werden. Eine Klärung

der Situation durch möglichst ausgedehnte Untersuchungen über die Zusammenhänge zwischen Reaktionstemperatur und Stereospezifität bei asymmetrischen Synthesen erscheint deshalb dringend geboten". – Quod erat demonstrandum.[*]

3.2. Addition of Alcohols to Ketenes Catalyzed by Polymer-Fixed Chiral Amines

The area studied intensively by *Pracejus*, amine-catalyzed addition of methanol to methylphenylketene **49**, has been interestingly extended by the work of *Yamashita* et al.[117–120] In their investigations they report on temperature-dependent stereoselectivity in the formation of **53**, using chiral amine catalysts bound to a polymeric matrix.[121–127]

Once again, it proved that for the vast majority of systems studied, two linear regions were found in the Eyring diagram, with an inversion point, though systems are also described for which a linear dependence of stereoselectivity in the chosen temperature region was observed.

In the light of the isoinversion relationship, the polymer-fixed chiral amine catalysts also show a zero-point line in the isoinversion diagram. The isoinversion temperature T_i determined from the gradient is identical to that found in the systems studied by *Pracejus* (T_i = 210 K).[91, 102–105]

3.3. Diastereoselective Addition of Alcohols to Ketenes

Anders, Ruch and *Ugi*[23a] have studied a diastereoselective variant of ester synthesis (8). They treated phenytrifluoromethylketene with racemic secondary alcohols in a non-catalyzed reaction. The stereoselective acylation of the alcohols served as an experimental test of the stereochemical structural model developed by the authors.[20–24] The temperature dependence of the diastereoselectivity was measured for two selected examples, and here, too, inversion points were observed in the Eyring diagram. Analysis in the sense of the isoinversion principle yields T_i = 259 K, a different value from the isoinversion temperature found for the catalytic variant of asymmetric ester synthesis. This is an indication that the mechanism of stereoselectivity is different for catalytic enantioselective and uncatalyzed diastereoselective ester syntheses.[294] *Jähme* and *Rüchardt*[274, 293] have also studied the addition of chiral secondary alcohols to methylphenylketene, but using achiral catalysts (such as pyridine and 1,4-diazabicyclo[2.2.2]octane). The authors report not only a rate acceleration, but also a "drastic increase in the stereoselectivity by addition of achiral bases". Analysis of the data for the diastereoselective addition of chiral alcohols to ketenes catalyzed by achiral amines leads to an isoinversion line with gradient T_i = 289 K.[292, 293]

[*] "If one compares the few available observations of temperature dependence in the stereospecificity of asymmetric syntheses, one has the surprising impression that differences in enthalpy and entropy in general work against each other, so that the reaction temperature determines which of the two factors dominates and decides the sign of the specificity. It remains to be seen whether this "rule" will hold for a larger number of reaction types; if so, this has important consequences for the interpretation of the steric course of asymmetric syntheses. The usual procedure today is to draw conclusions regarding configuration and conformation from the sign of the specificity at an arbitrarily chosen temperature, but this would then be questionable, or limited in applicability. Clarification of the situation by extensive studies on the connection between reaction temperature and stereospecificity in asymmetric synthesis seems, therefore, to be urgently required."

4. Asymmetric Amine Addition to Ketenes

As well as his detailed work on catalytic asymmetric ester synthesis, *Pracejus* also studied the nucleophilic addition of chiral primary amines **88** and **89** to the C=C double bond of unsymmetrical disubstituted ketenes **49**, **50** and **86**, yielding two diastereomeric amides **87** [Eq. (9)].[116, 128, 129]

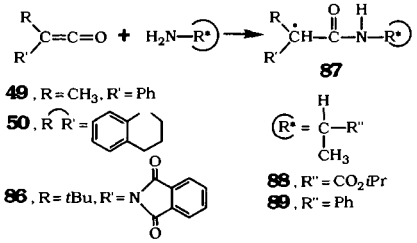

(9)

The stereoselective step of this stoichiometric, asymmetric synthesis consists of a proton transfer from the NH_2 group to the α-C-atom of the ketene component.[271] The chiral information is induced by the asymmetric C atom of the amine. If (*S*)-**89** is used in the reaction, then the newly formed chiral center in the major diastereomer will also display (*S*)-configuration, in almost every case. The diastereomeric amide with (*R*,*S*)-configuration is therefore the minor product (Fig. 23). The selectivity of this reaction is under purely kinetic control, since the diastereomeric amides formed under the reaction conditions given are configurationally stable and can therefore not be in thermodynamic equilibrium with each other.

Here too, the *de* values obtainable are determined not merely by the structures of the ketene and the chiral amine employed, but are also significantly temperature dependent. In addition, the solvent plays an important role. This reaction proceeds in quantitative yield throughout the temperature range studied, and no side product formation is observed.

4.1. The Influence of Temperature and Solvent

Table 7 gives an overview of the systems for which the temperature and solvent dependence of the diastereoselectivity have been studied.

If the data in Table 7 are evaluated in the form of Eyring diagrams, then in all but a few examples one finds two linear regions in the temperature-dependence curve, with an inversion point.

For the reaction of the ketene **50** with (*S*)-α-phenylethylamine **89** in chloroform, an inversion point is not observed within the temperature range studied (System 20, Table 7). Starting with methylphenylketene **49** in tetrahydrofuran, temperature-*in*dependent diastereoselectivity was found, within experimental error (System 7, Table 7).

Figure 21 shows the temperature-dependent stereoselectivity in a few typical systems from Table 7, in the form of an Eyring diagram.

Table 7. Overview of the ketenes and chiral amines whose temperature-dependent diastereoselectivity in Reaction (9) has been measured in various solvents.

No.	Ketene	Amine	Solvent	Ref.
1	**49**	**89**	methylcyclohexane	[116]
2	**49**	**89**	toluene	[116,128]
3	**49**	**89**	*p*-xylene	[116]
4	**49**	**89**	mesitylene	[116]
5	**49**	**89**	diisopropyl ether	[116]
6	**49**	**89**	diethyl ether	[116]
7	**49**	**89**	tetrahydrofuran	[116]
8	**49**	**89**	ethyl acetate	[116]
9	**49**	**89**	chloroform	[116]
10	**49**	**89**	dimethylformamide	[116]
11	**49**	**89**	triethylamine	[116]
12	**50**	**89**	methylcyclohexane	[116]
13	**50**	**89**	toluene	[116]
14	**50**	**89**	*p*-xylene	[116]
15	**50**	**89**	mesitylene	[116]
16	**50**	**89**	diisopropyl ether	[116]
17	**50**	**89**	diethyl ether	[116]
18	**50**	**89**	tetrahydrofuran	[116]
19	**50**	**89**	ethyl acetate	[116]
20	**50**	**89**	chloroform	[116]
21	**50**	**89**	dimethylformamide	[116]
22	**86**	**89**	toluene	[129]
23	**86**	**88**	toluene	[129]

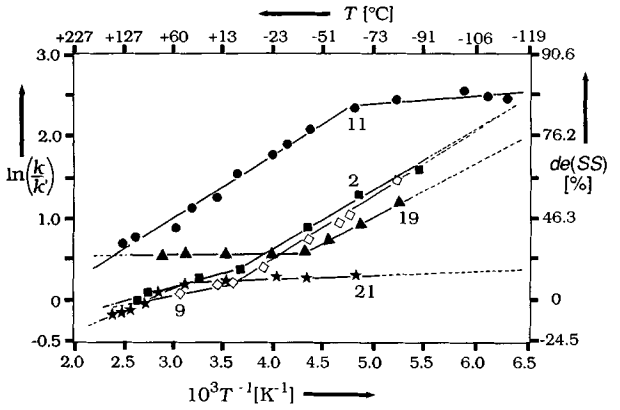

Fig. 21. Eyring diagram for a few typical systems from Table 7 (Systems 2, 9, 11, 19 and 21). The major diastereomer in all cases is the (*S,S*)-amide.

4.2. The Isoinversion Relationship for Asymmetric Amide Synthesis

From the gradient of the zero-point curve in the $\delta\Delta\Delta H^{\neq}/\delta\Delta\Delta S^{\neq}$ diagram (Fig. 22; correlation coefficient > 0.99), the isoinversion temperature $T_i = 276$ K may be determined. The systems with only one linear region lie at the zero point of the $\delta\Delta\Delta H/\delta\Delta\Delta S$ diagram.

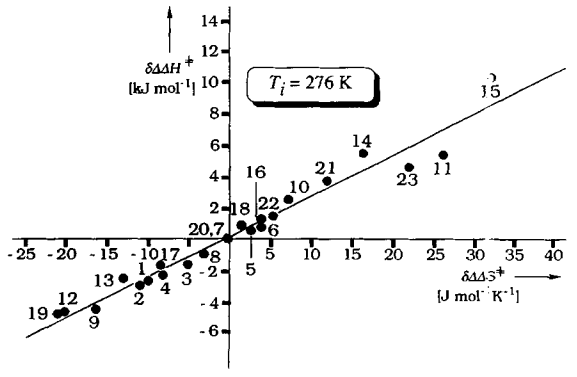

Fig. 22. Isoinversion line (correlation coefficient > 0.99) for stoichiometric asymmetric amide synthesis by Equation (9) ($T_i = 276$ K).

Because of the high overall rate of the reaction (in 0.1 M solution the conversion is quantitative in less than twenty seconds, even at temperatures below −100 °C), thorough mechanistic studies have not yet been undertaken. The authors propose a two-step mechanism (Fig. 23), analogous to catalytic, asymmetric ester synthesis.

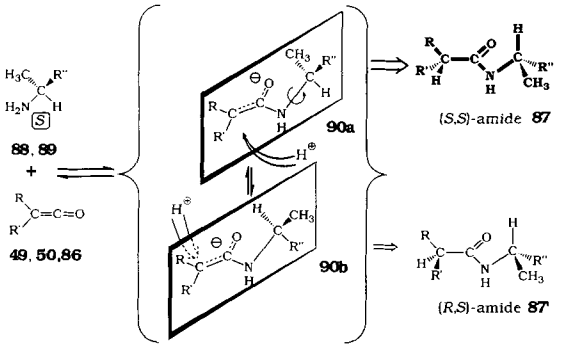

Fig. 23. Probable mechanism for stoichiometric, asymmetric amide synthesis according to Equation (9), with conformationally diastereomeric intermediates **90a, b** having an ammonium enolate structure.

In the initial step, an adduct with an ammonium enolate structure is formed. In the stereoselective step, a proton migration occurs from the N atom to the α-C-atom of the ketene unit. An ionic pair, which can exist in the conformations **90a** and **90b**, is favored as an intermediate. However, the resonance-stabilized anion **91** is also a plausible intermediate.[130]

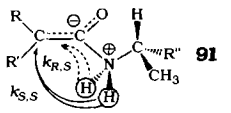

91

In both cases, however, the extent of stereoselectivity depends on the relative conformational arrangement of the amine moiety to the ketene part of the molecule.

At different temperatures, different conformations may be preferentially adopted, determined once more by enthalpy and entropy factors. Each conformation then opens into two competing diastereomeric reaction channels for proton transfer, whose cross-section is again temperature dependent, due to enthalpy and entropy effects.

Starting with this working hypothesis, *Pracejus* et al.[128, 129] describes intermediate **90a** as the preferred conformation for the low-temperature region ($T < T_{inv}$). This region depends on the solvent, but as a rule is determined by negative activation entropy differences and negative activation enthalpy differences ($\Delta\Delta H_2^{\neq}$, $\Delta\Delta S_2^{\neq} < 0$) for diastereomer formation. The influence of the activation parameters on conformer **90a** explains why the (*S,S*)-amide **87** is preferentially formed as the temperature falls.

For the high-temperature region ($T > T_{inv}$), conformation **90b** is assumed to be favored (compared to **90a**, the chiral group is rotated through 120°, so that the CH_3 group and the

hydrogen are staggered relative to the carbonyl group). In general, the influence of the activation parameters on **90b** show more negative activation entropy and activation enthalpy differences ($\Delta\Delta H_1^{\neq}$, $\Delta\Delta S_1^{\neq} \ll 0$), so that in some cases the diastereomeric (*R,S*)-amide **87′** can be formed in excess even at temperatures above 100 °C. According to *Pracejus*,[116, 128] of two sterically different, competing reactions, the more sterically hindered will normally be disfavored on energetic grounds (higher $\Delta H^{\neq}$), but favored on entropic ones (higher $\Delta S^{\neq}$).

At this point, it should be pointed out that the experimentally measurable differences in activation enthalpy and entropy of two competing reactions are generally complex values. They reflect not only the enthalpy and entropy differences of two diastereomeric transition states, but also the temperature dependence of the ratio of various conformational isomers in the starting material and products. The ratio of conformation-dependent diastereomeric intermediates also proves to be relevant, as does the temperature dependence of solvation equilibria (for reactions in solution). However, the fact that all the systems belong to the isoinversion line shows that despite the complexity of the activation parameter differences $\Delta\Delta H_{1,2}^{\neq}$ and $\Delta\Delta S_{1,2}^{\neq}$, their influence on the complex reaction may be represented simply. Here, too, one can state that: The enthalpic influence is repressed to the same extent as the gain in entropy influence, in a given temperature region.

The extreme solvent dependence of the reaction, and especially the characteristics of the temperature dependence of stereoselectivity, make it likely that polar intermediates play a part in the reaction mechanism. A concerted mechanism has also been discussed in the literature,[130] and is depicted schematically in Figure 24. It cannot, however, explain the

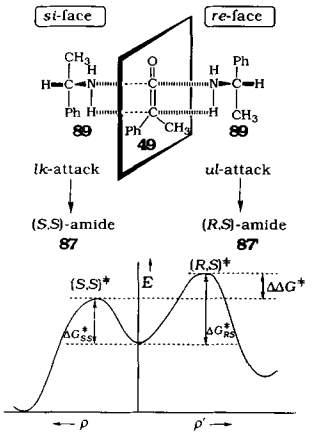

Fig. 24. Hypothetical concerted mechanism for stoichiometric asymmetric amide synthesis according to Equation (9) [130].

competing influence of enthalpy and entropy in the sense of the isoinversion relationship. In a concerted mechanism, the extent of stereoselectivity would depend solely on the difference in free activation enthalpy $\Delta G^{\neq}$ for *re*-directed versus *si*-directed attack. Inversion points in the Eyring diagram ought not to occur. The proposed concerted mechanism is therefore unlikely.

Ugi et al.[23] as well as *Ruch* et al. and *Youn*[273] have also studied the temperature dependence of diastereoselectivity in asymmetric amide synthesis (9). They treated phenyltrifluoromethylketene with phenylethylamine **89** and chiral α-ferrocenylalkylamines in a variety of solvents and also observed inversion points in the Eyring diagram. Independent analysis of this data also leads to an isoinversion relationship, with $T_i = 276$ K, a temperature identical with that for the systems studied by *Pracejus*.

5. Nucelophilic Substitution Reactions

In *Levene's* mechanistic study[131] of nucleophilic substitutions, inversion points were also observed in the temperature-dependent enantioselectivity of Reaction (10).[304] Chiral, secondary alcohols of type **92** were treated with gaseous HBr without a solvent, to afford bromides **93** and **93′**. The enantiomeric excess obtained, which also measures the ratio of retention to inversion, was determined by optical rotation. This is possible because below 0 °C the products do not racemize, and even above this temperature they do so only slowly.

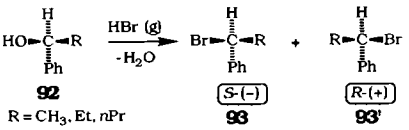

(10)

The reaction was carried out heterogeneously with gaseous HBr. In a homogeneous system, using a solvent, one observes complete S_N2-inversion in the temperature range − 80 °C to + 20 °C.

For the first two homologues of alcohol **92**, with R = Me and Et, the optical rotation of the product mixture falls with increasing temperature from maximum levorotation (retention) to 0° (at − 36 °C), and reaches a maximum dextrorotation (inversion) at − 30 °C. If the temperature is increased further, the rotation once again falls.

The temperature dependence of enantioselectivity is similar for compound **92**, with R = *n*Pr. Here, though, the measured rotations are all negative, so that only a minimum in the levorotation is observed (at − 20 °C).

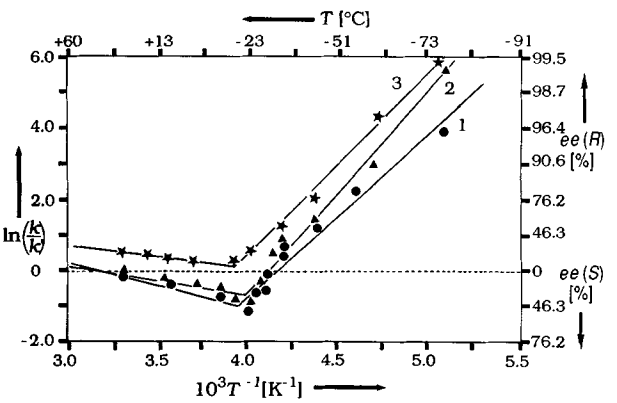

Fig. 25. Eyring diagram for the systems studied for Equation (10) (numbering as in Table 8).

All the systems in Equation (10) reveal two linear regions in the Eyring diagram, with the corresponding inversion points (Fig. 25). The activation entropy and enthalpy differences ($\Delta\Delta H^{\ddagger}_{1,2}$ and $\Delta\Delta S^{\ddagger}_{1,2}$) determined from the Eyring diagram, and the inversion temperatures T_{inv} are presented in Table 8. The gradient of the isoinversion curve obtained in Figure 26 yields an isoinversion temperature of $T_i = 250$ K.

Table 8. Activation energy differences $\Delta\Delta H^{\ddagger}_{1,2}$ and $\Delta\Delta S^{\ddagger}_{1,2}$ for the high- and low-temperature regions in reaction (10), with the inversion temperatures T_{inv}. Parameters $\delta\Delta\Delta H^{\ddagger}$ and $\delta\Delta\Delta S^{\ddagger}$ were determined from the above using Equations (4) and (5).

No.	R in **92**	$\Delta\Delta H_1^{\ddagger}$ / $\Delta\Delta H_2^{\ddagger}$ [kJ mol^{-1}]	$\delta\Delta\Delta H^{\ddagger}$ [kJ mol^{-1}]	$\Delta\Delta S_1^{\ddagger}$ / $\Delta\Delta S_2^{\ddagger}$ [J mol^{-1} K^{-1}]	$\delta\Delta\Delta S^{\ddagger}$ [J mol^{-1} K^{-1}]	T_{inv} [K](°C)
1	CH_3	+ 11.1 − 38.0	− 49.1	+ 36.6 − 161.4	− 198.0	248 (− 25)
2	Et	+ 7.2 − 47.4	− 54.5	+ 22.7 − 200.2	− 222.9	245 (− 28)
3	*n*Pr	+ 5.4 − 42.6	− 48.1	+ 21.5 − 172.3	− 193.9	248 (− 25)

The literature distinguishes between three idealized mechanisms of nucleophilic substitution: the S_N1, S_N2 and S_Ni mechanisms. The transition between the S_N1 and S_N2 mechanisms is a smooth one, depending on many marginal factors and leading to varying levels of inversion or retention. In addition, there is the rarer S_Ni mechanism, which leads to retention.

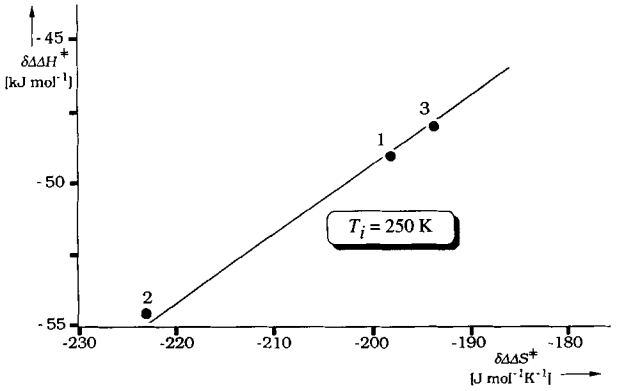

Fig. 26. Isoinversion diagram for nucleophilic substitution (10), with T_i = 250 K (correlation coefficient > 0.99).

In the case studied, it is this S_Ni mechanism that is observed in the low-temperature region. As well as the observed rate acceleration, this mechanism also allows isolation of the primary adduct **94** of alcohol E* and HBr (Fig. 27). At higher temperatures, however, this intermediate decomposes readily, so that the S_N2 or S_N1 mechanisms gain in importance, and inversion or a reduced level of retention is observed. The temperature-dependent interplay between the competing reaction channels of the S_N1, S_N2 and S_Ni mechanisms is illustrated schematically in Figure 27.

In the low-temperature region a high activation enthalpy and entropy is notable, which is responsible for formation of

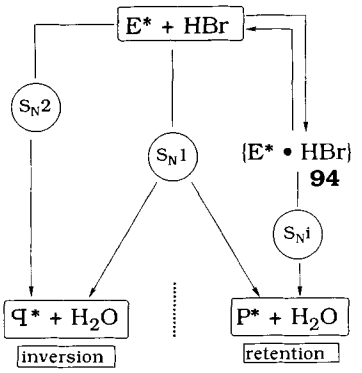

Fig. 27. Schematic diagram of the competing reaction channels of S_N1, S_N2 or S_Ni mechanisms, which lead to different ratios of retention and inversion according to weighting. The level of enantioselectivity is determined by which of the possible reaction channels dominates; the cross-section of this dominance is determined by the temperature-dependent interplay of activation enthalpy and activation entropy differences.

adduct **94**. In the high-temperature case both activation parameters are low, but a clear dependence on the structure of the alcohol **92** used may be seen. Obviously, for larger residues, the proportion of S_N2 reaction is reduced by steric hindrance, so that the extent of enantioselectivity in the high temperature region is reduced by the change from S_N2 to S_N1. This also explains the low levels of inversion for compound **92** with R = *n*Pr, where only levorotatory products are found.

6. Hydrogenations Catalyzed by Transition Metals

6.1. General

The catalytic hydrogenation of carbon–carbon or heteroatom–carbon multiple bonds to give one or more chiral centers is an intensively studied field of organic chemistry [Eq. (11)].[132–139, 144] Such hydrogenations can not only be

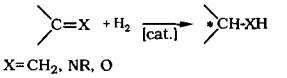

(11)

subdivided according to the phase of the catalyst (homogeneous[140–143] or heterogeneous catalysis[19, 132–135, 275]), but also according to the nature of chirality generation, as shown schematically in Figure 28 for C=C double bond hydrogenation, which is also useful.

On the one hand, the chiral information my be contained in the substrate itself, by suitable substitution of the prochiral unit. The use of an achiral catalyst then produces diastereomers (case B). In this case the chiral information is required in stoichiometric amounts. On the other hand, it is possible to convert double bonds into chiral centers with the help of chiral catalysts; the chiral information for generation of enantiomers then needs to be present in only substoichiometric amounts (case A). In this way, large amounts of an optically active compound can be synthesized, even though only a comparatively small amount of a chiral transition

metal catalyst is used. Because of this multiplication of chiral information, enantioselective catalysis has aroused interest in chemistry from beyond the traditional subject boundaries (chiral amplification).

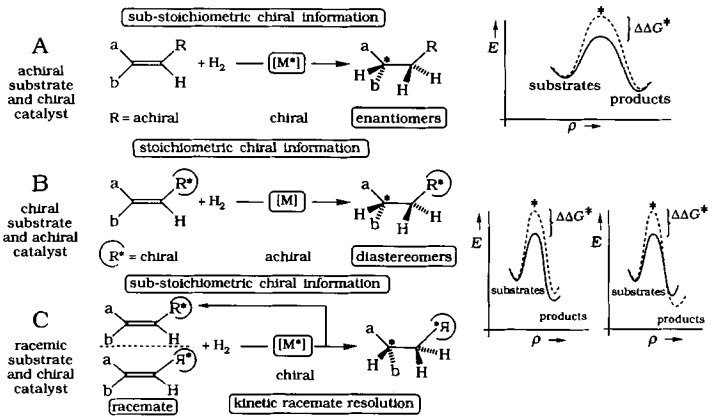

Fig. 28. Classification of catalytic C=C double bond hydrogenation according to the nature of chirality generation.

A further field for homogeneous hydrogenation in stereoselective synthesis lies in the kinetic resolution of racemates.[143, 145–146] For racemic starting materials, enantioselectivity in the course of hydrogenation leads to racemate resolution. In these experiments, the optical purity of the product decreases with time, while that of the starting material improves at the same rate (case C).

6.2. Enantioselective Catalytic Hydrogenation in the Homogeneous Phase

With respect to activity, selectivity, and mild reaction conditions, the present generation of homogeneous catalysts is quite comparable to enzymatic processes. In addition, hydrogenation in the homogeneous phase with substrates possessing several reactive groups can be carried out with a regioselectivity ("site specificity") which cannot generally be obtained with heterogeneous catalysts.

Although high optical inductions have also been achieved for particular substrates using monodentate, optically active phosphanes,[151] it was the transition to chelate-forming phosphanes that brought decisive improvements in optical yield.[152]

The great synthetic potential of homogeneous hydrogenation has been known since the sixties. *Noyori*[147] reported the first example of homogeneous enantioselective catalysis in organic chemistry with a transition metal system in 1966. In 1968, *Horner* et al.[148] and *Knowles* et al.[149] discovered independently of each other that prochiral olefins can be enantioselectively hydrogenated using rhodium complexes of the Wilkinson-catalyst type[150] with optically active phosphane ligands. The extraordinarily mild reaction conditions (room temperature, hydrogen at atmospheric pressure) and the possibility to hydrogenate dehydroamino acids and their esters to derivatives of amino acids with high enantioselectivity aroused great interest in homogeneous hydrogenation around the world. "The development of stereoselective homogeneous phase catalysis hydrogenation methods is one of the glorious chapters of synthetic organic chemistry."[132]

Systematic studies culminated a few years ago in the development of an industrial process for the synthesis of L-Dopa, a drug active against Parkinson's disease.[153, 154] In the following period, hundreds of optically active phosphanes and countless prochiral substrates were tested, not only in enantioselective hydrogenation, but also in transition metal catalyzed enantioselective hydrosilylation, hydroformylation, and similar reactions.[155–159]

In mechanistic studies of enantioselective homogeneous phase hydrogenation, these rhodium–chelate phosphane systems take the leading role, and dehydroamino acids (such as (*Z*)-α-acetaminoacrylic acid, itaconic acid, (*Z*)-α-*N*-acetylamino- and (*Z*)-α-*N*-benzoylaminocinnamic acid, and their esters) are by far the best investigated substrates for this reaction. These compounds have therefore established themselves as standard substrates for testing new ligand systems.[139, 160–166, 173] Scheme 2 shows a typical hydrogenation, that of (*Z*)-α-*N*-acetylaminocinnamic acid **95** and its methyl ester **96** leading to the phenylpropanoic acid derivates **97**/**97'**.

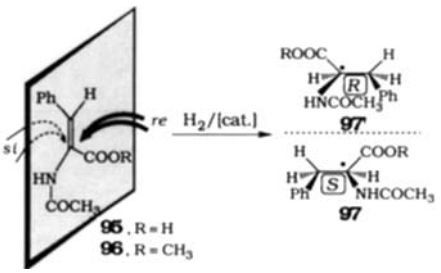

Scheme 2. Catalytic hydrogenation of **95** and **96**. Typical reaction conditions: 1 g of substrate in 20 mL of methanol, 1.1 bar H_2, 25 °C, 10 h, catalyst: substrate ≈ 1:200. **97** (R = H): $[\alpha]_D^{16} = +46.0$ ($c = 1.0$, EtOH); **97** (R = Me): $[\alpha]_D^{25} = +101$ ($c = 1.0$, $CHCl_3$).

6.2.1. *Mechanistic Considerations for Homogeneous, Rhodium-Catalyzed Hydrogenation*

Halpern's mechanistic studies on homogeneous hydrogenation show that for the achiral case the catalytic cycle may be divided into four fundamental steps. These are shown in simplified form in Figure 29 for the [Rh(diphos)]$^{\oplus}$-catalyzed hydrogenation of **96**.[167–171] The catalytic cycle has been confirmed by kinetic measurements and spectroscopic characterization of the intermediates observed for this example.

The catalyst precursor is the ionic diene adduct **98**. As hydrogen is taken up, the diene is saturated and substituted by solvent molecules, producing the solvated complex **99**. This represents the real starting point of the catalytic cycle. The first step is now the rapid establishment of an equilibrium to give the catalyst-substrate complex **100**, where the substrate is coordinated to the central atom through the double bond and the amide group. The second step, which is

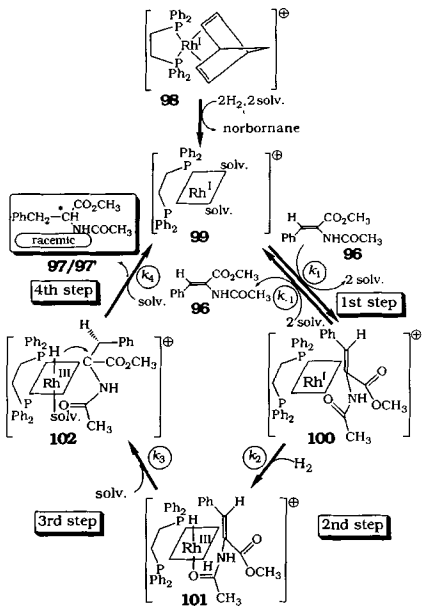

Fig. 29. The four basic steps in the catalytic cycle according to *Halpern* et al. [167–171], using as an example the [Rh(diphos)]$^{\oplus}$-catalyzed hydrogenation of **96**. The diagram shows the cycle for the production of only one enantiomer. Since an achiral catalyst is being used, the mirror-image catalytic cycle is equally justified, so that a racemate **97**/**97'** is produced. (solv. = solvent).

rate-determining at room temperature, consists of the irreversible oxidative addition of hydrogen to the central atom, forming the octahedral complex **101**. The irreversible transfer of a hydrogen atom to one of the sp^2-hybridized C-atoms leads to an alkylrhodium intermediate, which is converted into the octahedral σ-alkyl complex **102** by taking up a solvent molecule. Irreversible reductive elimination and release of the amino acid derivative then regenerates the active catalyst species for a repeat of the catalytic cycle. Kinetic measurements have shown that at temperatures below $-40\,^{\circ}C$, this final step is rate-determining, because of the high activation enthalpy. The kinetic parameters of the system studied are summarized from the literature[167] in Table 9.

Table 9. Rate constants and activation parameters for the [Rh(diphos)]$^{\oplus}$-catalyzed hydrogenation of **96** at 25 °C [167].

Step	k at 25 °C	$\Delta H^{\neq}$ [kJ mol^{-1}]	$\Delta S^{\neq}$ [J mol^{-1} K^{-1}]
1	$k_1 = 1.4 \times 10^4$ mol^{-1} s^{-1}	–	–
	$k_{-1} = 5.2 \times 10^{-4}$ s^{-1}	77	8.3
2	$k_2 = 1.0 \times 10^2$ mol^{-1} s^{-1}	26	−115.8
3	$k_3 > 1$ s^{-1}	–	–
4	$k_4 = 23$ s^{-1}	71	25

Depending on the type of catalyst, the substrate and the reaction conditions, however, the order of the individual steps has been disputed.[132, 135a, 163, 174–176] Thus, the reaction sequence depicted in Figure 30 (complexation of the substrate prior to oxidative addition) has been called the "unsaturated route" or "olefinic route"[167–171] (Path B in Fig. 30), whereas a mechanism in which the two steps are reversed is described as the "hydride route"[174–176] (Path A, Fig. 30).

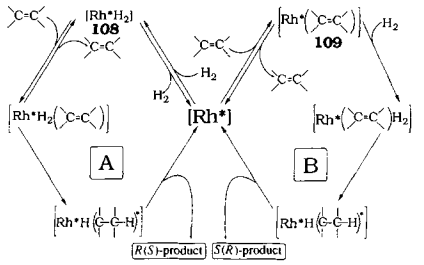

Fig. 30. According to catalyst type, substrate, and reaction conditions, homogeneous double bond hydrogenation is divided into the "unsaturated" or "olefin route" (Path B) and the "hydride route" (Path A). In reaction cycle B, the hydrogen is oxidatively added before complexation of the substrate as **109**, in cycle A the H_2-complex **108** is formed first ([Rh*] = chiral phosphanerhodium chelate complex).

For the enantioselective variant of the homogeneous hydrogenation of prochiral substrates, using rhodium catalysts containing chiral phosphane chelate ligands, the mechanistic scheme in Figure 29 must be altered such that each of the intermediates is present in two diastereomeric forms. Selectivity is derived here from two competing, diastereomeric reaction cycles. According to the mechanism presented in Figure 31, the stereochemistry of the product is fixed by the primary complexation of the substrate to the chiral catalyst. The extent of enantioselectivity in the overall reaction, however, is determined by the first irreversible step in the catalytic cycle, the oxidative addition of hydrogen.

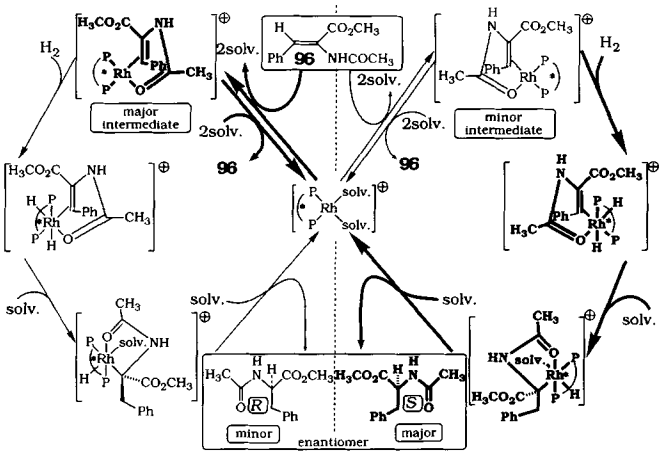

Fig. 31. Enantioselective variant of the "olefin route". The diagram shows the two diastereomeric catalytic cycles obtained when rhodium catalysts are used that contain chiral phosphane chelate ligands (P*P) (solv. = solvent).

Starting from the mechanism depicted in Figure 31, two borderline cases may be discussed. It is conceivable that the major enantiomer may be produced from a preferentially formed catalyst-substrate complex; alternatively, it may arise from the minor diastereomeric intermediate if the latter possesses far greater reactivity towards hydrogen than the major intermediate produced. The formation of the major enantiomer from the minor intermediate is probable, according to the mechanistic studies of *Halpern*. If these statements are transferred from the mechanistic diagrams of Figures 30 and 31 to the kinetic scheme of an isoinversion relationship (Fig. 13), then the asymmetric catalytic process may be represented in the simplified form shown in Scheme 3.[167, 170–172]

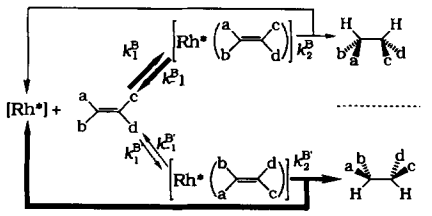

Scheme 3. Kinetic scheme of the catalytic asymmetric hydrogenation modeled on Figure 13.

Here, k_1^B and $k_1^{B'}$ represent the overall rate constants for formation of the diastereomeric catalyst-substrate adducts, while k_2^B and $k_2^{B'}$ are the sum of the rate constants for all the steps involved in formation of the hydrogenation products from the intermediates. The weighting of rate constants postulated by *Halpern* and indicated in Scheme 3 is represented schematically in Figure 15.

The enantiomeric excess that can be attained in the hydrogenation of prochiral olefins with chiral transition metal catalysts in homogeneous phase is influenced by the following parameters: the substrate (substitution pattern of the prochiral double bond), the catalyst complex (charge of the catalyst, central atom, nature of the ligands, e.g. monodentate/chelate ligands, nature of ligand chirality, nature of the coordinated phosphorous atom (phosphane, aminophosphane, phosphite etc.)) and the reaction conditions (solvent, temperature, H_2-pressure, added amine).

6.2.2. The Influence of Substrate Structure

Although the phosphanerhodium-catalyzed hydrogenation is one of the most elegant methods for synthesizing chiral compounds in high optical yields, the variety of possible substrates that can be used is very small.[132] Nonetheless, the correlation between substrate structure **96** and attainable enantiomeric excesses is a well studied area (Scheme 4).[160]

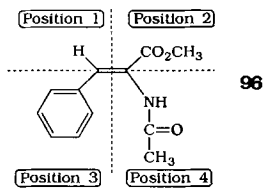

96

Scheme 4. Identification of substituent positions for analysis of the influence of the substrate structure on the enantiomeric excess in catalytic asymmetric hydrogenation.

Systematic studies have shown that the phenyl group in *position 3* of **96** can be replaced by all types of alkyl and aryl groups, and even by hydrogen.

The hydrogen atom in *position 1*, geminal to the phenyl group, cannot by substituted by any other functional group. Although (*E*)- and (*Z*)-isomeric substrates in a few cases yield the same product configuration, in many cases the (*Z*)-configurated substrate is hydrogenated faster and more selectively.[160, 177]

The functional group in the *2-position* must have electron-withdrawing character.[178] Carboxyl, carboxylate, carbonyl and cyano groups geminal to the amide group are all equally suitable for the generation of high enantiomeric excesses, though the free carboxyl group has been used most often in the past. For a variety of carboxylic esters, the *ee* value is not significantly affected by the steric requirements of the alcohol moiety.[179, 180] In a few cases, use of chiral alcohols has led to the observation of double induction.

The substituent situated in the *4-position* is the most important for achieving high enantiomeric excesses. Substituents such as NHCOR, OCOR or CH_2COOR possess a carbonyl group in the β-position to the double bond (β-carbonyl substituent). During complexation of the double bond and carbonyl functional groups to the rhodium, a chelate complex with structure **103**[160, 181] is then formed.

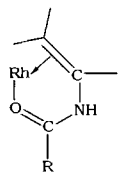

103

N-Acetyl- and *N*-benzoylenamines are usually preferred as substrates.[132]

6.2.3. The Influence of the Central Atom

In the area of homogeneously catalyzed double bond hydrogenation, rhodium complexes take a position ahead of all other transition metals with respect to activity and selectivity.[132] Chiral phosphaneruthenium complexes[182] are inferior to their rhodium analogues for hydrogenation reactions, and only a few examples of enantioselective double bond hydrogenation by cobalt[183] and titanium[184] complexes have been described. Cationic and neutral rhodium complexes, using the same phosphane ligands, yield different enantioselectivities, although no general correlation between the charge of the complex and attainable *ee* values has yet been observed.[132, 166]

6.2.4. The Influence of Ligand Structure

The carrier of the chiral information that is transferred to the substrate is the catalyst ligand system in the phosphane-rhodium complex.[155, 160] Model development has not been able to keep pace with the extensive experimental studies, so that asymmetric catalysis today still relies largely on empirical results.[132, 135, 156, 160] Nevertheless, a few guidelines can be recognized which optically active phosphorus-containing ligands must fulfill if high optical yields are to be attained in an asymmetric hydrogenation. Some of the factors that favor high enantioselectivities are, according to *Kagan*[267] and *Brunner*:[155] a) the use of bidentate ligands, b) the possibility of forming a conformationally rigid chelate ring, and c) aryl substitution on the phosphorus atoms of the chelate ligands.

From this point of view, factor (a) has an especially strong effect. Phosphorus chelate ligands are far more effective with respect to selectivity than monophosphanes.[139, 152] In com-

plexes with monodentate phosphanes, each rotamer relative to the metal–phosphorus bond is a separate catalyst species with an individual *R*/*S* selectivity. In complexes with chelate ligands, however, free rotation about the metal–phosphorus bond is abolished due to ring formation.

Most chiral 1,2-diphosphinoethanes carry their stereocenters in the carbon skeleton,[139] most effectively in the two-carbon chain connecting the phosphorus atoms.[132] In comparison, very few bisphosphanes are known with phosphorus atoms as stereocenters. One example of a ligand with chiral phosphorus atoms is the phosphane dipamp **105**.[163]

Examples of 1,2-diphosphinoethanes containing phosphorus and carbon stereocenters are even rarer in the literature. The bis(alkylphenylphosphino)pyrrolidines of type **106**, described by *Nagel* and *Rieger* et al.,[185, 186] are examples of these.

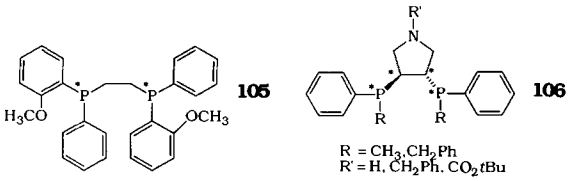

The vast majority of bisphosphanes form five- or seven-membered chelate rings with the rhodium.[132] Although efficient catalysts have now been found in both groups, the five-membered ring chelates still provide the greater number of highly selective catalyst systems.[139] Only very few chiral phosphane ligands have been described that build six-membered chelates.[142] Eight-membered and larger ring systems seem to be too flexible for effective chirality transfer.[132]

The five- and seven-membered rhodium chelate complexes that are mostly used are conformationally chiral[132, 173a] (Fig. 32) because of their non-planar conformation. The introduction of chiral ligands leads to a strongly favored preferred conformation. For a staggered five-membered-ring rhodium chelate complex, a λ-conformation (**106a**) or δ-conformation (**106b**)[187] is adopted, i.e. one of two conformations which behave like mirror images. Analogously, seven-membered chelate rings in the chair form take up a λ-conformation (**107a**) or δ-conformation (**107b**).[173a]

According to *Pavlov* et al.,[176, 185] a strict correlation must exist between catalyst conformation and the product configuration of the major enantiomer, since the chiral information is transferred to the substrate by the conformation of the chelate ring in the catalyst. In line with this argument, five-membered chelate ring complexes with λ-conformation (**106a**) and seven-membered chelates with chair-λ-conformation (**107a**) give an (*S*)-configuration in product **97**, starting from (*Z*)-*N*-acetylenamides **95**. In contrast, chelate rings with δ-conformation (**106b**) and chair-δ-conformation (**107b**) lead to the (*R*)-configurated products. Figure 32 illustrates schematically the stereochemical relationship between catalyst conformation and product configuration for bis(diphenylphosphane)rhodium complexes with a C_2-axis.[188]

In chelate complexes with chiral phosphorus atoms the configuration at the phosphorus atom merely influences the

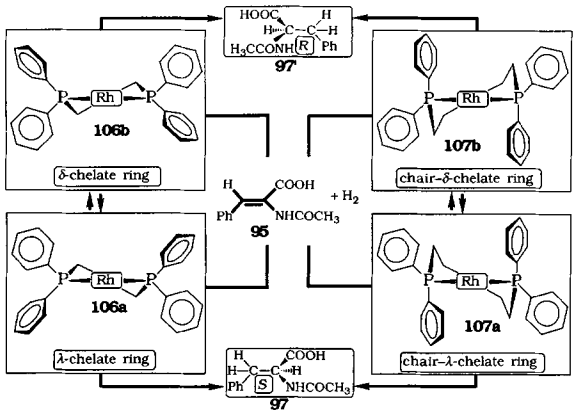

Fig. 32. Correlation between the conformation of chiral bisphosphanerhodium complexes and the product configuration of the major enantiomer in homogeneous double-bond hydrogenation.

extent of enantioselectivity, and the induced configuration in the major diastereomer remains the same.[185] The aryl substituents on the phosphorus atoms function as the actual agents of chirality transfer in asymmetric double bond hydrogenation. As a consequence of the staggered nature of the chelate ring, the phenyl groups may find themselves in either equatorial or axial position (see Fig. 32). Since the geminal phenyl rings lie almost next to one another, these two configurations are distinguished as "face exposed" or "edge exposed". The arrangement of the two phenyl groups on the phosphorus atom is therefore decided by a chirality which is determined by the shape of the chelate rings. The chiral information is then transferred from the centers of asymmetry in the chelate ring through the phosphorus phenyl groups to the catalytically active coordination sites on the metal.

According to *Brunner*,[155, 189] this chirality transfer from the ligand system must be associated with an "information smoothing" or even with a total loss of information.

From this hypothesis a concept was developed, whereby the inducing chiral center should be located directly at the site where the chirality transfer takes place. This idea of a direct interaction between the inducing chiral center and the coordination sites on the metal atom was then successfully realized for several systems, using molybdenum complexes.

The working model developed for catalytic asymmetric reactions, that of a catalyst-conformation directed product configuration,[176] displays a close relationship to the static shielding model for stoichiometric asymmetric synthesis described by *Schmierer* and *Helmchen*.[16]

On the basis of the extensive data collected, it is now possible to predict in some cases empirically which substrates and rhodium-ligand systems will lead to high enantiomeric excesses. At present, however, we cannot design an optimal catalyst system for a given substrate, or vice versa.[132, 160] Further, the selectivity of a catalyst depends largely on the reaction conditions chosen, which have to be experimentally determined for every catalyst–substrate combination.

6.2.5. *The Influence of the Solvent*

For many systems, considerable solvent effects are observed, since the mechanistic hypotheses described involve

solvent molecules in the catalytic cycle.[132, 162] (Hence, alcohols, especially methanol, and also benzene, benzene/alcohol mixtures, THF and water/alcohol mixtures have been used as solvents.) A direct correlation between a solvent property (e.g. dielectric constant) and attainable enantiomeric excess has been reported for only very few examples of homogeneous C=C double bond hydrogenation, so that solvent effects on a particular catalyst-substrate system may still be said to be unpredictable.

However, according to *Pavlov* et al., solvents with high dielectric constants inhibit the hydride route (Fig. 30, pathway A) significantly more than the reaction pathway B in Figure 30, with a consequent loss of selectivity.[176]

6.2.6. *The Influence of an Added Base*

The enantioselectivity of a particular catalyst for a given substrate is also influenced by the addition of a base (triethylamine is the most commonly used).[132, 138, 174, 175, 190, 191] In general, a reduction in selectivity is seen, which in some cases is quite considerable and can even lead to a stereoinversion of the major enantiomer.[175] The effect of added base is particularly catalyst-dependent, but also varies with substrate, and is not always clearly explicable. If unsaturated carboxylic acids are used as substrates, addition of a base will generate the anion, with the result that the equilibrium constant for catalyst-substrate complex formation will increase.[132]

According to *Ojima* et al.,[175] the olefin route may be favored over the hydride route in this manner, if one assumes that each of the two competing reaction pathways in Figure 30 leads preferentially to the opposite enantiomer. In addition, systems with added base show a different temperature and pressure dependence of the enantioselectivity.[175]

6.2.7. *The Influence of Temperature*

Data concerning the temperature dependence of attainable enantiomeric excesses at constant hydrogen pressure are only available for a few systems.[132, 160, 172, 289–291] However, it is known that the enantioselectivity of asymmetric hydrogenation is especially sensitive to temperature effects.

In several cases, an increase in enantiomeric excess is observed as the temperature falls.[161, 176, 192–194] However, catalyst-substrate systems have also been described which show the reverse behavior for optical yield, i.e., increasing temperature results in a rise in *ee* value.[174, 175] *Ojima* et al. report an improvement in optical yield from 0% to 60% on raising the temperature from 0 °C to 100 °C.[175]

One problematic aspect of temperature-dependent measurements is that reduced temperature generally leads to a severe loss of catalyst activity.[132] A loss of selectivity with a fall in temperature is explained by *Halpern*'s mechanistic theory on the origin of enantioselectivity in catalytic hydrogenation processes (Fig. 29) as follows.[170–172] High enantiomeric excesses are brought about in part by a rapid interconversion of the initial, reversibly formed catalyst-substrate complexes, compared with the reaction of these intermediates with hydrogen. In the ideal case, the starting material can, in this manner, be entirely converted into the major product enantiomer. Since the dissociation of the catalyst-substrate adduct has a larger activation enthalpy than H_2-addition (cf. $\Delta H^{\neq}$ to k_{-1} and k_2 in Table 9), at lower temperatures the interconversion process of the diastereomeric primary adducts will be "frozen", with the result that the major intermediate formed will have a higher probability of also reacting with hydrogen, leading to increased production of the minor hydrogenation product.

Ojima et al.,[175] on the other hand, explain an increase in enantioselectivity with increasing temperature as a favoring of the olefin route relative to the hydride pathway, since increasing temperature should inhibit the formation of the hydrido species [Rh*H_2] **108** (Fig. 30).[174]

The opposite temperature behavior, which has been observed by *Selke* and *Pracejus*,[194] for example, cannot be explained by the mechanistic interpretations of *Ojima* et al.[175] and *Halpern* et al.[170, 172]

Hydrogenation of amino acid precursors using carbohydrate phosphinites as chiral ligands showed a linear depen-

Table 10. Overview of the systems to determine the temperature dependence of enantioselectivity in catalytic C=C double bond hydrogenation (cod = cyclooctadiene, nbd = norbornadiene).

No.	Substrate E	Catalyst	Reaction conditions	Ref.
1	**95**	[Rh(cod)(P*P)]$^{\oplus}$ClO$_4^{\ominus}$	ethanol	[174a]
2	**95** [a]		p_{H_2} = 1 bar	[174a]
3	**96**	P*P =	[E]/[Rh] = 25	[174a]
4	**96** [a]			[174a]
5		[Rh(cod)(P*P)]$^{\oplus}$ClO$_4^{\ominus}$		[174b]
6		P*P =	ethanol p_{H_2} = 1.1 bar [E]/[Rh] = 50	[174b]
7				[174b]
8	**95**	[Rh(cod)(P*P)]$^{\oplus}$ClO$_4^{\ominus}$	ethanol	[174a]
9	**96**	P*P =	p_{H_2} = 1 bar [E]/[Rh] = 25	[174a]
10	**95**	[Rh(cod)(P*P)]$^{\oplus}$ClO$_4^{\ominus}$ P*P =	ethanol p_{H_2} = 1 bar [E]/[Rh] =100	[193a]
11		1/2 [Rh Cl(cod)]$_2$	ethanol p_{H_2} = 1 bar [E]/[Rh] =60	[193b]
12		[Rh(nbd)(P*P)]$^{\oplus}$PF$_6^{\ominus}$ P*P =	n-butanol p_{H_2} = 1 bar [E]/[Rh] =125	[289]
13		P*P =		[289]
14	**95**	1/2[Rh(nbd)$_2$]$^{\oplus}$BF$_4^{\ominus}$	ethanol p_{H_2} = 1 bar [E]/[Rh] =125	[192a]
15	**95**	1/2[Rh(nbd)$_2$]$^{\oplus}$BF$_4^{\ominus}$		[192a]
16		[Rh(P*P)$_2$]$^{\oplus}$BF$_4^{\ominus}$ P*P =	n-butanol/toluene=2/1 p_{H_2} = 1 bar [E]/[Rh] =300	[291]
17	**95**	[Rh(nbd)(P*P)]$^{\oplus}$ClO$_4^{\ominus}$	ethanol/benzene=1/1 p_{H_2} = 1.5 bar [E]/[Rh] =100	[290]
18	**95**	P*P =	ethanol/benzene=1/1 p_{H_2} = 10 bar [E]/[Rh] =100	[290]

[a] Addition of α-phenylethylamine as base; base/Rh catalyst = 3 : 1.

dence of enantioselectivity on temperature in the Eyring diagram, with a positive gradient ($\Delta\Delta H^{\neq}$ and $\Delta\Delta S^{\neq} < 0$).[194]

6.2.8. The Isoinversion Relationship for Homogeneous, Rhodium-Catalyzed Hydrogenation

Studies of temperature effects on catalytic hydrogenation have been carried out by several authors.[193, 289–291] The subject was investigated systematically by *Sinou* et al.[174] Table 10 lists the systems investigated. Here, too, plotting of the literature data (Fig. 33) gave two linear regions with an inversion point in the Eyring diagram for every system.

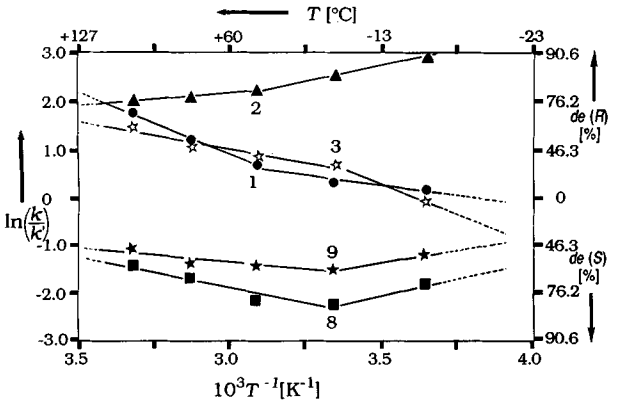

Fig. 33. Eyring diagram for the temperature-dependent *ee* values for Systems 1–3, 8 and 9 (Table 10), measured at constant pressure. The enantomeric excess was set equal to the optical yield. Ethanol was employed as solvent; at T = 100 °C, *n*-butanol served as solvent. The *ee* values were measured after complete conversion.

Analysis of the activation parameters in the sense of the isoinversion relationship yielded an isoinversion line with gradient T_i = 322 K (Fig. 34). This means that for a given pressure, optimal selectivity can be expected at this temperature for the homogeneous rhodium-catalyzed hydrogenation of prochiral substrates of type **96**.

Further, the existence of inversion points in temperature-dependent selectivity measurements teaches us that the temperature-dependent interplay of the overall rate constants in Scheme 3 determines the extent of enantioselectivity, under

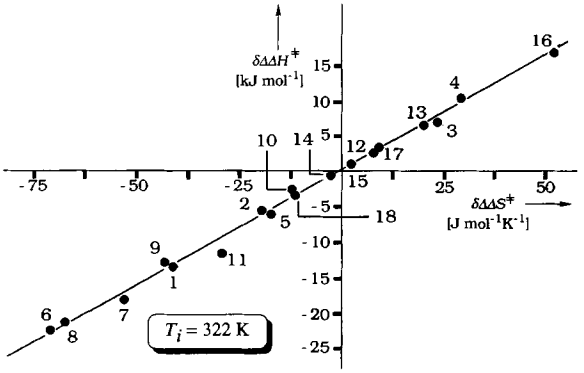

Fig. 34. $\delta\Delta\Delta H^{\neq}/\delta\Delta\Delta S^{\neq}$ diagram for the [Rh(cod)(P*P)]⊕-catalyzed hydrogenations in the homogeneous phase at constant hydrogen pressure (T_i = 322 K, correlation coefficient > 0.99).

given reaction conditions. The available data also reveal that the mechanistic statements regarding temperature-dependent selectivity by *Halpern* et al.[167–172] on the one hand, and *Ojima* et al.,[175] *Sinou* et al.[174] and *Pavlov* et al.[176] on the other may be valid for many systems in a particular temperature region, but they cannot explain simply a changed or inverse temperature dependence in another temperature range. Temperature does not have an isolated effect in one catalytic step, but in the dynamic model of the isoinversion relationship according to Scheme 3 it can lead to a reweighting of the enthalpy/entropy dominance in selectivity-determining partial steps.

6.2.9. The Influence of Hydrogen Pressure

Depending on substrate and catalyst structure, the hydrogen pressure may also have a significant influence on stereoselectivity at a given reaction temperature, since H_2-addition constitutes an important step in the catalytic cycle.[132, 196, 197] A series of systems are known where increasing hydrogen pressure leads to a loss of selectivity,[160, 174, 175, 185, 195] in some extreme cases even to an inversion of the configuration of the major enantiomer.[175] However, a few examples are also known where the stereoselectivity shows a reversed[176, 197] pressure dependence, or no dependence at all in the range measured.[176, 194] According to *Halpern* et al.,[160, 170, 172] the reduction in selectivity with increased pressure can be explained by an increased rate of hydrogen addition, with a simultaneous, relative decrease in the interconversion process between the two diastereomeric catalyst-substrate complexes. The stereochemistry is hence primarily determined by the initial step, and retrocleavage loses importance as a second selectivity level. For this mechanistic theory, the selectivity process requires low hydrogen pressures and high temperatures for high enantiomeric excesses. Since the activity of the catalyst increases considerably as the H_2-pressure rises, the loss of selectivity must be compensated for by an increase in reaction temperature.

Ojima et al.[175] and *Sinou* et al.[173] trace the loss of selectivity at higher hydrogen pressure to a contraselective favoring of the hydride route, with preferential formation of the [Rh*H_2] species **108** rather than the primary catalyst-substrate adduct **109** (see Fig. 30). However, neither selectivity mechanism can explain a changed or reversed pressure dependence of selectivity in the range studied.

6.2.10. The Pressure Analogue of the Isoinversion Relationship in Homogeneous, Rhodium-Catalyzed Hydrogenation

If *Ojima* and *Sinou*'s experimental data on pressure-dependent selectivity are plotted on a $\ln(k/k')/p$ diagram, then for a single system, two linear regions with an inversion point can again be recognized. The results from a selection of the systems listed in Table 11, where enantioselectivity has been measured with respect to temperature, are presented in Figure 35, in the form of a $\ln(k,k')/p$ diagram.

For pressure-dependent *ee*-value determinations, the gradient of a linear $\ln(k/k')/p$ correlation at a constant temperature gives, according to Equation (12), the activation vol-

Table 11. Overview of the systems studied by *Ojima* et al. [175], *Sinou* et al. [174] as well as *Nagel* and *Rieger* [185] to determine the enantioselectivity at constant temperature as a function of the hydrogen pressure.

No.	Substrate	P*P[a]	T[°C]	Ref.
1	**95**		25	[174a]
2 [b]	**95**		25	[174a]
3	**96**	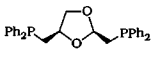	25	[174a]
4 [b]	**96**		25	[174a]
5 [c]	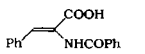	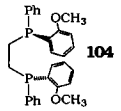 **104**	25	[175]
6			25	[175]
7			50	[175]
8 [c]	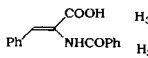	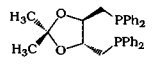	25	[175]
9			25	[175]
10			50	[175]
11 [c]	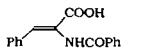	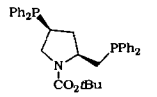	25	[175]
12			25	[175]
13			50	[175]
14 [c]	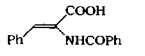	**104**	25	[175]
15			25	[175]
16			50	[175]
17 [c]	**95**	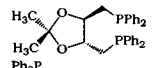	25	[175]
18	**95**		25	[175]
19	**95**		50	[175]
20 [c]	**95**	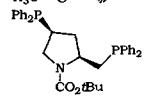	25	[175]
21	**95**		25	[175]
22	**95**		50	[175]
23	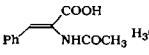	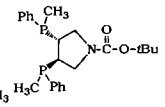	22	[185]
24		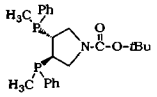	22	[185]
25	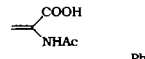		25	[174b]
26	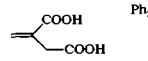	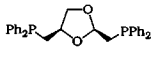	25	[174b]

[a] In the case of the Systems No. 1–13, 25 and 26 [(P*P)Rh(cod)]ClO_4 was used as catalyst, in the case of Systems No. 14–22 [(P*P)Rh(cod)Cl], and in the case of systems No. 23 and 24 [(P*P)Rh(cod)]BF_4. [b] In the Systems No. 2 and 4 α-phenylethylamine **89** was added to the catalyst in the ratio 3:1. [c] In the Systems No. 5, 8, 11, 14, 17 and 20 triethylamine was added in the ratio 2:1 to the catalyst.

ume difference $\Delta\Delta V^{\neq}$.[198–200] k, k' are the overall rate constants leading to the major and minor enantiomers respectively, in rhodium-catalyzed asymmetric hydrogenation.

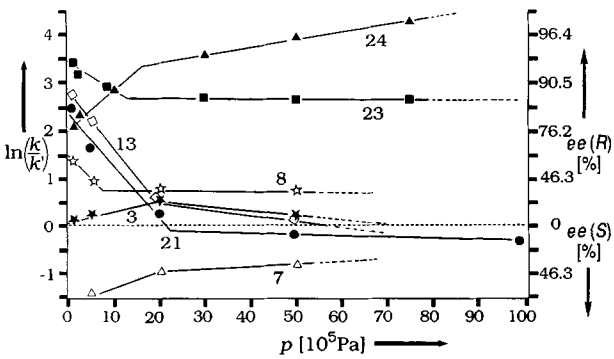

Fig. 35. $\ln(k/k')/p$ diagram for pressure-dependent *ee*-value measurements at constant temperature. A few selected systems are shown (Systems 3, 7, 8, 13, 21, 23, 24 in Table 11). An inversion pressure p_{inv} is assigned to the inversion point.

As for an Eyring diagram, in systems with two linear regions an inversion pressure p_{inv} may be assigned to the inversion point. This divides the pressure range into a high-pressure region ($p > p_{inv}$) and a low-pressure region ($p < p_{inv}$).

$$\Delta\Delta V^{\neq} = -RT\left(\frac{\partial \ln\left(\frac{k}{k'}\right)}{\partial p}\right)_T \tag{12}$$

The intercept on the ordinate at $p = 0$ in a $\ln(k/k')/p$ diagram corresponds to an activation entropy difference $\Delta\Delta S^{\neq}$ [Eq. (13)], analogously to the Eyring approach for stereoselective reactions. This demonstrates the formal equivalence of activation volume and activation enthalpy differences, and hence the formal equivalence of the parameters p and T^{-1}.

$$\lim_{p \to 0}\left(\ln\left(\frac{k}{k'}\right)\right) = \frac{\Delta\Delta S^{\neq}}{R} \tag{13}$$

The isoinversion principle derived from temperature-dependent selectivity measurements at constant pressure can also be applied for pressure-dependent selectivity measurements at constant temperature, by using Equation (14), which relates the activation volumes for the high- ($\Delta\Delta V_2^{\neq}$) and low-pressure ($\Delta\Delta V_1^{\neq}$) regions to each other.

$$\delta\Delta\Delta V^{\neq} = \Delta\Delta V_2^{\neq} - \Delta\Delta V_1^{\neq} \tag{14}$$

If one now plots the parameters $\delta\Delta\Delta V^{\neq}$ and $\delta\Delta\Delta S^{\neq}$ in a volume/entropy diagram, then here, too, the vast majority of systems[266] in Table 11 display a linear relationship. $\delta\Delta\Delta S^{\neq}$ can be calculated analogously to Equation 5 from the entropy values for the low- and high-pressure regions. The regression curve passes directly through the coordinate origin (Fig. 36).

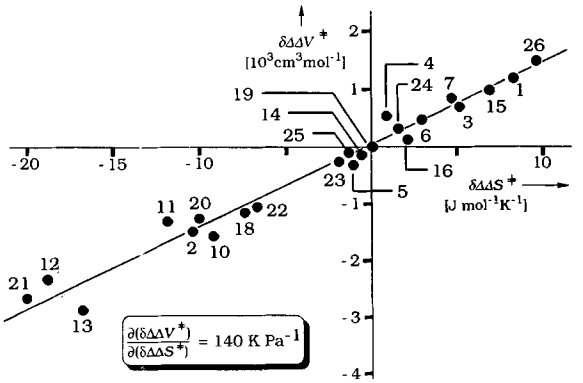

Fig. 36. $\delta\Delta\Delta V^{\neq}/\delta\Delta\Delta S^{\neq}$ diagram (correlation coefficient = 0.98) for the systems in Table 11. Systems 8, 9 and 17 have been disregarded in this diagram, as their deviations in the $\delta\Delta\Delta V^{\neq}/\delta\Delta\Delta S^{\neq}$ value were too high [266].

Figure 36 shows that a common relationship exists for the dominance change in the activation parameters $\Delta\Delta V_{1,2}^{\neq}$ and $\Delta\Delta S_{1,2}^{\neq}$ in the partial selectivity steps of homogeneous rhodium-catalyzed double bond hydrogenation. This relationship is independent of the *ee* value actually obtainable, and therefore also of the factors affecting the reaction-specific *ee* val-

ue, e.g. catalyst, substrate, added amine, temperature, and pressure.

The gradient of the line in Figure 36 is 140 K Pa^{-1}. The pressure analogue isoinversion diagram in Figure 36 yields an optimal pressure p_i for a given reaction temperature T in the selectivity process studied. (Eq. 15).

$$p_i = T\left(\frac{\partial(\delta\Delta\Delta V^{\neq})}{\partial(\delta\Delta\Delta S^{\neq})}\right)^{-1} \tag{15}$$

A comparison between the isoinversion relationship for temperature inversion (Fig. 34) and the isoinversion relationship for pressure inversion (Fig. 36) shows that here, too, p and T^{-1} are corresponding quantities, since the $\delta\Delta\Delta V^{\neq}/\delta\Delta\Delta S^{\neq}$ diagram (Fig. 36) incorporates the corresponding $\delta\Delta\Delta H^{\neq}/\delta\Delta\Delta S^{\neq}$ diagram, on the basis of Equation (16).

$$\delta\Delta\Delta H^{\neq} = \delta\Delta\Delta V^{\neq} \times p \tag{16}$$

From this it is clear that a pair of values exists (p_i/T_i), for which optimal selectivity will be observed for a given system [Eq. (17)].

$$p_i(T_i = 322\ \text{K}) = 2.3 \times 10^5\ \text{Pa} \tag{17}$$

6.3. Diastereoselective Heterogeneous Hydrogenation of the C=C Double Bond

Sheehan and *Chandler* have studied numerous examples of heterogeneous-phase asymmetric hydrogenation of the C=C double bond in chiral α,β-unsaturated amides of type **110**.[202] After removal of the chiral auxiliary, they obtained enantiomeric excesses between 6% and 39% [Eq. (18)]. Further works are described in Refs. [203–208].

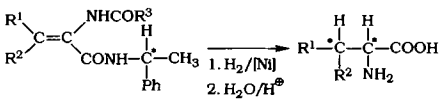

(18)

110 **a**, $R^1 = R^2 = R^3 = CH_3$ valine 39% *ee*
b, $R^1 = R^2 = CH_3$, R^3 = Ph valine 18% *ee*
c, R^1 = H, $R^2 = R^3$ = Ph phenylalanine 6% *ee*

To explain the steric course of the reaction, a model **111** was developed corresponding to the Prelog rule.[111] In this model, the carbonyl and the alkene units are arranged *trans* to each other , and the carbonyl group is fixed between the H atom and the methyl group of the chiral center in staggered conformation so that attack can occur from the sterically less hindered face.

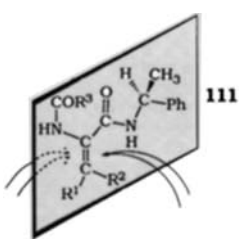

111

Harada and *Takasaki* have studied the temperature-dependence of the palladium-catalyzed hydrogenation of chiral *N*-acetyldidehydroalaninamides **112** in various solvents [Eq. (19)].[209]

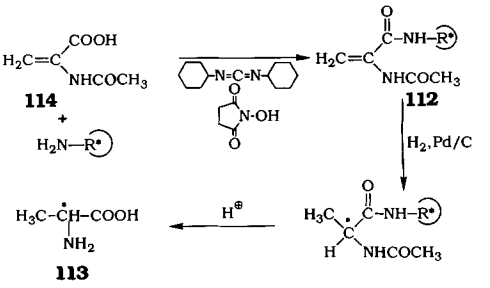

(19)

The enantiomeric excesses obtained for the product alanine **113** lie in the range 0 to 24%, while the chemical yield reaches 78–98%. The chiral *N*-acetyldidehydroalaninamides **112** were synthesized by the reaction of *N*-acetyldidehydroalanine **114** with the corresponding chiral amine and dicyclohexylcarbodiimide in the presence of *N*-hydroxysuccinimide.

Table 12 gives an overview of the systems studied and the solvents used.

Table 12. Overview of the systems whose stereoselectivity according to equation (19) has been studied with respect to temperature. The numbers assigned to the chiral amine components H_2N-(R•), with which **114** was allowed to react, and the solvents used, are as in Figure 38.

H_2N—(R•) \ Solvent	MeOH	EtOH	iPrOH	AcOEt
89	1	2	3	4
115	5	6	7	8
116	9	10	11	12

6.3.1. The Influence of Temperature and the Isoinversion Relationship for Diastereoselective, Heterogeneous C=C Double-Bond Hydrogenation

If one analyzes the published data on temperature-dependent stereoselectivity, one finds two linear regions and an inversion point here, too. Figure 37 shows the temperature dependence of several typical systems from Table 12.

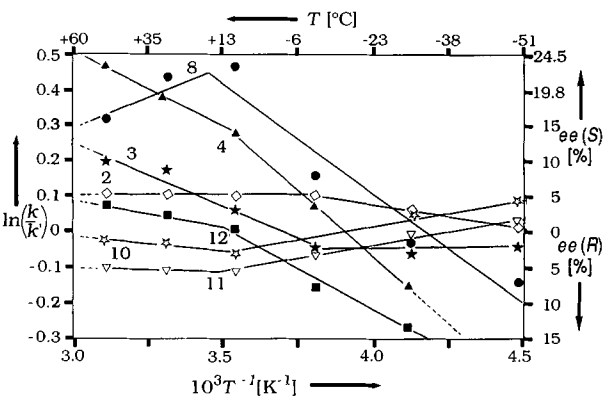

Fig. 37. Temperature-dependent course of stereoselectivity for a few typical systems (Systems 2–4, 8, 10, 11 and 12) from Table 12, in the form of an Eyring diagram.

Significantly better selectivities can be attained in catalytic hydrogenation when ethyl acetate is used as solvent, rather than alcohols. Further, it turns out that by varying the temperature a stereoinversion of the chiral C-atom in alanine may be achieved.

Analysis of the temperature-dependent selectivity in the sense of the isoinversion relationship gives a zero-point curve in the $\delta\Delta\Delta H^{\neq}/\delta\Delta\Delta S^{\neq}$ diagram, with $T_i = 293$ K (Fig. 38).

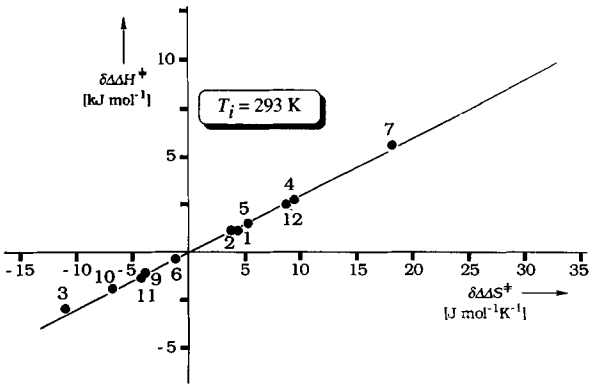

Fig. 38. The isoinversion line (correlation coefficient > 0.99) for heterogeneous, palladium-catalyzed hydrogenation of the C=C double bond in chiral amides of the type **110**, according to Equation (19) (Table 12).

The authors do not present a mechanistic model which could explain the temperature course of stereoselectivity. However, in the light of the isoinversion relationship, the following conclusions may be drawn: In the Eyring diagram, all the systems reveal generally small activation enthalpy differences and large activation entropy differences in both the high- and low-temperature regions. Throughout the temperature range studied, the stereoselectivity is largely determined by entropy effects, due to the complex equilibria responsible for formation of the diastereomeric, activated catalyst-substrate complexes. The relatively weak interactions which are responsible for adsorption of the substrate molecule onto the catalyst surface act to strengthen the unfavorable entropy term, so that overall the stereoselectivity attainable is only moderate. The molecular cause is presumably an equal weighting of the diastereomeric catalyst-substrate complexes with regard to formation and further reaction.

Ikeda and *Yamagishi* et al.[288] studied the diastereoselective hydrogenation of the C=C double bond in dehydrodipeptides[287] with achiral rhodium catalysts in homogeneous phase. The analysis of the data yields the isoinversion temperature $T_i = 308$ K.

6.4. Hydrogenolytic Asymmetric Transaminations (Heterogeneous Hydrogenation of the C=N Double Bond)

Numerous non-enzymatic, asymmetric syntheses of α-amino acids from the corresponding α-keto acid precursors have been reported in the literature.[210-222] A common feature of these reactions is the catalytic asymmetric reduction of a C=N double bond within a chiral starting compound.[223, 224]

Starting with a carbonyl compound (usually an α-keto acid) and an optically active amine, a chiral Schiff-base (**117**) is generated. This can then be converted into an optically active α-amino acid by catalytic reduction and subsequent hydrogenolytic cleavage of the C–N bond. The entire sequence is described as hydrogenolytic asymmetric transamination (Fig. 39),[225, 226] in analogy to biochemical processes.[232]

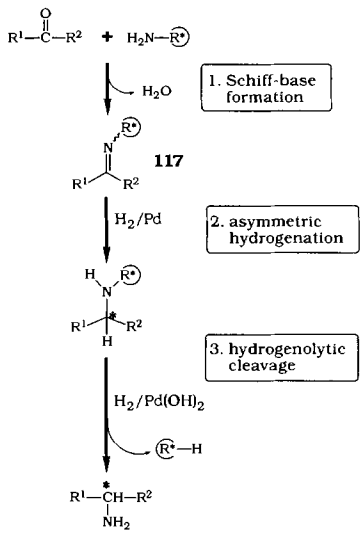

Fig. 39. Schematic diagram of hydrogenolytic asymmetric transamination. An optically active Schiff base **117** is generated from a keto component R–CO–R′ and a chiral amine H_2N-Ⓡ*. This is then hydrogenated in the stereoselective step, with heterogeneous palladium catalysis. Subsequent hydrogenolytic cleavage to remove the chiral auxiliary Ⓡ*–H yields an optically active amino acid derivative.

A fundamental disadvantage of this chemical chirality transfer from a chiral amine to a keto-compound is the loss of the original chirality carrier by cleavage of the C–N bond in the final step. Building on work by *Hiskey* and *Northrop*,[214, 219] who obtained amino acids from α-substituted benzylamines in optical purities of 12–81% and chemical yields of 20–80%, *Harada* et al.[210, 211, 215–217, 220–222, 227–231] carried out a very intensive study of the asymmetric transamination reaction. They showed that the attainable enantiomeric excesses in the product α-amino acids are dependent on the following parameters, if one starts from α-keto acids or α-keto esters and primary, α-substituted benzylamines or amino acid esters: the chiral amine component H_2N-R*,[223, 224] the nature of the α-keto acid derivative[223, 224] R^1-(C=O)-R^2 (R^1 = Me, R^2 = COOH or COOR′), the solvent,[221, 223, 224, 227–230] and the reaction temperature.[210, 211, 223, 224]

6.4.1 *The Influence of Amine and α-Keto Acid Structure*

The optical yields using α-phenylethylamine **89** are consistently higher than for the corresponding α-phenyl-*n*-propylamine **115** (cf., e.g., Nos. 4 and 8 in Fig. 37). The highest enantiomeric excess obtained so far has been with α-(1-naphthyl)ethylamine **116**. If the (*S*)-configuration amine is used in the reaction, the (*S*)-amino acid is usually obtained.

The *ee* values reached are very sensitive to the nature of the R^1 group in the keto component. However, no general-

ized correlation can be established between the size of the R^1 group and the *ee* value. With **89**, the following rankings were found for the R^1 residues: $CH_3 > CH_2COOH > C_2H_5 > Ph > CH_2Ph > CH_2CH_2COOH$. (" > " = higher *ee* values obtained under otherwise identical conditions). These rankings can be considerably changed, however, by altering the amine component.

The use of α-keto esters rather than the free acids has no significant effect on the enantiomeric purity of the amino acid synthesized (R^2 = COOH or COOR'), even if esters of chiral alcohols such as menthol **14** are employed (double induction). The (*E*)/(*Z*) ratio of the Schiff base **117** formed from the α-keto acid and the chiral amine ought to have no effect on the stereoselectivity.

6.4.2. *The Influence of Solvent and Temperature*

Hydrogenolytic transamination (Fig. 39) is very sensitive to solvent effects. If polar solvents (e.g. methanol, water) are used, lower enantiomeric excesses are generally found (30–50% *ee*) than for less polar solvents such as benzene, dioxane, ethyl acetate or tetrahydrofuran (60–80% *ee*). In many examples, a nearly linear relationship can be seen between the optical purity of the product amino acid and the dielectric constants of the solvent employed, under otherwise identical reaction conditions.

Asymmetric, palladium-catalyzed hydrogenation of the C=N double bond also shows a significant temperature effect.[210, 211, 228–230] Stereoinversion of the asymmetric reaction can be achieved merely by changing the temperature.

A series of systems exist which reveal only one linear region in the Eyring diagram for the temperature range studied.[211, 230] Others are also known, however, whose temperature-dependent stereoselectivity yields two linear regions with an inversion point.[210, 211, 228, 229, 285, 286] One example of a system whose temperature-dependent stereoselectivity is characterized by two linear regions is the hydrogenation of Schiff bases of type **117**, which can be synthesized from pyruvic acid or pyruvic acid esters and various chiral amines.[210, 211, 228, 229, 285]

Table 13 gives an overview of the systems studied. In Figure 40, some characteristic systems of temperature-dependent enantiomeric excess measurements are presented, both as an *ee* value/temperature diagram (top) and as the corresponding Eyring diagram (bottom).[210, 211]

Table 13. Overview of several systems whose stereoselectivity in the palladium-catalyzed hydrogenation of Schiff bases of type **117** has been studied with respect to temperature..

117

No.	R^1	R^2	Ⓡ*	Configuration at C* of Ⓡ*	Solvent	Ref.
1	CH_3	CO_2Et	CH(Ph)-CH_3	*R*	ethanol	[210]
2	CH_3	CO_2Et	CH(Ph)-CH_3	*S*	ethanol	[210]
3	CH_3	CO_2Et	CH(Ph)-Et	*R*	ethanol	[210]
4	CH_3	CO_2Et	CH(CH_3)-1-naphthyl	*S*	ethanol	[210]
5	CH_3	CO_2Et	CH(CH_3)-1-naphthyl	*R*	ethanol	[211]
6	CH_3	CO_2Et	CH(Ph)-CH_3	*R*	ethyl acetate	[210]
7	CH_3	CO_2Et	CH(Ph)-CO_2Et	*R*	methanol	[229]
8	CH_3	CO_2Et	CH(Ph)-CO_2Et	*R*	benzene	[229]
9	CH_3	CO_2H	CH(Ph)-CH_2OH	*R*	aqueous alkaline solution	[285]
10	Et	CO_2H	CH(Ph)-CH_2OH	*R*	ethanolic alkaline solution	[285]
11	CH_3	CO_2CH_3	CH(CH_3)-CO_2CH_3	*S*	methanol	[228]
12	CH_3	CO_2CH_3	CH(CH_3)-CO_2CH_3	*S*	ethyl acetate	[228]
13	CH_3	CO_2CH_3	CH(CH_3)-CO_2Et	*S*	methanol	[228]
14	CH_3	CO_2CH_3	CH(CH_3)-CO_2*i*Pr	*S*	methanol	[228]
15	CH_3	CO_2CH_3	CH(CH_3)-CO_2*t*Bu	*S*	methanol	[228]
16	CH_3	CO_2CH_3	CH(Et)-CO_2CH_3	*R*	methanol	[228]

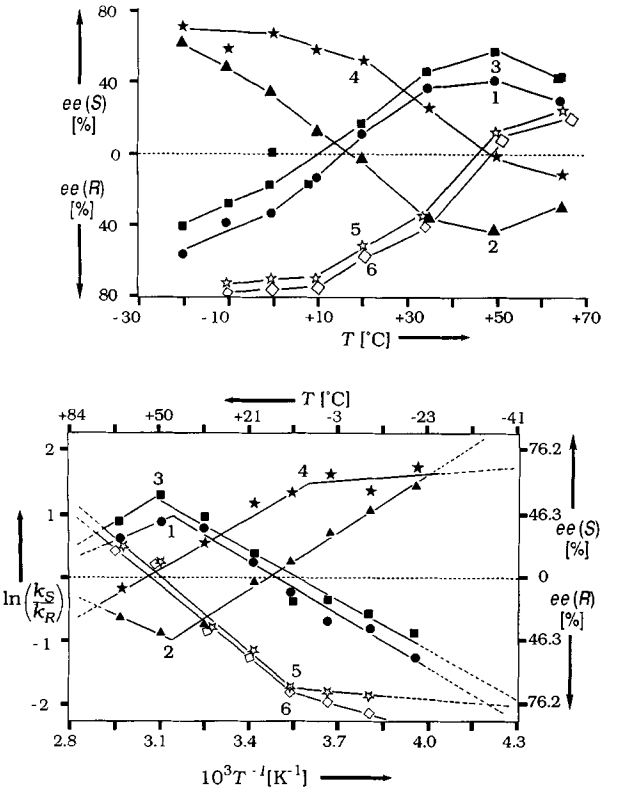

Fig. 40. Top: *ee* value/temperature diagram for the Systems 1–6 listed in Table 13. Bottom: Corresponding Eyring diagram for the Systems 1–6 listed in Table 13. To determine the enantiomeric excesses given, the alanine obtained after hydrogenolysis was converted into the corresponding dinitrophenyl derivative [210].

The results show very nicely that if chiral information carriers of opposite configuration are used (e.g. Systems 1 and 2, Table 13), an almost identical temperature dependence is observed, but with opposite sign. This is expected for enantiomers of equal optical purity.

With many systems, the influence of temperature can be used to achieve an inversion of stereochemistry at the newly formed chiral center. If one transforms the activation parameters $\Delta\Delta H^{\ddagger}_{1,2}$ and $\Delta\Delta S^{\ddagger}_{1,2}$ from the Eyring diagram into $\delta\Delta\Delta H^{\ddagger}$ and $\delta\Delta\Delta S^{\ddagger}$ values in the sense of the isoinversion relationship, then one also obtains an isoinversion diagram with a zero-point curve (T_i = 303 K, Fig. 41), independent of the solvent and the nature of the substituents R^1, R^2 and Ⓡ* in **117**.

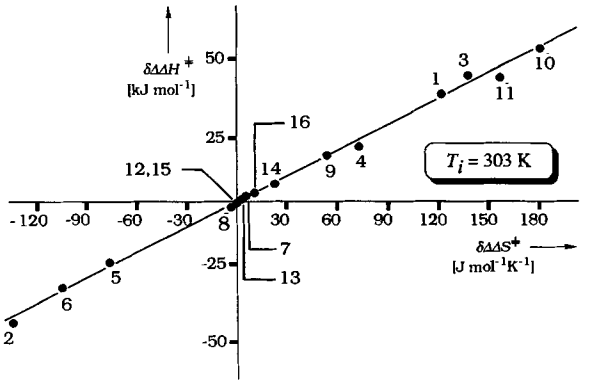

Fig. 41. The isoinversion line (correlation coefficient > 0.99) for hydrogenolytic transamination as in Figure 39 (T_i = 303 K); numbering of systems as in Table 13.

6.4.3. *Mechanistic Considerations on Hydrogenolytic Transamination in the Light of the Isoinversion Relationship*

The temperature and solvent dependence of stereoselectivity in palladium-catalyzed, hydrogenolytic, asymmetric transamination is explained by *Harada* as due to the appearance of intermediates **118**, which are in equilibrium with non-chelated particles **119** (Fig. 42),[210, 211, 215–217, 220, 221, 227–231] if Schiff bases of the type **117** ($R^1 = CH_3$, $R^2 = CO_2Et$) are used.

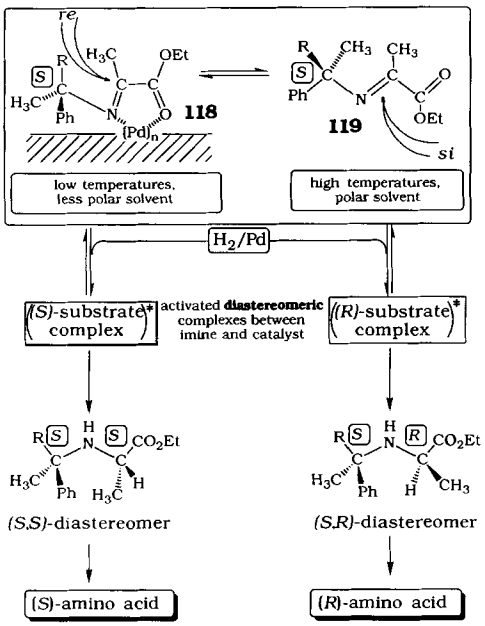

Fig. 42. Schematic diagram of the "chelation model" developed by *Harada* et al. showing the Schiff base **117** with $R^1 = CH_3$, $R^2 = CO_2Et$ as example.

In this theory, the imine **117** is fixed to the catalyst surface by formation of a five-membered chelate complex **118** before hydrogenation takes place. In the stereoselective hydrogenation step, an activated complex forms between this five-membered cyclic intermediate and the catalyst, such that the metal attacks the chelated species from the sterically less hindered face. In the example in Figure 42, attack takes place from the *re*-face of the fixed intermediate, so that one finally obtains the (*S*)-amino acid in excess. If the reaction temperature is increased, then the population of chelated intermediate **118** falls, because of the weak interaction between substrate and catalyst, and the proportion of the unfixed species **119** rises. In the stereoselective step the non-chelated intermediate **119** is also attacked from the sterically less hindered face, so that in the example given, an *si*-face attack takes place, and an (*R*)-amino acid is preferentially generated.

With the help of the equilibrium between chelated and unfixed intermediates, the influence of the solvent on stereoselectivity can also be explained.[221] In less polar solvents the formation of the five-membered chelate complex **118** is favored, partly because the electrostatic interaction between substrate and catalyst is more pronounced than in polar solvents, and partly because the substrate is less strongly solvated, increasing the tendency to form the chelate complex **118**. In polar solvents the reverse is true; the interaction between catalyst and substrate is weaker, and the formation of a chelate complex is hindered by stronger solvation of the substrate. According to the working hypothesis,[210, 211] the extent of stereoselectivity is determined by equilibrium between the chelated species and unfixed species, which takes place before the actual hydrogenation.

The chelation model developed by *Harada* et al.,[210, 211] which is generally applied to Schiff bases of the type **117**, does not, however, take into account the complex events in this heterogeneous reaction that are responsible for forming diastereomeric, activated complexes of substrate and catalyst. Complex equilibria between substrate and catalyst lead to two diastereomeric reaction channels, both for a chelated intermediate and for an unfixed species. The cross-section of these channels depends both on the temperature and on the solvent used. The preliminary equilibrium and the equilibria in the stereoselective step together determine the temperature course of stereoselectivity. If it were solely the equilibrium between chelated species and unfixed species that were responsible for the temperature dependence of stereoselectivity under otherwise identical conditions, then the Eyring diagram would contain merely one linear region, and large $\Delta\Delta H^{\ddagger}$ and even larger $\Delta\Delta S^{\ddagger}$ values would be expected. The influence of entropy is considerably larger in a chelation equilibrium than in a comparable conformation equilibrium. Indeed in each of the systems studied, a temperature interval was observed which was characterized by very large activation entropy differences. In this region, an equilibrium between fixed and unfixed particles may indeed be largely responsible for the temperature course of stereoselectivity. At the inversion temperature T_{inv}, i.e., at the changeover for entropy and enthalpy in the weighting of the selectivity process, the later equilibria between substrate and catalyst determine the temperature course. Here too, the fact that all systems belong to the isoinversion relationship teaches us that at particular temperature intervals the influence of enthalpy and entropy on a complex reaction course can be weighted differently. The observed temperature dependence of stereoselectivity cannot be explained by a change of mechanism, but by the temperature-dependent interplay of enthalpy and entropy in the selectivity-determining partial step concerned.

6.5. Catalytic Hydrogenation of the C=O Double Bond

In the case of the hydrogenation of methyl acetoacetate with modified Raney-nickel catalysts (modifying reagents: tartaric acid, amino acids) in heterogeneous phase the temperature dependence of enentioselectivity yields an isoinversion line with gradient $T_i = 321$ K.[272] Within experimental error, this value is identical to the T_i-value for homogeneous-phase rhodium-catalyzed hydrogenation.

The enantioselective hydrogenation of α-keto esters with chiral modified platinum catalysts in the heterogeneous phase yields the isoinversion temperature $T_i = 313$ K,[301] a slightly lower value. However, the use of homogeneous rhodium catalysts with constant type of substrate leads to $T_i = 229$ K.[302] In the palladium-catalyzed, heterogeneous hydrogenation of chiral α-keto amides $T_i = 291$ K is found. This is an example of a diastereoselective hydrogenation of the C=O double bond.[230, 303]

7. Further Examples of the General Applicability of the Isoinversion Principle in Chemistry

The isoinversion principle is not only applicable to stereoselective reactions. The following, randomly chosen examples show that this principle can apply whenever a selectivity process with competing reaction channels can be reduced to a simple scheme (Fig. 13), in which the starting materials are in equilibrium with reactive intermediates that can react in different ways. The partial steps differ in their activation enthalpy and entropy and therefore dominate in different temperature ranges, leading to an isoinversion relationship.

7.1. Temperature Dependence of Polymer Phosphorescence

Guillet et al.[233] have studied the temperature dependence of the phosphorescence intensity of polymer films. The inversion points that appear in the corresponding Eyring diagram result from transitions in the mobility of segments or side chains.[233] A knowledge of such transitions is interesting for an assessment of the material characteristics of polymers. During polymer film production, carbonyl groups arise by oxidation. These, like those already present, display an absorption maximum at 310 nm and a phosphorescence maximum at 460 nm.

One of the groups of polymers studied by *Guillet* et al.[233] is: polystyrene, carbonyl-containing copolymers of styrene and polystyrene-containing benzophenone (Table 14). The inversion points lie in a temperature range between 175 and 183 K (Fig. 43) and are therefore identical with the respective transition temperatures T_γ for the mobility of the phenyl moiety (rotation about the C–C single bond).

Table 14. Thermodynamic data for the transition in phenyl group mobility of polystyrene (PS(1), PS(2)), and copolymers of styrene and benzophenone-containing polystyrene.

No.	Polymer	ΔS_1 [J mol^{-1}K^{-1}]	ΔH_1 [kJ mol^{-1}]	Tγ [K]	ΔS_2 [J mol^{-1}K^{-1}]	ΔH_2 [kJ mol^{-1}]	$\delta\Delta S$ [J mol^{-1}K^{-1}]	$\delta\Delta H$ [kJ mol^{-1}]
1	PS-phenyl isopropenyl ketone	- 81.2	- 28.8	186	61.7	- 2.2	142.9	26.6
2	PS-phenyl vinyl ketone	- 61.3	- 24.9	185	65.7	- 1.4	127.0	23.5
3	PS-naphthyl(methacrylate)	- 64.6	- 22.3	190	11.1	- 8.0	75.7	14.3
4	PS-benzophenone	- 87.4	- 29.3	185	63.4	- 1.8	150.8	28.0
5	PS-5-hexen-2-one	- 80.8	- 23.2	171	43.0	1.9	123.8	21.1
6	PS-methyl vinyl ketone	- 81.7	- 21.3	176	16.5	- 4.1	98.2	17.2
7	PS-methyl isopropenyl ketone	- 87.7	- 22.2	181	17.8	- 3.1	105.5	19.1
8	PS (1)	- 77.7	- 19.3	176	22.3	- 1.7	100.0	17.6
9	PS (2)	- 83.1	- 19.7	172	21.9	- 1.6	105.0	18.1

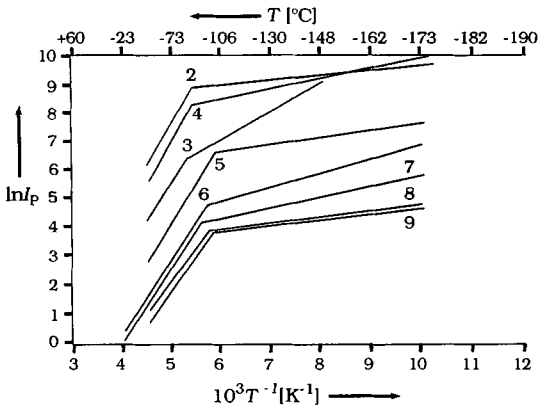

Fig. 43. Temperature-dependent phosphorescence intensities I_p measured for various polymers in Table 14, as an Eyring diagram (Systems 2–9). (The data points are too numerous to be shown individually.)

7.1.1. *The Causes of Temperature Dependence for Phosphorescence*

The simplified *Jablonski* scheme (Fig. 44) shows that the phosphorescence quantum yield ϕ_P is given by Equation (20).

$$\phi_P = \phi_{isc}\left(\frac{k_P}{k_P + k_Q}\right) \tag{20}$$

ϕ_{isc} is the quantum yield for intersystem crossing, k_P the phosphorescence rate, i.e., rate of $T_1 \rightarrow S_0$ transition, k_Q the total rate of all quenching processes.

Phosphorescence is quenched predominantly by oxygen diffusing into the system.[234] Although intersystem crossing (ϕ_{isc}) and phosphorescence (k_P) show a slight temperature dependence (entropy-determined), the temperature behavior of the quenching process (k_Q) is controlled by the temperature dependence of diffusion (enthalpy-determined). Because the weighting of the competing processes with respect to enthalpy and entropy differs, one of the two processes dominates in each of the temperature regions (Fig. 44).

If one considers the polymer film/oxygen system on a molecular scale, one finds that at temperature T_γ the phenyl

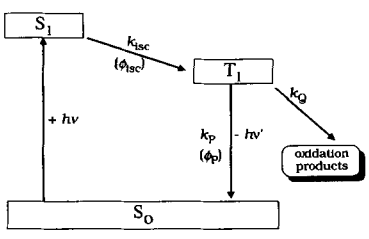

Fig. 44. Simplified Jablonski scheme for phosphorescence quenching. The equilibrium in the sense of the isoinversion principle is in this case a photostationary equilibrium. The irreversible reaction of excited species is here the formation of oxidation products by the quenching process.

rings of the styrene units become mobile. The tangled polymer then expands, and oxygen can diffuse in more rapidly. Since this system obeys the isoinversion principle (T_i = 188 K, Fig. 45), the transitions at T_y are all of the same type.

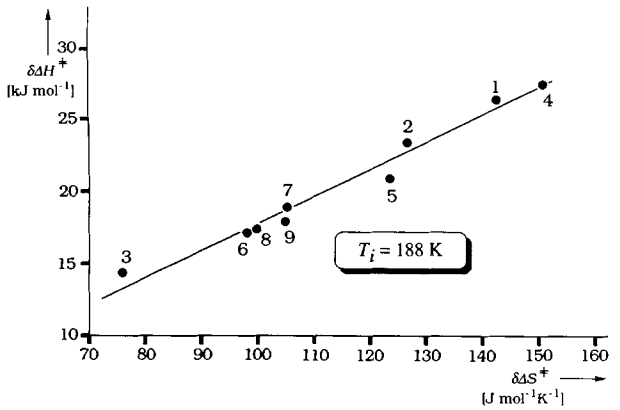

Fig. 45. Isoinversion diagram for the temperature-dependent phosphorescence of polystyrene-containing copolymers (Table 14). In this case the diagram is a $\delta\Delta H^*/\delta\Delta S^*$-diagram ($T_i$ = 188 K, correlation coefficient > 0.99).

The transition from one process to the other (phosphorescence and its quenching by oxygen) is associated with a distinct phase transition. Therefore T_{inv} is nearly equal for all systems. For simple mathematical reasons, in such a case $T_i \approx T_{inv}$. Because of the substraction of the activation parameters ($\delta\Delta H^{\neq}$, $\delta\Delta S^{\neq}$) during derivation of T_i the differences in the y ordinates vanish. In contrast to the examples mentioned so far in which the competing reactions produce different amounts of the two stereoisomeric products (two-dimensional process), in this case the two competing reactions determine only one variable quantity (ϕ_P). Therefore this process can be described as one-dimensional.

7.2. Photoisomerization of Nitrones to Oxaziridines

On irradiation, nitrones **120** isomerize to oxaziridines **121** [Eq. (21)],[243, 244] as was first observed by *Kalmet* and *Kaplan*.[235]

Oxaziridines **121** are generally unstable, and rearrange to the amides **122**. The reaction proceeds from an excited singlet state[236] of **120**, and the quantum yields are solvent and temperature dependent.[237, 238]

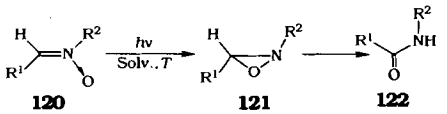

(21)

Thus, in benzene, for example, oxaziridines are formed, which in the dark re-isomerize to nitrones; in ethanol, amides are mainly observed.[239, 240]

Nitrones have been described, however, which yield exclusively oxaziridines, and where no side reactions have been observed. Examples of these are compounds **123**–**125**, which have been used by *Harada*, *Mori* and *Tanaka*[241] to study the temperature and solvent dependence of the quantum yields for the isomerization reaction.

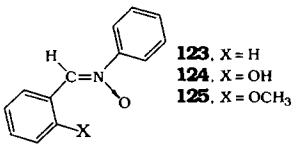

The compounds absorb in the range λ = 370–315 nm, and the only reaction steps observable are summarized in Scheme 5.

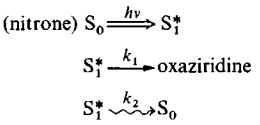

Scheme 5. Reaction steps of the isomerization **120** → **122**.

The quantum yield for photoisomerization of **123**–**125** in ethanol and cyclohexane at λ = 313 and 265 nm is presented in Table 15.

The quantum yield for **123** is lower in ethanol than in cyclohexane. This effect is interpreted as the result of intermolecular hydrogen bonding between ethanol and **123**, which accelerates the deactivation step k_2. On the other hand, it is interesting that the solvent effect for **124** is exactly the opposite. The quantum yield for **124** is higher in ethanol than in cyclohexane.

Table 15. Quantum yield ϕ for the photoisomerization of **123**–**125** in ethanol and cyclohexane after excitation at λ = 313 nm and 365 nm.

	123		**124**		**125**	
Solvent	λ_{max}	ϕ	λ_{max}	ϕ	λ_{max}	ϕ
ethanol	315	0.36	353	0.14	345	0.26
cyclohexane	320	0.52	370	0.04	341	0.27

This is explained by intramolecular H-bonding of **124** in cyclohexane, which quenches the excited singlet state of **124** most efficiently. The higher quantum yield in ethanol is then the result of conversion of the intra- to an intermolecular H-bond by the protic solvent, giving at least an average value of ϕ = 0.14.

Table 16 shows the quantum yield for the isomerization of compounds **123**–**125**, with respect to temperature.

Table 16. Quantum yield ϕ for the photoisomerization of **123**–**125** with respect to temperature.

Nitrone	Solvent	T[°C]	ϕ
123	ethanol	15	0.36
123	ethanol	- 90	0.36
124	ethanol	25	0.14
124	ethanol	- 100	0.25
124	pyridine	25	0.08
124	pyridine	- 35	0.10
124	diethyl ether	25	0.06
124	diethyl ether	- 60	0.07
125	ethanol	15	0.26
125	ethanol	- 90	0.26

From this, one can see that the quantum yields for **123** and **125** are clearly independent of temperature. Surprisingly, however, the value for **124**, in a variety of solvents, is higher at low temperature than at room temperature.

The Eyring diagram for the photoisomerization of **124** in various solvents shows significant inversion points at $-18\,^{\circ}C$ in ethanol, at $-4\,^{\circ}C$ in pyridine, and at $2\,^{\circ}C$ in diethyl ether (Fig. 46).

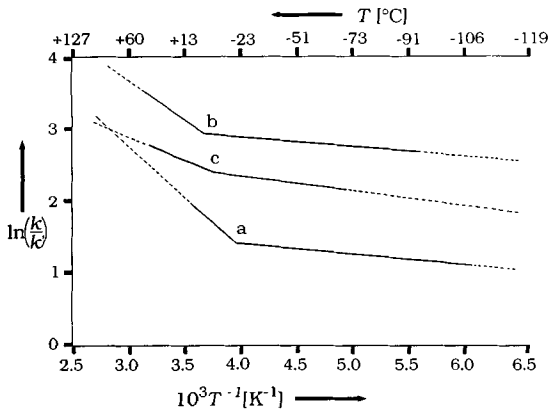

Fig. 46. Eyring diagram for the photoisomerization of **124** in the solvents a) ethanol, b) diethyl ether, and c) pyridine (Table 16). Here, the term $(1-\varphi)/\varphi$ is equivalent to the ratio $k/k' = k_1/k_2$ (Scheme 5). Hence, $\varphi = k_1/(k_1 + k_2)$. (The data points are too numerous to be shown individually.)

The authors concede that: "The sharp break in these curves is obviously indicative of a different mechanism" and "At present, it is impossible to tell what each line of different temperature dependence corresponds to individually..."

Since we suspected that the reason for the above situation was an isoinversion relationship, we analyzed the Eyring diagram published by the authors[241] in the sense of the isoinversion principle (Fig. 46).

7.2.1. The Isoinversion Relationship in the Photoisomerization of Nitrones

From the data in Figure 46 and the isoinversion line shown in Figure 47, $T_i = 260$ K may be calculated on the basis of the isoinversion principle.

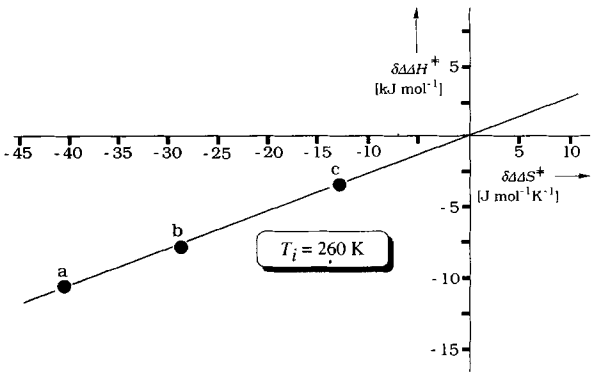

Fig. 47. Isoinversion line for the photoisomerization of **124** in a) ethanol, b) diethyl ether, and c) pyridine. ($T_i = 260$ K, correlation coefficient > 0.99).

Since neither of the nitrones **123** and **125** display temperature-dependent quantum yields in the photoisomerization to oxaziridines **121**, the authors[241] had already suspected that the change from an intra- to an intermolecular H-bond played a part in the "change of mechanism"—as they put it.

Indeed, in excited states, rapid deactivating processes via vibrational modes appear when an intermolecular H-bond is present in the molecule [242] (so-called "loose bolt effect"). However, from the applicability of the isoinversion principle to the photoisomerization of **124** it is obvious that this is

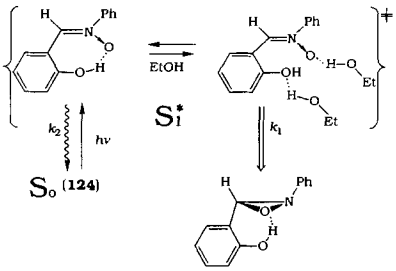

Fig. 48. Simplified reaction scheme for the photoisomerization of nitrones to oxaziridines. This represents the simplest kinetic model for an isoinversion relationship: $S_0 \underset{k_2}{\overset{h\nu}{\rightleftarrows}} S_1^* \xrightarrow{k_1}$ product.

again not a temperature-dependent change of mechanism in general, but a change in the weighting of the enthalpy and entropy terms of the same reaction. It is therefore not unexpected that the H-bonds in the excited state play a role in the mechanisms (Fig. 48).

7.3. The Oxidation of Thiols

The concurrent oxidation of two thiols of type **126** and **127** with molecular oxygen in binary solvent mixtures, catalyzed by triethylamine [Eq. (22)], has been intensively studied by

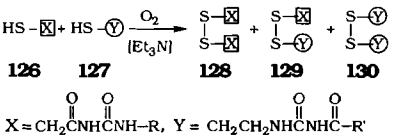

(22)

Endo et al.[248] as a model of "molecular recognition"[250] (Table 17).

Table 17. Overview of the thiols **126** and **127** used in Reaction (22).

HS-⊠ **126**	HS-Ⓨ **127**
X = CH₂CNHCNH-Ⓡ	Y = CH₂CH₂NHCNHC-Ⓡ
Ⓡ	Ⓡ
a R = *p*-$(H_3C)_2N$-C_6H_4	**a** R' = C_6H_5
b R = *n*Bu	**b** R' = *p*-$CH_3C_6H_4$
c *n*-C_5H_{11}	**c** R' = *p*-$C_2H_5C_6H_4$
	d R' = $(CH_2)_2CH(CH_3)_2$
	e R' = *n*-C_5H_{11}
	f R' = *n*Bu
	g R' = *cyclo*-C_6H_{11}
	h R' = $CH_2CH_2CH_2CH(CH_3)_2$

The starting thiols **126** and **127** consist of three structural units: the SH-group (reactive unit), the CONHCONH-group (formation of intermolecular hydrogen bonds) and an alkyl or aryl moiety, which is responsible for "molecular recognition".

For their investigations, the authors used 1:1 mixtures of thiols **126** and **127**, giving rise to the unsymmetrical disulfide (**129**) and the symmetrical disulfides (**128** and **130**). The selectivity of the reaction is described by the parameter P, which is defined for reaction (22) by Equation (23), where

$$P = \frac{n_u}{2n_s} = \frac{k_u}{2k_s} \tag{23}$$

n_u, n_s are the amounts of the unsymmetrical or symmetrical oxidation products **129**, or **128** and **130**, respectively, and k_u, k_s are the overall rate constants leading to the unsymmetrical and symmetrical oxidation products respectively.

The dependence of the selectivity on temperature was investigated for 13 systems (Table 18).[246, 247, 249] For Systems 5, 7 and 9 in Table 18, the reaction system was a heterogeneous water/ethanol binary mixture; in all other cases a homogeneous phase was employed.

Table 18. Overview of the systems whose selectivity in the Reaction (22) has been studied with respect to temperature.

No.	HS-[X] **126**	HS-(Y) **127**	Solvent
1	**a**	**a**	acetonitrile/water = 80/20
2	**a**	**b**	acetonitrile/water = 80/20
3	**a**	**c**	acetonitrile/water = 80/20
4	**a**	**d**	acetonitrile/water = 80/20
5	**a**	**e**	water/ethanol = 75/25
6	**a**	**e**	dioxane/ethanol = 75/25
7	**a**	**d**	water/ethanol = 75/25
8	**a**	**d**	dioxane/ethanol = 75/25
9	**b**	**f**	water/ethanol = 75/25
10	**b**	**f**	dioxane/ethanol = 75/25
11	**c**	**a**	acetonitrile/water = 58/42
12	**c**	**g**	acetonitrile/water = 58/42
13	**c**	**h**	acetonitrile/water = 58/42

If the results for these systems are transferred to an Eyring diagram (Fig. 49), then Systems 1–6, 8 and 11–13 yield two linear regions with an inversion point. For Systems 7, 9 and 10, the measurements were too few to permit interpretation. From the activation parameters determined for Systems 1–6, 8 and 11–13, an isoinversion line may be drawn, in the sense of the isoinversion principle (Fig. 50), with T_i = 314 K.

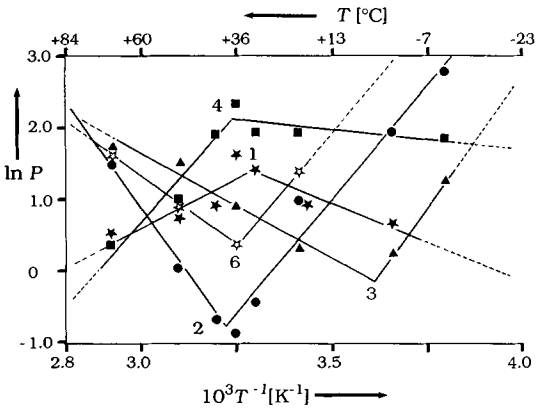

Fig. 49. Eyring diagram for the oxidation of thiols **126** and **127** according to Equation (22) (Systems 1–4 and 6 in Table 18). The selectivity parameter P is defined by Equation (23).

From a purely kinetic point of view, the symmetrical disulfides of type **128** would be expected clearly to dominate, since thiols **126** react most rapidly. However, preferential formation of the unsymmetrical disulfides of type **129** is observed, depending on the temperature and above all on structural variations in the thiol. Only for Systems 2, 9, 11 and 12 in Table 18 does one find minima with preferred formation of the symmetrical disulfides **128**. The thiols exist in the reaction medium as dimeric (**131a–c**) and tetrameric (**132a–e**) aggregates (Fig. 51).[247] Oxidation occurs at these aggregates, as is also demonstrated by the very negative activation entropies[246] of -214 to -189 JK^{-1}mol^{-1}. Since the thiol aggregates exist in a temperature- and substitution-dependent equilibrium, the selectivity is directed by these two parameters.

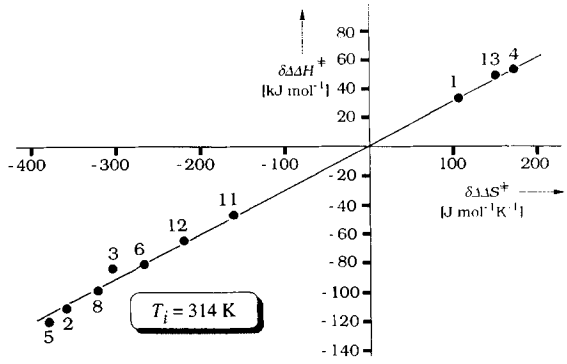

Fig. 50. Isoinversion line (T_i = 314 K correlation coefficient = 0.99) for the oxidation of the thiol pair **126**/**127** according to Equation (22) (for numbering see Table 18).

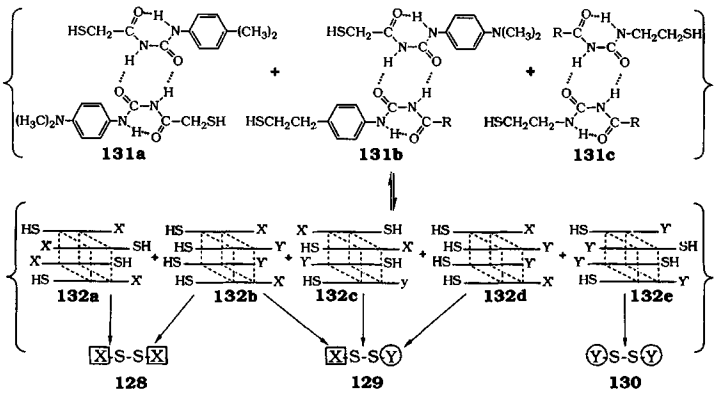

Fig. 51. Kinetic scheme for the oxidation of thiols of type **126** and **127**.

The temperature series presented shows that this example of "molecular recognition"[246] obeys the isoinversion principle. Intensive work on temperature-dependent selectivity in the oxidation of thiols **126** and **127** is expected to lead to important contributions to the understanding of "molecular recognition".

7.4. The Isoinversion Principle in Enzymatic Reactions

Enzyme reactions are classic examples of highly selective asymmetric reactions directed by optically active catalysts,[225, 270] where minimal amounts of "chiral information" are used to produce large quantities of optically active products. An enzyme molecule turns over its substrate 100 000 times per minute, and in a sense multiplies the information stored in it as optical activity by his factor.[251] However, both the activity and the stereoselectivity of this highly enantioselective, biological variant of "chiral amplification"[252] falls away rapidly with substrate variation.

On the basis of Michaelis-Menten kinetics (preliminary equilibrium between enzyme and substrate on the one hand and a substrate-enzyme complex on the other), isoinversion relationships ought to be observable here, too.[253] A suitable kinetic scheme for two competing products P and Q (e.g. stereoisomers) was proposed by *Wong* (Scheme 6).[254]

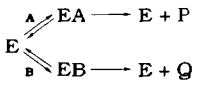

Scheme 6. Kinetic scheme for enzyme reactions, according to *Wong* [254]. E = enzyme; A, B = substrate; P, Q = products.

Inversion points T_{inv} are often observed in the Eyring diagram for enzyme activity.[255] However, except for compensation phenomena for denaturation of enzymes[263] insufficient data on any one system have appeared in the literature for a reliable isoinversion or compensation relationship to be constructed.

Application of the isoinversion relationship to enzymatic reactions will certainly lead to a better understanding of the selectivity process in these cases as well.

8. Outlook

As has been demonstrated, with the help of the isoinversion principle it is possible to interpret, assess and optimize selectivity phenomena in various areas of chemistry from a single point of view. To do so, the selectivity parameter in question must be measured with respect to the temperature and/or the pressure of the reaction.

The application of this principle to selectivity-producing reactions includes all those processes where the selectivity is generated at two or more levels. This is evident from the appearance of temperature inversion points T_{inv} in the relevant Eyring diagram. A lack of such inversion points may occur for the following reasons:

1. Selectivity is decided at only one level (e.g. Helmchen-Schmierer model; concerted reactions).
2. The inversion point corresponding to T_{inv} could lie outside the thermally tolerable measurement region for the reaction.
3. The enthalpy/entropy weighting could coincidentally be identical for the different selectivity levels.

It is now possible to create a flow chart for the application of the isoinversion principle to optimization of a selectivity parameter depending on the reaction temperature (Fig. 52). Similar considerations also hold for pressure-dependent selectivity processes (see Sections 6.2.9 and 6.2.10)

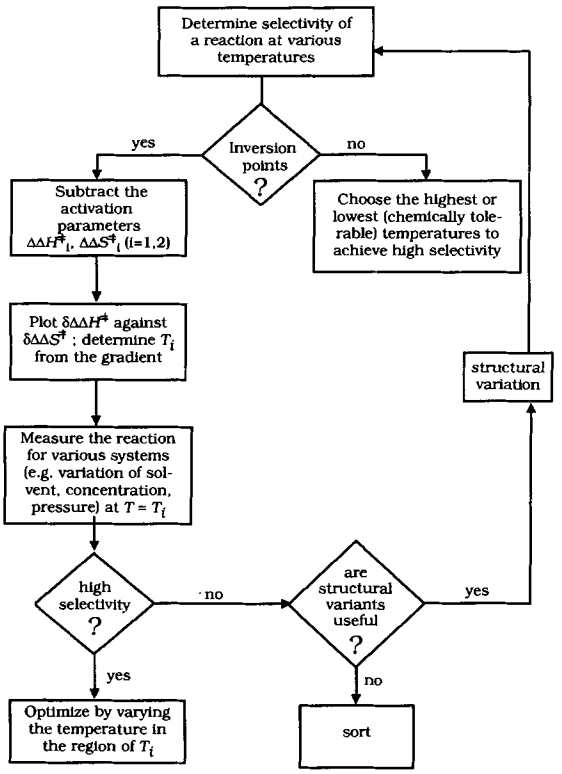

Fig. 52. Flow chart for the application of the isoinversion principle to optimization of a selectivity parameter, depending on the reaction temperature.

In addition to the reactions selected for this article, there are certainly numerous other phenomena[144b, 245, 281, 297, 298] which could be arranged and interpreted using the isoinversion principle, e.g. asymmetrically-directed hydrosilylation reactions,[155, 195, 259] or the problem of selectivity in hydroformylation reactions[256, 257] (branched/unbranched products, enantioselectivity).[258] Other examples that could be mentioned are asymmetric cyclopropanation reactions,[276] Diels-Alder reactions,[16, 295] the osmium-catalyzed asymmetric dihydroxylation[283] and asymmetric oxidation of sulfides to sulfoxides,[277] nucleophilic addition to the C=O double bond including the asymmetric reduction of ketones by metal hydride reagents,[278] stereoselective acylation of chiral amines by azlactones[279] as well as the four component condensation according to *Ugi*,[296] enantiomer separation on chiral GC-phases,[260] and various enantioselective photochemical reactions,[262, 280] especially the enantioselective protonation of photodienols catalyzed by chiral β-amino alcohols, which has been investigated by *Pete*.[261]

There are further examples of the application of the isoinversion principle other than stereoselective processes—for instance in the oxidative decomposition of methane to C_2-hydrocarbons catalyzed by metal oxides in heterogeneous phase[299] or the product-selective Lewis-acid cata-

lyzed polymerization of aromatic disulfides to poly(aryl sulfides).[300]

Herr Dr. H. Koch (Deutsche Shell GmbH) carried out the initial, pioneering studies on the asymmetric control of the Paternò-Büchi reaction and its temperature-dependence. We thank Herrn Dipl. Chem. M W. Plath, for his help in preparing Section 5. We are grateful to Herrn Dr. J. Runsink for important discussions on the interpretation of the mechanism of the Paternò-Büchi reaction and for carrying out extensive NMR analyses. Our thanks are due to the Fonds der Chemischen Industrie for supporting us with equipment and to Herrn Prof. Dr. K. H. Büchel and Herrn Dr. W. Draber of Bayer AG, Herrn Dr. R. Hopp of Haarmann and Reimer, and Herrn Prof. Dr. H. Offermanns of Degussa AG for generous donations of chemicals. We also thank Dr. W. Küsters of BASF AG for supporting our work with equipment. Finally, our special thanks go to Frau I. Voss for the preparation of the manuscript, and for her patience with us while doing so.

Received: March 12, 1990 [A 810 IE]
German version: *Angew. Chem. 103* (1991) 480
Translated by Dr. *M. Kertesz*, Zürich (Switzerland)

[1] a) L. Pasteur, Lectures before the Société Chimique de Paris on January 20 and February 3, 1860; b) *C.R. Hebd. Seances Acad. Sci. 26* (1848) 535; c) *Rev. Sci. Ser. 37* (1884) 2.
[2] J. H. van't Hoff, *Arch. Néerl. Sci. Exactes Nat. 9* (1874) 445.
[3] J.-A. Le Bel, *Bull. Soc. Chim. Fr. 22* (1874) 33.
[4] W. Marckwald, A. McKenzie, *Ber. Dtsch. Chem. Ges. 32* (1899) 2130.
[5] W. Marckwald, *Ber. Dtsch. Chem. Ges. 37* (1904) 1368.
[6] J. D. Morrison, H. S. Mosher: *Asymmetric Organic Reactions*, Prentice Hall, Englewood Clifts, NJ, USA 1971.
[7] M. Nógrádi: *Stereoselective Synthesis*, VCH, Weinheim 1986.
[8] Y. Izumi, A. Tai: *Stereodifferentiating Reactions*, Academic Press, New York 1977.
[9] a) D. J. Cram, F. A. Abd Elhafez, *J. Am. Chem. Soc. 74* (1952) 5828, 5851; b) D. J. Cram, K. R. Kopecky, *ibid. 81* (1959) 2748; c) N. N. Paddon-Row, N. G. Rondan, K. N. Houk, *ibid. 104* (1982) 7162; d) N. T. Anh, *Top. Curr. Chem. 88* (1980) 145; e) G. J. Karabatsos, *J. Am. Chem. Soc. 89* (1967) 1367; f) F. Vögtle, J. Francke, A. Aigner, D. Worsch, *Chem. Unserer Zeit 18* (1984) 203; g) M. Cherést, H. Felkin, N. Prudent, *Tetrahedron Lett. 1968*, 2199.
[10] V. Prelog, *Helv. Chim. Acta 36* (1953) 308.
[11] V. Prelog, H. L. Meier, *Helv. Chim. Acta 36* (1953) 320.
[12] W. G. Dauben, D. F. Dickel, O. Jeger, V. Prelog, *Helv. Chim. Acta 36* (1953) 325.
[13] a) V. Prelog, O. Ceder, M. Wilhelm, *Helv. Chim. Acta 38* (1955) 303; b) V. Prelog, E. Philbin, W. Watanabe, M. Wilhelm, *ibid. 39* (1956) 1086.
[14] V. Prelog, *Bull. Soc. Chim. Fr. 1956*, 987.
[15] a) J. C. Fiaud: (*Prelogs Method*) in H. B. Kagan (Ed.): *Stereochemistry*, Vol. 3, Thieme, Stuttgart 1977, p. 19; b) J. A. Berson, M. A. Greenbaum, *J. Am. Chem. Soc. 80* (1958) 445, 653; c) J. Weill-Raynal, J. Mathieu, *Bull. Soc. Chim. Fr. 1969*, 115; d) P. Parthasarathy, J. Ohrt, A. Horeau, J. P. Vigneron, H. B. Kagan, *Tetrahedron 26* (1970) 4705.
[16] G. Helmchen, R. Schierer, *Angew. Chem. 93* (1981) 208; *Angew. Chem. Int. Ed. Engl. 20* (1981) 205.
[17] G. Quinkert, H. Stark, *Angew. Chem. 95* (1983) 651; *Angew. Chem. Int. Ed. Engl. 22* (1983) 237.
[18] G. Quinkert, U. Schwartz, H. Stark, W.-D. Weber, F. Adam, H. Baier, G. Frank, G. Dürner, *Liebigs Ann. Chem. 1982*, 1999.
[19] Y. Izumi, *Angew. Chem. 83* (1971) 956; *Angew. Chem. Int. Ed. Engl. 10* (1971) 871.
[20] a) E. Ruch, I. Ugi, *Theor. Chim. Acta 4* (1966) 287; b) I. Ugi, *Z. Naturforsch. B 20* (1965) 405.
[21] a) E. Ruch, I. Ugi, *Top. Stereochem. 4* (1969) 99; b) J. Dugundji, I. Ugi, *Top. Curr. Chem. 39* (1973) 19.
[22] I. Ugi, *Chimia 19* (1965) 89.
[23] a) E. Anders, E. Ruch, I. Ugi, *Angew. Chem. 85* (1973) 16; *Angew. Chem. Int. Ed. Engl. 12* (1973) 25; b) E. Ruch, W. Hässelbarth, B. Richter, *Theor. Chim. Acta 19* (1970) 288; c) W. Hässelbarth, E. Ruch, *ibid. 29* (1973) 259; d) E. Ruch, D. J. Klein, *ibid. 63* (1983) 447; e) E. Ruch, *Acc. Chem. Res. 5* (1972) 49; f) E. Ruch, A. Schönhofer, *Theor. Chim. Acta 10* (1968) 91; g) E. Ruch, A. Schönhofer, I. Ugi, *ibid. 7* (1967) 420; h) E. Ruch, *ibid. 11* (1968) 183.
[24] a) I. Ugi, *Chimia 40* (1986) 340; b) J. Brandt, C. Jochum, I. Ugi, *Tetrahedron 33* (1977) 1353.
[25] a) K. Fukui (Theory of Orientation and Stereoselection), *React. Struct. Concepts Org. Chem. 2* (1975) 1; b) *Top. Curr. Chem. 15* (1970) 1.
[26] A. G. Griesbeck, *EPA Newsl. 28* (1986) 13.
[27] S. L. Schreiber, *Science 227* (1985) 857.
[28] H. Rau, *Chem. Rev. 83* (1983) 535.
[29] L. Horner, J. Klaus, *Liebigs Ann. Chem. 1979*, 1232.
[30] S. Jarosz, *Wiad. Chem. 37* (1983) 167.
[31] L. A. Paquette: (*Asymmetric Cycloaddition Reactions*) in J. D. Morrision (Ed.): *Asymmetric Synthesis*, Vol. 3, Academic Press, Orlando, FL, USA 1984, p. 455).
[32] a) H. Gotthardt, W. Lenz, *Angew. Chem. 91* (1979) 926; *Angew. Chem. Int. Ed. Engl. 18* (1979) 868; b) H. Gotthardt, W. Lenz, *Tetrahedron Lett. 1979*, 2879.
[33] M. Demuth, G. Mikhail, *Synthesis 1989*, 145.
[34] H. Koch, H.-D. Scharf, J. Runsink, H. Leismann, *Chem. Ber. 118* (1985) 1485.
[35] R. Pelzer, P. Jütten, H.-D. Scharf, *Chem. Ber. 122* (1989) 487.
[36] R. Pelzer, H.-D. Scharf, H. Buschmann, J. Runsink, *Chem. Ber. 122* (1989) 1187.
[37] H. Buschmann, H.-D. Scharf, N. Hoffmann, M. W. Plath, J. Runsink, *J. Am. Chem. Soc. 111* (1989) 5367.
[38] a) E. J. Corey, H. E. Ensley, *J. Am. Chem. Soc. 97* (1975) 6908; b) E. J. Corey, H. E. Ensley, J. W. Suggs, *J. Org. Chem. 41* (1976) 380; c) H. Herzog, H.-D. Scharf, *Synthesis 1986*, 420; d) H. E. Ensley, C. A. Parnell, E. J. Corey, *J. Org. Chem. 43* (1978) 1610; e) J. K. Whitesell, C. L. Liu, C. M. Buchanan, H. H. Chen, M. A. Milton, *ibid. 51* (1986) 551.
[39] a) H. Kipphardt, D. Enders, *Kontakte (Darmstadt) 1985*, No. 2, p. 37, and references cited therein; b) Merck-Schuchardt, MS-INFO 85-17 (8-phenylmenthol).
[40] a) J. W. Faller, D. L. Linebarrier, *J. Am. Chem. Soc. 111* (1989) 1937; b) F. J. A. Hundscheid, V. K. Tandon, P. H. F. M. Rouwette, A. M. van Leusen, *Recl. Trav. Chim. Pays-Bas 106* (1987) 159.
[41] W. Oppolzer, *Tetrahedron 43* (1987) 1969.
[42] W. Oppolzer, C. Chapuis, *Tetrahedron Lett. 25* (1984) 5383.
[43] a) W. Oppolzer, C. Chapuis, M. Guo, D. Reichlin, T. Godel, *Tetrahedron Lett. 23* (1982) 4781; b) W. Oppolzer, C. Chapuis, D. Dupuis, M. Guo, *Helv. Chim. Acta 68* (1985) 2100; c) S. M. Remiszewski, J. Yang, S. M. Weinreb, *Tetrahedron Lett. 27* (1986) 1853; d) W. Oppolzer, R. Moretti, T. Godel, A. Meunier, H. Löher, *ibid. 24* (1983) 4971; e) W. Oppolzer, T. Stevenson, *ibid. 27* (1986) 1139, f) W. Oppolzer, R. Pitteloud, G. Bernardinelli, K. Baettig, *ibid. 24* (1983) 4975; g) F. Kunisch, K. Hobert, P. Wenzel, *ibid. 26* (1985) 5433; h) G. Stork, N. A. Seccomano, *Nouv. J. Chim. 10* (1986) 677; i) R. Mortezaei, D. Awandi, F. Henin, J. Muzart, J.-P. Pete, *J. Am. Chem. Soc. 110* (1988) 4824.
[44] a) W. Oppolzer, C. Chapuis, G. Bernardinelli, *Tetrahedron Lett. 25* (1984) 5885; b) W. Oppolzer, P. Dudfield, T. Stevenson, T. Godel, *Helv. Chim. Acta 68* (1985) 212; c) W. Oppolzer, R. Moretti, G. Bernardinelli, *Tetrahedron Lett. 27* (1986) 4713; d) W. Oppolzer, J. Marco-Contelles, *Helv. Chim. Acta 69* (1986) 1699; e) W. Oppolzer, P. Dudfield, *Tetrahedron Lett. 26* (1985) 5037; f) W. Oppolzer, R. Moretti, *Helv. Chim. Acta 69* (1986) 1923; g) D. Crich, J. W. Davies, *Tetrahedron Lett. 28* (1987) 4205; f) M. A. Loreto, L. Pellacani, P. A. Tardella, *ibid. 30* (1989) 2975.
[45] a) H. C. Brown, N. R. Ayyangar, G. Zweifel, *J. Am. Chem. Soc. 86* (1964) 1071; b) H. C. Brown, A. K. Mandal, *J. Org. Chem. 42* (1977) 2996; c) H. C. Brown, P. K. Jadhav, A. K. Mandal, *Tetrahedron 37* (1981) 3547; d) H. C. Brown, B. Singaram, *J. Am. Chem. Soc. 106* (1984) 1797; e) H. C. Brown, J. Chandrasekharan, *J. Org. Chem. 51* (1986) 3394; f) H. C. Brown, P. K. Jadhav, B. Singaram (*Enantiomerically Pure Compounds via Chiral Organoboranes*) in R. Scheffold (Ed.): *Modern Synthetic Methods, Vol. 4*, Springer, Berlin 1986, p. 307; g) H. C. Brown, R. S. Randced, K. S. Bhat, M. Zaidlewicz, S. A. Weissman, P. K. Jadhav, P. T. Perumal, *J. Org. Chem. 53* (1988) 5513; h) H. C. Brown, B. Singaram, *Acc. Chem. Res. 21* (1988) 287; i) H. Takemura, N. Komeshima, I. Takahashi, S. Hashimoto, N. Ikota, K. Tomioka, K. Koga, *Tetrahedron Lett. 28* (1987) 5687.
[46] a) J. D. Morrison (Ed.): *Asymmetric Synthesis, Vol. 1–5*, Academic Press, Orlando, FL, USA 1983–1985; b) D. Enders, R. W. Hoffmann, *Chem. Unserer Zeit 19* (1985) 177, and references cited therein; c) H. S. Mosher, J. D. Morrison, *Science 221* (1983) 1013; d) W. Bartmann, B. Trost (Eds.): *Selectivity—a Goal for Synthetic Efficiency*, Verlag Chemie, Weinheim 1984; e) J. K. Whitesell, *Acc. Chem. Res. 18* (1985) 280; f) J. W. ApSimon, T. L. Collier, *Tetrahedron 42* (1986) 5157; g) S. G. Davies, J. M. Brown, A. J. Pratt, G. W. Fleet, *Chem. Br. 25* (1989) 259; h) J. M. Brown, S. G. Davies, *Nature 342* (1989) 631; i) J. K. Whitesell, *Chem. Rev. 89* (1989) 1581; j) K. Mori, *Tetrahedron 45* (1989) 3233.
[47] See Ref. [7], p. 275.
[48] S. Jarosz, A. Zamojski, *Tetrahedron 38* (1982) 1447.
[49] S. Jarosz, A. Zamojski, *Tetrahedron 38* (1982) 1453.
[50] H. Koch, *Dissertation*, Technische Hochschule Aachen 1984.
[51] A. Nehrings, H.-D. Scharf, J. Runsink, *Angew. Chem. 97* (1985) 882; *Angew. Chem. Int. Ed. Engl. 24* (1985) 877.
[52] A. I. Meyers, S. A. Fleming, *J. Am. Chem. Soc. 108* (1986) 306.
[53] M. Demuth, A. Palomer, H.-D. Sluma, A. K. Dey, C. Krüger, Y.-H.

Tsay, *Angew. Chem. 98* (1986) 1093; *Angew. Chem. Int. Ed. Engl. 25* (1986) 877.
[54] N. Hoffmannm, H.-D. Scharf, J. Runsink, *Tetrahedron Lett. 30* (1989) 2637.
[55] a) H. Herzog, H. Koch, H.-D. Scharf, J. Runsink, *Tetrahedron 42* (1986) 3547; b) H. Herzog, H. Koch, H.-D. Scharf, *Chem. Ber. 120* (1987) 1737.
[56] H. Koch, J. Runsink, H.-D. Scharf, *Tetrahedron Lett. 24* (1983) 3217.
[57] J. Runsink, H. Koch, A. Nehrings, H.-D. Scharf, E. Nowack, T. Hahn, *J. Chem. Soc. Perkin Trans 2 1988*, 49.
[58] M. Weuthen, H.-D. Scharf, J. Runsink, R. Vassen, *Chem. Ber. 121* (1988) 971.
[59] E. Paternò, G. Chieffi, *Gazz. Chim. Ital. 39* (1909) 341.
[60] G. Büchi, C. G. Inman, E. S. Lipinsky, *J. Am. Chem. Soc. 76* (1954) 4327.
[61] a) R. A. Caldwell, G.-W. Sovocool, R. P. Gajewski, *J. Am. Chem. Soc. 95* (1973) 2549; b) R. A. Caldwell, T. Majima, C. Pac, *ibid. 104* (1982) 629.
[62] N. J. Turro: *Modern Molecular Photochemistry*, Benjamin/Cummings, Menlo Park, CA, USA 1978.
[63] a) W. G. Dauben, L. Salem, N. J. Turro, *Acc. Chem. Res. 8* (1975) 41; b) N. J. Turro, P. A. Wriede, *J. Am. Chem. Soc. 92* (1970) 320; c) N. J. Turro, F. C. Dalton, K. Dawes, G. Farrington, R. Houtala, D. Morton, M. Morton, M. Niemczyk, N. Shore, *Acc. Chem. Res. 5* (1972) 92; d) N. J. Turro, *Pure Appl. Chem. 27* (1971) 679; e) J. C. Dalton, N. J. Turro, *Annu. Rev. Phys. Chem.* 21 (1970) 499.
[64] P. J. Wagner, *Top. Curr. Chem. 66* (1976) 3.
[65] S. C. Freilich, K. S. Peters, *J. Am. Chem. Soc. 103* (1981) 6255.
[66] S. C. Freilich, K. S. Peters, *J. Am. Chem. Soc. 107* (1985) 3819.
[67] a) D. R. Arnold, *Adv. Photochem. 6* (1968) 301; b) G. Jones II, *Org. Photochem. 5* (1981) 1; c) H. A. J. Carless in W. M. Horspool (Ed.): *Synthetic Organic Photochemistry*, Plenum, New York 1983, p. 425; d) K. M. Wilson, *Org. Photochem. 7* (1985) 339; e) R. A. Caldwell, D. Creed, *Acc. Chem. Res. 13* (1980) 45; f) S. L. Mattes, S. Farid, *ibid. 15* (1982) 80; g) U. Maharaj, M. A. J. Winnik, *J. Am. Chem. Soc. 103* (1981) 2328.
[68] H. Rau, *Chem. Rev. 83* (1983) 535.
[69] a) Y. Araki, *Carbohydr. Res. 58* (1977) C4-C6; b) Y. Araki, J.-i. Nogasawa, Y. Tschido, *J. Chem. Soc. Perkin Trans. 1 1981*, 12; c) S. L. Schreiber, A. H. Hoveyda, H.-J. Wu, *J. Am. Chem. Soc. 105* (1983) 660; d) S. L. Schreiber, K. Satake, *ibid. 105* (1983) 6723; e) S. L. Schreiber, K. Satake, *ibid. 106* (1984) 4186; f) S. L. Schreiber, A. H. Hoveyda, *ibid. 106* (1984) 7200; g) T. Koźluk, A. Zamojski, *Tetrahedron 39* (1983) 805; h) M. Braun, *Nachr. Chem. Tech. Lab. 33* (1985) 213.
[70] a) J. Saltiel, J. D'Agostino, E. D. Megarity, L. Metts, K. R. Neusberger, M. Wrighton, O. L. Zafiriou, O. C. Chapman, *Org. Photochem. 3* (1978) 1; b) L. G. Arnaut, S. J. Formosinho, *J. Photochem. 31* (1985) 315.
[71] a) R. M. Wilson, S. W. Wunderly, *J. Chem. Soc. Chem. Commun. 1974*, 461; b) W. Adam, U. Kliem, V. Lucchini, *Liebigs Ann. Chem. 1988*, 869; c) R. M. Wilson, S. W. Wunderly, *J. Am. Chem. Soc. 96* (1974) 7350; d) W. Adam, U. Kliem, V. Lucchini, *Tetrahedron Lett. 27* (1986) 2953; e) W. Adam, U. Kliem, T. Monsandl, E.-M. Peters, K. Peters, H. G. von Schnering, *J. Org. Chem. 53* (1988) 4986; f) W. Adam, U. Kliem, E.-M. Peters, K. Peters, H. G. von Schnering, *J. Prakt. Chem. 330* (1988) 391.
[72] M. Weuthen, *Dissertation*, Technische Hochschule Aachen 1987.
[73] R. Vassen, *Dissertation*, Technische Hochschule Aachen 1988.
[74] H. Buschmann, *Dissertation*, Technische Hochschule Aachen 1991.
[75] N. Hoffmann, *Diplomarbeit*, Technische Hochschule Aachen 1986.
[76] The diastereoselectivity of photochemical oxetane formation according to Equation (1) is characterized by the *de* value of the major oxetane and

$$de\,[\%] = \frac{c - c'}{c + c'} 100 = \frac{\sum_{i=1}^{n} (I_i - I_i')/(I_i + I_i')}{n} 100 \qquad (24)$$

determined from the ^{13}C-NMR spectrum according to (24), where c is the concentration of the major diastereomer, and c' the concentration of the minor diastereomer in the product mixture. Depending on the system, between 14 and 16 pairs of signals can be drawn on for determination of the *de* value. The *de* values given in Table 1 are averages of several independent measurements. By using this technique, the influence of nuclear Overhauser and spin relaxation effects can be kept to a minimum.
[77] a) B. M. Trost, D. O'Krongly, D. Belletine, *J. Am. Chem. Soc. 102* (1980) 7595; b) W. Oppolzer, M. Kurth, D. Reichlin, C. Chapuis, M. Mohnhaupt, F. Moffatt, *Helv. Chim. Acta 64* (1981) 2802.
[78] a) J. K. Whitesell, R. M. Lawrence, *Chimia 40* (1986) 318; b) J. K. Whitesell, H.-H. Chen, R. M. Lawrence, *J. Org. Chem. 50* (1985) 4663; c) J. K. Whitesell, R. M. Lawrence, H.-H. Chen, *ibid. 51* (1986) 4779.
[79] H. Herzog, H.-D. Scharf, *Synthesis 1986*, 788.
[80] G. Quinkert, H. G. Schmalz, E. M. Dzierzynsky, G. Dürner, J. W. Bats, *Angew. Chem. 98* (1986) 1023; *Angew. Chem. Int. Ed. Engl. 25* (1986) 992.
[81] M. W. Plath, *Dissertation*, Technische Hochschule Aachen 1991.
[82] a) The concepts of diastereo- and regioselectivity are used in the sense of *D. Seebach*'s definition. D. Seebach, *Angew. Chem. 91* (1979) 259; *Angew. Chem. Int. Ed. Engl. 18* (1979) 239; b) B. M. Trost, *Science 219* (1983) 4582.
[83] a) O. Exner in N. B. Charman, J. Shorter (Eds.): *Correlation Analysis in Chemistry: Recent Advances*, Plenum, New York 1978, p. 439–450; b) H. H. Jaffé, *Chem. Rev. 53* (1953) 191; c) C. D. Johnson: *The Hammett Equation*, Cambridge University Press *1973*.
[84] It should be noted here that in this correlation the rate constant quotients obtained from the diastereomeric excesses have been related to those of the unsubstituted system. This affects the ϱ value found, in that the σ values (defined as quotients of the equilibrium constants for the substituted or unsubstituted systems) are taken from references where they had been determined by direct quotient formation from the rate constants for substituted or unsubstituted systems.
[85] H. Buschmann, H.-D. Scharf, *Synthesis 1988*, 827.
[86] C. Rowland, L. Salem, *Angew. Chem. 84* (1972) 86; *Angew. Chem. Int. Ed. Engl. 11* (1972) 92.
[87] a) J. M. Vanest, R. H. Martin, *Recl. Trav. Chim. Pays-Bas 98* (1979) 113; b) G. L. Lange, C. Decicco, M. Lee, *Tetrahedron Lett. 28* (1987) 2833; c) J.-P. Pete, F. Hénin, R. Mortezaei, J. Muzart, O. Piva, *Pure Appl. Chem. 58* (1986) 1257; d) M. Demuth, *ibid. 58* (1986) 1233.
[88] a) H. Eyring, *J. Chem. Phys. 3* (1935) 107; b) S. Glasstone, K. J. Laidler, H. Eyring: *The Theory of Rate Processes*, McGraw-Hill, New York 1941.
[89] a) O. Exner in N. B. Charman, J. Shorter (Eds.): *Correlation Analysis in Chemistry: Recent Advances*, Plenum, New York 1978, p. 439; b) *Correlation Analysis of Chemical Data*, Plenum, New York 1988, p. 99; c) *Collect. Czech. Chem. Commun. 39* (1974) 515.
[90] J. E. Leffler, *J. Org. Chem. 20* (1955) 1202.
[91] H. Pracejus, *Justus Liebigs Ann. Chem. 634* (1960) 23.
[92] a) B. Giese, *Angew. Chem. 89* (1977) 162; *Angew. Chem. Int. Ed. Engl. 16* (1977) 125; b) *Acc. Chem. Res. 17* (1984) 438; c) B. Giese, J. Meister, *Angew. Chem. 90* (1978) 636; *Angew. Chem. Int. Ed. Engl. 17* (1978) 595; d) B. Giese, W.-B. Lee, J. Meister, *Liebigs Ann. Chem. 1980*, 725; e) B. Giese, *Angew. Chem. 92* (1980) 864; *Angew. Chem. Int. Ed. Engl. 19* (1980) 835; f) B. Giese, W.-B. Lee, C. Neumann, *ibid. 94* (1982) 320 and *21* (1982) 310; g) B. Giese, *ibid. 88* (1976) 159, 161, 723 and *15* (1976) 173, 174, 688.
[93] F. P. Price, L. P. Hammett, *J. Am. Chem. Soc. 63* (1941) 2387.
[94] a) P. Ooms, W. Hartmann, *Tetrahedron Lett. 28* (1987) 4271; b) S. H. Schroeter, C. M. Orlando, *J. Org. Chem. 34* (1969) 1181; c) S. H. Schroeter, *ibid. 34* (1969) 1188; d) S. M. Schroeter, *J. Chem. Soc. Chem. Commun. 1969*, 12; e) H. Dürr, P. Heitkämpfer, P. Herbst, *Synthesis 1972*, 261.
[95] P. S. Skell, M. S. Cholod, *J. Am. Chem. Soc. 91* (1969) 7131.
[96] a) R. Lumry, S. Rajender, *Biopolymers 9* (1970) 1125; b) P. Göldi, H. G. Elias, *Makromol. Chem. 153* (1972) 81; c) T. Yorozu, K. Hayashi, M. Irie, *J. Am. Chem. Soc. 103* (1981) 5480.
[97] The presence of an inversion point in temperature-dependent regioselectivity was not recognized by us in the original publication. [34] A new analysis of the original experimental data in the light of the isoinversion relationship, however, indicated the existence of an inversion point in the Eyring diagram.
[98] At this point, the usefulness in mechanistic studies of auxiliaries that yield diastereomeric excesses in the low to middle range should be noted. Middle range *de* values are especially sensitive to small variations in reactant structure and/or minor changes in reaction conditions [36, 37].
[99] a) J. K. Whitesell, A. Bhattacharga, K. Henke, *J. Chem. Soc. Chem. Commun. 1982*, 988; b) J. K. Whitesell, D. Deyo, A. Bhattacharga, *ibid. 1983*, 802; c) J. K. Whitesell, J. F. Carpenter, *J. Am. Chem. Soc. 109* (1987) 2839; d) J. K. Whitesell, D. James, J. F. Carpenter, *J. Chem. Soc. Chem. Commun. 1985*, 1449; e) J. K. Whitesell, H. A. Bhattacharya, C. M. Buchanan, H. H. Chen, D. Deyo, D. James, C. Liu, M. A. Minton, *Tetrahedron 42* (1986) 2993; f) see Ref. [39a].
[100] J. Mattay, *Tetrahedron 41* (1985) 2393, 2405.
[101] See Ref. [6], p. 40.
[102] H. Pracejus, H. Mätje, *J. Prakt. Chem. 296* (1964) 195.
[103] H. Pracejus, G. Kohl, *Justus Liebigs Ann. Chem. 722* (1969) 1.
[104] H. Pracejus, *Fortschr. Chem. Forsch. 8* (1967) 493.
[105] H. Pracejus, G. Wallura, *J. Prakt. Chem. 291* (1963) 33.
[106] G. Bredig, P. S. Fiske, *Biochem. Z. 46* (1912) 7.
[107] a) H. Wynberg, *Recl. Trav. Chim. Pays-Bas 100* (1981) 393; b) G. D. H. Dijkstra, R. M. Kellogg, H. Wynberg, *ibid. 108* (1989) 195; c) H. Wynberg, *Top. Stereochem. 19* (1989) 87.
[108] A. Tille, H. Pracejus, *Chem. Ber. 100* (1967) 196.
[109] V. Prelog, M. Wilhelm, *Helv. Chim. Acta 37* (1954) 1634.
[110] a) H. Wynberg, R. Helder, *Tetrahedron Lett. 1975*, 4057; b) K. Hermann, H. Wynberg, *J. Org. Chem. 44* (1979) 2238; c) see Ref. [107b].
[111] a) R. Helder, J. C. Hummelen, R. W. P. M. Laane, J. S. Wiering, H. Wynberg, *Tetrahedron Lett. 1976*, 1831; b) J. C. Hummelen, H. Wynberg, *Tetrahedron Lett. 1978*, 1089; c) H. Wynberg, B. Marsman, *J. Org. Chem. 45* (1980) 158; d) Y. Harigaya, H. Yamagucchi, M. Onde, *Heterocycles 15* (1981) 183; e) H. Pluim, H. Wynberg, *J. Org. Chem. 45* (1980) 2498.
[112] a) R. Helder, R. Arends, W. Bolt, H. Hiemstra, H. Wynberg, *Tetrahedron Lett. 1977*, 2181; b) H. Pracejus, F. W. Wilcke, K. Hanemann, *J. Prakt. Chem. 319* (1977) 219; c) N. Kobayashi, K. Iwai, *J. Am. Chem. Soc. 100*

(1978) 7071; d) H. Hiemstra, H. Wynberg, *ibid. 103* (1981) 417; e) N. Kobayashi, K. Iwai, *J. Org. Chem. 46* (1981) 1823.
[113] a) D. Borremann, R. Wegler, *Chem. Ber. 99* (1966) 1245; *ibid. 100* (1967) 1575; b) H. Wynberg, E. G. J. Staring, *J. Chem. Soc. Chem. Commun. 1984*, 1181.
[114] H. Pracejus, *Tetrahedron Lett. 1966*, 3809.
[115] a) H. Wynberg, *Chimia 43* (1989) 150; b) H. Alberts, H. Wynberg, *J. Am. Chem. Soc. 111* (1989) 7265.
[116] See Ref. [91].
[117] T. Yamashita, H. Yasueda, N. Nakamura, *Chem. Lett. 1974*, 585.
[118] T. Yamashita, H. Yasueda, Y. Miyauchi, N. Nakamura, *Bull. Chem. Soc. Jpn. 50* (1977) 1532.
[119] T. Yamashita, H. Yasueda, N. Nakatani, N. Nakamura, *Bull. Chem. Soc. Jpn. 51* (1978) 1183.
[120] T. Yamashita, H. Yasueda, N. Nakamura, *Bull. Chem. Soc. Jpn. 52* (1979) 2165.
[121] K. Herman, H. Wynberg, *Helv. Chim. Acta 60* (1977) 2208.
[122] N. Kobayashi, K. Iwai, *J. Am. Chem. Soc. 100* (1978) 7071.
[123] T. Yamashita, H. Yasueda, N. Nakamura, *Bull. Chem. Soc. Jpn. 51* (1978) 1247.
[124] N. Grubhofer, J. Schleith, *Naturwissenschaften 40* (1953) 508.
[125] K. Yamauchi, M. Kinoshita, M. Imoto, *Bull. Chem. Soc. Jpn. 44* (1971) 3186.
[126] C. P. Pinazzi, A. Menil, J. C. Rabadeux, A. Pleudeau, *J. Polym. Sci., Polym. Symp. No. 52* (1975) 1.
[127] H. Suda, R. Oda, *Kanazawa Daigaku Kogakubu Kiyo 2* (1960) 215.
[128] H. Pracejus, A. Tille, *Chem. Ber. 96* (1963) 854.
[129] S. Winter, H. Pracejus, *Chem. Ber. 99* (1966) 151.
[130] See Ref. [6], p. 276f.
[131] P. A. Levene, A. Rothen, *J. Biol. Chem. 127* (1939) 237.
[132] See Ref. [7], p. 53.
[133] See Ref. [6], p. 160ff. and 297ff.
[134] R. M. Williams: *Synthesis of Optically Active α-Amino Acids*, Pergamon, Oxford 1989, p. 230.
[135] a) H. B. Kagan in G. Wilkinson, F. G. A. Stone, W. E. Abel (Eds.): *Comprehensive Organometallic Chemistry, Vol. 8*, Pergamon, Oxford 1982, p. 463; b) B. Bosnich, *NATO Asi Ser. Ser. E 103* (1986); c) J. D. Morrison (Ed.): *Asymmetric Synthesis, Vol. 5*, Academic Press, Orlando, FL, USA 1985; d) P. Pino, G. Consiglio, *Pure Appl. Chem. 55* (1983) 1781; e) H. Brunner, *Kontakte (Darmstadt) 1981*, No. 3, p. 3; f) B. Bosnich, M. D. Fruyzuk, *Top. Stereochem. 12* (1981) 119.
[136] K. Hermann, *Nachr. Chem. Tech. Lab. 26* (1978) 651.
[137] H. Brunner, *Synthesis 1988*, 645.
[138] W. S. Knowles, *Acc. Chem. Res. 16* (1983) 106.
[139] H. Brunner, *Top. Stereochem. 18* (1988) 129.
[140] G. Wilke, H. Bönnemann, *Nachr. Chem. Tech. Lab. 28* (1980) 572.
[141] J. M. Brown, *Chem. Br. 1989*, 276.
[142] J. Falbe, H. Bahrmann, *Chem. Unserer Zeit 15* (1981) 37.
[143] J. M. Brown, *Angew. Chem. 99* (1987) 169; *Angew. Chem. Int. Ed. Engl. 26* (1987) 190.
[144] a) R. Noyori, M. Kitamura (Enantioselective Catalysis with Metal Complexes—an Overview) in R. Scheffold (Ed.): *Modern Synthetic Methods, Vol. 5*, Springer, Berlin 1989, p. 115; b) B. Bogdanovic, *Angew. Chem. 85* (1973) 1013; *Angew. Chem. Int. Ed. Engl. 12* (1973) 954; c) I. Ojima, N. Clos, C. Bastos, *Tetrahedron 45* (1989) 6901.
[145] J. M. Brown, *Chem. Ind. (London) 1988*, 612.
[146] H. B. Kagan, J. C. Fiaud, *Top. Stereochem. 18* (1988) 249.
[147] H. Nozaki, S. Moriuti, H. Takaya, R. Noyori, *Tetrahedron Lett. 1966*, 5239.
[148] L. Horner, H. Siegel, H. Büthe, *Angew. Chem. 80* (1968) 1034; *Angew. Chem. Int. Ed. Engl. 7* (1968) 942.
[149] a) W. S. Knowles, M. J. Sabacky, *J. Chem. Soc. Chem. Commun. 1968*, 1445; b) B. D. Vineyard, W. S. Knowles, M. J. Sabacky, *J. Mol. Catal 19* (1983) 159.
[150] J. A. Osborne, F. H. Jardine, Y. F. Yang, G. Wilkinson, *J. Chem. Soc. A 1966*, 1711.
[151] a) J. D. Morrison, R. E. Burnett, A. M. Aguiar, C. J. Morrow, C. Philips, *J. Am. Chem. Soc. 93* (1971) 1301; b) W. S. Knowles, M. J. Sabacky, B. D. Vineyard, *J. Chem. Soc. Chem. Commun. 1972*, 10; c) J. D. Morrison, W. F. Masler, *J. Org. Chem. 39* (1974) 270.
[152] a) T.-P. Dang, H. B. Kagan, *J. Chem. Soc. Chem. Commun. 1971*, 481; b) *J. Am. Chem. Soc. 94* (1972) 6429.
[153] a) W. S. Knowles, M. J. Sabacky, B. D. Vineyard, *Ann. N.Y. Acad. Sci. 172* (1970) 232, *ibid. 214* (1973) 119; b) *Chem. Eng. News 48* (1970) No. 29, p. 41, *ibid. 50* (1972) No. 6, p. 4; c) *Chem. Technol. 1972*, 590; d) *Adv. Chem. Ser. 132* (1974) 274; e) W. S. Knowles, M. J. Sabacky, B. D. Vineyard, D. J. Weinkauff, *J. Am. Chem. Soc. 97* (1975) 2567; f) Y. Izumi, I. Chibata, T. Itoh, *Angew. Chem. 90* (1978) 187; *Angew. Chem. Int. Ed. Engl. 17* (1978) 176.
[154] H. B. Kagan, *Bull. Soc. Chim. Fr. 1988*, 846.
[155] H. Brunner, *Angew. Chem. 95* (1983) 921; *Angew. Chem. Int. Ed. Engl. 22* (1983) 897.
[156] H. Brunner, *Chem. Unserer Zeit 14* (1980) 377.
[157] D. Valentine, Jr., J. W. Scott, *Synthesis 1978*, 329.
[158] H. B. Kagan, J. C. Fiaud, *Top. Stereochem. 10* (1978) 175.
[159] O. Consiglio, P. Pino, *Top. Curr. Chem. 105* (1982) 77.
[160] K. E. Koenig in Ref. [135c], p. 71.
[161] K. E. Koenig, G. L. Bachman, B. D. Vineyard, *J. Org. Chem. 45* (1980) 2362.
[162] M. D. Fryzuk, B. Bosnich, *J. Am. Chem. Soc. 99* (1977) 6262.
[163] B. D. Vineyard, W. S. Knowles, M. J. Sabacky, G. L. Bachman, D. J. Weinkauff, *J. Am. Chem. Soc. 99* (1977) 5946.
[164] R. R. Schrock, J. A. Osborn, *J. Am. Chem. Soc. 98* (1976) 2134, 3143.
[165] J. M. Brown, P. A. Chaloner, *J. Am. Chem. Soc. 102* (1980) 3040.
[166] M. D. Fryzuk, B. Bosnich, *J. Am. Chem. Soc. 100* (1978) 5491.
[167] J. Halpern, *Science 217* (1982) 401.
[168] C. R. Landis, J. Halpern, *J. Organomet. Chem. 250* (1983) 485.
[169] A. S. C. Chan, J. J. Pluth, J. Halpern, *J. Am. Chem. Soc. 102* (1980) 5952.
[170] J. Halpern, *Pure Appl. Chem. 55* (1983) 99.
[171] J. Halpern in Ref. [135c], p. 41.
[172] C. R. Landis, J. Halpern, *J. Am. Chem. Soc. 109* (1987) 1746, 6217.
[173] a) J. M. Brown, P. A. Chaloner, B. A. Murrer, D. Parker, *ACS Symp. Ser. 119* (1980) 1731; b) J. M. Brown, P. A. Chaloner, *J. Chem. Soc. Chem. Commun. 1980*, 344.
[174] a) D. Sinou, *Tetrahedron Lett. 22* (1981) 2987; b) D. Sinou, D. Lafont, G. Descotes, T. Dayrit, *Nouv. J. Chim. 7* (1983) 291.
[175] I. Ojima, T. Kogure, N. Yoda, *J. Org. Chem. 45* (1980) 4728.
[176] V. A. Pavlov, E. I. Klabunovskii, Yu. T. Struchkov, A. A. Volobaev, Yanovsky, *J. Mol. Catal. 44* (1988) 217.
[177] K. E. Koenig, W. S. Knowles, *J. Am. Chem. Soc. 100* (1978) 7561.
[178] a) K. E. Koenig, G. L. Bachman, B. D. Vineyard, *J. Org. Chem. 45* (1980) 2362; b) K. E. Koenig in J. R. Kosak, (Ed.): *Catalysis of Organic Reactions*, Marcel Dekker, New York 1984, p. 63–78.
[179] R. Glaser, J. Blumenfeld, M. Twaik, *Tetrahedron Lett. 1977*, 4639.
[180] R. Glaser, S. Geresh, J. Blumenfeld, B. Vanais, M. Twaik, *Isr. J. Chem. 15* (1976/77) 17.
[181] a) A. S. C. Chan, J. J. Pluth, J. Halpern, *Inorg. Chim. Acta 37* (1979) L477; b) J. M. Brown, R. Glaser, P. A. Chaloner, S. Geresh, *Tetrahedron 36* (1980) 815; c) J. M. Brown, D. Parker, *J. Org. Chem. 47* (1982) 2722.
[182] a) C. Botteghi, S. Gladiali, M. Bianchi, U. Matteoli, P. Frediani, P. G. Vergamini, E. Benedetti, *J. Organomet. Chem. 250* (1977) 221; b) G. Balavoine, T. P. Dang, C. Eskenazi, H. B. Kagan, *J. Mol. Catal. 7* (1980) 307; c) T. H. Johnson, L. A. Siegle, V. J. K. Chaffin, *J. Mol. Catal. 9* (1980) 307; d) E. R. James, R. S. McMillan, *Can. J. Chem. 55* (1977) 3927; e) K. Ohkubo, I. Terada, K. Yoshinaga, *Inorg. Nucl. Chem. Lett. 15* (1979) 421; f) K. Ohkubo, I. Terada, K. Sugahara, K. Yoshinaga, *J. Mol. Catal. 7* (1980) 421.
[183] a) A. Fischli, D. Süss, *Helv. Chim. Acta 62* (1979) 2361; b) A. Fischli, J. J. Daly, *ibid. 63* (1980) 1628; c) Y. Ohgo, K. Kobayashi, S. Takeuchi, J. Yoshimura, *Bull. Chem. Soc. Jpn. 45* (1972) 933; d) S. Takeuchi, Y. Ohgo, *ibid. 54* (1981) 2136.
[184] a) E. Cesarotti, R. Ugo, H. B. Kagan, *Angew. Chem. 91* (1979) 842; *Angew. Chem. Int. Ed. Engl. 18* (1979) 779; b) E. Cesarotti, R. Ugo, R. Vitiello, *J. Mol. Catal. 12* (1981) 63.
[185] U. Nagel, B. Rieger, *Organometallics 8* (1989) 1534.
[186] a) U. Nagel, *Angew. Chem. 96* (1984) 425; *Angew. Chem. Int. Ed. Engl. 23* (1984) 435; b) U. Nagel, E. Kinzel, J. Andrade, G. Prescher, *Chem. Ber. 119* (1986) 3326; c) U. Nagel, B. Rieger, *ibid. 121* (1988) 1123.
[187] The δ/λ conformation of the RhPCCP five-membered ring is defined as in the corresponding structural element MNCCN in numerous ethylenediamine complexes; cf. The Commission on the Nomenclature of Inorganic Chemistry of the International Union of Pure and Applied Chemistry, *Inorg. Chem. 9* (1970) 1.
[188] According to *Brown* et al., in seven-membered chelate rings the product configuration is determined by the chair or twist-boat conformation of the catalyst complex. Starting from (*Z*)-enamides, the chair conformation yields (*S*)-amino acids, whereas the twist-boat form leads to the (*R*)-enantiomer [173a].
[189] H. Brunner, *Acc. Chem. Res. 12* (1979) 250.
[190] a) K. Achiwa, *Tetrahedron Lett. 1977*, 3735; b) J. Kötter, G. Greber, *Chem. Ber. 113* (1980) 2323.
[191] a) K. Achiwa, *Chem. Lett. 1977*, 777; b) C. Cativiela, J. A. Mayoral, E. Melendez, R. Ulson, L. A. Oro, M. T. Pinillos, *React. Kinet. Catal Lett. 21* (1982) 173; c) J. M. Brown, P. A. Chaloner, G. Descotes, R. Glaser, D. Lafont, D. Sinou, *J. Chem. Soc. Chem. Commun. 1979*, 611.
[192] a) J. Bakos, I. Tóth, B. Heil, L. Markó, *J. Organomet. Chem. 279* (1985) 23; b) N. Ulrich, E. Kinzel, J. Andrade, G. Prescher, *Chem. Ber. 119* (1986) 3326.
[193] a) W. R. Cullen, Y. Sugi, *Tetrahedron Lett. 1978*, 1635; b) A. Uehara, T. Kubota, R. Tsuchiga, *Chem. Lett. 1983*, 441.
[194] R. Selke, H. Pracejus, *J. Mol. Catal. 37* (1986) 213.
[195] M. Čapka, J. Hetflejs, R. Selke, *React. Kinet. Catal. Lett. 10* (1979) 225.
[196] I. Ojima, T. Kogure, N. Yoda, *Chem. Lett. 1979*, 495.
[197] C. Valentini, E. Cernia, M. Fiorini, G. M. Giongo, *J. Mol. Catal. 23* (1984) 81.
[198] W. J. le Noble, *Chem. Unserer Zeit 17* (1983) 152.

[199] W. J. le Noble in R. van Eldik, J. Jones, (Eds.): *High Pressure Chemistry and Biochemistry*, Reidel, Dordrecht 1987, p. 279.
[200] T. Asano, W. J. le Noble, *Chem. Rev. 89* (1989) 549.
[201] R. Selke, *J. Organomet. Chem. 370* (1989) 249.
[202] J. C. Sheehan, R. Chandler, *J. Am. Chem. Soc. 83* (1961) 4795.
[203] M. Nakayama, G. Maeda, T. Kaneko, H. Katsura, *Bull. Chem. Soc. Jpn. 44* (1971) 1150.
[204] N. Izumiya, S. Lee, T. Kanmera, H. Aoyagi, *J. Am. Chem. Soc. 99* (1977) 8346.
[205] T. Kanmera, S. Lee, H. Aoyagi, N. Izumiya, *Tetrahedron Lett. 1979*, 4483.
[206] I. Ojima, T. Suzuki, *Tetrahedron Lett. 21* (1980) 1239.
[207] D. Meyer, J.-C. Poulin, H. B. Kagan, H. Levine-Pinto, J.-L. Morget, P. Fromageot, *J. Org. Chem. 45* (1980) 4680.
[208] K. Omura, T. Ito, A. Nakamura, *Chem. Lett. 1980*, 481.
[209] K. Harada, M. Takasaki, *Bull. Chem. Soc. Jpn. 57* (1984) 1427.
[210] K. Harada, T. Yoshida, *J. Org. Chem. 37* (1972) 4366.
[211] K. Harada in Ref. [135c], p. 345.
[212] F. Koop, C. Martius, *Z. Physiol. Chem. 258* (1939) 238.
[213] J. B. Herbst, E. A. Swart, *J. Org. Chem. 11* (1946) 368.
[214] R. G. Hiskey, R. C. Northrop, *J. Am. Chem. Soc. 83* (1961) 4798.
[215] K. Matsumoto, K. Harada, *J. Org. Chem. 31* (1966) 1956.
[216] K. Harada, *Nature 212* (1966) 1571.
[217] K. Harada, *J. Org. Chem. 32* (1967) 1790.
[218] A. Kandi, S. Mitsui, *Nippon Kaguka Zasshi 89* (1966) 183.
[219] R. G. Hiskey, R. C. Northrop, *J. Am. Chem. Soc. 87* (1965) 1753.
[220] K. Harada, K. Matsumoto, *J. Org. Chem. 32* (1967) 1794.
[221] K. Harada, K. Matsumoto, *J. Org. Chem. 33* (1968) 4467.
[222] K. Harada, T. Yoshida, *J. Chem. Soc. Chem. Commun. 1970*, 1071.
[223] See Ref. [7], p. 100.
[224] See Ref. [6], p. 302.
[225] J. Rétey, J. A. Robinson: *Stereospecifity in Organic Chemistry and Enzymology*, Verlag Chemie, Weinheim 1982, p. 169.
[226] Y. Tachibana, M. Ando, H. Kuzuhara, *Bull. Chem. Soc. Jpn. 56* (1983) 3652.
[227] K. Harada, T. Yoshida, *Bull. Chem. Soc. Jpn. 43* (1970) 921.
[228] K. Harada, S. Shiono, *Bull. Chem. Soc. Jpn. 57* (1984) 1367.
[229] K. Harada, Y. Kataoka, *Chem. Lett. 1987*, 791.
[230] K. Harada, T. Munegumi, *Bull. Chem. Soc. Jpn. 57* (1984) 3203.
[231] K. Harada, T. Kataoka, *Tetrahedron Lett. 1978*, 2103.
[232] Transamination plays a role in the biosynthesis and biodegradation of protein molecules. Aminotransferases make possible an amination/deamination exchange between keto acids (especially pyruvate) and glutamate, without the appearance of free ammonia. The coenzyme in amino-transferases is pyridoxal phosphate (Vitamin B_5).
[233] A. C. Somersall, E. Dau, J. E. Guillet, *Macromolecules 7* (1974) 233.
[234] J. E. Guillet in: M. A. Winnik (Ed.): *NATO ASI Ser., Ser. C 182* (1986) 467.
[235] M. J. Kamlet, L. A. Kaplan, *J. Org. Chem. 22* (1957) 576.
[236] K. Shinzawa, I. Ianaka, *J. Phys. Chem. 68* (1964) 1205.
[237] J. S. Splitter, M. Calvin, *J. Org. Chem. 20* (1955) 1086.
[238] J. S. Splitter, M. Calvin, *J. Org. Chem. 23* (1958) 651.
[239] L. Chardonnens, P. Heinrich, *Helv. Chim. Acta. 32* (1949) 656.
[240] A. Schönberg: *Präparative Organische Photochemie*, Springer, Berlin 1958.
[241] N. Harada, Y. Mori, I. Tanaka, *Mol. Photochem. 1* (1970) 153.
[242] A. Beckett, G. Porter, *Trans. Soc. Faraday 59* (1963) 2051.
[243] a) K. Koyana, I. Tanaka, *J. Phys. Chem. 69* (1965) 2545; b) K. Shinzawa, I. Tanaka, *ibid. 68* (1964) 1205.
[244] a) D. R. Boyd, R. M. Campbell, P. B. Coulter, J. Grimshaw, D. C. Neill, B. Jennings, *J. Chem. Soc. Perkin Trans. 1 1985*, 849; b) C. Bezzecki, D. Mostowicz, *J. Chem. Soc. Chem. Commun. 1975*, 244; c) J. S. Splitter, M. Calvin, *J. Org. Chem. 23* (1958) 651; d) J. S. Splitter, M. Calvin, *ibid. 30* (1965) 3427; e) D. R. Boyd, B. Jennings, R. Spratt, *Chem. Commun. 1970*, 745; f) J. S. Splitter, T.-M. Su, H. Ono, M. Calvin, *J. Am. Chem. Soc. 93* (1971) 4075.
[245] L. M. Jackman, B. C. Lange, *J. Am. Chem. Soc. 103* (1981) 4494.
[246] T. Endo, M. Hashimoto, T. Orii, M. M. Ito, *Bull. Chem. Soc. Jpn. 57* (1984) 1562.
[247] T. Endo, H. Takei, T. Isago, J. Kato, M. M. Ito, K. Guro, K. Akiyama, Y. Nakaijama, H. Kataoka, *J. Am. Chem. Soc. 111* (1989) 8166.
[248] T. Endo, *Top. Curr. Chem. 128* (1985) 91.
[249] T. Endo, H. Kashahara, S. Yugi, K. Tojima, M. M. Ito, M. Ogino, K. Kagino, *Chem. Lett. 1986*, 705.
[250] J. Rebeck, Jr., *Top. Curr. Chem. 149* (1988) 189; *Angew. Chem. 102* (1990) 261; *Angew. Chem. Int. Ed. Engl. 29* (1990) 245.
[251] A. L. Lehninger: *Biochemistry*, 2nd. Edit., Worth Publishers, New York 1977, p. 208.
[252] R. Noyori, *Chem. Soc. Rev. 18* (1989) 187; R. Noyori, M. Kitamura, *Angew. Chem. 103* (1991) 34; *Angew. Chem. 30* (1991) 49.
[253] a) J. Kraut, *Science 242* (1988) 533; b) S. A. Brenner, *Chem. Rev. 89* (1989) 789.
[254] C.-W. Wong, *Science 244* (1989) 1145.
[255] a) I. H. Segel, *Enzyme Kinetics*, Wiley, New York 1975; b) Y.-C. Chang, R. D. Scott, D. J. Graves, *Biochemistry 25* (1986) 1932; c) Y.-Y. Huang, T. Hara, S. Sligar, M. J. Coon, T. Kimura, *ibid. 25* (1986) 1390; d) V. Krasnobajew, R. Böniger, *Chimia 29* (1975) 123.
[256] a) C. U. Pittman, Jr., R. M. Hanes, *J. Am. Chem. Soc. 98* (1976) 5402; b) C. U. Pittman, Jr., A. Hirao, C. Jones, R. M. Hanes, Q. Ng, *Ann. N.Y. Acad. Sci. 295* (1977) 15; c) C. U. Pittman, Jr. in G. Wilkinson, F. G. A. Stone, W. E. Abel (Eds.): *Comprehensive Organometallic Chemistry*, Vol. 8, Pergamon, Oxford 1982, p. 569; d) T. Hayashi, M. Tanaka, Y. Ikeda, I. Ogata, *Bull. Chem. Soc. Jpn. 52* (1979) 2605; e) M. Tanaka, Y. Watanabe, T.-A. Mitsudo, Y. Takegami, *ibid. 47* (1974) 1698.
[257] a) B. Bosnich, M. D. Fryzuk, *Top. Stereochem. 12* (1980) 119; b) H. Siegel, W. Himmele, *Angew. Chem. 92* (1980) 182; *Angew. Chem. Int. Ed. Engl. 19* (1980) 178; c) Ref. [256]; d) L. Kollár, J. Bakos, I. Tóth, B. Heil, *J. Organomet. Chem. 350* (1988) 277.
[258] See Ref. [256d, e].
[259] a) K. Yamamoto, Y. Uramoto, M. Kumada, *J. Organomet. Chem. 31* (1971) C 9; b) T. Hayashi, M. Kumada, *Acc. Chem. Res. 15* (1982) 395; c) N. Langlois, T.-P. Dang, H. B. Kagan, *Tetrahedron Lett. 1973*, 4865; d) K. Felföldi, I. Kapocsi, M. Bartók, *J. Organomet. Chem. 362* (1989) 411.
[260] a) K. Watabe, R. Charles, E. Gil-Av, *Angew. Chem. 101* (1989) 195; *Angew. Chem. Int. Ed. Engl. 28* (1989) 192; b) V. Schurig, J. Ossig, R. Link, *ibid.* (1989) 197 and *28* (1989) 194.
[261] a) See Ref. [87]; b) O. Piva, J.-P. Pete, *Tetrahedron Lett. 31* (1990) 5157; c) O. Piva, R. Mortezaei, F. Hénin, J. Muzart, P.-P. Pete, *J. Am. Chem. Soc. 112* (1990) 9263; see also F. Hénin, J. Muzart, P.-P. Pete, A. M'boungou-M'passi, H. Rau, *Angew. Chem. 103* (1991) 460; *Angew. Chem. Int. Ed. Engl. 30* (1991) 416.
[262] J.-M. Vanest, R. H. Martin, *Recl. Trav. Chim. Pays-Bas 98* (1979) 113.
[263] R. R. Krug, W. G. Hunter, R. A. Grieger, *J. Phys. Chem. 80* (1976) 2335, 2341.
[264] a) [158]; b) J. C. Fiaud, A. Horeau, *Tetrahedron Lett. 1972*, 2565.
[265] According to *H. Wynberg*, the use of racemic auxiliaries for determining *de* values is only permissible to a first approximation. Because of the presence of chiral reagents, the medium itself becomes chiral, giving a chiral solvent effect. In a racemic system, the interactions of the enantiomers with each other (*R–R*, *R–S* and *S–S* interactions) can lead to differing asymmetric induction: H. Wynberg, B. Feringa, *Tetrahedron 32* (1976) 2831.
[266] The analysis of the data for pressure-dependent selectivity measurements must be treated with caution in some cases, since the experimental details for the measurements were not given in the literature. The appearance of the inversion points described could hence also be due to non-uniform experimental conditions. We thank *R. Selke* for this observation.
[267] a) H. B. Kagan, T.-P. Dang, *J. Am. Chem. Soc. 94* (1972) 6429; b) H. B. Kagan in [135c], p. 1.
[268] L. Salem, *J. Am. Chem. Soc. 95* (1973) 94.
[269] W. Linert, R. F. Jameson, *Chem. Soc. Rev. 18* (1989) 477.
[270] a) J. Rétey, J. A. Robinson: *Stereospecificity in Organic Chemistry and Enzymology*, Verlag Chemie, Weinheim 1982; b) T. W. Goodewin: *Essay in Biochemistry, Vol. 9*, Academic Press, New York 1973, p. 103.
[271] a) L. Duhamel, P. Duhamel, J.-C. Launay, J.-C. Plaquevent, *Bull. Soc. Chim. Fr. 1984*, 421; b) L. Horner, *Kontakte (Darmstadt) 1979*, No. 3; *ibid. 1980*, No. 1.
[272] a) Y. Izumi, M. Imaida, H. Fukawa, S. Akabori, *Bull. Chem. Soc. Jpn. 36* (1963) 155; b) Y. Izumi, S. Tatsumi, M. Imaida, S. Akabori, *ibid. 38* (1965) 1206; c) S. Tatsumi, *ibid. 41* (1968) 408; d) Y. Izumi, K. Matsunaga, S. Totsumi, M. Imaida, *ibid. 41* (1968) 2515; e) Y. Izumi, K. Okuda, *ibid. 44* (1971) 1330; f) F. Hiyashi, T. Ninomiya, Y. Izumi, *ibid. 44* (1971) 1333; g) Y. Izumi, S. Yajima, K. Ohkubo, K. K. Babievsky, *ibid. 44* (1971) 1416; h) Y. Izumi, T. Harada, T. Tanabe, K. Okuda, *ibid. 44* (1971) 1418; i) T. Harada, M. Imaida, Y. Izumi, *ibid. 44* (1971) 1419; j) T. Harada, *ibid. 53* (1980) 1019.
[273] J.-H. Youn, *Dissertation*, Technische Universität München 1986.
[274] J. Jähme, C. Rüchardt, *Angew. Chem. 93* (1981) 919; *Angew. Chem. Int. Ed. Engl. 20* (1981) 885.
[275] G. A. Somorja, *J. Phys. Chem. 94* (1990) 1013.
[276] a) H. Kanoi, H. Matsuda, *J. Mol. Catal. 29* (1985) 157; b) A. Nakamura, A. Konishi, Y. Tatsumo, S. Otsuka, *J. Am. Chem. Soc. 100* (1978) 3443, c) A. Nakamura, A. Konishi, R. Tsujitari, M. A. Kudo, S. Otsuka, *ibid. 100* (1978) 3449.
[277] A. Pitchen, E. Duñach, N. N. Deshmulch, H. B. Kagan, *J. Am. Chem. Soc. 106* (1984) 8188.
[278] a) J. P. Vigneron, I. Jacquet, *Tetrahedron 32* (1976) 935; b) C. Zioudrou, P. Chrysochou, *Tetrahedron Lett. 1972*, 5293; *Tetrahedron 33* (1977) 2103; d) T. J. Leitereg, D. J. Cram, *J. Am. Chem. Soc. 90* (1968) 4019; e) *ibid. 90* (1968) 4011; f) E. L. Eliel, S. Morris-Natschke, *ibid. 106* (1984) 2937; g) Y. Gault, H. Felkin, *Bull. Soc. Chim. Fr. 1960*, 1342; h) P. T. Lansbury, R. E. MacLeay, *J. Org. Chem. 28* (1963) 1940; i) M. Chérest, *Tetrahedron 36* (1980) 1593; j) R. Noyori, I. Tomino, Y. Tanimoto, N. Nishizawa, *J. Am. Chem. Soc. 106* (1984) 6709; k) G. M. Giongo, F. Di Gregorio, N. Palladino, W. Marconi, *Tetrahedron Lett. 1973*, 3195; l) O. Červinka, O. Bělovský, *Collect. Czech. Chem. Commun. 32* (1967) 3897;

m) G. P. Giacomelli, R. Menicayli, L. Lardicci, *J. Am. Chem. Soc. 97* (1975) 4009; n) G. P. Giacomelli, R. Menicayli, A. M. Caporusso, L. Lardicci, *J. Org. Chem. 43* (1978) 1790; o) G. P. Giacomelli, R. Menicayli, L. Lardicci, *ibid. 38* (1973) 2370; p) E. C. Ashby, S. H. Yu, *ibid. 35* (1970) 1034; q) H. Haubenstock, *Top. Stereochem. 14* (1983) 231; r) S. Niwa, K. Soai, *J. Chem. Soc. Perkin Trans. 1 1990*, 937; s) G. Muchow, Y. Vannoorenberghe, G. Buono, *Tetrahedron Lett. 28*, (1987) 6163.

[279] M. Balla-Tamasi, *Dissertation*, Technische Universität München 1974.

[280] a) J. Saltiel, A. D. Rousseau, A. Sykes, *J. Am. Chem. Soc. 94* (1972) 5903; b) S. Malkin, E. Fischer, *J. Phys. Chem. 68* (1964) 1153; c) *ibid. 66* (1962) 2482; d) U. Maharaj, M. A. Winnik, *J. Am. Chem. Soc. 103* (1981) 2328; e) J. D. Coyle, *J. Chem. Soc. Perkin Trans. 2 1972*, 683.

[281] a) L. T. Kanerva, E. K. Euranto, *J. Am. Chem. Soc. 104* (1982) 5419; b) D. Seebach, H.-O. Kalinowski, B. Bastani, G. Cross, H. Daum, H. Dörr, N. P. DuPreez, V. Ehrig, W. Langer, C. Nüssler, H.-A. Oei, M. Schmidt, *Helv. Chim. Acta 60* (1977) 301; c) H. E. Zimmermann, T. W. Cutshall, *J. Am. Chem. Soc. 81* (1959) 4305; d) M. Nitta, K. Aomura, K. Yamaguchi, *Bull. Chem. Soc. Jpn. 47* (1974) 2360; e) T. Baba, K. Nakamo, S. Nishiyama, S. Tsuruya, M. Masai, *J. Chem. Soc. Perkin Trans 2 1990*, 1113; f) W. Cocker, P. V. R. Shannon, P. A. Staniland, *J. Chem. Soc. C 1966*, 64; g) M. Srebnik, N. N. Joshi, H. C. Brown, R. B. Wetherill, *Isr. J. Chem. 29* (1989) 229; h) A. I. Meyers, G. Knaus, K. Kamata, M. E. Ford, *J. Am. Chem. Soc. 98* (1976) 567; i) T. Okawa, K. Harada, *J. Org. Chem. 37* (1972) 3286; j) K. Hiroi, K. Nakazawa, *Chem. Lett. 1980*, 1077.

[282] M. Vanderwalle, P. DeClercq, *Tetrahedron 41* (1985) 1767.

[283] a) K. Tomioka, M. Nakajima, Y. Iitaka, K. Koga, *Tetrahedron Lett. 29* (1988) 573; b) E. N. Jacobsen, I. Marko, M. B. France, J. S. Svendsen, K. B. Sharpless, *J. Am. Chem. Soc. 111* (1989) 737; c) J. S. M. Wai, I. Marko, J. S. Svendsen, M. G. Finn, E. N. Jacobsen, K. B. Sharpless, *ibid. 111* (1989) 1123; d) T. Oishi, M. Hirama, *J. Org. Chem. 54* (1989) 5834; e) E. J. Corey, P. D. Jardine, S. Virgil, P.-W. Yuen, R. D. Connell, *J. Am. Chem. Soc. 111* (1989) 9243; f) E. J. Corey, G. I. Lotto, *Tetrahedron Lett. 31* (1990) 2665.

[284] M. W. Plath, H.-D. Scharf, C. Raabe, C. Krüger, *Synthesis 1990*, 951.

[285] M. Tamura, S. Shiono, K. Karada, *Bull. Chem. Soc. Jpn. 62* (1989) 3838.

[286] K. Harada, S. Shiono, *Bull. Chem. Soc. Jpn. 57* (1984) 1040.

[287] M. Nakayama, G. Maeda, T. Kaneko, H. Katsura, *Bull. Chem. Soc. Jpn. 44* (1971) 1150.

[288] a) S. Ikeda, T. Yamagishi, M. Yamaguchi, M. Hida, *Bull. Chem. Soc. Jpn. 62* (1989) 3508; b) T. Yamagishi, S. Ikeda, M. Yatagai, M. Yamaguchi, M. Hida, *J. Chem. Soc. Perkin Trans. 1 1988*, 1787.

[289] D. P. Riley, R. E. Shumate, *J. Org. Chem. 45* (1980) 5187.

[290] V. Šunjić, I. Habuš, G. Snatzke, *J. Organomet. Chem. 370* (1989) 295.

[291] B. Ř. Jaḿes, D. Mǎhajan, *J. Organomet. Chem. 279* (1985) 31.

[292] U. Salz, C. Rüchardt, *Tetrahedron Lett. 23* (1982) 4017.

[293] J. Jähme, C. Rüchardt, *Tetrahedron Lett. 23* (1982) 4011.

[294] D. P. N. Satchell, R. S. Satchell, *Chem. Soc. Rev. 4* (1975) 231.

[295] a) D. Alonso, V. Branchadell, J. Font, A. Oliva, R. M. Ortuño, S. Sánchez-Ferrando, *Tetrahedron 46* (1990) 4371; b) D. Alonso, J. Orti, V. Branchadell, A. Oliva, R. M. Ortuño, J. Bertrán, J. Font, *J. Org. Chem. 55* (1990) 3060; c) O. Riant, H. B. Kagan, *Tetrahedron Lett. 30* (1989) 7403; d) J. Jurczak, A. Zamojski, *Tetrahedron 28* (1972) 1505; e) H. M. Walborsky, L. Barash, T. C. Davis, *Tetrahedron 19* (1963) 2333; f) T. Poll, A. F. Abdel Hady, R. Karge, G. Linz, J. Weetman, G. Helmchen, *Tetrahedron Lett. 30* (1989) 5595.

[296] a) I. Ugi, K. Offermann, H. Herlinger, D. Marquarding, *Justus Liebigs Ann. Chem. 709* (1967) 1; b) I. Ugi, *Angew. Chem. 94* (1982) 826; *Angew. Chem. Int. Ed. Engl. 21* (1982) 810; c) I. Ugi, G. Kaufhold, *Justus Liebigs Ann. Chem. 709* (1967) 11; d) D. Marquarding, P. Hoffmann, H. Heitzer, I. Ugi, *J. Am. Chem. Soc. 92* (1970) 1669.

[297] G. Wilke (Transition Metal Complexes as Catalysts in Organic Synthesis) in J. Streith, H. Prinzbach, G. Schill (Eds.): *Organic Synthesis—an Interdisciplinary Challenge*, Blackwell, Oxford 1985, p. 1.

[298] a) F. Franks, *Pure Appl. Chem. 59* (1987) 1189; b) F. Franks, P. J. Lillford, G. Robinson, *J. Chem. Soc. Faraday Trans. 1 85* (1989) 2417; c) S. J. Angyal, *Adv. Carbohyd. Chem. Biochem. 42* (1984) 15; d) S. J. Angyal, *Angew. Chem. 81* (1969) 172; *Angew. Chem. Int. Ed. Engl. 8* (1989) 157.

[299] a) G. J. Hutchings, M. S. Scurrell, J. R. Woodhouse, *Chem. Soc. Rev. 18* (1989) 251; b) G. J. Hutchings, J. R. Woodhouse, M. S. Scurrell, *J. Chem. Soc., Faraday Trans. 1 85* (1989) 2507.

[300] K. Yamamoto, S. Yoshida, H. Nishide, E. Tsuchida, *Bull. Chem. Soc. Jpn. 62* (1989) 3655.

[301] a) H. U. Blaser, H. P. Jalett, D. M. Monti, J. F. Reber, J. T. Wehrli, *Stud. Surf. Sci. Catal. 41* (1988) 153; b) J. T. Wehrli, A. Baiker, D. M. Monti, H. U. Blaser, H. P. Jalett, *J. Mol. Catal. 57* (1989) 245.

[302] C. Hatat, A. Karim, N. Kokel, A. Mortreux, F. Petit, *New J. Chem. 14* (1990) 141.

[303] K. Harada, T. Munegumi, *Bull. Chem. Soc. Jpn. 56* (1983) 2774.

[304] The results from *Savéant* reveal relevant points about the mechanism of the interaction of alkyl bromides with aromatic anion radicals and with low oxidation state iron porphyrins. The observation of inversion points in the Arrhenius diagram is explained in terms of single electron transfer and subsequent S_N2-like substitution: D. Lexa, J.-M. Savéant, K.-B. Su, D.-L. Wang, *J. Am. Chem. Soc. 110* (1988) 7617.

Chemical Sensors and Biosensors—Principles and Applications

By Karl Cammann,* Udo Lemke, Anja Rohen, Jürgen Sander, Hildegard Wilken and Babette Winter

Chemical and environmental engineering and biotechnology are among the fields now being transformed by continually increasing levels of automation. Whereas the objective in other sectors of industry is simply to increase efficiency, here considerations of system theory or safety demand a high level of automation. Either the processes are too complex and require multifunctional control with feedback, or an analysis of the safety requirements shows the necessity for a certain degree of redundancy in the safety measures, and for elimination of human error as a risk factor. With regard to quality control, cost-benefit analyses lead to striking conclusions which again indicate the need for highly automated, and above all reliable, systems to eliminate rejects. The crux of any automated system is the measurement and control technology; of central importance is the rapid, reliable, and in some cases continuous, measurement and interpretation of key processes or control variables. For this purpose a wide variety of recording instruments and sensors are used to give as accurate a picture as possible of the state of the system. It is obvious from this that the performance of the control system is critically dependent on the sensors. Errors in the measured quantities can become amplified in the control variables or, in dynamic systems, can lead to undesirable operating conditions. Moreover, as a consequence of great advances in microelectronics, "intelligent sensors" which can calibrate and control themselves will be one of the key technologies of the nineties. Unless fast and immediate information on the true current status of a system is available, microprocessors as control devices react blindly and unpredictably to errors in input information. New discoveries in the fields of electronic, electrochemical, and optical transducers are now being applied in heterogeneous catalysis and surface physics, and in biochemistry (enzymology and immunology); in these fields new chemical sensor principles are being tested, which could revolutionize instrumental methods of molecular analysis in particular, owing to their very favorable cost-performance relationship. This article aims to give an up-to-date overview of the current state of the art in these developments, with emphasis on their importance for analysis and their significance in relation to the chemist's interest in mechanisms for identifying substances.

1. Introduction[**]

1.1. Definitions

Following a definition which has been proposed under the relevant IUPAC Commission,[1] analytical chemical sensors are miniaturized transducers that selectively and reversibly respond to chemical compounds or ions and yield electrical signals which depend on the concentration. Interpreting this strictly, one only has a true sensor if concentration changes in both directions can be detected. These conditions are not in general satisfied by devices such as indicator tubes and test strips. Moreover, these cannot provide a continuous signal proportional to concentration, and according to another IUPAC discussion paper[2] they are better described as dosimeters. Similarly there is a consensus of opinion in the relevant IUPAC committees that a large analytical instrument (e.g. a mass spectrometer) used with an external probe or a flow injection system (FIA) cannot be regarded as a sensor, although in the case of integrated optics the dividing line between such devices and true sensors is blurred.

According to these nomenclature proposals biosensors can be regarded as a sub-group of chemical sensors in cases where biological recognition mechanisms or principles are used as a means of recognizing substances or molecules. Some types of "biomolecules" isolated from living systems, such as enzymes, antibodies, or receptors, are able to recognize chemical compounds with high specificity and can be adapted to generate signals. Biosensors are vastly superior to chemical sensors as regards selectivity. They would be the ideal sensors if their lifetime were not severely limited by stability problems.

1.2. History

When around the turn of the century it was discovered purely by accident, in the course of physiological studies on the properties of thin membranes, that certain types of glass were sensitive to pH,[3] the significance of this effect for the development of sensors with applications in analytical chemistry could not be foreseen. Subsequently by using suitably

[*] Prof. Dr. K. Cammann, Dipl.-Chem. U. Lemke, Dipl.-Chem. A. Rohen, Dipl.-Chem. J. Sander, Dipl.-Chem. H. Wilken, Dipl.-Chem. B. Winter
Lehrstuhl für Analytische Chemie/Institut
für Chemo- und Biosensorik der Westfälischen Wilhelms-Universität
Anorganisch-Chemisches Institut
Wilhelm-Klemm-Strasse 8, W-4400 Münster (FRG)

[**] The following abbreviations are used: Chem FET = chemical field-effect transistor; ENFET = enzymatically modified, ion-selective field-effect transistor; FET = field-effect transistor; FIA = flow injection analysis; ISE = ion-selective electrode; ISFET = ion-selective field effect transistor; PZ = piezoelectric crystal; SAW = surface acoustic wave.

designed pH electrodes made with glass membranes, it became possible for the first time to determine the hydrogen ion concentrations in aqueous solutions with high selectivity and remarkable precision,[4] a facility which proved extremely useful in guiding the development of early acid-base theories. However, it was not until 1935, when the first commercial electrometer amplifiers for measurements on high-resistance voltage sources became available (with the founding of Beckman Instruments by Prof. *A. O. Beckman*), that this brought about a major changeover from the optical pH indicator methods used previously to the much better potentiometric method, whose theoretical basis had been laid as early as 1889 by *Nernst*, in the equation named after him. The technique of electrometric pH measurements[5–7] subsequently became the most frequently used method in instrumental analysis, due to a large extent to further advances in measurement technology. A further breakthrough in chemical sensor technology came with the development in 1966 of ion-selective electrodes (ISEs) for calcium, fluoride, silver, and sulfide ions,[8, 9] and in 1967 for potassium ions;[10, 11] using these electrodes one could determine the relevant ions in a procedure analogous to a pH measurement. The knowledge gained during research in the field of ISEs led in the years that followed to the development of further electrodes for a number of different ions,[12, 13] so that nowadays a dozen cations and anions can be determined by direct potentiometric measurements (see Table 1).[14–16]

The technology of chemosensors was not confined to ion-selective potentiometry and other electrochemical methods of detection such as polarography, voltammetry, or amperometry, which gained considerably in importance as a result of the development of the gas-membrane-covered O_2 electrode by *Clark*.[17] Detection systems based on semiconductors, e.g. SnO_2, which can detect oxidizable gases, were first conceived in the 1970s.[18] Mass-sensitive systems incorporating piezoelectric crystals (PZ or quartz oscillator systems) and surface acoustic wave (SAW) devices were first reported in the mid-sixties as sensitive detectors for hydrocarbons in gas chromatography.[19] The first studies in the field of miniaturized fiber-optic sensors (optodes or optrodes) were published in 1975.[20, 21]

Enzyme electrodes were first described in 1962;[22] these depended for their selectivity on the enzymic breakdown of glucose, which could be arranged as an amperometric electrode, enabling glucose to be determined in physiological investigations. The term "biosensor" to describe enzyme-modified ion-selective electrodes first appeared in the analytical literature in 1977.[23] Biosensors are nowadays available commercially for many highly relevant substrates such as glucose, lactate, urea, penicillin, etc.

Table 1. Summary of the different types of electrodes, classified as conventional types and newer types.

Type of electrode	Species measured
Conventional electrodes	
glass membrane	$H^{\oplus}$ $Na^{\oplus}$, $Ag^{\oplus}$, $Li^{\oplus}$, $Cs^{\oplus}$, $Rb^{\oplus}$, $NH_4^{\oplus}$, $K^{\oplus}$, $Tl^{\oplus}$
liquid membrane	$Cu^{2\oplus}$, $Cl^{\ominus}$, $Mg^{2\oplus}$, $Ca^{2\oplus}$, $NO_3^{\ominus}$, $ClO_4^{\ominus}$, $UO_2^{2\oplus}$, $BF_4^{\ominus}$,
ion-exchange	organic cations and anions, some drugs
neutral carrier	$K^{\oplus}$, $Li^{\oplus}$, $H^{\oplus}$, $Ca^{2\oplus}$, $Mg^{2\oplus}$, $Na^{\oplus}$, $NH_4^{\oplus}$, $Sr^{2\oplus}$, $Ba^{2\oplus}$, $Cd^{2\oplus}$
crystal membrane	
single crystal	$F^{\ominus}$
polycrystalline	$S^{2\ominus}$, $Ag^{\oplus}$, $Hg^{2\oplus}$, $Cl^{\ominus}$, $Br^{\ominus}$
mixed crystal	$Cl^{\ominus}$, $Br^{\ominus}$, $I^{\ominus}$, $CN^{\ominus}$, $SCN^{\ominus}$, $Cd^{2\oplus}$, $Pb^{2\oplus}$, $Cu^{2\oplus}$
gas sensor based on ISE	CO_2, NH_3, H_2S, SO_2, HCN, HCl, HF, NO_x
Newer electrodes	
ISFET (ion-selective field-effect transistor)	H_2, H_2S, $H^{\oplus}$, $Li^{\oplus}$, $Na^{\oplus}$, $K^{\oplus}$, $NH_4^{\oplus}$, $Ca^{2\oplus}$, $Cl^{\ominus}$, $F^{\ominus}$
coated wire	$H^{\oplus}$, $Li^{\ominus}$, $Na^{\oplus}$, $K^{\oplus}$, $NH_4^{\oplus}$, $Ca^{2\oplus}$, $Fe^{3\oplus}$, $Cl^{\ominus}$, $Br^{\ominus}$, $I^{\ominus}$, $SCN^{\ominus}$, $SO_4^{2\ominus}$, $NO_3^{\ominus}$, $ClO_4^{\ominus}$, organic ions, amino acids, drugs
polymer matrix	$Cu^{2\oplus}$, $Mg^{2\oplus}$, $Ca^{2\oplus}$, $Cs^{\oplus}$, $Li^{\oplus}$, $Na^{\oplus}$, $K^{\oplus}$, $NH_4^{\oplus}$, $Co^{2\oplus}$, $NO_3^{\ominus}$, $S^{2\ominus}$
microelectrodes	$H^{\oplus}$, $K^{\oplus}$, $Na^{\oplus}$, $Li^{\oplus}$, $Ca^{2\oplus}$, $Mg^{2\oplus}$
film electrodes	$H^{\oplus}$, $K^{\oplus}$, $Na^{\oplus}$, $Li^{\oplus}$, $Cl^{\ominus}$

1.3. General Design Features of Chemo- and Biosensors

The essential principle of a chemo- or biosensor is described in terms of three basic components (Fig. 1). The most important component is the receptor (the recognition system), where in general an energetic interaction specific to the substance in question (the analyte) enables it to be recognized. The development of new recognition principles, or the improvement of known processes for this purpose, is a task for the chemist or physical chemist. Compared with this challenge the next stage is less difficult; the function of this second component of any chemo- or biosensor is to "relay" the substance-specific signal, in other words to transform an energy quantity into an electrical signal proportional to it.

Karl Cammann, born in 1939 in Düsseldorf, studied Chemistry at the Technical University of Munich after obtaining a degree in chemical engineering and working in industry (Beckman Instruments) for several years. His scientific advisor for the Diplom thesis was H. Gerischer; his Ph.D. advisor was G. Ertl (University of Munich). After postdoctoral positions with G. A. Rechnitz (State University of New York at Buffalo) and S. Mazur (University of Chicago) he accepted an assistant professorship for Analytical Chemistry at the University of Ulm. In 1986 he became an Associate Professor of Analytical Chemistry at the Technical University of Munich and shortly thereafter (1987) Full Professor of Analytical Chemistry at the Westfälische Wilhelms University of Münster (chair of Prof. F. Umland). His research interests lie in the field of selective chemical detectors and monitors. In 1987 he received two awards for the development of a new plasma-emission-spectroscopic GC-detector (Océ van der Grinten Pollution Control Award; Technology Transfer Award of the German Ministry for Education and Science).

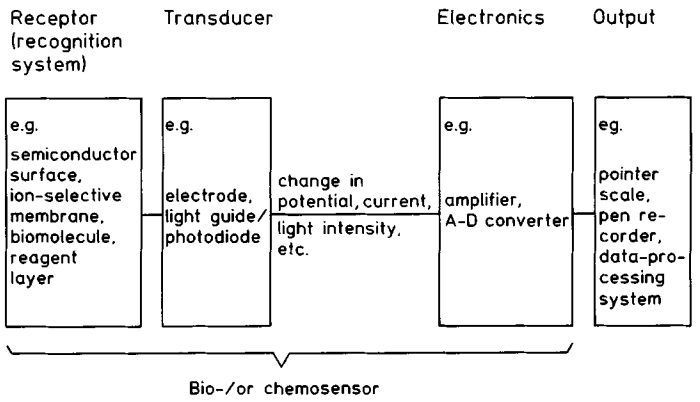

Fig. 1. Schematic arrangement of a chemo- or biosensor system.

This task is usually performed by one of a wide choice of familiar physical transducers. Often a third component, consisting of a further electronic unit (a preamplifier, impedance converter, multiplexer, analogue-to-digital converter, etc.) is placed directly after the transducer, to suppress as far as possible external influences caused by interfering electric or magnetic fields, or to feed the separate signals from several recognition systems simultaneously to the data processing unit through a single electrical connection.

Chemo- and biosensors can be classified according to the type of sensor element used for molecular recognition, or according to the type of transducer. If the emphasis is on analytical selectivity, the most important component is the recognition system. If on the other hand the limit of detectability or the signal-to-noise ratio is crucial, the critical component may be the physical or electronic transducer (see Table 2).

Table 2. Classification of chemo- and biosensors according to the type of transducer.

Type of transducer	Measuring principle or property measured
electrochemical	potentiometry
	amperometry
	voltammetry
	field effect (chemFET, ISFET)
electrical	surface conductivity (MOS)
	electrolyte conductivity
optical	fluorescence
	absorption
	reflection
	luminescence
	refractive index (surface plasmon resonance, SPR)
	light scattering
	evanescent wave
magnetic	paramagnetism
mass-sensitive	resonance frequency of a piezoelectric crystal (PZ)
	surface acoustic wave (SAW)
thermal	heat of reaction
	heat of adsorption

All chemo- and biosensors can be used directly for analyzing gases and liquids (the latter also includes suspensions or pastes) for specific ions or molecules, in concentrations varying from the ppb range to the percent range. As the sample preparation required for chemo- or biosensors of adequate selectivity is minimal, and the sensors are available at low cost, high rates of growth are forecast by all the market studies that have been carried out. For sensors that are less selective, it is still possible in many cases to design a comparatively inexpensive measuring instrument, by incorporating automatic sample preparation based on a chemical reaction which is selective, or on separation techniques. Flow injection analysis is especially valuable in this respect.[24]

2. Chemosensors

2.1. Electrochemical Sensors

2.1.1. Ion-Selective Electrodes

Till a few years ago ion-selective electrodes (including the glass pH electrode) were the most important class of chemosensors in economic terms, since at that time the "lambda-probe" for controlling three-way catalytic converters for automobiles was not yet produced in today's numbers because of the absence of legal requirements. In ion-selective potentiometry the data are processed using an extension of the Nernst equation derived empirically by *Nicolsky*.[25] This extended equation (a) relates the activity of the ion species to be determined and the measured voltage when an ISE half-cell is connected to a common reference electrode, taking into account the effects of all interfering components.

$$U = U^0 + \frac{RT}{z_M F} \ln \left[a_M + \sum_I K_{M-I}\, a_I^{z_M/z_I} \right] \qquad \text{(a)}$$

U = potential of the cell
U^0 = standard potential of the cell
R = universal gas constant
T = absolute temperature
F = Faraday constant
a_M = activity of the ion being measured
z_M = charge of the ion being measured (with appropriate sign)
K_{M-I} = selectivity coefficient (measured ion vs. interfering ion)
a_I = activity of the interfering ion
z_I = charge of the interfering ion (with appropriate sign)

The selectivity is described by the selectivity coefficient K_{M-I}, which unfortunately is not a constant, since it depends on the method used for the determination and on the concentrations of all the interfering species and the ion to be measured. For good ISEs it is of the order of 10^{-4}, which means that a 10^4-fold excess of the interfering ion would change the reading by a factor of 2 (i.e. an error of 100%). A new theoretical model of the mechanism for the selectivity in the potential generated at the phase boundary between the ion-selective membrane and the measured medium has been developed in the last few years.[26–30] This is based on the studies of *Koryta*[31] and others on electrochemical phenomena at the interface between two immiscible electrolytes, and also on results from studies on corrosion involving competing electrode reactions.

The basic principle of ion-*selective* potentiometry is the observation of an ion-*selective change* in the potential at the phase boundary. This in turn depends on the ion-selective change (or shift) of charge (or charge distribution) at this boundary, i.e., a significant transfer between the phases occurs only for the ion species in question. This requires that

certain energetic and geometrical variables be optimally matched.

If an uncharged ion-selective membrane electrode which satisfies the electrical neutrality condition is immersed in an electrolyte solution, a transfer of charge carriers occurs between the phases. The direction of this (membrane → solution or the reverse) is determined by the gradient of the chemical potential. When only one species of ion can selectively cross the boundary (this selectivity results, for example, from specific complex formation in liquid or PVC membranes, or from the dimensions of lattice sites in polycrystalline or semicrystalline materials), this selective transfer of charge carriers leads to a redistribution and an accumulation of charge at the phase boundary. This generates an electric field, thus counteracting the ion transfer which was at first energetically favored, so that eventually, under the combined influence of the electrostatic repulsion between similarly charged particles and the attractive forces due to the oppositely charged carriers left behind, the transfer of charge carriers ceases and the reverse reaction is favored. In the equilibrium state the microscopic ion currents passing in both directions through the phase boundary are equal, and the ion-selective potential difference that is thereby established is constant and can be measured. Externally the condition is one of zero current (a requirement for potentiometric measurement).

In terms of electrochemical kinetics the transport of charge carriers (measured ions) across the phase boundary between the electrode or ion-selective membrane and the solution corresponds to a directed electric current $\vec{i}$ or $\overleftarrow{i}$ (depending on whether the direction is from membrane to solution or the reverse). In the equilibrium state $\vec{i} = \overleftarrow{i} = i_0$. The current density j_0 ($= i_0/A$, A = area) is called the exchange current density (see Fig. 2). The two opposing current densities $\vec{j}$ and $\overleftarrow{j}$ maintain the ion-selective charge distribution at the phase boundary at a constant value. Furthermore, these microscopic ion-currents actually make it possible to measure the charge distribution at this interface, since in practice one cannot avoid drawing a current of 10^{-10} to 10^{-14} A in the measuring circuit, depending on the amplifier used, which corresponds to a net flow of 10^9 to 10^5 elementary charges per second. The ion-selective electrical potential generated at the phase boundary of such an ion sensor by selective charge separation is, of course, dependent on the concentration of the ionic species which can cross the boundary. The relationship between ion concentration and interfacial potential was derived theoretically by *Nernst* as long ago as 1889, in the brilliant work leading to the equation named after him. From the ion-exchange current density j_0, which can be determined experimentally, the recent theory predicts the selectivity of a potentiometric sensor. The potential in each case is determined by the ionic species that has the greatest exchange current density.

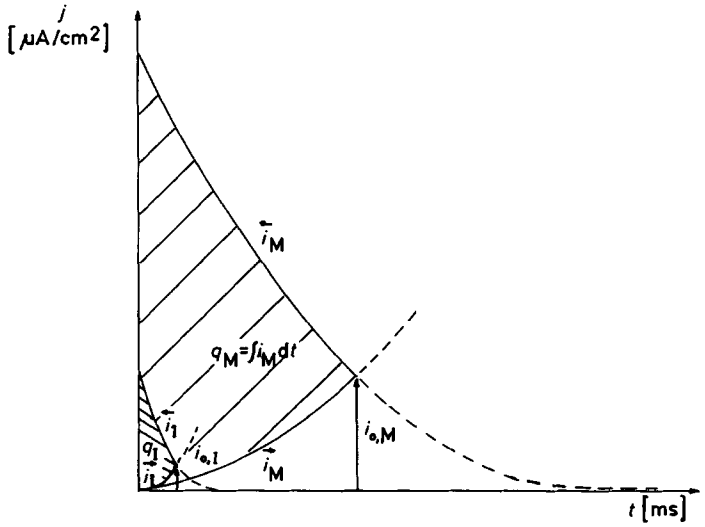

Fig. 2. Schematic representation of the forward and reverse currents $\vec{i}$ and $\overleftarrow{i}$ passing through the phase boundary; the selectivity is given by the ratio of the (equilibrium) charges q_M and q_1 for the measured and interfering ions respectively (see text).

Other reactions may take place at the phase boundary in parallel with the process described (because real solutions usually contain interfering ions in addition to those being measured). The thermodynamic equilibrium potentials for the individual electrode reactions (in this case, the parallel processes in which the measured and interfering ions cross the phase boundary between two ionic conductors), as in the case of corroding metal electrodes, may not be fully achieved. This results in deviations from the theoretical Nernst behavior. In order to achieve a high ion-exchange current density and thereby obtain the desired selectivity, appropriate changes can be made in the thermodynamic and kinetic variables. For example, introducing into the membrane an ionophore for a particular ion species causes an increase in the exchange current density, and therefore in the selectivity for that ion. The selectivity obtained in this way is probably due to a long-range ion–dipole interaction between this particular ion species in the solution and the ionophore in the membrane surface. It is conceivable that, specifically for the potential-determining ion species, an overlap of the energy barriers involved (desolvation and decomplexation activation-energy profiles) occurs, which results in the lowering of the effective activation energy for ion transfer over the entire phase boundary. This activation energy can also be expressed in electrochemical terms as an ion-transfer resistance. This in turn is inversely proportional to the exchange current density, and can be obtained, for instance, from impedance spectra.[32, 33]

The selectivity of all types of ion-selective membranes, the rapid establishment of the potential, even for thick membranes, and the abnormally large graph slopes in the U vs. $\log a$ diagram that are occasionally found (steeper than predicted by the Nernst factor preceding the logarithm of the activity of the measured ion, see Eq. (a)), can all be satisfactorily explained by this novel theoretical approach which also considers kinetic parameters. Numerous fundamental studies have been carried out in our research group since 1975 to determine the conditions that must be fulfilled for a particular ion to be potential-determining (and therefore able to be measured selectively). For every type of electrode the critical factor was the ratio of the exchange current density for the measured ion to that for the relevant interfering ion. In every case this ratio was equal to the potentiometrically measured selectivity coefficient in the extended form of the Nernst equation [Eq. (a)].

A comparison of good ion-selective electrodes reveals several common features. Firstly, they have a rather high poten-

tial-determining exchange current density for the measured ion at the phase boundary between the ion-selective membrane and the solution. Secondly, for solid membranes, there is a preferential ionic conductivity in regions near the surface (e.g., Ag_2S is a good conductor for $Ag^{\oplus}$ ions, and LaF_3 doped with $Eu^{2\oplus}$ is a good conductor for $F^{\ominus}$ ions). In PVC membranes with selective ionic charge carriers the preferred method is to use only ion–dipole interactions, as is evident from a glance at the list of so-called electroactive compounds that are available.[34] Apparently the course of the activation energy threshold for the transfer of ions from the membrane phase to the solution, together with the course of activation energy for the desolvation process, determines the intersection point (i.e., the effective energy of activation for the phase transition of the relevant ion).

The existence of a purely kinetic effect in favor of the ion being measured is a necessary, but not a sufficient, condition for a selective Nernst sensor which performs well and above all is stable over long periods. In addition there must be a certain degree of nonpolarizability. This quantity, as electrochemists use it, is, in simple terms, a measure of the ability of an electrochemical half-cell to maintain a constant potential regardless of the instantaneous current density at the interface. Good ion-selective electrodes, like good reference electrodes, have a relatively steep characteristic curve in the current vs. voltage diagram (C–V curve) for the ion being measured. Viewed from this standpoint, the interfering ions have characteristic C–V curves that are less steep than that for the ion being measured. If these ions are present in a solution together with the measured ions, according to our present state of knowledge a mixed potential is established, as is the case for corroding metal electrodes. This is determined predominantly by the equilibrium potential for that electrode reaction (transfer of ions between phases) which has the steepest C–V characteristic. To obtain a favorable C–V characteristic over as large a range of overpotential as possible, it is also necessary to take concentration polarization effects into account. Here higher concentrations of the measured ions in the membrane phase turn out to be beneficial; their diffusion from there into the solution, which has an unfavorable effect on the limits of detection, is hindered by complexation and by the charges of appropriately chosen counterions. This also has the advantage of increasing the buffer capacity for the chemical potential of the measured ions in the membrane phase. A detailed treatment of these aspects has been published.[35]

Ion-selective electrodes can be used as electrochemical half-cells in combination with suitable constant-potential reference electrodes for the quantitative determination of a wide range of substances (see Table 1). They can be classified according to the type of membrane, viz., glass, solid, liquid, or PVC membrane electrodes.[36, 37] Glass and solid membrane electrodes are robust and have a typical lifetime of several years, much longer than liquid or PVC membrane electrodes, which only remain effective for about six months, depending on the application, unless one is prepared to accept large sacrifices in sensitivity and selectivity. However, for the latter types of electrodes some manufacturers have introduced a modular design which allows the easy and rapid renewal of sensitive electrode elements. The most important types of ionophores required to make one's own selective PVC membranes are available commercially,[38] and are supplied complete with instructions; these were developed mainly by *Simon*'s research group in Zürich.

2.1.2 Ion-Selective Field Effect Transistors (ISFETs)

It was believed for a long time that in ion-selective field effect transistors, first described by *Bergveld*[39, 40] in 1970, we at last had a new generation of sensors which met all the requirements of miniaturizability, compatibility with microelectronics, and the capability for being mass-produced, with attendant cost savings. The now familiar production techniques of microelectronics seemed to offer prospects for developing chemosensors in the form of disposable mass-produced articles. Since then the initial euphoria has given way to a more realistic assessment, since these sensors still pose difficulties with regard to long-term stability and integration with miniaturized reference electrodes. Nevertheless, it is of interest to examine this class of sensors in a little more detail in the following discussion, since they bring together the disciplines of chemistry, electronics, and thin film technology, and they provide the basis for biochips.

An ISFET can be generally regarded as a very miniaturized version of an ion-selective half-cell with an in-built impedance converter. It can be used to determine the activity of not only individual ion species, for which ion-selective macro-electrodes are also available, but also—in the form of an enzyme-coated ISFET (biochip)—a wide variety of substrates. The transistors that are used can in most cases be made as very small devices, allowing the accommodation of several sensitive surfaces for detecting different ions or substrates on a single chip with an area of only a few mm^2. The entire electronic control circuit, including temperature compensation, can also be fitted on the same chip.

The basic building block of all ISFETs is a field effect transistor (FET), in which the metallic gate of a conventional transistor is replaced by an insulating layer, above which is an ion-selective layer. The value at any instant of the gating potential, which controls the current between the source and the drain, is determined by the activity of the ion species being measured, through the presence of the ion-selective surface film. Figure 3 shows the basic construction of an ISFET in a form which has certain advantages. Often, however, instead of measuring the variation of the source-to-drain current as a function of the activity of the measured ion

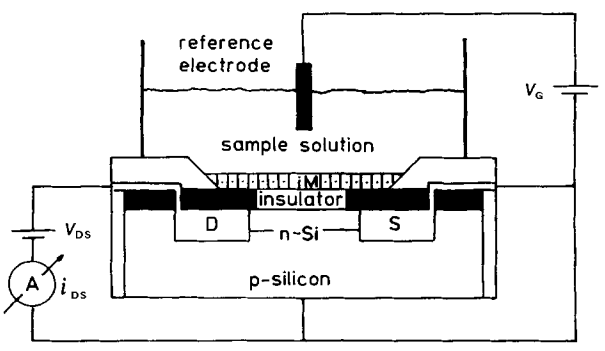

Fig. 3. Operating principle of an ISFET; the applied gate potential V_G controls the current i_{DS} flowing from source S to drain D.

species, one measures the control voltage that must be applied via a reference electrode to hold this current at a constant value; this makes it possible to maintain an optimal working point, chosen to reduce temperature effects.

In an ISFET the ion-selective PVC membrane, which is applied to the gate surface mainly by spin-coating, forms the sensor element, which recognizes specific substances. By using known electroactive compounds, all types of ion-selective PVC membrane electrodes can also be incorporated into ISFETs. However, problems with the adhesion of the plastic membrane to the gate surface result in contact difficulties, since the membrane which gives the selectivity becomes detached, usually after a few weeks. In a pH-ISFET[41-44] protons produce a field, whose intensity depends on the $H^{\oplus}$ concentration, at a thin film of SiO_2, Si_3N_4, Al_2O_3 or Ta_2O_5. A serious disadvantage of these materials is that in many cases they still have some sensitivity to light and redox systems. Also, the diffusion of impurities into the lower layers of the semiconductor, which are known to be sensitive to this, usually results in a slow drift of the measuring signal, of the order of a few mV per day.

The disadvantages mentioned, together with the fundamental problem of leakage-path formation in the insulation of the remaining transistor surfaces, which again causes drift in the readings before the device finally ceases to function, has so far prevented ISFETs from achieving a larger commercial success. However, recent developments in the area of electrolytic glazing offer some hope of improvements.[45] In the development of ISFETs work is already in progress on multisensor arrays[46, 47] in which several different ion-selective sensor elements controlling separate gates are integrated on a single chip. Here, however, one is approaching the limits of miniaturization technology. The spin-coating technique cannot lay down closely spaced regions of different selectivity less than 1 mm^2 in area. Experiments in which a common plasticized PVC membrane is laid down to cover all the gates before local regions above individual gate surfaces are doped with different electroactive compounds have also encountered problems, because diffusion of ionic carriers within the membrane smears out the ion selectivities.

It is also necessary to integrate into the ISFET a miniaturized reference electrode with long-term stability, in order to exploit fully the advantages of the device as a miniaturized chemosensor. If the dimensions of the salt-bridge elements are too small, resulting in only short-term resistance of the integrated reference electrode to invasion by potential-falsifying substances, it will only be possible to make disposable sensors. Here, however, it is important to investigate the possibility of using a conventional thick-film design for the electrodes, which might also be cheaper.

In this connection an interesting alternative to ISFETs are film electrodes produced using planar technology.[48] These too offer the advantages of miniaturized sensors which can be economically mass-produced. One commercially available system[49, 50] is based on the principle of zero-point potentiometry. In this one-shot disposable sensor, the measuring and reference systems are identical, and as the pair are made under identical conditions from the same materials the potential difference with the relevant membranes in contact with the same solution is zero. If one now deposits on one of the sensor surfaces a reference solution of known concentration, and on the other the solution to be tested (see Fig. 4), according to the Nernst equation the observed potential difference gives a direct measure of the concentration difference between the two solutions for the relevant measured ion species (concentration meter design). The errors that are pos

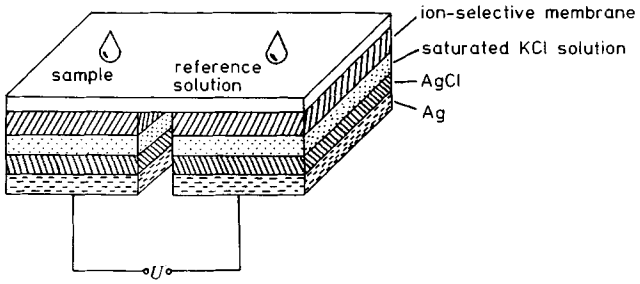

Fig. 4. Construction of a film sensor (Kodak), which works on the zero point potentiometry principle.

sible in difference methods of this sort (where no transport of samples is involved) are very small, as the problems with conventional reference electrodes (variations in potential due to diffusion), ageing effects, and electrode poisoning effects are avoided. However, continuous measurements are not possible with this device.

2.1.3. *Ion-Conducting Solid Electrolyte Sensors*

The lambda-probe, which has become familiar because of the three-way catalytic converter, is currently the most widely used of all electrochemical sensors. It enables the measurement of the residual oxygen content in the exhaust from internal combustion engines, making use of the selective ionic conductivity of the $O^{2\ominus}$ ion in yttrium-doped ZrO_2 at temperatures above 400 °C. A potentiometer device for measuring O_2 concentrations can be designed as a concentration cell, which allows the gaseous oxygen to be in equilibrium with the lattice oxygen in the solid electrolyte [reaction (1)].

$$O_2(g) + 4e^- \rightleftharpoons 2O^{2\ominus} \quad (1)$$

If there is a higher oxygen concentration on one side of the ZrO_2 membrane than on the other (i.e. on one side an oxygen partial pressure $p_{O_2}^{ref}$, for example, of the outside atmosphere or of a reference gas, and on the other side a partial pressure $p_{O_2}^{sample}$, for example, of the exhaust gas or other medium being analyzed), according to the Nernst equation a potential difference proportional to the logarithm of the ratio of the two oxygen pressures is set up [Eq. (b)].

$$U = \frac{RT}{4F} \ln \frac{p_{O_2}^{ref.}}{p_{O_2}^{sample}} \quad (b)$$

The selectivity of this sensor results from the fact that in ZrO_2 there is a selective conductivity for $O^{2\ominus}$ ions (similar to that for $F^{\ominus}$ ions in single crystals of LaF_3), which also determines the surface reaction. Figure 5 shows schematically the construction of a lambda-probe working on the potentio-

metric principle.[51, 52] With regard to the other analytical properties of the device, the same arguments as for ion-selective membrane electrodes apply here. The range of concentrations that can be measured is enormous (> 10 decades), provided that the current in the measuring circuit is considerably less than the exchange current for the redox reaction (a) at the platinum contact electrodes. The precision in this case also is limited to 0.1 mV, and at constant temperature this gives a relative precision of about 2% in the measured concentration. This accuracy is sufficient for the typical use in a three-way catalyst for automobiles; due to the logarithmic dependence of the signal according to the Nernst equation an immense potential difference results.

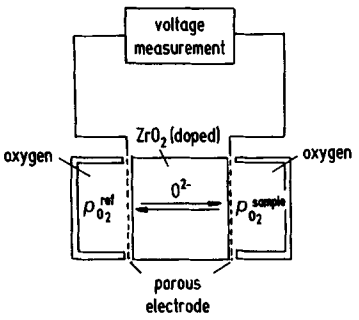

Fig. 5. Schematic representation of a lambda-probe, operated as a potentiometric sensor.

LaF_3, which has an appreciable ionic conductivity even at room temperature, has been found to be a suitable solid electrolyte for the determination of O_2 at room temperature.[53] In this material a change in potential is produced by $OH^{\ominus}$ and $HO_2^{\ominus}$ ions formed as intermediates, and this allows an indirect measurement of the O_2 concentration.[54]

High temperature solid electrolytes with $O^{2\ominus}$ conductivity can also be used at a constant oxygen concentration for detecting oxidizable substances, by making use of a second reaction that takes place at the electrodes. An example where this occurs is in the catalytic oxidation of NH_3 and the determination of chromium in molten steel,[55] by reaction (2).

$$3O^{2\ominus}(SIC) + 2Cr(metal) \longrightarrow Cr_2O_3(2nd\ phase) + 6e^-(metal) \quad (2)$$

(SIC = solid ionic conductor)

Here the $O^{2\ominus}$ ions moving in the solid electrolyte oxidize the chromium with the release of electrons, which can be measured as a change in potential. It has also been shown that silicon can be determined by a similar method when $ZrSiO_4$ is the solid ionic conductor.[56] A very compact sensor suitable for applications at these high temperatures (above 1600 °C) has recently been developed; this can be used for up to 10 h in molten steel.[57] Special sensors have also been developed for determining oxygen in liquid sodium, which is used in fast breeder reactors.[58, 59] In addition to withstanding high temperatures and mechanical loading, these sensors must also be resistant to radiation and corrosion by sodium.

Solid electrolyte sensors that have been developed for determining substances other than oxygen include especially those for SO_2/SO_3 and CO_2.[60] These consist for example, of $Li_2SO_4 + Ag_2SO_4$[57, 61–64] and have a working temperature of about 400 °C. The sensitivity of such sensors is in the range of 3 to 10^4 ppm of SO_3, and they are currently being tested for use in monitoring exhaust gases. The measurement of Cl_2 is also possible with surface-modified solid electrolytes, e.g. the ionic conductor $LiAlCl_4$ with its surface covered by a thin film of LiCl or $AlCl_3$. The cell voltage is determined by the partial pressure of chlorine, and obeys the Nernst equation.[65, 66]

2.1.4. *Amperometric Sensors*

To avoid the requirements for temperature constancy in the lambda-probe, and obtain a linear instead of a logarithmic relationship between signal and concentration with higher accuracy, which is essential in engines working with $\lambda > 1.0$, the sensor can alternatively be designed as a limiting current probe.[67, 68] This configuration, which can also be operated at temperatures below 400 °C, differs from the potentiometric form of a lambda-probe in that a current flows through the O_2 concentration cell as a result of an externally applied voltage ("pumping voltage"), thereby transporting oxygen from one side of the ZrO_2 membrane to the other (an "oxygen pump"). In front of the cathode there is a diffusion barrier (e.g. a porous ceramic layer), which the oxygen must traverse before being reduced and transported through the ZrO_2 to the anode (Fig. 6). If the applied voltage is chosen

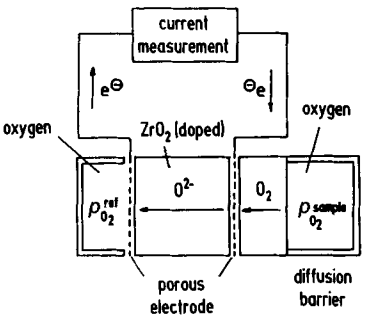

Fig. 6. Schematic representation of a lambda-probe operated as a limiting current sensor.

so that each oxygen molecule that arrives is immediately reduced at the cathode, a voltage-independent limiting current region is obtained, as in polarography. The current then flowing is directly proportional to the O_2 concentration to be measured, and the temperature coefficient is no longer given by the Nernst factor, but is determined by the properties of the diffusion barrier.[69]

The amperometric measuring principle has largely been used to advantage in industrial chemosensors for gases. The classic example of this is the Clark oxygen sensor.[17] The oxygen whose concentration is to be measured diffuses through a gas-permeable membrane 10 to 50 μm thick, which is made of polytetrafluoroethylene (Teflon) or a fluorinated ethylene–propylene copolymer (FEP) with a very high permeability to oxygen. Behind this membrane is an electrolyte solution containing chloride ions, in which are immersed a platinum or gold cathode as the working electrode

and an anode of Ag/AgCl as the constant potential counter-electrode (cf. Fig. 14). The reduction of the oxygen takes place at a working electrode potential of approximately -0.8 V relative to the Ag/AgCl electrode. The rate-limiting step is the diffusion of the oxygen through the gas-permeable membrane, and the rate of this depends on the gradient of the O_2 partial pressure across the membrane. The current is therefore determined primarily by the O_2 partial pressure. As the membrane is impermeable to liquids and electrolytes, the sensor can also be used to determine dissolved oxygen in liquids; in this case the dependence on the partial pressure must be noted. The sensor gives the same reading for air and for a liquid that is saturated with air! To obtain a reading which indicates the dissolved oxygen in $mg\,L^{-1}$ it is necessary to calibrate the sensor.

A disadvantage of most O_2 sensors based on this principle is that oxygen is consumed. When they are used in stationary liquids there may not be a sufficient flow of oxygen to the electrode (resulting in an oxygen-deficient layer in the liquid whose growth follows a $\sqrt{t}$ law), which gives readings that are too low. The solution being measured must therefore be stirred, but this leads to some extent to a dependence of the observed signal on the convection flow. The effects of this disadvantage (especially in biomedical applications) can be minimized by reducing the area of the working electrode, which in turn causes difficulties because the current then becomes very small. Efforts are now in progress to overcome this problem by using an array of ultramicroelectrodes (Fig. 7). The use individual electrodes as small as 1 μm in diameter, has led to such low reaction rates that the Brownian motion of the molecules together with the radial diffusion sphere ensures a sufficient oxygen supply. However, sensor technologies of this sort can only be put into effect with the most modern microelectronics manufacturing processes. Amperometric oxygen electrodes are widely used as transducers for many types of biosensors (see Table 7).

Many gas sensors for SO_2, CO and NO function on a similar principle. The measurement is based on the electrochemical oxidation of the relevant gas in the space separated off by the gas-permeable membrane.

The selectivity of amperometric sensors can be tailored to suit particular needs. Up to now the main technological use for amperometric chemosensors has been for measurements on gases, even though amperometry is also suitable for analyzing liquids, because of their limited selectivity. In the most commonly used aqueous electrolytic media, the usable voltage range extends over about 2 V. All substances that can be altered electrochemically, i.e. those that can be oxidized or reduced, which number many tens of thousands, are converted at voltages within this range. In the ideal case one can expect to distinguish ten substances at best in a voltammetric diagram by virtue of their different half-wave potentials.[70] The separation capacity achieved by the proper choice of a working electrode potential within the limiting current region for the substance to be determined is in general inadequate for the analysis of unknown liquids. However, if a gas-permeable membrane is interposed, the interfering substances are limited to gases that can permeate the membrane equally well, and also undergo electrochemical reactions under these conditions. In the case of the Clark O_2 sensor, for example, these are chlorine and some haloforms (CHX_3). These interferences can be even further reduced by a careful choice of the membrane material and the electrolyte. Occasionally a difference in electrochemical reversibility coupled with pulse techniques is also exploited to increase selectivity. The limit of detectability for amperometric gas sensors is determined by the noise level of the background current. Nevertheless, chemosensors for environmental applications (measurement of NO_x, SO_2 etc.) can be employed in the low ppm region without special signal-processing techniques.

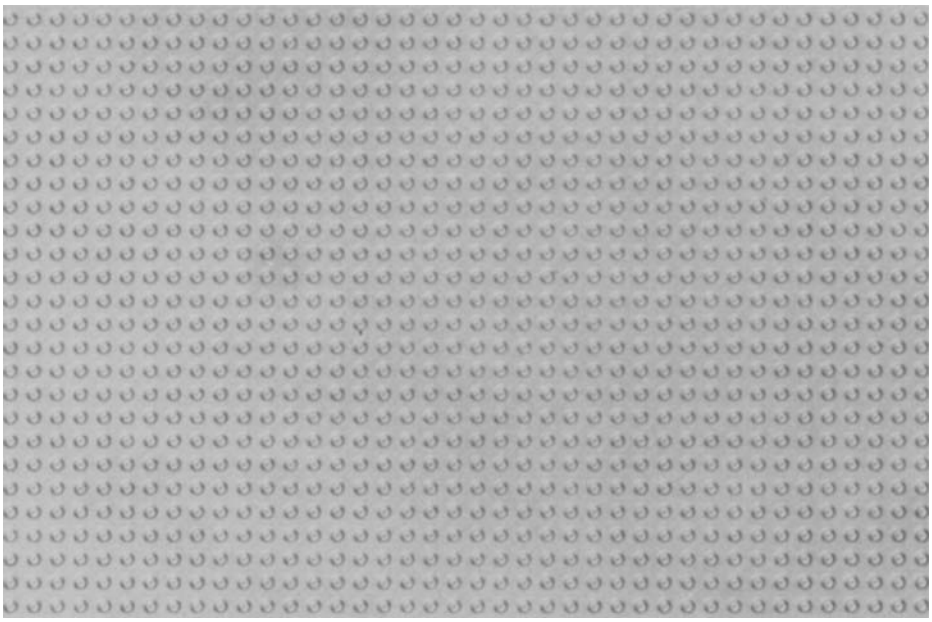

Fig. 7. Microelectrode array for amperometric determination of oxygen; the diameters of the platinum and silver electrodes are 1.5 μm and 20 μm respectively. [With permission of the Institut für Medizintechnik (IMT), Münster, FRG].

2.1.5. *Galvanic Sensors*

Amperometric measurements are also possible without an external current source, if a galvanic circuit is formed. The

best known example is the so-called internal electrolysis, in which $Cu^{2\oplus}$ ions are reductively deposited on a platinum wire mesh when this is connected to a zinc rod immersed in a zinc sulfate solution which is separated by a diaphragm from the solution containing the copper ions. Here again the driving force for the current which arises when zinc dissolves and copper ions are deposited on the platinum surface is the difference between the chemical potentials, or the energy difference between the two redox reactions in the electrochemical series. If in this example one connects a galvanometer externally between the zinc electrode and the platinum mesh, the current vs. time diagram obtained during the electrolysis has an exponential shape. The quantitative deposition of the $Cu^{2\oplus}$ ions on the platinum mesh is complete when the current has fallen to about 0.1% of its initial value. In this case, instead of using the gravimetric method, the amount of copper deposited can be calculated by Faraday's law from the total charge that has flowed (the integral of the current vs. time curve) as long as interference from side-reactions is absent. This coulometric procedure is one of the most precise absolute determination methods available, and requires no calibration. Coulometry is still an elegant method with exciting new possibilities for the development of intelligent sensors, and regrettably is too little used.

Over 25 years ago a coulometric measurement cell for SO_2 was proposed.[71] Subsequent advances in miniature electrochemical cells based on thin-film and thick-film technologies allow the easy application of such a cell as a chemosensor (Fig. 8). If the reaction is quantitative, a current of the order

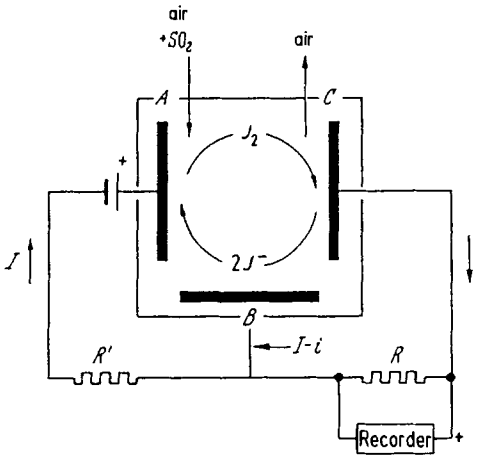

Fig. 8. "Fuel cell" detector for SO_2; a generation current flowing between electrodes A and B liberates free iodine, which then undergoes spontaneous reduction at electrode C, causing a current between electrodes B and C. In the absence of SO_2, this current is exactly equal to the generation current, and is registered by the recorder. The SO_2 whose concentration is to be measured reduces the reading by an amount given by the stoichiometry. (The symbol J is used here for iodine to avoid confusion with *I*, the symbol for current.)

of 1 μA, which is easily measurable, corresponds to an analyte reaction rate of only 10^{-10} mol s^{-1}! Here the selectivity is achieved by a preceding chemical reaction or membrane separation stage, either of which can nowadays easily be realized by means of a suitable layered structure. An "analytical fuel cell" of this kind has recently also appeared on the market in the form of an alcohol meter (for analysis of breath samples). As well as using the catalytic activity of noble metal electrodes, it is also possible, of course, to use enzymes to give increased selectivity. The H_2O_2, which is then often produced in quantities proportional to the amount of analyte, can also be easily determined coulometrically.

A galvanic measuring cell for the determination of oxygen in solutions has been well-known since the mid-1960s.[72] In contrast to the Clark sensor, the Mackereth oxygen sensor uses lead instead of silver as the anode material, and silver instead of platinum as the cathode material. This has the important advantage that a calibration in a blank solution (such as a saturated sulfide solution) is no longer necessary, since the electrodes produce no current in the absence of oxygen. For the internal electrolyte either sodium hydroxide or potassium hydrogen carbonate can be used.

2.2. Semiconductor Gas Sensors

Sensors based on semiconductors are often used in gas alarm devices. The underlying principle here depends on a transfer of electrons between a semiconductor surface and adsorbed gas molecules. This charge transfer results in an increase or decrease in the number of free charge carriers at the semiconductor surface, causing a change in conductivity which can be measured and is proportional to the number of reacting gas molecules present. Oxidizable gases such as hydrogen, hydrogen sulfide, carbon monoxide, and alkanes of low molecular mass reduce the surface conductivity of certain n-type semiconductors (SnO_2, ZnO etc.), which are used at temperatures between 100 and 600 °C. Reducible gases such as chlorine, oxygen, or ozone have an analogous effect on p-type semiconductors (NiO, CuO etc.). The mechanism of the electron transfer is still under intensive study and one possible model shown in Figure 9. When a gas molecule of

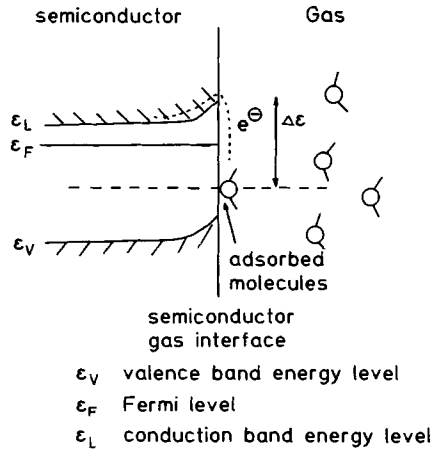

Fig. 9. Simplified mechanism of electron transfer at the semiconductor–gas interface.

the analyte approaches the surface of the semiconductor it first undergoes a weak physisorption. In the following step it can be either desorbed or chemisorbed with the transfer of an electron. The latter process causes a distortion of the valence

and conduction bands, and alters the electronic work function. Depending on the composition and the structure of the surface and on the interactions between the molecules and the surface, certain types of molecules can act preferentially. The selectivity of simple sensors of this kind, which can be easily and cheaply produced with thick film techniques (see Fig. 10), can be altered within certain limits using existing knowledge of heterogeneous catalysis. To obtain improved

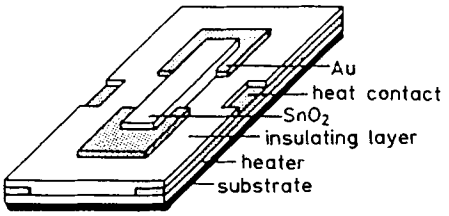

Fig. 10. Construction of a gas sensor of the SnO_2 thick-film type.

sensitivities and selectivities for particular applications, however, mechanistic studies of the kind used in heterogeneous catalysis research, requiring sophisticated and expensive equipment, are necessary, rather than the time-consuming trial-and-error methods of nonspecialists. Often the semiconductor surface is modified by introducing metals such as palladium, silver, or platinum, whose purpose is to weaken the O_2 double bond. The selectivity can be further increased to a certain extent by choosing the best operating temperature (Fig. 11). Nevertheless, the selectivities of these types of

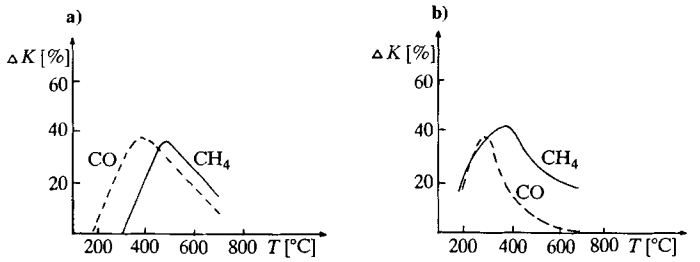

Fig. 11. Effects of temperature and of the presence of platinum on the selectivity of an SnO_2 gas sensor. a) Pure SnO_2 sensor, b) SnO_2 sensor with 1% platinum.

sensors based on semiconductors are often insufficient.[73] The surface composition, density of charge carriers, Fermi energy level, number of reactive centers at the surface, and even the extent of distortion of the bands, can be affected by the presence of other species (interfering molecules such as water, catalyst poisons etc.). This can cause changes in selectivity. These effects must be taken into account during calibration. A change in the selectivity, sensitivity (signal per unit concentration in the analyte) or zero point of the calibration line between carrying out the calibration and the analysis is inadmissable.

As it is a simple matter to modify the sensitivity, experiments are now in progress to use a sensor array in which each miniaturized individual sensor has a different sensitivity profile. Samples which contain interfering substances cause each individual sensor to give a different signal. By carrying out calibration measurements with different concentrations of the various interfering components, it should be possible, by a pattern recognition analysis, to use a special algorithm for the calculation of the true sample content. A simultaneous analysis on a mixture using such a sensor array should in principle enable the determination of every substance which has an effect on the signal, if more sensors than components to be analyzed are used. This has in fact been achieved for simple and well-defined mixtures.[74] Nevertheless, the analytical chemist with experience of industrial practice will harbour doubts about the feasibility of this method for real samples whose composition is generally unknown and continually changing. Taking the simplest form of an analytical function (c) is it possible to keep the parameters a and e constant between the calibration and the measurement? How can the algorithm take into account situations where interfering substances poison the sensors to differentor cause different drift phenomena? What are the consequences of "matrix effects" which cause the sensitivity e to vary from sample to sample?

$$s = a + ec \qquad (c)$$

s = analytical signal
a = intercept on the axis (blank value)
e = slope of the calibration function (sensitivity)
c = concentration of the analyte

Table 3 gives a summary of the most important materials currently used to make selective sensor elements for electrochemical sensors.

Table 3. Materials for selective chemosensor elements.

Sensor materials	Examples	Species detected	Refs.
glasses	Li_2O-BaO-SiO_2	$H^{\oplus}$	[5,6]
	Na_2O-Al_2O_3-SiO_2	$Na^{\oplus}$	[7]
synthetic polymers	PVC, silicone and PMMA membranes[a] with plasticizers and suitable carriers	e.g. $K^{\oplus}$, $Na^{\oplus}$, $Ca^{2\oplus}$, $Mg^{2\oplus}$, $NH_4^{\oplus}$, $NO_3^{\ominus}$	[14–16, 34,36–38]
	PTFE membranes for gas sensors	NH_3, CO_2, SO_2	[37]
solid	LaF_3	$F^{\ominus}$	[37]
		O_2	[53,54]
	ZrO_2 (lambda probe)	O_2	[51,52]
		Cr	[55]
	TiO_2, Nb_2O_5	O_2	
	$ZrSiO_4$	Si	[56]
	$Na_2SO_4 + Ag_2SO_4$	SO_2/SO_3	[57,60–64]
	Nasicon[b]	Na	[65]
		$Na^{\oplus}$	[66]
semi-conductors	Si, GaAs, SiC, SnO_2, ZnO, CuO	Oxidizing or reducing gases	[73,109–111]
metal oxide or nitride films	Al_2O_3, Si_3N_4, SiO_2, TiO_2 as insulators, electronic conductors and electroactive materials	$H^{\oplus}$, H_2, O_2	[73,109–111]

[a] Polylmethylmethacrylate. [b] $Na_{1+x}Zr_2Si_xP_{3-x}O_{12}$.

2.3. Fiber-Optic Sensors (Optodes)

Chemical information can also be translated into measurable signals through the interaction of electromagnetic radiation with the analyte. Spectroscopic analysis, spectrophoto-

metry, fluorimetry, and luminescence measurements are well-established and proven techniques. Their adaptation for performing in situ analyses with miniaturized probes that can be employed in the same way as chemosensors has come about through the application of modern light-guide technology. For use in conjunction with fiber optics a new class of sensors was developed, known as optodes (also as optrodes).[75-78] These optical sensors make use of changes in fluorescence, absorption, chemiluminescence, light scattering, polarization, Raman scattering, refractive index, or reflection, which at present are still detected by conventional optical or spectroscopic instruments. The light input is fed into the sample by a light-guide. The return path for the fluorescence emission or reflected light from the sample to the detector can be through the same light-guide or through a second branch (in a Y-branched light-guide). Figure 12 shows as an example the layout of a fiber-optic analytical system as commonly used for fluorescence measurements. The AC signal produced by a chopper is amplified frequency- and phase-selectively by a lock-in amplifier. This procedure makes it possible to measure delayed fluorescence as well (by the phase shift). Fluorescence and luminescence measurements give high sensitivity compared with other optical measurement methods and are therefore preferable for trace analysis.

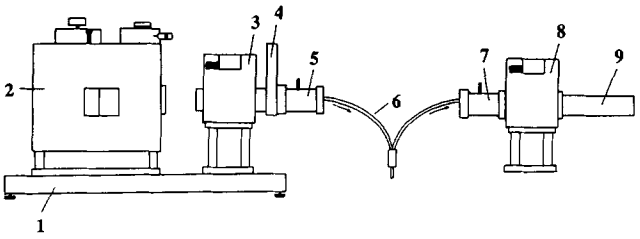

Fig. 12. Fiber-optic system for analysis by fluorescence measurements; the excitation unit (2) contains the light source (xenon or halogen lamp or laser) producing a beam which is passed through a monochromator (3), a chopper (4), and an optical coupler (5) into the light guide (6). The fluorescence radiation passes through a second light guide branch, coupler (7), and monochromator (8) to the detector (9), which consists of a photodiode or photomultiplier. (1) is the base plate.

Chemiluminescence measurements have an additional advantage, as they do not require an external light source. However, because chemiluminescence is a comparatively rare phenomenon, the method is mainly limited to systems such as H_2O_2/luminol.

The great advantage of fiber-optic sensors is that the measurements do not require a reference system, apart from comparison of the light intensities in the beam before and after it passes through the sample compartment (i.e. measuring I_0/I), or the use of a dual beam arrangement to compensate for fluctuations in the intensity of the light source. With the electrochemical sensors described earlier a second electrode giving a constant potential is always needed. Optodes can easily be miniaturized, as light-guides of suitably small diameter (e.g. 0.1 mm) are commercially available, although increasing miniaturization makes good coupling of the input radiation more difficult. Optodes can also be used in complex media such as blood. They are less susceptible to disturbance by electromagnetic fields and temperature changes than are potentiometric electrodes and semiconductor sensors. On the other hand, problems can arise from scattered and background light falling on optodes. In many cases these sensors can only be used within a small range of concentrations, like the spectroscopic analytical cuvette techniques on which they are usually based, and their selectivity is similar to that of those techniques. The detection limit also leaves room for future improvements, as it is restricted at present by the thinness of the optical films generally used for the measurements (see Table 4).

Despite all this, fiber-optic sensors are expected to emerge from their present status as research devices and find a place in industrial use in future; the flow-through cuvettes will probably be abandoned first. The types most studied are pH-optodes. The technique is based on the immobilization of an indicator dye at the end of the light-guide, which allows pH values to be determined by measuring fluorescence or absorption. Indicators that have been used include 8-hydroxypyrene-1,3,6-trisulfonate (HPTS) as well as conventional dyes such as eosin or phenyl orange.[79]

Such pH-optodes also form the basis for a range of gas sensors. For example, CO_2 and NH_3 optodes contain a pH optode immersed in a suitable internal solution behind a gas-permeable membrane, as in the analogous potentiometric sensors. The acidity or basicity of the above gases alters the pH of the internal solution by an amount related to the gas concentration to be measured. Such sensors are of particular interest for in vivo applications (blood, body fluids, etc.), since unlike electrochemical sensors they do not have electrical connections to voltage-carrying components.

The fields of application are similar for O_2 optodes, which work on the principle of direct fluorescence quenching. The mathematical basis of this type of sensor is given by the Stern–Volmer equation.[80] The fluorescence of an indicator such as decacyclene or perylene, which is immobilized on the tip of the light-guide, is partially quenched by oxygen. This effect can be used, after calibration, for the determination of O_2.

Some new developments are based on applying knowledge of the selectivity mechanism of ion-selective electrodes to fiber-optic systems. For example, valinomycin as a selective $K^{\oplus}$ carrier can be immobilized in a suitable matrix, together with a pH-sensitive indicator in its protonated form, so as to produce a membrane which can be attached to the tip of a light-guide. If this sensor is immersed in a solution containing $K^{\oplus}$ ions, these ions will preferentially enter the membrane phase, with the formation of a potassium–valinomycin complex. To maintain electrical neutrality $H^{\oplus}$ ions (as the most readily mobile ion species) move out of the membrane phase, causing a change in the absorption or fluorescence of the pH indicator in the membrane, which can easily be measured.[81]

In conclusion it should be noted that at present there are only a few manufacturers of optodes, and it will certainly take several more years before such fiber-optic analytical systems become as widely used as electrochemical sensors.

2.4. Mass-Sensitive Transducers

Chemosensors based on mass-sensitive transducers have been less thoroughly investigated, and their use has so far been restricted to special applications. The measuring prin-

ciple depends on the shift Δf in the characteristic frequency of a quartz oscillator due to a mass change Δm, which occurs when a layer of foreign material is deposited on its surface. The oscillation frequency is usually in the 9 to 14 MHz range, and the selectivity is obtained by coating the surface with an appropriate adsorbent. By using phthalocyanine, for example, planar-conjugated molecules and higher alcohols can be determined; in this case mass changes as small as 10^{-9} g can be detected.[82, 83] When working in vacuum the relationship between Δf and Δm is linear for small values of Δm and is given by the Sauerbrey equation [Eq. (d)].[84]

$$\frac{\Delta f}{f_0} = -\frac{\Delta m}{m} \qquad \text{(d)}$$

f_0 = resonance frequency in the unloaded condition
m = mass of the quartz crystal in the unloaded condition

The suitability of quartz oscillators for gas analysis has been demonstrated beyond doubt. Difficulties arise, however, in the search for selective ab- or adsorbents for particular analytes, and in compensation for the effects of moisture and other interfering deposits. Also it must be noted that the surface adsorption or film absorption are not usually reversible. Transducers of this type are potentially important for biosensors for gas phase use. At present, however, their high cost inhibits the development of practicable one-shot disposable sensors.

When quartz oscillator detectors are used directly in liquids[85, 86] without a drying stage before the mass-change measurement, the damping of the oscillations must also be taken into account [Eq. (e)].

$$\Delta f = f_0^{3/2} \left(\frac{\eta \rho}{\pi \mu_Q \rho_Q} \right)^{1/2} \qquad \text{(e)}$$

η = viscosity of the liquid
ρ = density of the liquid
μ_Q = shear modulus of the quartz
ρ_Q = density of the quartz

The latest studies,[87] which are based on an exact coulometric calibration, show that a 0.4 μm thick layer of the surrounding liquid moves with the quartz crystal surface during its oscillation. This makes exacting demands on the constancy of all the effects that shift the frequency. The layer of liquid that moves with the surface reduces the mass resolution (i.e. the ability to measure very small mass changes). It should also be mentioned here that a similar device is marketed for determining the densities of liquids; density changes of the order of a few parts per million can be detected.

Surface acoustic wave (SAW) detectors are devices in which acoustic waves are produced at the surface of a suitable material, by setting up appropriate resonance conditions between two surfaces. The resonance frequency is typically a few hundred MHz, and according to the Sauerbrey equation (d) this should result in greater sensitivity. However, this cannot be fully exploited, as it is only possible to measure the change in mass within a very thin layer between the two specially shaped electrodes. The selectivity is governed by the same considerations as above.

2.5. Applications of Chemosensors

The use of chemosensors in technology has grown enormously during the past decade. R & D in the field of chemosensors is being energetically pursued worldwide, but especially in Japan. The range of uses of conventional chemosensors extends from chemical process control technology through applications in clinical chemistry to municipal services. A field of special importance for chemosensors is environmental protection, where increased public awareness and ever stricter legislation make it increasingly necessary to set up on-line monitoring systems for environmentally significant gases such as NO, SO_2, NH_3, CO, or CO_2.[88–93]

The wide variety of chemosensors that have so far been developed means that in many cases the most suitable one for a particular application can be chosen from a number of alternative constructions. As an example Table 4 lists the various methods of measurement available for determining a single substance, in this case oxygen.

Table 4. Comparison of methods available for the determination of a single substance. Oxygen is used as example.

Sensor type	Principle	Measurement medium	Range
amperometry (*Clark*'s method)	amperometric arrangement with gas membrane	liquid or gas	0.1 ppm to 100 vol. %
potentiometry (principle of lambda-probe)	O_2 concentration cell with solid ionic conductor at elevated temperature	gas	1–100 vol. %
optical	e.g. quenching of fluorescence of an immobilized dye	oxygen dissolved in liquids	0.01 ppm–sat. solution
paramagnetic	deflection of a magnetic balance due to the paramagnetism of the O_2	gas	0.1–100 vol. %

The largest market for chemosensors at present is the automobile industry, which even in 1987 required over ten million oxygen sensors (lambda-probes) throughout the world for controlling the operating conditions of the three-way catalytic converter.

A similarly large market exists for semiconductor sensors based on SnO_2 for detecting oxidizable gases such as CO, NO_x and CH_4, which are used mainly in monitoring instruments (alarm devices) in underground garages, tunnels, and coal mines, and for measuring emissions in industry. Here the poor selectivity is not a serious disadvantage; on the contrary it gives extra safety. Conventional electrochemical sensors too are widely used in measurement and control technology, especially glass pH electrodes, of which about a million are produced every year throughout the world.[94]

The largest areas of use for conventional potentiometric sensors are in medicine and environmental technology. In clinical chemistry, for example, ion-selective sensors have many uses for measurements in biological media.[95–99]

They have been used successfully for some years to measure concentrations of individual ion species such as $Na^{\oplus}$, $K^{\oplus}$, $Ca^{2\oplus}$, and $Mg^{2\oplus}$ in blood. Unlike other methods of analysis such as atomic absorption spectroscopy (AAS), which always measure the total concentration of the ion species (both free and bound ions), ion-selective sensors allow a direct measurement of the activity of the free ion, which is the effective concentration and the only component that is relevant for medical diagnostic purposes.[100] Fluoride in urine and blood can be determined by, for example, a LaF_3 single crystal electrode, which gives an extremely high selectivity for $F^{\ominus}$. A knowledge of the fluoride concentration is important in the chemotherapeutic treatment of osteoporosis and kidney disease, and in the determination of the $F^{\ominus}$ content of the blood after the use of narcotics.[97]

The detection of traces of cyanide in blood is necessary during treatment of hypertonia with sodium pentacyanonitrosylferrate(II) (sodium nitroprusside), and this too can be carried out with an ion-selective electrode.

Iodide- and bromide-selective sensors are of interest in clinical toxicology, in connection with radioimmunological investigations into the functioning of the thyroid gland (using the iodine-131 isotope) and the administration of the bromine-containing sleeping drugs, ureides. Use of the latter often causes toxic effects due to metabolic dehalogenation and a dangerous build-up of $Br^{\ominus}$ ions.

In treating manic-depressive patients a control of the lithium content is of particular importance; this can be determined using ion-selective membrane electrodes which consist of PVC and a lithium ionophore such as ETH 1810 (*N*,*N*-dicyclohexyl-*N'*,*N'*-diisobutyl-*cis*-cyclohexane-1,2-dicarboxamide).

The non-invasive measurement of the transcutaneous blood CO_2 partial pressure is a technique that can be used to advantage in operations, in amputational surgery and in sport related medical practice. Here the sensor works on a principle analogous to that of other potentiometric gas sensors such as NH_3 or SO_2 detectors. It is essentially a pH probe consisting of a glass electrode and an Ag/AgCl reference electrode. The gas diffuses through a semipermeable membrane into an intermediate electrolyte, whose pH changes according to the gas partial pressure and is measured by the pH electrode. Figure 13 shows a sketch of the sensor.

The sensors that have been described are still used mainly for in vitro measurements, but the main research objective is to develop catheter needle electrodes for in vivo measurements. Figure 14 shows an example of an amperometric catheter electrode for measuring O_2 partial pressures.[101]

ISFETs have proved successful mainly in medical technology. Up to now pH-ISFETs have become commercially available and are used for determining acidity in blood and serum (whose normal pH value is 7.41) and other body fluids. Another technological application is in the photographic industry; here ISFETs are used in process control, to maintain important parameters such as the concentrations of $H^{\oplus}$ and $Ag^{\oplus}$ ions at constant levels.[102]

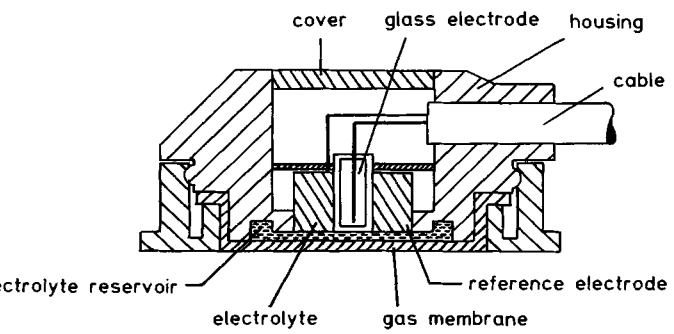

Fig. 13. Gas sensor for measuring CO_2 partial pressures in medical applications[95]; the sensor allows transcutaneous measurement of CO_2.

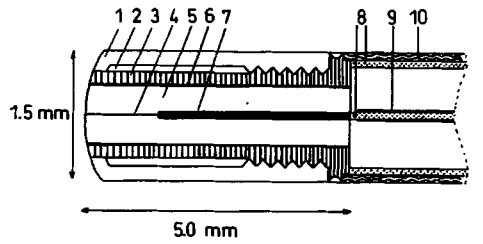

Fig. 14. Amperometric catheter sensor for measuring O_2 partial pressures [101]; (1) Teflon (PTFE) membrane and cap, (2) electrolyte space, (3) Ag/AgCl anode, (4) Pt cathode, (5) glass, (6) Araldite (epoxy resin), (7) platinum wire, (8) copper screening, (9) insulation, (10) cover tube.

The Ektachem film electrodes mentioned earlier (cf. Fig. 4) can be used as one-shot disposable sensors in medical applications. The Kodak Ektachem DT 60 is a commercially available system[49, 50, 103] and can be used for the determination of $K^{\oplus}$, $Na^{\oplus}$, $Cl^{\ominus}$ and other substances. Figure 15 shows a film sensor of this type for potassium.

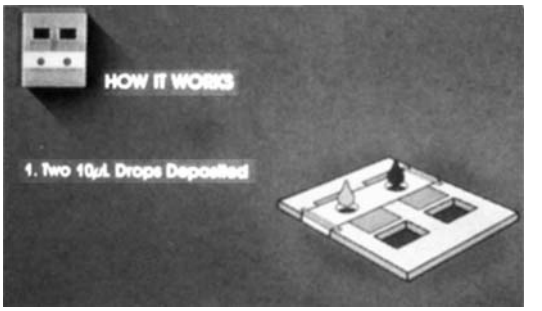

Fig. 15. Kodak DT 60 Ektachem system for the determination of potassium.

Potentiometric sensors can be used for environmental protection both in laboratory investigations and on-line applications. One task that they can perform is the continuous monitoring of $NO_3^{\ominus}$ and $NH_4^{\oplus}$ concentrations in groundwater and drinking water. This gives early warning of excessive concentrations in the water, allowing the necessary corrective measures to be applied quickly. Figure 16 is an example of a recorder trace obtained with a sensor used to monitor nitrate in drinking water. The trace shows immediately if the maximum legally permitted nitrate concentration of 50 mg L^{-1} (50 ppm) is exceeded. Here the technique of flow injection analysis (FIA) can be used, since the selectivity of the sensor makes a preliminary chromatographic separation unnecessary.[104]

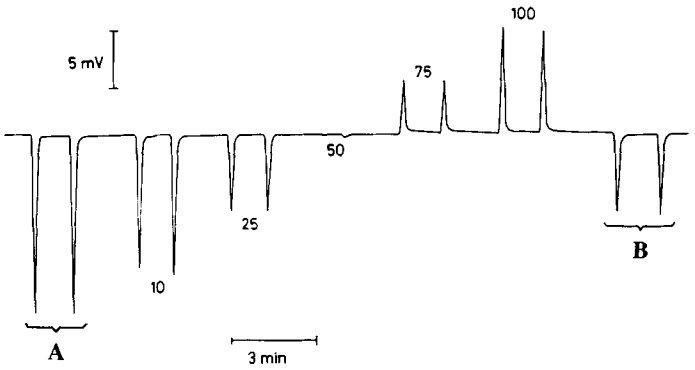

Fig. 16. Recorder trace obtained during the FIA monitoring of $NO_3^{\ominus}$ in drinking water; carrier electrolyte: 50 ppm $NO_3^{\ominus}$ in 0.01 M $NaH_2PO_4 \cdot H_2O$; flow rate: 3.0 mL min^{-1}; sample quantity: 0.3 mL in 0.01 M $NaH_2PO_4 \cdot H_2O$. The numbers represent the concentration of nitrate in mg L^{-1}; A: doubly distilled water; B: drinking water.

In process engineering, ion-selective sensors for $Ca^{2\oplus}$, $Na^{\oplus}$, $NH_4^{\oplus}$, or $Cl^{\ominus}$ can monitor the purity of boiler feed water in steam turbines;[105] with a glass electrode for $Na^{\oplus}$, ppb concentrations are detectable. Monitoring these concentrations is critically important in relation to boiler scale formation and turbine corrosion.

Table 5 lists important characteristics of the various types of sensors described here, such as the range of measurement, useful life and detection limits. ISEs that do not incorporate PVC membranes can also be used to a limited extent in nonaqueous media. For example, it is well known in the oil industry that impurities in crude oil feedstocks can adversely affect the refining process, and it is therefore essential to carry out continuous analyses.[106]

Table 6 gives a summary of some commercially available sensors.[107]

Table 6. Summary of commercially available sensors.

Supplier detector	Species detected	Range	Applications
AEG NO_x monitor	NO_x	0–600 ppm	vehicle exhausts, flue gases
MSI (Dräger) gas analyzing computer	O_2	0–20.9%	flue gases
	CO	0–1500 ppm	
	SO_2	0–1500 ppm	
	NO	0–1000 ppm	
	NO_2	0–200 ppm	
Unitronic (Figaro) gas monitor	CH_4	500–10,000 ppm	gas alarms (camping)
	C_3H_8	500–10,000 ppm	
	C_4H_{10}	500–10,000 ppm	
	CO	50–1000 ppm	gas alarms (garages, tunnels)
	NH_3	30–300 ppm	
	H_2S	5–100 ppm	gas alarms
	H_2O	0–100 ppm	humidity
Transducer Research, Inc. gas monitor	NO_2	10 ppb–50 ppm	gas alarms
	H_2S	0–1000 ppm	
	CO	0–1000 ppm	
Bran & Lübbe Ionometer	$Na^{\oplus}$	0–20 ppb	quality control monitoring liquids (maximum permitted concentrations)
	$Cl^{\ominus}$	0–100 ppb	
	$NH_3/NH_4^{\oplus}$	0–10 ppm	
	$F^{\ominus}$	0–10 ppm	
	$S^{2\ominus}$	0–30 ppm	

2.6. Development Trends

One should not overlook the fact that the majority of development work on sensors proceeds by methods that are still more or less empirical. Recently the most up-to-date research techniques, e.g., electrochemical impedance spectroscopy,[108] tracer methods, and surface analytical techniques[109–111] such as secondary ion mass spectrometry (SIMS), Auger electron spectroscopy (AES), or X-ray photoelectron spectroscopy (XPS, also known as ESCA), have been applied to optimize performance parameters such as selectivity, stability, dynamic behavior, reproducibility and sensitivity. These methods will at the same time provide a deeper insight into the mechanisms of functioning of the selective sensor elements.

A changing trend can now be seen in the technology of chemosensors, away from the hitherto conventional sensor design principle based on electrode-like structures, towards miniaturization with recognition systems and signal processing integrated in a single device.[112, 113] These developments can benefit from the existing technology of microelectronics. Besides savings in materials, this technology can also lead to considerable cost reductions through mass production, and may sometimes even result in sensors with improved proper-

Table 5. Characteristics of selected sensors.

Sensor	Species	Range	Detection limit	Sample form	Useful Life
ISFET	$H^{\oplus}$	pH 2–12	10^{-13} mol L^{-1}	liquid or paste	several weeks
ChemFET	$Na^{\oplus}$	$1-10^{-5}$ mol L^{-1}	$10^{-5.5}$ mol L^{-1}	liquid or paste	several weeks
ISE	$H^{\oplus}$	pH 0–14	10^{-14} mol L^{-1}	liquid or paste	years
	$Na^{\oplus}$	10^{-1}–10^{-5} mol L^{-1}	$10^{-5.5}$ mol L^{-1}	liquid or paste	years
	$F^{\ominus}$	10^{0}–10^{-6} mol L^{-1}	3×10^{-7} mol L^{-1}	liquid or paste	years
	$K^{\oplus}$	10^{-1}–$10^{-5.5}$ mol L^{-1}	10^{-6} mol L^{-1}	liquid or paste	months
	$NO_3^{\ominus}$	10^{0}–10^{-5} mol L^{-1}	5×10^{-6} mol L^{-1}	liquid or paste	months
film	$Na^{\oplus}$	10^{-5}–10^{-1} mol L^{-1}	10^{-5} mol L^{-1}	liquid or paste	disposable
electrode	$K^{\oplus}$	10^{-5}–10^{-1} mol L^{-1}	10^{-5} mol L^{-1}	liquid	sensor
Clark sensor	O_2	1–200 ppm	1 ppm	O_2 in solution	years
lambda-probe	O_2	1–100 vol. %	0.5 vol. %	gas	years
gas alarm	CO	1–100 vol. %	1 vol. %	gas	years
	H_2	1–100 vol. %	1 vol. %	gas	years
	Alkane	1–100 vol. %	1 vol. %	gas	years
fiber-optic (fluorescence)	$K^{\oplus}$	10^{-3}–10^{-1} mol L^{-1}	5×10^{-4} mol L^{-1}	liquid or paste	weeks
	O_2	10^{-3}–10^{0} mol L^{-1}	10^{-3} mol L^{-1}	O_2 in solution	months

ties. Physical sensors for a wide variety of variables are produced by these methods and are already well-known, while chemical sensors made in this way are just appearing on the market.

Thick-film technology offers an alternative way of integrating sensor recognition systems and subsequent signal processing on a single chip, and is within the financial budgets of medium-sized industrial concerns. A potentiometric hydrogen sensor based on thick-film technology and developed by the Battelle Institute is shown in Figure 17. The

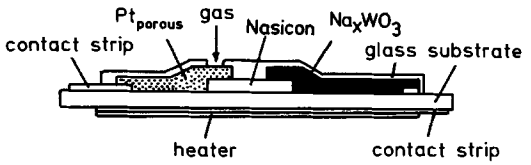

Fig. 17. Hydrogen sensor produced by thick-film technology[113] (see Text).

sensitive material is Nasicon ($Na_{1+x}Zr_2Si_xP_{3-x}O_{12}$), a solid ionic conductor which responds to hydrogen at elevated temperatures, but is a good $Na^{\oplus}$ sensor at room temperature and in solutions. This sensor based on Nasicon is at present one of only a few commercially available sensors made by thick-film technology.

3. Biosensors

A biosensor combines in a single sensor element the sensitivity of a chemosensor with the selectivity of a biological recognition mechanism. The great promise offered by such a combination has been the subject of increasing research efforts in the last few years, as is evident from the rapid growth in the number of publications in this area and the appearance of the first monographs on the topic.[114, 115] A number of different biosensors with biological or biochemical recognition systems coupled to various types of chemosensors have been demonstrated. Although to date biosensors have commercial importance only in medical technology, their use in future in other fields such as environmental monitoring and process engineering is likely. For this reason some relevant developments are described below.

Biosensors functioning on enzymic principles belong to the oldest generation of sensors in this category; they employ selective chemical reactions catalyzed by selected enzymes. The most effective method is to immobilize the relevant enzymes in or on the sensor element, which allows the device to be used repeatedly. Unfortunately the stability of enzymes immobilized in this way is at present rather limited, and consequently the lifetime at room temperature under working conditions varies between only a few days and several months, depending on the enzyme used and the immobilizing technique. However, if it is refrigerated and freeze-dried, an immobilized enzyme retains its activity almost indefinitely.

Another class of biosensors are immunosensors. These operate on a different principle, namely the selective association between antigens and antibodies. This specific biocomplex formation can be exploited in a number of ways as a means of analysis for one of the two partners. The methods that are of importance for the development of these sensors differ from those involved in radio immuno-assay (RIA), and are based either on enzymic immuno-assay (EIA) in combination with various detection methods (photometry, amperometry, or surface plasmon resonance), or on direct potentiometry.

Some of the systems under development function without isolation of biomolecules. In other words, these are enzymic biosensors in which biological materials such as intact cell cultures, tissue sections or microorganisms are used directly without purification; for immunosensors one uses intact receptors, receptor structures or reconstituted units.

As the development of biosensors follows on that of transducers or chemosensors, biosensors are not yet at such an advanced stage, and only a few types are commercially available at present. Nevertheless, some important advances have been achieved in each class of biosensors.

3.1. Monoenzyme Sensors

Monoenzyme sensors were the first biosensors to be developed, and are the best known. Here an enzyme is coupled to an optical or electrochemical chemosensor, which selectively detects one of the reaction partners of the substrate, or a reaction product. As early as the 1960s with the first enzyme electrodes, immobilization of the enzyme was a development goal. Although the immobilization technique is crucial to the behavior of the biosensor, it will not be considered in detail here. The situation is basically similar to that in bioreactors, where the aim is to achieve a high surface activity combined with a high durability; accordingly, the immobilization techniques used in biosensors are similar to those for bioreactors.[116–120] However, it must be said that many of the techniques are still far from giving reproducible results. Many preparative procedures evolved by trial and error, and if a breakthrough could be achieved in immobilization without loss of activity, many of the present disadvantages of biosensors would be overcome.

The modification of the coenzyme nicotinamide adenine dinucleotide ($NAD^{\oplus}$) can also be regarded as a type of immobilization.[121, 122] If the effective molecular mass of $NAD^{\oplus}$ is increased by reaction with polyethylene glycol (PEG) to give PEG-$NAD^{\oplus}$, the coenzyme can be immobilized behind a dialysis membrane, so that it can be used repeatedly after a recycling procedure.

Chemically preactivated membrane filters for simple and rapid immobilization of enzymes have recently become commercially available (Immunodyne, Gelman Sciences). The simplification of the procedure brought about by them could lead to a breakthrough in extending the storage life of biosensors. If a filter membrane freshly coated with the enzyme could be fitted to the sensor shortly before making a measurement, the cost of the biomaterial would be worthwhile in view of the great advantages of a rapid but selective measurement.

3.1.1. Electrochemical Biosensors

In the past the development of monoenzyme biosensors with different transducers was mainly limited to electro-

chemical sensors. This situation has now changed to some extent through the development of new optodes and of the technique of surface plasmon resonance. Biosensors with electrochemical transducers are still essentially restricted, owing to the nature of the products from enzymic reactions, to two methods of measurement, namely amperometry and potentiometry.

Amperometric Biosensors: The majority of biosensors used in research are of the amperometric type. Table 7 gives a short summary, which is by no means exhaustive, of the many different types of biosensors using conventional amperometry.

Table 7. Amperometric biosensors.

Substrate	Enzyme	Product(s) detected	Range	Refs.
alcohol, malate, formiate	dehydrogenase	NADH	10–150 mmol L^{-1} ; (5–100) × 10^{-6} mol L^{-1}	[121, 124]
choline	choline oxydase	H_2O_2	500 mmol L^{-1} [a]	[125]
ethanol	alcohol oxidase	H_2O_2	10 mg L^{-1} [a]	[114]
formaldehyde	formaldehyde dehydrogenase	NADH	10^{-6} mol L^{-1} [a]	[126]
glucose	glucose oxidase	H_2O_2	0–7 g L^{-1}	[127–135]
glutamine	glutaminase, glutamate oxidase	H_2O_2	0–25 mmol L^{-1}	[136]
glycerol	glycerol dehydrogenase	NADH, O_2		[137]
hypoxanthine	xanthine oxidase	H_2O_2	4–180 × 10^{-6} mol L^{-1}	[138, 139]
lactate	lactate oxidase	H_2O_2	1–40 mmol L^{-1}	[114]
oligosaccharides	glycoamylase, glucose oxidase	H_2O_2	0.1–2.5 mmol L^{-1}	[140]
phenol	polyphenol oxidase	quinone	–	[125]
inorganic phosphorus	nucleoside phosphorylase	O_2	–	[141]

[a] Only the upper limit is known.

In amperometric transducers, reaction partners or products of the enzymic reaction are directly reduced or oxidized at the working electrode, and the resulting current is measured. From this, on the basis of the stoichiometry, the quantity of the substrate that has reacted can be determined. As is evident from Table 7, the most commonly used transducers are based on the oxygen/hydrogen peroxide electrodes described in Section 2.1.4, since many enzymic reactions (e.g. those of the oxygenases) involve the consumption or production of oxygen. This consumption of O_2 or production of H_2O_2 is measured by an O_2 electrode.

In this area of development considerable time has been invested in the glucose sensor, which is based on reaction (3)

$$\beta\text{-D-glucose} + O_2 + H_2O \xrightarrow{GOD} \text{gluconic acid} + H_2O_2 \quad (3)$$

catalyzed by the enzyme glucose oxidase (GOD). In this selective reaction three concentration changes can be and have been used to determine the amount of material reacted:

1) the reduction in concentration of the cosubstrate (reduction in O_2),

2) the increase in H_2O_2 concentration, or

3) the concentration of the $H^{\oplus}$ ions generated by the dissociation of the gluconic acid.

Greater progress has been made in the area of in-vitro glucose measurements than in any other, which is not surprising in view of the large amount of research effort on this topic (about half of all the papers on biosensors are concerned with glucose measurements). Despite this, however, an implantable glucose sensor, which would be desirable in medical technology, is still not within sight. Implants need to have a lifetime of several years, because if it is shorter the added trauma for the patient as a result of more frequent operations is unacceptable. Up to now the lifetime of the enzyme GOD in synthetic glucose solutions has been at best about 100 days.[123] Among the problems which hinder applications are those arising from the nature of the cosubstrate (the quantity of O_2 available for reaction (3) limit the measurement range), from product inhibition, from the possibility of the enzyme being attacked by proteases, and from diffusion difficulties caused by encapsulation of the implant.

Other types of amperometric biosensors are those based on the detection of a coenzyme. Well over 100 enzymic reactions are known in which nicotinamide adenine dinucleotide ($NAD^{\oplus}$) functions as a coenzyme. The direct electrochemical reduction of $NAD^{\oplus}$ or oxidation of the reduced form NADH have both been successfully demonstrated,[142, 143] but owing to the very large overvoltage that must be applied (+ 0.7 to + 1.0 V vs. Ag/AgCl), the determination of both species is instead carried out with electron carriers (mediators), which work on the principle shown in Figure 18.[144–147] A similar situation exists for the coenzyme $NADP^{\oplus}$.

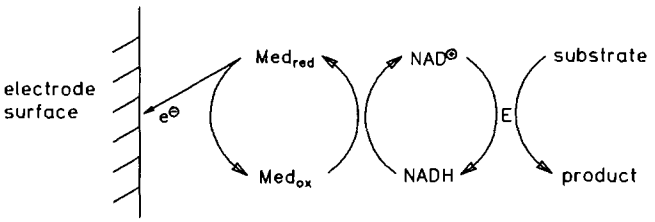

Fig. 18. Mediator-modified amperometric enzyme electrode.

The compounds used as mediators are reversible redox systems with high exchange current densities, often redox dyes such as methylene blue or thionine, or sometimes modified ferrocenes or hexacyanoferrates. The advantages of such a mediator are well-known: it reacts with the coenzyme $NAD^{\oplus}$ in a homogeneous solution without significant inhibition by kinetic factors, the mediator itself is electrochemically reversible, and it reacts at the electrode at a significantly lower potential than $NAD^{\oplus}$. Because of the lower working potential fewer interfering effects from other electrolyzable substances in the sample are expected.

Ferrocenes have also been used to effect the direct transfer of electrons between the enzyme and the electrode. A modified ferrocene serves as mediator between immobilized glucose oxidase and a graphite electrode.[148] This glucose sensor, developed at the Cranfield Institute of Technology (UK), is unaffected by O_2, as the ferrocene replaces oxygen as the cosubstrate. The sensor can therefore also be used in anaerobic media (e.g. in fermenters). In general the immobi-

Table 8. Potentiometric biosensors.

Substrate	Enzyme	Product(s)	Transducer	Range	Refs.
aspartam	L-aspartase	NH_3	NH_3 gas electrode	0.1–0.6 mmol L^{-1}	[149]
fats	lipase	fatty acids	pH electrode	5–50 10^{-6} mol/L^{-1}	[150, 151]
glucose	glucose oxidase	gluconic acid	pH electrode (pH ISFET)	0.12–2 g L^{-1}	[152]
urea	urease	$NH_4^{\oplus}$, CO_2	$NH_4^{\oplus}$ electrode pH electrode CO_2 gas sensor	0.01–10 mmol L^{-1}	[153–155]
nitrite	nitrite reductase	$NH_4^{\oplus}$	$NH_4^{\oplus}$ sensor	10^{-3} mol L^{-1}	[156, 157]
penicillin	penicillinase	$H^{\oplus}$	pH electrode	0.2–70 mmol L^{-1}	[158]
sulfate	sulfate reductase	$HS^{\ominus}$	Ag_2S ISE		[159]
antigen or antibody	partner of couple	antigen-antibody couple	$K^{\oplus}$ ISE	0–100 ppm	[187]

lization of mediators presents difficulties. An immobilization effective enough to prevent loss of the mediator from the transducer with time is usually accompanied by severe deactivation of that mediator.

Potentiometric Biosensors: Biosensors with potentiometric transducers can be used in any situation where protons are either generated or removed in the course of the enzymic reaction. Most types are based on a pH electrode, as can be seen from Table 8, which gives a short summary of potentiometric biosensors.

A pH measurement is an alternative way of following the glucose conversion reaction (eq. (3)) already described under amperometric biosensors. In this case the change in pH caused by the formation of gluconic acid is measured. Fats may be determined by measuring the change in pH caused by the formation of fatty acids, as listed in Table 8. Though still at the development stage,[151] this method seems to offer great promise, especially in view of the numerous potential applications in food technology. Recently stable lipases which even allow the determination of fats in organic solutions have been isolated.

The performance of all biosensors that work by means of a pH measurement is greatly affected by the buffer capacity of the sample solution. A lipophilic layer or membrane between the reaction zone and the buffer system decreases this dependence. Whereas with amperometric sensors, which consume some of the substance being determined during the course of the measurement, deposits of proteins formed on their surface attenuate the signal, with potentiometric sensors only the response time and not the magnitude of the signal is affected, since here the measurement does not consume the substance. This can be a crucial factor in the case of implants.

The conversion of aspartam by the enzyme L-aspartase is of interest in connection with the production and use of artificial sweeteners. The NH_3 generated in the reaction can be determined by the well-known NH_3 gas electrode. This type of electrode has also been used successfully for some time to determine urea in urine by means of the enzyme urease. The enzymic hydrolysis of urea [reaction (4)], like the oxidation of glucose, allows the use of various chemosensors as transducer.

$$CO(NH_2)_2 + 2\,H_2O \xrightarrow{\text{urease}} 2\,NH_4^{\oplus} + CO_3^{2\ominus} \quad (4)$$

In aqueous solution the reaction products give the pH-dependent equilibria (5) and (6), which provide further spe-

$$NH_4^{\oplus} + OH^{\ominus} \rightleftharpoons NH_3 + H_2O \quad (5)$$

$$CO_3^{2\ominus} + H^{\oplus} \rightleftharpoons HCO_3^{\ominus} \underset{-H^{\oplus}}{\overset{H^{\oplus}}{\rightleftharpoons}} CO_2 + H_2O \quad (6)$$

cies for which transducers are available. Potentiometric ISEs are available for two of the reaction products, the ammonium and carbonate ions. Furthermore, the gases NH_3 and CO_2 which may be produced depending on the pH in the reaction zone can be detected by means of the appropriate gas electrodes mentioned above.[160] A urea sensor as described here can be made in the form of a simple triple-membrane configuration as shown in Figure 19.

Conductometry is another electrochemical transducer principle which can be applied to biosensors, since the progress of an enzymic reaction can also be measured by the change in the resistivity of the solution. However, as well as lacking selectivity, this method suffers from the fundamental difficulty that only the total resistivity can be measured and the change in resistivity is caused not only by the reaction, but also by the introduction of an ion-containing medium. A difference method has been proposed by *Watson*.[161] Con-

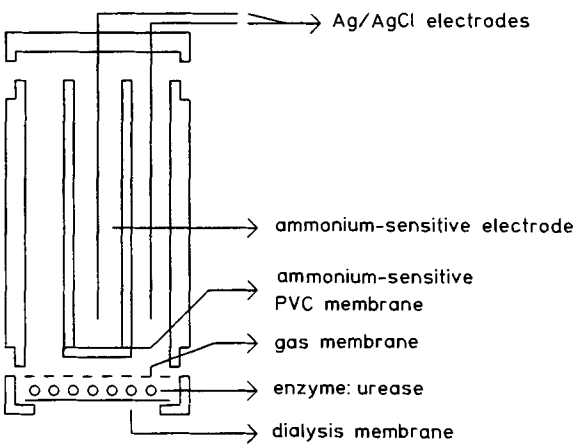

Fig. 19. Triple-membrane structure of, for example, a urea sensor.

ductometric biosensors for urea and for D-amino acids are described by *Rechnitz* et al.[162]

3.1.2. Biochips

The new microelectronic transducers are becoming increasingly important, as they make it possible to produce one-shot disposable biosensors. This offers a possible solution to the ever-present problems of poor storage properties and short lifetimes of biosensors. Even the problem of sterilization could be solved by sterile sensor elements which are introduced immediately before the measurement.

Special mention must be made here of ion-selective field effect transistors (ISFETs), whose small size, particularly, warrants their application as transducers in biosensors, as this factor is of great importance for catheter sensors in medical technology. Enzyme-modified ISFETs, known as ENFETs, consist in many cases of pH-sensitive ISFETs with an enzyme immobilized on their surface; this catalyzes the reaction of a substrate which generates or removes protons.

Examples of the use of ENFETs are the determination of glucose,[152, 163] urea, and penicillins,[158, 165] in which the appropriate enzymes were immobilized on the pH-sensitive surface of the ISFET with glutaraldehyde and bovine serum albumin, or in membranes. To compensate for errors caused by temperature fluctuations or by pH changes from effects other than the enzymic reaction, a differential measurement can be performed with two pH-ISFETs, one coated with the enzyme and one bare, as described in the first German patent for a biochip.[164]

Table 9. Enzymic sensors based on FETs. pH FETS serve as transducers.

Substrate	Enzyme	Product(s)	Range [10^{-3} M]	Refs.
glucose	GOD	gluconic acid	0–20	[163]
urea	urease	CO_2, $2NH_3$	0–6	[165]
penicillin G	penicillin G amidase	phenylacetic acid	1.5–50	[165]
penicillin	penicillinase	penicillic acid	0.2–20	[158]
triolein	lipase	fatty acids	0.6–3	[166]

The determination of triglycerides has also been performed by a differential measurement, with lipase immobilized in a polyvinylpyrrolidone membrane on the pH-sensitive surface of a pH-ISFET.[166] Table 9 gives a summary of the ENFETs that have been reported.

3.1.3. Optical Transducers

In addition to the well-proven electrochemical transducers, optical sensors have recently been exploited to an increasing extent for substrate recognition by enzymic reactions, since fiber-optic spectrophotometers and fluorimeters are now commercially available. The way in which these optical biosensors function will be described here with the help of a few examples.

Wolfbeis and *Trettnak*[167] have developed a biosensor for glucose determination using the reaction described in Eq. (3); this sensor contains as its transducer an oxygen optode which has already been described in Section 2.3. The glucose oxidase was bound to a nylon membrane by activated carboxyl groups (Immunodyne) and the membrane was attached to the surface of the optode.

Another approach of *Wolfbeis* et al.[168] is based on the intrinsic fluorescence of the enzyme concerned. Enzymes with FAD (flavine adenine dinucleotide) as prosthetic group change their fluorescence properties during the reaction with the substrate, because flavoproteins have different properties in their oxidized and reduced states. This change can be measured with optical fibers that have the enzyme held at their ends by a dialysis membrane. Experiments have been carried out on this system with glucose oxidase, lactate monooxygenase and cholesterol oxidase as enzymes.

An optical biosensor has been developed for controlling the biotechnological manufacture of penicillin. This sensor monitors the change in pH caused by the enzymic conversion of penicillin to penicillic acid; the measurement can be performed either electrochemically or optically.[169] For the latter the enzyme penicillinase was immobilized in a polymer together with a pH-indicator, as described in Section 2.3 for pH-optodes. Urea can be determined by an analogous method.[170]

These examples of optical sensors, which are summarized in Table 10, clearly illustrate that, like electrochemical biosensors, nearly all optical sensors depend on just a few basic principles, such as

1) the measurement of oxygen concentration by the fluorescence quenching of a dye (transducer: O_2 optodes),

2) pH-measurements (transducers: pH optodes), and

3) the determination of NADH fluorescence using a bifurcated light-guide.

Combining these measurement principles with different enzymes results in biosensors similar to those based on electrochemical transducers. There are no great differences in performance between them. Figure 20 shows the basic design features of an optical biosensor.

Table 10. Enzymic sensors based on optodes[a].

Substrate	Enzyme	Product	Transducer	Range [10^{-3} mol L^{-1}]	Refs.
ethanol	ADH/LDH	NADH	fiber-optic	0–1	[174]
glucose	GOD	D-gluconolactone	O_2 optode	0.1–20	[167]
urea	urease	ammonia	NH_3 optode	0.3–3	[170]
lactate	LMO	pyruvate	fiber-optic	0.5–1	[168]
penicillin	penicillinase	penicillic acid	pH optode	0.25–10	[169]

[a] Abbreviations: ADH = alcohol dehydrogenase; LDH = lactate dehydrogenase; GOD = glucose oxidase; LMO = lactate monooxygenase.

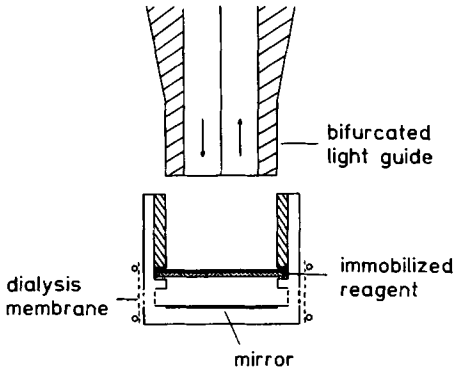

Fig. 20. Schematic arrangement of an optical biosensor.

3.1.4. Mass-Sensitive Transducers

A class of biosensors that have hitherto not been widely used are those based on piezoelectric crystals or surface acoustic wave (SAW) devices.[171] These provide a simple means of detecting changes in mass through the alteration in the resonance frequency of a crystal. If such a transducer is covered with a selectively adsorbing surface or absorbing film, the concentration of the ab- or adsorbed substance can be determined from the change in resonance frequency. Using a 9 MHz piezoelectric quartz crystal, for example, it is theoretically possible to measure mass changes as small as 10^{-9} g. *Guilbault* et al. describe sensors based on piezoelectric crystals coated with enzymes. The selectivity is provided by the formation of an enzyme-substrate complex, and the sensitivity is given by the stoichiometric mass increase given by the equation of the reaction. With immobilized formaldehyde dehydrogenase,[172] atmospheric formaldehyde concentrations in the range from 1 to 100 ppm can be detected, with choline esterase,[173] pesticides in the ppb range. Measurements in liquid media cause greater problems and are controversial. To maintain the theoretical sensitivity described in Equation (d), piezoelectric sensors should be subjected to a reproducible drying step in air before use.

3.2. Multienzyme Sensors

The repeated use of expensive coenzymes is possible if they are regenerated by a second enzyme.

The recycling method described by *Schepers* et al.[174] could be applied to many analytes. The fluorescence of the reduced coenzyme nicotinamide adenine dinucleotide (NADH) is measured in a flow-through cell using a fiber-optic device. The molecular mass of the $NAD^{\oplus}$ is increased by binding it onto polyethyleneglycol in order to trap it within the cell, together with an enzyme such as alcohol dehydrogenase, behind a dialysis membrane. When a second enzyme, e.g. lactate dehydrogenase, is also included behind this membrane, it becomes possible to regenerate the NADH by adding pyruvate. However, the need to add this reagent means that the device is no longer a sensor in the narrow sense, because a sensor should work without addition of reagents. Several enzymes, or even a whole enzyme series, could be necessary in cases where a single enzymic reaction step does not yield a substance which can be detected by a transducer.[114, 115]

3.3. Biosensors Based on Tissue Sections or Cell Cultures

Not only isolated enzymes but also entire groups of intact cells can be used as the basis for biosensors. Compared with the isolated enzymes, these often have the advantage of being active for longer periods, as the enzymes are kept in their natural environment. In this case an additional immobilization step for the coenzymes or cofactors is not necessary. However, such cell groups are often less selective, as they contain mixtures of enzymes.

Arnold and *Rechnitz*[175] published a table listing biosensors based on tissues and related materials. NH_3 or O_2 chemosensors are often used as transducers.

The principle of these devices will be explained by taking as an example a biosensor for hydrogen peroxide. As bovine liver contains relatively high concentrations of the enzyme catalase, a section of fresh tissue only 0.1 mm thick is immobilized with nylon mesh on the surface of a membrane-covered O_2 electrode. The hydrogen peroxide whose concentration is to be determined undergoes enzymic decomposition to oxygen and water, and the oxygen thus produced is measured amperometrically. This sensor is less sensitive to fluctuations in temperature and pH, and has a longer lifetime than a biosensor containing an isolated enzyme.[176] Another device of this kind which is frequently cited is the "bananatrode" which has been described by *Rechnitz* et al.[177] Here a thin slice of banana in front of an O_2 sensor is used as a detector for dopamine, which undergoes oxidation by the enzyme polyphenol oxidase present in bananas. The consumption of oxygen is then measured.

3.4. Microbial Biosensors

The majority of biosensors based on immobilized microorganisms function with amperometric oxygen sensors as transducers.[178] Biosensors for the determination of phosphate, nitrate, nitrite, sulfite, methane, and phenol have recently been described, but none has yet achieved a commercial breakthrough.

The determination of phosphate was performed with a sensor based on the microorganism *Chlorella vulgaris* in immobilized form. An O_2 optrode was used to measure the increase in the photocurrent on introducing phosphate. The photocurrent was found to be a function of the phosphate concentration in the range from 8 to 70 mmol L^{-1}.[179] *Karube*, *Kitagawa* et al.[180] have developed a microbiological sensor for alcohol using a pH ISFET as a transducer. For this the acetic acid bacterium *Gluconobacter suboxydans* was immobilized on the ISFET behind a gas-permeable membrane. Ethanol which diffuses in through the membrane is converted to acetic acid by the bacteria. This biosensor can be used for the determination of ethanol in the range from 3 to 70 mmol L^{-1}.

3.5. Immunosensors

Antibodies (Ab) and antigens (Ag) (or haptenes) bind specifically and strongly to each other. Techniques for following such reactions in order to determine one of the reac-

tion partners have up to now relied mainly on labeling one of the immunoreactands. This is the principle used in immunoassays, which are now indispensable in biochemical analysis. Immune reactions are subject to the limitations imposed by the law of mass action. In the equilibrium reaction between the free antigen (Ag) and the antibody (Ab) to form the antigen–antibody complex, the equilibrium ratio between the concentrations of the complex and of the free reaction partners is determined by the affinity constant K [Eq. (f)].

$$K = [AgAb]/[Ag][Ab] \quad (f)$$

In immunoassays quantitative determinations can be carried out by means of competitive binding tests or sandwich tests. In competitive tests labeled antigens are used. If radioactive labeling is used, the procedure is called a radioimmunoassay (RIA). If instead, an enzyme is covalently bound to the antigen (horseradish peroxidase or alkaline phosphatase are often used), the procedure is called enzyme immunoassay (EIA). The labeled antigen and the antigen to be assayed compete for the binding of the immobilized antibody, and the concentration of the antigen can be determined by comparison with a reaction of a known concentration of the pure antigen. Sandwich tests are carried out with labeled antibodies. When radioactive labeling is used the measurement is described as an immunoradiometric assay (IRMA), whereas if the antibody is attached to an enzyme it is called an enzyme-linked immunosorption assay (ELISA). The antigen which is to be determined binds to an antibody which is immobilized on a support, and is quantitatively determined by means of a second labeled antibody.

Both systems have important disadvantages. Purified antibodies and antigens are required. The calibration curves are only linear over a small concentration range. With radioactive labeling there are problems of waste management. Although an immunoassay is simple to perform, it involves a succession of stages, and often a separation step, requiring several hours of work.

In the last few years several immunosensors have been developed in which the immunological reaction is measured directly. These sensors use electrochemical, optical, or piezoelectric transducers or capacitance bridges. It should eventually be possible to perform the most important types of immunochemical analysis with disposable sensors.[181]

Enzyme immunoelectrodes comprise the transducer (electrode), the immune reaction system, and an enzyme indicator and are based on the usual EIA principles, except that the product of the enzyme-catalyzed reaction (often H_2O_2) is detected electrochemically and not by photometry.[182, 183]

Ion-selective membrane electrodes have also been used for the determination of antibodies. The method is described by *Rechnitz* et al.,[184] in which the corresponding antigen is covalently bound to an ionophore of the benzo-crown-ether group and immobilized in a PVC membrane to give an electrode sensitive to alkali metal ions. The change in the potential of the electrode which occurs on adding the appropriate antibody is caused by the alteration of the properties of the ionophore when the antibody binds to the antigen–ionophore complex. Another type of immunosensor is based on the antigen-induced change in the potential of a chemically modified semiconductor surface (TiO_2), the mechanism of which is still not understood.[185] Based on early fundamental studies on potentiometric immunosensors during the period 1978–89, the interdisciplinary research center for chemo- and biosensors at the Westfaelische Wilhelms University (FRG) has just elucidated the general mechanism of immunologically-induced changes in electrode potential.[186, 187] There are in principle many different antibodies for a particular antigen or haptene, so that a large variety of organic molecules can be selectively determined. If the remaining problems of standardization and storage life can be solved, this analytical technique should revolutionize at least molecular analysis, since a potentiometric immunoassay is fast, sensitive, and extremely economic.

Immunosensors based on mass-sensitive transducers (piezoelectric crystals and SAW devices) exploit the mass increase which results from the immune reaction.[188] Here again measurements in liquids present problems.

Immune reactions at surfaces also alter certain optical properties, on which optical sensors are based. One optical effect that can be used to determine antigens with immobilized antibodies is the change the resonance angle in surface plasmon resonance (SPR) spectroscopy[189] when immunocomplexation forms a film on a silicon or metal oxide base layer. Others are the change in light scattering from a coated glass surface when an immunocomplex is formed,[190] and changes in the reflection and absorption of a light beam (evanescent wave technique).[191]

A strict definition classifies immunosensors not as true sensors, but as dosimeters, because the immune reactions are not reversible. Under suitable conditions (e.g. by altering the pH) it is possible to break down the biocomplex to recover the antibody and the antigen, allowing a quasi-continuous measurement sequence.[186, 187]

A continuously operating type of immunosensor based on competitive reactions has been developed; here the analyte and a heterobifunctional complex compete for binding sites on an immobilized antibody.[192]

Nonspecific binding is a difficulty which limits the sensitivity of immunosensors in many applications. This problem has been investigated in detail by *Cullen* and *Lowe*.[193]

3.6. Biosensors Based on Receptors

A very promising approach is the development of biosensors in which individual receptors or receptor structures from living organisms are immobilized on transducers.[194] The advantages of receptors over enzymes, for example, lie in very high sensitivities and short response times. It is known, for example, that some marine species can recognize substances at concentrations as low as 10^{-13} mol L^{-1}. However, the problems of isolating receptor molecules and of their instability when immobilized are still so great, that this idea must be regarded at present as an interesting approach with potential for future developments.

A sensor for the determination of glucose which is based on a receptor protein has been developed by *Schultz* and *Meadows*.[195] This makes use of the competition between glucose and a glucose analogue, a dextran labeled with fluorescein isothiocyanate (FITC-dextran), for binding sites on

the glucose receptor protein concanavalin A labeled with rhodamine (Rh-Con A). FITC-dextran and Rh-Con A are sealed in a length of dialysis tube at the end of a bifurcated light guide with a diameter of 100 μm (Fig. 21). Light of a suitable wavelength excites FITC, which fluoresces. If the FITC is connected via the dextran to the Rh-Con A, the energy absorbed by the FITC is transmitted to the rhodamine, which then also fluoresces. If glucose diffuses

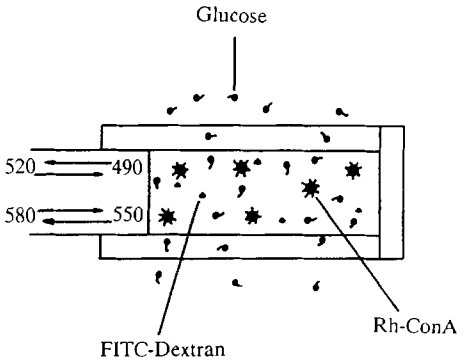

Fig. 21. Glucose sensor based on the use of a receptor[195]. The numbers represent the wavelengths (in nm) of the irradiating light (left) and fluorescent light (right).

through the dialysis membrane into the measuring cell, the dextran is partly displaced from its binding sites by the glucose and the measured FITC fluorescence increases, because less energy is transferred from FITC to rhodamine. From increase in fluorescence intensity the glucose concentration can be determined.

3.7. Applications of Biosensors

An important technological application of biosensors is the control of fermentation processes. Here it is desirable to measure continuously as far as possible, to ensure optimization of the fermentation process and to minimize the consumption of expensive nutrients. It is particularly important to monitor glucose, ethanol, lactate, cephalosphorins and penicillins.

Another area in which biosensors are used, is food technology and food testing. Of interest is the glucose content of wine and fruit drinks,[196] lactate production during milk processing,[197] and the freshness of fish, which is measured with a hypoxanthin sensor.[198]

An area of growing importance is monitoring the quality of water and effluents. Most of the sensors developed so far are based on the combination of microorganisms and transducers. Some sensors serve to determine individual constituents of water, such as phosphate, nitrite, and nitrate,[178] while others measure composite parameters through their inhibiting effects on microorganisms or enzymes. However, the latter are more like simple early warning systems (screening) than true sensors, as an alarm indication needs to be followed by a more precise analysis. Moreover, these systems work irreversibly. Such warning systems are used in particular to monitor pesticide contents or concentrations of heavy metal ions and the inhibition of the microorganisms is measured by the reduction in CO_2 production.[199] To obtain a quantity which can be related to the biological oxygen demand (BOD), changes in the respiratory rate of *Trichosporon cutaneum* are measured with an oxygen electrode.[200] A sensor of this type is already in routine operation in Japan.

A final example of a field in which biosensors are finding application is medical technology. The most frequently performed analyses are of glucose and lactate, and it is therefore in this area that the most intensive research is being undertaken. The desirability of in-vivo measurements, for example, to control an insulin pump, is giving impetus to the development of miniaturized biosensors. Here of utmost importance is the requirement that the reagents are biocompatible and physiologically harmless.

Already a few biosensors, based on electrochemical or optical transducers or on piezoelectric crystal measurements in the gas phase, are commercially available.

Analytical instruments have been developed to avoid some problems of biosensors. Here pretreatment of the samples can prolong the life of the sensor.

The early commercially available analytical instruments for medical technology are usually based on an oxygen or hydrogen peroxide electrode as a transducer, with an oxidase as the biochemical component. They permit analyses on whole blood for glucose content in the range from 0 to 30 mmol L^{-1} or lactate content from 0 to 15 mmol L^{-1}. A BOD-measuring instrument based on the BOD sensor described earlier is now also available.

A list of commercially available analytical instruments based on biosensors can be found in the article by *Owen*.[201]

4. Outlook

This article aimed to give a concise overview of the present state of development of chemical sensors that are already or might become important for chemical, medical, and environmental applications. However it does not claim to be exhaustive. In the field of biosensors alone there are, according to recent CAS on-line searches, over 3000 publications and over 300 patents, although there are at present barely a dozen types of commercially available sensors, of which more than a half are for glucose. One of the main reasons for this striking imbalance with regard to marketing success may be found in the low degree of interdisciplinary cooperation among scientists. Many of the publications go no further than demonstrating a reproducible effect observed for a single chemical substance. Often there is no investigation into the effects of interfering substances, nor an answer to the central analytical question: how accurately and reliably does the sensor measure the substance for which one is analyzing? Reports which only give information on reproducibility, measured on pure synthetic samples containing no interfering constituents, should be avoided in view of the present wealth of knowledge about sources of systematic errors. To an analytical chemist a report on the development of a new analytical method which tells one nothing about matrix effects, and therefore about its absolute accuracy (defined as coincidence with the true content in the sample) is like a report on a synthetic method for a new compound which was identified by elemental analysis alone (i.e. without

confirmation by universally recognized and indeed prescribed methods of modern structural analysis).

In the field of chemosensor development, as in that of ultra-trace analysis, there is a growing tendency to play down the importance of interfering effects. The disproportionately large amount of research effort devoted to the microelectronic aspects of modern transducers is pointless if not accompanied by a deeper understanding of the mechanisms by which substances are specifically recognized. The fundamental mechanisms of the molecular interactions taking place in these devices cannot be planned and optimized on purely engineering considerations; they depend on natural laws that one can use but cannot alter!

In summary it may be concluded that the development of sensors will advances further simply because there is a strong demand for it. The more research effort concentrated on the central problem of a selective molecular recognition, the quicker such advances will be achieved. Our present knowledge of mechanisms indicates that it is necessary to involve chemists from a wide variety of disciplines: theoretical, inorganic, organic, biochemical, analytical, and physico-chemical. The development of new sensors can only progress by an interdisciplinary approach, which must also include the collaboration of biologists, physicists, and medical scientists.

At this stage improvement in the transducer properties has a lower priority than improvement in the selectivity of chemosensors and the lifetime of biosensors. The transducers now available have adequate stability and sensitivity, and their full exploitation is prevented only by the laws of physical-chemistry or by shortcomings in the properties of the sensor elements.

The basic ideas of the novel approach to the theory of ion-selective electrodes described here were developed in 1975 by K. Cammann in his Ph.D. thesis. He would like to thank his academic teachers, Prof. Dr. G. Ertl and Prof. Dr. H. Gerischer, for many discussions and helpful suggestions. During a Humboldt-Fellowship, for which the Alexander von Humboldt Foundation is sincerely thanked, Prof. Dr. S. L. Xie could verify this far-reaching theory completely by means of the most modern experimental equipment. The basic research in this field during recent years was generously funded by the Deutsche Forschungsgemeinschaft (DFG) and the Fonds der Chemischen Industrie, which we have much appreciated. Grateful acknowledgement is also given to the Bundesministerium für Forschung und Technologie (BMFT) for its generous financial help to research in the field of biosensors at Münster. Last but not least, we owe a debt of gratitude to the State of Nordrhein–Westfalen, which is establishing a research institute for chemical sensors and biosensors (attached to the University of Münster) in cooperation with the Fraunhofer-Management-Gesellschaft (FhM). The aim of this interdisciplinary institute is to support applied research on all aspects of chemical sensing, including the development of complete measurement systems and monitoring equipment.

Received: February 26 (1990) [A 813 IE]
German Version: *Angew. Chem.* 103 (1991) 519
Translated by Dr. *T. K. Becconsall*, Gwynedd (Wales)

[1] A. Hulanicki, S. Glab, F. Ingman: *IUPAC Discussion Paper*, Commission V. I., Juli 1989.
[2] R. A. Durst, R. W. Murray, K. Izutsu, K. M. Kadish, L. R. Faulkner: *Draft IUPAC Report*, Commission V.5.
[3] M. Cremer, *Z. Biol. 47* (1906) 562.
[4] F. Haber, Z. Klemensiewicz, *Z. Phys. Chem. 67* (1909) 385.
[5] M. Dole: *The Glass Electrode, Methods, Applications and Theory*, Wiley, New York 1941.
[6] L. Kratz: *Die Glaselektrode und ihre Anwendungen*, Steinkopff, Frankfurt am Main 1950.
[7] G. Eisenman: *Glass Electrodes for Hydrogen and other Cations, Principles and Practice*, Dekker, New York 1967.
[8] J. W. Ross, M. S. Frant, *Science (Washington, D. C.) 154* (1966) 1553.
[9] M. S. Frant, J. W. Ross, „Ion-Sensitive Electrode and Method of Making and Using Same", *US-A 3672962* (1972).
[10] L. A. R. Pioda, V. Stankova, W. Simon, *Anal. Lett. 2* (1969) 665.
[11] W. Möller, W. Simon, „Ionenspezifisches Elektrodensystem", *DE-B 1648978* (1972).
[12] K. Cammann, *Fresenius Z. Anal. Chem. 216* (1966) 287.
[13] K. Cammann, *Naturwissenschaften 57* (1970) 298.
[14] K. Cammann: *Das Arbeiten mit ionenselektiven Elektroden*, 2nd ed. Springer, Berlin 1977.
[15] P. L. Bailey: *Analysis with Ion-Selective Electrodes*, 2nd ed. Heyden, London 1980.
[16] A. K. Covington: *Ion-Selective Electrode Methodology, Vol.1*, CRC, Boca Raton, FL 1979, p.1.
[17] L. C. Clark, „Electrochemical Device for Chemical Analysis", *US-A 2913386* (1959).
[18] T. Taguchi, K. Naoyoshi, „Gas-sensing element containing an electroconductivity-changing semiconductor material", *US-A 3625756* (1971).
[19] W. H. King, Jr., *Anal. Chem. 36*, (1964) 1735.
[20] D. W. Lübbers, N. Optitz, *Z. Naturforsch., C: Biosci. 30C* (1975) 532.
[21] T. M. Freeman, R. W. Seitz, *Anal. Chem. 50* (1978) 1242.
[22] L. C. Clark Jr., C. Lyons, *Ann. N. Y. Acad. Sci. 102* (1962) 29.
[23] K. Cammann, *Fresenius Z. Anal. Chem. 287* (1977) 1.
[24] J. Ruzicka, H. E. Hansen: *Flow Injection Analysis*, Wiley, New York 1981.
[25] B. P. Nicolsky, T. A. Tolmacheva, *Zh. Fiz. Khim. 10* (1937) 495.
[26] K. Cammann, *Ion-Sel. Electrodes, Conf. 1977* (1978) 297.
[27] K. Cammann, G. A. Rechnitz, *Anal. Chem. Symp. Ser. 22* (1985) 35.
[28] K. Camann, G. A. Rechnitz, *Ion-Sel. Electrodes 5, Proc. Symp. 5th* 1988 (1989) 31.
[29] K. Cammann, S.-L. Xie, *Ion-Sel. Electrodes, 5, Proc. Symp. 5th* 1988 (1989) 43.
[30] S.-L. Xie, K. Cammann, *Ion-Sel. Electrodes, 5, Proc. Symp. 5th* 1988 (1989) 639.
[31] J. Koryta, *Anal. Chem. Symp. Ser. 8* (1981) 53.
[32] S.-L. Xie, K. Cammann, *J. Electroanal. Chem. 229* (1987) 249.
[33] S.-L. Xie, K. Cammann, *J. Electroanal. Chem. 245* (1988) 117.
[34] D. Ammann, W. E. Morf, P. Anker, P. C. Meier, E. Pretsch, W. Simon, *Ion-Sel. Electrode Rev. 5* (1983)3.
[35] K. Cammann, *Top. in Curr. Chem. 128* (1985) 219.
[36] W. Simon, H.-R. Wuhrmann, M. Vasak, L. A. R. Pioda, R. Dohner, Z. Stefanac, *Angew. Chem. 82* (1970) 433; *Angew. Chem. Int. Ed. Engl. 9* (1970) 445.
[37] *Handbook of Electrode Technology*, Orion Research, Cambridge, MA 1982.
[38] *Selectophore, Ionophores for Ion-Selective Electrodes*, Firmenschrift der Fluka Chemie AG, Buchs (Switzerland) 1988.
[39] P. Bergveld, *IEEE Trans. Biomed. Eng. BME-17* (1970) 70.
[40] P. Bergveld, *IEEE Trans. Biomed. Eng. BME-19* (1972) 342.
[41] G. Koning, S. J. Schepel, *Anal. Chem. Symp. Ser. 17* (1983) 597.
[42] B. H. van der Schoot, P. Bergveld, M. Bos, L. J. Bousse, *Sens. Actuators 4* (1983) 252.
[43] L. J. Bousse, P. Bergveld, *Sens. Actuators 6* (1984) 65.
[44] D. Sobczynska, W. Torbicz, A. Olszyna, W. Wlosinki, *Anal. Chim. Acta 171* (1985) 357.
[45] H. H. van den Vlekkert, N. F. de Rooij, A. van den Berg, A. Grisel, *Sens. Actuators B1* (1990) 395.
[46] W. H. Ko, C. D. Fung, D. Yu, Y. H. Xu, *Anal. Chem. Symp. Ser. 17* (1983) 496.
[47] J. van der Spiegel, T. Lauks, P. Chan, D. Babic, *Sens. Actuators 4* (1983) 291.
[48] U. Lemke, K. Cammann, *Fresenius Z. Anal. Chem. 335* (1989) 852.
[49] C. Battaglia, J. Chang, D. Daniel, *US-A 4214968* (1980).
[50] D. P. Hamblen, C. P. Glover, S. H. Kim, *US-A 4053381* (1977).
[51] G. Hötzel, H. M. Wiedenmann, *Sens. Rep. 4* (1989) 32.
[52] J. P. Pohl, *GIT Fachz. Lab. 5* (1987) 379.
[53] B. C. LaRoy, A. C. Lilly, C. O. Tiller, *J. Electrochem. Soc. 120* (1973) 1668.
[54] S. Harke, H.-D. Wiemhöfer, W. Göpel, *Sens. Actuators B1* (1990) 188.
[55] Chromium Sensor Research Group, *7th Int. Conf. Solid State Ionics*, Hakone (1989), Abstr. No. 8aA-11.
[56] K. Gomyo, I. Sakaguchi, Y. Shin-ya, M. Iwase, *7th Int. Conf. Solid State Ionics*, Hakone (1989), Abstr. No. 8aA-12.

[57] Q. Liu in B. V. R. Chowdari, S. Radhakrishna (Ed.): *Proc. Int. Sem. Solid State Ionic Devices*, World Scientific – Asian Society for Solid State Ionics, Singapore 1988, p. 191.
[58] D. Jakes, J. Kral, J. Burda, M. Fresl, *Solid State Ionics 13* (1984) p. 164.
[59] M. R. Hobdell, C. A. Smith, *J. Nucl. Mater. 110* (1982) 125.
[60] a) K. T. Jacob, T. Matthews in T. Takahashi (Eds.): *High Conductivity Solid Ionic Conductors*, World Sci., Singapore 1989, p. 513; b) T. Maruyama, *Solid Stock Ionics 24* (1987) 281.
[61] W. L. Worrell in T. Seiyama (Eds.): *Chemical Sensor Technology, Vol.1*, Kodansha/Elsevier, Tokyo 1988, p. 97.
[62] W. L. Worrell, *Solid State Ionics 28/30* (1988) 1215.
[63] Q. G. Liu, W. L. Worrell in V. Kuduk, Y. K. Rao (Ed.): *Physical Chemistry of Extractive Metallurgy*, The Metallurgical Society, Warrington, PA 1985, p.387.
[64] C. M. Mari, M. Beghi, S. Pizzini, J. Faltemier, *Sens. Actuators B2* (1990) 51.
[65] P. C. Yao, D. J. Fray, *J. Appl. Electrochem. 15* (1985) 379.
[66] P. Fabry, J. P. Gros, J. F. Million-Brodaz, M. Kleitz, *Sens. Actuators 15* (1988) 33.
[67] T. Takeuchi, *Sens. Actuators 14* (1988) 109.
[68] T. Takeuchi in J. L. Aucouturier, J.-S. Cauhape, M. Destriau, P. Hagenmüller, C. Lucat, F. Menil, J. Portier, J. Salardenne (Eds.): *Proc. 2nd Int. Meet. Chem. Sensors*, University of Bordeaux, Bordeaux 1986, p.69.
[69] H. Jahnke, B. Moro, H. Dietz, B. Beyer, *Ber. Bunsenges. Phys. Chem. 92* (1988) 1250.
[70] K. Cammann in H. Naumer, W. Heller (Eds.): *Untersuchungsmethoden in der Chemie*, Thieme, Stuttgart 1986, p.110.
[71] R. Hersch, *Adv. in Anal. Chem. Instrum. 3* (1964) 183.
[72] F. J. H. Mackereth, *J. Sci. Instrum. 41* (1964) 38.
[73] W. Göpel, *Hard and Soft 8/9* (1988), special supplement: microperipherals, p. X.
[74] R. Müller, *Hard and Soft 11/12* (1989), special supplement: microperipherals, p. IV.
[75] O. S. Wolfbeis, *Appl. Flouresc. Technol. 1* (1989)1.
[76] S. M. Angel, *Spectroscopy (Eugene, Oregon) 2* (1987) 38.
[77] J. F. Alder, *Fresenius Z. Anal. Chem. 324* (1986) 372.
[78] H. H. Miller, T. B. Hirschfeld, *Engineers 718* (1987) 39.
[79] O. S. Wolfbeis, *Fresenius Z. Anal. Chem. 325* (1986) 387.
[80] M. Zander: *Fluorimetrie*, Springer, Berlin 1981.
[81] W. E. Morf, K. Seiler, P. R. Sorensen, W. Simon, in E. Pungor (Ed.): *Ion-Sel. Electrodes, 5, Proc. Symp. 5th* 1988 (1989) 141.
[82] S. Kurosawa, N. Kamo, D. Matsui, Y. Kobatake, *Anal. Chem. 62* (1990) 353.
[83] F. Dickert, *Hard and Soft 11/12* (1989), special supplement: microperipherals, p. VII.
[84] G. Sauerbrey, *Z. Phys. 155* (1959) 206.
[85] K. K. Kanazowa, J. G. Gordon II, *Anal. Chem. 57* (1985) 1770.
[86] R. Schuhmacher, *Angew. Chem. 102* (1990) 347; *Angew. Chem. Int. Ed. Engl. 29* (1990) 329.
[87] J. W. Schultze, A. Meyer, K. Saurbier, A. Thyssen in W. Günther, J. P. Matthes, H.-H. Perkampus (Eds.): *Instrumentalized Analytical Chemistry and Computer Technology*, GIT, Darmstadt 1990, p. 637.
[88] K. Cammann, *Hard and Soft 11/12* (1989), special supplement: microperipherals, p. I.
[89] K. Cammann, U. Lemke, J. Sander, *Hard and Soft 11/12* (1989), special supplement: microperipherals, p. II.
[90] K. Cammann, *Sens. Rep. 5* (1989) 16.
[91] K. Cammann in H. Krupp (Ed.): *Beitrag der Mikroelektronik zum Umweltschutz*, VDE-Verlag, Berlin 1988, S.433.
[92] A. Braat, *Adv. Instrum. 40* (1985) 1347.
[93] H. Warncke, *TM Tech. Mess. 52* (1985) 135.
[94] W. Göpel, F. Oehme, *Hard and Soft 3* (1987), special supplement: microperipherals, p. I.
[95] H. Schubert: *Sensorik in der medizinischen Diagnostik*, TÜV Rheinland, Köln 1989.
[96] P. Ulrich, *Das Mod. Lab. 3* (1987) 18.
[97] P. Ulrich: *Ionenselektive Analytik in der Klinischen Chemie*, Schriftenreihe der Colora Meßtechnik GmbH, Lorch, No.2 (1988).
[98] L. J. Russell, K. M. Rawson, *Biosensors 2* (1986) 301.
[99] S. J. Pace, *Sens. Actuators 1* (1981) 475.
[100] K. Cammann, *Instrum. Forsch. 9* (1982)1.
[101] J. G. Schindler, M. M. Schindler (Eds.): *Bioelektrochemische Membranelektroden*, de Gruyter, Berlin 1983.
[102] D. A. Thomason, *Anal. Proc. (London) 23* (1986) 293.
[103] O. Sonntag: *Trockenchemie*, Thieme, Stuttgart 1988.
[104] K. Cammann, *Fresenius Z. Anal. Chem. 329* (1988) 691.
[105] J. Mertens, P. van den Winkel, D. L. Massart, *Anal. Lett. 6* (1973) 81.
[106] R. P. Badoni, A. Jayaraman, Erdöl und Kohle-Erdgas-Petrochemie *41* (1988) 23.
[107] Infratest Industria, Marktübersicht, *Chemische und Biochemische Sensoren*, München 1989.
[108] R. Macdonald (Ed.): *Impedance Spectroscopy*, Wiley, New York 1987.
[109] W. Göpel, *TM Tech. Mess. 52* (1985) 47.
[110] W. Göpel, *TM Tech. Mess. 52* (1985) 92.
[111] W. Göpel, *TM Tech. Mess. 52* (1985) 175.
[112] U. Gerlach-Meyer, *Symposium Chemische Sensoren – Heute und Morgen*, Essen 1989.
[113] Batelle-Institut: *Sensoren: Miniaturisierung und Integration*, Studie, Frankfurt am Main 1987.
[114] F. Scheller, F. Schubert: *Biosensoren*, Birkhäuser, Basel 1989.
[115] A. P. F. Turner, I. Karube, G. S. Wilson (Eds.): *Biosensors*, Oxford Univ. Press, New York 1987.
[116] P. V. Sundaram, *Meth. Enzymol. 137* (1988) 288.
[117] H. Plainer, B. G. Sprössler, *Forum Mikrobiol. 5* (1987) 161.
[118] M. Nelboeck, D. Jaworek, *Chimia 29* (1975) 109.
[119] M. Shichiri, R. Kawamori, Y. Goriya, Y. Yamasaki, M. Nomura, N. Hakui, *Diabetologia 24* (1983) 179.
[120] M. Shichiri, *Horm. Metab. Res. Suppl. Ser. 20* (1988) 17.
[121] H.-L. Schmidt, R. Lammert, J. Ogbomo, T. Baumeister, J. Danzer, R. Kittsteiner-Eberle, *GBF Monogr. Ser. 13* (1989) 93.
[122] A. Malinauskas, J. J. Kulys, *Anal. Chim. Acta 98* (1978) 31.
[123] D. A. Gough: *Biosensors*, First World Congress, Singapore 1990.
[124] R. D. Schmidt, G. C. Chemnitius, *GBF Monogr. Ser. 13* (1989) 299.
[125] G. F. Hall, D. J. Best, A. P. F. Turner, *Enzyme Microb. Technol. 10* (1988) 543.
[126] K. Cammann, B. Winter, *Anal. Chem.*, in press.
[127] M. Niwa, K. Itih, A. Nagata, H. Osawa, *Tokai J. Exp. Clin. Med. 6* (1981) 403.
[128] G. Hanke, F. Scheller, A. Yersin, *Zentralbl. Pharm. Pharmakother. Laboratoriumsdiagn. 126* (1987) 445.
[129] A. P. F. Turner, J. Bradley, A. J. Kidd, P. A. Andersen, A. N. Dear, R. E. Ashby, *Analyst (London) 114* (1989) 375.
[130] H. Suzuki, *Fujitsu Sci. Tech. J. 25* (1989) 52.
[131] S. Gernet, M. Kondelka, N. F. De Rooji, *Sens. Actuators 17* (1989) 537.
[132] H. Gunasingham, K. P. Ang, R. Y. T. Teo, C. B. Tan, B. T. Tay, *Anal. Chim. Acta 221* (1989) 205.
[133] T. Weiss, K. Cammann, *GBF Monogr. Ser. 10* (1987) 267.
[134] K. Cammann, T. Weiss, *Horm. Metab. Res. Suppl. Ser. 20* (1988) 23.
[135] D. A. Gough, J. Y. Lucisano, H. S. Pius, *Anal. Chem. 57* (1985) 2351.
[136] G. Trott-Kriegeskorte, R. Renneberg, M. Pawlowa, F. Schubert, J. Hammer, V. Jäger, R. Wagner, R. D. Schmid, F. Scheller, *GBF Monogr. Ser. 13* (1989) 67.
[137] T. Kelly, G. Christian, *Analyst (London) 109* (1984) 453.
[138] A. Mulchandani, J. H. T. Luong, K. B. Male, *Anal. Chim. Acta 221* (1989) 215.
[139] J. Karube, R. D. Schmid, *GBF Monogr. Ser. 13* (1989) 107.
[140] R. Renneberg, R. D. Schmid, F. Scheller, G. Trott-Kriegestorte, M. Pawlowa, G. Kaiser, A. Warsinke, *GBF Monogr. Ser. 13* (1989) 59.
[141] E. Watanabe, H. Endo, K. Toyana, *Biosensors 3* (1988) 297.
[142] W. J. Blaedel, A. Jenkins, *Anal. Chem. 47* (1975) 1337.
[143] J. Moiroux, P. J. Elving, *Anal. Chem. 51* (1979) 346.
[144] L. Gorton, A. Torstensson, H. Jaegfeld, G. Johansson, *J. Electroanal. Chem. 161* (1984) 103.
[145] T. Ikeda, T. Shiraishi, M. Senda, *Agric. Biol. Chem. 52* (1988) 3187.
[146] A. P. F. Turner, *Methods Enzymol. 137* (1988) 90.
[147] A. P. F. Turner, *NATO ASI Ser. Ser. C226* (1988) 131.
[148] A. P. F. Turner, A. Cass, G. Davis, G. Francis, H. A. Hill, W. Aston, J. Higgins, E. Plotkin, L. D. Scott, *Anal. Chem. 56* (1984) 667.
[149] G. G. Guilbault, G. L. Lubrano, J. M. Kauffmann, G. J. Patriarche, *NATO ASI Ser. Ser. C226* (1988) 379.
[150] I. Satoh, I. Karube, S. Suzuki, *Anal. Chim. Acta 106* (1979) 369.
[151] K. Grebenkämper, *Diplomarbeit*, Universität Münster 1989.
[152] F. Honold, K. Cammann, *GBF Monogr. Ser. 10* (1987) 285.
[153] H. J. Moynihan, N.-H. L. Wang, *Biotechnol. Prog. 3* (1987) 90.
[154] G. G. Guilbault, M. Tarp, *Anal. Chim. Acta 73* (1974) 355.
[155] G. A. Rechnitz, D. S. Papastathopoulos, *Anal. Chim. Acta 79* (1975) 17.
[156] W. R. Hussein, G. G. Guilbault, *Anal. Chim. Acta 72* (1974) 381.
[157] C. H. Kiang, S. S. Kuan, G. G. Guilbault, *Anal. Chim. Acta 80* (1975) 209.
[158] J. Janata, S. Caras, *Anal. Chem. 52* (1980) 1935.
[159] G. G. Guilbault, R. Smith, J. G. Montalvo, *Anal. Chem. 41* (1969) 600.
[160] K. Cammann, *Fresenius Z. Anal. Chem. 287* (1977)1.
[161] L. D. Watson, *Biosensors 3* (1988) 101.
[162] S. Mikkelsen, G. A. Rechnitz, *Anal. Chem. 61* (1989) 1737.
[163] F. Honold, K. Cammann, *Horm. Metab. Res. Suppl. Ser. 20* (1988) 47.
[164] K. Cammann, F. Honold, *DE-A 3411448* (1984).
[165] U. Brand, B. Reinhardt, F. Rüther, T. Scheper, K. Schügerl, *GBF Monogr. Ser. 13* (1989) 127.
[166] M. Nakako, Y. Hanazato, M. Maeda, S. Shiono, *Anal. Chim. Acta 185* (1986) 179.
[167] W. Trettnak, M. J. P. Leiner, O. S. Wolfbeis, *Analyst (London) 113* (1988) 1519.
[168] O. S. Wolfbeis, W. Trettnak, *GBF Monogr. Ser. 13* (1989) 213.
[169] T. J. Kulp, I. Camins, S. M. Angel, C. Munkholm, D. R. Walt, *Anal. Chem. 59* (1987) 2849.
[170] M. A. Arnold, *GBF Monogr. Ser. 10* (1987) 223.

[171] W. M. Heckl, M. Thompson, *GBF Monogr. Ser. 13* (1989) 363.
[172] G. G. Guilbault, *Anal. Chem. 55* (1983) 1682.
[173] G. G. Guilbault, J. H. Luong, *J. Biotechnol. 9* (1988) 1.
[174] C. Schelp, T. Schepers, A. F. Bückmann, *GBF Monogr. Ser. 13* (1989) 263.
[175] M. A. Arnold, G. A. Rechnitz in [115], p. 30.
[176] M. Mascini, M. Jannelle, G. Palleschi, *Anal. Chim. Acta 138* (1982) 65.
[177] J. S. Sidwell, G. A. Rechnitz, *Biotechnol. Lett. 7* (1985) 419.
[178] R. Kindervater, R. D. Schmid, *Z. Wasser Abwasser-Forsch. 22* (1989) 84.
[179] M. Hikuma, T. Kubo, T. Yasuda, I. Karube, S. Suzuki, *Anal. Chem. 52* (1980) 1020.
[180] Y. Kitagawa, E. Tamiya, I. Karube, *Anal. Lett. 20* (1987) 81.
[181] *Biosensors*, First World Congress, Singapore 1990.
[182] G. A. Robinson, V. M. Cole, S. J. Rattle, G. C. Forrest, *Biosensors 2* (1986) 45.
[183] C. Gyss, C. Bourdillon, *Anal. Chem. 59* (1987) 2350.
[184] G. A. Rechnitz, M. Y. Keating, *Anal. Chem. 56* (1984) 801.
[185] Y. Yamamoto, S. Nagoaka, T. Tanaka, T. Shiro, K. Honma, H. Tsubomwa, *Proc. Int. Meet. Chem. Sens.*, Amsterdam (1983) 699.
[186] K. Cammann, H. Wilken, *Biosensors*, First World Congress, Singapore 1990.
[187] a) K. Cammann, C Sorg, German Offenlegungsschrift DE 3916432 A1 (1990); b) H. Wilken, *Dissertation*, Universität Münster 1991; c) H. Meyer, *Diplom Thesis*, Universität Münster 1991.
[188] H. Muramata, K. Kajiwara, E. Tamiya, I. Karube, *Anal. Chem. 59* (1986) 2760.
[189] R. P. H. Kooyman, H. Kolkmann, J. Greve, *GBF Monogr. Ser. 10* (1987) 295.
[190] I. Giaever, C. R. Keese, R. I. Ryves, *Clin. Chem. (Winston-Salem, N. C.) 30* (1984) 880.
[191] R. M. Sutherland, C. Dähne, J. F. Place, *Anal. Lett. 17* (1984) 43.
[192] J. S. Schramm, S. H. Pach, *Biosensors*, First World Congress, Singapore 1990.
[193] D. C. Cullen, C. R. Lowe, *Biosensors*, First World Congress, Singapore 1990.
[194] G. A. Rechnitz, *GBF Monogr. Ser. 10* (1987)3.
[195] D. Meadows, J. S. Schultz, *Talanta 35* (1988) 145.
[196] B. A. A. Dremel, B. P. H. Schaffar, R. D. Schmid, *Anal. Chim. Acta 225* (1989) 293.
[197] M. Mascini, D. Moscone, G. Palleschi, R. Pilloton, *Anal. Chim. Acta 213* (1988) 101.
[198] M. Suzuki, H. Suzuki, I. Karube, R. D. Schmid, *GBF Monogr. Ser. 13* (1989) 107.
[199] G. P. Evans, M. G. Briers, *Biosensors 2* (1986) 287.
[200] I. Karube, *Sci. Technol. Jpn 7/9* (1986) 32.
[201] V. M Owen, *NATO ASI Ser. Ser. C226* (1988) 329.

Optical Detection of Single Molecules in a Solid: A New Frontier in Optical Spectroscopy?

By *Dietrich Haarer** and *Lothar Kador**

On examining the emission spectrum of atomic hydrogen *Balmer* discovered a sequence of narrow spectral lines which didn't fit into the picture of classical physics. This observation triggered the birth of quantum mechanics. A comparable success story in molecular spectroscopy has not occurred since or, if there is such a story, the development stages have been smaller and less spectacular. This can be explained on the following grounds.

Firstly, larger molecules have a much larger variety of excited electronic states and, hence, the Hamiltonian cannot be solved without major approximations. Secondly, the molecular energy states in the condensed phase are, other than in diluted gases, not sharply defined but smeared out over a large energy interval due to intermolecular interactions. This phenomenon which smears out the well defined molecular states to broad, structureless bands is called inhomogeneous broadening.[1, 2] It is much more pronounced in amorphous materials than in ordered crystals. In spectroscopic experiments, it obscures the 'intrinsic' molecular information as is shown schematically in Figure 1. Recording

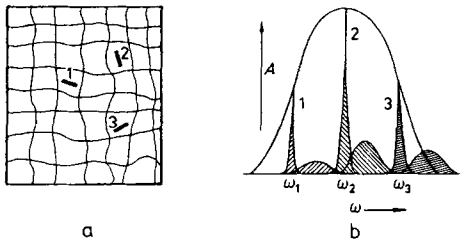

Fig. 1. Schematic representation of an ensemble of dye molecules in a disordered solid (a) and the corresponding distribution of their absorption frequencies (b)[11]. Although all the absorption lines belong to the same electronic transition of a set of identical molecules, their exact positions are affected by a variation of the dye–matrix interactions in the different local environments. In a straightforward optical experiment, the envelope of the full ensemble of lines yields the observed inhomogeneously broadened spectrum. A = absorption.

homogeneous, molecular absorption lines, i.e. absorption lines of single dopant molecules, has therefore until recently been an unfulfilled dream in the world of molecular spectroscopy.

In the past, scientists had to live with the above-mentioned 'nuisance' of inhomogeneous broadening and, hence, the success of straightforward optical spectroscopy in the solid state was rather limited. Following the advent of the laser with its unique capabilities of generating light of extremely narrow bandwidth or ultrashort pulses, a number of methods were devised as approaches to overcome this problem. They operate either in the time domain like two-pulse[3] and accumulated photon echo[4] or in the frequency domain like fluorescence line narrowing[5] and persistent spectral hole burning.[6, 7]

The experiments of the first group probe more or less all the absorbing centers in the inhomogeneous distribution and eliminate the differences of their absorption frequencies by sophisticated sequences of short light pulses, forcing the centers to emit coherent pulses of fluorescence radiation whose characteristics are solely determined by the homogeneous line shape. These methods are based on the similar technique of generating spin echoes in magnetic resonance.[8] They measure the homogeneous absorption linewidth on the time scales of picoseconds (two-pulse photon echo) and microseconds (accumulated photon echo) and are thus able to reveal fast time dependences which may occur in disordered matrices due to structural relaxation processes.[9, 10] On the other hand, it is difficult to decide with these methods if the limiting 'natural' linewidth, the homogeneous width, is really the same for all the molecules in the sample or if there is some distribution. In the latter case, the measurements yield an average value.

The second group of the above-mentioned experimental techniques selects and probes only a small subset of the absorbing centers whose transition frequencies are identical to within roughly one homogeneous linewidth. The common feature of these methods is that the sample is illuminated with laser light of very small bandwidth so that only those dye molecules are promoted to the excited state whose absorption lines are in resonance with the laser. Since the excitation frequency can be varied throughout the inhomogeneous distribution, it is possible to investigate correlations between optical properties of the dopant molecules and their exact transition frequencies. With the technique of persistent spectral hole burning[11, 12] it was shown, for instance, that in some dye–matrix systems the matrix-induced electric dipole moments of the absorbers,[13, 14] the pressure shifts of their transition frequencies,[15] and partly even the homogeneous linewidths[14, 16] vary with the position in the inhomogeneous band, i.e. with the solvent shift and, thus, the transition frequency. These results indicate that imperfections and disorder in a solid do not only influence the absorption frequencies but also a number of other properties of the dopant molecules. Therefore, the question arises as to whether at least a subset of absorbers with identical transition frequency is characterized by a number of coinciding physical parameters.

In order to address this point, several spectroscopic experiments of ultra-high sensitivity have been carried out during the past three years, which were aimed at detecting and probing very few or, ideally, only one single absorber in a solid at low temperatures. In vacuum, the spectroscopy of single metal ions trapped in Paul cages has meanwhile become a well-established technique[17] since the fluorescence signals of these particles can be detected very sensitively without any background light present. In condensed matter, the situation

[*] Prof. Dr. D. Haarer, Dr. L. Kador
Physikalisches Institut and Bayreuther Institut für Makromolekülforschung (BIMF) der Universität
Postfach 10 12 51, W-8580 Bayreuth (FRG)

 © VCH Verlagsgesellschaft mbH, W-6940 Weinheim, 1991 0570-0833/91/0505-0540 $ 3.50+.25/0

is distinctly more difficult. Due to diffraction effects, the probing light cannot be focussed to a volume much smaller than 1 μm^3 which still contains roughly 10^{10} matrix molecules. The latter give rise to Rayleigh and/or Raman scattering and, in fluorescence experiments, tend to obscure the desired signal of the dopant, the 'needle in the haystack'. Thus, the first ultra-sensitive measurement of this type[18] had a detection limit of five $Sm^{2\oplus}$ ions in a CaF_2 crystal. The excitation of the ions was hereby performed using a fixed-frequency laser. The first spectra of single molecules were recorded in an absorption experiment with a double-modulation technique.[19] The sample was a molecular host crystal of *p*-terphenyl doped with pentacene. Single absorption lines of dopant molecules were selected by tuning the laser frequency to positions way out in the wings of the inhomogeneous absorption band. The same system was subsequently investigated by a different group of researchers using an improved fluorescence technique.[20] They observed that some of their single-molecule signals disappeared and reappeared in the course of a few seconds and they explained this effect as being due to single-molecule hole burning. However, the latest investigation of pentacene in *p*-terphenyl[21] revealed a far more fascinating origin of the unstable signals. *Ambrose* and *Moerner* found that there are two classes of absorbing pentacene molecules in the crystal: Class I has stable absorption frequencies, whereas the transition lines of the Class II molecules jump spontaneously between two or more frequency positions.

Figure 2 shows a sequence of 22 fluorescence excitation spectra which were recorded successively in a spectral region around 592–593 nm. These data clearly indicate the presence of three Class I molecules whose fluorescence signals appear as stable ridges, and one absorber of Class II. The absorption frequency of the latter varies from one scan to the next. In fact, the corresponding absorption line can change its position several times in a 2-minute laser scan and, as a consequence, it gives rise to one or more broad fluorescence signals in some spectra and seems to be totally absent in others. No influence of the intensity of the probing light on the frequency jumps was detected.

This is the first report[21] of spectral diffusion of single molecules and, most interestingly, the effect was observed on a crystal rather than an amorphous sample. It shows that new and unexpected physical phenomena can be found in ultra-sensitive optical experiments which probe single, separate absorbing centers. In conventional site-selective techniques such as persistent spectral hole burning, these effects are not immediately visible since the optical experiment averages over many molecules.

So far, most of the extremely sensitive spectroscopic experiments which were capable of detecting signals from individual centers were performed on the molecular crystal *p*-terphenyl doped with pentacene. In several respects this system is ideally suited, because it is characterized by a large optical absorption cross section, narrow homogeneous lines, and an extremely low quantum yield for photochemical reactions. Similar conditions may be found in a number of other organic mixed crystals containing strongly absorbing dye molecules. It will be an experimental challenge, however, to apply such a technique to inorganic or amorphous systems, since the oscillator strengths of inorganic ions are usually smaller by several orders of magnitude and ions or molecules in glasses tend to exhibit far higher hole-burning quantum yields. On the other hand, the study of spectral-diffusion and hole-burning processes on a single-molecular level in a glass would certainly contribute to our present understanding of the amorphous state in general. Another interesting direction in which the experiments could be extended would be the investigation of single homogeneous lines close to the center of their absorption band rather than far out in the wings. For this purpose, samples of much lower dopant concentrations would have to be used. These measurements should reveal details about the dye–matrix interaction for molecules sitting in almost unperturbed equilibrium positions. However, the chemical purity of the samples will be of utmost importance in these investigations. The results obtained thus far on the pentacene/*p*-terphenyl system are very encouraging and can be considered as a step towards molecular spectroscopy as described by 'Molecular Hamiltonians'.

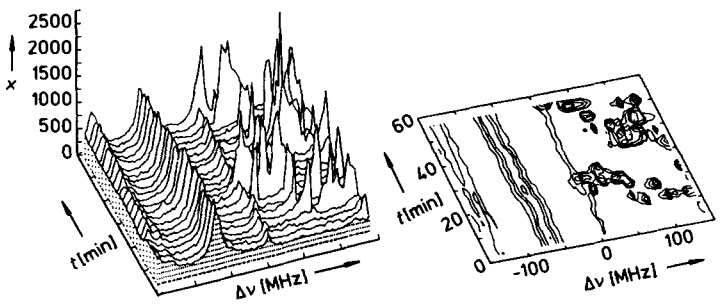

Fig. 2. Time dependence of the fluorescence excitation signals of single pentacene molecules in a *p*-terphenyl crystal[21]. Left: three-dimensional representation of 22 individual spectra which were recorded successively; x = number of photons per s; right: contour plot of the signal intensities as a function of excitation frequency and time. The recording time was 2 minutes for each spectrum.

German version: *Angew. Chem. 103* (1991) 553

[1] A. M. Portis, *Phys. Rev. 91* (1953) 1071.
[2] A. M. Stoneham, *Rev. Mod. Phys. 41* (1969) 82.
[3] N. A. Kurnit, I. D. Abella, S. R. Hartmann, *Phys. Rev. Lett. 13* (1964) 567.
[4] W. H. Hesselink, D. A. Wiersma, *Phys. Rev. Lett. 43* (1979) 1991.
[5] A. Szabo, *Phys. Rev. Lett. 27* (1971) 323.
[6] A. A. Gorokhovskii, R. K. Kaarli, L. A. Rebane, *Pis'ma Zh. Eksp. Teor. Fiz. 20* (1974) 474; *JETP Lett. (Engl. Transl.) 20* (1974) 216.
[7] B. M. Kharlamov, R. I. Personov, L. A. Bykovskaya, *Opt. Commun. 12* (1974) 191.
[8] A. Abragam: *The Principles of Nuclear Magnetism*, Clarendon, Oxford 1961; B. Blümich, *Chem. Unserer Zeit 24* (1990) 13.
[9] M. Berg, C. A. Walsh, L. R. Narasimhan, K. A. Littau, M. D. Fayer, *J. Chem. Phys. 88* (1988) 1564.
[10] A. Rebane, D. Haarer, *Opt. Commun. 70* (1989) 478.
[11] J. Friedrich, D. Haarer, *Angew. Chem. 96* (1984) 96; *Angew. Chem. Int. Ed. Engl. 23* (1984) 113.
[12] W. E. Moerner (Ed.): *Persistent Spectral Hole Burning: Science and Applications*, Springer, Berlin 1988.
[13] T. Sesselmann, L. Kador, W. Richter, D. Haarer, *Europhys. Lett. 5* (1988) 361.
[14] L. Kador, S. Jahn, D. Haarer, R. Silbey, *Phys. Rev. B41* (1990) 12215.
[15] S. Reul, W. Richter, D. Haarer, unpublished.
[16] A. A. Gorokhovskii, V. Kh. Korrovits, V. V. Pal'm, M. A. Trummal, *Chem. Phys. Lett. 125* (1986) 355.
[17] J. C. Bergquist, W. M. Itano, D. J. Wineland, *Phys. Rev. A 36* (1987) 428.
[18] R. Lange, W. Grill, W. Martienssen, *Europhys. Lett. 6* (1988) 499.
[19] L. Kador, D. E. Horne, W. E. Moerner, *J. Phys. Chem. 94* (1990) 1237.
[20] M. Orrit, J. Bernard, *Phys. Rev. Lett. 65* (1990) 2716.
[21] W. P. Ambrose, W. E. Moerner, *Nature 349* (1991) 225.

Bis(4,5-dihydrooxazolyl) Derivatives in Asymmetric Catalysis

By *Carsten Bolm**

The successful use of metal complexes for enantioselective catalysis is largely dependent on the structure and electronic properties of chiral ligands. These ligands should form an ideal, asymmetric environment at the catalytically active metal center, thereby allowing molecular recognition of the substrate and subsequent stereoselective reaction. To achieve efficient catalysis with high turnover numbers, the spatial requirements of the ligand must be minimized to avoid steric hindrance of the reaction partner. Especially the development and investigation of tailor-made, chiral mono- and bidentate phosphanes has led to a greater understanding of the prerequisites for chirality transfer.[1]

Nitrogen-containing chelating ligands are acquiring increasing importance in this respect. Their synthesis is often advantageous since the starting materials can be obtained in optically pure form from the "chiral pool". Thus, separation of enantiomers, as in the synthesis of optically active phosphanes, is no longer necessary. Because of their structural diversity and the wide-ranging possibilities for chemical modification and de novo synthesis, amino acids have become important nitrogen-containing building blocks for enantiomerically pure ligands.

In a paper that attracted much attention, *Masamune* et al. reported at the end of 1990 on the catalytic enantioselective cyclopropanation of alkenes [Eq. (a)] with copper complexes of C_2-symmetric bis(4,5-dihydrooxazolyl)methanes (**1**).[2] This article was shortly followed by further reports from other groups on syntheses, complexation properties, and asymmetric catalyses involving structurally very similar ligand systems.[3-8]

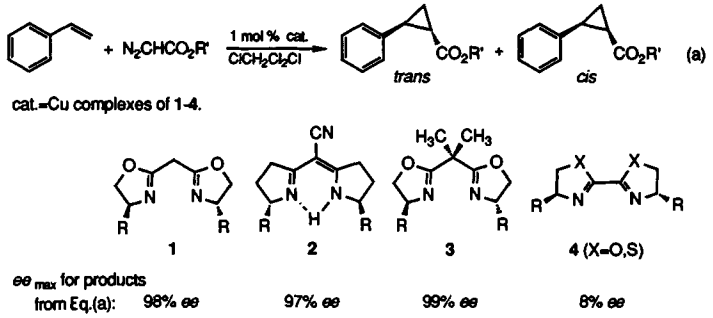

As early as 1986, *Pfaltz* et al. reported the synthesis of C_2-symmetric semicorrins (**2**) derived from pyroglutamic acids.[9a] The use of metal semicorrinato complexes allowed efficient control of the enantioselective cyclopropanation of olefins with diazo compounds (M = Cu; ee_{max} 97%) [Eq. (a)] as well as the asymmetric reduction of α,β-unsaturated carboxylic esters and amides with sodium borohydride (M = Co; up to 99% *ee*).[9]

The ligands used by *Masamune* et al., **1**, may be obtained directly from diethyl malonate and the corresponding β-amino alcohols in a reaction catalyzed by dichloromethylstannane.[2] Enantiopure β-amino alcohols are synthesized by racemization-free reduction of the corresponding amino acids. Deprotonation of **1** with *n*BuLi followed by addition of $CuCl_2$ gives the copper(II) complexes **5**, which can be purified by chromatography. The crystal structure of **5d** was determined by *Lehn* et al. in order to investigate the possibility of forming optically active, double-stranded helical complexes.[3] For the asymmetric catalytic cyclopropanation of olefins, **5** is activated by addition of phenylhydrazine.[2] The cyclopropanation of styrene with ethyl diazoacetate [Eq. (a), R' = Et] in the presence of **5a–5c** as catalysts occurs with good yields and high enantioselection. Two diastereomeric products are formed in a *trans*:*cis* ratio of about 2.5:1. The enantiomeric excess of the two enantiomers is strongly dependent on the substituents R on the ligand. The best results are obtained when the ligand bears bulky substituents such as *tert*-butyl (complex **5a**: *trans*, 90% *ee*; *cis*, 77% *ee*).[2]

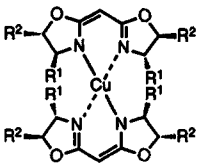

5a: R^1 = *t*Bu, R^2 = H
5b: R^1 = *i*Pr, R^2 = H
5c: R^1 = Ph, R^2 = H
5d: R^1 = CH_2OSi*t*BuMe$_2$, R^2 = Ph

The stereoselectivity is also influenced by the structure of the diazoacetate. Use of the chiral cyclopropanation reagent (−)-menthyl diazoacetate improves the diastereomeric ratio and increases the enantiomeric excess [*trans* (98% *ee*):*cis* (96% *ee*) = 86:14].

Evans et al. reported that copper complexes of **3** increase the enantioselectivity still further.[4] The geminal dimethyl groups prevent enolization of the ligand, which therefore reacts in *neutral* form with copper(I) triflate to give a catalytically active complex. In this case, the cyclopropanation of mono- and 1,1-disubstituted olefins with *achiral* diazoesters affords very high optical yields (up to 99% *ee* for styrene) and excellent *trans*/*cis* ratios (up to 94:6 for styrene). The reaction can be carried out at room temperature and 0.1 to 1 mol % of the complex is sufficient for efficient catalysis. The bis(dihydrooxazolyl)propanes **3**, which should form a six-membered ring chelate with copper ions, are more effective ligands than the tetrahydro-2,2'-bioxazoles **4**, for which only a five-membered ring chelate is expected.

For the enantioselective hydrosilylation of acetophenone [Eq. (b)], *Brunner* and *Obermann* reported the use of rhodium complexes with dihydrooxazolylpyridines (**6**) as nitrogen-containing chelating ligands in 1989.[10a,b] An enantiomeric excess of 83% was achieved with a complex prepared in situ from dihydrooxazolylpyridine (**6**, R = *t*Bu) and [{Rh(cod)Cl}$_2$]. The enantioselectivity is strongly dependent on the ligand/metal ratio, as well as on steric effects due to the reducing silane and to the substituents on the dihydroox-

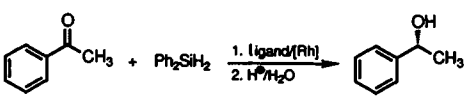

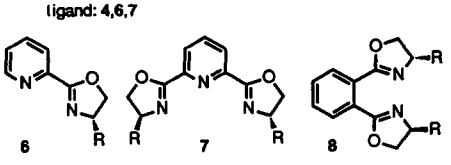

[*] Dr. C. Bolm
Institut für Organische Chemie der Universität
St. Johanns-Ring 19, CH-4056 Basel (Switzerland)

azole.[10a–c] Small structural changes have significant effects. Furthermore, dihydrooxazolylpyridine complexes of copper were found to catalyze the monophenylation of diols with triphenylbismuth diacetate. Optical yields of up to 50% *ee* were thereby achieved.[10d]

Nishiyama et al. introduced the concept of C_2 symmetry to this field with the synthesis of bis(4,5-dihydrooxazolyl)pyridines (**7**).[11] They react with rhodium trichloride to form 1:1 complexes, one of which, [**7** · $RhCl_3$] (R = *i*Pr), has been structurally characterized. After addition of Lewis acids, especially silver salts, these rhodium complexes containing **7** become efficient catalysts for the asymmetric hydrosilylation of ketones [Eq. (b)]. Use of 1 mol % of the rhodium complex followed by acidic workup affords optically active alcohols in good yields with enantiomeric excesses of up to 94%.

The tetrahydro-2,2′-bioxazoles **4** (X = O) were tested by *Helmchen* et al. as ligands in the rhodium-catalyzed asymmetric hydrosilylation of acetophenone [Eq. (b)].[6] The 1:1 complexes [**4** · {Rh(cod)PF_6}] and [Rh(cod) · **4**] (X = O, R = *i*Pr) show only low enantioselectivities. As found for the dihydrooxazolylpyridines of *Brunner* et al., the enantiomeric excess can be increased (up to 84% *ee* for **4**: Rh^I = 10:1 with X = O, R = Bn) by increasing the ligand/Rh^I ratio. Tetrahydro-2,2′-bithiazoles (**4**, X = S) also effect chirality transfer, but they are less effective (ee_{max} = 50% for **4** with X = S, R = Bn).

Bolm et al. synthesized structurally related 1,2-bis(4′,5′-dihydrooxazolyl)benzenes (**8**), which also act as ligands.[5] After addition of zinc or palladium chloride, they form 1:1 complexes, which were investigated in solution by NMR spectroscopy. The X-ray crystal structure analyses of a palladium and a zinc complex show that the metal salts are complexed through the nitrogen atoms of the ligand. The first attempts to carry out a catalytic reaction indicated that the complexes are not stable enough. Therefore, the addition of stabilizing ligands (such as phosphanes) is necessary.[5b]

The iron(III) complex of the bis(dihydrooxazolyl) propane **3** (R = Ph) catalyzes the Diels–Alder reaction of cyclopentadiene with the bidentate dienophile 3-acryloyl-1,3-oxazolidin-2-one [Eq. (c)].[7] *Corey* et al. reported that treatment of **3**

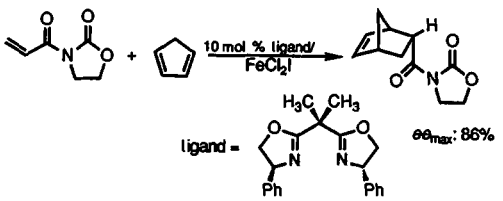

(c)

with $FeCl_2$ and iodine resulted in formation of an active complex, presumably [**3** · $FeCl_2I$], which catalyzes the formation of the *endo* cycloaddition product with high selectivity. The use of 10 mol % of the complex at −50 °C in dichloromethane/2-nitropropane results in an enantiomeric excess of 86% (*endo*:*exo* = 99:1). The catalytically active species is presumably [**3** · FeX_2]$^{\oplus}$ (X = Cl,I).

It is of little surprise that, after their investigations of C_2-symmetric semicorrin ligands,[9] the group of *Pfaltz* also employed bis(dihydrooxazolyl)alkanes as chiral ligands for enantioselective catalysis.[8] The results obtained for the asymmetric cyclopropanation of olefins with copper complexes of bis(dihydrooxazolyl)methanes (**1**) are in agreement with the results described by *Masamune* et al.[2] Two further metal-catalyzed reactions were investigated. The hydrogenation of aryl alkyl ketones [Eq. (d)] with an iridium complex

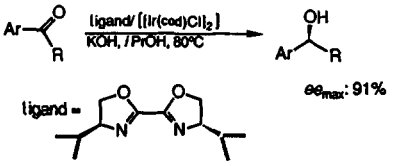

(d)

formed in situ from [{Ir(cod)Cl}$_2$] and tetrahydro-2,2′-bioxazole **4** (X = O, R = *i*Pr) gives optically active alcohols with enantiomeric excesses of between 47 and 91%. The corresponding complexes containing the anionic ligands **1** and **2** as well as the neutral compounds **3** (R = *i*Pr) and **4** (X = O, R = *t*Bu) do not exhibit catalytic activity.[8]

The nucleophilic allylic substitution of 1,3-diphenylprop-2-enyl acetate with sodium dimethyl malonate is catalyzed by 2 mol % of a palladium complex of tetrahydro-2,2′-bioxazole **4** (X = O, R = Bn) [Eq. (e)]. The product is obtained

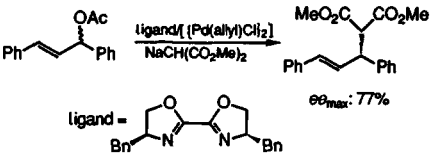

(e)

in good yield with an enantiomeric excess of 77%. Again, complexes containing bulky ligands such as **4** with *t*Bu show no activity under these conditions.[8]

The ready accessibility and the high structural variability of bis(dihydrooxazolyl) derivatives and tetrahydro-2,2′-bioxazoles make them attractive, very promising new ligand systems, which may be of importance for other metal-catalyzed processes as well. The successful use of chiral dihydrooxazoles in diastereoselective reactions by *Meyers* et al.[12] as well as the investigations of *Pfaltz* et al. and *Brunner* et al. on enantioselective catalysis with semicorrins[9] and dihydrooxazolylpyridines[10] have provided the groundwork for the development of these new classes of ligands.

German version: *Angew. Chem. 103* (1991) 556

[1] a) H. B. Kagan in J. D. Morrison (Ed.): *Asymmetric Synthesis, Vol. 5;* Academic Press, Orlando, FL, USA 1985, p. 1; b) H. Brunner, *Synthesis. 1988*, 645; c) R. Noyori, M. Kitamura in R. Scheffold (Ed.): *Modern Synthetic Methods, Vol. 5*, Springer, Berlin 1989, p. 115.
[2] R. E. Lowenthal, A. Abiko, S. Masamune, *Tetrahedron Lett 31* (1990) 6005.
[3] J. Hall, J.-M. Lehn, A. De Cian, J. Fischer, *Helv. Chim. Acta 74* (1991) 1.
[4] D. A. Evans, K. A. Woerpel, M. M. Hinman, M. M. Faul, *J. Am. Chem. Soc. 113* (1991) 726.
[5] a) C. Bolm, K. Weickhardt, M. Zehnder, T. Ranff, *Chem. Ber. 124* (1991) 1173; b) C. Bolm, K. Weickhardt, unpublished.
[6] G. Helmchen, A. Krotz, K.-T. Ganz, D. Hansen, *Synlett 1991*, 257.
[7] E. J. Corey, N. Imai, H.-Y. Zhang, *J. Am. Chem. Soc. 113* (1991) 728.
[8] D. Müller, G. Umbricht, B. Weber, A. Pfaltz, *Helv. Chim. Acta 74* (1991) 232.
[9] a) H. Fritschi, U. Leutenegger, A. Pfaltz, *Angew. Chem. 98* (1986) 1028; *Angew. Chem. Int. Ed. Engl. 25* (1989) 1005; b) A. Pfaltz in R. Scheffold (Ed.): *Modern Synthetic Methods, Vol. 5*, Springer, Berlin 1989, p. 199; c) A. Pfaltz, *Chimia 44* (1990) 202.
[10] a) H. Brunner, U. Obermann, *Chem. Ber. 122* (1989) 499; b) H. Brunner, P. Brandl, *J. Organomet. Chem. 390* (1990) C81; c) G. Balavoine, J. Clinet, I. Lellouche, *Tetrahedron Lett. 30* (1989) 5141; d) H. Brunner, U. Obermann, P. Wimmer, *Organometallics 8* (1989) 821.
[11] a) H. Nishiyama, H. Sakaguchi, T. Nakamura, M. Horihata, M. Kondo, K. Itoh, *Organometallics 8* (1989) 846; b) H. Nishiyama, M. Kondo, T. Hakamura, K. Itoh, *ibid. 10* (1991) 500.
[12] K. A. Lutomski, A. I. Meyers in J. D. Morrison (Ed.): *Asymmetric Synthesis, Vol. 3*, Academic Press, Orlando, FL, USA 1983, p. 213.

Monovalency of the Third Main-Group Elements: News from EX-Type Compounds

By *Peter Paetzold**

To start with divalent derivatives of the fourth main group elements, we can easily classify the structural diversity by taking the fluorides EF_2 as examples. The molecules, CF_2, SrF_2, GeF_2, SnF_2, and PbF_2, are stable in the gas phase at elevated temperatures. Higher molecular aggregates E_nF_{2n} may be held together either mainly by covalent E–E or mainly by polar E–F interactions. The C–C double bond of the volatile C_2F_4, metastable at room temperature with respect to disproportionation into C and CF_4 as well as to polymerization, represents an example of E–E interactions. On the other hand, in crystalline Sn_4F_8 an eight-membered ring Sn_4F_4 includes four bridging F atoms, while another four F atoms are terminally bonded to the Sn atoms and interact weakly with neighboring molecules. The solid compounds of the type EF_2 can also be differentiated according to covalent E–E interactions, as in poly(tetrafluoroethylene), and polar E–F interactions, as in ionic PbF_2.

Such a structural system turns up again, more or less, in the third main group with compounds of the type EX of elements E in the oxidation state + I. Solids with mostly ionic E–X interactions are found among the halides of the heavier elements in this group, InHal and TlHal, which crystallize in a CsCl, distorted NaCl, or α-TlI structure. On looking closer at InCl, for example, deviations from the ideal NaCl structure are detected that make some In–In interactions possible. Similarly, Tl–Tl interactions may be found in α-TlI. Solids with substantially covalent E–X interactions are represented by the organometallics $In(C_5H_5)$ and $Tl(C_5H_5)$, whose structure is characterized by zigzag chains of type **1** with cyclopentadienyl groups pentahapto bonded to each of two E atoms. A more complex example for a solid of type EX is provided by $Ga[GaCl_4]$ with long, predominantly ionogenic bonds between $Ga^{\oplus}$ and $GaCl_4^{\ominus}$ (318 pm) besides short, predominantly covalent bonds between Ga^{III} and Cl in the $GaCl_4$ tetrahedra (218 pm).

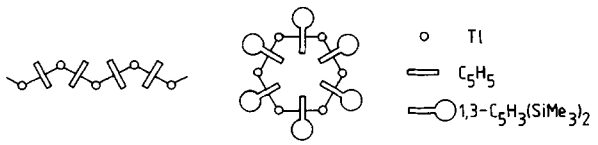

1 **2**

Molecules of the type E_nX_n containing E–X–E bridges are well known for thallium. An ideal example is represented by the cubane-type structure of $Tl_4(OR)_4$ in which each Tl is coordinated to three O atoms and vice versa (symmetry group T_d). The above-mentioned zigzag chains of $Tl(C_5H_5)$ with *trans* orientation within a Tl_4 chain fragment must give way to a *cis* orientation and hence to a ring structure when one side of the cyclopentadienyl moiety exhibits a high steric demand, as in $[Tl_6\{1,3\text{-}C_5H_3(SiMe_3)_2\}_6]$, which was found to be a six-membered ring compound of type **2**.[1] The molecule AlF in an argon matrix behaves in a way typical for the combination of a metal and a nonmetal: it dimerizes to give a four-membered ring with F bridges and not a molecule FAl=AlF with E–E bonds.[2]

Among dimeric molecules E_2X_2 with EE bonds, a linear chain of the type X–B=B–X is predicted in the case of boron, which would result in the occupation of symmetrically equivalent orthogonal π orbitals and thus a triplet ground state. For the heavier elements, a E=E double bond which is made up from two π bonds is also feasible, leading to a singlet ground state. The cyclopentadienides $(R_5C_5)EE(C_5R_5)$ (E = In, Tl; R = $PhCH_2$) have a well-known structure with a *trans* orientation of the η^5-ligands across the E–E axis (symmetry group C_i).[3] Since the In–In and Tl–Tl distance of 363 pm in each case is considerably longer than in the metals themselves (334 and 340 pm, respectively), the dimeric arrangement with weak E–E interactions may be caused mainly by steric factors. The reduction of $RBCl_2$ (R = $(Me_3Si)_3C$) by Na/K alloy gives a product, according to Equation (a), which makes an intermediate of the type RB=BR reasonable.[4]

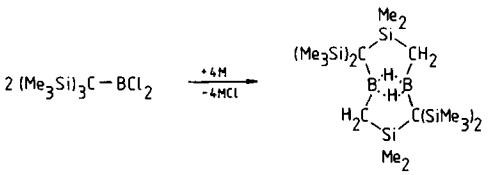

(a)

Molecules of the type E_nX_n (n > 2) are well-established in boron chemistry. Closed Δ-faced polyhedra, such as the tetrahedron, Δ-dodecahedron, and tricapped trigonal prism, were shown to represent the structures of B_4Cl_4, B_8Cl_8, and B_9Cl_9, respectively.[5] Since the number of polyhedral edges is larger than the number of electron pairs available for the cluster skeleton, these molecules belong to the class of nonclassical, electron-deficient compounds, which cannot be represented by structural formulas in which lines connecting neighboring atoms mean classical bonds set up by two electrons. Moreover, these molecules show electron-"hyperdeficiency", violating Wade's rules for the counting of cluster electrons, which stipulate n + 1 skeletal electron pairs for a closed polyhedron with n vertices. Only n pairs are available for B_nCl_n. The stability of these closed polyhedral boranes, in spite of their hyperdeficiency, had been ascribed to electronic effects exhibited by the chloro ligands. Recently, however, the tetrahedral structure of the molecule B_4tBu_4 (**3**) has been proven, which turned out to be unexpectedly stable

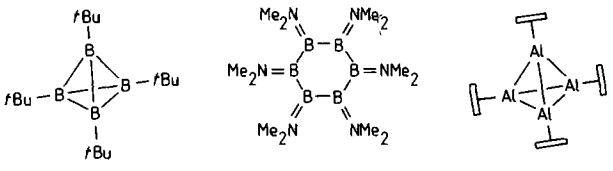

3 **4** **5**, = C_5Me_5

[*] Prof. Dr. P. Paetzold
Institut für Anorganische Chemie der Technischen Hochschule
Templergraben 55, W-5100 Aachen (FRG)

though lacking skeletal electrons as well as electron-rich ligands.[6] The amino groups of $B_6(NMe_2)_6$ (**4**) apparently determine the structure by their electron-donating effect: instead of an electron-deficient cluster structure, a six-membered ring of B atoms is present with six exocyclic B=N double bonds, for which the octet rule and a classical structural formula are valid.[7] The anionic closed polyhedral species $B_nH_n^{2\ominus}$ also obey Wade's rules, but need not be considered in this context, as the oxidation state of boron is lower than +1.

Little is known about molecules E_nX_n containing E–E bonds in the case of the heavier elements in the group. All the more fascinating, therefore, is the tetrahedral structure of the molecule $[Al_4(C_5Me_5)_4]$ (**5**) with C_5Me_5 groups that are bonded in a pentahapto manner to Al.[8] The average Al–Al bond length of 277 pm is shorter than in the metal (286 pm). In the related compound $[In_6(C_5Me_5)_6]$, an In_6 octahedron is distorted into a trigonal antiprism in which the C_5Me_5 groups, again pentahapto-bonded to In, are arranged in a propellerlike manner around a C_3 axis of the antiprism (symmetry group S_6).[9] The In–In bond lengths of 394–396 pm are so distinctly longer than in the metal (334 pm) that, different from the related aluminum species, only weak In–In interactions can be present. Mention should be made of the icosahedral anion $[Al_{12}iBu_{12}]^{2\ominus}$ as an example for the blossoming cluster chemistry of aluminum, even though this element is not entirely monovalent in this case.[10]

The monomeric molecules EX, finally, might be called "borylenes", "aluminylenes", "gallylenes", etc., or better—following IUPAC recommendations—boranediyls, alanediyls, gallanediyls, etc. The halides, EF, ECl, EBr, and EI, the spectroscopic properties of which have been thoroughly studied, are stable in the gas phase at elevated temperatures, with respect to disproportionation into E and $EHal_3$ (E = B, Al, Ga) or to crystallization as EHal (E = In, Tl). Gas phase structural analysis of the cyclopentadienides $In(C_5H_5)$, $In(C_5Me_5)$, and $Tl(C_5H_5)$ reveal that the ligands are again bound in a pentahapto fashion to E (symmetry group C_{5v}).

Experiments to trap boranediyls or alanediyls EX start from the postulated generation of such short-lived molecules in solution (e.g. on dehalogenation of $XEHal_2$ by alkali metals) or from the high-temperature generation in the gas phase of stable EX, which are then quenched and allowed to react at low temperature. The reduction of $(iPr_2N)BCl_2$ with Na/K alloy in aromatic hydrocarbons yields a variety of unexpected products; in benzene, for example, a triboraspiro[4.4]nonane is formed [Equation (b)].[11] The occurrence

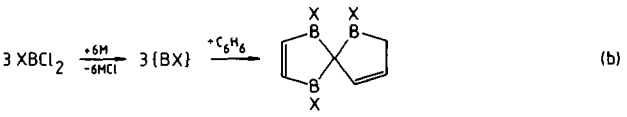

(b)

of such products may be rationalized by the formation of the reactive boranediyl BX (X = $NiPr_2$) that cleaves the arene. The molecule BF, formed by passing BF_3 over boron at

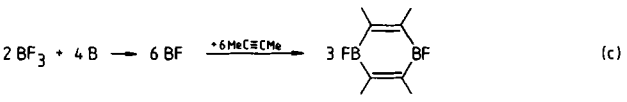

(c)

2000° C, may be reacted at low temperature with B_2F_4, CO, PF_3, or alkynes. Its reaction with 2-butyne, for instance, yields the corresponding diboracyclohexadiene, according to Equation (c).[12]

The molecule AlCl, easily formed from HCl and Al at nearly 1000° C, can be kept metastable at low temperature in a mixture of toluene and diethyl ether. This observation turned out to be fruitful for the chemistry of AlCl, though there is no structural evidence on the interactions between AlCl and the solvent molecules.[13] Similar to BF, AlCl in toluene–diethyl ether solution reacts with 2-butyne to give a dimetallacyclohexadiene, but in this case two six-membered rings are positioned above each other in such a way that the Al atoms of each form dihapto bonds to the double bonds of the other [Equation (d)].[14] The addition of 2,3-dimethylbutadiene to AlCl [Equation (e)] gives a product which has an S_6 axis. Six Al atoms at the vertices of a hexagon are connected by six Cl bridges lying alternately above and below the hexagon.[15] Finally the substitution of a Cl atom of AlCl

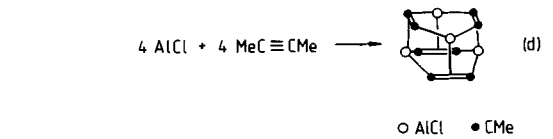

(d)

○ AlCl ● CMe

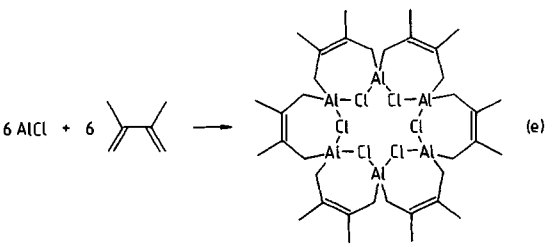

(e)

in solution seems to be a broadly applicable reaction. The treatment with $Mg(C_5Me_5)_2$, for example, yields the above-mentioned tetraaluminatetrahedrane, $Al_4(C_5Me_5)_4$, a molecule with a fascinating structure.

Monovalent gallium can be stabilized by hexahapto bonding to one, two, or even three aromatic six-membered rings. There are additional interactions of Ga^I with one or more halogen atoms of neighboring units of $Ga^{III}Cl_4$ or $Ga^{III}Br_4$. The bond lengths Ga^I-Hal are a good 100 pm longer than Ga^{III}-Hal. Chainlike associations may arise by linking Ga^I with two units of $GaCl_4$, as in the case of bis(η^6-mesitylene)-gallium(I)-tetrachlorogallate(III) (**6**),[16] but molecular associations are also known, such as for the [2.2.2]paracyclophane complex **7** in which the three lines from the central Ga atom to the centers of the *p*-phenylene rings are almost coplanar.

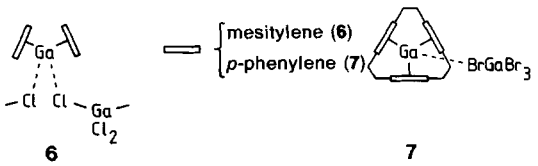

6 **7**

The boranediyls, alanediyls, and gallanediyls are no match for the carbenes, silanediyls, and germanediyls, in quantity

of available information. In terms of the structural diversity and the unorthodox reactivity, however, they outstrip the more conventional diyls of the fourth main group.

German version: *Angew. Chem. 103* (1991) 559

[1] S. Harvey, C. L. Raston, B. W. Skelton, A. H. White, M. F. Lappert, G. Srivastava, *J. Organomet. Chem. 328* (1987) C1.

[2] R. Ahlrichs, L. Zhengyan, H. Schnöckel, *Z. Anorg. Allg. Chem. 519* (1984) 155.

[3] a) H. Schumann, C. Janiak, J. Pickardt, U. Bömer, *Angew. Chem. 99* (1987) 788; *Angew. Chem. Int. Ed. Engl. 26* (1987) 789; b) H. Schumann, C. Janiak, F. Görlitz, J. Loebel, A. Dietrich, *J. Organomet. Chem. 363* (1989) 243.

[4] T. Mennekes, P. Paetzold, R. Boese, *Angew. Chem. 102* (1990) 909; *Angew. Chem. Int. Ed. Engl. 29* (1990) 899.

[5] J. A. Morrison in J. F. Liebman, A. Greenberg, R. E. Williams (Hrsg.): *Advances in Boron and the Boranes*, VCH, Weinheim 1988, p. 151.

[6] T. Mennekes, P. Paetzold, R. Boese, D. Bläser, *Angew. Chem. 103* (1991) 199; *Angew. Chem. Int. Ed. Engl. 30* (1991) 173.

[7] H. Nöth, H. Pommerening, *Angew. Chem. 92* (1980) 481; *Angew. Chem. Int. Ed. Engl. 19* (1980) 482.

[8] C. Dohmeier, C. Robl, M. Tacke, H. Schnöckel, *Angew. Chem. 103* (1991) 594; *Angew. Chem. Int. Ed. Engl. 30* (1991), 564.

[9] O. T. Beachley, Jr., R. Blom, M. R. Churchill, K. Faegri, Jr., J. C. Fettinger, J. C. Pazik, I. Victoriano, *Organometallics 8* (1989) 346.

[10] W. Hiller, K.-W. Klinkhammer, W. Uhl, J. Wagner, *Angew. Chem. 103* (1991) 182; *Angew. Chem. Int. Ed. Engl. 30* (1991) 179.

[11] A. Meller, D. Bromm, W. Maringgele, A. Heine, D. Stalke, G. M. Sheldrick, *J. Chem. Soc. Chem. Commun. 1990*, 741.

[12] P. L. Timms, *J. Am. Chem. Soc. 90* (1968) 4585.

[13] M. Tacke, H. Schnöckel, *Inorg. Chem. 28* (1989) 2895.

[14] H. Schnöckel, M. Leimkühler, R. Lotz, R. Mattes, *Angew. Chem. 98* (1986) 929; *Angew. Chem. Int. Ed. Engl. 25* (1986) 921.

[15] C. Dohmeier, R. Mattes, H. Schnöckel, *J. Chem. Soc. Chem. Commun. 1990*, 358.

[16] H. Schmidbaur, U. Thewalt, T. Zafiropoulos, *Chem. Ber. 117* (1984) 3381.

[17] H. Schmidbaur, R. Hayer, B. Huber, G. Müller, *Angew. Chem. 99* (1987) 354; *Angew. Chem. Int. Ed. Engl. 26* (1987) 338.

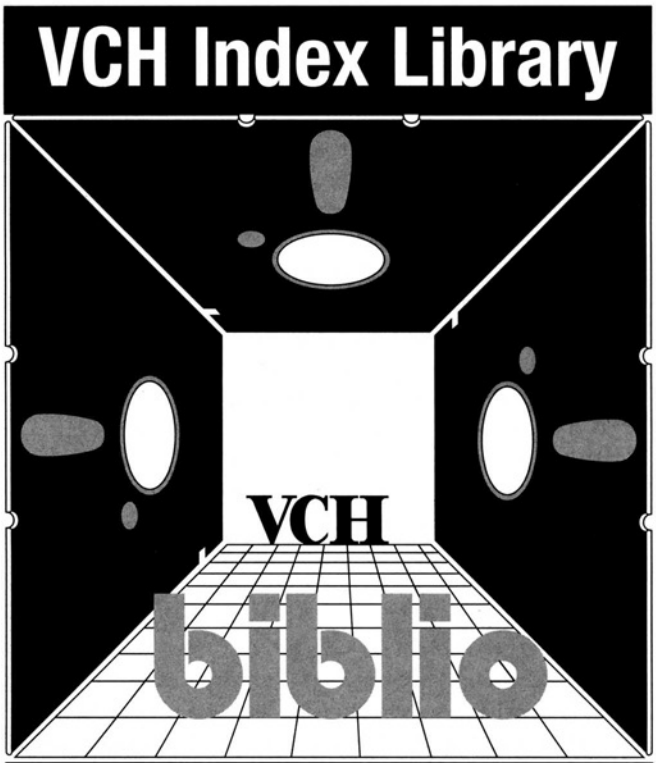

The electronic index comes with the search module of the literature-management program, VCH Biblio. You can use this index on all PCs running with MS-DOS.

ANGEWANDTE CHEMIE
International Edition in English

Soon available

At the press of a button

The annual index of "Angewandte" is soon available on 5 1/4" and 3 1/2" diskettes.

Yearly updates will keep this invaluable electronic library complete. You can search the cumulative contents in mere seconds.

Price: ca. DM 34.00 plus shipping and handling.

Special news! In honor of the 30th anniversary of "Angewandte Chemie I.E." the cumulative index will also be available on diskette.

VCH
Software
P.O. Box 101161
D-6940 Weinheim

VCH

Communications may be submitted in English *or* in German. Further details regarding the submission of communications can be found in the "Notice to Authors" reproduced in the January issue of the journal. Copies thereof may be obtained from the editorial office upon request.

Bis(η^6-phosphabenzene)vanadium: Synthesis, Structure, Redox Properties, and Conformational Flexibility**

By *Christoph Elschenbroich,* Mathias Nowotny, Bernhard Metz, Werner Massa, Jens Graulich, Karl Biehler,* and *Wolfgang Sauer*

Dedicated to Professor Kurt Dehnicke on the occasion of his 60th birthday

The unsubstituted heteroarenes analogous to pyridine namely phospha-, arsa-, stiba-, and bismabenzenes,[2] a class of compounds that has been developed by *Ashe III*, offer the coordination chemist a rich field of activity. The heterocycles C_5H_5E (E = element of group 15) are ambidentate, since, in principle, they can bind to metals via the lone σ-electron pair at E (η^1) and/or via the π-electron sextet (η^6). In the case of the pyridine ligand σ-coordination clearly predominates, since bis(η^6-pyridine)chromium **1** can be obtained only if complexation is effected via an intermediate in which the N atom is sterically blocked by neighboring trimethylsilyl groups.[1] In the synthesis of bis(η^6-arsabenzene)chromium

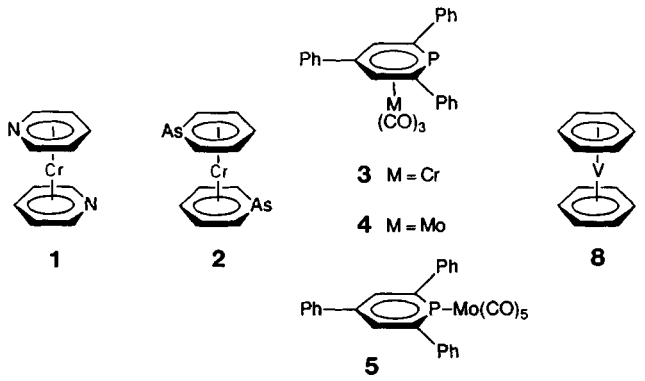

1 **2** **8**

5

2 this shielding is unnecessary.[3] η^6-Coordination of phosphabenzene—albeit only in ring-substituted form—is exemplified by a few ternary complexes[4] (first example: tricarbonyl(2,4,6-triphenyl-η^6-phosphabenzene)chromium **3**[4a]). The readiness of phosphabenzene to undergo η^6-coordination manifests itself, inter alia, in that on heating the η^1-complex **5** rearranges almost quantitatively to the η^6-complex **4**.[4b] We therefore engaged in the synthesis of binary phosphabenzene-transition-metal complexes and report here on the first representative of this series.[5] In order to study a possible conformational preference unaffected by steric effects we have chosen unsubstituted phosphabenzene **6** as ligand.[6]

Metal atom–ligand cocondensation affords bis(η^6-phosphabenzene)vanadium **7** in the form of reddish-brown, sublimable crystals, whose air-sensitivity is noticeably reduced compared to that of the free ligand **6** [Eq. (a)]. The robust

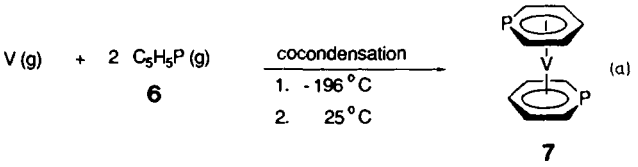

ness of the metal–ligand bond in **7** is reflected in the thermal stability (m.p. 210 °C) and the appearance of the molecular ion $7^{\oplus}$ in the mass spectrum as base peak. Anaerobically prepared solutions of **7** in aromatic solvents are storable without decomposition for several hours when exposed to air, whereas both bis(η^6-benzene)vanadium **8** as well as free phosphabenzene are oxidized instantaneously. This observation is consistent with the cyclovoltammetrically determined redox potentials (Fig. 1, Table 1), which feature the anodic shifts $\Delta E_{1/2}$ ($7^{\ominus}/7$, $8^{\ominus}/8$) = + 0.72 V and $\Delta E_{1/2}$ ($7/7^{\oplus}$, $8/8^{\oplus}$) = + 0.53 V.[8] That the shifts for reduction and oxidation of the pair **7**, **8**, in contrast to those of the pair **7**, **6** are very similar follows from the electronic structure of the bis(arene)vanadium complex ($\ldots e_2^4 a_{1g}^1$), according to which both reduction and oxidation of **7** as well as **8** involve the same redox orbital a_{1g}.

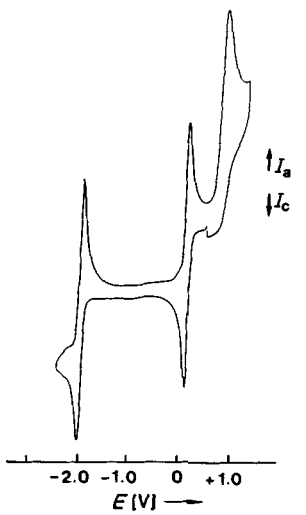

Fig. 1. Cyclic voltammogram of **7** in DME/$(n\text{-Bu})_4NClO_4$ (0.1 M), glassy carbon electrode, $T = -48$ °C, $v = 50$ mVs^{-1}.

[*] Prof. Dr. C. Elschenbroich, Dipl.-Chem. M. Nowotny, Dipl.-Chem. B. Metz, Prof. Dr. W. Massa, Dipl.-Chem. J. Graulich, K. Biehler, W. Sauer
Fachbereich Chemie der Universität
Hans-Meerwein-Strasse, W-3550 Marburg (FRG)

[**] Metal-π-Complexes of Heteroarenes, Part 3. This work was supported by the Deutsche Forschungsgemeinschaft, the Fonds der Chemischen Industrie, and the NATO Scientific Affairs Division.—Part 2: [1].

Table 1. Cyclovoltammetric data for **6**–**8**.

	$E_{1/2}(M^{\ominus}/M)$ [V] [b]	ΔE_p[mV] [b,i]	r[c]	$E_{1/2}(M/M^{\oplus})$ [V]	ΔE_p[mV] [b]	r[c]	$E_{pa}(M^{\oplus}/M^{2\oplus})$ [V] [e]
6[a]	−2.27[f]	100	0.56	−1.05[d]			−0.14[d]
7[a]	−1.99[j]	80	1.10	0.18[h]	44	1.00	1.02[e]
8[a]	−2.71[g]	74	0.93	−0.35[h]	66	1.00	0.24[e]

[a] In DME/(n-Bu)$_4$NClO$_4$ (0.1 M) at glassy carbon vs. saturated calomel electrode, $v = 50\,mVs^{-1}$, data for **8** from [8]; [b] $E_{1/2} = (E_{pa} + E_{pc})/2$, $\Delta E_p = E_{pa} - E_{pc}$; [c] $= I_{pc}/I_{pc}$; [d] irreversible oxidation of a secondary product of the partially reversible reduction (ECE mechanism); [e] irreversible oxidation; [f] chemically only partially reversible reduction; [g] reversible at $-48 < T < +25\,^{\circ}C$; [h] reversible at $T = -48\,^{\circ}C$, irreversible at $T = 25\,^{\circ}C$; [i] expected value: $\Delta E_p = 2.2\,RT/nF = 42$ mV; [j] quasireversible.

The phosphorus heteroatom has a much stronger influence on the electron affinity of the free arene than in the complex-bound arene. This manifests itself in the redox potentials [$E_{1/2}$ ($C_6H_6^{\ominus}/C_6H_6$) = −3.42,[9] $E_{1/2}$ ($C_5H_5P^{\ominus}/C_5H_5P$) = −2.27; $\Delta E_{1/2}$ = +1.15 V] and in the electron-transmission spectra (ETS), which indicate that in the gas phase anion states for phospha-, arsa- and stibabenzene are binding.[10] Replacement of CH by E (E = P,As,Sb,Bi) modifies the electronic structure through the change in electronegativity and the reduction in the resonance integral β_{CE} as a result of increasing bond length. Figure 2 depicts the changes in the π-orbital energies for the benzene/phosphabenzene pair, whereby step ① outlines the removal of the

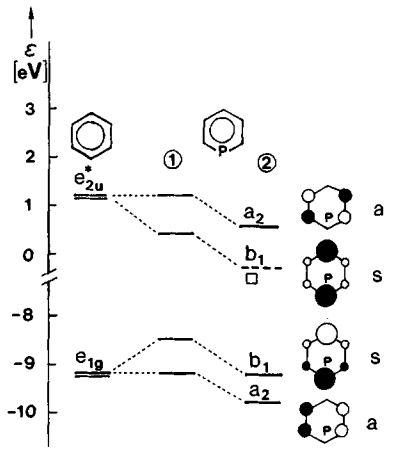

Fig. 2. Correlation diagram of the frontier orbitals for benzene and phosphabenzene, modified as described in [10]. ① Removal of the degeneracy as a result of the variation in the resonance integrals, $\beta_{CC} > \beta_{CP}$. ② Decrease in energy caused by increasing effective π-orbital electronegativity $\chi^{\pi}_C < \chi^{\pi}_P$ [11]. The positions on the energy scale are taken from PE [18] and ETS [20] measurements. □ Position inaccessible by ETS, since anionic state is binding.

degeneracies of e_{1g} and e^*_{2u} and step ② indicates the decrease in the energies of the π-MO caused by the inductive perturbation of the p_z orbital on the phosphorus atom.[11] With regard to the coordination properties, this means that phosphabenzene (relative to benzene) is a ligand with comparable π-donor but higher π-acceptor strength. Thus the central vanadium atom in **7** should carry a more positive partial charge than in **8**, and the anodic shifts $\Delta E_{1/2}$ ($7^{\ominus}/7$, $8^{\ominus}/8$) and $\Delta E_{1/2}$ ($7/7^{\oplus}$, $8/8^{\oplus}$) are plausible.[12]

Under this premise the EPR data are, at first sight surprising: the hyperfine coupling constants $a(^{51}V)$, $A_z(^{51}V)$ and $A_{x,y}(^{51}V)$ in **7** are larger and the couplings $a(^1H)$ are smaller than the corresponding values a, $A_{\parallel}$ and $A_{\perp}$ in **8**, even though **7** bears ligands with stronger acceptor properties (Fig. 3. and Table 2). This, however, is only an apparent contradiction, since the SOMO in **7** and **8** is almost void of ligand contributions. Rather, the increased $\delta^{\oplus}$ charge on the central metal atom in **7** leads to a contraction of the V($3d_{z^2}$) orbital, a weaker overlap V($3d_{z^2}$)-ligand (a_{1g}, σ), more effective spin polarization $(3d_{z^2})^1/(ns)^2$ of inner shells,[13] and thus to an increased Fermi contact interaction with the vanadium nucleus. The EPR spectrum of **7** in a glassy solution features an orthorhombic g-tensor (Fig. 3). The resolution of g_x and g_y (z axis = sandwich axis) shows that the frequency of ring rotation at 120 K in the rigid phase must be smaller than $5 \times 10^7\,s^{-1}$ (i.e. $\Delta g_{x,y}$ in frequency units). Thus, the EPR signal could be caused either by superposition of the spectra

Table 2. EPR spectroscopic data of **7**.

	T[K]⟨g⟩	g_x[a]	g_y	g_z[b]	a[c]	(^{51}V) A_x[a]	A_y	A_z[b]	a[c]	(^{1}H) $A_{x,y}$	A_z[b]
7[d]	300	1.9874			7.03						
	120		1.9745	1.9840	2.002	10.66	8.77	1.66	0.35		
7[e]	300		1.9801	1.9801	2.002	9.39	9.39	2.30		0.37	0.3
	38		1.9764	1.9814	2.002	10.55	8.78	1.76			

[a] x,y assignment uncertain; [b] calculated according to $g_z = 3g - (g_x + g_y)$ or $A_z = 3a - (A_x + A_y)$; [c] cf. **8**: $a(^{51}V) = 6.35$ mT; $A_{\perp}(^{51}V) = 9.2$ mT; $A_{\parallel}(^{51}V) = 0.65$ mT; $a(^1H) = 0.40$ mT; [d] in liquid and rigid DME respectively, coupling constants in mT; [e] in [2.2]paracyclophane as mixed crystal powder, coupling constants in mT.

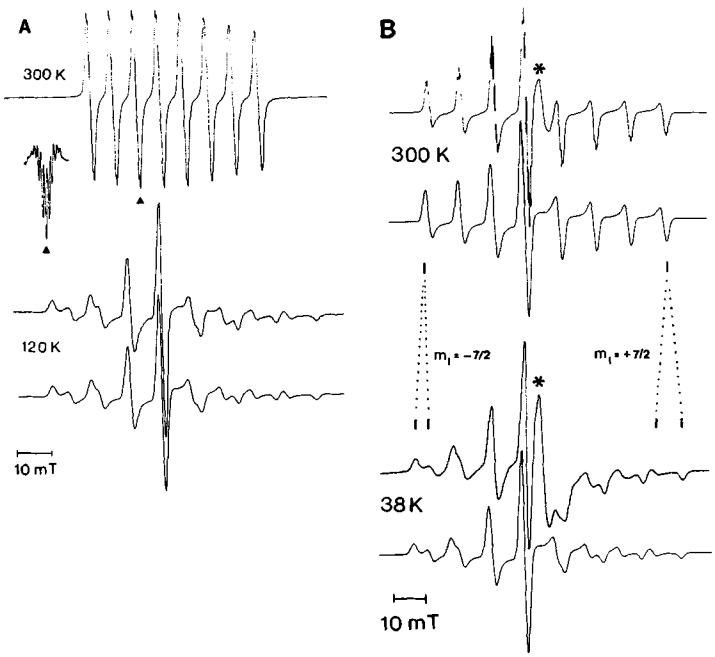

Fig. 3. EPR spectra of **7**, X-band, at various temperatures; lower traces are simulated [17]. Left **A**: In DME, liquid or rigid solution; right **B**: as mixed crystal powder (≈ 1 % **7** in [2.2]paracyclophane **9**). * Exchange narrowed signal of microcrystallites of pure **7**.

of two different rotameric forms of **7** each with an axial g tensor, or by the presence of a single rotamer **7** with a non-axial g tensor.[14] In both cases the excitation of ring rotation should lead to removal of the inequivalencies in the x,y planes. As a matrix which permits variation of temperature over a wide range we have chosen [2.2]paracyclophane **9**, which is structurally related to **7**.[15] Indeed, EPR powder spectra of mixed crystals (ca. 1% **7** in **9**) at 120 K furnish orthorhombic and at 293 K tetragonal g- and ^{51}V-hyperfine tensors (Fig. 3). Coalescence (A_x, A_y) $\rightarrow A_\perp$(^{51}V) for the low field components ($m_I = -7/2$) occurs at $T_c \approx 170$ K and for the high field components ($m_I = +7/2$) at $T_c \approx 220$ K. Hence, the rotational barrier in the heteroarene complex **7** is comparable with that in the homoarene complex **8**[15] and is largely determined by packing forces. This conclusion is further supported by the fact that a complete suppression of the ring rotation is effected at substantially lower temperature in the mixed crystal than in glassy solution (Fig. 3). Since the molecular dimensions of the host **9**[16] exceed those of the guest **7**, the latter should experience relatively slight matrix-induced hindrance to internal rotation.

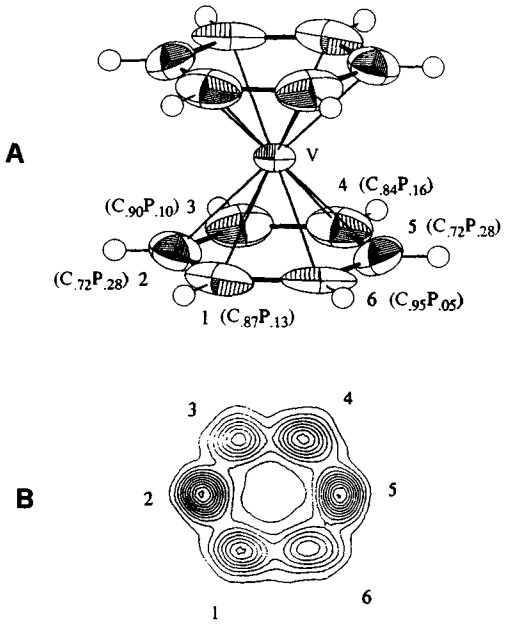

Fig. 4. **A**: ORTEP plot of a molecule of **7** in the crystal with data of the C:P occupation. Thermal ellipsoids at the 50% probability level. Important bond lengths [pm] and angles [°] (because of disorder the probable errors have to be set higher than derived from the standard deviations): (C,P)1-(C,P)2 158.3(5), (C,P)1-C6 158.1(6), (C,P)2-C3 154.5(5), C3-(C,P)4 159.1(6), (C,P)4-(C,P)5 154.7(5), (C,P)5-C6 147.8(5), mean: 155.4 pm; ring angles at (C,P)1 121.7(3), (C,P)2 112.8(3), C3 124.9(3), (C,P)4 119.4(3), (C,P)5 117.6(3), C6 123.6(3), V-(C,P)1 225.1(4), V-(C,P)2 231.7(3), V-C3 222.9(4), V-(C,P)4 227.1(3), V-(C,P)5 232.0(3), V-C6 225.5(4) pm, mean V-(C,P) 227.4 pm. **B**: Observed electron densities (F_0 Fourier section) in the "best" ring plane of **7**. Intervals of the contour lines 0.5, beginning at 0.5 e/ Å^3.

In order to clarify whether a certain conformation is preferred in the single crystal of **7** we have carried out an X-ray structure analysis.[18] It led to a very similar unit cell and the same space group type $P2_1/n$ as in the chromium complexes bis(η^6-pyridine)chromium **1**[1] and bis(η^6-arsabenzene)-chromium **2**[3] studied previously. As anticipated, **7**, like **1** and **2**, shows disorder of the heteroatom in the ring (Fig. 4). However, the three disorder models differ significantly.[19] Interestingly, the only common structural interpretation, which includes the compounds **1**, **2** and **7**, is that of an orientational disorder of the antiperiplanar conformation.[19]

Received: December 10, 1990 [Z 4314 IE]
German version: *Angew. Chem. 103* (1991) 601

CAS-Registry number:
7, 132749-46-7; **8**, 12129-72-5; V, 7440-62-2; C_5H_5P, 289-68-9.

[1] C. Elschenbroich, J. Koch, J. Kroker, M. Wünsch, W. Massa, G. Baum, G. Stork, *Chem. Ber. 121* (1988) 1983.
[2] a) A. J. Ashe III, *Acc. Chem. Res. 11* (1978) 153; b) A. J. Ashe III, *Top. Curr. Chem. 105* (1982) 125.
[3] C. Elschenbroich, J. Kroker, W. Massa, M. Wünsch, A. J. Ashe III, *Angew. Chem. 98* (1986) 562; *Angew. Chem. Int. Ed. Engl. 25* (1986) 571.
[4] a) J. Deberitz, H. Nöth, *Chem. Ber. 103* (1970) 2541; H. Vahrenkamp, H. Nöth, *Chem. Ber. 105* (1972) 1148; b) J. Deberitz, H. Nöth, *Chem. Ber. 106* (1973) 2222; c) K. C. Nainan, C. T. Sears, *J. Organomet. Chem. 148* (1978) C 31; d) F. Nief, C. Charrier, F. Mathey, M. Simalty, *J. Organomet. Chem. 187* (1980) 277; e) J. Fischer, A. de Cian, F. Nief, *Acta Crystallogr. Sect. B 37* (1981) 1067; f) K. Dimroth, H. Kaletsch, *Organomet. Chem. 247* (1983) 271.
[5] Bis(2,4,6-*tert*-butyl-η^6-phosphabenzene)chromium was first prepared in 1984 and was characterized by ^{1}H-NMR and ^{31}P-NMR spectroscopy as well as by cyclic voltammetry: E. Bilger, *Dissertation*, Marburg 1984; C. Elschenbroich, E. Bilger, unpublished results.
[6] Experimental procedure: The wall of a cocondensation reactor equipped with an electron beam heated metal-vapor source was cooled to -196 °C and coated with 40 mL of methylcyclohexane. Vanadium (0.66 g, 12.9 mmol) and phosphabenzene **7b** (2.3 g, 23.9 mmol) were then condensed onto the wall at 5×10^{-6} mbar and an electron-beam power of 490 W within 2 h. After equalization of pressure (N_2) and warming to 25 °C the dark-brown cocondensate was filtered through a G4 frit and the filtrate evaporated to dryness. For removal of colloidal metal the residue was extracted with methylcyclohexane, the extract evaporated to dryness, and the residue taken up in 5 mL of toluene. After adding a layer of hexane (5 mL), 26 mg (0.11 mmol, ca. 1%) of **7** crystallized at + 4 °C in the form of dark-brown rhombs (m.p. 201 °C). UV/VIS (methylcyclohexane): λ_{max}[nm](ε): 311 (7150), 333 (8300), 447 (975), 675 (75); MS (EI, 70 eV): m/z 234 ($M^{\oplus}$, 100%), 147 ($M^{\oplus}$-C_5H_5P, 90.5), 51 ($V^{\oplus}$, 91.3).
[7] a) F. G. N. Cloke, M. L. H. Green, *J. Chem. Soc. Dalton Trans. 1981*, 1938; b) A. J. Ashe III, *J. Chem. Soc. 93* (1971) 3293; A. J. Ashe III, University of Michigan, Ann Arbor, USA, private communication.
[8] Concerning the redox potentials of $(C_6H_6)_2M$ and (C_5H_5) $(C_7H_7)M$ (M = V, Cr) see C. Elschenbroich, E. Bilger, B. Metz, *Organometallics*, in press.
[9] J. Mortensen, J. Heinze, *Angew. Chem. 96* (1984) 64; *Angew. Chem. Int. Ed. Engl. 23* (1984) 84.
[10] P. D. Burrow, A. J. Ashe III, D. J. Bellville, K. D. Jordan, *J. Am. Chem. Soc. 104* (1982) 425.
[11] In such considerations, effective π-orbital electronegativities χ_E^π are to be used instead of the Pauling electronegativity values. The χ_E^π values for P, As, Sb are higher than for C; compare J. Waluk, H.-P. Klein, A. J. Ashe III, J. Michl, *Organometallics 8* (1989) 2804.
[12] According to EPR spectroscopic measurements the redox orbital a_{1g} in the case of **7** and **8** has almost exclusively metal $3d_{z^2}$ character. The anodic shifts $\Delta E_{1/2}$ for unsymmetrical sandwich complexes (C_5H_5) $(C_7H_7)M$ relative to the symmetrical forms $(C_6H_6)_2M$ are explained in an analogous way [8].
[13] B. A. Goodman, J. B. Raynor, *Adv. Inorg. Chem. Radiochem. 13* (1970) 136.
[14] In order to decide between these alternatives additional measurements using multiple resonance methods (TRIPLE, ENDOR-induced EPR) are required; C. Elschenbroich et al., unpublished results.
[15] a) A. Schweiger, R. Wolf, H. H. Günthard, J. H. Ammeter, E. Deiss, *Chem. Phys. Lett. 71* (1980) 117; b) R. Wolf, A. Schweiger, H. H. Günthard, *Mol. Phys. 53* (1984) 585.
[16] H. Hope, J. Bernstein, K. N. Trueblood, *Acta Crystallogr. Sect. B 28* (1972) 1733.
[17] Programm POWDER, C. Daul, C. W. Schläpfer, B. Mohos, J. Ammeter, E. Gamp, *Comput. Phys. Commun. 91* (1981) 385.
[18] Crystal structure determination of **7**: A blackish-brown crystal (ca. $0.2 \times 0.2 \times 0.1$ mm), after orienting film exposures, was measured on a CAD4 diffractometer, Enraf-Nonius, $Mo_{K\alpha}$ radiation, graphite monochromator at -80 °C. The monoclinic unit cell ($a = 651.2(1)$, $b = 782.2(1)$, $c = 977.6(2)$ pm, $\beta = 97.13(1)°$ was determined on the basis of 25 reflections with $\theta > 12°$. The space group is $P2_1/n$, $Z = 2$. The structure was solved with Patterson and difference Fourier syntheses and, owing to different electron densities at the six ring atom positions, described and refined using a disorder model (the ring positions display varying P/C occupation). The relative occupation ratios were calculated from the maxima of a Fourier synthesis, the P fraction for the lowest maximum was

varied iteratively in the refinement until an equivalent isotropic displacement factor comparable with that at the other positions resulted. For each ring position in the disorder model so obtained the C:P ratio was fixed, an anisotropic displacement factor refined together with the atomic positions, and—corresponding to the C fraction—an H atom was introduced "riding" at a calculated position with a common isotropic displacement factor ($U = 0.09$ Å^2). The refinement converged well and led (considering the positional disorder) to reasonable displacement factors. Using the weights $w = 1/\sigma^2(F_0)$ and after introduction of an extinction correction the residuals $R = 0.054$, $wR = 0.037$ resulted for 920 observed reflections with $F_0 > 4\sigma$. Further details of the crystal structure investigation are available on request from the Fachinformationszentrum Karlsruhe, Gesellschaft für wissenschaftlich-technische Information mbH, W-7514 Eggenstein-Leopoldshafen 2 (FRG), on quoting the depository number CSD-55147, the names of the authors, and the journal citation.

[19] Whereas the N atom in **1** occupies the 1,3 positions (50/50 ratio) and in **2** As occupies the 1,4 positions, the electron density distribution in the ring of **7** (Fig. 4) shows that the P atom, like in the As-analogue of chromium, is preferentially located at the 1,4-positions, but that differing and smaller fractions of P are located on all other ring positions. Because of superposition of several orientations of a distorted six-membered ring, varying bond lengths from 148 to 159 pm are encountered, whereby the mean value (155.4 pm) lies well above the mean of the bond lengths in free phosphabenzene (150.7 pm) [2]. This is plausible since, because of its higher number of electrons the P atom "prevails" more strongly during the superposition of C and P atoms than corresponds to its percentage. The deviations of a "best plane" through the six ring atom positions of **7** are less than 0.3 pm and thus indicate planarity. The V atom is located 166(1) pm above the ring plane, its distance from the ring atoms is on the average 227.4 pm. The second ring is generated through the symmetry center in the V atom, i.e. is parallel to the other ring and is in the eclipsed orientation. Since pairwise oppositely disposed positions in the ring are occupied to about the same extent by P, the disorder model is compatible both with the assumption—with varying contribution—of differently oriented molecules with antiperiplanar and with synperiplanar conformation. The exclusive presence of a synclinal conformation is ruled out by the different extent of occupation of the "*meta*" positions; an admixture cannot by ruled out, however.

[20] C. Batich, E. Heilbronner, V. Hornung, A. J. Ashe III, D. T. Clark, U. T. Cobley, D. Kilcast, I. Sanlan, *J. Am. Chem. Soc. 98* (1973) 928.

Cp'_2TiS_5O and Cp'_2TiOS_5—Isomeric Titanocene Complexes with Two Novel S-O Chelate Ligands ($Cp' = \eta^5$-$CH_3C_5H_4$)**

By *Ralf Steudel,* Andreas Prenzel,* and *Joachim Pickardt*

S_8O and other cyclic sulfur oxides can be prepared by oxidation of sulfur rings with trifluoroperoxoacetic acid [Eq. (a)].[1] They contain the group –S–S(O)–S–, which can also be incorporated into organic compounds by condensation of thiols or thiolates with thionyl chloride, whereby sulfane oxides are formed [Eq. (b)].[2]

$$cyclo\text{-}S_n + CF_3CO_3H \longrightarrow S_nO + CF_3CO_2H \quad (a)$$
$$n = 6\text{–}10$$

$$2\,RSH + Cl_2SO \longrightarrow R\text{-}S\text{-}S(O)\text{-}S\text{-}R + 2\,HCl \quad (b)$$
$$R = Aryl$$

Unfortunately these reactions are not suitable for the preparation of inorganic or organic heterocyles with the group –S–S(O)–S– according to Equation (a) or of chain-like sulfane oxides with essentially more than three sulfur atoms according to Equation (b). We report here on the first synthesis of a polysulfide oxide complex of titanocene, which should enable the -S_5O- group to be incorporated into chain-like or ringlike compounds, i.e. analogously to the use of Cp_2TiS_5 ($Cp = \eta^5$-C_5H_5) for the synthesis of ring- and chain-like polysulfur compounds.[3]

The dinuclear titanocene complex $Cp_4Ti_2S_4$ **1**[4] reacts spontaneously with thionyl chloride in the ratio 1:1 at 0 °C in CS_2 to give the titanocene dichloride **2** and the pentasulfide oxide complex **3**, which is sparingly soluble in CS_2 and precipitates in the form of red crystals (m.p. 105 °C, decomp.)[5] [Eq. (c)].

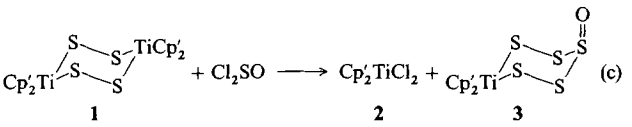

1 **2** **3**

Solid **3**, in contrast to the decomposable *cyclo*-sulfur oxides S_nO, is stable at 20 °C in air. The IR spectrum of **3** (KBr pellet) shows the SO stretching vibration as a very strong band at 1094 cm^{-1}, an unequivocal indication of the –S–S(O)–S– group, as ν(SO) for S_8O appears at almost exactly the same wave number.[6] Since the SSO deformation vibration of **3** (380 cm^{-1}) also appears at exactly the same wave number as in S_8O, it can be assumed that the O atom in **3**, as in S_8O, is in the axial position, which is stabilized by the anomeric effect.

The EI mass spectrum of **3** (sample temperature 140 °C) does not show a peak for the molecular ion $M^{\oplus}$, but peaks for the characteristic fragments $[M - S_2O]^{\oplus}$ and $[M - S_3O]^{\oplus}$; the base peak is $S_2^{\oplus}$. The elimination of S_2O and S_3O is also typical for *cyclo*-sulfur oxides S_nO.[1] The ^{1}H-NMR spectrum of **3** in $CDCl_3$ (400 MHz) shows two singlets at $\delta = 2.012$ and 2.466 for the methyl groups and four triplets at 5.863, 5.911, 6.277 and 6.398 for the aromatic ring protons. Thus, with respect to the number of lines, this spectrum corresponds exactly to the ^{1}H-NMR spectrum of Cp'_2TiS_5,[7] i.e. the TiS_5O ring in **3** must have a mirror plane. As to be expected from the synthesis, **3** is present as $Cp'_2Ti(\mu\text{-}S_2)_2S{=}O$ and not as $Cp'_2Ti(\mu\text{-}S)(\mu\text{-}S_3)S{=}O$, since the ring protons of the unsymmetrical compound would have to give eight quartet signals.

3 is readily soluble in $CHCl_3$, CH_2Cl_2 and THF, but the solutions decompose within 45 min at 20 °C, whereby **3** is converted via ring expansion into the isomeric complex **4** [Eq. (d)].

$$Cp'_2TiS_5O \xrightarrow{CH_2Cl_2} Cp'_2TiOS_5 \quad (d)$$
3 **4**

This reaction can be monitored by means of reversed phase HPLC,[8] since **4** has a significantly greater retention time than the obviously more polar **3**; further reaction products are not formed (eluent: CH_3OH; stationary phase: octadecylsilane). The UV absorption spectra of **3**, **4**, and—for comparison—of Cp'_2TiS_5 **5** were measured immediately after the chromatographic separation.[8] Whereas the spectra of **3** and **5** are, as expected, very similar, that of **4** shows a marked shift of the absorption at ca. 300 nm (Table 1).

4 crystallizes from CH_2Cl_2/hexane in the form of dark-brown, rhomboidal, monoclinic, air-stable crystals,[9] which

[*] Prof. Dr. R. Steudel, Dipl.-Chem. A. Prenzel, Prof. Dr. J. Pickardt
Institut für Anorganische und Analytische Chemie der
Technischen Universität, Sekr. C 2
Strasse des 17. Juni 135, W-1000 Berlin 12 (FRG)

[**] Sulfur Compounds, Part 137. This work was supported by the Deutsche Forschungsgemeinschaft and by the Verband der Chemischen Industrie. We thank Priv.-Doz. Dr. *J. Jakupovicz* and Dipl.-Chem. *J. Albertsen* for recording the NMR and mass spectra.—Part 136: R. Steudel, B. Plinke, D. Jensen, F. Baumgart, *Polyhedron*, in press.

Table 1. Absorption spectra of **3**–**5** in methanol (range: 220–600 nm, relative extinctions in brackets).

Cp'_2TiS_5O **3**	Cp'_2TiOS_5 **4**	Cp'_2TiS_5 **5**
240 (100)	240 (100)	240 (100)
310 (33; shoulder)	328 (38)	310 (41)
484 (4)	482 (3)	486 (8)

were characterized X-ray crystallographically.[10] The novel chelate ligand OS_5 in **4** is bound to the metal via the O atom and one S atom, whereby a seven-membered ring with C_1 symmetry is formed (Fig. 1.). In this ring the torsion angles vary between 22.5° (Ti–O–S–S) and 88.0° (S1–S2–S3–S4), the motif (signs of the torsion angles) is + + − + − + −. Other than in the case of *cyclo*-heptasulfur[11] there is no torsion angle close to 0°.

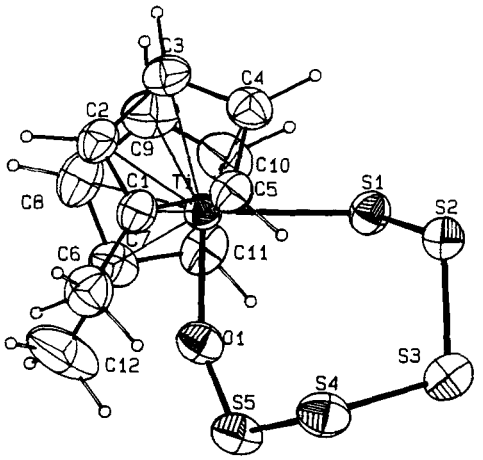

Fig. 1. Structure of **4** in the crystal. Selected bond lengths [pm], angles and torsion angles [°]: Ti-O1 194.6, Ti-S1 246.7, S1-S2 204.5, S2-S3 204.4, S3-S4 208.1, S4-S5 199.9, S5-O1 152.9; O1-Ti-S1 92.3, Ti-S1-S2 111.8, S1-S2-S3 106.5, S2-S3-S4 105.7, S3-S4-S5 106.2, S4-S5-O1 110.9, S5-O1-Ti 154.8; O1-Ti-S1-S2 −70.8, Ti-S1-S2-S3 84.9, S1-S2-S3-S4 − 81.0, S2-S3-S4-S5 88.0, S3-S4-S5-O1 −79.5, S4-S5-O1-Ti 22.5, S5-O1-Ti-S1 39.8.

The seven covalent bonds in the ring are of different bond order: the Ti–S bond (246.7 pm) is somewhat longer than in Cp_2TiS_5 (243 pm);[12] the Ti–O bond (194.6 pm) is substantially longer than in $(Cp_2ClTi)_2O$ (184 pm) or analogous Cp_2Ti alkoxy compounds.[13]

The S–O bond (152.9 pm) lies between S–O single bonds (e.g. 163–165 pm in $(CH_3O)_2S$ and $(CH_3O)_2S_2$[14]) and S=O double bonds (e.g. 143 pm in SO_2). The S–S bond lengths (199.9–208.1 pm) fluctuate about the value of the single bond (205 pm),[15] whereby, as usual,[11,15] the longest bond (S3–S4) is adjacent to the shortest bond (S4–S5).

The ^{1}H-NMR spectrum of **4** in CD_2Cl_2 at 20 °C shows a single sharp singlet at $\delta = 2.14$ for the two methyl groups, which can only be explained in terms of a rapid inversion (pseudorotation) of the $TiOS_5$ ring on the NMR time scale. At − 10 °C, this singlet is strongly broadened, and at − 40 °C two sharp singlets are observed at $\delta = 2.0$ and 2.1 as well as eight quartets in the range $\delta = 5.4$–7.5 for the aromatic ring protons.[9] At this temperature the metallacycle is conformationally rigid. The appearance of eight quartets is characteristic for unsymmetrical titanocene complexes with two $CH_3C_5H_4$ ligands (e.g. $Cp'_2TiSe_3S_2$[16] and $Cp_2'(\mu\text{-}S)(\mu\text{-}S_3)CH_2$[17]). In the IR spectrum of **4** the SO stretching vibration is observed at 868 cm^{-1} (KBr pellet).

At present one can only speculate on the mechanism of the isomerization **3** → **4**: during a transition of the presumably chair-shaped TiS_5 ring of **3** into the boat conformation, Ti–O contacts can occur, which lead to rupture of a Ti–S bond and the rearrangement of some S–S bonds, whereby the oxophilicity of the titanium atom is apparently the driving force. Preliminary experiments show that **3** reacts similarly to Cp_2TiS_5 with S–Cl compounds, affording access to compounds containing –S-S–S(O)–S–S groups which could not be prepared hitherto. These reactions proceed more rapidly than the isomerization.

Received: December 14, 1990 [Z 4328 IE]
German version: *Angew. Chem. 103* (1991) 586

[1] R. Steudel, J. Latte, *Angew. Chem. 86* (1974) 648; *Angew. Chem. Int. Ed. Engl. 13* (1974) 603; R. Steudel, *ibid. 88* (1976) 854–855 and *15* (1976) 772–773; R. Steudel, J. Steidel, *ibid. 90* (1978) 134–135 and *17* (1978) 134–135; R. Steudel, T. Sandow, *ibid. 90* (1978) 644–645 and *17* (1978) 611–612; R. Steudel, T. Sandow, J. Steidel, *Z. Naturforsch. B 40* (1985) 594–600.

[2] L. Field, W. B. Lacefield, *J. Org. Chem. 31* (1966) 3555–3561; P. W. Schenk, R. Steudel, J. Bilal, *Angew. Chem. 78* (1966) 717; *Angew. Chem. Int. Ed. Engl. 5* (1966) 673; *Z. Anorg. Allg. Chem. 353* (1967) 250–258; R. Steudel, G. Scheller, *Z. Naturforsch. B 24* (1969) 351–352; H. E. Simmons, R. D. Vest, D. C. Blomstrom, J. R. Roland, T. L. Cairns, *J. Am. Chem. Soc. 84* (1962) 4746–4756, 4772–4781; R. Steudel, P. Luger, H. Bradaczek, *Chem. Ber. 110* (1977) 3553–3560; R. Steudel, *Phosphorus Sulfur 23* (1985) 33–64.

[3] Reviews: M. Schmidt, *Angew. Chem. 85* (1973) 474–484; *Angew. Chem. Int. Ed. Engl. 12* (1973) 445–455; R. Steudel, *Top. Curr. Chem. 102* (1982) 149–176; R. Steudel in I. Haiduc and D. B. Sowerby (Eds.): *"The Chemistry of Inorganic Homo- and Heterocycles", Vol. 2*, Academic Press, London 1987, p. 737–768; H. Schmidt, R. Steudel, *Z. Naturforsch. B 45* (1990) 557–558.

[4] C. M. Bolinger, J. E. Hoots, T. B. Rauchfuss, *Organometallics 1* (1982) 223–225.

[5] Preparation of **3**: a stirred solution of $Cp'_4Ti_2S_4$ (*100 mg, 0.185 mmol*) *in* CS_2 (28 mL) was treated at 0 °C with a solution of $SOCl_2$ (22 mg, 0.185 mmol) in CS_2. After 10 min the precipitated Cp'_2TiS_5O was recovered by suction, washed with *n*-pentane, and immediately dried in vacuo. Yield 38 mg (54% of theory). Correct C,H analysis.

[6] R. Steudel, *Z. Naturforsch. B 25* (1970) 156–165; R. Steudel, M. Rebsch, *J. Mol. Spectrosc. 51* (1974) 334–340; R. Steudel, D. F. Eggers, *Spectrochim. Acta A 31* (1975) 871–877.

[7] Cp'_2TiS_5 shows singlets at $\delta = 2.00$ and 2.26 as well as four multiplets in the range $\delta = 5.92$–6.18 (in $CDCl_3$): C. M. Bolinger, T. B. Rauchfuss, *Inorg. Chem. 21* (1982) 3947–3954.

[8] Separating column: 10C18 Radial-Rak (Waters): UV spectra: Diode array detector 990 (Waters; 512 diodes, range 190–800 nm) with NEC-APC-III computer.

[9] Preparation of **4**: a stirred solution of $Cp'_4Ti_2S_4$ (1 g, 1.85 mmol) in CH_2Cl_2 (150 mL) was treated with a solution of $SOCl_2$ (220 mg, 1.85 mmol) in CH_2Cl_2 (3.5 mL). After 45 min the dark-brown solution was separated chromatographically (150 g silica gel 40 (Merck), $l = 60$ cm) and eluted with CH_2Cl_2. The first 500 mL were evaporated down to 25 mL in vacuo, treated with 25 mL hexane, and cooled to − 60 °C, whereupon **4** crystallized out. Yield: 142 mg (20% theoretical). Correct C,H analysis EI-MS (180 °C sample temperature): no molecular peak, $[M-SO]^{\oplus}$, $[M-S_2O]^{\oplus}$ and $[M-S_3O]^{\oplus}$ observed, base peak: $S_8^{\oplus}$. ^{1}H NMR (CD_2Cl_2, − 40 °C, 400 MHz): $\delta = 2.083$, 2.036(s), 5.458, 5.645, 6.061, 6.438, 6.52, 6.734, 7.453 (q).

[10] Crystal structure analysis of **4**: space group $P2_1/n$ (No. 14); $a = 738.5(5)$, $b = 1606.8(6)$, $c = 1317.8(7)$ pm, $\beta = 95.27(9)°$, $V = 1557.1 \times 10^6$ pm^3, $Z = 4$, $\varrho_{calcd} = 1.63$ g cm^{-3}, $\mu(Mo_{K\alpha}) = 11.0$ cm^{-1}, diffractometer Enraf-Nonius CAD4, room temperature, $Mo_{K\alpha}$ radiation ($\lambda = 71.069$ pm), $2\theta \leq 50°$, 2436 independent reflections, 1694 with $I \geq 2\sigma(I)$, empirical absorption correction, solution of structure by Patterson methods, refinement with anisotropic temperature factors for all atoms except hydrogen, the CH bonds were calculated and not refined: 180 parameters, $R = \Sigma(\|F_o\| - \|F_c\|)/\Sigma|F_o| = 0.0436$. Further details of the crystal structure

investigation are available on request from the Fachinformationszentrum Karlsruhe, Gesellschaft für wissenschaftlich-technische Information mbH, W-7514 Eggenstein-Leopoldshafen 2 (FRG), on quoting the depository number CSD-55148, the names of the authors, and the journal citation.
[11] R. Steudel, J. Steidel, J. Pickardt, F. Schuster, R. Reinhardt, *Z. Naturforsch. B 35* (1980) 1378–1383.
[12] E. F. Epstein, I. Bernal, H. Köpf, *J. Organomet. Chem. 26* (1971) 229–245; E. G. Muller, J. L. Petersen, L. F. Dahl, *ibid. 111* (1976) 91–112.
[13] Y. LePage, J. D. McCowan, B. K. Hunter, R. D. Heyding, *J. Organomet. Chem. 193* (1980) 201–207; J. C. Huffman, K. C. Moloy, J. A. Marsella, K. G. Caulton, *J. Am. Chem. Soc. 102* (1980) 3009–3014.
[14] E. Baumeister, H. Oberhammer, H. Schmidt, R. Steudel, *Heteroatom Chem.*, in press, and unpublished results.
[15] R. Steudel, *Angew. Chem. 87* (1975) 683–692; *Angew. Chem. Int. Ed. Engl. 14* (1975) 655–663.
[16] M. Papavassiliou, *Dissertation*, Technische Universität Berlin 1990.
[17] D. M. Giolando, T. B. Rauchfuss, *Organometallics 3* (1984) 487–489.

Proof of Strong S–H···S Bridges in $[Ru(SH_2)(PPh_3)('S_4')]\cdot THF$, the First H_2S Complex Characterized by X-Ray Crystallography **

By *Dieter Sellmann,* Peter Lechner, Falk Knoch,* and *Matthias Moll*

The interaction of H_2S, $HS^{\ominus}$ and $S^{2\ominus}$ with transition metals is a primary step in the formation of ores and in the construction of the $[M_xS_y]$ clusters in enzymes like ferredoxines or nitrogenases. Here, as in the metal-enzyme catalyzed $SO_4^{2\ominus}/H_2S$ transformation in the biological sulfur cycle, H_2S complexes are assumed to be intermediates. Because of their extreme reactivity,[1, 2a] such complexes could be detected,[2b, f, g] or isolated,[2a–e] only in exceptional cases in the past, but never be studied by X-ray crystallography. In this respect they differ from the numerous well-characterized H_2O complexes.

$$[Ru(PPh_3)('S_4')] \xrightarrow[5\ min]{H_2S/-70\,^{\circ}C} [Ru(SH_2)(PPh_3)('S_4')]\ \mathbf{1} \qquad (a)$$

We have now succeeded in obtaining the H_2S complex $[Ru(SH_2)(PPh_3)('S_4')]$ **1** from $[Ru(PPh_3)('S_4')]$[3] (eq. (a)), which could be characterized by X-ray crystallography (Fig. 1a).[4] Compound **1** precipitates as **1**·THF on recrystallization from H_2S-saturated THF as yellow-orange crystals and can be ionized in a mass spectrometer without decomposition. In contrast to the highly labile solvent-free **1**, **1**·THF is stable at 25 °C and loses H_2S slowly in vacuum only. Both compounds are rapidly oxidized by O_2 to turquoise-colored $[(\mu\text{-}S_2)\{Ru(PPh_3)('S_4')\}_2]$[5] (Eq. (b)).

$$2\,[Ru(SH_2)(PPh_3)('S_4')]\ \mathbf{1} \xrightarrow[-2H_2O]{O_2} [(\mu\text{-}S_2)\{Ru(PPh_3)('S_4')\}_2] \qquad (b)$$

In the unit cell of **1**·THF, two enantiomers are each associated via two S–H···S bridges to a cyclic dimer containing an inversion center. In addition each H_2S ligand is bound to a THF molecule via one S–H···O bridge (Fig. 1, bottom). The position of the H_2S hydrogen atoms were localized by difference Fourier synthesis.

The Ru atoms are each surrounded by five sulfur and one phosphorus atom in a pseudo-octahedral geometry. The angles in the coordination polyhedron are all close to 90 or 180° and do not exhibit anomalies. The Ru–S distances (236.1(5)–239.7(5) pm) and the Ru–P distance (232.4(5) pm) are typical for these complexes. Only the Ru1–S3 distance in *trans* position to the H_2S ligand is clearly shorter (229.3(5) pm); comparison with other $[Ru(L)(PPh_3)('S_4')]$ complexes[6] suggests a stronger Ru → S (thioether) π acceptor bond.

The S–H···S bridges in **1**·THF are of particular interest (Fig. 1, bottom). For the first time the existence of these bridges in H_2S complexes could be proved by X-ray crystallography. They are very strong in comparison with the usually weak S–H···S bridges (e.g., in H_2S: $\Delta H_f^{298} = 7\ kJ\ mol^{-1}$[7]).

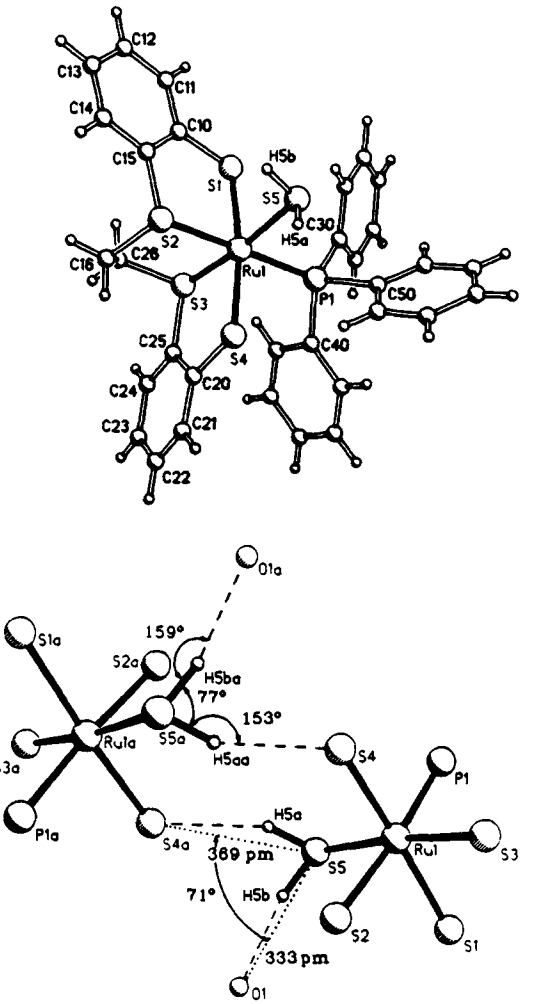

Fig. 1. Top: Structure of **1**·THF in the crystal (THF omitted); bottom: S–H···S and S–H···O hydrogen bridges in **1**·THF.

The strongest S–H···S bridges known as yet ($\Delta H_f^{298} \approx 12\ kJ\ mol^{-1}$[8]) were found in dithiophosphinic acids, which have S···S distances of 375 to 384 pm, ν(SH) between 2340 and 2400 cm^{-1} (KBr) and S–H···S angles in the range 159 to 173°.[9] In comparison, the calculated S–H···S limiting

[*] Prof. Dr. D. Sellmann, Dipl.-Chem. P. Lechner, Dr. F. Knoch, Dr. M. Moll
Institut für Anorganische Chemie II der Universität Erlangen-Nürnberg
Egerlandstrasse 1, W-8520 Erlangen (FRG)

[**] $('S_4')^{2\ominus}$ = 2,2'-(ethylenedithio)bis(thiophenolate). Transition Metal Complexes with Sulfur-Containing Ligands, Part 64. This work was supported by the Deutsche Forschungsgemeinschaft, the Fonds der Chemischen Industrie, and Degussa AG, Hanau (gift of $RuCl_3\cdot xH_2O$). Part 63: D. Sellmann, M. Geck, F. Knoch, M. Moll, *Inorg. Chim. Acta*, in press.

distance is ca. 439 pm,[9a] and the ν(SH) in gaseous H_2S occur at 2615 and 2628 cm^{-1}.[10] The angle formed by the S–H···S bridge in **1**·THF is 153°, the sum of the distances S5–H5a and H5a–S4a is 378 pm and the distance S5–S4a 369 pm. In particular this extremely short distance indicates that the S–H···S bridges in **1**·THF must be exceptionally strong; this is corroborated by the ν(SH···S) at 2290 cm^{-1} (KBr) that is the lowest frequency observed for S–H···S bridges as yet. In H_2S complexes without hydrogen bridges, the ν(SH) appear at significantly higher wavenumbers (2590 to 2510 cm^{-1}). Compound **1**·THF shows in contrast to **1** a ν(S–H···O) at 2410 cm^{-1}, which together with the short S···O distance of 333 pm indicates that the S–H···O bridges are also strong.[11]

^{1}H NMR spectroscopic evidence for SH protons in **1**·THF can only be obtained by using solutions of freshly prepared **1** in H_2S-containing mixtures of CD_2Cl_2/[D_8]THF (1:2). Besides the signal of free H_2S ($\delta = 1.00$), a signal for the protons of the H_2S ligand at $\delta = 1.96$ is observed. When the sample is oxidized by air, the signal for the H_2S ligand decreases and splits, until it finally can no longer be detected. In the ^{1}H NMR spectrum of the corresponding D_2S complex [$Ru(SD_2)(PPh_3)('S_4')$] it does not appear.[12]

1·THF thus shows that H_2S in complexes with a sulfur-dominated coordination sphere is stabilized by strong hydrogen bonds. Their strength results on one hand from the high charge density in the [RuS] framework, through which the thiolate donors become good H acceptors, and on the other from the large polarity of the S–H bond in coordinated H_2S. The short S···S distance and the low frequency of ν(S–H···S) confirm that S–H···S bridges can be significantly more stable than hitherto suspected. This result is of considerable interest, because S–H···X bridges (X = N, O, S) in ferredoxines and most other metal-sulfur enzymes, influence redox potentials and equilibrium configurations, and thereby reactivities.[13]

Experimental Procedure

All procedures were conducted in an H_2S atmosphere under strict O_2 and H_2O exclusion. 10 mL of H_2S was condensed onto 830 mg (1.24 mmol) of [$Ru(PPh_3)('S_4')$] at −196 °C in a Schlenk tube. Slow warming of the mixture to −70 °C gave a red suspension, which rapidly turned into a clear yellow solution. Concentration to 1 mL at −60 °C caused precipitation of yellow **1**. Careful dissolution in 30 mL of cold (−50 °C) THF and slow addition of 30 mL pentane (−10 °C) with stirring yielded finely crystalline **1**·THF, which was separated, washed with pentane/THF (10:1) and dried in a stream of H_2S gas. Correct elemental analysis. 745 mg (77%) yield. ^{1}H NMR of **1** (270 MHz, CD_2Cl_2/[D_8]THF (1:2), TMS): δ = 7.67–6.40 (23 H, m, C_6H_4, PPh_3), 2.85–2.35 (4H, m, C_2H_4), 1.96 (2H, s, SH); ^{31}P{^{1}H} NMR of **1** and **1**·THF (109 MHz, CD_2Cl_2/[D_8]THF (1:2), H_3PO_4): δ = 42.2; FD-MS: *m/z* 706 ([$Ru(SD_2)(PPh_3)('S_4')$]: *m/z* 708). Single crystals were obtained from a saturated solution of freshly synthesized **1** in THF at 0 °C by layering with the same volume of pentane.

Received: December 17, 1990 [Z 4333 IE]
German version: *Angew. Chem. 103* (1991) 599

[1] H. Vahrenkamp, *Angew. Chem. 87* (1975) 363; *Angew. Chem. Int. Ed. Engl. 14* (1975) 322.
[2] a) C. G. Kühn, H. Taube, *J. Am. Chem. Soc. 98* (1976) 689; b) M. Herberhold, G. Süss, *Angew. Chem. 88* (1976) 375; *Angew. Chem. Int. Ed. Engl. 15* (1976) 366; c) P. J. Harris, S. A. R. Knox, R. J. McKinney, F. G. A. Stone, *J. Chem. Soc. Dalton Trans. 1978*, 1009; d) G. Urban, K. Sünkel, W. Beck, *J. Organomet Chem. 290* (1985) 329; e) K. Raab, W. Beck, *Chem. Ber. 118* (1985) 3830; f) D. Morelli, A. Segre, R. Ugo, G. La Monica, S. Genini, F. Conti, E. Bonati, *J. Chem. Soc. Chem. Commun. 1967*, 524; g) J. Amarasekera, T. B. Rauchfuß, *Inorg. Chem. 28* (1989) 3875.
[3] D. Sellmann, I. Barth, M. Moll, *Inorg. Chem. 29* (1990) 176.
[4] X-ray structure analysis: diffractometer Nicolet R3m/V, T = 200 K, ($Mo_{K\alpha}$) graphite monochromator, ω scan, $3° < 2\theta < 54°$, direct methods (SHELXTL-PLUS), 7662 reflections, 6662 independent and 4759 with $F > 6\sigma(F)$. Non-hydrogen atoms anisotropically refined, SH_2 hydrogen atoms found by difference Fourier synthesis and fixed during refinement. 401 refined parameters, $R = 0.065$, $R_w = 0.056$, $P2_1/c$, $a = 1124.7(9)$, $b = 1378.5(14)$, $c = 2274.0(16)$ pm, $\beta = 97.06(6)°$, $V = 3499(5) \times 10^6$ pm^3, $\rho_{calc} = 1.48$ g cm^{-3}, $Z = 4$. Further details of the crystal structure investigation may be obtained from the Fachinformationszentrum Karlsruhe, Gesellschaft für wissenschaftlich-technische Information mbH, W-7514 Eggenstein-Leopoldshafen 2 (FRG) on quoting the depository number CSD-320193, the names of the authors and the journal citation. Important distances [pm] and angles [°]: S5-H5a 119, S5-H5b 121, Ru1-S1 239.7(5), Ru1-S2 236.1(5), Ru1-S3 229.3(5), Ru1-S4 239.3(5), Ru1-S5 239.9(5), Ru1-P1 232.4(5), H5a-S4a 258, H5b-O1 216; Ru1-S5-H5a 102, Ru1-S5-H5b 121, H5a-S5-H5b 77, S1-Ru1-S5 87.4(1), S2-Ru1-S5 87.9(1), S3-Ru1-S5 174.1(1), S4-Ru1-S5 97.6(1), S5-Ru1-P1 88.9(1), Ru1-S4-H5aa 129, S5-H5aa-S4a 153, S5-H5b-O1 159.
[5] D. Sellmann, I. Barth, *Inorg. Chim. Acta 164* (1989) 171.
[6] Cf: D. Sellmann, I. Barth, F. Knoch, M. Moll, *Inorg. Chem. 29* (1990) 1822, and references quoted therein.
[7] S. Singh, C. N. R. Rao, *J. Phys. Chem. 71* (1967) 1074.
[8] R. R. Shagidullin, I. P. Lipatova, L. I. Vachugova, R. A. Cherkasov, F. Kh. Khairutdinova, *Izv. Akad. Nauk SSSR Ser. Khim. 1972*, 847.
[9] a) B. Krebs, *Angew. Chem. 95* (1983) 113; *Angew. Chem. Int. Ed. Engl. 22* (1983) 113; b) B. Krebs, G. Henkel, *Z. Kristallogr. 179* (1987) 373.
[10] H. C. Allen, Jr., L. R. Blaine, E. K. Plyler, *J. Chem. Phys. 24* (1956) 35.
[11] R. D. Amos, *Chem. Phys. 104* (1986) 145.
[12] The D_2S required for the synthesis of [$Ru(SD_2)(PPh_3)('S_4')$] was prepared from Na_2S and D_2SO_4 (50% in D_2O), condensed into a Schlenk tube at −78 °C and dried over 4 Å molecular sieves.
[13] A. Nakamura, N. Ueyama in L. Que (Ed.): *Metal Clusters in Proteins*, Am. Chem. Soc., Columbus, OH, USA 1988, Kap. 14.

Bicyclic P_6 as Complex Ligand**

By *Otto J. Scherer,* Bernd Werner, Gert Heckmann,* and *Gotthelf Wolmershäuser*

Dedicated to Professor Marianne Baudler on the occasion of her 70th birthday

If one considers the opening of one edge and one bond of the double bond of the as yet unknown hexaphosphabenzvalene **A**[1] by a four-electron reduction, the formally bicyclic $P_6^{4\ominus}$ anion **B** is formed. The cothermolysis of the butadiene

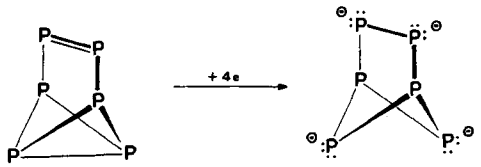

A **B**

complex **1** and P_4 leads in about 30% yield to the binuclear thorium complex **2** with a new structure variant of the P_6 ligand.[2]

$$[Cp''_2Th(\eta^4\text{-}C_4H_6)] \xrightarrow[\text{ca. 100 °C, ca. 20 h}]{P_4,\ \text{toluene}} [Cp''_2Th(\mu, \eta^3, \eta^3\text{-}P_6)ThCp''_2]$$

1 **2**

$Cp'' = \eta^5$-1,3-tBu$_2$C$_5$H$_3$

The reaction of **1** with P_4 in the presence of $MgCl_2$ affords the binuclear complex **3** in about 80% yield. In this complex

[*] Prof. Dr. O. J. Scherer, Dipl.-Chem. B. Werner, Dipl.-Chem. G. Heckmann [+], Dr. G. Wolmershäuser [+]
Fachbereich Chemie der Universität
Erwin-Schrödinger-Strasse, W-6750 Kaiserslautern (FRG)
[+] X-ray crystallography

[**] This work was supported by the Fonds der Chemischen Industrie.

the oxidation state of IV, which is almost the only occurring state for thorium, is possible if the unsubstituted phosphorus ligand is described as *cyclo*-$P_3^{3\ominus}$, a formulation isoelectronic with *cyclo*-S_3.[3]

$$2\,\mathbf{1} \xrightarrow[\text{toluene, ca. 100 °C, ca. 20 h}]{P_4,\ 1/2\,MgCl_2(OEt_2)} \underset{\mathbf{3}}{[Cp''_2Th(\mu,\eta^3\text{-}P_3)Th(Cl)Cp''_2]}$$

The extremely air-sensitive crystals of the amber-colored **2** or yellow-orange **3** are very soluble in dichloromethane, soluble in toluene, but only slightly soluble in hexane.

The ^{31}P NMR spectrum[4] reveals an AA'MM'Q_2 system for **2**; for **3** a broad singlet is observed at 293 K, which splits into an A_2B system at 193 K (see Fig. 2). The rotation barrier of the *cyclo*-P_3 unit is ca. 44 kJ mol^{-1}.[4]

The X-ray structure[5] shows that **2** is a cage compound, in which the Th_2P_6 framework consists of a P_6 bicycle (similar to **B**) with the thorium atoms capping the five-membered rings (Fig. 1). As in the structurally related tricyclic

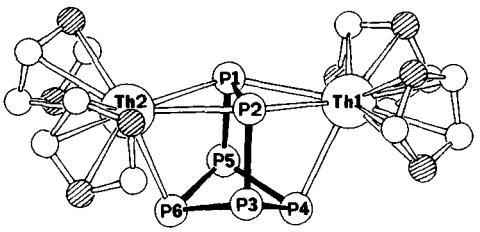

Fig. 1. Structure of **2** in the crystal. Selected bond lengths [Å] and angles [°]: Th1-P1 2.878(7), Th1-P2 2.921(7), Th1-P4 2.840(7), Th2-P1 2.919(7), Th2-P2 2.899(7), Th2-P6 2.847(7), Th1-Cp'' (center) 2.55/2.58, Th2-Cp'' (center) 2.57/2.57, P1-P2 2.183(10), P2-P3 2.271(9), P1-P5 2.281(10), P3-P4 2.235(10), P3-P6 2.227(11), P5-P4 2.228(10), P5-P6 2.212(10), P3···P5 3.01, P4···P6 2.97; P1-Th1-P2 44.2(2), P2-Th1-P4 73.6(2), P1-Th1-P4 74.9(2), P1-Th2-P2 44.1(2), P2-Th2-P6 74.8(2), P1-Th2-P6 73.0(2), Th1-P1-Th2 134.1(2), Th1-P2-Th2 133.0(3), Th1-P1-P2 68.9(3), Th2-P1-P2 67.5(3), Th1-P2-P1 66.9(3), Th2-P2-P1 68.5(39), Th1-P1-P5 85.6(3), Th2-P1-P5 88.9(3), Th1-P2-P3 88.8(3), Th2-P2-P3 85.2(3), Th1-P4-P3 91.5(3), Th1-P4-P5 87.5(3), Th2-P6-P3 87.3(3), Th2-P6-P5 92.2(3), P1-P2-P3 100.0(4), P2-P1-P5 100.9(4), P2-P3-P4 100.0(4), P2-P3-P6 101.7(4), P1-P5-P4 101.0(4), P1-P5-P6 99.4(4), P4-P3-P6 83.5(4), P4-P5-P6 84.0(4), P3-P4-P5 84.8(4), P3-P6-P5 85.4(4). ⊘ = C*t*Bu.

polyphosphane $P_6(C_5Me_5)_2$ (**4**),[6, 7b] the P_1-P_2 bond of 2.18 Å is the shortest. (In **4** an η^1-C_5Me_5 substituent is bonded to each of these atoms.) The P2–P3 distance of 2.27 and P1–P5 distance 2.28 Å are distinctly longer than the corresponding 2.19 Å in **4**.[6, 7b] The average of 2.225 Å for the remaining four P–P bond lengths (P3 to P6) differs only minimally from the $\bar{d}$(P–P) = 2.21 Å of the P_4 molecule. The P_6R_4 compounds **5a** (R = *t*Bu)[7a] and **5b** (R = C_5Me_5),[7b] which have been characterized by X-ray crystallography, and which have a five-membered ring with an annelated three-membered ring as P_6 framework,[7c] give values for $\bar{d}$(P–P) of 2.195 Å for **5a** and 2.221 Å for **5b**.[7b] The Th–P bond lengths in **2** (2.84 to 2.92 Å, Fig. 1) lie in the range for thorium phosphido complexes.[8] Although the atoms Th1 P1 P2 Th2 (dihedral angle = 165.1°) lie almost in a plane, the dihedral angle between the planes defined by P3 P5 P4 and P3 P5 P6 is 129.9°.

The X-ray structure[5] of **3** (Fig. 2) shows that the distance from Th1 to the center of the P_3 ring is 2.57 Å, ca. 0.1 Å shorter than the corresponding distance to Th2 of 2.68 Å. Accordingly the Th1–P1 distance of 2.81 Å is the shortest and the Th2–P1 distance of 2.99 Å the longest Th–P distance in the molecule. The average P–P distance of 2.185 Å in the almost equilateral P-triangle (2 × 2.192, 1 × 2.171 Å) is slightly longer than the calculated 2.174 Å for *cyclo*-$P_3^{\ominus}$[3c] and comparable with those for the [(triphos)M(μ,η^3-P_3)M(triphos)]$^{n\oplus}$ class of substances where, for example, M = Co, n = 2, and triphos = $CH_3C(CH_2PPh_2)_3$.[9] The coordination environment of Th1 (sum of the angles Th1Cp''Cp''*cyclo*-P_3(center) = 356°) differs only minimally from the exactly trigonal-planar environment of the Th atom in [Th{η-$C_5H_3(SiMe_3)_2$}$_3$],[10] while Th2 occupies a distorted tetrahedral site formed by the four ligands Cl, Cp'', Cp'', *cyclo*-P_3(center). The Cl ··· P1 and Cl ··· P2 distances of 3.76 and 3.66 Å respectively are nonbonding.

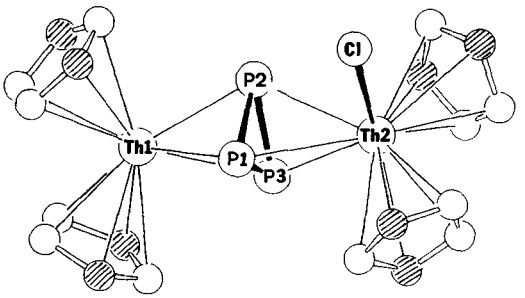

Fig. 2. Structure of **3** in the crystal. Selected bond lengths [Å] and angles [°]: Th1-P1 2.809(6), Th1-P2 2.898(7), Th1-P3 2.892(6), Th2-P1 2.994(7), Th2-P2 2.974(8), Th2-P3 2.910(6), Th2-Cl 2.675(5), Th1-Cp'' (center) 2.54/2.54, Th2-Cp'' (center) 2.59/2.605, P1-P2 2.171(9), P2-P3 2.192(9), P1-P3 2.192(8), P1-Th1-P2 44.7(2), P2-Th1-P3 44.5(2), P1-Th1-P3 45.2(2), P1-Th2-P2 42.7(2), P2-Th2-P3 43.7(2), P1-Th2-P3 43.6(2), P1-Th2-Cl 82.9(2), P2-Th2-Cl 80.5(2), P3-Th2-Cl 120.1(2). ⊘ = C*t*Bu.

Experimental Procedure

2 [3]: 2.00 g (3.12 mmol) of **1** [11], dissolved in 10 mL toluene, and 0.77 g (6.24 mmol) P_4 [and 0.16 g (0.94 mmol) $MgCl_2(OEt_2)$] were stirred in a sealed Schlenk tube at 100 °C for 20 h (tested for completion with ^1H NMR). The orange-red solution slowly darkened. After removal of the solvent in vacuum and subsequent sublimation of P_4 (0.01 Torr, 60 °C, 1 h), the solid, red-brown residue was washed (only for **2**) several times with 5 mL portions of cold hexane. **2** precipitated as a yellow powder (purity > 90 %, determined by ^1H NMR spectroscopy). The solid was taken up in toluene and filtered through filter flakes [for **3**, a small amount of a red-brown solid precipitated, which was insoluble in the common organic solvents] and crystallized at −18 °C. Yield: 0.66 g (31 %) [1.64 g (81 %)] amber-colored [yellow-orange] crystals [amongst them intergrowing needles].

Received: November 12, 1990 [Z 4276 IE]
German version: *Angew. Chem. 103* (1991) 562
Publication delayed at authors' request

[1] Theoretical studies were performed on P_6-isomers of hexaphosphabenzene, hexaphosphaprismane and hexaphospha-Dewar benzene. R. Janoschek, *Chem. Ber. 122* (1989) 2121, and references cited therein.

[2] Latest review: O. J. Scherer, *Angew. Chem. 102* (1990) 1137; *Angew. Chem. Int. Ed. Engl. 29* (1990) 1104.

[3] For ab initio studies see: a) J. E. Rice, R. D. Amos, N. C. Handy, T. J. Lee, H. F. Schaefer III, *J. Chem. Phys. 85* (1986) 963; b) J. K. Burdett, C. J. Marsden, *New J. Chem. 12* (1988) 797; c) T. P. Hamilton, H. F. Schaefer III, *Chem. Phys. Lett. 166* (1990) 303.

[4] ^{31}P NMR (162 MHz, 85 % H_3PO_4 ext.); **2** (293 K, [D_8]toluene): AA'M M'Q_2 system (AA' = P3P5, MM' = P1P2, Q = P4P6), $\delta(P_{AA'})$ = 125.3 ("q"), $\delta(P_{MM'})$ = 18.4 (degenerate AA'MM' subspectrum), $\delta(P_Q)$ = −41.9(t), $^1J(AQ) = {}^1J(A'Q)$ = $^1J(A'Q)$ = 200 Hz, $^1J(MM')$ = 159 Hz, $^1J(AM) = {}^1J(A'M')$ = 239 Hz, $^2J(M'Q) = {}^2J(M'Q)$ = 0.5 Hz, $^2J(AM') = {}^2J(A'M)$ = 12 Hz, $^2J(AA')$ = 1.0 Hz. Spectrum simulation (PANIC program, version 850501.1, Bruker), Basic parameters: $^1J(AQ) = {}^1J(A'Q)$ = 200 Hz, $^1J(MM')$ and $^1J(AM) = {}^1J(A'M')$ from the calculation of the degenerate AA'MM' subspectrum ($^2J(AA')$ = 0); **3** (293 K, CD_2Cl_2): δ = −75.7 (s, $\Delta\nu_{1/2}$ = 300 Hz), 193 K: A_2B system (A = P1P2, B = P3), $\delta(P_A)$ = −69.7(d), $\delta(P_B)$ = −94.5(t), $^1J(AB)$ = 166.7 Hz, T_c = 263 ± 5 K, $\Delta G^{\ddagger}_{T_c}$ = 44 ± 3 kJ mol^{-1}—^1H NMR (400 MHz, 293 K, C_6D_6), *2*: δ = 6.27 (dd, br., 4H), 6.11 (dd, br., 4H), 5.50

(dd, br., 4H), ^3J(HH) ≈ ^4J(HH) ≈ 2 Hz, 1.65 (s, 36H), 1.29 (s, 36H); **3**: Two symmetry-equivalent Cp″ ligands per thorium; Cp″ on Th2 with diastereotopic groups, Cp″ on Th1: $\delta = 7.1$ (t, 2H), 5.78 (d, ^4J(HH) = 2.6 Hz), 1.38 (s, 36H), Cp″ on Th2: $\delta = 6.39$ (dd, 2H), 6.13 (dd, 2H), 6.09 (dd, 2H), ^3J(HH) ≈ ^4J(HH) ≈ 1.6 Hz, 1.67 und 1.65 (s, 18H).

[5] a) **2**, which contains three molecules of toluene, forms monoclinic crystals; $P2_1/c$; $a = 11.263(2)$, $b = 18.838(2)$, $c = 34.974(5)$ Å; $\beta = 95.96(2)°$; $Z = 4$; 6779 independent reflections ($Mo_{K\alpha}$: $1.5° \leq \theta \leq 20°$), 3983 with $I \geq 2\sigma(I)$; 281 parameters, $R = 0.060$, $R_w = 0.065$ [5c]; b) **3** forms orthorhombic crystals; $P2_12_12_1$; $a = 18.194(1)$, $b = 26.246(3)$, $c = 11.714(1)$ Å; $Z = 4$; 4292 independent reflections ($Mo_{K\alpha}$: $1.5° \leq \theta \leq 23°$), 3113 with $I \geq 2\sigma(I)$; 263 parameters, $R = 0{,}047$, $R_w = 0{,}046$ [5c]; c) Solution and refinement of the structures with the program systems SHELX-76 and SHELXS-86. Further details of the crystal structure investigation may be obtained from the Fachinformationszentrum Karlsruhe, Gesellschaft für wissenschaftlich-technische Information mbH, W-7514 Eggenstein-Leopoldshafen 2 (FRG) on quoting the depository number CSD-55098, the names of the authors and the journal citation.

[6] P. Jutzi, R. Kroos, A. Müller, M. Penk, *Angew. Chem. 101* (1989) 628; *Angew. Chem. Int. Ed. Engl. 28* (1989) 600.

[7] a) M. Baudler, Y. Aktalay, K.-F. Tebbe, T. Heinlein, *Angew. Chem. 93* (1981) 1020; *Angew. Chem. Int. Ed. Engl. 20* (1981) 967; b) P. Jutzi, R. Kroos, A. Müller, H. Bögge, M. Penk, *Chem. Ber. 124* (1991) 75 c) also known is the $P_6(t\text{Bu})_4$-isomer with two P_3 rings joined by a σ bond: M. Baudler, B. Makowka, *Angew. Chem. 96* (1984) 976; *Angew. Chem. Int. Ed. Engl. 23* (1984) 987.

[8] For example: D. A. Wrobleski, R. R. Ryan, H. J. Wasserman, K. V.-Salazar, R. T. Paine, D. C. Moody, *Organometallics 5* (1986) 90; J. M. Ritchey, A. J. Zozulin, D. A. Wrobleski, R. R. Ryan, H. J. Wasserman, D. C. Moody, R. T. Paine, *J. Am. Chem. Soc. 107* (1985) 501; P. J. Hay, R. R. Ryan, K. V. Salazar, D. A. Wrobleski, A. P. Sattelberger, *ibid. 108* (1986) 313.

[9] Review: M. Di Vaira, L. Sacconi, *Angew. Chem. 94* (1982) 338; *Angew. Chem. Int. Ed. Engl. 21* (1982) 330.

[10] P. C. Blake, M. F. Lappert, J. L. Atwood, H. Zhang, *J. Chem. Soc. Chem. Commun. 1986*, 1148.

[11] B. Werner, O. J. Scherer, unpublished.

Diastereoselective Enzymatic Aldol Additions: L-Rhamnulose and L-Fuculose 1-Phosphate Aldolases from *E. coli***

By *Wolf-Dieter Fessner*, Gudrun Sinerius, Achim Schneider, Matthias Dreyer, Georg E. Schulz, Josefa Badía,* and *Juan Aguilar*

Aldolases hold great promise as catalysts for organic synthesis, since enzyme-catalyzed C-C bond formations proceed with a high degree of enantio- and diastereoselectivity, which is rarely rivaled by classical synthetic methodology.[1] Particularly, four complementary aldolases are known in carbohydrate metabolism (Scheme 1) which catalyze the asymmetric addition of dihydroxyacetone phosphate (DHAP) to L-lactaldehyde or D-glyceraldehyde 3-phosphate to generate a unique product each, namely only one of the four possible diastereomeric configurations. D-Fructose 1,6-bisphosphate aldolase (FruA) has been shown to accept a broad range of aldehydes as substrate.[2] The development of the full potential value of DHAP aldolases into a general and efficient methodology for asymmetric synthesis will largely depend on the availability of the whole tetrad of enzymes. This would allow the creation of all four possible diastereomers at will in a building block fashion by simply selecting a suitable aldehyde and the correct enzymic catalyst. Here we report the subcloning, overexpression, isolation, and application in synthesis of two bacterial DHAP aldolases, the L-rhamnulose (RhuA; EC 4.1.2.19) and L-fuculose 1-phosphate aldolases (FucA; EC 4.1.2.17) of *E. coli*, which likewise accept a useful range of structurally diverse aldehydes, but provide products which are stereochemically distinct from those generated by FruA.

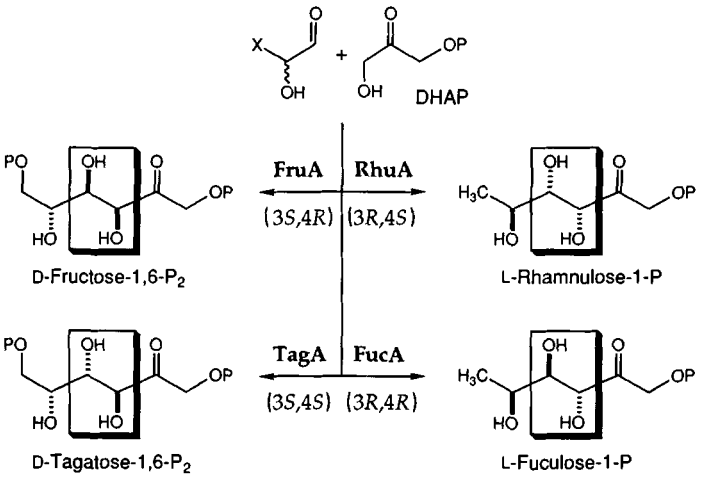

Scheme 1. Product stereochemistries generated by the four complementary DHAP aldolases (P = orthophosphate ester). FruA = D-fructose 1,6-bisphosphate aldolase, X = CH_2OP; RhuA = L-rhamnulose 1-phosphate aldolase, X = CH_3; TagA = D-tagatose 1,6-bisphosphate aldolase, X = CH_2OP; FucA = L-fuculose 1-phosphate aldolase, X = CH_3.

Cells of *E. coli* K-12 are able to grow on L-rhamnose or L-fucose as the sole sources of carbon and energy by two parallel, inducible pathways, each of which capitalizes on the aldol cleavage of the C_6 sugar by the action of RhuA or FucA. To generate the large amounts of the enzymes required for preparative utilization, separate overexpression systems were constructed. For RhuA, a *Bam*HI–*Hin*dIII genome fragment of 3.3 kilobase, which contained the complete structural *rhaD* gene encoding for the aldolase, was subcloned into the pUC18 vector.[3] A *rec*A derivative of *E. coli* strain ECL40 was transformed with the recombinant plasmid from which the enzyme was constitutively overexpressed relative to wild-type cells by a factor of ca. 15 (0.4 U mg^{-1} in crude cell extracts with a total of 400 U from 1 L of culture[4]) when grown in 1% CAA medium supplemented with ampicillin (100 μg mL^{-1}).[5] The structural gene for FucA was subcloned by introducing *Eco*RI–*Pst*I restriction sites according to standard PCR protocols from plasmid pfuc41a[6] into a pUC18-derived expression vector,[7] where it came under control of the *tac* promoter. Cells of *E. coli* strain HB101 transformed with this recombinant plasmid overexpressed FucA protein by a factor of 20 relative to wild-type cells (5 U mg^{-1} in crude cell extracts with a total of 900 U from 1 L of culture[4]) upon induction with 0.5 mM isopropyl-β-D-thiogalactopyranoside (IPTG).[8]

[*] Dr. W.-D. Fessner, Dipl.-Chem. G. Sinerius, Dipl.-Chem. A. Schneider, Dipl.-Chem. M. Dreyer, Prof. Dr. G. E. Schulz
Institut für Organische Chemie und Biochemie der Universität
Albertstrasse 21, W-7800 Freiburg (FRG)
Dr. J. Badía, Prof. Dr. J. Aguilar
Department of Biochemistry, School of Pharmacy,
University of Barcelona
Barcelona 08028 (Spain)

[**] Enzymes in Organic Synthesis, part 1. This research was supported by the Deutsche Forschungsgemeinschaft (Grant Fe 244/2-1), the Wissenschaftliche Gesellschaft Freiburg, and the Fonds der Chemischen Industrie and the Comisión Asesora de Investigación Científica y Técnica (Grant PB 85-0084). We gratefully acknowledge the generous gift of bacterial strains and plasmid DNA harboring the *fuc* genes by Prof. Dr. *E. C. C. Lin* and Dr. *Y.-M. Chen* of Harvard Medical School, Boston, and a preprint of ref. [8] obtained from Dr. *A. Ozaki*.

The enzymes were purified to homogeneity (one band upon SDS polyacrylamide gel electrophoresis or upon isoelectric focusing; no FruA activity detectable) in $\geq 60\%$ (for RhuA) or $\geq 40\%$ (for FucA) overall yields by similar three-step preparations consisting of ion exchange, hydrophobic interaction, and gel-permeation chromatography. Both catalytically active aldolases appear to be homotetramers with a subunit molecular weight of 30 kDa (RhuA)[3] and 25 kDa (FucA).[6] In a pure state, both enzymes readily form crystals (RhuA: rods or rectangular platelets form $\geq 10\%$ $(NH_4)_2SO_4$ solution; FucA: square platelets from 22% $(NH_4)_2SO_4$ solution at pH 7.8) that are suitable for X-ray analyses.

The stereoselectivity and substrate tolerance of purified enzymes were determined in two series of preparative syntheses, each employing a range of representative achiral and homochiral aldehydes **1**–**13** as substrate analogues (Table 1). All reaction rates, as determined by separate enzymic assays, were found to be sufficiently fast to allow an efficient and economical conversion of DHAP.[9] Reactions were carried out on 1–20 mmol scales at which nonoptimized isolated yields typically amounted to 70–90%. Diastereomeric composition was analyzed by high-field ^{1}H-NMR spectroscopy of crude reaction products. In addition, products were purified by ion-exchange chromatography[10] and were identified either by comparison with authentic samples, which were available from another study,[11] or by comparison with enantiomeric material obtained from respective FruA-catalyzed reactions.

All single or major diastereomers obtained from RhuA reactions were indistinguishable from analogous material generated by FruA, except for the opposite optical rotation. This confirms that RhuA generates vicinal diol units having the absolute (3*R*,4*S*)-*trans* configuration ("L-*threo*") as opposed to the (3*S*,4*R*)-*trans* stereochemistry ("D-*threo*") formed by FruA. In contrast, all the single diastereomers obtained from FucA-catalyzed reactions with achiral or homochiral hydroxaldehydes **1**–**5** were disparate to those produced upon FruA or RhuA catalysis. This corroborates that FucA generates vicinal diol units having a *cis* instead of a *trans* relationship among the hydroxyl substituents around the C3–C4 bond. Product identity, and thereby the common absolute (3*R*,4*R*) configuration ("D-*erythro*"), was unambiguously established by comparison with authentic samples.[11]

Within the limits of detection by high-field ^{1}H and ^{13}C NMR ($\leq 3\%$), enzymes RhuA and FucA both formed only single diastereomers from hydroxyaldehydes **1**–**5**, which suggests that the typifying magnitude of diastereoselectivity in the formation of L-rhamnulose or L-fuculose 1-phosphate (**16** and **17** respectively) is usually well conserved with related polar substrate analogues. Thus, these entries provide a straightforward, highly stereocontrolled access to phosphates of less common or nonnatural sugars like L-xylulose (**14**), D-sorbose (**18**), L-fructose (**20**), D-ribulose (**15**), D-psicose (**19**), L-tagatose (**21**), or corresponding 5-deoxy derivatives (**22**, **23**). The phosphorylated compounds are of interest in studies of carbohydrate metabolism[12] and are additionally a stable source for the free sugars.[2]

In experiments employing RhuA with a series of nonpolar aliphatic aldehydes **7**–**10**, however, in addition to the expected deoxysugars **25**, **27**, **29**, and **31**, the formation of varying amounts of a second stereoisomer was detected by the distinctive signals of 3-/4-H in high-field proton NMR spectra (Fig. 1). The wrong diastereomers, formed in larger amounts the smaller the substituent size (maximum of ca. 30% for acetaldehyde), were determined to be of opposite stereochemistry at C-4 (e.g. **26**) by their identity with corresponding FucA-derived materials and hence must have emerged due to imperfect guidance of the aldehyde approach. Apparently, the active site is so constructed that a more stringent binding occurs for hydrogen-bonding than for non-hydrogen-bonding substituents within the aldehyde part. Although highly selective with acetaldehyde **7** (95:5 ratio), FucA proved less selective with the sterically more demanding isobutyraldehyde **10** (70:30). These results accentuate the difficulty of demonstrating applicability of enzymic catalysts for synthesis by only assaying for substrate conversion[8]

Table 1. RhuA/FucA-catalyzed enzymic syntheses of ketose 1-phosphates[a]

Aldehyde	Formula	Product Configuration *trans*	*cis*	Enzyme	Diastereomer Ratio *trans* : *cis*	Yield [%] [b]	Relative Rate [%] [c]
1, glycolaldehyde	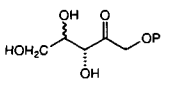	**14**	**15**	RhuA	≥ 97 : 3	82	43
				FucA	≤ 3 : 97	85	38
2, L-lactaldehyde	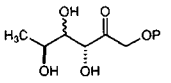	**16**	**17**	RhuA	≥ 97 : 3	95	100
				FucA	≤ 3 : 97	83	100
3, D-glyceraldehyde	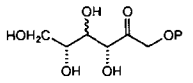	**18**	**19**	RhuA	≥ 97 : 3	84	42
				FucA	≤ 3 : 97	82	28
4, L-glyceraldehyde	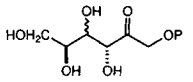	**20**	**21**	RhuA	≥ 97 : 3	91	41
				FucA	≤ 3 : 97	86	17
5, 3-hydroxypropionaldehyde	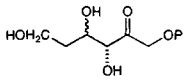	**22**	**23**	RhuA	≥ 97 : 3	73	29
				FucA	≤ 3 : 97	78	11
6, formaldehyde	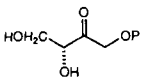	**24**		RhuA	–	(81)	22
				FucA	–	(73)	44
7, acetaldehyde	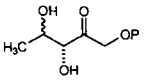	**25**	**26**	RhuA	69 : 31	(84)	32
				FucA	5 : 95	(54)	14
8, propionaldehyde	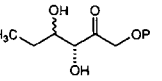	**27**	**28**	RhuA	90 : 10	(89)	50
9, *n*-butyraldehyde	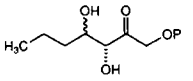	**29**	**30**	RhuA	83 : 17	(82)	48
10, *i*-butyraldehyde	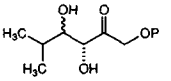	**31**	**32**	RhuA	97 : 3	(88)	22
				FucA	30 : 70	(58)	20
11, 3,3-diethoxypropionaldehyde	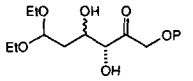	**33**	**34**	FucA	≤ 3 : 97	(68)	31
12, succinic semialdehyde	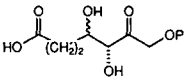	**35**	**36**	FucA	≤ 3 : 97	(80)	19
13, pyridine 2-carbaldehyde	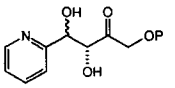	**37**	**38**	FucA	≤ 3 : 97	(43)	39

[a] For conditions, see *Experimental*. P = orthophosphate ester. Denotation of absolute configurations at C-4: *trans* |||, *cis* –. [b] Determined as crystalline bis(cyclohexylammonium) salts; values in parentheses refer to noncrystallizing bis(triethylammonium) salts of diastereomers[10]. [c] Rate for L-lactaldehyde is set at 100%. Initial rates were determined by assaying for remaining DHAP in aliquots which were taken in 1 min intervals from reaction mixtures containing 5 mM DHAP, 50 mM aldehyde and an appropriate quantity of purified aldolase.

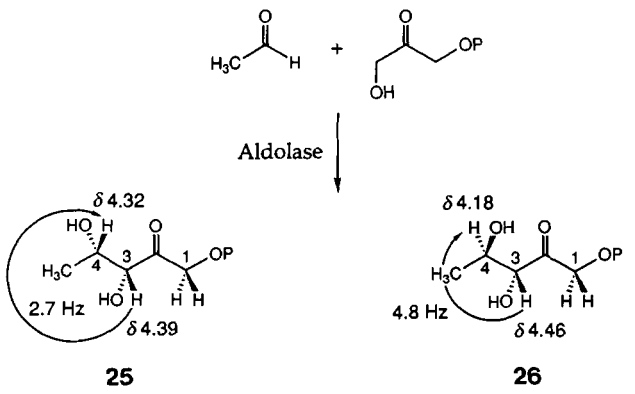

Fig. 1. Exemplary ^{1}H NMR data (400 MHz, D_2O, pH 7.0) for diastereomeric aldol adducts **25** (*trans*) and **26** (*cis*).

without analyzing the product composition thoroughly for every case as well.

The breadth of substrate tolerance is exemplified by additional FucA-catalyzed reactions of DHAP with some representative aldehydes **11**–**13** as substrate analogues that incorporate a number of functional groups typical for those useful in synthesis. The level of diastereoselectivity was found to be generally better than 97%. While we have been unable so far to rigorously assign the absolute configurations of products **34**, **36**, and **38** due to limitations in unambiguous comparison samples, it may safely be assumed from mechanistic considerations[13] that the absolute configuration at C-3 will be conserved throughout with any DHAP aldolase. For similar reasons, a rather narrow restriction for DHAP analogues has to be expected.

Both purified microbial aldolases display excellent stability in the presence of low levels of $Zn^{2\oplus}$ ions ($\leq$ 1 mM), with estimated half-lives at room temperature of several weeks and negligible inactivation during storage at 4°C for months. In addition, the enzymes tolerate remarkable proportions of organic cosolvents, e.g., 30–50% of ethanol, DMF, or DMSO (Fig. 2).

In summary, this data demonstrates that both RhuA and FucA accept a significant variety of aldehydes as substrate analogues for the efficient, highly enantio- and diastereocontrolled de-novo synthesis of carbohydrates, related polyhydroxy compounds, and phosphorylated derivatives. Although diastereoselectivity may be biased for certain substrate classes and may require careful choice of substitution patterns, the accessibility and broad applicability make these aldolases valuable enzymic catalysts for organic synthesis.

In general, the methodology of enzymic aldol addition benefits from the high level of catalytic asymmetric induction for two stereocenters at the same time, the mild reaction conditions, and the fact that no protection of functional groups is required. Nevertheless, practical limitations still remain in the control of the fourth, as yet inaccessible (3*S*,4*S*)-*cis*("L-*erythro*") aldol diastereochemistry and the inherent restriction to ketose-type products.[14] Efforts are now being directed at making the TagA as well as supplementary ketose → aldose isomerases available by recombinant DNA techniques.

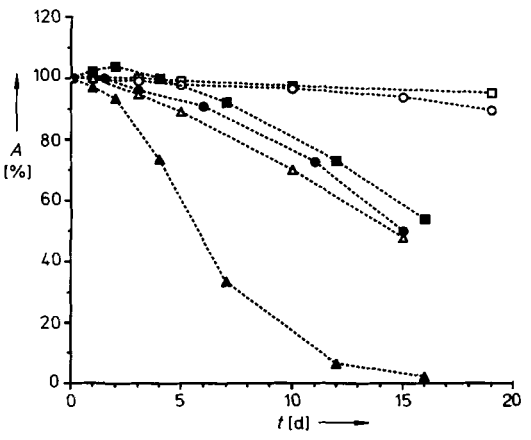

Fig. 2. Stabilities of the aldolases in phosphate buffer (50 mM; 0.5 mM $ZnCl_2$; pH 7.2; ca. 1 U mL^{-1}) at 25°C, determined by assays according to [4]. Examples are a) □ RhuA; b) ○ RhuA, 30% EtOH; c) △ RhuA, 50% DMSO; d) ■ FucA; e) ● FucA, 30% DMSO; f) ▲ FucA, 30% DMF.

Experimental

An aqueous solution of D-glyceraldehyde **3** (25 mmol in 300 mL) was combined with a solution of DHAP[9] (20 mmol in 200 mL) freshly adjusted to pH 6.8. The mixture was incubated with RhuA (100 U) at room temperature for 24 h with monitoring of conversion by thin-layer chromatography (2-propanol/sat. ammonia/water 6:4:2) and enzymic assay for DHAP. The product was isolated by passage through an ion-exchange column (Dowex AG1-X8, $HCO_3^{\ominus}$; 100 mL) and consecutive elution with 200 mM triethylammonium bicarbonate solution. After ion exchange with Dowex AG50W-X8 ($H^{\oplus}$) and neutralization with cyclohexylamine, the product was crystallized from aqueous ethanol (90%) to afford colorless crystals of α-D-sorbopyranose 1-phosphate bis(cyclohexylammonium) salt (**18**); yield: 7.71 g (84%); m.p. 158°C (dec); $[\alpha]_D^{20} = +8.0$ (H_2O, c = 1); ^{1}H NMR (400.1 MHz, D_2O, TSPNa, pH 7.0) δ = 3.56 (d, 3-H), 3.62–3.76 (m, 4-, 5-, 6-H), 3.78 (dd, 1-H_A), 3.87 (dd, 1-H_B); ^{13}C NMR (100.6 MHz, D_2O, CH_3CN, pH 7.0) δ = 62.2 (C-6), 66.5 (C-1, J(C-P) = 3.7 Hz), 70.0 (C-5), 71.2 (C-4), 74.0 (C-3), 98.1 (C-2, J(C-P) = 7.3 Hz).

Received: December 12, 1990
Revised: February 13, 1991 [Z 4322/4323 IE]
German version: *Angew. Chem. 103* (1991) 596

CAS Registry numbers:
1, 141-46-8; **2**, 3913-64-2; **3**, 453-17-8; **4**, 497-09-6; **5**, 2134-29-4; **6**, 50-00-0; **7**, 75-07-0; **8**, 123-38-6; **9**, 123-72-8; **10**, 78-84-2; **11**, 6367-37-9; **12**, 692-29-5; **13**, 1121-60-4; **14**, 2547-08-2; **15**, 7721-50-8; **16**, 444-09-7; **17**, 92418-41-2; **18**, 2650-47-7; **19**, 92418-40-1; **20**, 19456-80-5; **21**, 133007-25-7; **22**, 132959-24-1; **23**, 132959-25-2; **24**, 2547-10-6; **25**, 89195-02-8; **26**, 133007-26-8; **27**, 132959-26-3; **28**, 132959-27-4; **29**, 132959-28-5; **30**, 132959-29-6; **31**, 132959-30-9; **32**, 132959-31-0; **33**, 132959-32-1; **34**, 132959-33-2; **35**, 132959-34-3; **36**, 132959-35-4; **37**, 132959-36-5; **38**, 132959-37-6; DHAP, 57-04-5; L-rhamulose 1-phosphate aldolase, 9054-58-4; L-fuculose-1-phosphate aldolase, 9024-54-8.

[1] a) G. M. Whitesides, C.-H. Wong, *Angew. Chem. 97* (1985) 617–638; *Angew. Chem. Int. Ed. Engl. 25* (1985) 617–638; b) E. J. Toone, E. S. Simon, M. D. Bednarski, G. M. Whitesides, *Tetrahedron 45* (1989) 5365–5422.

[2] a) M. D. Bednarski, E. S. Simon, N. Bischofberger, W.-D. Fessner, M.-J. Kim, W. Lees, T. Saito, H. Waldmann, G. M. Whitesides, *J. Am. Chem. Soc. 111* (1989) 627–635; b) J. R. Durrwachter, D. G. Drueckhammer, K. Nozaki, H. M. Sweers, C.-H. Wong, *ibid. 108* (1986) 7812–7818; c) C. H. von der Osten, A. J. Sinskey, C. F. Barbas, R. L. Pederson, Y.-F. Wang, C.-H. Wong, *ibid. 111* (1989) 3924–3927; d) A. Straub, F. Effenberger, P. Fischer, *J. Org. Chem. 55* (1990) 3926–3932; e) M. Schultz, H. Waldmann, H. Kunz, W. Vogt, *Liebigs Ann. Chem. 1990*, 1019–1024; f) H. P. Brockamp, M. R. Kula, *Tetrahedron Lett. 31* (1990) 7123–7126.

[3] J. Badía, L. Baldomá, J. Aguilar, A. Boronat, *FEMS Microbiol. Lett. 65* (1989) 253–258.

[4] 1 Unit catalyzes the cleavage of 1 μmol of L-ketose 1-phosphate per minute at 25°C; assayed photometrically by coupling to glycerophosphate dehydrogenase-catalyzed NADH oxidation.

[5] Based on the *N*-terminal amino acid sequence (E. Schiltz, W.-D. Fessner, unpublished results), the corresponding reading frame and initiating DNA sequence coding for the RhuA enzyme have been identified (J. Aguilar et al., unpublished results). This information has enabled the construction of a *tac*-promoter-controlled expression system similar to the one described for FucA (G. Sinerius, W.-D. Fessner, unpublished results).

[6] Y.-M. Chen, Z. Lu, E. C. C. Lin, *J. Bacteriol. 171* (1989) 6097–6105.

[7] K. Proba, *Dissertation*, University of Freiburg, in preparation. The correct sequence of the *fucA* insert was verified by complete dideoxy sequencing; M. Dreyer, *Diploma thesis*, University of Freiburg 1991.

 © *VCH Verlagsgesellschaft mbH, W-6940 Weinheim, 1991* *0570-0833/91/0505-0557 $ 3.50+.25/0*

[8] Overexpression of FucA and substrate assays with unpurified enzyme have recently been reported for a limited number of aldehydes: A. Ozaki, E. J. Toone, C. H. von der Osten, A. J. Sinskey, G. M. Whitesides, *J. Am. Chem. Soc. 112* (1990) 4970–4971.

[9] DHAP was prepared chemically according to the literature procedure (F. Effenberger, A. Straub, *Tetrahedron Lett. 28* (1987) 1641–1644), but employing the corresponding methyl acetals. By this modification, $\geq 95\%$ purity is achieved in the product and $\leq 5\%$ formation of inorganic phosphate (as compared with 80% purity, 20% P_i). G. Sinerius, A. Schneider, *Diploma thesis*, University of Freiburg 1990.

[10] All products were characterized by spectral data (^1H, ^{13}C NMR, IR). In addition, satisfactory analytical data (C, H, P) were obtained for crystalline compounds.

[11] Obtained by enzymic phosphorylation of corresponding ketosugars. A. Schneider, J. Badía, W.-D. Fessner, unpublished results.

[12] J. Badía, R. Gimenez, L. Baldomá, E. Barnes, W.-D. Fessner, J. Aguilar, *J. Bacteriol.*, in press.

[13] D. J. Hupe in M. I. Page, A. Williams (Eds.): *Enzyme Mechanisms*, The Royal Society of Chemistry, London 1987, p. 324–332.

[14] A synthesis of aldoses from dialdehyde derivatives, incorporating reconstruction and formal "inversion" of stereochemical descriptors, has also been proposed: C. W. Borysenko, A. Spaltenstein, J. A. Straub, G. M. Whitesides, *J. Am. Chem. Soc. 111* (1989) 9275–9276.

Chromoionophoric Pyridinium-*N*-phenolate Betaine Dyes**

By *Christian Reichardt** and *Siamak Asharin-Fard*

The pyridinium-*N*-phenolate betaine dye **1** is solvatochromic, thermochromic, piezochromic, and halochromic, i.e. the longest wavelength absorption band in the UV-vis solution spectrum is dependent on the polarity of the solvent, the temperature of the solution, the external pressure, and the nature and concentration of an added electrolyte.[1] The exceptionally large negative solvatochromism of **1** was used to define an empirical parameter for solvent polarity, the $E_T(30)$ values.[1, 2] The application of the betaine dye **2**, which is more soluble in water, recently enabled the empirical determination of the polarity of aqueous electrolyte solutions.[3] Both betaine dyes show a *true general* (*nonspecific*) *halochromism*.[3, 4]

The extreme sensitivity of the long-wavelength absorption band in the UV-vis spectrum of **1** to a slight change in surrounding medium suggests that the introduction of crown ether substituents in the phenolate moiety of **1** would create a chromoionophoric,[5] cation-selective betaine dye displaying true halochromism.[4] A study of the UV-vis spectroscopic properties of such halochromic betaine dyes in aqueous and nonaqueous media would be interesting. We describe here the synthesis and cation-selective true halochromism of the betaine dyes **3**–**5**, which have several advantages over the chromoionophoric dyes known to date.[6]

In our improved synthesis,[7] a solution of 2,6-bis(bromomethyl)anisol and tri-, tetra-, or pentaethylene glycol and sodium hydride in THF is transformed into the crown ether substituted anisols **6** (yields 38–50%) and demethylated with lithium iodide in boiling pyridine to give **7** (yields 60–86%). The careful nitration of **7** with potassium nitrite in dilute nitric acid at room temperature to the 4-nitrophenols **8** (yields 73–86%), followed by catalytic reduction with hydrogen in methanol to the extremely oxidation-sensitive 4-aminophenols **9** (yields 93–99%) and treatment immediately thereafter with 2,4,6-triphenylpyrylium tetrafluoroborate in dichloromethane/AcOH affords (4-hydroxyphenyl)pyridinium salts (yields 80–84%), which are deprotonated practically quantitatively to the betaine dyes **3**–**5** by a basic ion-exchange resin (Amberlyst A-21) suspended in dichloromethane. The other common deprotonation with sodium methanolate in methanol does not yield salt-free betaines **3**–**5**, because of their excellent cation-complexing properties!

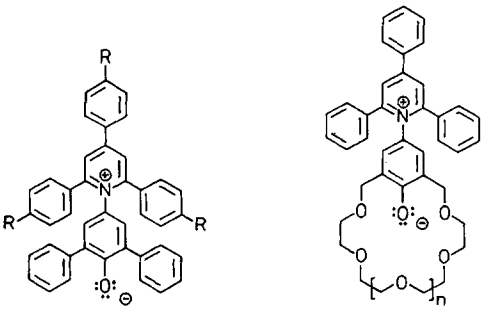

1 (R = H)
2 (R = SO_2CH_3)

3 (n=0): [15] crown-4-betaine
4 (n=1): [18] crown-5-betaine
5 (n=2): [21] crown-6-betaine

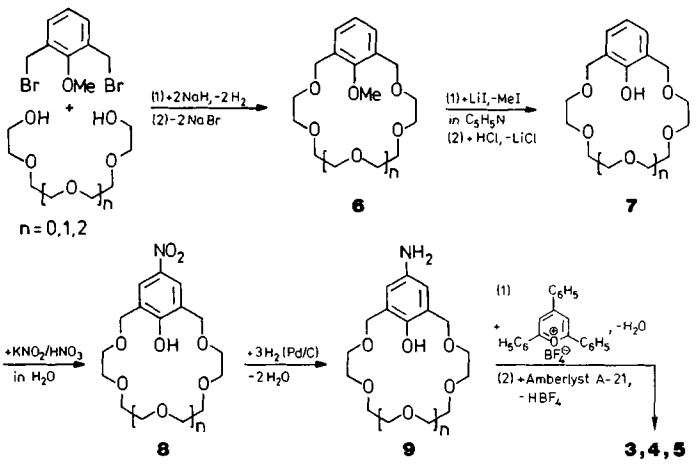

Like **1** and **2**, the dyes **3**–**5** show a pronounced negative solvatochromism. Thus changing from chloroform ($\lambda_{max} = 668$ nm) to water ($\lambda_{max} = 433$ nm), the long wavelength UV-vis absorption band of the [18]crown-5-betaine **4** undergoes a hypsochromic shift of 235 nm(!). The corresponding molar transition energies E_T[8] of the betaines **3**–**5** correlate linearly with the $E_T(30)$ values of the standard betaine **1**.

The pronounced cation-selective negative halochromism[4] of the new chromoionophoric[5] betaine dyes **3**–**5** can be demonstrated by a test-tube experiment: treatment of a ca. 10^{-3} M solution of **4** in acetonitrile with 10^{-2} M potassium iodide causes a distinct color change from violet ($\lambda_{max} = 583$ nm) to dark red ($\lambda_{max} = 529$ nm; $\Delta\lambda = -54$ nm). The long-wavelength UV-vis band of the betaines **1**–**5** is caused by an intramolecular charge-transfer(CT) transition, through which charge is transported from the phenolate to

[*] Prof. Dr. C. Reichardt, Dipl.-Chem. S. Asharin-Fard
Fachbereich Chemie und Wissenschaftliches Zentrum
für Materialwissenschaften der Universität
Hans-Meerwein-Strasse, W-3550 Marburg (FRG)

[**] Part 17 on Pyridinium *N*-phenoxide Betaines and Their Application for the Characterization of Solvent Polarities. This work was supported by the Deutsche Forschungsgemeinschaft and the Fond der Chemischen Industrie. Part 16: S. Spange, M. Lauterbach, A.-K. Gyra, C. Reichardt, *Liebigs Ann. Chem. 1991*, 323.

the pyridinium moiety.[1, 2] This band disappears on protonation of the phenolate-*O* atom. The crown-ether-mediated complexation of the phenolate moiety of **3**–**5** by suitable cations introduces a hypsochromic shift of the CT band, because the $O^{\ominus}/M^{\oplus}$ interaction increases the ionization energy of the electron donor moiety, while the electron affinity of the electron acceptor moiety is unaffected.

Systematic variation of the cation ($Na^{\oplus}$, $K^{\oplus}$, $Rb^{\oplus}$, $Cs^{\oplus}$, and $nBu_4N^{\oplus}$ as iodides) and anion ($F^{\ominus}$, $Cl^{\ominus}$, and $I^{\ominus}$, as potassium salts) in the solvents methanol, acetonitrile, and propylene carbonate (ca. 10^{-3} M betaine + 10^{-2} M salt) shows that the halochromism of **3**–**5** is selective for cations but hardly dependent on the anion. With tetra-*n*-butylammonium iodide in methanol or acetonitrile, a significantly smaller, but for these three compounds practically equally large, hypsochromic band shift is obtained for all **3**–**5** because of a nonspecific general salt effect (general halochromism[3]).

It follows from the dependence of the λ_{max} shifts of **3**–**5** in methanol on the size of the alkali metal ion of the iodide salt added (Fig. 1) that [15]crown-4-betaine **3** complexes preferably with $Na^{\oplus}$, [18]crown-5-betaine **4** with $K^{\oplus}$, and [21]crown-6-betaine **5** with $Cs^{\oplus}$. Treatment of the $Na^{\oplus}$-

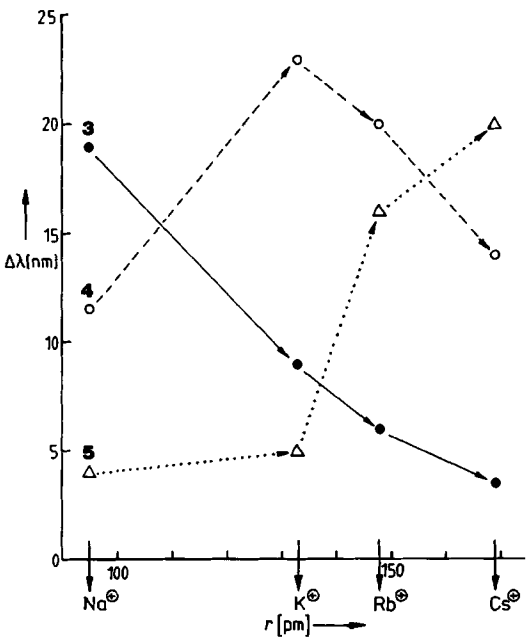

Fig. 1. Halochromism of **3**–**5** in methanol at 25 °C as a function of the Pauling cation radius *r* of the alkali metal iodides NaI, KI, RbI, and CsI (betaine concentration ca. 10^{-3} M; salt concentration 10^{-2} M). $\Delta\lambda = \lambda_{max}$(free of salt) – λ_{max}(with salt).

selective **3** in methanol with a mixture of Na, K, Rb, and Cs iodide, causes a hypsochromic λ_{max} shift as if NaI alone were added. On addition of lithium and alkaline earth metal salts to solutions of **3**–**5** in methanol or acetonitrile, the long-wavelength halochromic CT absorption band disappears, which corresponds to a more intense cation complexation by the phenolate moiety similar to the effect of protonation (formation of contact ion pairs).

Conclusion: The crown-ether-substituted betaine dyes **3**–**5** show, in contrast to several other chromoionophores,[6] a cation-selective negative halochromism,[4] which is manifested as a hypsochromic shift of the long-wavelength CT absorption band of the pyridinium-*N*-phenolate chromophore on addition of salt. As this absorption band lies in the visible spectral region, the cation-induced color changes can be followed easily by eye, which suggests an application of these new chromoionophores as cation indicators.

Experimental Procedure

The spectra were recorded on Hitachi U-3410 (UV/vis), Bruker AC-300 (^1H and ^{13}C NMR), and Varian MAT 711 (MS-FD) spectrometers. All compounds gave correct elemental analyses and were completely characterized by spectroscopy.

3: 1.00 g (3.1 mmol) of **8** (n = 0)[7] in 40 mL anhydrous methanol is reduced with hydrogen at normal pressure (H_2 consumption ca. 230 mL) after addition of 40 mg palladium on activated carbon (0.1 g per g carbon). Removal of the catalyst by filtration and the solvent by distillation under inert gas (N_2) affords 0.90 g (99%) of the aminophenol **9** (n = 0) as bright yellow crystals, which darken immediately on oxidation in air and therefore must be treated further without delay: To a suspension of 0.81 g (2.00 mol) of 2,4,6-triphenylpyrylium tetrafluoroborate [9] in 5 mL dried, N_2-saturated dichloromethane is added, while stirring under N_2, 0.90 g (3.10 mmol) of **9** (n = 0). After 1.5 h stirring at room temperature, 0.10 mL glacial acetic acid is added. The mixture is stirred for 4 h, whereupon 300 mL diethylether is added dropwise, the bright yellow precipitate filtered off, dried over P_4O_{10}, and precipitated from a solution in 5 mL acetone by addition of 15 mL diethylether. 1.10 g of "protonated" **3** (82%, **3**·HBF4) as bright yellow, finely crystalline powder (m.p. 207–209 °C) was obtained, whose composition according to elemental analysis still included 0.5 equiv water. MS(FD): *m/z* 574 [$M^{\oplus}$ – BF_4, 100%]. UV/vis(acetonitrile): λ_{max}[nm](ε)=306(32580). A solution of 0.50 g (0.75 mmol) **3**·HBF_4 in 10 mL dried dichloromethane was treated with 2.00 g Amberlyst A-21 (Serva) and stirred for 3.5 h at room temperature. The dark blue solution was filtered, the solvent distilled off, and the residue dried at 35 °C/0.01 Torr over P_4O_{10} in a drying pistol. Black-red, very hygroscopic crystals of **3** (0.41 g, 97%) were obtained (m.p. 135–139 °C), whose composition according to elemental analysis still includes 1 mol dichloromethane. UV/vis(acetonitrile): λ_{max}[nm](ε) = 581(330), 305(29920).

The betaine dyes **4** and **5** were prepared analogously.

Received: November 30, 1990 [Z4300 IE]
German version: Angew. Chem. 103 (1991) 614

[1] C. Reichardt, E. Harbusch, R. Müller in I. Bertini, L. Lunazzi, A. Dei (Eds.): *Advances in Solution Chemistry*, Plenum, New York 1981, p. 275–293.

[2] a) C. Reichardt, *Angew. Chem. 91* (1979) 119; *Angew. Chem. Int. Ed. Engl. 18* (1979) 98; b) *Solvents and Solvent Effects in Organic Chemistry*, 2. Ed., VCH Verlagsgesellschaft, Weinheim 1988, p. 287 ff, 363 ff.

[3] C. Reichardt, G. Schäfer, P. Milart, *Collect. Czech. Chem. Commun. 55* (1990) 97.

[4] Following a proposal of *A. von Baeyer* and *V. Villiger* (*Ber. Dtsch. Chem. Ges. 35* (1902) 1189), halochromism means the color change of a dissolved compound on addition of acid or base during which a chemical reaction transforms a colorless compound into a colored one. In contrast to this trivial halochromism, the true halochromism of dyes like **1** and **2** refers to a color change on addition of an electrolyte to the dye solution not accompanied by a chemical change. We have suggested the term "negative (positive) true halochromism" for a hypsochromic (bathochromic) shift of the UV/vis absorption band of a dissolved substance on increasing electrolyte concentration, when this shift is *not* caused by a chemical change of the chromophore: C. Reichardt, E. Harbusch-Görnert, G. Schäfer, *Liebigs Ann. Chem. 1988*, 839; see also [3].

[5] Chromoionophores are dye molecules which contain chromophoric and ionophoric units. Such an ionophore can complex ions with concomittant color change: a) J. P. Dix, F. Vögtle, *Chem. Ber. 114* (1981) 638 (cf. footnote 2); b) A. Villiger, W. E. Morf, W. Simon, *Helv. Chim. Acta 66* (1983) 1078. Ionophores are neutral macrocyclic molecules (or parts of molecules) which form complexes with ions, and as carriers transport them through biological membranes: B. C. Pressman: "Alkali Metal Chelators – the Ionophors" (*Inorg. Biochem. Vol. 1* (1973) 203). This term was chosen somewhat unfortunately, because previously ionophores referred to ionic compounds which—in contrast to ionogenes—consist of ions in the crystal, in the melt, and in solution: R. Fuoss, *J. Chem. Educ. 32* (1955) 527.

[6] a) M. Takagi, K. Ueno, *Top. Curr. Chem. 121* (1984) 39; b) E. Weber, *Kontakte (Darmstadt) 1984*, No. 1, p. 26; c) H.-G. Löhr, F. Vögtle, *Acc. Chem. Res. 18* (1985) 65; d) T. Kaneda, *Yuki Gosei Kagaku Kyokaishi 46* (1988) 96; *Chem. Abstr. 108* (1988) 160414q.

[7] C. M. Browne, G. Ferguson, M. A. McKervey, D. L. Mulholland, T. O'Connor, M. Parvez, *J. Am. Chem. Soc. 107* (1985) 2703.

[8] *T*ransition *E*nergy E_T[kcal mol^{-1}] = $hc\tilde{\nu}N_A$ = 28591/λ_{max}[nm] [1, 2].

[9] K. Dimroth, C. Reichardt, K. Vogel, *Org. Synth. Collect. Vol. 5* (1973) 1135.

Stoichiometric Mono *N*-Functionalization of Tetraazamacrocycles via Phosphoryl-Protected Intermediates**

By *Ayoub Filali, Jean-Jacques Yaouanc,* and *Henri Handel**

Owing to the cost of polyazacrowns, a stoichiometric and direct method to introduce mono *N*-functionalization is needed.[1] During the past ten years, some phosphorous P^{III}- and P^{V}-containing tetraazamacrocycles have been reported,[2] but they have surprisingly not yet found any synthetic application. Our previous studies on selective mono *N*-alkylation of tetraazamacrocycles[3] prompted us to consider the P^{V}-phosphorylated macrocycles as potential precursors of monofunctionalized tetraazamacrocycles, since they could be seen as cyclic analogues of hexamethylphosphoric triamide containing, besides three inert nitrogen atoms, a free nitrogen atom available for further reaction.

We now report the reaction of these phosphorylated macrocycles with some electrophiles RX giving rise to mono *N*-functionalized ligands after removal of the phosphoryl protection, as depicted in Scheme 1.

The polyaminophosphoranes **1** were obtained according to a previously described reaction by transaminating hexamethylphosphoric triamide with the appropriate tetraazacycloalkane. As noted by *Atkins* and *Richman*[2a] these compounds exist as P^{III}/P^{V} tautomers. After oxidation with CCl_4, the resulting phosphonium salts **2** were hydrolyzed with sodium hydroxide to yield quantitatively the oxides **3**. The action of a suitable electrophile gave finally, after hydrolysis of the intermediate **4**, the desired mono *N*-substituted macrocycles **5**.

In general, the reaction of alcohols with the phosphonium salts **2** leads to a stable, distillable pentacoordinated alkoxyphosphorane **6**;[2b] nevertheless, in the special case of activated alcohols like benzyl, allyl, or propargyl alkohols we observed that **6** isomerized to the *N*-alkylated intermediates **4**. Using this principle we alkylated a series of tetraazamacrocycles (Table 1). When applied to less symmetrical azamacrocycles (for instance isocyclam "3322"), this method led to a mixture of regioisomers which are not easily separable by usual techniques. It is thus better suited to symmetrical macrocycles.

This easy-to-run process constitutes a powerful and stoichiometric method of preparing the mono *N*-functionalized tetraazamacrocycles.

Table 1. Mono *N*-functionalization of tetraazamacrocycles.

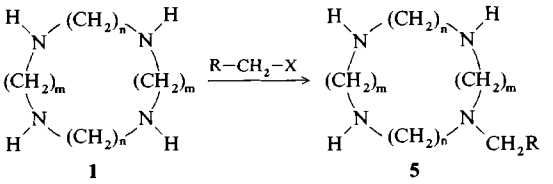

1 **5**

1	n	m	R	X	Yield [%]	$\delta(^1H)$ [a]	m/z ($M^{\oplus}$)
cyclen (2222)	2	2	C_6H_5	Br	90	3.7	262
			C_6H_5	OH	80		
cyclam (2323)	2	3	C_6H_5	Br	96	3.6	290
			C_6H_5	OH	92		
			$H_2C=CH$	Br	80	3.1	240
			$H_2C=CH$	OH	75		
			$HC\equiv C$	Br	92	3.5	238
			$HC\equiv C$	OH	83		
			Fc [b]	Cl	80	3.6	384
			Fc [b]	OH	85		
			$C_6H_5CH_2$	Br	86	[c]	304
			$C_6H_5(CH_2)_2$	Br	75	[c]	318
			n-$C_{11}H_{23}$	Br	75	[c]	368
"3333"	3	3	C_6H_5	Br	90	3.5	318
			C_6H_5	OH	80		
"3434"	3	4	C_6H_5	Br	92	3.5	346

[a] Signal of the exocyclic N-CH_2 group. [b] Fc = ferrocenyl. [c] Masked by the endocyclic N-CH_2 signal.

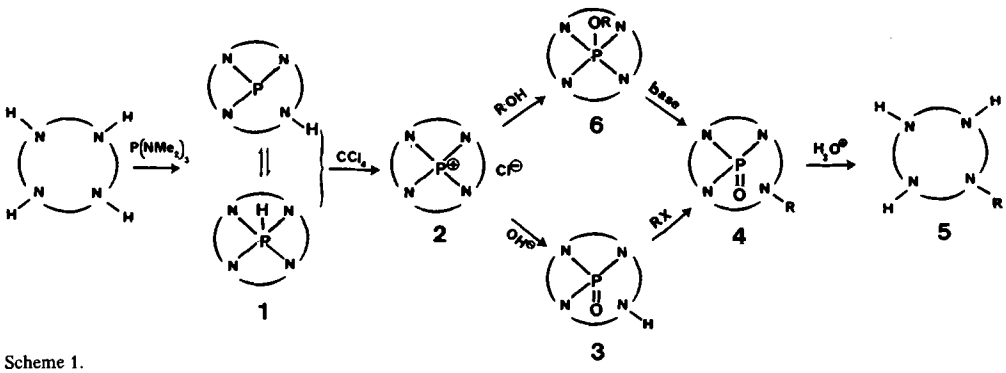

Scheme 1.

Experimental Procedure

General Procedure

The tetraazamacrocycle **1** (1.0 mmol) in dry toluene (30 mL) was refluxed under nitrogen with hexamethylphosphoric triamide (1.0 mmol) until dimethylamine evolution ceased. After cooling to 0–5 °C, excess CCl_4 was added upon which a white solid separated. The solvent was removed under reduced pressure and the remaining crude phosphonium salt **2** treated with 2 N sodium hydroxide (5 mL). The aqueous phase was extracted with $CHCl_3$ (2 × 50 mL); the combined organic phases were dried and finally concentrated to dryness in vacuo giving the crude phosphorylated tetraazamacrocycle **3** pure enough for the next reaction.[4]

To a solution of **3** (1.0 mmol) in dry DMF (20 mL) was added an excess of dry Na_2CO_3 and the mixture heated to 100 °C. The alkylating agent (1.0 mmol) was

[*] Prof. H. Handel, Dr. J. J. Yaouanc, A. Filali
Unité de Recherche Associée au CNRS N°322
Chimie, Electrochimie et Photochimie Moléculaires
Faculté des Sciences et Techniques
6, avenue le Gorgeu, F-29287 Brest (France)

[**] This work was supported by the Centre National de la Recherche Scientifique.

introduced by syringe and the temperature maintained at 100 °C for 2 hours. After cooling to room temperature, the solvent was removed in vacuo. The resulting residue was taken up in 3 N HCl (10 mL) and refluxed for 10 hours. The pH was then carefully adjusted to 12 with NaOH pellets. After extraction with $CHCl_3$ (2 × 50 mL), drying of the combined organic phases, and evaporation of the solvent, the pure mono *N*-alkylated tetraazamacrocycle was obtained, generally as an oily residue.

Modified Procedure: direct alkylation of the phosphonium salt **2**

The suspension of **2** in toluene was treated with the required alcohol (1.0 mmol) (Scheme 1), the solvent was removed and replaced by dry DMF (20 mL), an excess of Na_2CO_3 was added, and the mixture was heated at 100 °C for 2 hours. The subsequent work-up was as described above. All the mono *N*-alkylated tetramines gave satisfactory IR, MS, and ^1H NMR data.

Received: November 12, 1990 [Z 4277 IE]
German version: *Angew. Chem. 103* (1990) 563

[1] a) K. E. Krakowiak, J. S. Bradshaw, R. M. Izatt, *J. Org. Chem. 55* (1990) 3364; b) T. A. Kaden in F. Vögtle, F. Weber (Eds.): *Host Guest Complex Chemistry Vol. III*, Springer, Berlin 1984, p. 157; c) I. M. Helps, D. Parker, T. R. Morphy, J. Chapman, *Tetrahedron 45* (1989) 219.

[2] a) T. J. Atkins, J. E. Richman, *Tetrahedron Lett. 52* (1978) 5149; b) J. E. Richman, J. J. Kubala, *J. Am. Chem. Soc. 105* (1983) 749; c) J. E. Richman, R. B. Flay, O. D. Gupta, *ACS. Symp. Ser. 171* (1981) 271; d) J. M. Dupart, A. Grand, J. G. Riess, *J. Am. Chem. Soc. 108* (1986) 1167; e) F. Bouvier, J. M. Dupart, A. Grand, J. G. Riess, *Inorg. Chem. 26* (1987) 2090.

[3] H. Handel, H. Chaumeil, European patent, 88 400 839.2. (1988), CNRS.

[4] The P=O derivative of "3434" exhibits a ^{31}P NMR signal at $\delta = -18.4$; for other phosphorylated macrocycles, see ref. [2c].

Benzene Bis(diazocyanides)—the First Acceptors of the Inverse Wurster Type for Conductive Organic Materials**

By *Hartmut Almen, Thomas Bauer, Siegfried Hünig,* Vladimir Kupčik, Uwe Langohr, Tobias Metzenthin, Klaus Meyer, Harald Rieder, Jost Ulrich von Schütz, Ekkehart Tillmanns,* and *Hans Christoph Wolf*

Tetracyanoquinodimethane(TCNQ)[1] and *N,N'*-dicyanoquinonediimine(DCNQI)[2] and derivatives thereof (**1** and **2** respectively) have proved to be the most important organic electron acceptors for charge-transfer(CT) complexes or radical anion salts with electrical conductivity. Both types of compound form two-stage reversible redox systems and thus belong to the Wurster type, in which the defined acceptor end groups are connected to the six membered π ring system in such a way that the oxidized stage has quinone character.[3] We wondered whether the as yet unused two-stage redox systems of inverse Wurster type, that is, with aromatic oxidized stage[3] (see Scheme 2), is also suitable as acceptor for conductive organic materials.

The benzene-1,4-bis(diazocyanides) **3** (dicyanazobenzene [DCNAB]) appeared to be promising candidates, since the

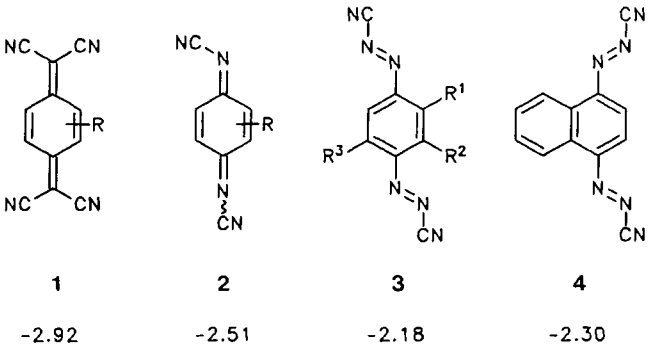

Scheme 1. Organic electron acceptors and their LUMO energies calculated with MNDO-AM1 for the parent compounds.

LUMO energy as calculated by MNDO-AM1[4] (Scheme 1) of the almost planar structure lies in a similarly favorable range to the tried and tested compounds **1** and **2**.[5] It was, however, doubtful whether the orbital symmetry of **3**, which is vastly different from that of the quinones, would allow the stacking in the crystal essential for conduction.

We now use the first examples, which also include naphthalene-1,4-bis(diazocyanide) **4**, to show that these compounds, besides having spectroscopically detectable radical anions[6], not only form fully reversible two stage redox systems of the inverse Wurster type,[3] but are also potent acceptors in conductive CT complexes and radical anion salts.[7]

Table 1 shows that the redox potentials of **3** and **4** lie in the same region as those of TCNQ, **1**(R = H) and DCNQI, **2** (R = H). The semiquinone formation constants of lg K_{SEM} =

Table 1. Redox potentials E_1 and E_2 determined by cyclic voltammetry (Pt electrode vs. Ag/AgCl/CH_3CN, electrolyte nBu$_4$NBF$_4$) and semiquinone formation constants lg K_{SEM} of **1**–**4** (see also Scheme 2.)

	R^1	R^2	R^3	E_1 [V]	E_2 [V]	lg K_{SEM}
3a	Me	H	Me	− 0.15	+ 0.20	5.92
3b	H	H	H	− 0.15	+ 0.22	6.10
3c	Cl	H	Cl	+ 0.07	+ 0.47	6.82
4				− 0.01	+ 0.32	6.49
1 (R = H) [5]				− 0.28	+ 0.39	11.42
2 (R = H) [5]				− 0.25	+ 0.39	10.75

5.92–6.82 are still very large, although a factor of ca. 10^4 smaller than in TCNQ and DCNQI. That is predictable, because the Coulomb repulsion in the longer systems of **3** and **4** (they contain two more atoms) has less effect on the gain of electrons.[8] Surprisingly, a higher acceptor capacity (LUMO = 2.30 eV) is calculated for **4** than for **3b**, which is also reflected in a higher reducibility (E_2 = + 0.32 V). The opposite is true for the transition from DCNQI to the corresponding naphthalene derivate.[5]

Furthermore, the MNDO-AM1 calculations show that during the reduction (OX → SEM → RED) **3b** indeed assumes progressively a quinoid structure. Thus the exocyclic C_{aryl}–N single bond becomes shorter on gain of electrons (144 (OX) via 138 (SEM) to 133 pm (RED)); the bond between C2 and C3 also shortens (139 (OX), 137 (SEM), 135 pm (RED)). The corresponding experimentally determined bond lengths in DCNQI are 130 (C–N) and 134 pm (C=C).[9]

On combining solutions of **3** or **4** with solutions of tetrathiofulvalenes(TTF) or tetramethyltetraselenafulvalenes-

[*] Prof. Dr. S. Hünig, Dipl.-Chem. T. Metzenthin
Institut für Organische Chemie der Universität
Am Hubland, W-8700 Würzburg (FRG)
Dipl.-Phys. U. Langohr, Dipl.-Phys. K. Meyer, Dipl.-Phys. H. Rieder, Dr. J. U. von Schütz, Prof. Dr. H. C. Wolf
3. Physikalisches Institut der Universität Stuttgart
Dipl.-Min. H. Almen, Dipl.-Min. T. Bauer, Prof. Dr. E. Tillmanns
Mineralogisches Institut der Universität Würzburg
Prof. Dr. V. Kupčik
Mineralogisch-Kristallographisches Institut der Universität Göttingen

[**] This work was supported by the Volkswagen-Stiftung and the Fonds der Chemischen Industrie. *T. Metzenthin* thanks the Fonds der Chemischen Industrie for a study grant.

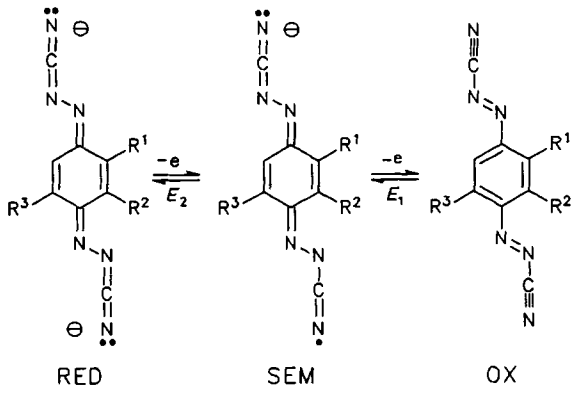

Scheme 2. Redox systems **3** and **4**.

(TMTSF), black CT complexes crystallize, the majority of which have a high powder conductivity (Table 2), so that they compare well with the CT complexes of TCNQ[10] and DCNQI.[11]

Table 2. Powder conductivities σ of CT complexes with **3** or **4** as acceptor.

Acceptor	Donor [a]	m:n [b]	σ [S cm^{-1}]
3a	TTF	1:1	120 [c]
3b	TTF	1:1	3×10^{-1}
3b	TMTTF	1:1	3×10^{-3} [c]
3c	DBTTF	1:2	2×10^{-5}
3c	TTF	1:1	2×10^{-4}
3c	TMTTF	1:2	1×10^{-2}
3c	TMTSF	1:2	4×10^{-2}
4	TTF	1:1	1
4	TMTTF	1:1	1

[a] TMTTF = tetramethyltetrathiafulvalene, DBTTF = dibenzotetrathiafulvalene. [b] Ratio Acceptor: Donor derived from elemental analysis. [c] Single crystal conductivities.

Thus segregated donor and acceptor stacks can also be assumed for the new CT complexes.[12] This characteristic arrangement for conductive CT complexes was confirmed by a crystal structure analysis of the **3a**/TTF complex (for which

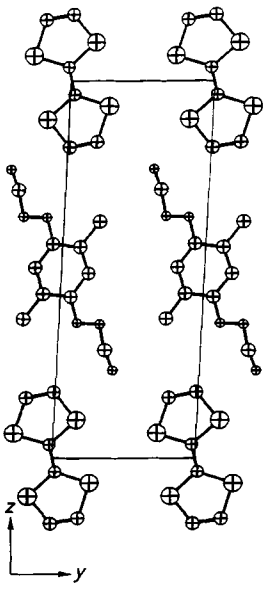

Fig. 1. Structure of **3a**/TTF in the crystal; projection along [100]; space group $P\bar{1}$, $a = 3.76$, $b = 6.54$, $c = 18.12$ Å, $\alpha = 87.0$, $\beta = 85.8$, $\gamma = 87.7°$.

$\sigma = 120$ S cm^{-1}).[13] A preliminary picture could be obtained by synchrotron–X-ray radiation. Figure 1 shows the projection onto the yz plane. Although the poor quality of the crystals, and therefore of the crystal data, has not yet enabled the determination of the atomic coordinates in the x direction with satisfactory accuracy, the small lattice constant of 3.76 Å allows only one molecular unit per unit cell, so that the separate arrangement of donor and acceptor stacks is assured.

The temperature dependence of the conductivity of this compound (Fig. 2, top) corresponds with that of a metal-like semiconductor with a small band gap of $\Delta E \approx 40$ meV. This value results from the charge carrier concentration C, which could be followed in the electron spin resonance experiments (Fig. 2, bottom) down to very low temperatures. The small

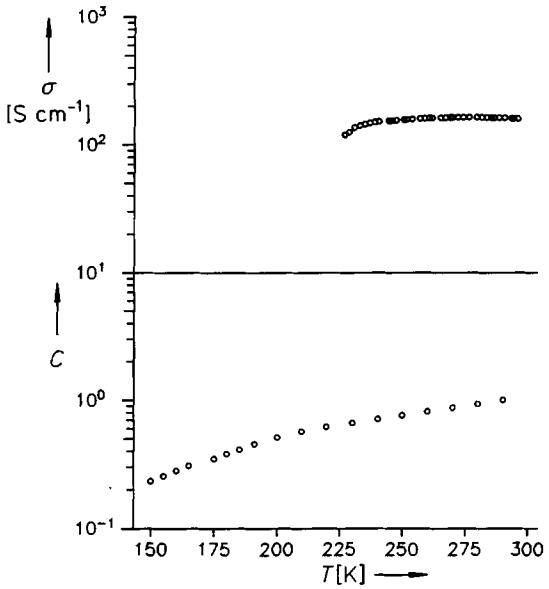

Fig. 2. Top: Temperature dependence of the single crystal conductivity of **3a**/TTF. All crystals break at $T < 215$ K. Bottom: Normed spin carrier concentration $C = \chi T/300\chi_{300K}$ as function of the temperature.

ESR signal width of 2 Gauss at 300 K is a strong indication that the **3a** stack is the dominant factor in conductivity, because when the charge carriers in such complexes come into contact with sulfur atoms of the TTF stack, the signal widths are usually at least 6–100 Gauss.[14]

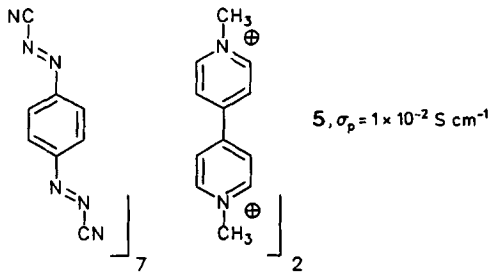

Example **5** shows that conductive radical ion salts can also be formed from the new acceptor types. This proves that acceptors of the inverse Wurster type can assume the role of those of normal Wurster type used till now.[15] These results have prompted us to synthesize further derivatives of **3** and to test them in conducting materials.

Experimental Procedure

Reaction of **3a** with TTF: 21 mg (100 μmol) **3a** in a mixture of 0.5 mL dry dichloromethane and 0.5 mL acetonitrile is treated at room temperature with a solution of 30 mg (147 μmol) TTF in 1 mL acetonitrile. Immediately a dark precipitate forms. After 45 min at 0 °C, filtration and drying over silica gel yields 36 mg (86%) green-golden needles. M.p. 146 °C (dec.). IR(KBr): $\nu = 2100\ cm^{-1}$. UV/vis (CH_3CN): $\lambda_{max}(\lg \varepsilon)$ = 226(sh, 3.989), 321(4.256), 360(4.416), 572 nm(2.739).

Received: December 7, 1990 [Z4312 IE]
German version: *Angew. Chem. 103* (1991) 608

CAS Registry numbers:
3a, 132556-13-2; **3a** · TTF, 132566-16-6; **3b**, 132619-62-6; **3b** · TTF, 132619-63-7; **3b** · TMTTF, 132619-64-8; **3c**, 132566-14-4; **3c** · DBTTF, 132566-17-7; **3c** · TTF, 132590-84-2; **3c** · TMTTF, 132590-85-3; **3c** · TMTSF, 132566-18-8; **4**, 132566-15-5; **4** · TTF, 132566-19-9; **4** · TMTTF, 132566-20-2.

[1] a) J. Ferraris, D. O. Cowan, V. Walatka, Jr., J. H. Perlstein, *J. Am. Chem. Soc. 95* (1973) 948; b) D. S. Acker, W. R. Hertler, *ibid. 84* (1962) 3370; c) L. B. Coleman, M. J. Cohen, D. J. Sandman, F. G. Yamagishi, A. F. Garito, A. J. Heeger, *Solid State Commun. 12* (1973) 1125.
[2] S. Hünig, *Pure Appl. Chem. 62* (1990) 395; P. Erk, S. Hünig, *Adv. Mater.*, in press.
[3] K. Deuchert, S. Hünig, *Angew. Chem. 90* (1978) 927; *Angew. Chem. Int. Ed. Engl. 17* (1978) 875.
[4] a) M. J. S. Dewar, E. G. Zoebisch, H. F. Healy, J. J. P. Stewart, *J. Am. Chem. Soc. 107* (1985) 3902; b) QCPE Program No. 527.
[5] A. Aumüller, S. Hünig, *Liebigs Ann. Chem. 1986*, 165.
[6] I. Ya. Kachkurova, L. D. Ashkinadse, U. Kh. Shamsutdinova, L. A. Kazitsyna, *Zh. Org. Khim. 23* (1987) 1831.
[7] Presented in part at ICSM '90 (*Int. Conf. Sci. Technol. Synth. Met.*), September 1990, Tübingen.
[8] a) S. Hünig, D. Scheutzow, P. Cársky, R. Zahradnik, *J. Phys. Chem. 75* (1971) 335; b) S. Hünig, H. Berneth, *Top. Curr. Chem. 92* (1980) 1–44.
[9] G. D. Andreetti, S. Bradamante, P. C. Bizzarri, G. A. Pagani, *Mol. Cryst. Liq. Cryst. 120* (1985) 309.
[10] R. C. Wheland, J. L. Gillson, *J. Am. Chem. Soc. 98* (1976) 3916.
[11] A. Aumüller, P. Erk, H. Meixner, S. Hünig, J. U. von Schütz, H.-P. Werner, *Liebigs Ann. Chem. 1987*, 997.
[12] A CT complex with mixed donor/acceptor stacks was also obtained E. Tillmanns, S. Hünig, T. Metzenthin, H. Rieder, J. U. von Schütz, H. C. Wolf, *Acta Crystallogr. Sect. C.*, in press.
[13] S. Hünig, P. Erk, E. Günther, H. Meixner, T. Metzenthin, J. U. von Schütz, M. Bair, H.-J. Groß, U. Langohr, S. Söderholm, H.-P. Werner, H. C. Wolf, E. Tillmanns, *Synth. Met.*, in press.
[14] J. Tomkiewicz, *Phys. Rev. B 19* (1979) 4038.
[15] In 1,4-bis(tricyanovinyl)benzene a two-stage redox system of the inverse Wurster type is also present, whose redox potentials are similar to those of compound **3**. Neither stoichiometry nor physical properties are known for its TTF salt, which exists in at least two phases: F. Wudl, P.-M. Allemand, P. Delhaes, Z. Soos, H. Hinkelmann, *Mol. Cryst. Liq. Cryst. 171* (1989) 179–182.

A New Route to Aromatic Diazocyanides**

By *Siegfried Hünig** and *Tobias Metzenthin*

Benzene-1,4-bis(diazocyanide) and naphthalene-1,4-bis(diazocyanide) belong, as the previous communication shows,[1] not only to the reversible two-stage redox systems, but also to the first acceptors of the inverse Wurster type for conductive organic materials.[2] We therefore required a flexible synthesis route for this class of compounds.

The problem appeared to be very simple to solve along the lines of the classical synthesis of arene diazocyanides **1** according to *Hantzsch* et al.[3] (Eq. (a)). Many compounds have been prepared in this way, especially for the study of *syn/anti* isomerism.[4]

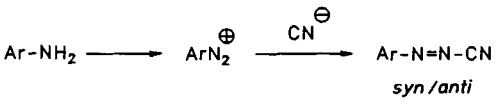

(a)

1

The arene bis(diazocyanides) **4** could indeed be synthesized from some *p*-phenylenediamines **2** via the bis(diazonium) salts **3**[5] (Eq. (b)). It was, however, necessary to isolate the labile and occasionally explosive salts **3** and to extract the diazocyanides **4**, which form in the reaction with cyanide, continuously into chloroform in order to suppress a further addition of cyanide at the nitrile group.[4a,d] Even under these conditions the yields are only 10–50%. A more serious disadvantage is that some bis(diazonium) salts (e.g. **3d**, $R^1 = R^3 = Me$; $R^2 = R^4 = H$) can be isolated only in impure state or sometimes not at all.

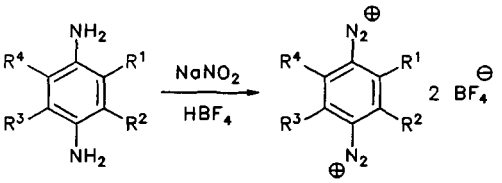

2 **3**

(b)

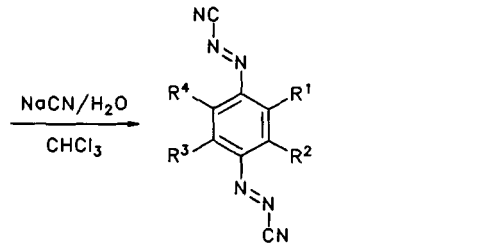

4

a, R^1-R^4 = H; **b**, $R^2 = R^4 = H$, $R^1 = R^3 = Cl$; **c**, $R^1R^2 = (CH)_4$, $R^3 = R^4 = H$

Therefore we searched for a synthesis of **4** in which the isolation of the bis(diazonium) salts was unnecessary and the diazocyanide function could be formed without further reaction with excess cyanide. We describe now a general route to the diazocyanides **1**, which can also be applied in the case of the difunctional derivatives **4**[6] without these difficulties.

This route requires first the nitrosation of *N*-aryl amides **5** to the *N*-nitroso derivatives **6** by known methods,[7] whose rearrangement to the *O*-aryldiazo esters **7** was studied thoroughly, in particular by *Huisgen* et al.[8] The thermal rearrangement in the presence of trimethylsilylcyanide in an organic solvent affords the desired diazocyanides **1**, in good yields after their easy separation from the trimethyl esters **8** (e.g., for 4-chlorobenzenediazocyanide,[4a] 60% after sublimation; see Scheme 1).

The conversion **7** → **1** is apparently very rapid, because the competing intramolecular reaction of the methyl group in an *o*-substituted arene, which leads smoothly to indazoles, is not observed. (The same is true for **10** → **4**.)

[*] Prof. Dr. S. Hünig, Dipl.-Chem. T. Metzenthin
Institut für Organische Chemie der Universität
Am Hubland, W-8700 Würzburg (FRG)

[**] This work was supported by the Volkswagen-Stiftung and the Fonds der Chemischen Industrie.

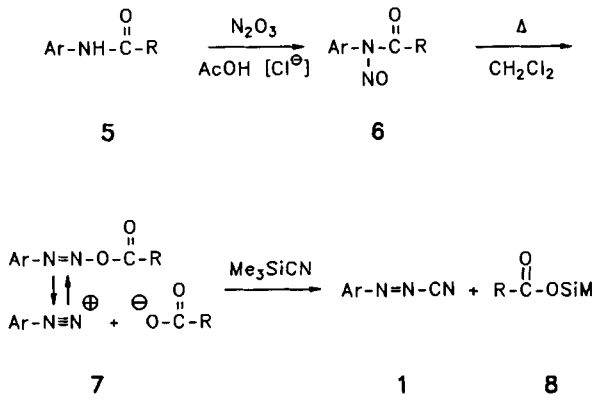

Scheme 1. Ar = C_6H_5; *p*-ClC_6H_4, R = CH_3.

The extension of steps **5** → **7** to the bifunctional derivatives failed at first because of the low solubility of the bis(acylamines) **9**. Whereas the solubilities when R = Me, Et, *n*Pr, *i*Bu, and *t*Bu hardly differ, the bis(acylamines) **9** with R = CH_2OMe were very soluble and could be nitrosated in the usual way in 70–95% yield (Scheme 2). The methoxyacetyl residue gave the added advantage that the dinitroso derivatives **10** then could easily be handled at room temperature and rearranged only in boiling dichloromethane. The high temperatures involved cause the bis(diazocyanides) **4** to precipitate exclusively as *trans* isomers.

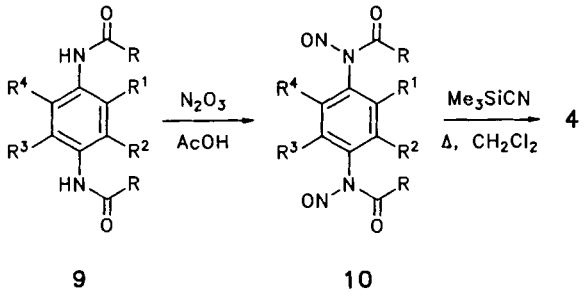

Scheme 2. Synthesis of bis(diazocyanides) **4**. Optimal R: CH_2OMe. Yields: 62% **4c**, 68% **4d**.

The proposed route for the introduction of the diazocyanide function into arenes is thus a clear improvement over the classical method, at least for the difunctional derivatives **4**. At the same time it represents a new trapping reaction for the *O*-diazoesters formed by rearrangement.

Experimental Procedure

4d: Into a heated flask is placed a solution of 1.50 g(4.43 mmol) **10d** [7,10] in 80 mL dried dichloromethane and 20 mL trimethylsilylcyanide (Aldrich). The mixture is heated in a fume hood for 4 h at 50 °C, whereupon the solvent and trimethylsilyl cyanide is distilled off at 1 torr. The residue is dried for 0.5 h at 0.1 Torr, taken up in dichloromethane, and quickly filtered over silica gel (0.032–0.063 mm). The eluant is evaporated to dryness and the product dried under vacuum (oil pump). Yield: 635 mg deep red crystals of **4d**, m.p. 171 °C(dec.). – IR(KBr): $\tilde{\nu}$ [cm^{-1}] = 3090(CH), 3030(CH), 2180 (C≡N), 1475, 1380, 1360, 1300, 1150, 910. UV(CH_3CN): λ_{max} [nm] (lgε) = 208 (4.23), 227 (sh, 3.88), 361 (4.44). ^1H NMR (200 MHz, $CDCl_3$): δ = 2.72 (s, 6H, CH_3), 7.58 (s, 2H, H_{aryl}). ^{13}C NMR(50.3 MHz, $CDCl_3$): δ = 17.39 (q, CH_3), 115.20 (s, CN), 117.26 (d, C-3,6), 141.31 (s, C-2,5), 155.23 (s, C-1,4).

Received: December 7, 1990 [Z4313 IE]
German version: *Angew. Chem. 103* (1991) 610

[1] H. Almen, T. Bauer, S. Hünig, V. Kupčik, U. Langohr, T. Metzenthin, K. Meyer, H. Rieder, J. U. von Schütz, E. Tillmanns, H. C. Wolf, *Angew. Chem. 103* (1991) 608; *Angew. Chem. Int. Ed. Engl. 30* (1991) 561.
[2] K. Deuchert, S. Hünig, *Angew. Chem. 90* (1978) 927; *Angew. Chem. Int. Ed. Engl. 17* (1978) 875.
[3] A. Hantzsch, O. W. Schulze, *Ber. Dtsch. Chem. Ges. 28* (1895) 666.
[4] a) M. F. Ahern, A. Leopold, J. R. Beadle, G. W. Gokel, *J. Am. Chem. Soc. 104* (1982) 548; b) T. Ignasiak, J. Suszko, B. Ignasiak, *J. Chem. Soc. Perkin Trans. 1 1975*, 2122; c) V. Sterba in S. Patai (Hrsg.): *The Chemistry of Diazonium- and Diazogroups*, Wiley, New York 1978, p. 91; d) R. Pütter in *Methoden Org. Chem. (Houben-Weyl) 4th Ed. Vol. 10/3*, Thieme, Stuttgart 1965, p. 595.
[5] According to the synthesis of **4a**: I. Ya. Kachkurova, L. D. Ashkinadse, M. Kh. Shamsutdinova, L. A. Kazitsyna, *Zh. Org. Khim. 23* (1987) 1831.
[6] All new compounds were characterized by IR, ^1H NMR, ^{13}C NMR, and mass spectra, and elemental analyses..
[7] Cf. for example. J. W. Haworth, D. H. Hey, *J. Chem. Soc. 1940*, 361. Here the synthesis of *N,N'*-(1,4-phenylene)bis(*N*-nitrosoacetamide) is described.
[8] R. Huisgen, L. Krause, *Justus Liebigs Ann. Chem. 574* (1951) 157.
[9] R. Huisgen, H. Nakaten, *Justus Liebigs Ann. Chem. 573* (1951) 181.
[10] Synthesis of **10d** according to [7]; yellow crystalline powder, which explodes under strong heating. IR(KBr): $\tilde{\nu}$ [cm^{-1}] = 3010, 2980, 2950, 2920, 2820, 1730, 1530, 1400, 1290, 1115, 1055, 935, 890, 770, 660. ^1H NMR($CDCl_3$): δ = 1.87 (s, 6H, CCH_3), 3.64 (s, 6H, OCH_3), 5.06 (s, 4H, $COCH_2$), 6.77 (s, 2H, H_{aryl}).

The Tetrameric Aluminum(I) Compound $[\{Al(\eta^5\text{-}C_5Me_5)\}_4]$**

By *Carsten Dohmeier, Christian Robl, Matthias Tacke,* and *Hansgeorg Schnöckel**

Gaseous, low-valent aluminum compounds have been known for a long time. *Klemm* et al. reported in 1948 already[1] the formation of gaseous AlCl during the reaction of Cl_2 with Al at 1000 °C. The first structural investigations on compounds with low-valent aluminum and Al–Al bonds are fairly recent. *Nesper* et al [2] prepared solid Al_7Te_{10} and *Uhl* the first molecular compound with an Al–Al bond: R_2Al–AlR_2(R = $CH(SiMe_3)_2$) **1**.[3]

For some time we have been studying the high temperature molecule AlCl,[4] its stabilization, and applications in preparative chemistry. The application of cryochemical methods enabled the preparation of unusual compounds of the trivalent aluminum from AlCl and unsaturated organic molecules.[5] Recently we prepared and identified a solution of AlCl which is metastable at −78 °C in the mixed solvent toluene/diethylether.[6] The first compound of monovalent aluminum stable at room temperature could be synthesized by treatment of this solution with $[Mg(C_5Me_5)_2]$ (eq. (a)).

$$\underset{\mathbf{2}}{4(AlCl \cdot x\,Et_2O)} + \underset{\mathbf{3}}{2[Mg(C_5Me_5)_2]} \xrightarrow{\text{toluene/}Et_2O} \underset{\mathbf{4}}{[\{Al(C_5Me_5)\}_4]} + 2(MgCl_2 \cdot 2Et_2O) + (4x-4)\,Et_2O \qquad \text{(a)}$$

The constitution of the (η^5-pentamethylcyclopentadienyl)-aluminum(I) **4** was confirmed by X-ray crystallography (Fig. 1).[7] The four aluminum atoms form a regular tetrahedron. Each pentamethylcyclopentadienyl ring is η^5-coordinated to an aluminum atom, whereby the planes of the C_5Me_5 rings are, in good approximation, parallel to the opposite base of the tetrahedron. The average Al–C distance is

[*] Prof. Dr. H. Schnöckel, C. Dohmeier, Dr. C. Robl, Dr. M. Tacke
Institut für Anorganische Chemie der Universität
Meiserstrasse 1, W-8000 München (FRG)
[**] This work was supported by the Deutsche Forschungsgemeinschaft and the Fonds der Chemischen Industrie.

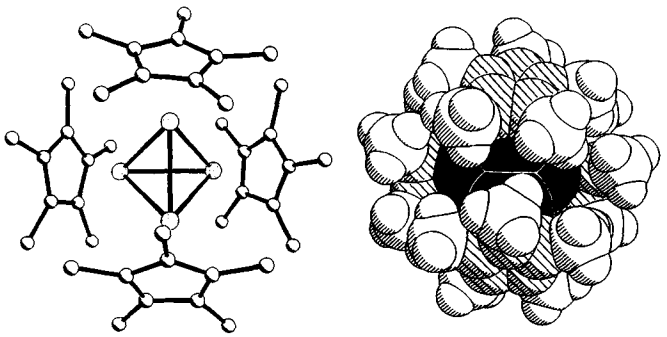

Fig. 1. Left: Structure of **4** in the crystal (hydrogen atoms omitted.) Selected distances [pm] and angles [°] (standard deviations in parentheses): ($d_{max}/d_{min}/\bar{d}$) Al-Al (277.3 (4)/276.7 (5)/276.9), Al-C_{Ring} (229.2 (13)/237.8 (11)/233.4), Al-Cp_{center} (203.2/199.7/201.5), Al-Al-Al (60.1 (1)/59.9 (1)/60.0). Right: Space-filling model of 4; Al atoms are black, C atoms hatched, and methyl-C and hydrogen atoms white.

233.4 pm and is thereby comparable with that in **3** (234.8 pm).[8]

The average Al–Al distance of 276.9 pm lies between that of **1** (266.0 pm) and of metallic aluminum (286 pm). This intermetallic distance distinguishes the aluminum compound from other oligomeric and polymeric M^I–η^5-C_5Me_5 compounds (M = In, Tl). In the octahedral cluster [In(η^5-C_5Me_5)]$_6$,[9] the In–In distances are 394.2 and 396.3 pm and therefore significantly longer than in In metal (394, 336 pm). Shorter metal atom distances are found in "dimeric" [In{η^5-$C_5(CH_2Ph)_5$}] (363.1 pm).[10] In the structurally analogous thallium compound, [Tl{η^5-$C_5(CH_2Ph)_5$}],[11] the distance between thallium atoms is 363.2 pm, in metallic thallium 336 and 343 pm. [Tl(η^5-C_5Me_5)][12] forms a polymeric chain of alternating thallium atoms and C_5Me_5 rings. In this compound the distance between chains is so large (641 pm) that a Tl–Tl interaction can be excluded. Thus, the interactions between the aluminum atoms in **4** are significantly larger than in the known cyclopentadienyl compounds of monovalent indium or thallium.

In the FT Raman spectrum of solid **4**, a broad band is observed at 377 cm^{-1},[14] which we assign to the breathing vibration (A_1) of the Al_4 tetrahedron. The Al–Al frequency of **1** lies at 373 cm^{-1}.[3] In spite of the weak bonding in the Al_4 species relative to the Al–Al bond in **1**, the frequencies agree. This can be explained by different vibration equations.[15]

The ^{27}Al NMR spectrum (70.4 MHz, external standard $[Al(H_2O)_6]^{3\oplus}$) of a solution of **4** in benzene exhibits a sharp signal at $\delta = -80.8$ ($\omega_{1/2} = 170$ Hz). This is to our knowledge the highest known chemical shift for an aluminum nucleus. The structure and reactions of **4** in solution are at present under investigation.

The compound [{Al(η^5-C_5Me_5)}$_4$] **4** presented here is the first molecular aluminum(I) compound stable under normal conditions, whose structure could be determined by diffraction methods and the third example (after In and Tl) of a $M^I(C_5Me_5)$ compound of the third main group elements. After the successful synthesis of **4** one expects that the missing members [B(C_5Me_5)] and [Ga(C_5Me_5)] can be prepared along similar lines.

Experimental Procedure

To a solution of 3.3 mmol **2** in 13 mL toluene at −78 °C is added dropwise a solution of 1.5 mmol **3** in 10 mL toluene. 214 mg(44%) yellow octahedral crystals of **4** are isolated from the resulting deep red solution at −25 °C. The product is air- and moisture-sensitive.

Received: December 17, 1990 [Z4329 IE]
German version: *Angew. Chem. 103* (1991) 594

CAS Registry numbers:
2 (x = 3), 132645-88-6; **3**, 74507-64-5; **4**, 132645-87-5.

[1] W. Klemm, E. Voss, K. Geiersberger, *Z. Anorg. Allg. Chem. 256* (1948) 15.
[2] R. Nesper, J. Curda, *Z. Naturforsch. B 42* (1987) 577.
[3] W. Uhl, *Z. Naturforsch. B 43* (1988) 1113.
[4] a) H. Schnöckel, *Z. Naturforsch. B 31* (1976) 1291; b) H. Schnöckel, *J. Mol. Struct. 50* (1978) 275.
[5] a) H. Schnöckel, M. Leimkühler, R. Lotz, R. Mattes, *Angew. Chem. 98* (1986) 929; *Angew. Chem. Int. Ed. Engl. 25* (1986) 921; b) C. Dohmeier, R. Mattes, H. Schnöckel, *J. Chem. Soc. Chem. Commun. 1990*, 358.
[6] M. Tacke, H. Schnöckel, *Inorg. Chem. 28* (1989) 2895.
[7] X-ray analysis: $C_{40}H_{60}Al_4$, triclinic, space group $P\bar{1}$ (No. 2), a = 1095.3(2), b = 1101.2(3), c = 1828.8(4) pm, α = 83.83(2), β = 83.88(2), γ = 66.80(2)°, $V = 2010.6 \times 10^6$ pm^3, $Z = 2$, $\varrho_{ber} = 1.07$ g cm^{-3}, $F(000)$ = 704, $\mu = 1.4$ cm^{-1} ($Mo_{K\alpha}$), 295 K, ω-scan, $\theta_{max} = 25°$, scan speed 2.93–14.65 deg min^{-1}, scan width 1.2°, Siemans R3m/V diffractometer, graphite monochromator, 7665 reflections of which 6966 are symmetry independent, $R_{int} = 0.0240$; 4891 reflections with $|F| > 3\sigma(|F|)$ were considered observed. Calculations with SHELXTL-Plus, 374 parameters including an isotropic extinction parameters were refined, H atoms geometrically positioned, non-hydrogen atoms anisotropically refined with the exception of C(21)–C(30); $R = 0.1227$, $R_w = 0.0970$, $R_g = 0.0801$, $w = 1/\sigma^2(F)$. Extremes of the final difference fourier synthesis + 1.1/ − 0.5 × 10^{-6}pm^{-3}. Further details of the crystal structure investigation may be obtained from the Fachinformationszentrum Karlsruhe, Gesellschaft für wissenschaftlich-technische Information mbH, W-7514 Eggenstein-Leopoldshafen 2 (FRG) on quoting the depository number CSD-55176, the names of the authors and the journal citation.
[8] R. A. Andersen, J. M. Boncella, C. J. Burns, R. Blom, A. Haaland, H. V. Volden, *J. Organomet. Chem. 312* (1986) C49.
[9] a) O. T. Beachley, Jr., R. Blom, M. R. Churchill, K. Faegri, Jr., J. C. Fettinger, J. C. Pazik, L. Victoriano, *Organometallics 8* (1989) 346; b) O. T. Beachley, Jr., M. R. Churchill, J. C. Fettinger, J. C. Pazik, L. Victoriano, *J. Am. Chem. Soc. 108* (1986) 4666.
[10] H. Schumann, C. Janiak, F. Görlitz, J. Loebel, A. Dietrich, *J. Organomet. Chem. 363* (1989) 243.
[11] H. Schumann, C. Janiak, J. Pickardt, U. Börner, *Angew. Chem. 99* (1987) 788; *Angew. Chem. Int. Ed. Engl. 26* (1987) 789.
[12] H. Werner, H. Otto, H. J. Kraus, *J. Organomet. Chem. 315* (1986) C57.
[13] FT Raman spectrum of **4** (Bruker FRA 106 (Nd:YAG laser 1.06 μ)) [cm^{-1} (rel. int.)]: 2910(10), 2859(4), 2721(2), 1486(2), 1431(5), 1179(1), 601(3), 559(2), 377(broad, 4), 124(5).
[14] The large half-height width possibly results from overlapping of bands.
[15] The G matrix element in an Al_4 tetrahedron is twice as large as that for an Al–Al unit. The F matrix element contains besides the Al–Al force constant interaction force constants for the Al_4 unit; cf. E. B. Wilson, J. C. Decius, P. C. Cross, *Molecular Vibrations*, McGraw-Hill, New York 1955.
[16] *Note added in proof (March 14, 1991):* In the recently prepared dodecaaluminate $K_2[Al_{12}iBu_{12}]$ the Al–Al distance is 268 pm: W. Hiller, K. W. Klinkhammer, W. Uhl, J. Wagner, *Angew. Chem. 103* (1991) 182, *Angew. Chem. Int. Ed. Engl. 30* (1990) 179.

Difference Electron Densities in a Spiropentene**

By *Hermann Irngartinger,** and *Stefan Gries*

Dedicated to Professor Heinz A. Staab on the occasion of his 65th birthday

Spiropentene ranks among the most strained organic molecules known. The calculated strain energy lies between 82.1 and 92.3 kcal mol^{-1}.[1, 2] To prove that the bonds are bent,

[*] Prof. Dr. H. Irngartinger
Organisch-chemisches Institut
der Universität
Im Neuenheimer Feld 270, W-6900 Heidelberg (FRG)

[**] This work was supported by the Deutsche Forschungsgemeinschaft and the Fonds der Chemischen Industrie.

we determined the difference electron density of the crystalline spiropentene derivative, dimethyl 4,5-diphenyl-4-spiropentene-(*E*)-1,2-dicarboxylate **1**, by low temperature X-ray diffraction measurements (105 K) according to the X-X method.[3]

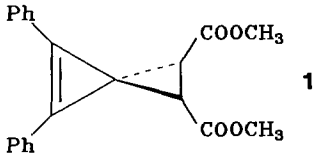

The spiropentene **1** was synthesized by carbenoid-addition techniques.[5] As in spiropentanes,[6] the central bonds in spiropentene **1** are shorter than the peripheral C–C single bonds (Fig. 1). Because of the large strain and the conjugation with both phenyl rings, the C–C double bond in 1 (C4–C5: 1.311 Å) is longer than in cyclopropene (from microwave spectroscopy: 1.296 Å[7]). The conditions for conjugation with both phenyl rings are favorable, because the dihedral angles are only 6.0° and 11.3°.

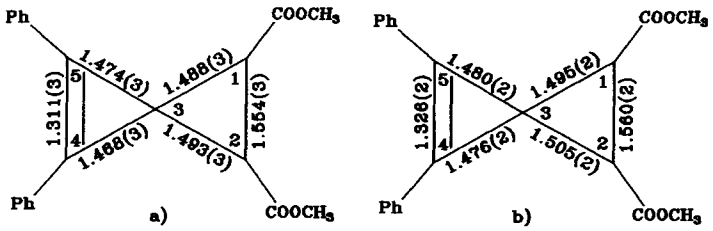

Fig. 1. Bond lengths (Å) of the spiropentene **1**: a) at room temperature (293 K), b) at 105 K.

The peripheral bond C1–C2 in **1** is longer than in spiropentane.[6] As in the cyclopropane derivatives[8] this bond is lengthened by the electron-withdrawing properties of the ester groups (Fig. 1). The two ester groups deviate by only 0.3° and 5.3° from a bisecting orientation, which allows an optimal interaction between the orbitals of the substituents and the Walsh orbitals of the three-membered ring. The electronic effects on the central bonds C1–C3 and C2–C3 weaken each other, since these bonds are in geminal and distal positions, respectively. Therefore, on comparison with spiropentane[6] no significant differences in these bond lengths can be observed. The interatomic distances at low temperature are longer than at room temperature, because the shortening effects due to libration and to the influence of the bonding electrons are minimal (Fig. 1).

All the single bonds of the spiropentene **1** are strongly bent, which is easily recognized in the shifts of the electron density maxima relative to the bond axes (Fig. 2). The bending of the bonds in spiropentanes is of the same order of magnitude.[6] Significantly more pronounced bending in the saturated three-membered ring of **1** relative to the less strained cyclopropane[9] and its derivatives[9, 10] could not be observed within experimental error.

The C4–C5 bond has a very high degree of bending compared with other strained double bonds. The density maximum is shifted significantly from the bond axis (0.18 Å, angle between bond axis and the line connecting the atom and the electron density maximum: 15°). The bending is more pronounced than in the double bonds of the four-membered ring system of cyclobutadiene (0.08 Å and 8° respectively[11]). In benzocyclopropenes the bending is greater as a result of the reduced bond order.[12] Strong deformations of the bonds in spiropentane and spiropentene are also predicted by quantum mechanical calculations.[2, 13]

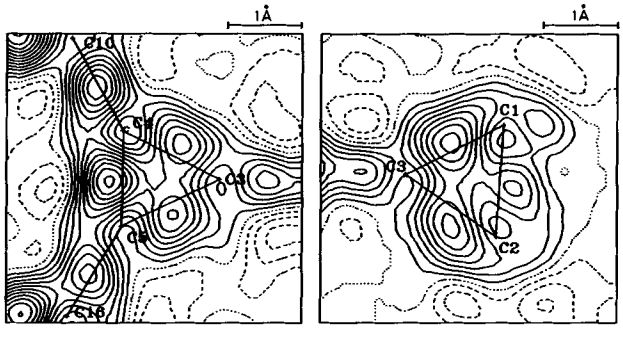

Fig. 2. Difference electron density map of the planes containing the cyclopropene (C3, C4, C5) and cyclopropane (C1, C2, C3) rings of spiropentene **1**. Contour interval 0.05 e/Å^{-3}. Standard deviation of the difference density outside the atomic positions 0.03–0.04 e/Å^{-3}. Zero density line dotted, negative electron densities dashed.

Received: January 11, 1990 [Z 4380 IE]
German version: *Angew. Chem. 103* (1991) 595

CAS Registry number:
1, 132856-63-2.

[1] J. Kao, L. Radom, *J. Am. Chem. Soc. 100* (1978) 760.
[2] Z. B. Maksić, K. Kovačević, A. Maguš, *J. Mol. Struct. 85* (1981) 9.
[3] Crystallographic data at room temperature and 105 K: a) Room temperature: colorless prisms from ethanol/ether, $a = 11.637(2)$, $b = 17.548(3)$, $c = 17.692(3)$ Å; orthorhombic space group *Pbca*; $Z = 8$, $\rho_{calcd} = 1.23$ Mg m^{-3}, crystal size 0.5^3 mm^3; $Mo_{K\alpha}$ radiation, Enraf-Nonius CAD4 diffractometer, graphite monochromator $\sin\theta/\lambda < 0.66$ Å^{-1}, 3868 independent reflections, of which 1719 observed ($I > 2.5\sigma(I)$). Refinement: C, O anisotropically, H isotropically, $R = 0.04$. b) Low temperature (105 K): $a = 11.427(2)$, $b = 17.476(2)$, $c = 17.617(3)$ Å, $\rho_{calcd} = 1.27$ Mg m^{-3}, crystal size 0.45^3 mm^3; three ($2° \le \theta \le 28°$) and four ($28° \le \theta \le 55°$) independent sets of data with a total of 18 269 reflections were measured. In the high order region only strong reflections ($|F(hkl)| > 3$) were collected. After averaging ($R_{int} = 0.029$) 7173 independent reflections remained, of which 6074 reflections were treated as observed ($I > 2.5\sigma(I)$) in the range to $\sin\theta/\lambda = 1.15$ Å^{-1}. Refinement (C,O anisotropically) with 3003 high order reflections ($\sin\theta/\lambda = 0.66$–1.15 Å^{-1}), R = 0.052. Parameters of the H atoms from the refinement with low order reflections ($\sin\theta/\lambda < 0.66$ Å^{-1}). Hirshfeld test [4]: average difference of the anisotropic displacement parameters along the bonds 0.0008 Å^2. Further details of the crystal structure investigation may be obtained from the Fachinformationszentrum Karlsruhe, Gesellschaft für wissenschaftlich-technische Information mbH, W-7514 Eggenstein-Leopoldshafen 2 (FRG) on quoting the depository number CSD-55258, the names of the authors and the journal citation.
[4] F. L. Hirshfeld, *Acta Crystallogr. Sect. A 32* (1976) 239.
[5] M. W. Jones, M. E. Stowe, E. E. Wells, Jr., E. W. Lester, *J. Am. Chem. Soc. 90* (1968) 1849.
[6] R. Boese, D. Bläser, K. Gomann, U. H. Brinker, *J. Am. Chem. Soc. 111* (1989) 1501; G. Dallinga, R. K. van der Draai, L. H. Toneman, *Recl. Trav. Chim. Pays-Bas 87* (1968) 897.
[7] W. M. Stigliani, V. W. Laurie, J. C. Li, *J. Chem. Phys. 62* (1975) 1890.
[8] F. H. Allen, *Acta Crystallogr. Sect. B 36* (1980) 81.
[9] D. Nyveldt, A. Vos, *Acta Crystallogr. Sect. B 44* (1988) 289, 296.
[10] A. Hartmann, F. L. Hirshfeld, *Acta Crystallogr. 20* (1966) 80.
[11] H. Irngartinger, M. Nixdorf, *Chem. Ber. 121* (1988) 679.
[12] D. Bläser, R. Boese, W. A. Brett, P. Rademacher, H. Schwager, A. Stanger, K. P. C. Vollhardt, *Angew. Chem. 101* (1989) 209; *Angew. Chem. Int. Ed. Engl. 28* (1989) 206.
[13] K. B. Wiberg, R. F. W. Bader, C. D. H. Lau, *J. Am. Chem. Soc. 109* (1987) 985; Z. B. Maksić, K. Kovačević, *J. Org. Chem. 39* (1974) 539.

Highly Stable Liposomes Derived from Perfluoroalkylated Glycerophosphocholines**

By *Catherine Santaella, Pierre Vierling,* and *Jean G. Riess**

Dedicated to Professor Rolf Appel on the occasion of his 70th birthday

Vesicles formed from phospholipids (liposomes) provide chemical models for the study of biological membrane functions[1] as well as challenging drug carrier and delivery systems.[2] Vesicles made from pure phospholipids, however, have low stability. The development of more stable membranes usually requires multicomponent systems and elaborate formulations resulting in increased complexity.[3] Natural soybean or egg-yolk phospholipid (EYP) mixtures are also routinely used as surfactants in injectable preparations such as fat emulsions for parenteral nutrition,[4] emulsions of fluorocarbons to be used as artificial oxygen carriers and contrast agents,[5] and drug delivery systems.[6] However, these phospholipids have limitations owing to their biological origin (complex, not exactly reproducible mixtures) and to their chemical nature (hydrolizable and oxidizable). Moreover, they leave little leeway for varying the properties of vesicles and emulsions, and further additives such as cholesterol are generally needed to achieve practical shelf lives.

Future progress will aim at obviating these limitations and therefore at developing new lines of biocompatible membrane- and vesicle-forming amphiphiles, which may also be used as surfactants or co-surfactants for injectable fluorocarbon emulsions. Accordingly, we have synthesized analogues of phosphatidylcholines, the main components of natural EYPs[7] (Scheme 1), in which the natural fatty acid tails are

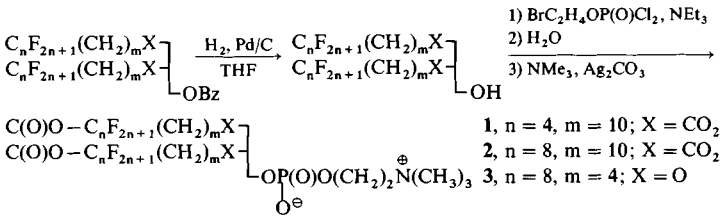

Scheme 1. Synthetic pathway for the preparation of F-alkyl GPCs **1**–**3**.

replaced by saturated chains (to avoid oxidation) terminated by perfluoroalkylated chains, and linked to the glycerophosphocholine polar head through an ester (**1** and **2**) or an ether junction (to avoid hydrolysis) (**3**). The perfluoroalkylated tails were expected to increase the hydrophobicity of the membrane lipids, which usually leads to improved stability of the vesicle shell,[8] and their fluorophilicity, which should facilitate and stabilize the dispersion of fluorocarbons in water.

We report here that the *pure* perfluoroalkylated glycerophosphocholine (F-alkyl GPC) esters **1**, **2** and ether **3** do effectively form highly stable liposomes without any secondary additive, and that these vesicles can be heat-sterilized under the standard norms of the Food and Drug Administration. Their shelf-life is considerably higher (months vs. days) than that of the vesicles formed by their hydrocarbon analogue 1,2-dipalmitoyl 3-*rac*-glycerophosphocholine (DPPC, **4**). Some preliminary data on their biocompatibility and on their ability to emulsify fluorocarbons are also given.

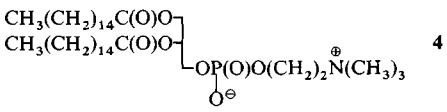

4

Like their hydrocarbon analogue **4**, the F-alkyl GPCs **1** to **3** are insoluble but dispersible in water, on application of standard procedures such as sonication. Concentrations as high as, or even higher than 200 g L^{-1} of F-alkyl GPC could be attained. Electron microscopy of these dispersions after freeze fracture (exemplified for **1** in Fig. 1a) shows that they consist of vesicles. These vesicles[9] have average sizes (60–200 nm, by light scattering spectroscopy (LSS) after brief sonication) in the range of those formed by natural or synthetic phospholipids in similar conditions.[10]

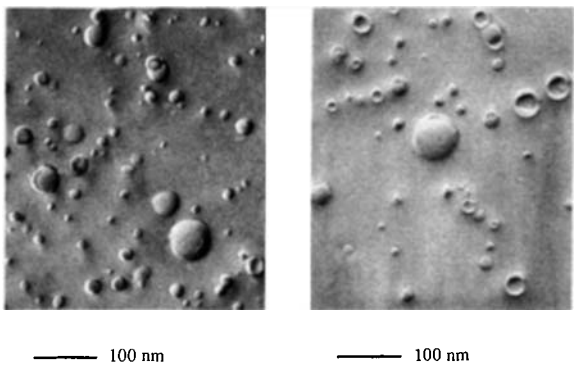

Fig. 1. Unilamellar and multilamellar vesicles made from F-alkyl GPC **1**. Left: before sterilization; right: after sterilization (121 °C, 15 min, 10^5 Pa)

Two issues are of major importance in the technology of liposomes and injectable emulsions for medical purposes: their resistance to sterilization and their in vitro storage stability.[11] Electron microscopy after freeze fracture (Fig. 1) showed that the vesicles formed by the F-alkylated amphiphiles **1** were morphologically not affected by thermal sterilization (121 °C, 15 min, 10^5 Nm^{-2} 10^5 Pa. LSS measurements also established that no significant modification of the average particle sizes had occurred (Table 1). By contrast, when a dispersion of **4** was prepared under the same conditions, a new population of much larger-sized vesicles (1150 nm diameter) appeared and became predominant upon sterilization.

Most remarkable is the fact that the F-alkyl GPC dispersions can be stored at room temperature for several months without sedimentation or any other visible change. LSS measurements showed that only a limited particle size increase had occurred after five or ten months for sterilized dispersions of F-alkyl GPC esters **2** and **1** respectively (Table 1). Likewise, dispersions of the F-alkyl GPC ether **3** have been stored (without sterilization) for 1.5 years without sedimentation or other visible changes. However, particle size measurements show that two populations of liposomes had

[*] Prof. J. G. Riess, C. Santaella, Dr. P. Vierling
Laboratoire de Chimie Moléculaire, Unité associée au CNRS
Université de Nice-Sophia Antipolis,
F-06034 Nice Cedex (France)

[**] We acknowledge the generous support of the Centre National de la Recherche Scientifique (CNRS) and the Agence de Transferts de Technologies Avancées (ATTA) throughout this research.

formed (53 nm and 207 nm). The absence of large particles ($> 1\ \mu m$), especially with **1**, indicates that the fusion of vesicles during storage is very slow. The behavior of **1**, **2** and **3** thus contrasts strongly with that of DPPC (**4**) whose liposomal dispersions, whether sterilized or not, can only be stored for a few days. When prepared by sonication or French press extrusion the latter were shown to retain their original sizes and integrity for 48 h at most.[12] When treated in the same way as the F-alkyl GPC, heat-sterilized dispersions of DPPC vesicles (3% w/w) displayed already after two days an increase in turbidity and a fluffy aspect which indicated the formation of larger particles and precluded valid LSS particle size measurements; an irreversible sedimentation was observed after six days at room temperature.

Table 1. Particle sizes D after preparation (left), sterilization (center), and ageing (right) at 25 °C of dispersions of F-alkyl GPC (**1**, **2**, **3**) and DPPC (**4**)[a].

Compound	D [nm] [a]	Amount [%]	D [nm] [a]	Amount [%]	D [nm] [a]	Amount [%]	Age days
1[b]	133 (broad)	100	133 (50)	100	21 (5)	4	**100**
					139 (22)	96	
					42 (13)	14	**300**
					121 (33)	86	
2[b]	121 (43)	100	147 (90)	100	183 (100)	100	**150**
3[c]	106 (72)	100	–	–	53 (16)	36	**600**
					207 (53)	64	
4[b]	60 (23)	43	51 (19)	26	irreversible opaque		**6**
	260 (70)	57	140 (20)	14	precipitate		
			1150 (230)	60			

[a] Standard deviations [nm] in parentheses. [b] Sterilized dispersion of 3% (w/w) of **1**, **2**, or **4** in either water, NaCl (0.9%) or Hepes buffer (10^{-2} M). No difference in size or size distribution was observed whatever the aqueous phase. [c] Nonsterilized dispersion of **3** at 6% (w/w) concentration in NaCl (0.9%).

The remarkably long shelf life of the F-alkyl GPC vesicles indicates that their membrane is highly stable. Apparently the partial replacement of hydrocarbon chains by fluorinated ones resulted in sufficient increase of the hydrophobic interactions[8] to counterbalance any destabilizing effect[13] arising from lower intermolecular interactions and an increase of steric repulsions between the fluorinated chains.

With the new F-alkyl GPCs as emulsifier, stable emulsions of 50% (w/v) of perfluorodecalin, a fluorocarbon rather difficult to emulsify, can be readily prepared using sonication.[14] Compound **2** was compared to EYP and to hydrogenated EYP (Lecinol®, which, because it is saturated, is structurally closer to **2** than EYP). Both EYP and Lecinol are mixtures of amphiphiles and are therefore known to be considerably more efficacious emulsifiers than any single phospholipid. It is therefore noteworthy that **2** when used alone was significantly more effective than Lecinol (which failed in the emulsification of perfluorodecalin), and was nearly as efficient as the natural EYP mixture. Thus, for example, 50/50 (w/v) emulsions of perfluorodecalin were prepared with 32.5 mM of surfactant. The emulsions prepared from EYP in a phosphate buffer had an average particle size of 0.24 μm (76% < 0.40 μm, no particle larger than 1.1 μm) after preparation, 0.23 μm (79% < 0.40 μm, 3% > 1.1 μm) after sterilization, and 0.31 μm (67% < 0.40 μm, 3.5% > 1.1 μm) after one month at 25 °C; in comparison, when **2** was used as the surfactant the average particle sizes were 0.24 μm (85% < 0.40 μm, 0% > 0.95 μm) after preparation, 0.32 μm (73% < 0.40 μm, 0% > 1.1 μm) after sterilization, and 0.36 μm (58% < 0.40 μm, 0% > 1.1 μm) after ageing at 25 °C. Further improvement in stability of such emulsions is expected when mixtures of F-alkyl phospholipids, or mixtures of F-alkyl GPCs with other surfactants, are used.

As the F-alkyl GPCs are destined for in vivo applications, preliminary biological tests, including effect on cell cultures, hemolytic activity, and acute toxicity in mice, were undertaken.[15] Compounds **1** to **3**, in the form of dispersions, did not perturb the growth or viability of lymphoblastoid Namalva cell cultures. It is particularly remarkable that no hemolytic effect on a suspension of human red blood cells was detected, even at high concentrations (for example 60 g L^{-1} of **2**), while saturated hydrocarbon phosphatidylcholines of similarly low chain lengths (eight to twelve carbon atoms) are definitely hemolytic,[16] (for example a 1 g L^{-1} dispersion of 1,2-dilauryl-3-*rac*-glycerophosphocholine). Preliminary in vivo tests indicate that the intravenous LD_{50} in mice are higher than 2500 mg kg^{-1} body weight (no death among ten animals after one month observation). Although these synthetic phospholipids are racemic, the non-natural D-isomer apparently does not lead to any acute toxicity, at least not in these initial screening tests.

Received: November 23, 1990 [Z 4278]
German version: *Angew. Chem. 103* (1990) 584

[1] J. H. Fendler: *Membrane Mimetic Chemistry*, Wiley, New York 1982.
[2] G. Gregoriadis: *Liposomes as Drug Carriers: Recent Trends and Progress*, Wiley, Chichester 1988.
[3] To overcome this stability problem, various membrane-forming amphiphiles and polymeric systems have also been developed: for a review see H. Ringsdorf, B. Schlarb, J. Venzmer, *Angew. Chem. 100* (1988) 117–162; *Angew. Chem. Int. Ed. Engl. 27* (1988) 113–158.
[4] A. Wretlind, *JPEN J. Parenter. Enteral. Nutr. 5* (1981) 230–235.
[5] J. G. Riess, M. LeBlanc in K. C. Lowe (Ed.): *Blood Substitutes: Preparation, Physiology and Medical Applications*, Horwood, Chichester 1988, p. 94–129; D. C. Long, D. M. Long, J. Riess, R. Follana, A. Burgan, R. F. Mattrey in T. M. S. Chang, R. P. Geyer (Ed.): *Blood Substitutes*, Dekker, New York 1989, p. 441–442.
[6] G. Lopez-Berestein, I. J. Fidler: *Liposomes in the Therapy of Infectious Diseases and Cancer*, A. R. Liss, New York 1988.
[7] F. Jeanneaux, M. P. Krafft, C. Santaella, P. Vierling, and J. G. Riess, EP-B 90/0099, US-A 542,227. The starting perfluoroalkylated iodides were a gift from Atochem. The purity of the phospholipids was checked by TLC and HPLC analysis. Their formulas are supported by their elemental analysis, ^1H, ^{31}P, ^{13}C, ^{19}F NMR and IR spectroscopy.
[8] P. Mukerjee, *J. Phys. Chem. 85* (1981) 2298–2303.
[9] Dispersions of phospholipids were prepared by hydrating the powdered or thin-layered lipid with water, NaCl (0.9%) or Hepes buffer (10^{-2} M) for ten minutes above the phase transition temperature of the lipid, shaken for 1 min to produce a coarse dispersion, which was then sonicated briefly (2 to 5 min, Branson B30 sonifier, titanum probe 15 mm, dial 5, pulse 50). Sterilization was achieved by autoclaving the samples (5 ml) for 15 min at 121 °C under 10^5 Pa. Particle sizes and size distributions were determined by light scattering on a Coulter N4SD Sub-Micron Particle Analyser.
[10] D. Chapman in G. Gregoriadis (Ed.): *Liposomes Technology: Preparation of Liposomes 1* CRC Press, Boca Raton, Fl, USA 1986, p. 11–17.
[11] L. Rao in G. Gregoriadis (Ed.): *Liposomes Technology: Preparation of Liposomes 1*, CRC Press, Boca Raton, Fl, USA 1986, p. 247–257.
[12] a) Y. K. Levine, A. G. Lee, N. J. Birdsall, J. C. Metcalfe, J. D. Robinson, *Biochim. Biophys. Acta 291* (1979) 592–607; b) Y. Barenholz, D. Gibbes, B. J. Littman, J. Goll, T. E. Thomson, F. D. Garlson, *Biochemistry 16* (1977) 2806–2810.
[13] W. R. Hargreaves, D. W. Deamer, *Biochemistry 18* (1978) 3759–3768.
[14] The emulsions were prepared in a phosphate buffer by sonication according to M. P. Krafft, J. P. Rolland, P. Vierling, J. G. Riess, *New. J. Chem. 14* (1990) 869–875. Average particle sizes (± 5%) were measured by a centrifugal sedimentation method coupled with optical density measurements (Horiba Capa 700).
[15] The biological tests were performed according to L. Zarif, J. Greiner, S. Pace, J. G. Riess, *J. Med. Chem. 33* (1990) 1262–1269.
[16] F. C. Reman, R. A. Demel, J. de Gier, L. L. M. Van Deenen, H. Eibl, O. Wesphal, *Chem. Phys. Lipids 3* (1969) 221–233.

Direct Observation of Streptavidin Specifically Adsorbed on Biotin-Functionalized Self-Assembled Monolayers with the Scanning Tunneling Microscope**

By *Lukas Häussling, Bruno Michel,* Helmut Ringsdorf,** and *Heinrich Rohrer*

Molecular recognition, i.e. the specific and selective interaction between host and guest molecules, is of critical importance not only in biology, but also in materials science for the molecular architecture of organized materials.[1]

Scanning tunneling microscopy (STM) and related methods[2] facilitate direct investigation of adsorbed molecules.[3-6] A broad spectrum of organic molecules can be bound by functionalized chemisorbed monolayers to conducting surfaces for subsequent study with the STM.

Binding of biotin (vitamin H) by the bacterial protein streptavidin is a model case of molecular recognition for the following reasons: 1) The binding constant ($K_a = 10^{15}$ L mol^{-1}) is extremely high and very specific. 2) Biotin can easily be functionalized and its binding properties are only slightly influenced by this process.[7] 3) Streptavidin has four binding sites for biotin situated on two opposite sides of the tetrameric protein. It can thus be used to link two different functions in the new molecular complex.

Since two-dimensional crystallization of fluorescence-marked streptavidin was recently achieved[8] on biotinylated lipid monolayers, we became interested in the analogous experiment on so-called "self-assembled monolayers" (see Scheme 1). *Nuzzo* and *Allara*[9a] as well as *Sagiv*[9b] showed that such films adsorbed from isotropic solutions onto solid supports are indeed monolayers with nearly perfect two dimensional organization. It was shown for the chemisorption of thiols and disulfides onto gold surfaces[10] that these self-assembled monolayers are well suited to functionalize metallic surfaces on a larger scale.

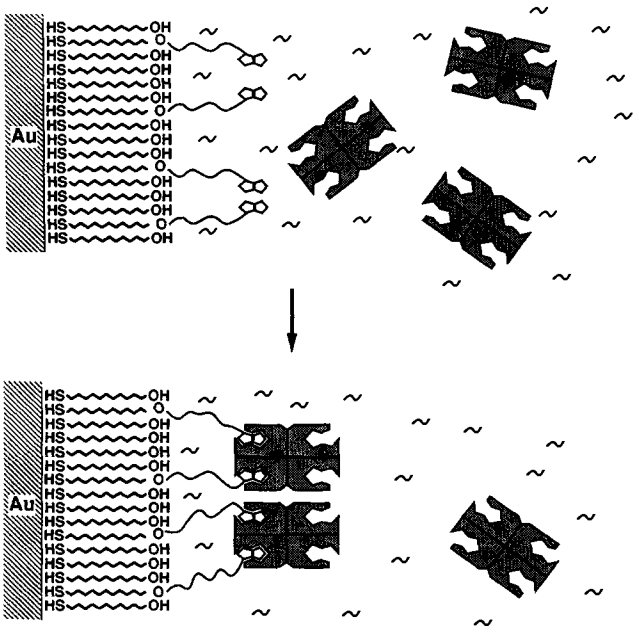

Scheme 1. Surface recognition on a mixed monolayer of **1** and **3** by streptavidin.

In order to perform the recognition reaction between biotin and streptavidin on functionalized gold surfaces, we synthesized the thiols **1** and **3**, and disulfide **2**.[11] 11-Mercaptoundecanol **1** was chemisorbed from a solution onto gold (111),[13] and the contact angle measured (Table 1). Figure 1 shows the STM picture of a chemisorbed monolayer of **1** on gold (111): a smooth surface with randomly distributed depressions[14] (bare gold shows none of these depressions).

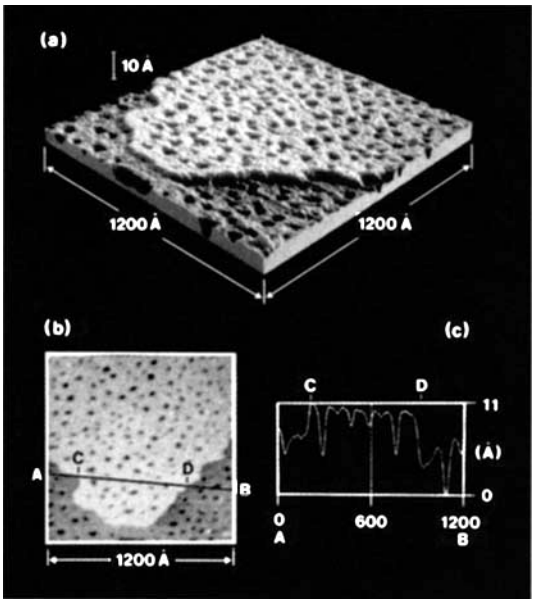

Fig. 1. Monolayer of **1** chemisorbed from a 2.1×10^{-4} M solution in ethanol on gold (111); imaging conditions: tungsten tip, 200 mV and 100 pA. a) Three-dimensional image with simulated illumination. b) Top view of a) in gray-scale scheme with a vertical dimension of 24 Å from black to white. c) Cross-section along line AB with an additional monolayer of gold from C to D.

The smooth parts cover approximately 95% of the surface (by STM analysis). The new organic surface exhibits the same terraced structure (e.g., step height and sharpness) as the uncovered gold films. The depressions have lateral dimensions of up to 35 Å and a maximum depth of 11 Å (cf. Fig. 1 b and c). We conclude that the gold substrate is covered by a densely packed monolayer of **1** except for the depressions. These are either empty or contain loosely packed molecules which yield laterally to the scanning tip. We note further that the observed 95% coverage also corresponds to the ratio of the area requirement of perpendicular paraffin chains to that of a $\sqrt{3} \times \sqrt{3}$ superlattice[15] of sulphur atoms on gold (111), i.e., densely packed sulfur atoms on the gold surface and a consequent loose packing of a certain percentage of the hydrocarbon chains.

Following the same procedure, the bisbiotin disulfide **2** was adsorbed (see Table 1). The biotin-functionalized gold surface was then dipped into the protein solution[16]; still no proteins were detectable with the STM, even after an incubation period of 12 hours.

Weber et al.[17] showed that the reason for the high binding constant of biotin to streptavidin is that the biotin molecule is completely engulfed by the protein. Therefore, streptavidin cannot bind tightly to a monolayer of **2** chemisorbed

[*] Dr. B. Michel, Dr. H. Rohrer
IBM Research Division, Zürich Research Laboratory
Säumerstrasse 4, CH-8803 Rüschlikon (Switzerland)
Prof. H. Ringsdorf, Dipl. Chem. L. Häussling
Institut Organische Chemie der Universität
J. J.-Becher-Weg 20, W-6500 Mainz (FRG)

[**] We thank Mrs. *G. Bender* for her enthusiastic help with the syntheses, and Mr. *H.-G. Batz* (Boehringer, Mannheim) for a gift of streptavidin

on gold, because of steric hindrance and limited mobility of the densely packed biotin molecules. This steric hindrance can be overcome by "diluting" the biotin functionalities on the gold surface by means of coadsorption of an unfunctionalized thiol or disulfide. The mobility can be increased by the introduction of a long hydrophilic spacer as with mercaptobiotin **3** (Scheme 1).

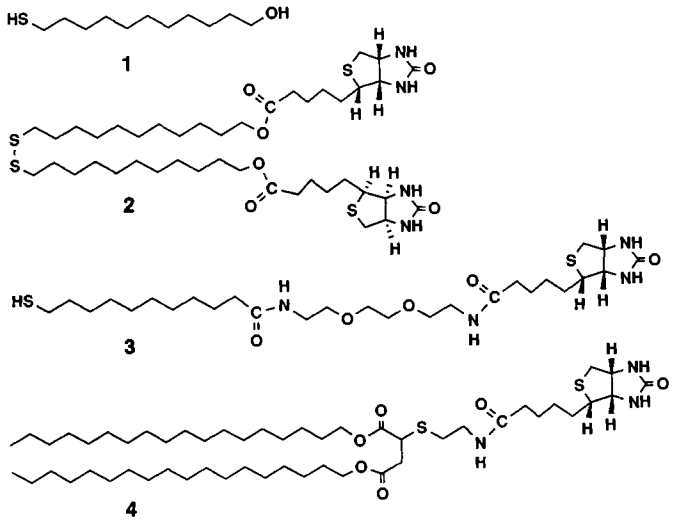

Table 1. Contact angles of water with chemisorbed thiols on gold(111) surfaces [12].

Compound	Adsorption time [h]	θ_{adv} [°] [a]	θ_{re} [°] [a]
1	14	42	7
2	5	66	25
3	18	52	20
1/3 2:1	21	60	18
1/3 50:1	24	35	8
Gold (111)	–	70–80	38–50

[a] adv = advancing, re = receding

Compound **3** was chemisorbed from pure solution and mixtures with mercaptoundecanol **1** on gold (111) surfaces. The monolayer of pure **3** is wetted sufficiently by water (Table 1); a periodicity of 10 Å in one direction and 20 Å in the perpendicular direction is visible in the STM (not shown). Figure **2** shows a mixed monolayer obtained by coadsorption from a solution of **1** and **3** (2:1). This monolayer exhibits marked depressions with lateral dimensions of 120 Å and a depth of approximately 3 Å. We associate this with a difference in length of the two components, the depth of the depressions indicating that the protruding spacer with the biotin lies flat on the densely packed alkane layer. Occasionally, we observe a periodicity of 7.5×10 Å which is in agreement with the length and width of the protruding hydrophilic part of **3**. This, however, requires a much larger ratio of **1/3** in the adsorbed monolayer than in the original solution (i.e. **3** adsorbs slower than **1**).

A mixed monolayer chemisorbed from a solution of **1** and **3** in the ratio 50:1 was incubated with a buffered protein solution[16] for 72 h at room temperature, subsequently removed and rinsed thoroughly with diluted buffer. The individual proteins are visible in the STM image (Fig. 3), especially in the profile along AB (Fig. 3b). The width of 45 Å is in accordance with values in the literature ($42 \times 42 \times 56$ Å)[17] (lattice constant 80 Å).[18] We observed regions free of

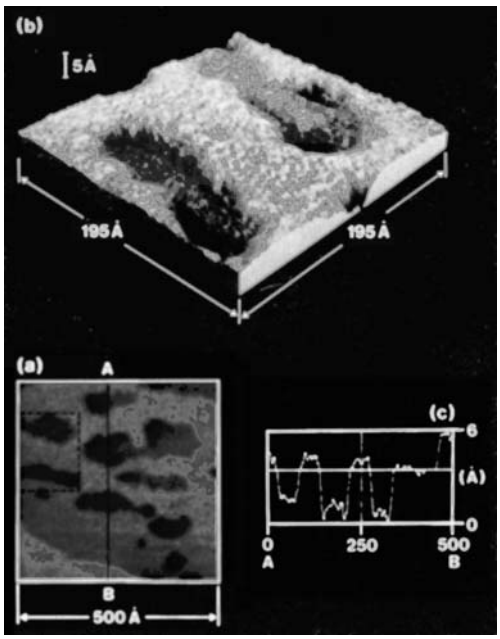

Fig. 2. Chemisorbed monolayer of **3** and **1** (1:2) on gold (111); imaging conditions as in Figure 1. a) Top view in gray-scale scheme with a vertical dimension of 54 Å from black to white. b) Three-dimensional image of the zone marked in a) with simulated illumination. c) Cross-section along line AB; B has an additional monolayer of gold.

protein as well as areas covered with several layers; true monolayer coverage was rarely found. The mobilities of both the chemisorbed biotin and proteins docked to it are apparently rather small, causing lateral and vertical disorder of the proteins.

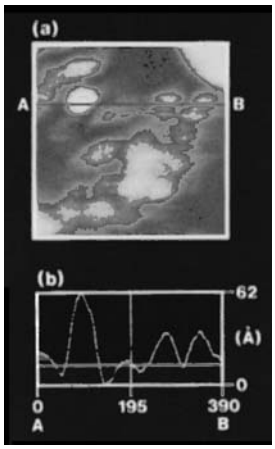

Fig. 3. Streptavidin docked onto a chemisorbed monolayer consisting of **3** and **1** (1:50); imaging conditions as in Figure 1. a) Top view in gray-scale scheme with a vertical dimension of 140 Å from black to white. b) Cross-section along line AB.

To demonstrate the effect of steric hindrance, lateral and especially vertical mobility in the underlying self-assembled monolayers, we spread the bisbiotin disulfide **2** on buffer solution[16] in a Langmuir trough. Figure 4 shows the pressure area diagram of this compound. We incubated these monolayers with streptavidin at two surface pressures for 30–60 minutes at room temperature. The film of oriented bisbiotinylated disulfide **2** and bound streptavidin was then

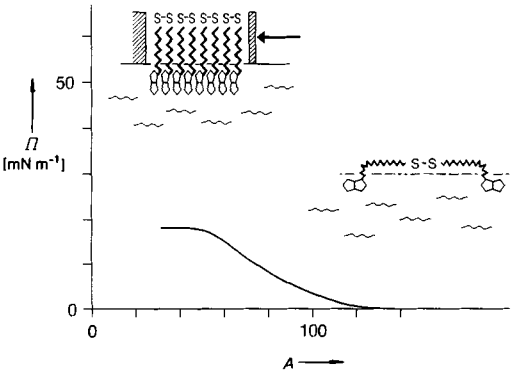

Fig. 4. Pressure area diagram of **2** at 20 °C on water. A = area in Å per molecule, Π = surface pressure.

transferred to the gold support by the Langmuir-Schäfer technique. Figure 5a shows the STM picture of the layer obtained after incubating a monolayer of **2** for 30 minutes with streptavidin at 1 mN m^{-1} in the liquid analogous phase. It shows terraces of about 3 Å in height caused by steps in the gold substrate, and in the background a large protein aggregate several hundred angstroms high (Fig. 5b).

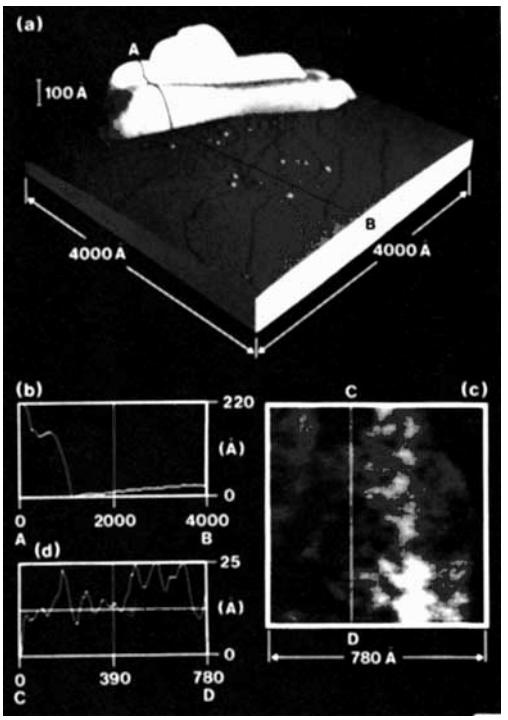

Fig. 5. Compound **2** spread over NaCl/Tris-HCl (each 10 mM), pH 7, incubated with streptavidin and transferred to gold (111); imaging conditions: gold tip, 200 mV and 100 pA. a) Three-dimensional image of an area with a streptavidin aggregate grown in the liquid analogous phase at 1 mN m^{-1}, with simulated illumination. b) Cross-section along line AB; the steps in the right-hand side of the image correspond to monoatomic gold steps. c) Top view with streptavidin docked on a monolayer of **2** in the gas analogous phase with a vertical dimension of 50 Å from black to white. d) Cross-section along line CD.

This needle-shaped type of aggregation has not been observed previously,[8, 18] but the protein concentration used in this experiment was much higher than before. Figure 5c shows the STM image of a monolayer composed of **2** and streptavidin, which was kept at 0 mN m^{-1} (gas analogous phase) during an incubation time of one hour. Here, however, small patches of proteins show tetragonal symmetry, similar to the two-dimensional structures found with biotinylated lipid monolayers at the air–water interface.[8, 18]

To compare the epifluorescence microscopy experiments of *Blankenburg* et al.[8, 18] with the recognition reaction at self-assembled monolayers on solid surfaces, we spread the biotin lipid **4** on a buffer solution[16] and compressed it to 4 mN m^{-1} (solid analogue packing). Compound **4** forms solid analogue packed monolayers and thus can be more easily imaged by scanning tunneling microscopy. In addition it could be shown by parallel monolayer experiments, that this biotin lipid leads to many small protein domains at the gas water interface, which are also more suitable for STM experiments.

The subphase below this monolayer was then exchanged by a solution of streptavidin (1 μM) in the same buffer. After an hour at room temperature, this film was transferred to a gold (111) surface by the Langmuir-Schäfer technique and investigated with STM. Figure 6a shows the typical structure of the streptavidin aggregates, which have a two fold symmetry, stretched shape and characteristic grooves in the short sides. Most aggregates are 100–120 Å thick, corresponding to two layers of streptavidin; only few of the protein aggregates are true monolayers, as demonstrated by the trace of the line AB in Figure 6b corresponding to two double layered protein aggregates on the left and a single layer protein aggregate on the right. Figure 6c displays a close-up of the groove of such a protein aggregate. The cross-section CD in Figure 6d displays top left three protein

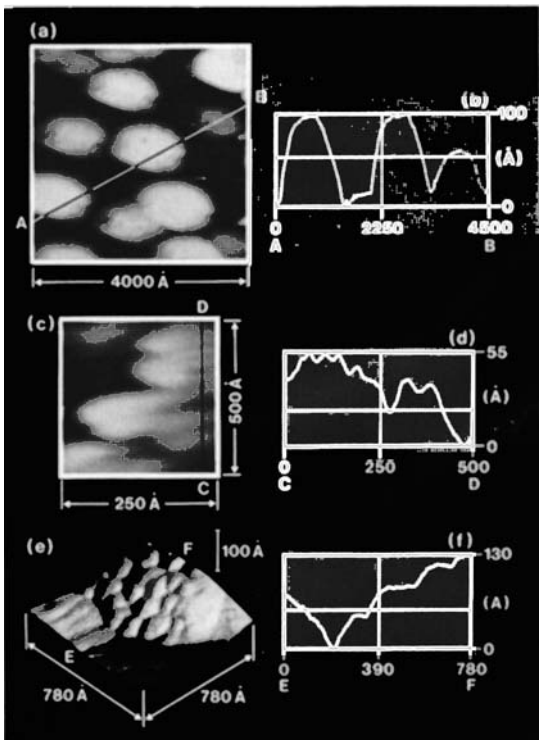

Fig. 6. Biotin lipid **4** spread over NaCl/Tris-HCl solution (each 10 mM), pH 7, exchanged with a subphase of streptavidin and transferred to gold (111); imaging conditions as in Figure 1. a) Top view of streptavidin aggregates in gray scale scheme, the vertical dimension is 100 Å from black to white. b) Cross-section along line AB. c) Close up of a top view of a groove area of one of the aggregates in a), shown in grayscale scheme; the vertical dimension in 55 Å from black to white. d) Cross section along line CD. e) Three dimensional image with simulated illumination of the edge of a multilayered protein aggregate. f) Cross-section along line EF.

molecules next to each other with lateral dimensions of about 40 Å. On the right are two protein molecules with a spacing in between, this time corresponding to the 80 Å lattice constant found in monolayer experiments.[18] The overall irregularity in the packing points to the fact that the protein aggregates are not perfectly ordered. In Figures 6e and the cross-section 6f, part of a 400–500 Å thick aggregate of streptavidin is shown. This thickness corresponds to about 8 layers of streptavidin, four of which are visible in the image (Fig. 6f). Such multilayered streptavidin aggregates at lipid monolayers have not been observed previously. This may be due to the unusually high concentration of streptavidin used in the incubation solution.

Chemisorbed self-assembled monolayers, e.g. of mercaptoundecanol **1**, possess sufficient adhesion to the substrate to allow the tunneling tip to scan over them without significant displacement of the molecules. This is in contrast to monolayers of fatty acids or lipids, whose mobility on solids is too high to resist repulsive or attractive tip interaction. We confirmed the surface coverage postulated from contact angle measurements,[9, 10] even though the microstructure of the layer is quite heterogeneous. Unlike Langmuir monolayers on water, however, chemisorbed monolayers on solids exhibit only limited lateral and no vertical mobility.[19] Only after three days incubation could we detect proteins docked directly to the functionalized solid, whereas the same process on a monolayer formed in a Langmuir trough took less than one hour.

Nevertheless, upon imaging with the STM, the insufficient adhesion of such transferred Langmuir-Blodgett monolayers poses a problem. Good adhesion can be obtained by compounds of type **2**, which can be spread on a liquid surface and whose transferred monolayers are chemically bound by the solid support. However, the fact that imaging of protein aggregates on solid surfaces is possible at all is very promising for investigations of functionalized solid surfaces.

Received: October 8, 1990.
Revised version: February 1, 1991 [Z 4235 IE]
German version: *Angew. Chem. 103* (1990) 568

CAS Registry numbers:
1, 73768-94-2; **2**, 132722-88-4; **3**, 132722-89-5; **4**, 122567-71-9; 11-bromoundecanol, 1611-56-9; 11-bromoundecanoic acid, 2834-05-1; 1,8-diamino-3,6-dioxaoctane, 929-59-9; streptavidin, 9013-20-1.

[1] a) J. M. Lehn, *Angew. Chem. 100* (1988) 91; *Angew. Chem. Int. Ed. Engl. 27* (1988) 89; b) H. Ringsdorf, B. Schlarb, J. Venzmer, *ibid. 100* (1988) 117 and *27* (1988) 113.
[2] R. J. Behm, N. Garcia, H. Rohrer (Eds.): *Scanning Tunneling Microscopy (STM) and Related Methods (NATO ASI Series E 184* (1991)).
[3] G. Travaglini, H. Rohrer, M. Amrein, H. Gross, *Surf. Sci. 181* (1987) 514.
[4] J. S. Foster, J. E. Frommer, *Nature 333* (1987) 542.
[5] a) M. Amrein, A. Stasiak, H. Gross, E. Stoll, G. Travaglini, *Science (Washington, DC) 240* (1988) 5124; b) M. Amrein, R. Dürr, A. Stasiak, H. Gross, G. Travaglini, *ibid. 243* (1989) 1708.
[6] a) D. P. E. Smith, H. Hörber, C. Gerber, G. Binnig, *Science (Washington DC) 245* (1989) 43; b) B. Michel, G. Travaglini, H. Rohrer, C. Joachim, M. Amrein, *Z. Phys. B 76* (1989) 99.
[7] M. Wilcheck, E. Bayer, *Trends Biochem. Sci. 14* (1989), 408; *Anal. Biochem. 171* (1988) 1.
[8] R. Blankenburg, P. Meller, H. Ringsdorf, C. Salesse, *Biochemistry 28* (1989) 8214.
[9] a) R. G. Nuzzo, D. L. Allara, *J. Am. Chem. Soc. 105* (1983) 4481; b) J. Sagiv, *ibid. 102* (1980) 92.
[10] a) C. D. Bain, G. M. Whitesides, *Science (Washington DC) 240* (1988) 62; b) C. D. Bain, J. Evall, G. M. Whithesides, *J. Am. Chem. Soc. 111* (1989) 7155; c) *ibid. 111* (1989) 7164; d) C. D. Bain, G. M. Whitesides, *Angew. Chem. Adv. Mater. 101* (1989) 522; *Angew. Chem. Int. Ed. Engl. Adv. Mater. 28* (1989) 506; *Adv. Mater. 4* (1989) 110.
[11] Compound **4** has been described in [8]. Compounds **1**–**3** were synthesized as follows: **1**: 11-bromoundecanol (Merck) was converted with sodium thiosulfate into the corresponding Bunte salt. The crystalline product was filtered off, recrystallized from ethanol, subjected to acid hydrolysis, and recrystallized from *n*-hexane to yield **1** (95%). **2**: The Bunte salt of 11-bromoundecanol was converted into the symmetric disulfide following the description by *Milligan* and *Swan* [22] (98% yield). The disulfide was isolated and esterified with a small surplus of a-biotin, following the method of *Steglich* et al. [23]. The reaction mixture was separated chromatographically to produce pure **2** with a yield of 13%. **3**: The activated ester of 11-bromoundecanoic acid was treated with a surplus of 1,8-diamino-3,6-dioxaoctane (German Texaco) and unchanged amine was removed. The intermediate product was treated with biotin-active ester and the product was isolated. The bromide was converted into the corresponding Bunte Salt and subjected to acid hydrolysis. Flash chromatography ($CHCl_3/CH_3OH$ 1:1) yielded **3** (3% yield pure according to NMR spectrum).
[12] To characterize the gold-coated substrates quickly and easily, the contact angle of a drop of water was measured at the three-phase line between air, water, and solid. Liquid was pumped into the drops with a micrometer-driven glass syringe. We measured the constantly advancing or receding contact angles. The contact angles were measured with the contact angle microscope GI (Krüss Inc., Hamburg, FRG).
[13] As substrate for chemisorption and the STM measurements, epitaxially grown gold on freshly cleaved mica was used. The mica was cleaved in air and rinsed immediately with millipore water. 2500 Å of gold was evaporated onto it at a pressure of $< 10^{-7}$ mbar. The gold was evaporated at a rate of 5 Å/s onto the mica, which was heated to 300 °C before and during the evaporation [21]. The surface shows (111) crystal faces which are atomically flat over regions of > 1000 Å.
[14] The STM investigations were performed under normal conditions in air with a Bioscope STM [20]. The images shown were recorded at a tunneling current (I_t) of 100 pA and a tunneling voltage (V_t tip to sample) of + 200 mV. Using both electrochemically etched gold and also tungsten tips, we obtained essentially the same results.
[15] R. G. Nuzzo, E. M. Korenic, L. H. Dubois, *J. Chem. Phys. 93* (1990) 767.
[16] 10–100 μM streptavidin in 10 mM Tris-HCl, 10 mM NaCl, pH 7.4.
[17] P. C. Weber, D. H. Ohlendorf, J. J. Wendoloski, F. R. Salemme, *Science (Washington DC) 243* (1989) 85.
[18] a) M. Ahlers, R. Blankenburg, D. W. Grainger, P. Meller, H. Ringsdorf, C. Salesse, *Thin Solid Films 180* (1989) 93; b) S. A. Darst, M. Ahlers, P. H. Meller, E. W. Kubalek, R. Blankenburg, H. O. Ribi, H. Ringsdorf, R. D. Kornberg, *Biophys. J.*, in press.
[19] K. L. Wolf: *Physik und Chemie der Grenzflächen, Vol. 2*, Springer, Berlin 1959, p. 143.
[20] B. Michel, G. Travaglini, *J. Microsc. (Oxford) 151* (1988) 681.
[21] V. M. Hallmark, S. Chiang, J. F. Rabolt, J. D. Swalen, R. J. Wilson, *Phys. Rev. Lett. 59* (1987) 2879.
[22] B. Milligan, J. Swan, *J. Chem. Soc. 1962* (1962) 2172.
[23] W. Steglich, B. Neises, *Angew. Chem. 90* (1978) 556; *Angew. Chem. Int. Ed. Engl. 17* (1978) 522.

The High-Yield Synthesis and Characterization of the First Porphyrin–Cyclam Dinucleating Ligand and Its Iron(III)/Copper(II) Complex **

By *Véronique Bulach, Dominique Mandon** and *Raymond Weiss**

Access to homo- or heterobimetallic porphyrin complexes by simple and high-yield pathways is of special interest, not only in the field of synthetic analogues of active sites in biological processes, but in many other different areas where metalloporphyrins are involved, such as catalysis, redox processes, mixed-valence chemistry, or even selective cleavage of DNA.[1–4]

[*] Prof. Dr. R. Weiss, Dipl.-Chem. V. Bulach, Dr. D. Mandon
Laboratoire de Cristallochimie et Chimie Structurale
URA CNRS 424
Institut Le Bel, Université Louis Pasteur
4, Rue Blaise Pascal, F-67070 Strasbourg Cedex (France)

[**] This work was supported by the Centre National de la Recherche Scientifique. We are indebted to Dr. *E. Bill* and Prof. *A. X. Trautwein* (Medizinische Universität Lübeck, Germany) for the ESR measurements and spectrum simulation; we thank Dr. *M. Momenteau* for helpful discussions. *R. W.* thanks the Alexander von Humboldt Foundation for financial support.

Among the variety of polymetallic enzymes, one of the most remarkable is cytochrome c oxidase,[5] in which one iron(cyt_a) and one copper (Cu_A) interact with the cyt_{a3}–Cu_B heme-iron–copper pair to catalyze the reduction of dioxygen to water in protic media ($O_2 + 4H^{\oplus} + 4e^{\ominus} \rightarrow 2H_2O$, $E_o = +1.23$ V vs NHE).

So far the structure of this enzyme has not been unambiguously established. Whereas cyt_a and Cu_A seem to act as electron carriers, the cyt_{a3}–Cu_B pair is probably responsible for the complexation, reduction, and cleavage of the dioxygen molecule. In the oxidized state, this pair displays magnetic and ESR properties consistent with a ground spin state of $S = 2$, arising from a strong antiparallel coupling ($-J > 200\ cm^{-1}$) between the high-spin ferric iron and the cupric system, and suggesting the involvement of an endogenous or exogenous bridging ligand. The most recent EXAFS studies indicate that the Cu–Fe distance in cyt_{a3}–Cu_B is close to 3 Å.[6]

Access to heterobimetallic species is generally achieved either by self-assembling[7] methods, which requires work with reactive precursors, or by design of a chelating ligand covalently attached to a porphyrin;[8] nevertheless, only a few examples of such a chelating ligand are known, and efficient selective metalation has to be carried out.

To fulfill the requirements of thermal stability in the solid state as well as in solution and the relative proximity of the two metal centers combined with flexibility of the system, we have developed a modeling strategy involving the coupling of the 1,4,8,11-tetraazacyclotetradecane (cyclam)—a macrocycle which forms very stable complexes with transition metals and is easily functionalized[9]—with the *meso*-mono(*o*-aminophenyl)triphenylporphyrin[10] (*o*-$MAPTPH_2$) by a lateral arm, which allows a free rotation of the two macrocycles relative to each other and therefore introduces important flexibility. We report in this paper the high-yield synthesis and characterization of the first porphyrin–cyclam dinucleating ligand (Fig. 1), as well as a synthetic pathway leading to the corresponding heterobimetallic complexes of this ligand.

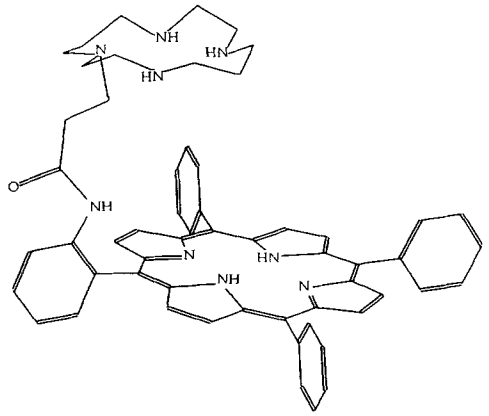

Figure 1. Structure of the porphyrin-cyclam ligand, 3.

Treatment at 0 °C of a dichloromethane solution of *o*-$MAPTPH_2$ **1** with one equivalent of acryloyl chloride affords, after extraction, chromatography, and crystallization (CH_2Cl_2/hexane), the new prophyrin **2**, monofunctionalized by an activated olefin, in 70% yield. This functional group reacts with secondary amines under mild conditions:[11] indeed, the complete reaction of **2** with an excess of cyclam is achieved within three days simply by stirring the two reagents in CH_2Cl_2 at room temperature (Scheme 1). After extraction and chromatographic procedures (dextran-type stationary phase), the porphyrin **3** with appended cyclam[12] can be crystallized from CH_2Cl_2/*n*-hexane, with a 67% yield. ^1H and ^{13}C NMR spectroscopy confirms the structure of this bisheteromacrocycle (Fig. 2a): the 12 nonequivalent methylene groups appear in the ^1H NMR spectrum at $0.1 \leq \delta \leq 1.8$, upfield from the corresponding signals in tetrasubstituted free macrocyle[13] ($1.7 \leq \delta \leq 2.8$), indicating an important interaction of the cyclam with the porphyrin core. Variable temperature experiments have been carried out between 293 and 215 K. Below 243 K the pyrrole signals

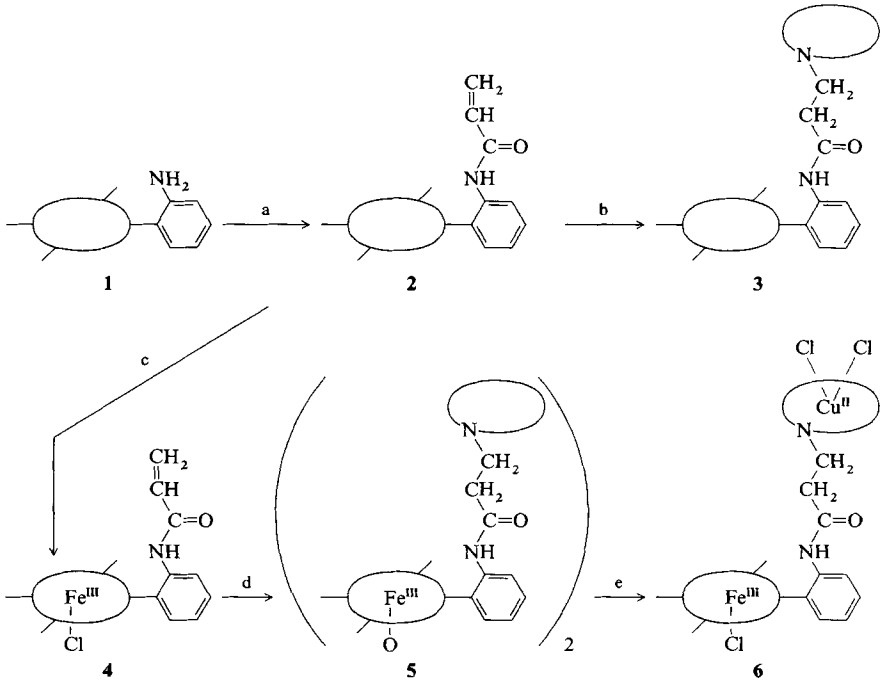

Scheme 1. a) $ClCOCH{=}CH_2$, 0 °C, 1 h, CH_2Cl_2; b) cyclam, excess, RT, 3 days, CH_2Cl_2; c) $FeCl_2$, 3 days, RT, THF; d) cyclam, excess, RT, 1 day, CH_2Cl_2; e) $CuCl_2 \cdot 2H_2O$, reflux, 2 days, THF/H_2O 50/50; then HCl. Large ellipses represent porphyrin; ellipses containing N, the cyclam moiety.

are split into two components (Fig. 2b), as previously reported for some more rigid, functionalized porphyrins.[14] Moreover, the upfield shift of the methylene protons, although significant, is less marked at low temperature. These observations suggest that free rotation of the cyclam relative to the porphyrin is reduced at low temperature.

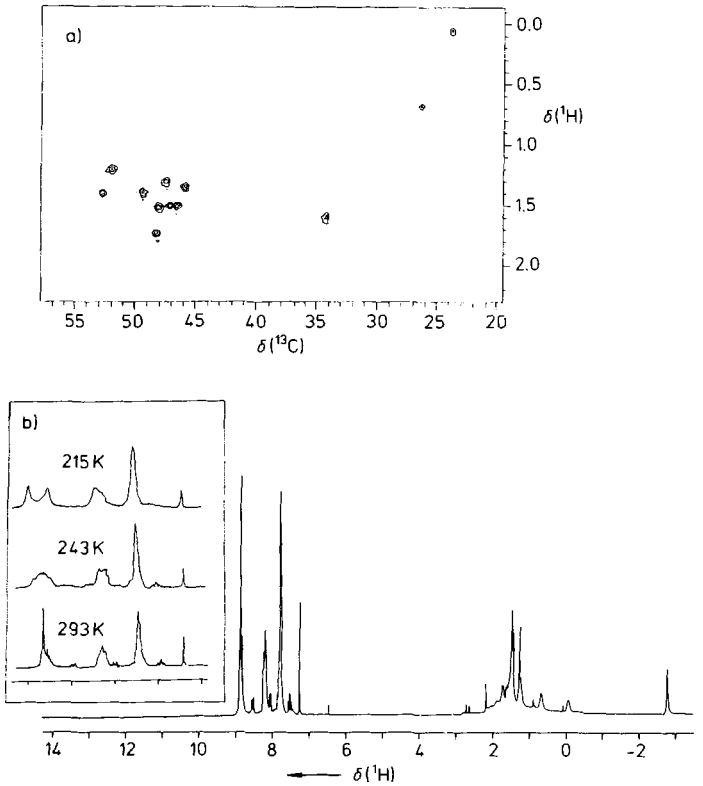

Figure 2. a) 2D NMR spectrum ($^1H/^{13}C$ correlation) for **3** ($CDCl_3$, RT), showing the 12 nonequivalent methylene groups. b) ^1H NMR ($CDCl_3$, RT) spectrum of **3**, and temperature dependence of the region from $\delta = 6$ to 10.

Access to binuclear systems is now anticipated, by metalation of the two coordination sites in **3**. Nevertheless, if *hetero*bimetallic systems have to be synthesized, statistic metalation of both macrocycles might occur, even if 1 equivalent of metal is used initially, leading to tedious separation procedures. To avoid this problem we have investigated the reactivity of the cyclam ligand with the appended olefin of the metalated porphyrin **4**:[15] indeed, this reaction in CH_2Cl_2 is achieved within 24 hours, faster than with **2** under the same conditions. After workup, the microcrystalline material **5** is obtained from dichloromethane/*n*-hexane in 60% yield. Spectroscopic investigations of this material (UV/VIS(CH_2Cl_2): λ_{max} [nm] = 410 (Soret band), 570, 615; ESR (CH_2Cl_2, 4.2 K): nonactive; ^1H NMR (CD_2Cl_2, 25 °C, TMS): $\delta_{pyrrole} = 13.8$) indicate that **5** is a μ-oxoiron(III)-porphyrin dimer. Treatment of **5** with hydrochloric acid and recrystallization yielded the corresponding high-spin chloroferriporphyrin **5'** as an hygroscopic, microcrystalline solid, in which the cyclam is in its fully protonated form (UV/VIS(CH_2Cl_2): λ_{max} [nm] = 418 (Soret band), 505, 575, 660; ESR (CH_2Cl_2, 4.2 K): $g_\perp = 6$, $g_\parallel = 2$; ^1H NMR (CD_2Cl_2, 25 °C, TMS): $\delta_{pyrrole} = +80.0$).

The cyclam ligand in **5** can be easily metalated by refluxing with an excess of cupric chloride in a 50/50 THF/water mixture for 48 hours. After extraction, chromatography on a dextran-type stationary phase, and treatment with hydrochloric acid, a stable microcrystalline solid can be isolated in a 65% yield. Mass spectroscopy measurements (FAB$^\oplus$, nitrobenzyl alcohol (NBA)) indicate that it is chloroiron(III) porphyrin–dichlorocopper(II) cyclam complex **6** (characteristic fragments: m/z = 1105.02 (**6**$^\oplus$), 1072.0 (**6**$-Cl^\ominus$), 1035.1 (**6**$-2\,Cl^\ominus$), and 1000.1 (**6**$-3\,Cl^\ominus$). ^1H NMR ($CDCl_3$, 25 °C, TMS) as well as optical spectroscopy display typical ferric high-spin features ($\delta_{pyrrole} = +80.0$ and λ_{max} [nm] = 420 (soret band), 505, 575, 660 nm). The X band ESR spectrum of **6**, run at 10 K in frozen THF solution, displays a signal at $g = 6.0$ together with a signal close to $g = 2$. This spectrum can be simulated (see Fig. 3) as a superimposition of two independent subspectra corresponding to an axial high-spin iron(III) complex ($g_\perp = 6$ and $g_\parallel = 2$, line width = 45 G), and a slightly rhombic copper(II) derivative ($g_z = 2.25$, $g_y = 2.05$, $g_x = 2.04$, line width = 150 G), in a 1:1 Fe(III)/Cu(II) ratio. The lack of magnetic interaction between the two paramagnetic centers in **6** is presumbably due to their separation in space and to the absence of any bridging ligand between the two metals[16] in this molecule.

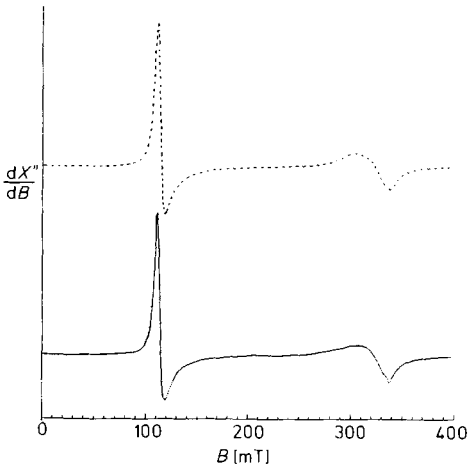

Figure 3. Simulated (dashed line) spectrum of a high-spin Fe^{III}porphyrin/Cu^{II} complex (1:1) and experimental (solid line) spectrum of **3** (10.0 K, THF).

In conclusion, the very mild conditions involved in the addition of secondary amines to activated olefins allow the preparation of the first linked-cyclam porphyrin ligand, and provide an easy access to a heterobimetallic iron(III)–copper(II) derivative. Reactions with bridging ligands, as well as extension of this strategy to other metals, is presently under investigation. Compound **3** is a lipophylic porphyrin linked by a flexible arm to a hydrophilic macrocycle. Appropriate selection of the olefin substituent should lead to species displaying different flexibility features; also, choice of aryl groups on the porphyrin,[17] as well as substitution of the cyclam moiety, would allow variation in the hydrophilicity of the system.

Experimental

2: ^1H NMR (200 MHz, $CDCl_3$, TMS): $\delta = 8.9$ (m, 8H; β pyrrole), 8.3 (m, 6H; *o*-phenyl), 7.9 (d, 1H; *o*-phenyl subst.), 7.8 (m, 9H; *m,p*-phenyl) 7.1 (m, 2H; *p*-phenyl subst.; *m'*-phenyl subst), 7.6 (t, 1H; *m*-phenyl subst.), 6.8 (s, 1H; NHC=O), 5.7 (m, 1H; $CH{=}CH_2$), 4.9 (m, 2H; $CH{=}CH_2$), -2.77 (NH pyrrole); IR (Nujol) $\tilde{\nu}$, [cm^{-1}] = 1692 (C=O); MS (FAB$^\oplus$, tetraglyme): m/z 684.5 (**2**$^\oplus$); correct elemental analyses (C, H, N).

3: ^{1}H NMR (200 MHz, $CDCl_3$, TMS): δ = 8.9 (m, 8H; β pyrrole), 8.5 (d, 1H; *o*-phenyl), 8.2 (m, 6H; *o*-phenyl), 8.0 (d, 1H; *m'*-phenyl), 7.8 (m, 10H; *p,m*-phenyl; *p'*-phenyl), 7.5 (t, 1H; *m*-phenyl), − 2.8 (NH pyrrole), 1.9–0.0 (6 m, 28H; CH_2, $3H_2O$, N*H*C=O, cyclam and lateral arm); ^{13}C NMR (50.33 MHz, $CDCl_3$, TMS): δ = 170.8 (C=O), 140.7 (α-pyrrole), 142.1, 141.9, 139.0 (C *meso*), 135.0 (*o*-phenyl subst.), 134.6 (*o*-phenyl), 132.2, 131.9, 131.4, 130.7, 129.2 (β-pyrrole), 129.4 (*p*-phenyl subst.), 127.9 (*p*-phenyl), 126.8 (*m*-phenyl), 122.9 (*m*-phenyl subst.), 122.2 (*m'*-phenyl subst.), 120.9, 120.5 (*ipso*-phenyl), 52.7, 51.3, 49.1, 48.2, 47.8, 47.4, 47.2, 47.0, 46.1, 34.3, 27.3, 23.5 (12 CH_2, cyclam and lateral arm); IR (Nujol) $\tilde{\nu}$, [cm^{-1}] = 1680(C=O); MS (FAB$^{\oplus}$, NBA): *m/z* 884.4 (**3**$^{\oplus}$); correct elemental analyses (C, H, N).

4: ^{1}H NMR (200 MHz, $CDCl_3$, TMS): δ = 86, 81, 78 (broad, 8H; β-pyrrole), 16.1 (6H; *m*-phenyl), 13.3 (1H; *m*-phenyl subst.), 12.8 (6H; *o*-phenyl), 12.2 (1H; *o*-phenyl subst.), 8.1 (3H, *p*-phenyl), 7.8 (1H; *p*-phenyl subst.); IR (Nujol) $\tilde{\nu}$[cm^{-1}] = 1689 (C=O); correct elemental analyses (C, H, N).

5: ^{1}H NMR (200 MHz, $CDCl_3$, TMS): δ = 13.8 (broad, 8H; β-pyrrole), 8.4, 7.7 (broad, phenyl); ESR (4.2 K, CH_2Cl_2): diamagnetic, ca. 1% high-spin contamination. MS (FAB$^{\oplus}$, NBA): *m/z* 1892.5 (**5**$^{\oplus}$).

5': ^{1}H NMR (200 MHz, $CDCl_3$, TMS): δ = 80 (broad, 8H; β-pyrrole), 13.3 (broad, *m*-phenyl), 12.8 (broad, *o*-phenyl), 7.8 (broad, *p*-phenyl); ESR (4.2 K, CH_2Cl_2): $g_{\perp}$ = 6, $g_{\parallel}$ = 2; IR (Nujol) $\tilde{\nu}$[cm^{-1}] = 1670 (C=O); MS (FAB$^{\oplus}$, NBA): *m/z* 973.6 (**5'**$^{\oplus}$−4HCl). correct elemental analyses (C, H, N).

6: ^{1}H NMR (200 MHz, $CDCl_3$, TMS): δ = 80 (broad, 8H; β-pyrrole), 13.5, 12.1, 7.1 (broad, phenyl); ESR 10 K, THF) $g_{\perp}$ = 6, ferric; $g_{\parallel}$ = 2, ferric, cupric cyclam; IR (Nujol) $\tilde{\nu}$[cm^{-1}] = 1680 (C=O); MS (FAB$^{\oplus}$, NBA): *m/z* 1105.2 (**6**$^{\oplus}$), 1072.0 (**6**−Cl$^{\ominus}$), 1035.1 (**6** − 2Cl$^{\ominus}$), 1000.1 (**6**-3 Cl$^{\ominus}$). Correct elemental analyses (C, H, N).

Received: December 20, 1990 [Z 4341 IE]
German version: *Angew. Chem. 103* (1990) 611

CAS Registry numbers:
1, 69082-94-6; **2**, 127049-74-5; **3**, 132938-11-5; **4**, 132911-21-8; **5**, 132911-22-9; **5'**, 132911-24-1; **6**, 132911-23-0; ClCOCH=CH_2, 814-68-6; cyclam, 295-31-4; cytochrome oxidase, 9001-16-5

[1] L. Stryer, *Biochemistry, 3rd Ed.*, Freeman & Co, New York 1988; J. A. Ibers, R. H. Holm, *Science 209* (1980) 223–235; R. J. P. Williams, *J. Mol. Catal. 30* (1985) 1–26; O. Kahn, *Struct. Bonding (Berlin) 68* (1987) 89–167.

[2] H. Nishihara, K. Pressprich, R. W. Murray, J. P. Collman, *Inorg. Chem. 29* (1990) 1000–1006; R. D. Arasasingham, T. C. Bruice, *ibid. 29* (1990) 1422–1427; M. Perrée-Fauvet, A. Gaudemer, J. Bonvoisin, J. J. Girerd, C. Boucly-Goester, P. Boucly, *ibid. 28* (1989) 3533–3538.

[3] J. T. Groves, P. Viski, *J. Am. Chem. Soc. 111* (1989) 8537–8538; D. Ostovic, T. C. Bruice, *ibid. 111* (1989) 6511–6517; W.-H. Leung, C.-M. Che, *ibid. 111* (1989) 8812–8818.

[4] D. L. Banville, L. G. Marzilli, J. A. Strickland, W. D. Wilson, *Biopolymers 25* (1986) 1837–1858; M. J. Carvlin, R. J. Fiel, *Nucleic Acids Res. 11* (1983) 6121–6139; R. F. Pastenack, E. J. Gibbs, J. J. Villafranca, *Biochemistry 22* (1983) 5409–5417; for more recent work: J. Bernadou, G. Pratviel, F. Bennis, M. Girardet, B. Meunier, *ibid. 28* (1989) 7268–7275.

[5] For a recent review, see: BO. G. Malmström, *Chem. Rev. 90* (1990) 1247–1260.

[6] R. A. Scott, *Ann. Rev. Biophys. Chem. 18* (1989) 137–158.

[7] R. J. Saxton, L. W. Olson, L. J. Wilson, *J. Chem. Soc. Chem. Commun. 1982*, 984–986; B. R. Serr, C. E. L. Headford, O. P. Anderson, C. M. Elliot, C. K. Schauer, K. Akabori, K Spartalian, W. E. Hatfield, B. R. Rohrs, *Inorg. Chem. 29* (1990) 2663–2671; G. P. Gupta, G. Lang, C. A. Koch, B. Wang, W. R. Scheidt, C. Reed, *ibid. 29* (1990) 4234–4239.

[8] C. K. Chang, M. S. Koo, B. Waerd, *J. Chem. Soc. Chem. Commun. 1982*, 716–719; C. K. Chang, *J. Am. Chem. Soc. 99* (1977) 2819–2822; M. J. Gunter, K. J. Berry, K. S. Murray, *ibid. 106* (1984) 4227–4235.

[9] T. A. Kaden, *Top. Curr. Chem. 128* (1984) 157–179; T. A. Kaden, *Comments Inorg. Chem. 10* (1990) 25–36.

[10] J. P. Collman, J. I. Brauman, K. M. Doxsee, T. R. Halbert, E. Bunnenberg, R. E. Linder, G. N. LaMar, J. Del Gaudio, G. Lang, K. Spartalian, *J. Am. Chem. Soc. 102* (1980) 4182–4192.

[11] J. March, *Adv. Org. Chem., 3rd Ed.* Wiley Interscience Publishers, New York 1985 pp. 689–691.

[12] In its fully protonated form as a chloride salt, **3** is soluble in water.

[13] Chemical shifts of the methylene groups in the tetra-*N*-methylpropionate derivative of the cyclam. V. Bulach, D. Mandon, R. Weiss, unpublished results.

[14] M. Momenteau, B. Loock, C. Tetreau, D. Lavalette, A. Croisy, C. Schaeffer, C. Huel, J. M. Lhoste, *J. Chem. Soc. Perkin Trans. 2 1987*, 249–257; B. Boitrel, A. Lecas, Z. Renko, E. Rose, *New. J. Chem. 1989*, 73–99 and references therein; J. Almog, J. E. Baldwin, R. L. Dyer, M. Peters, *J. Am. Chem. Soc. 97* (1975) 226–227.

[15] For metalation procedures, see: J. P. Collman, R. G. Gagne, C. A. Reed, T. H. Halbert, G. Lang, W. T. Robinson, *J. Am. Chem. Soc. 96* (1975) 1427–1439.

[16] It is not clear whether the chlorine atom ligated to the iron is on the same side as the substituent, or not; on the other hand, the chlorocupric moiety may have a *cis* configuration at the opposite side of the porphyrin. For copper dichloride/cyclam complexes, see: B. Bosnisch, *Inorg. Chem. 4* (1965) 1102–1107.

[17] For example, tetrapyridinyl porphyrin salts are well-known as water-soluble compounds: P. Hambright, E. B. Fleischer, *Inorg. Chem. 9* (1970) 1757–1761.

Strategy for the Synthesis of Tube-Shaped Molecules**

By *Fritz Vögtle,* Axel Schröder* and *Detlef Karbach*

Molecules whose structures[1] and functions[2] closely resemble and imitate those of well-known macroscopic objects have repeatedly motivated new developments in synthetic chemistry.[3] Some eight years ago we commented on tube-shaped molecules of type **I**, whose synthesis still presents a challenge to the preparative chemist.[4] The molecular ribbons,[5] belts or collars[6] which have in the meantime become well known provide some progress but all contain merely "classic" 1,2-coupled double bonds or *ortho*-condensed benzene rings.

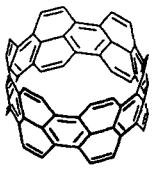

I

The aim of our studies was to develop a generally applicable entry to longer tube-shaped molecules. Thus far no synthetic concept has been reported concerning molecular tubes, which are of interest not only for the encapsulation of guest compounds but also as channels for the transport of ions and neutral molecules. Prerequisite for subsequent host/guest matching is a variable repetitive synthetic strategy with several reproducible steps as we have used in connection with the first cascade-like synthesis.[7]

The difficulties in the synthesis were encountered in particular in the development of isolable yet reactive tetrafunction-

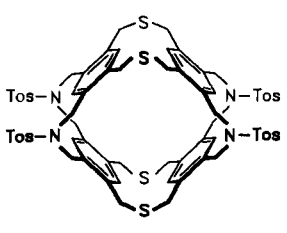

1a

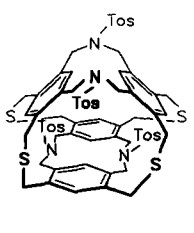

1b

[*] Prof. Dr. F. Vögtle, Dipl.-Chem. A. Schröder, Dipl.-Chem. D. Karbach
Institut für Organische Chemie und Biochemie der Universität
Gerhard-Domagk-Strasse 1, W-5300 Bonn 1 (FRG)

[**] This work was supported by the Fonds der Chemischen Industrie. We thank Herr *C. Schmidt* and Dr. *G. Eckhardt* for recording the NMR and MS spectra, respectively.

alized cyclization components. Key building blocks for the synthesis of the desired tube-shaped compounds **1** are tetrasubstituted monocycles such as the [3.3]phanes **3**, which are obtainable by "cyclizing elongation" of fourfold functionalized benzene building blocks of type **2**.

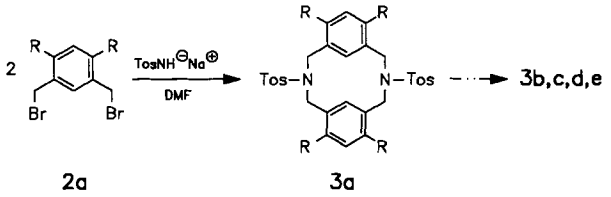

2a **3a**

	2a/3a	3b	3c	3d	3e
R	CO_2Et	CH_2OAc	CH_2OH	CH_2Br	CH_2SH

Although the synthesis of the building blocks **4a–c** and **5a–c** (with sulfide bridges) was possible, the key compounds **4d, e** and **5d, e** could not be prepared because of the sparing solubility of **4c** and **5c** and their low stability towards acidic reagents (e.g. HBr/glacial acetic acid, PBr_3, $SOBr_2$).[8]

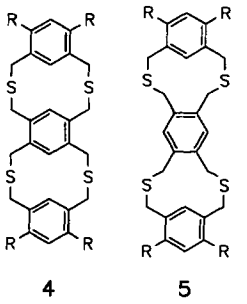

4 **5**

	R
a	CO_2Et
b	CH_2OAc
c	CH_2OH
d	CH_2Br
e	CH_2SH

Isolation of the cyclization components **3d** and **3c** was possible only after exchange of the sulfide sulfur atoms in the bridges by *N*-Tos (Tos = *p*-$SO_2C_6H_4CH_3$).

Although cyclization of **3d** with the easily accessible, fourfold functionalized building block **6b** of the metacyclophane type used in the first experiments did not lead to the desired compound because of side reactions, we were able to detect macrocyclizations of **3d** with 1,2,4,5-tetrakis(mercaptomethyl)benzene **7b** and 3,3′,5,5′-tetrakis(mercaptomethyl)-biphenyl **8b** mass spectroscopically.

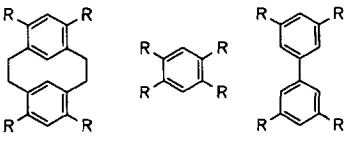

6a,b **7a,b** **8a,b**

a: R = CH_2Br, b: R = CH_2SH

In the following we discuss what we consider the most important cyclization in this context, **3d** + **3e** → **1**. It was carried out as a two-component reaction according to the dilution principle[9] (by simultaneous dropwise addition of the components **3d** and **3e** to a suspension of Cs_2CO_3 in benzene/ethanol).

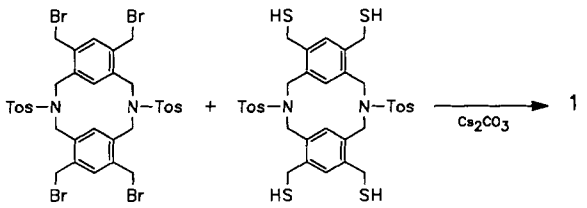

3d **3e**

In principle, in macrocyclizations of this type two isomers can be formed: tube-shaped molecules such as **1a** and less formally tube-shaped isomers such as **1b** with a "crossed" arrangement of the [3.3]phane building blocks. Isolation of one of the isomers of **1** was remarkable easy after flash chromatography of the crude product on silica gel (eluent $CHCl_3$/ethyl acetate 2/1, v/v) and crystallization from dichloromethane/*n*-hexane (colorless crystals, m.p. 280 °C (decomp.), yield 3.4%). Whereas the isomer isolated in this way was obtained in pure form in 50 mg amounts, a second isomer could not be found even upon careful work-up by means of HPLC (inter alia Nucleosil-CN phase 5 μm; eluent CH_2Cl_2/CH_3CN 1/1, v/v).

Due to the poor quality of the otherwise well-formed crystals[10] it was not possible to differentiate by an X-ray structure analysis which isomer had been formed. The formation of one of the two isomers **1a/1b** could, however, be confirmed ^{1}H-NMR spectroscopically and by FAB mass spectrometry [m/z = 1325.3 ($M^{\oplus}$ + H)]; the assignment of the isolated isomers as **1a** or **1b** was at first difficult because of the similarity of the two structures. 90-MHz ^{1}H-NMR spectra of the isolated isomer at room temperature show broadened signals, which are sharper and in each case doubled in the 200-MHz and 400-MHz spectra. Thus, at 20 °C, the 400-MHz spectrum shows four AB systems (CD_2Cl_2: δ = 5.05(br) and 3.15(br), 5.0(d), and 4.6(d), 4.3(d) and 3.2(d), 3.85(d) and 3.65(d); assignment by double resonance experiments) for the protons of the methylene bridges and four signals (δ = 8.75(s, $H_{b,c}$) 6.7(s, $H_{a,d}$), 6.65(s, $H_{a,d}$), and 6.35(s, $H_{b,c}$) for the protons of the benzene rings.

Noteworthy is the signal for the protons of the benzene rings at δ = 8.75, whose extreme downfield position prompted us to assign the structure **1a** to the compound isolated, since only the hydrogen atoms H_b and H_c of this isomer should show such a shift. On the basis of a comparison with known cyclophanes[11] and taking into consideration the influence of the magnetic anisotropism of the neighboring benzene ring[12] all other hydrogen atoms of **1a** and **1b** should absorb at higher field.[13]

This assignment is also consistent with observations made in other cyclophane syntheses, which show that cyclizations can be accomplished when the functional groups of the precursors (here **3d** and **3e**) fit together spatially (principle of rigid groups).[14] This is to be expected all the more if the two reactants are oriented parallel to each other, i.e. formation of the crossed isomer **1b** is not favored. We therefore assume that the cyclic compound isolated is **1a**.

Remarkably, the ^{1}H-NMR spectrum of the compound is temperature dependent. At 160 °C only two AB systems are observed for the protons of the methylene bridges (90 MHz, $C_2D_2Cl_4$; δ = 4.8 (d, CH_2-N) and 4.2 (d, CH_2–N) and 3.9 (d, CH_2-S) and 3.5 (d, CH_2–S) and only two signals for the protons of the benzene rings (δ = 7.5 (s, $H_{b,c}$) and 6.7 (s, $H_{a,d}$). It follows, therefore, that **1a** is present in the less symmetric conformation **A** at room temperature and slowly transforms (on the NMR time scale) into the conformer **B**.

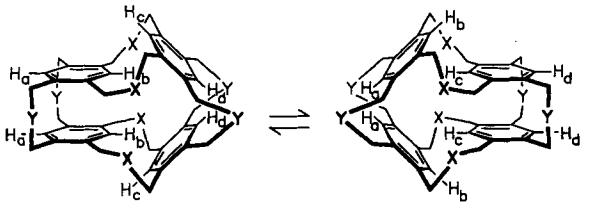

A X, Y = S, N-tos B

1a

The barrier for this process is ca. 65–70 kJ mol^{-1} (with $T_c = 70\,^{\circ}C$ and $\Delta\nu = 215$ Hz for H_b and H_c).

1a, "a short molecular tube" is comparatively easily accessible since the starting compounds are readily synthesized. Its cavity is large enough to accomodate a benzene molecule. By suitable choice of other tetrafunctionalized building blocks it should be possible in analogous way (if necessary with subsequent extrusion of the bridge heteroatoms) to prepare further tube-shaped "endoreceptors" (longer, expanded ring hydrocarbons, Möbius strips), the cavities of which are enclosed as by cell walls.

Received: December 18, 1990 [Z 4339 IE]
German version: *Angew. Chem. 103* (1991) 582

CAS Registry numbers:
1, 133071-04-2; **3d**, 133043-80-8; **3e**, 133043-81-9.

[1] See for example "Platonische Körper"; review: F. Vögtle: *Reizvolle Moleküle der Organischen Chemie*, Teubner, Stuttgart 1989.
[2] For example "octopus molecules"; see F. Vögtle, E. Weber, *Angew. Chem. 86* (1974) 896; *Angew. Chem. Int. Ed. Engl. 13* (1974) 814.
[3] Dendrimers: D. A. Tomalia, A. M. Naylor, W. A. Goddard III, *Angew. Chem. 102* (1990) 119; *Angew. Chem. Int. Ed. Engl.* 29 (1990) 138; A. Nickon, E. F. Silversmith: *Organic Chemistry—The Name Game*, Pergamon, New York 1987.
[4] F. Vögtle, *Top. Curr. Chem. 115* (1983) 157.
[5] D. M. Walba, *Tetrahedron 41* (1985) 3161.
[6] F. H. Kohnke, A. M. Z. Slawin, J. F. Stoddart, D. J. Williams, *Angew. Chem. 99* (1987) 941; *Angew. Chem. Int. Ed. Engl. 26* (1987) 892; P. R. Ashton, N. S. Isaacs, F. H. Kohnke, A. M. Z. Slawin, C. M. Spencer, J. F. Stoddart, D. J. Williams, *ibid. 100* (1988) 981 bzw. *27* (1988) 966; cf. also "deltaphane": H. C. Kang, A. W. Hanson, B. Eaton, V. Boekelheide, *J. Am. Chem. Soc. 107* (1985) 1979.
[7] E. Buhleier, W. Wehner, F. Vögtle, *Synthesis 1977*, 155; cf. also E. Vogel, H. M. Deger, J. Sombroek, J. Palm, A. Wagner, J. Lex, *Angew. Chem. 92* (1980) 43; *Angew. Chem. Int. Ed. Engl. 19* (1980) 41; cf. also [6].
[8] A. Schröder, *Diplomarbeit*, Universität Bonn 1988; D. Karbach, *Diplomarbeit*, Universität Bonn 1990.
[9] P. Knops, N. Sendhoff, H.-B. Mekelburger, F. Vögtle, *Top. Curr. Chem.*, in press.
[10] We thank Herrn Doz.-Dr. *K. Rissanen*, Universität Jyväskylä, Finnland, for these experiments.
[11] Review: F. Vögtle: *Cyclophan-Chemie*, Teubner, Stuttgart 1990.
[12] C. W. Haigh, R. B. Mallion, *Org. Magn. Reson. 4* (1972) 203.
[13] An assignment by nuclear Overhauser effects is not possible because of the symmetry of the isomers.
[14] P. Knops, F. Vögtle, *Chem. Ber.*, in press.

Se_4N_2, a Novel Selenium Nitride

By *Kurt Dehnicke,* Fritjof Schmock, Klaus F. Köhler,* and *Gernot Frenking*

The only binary nitride of selenium reported thus far is the highly explosive tetraselenium tetranitride **1**,[1] whose crystal structure analysis[2] revealed strong intermolecular Se···N contacts between the cage molecules, thus making its insolubility in all solvents understandable. This property, and its explosivity, limit its application as a preparative reagent severly compared to that of the well-investigated tetrasulfur tetranitride **2**.[3] Therefore only very few preparative applications of **1** have been reported.[4–7]

Se_4N_4 S_4N_4 Se_4N_2 S_4N_2
1 **2** **3** **4**

In the search for less sensitive selenium nitrides we found an entry to the previously unknown tetraselenium dinitride **3** in the reaction of diselenium dichloride with trimethylsilylazide in dichloromethane [Eq. (a)].

$$2Se_2Cl_2 + 4Me_3SiN_3 \longrightarrow \underset{\mathbf{3}}{Se_4N_2} + 5N_2 + 4Me_3SiCl \qquad (a)$$

It is formed almost quantitatively as a black, finely crystalline powder, whose thermal and mechanical stability is greater by far than that of **1**. It can be handled with ease at room temperature, but on heating to 80 °C it decomposes explosively; it also explodes when struck with a hammer. These properties are comparable with those of **2**.[2] In contrast to the hydrolysis-insensitive **1**,[1] **3** slowly decomposes with disproportionation on exposure to moisture, forming red Se_8 and ammonium hydrogen selenite.

The IR spectrum of **3** shows a sequence of bands corresponding to that shown by the crystallographically characterized tetrasulfur dinitride **4**,[8, 9] so that we assume an analogous molecular structure with C_s symmetry for **3**.

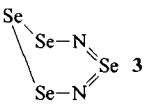

3

According to the irreducible representations, this model requires twelve IR-active fundamental vibrations, of which seven belong to the symmetry type A′ and five to the symmetry type A″. Of these six are stretching vibrations (3A′, 3A″) and six are deformation vibrations.[10] With the assumption of coincidental degeneration of the deformation vibration at 281 cm^{-1}, which is supported by the ab initio calculation, this expectation is fulfilled (Table 1). Consistent with the different bond orders Se=N and Se–N two pairs of stretching vibrations appear at 828 and 792 cm^{-1} and at 584 and 571/554 cm^{-1}, of which the A″ band splits by Fermi reso-

Table 1. Calculated (3-21G*) and observed vibration frequencies ν[cm^{-1}], calculated intensities [kmmol^{-1}] and assignments for Se_4N_2 (C_s symmetry).

3-21G*			Experimental		Vibration
ν	Symmetry type	Int.	ν	Int.	
96	A′	1	105	vw	
120	A″	11	126	st	δ(SeSeSe)
155	A′	1	169	st	
238	A″	1	244	st	
290	A′	1	281	vst	δ(SeNSe)
290	A′	9			
311	A″	23	325	m	$\nu_{as}(SeSe_2)$
366	A′	7	352	sh, w	$\nu_s(SeSe_2)$
515	A″	73	554 / 571	st	ν_{as}(Se-N)
572	A′	45	584	m	ν_s(Se-N)
1055	A′	24	792	w	ν_s(Se-N_2)
1068	A″	122	828	st	$\nu_{as}(SeN_2)$

[*] Prof. Dr. K. Dehnicke, F. Schmock, Dipl.-Chem. K. F. Köhler, Prof. Dr. G. Frenking
Fachbereich Chemie der Universität
Hans-Meerwein-Strasse, W-3550 Marburg (FRG)

nance with the deformation vibration at 281 cm^{-1} into a doublet. This finding correlates very well with the IR spectrum of **1**, in which the Se–N bond order is 1.5 and the two highest frequency stretching vibrations lie at 800 and 788 cm^{-1}.[11] The two resulting bands at 352 and 325 cm^{-1} in the IR spectrum of **3** can then be freely assigned to the two Se–Se stretching vibrations.

This interpretation is confirmed by an ab initio[13] calculation carried out with the 3-21G* all-electron basis set[12] (Table 1). With exception of the two highest-frequency vibrations the agreement with the experimental data is satisfactory. The deviations are due both to the harmonic approximation, with which the calculations are additionally restricted to the approximations of the Schrödinger equation, as well as to the neglection of strong intermolecular interactions, as are also reflected in the low solubility of **3**.

The results of the optimization of the geometry of **3**, which were carried out both with the 3-21G* program as well as with an effective core potential,[12] lead to a chair-shaped structure with C_s symmetry (Fig. 1) which closely resembles

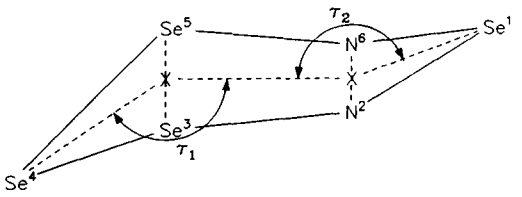

	3-21G*	LANL1DZ+P
Se^1-N^2	168.1	167.2
N^2-Se^3	182.6	181.8
Se^3-Se^4	235.1	236.3
$<N^2Se^1N^6$	119.1	118.4
$<Se^3Se^4Se^5$	99.0	99.5
τ_1	121.9	123.1
τ_2	175.8	176.1
E_{tot}	−9699.4622	−144.8618

Fig. 1. Optimized geometry of **3**. Bond lengths in pm, bond angles in degrees, total energy E_{tot} in Hartree.

that of the valence isomer **4**.[9, 14] The folding of the SeN_2 unit is very slight, $\tau = 176°$ (**4**: 177°[14]). The dihedral angle τ_1 in the case of **3** (121.9° and 123.1°, respectively) is calculated as being somewhat smaller than for **4** (124.2° and 125.0°, respectively[14]). The calculations also give two short Se–N bonds ($\approx$ 168 pm) and two long Se–N distances ($\approx$ 182 pm) corresponding to double and single bonds.[1]

Experimental procedure

A solution of diselenium dichloride (1.64 g) in anhydrous dichloromethane (20 mL) was cooled to −30 °C and treated dropwise with occasional shaking with a solution of trimethylsilylazide (1.70 g) in dichloromethane (10 mL). The mixture was allowed to warm slowly to room temperature and the black, fine precipitate filtered off under dry nitrogen, washed with dichloromethane, and dried in vacuo. Yield 1.14 g (92%).

Warning: Explodes on heating to 80 °C and on subjection to mechanical stress.

Received: November 30, 1990 [Z 4304 IE]
German version: *Angew. Chem. 103* (1991) 564

[1] *Gmelin Handbuch der anorganischen Chemie, Selenium, Suppl. Vol. B 1*, 8th Edit., Springer, Berlin 1981.
[2] H. Bäringhausen, T. von Volkmann, J. Jander, *Acta Crystallogr. 21* (1966) 571.
[3] *Gmelin Handbuch der anorganischen Chemie, Sulfur-Nitrogen Compounds, Part 2*, 8th Edit., Springer, Berlin 1985.
[4] J. Adel, A. El-Kholi, W. Willing, U. Müller, K. Dehnicke, *Chimia 42* (1988) 70.
[5] J. Adel, K. Dehnicke, *Chimia 42* (1988) 413.
[6] P. F. Kelly, A. M. Z. Slawin, D. J. Williams, J. D. Woollins, *J. Chem. Soc. Chem. Commun. 1989*, 408.
[7] I. P. Parkin, J. D. Woollins, *J. Chem. Soc. Dalton Trans. 1990*, 925.
[8] R. W. H. Small, A. J. Banister, Z. V. Hauptman, *J. Chem. Soc. Dalton Trans. 1981*, 2188.
[9] T. Chivers, P. W. Codding, W. G. Laidlaw, S. W. Liblong, R. T. Oakley, M. Trsic, *J. Am. Chem. Soc. 105* (1983) 1186.
[10] J. Weidlein, U. Müller, K. Dehnicke: *Schwingungsspektroskopie*, 2nd Edit., Thieme, Stuttgart 1988.
[11] J. Adel, C. Ergezinger, R. Figge, K. Dehnicke, *Z. Naturforsch. B 43* (1988) 639.
[12] For N, in all calculations using the standard Dunning/Huzinaga split-valence 3s2p basis set. T. H. Dunning, P. J. Hay in H. F. Schaefer III (Ed.): *Modern Theoretical Chemistry*, Plenum, New York 1976, p. 1–28. In the all-electron calculations, for Se the Huzinaga basis set (4333/433/4) was split to (43321/4321/41*), with an exponent of 0.338 for the set of six d-polarization functions. The LANL1DZ + P calculations embrace the LANL1DZ effective core potential implemented in Gaussian 88 with a double zeta basis set for the valence electrons: W. R. Wadt, P. J. Hay, *J. Chem. Phys. 82* (1985) 284, as well as an additional set of d-polarization functions on Se with an exponent of 0.338.
[13] The calculations were carried out with the program Gaussian 88: M. J. Frisch, M. Head-Gordon, H. B. Schlegel, K. Raghavachari, J. S. Binkley, C. Gonzalez, D. J. DeFrees, D. J. Fox, R. A. Whiteside, R. Seeger, C. F. Melius, J. Baker, R. Martin, L. R. Kahn, J. J. P. Stewart, E. M. Fluder, S. Topiol, J. A. Pople, Gaussian Inc., Pittsburgh, PA (USA) 1988.
[14] K. F. Köhler, G. Frenking, unpublished.

Conformational Preference of 2-Triphenylphosphonio-1,3-Dithianes: Competition Between Steric and Anomeric Effects

By *Marian Mikołajczyk,* Piotr Graczyk, Michal W. Wieczorek* and *Grzegorz Bujacz*

Dedicated to Professor Rolf Appel on the occasion of his 70th birthday

There has been considerable interest in the conformation of 1,3-diheteroanes containing phosphoryl and related groups at the anomeric carbon atom, as well as in understanding the origin of the anomeric effect operating in these systems.[1, 2] Perhaps the most interesting recent observation is that the phosphoryl group favors the axial conformation in 2-phosphoryl 1,3-dithianes **1**, but strongly prefers the equatorial position in 1,3-dioxanes[3, 4] and 1,3-oxathianes **2**.[4, 5] The magnitude of the anomeric effect in **2**, estimated recently by *Juaristi*,[6] was found to be quite substantial and close to 3 kcal mol^{-1}.

Because the anomeric effect is very often rationalized in terms of electrostatic effects (dipole-dipole interactions),[7] we investigated the conformations of 1,3-dithianes containing the triphenylphosphonium group at C2 where the phosphorus atom formally bears a positive charge. Conforma-

[*] Prof. Dr. M. Mikołajczyk, P. Graczyk
Centre of Molecular and Macromolecular Studies
Polish Academy of Sciences
PL-90-363 Łódź, Sienkiewicza 112 (Poland)
Dr. M. W. Wieczorek, G. Bujacz
Institute of Technical Biochemistry, Technical University, Łódź (Poland)

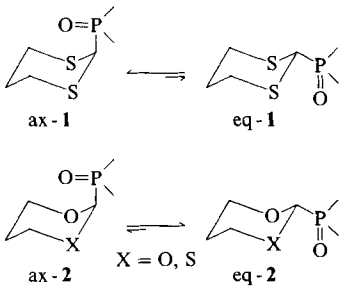

tional studies of this type of compounds are also interesting in view of the reverse anomeric effect observed for the ammonium-substituted six-membered heterocycles.[8] With this in mind we prepared the conformationally labile 2-triphenylphosphonio-1,3-dithianes **3** and **4** and two diastereomeric pairs of 2-triphenylphosphonio-1,3-dithianes, **5** and **6**, from the corresponding 2-chloro-1,3-dithianes and triphenylphosphane (Scheme 1).

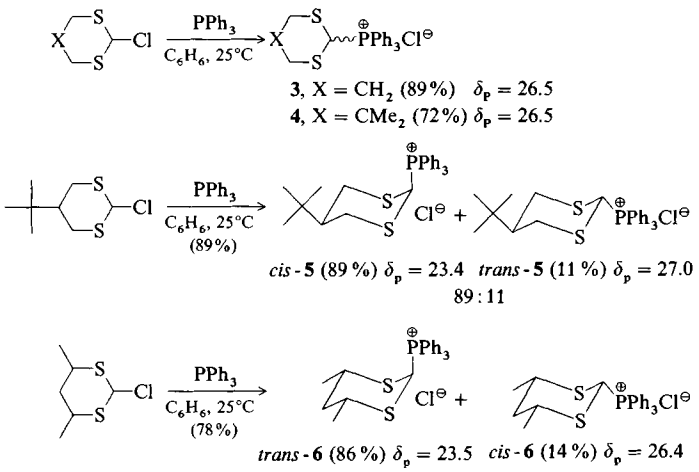

Scheme 1.

The major diastereomer was isolated in a pure state from the mixture of two diastereomeric dithianes, *cis*- and *trans*-**5**, by careful crystallization from DMF/ether.[9] Its *cis* geometry was established by X-ray analysis,[10] (Fig. 1) which also revealed that this isomer exists in a chair conformation in which the triphenylphosphonium group at C1 is in an axial and the *tert*-butyl group at C3 in an equatorial position (numbers refer to Fig. 1). The phenyl ring lying over the

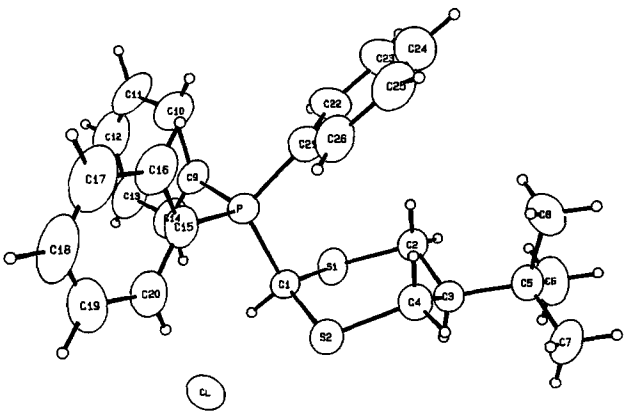

Figure 1. A three-dimensional view of the structure of *cis*-**5** in the crystal. Important bond lengths [Å] and bond angles [°]: S(1)–C(1) 1.798(4) S(2)–C(1) 1.807(4), C(1)–P 1.817(4); S(1)–C(1)–S(2) 115.9(2), S(1)–C(1)–P 111.4(2), S(2)–C(1)–P 114.0(3)

dithiane ring is almost parallel to the plane formed by the S1, S2, C2 and C4 atoms. The distances between this phenyl ring and two axial hydrogens at C2 and C4 are 2.642 and 2.576 Å, respectively.

When a concentrated DMF solution of a mixture of *cis*-**5** and *trans*-**5** (89:11) was heated for a few minutes, the diastereomeric ratio was changed in favor of *trans*-**5** indicating that the *trans* isomer is thermodynamically more stable. By crystallization of this mixture containing ca. 60% of *trans*-**5** from DMF/ether we were able to obtain *trans*-**5** of 95% diastereomeric purity. Similarly, in the synthesis of **6** the less thermodynamically stable isomer was the predominant product (*trans*:*cis* 86:14).

The ^{1}H-NMR spectrum (300.13 MHz, CD_2Cl_2) of *cis*-**5** revealed that the *t*Bu signal ($\delta = 0.59$) is slightly shielded due to the anisotropic effect of the phenyl ring located over the heterocyclic 1,3-dithiane ring. Even more pronounced shielding ($\Delta\delta \approx 1$) is observed for the axial hydrogens at C4 and C6 in *cis*-**5** and *trans*-**6**. While in the 1,3-dithianes without PPh_3 substituents these proton signals occur at $\delta = 2.63$ (5-*tert*-butyl-1,3-dithiane) and 2.83 (*cis*-4,6-dimethyl-1,3-dithiane), in *cis*-**5** and *trans*-**6** the relevant chemical shifts are $\delta = 1.64$ and 1.79, respectively. The two-proton, deceptively simple doublet at $\delta = 2.4$ ($J = 10.9$ Hz) in *cis*-**5** may be tentatively assigned to the equatorial methylene protons. Since the chemical shifts of the methine proton at C5 and axial methylene protons are almost the same ($\delta = 1.64$), the first-order approximation cannot be applied, and the coupling constant values cannot be simply extracted from the spectrum. In contrast, the proton spectrum of *trans*-**5** showed well-separated signals for all protons. Thus, the *tert*-butyl signal occurred at $\delta = 0.92$, and the equatorial and axial methylene protons at $\delta \approx 2.9$ and 3.8, respectively. The equatorial position of the *tert*-butyl group was confirmed by the *trans*- and *gauche*-coupling constants of $^3J_{H-H} = 11.3$ and 2.2 Hz, respectively, between the methine and methylene protons. Based on the splitting pattern, the signals at $\delta = 2.87$ were assigned to the equatorial protons and the downfield resonance at $\delta = 3.81$ to the axial ones. Similarly, the axial protons at C4 and C6 in *cis*-**6** are shifted to lower field ($\delta \approx 4.08$).[11] The equatorial position of the triphenylphosphonium group in *cis*-**6** was also supported by the long-range coupling constant ($^5J_{H-P} = 4.1$ Hz) between the equatorial proton at C5 and phosphorus.

The ^{13}C-NMR spectrum (75.47 MHz, CD_2Cl_2) of *cis*-**5** and *trans*-**6** showed no coupling between phosphorus and C4 or C6. Such coupling is expected for the synclinal (*gauche*) arrangement of the C-S-C-P fragment. In both cases the γ-effect is negative (-4.48 for *cis*-**5** and -3.55 for *trans*-**6**), as was found earlier for the axially substituted 2-phosphoryl-1,3-dithianes.[12] The ^{13}C-NMR spectra of the more stable diastereomers *trans*-**5** and *cis*-**6** revealed long-range coupling constants of $^3J_{C-P} = 7.5$ and $^3J_{C-P} = 7.4$ Hz, respectively, in agreement with the antiperiplanar arrangement of the C4,6–S and C2–P bonds. As would be expected by analogy with the equatorially substituted 2-phosphoryl-1,3-dithianes,[12] the values for the γ-effect are positive (1.09 and 1.14 for *trans*-**5** and *cis*-**6**, respectively).

Both ^{1}H and ^{13}C-NMR spectra of the conformationally mobile dithianes **3** and **4** strongly suggest that the conformation in which the PPh_3 group is in the equatorial position predominates in solution. Thus, in the ^{1}H-NMR spectrum of **4** the methylene protons appear at $\delta = 2.3$ and 3.6. Because the coupling constant with phosphorus ($^4J_{H-P} = 4.9$ Hz) is observed in the upfield part of the spectrum, this signal was assigned to the equatorial protons. In the ^{13}C-NMR spectra of **3** and **4**, the methylene carbons C4 (C6) are coupled with

 © VCH Verlagsgesellschaft mbH, W-6940 Weinheim, 1991 0570-0833/91/0505-0579 $ 3.50+.25/0

phosphorus ($^3J_{C-P}$ = 6.2 and 5.7 Hz, respectively) indicating an antiperiplanar conformation of the C-S-C-P fragment and hence the prevailing equatorial position of the triphenylphosphonium group in solution. The γ-effect values (+ 0.135 and − 0.26 for **3** and **4**, respectively) are also in accord with this interpretation.

Chemical equilibration (CD_2Cl_2, Et_3N, 293 K, ^{31}P-NMR assay) of the conformationally fixed diastereomeric dithianes **5** and **6**, initiated from both sides, allowed us to estimate the following equilibrium constants and ΔG° values: $K = 1.74$, $\Delta G^\circ_{293} = -0.32$ kcal mol^{-1} for **5** and $K = 6.10$, $\Delta G^\circ_{293} = -1.05$ kcal mol^{-1} for **6**. The K and ΔG° values for conformational equilibria of the labile derivatives **3** and **4** were calculated using the Eliel equation[13] with the assumption that the value of the γ-effect on ^{13}C-NMR chemical shifts in these systems is the weighted average value of those for the model diastereomeric dithianes **5** or **6**. In this way the following values were obtained: $K = 4.84$, $\Delta G^\circ_{293} = -0.92$ kcal mol^{-1} for **3**, $K = 3.14$, $\Delta G^\circ_{293} = -0.66$ kcal mol^{-1} for **4** using *cis*- and *trans*-**5** as models; $K = 3.65$, $\Delta G^\circ_{293} = -0.75$ kcal mol^{-1} for **3** and $K = 2.35$, $\Delta G^\circ_{293} = -0.50$ kcal mol^{-1} for **4** using *trans*- and *cis*-**6** as models. Moreover, the ^{31}P-NMR spectrum of **4** at 190 K showed two singlets at $\delta = 22.0$ and 26.2 which can be assigned to the axial and equatorial conformers of **4**, respectively. Since their intensity ratio was 1:2.5, the equilibrium constant $K_{190} = 2.5$.[14] This value corresponds to $\Delta G^\circ_{190} = -0.35$ kcal mol^{-1} and is close to the calculated value.

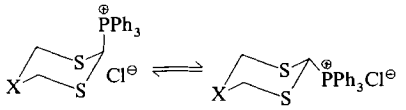

ax-**3** X = CH_2 eq-**3**
ax-**4** X = CMe_2 eq-**4**

The data presented above indicate a surprisingly small equatorial preference for the bulky triphenylphosphonium group in the 1,3-dithiane ring.[15] Most probably, in this case a considerable anomeric effect that partially compensates for 1,3-diaxial repulsive interactions is also operating.[16]

The diversity of the K (and ΔG°) values determined experimentally or calculated for the 2-triphenylphosphonio-1,3-dithianes **3**–**6** is most probably due to the solvent effect on conformational equilibria of the variously substituted 1,3-dithiane rings, which should also differ, although to a small extent, in some structural parameters. The solvent effect may play an important role, especially in the systems investigated when steric and anomeric effects act in opposite directions. Therefore even a small disturbance of this balance by the solvent-solute interactions may substantially affect K and ΔG° values.[17]

With regard to the origin of the anomeric effect in the system described above, three mechanisms can be taken into account. The first, commonly accepted one may involve $n_S \rightarrow \sigma^*_{C-P}$ conjugation.[8] The second, proposed recently by *Juaristi*,[2] is based on a through-space 3p–3d electron donation from sulfur to phosphorus in the axial conformation. Finally, in our opinion, the equatorial position of the triphenylphosphonium group may be destabilized by repulsive interactions between lone electron pairs on the endocyclic sulfur atoms and π-electrons of the phenyl ring. Further experiments to test this hypothesis are in progress.

Received: November 2, 1990;
revised: January 17, 1991 [Z 4265 IE]
German version: *Angew. Chem. 103* (1991) 604

CAS Registry numbers:
3, 63822-67-3; **4**, 132832-88-3; *cis*-**5**, 132832-89-4; *cis*-**5** · DMF, 132832-91-8; *trans*-**5**, 132854-65-0; *cis*-**6**, 132882-71-4; *trans*-**6**, 132832-90-7.

[1] M. Mikołajczyk, *Pure Appl. Chem. 57* (1987) 983.
[2] E. Juaristi, *Heteroatom Chem. 1* (1990) 267.
[3] M. Mikołajczyk, P. Graczyk, M. W. Wieczorek, G. Bujacz, Y. T. Struchkov, M. Y. Antipin, *J. Org. Chem. 53* (1988) 3609.
[4] E. Juaristi, A. Flores-Vela, V. Labastida, M. Ordonez, *J. Phys. Org. Chem. 2* (1989) 349.
[5] M. Mikołajczyk, P. Graczyk, M. W. Wieczorek, G. Bujacz, *Tetrahedron Lett. 29* (1988) 6801.
[6] E. Juaristi, A. Flores-Vela, V. Labastida, *J. Org. Chem. 54* (1989) 5191.
[7] J. T. Edward, *Chem. Ind. (London) 1955*, 1102.
[8] A. J. Kirby: *The Anomeric Effect and Related Stereoelectronic Effects at Oxygen*, Springer, Berlin 1983.
[9] *cis*-**5** crystallized as a 1:1 complex with dimethylformamide, m.p. 195–200 °C. An X-ray analysis was carried out on crystals of this complex.
[10] Crystal data of *cis*-**5** · DMF: $C_{29}H_{27}ONS_2PCl$ (545.14), monoclinic; space group $P2_1/n$; $a = 10.282(2)$, $b = 19.169(2)$, $c = 14.908(2)$ Å, $\beta = 91.36(1)^\circ$, $V = 2937.3(8)$ Å^3; $Z = 4$; $\mu(Mo_{K\alpha}) = 3.6$ cm^{-1}, $\rho_{exp} = 1.28$ g cm^{-3}. No. of reflections measured: 6950; no. of unique reflections: 6377. CAD4 diffractometer. Lattice constants refined by least-squares fit of 25 reflections in the range $\theta = 10.23$–12.89°. Solution by SHELXS-86 program. 4511 observed reflections [$I > 3\sigma(I)$], full matrix least-squares using F's; $R = 0.063$, $R_w = 0.068$, for 316 refined parameters. Further details of the crystal structure investigation may be obtained from the Fachinformationszentrum Karlsruhe, Gesellschaft für wissenschaftlich-technische Information mbH, W-7514 Eggenstein-Leopoldshafen 2 (FRG), on quoting the depository number CSD-55058, the names of the authors, and the journal citation.
[11] In 5-*tert*-butyl-1,3-dithiane and 4,6-dimethyl-1,3-dithiane the signals for the axial protons at C4 and C6 occur at $\delta = 2.63$ and 2.84, respectively. Thus, the deshielding effect exerted by the equatorial triphenylphosphonium group is $\Delta\delta = 1.18$ and 1.24 for **5** and **6**, respectively.
[12] M. Mikołajczyk, P. Graczyk, P. Bałczewski, *Tetrahedron Lett. 28* (1987) 573.
[13] E. Eliel, *Chem. Ind. (London) 1959*, 568.
[14] The K_{190} value should be somewhat larger than K_{293}: therefore **6** would be the better reference system.
[15] X-ray structure analysis of **4** showed that the PPh_3 group is located in an axial position in the solid state.
[16] Although the magnitude of the anomeric effect in 2-triphenylphosphonio-1,3-dithianes cannot be calculated, because of the absence of the A-value for the corresponding cyclohexane, it is possible to estimate its value by assuming that the triphenylphosphonium group is larger than the diphenylthiophosphinoyl one. The A-value for the latter was found by *Juaristi* et al. [2] to be 3.61 kcal mol^{-1}. Therefore, an anomeric effect in **5** and **6** should be at least 2.5 kcal mol^{-1}. The synthesis of the desired triphenylphosphoniocyclohexanes is currently under way in this laboratory.
[17] Similar diversity of K and ΔG° values (up to 0.25 kcal mol^{-1}) was observed by *Tschierske* et al. (see ref. [18]).
[18] C. Tschierske, H. Köhler, Z. Zaschke, E. Kleinpeter, *Tetrahedron 45* (1989) 6987.

Carbonyl(pentaphosphacyclopentadienyl)–Transition Metal Complexes (M = Cr, Mo, W, Mn) through Directed Syntheses with *cyclo*-$P_5^\ominus$ **

By *Marianne Baudler** and *Thomas Etzbach*

Dedicated to Professor Rolf Appel on the occasion of his 70th birthday

A few years ago we reported on the formation of the pentaphosphacyclopentadienide ion, *cyclo*-$P_5^\ominus$ (**1**), upon the nucleophilic fission of white phosphorus, and on the preparation of

[*] Prof. Dr. M. Baudler, Dipl.-Chem. T. Etzbach
Institut für Anorganische Chemie der Universität
Greinstrasse 6, W-5000 Köln 41 (FRG)

[**] Contributions to the Chemistry of Phosphorus, Part 216. This work was supported by the Deutsche Forschungsgemeinschaft and the Fonds der Chemischen Industrie. Part 215: M. Baudler, T. Etzbach, *Chem. Ber.*, in press.

pure LiP_5/THF and NaP_5/[18]crown-6/THF solutions.[1-4] Recently, we have also obtained surprisingly stable KP_5/DMF solutions through degradation of red phosphorus with potassium dihydrogenphosphide in dimethylformamide (DMF).[5]

1

Because of its electronic structure (resonance-stabilized 6π electron system), **1** can be bound in transition metal complexes as an (η^5-P_5) ligand. The first examples, described recently by *Scherer*,[6] are the sandwich and triple decker complexes [(η^5-P_5)M(η^5-C_5Me_4R)] (M = Fe, Ru; R = Me, Et) and [(η^5-C_5Me_5Cr)$_2$(μ,η^5-P_5)], respectively, which were prepared from white phosphorus by cothermolysis with suitable starting complexes. In the case of the mixed sandwich complex [(η^5-P_5)Fe(η^5-C_5Me_5)], we also realized the directed synthesis from LiP_5, LiC_5Me_5, and $FeCl_2$.[3] All the *cyclo*-P_5 complexes known to date have an additional (η^5-$C_5R^1_4R^2$) ligand (R^1 = R^2 = Me, H; R^1 = Me(H), R^2 = Et(Me)) at the metal center. Attempts to prepare metallocene analogues with two P_5 ligands led, without exception, to high molecular weight solids which appeared amorphous under X-ray examination. Their formation can presumably be attributed to the additional coordination capability of the λ^3-phosphorus via the lone pair.[7] We have now achieved the directed synthesis of the first mixed carbonyl(pentaphosphacyclopentadienyl)-metal complexes through thermal ligand exchange reactions, using **1** as a synthetic reagent (Scheme 1).

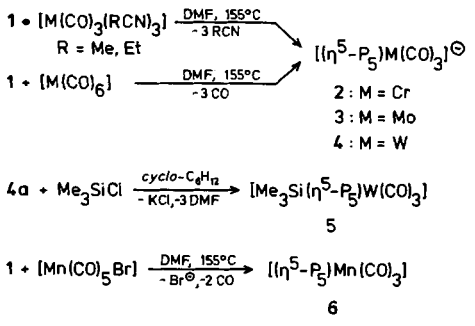

Scheme 1. Thermal ligand-exchange reactions with **1**. Compounds **4a**: [K(dmf)$_3$] [(η^5-P_5)W(CO)$_3$]; **4b**: Li[(η^5-P_5)W(CO)$_3$].

During the reaction of **1** with tris(nitrile)tricarbonyl complexes of chromium, molybdenum or tungsten, the corresponding tricarbonyl(pentaphosphacyclopentadienyl)metalate ions **2**–**4** form on exchange of the three nitrile ligands. Their formation occurs via intermediates which were not further characterized, but could be detected by ^{31}P NMR spectroscopy in the early stages of the reaction, especially at room temperature. The use of the complex in which R = Et and of the KP_5/DMF solution[5] is particularly favorable because of their stability. With prolonged reaction times (24 h), the substitution of three carbonyl ligands of the corresponding hexacarbonyl-metal complexes can also be achieved by **1** using KP_5/DMF solution. At the same time small amounts of by-products, very probably multinuclear P_5 complexes, are formed in addition to **2**–**4**. Compound **4** was isolated in the form of the salts **4a** (dark brown, honeylike) and **4b** (brown powder). Compound **4b** is significantly more sensitive to oxidation than **4a**. The solutions of **2** and **3** in DMF or THF are also brown. In suspension **4a** reacts smoothly with chloro(trimethyl)silane to yield the silyl derivative **5** (colorless, volatile oil). The reaction of KP_5/DMF solution with bromo(pentacarbonyl)manganese(I) affords tricarbonyl(pentaphosphacyclopentadienyl)manganese (pentaphosphacymantrene) (**6**), a volatile, pale yellow solid which was separated from saltlike by-products by extraction with THF. In the mass spectrum of **6**, the signals of the characteristic fragment ions $Mn(CO)_nP_5^{\oplus}$ (n = 2–0), formed by loss of CO, occur besides the signal for the $M^{\oplus}$ ion (m/z = 294).

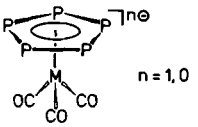

Scheme 2. Complexes with C_{3v} symmetry; M = W, Mo, Cr, Mn.

Proof of the constitution of **2**–**6** is provided by the spectroscopic data. In the ^{31}P-NMR spectrum of each, a singlet appears (**2**: δ = 163.4; **3**: δ = 141.6; **4**: δ = 105.2, $^1J(^{31}P,^{183}W)$ = 11.9 Hz; **6**: δ = 126.7), which lies in the same region as the signals of the pentaphosphametallocenes.[6] In the case of the metalate ions **2**–**4**, the position of the signal is practically independent of the counterion ([K(dmf)$_3$]$^{\oplus}$, Li$^{\oplus}$); in the case of the silyl compound **5** (δ = −23.4), the electropositive substituent causes an additional shielding. The strongly negative coordination shift[8] in **2**–**6** compared to free **1** (δ = +470[1,5]) is a general feature of π-phosphaarene complexes.[9] The ^{13}C-NMR signal of the CO ligands of **4** (δ = 218.7, $^1J(^{13}C,^{183}W)$ = 3.5 Hz, ^2J(C,P) = 1.7 Hz) lies in the normal range; the small ^{13}C,^{183}W coupling constant is remarkable. The ^{1}H-NMR signal of the Me_3Si group of **5** (δ = −0.55) has a very similar chemical shift as in the corresponding cyclopentadienyl complex.[10]

In the IR spectrum of **4** and **6**, the two intense CO bands that are typical for [M(CO)$_3$] fragments with undisturbed C_{3v} symmetry appear. Their position is significantly shifted with respect to that of the corresponding cyclopentadienyl complex:[11,12] for **4** to larger, and for **6** to smaller wave numbers. Obviously, **1** and $C_5H_5^{\ominus}$ have a markedly different donor/acceptor behavior.

All spectroscopic findings confirm a structure for **2**–**6** analogous to the corresponding cyclopentadienyl complexes. It is to be expected that numerous other *cyclo*-P_5 complexes may be prepared through directed synthesis reactions with **1**.

Experimental Procedure

4a: 30 mL (1.13 mmol) of a 3.8×10^{-2} M KP_5 solution in DMF [5] was added dropwise under inert gas with vigorous stirring within 5 min to [W(CO)$_3$(EtCN)$_3$] [13] (4.0 g, 9.24 mmol, excess). Thereafter the mixture was heated to boiling for 30 min. The dark brown solution was cooled to room temperature and monitored by ^{31}P NMR spectroscopy, which confirmed a quantitative reaction of KP_5. Removal of DMF and excess starting complex at 50 °C in vacuo (oil pump) gave 0.71 g of **4a** (92%, based on KP_5). IR (in DMF, selected data): $\tilde{\nu}$[cm^{-1}] = 1988 vs (CO, A_1), 1886 vs (CO, E); correct elemental analysis.

4b: [W(CO)$_3$(EtCN)$_3$] (0.35 g, 0.82 mmol, excess) in THF (10 mL) was added dropwise with vigorous stirring within 15 min to 125 mL (0.088 mmol) of a 7×10^{-4} M LiP_5 solution in THF [1], whereupon a brown precipitate separated. After stirring for a further 30 min, the colorless solution was siphoned off, the solid washed with THF (3×10 mL) and dried in vacuo (oil pump); yield 36 mg **4b** (96%, based on LiP_5). Correct elemental analysis.

5: A suspension of **4a** (2.0 g, 2.94 mmol) in cyclohexane (5 mL) was stirred with chloro(trimethyl)silane (1.3 g, 11.93 mmol) for 24 h at room temperature. Sep-

aration of the colorless reaction solution from unchanged **4a** and removal of the solvent under vacuum afforded 0.70 g **5** (48%, based on **4a**).
6: 10 mL (0.38 mmol) of a 3.8×10^{-2} M KP_5 solution in DMF [5] was added dropwise under inert gas with vigorous stirring within 5 min to $[Mn(CO)_5Br]$ (0.85 g, 3.09 mmol, excess). After 24 h stirring at the boiling point, the solvent of the red-brown solution was removed in vacuo at room temperature. The residue was stirred with THF (5 mL) for 12 h and the solvent removed completely from the colorless extract; yield 27 mg **6** (23%, based on KP_5). IR (in THF, selected data): $\tilde{\nu}$[cm^{-1}] 1960 s (CO, A_1), 1778 s (CO, E).

Received: December 3, 1990 [Z 4306 IE]
German version: *Angew. Chem. 103* (1991) 590

CAS Registry numbers:
2, 132622-41-4; **3**, 132622-42-5; **4a**, 132622-45-8; **4b**, 132622-46-9; **5**, 132622-47-0; **6**, 132622-48-1; $[Mn(CO)_5Br]$, 14516-54-2; $[Cr(CO)_6]$, 13007-92-6; $[Mo(CO)_6]$, 13939-06-5; $[W(CO)_6]$, 14040-11-0; $[W(CO)_3(MeCN)_3]$, 16800-47-8; $[W(CO)_3(EtCN)_3]$, 84580-21-2; $[Cr(CO)_3(EtCN)_3]$, 91513-88-1; $[Cr(CO)_3(MeCN)_3]$, 16800-46-7; $[Mo(CO)_3(EtCN)_3]$, 103933-26-2; $[Mo(CO)_3(MeCN)_3]$, 15038-48-9; Me_3SiCl, 75-77-4.

[1] M. Baudler, D. Düster, D. Ouzounis, *Z. Anorg. Allg. Chem. 544* (1987) 87.
[2] M. Baudler, *Angew. Chem. 99* (1987) 429; *Angew. Chem. Int. Ed. Engl. 26* (1987) 419.
[3] M. Baudler, S. Akpapoglou, D. Ouzounis, F. Wasgestian, B. Meinigke, H. Budzikiewicz, H. Münster, *Angew. Chem. 100* (1988) 288; *Angew. Chem. Int. Ed. Engl. 27* (1988) 280.
[4] M. Baudler, D. Ouzounis, *Z. Naturforsch. B 44* (1989) 381.
[5] M. Baudler, T. Etzbach, *Chem. Ber.*, in press.
[6] Reviews: O. J. Scherer, *Angew. Chem. 102* (1990) 1137; *Angew. Chem. Int. Ed. Engl. 29* (1990) 1104; *Comments Inorg. Chem. 6* (1987) 1; *Nachr. Chem. Tech. Lab. 35* (1987) 1140, and references cited therein.
[7] See also: J. A. Chamizo, M. Ruiz-Mazón, R. Salcedo, R. A. Toscano, *Inorg. Chem. 29* (1990) 879.
[8] Coordination chemical shift $\Delta = \delta_{complex} - \delta_{ligand}$; S. O. Grim, D. A. Wheatland, W. McFarlane, *J. Am. Chem. Soc. 89* (1967) 5573.
[9] See for example: a) J. Deberitz, H. Nöth, *Chem. Ber. 103* (1970) 2541; b) F. Mathey, A. Mitschler, R. Weiss, *J. Am. Chem. Soc. 100* (1978) 5748.
[10] W. Malisch, M. Kuhn, *Chem. Ber. 107* (1974) 979.
[11] J. E. Ellis, E. A. Flom, *J. Organomet. Chem. 99* (1975) 263.
[12] I. J. Hyams, R. T. Bailey, E. R. Lippincott, *Spectrochim. Acta Part A 23* (1967) 273.
[13] G. J. Kubas, *Inorg. Chem. 22* (1983) 692.

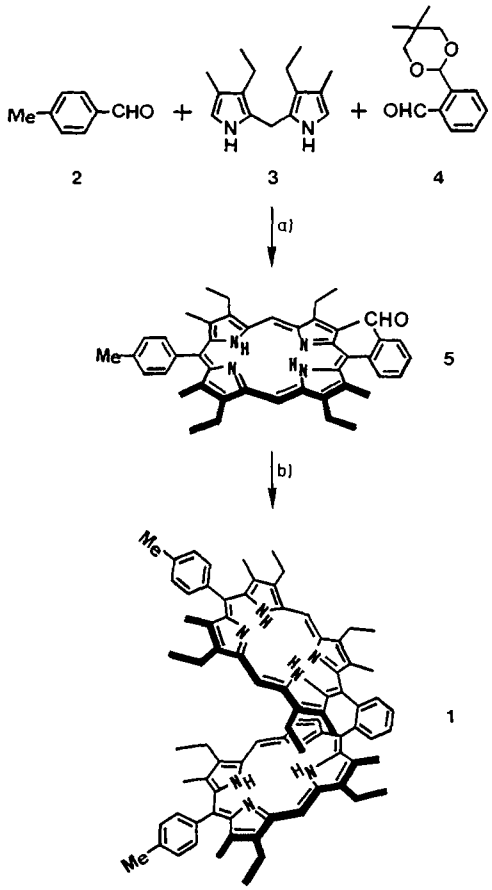

Scheme 1. a) 1. CCl_3CO_2H, CH_3CN, room temperature, 16 h; 2. *p*-chloranil, THF, room temperature, 5 h; 3. CF_3CO_2H, 10% H_2SO_4, reflux, 1 h (35% yield). b) 1. **3** + **4**, CCl_3CO_2H, CH_3CN, room temperature, 10 h; 2. *p*-chloranil, THF, 3 h (48% yield).

A 1,2-Phenylene-Bridged Porphyrin Dimer—Synthesis, Properties, and Molecular Structure**

By *Atsuhiro Osuka,* Satoshi Nakajima, Toshi Nagata, Kazuhiro Maruyama,** and *Koshiro Toriumi*

The X-ray structure analyses of photosynthetic reaction centers (RCs) of bacteria have stimulated extensive studies of model compounds.[1] These included coupled diporphyrins, the study of which should clarify the role of the special pair (SP) acting as primary electron donor in the reaction center. Two important criteria for a synthetic analogue of SP are 1) an energetically lower S_1-state and 2) a lower one-electron oxidation potential.[2] One of the central issues is under discussion is: how porphyrin-porphyrin interactions influence the electronic properties of the dimer. Herein, we describe the synthesis, X-ray crystallography, and physical properties of the novel 1,2-phenylene-bridged porphyrin dimer **1**-Zn_2,[3] which meets the criteria mentioned above.[4] The synthetic route is illustrated in Scheme 1. Formyl-substituted porphyrin **5**, which was obtained from the cross-condensation of *p*-tolualdehyde **2**, dipyrrylmethane **3**, and mono-protected phthalaldehyde **4**, was again cyclized with **2** and **3** to give the dimer **1** in 48% yield.

Small red crystals of **1**-Zn_2 were grown by slow evaporation of a dichloromethane/hexane solution. Figure 1 shows the molecular structure of **1**-Zn_2.[5, 6] The most remarkable

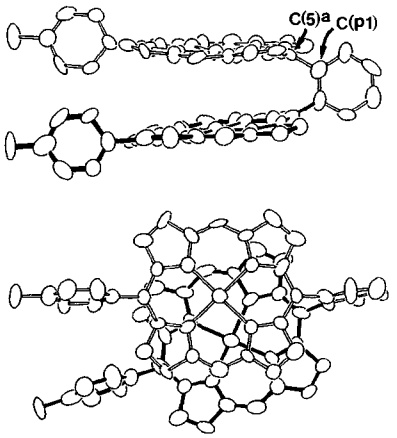

Fig. 1. Molecular structure of **1**-Zn_2. Above: side view; below: top view. Peripheral alkyl groups are omitted for clarity.

[*] Prof. A. Osuka, Prof. K. Maruyama, S. Nakajima, and T. Nagata
Department of Chemistry, Faculty of Science,
Kyoto University Kyoto 606 (Japan)
Prof. K. Toriumi,
Institute for Molecular Science,
Okazaki National Research Institutes, Okazaki, 444 (Japan)

[**] Support of this work by a grant-in-aid for Specially Promoted Research from the Ministry of Education, Science, and Culture of Japan (No. 02102005) and by Nissan Science Foundation is gratefully acknowledged.

Table 1. Physical properties of **1** and **1**-Zn_2.

Porphyrin	Absorption [a] λ_{max}[nm] Soret band	Q-bands	Fluorescence [a] λ_{max}[nm]	Stokes shift [c] [cm^{-1}]	$E(S_1)$ [b] [cm^{-1}]	$E_{1/2}$ [c] [V]
1	381	518.5 591.5 638.5	671 727	760	15300	0.15 [d] 0.49 [d] 0.38 [d] 0.65 [d]
6	407	505.5 540.0 573.5 624.5	628 693	90	16000	0.21 0.54
1-Zn_2	395	545.0 560.5 610.0	652	1060	15900	0.01 0.21 0.41 0.54
6-Zn	407	537.5 572	578 630	180	17400	0.17 0.37

[a] In CH_2Cl_2 [b] Energy of the lowest singlet excited state. [c] Oxidation potentials (vs. ferrocene/ferrocenium) measured by cyclic voltammetry at a Pt electrode in CH_2Cl_2 containing 0.1 M n-Bu_4NClO_4 at 20°C. [d] Peak potentials.

structural feature is that, though the two porphyrin rings are bridged by the 1,2-phenylene moiety, they tend to closely overlap each other and assume an almost parallel conformation (dihedral angle 6.6°). This overlapping conformation appears to increase the van der Waals interaction of the two porphyrin rings. The average interplanar separation between the two rings is 3.43 Å, which is similar to the reported value of 3.45 Å in biphenylene-bridged Cu_2-diporphyrin,[6b] and 3.52 Å in Cu_2-"hexyldiporphyrin-7".[6c] The interplanar separations between the neighboring molecules (3.61 Å and 4.92 Å) are larger than the intramolecular separation. This fact indicates that the parallel conformation is induced by the attractive intramolecular interactions between the two porphyrin rings. A large strain is generated at the C5a-Cp1 bond by this "enforced" parallel structure, but is dispersed widely over the whole porphyrin ring. The second interesting feature is the rotation of the two porphyrin rings about the phenylene bridge (by 22.7°) rather than an exact "stacked" conformation. This offset geometry may be the result of electrostatic interactions between the two porphyrin rings.[7] The ^{1}H-NMR data provide information about the structure of **1** and **1**-Zn_2 in solution. The large upfield shifts of the NH and *meso* protons in the dimers indicate that a parallel conformation is present even in solution. However, the ^{1}H-NMR spectra of **1** and **1**-Zn_2 contain only half the number of signals predicted by the crystal structure of **1**-Zn_2, indicating that a very rapid switching between the two conformations must take place.

The absorption and fluorescence properties of **1** and **1**-Zn_2 are listed in Table 1, together with the data for the monomers **6** and **6**-Zn for comparison. Strong excitonic interactions are observed for the diporphyrins **1** and **1**-Zn_2, i.e. blue-shifted Soret bands, red-shifted Q-bands, and broad red-shifted fluorescence.[8] **1** and **1**-Zn_2 exhibit relatively large Stokes shifts, (760 and 1060 cm^{-1}, respectively), suggesting nuclear geometric changes in their excited states. The characteristic vibrational mode of Zn-porphyrin is no longer observed in the relatively broad fluorescence band of **1**-Zn_2, which is reminiscent of the emission from an excimer of condensed aromatics. The relative fluorescence quantum yields of **1** and **1**-Zn_2 are 0.25- and 0.087-fold those of the corresponding monomers. On the basis of the absorption and fluorescence spectra, the energy levels of the S_1-states of **1** and **1**-Zn_2 were estimated to be lower by ca. 700 and 1500 cm^{-1} respectively than the corresponding monomer. The reduced fluorescence quantum yield indicates the presence of additional nonrediative decaying channels in the S_1-state of **1**-Zn_2. However, the shape and intensity of the fluorescence of **1**-Zn_2 were not significantly altered by the solvent polarity (from C_6H_6 to CH_3CN). This suggests that excimer interactions are more important than charge transfer interactions in the S_1 state of **1**-Zn_2.

Cyclic voltammetry of **1**-Zn_2 in CH_2Cl_2 solution, using (n-Bu_4N)ClO_4 as supporting electrolyte, reveals four reversible oxidation waves (Table 1). It is reasonable to assign the wave at 0.01 V to the one-electron oxidation of the neutral Zn-porphyrin ($E^+_{1/2}$(ZnP–ZnP$^{\oplus}$/ZnP–ZnP)). Therefore, it is concluded that **1**-Zn_2 undergoes reversible one-electron oxidation 160 mV more easily than **6**-Zn.

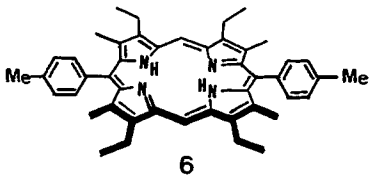

6

In conclusion, the strong interactions in **1**-Zn_2 result in a decrease both in the energy of the S_1-state and in the one-electron oxidation potential, which make it a promising candidate for the electron donor in an artificial photosynthetic reaction center involving oligomeric porphyrins.

Experimental Procedure

1: The formyl-substituted porphyrin **5** (249 mg, 0.37 mmol) and *p*-tolualdehyde **4** (175 mg, 1.455 mmol) were dissolved in CH_3CN (20 mL) containing trichloroacetic acid (131 mg, 0.8 mmol). Then, the dipyrrylmethane **3** (422 mg, 1.83 mmol) in CH_3CN (3 mL) was added, and the mixture was stirred for 19 h (in the dark, under nitrogen). *p*-Chloranil (662 mg, 2.69 mmol) in THF (30 mL) was added, and stirring was continued for 3 h. After work-up in the usual way, the porphyrin products were separated by flash column chromatography, giving **1**. Yield 48% based on the amount of **5** used (215 mg): ^{1}H NMR (400 MHz, $CDCl_3$, 25°C, TMS): δ = −6.31 (broad, NH, 2H), −5.77 (br, NH, 2H), 1.32 (t, 12H), 1.53 (t, 12H), 3.3–3.6 (m, 16H), 2.35 (s, Me, 12H), 2.81 (s, Ar–Me, 6H), 2.91 (s, Me, 12H), 7.28 (dd, J = 2 and 7.8 Hz, 2H), 7.36 (d, J = 7 Hz, 2H), 7.76 (d, J = 7 Hz, 2H), 8.17 (dd, J = 3.8 and 5.8 Hz, 2H), 8.26 (dd, J = 7.3 and 2 Hz, 2H), 8.39 (s, *meso*-H, 4H), and 9.00 (dd, J = 3.4 and 5.4 Hz, 2H) ppm. FAB MS: m/z 1211 ($M^{\oplus}$ + 1).

1-Zn_2: ^{1}H NMR (400 MHz, $CDCl_3$, 25°C, TMS): δ = 1.28 (t, Et, 12H), 1.53 (t, Et, 12H), 2.30 (s, Me, 12H), 2.79 (s, Ar–Me, 6H), 2.90 (s, Me, 12H), 3.4–3.6 (m, Et, 16H), 7.10 (dd, J = 2 and 7.5 Hz, 2H), 7.29 (dd, J = 2 and 7.5 Hz, 2H), 7.77 (dd, J = 2 and 7.5 Hz, 2H), 8.11 (t, J = 7 Hz, 2H), 8.33 (s, *meso*-H, 4H), 8.35 (dd, J = 2 and 7.5 Hz, 2H), 8.93 (dd, J = 3.8 and 6 Hz, 2H) ppm. FAB MS: m/z 1341 ($M^{\oplus}$ + 1).

Received: November 12, 1990 [Z 4274 IE]
German version: *Angew. Chem.* *103* (1991) 579

CAS Registry numbers:
1, 132911-80-9; **1**-Zn_2, 132938-18-2; **2**, 104-89-0; **3**, 92415-30-0; **4**, 106456-88-6; **5**, 132938-17-1.

[1] M. R. Wasielewski in M. A. Fox and M. Chanon (Eds.): *Photoinduced Electron Transfer*, Elsevier, Amsterdam and 1988, part A, p 161.
[2] J. Breton and A. Vermeglio (Eds.): *The Photosynthetic Bacterial Reaction Centers, Structure and Dynamics*, NATO Series A 149, Plenum Press, New York and 1988.
[3] Recently, a 1,2-phenylene-bridged tetraphenylporphyrin dimer was synthesized: H. Meier, Y. Kobuke, S. Kugimiya, *J. Chem. Soc. Chem. Commun. 1989*, 923.
[4] J. A. Cowan, J. K. M. Sanders, *J. Chem. Soc. Perkin Trans 1 1987*, 2395. C. A. Hunter, J. K. M. Sanders, A. J. Stone, *Chemical Physics 133* (1989) 395.
[5] Crystal data of **1**-Zn: triclinic, space group $P\bar{1}$, $a = 19.44(1)$ Å, $b = 19.53(1)$ Å, $c = 15.023(5)$ Å, $\alpha = 100.95(5)°$, $\beta = 104.38(4)°$, $\gamma = 129.54(3)°$, $V = 3769(5)$ Å^3, $Z = 2$; $\varrho_{calcd} = 1.31$ g cm^{-1}; $\mu(Mo_{K\alpha}) = 0.832$ mm^{-1}. Intensity data were collected on an ENRAF NONIUS CAD4 diffractometer with graphite monochromated $Mo_{K\alpha}$ radiation ($\lambda = 0.71073$ Å). A crystal with dimensions $0.40 \times 0.12 \times 0.03$ mm was used. The structure was solved by a conventional heavy-atom method, and refined on F by a block-diagonal least-squares technique to $R = 0.079$, $R_w = 0.082$ and $S = 1.56$ for 2842 independent reflections ($2\theta < 40°$, $|F_o| > 3\sigma(F_o)$). Weighting scheme is $W = [\sigma_c^2 + (0.04 \times |F_o|)^2]^{-1}$. Further details of the crystal structure investigation are available on request from the Director of the Cambridge Crystallographic Data Center, University Chemical Laboratory, Lensfield Road, Cambridge CB21EW, on quoting the full literature citation.
[6] So far, the structures of only five porphyrin dimers have been determined by the X-ray diffraction method; a) J. P. Collman, A. O. Chong, G. B. Jameson, R. T. Oakley, E. Rose, E. R. Schmittou, and J. A. Ibers, *J. Am. Chem. Soc. 103* (1981) 516; b) J. P. Fillers, K. G. Ravichandran, I. Abdalmuhdi, A. Tulinsky, C. K. Chang, *ibid. 108* (1986) 417; c) M. H. Hatada, A. Tulinsky, C. K. Chang, *ibid. 102* (1980) 7115; d) J. L. Sessler, M. R. Johnson, T.-Y. Liu, *Tetrahedron 45* (1989) 4767.
[7] C. A. Hunter, J. K. M. Sanders, *J. Am. Chem. Soc. 112 (1990) 5525*, and references cited therein.
[8] Recently several monomeric non-planar porphyrins were reported to exhibit similar red-shifted Q-bands and reduced oxidation potentials; a) K. M. Barkigia, L. Chantranupong, K. M. Smith, J. Fajer, *J. Am. Chem. Soc. 110* (1988) 7566; b) C. J. Medforth, M. D. Berber, K. M. Smith, J. A. Shellnutt, *Tetrahedron Lett., 31* (1990) 3719. However, the porphyrin ring in **1**-Zn_2 is rather flat, indicating that its unusual properties are not due to the porphyrin ring distortion but mainly due to the strong interactions between the two porphyrin rings.

A Complex with Three-Coordinate Tungsten Atom: [(silox)$_2$W=N*t*Bu](silox = *t*Bu$_3$SiO)**

By *Daniel F. Eppley, Peter T. Wolczanski,** and *Gregory D. Van Duyne*

The application of sterically demanding ligands often permits the isolation of low-coordinate transition metal complexes. Recently, the utilization of bulky imido and siloxido ligands led to the synthesis of [Ta(silox)$_3$] (silox = *t*Bu$_3$SiO)[1] and [Os{=N-2,6-*i*Pr$_2$C$_6$H$_3$)}$_3$],[2] both rare examples of three-coordinate, third row compounds. Herein we describe the preparation and structure of [(silox)$_2$W=N*t*Bu] **3**. To our knowledge, this imido complex is the first example of a three-coordinate tungsten species.[3]

Thermolysis of [(*t*BuNH)$_2$W(=N*t*Bu)$_2$][4] and 2.0 equiv of (silox)H[5] in benzene afforded *t*BuNH$_2$ and colorless [(silox)$_2$W(=N*t*Bu)$_2$] **1** in 81% yield upon crystallization from hexane [Eq. (a)]. Treatment of **1** with 3.0 equiv of HCl in C_6H_6 eliminated [*t*BuNH$_3$]Cl and provided light-yellow [(silox)$_2$Cl$_2$W=N*t*Bu] **2** in 88% yield after crystallization from hexane [Eq. (b)]. Reduction of **2** with Mg dust in diethyl ether generated a dark green solution. Removal of the Et_2O, followed by filtration and crystallization from hexanes, produced three-coordinate [(silox)$_2$W=N*t*Bu] **3** as emerald-green crystals in 91% yield [Eq. (c)]. The bis(silox-imido) complex **3** is stable as a solid, but unstable in benzene or hydrocarbon solutions. Cryoscopic molecular weight measurements of **3** were precluded by its slow decomposition ($t_{1/2} \approx 1$ h), but ^{1}H-NMR and IR spectra (ν(W=N) = 1295 cm^{-1}) were indicative of a diamagnetic, monomeric imido complex.[6]

$$[(t\text{BuNH})_2\text{W}(=\text{N}t\text{Bu})_2] + 2\,\text{H(silox)} \xrightarrow[-\,2\,t\text{BuNH}_2]{C_6H_6,\ >3\text{d},\ 90\,^\circ\text{C}} \underset{\mathbf{1}}{[(\text{silox})_2\text{W}(=\text{N}t\text{Bu})_2]} \quad \text{(a)}$$

$$\underset{\mathbf{1}}{[(\text{silox})_2\text{W}(=\text{N}t\text{Bu})_2]} + 3\,\text{HCl} \xrightarrow[-\,[t\text{BuNH}_3]\text{Cl}]{C_6H_6,\ 3.5\text{d},\ 110\,^\circ\text{C}} \underset{\mathbf{2}}{[(\text{silox})_2\text{Cl}_2\text{W}=\text{N}t\text{Bu}]} \quad \text{(b)}$$

$$\underset{\mathbf{2}}{[(\text{silox})_2\text{Cl}_2\text{W}=\text{N}t\text{Bu}]} \xrightarrow[-\,\text{MgCl}_2]{\text{Mg},\ \text{Et}_2\text{O},\ 25^\circ,\ 7\text{h}} \underset{\mathbf{3}}{[(\text{silox})_2\text{W}=\text{N}t\text{Bu}]} \quad \text{(c)}$$

The structure of **3** was confirmed via single crystal X-ray diffraction studies (monoclinic, $P2_1/c$, $R = 0.078$, $R_w = 0.092$), although the bond distances and angles reflect some imprecision due to the disorder of all peripheral *t*Bu groups.[7] Similar disorder problems have been observed in other complexes with the silox-ligand.[1, 8] As Figure 1 shows, the (SiO)$_2$W=NC framework of **3** is nearly trigonal planar, with a slight distortion toward a T-shape. Relatively short W–O (1.826(16), 1.814(15) Å) and W=N (1.658(17) Å) bonds are observed,[6] consistent with a low-coordinate, electrophilic metal center. The steric requirements of the silox ligands[9] render the O1–W–O2 angle (127.4(6)°) greater than the O1–W–N (115.7(8)°) and the O(2)–W–N (116.8(8)°) angles. The W–O1–Si1 (177.8(8)°), W–O2–Si2 (169.7(10)°) and W=N–C (175.3(16)°) angles manifest minimal deviations from linearity; thus, electronic effects that maximize O(pπ) → W(sπ) and N(pπ) → W(dπ) bonding may play consequential roles.[10] Provided the linearity of the W–O–Si and W=N–C linkages can be attributed to the maximum π-donation of oxygen and nitrogen filled p-orbitals, the valence shell of tungsten contains 20e. As in the related d^2 complexes, [Os{=N(2,6-*i*PrC$_6$H$_3$)}$_3$] and [Ta(silox)$_3$], 2e reside in a non-bonding π-type ligand-based orbital, thus the complex possesses at most 18e.[2] Due to the lower symmetry (C_{2v}), this orbital has greater oxygen than nitrogen character.

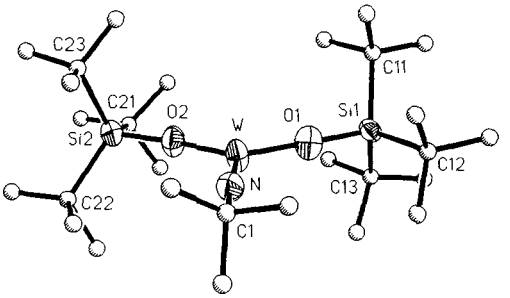

Fig. 1. Structure of **3** in the crystal. The inner coordinate sphere is depicted with 40% vibration ellipsoids, while the best model of the disordered peripheral *t*Bu groups is illustrated by isotropic spheres.

Simple σ-donors, such as THF, do not bind to **3** because of a significant 4e repulsion between a σ-donor orbital and

[*] Prof. P. T. Wolczanski,[+] D. F. Eppley, Dr. G. D. Van Duyne
Cornell University,
Department of Chemistry, Baker Laboratory
Ithaca, NY 14853 (USA)
[+] Alfred P. Sloan Foundation Fellow, 1987–89.
[**] This work was supported by the Air Force Office of Sponsored Research and the National Science Foundation.

the d_{z^2} orbital of the metal,[1] yet π-accepting ligands readily form adducts. Exposure of **3** to either ethylene or 2-butyne[11] generated the orange and colorless four-coordinate

$$[(silox)_2W{=}NtBu] + L \xrightarrow{\text{hexane, } 25^\circ,\ 1.5\,h} [(silox)_2LW = NtBu] \qquad (d)$$

4, L = C_2H_4; **5**, L = Me_2C_2

$[(silox)_2LW{=}NtBu]$ derivatives **4** and **5** respectively [Eq. (d)]. ^{1}H- and ^{13}C-{^{1}H}-NMR spectra indicate that the ethylene is bound with its carbons parallel to the two oxygens, and variable temperature ^{1}H-NMR studies indicate that the barrier to rotation is 15.3 kcal mol^{-1} (T_{coal} = 69 °C). This is the orientation expected from comparisons with analogous $[(RO)_2(R'N)W{=}CHR'']$ complexes,[12] hence the 2-butyne is presumed to coordinate in similar fashion. Further reactivity studies of **3** and related derivatives are currently underway.

Experimental Procedure

All operations were performed using glovebox (N_2) or high vacuum line (Ar) techniques. Ethereal and hydrocarbon solvents were dried over Na/benzophenone and twice distilled. Satisfactory C and H analysis were obtained for all isolated species.

1: 50 mL of benzene was distilled into a glass bomb reactor containing $[(tBuNH)_2W(=NtBu)_2]$ (8.53 g, 18.1 mmol) and (silox)H (7.85 g, 36.3 mmol) at −78 °C. The mixture was heated and stirred for 3 d at 90 °C, then checked by ^{1}H NMR. Additional (silox)H (≈ 2 g) and further heating (≈ 1 d) was occasionally required. The benzene was removed, hexane added, and the solution filtered and cooled to −78 °C. Yield of colorless microcrystalline **1**: 11.04 g (81%). ^{1}H NMR (C_6D_6): δ = 1.26 (s, 54H, silox), 1.42 (s, 18H, *t*Bu); ^{13}C{^{1}H}-NMR: δ = 23.94 (SiC), 30.21 ($SiC(CH_3)_3$), 33.79 ($NC(CH_3)_3$), 66.50 (NC). IR (nujol): ν(W = N) = 1215, 1245 cm^{-1}.

2: 30 mL of benzene was distilled into a glass bomb reactor containing 6.87 g (9.08 mmol of **1**). HCl gas (27.24 mmol) was then passed at −196 °C into the bomb reactor, which was heated and stirred for 3.5 d at 110 °C. The benzene and residual HCl were removed, 50 mL of hexane added, and the solution filtered and cooled (−78 °C) to yield 5.47 g (88%) of pale yellow, crystalline **2**. ^{1}H NMR (C_6D_6): δ = 1.28 (s, 9H, *t*Bu), 1.34 (s, 54H, silox); ^{13}C{^{1}H}-NMR: δ = 24.82 (SiC), 30.28 ($NC(CH_3)_3$), 30.48 ($SiC(CH_3)_3$), 75.23 (NC). IR (nujol): ν(W = N) = 1280 cm^{-1}.

3: 25 mL of diethyl ether was distilled into a flask containing **2** (3.10 g, 4.10 mmol) and Mg dust (440 mg, 19.1 mmol) at −78 °C. The solution was stirred at 25 °C for 7 h and the ether removed to yield a crusty green solid. Hexane (25 mL) was added and the solution filtered and cooled to −78 °C to give 2.57 g (91%) of emerald-green **3**. ^{1}H NMR (C_6D_{12}): δ = 1.15 (s, 54H, silox), 1.74 (s, 9H, *t*Bu). IR (nujol): ν(W=N) = 1295 cm^{-1}.

4: 10 mL of hexane was distilled into a glass bomb containing 448 mg (0.653 mmol) of **3**. Ethylene (0.656 mmol) was then added at −196 °C. The solution was stirred for 1 h at 25 °C and cooled to −78 °C, yielding 208 mg (45%) of orange, microcrystalline **4**. ^{1}H NMR (C_6D_{12}): δ = 1.14 (s, 54H, silox), 1.32 (s, 18H, *t*Bu), 1.64 (br m, 2H, *H*HC=C*H*H), 2.83 (br m, 2H, H*H*C=CH*H*); ^{13}C{^{1}H}-NMR (C_6D_6): δ = 23.36 (SiC), 30.31 ($SiC(CH_3)_3$), 31.09 ($NC(CH_3)_3$), 52.51 (C_2H_4). IR (nujol): ν(W=N) = 1295 cm^{-1}.

5: 8 mL of hexane was distilled into a glass bomb containing 598 mg, (0.872 mmol) of **3**. Ca. 3 mL of 2-butyne (60 mmol) was then added at −78 °C. The resulting brown solution was stirred for 1.5 h at 25 °C, filtered and cooled to 0 °C, yielding 215 mg (33%) of colorless **5**. ^{1}H NMR (C_6D_6): δ = 1.17 (s, 18H, *t*Bu), 1.29 (s, 54H, silox), 2.59 (t, *J*(WH) = 5 Hz, 6H, Me_2); ^{13}C{^{1}H}-NMR: δ = 20.83 (Me_2), 23.77 (SiC), 30.50 ($SiC(CH_3)_3$), 32.99 ($NC(CH_3)_3$), 68.34 (NC), 199.73 (C≡C). IR (nujol): ν(W=N) = 1281 cm^{-1}.

Received: November 27, 1990 [Z 4295 IE]
German version: *Angew. Chem. 103* (1991) 616

CAS Registry numbers:
1, 132912-03-9; **2**, 132912-04-0; **3**, 132912-05-1; **4**, 132912-01-7; **5**, 132912-02-8; $[(tBuNH)_2W(=NtBu)_2]$, 132912-06-2.

[1] D. R. Neithamer, R. E. LaPointe, R. A. Wheeler, D. S. Richeson, G. D. Van Duyne, P. T. Wolczanski, *J. Am. Chem. Soc. 111* (1989) 9056.
[2] J. T. Anhaus, T. P. Kee, M. H. Schofield, R. R. Schrock, *J. Am. Chem. Soc. 112* (1990) 1642.
[3] For syntheses and discussions of four-coordinate tungsten, see: a) D. S. Williams, M. H. Schofield, J. T. Anhaus, R. R. Schrock, *J. Am. Chem. Soc. 112* (1990) 6728; b) R. H. Cayton, M. H. Chisholm, D. L. Clark, C. E. Hammond, *ibid. 111* (1989) 2751.
[4] W. A. Nugent, R. L. Harlow, *Inorg. Chem. 19* (1980) 777.
[5] a) M. Weidenbruch, H. Pesel, W. Peter, R. Steichen, *J. Organomet. Chem. 141* (1977) 9; b) E. M. Dexheimer, L. Spialter, L. D. Smithson, *ibid. 102* (1975) 21.
[6] W. A. Nugent, J. M. Mayer: *Metal-Ligand Multiple Bonds*, Wiley, New York 1988.
[7] Further details of the crystal structure investigation may be obtained from the Fachinformationszentrum Karlsruhe, Gesellschaft für wissenschaftlich-technische Information mbH, W-7514 Eggenstein-Leopoldshafen 2 (FRG), on quoting the depository number CSD-55093, the names of the authors, and the journal citation.
[8] a) D. R. Neithamer, L. Párkányi, J. F. Mitchell, P. T. Wolczanski, *J. Am. Chem. Soc. 110* (1988) 4421; b) D. R. Neithamer, Ph.D. Thesis, Cornell University 1989; c) Katharine J. Covert, Ph.D. Thesis, Cornell University 1990.
[9] R. E. LaPointe, P. T. Wolczanski, G. D. Van Duyne, *Organometallics 4* (1985) 1810.
[10] For an alternative viewpoint, see: B. D. Steffey, P. E. Fanwick, I. P. Rothwell, *Polyhedron 9* (1990) 963.
[11] A. J. Nielson, P. C. Ware, *Polyhedron 9* (1990) 603.
[12] R. R. Schrock, R. T. DePue, J. Feldman, K. B. Yap, D. C. Yang, W. M. Davis, L. Park, M. DiMare, M. Schofield, J. Anhaus, E. Walborsky, E. Evitt, C. Krüger, P. Betz, *Organometallics 9* (1990) 2262.

Synthetic Strategy for the Coupling of the Calicheamicin Oligosaccharide with Aglycons: Synthesis of Dynemicin A–Calicheamicin Hybrid Structures**

By *K. C. Nicolaou,* E. P. Schreiner* and *W. Stahl*

Studies in the area of enediyne antibiotics[1-3] recently reported from these laboratories include the total synthesis[4] of the oligosaccharide fragment of calicheamicin γ_1^I and the construction[5] of a number of dynemicin A models. Crucial to a successful total synthesis of calicheamicin γ_1^I is the stereoselective coupling of the oligosaccharide and agly-

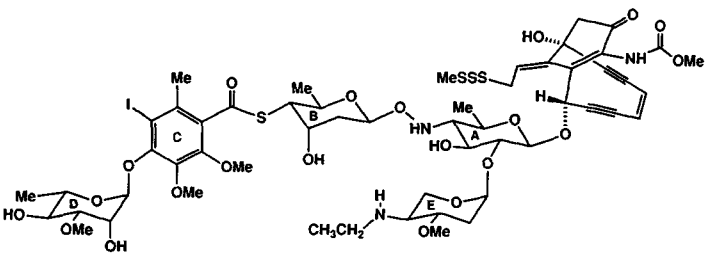

Calicheamicin γ_1^I

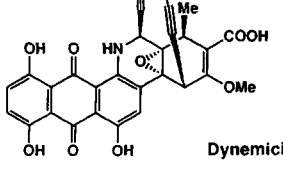

Dynemicin A

[*] Prof. K. C. Nicolaou, E. P. Schreiner, Dr. W. Stahl
Department of Chemistry
Research Institute of Scripps Clinic
10666 N. Torrey Pines Road, La Jolla, California 92037 (USA)
and
Department of Chemistry
University of California, San Diego
La Jolla, California 92093 (USA)

[**] This work was financially supported by the National Institutes of Health (USA) and the National Science Foundation (USA). *W. S.* is a Feoder Lynen Postdoctoral Fellow of the Alexander von Humboldt Foundation (1990–1991).

con fragments under mild conditions that will ensure the survival of sensitive functionalities. In this communication we report a) a synthetic strategy that addresses the stereoselective connection of the calicheamicin γ_1^I oligosaccharide and aglycon fragments, and b) the construction of novel calicheamicin γ_1^I–dynemicin A hybrid structures.

To test a possible scenario for the stereoselective coupling of the calicheamicin γ_1^I oligosaccharide and aglycon fragments, model **18** (Scheme 2) was chosen for synthesis. The key intermediate **6** was synthesized from D-fucose as outlined in Scheme 1. Thus, D-fucose (**1**) was acetylated to form te-

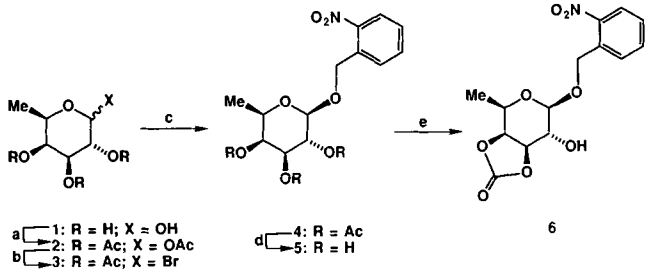

Scheme 1: Synthesis of intermediate **6**; reagents and conditions: a) 6.0 eq Ac_2O, 8.0 eq NEt_3, 4-dimethylaminopyridine (DMAP) cat., CH_2Cl_2, 0–25 °C, 2 h, 98%; b) HBr (30%) in HOAc, 0 °C, 0.5 h; c) 1.3 eq HOBn-NO_2, 1.3 eq $AgCO_3$, 3 Å molecular sieves, CH_2Cl_2, 25 °C, 16 h, 65% from **2**; d) NaOMe cat., MeOH, 25 °C, 3 h, 95%; e) 2.5 eq CDI, MeCN, reflux, 2 h, 90%.

traacetate **2**, which was converted into the anomeric bromide **3**. Glycosylation with *o*-nitrobenzyl alcohol afforded compound **4** (63% overall yield). Deacetylation of **4** led to **5**, which reacted selectively with carbonyl diimidazole (CDI) to afford the requisite ring A intermediate **6** in 86% overall yield.

Intermediate **6** was then coupled[6] to glycosyl fluoride **7**[7] (Scheme 2) with $AgClO_4$–$SnCl_2$ catalyst, leading stereoselectively to disaccharide **8** as the major anomer (80% yield, ca. 5:1 ratio of anomers). Chromatographic purification of **8** followed by removal of the carbonate protecting group ($NaH/HOCH_2CH_2OH$, 90%) and treatment with $n$$Bu_2SnO$-$Br_2$[8] led to hydroxyketone **10** (65% yield plus 17% **9**) via intermediate **9**. Oxime formation with *o*-benzylhydroxylamine under acid conditions led to **11** (90%, single geometrical isomer of unassigned stereochemistry), which was silylated under standard conditions to furnish compound **12** (90%). Photolytic cleavage[9] of the *o*-nitrobenzyl group from **12** (THF/H_2O, 15 min) produced lactol **13** in 95% yield. Treatment of **13** with NaH–$Cl_3CC{\equiv}N$ in CH_2Cl_2[10] for 2 h at 25 °C resulted in the formation of the α-trichloroacetimidate **14** in 98% yield. Reaction of benzyl alcohol (2.0 equiv) with trichloroacetimidate **14** under Schmidt conditions[10] [$BF_3 \cdot Et_2O$, CH_2Cl_2, $-60 \rightarrow -30$ °C] resulted in stereoselective formation of the β-glycoside **15** (79% yield) together with its anomer (16%, separated by chromatography; ^{1}H NMR, 500 MHz, C_6D_6: **15**: $J_{1/2} = 6.5$ Hz, *epi*-**15**: $J_{1,2} = 2.4$ Hz). On the other hand, treatment of lactol **13** with diethylaminesulfurtrifluoride (DAST) led to the glycosyl fluoride **13a** in 90% yield (ca. 1:1 anomeric mixture). Reaction of **13a** with benzyl alcohol in the presence of silver silicate[11]/$SnCl_2$ resulted in the formation of the β-glycoside **15** and its anomer in 85% (ca. 1:1 anomeric mixture). Generation of intermediate **17** via **16** proceeded smoothly under standard deprotection conditions. Finally, exposure of **17** to Ph_2SiH_2 in the presence of $Ti(OiPr)_4$ resulted in the formation of the target **18**[12] as the only detectable product (92% yield). Interestingly, reduction of **17** with $NaCNBH_3/H^{\oplus}$ led predominantly to the 4-epimer of **18** (90% yield). The stereochemical assignments of **18** and *epi*-**18** at C-4 were based on ^{1}H NMR coupling constants (^{1}H NMR, 500 MHz, C_6D_6, **18**: $J_{3,4} = 9.5$, $J_{4,5} = 9.5$ Hz; *epi*-**18**: $J_{3,4} = 1.9$, $J_{4,5} = 1.5$ Hz).

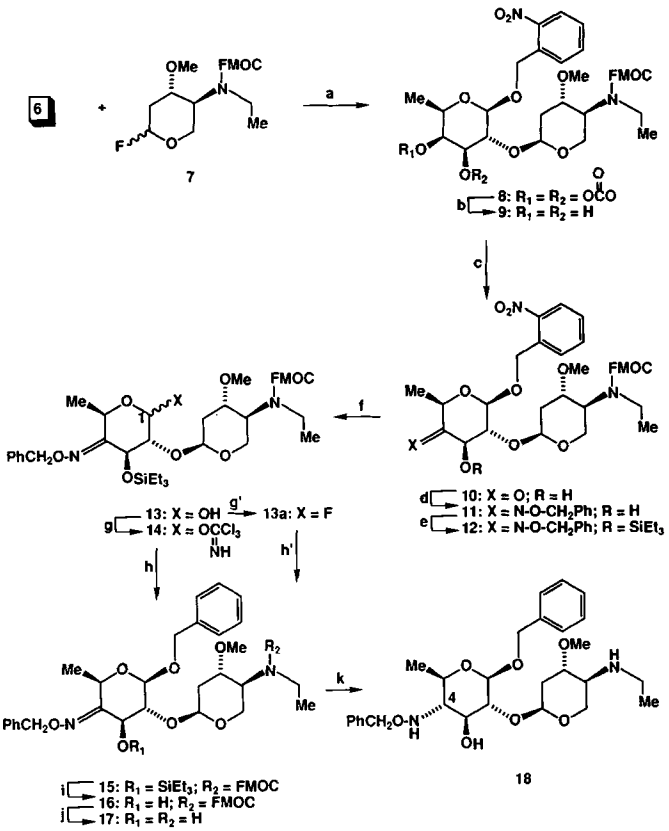

Scheme 2: Synthesis of benzyl glycoside model **18**; reagents and conditions. a) 1.2 eq of **7**, 2.5 eq $AgClO_4$, 2.5 eq $SnCl_2$, THF, −90 to −10 °C, 6 h, 80%, (α:β ca 5:1); b) NaH cat., $HOCH_2CH_2OH$/THF (1:10), 0 °C, 0.5 h, 90%; c) 1.05 eq $n$$Bu_2SnO$, MeOH, reflux, 1 h, then 1.0 eq Br_2, 1.0 eq $n$$Bu_3SnOMe$, CH_2Cl_2, 25 °C, 2 h, 65% + 17% starting material **9**; d) 1.1 eq $BnONH_2$, pyridinium-*p*-toluenesulfonate (PPTS) cat., benzene, 25 °C, 0.5 h, 90%; e) 1.0 eq Et_3SiOTf, 1.2 eq 2,6-lutidine, CH_2Cl_2, 0 °C, 0.5 h, 98%; f) *hv*, THF/H_2O (9:1), 0 °C, 15 min, 95%; g) NaH cat., CCl_3CN/CH_2Cl_2 (1:12), 25 °C, 2 h, 98%; g') 3.0 eq DAST, THF, −78 to 0 °C, 1 h, 90%; h) 2.0 eq BnOH, 1.0 eq $BF_3 \cdot OEt_2$, CH_2Cl_2, −60 to −30 °C, 95%, (α:β ca 1:5); h') 1.2 eq BnOH, 1.2 eq silver silicate, $SnCl_2$ cat., CH_2Cl_2, 25 °C, 3 h, 85%; i) excess HF · py, CH_2Cl_2/THF (7:1), 0 °C, 20 min, 98%; j) Et_2NH/THF (1:1), 25 °C, 2 h, 98%; k) excess $Ti(OiPr)_4$, excess Ph_2SiH_2, CH_2Cl_2, 25 °C, 1 h, 92%. FMOC = fluoroenylmethoxy-carbonyl.

As an application of this strategy, the calicheamicin-dynemicin A hybrid structures **26a** and **26b** (Scheme 3) were targeted starting with the recently reported model system **19**.[5] Thus, coupling of **19** with ethyl bromoacetate under basic conditions led to derivative **20** (60% yield), which was converted to primary alcohol **22** (80% overall yield) by: 1) ester hydrolysis, 2) 2-pyridyl thiolester formation, and 3) reduction. Coupling of **22** (1.2 equiv) with trichloroacetimidate **14** under the influence of $BF_3 \cdot Et_2O$ as described above led to the formation of two major products (70%, ca. 1:1 ratio) and two minor products (14%, ca. 1:1 ratio) which were separated by chromatography. The major isomers were proven to be the diastereomeric β-glycosides **23a** ($R_f = 0.12$, silica, 20% ethyl acetate in petroleum ether) and **23b** ($R_f = 0.10$, silica, 20% ethyl acetate in petroleum ether) [^{1}H

NMR, 500 MHz, C_6D_6: **23a**: $J_{1,2} = 6.5$ Hz; **23b**: $J_{1,2} = 6.5$ Hz], and the minor isomers the anomers of **23a** and **23b** at C-1 [^{1}H NMR, 500 MHz, C_6D_6: *epi*-**23a**, $J_{1,2} = 2.4$ Hz; *epi*-**23b**, $J_{1,2} = 2.4$ Hz]. Sequential deprotection of **23a** and **23b** as described above for **15** led to oximes **25a** and **25b** via intermediates **24a** and **24b** respectively. Finally, reduction of **25a** and **25b** under the $Ph_2SiH_2/Ti(OiPr)_4$ conditions led exclusively to the targeted compounds **26a**[12] and **26b**[12] respectively (90% yield). The C-4 configuration of **26a** and **26b** was again based on the coupling constants $J_{4,3} = 9.5$ and $J_{4,5} = 9.5$ Hz for the newly installed H-4. Structures **23a**–**26a** and **23b**–**26b** are interchangeable, since the absolute stereochemistry of the aglycons has not been determined.

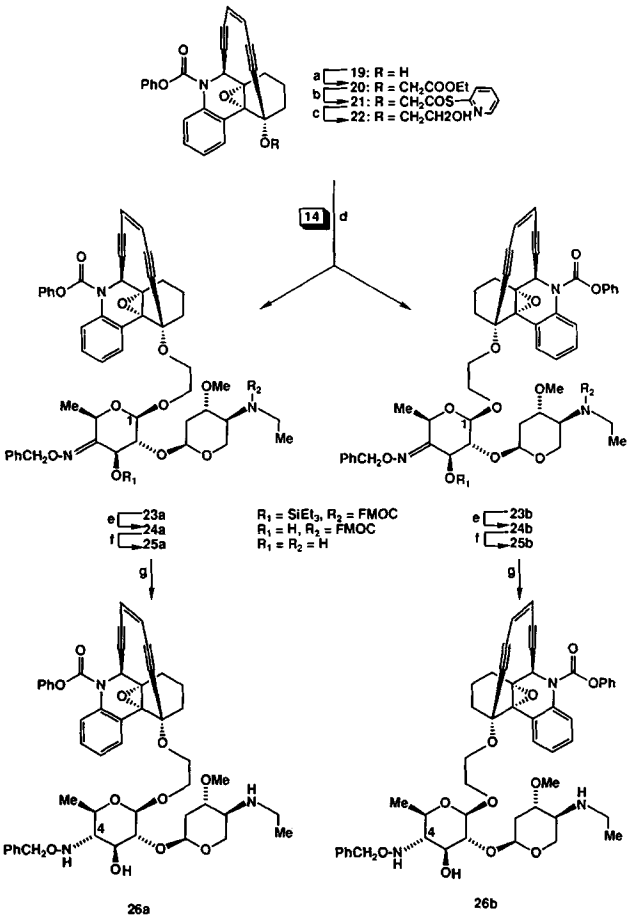

Scheme 3: Synthesis of calicheamicin-dynemicin A models **26a** and **26b**; reagents and conditions: a) 3.0 eq $BrCH_2CO_2Et$, 2.0 eq $CsCO_3$, 1.0 eq 18-crown-6, MeCN, 50 °C, 5 h, 60%; b) 2.0 eq LiOH, THF/H_2O (1:1), 0.5 h; then 1.1 eq $(pyS)_2$, 1.1 eq PPh_3, CH_2Cl_2, 25 °C, 0.5 h, 92%; c) 5.0 eq $NaBH_4$, CH_2Cl_2/*i*PrOH (1:1), 25 °C, 20 min, 92%; d) 0.83 eq **14**, $BF_3 \cdot OEt_2$ cat., CH_2Cl_2, −60 to −40 °C, 1 h, 84%, (α:β ca 5:1), e) excess HF · py, CH_2Cl_2/THF (7:1), 0 °C, 20 min, 98%; f) Et_2NH/THF (1:1), 25 °C, 2 h, 98%; g) excess $Ti(OiPr)_4$, excess Ph_2SiH_2, CH_2Cl_2, 25 °C, 1 h, 90%.

These successful coupling reactions demonstrate a) the facile resolution of racemic aglycons such as **22** using enantiomerically pure carbohydrate chains, and b) the survival of the highly sensitive functionalities present in the enediyne antibiotics under the reaction conditions. Furthermore, the C-4 nitrogen functionality of the calicheamicin skeleton may be stereoselectively installed in these systems under mild conditions. Finally, the synthesized model systems are novel and potentially biologically active enediyne compounds. It is hoped that the described chemistry will be valuable in the total synthesis of calicheamicin γ_1^I and in the construction of further hybrid molecules within the enediyne class.

Received: December 13, 1990 [Z 4327 IE]
German version: *Angew. Chem. 103* (1990) 566

CAS Registry numbers:
1, 3615-37-0; **2**, 51921-33-6; **3**, 69483-13-2; **4**, 132938-41-1; **5**, 132938-42-2; **6**, 132938-43-3; **7**, 133006-26-5; **8** (α anomer), 132938-44-4; **8** (β anomer), 132938-60-4; **9**, 132938-45-5; **10**, 132938-46-6; **11**, 132938-47-7; **12**, 132938-48-8; **13**, 132958-86-2; **13a** (α anomer), 132938-62-6; **13a** (β anomer), 132938-63-7; **14**, 132938-49-9; **15** (α anomer), 132958-88-4; **15** (β anomer), 132938-50-2; **16**, 132938-51-3; **17**, 132938-52-4; **18**, 132938-53-5; **18** (4-epimer), 132938-61-5; **19**, 130031-63-9; **20**, 132938-54-6; **21**, 132938-55-7; **22**, 132938-56-8; **23a** (α anomer), 133006-27-6; **23a** (β anomer), 132938-57-9; **23b** (α anomer), 133006-28-7; **23b** (β anomer), 133006-29-8; **24a**, 132938-58-0; **24b**, 133006-30-1; **25a**, 132938-59-1; **25b**, 133007-23-5; **26a**, 132958-87-3; **26b**, 133007-24-6; calicheamicin γ_1^I, 108212-75-5; ethyl bromoacetate, 105-36-2; dynemicin A, 124412-57-3.

[1] a) J. Golik, J. Clardy, G. Dubay, G. Groenewold, H. Kawaguchi, M. Konishi, B. Krishnan, H. Ohkuma, K. Saitoh, T. W. Doyle, *J. Am. Chem. Soc. 109* (1987) 3461; b) J. Golik, G. Dubay, G. Groenewold, H. Kawaguchi, M. Konishi, B. Krishnan, H. Ohkuma, K. Saitoh, T. W. Doyle, *ibid. 109* (1987) 3462.

[2] a) M. D. Lee, T. S. Dunne, M. M. Siegel, C. C. Chang, G. O. Morton, D. B. Borders, *J. Am. Chem. Soc. 109* (1987) 3464; b) M. D. Lee, T. S. Dunne, C. C. Chang, G. A. Ellestad, M. M. Siegel, G. O. Morton, W. J. McGahren, D. B. Borders, *ibid. 109* (1987) 3466.

[3] M. Konishi, H. Ohkuma, K. Matsumoto, T. Tsuno, H. Kamei, T. Miyaki, T. Oki, H. Kawagushi, G. D. VanDuyne, J. Clardy, *J. Antibiot. 42* (1989) 1449; b) M. Konishi, H. Ohkuma, T. Tsuno, T. Oki, G. D. VanDuyne, J. Clardy, *J. Am. Chem. Soc. 112* (1990) 3715.

[4] K. C. Nicolaou, R. D. Groneberg, T. Miyazaki, N. A. Stylianides, T. J. Schultze, W. Stahl, *J. Am. Chem. Soc. 112* (1990) 8193; K. C. Nicolaou, R. D. Groneberg, *ibid. 112* (1990) 4085.

[5] K. C. Nicolaou, C.-K. Huang, A. L. Smith, S. V. Wendeborn, *J. Am. Chem. Soc. 112* (1990) 7416; K. C. Nicolaou, A. L. Smith, S. V. Wendeborn, C.-K. Huang, *ibid. 113* (1991) in press. For another approach to a dynemicin A model, see: J. A. Porco, Jr., F. J. Schoenen, T. J. Stout, J. Clardy, S. L. Schreiber, *ibid. 112* (1990) 7410.

[6] T. Mukaiyama, Y. Muria, S. Shode, *Chem. Lett. 1981*, 431; K. C. Nicolaou, R. E. Dolle, D. P. Papahatjis, J. L. Randall, *J. Am. Chem. Soc. 106* (1984) 4159.

[7] K. C. Nicolaou, R. D. Groneberg, N. A. Stylianides, T. Miyazaki, *J. Chem. Soc. Chem. Commun. 1990*, 1275.

[8] S. David, A. Theiffry, *J. Chem. Soc. Perkin Trans 1 1979*, 1568.

[9] U. Zenhavi, B. Amit, A. Patchornik, *J. Org. Chem. 37* (1972) 2281; U. Zenhavi, A. Patchornik, *ibid. 37* (1972) 2285; E. Ohtsuka, S. Tanaka, M. Ikehara, *J. Am. Chem. Soc. 100* (1978) 8210; V. N. R. Pillai, *Synthesis 1980*, 1.

[10] G. Grandler, R. R. Schmidt, *Carbohydr. Res. 135* (1985) 203; R. R. Schmidt, *Angew. Chem. 98* (1986) 213; *Angew. Chem. Int. Ed. Engl. 25* (1986) 212.

[11] H. Paulsen, O. Lockhoff, *Chem. Ber. 114* (1981) 3102.

[12] All new compounds exhibited satisfactory spectral and analytical and/or exact mass data. Yields refer to spectroscopically and chromatographically homogenous materials. Selected physical properties for compounds **18**, **26a** and **26b** (Ar = aryl). **18**: pale yellow oil; $R_f = 0.31$ (silica, 10% methanol in dichloromethane), $[\alpha]_D^{25} = -49.2$ ($c = 0.66$, $CHCl_3$); ^{1}H NMR (500 MHz, C_6D_6): $\delta = 7.56$ (d, 2H, $J = 7.6$ Hz, Ar), 7.32–7.13 (m, 8H, Ar), 5.88 (br. s, 1H, OH), 5.86 (s, 1H, E-1), 5.75 (br. s, 1H, O-NH), 4.99 (d, 1H, $J = 11.7$ Hz, CH_2Ph), 4.67 (d, 1H, $J = 11.7$ Hz, CH_2Ph), 4.54–4.47 (m, 3H, A-1, CH_2Ph-hydroxylamine), 4.32 (dd, 1H, $J = 10.8$, 9.2 Hz, E-5ax), 4.04 (dd, 1H, $J = 9.5$, 9.5 Hz, A-3), 4.02–3.94 (m, 1H, E-3), 3.90 (dd, 1H, $J = 10.8$, 4.7 Hz, E-5eq), 3.88 (dd, 1H, $J = 9.5$, 7.6 Hz, A-2), 3.57 (dq, 1H, $J = 9.5$, 6.0 Hz, A-5), 3.23 (s, 3H, OCH_3), 2.82 (ddd, 1H, $J = 9.2$, 9.2, 4.7 Hz, E-4), 2.57–2.42 (m, 3H, E-2eq, NCH_2), 2.34 (dd, 1H, $J = 9.5$, 9.5 Hz, A-4), 1.54 (dd, 1H, $J = 10.2$, 10.2 Hz, E-2ax), 1.36 (d, 3H, $J = 6.0$ Hz, A-6), 0.99 (t, 3H, $J = 6.5$ Hz, NCH_2CH_3); IR ($CHCl_3$): $\tilde{\nu}_{max} = 2964$, 2932, 1456, 1095, 1071 cm^{-1}; HRMS calcd for $C_{28}H_{40}N_2O_7$ (M + Cs$^{\oplus}$) 649.1890; found 649.1900. **26a**: pale yellow oil; $R_f = 0.39$ (silica, 10% methanol in dichloromethane), $[\alpha]_D^{25} = -87.3$ ($c = 0.48$, $CHCl_3$), ^{1}H NMR, (500 MHz, C_6D_6): $\delta = 8.97$ (dd, 1H, $J = 4.2$, 0.7 Hz, dyn-Ar), 7.52 (m, 1H, dyn-Ar), 7.41–6.98 (m, 12H, 11 Ar, propargylic H), 6.98 (dd, 1H, $J = 7.1$, 7.1 Hz, dyn-Ar), 5.89 (bs, 1H, OH), 5.83 (br. s, 1H, O-NH), 5.78 (s, 1H, E-1), 5.28 (d, 1H, $J = 10.0$ Hz, vinylic H), 5.10 (dd, 1H, $J = 10.0$, 1.7 Hz, vinylic H), 4.58–4.51 (m, 2H, CH_2Ph), 4.50 (d, 1H, $J = 7.4$, A-1), 4.48–4.40 (m, 1H, E-5ax), 4.25–4.17 (m, 1H, E-5eq),

4.13–4.02 (m, 3H, A-3, OCH_2CH_2O), 4.01–3.94 (m, 1H, OCH_2CH_2O), 3.93–3.90 (m, 1H, E-3), 3.77 (dd, 1H, J = 9.5, 7.3 Hz, A-2), 3.69–3.52 (m, 1H, A-5), 3.26 (s, 3H, OCH_3), 2.78–2.66 (m, 2H, E-4, NCH_2), 2.65–2.57 (m, 1H, NCH_2), 2.47 (dd, 1H, J = 12.0, 2.2 Hz, E-2eq), 2.44 (dd, 1H, J = 9.5, 9.5 Hz, A-4), 2.31 (dd, 1H, J = 14.5, 6.5 Hz, dyn-CH_2), 2.04 (d, 1H, J = 6.7 Hz, dyn-CH_2), 1.95–1.83 (m, 4H, CH_2), 1.43 (dd, 1H, J = 14.5, 9.3 Hz, E-2ax), 1.33 (d, 3H, J = 6.1 Hz, A-6), 1.04 (t, 3H, J = 6.5 Hz, NCH_2CH_3); IR ($CHCl_3$) $\tilde{\nu}_{max}$ = 2965, 2931, 1733, 1380, 1323, 1146, 1098, 1071 cm^{-1}; HRMS calcd for $C_{49}H_{55}N_3O_{11}$ (M + $Cs^{\oplus}$) 994.2891; found 994.2904. **26b**: pale yellow oil; R_f = 0.38 (silica, 10% methanol in dichloromethane), $[\alpha]_D^{25}$ = + 125.7 (c = 0.68, $CHCl_3$), ^1H NMR (500 MHz, C_6D_6): δ = 8.93 (dd, 1H, J = 4.2, 0.7 Hz, dyn-Ar), 7.56 (dd, J = 7.4, 1.4 Hz, dyn-Ar), 7.32–7.02 (m, 12H, 11 Ar, propargylic H), 6.90 (dd, 1H, J = 7.1, 7.1 Hz, dyn-Ar), 5.90 (br. s, 1H, O-NH), 5.88 (br. s, 1H, OH), 5.82 (s, 1H, E-1), 5.29 (d, 1H, J = 10.2 Hz, vinylic H), 5.11 (dd, 1H, J = 10.2, 1.7 Hz, vinylic H), 4.56–4.51 (m, 2H CH_2Ph), 4.49 (dd, 1H, J = 11.1, 9.0 Hz, E-5ax), 4.48 (d, 1H, J = 7.4 Hz, A-1), 4.22–4.17 (m, 2H, OCH_2CH_2O), 4.14 (dd, 1H, J = 11.1, 4.7 Hz, E-5eq), 4.09 (dd, 1H, J = 9.5, 9.5 Hz, A-3), 4.06–4.01 (m, 1H, OCH_2CH_2O), 3.93–3.88 (m, 1H, OCH_2CH_2O), 3.87–3.81 (m, 1H, E-3), 3.78 (dd, 1H, J = 9.5, 7.1 Hz, A-2), 3.58 (dq, 1H, J = 9.5, 6.1 Hz, A-5), 3.27 (s, 3H, OCH_3), 2.84 (ddd, 1H, J = 9.0, 9.0, 4.7 Hz, E-4), 2.77 (m, 2H, N-CH_2), 2.54 (dd, 1H, J = 12.2, 2.5 Hz, E-2eq), 2.42 (dd, 1H, J = 9.5, 9.5 Hz, A-4), 2.30 (dd, 1H, J = 14.6, 10.5 Hz, dyn-CH_2), 2.06 (dd, 1H, J = 14.6, 7.1 Hz, dyn-CH_2), 1.97–1.83 (m, 4H, dyn-CH_2), 1.51 (dd, 1H, J = 12.2, 9.2 Hz, E-2ax), 1.33 (d, 3H, J = 6.1 Hz, A-6), 1.10 (t, 3H, J = 6.5 Hz, NCH_2CH_3); IR ($CHCl_3$): $\tilde{\nu}_{max}$ = 2962, 2957, 2929, 1733, 1386, 1323, 1146, 1097, 1070 cm^{-1}; HRMS calcd for $C_{49}H_{55}N_3O_{11}$ (M + $Cs^{\oplus}$) 994.2891; found 994.2904.

Formation of a Cluster Sheath around a Central Cluster by a "Self-Organization Process": the Mixed Valence Polyoxovanadate $[V_{34}O_{82}]^{10\ominus}$ **

By *Achim Müller,* Ralf Rohlfing, Joachim Döring,* and *Michael Penk*

Studies on the properties of mixed valence species are of importance in catalysis research, geochemistry, and above all biochemistry, but also in general for material sciences.[1, 2]

The title compound, a high-nuclearity mixed valence binary cluster anion which is of interest topologically, magnetochemically, and by pre-formation of a solid state structure, could be prepared as the potassium salt **1** by reduc-

$K_{10}[V^{IV}_{16}V^{V}_{18}O_{82}] \cdot 20H_2O$ **1**

tion of an aqueous potassium vanadate solution, and could be characterized by elemental analysis (including manganometric titration of the V^{IV} content and thermogravimetric determination of the water of crystallization), IR spectroscopic and magnetic measurements, as well as single-crystal X-ray structure analysis.[3]

1 crystallizes in the triclinic space group $P\bar{1}$. Its cluster anion $[V_{34}O_{82}]^{10\ominus}$ displays approximate D_{2d} symmetry (Fig. 1a) and consists of an ellipsoid-shaped $V_{30}O_{74}$ sheath, which is formed by linking 30 tetragonal VO_5 pyramids, and a central $\{V_4O_4\}O_4$ cube. This means that assemblage of the VO_5 pyramids results in a shell which fits the distorted, central V_4O_4 cube (and its four terminal O atoms, Fig. 1b). The two identical halves of the $V_{30}O_{74}$ shell are, as demanded by the

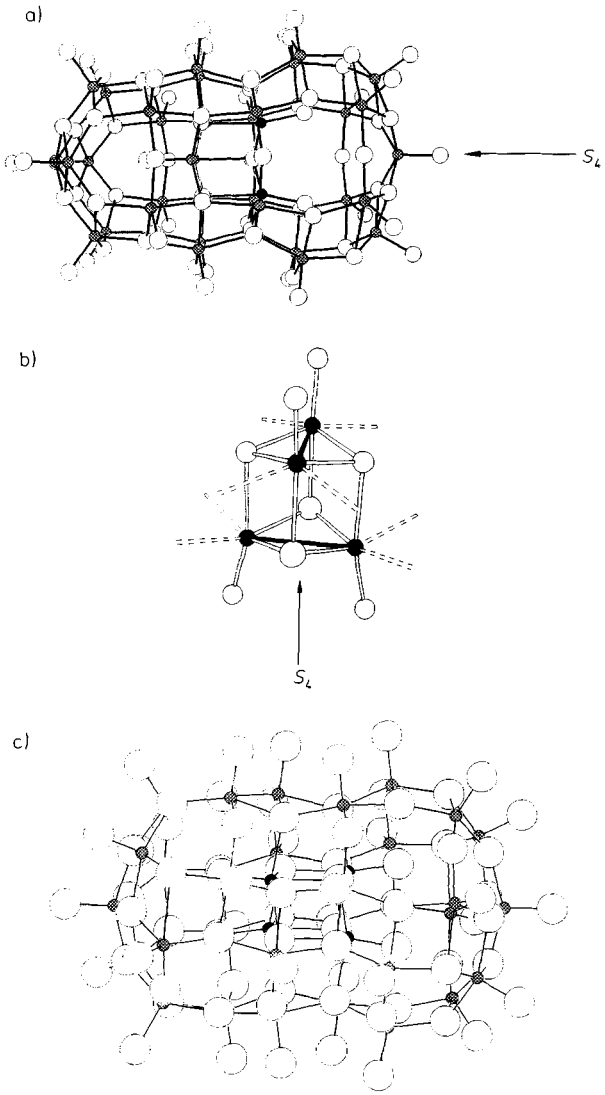

Fig. 1a) Structure of the $[V_{34}O_{82}]^{10\ominus}$ anion in the crystal of **1** (view perpendicular to the virtual S_4 axis); b) structure of the central $\{V^{IV}_4O_4\}O_4$ unit of **1** (V^{IV}-μ_3-O 192–196 and 220–222 pm) with two (in bold print) V–V bonds (265 pm) and (indicated) V–O bonds to the shell (205–210 pm; with approximate D_{2d} symmetry corresponding to the rotation of the two cluster halves with respect to each other; c) demonstration of the (approximative) layers of the oxygen atoms of **1** (for clarification of the transition to the solid-state structure; view perpendicular to the virtual S_4 axis, but rotated by 45° compared to (a). V = grey, V^{IV} = black, O = white.

geometry of the central cube, rotated by 90° with respect to each other (Fig. 1a).

Topologically the anion can be described in a simplified way as follows: each of the $V_{15}O_{37}$ halves contains 20 of the 24 O atoms of the O_{24} rhombicuboctahedron, a basic unit for many aspects of polyoxometalate chemistry (twelve square {110} faces and six {100} faces as well as eight {111} triangles), which form the μ_2-O atoms, e.g., in an α-Keggin ion.[4] Nine of the twelve occupied {110} faces and two of the unoccupied {100} faces in the Keggin ion are capped by a V=O group. In addition a novel form of capping occurs: above two {110} faces of the Keggin ion, each of which is flanked by two {111} triangles, the V=O group is replaced by an O=V–O–V=O group.

Also remarkable is that the anion, with exception of two $\{V_3O_7\}$ units at the poles, can be regarded as a distorted section of the NaCl lattice (which is also present in the VO_x defect structure, cf. Ref. [6]). The oxygen atoms form ap-

[*] Prof. Dr. A. Müller, Dipl.-Chem. R. Rohlfing, Dr. J. Döring, Dipl.-Chem. M. Penk
Fakultät für Chemie der Universität
Postfach 8640, W-4800 Bielefeld 1 (FRG)

[**] We thank Prof. Dr. *K. Wieghardt*, Prof. Dr. *W. Haase*, and Prof. Dr. *E. Pedersen* for carrying out the magnetic measurements, and Dr. *H. Bögge* for help with the X-ray structure analysis.

proximately a cubic close packing arrangement whose octahedral holes are occupied by the V centers but, as expected, in each case clearly displaced towards the terminal O atoms (transition to the solid-state structure; Fig. 1c).

In the formally neutral, central $\{V_4O_4\}O_4$ unit there are, according to the calculated bond valence sums,[5] four localized V^{IV} centers, which in accord with an "exact electron count" form two covalent V–V bonds of 265 pm in length (Fig. 1b). Also novel are the four terminal V=O bonds (162–166 pm) of the enclosed cube, which stabilize a "cluster in a cluster" (regarding the tendency of formation see below).

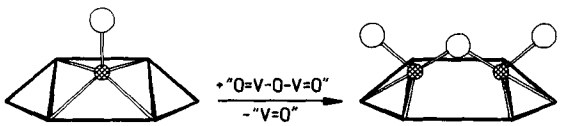

α-Keggin ion

In contrast, the V–V distances in the shell (Table 1) lie in the range of values reported for most known reduced polyvanadates.[4] The bond valence sums for the atoms of the shell indicate a "delocalization" of the remaining twelve V^{IV} centers (the manganometric titration affords 16 V^{IV} centers per formula unit),[5] whereby, as in almost all other reduced V–O clusters,[4] an antiferromagnetic coupling exists (Table 1).

Due to the two very short V–V distances (quasi-diamagnetism) the spin-spin coupling in the central cube should be comparable with that in the monoclinic VO_2[6] and more pronounced than in the $[V_{19}O_{41}(OH)_9]^{8\ominus}$ cluster in **2**[8,9] containing exactly six very strongly antiferromagnetically coupled V^{IV}–V^{IV} pairs ("weak chemical bonding"[7]; number of V^{IV}–V^{IV} pairs n/2(!), n = number of 3d electrons), whereby **2** contains a further seven localized V^{V} centers.[10]

A relatively large number of comparable V–V distances leads, as in many known V–O clusters, e.g. the $[V_{18}O_{42}(SO)_4]^{8\ominus}$ anion in **3**,[11] to weaker antiferromagnetic coupling, i.e. with decreasing temperature to a smaller lowering of the μ_{eff} value (here: n/2 < number of the almost equivalent V–V contacts). This applies to an equal extent for the shell of **1**, but also for the total magnetism of the compound (because of the quasi-diamagnetism of the central unit). The anions in **1**, **2**, and **3** are molecular electronic models for the monoclinic and tetragonal VO_2 phase;[6] for the tetragonal phase, however, only in a limited sense because of the conduction electrons and the resulting virtually *T*-independent Landau diamagnetism and Pauli paramagnetism—both albeit with relatively small contribution. The relevant distances and μ_{eff} data for all the species discussed are listed in Table 1.

The breadth of variation from weak exchange interactions (in the case of **3** and the majority of known V–O species[4]), through very strong exchange interactions (in the case of **2**) to relatively strongly covalent bonds (in the case of **1** and monoclinic VO_2) is unique in clusters with exclusively "classical" ligands such as $O^{2\ominus}$. The magnetic properties correlate unequivocally with the bond data and with the presence of V^{IV}–V^{IV} pairs (as "spin traps").

Generally, very different high nuclearity V–O clusters can be generated by assemblage of a cluster shell formed from tetragonal VO_5 pyramids around a central unit (template),[17] which is added before the reaction or, as here, formed during the course of the synthesis. In the present case the ellipsoid-shaped structure as well as the distorted NaCl-type V–O lattice is determined by the formally neutral $\{V_4^{IV}O_4\}O_4$ center (with the stoichiometry of amphoteric VO_2!). The latter is probably formed from the reaction solution with attachment to the shell, and then as "pseudo template," non-existent in isolated form, influences the structure of the cluster with regard to its size and shape in a self-organization process,[16] whereby the cluster shell halves are rotated by 90° with respect to each other (Fig. 1a, b). At the same time the symmetry of the central unit is correspondingly lowered from T_d to approximate D_{2d}.

Table 1. Relationships between V–V distances and magnetic properties of V–O species.

V–O Species	V–V Distances [pm]	μ_{eff} [μ_B] (in brackets per V^{IV} center) [f]
$K_{10}[V_{34}O_{82}] \cdot 20H_2O$ **1**	265 (two V^{IV}-V^{IV} pairs in the cube) [a] 292–315 (V^{IV}/V^{V} shell) [b]	4.8 (1.2) at 290 K 3.8 (1.0) at 80 K [c] (weak *T* dependence)
$(NH_4)_8[V_{19}O_{41}(OH)_9] \cdot 11H_2O$ [8] **2**	290–300 (six V^{IV}-V^{IV}-pairs) [a] 330–360 (V^{IV}-V^{IV}, V^{IV}-V^{V})	3.1 (0.9) at 290 K 1.1 (0.3) at 80 K [c] (strong *T* dependence)
$(NH_4)_8[V_{18}O_{42}(SO_4)] \cdot 25H_2O$ [11] **3**	291 [b] (no localized V^{IV}-V^{IV} pairs) [d]	4.0 (1.2) at 290 K 2.8 (0.8) at 80 K [c] (weak *T* dependence)
VO_2 (monoclinic, 298 K) [14]	262 (V^{IV}-V^{IV}-pairs) [a] 317 (between the pairs)	0.4 at 293 K [6, 15]
Δ		Δ (strong *T*-dependence at the phase transition)
VO_2 (tetragonal, 351 K) [14]	285 (no pairs)	1.4 [e] at 353 K [6, 15]

[a] Numbers of pairs = n/2 with n = number of 3d electrons and practically covalent bonds in **1** and monoclinic VO_2. [b] As well as longer distances. [c] This work. [d] 12 V^{IV} centers not localized; in the corresponding $Na_6[V_{18}O_{42}H_9(VO_4)] \cdot 21H_2O$ [11] (as in the tetragonal VO_2) *only* localized V^{IV} centers are present in the shell (number of electrons n = number of V centers). [e] The relatively small proportion of Pauli spin paramagnetism is proportional to the density of states of the conduction electrons at the Fermi edge, whereby the *T*-dependence of χ above the phase transition also proves the presence of strong exchange interactions [6]. [f] Correction for diamagnetic, but not TIP portions.

The $VO^{n\oplus}$ unit resembles $Fe^{n\oplus}$ centers in its chemical behavior (cf. the biochemically relevant incorporation of $VO^{2\oplus}$ into the biological Fe-transport and storage proteins transferrin and ferritin, respectively[12] and the existence of aggregated Fe–O clusters in the ferritin with ca. 4000 Fe centers). It would therefore also be of interest to synthesize high-nuclearity mixed V/Fe–O clusters. In this connection it should be emphasized that a knowledge of the mechanistic aspects of the mode of action of transferrin and ferritin is also of fundamental importance from the medicinal point of view[13] (for instance in the case of rheumatic arthritis).

Experimental

KVO_3 (3.45 g, 25.0 mmol) was dissolved in H_2O (50 mL) at 90 °C in a 100-mL Erlenmeyer flask covered with a watch glass. The clear solution was then treated with 182 μL of hydrazinium hydroxide (100%, 3.75 mmol) and kept at 90 °C. After 1 h, the pH of the now deep-black solution was adjusted to 3.8 by addition of glacial acetic acid. After a further 2 h the solution was filtered hot, the filtrate kept at 90 °C for 3 h and finally cooled to room temperature. After storage for 1 d the precipitated black, needle-shaped crystals were filtered off, washed with a little 50% aqueous 2-propanol, and dried in air. Yield: ca. 1 g (53% of the theoretical referred to V). IR data (solid/KBr pellet):

$\tilde{\nu}$[cm^{-1}] = 990 (vs, sheath), 890 (s, cube) (ν(V=O_{term})); 745 (s), 615 (vs) (ν_{as}(V–O–V)).

Received: November 12, 1990 [Z 4275 IE]
German version: *Angew. Chem. 103* (1991) 575

CAS Registry numbers:
1, 132938-06-8; $K_5(NEt_3H)_5[V_{34}O_{82}]$, 133039-81-3; KVO_3, 13769-43-2.

[1] D. B. Brown (Ed.): *Mixed-Valence Compounds, Theory and Applications in Chemistry, Physics, Geology and Biology*, Reidel, Dordrecht 1980.

[2] A. Müller, E. Krickemeyer, M. Penk, H.-J. Walberg, H. Bögge, *Angew. Chem. 99* (1987) 1060; *Angew. Chem. Int. Ed. Engl. 26* (1987) 1045.

[3] **1**: $P\bar{1}$, a = 1267.9(6), b = 1755.3(8), c = 2366.6(6) pm, α = 73.36(3), β = 86.36(3), γ = 76.83(3)°, V = 4914(3) 10^6 pm^3, Z = 2, ϱ_{calcd} = 2.57 g cm^{-3}; solution by direct methods, R = 0.083 for 8551 independent reflections ($F_0 > 4\sigma(F_0)$). Some V centers show a transition from distorted square-pyramidal to distorted tetrahedral coordination with an additional longer bond and four show to a lesser extent a disorder of pyramids and distorted tetrahedra. $K_5(NEt_3H)_5[V_{34}O_{82}] \cdot 8H_2O$, also prepared by us, does not show this disorder, but a very strong unresolvable disorder in the cation/water of crystallization lattice. Further details of the crystal structure investigation are available on request from the Fachinformationszentrum Karlsruhe, Gesellschaft für wissenschaftlich-technische Information mbH, W-7514 Eggenstein-Leopoldshafen 2 (FRG), on quoting the depository number CSD-55095, the names of the authors, and the journal citation.

[4] a) M. T. Pope, A. Müller, *Angew. Chem. 103* (1991) 56; *Angew. Chem. Int. Ed. Engl. 30* (1991) 34; b) A. Müller, M. Penk, R. Rohlfing, E. Krickemeyer, J. Döring, *ibid. 102* (1990) 927 and *29* (1990) 926, and references cited therein; c) A. Müller, J. Döring, H. Bögge, *J. Chem. Soc. Chem. Commun. 1991*, 273.

[5] The bond valence sums for the V atoms were calculated using the expression $\sum_i n_i = \sum_i (d(V\text{-}O_i)/178)^{-5.15}$ (cf. I. D. Brown, K. K. Wu, *Acta Crystallogr. Sect. B 32* (1976) 1957) (V_4O_4 cube: 4.1).

[6] In monoclinic VO_2 (low-temperature modification with distorted rutile structure) the V–V distances along the c-axis are not, as in TiO_2, of equal length but alternately short and long (covalent V^{IV}–V^{IV} bond formation) and, as a result, very small and almost T-independent μ_{eff} values are found; compare known values for polyacetylene. On heating above 67.5 °C the V^{IV}–V^{IV} pairs "break apart" with consequences for the structure (transition into the tetragonal rutile structure of VO_2 with antiferromagnetic behavior), the magnetism (jump for χ and μ_{eff}; Table 1), the conductivity (transition from semiconductor into a metallic conductor), and other physical properties. Also fascinating is the "mechanical breakage" of the V–V bonds in very small particles, which manifests itself in monoclinic VO_2 in an increase of the susceptibility. V–O phases, including the defect systems VO_x (x = 0.8–1.3) are of exceptional interest from the physical point of view (cf. D. L. Kepert: *The Early Transition Metals*, Academic Press, London 1972, p. 192; J. B. Goodenough: *Les Oxydes Des Métaux De Transition*, Gauthiers-Villards, Paris 1973, p. 143, 297; A. Wold in L. V. Interrante (Ed.): *Extended Interactions between Metal Ions in Transition Metal Complexes (ACS Symp. Ser.) 5* (1974) 5, and P. A. Cox: *The Electronic Structure and Chemistry of Solids*, Oxford University Press, Oxford 1987, p. 173.

[7] W. E. Hatfield in R. D. Willet, D. Gatteschi, O. Kahn (Eds.): *Magneto-Structural Correlations in Exchange Coupled Systems*, Reidel, Dordrecht 1985, p. 558.

[8] A. Müller, M. Penk, E. Krickemeyer, H. Bögge, H.-J. Walberg, *Angew. Chem. 100* (1988) 1787; *Angew. Chem. Int. Ed. Engl. 27* (1988) 1719.

[9] In this case the magnetism can be described with the help of the Hamiltonian $H = -2\sum_i J_{i,i+1} \cdot \hat{S}_i \cdot \hat{S}_{i+1}$. The coupling constant J is a measure of the strength of the exchange interaction (cf. F. E. Mabbs, D. J. Machin: *Magnetism and Transition Metal Complexes*, Chapman and Hall, London 1973, p. 177).

[10] The structurally enforced formation of V^{IV}–V^{IV} pairs (but without strong covalent bonding) as in **2** generally effects a significantly stronger temperature dependence of the μ_{eff} values, so that at low, but nevertheless for the magnetochemist still relatively high temperatures, almost exclusively the S = 0 (singlet) state is populated (Table 1; accordingly relatively large difference in energy between the triplet and singlet state (pair consideration), which corresponds to a high Néel temperature (T_N (**2**) > 300 K) and a large J value).

[11] A. Müller, J. Döring, H. Bögge, E. Krickemeyer, *Chimia 42* (1988) 300.

[12] D. Rehder, *Angew. Chem. 103* (1991) 152; *Angew. Chem. Int. Ed. Engl. 30* (1991) 148.

[13] See e.g. M. de Soua, J. H. Brock (Eds.): *Iron in Immunity, Cancer and Inflammation*, Wiley, New York 1989.

[14] J. M. Longo, P. Kierkegaard, *Acta Chem. Scand. 24* (1970) 420; K. V. K. Rao, S. V. N. Naidu, L. Iyengar, *J. Phys. Soc. Jpn. 23* (1967) 1380.

[15] W. Rüdorf, G. Walter, J. Stadler, *Z. Anorg. Allg. Chem. 297* (1958) 1.

[16] For self-organization phenomena (theoretical aspects and examples in chemistry) cf. I. Prigogine: *From Being to Becoming—Time and Complexity in the Physical Sciences*, W. H. Freeman, New York 1980; as well as A. Dress, H. Hendrichs, G. Küppers (Eds.): *Selbstorganisation*, Piper, München 1986 (with a general definition of self-organization in the article of B.-O. Küppers, p. 81).
The term "self-organization" is used here for the spontaneous formation of ordered structures from a primary generated unit, which has an amplifying and regulating influence on the sequential processes; cf. J.-M. Lehn, *Angew. Chem. 100* (1988) 91; *Angew. Chem. Int. Ed. Engl. 27* (1988) 89; J.-M. Lehn, A. Rigault, *ibid. 100* (1988) 1121 and *27* (1988) 1095.

[17] See also A. Müller, *Nature*, in press.

Synthesis of Prothymosin α (ProTα)—a Protein Consisting of 109 Amino Acid Residues**

By *Kleomenis Barlos**, *Dimitrios Gatos*, and *Wolfram Schäfer*

The synthesis of proteins using either the solid phase technique or the fragment condensation technique in solution is still a difficult task, even when extremely pure amino acid derivatives and efficient coupling and deblocking procedures are used. Indeed only a few protein syntheses such as for ribonuclease,[1] interleukin 3,[2] ubiquitin,[3] and angiogenin[4] have been described. Biotechnological procedures seem to be more effective,[5] but this technique can only be used for proteins with biologically codable structural information. Nevertheless, large peptides and proteins are becoming increasingly important, especially in the areas of immunology and cancer therapie.[6a] The development of a generally applicable strategy for protein synthesis which allows to check the synthesis at each step and which yields very pure proteins is therefore of considerable interest.[6b]

Such a synthesis could be accomplished, as postulated earlier,[7] by sequential coupling of totally blocked peptide fragments to a resin. In order to check the progress of the synthesis after each peptide coupling, the new peptide fragment may be split off from the resin for analysis and purification if necessary. Peptide fragments whose side chains are blocked by easily removable *tert*-butyl- and triphenylmethyl (trityl) type groups should be prepared quickly and with the highest possible yield and purity. At present this seems to be only possible by using the solid phase technique with specially prepared resins.

After testing a series of acid labile resins of the diphenylmethyl- and triphenylmethyl-type[8, 9] the 2-chlorotriphenylmethyl (trityl) resin **2**[8] turned out to be especially suitable. The most important properties of this resin are: a) the quick, high yield coupling of the C-terminal amino acid to the resin. The reaction of Fmoc amino acids with **2** is accomplished in dichloromethane and diisopropyl(ethyl)amine (DIEA) within 25 min at room temperature. Because the esterification does not need electrophilic activation of the amino acid, the reaction proceeds without racemization. b) The large volume of the chlorotrityl group prevents completely the forma-

[*] Prof. Dr. K. Barlos, Dr. D. Gatos
Chemistry Department, University of Patras
GR-Patras (Greece)
Prof. Dr. W. Schäfer
Max Planck Institut für Biochemie
W-8033 Martinsried (FRG)

[**] This study was sponsored by the Greek Ministry for Industry Energy and Research (*K. B.*) and the Bundesministerium für Forschung und Technologie (PTb 038824) (*W. S.*). We thank Dr. *C. N. Baxevanis* and Dr. *M. Papamihail* (Department of Immunology, Anitcancer Institute, Athen), for testing the biological activity of the synthetic ProTα.

tion of diketopiperazines during the dipeptide step in the SPPS procedure. This is still an unsolved problem especially in the synthesis of peptides with C-terminal glycine and proline; these amino acids are used preferentially for fragment couplings because of their optical stability. c) The stability of the ester bond between the C-terminal amino acid and the resin during peptide extension. This was confirmed by the synthesis of several peptides which were always isolated in high yield. d) The splitting of the peptides from the 2-chlorotrityl resin is done under very mild conditions, for example with acetic acid/trifluoroethanol/dichloromethane (1:1:8) (splitting solution) for a few minutes, and without loss of any of the side chain blocking group.

As a first example of a protein synthesis with resin **2** we prepared human prothymosin α (ProTα[10]), which is shown in Figure 1 in protected and resin-bound form. ProTα is 109 amino acid residues long. It is widely distributed in human cells,[11-13] protects against infection from *Candida albicans*[11,14] and systemic lupus erythematosus,[15] induces the enhanced secretion of interleukin[16] and MIF (migrating inhibition factor),[11] activates monocytes and T-lymphocytes, is a strong immunomodulator,[17] and seems to be necessary for cell division.[18] To establish its therapeutic potential ProTα should be available in larger amounts.

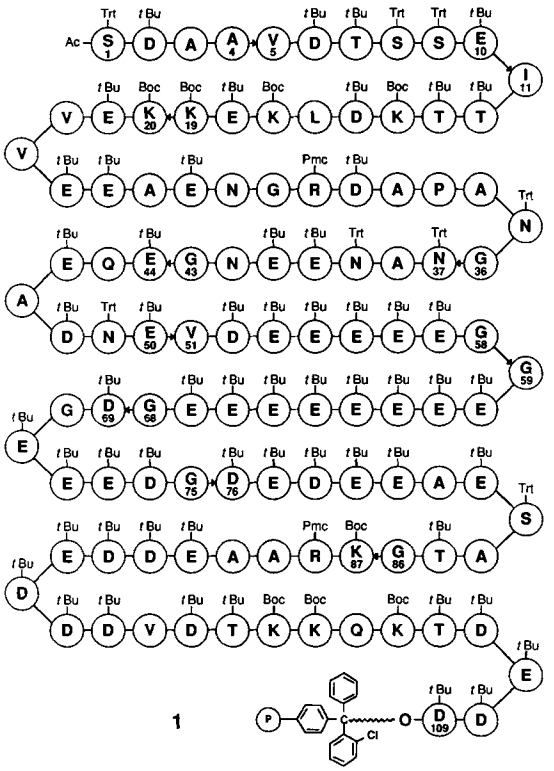

Fig. 1. Sequence of prothymosin α (ProTα), including side chain blocking group, bound to the 2-chlorotrityl resin; arrows indicate the coupling positions for the fragment condensation. Ac = acetyl, Trt = trityl, Boc = *tert*-butoxycarbonyl, Pmc = 2,2,5,7,8-pentamethylchroman-6-sulfonyl.

The synthesis of ProTα was carried out follows: reaction of Fmoc-Asp(*t*Bu)OH (0.1 mmol) with **2** (1 g, 1.6 mmol Cl) and DIEA (2 mmol) in dichloromethane yielded resin **3** with a substitution density of 0.09 mmol amino acid per gram (Fig. 2, top). According to our experience such a low substitution density is most important for good coupling yields during the synthesis of large peptides (for example of **4**) and

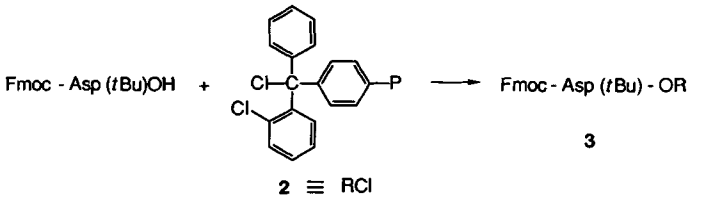


```
   76
H-Asp(tBu)-Glu(tBu)-Asp(tBu)-Glu(tBu)-Glu(tBu)-Ala-Glu(tBu)-
  Ser(X)-Ala-Thr(tBu)-Gly-Lys(Boc)-Arg(Pmc)-Ala-Ala-Glu(tBu)-
  Asp(tBu)-Asp(tBu)-Glu(tBu)-Asp(tBu)-Asp(tBu)-Asp(tBu)-Val-
  Asp(tBu)-Thr(tBu)-Lys(Boc)-Lys(Boc)-Gln-Lys(Boc)-Thr(tBu)-
                          109
  Asp(tBu)-Glu(tBu)-Asp(tBu)-Asp(tBu)-OR                    4

      69                                                75
Fmoc-Asp(tBu)-Gly-Glu(tBu)-Glu(tBu)-Glu(tBu)-Asp(tBu)-Gly-OH  5

      59              68
Fmoc-Gly-[Glu(tBu)]8-Gly-OH                                   6

      51                          58
Fmoc-Val-Asp(tBu)-[Glu(tBu)]5-Gly-OH                          7

      44                                              50
Fmoc-Glu(tBu)-Gln-Glu(tBu)-Ala-Asp(tBu)-Asn(Trt)-Glu(tBu)-OH  8

      37                                          43
Fmoc-Asn(Trt)-Ala-Asn(Trt)-Glu(tBu)-Glu(tBu)-Asn-Gly-OH       9

      30                                      36
Fmoc-Arg(Pmc)-Asp(tBu)-Ala-Pro-Ala-Asn(Trt)-Gly-OH            10

      20
Fmoc-Lys(Boc)-Glu(tBu)-Val-Val-Glu(tBu)-Glu(tBu)-Ala-Glu(tBu)-
        29
     Asn-Gly-OH                                               11

      11
Fmoc-Ile-Thr(tBu)-Thr(tBu)-Lys(Boc)-Asp(tBu)-Leu-Lys(Boc)-
            19
     Glu(tBu)-Lys(Boc)-OH                                     12

       1
Fmoc-Ser(X)-Asp(tBu)-Al-Ala-Val-Asp(tBu)-Thr(tBu)-Ser(X)-
           10
     Ser(X)-Glu(tBu)-OH                                       13

   4,13: a, X= Trt; b, X= tBu
```

Fig. 2. Synthesis of peptide fragments for the synthesis of ProTα.

also to achieve optimal reaction conditions during the fragment condensation reactions. Starting with **3** we synthesized the ProTα (76–109) fragment **4**. After preactivation with 1-hydroxybenzotriazole (1-HOBt) and dicyclohexylcarbodiimide (DCC) a threefold molar excess of Fmoc amino acids were used. Removal of the Fmoc protective groups was carried out by incubation in 20% piperidine in DMF. The completness of the coupling was proved by the Kaiser test. The totally blocked peptide fragments **5**–**13** were prepared in an analogous manner. The resins had substitution densities of 0.4–0.6 mmol amino acid per gram of resin. The blocked peptides were recovered in yields greater than 90% after 60 min incubation in the splitting solution as described above. Purity was checked by HPTLC and RP-HPLC. We found a purity of > 98% for fragments **5**, **6**, **7** and **9**, > 96% for **8** and **10** and > 90% for **11** and **12**. Despite the high purity, the peptides were further purified by column chromatography (silica gel 60, 240–400 mesh, Merck; eluant: mixtures of chloroform, methanol and acetic acid). In order to remove completely traces of adsorbed acetic acid, the peptides were dissolved in trifluoroethanol, precipitated with water and dried. Because of their low solubility fragments **13a** and **13b** could not be analyzed by HPLC. The structure of the blocked peptides were confirmed by FAB-MS, Xe,

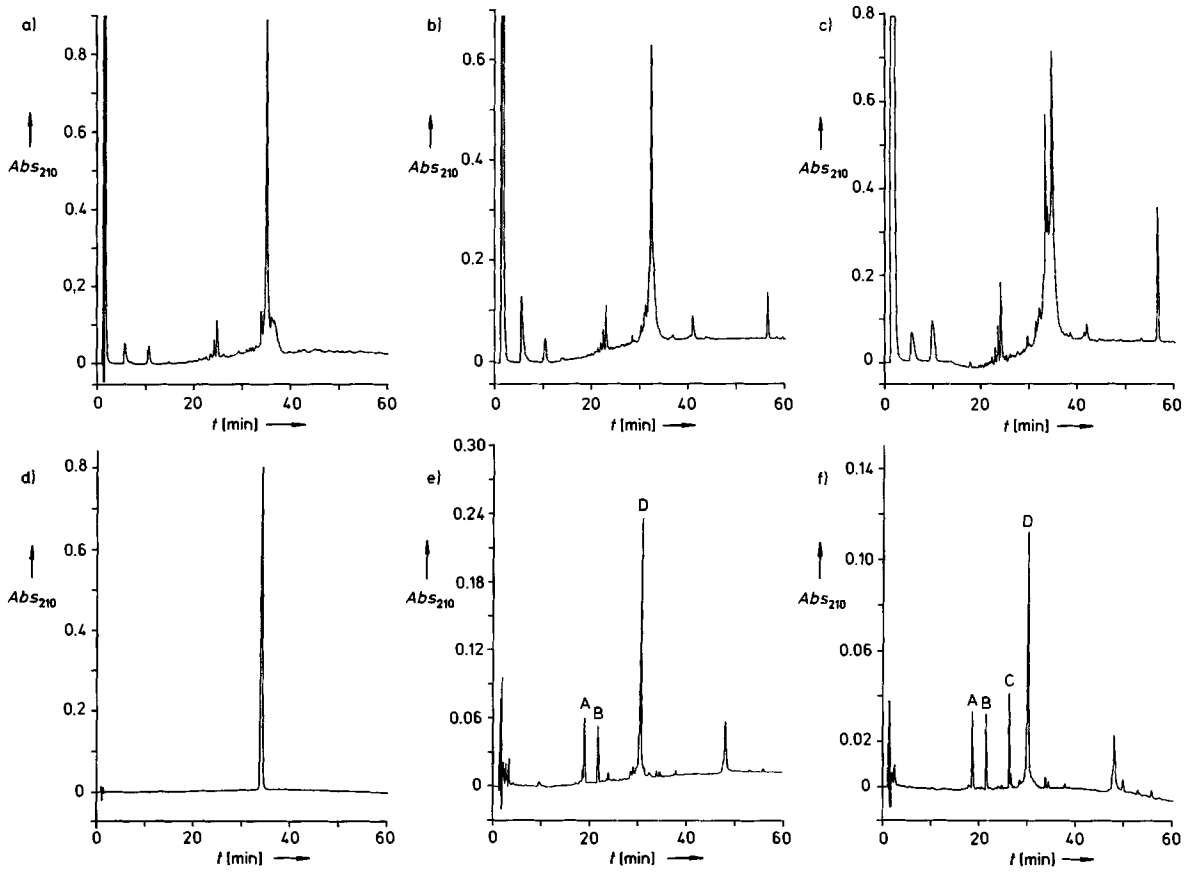

Fig. 3. HPLC: a) raw material of the deblocked ProTα (11–109), b) same for de-acetyl-ProTα, c) same after acetylation of the mixture of ProTα (11–109) and ProTα (1–109); d) ProTα after HPLC purification; e) tryptic digest of ProTα (11–109); f) same of ProTα. Conditions: Nucleosil C-8 (4.6 × 25 mm); flow 1 ml/min, 5 min isocrat., then from 100% A to 100% B in 60 min. A: 0.1% TFA in water, B: 0.1% TFA in acetonitrile for 3a–c; A 0.06% TFA in water, B 0.054% TFA in acetonitrile for 3d–f; detection at 210 nm. Components eluting after 40 min in 3b, c are partially blocked peptides, those which are eluted in e and f after 48 min are components of the trypsin preparation.

9 kV, ca. 50 μA or LSIMS, $Cs^{\oplus}$, 20 kV, 4 μA, matrix *m*-nitrobenzyl alcohol (NBA) or NBA/glacial acetic acid. The actual molecular weights of the peptide fragments were as expected.

The synthesis of blocked ProTα was established by sequential condensation of the fragments **5**–**13** with fragment **4** immobilized on the resin via the ester bond. A fivefold excess of blocked fragment/1-HOBt/DCC (1:1.5:1) in dimethyl sulfoxide was used. The coupling reactions were followed by HPTLC and Kaiser test; the reactions were complete after 6–18 h. After each coupling reaction a small aliquot of peptide ester resin was withdrawn, the peptide split from the resin and the protective groups removed from the side chains by treatment with trifluoroacetic acid/water (95:5). HPLC analyses of the recovered material confirmed the high yield of the coupling reactions until ProTα (11–109) (Fig. 3). Fragment **13a**, because of its low solubility in dimethyl sulfoxide could only be coupled to the immobilized ProTα (11–109) with 55% yield (Fig. 3b). Replacing the *tert*-butyl groups of serine against trityl groups improved the solubility of **13b** in dimethyl sulfoxide, but the coupling yield was not improved because the benzotriazolyl ester of **13b** precipitated during the reaction.

The resin-bound product mixture from the last fragment condensation, which was primarily de-acetyl-ProTα and unchanged ProTα (11–109), was acetylated with a 10-fold excess of acetic anhydride/DIEA in dimethyl formamide (Fig. 3c). After removal of the side-chain protective groups, the overall ProTα was isolated by HPLC in 11% yield from the product mixture (Fig. 3d). The identities of ProTα and the other peptides ProTα (87–109), (59–109), (11–109) which were obtained in > 55% yield were verified through amino acid analyses. ProTα and ProTα (11–109) were digested with trypsin and the expected peptide products were obtained (Fig. 3e, f); the main fragments (89–109), (21–30) and acetyl-(1-14) were isolated by HPLC and identified by FABMS. Because of its high acidity, fragment (31–87) and ProTα itself could not be analyzed by FABMS.

The biological activity of synthetic prothymosin α was tested with the auto-MLR-reaction (autologous multiple lymphocyte reaction)[16] using T-lymphocytes from healthy human donors. The immune response was enhanced by a factor of 1.7; using the same test system an enhancement factor of 1.5 was observed with prothymosin α from rat thymus.

Received: September 20, 1990 [Z 4194 IE]
German version: *Angew. Chem. 103* (1991) 572

[1] R. B. Merrifield, *Angew. Chem. 97* (1985) 801; *Angew. Chem. Int. Ed. Engl. 24* (1985) 799.
[2] I. Clark-Lewis, R. Aebershold, H. Ziltener, J. W. Schrader, L. E. Hood, S. B. H. Kent, *Science 231* (1986) 134.
[3] R. Ramage, J. Green, O. M. Ogounjobi, *Tetrahedron Lett. 30* (1989) 2149.
[4] T. Kimura, N. Chino, M. Takai, S. Kumagaye, H. Kuroda, S. Sakakibara in S. Sakakibara (Ed.): *The Second Akabori Conference*, Protein Research Foundation, Osaka 1988, p. 63; T. Kimura, N. Chino, S. Kumagaye, H. Kuroda, F. Emura, S. Sakakibara in E. Wünsch (Ed.): *The Third Akabori Conference*, Max Planck Institut für Biochemie, Martinsried 1989, p. 35; T. Kimura, N. Chino, S. Kumagaye, H. Kuroda, I. Emura, S. Sakakibara, *Biochem. Soc. Trans. 18* (1990) 1297.

[5] H. Yasueda, K. Nagase, A. Hosoda, Y. Akiyama, *Biotechnology 8* (1990) 1036.
[6] a) H. Quadbeck-Seeger, *Angew. Chem. 102* (1990) 1213; *Angew. Chem. Int. Ed. Engl. 29* (1990) 1177; E. Bayer, *ibid. 103* (1991) 117 and *30* (1991) 113.
[7] E. Atherton, E. Brown, G. Priestkey, R. C. Sheppard, B. J. Williams in D. H. Rich, E. Gross (Ed.): *Peptides: Structure and Function*, Pierce Chemical Company, Rockford, IL, USA 1981, p. 163; E. Atherton, A. Dryland, R. C. Sheppard, J. D. Wade in V. J. Hruby, D. H. Rich (Eds.): *Peptides: Structure and Function*, Pierce Chemical Company, Rockford, IL, USA 1983, p. 45.
[8] K. Barlos, D. Gatos, J. Kallitsis, G. Papaphotiu, P. Sotiriu, Y. Wenquing, W. Schäfer, *Tetrahedron Lett. 30* (1989) 3943; K. Barlos, D. Gatos, S. Kapolos, G. Papaphotui, W. Schäfer, Y. Wenquing, *ibid. 30* (1989) 3947.
[9] K. Barlos, D. Gatos, J. Kallitsis, D. Papaioannou, P. Sotiriou, W. Schäfer, *Liebigs Ann. Chem. 1987*, 1031; K. Barlos, D. Gatos, J. Hondrelis, J. Matsoukas, G. J. Moore, W. Schäfer, P. Sotiriou, *ibid. 1989*, 951.
[10] A. A. Haritos, G. J. Goodall, B. L. Horecker, *Methods Enzymol. 116* (1985) 255.
[11] L. X. Pan, A. A. Haritos, J. Wideman, T. Komiyama, M. Chang, S. Stein, S. B. Salvin, B. L. Horecker, *Arch. Biochem. Biophys. 250* (1986) 198.
[12] W. H. Eschenfeldt, R. E. Manrow, M. S. Krug, S. L. Berger, *J. Biol. Chem. 264* (1989) 7546.
[13] A. A. Haritos, O. Tsolas, B. L. Horecker, *Proc. Natl. Acad. Sci. USA 81* (1984) 1391.
[14] J. Caldarelle, G. J. Goodall, A. M. Felix, E. P. Heimer, S. B. Salvin, B. L. Horecker, *Proc. Natl. Acad. Sci. USA 80* (1983) 7424.
[15] C. N. Baxevanis, G. J. Reclos, H. Papamihail, C. G. Tsokos, *Immunopharmacol. Immunotoxicol. 9* (1988) 429.
[16] C. N. Baxevanis, G. J. Reclos, M. Economou, P. Arsenis, A. Katsiyiannis, K. Seferiades, G. Papadopoulos, O. Tsolas, M. Papamichail, *Immunopharmacol. Immunotoxicol. 10* (1988) 443.
[17] C. N. Baxevanis, E. Anastasopoulos, G. J. Reclos, M. Papamichail, *J. Neuroimmunol. 27* (1990) 141.
[18] A. R. Sburlati, R. E. Manrow, S. L. Berger, *Proc. Natl. Acad. Sci. 88* (1991) 253.

Palladium(II)-Induced Conversion of α-Acetoxyalkynes into α,β-Unsaturated α-Acetoxyketones; a Novel Access to α-Diketones.

By *Rainer Mahrwald* and *Hans Schick**

Allyl acetates of type **1** rearrange in tetrahydrofuran at room temperature (RT) in the presence of bis(acetonitrile)palladium(II) chloride $[PdCl_2(CH_3CN)_2]$ in an equilibrium reaction to form the isomeric allyl acetates of type **2**.[1] This [3,3]-sigmatropic rearrangement, which takes place

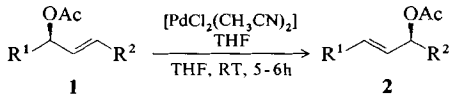

1 **2**

with chirality transfer, has been used, for instance, for the construction of the (1*E*,3*S*)-3-hydroxyoct-1-enyl side chain of prostaglandins.[2-6] While investigating this reaction we observed by chance that a propargyl acetate (α-acetoxyalkyne) of type **3** is converted into an α-acetoxyenone of type **4**. Since the behavior of α-acetoxyalkynes of type **3** has not yet been studied systematically under these conditions,[7-9] we looked into the problem.

On treatment with an equimolar amount of bis(acetonitrile)palladium(II) chloride in aqueous tetrahydrofuran at 20 °C, the α-acetoxyalkynes **3a–d** are converted within three hours into the α-acetoxyenones **4a–d**. The yield of pure product is 45–75%. The reaction is accompanied by the precipitation of metallic palladium and the formation of hydrochloric acid. The structures of **4a–d** are deduced from the ^{13}C- and ^1H-NMR spectra, mass spectra, and the elemental analyses.

Although the reaction was performed under argon, the compounds **4a–d** contain one more oxygen atom than the starting compounds **3a–d**. The conditions for the transfor-

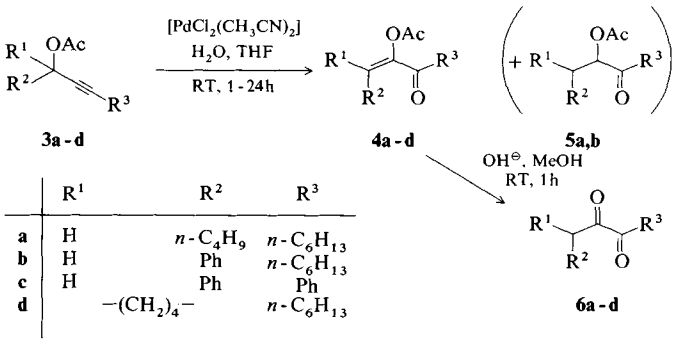

	R^1	R^2	R^3
a	H	n-C_4H_9	n-C_6H_{13}
b	H	Ph	n-C_6H_{13}
c	H	Ph	Ph
d	$-(CH_2)_4-$		n-C_6H_{13}

mation of **3a** into **4a** were studied more closely to discover the origin of this oxygen atom. On strict exclusion of air and water in dried THF, no trace of the α-acetoxyenone **4a** is observed even after many days. A thin-layer chromatographic study of the reaction solution reveals that **3a** ($R_f = 0.66$)[10] is completely converted into a substance with higher polarity ($R_f = 0.26$), which is not the α-acetoxyenone **4a** ($R_f = 0.43$), and which does not change even after two days in the solution. There is also no change if the argon is replaced by rigorously dried oxygen and the solution stirred vigorously for a further 24 h. The formation of **4a** is only observed when an equimolar amount of water is added. As the formation of **4a** on addition of water does not depend on whether the reaction is performed under an argon or oxygen atmosphere, the oxygen atom must, in the case of an argon atmosphere at least, stem from water.

A reaction of **3a** with only 0.15 to 0.20 equivalents of $[PdCl_2(CH_3CN)_2]$, in dried tetrahydrofuran at 20 °C and with strict exclusion of air and moisture, affords quantitatively after 24 h a mixture (1:1) of **4a** and **5a**. The surprising formation of the α-acetoxyketone **5a** is explained most easily by a hydrogen addition to the α-acetoxyenone **4a**. The tendency to add hydrogen decreases from **4a** through **4b** to **4c**. Although the palladium(II)-induced transformation of **3b** into **4b** in the presence of catalytic amounts of $[PdCl_2(CH_3CN)_2]$ affords **4b** and **5b** in the ratio 7:3, compound **3c** under the same conditions yields exclusively **4c**. The formation of the hydrogenation products **5a** and **5b** is suppressed in the presence of an equimolar amount of cyclohexene.

The catalytic cycle sketched in Scheme 1 reflects our preliminary understanding of the palladium(II)-induced transformation of the α-acetoxyalkynes **3** into the α-acetoxyenones **4**. The regeneration of $PdCl_2$ from HPdCl and HCl is only possible if hydrogen is formed in this reaction. Although this could not be detected analytically, the α-acetoxyketones **5a** and **5b** and the suppression of their formation in the presence of cyclohexene may be considered as indications that hydrogen is formed.

The proposal for the mechanism must be confirmed by further studies. Recently other authors[11] reported that during the palladium(II)-induced transformation of α-acetoxyalkynes into α-acetoxyenones oxygen can purposely be

[*] Prof. Dr. H. Schick, Dr. R. Mahrwald
Zentralinstitut für Organische Chemie
Rudower Chaussee 5, O-1199 Berlin-Adlershof (FRG)

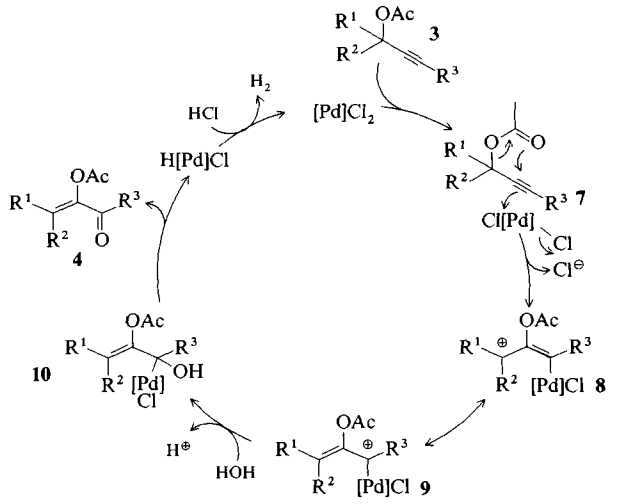

Scheme 1. [Pd] = $Pd(CH_3CN)_2$

added as oxidizing agent. This does not conflict with our results obtained in the absence of oxygen, but may represent an alternative pathway.[12]

The α-acetoxyenones **4** obtained by palladium(II)-induced conversion of the α-acetoxyalkynes **3** were used in further synthesis steps. For instance, **4a–d** can be readily converted into the α-diketones **6a–d** through hydrolysis with a basic ion-exchanger as expected.

Experimental Procedure

4a: 1.0 g (4.2 mmol) of 5-acetoxytridec-6-yne **3a** was dissolved in 20 mL of dried THF and treated with 1.1 g (4.2 mmol) of $[PdCl_2(CH_3CN)_2]$[13]. The bright yellow suspension was stirred under inert gas for about 1 h at 20 °C till the palladium complex dissolved. The solution was then dark brown to black. After the addition of 76 μL (4.2 mmol) of water the mixture was stirred for a further 3–4 h at 20 °C. At this stage **3a** could no longer be detected by thin-layer chromatography. 10 mL of saturated aqueous $NaHCO_3$ solution was added, and after extraction with diethyl ether and drying with Na_2SO_4, the solvent was removed in vacuum. The residue was purified by flash chromatography[14] on silica gel. Yield: 780 mg (72.5%) of **4a** as colorless oil. TLC (silica gel, hexane/acetone 95:5): $R_f = 0.43$; ^1H NMR ($CDCl_3$, 80 MHz): $\delta = 0.82$ and 0.86 (2 m, 6H; 1-H, 13-H), 2.20 (s, 3H; CH_3CO), 6.30 (t, $J = 10$ Hz, 1H, 5-H); ^{13}C NMR (75 MHz, [D_8]THF): $\delta = 13.93$, 14.18, 22.99, 23.20, 24.57, 25.10, 25.64, 26.26, 29.52, 32.42, 37.33, 131.14, 147.20, 168.34, 193.27. MS (EI, 70 eV): m/z 212 (100), 142 (50), 113 (35), 99 (40).

6d: 252 mg (1 mmol) of **4d** was dissolved in 20 mL of methanol and stirred with 10 g of the basic ion-exchange resin SBW for 1 h at 20 °C. The ion-exchange resin was removed by filtration, the solvent evaporated under reduced pressure, and the product purified by flash chromatography[14] on silica gel with hexane/acetone (95:5) as eluant. Yield: 134 mg (64%) colorless oil. TLC (silica gel, hexane/acetone 97:3, developed three times): $R_f = 0.71$. ^1H NMR (20 MHz, $CDCl_3$): $\delta = 14.00$, 22.53, 26.63, 29.07, 31.58, 36.21, 44.02, 46.52, 49.52, 109.87, 119.38, 167.92, 200.70. MS (EI, 70 eV): m/z 209 ($M^{\oplus}-1$, 10%), 194 (4), 113 (25), 94 (40), 55 (100).

Received: May 14, 1990
Revised: January 2, 1991 [Z 3958 IE]
German version: *Angew. Chem. 103* (1991) 577

CAS Registry numbers:
3a, 132938-21-7; **3b**, 132938-22-8; **3c**, 93321-44-9; **3d**, 132938-23-9; **4a**, 132938-24-0; **4b**, 132938-25-1; **4c**, 132938-26-2; **4d**, 132938-27-3; **5a**, 105824-00-8; **5b**, 132938-28-4; **6a**, 125285-58-7; **6b**, 132938-29-5; **6c**, 23464-17-7; **6d**, 132938-30-8; $[PdCl_2(CH_3CN)_2]$, 14592-56-4.

[1] Review: L. E. Overman, *Angew. Chem. 96* (1984) 565; *Angew. Chem. Int. Ed. Engl. 23* (1984) 579.
[2] P. A. Grieco, T. Takigawa, S. L. Bongers, H. Tanaka, *J. Am. Chem. Soc. 102* (1980) 7588.
[3] R. Mahrwald, F. Theil, V. I. Mel'nikova, H. Schick, K. K. Pivnitsky, *Zh. Org. Khim. 22* (1986) 1647.
[4] U. Hofmann, C. O. Meese, M. Hecker, V. Ullrich, *Tetrahedron Lett. 28* (1987) 5655.
[5] S. J. Danishefsky, M. Paz Cabal, K. J. Chow, *J. Am. Chem. Soc. 111* (1989) 3456.
[6] R. Mahrwald, H. Schick, K. K. Pivnitsky, S. Schwarz, *J. Prakt. Chem. 332* (1990) 403.
[7] J. Tsuji: *Organic Synthesis with Palladium Compounds*, Springer, Berlin 1980.
[8] R. F. Heck: *Palladium Reagents in Organic Synthesis*, Academic, London 1985.
[9] A. C. Oehlschlaeger, P. Mishra, S. Dhami, *Can. J. Chem. 62* (1984) 791.
[10] The thin-layer chromatography (TLC) was performed with precoated HPTLC plates (E. Merck, Kieselgel 60) and hexane/acetone (95:5) as mobile phase.
[11] H. Kataoka, K. Watanabe, K. Goto, *Tetrahedron Lett. 31* (1990) 4181.
[12] We discussed our results in September 1989 with Prof. *J. Tsuji*.
[13] L. S. Hegedus, R. E. Williams, M. A. Mcguire, T. Hayashi, *J. Am. Chem. Soc. 102* (1980) 4973.
[14] W. C. Still, M. Kahn, A. Mitra, *J. Org. Chem. 43* (1978) 2923.

A Cyclic Methyleneborane with Trapezoidal Geometry**

By *Andrea Höfner, Bernd Ziegler, Ralf Hunold, Peter Willershausen, Werner Massa,* and *Armin Berndt**

Dedicated to Professor Kurt Dehnicke on the occasion of his 60th birthday

On attempting to transform the 1,2-dichloroboranes(4) **1a, b**[1] into the corresponding 1,2-difluoro compounds with lithium fluoride according to the method of *Kaufmann* et al.[2] we obtained the 1,1-difluoroboranes(4) **2a, b**.[3] Reaction of **2a** with the dilithium compounds **3a, b**[1,4] led to the orange-red compounds **4a, b** (Scheme 1), the first methyleneboranes bearing an acceptor substituent on the dicoordinat-

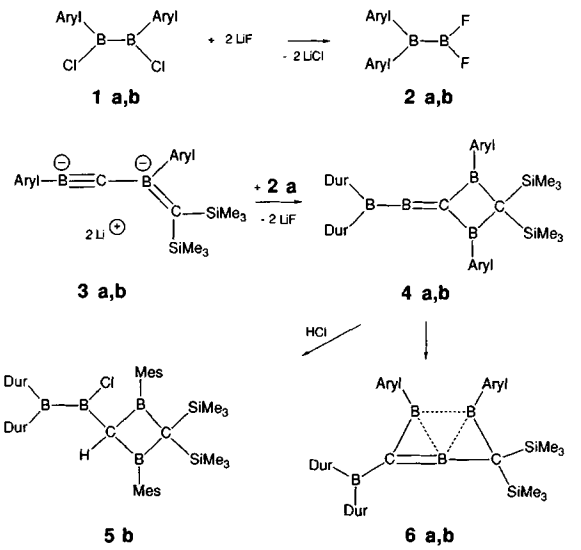

Scheme 1. **a**: Aryl = Dur (2,3,5,6-tetramethylphenyl); **b**: Aryl = Mes (2,4,6-trimethylphenyl).

[*] Prof. Dr. A. Berndt, A. Höfner, Dr. B. Ziegler, Dr. R. Hunold, Prof. Dr. W. Massa, P. Willershausen
Fachbereich Chemie der Universität
Hans-Meerwein-Strasse, W-3550 Marburg (FRG)

[**] This work was supported by the Deutsche Forschungsgemeinschaft and the Fonds der Chemischen Industrie.

Table 1. Some physical data of compounds **2a**, **4b**, **5b** and **6a** [a]. Standard for ^{1}H- and ^{13}C NMR spectra TMS, for ^{11}B-NMR spectra $BF_3 \cdot OEt_2$.

2a: colorless crystals, m.p. = 75 °C, yield: 92%. – ^{1}H NMR (100 MHz, $CDCl_3$, 25 °C): δ = 2.21 (s, 24 H, CH_3), 7.02 (s, 2 H, *p*-H); ^{13}C NMR (25 MHz, $CDCl_3$, 25 °C): δ = 19.2, 19.7 (each 4 C, CH_3), 133.9, 134.4, 136.1 (C_{sp^2}), 145.1 (br., 2 C, *i*-C); ^{11}B NMR (96 MHz, $CDCl_3$, 25 °C): δ = 29, 82 ($\nu_{1/2}$ each $\approx$ 700 Hz).

4b: orange-red crystals, m.p. = 150 °C (dec.), yield: NMR-spectroscopically ca. 95%. – ^{1}H NMR (300 MHz, C_6D_6, 25 °C): δ = 0.29 (s, 18 H, $Si(CH_3)_3$), 1.91, 2.06 (each s, each 12 H, *o*- and *m*-CH_3), 2.16 (s, 6 H, *p*-CH_3), 2.39 (s, 12 H, *o*-CH_3(Mes)), 6.68 (s, 4 H, *m*-H), 6.79 (s, 2 H, *p*-H); ^{13}C NMR (100 MHz, CD_2Cl_2, – 40 °C): δ = 4.5 (q, 6 C, $Si(CH_3)_3$), 19.7, 20.0 (each q, each 4 C, *o*- and *m*-CH_3), 21.1 (q, 2 C, *p*-CH_3), 24.8 (q, 4 C, *o*-CH_3), 62.5 (s, 1 C, CSi_2), 128.0 (d, 4 C, *m*-C, (Mes)), 132.1 (br. s, 1 C, CB_3), 134.0, 136.4 (each s, each 4 C, *o*- and *m*-C), 134.1 (d, 2 C, *p*-C (Dur)), 136.9 (s, 2 C, *p*-C (Mes)), 138.7 (s, 4 C, *o*-C (Mes)), 140.5, 144.3 (each s, each 2 C, *i*-C); ^{11}B NMR (96 MHz, toluene, 90 °C): δ = 62, 76 ($\nu_{1/2} \approx$ 590, 1260 Hz).

5b: pale yellow crystals, m.p. = 160 °C (dec.), yield: NMR-spectroscopically ca. 95%. – ^{1}H NMR (300 MHz, $CDCl_3$, 25 °C): δ = 0.07, 0.25 (each s, each 9 H, $Si(CH_3)_3$), 1.82, 2.11 (each s, each 12 H, *o*- and *m*-CH_3), 2.20 (br. s, 12 H, *o*-CH_3), 2.31 (s, 6 H, *p*-CH_3), 3.71 (s, 1 H, CHB_3), 6.74 (s, 4 H, *m*-H), 6.89 (s, 2 H, *p*-H); ^{13}C NMR (75 MHz, $CDCl_3$, 25 °C): δ = 4.5, 5.8 (each q, each 3 C, $Si(CH_3)_3$), 19.8, 20.2 (each q, each 4 C, *o*- and *m*-CH_3), 20.9 (q, 2 C, *p*-CH_3), 24.8 (br. q, 4 C, *o*-CH_3), 72.3 (s, 1 C, CSi_2), 79.5 (d, 1 C, CB_3, $^1J(^{13}C, ^1H)$ = 101.4 Hz), 127.7 (d, 4 C, *m*-C), 132.7 (d, 2 C, *p*-C), 133.4, 135.3, 137.2 (each s, each 4 C, *o*- and *m*-C), 136.8 (s, 2 C, *p*-C), 139.3, 146.7 (each br. s, each 2 C, *i*-C); ^{11}B NMR (96 MHz, toluene, 80 °C): δ = 75, 85 ($\nu_{1/2} \approx$ 1100, 1700 Hz).

6a: colorless crystals, m.p. > 230 °C, yield: NMR-spectroscopically ca. 70%. – ^{1}H NMR (300 MHz, $CDCl_3$, 25 °C): δ = 0.03 (s, 18 H, $Si(CH_3)_3$), 1.57, 1.92, 1.96, 2.00 (each s, each 6 H, *o*- and *m*-CH_3), 2.17 (s, 24 H, *o*- or *m*-CH_3), 6.68, 6.82 (each s, each 1 H, *p*-H), 6.90 (s, 2 H, *p*-H); ^{13}C NMR (100 MHz, $CDCl_3$, 25 °C): δ = 2.4 (q, 6 C, $Si(CH_3)_3$), 19.7, 20.0 (each q, each 2 C, CH_3), 19.8, 22.3 (each br. q, each 2 C, CH_3), 20.2 (q, 4 C, CH_3), 23.0 (br. q, 4 C, CH_3), 31.9 (br. s, 1 C, CSi_2), 130.4, 132.9 (each d, each 1 C, *p*-C), 131.3 (d, 2 C, *p*-C), 131.9, 133.1, 136.37, 136.43 (each s, each 2 C, *o*- resp. *m*-C), 133.0, 134.9 (each s, each 4 C, *o*- resp. *m*-C), 138.9; 150.5 (each br. s, each 1 C, *i*-C), 140.1 (br. s, 1 C, CB_3), 145.6 (s, 2 C, *i*-C); ^{11}B NMR (96 MHz, toluene, 25 °C): δ = 23, 33, 71 ($\nu_{1/2} \approx$ 1445, 1700, 2975 Hz).

[a] **2b** has NMR data similar to those of **2a**; **4a** and **6b** were identified on the basis of their NMR data similarly to **4b** and **6a** in a mixture with by-products.

ed boron atom—as shown by the NMR data (Table 1) and the crystal structure of the HCl-adduct **5b**.[5]

Whereas the methyleneboranes corresponding to **4a**, **b**,[6] which bear the substituents mesityl or duryl (2,3,5,6-tetramethylphenyl) on the dicoordinated boron atom instead of the boryl residue, are stable at room temperature, **4a**, **b** transform in solution within days (**4a**) or weeks (**4b**) into a mixture of compounds which contain as major components **6a** and **6b**, respectively, the first cyclic methyleneboranes. **6a** crystallizes from hexane in the form of colorless platelets. Figure 1 shows the structure of **6a** in the crystal.[7]

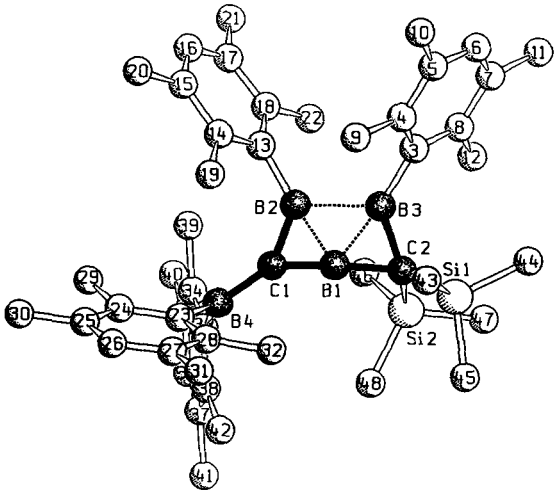

Fig. 1. SCHAKAL drawing of the structure of **6a** in the crystal. Projection on the B1,B2,B3 plane. Important bond lengths [pm] and angles [°]: B1-C1 142.5(5), C1-B2 149.5(5), B2-B3 193.3(6), B3-C2 155.8(5), C2-B1 154.5(5), B1-B2 166.2(6), B1-B3 170.4(6), C1-B4 152.0(5), B2-C13 157.6(5), B3-C3 158.1(5), C2-Si1 188.2(3), C2-Si2 191.1(3); C1-B1-C2 170.9(4), B1-C1-B2 69.3(3), B1-C2-B3 66.6(2), B1-C2-Si1 123.8(2), B1-C2-Si2 101.9(2); B2-C1-B1-B3 – 0.5(4), B1-C1-B2-B3 0.3(3), C1-B2-B1-B3 179.6(3), B3-C2-B1-B2 10.9(3), B1-C2-B3-B2 – 8.0(3), B2-B3-B1-C2 170.6(3), B2-C1-B4-C23 – 85.2(6), B2-C1-B4-C33 96.4(6).

The four-membered ring compound **4a** with two exocyclic boron atoms bound together is converted into the five-membered ring compound **6a** with only one exocyclic boron atom. It has an unusual shape for a five-membered ring, namely trapezoidal: B1,C1,B2 and B3 lie in a plane, which is inclined at an angle of only 9° to the plane through B1,C2,B3. The didurylboryl group, which is bound to the dicoordinated boron atom in **4a**, is attached to the carbon atom of the B=C double bond in **6a**. The carbon atom with the two trimethylsilyl groups, which in **4a** has two duryl-substituted boron atoms as neighbors, has only one such boron atom as neighbor in **6a**, the other is the almost linearly (171°) coordinated B of the B=C double bond.

The transformation **4** → **6** can readily be explained in terms of the intermediates **7** through **9** or **8** and **9**. The very high deficiency of electrons at the dicoordinated boron atom in **4** is compensated for by a shift of the σ electrons of a C_{sp^2}–B_{ring} bond to this center, i.e. rearrangement to **7**, the very high deficiency of electrons at the dicoordinated C atom of the diborylcarbene **7** by a shift of the σ electrons of the exocyclic B–B bond to the carbene C-atom, i.e. by rearrangement to **8**. Probably both rearrangements take place synchronously (dyotropically[8]), without formation of **7** as an intermediate.

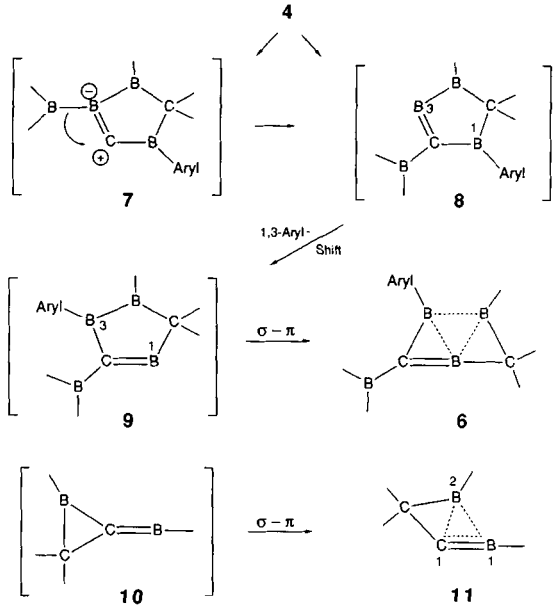

Subsequent 1,3-migration of an aryl group in **8** from the tri- to the di-coordinated boron atom—a reaction characteristic for C-borylmethylene boranes[9]—leads to **9**, which already has the same skeletal framework as **6**. The distortion of **9** to the trapezoidal arrangement of **6** with an almost linearly coordinated boron atom of the B=C double bond is the consequence of strong σ-π interaction between the dicoordinated boron atom as π-electron deficient center and the σ electrons of the oppositely disposed B–B bond. The three-center, two-electron bond formed thereby (B1, B2, B3) with

a long (193.3 pm) B2–B3 distance belongs to the simplest with three boron atoms.[10] A similarly strong distortion of the molecular geometry by σ-π interaction as in **9** → **6** is also found in **10** → **11**.[11] In **6** the B=C double bond (142.5 pm) is longer than in H_2C=B–H (138 pm[12]). This is the result of the π–π delocalization characteristic for[6, 9] *C*-boryl-methyleneboranes,[13] which also explains the short C1–B2 distance of 149.5 pm. A similar bond situation as for the framework atoms B1,C1,B2 of **6a** is also found in **12**.[14]

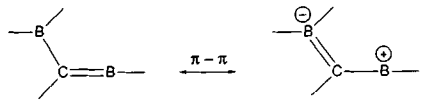

Since the planes through B1,C1,B2 and C23,B4,C33 in **6a** form an angle of 85°, π–π delocalization to the exocyclic boryl substituents is ruled out. The nevertheless remarkably short C1–B4 distance of 152 pm can be explained—like the short exocyclic B–C distance (150 pm) in *C*-borylborirene 13[15]—in terms of C–B hyperconjugation between the strained C1–B2 and C1–B1 σ bonds and the p-orbital at the exocyclic boron atom. Finally, the small B1–C2–Si2 angle of

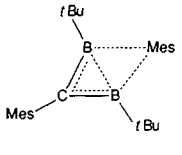

12

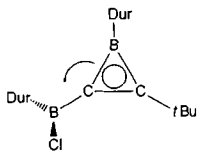

13

102° (B1–C2–Si1 124°) together with the long C2–Si2 distance of 191 pm (C2–Si1 188 pm) indicate C–Si hyperconjugation of this σ bond with the p-orbital of B1, which is positively charged by the above discussed π-π interaction.

In the structure of **6** strong and very strong variants of σ-π interactions participate in hyperconjugation and bridging. In addition, variants of their extreme form participate in the rearrangement which leads to formation of **6**.

Received: October 22, 1990 [Z 4247 IE]
German version: *Angew. Chem. 103* (1991) 580
Publication delayed at authors' request

CAS-Registry number:
2a, 132645-80-8; **2b**, 132645-81-9; **3a**, 120637-66-3; **3b**, 114958-96-2; **4a**, 132645-82-0; **4b**, 132645-83-1; **5b**, 132645-84-2; **6a**, 132645-85-3; **6b**, 132645-86-4.

[1] R. Hunold, J. Allwohn, G. Baum, W. Massa, A. Berndt, *Angew. Chem. 100* (1988) 961; *Angew. Chem. Int. Ed. Engl. 27* (1988) 961. **1a** is accessible analogously to **1b** from duryllithium.
[2] G. Bir, W. Schacht, D. Kaufmann, *J. Organomet. Chem. 340* (1988) 267.
[3] We thank Dr. *W. Storch*, Universität München, for the first hint of the constitution of **2a, b**.
[4] J. Allwohn, M. Pilz, R. Hunold, W. Massa, A. Berndt, *Angew. Chem. 102* (1990) 1084, *Angew. Chem. Int. Ed. Engl. 29* (1990) 1032.
[5] A. Höfner, *Dissertation*, Universität Marburg 1991.
[6] R. Hunold, M. Pilz, J. Allwohn, A. Stadler, W. Massa, P. von R. Schleyer, A. Berndt, *Angew. Chem. 101* (1989) 759; *Angew. Chem. Int. Ed. Engl. 28* (1989) 781.
[7] X-ray structure analysis of **6a**: $C_{48}H_{70}Si_2B_4$, space group $P2_1/c$; $Z = 4$; $a = 1158.5(3)$, $b = 1870.0(2)$, $c = 2249.1(6)$ pm, $\beta = 101.97(1)°$; $\varrho_{calcd} = 1.04$ g cm^{-3}; 6263 reflections measured on a four-circle diffractometer (CAD4, Enraf-Nonius) with $Cu_{K\alpha}$ radiation at 220 K; of 5910 independent reflections 4635 with $F_o > 2\sigma(F_o)$ were used for the structure determination; solution by direct methods; refinement to $R = 0.057$, $wR = 0.039$ (weighting $w = 1/\sigma^2(F_o)$); no absorption correction $\mu = 8.7$ cm^{-1}; all H atoms could be located from difference Fourier syntheses, but were incorporated in the calculation with a "riding" model on their bonding partners with groupwise common isotropic temperature factors. Anisotropic temperature factors were used for all other atoms (491 parameters). Further details of the crystal investigation are available on request from the Fachinformationszentrum Karlsruhe, Gesellschaft für wissenschaftlich-technische Information mbH, W-7514 Eggenstein-Leopoldshafen 2 (FRG), on quoting the depository number CSD-55032, the names of the authors, and the journal citation.
[8] M. T. Reetz, *Adv. Organomet. Chem. 16* (1977) 33.
[9] J. Allwohn, R. Hunold, M. Pilz, R.-G. Müller, W. Massa, A. Berndt, *Z. Naturforsch. B 45* (1990) 290 and unpublished results.
[10] Another simple example was reported in this journal recently: P. Paetzold, B. Redenz-Stormanns, R. Boese, M. Bühl, P. von R. Schleyer, *Angew. Chem. 102* (1990) 1059; *Angew. Chem. Int. Ed. Engl. 29* (1990) 1059.
[11] C. Wieczorek, J. Allwohn, G. Schmidt-Lukasch, R. Hunold, W. Massa, A. Berndt, *Angew. Chem. 102* (1990) 435; *Angew. Chem. Int. Ed. Engl. 29* (1990) 398.
[12] P. von R. Schleyer, D. Kost, *J. Am. Chem. Soc. 110* (1988) 2105.
[13] This π-π delocalization also leads to a lengthening of the C1–B1 bond and a shortening of the C1–B2 bond in **11**. These changes, however, are compensated, or overcompensated by the opposite effects of the σ-π interaction (C1–B2: 154.5): the C1–B1 bond (135.1 pm) is *shorter* than in H_2C=B–H (138 pm).
[14] M. Pilz, J. Allwohn, W. Massa, A. Berndt, *Angew. Chem. 102* (1990) 436; *Angew. Chem. Int. Ed. Engl. 29* (1990) 399.
[15] A. Höfner, B. Ziegler, W. Massa, A. Berndt, *Angew. Chem. 101* (1989) 188; *Angew. Chem. Int. Ed. Engl. 28* (1989) 186.

A Stable Os^0 16-Electron Complex: Synthesis and Structure of $[OsCl(NO)(PiPr_3)_2]$**

By *Helmut Werner,* Annette Michenfelder,* and *Michael Schulz*

Dedicated to Professor Siegfried Hünig on the occasion of his 70th birthday

d^8-Metal complexes with 16-electron configuration, e.g. the Wilkinson catalyst $[RhCl(PPh_3)_3]$, or the active intermediate $[HCo(CO)_3]$ in the oxo synthesis, play a decisive role in various homogeneous catalytic processes.[1] Whereas numerous compounds of the d^8-systems Rh^I, Ir^I, Ni^{II}, Pd^{II}, Pt^{II} and Au^{III} having the composition $[ML_4]$ (L = monodentate ligand) have already been reported it has so far not been possible to prove the existence of a corresponding osmium(0) complex that is stable under normal conditions. We report here on the synthesis and reactivity of $[OsCl(NO)(PiPr_3)_2]$ **1** as the first structurally characterized $[OsL_4]$ complex.[3]

The 18-electron compound $[OsCl(NO)(PPh_3)_3]$, which was first synthesized by *Roper* et al., and used, inter alia, for the preparation of carbene, sulfur dioxide, and disulfur oxide complexes,[5, 6] reacts with excess triisopropylphosphane at room temperature with complete removal of the PPh_3 ligands to give **1** in almost quantitative yield.[7] The ^{1}H-NMR data (*one* doublet of virtual triplets for the $PCHCH_3$ protons) point to a square-planar configuration with *trans* $PiPr_3$ ligands. This is confirmed by the X-ray structure analysis of **1**[8] [angles [°]: P–Os–N 89.8(2), P–Os–Cl 90.53(5), N–Os–Cl 178.7(3), Os–N–O 179.5(6). As already indicated from space group and unit cell content, the Os atom lies on the crystallographic center of symmetry, resulting in a 1:1 disorder of

[*] Prof. Dr. H. Werner, Dipl.-Chem. A. Michenfelder, Dipl.-Chem. M. Schulz
Institut für Anorganische Chemie der Universität
Am Hubland, W-8700 Würzburg (FRG)

[**] This work was supported by the Deutsche Forschungsgemeinschaft (SFB 347), the Fonds der Chemischen Industrie, and Degussa AG.

the Cl and NO ligands. Due to the disorder, the Os–Cl, Os–N and N–O distances are subject to a relatively high uncertainty, which is not revealed in the standard deviations. Disorders of this type are apparently characteristic for square-planar complexes of the composition *trans*-[MCl(L)($P\mathit{i}Pr_3$)$_2$], as shown by the structural analyses of [RhCl(O_2)($P\mathit{i}Pr_3$)$_2$],[9] [RhCl(N_2)($P\mathit{i}Pr_3$)$_2$],[9, 10] [IrCl(CO)($P\mathit{i}Pr_3$)$_2$],[11] and [IrCl(SO)($P\mathit{i}Pr_3$)$_2$].[12]

In contrast to the isoelectronic compound *trans*-[IrCl(CO)($P\mathit{i}Pr_3$)$_2$],[13] complex **1** reacts not only with Lewis acids but also with Lewis bases. The reactions carried out so far, which splendidly document the electronic and coordinatively unsaturated character of the osmium complex, are shown in Scheme 1. The transition from the 16-electron con-

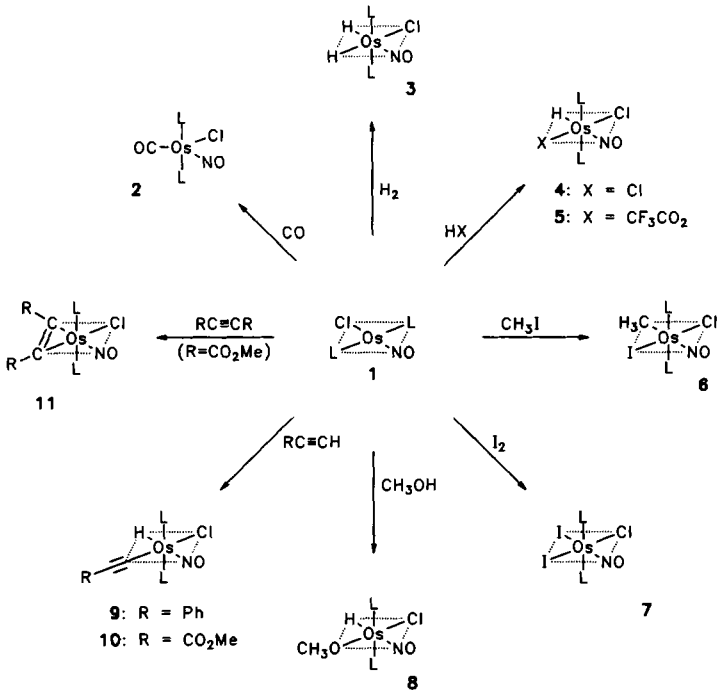

Scheme 1. Reactions of **1**; L = $P\mathit{i}Pr_3$.

figuration in **1** to the 18-electron configuration in **2**–**11** is accompanied by a characteristic color change from dark-green (**1**) to yellow (**2**–**8**) or red (**9**–**11**). The ^{1}H-NMR spectra of **5**, **6** and **8**–**11** each show two signals for the diastereotopic PCHCH_3 protons of the triisopropylphosphane ligands, thus confirming the proposed structure with four different bonding partners in the basal plane of the octahedron. The reaction of **1** with methanol leading to **8**[7] in almost quantitative yield is remarkable, since alkoxo(hydrido)osmium(II) complexes are, to our knowledge, unknown. A rearrangement of **9** and **10** to the isomeric vinylidene compounds [OsCl(NO)(=C=CHR)($P\mathit{i}Pr_3$)$_2$] cannot be achieved thermally (up to ca. 60 °C); the structurally related iridium complexes [IrHCl(C≡CR)(CO)($P\mathit{i}Pr_3$)$_2$] are similarly inert.[13b]

Experimental

1: To a suspension of 847 mg (0.81 mmol) of [OsCl(NO)(PPh_3)$_3$] in 15 mL of toluene was added 0.4 mL (2.0 mmol) of $P\mathit{i}Pr_3$ and the mixture stirred for 10 min at 25 °C. The solution was concentrated to ca. 3 mL in vacuo and treated with 5 mL of hexane. A dark-green, microcrystalline solid was formed; yield 384 mg (82%).—**2**: By passage of CO gas (ca. 1 min) into a solution of **1** in toluene; yellow solid; m.p. 101 °C (decomp.); yield 85%.—**3**: By passage of H_2 (ca. 2 min) into a solution of **1** in toluene; bright yellow solid; m.p. 102 °C; yield 92%.—**4**: A solution of 91 mg (0.16 mmol) of **1** in 7 mL of toluene was treated dropwise with an ethereal solution of HCl until a color change from green to yellow occurred. After removal of the solvent and repeated washing of the residue with cold ether, there remained a yellow solid; m.p. 126 °C (decomp.); yield 87 mg (89%).—**5**: A solution of 89 mg (0.15 mmol) of **1** in 7 mL of toluene was treated with 12 µL (0.16 mmol) of CF_3CO_2H. The solvent was removed in vacuo, the residue extracted with ether, the extract evaporated to dryness, and the resulting yellow residue washed with hexane; m.p. 82 °C (decomp.); yield 81 mg (78%).—**6**: From **1** and CH_3I in toluene; after extraction with hexane and removal of the solvent an orange-yellow solid was obtained; m.p. 125 °C (decomp.); yield 76%.—**7**: From **1** and I_2 in toluene; yellow solid; m.p. 186 °C (decomp.); yield 97%.—**8**: A suspension of 127 mg (0.22 mmol) of **1** in 15 mL of methanol was heated at 60 °C for 3 h. After cooling, the solution was concentrated to ca. 5 mL and cooled to − 40 °C; yellow crystals; m.p. 110 °C (decomp.); yield 121 mg (90%).—**9**: From **1** and PhC_2H in toluene; reaction time 4 h at 25 °C; bright red solid; m.p. 162 °C (decomp.); yield 94%.—**10**: From **1** and methyl propiolate in toluene; duration of reaction 3 h at 25 °C. After evaporation of the solvent, extraction with ether, and removal of the solvent a red solid was obtained; m.p. 131 °C (decomp.); yield 74%.—**11**: From **1** and $C_2(CO_2Me)_2$ in toluene; red solid; m.p. 51 °C; yield 75%.

Received: November 23, 1990 [Z 4291 IE]
German version: *Angew. Chem. 103* (1991) 617

CAS Registry numbers:
1, 132621-17-1; **2**, 132621-18-2; **3**, 132621-19-3; **4**, 132621-20-6; **5**, 132621-21-7; **6**, 132621-22-8; **7**, 132621-23-9; **8**, 132621-24-0; **9**, 132621-25-1; **10**, 132621-26-2; **11**, 132621-27-3; OsCl(NO)(PPh_3)$_3$, 86645-90-1; $C_2(CO_2Me)_2$, 762-42-5; $P\mathit{i}Pr_3$, 6476-36-4; PhC_2H, 536-74-3; $HC_2(CO_2Me)$, 922-67-8.

[1] a) J. P. Collman, L. S. Hegedus, J. R. Norton, R. G. Finke: *Principles and Applications of Organotransition Metal Chemistry*, 2nd Edit., University Science Books, Mill Valley, CA, USA 1987; b) G. W. Parshall: *Homogeneous Catalysis*, Wiley, New York 1980; c) C. Elschenbroich, A. Salzer: *Organometallchemie*, Teubner, Stuttgart 1988, Chap. 17.

[2] a) F. A. Cotton, G. Wilkinson: *Anorganische Chemie*, 4th Edit., Verlag Chemie, Weinheim 1982, Chap. 4; b) F. Kober: *Grundlagen der Komplexchemie*, Salle, Frankfurt and Sauerländer AG, Aarau 1979, Chap. 13.

[3] *Stiddard* and *Townsend* [4] have synthesized an extremely reactive compound [RuCl(NO)(PPh_3)$_2$] comparable with **1** by reduction of [$RuCl_3$(NO)(PPh_3)$_2$] with Zn or Zn/Cu. In subsequent reactions it was not isolated but only prepared in situ [4b, c]; its structure is not known.

[4] a) M. H. B. Stiddard, R. E. Townsend, *J. Chem. Soc. Chem. Commun. 1969*, 1372; b) J. Reed, C. G. Pierpont, R. Eisenberg, *Inorg. Synth. 16* (1976) 21; c) C. J. Jones, J. A. McCleverty, A. S. Rothin, *J. Chem. Soc. Dalton Trans. 1985*, 401.

[5] a) A. F. Hill, W. R. Roper, J. M. Waters, A. H. Wright, *J. Am. Chem. Soc. 105* (1983) 5939; b) W. R. Roper, *J. Organomet. Chem. 300* (1986) 167; c) M. A. Gallop, W. R. Roper, *Adv. Organomet. Chem. 25* (1986) 121.

[6] M. Herberhold, A. F. Hill, *J. Organomet. Chem. 387* (1990) 323.

[7] Spectroscopic data [without ^{1}H NMR for $P\mathit{i}Pr_3$-Ligands; ^{31}P{^{1}H} NMR (36.2 MHz, C_6D_6)]. **1**: IR (KBr): $\tilde{\nu}$ = 1700 cm^{-1} (NO); ^{31}P NMR: δ = 37.82 (s).—**2**: IR (KBr): $\tilde{\nu}$ = 1895 (CO), 1755 cm^{-1} (NO); ^{31}P NMR: δ = 23.65(s).—**3**: IR (KBr): $\tilde{\nu}$ = 2130, 2050 (OsH), 1713 cm^{-1} (NO); ^{1}H NMR (90 MHz, C_6D_6): δ = − 2.16 (dt, J(PH) = 14.3, J(HH) = 7.3 Hz, 1H, OsH), − 10.03 (dt, J(PH) = 23.4, J(HH) = 7.3 Hz, 1H, OsH); ^{31}P NMR: δ = 30.68 (s; dd in off-resonance).—**4**: IR (KBr): $\tilde{\nu}$ = 2160 (OsH), 1780 cm^{-1} (NO); ^{1}H NMR (60 MHz, C_6D_6): δ = − 5.40 (t, J(PH) = 14.5 Hz, OsH); ^{31}P NMR: δ = 13.56 (s; d in off-resonance).—**5**: IR (KBr): $\tilde{\nu}$ = 2205 (OsH), 1805 (NO), 1688 cm^{-1} (OCO); ^{1}H NMR (60 MHz, C_6D_6): δ = −7.83 (t, J(PH) = 15.0 Hz, OsH); ^{31}P NMR: δ = 21.12 (s; d in off-resonance).—**6**: IR (KBr): $\tilde{\nu}$ = 1775 cm^{-1} (NO); ^{1}H NMR (60 MHz, C_6D_6): δ = 2.68 (t, J(PH) = 4.3 Hz, $OsCH_3$); ^{31}P NMR: δ = − 15.73 (s).—**7**: IR (KBr): $\tilde{\nu}$ = 1792 cm^{-1} (NO); ^{31}P NMR: δ = − 19.81 (s).—**8**: IR (KBr): $\tilde{\nu}$ = 2098 (OsH), 1750 cm^{-1} (NO); ^{1}H NMR (90 MHz, C_6D_6): δ = 3.92 (t, J(PH) = 1.8 Hz, OCH_3), − 6.04 (t, J(PH) = 14.5 Hz, OsH); ^{31}P NMR: δ = 18.50 (s; d in off-resonance).—**9**: IR (KBr): $\tilde{\nu}$ = 2205 (OsH), 2115 (C≡C), 1795 cm^{-1} (NO); ^{1}H NMR (90 MHz, C_6D_6): δ = 7.11 (m, C_6H_5), − 0.72 (t, J(PH) = 23.5 Hz, OsH), ^{31}P NMR: δ = 18.21 (s; d in off-resonance).—**10**: IR (KBr): $\tilde{\nu}$ = 2095 (OsH), 2075 (C≡C), 1748 (NO), 1680 cm^{-1} (OCO); ^{1}H NMR (60 MHz, C_6D_6): δ = 3.41 (s, CO_2CH_3), − 0.73 (t, J(PH) = 22.7 Hz, OsH); ^{31}P NMR: δ = 19.41 (s; d in off-resonance).—**11**: IR (KBr): $\tilde{\nu}$ = 1730 (NO), 1692, 1671 cm^{-1} (OCO), ν(C≡C) superposed by ν(NO); ^{31}P NMR: δ = − 4.53 (s).

[8] Crystals from toluene (− 30 °C); crystal dimensions 0.4 × 0.4 × 0.7 mm; monoclinic, space group $P2_1/c$, Z = 2; a = 8.114(1), b = 8.958(1), c = 16.662(2) Å, β = 93.00(1)°, V = 1209.5 Å^3, ρ_{calcd} = 1.58 g cm^{-3};

$4° \leq 2\theta \leq 60°$ ($Mo_{K\alpha}$, $\lambda = 0.71069$ Å, graphite monochromator, $\omega/2\theta$-scan); 3347 independent reflections Lp and empirical absorption correction ($\mu = 55.3\ cm^{-1}$, ψ scan method, min. transmission 92%); Patterson method (SHELXS-86), refinement with program packet SDP (Enraf-Nonius), hydrogen atoms calculated for ideal geometry, varied according to a riding method; $R = 0.016$, $R_w = 0.019$ for 2476 structure factors ($I_o > 3\sigma(I_o)$); residual electron density 0.78 e Å^{-3}. Further details of the X-ray structure analysis are available on request from the Fachinformationszentrum Karlsruhe, Gesellschaft für Wissenschaftlich-technische Information mbH, W-7514 Eggenstein-Leopoldshafen 2 (FRG), on quoting the depository number CSD-54991, the names of the authors, and the journal citation.

[9] C. Busetto, A. D'Alfonso, F. Maspero, G. Perego, A. Zazzetta, *J. Chem. Soc. Dalton Trans. 1977*, 1828.

[10] D. L. Thorn, T. H. Tulip, J. A. Ibers, *J. Chem. Soc. Dalton Trans. 1979*, 2022.

[11] L. Dahlenburg, A. Yardimcioglu, *J. Organomet. Chem. 291* (1985) 371.

[12] W. A. Schenk, J. Leissner, C. Burschka, *Angew. Chem. 96* (1984) 787; *Angew. Chem. Int. Ed. Engl. 23* (1984) 806.

[13] Preparation: a) W. Strohmeier, T. Onoda, *Z. Naturforsch. B 23* (1968) 1377; b) H. Werner, A. Höhn, *Z. Naturforsch. B 39* (1984) 1505.

Hexanuclear Ferric Complex with a Novel $S = 5$ Ground State**

By *Daniel F. Harvey,* Cheryl A. Christmas, James K. McCusker, Paula M. Hagen, Raj K. Chadha,* and *David N. Hendrickson**

Oxo-bridged iron complexes have been found to exist in a variety of metalloproteins.[1] Studies of the oligomerization of lower nuclearity oxo Fe^{III} units have resulted in the preparation of higher nuclearity oxo-iron complexes.[2] In all of these high-spin Fe^{III} complexes, oxo, hydroxo or alkoxo bridges have been found to support *only* antiferromagnetic pairwise interactions between Fe^{III} ions. In this communication we report that the chelating ligand 1,1-bis(*N*-methylimidazol-2-yl)ethanol **1** reacts with the acetato-oxo Fe^{III}_3-complex **2** to give the hexanuclear Fe^{III} complex **3**. Complex **3** has been found to have novel magnetic properties. Even though all six iron ions are high-spin Fe^{III} ions, complex **3** has an $S = 5$ ground state.

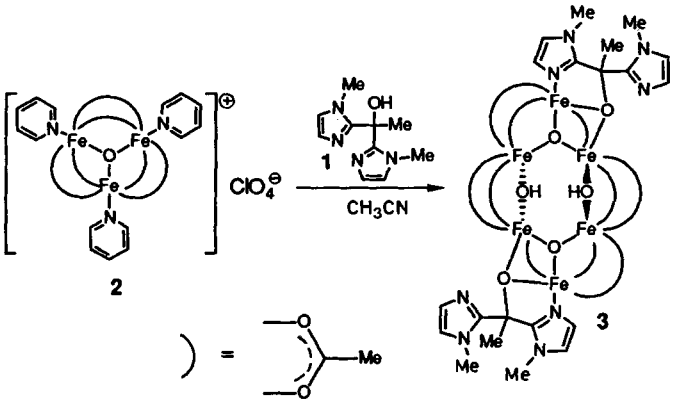

[*] Prof. Dr. D. F. Harvey, Prof. Dr. D. N. Hendrickson, C. A. Christmas, J. K. McCusker, P. M. Hagen, Dr. R. K. Chadha
Department of Chemistry-0506
University of California at San Diego
La Jolla, California 92093-0506 (U.S.A)

[**] This work is supported by the U.S. National Institutes of Health (GM39972 to *D. F. H* and HL13652 to *D. N. H*) and the American Cancer Society (*D. F. H*).

Addition of 3.1 equivalents of **1** to a stirred acetonitrile solution of 1 equivalent of $[Fe_3O(OAc)_6(py)_3]ClO_4$ **2** gave a dark brown solution. After 20 minutes the solution was concentrated in vacuo and a brown oil was obtained. Addition of CH_2Cl_2 to the brown oil gave a brown solution, which was kept in an open flask at room temperature. Upon slow evaporation of solvent, red block-like crystals of $\mathbf{3} \cdot 8CH_2Cl_2$ suitable for characterization by X-ray crystallography were obtained.[3] Further drying gave $\mathbf{3} \cdot CH_2Cl_2$ in 40% yield[4] which was used for the magnetization studies. The X-ray crystal structure of **3** is shown in Figure 1. Com-

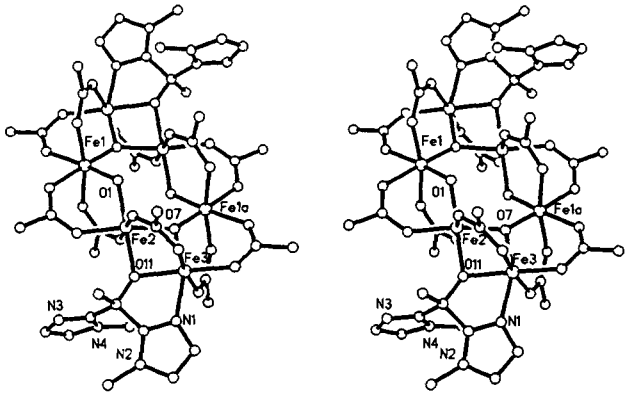

Fig. 1. Stereoview of **3**. H atoms and solvent molecules (CH_2Cl_2) have been omitted for clarity. Selected bond lengths [Å] and angles [°]: Fe1a-O7, 1.873(4); Fe2-O7, 1.963(3); Fe3-O7, 1.908(5); Fe3-N1, 2.111(6); Fe1-O1, 1.977(4); Fe2-O1, 1.948(4); Fe2-O11, 2.014(5); Fe3-O11, 2.021(3). Fe1a-O7-Fe2, 137.9(3); Fe2-O7-Fe3, 100.2(2); Fe1a-O7-Fe3, 119.7(2); Fe1-O1-Fe2, 123.5(2); Fe3-O11-Fe2, 94.8(2); 07-Fe3-N1, 157.7(1).

plex **3** possesses a center of inversion and has three unique Fe^{III} centers. Iron atoms Fe1 and Fe2 both have only oxygen ligation whereas Fe3 has both oxygen and nitrogen ligation. Fe1 is bound to one μ_3-oxo, one μ_2-hydroxo, and four acetato oxygen atoms. Fe2 has the same coordination as Fe1 except one of the acetate oxygen atoms is replaced by a μ_2-O-bound, deprotonated ligand **1**. Fe3 (like Fe2) has only three μ_2-acetato oxygen atoms in its coordination sphere. The remaining coordination sites of Fe3 are filled by one of the imidazole rings of the ligand **1** and its μ_2-alkoxide function. The second imidazole ring of **1** is not bound to any of the iron centers. This structure may be viewed as two Fe^{III}_3 μ_3-oxo scalene triangles bridged by four μ_2-acetato and two μ_2-hydroxo ligands. The four central ions (Fe1, Fe2, Fe1a, and Fe2a) are planar with one μ_2-hydroxo bridging above the plane and the other below the plane.

Two similar Fe_6 complexes have recently been reported. The structure of **3** is quite similar to that of $[Fe_6O_2(OH)_2(O_2CCMe_3)_{12}]$ **4**[2f] but is fundamentally different than $[Fe_6O_2(OH)_2(O_2CPh)_{12}(1,4\text{-dioxane})(OH_2)]$ **5**.[2g, h] In **4**, the two peripheral irons are five-coordinate and all of the carboxylate ligands are pivalates. Complex **5** contains bridging carboxylates between the edges of the trinuclear subunits that face one another. In **5**, both of the bridging hydroxides are on the same side of the iron plane, whereas in **3** and **4** the bridging hydroxides are on opposite faces.

The unusual magnetic properties of complex **3** are summarized in Figure 2. At 10.0 kG the magnetic moment (μ_{eff}) per molecule gradually increases from 9.21 μ_B at 346.1 K to a maximum of 10.89 μ_B at 20.00 K, where it plateaus before it decreases to a value of 10.44 μ_B at 6.00 K. The increase in μ_{eff} as the temperature is decreased is unprecedented for com-

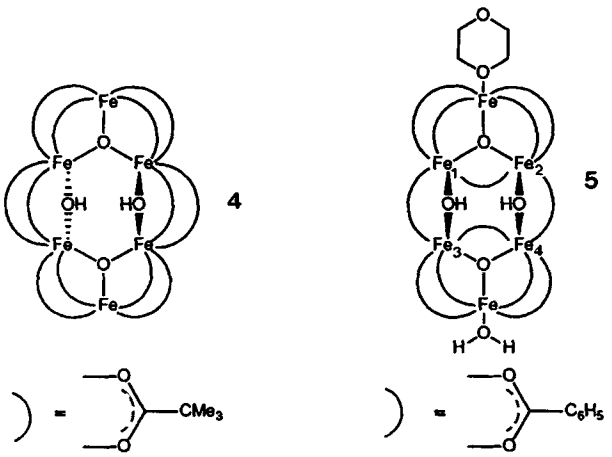

plexes comprised of only high-spin Fe^{III} ions. Zero-field Mössbauer spectra at 300 and 200 K can be fit with parameters consistent with high-spin Fe^{III} ions.[5]

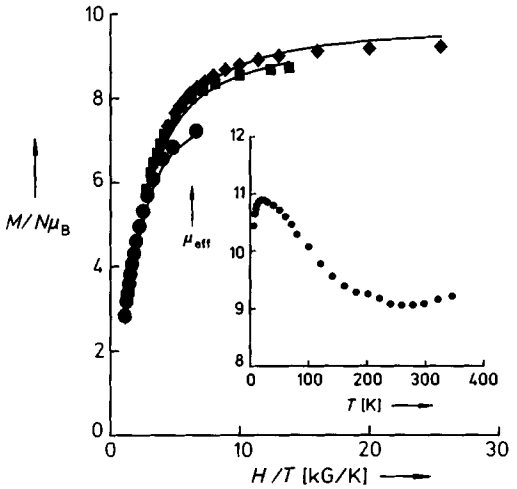

Fig. 2. Plot of the reduced magnetization ($M/N\mu_B$) of a polycrystalline sample of complex $3 \cdot CH_2Cl_2$ versus H/T, whereby the values for H are ●, 10.0; ■, 25.0; and ◆, 40.0 kG. The solid lines result from a fit of all data to a spin Hamiltonian for an $S = 5$ state. The inset shows a plot of effective magnetic moment μ per molecule [μ_B] versus temperature for complex **2** in an applied field of 10.0 kG.

The spin of the ground state of a Fe_6^{III} complex could range from $S = 0$ to $S = 15$. However, from the literature[2] it would be expected that pairwise antiferromagnetic interactions in a Fe_6^{III} complex would give an $S = 0$ ground state. In fact, complex **5** has been reported[2g,h] to have an $S = 0$ ground state. The plot of μ_{eff} versus temperature in Figure 2 is strongly suggestive of a complex with an $S = 5$ ground state, which would be expected to give a spin-only value of 10.95 μ_B/molecule for a Fe_6^{III} complex. Substantiation of this unusual ground state was obtained by field-dependent magnetization measurements. It should be mentioned that due to the topology of complex **3** it is *not* possible to use the Kambe operator replacement technique[6] to derive an eigenvalue energy level expression for complex **3**. Thus, to fit the 10.0 kG susceptibility data and to extract exchange parameters for pairwise $Fe^{III} \cdots Fe^{III}$ interactions in complex **3** would require on each iteration diagonalization of a 46 656 × 46 656 matrix.

However, the isofield magnetization data (1.51–9.04 K at 10.0 kG; 1.81–9.00 K at 25.0 kG; 1.57–9.04 K at 40.0 kG) shown in Figure 2 definitively establish that the ground state of complex **3** has $S = 5$. At the highest field employed, the reduced magnetization, $M/N\mu_B$ (N is Avagadros number and μ_B is the Bohr magneton) is saturating at $\approx 9.2\,\mu_B$. The solid lines show how well the data can be fit by assuming a theoretical model with an $S = 5$ ground state experiencing axial zero-field interactions ($D\hat{S}_z^2$). The three isofield data sets are simultaneously fit [diagonalization of two $(2S + 1) \times (2S + 1)$ matrices on each iteration] with parameters $g = 1.94$ and $D = 0.22\ cm^{-1}$ for $S = 5$. Fits with $S = 4$ and 6 spin Hamiltonian matrices give unreasonable g values of 2.39 and 1.63, respectively. It is thus clear that complex **3** has a $S = 5$ ground state.

The unusual $S = 5$ ground state for complex **3** can be rationalized as a manifestation of spin frustration. By "spin frustration" we refer to an effect whereby the interplay of various exchange pathways results in spin vector alignments which deviate from those anticipated based upon the intrinsic nature of the pairwise exchange interactions. It is well documented[7] that triangular trinuclear complexes can exhibit spin frustration. For example, consider the exchange interactions in an isosceles Fe_3^{III} triangle: When both J and J'

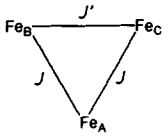

are negative and $J/J' > 2$, the ground state has $S = 5/2$. The dominance of the two J-type interactions leads to a frustration in the $Fe_B \cdots Fe_C$ interaction and a net parallel alignment of the spin vectors on Fe_B and Fe_C despite the fact that the interaction between these two ions is antiferromagnetic. Spin frustration in higher nuclearity complexes is *not* as well documented.[8] The $S = 5$ ground state for the Fe_6^{III} complex **3** and $S = 0$ ground state for the analogous complex **5** can be rationalized by differing degrees of spin frustration. One possibility is shown in the schematic drawings (Scheme 1). In

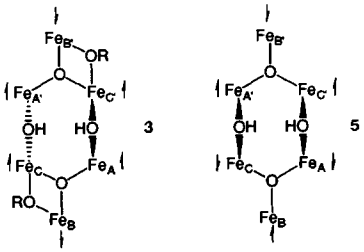

Scheme 1. Description of the groundstate of **3** ($S = 5$) and **5** ($S = 0$). The arrows indicating spin vectors merely reflect orientations, not absolute magnitudes.

both complexes the interaction propagated by the hydroxo bridges is assumed to be the weakest pairwise exchange interaction. In complex **3**, the presence of the μ_2-OR group breaks the symmetry of the pairwise interactions within the iron triangle. If any one of these interactions is sufficiently strong, frustration of the weak antiferromagnetic μ-$OH^{\ominus}$ pathway may occur, resulting in a net spin alignment of the spin vectors on these ions and an $S = 5$ ground state. On the other hand, perhaps any one interaction is not so dominating in complex **5**, then all three Fe^{III} ions (A, B and C) in each

triangle are comparably involved in a mutual spin polarization which would tend to give an $S = 0$ ground state.

Received: January 2, 1991 [Z 4365 IE]
German version: *Angew. Chem. 103* (1991) 592

[1] a) S. J. Lippard, *Chem. Br. 22* (1986) 222–227; b) S. J. Lippard, *Angew. Chem. 100* (1988) 353–371; *Angew. Chem. Int. Ed. Engl. 27* (1988) 344–361; c) L. Que, Jr., R. C. Scarrow, *Metal Clusters in Proteins* (*ACS Symposium Ser. 372* (1988) 152–178); d) P. C. Wilkins, R. G. Wilkins, *Coord. Chem. Rev. 79* (1987) 195–214; e) B.-M. Sjöberg, A. Gräslund, *Adv. Inorg. Biochem. 5* (1983) 87–110; f) E. C. Thiel, *Metal Clusters in Proteins* (*ACS Symposium Ser. 372* (1988) 179–195).

[2] Fe_3-complexes see a) S. J. Lippard, S. M. Gorun, *J. Am. Chem. Soc. 107* (1985) 4568–4570; b) S. M. Gorun, G. C. Papaefthymiou, R. B. Frankel, S. J. Lippard, *ibid. 109* (1987) 4244–4255; Fe_4-complexes see: c) S. M. Gorun, S. J. Lippard, *Inorg. Chem. 27* (1988) 149–156, and references therein; d) S. Drüeke, K. Wieghardt, B. Nuber, J. Weiss, E. L. Bominaar, A. Sawaryn, H. Winkler, A. X. Trautwein, *ibid. 28* (1989) 4477–4483, and references therein; e) J. L. Sessler, J. W. Sibert, V. Lynch, *ibid. 29* (1990) 4143–4146; Fe_6 complex: f) A. S. Batsanov, Yu. T. Struchkov, G. A. Timko, *Koord. Khim. 14* (1988) 266–270; g) W. Micklitz, S. J. Lippard, *Inorg. Chem. 27* (1988) 3067–3069; h) W. Micklitz, S. G. Bott, J. G. Bensten, S. J. Lippard, *J. Am. Chem. Soc. 111* (1989) 372–374; i) K. Hegetschweiler, H. Schmalle, H. M. Streit, W. Schneider, *Inorg. Chem. 29* (1990) 3625–3627; for an example of an Fe_8 complex see: j) K. Wieghardt, K. Pohl, I. Jibril, G. Huttner, *Angew. Chem. 96* (1984) 66–67; *Angew. Chem. Int. Ed. Engl. 23* (1984) 77–78; For examples of Fe_{11} complexes see: k) S. M. Gorun, G. C. Papaefthymiou, R. B. Frankel, S. J. Lippard, *J. Am. Chem. Soc. 109* (1987) 3337–3348, and references therein.

[3] X-ray structure data: triclinic, spacegroup $P\bar{1}$, $a = 12.167(2)$ Å, $b = 12.921(4)$ Å, $c = 15.394(4)$ Å, $\alpha = 114.41(2)°$, $\beta = 97.641(15)°$, $\gamma = 102,17(2)°$, $V = 2087.4$ Å^3, $Z = 1$, data collected $4.0° \leq 2\theta \leq 45.0°$, 4179 unique reflections with $F > 6.0\sigma(F)$, $R = 0.046$, $R_w = 0.059$. Further details of the crystal structure investigations are available on request from the Director of the Cambridge Crystallographic Data Center, University Chemical Laboratory, Lensfield Road, GB-Cambridge CB2 1EW (U. K.), on quoting the complete journal citation.

[4] Satisfactory elemental analysis for $Fe_6Cl_2O_{26}N_8C_{41}H_{60}(3{\cdot}CH_2Cl_2)$.

[5] Mössbauer hyperfine parameters for two doublets in area ratio of 1:2 (values relative to iron foil): 300 K: δ [0.406(6), 0.383(3) mm/s]; ΔE_Q [1.056(11), 0.729(5) mm/s]. 200 K: δ [0.510(6), 0.350(14) mm/s]; ΔE_Q [1.061(12), 0.78(3) mm/s].

[6] K. Kambe, *J. Phys. Soc., Jpn. 5* (1950) 48.

[7] S. Ghose, A. W. Hewat, M. Pinkney, *Solid State Communications 74* (1990) 413, and references therein.

[8] a) J. K. McCusker, J. B. Vincent, E. A. Schmitt, M. L. Mino, K. Shin, D. K. Coggin, P. M. Hagen, J. C. Huffman, G. Christou and D. N. Hendrickson, *J. Am. Chem. Soc. 113* (1991) 3012–3021; b) J. K. McCusker, E. A. Schmitt and D. N. Hendrickson in D. Gatteschi, (Ed.): *Magnetic Molecular Materials*, Kluwer Academic Publishers, in press.

Isoselective Relationship for the Stereoselectivity of the Transfer of Hydrogen Atoms to Cyclic Alkyl Radicals**

By *Bernd Giese*,* *Hassan Farshchi, Jörg Hartmanns, and Jürgen O. Metzger**

With the increasing use of radical reactions in organic synthesis a more detailed understanding of the reactivities and selectivities is of decisive importance.[1] Especially important is an exact knowledge of the stereoselectivity of hydrogen transfer and the possibility of controlling it, since this reaction is frequently the decisive product-forming step in radical reactions.[2]

Using the π-alkenyl radical **1** as example we have shown that the stereoselectivity of hydrogen transfer to give (*Z*)-**2** and (*E*)-**2** can be steered by both variation of the H donor RH as well as by the temperature, and that it obeys the

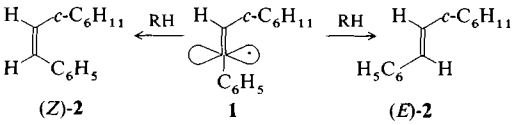

(*Z*)-**2** **1** (*E*)-**2**

isoselective relationship (a) with an isoselective temperature T_{iso} of 60–80 °C.[3] At this isoselective temperature, variation of the H donor has no influence on the selectivity.[4a]

$$T_{iso} = \frac{\delta(\Delta H_E^{\ddagger} - \Delta H_Z^{\ddagger})}{\delta(\Delta S_E^{\ddagger} - \Delta S_Z^{\ddagger})} \qquad \text{(a)}$$

Such isoselective realtionships are of practical importance, but also enable us to assess the selectivity of a series of reactions over a large temperature range and possibly to anticipate reversal of selectivity as a function of the temperature.[4] In addition, the occurrence of an isoselective relationship points to a common reaction mechanism. Hitherto a series of reactions in which isoselectivity occur, were experimentally measured with variation of only one reaction partner.[4a] We have now for the first time, by H trapping with the radical **4**, measured a series of reactions, which upon variation of both reaction partners—radical **4** and H donor RH—leads to a single isoselective relationship (Scheme 1).

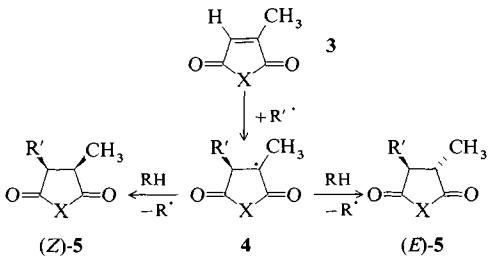

Scheme 1. X = O, PhN; RH = Bu_3SnH, PhMe, PhEt, c-C_6H_{12}; R′:Me (**a**), n-C_6H_{13} (**b**), $PhCH_2$ (**c**), c-C_6H_{11} (**d**), PhCH(Me) (**e**).

The radicals **4** were obtained by addition of a radical R′· to methylmaleic anhydride or *N*-phenyl(methyl)maleimide **3**. Transfer of H from H donors RH to the planar π-alkyl radical **4** leads to formation of (*Z*)-**5** and (*E*)-**5**, whose ratio was determined in the temperature range 0–400 °C. The stereoselectivity of the H transfer is significantly greater with the alkyl radical **4** than with the alkenyl radical **1** as acceptor. It is strongly influenced by the β-substituent R′, by the H donor and by the temperature, but is largely independent of whether **3** is employed as the *N*-phenylimide or the anhydride (Table 1).

Since the approach of the H donor RH upon **4** from the *anti*-side with respect to R′ is less hindered than from the *syn*-side, the activation enthalpy for the formation of (*Z*)-**5** is 3.5–10.9 kmol^{-1} lower than for the formation of (*E*)-**5**.

[*] Priv.-Doz. Dr. J. O. Metzger, Dr. J. Hartmanns
Fachbereich Chemie der Universität
Carl-von-Ossietzky-Strasse 9–11, W-2900 Oldenburg (FRG)
Prof. Dr. B. Giese
Institut für Organische Chemie der Universität
St.-Johanns-Ring 19, CH-4056 Basel (Switzerland)
Dr. H. Farshchi
Institut für Organische Chemie der Technischen Hochschule Darmstadt
Petersenstr. 22
W-6800 Darmstadt (FRG)

[**] This work was supported by the Deutsche Forschungsgemeinschaft.

Table 1. Activation parameters for the stereoselectivity of the transfer of H to the alkyl radicals **4** and ratio of the products [(*Z*)-**5**]:[(*E*)-**5**].

No.	4	RH	$\Delta\Delta H^{\neq}$ [e] [kJ mol^{-1}]	$\Delta\Delta S^{\neq}$ [e] [J mol^{-1}K^{-1}]	[(*Z*)-**5**]:[(*E*)-**5**]]	*T* [°C]
1	**a**[a]	Bu_3SnH	5.1 ± 0.3	8.6 ± 0.8	3.0:1[c]	0–140[7]
2	**b**[a]	Bu_3SnH	5.4 ± 0.3	9.0 ± 1.2	3.0:1[c]	0–110[7]
3	**c**[a]	Bu_3SnH	5.7 ± 0.7	11.3 ± 2.1	3.5:1[c]	0–80 [7]
4	**d**[a]	Bu_3SnH	8.2 ± 0.5	14.3 ± 1.5	5.6:1[c]	0–140[7]
5	**d**[b]	Bu_3SnH	9.4 ± 1.2	16.6 ± 3.7	6.7:1[c]	0–110[7]
6	**d**[b]	*c*-C_6H_{12}	9.7 ± 0.3	15.2 ± 0.7	1.91:1[d]	180–400[8]
7	**d**[b]	*c*-C_6H_{12}	10.9 ± 0.6	17.6 ± 1.2	1.96:1[d]	200–260[8]
8	**c**[a]	PhMe	3.5 ± 0.2	7.0 ± 0.5	1.04:1[d]	180–260[8]
9	**e**[a]	PhEt	4.8 ± 0.4	8.7 ± 0.8	1.18:1[d]	180–260[8]

[a] X = PhN. [b] X = O. [c] 20 °C. [d] 200 °C. [e] In each case the value for (*E*)-**5** − the value for (*Z*)-**5**.

Thereby, the energy difference $\Delta H^{\neq}((E)\text{-}5) - \Delta H^{\neq}((Z)\text{-}5)$ with the same H donor tributyltin hydride increases with increasing size of the β-substituent R′ from 5-6 (methyl, *n*-hexyl,benzyl) to 8.2 kJ mol^{-1} (cyclohexyl), and accordingly the stereoselectivity increases. Since also the differences in the activation entropies increase in the same direction from 9 (methyl, *n*-hexyl) through 11.3 (benzyl) to 14.3 J mol^{-1} K^{-1} (cyclohexyl), the compensation of the activation enthalpies and activation entropies leads to an isoselective temperature[4a] of 750 K with $[(Z)\text{-}5]/[(E)\text{-}5] = 0.72 + 0.07$ (Fig. 1). At this temperature, which lies outside the measurement range, the radicals **4a**–**4d** (X = PhN) react with the H donor tributyltin hydride (Experiments 1–4) with the same stereoselectivity.

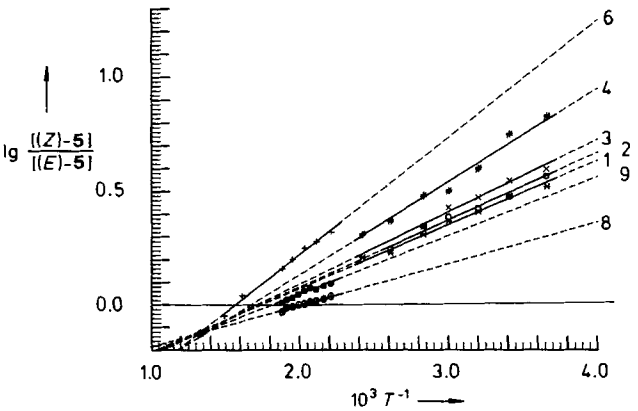

Fig. 1. Temperature dependence of the stereoselectivity of the H transfer to the alkyl radicals **4** by Bu_3SnH, *c*-C_6H_{12}, PhMe and PhEt. The numbers on the Arrhenius curves correspond to the experiment numbers in Table 1. The unbroken portions of the curves demarcate the ranges of measurement (cf. Table 1).

The H transfer from toluene to **4c** (X = PhN), from ethylbenzene to **4e** (X = PhN), and from cyclohexane to **4d** (X = O) (Experiments 8, 9, and 6) obey the same isoselective relationship as the H transfer from tributyltin hydride to the radical **4** (Fig. 1). This is a remarkable result, since it shows that the reactions of five sterically differently shielded radicals **4** with four differently reactive H donors RH[5] obey a common isoselective relationship. It can therefore be concluded that the stereoselectivity of the H transfer is determined by the steric interaction between H donor and β-substituent in radical **4**. The finding that **4c** (X = PhN) reacts more selectively with the H donor tributyltin hydride (Experiment 3) than with the much less reactive toluene, is surprising, since the difference in the steric shielding by R′ should have all the more stronger effect on the activation energies the less reactive the H donor is.[3a] Our result—a further deviation from the reactivity–selectivity principle[6]—shows that the steric effect of tributyltin hydride on **4c** (X = PhN) is greater than that of toluene in the transition state of the H transfer, so that the above effect is overcompensated. In contrast, in the case of the radical **4d** (Experimental pairs 4 and 7 as well as 5 and 6), the expected behavior is observed even when the differences are smaller than in the case of the alkenyl radical **1**.[3]

The temperature dependence of the stereoselectivity with incorporation of the isoselective point is shown in Figure 1. The selectivity $\lg\{[(Z)\text{-}5]/[(E)\text{-}5]\}$ decreases as expected with increasing temperature, and between 475 K (Experiment 8) and 638 K (Experiment 6) is equal to zero. Above these temperatures the selectivity increases again, and entropically favored preferentially (*E*)-**5** is formed. This reversal of selectivity lies within the range of measurement in the case of Experiments 6–9, and could therefore be measured directly.

Our investigations on the alkyl radicals **4** show that the stereoselectivity of radical hydrogen transfer reactions can be controlled by variation of the β-substituent, the H donor, and the reaction temperature. These results are important for the planning of syntheses in which the subsequent H transfer takes place at a prochiral center.

Received: November 16, 1990 [Z 4283 IE]
German version: *Angew. Chem. 103* (1991) 619

CAS Registry numbers:
3 (X = O), 616-02-4; **3** (X = PhN), 3120-04-5; **4a** (X = PhN), 132750-69-7; **4b** (X = PhN), 132750-70-0; **4c** (X = PhN), 132750-71-1; **4d** (X = PhN), 132750-72-2; **4d** [b] (X = O), 65149-70-4; **4e** (X = PhN), 132750-73-3; (*E*)-**5a** (X = PhN), 35393-95-4; (*Z*)-**5a** (X = PhN), 6144-74-7; (*E*)-**5b** (X = PhN), 132750-74-4; (*Z*)-**5b** (X = PhN), 132750-78-8; (*E*)-**5c** (X = PhN), 132750-75-5; (*Z*)-**5c** (X = PhN), 132750-79-9; (*E*)-**5d** (X = PhN), 132750-76-6; (*Z*)-**5d** (X = PhN), 132750-80-2; (*E*)-**5d** (X = O), 65424-96-6; (*Z*)-**5d** (X = O), 65424-93-3; **5e** (X = PhN), 132750-77-7.

[1] M. Regitz, B. Giese (Eds.): *C-Radikale (Methoden Org. Chem. (Houben-Weyl) 4th Ed., Vol. E19a* (1989)); B. Giese: *Radicals in Organic Synthesis: Formation of Carbon-Carbon Bonds,* Pergamon, Oxford 1986; further reviews: D. J. Hart, *Science (Washington D. C.) 223* (1984) 883; M. Ramaiah, *Tetrahedron 43* (1987) 3541; W. P. Neumann, *Synthesis 1987*, 665; D. P. Curran, *ibid. 1988*, 417, 489.

[2] B. Giese, *Angew. Chem. 101* (1989) 993; *Angew. Chem. Int. Ed. Engl. 28* (1989) 969, and references cited therein.

[3] a) B. Giese, J. A. González-Gómez, S. Lachhein, J. O. Metzger, *Angew. Chem. 99* (1987) 475; *Angew. Chem. Int. Ed. Engl. 26* (1987) 479; b) see also L. A. Singer *Sel. Org. Transform. 2* (1972) 239; O. Simamura, *Top. Stereochem. 4* (1969) 1.

[4] a) B. Giese, *Acc. Chem. Res. 17* (1984) 438; b) see also H. Buschmann, H.-D. Scharf, N. Hoffmann, P. Esser, *Angew. Chem. 103* (1991) 480; *Angew. Chem. Int. Ed. Engl. 30* (1991), 477.

[5] The rate constants for the transfer of H to primary alkyl radicals were determined for tributyltin hydride, ethylbenzene, toluene, and cyclohexane at 100 °C to be 8.3×10^6, 1.3×10^3, 4.2×10^2, and 16×10^2 M^{-1}s^{-1}, respectively: C. Chatgilialoglu, K. U. Ingold, J. C. Scaiano, *J. Am. Chem. Soc. 103* (1981) 219; V. E. Agabekov, N. L. Budeiko, E. T. Denisov, N. I. Mitskovich, *React. Kinet. Catal. Lett. 7* (1972) 437; P. J. Boddy, E. W. R. Steacie, *Can. J. Chem. 39* (1961) 13.

[6] B. Giese, *Angew. Chem. 89* (1977) 162; *Angew. Chem. Int. Ed. Engl. 16* (1977) 125.

[7] A mixture of one equivalent of alkyl iodide or alkyl bromide R′Y, two equivalents of tributyltin hydride, two equivalents of alkene **3**, and 0.1 equivalent of azobisisobutyronitrile in toluene was irradiated for 5–30 min or heated, and the ratio of the products [(*Z*)-**5**]:[(*E*)-**5**] determined gas chromatographically.

[8] **3** and the H-donor, which concomitantly supplies R′, (molar ratio 1:1000) contained in pyrex ampoules below the critical temperature of the H donor[9], in a high-pressure/high-temperature flow reactor above the critical temperature[9] were allowed to react in the absence of air. The reaction time was so chosen that the conversion sufficed for determination of the sterisomeric ratio even though no isomerization was detectable. The ratio [(*Z*)-**5**]:[(*E*)-**5**] was determined by capillary gas chromatography with on-column injection.

[9] J. Hartmanns, K. Klenke, J. O. Metzger, *Chem. Ber. 119* (1986) 488.

Helical Semiquinones: Proof of Chirality by ENDOR Spectroscopy**

By *Manfred Mäurer, Klaus Scheffler, Hartmut B. Stegmann,** and *Albrecht Mannschreck*

4,5-Disubstituted phenanthrenequinones **II** are helical and therefore, in contrast to the unsubstituted species **I**, chiral. The twist is mainly caused by the repulsion between the substituents in 4,5 positions. The nonbonding oxygen-oxygen interaction adds a smaller contribution.[1] For the methyl substituted compounds the free activation enthalpy of racemization lies between 94 and 131 kJ mol^{-1}, that is, the enantiomers can be separated at room temperature by liquid chromatography (LC).[1] The corresponding semiquinones are also expected to have a twisted ground state and a relatively high enantiomerization barrier. EPR and ENDOR studies of thallium complexes of these semiquinones show smaller values of the thallium coupling constants for the nonplanar species than for the planar ones.[2] An estimate of the height of the enantiomerization barrier was not possible by this method.

The helical form of these semiquinones has now been proved by ENDOR spectroscopic studies of the diastereomeric radicals, which were prepared by reduction of the corresponding quinones with prochiral auxiliaries. The 2,2'-biphenyldiyl(*p*-tolyl)tin chloride **B** provides a suitable probe.[3] For comparison, triphenyltin chloride **A** was also used. **A** and **B** react with quinones, whereby in each case an aryl substituent is lost and semiquinone chelates of trigonal-bipyramidal, pentacoordinate tin are formed, in which the bidentate ligand takes up axial-equatorial positions because of the ring strain.[3] Thus the chlorine atom in chelates with **B** must occupy an equatorial position, and tin is therefore a chiral center. When **A** is used, the chlorine atom, as an electronegative substituent, is bound axially, and the organometallic component is achiral. Studies of the corresponding benzoquinone complexes have shown[3] that the permutation isomerization at room temperature is slow on the EPR time scale.

Since the behavior of these paramagnetic complexes is determined by the central atom, a similar situation is anticipated with the phenanthrenesemiquinones. In order to distinguish between the spectral properties of the diastereomers and "nonchiral" effects, planar as well as helical phenanthrene quinones[4] were treated with **A** and **B** (in **7** the positions 3 and 4 as well as 5 and 6 are linked by dioxymethylene bridges).

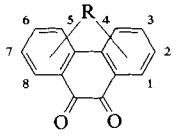

	$R^{1/8}$	$R^{2/7}$	$R^{3/6}$	$R^{4/5}$
1	H	H	H	H
2	H	H	CH_3	H
3	H	H	H	CH_3
4	H	H	CH_3	CH_3
5	H	CH_3	H	CH_3
6	H	CH_3	CH_3	CH_3
7	H	H	$-O-CH_2-O-$	

The EPR spectra are only partly resolved, and the large number of coupling nuclei prevents a complete interpretation (Fig. 1). In all cases they are symmetric and the g factors

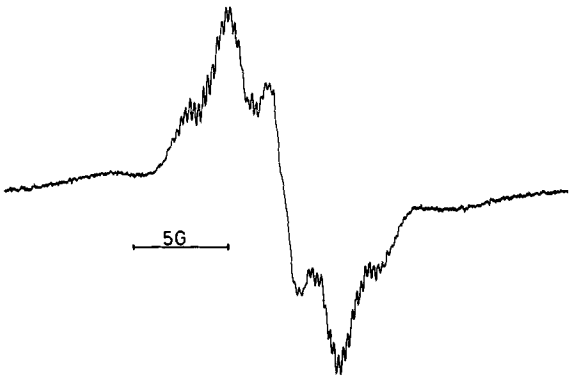

Fig. 1. EPR spectrum of **5B** in toluene at room temperature.

vary only slightly (e.g. $g_{1A} = 2.00339$ and $g_{1B} = 2.00341$). The ^1H coupling constants were obtained from ENDOR spectra at various temperatures (Table 1).

The assignment of the coupling constants in phenanthrene semiquinones is known[2, 5] and can be applied to the tin chelates. This was confirmed by the determination of their relative signs. This means large values of the coupling constants for the positions 1, 3, 6, and 8, but small ones for the positions 2, 4, 5, and 7. However, the equivalence of the positions 1/8, 2/7, 3/6, and 4/5 is lifted in the tin complexes, because the semiquinones are axial-equatorially bound. Thus for each of the radicals **1A–6A** with achiral tin components four small ($|a| < 1$ G) and four large ($|a| > 1$ G) couplings are expected. The complexes **1B** and **2B** must behave completely analogously, as in these cases the phenanthrene moiety is achiral. The ENDOR spectra of these compounds do not, however, show the theoretical number of lines in all cases because of coincidental degeneracy; nevertheless there are always enough lines to exclude rapid permutation isomerization.

The spectra of the radicals **3B–5B** at 213 K show up to seven large couplings (Table 1 and Fig. 2, top spectrum), so that the diastereomeric complexes, which arise from a combination of helical semiquinones with chiral organometallic

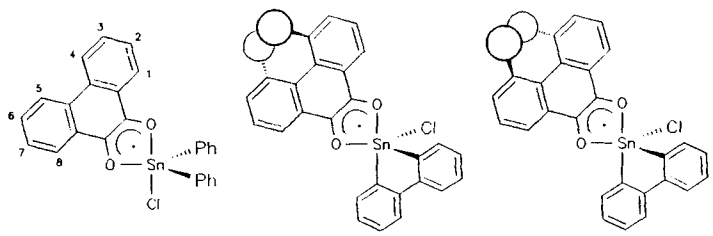

IA (*P,S*)-IIB (*M,S*)-IIB

[*] Prof. Dr. H. B. Stegmann, M. Mäurer, Prof. Dr. K Scheffler
Institut für Organische Chemie der Universität
Auf der Morgenstelle 18, W-7400 Tübingen 1 (FRG)
Prof. Dr. A. Mannschreck
Institut für Organische Chemie der Universität Regensburg (FRG)

[**] This work was supported by the Deutsche Forschungsgemeinschaft and the Fonds der Chemischen Industrie. ENDOR = Electron Nuclear Double Resonance.

Table 1. ENDOR data of **1A–7B** [a].

Radical	T [K]	^{1}H Couplings [G], assigned to the positions 2,4,5,7				1,3,6,8						
1A	213	0.26	0.38	0.49	0.63	1.72	2.27	2.34				
	253	0.26	0.39	0.50	0.63	1.71	2.27	2.35				
1B	213	0.24	0.35	0.51	0.64	1.66	2.26	2.36				
	253	0.24	0.34	0.52	0.64	1.65	2.28	2.37				
2A	213	0.16	0.41	0.66		1.73	2.00	2.26	2.72			
	253	0.16	0.41	0.66		1.72	1.99	2.25	2.71			
2B	213	0.15	0.40	0.67		1.67	1.91	2.26	2.72			
	253	0.13	0.41	0.67		1.65	1.91	2.27	2.71			
3A	213	0.24	0.45	0.73		1.81	1.94	2.50	2.58			
	253	0.24	0.46	0.73		1.80	1.93	2.49	2.57			
3B	213	0.24	0.47	0.73		1.71	1.84	1.93	2.53	2.60		
	253	0.24	0.47	0.74		1.71	1.85	2.53				
4A	213	0.27	0.48	0.74		1.93	2.06	2.53	2.81			
	253	0.27	0.49	0.75		1.90	2.05	2.52	2.80			
4B	213	0.26	0.49	0.74		1.82	1.92	2.03	2.47	2.56	2.75	2.85
	253	0.25	0.50	0.75		1.82	1.96	2.52	2.80			
5A	213	0.24	0.46	0.71		1.77	1.98	2.46	2.58			
	253	0.24	0.45	0.71		1.75	1.97	2.45	2.57			
5B	213	0.23	0.46	0.72		1.67	1.75	1.87	1.95	2.44	2.52	2.61
	253	0.23	0.46	0.71		1.68	1.89	2.47	2.58			
6A [b]	213	0.24	0.46	0.50	0.72	1.92	2.12	2.49	2.89			
	253	0.24	0.47	0.72		1.91	2.09	2.50	2.87			
7A [c]	213	0.63	0.82	0.92	1.17	2.50	3.19					
	253	0.62	0.84	1.12		2.47	3.18					
7B [c]	213	0.60	0.82	1.10		2.41	3.16					
	253	0.59	0.81	1.05		2.38	3.16					

[a] All compounds were studied in toluene. The experimental error in proton couplings is ca. 0.02 G, and the difference between two couplings of a diastereomeric pair 0.01 G. In some spectra an additional small coupling of 0.03 to 0.05 G is observed, which is assigned to the aryl protons at tin. [b] **6B** gave no reproducible ENDOR spectra. [c] The couplings up to 1.2 G were assigned to positions 2 and 7 and to the methylene protons, the couplings > 1.2 G to positions 1 and 8.

components, can be recognized by their different proton couplings. Theoretically, in the case of the diastereomeric pairs of enantiomers *M,R/P,S* and *P,R/M,S* four splittings with $|a| > 1$ G are expected, for each species, leading to a total of eight large couplings. They could, however, not be resolved completely. Nevertheless, in all examples the number of experimentally observed splittings is higher than four.

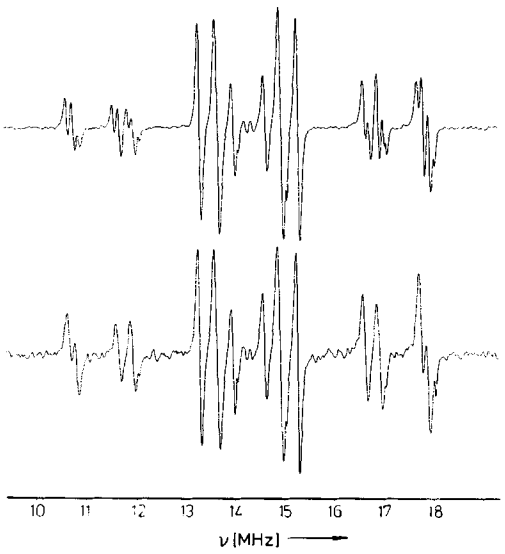

Fig. 2. ENDOR spectra of **5B** in toluene at 213 K (top) and 253 K (bottom).

The coupling constants of the diastereomers differ by ca. 100 mG, which is about 5% of the total. Such small differences can not be found for couplings with $|a| < 1$ G because of the line widths (Fig. 2, top spectrum). At 233 K only a maximum of four incompletely resolved peaks were observed in the range where large couplings are to be found. At 253 K nothing suggests the presence of diastereomers of **3B–5B** any more (Fig. 2, bottom spectrum). As the line widths are largely independent of temperature, the conclusion is that already at 253 K a rapid interconversion between the diastereomers takes place. The free activation enthalpy is estimated from the coalescence temperature of ca. 240 K to be approximately 33 kJ mol^{-1}.

Since the permutation isomerization at tin could be excluded, a rapid conformational interchange at the phenanthrene moiety must be assumed. Thus the barrier for the enantiomerization of the semiquinones must have been substantially lowered on going from the phenanthrene quinone to the semiquinone chelate. The change in the double-bond character between C4a and C4b, less twisting of the ligand by chelate formation, the decrease of the O–O distance and the concomitant stretching of the C4a–C4b bond are perhaps reasons for the lower barrier.

In the radical **7A** only two large proton couplings are observed, which must be assigned to the hydrogen atoms in positions 1 and 8. The diastereomeric effects should therefore be particularly easy to detect when comparing **7A** with **7B**. With ^{1}H NMR spectroscopy and LC, however, no proof for the helicity of 7 could be found.[1b] This is in good agreement with the EPR studies on the thallium complexes.[2b] Correspondingly, the barrier for enantiomerization of the semiquinone chelate is now so low that no evidence for diastereomers can be found, even at 213 °C.

Till now different EPR couplings of diastereomeric radicals were rationalized mainly on the grounds of different hyperconjugation angles of corresponding β protons.[6, 7] As compounds **3B–5B** have either α protons or freely rotatable methyl groups to serve as probes, this explanation cannot hold for the helical phenanthrene quinones. Therefore the differences must be caused by the spin polarization and/or the spin density distribution. Since the diastereomers **4B** differ in both their α and their β couplings, it is more likely that the stereomers have different distribution functions for the free electron. A possible reason for this is the different orientation of the Cl atom in relation to the π electron system of the phenanthrene moiety and the resulting difference in orbital interaction.

Experimental Procedure

The samples were prepared by mixing approximately equivalent amounts of quinone and organotin chloride in toluene in an EPR tube and flushing with nitrogen for several minutes. In some cases the sample was also irradiated with light from a mercury vapor lamp. The EPR spectra were recorded on a Varian E 12 EPR spectrometer, ENDOR and TRIPLE spectra on a Varian E line EPR spectrometer fitted with a Bruker ENDOR ER 810 unit and Bruker ER 140 data system (typical instrument parameters: microwave output 5 mW, RF output 7 dB, 500 W, modulation 30 kHz, 20 scans).

Received: December 21, 1990 [Z 4352 IE]
German version: *Angew. Chem. 103* (1991) 588

CAS Registry numbers:
1A, 132776-44-4; **1B**, 132776-51-3; **2A**, 132776-45-5; **2B**, 132776-52-4; **3A**, 132776-46-6; **3B**, 132776-53-5; **4A**, 132776-47-7; **4B**, 132776-54-6; **5A**, 132776-48-8; **5B**, 132776-55-7; **6A**, 132776-49-9; **7A**, 132776-50-2; **7B**, 132776-56-8.

[1] a) A. Mannschreck, E. Hartmann, H. Buchner, D. Andert, *Tetrahedron Lett. 28* (1987) 3479; b) E. Hartmann, *Dissertation*, Universität Regensburg 1988.
[2] a) H. B. Stegmann, H. Dao-Ba, M. Mäurer, K. Scheffler, H. Buchner, E. Hartmann, A. Mannschreck, *Magn. Reson. Chem. 26* (1988) 547; b) H. Dao-Ba, *Dissertation*, Universität Tübingen 1987.
[3] H. B. Stegmann, M. Sadowski, P. Schuler, K. Scheffler, *J. Organomet. Chem. 339* (1988) 81.
[4] The phenanthrenequinones were provided by H. Buchner (*Dissertation*, Universität Regensburg 1988, p. 155; **2**), E. Hartmann (see [1b]; **3**, **4**, **5**), R. Allmeier (Universität Regensburg; **6**), and F. Dallacker and M. T. Sommer (*Chem.-Ztg. 108* (1984) 329; **7**).
[5] B. Kirste, *Habilitationsschrift*, Freie Universität Berlin 1985; *Magn. Reson. Chem. 25* (1987) 166.
[6] Y. Kotake, K. Kuwata, E. G. Janzen, *J. Phys. Chem. 83* (1979) 3024 and references cited therein.
[7] M. Mäurer, H. B. Stegmann, *Chem. Ber. 123* (1990) 1679.

Ab initio Calculations on the $(ClAuPH_3)_2$ Dimer with Relativistic Pseudopotential: Is the "Aurophilic Attraction" a Correlation Effect?

By *Pekka Pyykkö** and *Yongfang Zhao*

Schmidbaur et al. and *Jansen*[1,2] have recently found empirical evidence for an $Au^I \cdots Au^I$ "aurophilic" attraction of about -30 kJ/mol (-0.011 a.u.), leading to secondary metal–metal bond lengths of about 300–340 pm. A 5d6s6p hybridization,[3] analogous to the 3d4s4p one discussed for $Cu \cdots Cu$,[3a] was proposed as a possible mechanism. No earlier ab initio calculations are known to us.

We therefore carried out calculations with GAUSSIAN 90 on a $(ClAuPH_3)_2$ dimer in parallel (C_{2v}), perpendicular (C_2) and antiparallel (C_{2h}) configuration (Scheme 1). The 5d6s6p double-zeta, 11 valence-electron "LANL1DZ" quasirelativistic pseudopotential of *Hay* and *Wadt*[4] is used in Gaussian 90 at HF, MP2 and MP3 levels. For Au_2 this potential gives a calculated R_e of 267.1, 264.9 and 265.9 pm at the Hartree-Fock (HF), MP2 and MP3 level, respectively, compared to the experimental value of 247.2 pm.[5]

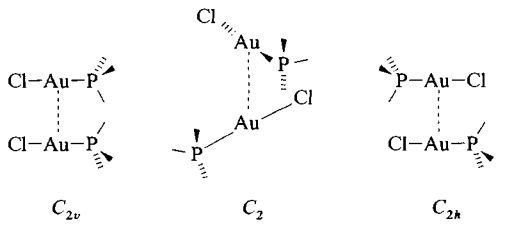

Scheme 1. Calculated configuration of $(ClAuPH_3)_2$.

The C_{2v} and C_{2h} HF curves in Figure 1a are dominated by electrostatic dipole–dipole interactions, dependent on the orientation chosen. In the crossed, C_2 case, a weak attraction of about -0.02 Hartree is found. The Au–Au overlap populations are small and negative for all three geometries (-0.026 for C_2 symmetry at $R = 350$ pm). Thus, the experimental attraction is not reproduced at the HF level. Note the existence of the attraction for both planar and rotated, symmetrical $(LAuL)_2$ systems,[2] where no dipole–dipole interactions occur. The first non-vanishing electrostatic term is the quadrupole–quadrupole one.

The MP2 and MP3 curves in Figure 1b closely agree, suggesting convergence of the Møller-Plesset perturbation series. Correlation effects are attractive for all three geometries and lead to comparable attractive wells for the C_2 and C_{2h} geometries. The parallel, C_{2v} curve still remains repulsive. The C_2 (MP2) well depth of -0.019 Hartree at 300 pm, is comparable with *Schmidbaur*'s surmised interaction. In the antiparallel case, the depth of the (MP2) minimum is -0.026 Hartree at 370 pm.

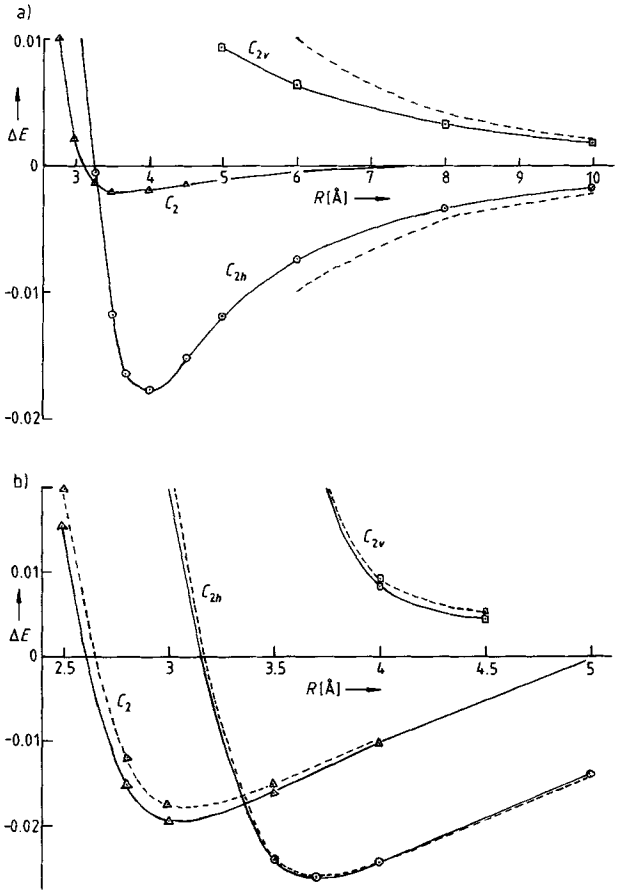

Fig. 1. Calculated interaction energies ΔE [Hartree] for the dimer $ClAuPH_3$ in parallel (C_{2v}), perpendicular (C_2) and antiparallel (C_{2h}) configurations. The two Cl-Au-P-"H" planes of the C_2 case are parallel (see Scheme 1). R = Au–Au. a) — HF calculation; - - - classical dipole-dipole interaction corresponding to the HF dipole moment μ (of the monomer $\pm \mu^2/R^3$). b) — MP2; - - - MP3.

Experimentally the Au–A distance is 344.0(1) pm in the antiparallel dimer of **1**,[6] 336 pm in **2** with almost perpendicular P–Au–Cl unit,[7a] 300 pm in **3**, in which the phosphino groups are covalently bound,[1] and on average 313 pm in **4**.[7b] The two compounds **3** and **4** with parallel P–Au–Cl units give an impression of dipole repulsion and Au–Au attraction.

We have only tried to analyze the nature of the correlation effects by omitting the Au 6p functions from the base in a single case, the C_{2h} geometry for $R = 370$ pm. This diminished the ΔE_{corr} in Table 1 from -0.0097 to -0.0033 Hartree suggesting a 5d-6p correlation.

If Au is replaced by Ag, the C_2 MP2 well depth diminishes from -0.0194 Hartree at R = 300 pm to -0.0115 Hartree

[*] Prof. Dr. P. Pyykkö, Assoc. Prof. Y.-F. Zhao [+]
Department of Chemistry, University of Helsinki, Et Hesperiankatu 4, SF-00100 Helsinki (Finland)
[+] Present and permanent address: Institute of Atomic and Molecular Physics, Jilin University, 130023 Changchun (P. R. China).

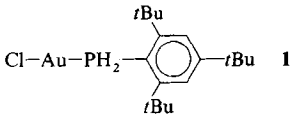

1

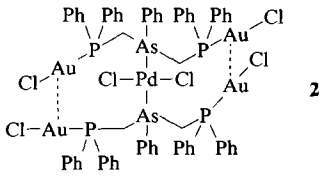

2

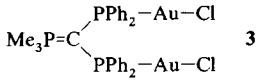

3

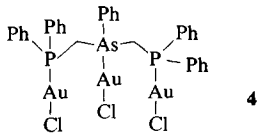

4

at $R' = 320$ pm. As the difference between gold and silver is mainly attributed to relativistic effects,[8] they seem to be important, as originally presumed.[1]

Table 1. The interaction energies ΔE and correlation contributions ΔE_{corr}[Hartree] for two monomers in the C_{2h} configuration with $R = 370$ pm, calculated with and without Au 6p functions in the basis set.

	ΔE(HF)	ΔE(MP2)	ΔE_{corr}
With 6p	− 0.165	− 0.0261	− 0.0097
Without 6p	− 0.0199	− 0.0232	− 0.0033

We conclude that the expected attraction is indeed there, but caused by correlation effects and strengthened by relativitic effects, rather than caused by hydridization. A similar conclusion on considerable correlation shortening of the Cu ··· Cu distance was found by *Kölmel* and *Ahlrichs*.[7] An extended Hückel hybridization picture[3] only holds in the allegorical sense that EHT include correlation effects. The eventual role of these correlation effects in the $(XAu_n)^{m\oplus}$ clusters, which were already calculated at the HF level,[10] remains to be studied. So do the systematic trends of the Au–Au distances and the detailed analysis of the correlation.

Received: November 27, 1990 [Z 4296 IE]
German verison: *Angew. Chem. 103* (1991) 622

CAS Registry numbers:
$ClAuPH_3$, 132912-07-3; Au, 7440-57-5.

[1] H. Schmidbaur, W. Graf, G. Müller, *Angew. Chem. 100* (1988) 439; *Angew. Chem. Int. Ed. Engl. 27* (1988) 417.
[2] H. Schmidbaur, *Gold Bull. 23* (1990) 11; M. Jansen, *Angew. Chem. 99* (1987) 1136; *Angew. Chem. Int. Ed. Engl. 26* (1987) 1098.
[3] a) P. K. Mehrotra, R. Hoffmann, *Inorg. Chem. 17* (1978) 2187; b) Y. Jiang, S. Alvarez, R. Hoffmann, *ibid. 24* (1985) 749; c) K. M. Merz, Jr., R. Hoffmann, *ibid. 27* (1988) 2120; d) A. Dedieu, R. Hoffmann, *J. Am. Chem. Soc. 100* (1978) 2074.
[4] P. J. Hay, W. R. Wadt, *J. Chem. Phys. 82* (1985) 270.
[5] K. P. Huber, G. Herzberg: *Constants of Diatomic Molecules*, Van Nostrand, New York 1979.
[6] H. Schmidbaur, G. Weidenhiller, O. Steigelmann, G. Müller, *Chem. Ber. 123* (1990) 285.
[7] a) A. L. Balch, E. Y. Fung, M. M. Olmstead, *Jnorg. Chem. 29* (1990) 3203; b) *J. Am. Chem. Soc. 112* (1990) 5181.
[8] J. P. Desclaux, P. Pyykkö, *Chem. Phys. Lett. 39* (1976) 300; P. Pyykkö, J. P. Desclaux, *Acc. Chem. Res. 12* (1979) 276.
[9] C. Kölmel, R. Ahlrichs, *J. Phys. Chem. 94* (1990) 5536.
[10] P. Pyykkö, Y. Zhao, *Chem. Phys. Lett.* (in press).
[11] In the caluclations on the Cray X-MPEA/432 at the Center for Scientific Computing, Espoo (Finland), the following parameters were used for the monomer $ClAuPH_3$: Cl-Au 229, Au-P 224, P-H 136 pm, Au-P-H 122.53°.

A Novel Phosphorus Chalcogenide: P_2Se_5 **

By *Roger Blachnik,* Hans-Peter Baldus, Peter Lönnecke,* and *Bruce W. Tattershall**

Dedicated to Professor Marianne Baudler on the occasion of her 70th birthday

P_4E_3[1, 2] and its derivatives α-$P_4E_3X_2$ **1** and β-$P_4E_3X_2$ (E = S, Se; X = halogen, pseudohalogen or similar groups)[3–6] contain four phosphorus atoms in an approximately tetrahedral arrangement. Replacement of one PI group of $P_4Se_3I_2$ by Se affords the structurally similar P_3Se_4I **2**,[7] while replacement of both PI groups by Se affords P_2Se_5 **3**, described here. The bicyclic species **3** contains only two three-coordinate phosphorus atoms, in bridgehead positions.

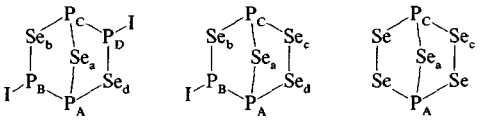

1 **2** **3**

The selenide **3** was observed as a decomposition product of the monoiodide **2** in CS_2 solutions. By annealing a P_2Se_5 glass above the glass temperature and prolonged extraction with CS_2, we have now been able to prepare **3** in pure form. **3** crystallizes as black needles and can be recrystallized from CS_2.[8]

For determination of the structure the ^{31}P- and ^{77}Se-NMR spectra of **3** were analyzed and the coupling constants compared with those of the known compounds **1** and **2**. Three kinds of isotopomers of **3** were observed in the ^{31}P-NMR spectrum: the ^{31}P-resonance signal of the ^{77}Se-free isotopomers **3** at $\delta = 104.95$ is flanked by two ^{77}Se satellite spectra (Fig. 1), which are due to a differing occupation of Se positions in P_2Se_5 by ^{77}Se. The isotopomers **3c**, which contain ^{77}Se nuclei in the diselenide bridges (Se_c), give rise to ABX spin systems; the isotopomers **3a**, with ^{77}Se in the monoselenide bridges (Se_a), give rise to A_2X spin systems. The measured ratio of integrals of the satellite spectra (**3c**:**3a** = 4.02:1) correlates well with the expected ratio of

[*] Prof. Dr. R. Blachnik, Dr. H.-P. Baldus, Dipl. Chem. P. Lönnecke
Institut for Anorganische Chemie (FB Biologie-Chemie) der Universität Barbarastr. 7, W-4500 Osnabrück (FRG)
Dr. B. W. Tattershall
Department of Chemistry, The University
Newcastle upon Tyne NE1 7RU (UK)

[**] This work was supported by the DAAD (ARC Program) and the Deutsche Forschungsgemeinschaft. We thank Dr. *M. N. S. Hill* (Newcastle) for obtaining the NMR spectra.

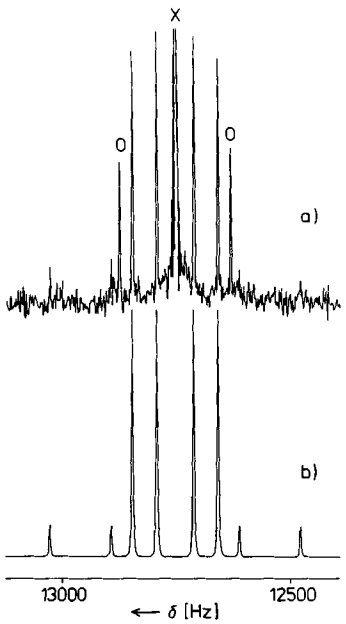

Fig. 1. ^{31}P-NMR spectrum of P_2Se_5 at 121.5 MHz. a) Observed spectrum (X: isotopomers **3** without ^{77}Se. O: isotopomers **3a**). b) Calculated spectrum of isotopomers **3c**.

4:1. The four intense signals of the AB part in the ^{31}P-NMR spectrum, and the three intense signals of the X part in the ^{77}Se-NMR spectrum (Fig. 2), are easily recognizable for the isotopomers **3c**, as is the ^{31}P doublet of the A_2X spin system of isotopomers **3a**. To find all of the less intense signals, long measuring times (^{31}P, 16 h; ^{77}Se 64 h), saturated solutions, and 10-mm NMR tubes had to be used. The spectra of **3a** and **3c** were fitted by computer[9] to yield the NMR parameters.[8]

The coupling constants $^2J(P_AP_C)$ increase monotonically (87.2 for **1**, 121.0 for **2**, and 181.0 Hz for **3c**), as the replacement of P_D and/or P_B by the larger selenium atoms widens the bond angle at Se_a. The ^1J(PSe) couplings to Se_a show a similar trend: -279.6 ($^1J(P_ASe_a)$ in the α-$P_4Se_3I_2$ isotopomers **1a**), -267.6 (mean value of $^1J(P_ASe_a)$ and $^1J(P_CSe_a)$ in the P_3Se_4I isotopomers **2a**) and -243.5 Hz ($^1J(P_ASe_a)$ in the P_2Se_5 isotopomers **3a**). Similar, albeit less extreme, changes are observed when sulfur is replaced by selenium, or phosphorus replaced by arsenic, in P_4S_3 compounds.[10] The $^1J(P_CSe_c)$ coupling in the isotopomers **3c** (-283.6 Hz) is very similar to that in the P_3Se_4I isotopomers **2c** (-286.1 Hz). In solutions of **2** at room temperature an intramolecular exchange takes place which can be suppressed only at low temperatures.[7] The solubility of **2** in CS_2 is then, however, so sparing that the parameter $^2J(P_ASe_c)$ is not determinable. The corresponding values of $^2J(P_ASe_c)$ for P_3Se_4Cl and P_3Se_4Br are 17.0 and 16.5 Hz respectively, which are comparable with the corresponding coupling in isotopomers **3c** (14.7 Hz). The secondary isotope shifts for **3** correlate well with those of α-$P_4Se_3I_2$ [$^1\Delta P_A(Se_a) = 0.0062$, $^1\Delta P_C(Se_b) = 0.0047$ and $^2\Delta P_A(Se_b) = 0.0024$ ppm].

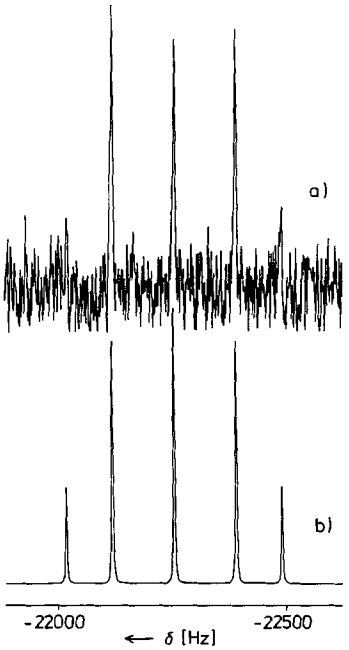

Fig. 2. ^{77}Se-NMR spectrum of isotopomers **3c** at 57.3 MHz. a) Observed and b) calculated spectrum.

Berzelius[11] presumed the existence of P_2Se_5, and there has been no lack of attempts[12] to prepare the compound by direct synthesis from the elements. In all the cases so far it was formed as an amorphous insoluble solid, whose structure was first investigated only recently. *Monteil* and *Vincent*[13] concluded that, in analogy to P_4S_{10}, a P_2Se_5 glass of P_4Se_{10} moieties should be formed. To support this hypothesis an IR absorption band at 500 cm^{-1} was assigned to a P=Se double bond. This band becomes more intense through the action of water vapor on crystalline P_2Se_5 and on glasses which were prepared according to *Monteil* and *Vincent* from P_4Se_3 and Se, and it should probably be assigned to a decomposition product. ^{77}Se-isotopomers of P_4Se_{10} would give NMR spectra with the spin systems AB_3X (exocyclic ^{77}Se) and A_2B_2X (endocyclic ^{77}Se), with which the ^{31}P- and ^{77}Se-NMR signals observed for our soluble product are not reconcilable. Moreover, ions with a higher m/z ratio than the molecular ion $P_2Se_5^{\oplus}$ were not observed in mass spectra of P_2Se_5 solutions. The first detailed investigation of the structure of P-Se glasses was carried out by *Price* et al.[14] According to their observations a P_2Se_5 glass consists predominantly of P_4Se_5 moieties, which are coupled to each other via selenium atoms or chains. They could unequivocally rule out P_4Se_{10} moieties. We presume that in the polymeric matrix of such glasses, isolated P_2Se_5 molecules or very similar, less cross-linked moieties are present which can be removed from the matrix by extraction with CS_2.

The phosphorus selenide **3** (P and Se in the stoichiometric ratio 2:5) does not have a P_4X_{10} structure. It exhibits a different type of structure from other phosphorus-chalcogen systems. An increase in chalcogen content in the phosphorus-selenium system does not lead to a larger coordination number of the phosphorus due to exocyclic selenium atoms, but instead the threefold coordination of the phosphorus remains unchanged, and the increased selenium content appears in the form of two diselenium bridges.

Experimental

Red phosphorus (0.762 g; 24.6 mmol; Knapsack) and selenium (4.858 g; 61.5 mmol; Retorte) were sealed in an evacuated quartz ampoule. A homogeneous melt was obtained by heating for ten days at 400 °C. The ampoule was quenched in ice-water, the product pulverized, resealed, and annealed for four months above the glass temperature of 100 °C. The subsequent CS_2-extraction was accomplished by several days stirring of the pulverized product with 200 mL CS_2 at room temperature. Filtration of the straw colored solution and cooling to -50 °C afforded the first crystal fraction. The supernatant liquid was reunited with the crude product and the extraction repeated five times. All

operations were carried out under inert gas. Yield: 0.32 g P_2Se_5 **3** (5.62% of the roretical).

Received: October 1, 1990 [Z 4220 IE]
German version: *Angew. Chem. 103* (1991) 620

[1] Y. C. Leung, J. Waser, S. van Houten, A. Vos, G. A. Wiegers, E. H. Wiebenga, *Acta Crystallogr. 10* (1957) 574.
[2] E. Keulen, A. Vos, *Acta Crystallogr. 12* (1959) 323.
[3] G. W. Hunt, A. W. Cordes, *Inorg. Chem. 10* (1971) 1935.
[4] G. J. Penney, G. M. Sheldrick, *Acta Crystallogr. Sect. B 26* (1970) 2092.
[5] R. Blachnik, G. Kurz, U. Wickel, *Z. Naturforsch. B 39* (1984) 778.
[6] B. W. Tattershall, *J. Chem. Soc. Dalton Trans.* 1987, 1515.
[7] R. Blachnik, W. Buchmeier, C. Schneider, U. Wickel, *Z. Naturforsch. B 42* (1987) 47.
[8] **3**: IR(CsI): ν[cm^{-1}] = 500 m, 389 s, 358 vs, 322 w, 310 s, 245 w, 220 w. ^{31}P NMR (121.5 MHz, 85% H_3PO_4, CS_2, 25 °C): δ = 104.95; ^{77}Se NMR (57.3 MHz, sat. H_2SeO_3, CS_2, 25 °C): δ = − 408.24 (Se(a)), − 388.28 (Se(c));, ^1J(P(A)Se(a)) = − 243.49(6) Hz, ^1J(P(C)Se(c)) = − 283.6(3) Hz, ^2J(P(A)Se(c)) = 14.7(7) Hz, ^2J(P(A)P(C)) = 181.0(2) Hz; secondary isotope shifts of the ^{77}Se-containing isotopomers, relative to the ^{31}P main spectrum: $^1\Delta$P(A)(Se(a)) = + 0.0046, $^1\Delta$P(C)(Se(c)) = + 0.0044 and $^2\Delta$P(A)(Se(c)) = + 0.0013 ppm. MS (EI, 70 eV): *m/z* 458 ($P_2Se_5^{\oplus}$, 13%), 300 ($P_2Se^{\oplus}$, 24), 222 ($P_2Se_2^{\oplus}$, 5), 191 ($PSe_2^{\oplus}$, 9), 160 ($Se_2^{\oplus}$, 20), 142 ($P_2Se^{\oplus}$, 13) 111 ($PSe^{\oplus}$, 100).
[9] Programm *NUMARIT*, S.E.R.C. NMR. Program Library, Daresbury.
[10] B. W. Tattershall, R. Blachnik, H. P. Baldus, *J. Chem. Soc. Dalton Trans. 1989*, 977.
[11] J. J. Berzelius in *Gmelins Handbuch der anorganischen Chemie*, System No. 9–12, Verlag Chemie, Leipzig 1942, p. 244.
[12] M. V. Kudchadker, R. A. Zingaro, K. J. Irgolic, *Can. J. Chem. 46* (1968) 1415.
[13] Y. Monteil, H. Vincent, *Z. Anorg. Allg. Chem. 428* (1977) 259.
[14] D. L. Price, M. Misawa, S. Susman, T. I. Morrison, G. K. Shenoy, M. Grimsditch, *J. Non-Cryst. Solids 66* (1983) 443.

Blocking of Acidic Centers upon Hydrothermal Dealumination of ZSM-5 Zeolites

By *Manfred Richter**

Treatment of the ZSM-5 zeolites with water vapor at high temperatures removes aluminum from lattice positions and thus reduces the concentration of acidic Brønsted centers.

The question whether the extra-lattice aluminum species (Al_{ex}) block acidic centers of the lattice during the dealumination is controversial. *Vogt* et al.,[1] e.g., reported an increase in the concentration of acidic centers after dealumination with HCl in the case of the zeolite ZSM-5. Apparently, the acid treatment leads to the extraction of Al_{ex} and thus to exposure of lattice Brønstedt centers. *Mavrodinova* et al. report analogous findings in the case of the zeolite US-Y: on the basis of the NH_3 thermodesorption, after extraction of Al_{ex} both an increase of the total concentration of acidic centers as well as a modification of the distribution of acidity is observed. The authors concluded that Al_{ex} species partially neutralize lattice Brønsted centers. In the case of the ZSM-5 zeolites T3 and HS 30 (Chemie AG, Bitterfeld), which were synthesized without organic templates, IR spectroscopic investigations and NH_3-thermodesorption[3, 4] show that neither a further dealumination occurs nor does the number of acidic centers increase upon extraction of hydrothermally dealuminated samples with 1 M HNO_3. However, the isomerization of *m*-xylene on samples treated this way leads to higher conversions and to a modified isomeric ratio (smaller amount of *p*-xylene), i.e. to a diminished shape selectivity.[5, 6] This is explained in terms of a partial extraction of Al_{ex} and the associated exposure of blocked centers on the inner and outer surfaces of the zeolite.[6] Since the reaction of *m*-xylene on ZSM-5 zeolites is disguised by internal mass transport effects,[5] which vary according to the concentration of Al_{ex}, it cannot be decided on the basis of activity and selectivity data whether the blocking of acidic centers by Al_{ex} or the exposure of such centers is responsible for the effects observed during the extraction.

The present communication demonstrates for the ZSM-5 zeolites discussed in Refs. [3–6], by checking their catalytic activity, that the extraction of Al_{ex} does not expose acidic centers, and therefore the prior hydrothermal dealumination has not blocked acidic centers. The isomerization of *m*-xylene and the conversion of ethylbenzene served as test reactions. Due to the smaller kinetic diameter of the ethylbenzene the latter reaction is not disguised by internal mass transport effects.

Starting from the NH_4-form of the template-free synthesized ZSM-5 zeolite HS 30, samples with various degrees of dealumination by hydrothermal treatment were prepared and the catalytic activity of the dealuminated samples and of the untreated zeolite were determined, both without as well as after extraction with 2 M HNO_3 (385 K, 2 h). Further details of the experimental determination of the Si/Al(lattice) ratio, of the acidity characterization, and of the measurements of the catalytic activity are given in the References [4–6, 8]. The samples investigated here are listed in Table 1.

Table 1. Zeolite samples investigated[a]

Sample	1	2	3	4
Treatment	2 h, 775 K	hydrothermal treatment at 775 K		
	shallow bed	1 h[b]	3 h	6 h
Si/Al (lattice)	20.0	31.0	51.5	75.4
Al_{ex} (total)[c]	0.088	0.359	0.562	0.660
Al_{ex} (extr.)[d]	0.021	0.025	0.11	0.153

[a] Starting material was the ZSM-5 zeolite H530 in the NH_4-form, Si/Al (lattice) = 20. [b] Additional calcination 2 h at 775 K under shallow bed conditions (ca. 2 cm layer height). [c] Concentration of Al_{ex} after dealumination, data in mmol Al g^{-1}, total Al content 0.871 mmol g^{-1}. [d] Amount of the soluble Al_{ex} in mmol g^{-1} after extraction with 2 M HNO_3 (385 K, 2 h).

The isomerization of *m*-xylene on the zeolite samples shows (Fig. 1a) that at Si/Al (lattice) ratios > 30 the conversions decrease, the extraction of about 20% of Al_{ex} (cf. Table 1) however increase the conversions by maximally 20%. Since a loss of activity on continuing dealumination is unavoidable (the concentration of acidic centers is reduced by the transformation of Al of the zeolite lattice into Al_{ex}), the influence of an additional blocking of acidic centers by Al_{ex} cannot be estimated. The higher activity of the extracted samples would be reconcilable with the concept that the extraction of Al_{ex} exposes acidic centers. The lower shape selectivity after the extraction (lower *p*-/*o*-xylene ratio (Fig. 2) would come about by the exposure of blocked centers on the outer zeolite surface, which is not shape-selective. This interpretation is not tenable however if one takes into consideration the results of the ethylbenzene conversion under the same conditions (Fig. 1b). In the case of the ethylbenzene conversion an extraction of acid-soluble Al_{ex} species has no recognizable influence on the activity of the samples, i.e. acidic centers are apparently not exposed by the extraction.

[*] Dr. M. Richter
Institut für Physikalische Chemie, Bereich Katalyse
Rudower Chaussee 5, O-1199 Berlin-Adlershof (FRG)

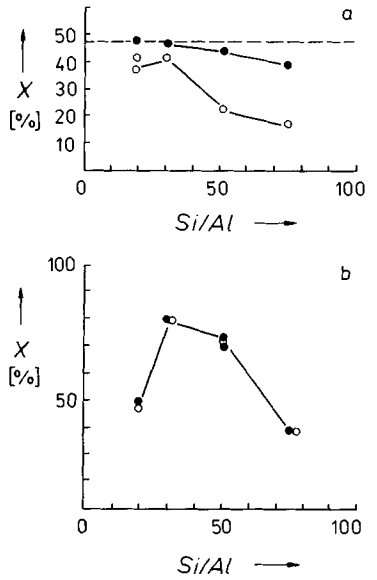

Fig. 1. Dependence of the conversion X of *m*-xylene (a) and ethylbenzene (b) on the Si/Al (lattice) ratio of the ZSM-5 zeolites. o samples dealuminated, not extracted, • samples dealuminated, extracted. Reaction conditions: normal pressure flow reactor, carrier gas N_2 (10 L h^{-1}, 1 vol % C_8), 1 g zeolite (without binder), reaction temperature 623 K. – – – thermodynamic equilibrium conversion of the *m*-xylene at 623 K [12].

A blocking of these centers by the Al_{ex} species formed in the hydrothermal dealumination can therefore be ruled out (under the plausible assumption that both test reactions take place, in principle, at the same acidic centers). The activity maximum, which is observed for all samples in dependence on the Si/Al ratio, could, as in the case of *n*-hexane conversion on the H form of ZSM-5,[9, 10] be attributed to a special

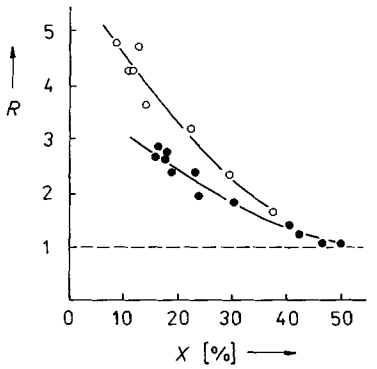

Fig. 2. Ratio R of the *p*-/*o*-xylene formation as a function of the *m*-xylene conversion for Sample 4. o sample dealuminated, not extracted, • sample dealuminated, extracted. Reaction temperature 573 K. Conversion was changed by variation of residence time. – – – thermodynamic equilibrium value at 573 K [12].

interaction of the substrate with Brønsted centers and Al_{ex} species. Since the dependence of the activity on the Si/Al (lattice) ratio of the zeolite does not change, even after extraction of the soluble Al_{ex} species, it is conceivable, as in the case of the substrate *n*-hexane, that insoluble Al_{ex} species are decisive for the modified interaction of the substrate with the active centers. Hence, the following conclusions can be drawn:

1. The modification of activity/selectivity in the isomerization of *m*-xylene is only apparently determined by a blocking or exposure of acidic centers on the internal/external surfaces of the ZSM-5 zeolites.

2. The results of the ethylbenzene conversion confirm the IR spectroscopic[3, 4] and the NH_3-desorption data:[4] an extraction of Al_{ex} neither exposes acidic centers nor leads to the formation of new acidic sites.

3. The modification of activity/selectivity in the isomerization of *m*-xylene is obviously a result of the mass transport influenced by Al_{ex}. This not only concerns the diffusion of the isomers but also the movement of *m*-xylene in the pore system. The reaction takes place in the range of internal diffusion as is suggested by the activation energy for the *m*-xylene conversion.[5] Since *p*-/*o*-xylene values above the thermodynamic equilibrium ratio (Fig. 2) are also observed on the extracted catalysts, the mass transport barriers are still not completely removed with the removal of the acid-soluble Al_{ex} species.

Received: December 20, 1990 [Z 4348 IE]
German version: *Angew. Chem. 103* (1991) 606

[1] F. Vogt, K.-P. Wendtlandt, J. J. Isakov, T. A. Isakova, C. M. Minacev, *Z. Anorg. Allg. Chem. 563* (1988) 127–135.
[2] V. Mavrodinova, V. Penchev, U. Lohse, H. Stach, *Zeolites 9* (1989) 197–202.
[3] E. Löffler, C. Peuker, H.-G. Jerschkewitz, *Catal. Today 3* (1988) 415–420.
[4] G. Öhlmann, H.-G. Jerschkewitz, G. Lischke, B. Parlitz, M. Richter, R. Eckelt, *Z. Chem. 28* (1988) 161–168.
[5] M. Richter, W. Fiebig, H.-G. Jerschkewitz, G. Lischke, G. Öhlmann, *Zeolites 9* (1989) 238–246.
[6] U. Kürschner, H.-G. Jerschkewitz, E. Schreier, J. Völter, *Appl. Catal. 57* (1990) 167–177.
[7] Starting from the NH_4-form of the zeolite, the hydrothermal treatment is accomplished by passage of water vapor (ca. 1.5 mol h^{-1}) at 775 K for the times quoted in Table 1. In the case of shorter hydrothermal treatment an additional calcination was necessary for complete conversion of the NH_4-form into the H-form. The H-form of the non-dealuminated sample was prepared by thermal decomposition of the NH_4-form.
[8] W. Schwieger, K.-H. Bergk, E. Alsdorf, U. Lohse, B. Parlitz, *Z. Phys. Chem. (Leipzig) 271* (1990) 243–257.
[9] R. M. Lago, E. O. Haag, R. J. Mikovsky, D. H. Olson, S. D. Hellring, K. D. Schmidt, G. I. Kerr in L. Murakami, A. Iijima, J. P. Ward (Hrsg.): *New Developments in Zeolite Science and Technology (Proc. 7th Int. Zeolite Conf. Tokyo 1986)* Elsevier, Amsterdam 1986, S. 677–687.
[10] V. L. Zholobenko, L. M. Kustov, V. B. Kazansky, E. Loeffler, U. Lohse, C. Peuker, G. Öhlmann, *Zeolites 10* (1990) 304–306.
[11] E. Brunner, H. Ernst, D. Freude, M. Hunger, H. Pfeifer, *Stud. Surf. Sci. Catal. 49* (1989) 623–632.
[12] W. W. Kaeding, C. Chu, L. B. Young, B. Weinstein, S. A. Butter, *J. Catal. 67* (1981) 159–174.

Book Reviews are written by invitation from the editor. Suggestions for books to be reviewed and for book reviewers are welcome. Publishers should send brochures or (better) books to the following address: Redaktion Angewandte Chemie, Postfach 101161, W-6940 Weinheim, Federal Republic of Germany. The editor reserves the right of selecting which books will be reviewed. Uninvited books not chosen for review will not be returned.

International Encyclopedia of Composites. Volumes 1 and 2. (Six-volume work). Edited by *S. M. Lee*. VCH Publishers, New York/VCH Verlagsgesellschaft, Weinheim 1990. Vol. 1: xvi, 563 pp., hardcover, £ 170.00 (subscription price: £ 156.00).—ISBN 0-89573-731-0/3-527-27947-4. Vol. 2: xii, 524 pp., hardcover, £ 170.00 (subscription price: £ 156.00).—ISBN 0-89573-732-9/3-527-27948-2 (set: 0-89573-290-5/3-527-26852-9)

The field of composites is one of the main research topics of modern materials science. Major advances have been made in the last decade, resulting in a great diversification of this area of research into many different directions. The factors that have led to this are firstly the considerable advances that have occurred in the production of reinforcing fibers with extraordinary mechanical properties, and secondly the development of new matrix materials and special techniques for producing composites reinforced with fibers, platelets and particles. Fundamental studies on the relationships between the properties of the separate components and those of the composite have provided an important stimulus for composites research. In many fields of application the superiority of composites over conventional materials is so great that one can with justification speak of the beginning of a composites era.

The rapid developments in the area of composites have led to a rapid growth in the number of publications concerned with a wide variety of scientific disciplines. The fact that these publications are so widely scattered makes it difficult to monitor the literature effectively and to coordinate the different disciplines and directions of research. Modern composites technology is the result of many diverse contributions from inorganic, organic and macromolecular chemistry, from research on ceramics and metals, and from mechanical engineering and textile technology. This encyclopedia of composites aims to provide scientists interested in this area with a broad and detailed survey of the current state of research and development. It contains contributions from more than 300 experts engaged in a wide variety of research activities, thus ensuring a comprehensive coverage of the many different aspects of research and development.

The topics treated in these first two volumes range from "Acetal Resins and Composites" to "Joining Polymeric Composites: Adhesives". The majority of the 77 contributions are from industrial research laboratories. Consequently the main emphasis is on results of applied research and on practical aspects of the manufacture of composites and their applications in structural components. When one reflects that large numbers of scientists in Europe and Japan are working in the area of composites, it is surprising that about 90% of the articles in this encyclopedia are from the USA, and there is not a single one from Japan. From this standpoint the name "International Encyclopedia" is not entirely accurate. It is also noticeable that even with most of the experts being drawn from the USA it has not always been possible, at least in some of the areas, to engage the services of those with the highest international reputations.

Despite this restricted selection of authors, most of the contributions have a high information content. The work offers a comprehensive overview for the newcomer to the field of composites, while specialists in particular aspects can use it to broaden their knowledge to include areas outside their immediate experience. The bibliographies attached to the individual articles are extensive in some cases, and enable readers to pursue their own special lines of interest within the topics covered. The encyclopedia can be especially recommended for materials research centers that are mainly concerned with applications-orientated work and engineering aspects.

Wilhelm Ruland [NB 1107 IE]
Fachbereich Physikalische Chemie
und Zentrum für Materialwissenschaft
der Universität Marburg (FRG)

General Chemistry. International Student Edition. By *P. W. Atkins*. Scientific American Inc., 1989 (Suppliers: W. H. Freeman, Oxford). 989 pp., paperback, £ 16.95.—ISBN 0-7167-2053-1

If you should happen to come across this textbook in a bookshop or at a book fair, stop and take a look inside it. It will prove worthwhile! As one who appreciates aesthetic presentation you will admire the exemplary typography and the overall arrangement, and as a scientist used to presenting information visually you will take pleasure in the hundreds of impressive color illustrations, ranging from molecular models that convey a three-dimensional picture, through sectional diagrams of industrial plants, to vivid representations of reaction sequences. The many brilliant photographs would justify a book in themselves; they range from the Crab nebula, the planet Earth and the hole in its ozone layer, and the launching of the space shuttle Atlantis, via a picture of a student holding a plastic cube to show the molar volume of an ideal gas, the coloration of a flame by alkali metal atoms, and indicator solutions on both sides of the transition point, through to a Tiffany glass window, the Stanford linear accelerator and electromicrographs of a silicon surface and of the retina of the eye. In short, leafing through this book will reveal an introduction to chemistry for first-year science students which is exemplary in its quality of production and in the care that has been devoted to presenting information in visual form.

The contents are arranged under five main topics: "Matter and Reactions", "Atoms, Molecules and Ions", "Rates and Equilibrium", "The Elements" and "Organic Chemistry". The book as a whole consists of sections headed "Contents in Brief", "Table of Contents", including "Worked Examples", "Preface" with a note "To the Student", then the above-listed sections grouped under "General Chemistry", followed by "Appendix I: Mathematical Information",

"Appendix II: Experimental Data", "Glossary", "Answers to Odd-Numbered Numerical Exercises", and a detailed "Index" with over 3600 entries. Each of the 24 individual sections has a separate title page, its own introduction, a summary at the end and numerous exercise problems.

As a representative example we may take the topic "Atoms, Molecules and Ions" and consider the treatment in detail. This section consists of three chapters headed "Atomic Structure and the Periodic Table", "The Chemical Bond" and "The Shapes of Molecules". The starting point is the structure of the hydrogen atom, whose emission spectrum is described in the context of the total electromagnetic spectrum, and also in relation to the definition of the photoelectric effect and the ionization threshold. After introducing the de Broglie equation and the Heisenberg uncertainty principle, quantum numbers and the related orbital functions are described. A discussion of atoms with many electrons, their effective nuclear charges and their electron configurations leads to the Periodic System of the elements, quoting selected experimental data on atomic and ionic radii, ionization energies and electron affinities to illustrate the points. The distinction between metals and non-metals, classified into s-, p- and d-block elements, is discussed in terms of their characteristic "periodic" properties and reactions. The formation of ion pairs and ionic lattices is then discussed, illustrated by thermodynamic data and with the help of Born-Haber cycles in some cases, together with "variable valence" effects. Covalent bonds are introduced via the octet rule and are described in terms of Lewis structures; these concepts are related to real situations with the help of space-filling molecular models. The topic of bond enthalpies and lengths leads into a detailed discussion of charge distributions (illustrated in some cases by dipole moments). The third chapter—"The Shapes of Molecules"—begins with arguments based on the repulsion between electron pairs. Regrettably, the author has decided against introducing simple point-group symmetries, and instead devotes an unnecessary amount of space to the fictional description in terms of hybridization. The molecular orbital considerations that follow could with advantage have taken symmetry-adapted bonding orbitals as a starting point rather than partially hybridized atomic orbitals. On the other hand one welcomes the correct discussion of diatomic molecules (with $2p_\pi < 2p_\sigma$) and the description of electron delocalization in terms of molecular orbitals, especially for electron-deficient compounds. Altogether the three chapters contain 278 (!) exercise problems. Despite the comments above regarding alternative ways of presenting concepts, the section viewed as a whole is a lucid and unified introduction to the various aspects of the chemical bond, supported by experimental data, and can therefore be recommended for first-year students. It also provides an excellent foundation for the sections that follow dealing with liquids, solids and solutions.

The sections on "General Chemistry", which include those on chemical kinetics, equilibria, acids and bases and electrochemistry, are clearly presented, mainly experimentally orientated, well illustrated, and mostly excellent from a teaching standpoint. In the opinion of this reviewer, and also of other chemists (see, for example, *Chemistry in Britain 1990,* 357), it is in these that the main strength of the textbook lies. Other textbooks competing for acceptance by students will find them difficult to match.

It is less easy to evaluate the later and rather meager chapters of the book, on "The Elements" (divided into those of the s-, p- and d-blocks with a mere 28, 64 and 32 pages respectively), and on nuclear chemistry and organic chemistry, both of which are likewise disproportionately short, with 32 and only 80 (!) pages respectively. The treatment of organic chemistry is certainly too brief, its length being more appropriate to schools than to first-year undergraduate classes. Without going into further detail, however, one can be more positive about the inorganic part. The clarity of the text and the exemplary visual presentation extend throughout the description of the typical compounds of the various elements, and although the examples are few in number they are chosen with a high degree of topicality. Nevertheless, for the next edition of the book, which must certainly already be at the planning stage, it would be desirable to considerably enlarge the coverage of this field. In this way university teachers, who will probably be very pleased with the general chapters, could be relieved of the necessity to recommend in addition a second textbook orientated more towards chemical substances.

To sum up, if you happen to come across this excellent textbook for first-year science students, allow yourself time to have a closer look at it...

Hans Bock [NB 1128 IE]
Institut für Anorganische Chemie
der Universität Frankfurt am Main (FRG)

Spectroscopy of Matrix Isolated Species. (Series: Advances in Spectroscopy, Vol. 17). By *M. J. Almond* and *A. J. Downs*. Edited by *R. J. H. Clark* and *R. E. Hester*. Wiley, Chichester 1989. xiv, 511 pp., hardcover, £ 111.00.—ISBN 0-471-92170-X

The development of almost every new technique follows a characteristic pattern: the pioneering phase is followed by a period of rapid expansion during which many different laboratories test the limits of the method, then comes a much quieter phase of consolidation. The founding fathers of the technique then go into retirement, their sons are now firmly established, but for the grandsons the technique has become a routine procedure.

This sequence of events applies to matrix isolation spectroscopy. The matrix technique has now become a standard part of the textbooks, and specialists from all over the world have had their seventh successive conference. The doyen of the technique, *Georg Pimentel*, whose pioneering experiments over the last 35 years have had such a great influence and attracted so much interest, died prematurely in the early part of 1989.

This book is the seventeenth in the series "Advances in Spectroscopy". It differs from the normal pattern in being devoted to a single topic, matrix spectroscopy, which is treated by two British authors, *Matthew J. Almond* and *Anthony J. Downs*, in a main text of 185 pages together with many figures. Two-thirds of the book's 511 pages consist of a tabulation of the species investigated between 1977 and 1986, together with a bibliography of 60 pages containing 2250 literature references.

As is so often the case, this is the right book at the wrong time. If it had been published in 1987, or even early in 1988, the impressive and diligent compilation of the bibliography alone would have allowed one to overlook the weak points. However, it has appeared in 1989. In the previous year *David W. Ball* and his collaborators at Rice University in Houston published their excellent "Bibliography of Matrix Isolation Spectroscopy: 1954–1985" (Rice University Press), which is also available as a DBase file on floppy disk. Two years earlier *Martin Moskovits* covered the subject of atoms and small clusters in the book "Metal Clusters" (Wiley-Inter-

science), and the same author in collaboration with *Lester Andrews* published the book "Chemistry and Physics of Matrix-Isolated Species" (North-Holland).

In comparison with these works the weaknesses of the present book cannot be ignored; to the well-informed reader it seems more like a patchwork rug than the product of a single hand. However, even a patchwork rug has its charm.

The introductory chapter (14 pp.) describes the history of matrix isolation; seven of the pages are devoted to a list of all the main books and review articles on the subject, with their titles and the topics covered. Here a disadvantage of the computerized literature searching system becomes apparent: although many obscure papers are cited, some important ones are missing—for example, there is no reference to the book "Cryochemistry" by *Gleb. B. Sergeev* and *Vladimir A. Batyuk* (Mir Publishers, Moscow, 1978), which is the Soviet matrix spectroscopists' "bible". As in many review articles written in the Western world, the coverage of publications originating from the Eastern block is incomplete.

The experimental techniques of matrix isolation spectroscopy have changed little since the publication of the classic works by *Moskovits* and *Ozin* and by *Hallam*. Therefore the second chapter treats the problems of and recent results from the relevant spectroscopic techniques in a condensed form. A three-page table again lists the most important publications. Together with a series of large-format figures the chapter comes to a total of 23 pages.

Chapter 3 (17 pp.) deals with problems of energy transfer in matrices and includes several full-page figures. As a comparison the same topic in the book by *Andrews* and *Moskovits* takes up 33 closely printed pages. The following chapter treats matrix photochemistry in rather more detail; here the authors must be given credit for describing, though briefly and at third hand, the techniques of photolysis in liquid inert gases and flash photolysis with infrared detection that were developed in the early 1980s.

Chapter 5 discusses hydrogen-bonded species and isomerization processes within the matrix, and Chapter 6 deals with ionic and high-energy molecules. The next chapter, on atoms and small clusters, went to press at a time when the subject had already been covered in a book and several review articles. This is probably why the authors decided to confine their discussion to resonance Raman studies of dimers and trimers and to the iron cocondensation experiments of *Margrave*'s group in Houston. Regrettably there is no mention of the studies on bimetallic clusters that were carried out during the period covered by the report.

The subject of Chapter 8, astrochemistry and atmospheric processes, is one on which only a few groups are working. For this reason it is all the more pleasing to find it discussed here, as a striking illustration of the interdisciplinary application possibilities of the matrix technique.

The rest of the book is almost entirely occupied by four tables which list for each species the method of preparation, the spectroscopic detection method, the main results and the literature references. However, the order of presentation seems a little unsystematic. Thus the reader is left to decide whether to search for a desired molecule among the inorganic species (Table 7, 93 pp.), the organometallic species (Table 8, 41 pp.), or the organic species (Table 9, 95 pp.), or possibly even among the molecular complexes (Table 10, 18 pp.). In cases of doubt it is worth trying a permutation (AgCr appears under CrAg, for example), or better still to look in the more clearly arranged matrix bibliography of *Ball* et al. The literature citations, of which there are nearly 2250, numbered in the sequence of the atoms and molecules under discussion, would undoubtedly be more useful and easier to check if a different method of indexing were used, e.g. by first-named author. It remains a mystery why 63 of the references are listed separately in the middle of the book.

Summary: The book is useful subject to certain limitations, but is not very suitable for beginners in matrix isolation spectroscopy. Nevertheless, as part of the "Advances in Spectroscopy" series it has a place in scientific libraries. For the specialist its strength lies in the critical summaries of research results.

Werner E. Klotzbücher [NB 1109 IE]
Max-Planck-Institut für Strahlenchemie,
Mülheim (FRG)

Houben-Weyl. Methoden der Organischen Chemie. Band E 19a, Parts 1 and 2. C-Radikale. Edited by *M. Regitz* and *B. Giese*. Thieme, Stuttgart 1989. Part 1: pp. 1–716; Part 2: pp. 717–1567, hardcover DM 1960.00 (subscription price: DM 1764.00).—ISBN 3-13-218904-9

Supplementary Volume 19 of "Houben-Weyl" is devoted to "low-valency carbon compounds", i.e. carbon radicals, cations and anions together with carbenes. The preparative chemistry of a class of compounds that in most cases cannot be isolated or even observed—can this really be a true "Houben-Weyl"?

As the opening to this new series on methods for the preparation and conversion of reactive intermediates, Volume 19a, Parts 1 and 2, deals with carbon radicals. This is an indication that the editors of Houben-Weyl attach a particularly high importance to these species, which is not surprising in view of the rapid developments that have occurred in free radical chemistry during the last decade, and the considerable stimulus that this has given to organic synthesis and will continue to do in the future. To anticipate the verdict: since the well-proven Houben-Weyl principle of placing applications to preparative chemistry in the foreground, while keeping the treatment of individual compounds in the background, has been consistently applied, the question posed above can be answered with an unequivocal "yes".

The contents of the volume on carbon radicals are divided into three parts. First there is a brief introduction, in textbook style, to the principles and special features of free radical chemistry (*B. Giese*). This is followed by a section on methods for generating free carbon radicals (*J. O. Metzger*). The last section, which is the most important and the most voluminous, describes the conversion of radicals into products belonging to a wide variety of compound classes (C-X: *J. O. Metzger*; C-C: *A. Ghosez, B. Giese, W. Mehl, H. Zipse*).

This book is therefore unusual in the context of the series, not only because it treats species that are characteristically short-lived, but also because it includes a general discussion of the special properties of these compounds and the factors controlling their reactivities and selectivities, in a separate section orientated towards the non-specialist. The introduction outlines general principles for the successful use of free radical reactions in synthesis, briefly referring to elementary methods for generating and detecting free radicals, and listing some values of activation parameters, ESR coupling constants for typical radicals, and half-lives of commonly used initiators; concepts explained include orbital interactions and even "radical clock" reactions.

After a detailed account of C-X homolytic reactions useful for preparing radicals, the long main section details the wide range of applications of free radical reactions in organic synthesis for a great variety of conversions. The very detailed

breakdown into subsections, with sometimes as many as eight levels of subheadings, means that after a little practice one can unerringly find the possible ways of synthesizing a compound of the type R-Y from R-X by breaking bonds and forming new ones. By varying X and Y virtually the entire range of the periodic system is systematically covered; however, the main emphasis is on inter- and intramolecular carbon-carbon linkages. This treatment is clearly orientated towards the needs of the synthetic chemist, whose main interest is in the selective interconversion of functional groups or in the build-up of carbon skeletons. Admittedly the mainly educt-orientated structure of the text is a disadvantage in the latter case, since a product-orientated search can easily lead to confusion owing to the large number of potential precursors. A similarly undesirable effect results from the breakdown into the volume parts, which seems rather arbitrary and causes an unnecessary fragmentation of the treatment of C-C bond formation.

All the subsections are illustrated by clear formula schemes, following the usual high standard of Houben-Weyl. The high utility value is further enhanced by the many tables and experimental protocols; the many individual results that are here cited and evaluated would otherwise only be accessible at the cost of much tedious searching through the original papers. The coverage is unusually up-to-date for such a bulky work; many very recent developments are included, and the literature references extend up to the end of 1988 (and this does not merely apply to the authors' own publications!). The homogeneous presentation of the material, despite the considerable size of the work, is explained by the limited number of authors.

The volumes contain few printing errors (Hun*d*sdiecker? p. 143) and the figures are rich in detail, even though not completely free of errors (e.g. the nonsensical Scheme 2 on page 42). Without wishing to be too petty, the critical comments that follow are offered more with the aim of showing that the reviewer has been conscientious. As an innovation aimed at greater visual clarity, free radical reactive centers have been emphasized in structural formulas by using bold type (**C**·). One has to get used to this device, which can be rather confusing at times, since on the one hand the incoming or departing radical carriers (heteroradicals; R·) are not labeled, and on the other hand the use of bold type for the carbon radical carriers themselves is often not consistently applied (sometimes within single formula schemes, sometimes through entire passages). A similar criticism applies to the use of bold type to emphasize compound names in the text. The statement on page 22 that ab initio calculations on small molecules are nowadays sufficiently reliable to provide an indication of the stabilities of free radicals ("... so vertrauenswürdig, daß ihre Ergebnisse für die Kenntnis von Radikal-Stabilitäten brauchbar sind") is too sloppy and misleading. It would have been desirable to be more specific here, especially since modern computational methods at a sufficiently high level of sophistication have now become more than a mere alternative to experimental measurements for quantitatively determining the molecular properties of transient species and those that are highly reactive and difficult to handle. It is annoying to find that the discussion of the Cope reaction (p. 135), although relevant to the topic, adopts a dubious one-sided position in favor of a diradical mechanism. Also, on the same page, the (singlet) diradical structure for the *Berson* 1,4-diradicals (3,4-dimethylfuran-3′,4′-diyl and 3,4-dimethylthiophen-3′,4′-diyl) is uncritically perpetuated, without referring to the dipolar canonical structures which are at least equally plausible.

As a valuable addition to the chemical literature, this volume it deserves a wide readership. However, the fact that it is in German, in common with the rest of the series, may be a disadvantage, even though the very systematic manner of presentation and the generous provision of formula schemes enable non-German readers to make some limited use of it. Can a publishing house still afford to continue the anachronism whereby, through publishing a work exclusively in German, it reaches only an elite and severely restricted readership? This applies especially when, as in this case, it treats a highly topical subject for which there is (as yet) no equivalent in English.

One can thus sum up by saying that with this volume yet another extremely useful "true Houben-Weyl" has been added to the series; it is of the usual high quality as regards content and production, which of course has its (very high) price. Despite the latter, it should find a place in every good chemical library.

Wolf-Dieter Fessner [NB 1103 IE]
Institut für Organische Chemie und Biochemie
der Universität Freiburg (FRG)

Registered names, trademarks, etc. used in this journal, even when not marked as such, are not to be considered unprotected by law.

© VCH Verlagsgesellschaft mbH, W-6940 Weinheim, 1991. – Printed in the Federal Republic of Germany by Konrad Triltsch Druck- und Verlagsanstalt Würzburg.

All rights reserved (including those of translation into foreign languages). No part of this issue may be reproduced in any form — by photoprint, microfilm, or any other means — nor transmitted or translated into a machine language without written permission from the publishers. Only single copies of contributions, or parts thereof, may be made for personal use. This journal was carefully produced in all its parts. Nevertheless, authors, editors and publisher do not warrant the information contained therein to be free of errors. Readers are advised to keep in mind that statements, data, illustrations, procedural details or other items may inadvertently be inaccurate.

Valid for users in the USA: The appearance of the code at the bottom of the first page of an article (serial) indicates the copyright owner's consent that copies of the article may be made for personal or internal use, or for the personal or internal use of specific clients. This consent is given on the condition, however, that the copier pay stated per-copy fee through the Coypright Clearance Center, Inc. (CCC), for copying beyond that permitted by Sections 107 or 108 of the U.S. Copyright Law. This consent does not extend to other kinds of copying, such as copying, for general distribution, for advertising or promotional purposes, for creating new collective works, or for resale. For copying from back volumes of this journal see 'Permissions to Photo-Copy: Publisher's Fee List' of the CCC.

Editorial office: Postfach 10 11 61, W-6490 Weinheim, Federal Republic of Germany, Telephone (06201) 60 23 15, Telex 465 516 vchwh d, Telefax (06201) 602 328, E-Mail Z16@DHDURZ2 in Earn Bitnet.

Editor: *Peter Gölitz*

Associate editors: *D. I. Loewus, K. J. Schneider, A. Stimson.* **Editorial assistant:** *E. Schweikart*

Publishers: VCH Verlagsgesellschaft mbH. (Managing Directors: *Hans Dirk Köhler, Dr. Hardy G. Sehrt.*), Pappelallee 3, W-6940 Weinheim, Federal Republic of Germany.

Advertising office (Advertising Manager *R. J. Roth*): Postfach 10 11 61, W-6940 Weinheim, Federal Republic of Germany, Telephone (0 62 01) 60 61 36, Telex 4 67 155, Telefax (0 62 01) 606 156.

ANGEWANDTE CHEMIE
International Edition in English
Volume 30 · Number 6
June 1991
Pages 613–722

Chemically Modified Oligonucleotides as Probes and Inhibitors

By Uwe Englisch* and Dieter H. Gauss*

Oligonucleotides bind specifically to single-stranded nucleic acids to form a double helix if there is a complementary antiparallel nucleotide sequence. In addition, certain oligonucleotides bind specifically to a variety of proteins. Therefore, biological processes involving these nucleic acids or proteins can be modulated (normally inhibited) by addition of the respective oligonucleotides. The effects of these oligonucleotides and the fields of potential application can be broadened by the introduction of chemically modified nucleotides. For instance, replacing oligonucleotide phosphate groups by methylphosphonates results in the loss of one negative charge per nucleotide and the oligonucleotide becomes more lipophilic. An oligonucleotide carrying a reactive group can modify its binding partner. An oligonucleotide covalently linked to a dye can be localized in a biological specimen. Oligonucleotides attached to an enzyme can be detected in very small amounts since the enzyme can catalyze the formation of large amounts of the substance assayed (e.g., a fluorescent product). An important biochemical application is the detection and localization of a messenger RNA or its gene. Medical applications include the detection of bacterial or viral sequences. There is also great interest in inhibiting the translation of messenger RNA and the transcription and replication of DNA. So-called antisense oligonucleotides are currently being used for the inhibition of protein biosynthesis and of reverse transcription of retroviruses.

1. Design, Synthesis, and Testing of Modified Oligonucleotides as Therapeutic Agents: Psoralen-modified Oligonucleotides

Double-stranded nucleic acid is generally considered to be in an arrested state in a living cell. In contrast, single-stranded RNA and DNA usually undergo active processing; for example, DNA is replicated and transcribed and RNA, as messenger RNA, is used as template for protein biosynthesis. Oligonucleotides of complementary and antiparallel sequence can bind to these single-stranded tracts (e.g., **1**),

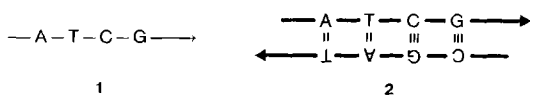

1 **2**

establishing new double-helical tracts (**2**) via Watson–Crick base-pairing (**3** + **4** → **5**).

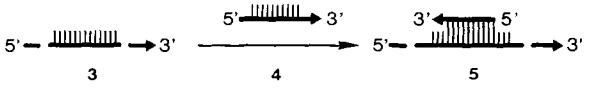

This binding obviously can find two different applications. Labeled oligonucleotide allows detection of the complementary sequence in solution. In addition, the complementary sequence can be localized in an extract, a cell, or a tissue. Thus, oligonucleotides can be used for identification of specific sequences. Oligonucleotides can also be used for inhibition. In this case the function of a single-stranded sequence is decreased or totally suppressed as the single-stranded region is converted into an inactive double strand. This principle of regulation occurs in nature, where the regulatory agent is usually called antisense RNA (for reviews

[*] Dr. U. Englisch, Dr. D. H. Gauss
Max-Planck-Institut für experimentelle Medizin, Abteilung Chemie
Hermann-Rein-Strasse 3, W-3400 Göttingen (FRG)

 © VCH Verlagsgesellschaft mbH, W-6940 Weinheim, 1991 0570-0833/91/0606-0613 $ 3.50+.25/0

see Refs. [1–6]); correspondingly, synthetic products that mimic this sort of regulation are called antisense oligonucleotides.

However, the use of synthetic, unmodified oligonucleotides in living cells to mimic antisense RNA faces the following obstacles:

1. Oligonucleotides, which carry one negative charge per phosphate group, do not easily pass through the mainly lipophilic cell membrane.
2. In cells many nucleases rapidly degrade oligonucleotides.
3. The stability of a duplex formed from an RNA or DNA tract and an oligonucleotide of medium chain length is not very high; thus, the half-life is often considerably lower than desired.

1.1. Modified Oligonucleotides

Whereas unmodified oligonucleotides have not proven very successful in modulating biochemical processes in living cells (for reviews see Refs. [7–9]), chemically modified oligonucleotides should be able to surmount the above-mentioned obstacles.

1. Increasing the hydrophobicity of an oligonucleotide should improve its uptake since membranes largely consist of lipids and lipophilic proteins. On the other hand, high lipophilicity could destroy the antisense activity owing to tight binding of the oligonucleotide in the cell membrane or any other lipophilic cell compartment. Moreover, an oligonucleotide must be sufficiently water soluble both outside and inside the cell.
2. Since nucleases cleave the sugar-phosphate backbone of an oligonucleotide, suitable modifications of these moieties could increase the stability toward nucleases. For example, cleavage of the internucleotide link could be prevented by modification of the ribose or phosphate moiety. Alternatively, access of nucleases to the internucleotide link could be sterically hindered by a bulky group. However, since the nucleobases can also strongly influence the structure of a nucleic acid, even nucleobase modifications can decrease cleavage by nucleases.
3. Upon hybridization of two complementary sequences (for reviews see Refs. [10, 11]), the formation of each hydrogen bond and the stacking of each nucleobase releases a small amount of energy. The total energy determines the stability of the double helix. The stability varies only slightly for formation of a "ribo" or "deoxy" duplex (homo duplex) or a hetero duplex. (Therefore, most of the experiments mentioned can be done with ribo- and deoxyoligonucleotides. In general, deoxyoligonucleotides are easier to prepare and handle). Stable duplexes are not formed with short oligonucleotides, and long oligonucleotides have the tendency to bind unspecifically. With oligonucleotides of appropriate length, oligonucleotide binding may depend on only one additional or missing nucleotide or on only one mispair. In these cases physical parameters such as temperature and ionic strength play an important role. Under physiological conditions double-helical stretches longer than about 15 base pairs are quite stable; under extraordinary conditions double-helical regions containing only five base pairs are sometimes stable. Hybridization can be modulated by chemically modifying the oligonucleotide; for example, changes in the nucleobases can improve pairing or stacking, and intercalating substituents can be tethered to the oligonucleotide. Ultimately, the use of an appropriately substituted oligonucleotide may result in covalent linkage between the two strands of a duplex. It is essential, however, that the additional energy (for example, that released on intercalation) not be so high that the sequence-dependent hybridization becomes negligible.

Uwe Englisch, born in 1954 in Oldenburg, studied biochemistry at the University of Michigan, USA, and chemistry at the Universität Göttingen. He received his doctorate in 1983 under F. Cramer. Since 1984 he has been employed at the Max-Planck-Institut für experimentelle Medizin, where he has been a group leader since 1987. His fields of interest are the molecular biology and biochemistry of transfer RNA as well as the synthesis and application of modified oligonucleotides in molecular biology.

Dieter Gauss, born in 1933 in Stuttgart, studied chemistry and medicine at the Universität Tübingen and received his doctorate in biochemistry in 1967 under G. Weitzel. Since then he has worked in the chemistry department (director: Prof. Dr. F. Cramer) at the Max-Planck-Institut für experimentelle Medizin. His regular duties include library and information technologies.

1.2. Synthesis

Oligonucleotides (**11**) can be synthesized (using several protocols) by commercially available automated synthesizers starting with suitably phosphorylated, protected, and activated nucleosides (**6**–**10**) (for reviews see Refs. [8, 12–17]).

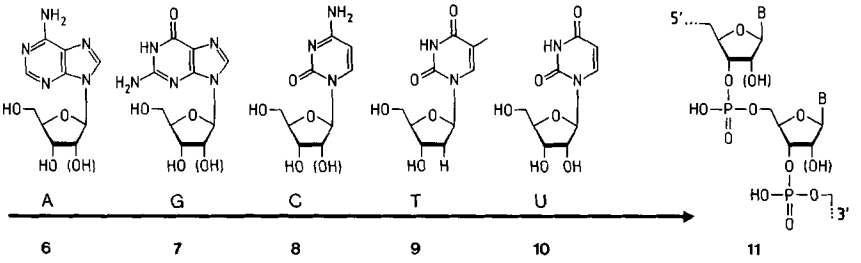

The syntheses of modified oligonucleotides do not require major changes in the normal automated elongation steps. One of the usual nucleotide building blocks can be replaced in any given synthesis cycle by a modified nucleotide derivative. This derivative can bear the desired modification or may be an intermediate which is converted into the final product later on. In the simplest case only the last step of an oligonucleotide synthesis requires a modified substance, as exemplified by one of the syntheses of psoralen-modified oligonucleotides.[18] Typically, the oligonucleotide is elongated according to the phosphoramidite method on a solid support in the 3'-to-5' direction (**12** → **13**). Compound **14**, a

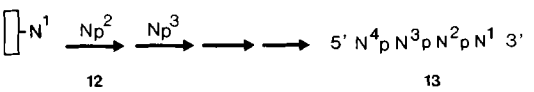

derivative of 4,5',8-trimethylpsoralen, is used instead of a nucleotide derivative in the last step. Cleavage of the product from the solid support and cleavage of the protecting groups yields the psoralen-modified oligonucleotide **15**.[*]

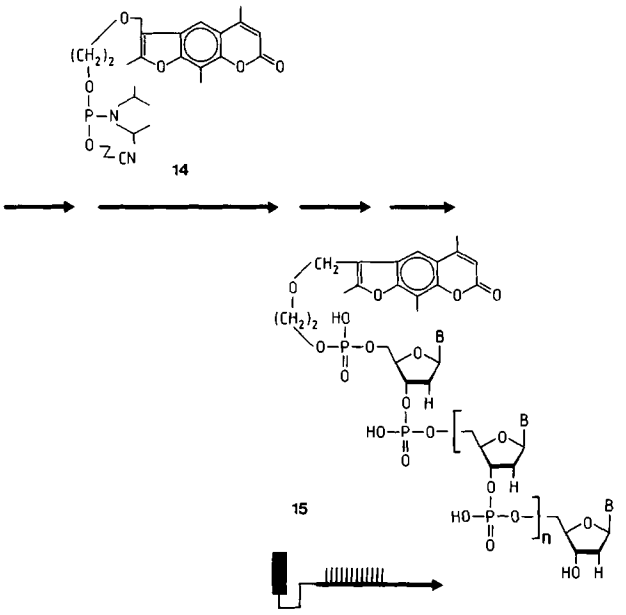

[*] All psoralen-modified compounds discussed here contain the psoralen derivative shown in **14**–**16**.

Another preparation of psoralen-modified oligonucleotides (**17**) uses the adenosine derivative **16** in a phosphoramidite solid-support synthesis.[19]

Thus, any adenosine in a sequence can be replaced by the psoralen-modified adenosine. Additional protocols describing covalent psoralen–oligonucleotide couplings[20–22] use other building blocks and synthetic schemes, although essentially the same as those described above.

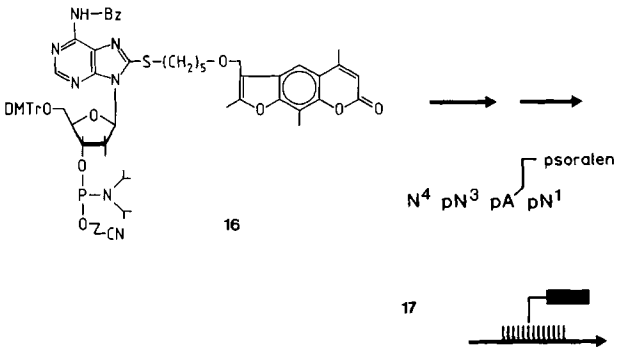

1.3. Psoralen and Psoralen-modified Oligonucleotides

Psoralen is found in plant extracts that have been used for 3000 years to treat skin and tumor diseases (for reviews see Refs. [23–25]). Psoralen intercalates between two base pairs of DNA as shown by **18**, thereby inhibiting transcription and replication of DNA. Upon irradiation of this adduct with UV light (300–400 nm) psoralen can form covalent linkages to neighboring thymidines (see **19**) through both the furan and pyran moiety; thus, the inhibitory effect is long-lasting.

Psoralen-modified oligonucleotides (**21**) are expected to be considerably better drugs than psoralen (which obviously binds to DNA unspecifically), since hybridization of the oligonucleotide to the complementary sequence (**20**) places the psoralen at a specific position in the DNA (see **22**). This DNA tract should then be inactivated. A potential application would be the inactivation of a DNA tract known to be transcribed in tumor cells but not in nontransformed cells.

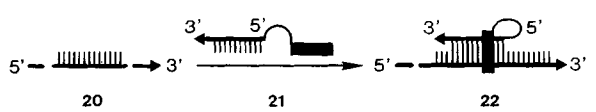

In vitro experiments have shown that this strategy is reasonable. After hybridization, a psoralen-modified oligonucleotide and its complementary oligonucleotide (see **23**) were

23

covalently linked by irradiation. As expected, the covalently linked oligonucleotides remain together under denaturing chromatographic conditions.[18, 19] The inhibition of transcription and translation by psoralen-modified oligonucleotides has also been described.[20, 21, 26, 27]

Especially important is the length of the linker between the substituent (e.g., psoralen) and the oligonucleotide. If no linker is there, the substituent has limited flexibility for interaction, whereas a so-called spacer enhances the ability of the substituent to interact with the complementary oligonucleotide. Without a spacer some interactions or reactions are impossible; a well-designed spacer—regularly three to twenty atoms in length—enables a substituent to contact exclusively the desired site. Usually, however, the substituent comes in contact with more than one nucleotide. The subsequent reactions, which involve a characteristic stretch of nucleotides, are classified as having high or low regioselectivity, as symbolized by large or small arrows pointing to specific sites in the complementary oligonucleotide.

Psoralen-modified oligonucleotides exhibit greater hydrophobicity and are expected to be more resistant to nuclease digestion owing to the bulky psoralen residue. Both these properties are increased further in another family of psoralen-modified oligonucleotides where the charged phosphate groups are replaced by uncharged methylphosphonate groups.[20, 21] After hybridization, the length of the spacer governs the possible site of intercalation. In compound **15**, the spacer is eight atoms long; thus, the choice of an intercalation site is limited. The sequence of this oligonucleotide is specifically designed so that, after hybridization (see **23**), the psoralen intercalates between thymine residues where the cross-linking photoreaction can occur (see **23** and **18/19**). The coupling of the two thymine residues to the psoralen can be reversed by UV irradiation (< 300 nm). In addition, if the linker between the psoralen and the oligonucleotide contains a disulfide bridge, this bridge can easily be cleaved by a standard reduction procedure.[22]

1.4. Modified Oligonucleotides as Substrate Analogues

A third way of applying modified oligonucleotides is to use them as substrate analogues for nucleases, polymerases, and other enzymes or to use them to bind proteins. For these studies the oligonucleotides need not be in a single-stranded form but can be used as duplexes. Thus, possible applications include investigations of reaction mechanisms (e.g., those of restriction endonucleases), labeling (e.g., upon sequencing), and modulations of regulatory cycles.

1.5. Literature

Oligonucleotides—with or without chemical modification—are the subject of more than 3000 publications. Thus, unmodified and modified oligonucleotides have been reviewed critically several times. For instance, their chemistry,[7, 9] their role in enzymatic replication,[28] their inhibition of gene expression in extracts as well as in cell cultures,[9, 29–35] and their application as antineoplastic drugs has been reviewed.[36–38] Also, their use to identify nucleic acids and proteins[39] and their application in medical diagnosis have been discussed critically.[40] In this article we report on those fields with publications in recent years (up to the middle of 1990). Even with this restriction only selected citations can be given. The reader may refer to other publications, in particular several comprehensive reviews.[7, 9, 30–35, 37–40]

2. Inhibition of the Function of RNA and DNA by Modified Oligonucleotides

Psoralen-modified oligonucleotides, which were used as examples in the introduction, are a subgroup of oligonucleotides designed for inhibiting the function of RNA or DNA. Numerous other subgroups of potentially inhibitory oligonucleotides exist. In this article the following five examples are dealt with: (1) acridine oligonucleotides, which belong to the group of oligonucleotides bearing intercalators (for a review see Ref. [41]), (2) modified oligonucleotides able to establish a covalent linkage to the complementary strand (or to a protein), (3) modified oligonucleotides equipped to cleave the complementary strand, (4) oligonucleotides carrying tumor-inhibiting platinum complexes, and (5) oligonucleotides potentially inhibiting virus proliferation.

2.1. Acridine-modified Oligonucleotides

Acridine oligonucleotides (for reviews see Refs. [42, 43]) are comparable to psoralen oligonucleotides in that the acridine moiety is also able to intercalate. Since acridine is similar in size and chemical properties to psoralen, the amount of energy released upon intercalation of acridine is also similar to that of psoralen. In contrast, reversible photoreaction occurs only with psoralen. The acridine moiety (normally derived from 9-amino-6-chloro-2-methoxyacridine, see **28**) can be linked to several different sites of an oligonucleotide, following one of the standard coupling procedures; possible sites are the 3'-phosphate (**24**),[44] the 5'-phosphate (**25**),[45, 46] both phosphates (**26**),[45] and an internal phosphate (**27**).[45, 47] In each case the reactive group of

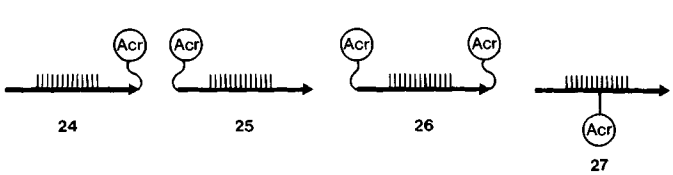

acridine is the amino moiety. The binding of these oligonucleotides to nucleic acids and the intercalation of the acridine residue are well documented by NMR[48, 49] using short nucleic acid fragments. A typical example is compound **28**,[48]

which is modified by a neopentyl residue to render the oligonucleotide more lipophilic and to inhibit nuclease attack by steric hindrance.[48] Besides compound **28** there are

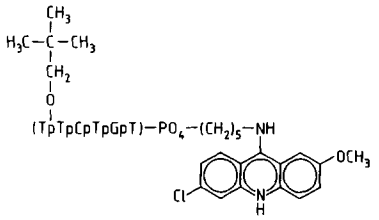

28

further acridine oligonucleotides with a second modification, such as phosphorothioate groups[46, 50] or 3′-phosphate triesters carrying an additional positive charge[51] or a photoreactive group.[52] These acridine oligonucleotides exhibit biological activity in several assays (e.g., the inhibition of translation of β-globin mRNA[46, 53] or trypanosomal mRNA[54]). Furthermore, the proliferation of certain viruses, such as influenza virus[55] and simian-40 virus,[52] and of bacteriophages[56] is inhibited. Acridine oligonucleotides not only bind to nucleic acid single strands to form duplexes but can also bind to double-stranded DNA yielding triple helices[52, 57] (see Section 5). In these cases, the acridine is also known to intercalate between the nucleobases.

The stability of acridine oligonucleotides towards digestion by cell nucleases dramatically increases when the oligonucleotide is synthesized from the α anomers of nucleosides (**30** instead of **29**).[58–61] Because of the increased stability toward nucleases, the inhibitory potency of these substances also increases.[62]

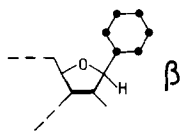

29

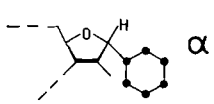

30

In normal nucleic acid duplexes, with both strands consisting of β anomers, the strands are base-paired in an antiparallel direction. In duplexes where one strand consists of α anomers and the other strand contains β anomers, the strands are base-paired in the parallel direction.[58, 61] These duplexes can be quite stable, in particular the one formed between an α-deoxyoligonucleotide and β-RNA; however, the stability is also sequence-dependent.[63] The disadvantage of α-oligonucleotides (and of methylphosphonate oligonucleotides as well) is that they do not activate RNase H[62] (see Section 2.4). Thus, the inhibitory effect rests solely on duplex formation and there is no enzymatic hydrolysis of the complementary RNA strand.

Oligonucleotides containing α anomers of nucleosides have not only been described for acridine oligonucleotides (for a review see Ref. [64]).[65–68] Antisense α-oligonucleotides, without a second modification, are reported to inhibit the reverse transcription of human immunodeficiency virus,[65, 66] the synthesis of β-globin,[67] and the cleavage of RNA by RNase H.[65, 68] In another group of substances, similar to acridine α-oligonucleotides, oligonucleotides of α anomers are coupled with a second functional agent, such as proflavin,[69] or are modified with a *p*-azidophenacyl group.[61, 70] Both of these oligonucleotides can undergo photochemical cross-linking reactions (see Section 2.2).

2.2. Covalent Linkage of Modified Oligonucleotides with the Complementary Strand

Another possibility to increase the inhibitory effect of hybridization of an oligonucleotide to an RNA or DNA single strand is to modify the oligonucleotide (**32**) so that, after hybridization, a covalent linkage to the complementary strand is formed (**31** + **32** → **33**). Thus, the resulting duplex has a long life (for reviews see Refs. [71, 72]).

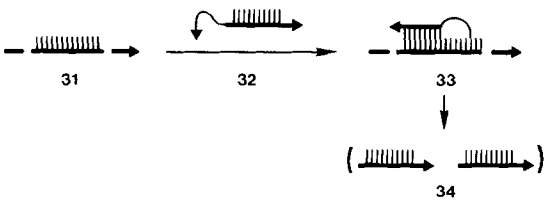

A typical oligonucleotide is **35**;[73] the alkylating functional group is tethered to the oligonucleotide via the 2′- and 3′-hydroxyl groups of the 3′-terminal ribose. The 5′-phenazinium group is incorporated to improve the binding after hybridization but prior to covalent linking (compare Section 2.1). Oligonucleotides of this sort can inactivate the function of single-stranded DNA,[74, 75] of double-stranded DNA,[76] and of phages or viruses.[73] Most frequently, alkylation of a guanine nucleobase of the target nucleic acid occurs, followed by strand breakage (**33** → **34**).[73, 75] Instead of a phenazinium moiety, a cholesterol moiety can be tethered to such oligonucleotides;[77] the uptake into cells is thereby considerably improved, whereas hybridization and binding do not change dramatically.

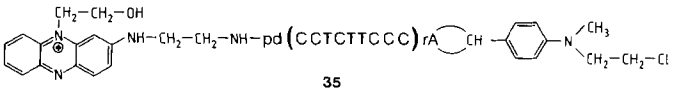

35

There are many other functional groups that allow analogous linking reactions (e.g., the *p*-azidophenacyl group,[61, 70] the proflavin residue,[69] the azidoproflavin residue,[78] a 5-azido-substituted uridine residue,[79, 80] a 5-methyl-N^4,N^4-ethanocytidine residue,[81] and a naphthoquinone derivative[82]). The first four groups and the last group require irradiation for cross-linking to occur, similar to the psoralen oligonucleotides (see Section 1.3). Finally, a nucleic acid strand and a (modified) oligonucleotide can become covalently linked by a third compound, such as a platinum complex.[83] A modified oligonucleotide may also be covalently linked to a protein.[79, 84–86] This cross-linking is reversible if the modified oligonucleotide is linked via a disulfide bridge to a cysteine of the protein.[86]

If they can be developed up to the stage of drugs, these reagents are expected to exhibit the most intensive and long-lasting inhibition, for example towards viruses.

2.3. Cleavage of the Complementary Strand by a Modified Oligonucleotide

Another possibility to prolong the inhibitory effect due to hybridization of an oligonucleotide to a nucleic acid strand rests on triggering a strand break in the complementary strand (**36**). This can be effected by activating a nuclease within the cell (see Section 2.4)—the duplex that forms then has to fulfill certain structural requirements—or it can be effected by the oligonucleotide itself. In the simplest case a cleaving enzyme is linked to an oligonucleotide (**37**),[87, 88] for example a ribonuclease to a deoxyoligonucleotide; following hybridization (see **38**), the enzyme cleaves the complementary RNA strand (see **39**). There is another group of reagents effecting the cleavage of the complementary strand by a complexed metal ion linked to the oligonucleotide through a spacer.

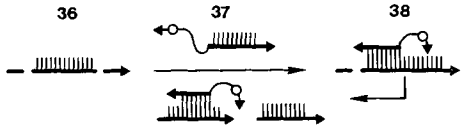

39

Oligonucleotides bearing iron porphyrin complexes[89, 90] or iron EDTA complexes[91–93] can cleave single-stranded DNA[89–94] or RNA (porphyrin;[94] EDTA[95]). Additionally, double-stranded DNA can be cleaved by an iron EDTA complex via triple-strand formation.[96–98] Furthermore, a copper phenanthroline complex has been attached as reactive moiety to an oligonucleotide to cleave single-stranded DNA[99, 100] and RNA[101] and double-stranded DNA,[102] a typical example being compound **40**.[101]

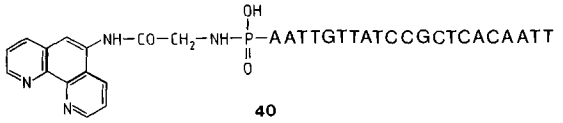

40

These metal-catalyzed cleavage reactions do not cleave in *one* step to *one* well-defined product. Rather, secondary reactions and side reactions are observed. Therefore, a therapeutic application in living cells does not seem possible. Strand cleavages of the complementary strand also can originate from completely different reactions, namely, those following photochemical reactions and/or various alkylation reactions.[7, 61, 69, 70, 78, 103, 104] Ellipticin oligonucleotides (**41**)

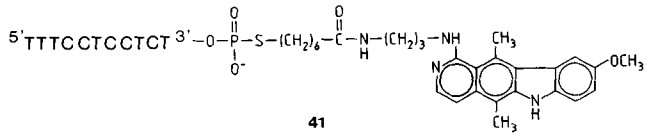

41

are reported to cleave both strands of a double-stranded DNA, a triple strand being the reactive intermediate.[104]

An important application of this type of cleavage reaction would be the preparation of artificial specific endonucleases capable of cutting single strands of RNA or DNA at specific internucleotide bonds. Natural restriction endonucleases need double-stranded DNA as substrate and the enzyme needed for cleavage at a specific site is often not available. Specific RNA cleaving enzymes are generally not available. Since gene technology requires the cleavage of nucleic acids with high selectivity, such artificial scissors need considerable improvement to be applicable.

2.4. Cleavage of the Complementary Strand by RNase H Triggered by a Modified Oligonucleotide

Scission of only one strand in a duplex occurs in biological processes such as repair events, in which a stretch of one strand is excised and the gap is refilled, or initiation of replication, after which the primer, a ribooligonucleotide, is digested separately. In each case the structure of the duplex, which deviates from that of a normal duplex, triggers an enzyme. Therefore, hybridization of an oligonucleotide to a single strand (or to a double strand with a single-strand tract) might mimic such a structure. For instance, a naturally occurring enzyme might be triggered to cleave a phosphodiester bond at a certain nucleotide, which would depend on the sequence of the oligonucleotide used. An example is RNase H, which cleaves RNA after hybridization of the RNA single strand (**42**) with a deoxyoligonucleotide (**42** → **43** → **44** → **45**).

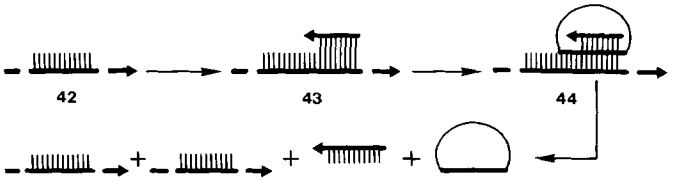

45

This sort of cleavage can be effected with unmodified deoxyoligonucleotides[105–108] and with some modified oligonucleotides (e.g., phosphorothioate oligonucleotides). However, methylphosphonate oligonucleotides and phosphoramidate oligonucleotides (or oligonucleotides containing longer tracts of these groupings) do not stimulate cleavage by RNase H.[107, 108] Another series of modified oligonucleotides able to trigger RNase H cleavage are constructed in a nonuniform manner in order to direct the cleavage of the complementary strand to one specific internucleotide bond. Such oligonucleotides have a ribo part and a deoxy part, linked in some cases by a pyrophosphate group instead of a phosphate group[109] or they contain a longer 2′-O-methylated ribo part followed by a short deoxy sequence.[110] Furthermore, a deoxy sequence containing two to four nucleotides can be inserted into a ribooligonucleotide[111] or either a methylphosphonate oligonucleotide[112] or a phosphorothioate deoxy stretch can be placed in a methylphosphonate oligonucleotide.[108] These oligonucleo-

tides for the most part cleave one specific internucleotide bond. This is particularly evident in **46** and **47**. When 2′-*O*-methylribonucleotides (**47**) instead of deoxynucleotides (**46**) flank the central deoxyoligonucleotide stretch,[113] cleavage occurs at only one internucleotide bond.

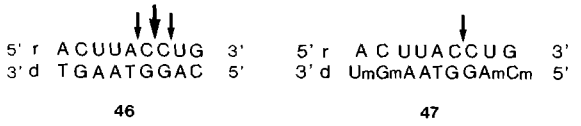

46 **47**

These enzymatic cleavage reactions at any desired internucleotide bond appear particularly promising for application in molecular biology and gene technology (see Section 2.3). Finally, it should be mentioned that most of the anti-messenger oligonucleotides do not only inhibit by hybridization but also by activating RNase H.

2.5. Antineoplastic Platinum Compounds

Cisplatin, *cis*-$[Pt(NH_3)_2Cl_2]$ (for a review see Ref. [114]) and some other platinum compounds[115] are used as antineoplastic drugs, although their detailed mechanism is still unknown. These platinum compounds form DNA adducts (without intercalation), binding especially to two neighboring guanosine residues of one strand, thereby bending the DNA.[116–120] In a model experiment an oligonucleotide containing two neighboring guanosine residues was allowed to react with cisplatin to give an oligonucleotide containing the stretch *cis*-$[Pt(NH_3)_2dGpG]$ (see **48**) and then cloned into DNA. The function of the platinum-carrying single strand was largely suppressed,[121] thus indicating that such inhibition could be the mechanism of the antineoplastic platinum compound.

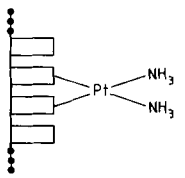

48

There are other examples of nucleic acids being bent by agents or chemical modifications such as the formation of thymine dimers (see Section 4.2) in DNA. Unmodified DNA, too, can be bent, in particular when it contains A·T stretches, the A_n sequences of which lie on one side of the helix (see Sections 4 and 5). The bending plays an important role for DNA structure and function (not discussed here).

2.6. Modified Oligonucleotides as Potential Inhibitors of Virus Proliferation

The inhibition of gene expression by modified oligonucleotides has been mentioned above and also has been reviewed elsewhere in terms of substances[122, 123] or effects[35, 43, 124] (e.g., inhibition of oncogene expression[36]). In this article the structure and function of some antiviral oligonucleotides will be discussed. Since phosphate-modified oligonucleotides are of particular interest, a compilation of some important and/or recently published classes of phosphate-modified oligonucleotides is given (**49**–**64**). These compounds range from substances with only one atom exchanged (e.g., phosphorothioates) to those in which the whole sugar-phosphate backbone is replaced by another backbone (not discussed here).

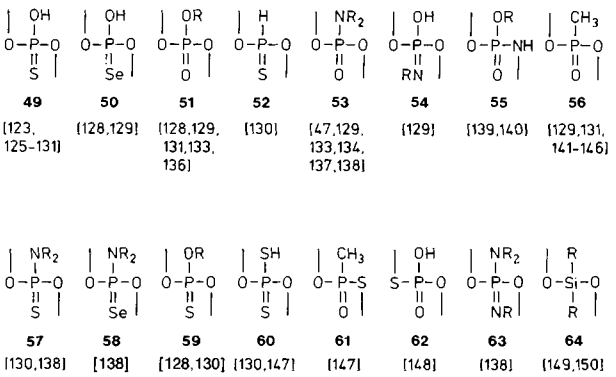

49	**50**	**51**	**52**	**53**	**54**	**55**	**56**
[123, 125–131]	[128,129]	[128,129, 131,133, 136]	[130]	[47,129, 133,134, 137,138]	[129]	[139,140]	[129,131, 141–146]

57	**58**	**59**	**60**	**61**	**62**	**63**	**64**
[130,138]	[138]	[128,130]	[130,147]	[147]	[148]	[138]	[149,150]

The oldest, and perhaps most important, class of phosphate-modified oligonucleotides comprises phosphorothioate oligonucleotides (**49**) (for reviews see Refs. [123, 125–127]).[128–131] Like natural nucleic acids, these substances have one negative charge per nucleotide unit. In contrast, methylphosphonates (**56**) have lost this charge and therefore pass more easily through cell membranes. The properties of oligonucleotides are still more fine-tuned in some oligonucleotides, such as those with CHF_2 instead of CH_3 groups.[132] In some cases the modification changes the whole character of the oligonucleotide; examples include triesters (**51**) in which the substituent is lipophilic[133] or, for amidates (**53**), carries a positive charge ($R = -X-NR_3^{\oplus}$)[133, 134] or can bear a group suitable for intercalation.[47] Exchange of an oxygen atom belonging to the backbone can be carried out either 5′ or 3′ to the phosphorus atom (**55**, **61**, **62**). The Si-containing substances (**64**) are one simple example of the large family of non-phosphorus-containing compounds (not reviewed here).

Replacing one of the nonbridging oxygen atoms of phosphorus with CH_3 or SH, for example, creates a new stereogenic center. With n modified centers one obtains 2^n isomers. These isomers are distinguished by enzymes. On hybridization, these isomers bind differently to the target sequence (a substituent may protrude into the major or minor groove of the resulting duplex) and hence the stability of the duplexes and their biological activity differ. For these reasons stereoselective syntheses of modified oligonucleotides (for reviews see Refs. [7, 39, 135]) have been developed and the biological activities of the isomers have been tested separately (not reviewed here).

A considerable number of modified oligonucleotides have been tested as inhibitors of the proliferation of HIV (human immunodeficiency virus) or of other viruses and phages. They were first tested in an in vitro assay to determine whether the formation of viruses or phages or subparticles

thereof was diminished or whether the expression of a single viral protein was inhibited. Inhibitory effects were found for the following oligonucleotides: acridine oligonucleotides towards T4 phages,[56] polylysine oligonucleotides towards vesicular stomatitis virus (VSV),[151,158] methylphosphonate oligonucleotides towards VSV, simian-40 virus (SV 40), and herpes viruses,[144,152] and phosphorothioate oligonucleotides towards herpes viruses.[153] Analogous effects against HIV were found using phosphorothioate oligonucleotides[154,155] and oligonucleotides containing α anomers[65,66] (see Section 2.1). The phosphorothioate oligonucleotides have proven to be less toxic and more inhibitory than the corresponding seleno oligonucleotides.[156] An inhibitory effect against HIV[66,154,155] and herpes viruses[153] was also detected using S-dC-28, a phosphorothioate-containing deoxyoligocytidylic acid (and some further related modified homooligonucleotides[137]). This is surprising since there is no complementary sequence in the virus for these oligonucleotides. In these cases the reverse transcriptase or viral polymerase seems to be the target for the oligonucleotide. Inhibitory transcription initiation complexes, not formed according to the antisense principle, are probably involved here. Nonetheless, this is very interesting since reverse transcriptase does not exist in normal eukaryotic cells and is therefore a suitable target enzyme for drugs.

The second step towards drug development is to assay potential antisense oligonucleotides in cell cultures. Two viral systems, HIV and VSV, have been rigorously tested. In addition, the inhibition of influenza viruses by acridine oligonucleotides,[55] of herpes viruses and SV 40 viruses by methylphosphonate oligonucleotides[144,157] and acridine oligonucleotides,[52] and of coliphages by alkylating oligonucleotides[73] has been investigated. Methylphosphonate oligonucleotides,[144,152] polylysine oligonucleotides,[151,158–160] and lipid-substituted oligonucleotides[161] have proven effective against VSV. Towards HIV, in cell culture, an inhibition was found for deoxyoligonucleotides with phosphoramidate,[137,162] phosphorothioate,[137,162–165] or methylphosphonate groups.[162] Similar results were found for oligonucleotides carrying polylysine moieties[166] and for ribooligonucleotides with phosphorothioate or 2′-*O*-methyl groups.[167] In these cases the oligonucleotides are complementary to viral sequences and it is well established that the inhibition is the result of antisense effects. Oligonucleotides (with or without phosphorothioates) carrying a cholesterol moiety exhibit considerable anti-HIV activity. However, this activity is not due to the antisense principle.[168] Comparison of unmodified and phosphorothioate-modified oligonucleotides that contained antisense sequences and random sequences clearly showed that antisense phosphorothioate oligonucleotides are the most powerful agents[165] in accordance with earlier studies.[73,157,167]

Although antiviral effects have been demonstrated unambiguously, their origin is still largely unclear—at least two mechanisms, one following the antisense principle and another based on the initiation of transcription are involved. Perhaps still more mechanisms will emerge. To date, modified oligonucleotides have not been used clinically; however, clinical trials have been started. Once found, an inhibitory system will probably be adapted for use against additional viruses. Formula **65** shows part of a methylphosphonate oligonucleotide.[144] Suitable combinations of phosphate (p) and methylphosphonate (p) groups, as shown by the oligonucleotides **66**, should allow the oligonucleotide properties (e.g., hydrophobicity and charge distribution) to be modulated in order to obtain antiviral drugs.

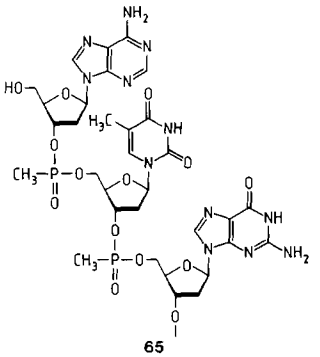

65

Ap ApTp Ap Cp Cp Tp Cp A
Cp Cp Ap Gp GpT
Gp Gp Tp Ap Ap G
Tp Tp Tp Tp Tp T

66

A promising modification to improve uptake into cells is the linkage of polylysine moieties to potentially virus-inhibiting oligonucleotides;[151,158–161,166] for example, $lysine_{100}$ was attached to an oligonucleotide containing 15 nucleotides.[159] These oligonucleotides exhibit good inhibitory activity in cells infected with VSV[151,158–161] or HIV.[166] In some cases, however, they were found to be toxic. Oligonucleotides coupled with peptides of nonuniform sequence have also been prepared[169,170] but their antiviral application has not yet been fully investigated.

Derivatives of 2′-5′ oligoadenylates are a separate class of antiviral substances which will not be discussed further here. They do not act according to the antisense principle (for reviews see Refs. [171,172]).[158,173,174]

3. Identification and Localization of RNA or DNA Sequences with Modified Oligonucleotides

The presence of a certain RNA or DNA sequence can be determined by hybridizing a complementary oligonucleotide to it. The oligonucleotide—after separation from unbound oligonucleotide—is recognized via a label. Unmodified oligonucleotides (for reviews see Refs. [39,175–179]) are radioactively labeled and modified oligonucleotides, in the simple cases, are substituted with a colored, chemiluminescent, or fluorescent marker (**67** + **68** → **69**). Suitable sub-

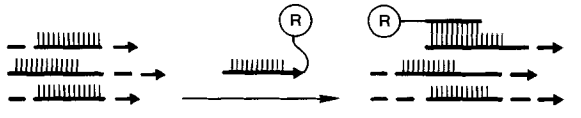

67 **68** **69**

stituents used for this purpose are fluorescein,[180–187] isoluminol,[180] rhodamine compounds,[180,188] a ruthenium bathophenanthroline complex,[189] and a pyrene derivative.[182] The linkage of the dye (e.g., **71**) to the oligonucleotide can be accomplished in many ways, for example via the 3′-phosphate (**70** + **71** → **72**).[183] After detection of a given

RNA or DNA sequence, it can be immediately isolated by known procedures.[39, 179]

Another approach is to attach antigenic groupings to the oligonucleotide. After hybridization of the oligonucleotide to the target sequence, binding of the antibody to the oligonucleotide, and suitable staining, the target sequence

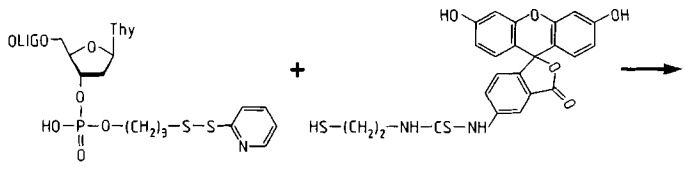

70 71

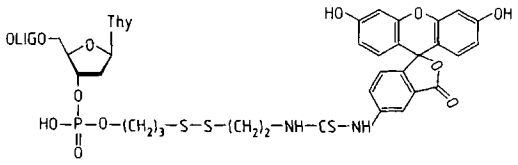

72

can be visualized by electron microscopy. This protocol was used, for instance, to pinpoint some ribosomal areas via the antigenic determinants 2,4-dinitrophenyl and isopentenyladenosyl.[190, 191]

3.1. Enzyme-linked Oligonucleotide Probes

Enzyme-linked oligonucleotide probes can be used for the recognition of an RNA or DNA sequence with high precision, comparable to that of radioactively labeled compounds. The enzyme is designed to multiply a signal, such as the production (or disappearance) of a colored or fluorescent product (**73** + **74** → **75**). The enzyme can be linked to the

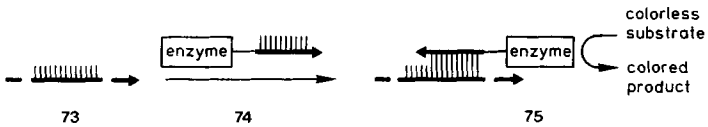

73 74 75

oligonucleotide directly or, alternatively, the enzyme can be linked to any agent which immediately or in situ binds to the enzyme. In the first case an enzyme and an oligonucleotide might be linked through a bifunctional reagent[192–197] or by UV irradiation;[198] normally, a spacer of about 30 atoms in length is used. Compound **76**[196] is an appropriate example, where the oligonucleotide was constructed to hybridize to a sequence of phage M13mp8 (see **77**).

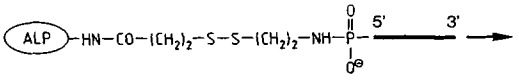

76

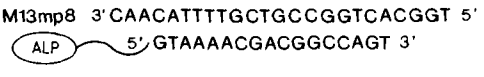

77

In this case alkaline phosphatase (ALP) is linked to an oligonucleotide (**76**). After hybridization, the ALP-catalyzed degradation of *p*-nitrophenyl phosphate to *p*-nitrophenol allows colorimetric detection of the phage sequence.[194–196] Alternatively, alkaline phosphatase can initiate the formation of a dye of 5-bromo-4-chloroindolyl phosphate (BCIP) and nitroblue tetrazolium (NBT),[193, 196] also assayed colorimetrically. This enzyme can also cleave 4-methylumbelliferone phosphate, which releases a fluorescent product.[193, 194, 196] When peroxidase is used as oligonucleotide-linked enzyme, dye formation from the reaction of *o*-phenylenediamine and hydrogen peroxide is assayed.[180]

The enzyme need not be linked directly to the oligonucleotide. Instead, the oligonucleotide can be coupled to any agent which in situ binds the enzyme. The antibody variation of this system requires that the oligonucleotide carry an antigenic substituent such as digoxigenin,[199, 200] 5-bromo-2′-deoxyuridine,[201] fluorescein,[181] or DNA protein A.[198] An antibody linked to the enzyme then binds to the antigenic group and the enzyme generates a signal (**78** + **79** → **80**).

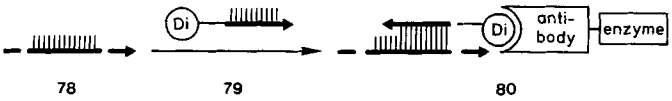

78 79 80

Among these assay systems, the most widely used is the system biotin–(strept)avidin (see Section 3.2).

3.2. The System Oligonucleotide–Biotin–Avidin–XXX

Biotin-linked oligonucleotides in solutions, extracts, or tissue specimens form very tight and specific aggregates of the biotin group (**81**) and the protein avidin or streptavidin. Avidin can be easily coupled to further agents suitable for recognition, such as alkaline phosphatase or peroxidase (see **82**). In either case a chromogen is converted into a chromophore or vice versa (see Section 3.1).

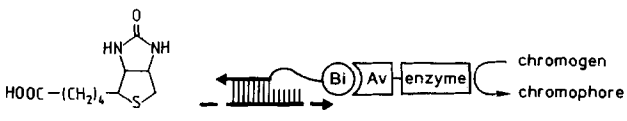

81 82

The linking of biotin (Bi) to an oligonucleotide—normally through a spacer of about 10 atoms—can be accomplished chemically or enzymatically. In a simple protocol biotin and the oligonucleotide are linked unspecifically through a bifunctional reagent[202] or photochemically.[203] Most of the coupling procedures published, however, form specific linkages so that the number of biotin residues per oligonucleotide is known. In most cases a nucleotide derivative already substituted with all or part of the spacer is used in conjunction with an automated oligonucleotide synthesis. The oligonucleotide is biotinylated after the synthesis is complete. Suitable nucleotide derivatives are 8-substituted adenosine,[204] 5-substituted 2′-deoxyuridine,[182, 205] the

so-called biotin-11-dUMP (examples **83**,[205] B or Bi = biotinyl), and cytidine substituted at the exocyclic amino group.[182, 206, 207] Furthermore, biotinylation can use a terminal phosphate group[184, 208, 209] or a terminal hydroxyl group[192] (examples **84**, **85**) for attachment. Finally, biotinylation of oligonucleotides (synthesized or isolated) also can be successfully accomplished by adding a biotin-carrying nucleotide to an oligonucleotide using an appropriate polymerase[210, 211] or the enzyme terminal nucleotidyltransferase.[181, 212]

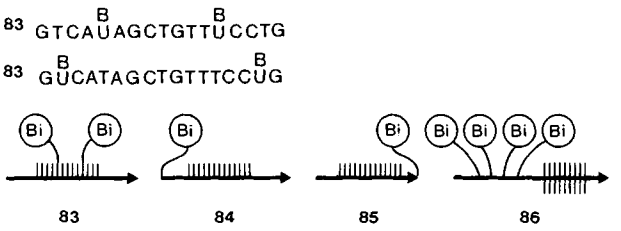

Oligonucleotide **86** is composed of a deoxy stretch of four biotinylated cytidine phosphates and a ribo stretch of 2′-*O*-methylribonucleotides (see **122** in Section 5). This modified oligonucleotide combines good recognition with good stability towards nucleases.[207] Oligonucleotides with this typical structure have been used successfully for recognition and inhibition even in complex biological processes, such as the splicing process on the spliceosome.[213, 214]

The synthesis of many biotinylated oligonucleotides has encouraged their use in nucleic acid recognition assays. The sensitivity of this system is always very good when one of the detection systems mentioned above or immunofluorescence assays are used.[215]

The detection assays described in Sections 3, 3.1, and 3.2 are not restricted to applications in molecular biology (for a review see Ref. [216]), where they have been used to detect genes or gene fragments,[215, 217, 218] find enterotoxin genes[181, 219] or sequences originating from enterotoxic *E. coli*,[195] localize RNA,[220] and prove the presence of viruses.[181, 221] They have also become more and more important in biology, where they have been used for classification in phylogeny and for detection of microorganisms,[188] and in medicine as well (for a review see Ref. [40]), where they have found application in the diagnosis of viral infections by detection of viral sequences in specimens (for a review see Ref. [222]), the detection of other infections,[222] of genetic diseases,[40, 222] and of neoplastic diseases,[40] and the identification of persons.[40] Under optimal assay conditions these assays are sensitive enough to detect one nucleobase exchange in a target sequence.[192]

4. Modified Oligonucleotides as Substrates for Nucleases and Polymerases

A third way of applying modified oligonucleotides is to use them as substrate analogues of nucleases, polymerases, and other enzymes and for interaction with nonenzyme proteins. The examples described here show how modified oligonucleotides contribute to the elucidation of the mechanisms of restriction endonucleases and to the manipulation of these enzymes. Also discussed is work on mutation processes initiated by apurinic DNA stretches or thymine dimers in DNA as well as sequencing techniques using fluorescence indicators.

One of the easiest modifications of an oligonucleotide that is a substrate for a given nuclease is to change the ribose-phosphate backbone (see Sections 2.1 and 2.6). Indeed, the mechanisms of numerous nucleases were (and still are) investigated with backbone-modified oligonucleotides,[7] most often phosphorothioate analogues.[124–126] However, the role of the nucleobases is not restricted to defining the sequence. The recognition of a nucleic acid by an enzyme, whether a nuclease or a polymerase, is additionally determined by the helix diameter, the length of the repeating unit, the tilt and twist of the nucleobase, and further parameters, all of which are dependent on the nature of the nucleobases. Therefore, some of the nucleobases introduced into oligonucleotides in recent years will first be discussed before turning to the restriction endonucleases.

Inosine can be inserted opposite all four regular nucleobases without disrupting the double helix. Therefore, oligonucleotides containing 2′-deoxyinosine (dI, **88**)[223–227] are suitable as polyvalent probes. Oligonucleotides containing 2′-deoxynebularine (dNeb, **89**)[228] or 2′-deoxyxanthosine (dXao, **90**)[228] can act similarly. Double helices containing these nucleobases are generally less stable than those with normal nucleobases. In contrast, the helix stability is increased by inserting 2-amino-2′-deoxyadenosine (n^2dA, **92**)[226, 229, 230] as well as by introducing **105**, a fluorescent pyridopyrimidine which is able to pair with guanine and adenine.[231] In another series of oligonucleotides, the aromatic nuclei of the nucleobases are modified; examples include 7-deaza-2′-deoxyguanosine (c^7dG, **93**),[232] 7-deaza-2′-deoxyadenosine (c^7dA, **94**; also called 2′-deoxytubercidine),[233–237] 7-deaza-8-aza-2′-deoxyadenosine (z^8c^7dA, **95**),[235, 238, 239] 7-deaza-8-aza-2′-deoxyguanosine (z^8c^7dG, **96**),[239] and 3-deaza-2′-deoxyadenosine (c^3dA, **97**).[240] Some of these oligonucleotides have additional modifications, namely, N^6-methylation (as in **94** and **95**)[241] and glycosidic linkages to N-8 instead of N-9.[238, 241] The latter compounds, in particular, are specifically designed tools for DNA structure and function studies (e.g., DNA bending and recognition by proteins).

Pyrimidine nucleoside analogues of 2′-deoxycytidine (**98**) and thymidine (**100**) each lacking the functional group *para* to the glycosidic linkage (**99** and **101**, respectively)[242] were synthesized in order to quantify the contribution of these functional groups to duplex stability. Additional modified pyrimidine nucleosides incorporated into oligonucleotides are O^4-methyl- or O^4-ethylthymidine (m^4T or et^4T, **102**),[243] 2′-deoxyuridine (dU, **103**),[227] 5-methylcytidine (m^5dC, **104**),[227, 244] the pyridopyrimidine nucleoside mentioned already (**105**[231]) and a similar compound which is able to pair with several nucleobases (**106**[245]), 5-putrescinylthymidine (**107**) as well as some other 5-substituted thymidines,[246] which occur in bacteriophages and inhibit nuclease digestion, and an oligonucleotide with 5-azacytidine (z^5dC, **108**) (or 5,6-dihydro-5-azacytidine[247]); thus, the pyrimidine field, too, presents compounds modified in the aromatic nucleus of the nucleobases.

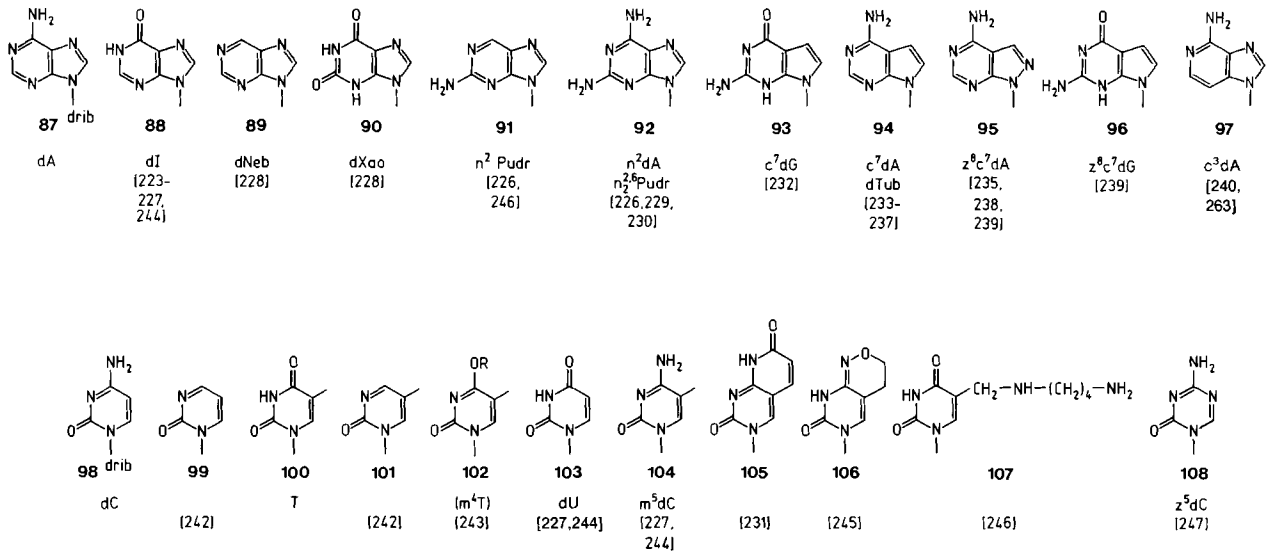

Furthermore, there are a series of double-helical nucleic acid analogues[28, 248, 249] based on artificial base pairs (not described here). Recent work has provided nucleobase analogues sufficiently voluminous to replace a complete base pair;[249] the fitting of these voluminous nucleobase analogues into DNA may be related to the intercalation of polycyclic aromatic compounds.

4.1. Recognition Sequences and Cleavage Sites of Restriction Endonucleases

Restriction endonucleases—about 600 enzymes have been characterized—differ from simple nucleases in that they cleave double-stranded DNA only at those internucleotide linkages coded for by their respective recognition sequences (**109**–**111**).

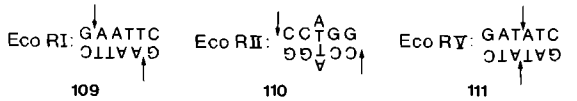

The mechanism of cleavage by restriction endonucleases as well as the structure of the recognition sequence can be studied with modified oligonucleotides as substrate analogues. Phosphate-modified oligonucleotides (containing pyrophosphate, triester, or phosphorothioate moieties),[148, 250–252] sugar-modified oligonucleotides (containing ribose or xylose moieties),[250, 251, 253] and nucleobase-modified oligonucleotides have been used. The latter include pyrimidine nucleobases with or without 5-methyl groups[250, 254–258] or with further substitutions (e.g., thio, bromo, alkyl, fluoro, or cyano groups),[250, 251, 253, 254, 257, 259–261] methylated purine nucleobases,[258, 260, 262, 263] and purine moieties with modified functional groups[230, 260, 263–265] or modified aromatic nuclei.[235, 236, 238, 240, 241, 262, 263, 265] The compilations of the oligonucleotides **112** and **113** display one oligonucleotide in which two thymidines are replaced by uridines or uridine derivatives (**112**)[259] and three adenosine-containing oligonucleotides in which adenosines are replaced by 7-deazaadenosines (**113**).[236]

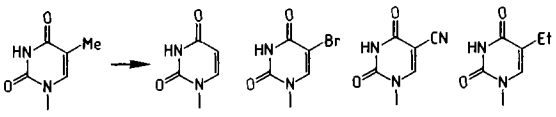

GGAGATCTCC	GGAGATCTCC
GGAGATCUCC	GGAGAUCTCC
GGAGATCbr⁵UCC	GGAGAbr⁵UCTCC
GGAGATCcn⁵UCC	GGAGAcn⁵UCTCC
GGAGATCet⁵UCC	GGAGAet⁵UCTCC

112

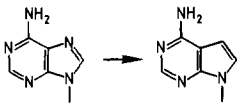

GGAATTCC	CGCGAATTCGCG	GTAGAATTCTAC
GGc⁷AATTCC	CGCGc⁷AATTCGCG	GTAGc⁷AATTCTAC
GGAc⁷ATTCC	CGCGAc⁷ATTCGCG	GTAGAc⁷ATTCTAC
GGc⁷Ac⁷ATTCC	CGCGc⁷Ac⁷ATTCGCG	GTAGc⁷Ac⁷ATTCTAC
		GTc⁷AGAATTCTAC
		GTAGAATTCTc⁷AC

113

A number of functional groups have been identified as essential recognition elements for identification and cleavage of deoxy duplexes by restriction endonucleases (e.g., the exocyclic amino groups of adenine and cytosine, the N-7 of adenine, and the methyl group of thymine are essential contact points for the enzyme Eco RV[265] and another known series of functional groups are essential for the enzyme Eco RI[260]). Despite a detailed search for essential functional groups that, when modified, prevent an oligonucleotide from being cleaved, the general result of modifications of

functional groups in deoxyoligonucleotide duplexes is to change the substrate properties of these duplexes. Therefore, a more valid statement is that recognition and cleavage subtly depend on the whole three-dimensional structure of the recognition sequence. Many times, after a modification and subsequent incubation with a restriction endonuclease, cleavage of a deoxyoligonucleotide duplex is not completely suppressed but only slowed down or limited to one strand. The site-directed mutagenesis procedure of *Eckstein* et al.[126, 127] is based on the inability of a restriction endonuclease to hydrolyze a phosphorothioate-containing strand of a double-helical DNA substrate.

4.2. Polymerases and Oligonucleotides Containing Apurinic/Abasic Stretches or Thymine Dimers

The numerous interactions of polymerases, ligases, etc., with RNA or DNA can be mimicked with (modified) oligonucleotides. Thus, experiments to discover mechanistic details can be designed and biological regulation circuits can be influenced by using modified oligonucleotides. In this article, oligonucleotides with abasic stretches and oligonucleotides containing thymine dimers will be discussed, owing to their importance in mutation events.

Apurinic or abasic nucleotides or stretches of nucleotides (**115**) play an important role in biology since breakage of the glycosidic linkage can occur under in vivo conditions. These sites of abasic RNA or DNA must therefore be digested or repaired in order to avoid mutations (for a review see Ref. [266]). Abasic[267–270] and apurinic[271–274] oligonucleotides can be used as model substrates for nucleases and polymerases.

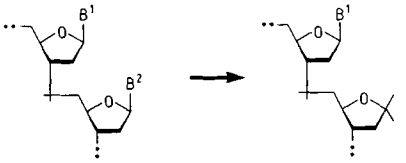

114 115

Abasic oligonucleotides lack one or several nucleobases. One way of preparing these oligonucleotides is to cleave nucleobases from the complete oligonucleotide.[268, 271] The other approach is oligonucleotide syntheses in which one or several steps use sugar-phosphate building blocks without nucleobases.[267, 270, 273, 274] The structure of a series of these oligonucleotides has been thoroughly investigated by NMR, CD, and IR;[267, 273, 274] these substances have a gap in the nucleobase sequence and, accordingly, their structures deviate from those of normal oligonucleotides. Preparatively, the abasic sites within an oligonucleotide can be used for triggering chain cleavage (by alkaline agents[272]) or for introducing reporter moieties (via amino groups of the reporter compounds[274–276]). In biological test systems containing abasic oligonucleotides and nucleases or polymerases, unusual reaction intermediates are produced or the enzymes are completely inhibited.

Thymine dimers (**117**) are the most important reaction product formed upon irradiation of DNA. In this reaction, two thymines belonging to the same strand and nucleobase stack are linked by formation of a cyclobutane moiety (**116** → **117**). The standard DNA functions are thereby inhibited. In vivo a DNA stretch modified in this way will be subject to repair. A number of oligonucleotides containing thymine dimers have been prepared, either by irradiation of unmodified oligonucleotides[277–279] or by synthesis of oligonucleotides incorporating preformed thymine dimers.[280, 281] These oligonucleotides have been used for

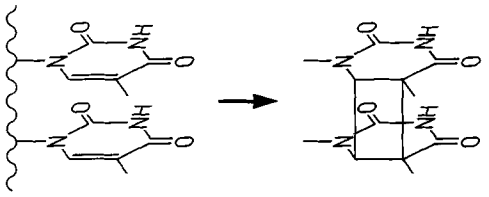

116 117

structural analyses[282–285] in order to elucidate the structure of DNA containing thymine dimers[286] (thymine dimers bend DNA; compare Section 2.5) or for studying DNA repair[277, 287] and mutagenesis[279] (in cases of incomplete or lacking repair).

4.3. Sequencing with Fluorescent Dyes Instead of Radioactive Isotopes

Sequencing techniques are under development with several different goals (for a review see Ref. [288]). First, there is a need for machine-readable sequencing gels[289–291] and for sequencing systems suitable for rare and artificial nucleotides.[292] Second, methods to obtain nucleotide sequences from very small amounts of material (mass spectrometry systems) are a target of research. Third, nonradioactive sequencing systems based on fluorescence spectroscopy are under development. The fluorescent label (e.g., rhodamine or fluorescein) can be linked to the primer.[189, 291, 293–297] After chromatographic separation of all oligonucleotides, the label is linked to the 5′ terminus of every oligonucleotide (**118** → **119**). Alternatively, the fluorescent dye can be coupled to that nucleotide terminating the chain, in which case all oligonucleotides are 3′-labeled[290, 298, 299] (**120** → **121**).

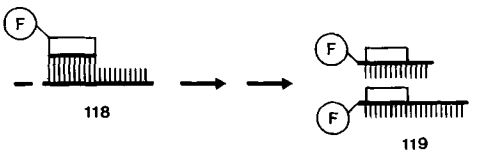

118 119

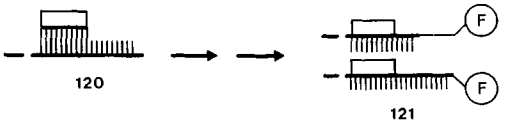

120 121

5. Summary and Outlook

A number of applications of modified oligonucleotides have been described in this article; many other applications have not been mentioned, such as those in the field of artificial enzymes or ribozymes. Other oligonucleotides of great interest include cyclic,[300-302] branched,[303-306] magnetic,[307] catalytic,[308, 309] and bent oligonucleotides[226, 227, 233, 234, 244, 286] (compare Sections 2.5 and 4), oligonucleotides carrying spin labels,[310] oligonucleotides suitable for immobilization of nucleic acids,[311, 312] oligonucleotides capable of binding heavy metals for X-ray analyses[295, 313] or for electron microscopy,[314] and antigenic or antigenic-response-modulating[315] oligonucleotides.

Modified oligonucleotides have been developed so far as substrate analogues, for identification, and as antisense oligonucleotides. A few applications as substrate analogues have been discussed above. The use of modified oligonucleotides to identify and localize nucleic acids has become a routine procedure. However, so far no modified oligonucleotide has been used as therapeutic agent. This would be particularly desirable since sequence-specific access to a given RNA or DNA stretch can be accomplished only with an antisense oligonucleotide or a protein (repressor, antibody, restriction endonuclease). To date such proteins cannot be designed or synthesized. In contrast, oligonucleotides can be synthesized and the mechanism of the inhibitory action of oligonucleotides via base-pairing is well understood. Three practical problems, already mentioned above, block application of a modified oligonucleotide as therapeutic agent: poor uptake into cells, digestion by cell nucleases, and short lifetime of the duplex formed. Nuclease-resistant oligonucleotides can be constructed. The lifetime of the duplex can be increased in several ways. For example, a covalent linkage can be formed between the two strands of a duplex. In addition, the methods to induce a strand scission in the complementary strand are well worked out. The problem that still needs attention is insufficient uptake of oligonucleotides into cells. (An alternative would be to transcribe an appropriate oligonucleotide from an artificial gene in the cell, but this approach is not possible at present.)

There is little knowledge regarding the mechanism of uptake.[131] Perhaps charged oligonucleotides, whether modified or not, are taken up by an active transport mechanism.[316, 317] Uncharged oligonucleotides, if considerably more lipophilic, also might be transported by passive mechanisms. The concentrations of oligonucleotides required in the cell culture medium for an effective inhibition of virus proliferation in virus-infected cells range from 0.5 to 30 μM for phosphorothioate oligonucleotides. In comparison, methylphosphonate oligonucleotides need 50–200 μM concentrations (see Section 2.6), perhaps owing to their lower water solubility or the lack of activation of RNase H. The concentration of the oligonucleotide inside the cell is considered to be roughly 10% of that outside the cell;[318] the uptake occurs in the range of minutes to hours. In addition, oligonucleotides can enter the nucleus[77] since oligonucleotides directed to bind to splice regions show inhibitory effects.[144, 157, 162, 213] In general, however, knowledge regarding distribution of oligonucleotides within the cell compartments is rather sketchy.[319] These data for in vivo systems largely agree with the in vitro finding that to yield an inhibition of 80–90% the molar relation of oligonucleotide to target sequence must range from 1000:1 to 5:1.[27] The uptake problem urgently needs more attention. For artificial therapeutic agents additional oligomer delivery systems are being considered, such as the inclusion of oligonucleotides in liposomes. Such particles, via an antigen–antibody reaction,

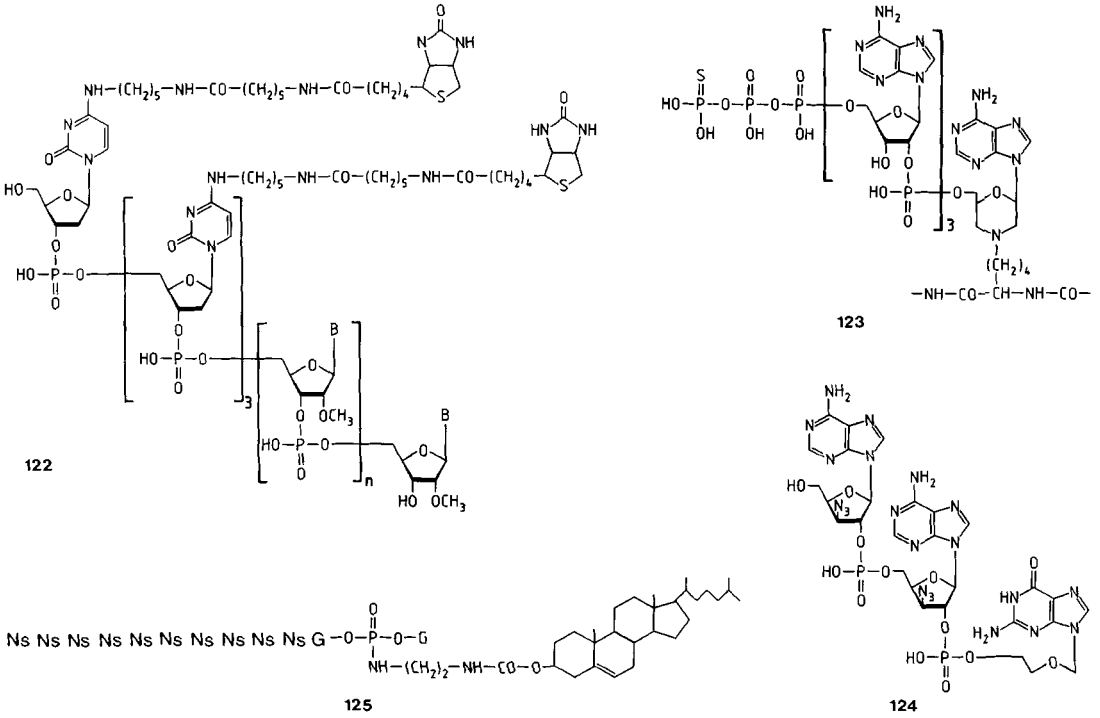

might even be selectively transported to one target tissue.[320] An oligonucleotide can also be linked to a protein (for example, interleukin[321]) and then internalized through the receptor specific for the protein. Some further artificial uptake systems are under development.[38]

In theory, the concentration of oligonucleotide needed for inhibition at the level of transcription would be considerably smaller than at the level of translation, since the concentration of the target nucleic acid is by far lower at the transcription level. On the translation level inhibition by an oligonucleotide generally means the formation of a duplex of a single-stranded messenger RNA and an oligonucleotide. In contrast, transcription principally starts from double-stranded DNA. The formation of a triple-helix structure as an inhibitory entity is documented for polypurine and polypyrimidine stretches of DNA (which occur in control regions of eukaryotic genes; for an example see Ref. [322]) and for oligothymidylates or similar oligonucleotides.[57, 76, 96, 97, 102] In contrast, triple-helix formation with variable sequences has not been established[323] and no successful inhibition via such a triple helix has been reported (for a review see Ref. [324]).

Another prerequisite for selecting a drug out of the many prepared oligonucleotides is to test each oligonucleotide in many biological systems. So far, however, each oligonucleotide synthesized has usually been tested in only one biological system. Obviously, an oligonucleotide will exhibit different properties in different biological test systems (e.g., normal and neoplastic tissues or normal and infected cells). Establishing and compiling such data might reveal some general rules. The rules—in the sense of rational drug design—might then describe how to increase at least the uptake, nuclease resistance, and duplex stability of a modified oligonucleotide without increasing properties, such as toxicity (for reviews see Refs. [7, 31–34, 37, 40, 325]).

Modified oligonucleotides will continue to be a field of exciting research with the ultimate goal of clinical application. Probably, those oligonucleotides that are able to escape all the "traps" in the cells must deviate considerably from unmodified oligonucleotides; that is, they must be modified in several ways. Typical examples may be a biotin-carrying oligonucleotide (**122**),[207] a 5′-γ-phosphorothioate(2′-5′)A_4-poly(Lys) construct (**123**),[174] a trinucleotide analogue (**124**)[326] with three modifications (designed to release the antiviral compound acyclovir monophosphate within the cell[327]), and a cholesterol-phosphorothioate oligonucleotide (**125**).[168]

The authors would like to imagine an oligonucleotide that is hydrophobic in the uptake step, then changes its properties through contact with RNase, for example, so that, in a highly reactive state, it forms a covalent dead-end complex. Certainly, organic chemistry should be able to synthesize such an oligonucleotide.

The authors thank Ute Rust for typing this manuscript and Dr. W. Freist and Dr. H. Rosemeyer for critically reading it.

Received: December 13, 1989;
supplemented: December 21, 1990 [A 816 IE]
German version: *Angew. Chem. 103* (1991) 629

[1] M. Inouye, *Gene 72* (1988) 25.
[2] R. W. Simons, N. Kleckner, *Annu. Rev. Genet. 22* (1988) 567.
[3] R. Frankham, *J. Theor. Biol. 135* (1988) 85.
[4] B. Polisky, *Cell (Cambridge, Mass.) 55* (1988) 929.
[5] A. R. van der Krol, J. N. M. Mol, A. R. Stuitje, *Gene 72* (1988) 45.
[6] R. W. Simons, *Gene 72* (1988) 35.
[7] J. S. Cohen (Ed.): *Oligodeoxynucleotides, Antisense Inhibitors of Gene Expression*, Macmillan, London 1989.
[8] K. Itakura, J. J. Rossi, R. B. Wallace, *Annu. Rev. Biochem. 53* (1984) 323.
[9] E. Uhlmann, A. Peyman, *Chem. Rev. 90* (1990) 543.
[10] J. E. Hearst, *Annu. Rev. Phys. Chem. 39* (1988) 291.
[11] J. Sambrook, E. F. Fritsch, T. Maniatis: *Molecular Cloning, 2nd ed.*, Chapter 11: "Synthetic Oligonucleotide Probes," Cold Spring Harbor Lab. 1989.
[12] J. W. Engels, E. Uhlmann, *Angew. Chem. 101* (1989) 733; *Angew. Chem. Int. Ed. Engl. 28* (1989) 716.
[13] R. Wu, L. Grossmann (Eds.): *Methods Enzymol. 154* (1987) 221–236, Section III: "Chemical Synthesis and Analysis of Oligonucleotides."
[14] S. A. Narang (Ed.): *Synthesis and Applications of DNA and RNA*, Academic, Orlando 1987.
[15] M. J. Gait (Ed.): *Oligonucleotide Synthesis*, IRL Press, Oxford, 1984.
[16] H. G. Gassen, A. Lang (Eds.): *Chemical and Enzymatic Synthesis of Gene Fragments*, Verlag Chemie, Weinheim 1982.
[17] M. H. Caruthers in [7], pp. 7–24.
[18] U. Pieles, U. Englisch, *Nucleic Acids Res. 17* (1989) 285.
[19] U. Pieles, B. S. Sproat, P. Neuner, F. Cramer, *Nucleic Acids Res. 17* (1989) 8967.
[20] B. L. Lee, K. R. Blake, P. S. Miller, *Nucleic Acids Res. 16* (1988) 10681.
[21] B. L. Lee, A. Murakami, K. R. Blake, S.-B. Lin, P. S. Miller, *Biochemistry 27* (1988) 3197.
[22] J. Teare, P. Wollenzien, *Nucleic Acids Res. 17* (1989) 3359.
[23] G. D. Cimino, H. B. Gamper, S. T. Isaacs, J. E. Hearst, *Annu. Rev. Biochem. 54* (1985) 1151.
[24] E. Moustacchi, *Arch. Toxicol. Suppl. 12* (1988) 26.
[25] J. E. Hearst, *Chem. Res. Toxicol. 2* (1989) 69.
[26] U. Englisch, F. Benseler et al., unpublished.
[27] A. Wolf, U. Pieles, U. Englisch et al., unpublished.
[28] P. Strazewski, C. Tamm, *Angew. Chem. 102* (1990) 37; *Angew. Chem. Int. Ed. Engl. 29* (1990) 36.
[29] See [7], Chapter 3–5, 7.
[30] P. O. P. Ts'o, P. S. Miller, L. Aurelian, A. Murakami, C. Agris, K. R. Blake, S. B. Lin, B. L. Lee, C. C. Smith, *Ann. N.Y. Acad. Sci. 507* (1987) 220.
[31] P. S. Miller, P. O. P. Ts'o, *Annu. Rep. Med. Chem. 23* (1988) 295.
[32] C. A. Stein, J. S. Cohen, *Cancer Res. 48* (1988) 2659.
[33] J. J. Toulmé, C. Hélène, *Gene 72* (1988) 51.
[34] C. J. Marcus-Sekura, *Anal. Biochem. 172* (1988) 289.
[35] J. S. Cohen, *Trends Pharmacol. Sci. 10* (1989) 435.
[36] L. M. Neckers in [7], pp. 211–232.
[37] D. M. Tidd, *Anti-Cancer Res. 10* (1990) 1169.
[38] G. Zon, *Pharm. Res. 5* (1988) 539.
[39] C. G. Miyada, A. B. Studencki, R. B. Wallace in [14], pp. 207–227.
[40] B. S. Reckmann, *Nachr. Chem. Tech. Lab. 37* (1989) 692.
[41] H. W. Zimmermann, *Angew. Chem. 98* (1986) 115; *Angew. Chem. Int. Ed. Engl. 25* (1986) 115.
[42] N. T. Thuong, U. Asseline, T. Montenay-Garestier in [7], pp. 25–51.
[43] C. Hélène, J. J. Toulmé in [7], pp. 137–172.
[44] U. Asseline, M. Delarue, G. Lancelot, F. Toulmé, N. T. Thuong, T. Montenay-Garestier, C. Hélène, *Proc. Natl. Acad. Sci. USA 81* (1984) 3297.
[45] U. Asseline, N. T. Thuong, *Nucleosides Nucleotides 7* (1988) 431.
[46] K. Mori, C. Subasinghe, C. A. Stein, J. S. Cohen, *Nucleosides Nucleotides 8* (1989) 649.
[47] A. Jäger, M. J. Levy, S. M. Hecht, *Biochemistry 27* (1988) 7237.
[48] G. Lancelot, J.-L. Guesnet, U. Asseline, N. T. Thuong, *Biochemistry 27* (1988) 1265.
[49] G. Lancelot, N. T. Thuong, *Biochemistry 25* (1986) 5357.
[50] C. A. Stein, K. Mori, S. L. Loke, C. Subasinghe, K. Shinozuka, J. S. Cohen, L. M. Neckers, *Gene 72* (1988) 333.
[51] U. Asseline, N. T. Thuong, C. Hélène, *J. Biol. Chem. 260* (1985) 8936.
[52] F. Birg, D. Praseuth, A. Zerial, N. T. Thuong, U. Asseline, T. Le Doan, C. Hélène, *Nucleic Acids Res. 18* (1990) 2901.
[53] C. Cazenave, N. Loreau, N. T. Thuong, J. J. Toulmé, C. Hélène, *Nucleic Acids Res. 15* (1987) 4717.
[54] P. Verspieren, A. W. C. A. Cornelissen, N. T. Thuong, C. Hélène, J. J. Toulmé, *Gene 61* (1987) 307.
[55] A. Zerial, N. T. Thuong, C. Hélène, *Nucleic Acids Res. 15* (1987) 9909.
[56] J. J. Toulmé, H. M. Krisch, N. Loreau, N. T. Thuong, C. Hélène, *Proc. Natl. Acad. Sci. USA 83* (1986) 1227.
[57] J.-S. Sun, J.-C. François, T. Montenay-Garestier, T. Saison-Behmoaras, V. Roig, N. T. Thuong, C. Hélène, *Proc. Natl. Acad. Sci. USA 86* (1989) 9198.
[58] J.-S. Sun, U. Asseline, D. Rouzaud, T. Montenay-Garestier, N. T. Thuong, C. Hélène, *Nucleic Acids Res. 15* (1987) 6149.

[59] N. T. Thuong, U. Asseline, V. Roig, M. Takasugi, C. Hélène, *Proc. Natl. Acad. Sci. USA 84* (1987) 5129.
[60] N. T. Thuong, M. Chassignol, *Tetrahedron Lett. 29* (1988) 5905.
[61] D. Praseuth, M. Chassignol, M. Takasugi, T. Le Doan, N. T. Thuong, C. Hélène, *J. Mol. Biol. 196* (1987) 939.
[62] C. Hélène, N. T. Thuong, *Biochem. Pharmacol. 37* (1988) 1797.
[63] J. Paoletti, D. Bazile, F. Morvan, J.-L. Imbach, C. Paoletti, *Nucleic Acids Res. 17* (1989) 2693.
[64] B. Rayner, C. Malvy, J. Paoletti, B. Lebleu, C. Paoletti, J.-L. Imbach in [7], pp. 119–136.
[65] J.-L. Imbach, B. Rayner, F. Morvan, *Nucleosides Nucleotides 8* (1989) 627.
[66] R. Pauwels, Z. Debyser, J. Balzarini, M. Baba, J. Desmyter, B. Rayner, F. Morvan, J. L. Imbach, E. De Clercq, *Nucleosides Nucleotides 8* (1989) 995.
[67] J.-R. Bertrand, J.-L. Imbach, C. Paoletti, C. Malvy, *Biochem. Biophys. Res. Commun. 164* (1989) 311.
[68] C. Gagnor, B. Rayner, J.-P. Leonetti, J.-L. Imbach, B. Lebleu, *Nucleic Acids Res. 17* (1989) 5107.
[69] D. Praseuth, T. Le Doan, M. Chassignol, J.-L. Decout, N. Habhoub, J. Lhomme, N. T. Thuong, C. Hélène, *Biochemistry 27* (1988) 3031.
[70] D. Praseuth, L. Perrouault, T. Le Doan, M. Chassignol, N. T. Thuong, C. Hélène, *Proc. Natl. Acad. Sci. USA 85* (1988) 1349.
[71] D. G. Knorre, V. V. Vlassov, V. F. Zarytova in [7], pp. 173–196.
[72] V. V. Vlassov, A. A. Godovikov, N. D. Kobets, A. S. Ryte, L. V. Yurchenko, A. G. Bukrinskaya, *Adv. Enzyme Regul. 24* (1985) 301.
[73] V. V. Vlassov, V. F. Zarytova, I. V. Kutyavin, S. V. Mamaev, *FEBS Lett. 231* (1988) 352.
[74] I. V. Kutyavin, M. A. Podyminogin, Y. N. Bazhina, O. S. Fedorova, D. G. Knorre, A. S. Levina, S. V. Mamayev, V. F. Zarytova, *FEBS Lett. 238* (1988) 35.
[75] V. V. Vlassov, V. F. Zarytova, I. V. Kutyavin, S. V. Mamaev, M. A. Podyminogin, *Nucleic Acids Res. 14* (1986) 4065.
[76] V. V. Vlassov, S. A. Gaidamakov, V. F. Zarytova, D. G. Knorre, A. S. Levina, A. A. Nikonova, L. M. Podust, O. S. Fedorova, *Gene 72* (1988) 313.
[77] A. S. Boutorin, L. V. Guskova, E. M. Ivanova, N. D. Kobetz, V. F. Zarytova, A. S. Ryte, L. V. Yurchenko, V. V. Vlassov, *FEBS Lett. 254* (1989) 129.
[78] T. Le Doan, L. Perrouault, D. Praseuth, N. Habhoub, J.-L. Decout, N. T. Thuong, J. Lhomme, C. Héléne, *Nucleic Acids Res. 15* (1987) 7749.
[79] R. K. Evans, J. D. Johnson, B. E. Haley, *Proc. Natl. Acad. Sci. USA 83* (1986) 5382.
[80] R. K. Evans, B. E. Haley, *Biochemistry 26* (1987) 269.
[81] T. R. Webb, M. D. Matteucci, *Nucleic Acids Res. 14* (1986) 7661.
[82] M. Chatterjee, S. E. Rokita, *J. Am. Chem. Soc. 112* (1990) 6397.
[83] B. C. F. Chu, L. E. Orgel, *Nucleic Acids Res. 18* (1990) 5163.
[84] T. P. Brent, J. S. Remack, *Nucleic Acids Res. 16* (1988) 6779.
[85] T. S. Godovikova, M. A. Grachev, J. V. Kutyavin, J. G. Tsarev, V. F. Zarytova, E. F. Zaychikov, *Eur. J. Biochem. 166* (1987) 611.
[86] B. C. F. Chu, L. E. Orgel, *Nucleic Acids Res. 16* (1988) 3671.
[87] R. N. Zuckermann, D. R. Corey, P. G. Schultz, *J. Am. Chem. Soc. 110* (1988) 1614.
[88] D. R. Corey, D. Pei, P. G. Schultz, *J. Am. Chem. Soc. 111* (1989) 8523.
[89] T. Le Doan, L. Perrouault, M. Chassignol, N. T. Thuong, C. Hélène, *Nucleic Acids Res. 15* (1987) 8643.
[90] E. I. Frolova, E. M. Ivanova, V. F. Zarytova, T. V. Abramova, V. V. Vlassov, *FEBS Lett. 269* (1990) 101.
[91] B. C. F. Chu, L. E. Orgel, *Proc. Natl. Acad. Sci. USA 82* (1985) 963.
[92] E. B. Brosalina, V. V. Vlassov, S. A. Kazakov, *Bioorg. Khim. 14* (1988) 125.
[93] G. B. Dreyer, P. B. Dervan, *Proc. Natl. Acad. Sci. USA 82* (1985) 968.
[94] T. Le Doan, L. Perrouault, C. Hélène, M. Chassignol, N. T. Thuong, *Biochemistry 25* (1986) 6736.
[95] A. S. Boutorin, V. V. Vlassov, S. A. Kazakov, I. V. Kutiavin, M. A. Podyminogin, *FEBS Lett. 172* (1984) 43.
[96] M. Boidot-Forget, M. Chassignol, M. Takasugi, N. T. Thuong, C. Hélène, *Gene 72* (1988) 361.
[97] H. E. Moser, P. E. Dervan, *Science (Washington, D.C.) 238* (1987) 645.
[98] S. A. Strobel, P. B. Dervan, *J. Am. Chem. Soc. 111* (1989) 7286.
[99] J.-C. François, T. Saison-Behmoaras, M. Chassignol, N. T. Thuong, J.-S. Sun, C. Hélène, *Biochemistry 27* (1988) 2272.
[100] C. H. B. Chen, D. S. Sigman, *Proc. Natl. Acad. Sci. USA 83* (1986) 7147.
[101] C. H. B. Chen, D. S. Sigman, *J. Am. Chem. Soc. 110* (1988) 6570.
[102] J. C. François, T. Saison-Behmoaras, C. Hélène, *Nucleic Acids Res. 16* (1988) 11 431.
[103] B. L. Iverson, P. B. Dervan, *J. Am. Chem. Soc. 109* (1987) 1241.
[104] L. Perrouault, U. Asseline, C. Rivalle, N. T. Thuong, E. Bisagni, C. Giovannangeli, T. Le Doan, C. Hélène, *Nature (London) 344* (1990) 358.
[105] O. B. Stepanova, V. G. Metelev, N. V. Chichkova, V. D. Smirnov, N. P. Rodionova, J. G. Atabekov, A. A. Bogdanov, Z. A. Shabarova, *FEBS Lett. 103* (1979) 197.
[106] J. Shuttleworth, G. Matthews, L. Dale, C. Baker, A. Colman, *Gene 72* (1988) 267.
[107] P. J. Furdon, Z. Dominski, R. Kole, *Nucleic Acids Res. 17* (1989) 9193.
[108] S. Agrawal, S. H. Mayrand, P. C. Zamecnik, T. Pederson, *Proc. Natl. Acad. Sci. USA 87* (1990) 1401.
[109] K. J. Atabekov, L. G. Tyulkina, O. V. Karpova, V. G. Metelev, N. P. Rodionova, Z. A. Shabarova, J. G. Atabekov, *FEBS Lett. 232* (1988) 96.
[110] S. Shibahara, S. Mukai, T. Nishihara, H. Inoue, E. Ohtsuka, H. Morisawa, *Nucleic Acids Res. 15* (1987) 4403.
[111] J. R. Wyatt, G. T. Walker, *Nucleic Acids Res. 17* (1989) 7833.
[112] R. S. Quartin, C. L. Brakel, J. G. Wetmur, *Nucleic Acids Res. 17* (1989) 7253.
[113] H. Inoue, Y. Hayase, S. Iwai, E. Ohtsuka, *FEBS Lett. 215* (1987) 327.
[114] A. Pasini, F. Zunino, *Angew. Chem. 99* (1987) 632; *Angew. Chem. Int. Ed. Engl. 26* (1987) 615.
[115] N. P. Johnson, P. Lapetoule, H. Razaka, G. Villani, *Assoc. Int. Cancer Res. Symp. 4* (1985) 1.
[116] L. Marrot, M. Leng, *Biochemistry 28* (1989) 1454.
[117] M. F. Anin, M. Leng, *Nucleic Acids Res. 18* (1990) 4395.
[118] C. J. van Garderen, H. van den Elst, J. H. van Boom, J. Reedijk, L. P. A. van Houte, *J. Am. Chem. Soc. 111* (1989) 4123.
[119] S. E. Sherman, D. Gibson, A. H. Wang, S. J. Lippard, *J. Am. Chem. Soc. 110* (1988) 7368.
[120] T. P. Kline, L. G. Marzilli, D. Live, G. Zon, *Biochem. Pharmacol. 40* (1990) 97.
[121] L. J. Naser, A. L. Pinto, S. J. Lippard, J. M. Essigmann, *Biochemistry 27* (1988) 4357.
[122] P. S. Miller in [7], pp. 79–95.
[123] C. A. Stein, J. S. Cohen in [7], pp. 97–117.
[124] J. Goodchild in [7], pp. 53–77.
[125] F. Eckstein, *Angew. Chem. 95* (1983) 431; *Angew. Chem. Int. Ed. Engl. 22* (1983) 423.
[126] F. Eckstein, G. Gish, *Trends Biochem. Sci. 14* (1989) 97.
[127] D. B. Olsen, F. Eckstein, *Proc. Natl. Acad. Sci. USA 87* (1990) 1451.
[128] B. Uznanski, A. Wilk, W. J. Stec, *Tetrahedron Lett. 28* (1987) 3401.
[129] M. J. Nemer, K. K. Ogilvie, *Tetrahedron Lett. 21* (1980) 4149.
[130] J. Nielsen, W. K.-D. Brill, M. H. Caruthers, *Tetrahedron Lett. 29* (1988) 2911.
[131] C. J. Marcus-Sekura, A. M. Woerner, K. Shinozuka, G. Zon, G. V. Quinnan, *Nucleic Acids Res. 15* (1987) 5749.
[132] D. E. Bergstrom, P. W. Shum, *J. Org. Chem. 53* (1988) 3953.
[133] R. L. Letsinger, S. A. Bach, J. S. Eadie, *Nucleic Acids Res. 14* (1986) 3487.
[134] R. L. Letsinger, C. N. Singman, G. Histand, M. Salunkhe, *J. Am. Chem. Soc. 110* (1988) 4470.
[135] M. Koziolkiewicz, B. Uznanski, W. Stec, G. Zon, *Chem. Scr. 26* (1986) 251.
[136] H. M. Moody, M. H. P. van Genderen, L. H. Koole, H. J. M. Kocken, E. M. Meijer, H. M. Buck, *Nucleic Acids Res. 17* (1989) 4769.
[137] S. Agrawal, J. Goodchild, M. Civeira, A. H. Thornton, P. S. Sarin, P. C. Zamecnik, *Proc. Natl. Acad. Sci. USA 85* (1988) 7079.
[138] M. J. Nemer, K. K. Ogilvie, *Tetrahedron Lett. 21* (1980) 4153.
[139] R. L. Letsinger, W. S. Mungall, *J. Org. Chem. 35* (1970) 3800.
[140] M. Mag, J. W. Engels, *Nucleic Acids Res. 17* (1989) 5973.
[141] R. S. Quartin, J. G. Wetmur, *Biochemistry 28* (1989) 1040.
[142] Z. J. Lesnikowski, M. Jaworska, W. J. Stec, *Nucleic Acids Res. 16* (1988) 11 675.
[143] A. Murakami, K. R. Blake, P. S. Miller, *Biochemistry 24* (1985) 4041.
[144] P. S. Miller, C. H. Agris, L. Aurelian, K. R. Blake, A. Murakami, M. P. Reddy, S. A. Spitz, P. O. P. Ts'o, *Biochimie 67* (1985) 769.
[145] D. M. Tidd, P. Hawley, H. M. Warenius, I. Gibson, *Anti-Cancer Drug Des. 3* (1988) 117.
[146] L. J. Maher, B. J. Dolnick, *Nucleic Acids Res. 16* (1988) 3341.
[147] W. K.-D. Brill, M. H. Caruthers, *Nucleosides Nucleotides 8* (1989) 1011.
[148] R. Cosstick, J. S. Vyle, *Tetrahedron Lett. 30* (1989) 4693.
[149] H. Seliger, G. Feger, *Nucleosides Nucleotides 6* (1987) 483.
[150] J. F. Cormier, K. K. Ogilvie, *Nucleic Acids Res. 16* (1988) 4583.
[151] G. Degols, J.-P. Leonetti, C. Gagnor, M. Lemaitre, B. Lebleu, *Nucleic Acids Res. 17* (1989) 9341.
[152] C. H. Agris, K. R. Blake, P. S. Miller, M. P. Reddy, P. O. P. Ts'o, *Biochemistry 25* (1986) 6268.
[153] W. Gao, C. A. Stein, J. S. Cohen, G. E. Dutschman, Y.-C. Cheng, *J. Biol. Chem. 264* (1989) 11 521.
[154] M. Matsukura, K. Shinozuka, G. Zon, H. Mitsuya, M. Reitz, J. S. Cohen, S. Broder, *Proc. Natl. Acad. Sci. USA 84* (1987) 7706.
[155] C. Majumdar, C. A. Stein, J. S. Cohen, S. Broder, S. H. Wilson, *Biochemistry 28* (1989) 1340.
[156] K. Mori, C. Boiziau, C. Cazenave, M. Matsukura, C. Subasinghe, J. S. Cohen, S. Broder, J. J. Toulmé, C. A. Stein, *Nucleic Acids Res. 17* (1989) 8207.
[157] C. C. Smith, L. Aurelian, M. P. Reddy, P. S. Miller, P. O. P. Ts'o, *Proc. Natl. Acad. Sci. USA 83* (1986) 2787.

[158] M. Lemaître, C. Bisbal, B. Bayard, B. Lebleu, *Nucleosides Nucleotides 6* (1987) 311.
[159] M. Lemaître, B. Bayard, B. Lebleu, *Proc. Natl. Acad. Sci. USA 84* (1987) 648.
[160] J.-P. Leonetti, G. Degols, P. Milhaud, C. Gagnor, M. Lemaître, B. Lebleu, *Nucleosides Nucleotides 8* (1989) 825.
[161] R. G. Shea, J. C. Marsters, N. Bischofberger, *Nucleic Acids Res. 18* (1990) 3777.
[162] S. Agrawal, J. Goodchild, M. Civeira, P. S. Sarin, P. C. Zamecnik, *Nucleosides Nucleotides 8* (1989) 819.
[163] M. Matsukura, G. Zon, K. Shinozuka, C. A. Stein, H. Mitsuya, J. S. Cohen, S. Broder, *Gene 72* (1988) 343.
[164] M. Matsukura, G. Zon, K. Shinozuka, M. Robert-Guroff, T. Shimada, C. A. Stein, H. Mitsuya, F. Wong-Staal, J. S. Cohen, S. Broder, *Proc. Natl. Acad. Sci. USA 86* (1989) 4244.
[165] S. Agrawal, T. Ikeuchi, D. Sun, P. S. Sarin, A. Konopka, J. Maizel, P. C. Zamecnik, *Proc. Natl. Acad. Sci. USA 86* (1989) 7790.
[166] M. Stevenson, P. L. Iversen, *J. Gen. Virol. 70* (1989) 2673.
[167] S. Shibahara, S. Mukai, H. Morisawa, H. Nakashima, S. Kobayashi, N. Yamamoto, *Nucleic Acids Res. 17* (1989) 239.
[168] R. L. Letsinger, G. Zhang, D. K. Sun, T. Ikeuchi, P. S. Sarin, *Proc. Natl. Acad. Sci. USA 86* (1989) 6553.
[169] J. Haralambidis, L. Duncan, G. W. Tregear, *Tetrahedron Lett. 28* (1987) 5199.
[170] E. Kuyl-Yeheskiely, C. M. Dreef-Tromp, A. Geluk, G. A. van der Marel, J. H. van Boom, *Nucleic Acids Res. 17* (1989) 2897.
[171] E. De Clercq, *Nucleosides Nucleotides 4* (1985) 3.
[172] I. M. Kerr, *J. Interferon Res. 7* (1987) 505.
[173] D. C. Montefiori, R. W. Sobol, S. W. Li, N. L. Reichenbach, R. J. Suhadolnik, R. Charubala, W. Pfleiderer, A. Modliszewski, W. E. Robinson, W. M. Mitchell, *Proc. Natl. Acad. Sci. USA 86* (1989) 7191.
[174] C. Bisbal, M. Silhol, M. Lemaître, B. Bayard, T. Salehzada, B. Lebleu, T. D. Perrée, M. G. Blackburn, *Biochemistry 26* (1987) 5172.
[175] C. G. Miyada, R. B. Wallace, *Methods Enzymol. 154* (1987) 94.
[176] W. I. Wood, *Methods Enzymol. 152* (1987) 443.
[177] N. A. Spoerel, F. C. Kafatos, *Methods Enzymol. 152* (1987) 588.
[178] R. B. Wallace, C. G. Miyada, *Methods Enzymol. 152* (1987) 432.
[179] A. A. Reyes, R. B. Wallace, *Genet. Eng. (London) 6* (1984) 157.
[180] M. S. Urdea, B. D. Warner, J. A. Running, M. Stempien, J. Clyne, T. Horn, *Nucleic Acids Res. 16* (1988) 4937.
[181] A. Kumar, P. Tchen, F. Roullet, J. Cohen, *Anal. Biochem. 169* (1988) 376.
[182] J. Telser, K. A. Cruickshank, L. E. Morrison, T. L. Netzel, *J. Am. Chem. Soc. 111* (1989) 6966.
[183] R. Zuckermann, D. Corey, P. Schultz, *Nucleic Acids Res. 15* (1987) 5305.
[184] V. K. Kansal, T. Huynh-Dinh, J. Igolen, *Tetrahedron Lett. 29* (1988) 5537.
[185] K. A. Cruickshank, D. L. Stockwell, *Tetrahedron Lett. 29* (1988) 5221.
[186] J. Haralambidis, M. Chai, G. W. Tregear, *Nucleic Acids Res. 15* (1987) 4857.
[187] T. Tanaka, Y. Yamada, M. Ikehara, *Chem. Pharm. Bull. 36* (1988) 1386.
[188] R. I. Amann, L. Krumholz, D. A. Stahl, *J. Bacteriol. 172* (1990) 762.
[189] W. Bannwarth, D. Schmidt, *Tetrahedron Lett. 30* (1989) 1513.
[190] L. S. Lasater, P. A. Cann, D. G. Glitz, *J. Biol. Chem. 264* (1989) 21 798.
[191] L. S. Lasater, L. Montesano-Roditis, P. A. Cann, D. G. Glitz, *Nucleic Acids Res. 18* (1990) 477.
[192] A. M. Alves, D. Holland, M. D. Edge, F. J. Carr, *Nucleic Acids Res. 16* (1988) 8722.
[193] J. L. Ruth, E. Jablonski, *Nucleosides Nucleotides 6* (1987) 541.
[194] E. Jablonski, E. W. Moomaw, R. H. Tullis, J. L. Ruth, *Nucleic Acids Res. 14* (1986) 6115.
[195] P. Li, P. P. Medon, D. C. Skingle, J. A. Lanser, R. H. Symons, *Nucleic Acids Res. 15* (1987) 5275.
[196] A. Murakami, J. Tada, K. Yamagata, J. Takano, *Nucleic Acids Res. 17* (1989) 5587.
[197] S. S. Ghosh, P. M. Kao, D. Y. Kwoh, *Anal. Biochem. 178* (1989) 43.
[198] J. Czichos, M. Köhler, B. Reckmann, M. Renz, *Nucleic Acids Res. 17* (1989) 1563.
[199] W. S. Young, *Neuropeptides (Edinburgh) 13* (1989) 271.
[200] H. Zischler, R. Schäfer, J. T. Epplen, *Nucleic Acids Res. 17* (1989) 4411.
[201] J. F. R. Ramalho-Ortigao, G. F. Jirikowski, H. Seliger, *Nucleosides Nucleotides 8* (1989) 805.
[202] A. H. Al-Hakim, R. Hull, *Biochem. J. 251* (1988) 935.
[203] E. L. Sheldon, D. E. Kellogg, R. Watson, C. H. Levenson, H. A. Erlich, *Proc. Natl. Acad. Sci. USA 83* (1986) 9085.
[204] J.-P. Roduit, J. Shaw, A. Chollet, A. Chollet, *Nucleosides Nucleotides 6* (1987) 349.
[205] A. F. Cook, E. Vuocolo, C. L. Brakel, *Nucleic Acids Res. 16* (1988) 4077.
[206] R. Kierzek, W. T. Markiewicz, *Nucleosides Nucleotides 6* (1987) 403.
[207] B. S. Sproat, A. I. Lamond, B. Beijer, P. Neuner, U. Ryder, *Nucleic Acids Res. 17* (1989) 3373.
[208] T. Kempe, W. I. Sundquist, F. Chow, S.-L. Hu, *Nucleic Acids Res. 13* (1985) 45.
[209] B. C. F. Chu, L. Orgel, *DNA 4* (1985) 327.
[210] P. R. Langer, A. A. Waldrop, D. C. Ward, *Proc. Natl. Acad. Sci. USA 78* (1981) 6633.
[211] A. Murasugi, R. B. Wallace, *DNA 3* (1984) 269.
[212] L. K. Riley, M. E. Marshall, M. S. Coleman, *DNA 5* (1986) 333.
[213] S. M. L. Barabino, B. S. Sproat, U. Ryder, B. J. Blencowe, A. I. Lamond, *EMBO J. 8* (1989) 4171.
[214] B. J. Blencowe, B. S. Sproat, U. Ryder, S. M. L. Barabino, A. I. Lamond, *Cell (Cambridge, Mass.) 59* (1989) 531.
[215] E. Viegas-Pequignot, B. Dutrillaux, H. Magdelenat, M. Coppey-Moisan, *Proc. Natl. Acad. Sci. USA 86* (1989) 582.
[216] A. K. Basu, J. M. Essigmann, *Chem. Res. Toxicol. 1* (1988) 1.
[217] N. Gregersen, V. Winter, K. B. Petersen, J. Koch, S. Kolvraa, N. Rüdiger, E.-M. Heinsvig, L. Bolund, *Clin. Chim. Acta 182* (1989) 151.
[218] L. L. Tilzer, E. G. Concepcion, *Am. J. Clin. Pathol. 91* (1989) 464.
[219] X. Saez-Llorens, L. M. Guzman-Verduzco, S. Shelton, J. D. Nelson, Y. M. Kupersztoch, *J. Clin. Microbiol. 27* (1989) 1684.
[220] A.-F. Guitteny, B. Fouque, C. Mougin, R. Teoule, B. Bloch, *J. Histochem. Cytochem. 36* (1988) 563.
[221] H. E. Hopp, L. Giavedoni, M. A. Mandel, A. Arese, B. Orman, F. B. Almonacid, H. N. Torres, A. N. Mentaberry, *Arch. Virol. 103* (1988) 231.
[222] D. T. Kingsbury, *Trends Biotechnol. 5* (1987) 107.
[223] Y. Kawase, S. Iwai, E. Ohtsuka, *Chem. Pharm. Bull. 37* (1989) 599.
[224] F. H. Martin, M. M. Castro, F. Aboul-ela, I. Tinoco, *Nucleic Acids Res. 13* (1985) 8927.
[225] E. Ohtsuka, S. Matsuki, M. Ikehara, Y. Takahashi, K. Matsubara, *J. Biol. Chem. 260* (1985) 2605.
[226] S. Diekmann, E. von Kitzing, L. McLaughlin, J. Ott, F. Eckstein, *Proc. Natl. Acad. Sci. 84* (1987) 8257.
[227] P. J. Hagerman, *Biochemistry 29* (1990) 1980.
[228] R. Eritja, D. M. Horowitz, P. A. Walker, J. P. Ziehler-Martin, M. S. Boosalis, M. F. Goodman, K. Itakura, B. E. Kaplan, *Nucleic Acids Res. 14* (1986) 8135.
[229] B. L. Gaffney, L. A. Marky, R. A. Jones, *Tetrahedron 40* (1984) 3.
[230] A. Chollet, E. Kawashima, *Nucleic Acids Res. 16* (1988) 305.
[231] H. Inoue, A. Imura, E. Ohtsuka, *Nucleic Acids Res. 13* (1985) 7119.
[232] F. Seela, H. Driller, *Nucleic Acids Res. 13* (1985) 911.
[233] F. Seela, H. Berg, H. Rosemeyer, *Biochemistry 28* (1989) 6193.
[234] F. Seela, H. Rosemeyer, T. Grein, *Nucleosides Nucleotides 9* (1990) 411.
[235] F. Seela, U. Bindig, H. Driller, W. Herdering, K. Kaiser, A. Kehne, H. Rosemeyer, H. Steker, *Nucleosides Nucleotides 6* (1987) 11.
[236] F. Seela, A. Kehne, *Biochemistry 26* (1987) 2232.
[237] M. J. McLean, F. Seela, M. J. Waring, *Proc. Natl. Acad. Sci. USA 86* (1989) 9687.
[238] F. Seela, K. Kaiser, *Helv. Chim. Acta 71* (1988) 1813.
[239] F. Seela, H. Driller, K. Kaiser, H. Rosemeyer, H. Steker, *Nucleosides Nucleotides 8* (1989) 789.
[240] R. Cosstick, X. Li, D. K. Tuli, D. M. Williams, B. A. Connolly, P. C. Newman, *Nucleic Acids Res. 18* (1990) 4771.
[241] F. Seela, K. Kaiser, U. Bindig, *Helv. Chim. Acta 72* (1989) 868.
[242] B. Gildea, L. W. McLaughlin, *Nucleic Acids Res. 17* (1989) 2261.
[243] Y.-Z. Xu, P. F. Swann, *Nucleic Acids Res. 18* (1990) 4061.
[244] H.-S. Koo, D. M. Crothers, *Biochemistry 26* (1987) 3745.
[245] P. K. T. Lin, D. M. Brown, *Nucleic Acids Res. 17* (1989) 10 373.
[246] T. Takeda, K. Ikeda, Y. Mizuno, T. Uede, *Chem. Pharm. Bull. 35* (1987) 3558.
[247] A. J. Goddard, V. E. Marquez, *Nucleosides Nucleotides 8* (1989) 1015.
[248] J. A. Piccirilli, T. Krauch, S. E. Moroney, S. A. Benner, *Nature (London) 343* (1990) 33.
[249] N. Bischofberger, M. D. Matteucci, *J. Am. Chem. Soc. 111* (1989) 3041.
[250] E. A. Kubareva, C.-D. Pein, E. S. Gromova, S. A. Kuznezova, V. N. Tashlitzki, D. Cech, Z. A. Shabarova, *Eur. J. Biochem. 175* (1988) 615.
[251] Z. A. Shabarova, *Biochimie 70* (1988) 1323.
[252] M. Koziolkiewicz, B. Uznanski, W. J. Stec, *Nucleosides Nucleotides 8* (1989) 185.
[253] D. Cech, C.-D. Pein, E. A. Kubareva, E. S. Gromova, T. S. Oretskaya, Z. A. Shabarova, *Nucleosides Nucleotides 7* (1988) 585.
[254] A. A. Yolov, M. N. Vinogradova, E. S. Gromova, A. Rosenthal, D. Cech, V. P. Veiko, V. G. Metelev, V. G. Kosykh, Y. I. Buryanov, A. A. Bayev, Z. A. Shabarova, *Nucleic Acids Res. 17* (1989) 8083.
[255] J. Benhattar, J. Jiricny, *Nucleic Acids Res. 16* (1988) 4160.
[256] A. Fliess, H. Wolfes, A. Rosenthal, K. Schwellnus, H. Blöcker, R. Frank, A. Pingoud, *Nucleic Acids Res. 14* (1986) 3463.
[257] B. A. Connolly, P. C. Newman, *Nucleic Acids Res. 17* (1989) 4957.
[258] A. Ono, T. Ueda, *Nucleic Acids Res. 15* (1987) 219.
[259] T. Hayakawa, A. Ono, T. Ueda, *Nucleic Acids Res. 16* (1988) 4761.
[260] C. A. Brennan, M. D. van Cleve, R. I. Gumport, *J. Biol. Chem. 261* (1986) 7270.
[261] H. Wolfes, A. Fliess, F. Winkler, A. Pingoud, *Eur. J. Biochem. 159* (1986) 267.
[262] F. Seela, H. Driller, *Nucleosides Nucleotides 8* (1989) 1.
[263] A. Ono, T. Ueda, *Nucleic Acids Res. 15* (1987) 3059.
[264] L. W. McLaughlin, T. Leong, F. Benseler, N. Piel, *Nucleic Acids Res. 16* (1988) 5631.

[265] A. Fliess, H. Wolfes, F. Seela, A. Pingoud, *Nucleic Acids Res. 16* (1988) 11 781.
[266] L. A. Loeb, *Cell (Cambridge, Mass.) 40* (1985) 483.
[267] S. Pochet, T. Huynh-Dinh, J.-M. Neumann, S. Tran-Dinh, S. Adam, J. Taboury, E. Taillandier, J. Igolen, *Nucleic Acids Res. 14* (1986) 1107.
[268] L. S. Kappen, C.-Q. Chen, I. H. Goldberg, *Biochemistry 27* (1988) 4331.
[269] M. Takeshita, C. N. Chang, F. Johnson, S. Will, A. P. Grollman, *J. Biol. Chem. 262* (1987) 10171.
[270] R. Eritja, P. A. Walker, S. K. Randall, M. F. Goodman, B. E. Kaplan, *Nucleosides Nucleotides 6* (1987) 803.
[271] G. R. Stuart, R. W. Chambers, *Nucleic Acids Res. 15* (1987) 7451.
[272] T. Horn, M. S. Urdea, *Nucleic Acids Res. 16* (1988) 11 559.
[273] J. Raap, C. E. Dreef, G. A. van der Marel, J. H. van Boom, C. W. Hilbers, *J. Biomol. Struct. Dyn. 5* (1987) 219.
[274] J.-J. Vasseur, B. Rayner, J.-L. Imbach, *Biochem. Biophys. Res. Commun. 134* (1986) 1204.
[275] J.-J. Vasseur, B. Rayner, J.-L. Imbach, S. Verma, J. A. McCloskey, M. Lee, D. K. Chang, J. W. Lown, *J. Org. Chem. 52* (1987) 4994.
[276] J.-R. Bertrand, J.-J. Vasseur, B. Rayner, J.-L. Imbach, J. Paoletti, C. Paoletti, C. Malvy, *Nucleic Acids Res. 17* (1989) 10307.
[277] T. Inaoka, M. Ishida, E. Ohtsuka, *J. Biol. Chem. 264* (1989) 2609.
[278] V. V. Demidov, V. N. Potaman, *J. Chromatogr. 285* (1984) 135.
[279] S. K. Banerjee, R. B. Christensen, C. W. Lawrence, J. E. Le Clerc, *Proc. Natl. Acad. Sci. USA 85* (1988) 8141.
[280] J.-S. Taylor, I. R. Brockie, C. L. O'Day, *J. Am. Chem. Soc. 109* (1987) 6735.
[281] J.-S. Taylor, I. R. Brockie, *Nucleic Acids Res. 11* (1988) 5123.
[282] F. N. Hayes, D. L. Williams, R. L. Ratliff, A. J. Varghese, C. S. Rupert, *J. Am. Chem. Soc. 93* (1971) 4940.
[283] S. N. Rao, J. W. Keepers, P. Kollman, *Nucleic Acids Res. 12* (1984) 4789.
[284] J. Kemmink, R. Boelens, T. M. G. Koning, R. Kaptein, G. A. van der Marel, J. H. van Boom, *Eur. J. Biochem. 162* (1987) 37.
[285] J. Kemmink, R. Boelens, T. M. G. Koning, G. A. van der Marel, J. H. van Boom, R. Kaptein, *Nucleic Acids Res. 15* (1987) 4645.
[286] I. Husain, J. Griffith, A. Sancar, *Proc. Natl. Acad. Sci. USA 85* (1988) 2558.
[287] I. Husain, A. Sancar, *Nucleic Acids Res. 15* (1987) 1109.
[288] R. Wu (Ed.): *Methods Enzymol. 155* (1987) 51–331, Section II: "Rapid Methods for DNA Sequence Analysis."
[289] G. Gish, F. Eckstein, *Science (Washington, D.C.) 240* (1988) 1520.
[290] G. L. Trainor, F. W. Hobbs, A. J. Cocuzza, P. N. Confalone, *Nucleic Acids Symp. Ser. 20* (1988) 119.
[291] J. A. Brumbaugh, L. R. Middendorf, D. L. Grone, J. L. Ruth, *Proc. Natl. Acad. Sci. USA 85* (1988) 5610.
[292] A. Rosenthal, H. Billwitz, A. Kehne, F. Seela, *Nucleic Acids Res. 16* (1988) 1631.
[293] L. M. Smith, R. J. Kaiser, J. Z. Sanders, L. E. Hood, *Methods Enzymol. 155* (1987) 260.
[294] L. M. Smith, *Genet. Eng. (London) 10* (1988) 91.
[295] B. S. Sproat, B. Beijer, P. Rider, P. Neuner, *Nucleic Acids Res. 15* (1987) 4837.
[296] W. Ansorge, B. Sproat, J. Stegemann, C. Schwager, M. Zenke, *Nucleic Acids Res. 15* (1987) 4593.
[297] P. Richterich, *Nucleic Acids Res. 17* (1989) 2181.
[298] D. A. Amorese, A. M. Hochberg, *Am. Biotechnol. Lab. 7* (1989) 38.
[299] J. M. Prober, G. L. Trainor, R. J. Dam, F. W. Hobbs, C. W. Robertson, R. J. Zagursky, A. J. Cocuzza, M. A. Jensen, K. Baumeister, *Science (Washington, D.C.) 238* (1987) 336.
[300] E. de Vroom, H. J. G. Broxterman, L. A. J. M. Sliedregt, G. A. van der Marel, J. H. van Boom, *Nucleic Acids Res. 16* (1988) 4607.
[301] S. Barbato, L. de Napoli, L. Mayol, G. Piccialli, C. Santacroce, *Tetrahedron Lett. 28* (1987) 5727.
[302] M. V. Rao, C. B. Reese, *Nucleic Acids Res. 17* (1989) 8221.
[303] M. Sekine, J. Heikkila, T. Hata, *Tetrahedron Lett. 28* (1987) 5691.
[304] N. Balgobin, X.-X. Zhou, J.-M. Vial, A. Nyilas, A. Földesi, J. Chattopadhyaya, *Nucleosides Nucleotides 8* (1989) 793.
[305] M. J. Damha, S. Zabarylo, *Tetrahedron Lett. 30* (1989) 6295.
[306] T. Horn, M. S. Urdea, *Nucleic Acids Res. 17* (1989) 6959.
[307] V. Lund, R. Schmid, D. Rickwood, E. Hornes, *Nucleic Acids Res. 16* (1988) 10861.
[308] J. Visscher, C. G. Bakker, R. Vanderwoerd, A. W. Schwartz, *Science (Washington, D.C.) 244* (1989) 329.
[309] J.-P. Perreault, T. Wu, B. Cousineau, K. K. Ogilvie, R. Cedergren, *Nature (London) 344* (1990) 565.
[310] E. A. M. de Jong, J. P. M. van Duynhoven, B. J. M. Harmsen, G. I. Tesser, R. N. H. Konings, C. W. Hilbers, *J. Mol. Biol. 206* (1989) 133.
[311] J. N. Kremsky, J. L. Wooters, J. P. Dougherty, R. E. Meyers, M. Collins, E. L. Brown, *Nucleic Acids Res. 15* (1987) 2891.
[312] R. Bischoff, J. M. Coull, F. E. Regnier, *Anal. Biochem. 164* (1987) 336.
[313] R. D. Sheardy, N. C. Seeman, *J. Org. Chem. 51* (1986) 4301.
[314] B. S. Sproat, B. Beijer, P. Rider, *Nucleic Acids Res. 15* (1987) 6181.
[315] Y. Borel, H. Borel, *J. Clin. Invest. 82* (1988) 1901.
[316] L. A. Yakubov, E. A. Deeva, V. F. Zarytova, E. M. Ivanova, A. S. Ryte, L. V. Yurchenko, V. V. Vlassov, *Proc. Natl. Acad. Sci. USA 86* (1989) 6454.
[317] S. L. Loke, C. A. Stein, X.-H. Zhang, K. Mori, M. Nakanishi, C. Subasinghe, J. S. Cohen, L. M. Neckers, *Proc. Natl. Acad. Sci. USA 86* (1989) 3474.
[318] P. C. Zamecnik, J. Goodchild, Y. Taguchi, P. S. Sarin, *Proc. Natl. Acad. Sci. USA 83* (1986) 4143.
[319] M. Ceruzzi, K. Draper, J. Schwo, *Nucleosides Nucleotides 9* (1990) 679.
[320] J.-P. Leonetti, P. Machy, G. Degols, B. Lebleu, L. Leserman, *Proc. Natl. Acad. Sci. USA 87* (1990) 2448.
[321] A. Chollet, *Nucleosides Nucleotides 9* (1990) 957.
[322] U. Englisch, S. Englisch, P. Markmeyer, J. Schischkoff, H. Sternbach, H. Kratzin, F. Cramer, *Biol. Chem. Hoppe-Seyler 368* (1987) 971.
[323] M. Cooney, G. Czernuszewicz, E. H. Postel, S. J. Flint, M. E. Hogan, *Science (Washington, D.C.) 241* (1988) 456.
[324] P. B. Dervan in [7], pp. 197–210.
[325] G. Zon in [7], pp. 233–247.
[326] P. Herdewijn, R. Charubala, R. Pauwels, E. De Clercq, W. Pfleiderer, *Nucleosides Nucleotides 6* (1987) 441.
[327] G. B. Elion, *Angew. Chem. 101* (1989) 893; *Angew. Chem. Int. Ed. Engl. 28* (1989) 1970.

Molecular Structures from Density Functional Calculations with Simulated Annealing

By Robert O. Jones*

The geometrical structure of any aggregate of atoms is one of its basic properties and, in principle, straightforward to predict. One chooses a structure, determines the total energy E of the system of electrons and ions, and repeats the calculation for all possible geometries. The ground state structure is that with the lowest energy. A quantum mechanical calculation of the exact wave function Ψ would lead to the total energy, but this is practicable only in very small molecules. Furthermore, the number of local minima in the energy surface increases dramatically with increasing molecular size. While traditional ab initio methods have had many impressive successes, these difficulties have meant that they have focused on systems with relatively few local minima, or have used experiment or experience to limit the range of geometries studied. On the other hand, calculations for much larger molecules and extended systems are often forced to use simplifying assumptions about the interatomic forces that limit their predictive capability. The approach described here avoids both of these extremes: Total energies of predictive value are calculated *without* using semi-empirical force laws, and the problem of multiple minima in the energy surface is addressed. The density functional formalism, with a local density approximation for the exchange-correlation energy, allows one to calculate the total energy for a given geometry in an efficient, if approximate, manner. Calculations for heavier elements are not significantly more difficult than for those in the first row and provide an ideal way to study bonding trends. When coupled with finite-temperature molecular dynamics, this formalism can avoid many of the energetically unfavorable minima in the energy surface. We show here that the method leads to surprising and exciting results.

1. Introduction

A knowledge of the exact wave function Ψ of an interacting system of electrons and ions would allow one to determine many quantities of interest, including the total energy E (Eq. 1), where $\mathscr{H}$ is the Hamiltonian of the system. Calcu-

$$E = \langle \Psi | \mathscr{H} | \Psi \rangle / \langle \Psi | \Psi \rangle \tag{1}$$

lations of this type can be carried out for systems with very few electrons, the most familiar example being the hydrogen atom. However, approximations for Ψ are generally unavoidable, and are usually based on the variational principle of *Rayleigh* and *Ritz*: If $|\Phi\rangle$ is an approximate wave function, then Equation 2 is valid, where E_{GS} is the exact energy of the ground state.

$$\langle \Phi | \mathscr{H} | \Phi \rangle / \langle \Phi | \Phi \rangle \geq E_{GS} \tag{2}$$

The simplest form of a many-particle wave function is that of *Hartree* (1928), who represented Φ as a product of single-electron functions (Eq. 3), where each ϕ_i satisfies a

$$|\Phi\rangle = \phi(\boldsymbol{r}_1)\,\phi_2(\boldsymbol{r}_2) \ldots \phi_n(\boldsymbol{r}_n) \tag{3}$$

Schrödinger equation whose potential term is given by the mean field of all other electrons (Eq. 4). V_{ext} is the external

$$(-\tfrac{1}{2}\nabla^2 + V_{ext} + \varphi)\phi_i(\boldsymbol{r}_i) = \varepsilon_i \phi_i(\boldsymbol{r}_i) \tag{4}$$

field of the nuclei, and the Coulomb potential φ is determined by solving Poisson's equation (we use atomic units, i.e., the unit of charge is the electron charge e, of distance the Bohr radius a_0, and of mass the electron mass m). Replacing the product by a single (Slater) determinant—the Hartree–Fock (HF) approximation—leads to an additional "exchange" potential, without changing the single-particle picture. Although this has been the basic method of atomic and molecular physics for many years, a single determinant does not generally lead to a satisfactory value of the total energy. While a linear combination of determinants ("configuration interaction", CI) should lead in principle to an exact wave function and energy, the numerical effort required increases explosively with increasing electron number.

These arguments apply to a *one* geometry, that is, for a particular set of internal coordinates of a system. If we have N atoms in an aggregate ($N > 2$), the total number of internal coordinates is $3N - 6$, since the internal energy of the aggregate is independent of any translational or rotational motion. With so many independent interatomic degrees of freedom, the scale of the problem is clear: 1) Finding the energy minimum by calculating the exact energy for all possible geometries is impracticable, since it would require a vast number of calculations in a system where *one* is difficult! 2) The ability to locate the closest minimum to a particular geometry would simplify the calculations greatly, particularly if the number of possible isomers is small. In general, however, it is difficult to predict the most stable structure, since the number of local minima in the energy surface can be very large indeed.

The enumeration of topologically different isomers consistent with a given chemical formula is one of the oldest problems in theoretical chemistry. In 1874, only a decade after the

[*] Dr R. O. Jones
Institut für Festkörperforschung
Forschungszentrum Jülich, W-5170 Jülich (FRG)

chemical bond was first denoted by a line joining the nuclei, *Cayley*[1] showed that the number of isomers could grow rapidly with increasing N, and much work in the intervening period has confirmed this. *Hoare* and *McInnes*,[2] for example, located all the minima in small aggregates with simple, pairwise interatomic interactions, and found a rapid, perhaps exponential, increase in their number with increasing N. In fact, for aggregates of identical atoms interacting with a pairwise potential, *Wille* and *Vennik*[3] have shown that there is no known algorithm for determining the ground state energy and structure that grows with time as a power of N. Such problems are classified as "NP—hard"[4] and are termed intractable. It is indeed sobering when mathematicians derive such a result. Moreover, the parameters in force laws such as those used by *Hoare* and *McInnes* are usually derived from experiment, and one cannot be sure that the results are not affected by the choice of parameters.

This discussion shows that there are two distinct problems to be solved, and the difficulties are multiplicative in nature. The approach we now describe addresses both aspects. First, the density functional formalism provides a numerically efficient scheme for calculating the ground state energy of the interacting system of ions and electrons without attempting to calculate the wave function Ψ. Second, we use the strategy of simulated annealing (SA) to determine low-lying energy minima. We show that, even in small molecules, there are energetically favorable structures that had not been found on the basis of experiment or intuition. In Section 2 we outline the density functional (DF) formalism and discuss the form of the exchange–correlation energy E_{xc} and local density approximations to it. The results of local spin density (LSD) calculations given in Section 3 illustrate the level of accuracy to be expected, and we show in Section 4 how DF calculations can be combined with molecular dynamics. We present some applications in Section 5 and our concluding remarks in Section 6.

2. Density Functional Formalism

2.1. Formal Basis

The basic theorems of the density functional formalism were derived by *Hohenberg* and *Kohn*.[5] They showed that:

1) Ground state (GS) properties of a system of electrons and ions in an external field V_{ext} can be determined from a knowledge of the electron density $n(\boldsymbol{r})$ *alone*. The total energy E is such a functional of the density, that is, $E = E(n)$.

2) $E(n)$ satisfies the variational principle $E(n) \geq E_{GS}$, and the density for which the equality holds is the ground state density n_{GS}.

A simple and general proof of these assertions has been given by *Levy*.[6]

The step to a practical scheme for energy calculations resulted from the observation by *Kohn* and *Sham*[7] that the minimization of $E(n)$ can be simplified if we write E as in

$$E(n) = T_0(n) + \int d\boldsymbol{r}\, n(\boldsymbol{r})\,(V_{ext}(\boldsymbol{r}) + \tfrac{1}{2}\varphi(\boldsymbol{r})) + E_{xc}(n) \qquad (5)$$

Equation 5. Here T_0 is the kinetic energy that a system with density n would have in the absence of electron–electron interactions, $\varphi(\boldsymbol{r})$ is the Coulomb potential, and the remainder E_{xc} is our definition of the exchange–correlation energy. The variational principle now yields Equation 6, where μ is the Lagrange multiplier associated with the requirement of constant particle number.

$$\frac{\delta E(n)}{\delta n(\boldsymbol{r})} = \frac{\delta T_0}{\delta n(\boldsymbol{r})} + V_{ext}(\boldsymbol{r}) + \varphi(\boldsymbol{r}) + \frac{\delta E_{xc}(n)}{\delta n(\boldsymbol{r})} = \mu \qquad (6)$$

Equation 6 applies to the interacting system of electrons and ions. The solution of the corresponding equation for a system of noninteracting particles, Equation 7, can be found

$$\frac{\delta E(n)}{\delta n(\boldsymbol{r})} = \frac{\delta T_0}{\delta n(\boldsymbol{r})} + V(\boldsymbol{r}) = \mu \qquad (7)$$

by solving the Schrödinger equation, Equation 8a. The density is given by Equation 8b, where the sum runs over orbitals i with occupation numbers f_i. The problems (6) and (7)

$$(-\tfrac{1}{2}\nabla^2 + V(\boldsymbol{r}))\,\psi_i(\boldsymbol{r}) = \varepsilon_i \psi_i(\boldsymbol{r}) \qquad (8a)$$

$$n(\boldsymbol{r}) = \sum_i f_i |\psi_i(\boldsymbol{r})|^2 \qquad (8b)$$

are mathematically identical, provided that $V(\boldsymbol{r})$ is defined according to Equation 9. This condition can be satisfied in practice by a "self-consistency" cycle: From a starting value of n we compute $V(\boldsymbol{r})$ and the n' that results, and continue this procedure until $n = n'$.

$$V(\boldsymbol{r}) = V_{ext} + \Phi(\boldsymbol{r}) + \frac{\delta E_{xc}(n)}{\delta n(\boldsymbol{r})} \qquad (9)$$

Robert O. Jones was born in 1941 in Kojonup, Western Australia. He graduated in 1963 from the University of Western Australia, Perth, and obtained his Ph.D. in 1967 from the University of Cambridge, England, under V. Heine. From 1967 to 1970 he worked as Research Associate, Laboratory of Atomic and Solid State Physics, Cornell University, Ithaca, NY, USA and since 1970 as Scientist at the Forschungszentrum Jülich (KFA). In 1975 he was NORDITA Professor at the Chalmers Technical University, Göteborg, Sweden and has been Fellow of the Australian Institute of Physics since 1978.

The problem of determining the total energy of a system of electrons and ions has therefore been reduced to the solution of a single-particle equation of Hartree form (cf. Eq. 4), leading to the energy and electron density of the lowest state and all quantities derivable from them. This method can be extended to the lowest energy state of a given symmetry by restricting the variation to densities compatible with the corresponding symmetry quantum numbers.[8] In the form of Equations 8 and 9, density functional theory is an *orbital* theory and it shares the main advantage of the Hartree–Fock method, namely the interpretation of the results in a single-particle picture. In contrast to the HF potential, however, the effective potential $V(\boldsymbol{r})$ has a *local* dependence on the density.

This situation may seem to be almost too good to be true. Before celebrating, however, we should note the following:

1) The total energy E of the most stable state of a given symmetry is found by solving equations describing a fictitious system of noninteracting "electrons", and the eigenvalues ε_i and eigenfunctions ψ_i in Equation 8 can *not* be viewed as excitation energies and wave functions of the interacting system. The use of such fictitious systems leads to additional complications, since it is not always possible to draw an unambiguous connection between the states of the interacting and noninteracting systems. In the latter, the f_i will be compatible with a single determinant—or at most a small number of determinants—of the same symmetry.[9]

2) While in the energy expression (5) T_0, the electron–ion and electron–electron interaction energies can readily be evaluated, E_{xc} is *defined* only as the difference between the sum of these terms and the exact energy. It is a small but far from negligible part of the total energy of atoms and molecules. Moreover, if there is no simple expression for E_{xc}, how do we determine in practice its functional derivative in Equation 6? Approximations to E_{xc} therefore play an essential part in applications of DF theory, and we now study its form in more detail.

2.2. Exchange–Correlation Energy

The connection between the noninteracting and interacting systems—both of density $n(\boldsymbol{r})$—can be drawn simply by considering an electron–electron interaction $\lambda\phi$ and increasing λ slowly from 0 to 1. One can use this construction to derive an exact expression (10) for E_{xc},[8] in which n_{xc} is defined as in Equation 11. The pair-correlation function $g(\boldsymbol{r}, \boldsymbol{r}', \lambda)$ describes the fact that an electron at point $\boldsymbol{r}$ reduces the probability of finding one at $\boldsymbol{r}'$, so that E_{xc} can be viewed as the interaction between $n(\boldsymbol{r})$ and the exchange–correlation hole $n_{xc}(\boldsymbol{r})$. This picture is, of course, very similar to that of the exchange hole introduced by *Slater* for electrons of parallel spin.[10]

$$E_{xc} = \frac{1}{2}\int d\boldsymbol{r}\, n(\boldsymbol{r}) \int d\boldsymbol{r}' \frac{1}{|\boldsymbol{r}-\boldsymbol{r}'|} n_{xc}(\boldsymbol{r}, \boldsymbol{r}'-\boldsymbol{r}) \tag{10}$$

$$n_{xc}(\boldsymbol{r}, \boldsymbol{r}'-\boldsymbol{r}) \equiv n(\boldsymbol{r}') \int_0^1 d\lambda (g(\boldsymbol{r}, \boldsymbol{r}', \lambda) - 1) \tag{11}$$

The isotropic nature of the Coulomb interaction suggests the variable substitution $\boldsymbol{R} \equiv \boldsymbol{r}' - \boldsymbol{r}$ in (10), leading to Equation 12.[8] E_{xc} depends only on the spherical average of

$$E_{xc} = \frac{1}{2}\int d\boldsymbol{r}\, n(\boldsymbol{r}) \int_0^\infty d\boldsymbol{R}\, R^2 \frac{1}{R}\int d\Omega\, n_{xc}(\boldsymbol{r}, \boldsymbol{R}) \tag{12}$$

$n_{xc}(\boldsymbol{r}, \boldsymbol{R})$, so that approximations for it can give an accurate value even if the description of the nonspherical parts of n_{xc} is very poor. Furthermore, a sum rule following from the definition of the pair-correlation function requires that the exchange–correlation hole contain one electron, that is, for all $\boldsymbol{r}$, Equation 13 is valid. If we consider $-n_{xc}(\boldsymbol{r}, \boldsymbol{r}'-\boldsymbol{r})$ as

$$\int d\boldsymbol{r}'\, n_{xc}(\boldsymbol{r}, \boldsymbol{r}'-\boldsymbol{r}) = -1 \tag{13}$$

a normalized weight factor and define locally the radius of the exchange–correlation hole (Eq. 14), Equation 15 follows.

$$\left\langle \frac{1}{\boldsymbol{R}} \right\rangle_{\boldsymbol{r}} = -\int d\boldsymbol{r}\, \frac{n_{xc}(\boldsymbol{r}, \boldsymbol{R})}{|\boldsymbol{R}|} \tag{14}$$

$$E_{xc} = -\frac{1}{2}\int d\boldsymbol{r}\, n(\boldsymbol{r}) \left\langle \frac{1}{\boldsymbol{R}} \right\rangle_{\boldsymbol{r}} \tag{15}$$

Provided the sum rule (13) is satisfied, E_{xc} depends only weakly on the details of n_{xc} and is determined by the first moment of a function whose second moment is known exactly.

The experience of the last twenty years shows that the exact exchange–correlation energy functional $E_{xc}(n(\boldsymbol{r}))$ must be extremely complicated. The calculation of correlation functions (see Eq. 11, for example) generally requires the knowledge of the exact wave function. Nevertheless, the above argument shows that simple, useful approximations to E_{xc} may exist. The practical necessity of approximating E_{xc} is an essential difference between the density functional and configuration interaction approaches. While the latter seeks an exact numerical solution of the Schrödinger equation and precise values of related quantities, even the best solution of the DF equations can only reflect the accuracy of the approximation used for E_{xc}. Furthermore, while the CI approach can be improved systematically by increasing the number of determinants and basis functions, a corresponding scheme for improving the accuracy of LD calculations is presently not known.

2.3. Local Density Approximations for E_{xc}

Local density calculations have a long history in condensed matter physics, where a special role has been played by the approximate exchange potential introduced by *Slater*.[10] It is sometimes overlooked that *Slater*'s derivation was based on the concept of the exchange-hole discussed above, and not on the particular form of the exchange energy density obtained for a homogeneous electron gas. The approximation for E_{xc} in most widespread use today is the local spin density (LSD) approximation (16). Here $\varepsilon_{xc}(n_\uparrow, n_\downarrow)$ is

$$E_{xc}^{LSD} = \int d\boldsymbol{r}\, n(\boldsymbol{r})\, \varepsilon_{xc}(n_\uparrow(\boldsymbol{r}), n_\downarrow(\boldsymbol{r})) \tag{16}$$

the exchange and correlation energy per particle of a homogeneous, spin-polarized electron gas with spin-up and spin-

down densities $n_\uparrow$ and $n_\downarrow$, respectively. This approximation is free of adjustable parameters—ε_{xc} is taken from the best available calculations for the uniform electron gas—and its use can be justified in systems with small departures from homogeneity. Density distributions are far from homogeneous in atoms, molecules, and most solids, and the usefulness of the approximation relies on arguments such as those in Section 2.2. The approximation satisfies the sum rule (13); more details are given in the review article by *Jones* and *Gunnarsson*.[11]

3. DF Calculations with Local Density Approximations

Density functional calculations with the LSD approximation are common in extended systems, and the results show some general features. Equilibrium geometries are given reliably in most materials, and energy variations in the neighborhood of local minima are described well, so that vibration (phonon) frequencies are generally in reasonable agreement with experiment. In this section, we select examples from the applications to molecular systems[11] to indicate the level of accuracy to be expected in such systems. They illustrate two strengths of the method: the ability to study molecules containing elements from the whole periodic table, and the advantages of an interpretation based on a single-particle picture. They also demonstrate the tendency of LD calculations to overestimate strengths of bonds involving sp orbitals.

3.1. First-row Diatomic Molecules

Diatomic molecules of first-row atoms Li–F have served as a testing ground for numerous methods of electronic structure calculation. In Table 1 we compare measured potential well depths[12] in first-row dimers (homonuclear diatomic molecules) with values calculated using Hartree–Fock,[13] and local spin density approximations for E_{xc} and E_x (exchange only).[7, 14, 15] The HF approximation leads to substantial underestimates of the binding energies, particularly for singlet ground states. The LSD values overestimate the stability of these molecules, particularly beyond carbon in this row, although the deviations from experiment are small for H_2 and Li_2. In cases where it leads to an energy minimum, the HF approximation usually leads to a small underestimate of the equilibrium interatomic separations. The values for r_e calculated using the LSD approximations are generally in good agreement with experiment. An overestimate of 1–2% is common.[15, 16] Ground state vibration frequencies are correspondingly low. The dipole moment of CO and its variation with internuclear separation are given significantly better by the LSD approximation than by HF calculations.[17]

Table 1. Experimental and calculated well depths [eV] for the experimental ground states of the first-row dimers.

Molecule	Expt [a]	LSD [b]	XO [b, c]	HF [d]
H_2	4.75	4.91	3.59	3.64
Li_2	1.07	1.01	0.21	0.17
Be_2	0.10	0.50	0.43	[e]
B_2	3.09	3.93	3.79	0.89
C_2	6.32	7.19	6.00	0.79
N_2	9.91	11.34	9.09	5.20
O_2	5.22	7.54	7.01	1.28
F_2	1.66	3.32	3.04	−1.37

[a] For Be_2 from Ref. [25], otherwise Ref. [12]. [b] Ref. [15]. [c] Local density calculations with exchange only. [d] Total energies for experimental geometries from Ref. [13]. [e] HF calculations for Be_2 give a purely repulsive energy curve.

3.2. Alkaline Earth Dimers Be_2, Mg_2, Ca_2 ...

While the LSD and HF approximations generally lead to similar bond lengths in first-row molecules, Be_2 is quite different. The lowest-lying state in the alkaline earth dimers ($^1\Sigma_g^+[1\sigma_g(\uparrow\downarrow)\,1\sigma_u(\uparrow\downarrow)]$) has equal occupancies of bonding and antibonding orbitals, and Hartree–Fock calculations[18] lead to repulsive curves. Bonds in these molecules have often been referred to as Van der Waals bonds, in the expectation that the bond strength increases monotonically $Be_2 \rightarrow Mg_2 \rightarrow Ca_2$ ... with increasing atomic polarizabilities. The earliest CI calculations supported this picture, since they predicted for Be_2 a very weak bond with an equilibrium separation near $9a_0$.[19]

The local density approximation gives qualitatively different results and a different picture of bonding in this homologous series.[20] The energy curves show minima in all cases, and the equilibrium separations in Mg_2 and Ca_2 agree well with measured values. The bond length in Be_2 (4.86 a_0) was found to be much shorter than in CI calculations. Most striking, however, is the variation in bond energies shown in Figure 1. The bond in Be_2 is *stronger* than in Mg_2, and the variation with atomic number parallels the irregular behavior observed in the bulk cohesive energies (Fig. 1, experiment: ref. [21]; LD calculations: ref. [22]). The bond energies in the molecules and solids are overestimated by the LD approximation in those cases where experimental values are

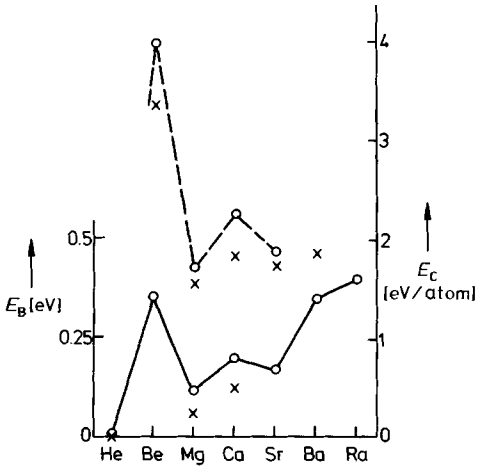

Fig. 1. Bond energies E_B calculated for the $^1\Sigma_g^+$ state of alkaline earth dimers (full curve, left scale, Ref. [20]) and cohesive energies of bulk materials (broken curve, right scale, ref. [22]). Experimental values Refs. [12] and [21]) are given as crosses.

known. The error is significant in Be_2, as we show in Table 2, where we include the results of more recent LD and CI calculations[23, 24] and gas-phase experimental results.[25] The DF and experimental equilibrium separations are in very good agreement, and the extensive CI calculations reproduce both the well depth and equilibrium separation satisfactorily.

Table 2. Experimental and calculated spectroscopic constants of Be_2 ($^1\Sigma_g^+$).

	r_e [a_0]	ω_e [cm^{-1}]	D_e [eV]
Experiment [25]	4.658	223.4	ca. 0.11
CI[24]	4.73 ± 0.03	...	0.09 ± 0.01
CI[23]	4.78	...	0.10[a]
CI[19]	4.9	...	0.04
LD-LMTO[b]	4.67	360	0.48
LD-LCAO[15]	4.63	362	0.50

[a] Estimated. [b] R. O. Jones, unpublished results (1982).

To discuss the bonding in this homologous series, it is useful to consider the valence orbitals (Fig. 2) of the atoms. With the exception of He_2, there is a substantial overlap between the electron densities on the two atoms, particularly in Be_2. Furthermore, the radial extent of the orbitals does not increase smoothly with core size, but shows a "secondary periodicity". For example, the valence s orbital in Mg is not

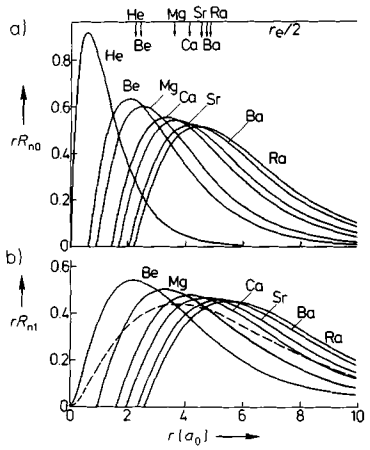

Fig. 2. Radial valence orbital functions for helium and alkaline earth atoms: a) s functions for the ^1S (ns^2) states, b) p functions for the ^3P (ns^1np^1) state. The dashed curve is the 2p function of He (1s2p). The arrows denote half of the calculated equilibrium separation ($r_e/2$) in each dimer [20].

much more extended than that in Be. The 2p functions in the Mg core have no repulsive (orthogonalization) effect on the 3s function and are sufficiently extended that the additional core charge is incompletely screened. A similar orbital compression is evident in Sr and Ra, where 3d and 4f functions enter the core for the first time. The unoccupied p orbitals are generally more extended than the s valence functions, but Figure 2 shows that Be is an exception. The similar extent of the 2s and 2p orbitals suggests that sp mixing will be favored. This picture is in accord with the pseudopotential theory of cohesion in the bulk: a stronger sp hybridization (and larger band gap) in Be than in Mg, and increasing sd hybridization with increasing atomic number. It is encouraging that the trends predicted by the DF calculations, particularly the relative strength of the bond in Be_2, were confirmed by both exhaustive CI calculations and by experiment.

3.3. Diatomic Molecules of the Fourth Main Group: C_2, Si_2, Ge_2

The absence of core p states, the strong attractive potential experienced by the 2p states, and their relatively compact nature apply to all first-row atoms. As a consequence, their bonding properties differ qualitatively from those of atoms in the remainder of the periodic table. The experimental ground state in C_2, for example, is $^1\Sigma_g^+$, and the excitation energy ($T_e = 0.09$ eV) to the $^3\Pi_u(2\sigma_g\pi_u^3)$ is very small.[12] The remarkable ease of the $\sigma_g \rightarrow \pi_u$ transfer is not found in the heavier dimers of this group; these have $^3\Sigma_g^-(2\sigma_g^2 1\pi_u^2)$ ground states, excitation energies of 1.0 to 1.5 eV to the $^1\Sigma_g^+$ state ($1\pi_u^4$), and substantially weaker π bonds.[26]

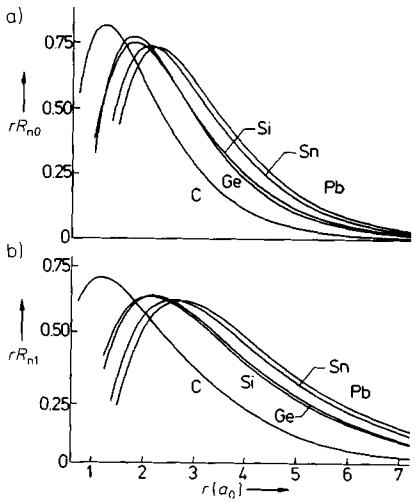

Fig. 3. Radial valence orbital functions for atoms of the fourth main group: a) s functions, b) p functions.

The radial functions of the valence orbitals of these elements (Fig. 3) show a similar behavior to that discussed above. The valence functions of Si and Ge are remarkably

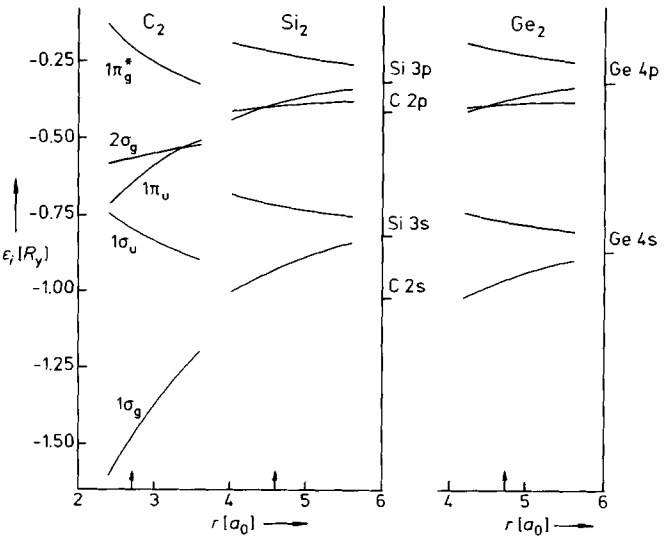

Fig. 4. Dependence of the self-consistent eigenvalues for $^3\Sigma_g^-$ state of C_2, Si_2, and Ge_2 on the interatomic distance r. The valence eigenvalues for the isolated atoms are given and the arrows on the r axis denote half of the calculated equilibrium separation ($r_e/2$) in each case.

similar, since the relatively diffuse 3d core density in Ge screens the additional nuclear charge imperfectly. This is reflected in very similar bulk properties, such as ground state geometries, and in the eigenvalues of Si_2 and Ge_2 shown in Figure 4. The C_2 eigenvalues reflect the compact valence p function and show why the multiplet structure is so different. The $^1\Sigma_g^+$ state obtained by placing four electrons in the π_u orbital has a very similar energy to the $^3\Sigma_g^-$ state obtained by transferring two electrons to the $2\sigma_g$ orbital. The eigenvalues in Figure 4 suggest that occupancy of the latter orbital will be favored in the heavier dimers, resulting in weaker π bonds. The consequences for the formation of simple saturated molecules have been discussed by *Harris* and *Jones*.[26]

3.4. Triatomic Molecules of the Sixth Main Group: O_3, SO_2

As a further example, we study the energy hypersurfaces of O_3 and SO_2,[27] which have ground states with $^1A_1(C_{2v})$ symmetry and similar bond angles (116.8° and 119.4°, respectively). Although the absorption spectrum of ozone has been studied in detail, particularly for ultraviolet radiation, little experimental information is available on the excited state energy surfaces, and theoretical studies have been essential. Attention has been focused in the past on the presence of two minima in the $^1A_1$ energy hypersurfaces and the energy difference between them. The HF approximation gives a qualitatively incorrect ordering of the low-lying states of O_3, since there are two configurations with substantial contributions to the ground state wave function.

In Figure 5 we show the energy hypersurfaces for low-lying states of ozone. DF calculations reproduce the ground

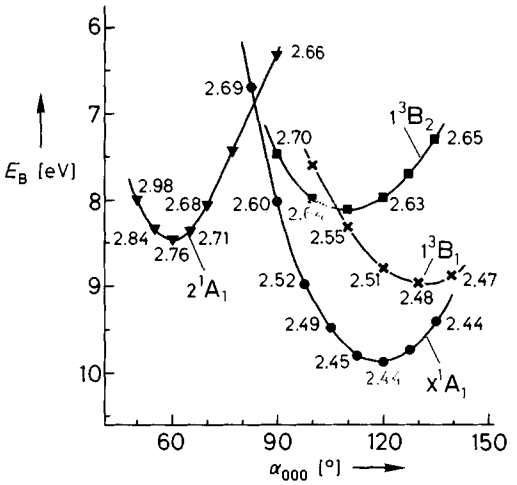

Fig. 5. Energy surfaces for low-lying states of O_3. α = bond angle. The values on the curves give the bond lengths [a_0] that optimize the energy for each angle α.

state geometry well, and the excitation energy between the two $^1A_1$ minima (1.4 eV) is in reasonable agreement with the most recent CI calculations, which give results between 1.0 eV and 1.4 eV.[27] In both O_3 and SO_2, the bond lengths increase in the order $x^1A_1 \rightarrow 1^3B_1 \rightarrow 1^3B_2 \rightarrow 2^1A_1$, and the bond angles in the order $2^1A_1 \rightarrow 1^3B_2 \rightarrow x^1A_1 \rightarrow 1^3B_1$. However, there are qualitative differences between the energy ordering of the states. In particular, the excitation from the ground state to the low-lying triplet states requires substantially more energy for SO_2 than for O_3, and the energy separation between the two $^1A_1$ states (4.1 eV) is almost three times as large for SO_2.

These differences can be related to the larger radius of the sulfur atom and the higher energy of the p orbital.[27] The ground state (x^1A_1) has the valence configuration $1a_2^2 3b_2^2 4a_1^2 2b_1^0$, and the 2^1A_1 state corresponds to the excitation ($3b_2^2 \rightarrow 2b_1^2$). While the $1a_2$ and $3b_2$ orbitals have significant contributions only from the outer (oxygen) atoms, the higher-lying $4a_1$ and $2b_1$ orbitals have a strong contribution from the central atom (O in O_3, S in SO_2). The eigenvalue spread in SO_2 is therefore much larger, so that the large excitation energy $x^1A_1 \rightarrow 2^1A_1$ in SO_2 reflects simply the double excitation to the high-lying $2b_1$ orbital.

The above molecules are only a small sample of those that have been studied with the DF method. Nevertheless, they illustrate some general features of the results. As in extended systems, equilibrium geometries and vibration frequencies are described satisfactorily, even in molecules—such as Be_2 and O_3—where the Hartree–Fock method gives qualitatively incorrect results. While energy variations near equilibrium geometries are given satisfactorily, this is not true of all regions of configuration space. The errors in the dissociation energies of first-row diatomic molecules and the ozone family (up to ca. 2 eV), for example, are unacceptably large and have contributed to the motivation behind the search for improved approximations.[11] The single-particle picture and the relative ease of performing calculations for elements with large atomic numbers is very useful in understanding the differences between first-row and heavier elements. A discussion on similar lines was presented subsequently by *Kutzelnigg*.[28]

4. The Molecular Dynamics/Density Functional Approach

While we cannot expect to be able to determine the exact ground state if the energy hypersurface has many local minima, it is essential to develop methods for avoiding energetically unfavorable local minima. *Kirkpatrick* et al.[29] noted that this can be achieved by allowing the system to evolve at finite temperature and implemented this "simulated annealing" strategy using a Monte Carlo sampling. Molecular dynamics (MD) provides an alternative, and *Car* and *Parrinello*[30] showed that it could be combined with the density functional (DF) scheme for calculating total energies. The use of the LSD approximation for the exchange–correlation energy avoids the parameterization of the interatomic forces common in MD schemes,[31] and should give a reliable description of energy variations for large regions of configuration space.

To perform geometry optimization using DF calculations, we face two minimization problems: The total energy must be minimized for each geometry by varying the density (the solution of Eq. 7), and the geometry with the lowest energy must be found. This is done conveniently by viewing E as a

function of two interdependent sets of degrees of freedom, $\{\psi_i\}$ and $\{\boldsymbol{R}_I\}$, and using standard MD techniques (Eq. 17, where Z_I are the ionic charges).[30]

$$E(\{\psi_i\}, \{\boldsymbol{R}_I\}) = \sum_i \left\langle \psi_i(\boldsymbol{r}) \left| -\frac{\nabla^2}{2} \right| \psi_i(\boldsymbol{r}) \right\rangle + \int d\boldsymbol{r} n(\boldsymbol{r}) \left(V_{ext}(\boldsymbol{r}, \{\boldsymbol{R}_I\}) + \tfrac{1}{2}\varphi(\boldsymbol{r})\right) + E_{xc}(n(\boldsymbol{r})) + \frac{1}{2} \sum_{I \neq J} \frac{Z_I Z_J}{|\boldsymbol{R}_I - \boldsymbol{R}_J|} \quad (17)$$

The energy minimization required for structure determination can be performed using standard MD techniques,[30] since the evolution of the system of electrons and ions is reproduced exactly by the evolution of a dynamic system defined by the Lagrangian (18) and the equation of motion 19a and 19b. M_I and $\boldsymbol{R}_I$ denote the ionic masses and

$$\mathscr{L} = \sum_i \mu_i \int_\Omega d\boldsymbol{r} |\dot{\psi}_i^* \psi_i| + \sum_I \tfrac{1}{2} M_I \dot{\boldsymbol{R}}_I^2 - E(\{\psi_i\}, \{\boldsymbol{R}_I\}) + \sum_{ij} \Lambda_{ij} \left(\int_\Omega d\boldsymbol{r} \psi_i \psi_j^* - \delta_{ij}\right) \quad (18)$$

$$\mu_i \ddot{\psi}_i(\boldsymbol{r}, t) = -\frac{\delta E}{\delta \psi^*(\boldsymbol{r}, t)} + \sum_k \Lambda_{ik} \psi_k(\boldsymbol{r}, t) \quad (19a)$$

$$M_I \ddot{\boldsymbol{R}}_I = -\nabla_{\boldsymbol{R}_I} E \quad (19b)$$

coordinates, μ_i are fictitious "masses" associated with the electronic degrees of freedom, dots denote time derivatives, and the Lagrangian multipliers Λ_{ij} are introduced to satisfy the orthonormality constraints on the $\psi_i(\boldsymbol{r}, t)$. From these orbitals and the resultant density $n(\boldsymbol{r}, t) = \sum_i |\psi_i(\boldsymbol{r}, t)|^2$ we use Equation 17 to evaluate the total energy E, which acts as the classical potential energy in the Lagrangian function 18. The artificial Newton's dynamics for the electronic degrees of freedom, together with the assumption $\mu_i \ll M_I$, prevent transfer of energy from the classical to the quantum degrees of freedom, even for long simulations.

5. Applications of the MD/DF Scheme to Molecules

MD/DF calculations have been performed for several families of molecules containing main-group elements, using a large unit cell with periodic boundary conditions to guarantee a weak interaction between the molecules. We give some examples here to show the value of the approach in several contexts.[32] The scattering properties of the individual atoms are described by nonlocal pseudopotentials, and the eigenfunctions ψ_i are expanded in a plane wave basis. We set the velocities $\dot{\psi}_i$ and $\dot{\boldsymbol{R}}$ equal to zero for an arbitrary starting geometry, and use an efficient self-consistent iterative diagonalization technique to determine those ψ_i that minimize E. With the electrons initially in their ground state, the dynamics (Eq. 19a and b) generate Born–Oppenheimer (BO) trajectories without the need for additional diagonalization/self-consistency cycles for the electrons. In the present applications, the minimum of the potential energy surfaces can be found by alternating MD calculations at finite temperature with steepest descents (or conjugate gradient) determinations of the nearest local minimum. Further details are given in the original papers.

5.1. Sulfur Clusters S_n

The elements of the sixth main group provide some of the best characterized of small atomic clusters. These elements are unique in that many allotropes comprise regular arrays of well-separated ring molecules, and X-ray structure analyses have been performed for S_n, $n = 6$–$8, 10$–$13, 18, 20$, and Se_n, $n = 6, 8$. S_9 has been found as microcrystals, and S_{18} exists in two distinct forms. Several mixed crystals of the form Se_nS_m and a range of sulfur oxides and ions are also known. The preparation and structure of these clusters has been reviewed by *Steudel*.[33]

The theoretical results for sulfur clusters S_2 to S_{13}[34] show that it is possible to determine low-lying energy minima even if the starting geometries are far from correct: linear chains in S_3 to S_6 and nearly planar rings in S_7 to S_{13}. The final structures agreed well with experiment in all cases where X-ray data were available. For example, the D_{3d} symmetry in S_{12} (Fig. 6b) is reproduced very closely, and the structural parameters (bond length $d = 3.97 a_0$, bond angle $\alpha = 106°$, dihedral angle $\gamma = 88°$) are in good agreement with measured values ($3.88 a_0$, $\alpha = 106.2°$, $\gamma = 87.2°$). The discrepancy in bond length is reduced by using a more accurate pseudopotential, as shown by calculations for the D_{4d} form of S_8, where the structure ($d = 3.900 a_0$, $\alpha = 108.5°$, $\gamma = 98.1°$) is very close to the experimental result ($d = 3.893 \pm 0.006 a_0$, $\alpha = 108.0 \pm 0.7°$, $\gamma = 98.3 \pm 2.1°$).[35]

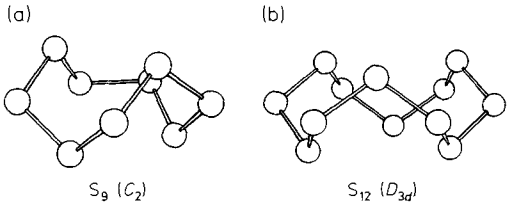

Fig. 6. Structures of a) S_9 and b) S_{12}.

Cases where the most stable isomers are not yet known are of particular interest. There is no experimental information on S_4 and S_5, for example, and S_9 has only been prepared as crystallites that are too small for X-ray diffraction analysis. The most stable S_4 isomer in our calculations was an unusual rectangular structure made up of two weakly interacting dimers. This minimum of the energy surfaces is very shallow and it is easy to distort the molecule. The detailed ab initio calculations of *Raghavachari* et al.[36] support our assignment of the ground state. This is also true in S_9, where we found a ground state isomer with C_2 symmetry (Fig. 6a) as well as several local minima with C_s symmetry with energies > 0.2 eV higher. The calculated ground state structure is consistent with measured Raman spectra, which indicate narrow ranges of bond lengths and bond angles, and dihedral angles in the range 70–130°.

5.2. Structural Change in S_7O

A surprising example of structural optimization is provided by the S_7O molecule.[37] In the course of the simulation

shown in Figure 7—1200 time steps at $T = 2000\,K$—the molecule changed from one with a stable local minimum and a ring structure similar to that in S_8 (Fig. 7a) to a structure with different topology: an oxygen atom outside the S_7 structure (Fig. 7i). The structure found on reducing the temperature slowly to $T = 0\,K$ (Fig. 7j) agrees well with the experimental ground state.[37] The entire structural change

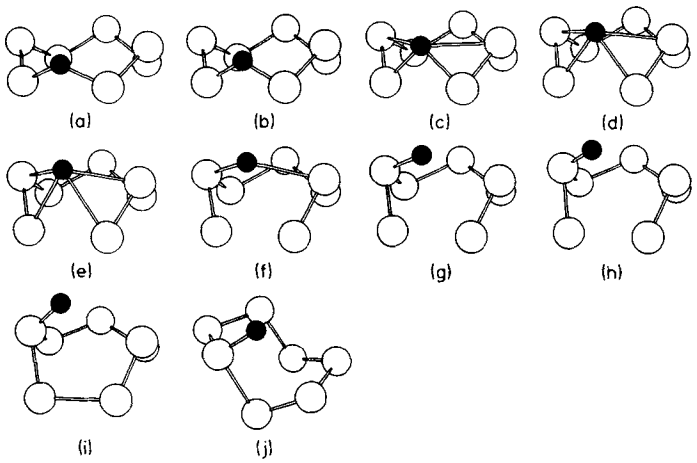

Fig. 7. Evolution of S_7O from ring (a) to ground state structure (j). The time difference between successive frames is 1.1×10^{-14} s.

(including cooling) took only about 8000 time steps ($< 10^{-12}$ s), although the energy barrier between ring and ground state structures is ca. 5 eV and the energy difference only about 0.2 eV. This shows just how efficient molecular dynamics can be in generating geometrical configurations.

5.3. Isomers of Se_2S_6, Se_6S_2

Sulfur and selenium have much in common, and binary systems have been studied extensively in the vapor phase[38, 39] and as liquids and as solid solutions.[40–42] The different species tend to crystallize together, leading to structures with sulfur and selenium atoms distributed over the atomic sites.[43] The possible complexity is evident in the eight-membered rings S_nSe_{8-n}, where thirty different crown-shaped isomers can occur. Apart from the intrinsic interest in molecules of the form Se_mS_n, an understanding of their structures could provide insight into the structures of related liquid and amorphous materials, including Se itself.

The interconversion of various Se_nS_m isomers and ring–chain equilibration processes involves reactions of the type in (20). This reaction is endothermic in the liquid.[44] For

$$\text{–S–S–} + \text{–Se–Se–} \longrightarrow 2\ \text{–Se–S–} \qquad (20)$$

diatomic S–Se molecules in the gas phase,[45] the measured enthalpy change is $+7.9 \pm 6.7\,kJ\,mol^{-1}$ and the sum of the dissociation energies on the left side of (20) is greater than the sum on the right. Theoretical predictions of the relative stability of different isomers are difficult to make,[46] and it is natural to ask whether DF calculations can describe reliably the small energy differences involved.

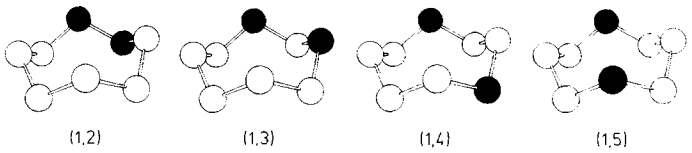

Fig. 8. Possible cyclic structures for Se_2S_6 and Se_6S_2. The numbers in parentheses indicate the positions of the two atoms of the minority element.

Calculations have been carried out on seven- and eight-membered rings of the type Se_mS_n,[47] starting with the ground state structures of S_7 (C_s) or S_8 (D_{4d}). The eight-membered rings are characterized by small deviations from the crown-shaped (D_{4d}) structures, and the possible cyclic structures in Se_2S_6 and Se_6S_2 are shown in Figure 8. The results for these molecules show several remarkable features, illustrated by the structural parameters for Se_2S_6 given in Table 3. In all eight structures, the bond lengths (d_{S-S}, d_{S-Se}, d_{Se-Se}) are the same to within 0.02 a_o (3.93 a_o, 4.21 a_o, 4.44 a_o), and d_{S-S} and d_{Se-Se} are the same as found previously for the ring structures of S_8 and Se_8. The (1,2) isomers are the most stable in both Se_2S_6 and Se_6S_2, and the energies of the other three structures are ca. 0.08 eV higher and degenerate to within $\pm$ 3 meV in each case. We now show that these findings can be understood in terms of a very simple model.

Table 3. Molecular parameters $d[a_o]$, α and γ[°] for all isomers of Se_2S_6 (see Fig. 8). Bond lengths between atoms i and j are denoted by d_{ij}, bond angles at atom i by α_i and dihedral angles at bond ij by γ_{ij}.

	Isomer [symmetry]			
	(1,2) [C_2]	(1,3) [C_s]	(1,4) [C_2]	(1,5) [C_{2v}]
d_{12}	4.42	4.20	4.20	4.21
d_{23}	4.21	4.20	3.92	3.93
d_{34}	3.92	4.20	4.21	3.93
d_{45}	3.93	3.93	4.21	4.21
d_{56}	3.95	3.93	3.93	4.21
d_{67}	3.93	3.93	3.92	3.92
d_{78}	3.92	3.93	3.93	3.93
d_{81}	4.21	4.20	4.21	4.21
α_1	105.9	106.1	106.7	106.7
α_2	105.8	108.1	108.2	108.9
α_3	108.1	106.2	108.2	108.6
α_4	108.8	108.4	106.7	108.4
α_5	109.1	108.7	108.5	106.5
α_6	109.2	109.2	108.7	109.2
α_7	108.8	108.7	108.8	108.7
α_8	108.2	108.5	108.6	108.5
γ_{12}	96.8	98.0	98.3	99.1
γ_{23}	97.2	96.6	97.8	96.6
γ_{34}	97.6	96.1	96.3	98.2
γ_{45}	100.6	100.4	99.1	100.5
γ_{56}	102.9	102.1	101.1	99.0
γ_{67}	100.5	100.4	98.9	96.5
γ_{78}	97.5	99.0	99.1	97.7
γ_{81}	97.3	97.6	99.1	100.4

The transferability of the bond lengths and the known connection between bond length and bond strength[26] suggest that we can associate with each bond type a contribution to the binding energy, E_{S-S}, E_{S-Se}, and E_{Se-Se}. This leads to (21) for the (1,2) structure in Se_2S_6 and to (22) for all remain-

$$E_{12} = E_{Se-Se} + 2E_{S-Se} + 5E_{S-S} \qquad (21)$$

$$E_{13} = E_{14} = E_{15} = 4E_{S-Se} + 4E_{S-S} \qquad (22)$$

ing structures. This argument predicts that the energies of the last three structures will be equal, and will differ from the energy of the (1,2) structure by ΔE (23).

$$\Delta E = E_{Se-Se} + E_{S-S} - 2E_{S-Se} \quad (23)$$

If we apply the same argument to the Se_6S_2 structures, Equations 21–23 still apply when S and Se are interchanged. This explains why the energy orderings in Se_2S_6 and Se_6S_2 are the same, and why the most stable (1,2) isomers are separated from three structures with almost identical energies. The separation in the present calculations (ca. 0.08 eV, 7.4 kJ mol^{-1}) is consistent with the endothermic reaction (20) and in reasonable agreement with the measured heats of reaction in the gas and liquid phases.

In spite of its simplicity, this model—based on a very careful geometry optimization—gives results that agree with trends found in recent measurements, particularly the relative abundance of structures in which the minority atoms are adjacent. The symmetry between the energy ordering of the isomers of Se-rich and S-rich molecules is perturbed, of course, by differences between the elements such as the atomic radius, but the essential features should be unchanged. The trend to segregation of minority components could also occur in the disordered liquid and amorphous states. Segregation in this model is a consequence of the sign of ΔE in Equation 23, and other systems with a small value of ΔE or with one of opposite sign would behave differently.

5.4. Phosphorus Clusters P_n

The structural variety shown by phosphorus exceeds that of all elements other than sulfur and perhaps boron, and there have been many studies of its crystalline and amorphous forms.[48, 49] A problem of continuing interest in gas-phase clusters has been the detection of only P_2, P_3, P_4, and (possibly) P_8 in the vapor phase at high temperatures.[50] There have been numerous speculations about the apparent absence of heavier clusters,[51] and several calculations indicate that the cubic form of P_8 is less stable than two P_4 tetrahedra.[52, 53] Recently, *Martin*[54] was able to detect by mass spectroscopy P_n molecules up to $n = 24$ in a low-temperature beam. In spite of this, almost nothing is known about the structure of clusters with $n > 4$.

MD/DF calculations have been performed on phosphorus clusters up to P_{10},[55] and calculated and experimental geometries and vibration frequencies agree well in those cases (P_2, P_4) where the latter are known. In the larger clusters there were several unexpected findings: 1) Although the tetrahedral structure is energetically favored in P_4, there is a large "basin of attraction" for a D_{2d} "roof" structure, that is, this structure is the closest minimum for a large region of configuration space. 2) The roof structure is a prominent feature in the low-lying isomers in P_5 to P_8. The most stable isomers found in P_5, P_6, and P_7 have a P_4-roof with an additional one, two, and three atoms, respectively.

The two forms of P_8 shown in Figure 9 are energetically more stable than the cubic structure. The structure in Figure 9a shows again the preference for the "roof" structure (two such units are bonded together), and the isomer shown in Figure 9b was the most stable we found. It can most easily be understood as a (distorted) cube with one bond rotated through 90° and is ca. 40 kcal mol^{-1} more stable than the cubic form. This "wedge" or "cradle" structure is found as a structural unit in violet (monoclinic, Hittorf) phosphorus.[56]

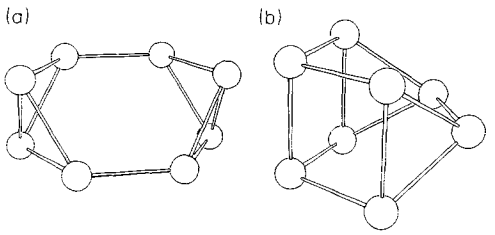

Fig. 9. Two isomers of P_8.

There is a pronounced analogy between the structures of the P_8 isomers and those of the corresponding isoelectronic hydrocarbons C_8H_8. The cubic form of the latter (cubane) has been prepared by *Eaton* and *Cole*,[57] and can be converted catalytically to the wedge-shaped form cuneane.[58] The third possible isomer of C_8H_8 (analogous to Fig. 9a) was estimated to have a strain energy intermediate between the other two, in agreement with the energy ordering we found in the P_8 isomers.[55]

The results for the P_n clusters show two particularly interesting features: 1) The presence of a large basin of attraction for the energetically unfavorable roof structure in P_4. This shows that the most favorable structures are not necessarily surrounded by the most extensive minima in the energy surfaces. 2) The existence of two isomers of P_8 that are more stable than the cubic form. Although attention had been focused for many years exclusively on the last, our finite-temperature simulation led almost immediately to more stable forms. The lowest energy for P_8 lies ca. 0.5 eV below the energy of two P_4 tetrahedra in the LD calculations. It would be interesting to see the energy difference found using ab initio methods.

5.5. Aluminum Clusters Al_n

The calculations for the sulfur and phosphorus clusters reproduce known structures satisfactorily. This is also true for small aluminum clusters, where spectroscopic data are available for Al_2, and ab initio calculations have been performed for a limited range of geometries up to Al_6.[59] If we can reproduce known structures of small clusters with our methods, we may have confidence in our predictions for larger clusters of these elements. Aluminum is a prototype "simple metal" of the condensed matter theorist, which is characterized by a weak electron–ion interaction and a valence electron charge distribution that is nearly uniform. It is natural then that calculations of the electronic structure of Al clusters have often used a "spherical jellium" model,[60] where both the electron density and the positive-ion distribution are assumed to be uniform inside a sphere of appropriate size. The focus in such calculations has been on particularly stable electronic configurations with "magic numbers" of electrons.

MD/DF calculations up to $n = 10$ give structures for $n = 2-4$ in good agreement with other calculations, and a satisfactory description of variations in ionization energies. There were, however, some unexpected results for larger clusters,[61] including the existence of a class of energetically favorable structures that can by no means be viewed as spherical. Figure 10 shows three such structures for Al_8. They can be viewed as distorted planar arrays of approximately equilateral triangles, connected so that adjacent triangles are either nearly coplanar (dihedral angle near zero) or have dihedral angles ca. 35°–55°. These features are also apparent in bulk aluminum (the face-centered-cubic structure comprises equilateral triangles with dihedral angles zero or 54.7°) and in the α form of the neighboring boron-group element gallium, as shown in Figure 10d. There are, of course, many possible structures of this type in molecules of finite extent. It is surprising, nevertheless, that DF calculations show that they are of comparable stability to the more compact "metallic" structures of Al_8. The structure shown in Figure 10c was, in fact, the most stable found in this molecule.

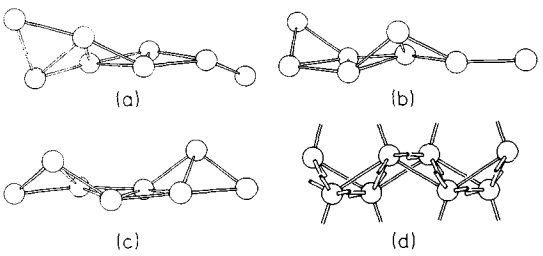

Fig. 10. a)–c) Three isomers of Al_8. d) Crystal structure of α-Ga.

We have noted above how useful the DF approach has been in finding trends in families of molecules, and in relating them to single-particle properties such as the valence orbital. This is also true in the elements of the third main group. We find that the bonds in gallium clusters are generally shorter than the corresponding bonds in aluminum clusters, and that this can again be correlated with the range of the valence orbitals.[61]

6. Concluding remarks

Theory should be able to contribute much to the determination of molecular structures. The calculation of the energy surfaces and the location of low-lying minima should lead to the most stable isomers, but there are severe problems: The determination of the energy E from the exact wave function is impracticable in all but the smallest molecules, and there are usually many local minima in the energy surface.

The approach described here addresses both aspects. The density functional formalism, with the local spin density approximation for the exchange–correlation energy, enables us to carry out energy calculations in an efficient manner, and the use of finite temperature molecular dynamics prevents the molecule becoming trapped in unfavorable energy minima. The results have been encouraging. The structures of small clusters of sulfur are described well and, in the case of S_7O, we can simulate structural changes involving a high energy barrier. The final structure (an O atom outside an S_7-ring) is in good agreement with the structure determined by X-ray diffraction. The heterocyclic ring molecules Se_mS_n are characterized by structures with very small energy differences and energy barriers that are small on a thermal scale. The calculations led in this case to a simple model of the energy differences in mixed Se–S ring structures and predictions for molecules for which calculations have not yet been performed. In the case of phosphorus clusters, we predict structures with plausible trends and with an interesting analogy to isoelectronic hydrocarbons $(CH)_n$. In Al_n clusters we have found a class of energetically favorable structures that was quite unexpected. There have been so many surprises, in fact, that one can only assume that many calculations using other methods have overlooked important minima in molecular energy surfaces. The number of minima and the fact that many can have comparable stability show how difficult it is to determine structures on the basis of "chemical intuition" alone. There is little doubt that other methods of calculating electronic structures would benefit from the implementation of simulated annealing.

The successes of this approach should not lead us to overlook its limitations. Even the most careful calculation reflects the approximations used, and the LSD approximation is an essential part of most of the calculations performed so far. Overestimates in the binding energy are evident in all the molecules discussed above, and there are indications that an inadequate description of exchange energy differences is an important factor.[111] Improved approximations would be useful, if implemented in a systematic way, but attempts in this direction have had mixed success. Moreover, there are many local minima in the energy surfaces even for clusters containing less than 10 atoms. The implementation of molecular dynamics techniques does not change this, and no method can guarantee finding the global energy minimum, or even all of the most important minima. The development of alternative optimization schemes and of simplified energy functionals[62] will be important in the future.

Density functional calculations are common in condensed matter physics and it is not surprising that workers from this field have played the major role in theoretical developments and in molecular applications. In fact, density functional methods have been slow to find favor amongst chemists. The coupling to molecular dynamics has opened up perspectives not currently available to some of the traditional methods of theoretical chemistry, and—perhaps in conjunction with these methods—the prospects of applications to many problems of chemical interest are very good.

I have benefited greatly from collaboration over the years with O. Gunnarsson, J. Harris, and D. Hohl, and from discussions with many colleagues. Special thanks are due to the developers of the MD/DF method, R. Car and M. Parrinello, and to G. Eilenberger for critical remarks on the manuscript.

Received: October 5, 1990 [A 818 IE]
German version: *Angew. Chem. 103* (1991) 647

[1] A. Cayley, *Philos. Mag. (4) 47* (1874) 444.
[2] M. R. Hoare, J. A. McInnes, *Adv. Phys. 32* (1983) 791.
[3] L. T. Wille, J. Vennik, *J. Phys. A 18* (1985) L419, L1113.

[4] M. R. Garey, D. S. Johnson: *Computers and Intractability: A Guide to the Theory of NP-Completeness*, Freeman, San Francisco 1979; NP-complete means nondeterministic polynomial time complete [29].
[5] P. Hohenberg, W. Kohn, *Phys. Rev. 136* (1964) B864.
[6] M. Levy, *Proc. Natl. Acad. Sci. USA 76* (1979) 6062.
[7] W. Kohn, L. J. Sham, *Phys. Rev. 140* (1965) A1133.
[8] O. Gunnarsson, B. I. Lundqvist, *Phys. Rev. (B) 13* (1976) 4274; see also J. Harris, R. O. Jones, *J. Phys. F4* (1974) 1170.
[9] J. Harris, *Phys. Rev. A 29* (1984) 1648.
[10] J. C. Slater, *Phys. Rev. 81* (1951) 385; *ibid. 82* (1951) 538.
[11] For a review on the formalism and some applications see R. O. Jones, O. Gunnarsson, *Rev. Mod. Phys. 61* (1989) 689.
[12] K. P. Huber, G. Herzberg: *Molecular Spectra and Molecular Structure. IV. Constants of Diatomic Molecules*, Van Nostrand Reinhold, New York 1979.
[13] P. E. Cade, A. C. Wahl, *At. Data Nucl. Data Tables 13* (1974) 339.
[14] R. Gáspár, *Acta Phys. Hung. 3* (1954) 263.
[15] G. S. Painter, F. W. Averill, *Phys. Rev. B 26* (1982) 1781.
[16] A. D. Becke, *J. Chem. Phys. 84* (1986) 4524.
[17] See, for example, O. Gunnarsson, J. Harris, R. O. Jones, *J. Chem. Phys. 67* (1977) 3970.
[18] M. R. A. Blomberg, P. E. M. Siegbahn, B. O. Roos, *Int. J. Quantum Chem. Quantum Chem. Symp. 14* (1980) 229.
[19] M. R. A. Blomberg, P. E. M. Siegbahn, *Int. J. Quantum Chem. 14* (1978) 583.
[20] R. O. Jones, *J. Chem. Phys. 71* (1979) 1300.
[21] K. A. Gschneidner, Jr., *Solid State Phys. 16* (1964) 276.
[22] V. L. Moruzzi, J. F. Janak, A. R. Williams: *Calculated Electronic Properties of Metals*, Pergamon, New York 1978.
[23] R. J. Harrison, N. C. Handy, *Chem. Phys. Lett. 98* (1983) 97.
[24] B. H. Lengsfield III, A. D. McLean, M. Yoshimine, B. Liu, *J. Chem. Phys. 79* (1983) 1891.
[25] V. E. Bondybey, J. H. English, *J. Chem. Phys. 80* (1984) 568.
[26] J. Harris, R. O. Jones, *Phys. Rev. A 18* (1978) 2159; *ibid. 19* (1979) 1813.
[27] R. O. Jones, *J. Chem. Phys. 82* (1985) 325.
[28] W. Kutzelnigg, *Angew. Chem. 96* (1984) 262; *Angew. Chem. Int. Ed. Engl. 23* (1984) 272.
[29] S. Kirkpatrick, C. D. Gelatt, M. P. Vecchi, *Science 220* (1983) 671.
[30] R. Car, M. Parrinello, *Phys. Rev. Lett. 55* (1985) 2471.
[31] F. Stillinger, T. A. Weber, R. A. LaViolette, *J. Chem. Phys. 85* (1986) 6460.
[32] See also R. Car, M. Parrinello, *Phys. Rev. Lett. 60* (1988) 204; P. Ballone, W. Andreoni, R. Car, M. Parrinello, *ibid. 60* (1988) 271.
[33] R. Steudel, *Stud. Inorg. Chem. 5* (1984) 3.
[34] D. Hohl, R. O. Jones, R. Car, M. Parrinello, *J. Chem. Phys. 89* (1988) 6823.
[35] R. O. Jones, D. Hohl, *Int. J. Quantum Chem. Quantum Chem. Symp. 24* (1990) 141.
[36] K. Raghavachari, C. M. Rohlfing, J. S. Binkley, *J. Chem. Phys. 93* (1990) 5862.
[37] D. Hohl, R. O. Jones, R. Car, M. Parrinello, *J. Am. Chem. Soc. 111* (1989) 825.
[38] R. Cooper, J. V. Culka, *J. Inorg. Nucl. Chem. 29* (1967) 1217.
[39] M. Schmidt, E. Wilhelm, *Z. Naturforsch. B 25* (1970) 1348.
[40] R. Steudel, E. M. Strauss: *The Chemistry of Inorganic Homo- and Heterocycles, Vol. 2*, Academic, London 1987, p. 769.
[41] R. Steudel, R. Laitinen, *Top. Curr. Chem. 102* (1982) 177.
[42] H. Bitterer (Ed.): *Selenium, Gmelin Handbuch der Anorganischen Chemie, Ergänzungsband B2*, Springer, Berlin 1984.
[43] R. Laitinen, L. Niinistö, R. Steudel, *Acta Chem. Scand. Ser. A 33* (1979) 737.
[44] T. Maekawa, T. Yokokawa, K. Niwa, *Bull. Chem. Soc. Jpn. 46* (1973) 761.
[45] J. Drowart, S. Smoes, *J. Chem. Soc. Faraday Trans. 2 73* (1977) 1755.
[46] R. Laitinen, T. Pakkanen, *J. Mol. Struct. THEOCHEM. 91* (1983) 337; *ibid. 124* (1985) 293.
[47] R. O. Jones, D. Hohl, *J. Am. Chem. Soc. 112* (1990) 2590.
[48] J. Donohue: *The Structures of the Elements*, Wiley, New York 1974, Chap. 5 (boron group), 8 (nitrogen group), 9 (oxygen group).
[49] D. E. C. Corbridge: *Phosphorus. An Outline of its Chemistry, Biochemistry and Technology*, Elsevier, Amsterdam 1985.
[50] J. D. Carette, L. Kerwin, *Can. J. Phys. 39* (1961) 1300.
[51] H. Bock, H. Müller, *Inorg. Chem. 23* (1984) 4365.
[52] K. Raghavachari, R. C. Haddon, J. S. Binkley, *Chem. Phys. Lett. 122* (1985) 219.
[53] R. Ahlrichs, S. Brode, C. Ehrhardt, *J. Am. Chem. Soc. 107* (1985) 7260.
[54] T. P. Martin, *Z. Phys. D 3* (1986) 221.
[55] P_2 to P_8: R. O. Jones, D. Hohl, *J. Chem. Phys. 92* (1990) 6710.
[56] H. Thurn, H. Krebs, *Acta Crystallogr. Sect. B 25* (1969) 125.
[57] P. E. Eaton, T. W. Cole, Jr., *J. Am. Chem. Soc. 86* (1964) 962, 3157.
[58] L. Cassar, P. E. Eaton, J. Halpern, *J. Am. Chem. Soc. 92* (1970) 6366.
[59] T. H. Upton, *J. Chem. Phys. 86* (1987) 7054; L. G. M. Petterson, C. W. Bauschlicher, Jr., T. Halicioglu, *J. Chem. Phys 87* (1987) 2205, and references cited therein.
[60] For a review, see W. A. deHeer, W. D. Knight, M. Y. Chou, M. L. Cohen, *Solid State Phys. 40* (1987) 94.
[61] R. O. Jones, unpublished results.
[62] See, for example, J. Harris, D. Hohl, *J. Phys. Condens. Matter 2* (1990) 5161, and references cited therein.

Spectroscopy of Fluid Phases—The Study of Chemical Reactions and Equilibria up to High Pressures

By Michael Buback*

The properties of fluid phases can be altered considerably by the external conditions. Phase equilibria and chemical equilibria can be greatly affected, and it is possible to carry out chemical reactions by exploiting the special properties of compressed fluid phases. The use of high pressure in chemical reactions is of considerable diagnostic and preparative value. Applied research is directed towards elucidating the details of existing technical high pressure processes and to the development of novel fluid phase reactions where the application of high pressure is able to induce selectivity. In order to pursue these lines of research, and to study structure and dynamics throughout the entire range from gaseous to liquidlike states, it is important to have spectroscopic methods for characterizing systems at high pressures and temperatures. This article is concerned with quantitative absorption spectroscopy in the infrared to the ultraviolet spectral region at pressures up to about 7 kbar and temperatures up to 900 K.

1. Introduction

The application of pressure to gaseous substances causes a significant reduction in the intermolecular distances. At pressures greater than 1000 bar all substances exist in dense states. In the kbar pressure range one probes intermolecular effects, and at very high pressures significant intramolecular effects occur, such as changes in the structures of the molecules or the formation of ionic or metallic states.[1,2]

For the chemist the study of fluid phases at pressures up to several kbar is of particular interest, especially with regard to possible preparative applications. The pressure–temperature diagram shown in Figure 1 indicates in a qualitative way[1] the behavior of a substance in the fluid, i.e. nonsolid, region. The density of packing of the circles is proportional to the density of the substance. In the bottom left part of the diagram the vapor-pressure curve, which extends to the critical point, divides the (condensed) liquid phase from the gaseous phase. At very high pressures the fluid region is bounded by the melting-pressure curve (not shown in the figure). In the literature[3] the region where temperature and pressure are both supercritical ($T > T_c, p > p_c$) is sometimes treated as a special region, that of the "supercritical fluid".

Figure 1 indicates that high-pressure experiments at supercritical temperatures offer special advantages: one can alter the density of a substance continuously from a gaseous to a liquidlike state, and if suitable physical measurement techniques are available, one can investigate the structure and dynamics over a wide range in the fluid state. It is important for practical applications that in supercritical fluid phases, properties such as the viscosity, dielectric constant, and heat-transfer coefficients vary considerably. This behavior has been studied in particular detail for supercritical water.[2,4–6]

When the pressure and temperature can be varied over a wide range, it is possible to produce large changes in the positions of the phase boundaries, and therefore also in solubilities. The chemist would like to influence chemical equilibria and reactions by applying high pressure. Kinetic experiments focus on the study of reaction mechanisms[7] including fast elementary processes, as well as on the use of high pressures for the development of new reaction routes or new products. In reactions that involve complex kinetic mechanisms, a difference between the pressure dependence of individual reaction steps can sometimes be exploited to achieve a pressure-induced selectivity.[8]

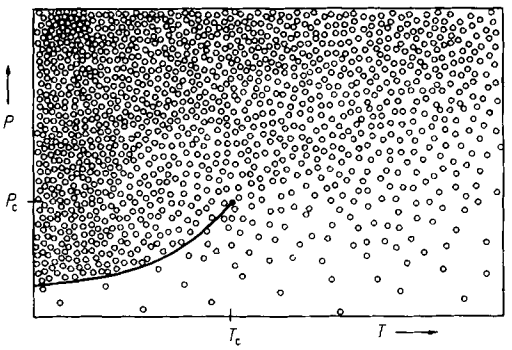

Fig. 1. Pressure-temperature diagram representing the density of a simple substance; p_c: critical pressure, T_c: critical temperature.

For measuring the effects of pressure, it is very useful to be able to perform quantitative analyses under high-pressure conditions. Particularly suitable methods for this are infrared and near infrared (near-IR) spectroscopy, but spectroscopy in the visible and ultraviolet regions also has some important applications. This article is concerned with measurements on fluid phases under conditions of both high pressure and temperature.

Section 2 describes sample cells that can be used for measurements at wavelengths throughout the range from IR to UV, with pressures up to 7000 bar and temperatures up to 900 K in some cases. Section 3 describes the changes in the vibrational spectra of pure substances over a wide range of densities. Section 4 contains examples of the use of quantitative absorption spectroscopy to study equilibria in fluid phases. In Section 5 the capabilities of quantitative absorption vibrational spectroscopy as a means of investigating pressure-induced reactivity and selectivity in chemical reactions are illustrated by examples. Section 6 shows how quan-

[*] Prof. Dr. M. Buback
Institut für Physikalische Chemie der Universität
Tammannstrasse 6, W-3400 Göttingen (FRG)

titative vibrational spectroscopy can be used very effectively for a direct study of industrial processes carried out at high pressures, taking free-radical polymerizations as an example.

2. Experimental Arrangements for Absorption Spectroscopy at High Pressures and Temperatures

Cells for fluid phase spectroscopy require windows that can withstand high pressures and can be used over as wide a spectral range as possible. It is necessary to be able to observe at least one characteristic absorption band for each relevant species in the system. For components whose concentration undergoes large changes during the course of the high-pressure reaction the ability to record several bands with widely different molar absorption coefficients is desirable.

The books by *Isaacs*[9] and by *Sherman* and *Stadtmuller*[10] contain detailed descriptions of high-pressure optical cells, including not only hydrostatic pressure cells but also other designs for measurements on solids, e.g. diamond-anvil cells. Only a few of these cell types are suitable for quantitative spectroscopic measurements in the fluid phase under conditions of simultaneous high pressure and high temperature. Cells with these capabilities that can be used up to 7 kbar and 900 K have been developed chiefly by *Franck*'s group at the University of Karlsruhe.[11] A basic design for such a high-pressure optical cell is described here.

The sealing of the optical window is based on the Poulter principle,[12] which is a modification of *Bridgman*'s unsupported area principle. The arrangement is shown in Figure 2. The window (2) rests on the optically flat polished surface (3) of a hollow steel ram (4) with a cylindrical bore. The high pressure side is denoted by P and the atmospheric pressure side by A. The pressure on the seating face (3) exceeds that at P by the factor $(d_1^2/d_1^2 - d_2^2)$, the ratio of the total surface area to the supported surface area, with the result that the arrangement is self-sealing at this interface. A sealing ring of poly(tetrafluoroethylene) (PTFE) film or gold foil inserted between the window and the steel seating compensates for any irregularities at the two surfaces. The high-pressure window is held under compression by a cap (1), to ensure effective sealing even at low pressures. The choice of the material for the cap is determined essentially by the working temperature. Stainless steel is suitable to 650 K. At higher temperatures it is important that the thermal expansion coefficient of

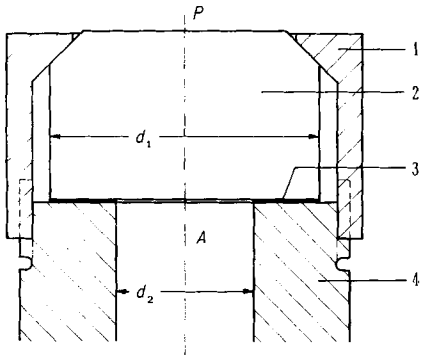

Fig. 2. Sealing arrangement of the high-pressure optical window; 1: cap, 2: window, 3: polished front surface of the ram with sealing ring in position, 4: steel ram; P: high-pressure side, A: atmospheric pressure, d_1: window diameter, d_2: diameter of free area available for passage of beam.

the material of the cap should be well matched to that of the window; for example, niobium is a suitable cap material for use with a sapphire window. This ensures that the compressional stress in the window remains sufficient up to high temperatures, giving good sealing even at low pressures.

Figure 3 shows a sample cell designed for pressures up to 3500 bar and temperatures up to 550 K. The two high-pressure optical windows (1) are supported on stainless steel rams (5) in accordance with the Poulter principle. Each ram is pressed against the body of the cell by a flange (3), which is secured by several bolts (2). The optical path length is determined by the distance between the inner surfaces of the high-pressure windows. Holes are drilled perpendicular to the axis of the cylindrical cell for introducing the sample and allowing one or more sheathed thermocouples (6) to be in-

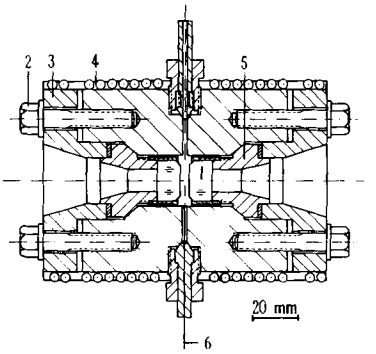

Fig. 3. High-pressure optical cell; 1: window, 2: retaining bolt, 3: flange, 4: heating coil, 5: stainless steel ram, 6: sheathed thermocouple.

Michael Buback was born in 1945 in Nobitz near Altenburg (Thüringen) and from 1963 studied chemistry at the University (Technische Hochschule) of Karlsruhe, gaining his doctorate in 1972 under Professor Ernst Ulrich Franck. Following his habilitation in 1978 he was awarded a Heisenberg fellowship by the Deutsche Forschungsgemeinschaft. In 1981 he took up the position of Professor of Applied Physical Chemistry at the University of Göttingen. He was awarded the Carl Duisberg Memorial Prize by the Gesellschaft Deutscher Chemiker, and in 1989 received the Dechema Prize from the Max Buchner Research Foundation. His special fields of interest are the kinetics and selectivity of reactions in fluid phases up to high pressures and temperatures, the study of free-radical polymerizations, especially using excimer laser initiation, and the development of absorption spectroscopy techniques for quantitative investigations of fluid systems under extreme conditions.

serted. The cell is heated from the outside by a resistive heating element (4) which may be mounted in a brass support.

For measurements requiring good optical transparency in the range from about 2000 cm^{-1} to 50 000 cm^{-1} at pressures up to 10 kbar, sapphire is unrivalled as a high-pressure, high-temperature window material, especially since it is also very resistant to chemical attack. In the wavenumber range below 2000 cm^{-1} windows made of polycrystalline silicon (down to 1450 cm^{-1}) or CaF_2 single crystals[13] (down to 1000 cm^{-1}) can be used. The maximum working pressures with these materials are 3 kbar and 2 kbar respectively. For still lower wavenumbers extending into the far infrared region one can use windows made of diamond (type IIa), or in some cases of quartz or silicon. Further information on high-pressure window materials can be found in the paper by *Ferraro* and *Basile*[14] and in relevant books.[10, 11]

High-pressure, high-temperature optical cells, based on the principles sketched in Figures 2 and 3, have also been developed for several special applications.[11, 15] These allow higher pressures to be reached by reducing the internal diameter of the cell[11, 16] or enable the separation of the sample under investigation from the pressurizing medium by a stainless steel bellows inside the optical cell.[11, 17, 18] Particular problems arise when attempting quantitative IR spectroscopic measurements on pure substances at very high pressures. Here path lengths need to be as short as several μm, and these distances are comparable with the changes in path length caused by altering the pressure and temperature in sample cells of the type shown in Figure 3. Considerable difficulties also arise in joining together the parts of such optical cells for working with path lengths shorter than 0.1 mm. These difficulties can be overcome by using cells in which the path length can be adjusted from outside while the cell is under pressure.[19] In this case two spectra are recorded under the same measurement conditions but with different path lengths; one of these serves as the sample spectrum and the other as a reference spectrum. The difference between the path lengths can be accurately determined.

The walls of the vessel, which are of stainless steel and can contain large amounts of nickel, cobalt, molybdenum, or other catalytically active constituents (e.g., German Standard No. 2.4668), can substantially influence the course of chemical reactions. This problem can be avoided by a procedure introduced by *le Noble*, in which the system under investigation is contained in an inner cell of quartz with a movable piston which is ground to give a close fit.[20] A recently introduced alternative method uses a PTFE container into which the reaction mixture is sealed by welding. The PTFE inner cell has a wall thickness of about 0.1 mm and the analyzing light beam readily passes through it. It is fitted into the high-pressure cell in such a way that it is in direct contact with the inner faces of the two high-pressure windows.[16, 21]

3. Absorption Spectra of Pure Substances in Fluid States

Experimental arrangements of the types described in Section 2 can be used to measure absorption spectra in the far infrared (far-IR) to the UV range. The far-IR spectra of condensed phases arise mainly from hindered rotations and intermolecular librational motions. *Bohn* and *Franck*[22] have demonstrated the continuous transition that occurs between these two types of motions in monochlorodifluoromethane on passing from the gaseous to the liquidlike state at a constant supercritical temperature. However, the far-IR spectrum is not very useful for determining the composition of fluid systems. The UV spectrum too is generally of little use for quantitative analysis, since the absorption bands of electronic transitions are broad and not very specific, so that qualitative and quantitative analyses are only advantageous in systems where the components are few in number and very different. A totally different situation prevails in the region of the fundamental, overtone, and combination frequencies of molecular vibrations: here, in the IR and near infrared (near-IR), one finds a wealth of characteristic absorption bands. The proven suitability of this spectral region for qualitative and quantitative analysis of gases, liquids, and solids under normal conditions should apply equally to studies on fluid phases up to high pressures and temperatures. Some IR and near-IR spectra of polar and nonpolar pure compounds in fluid phases are described below.

Figure 4 shows a plot of the molar absorption coefficient ε for the O–D stretching vibration in HDO at 673 K (above T_c = 647 K) for densities ranging from 0.01 to 0.90 g cm^{-3}, taken from the results of *Franck* and *Roth*[23], which extended up to 773 K and 4 kbar. Here $\varepsilon = A/cl$, in which A is the

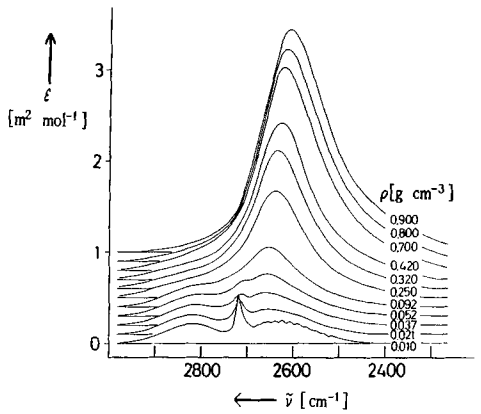

Fig. 4. Molar absorption coefficient ε for the O–D stretching vibration in HDO at 673 K and various densities ϱ.

logarithmic absorbance (decade scale), c is the concentration or density, and l is the path length. The bands are shifted slightly relative to each other along the baseline. At the lowest density the pressure-broadened spectrum observed is the envelope of the P, Q, and R branches. At higher pressures the spectrum changes to a strong broad band without shoulders.

Figure 5 shows how the vibrational spectrum of pure hydrogen chloride at 373 K (above T_c = 324 K) varies with the density.[24] At the lowest density (0.0065 g cm^{-3}) one observes the familiar spectrum with the P and R branches. With increasing density the rotational structure is lost, and at the highest density one again finds a single band, which is essentially symmetrical.

Figures 4 and 5 confirm that, as a result of dynamic and static effects, the infrared spectrum changes appreciably with

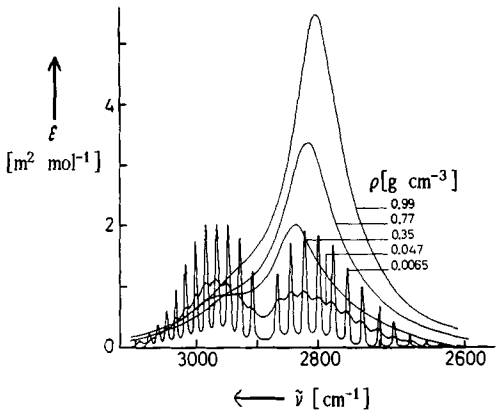

Fig. 5. Molar absorption coefficient ε for pure hydrogen chloride at 373 K and various densities ϱ.

the pressure or density. For these two polar compounds the vibrational intensity $B = \int \varepsilon(\tilde{\nu})\,d\tilde{\nu}$ increases markedly with increasing density, and the absorption maximum is shifted in the direction of smaller wavenumbers. In Figure 6 the shift of the band maximum to longer wavelengths for the O–D stretching mode of HDO and the H–Cl mode is plotted as a function of the "reduced" density ϱ/ϱ_c, where ϱ_c is the critical density for each substance; here the shifts are expressed as $\Delta\tilde{\nu} = \tilde{\nu}_{gas} - \tilde{\nu}_{max}$, i.e. the shift relative to the position in the gas phase. For both compounds $\Delta\tilde{\nu}$ is strongly dependent on the density at a given constant temperature. For a constant density, in the case of HCl, $\Delta\tilde{\nu}$ shows only a slight temperature-dependence, whereas in HDO the band maximum of the O–D stretching mode shifts considerably with temperature. However, above 673 K the stretching mode in HDO behaves in a similar way to the HCl stretching vibration, showing only a small effect on the band position when the temperature is increased further to 773 K. The behavior shown in Figure 6 for HCl can be regarded as typical for a normal dipolar liquid, whereas a strong temperature-dependence of $\Delta\tilde{\nu}$ at constant density, as observed for water up to about 573 K (Fig. 6), is regarded as an indication of significant hydrogen-bonding effects.[24] According to this criterion the behavior of water at supercritical temperatures, even in a highly condensed phase, resembles that of a normal dipolar liquid.

When the vibrational intensity B changes with the density and—as in the case of water—with the temperature, the absorbance $A(\tilde{\nu}) = \varepsilon(\tilde{\nu})cl$, as obtained directly from experimental absorption spectra, does not allow concentrations to be determined reliably, even if the path length l is accurately known. However, as we shall see below, polar fluids have overtone and combination bands for which the vibrational intensities show little or no dependence on density and temperature.

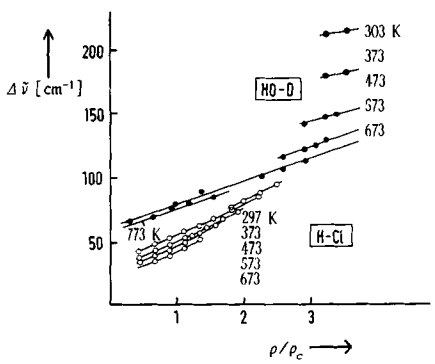

Fig. 6. The shift $\Delta\tilde{\nu} = \tilde{\nu}_{gas} - \tilde{\nu}_{max}$ of the band maximum (in wavenumber units) for the H–Cl vibration (lower curves) and the O–D vibration in HDO (upper curves) as a function of the reduced density ϱ/ϱ_c at various temperatures.

Figure 7 shows the vibrational intensity $B(0 \rightarrow 2)$ of the first overtone $(0 \rightarrow 2)$ absorption of pure CO over a wide range of densities at temperatures from 293 to 500 K.[25] The dependence of $B(0 \rightarrow 2)$ on density is quite different from the behavior of the absorption bands of strongly polar fluids (Figs. 4 and 5); it changes by only a few percent, and is independent of the temperature, at least between 293 and 500 K. Thus one has favorable conditions for the quantitative spectroscopic determination of CO over a wide range of fluid states. The same also applies for the fundamental mode IR absorption $(0 \rightarrow 1)$[26] at 2150 cm^{-1}, and with slight restrictions, also for the second overtone $(0 \rightarrow 3)$[25], which gives an absorption at about 6350 cm^{-1}.

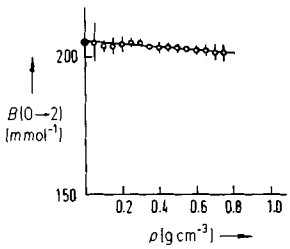

Fig. 7. Dependence of the vibrational intensity $B(0 \rightarrow 2)$ on density for the first overtone absorption in pure CO at temperatures between 293 and 500 K; ●: value from Ref. [27].

Further evidence that intermolecular interactions only weakly influence the vibrational spectrum of CO is provided by the band shapes in the condensed phase, which can be well described using the parameters of the gas phase spectrum. For this, a model developed by *Bouanich* et al. can be used,[27, 28] in which the band contour, expressed as the reduced molar absorption coefficient $\varepsilon_n(\tilde{\nu}) = \varepsilon(\tilde{\nu})/B(0 \rightarrow n)$, is calculated as a summation over the individual rotational–vibrational lines of the gas phase spectrum. These lines are assumed to have a modified Lorentzian shape with a half-width proportional to the density. The model contains only one adjustable parameter, which has the effect of varying the band shape of the individual lines between a Lorentzian and a nearly Gaussian function.

The spectra calculated using this model (data points in Fig. 8) are in very good agreement with the experimentally observed spectra (solid curves in the figure) for the fundamental mode and the first and second overtones at moderately high densities (0.1 $g\,cm^{-3}$) throughout the temperature range investigated (up to 500 K).[25] The first overtone region depicted in Figure 8 shows that at higher densities (up to 0.3 $g\,cm^{-3}$) the experimental curves for the P-branch are still very well described by the model, while the agreement for the R-branch is just barely satisfactory. In liquidlike states (densities around 0.6 $g\,cm^{-3}$) discrepancies of as much as 10% in the P-branch and 20% in the R-branch are found.[25] Since a density of 0.3 $g\,cm^{-3}$ at 500 K corre-

sponds to a pressure of about 600 bar, the conclusion from Figure 8 is that this model which, apart from one adjustable parameter, is based solely on the spectroscopic data from the gas phase spectrum, is applicable over quite a broad range of pressures and temperatures.

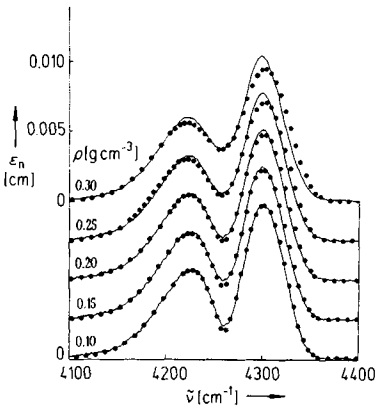

Fig. 8. Comparison of observed line shapes (——) with those calculated from Ref. [27] (●) for the first overtone absorption of pure CO at 500 K and various densities ϱ.

Similar studies of the density-dependent band shapes have been carried out for pure CO_2 in the region from 3200 to 7400 cm^{-1}.[29, 30] In this case the overlapping of several vibrational bands, and particularly a vibrational coupling by Fermi resonance must be taken into account. For some of the CO_2 modes, such as the $3\nu_3$ overtone, the wavenumber position of the band maximum does not continue to move downwards at very high densities, and at the highest attainable densities a shift in the opposite direction starts to occur. Effects of this kind are known from studies by *Drickamer* et al.,[31, 32] and are attributed to the influence of repulsive interactions.

The IR spectra of the fundamental stretching modes in water (Fig. 4) and hydrogen chloride (Fig. 5), and also in ammonia,[33] are not very suitable for quantitative analytical purposes, as the vibrational intensities vary considerably with changes in densities from the gaseous phase to liquidlike states. In contrast, carbon monoxide,[25, 26] carbon dioxide,[29, 30] ethylene,[34–36] and *n*-heptane[37] have several bands in the IR and near-IR whose intensities remain constant or change by only a few percent when the density or temperature is altered over a broad range in the fluid state. In the near-IR, even polar substances have combination and overtone bands whose vibrational intensities show little or no variation with density and temperature. This behavior has been observed for the O–H stretching modes in water by *Luck*[38] and in alcohols by *Luck* and *Ditter*.[39] Figure 9 shows a series of absorption spectra for pure NH_3 at 523 K at densities from 0.025 to 0.525 g cm^{-3}.[40] The band with a maximum at 4400 cm^{-1} is assigned to the combination frequency $\nu_2 + \nu_3$ and that at 5000 cm^{-1} to $\nu_3 + \nu_4$.[40, 41] When the absorption spectra of Figure 9 are integrated and normalized to a standard path length and concentration, the resulting vibrational intensity B is found to be independent of the density within the limits of accuracy of the measurements. In contrast, the values of B measured in the region of the N–H fundamental stretching modes (ca. 3200 cm^{-1}) alter by about 300% on going from the gas phase to a liquidlike phase. Thus the near-IR region, which has the additional advantage of greater path lengths, is very well suited for quantitative measurements on fluids. For nonpolar compounds and those that are only weakly polar the combined use of the IR and near-IR spectra brings considerable analytical advantages, as illustrated below for the example of the ethylene–polyethylene system.

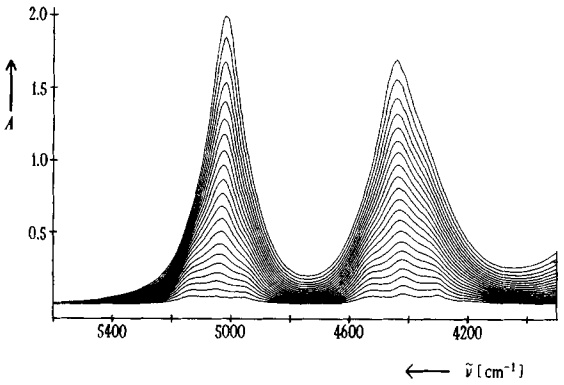

Fig. 9. Original traces obtained in measurements of the near-IR absorbance A of pure ammonia at 523 K and various densities ϱ, increasing from 0.025 g cm^{-3} (lowest curve) in steps of 0.025 g cm^{-3} to 0.525 g cm^{-3}.

Figure 10 shows selected IR and near-IR bands in the range 2000 to 12 000 cm^{-1} for dense fluid ethylene (E) under high pressure and for polyethylene (PE). In order of increasing wavenumber the four absorption regions shown are assigned to the fundamental C–H stretching mode and the first, second, and third overtones. However, this is only a rough classification, since the near-IR absorption is largely determined by combination modes.[34, 35] In ethylene, for example, all the odd-numbered overtones are forbidden on symmetry grounds.

For quantitative analysis on compressed fluid phases by IR and/or near-IR spectroscopy, it is highly advantageous that the molar absorption coefficient ε varies by several orders of magnitude in an extended wavenumber range such as the one shown in Figure 10 (which can be recorded in less than one second on a Fourier transform spectrometer). The relationship $A(\tilde{\nu}) = \varepsilon(\tilde{\nu})cl$ leads directly to two types of applications: 1) Measurement of the entire spectrum allows the

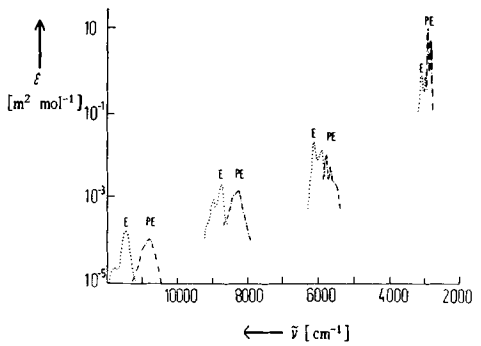

Fig. 10. Molar absorption coefficient ε for selected bands of compressed fluid ethylene (E) and of polyethylene (PE) between 2000 and 12 000 cm^{-1}.

detection of low concentrations with high spectroscopic sensitivity (high ε) from data for the fundamental mode region, while components present in relatively high concentrations can be measured in the less sensitive near-IR region. Thus use of a large spectral region greatly increases the range of concentrations that can be measured in a single experiment, and the entire course of a reaction can be followed up to a high percentage conversion. This is especially useful in high-pressure experiments. For example, in the early stages of a high-pressure polymerization the monomer, which is at first the only component or in overwhelming excess, is measured by a higher overtone, while the polymer, initially present only in trace amounts, is detected by the fundamental mode; during the middle stage the monomer and polymer are monitored by their first or second overtones; then as the reaction nears complete conversion, the polymeric product is measured by a higher overtone and the monomer, now present only in a low concentration, by the fundamental mode. Analytical possibilities of this kind exist for nearly all substances, provided that the absorption bands of the starting material and the product are sufficiently separated, because the absorption intensities always decrease rapidly the higher the overtones. 2) The large differences in the absorption intensities enable the selection of regions of the spectrum to measure concentrations in fluid systems with widely different optical path lengths, and therefore in reactors of different dimensions. For ethylene at a density of about 0.5 g cm^{-3}, which is typical in high-pressure polymerization reactions, the optical path lengths l needed to give an absorbance value $A = 1$ at the band maximum in each case are as follows: for the fundamental mode at 3000 cm^{-1}, $l = 0.05$ mm; for the first overtone at 6000 cm^{-1}, $l = 1.1$ mm; for the second overtone at 9000 cm^{-1}, $l = 12.5$ mm; for the third overtone at 11 500 cm^{-1}, $l = 140$ mm.

4. Fluid Phase Equilibria

The ability to determine the nature and concentration of species of interest in fluid phases directly by spectroscopic measurements can be used in many ways. Some examples of applications to the study of fluid phase equilibria are described below.

A knowledge of the positions of phase boundaries in fluid mixtures is of considerable scientific and technological importance. The two standard methods for determining phase behavior are the synthetic and the analytical method, based on repeated sampling.[42] A procedure based on near-IR measurements was first used by *Nees*[17,43] in studies on the ethylene–polyethylene system at pressures up to 3000 bar and temperatures up to 573 K. *Schneider* et al.[44] determined the solubilities of adamantane, octacosane, and squalane in fluid CO_2 by near-IR spectroscopy at pressures up to 1000 bar. The solubility of anthracene in a number of fluid phases at pressures up to 3000 bar and temperatures up to 550 K was studied by *Rößling* and *Franck*[45] by quantitative UV spectroscopy. The same method was also successful in the determination of the solubility of caffeine in fluid CO_2.[46]

Quantitative spectroscopy in the visible and UV range can be used to investigate complex equilibria in aqueous solutions up to high pressures and temperatures.[47–49] Figure 11 shows measurements by *Lüdemann* and *Franck*[48] of the molar absorption coefficient ε for 0.005 M cobalt(II) bromide in an aqueous solution (4 M) of NaBr at 6 kbar and temperatures from 298 to 773 K. At temperatures up to 473 K the cobalt is present mainly in the form of the pink octahedral hexaquacobalt complex (band maximum at 500 nm). At higher temperatures the solutions are blue. The band at 700 nm is assigned to the tetrahedral tribromomonoaquacobalt complex.

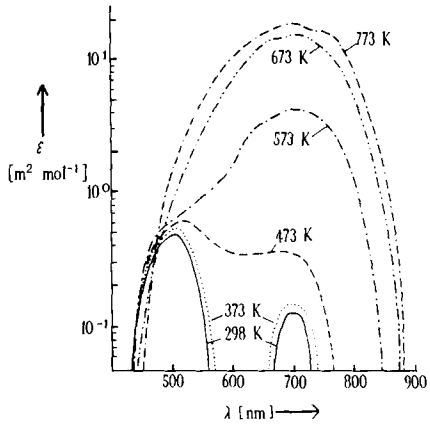

Fig. 11. Molar absorption coefficient ε for 0.005 M $CoBr_2$ in an aqueous solution of NaBr (4 M) at 6 kbar and temperatures from 298 to 773 K.

Studies on aqueous solutions of cobalt(II) halides diluted without further addition of sodium halide show that here too the dominant form up to 573 K is the pink octahedral hexaquacobalt complex.[47] At higher temperatures and moderately high pressures (about 1000 bar) the dominant species is the blue tetrahedral dichlorodiaqua complex with an absorption maximum at 680 nm. On increasing the pressure, e.g. to 6 kbar, it is found that at 773 K the pink-to-blue color change can be reversed. A review of the formation of metal complexes in aqueous solutions can be found in the publication by *Seward*.[49]

Quantitative IR spectroscopy has been used to study the effects of pressure and temperature on the equilibria between monomers and cyclic dimers in dilute solutions of carboxylic

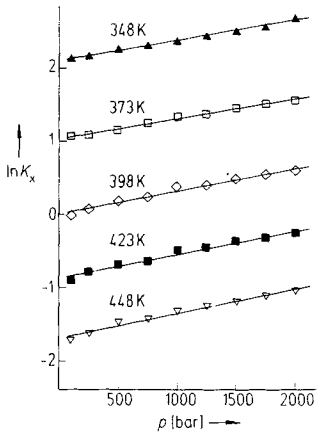

Fig. 12. Dependence of the equilibrium constant K_x on pressure for the dimerization of pivalic acid as a solution in *n*-heptane (1.0×10^{-2} M) at various temperatures.

acids.[50-52] Characteristic absorption bands for the two species without significant overlapping occur in the regions of the C=O and O-H stretching fundamentals. The intensities of the vibrational bands for the monomer and dimer in the C=O region are found to be independent of pressure and temperature, and can therefore be used to measure concentrations and hence determine equilibrium constants. Results obtained by this method for pivalic acid dissolved in heptane at temperatures from 348 to 448 K and pressures up to 2000 bar are shown in Figure 12; here the equilibrium constant is defined as $K_x = x_D/x_M^2$, where x_D and x_M are the mole fractions of the dimer and monomer respectively.[50]

Figure 13 shows the intensities of the O-H stretching modes for pivalic acid (monomer and dimer) referred to 1 mole of the monomer. The values for the monomer

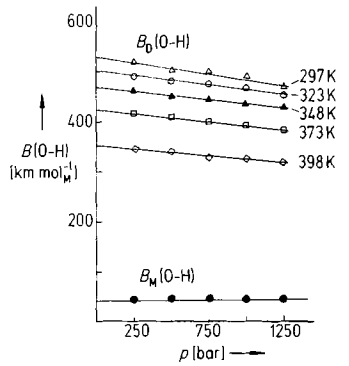

Fig. 13. Vibrational intensities B_M(O-H) and B_D(O-H) for the monomer and the cyclic dimer respectively of pivalic acid (5.0×10^{-2} M in CCl_4) as a function of the pressure p at various temperatures.

(B_M(O-H)) are independent of pressure and temperature within the limits of accuracy. On the other hand the values for the dimer (B_D(O-H)), which are greater by an order of magnitude, decrease with increasing temperature and—to a lesser extent—with increasing pressure.[50] This observation suggests that the nature of the dimer present in the equilibrium mixture changes with temperature and pressure. Figure 13 also provides a further example of the high sensitivity of the fundamental intramolecular O-H stretching mode as an indicator of intermolecular interactions (cf. Fig. 4).

From the pressure dependence of the equilibrium constant K the dimerization volume change $\Delta V = -(\delta(RT\ln K)/\delta p)_T$

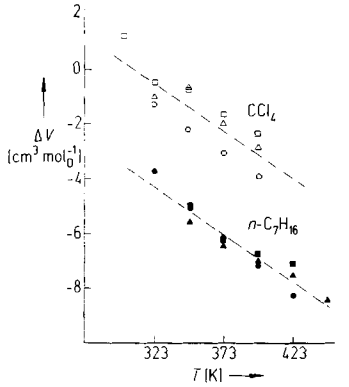

Fig. 14. Temperature dependence of the dimerization volume change ΔV for acetic acid (○), benzoic acid (□) and pivalic acid (△) in CCl_4 (open symbols) and in n-heptane (filled symbols).

can be determined. In Figure 14 ΔV is plotted as a function of the temperature for several carboxylic acids. The equilibrium constant represents $K_c = c_D/c_M^2 = K_x/c$ (where c = total concentration of carboxylic acid). In both solvents (CCl_4 and n-heptane) ΔV increases with decreasing temperature. A CCl_4 solution of benzoic acid yields a positive value for ΔV at room temperature, indicating that increasing pressure favors a dissociation of the cyclic dimer into monomer molecules. In order to explain the temperature dependence of ΔV it is assumed that at lower temperatures the dimers have a more stable planar structure with a greater volume, whereas at higher temperatures dimers with less perfect structures and a lesser degree of planarity are present. The latter species occupy a smaller volume, and consequently at higher temperatures increasing pressure always favors dimer formation.

5. Chemical Conversions in Fluid Phases

The review article by *Asano* and *le Noble*[7a] and the more recent review by these authors together with *van Eldik*[7b] provide a very good account of the many different types of investigations of chemical reactions at high pressures. The extensive field of high-pressure organic syntheses has also been covered in two review articles by *Matsumoto* et al.[53, 54] Preparative aspects of chemical reactions at high pressures are treated in the articles by *Jurczak*[55] and *Klärner*.[8] However, up to now there have been only a few cases where reaction kinetics have been studied directly by quantitative high-pressure absorption spectroscopy, although this method enables one to make very detailed observations and to recognize and study even quite complex reaction sequences.

The use of quantitative spectroscopic methods to study high-pressure reactions will first be illustrated by some examples of hetero-Diels–Alder reactions. The reactions of enamine carbaldehydes and enamino ketones with various vinyl ethers have been studied.[16, 21, 56-58] Figure 15 shows absorbance difference spectra in the region of the N-H

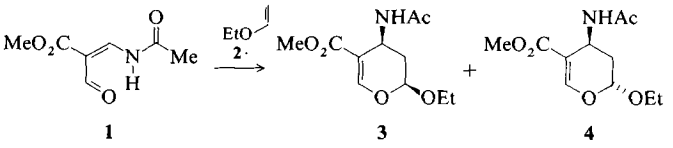

1 3 4

stretching modes recorded during the reaction of **1** and **2** at 333 K and 1500 bar in CH_2Cl_2 solution, yielding the diastereomeric products **3** and **4**. The traces were obtained by subtracting the first spectrum, recorded after establishing the experimental conditions, from each of the spectra recorded thereafter; this eliminates the absorptions of the solvent and of groups that do not change absorption during the reaction. With this difference procedure the products give positive absorbances and the diene starting compound gives negative absorbances. In some solvents it is possible to observe separate N-H stretching bands for the two diastereomeric products.[16, 21]

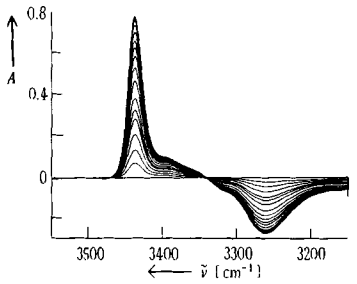

Fig. 15. Infrared difference spectra (see text) in the region of the N–H stretch during the reaction of **1** and **2** in CH_2Cl_2 at 333 K and 1500 bar.

Quantitative spectroscopy in the region of the carbonyl stretching modes has been used to investigate the Diels–Alder reactions of **2** with enamino ketones of the general structure **5**, yielding the diastereomeric dihydropyrans **6a–d** and

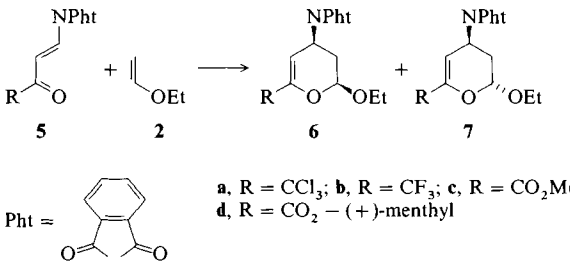

a, R = CCl_3; **b**, R = CF_3; **c**, R = CO_2Me; **d**, R = CO_2 – (+)-menthyl

7a–d.[21, 57] The formation of the *cis* adducts **6** is thought to occur via an *endo* intermediate and that of the *trans* adducts **7** via an *exo* intermediate. In the presence of an excess of ethyl vinyl ether (**2**) over the diene, the spectroscopically measured concentration data have been used to determine rate coefficients k by a modified *Kezdy–Swinbourne* procedure.[16, 21, 59] Figure 16 shows the pressure dependence of k

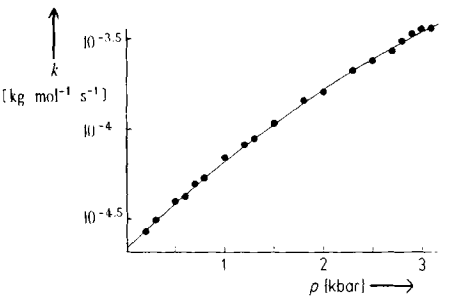

Fig. 16. Dependence of the rate coefficient k on pressure for the cycloaddition reaction of **5b** and **2** in CH_2Cl_2 at 318 K.

for the cycloaddition reaction of **5b** and **2** in CH_2Cl_2 at 318 K. Figure 17 shows the temperature dependence of k for the cycloaddition of **5a** and **2** in CH_2Cl_2 at 1000 bar.

In all these experiments the reaction solution was contained in a sealed, thin-walled PTFE cell, as described in Section 2, to avoid catalytic effects from the stainless steel walls of the autoclave. In each case the kinetic measurements were followed by HPLC measurements on the reaction mixture when the conversion was nearly or fully completed, to determine the ratio of the concentrations of the two diastereomers **6** and **7**. From the pressure and temperature dependence of this ratio one can directly obtain the quantities $\Delta\Delta V^{\neq}$ and $\Delta\Delta H^{\neq}$ which are the differences between the activation volumes and activation enthalpies for the reaction channels leading to the two diastereomers.[16, 56–58] For the reaction of **5a** with **2** the difference between the activation volumes is especially large, $\Delta\Delta V^{\neq} = 5.9 \pm 0.5\ cm^3\ mol^{-1}$.

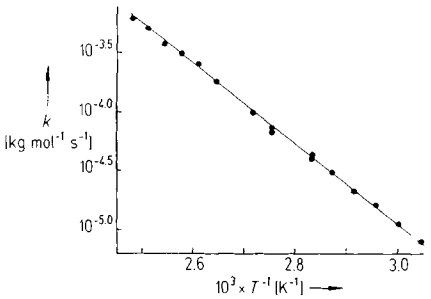

Fig. 17. Dependence of the rate coefficient k on temperature for the cycloaddition reaction of **5a** and **2** in CH_2Cl_2 at 1000 bar.

In Figure 18 the percentage yield of the *cis* diastereomer **6a** from the reaction of **5a** with **2** is plotted as a function of pressure for a range of temperatures. The solid curves were obtained from the experimentally measured selectivity data (filled circles), partly by extrapolation. With increasing pressure and decreasing temperature the reaction becomes increasingly selective in favor of the *cis* diastereomer. Thus at

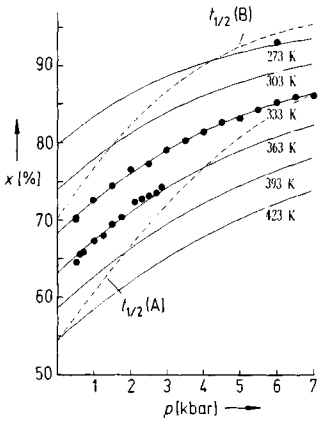

Fig. 18. Percentage yield x of the *cis* diastereomer **6a** in the cycloaddition reaction of **5a** and **2** in CH_2Cl_2 as a function of pressure at various temperatures. The broken lines correspond to reaction half-lives of $t_{1/2}(A) = 15$ minutes and $t_{1/2}(B) = 6$ days for the chosen concentrations. These times encompass the range of "reasonable" values in reactions with on-line spectroscopic detection.

273.5 K and 6 kbar one obtains **6a** and **7a** in the ratio 13.6 to 1.0, compared with a ratio of 1.67 to 1.00 at atmospheric pressure and 363 K. The dashed curves contain information obtained from kinetic measurements as a function of time. The lower of these two curves (labeled $t_{1/2}(A)$) intersects the solid curves at the pressure and temperature values corresponding to a half-life of 15 minutes at the concentrations present in the experiment. The upper curve ($t_{1/2}(B)$) corresponds to the intersection points for a half-life of 6 days.

From the rate coefficients k one can calculate similar dashed curves for any given reaction conditions. Figure 18 indicates that at atmospheric pressure and 273 K, an 80% yield of **6a** should be obtainable. The corresponding half-life is about 1.5 years. The data in this figure show that high pressure provides two advantages: firstly, at a given temperature a higher pressure gives increased selectivity; secondly, raising the pressure significantly increases the rate of the cycloaddition reaction, so that satisfactory reaction rates are achieved at lower temperatures. Thus the advantage of increased selectivity at lower temperature can also be exploited. By further increasing the pressure and reducing the temperature it should be possible to achieve high selectivities.

A further example of the use of quantitative absorption spectroscopy in fluid phases is seen in Figure 19, which shows infrared absorption spectra measured in the carbonyl stretching region during the decomposition of *tert*-butylperoxypivalate dissolved in *n*-heptane at 353 K and 2000 bar.[60] The peroxide band at 1775 cm^{-1} decays, and the absorption at 2340 cm^{-1} due to CO_2 that is formed increases. The growing absorption at 1725 cm^{-1} is assigned to acetone. From measurements in the O–H stretching region between 3500 and 3700 cm^{-1} the formation of *tert*-butanol and (in smaller amounts) pivalic acid during the decomposition can also be detected.[60] Such measurements provide access to the kinetics of the decomposition, and to direct observation of several reaction pathways and their dependence on the pressure and temperature. The spectroscopic method can also be used to measure the efficiencies of initiators in free-radical polymerizations.[61] Experiments of the kind shown in Figure 19 have already been carried out for di-*tert*-butyl peroxide,[62] dioctanoyl peroxide,[61] dibenzoyl peroxide,[61] and *tert*-butylperoxybenzoate.[63]

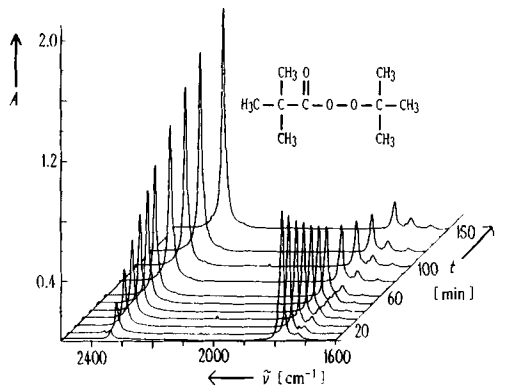

Fig. 19. Infrared absorption spectra recorded during the thermal decomposition of *tert*-butylperoxypivalate in *n*-heptane at 353 K and 2000 bar.

6. Free-Radical Polymerizations at High Pressures

The high pressure polymerization of ethylene and various copolymerization reactions of ethylene with polar comonomers are of special technical importance. The scientific interest in these reactions is directed mainly towards determining individual rate coefficients over a wide range of pressure, temperature, and degree of conversion, and as a function of the radical chain length. For such investigations the ability to make direct spectroscopic observations during polymerization is of great value.

Figure 20 shows a series of spectra measured in the region of the second overtone of the C–H stretching vibration during the homopolymerization of ethylene at 463 K and an initial pressure of 2630 bar.[64] The progress of the reaction can be measured both by the reduction in the ethylene absorbance at 8730 and 8960 cm^{-1} and by the growth of the polyethylene absorbance at 8260 cm^{-1}. The spectra in Figure 20 cover a range extending to about 80% conversion. In the case of ethylene–acrylic ester copolymerizations, the concentration of the acrylate comonomer can be measured from its C=C stretching band (the corresponding vibration in ethylene is inactive); in butyl acrylate, for example, this occurs at 1630 cm^{-1}.[65] The extended IR and near-IR region also contains other bands that are suitable for quantitative analysis. The high-pressure spectroscopic method has also been used in studies of the copolymerization of ethylene with carbon monoxide[66] and with acrylonitrile,[67] and of the homopolymerization of styrene[68] and of methylmethacrylate.[69]

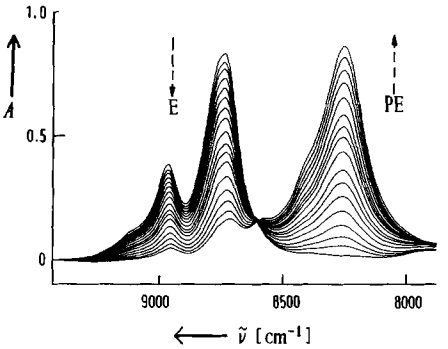

Fig. 20. Near-IR absorbance spectra recorded during the free-radical polymerization of ethylene at 463 K and 2630 bar (E: ethylene, PE: polyethylene).

The use of excimer lasers for initiating free-radical polymerizations, in conjunction with IR or near-IR spectroscopy for detection, has proved to be a very effective method for determining kinetic parameters under a wide range of conditions. Two procedures have been used. The first (Method 1) involves time-resolved measurements, in the microsecond to millisecond range, of the growth of macromolecules initiated by a single pulse of about 20 ns duration from an excimer laser.[70, 71] In the second procedure (Method 2) the progress of the polymerization is measured at intervals, after applying sequences of excimer laser pulses varying the number of pulses and the pulse repetition frequency.[64, 72] In this case each pulse train is followed by a measurement of the IR and near-IR spectrum over a broad range of wavenumbers using a Fourier transform spectrometer. In experiments based on Method 1 the measurements are made at a fixed wavelength. Figure 21 shows a signal recorded in this way for an ethylene polymerization at 463 K and 2550 bar. At t = 0 a KrF laser pulse of 248 nm wavelength was applied to the reaction mixture already containing 9.5% polyethylene. The resulting conversion to polyethylene, measured by the near-IR ab-

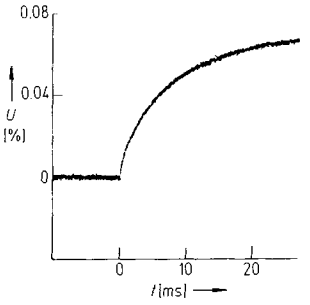

Fig. 21. Time resolved near-IR measurement (at $8258 \pm 5\,cm^{-1}$) of the monomer conversion U induced by a single pulse from a KrF excimer laser (248 nm) in an ethylene polymerization at 463 K and 2550 bar (degree of conversion already existing before this particular pulse experiment starts: 9.5%).

sorption at $8258 \pm 5\,cm^{-1}$ (cf. Fig. 20) with a time resolution of 10 μs, is less than 0.1%. The recorded signal was processed by fitting the curve to Equation (a), which describes the amount of polymerization induced by the laser pulse.[70] Here $c_M(t=0)$ and $c_M(t)$ are the monomer concen-

$$\frac{c_M(t)}{c_M(t=0)} = (2k_t c_R(t=0)t + 1)^{-0.5k_p/k_t} \quad \text{(a)}$$

trations at the instant when the pulse is applied and at a time t later, k_p and k_t are the rate coefficients for the propagation and termination reactions respectively, and $c_R(t=0)$ is the initial instantaneous concentration of growth-initiating primary free radicals produced by the laser pulse, which is related to the primary quantum yield φ_i by Equation (b), where

$$c_R(t=0) = 2\,\varphi_i n_{abs} V^{-1} \quad \text{(b)}$$

n_{abs} is the number of absorbed quanta and V is the volume of the sample.

The pulse experiment has certain important advantages. The kinetic parameters k_p/k_t and $k_t\varphi_i$ obtained directly by fitting the data to Equation (a) are very well resolved as functions of the degree of conversion, since the polymerization induced by each pulse is very small. As the formation of all the radicals, and thus the initiation of growth, occurs simultaneously, the radicals present at a given time t after the pulse have a very narrow size distribution, provided that transfer reactions are insignificant. This enables one to obtain information about kinetic parameters for radicals of different chain lengths.[70, 73] Method 2 also yields values of k_p/k_t and $k_t\varphi_i$, but does not give comparable resolution as a function of the degree of conversion; moreover, the pulse repetition frequencies that can currently be attained are insufficient to enable one to study the dependence of the rate coefficients on chain length.

In Figure 22 the primary kinetic parameters $k_t\varphi_i$ and k_p/k_t obtained from excimer laser experiments[70, 74] are plotted as functions of the conversion U for the high-pressure free-radical polymerization of ethylene at 503 K and 2550 bar. It can be seen that $k_t\varphi_i$ decreases with the degree of conversion, at first quite rapidly, then at a slower rate, and again rapidly at high degrees of conversion, with an overall reduction of about three orders of magnitude to 80% conversion ($U = (c_M^0 - c_M)/c_M^0 = 0.8$, where c_M^0 refers to zero conversion). In the case of k_p/k_t we find an increase with the degree of conversion, at first rapid then slower. The change (increase) in k_p/k_t to 80% conversion is much smaller than the change (decrease) in $k_t\varphi_i$. Before discussing the data in Figure 22 it is useful to examine the behavior of the quantity

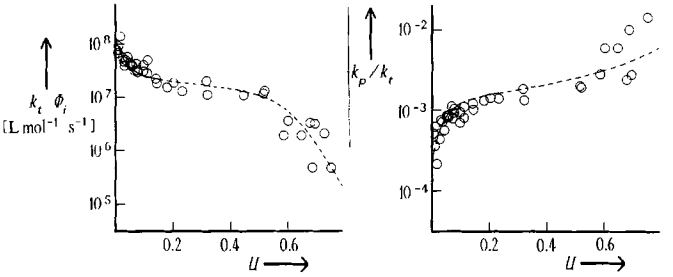

Fig. 22. Kinetic parameters for the free-radical polymerization of ethylene at 503 K and 2550 bar plotted as functions of the degree of conversion. Left: the product $k_t\varphi_i$ of the termination rate coefficient k_t and the primary quantum yield φ_i; right: the quotient k_p/k_t (k_p = propagation rate coefficient).

$k_p\varphi_i$ obtained by multiplying together the values of $k_t\varphi_i$ and k_p/k_t from experiments performed by Method 1. This product is plotted in Figure 23 for the polymerization of ethylene at 503 K and 2550 bar. Over a considerable range extending to about 50% conversion, $k_p\varphi_i$ is found to remain constant within the range of experimental error. At higher degrees of conversion the value falls steeply. It is unlikely that in the range from 0% to 50% conversion, over which the viscosity of the medium increases by about five orders of magnitude, k_p and φ_i change in such a way that their product remains constant, and the results shown in Figure 23 must therefore mean that k_p and φ_i both remain constant under the chosen conditions of pressure and temperature. It follows from this that where independent information is available on either k_p or φ_i within this range of conversion, one can determine all three quantities, k_p, k_t, and φ_i.

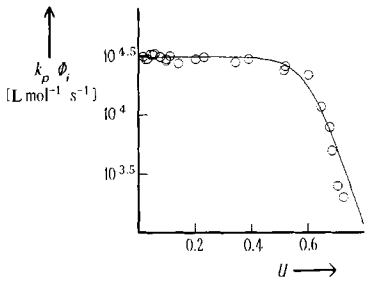

Fig. 23. The product $k_p\varphi_i$ for the free-radical polymerization of ethylene at 503 K and 2550 bar as a function of the degree of conversion.

Measurements show that φ_i [see Eq. (b)] has a value close to 1.[72] It is assumed that this value continues to apply beyond 50% conversion, and $k_p\varphi_i$ in Figure 23 can therefore be regarded as identical to k_p. One should be able to describe this k_p curve using the equation given in the literature for a diffusion-controlled propagation rate coefficient [Eq. (c)].[75, 76] Here $k_{p,0}$ is the (chemical) propagation rate

$$k_p = \frac{1}{k_{p,0}} + \frac{1}{k_{p,D}} \quad \text{(c)}$$

coefficient without any influence from diffusion control and $k_{p,D}$ describes the diffusion-controlled contribution. It is assumed that $k_{p,D}$ is inversely proportional to the viscosity of the solution [Eq. (d)]. The quantity $\eta_r = \eta/\eta_0$ is the relative

$$k_{p,D} = k^0_{p,D}/\eta_r \tag{d}$$

viscosity for the conditions of the experiment, expressed relative to the viscosity η_0 of the pure monomer under the same conditions. Equation (d) is based on the questionable assumption that bulk viscosity is a relevant transport parameter for the elementary processes under consideration (see also Eq. (h) below). An essential reason for introducing η_r is that a few high-pressure, high-temperature viscosities are available from the literature, whereas monomer, polymer, and especially free-radical diffusion coefficients are not yet known. From Equations (c) and (d) we obtain Equation (e).[77] This simple kinetic relationship, together with the

$$k_p = (k^{-1}_{p,0} + \eta_r/k^0_{p,D})^{-1} \tag{e}$$

data given by *Ehrlich* and *Woodbrey*[78] for the viscosity of the ethylene–polyethylene system, leads to the solid line in Figure 23. The relative viscosities were calculated using Equation (f), which is approximately valid for the particular

$$\log \eta_r = 5.39\,U + 3.70\,U^{0.5} \tag{f}$$

reaction conditions. It is important to note that the viscosity depends on both the degree of conversion *and* the properties of the polymer that is formed (described, for example, by its intrinsic viscosity). Thus viscosities should be taken from experiments under identical or at least similar polymerization conditions.

The rate coefficient k_t for the chain-termination reaction is several orders of magnitude greater than k_p, and the termination reaction is usually already diffusion-controlled in the initial stages of the polymerization. The termination process may be regarded as a multistage reaction consisting of three steps: translational diffusion (TD) of two radicals, segmental diffusion (SD) bringing the radical centers into direct contact, and lastly the chemical reaction (CR). The kinetics should be represented by Equation (g).[79] The rate coefficient for the translational diffusion step is assumed to be inversely proportional to the viscosity of the medium [Eq. (h)].

$$\frac{1}{k_{t,D}} = \frac{1}{k_{TD}} + \frac{1}{k_{SD}} + \frac{1}{k_{CR}} \tag{g}$$

$$k_{TD} = k^\circ_{TD}/\eta_r \tag{h}$$

It turns out that Equation (g) is not adequate to describe the entire range of conversion. At high degrees of conversion and high viscosities, where the center-of-mass motions of the radicals are largely suppressed, the values calculated for k_{TD}, and therefore for $k_{t,D}$, are too low. Under these conditions termination occurs mainly through a "reaction diffusion" mechanism, as was first shown by *Schulz*.[80] Radical chain ends come into contact with each other through propagational growth reactions within the monomer matrix in which they are embedded.[76, 77, 80, 81] The rate coefficient for this process is proportional to k_p and to the monomer concentration c_M, i.e. to $(1 - U)$, where, as before, $U = (c^\circ_M - c_M)/c^\circ_M$; it is given by Equation (i) where C_{RD} is the reaction diffusion constant.

$$k_{t,RD} = C_{RD} k_p (1 - U) \tag{i}$$

Termination occurs by the parallel mechanisms of diffusion-controlled termination ($k_{t,D}$) and reaction diffusion ($k_{t,RD}$) [Equation (j)].

$$k_t = k_{t,D} + k_{t,RD} \tag{j}$$

By inserting into Equation (j) the expressions (e) and (g)–(i), and assuming that $k_{CR} \gg k_{TD}, k_{SD}$, we obtain the overall termination rate coefficient k_t [Eq. (k)].

$$k_t = \frac{1}{k^{-1}_{SD} + \eta_r/k^0_{TD}} + \frac{C_{RD}\cdot(1-U)}{k^{-1}_{p,0} + \eta_r/k^0_{p,D}} \tag{k}$$

Various simplifying approximations[77] can be applied to this equation depending on the system. For example, in the ethylene high-pressure polymerization reaction k_{SD} is usually, much greater than k_{TD}, so that the term k^{-1}_{SD} in Equation (k) can be neglected. The resulting simplified equation yields the broken curve in Figure 22 (left) and gives a very reasonable fit to the experimental points for $k_t\varphi_i$.

The transition between regions in which k_t and k_p show little change and rapid change with the degree of conversion indicates a change in the mechanism controlling the kinetics. In ethylene, for example, k_t (Fig. 22, left) is, at low degrees of conversion, initially controlled by translational diffusion, and later by reaction diffusion, and at high degrees of conversion the diffusion control of k_p has a significant effect on the termination reaction (see Equation (i), in which C_{RD} is assumed to be independent of the degree of conversion).

The kinetic relationships arrived at on the basis of spectroscopic studies of the dependence of k_t and k_p on degree of conversion [e.g. Eq. (k)] can also be applied to the free-radical polymerization of other monomers. This is illustrated in Figure 24, which shows results for butyl acrylate (BA) and methyl methacrylate (MMA). The data for BA are from our excimer laser experiments at 383 K,[82] while the results for MMA are a combination of literature data for 273 K[83] and

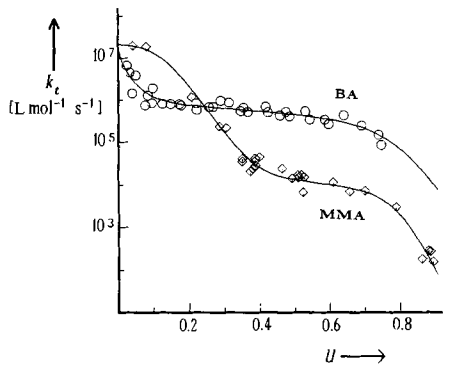

Fig. 24. The termination rate coefficient k_t as a function of the degree of conversion for the free-radical polymerization reactions of butyl acrylate (BA) at 383 K [82] and methyl methacrylate (MMA) at 273 K [83] and 323 K [84].

323 K.[84] The dependence of k_t on degree of conversion for BA is closely related to that for ethylene. For MMA, however, there are substantial differences, because at low conversion k_t is limited by segmental diffusion. The subsequent rapid decrease in k_t indicates that here the limiting mechanism is translational diffusion. This is followed by regions in which reaction diffusion, and finally at very high conversion, diffusion-controlled propagation, are the dominant mechanisms. The steep fall of k_t in the region of 20 to 40% conversion, closely related to the *Norrish–Trommsdorff* effect, can be understood in terms of the model represented by Equation (k) as being due to the much slower termination by reaction diffusion here compared with BA and ethylene (k_p and C_{RD} in Eq. (i) are considerably smaller for MMA[77]). Because of this the translational diffusion, which decreases with increasing viscosity, controls the overall termination reaction up to a higher degree of conversion. The solid lines in Figure 24 show that Equation (k) accounts very well for the experimental data for both monomers over this wide range of the degree of conversion, in which the viscosity increases by many orders of magnitude [see Eq. (f)].

The parameters in the kinetic model described by Equation (k) are mainly concerned with the initial stage of the polymerization (near-zero conversion) and have a physical meaning ($k_{p,0}$, $k^0_{p,D}$, k^0_{TD}, k_{SD}). The description of the dependence on degree of conversion is reduced to (at least) one measurement to determine C_{RD} and an independent measurement or estimation of the reduced viscosity during the polymerization.[77] The representation of free-radical rate coefficients in an extended conversion range by Eq. (k) is quite remarkable. The model should certainly be further extended and refined. It should always be kept in mind that the kinetics at a given conversion, temperature, and pressure depend on the history of the particular system, because the rate coefficients can change with U, T, and p, which in turn affects polymer properties and thus transport processes.

The technique of using an excimer laser to induce the reaction is not only of great importance for basic studies of high-pressure free-radical polymerizations, but also offers some interesting prospects for technological applications. These concern possibilities such as polymerization of pure monomers without the use of additives (initiators or chain transfer agents), and effective external control of the progress of a polymerization and to some extent also of the properties of the polymer produced. Studies that are already well advanced for ethylene homopolymerization could be extended to include high-pressure copolymerizations involving ethylene. Systems that have already been investigated in some detail are ethylene–carbon monoxide,[66] ethylene–acrylonitrile,[67] and ethylene–butyl acrylate.[65]

7. Summary and Outlook

Techniques are now available for measuring absorption spectra in the range from the IR to the UV on fluid systems at pressures up to 7000 bar and temperatures up to 900 K. At only moderately high temperatures, this pressure range can be extended still higher, and conversely, moderate pressures allow higher temperatures to be reached. For example, in studies of fluid metals at pressures up to 2500 bar, it has been possible to record spectra at temperatures up to 2000 K.[85]

These methods enable one to study equilibria and reactions throughout the whole field of organic, inorganic, and macromolecular chemistry. Some reactions of inorganic complex species in liquid solutions have already been systematically studied by high-pressure spectroscopy,[86] and it is expected that the range of the measurements can be extended to include fluid states at higher temperatures. Also spectroscopic studies in biochemistry[87] and geochemistry[15,49] will become increasingly important. Whereas high-pressure high-temperature absorption spectroscopy has up to now been used mainly for qualitative and quantitative analysis of fluid systems, the technique will in future be used increasingly for fundamental studies of ultra-fast elementary chemical processes; here systematic investigations of the pressure- und temperature-dependence of different representative reactions should provide a method for thoroughly testing theoretical reaction models. This is illustrated by the work of *Troe*, *Schroeder*, and collaborators,[88,89] who have used pump-and-probe absorption spectroscopy with picosecond and subpicosecond time resolution to follow fast reactions, especially isomerizations, directly. An example of such measurements is an investigation of the isomerization of diphenylbutadiene in ethane at 298 bar and 354 K; the lower curve of Figure 25 shows the transient absorption of the S_1 state of diphenylbutadiene at 616 nm after excitation by a picosecond pulse at 308 nm (at $t = 0$).[88] The kinetics of the reaction can be determined directly from the exponential decay curve corresponding to the population of the S_1 state.

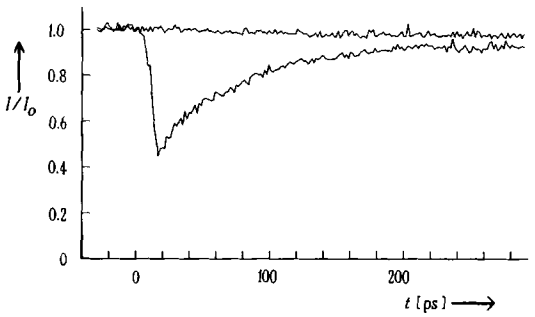

Fig. 25. Transient absorption of the S_1 state of diphenylbutadiene at 616 nm following excitation by a picosecond laser pulse at 308 nm; reaction in ethane at $p = 298$ bar and $T = 354$ K (upper curve was recorded without laser pulse excitation).

Isomerization kinetics of the kind shown in Figure 25 have also been measured for *trans*-stilbene in a wide variety of liquid and supercritical solvents at pressures up to 7000 bar and temperatures up to 425 K.[89] An important result of these studies is that by combining standard equations of the theory of unimolecular reactions with the hydrodynamic Kramers model one obtains a satisfactory description of the experiments under nearly all conditions, provided that the effects of the multidimensionality of the barrier region of the potential energy hypersurface on the dynamics are taken into account. High-pressure high-temperature spectroscopy, especially when used in combination with pulsed laser experiments, will make important contributions to investigations

of other elementary reactions in future. The method is of great importance for studying the kinetics and selectivity of chemical processes over a wide range of fluid states. Interest in potential technological applications is centered on the search for new reaction routes and new products; the ability to study existing fluid phase processes under reaction conditions is already proving to be very important from a practical standpoint.

The studies carried out in the author's own laboratory and described in this article were generously supported by the Deutsche Forschungsgemeinschaft (SFB 93: "Photochemie mit Lasern") and by the Fonds der Chemischen Industrie. The author thanks Dr. J. Schroeder for additions to the manuscript, and Dr. H.-P. Vögele for his support in completing this work.

Received: January 16, 1991 [A 817 IE]
German version: *Angew. Chem. 103* (1990) 658
Translated by Dr. J. K. Becconsall, Gwynedd (Wales)

[1] E. U. Franck, *Ber. Bunsenges. Phys. Chem. 73* (1969) 135–142.
[2] K. Tödheide, *Naturwissenschaften 57* (1970) 72–82.
[3] K. D. Bartle in R. M. Smith (Ed.): *Supercritical Fluid Chromatography*, Royal Soc. Chem., London 1988, p. 2.
[4] K.-H. Dudziak, E. U. Franck, *Ber. Bunsenges. Phys. Chem. 70* (1966) 1154.
[5] K. Heger, Dissertation, Karlsruhe 1969; K. Heger, M. Uematsu, E. U. Franck, *Ber. Bunsenges. Phys. Chem. 84* (1980) 758–762.
[6] K. Tödheide in F. Franks (Ed.). *Water—A Comprehensive Treatise, Vol. 1*, Plenum, New York 1972, pp. 464–514.
[7] a) T. Asano, W. J. le Noble, *Chem. Rev. 78* (1978) 407–489; b) R. van Eldik, T. Asano, W. J. le Noble, *Chem. Rev. 89* (1989) 549–688.
[8] F.-G. Klärner, *Chem. Unserer Zeit 23* (1989) 53–63.
[9] N. S. Isaacs: *Liquid Phase High Pressure Chemistry*, Wiley, Chichester 1981.
[10] W. F. Sherman, A. A. Stadtmuller: *Experimental Techniques in High-Pressure Research*, Wiley, Chichester 1987.
[11] M. Buback, *Phys. Chem. Earth, 13/14*, 1981, pp. 345–360.
[12] T. C. Poulter, *Phys. Rev. 40* (1932) 860–869.
[13] M. Buback, E. U. Franck, H. Lendle, *Z. Naturforsch. A 34*, (1979) 1489–1495.
[14] J. R. Ferraro, L. J. Basile, *Appl. Spectrosc. 28* (1974) 505–517.
[15] M. Buback, D. A. Crerar, L. M. Vogel-Koplitz in G. C. Ulmer, H. L. Barnes (Eds.): *Hydrothermal Experimental Techniques*, Wiley-Interscience, New York 1987, pp. 333–359.
[16] W. Tost, Dissertation, Göttingen 1988.
[17] F. W. Nees, M. Buback, *Ber. Bunsenges. Phys. Chem. 80* (1976) 1017–1023.
[18] M. Buback, H. Lendle, *Makromol. Chem. 184* (1983) 193–206.
[19] M. Buback, *Z. Naturforsch. A 32* (1977) 1295–1300.
[20] W. J. le Noble, R. Schlott, *Rev. Sci. Instrum. 47* (1976) 770.
[21] M. Buback, W. Tost, L. F. Tietze, E. Voß, *Chem. Ber. 121* (1988) 781–785.
[22] M. A. Bohn, E. U. Franck, *Ber. Bunsenges. Phys. Chem. 92* (1988) 850–859.
[23] E. U. Franck, K. Roth, *Discuss. Faraday Soc. 43* (1967) 108–114.
[24] M. Buback, E. U. Franck, *Ber. Bunsenges. Phys. Chem. 75* (1971) 33–39.
[25] M. Buback, J. Schweer, H. Tups, *Ber. Bunsenges. Phys. Chem. 89* (1985) 545–550.
[26] M. Buback, J. Schweer, H. Tups, *Z. Naturforsch. A 42* (1987) 267–271.
[27] J. P. Bouanich, Nguyen-Van-Thanh, H. Strapelias, *J. Quant. Spectrosc. Radiat. Transfer 26* (1981) 53.
[28] J. P. Bouanich, Nguyen-Van-Thanh, I. Rossi, *J. Quant. Spectrosc. Radiat. Transfer 30* (1983) 9–15.
[29] M. Buback, J. Schweer, H. Tups, *Z. Naturforsch. A 41* (1986) 505–511.
[30] M. Buback, J. Schweer, H. Tups, *Z. Naturforsch. A 41* (1986) 512–518.
[31] A. M. Benson, H. G. Drickamer, *J. Chem. Phys. 27* (1957) 1164.
[32] R. R. Wiederkehr, H. G. Drickamer, *J. Chem. Phys. 28* (1958) 311.
[33] M. Buback, E. U. Franck, *J. Chim. Phys. 72* (1975) 601–606.
[34] M. Buback, F. W. Nees, *Ber. Bunsenges. Phys. Chem. 80* (1976) 650–656.
[35] F. W. Nees, M. Buback, *Z. Naturforsch. A 31* (1976) 1690–1695.
[36] M. Buback, I. Heym, *Ber. Bunsenges. Phys. Chem. 84* (1980) 245–250.
[37] M. Buback, A. A. Harfoush, *Z. Naturforsch. A 38* (1983) 528–532.
[38] W. A. P. Luck, *Ber. Bunsenges. Phys. Chem. 69* (1965) 626–637.
[39] W. A. P. Luck, W. Ditter, *Ber. Bunsenges. Phys. Chem. 72* (1968) 365–374.
[40] S. Rohde, *Diplomarbeit*, Göttingen 1989.
[41] G. Herzberg: *Infrared and Raman Spectra of Polyatomic Molecules*, Van Nostrand, New York 1945.
[42] G. M. Schneider in B. Le Neindre, B. Vodar (Eds.): *Experimental Thermodynamics, Vol. 2*, Butterworths, London 1975, pp. 787–801.
[43] F. W. Nees, *Dissertation*, Karlsruhe 1978.
[44] I. Swaid, D. Nickel, G. M. Schneider, *Fluid Phase Equilibria 21* (1985) 95–112.
[45] G. L. Rößling, E. U. Franck, *Ber. Bunsenges. Phys. Chem. 87* (1983) 882–890.
[46] H. Ebeling, E. U. Franck, *Ber. Bunsenges. Phys. Chem. 88* (1984) 863–865.
[47] H. D. Lüdemann, E. U. Franck, *Ber. Bunsenges. Phys. Chem. 71* (1967) 455–460.
[48] H. D. Lüdemann, E. U. Franck, *Ber. Bunsenges. Phys. Chem. 72* (1968) 514–523.
[49] T. M. Seward, *Phys. Chem. Earth, 13/14* (1981) 113–132.
[50] E. M. Borschel, M. Buback, *Z. Naturforsch. A 42* (1987) 187–196.
[51] R. Barraza, E. M. Borschel, M. Buback, *Z. Naturforsch. A 42* (1987) 406–412.
[52] E. M. Borschel, M. Buback, *Z. Naturforsch. A 43* (1988) 207–214.
[53] K. Matsumoto, A. Sera, T. Uchida, *Synthesis 1985*, 1–26.
[54] K. Matsumoto, A. Sera, *Synthesis 1985*, 999–1027.
[55] J. Jurczak, *Physica 139/140 B* (1986) 709–716.
[56] L. F. Tietze, T. Hübsch, E. Voß, M. Buback, W. Tost, *J. Am. Chem. Soc. 110* (1988) 4065–4066.
[57] M. Buback, W. Tost, T. Hübsch, E. Voß, L. F. Tietze, *Chem. Ber. 122* (1989) 1179–1186.
[58] J. Oelze, *Diplomarbeit*, Göttingen 1990.
[59] F. J. Kezdy, J. Jaz, A. Bruylants, *Bull. Soc. Chim. Belg. 67* (1958) 687; E. S. Swinbourne, *J. Chem. Soc. 2* (1960) 2371.
[60] M. Buback, H. Lendle, *Z. Naturforsch. A 36* (1981) 1371–1377.
[61] E. Schmid, *Dissertation*, Göttingen 1991.
[62] M. Buback, H. Lendle, *Z. Naturforsch. A 34* (1979) 1482–1488.
[63] A. Drefahl, *Diplomarbeit*, Göttingen 1984.
[64] H. Brackemann, M. Buback, H.-P. Vögele, *Makromol. Chem. 187* (1986) 1977–1992.
[65] U. Hain, *Dissertation*, Göttingen 1991.
[66] M. Buback, H. Tups, *Physica 139/140 B* (1986) 626–628; H. Tups, *Dissertation*, Göttingen 1986.
[67] H. Brackemann, M. Buback, *Makromol. Chem. Rapid Commun. 10* (1989) 283–286; H. Brackemann, M. Buback, *Makromol. Chem. 190* (1989) 3073–3084.
[68] B. Huckestein, *Dissertation*, Göttingen 1991; B. Ludwig, *Diplomarbeit*, Göttingen 1991.
[69] S. Beuermann, *Diplomarbeit*, Göttingen 1990.
[70] M. Buback, J. Schweer, *Z. Phys. Chem. (Munich) 161* (1989) 153–165; J. Schweer, *Dissertation*, Göttingen 1988.
[71] M. Buback, H. Hippler, J. Schweer, H.-P. Vögele, *Makromol. Chem. Rapid Commun. 7* (1986) 261–265.
[72] M. Buback, B. Huckestein, U. Leinhos, *Makromol. Chem. Rapid Commun. 8* (1987) 473–479.
[73] M. Buback, J. Schweer, *Makromol. Chem. Rapid Commun. 9* (1988) 699–704.
[74] M. Buback, B. Degener, H. Hippler, B. Huckestein, J. Schweer, unpublished results.
[75] M. J. Ballard, D. H. Napper, R. G. Gilbert, D. F. Sangster, *J. Polym. Sci. Polym. Chem. Ed. 24* (1986) 1027; M. J. Ballard, R. G. Gilbert, D. H. Napper, P. J. Pomery, P. W. O'Sullivan, J. H. O'Donnell, *Macromolecules 19* (1986) 1303.
[76] S. K. Soh, D. C. Sundberg, *J. Polym. Sci. Polym. Chem. Ed. 20* (1982) 1299, 1315, 1331, 1345.
[77] M. Buback, *Makromol. Chem. 191* (1990) 1575.
[78] P. Ehrlich, J. C. Woodbrey, *J. Appl. Polym. Sci. 13* (1969) 117.
[79] S. W. Benson, A. M. North, *J. Am. Chem. Soc. 84* (1962) 935.
[80] G. V. Schulz, *Z. Phys. Chem. (Munich) 8* (1956) 290.
[81] G. T. Russell, D. H. Napper, R. G. Gilbert, *Macromolecules 21* (1988) 2133.
[82] M. Buback, B. Degener, B. Huckestein, *Makromol. Chem. Rapid Commun. 10* (1989) 311; B. Degener, *Dissertation*, Göttingen 1991; B. Huckestein, *Dissertation*, Göttingen 1991.
[83] R. Sack-Kouloumbris, G. Meyerhoff, *Makromol. Chem. 190* (1989) 1133.
[84] M. J. Ballard, D. H. Napper, R. G. Gilbert, *J. Polym. Sci. Polym. Chem. Ed. 22* (1984) 3225.
[85] H. Uchtmann, F. Hensel, *Proc. Int. Conf. High Pressures 4th 1975*, pp. 591–595.
[86] R. van Eldik (Ed.): *Inorganic High Pressure Chemistry—Kinetics and Mechanisms*, Elsevier, Amsterdam 1986.
[87] R. van Eldik, J. Jonas (Eds.): *High Pressure Chemistry and Biochemistry*, Reidel, Dordrecht 1987.
[88] C. Gehrke, J. Schroeder, D. Schwarzer, J. Troe, F. Voß, *J. Chem. Phys. 92* (1990) 4805–4816.
[89] J. Schroeder, D. Schwarzer, J. Troe, F. Voß, *J. Chem. Phys. 93* (1990) 2393–2404.

The Chemistry of Rose Pigments

By Conrad Hans Eugster* and Edith Märki-Fischer

In this article we present a survey of the pigments found in the flowers and fruits of old and modern varieties of roses. The yellow colors are produced by carotenoids, the reds by anthocyanins, and the modern oranges by a mixture of the two. The great structural diversity of the carotenoids contrasts with a surprisingly small number of anthocyanins. For the carotenoids found in roses, a clear correspondence exists between the structure and the breeding partners used; the old yellow roses, which arose from crosses with Chinese varieties, mainly contain carotenoids from early stages in the biosynthesis, while in the modern yellow roses, which are descended from Central Asian *foetida* types, hydroxylations, epoxidations, and epoxide transformations readily occur. A recently elucidated carotenoid degradation sequence follows the scheme $C_{40} \rightarrow C_{13} + C_{27} \rightarrow C_{13} + C_{14}$. The C_{13} compounds are odoriferous substances that contribute to the scent of roses. In the physiological pH region, copigmentation with flavonol glycosides is crucial for stabilization of the anthocyanin chromophores. Many roses, including the "apothecary's rose", which was once used medicinally, contain large amounts of strongly astringent ellagitannins, monosaccharide esters of gallic acid.

1. Introduction

The word "rose" is laden with meaning and evokes different images for everyone. These range from the fragrance of roses to the fine-sounding name of rosebushes in our own or a neighbor's garden, or in rosariums throughout the world; they include cut roses as gifts or for decorating the table on festive occasions, but also the symbolism of roses,[1] their role in history, architecture, heraldry, painting, and literature, especially valuable, old illuminated works.[2] Possibly they also encompass rose societies and their journals, as well as the breeding, propagation, trade, and uses of roses in horticulture.[3]

All garden roses are descended from wild roses (botanical roses consist of species and their natural hybrids). Selection, mutation, and hybridization have gradually led to a large number of garden roses (varieties are genetically identical plants which are propagated vegetatively). In *Jaeger*'s *Rosenlexikon*,[4] some 15000 varieties are described, while *Modern Roses*[5] includes some 14000 old and new registered varieties.[6] Specialists estimate the total number of garden rose varieties bred to date at 50000.[3b] Even though many varieties, especially the more modern ones, disappear again after a few decades, the rose is still the only garden plant where the results of so many hybridizations have been retained. The development of some varieties reaches back into the late Middle Ages.[7] This unique situation has never yet been used for a comparative scientific study.

Garden roses and wild roses possess three structurally distinct groups of pigments: chlorophylls, flavonoids (including anthocyanins), and carotenoids. Yellow colors were unknown in old European garden roses; the flowers of the classical provins, alba, damask, cabbage, and moss roses were always white, pink, or red, in all their variations. The advent of yellow in garden roses, from about 1820 on, was greeted with great enthusiasm, as can be seen in old books on roses. Today, we find the illustrations and descriptions in those books correspondingly exaggerated. The development of yellow colors up to the present day will be explored in detail in Section 7.7.

[*] Prof. Dr. C. H. Eugster, Dipl.-Chem. E. Märki-Fischer
Organisch-chemisches Institut der Universität
Winterthurerstrasse 190, CH-8057 Zürich (Switzerland)

2. Carotenoids in Roses

2.1. General Considerations

The assumption that the yellow pigmentation of rose petals is due to flavonol glycosides has persisted up to the present day.[8] It is only since 1963 that qualitative tests (solubility in ether, blue staining with $SbCl_3$, etc.) have led to the proposal that carotenoids are present.[9] With one exception,[9b] identification was never attempted. In fact, all rose flowers, including yellow ones, contain quite a lot of flavonoids. However, only when they are present in high concentrations, together with carotenoids, do they contribute to visible absorption, giving rise to a bronze color.[10] This has been proven experimentally for 'William Allen Richardson' (*Ducher*, 1878) and 'Whisky Mac' (*Tantau*, 1967),[11, 12] whose flowers are brownish yellow.

Carotenoids are widely distributed in the anthers of roses. Their function is still a mystery. Moreover, some carotenoids in the anthers have not yet been found in the petals (see Section 2.2).

Our studies on about 40 different yellow or yellowish rose varieties and species have led to the identification of about 75 carotenoids[13] (Fig. 1). The individual structures will be described in more detail in the following sections.

2.2 Analysis and Identification

In 1977, our first analysis of the carotenoids from the yellow rose *R. foetida*, using classical adsorption chromatography, led to the identification of seven carotenoids.[13a] Seven years later, a further study of material from the same

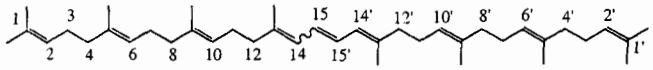

1, 1a, phytoene, λ_{max}=275/285/298

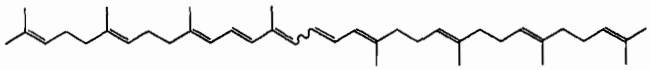

2, 2a, phytofluene, λ_{max}=331/347/367

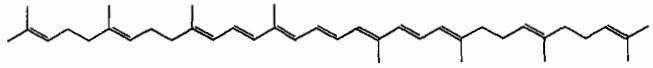

3, 3a, 3b, ζ-carotene, λ_{max}=379/400/424

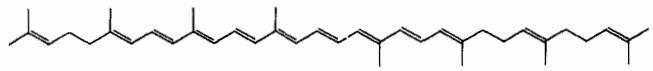

4, 4a, 4b, neurosporene, λ_{max}=416/438/468

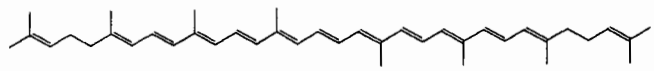

5, 5a - 5e, lycopene, λ_{max}=444/470/501

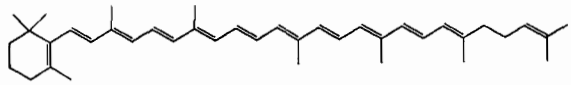

6, 6a, β,ψ-carotene (formerly γ-carotene), λ_{max}=435/459/489

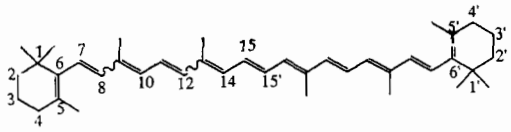

7, 7a, 7b, β,β-carotene, λ_{max}=450/478

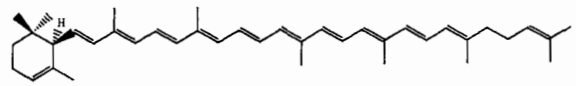

8, 8a, ε,ψ-carotene (formerly α-carotene), λ_{max}=420/444/472

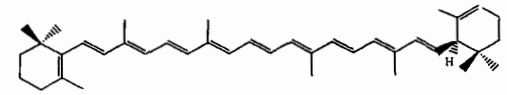

9, β,ε-carotene (formerly δ-carotene), λ_{max}=429/455/484

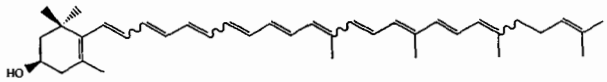

10, 10a - 10e, *rubixanthin ((5'Z)-gazaniaxanthin)*, λ_{max}=435/460/491

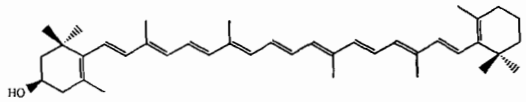

11, 11a - 11c, β-kryptoxanthin, λ_{max}=450/478

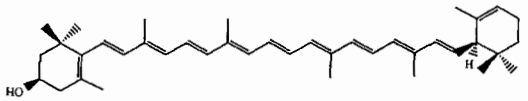

12, α-kryptoxanthin (formerly zeinoxanthin), λ_{max}=420/444/472

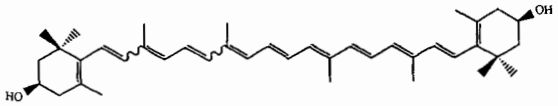

13, 13a, 13b, zeaxanthin, λ_{max}=450/478

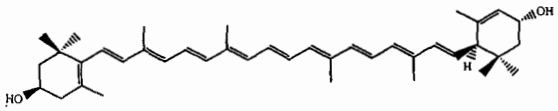

14, lutein (formerly xanthophyll), λ_{max}=420/444/472

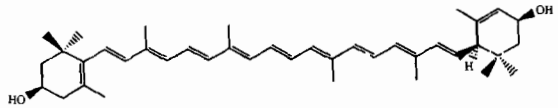

15, 3'-epilutein (formerly calthaxanthin), λ_{max}=420/444/472

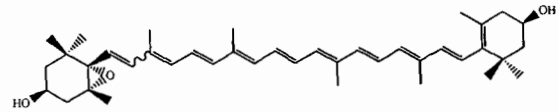

16, 16a, antheraxanthin, λ_{max}=422/445/473

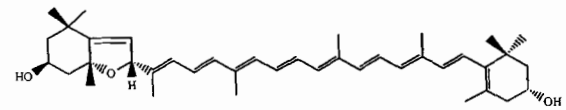

17, (8*R*)-mutatoxanthin, λ_{max}=403/426/451

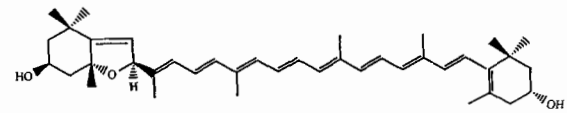

18, (8*S*)-mutatoxanthin, λ_{max}=404/427/452

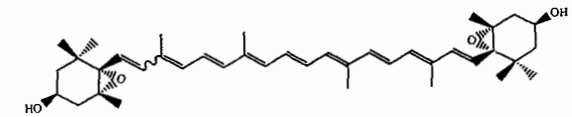

19, 19a, violaxanthin, λ_{max}=415/438/468

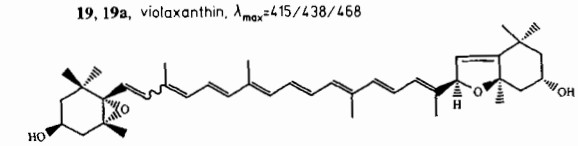

20, 20a, (8*R*)-luteoxanthin, λ_{max}=398/422/448

Fig. 1. Carotenoids isolated from roses and their bands in the visible (λ_{max} in nm). Formula numbers with letters indicate all-*Z* compounds; those without letters are *E* isomers. The position of the *E* double bond is given by a wavy line from the preceding single bond; that is, a wavy line from C(14) to C(15) indicates the presence of a (15*Z*,15'*Z*) double bond. Note that not only mono-*Z*-carotenoids can occur, but that di-*Z* compounds, etc., are also found.

plant, using more refined techniques, allowed us to identify nearly 40 components.[13d] This was primarily due to the introduction of new HPLC methods, which, together with high-field NMR and other spectroscopic techniques permit us to analyze even very minor components. Comparison with standard compounds, which we have synthesized parallel to the isolation studies, was also helpful. It quickly became obvious that, in submilligram amounts, the isolates

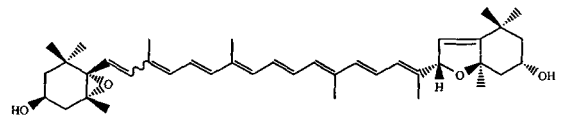

21, 21a, (8*S*)-luteoxanthin, λ_{max}=398/422/448

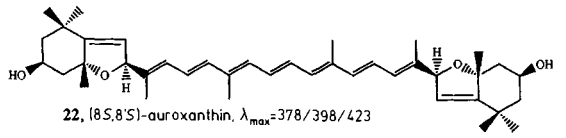

22, (8*S*,8'*S*)-auroxanthin, λ_{max}=378/398/423

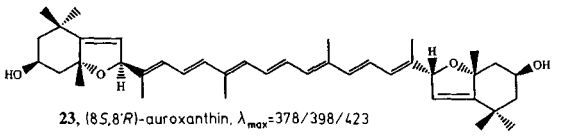

23, (8*S*,8'*R*)-auroxanthin, λ_{max}=378/398/423

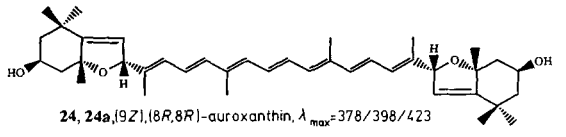

24, 24a,(9*Z*),(8*R*,8*R*)-auroxanthin, λ_{max}=378/398/423

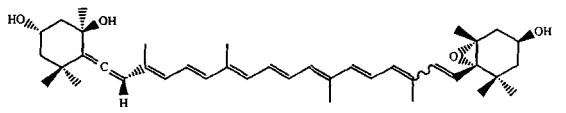

25, 25a, neoxanthin (formerly trollixanthin, foliaxanthin), λ_{max}=415/438/468

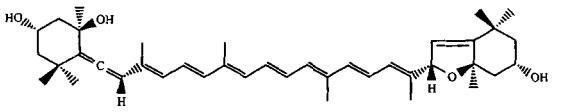

26, (8'*S*)-neochrome (*trollichrome*), λ_{max}=398/422/448

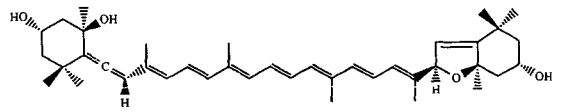

27, (8'*R*)-neochrome (trollichrome), λ_{max}=398/422/448

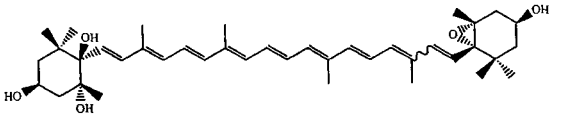

28, 28a, latoxanthin, λ_{max}=417/440/468

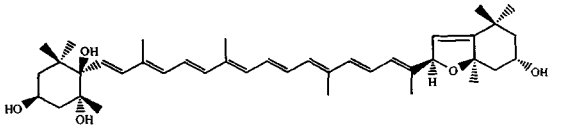

29, (8'*R*)-latochrome, λ_{max}=398/422/448

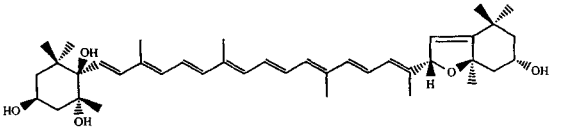

30, (8'*S*)-latochrome, λ_{max}=398/422/448

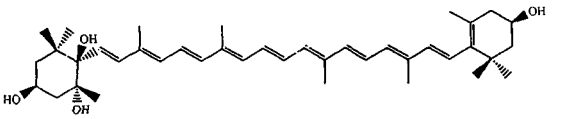

31, karpoxanthin, λ_{max}=420/444/472

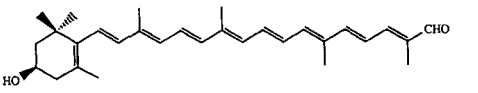

32, β-citraurin, λ_{max} = 445/470

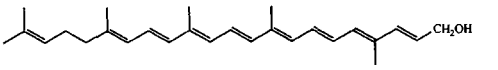

33, 10'-apolycopen-10'-ol, λ_{max}=392/414/441

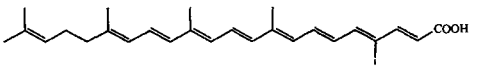

34, 10'-apolycopene-10'-carboxylic acid, λ_{max}=415/437/465

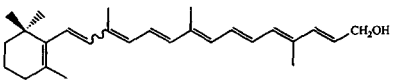

35, 35a, 10'-apo-β-caroten-10'-ol, λ_{max}=378/398/418

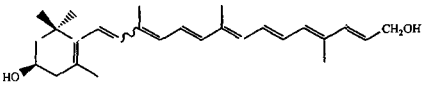

36, 36a, 10'-apo-zeaxanthin-10'-ol (galloxanthin), λ_{max}=378/398/418

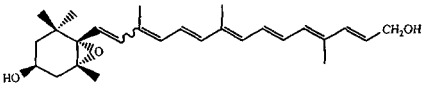

37, 37a, sinensiaxanthin, λ_{max}=373/393/418

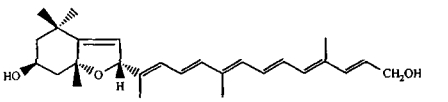

38, 38a (9*Z*),(8*R*)-sinensiachrome, λ_{max}=351/370/398

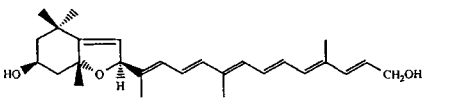

39, 39a (9*Z*),(8*S*)-sinensiachrome, λ_{max}=351/370/398

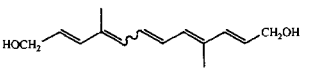

40, 40a, rosafluene, λ_{max}=323/338/358

Fig. 1. Continued.

always contained contaminants that made the interpretation of the spectra very difficult. The most urgent question concerned the steric configurations of the 5,6- and 5,8-epoxides, large amounts of which are present in the more modern rose varieties.[14] The commonly used constitutional terms "aurochrome", "luteoxanthin", and "auroxanthin" concealed numerous stereoisomers which had not yet been identified. Thus, "auroxanthin" contains three pairs of constitutionally identical chiral centers. An all-*E* configuration would lead to a total of twenty possible diastereoisomers (sixteen enan-

tiomeric pairs and four *meso* forms). If there is just a single, noncentral *Z* double bond, the numbers of isomers rises to thirty-two enantiomeric pairs! Even if biogenetic arguments are used to justify 3*S*,5*S*,3′*S*,5′*S* chirality, numerous isomers remain to be identified. Noteworthy in this connection is the surprising presence of 3′-epilutein (**15**) in the anthers of *R. gallica officinalis* and other roses.[131] If the usual precautions are taken (material as fresh as possible, degassed solvents, avoidance of direct light, rapid work, inert atmosphere (whenever possible), then the isolation of carotenoids from flowers presents no great difficulties. The lability of the 5,6-epoxides towards acids must be noted. We always add sufficient quantities of finely powdered $CaCO_3$ to the material to be extracted. Before chromatography, phytosterols are precipitated from acetone solution by cooling. Preliminary purification of the saponified carotenoids is usually carried out on silica (Merck, 40–63 μ) using hexane/ether or hexane/acetone mixtures containing 0.05% Et(*i*Pr)$_2$N (beware of possible acetone condensation with aldehydes!). For small amounts we also use silica plates (e.g., Merck 60, F254, 0.25 or 0.5 mm). When major components are present, these must be removed by crystallization (check by HPLC!).

The subsequent HPLC separations were performed as follows: hydrocarbons on Spherisorb ODS-5μ with acetonitrile/THF mixtures or on Spherisorb NH_2-5μ with hexane/Et(*i*Pr)$_2$N; fractions with monohydroxy, dihydroxy, hydroxyepoxy, neoxanthin, and latoxanthin polarity were each purified separately on Spherisorb S-5 CN with hexane containing 0.1% Et(*i*Pr)$_2$N and a gradient of various dichloromethane/methanol mixtures.[13, 15]

For conclusive identification of rare carotenoids or those only present in trace amounts it is necessary to record UV/VIS, NMR, mass, and CD spectra and to carry out cochromatography with authentic samples. A library of spectra is extremely useful here; compilations of UV/VIS,[16] NMR,[17] CD,[18] and mass spectra[17a, 19] are available.

3. White Roses

The petals of white roses reflect a large proportion of the incident light. They are therefore more or less free of compounds that absorb light of wavelength 400–700 nm. Nonetheless, the petals are not transparent. This is due to the many air-filled spaces between the cells, the so-called intracellular spaces. When the air is displaced, for example, by dipping a petal into acetone, the luster und reflection are rapidly diminished. On the other hand, the petals contain significant amounts of UV-absorbing substances, above all large amounts of flavonol glycosides. Up till now, these have only been studied in a very few varieties; thus, 'Niphetos' (*Bougère*, 1843) contains a great deal of quercetin, some isoquercetin, rutin, spireoside, and other, unknown flavonoids (see Section 8.5.2).

Table 1. Carotenoids in white roses.

Roses	Content	*N* [b]	HC [c]	OH [d]	Amount [%] epoxides	AC [e]
R. pimpinellifolia	5.8	29	56 (**1**,**2**)	22 (**14**)	17	5
'Sombreuil' (*Robert*, 1850)	3.8	32	80 (**1**,**2**)	6.8	9.9	1.4
'Virgo' (*Mallerin*, 1947)	8.6	15	94 (**1**,**2**)	2.2	0.7	2.9

[a] Milligrams of carotenoids per 100 g of dried petals. [b] *N* = number of identified carotenoids. [c] HC = hydrocarbons; main carotenoids in parentheses. [d] Xynthophylls. [e] AC = apocarotinols.

More is known about the carotenoids[12] (Table 1). All the white roses we have studied contain significant amounts of carotenoids; examples include *R. pimpinellifolia*, 'Niphestos', 'Mme Plantier' (*Plantier*, 1835), 'Alberic Barbier' (*Barbier*, 1900), 'Yvonne Barbier' (*Turbat*, 1910), 'Nevada' (*Dot*, 1927), 'Virgo' (*Mallerin*, 1947). 'Iceberg' = 'Schneewittchen' (*Kordes*, 1958), although colorless hydrocarbons predominate. The few colored carotenoids also found presumably come from the base of the petals. Even epoxides are present. The apocarotenols, which comprise primarily esterified rosafluene (**40**), are remarkable.[13h] Rosafluene, like phytofluene (**2**), has a fluorescence emission maximum in the blue-green (λ_{ex} = 359 nm, $\lambda_{em} \approx$ 525 nm). If the apocarotenols are present in sufficient amounts and their fluorescence is not quenched, these compounds act as natural brighteners. Rosafluene is a catabolite of any carotenoid from ζ-carotene onwards (see Section 7.6). For the determination of the degree of whiteness in roses, see Ref. [13i]. Beautiful examples of white roses are shown in Figure 2.

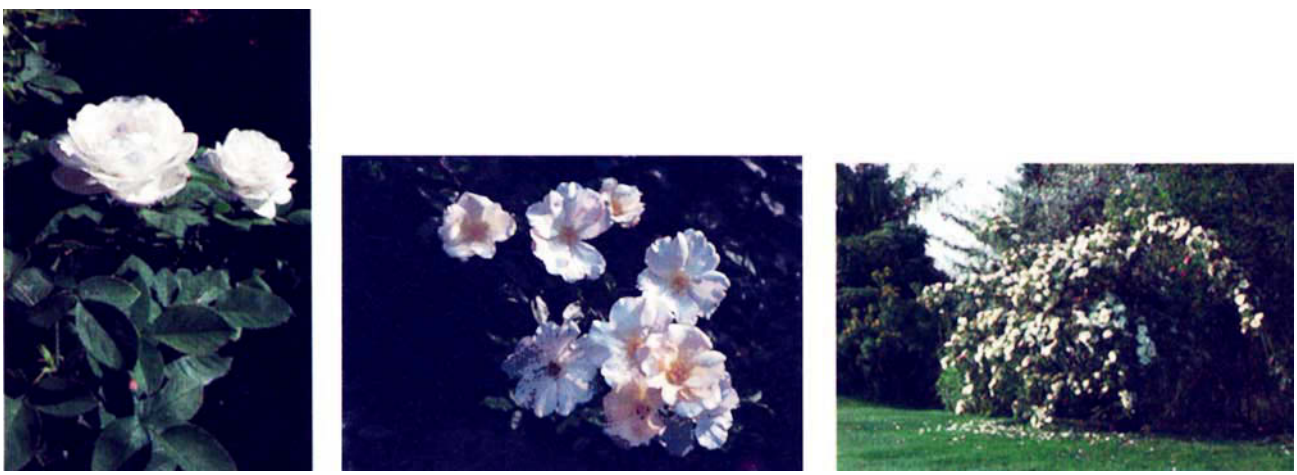

Fig. 2. Left: 'Merveille de Lyon' (1:5.5 scale; bush rose, *Pernet Père*, 1882), in which pigment synthesis is practically fully blocked. Middle: 'Schneeschirm' (1:5; small shrub, *Tantau*, 1946). Right: 'Nevada' (shrub, *Pedro Dot*, 1927). Temperature-dependent, partial pigment synthesis occurs in both 'Schneeschirm' and 'Nevada'.

4. Green Roses

Roses with green petals are very rare. The best-known example is *R. chinensis viridiflora* (Fig. 3), which is said to have arisen by mutation in South Carolina in 1833.[20] Its pale green, often lightly russet flowers doubtless contain chlorophylls, but no detailed studies have been performed.

Fig. 3. *Rosa chinensis viridiflora* (1:5 scale).

Various modern, white roses occasionally reveal a definite green tinge, such as 'Green Ice' (*Moore*, 1971), 'Greensleeves' (*Harkness*, 1980), and 'White Success' (*Jelly*, 1985). These, too, presumably contain chlorophylls.

5. The Structure of Rose Carotenoids

Most of the carotenoids listed in Figure 1 also occur in other yellow, carotenoid-containing flowers, but in no other case has such a detailed analysis been made. The large number of epoxides, the many *Z*/*E* isomers, and the multitude of apocarotenoids are novel and should be stressed. The absolute configurations of chiral carotenoids given in the formulas have in some cases been determined parallel to the studies on roses; for example, the structure of the C(5),C(6) diols in latoxanthin (**28**), latochrome (**29**), karpoxanthin (**31**),[13d, 21] neoflor,[22] and other carotenoids with triol end groups.[23] This also applies to the 5,6-epoxy[14, 24] and 5,8-epoxy end groups.[14, 24c, 25]

The most fundamental of these studies was the determination of the absolute configuration of C(6) in the ε end group,[26] of OH-C(3) in the zeaxanthin end group,[24a] and of OH-C(3′) in lutein (**14**)[27a] and 3′-epilutein (**15**)[27b] as well as the allene configuration in neoxanthin (**25**) and its relatives.[28] These are all distinguished by characteristic spectral and chiroptical data and can now be easily recognized in isolates. Positional isomerism in *Z*/*E*-isomeric carotenoids can readily be determined by NMR methods.[17] Often, this can also be inferred from the so-called *cis* peak.[29]

6. The Synthesis of Standard Carotenoids for Comparison Purposes

As mentioned in Section 2.2, minor rose carotenoids have been synthesized for comparison in order to confirm their structures. The syntheses leading to optically active end groups will be described briefly here; more detailed information on the construction of the polyene chains can be found in Ref. [30].

Optically active carotenoids with an ε end group, such as β,ε-carotene (**9**), were prepared from the enantiomers of α-ionone (**41** and *ent*-**41**, Scheme 1). These were always obtained by racemate resolution of the diastereomeric menthylhydrazones according to Ref. [31] modified as in Ref. [32a]. Straightforward transformations of **41** led to **42**, which was hydrolyzed to give the corresponding glycol.[32b] For the synthesis of oxygenated carotenoids, such as zeaxanthin (**13**), (4*R*,6*R*)-4-hydroxy-2,2,6-trimethylcyclohexanone (**43**) has become important[33] and is now produced industrially. For example, **43** can be converted into 3-hydroxy-β-ionone (**44**),[34] which is otherwise difficult to synthesize. The synthesis of the triol end group **45** is described in Ref. [23]. The violaxanthin end group **47** was obtained from **46**, which, in

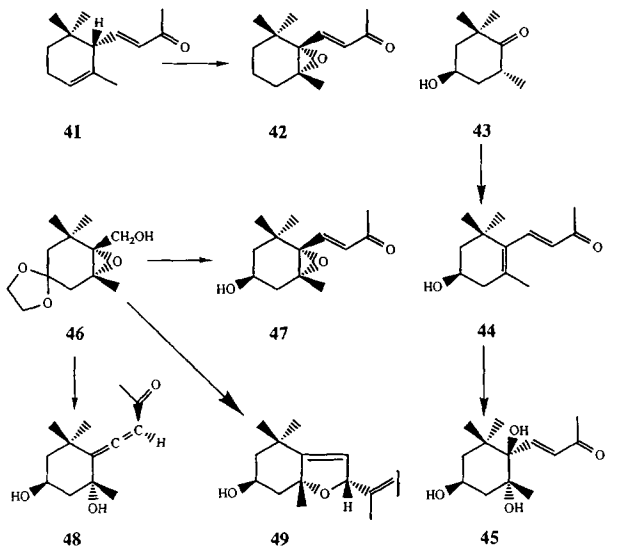

Scheme 1.

turn, was prepared by enantioselective epoxidation of a β-cyclogeraniol derivative,[35] using the Katsuki–Sharpless procedure.[36] Compound **46** also proved to be a suitable starting material for the synthesis of allenic end groups such as **48**[37] and of the auroxanthin end group **49**.[38] The way was thus open for synthesis of neoxanthin (**25**), one of the most abundant carotenoids found in green plants. These results show that the study of rose pigments has led to results whose importance extends far beyond the boundaries of this field.

7. Biogenesis of Carotenoids in Rose Flowers

If we attempt to summarize the results presented in Sections 2, 3, and 5, one solution is to classify them in a bio-

genetic sequence. This biogenesis has been worked out for plants other than roses,[39] but ought also to be valid for roses, at least in outline. The most important steps, besides the catabolic reactions discovered in roses, are shown in Scheme 2, though Z/E isomerism has been largely ignored. In recent years, however, it has become clear, thanks to improved methods of separation, that these isomers are not artifacts of workup. Phytoene (**1**) is genuinely a 15*Z* compound. In roses, we have found a mixture of (15*Z*)-**1** and (15*E*)-**1**. With the exception of those at C(1) and C(1′), all the

1. Acetyl-CoA → C_{40} → **1** (phytoene)
2. Dehydrogenations: **1** → **2** → **3** → **4** → **5**
   2.1. Degradation reactions
3. Cyclizations
   3.1. (all-*E*)-**5** → **6** → **7**
   3.2. (5*Z*)-**5**(?) → **8** → ε,ε-carotene
   3.3. Degradation reactions
4. Hydroxylations: for example **6** → **10**; **9** → **12** → **14**
   7 → **11** → **13**
   4.1. Degradation reactions
5. Epoxidations
   5.1. Degradation reactions
6. Epoxide transformations
   6.1. 5,8-Epoxides
   6.2. Hydrolysis
   6.3. Allene formation
   6.4. Degradation reactions

Scheme 2. The most important steps in carotenoid biosynthesis and transformation.

other trisubstituted double bonds have *E* configuration. Nonetheless, most of the Z/E-isomeric carotenoids that have been investigated in this respect show isomerism at one or more of the trisubstituted double bonds, possibly due to a new isomerization for each step of carotenoid biosynthesis. However, the isomerization described by *Pattenden* et al.[40] is also possible. This occurs during the dehydrogenation step, so that the double bond moving into conjugation can assume *Z* configuration. However, this theory leads to a cascade of different biosynthetic pathways, each with Z/E-isomeric intermediates.

7.1. Biogenetic Step 2

Carotenoids **1**–**5** are found in most rose flowers in variable, but also characteristic amounts. In white roses, the dominant compounds are phytofluene and occasionally ζ-carotene, as mentioned in Section 3. Hence, the biosynthesis is strongly inhibited at the level of the desaturating enzymes. The products of carotene catabolism found in white roses, rosafluene (**40**) and geranylacetone (**60**, see Table 2) demonstrate that even ζ-carotene is degraded.

The colored hydrocarbons neurosporene (**4**) and lycopene (**5**) only occur in minute amounts in roses. This not only indicates a gap in the possible palette of colors in these flowers, but also shows that **4** and **5** are very rapidly consumed in the following step. Therefore, cyclases are active in non-white roses. They are clearly much more active than in the rosehips of many species, where lycopene (**5**) can be the major pigment (see Section 11).

7.2. Biogenetic Step 3

Lycopene (**5**) is a proven substrate for the cyclases, though neurosporene (**4**) may also be used.[39] Here, the pathways branch, leading to carotenoids with a β end group and those with an ε end group, clearly recognizable in **6** and **8**, respectively. Our interpretation of this phenomenon is that it is due to the differing configurations at C(5); (5*E*)-lycopene leads to **6**, whereas the 5*Z* isomer gives rise to **8**.[41] Various incorporation experiments in other organisms have shown[42] that the terminal methyl groups in **5** retain their identity during the proton-catalyzed ring closure, which therefore proceeds stereoselectively. The same is true for **8**, though with a different folding of (5*Z*)-**5**. This ring closure generates a chiral center at C(6), which possesses *R* chirality in all higher plants studied to date.[43]

7.3. Biogenetic Step 4

As in all higher plants, hydroxylation occurs in roses only on cyclic end groups, at C(3) or C(3′). To date, exclusively 3*R* chirality has been found at the β end groups, while at ε rings the reverse configuration appears (owing to the sequence rules this is also 3*R*). So far, the only exception is 3′-epilutein (**15**),[13] which, however, always occurs together with lutein (**14**) and is produced by a redox process with an oxo compound as intermediate.[27b] There are as yet no indications that hydroxylations of carotenoids can take place at a later biogenetic stage. Rubixanthin (**10**) is found primarily in rosehips.

7.4. Biogenetic Step 5

The 5,6-epoxides antheraxanthin (**16**) and violaxanthin (**19**) are found in large amounts in roses; the other 5,6-epoxides **25**, **28**, and **37** are products of subsequent reactions. Epoxidation thus occurs preferentially at hydroxylated β end groups. We have not yet been able to identify epoxides of hydrocarbons such as β,β-carotene.[44] The epoxide oxygen atom is derived from O_2 and is presumably introduced via the so-called violaxanthin cycle [Eq. (a)].[45]

$$\text{zeaxanthin (13)} \underset{h\nu}{\overset{\text{dark}}{\rightleftharpoons}} \text{antheraxanthin (16)} \underset{h\nu}{\overset{\text{dark}}{\rightleftharpoons}} \text{violaxanthin (19)} \quad \text{(a)}$$

Since some yellow roses have total epoxide levels of > 80%, the violaxanthin cycle appears to be disrupted. The 5,6-epoxides always have 5*R*,6*S* chirality; introduction of the oxygen atom therefore takes place from the opposite face to the hydroxyl group.

Although hydroxylation at C(3) does not alter the light absorption of the polyene system, the epoxidation shifts it significantly to shorter wavelengths, that is from the orange

region of the visible into the yellow. At the same time, epoxidation makes the molecule labile, especially towards acids.

7.5. Biogenetic Step 6

The acid-catalyzed transition from the 5,6- to the 5,8-epoxides is an important epoxide rearrangement (Scheme 3). It can take place even in the intact plant, for example, during chromoplast senescence, but occurs very readily on insufficiently careful workup (cf. Section 2.2). The configuration at C(5) is retained during the rearrangement, except for compounds like **47**, where hydrolysis occurs with inversion at C(6).[32b, 46] A new chiral center is formed at C(8); hence, all acid-catalyzed, nonenzymatic epoxide rearrangements afford a mixture of diastereomers. C(8) is especially easily oxidized in the furanoid epoxides **51** and **52**. Peroxidation and rearrangement leads to lactones of type **53**, which contribute, for example, to the aroma of tea.

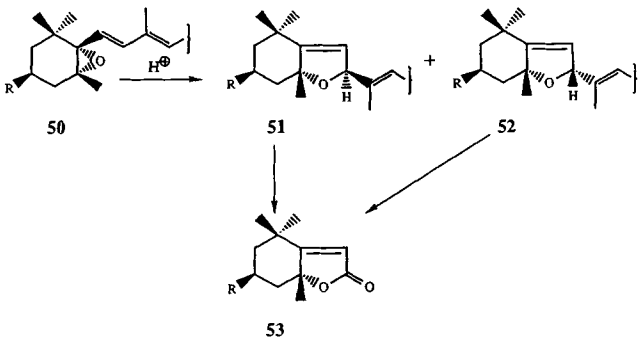

Scheme 3. R=H, OH, OAc.

The rearrangement of the 5,6- to the 5,8-epoxides also leads to a shortening of the chromophoric system. The first step, from **19** to **20**/**21**, shifts the absorption maximum 20 nm to shorter wavelengths, while the second step, leading to the auroxanthins **22**–**24**, yields a further 25-nm shift. This affords a pure, somewhat greenish yellow of high saturation. For pure yellow colors, without any trace of red. the epoxide rearrangement is of great importance.

Recently, the hydrolysis of carotenoid-5,6-epoxides in flowers and fruits has also been discovered. The 5,6-diols produced are highly polar compounds. This is one reason for their late discovery; latoxanthin (**28**) and latochrome (**29**) in 1983,[13b, 13d] karpoxanthin (**31**) in 1985[13b, 21, 47a] (for others see Refs. [47b, c]). The 5,6-diols are presumably substrates of further catabolic reactions.

The transformation of violaxanthin (**19**) into allenes **25**–**27** is a very strange one and as yet mechanistically unexplained. Any theories proposed must take into account the uniform *S*-axial chirality observed in the allene bond to date.

7.6. Carotenoid Catabolism in Roses

Our findings show that, besides citrus fruits,[48] rose flowers are also a relatively rich source of degraded carotenoids. In total, we have isolated fifteen apocarotenoids, including stereoisomers, and characterized their structures. These compounds include β-citraurin (**32**), usually a trace component in the flowers of various roses. We were able to isolate quite large amounts from the Chinese shrub rose *R. hugonis* and from the bush roses 'Piccadilly' (*S. McGredy*, 1960) and 'Alexander' (*Harkness*, 1972).[12] The 10′-apolycopene derivatives **33** and **34** were first found by us in the famous old climber 'Maréchal Niel', whose large, gloriously scented flowers are primrose yellow owing to the presence of **33**, as long as the plants flower in a greenhouse. In the open air (i.e., in direct sunlight), the blooms are yellow with a tinge of green, owing to the replacement of **33** by **34**.[13f] Both compounds are especially prevalent in old noisette hybrids and in tea roses such as 'Safrano' (*Beauregard*, 1839), but even modern roses such as 'Alexander' and 'Elina' (= 'Peaudouce', *P. Dickson*, 1985) contain significant quantities.

10′-Apo-β-caroten-10′-ol (**35**) and 10′-apozeaxanthin-10′-ol (**36**) have been found in several old and modern garden roses.[12, 13e, 13g] Compound **35** is novel, as are **33** and **34**, but **36** is already known under the name galloxanthin and has previously been isolated from the retina of birds. Apparently, birds and roses possess similar carotenoid-cleaving enzymes.

The epoxides sinensiaxanthin (**37**) and the sinensiachromes **38** and **39** are widespread in fruits, where they give rise to the yellow color of the flesh in apple varieties such as "Golden Delicious", for example. The structures, synthesis, and purification of the multiple stereoisomers present have, however, only been studied in connection with roses.[13g, 38] Sinensiaxanthins and sinensiachromes are found in many white, yellow, or orange roses, usually together with the stereoisomeric violaxanthins and auroxanthins, from whose cleavage they arise.

The colorless, highly fluorescent C_{14} compound rosafluene (**40**), mentioned briefly in Section 3, is most remarkable. Rosafluene occurs as an ester and possesses extremely similar characteristics to phytofluene (**2**). It is very unstable, especially as the free alcohol. We have found it in numerous old and modern roses, with relatively high amounts in 'Piccadilly', 'Alexander', and 'Penelope' (*Pemberton*, 1924).

With the exception of **34** and **40**, the apocarotenoids found are all C_{27} alcohols. They are definitely carotenoid metabolites and arise by cleavage at C(9) and/or C(9′). The apocarotenoids from roses are not aldehydes but the corresponding alcohols, just as is the case with Car(15,15′) dioxygenase. This enzyme cleaves β,β-carotene (**7**) to retinal, a C_{20} compound which is stored after reduction as the alcohol (retinol, Vitamin A_1). Presumably aldehydes also occur, but because of the very small amounts present, they have not yet been identified.[12]

An analysis of the products shows that the postulated Car(9,10:9′,10′) dioxygenase is not specific for end groups. It cleaves excentrically according to Equation (b). The widespread occurrence of rosafluene (**40**) indicates that the enzyme can also cleave the C_{27} compounds a second time.

$$C_{40} \rightarrow C_{13} + C_{27} \longrightarrow C_{13} + C_{14} \qquad \text{(b)}$$

Recently, we have begun to identify the postulated C_{13} compounds in Equation (b).[50] Our results (Table 2) con-

Table 2. C_{13} compounds in the "headspace" of rose flowers [a].

Rose variety	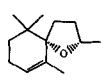 54	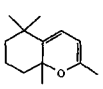 55	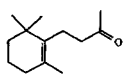 56	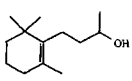 57	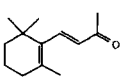 58	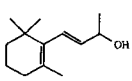 59	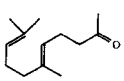 60	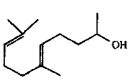 61
'Sombreuil' (*Robert*, 1850) cream white	0.1–0.3	0.2–0.3	0.2–1.0	0.4–1.0	1.0–3.0	1.0–2.0	0.02–0.05	–
'Maréchal Niel' (*Pradel*, 1864) golden yellow to bright yellow	0.1–0.3	0.3–0.5	1.5–3.0	0.5–1.0	2.0–4.0	0.5–1.5	0.2–0.4	0.02–0.05
'Sutter's Gold' (*Swim*, 1950), gold-orange [b]	trace	trace	0.3–0.6	0.05–0.1	0.1–0.2	–	0.05–0.1	?
'King's Ransom' (*Morey*, 1961) golden yellow	0.1–0.2	–	1.5–2.5	0.1–0.3	0.05–0.1	–	0.7–1.2	?
'Rose Dot' (*Dot*, 1962) red/white [b]	–	–	0.1–0.4	0.1–0.4	0.3–0.7	0.1–0.4	0.02–0.05	?
'Duftwolke' (*Tantau*, 1963), coral red	–	–	0.2–0.4	0.3–0.5	0.3–0.5	–	0.02–0.05	?

[a] Percent amount in the headspace of the blossom. The amount depends on the time of day. [b] Carotenoids and anthocyanins occur together in the petals.

vincingly show the other side of the carotenoid catabolism under discussion. The detection of acyclic C_{13} ketones and alcohols is also important. If the latter were stored in the form of glycosides, they would not be detectable by gas chromatography.[51]

In summary, the degradation starts with ζ-carotene (**3**) and includes all the end groups in Figure 1 found in roses to date[52] (Table 3).

Table 3. Products of the Car(9,10:9',10') dioxygenase reactions.

Substrate	C_{13} found	C_{27} found	C_{14} possible
ζ-Carotene **3**	**60/61**	?	+
Neurosporene **4**	?	?	+
Lycopene **5**	?	**33/34**	+
β,β-Carotene **7**	**55–59**	**35**	+
ε,ψ-Carotene **8**	**54**	?	+
β,ε-Carotene **9**	**54**	**35**	+
Zeaxanthin **13**	?	**36**	+
Violaxanthin **19**	?	**37**	+
Auroxanthin **22–24**	?	**38/39**	+
Neoxanthin **25**	?	presumed	+

The results presented in Tables 2 and 3 complete the picture of our pigment analyses of carotenoid-containing roses. Originally, carotenoids may have served in the plant's showpiece as a means of communication with potential pollinators. Then followed the degradation of carotenoids to aroma compounds and to other substances with many different physiological qualities, whose significance is still unclear to us. If one also remembers the fundamental role of carotenoids in photosynthesis, then it is clear that all in all they are the most multifaceted of all natural product groups.

7.7. Carotenoids and the Genealogy of Garden Roses

Old European garden roses, that is, those before 1830, had flowers that were white or red (in many shades). The only exceptions were a few botanical roses which had been introduced to Europe centuries earlier: *R. hemisphaerica* with its full, sulfur-yellow flowers, *R. foetida* (also called *R. lutea* by later authors, the so-called Austrian briar), with a simple, bright yellow flower, and *R. foetida bicolor* (Austrian copper), also with a simple flower, but in two colors, yellow outside and red within. They all originated in central Asia and possibly represent cultivated forms of the original species. *R. hemisphaerica* is often to be seen in old floral still-life paintings. Remarkably, no hybrids between these roses and the old European garden roses are known, although they have been grown in gardens for centuries. The same is true of the yellowish-flowering varieties of *R. pimpinellifolia*. Only after 1800, when several cultivated forms of Chinese roses, including the yellow 'Park's Yellow Tea-scented China'[53] were introduced, did crossings lead to a gradual expansion of the color scale (Fig. 4). 'Park's Yellow' was of crucial importance for the yellow shades. Unfortunately, it has died out[54] and is not available for analysis. On looking through old rose lists one notices that yellow flowers were commoner in noisette roses than in tea roses. These were usually pink on a yellow base or vice versa. Noisette roses arose from crosses with *R. moschata*, which had an as yet unknown effect on the flower color. Famous yellow roses were 'Elise Sauvage' (*Millez*, 1818, tea rose, pale yellow with an orange center[55]), 'Jaune Desprez' (*Desprez*, 1830, noisette, yellow and pink), 'Solfaterre' (*Boyau*, 1843, noisette, sulfur yellow), and the varieties listed in Table 4.

One can see that breeders have always aimed for a purer and more saturated yellow, a development which culminated in 'Maréchal Niel'. Nonetheless, the yellow color in most of these roses was unstable and faded a great deal during flowering. One exception was *R. x harisonii* (*x* indicates a hybrid), which only flowers once. The red roses developed much more rapidly than the yellow varieties and gave rise to the new rose classes of portland, bourbon, and hybrid perpetuals. Among the roughly 4000 hybrid perpetual varieties, there was not a single yellow rose! Even the tea hybrids, which developed slowly from ca. 1850—one of the most important classes today—displayed only very few good yellow varieties before 1900. The emergence of varieties with an intense, highly saturated yellow did not begin till 1900, with the breeding of 'Soleil d'Or' (*Jean Pernet-Ducher*, Lyon), a hybrid of *R. foetida persiana* (Fig. 5) and a red hybrid perpetual. Predecessors such as 'Gottfried Keller' (*Hermann*

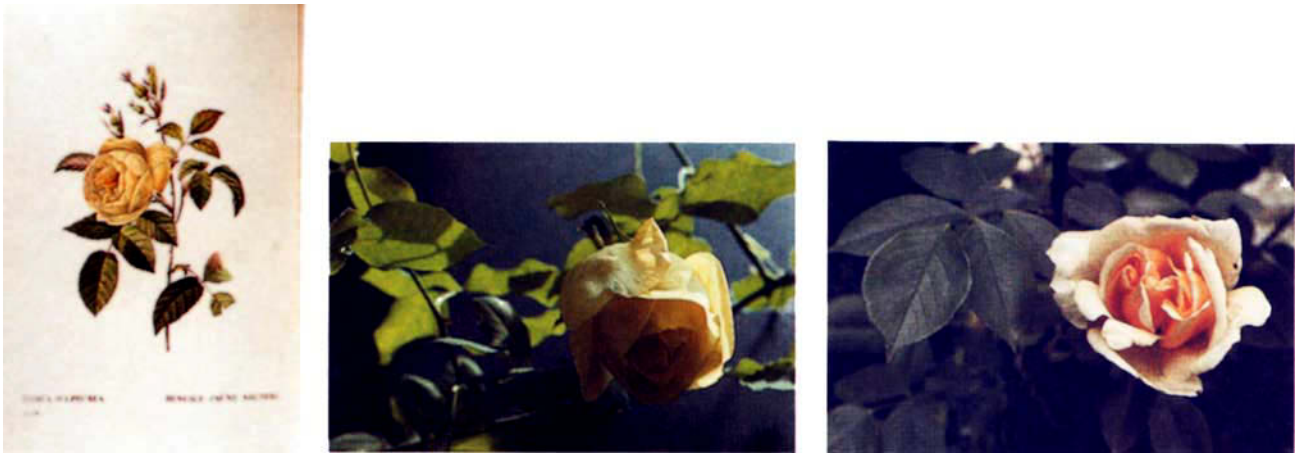

Fig. 4. Old yellow garden roses with carotenoid biogenesis steps 1–3 and pronounced degradation reactions. Left: 'Park's Yellow' (1:3.5, died out; photo taken from P. J. Redouté: Les Roses, 3rd ed. 1828; a specimen from the *Jardin botanique de la Ville* de Genève; parent of the old yellow garden roses). Middle: 'Maréchal Niel' (1:2.5; climber, *Pradel*, 1864; most famous of the old yellow garden roses). Right: 'William Allen Richardson' (1:2.2; rambler, *Ducher*, 1878); carotenoids concentrated in the center; become almost white owing to degradation.

Müller, 1894) had practically no effect on the development of modern yellow varieties.

We have analyzed forty old and modern varieties of yellow garden rose and several important species.[12] In Table 4, some results of this study are presented. The data allow the following conclusions to be drawn:

1. Old, yellow, garden roses that have the Chinese cultivars and above all 'Park's Yellow' and *R. moschata* in their pedigree display an incomplete carotenoid biosynthetic pathway; hydrocarbons at step 2 are accumulated, though usually without neurosporene (**4**) and lycopene (**5**). As a rule, there is a pronounced inhibition of the

Table 4. Analyses of selected examples of old and modern roses.

Rose variety	Introduction	Color	*N* [b]	Content [c]	Amount [%] HC [d]	OH [e]	Epx. [f]	AC [g]	MC [h]
R. foetida [i]	ca. 1540	highly saturated yellow	36	151	2.2	9.9	86.6	trace	**19** (58,3%), **20/21** (15,4%)
R. x harisonii (Harison)	ca. 1830	yellow	35	100	5.6	16.1	72	3.4	**20/21** (31%)
'Safrano' (*Beauregard*) [k]	1839	yellow to red (Cy, Chrys)	20	10–15	55.2	5.4	4.1	19.9	acycl. HC (34%), **7** (21%)
R. odorata x pseudindica	ca. 1845	yellow/pink (Cy, Chrys, Pä)	33	56	74	17.1	8.5	ca. 1	**7** (72%)
'Gloire de Dijon' [k] *(Jacotot)*	1853	yellow, tinged with pink (Cy, Chrys)	17	50	73.6	3.6	0	20.7	acycl. HC (65%), **33/34** (20.7%)
'Maréchal Niel'	1864	primrose yellow (Cy, Chrys)	14	24	70.5	0.5	0	21.5	acycl. HC /70.5%), **33** (21%)
'William Allen Richardson' *(Ducher)*	1878	leather yellow to orange	30	38	58	10	27	4.1	**7** (53%)
'Alister Stella' Gray (*Gray*)	1894	saffron yellow to orange	26	32	79.7	9.1	9.4	1.8	**7** (72%)
'Gottfried Keller' (*Müller*)	1894	yellow tinged with pink (Cy, Chrys, Pä, Pel)	42	50	7	36.2	55.8	0.5	**13** (25.5%), **20/21** (18.3%)
'Soleil d'Or' (*Pernet-Ducher*)	1900	yellow and red (Cy, Chrys)	41	130	20.4	10.1	63	5	**19** (23.7%), **20/21** (14.8%)
'Star of Persia' (*Pemberton*)	1919	golden yellow to ochre	31	70	3.0	9.1	83.3	2.6	**19** (40%), **20/21** (22.9%)
'Lawrence Johnston'	1923	yellow	35	123	13.6	9	74	3.4	**22/23/24** (23%), **20/21** (16%)
'Mme. A. Meilland' (*Meilland*)	1945	bright yellow with pink (Cy)	46	3	21.3	27.5	47.4	2	**19** (21.3%), **7** (19%), **13** (15%)
'Sutter's Gold' (*Swim*)	1950	golden yellow with orange (Cy, Chrys)	34	19	25.5	16.7	56.7	trace	**22/23/24** (25%), **20/21** (15.5%)
'Allgold' [l] (*Le Grice*)	1958	yellow (Cy, Chrys)	37	125	15.3	7	76	0.5	**22/23/24** (17%), **20/21** (24%)
'Whisky Mac' (*Tantau*)	1967	variable bronzy yellow (Cy, Chrys, Pel)	45	53	30.5	25	35.2	10.3	**11** (13%), **7** (11%)
'Gold Bunny' (*Meilland*)	1978	lemon yellow	33	115	8	12	76.1	2.3	**22/23/24** (25%), **20/21** (22%)
'Elina' ('Peaudouce') (*Dickson*)	1985	pale yellow to ivory	30	23	8	14.4	70.2	6.8	**22/23/24** (52.8%)

[a] The most important anthocyanins in parentheses; Cy = cyanidin-3,5-diglucoside, Chrys = cyanidin-5-glucoside, Pä = peonidin-3,5-diglucoside, Pel = pelargonidin-3,5-diglucoside. [b] *N* = number of carotenoids identified; *Z*/*E* isomers counted separately. A quantitative analysis was carried out for each of the rose varieties listed. [c] Carotenoid content in mg per 100 g dry weight. [d] HC = hydrocarbon s; based on carotenoids = 100%. [e] Mono- and dihydroxylated carotenoids. [f] C_{40} epoxides. [g] AC = apocarotenoids. [h] *Z*/*E*-isomeric carotenoids of the same type counted together. MC = main carotenoids. [i] *R. foetida persiana* and *R. ecae* show practically identical results. [k] Results of low accuracy. [l] Our results are completely different from those in [9b].

Fig. 5. Representatives of *foetida* wild roses that were most important for the breeding of modern, yellow roses. Left: *R. foetida bicolor* (1:2.2), known in Europe since the Middle Ages. Middle: *R. foetida* (1:3), originated in middle Asia, first described by *Conrad Gessner* in 1561 and *Matthias Lobelius* in 1581. Right: *R. foetida persiana* (1:3), introduced from middle Asia in 1837. Characteristic of all is the high content of carotenoids, especially those arising at biogenetic step 6, and a weak catabolism. Thus, these carotenoids are very stable toward light. The main anthocyanin in *R. foetida bicolor* is peonin.

desaturating enzymes, and catabolic reactions are prominent.

2. One exception is *R. odorata x pseudindica*, which has the ability to carry out cyclization (step 3). Unfortunately, it was never used for breeding.
3. Garden roses with pure, stable and strongly saturated yellows emerged only by crossing in of roses of the *foetida* group (Fig. 6), especially *R. foetida persiana*. They contain a complete carotenoid biogenetic sequence; step 5 is pronounced. Degradation reactions are minimal.
4. Carotenoid analysis shows that *R. x harisonii* is descended from *R. pimpinellifolia* and *R. foetida*.
5. Modern, light yellow rose varieties such as 'Mme Meilland' (*Meilland*, 1945) or 'Elina' combine a complete carotenoid biogenetic pathway with enhanced Car(9,10:9′,10′) dioxygenase activity.

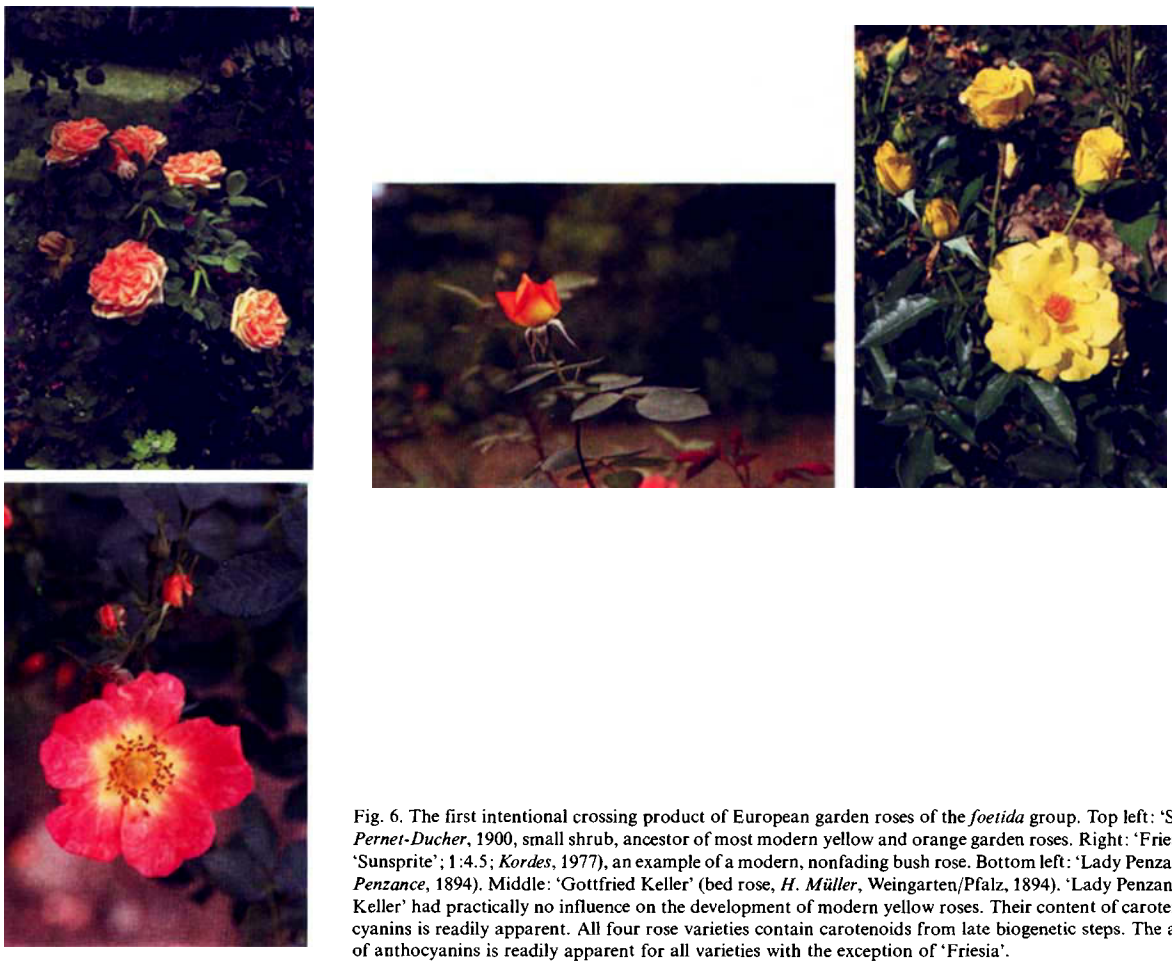

Fig. 6. The first intentional crossing product of European garden roses of the *foetida* group. Top left: 'Soleil d'Or' (1:6.5; *Pernet-Ducher*, 1900, small shrub, ancestor of most modern yellow and orange garden roses. Right: 'Friesia' (= 'Korresia', 'Sunsprite'; 1:4.5; *Kordes*, 1977), an example of a modern, nonfading bush rose. Bottom left: 'Lady Penzance' (1:2.5; shrub, *Penzance*, 1894). Middle: 'Gottfried Keller' (bed rose, *H. Müller*, Weingarten/Pfalz, 1894). 'Lady Penzance' and 'Gottfried Keller' had practically no influence on the development of modern yellow roses. Their content of carotenoids and anthrocyanins is readily apparent. All four rose varieties contain carotenoids from late biogenetic steps. The additional content of anthocyanins is readily apparent for all varieties with the exception of 'Friesia'.

8. Anthocyanins in Roses

8.1. General Considerations

Anthocyanins are more important than carotenoids for the colors of roses, because their light absorption extends over a greater part of the spectrum. At short wavelengths, the orange almost coincides with that of the carotenoids, while at long wavelengths the color extends to a pale mauve. The properties of anthocyanins could hardly be more different from those of the carotenoids; they are hydrophilic and are generally dissolved in the cell sap. Analytical studies on rose anthocyanins began as early as 1915 with the classical work of *Willstätter* and *Nolan* on the isolation of cyanin (**66**) from dried "flores rosae gallicae rubrae".[56] In 1934, pelargonin (**62**) was isolated for the first time from the new, orange scarlet variety 'Gloria Mundi' (*de Ruiter*, 1929);[57] this was followed in 1961 by peonin (**71**) from *R. rugosa* and its hybrids[58] as well as the 3-glucosides **63** and **68**.[9a] For systematic analytical studies of hundreds of hybrids and species, see Refs. [9a, 59]. Our own HPLC studies of roughly 160 varieties and botanical roses have led to the identification of five to six further anthocyanins and anthocyanidins.[60] The structures of the anthocyanins so far identified in rose petals are shown in Figure 7.

Table 5. Spectrophotometric determination of anthocyanins.

Rose variety	Flower color	Anthocyanin	Content [a]
'Mister Lincoln' (*Swim & Weeks*, 1964)	dark red	**66** (little **67**, **68**)	0.6
'Papa Meilland' (*Meilland*, 1963)	dar red	**66**	0.3
R. rugosa rubra	violet-pink	**71** (little **72**, **73**)	0.25
'Veilchenblau' (*Schmidt*, 1909)	lilac with white	**66**	0.1
'Better Times' (*Hill*, 1934)	cherry red	**66** (+ ?)	1.3–1.8 [b]
'Maria Callas' (*Meilland*, 1965)	dark pink	**66** (little **67**)	0.1
'Queen Elizabeth' (*Lammerts*, 1954)	light pink	**66** (little **72**)	0.03

[a] % of fresh weight, calculated with $\varepsilon = 37000$ for **66** and 25000 for **71** in 1% trifluoroacetic acid in $MeOH/H_2O = 1:1$. [b] Content in epidermis cells [61].

anthocyanins on acid treatment, are not present in significant amounts, since there is no visible deepening of the color during extraction of pink roses. The noncorrelation between flower color and the light absorption of the flavylium cations (Fig. 12) responsible will be discussed in Section 8.5.

8.2. Pelargonin in Roses

Pelargonin (**62**; see Fig. 8) did not appear in roses in color-determining concentrations until 1929. In other garden plants, such as pelargoniums and geraniums, it had been known for years. However, analysis shows that pelargonin is hardly ever formed on its own, but is accompanied in almost all scarlet roses by cyanin (**66**). 'Gloria Mundi' is one of the very few roses that contains almost pure pelargonin (Fig. 8). Since then, the unexpected appearance of **62** in roses has been traced by many authors (cf. Ref. [62]) to a mutation. Now, however, analyses show[9a, f] that even very old varieties contain significant amounts of **62**; examples are *R. centifolia muscosa* (moss rose, appeared before 1750), 'Königin von Dänemark' (*Booth*, 1816, alba hybrid?), 'Général Jaqueminot' (*Roussel*, 1853, hybrid perpetual), 'Crimson Rambler' (Japan, pre 1890, multiflora hybrid), and 'Soleil

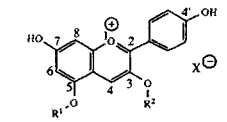

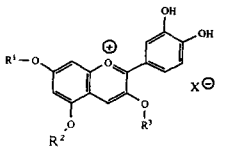

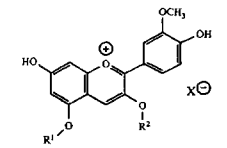

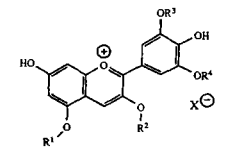

	λ_{max} [nm]
62: $R^1 = R^2 =$ β-D-glucose; pelargonin	497
63: $R^1 =$ H, $R^2 =$ β-D-glucose, callistephin	501
64: $R^1 =$ β-D-glucose, $R^2 =$ H	507
(**65**: $R^1 = R^2 =$ H, pelargonidin)	511
66: $R^1 =$ H, $R^2 = R^3 =$ β-D-glucose, cyanin	513
67: $R^1 = R^3 =$ β-D-glucose, $R^2 =$ H	
68: $R^1 = R^2 =$ H, $R^3 =$ β-D-glucose, chrysanthemin	517
69: $R^1 = R^3 =$ H, $R^2 =$ β-D-glucose	519
70: $R^1 = R^2 = R^3 =$ H, cyanidin	525
71: $R^1 = R^2 =$ β-D-glucose, peonin	515
72: $R^1 =$ H, $R^2 =$ β-D-glucose, oxycoccicyanin	517
73: $R^1 =$ β-D-glucose, $R^2 =$ H	521
74: $R^1 = R^2 =$ H, peonidin	527
75, $R^1 = R^2 =$ β-D-glucose, $R^3 = R^4 = CH_3$, malvin	
Not yet identified in rose petals.	

Fig. 7. Anthocyanins identified in rose flowers. The flavylium cations stable at low pH are shown.

Only glucose is used for glycosidation, and the 3,5-diglucosides are the dominant pigments. All the others are minor components and play only an occasional color-determining role in pink flowers. Whether other glycosides occur in the nonidentified trace components is not yet known. They may be important for breeding. The absence of delphinidin derivatives (e.g., **75**) is most important, since the hope of a blue rose vanishes with them.

A qualitative relationship exists between the intensity and saturation of petal coloration and the anthocyanin content (Table 5; see also the older analyses in Ref. [61]).

Less colored precursors of anthocyanins such as chalcones (**79**) and hydrates (**78**) (see Scheme 5), which can re-form

Fig. 8. 'Gloria Mundi' (1:2.5; *de Ruiter*, 1929); the first garden rose in which mainly pelargonin is responsible for the color.

d'Or'. In contrast to the views of Refs. [9a, d], we also found pelargonin in botanical roses, such as *R. pendulina*, *R. willmottiae*, *R. rugosa*, *R. pomifera*, and *R. gallica versicolor*. These are species that originate in quite different parts of the world and are members of different botanical sections of the subgenus *Eurosa*. This can be explained by referring to the general biosynthetic scheme for flavonoids, modified according to Ref. [63] (Scheme 4 and Fig. 9). It shows that there

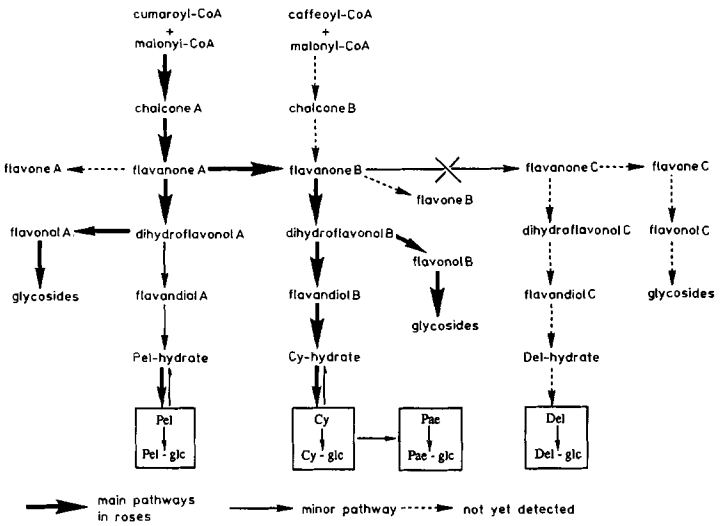

Scheme 4. Flavonoid biogenesis, modified from [63]: ⟶, major pathways in roses; ⟶, minor pathways; - - ⟶, not yet detected in roses. The abbreviations refer to Figure 7. PeL = compounds of the type **62**–**65**, Cy = **66**–**70**, Pae = **71**–**74**, Del = **75**, glc = D-glucose.

is no immediate connection between pelargonin, cyanidin, and delphinidin, but that they represent different branches from a series of precursors. Pelargonidin only occurs if the reduction of dihydroflavonol A to flavandiol A is *not* inhibited, while the hydroxylation of flavanone A to flavanone B is blocked. How the formation of flavonol A is correlated to pelargonidin is not yet known.

With pelargonin one also always finds some of the 3-glucoside (callistephin, **63**; see Fig. 7). The 5-glucoside **64** is very rare; it occurs, for instance, in 'Super Star' (*Tantau*, 1960). We assume that pelargonidin also arose spontaneously in other breeding strains not related to 'Gloria Mundi' and its relatives, such as 'Independence' (= 'Kordes Sondermeldung', *Kordes*, 1951).

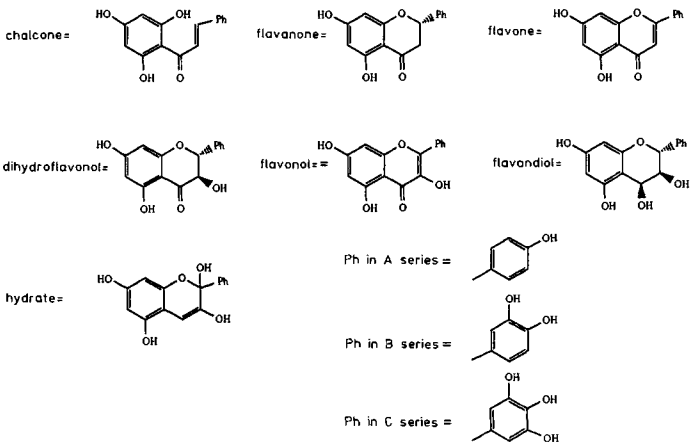

Fig. 9. Key to Scheme 4.

8.3. Cyanin in Roses

Cyanin (**66**) is the most important pigment in red roses. Often it is accompanied by smaller quantities of chrysanthemin (**68**). We have only found a few varieties where the ratio **68**:**66** is greater than 1, for example, in the old bourbon rose 'Souvenir de la Malmaison' (*Béluze*, 1843) and in the climbers 'François Juranville' (*Barbier*, 1906) and 'Dorothy Perkins' (*Jackson* and *Perkins*, 1901). As the cherry red flowers of the latter variety show, high levels of chrysanthemin can yield surprising red shades. We found the 5-glucoside **69** quite often, but always in low amounts. Cyanidin (**70**) and the 3,7-diglucoside (**67**) are rare. The well-known paradox that cyanin is present in both red and purple flowers is also true for roses; the mauve-colored 'Blue Moon' (= 'Mainzer Fastnacht', *Tantau* 1964) and 'Veilchenblau' (Fig. 10) both contain almost pure cyanin. For a possible explanation, see Section 8.5. A direct synthesis of cyanidin from caffeoyl-CoA in roses cannot be excluded, as it has not been studied (see Scheme 4).

8.4. Peonin in Roses

The earlier assumption that peonin (**71**) is typical for *R. rugosa* and *rugosa* hybrids must today be modified. More recent studies[9a, 60, 64] show a broad distribution in the sections Cinnamoneae, namely, *R. arkansana*, *R. acicularis*, and *R. x dulcissima* (all from North America), and *R. moyesii*, *R. multibracteata*, and *R. sweginzowii macrocarpa* (all from China), the Caninae (*R. canina*, *R. glauca*, and *R. pomifera*; all European), and the Pimpinellifoliae (*R. foetida bicolor*!). The mysterious 'Crimson Rambler' and 'Königin von Dänemark' also contain unexpectedly high levels of peonin, which throws new light on their unknown pedigrees.

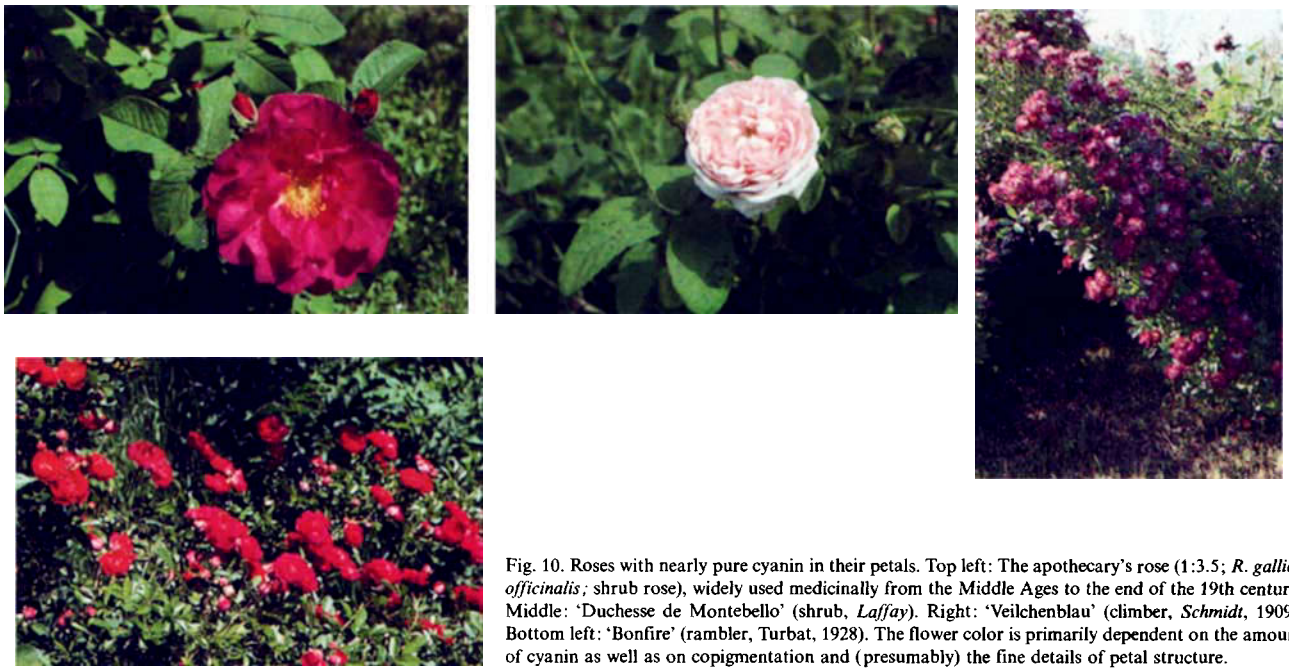

Fig. 10. Roses with nearly pure cyanin in their petals. Top left: The apothecary's rose (1:3.5; *R. gallica officinalis;* shrub rose), widely used medicinally from the Middle Ages to the end of the 19th century. Middle: 'Duchesse de Montebello' (shrub, *Laffay*). Right: 'Veilchenblau' (climber, *Schmidt*, 1909). Bottom left: 'Bonfire' (rambler, Turbat, 1928). The flower color is primarily dependent on the amount of cyanin as well as on copigmentation and (presumably) the fine details of petal structure.

Pure peonin is not found even in *R. rugosa rubra*; it is accompanied by much cyanin. The richest source of almost pure peonin is the old shrub rose 'Hansa' (*Schaum* and *Van Tol*, 1905; Fig. 11). Its mauve-red flowers show what can be achieved by high levels of pure peonin! Rarely have we found the 3- or 5-glycosides **72** (oxycoccicyanin) and **73**, or free peonidin (**74**).

8.5. The Stabilization of the Anthocyanin Chromophore in Roses

8.5.1. General Considerations

The sap of the anthocyanin-containing epidermis cells of the cerise-red 'Better Times' has a pH of 3.7–4.2, as deter-

Fig. 11. Peonin-dominated flower colors. Left: 'Frau Dagmar Hartopp' (1:2.5; small shrub, *Hastrup*, ca. 1914). Right: 'Hansa' (1:3; shrub rose, *Schaum* and *van Tol*, 1905).

The Austrian copper (*R. foetida bicolor*) contains surprising amounts of peonin, as already mentioned.[9a, 60] If its progeny contain anthocyanins—which is not always the case—they always include peonin. An example is 'Lady Penzance' (*Penzance*, 1894), a shrub rose bearing coppery red flowers with a yellow center (see Fig. 6). However, a connection between *rugosa* type and the peonin content of the flowers need not exist. Thus, analysis of the flowers of 'Conrad Ferdinand Meyer' (*H. Müller*, 1899) shows them to be free of peonin.

Peonin is probably derived from cyanin.[63] Whether the methylation occurs at the level of the cyanidin or only at its glucosides is unknown. A direct route starting from activated ferulic acid (3-*O*-methylcaffeoyl CoA) is also possible.

mined by spectrometric microtechniques.[61c] Within three days, this rises to 4.4–4.5, and the petals take on a slightly bluish tinge. In this pH range, pure flavylium ions are mostly transformed into the colorless hydrates **78** or the yellow chalcones **79** (Scheme 5), since the intermediate quinone methides **77** are so electrophilic that they do not survive in aqueous solution.[65] Hence, the question of stabilization arises for all anthocyanin pigments in plant organs, and a great many studies have been devoted to the subject, especially recently.[66] The interpretations given are selectively true for certain plants and to various extents: complex formation between anthocyanins and flavonoids with metal ions,[66a, 66b] intramolecular stacking,[66a, 66b] association (copigmentation) with the related chalcone,[67] stacking by

self-association,[66c] copigmentation with flavonols and related compounds.[66] Which of these are true for roses?

Metal complexes with anthocyanins and flavonoids have not yet been detected. These would be most likely for lilac or mauve varieties. In any case, studies of 'Veilchenblau' showed that the isolable, intense blue-violet fractions are very unstable and do not correspond[60] to the types described by *Goto* et al.[66] Intramolecular stacking appears when the glycosyl residues on the anthocyanidin (disaccharides!) are esterified to cinnamic acids. This shields the pyrylium ring from nucleophilic attack at C(2) and hence protects the anthocyanin chromophore. In roses, neither disaccharide glycosides nor esters of phenylpropanoid acids have been found, so that this form of stabilization must be disregarded. Copigmentation with the related chalcone,

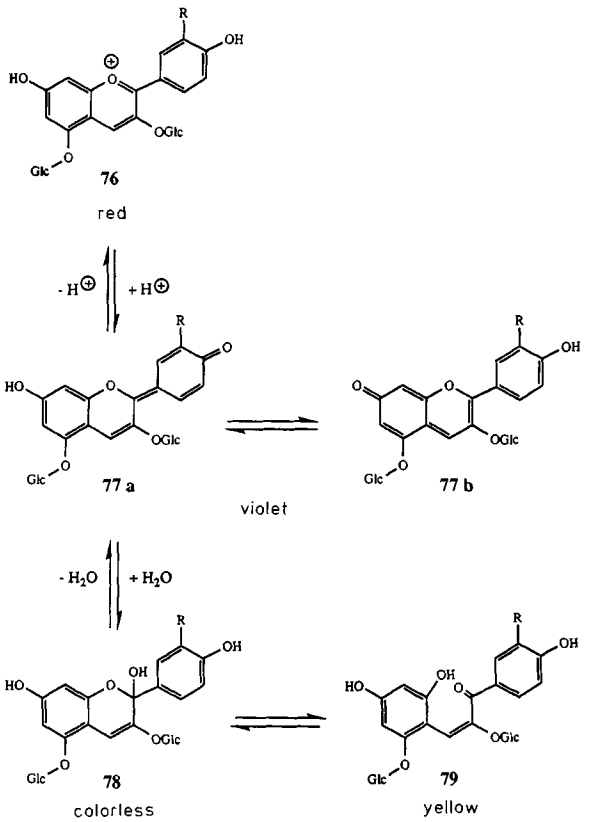

Scheme 5. R=H, OH, OCH_3.

which is in equilibrium with the anthocyanin, leads in vitro, in a 1:1 ratio, to significant stabilization, with bathochromic and hyperchromic effects.[67] This stabilization mechanism was suggested only recently and cannot be excluded for roses. However, it would lead to a great increase in the extinction on acidification, due to a shift of the equilibria towards the flavylium cation (Scheme 5), and this has not yet been observed.

Stacking by self-association has been demonstrated in in vitro experiments by deviation from the Lambert–Beer relationship and by strong exciton couplings in the circular dichroism spectrum. $Al^{3\oplus}$ salts may also play a role here.[68] This phenomenon could be important in roses with high anthocyanin content, but proof is lacking.

8.5.2. Copigmentation in Roses

From our current knowledge, copigmentation is the most important process for stabilization of rose anthocyanin chromophores. It consists of a loose association between a flavylium cation or quinone methide and a flavonol or related compound and is only observed in aqueous medium. To date, no such loose complexes have been isolated. This association has several consequences: shifting of the anthocyanin equilibria in Scheme 5 towards **76** and/or **77**; stabilization of the light absorption in the visible even in the physiological pH range; a shift in the visible maximum towards longer wavelengths; an increase in the extinction compared to a solution without copigment (see Fig. 12). Copigmentation effects are proportional to the concentration of the copigment. Initial studies of the copigments in 'Better Times' revealed a series of flavonol glycosides,[61c] including kaempferol-3-*O*-β-D-glucoside, a xyloside, quercitrin (**84**), and a quercitrin glucoside, arabinoside, and glucuronoside.

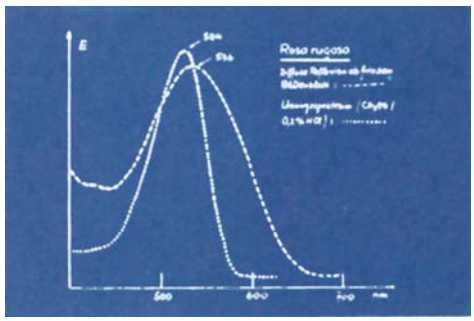

Fig. 12. Copigmentation effect for peonin: Absorptions of the pigment from *Rosa rugosa* in solution (···, in CH_3OH/0.2% HCl) and of its diffuse reflectance from fresh petals (----).

Recent studies on 'Veilchenblau' and 'Papa Meilland' have confirmed the wealth of flavonol glucosides present.[13k, 60a] Compounds **80**–**84** were identified in both these varieties (Fig. 13). They also occur in numerous white, yellow, and red roses in quite different proportions and mixed with other, not yet identified flavonoids. Spireoside (**82**) displays an especially strong copigmentation effect. At pH 4.7 and in a cyanin/spireoside ratio of 1:1, λ_{max} is shifted by 18 nm to longer wavelenghts; at a 1:2 ratio the shift is as great as 27 nm.[69] More detailed studies of roses with respect to their flavonol glycosides and other, as yet unknown copigments will be most worthwhile.

9. Tannins in Rose Petals

As many rose lovers know, chewing a rose petal produces an astringent effect in the mouth. The assumption that tannins occur in roses is an old one. Tannins have even been considered as possible stabilizers of the anthocyanin chromophore.[70] A more detailed study has now revealed that rose flowers contain a great many *ellagitannins*.[13k] These are esters of gallic acid (3,4,5-trihydroxybenzoic acid) and its oxidation products with monosaccharides.[71] Compounds

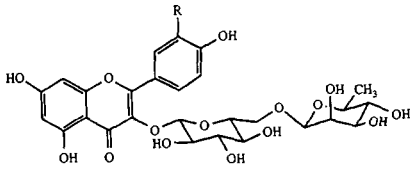

80, R = OH (rutin)
81, R = H (nicotiflorin)

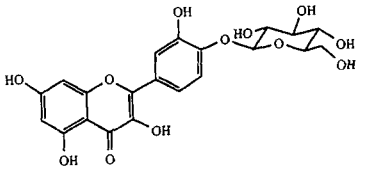

82 (spireoside)

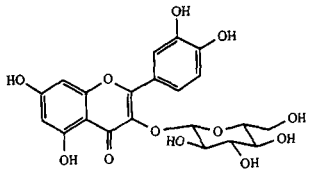

83 (isoquercitrin)

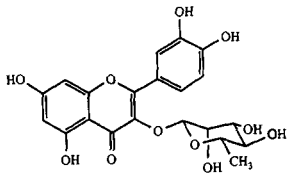

84 (quercitrin)

Fig. 13. Flavonol glycosides identified in roses.

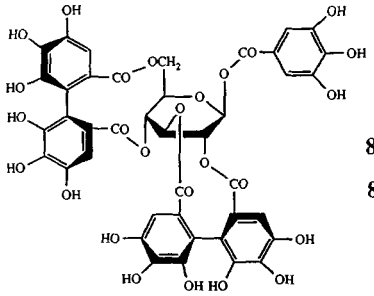

85, R=OH (eugeniin)
86, R=β-*O*-galloyl (tellimagrandin I)

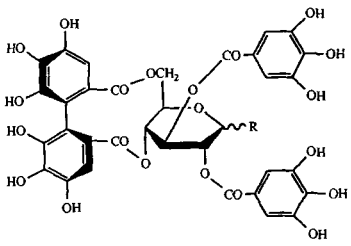

87 (casuarictin)

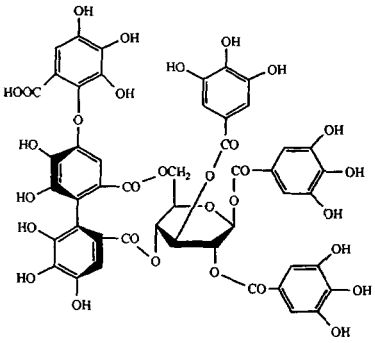

88 (rugosin A)

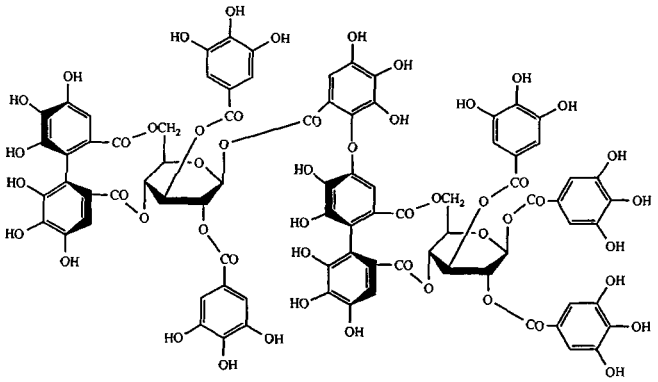

89 (rugosin D)

Fig. 14. Ellagitannins identified in rose petals.

85–89 were identified in 'Papa Meilland' and compound **86** in 'Veilchenblau' (Fig. 14). Ellagitannins are widespread and occur in high concentrations in all rose varieties. Many still await identification.

The presence of ellagitannins offers the first rational explanation for the long-standing medicinal use of dried rose petals. The apothecary's rose (*R. gallica officinalis*), in particular, has been used to treat diarrhoea, bleeding, and all kinds of inflammations.[72]

Compounds **85–89** display very little copigment effect. Though anthocyanins do not bleach in their presence, they lose their distinct maxima in the visible.

The trihydroxylated benzene ring of gallic acid is most remarkable! If this hydroxylation were to take place on anthocyanins to yield, for example, **75**, then the path to blue roses would lie open. It follows, therefore, the gallic acid and the flavonoids are synthesized by different routes.

10. Orange Roses

In recent decades, the breeding of orange roses has been strongly promoted. These modern varieties give particularly bright colors when planted in large beds; their shades lie somewhere in the overlap region between yellow and red. The almost uniform coloration is remarkable in these roses and is quite different from that of the yellow-red, two-tone roses. In the latter, carotenoids and anthocyanins show quite clear local differences in concentration. A good example is the Austrian copper (*R. foetida bicolor*), which has carotenoids on the outside and anthocyanins on the inside of the petals. In modern orange garden roses, this differentiation is absent. Pigment analysis shows that the saturation of the yellow cannot be explained by the presence of high levels of pelargonin (**62**): the new orange roses contain easily detectable quantities of carotenoids and high levels of anthocyanins (Table 6, Fig. 15). Even though the carotenoids are concentrated in the base of the petal, they are easily detectable in the blade by reflection spectroscopy; in vivo, 'Alexander' shows a reflection maximum at 425/445 nm, typical of carotenoids. Two further examples demonstrate how strongly carotenoids influence the color: flowers of the old rose 'Daily Mail Rose' (= 'Mme Edouard Herriot', *Pernet-*

Fig. 15. Modern orange-red roses in which the brightness of the pigments is increased by the presence of carotenoids. The most important anthocyanin is pelargonin. Left: 'Ville de Zürich' (1:3.8; bush rose, *Gaujard*, 1967). Right: 'Orangeade' (1:3.7; bush rose, *McGredy*, 1959).

Ducher, 1913) show almost uniform areas of a strong, coppery orange, and the same is true for the bright orange rose 'Louis de Funè' (*Meilland*, 1984). To our surprise, the anthocyanin content of both of these comprises practically pure cyanin, and the coppery orange is due to a mixture with carotenoids.

Table 6. Anthocyanins and carotenoids in orange-red roses.

Variety	Anthocyanins	Carot. [a]	*N* [b]	MC [c]
'Sarabande' (*Meilland*, 1957)	**62** + **63** (ca. 1:1)	1.5	16	**7**, **10**, **14**
'Super Star' (*Tantau*, 1960)	**62** + **66** (ca. 3:2)	1.6	21	**7**, **13**, **22–24**
'Orange Bunny' (*Meilland*, 1980)	**62** + **66** (ca. 2:1)	1.0	17	**7**, **10**, **14**

[a] Carotenoids: mg per 100 g dry weight. [b] *N* = number of carotenoids identified. [c] M_C = main carotenoids.

The physiological conditions that allow such an intimate mixture of pigments with such different solubility characteristics, and yet give a uniform coloration, are unknown.

A development is therefore in progress which, according to measurement of color and analytic findings, has not yet reached a conclusion. This is shown by a comparison between modern orange varieties of garden roses and the nasturtium (*Tropaeloum majus*), an old garden plant. Its flowers also contain the usual carotenoids and anthocyanins.[73] Nevertheless, its orange attains a higher saturation of the yellow than has yet been found in any comparable variety (Table 7).

Table 7. Measurement of color (CIELAB).

Flowers	L* [a]	+ a* [b]	+ b* [c]
'Super Star'	51–55	56–58	48–55
'Orange Bunny'	54	58	53–55
'Alexander'	56	54	51
Nasturtium (orange)	52–53	55–57	80–83

L*, measure of lightness; a*, measure of color saturation on the red-green axis; b*, measure of color saturation on the yellow-blue axis.

11. Pigments of Rosehips

Rosehips come in many different colors, shapes, and sizes. The flesh is colored a lively yellow, orange, pink, red, brown, or deep black by carotenoids and anthocyanins. Chemical studies on these pigments began in 1913, many years before carotenoid structures were known.[74] It is striking that they only concerned the hips of botanical roses; perhaps, especially in more recent times, this has been due to an interest in their possible content of provitamin A_1.[75] The published results are difficult to evaluate, because of often inadequate purification and identification procedures. Table 8 contains some relevant, recent results.[12, 76] The dominance of lycopene (**5**) and β,β-carotene (**7**) can be seen, also occasionally of rubixanthin (**10**) and lutein (**14**). In contrast to rose flowers, epoxides are almost completely absent; in *R. pomifera* only 3–4% of the total content consisted of epoxides, including the stereoisomeric mutatoxanthins (**17**, **18**), which are only found in traces in flowers if at all.

Table 8. Carotenoid content of rosehips.

Rose	Content [a]	*N* [b]	Main carotenoids [c]	Ref.
R. canina	1.2–2.5	14	**5**, **7**, **10**	[76a]
	133 [d]	11	**5**, **7**, **10**	[76b]
R. moyesii	22.4	10	**5**, **7**, **10**, **11**(?), **13**, **14**	[76a]
R. rubrifolia	8.8	11	**5**, **7**, **10**	[76a]
R. rubiginosa	162 [d]	8	**5**, **10**	[76b]
R. pomifera	6.2	43 [e]	**5**, **7**, **10**, **13**	[13b]
'American Pillar' (*van Fleet*, 1902)	2	17	**5**, **7**, **14**	[12]
'Golden Wings' (*Shepherd*, 1956)	6.1	15	**7**, **14**	[12]
'Sarabande' (*Meilland*, 1957)	5.4	16	**7**	[12]

[a] mg carotenoids per 100 g fresh weight. [b] *N* = number of carotenoids identified. [c] HC = main carotenoids. [d] mg in dried rosehip flesh. [e] Analyzed by HPLC.

The anthocyanins in rose hips have hardly been studied at all. The conspicuously black hips of *R. pimpinellifolia* contain almost pure chrysanthemin (**68**), according to *Demi-*

na[77] and demonstrate in extremis how important it is to identify the copigments that are presumably responsible for the black color.

12. The Dream of a Blue Rose

Many breeders and even more rose fanciers have dreamed of a blue rose—to the disapproval of more traditional rose lovers. However, violet-red roses have existed for a long time; for example, 'Tuscany' (gallica hybrid, pre-1600), 'Cardinal de Richelieu' (*Laffay*, 1840), and several others from the hybrid perpetuals, such as 'Reine des Violettes' (*Millet-Malet*, 1860). The roses tending most to violet are, however, 'Veilchenblau', a climbing rose with large inflorescences full of small, simple, lilac-colored individual flowers, and 'General Stefanik' (*J. Böhm*, 1931), a dwarf hybrid perpetual. In the former, 'Crimson Rambler' may have given rise to the violet color, in the latter *R. rugosa*. The hybrid polyantha 'Baby Faurax' (*Lille*, 1924) appeared later, as did the pale lilac tea hybrid 'Blue Moon' and many others. No breakthrough has been achieved to date.

The anthocyanins detected so far leave little hope for breeding a blue rose by conventional methods. With peonidin (**74**) as a basis, a rose with sky-blue flowers like those of *Ipomoea coerulea* (morning glory) would be possible if the requirement for intramolecular pigmentation (stacking with disaccharides and caffeic acid esters[78]) were fulfilled. With cyanidin (**70**), one can fall back on a comparison with cornflowers. Here, too, suitable glycosidation, acylation, and complex formation with cations would be required (see Section 8.5.1).

In Section 9 it was mentioned that rose petals are full of gallic acid esters. Could this hydroxylation activity be redirected to ring B of cyanidin? Otherwise, only the gene-technological path remains, with introduction of suitable genes from *Petunia*, for example. A far-fetched idea? One must not forget that a successful breeder could expect to receive several millions in licence fees for a good blue rose.[79]

13. Epilog

Our studies of rose pigments bring some more light into the long history of rose breeding. Roses are still full of unsolved puzzles, however. We would like to prompt young researchers to take them on with further scientific methods. Roses are also of great economic importance.[80] Moreover, our investigations have revealed gaps in the color range of current varieties. In yellow roses, the degree of the saturation of the color of the *foetida* group has still not been reached; an improvement in the lycopene, β,β-carotene, or rubixanthin content could produce quite new shades (compare tomatoes, corollas of narcissus with about 1.5% β,β-carotene, and rosehips); an increase in the content of chrysanthemin (**68**) would afford purer und more powerful red shades.

The analysis of rose carotenoids has furnished more insight into the genealogy of garden roses than bare the anthocyanins, where the small number of structures is a disadvantage. The identification of trace components, especially flavonol glycosides and other copigments, could help. Above all, the copigments must be studied more intensively. To date, breeders have always oriented themselves by the anthocyanin colors expressed and have ignored (or have been unable to consider) the copigments that are required for stabilization of the color and which are also passed on genetically. Scientifically, a study of carotenoid-degrading enzymes is also long overdue; roses constitute a readily available starting material, and well-developed procedures for analyzing the cleavage products are known.

We thank the Swiss National Science Foundation for financial support of our studies. The Ministry of Education (Canton Zürich) made possible the installation of a rose garden close to the Institute. Our thanks also go to the members of our research group for expert collaboration. We thank the rosarians K. Hauenstein (Rafz), K. Herter (Nussbaumen), R. Huber (Dottikon), Hauser (Vaumarcus), D. Woessner (Neuhausen), P. Täckelburg, and H. Vonholdt (Sangerhausen rosarium) for their help in procuring the roses. We are grateful to J. Klitscher (D-Klein Offenseth-Sparrieshoop) for statistical data.

Received: Dezember 27, 1990 [A 819 IE]
German version: *Angew. Chem. 103* (1991) 671
Translated by Dr. *Michael Kertesz*, Zürich

[1] G. Heinz-Mohr, V. Sommer: *Die Rose: Entfaltung eines Symbols*, Diederich, München 1988.

[2] The bibliography of K. L. Stock: *Rose Books*, Wheldon & Wesley, Codicote, Hitchin, Great Britain 1984, characterizes 3279 works.

[3] A large number of books on roses are available. The following books are recommended: a) G. Krüssmann: *Rosen, Rosen, Rosen*, Paul Parey, Berlin 1974; b) D. Woessner: *Rosen für den Garten*, Ulmer, Stuttgart 1988; c) A. Jacob, H. Grimm, W. Grimm, B. Müller: *Alte Rosen and Wildrosen*, Ulmer, Stuttgart 1990; d) R. Genders: *Die Rose*, Albert Müller, Rüschlikon-Zürich 1978; e) Fördergesellschaft "Grün ist Leben", *BdB-Handbuch Teil IV: Rosen*, Klett Flora-Druck, Leinfelden-Echterdingen 1986; f) H. Noack: *Wild- and Parkrosen*, Neumann-Neudamm, Melsungen 1989. g) Rose books in the English language: L. Hollis: *Beginner's Guide to Rose Growing*, Pelham Books, London 1971; N. Young: *The Complete Rosarian*, Hodder and Stoughton, London 1971; J. Harkness: *Roses*, Dent & Sons, London 1978; M. Gibson: *The Book of the Rose*, MacDonald and Jane's, London 1980; P. Beales: *Classic Roses*, Collins Harville, London 1985; J. Fisher: *The Companion to Roses*, Viking, Penguin Books, Harmondsworth, England 1986; P. Harkness: *Modern Roses*, Century London 1988; H. Le Rougetel: *A Heritage of Roses*, Unwin Hyman, London 1988; D. Austin: *The Heritage of the Rose*, Antique Collector's Club, Woodbridge, England, 1988. For the history of garden roses, see especially: F. Love Keays: *Old Roses*, MacMillan, New York 1935; E. A. Bunyard: *Old Garden Roses*, Country Life, London 1936; R. E. Shepherd: *History of the Rose*, MacMillan, New York 1954; Ann Wiley, *Endeavour (London) 1955*, 181; *J. R. Hortic. Soc. 1954*, 555; *ibid. 1955*, 8, 77; C. C. Hurst in G. S. Thomas (Ed.): *The old shrub roses*, Dent, London 1971, p. 57; Charlotte Testu: *Les Roses anciennes*, Flammarion, Paris 1984.

[4] A. Jaeger: *Rosenlexikon* (1936), Zentralantiquariat der DDR, Leipzig 1970, and G. Weiland, Lübeck 1970.

[5] McFarland in C. E. Meikle (Ed.): *Modern Roses 8*, Harrisburg, PA, USA 1980.

[6] Many varieties that are now scarcely available are no longer included in the newest edition of P. A. Haring (Ed.): *Modern Roses 9*, The Am. Rose Soc., Shreveport, LA, USA 1986.

[7] The world's largest rose museum, the Rosarium Sangerhausen (Sachsen-Anhalt), preserves some 6500 old and more modern varieties.

[8] Compare, for example, J. B. Harborne, G. Rowley, *Rose Annual (England) 1959*, 47; *Gardener's Chronicle (England) 1958*, 427 and information in numerous recent books on roses.

[9] a) K. Arisumi, *Gakugei Zasshi Kyushu Daigaku Nogakubu 20* (1963) 131; *ibid. 21* (1964) 169; *Yamaguchi Daigaku Nogakubu Gakujutsu Hokoku 19* (1968) 1173; b) L. R. G. Valadon, R. S. Mummery, *Phyton (Buenes Aires) 25* (1968) 157; c) C. V. Raman, *Curr. Sci. 38* (1969) 503; d) M. C. Jain, T. R. Seshadri, R. K. Trikha, *J. Ind. Res. (India) 30* (1971) 77; e) M. Yokoi,

N. Saitô, *Phytochemistry 12* (1973) 1783; f) D. P. de Vries, H. A. van Keulen, J. W. de Bruyn, *Euphytica 23* (1974) 447.
[10] Only higly oxygenated and methylated flavonols give rise to yellow colors in flowers and pollen; cf. R. Wiermann, E. Wollenweber, C. Rehse, *Z. Naturf. C 36* (1981) 204; J. B. Harborne, *Phytochemistry 20* (1981) 1117.
[11] The names of rose varieties are usually given with the name of the breeder (or the company) and the year of their entry onto the market. Variations occur, depending on the country concerned.
[12] E. Märki-Fischer, C. H. Eugster, unpublished results.
[13] a) R. Buchecker, C. H. Eugster, *Helv. Chim. Acta 60* (1977) 1754; b) E. Märki-Fischer, U. Marti, R. Buchecker, C. H. Eugster, *ibid. 66* (1983) 494; c) C. H. Eugster in L. Günthart (Ed.): *Linger Golden Light*, Carnegie-Mellon University, Hunt Institute for botanic Documentation, Pittsburg 1984, p. 195; German: *Verweile schönes Licht*, Rote Rose, CH-Regensberg 1986; d) E. Märki-Fischer, R. Buchecker, C. H. Eugster, *Helv. Chim. Acta 67* (1984) 2143; e) E. Märki-Fischer, C. H. Eugster, *ibid. 70* (1987) 1988; f) E. Märki-Fischer, P. Uebelhart, C. H. Eugster, *ibid. 70* (1987) 1994; g) E. Märki-Fischer, C. H. Eugster, *ibid. 71* (1988) 24; h) *ibid. 71* (1988) 1491; i) C. H. Eugster, *Rosa Helvetica 4/5* (1988/1989), 9; k) K. Nayeshiro, C. H. Eugster, *Helv. Chim. Acta 72* (1989) 985; l) E. Märki-Fischer, C. H. Eugster, *ibid. 73* (1990) 1205.
[14] Compare the reviews of a) C. H. Eugster, *Pure Appl. Chem. 57* (1985) 639; b) C. H. Eugster in N. I. Krinsky, M. M. Mathews-Roth, R. F. Taylor (Eds.): *Carotenoids, Chemistry and Biology*, Plenum, New York 1989, p. 1; c) J. Szabolcs, *ibid.* p. 39.
[15] P. Rüedi, *Pure Appl. Chem. 57* (1985) 793.
[16] B. D. Davies in T. W. Goodwin (Ed.): *Chemistry and Biochemistry of Plant Pigments, Vol. 2*, Academic, New York 1976, p. 38.
[17] a) W. Vetter, G. Englert, N. Rigassi, U. Schwieter in O. Isler, H. Gutmann, U. Solms (Eds.): *Carotenoids*, Birkhäuser, Basel 1971, p. 189; b) G. Englert in G. Britton, T. W. Goodwin (Eds.): *Carotenoid Chemistry and Biochemistry*. Pergamon, Oxford 1982, p. 107; c) *Pure Appl. Chem. 57* (1985) 801.
[18] a) K. Noack, A. J. Thomson, *Helv. Chim. Acta 62* (1979) 1902; b) V. Sturzenegger, R. Buchecker, G. Wagnière, *ibid. 63* (1980) 1074; c) K. Noack in G. Britton, T. W. Goodwin (Eds.): *Carotenoid Chemistry and Biochemistry*, Pergamon, Oxford 1982, p. 135.
[19] a) C. R. Enzell, *Pure Appl. Chem. 20* (1969) 497; b) H. Budzikiewicz in G. Britton, T. W. Goodwin (Eds.): *Carotenoid Chemistry and Biochemistry*, Pergamon, Oxford 1982, p. 155; M. E. Rose, *ibid.* p. 167.
[20] G. S. Thomas: *Shrub Roses of Today*, Dent, London 1967, p. 122.
[21] E. Märki-Fischer, C. H. Eugster, *Helv. Chim. Acta 68* (1985) 1704.
[22] E. Märki-Fischer, C. H. Eugster, *Helv. Chim. Acta 73* (1990) 1637.
[23] R. Buchecker, U. Marti, C. H. Eugster, *Helv. Chim. Acta 67* (1984) 2043.
[24] a) L. Bartlett, W. Klyne, W. P. Mose, P. M. Scopes, G. Galasko, A. K. Mallams, B. C. L. Weedon, J. Szabolcs, G. Tóth, *J. Chem. Soc. C 1969*, 2527; b) H. Cadosch, C. H. Eugster, *Helv. Chim. Acta 57* (1974) 1466; c) E. Märki-Fischer, C. H. Eugster, G. Englert, K. Noack, M. Vecchi, *Helv. Chim. Acta 65* (1982) 2198; d) M. Acemoglu, C. H. Eugster, *Helv. Chim. Acta 67* (1984) 184; e) L. Bicudo de Almeida, M. De Vuono Camargo Penteado, G. Britton, P. Uebelhart, M. Acemoglu, C. H. Eugster, *ibid. 71* (1988) 31.
[25] a) D. Goodfellow, G. P. Moss, J. Szabolcs, G. Tóth, B. C. L. Weedon, *Tetrahedron Lett. 1973*, 3925; b) K. Bernhard, G. P. Moss, G. Tóth, B. C. L. Weedon, *ibid. 1976*, 115; c) H. Cadosch, U. Vögeli, P. Rüedi, C. H. Eugster, *Helv. Chim. Acta 61* (1978) 783, 1511; d) M. Acemoglu, R. Prewo, J. H. Bieri, C. H. Eugster, *ibid. 67* (1984) 175; e) E. Märki-Fischer, R. Buchecker, C. H. Eugster, *ibid. 67* (1984) 461; f) M. Acemoglu, C. H. Eugster, *ibid. 67* (1984) 471, 2226; g) L. Bicudo de Almeida, M. De Vuono Camargo Penteado, K. L. Simpson, G. Britton, M. Acemoglu, C. H. Eugster, *ibid. 69* (1986) 1554.
[26] R. Buchecker, R. Egli, H. Regel-Wild, C. Tscharner, C. H. Eugster, G. Uhde, G. Ohloff, *Helv. Chim. Acta 56* (1973) 2548.
[27] a) R. Buchecker, P. Hamm, C. H. Eugster, *Helv. Chim. Acta 57* (1974) 631; b) R. Buchecker, C. H. Eugster, *ibid. 62* (1979) 2817.
[28] a) T. E. De Ville, M. B. Hursthouse, S. W. Russell, B. C. L. Weedon, *J. Chem. Soc. Chem. Commun. 1969*, 1311; b) J. R. Hlubucek, J. Hora, S. W. Russell, T. P. Toube, B. C. L. Weedon, *J. Chem. Soc. Perkin Trans. 1 1974*, 8.
[29] L. Zechmeister in L. Zechmeister (Ed.): *Fortschritte der Chemie organischer Naturstoffe*, Springer, Wien 1960, p. 224.
[30] H. Mayer, O. Isler in O. Isler, H. Gutmann, U. Solms (Eds.): *Carotenoids*, Birkhäuser, Basel 1971, p. 325.
[31] H. Sobotka, E. Bloch, H. Cahnmann. E. Feldbau, E. Rosen, *J. Am. Chem. Soc. 65* (1943) 2061.
[32] a) A. Haag, W. Eschenmoser, C. H. Eugster, *Helv. Chim. Acta 63* (1980) 10; b) M. Acemoglu, W. Eschenmoser, C. H. Eugster, *ibid. 64* (1981) 2691.
[33] H. G. W. Leuenberger, W. Boguth, E. Widmer, R. Zell, *Helv. Chim. Acta 59* (1976) 1832.
[34] a) H. Mayer, *Pure Appl. Chem. 51* (1979) 535; b) A. Rüttimann, H. Mayer, *Helv. Chim. Acta 63* (1980) 1456.
[35] M. Acemoglu, P. Uebelhart, M. Rey, C. H. Eugster, *Helv. Chim. Acta 71* (1988) 931.
[36] E. Rossiter, T. Katsuki, K. B. Sharpless, *J. Am. Chem. Soc. 103* (1981) 464.
[37] A. Baumeler, W. Brade, A. Haag, C. H. Eugster, *Helv. Chim. Acta 73* (1990) 700.
[38] P. Uebelhart, C. H. Eugster, *Helv. Chim. Acta 71* (1988) 1983.
[39] The following selected books are recommended: a) T. W. Goodwin: *The Biochemistry of the Carotenoids, Vol. I, Plants*, Chapman and Hall, London 1980; b) T. W. Goodwin in O. Isler, H. Gutmann, U. Solms (Eds.): *Carotenoids*, Birkhäuser, Basel 1971, p. 577; c) G. Britton in T. W. Goodwin (Ed.): *Plant Pigments*, Academic, London 1988, p. 133; d) B. H. Davies in F.-C. Czygan: *Pigments in Plants*, Fischer, Stuttgart 1980, p. 31.
[40] J. M. Clough, G. Pattenden, *J. Chem. Soc. Chem. Commun. 1979*, 616.
[41] a) C. H. Eugster, *Pure Appl. Chem. 51* (1979) 463; b) H. P. Märki, C. H. Eugster, *Helv. Chim. Acta 64* (1981) 1257.
[42] a) G. Britton, *Pure Appl. Chem. 57* (1985) 701; b) S. Mohanty: *Stereochemie des biologischen Ringschlusses bei Carotinoiden, Dissertation*, Universität Zürich 1988.
[43] ε,ψ-carotene **8**: R. Buchecker, C. H. Eugster, *Helv. Chim. Acta 54* (1971) 327; β,ε-carotene **9**: [26]; α-zeacarotene: R. Buchecker, C. H. Eugster, *Helv. Chim. Acta 56* (1973) 1124; ε,ε-carotene: *ibid. 56* (1973) 2548; lutein: [27]; α-kryptoxanthin **12**: [24a]; fritschiellaxanthin and α-doradexanthin: R. Buchecker, C. H. Eugster, A. Weber, *Helv. Chim. Acta 61* (1978) 1963; see also [41a].
[44] The plentiful occurrence of β,β-carotene mono- and diepoxides, quoted often by *Valadon* and *Mummery*, (see, e.g., [9b]) could not be confirmed by us.
[45] A. Hager in F.-C. Czygan (Ed.): *Pigments in Plants*, Fischer, Stuttgart 1980, p. 57.
[46] For the mechanism of epoxide rearrangement, see: P. Uebelhart, A. Baumeler, A. Haag, J. H. Bieri, C. H. Eugster, *Helv. Chim. Acta 69* (1986) 816.
[47] a) E. Märki-Fischer, C. H. Eugster, *Helv. Chim. Acta 68* (1985) 1708; b) R. Buchecker, S. Liaaen-Jensen, *Phytochemistry 16* (1977) 729; c) E. Märki-Fischer, C. H. Eugster, *Helv. Chim. Acta 73* (1990) 1637.
[48] a) I. Stewart, *J. Agric. Food. Chem. 25* (1977) 1132; b) H. Pfander (Ed.): *Key to Carotenoids*, Birkhäuser, Basel 1987.
[49] a) G. Wald, *J. Gen. Physiol. 31* (1948) 377; b) T. H. Goldsmith, J. S. Collins, S. Licht, *Vision Res. 24* (1984) 1661.
[50] R. Kaiser, C. H. Eugster, unpublished work. We thank *Roman Kaiser* (Givaudan Res. (Comp. Ltd., CH-Dübendorf) for allowing us to use his gas-chromatographic analyses of selected roses.
[51] Compare the occurrence of the glucosidated allenic C_{13} compounds from neoxanthin (**25**) in various plants: S. Shimizu, T. Miyase, A. Ueno, K. Usmanghani, *Phytochemistry 28* (1989) 3399.
[52] We have good evidence that the C_{27} alcohol from **25** also occurs in roses [12].
[53] Picture of *R. indica sulphurea* in P. J. Redouté: *Les Roses*, 3rd ed., Dufart, Paris 1828-1829, Picture No. 10.
[54] For another opinion see *P. Beales: Classic Roses*, Collins Harvill, London 1985, p. 356; picture in H. Le Rougetel: *A Heritage of Roses*, Unwin Hyman, London 1988, p. 43.
[55] Picture in H. Curtis: *Beauties of the Rose, Vol. 1*, Lavars, Bristol 1850, No. 9.
[56] R. Willstätter, T. J. Nolan, *Liebigs Ann. Chem. 408* (1915) 1.
[57] G. M. Robinson, R. Robinson, *Biochem. J. 28* (1934) 1712.
[58] J. Harborne, *Experientia 17* (1961) 72.
[59] M. Yokoi, N. Saitô, Y. Kawabata, Sh. Suzuki, H. Hirabayashi, *Chiba Daigaku Engeigakubu Gakujutsu Hokoku 1979*, 1.
[60] a) C. H. Eugster, A. Baumeler, U. Grunder, unpublished results; b) Whenever possible, our analyses were carried out with fresh petals, since it was observed that even drying could give rise to changes in composition.
[61] a) R. Willstätter, H. Mallison, *Liebigs Ann. Chem. 408* (1915) 147; b) G. M. Robinson, *J. Am. Chem. Soc. 61* (1939) 1606; c) S. Asen, K. H. Norris, R. N. Stewart, *J. Am. Soc. Hortic. Sci. 96* (1971) 770.
[62] R. Scott-Moncrieff, *J. Genet. 32* (1936) 117.
[63] a) K. F. F. Kho, *Phytochemistry 17* (1978) 245; b) B. Ruhnau, G. Forkmann, *ibid. 27* (1988) 1035; c) W. Heller, G. Forkmann in J. B. Harborne (Ed.): *The Flavonoids*, Chapman and Hall, London 1988, p. 399; W. Heller in V. Cody, E. Middleton, J. B. Harborne (Eds.): *Plant Flavonoids in Biology and Medicine*, A. R. Liss, New York 1986, p. 25; H. Griesbach in P. Markakis (Ed.): *Anthocyanins as Food Colors*, Academic, New York 1982, p. 69.
[64] H. H. Marshall, *J. Am. Soc. Hortic. Sci. 100* (1975) 336.
[65] R. Brouillard, *Phytochemistry 22* (1983) 1311.
[66] a) T. Goto, *Prog. Chem. Org. Nat. Prod. 52* (1987) 113; b) T. Goto, T. Kondo, *Angew. Chem. 103* (1991) 17; *Angew. Chem. Int. Ed. Engl. 30* (1991) 17; c) S. Asen, R. N. Stewart, K. H. Norris, *Phytochemistry 11* (1972) 1139; d) Y. Osawa in P. Markakis (Ed.): *Anthocyanins as Food Colors*, Academic, New York 1982, p. 41.
[67] a)P.Rüedi, B. Hutter-Beda, *Bull. Liaison Groupe Polyphenols 15* (1990) 332; b) B. Hutter-Beda, *Dissertation*, Universität Zürich 1991; c) L.-J. Chen, G. Hrazdina, *Phytochemistry 20* (1981) 297.
[68] T. Goto, H. Tamura, T. Kondo, *Tetrahedron Lett. 28* (1987) 5907.

[69] In Table 2 of [13k], the formula numbers **2** (for spireoside) and **3** (for quercitrin) have been erroneously exchanged throughout.
[70] a) R. Willstätter, E. H. Zollinger, *Liebigs Ann. Chem. 412* (1916) 195; b) G. M. Robinson, R. Robinson, *Biochem. J. 25* (1931) 1687.
[71] Reviews: a) T. Okuda, *J. Nat. Prod. 52* (1989) 1; b) T. Okuda, T. Yoshida, K. Mori, T. Hatano, *Heterocycles 15* (1981) 2; c) E. Haslam in T. Swain, J. B. Harborne, C. F. van Sumere (Eds.): *Recent Advances in Phytochemistry Vol. 12*, Plenum, New York 1979, p. 475; d) *Prog. Chem. Org. Nat. Prod. 41* (1982) 1.
[72] For the medicinal use of rose flowers see a) M. Boitard, *Manuel complet de l'amateur de roses*, Roret, Paris 1836, p. 50; b) M. Touw, Roses in the Middle Ages, *Econ Bot. 36* (1982) 71; for the biological effect of ellagitannins, see [71].
[73] Pelargonidin-3-*O*-gentiobioside, zeaxanthin (**13**), its *O,O'*-dipalmitate, auroxanthin, and flavoxanthin have been identified: A. Sykut, *Chem. Abstr. 66* (1966) 5866.
[74] The literature is summarized in [13b, 39a].
[75] The remark is necessary, since an aqueous infusion of rosehips, the popular rosehips tea, does not of course gain its red color from carotenoids—they are quite insoluble in water—but from the addition of anthocyanin-containing flowers.
[76] a) T. W. Goodwin, *Biochem. J. 62* (1956) 346; b) G. Toth, J. Szabolcs, *Acta Chim. Acad. Sci. Hung. 64* (1970) 393.
[77] T. G. Demina, *Sib. Otd. Akad. Nauk SSSR. Ser. Biol. Med. Nauk 2* (1966) 133.
[78] a) S. Asen, R. N. Stewart, K. H. Norris, *Phytochemistry 16* (1977) 1118; b) T. Goto, T. Kondo, H. Imagawa, S. Takase, M. Atobe, I. Miura, *Chem. Lett. 1981*, 883; c) T. Goto, T. Kondo, H. Imagawa, I. Miura, *Tetrahedron Lett. 22* (1981) 3213.
[79] A. V. Roberts, J. Humphreys, *Rose Ann. (London) 1980*, 133.
[80] A large rose company in Germany makes roughly 100 000 crosses annually, which give to some 250 000 seedlings. Of these, three to five come onto the market as new varieties, after the required testing. In addition, old and new varieties are propagated; in Germany this amounts to about 30 million rose plants every year. The world production is unknown, but is presumably over 150 million. The number of cut roses produced from rose plantations is also enormous; the area of cultivation worldwide is > 3000 hectares.

Metalla-enes and Metalla-ynes—from Small Molecules to Infinite Polymers

By *Malcolm H. Chisholm**

Conjugated organic π-systems in rings, chains, and polymers have long been of interest in terms of their structure and bonding. The delocalized π-systems endow these materials with enhanced electrical conductivities and nonlinear optical responses.[1] Multiple bonding between metal atoms[2] and between metal atoms and carbon, nitrogen, or oxygen atoms[3] form the basis for innumerable possibilities for molecular design of metalloorganic analogues. In the small molecules $[\{(CO)_5Re\}_2C_2]$,[4] $[\{(tBu_3Si)_3Ta\}_2C_2]$,[5] and $[\{(tBuO)_3W_2\}_2C_2]$[5,6] we find a central linear M-C-C-M moiety with distances and electronic structure consistent with the valence bond descriptions shown in **1**, **2**, and **3** below.

$M-C\equiv C-M$ $M=C=C=M$ $M\equiv C-C\equiv M$

1 **2** **3**

The *trans*-bis(acetylide) complexes of platinum depicted by **4**, where D and A represent π-donor and π-acceptor groups, respectively, have been synthesized and shown to exhibit second-order nonlinear optical behavior.[7] Polymeric species of the type shown in **5** were first reported by *Takahashi* and co-workers[8] and have been shown to have nonlinear optical (large $\chi^{(3)}$)[9] and liquid-crystalline properties.[10]

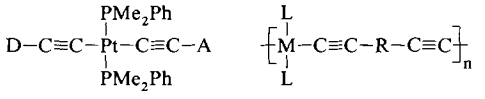

4 **5**

Two recent independent reports described the synthesis of related rhodium polymers. *Lewis* and co-workers[11] at Cambridge showed that the use of bis(trimethylstannyl)diyne $Me_3SnCC-R-CCSnMe_3$ in the reaction sequence (a) generated the polymer **6**. *Marder* and co-workers[12] at Waterloo, Canada, found that the reaction between a 1:1 mixture of $Rh(PMe_3)_4Me$ and $HC\equiv C-C_6H_4-C\equiv CH$ yielded **7** with the elimination of methane.

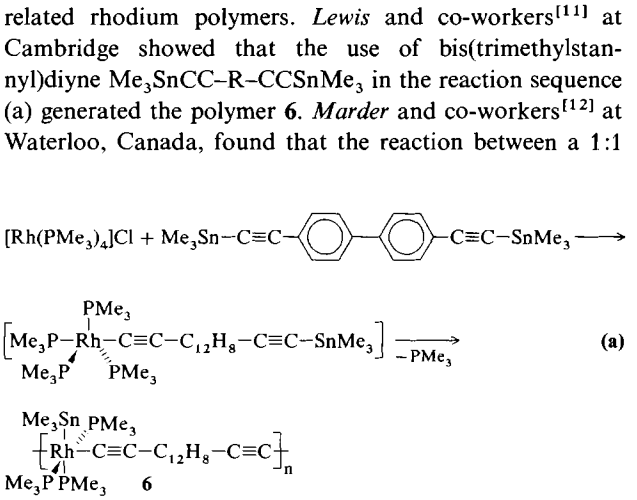

(a)

6

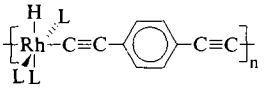

7, L = P*n*Bu$_3$

The solubilities of the two rhodium alkynyl polymers **6** and **7** were very similar as were the values of $\nu_{C\equiv C}$ (2080 cm^{-1}). The crystal structure of the bridged rhodium compound shown in **8** provides a structural model for a segment of one of these rigid-rod or stiff-chain polymers.[13]

$[(Me_3P)_4Rh-C\equiv C-C_6H_4-C\equiv C-Rh(PMe_3)_4]$ **8**

The Cambridge group reported that the use of $Me_3SnCC-R-CCSnMe_3$, $R=p\text{-}C_6H_4-C'_6H_4\text{-}p$, in Equation (b) led to polymers with average molecular weights of *ca.* 100000, somewhat higher than that reported in the original preparation by the Japanese workers.[8]

$$trans\text{-}(PBu_3)_2MCl_2 + Me_3Sn-C\equiv C-R-C\equiv C-SnMe_3 \longrightarrow 1/n\ \{M\equiv C-C-R-C\equiv C\}_n + 2\ Me_3SnCl \quad (b)$$

The nitrides $(tBuO)_3M\equiv N$, where M = Mo or W, crystallize in noncentrosymmetric space groups ($P6_3cm$, $P6_3$) and contain infinite chains of alternating short (ca. 1.7 Å) and long (2.7 Å) M–N bonds corresponding formally to triple and single (or dative) bonds as shown in **9**.[14]

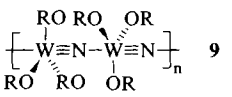

9

Hopkins and co-workers[15] recently reported that time-resolved spectroscopic analysis of the light emitted by powdered samples of $[(tBuO)_3M\equiv N)]_\infty$ showed nonlinear optical activity (a second harmonic generation, SHG). The relative yield of the SHG was only ca. 30% of that of urea. These efficiencies are surprisingly modest since these compounds should in principle possess large molecular hyperpolarizabilities (β), as predicted from the $\beta \propto L^3$ dependence of this property on the conjugated chain length (L).

Crystals of these nitride polymers were also found to be highly emissive at low temperature (77 K) and have extremely long excited-state lifetimes. That for molybdenum ($\tau = 750$ µs) was amongst the longest known of any transition-metal-containing complex (indicative that emission is a

[*] Prof. M. H. Chisholm
Department of Chemistry, Indiana University
Bloomington, IN 47405 (USA)

 © VCH Verlagsgesellschaft mbH, W-6940 Weinheim, 1991 0570-0833/91/0606-0673 $ 3.50+.25/0

spin-forbidden process). The vibronic structure allowed a simple estimate of the M≡N–M distortion (ca. 0.2 Å) for the excited states. This is consistent with an earlier band calculation on the hypothetical infinite linear polymer $[W(OH)_3N]_\infty$ that placed the valence and conduction bands are correspondent with the W≡N σ/π (occupied) and W–N π^* (empty) orbitals of the monomer $W(OH)_3N$.[16]

These recent findings serve to highlight some of the interests that surround a growing class of materials containing metal ions in conjugated systems: metalla-enes and metallaynes.

German version: *Angew. Chem. 103* (1991) 690

[1] See for example: D. J. Williams, *Angew. Chem. 96* (1984) 637; *Angew. Chem. Int. Ed. Engl. 23* (1984) 690; D. S. Chemla, J. Zyss (Eds.): *Non-Linear Optical Properties of Organic Molecules and Crystals, Vol. 1 and 2*, Academic, Orlando, FL, USA 1987; *Organic Materials for Non-Linear Optics (Spec. Publ. No. 69)* The Royal Society of Chemistry, London 1989; P. N. Prasad, D. R. Ulrich (Eds.): *Non-Linear Optical and Electronactive Polymers*, Plenum, New York 1988; J. R. Ferraro, J. M. Williams: *Introduction to Synthetic Electrical Conductors*, Academic, Orlando, FL, USA 1987, Ch. 3; T. A. Stotheim (Ed.): Handbook of Conducting Polymers, Marcel Dekker, New York, 1986.

[2] F. A. Cotton, R. A. Walton: *Multiple Bonds Between Metal Atoms*, Wiley, New York 1982.

[3] W. A. Nugent, J. M. Meyer: *Metal–Ligand Multiple Bonds*, Wiley, New York 1988.

[4] J. Heidrich, M. Steimann, M. Appel, W. Beck, J. R. Phillips, W. C. Trogler, *Organometallics 9* (1990) 1296.

[5] D. R. Neithamer, R. E. LaPointe, R. A. Wheeler, D. S. Richeson, D. G. Van Dwyne and P. T. Wolczanski, *J. Am. Chem. Soc. 111* (1989) 9054.

[6] K. G. Caulton, M. H. Chisholm, J. C. Huffman, E. M. Lobkovsky, Z. Xue, *Organometallics*, unpublished results.

[7] T. B. Marder, G. Lesley, Z. Yuan, H. B. Fyfe, P. Chow, G. Stringer, I. R. Jobe, N. J. Taylor, I. D. Williams, S. K. Kurtz, *ACS Symp. Ser. 455* (1991) 605.

[8] S. Takahashi, H. Morimoto, E. Murato, S. Kataoka, K. Sonogashira, N. Hagihara, *J. Polym. Sci. Polym. Chem. Ed. 20* (1982) 565.

[9] C. C. Frazier, S. Guha, W. P. Chem, M. P. Cockerham, P. L. Porter, E. A. Chanchard, C. H. Lee, *Polymer 24* (1987) 553.

[10] S. Takahasi, Y. Takai, H. Morimoto, K. Sonogashira, N. Hagihara, *Mol. Cryst. Liq. Cryst. 32* (1982) 139.

[11] S. J. Davies, B. F. G. Johnson, M. S. Khan, J. Lewis, *J. Chem. Soc. Chem. Commun. 1991*, 187.

[12] H. B. Fyfe, M. Mlekuz, D. Zargarian, N. J. Taylor, T. B. Marder, *J. Chem. Soc. Chem. Commun. 1991*, 188.

[13] M. Ballauff, *Angew. Chem. 101* (1989) 261; *Angew. Chem. Int. Ed. Engl. 28* (1989) 253.

[14] M. H. Chisholm, D. M. Hoffman, J. C. Huffman, *Inorg. Chem. 22* (1983) 2903; D. M. T. Chan, M. H. Chisholm, K. Folting, J. C. Huffman, N. S. Marchant, *ibid. 25* (1986) 4170.

[15] T. P. Pollagi, T. C. Stoner, R. F. Dallinger, T. M. Gilbert, M. D. Hopkins, *J. Am. Chem. Soc. 113* (1991) 703.

[16] R. A. Wheeler, M. H. Whangbo, T. Hughbanks, R. Hoffmann, J. K. Burdett, T. A. Albright, *J. Am. Chem. Soc. 108* (1986) 2222; R. A. Wheeler, R. Hoffmann, J. Strahle, *ibid. 108* (1986) 5381.

Stable Carbenes—Illusion or Reality?

By *Manfred Regitz**

Carbenes (**1**) are divalent carbon compounds with two nonbonding electrons on one carbon atom. The electron spins can be either antiparallel (singlet, **1a**) or parallel (triplet, **1b**). Carbenes are regarded as short-lived and highly reactive and they play a prominent role in the broad field of reactive intermediates. They are especially fascinating because chemists used to thinking in terms of the tetravalency of carbon are confronted with a radical change in perspective and with a bewildering array of reactions.

1 **1a** **1b**

Retrospect: Attempts to obtain the parent compound, methylene, by dehydration of methanol date from the first half of the last century, when the compound was thought to be stable.[1] Although such efforts seem daring today, it should be recalled that the tetravalency of carbon was not an established fact at that time. There were many subsequent attempts, all in vain, to find "bottle-able carbenes". Milestones on the route leading to recognition of the true character of carbenes as reactive intermediates included the work of *H. Staudinger* (decomposition of diazo compounds and ketenes, 1911–1916), *H. Meerwein* (C–H insertion of carbenes, 1942), *J. Hine* (α elimination of haloforms, 1950), and *W. von E. Doering* (addition of dihalocarbenes to olefins, 1956), who also coined the name. These developments led to an explosive growth in our knowledge of carbenes, a subject treated in several important monographs.[2] Even a standard handbook of organic synthesis has had to include carbenes in its palette of synthetically useful species.[3]

Stabilization of Carbenes: The electron deficiency due to the sextet on the carbene carbon can be partly relieved by donor substituents. Thus, carbon monoxide (**2**) and isocyanides (**3**), formulated as neutral species, can also be included in the definition of carbenes given above. In these cases, however, the heteroatom compensates for the electron deficiency on the divalent carbon. Of course, it would be erroneous to speak here of stable carbenes, even though

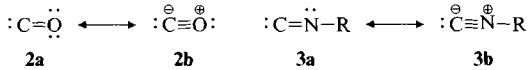

2a **2b** **3a** **3b**

carbene behavior, such as [2 + 1] and [4 + 1] cycloadditions, is observed. The so-called nucleophilic carbenes such as 1,3-diphenylimidazolidin-2-ylidene (**5**) and 1-methyl-1,3-benzthiazolin-2-ylidene (**8**) are more relevant to the question

[*] Prof. Dr. M. Regitz
Fachbereich Chemie der Universität
Erwin-Schrödinger-Strasse, W-6750 Kaiserslautern (FRG)

at hand. The former can be generated by thermal α elimination from **4**,[4] for example; the latter can be generated by deprotonation of cation **7**.[5] Both species have been trapped by numerous electrophiles.[3]

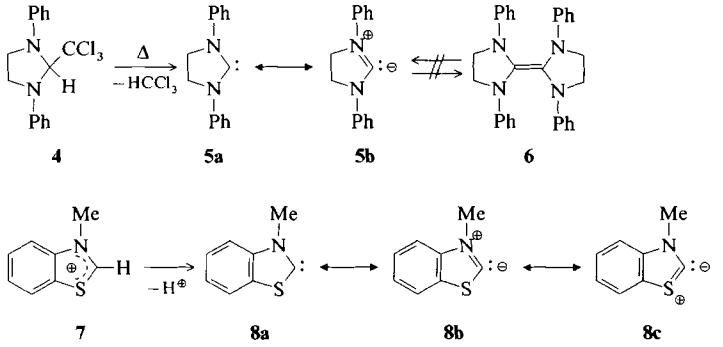

4 **5a** **5b** **6**

7 **8a** **8b** **8c**

The assumption that the "Wanzlick olefin" **6**, despite many indications to the contrary from its reactive behavior, exists in equilibrium with carbene **5** at about 150 °C is not supported by crossing experiments.[6] Similarly, the product obtained on deprotonation of **7** proved to be the dimer of carbene **8** rather than **8** itself.[5] Despite stabilization by donor substituents (**5a** ↔ **5b** and **8a** ↔ **8b** ↔ **8c**), both species still behaved as reactive intermediates. Nonetheless, the possibilities discussed here for thermodynamic stabilization of carbenes, together with steric shielding of the reaction center, play a crucial role in answering the question posed in the title. Recently, the groups of *G. Bertrand* in Toulouse and *A. J. Arduengo* in Wilmington, Delaware, published exciting results that have revived the discussion.

Bertrand's Carbene: The starting point in this development was the observation made by *T. Curtius* over 100 years ago that α-bis(diazo) compounds spontaneously lose N_2 to give acetylenes [Eq. (a)]. Combination of this fact with the

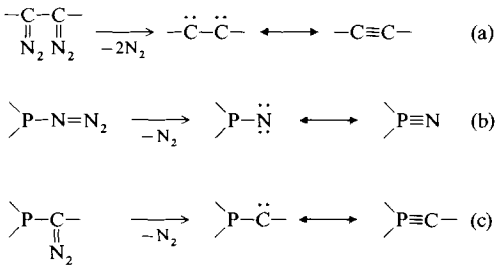

knowledge that low-coordinate phosphorus can engage in double- and triple-bond formation[7] leads logically to the question whether the species formed on loss of N_2 from azidophosphanes are best characterized as nitrenes or as phosphanitriles [Eq. (b)]. The experiments—1,2 additions, [3 + 2] cycloadditions, cyclooligomerizations[8]—support unequivocally an intermediate with multiple-bond character. The formulation of a corresponding carbene intermediate was obvious [Eq. (c)]. It required, however, the synthesis of phosphinodiazo compounds.

The model diazo compound **9** was synthesized from lithiated diazotrimethylsilylmethane and chlorobis(diisopropylamino)phosphane.[9, 10] Thermolysis of **9** at 160 °C afforded a spectroscopically and analytically well-characterized, distillable red oil in 80% yield.[10] The title of the published results, "Synthesis of a Stable λ^3-Phosphinocarbene-λ^5-phosphaacetylene", points to both the carbene *and* acetylene character.

The initial studies of its reactivity showed that **10** can undergo 1,2 addition of chlorotrimethylsilane, for example, **10** → **11**, although an alternative mechanism involving insertion of **10** into the Si–Cl bond followed by C → P Cl shift must also be considered.[10] On the other hand, the result of [3 + 2] addition of trimethylsilyl azide to **10** is unequivocal. The initially formed cycloadduct has been detected by NMR spectroscopy before it undergoes ring opening to give the diazo compound **12**.[10] Reactivity typical of carbenes has also been observed for **10**. Thus, it undergoes intramolecular

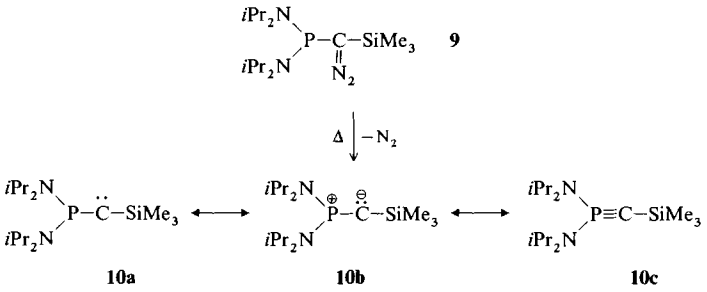

9

10a **10b** **10c**

C–H insertion, albeit at 300°, to form the tetrahydro-1,2-diazophosphole **13**;[10] thermodynamic stabilization (**10a** ↔ **10b** ↔ **10c**) carries a price! Finally, the stereospecific [2 + 1] cycloaddition of **10** to electron-poor olefins such as dimethyl fumarate (**10** → **14**) demonstrates its character as a nucleo-

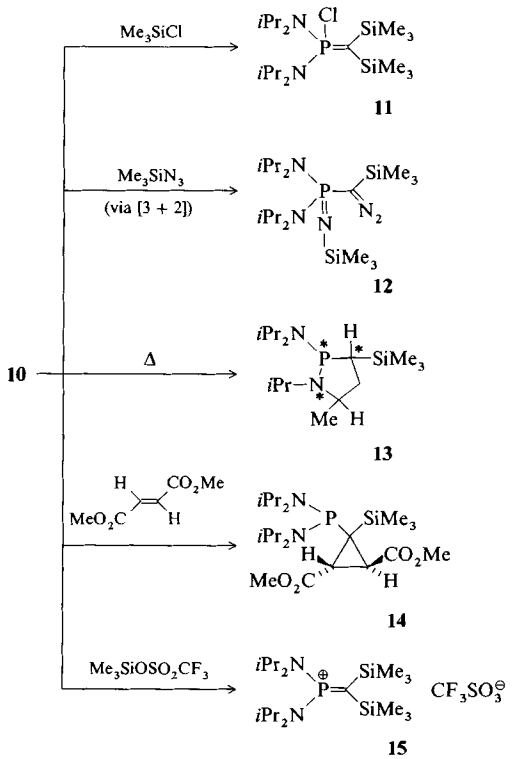

11 **12** **13** **14** **15**

philic carbene.[11,12] This character also accounts for its silylation to give the methylenephosphonium fluoromethanesulfonate **15**.[13] A preliminary conclusion, based only on the reactivity of **10**, is that the nonbonding electrons on phosphorus are involved in stabilizing **10**, as shown by formula **10b**. The silyl group also acts to stabilize the negatively charged center. Moreover, steric shielding presumably plays a role as well. If it is possible to synthesize a crystalline member of this class, the crystal structure analysis will reveal still more about its character.

Arduengo's Carbene: "A Stable Crystalline Carbene" is the title of a communication that appeared at the beginning of the year and reported on compound **17**, which melts only at 240–241 °C. It was obtained as colorless crystals on deprotonating bis(adamantyl)imidazolium chloride (**16**) with sodium hydride in the presence of catalytic amounts of dimethyl sulfoxide anion.[14,15]

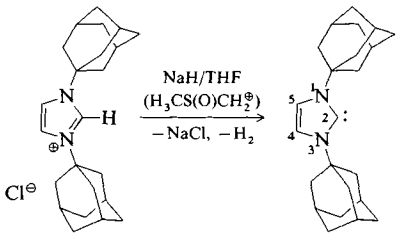

16 **17**

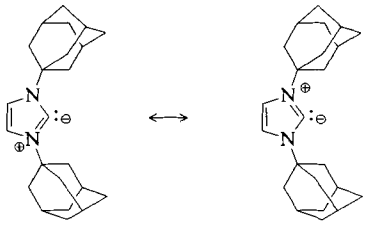

17a **17b**

Analytical and spectroscopic data support unambiguously the structure of **17**. In the ^{13}C NMR spectrum, for example, the carbene carbon gives rise to a very low-field signal ($\delta = 211.43$); the molecular mass was determined by electron impact fragmentation. The crystal structure analysis revealed several salient features that indicate the nature of the carbene. The bond angle at the carbene center (102.2°) is appreciably smaller than the corresponding angle in imidazolium salts of type **16** (108.5–109.7°), in very good agreement with the values calculated for π-donor-substituted singlet carbenes. The N1–C2 and N3–C2 bonds (1.367 and 1.373 Å) are significantly longer than those of imidazolium salts (1,32 Å). This also holds for the N1–C5 and N3–C4 distances, although the effect here is less pronounced. These findings indicate that the π delocalization in **17** is smaller than in **16**. In agreement with this conclusion, the signals of the olefinic hydrogens of **16** ($\delta = 7.92$) are shifted to higher field on going to **17** ($\delta = 6.91$).

The donor character of the N–C=C–N structural unit (**17a** ↔ **17b**) on the one hand and the σ-electronegativity effect of the two heteroatoms on the other are the factors responsible for the thermodynamic stabilization of **17**. However, the importance of the resonance structures **17a** and **17b** appears to be very limited, since the calculated charge on C2 is only − 0.08 e. Furthermore, the kinetic stabilization due to the two adamantyl moieties plays an important role. They make it possible to isolate this almost true carbene. Work in *Arduengo*'s laboratory should soon answer the question whether this stabilization affects the typical carbene reactivity expected of such a species.

Thermodynamic and kinetic stabilization have once again proved to be concepts useful for the isolation of "bottleable" reactive intermediates. The title question is thereby answered. Clearly, however, the electronic relationships and reactivity will be somewhat changed in such species.

German version: *Angew. Chem. 103* (1991) 691

[1] See W. Kirmse: *Carbene, Carbenoide und Carbenanaloge*, Verlag Chemie, Weinheim 1969, p. 6 ff.

[2] W. Kirmse: *Carbene Chemistry*, 2nd ed., Academic Press, New York 1971; M. Jones, R. A. Moss: *Carbenes I*, Wiley, New York 1973; R. A. Moss, M. Jones, *Carbenes II*, Wiley, New York 1975.

[3] M. Regitz (Ed.): *Houben-Weyl, Methoden der Organischen Chemie, E19b*, Thieme, Stuttgart 1989.

[4] H. W. Wanzlick, E. Schikora, *Angew. Chem. 72.* (1960) 494; *Chem. Ber. 94* (1961) 2389.

[5] H. Quast, S. Hünig, *Angew. Chem. 76* (1964) 989; *Angew. Chem. Int. Ed. Engl. 3* (1964) 800; *Chem. Ber. 99* (1966) 2017.

[6] Short review: R. W. Hoffmann, *Angew. Chem. 80* (1968) 823; *Angew. Chem. Int. Ed. Engl. 7* (1968) 754.

[7] M. Regitz, O. J. Scherer (Eds.): *Multiple Bonds and Low Coordination in Phosphorus Chemistry*, Thieme, Stuttgart 1990.

[8] G. Sicard, A. Baceiredo, G. Bertrand, J.-P. Majoral, *Angew. Chem. 96* (1984) 459; *Angew. Chem. Int. Ed. Engl. 23* (1984) 459; A. Baceiredo, G. Bertrand, J.-P. Majoral, G. Sicard, J. Jaud, J. Galy, *J. Am. Chem. Soc. 106* (1984) 6088; see also J.-P. Majoral in [7], p. 455 ff.

[9] A. Baceiredo, G. Bertrand, G. Sicard, *J. Am. Chem. Soc. 107* (1985) 4781.

[10] A. Igau, H. Grützmacher, A. Baceiredo, G. Bertrand, *J. Am. Chem. Soc. 110* (1988) 6463.

[11] A. Igau, A. Baceiredo, G. Trinquier, G. Bertrand, *Angew. Chem. 101* (1989) 617; *Angew. Chem. Int. Ed. Engl. 28* (1989) 621.

[12] Further support is provided by the formation of ketenimines from **10** and **9** with other amino groups and *tert*-butyl isocyanide; see [10] and G. R. Gilette, A. Baceiredo, G. Bertrand, *Angew. Chem. 102* (1990) 1431; *Angew. Chem. Int. Ed. Engl. 29* (1990) 1429; G. Bertrand, A. Igau, A. Baceiredo, H. Grützmacher, *Phosphorus, Sulfur Silicon Relat. Elem. 49/50* (1990) 301. For other reactions see G. Bertrand in [7], p. 443 ff.

[13] A. Igau, A. Baceiredo, H. Grützmacher, H. Pritzkow, G. Bertrand, *J. Am. Chem. Soc. 111* (1989) 6853. For other reactions see G. Bertrand in [7], p. 443 ff.

[14] A. J. Arduengo, R. L. Harlow, M. Kline, *J. Am. Chem. Soc. 113* (1991) 361.

[15] First comparison of **10** and **17**: R. Dagani, *Chem. Eng. News 69* (1991) No 4, p. 19.

Novel Polymeric Materials from Monodisperse Copolypeptides by Biotechnological Methods**

By *Helmut Ritter**

The multiplicity of chemical methods that has been described and employed for the synthesis of peptides impressively demonstrates that an ideal synthetic method is apparently still lacking. Emil Fischer already recognized this need at an earlier date, and neatly summed up the situation at that time with the poignant remark "der Ochs kann's besser" ("the ox can do it better"). Meanwhile, however, there has been a change of approach with increasing application of biotechnological methods, and success has not only been reported in the pharmaceutical and agricultural sectors, but quite topically a first breakthrough is also recognizable in the directed preparation of novel and interesting protein materials with predetermined structures.[1]

The effort to realize the kinetically and thermodynamically controlled synthesis of peptides, not only by more improved chemical methods but also biocatalytically using free or supported enzymes has long surpassed the stage of an experimental exercise, and, e.g. in the case of racemization-free preparation of the sweetener aspartame (Asp–Phe) with thermolysin, has found industrial use.[2] As an extension to the widely developed synthesis of peptides on polymer supports[3] we are currently also concerned with the employment of pure enzymes, e.g. α-chymotrypsin, for the coupling of peptides to side chains in comblike structured polymers.[4]

The use of the enzyme apparatus of whole cells has recently led to the synthesis of chiral polyesters with the side chains containing phenyl groups and fluorine atoms. The molecular weights of such polyesters generated by *Pseudomonas oleovorans* reached $\bar{M}_w$ values of up to 350000.[5]

The procedure recently elaborated by *Tirell* et al. for the directed synthesis of proteins with predetermined molecular weights and repetitive sequences by gene manipulation provides a completely new entry to materials similar to naturally occurring proteins (e.g. silk or elastin) and having interesting properties such as elasticity in fibers or the adhesiveness of excretory products of certain types of mussels. Whereas biotechnologically produced enzymes or hormones exhaust the full spectrum of the twenty common amino acids, the new biomaterials consist of only few repeating amino acids. This means, however, that the respective DNAs and mRNAs must to a large extent also be built up in a repeating fashion. Since this simple regular structural assemblage presents problems, e.g. stiffening of the mRNA by secondary hydrogen bonds, whereby translation is made difficult, the genetic code was alternatingly varied. For example, the coding of glycine was alternatingly carried out by GCT and GGC, that of alanine by GCC and GCT. In order to keep the errors in the gene synthesis as small as possible DNA sequences were first prepared by conventional chemical methods with two repeat units, e.g. of a nonapeptide, and these subsequently cloned by insertion in a plasmid which was introduced into *Escherichia coli* as host cell and reproduced. The DNA segments amplified in this way were coupled to a series of multimers by self ligation and recloned with *E. coli* in nutrient containing antibiotics. Individual colonies were separately further reproduced and the respective molecular weight of the protein produced therefrom ascertained by gel electrophoresis. Staggered monodisperse proteins with predetermined molecular weights can be produced in large amounts (ca. 40 mgL^{-1}) from the separate cultures. A copolypeptide with exactly 14 repeat units of the undecapeptide sequence **1** was very effectively prepared by the above-mentioned simple, general method.[1]

$$-(AlaGly)_4ProGluGly- \quad \mathbf{1}$$

The novel "polycondensate" has a glass temperature of 182°C and decomposes above ca. 250°C. Homogeneous films can be readily cast from formic acid solution. The respective oligonucleotide **2** containing 82 base pairs was synthesized on a support using the phosphoramidite method.

For comparison the chemical synthesis of a protein with repeating nonapeptide units was also carried out in a rather tedious way according to Scheme 1.[6] The total yield after

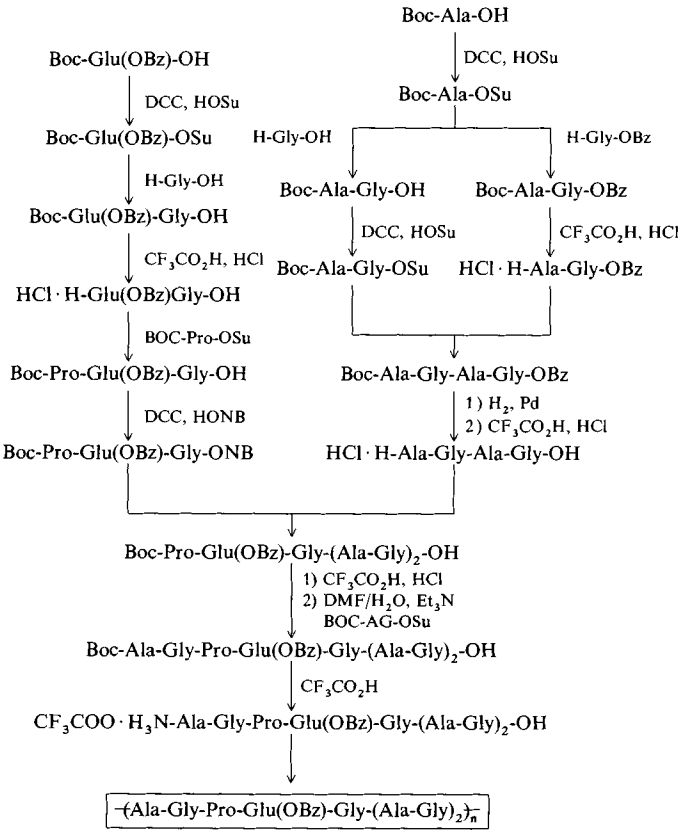

Scheme 1. Conventional peptide chemical method for the synthesis of a protein with repeating nonapeptide sequences. DCC = dicyclohexylcarbodiimide, HOSu = *N*-hydroxysuccinimide, HONB = *N*-hydroxy-5-norbornene-2,3-dicarboximide.

[*] Prof. Dr. H. Ritter
Bergische Universität-GH Wuppertal
Fachbereich 9
Gausstrasse 20, W-5600 Wuppertal (FRG)

[**] I thank Professor Dr. *W. Reineke*, Wuppertal, for valuable information.

18 steps was only 11% in the conventional method. The presence of a polydisperse mixture having only a relatively small molecular weight of ca. 10000 was established by gel chromatography.

According to recent findings,[1] the entry to proteins with repeating amino acid sequences by biotechnological methods seems to be very promising. The great efforts made to prepare materials with such relatively simple structures is justified in particular by the fact that applications in medicine are now already recognizable. Thus, e.g., block cocondensates containing repeating amino acid sequences which are analogues of silk, and sequences which are capable of binding strongly to cell surfaces, may be useful for the "adhesion" of individual cells to give large aggregates such as is required, e.g., in cases of severe burning. The coupling of hard and soft segments of appropriate repeating structural amino acid sequences is considered as the reason for the high elasticity of spider's silk.

The materials now accessible biotechnologically should show similar properties in blocklike coupling and be of particular interest in the form of films for covering wounds or coatings for implants.[7] The route outlined by *Tirrell* et al. for the synthesis of proteins which contain few repetitive amino acid sequences and have a predetermined molecular weight has proven better than classical methods as regards outlay and results. Hence, polymer chemists and protein chemists now have new materials on hand that should be further convertible by chemical and enzymatic processes, e.g. into block and graft cocondensates. Finally, there remains the question as to what extent the structural variants of the monodisperse proteins can be further enlarged, e.g. by fluorinated amino acids in the nutrient.

German version; *Angew. Chem. 103* (1991) 694

[1] H. S. Creel, M. J. Fournier, T. L. Mason, D. A. Tirrell, *Macromolecules 24* (1991) 1213.
[2] H. D. Jakubke, P. Kuhl, A. Könnecke, *Angew. Chem. 97* (1985) 79; *Angew. Chem. Int. Ed. Engl. 24* (1985) 85.
[3] E. Bayer, *Angew. Chem. 103* (1991) 117; *Angew. Chem. Int. Ed. Engl. 30* (1991) 113.
[4] H. Rehse, H. Ritter, *Makromol. Chem. 189* (1988) 529; M. Gormanns, H. Ritter, *ibid. 192* (1991) p. 745.
[5] K. Fritzsche, R. W. Lenz, R. C. Fuller, *Makromol. Chem. 191* (1990) 1957; C. Abe, Y. Taima, Y. Nakamura, Y. Doi, *Polym. Commun. 31* (1990) 404.
[6] K. P. McGrath, D. A. Tirrell, M. Kawai, T. L. Mason, M. J. Fournier, *Biotechnol. Prog. 6* (1990) 188.
[7] D. A. Tirrell, Amherst, MA, USA, private communications.

C_{60}: From Soot to Superconductors

By *François Diederich** and *Robert L. Whetten*

In 1990, a team of astronomers led by *Krätschmer* and *Huffman*[1] reported that the new allotrope of carbon C_{60} (buckminsterfullerene, so named after Buckminster Fuller, an architect renowned for his geodesic domes)[2] can be produced in macroscopic quantities through resistive heating of graphite under inert atmosphere. In an *Angewandte Chemie* Highlight article in January 1991, *Fraser Stoddart* summarized the early results in the vigorous worldwide research efforts that were triggered by this surprising development.[3] Only half a year later, a series of exciting new findings require that yet another Highlight article be written (closing date May 20, 1991).

X-ray Crystal Structure Analysis of Osmylated C_{60}

Although the icosahedral-cage structure of C_{60} was strongly suggested by ^{13}C NMR[3], IR[3-6], Raman[6], and photoelectron spectroscopy,[7] as well as by scanning tunneling microscopy (STM) imaging,[8-10] the ultimate confirmation and detailed parameters of the soccerball-shaped framework had to await X-ray crystallography. However, rapid isotropic rotational motion of the orderly packed spherical molecules in the crystal to temperatures down to 100 K[11,12] have so far prevented a successful high resolution X-ray crystal structure analysis. To break the symmetry of C_{60} and prevent its rapid spinning in the crystal, *Hawkins* et al. prepared by osmylation [Eq. (a)] a remarkable 1:1

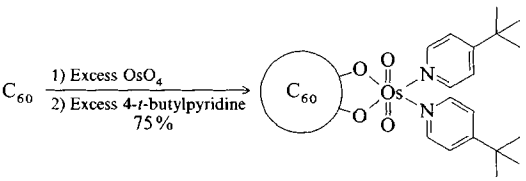

(a)

C_{60}–osmium tetraoxide adduct.[13,14] The crystal structure of this adduct was subsequently solved by the Berkeley group and clearly confirms the soccerball structure of C_{60}, composed of 20 six-membered rings fused to 12 five-membered rings (Fig. 1).[14] All tricoordinate carbon atoms of C_{60} are pyramidalized and lie at an average distance of 3.512(3) Å from the center of the sphere. The unfunctionalized five- and six-membered rings are all planar within ± 0.05 Å. The two bond lengths in these rings are 1.388(9) Å for the fusion between two six-membered rings and 1.432(5) Å for the fusion between a six- and a five-membered ring. Values of 1.40 (± 0.015) Å and 1.45 (± 0.015) Å were determined for the two bond lengths in C_{60} by solid-state ^{13}C NMR.[15]

[*] Prof. Dr. F. Diederich, Prof. R. L. Whetten
Department of Chemistry and Biochemistry
University of California, Los Angeles, CA 90024-1569 (USA)

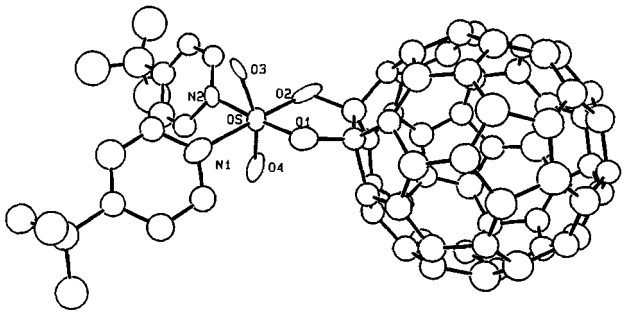

Fig. 1. Structure of the C_{60}–osmium tetraoxide–di(*p-tert*-butylpyridine) adduct in the crystal [16].

Reactivity of C_{60}

The chemistry of C_{60} promises to develop rapidly in the coming months. Initial reactivity studies with this fully delocalized closed-shell molecule[17] might have been of limited success since they probably relied too much on analogy to the chemistry of polycyclic aromatic hydrocarbons. However, C_{60} differs in many aspects from these planar molecules and shows "ambiguous"[18] aromatic character. The C_{60} structural framework is highly stable. Ion-beam collision experiments, in which $C_{60}^{\oplus}$ or $C_{60}^{\ominus}$ collide with silicon or graphite surfaces at speeds up to 50 000 km per hour ($\hat{=}$ 250 eV impact energy) show high inelasticity of the ions, but no evidence for impact-induced fragmentation.[19] This behavior differs from those of any other molecule or similar-sized cluster ions that have been tested, including benzene and naphthalene ions, which show fragmentation under these drastic conditions. The electronic properties predicted by *Elser* and *Haddon*[20] were confirmed. C_{60} possesses a vanishingly small π-electron ring-current magnetic susceptibility χ, far below that of graphite or benzene, resulting from accidental cancellation of the diamagnetic and paramagnetic contributions to χ.[18, 21] Electrochemical studies showed that C_{60} is a very strong oxidizing agent, comparable to methyl viologen and flavin chromophores, and its first reduction potential ($E^{\circ} = -180$ mV in THF against Ag/AgCl) is at least 1 V more positive than those of most polycyclic aromatic hydrocarbons.[3, 4, 22] This electron-deficient character of C_{60} determines much of the chemistry that is currently being pursued. C_{60} does not react with electrophiles or as a diene in Diels–Alder and other cycloadditions. Rather, it is easily reduced and reacts readily with nucleophilic agents.[23, 24] In an exploratory investigation, *Olah* et al. obtained deep red-brown solutions of diamagnetic polyanions of C_{60} upon reaction with lithium in THF.[23] Subsequent alkylation with methyl iodide led to polymethylated C_{60}; according to mass spectrometric analysis, one or more (all the way up to 24) methyl groups were covalently added to the sphere. *Wudl* et al. observed multiple additions of amine nucleophiles to C_{60} and were able to prepare polyaminated derivatives that are soluble in water.[24] In sharp contrast to rigid aromatic polycycles, C_{60}, upon excitation, exhibits no significant fluorescence or phosphorescence despite a richly structured optical spectrum in the red and violet regions;[25–27] luminescence observed for neat C_{60} films is probably due to solid-state interactions between spheres.[28] Besides being a strong oxidizing agent, C_{60} is a potent sensitizer of singlet oxygen and, therefore, should be handled with caution.[25]

Superconductivity of Alkali-Metal-Doped C_{60}

Recent reports from AT&T Bell Laboratories on the conductivity and superconductivity of C_{60} are breakthrough results with potentially significant technological implications.[29, 30] Today, doped C_{60} is the molecular superconductor with by far the highest onset temperature of superconductivity T_c. It is not difficult to predict in view of extremely rapid developments that the following information might well be outdated when this article is published.

Earlier, the *Wudl* group used C_{60}'s high electron affinity to prepare a crystalline semiconducting (10^{-5}–10^{-7} Scm^{-1}) $Ph_4P^{\oplus}/C_{60}^{\ominus}$ salt by bulk electrolysis.[31] *Haddon* et al. found that C_{60} films doped with alkali-metal vapor become organic metals that exhibit conductivities at ambient temperature comparable to those of *n*-type doped polyacetylene (100 Scm^{-1} for Rb/C_{60} and 500 Scm^{-1} for K/C_{60}).[29] Doping is presumed to occur in the tetrahedral interstices between C_{60} molecules. Soon after, a report from the same laboratory appeared on the superconductivity of potassium-doped C_{60}, both in forms of thin films and polycrystalline powders.[30] The powder samples showed a well-defined, yet small (circa 1%), diamagnetic shielding (Meissner effect) with an onset temperature T_c of 18 K. The C_{60} group at the University of California in Los Angeles (UCLA) subsequently characterized the composition of the stable superconductive phase as K_3C_{60}, and $T_c = 19.3$ K.[32] Controlled sample preparation raised the Meissner effect to above 40% of the perfect diamagnetic shielding, which is a high value for a powder sample. This should probably be regarded as a stoichiometric compound ($K_3^{\oplus}C_{60}^{3\ominus}$) rather than a doped molecular solid. The UCLA group also found that Rb_xC_{60} shows an even higher onset temperature for superconductivity ($T_c = 30$ K); diamagnetic shielding was 7% at the time of manuscript preparation.[32] An onset temperature of $T_c = 28$ K for a Rb-doped C_{60} sample was measured by the Bell Lab group.[33] Theoretical models for the superconductivity of doped fullerenes are already appearing.[34]

The Fullerene and Heterofullerene Family

Buckminsterfullerene (C_{60}) and C_{70}, whose ellipsoidal-cage structure with D_{5h}-symmetry is now firmly supported by a variety of spectroscopic methods,[3, 4–6, 22, 35] are both major, but not the only products that can be isolated from

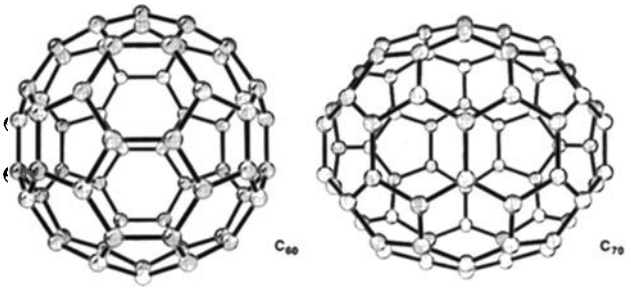

 © VCH Verlagsgesellschaft mbH, W-6940 Weinheim, 1991 0570-0833/91/0606-0679 $ 3.50+.25/0

the toluene-soluble fraction of the fluffy soot produced by resistive heating of graphite. By repeated chromatography on alumina, *Diederich* et al.[36] obtained small quantities of C_{76}, C_{84}, C_{90}, and C_{94}, which, like C_{60} and C_{70}, are members of the same family of hollow-cage all-carbon molecules called the fullerenes.[37] In addition, they also showed that the toluene-insoluble fraction of the soot contains a variety of larger fullerenes in the range between C_{100} and C_{212} that dissolve in boiling 1,2,4-trichlorobenzene.[36, 38] The structures of the higher fullerenes above C_{70} have yet to be determined. The UCLA group also isolated $C_{70}O$, a stable oxide of D_{5h}-C_{70} with the oxygen atom covalently attached to the convex external surface of the ellipsoid.[36] Apparently, this oxide forms from trace oxygen impurities in the helium gas used as the inert atmosphere during the resistive heating process. A recent study by *Smalley* et al. suggests the existence of heterofullerenes, and it should not take long before such compounds are actually isolated.[39] Supersonic beams produced by laser vaporization of a graphite pellet containing boron nitride powder were found to contain heterofullerenes, e.g. $C_{58}B_2$ and $C_{59}B$, in which presumably one or more atoms of the soccerball are replaced by a boron atom. The doped carbon balls are Lewis acidic and readily chemisorb one ammonia molecule per boron atom.

It is obvious from this short account that research on C_{60} and the other fullerenes is about to revolutionize chemistry within a rather short period of time. Since these new materials are readily prepared[3, 22, 40] as well as commercially available,[41] the exploration of their tremendous basic research and technological perspectives is now limited only by the imagination of the individual investigators.[42]

German version: *Angew. Chem. 103* (1991) 695

[1] W. Krätschmer, L. D. Lamb, K. Fostiropoulos, D. R. Huffman, *Nature (London) 347* (1990) 354.

[2] H. W. Kroto, J. R. Heath, S. C. O'Brien, R. F. Curl, R. E. Smalley, *Nature (London) 318* (1985) 162.

[3] J. F. Stoddart, *Angew. Chem. 103* (1991) 71; *Angew. Chem. Int. Ed. Engl. 30* (1991) 70. For a more recent account see: J. S. Miller, *Adv. Mater. 3* (1991) 262.

[4] D. M. Cox, S. Behal, M. Disko, S. M. Gorun, M. Greaney, C. S. Hsu, E. B. Kollin, J. Millar, J. Robbins, W. Robbins, R. D. Sherwood, P. Tindall, *J. Am. Chem. Soc. 113* (1991) 2940.

[5] J. P. Hare, T. J. Dennis, H. W. Kroto, R. Taylor, A. W. Allaf, S. Balm, D. R. M. Walton, *J. Chem. Soc. Chem. Commun. 1991*, 412.

[6] D. S. Bethune, G. Meijer, W. C. Tang, H. J. Rosen, W. G. Golden, H. Seki, C. A. Brown, M. S. de Vries, *Chem. Phys. Lett. 179* (1991) 181.

[7] D. L. Lichtenberger, K. W. Nebesny, C. D. Ray, D. R. Huffmann, L. D. Lamb, *Chem. Phys. Lett. 176* (1991) 203.

[8] R. J. Wilson, G. Meijer, D. S. Bethune, R. D. Johnson, D. D. Chambliss, M. S. de Vries, H. E. Hunziker, H. R. Wendt, *Nature (London) 348* (1990) 621.

[9] J. L. Wragg, J. E. Chamberlain, H. W. White, W. Krätschmer, D. R. Huffman, *Nature (London) 348* (1990) 623.

[10] Y. Z. Li, J. C. Patrin, M. Chandler, J. H. Weaver, L. P. F. Chibante, R. E. Smalley, *Science (Washington D. C.) 252* (1991) 547.

[11] C. S. Yannoni, R. D. Johnson, G. Meijer, D. S. Bethune, J. R. Salem, *J. Phys. Chem. 95* (1991) 9.

[12] R. Tycko, R. C. Haddon, G. Dabbagh, S. H. Glarum, D. C. Douglass, A. M. Mujsce, *J. Phys. Chem. 95* (1991) 518.

[13] J. M. Hawkins, T. A. Lewis, S. D. Loren, A. Meyer, J. R. Heath, Y. Shibato, R. J. Saykally, *J. Org. Chem. 55* (1990) 6250.

[14] J. M. Hawkins, A. Meyer, T. A. Lewis, S. Loren, F. J. Hollander, *Science (Washington D. C.) 252* (1991) 312.

[15] C. S. Yannoni, P. P. Bernier, D. S. Bethune, G. Meijer, J. R. Salem, *J. Am. Chem. Soc. 113* (1991) 3190.

[16] We thank Professor *J. M. Hawkins*, Univ. of California, Berkeley, for providing the picture of the X-ray crystal structure analysis.

[17] R. C. Haddon, L. E. Brus, K. Raghavachari, *Chem. Phys. Lett. 125* (1986) 459.

[18] R. C. Haddon, L. F. Schneemeyer, J. V. Waszczak, S. H. Glarum, R. Tycko, G. Dabbagh, A. R. Kortan, A. J. Muller, A. M. Mujsce, M. J. Rosseinsky, S. M. Zahurak, A. V. Makhija, F. A. Thiel, K. Raghavachari, E. Cockayne, V. Elser, *Nature (London) 350* (1991) 46.

[19] R. D. Beck, P. St. John, M. M. Alvarez, F. Diederich, R. L. Whetten, *J. Phys. Chem.*, in press.

[20] V. Elser, R. C. Haddon, *Nature (London) 325* (1987) 792.

[21] R. S. Ruoff, D. Beach, J. Cuomo, T. McGuire, R. L. Whetten, F. Diederich, *J. Phys. Chem. 95* (1991) 3457.

[22] P. M. Allemand, A. Koch, F. Wudl, Y. Rubin, F. Diederich, M. M. Alvarez, S. J. Anz, R. L. Whetten, *J. Am. Chem. Soc. 113* (1991) 1050.

[23] J. W. Bausch, G. K. Surya Prakash, G. A. Olah, D. S. Tse, D. C. Lorents, Y. K. Bae, R. Malhotra, *J. Am. Chem. Soc. 113* (1991) 3205.

[24] Professor *F. Wudl*, cited in: I. Amato: "Buckyballs, Hairyballs, Dopeyballs", *Science (Washington, D. C.) 252* (1991) 646.

[25] J. W. Arbogast, A. P. Darmanyan, C. S. Foote, Y. Rubin, F. N. Diederich, M. M. Alvarez, S. J. Anz, R. L. Whetten, *J. Phys. Chem. 95* (1991) 11.

[26] R. E. Haufler, L.-S. Wang, L. P. F. Chibante, C. Jin, J. Conceicao, Y. Chai, R. E. Smalley, *Chem. Phys. Lett. 179* (1991) 449.

[27] M. R. Wasielewski, M. P. O'Neil, K. R. Lykke, M. J. Pellin, D. M. Gruen, *J. Am. Chem. Soc. 113* (1991) 2774.

[28] C. Reber, L. Yee, J. McKiernan, J. I. Zink, R. S. Williams, W. M. Tong, D. A. A. Ohlberg, R. L. Whetten, F. Diederich, *J. Phys. Chem.* 95 (1991) 2127.

[29] R. C. Haddon, A. F. Hebard, M. J. Rosseinsky, D. W. Murphy, S. J. Duclos, K. B. Lyons, B. Miller, J. M. Rosamilia, R. M. Fleming, A. R. Kortan, S. H. Glarum, A. V. Makhija, A. J. Muller, R. H. Eick, S. M. Zahurak, R. Tycko, G. Dabbagh, F. A. Thiel, *Nature (London) 350* (1991) 320.

[30] A. F. Hebard, M. J. Rosseinsky, R. C. Haddon, D. W. Murphy, S. H. Glarum, T. T. M. Palstra, A. P. Ramirez, A. R. Kortan, *Nature (London) 350* (1991) 600.

[31] P.-M. Allemand, G. Srdanov, A. Koch, K. Khemani, F. Wudl, Y. Rubin, F. Diederich, M. M. Alvarez, S. J. Anz, R. L. Whetten, *J. Am. Chem. Soc. 113* (1991) 2780.

[32] K. Hoiczer, O. Klein, S.-M. Huang, R. B. Kaner, K.-J. Fu, R. L. Whetten, F. Diederich, *Science (Washington, D. C.) 252* (1991) 1154.

[33] M. J. Rosseinsky, A. P. Ramirez, S. H. Glarum, D. W. Murphy, R. C. Haddon, A. F. Hebard, T. T. M. Palstra, A. R. Kortan, S. M. Zahurak, A. V. Makhija, *Phys. Rev. Lett.* May 27, 1991.

[34] S. Chakravarty, S. Kivelson, *Phys. Rev. Lett.* submitted.

[35] R. D. Johnson, G. Meijer, J. R. Salem, D. S. Bethune, *J. Am. Chem. Soc. 113* (1991) 3619.

[36] F. Diederich, R. Ettl, Y. Rubin, R. L. Whetten, R. Beck, M. Alvarez, S. Anz, D. Sensharma, F. Wudl, K. C. Khemani, A. Koch, *Science (Washington, D. C.) 252* (1991) 548.

[37] H. Kroto, *Pure Appl. Chem. 62* (1990) 407; R. E. Smalley, *Sciences (N.Y.) 31* (1991) No. 2, p. 22.

[38] D. Ben-Amotz, personal communication.

[39] T. Guo, C. Jin, R. E. Smalley, *J. Phys. Chem.*, in press. see also ref. [24].

[40] A simple benchtop reactor for the preparation of fullerenes has been developed: A. Koch, K. C. Khemani, F. Wudl, *J. Org. Chem.*, in press.

[41] Commercial sources of fullerenes: a) Texas Fullerenes Corporation, 2415 Shakespeare, Suite 5, Houston, TX 77030-1038 (Tel. 713-227-9003, FAX 713-686-5139). Crude Soot: 20 $ per gram, 10 $ with University discount. Benzene-soluble extract (mainly C_{60} and C_{70}): 500 $ per gram. Pure C_{60}: 6 $ per milligram. b) Materials and Electrochemical Research (MER) Corporation, 7960 S. Kolb Road, Tucson, AZ 85706 (Tel. 602-574-1980, FAX 602-574-1983). Crude Soot: 80 $ per gram. C_{60}/C_{70} mixture: $ 1250 per gram. c) Research Materials Incorporated, 1667 Cole Blvd., Building 19, Suite 400, Golden, CO 80401 (Tel. 303-238-9369, FAX 303-237-1103). All three companies deliver worldwide.

[42] Editorial note: We have just learnt of some exciting results of a group at the Laboratory for Research on the Structure of Matter, University of Pennsylvania, Philadelphia, PA 19104. In press are the following articles: Fluorinated Fullerenes (H. Selig, C. Lifshitz, T. Peres, J. E. Fischer, A. B. Smith III, A. R. McGhie, W. J. Romanow, J. P. McCauley, Jr., *J. Am. Chem. Soc.*); Orientational Ordering Transition in Solid C_{60} (P. A. Heiney, J. E. Fischer, A. R. McGhie, W. J. Romanow, A. M. Denenstein, J. P. McCauley, Jr., A. B. Smith III, D. E. Cox, *Phys. Rev. Lett.*); Compressibility of Solid C_{60} (J. E. Fischer, P. A. Heiney, A. R. McGhie, W. J. Romanow, A. M. Denenstein, J. P. McCauley, Jr., A. B. Smith III, *Science (Washington, D. C.)*); Structure and Bonding in Alkali-Metal-Doped O_{60} (O. Zhou, J. E. Fischer, N. Coustel, S. Kycin, Q. Zhu, A. R. McGhie, W. J. Romanow, J. P. McCauley Jr., A. B. Smith III, D. E. Cox, *Nature (London)*).

Communications may be submitted in English *or* in German. Further details regarding the submission of communications can be found in the "Notice to Authors" reproduced in the January issue of the journal. Copies thereof may be obtained from the editorial office upon request.

[14]Annulenequinones with Anthraquinone Periphery: "Isopyrenequinone" **

By *Emanuel Vogel,* Lutz Schmalstieg, Peter Henk, Oswald Wilmes, Johann Lex, Rolf Gleiter,** and *Michael Langer*

Anthraquinone **1**, the weakly quinonoid, very stable oxidation product of anthracene is the parent compound of many industrially important carbonyl dyes and pigments.[1] The significance of **1** in dye chemistry aroused our interest in the [14]annulenequinones *syn*- and *anti*-bishomoanthraquinone **2** and **3**, respectively, *syn*-1,6:8,13-ethanediylidene[14]annulene-7,14-dione **4**, and "isopyrenequinone" (azuleno[2,1,8-*ija*]azulene-5,10-dione) **5** (Scheme 1), which are structurally closely related to **1** through the anthraquinone periphery, yet, in part, differ considerably from it with regard to the π-electron system.

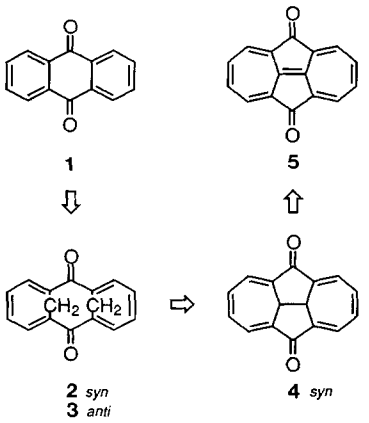

Scheme 1. Conceptual interrelationship of **1** and [14]annulenequinones **2**–**5**.

After having been able to synthesize **2** and **3**, and to demonstrate in the case of **2** that its redox behavior is comparable with that of **1**,[2] we can now also report the successful preparation of **5**, the availability of which concomitantly opens an entry to **4**.

A chance to obtain **5** was provided by the oxidation of isopyrene (azuleno[2,1,8-*ija*]azulene) **6**, modeled on the anthracene–anthraquinone conversion.[1] This nonbenzenoid (and non-alternating) aromatic hydrocarbon can be described as a resonance hybrid in which, according to spectroscopic and structural data, the resonance structure **6** has special weight.[3] Isopyrene may therefore be considered, to a first approximation, as a bridged [14]annulene with a central C=C unit as a perturbation. As already demonstrated, the highest occupied orbital (HOMO) of **6** shows significant orbital coefficients only at C-5, C-10, C-10b, and C-10c, so that electrophiles should attack the hydrocarbon preferentially at these positions.

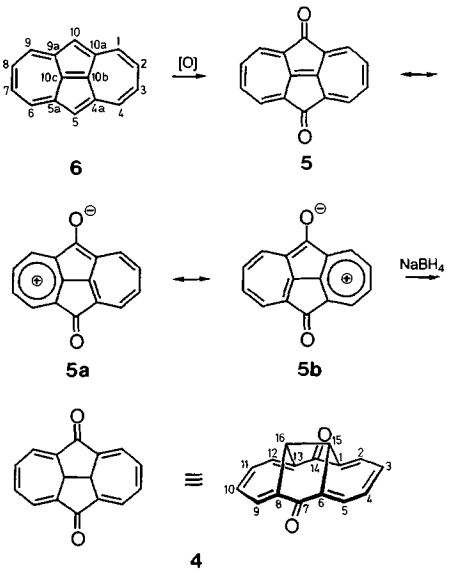

Consistent with predictions based on the HOMO orbital coefficients, the relatively reactive **6** can be converted with a series of oxidizing agents into the desired isopyrenequinone **5** (5-/10-attack) and/or into 1,6:8,13-ethanediylidene[14]annulene derivatives (oxidative addition at the C-10b–C-10c bond),[4] whereby it depends on the oxidizing agent and conditions whether only one or both reaction routes are followed. According to observations made so far, **5** is best

Table 1. Selected physical data of **4** and **5**.

4: ^{1}H NMR (300 MHz, $CDCl_3$): $\delta = 4.06$ (s, 2H, H-15,16), 6.85 and 7.04 (AA'BB', 8H, H-3,4,10,11 and H-2,5,9,12, $^3J_{2,3} = 6.3$, $^4J_{2,4} = 0.7$, $^5J_{2,5} = 0.5$, $^3J_{3,4} = 11.3$ Hz); ^{13}C NMR (75.5 MHz, $CDCl_3$): $\delta = 39.57$, 127.27, 135.13, 136.68, 189.38; MS (70 eV): *m/z* 234 ($M^{\oplus}$, 8%), 206 (25), 178 (100); IR (CsI): $\tilde{\nu} = 1679\ cm^{-1}$ (C=O); UV/VIS (dioxane): λ_{max} [nm] (ε) = 222 (10500), 262 (1800), 304 (30400), 345 (9400), 464 (600), 626 (60)

5: ^{1}H NMR (300 MHz, $CDCl_3$): $\delta = 7.60$ and 8.12 (AA'BB', 8H, H-2,3,7,8 and H-1,4,6,9, $^3J_{1,2} = 10.8$, $^4J_{1,3} = 0.5$, $^5J_{1,4} = 1.2$, $^3J_{2,3} = 9.4$ Hz); ^{13}C NMR (75.5 MHz, $CDCl_3$): $\delta = 131.88$, 135.54, 136.87, 158.37, 180.05; MS (70 eV): *m/z* 232 ($M^{\oplus}$, 72%), 204 (12), 176 (100); IR (CsI): $\tilde{\nu} = 1641$, 1590, 1551 cm^{-1} (C=O and C=C); UV/VIS (CH_2Cl_2): λ_{max} [nm] (ε) = 240 (37000), 269 (5900), 359 (30000), 387 (11000), 410 (19500), 570 (8500), 620 (52000); ^{1}H NMR (300 MHz, CD_2Cl_2/CF_3COOH): $\delta = 8.35$ and 8.66 (AA'BB', 8H, H-2,3,7,8 and H-1,4,6,9, $^3J_{1,2} = 10.7$, $^4J_{1,3} = 0.5$, $^5J_{1,4} = 1.0$, $^3J_{2,3} = 9.5$ Hz); ^{13}C NMR (75.5 MHz, CD_2Cl_2/CF_3COOH): $\delta = 132.85$, 136.99, 141.94, 157.38, 174.46; UV/VIS (96% H_2SO_4): λ_{max} [nm] (ε) = 247 (35000), 261 (38000), 382 (18300), 515 (11200), 557 (33000)

[*] Prof. Dr. E. Vogel, Dr. L. Schmalstieg, Dr. P. Henk, Dr. O. Wilmes, Dr. J. Lex
Institut für Organische Chemie der Universität
Greinstrasse 4, W-5000 Köln 41 (FRG)
Prof. Dr. R. Gleiter, Dr. M. Langer
Institut für Organische Chemie der Universität
Im Neuenheimer Feld 270, W-6900 Heidelberg (FRG)

[**] This work was supported by the Minister für Wissenschaft und Forschung des Landes Nordrhein-Westfalen (FRG).

accessible when *m*-chloroperbenzoic acid (MCPBA) is used as oxidizing agent[5] and the reaction is carried out as follows: a solution of isopyrene **6** (100 mg, 0.5 mmol) in ether (50 mL) is treated with a solution of eight equivalents of MCPBA in 20 mL of ether at 0° C in the presence of sodium hydrogen carbonate as buffer (840 mg).[6] The reaction mixture is stirred for 90 min at this temperature and then transferred to a silica gel column[7] and the oxidation products chromatographed with dichloromethane/ethyl acetate (1:1) as eluent. Two fractions are obtained, first a brown one and then an intensely blue one,[8] the latter of which contains the desired isopyrenequinone **5**. After threefold crystallization from dichloromethane/ether (1:2), compound **5** precipitates in the form of black-violet needles with a copperlike luster [no decomposition up to 300 °C, yield 20%].

Isopyrenequinone **5** was characterized by NMR, IR, UV/VIS and mass spectra (Table 1), X-ray structure analysis, and cyclic voltammetry. The ^{1}H-NMR spectrum, which shows only the signals of two equivalent AA'BB' systems at $\delta = 8.12$ (H-1,4,6,9) and 7.60 (H-2,3,7,8) with $^3J_{1,2} = 10.8$, $^3J_{2,3} = 9.4$, $^4J_{1,3} = 0.5$ and $^5J_{1,4} = 1.2$ Hz, is indeed consistent with the assumed D_{2h} symmetry of the compound, but the chemical shifts and the vicinal coupling constants are not reconcilable with a heptafulvenoid molecule as formulated in **5**. If the bonding situation in the isopyrenequinone were comparable with that in a heptafulvalene[9] then the ^{1}H-NMR signals would have to appear at noticeably higher field, despite the presence of the carbonyl groups, whereas for the vicinal coupling constants one should expect—judging from the situation in heptafulvalene reference compounds[10]—a strong alternation in the sense of $^3J_{2,3} > {}^3J_{1,2}$. As a matter of fact, however, it is observed in the case of **5** that $^3J_{1,2}$ is even somewhat greater than $^3J_{2,3}$. The measured ^{1}H-NMR parameters become understandable if isopyrenequinone is regarded as a resonance hybrid in which the polar tropylium resonance structures **5a** and **5b** make a relatively high contribution.

The description of **5** as a resonance hybrid with contributing tropylium resonance structures **5a** and **5b**, as suggested by the ^{1}H-NMR spectrum, finds support in the outcome of the X-ray structure analysis[11] (Fig. 1). In the crystal, the molecule is almost planar (maximum deviation from the mean plane: 0.027 Å) and has, within the limit of error, D_{2h} symmetry. Convincing arguments in favor of **5a**/**5b** as resonance structures are provided mainly by the following observations: 1) the C–C bond lengths in the perimeter segments C-10a, C-1 to C-4, C-4a and C-5a, C-6 to C-9, C-9a lie approximately within the range of lengths found in aromatic C–C bonds. Their alternation, which is the inverse of that which was established for the corresponding bond lengths in **2** and **4**, could be largely due to strain effects; 2) the central C–C bond (1.441 Å) has approximately the character of an sp^2–sp^2 single bond, as required for a partial bond equalization in the seven-membered ring moieties. Since the length of the central C–C bond in **6** is only 1.354 Å,[3c] the latter finding is particularly informative.

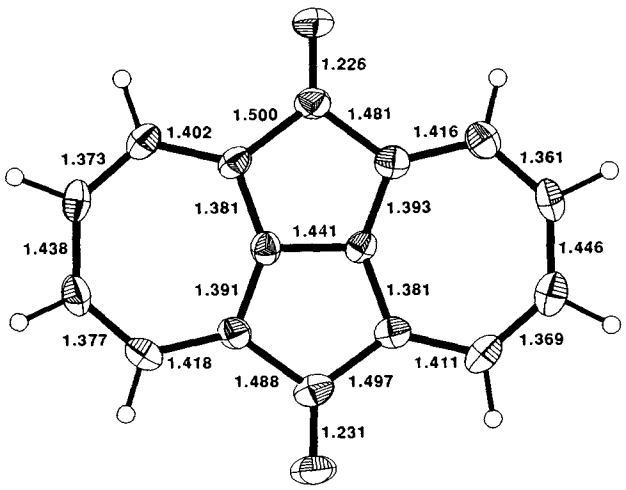

Fig. 1. Structure of **5** in the crystal. Bond lengths [Å]; standard deviation ca. 0.006 Å. Vibration ellipsoids drawn at the 40% probability level.

The troponoid nature of **5** implicated by the tropylium resonance structures manifests itself chemically in that the compound is relatively strongly basic and, analogously to tropone,[12] forms a stable monohydroperchlorate upon reaction with perchloric acid in dichloromethane. This salt, which is isolable in crystalline form [reddish-violet needles (from dichloromethane); no decomposition up to 300 °C], apparently undergoes a rapid proton exchange in solution, since its ^{1}H-NMR spectrum has the same form as that of **5** (two equivalent AA'BB' systems), but all signals are shifted downfield by $\Delta\delta \approx 0.5$. The UV/VIS spectrum of **5** in 96% sulfuric acid resembles that of the hydrocarbon **6** in the same solvent, for which a monoprotonation in the 5-/10-position is confirmed NMR spectroscopically under these conditions.[13]

5 is readily reduced to 5,10-diacetoxy-azuleno[2,1,8-*ija*]-azulene [brownish-black needles (dichloromethane/hexane); slow decomposition above 180 °C; yield 50%] upon reaction with zinc/acetic anhydride in pyridine.

Cyclovoltammetric measurements carried out on **5** showed that the dicarbonyl compound, as is typical for quinones, can be reduced in two reversible one-electron transitions via the semiquinone radical anion to the dianion. Information about the corresponding reduction potentials, including those of *p*-benzoquinone, **1**, **2**, and **4**, is given in Table 2.

Table 2. Comparison of experimentally determined reduction potentials of *p*-benzoquinone, **1**, **2**, **4**, and **5** [a].

Compound	E_1 [V]	E_2 [V]	$E_2 - E_1$ [V]	$E_1 + E_2$ [V]	ε(LUMO) [eV]	J_{LUMO} [eV]	Ref.
p-benzoquinone	−0.23	−1.15	−0.92	−1.38	−1.03	6.23	[2]
1	−0.64	−1.39	−0.75	−2.03	−0.62	5.05	[2]
2	−0.78	−1.01	−0.23	−1.79	−0.48	4.56	[2]
4	−0.32	−0.72	−0.40	−1.04	−0.95	4.65	
5	−0.46	−0.94	−0.48	−1.40	−0.76	4.40	

[a] Measuring conditions: dimethylformamide (DMF) as solvent, in the case of **5** dichloromethane, with 0.1 M nBu$_4$NPF$_6$ under argon. Glassy carbon working electrode, Ag/AgCl reference electrode (**5**: calomel electrode) and Pt as counter electrode. Scan rate 15 mVs^{-1}. Oxidation potential for ferrocene $E_{1/2}$ = 0.705 V in DMF, 0.455 V under the conditions as for **5**.

In the case of **4** and **5** the first reduction potential is significantly less negative than in the case of **1** and **2**. Also, the dianion is formed more readily in the case of **4** and **5** than in the case of the reference compounds. It can be concluded from Table 2 that the E_1 values of the quinones correlate with the energies of the LUMOS calculated by the MINDO/3 method. That the difference between E_1 and E_2 observed in the case of **2**–**5** is smaller than in the case of **1** could, in the first instance, be due to a reduced coulomb interaction of the electrons in the LUMO (cf. J_{LUMO} in Table 2).[14] This can be explained in terms of an increased π/σ interaction in the case

of **2** and **4**,[2] and in terms of an increased conjugative interaction between the hydrocarbon framework and the CO groups (**5a**/**5b**) in the case of **5**.

Among the chemical reactions of **5**, that which deserves special attention, aside from the protonation and reductive acetylation already mentioned, is its reduction with sodium borohydride in methanol/dichloromethane. The reaction product formed thereby—formally with saturation of the central C=C bond—is the 10b,10c-dihydro compound, the no longer planar *syn*-1,6:8,13-ethanediylidene[14]annulene-7,14-dione **4** [red rhombs (from acetone/hexane); slow decomposition above 165 °C; yield 20%]; when dissolved in concentrated sulfuric acid, **4** is re-oxidized by atmospheric oxygen to **5**. If one assumes a relatively high contribution of the tropylium resonance structures to **5**, then the initial step of the observed hydrogenation might be interpreted as a nucleophilic addition of a hydride ion at C-10b (or C-10c).[15] Proof of the structure of **4** is based not only on the spectra (Table 1) and their analogy to those of **2**, but also on an independent synthesis of this new [14]annulenequinone, which, together with the structure and electrochemical investigations on **4**, will be reported upon in a separate communication.[16]

Received: September 27, 1990 [Z 4208 IE]
German version: *Angew. Chem. 103* (1991) 699

CAS Registry numbers:
4, 133228-91-8; **5**, 109324-40-5; **5**·$HClO_4$, 133228-90-7; **6**, 3526-04-3; 16-*m*-chlorobenzoyloxy-15-hydroxy-1,6:8,13-ethanediylidene[14]annulene, 133228-87-2; azuleno[2,1,8-*ija*]azulene-3,5-dione, 133228-88-3; azuleno[2,1,8-*ija*]azulene-1,5-dione, 133228-89-4; 5,10-diacetoxyazuleno[2,1,8-*ija*]azulene, 133228-92-9.

[1] O. Bayer, *Methoden Org. Chem. Houben-Weyl (4th Ed.) Vol. 7/3c, 1979*; S. Patai (Ed.): *The Chemistry of the Quinonoid Compounds, Part 1/2*, Wiley, London 1974; S. Patai (Ed.): *The Chemistry of the Quinonoid Compounds, Part 1/2*, Wiley, London 1988; H. Zollinger: *Color Chemistry*, VCH, Weinheim 1987.

[2] E. Vogel, S. Böhm, A. Hedwig, B. O. Hergarten, J. Lex, J. Uschmann, R. Gleiter, *Angew. Chem. 98* (1986) 1001; *Angew. Chem. Int. Ed. Engl. 25* (1986) 1000.

[3] a) Synthesis: H. Reel, E. Vogel, *Angew. Chem. 84* (1972) 1064; *Angew. Chem. Int. Ed. Engl. 11* (1972) 1013; E. Vogel, H. Wieland, L. Schmalstieg, J. Lex, *ibid. 96* (1984) 717 and *23* (1984) 717; see also K. Fujimori, N. Morita, M. Yasunami, T. Asao, K. Takase, *Tetrahedron Lett. 24* (1983) 781; b) spectroscopy: K. Müllen, H. Reel, *Helv. Chem. Acta 56* (1973) 363; J. Kolc, J. Michl, E. Vogel, *J. Am. Chem. Soc. 98* (1976) 3935; C. Batich, E. Heilbronner, E. Vogel, *Helv. Chim. Acta 57* (1974) 2288; c) molecular structure see [3a], second citation.

[4] E. Vogel, L. Schmalstieg, H.-J. Weyer, R. Gleiter, *Chem. Lett. 1987*, 33.

[5] For the electrophilic hydroxylation of arenes with peracids (examples for subsequent oxidation to quinones) see R. Taylor: *Electrophilic Aromatic Substitutions*, Wiley, Chichester, England 1990, p. 327.

[6] The commercially available 80–85% MCPBA used was washed with a phosphate buffer (pH 7) before the reaction. After drying to constant weight in an oil-pump vacuum the peracid content was 97–99%. See also N. N. Schwartz, J. H. Blumbergs, *J. Org. Chem. 29* (1964) 1976.

[7] An aqueous work-up is to be avoided, since this leads to considerable loss in yield in the case of **5**.

[8] The following by-products can be isolated from the brown fraction after washing with saturated sodium hydrogen carbonate solution and repeated chromatography on silica gel: 1) 16-*m*-chlorobenzoyloxy-15-hydroxy-1,6:8,13-ethanediylidene[14]annulene [orange colored prisms (from dichloromethane/ether); m.p. 160–163 °C (decomp.); yield 2%], 2) azuleno[2,1,8-*ija*]azulene-3,5-dione [black needles (from dichloromethane/pentane); decomposition above 180 °C; yield 1%], 3) azuleno[2,1,8-*ija*]azulene-1,5-dione [black needles (from dichloromethane/pentane); decomposition above 200 °C; yield 5%].

[9] W. M. Jones, C. L. Ennis, *J. Am. Chem. Soc. 91* (1969) 6391; R. Thomas, P. Coppens, *Acta Crystallogr. Sect. B28* (1972) 1800.

[10] E. Vogel, B. Neumann, W. Klug, H. Schmickler, J. Lex, *Angew. Chem. 97* (1985) 1044; *Angew. Chem. Int. Ed. Engl. 24* (1985) 1046.

[11] **5**: $C_{16}H_8O_2$, no decomposition up to 300 °C, crystals from dichloromethane, orthorhombic, space group $P2_12_12_1$, $Z = 4$, $a = 3.854(1)$, $b = 13.338(3)$, $c = 20.015(5)$ Å, $\varrho_{calcd} = 1.499\ g\,cm^{-3}$, intensity measurements on an Enraf-Nonius CAD-4 four-circle diffractometer [room temperature, $\lambda_{Mo} = 0.71069$ Å, θ_{Mo} (max) = 27°]; refinement (C,O anisotropic, H isotropic) taking into consideration 627 reflections with $F_o > 4\sigma(F_o)$; $R = 0.042$; $R_w = 0.042$. Further details of the crystal structure investigation are available on request from the Fachinformationszentrum Karlsruhe, Gesellschaft für wissenschaftlich-technische Information mbH, W-7514 Eggenstein-Leopoldshafen 2 (FRG), on quoting the depository number CSD-55355, the names of the authors, and the journal citation.

[12] K. M. Harmon, A. B. Harmon, T. T. Coburn, J. M. Fisk, *J. Org. Chem. 33* (1968) 2567.

[13] L. Schmalstieg, *Dissertation*, Universität Köln 1987.

[14] P. Carsky, S. Hünig, D. Scheutzow, R. Zahradnik, *Tetrahedron 25* (1969) 4781.

[15] Examples of the hydrogenation of C=C double bonds in Michael systems with complex hydrides are to be found in E. Schenker, *Angew. Chem. 73* (1961) 81; H. C. Brown, S. Krishnamurthy, *Tetrahedron 35* (1979) 567.

[16] The marked difference in the redox behavior of **2** and **4**—as a result of a strongly planarized perimeter in the case of **4**—should already be pointed out here.

σ-Homoacenaphthylene and π-Homoacenaphthene **

By *Roland Arnz, José Walkimar de M. Carneiro, Wolfgang Klug, Hans Schmickler, Emanuel Vogel,* Rolf Breuckmann,* and *Frank-Gerrit Klärner**

Dedicated to Professor Wolfgang R. Roth on the occasion of his 60th birthday

More than 25 years ago, in the course of our studies concerning the cycloheptatriene-norcaradiene structural problem, we discovered the 10π-electron Hückel system 1,6-methano[10]annulene **1**.[1] Since then almost the entire armory of physical instrumentation available to the organic chemist has been mobilized[2] to gain closer insight into the subtle bonding situation in this hydrocarbon, which can be regarded as an aromatic homologue of benzene. Spectroscopic and structural findings reinforce the assumption, based on model considerations, that homoconjugation across the carbon atoms 1 and 6 contributes significantly to the electronic stability of the molecule.[2e] Consequently, there is a certain justification for **1** being alternatively termed "π-homonaphthalene".[3]

1 **2**

According to ab initio calculations,[4] as regards free energy **1** is favored over its olefinic "bisnorcaradiene" valence tautomer **2** by only 4.5 kcal mol^{-1} [4a]—a value which closely corresponds to that for the tautomerism cycloheptatriene ⇄ norcaradiene.[5] The hereby aroused expectation

[*] Prof. Dr. E. Vogel, Dr. R. Arnz, J. W. de M. Carneiro, Dr. W. Klug, Dr. H. Schmickler
Institut für Organische Chemie der Universität
Greinstrasse 4, W-5000 Köln 41 (FRG)
Prof. Dr. F.-G. Klärner, R. Breuckmann
Fakultät für Chemie der Universität
Postfach 102148, W-4630 Bochum 1 (FRG)

[**] This work was supported by the Minister für Wissenschaft und Forschung des Landes Nordrhein-Westfalen (FRG). *J. W. de M. Carneiro* thanks the Brazilian Government for a Conselho Nacional de Desenvolvimento Cientifico e Tecnologico grant (CNPq).

that the postulated arene-olefin equilibrium $\mathbf{1} \rightleftarrows \mathbf{2}$[6] responds to acceptor substituents on the methylene carbon atom[7] in the same way as the cycloheptatriene–norcaradiene equilibrium could be impressively demonstrated a few years ago: 1,6-methano[10]annulene-11,11-dicarbonitrile[8] exists, analogously to cycloheptatriene-7,7-dicarbonitrile,[9] exclusively as norcaradiene valence tautomer (>99%).

With the intention of exploring the limits of existence of 1,6-methano[10]annulenes, in the present study we examined what influence a *peri*-CH_2–CH_2 or *peri*-CH=CH bridge has on the equilibrium $\mathbf{1} \rightleftarrows \mathbf{2}$. Force field calculations (MM2 ERW)[10] revealed that a *peri*-CH_2–CH_2 bridge has virtually no effect on the enthalpy difference between 1,6-methano[10]annulene and norcaradiene valence tautomer, while a *peri*-CH=CH bridge alters this energy difference by no less than 10 kcal mol^{-1} in the sense of a stabilization of the norcaradiene valence tautomer. Unlike a *peri*-CH_2–CH_2 bridge, a *peri*-CH=CH bridge should therefore shift the equilibrium far on the side of the norcaradiene form.

Consistent with these calculations we now established that 2,10-etheno-1,6-methano[10]annulene **8** mainly exists as the norcaradiene valence tautomer **9**—here referred to as "σ-homoacenaphthylene"; 2,10-ethano-1,6-methano[10]annulene **10**, on the other hand, is present practically only as such ("π-homoacenaphthene"), with total exclusion of **11**.

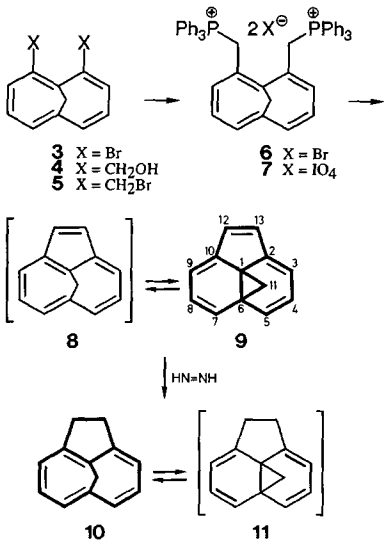

8 9 10 11

Scheme 1. **3** → **4**: *n*BuLi/hexane, ether, −40°C → −10°C, then CH_2O, 1 h reflux, 70%; **4** → **5**: PBr_3/benzene, 0°C, then 65°C, 1 h, 75%; **5** → **6**: PPh_3, dimethylformamide (DMF), 3 h, 100°C, 95%; **6** → **7**: $NaIO_4$, H_2O, 10°C, 80%; **7** → **8**/**9**: $NaNH_2/NH_3$, −40°C, then 3 h NH_3 reflux, 41%. Important physical data of **4**–**7**, **9** and **10** are collected in Table 2.

Of the conceivable entries to **8**/**9**, the periodate oxidation of the resonance-stabilized diylide derived from the diphosphonium salt **6**, which is modeled after the Bestmann acenaphthylene synthesis,[11] seemed most promising, since the reaction conditions largely allow for the presumed thermal instability of the product (tendency to undergo the norcaradiene "walk"-rearrangement). Starting from the readily available 2,10-dibromo-1,6-methano[10]annulene **3**,[12] the diphosphonium bromide **6** can be obtained in a conventional way via the 2,10-bis(hydroxymethyl)-1,6-methano[10]annulene **4** and the corresponding dibromide **5** as isolated intermediates. When **6**, dissolved in hot water, was added to a cold saturated aqueous solution of sodium periodate the diperiodate **7** immediately separated as a yellow microcrystalline compound. In order to bring about intramolecular C=C bond formation leading to **8**/**9**, the diperiodate **7** was treated with sodamide in liquid ammonia under the conditions as described for similar cases.[11] After addition of pentane to the reaction mixture, the product was worked up in the usual way at 0°C and finally distilled in a high vacuum (4×10^{-5} torr, bath temperature 0°C, trap cooled to −78°C). **8**/**9** separated as an orange-yellow crystalline solid (m.p. ≈ 5°C, yield 41%).

The position of the equilibrium between **8** and **9** as well as between **10** and **11** (see later) follows from NMR spectroscopic comparisons, in which, aside from **1**, the compounds 2,10-propano-1,6-methano[10]annulene **12**[13] and tricyclo[4.3.1.0^{1,6}]deca-2,4-diene **13**[14] serve as reference compounds for the [10]annulene- and norcaradiene-valence tautomers.

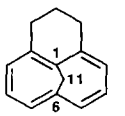

12

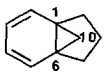

13

The exclusive presence of **9** was already indicated by the ^{1}H-NMR spectrum, since the signals of the vinylic protons H-3 to H-5 and H-7 to H-9 appear at relatively high field [$\Delta\delta$ = 1.2 (mean value), with respect to **12**] and the vicinal coupling constants $^3J_{3,4}$ and $^3J_{4,5}$ correlate perfectly with the corresponding couplings in cyclohexa-1,3-dienes. The presence of **9** is even more convincingly demonstrated by the ^{13}C-NMR spectrum (Fig. 1), which, from experience, responds particularly sensitively to a σ/π bond change in valence tautomers. It is found that **9** not only compares very well with **13** regarding the position of the C1 and C6 signals, but also shows a ^{13}C-^{1}H coupling constant for C11 which is typical for cyclopropane C-atoms (160–170 Hz) (Table 1).

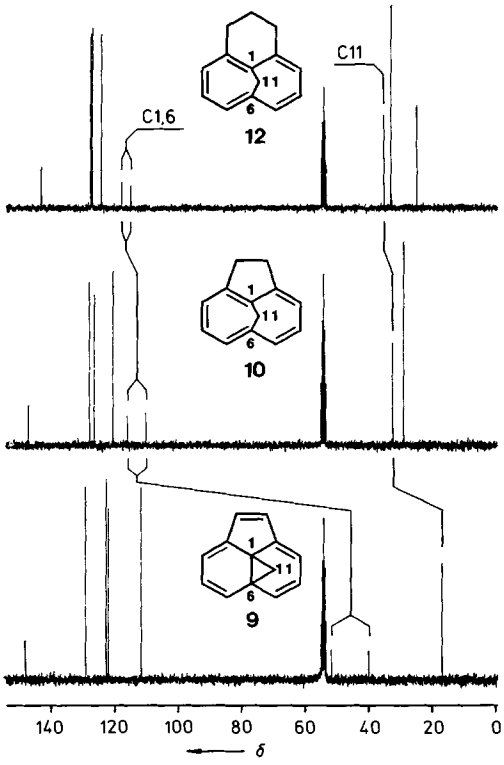

Fig. 1. ^{13}C-NMR spectra of **12**, **10**, and **9** (75.5 MHz, CD_2Cl_2).

Table 1. Selected ^{13}C-NMR data of **12**, **10**, **9** (75.5 MHz, CD_2Cl_2) and **13** [14] (22.6 MHz, CCl_4, $CDCl_3$); couplings in Hz.

	12	**10**	**9**	**13**
δ(C1) [a]	117.17	115.41	51.14	37.70
δ(C6) [a]	114.32	109.53	39.58	
δ(C11)	34.50	31.85	16.71	15.40 [b]
^1J(C11, H)	141.5	146.2	167.3	161.0 [b]

[a] Assignment not certain. [b] For C10.

Upon reaction with diimine, generated from the potassium salt of the azodicarboxylic acid with acetic acid in dichloromethane, σ-homoacenaphthylene **9** is selectively hydrogenated to the 12,13-dihydro compound, which, after chromatography on silica gel is obtained in the form of yellow crystals [m.p. 38°C (from methanol); yield 30%]. Interestingly, the product proved to be almost exclusively π-homoacenaphthene **10**, which means that the hydrogenation of **9** entails saturation of the *peri* double bond with a complete reversal of the bisnorcaradiene–1,6-methano[10]annulene equilibrium. The drastic shift of the equilibrium is evident from characteristic changes in the ^{1}H-NMR spectrum, particularly in the downfield shift of the signals of H-3,4,5,7,8,9 by $\Delta\delta = 0.88$ (mean value) and the approximate equalization of $^3J_{3,4}$ and $^3J_{4,5}$, but manifests itself most impressively in the ^{13}C-NMR spectra of the two compounds (Table 1). As can be seen from Figure 1, the signals of C1,6 and C11 are shifted downfield so much in the transition from **9** to **10**, that they now almost coincide with the corresponding signals of **12**, which can be regarded as the optimal [10]annulene reference compound for **10**.

The difference between **9** and **10** regarding type of structure[15] is also reflected in the chemical behavior of the two compounds, particularly in their tendency to undergo the norcaradiene walk rearrangement upon thermolysis.[16] The walk rearrangement of **9**, initiated by the homolytic cleavage of the cyclopropane bond C6–C11,[17] already takes place at 120°C [$\Delta G^{\neq}$ (determined ^{1}H-NMR spectroscopically) = 33.0 kcal mol^{-1} in benzene], whereas the corresponding isomerization of **10** requires temperatures around 250°C [$E_A = 41.7 \pm 0.5$ kcal mol^{-1}, lg$A = 14.3 \pm 0.2$ (gas phase)]. An increase in the activation barrier of the rearrangement in the case of **10** is consistent with expectation, since here the migration of the CH_2 bridge is preceded by the endothermal formation of the bisnorcaradiene **11**.[18]

Received: September 27, 1990 [Z 4209 IE]
German version: *Angew. Chem. 103* (1991) 702

Table 2. Selected physical data of **4**–**7**, **9**, **10** and **12**.

4 [19]: m.p. 128–129°C (from methanol); ^{1}H NMR (300 MHz, $CDCl_3$): $\delta = 7.47$ (d, 2H, $J = 8.7$ Hz), 7.19 (d, 2H, $J = 9.4$ Hz), 7.09 (dd, 2H), 4.98 (d, 2H, $J = 13.3$ Hz), 4.86 (d, 2H), 4.82 (s, 2H), −0.60 (s, 2H); IR (KBr): $\tilde{\nu}$ = 3212, 3042, 2948, 1209, 1183, 1099, 1058, 1014, 961, 785 cm^{-1}; UV/VIS (CH_3OH): λ_{max} [nm] (ε) = 262 (65400), 311 (8100), 377 (220)

5: m.p. 121°C (from benzene); ^{1}H NMR (300 MHz, $CDCl_3$): $\delta = 7.48$ (d, 2H, $J = 8.9$ Hz), 7.35 (d, 2H, $J = 9.5$ Hz), 7.18 (dd, 2H), 5.12 (d, 2H, $J = 11.0$ Hz), 5.08 (d, 2H), −0.56 (s, 2H); IR (KBr): $\tilde{\nu}$ = 3044, 2952, 1465, 1447, 1333, 1284, 1221, 1199, 1138, 782 cm^{-1}; UV/VIS (CH_3OH): λ_{max} [nm] (ε) = 262 (61200), 312 (7600), 376 (210)

6: m.p. 163–165°C (from water); ^{1}H NMR (300 MHz, CD_2Cl_2): $\delta = 7.71$ (m, 18H), 7.60 (m, 12H), 7.26 (d, 2H, $J = 7.3$ Hz), 6.85 (d, 2H, $J = 9.6$ Hz), 6.73 (dd, 2H), 5.74 (dd, 2H, J(H,H) = 16.0, J(P,H) = 16.4 Hz), 5.68 (dd, 2H), −0.97 (s, 2H); IR (KBr): $\tilde{\nu}$ = 3040, 1613, 1586, 1438, 1110, 995, 794, 743, 727, 689 cm^{-1}; UV/VIS (CH_2Cl_2): λ_{max} [nm] (ε) = 228 (54200), 270 (35000), 329 (7800)

7: m.p. 109°C (decomp.); ^{1}H NMR (300 MHz, CD_2Cl_2): $\delta = 7.77$ (m, 6H), 7.57 (m, 24H), 7.31 (d, 2H, $J = 7.5$ Hz), 6.78 (d, 2H, $J = 9.6$ Hz), 6.74 (dd, 2H), 5.32 (dd, 2H, J(H,H) = 16.0, J(P,H) = 16.4 Hz), 5.21 (dd, 2H), −0.91 (s, 2H); IR (KBr): $\tilde{\nu}$ = 3049, 1584, 1481, 1436, 1107, 994, 841, 739, 725, 685 cm^{-1}; UV/VIS (CH_2Cl_2): λ_{max} [nm] (ε) = 228 (65900), 270 (37100), 329 (8600)

9: m.p. ≈ 5°C; ^{1}H NMR (300 MHz, CD_2Cl_2): $\delta = 6.29$ (s, 2H, $J = 5.1$ Hz), 6.00 (dd, 2H), 5.99 (d, 2H, $J = 9.2$ Hz), 5.79 (d, 2H, $J = 6.0$ Hz), 0.94 (s, 2H); ^{13}C NMR (75.5 MHz, CD_2Cl_2): $\delta = 147.73$, 128.92, 122.46, 121.76, 111.42, 51.14, 39.58, 16.71 (J(C11, H) = 167.3 Hz); MS (70 eV): m/z 166 ($M^{\oplus}$, 40%), 165 ($M^{\oplus}$ − H, 100%); UV/VIS (pentane): λ_{max} [nm] (ε) = 273 (7250), 332 (710) sh, 406 (1260) (extinctions with an error of ca. 15%)

10: m.p. 38°C (from methanol); ^{1}H NMR (300 MHz, CD_2Cl_2): $\delta = 7.00$ (d, 2H, $J = 9.4$ Hz), 6.83 (dd, 2H), 6.58 (d, 2H, $J = 8.7$ Hz), 3.40 (m, 2H), 2.75 (m, 2H), 0.36 (s, 2H); ^{13}C NMR (75.5 MHz, CD_2Cl_2): δ = 146.74, 127.39, 125.83, 119.94, 115.41, 109.53, 31.85 (J (C11, H) = 146.2 Hz), 28.38; MS (70 eV): m/z 168 ($M^{\oplus}$, 57%), 167 ($M^{\oplus}$ − H, 61%), 153 ($M^{\oplus}$ − CH_2−H, 100%); IR (film): $\tilde{\nu}$ = 3037, 2934, 2848, 1509, 1436, 1226, 894, 860, 765 cm^{-1}; UV/VIS (cyclohexane): λ_{max} [nm] (ε) = 255 (30200), 310 (5250), 390 (620)

12: m.p. 40–41°C (from methanol); ^{1}H NMR (300 MHz, CD_2Cl_2): $\delta = 7.28$ (d, 2H, $J = 8.9$ Hz), 7.00 (dd, 2H), 6.91 (d, 2H, $J = 9.0$ Hz), 3.25 (m, 2H), 2.45 (m, 2H), 2.34 (m, 1H), 2.12 (m, 1H), −0.42 (s, 2H); ^{13}C NMR (75.5 MHz, CD_2Cl_2): δ = 142.69, 126.96, 126.49, 123.61, 117.17, 114.32, 34.50 (J (C11, H) = 141.5 Hz), 32.34, 24.20; MS (70 eV): m/z 182 ($M^{\oplus}$, 42%), 167 ($M^{\oplus}$ − CH_2−H, 100%), 152 ($M^{\oplus}$ − $2CH_2$−2H, 53%); IR (film): $\tilde{\nu}$ = 3037, 2941, 2826, 1447, 1423, 1412, 1248, 867, 774 cm^{-1}; UV/VIS (cyclohexane): λ_{max} [nm] (ε) = 258 (56800), 313 (6600), 393 (428) sh, 398 (450), 410 (328) sh

[1] E. Vogel, H. D. Roth, *Angew. Chem. 76* (1964) 145; *Angew. Chem. Int. Ed. Engl. 3* (1964) 228; E. Vogel, *Spec. Publ. Chem. Soc. 21* (1967) 113; *Pure Appl. Chem. 20* (1969) 237.

[2] a) X-ray structure analyses: M. Dobler, J. D. Dunitz, *Helv. Chim. Acta 48* (1965) 1429; R. Bianchi, T. Pilati, M. Simonetta, *Acta Crystallogr. Sect. B36* (1980) 3146; T. Pilati, M. Simonetta, *ibid. B32* (1976) 1912; b) ^{1}H-NMR: H. Günther, *Z. Naturforsch. B20b* (1965) 948; c) ^{13}C NMR: H. Günther, H. Schmickler, H. Königshofen, K. Recker, E. Vogel, *Angew. Chem. 85* (1973) 261; *Angew. Chem. Int. Ed. Engl. 12* (1973) 243; A. V. Kemp-Jones, A. J. Jones, M. Sakai, C. P. Beeman, S. Masamune, *Can. J. Chem. 51* (1973) 767; d) ESR: F. Gerson, E. Heilbronner, W. A. Böll, E. Vogel, *Helv. Chim. Acta 48* (1965) 1494; e) UV/VIS: H.-R. Blattmann, W. A. Böll, E. Heilbronner, G. Hohlneicher, E. Vogel, J.-P. Weber, *ibid. 49* (1966) 2017; f) photoelectron spectrum: R. Boschi, W. Schmidt, J.-C. Gfeller, *Tetrahedron Lett. 1972*, 4107; g) dipole moment: W. Bremser, H. T. Grunder, E. Heilbronner, E. Vogel, *Helv. Chim. Acta 50* (1967) 84; h) bond enthalpy: W. Bremser, R. Hagen, E. Heilbronner, E. Vogel, *ibid. 52* (1969) 418; W. R. Roth, M. Böhm, H.-W. Lennartz, E. Vogel, *Angew. Chem. 95* (1983) 1011; *Angew. Chem. Int. Ed. Engl. 22* (1983) 1007.

[3] For nomenclature, see: H. W. Whitlock, Jr., P. F. Schatz, *J. Am. Chem. Soc. 93* (1971) 3837.

[4] a) D. Cremer, B. Dick, *Angew. Chem. 94* (1982) 877; *Angew. Chem. Int. Ed. Engl. 21* (1982) 865; b) L. Farnell, L. Radom, *J. Am. Chem. Soc. 104* (1982) 7650; c) R. C. Haddon, K. Raghavachari, *J. Am. Chem. Soc. 107* (1985) 289.

[5] M. B. Rubin, *J. Am. Chem. Soc. 103* (1981) 7791; H. Frauenrath, M. Kapon, M. B. Rubin, *Isr. J. Chem. 29* (1989) 307.

[6] H. Günther, H. Schmickler, W. Bremser, F. A. Straube, E. Vogel, *Angew. Chem. 85* (1973) 585; *Angew. Chem. Int. Ed. Engl. 12* (1973) 570; H. Günther, H. Schmickler, *Pure Appl. Chem. 44* (1975) 807.

[7] R. Hoffmann, *Tetrahedron Lett. 1970*, 2907; H. Günther, *ibid. 1970*, 5173.

[8] E. Vogel, T. Scholl, J. Lex, G. Hohlneicher, *Angew. Chem. 94* (1982) 878; *Angew. Chem. Int. Ed. Engl. 21* (1982) 869; R. Bianchi, T. Pilati, M. Simonetta, *Acta Crystallogr. Sect C39* (1983) 378.

[9] E. Ciganek, *J. Am. Chem. Soc. 87* (1965) 652; *ibid. 89* (1967) 1454; C. J. Fritchie, *Acta Crystallogr. 20* (1966) 27.

[10] W. R. Roth, O. Adamczak, F. Bauer, H.-W. Lennartz, unpublished (we thank Professor *Roth* for permission to use the program). Also according to AM1 calculations the bisnorcaradiene **9** is more stable than the valence tautomeric [10]annulene **8** (with C_s symmetry), whereas a higher stability is determined for **10** than for **11**. For details of the method see M. J. S. Dewar, E. G. Zoebisch, E. F. Healy, J. J. P. Stewart, *J. Am. Chem. Soc. 107* (1985) 3902.

[11] H. J. Bestmann, R. Armsen, H. Wagner, *Chem. Ber. 102* (1969) 2259.

[12] E. Vogel, W. A. Böll, M. Biskup, *Tetrahedron Lett. 1966*, 1569.

[13] **12** (Table 2) was obtained by reduction of 2,10-(1'-oxo-propano)-1,6-methano[10]annulene [K. Nakasuji, M. Katada, I. Murata, *Tetrahedron Lett. 1978*, 2515; R. Neidlein, H. Zeiner, *Chem. Ber. 115* (1982) 3353] with $LiAlH_4/AlCl_3$, J. Pinger, *Diplomarbeit*, Universität Köln 1983.

[14] E. Vogel, W. Wiedemann, H. D. Roth, J. Eimer, H. Günther, *Liebigs Ann. Chem. 759* (1972) 1; H. Schmickler, *Dissertation*, Universität Köln 1974.

[15] According to the X-ray structure analysis, **10** is also present as [10]annulene valence tautomer in the crystal. Moreover, the analysis shows quite clearly that the deformation of the annulene ring and reduction in the C1–C6 distance deduced from models of **10** are consistent with the geom-

etry of the molecule (C1–C6: 2.121 Å compared to 2.235 Å in **1**). Apart from that, in the case of **10** one finds an asymmetry in the lengths of the C–C bonds caused by the *peri*-bridge, both in the CH_2 bridge (shortening of C1–C11 to 1.45 Å and lengthening of C6–C11 to 1.51 Å referred to the C1–C11/C6–C11 bond lengths of 1.485 Å in **1**) as well as in the annulene ring; slight deviations from the expected C_s symmetry of the molecule could be due to packing effects (according to studies in collaboration with *J. Lex*). Details of the crystal structure investigation are available on request from the Fachinformationszentrum Karlsruhe, Gesellschaft für wissenschaftlich-technische Information mbH, W-7514 Eggenstein-Leopoldshafen 2 (FRG), on quoting the depository number CSD-55354, the names of the authors, and the journal citation.

[16] Review: F.-G. Klärner, *Top. Stereochem. 15* (1984) 1.

[17] For a detailed discussion of the walk-rearrangement of **9** and **10** see: R. Arnz, *Dissertation*, Universität Köln 1989.

[18] Apart from the mentioned enthalpy effect, the still unknown influence of the *peri*-double bond on the dissociation energy of the C6–C11 bond in **9** has to be taken into account for the difference in reactivity of **9** and **10**. Other than in **9**, the walk-rearrangement initiated by cleavage of the C1–C11 bond also takes place in the case of **10** [$E_A = 43.5 \pm 1.9$ kcal mol^{-1}; $\lg A = 14.4 \pm 0.8$ (gas phase)].

[19] Alternative synthesis of **4**: H. Klenk, W.-D. Stohrer, F. Effenberger, *Chem. Ber. 109* (1976) 777.

Synthesis and Characterization of P-containing ZSM-5 Zeolites

By *Wladimir Reschetilowski,* Brit Meier, Michael Hunger, Baldur Unger,* and *Klaus-Peter Wendlandt*

Zeolites of the Pentasil type can be modified in various ways by incorporation of different elements in the aluminosilicate lattice, both under the conditions of hydrothermal synthesis as well as by post-treatment or impregnation.[1] Often very little is known of the bond order of these elements in the zeolite.

The aim of the present study was to prepare a series of P-containing zeolites with ZSM-5 structure (P-ZSM-5) by direct synthesis and to characterize them NMR spectroscopically as well as by adsorptive and catalytic measurements.

Silicon-rich P-ZSM-5 zeolites with variable P content were synthesized in laboratory autoclaves under the conditions used for the synthesis of ZSM-5[2] by hydrothermal crystallization of a reaction mixture of water glass, aluminum sulfate and phosphoric acid with the addition of *n*-propylamine. The reaction temperature was 170 °C and the duration of crystallization 55 h. The product was thoroughly washed with distilled water, dried, and tempered at 500 °C over the course of 6 h. The freshly calcined product was converted into the H-form by ion-exchange with a 0.5 N NH_4NO_3 solution at 80 °C for 3 h. The ion-exchange was followed by thermal deammonization at 500 °C over the course of 4 h.

The composition of the modified P-ZSM-5 zeolite was determined by electron probe microanalysis and with the help of ^{27}Al-MAS-NMR spectroscopy (MAS = magic angle spinning). The measurement of the isopiestic H_2O adsorption capacity of the sample tempered at 500 °C was performed at 20 °C. The catalytic properties of the P-ZSM-5 zeolites in the H-form were investigated in the acid-catalyzed cracking reaction of *n*-hexane in an integral flow reactor at normal pressure and at a reaction temperature of 300 °C. Taking a first-order rate law as basis, reaction rate constants could be determined which were used to establish the catalytic activity and the tendency of zeolite samples employed to deactivate according to the equation $1/k = 1/k_0 + B\tau$[3] (k and k_0 = reaction rate constants at time τ and $\tau = 0$; τ = time on stream; B = deactivation parameter).

The P contents, Si/Al ratios, results of adsorption and ^{1}H-MAS-NMR investigations and the catalytic measurements are summarized in Table 1.

Table 1. P-ZSM-5 zeolites investigated in the H-form and results of the adsorption, ^{1}H-MAS-NMR and catalytic measurements.

Sample No.	P per unit cell	Si/Al	A_{H_2O} [cm^3 g^{-1}]	SiOH/POH [10^{19} g^{-1}]	Si–OH–Al [10^{19} g^{-1}]	k_0[a]	B[b]
1	0	15	0.19	10	50	1.71	0.005
2	0.14	30	0.18	8.5	38	0.51	0.032
3	0.4	31	0.16	11	41	0.36	0.043
4	0.5	30	0.16	13	37	0.28	0.089
5	0.8	30	0.14	10	38	0.12	0.355

[a] k_0 = rate constant at time $\tau = 0$ in mol MPa^{-1} g^{-1} h^{-1}. [b] B = deactivation factor in MPa g mol^{-1}.

The ^{31}P-MAS-NMR signal of the P-ZSM-5 samples synthesized is shifted to lower range compared to the ^{31}P-NMR signal of H_3PO_4 and lies at $\delta = -2.5$. Together with the significantly reduced H_2O adsorption capacity in the samples with the highest P content this can be regarded as a further indication that the phosphate groups in the synthesized products are linked to the aluminosilicate framework preferentially in the form of dihydrogen phosphate groups. Hence, the geminal P–OH groups protruding into the channeling of the framework fill a part of the pore volume which would otherwise be available for an unhindered H_2O adsorption.

^{1}H-MAS-NMR measurements show that the phosphorus-free reference sample (Sample 1) contains bridging OH groups ($\delta = 4.2 \pm 0.1$) in a concentration of 50×10^{19} g^{-1} (Table 1). The concentration of the SiOH/POH groups ($\delta = 2.0 \pm 0.2$), whose differentiation is not possible, is 10×10^{19} g^{-1} and hardly changes on transition to P-containing ZSM-5 zeolites (Samples 2 to 5); the concentration of bridging OH groups clearly increases thereby to 40×10^{19} g^{-1} independently of the P content.

It seems plausible that the bridging OH groups determine the catalytic activity in proton-catalyzed reactions since the reference sample, which has the largest concentration of Si–OH–Al groups, shows the highest catalytic activity in the cracking of *n*-hexane (Table 1). It seems surprising at first sight that the P-ZSM-5 samples exhibit differing catalytic activity despite the almost equal concentration of acidic OH groups: an increase in the P content in P-ZSM-5 zeolites with unchanged Si/Al ratio in the zeolite framework leads to a reduction of the catalytic activity and a poorer activity-time behavior. Apparently the acid-strength distribution of the acidic OH groups is shifted more and more in favor of weakly acidic Brønsted acid centers with increasing P content, and results in a reduced catalytic activity. This explanation is consistent with the observation of *Lercher* et al.[4] that the concentration of strongly acidic Brønsted acid centers decreases and that of the weakly acidic centers increases when the number of the dihydrogen phosphate groups in the zeo-

[*] Doz. Dr. W. Reschetilowski
Dechema-Institut
Theodor-Heuss-Allee 25, W-6000 Frankfurt am Main 97 (FRG)
Dipl.-Chem. B. Meier, Dr. M. Hunger
Fachbereiche Chemie und Physik der Universität Leipzig
O-7010 Leipzig (FRG)
Dr. B. Unger, Doz. Dr. K.-P. Wendtlandt
Fachbereich Chemie der Technischen Hochschule Leuna-Merseburg
O-4200 Merseburg (FRG)

lite surface is increased. This then also explains the increased tendency to deactivation observed on the P-ZSM-5 zeolite samples investigated. Both a rapid "fatiguing" of the catalytically active centers as a result of coking as well as blocking of the pores following deposition of coke can be regarded as the cause of the rapid deactivation at high P contents in the zeolite.

Received: December 20, 1990 [Z 4347 IE]
German version: *Angew. Chem. 103* (1991) 728

CAS Registry numbers:
H_2O, 7732-18-5; water glass, 1344-09-8; aluminum sulfate, 10043-01-3; phosphoric acid, 7664-38-2; *n*-propylamine, 107-10-8; *n*-hexane, 110-54-3.

[1] Reviews: a) M. Tielen, M. Geelen, P. A. Jacobs, *Proc. Int. Symp. Zeolite Catal., Acta Phys. Chem. 31* (1985) 1–18; b) J. Weitkamp, S. Ernst, H. Dauns, E. Gallei, *Chem. Ing. Tech. 58* (1986) 623–632; c) K. G. Ione, L. A. Vostrikova, *Usp. Khim. 56* (1987) 393–427; d) W. Hölderich, M. Hesse, F. Näumann, *Angew. Chem. 100* (1988) 232–251; *Angew. Chem. Int. Ed. Engl. 27* (1988) 226–246.
[2] H. Bremer, W. Reschetilowski, D. Q. Son, K.-P. Wendlandt, P.-E. Nau, F. Vogt, *Z. Chem. 21* (1981) 77–78.
[3] W. Reschetilowski, H. Siegel, B.-H. Maschke, *Z. Anorg. Allg. Chem. 573* (1989) 231–239.
[4] A. Jentys, G. Rumplmayr, J. A. Lercher, *Appl. Catal. 53* (1989) 299–311.

Synthesis of Heterocycles by Tandem Reactions: Beckmann Rearrangements/Allylsilane Cyclizations**

By *Dieter Schinzer** and *Yunxin Bo*

Diastereoselective cyclization reactions leading to five- to eight-membered rings by intramolecular Sakurai reactions have proven to be a very useful preparative strategy.[1] Herein, we now describe for the first time the use of this method for the synthesis of heterocycles by tandem reactions of functionalized oximes. The starting compounds necessary for this purpose, such as **1** and **2** (R = H), are readily accessible by alkylation of simple oximes.[2] By stirring in chloroform (acid actalysis) they can also be converted into the (*E*)-configurated isomers **3** and **4**, respectively ((*Z*) : (*E*) ratio ca. 2.5 : 1). Reaction with mesyl chloride affords the corresponding methanesulfonates **1**–**4** (R = Ms).

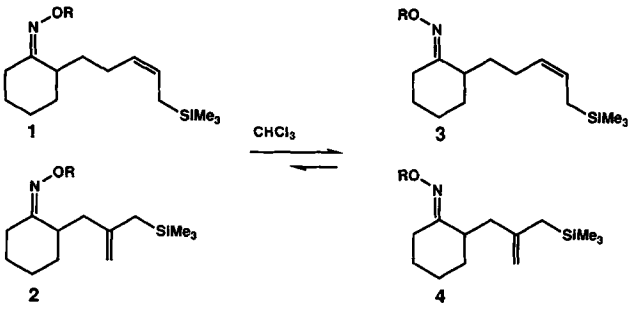

When the compounds **1** and **2** (R = Ms) are allowed to react with four equivalents of DIBAH[3] (diisobutylaluminum hydride) in methylene chloride at low temperature (−78 °C to 0 °C), the heterocycles **6** and **8**, derivatives of azepane, are obtained in a tandem reaction.

In this reaction sequence DIBAH apparently reacts initially as a mild Lewis acid and induces a stereoselective Beckmann rearrangement[4] to give the ring-expanded intermediates **5** and **7**, which are trapped in situ and regioselectively by the electron-rich allylsilane. In the last reaction step the imines are reduced stereoselectively to the secondary amines **6** and **8**, respectively. We are thus in a position to prepare precursors for the syntheses of azepine alkaloid systems stereoselectively in a one-pot reaction.[5]

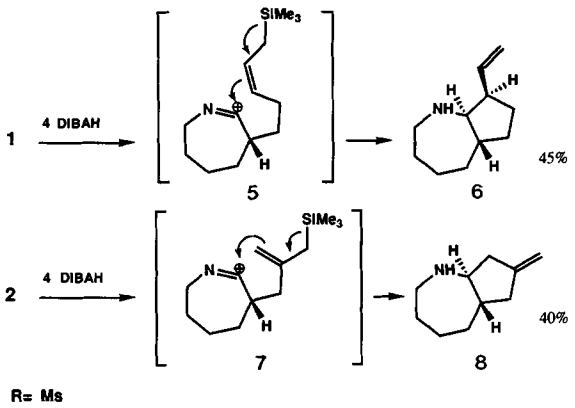

The analogous reaction of the (*E*)-configurated oximes **3** and **4** leads, when R = Ms, to their decomposition; in contrast, with R = H we surprisingly isolated **10** and **12**, heterocycles of the perhydroquinoline type, and not the expected 1,3-annelated products. Apparently the allylsilane-cyclization is now more rapid than the Beckmann rearrangement—in contrast to **1** and **2**, where, for steric and stereoelectronic reasons, a Beckmann rearrangement takes place first—so that the oxime nitrogen atom is now incorporated directly into the ring being formed. This is to our knowledge the first case in which an allylsilane reacts with a positively charged nitrogen atom.

Here too, a polarization of the NO bond by DIBAH most likely takes place first. In the cyclization step the Beckmann rearrangement cannot compete with the allylsilane cyclization; it is therefore suppressed and the cyclization to the six-membered ring ensues via the intermediates **9** and **11**. Subsequently, these are reduced in situ to give the heterocycles **10** and **12**, respectively.[5–7]

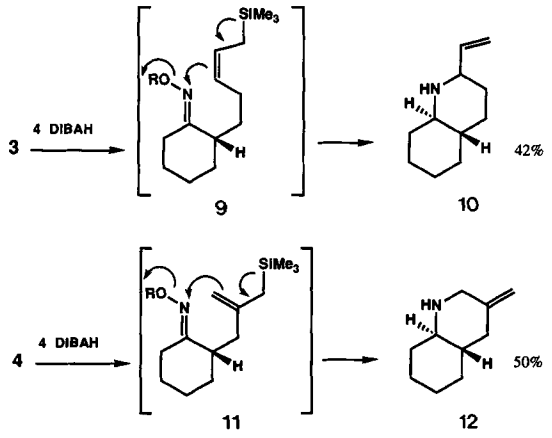

[*] Prof. Dr. D. Schinzer, Y. Bo
Institut für Organische Chemie der Technischen Universität
Hagenring 30, W-3300 Braunschweig (FRG)

[**] This work was supported by the Volkswagen-Stiftung and the Fonds der Chemischen Industrie.

The stereoselective reaction sequences presented here enable the synthesis of numerous heterocyclic ring systems. Depending upon the oxime system used, the reaction sequences lead with ring expansion to products of the azepane type or by direct cyclization to products of the perhydroquinoline type, whereby the functionalization of the heterocycle formed is determined by the allylsilane-substituent. Considering the number of steps involved in a one-pot reaction the yields of 40–50% obtained are very good. An analogous reaction could be carried out with cyclopentanone, however we have not yet been able to establish the relative configurations of the products.

Received: January 24, 1991 [Z 4402 IE]
German version: *Angew. Chem. 103* (1991) 727

CAS Registry numbers:
1 (R = Ms), 133228-28-1; **2** (R = Ms), 133228-29-2; **3** (R = H), 133228-30-5; **4** (R = H), 133228-31-6; **5**, 133228-32-7; **6**, 133228-33-8; **7**, 133228-34-9; **8**, 133228-35-0.

[1] D. Schinzer, *Synthesis 1988*, 263.
[2] M. E. Jung, P. A. Blair, J. A. Lowe, *Tetrahedron Lett. 1976*, 1439.
[3] E. Winterfeldt, *Synthesis 1975*, 617.
[4] K. Maruoka, T. Miyazaki, M. Ando, Y. Matsumura, S. Sakane, K. Hattori, H. Yamamoto, *J. Am. Chem. Soc. 105* (1983) 2831.
[5] All the new products were characterized by standard methods. The configurations were determined NMR spectroscopically by 600-MHz COSY experiments, C/H correlations, and NOE effects. Due to the flexibility of the seven-membered ring the *trans*-coupling of the seven-membered rings in **6** and **8** could not be established with certainty. This was possible, however, from model considerations. The relative configuration of the ethenyl group could be determined by NOE effects. We thank Dr. *V. Wray*, Gesellschaft für biotechnologische Forschung (GBF), Braunschweig-Stöckheim, for the NMR measurements.
[6] The configuration of the ethenyl group in **7** could not be determined; however, only one diastereomer is formed. The *trans* configuration of the six-membered ring follows unequivocally from the coupling constants.
[7] The reaction described does not implicate any mechanism, but merely contributes to an elucidation of the product formation.

Oxidative Cleavage of Triethylenetetramine (trien) to Yield Diethylenetriamine (dien): Structure of the Mn^{II}/Mn^{III} Heptanuclear Complex $[Mn_7(trien)_2(dien)_2O_4(OAc)_8](PF_6)_4 \cdot 2H_2O$ **

By *Rajumati Bhula* and *David C. Weatherburn**

Polynuclear manganese complexes where the metal is in oxidation states III, IV, V have interesting spectroscopic and magnetic properties. Such complexes can serve as useful models for manganese-containing biomolecules.[1–4] We are investigating manganese complexes of linear polyamine ligands and have described complexes of manganese(III) with diethylenetriamine (dien)[5] and Mn^{III}, and mixed-valent Mn^{III}/Mn^{IV} complexes with 1,5,8,12-tetraazadodecane (3,2,3-tet).[6] Extension of these studies to reactions with the ligand triethylenetetramine (trien) resulted in the isolation of a species which indicates that under certain experimental conditions oxidation of the polyamine ligands can occur.

Reaction of trien with manganese(III) acetate and sodium acetate in methanol solution, followed by the addition of NH_4PF_6, results in the precipitation of red needles of a novel septanuclear manganese salt (**1**). The same compound can be prepared from manganese(II) acetate with essentially the

$[Mn_7(trien)_2(dien)_2O_4(OAc)_8](PF_6)_4 \cdot 2H_2O$ **1**

same procedure. Figure 1 shows the arrangement of the manganese atoms in the cation.[7] Mn1 lies on an inversion

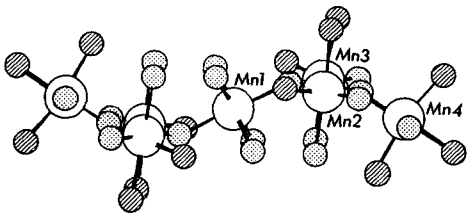

Fig. 1. Arrangement of the manganese atoms and the atoms coordinated to manganese in the cation of **1**. ◎ = N, ○ = O.

center. The overall shape of the cation is best described as two $[Mn_4(\mu_3\text{-}O)_2]$ units, the familiar 'butterfly' moiety,[6, 8–10] which share a manganese atom, Mn1, at the wing-tip. Figure 2 shows the asymmetric unit of the cation. Charge requirements indicate that probably six Mn^{III} ions and one Mn^{II} ion are present in the complex cation. The bond distances to Mn1 suggest that this is the Mn^{II} center and that the complex is valence trapped. Bond distances between the μ_3-oxo and μ_2-acetato oxygens and Mn2, Mn3, and Mn4 are comparable to those observed for Mn^{III} centers in similar complexes.[5, 6, 8–16]

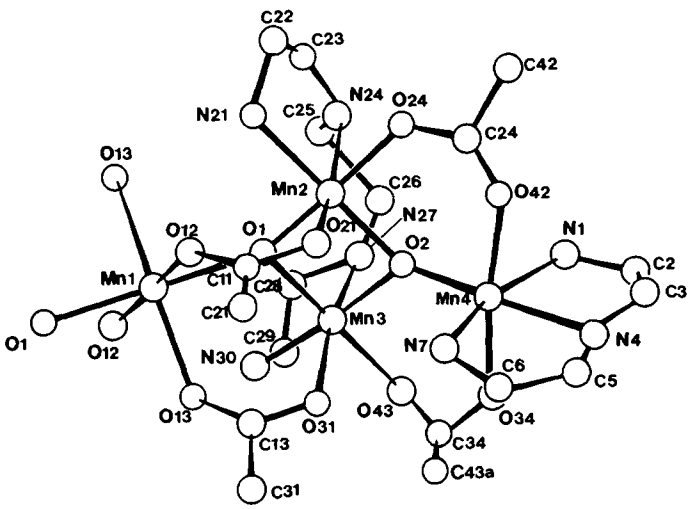

Fig. 2. Structure of the asymmetric unit of the cation of **1** showing the numbering system used.

The Mn2–N and Mn3–N bond distances are notable in that there are short bonds to the primary amines and long bonds to the secondary amines. The magnitude of the distortion is much greater than is usually observed for Mn^{III} centers so that steric constraints imposed on the trien ligand as it bridges the two metal ions rather than Jahn–Teller distortion are probably responsible. The Mn–O_{oxo} bond is *trans* to the short Mn–N bond. A similar lack of a structural *trans*

[*] Dr. D. C. Weatherburn, Dr. R. Bhula
Department of Chemistry, Victoria University of Wellington
P. O. Box 600, Wellington, New Zealand.

[**] This research was supported by a grant from the Internal Grants Committee of Victoria University. We wish to thank Dr. *W. T. Robinson* of the University of Canterbury for collecting the X-ray data set.

influence of the Mn–O_{oxo} bond has been noted previously.[15] The Mn4–N bond distances are in accord with normal Jahn–Teller distorted Mn^{III} centers.[6, 15]

The ESR spectrum of **1** has been measured in a frozen DMF solution. A six-line spectrum centered at $g = 1.97$, $A = 100$ G, was observed together with a small broad feature at $g = 3.9$. This spectrum is consistent with other reported spectra for mixed-valence Mn^{II}/Mn^{III} complexes.[16]

Table 1. Selected bond distances [Å] in the cation of **1**.

Mn1	Mn2	3.601(3)	Mn1	Mn3	3.551(3)
Mn2	Mn3	2.781(4)	Mn3	Mn4	3.344(5)
Mn2	Mn4	3.418(4)	Mn1	O1	2.208(11)
Mn1	O12	2.148(13)	Mn1	O13	2.167(12)
Mn2	O1	1.836(12)	Mn2	O2	1.924(12)
Mn2	O21	2.258(13)	Mn2	O24	1.950(14)
Mn2	N24	2.385(17)	Mn2	N21	2.101(15)
Mn3	O1	1.864(12)	Mn3	O2	1.914(13)
Mn3	O31	2.263(14)	Mn3	O34	1.987(14)
Mn3	N27	2.378(18)	Mn3	N30	2.059(16)
Mn4	O2	1.830(12)	Mn4	O42	2.156(15)
Mn4	O43	2.171(18)	Mn4	N1	2.078(14)
Mn4	N4	2.069(15)	Mn4	N7	2.147(15)

An unexpected feature of the isolated complex (**1**) is the presence of the dien ligand. The trien used in the preparation was carefully purified by a standard procedure[17] and no detectable quantity of dien (gas chromatography and mass spectra) was present in the starting material. In contrast, the mother liquor from which **1** was isolated contained significant quantities of both dien and trien ligands. We suggest that under the 'acidic' conditions provided by NH_4PF_6, the trien is oxidized to an imine intermediate, which is then hydrolyzed to give dien. A ^{13}C NMR spectrum of a CH_2Cl_2 extract of the mother liquor showed resonances assigned to both trien and dien. Other peaks present were an extra resonance in the C–N region ($\delta = 49.5$) and a carbonyl resonance ($\delta = 173.2$). These resonances suggest that the $C_2H_4NH_2$ residue cleaved from the trien has formed glycine. The ultimate oxidant is oxygen from the air as no dien can be detected in solutions which have been reacted in the absence of air. Mixed-valent Mn^{III}/Mn^{IV} complexes can be isolated from more basic solutions containing a similar tetraamine[6] so that high-valent manganese complexes are probably responsible for the oxidation reaction. Whether the oxidation proceeds before or after complexation to manganese has not been established; both Mn^{II} and Mn^{III} ions are labile so that uncoordinated dien present in the mother liquor cannot be taken as evidence for a pathway involving oxidation of the uncoordinated ligand. Oxidative dehydrogenation of coordinated ligands has been observed previously for complexes of Co^{II}, Ni^{II}, and Fe^{II},[18] and coordinated dioxygen has been implicated as the oxidant. In this context it is interesting that the center of Photosystem-II preparations which evolves oxygen is capable of oxidizing both primary and secondary amines,[19] and recent evidence suggests that the $S_2 \rightarrow S_3$ transition occurring in Photosystem-II corresponds to the oxidation of histidine.[20]

Experimental Section

$Mn(OAc)_3$ (0.5 g, 0.002 mmol) and NaOAc (0.3 g, 0.0036 mmol) were dissolved in methanol (25 mL) and the solution heated to 60 °C. Trien (0.3 g, 0.002 mmol) was added and the solution became a deep green color. Addition of solid NH_4PF_6 (0.5 g, 0.003 mmol), followed by further heating to dissolve the solid, gave a light orange solution. Upon cooling in air the solution developed a deep red color and red needles crystallized out overnight. If the reaction is carried out in the absence of air, it does not proceed beyond the light orange solution stage. Correct elemental analysis (C, H, N, P, F, Mn) for $C_{36}H_{90}N_{14}O_{22}P_4F_{24}Mn_7$. Crystals suitable for the structural analysis were isolated from the reaction mixture.

Received: December 3, 1990 [Z 4307 IE]
German version: *Angew. Chem. 103* (1991) 715

CAS Registry numbers:
1, 133445-39-3; trien, 112-24-3; dien, 111-40-0.

[1] K. Wieghardt, *Angew. Chem. 101* (1989) 1179; *Angew. Chem. Int. Ed. Engl. 28* (1989) 1153.
[2] J. B. Vincent, G. Christou, *Adv. Inorg. Chem. 33* (1989) 197.
[3] G. Christou, *Acc. Chem. Res. 22* (1989) 328.
[4] R. H. Crabtree, G. W. Brudvig, *Prog. Inorg. Chem. 37* (1989) 99.
[5] R. Bhula, G. J. Gainsford, D. C. Weatherburn, *J. Am. Chem. Soc. 110* (1988) 7550.
[6] R. Bhula, S. Collier, W. T. Robinson, D. C. Weatherburn, *Inorg. Chem. 29* (1990) 4027.
[7] Crystal data of **1**: $M_r = 2035.7$, monoclinic, space group $P2_1/n$, $a = 10.263(4)$, $b = 18.922(6)$, $c = 20.007(8)$ Å, $\beta = 92.39(3)°$, $V = 3882(3)$ Å^3, $Z = 2$, $\lambda(Mo_{K\alpha}) = 0.71069$ Å, crystal dimensions $0.76 \times 0.36 \times 0.14$ mm, $F(000)$ 1930, $\mu = 16.02$ cm^{-1}. 5578 reflections were collected (− 120 °C, ω scans in the $4° \leq 2\theta \leq 45°$ range) 4647 were unique, 2825 with $I \geq 3\sigma(I)$ were used in the refinement. Cell parameters were obtained from 25 accurately centered reflections in the $12.4° \leq 2\theta \leq 29°$ range. Three intensities were monitored every 100 reflections; no significant variation. Lorentz polarization, and empirical absorption corrections (ω scans) were applied (T_{max} 0.775, T_{min} 0.731). Structure solved with SHELXS using heavy atom methods and subsequent difference Fourier maps using SHELX-76. Neutral atom scattering factors, full-matrix least-squares refinement with 393 parameters and a fixed weight of 0.0006 gave $R = 0.0927$ ($R_w = 0.0889$). The Mn and P atoms, and the O and N atoms bound to Mn were refined anisotropically, all other atoms (including hydrogens at calculated positions) were refined isotropically. Both $PF_6^{\ominus}$ anions in the asymmetric unit exhibited disorder. In the final cycles of the refinement these $PF_6^{\ominus}$ groups were treated as rigid groups with four of the six fluorine atoms bound to *P*1 refined with partial occupancies over two sites (occupancy 0.64, 0.36) while all fluorines around *P*2 were refined as two sets (occupancy 0.57, 0.43). There is also evidence for some disorder in the positions of one of the methyl carbons, C43, and in one of the chelate rings of the dien molecule. Max. shift/esd = 0.3 for *P*1, max. peak in final difference map = 0.88 e Å^{-3}, 1.67 Å from *P*2. Further details of the crystal structure determination are available from the Director of the Cambridge Crystallographic Data Centre, University Chemical Laboratory, Lensfield Road, GB-Cambridge CB2 1 EW (UK) upon quoting the full journal citation.
[8] J. B. Vincent, C. Christmas, H.-R. Chang, Q. Li, P. D. W. Boyd, J. C. Huffman, D. N. Hendrickson, G. Christou, *J. Am. Chem. Soc. 111* (1989) 2086.
[9] E. Libby, K. Folting, J. C. Huffman, G. Christou, *J. Am. Chem. Soc. 111* (1989) 5354.
[10] C. Christmas, J. B. Vincent, H.-R. Chang, J. C. Huffmann, G. Christou, D. N. Hendrickson, *J. Am. Chem. Soc. 110* (1988) 823.
[11] M. K. Chan, W. H. Armstrong, *J. Am. Chem. Soc. 111* (1989) 9121.
[12] P. A. Goodson, A. R. Oki, J. Glerup, D. J. Hodgson, *J. Am. Chem. Soc. 112* (1990) 6248.
[13] J. B. Vincent, G. Christou, *Inorg. Chim. Acta 136* (1987) L41; H. Diril, H.-R. Chang, M. J. Nilges, X. Zhang, J. A. Potenza, H. J. Schugar, S. S. Isied, D. N. Hendrickson, *J. Am. Chem. Soc. 111* (1989) 5102.
[14] R. J. Kulawiec, R. H. Crabtree, G. W. Brudvig, G. K. Shulte, *Inorg. Chem. 27* (1988) 1309.
[15] U. Bossek, K. Wieghardt, B. Nuber, J. Weiss, *Inorg. Chim. Acta 165* (1989) 123.
[16] X. Li, D. P. Kessissoglou, M. L. Kirk, C. J. Bender, V. L. Pecoraro, *Inorg. Chem. 27* (1988) 1; D. P. Kessissoglou, M. L. Kirk, C. A. Bender, M. S. Lah, V. L. Pecoraro, *J. Chem. Soc. Chem. Commun. 1989*, 84; H.-R. Chang, S. K. Larsen, P. D. W. Boyd, C. G. Pierpont, D. N. Hendrickson, *J. Am. Chem. Soc. 110* (1988) 4565.
[17] H. B. Jonassen, G. T. Strickl, *J. Am. Chem. Soc. 80* (1958) 312.
[18] A. K. Basak, A. E. Martell, *Inorg. Chem. 27* (1988) 1984, and references cited therein.
[19] W. F. Beck, J. Sears, G. W. Brudvig, R. J. Kulawiec, R. H. Crabtree, *Tetrahedron 45* (1988) 4903.
[20] A. Bousacc, J.-L. Zimmermann, A. W. Rutherford, J. Lavergne, *Nature (London) 347* (1990) 303.

 © *VCH Verlagsgesellschaft mbH, W-6940 Weinheim, 1991* *0570-0833/91/0606-0689 $ 3.50+.25/0*

Dichloro(pentamethylcyclopentadienyl)ruthenium—Novel Dichotomy in a Molecular Structure**

By *Ulrich Kölle,* Janusz Kossakowski, Norbert Klaff, Lars Wesemann, Ulli Englert,* and *Gerhard E. Heberich*

The title complex $[\{Cp^*RuCl_2\}_2]$, **1** ($Cp^* = \eta^5$-C_5Me_5),[1,2] is a much-used reagent in the preparation of Cp*Ru sandwich and, in particular, half-sandwich complexes.[3–7] Although the solubility of the complex in halogenated hydrocarbons and the molar mass in chloroform (as determined by osmometric methods[6b]) speaks against the existence of a polymer, the compound is always seen as such.[8] We report on the structure of **1**[9] and analogous complexes $[\{Cp'RuCl_2\}_2]$ ($Cp' = \eta^5$-C_5Me_4Et) **2**[10] and the bromine derivative $[\{Cp^*RuBr_2\}_2]$ **3**.[6b]

In the preparation from $RuCl_{3(aq)}$ and Cp*H in methanol[1] or ethanol,[2] **1** precipitates as a red-brown, microcrystalline powder, which for some time thwarted attempts at crystallization. Crystals suitable for X-ray crystallography were finally obtained by diffusion of ether into a concentrated dichloromethane solution of **1**, after purification of an ether/dichloromethane solution by chromatography on silylated silica gel.[12] For compounds **2** and **3** the chromatographic procedure is unnecessary.

The structure determination[13–15] showed that all three compounds were dimers, as anticipated. A pecularity of the crystals of **1** was the equal distribution of forms **1a** and **1b** (Fig. 1), which have distinctly different Ru–Cl distances and

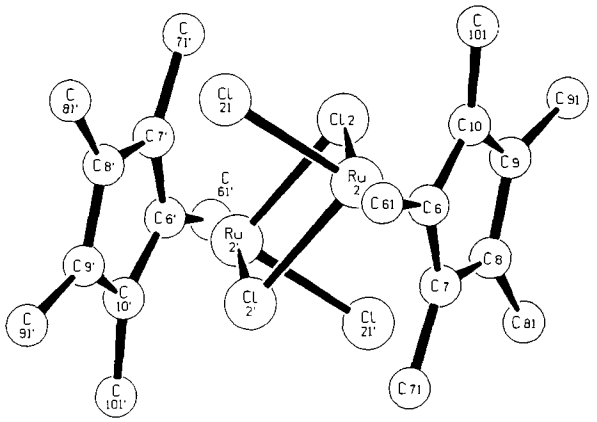

Fig. 1. Schakal picture of the structure of the isomer **1b** in the crystal.

Ru-Cl-Ru angles, and Ru–Ru distances of 2.93 and 3.75 Å (Fig. 2), and are located at positions 000 and $0\frac{11}{22}$ (**1a**) and $\frac{111}{222}$ and $\frac{1}{2}00$ (**1b**) of the monoclinic unit cell. The bonding parameters of **1a** and **1b** differ enough to justify the term "deformational isomerism". The molecular geometries of the compounds **2** and **3**, where crystals consist of only one form, correspond to isomer **1a** (Table 1).

The different Ru–Ru distances in the isomers suggest a strong exchange interaction between the unpaired spins of the d^5 low-spin Ru centers[16] in **1a**, but not in **1b**, where the metal–metal distance is similar to the nonbonding Rh–Rh distance in the analogous Rh complex $[\{Cp^*RhCl_2\}_2]$ **4**

[*] Prof. Dr. U. Kölle, Dr. J. Kossakowski, Dr. N. Klaff, Dr. L. Wesemann, Dr. U. Englert, Prof. Dr. G. E. Herberich
Institut für Anorganische Chemie der Technischen Hochschule
Professor-Pirlet-Strasse 1, W-5100 Aachen(FRG)

[**] This work was supported by the Deutsche Forschungsgemeinschaft and the Fonds der Chemischen Industrie. We thank the company Johnson-Matthey for a gift of $RuCl_3$.

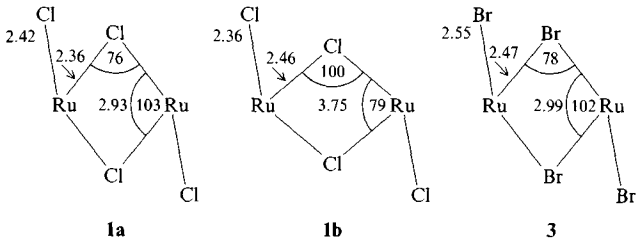

Fig. 2. Ru–halogen bond lengths [Å] and angles [°] of **1a**, **1b**, and for comparison **3b**.

(3.712 Å[17]). This isomer should thus be paramagnetic. This interpretation is supported by solid-state CP/MAS NMR spectroscopy on **1**.[18] The ^1H and ^{13}C NMR spectra each show two resonance signals ($\delta = 2$ and 18, and $\delta = 13$ and 246, respectively), which can be attributed to the deformational isomers. The low-field signals show the temperature proportionality characteristic of NMR signals of paramagnetic compounds. In contrast to the IR spectrum of **4**, in the case of **1** (CsI pellet) the bands assigned to the M–Cl vibrational modes at 292/309 and 260/275 cm^{-1} are split. This correlates with the different distances between the Ru atoms and the terminal chloro ligands in **1a** and **1b** (Table 1).

Table 1. Distances [Å] and bond angles [°] in **1**–**3**[a].

	1a	**1b**	**2**	**3**
Ru-Ru	2.930(1)	3.752(1)	2.9256(3)	3.098(2)
Ru-X_T	2.418(2)	2.365(2)	2.3619(6)	2.543(2)
Ru-X_B	2.366(1)	2.445(1)	2.4147(6)	2.479(2)
R-C_{Cp}[b]	2.191	2.173	2.191	2.178 2.194
Ru-X_B-Ru[b]	76.50(4)	100.24(5)	76.53(2)	76.25
X_B-Ru-X'_B[b]	103.50(4)	79.76(5)	103.47(2)	102.76
X_T-Ru-X_B[b]	89.99(6)	91.50(6)	89.56(2)	90.30

[a] X_T = terminal halogen, X_B = bridging halogen, C_{Cp} = C atom of the C_5 ligand. [b] Average values.

Finally the existence of a diamagnetic and a paramagnetic isomer explains the temperature dependence of the ^1H NMR signals of **1** and **2**, and to a lesser extent of **3**, in solution (Fig. 3). In dichloromethane a resonance signal which shifts reversibly with temperature in the range 109–350 K between $\delta = 1.6$ and 8,[19] accompanied by corresponding changes in line width (2.7 Hz at 190 K, 41 Hz at 350 K), is observed. Susceptibility measurements on solid samples of **1**[16] revealed an almost constant effective magnetic moment in the relevant temperature range (2.24 μ_B at 295 K, 2.22 μ_B at 95 K). Thus the temperature dependence of the chemical shift can only be caused by a dissociation into paramagnetic monomers or a temperature-dependent equilibrium between the deformational isomers **1a**/**1b**. Since we could not detect a concentration dependence of the chemical shift as predicted for a dissociation into monomers,[20] the second explanation apparently takes precedence, at least in the temperature range up to room temperature; **1b** is the less energetic form.[21] This means that the isomers also exist in solution. The same argument holds for **2**. In this case the four ^1H NMR signals in CD_2Cl_2 show an analogous temperature dependence, although only one form is present in the crystal. Apparently the often more favorable packing of the tetramethylethyl ligand prevents two isomers from crystallizing. Similar behavior is inferred for **3** above room temperature

(Fig. 3). The NMR spectrum of the bromine compound suggests that it is diamagnetic; a paramagnetic form would be substantially more energetic.

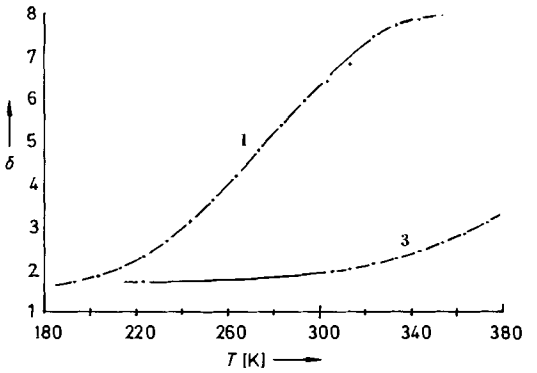

Fig. 3. Temperature dependence of the ^{1}H NMR chemical shift of **1** and **3**. Solvent CD_2Cl_2; standard: CH_2Cl_2, external ($\delta = 5.32$)

The deformational isomerism observed in crystals of **1** can be understood as a transition from magnetically interacting to noninteracting edge-sharing octahedra. The metal–metal distances in a large number of dimeric complexes[22] cluster around 2.8 Å where interaction is present (d^1–d^5) and around 3.7 Å where it is not. The d^5-d^5 low spin configuration in **1** is expected to lead to a rather weak interaction between the metal centers. As a result both molecular geometries, namely that dominated by the weak Ru–Ru bond and that by the repulsion between the Cl ligands, can coexist.

Received: October 8, 1990 [Z4234 IE]
German version: *Angew. Chem. 103* (1991) 732

CAS Registry numbers:
1, 130273-60-8; **2**, 133191-77-2; **3**, 133227-84-6; $RuCl_3$(aq), 14898-67-0; C_5Me_4EtH, 57693-77-3.

[1] T. Don Tilley, R. H. Grubbs, J. E. Bercaw, *Organometallics 3* (1984) 274.
[2] N. Oshima, H. Suzuki, Y. Moro-Oka, *Chem. Lett. 1984*, 1161.
[3] a) M. Hidai, K. Imagawa, G. Cheng, Y. Mizobe, Y. Wakatsuki, H. Yamazaki, *Chem. Lett. 1986*, 1299; b) N. Oshima, H. Suzuki, Y. Moro-Oka, H. Nagashima, K. Itoh, *J. Organomet. Chem. 314* (1988) C46; c) H. Suzuki, H. Omoro, Y. Moro-Oka, *Organometallics 7* (1988) 2579.
[4] a) B. K. Campion, R. H. Heyn, T. Don Tilley, *J. Chem. Soc. Chem. Commun. 1988*, 278; b) S. D. Loren, B. K. Campion, R. H. Heyn, T. Don Tilley, B. E. Bursten, K. W. Luth, *J. Am. Chem. Soc. 111* (1989) 4712; c) B. K. Campion, R. H. Heyn, T. Don Tilley, *Organometallics 9* (1990) 1106.
[5] a) P. J. Fagan, M. D. Ward, J. C. Calabrese, *J. Am. Chem. Soc. 111* (1989) 1698; b) M. D. Ward, P. J. Fagan, J. C. Calabrese, D. C. Johnson, *ibid. 111* (1989) 1719; c) P. J. Fagan, W. S. Mahoney, J. C. Calabrese, *Organometallics 9* (1990) 1843.
[6] a) U. Kölle, J. Kossakowski, *J. Chem. Soc. Chem. Commun. 1988*, 459; b) U. Kölle, J. Kossakowski, *J. Organomet. Chem. 362* (1989) 383; c) U. Kölle, J. Kossakowski, R. Boese, *ibid. 378* (1989) 449; d) U. Kölle, M. H. Wang, *Organometallics 9* (1990) 195; e) U. Kölle, B.-S. Kang, G. Raabe, C. Krüger, *J. Organomet Chem. 386* (1990) 261; f) U. Kölle, B.-S. Kang, U. Thewalt, *ibid. 386* (1990) 267; g) U. Kölle, J. Kossakowski, G. Raabe, *Angew. Chem. 102* (1990) 839; *Angew. Chem. Int. Ed. Engl. 29* (1990) 773.
[7] B. Chaudret, F. A. Jalon, *J. Chem. Soc. Chem. Commun. 1988*, 711.
[8] Cf. *Aldrichimica Acta 23* (1990) 26, and references cited therein.
[9] Cf. U. Kölle, N. Klaff, L. Wesemann, G. E. Herberich, *Abstr. 22. Hauptversammlung GDCh*, Bonn 1989.
[10] Compound **2** is formed analogously to **1** from $RuCl_{3(aq)}$ and C_5Me_4EtH in methanol. ^{1}H NMR (CD_2Cl_2, 25 °C): $\delta = 6.52(30)$ (CH_3), 6.11(30) (CH_3), 4.65(12) (CH_2CH_3), 3.60(35) (CH_2CH_3). The values in parentheses are line widths in Hz.
[11] Rapid crystallization from CH_2Cl_2/Et_2O yielded rhombic crystals which were studied under the diffractometer, as well as needles which gave only weak reflections. We cannot exclude the possibility that the substance is dimorphic.
[12] Silica gel (Merck-60) was treated with Me_3SiCl, filtered by suction, washed, and dried.
[13] **1**: Space group $P2_1/c$, $Z = 8/2$; $a = 16.754(4)$, $b = 9.192(4)$, $c = 15.828(4)$ Å, $\beta = 109.59(2)°$, $V = 2296.4(3)$ Å^3, $\mu = 17.654$ cm^{-1}; ENRAF-Nonius-CAD4, $Mo_{K\alpha}$ ($\lambda = 0.7107$ Å, graphite monochromator), 4896 reflections, ω scan with $0 < 2\theta < 30°$; empirical absorption correction; structure solved by Patterson and difference Fourier methods, anisotropic refinement of all non-hydrogen atoms, H atoms as riding atoms; $R = 0.036$, $R_w = 0.044$ with $w = 1/\sigma^2(F_0)$ for 235 variables with 3027 independent reflections $I > 3\sigma(I)$[15b].
[14] **2**: Space group $P2_1/n$, 1, $Z = 2$; $a = 7.983(6)$, $b = 14.816(3)$, $c = 11.123(3)$ Å, $\beta = 109.64(3)°$, $V = 1237(2)$ Å^3, $\mu = 16.43$ cm^{-1}; ENRAF-Nonius CAD4, $Mo_{K\alpha}$ ($\lambda = 0.7093$ Å, graphite monochromator), 4532 reflections ω scan with $3 < 2\theta < 29°$; empirical absorption correction; structure solved by Patterson and difference Fourier methods, anisotropic refinement of all non-H atoms, H atoms as riding atoms; $R = 0.027$, $R_w = 0.035$ with $w = 1/\sigma^2(F_0)$ for 127 variables with 2820 independent reflections with $I > 2\sigma(I)$[15b].
[15] a) **3**: Space group $P2_1/c$, $Z = 6$; $a = 8.353(4)$, $b = 15.526(4)$, $c = 27.876(6)$ Å, $\beta = 92.14(3)$, $V = 3612.6(38)$ Å^3, $\mu = 89.089$ cm^{-1}; ENRAF-Nonius CAD4, $Mo_{K\alpha}$ ($\lambda = 0.7107$ Å, graphite monochromator), 11 565 reflections (4784 independent), ω scan with $0 < 2\theta < 30°$; empirical absorption correction; structure solved by Patterson and difference Fourier methods, anisotropic refinement of all non-H atoms, H-atoms as riding atoms; $R = 0.064$, $R_w = 0.074$ with $w = 1/\sigma^2(F_0)$ für 235 Variable at 3019 unabhängigen Reflexen with $I > 3\sigma(I)$[15b]. b) Further details of the crystal structure investigation may be obtained from the Fachinformationszentrum Karlsruhe, Gesellschaft für wissenschaftlich-technische Information mbH, W-7514 Eggenstein-Leopoldshafen 2 (FRG) on quoting the depository number CSD-55259, the names of the authors and the journal citation.
[16] For the susceptibility measurements (Faraday balance, 3.4–328 K), rhombic crystals were selected from a sample crystallized as described. The unit cell dimensions were checked on the diffractometer, and the sample crushed and sealed in a quartz ampul under argon. (H. Lueken, U. Kölle, unpublished results.)
[17] M. W. Churchill, S. A. Julis, F. J. Rotella, *Inorg. Chem. 16* (1977) 1137.
[18] R. Benn, H. Grondey, U. Kölle, *J. Magn. Reson. 89* (1990) 375.
[19] Recorded in a double walled NMR tube, with solution of **1** in the inner tube and a mixture of $CHCl_3/CDCl_3$ as standard in the outer tube.
[20] From the average chemical shift ($\delta = 5.0$) of a 0.1 M solution of **1** in $CDCl_3$ at 306 K and the values for the diamagnetic dimer ($\delta = 2$) and a hypothetical paramagnetic monomer ($\delta = 25$), an equilibrium constant of $K = [mon]^2/[dim] = 2 \times 10^{-3}$ M can be calculated. A dilution from 10^{-1} to 1.2×10^{-2} M should shift the NMR signal by $\Delta\delta = 4.2$. The shift is only $\Delta\delta = 0.1$, close to the error limit.
[21] The fit of a two-component model to the curve of Figure 2 yielded the following parameters: $\delta_{(dia)} = 1.4$, $\delta_{(para)} = C/T$ where $C = 6500$ K^{-1}, $\Delta H^* = 15$ kJ mol^{-1}, $\Delta S^* 40.5$ J mol K.
[22] F. A. Cotton, *Polyhedron 6* (1987) 667.

Synthesis and Structure of the Novel Ga_3P_3 Ring Compound $[(2,4,6\text{-}Ph_3C_6H_2)GaP(cyclo\text{-}C_6H_{11})]_3$**

By *Håkon Hope, Doris C. Pestana,* and *Philip P. Power**

Multiple bonding between elements of the main groups 3 and 5 and related species has been one recent focus of research in this laboratory.[1–9] Part of this work has involved the synthesis of various types of novel six-membered, quasi aromatic rings such as $(RBPR')_3$,[2,4] $(RAlNR')_3$,[5] $(GeNR)_3$,[6] $(RZnER')_3$ (E = S,[7,9] Se,[8] and R,R′ = large alkyl or aryl substituent). All of these rings have displayed structural properties (for example, planarity and shortened, equivalent ring bonds) that are suggestive of some aromatic character. The experimental results have also been supported by calculations that indicate varying degrees of stabilization owing to π-electron delocalization.[10] A feature of these compounds is that, with the exception of the zinc–sulfur and

[*] Professor Philip P. Power, Professor H. Hope, D. C. Pestana
Department of Chemistry, University of California
Davis, California 95616 (USA)

[**] This work was supported by the National Science Foundation.

the zinc–selenium species, the rings invariably involve an element from the first row such as B or N. Rings composed exclusively of heavier main-group elements, where all the ring members are three coordinate, so that the possibility of extensive delocalization is preserved, are currently unknown.[11] In this paper the synthesis and structure of the first example of such a ring, involving only three-coordinate heavier main-group elements, is reported.

$[TriphGaP(C_6H_{11})]_3$ **1**, triph = $2,4,6\text{-}Ph_3C_6H_2$

The title compound (**1**) was synthesized in moderate yield by treatment of $triphGaCl_2$ with $Li_2P(cyclo\text{-}C_6H_{11})$ in an Et_2O/toluene solution. The ^1H and ^{13}C NMR spectra of **1** indicate that equal amounts of triph and C_6H_{11} are present. In addition, the ^{31}P NMR spectrum displays a single resonance at $\delta = -61$. The structure[12] of **1** was determined by X-ray crystallography (Fig. 1). The core involves a non-

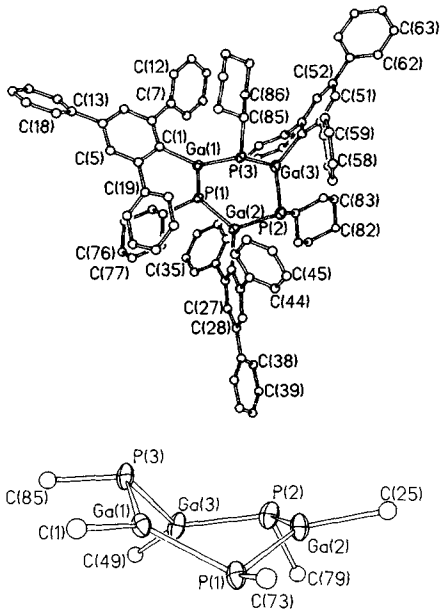

Figure 1. Schematic drawing of **1** (top) and the Ga_3P_3 core (bottom); H atoms are omitted for clarity. Bond distances (Å) and angles (°): Ga(1)–P(1) 2.286(4), Ga(1)–P(2) 2.283(4), Ga(2)–P(1) 2.279(4), Ga(2)–P(2) 2.338(5), Ga(3)–P(2) 2.291(3), Ga(3)–P(3) 2.302(3), Ga(1)–C(1) 2.004(9), Ga(2)–C(25) 1.992(11), Ga(3)–C(49) 2.019(13), P(1)–C(73) 1.863(14), P(2)–C(79) 1.892(12), P(3)–C(85) 1.880(15); Ga(1)-P(1)-C(73) 108.5(3), Ga(1)-P(1)-Ga(2) 108.3(2), Ga(2)-P(1)-C(73) 114.3(4), Ga(2)-P(2)-C(79) 104.2(4), Ga(2)-P(2)-Ga(3) 103.9(2), Ga(3)-P(2)-C(79) 107.6(5), Ga(1)-P(3)-C(85) 110.8(4), Ga(1)-P(3)-Ga(3) 104.3(1), Ga(3)-P(3)-C(85) 114.3(4), P(1)-Ga(1)-P(3) 118.6(1), P(1)-Ga(2)-P(2) 120.6(2), P(2)-Ga(3)-P(3) 114.7(2).

planar ring comprising three Ga and three P atoms. All the ring members are three-coordinate. The Ga–P bond lengths average ca. 2.3 Å. Although the Ga centers have almost planar coordination, the geometry at the P atoms is pyramidal and the sum of the angles at the P centers varies from 315.7° to 331.1°. Moreover, this sum may be correlated with the relevant Ga–P bond lengths. Thus the shortest Ga–P distances are associated with the flattest phosphorus center at P(1). The P–C, Ga–C, and C–C distances are unremarkable. The angle between each GaP_2C plane and the plane of the corresponding phenyl substituents is 82° for Ga(1), 64.3° for Ga(2), and 65.7° for Ga(3).

The structure of **1** is interesting for several reasons. It is the first well-characterized compound that has a ring consisting exclusively of three-coordinate, heavier main-group elements. In addition, the Ga–P bond length, 2.3 Å, is the shortest that has been observed to date.[13] It is significantly shorter than the Ga–P distance (2.338(1) Å) seen in the Ga_2P_2-ring species **2**.[11] Presumably, the longer distance in

$[\{2,6\text{-}(CH_2NMe_2)_2C_6H_3\}GaPSiPh_3]_2$ **2**

2 is due to the four-coordinate nature of the Ga center. The most significant structural feature of **1** concerns the nonplanarity of the Ga_3P_3 array and the P centers. The puckering indicates that delocalization in the Ga_3P_3 ring is not extensive. This view is supported by the upfield chemical shift($\delta = -61$) observed in the ^{31}P NMR spectrum. Had the amount of the delocalization of the P lone pairs onto Ga been large, a downfield chemical shift of $\delta \approx +50$ similar to those observed in the $(RBPR')_3$ rings[2,4] would have been expected. Thus the structural and spectroscopic data for **1** point to a sharp contrast in bonding with respect to the closely related planar B_3P_3 rings,[2,4] which were calculated to have greater delocalization than borazine.[10] It may be concluded that the energy gained by forming Ga–P π bonds is insufficient to overcome the high inversion barrier at phosphorus. Competition between these two factors exerts a considerable influence on B–P multiple bonding.[4] In this Ga–P system, at least, the inversion barrier appears to be dominant. Suitable variations of the substituents or replacement of Ga by the more electropositive Al will probably result in a planar array.

The stoichiometry and structure of **1** has proved that an earlier prediction, arising from the synthesis of the cluster **3**[14]

$[Ga_4(trip)_3\{P(1\text{-}ad)\}_4P(H)(1\text{-}ad)]$ **3**, trip = $2,4,6\text{-}i\text{-}Pr_3C_6H_2$, 1-ad = 1-adamantyl

of the existence of species such as $(RPGaR')_3$ is correct. Efforts to synthesize further examples of these and related species are under way.

Experimental Procedure

Under anaerobic and anhydrous conditions, a hexane solution of *n*BuLi (6.25 mL, 1.6 M) was added dropwise to an Et_2O solution of $H_2P(C_6H_{11})$ (0.61 mL, 5 mmol) with cooling in an ice bath. The yellow suspension was then stirred for a further 2 h. This was added by a double-tipped needle to a toluene/Et_2O (20 mL) solution of $triphGaCl_2$ derived from $GaCl_3$ (0.88 g, 5 mmol) and $triphLi(Et_2O)_2$ (2.3 g, 5 mmol)[15]. The addition produced a yellow solution which was filtered after 12 h stirring. The volume was reduced to ca. 15 mL and filtered again. Cooling to −20 °C afforded the product **1** as almost colorless, pale yellow crystals. Yield: 1.1 g, 45%; heating produces apparent desolvation at ca. 155 °C and decomposition above 200 °C.

Received: December 10, 1990 [Z 4315 IE]
German version: *Angew. Chem. 103* (1990) 726

[1] R. A. Bartlett, X. Feng, P. P. Power, *J. Am. Chem. Soc. 108* (1986) 6817.
[2] H. V. R. Dias, P. P. Power, *Angew. Chem. 99* (1987) 1320; *Angew. Chem. Int. Ed. Engl. 26* (1987) 1270; *J. Am. Chem. Soc. 111* (1989) 144.
[3] M. A. Petrie, S. C. Shoner, H. V. R. Dias, P. P. Power, *Angew. Chem. 102* (1990) 1061; *Angew. Chem. Int. Ed. Engl. 29* (1990) 1033.
[4] P. P. Power, *Angew. Chem. 102* (1990) 527; *Angew. Chem. Int. Ed. Engl. 29* (1990) 449.
[5] K. M. Waggoner, H. Hope, P. P. Power, *Angew. Chem. 100* (1988) 1765; *Angew. Chem. Int. Ed. Engl. 27* (1988) 1699.
[6] R. A. Bartlett, P. P. Power, *J. Am. Chem. Soc. 112* (1990) 3660.

[7] M. M. Olmstead, P. P. Power, S. C. Shoner, *J. Am. Chem. Soc. 113* (1991) 3379.
[8] K. Ruhlandt-Senge, P. P. Power, unpublished results.
[9] P. P. Power, *J. Organomet. Chem. 400* (1990) 49.
[10] W. H. Fink, J. J. Richards, *J. Am. Chem. Soc. 113* (1991) 3393.
[11] A. H. Cowley, R. A. Jones, M. A. Mardones, J. Ruiz, J. L. Atwood, S. G. Bott, *Angew. Chem. 102* (1990) 1169; *Angew. Chem. Int. Ed. Engl. 29* (1990) 1150. This paper describes the structure of a four-membered Ga_2P_2 ring compound $[\{2,6\text{-}(CH_2NMe_2)_2C_6H_3\}GaPS{:}Ph_3]_2$ (**2**) with four-coordinate Ga and three-coordinate P centers.
[12] Crystal data for **1** at 120 K ($Cu_{K\alpha}$ radiation $\lambda = 1.54178$ Å): $a = 12.819(2)$, $b = 17.445(3)$, $c = 20.107(3)$ Å, $\alpha = 101.10(1)$, $\beta = 107.92(1)$, $\gamma = 90.57(1)°$, $Z = 2$, triclinic, space group $P\bar{1}$, $\varrho_{calcd} = 1.294$ g cm^{-3}, $V = 4186.3(12)$ Å^3, 5251 unique observed data ($I > 2\sigma I$), $R = 0.091$. Data were obtained on a Siemens P3R diffractometer with a locally modified LT-2 low-temperature apparatus and a rotating anode. The structure contains molecules of Et_2O and toluene in its lattice. Further details of the crystal structure may be obtained from the Fachinformationszentrum für Energie, Physik, Mathematik, GmbH, W-7514 Eggenstein-Leopoldshafen 2 (FRG), on quoting the depository number CSD-55145, the names of the authors and the journal citation.
[13] Many references to the structures of the compounds of main groups 3 to 5 and their use as semiconductor precursors have been assembled in the review: A. H. Cowley, R. A. Jones, *Angew. Chem. 101* (1989) 1235; *Angew. Chem. Int. Ed. Engl. 28* (1989) 1028.
[14] K. M. Waggoner, S. M. Parkin, D. C. Pestana, H. Hope, P. P. Power, *J. Am. Chem. Soc. 113* (1991) 3597.
[15] M. M. Olmstead, P. P. Power, *J. Organomet. Chem.*, in press.

One-Step Synthesis of Organolanthanide(II) Complexes from the Metal**

By *Anja Recknagel* and *Frank T. Edelmann**

The organometallic chemistry of the divalent lanthanides has developed into a fascinating research area in the past ten years.[1] The decamethylmetallocene derivatives of samarium, europium, and ytterbium play a central role in this area. A prominent example is the unusually reactive THF adduct of decamethylsamarocene, $[Cp^*_2Sm(thf)_2]$.[2] This compound, first prepared by *Evans* et al., reacts with a number of substrates to yield organosamarium(III) complexes.[1c] The range of novel reactions of $[Cp^*_2Sm(thf)_2]$ stretches from the reductive CO trimerization[3] through the dimerization of phosphaalkynes[4] to the formation of the first complex of an f-block element containing an N_2 ligand.[5]

Cyclopentadienyl complexes of the divalent lanthanides are usually obtained in two-step syntheses.[1] The reaction of lanthanide(II) iodide with alkali cyclopentadienide has often proved its worth in the preparation of complexes such as $[Cp^*_2Sm(thf)_2]$, $[Cp^*_2Yb(Et_2O)]$ and $[\{(Me_3Si)_2C_5H_3\}_2Sm(thf)]$.[6] A further method is the reduction of bis(cyclopentadienyl)lanthanide(III) halides with alkali metals.[1] We report here on a new, direct synthesis of organolanthanide(II) complexes from the metal, in which the organic ligand is formed in situ.

On treatment of a suspension of activated samarium or ytterbium powder in THF with two equivalents of 6,6-dimethylfulvene, the solution becomes intensely red (Yb) or violet (Sm) after an induction period of ca. 2–4 h. After further stirring for 24 h at room temperature, the metal has almost completely dissolved. The organolanthanide(II) complexes **1** (Ln = Sm, 46%) and **2** (Ln = Yb, 75% yield) can be isolated from the filtered reaction solutions. Apparently the difunctional C_2-bridged bis(cyclopentadienyl) ligand $[Me_4C_2(C_5H_4)_2]^{2\ominus}$ is formed by reduction and subsequent dimerization of 6,6-dimethylfulvene during the reaction (Scheme 1). The compounds **1** (deep violet crystals) and **2**

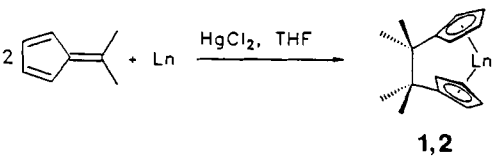

1,2

Scheme 1. **1**: Ln = Sm, **2**: Ln = Yb.

(dark red crystals) are very air-sensitive and soluble in THF, but sparingly soluble in hexane. The EI mass spectra of the complexes exhibit a peak with high intensity for the molecular ion of the unsolvated species $[\{Me_4C_2(C_5H_4)_2\}Ln]$. The chemical analyses and ^1H NMR spectra also show that the complexes **1** and **2** contain no coordinated THF. A comparable reaction is known for the alkaline earth metals: a reaction of magnesium and 6,6-dimethylfulvene in THF/CCl_4 yields the bis-Grignard reagent $[Me_4C_2(C_5H_4MgCl)_2]\cdot 4\,THF$, which in contrast to **1** and **2** is insoluble in THF.[7] It is still not clear whether the heavier alkaline earth metals also react with fulvenes in a similar manner.

The new organolanthanide(II) complexes **1** and **4** should be as reactive as their Cp* analogues. Compound **1**, for example, is converted extremely easily with *tert*-butylchloride into the organosamarium(III) complex **3**. This yellow,

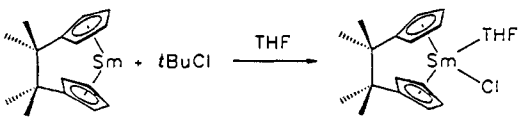

1 **3**

thermally very stable compound was characterized by spectroscopy and elemental analysis. The EI mass spectrum shows the molecular ion peak at $m/z = 471$, whose isotope pattern coincides with that calculated for $C_{20}H_{28}ClOSm$. The easy access to the lanthanide(II) complexes **1** and **2** makes them attractive starting materials for organometallic synthesis. Only a small step is needed from compounds of type **3** to potentially catalytically active organolanthanide(III) complexes.

Experimental Procedure

Because of the extreme air-sensitivity of the compounds described here, all reactions were performed under purified nitrogen in dry, oxygen-free solvents. **1**: To a suspension of Sm powder (2.00 g, 13.3 mmol) in THF (20 mL) was added $HgCl_2$ (ca. 100 mg), and the mixture was stirred for 2 h at 20 °C. Dropwise addition of 6,6-dimethylfulvene[8] (1.41 g, 13.3 mmol) in THF (100 mL) and further stirring at room temperature for 24 h yielded a deep violet solution, which was filtered through a thin Celite layer. The filtrate was concentrated to 50 mL, and crystallization at −25 °C afforded deep violet crystals (2.21 g, 46%). M.p. 158 °C; correct elemental analysis (C,H); IR (Nujol): $\tilde{\nu}$[cm^{-1}] = 1261 m, 1040 s, 896 m, 765 s; EI-MS: *m/z* 364 ($M^{\oplus}$, 24%), 259 ($[Me_2C(C_5H_4)]Sm^{\oplus}$, 18), 91 ($MeC(C_5H_4)^{\oplus}$, 100); ^1H NMR (80 MHz, [D$_8$]THF): δ = 15.5–15.0 (m, 8H, C_5H_4), 6.6 (s, br, $\nu_{1/2}$ = 30 Hz, 12H, Me). **2**: Analogously, a deep red crystalline solid (3.34 g, 46%) is obtained from Yb powder (2.00 g, 11.6 mmol) and 6,6-dimethylfulvene (1.22 g, 11.6 mmol). M.p. 142 °C; correct elemental analysis (C,H); IR (Nujol) $\tilde{\nu}$[cm^{-1}] = 1261 m, 1034 s, 880 m, 802 m, 728 vs; EI-MS: *m/z* 386 ($M^{\oplus}$, 87%), 279 $[Me_2C(C_5H_4)]Yb^{\oplus}$, 72), 91 ($MeC(C_5H_4)^{\oplus}$, 100); ^1H NMR (80 MHz, [D$_8$]THF): δ = 5.90–

[*] Dr. F. T. Edelmann, Dipl.-Chem. A. Recknagel
Institut für Anorganische Chemie der Universität
Tammannstrasse 4, W-3400 Göttingen (FRG)

[**] We thank Prof. Dr. *H. W. Roesky* for his generous support of this work. F. T. E. thanks the Deutsche Forschungsgemeinschaft for a habilitation scholarship.

4.42 (m, 8H, C_5H_4), 1.17 (s, br, $\nu_{1/2}$ = 6 Hz, 12H, Me). **3**: A THF solution of **1** is prepared from Sm powder (2.00 g, 13.3 mmol) and 6,6-dimethylfulvene (1.41 g, 13.3 mmol) and treated with *t*BuCl (1.18 g, 12.8 mmol) directly after filtration. The mixture was stirred at room temperature for 12 h before the orange solution was evaporated to dryness. Recrystallization of the residue from toluene (ca. 30 mL) affords a yellow crystalline powder (2.50 g, 40%), which decomposes at 260 °C. Correct elemental analysis (C,H); IR (Nujol): $\tilde{\nu}$[cm^{-1}] = 1258 s, 1045 s, 853 m, 785 m, 609 m; EI-MS: *m/z* 471 ($M^{\oplus}$, 12%), 364 ([$Me_4C_2(C_5H_4)_2$]$Sm^{\oplus}$, 27), 259 ([$Me_2C(C_5H_4)$]$Sm^{\oplus}$, 100); ^{1}H NMR (80 MHz, C_6D_6): δ = 15.9 (m, 4H, THF), 8.7 (m, 4H, THF), 7.1 (m, 8H, C_5H_4), 1.2 (s, br, 12H, Me).

Received: January 24, 1991 [Z4400 IE]
German version: *Angew. Chem. 103* (1991) 720

CAS Registry numbers:
1, 133165-05-6; **2**, 133165-06-7; **3**, 133165-07-8; Sm, 7440-19-9; Yb, 7440-64-4; 6,6-dimethylfulvene, 2175-91-9.

[1] Reviews: a) H. Schumann, *Angew. Chem. 96* (1984) 475; *Angew. Chem. Int. Ed. Engl. 23* (1984) 474; b) W. J. Evans, *Adv. Organomet. Chem. 24* (1985) 131; c) W. J. Evans, *Polyhedron 6* (1987) 803; d) I. P. Beletskaya, G. Z. Suleimanov, *Metalloorg. Khim.* 1 (1988) 3.
[2] a) W. J. Evans, I. Bloom, W. E. Hunter, J. L. Atwood, *Organometallics 4* (1985) 112; b) W. J. Evans, J. W. Grate, I. Bloom, W. E. Hunter, J. L. Atwood, *J. Am. Chem. Soc. 107* (1985) 3728.
[3] W. J. Evans, J. W. Grate, L. A. Hughes, H. Zhang, J. L. Atwood, *J. Am. Chem. Soc. 107* (1985) 941.
[4] A. Recknagel, D. Stalke, H. W. Roesky, F. T. Edelmann, *Angew. Chem. 101* (1989) 496; *Angew. Chem. Int. Ed. Engl. 28* (1989) 445.
[5] W. J. Evans, T. A. Ulibarri, J. W. Ziller, *J. Am. Chem. Soc. 110* (1988) 6877.
[6] W. J. Evans, R. A. Keyer, J. W. Ziller, *J. Organomet. Chem. 394* (1990) 87.
[7] H. Schwemmlein, H. H. Brintzinger, *J. Organomet. Chem. 254* (1983) 69.
[8] W. Freiesleben, *Angew. Chem. 75* (1963) 576; *Angew. Chem. Int. Ed. Engl. 2* (1963) 396.

β-Alkyl and β-Alkyl-α-Hydroxy Carboxylic Acid Derivatives from Radical or Ionic 1,4 Addition of Dialkylaluminum Chlorides to α,β-Unsaturated *N*-Acyl Urethanes**

By *Karola Rück* and *Horst Kunz**

Dedicated to Professor Leopold Horner

Chiral β-branching carboxylic acids are interesting building blocks for syntheses of natural products. The same is true of β-alkyl α-hydroxy carboxylic acid derivatives, which have, in comparison with the products of aldol reactions on enolates, the opposite α- and β-substituent pattern. Recently we reported a new access to chiral β-alkyl carboxylic acids by 1,4 addition of dialkylaluminum halides to α,β-unsaturated *N*-acyl urethanes.[1] A particular feature of this reaction is the smooth transfer of the alkyl group to the acceptor by diethylaluminum chloride but not by dimethylaluminum chloride under the same conditions. Dimethylaluminum chloride will catalyze the 1,4 addition of higher alkyl homologues. In contrast to our results,[1] *Evans* et al.[2a] observed that during Diels–Alder reactions, 1,4 additions of organoaluminum compounds do occur, but as side reactions and not only with Et_2AlCl but also with Me_2AlCl.

We therefore studied more closely the new reaction of the chiral oxazolidinones used by *Evans* on α,β-unsaturated acyl derivatives (**1**). Compounds **1** react with Et_2AlCl (**2**) under 1,4 addition, as do the oxazinone derivatives of xylofuranose[1] (Scheme 1). Treatment with 4 equivalents of **2** in a toluene/*n*-hexane solution with exclusion of oxygen at −78 °C yields the ethyl-substituted derivative **3** in high yield and with a high diastereomeric ratio in favor of the *S* configurated product (93:7). Under the same conditions Me_2AlCl (**4**) did not react, despite raised temperatures (−20 °C). In the presence of air, however, a slow reaction was observed. A useful preparative reaction is the 1,4 addition of **4** to acceptors (**1**) on photochemical induction (λ_{max} = 254 nm), which yields branched β-(methyl acyl) oxazolidinones.

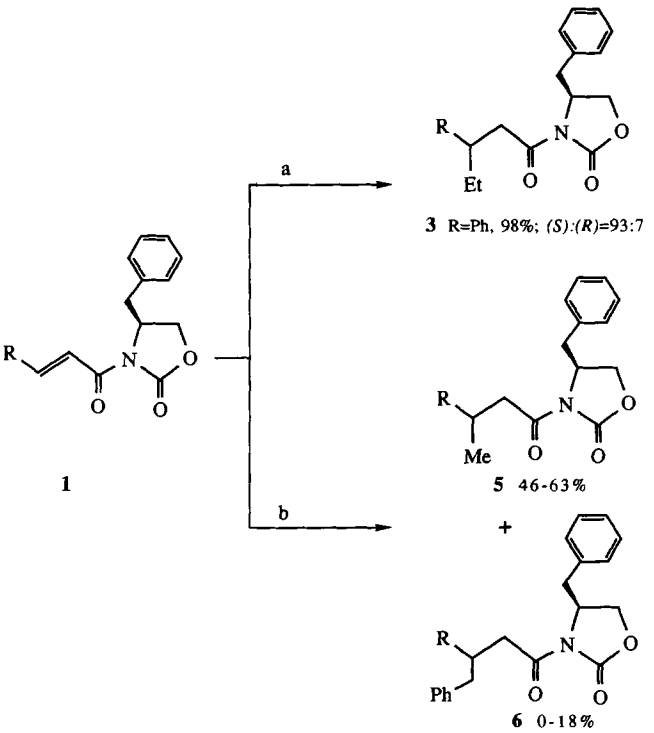

Scheme 1. a) Et_2AlCl (**2**, 4 equiv, 1 M) in *n*-hexane/toluene at −78 °C under argon. b) Me_2AlCl (**4**, 4 equiv) in *n*-hexane/toluene, 5 h irradiation. Total reaction time 30–48 h.

This indicates that the methyl transfer takes place by a radical mechanism, and indeed, can be completely inhibited by 5 mol % galvinoxyl.[3] The formation of **6** on addition of benzyl radicals also confirms the radical nature of the process. Radical reactions of the strong Lewis acid **4** with polar compounds such as **1** were till now unknown.[4] The stereoselectivity of the radical methyl transfer lies between 4:1 and 12:1 (Table 1). The separation of the diastereomeric ethyl compounds **3**,[5] as well as for the aromatic compounds **5b**

Table 1. Diastereoselective radical 1,4 addition of Me_2AlCl (**4**) to the acceptor **1** on irradiation for 5 h.

R (**1**)	*T*/*t* [a]	Prod.	Yield [b]	(*S*):(*R*) [c]	**6** [d]
*n*Pr	−45/31	**5a**	61	19:81	-
C_6H_5	−20/48	**5b**	63	88:12	10
C_6H_5	−40/30	**5b**	56	92:8	15
p-C_6H_4Cl	−45/35	**5c**	46	90:10	18 [e]

[a] *T* = Reaction temperature [°C], *t* = reaction time [h]; [b] yield [%] after flash chromatography; [c] diastereomeric ratio determined by HPLC on RP-18 in MeOH/H_2O mixtures and ^{1}H NMR spectroscopy (400 MHz, $CDCl_3$); [d] yield of the minor product **6** [%]; [e] according to the ^{1}H NMR spectrum (400 MHz) of the crude product **6c**, the diastereomeric ratio is 82:18.

[*] Prof. Dr. H. Kunz, Dipl.-Chem. K. Rück
Institut für Organische Chemie der Universität
Johann-Joachim-Becher-Weg 18–20, W-6500 Mainz (FRG)

[**] This work was supported by the Fonds der Chemischen Industrie. *K. R.* is grateful for a study grant from the Fonds der Chemischen Industrie and for a grant from the Adolf-Todt-Stiftung.

($R = C_6H_5$) and **5c** ($R = p\text{-}C_6H_4Cl$), can be achieved by flash chromatography.[6] Hydrolysis of the diastereomeric mixture of **5b** yields predominantly (*S*)-3-phenylbutyric acid.[7]

We have extended the radical transfer of a methyl group from Me_2AlCl to a cascadelike double functionalization of the α,β-unsaturated carboxylic acid derivatives (**1**) to yield β-methyl α-hydroxy carboxylic acid derivatives. Interestingly, the aluminum enolate intermediates **7**, which are formed stereoselectively in the radical process, react more smoothly with triplet oxygen than with polar oxidizing agents to form the target compounds **8**–**11**. Till now the alkali enolates could not be satisfactorily oxidized to α-hydroxy carbonyl compounds with oxygen,[8] a reaction which could also be achieved stereoselectively[9–11] with *N*-sulfonyl oxaziridine[12] and a MoO_5/pyridine/hexamethylphosphoric triamide complex.[13]

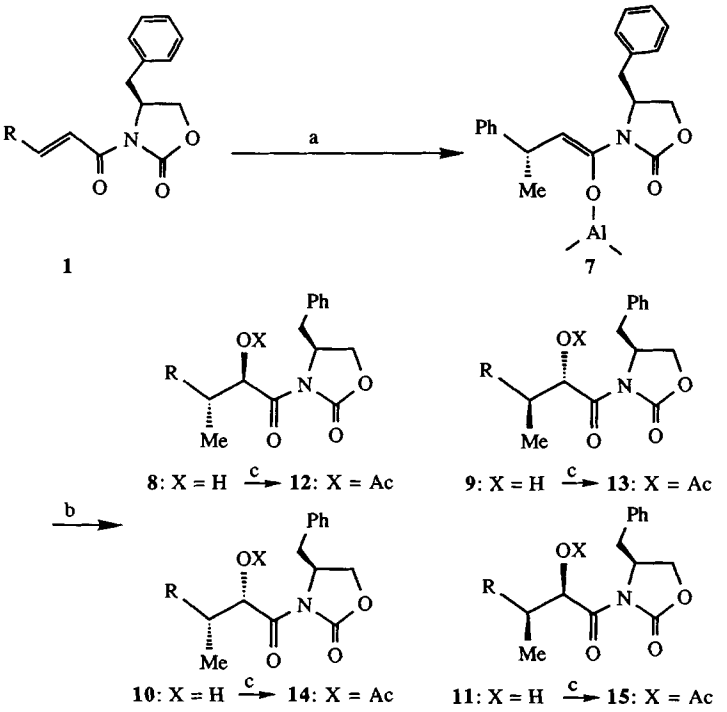

Scheme 2. a) Me_2AlCl (**4**, 4 equiv) in *n*-hexane/toluene is irradiated for 5 h and allowed to react for 24 h thereafter without irradiation at −40 °C. b) Oxidation: passage of oxygen for 1 h; thereafter allowed to react for 48–72 h. c) Acylation with Ac_2O, DMAP.

To perform the reaction sequence the compounds **1** (see Table 2) were irradiated in the presence of **4** (4 equiv, 1 M in *n*-hexane) in toluene at −40 °C with a mercury immersion lamp ($\lambda_{max} = 254$ nm) for 5 h (Scheme 2). The mixture was allowed to react without irradiation for 24–48 h, after which dry air was passed through the solution for 1 h at the same temperature. The reaction was quenched after a total of 72–96 h by hydrolysis with NH_4Cl solution and the diastereoisomers of (β-methyl α-hydroxy acyl) oxazolidine (**8**–**11**), were isolated after flash chromatography with petroleum ether/ethyl acetate in yields of 50–92%. The *syn*/*anti* product ratio was determined by ^1H NMR spectroscopy directly from the crude product.[14] After acetylation of the crude product with Ac_2O/DMAP (4-dimethylaminopyridine)[15] at 0 °C in dichloromethane, the ratio of the diastereomeric *O*-acylated hydroxy carboxylic acid derivatives **12**–**15** were

Table 2. Synthesis of (β-methyl α-hydroxy acyl) oxazolidinones **8**–**11**.

	R	*T*/*t* [a]	Products	Yield [b]	**12** (*R*,*R*)	**13** (*S*,*S*)	**14** (*R*,*S*)	**15** [c] (*S*,*R*)
1a	*n*-Pr	−40/108	**8a**–**11a**	82	48.8	8.4	26.1	16.7
1b	C_6H_5	−40/80	**8b**–**11b**	50	77	12	6.5	4.5
1c	$p\text{-}C_6H_4Cl$	−45/72	**8c**–**11c**	55	78.3	13.8	5.9	2.0
1d	C_2H_5	−55/81	**8d**–**11d**	48	50.4	8.9	26.9	13.8
1e	CH_3	−40/96	**8e**/**11e**–**9e**/**10e**	92	(*R*):(*S*) = 67:33 [d]			

[a] *T* = Reaction temperature [°C], *t* = reaction time [h]; [b] yield [%] after flash chromatography in petroleum ether/ethyl acetate mixtures, [c] diastereomeric ratio determined by HPLC on RP columns in MeOH/H_2O or by ^1H NMR spectroscopy (400 MHz, $CDCl_3$) of the *O*-acylated Derivatives **12**–**15**; [d] see [22].

determined by analytical HPLC (Table 2). The results agreed with the ratios obtained by ^1H NMR spectroscopy.[16] The diastereomers **8**–**11** were separated by flash chromatography. In each case the *anti* configuration was assigned to the major diastereomer **8a**–**d** and **12a**–**d**, since their ^1H NMR spectra showed the larger coupling constant $J_{\alpha/\beta}$ for the signals of the acyl side chain.[17] This was also true for the diastereomers **9a**–**d** and **13a**–**d**. The structure assignment was confirmed, since the absolute configurations of the diasteromers **9d** and **13d**, and their place in the *anti* series, could be proved by comparison of the ^1H NMR spectrum with that of an authentic sample isolated from L-isoleucine.[18]

The decisive step in the stereoselection of this reaction sequence is the initial 1,4 addition of the methyl group. The chiral center formed by this 1,5 induction in the β-position of the enolate **7** controls the following enolate oxidation. Thus for the aryl-substituted enolates **7b**, **c**, the (β*S*/4*S*) diastereomers form the matched pair in the intramolecular double stereodifferentiation. They react with oxygen with high stereoselectivity ($R:S \approx 93:7$) preferentially to the β*R*,α*R* diastereomers **8b**, **c**.[19] The β*R*,4*S* enolates represent the mismatched pair for the subsequent α-oxidation. Their oxidation shows low stereoselectivity ($R:S \approx 1:4$[20]). Stereoselectivity amongst the aliphatic examples **7a**, **d** of the 1,4-methyl addition, and in particular the inducing influence of the newly formed chirality center, is substantially smaller.[20]

Although the reaction mechanism needs further clarification, no long-lived hydroperoxides are formed during the oxidation process. Such alkylaluminum peroxides would undergo a rapid intra- or intermolecular reaction to alkoxyaluminum compounds.[21] This explains why in our reaction sequence the free hydroxy carboxylic acid derivatives **8**–**11** are isolable directly after hydrolysis. Furthermore, the example of **1e** (R = Me) makes it clear that the actual oxida-

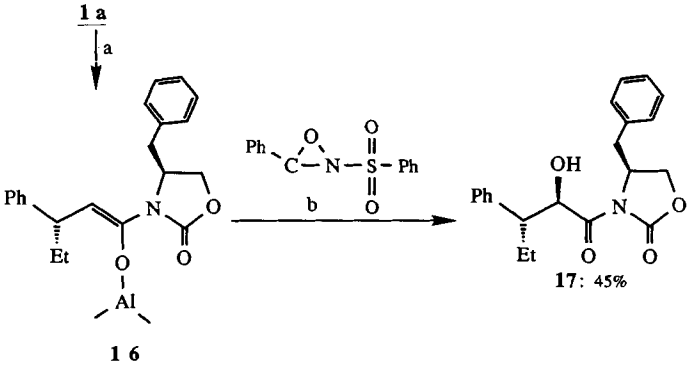

Scheme 3. a) Et_2AlCl (**2**, 4 equiv) in *n*-hexane/toluene at −78 °C, 9 h reaction time. b) Reaction temperature of −78 to +5 °C, 15 h reaction time. **17**: *anti*/*syn* ratio > 95:5, (β*R*):(β*S*) ≈ 9:1.

tion of the aluminum enolate is hardly influenced by the oxazolidinone auxillary in **7**. In this case the *R*-hydroxy carboxylic acid derivative is formed in only slight excess.[22]

The described double functionalization of the unsaturated acyl oxalidinones **1** gains a significant extension in that the ionic transfer of higher homologue alkyl groups from alkylaluminum halides to these acceptors[1] can be followed by an oxidation. These ionic processes afford enolates such as **16** (Scheme 3), whose subsequent oxidation with atmospheric oxygen, in contrast to that of **7**, is unsatisfactory. It is significant that with *N*-sulfonyl oxaziridine, which reacts ionically,[12] **16** reacts with high *anti*-selectivity to form the diastereoisomer **17** of the β-ethyl α-hydroxy carboxylic acid in 85% yield.

Received: January 28, 1991 [Z4404/4405 IE]
German version: *Angew. Chem. 103* (1991) 712

[1] a) H. Kunz, K.-J. Pees, *J. Chem. Soc. Perkin. Trans. 1 1989*, 1169; b) K. J. Pees, *Dissertation*, Universität Mainz, 1988.
[2] a) See footnotes 11 and 21 in D. A. Evans, K. T. Chapman, J. Bisaha, *J. Am. Chem. Soc. 110* (1988) 1238; b) D. A. Evans, T. C. Britton, J. A. Ellmann, *Tetrahedron Lett. 28* (1987) 6141.
[3] H. J. Shine, J. A. Waters, D. M. Hoffmann, *J. Am. Chem. Soc. 85* (1963) 3613.
[4] For a description of a radical-initiated reaction of tri-*n*-propylaluminum with enones, see: G. W. Kabalka, R. F. Daley, *J. Am. Chem. Soc. 95* (1973) 4428.
[5] (*S*)-**3c**: M.p. = 91 °C; $[\alpha]_D^{22} = +62.9$ ($c = 1.2$; $CHCl_3$); ^1H NMR (400 MHz, $CDCl_3$): $\delta = 4.45$ (m, 1H, C*H*N-Oxazolidinone), 3.38 (dd, 1H, $J_{vic} = 9.0$ Hz, $J_{gem} = 16.2$ Hz, CH_a(C = O)N).
[6] (*S*)-**5b**: M.p. = 85 °C; $[\alpha]_D^{22} = +84.0$ ($c = 0.2$; $CHCl_3$); ^1H NMR (400 MHz, $CDCl_3$): $\delta = 4.53$ (m, 1H, C*H*N-Oxazolidinone), 3.36 (dd, 1H, $J_{vic} = 8.0$ Hz, $J_{gem} = 16.0$ Hz, CH_a(C = O)N); (*S*)-**5c**: m.p. = 96 °C; $[\alpha]_D^{22} = +66.3$ ($c = 1.0$; $CHCl_3$); ^1H NMR (400 MHz, $CDCl_3$): $\delta = 4.55$ (m, 1H, C*H*N-Oxazolidinone), 3.32 (dd, 1H, $J_{vic} = 8.1$ Hz, $J_{gem} = 16.0$ Hz, CH_a(C = O)N).
[7] 3-Phenylbutyric acid from diastereomeric mixture **5b**: $[\alpha]_D^{22} = +39.9$ ($c = 1.0$, benzene); (*S*)-3-phenylbutyric acid: $[\alpha]_D^{25} = +54.4$ ($c = 1.4$, benzene). G. Sörlin, G. Bergson, *Ark. Kemi 29* (1969) 593, 606.
[8] a) J. N. Gardner, F. E. Carbon, O. Guoi, *J. Org. Chem. 33* (1968) 3294; b) H. H. Wasserman, B. H. Lipshutz, *Tetrahedron Lett. 1975*, 1731.
[9] D. Boschelli, A. B. Smith, O. D. Stringer, R. H. Jenkins, Jr., F. A. Davis, *Tetrahedron Lett. 22* (1981) 4385.
[10] R. Gamboni, P. Mohr, N. Waespe-Sarcevic, C. Tamm, *Tetrahedron Lett. 26* (1985) 203.
[11] D. A. Evans, M. M. Morrissey, R. L. Dorow, *J. Am. Chem. Soc. 107* (1985) 4346.
[12] a) F. A. Davis, L. C. Vishawakarma, J. M. Billmers, J. Finn, *J. Org. Chem. 49* (1984) 3241; b) F. A. Davis, A. C. Sheppard, *Tetrahedron 45* (1989) 5729.
[13] E. Vedejs, S. Larsen, *Org. Synth. 64* (1985) 127.
[14] *anti*-**8b/9b**: ^1H HMR (400 MHz, $CDCl_3$): $\delta = 5.3$ (dd, 1H, $J = 5.8$ Hz, C*H*OH); *syn*-**10b/11b**: ^1H NMR (400 MHz, $CDCl_3$): $\delta = 5.25$ (dd, 1H, $J = 3.3$ Hz, C*H*OH).
[15] W. Steglich, G. Höfle, *Angew. Chem. 81* (1969) 1001; *Angew. Chem. Int. Ed. Engl. 8* (1969) 981.
[16] **12b/13b/14b/15b**: ^1H NMR (400 MHz, $CDCl_3$): $\delta = 6.27$ (d, $J = 6$ Hz, C*H*OAc, **15a**); $\delta = 6.17$ (d, $J = 6$ Hz, C*H*OAc, **14a**); $\delta = 6.13$ (d, $J = 7.5$ Hz, C*H*OAc, **12a**); $\delta = 6.10$ (d, $J = 7.5$ Hz, C*H*OAc, **13a**).
[17] Cf. the assignment of *syn*/*anti*-α-hydroxy-β-alkyl ketones in S. Hünig, C. Marschner, *Chem. Ber. 122* (1989) 1329.
[18] (2*S*,3*S*)-*O*-Acetyl-2-hydroxy-3-methylvaleric acid is prepared from L-isoleucine (isoamyl nitrite, glacial acetic acid, sodium acetate, 15 °C, 48 h, 53%, b.p. = 85 °C/3 × 10^{-2} mbar, $[\alpha]_D^{22} = -14.0$ ($c = 1.25$; $CHCl_3$) [P. A. Plattner, K. Vogler, R. O. Studer, P. Quitt, W. Keller-Schierlein, *Helv. Chim. Acta 46* (1963) 927] and transformed after conversion into the acid chloride ($SOCl_2$, b.p. = 89 °C/18 torr, 91%) into (4*S*)-3-(2*S*,3*S*)-(*O*-Acetyl-2-hydroxy-3-methyl-1-oxopentyl)-4-(phenylmethyl)-2-oxazolidinone[6,5][M.p. 77 °C; $[\alpha]_D^{22} = +47.7$ ($c = 1.0$, $CDCl_3$); ^1H NMR (200 MHz, $CDCl_3$): $\delta = 5.89$ (d, 1H, $J_{2',3'} = 4.2$ Hz; C*H*OAc); 96%].
[19] Diastereoselectivitity of the enolate oxidation: (β*R*,4*S*)-**7b**: 92:8 (*R*:*S*) matched pair, (β*S*,4*S*)-**7b**: 27:73 (*R*:*S*) mismatched pair; (β*R*,4*S*)-**7c**: 93:7 (*R*:*S*) matched pair, (β*S*,4*S*)-**7c**: 13:87 (*R*:*S*) mismatched pair.
[20] Diastereoselectivitity of the enolate oxidation: (β*R*,4*S*)-**7a**: 64:36 (*R*:*S*); (β*S*,4*S*)-**7a**: 67:33 (*R*:*S*).
[21] a) A. G. Davis, C. D. Hall, *J. Chem. Soc.* (1963) 1192; b) A. G. Davis, B. P. Roberts, *J. Chem. Soc. B 1968*, 1074.
[22] (4*S*)-(2-hydroxy-3-methyl-1-oxobutyryl)-4-(phenylmethyl-2-oxazolidinone) in diastereomeric ratio 67:33 (2*R*:2*S*). After separation of the diastereomers by flash chromatography and removal of the auxillary [2b], the optical rotation for the minor component is $[\alpha]_D^{25} = +12$ ($c = 1.0$; $CHCl_3$), which thus identified as L-α-hydroxyisovaleric acid by comparison with the literature value $[\alpha]_D^{14} = 16.9$ ($c = 1.0$; $CHCl_3$); see A. H. Cook, S. F. Cox, T. H. Farmer, *J. Chem. Soc. 1949*, 1026.

Direct Assignment of Absolute Configuration of Chiral Alkyl Gluconamides by Wettability Measurements

By *Jinn-Lung Wang, Meir Lahav,* Leslie Leiserowitz**

Dedicated to Professor Vladimir Prelog on the occasion of his 85th birthday

For a century, from the milestone experiment of *Pasteur*[1] in 1848 on the manual separation of the two enantiomorphs of $NaNH_4$ tartrate tetrahydrate, till 1951, when *Bijvoet*[2] directly assigned the absolute configuration of crystals by anomalous X-ray scattering only relative stereochemistry was considered. In the absence of anomalous X-ray scattering, one cannot differentiate by conventional X-ray diffraction, in accordance with Friedel's law, between a chiral crystal structure and its mirror image.[3] Recently, several independent methods for assignment of absolute molecular configuration were proposed, including the use of tailor-made molecular additives for inducing controlled morphological changes in crystals,[4] crystal etching,[5] and reduction of symmetry in crystals,[6] as well as gas/solid reactions[7] and ferroelectric measurements in liquid crystals.[8]

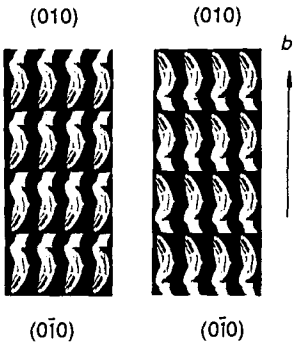

Scheme 1. The principle used to determine the absolute configuration of chiral molecules.

These methods involve the principle of fixing the orientation of the constituent chiral molecules vis-à-vis the polar axis, or axes, of the crystal and subsequently determining the absolute configuration of the chiral molecules. This principle is depicted schematically in Scheme 1. The fingers of the hands are exposed at the (010) face for the right-handed "molecules" and, by symmetry, at the (0$\bar{1}$0) face for the left-handed "molecules". Thus, by determining at which face

[*] Prof. Dr. M. Lahav, Prof. Dr. L. Leiserowitz, J.-L. Wang
Department of Structural Chemistry
Weizmann Institute of Science
Rehovot 76100 (Israel)

of the crystal specimen the fingers or wrists are exposed, one may assign the handedness of the constituent molecules.

In the course of studies on induced freezing of supercooled water via structured surfaces, we investigated crystals of the class of chiral resolved alkyl gluconamides $H(CH_2)_nNHCO(CHOH)_4CH_2OH$ ($n = 7-10$). We noticed that the molecular packing arrangements, crystal morphology, and cleavage properties of the entire class permit a direct determination of the absolute configuration of the molecules by simple wettability measurements at opposite hemihedral faces of the crystals.

Saenger et al. recently reported the crystal structures of chiral resolved alkyl gluconamides.[9] Compounds with an odd number of carbon atoms in the hydrocarbon chain crystallize in space group $P1$ with one molecule per unit cell (Fig. 1 a); compounds with an even number of carbon atoms appear in space group $P2_1$ with two molecules per unit cell (Fig. 1 b).

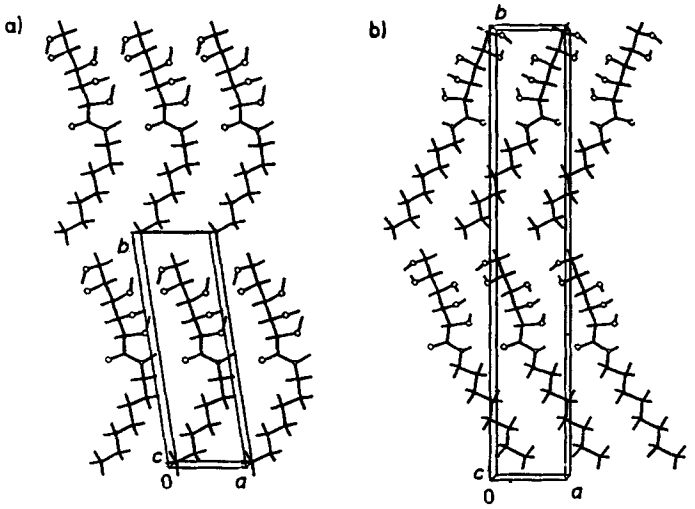

Fig. 1. Head-to-tail packing arrangements of alkyl gluconamides in the crystal. a) *N*-*n*-heptyl-D-gluconamide, space group $P1$. b) *N*-*n*-octyl-D-gluconamide, space group $P2_1$.

For both the n odd and even series, the molecules form layers by translation symmetry only. Within each layer the molecules are interlinked by hydrogen bonds at the gluconamide moiety and by methylene–methylene contacts at the alkyl side. The layers are similar in structure for the whole class of compounds (Fig. 1) and are stacked head-to-tail in a polar arrangement either by translation for n odd or by twofold screw symmetry for n even. The crystals form {010} plates whose faces are parallel to the molecular layers. Thus, the ω-CH_3 group at the hydrophobic end of the molecule emerges at one {010} face of the crystal plate and the terminal CH_2OH moiety at the opposite face, with the hydroxyl oxygen oriented such that its lone pair protrudes from the crystal surface. For sugars of D configuration the $(0\bar{1}0)$ face of the crystal plate is hydrophobic and the opposite (010) face is hydrophilic. The reverse situation holds for molecules of L configuration. Thus, the assignment of the hydrophobic–hydrophilic character of the plate faces by simple wettability measurements would fix the sense of polarity of the crystal and subsequently the absolute configuration of the sugar molecules.

The contact angle between a liquid drop and a flat solid surface reflects the difference between cohesion forces of the liquid and the adhesion forces to the solid surface. Systematic studies of contact angle measurements on a variety of surfaces, including those of crystals, monolayers, and polymers, have demonstrated that the contact angle depends primarily on the groups constituting the exposed surface, with some modulation by the presence of polar groups embedded below the surface.[10-12] These studies have led to a correlation between contact angle and the hydrophobic or hydrophilic nature of the surface. Therefore, a pronounced difference was expected for the contact angles for the two opposite (010) and $(0\bar{1}0)$ hemihedral faces of the alkyl gluconamide crystals.

The advancing contact angle α for this class of crystals was measured with three different solvents: water, glycerol, and ethylene glycol. Advantage was taken of the intrinsic property of these crystals to cleave along the {010} face and so provide clean, fresh surfaces. The results are given in Figure 2. The contact angles can be classified into two distinct groups; the angles range in value from 75 to 87° at the $(0\bar{1}0)$ face and from 44 to 56° at the opposite (010) face. The average difference in contact angle at the two opposite faces for the three solvents and the four compounds is 32°.

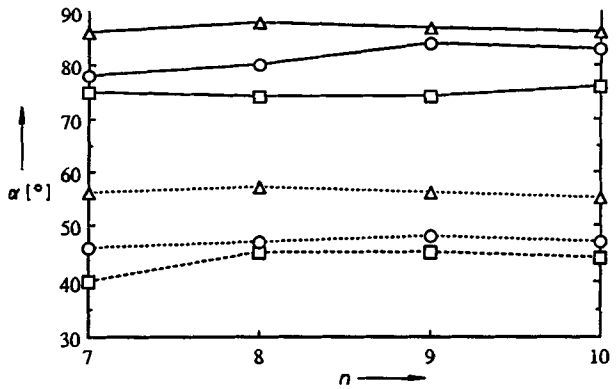

Fig. 2. Advancing contact angles α of the {010} faces of *N*-alkyl-D-gluconamide crystals ($n = 7-10$). △=glycerol, ○=water, □=glycol, —— = contact angles at the $(0\bar{1}0)$ face, – – – = contact angle at the (010) face.

These results may be compared with contact angle measurements on model surfaces of known hydrophilic and hydrophobic character.[13] As a hydrophilic surface, we made use of 1,9-nonanediol, which crystallizes as thick plates in which the molecules are arranged in layers. The two dominant faces of the platelike crystals expose hydroxyl groups. The contact angle for the water was 44°, comparable to the average contact angle of 46° for the (010) face of the alkyl gluconamides. As a model for the hydrophobic face, we prepared Langmuir–Blodgett films of an alkyl gluconamide (n=18) which forms a Z-type multilayer[14] and whose exposed faces were thus hydrophobic. The average value for each of the three solvents glycerol, ethylene glycol, and water were 95, 82, and 79°, respectively, comparable to the average contact angle on the $(0\bar{1}0)$ face of the alkyl-gluconamide crystals.

All these results are completely consistent with the assignment that the $(0\bar{1}0)$ face of the alkyl gluconamides is hydrophobic and the (010) face hydrophilic. This assignment fixes the absolute configuration of the chiral gluconamide molecules to be the D configuration as expected.

Thus, there are now available a variety of chemical methods, including simple wettability measurements, for the direct assignment of absolute configuration of chiral molecules

in crystals. The importance therein lies not only in the fact that we may directly correlate macroscopic chemical behavior with molecular chirality, but also in the educational value of the method, particularly for students of organic chemistry who find the usual method of anomalous X-ray scattering too esoteric.

Received: January 7, 1991 [Z4376IE]
German version: *Angew. Chem. 103* (1991) 698

CAS Registry numbers:
N-heptyl-D-gluconamide, 18375-60-5; *N*-octyl-D-gluconamide, 18375-61-6; *N*-nonyl-D-gluconamide, 5438-32-4; *N*-decyl-D-gluconamide, 18375-62-7; water, 7732-18-5; glycerol, 56-81-5; glycol, 107-21-1.

[1] L. Pasteur, *Ann. Chim. Phys. Ser. 324* (1848) 442.
[2] J. M. Bijvoet, A. F. Peerdeman, A. J. van Bommel, *Nature 168* (1951) 271.
[3] J. Dunitz: *X-Ray Analysis and the Structure of Molecules*, Cornell University Press 1979, pp. 129–148.
[4] a) L. Addadi, Z. Berkovitch-Yellin, I. Weissbuch, M. Lahav, L. Leiserowitz, *Top. Stereochem. 16* (1986) 1–85; b) Z. Berkovitch-Yellin, L. Addadi, M. Idelson, L. Leiserowitz, M. Lahav, *Nature 296* (1982) 27–34; c) I. Weissbuch, L. Addadi, Z. Berkovitch-Yellin, E. Gati, S. Weinstein, M. Lahav, L. Leiserowitz, *J. Am. Chem. Soc. 105* (1983) 6615–6621.
[5] L. J. Shimon, M. Lahav, L. Leiserowitz, *Nouv. J. Chim. 10* (1986) 723–737.
[6] M. Vaida, L. J. Shimon, Y. Weisinger-Lewin, F. Frolow, M. Lahav, L. Leiserowitz, R. K. McMullan, *Science 241* (1988) 1475–1479.
[7] I. C. Paul, D. Y. Curtin in G. R. Desiraju (Ed.): *Organic Solid State Chemistry*, Elsevier, Amsterdam 1987, pp. 331–370.
[8] D. M. Walba, H. A. Razavi, N. A. Clark, D. S. Parmar, *J. Am. Chem. Soc. 110* (1988) 8686–8691.
[9] a) V. Zabel, A. Müller-Fahrnow, R. Hilgenfeld, W. Saenger, B. Pfannemüller, V. Enkelmann, W. Welte, *Chem. Phys. Lipids 39* (1986) 313–327; b) A. Müller-Fahrnow, R. Hilgenfeld, H. Hesse, W. Saenger, *Carbohydr. Res. 176* (1988) 165–174.
[10] W. A. Zisman in F. M. Fowkes (Eds.): *Contact Angles, Wettability and Adhesion (Adv. Chem. 43* (1964) 1–51).
[11] M. D. Wilson, G. S. Ferguson, G. M. Whitesides, *J. Am. Chem. Soc. 112* (1990) 1244–1245.
[12] R. Maoz, J. Sagiv, *J. Colloid Interface Sci. 100* (1984) 465–496.
[13] A large body of data is available on contact angle measurements of polymers, thin films, and crystals. From these works a correlation has been made between the contact angle and the hydrophobic-hydrophilic nature of the surface.
[14] R. Popovitz-Biro, K. Hill, E. Shavit, D. J. Hung, M. Lahav, L. Leiserowitz, J. Sagiv, H. Hsiung, G. R. Meredith, H. Vanherzeele, *J. Am. Chem. Soc. 112* (1990) 2498–2506.

Tetraethynylethene **

By *Yves Rubin, Carolyn B. Knobler,* and *François Diederich* *

Dedicated to Professor Heinz A. Staab on the occasion of his 65th birthday

Despite the enormous importance of acetylene and ethylene in chemistry, the tetraalkynylethene system has received little attention so far.[1] Our research on molecular and polymeric carbon allotropes has led us to isolate tetraethynylethene (**4a**), the ultimate and hitherto elusive member of this class.[2–4] We believe that the preparation of **4a**, the only known isomer of molecular formula $C_{10}H_4$, is important for several reasons: (1) Compound **4a** and its substituted derivatives are interesting examples of cross-conjugated π systems.[1] (2) Tetraethynylethene (**4a**) is a direct precursor of new carbon networks.[5, 6] (3) Double Bergman cyclization[7] of **4a** could provide a convenient route to poly(*peri*-naphthalenes), which have been predicted to pos-

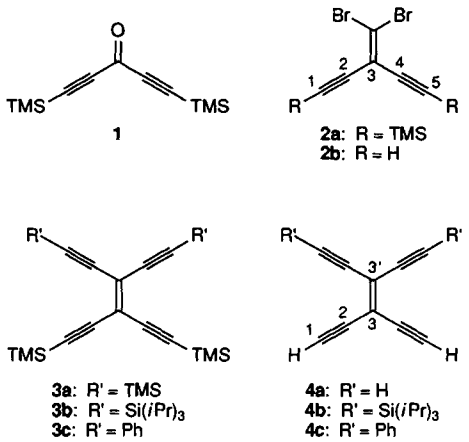

Table 1. Selected spectroscopic data for **2a**, **2b**, **3a–3c**, and **4a–4c**. ^1H and ^{13}C NMR spectra were recorded at 360 MHz and 90.6 MHz, respectively.

2a: Yield 66%; oil. FT-IR (CCl_4): $\tilde{\nu}$ = 2156, 2133 (C≡C) cm^{-1}. ^1H NMR ($CDCl_3$): δ = 0.23 (s). ^{13}C NMR ($CDCl_3$): δ = −0.45, 100.1, 102.6, 110.5, 114.3.

2b: Yield 65%; m.p. > 35 °C. FT-IR (CCl_4): $\tilde{\nu}$ = 3306 (≡CH), 2117 (C≡C) cm^{-1}. ^1H NMR ($CDCl_3$): δ = 3.52 (s). ^{13}C NMR ($CDCl_3$) [a]: δ = 79.5 (dd, ^2J = 50.7, ^4J = 1.4 Hz; C-2,4), 84.4 (d, ^1J = 256.7 Hz; C-1.5), 111.7 (t, ^4J = 3.6 Hz; CBr_2), 112.5 (t, ^3J = 4.9 Hz; C-3).

3a [1b]: Yield 88%; m.p. 199–201 °C (lit. m.p. 203–205 °C). FT-IR (CCl_4): $\tilde{\nu}$ = 2164, 2145 (C≡C) cm^{-1}. ^{13}C NMR ($CDCl_3$): δ = −0.2, 101.0, 105.3, 118.8. UV/VIS (MeOH): λ_{max} = 214 (ε = 15600), 224 (18300), 262 sh (8590), 270 (10800), 285 (10200), 315 sh (15600), 326 (24800), 335 (30300), 350 (39400 nm).

3b: Yield 65%; m.p. 156–157 °C. FT-IR (CCl_4): $\tilde{\nu}$ = 2159, 2143 (C≡C) cm^{-1}. ^1H NMR ($CDCl_3$): δ = 0.20 (s, 18H, $SiMe_3$), 1.10 (s, 42H, $CH(CH_3)_2$). ^{13}C NMR ($CDCl_3$): δ = −0.34, 11.2, 18.7, 101.2, 102.2, 103.7, 104.7, 117.0, 118.9. UV/VIS (MeOH): λ_{max} = 213 (ε = 14800), 223 (16100), 274 (10800), 288 (10700), 316 sh (16200), 328 (26700), 336 (32700), 351 (44900) nm.

3c: Yield 61%; m.p. 112.5–113.5 °C. FT-IR (CCl_4): $\tilde{\nu}$ = 2199, 2143 (C≡C), 1596 (C=C) cm^{-1}. ^{13}C NMR ($CDCl_3$): δ = −0.26, 87.0, 99.1, 101.3, 105.1, 116.6, 119.5, 122.4, 128.3, 129.1, 131.8. UV/VIS (MeOH): λ_{max} = 219 sh (ε = 20800), 225 (23300), 238 sh (17400), 245 sh (16800), 249 sh (16400), 271 sh (20900), 278 (23100), 283 sh (22500), 295 (22800), 358 (30500), 372 (31500), 380 sh (29700) nm.

4a: Yield 87%; m.p. > 30 °C (dec). FT-IR (CCl_4): $\tilde{\nu}$ = 3307 (≡C-H), 2102 (C≡C), 1634 (C=C), 653, 632 (≡C-H_{bend}) cm^{-1}. ^1H NMR ([D_6]acetone): δ = 4.38 (s). ^{13}C NMR ([D_6]acetone) [a]: δ = 80.1 (d, ^2J = 50.6 Hz; C-2), 89.8 (d, ^1J = 257.4 Hz; C-1), 119.1 (m, C-3). UV/VIS (MeOH) [b]: λ_{max} = 242 sh (ε = 4860), 250 (5290), 264 (5500), 286 sh (13800), 295 sh (19800), 301 (22900), 313 (25800) nm. HR-MS: *m/z* ($M^{\oplus}$, $C_{10}H_4$), calcd 124.0313, obsd 124.0311.

4b: Yield 99%; oil. IR (CCl_4): $\tilde{\nu}$ = 3302 (≡C-H), 2152, 2096 (C≡C) cm^{-1}. ^1H NMR ($CDCl_3$): δ = 1.10 (s, 42H, $CH(CH_3)_2$), 3.49 (s, 2H, ≡CH). ^{13}C NMR ($CDCl_3$) [a]: δ = 11.2 (dm, ^1J = 119.7 Hz; $CH(CH_3)_2$), 18.5 (qm, ^1J = 126.3 Hz; $CH(CH_3)_2$), 80.2 (dd, ^2J = 49.7, ^4J = 1.7 Hz; C-2), 86.5 (d, ^1J = 255.3 Hz, C-1), 102.7 (s), 102.9 (s), 115.6 (t, ^3J = 5.0 Hz; C-3), 121.4 (t, ^4J = 2.9 Hz; C-3'). UV/VIS (MeOH) [b]: λ_{max} = 217 (ε = 11600), 273 sh (10200), 288 (12400), 303 sh (15600), 314 sh (24100), 320 (27500), 334 (34300) nm. HR-MS: *m/z* ($M^{\oplus}$, $C_{28}H_{44}Si_2$), calcd 436.2981, obsd 436.2966.

4c: oil [c]. FT-IR (CCl_4): $\tilde{\nu}$ = 3307 (≡CH), 2196 (C≡C), 1598 (C=C) cm^{-1}. ^1H NMR ([D_6]acetone): δ = 4.11 (s, 2H; ≡CH), 7.35–7.45 (m, 6H; Ph), 7.5–7.55 (m, 4H; Ph). ^{13}C NMR ([D_6]acetone): δ = 80.8, 86.7, 88.6, 99.5, 115.6, 120.7, 122.5, 129.0, 129.9, 132.3. UV/VIS (MeOH): λ_{max} = 229 (ε = 17200), 237 (17300), 241 sh (17100), 248 sh (15900), 267 sh, (18000), 274 (20600), 280 (20600), 290 (22400), 350 (30700), 361 sh (26300) nm. HR-MS: *m/z* ($M^{\oplus}$, $C_{22}H_{12}$), calcd 276.0939, obsd 276.0932.

[a] Gated decoupling. [b] Solutions of **4a–4c** were obtained from solutions of **3a–3c** of known concentration in MeOH by treatment with 5 mg of K_2CO_3 for 10 min, followed by addition of 10 μL of 36% HCl. Absorption coefficients ε based on quantitative deprotection of TMS groups. [c] Neat oil polymerized within 5 s.

[*] Prof. F. Diederich, Y. Rubin, C. B. Knobler
Department of Chemistry and Biochemistry
University of California
Los Angeles, CA 90024-1569 (USA)

[**] We thank the National Science Foundation for support of this work. According to IUPAC rules, the name of the title compound is 3,4-diethynyl-3-hexene-1,5-diyne.

sess a low-lying band gap.[8] (4) Finally, derivatives of **4a** could show the potent anticancer activity observed for strained *cis*-enediynes.[9]

A general synthetic route to **4a** and its derivatives **4b** and **4c** required the preparation of the differentially protected tetraalkynylethenes **3a**–**3c** (Table 1). Accordingly, 1,5-bis(trimethylsilyl)-1,4-pentadiyn-3-one (**1**)[10] was converted into the dibromomethylene derivative **2a** with CBr_4/PPh_3.[11] The $[Pd(PPh_3)_4]$-catalyzed alkynylation of **2a** was successfully carried out with trimethylsilylacetylene, triisopropylsilylacetylene, and phenylacetylene in the presence of CuI and *n*-butylamine in benzene (25 °C) to give **3a**,[1b] **3b**, and **3c**, respectively.[12] Removal of the trimethylsilyl groups in **2a** and **3a**–**3c** with catalytic amounts of K_2CO_3 in methanol smoothly afforded the free alkynes **2b** and **4a**–**4c** in essentially quantitative yields. The lower isolated yields for **2b** and **4a** reported in Table 1 are due to material loss occurring upon drying these highly volatile compounds.

Tetraethynylethene (**4a**) is fairly soluble in pentane and crystallizes out of this solvent at −10 °C as white plates. At 25 °C, **4a** becomes rapidly brown even in the absence of oxygen and polymerizes to a black solid with metallic luster; the same process happens slowly in solution to give a brown precipitate. Similarly, the triisopropylsilyl derivative **4b** decomposes at 25 °C in the neat state, although more slowly than **4a**. A dramatic instability is observed for **4c**: the neat oil polymerizes to a black hard mass in a matter of a few seconds. Therefore, all manipulations with this compound were made in solution.

The gated decoupled ^{13}C NMR spectrum of **4a** in [D_6]acetone shows only three absorptions with the expected CH coupling constants for the alkyne carbons. The remarkably simple FT-IR spectrum of **4a** in CCl_4 shows a characteristic strong C–H stretching band at 3307 cm^{-1}, together with a weak C≡C stretching band at 2102 cm^{-1} (Fig. 1). The

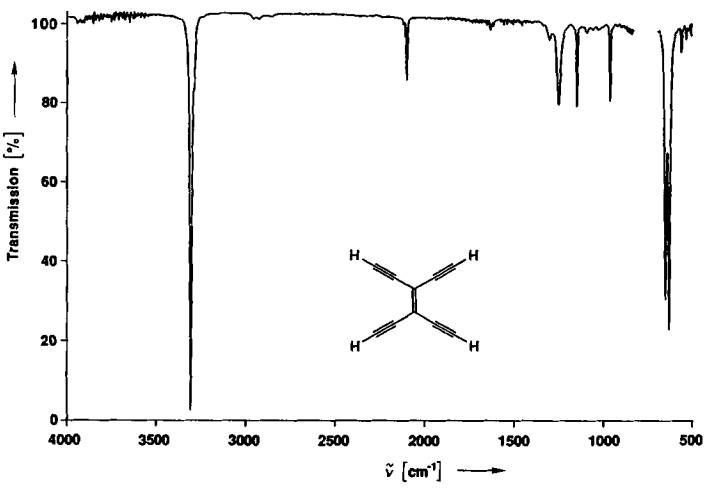

Fig. 1. FT-IR spectrum of **4a** in dilute CCl_4 solution.

strong absorptions at 653 and 632 cm^{-1} are due to the coupled C–H bending modes in **4a**. The UV spectrum of **4a** in MeOH is very similar to the one of its $SiMe_3$-substituted derivative **3a**,[1b] although the absorption bands for **4a** are shifted 20–35 nm to higher energy and are somewhat broader (Fig. 2).

An X-ray structure analysis was performed with the stable derivative **3a** (Fig. 3).[13, 14] The molecule is nearly planar: the maximum deviation from the least-squares plane through

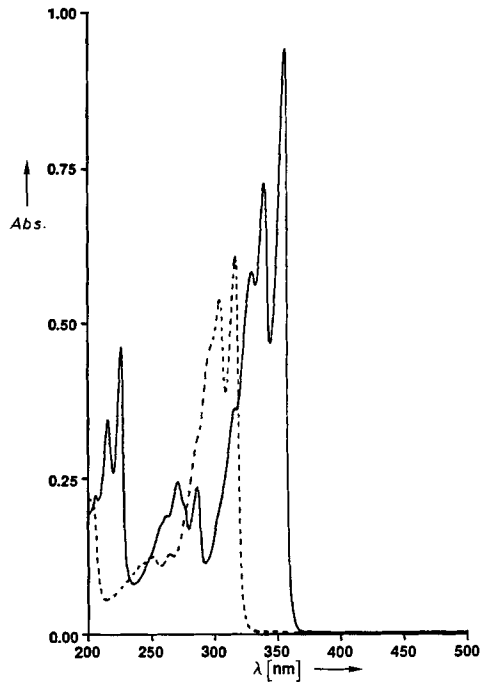

Fig. 2. Electronic absorption spectra of **3a** (——) and **4a** (---) in MeOH, $T = 25$ °C, $d = 1$ cm, $[\mathbf{3a}] = [\mathbf{4a}] = 2.33 \times 10^{-5}$ M.

the tetralkynylethene framework including the four silicon atoms is 0.032(9) Å. The tetralkynylethene framework itself is planar within 0.007(8) Å. The molecule is slightly distort-

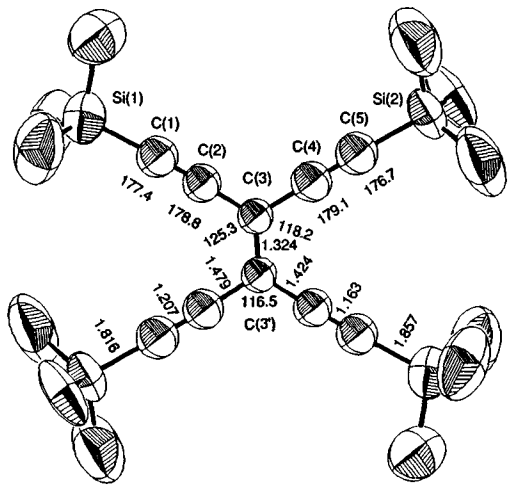

Fig. 3. X-ray crystal structure of **3a**.

ed: the C3′–C3–C2 angle is 125.3(7)°, a value similar to those calculated for other unstrained *cis*-enediynes,[15] while the C3′–C3–C4 angle is unusually small, with a value of 118.2(7) Å. This distortion presumably results from crystal packing effects in the solid.[4] The bond lengths in **3a** are within the normal range for C=C and C≡C bonds.

Experimental Procedure

4a: A solution of tetrakis[(trimethylsilyl)ethynyl]ethene (**3a**) (1.25 g, 3.0 mmol) in 50 mL of methanol was stirred with solid K_2CO_3 (200 mg) for 15 min at 25 °C. The mixture was poured into pentane/water with stirring, and the organic phase was washed with more water and dried with $MgSO_4$ and silica gel. Evaporation at ≤25 °C gave 325 mg (87%) of **4a** as volatile white platelets,

which became brown within 2 min. Solutions of **4a** in Et_2O were conveniently stored for more than two months at $-5\,^{\circ}C$.

Received: February 20, 1991 [Z 4457 IE]
German version: *Angew. Chem. 103* (1991) 708

[1] a) Y. Hori, K. Noda, S. Kobayashi, H. Taniguchi, *Tetrahedron Lett. 1969*, 3563; b) H. Hauptmann, *Angew. Chem. 87* (1975) 490; *Angew. Chem. Int. Ed. Engl. 14* (1975) 498.
[2] a) F. Diederich, Y. Rubin, C. B. Knobler, R. L. Whetten, K. E. Schriver, K. N. Houk, Y. Li, *Science (Washington, D.C.) 245* (1989) 1088; b) Y. Rubin, M. Kahr, C. B. Knobler, F. Diederich, C. L. Wilkins, *J. Am. Chem. Soc. 113* (1991) 495.
[3] H. Hopf, M. Kreutzer, *Angew. Chem. 102* (1990) 425; *Angew. Chem. Int. Ed. Engl. 29* (1990) 393.
[4] For the synthesis of hexaethynylbenzene see: R. Diercks, J. C. Armstrong, R. Boese, K. P. C. Vollhardt, *Angew. Chem. 98* (1986) 270; *Angew. Chem. Int. Ed. Engl. 25* (1986) 268.
[5] a) R. H. Baughman, E. Eckhardt, M. Kertesz, *J. Chem. Phys. 87* (1987) 6687; b) A. T. Balaban, *Computers Math. Applic.* (1989) 397.
[6] a) T. X. Neenan, G. M. Whitesides, *J. Org. Chem. 53* (1988) 2489, and references cited therein; b) T. X. Neenan, M. R. Callstrom, L. M. Scarmoutzos, K. R. Stewart, G. M. Whitesides, V. R. Howes, *Macromolecules 21* (1988) 3525.
[7] T. P. Lockhart, P. B. Comita, R. G. Bergman, *J. Am. Chem. Soc. 103* (1981) 4082.
[8] a) A. Bohnen, K. H. Koch, W. Lüttke, K. Müllen, *Angew. Chem. 102* (1990) 548; *Angew. Chem. Int. Ed. Engl. 29* (1990) 525; b) J. L. Brédas, R. H. Baughman, *J. Chem. Phys. 83* (1985) 1316.
[9] a) K. C. Nicolaou, C.-K. Hwang, A. L. Smith, S. V. Wendeborn, *J. Am. Chem. Soc. 112* (1990) 7416; b) J. A. Porco, Jr., F. J. Schoenen, T. J. Stout, J. Clardy, S. L. Schreiber, *ibid. 112* (1990) 7410, and references cited therein.
[10] H. Hauptmann, *Tetrahedron 32* (1976) 1293.
[11] G. H. Posner, G. L. Loomis, H. S. Sawaya, *Tetrahedron Lett.* (1975) 1373.
[12] K. P. C. Vollhardt, L. S. Winn, *Tetrahedron Lett. 26* (1985) 709.
[13] X-ray crystal data for **3a** ($C_{22}H_{36}Si_4$); $M_r = 412.87$, orthorhombic space group *Pcab*, $Z = 4$; $a = 12.927(2)$, $b = 13.057(2)$, $c = 18.004(3)$ Å, $V = 3039$ Å^3, $Cu_{K\alpha}$ radiation, $2\theta \leq 115°$, 2079 unique reflections. The structure was solved by statistical methods (SHELX-86), yielding $R = 0.080$, $R_w = 0.099$ for 864 independent reflections with $I > 3\sigma(I)$. Further details of the crystal structure investigations are available on request from the Director of the Cambridge Crystallographic Data Centre, University Chemical Laboratory, Lensfield Road, GB-Cambridge CB2 1EW (UK), on quoting the full journal citation. A similar X-ray structure analysis was performed with compound **3b** at 25°C: the tetraalkynylethene framework could easily be located, but highly disordered triisopropylsilyl groups prevented further refinement.
[14] *H. Hopf* et al. have independently carried out an X-ray structure analysis of tetraphenylethynylethene: *Chem. Ber. 124* (1991), No. 6.
[15] Y. Li, Y. Rubin, F. Diederich, K. N. Houk, *J. Am. Chem. Soc. 112* (1990) 1618.

Mononuclear Silylvinylidene Rhodium Complexes from Silylalkynes: The $SiMe_3$ Migration as an Alternative to the [1,2]-H Shift**

By *Dirk Schneider* and *Helmut Werner**

Dedicated to Professor Rolf Appel on the occasion of his 70th birthday

The rearrangement of 1-alkynes to vinylidenes in the coordination sphere of a transition metal has been intensively investigated in recent years.[1, 2] The general reaction, as shown in Equation (a), is often inhibited for kinetic reasons, in particular if both the starting material (**1**) and the product (**2**) are 18-electron species.[3] However, if ML_n is $[RhCl(PiPr_3)_2]$ or $[IrCl(PiPr_3)_2]$, a smooth transformation takes place;[4, 5] in this case, the isolation of intermediates of composition $[MH(C{\equiv}CR)Cl(PiPr_3)_2]$ supports the assumption[1a] that the rearrangement occurs stepwise.

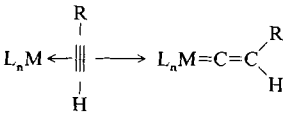

(a)

1 **2**

Almost nothing is known about the conversion of a disubstituted alkyne, $RC{\equiv}CR'$, into the isomeric vinylidene, $:C{=}CRR'$, in the vicinity of one metal center.[1, 6] We report here that with silylalkynes, $RC{\equiv}CSiMe_3$, such a reaction takes place in the coordination sphere of rhodium and that, independent of the substituent R, the [1,2]-$SiMe_3$ migration proceeds analogously to the [1,2]-H shift.

Complex **3**[7] does not react with an equimolar amount of bis(trimethylsilyl)acetylene (**4a**). If, however, a larger excess of **4a** is added to a pentane solution of **3** at $-20\,^{\circ}C$, a quick color change from violet to orange-red is observed. After a few minutes, the solution turns violet again. Upon workup and recrystallization at low temperatures dark violet crystals of **6a** are isolated; the spectroscopic data of **6a** (Table 1) confirm the structure shown in Scheme 1. The most typical

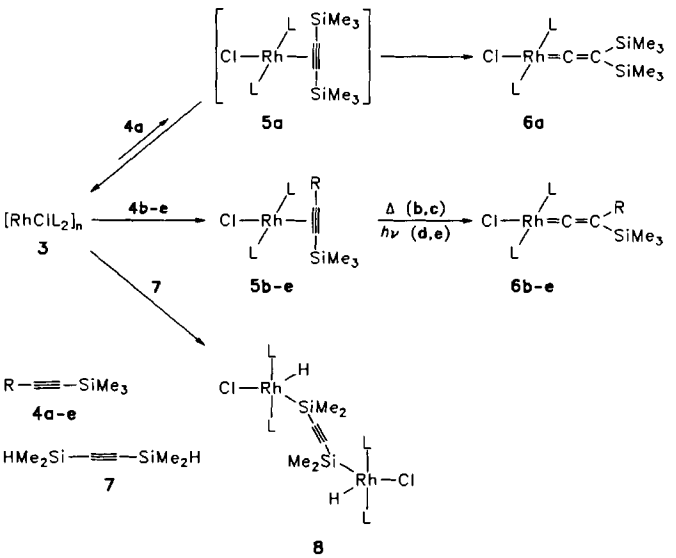

Scheme 1. L = $PiPr_3$; **4**: **a**, R = $SiMe_3$; **b**, R = Me; **c**, R = Ph; **d**, R = CO_2Et; **e**, R = CO_2SiMe_3.

features of the spectra, the position of the ^{13}C NMR signal of the α-carbon atom of the vinylidene ligand[1] and the appearance of a sharp triplet in the ^{29}Si NMR spectrum, support the equivalence of the $SiMe_3$ groups. If, after the addition of the alkyne, the reaction solution is worked up immediately at $-78\,^{\circ}C$, an orange solid (**5a**) can be isolated; its IR spectrum [$\nu(C{\equiv}C) = 1832\,cm^{-1}$] indicates the presence of a coordinated alkyne. Compound **5a** is extremely labile and, even in the solid state, rearranges to give the isomer **6a**.

[*] Prof. Dr. H. Werner, Dipl.-Chem. D. Schneider
Institut für Anorganische Chemie der Universität
Am Hubland, W-8700 Würzburg (FRG)

[**] This work was supported by the Deutsche Forschungsgemeinschaft, the Fonds der Chemischen Industrie, and Degussa AG. We thank *R. Lass* and Dr. *J. Wolf* for some valuable comments.

Table 1. Spectroscopic data for **5b–5e** and **6a–6e** (^{1}H and ^{13}C NMR data of the P*i*Pr$_3$ ligands only for **5b** and **6b**). NMR spectra at 200 MHz (^{1}H), 50.3 MHz (^{13}C), 17.8 MHz (^{29}Si), and 36.2 MHz (^{31}P), always in C_6D_6. IR spectra in hexane, only for **5d** in toluene and for **6e** in THF.

5b: IR: $\tilde{\nu}$ = 1848 cm^{-1} (C≡C). ^{1}H NMR: δ = 2.33 (m, PC*H*), 2.31 (d, J(RhH) = 0.5 Hz, ≡CCH_3), 1.35 (dvt, J(HH) = 6.9, N = 13.5 Hz, PCHCH_3), 1.19 (dvt, J(HH) = 6.2, N = 12.9 Hz, PCHCH_3), 0.24 (s, SiMe$_3$). ^{13}C NMR: δ = 112.97 (d, J(RhC) = 16.7 Hz), 62.06 (d, J(RhC) = 14.3 Hz), both signals for alkyne-C atoms, 23.03 (vt, N = 15.8 Hz, P*C*H), 21.01, 19.80 (both s, PCH*C*H$_3$), 15.99 (s, ≡C*C*H$_3$), 1.80 (s, SiMe$_3$). ^{31}P NMR: δ = 32.78 (d, J(RhP) = 118.7 Hz)

5c: IR: $\tilde{\nu}$ = 1805 cm^{-1} (C≡C). ^{1}H NMR: δ = 7.05 (m, C_6H_5), 0.33 (s, SiMe$_3$). ^{13}C NMR: δ = 132.22, 131.05, 130.51 (all s, *C*$_6$H$_5$, one other signal covered by the solvent), 117.00 (dt, J(RhC) = 18.3, J(PC) = 3.2 Hz), 77.92 (d, J(RhC) = 14.4 Hz), both signals for alkyne-C atoms, 1.64 (s, SiMe$_3$). ^{31}P NMR: δ = 31.20 (d, J(RhP) = 115.8 Hz)

5d: IR: $\tilde{\nu}$ = 1805 (C≡C), $\tilde{\nu}$ = 1695, 1685 cm^{-1} (C=O). ^{1}H NMR: δ = 4.09 (q, J(HH) = 7.1 Hz, CH_2CH$_3$), 1.07 (t, J(HH) = 7.1 Hz, CH$_2$CH_3), 0.35 (s, SiMe$_3$). ^{13}C NMR: δ = 155.35 (s, *C*O$_2$Et), 106.61 (dt, J(RhC) = 20.2, J(PC) = 3.6 Hz), 100.82 (d, J(RhC) = 14.6 Hz), both signals for alkyne-C atoms, 60.40 (s, *C*H$_2$), 14.27 (s, CH$_2$*C*H$_3$), 0.75 (s, SiMe$_3$). ^{31}P NMR: δ = 34.01 (d, J(RhP) = 114.3 Hz)

5e: IR: $\tilde{\nu}$ = 1805 (C≡C), $\tilde{\nu}$ = 1675, 1663 cm^{-1} (C = O). ^{1}H NMR: δ = 0.34, 0.33 (both s, SiMe$_3$). ^{29}Si NMR: δ = 22.59 (s, CO$_2$SiMe$_3$), − 13.17 (s, ≡CSiMe$_3$). ^{31}P NMR: δ = 33.97 (d, J(RhP) = 114.3 Hz)

6a: IR: $\tilde{\nu}$ = 1624 cm^{-1} (C=C). ^{1}H NMR: δ = 0.24 (s, SiMe$_3$). ^{13}C NMR: δ = 272.00 (dt, J(RhC) = 58.9, J(PC) = 13.7 Hz, Rh = *C*), 89.71 (dt, J(RhC) = 14.7, J(PC) = 4.2 Hz, = *C*R$_2$), 2.87 (s, SiMe$_3$), from SiMe$_3$ satellites: J(SiC) = 52.6 Hz. ^{29}Si NMR: δ = − 14.49 (t, J(PSi) = 2.2 Hz). ^{31}P NMR: δ = 41.10 (d, J(RhP) = 140.7 Hz)

6b: IR: $\tilde{\nu}$ = 1647 cm^{-1} (C=C). ^{1}H NMR: δ = 2.72 (m, PC*H*), 1.74 (t, J(PH) = 1.9 Hz, = CCH_3), 1.33 (dvt, J(HH) = 7.0, N = 13.4 Hz, PCHCH_3), 1.32 (dvt, J(HH) = 6.9, N = 13.3 Hz, PCHCH_3), 0.10 (s, SiMe$_3$). ^{13}C NMR: δ = 280.25 (dt, J(RhC) = 57.8, J(PC) = 15.3 Hz, Rh = *C*), 92.81 (dt, J(RhC) = 15.3, J(PC) = 4.9 Hz, = *C*RR'), 23.95 (vt, N = 19.0 Hz, P*C*H), 20.56 (s, PCH*C*H$_3$, diastereotopic splitting not resolved), 1.37 (s, = C*C*H$_3$), − 0.91 (s, SiMe$_3$). ^{31}P NMR: δ = 41.44 (d, J(RhP) = 136.3 Hz)

6c: IR: $\tilde{\nu}$ = 1642 cm^{-1} (C=C). ^{1}H NMR: δ = 7.64 (m, 2 H of C_6H_5), 7.04 (m, 3 H of C_6H_5), 0.37 (s, SiMe$_3$). ^{13}C NMR: δ = 286.68 (dt, J(RhC) = 60.7, J(PC) = 14.7 Hz, Rh = *C*), 128.42, 127.58, 125.65 and 124.93 (all s, C_6H_5), 106.44 (dt, J(RhC) = 14.5, J(PC) = 4.9 Hz, = *C*RR'), 1.13 (s, SiMe$_3$). ^{29}Si NMR: δ = − 15.86 (t, J(PSi) = 1.8 Hz). ^{31}P NMR: δ = 41.62 (d, J(RhP) = 136.3 Hz)

6d: IR: $\tilde{\nu}$ = 1675 (C=O), $\tilde{\nu}$ = 1585 cm^{-1} (C=C). ^{1}H NMR: δ = 4.03 (q, J(HH) = 7.1 Hz, CH_2), 1.03 (t, J(HH) = 7.1 Hz, CH$_2$CH_3), 0.39 (s, SiMe$_3$). ^{13}C NMR: δ = 284.13 (dt, J(RhC) = 63.1, J(PC) = 13.1 Hz, Rh = *C*), 159.40 (s, *C*O$_2$Et), 105.71 (dt, J(RhC) = 15.3, J(PC) = 4.4 Hz, = *C*RR'), 59.85 (s, *C*H$_2$), 14.47 (s, CH$_2$*C*H$_3$), 0.19 (s, SiMe$_3$). ^{31}P NMR: δ = 43.08 (d, J(RhP) = 136.3 Hz)

6e: IR: $\tilde{\nu}$ = 1675 (C=O), $\tilde{\nu}$ = 1580 cm^{-1} (C=C). ^{1}H NMR: δ = 0.35, 0.31 (both s, SiMe$_3$). ^{13}C NMR: δ = 284.82 (dt, J(RhC) = 62.1, J(PC) = 13.8 Hz, Rh = *C*), 159.62 (s, *C*O$_2$SiMe$_3$), 104.70 (dt, J(RhC) = 15.3, J(PC) = 4.4 Hz, = *C*RR'), 0.06 and 0.03 (both s, SiMe$_3$). ^{29}Si NMR: δ = 20.74 (s, CO$_2$*Si*Me$_3$), − 11.32 (t, J(PSi) = 1.5 Hz, = C*Si*Me$_3$). ^{31}P NMR: δ = 43.52 (d, J(RhP) = 136.3 Hz)

The reaction of **3** with **4b–e** leads, in some cases almost quantitatively, to the silylalkyne rhodium complexes **5b–e** (Scheme 1), which, in contrast to **5a**, are stable at room temperature. Upon warming in pentane or hexane, only **5b, c**, but not **5d, e**, react to give the isomers **6**. On the other hand, the conversion of **5d,e** into the corresponding silylvinylidene complexes **6** proceeds photochemically; the yields are 55–60%. Attempts to observe a stepwise reaction sequence involving an acetylide(silyl)metal compound as intermediate failed. The reason for the different behavior of **5b,c** on one hand and of **5d,e** on the other is not yet clear; the positions of the charge-transfer (CT) and $\pi-\pi^*$ bands in the UV spectra of **5c** and **5d** are almost the same.

The properties of the violet, moderately air-stable solids **6b–e** are similar to those of **6a** and the previously described complexes *trans*-[RhCl(=C=CHR) (P*i*Pr$_3$)$_2$] (R = H, Me, *t*Bu, Ph, CO$_2$Me).[4] However, a characteristic difference is the presence of two sets of signals for the protons and the carbon atoms of the phosphane-CH$_3$ groups in the ^{1}H and ^{13}C NMR spectra of **6b–e** even at room temperature, indicating a hindered rotation of the vinylidene ligand around the Rh–C bond. We assume that the reason for this is steric hindrance between the two substituents on the β-carbon atom of the vinylidene and the bulky P*i*Pr$_3$ ligands. For the known complexes *trans*-[RhCl(= C=CHR) (P*i*Pr$_3$)$_2$] a comparable restriction of the rotation at 25 °C cannot be detected.[4]

The C–Si bond in **6a–e** can easily be cleaved by proton sources. After chromatography of benzene or hexane solutions of the silylvinylidene complexes on Al_2O_3 (activity grade III), not the original compounds but the desilylated complexes *trans*-[RhCl(= C=CHR) (P*i*Pr$_3$)$_2$][4] are eluted. If alumina deactivated with D_2O is used, the deuterated derivatives *trans*-[RhCl(= C=CDR) (P*i*Pr$_3$)$_2$] are obtained.

Surprisingly, the behavior of the SiMe$_2$H-substituted alkyne **7** toward **3** is completely different from that of the SiMe$_3$ analogue **4a**. It reacts with **3** under the same conditions as used for the synthesis of **6a** (in pentane) to form the binuclear compound **8**.[8] The oxidative addition of the Si–H bond to the metal center is obviously preferred over π coordination. Mononuclear rhodium complexes of composition [RhH(SiX$_3$) (Y) (PPh$_3$)$_2$] (Y = Cl, Br, I; X = Cl, OEt, Me, Et, Ph) are known[9] but, for X = alkyl, are unstable in solution.

Using silylalkynes as starting materials for the preparation of vinylidene complexes is probably not restricted to rhodium.[10] Recently, *Vahrenkamp* and co-workers showed that treatment of [Ru$_3$(CO)$_{11}$] with **4b** gave the alkyne-bridged cluster [RuCo$_2$(CO)$_9$(μ_3-MeC≡CSiMe$_3$)] accompanied by the rearranged complex [RuCo$_2$(CO)$_9$(μ_3-C=C(Me)SiMe$_3$].[11] No vinylidene complex is obtained from [RuCo$_2$(CO)$_{11}$] and **4a**; instead, a cluster fragmentation takes place. In contrast, at rhodium as metal center, the course of the reaction is clear for all the silylalkynes used so far. The ease of the [1,2]-SiMe$_3$ shift is particularly noteworthy because such a process only occurs under extreme thermal conditions for free alkynes.[12]

Experimental Procedure

6a: A solution of **3** (287 mg, 0.63 mmol) in pentane (25 mL) was treated at − 20 °C with **4a** (1 mL). A spontaneous color change from violet to orange-red occurred and in a few minutes, the solution became violet again. The solvent was removed in vacuo and the oily residue was dissolved in hexane (3 mL). On cooling the solution to − 78 °C, dark violet crystals were obtained: yield 242 mg (61%); m.p. 72 °C (dec.). **5b–e**: A solution of **3** (397 mg, 0.87 mmol) in pentane (30 mL) was treated at 0 °C with an equimolar amount of **4b–e** and then stirred for 30 min at room temperature. Workup as described for **6a**; orange-yellow crystals: **5b**, yield 53%; m.p. 86 °C (dec.); **5c**, yield 57%; m.p. 86 °C (dec.); **5d**, yield 84%; m.p. 69 °C (dec.); **5e**, yield 89%; m.p. 74 °C (dec.). **6b**: A solution of **5b** (171 mg, 0.30 mmol) in pentane (20 mL) was stirred for 6 h at 35 °C. After concentration of the solution to about 3 mL and cooling to − 78 °C, dark violet crystals were isolated: yield 53%; m.p. 83 °C (dec.). **6c**: Prepared analogously to **6b**, but **5c** was stirred for 25 h at 60 °C in hexane: yield 67%; m.p. 97 °C (dec.). **6d**: A solution of **5d** (189 mg, 0.30 mmol) in benzene (20 mL) was irradiated for about 5 h at room temperature; the color changed from orange to red-violet. Workup as described for **6a**: yield 54%; m.p. 116 °C (dec.). **6e**: As described for **6d**: yield 59%; m.p. 107 °C (dec.). **8**: A solution of **3** (397 mg, 0.87 mmol) in pentane (30 mL) was treated at 0 °C with an equimolar amount of **7**. The bright yellow solid that precipitated was washed with pentane and dried in vacuo: yield 415 mg (90%); m.p. 102 °C (dec.). Satisfactory elemental analyses were obtained for all compounds.

Received: January 2, 1991 [4367 IE]
German version *Angew. Chem. 103* (1991) 710

[1] a) M. I. Bruce, A. G. Swincer, *Adv. Organomet. Chem. 22* (1983) 59; b) M. I. Bruce, *Chem. Rev. 91* (1991) 197; c) A. B. Antonova, A. A. Johansson, *Usp. Khim. 58* (1989) 1197; d) H. Werner, *Angew. Chem. 102* (1990) 1109; *Angew. Chem. Int. Ed. Engl. 29* (1990) 1077.

[2] For the rearrangement of 1-alkynes in vinylidenes on metal clusters see: a) E. Roland, W. Bernhardt, H. Vahrenkamp, *Chem. Ber. 118* (1985) 2858; b) T. Albiez, W. Bernhardt, C. von Schnering, E. Roland, H. Bantel, H. Vahrenkamp, *ibid. 120* (1987) 141; c) H. Vahrenkamp in H. Werner, G. Erker (Eds.): *Organometallics in Organic Synthesis 2*, Springer, Heidelberg 1989, p. 235.
[3] Theoretical studies: a) N. M. Kostić, R. F. Fenske, *Organometallics 1* (1982) 974; b) J. Silvestre, R. Hoffmann, *Helv. Chim. Acta 68* (1985) 1461.
[4] M = Rh: a) H. Werner, J. Wolf, F. J. Garcia Alonso, M. L. Ziegler, O. Serhadli, *J. Organomet. Chem. 336* (1987) 397; b) H. Werner, F. J. Garcia Alonso, H. Otto, J. Wolf, *Z. Naturforsch. B43* (1988) 722; c) H. Werner, U. Brekau, *ibid. B44* (1989) 1438.
[5] M = Ir: a) F. J. Garcia Alonso, A. Höhn, J. Wolf, H. Otto, H. Werner, *Angew. Chem. 97* (1985) 401; *Angew. Chem. Int. Ed. Engl. 24* (1985) 406; b) A. Höhn, H. Otto, M. Dziallas, H. Werner, *J. Chem. Soc. Chem. Commun. 1987*, 852; c) A. Höhn, H. Werner, *J. Organomet. Chem. 382* (1990) 255.
[6] *Sakurai* et al. mentioned in a preliminary communication that the macrocyclic trisalkyne [-O-$SiMe_2$-C≡C-$SiMe_2$-]$_3$ reacts with [$C_5H_5Mn(CO)_3$] to give a vinylidene manganese complex; no details are known: H. Sakurai, K. Hirama, Y. Nakadaira, C. Kabuto, *J. Am. Chem. Soc. 109* (1987) 6880.
[7] a) Isolation: H. Werner, J. Wolf, A. Höhn, *J. Organomet. Chem. 287* (1985) 395; b) **3** is monomeric in benzene [M_r(calcd) = 458.85; M_r(found) = 498] but a dimer in the solid state. For X-ray structural analysis see: J. Haas, *Dissertation*, Universität Kaiserslautern 1990. We thank Prof. *P. Binger* for this information.
[8] Spectroscopic data: IR (KBr): ν = 2108 cm^{-1} (RhH). ^1H NMR (C_6D_6, 200 MHz): δ = 2.71 (m, PC*H*), 1.35 (dvt, J(HH) = 7.0, N = 13.9 Hz, $PCHCH_3$), 1.25 (dvt, J(HH) = 6.6, N = 13.5 Hz, $PCHCH_3$), 0.93 (s, $SiMe_2$), − 16.34 (dt, J(RhH) = 21.5, J(PH) = 13.1 Hz, Rh*H*). ^{29}Si NMR (CD_2Cl_2, − 35 °C, 17.8 MHz): δ = 14.52 (dt, J(RhSi) = 36.4, J(PSi) = 9.7 Hz); ^{31}P NMR (CD_2Cl_2, − 35 °C, 36.2 MHz): δ = 44.74 (d, J(RhP) = 115.7 Hz, dd in off-resonance).
[9] R. N. Haszeldine, R. V. Parish, D. J. Parry, *J. Chem. Soc. (A) 1969*, 683.
[10] On photolysis of *trans*-[IrCl(C_8H_{14})($PiPr_3$)$_2$] and **4d**, most probably the vinylidene complex *trans*-[IrCl(= C=C($SiMe_3$)CO_2Et) ($PiPr_3$)$_2$] is formed: R. Lass, *Diplomarbeit*, Universität Würzburg, in preparation.
[11] H. Bantel, A. K. Powell, H. Vahrenkamp, *Chem. Ber. 123* (1990) 661.
[12] a) M. Karpf, A. S. Dreiding, *Helv. Chim. Acta 62* (1979) 1852; b) T. J. Barton, B. L. Groh, *Organometallics 4* (1985) 575.

Furfural as a Marker of DNA Cleavage by Hydroxylation at the 5′ Carbon of Deoxyribose**

By *Geneviève Pratviel, Marguerite Pitié, Jean Bernadou,** and *Bernard Meunier**

Besides naturally occurring nucleases which cleave DNA by phosphodiester bond hydrolysis, there is a growing interest in synthetic compounds that show DNA-cleaving activity.[1] The common feature of these systems is an oxidative attack on the sugars of the DNA backbone. DNA degradation is initiated by the abstraction of an H atom from a C–H bond of a deoxyribose, as also observed in DNA cleavage by radiolysis.[2, 3] The C–H bond cleaved depends on the DNA cleaver used. C4′–H is the major target of iron-bleomycin,[4] whereas the bis(*o*-phenanthroline)copper attacks at C1′–H.[1, 5] A hydrogen atom is abstracted from C5′–H′ (or H″) by neocarzinostatin and drugs related to calicheamicin.[6, 7] In the case of neocarzinostatin, two other minor routes of DNA sugar attack have also been described: at C1′ with cytosine release[8, 9] and at C4′ with thymine release.[10] A minor pathway at C1′ was also proposed in the bleomycin degradation of the hybrid poly(dA)·poly(rU).[11]

The artificial nuclease we used is a cationic manganese porphyrin, *meso*-tetrakis (*N*-methylpyridinium-4-yl)porphyrinatomanganese(III) pentaacetate (Mn-TMPyP), that has been shown to interact with DNA in the minor groove.[12] In the presence of a water-soluble oxygen-atom donor, such as $KHSO_5$, potassium monopersulfate, or magnesium monoperphthalate (MMPP), a high-valent manganese oxo porphyrin complex (reminiscent of the activated form of cytochrome P-450 capable of activating the C–H bond of saturated compounds) is generated in the close vicinity of DNA. Subsequent DNA cleavage is observed for nanomolar concentrations of the metalloporphyrin.[13] Previous analysis of the reaction products on a simplified model of DNA, polyadenylic acid or poly(dA), led us to propose the sugar C1′–H bond as the main target of this artificial nuclease.[14]

We wish to report here that, depending on the type of DNA substrate, the Mn-TMPyP/$KHSO_5$ system can hydroxylate deoxyriboses at the C1′ and/or C5′ carbon. The C1′ route has been confirmed through the release of 5-methylene-2-furanone (5-MF) as the product of deoxyribose oxidation.[5, 14] Evidence for the C5′ route is provided by the release of another oxidized sugar residue, furfural (FUR). To our knowledge, this is the first identification of furfural as a marker of hydroxylation at the 5′ carbon of deoxyribose in oxidative DNA cleavage. The quantitative comparison of the FUR/5-MF ratio is indicative of the relative reactivities of the activated Mn-TMPyP complex towards C5′ and C1′.

A typical experiment consisted of preincubation of DNA substrate (700 μM nucleotides) with Mn-TMPyP (35 μM) in 50 μL of pH 8 phosphate buffer (34 mM) and NaCl (100 mM) for 15 minutes. The reactions were initiated by the addition of $KHSO_5$ (2 mM). After 3 minutes at room temperature, the reactions were stopped by addition of pH 8 Hepes buffer (100 mM).[13b] Concentrations in brackets are final concentrations. The products released were analyzed by HPLC, either after 3 minutes at 20 °C or after a heating step at 90 °C for 15 minutes. Examples of HPLC chromatograms are shown in Figure 1 and the results are summarized in Table 1. The free bases are released at ambient temperature. No guanine is observed because of its high oxidizability under the experimental conditions. After heating, two other products were detected and have been identified as 5-MF[5, 14] and FUR by HPLC (Fig. 1) and by GC/MS.[15] The appearance of FUR correlates with an enhanced release of the corresponding bases during heating. Some of the variations in the results are

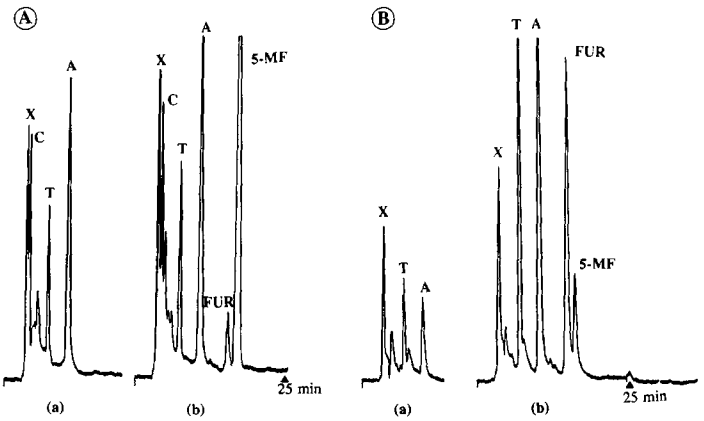

Fig. 1. Chromatograms of products released during the reaction of Mn-TMPyP/$KHSO_5$ with CT DNA, Ⓐ, and poly(dA)·poly(dT), Ⓑ, after 3 min at 20 °C (a) and 15 min at 90 °C (b). Nucleosil C_{18} 5 μ column eluted with 0.1 M triethylammonium acetate, pH 6.5, 5% acetonitrile, 0.5 mL min^{-1}; UV detection at λ = 254 nm (X: porphyrin degradation product).

[*] Prof. Dr. J. Bernadou, Dr. B. Meunier, Dr. G. Pratviel, M. Pitié
Laboratoire de Chimie de Coordination du CNRS
205 route de Narbonne
F-31077 Toulouse Cedex (France)

[**] The financial support of the Centre National de la Recherche Scientifique, "Association pour la Recherche sur le Cancer" (ARC, Villejuif), the Université Paul Sabatier, and the Région Midi-Pyrénées is gratefully acknowledged.

Table 1. Release of free bases, 5-MF, and FUR during oxidative degradation of various DNA substrates catalyzed by Mn-TMPyP/$KHSO_5$ [a].

	Before heating [b]			After heating [b]					
	A	C	T	A	C	T	FUR	5-MF	% [c]
poly(dA) [d]	13±4	–	–	20±5	–	–	2.5±1	6±2	29
poly(dT)	–	–	77±11	–	–	97±18	9±2	65±14	12
poly(dC)	–	49±6	–	–	58±16	–	3±1	34±11	8
poly[d(A-T)·d(A-T)]	26±3	–	17±3	45±5	–	42±4	37±4	21±4	64
poly(dA)·poly(dT)	11±1	–	15±4	39±2	–	50±3	57±1	12±2	83
poly[d(G-C)·d(G-C)]	–	64±8	–	–	75±8	–	3±1	44±8	6.5
poly(dG)·poly(dC)	–	71±20	–	–	92±17	–	3.5±1	63±12	5.5
CT DNA	32±4	30±5	17±1	35±2	35±2	24±4	8±1	59±6	12

[a] For reaction conditions see text. [b] All values (μM) represent the mean standard deviation from three measurements. Free G, owing to its high oxidizability, was not found in these experiments. [c] % = 100 × [FUR]/[5-MF] + [FUR]. [d] Poly(dG) was not tested owing to its special polymerization process in solution.

due to degradation of the bases through partial or, for guanine, complete oxidation by Mn-TMPyP/$KHSO_5$; also, FUR and 5-MF are slightly unstable. The quantitative results for the products listed in Table 1 should be supplemented by further kinetic studies. However, preliminary kinetic data indicate that our conclusions are largely valid. The last column of Table 1 reflects the ratio of attack at C5′ versus C1′. C1′ is still the main hydroxylation site for calf thymus DNA (CT DNA) and G-C polymers (the percent attack at C5′ is 12, 6, and 7% for CT DNA, poly(dG)·poly(dC), and poly[d(G-C)·d(G-C)][*]). Highly selective attack at C5′ is observed for A-T polymers (the percent attack at C5′ is 64 and 83% for poly[d(A-T)·d(A-T)] and poly(dA)·poly(dT), which suggests that the mechanism of DNA cleavage is highly sequence-dependent.

The molecular mechanism proposed to account for these product distributions is presented in Scheme 1. Hydroxylation of the C1′ carbon induces spontaneous release of the corresponding free base. Two subsequent βeliminations lead to 5-MF and leave two DNA strands terminated by phosphate groups. The first βelimination creates a 5′-phosphate end. This reaction probably takes place at ambient temperature because the addition of $NaBH_4$ before heating prevents the 5-MF release ($NaBH_4$ was allowed to react for 30 minutes and then was completely destroyed by acetone before increasing the temperature). $NaBH_4$ should not react with intermediate **I** but rather with **II** (Scheme 1).[16] On the other hand, hydroxylation of the C5′ carbon gives a C5′ aldehyde at one strand terminus and a 3′-phosphate at the other at ambient temperature. Upon heating, two βeliminations result in the formation of FUR, free base, and a 5′-phosphate terminus.

Both routes give rise to the same phosphate termini but not in the same order, and the sugar degradation products are different. In both cases a DNA single-strand break is created at ambient temperature.

DNA models suggest that the distance between H1′ on one strand and either H1′ or H5′ (or H5″) of deoxyribose (shifted by two or three base pairs in the direction of the 3′ end) on the opposing strand are very close. Thus, it is not so surprising that small changes in the interaction of the cleaving reagent with the DNA minor groove direct the reactivity from one target to the other.

Our results show that furfural is a convenient marker of the C5′ hydroxylation of DNA deoxyribose, just as 5-MF was previously shown to be a marker of the C1′ hydroxylation.[5, 14, 17] These two targets (C1′ on one strand and C5′ on the other strand) are often involved in bifunctional DNA-cleaving agents. When one active part of the molecule points inside the minor groove at C1′ of one DNA strand, the second active part is close to C5′, which is at the entrance of the minor groove on the other strand. The biradical intermediate of neocarzinostatin is an example. For manganese porphyrin complexes a similar explanation applies if the orientation of the axial ligand is colinear with the C1′–C5′ axis and the possible formation of the active manganese-oxo species at one of the two axial positions in *trans* configuration is also considered. Such subtle changes in the geometry of the interactions between cleaving reagent and DNA should give rise to dramatic changes in the selectivity of C–H bond activation of the deoxyribose units within the minor groove of DNA.

[*] d(G-C) represents an alternating copolymer consisting of guanine and cytosine deoxynucleotides; poly[d(G-C)·d(G-C)] is the hybrid formed from two such copolymers.

Received: December 27, 1990 [Z 4359 IE]
German version: *Angew. Chem. 103* (1991) 718

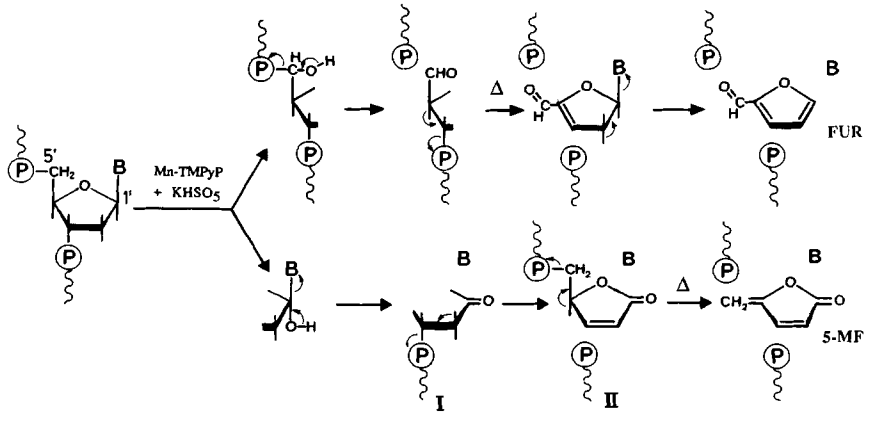

Scheme 1. Proposed mechanism for the cleavage of DNA after hydroxylation of deoxyribose by Mn-TMPyP/$KHSO_5$.

 © *VCH Verlagsgesellschaft mbH, W-6940 Weinheim, 1991* *0570-0833/91/0606-0703 $ 3.50+.25/0*

CAS Registry numbers:
Mn-TMPyP, 110989-01-0; FUR, 98-01-1; poly(dA), 25191-20-2; poly(dT), 25086-81-1; poly(dC), 25609-92-1; poly(dA) · poly(dT), 24939-09-1; poly(dG) · poly(dC), 25512-84-9; poly[d(A-T) · d(A-T)], 26966-61-0; poly[d(G-C)-d(G-C)], 36786-90-0; deoxyribonuclease, 9003-98-9; desoxyribose, 533-67-5.

[1] D. S. Sigman, *Biochemistry 29* (1990) 9097.
[2] C. von Sonntag: *The Chemical Basis of Radiation Biology*, Taylor and Francis, London 1987, pp. 167–193.
[3] J. Cadet, R. Téoule, *Bull. Soc. Chim. Fr. 1975*, 891.
[4] a) S. M. Hecht, *Acc. Chem. Res. 19* (1986) 383; b) J. Stubbe, J. W. Kozarich, *Chem. Rev. 87* (1987) 1107.
[5] T. E. Goyne, D. S. Sigman, *J. Am. Chem. Soc. 109* (1987) 2846.
[6] I. H. Goldberg, *Free Radical Biol. Med. 3* (1987) 41.
[7] N. Zein, A. M. Sinha, W. J. McGahren, G. A. Ellestad, *Science (Washington DC) 240* (1988) 1198.
[8] L. S. Kappen, I. H. Goldberg, *Biochemistry 28* (1989) 1027.
[9] L. S. Kappen, I. H. Goldberg, S. H. Wu, J. Stubbe, L. Worth. J. W. Kozarich, *J. Am. Chem. Soc. 112* (1990) 2797.
[10] I. Saito, H. Kawabata, T. Fujiwara, H. Sugiyama, T. Matsuura, *J. Am. Chem. Soc. 111* (1989) 8302.
[11] C. R. Krishnamoorthy, D. E. Vanderwall, J. W. Kozarich, J. Stubbe, *J. Am. Chem. Soc. 110* (1988) 2008.
[12] B. Ward, A. Skorobogaty, J. C. Dabrowiak, *Biochemistry 25* (1986) 7827.
[13] a) E. Fouquet, G. Pratviel, J. Bernadou, B. Meunier, *J. Chem. Soc. Chem. Commun. 1987*, 1169; b) J. Bernadou, G. Pratviel, F. Bennis, M. Girardet, B. Meunier, *Biochemistry 28* (1989) 7268; c) G. Pratviel, J. Bernadou, M. Ricci, B. Meunier, *Biochem. Biophys, Res. Commun. 160* (1989) 1212; d) R. B. Van Atta, J. Bernadou, B. Meunier, S. M. Hecht, *Biochemistry 29* (1990) 4783.
[14] J. Bernadou, B. Lauretta, G. Pratviel, B. Meunier, *C. R. Acad. Sci. Ser. 3 309* (1989) 409.
[15] A 50-μL sample was prepared as described in the text with poly(dA) · poly(dT) as DNA substrate. After the heating step, it was extracted with 300 μL of diethyl ether and the solvent was concentrated before injection in the GC/MS apparatus. GC/MS analyses were carried out with a Hewlett Packard 5890 gas chromatograph interfaced to a Hewlett Packard 5970 mass spectrometer. Gas-chromtography was carried out on a silica capillary column (12.5 m × 0.20 mm inner diameter) coated with cross-linked methylsilicone. Isothermal separation was performed at 80 °C, with the injector and interface maintained at 210 °C. Mass spectra were taken at 70 eV. In the heated sample a product with a GC retention time identical to an authentic sample of FUR gave a mass spectrum with a molecular peak (96) and fragmentations corresponding to FUR.
[16] L. S. Kappen, I. H. Goldberg, *Biochemistry 27* (1988) 4331.
[17] The hydroxylation of the sugar C1′–H bond has also been described for γ-irradiation of DNA [2, 3]. However, without the thermal step(s) (formation of 5-MF from intermediate **I** of Scheme 1) but after acid hydrolysis of DNA, deoxyribonolactone, not 5-MF, is the observed sugar oxidation product.

The Structure of "Organic Permanganate"

By *Maree L. Burgess, Donald C. Craig,* and *Michael J. Gallagher**

Over 120 years ago *Jena* reported[1] that the distillation of benzilic acid (**1**) gave a red-brown (actually "rotbraunes, empyreumatisch riechendes") oil. Other workers[2, 3] subsequently confirmed the formation of a deeply colored product in addition to carbon dioxide, diphenylacetic acid, and benzophenone. In 1911 *Staudinger*[4] showed that the dilactone **2** was formed on gentle heating and this decomposed at higher temperatures to give carbon dioxide, diphenylketene, and benzophenone as well as a deep red resin presumed to arise by polymerization of diphenyl ketene.

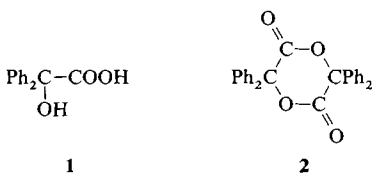

1 **2**

Eventually, in 1928, *Langenbeck* and *Langenbeck*[5] obtained from the pyrolysis mixture permanganate-colored crystals which they considered to be a dimer of diphenylketene on the basis of microanalysis and molecular weight data. As *Staudinger* had already obtained a colorless dimer of the ketene, the *Langenbecks* proposed that their dimer was in fact tetraphenylcyclobutanedione. There is, however, no obvious reason why this should be colored and almost immediately *Wittig* and *Lupin*[6] suggested an open-chain diradical variant. *Müller*[7] subsequently showed that the crystals were not paramagnetic, casting doubt on this interpretation, which was already considered unlikely as the compound is quite stable in air. Further studies[8, 9] over a number of years and using a variety of physical techniques failed to resolve the nature of this intriguing chromophore. We now report its structure.

Repetition of the *Langenbecks*' preparation, or *LeFevre*'s modification, afforded deep black-red crystals which possessed a pronounced purple cast by reflected light. The mass spectral molecular weight ($M = 374$)[10] immediately excluded all previous structures based on a dimer of diphenylketene ($M = 386$). ^1H and ^{13}C NMR spectra[10] were not particularly informative, though the latter showed only a single carbonyl absorption which was in the ester/lactone range ($\delta = 169.4$), suggesting that the chromophore was not quinonoid. A single-crystal X-ray analysis[11] has shown the structure to be the *p*-quinodimethane derivative **3** related to *Thiele*'s orange-yellow hydrocarbon **4**,[12] whose crystal structure has been recently determined.[13]

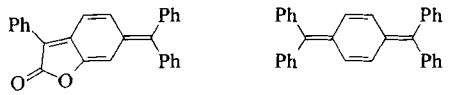

3 **4**

The structures of **3** and **4** are very similar, with distinct bond alternation and twisting of the Ph_2C group by ca. 15°, though of course **3** lacks the symmetry of **4**. The major difference is that **3**, excluding the phenyl groups, is significantly less planar than **4**. All atoms in the core of the molecule are displaced in the same direction (above the plane of the diagram) from the almost perfect plane through C1-C2-C4-C5-O1, the largest deviations being ca. 0.17 Å for C7 and C9.

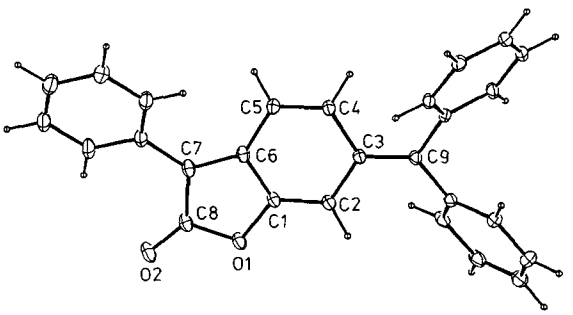

Fig. 1. Molecular structure of **3** (ORTEP). Selected bond lengths [Å] and angles [°]: C1-C2 1.346(3), C4-C5 1.353(3), C2-C3 1.448(3), C5-C6 1.422(3), C6-C7 1.387(3), C1-C6-C7 107.7(2), C2-C3-C9 122.1(2).

[*] Prof. M. J. Gallagher, M. L. Burgess, D. C. Craig
School of Chemistry, University of New South Wales
P.O. Box 1, Kensington, 2033 NSW (Australia)

[**] We thank the School of Chemistry for the award of a summer scholarship to *M. L. B.*

The bathochromic shift in the UV spectrum of **3** (λ_{max} = 463 nm in dioxane[9]) compared with **4** (λ_{max} = 426 nm in dioxane[14]) presumably reflects the extended conjugation resulting from formation of the furanone ring and the lower twist angle (ca. 27°) of the phenyl group on C7 compared with those for **4** (mean value ca. 43°).

A possible route to this compound is via the attack of diphenylcarbene on benzilic acid (Scheme 1).

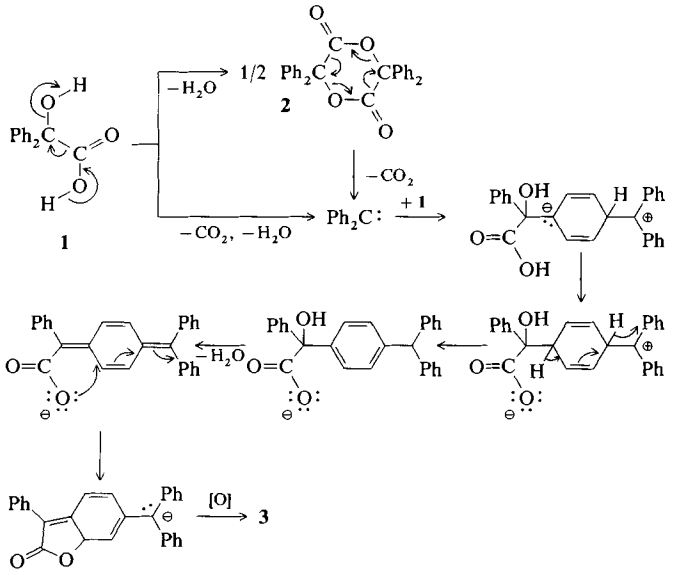

Scheme 1. Possible mechanism for the formation of **3**

Cyclization and oxidation to form the furanone ring system could occur either before or after formation of the chromophore and the carbene may be envisaged as arising from **1** or **2** by pyrolysis.

Experimental Procedure

A mixture of benzilic acid (5 g) and anhydrous sodium carbonate (0.1 g) was heated rapidly and briefly (ca. 2 min) with a Bunsen flame. After cooling, the virtually black residue was dissolved in chloroform and washed with aqueous sodium bicarbonate and water. The dried extract was concentrated and chromatographed over silica gel (200 g) and eluted with chloroform. The second band off the column comprised a mixture of **3** and the dilactone **2**. A pure sample of **3** was obtained by recrystallization from a mixture of chloroform and ethanol (m.p. 168–172°; lit. [5, 9], 168°/169°). The yield was low, closer to that reported by *Le Fevre* (ca. 3%) [9] than by the *Langenbecks* (ca. 10%).

Received: December 17, 1990 [Z 4335 IE]
German version: *Angew. Chem. 103* (1991) 723

CAS Registry numbers:
1, 76-93-7; **2**, 467-32-3; **3**, 4815-07-0.

[1] A. Jena, *Justus Liebigs Ann. Chem. 155* (1870) 77–89.
[2] H. Klinge, O. Standke, *Ber. Dtsch. Chem. Ges. 22* (1889) 1211–1215.
[3] J.U. Nef, *Justus Liebigs Ann. Chem. 298* (1897) 202–374.
[4] H. Staudinger, *Ber. Dtsch. Chem. Ges. 44* (1911) 543–547.
[5] W. Langenbeck, H. Langenbeck, *Ber. Dtsch. Chem. Ges. 61* (1928) 938–942.
[6] G. Wittig, F. Lupin, *Ber. Dtsch. Chem. Ges. 61* (1928) 1627–1634.
[7] E. Müller, *Ber. Dtsch. Chem. Ges. 68* (1935) 1883–1887.
[8] A. Schonberg, A. Sina, *J. Chem. Soc. 1947*, 175–176.
[9] R.S. Armstrong, R.J.W. Le Fevre, *Aust. J. Chem. 10* (1957) 34–39.
[10] ^{1}H NMR (500 MHz, $CDCl_3$, 25°C, TMS): δ = 6.81 (d, J = 1.65 Hz, 1H; CH), 7.11 (dd, J = 1.65, 9.5 Hz, 1H; CH), 7.24–7.29 (m, ca. 6H), 7.34–7.47 (m, ca. 10H). ^{13}C NMR (125.5 MHz, $CDCl_3$, 25°C, TMS): δ = 102.6 (CH), 114.6 (C), 119.3 (CH), 128.4–134.2 (9 peaks, CH), 139.5 (C), 140.7 (C), 141.1 (C), 151.1 (C), 156.6 (C–O), 169.4 (C=O). MS (70 eV): *m/z* 374 ($M^{\oplus}$, 100%), 345 ($M^{\oplus}$ − 29, 40), 317 (15), 312 (12), 286 (15), 241 (14), 239 (15).
[11] Reflection data were measured with an Enraf-Nonius CAD-4 diffractometer in $\theta/2\theta$ scan mode using nickel-filtered copper rediation (λ = 1.5418 Å) and the structure was determined by direct phasing and Fourier methods using MULTAN80 [15] and refined using BLOCKLS, a local version of ORFLS [16]. $C_{27}H_{18}O_2$, M = 374.4, monoclinic, space group $P2_1/c$; a = 15.226 (2), b = 7.727 (1), c = 19.052 (3) Å, β = 118.38 (1)°, V = 1972.1 (5) Å^3, ρ_{calcd} = 1.26 g cm^{-3}, Z = 4, μ_{Cu} = 5.82 cm^{-1}. Crystal size, 0.14 by 0.26 by 0.31 mm; $2\theta_{max}$ = 120°. Out of 2918 unique reflections, 2295 were considered observed, R/R_w = 0.046/0.068. Further details of the crystal structure investigation are available on request from the Director of the Cambridge Crystallographic Centre, University Chemical Laboratory, Lensfield Rd., GB-Cambridge, CB2 1EW (UK), on quoting the full journal citation.
[12] J. Thiele, H. Balthorn, *Ber. Dtsch. Chem. Ges. 37* (1904) 1463.
[13] L.K. Montgomery, J.C. Huffman, E.A. Jurczak, M.P. Grendze, *J. Am. Chem. Soc. 108* (1986) 6004–6011.
[14] A. Pullmann, B. Pullmann, E.D. Bergmann, G. Berthier, E. Fischer, D. Ginsburg, Y. Hershberg, *Bull. Soc. Chim. Fr. 1951*, 707–713.
[15] J. Main: *MULTAN80*, University of York, England 1980.
[16] W.O. Busing, K.O. Martin, H.A. Levy: *ORFLS*, Oak Ridge National Laboratory, TN, USA 1962.

Synthesis of β,γ-Unsaturated D-α-Amino Acids from L-Cysteine**

By *Rudolf O. Duthaler**

Despite numerous new methods for the synthesis of α-amino acids in enantiomerically pure form,[1] there are only a few stereoselective routes to the sensitive β,γ-unsaturated amino acids,[2] which are of interest as enzyme inhibitors[3] or conformationally constrained receptor antagonists.[4] The L enantiomers are obtained conveniently by enzymatic resolution of racemates (e.g., Ref. [2f]). The D enantiomers **1** (for R see Table 1), on the other hand, can be synthesized from L-serine (**2**, R′ = H) (e.g., Ref. [2g, h, j, 4a]). A favored intermediate for this strategy is the astonishingly stable 4-formyloxazolidinone **3** introduced by *Garner* et al.[5] (Scheme 1). However, the oxidation of the hydroxymethyl group to the carboxylic acid is a pivotal disadvantage of this sequence, especially in the case of unsaturated compounds, because Pt/O_2[6] and Cr^{VI} reagents,[2h, 4a] the only means for this

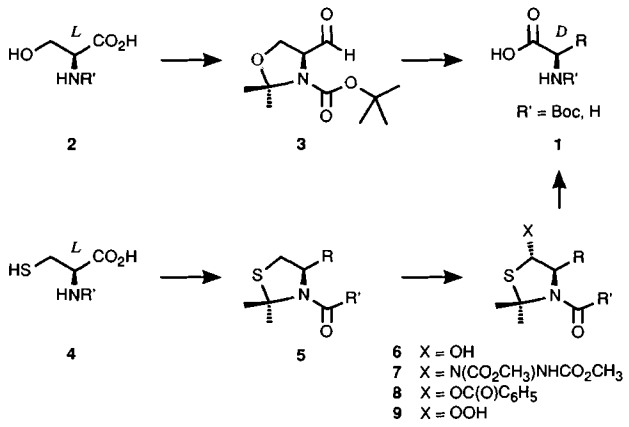

Scheme 1. Transformation of L-serine and L-cysteine to D-amino acids (for R see Table 1).

[*] Dr. R.O. Duthaler
Central Research Laboratories, Ciba-Geigy AG
Post Office Box, CH-4002 Basel (Switzerland)

[**] This work was presented at the autumn meeting of the Swiss Chemical Society and the Association of Swiss Chemists, October 19, 1990, in Bern; cf. *Abstracts of Communications and Posters*, p. 30.

transformation, are unacceptable, at least in industrial production, for economical and ecological reasons (low yields, price, toxicity, risks).[7] The *N*-acylthiazolidines **5**, derived from L-cysteine (**4**), offer an attractive alternative, since they can be oxidized by a variety of methods to stable hemithioacetals (**6**) or precursors thereof (**7**, **8**, and **9**).[8] We have now demonstrated that the elegant $^1O_2$ oxidation introduced by *Ando* et al.[8d-f] is compatible with substrates bearing *tert*-butyloxycarbonyl (Boc) protecting groups as well as with unsaturated substrates. Further, the hydroperoxides **9** can be transformed readily into 5-thiazolidinones, which, upon hydrolysis, afford β,γ-unsaturated D-amino acids of high enantiomeric purity (Scheme 1).

N-Boc-2,2-dimethylthiazolidine-4-carboxylate (**10**)[8a, 9] is transformed via amide **11** into the aldehyde **12**, an intermediate for the thiazolidines **5d**–**k**[10] (Scheme 2, Table 1).

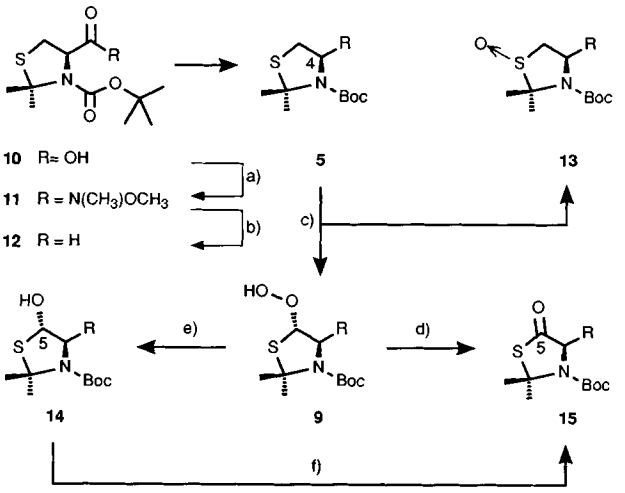

Scheme 2. Synthesis and singlet O_2 oxidation of *N*-Boc-thiazolidines. a) *N*-Methoxy-*N*-methylamine/dicyclohexylcarbodiimide/EtOAc, room temperature (RT) (74%); b) $LiAlH_4/Et_2O$, 0°C (95%); c) *meso*-tetraphenylporphyrin (1–2 ppt)/O_2/*hv* (125 W, halogen)/THF, −78°C; d) Ac_2O/Et_3N/THF, −78°C; e) Ph_3P/THF, −78°C to RT, f) DMSO/oxalyl chloride/$EtNiPr_2$/CH_2Cl_2, −78°C to RT.

Table 1. Transformation of thiazolidines **5** to **14** and **15**[a].

Compd. R		Red. $(Ph)_3P$ **14**[%][b]	**13**[%][c]	Ac_2O/Et_3N **15**[%][b]	Swern oxid. **15**[%][b,d]
11	$-C(O)N(CH_3)OCH_3$	86	4	72 [e]	68 (58)
5a	$-CO_2CH_3$	57	–	73 [f]	7 (4)
5b	$-CO_2tBu$	74	–	71 [g]	66 (49)
5c	$-H$	40 [h]	23	–	–
5d	$-CH=CHCH_3$	(*Z*) 66	23	70	92 (60)
		84 [i]	4	–	–
		0 [j]	56	–	–
5e	$-CH=C(CH_3)_2$	75	–	–	–
5f	$-CH=CHCH_2Si(CH_3)_3$	(*Z*) 71	–	–	–
5g	$-CH=CHCH_2Si(CH_3)_3$	(*E*) 77	–	–	–
5h	$-CH=C(CH_3)CH_2OH$	(*E*) 63	–	61 [k]	–
5i	$-CH=C(CH_3)CH_2Br$	(*E*) 47	–	57	–
5j	$-CH=C(CH_3)CH_2P(O)(OiPr)_2$	(*E*) 66	–	80	91 (60)
5k	$-CH=C(CF_3)CH_2P(O)(OiPr)_2$	(*E*) 62	–	–	76 (47)

[a] Structures and reaction conditions are given in Scheme 2. [b] The yields are not optimized, with the exception of **11**, **5d**, and **5j**. [c] The polar sulfoxides **13** (mixtures of epimers) have usually not been isolated, since the separation from $(Ph)_3PO$ is difficult. [d] The overall yield of **15** from **5** (or **11**) via **14** is given in parentheses. [e] $[\alpha]_D = -145°$ ($c = 0.58$, $CHCl_3$), the optical purity is most probably ≥ 95%, since this β-dicarbonyl compound is racemized less readily than the corresponding 5-thiazolidinone from **15d** (cf. [21]), which is isolated with ≥ 95% *ee*. [f] Racemic, $[\alpha]_D = 0$. [g] $[\alpha]_D = -18°$ ($c = 0.3$ $CHCl_3$), presumably of low optical purity. [h] Reaction in toluene. [i] Reaction in $tBuOCH_3$. [j] Reaction in CH_2Cl_2. [k] The alcohol function was protected temporarily as its trimethylsilyl ether.

$^1O_2$ oxidation leads then to the hydroperoxides **9**; the only side products of these otherwise clean reactions are the sulfoxides **13** corresponding to the "normal" course of sulfide oxidation.[12] After reduction of **9** with triphenylphosphane, the hemiacetals **14** can be isolated in satisfactory yields by chromatography. Crucial for the feasibility of this method as opposed to other $^1O_2$ processes,[13] are its mildness and the high substrate concentrations (12% wt/vol.) tolerated. This allows application to reactive substrates (**5i**) or compounds otherwise sensitive to $^1O_2$ oxidation (**5e**–**g**). As demonstrated by the examples **5j**,**k**, complex side chains can be constructed in analogy to the serine method.[2g, h, j, 4a] Bulky substituents at N(3) and C(4) appear to increase the rate of oxidation and favor the formation of **9** and therefore **14** (cf. Table 1, **11**, **5a**–**c**).[14] The effect of solvent, normally THF, has been investigated for **5d**. Whereas more hydroperoxide **9** is formed in *tert*-$BuOCH_3$ at the expense of **13**, the sulfoxides **13** are the sole products in CH_2Cl_2.

The 5-hydroxythiazolidines **14** are amenable to oxidation by the method of *Swern* et al.[15] with the exception of the product obtained from **5a**. Preferable, however, would be a direct transformation of the hydroperoxides **9** to the 5-thiazolidinones **15**. While such formal eliminations of water are known for various secondary alkyl hydroperoxides,[16] no such transformation of an α-thioalkylhydroperoxide has been reported yet. After many unsuccessful experiments[17] it was found surprisingly that, for all cases studied so far, a clean transformation of the hydroperoxides **9** to **15** can be effected by Ac_2O/Et_3N at −78°C. The yields are significantly better than those of the two-step procedure via **14** (Scheme 2, Table 1). Unwanted acetylations of alcohols like **5h** can be avoided by temporary protection as silyl ethers.

The final transformation to D-amino acids has been optimized for the thiol lactone **15d** (Scheme 3). Treatment with LiOH gives the *N*-Boc-protected acid **16** with 78% *ee*;[18] the amide **17**[19] is obtained with dimethylaluminum amide.[20] Since the thiol lactone **15d** is slowly racemized by Et_3N at temperatures above −30°C,[21] partial racemization upon cleavage with nucleophiles can be expected. Acid-catalyzed hydrolysis is therefore preferable. Treatment with Me_3SiBr/phenol to afford **18**, in analogy to Ref. [22], is the best method for the removal of the Boc protection. In Me_3SiBr/CH_3OH, **18** is then slowly transformed (one week) into methyl ester **19** (≥ 99% *ee*).[11, 23] Water in turn effects the hydrolysis of **18** to **20** (86% *ee*) in nine days without acid catalyst. The 5-thiazolidinone **18**, however, is cleaved more efficiently (one to two days) in 1 N HCl, affording the product **20** with higher optical purity (94–96% *ee*).[24] Compared to enzymatic methods (e.g., Ref. [2f]), this type of transfor-

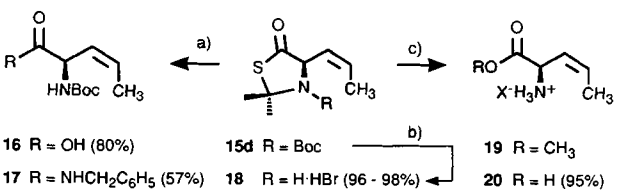

Scheme 3. Transformation of 5-thiazolidinones to D-amino acids. a) LiOH/H_2O-THF (→ **16**, 78% *ee*); $(CH_3)_2AlNHCH_2C_6H_5$/toluene (→ **17**); b) $(CH_3)_3SiBr$ (2 equiv.)/phenol (6 equiv.)/CH_2Cl_2; c) $CH_3OH/(CH_3)_3SiBr$ or $(CH_3)_3SiCl$ (→ **19**, ≥ 99% *ee*); 1 N HCl (→ **20**, 95% *ee*).

mation gives D-amino acids of similar quality but with fewer structural restrictions. This new route offers advantages over the synthetic methods so far available,[1, 2] especially when sensitive compounds are involved. In addition to D enantiomers, racemization of either aldehyde **12**[10] or 5-thiazolidinones **15**[21] allows the preparation of racemic amino acids. Thanks to improved methods for the preparation of D-cysteine,[25] L enantiomers can be obtained with little more effort.

Received: January 14, 1991 [Z 4386 IE]
German version: *Angew. Chem. 103* (1991) 729

CAS Registry numbers:
5a, 5317-16-8; **5b**, 133228-51-0; **5c**, 133228-52-1; **5d**, 133228-53-2; **5e**, 133228-54-3; **5f**, 133228-55-4; **5g**, 133228-56-5; **5h**, 133228-57-6; **5i**, 133228-58-7; **5j**, 133228-59-8; **5k**, 133270-04-9; **10**, 5317-15-7; **11**, 133228-60-1; **12**, 133228-61-2; **13c**, 133228-62-3; **13d**, 133228-63-4; **14** (R = CONMeOMe), 133228-64-5; **14a**, 133320-17-9; **14b**, 133228-65-6; **14c**, 133228-66-7; **14d**, 133228-67-8; **14e**, 133228-68-9; **14f**, 133228-69-0; **14g**, 133228-70-3; **14h**, 133228-71-4; **14i**, 133228-72-5; **14j**, 133228-73-6; **14k**, 133228-74-7; **15** (R = CONMeOMe), 133228-75-8; **15a**, 133228-76-9; **15b**, 133228-77-0; **15d**, 133228-78-1; **15h**, 133228-79-2; **15i**, 133228-80-5; **15j**, 133228-81-6; **15k**, 133228-82-7; **16**, 125700-59-6; **17**, 133228-83-8; **18**, 133228-84-9; **19**, 133228-85-0; **20**, 133228-86-1; *N*-methoxy-*N*-methylamine, 1117-97-1; L-cysteine, 52-90-4.

[1] a) U. Schöllkopf, *Top. Curr. Chem. 109* (1983) 65–84; b) K. A. Kochetkov, V. M. Belikov, *Russ. Chem. Rev. (Engl. Transl.) 56* (1987) 1045–1067; c) α-Amino-Acid Synthesis, Tetrahedron Symposium in Print No. 33, *Tetrahedron 44* (1988) 5253–5605; d) D. Seebach, E. Dziadulewics, L. Behrendt, S. Cantoreggi, R. Fitzi, *Liebigs. Ann. Chem. 1989*, 1215–1232; e) R. M. Williams, *Synthesis of Optically Active α-Amino Acids*, Pergamon Press Oxford 1989; f) D. A. Evans, T. C. Britton, J. A. Ellman, R. L. Dorow, *J. Am. Chem. Soc. 112* (1990) 4011–4030; g) W. Oppolzer, O. Tamura, *Tetrahedron Lett. 31* (1990) 991–994.

[2] a) D. D. Keith, J. A. Tortora, K. Ineichen, W. Leimgruber, *Tetrahedron 31* (1975) 2633–2636; b) U. Schöllkopf, J. Nozulak, U. Groth, *ibid. 40* (1984) 1409–1417; c) T. Itaya, A. Mizutani, *Tetrahedron Lett. 26* (1985) 347–350; d) T. Weber, R. Äschimann, T. Mätzke, D. Seebach, *Helv. Chim. Acta 69* (1986) 1365–1377; e) R. M. Williams, W. Zhai, *Tetrahedron 44* (1988) 5425–5430; f) L. Havliček, J. Hanuš, *Radioisotopy 29* (1988) 157–163; g) P. L. Beaulieu, P. W. Schiller, *Tetrahedron Lett. 29* (1988) 2019–2022; h) N. A. Sasaki, Ch. Hashimoto, R. Pauly, *ibid. 30* (1989) 1943–1946; i) J. E. Baldwin, M. G. Moloney, M. North, *Tetrahedron 45* (1989) 6319–6330; j) M. P. Sibi, P. A. Renhowe, *Tetrahedron Lett. 31* (1990) 7407–7410.

[3] a) R. R. Rando, *Acc. Chem. Res. 8* (1975) 281–288; b) R. H. Abeles, A. L. Maycock, *ibid. 9* (1976) 313–319; c) C. Walsh, *Tetrahedron 38* (1982) 871–909; d) J. R. Sufrin, J. B. Lombardini, D. D. Keith, *Biochem. Biophys. Res. Commun. 106* (1982) 251–255.

[4] a) H. Allgeier, C. Angst, G. Bold, R. Duthaler, R. Heckendorn, A. Togni, *EP-A* 302826 (1989), *Chem. Abstr. 112* (1990) 139560g; b) G. E. Fagg, H. R. Olpe, M. F. Pozza, J. Baud, M. Steinmann, M. Schmutz, C. Portet, P. Baumann, K. Thedinga, *Br. J. Pharmacol. 99* (1990) 791–797.

[5] a) P. Garner, *Tetrahedron Lett. 25* (1984) 5855–5858; b) P. Garner, J. M. Park, *J. Org. Chem. 52* (1987) 2361–2364.

[6] P. J. Maurer, H. Takahata, H. Rapoport, *J. Am. Chem. Soc. 106* (1984) 1095–1098.

[7] As described recently (W. D. Lubell, T. F. Jamison, H. Rapoport, *J. Org. Chem. 55* (1990) 3511–3522), such an oxidation of a compound with a triple bond is effected by transformation to an unstable α-amino aldehyde with *N*-chlorosuccinimide/Me_2S, followed by $NaClO_2$ oxidation. It is questionable, however, whether this procedure is applicable to olefinic substrates..

[8] a) R. B. Woodward, *Science 153* (1966) 487–493; b) J. E. Baldwin, A. Au, M. Christie, S. B. Haber, D. Hesson, *J. Am. Chem. Soc. 97* (1975) 5957–5958; c) M. Iwakawa, B. M. Pinto, W. A. Szarek, *Can. J. Chem. 56* (1978) 326–335; d) T. Takata, K. Hoshino, E. Takeuchi, Y. Tamura, W. Ando, *Tetrahedron Lett. 25* (1984) 4767–4770; e) T. Takata, Y. Tamura, W. Ando, *Tetrahedron 41* (1985) 2133–2137; f) T. Takata, L. Huang, W. Ando, *Chem. Lett. 1985*, 1705–1708; g) N. Tokitoh, Y. Igarashi, W. Ando, *Tetrahedron Lett. 28* (1987) 5903–5906; h) D. Seebach, A. Jeanguenat, J. Schmidt, T. Mätzke, *Chimia 43* (1989) 314–317.

[9] D. S. Kemp, R. I. Carey, *J. Org. Chem. 54* (1989) 3640–3646.

[10] The aldehyde **12**, obtained in about 50% overall yield from L-cysteine-HCl (92–97% *ee*, capillary GLC, Chirasil-Val* [11]), shows a somewhat higher tendency for racemization than **2** but otherwise similar properties [5]. The transformations of **12** to the thiazolidines **5d–k** will be published later.

[11] H. Frank, G. J. Nicholson, E. Bayer, *Angew. Chem. 90* (1978) 396–398; *Angew. Chem. Int. Ed. Engl. 17* (1978) 363.

[12] a) G. O. Schenck, C. H. Krauch, *Angew. Chem. 74* (1962) 510; b) C. S. Foote, J. W. Peters, *J. Am. Chem. Soc. 93* (1971) 3795–3796; c) K. Nahm, C. S. Foote, *ibid. 111* (1989) 1909–1910; d) E. L. Clennan, X. Chen, *ibid. 111* (1989) 8212–8218.

[13] A. A. Frimer (Ed.): *Singlet O_2 Vol. II/III*, CRC Press, Boca Raton, FL, USA 1987.

[14] Under comparable conditions, **11** (10 g) is oxidized within about 2 h, **5d** (8.4 g) within about 18 h.

[15] A. J. Mancuso, D. S. Brownfain, D. Swern, *J. Org. Chem. 44* (1979) 4148–4150.

[16] a) G. O. Schenck, O.-A. Neumüller, W. Eisfeld, *Liebigs Ann. Chem. 618* (1958) 202–210; b) E. D. Mihelich, D. J. Eickhoff, *J. Org. Chem. 48* (1983) 4135–4137; c) G. Rousseau, P. Le Perchec, J. M. Conia, *Synthesis 1978*, 67–70; d) R. S. Drago, R. Riley, *J. Am. Chem. Soc. 112* (1990) 215–218.

[17] This is explained by the very restricted choice of reagents tolerated for this process. No trace of **15** is observed upon replacement of Et_3N by $EtNiPr_2$ or of Ac_2O by sulfonyl chlorides, isocyanates, or acylimidazolides.

[18] $[\alpha]_D = -100$ ($c = 2.2$, CH_3OH), 78% *ee* (capillary GLC [11]); Lit. [2h]: $[\alpha]_D = -102$ ($c = 2$, CH_3OH), ≥ 97% *ee*(!) (NMR, 2-methoxy-2-(trifluormethyl)phenacetylamide.

[19] $[\alpha]_D = -57$ ($c = 0.5$, $CHCl_3$); the optical purity has not been determined.

[20] J. I. Levin, E. Turos, St. M. Weinreb, *Synth. Commun. 12* (1982) 989–993.

[21] Racemic **15d** can be isolated in 93% yield after boiling for 20 h in Et_3N/CH_2Cl_2 (cf. Table 1 [e]).

[22] E. Kaiser, Sr., J. P. Tam, T. M. Kubiak, R. B. Merrifield, *Tetrahedron Lett. 29* (1988) 303–306.

[23] $[\alpha]_D = -174$ ($c = 0.44$, CH_3OH), crude product (hydrobromide).

[24] $[\alpha]_D = -283$ ($c = 0.27$, AcOH); 94% *ee* (capillary GLC [11] of the *N*-Boc methyl ester); Lit. [2f]: $[\alpha]_D = +275$ ($c = 0.16$, AcOH), L enantiomer, enzymatic resolution.

[25] a) T. Shiraiwa, K. Kataoka, S. Sakata, H. Kurokawa, *Bull. Chem. Soc. Jpn. 62* (1989) 109–113; b) T. Shiraiwa, H. Tazoh, M. Sunami, Y. Sado, H. Kurokawa, *ibid. 60* (1987) 3985–3990.

Facile N–H Cleavage of Ammonia**

By *Robert Koelliker* and *David Milstein**

Ammonia is one of the most abundant and useful industrial chemicals[1] and its direct, catalytic functionalization with organic substrates, such as olefins, is of much current interest.[2] Most of the chemistry of ammonia is dominated by its nucleophilicity. Our strategy is to develop new modes of reactivity based on oxidative addition of ammonia to a metal center yielding, in the first step, amido hydride complexes. Such an N–H activation approach has already led to catalytic stereoselective addition of aniline to norbornene.[3]

Examples of oxidative addition of ammonia to a metal center in solution are rare.[4] We now report that, upon coordination of ammonia to a low-valent metal olefin complex, the metal center may become electron-rich enough, even in the absence of other strong σ donors, to induce N–H cleavage of a subsequent incoming ammonia molecule. This oxidative addition process takes place under exceedingly mild conditions and leads to complexes of interest in their own right.

When a slurry of the Ir^I complex **1** in THF is treated with excess ammonia at 25 °C, a homogeneous red solution containing mainly the adduct **2** is immediately formed.[5] After two minutes at 25 °C (or 18 hours at −50 °C) a yellow precipitate starts to form. Isolation of the precipitate after two hours under an NH_3 pressure of 35000 Pa reveals that it consists of the Ir^{III} complexes **3b** and **4b** in the ratio of 1:3 (combined yield 32% based on **1**[6]). Complex **5** can be iso-

[*] Prof. Dr. D. Milstein, Dr. R. Koelliker
Department of Organic Chemistry
The Weizmann Institute of Science
Rehovot 76100 (Israel)

[**] This work was supported by the US-Israel Binational Science Foundation and by the Israel Academy of Sciences and Humanities.

lated from the red mother liquor in 32% yield.[6] When ND_3 is used, the corresponding Ir-D complexes are formed (as detected by IR and ^{2}H NMR), thus excluding participation of C–H activation processes. Anion exchange of complexes **3** and **4** with $NaPF_6$ leads to the more soluble complexes **3a** and **4a**, which were identified by ^{1}H and ^{13}C NMR, as well

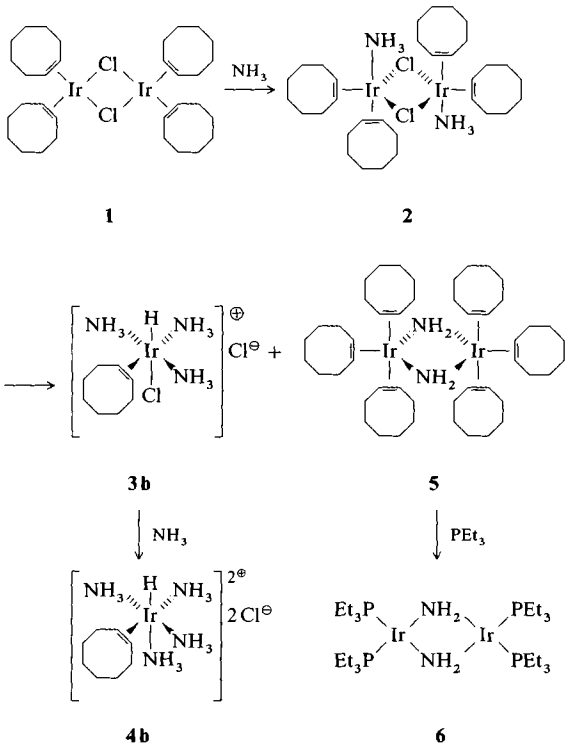

as by ^{2}H and ^{15}N NMR of the labeled complexes obtained from the reaction with NH_3 and $^{15}NH_3$, respectively. ^{15}N NMR of a representative product mixture of **3a** and **4a** is shown in Figure 1. The ammine ligand *trans* to the hydride in **4a** appears as a doublet of quartets as a result of coupling with both the N–H protons and the hydride ligand.

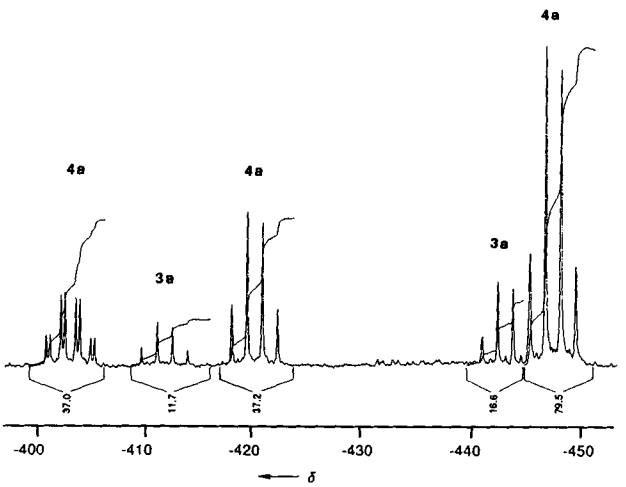

Fig. 1. ^{1}H-coupled ^{15}N NMR spectra of a mixture of **3a** and **4a** in THF.

Complexes **3** and **4** are the first reported ammine olefin hydride complexes. The fairly unusual *cis* arrangement of olefin and hydride ligands is probably thermodynamically favored in this electron-rich system over that of the corresponding alkyl complex because of stabilization provided by back-donation to the olefin, the only π acceptor present.

Reaction of the monocationic complex **3a** with ammonia leads to the dicationic **4a**, indicating that **3b** is probably an intermediate in the formation of **4b**. The unexpected displacement of the chloride rather than the olefin ligand and the retention of the *cis* arrangement of olefin and hydride ligands, even in the presence of added ammonia, are again a reflection of considerable back-donation to the olefin, promoted by the strong σ-donor character of the ammine ligand and its inability to participate in π back-bonding.

In the coupled ^{15}N NMR spectrum at $-50°$, the air-sensitive Ir^I complex **5** exhibits only one triplet at $\delta = -372.8$ ($J = 68.6$ Hz), indicating one type of bridging NH_2 ligand. The $^{13}C\{^1H\}$ NMR spectrum shows one broad signal for the olefinic carbons even at $-30°C$, compatible with fluxional behavior. Complex **5** is the first reported amido olefin complex. Its saturated nature in solution, which is uncommon for a d^8 complex, and its surprising substitutional stability towards excess ammonia may both reflect the high electron density on this Ir^I amide complex. In contrast, facile substitution of the cyclooctene ligand occurs by the soft PEt_3, leading to complex **6**, which is also obtained by deprotonation of **7** with lithium diisopropylamide.[7] The difference in substitutional activity of ammonia and PEt_3 is likely to be influenced by π back-bonding to the phosphane.

Table 1. Selected physical data for compounds **2**, **3a**, **4a**, **5**, and **6** [a].

2: IR (Nujol): $\tilde{\nu}$[cm^{-1}] = 3296(s), 3230(s), 3172(s) (ν(NH), ν(NH)/ν(ND) = 1.34). ^{1}H NMR: $\delta = 2.02$ (br, NH_3), $^{13}C\{^1H\}$ NMR: $\delta = 69.9$ (br), 55.5 (br), 30.9 (br, 2C), 29.8, 28.6, 26.9, 26.5. ^{15}N NMR: $\delta = -377.3$ (q, $J = 70.1$ Hz).
3a: ^{1}H NMR ([D$_8$]THF): $\delta = -19.66$ (s, 1H), 2.96 (s, br, 6H; $^{15}NH_3$:d, $J = 70.4$ Hz), 4.18 (s, br, 3H; $^{15}NH_3$:d, $J = 71.0$ Hz). ^{2}H NMR: $\delta = -19.39$ (s). $^{13}C\{^1H\}$ NMR ([D$_8$]THF): $\delta = 63.6$, 31.6, 27.3, 26.9. ^{15}N NMR: $\delta = -411.8$ (q, 1N, J(NH) = 71.2 Hz), -442.8 (q, 2N, J(NH) = 70.3 Hz).
4a: IR (neat) $\tilde{\nu}$[cm^{-1}] = 3367(s), 3305(s) (ν(N–H), ν(NH)/ν(ND) = 1.34); 2928(s), 2859(s) (ν(C–H); 2209(m) (ν(Ir–H), ν(IrH)/ν(IrD) = 1.38); 1633(m) (δ(N–H)). ^{1}H NMR ([D$_8$]THF): $\delta = -18.05$ (s, 1H; $^{15}NH_3$: d, $J = 19.1$ Hz), 3.04 (s, br, 6H; $^{15}NH_3$:d, $J = 70.3$ Hz), 3.63 (s, br, 3H; $^{15}NH_3$:d, $J = 68.5$ Hz), 4.35 (s, br, 3H; $^{15}NH_3$:d, $J = 70.6$ Hz). ^{2}H NMR: $\delta = -17.74$(s). $^{13}C\{^1H\}$ NMR ([D$_8$]THF): $\delta = 63.7$, 31.3, 26.9, 26.7. ^{15}N NMR: $\delta = -403.2$ (dq, 1N, J(NH) = 68.6 Hz, J(NIrH) = 18.9 Hz), -420.0 (q, 1N, J(NH) = 70.8 Hz), -447.2 (q, 2N, J(NH) = 70.1 Hz).
5: IR (Nujol): $\tilde{\nu}$[cm^{-1}] = 3393w, 3270w, 3252w (ν(N–H); ν(NH)/ν(ND) = 1.34 and 1.36. ^{15}N NMR: ($-50°C$): $\delta = -372.8$ (t, J(NH) = 68.6 Hz). $^{13}C\{^1H\}$ NMR: $\delta = 60.5$(br), 31.1, 30.2, 27.0. ^{1}H NMR: $\delta = 1.03$ (s, br, 2H, mit $^{15}NH_3$: d, $J = 67.9$ Hz), 1.2–2.4 (m, 42H).
6: ^{15}N NMR: $\delta = -415.2$ (tt, J(NH) = 68.3 Hz, J(PN) = 32 Hz. $^{31}P\{^1H\}$ NMR (THF): $\delta = +3.5$ (s; ^{15}N:d, $J = 31.0$ Hz).

[a] The standard for ^{1}H (270 MHz), ^{13}C (125.76 MHz), and ^{2}H NMR (41.45 MHz) spectra was ext. TMS; for ^{15}N NMR (50.70 MHz) spectra, ext., neat CH_3NO_2; for ^{31}P NMR (109.29 MHz) spectra, ext. 85% H_3PO_4, internal capillary in the corresponding solvent. ^{2}D NMR and ^{15}N NMR were recorded from complexes obtained from reactions with ND_3 and $^{15}NH_3$, respectively [10]. Unless otherwise stated, ^{1}H and ^{13}C NMR spectra were recorded for C_6D_6 solutions, ^{2}H NMR spectra for THF solutions, and ^{15}N NMR spectra for THF/[D$_8$]THF solutions.

$[\{Ir(PEt_3)_2(\mu\text{-}NH_2)(NH_3)(H)\}_2]Cl_2$ **7**

Although ammine complexes of late transition metals are quite common,[8] especially in high oxidation states, they have not been reported to undergo N–H activation in the absence of other σ-donor ligands. Indeed, starting with a low-oxidation-state precursor containing loosely bound ligands, we observed novel reactivity which is strongly influenced by the σ-donor properties of ammonia. This leads to

uncommon complexes with unique features. The overall reactivity pattern observed here is substantially different from that of electron-rich Ir^I phosphane complexes with ammonia,[4c] perhaps because of the better ability of phosphanes to stabilize the soft Ir^I metal center and the steric constraints imposed by these ligands. Indeed, the reaction described here, which occurs even at $-50\,^{\circ}C$, is to our knowledge the fastest reported ammonia oxidative addition to a transition-metal center in solution.[9]

We are currently studying the mechanism and scope of this unusual N–H cleavage process and the chain of events leading to the final products. The advantages of using ammonia as both a substrate and ligand for potential catalysis is also being explored.

Received: December 28, 1990 [Z4363IE]
German version: *Angew. Chem. 103* (1991) 724

[1] F. T. Campbell, R. Pfefferkorn, J. F. Rounsaville (Eds.): *Ullmanns Encyclopedia of Industrial Chemistry, Vol. A2*, 5th ed., VCH, Weinheim 1985; pp. 228–230.

[2] Reviews: a) J. J. Brunet, D. Neibecker, F. Niedercorn, *J. Mol. Catal. 49* (1989) 235–259; b) D. Steinborn, R. Taube, *Z. Chem. 26* (1986) 349–359.

[3] A. L. Casalnuovo, J. C. Calabrese, D. Milstein, *J. Am. Chem. Soc. 110* (1988) 6738–6744.

[4] a) M. M. Banaszak Holl, P. T. Wolczanski, G. D. Van Duyne, *J. Am. Chem. Soc. 112* (1990) 7989–7994; b) H. W. Roesky, Y. Bai, M. Noltemeyer, *Angew. Chem. 101* (1989) 788–789; *Angew. Chem. Int. Ed. Engl. 28* (1989) 754–755; c) A. L. Casalnuovo, J. C. Calabrese, D. Milstein, *Inorg. Chem. 26* (1987) 971–973; d) J. E. Bercaw, D. L. Davies, P. T. Wolczanski, *Organometallics 5* (1986) 443–450; e) G. L. Hillhouse, J. E. Bercaw, *J. Am. Chem. Soc. 106* (1984) 5472–5478; f) G. Süss-Fink, *Z. Naturforsch. B 35* (1980) 454–457; g) J. N. Armor, *Inorg. Chem. 17* (1978) 203–213; h) E. G. Bryan, B. F. G. Johnson, J. Lewis, *J. Chem. Soc. Dalton Trans. 1977*, 1328–1330.

[5] We also observe a small amount of the monomeric, square-planar complex *cis*-$[(C_8H_{14})_2Ir(NH_3)Cl]$, which exhibits sharp vinylic ^{13}C NMR signals, as opposed to the broad ^{13}C NMR signals of **2**. The broadness is probably a result of fluxional behavior expected in a trigonal-bipyramidal complex. Free cyclooctene is not observed (^1H NMR), thus excluding dissociative equilibria.

[6] The maximum theoretical yield is 50%.

[7] A. L. Casalnuovo, private communication.

[8] D. A. House in R. D. Gillard, J. A. McCleverty (Eds.): *Comprehensive Coordination Chemistry, Vol. 2*, Pergamon, Oxford 1987, pp. 26–28.

[9] A mechanism based on deprotonation of an ammine ligand by ammonia is highly unlikely since (1) deprotonation of Ir^{III}-NH_3 would be preferred over that of Ir^I-NH_3 and formation of at least some Ir^{III}-NH_2 would be expected, but none is observed, (2) the Ir^{III}-NH_3 complexes **3** and **4** do not undergo deprotonation even in the presence of a large excess of ammonia, (3) reaction of **4a** with $KN(SiMe_3)_2$ leads to deprotonation of Ir-H (and not of Ir-NH_3), and (4) equivalent amounts of Ir^{III} and Ir^I complexes are formed, regardless of the ammonia concentration employed.

[10] Complexes **4a**, **5**, and **6** were obtained as pure solids. Complex **2** was isolated together with minor amounts of its monomer. Complex **3a** was obtained in a mixture with **4a**. The structures of **3a** and **4a** were further confirmed by substitution reactions with PEt_3.

Methylene Phosphonium Ions**

By *Hansjörg Grützmacher** and *Hans Pritzkow*

Stable silaethenes **1**[1] and phosphinoboranes **2**[2] are well-known. In contrast, the methylenephosphonium ion **3**, which is isostructural with these compounds, could only recently be completely characterized.[3] Although for steric reasons the halves of the molecule are twisted through 60° relative to one another, the P–C distance of 1.62 Å is very short, which can be attributed to strong electrostatic interactions.[4] Variation of the substituents at the P or C atom, or both, should change the character of the P–C bond. Thus the synthesis of P-alkylated methylene phosphonium ions, which we now report, is interesting.

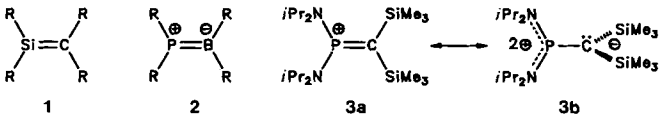

1 **2** **3a** **3b**

The reaction of lithiobis(trimethylsilyl)methane **4**[5] with di-*tert*-butylchlorophosphane **5** in THF afforded quantitatively phosphane **6**.[6] Oxidation of this compound with CCl_4[7] in hexane led to loss of $CHCl_3$ and the concomitant formation of the chloro-substituted phosphorus ylide **7**, whereas the reaction at $-78\,^{\circ}C$ in CH_2Cl_2 yielded ylide **8** exclusively, with loss of Me_3SiCCl_3. The abstraction of chloride from $(iPr_2N)_2ClP^{\oplus}$–$C^{\ominus}(SiMe_3)_2$ by aluminum trichloride to form **3** was not successful,[9] but the corresponding reactions with **7** and **8** yielded the desired methylene phosphonium ions **9** and **10**, respectively.[10]

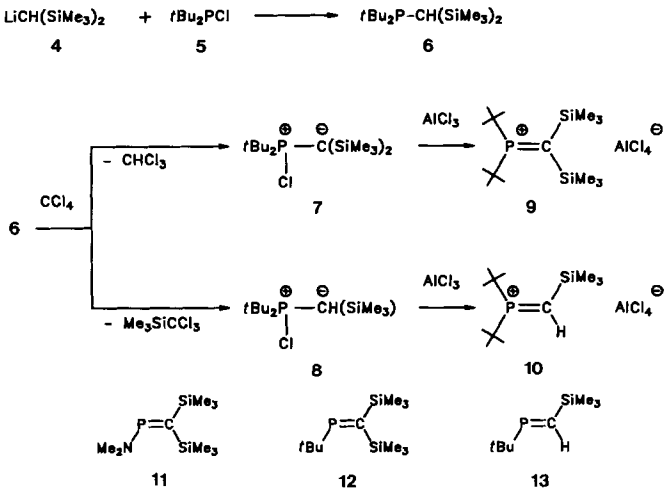

4 **5** **6** **7** **8** **9** **10** **11** **12** **13**

Rapid workup of the reaction mixtures at temperatures below $-30\,^{\circ}C$ allowed the isolation of **9** and **10** as colorless, crystalline solids. They may be stored in the solid state at $-30\,^{\circ}C$, but decompose in dichloromethane solution.

The NMR spectra of **9** and **10** differ greatly from those of **3** (Table 1). The resonance signal of both the phosphorus

Table 1. Selected NMR data of **3**, **9**, **10**, **11**, **12**, and **13** [a].

Cmpd.	$\delta(^{31}P)$	$\delta(^{13}C)$	$^1J(CP)$ [Hz]	Ref.
3	130.8	76.5	87.6	[3]
9	258.7	178.8	8.6	
10	245.4	149.6	45.2	
11	330.2	128.6	76.8	[11]
12	438.7	194.4	94.3	[12]
13	328.2	–	–	[13]

[a] For a complete list of the NMR data for **9** and **10**, see ref. [10].

[*] Dr. H. Grützmacher, Dr. H. Pritzkow
Anorganisch-chemisches Institut der Universität
Im Neuenheimer Feld 270, W-6900 Heidelberg

[**] This work was supported by the Dr. Otto Röhm Gedächtnisstiftung, the Deutsche Forschungsgemeinschaft, the Fonds der Chemischen Industrie and by Prof. W. Sundermeyer and Prof. G. Huttner. We thank Prof. R. Ahlrichs sincerely for helpful discussions.

atom and the carbon atom of the double bond are strongly shifted to lower field relative to **3**. Comparison with **11**,[11] **12**,[12] and **13**[13] shows that the chemical shifts of the sp^2 carbon atoms in **9** and **10** lie among the typical values for phosphaalkenes. Predictably, the ^{31}P NMR signals of **9** and **10** are strongly shifted to higher field with respect to the corresponding signals in **12** and **13**, as a result of the increase in the coordination number of the phosphorus atom. On the grounds of these NMR data, **9** and **10** may be considered analogues of olefins, while in **3** interaction with the lone pairs of the amino groups compensates for the electron deficiency at the phosphorus atom. The "double bond" between the phosphorus and carbon atoms in **3** has a pronounced ylide character.

Because of the facile decomposition of **9** and **10** in solution, only crystals of **10** have been obtained, though in poor quality, by rapid crystallization from *n*-hexane/CH_2Cl_2. The X-ray structure analysis[14] could give only qualitative information about the molecular geometry, but indicates that the phosphorus atom is in an almost planar environment (sum of the bond angles: 359°C) and the halves of the molecule are twisted 11° relative to one another. The length of the P–C double bond is 1.69(4) Å, which lies in the range typical of phosphaalkenes. The cations and anions are separated in the crystal (shortest P–Cl distance: 3.9 Å).

Remarkably, in both the ^1H and ^{13}C NMR solution spectra of **10**, even at temperatures as low as −90 °C, the signals of the *tert*-butyl groups are equivalent, from which we conclude that the rotational barrier for the P–C multiple bond is unusually low compared with phosphaalkenes.

The reactivities of **3**, **9**, and **10** also differ widely. Whereas only nucleophilic attack on the phosphorus atom is available to **3**,[3] **9** and **10** react rapidly with 2,3-dimethylbutadiene at room temperature, in spite of steric hindrance of the P–C bond. (The reaction of **10** is exothermic!) The product from **9** in this reaction is predominantly **14**, formed by an ene reaction, while the sterically less hindered **10** undergoes exclusively a [2+4] cycloaddition to yield **15**.[15] The ene reaction is, to our knowledge, not yet described for phosphaalkenes, but is often observed in the chemistry of the silaethenes **1** and underlines their close relationship to **9** and **10**.[16]

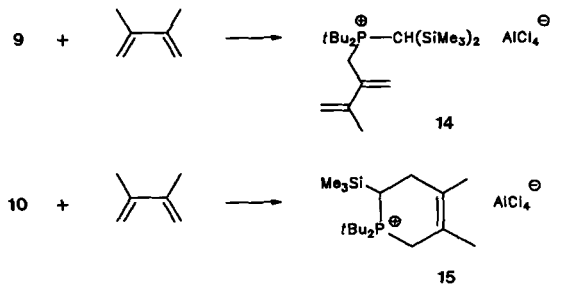

Received: January 11, 1991 [Z4379 IE]
German version: *Angew. Chem. 103* (1991) 721

CAS Registry numbers:
6, 89982-67-2; **7**, 133474-11-0; **8**, 81176-02-5; **9**, 133474-13-2; **10**, 133474-15-4; **14**, 133474-17-6; **15**, 133474-19-8; CCl_4, 56-23-5; 2,3-dimethylbutadiene, 513-81-5.

[1] A. G. Brook in E. Block (Eds.): *Heteroatom Chemistry*, VCH Publishers, New York 1990, p. 105; G. Raabe, J. Michl in S. Patai, Z. Rappoport (Eds.): *The Chemistry of Organic Silicon Compounds*, Wiley, Chichester 1989, p. 1015; N. Wiberg, *J. Organomet. Chem. 272* (1984) 141.

[2] P. P. Power, *Angew. Chem. 102* (1990) 527; *Angew. Chem. Int. Ed. Engl. 29* (1990) 449.

[3] A. Igau, A. Bacereido, H. Grützmacher, H. Pritzkow, G. Bertrand, *J. Am. Chem. Soc. 111* (1989) 6853.

[4] M. Ehrig, H. Horn, C. Kölmel, R. Ahlrichs, *J. Am. Chem. Soc.*, in press.

[5] N. Wiberg, G. Wagner, G. Müller, J. Riede, *J. Organomet. Chem. 271* (1984) 381.

[6] B.-L. Li, R. H. Neilson, *Inorg. Chem. 23* (1984) 3665. Pure **6** has a melting point of 44°C.

[7] O. I. Kolodiazhnyi, *Z. Chem. 29* (1989) 396, and references cited therein. Product distributions that are solvent dependent are well known for the reaction of phosphanes with CCl_4: R. Appel, F. Knoll, W. Michel, W. Morbach, H. D. Wihler, H. Veltmann, *Chem. Ber. 109* (1976) 58.

[8] O. I. Kolodiazhnyi, *Zh. Obshch. Khim. 51* (1981) 2466.

[9] H. Grützmacher, unpublished results; see also: R. Appel, R. Schmitz, Chem. Ber. 116 (1983) 3521.

[10] Preparative details: **7**: Compound **6** (3.04 g, 10 mmol) was dissolved in dry, degassed *n*-hexane (20 mL), and CCl_4 (4.62 g, 30 mmol) was added at −78°C. The reaction vessel was then warmed to room temperature and stirred for 3 h. Thereafter all volatile components were removed under vacuum, CH_3CN (10 mL) was added to the bright yellow, oily residue, and the mixture was solidified at −30 °C. Further purification of **7** can be achieved by sublimation at 100°C/10^{-1} Torr. M.p. 127°C; $^{31}P\{^1H\}$ NMR (C_6D_6): $\delta = 105.9$; ^{13}C NMR (C_6D_6): $\delta = 8.5$ (d, $^3J(PC) = 3.7$ Hz, $^1J(SiC) = 52.9$ Hz, $SiCH_3$), 27.65 (d, $^1J(PC) = 130.1$ Hz, $P^{\oplus}$-$C^{\ominus}$), 28.68 (d, $^2J(PC) = 3.5$ Hz, CCH_3), 44.3 (d, $^1J(PC) = 39.3$ Hz, CMe_3); ^1H NMR (C_6D_6): $\delta = 0.46$ (s, 18H, $SiCH_3$), 1.12 (d, $^3J(PH) = 16.4$ Hz, 18H, CCH_3); ^{29}Si NMR ($CDCl_3$, $T = 230$ K): $\delta = -2.43$ (d, $^2J(PSi) = 1.8$ Hz), −11.33 (d, $^2J(PSi) = 23.3$ Hz). MS (EI, 70 eV): *m/z* 338 ($M^{\oplus}$, 5%), 323 ($M^{\oplus}-CH_3$, 7.5), 267 (5), 226 (7), 211 (9), 147 (11), 120 (13), 73 (Me_3Si, 46), 57 (Me_3C, 100). **9**: Compound **7** (1 g, 3 mmol) was dissolved in CH_2Cl_2 (10 mL) and added dropwise by syringe to a suspension of freshly sublimed $AlCl_3$ (0.45 g, 3.4 mmol) at −78 °C. The resulting pale yellow solution was stirred for 10 min and then rapidly separated from unreacted $AlCl_3$ by filtration without warming. The solvent was thereafter removed in vacuum at −30–−10 °C. The crystalline residue was washed with *n*-hexane and dried in vacuum; yield 80–90%. ^{13}C NMR (CD_2Cl_2): $\delta = 5.1$ (d, $^3J(PC) = 6$ Hz, $^1J(SiC) = 54.5$ Hz, $SiCH_3$), 31.4 (s, CCH_3), 54.6 (d, $^1J(PC) = 8.7$ Hz, CMe_3), 178.8 (d, $^1J(PC) = 8.6$ Hz, P = C); ^1H NMR (CD_2Cl_2): $\delta = 0.48$ (s, 18H, $SiCH_3$) 1.75 (d, $^3J(PH) = 18.5$ Hz, 18H, CCH_3); ^{27}Al NMR (CD_2Cl_2): $\delta = 103.6$. **10**: Analogous to **9**, from **8** (1 g, 3.7 mmol) and $AlCl_3$ (0.56 g, 4.2 mmol). ^{13}C NMR (CD_2Cl_2): $\delta = 1.2$ (d, $^3J(PC) = 6.3$ Hz, $SiCH_3$), 30.3 (d, $^2J(PC) = 1.4$ Hz, CCH_3), 47.5 (d, $^1J(PC) = 10.6$ Hz, CMe_3), 149.6 (d, $^1J(PC) = 45.2$ Hz, P = C); ^1H NMR (CD_2Cl_2): $\delta = 0.11$ (d, $^4J(PH) = 1$ Hz, 9H, $SiCH_3$), 1.43 (d, $^3J(PH) = 18.8$ Hz, 18H, CCH_3), 7.75 (d, $^2J(PH) = 36.7$ Hz, 1H, CH); ^{27}Al NMR (CD_2Cl_2): $\delta = 103.6$. The chloride abstraction from **7** or **8** failed with $GaCl_3$ or $SbCl_5$.

[11] R. J. Thoma, C. A. Prieto, R. H. Neilson, *Inorg. Chem. 27* (1988) 784.

[12] K. Issleib, H. Schmidt, C. Wirkner, *Z. Anorg. Allg. Chem. 473* (1981) 85.

[13] I. F. Lutsenko, A. A. Prishchenko, A. A. Borisenko, Z. S. Novikova, *Dokl. Akad. Nauk. SSSR 256* (1981) 1401.

[14] Thin colorless flakes, poor crystal quality, space group *Pbcb*, $a = 12.90(1)$, $b = 16.51(1)$, $c = 21.17(2)$ Å, $V = 4510$ Å^3, $Z = 8$; 550 observed reflections with $I > 2\sigma(I)$ (*tert*-butyl and trimethylsilyl groups and $AlCl_4^{\ominus}$ as rigid groups, Al, Cl, P, and Si refined anisotropically, C isotropically; 85 parameters, $R = 0.15$).

[15] **14**: m.p. = 144°C. $^{31}P\{^1H\}$ NMR ($CDCl_3$): $\delta = 61.4$. Another signal of low intensity (8%) at $\delta = 53.4$ can be assigned to the corresponding [2+4] cycloadduct. Cf. ^{31}P NMR signal of **15**. ^{13}C NMR ($CDCl_3$): $\delta = 6.0$ (d, $^3J(PC) = 2.3$ Hz, $SiCH_3$), 6.5 (d, $^1J(PC) = 9.1$ Hz, $CHSi_2$), 21.2 (s, CH_3), 25.1 (d, $^1J(PC) = 42.8$ Hz, PCH_2), 29.1 (s, CCH_3), 37.7 (d, $^1J(PC) = 35.1$ Hz, CMe_3), 115.5 (s, $H_2C=CMe$-), 118.1 (d, $^3J(PC) = 4.5$ Hz, $H_2C=CMe$-), 138.6 (d, $^3J(PC) = 7.0$ Hz, $H_2C=CCH_2$), 142.3 (d, $^2J(PC) = 8.9$ Hz, $H_2C=CCH_2$); ^1H NMR ($CDCl_3$): $\delta = 0.52$ (s, 18H, $SiCH_3$), 1.28 (d, $^2J(PH) = 22.8$ Hz, 1H, $CHSi_2$), 1.56 (d, $^3J(PH) = 15.4$ Hz, 18H, CCH_3), 2.00 (s, 3H, CH_3), 3.20 (d, $^2J(PH) = 12.3$ Hz, 2H, CH_2), 5.21 (s, 1H, *H*HC=), 5.23 (s, 1H, H*H*C=), 5.27 (s, 1H, *H*HC=), 5.72 (s, 1H, H*H*C=); ^{27}Al NMR ($CDCl_3$): $\delta = 102.3$ **15**: m.p. = 169°C. $^{31}P\{^1H\}$ NMR (CD_2Cl_2): $\delta = 55.8$; ^{13}C NMR (CD_2Cl_2): $\delta = 1.2$ (d, $^3J(PC) = 1.6$ Hz, $SiCH_3$), 16.1 (d, $^1J(PC) = 34.9$ Hz, CHSi), 19.8 (d, $^4J(PC) = 1.9$ Hz, CH_3), 20.3 (d, $^3J(PC) = 7.0$ Hz, CH_3), 21.6 (d, $^1J(PC) = 40.1$ Hz, PCH_2), 27.4 (s, CCH_3), 27.6 (s, CCH_3), 32.6 (d, $^2J(PC) = 7.3$ Hz, CH_2), 34.5 (d, $^1J(PC) = 36.1$ Hz, CMe_3), 35.6 (d, $^1J(PC) = 35.4$ Hz, CMe_3), 120.3 (d, $^3J(PC) = 8.4$ Hz, = C), 133.7 (d, $^2J(PC) = 8.2$ Hz, = C); ^1H NMR (CD_2Cl_2): $\delta = 0.31$ (s, 9H, $SiCH_3$), 1.11 (ddd, $^2J(PH) = 31.4$ Hz, $^3J(HH) = 12.5$ Hz, $^3J(HH) = 3.4$ Hz, 1H, CHSi), 1.26 (d, $^3J(PH) = 15.0$ Hz, 9H, CCH_3), 1.39 (d, $^3J(PH) = 15.2$ Hz, 9H, CCH_3), 1.70 (s, 3H, CH_3), 1.79 (s, 3H, CH_3), 2.10–2.44 (m, 2H, CH_2), 2.55 (d, $^2J(PH) = 11.0$ Hz, 2H, CH_2); ^{29}Si (CD_2Cl_2): $\delta = 8.0$ (d, $^2J(PSi) = 15.15$ Hz); ^{27}Al NMR ($CDCl_3$): $\delta = 102.3$.

[16] With silaethenes the [2+4] cycloaddition product is often observed in a mixture with products of the ene reaction; see, for example, N. Wiberg, M. Link, G. Fischer, *Chem. Ber. 122* (1989) 409

Effects of Perturbed Symmetry: Low-Melting Stable Mesogens Based on *ortho*-Palladated Imines**

By *María Jesús Baena, Pablo Espinet,* María Blanca Ros,* and *José Luis Serrano**

Among the rapidly growing family of metallomesogens (liquid crystals containing coordinated metals),[1] a minority are organometallic compounds. Cyclometalated palladium complexes derived from azobenzenes,[2] azomethines,[3] azines,[4] or related ligands[5] are a distinct subclass mostly constituted by halogen-bridged dimers, which can be further elaborated. Thus, replacement of the halide by carboxylate has provided mesogens based on a novel open-book molecular shape.[4] Such mesogens offer a novel approach to introducing ferroelectric properties as well as [6] the possibility of tuning the mesogenic properties by varying the bridging carboxylate.[7]

A drawback of these cyclopalladated systems is their high melting and clearing temperatures (usually > 130 and $> 200°$ C, respectively), which cause thermal decomposition of the products during prolonged studies. In the azomethine and azine systems, moreover, there is a clear predominance of smectic mesophases, and nematic mesophases are a rarity.

Both properties suggest that excellent packing of the molecules in these systems leads to high lattice energies and ordered mesophases. Consequently, perturbing the highly symmetric molecular shape might lead to lower melting points and less ordered mesophases. We describe here a successful application of this idea. A different approach to this idea of producing asymmetry in the long molecular axis of a rodlike molecule[8] has yielded low-melting mesogens, but their properties cannot be compared with the corresponding symmetrical molecules.

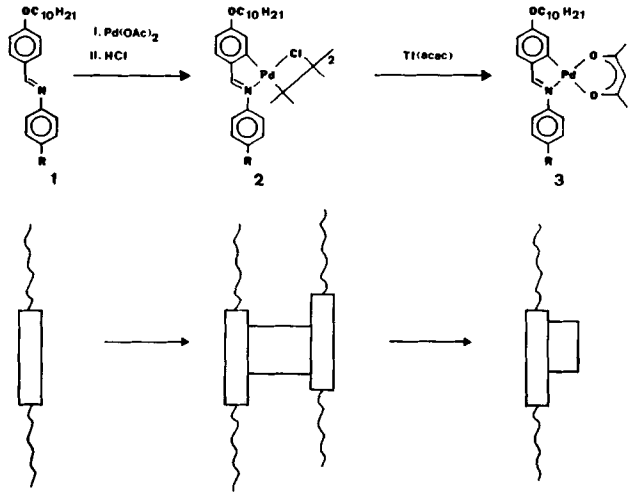

Scheme 1. Syntheses and sketch of molecular shapes of **1**–**3**. **a**, R = H; **b**, R = OC_2H_5; **c**, R = O-*n*-C_6H_{13}; **d**, R = O-*n*-$C_{10}H_{21}$.

[*] Prof. Dr. Espinet, M.J. Baena
Química Inorgánica, Facultad de Ciencias, Universidad de Valladolid
E-47005 Valladolid (Spain)
Prof. Dr. J.L. Serrano, Dr. M.B. Ros
Química Orgánica, Faculted de Ciencias-I.C.M.A. Unversidad de Zaragoza-C.S.I.C.
E-50009 Zaragoza (Spain)

[**] This work was supported by the European Community (Twinning Grant ST2J-0387C) and the Comisión Interministerial de Ciencia y Tecnologica (CICYT, Spain, Project PB86-0028 and MAT88-0324-C02-01)). *M.J. Baena* thanks IBERDUERO for a studentship.

Azomethines **1** were *ortho*-palladated to give the binuclear complexes **2** and these were treated with Tl(acac) (acac = acetylacetonate) to give the mononuclear species **3** (Scheme 1). All the compounds gave elemental analyses, ^{1}H NMR spectra, and IR spectra in full agreement with the proposed structures. The chemical transformations result in changes in molecular shape from the rodlike (or I-shaped) molecules **1** to the H-shaped (or ladderlike) binuclear complexes **2** and finally to the P-shaped (or "humpbacked") mononuclear compounds **3**.

The thermotropic behavior of **1**, **2**, and **3** was studied by optical microscopy and differential scanning calorimetry (DSC). Their thermal data are summarized in Table 1. The

Table 1. Temperature and enthalpy data for **1**–**3**.

Compound	Transition [a]	T [°C]	ΔH [kJ mol^{-1}]
1a	C-I	63.9	45.1
1b	C-N	101.3	48.6
	N-I	115.5	1.5
	N-S_A [b]	92.6	−0.7
1c	C-S_C	91.9	43.7
	S_C-S_A	111.8	
	S_A-N	112.7	
	N-I	113.2	7.0 [c]
	S_C-S_F [b]	91.4	−2.7
1d	C-S_C	102.9	52.0
	S_C-I	111.9	10.5
2a	C-I	185.6	59.1
	I-S_A [b]	177.8	−2.8
2b	C-C′	100.3	32.8
	C′-S_A	172.3	26.9
	S_A-I	274.0 (dec.)	
2c	C-C′	74.1	43.0
	C′-S_A	146.1	24.0
	S_A-I	268.2 (dec.)	
	S_A-S_C [b]	140.0 [d]	
2d	C-C′	124.2	15.1
	C′-S_C	132.7	31.5
	S_C-S_A	204.0 [d]	
	S_A-I	242.8 (dec.)	
3a	C-I	104.7	46.0
3b	C + C′-C + N	99.1	41.0
	C + N-N	108.9	0.2
	N-I	117.8	0.9
3c	C-S_A	84.0	38.4
	S_A-N	118.5	0.5
	N-I	124.8	1.3
3d	C-S_A	74.3	58.3
	S_A-I	128.0	5.8

[a] C, crystal; N, nematic; S_A, smectic A; S_C, smectic C; S_F, smectic F; I, isotropic liquid. [b] Monotropic transition. [c] Combined enthalpies. [d] Optical microscopy data.

nematic phase (N) of complexes **3** was assigned on the basis of their optical textures. The photomicrograph of the nematic phase of **3c** at 121°C (Fig. 1) shows the characteristic[9] two- and four-brush isogyres at the termination of disclination lines. Smectic A (S_A) and C (S_C) phases are observed showing optical mielinic, focalconic, and schlieren textures similar to those of classical rodlike organic compounds but more viscous.

The free ligands **1** are typical calamitic compounds, like other previously described azomethines,[3, 10] and all except **1a** are mesogenic. Except **3a**, all the palladium complexes are also liquid crystals (Fig. 2). The binuclear complexes **2** show the behavior typical of this type of molecule: they exhibit high melting ($> 130°$ C) and clearing ($> 180°$ C) temperatures and decomposition generally occurs at the clearing point.

A dramatic change in properties is observed in the corresponding mononuclear complexes **3**, which give rise to

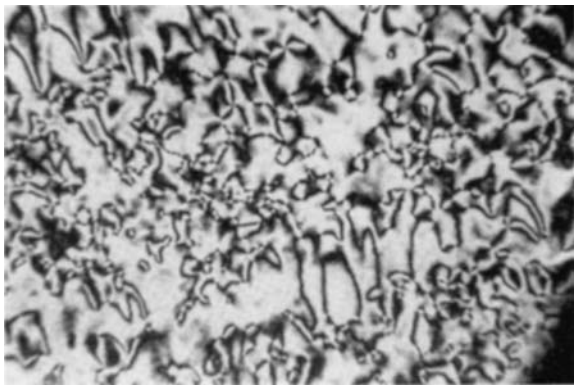

Fig. 1. Photomicrograph of **3c** in its nematic phase at 121°C viewed between crossed polars.

mesophases at temperatures below 90°C, about 50°C lower than the parent binuclear compounds **2**. The clearing temperatures are lowered to about 125°C with the consequence that the compounds can be taken from the crystalline to the isotropic state repeatedly without decomposition. This is important with respect to their eventual processability.

A second noticeable property of the mononuclear complexes **3** is the consistent occurrence of nematic (N) mesophases, which is unusual in the *ortho*-palladated binuclear species **2** we have previously described.[3] (The accessibility of a nematic phase facilitates ordered arrangements in liquid-crystal-based devices.) Broadly speaking, a decrease of order in the mesophase is observed such that S_C behavior in **2** leads to S_A behavior in **3**, and S_A behavior in **2** leads to N behavior in **3**. Thus, the only previously reported[5] acac mononuclear complex containing an *ortho*-palladated phenyl-substituted pyrimidine ligand was monotropic (S_A), whereas its parent binuclear complex displayed an enantiotropic (S_A) mesophase.

Moving from I-shaped "one-dimensional" molecules **1** to highly symmetrical H-shaped "two-demensional" structures **2** greatly increases the range of mesogenic behavior, but at the expense of high transition temperatures and a scarcity of nematic phases. The new P-shaped "two-dimensional" symmetry-perturbed mononuclear species **3** are an excellent compromise, since they show mesophase ranges broader than the free ligands, melting temperatures even lower than the free ligands, and a less complex mesogenic behavior. The complete family of I-, H-, and P-shaped mesogens, which can be extended to many related complexes, offers a very promising horizon in the tailoring of mesogenic materials.

Received: December 18, 1990 [Z 4339 IE]
German version: *Angew. Chem. 103* (1991) 716

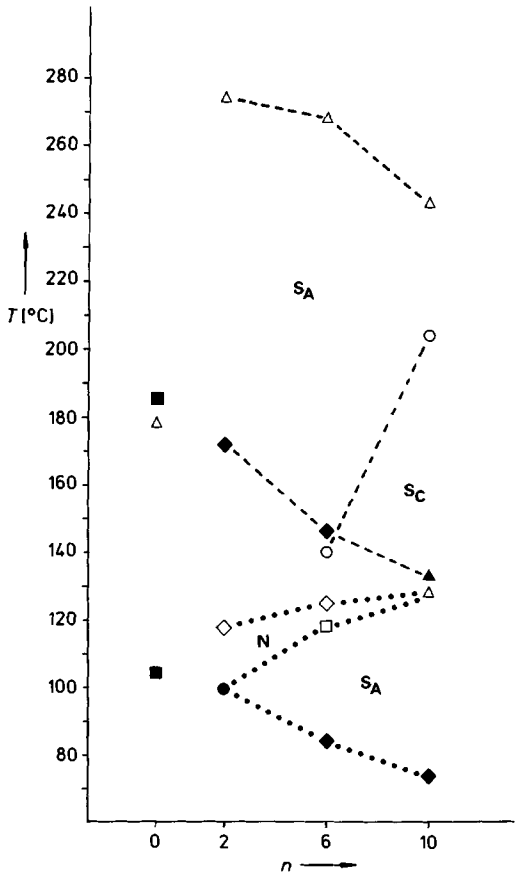

Fig. 2. Transition temperatures of the palladium complexes **2** (– – –) and **3** (····) as a function of the organic ligand **1** (n is the number of C atoms in the substituent R). **1a**, n = 0; **1b**, n = 2; **1c**, n = 6; **1d**, n = 10. ■, C-I; ●, C-N; ◆, C-S_A; ▲, C-S_C; □, S_A-N; ○, S_C-S_A; ◇, N-I; △, S_A-I.

[1] Review: A. M. Giroud-Godquin, P. M. Maitlis, *Angew. Chem. 103* (1991) 370–398; *Angew. Chem. Int. Ed. Engl. 30* (1991) 375–402, and references cited therein.
[2] M. Ghedini, M. Longeri, R. Bartolino, *Mol. Cryst. Liq. Cryst. 84* (1982) 207–211; M. Ghedini, S. Armentano, R. Bartolino, F. Rustichelli, G. Torquati, N. Kirov, M. Petrov, *ibid. 151* (1987) 75–91.
[3] J. Barberá, P. Espinet, E. Lalinde, M. Marcos, J. L. Serrano, *Liq. Cryst. 2* (1987) 833–842; M. Marcos, M. B. Ros, J. L. Serrano, *ibid. 3* (1988) 1129–1136; M. B. Ros, N. Ruiz, J. L. Serrano, P. Espinet, *ibid. 9* (1991) 77–86.
[4] P. Espinet, E. Lalinde, M. Marcos, J. Pérez, J. L. Serrano, *Organometallics 9* (1990) 555–560.
[5] M. Ghedini, D. Pucci, *J. Organomet. Chem. 395* (1990) 105–112.
[6] P. Espinet, J. Etxebarria, M. Marcos, J. Pérez, A. Remón, J. L. Serrano, *Angew. Chem. 101* (1989) 1076–1078; *Angew. Chem. Int. Ed. Engl. 28* (1989) 1065–1066.
[7] P. Espinet, J. Pérez, M. Marcos, M. B. Ros, J. L. Serrano, J. Barberá, A. M. Levelut, *Organometallics 9* (1990) 2028–2033.
[8] J. P. Rourke, F. P. Fanizzi, N. J. S. Salt, D. W. Bruce, D. A. Dunmur, P. E. Maitlis, *J. Chem. Soc. Chem. Commun. 1990*, 229.
[9] D. Demus, L. Ritcher: *Textures of Liquid Crystals*, Verlag Chemie, Weinheim 1978.
[10] D. Demus, H. Demus, H. Zaschke: *Flüssige Kristalle in Tabellen I*, VEB Deutscher Verlag für Grundstoffindustrie, Leipzig 1974, p. 97–98; D. Demus, H. Zaschke: *Flüssige Kristalle in Tabellen II*, VEB Deutscher Verlag für Grundstoffindustrie, Leipzig 1984, p. 199.

Chemoenzymatic Syntheses of ω-Ureido D-Amino Acids**

By *Karlheinz Drauz,* Matthias Kottenhahn, Kyriakos Makryaleas, Herbert Klenk*, and *Michael Bernd*

Dedicated to Professor Heinz A. Staab on the occasion of his 65th birthday

The D-amino acids are of great importance in the synthesis of biologically active substances. Compounds such as D-

[*] Dr. K. Drauz, Dr. M. Kottenhahn, Dr. K. Makryaleas, Dr. H. Klenk
Degussa AG, Fachbereich Organische und Biologische Chemie
Postfach 1345, W-6450 Hanau 1 (FRG)
Dr. M. Bernd
Asta Pharma AG, Abteilung CFW

[**] Amino Acid Transformation, Part 7. This work was supported by Recordati-De. Bi., Milan (donation of the *Agrobacterium radiobacter* culture). Part 6: K. Drauz, U. Groeger, M. Schäfer, H. Klenk, *Chem. Ztg. 115* (1991), in press.

Table 1. LH-RH agonists and antagonists[a]. The table shows some of the variations in the peptide sequence.

LH-RH	1 Glp	2 His	3 Trp	4 Ser	5 Tyr	6 Gly	7 Leu	8 Arg	9 Pro	10 Gly	NH_2
Agonists											
Buserelin						D-Ser(*t*Bu)					
Naferelin						D-2-Nal					
Lutrelin						D-Trp	*N*-MeLeu		Pro-NHC_2H_5 (1–9)		
Leuprolide						D-Leu					
Tryptorelin						D-Trp			Pro-NHC_2H_5 (1–9)		
Goserelin						D-Ser(*t*Bu)					
Histrelin						D-His(Bzl)			Pro-NHC_2H_5 (1–9)		
Antagonists											
SB-075	Ac-D-(2-Nal)-*p*-Cl-D-Phe-D-(3-Pal)					D-Cit					
Antide	Ac-D-(2-Nal)-*p*-Cl-D-Phe-D-(3-Pal)				Lys(Nic)	D-Lys(Nic)		Lys(*i*Pr)		D-Ala-NH_2	
Hoe 2013	Ac-D-(2-Nal)-*p*-Cl-D-Phe-D-Trp					D-Ser(Rha)				Azagly-NH_2	

[a] Glp = pyroglutamic acid, 2-Nal = 2'-naphthylalanine, 3-Pal = 3'-pyridylalanine, Nic = nicotinoyl, Rha = rhamnosyl.

phenylglycine and the corresponding 4-OH derivative, D-serine, and D-thienylglycine are incorporated into the side chains of important β-lactam antibiotics;[1] D-valine is one of the starting materials used to prepare the pyrethroid fluvalinate.[2] Rapid progress in the development of active peptides, in particular, requires the ready availability of a large number of structurally diverse D-amino acids.[3] Candidates include the D enantiomers of protein amino acids, of other naturally occurring amino acids, and of amino acids not present in nature.

Recently, therapeutic concepts based on influencing the formation of releasing hormones have been developed. A prominent example is the decapeptide LH-RH (luteinizing hormone releasing hormone or gonadorelin), a member of the liberin family that is formed in the hypothalmus. LH-RH induces release of gonadotropins, that is, the sex hormones follitropin (FSH) and lutropin (LH).

Potent LH-RH agonists and antagonists have potential use in treating sex-hormone-dependent diseases such as breast and prostate cancer as well as endometriosis.[4] In particular, recently developed LH-RH antagonists are capable of blocking the LH-RH receptors and reducing the release of LH and FSH immediately after the start of therapy. The first-generation drugs were unsuitable for therapy because they strongly induced the release of histamines and thus caused allergic reactions. Variation of the peptide sequence, especially the incorporation of nonproteinogenic D-amino acids at various positions, resulted in a marked reduction in the side effects. The most important LH-RH agonists and antagonists are summarized in Table 1.

The synthesis of the releasing hormone antagonist SB075, which is at the stage of clinical development, requires D-citrulline (D-Cit, **1**), an ω-ureido D-amino acid not found in nature.[5] Preparation of D-Cit by asymmetric synthesis poses problems; classical enantiomer separation necessitates a good route to racemic citrulline, which can only be obtained with difficulty from L-Cit or other precursors owing to the considerable formation of side products. We therefore sought to prepare D-Cit via the simplest possible route starting from an inexpensive, chiral amino acid.

Racemic amino acid hydantoins can often be converted practically quantitatively into D-amino acids by a system consisting of D-hydantoinase and carbamoylase.[6] The function of hydantoinases in vivo is to degrade nucleobases. These enzymes have therefore been classified as dihydropyrimidine amidohydrolases (E. C. 3.5.2.2). The hydantoinase/carbamoylase systems have only been used up to now in the large-scale production of D-phenylglycine and D-*p*-hydroxyphenylglycine, which may be employed in turn to prepare other aromatic as well as simple aliphatic D-amino acids. Nothing has been reported on the substrate specificity with respect to the side chain of amino-functionalized hydantoins.[7]

We also used this strategy for the synthesis of D-Cit. D-Cit may formally be derived form L-ornithine (**2**), which has the same number of C atoms and is accessible by enzymatic cleavage of the inexpensive protein amino acid L-arginine (**3**) (Scheme 1). Reaction of **2** with two equivalents of cyanate yields the α,ω-bisureido compound **4**, which can also be obtained from L-Cit and one equivalent of cyanate. Under acid conditions, **4** is converted into the 5-(3-ureidopropyl) hydantoin (citrulline hydantoin, **5**). Surprisingly, our hydantoinase/carbamoylase system, obtained from the strain *Agrobacterium radiobacter*, accepts this substrate[8] and affords D-citrulline in good chemical and optical yields.

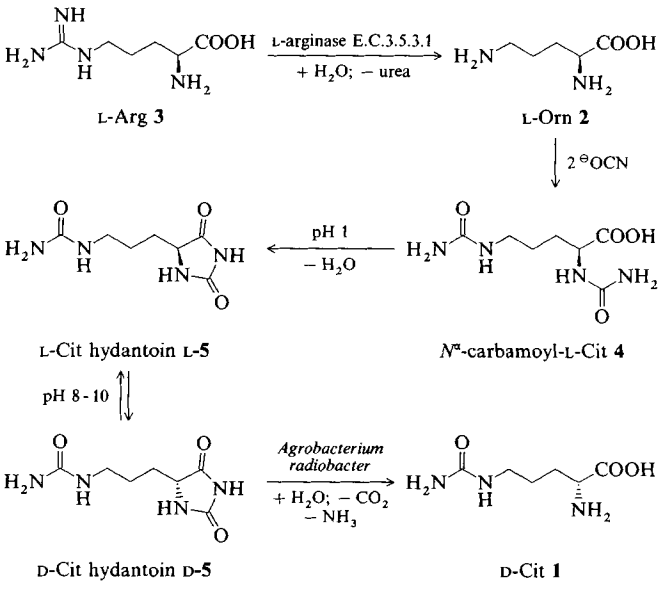

Scheme 1.

Hydantoins that are sufficiently acidic undergo chemical racemization under the alkaline reaction conditions. In the presence of racemases, the reaction can also be catalyzed enzymatically. Thus, D-amino acids may be obtained from L-hydantoins. In principle, this reaction offers a method of configuration reversal.

Table 2. Preparation of ω-ureido D-amino acids.

Hydantoin	D-amino acid	Yield [%] [a]	Content of D [b]
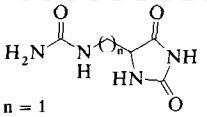	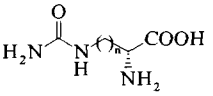		
n = 1	D-albizziin [10]	69	>99
n = 2	D-4-ureido-2-amino-butyric acid [11]	73	98–99.8
n = 3	D-citrulline [12]	79	96–99.8
n = 4	D-homocitrulline [13]	70	60
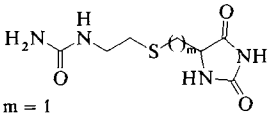	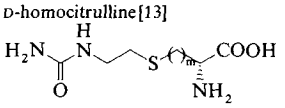		
m = 1	D-ω-ureido-AEC [c]	71	98–99.8
m = 2	D-ω-carbamoylthialysine [14]	78	98–99.8

[a] Yield of isolated product [%]. [b] Amount of D enantiomer [%], determined by comparison with literature data or by chromatography with the racemic compounds for comparison [10–14]; the ranges refer to different runs. [c] AEC = *S*-aminoethylcysteine.

Furthermore, we desired to determine the spectrum of substrates accepted by this biocatalyst. Readily obtainable racemic or L-α,ω-diamino carboxylic acids were converted into hydantoins analogous to **5**[9] and subjected to biotransformation (Table 2).

This approach provides a series of interesting ω-ureido δ-amino acids that are chemically synthesized only with difficulty and are not obtainable at all through fermentation. These examples show the advantages of combining chemical and enzymatic steps in the preparation of enantiomerically pure amino acids unknown in nature.

Experimental Procedure

Summary of the synthesis of D-citrulline (**1**, $C_6H_{13}N_3O_3$, M = 175.19) [15]: A solution of **5** (4 g, 22.8 mmol), prepared according to [9], in water (55 mL) was adjusted to pH 8.4 by addition of concentrated aqueous sodium hydroxide. The solution was then degassed by agitating in a mechanical shaker at 40 °C for 10 min, treated with the bacterial culture (*Agrobacterium radiobacter*, 0.5 g) under N_2, degassed once again, and then sparged with N_2. The vessel was shaken for 24 h at 40 °C under N_2 at 6 bar and then for 24 h at 40 °C under normal pressure before cooling it and adjusting the pH of the solution to pH 9. The solid portion of the culture was separated by centrifugation and the remaining liquid was treated with charcoal to clear the solution. Yield in solution 95%. Isolation was accomplished by filtering the solution through a strongly acidic ion exchanger (Merck, IR 120) and eluting the product with 5% aqueous NH_3. The solution thereby obtained was evaporated and the residue was dissolved in a small amount of water. Addition of ethanol precipitated the product. 3.4 g (85%), m.p. 215–218 °C (dec.), $[\alpha]_D^{20}$: +22 (c = 2 in 1 N HCl) ^{1}H NMR (250 MHz, D_2O): δ = 3.73 (m, 1H, Hα), 3.1 (m, 2H, Hγ); 1.4–2.0 (2 × m, each 2H, Hβ + Hγ).

Received: February 14, 1991 [Z 4441 IE]
German version: *Angew. Chem. 103* (1991) 704

[1] A. Kleemann, J. Engel: *Pharmazeutische Wirkstoffe; Synthesen, Patente, Anwendungen, Band 5*, 2nd ed. and supplement 1982–1987, Thieme, Stuttgart 1982 and 1987; A. Kleemann, H. J. Roth: *Arzneistoffgewinnung*, Thieme, Stuttgart 1983; H. J. Roth, A. Kleemann: *Arzneistoffsynthese*, Thieme, Stuttgart 1982.
[2] C. A. Henrik, B. A. Garcia, G. B. Staal, D. C. Cerf, R. J. Anderson, K. Gill, H. R. Chinn, J. N. Labovitz, M. M. Leippe, S. L. Woo, R. L. Carney, D. C. Gordon, G. K. Kohn, *Pestic. Sci. 11* (1980) 224; R. J. Anderson, K. G. Adams, C. A. Henrik, *J. Agric. Food Chem. 33* (1985) 508.
[3] B. W. Bycroft, *Amino Acids Pept. Proteins 7* (1976) 333; J. S. Davies, *ibid. 20* (1989) 129, and references cited therein.
[4] A. S. Dutta, *Drugs of the Future 13* (1988) 43.
[5] S. Bajusz, V. J. Csernus, T. Janaky, L. Bokser, M. Fekete, A. V. Schally, *Int. J. Pept. Protein Res. 32* (1988) 425.
[6] A. Möller, C. Syldatk, M. Schulze, F. Wagner, *Enzyme Microb. Technol. 10* (1988) 618; C. Syldatk, A. Läufer, H. Höke, F. Wagner, *Forum Mikrobiol. 11* (1988) 224; C. Syldatk, D. Cotoras, A. Möller, F. Wagner, *Biotech Forum 3* (1986) 10.
[7] C. Syldatk, A. Läufer, R. Müller, H. Höke, *Adv. Biochem. Eng. Biotechnol. 41* (1990) 29.
[8] R. Olivieri, E. Fascetti, L. Angelini, L. Degen, *Enzyme Microb. Technol. 1* (1979) 201.
[9] F. A. Hoppe-Seyler, *Hoppe-Seyler's Z. Physiol. Chem. 214* (1933) 267, 268, 270.
[10] A. Kjaer, P. Olesen Larsen, G. Gmelin, *Experimentia 15* (1959) 253.
[11] J. Rudinger, K. Poduska, M. Zaoral, *Collect. Czech. Chem. Commun. 25* (1960) 2022.
[12] A. C. Kurtz, *J. Biol. Chem. 180* (1949) 1254.
[13] A. C. Kurtz, *J. Biol. Chem. 180* (1949) 1261.
[14] G. Kalopissis, G. Manoussos, US Patent 3950542 (1976) L'Oreal S. A.
[15] K. Makryaleas, K. Drauz, EP Pat. Appl. 0400638 (1990) Degussa AG.

2,3,6,7-Tetramethoxythianthrene Dication: An "Aromatic" π System "Gives Up the Ghost"**

By *Hans Bock*,* *Andreas Rauschenbach*, *Klaus Ruppert*, and *Zdenek Havlas*

Dedicated to Edgar Heilbronner on the occasion of his 70th birthday

Well over half a century ago, *E. Hückel* proposed the (4n + 2)-electron rule for cyclic π systems. Since then, this simple and fascinating concept[1] has stimulated the syntheses of a great variety of novel molecules and molecular ions, which in lab jargon are frequently termed aromatic (Greek: aromatikos = herbal smelling) and which, according to numerous experimental data as well as quantum-chemical results, are distinguished by an energetically favorable electron distribution.[2] Deviations from the optimum number of electrons, therefore, should inflict severe perturbations and, as is known for redox reactions of other organic compounds, result in surprising structural changes.[3]

For a model compound, we have selected 2,3,6,7-tetramethoxythianthrene (TMT, Scheme 1),[4a, b] which, unlike the related hydrocarbon anthracene with 14 π electrons, is not

[*] Prof. Dr. H. Bock, Dipl.-Chem. A. Rauschenbach, Dipl.-Chem. K. Ruppert, Dr. Z. Havlas [+]
Institut für Anorganische Chemie der Universität
Niederurseler Hang, W-6000 Frankfurt am Main (FRG)
[+] Permanent address: Dr. Z. Havlas, Institut of Organic Chemistry and Biochemistry of the Czechoslovakian Academy of Sciences, Flemingova Nam. 2, CS-16610 Prague 6 (Czechoslovakia)

[**] Structures of Sterically Overcrowded or Charge-Perturbed Molecules, Part 6. This research was supported by the Land Hessen, by the Fonds der Chemischen Industrie, and by the Alexander von Humboldt-Stiftung (*Z.H.*) Parts 5: H. Bock, I. Göbel, Z. Havlas, H. Oberhammer, S. Liedle, *Angew. Chem. 103* (1991) 193; *Angew. Chem. Int. Ed. Engl. 30* (1991) 187.

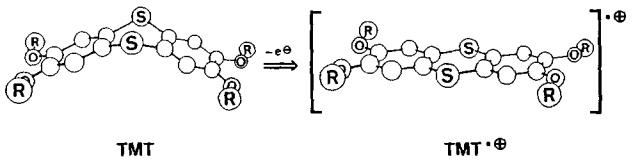

TMT $\qquad$ TMT$^{\cdot\oplus}$

Scheme 1. Structures of TMT and its radical cation.

planar. Since sulfur substitution increases the number of π electrons by 2, TMT shows the same "butterfly"-like folding of its skeleton as the parent compound $C_{12}H_8S_2$.[4c]

Its one-electron oxidation by $NO^{\oplus}SbCl_6^{\ominus}$ or I_2 yields a blue radical cation, $TMT^{\cdot\oplus}$, the tricyclic skeleton of which is flattened[4d] even though the "ideal" 14-π-electron configuration is still exceeded by 1. Cyclic voltammetric measurements[4e] under aprotic conditions and at enhanced recording speed[4f] reveal, in addition to the first half-wave potential at + 0.88 V, a second reversible oxidation at + 1.27 V (Fig. 1).

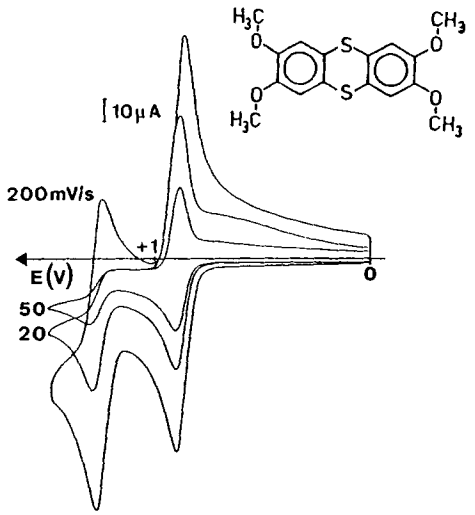

Fig 1. Cyclic voltammograms of TMT in Al_2O_3-dried H_2CCl_2 under argon at 293 K (electrolyte 0.1 M $Bu_4N^{\oplus}ClO_4^{\ominus}$, glassy carbon electrode vs. SCE, recording speed 20 to 200 mV s^{-1}, each ΔE 60 mV).

What structural changes will result on the removal of a second electron to produce the dication $TMT^{2\oplus}$?[4f, g]

Reaction of TMT with $SbCl_5$ in H_2CCl_2 under argon and under aprotic conditions ($c_{H^{\oplus}} < 1$ ppm) yields a green solution, from which, after several days at 5 °C, rhombuses with a metallic luster crystallize. The crystals are black, but dark red when viewed against light. Their low-temperature structure determination[6] provides an unexpected result (Fig. 2).

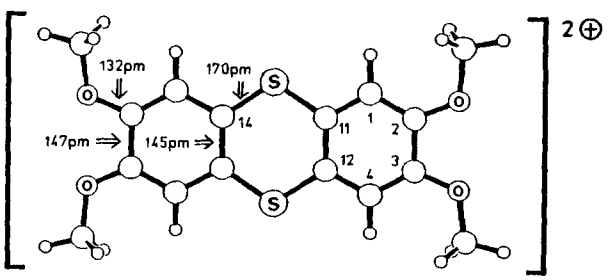

Fig. 2. Molecular structure of $TMT^{2\oplus}$ [6]. Important distances [pm ± 0.8] and angles [° ± 0.3] (average values): C2-C3 147.2, C11-C12 145.3, C1-C2 138.7, C1-C11 140.1, C11-S 169.5 C2-O 131.5, C11-S-C14 109.9, S-C11-C1 115.1, C11-C1-C2 120.4, C1-C2-O 126.8, C2-O-C_{Me} 118.7.

The dication $TMT^{2\oplus}$, which has 14 π electrons in the three annelated six-membered rings does not exhibit the "aromatic" character expected. Instead, the π molecular skeleton is extended by the methoxy oxygens to include altogether 18 centers; the O–C and C–S bonds are shortened to 132 and 170 pm and the ring C–C bonds shown in Figure 2 are elongated to 147 and 145 pm. Comparison with the corresponding C–X bond distances of both TMT[4b] and $TMT^{\cdot\oplus}$ suggests that the structure of $TMT^{2\oplus}$ consists of two fourfold C–C-connected and positively charged chains, H_3CO-CCC-$S^{\oplus}$-CCC-OCH_3 (Scheme 2; Table 1).

Table 1. Bond lengths [pm] in TMT, $TMT^{\cdot\oplus}$, and $TMT^{2\oplus}$. Numbering shown in Figure 1.

	C2-C3	C11-C12	C1-C2	C1-C11	C11-S	C2-O
TMT	141.0	138.3	138.0	139.7	177.6	136.9
$TMT^{\cdot\oplus}$	143.0	139.5	136.2	140.0	172.3	134.9
$TMT^{2\oplus}$	147.2	145.3	138.7	140.1	169.5	131.5

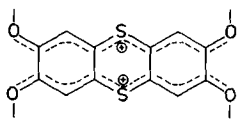

Scheme 2. Structural proposal for $TMT^{2\oplus}$ based on comparison of the bond lengths of TMT, $TMT^{\cdot\oplus}$, and $TMT^{2\oplus}$ (Table 1).

This assumption is supported by geometry-optimized MNDO calculations,[7] which reproduce satisfactorily both the structure (e.g., C2-C3 = 148 pm) and the color ($\tilde{\nu}_m^{exp.} = 14100\ cm^{-1}$, $\tilde{\nu}_m^{calcd} = 13700\ cm^{-1}$) of the dication $TMT^{2\oplus}$. Furthermore, the charge distributions calculated for the species TMT, $TMT^{\cdot\oplus}$, and $TMT^{2\oplus}$ (Scheme 3) demonstrate a localization of the positive charges predominantly at the electron-rich sulfur centers and, to a lesser extent, around the methoxy oxygens, which possess the highest effective nuclear charge within the system.

In addition, the electron densities, which decrease significantly especially at the outer ring centers, provide a plausible explanation for the elongation of the C2–C3 and C11–C12 distances by 7 pm each (see Table 1).

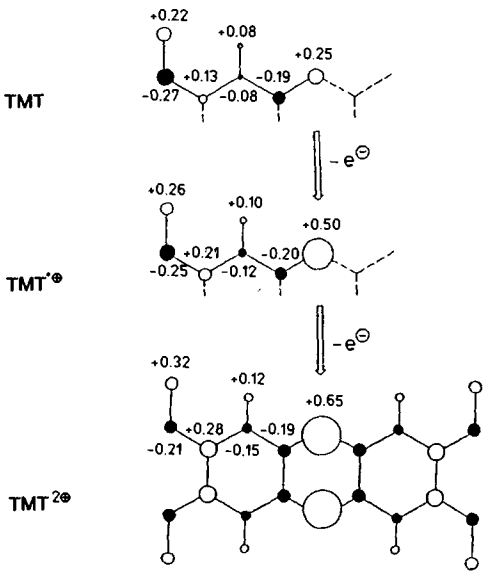

Scheme 3. Calculated charge distribution in TMT, $TMT^{\cdot\oplus}$, and $TMT^{2\oplus}$.

The structural (Table 1) and quantum-chemical (Scheme 3) observations for $TMT^{2\oplus}$ can be discussed in terms of the well-known "cyanine concept". On the basis of UV/VIS data and HMO calculations,[8] the formation of chainlike π subsystems was first proposed 25 years ago for π systems with subunits which contain an even number of π electrons distributed over an odd number of π centers[3a, b, 9]. In the meantime, such distortions have been confirmed many times over by structure determinations. From this point of view, the dications of suitably donor-substituted ethene derivatives[3a, 9a] and the dianions of suitably acceptor-substituted[3b] ethene derivatives formally consist of two cyanine-like three-center subsystems, $(R_2N)_2C^{\oplus}$ and $(H_5C_6)_2C^{\ominus}$, each with 4 π electrons, which are connected by C–C single bonds and twisted by 76°[3a, 9a] and 56°, respectively.[3b] The surprising structures of the 1,2,4,5-tetrakis(dimethylamino)benzene dication[9a] and the dipotassium salt of 2,5-dihydroxy-*p*-benzoquinone[9b] are also rationalized by the existence of two cyanine subunits, $R_2N^{\delta\oplus}$-CCC-$^{\delta\oplus}NR_2$ and $^{\delta\ominus}$O-CCC-$O^{\delta\ominus}$, respectively, containing five centers and six electrons, which are connected by C–C single bonds of 153 and 154 pm length, respectively. Despite the three annelated six-membered rings in $TMT^{2\oplus}$ and although two more π electrons would have to be removed to generate two complete cyanine subsystems, the formation of two positively charged chains connected by elongated C–C bonds, H_3CO-CCC-$S^{\oplus}$-CCC-OCH_3, wins over an increased cyclic π delocalization.

Altogether, the cyanine concept[8] constitutes a general and powerful structure perturbation principle.[10] With quite some excitement one may look forward to the skeletal distortions predicted by this old rule of thumb in other organic salts[11] prepared by appropriate redox reactions.

Received: January 14, 1991 [Z 4385 IE]
German version: *Angew. Chem. 103* (1991) 706

[1] See, for example, E. Heilbronner, H. Bock: *Das HMO-Modell und seine Anwendung, Band I to III*, Verlag Chemie, Weinheim 1968–1970; *The HMO Model and Its Application*, Wiley, New York 1975/1976.

[2] Summaries from a current point of view are provided, for example, by the lectures at the Int. Symp. on "Novel Aromatic Compounds", Osaka, Japan, 1989, published in *Pure Appl. Chem. 62/3* (1990); our own contribution is found in pp. 383–394. Cf. also the essay dedicated to *E. Hückel* on occasion of his 80th birthday: "Molecular States and Molecular Orbitals", H. Bock, *Angew. Chem. 89* (1977) 631; *Angew. Chem. Int. Ed. Engl. 16* (1977) 613, and references cited therein.

[3] Cf., e.g., a) twisted tetrakis(dimethylamino)ethene dication (H. Bock, K. Ruppert, K. Merzweiler, D. Fenske, H. Goesmann, *Angew. Chem. 101* (1989) 1715; *Angew. Chem. Int. Ed. Engl. 28* (1989) 1684, b) twisted tetraphenylethene dianion containing an intermolecular dibenzene Na sandwich (H. Bock, K. Ruppert, D. Fenske, *ibid. 101* (1989) 1717 and 28 (1989) 1685) as well as additional contact ion pairs, c) tetraphenylallylsodium containing an intramolecular dibenzene Na sandwich (H. Bock, K. Ruppert, D. Fenske, Z. Havlas, *ibid. 102* (1990) 1095 and *29* (1990) 1042) or 1,1,4,4-tetraphenylbutane-1,4-diyldisodium with chain structure (H. Bock, K. Ruppert, Z. Havlas, W. Bensch, W. Hönle, H. G. v. Schnering, *Angew. Chem.*, in press; *Angew. Chem. Int. Ed. Engl.*, in press).

[4] a) Preparation: G. Klar, T. Weiß, *Liebigs. Ann. Chem. 1978*, 785; b) Structure: G. Klar, W. Hinrichs, J. Riedel, *J. Chem. Res. 1982*, 334; c) I. Rowe, B. Post, *Acta Crystallogr. 11* (1958) 372; d) G. Klar, W. Hinrichs, P. Berges. *Z. Naturforsch. B42* (1987) 169 (the interplanar angles are 180° in $TMT^{\cdot\oplus}SbCl_6^{\ominus}$ and 172° in $TMT^{\cdot\oplus}$ ($I^{\ominus}$); e) G. Klar, K. W. Stender, *Z. Naturforsch. B40* (1985) 774; f) A. Rauschenbach, *Diplomarbeit*, Universität Frankfurt 1990; g) For evidence on the oxidation to the dication see [4a] and references cited therein.

[5] a) The oxidizing agent is presumably the chloromethyl carbocation formed by the reaction $SbCl_5 + H_2CCl_2 \rightarrow SbCl_6^{\ominus} + H_2CCl^{\oplus}$; oxidation potential $E_{1/2}^{ox} \approx +1.6$ V (H. Bock, U. Lechner-Knoblauch, *J. Organomet. Chem. 294* (1985) 295); b) Preparation: $SbCl_5$ (1.2 g, 4 mmol) in 50 mL of H_2CCl_2 was added at room temperature and under Ar to a solution of TMT (670 mg, 2 mmol) in 50 mL of H_2CCl_2 dried by treatment with Al_2O_3, which had been heated to high temperature. The solution instantly turned green. The amorphous precipitate was filtered off under Ar. Its H_2CCl_2 solution, saturated at 40 °C, was kept for 1 day at 20 °C and then cooled to 5 °C. After 1 week, black rhombuses crystallized; on viewing in front of a cool-light lamp, the crystals shine dark red.

[6] Crystal structure analysis: $TMT^{2\oplus}$ (661.88 g mol^{-1}), $a = 963.4(5)$, $b = 2502.3(12)$, $c = 1350.2(7)$ pm, $\beta = 97.6(3)°$; $V = 3226.4 \times 10^6$ pm^3 (200 K), $P2_1/n$, $Z = 4$, $\mu(Mo_{K\alpha}) = 27.48$ cm^{-1}, Siemens AED II with graphite monochromator, $3° < 2\theta < 50°$, 5094 registered reflections, of which 3478 are independent with $I > 1.5\,\sigma(I)$; $R = 0.0524$, $R_w = 0.0530$ ($\omega = 1.6648/\sigma^2(F) + 0.002594\,F^2$). All C, O, S, Cl, and Sb atoms refined anisotropically, all H atoms of thianthrene refined with fixed temperature factor (0.5), all methyl protons refined with common temperature factor within a "rigid-body" model. Average values for additional bond distances [pm ± 0.8] and angles [° ± 0.3]: O-C(H_3) 146.6 S-C 11-C12 125.2, C1-C11-C12 119.9, C3-C2-O 113.4, Sb-Cl 237.3, Sb-Cl 234.8, Cl-Sb-Cl 179, Cl···H 280. The $TMT^{2\oplus}$ dications are stacked layerlike in the lattice; their average separation is 450 pm. Additional details of the crystal structure investigation can be obtained from the Fachinformationszentrum Karlsruhe, Gesellschaft für wissenschaftlich-technische Information mbH, W-7514 Eggenstein-Leopoldshafen 2 (FRG), by quoting the depository number CSD-55289, the names of the authors, and the literature citation.

[7] Extensive MNDO and especially PM3 calculations yield inter alia the following results: The structure optimizations based on at least C_{2v} symmetry and planar dimethoxybenzene units predict for the neutral compound TMT an interplanar angle γ of about 150° between the two molecular halves; this value significantly exceeds the experimental value of 131°[4b]. Altogether, however, a rather shallow double minimum potential with a barrier of only approximately 5 kJ mol^{-1} results for the flattening to $\gamma = 180°$ and, therefore, the planar structure of the radical cation [4b] can be readily explained by crystal effects only. For the radical cation $TMT^{\cdot\oplus}$ and the dication $TMT^{2\oplus}$ planar tetraoxothianthrene skeletons were calculated. The respective PM3 enthalpies of formation ΔH_f[kJ mol^{-1}] are −311 for TMT, +406 for $TMT^{\cdot\oplus}$, and +1501 for $TMT^{2\oplus}$. Therefore, adiabatic ionization energies $IE_1^a(TMT \rightarrow TMT^{\cdot\oplus}) \approx 7.4$ eV and $IE_2^a(TMT^{\cdot\oplus} \rightarrow TMT^{2\oplus}) \approx 11.4$ eV result. The first vertical ionization energy of tetramethoxythianthrene is predicted according to Koopmans' theorem to be $IE_1^v \approx -\varepsilon_1^{PM3} = 8.0$ eV. In addition, PM3/CI calculations based on altogether 100 configurations yield the following energies for the long-wavelength excitations within the visible spectral region state assignments in brackets: $\tilde{\nu}_{m,1} \approx 13\,700$ cm^{-1} ($\pi \rightarrow \pi^*$, $b_{1g} \times b_{3u} = B_{2u}$), $\tilde{\nu}_{m,2} = 15\,900$ cm^{-1} ($\pi \rightarrow \pi^*$, $b_{3u} \times b_{3u} = Ag$), $\tilde{\nu}_{m,3} = 16\,300$ cm^{-1} ($\pi \rightarrow \pi^*$, $b_{2g} \times b_{3u} = B_{1u}$).

[8] S. Dähne, D. Leupold, *Angew. Chem. 78* (1966) 1029, *Angew. Chem. Int. Ed. Engl. 5* (1966) 984; cf. also S. Dähne, F. Moldenhauer, *Prog. Phys. Org. Chem. 15* (1985) 1–130, and references cited therein.

[9] a) K. Elbl, C. Krieger, H. A. Staab, *Angew. Chem. 98* (1986) 1024; *Angew. Chem. Int. Ed. Engl. 25* (1986) 1023; *ibid* 102 (1990) 183 and 29 (1990) 211; b) S. Kulpe, *J. Prakt. Chem. 316* (1974) 353; cf. also S. Kulpe, D. Leupold, S. Dähne, *Angew. Chem. 78* (1966) 639; *Angew. Chem. Int. Ed. Engl. 5* (1966) 699.

[10] We want to thank the two referees without aromatically clouded spectacles for their valuable comments on cyanine perturbations of organic molecular ions.

[11] For instance, the dication of tetrakis(dimethylamino)-*p*-benzoquinone shows a twist conformation of the two cyanine subunits $^{\delta\ominus}N$-C-C(O)-C-$N^{\delta\oplus}$ (H. Bock, K. Ruppert, C. Näther, Z. Havlas, unpublished).

Nickel-catalyzed Cyclotrimerization of Malononitrile: The Dicyanomethanide-bridged, Anionic Ni^{II} Complex $[\{Ni(C_5F_5)_2(\mu\text{-NCCHCN})\}_2]^{2\ominus}$**

By *Gregorio López,* Gregorio Sánchez, Gabriel García, José Ruiz, Joaquín García, M. Martínez-Ripoll, A. Vegas,* and *Juan A. Hermoso*

The α-methylene group in malononitrile is sufficiently acidic to afford the dicyanomethanide anion, $[CH(CN)_2]^{\ominus}$,

[*] Prof. G. López, Dr. G. Sánchez, Dr. G. García, Dr. J. Ruiz, J. García
Departamento de Química Inorgánica
Universidad de Murcia
E-30071 Murcia (Spain)
Prof. M. Martínez-Ripoll, Dr. A. Vegas, J. A. Hermoso
Instituto de Química-Física "Rocasolano"-CSIC, Madrid

[**] This work was supported by the Dirección General de Investigación Científica y Técnica (project PB87–0690). *J.G.* thanks the Dirección Regional de Educación y Universidad de Murcia for a research grant.

which may be represented by the resonance structures **A**. Transition-metal complexes with the dicyanomethanide ion have been reported;[1] they usually contain a dicyanomethyl–metal linkage as in **B**. In some rhodium and iridium complexes the monocyanoketenimine structure **C** has been assigned on the basis of IR data.[1a] Some ruthenium complexes containing either monodentate malononitrile or bridging substituted malononitrile have also been described.[2]

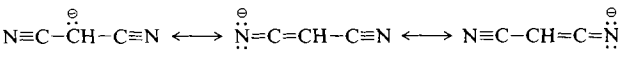

A

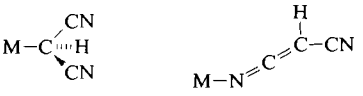

B **C**

Recently, the synthesis of a number of new hydroxo-bridged binuclear complexes of nickel, palladium, and platinum has been reported.[3] These complexes have potential utility in organic and organometallic synthesis.[4]

In the course of our research into the chemistry of $[\{R_2M(\mu\text{-}OH)\}_2]^{2\ominus}$-type complexes (M=Ni, Pd, Pt), we have found that the nickel complex ($R=C_6F_5$)[5] can be used as an efficient catalyst for the cyclotrimerization of malononitrile [Eq. (a)]. The isolated product[6] was identified as the so-called Trimer I of malononitrile.[7]

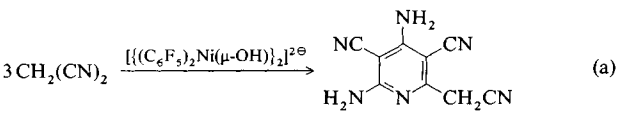

(a)

The high basicity of the OH bridges in the hydroxo-nickel complex (its ^{1}H NMR spectrum shows the OH resonance at $\delta = -5.74$) should facilitate the formation of $[CH(CN)_2]^{\ominus}$; the carbanion can then react further to produce an anionic dimer, and the reaction of this with a third malononitrile molecule (and abstraction of one proton) produces the trimer.[8]

The reaction of the hydroxo-bridged nickel complex with malononitrile (molar ratio 1:2) in dichloromethane leads to the formation of an unprecedented binuclear nickel complex containing a bridging $[CH(CN)_2]^{\ominus}$ ligand [Eq. (b)].

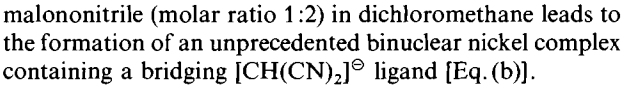

(b)

1

The conductance of **1** in acetone solution corresponds to that of a 2:1 electrolyte[9] and the ^{19}F NMR spectrum indicates that the two C_6F_5 groups are equivalent. The IR spectrum of **1** shows two bands in the $\nu(C\equiv N)$ region at lower energy than in free malononitrile (at 2270 cm^{-1})[10] (see *Experimental Procedure*).

An X-ray crystal structure determination of **1**[11] revealed the anion structure shown in Figure 1. The Ni atoms are coordinated in a distorted square-planar arrangement, the deviations from the plane towards a tetrahedral disposition being $\pm$ 0.01 Å. The average Ni–C_6F_5 bond length of 1.89(1) Å is in good agreement with those reported for other binuclear nickel complexes containing the C_6F_5 group.[12]

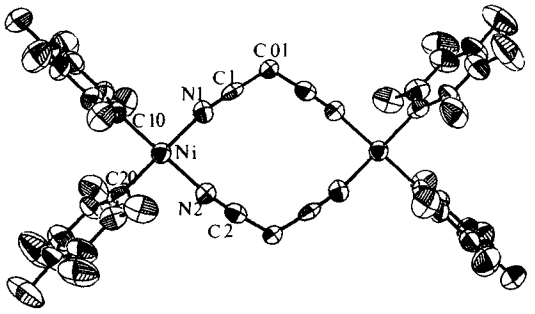

Fig. 1. Centrosymmetric anion structure of **1** (ORTEP). Selected bond lengths [Å] and angles [°]: Ni-C10 1.88(1), Ni-C20 1.90(1), Ni-N1 1.87(1), Ni-N2 1.89(1), Ni-C1 1.14(1), N2-C2 1.15(2), C1-C01 1.39(2), C2'-C01 1.36(2); N1-Ni-C10 92.7(4), C10-Ni-C20 88.4(4), C20-Ni-N2 92.0(4), N2-Ni-N1 87.0(4), Ni-N1-C1 170.3(7), Ni-N2-C2 170.5(8), N1-C1-C01 175(1), C1-C01-C2' 118.9(9). The atoms labeled with a prime sign are generated by reflection of the corresponding atoms through a crystallographic inversion center.

The C1–C01–C2' angle (118.9(9)°) and the C–C distances in the bridge indicate that the C01 atom is sp^2 hybridized. Taking into further account the C–N distances, the best description of the coordinated $[CH(CN)_2]^{\ominus}$ ion should assign an electron pair to a bonding molecular orbital extending over the whole NCCCN skeleton. The value of 170.4(8)° for the Ni–N–C angle is consistent with the above description. Thus, the twelve-membered ring Ni(μ-NC-CHCN)$_2$Ni may be represented as depicted in **D**.

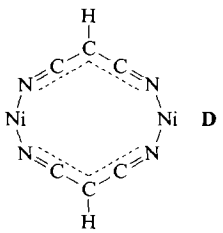

D

Experimental Procedure

Malononitrile (0.010 g, 0.153 mmol) was added to a solution of $(NBu_4)_2$-$[\{(C_6F_5)_2Ni(\mu\text{-}OH)\}_2]$ (0.1 g, 0.077 mmol) in CH_2Cl_2 (5 mL) and the mixture was stirred at room temperature for 30 min, whereupon a yellow solid precipitated. The isolated compound was identified as **1** (84% yield). Correct C,H,N elemental analysis. M.p. 209 °C (dec.) Λ_e [S cm^2 mol^{-1}] = 164 × 10^{-4} M acetone solution. IR (Nujol): $\tilde{\nu}$(CN) = 2215(s), 2160(br,s); $\nu(C_6F_5)$ = 1630(m), 1495(vs), 1055(vs), 950(vs), 780(s) cm^{-1}. UV/VIS(acetone): λ_{max}[nm](ε) = 421 (1390). ^{1}H NMR (200 MHz, [D$_6$]-acetone TMS): δ = 1.66 (s, 2H, CH), and additional peaks from $[NBu_4]^{\oplus}$ at δ = 3.47, 1.86, 1.45, 0.97. ^{19}F NMR (80 MHz, $CFCl_3$): δ = – 116.1 (dd, 8F, $J(o\text{-}m)$ = 29.3 Hz, $J(o\text{-}o)$ = 4.8 Hz, *o*-F), – 165.3 (t, 4F, $J(m\text{-}p)$ = 19.3 Hz, *p*-F), – 167.2 (m, 8F, *m*-F).

Received: November 27, 1990 [Z 4294 1E]
German version: *Angew. Chem. 103* (1991) 733

CAS Registry numbers:
1, 133228-27-0; $(NBu_4)[(C_6F_5)_2Ni(\mu\text{-}OH)_2]$, 125963-03-3; $CH_2(CN)_2$, 109-77-3.

[1] a) W. H. Badley, P. Choudhury, *J. Organomet. Chem. 60* (1973) C74; b) K. Suzuki, S. Nakamura, *Inorg. Chim. Acta 25* (1977) L21, and references cited therein; c) K. Suzuki, M. Sakurai, *ibid. 32* (1979) L3; d) T. G. Appleton, M. A. Bennett, *Inorg. Chem. 17* (1978) 738.

[2] a) G. S. Ashby, M. I. Bruce, I. B. Tomkins, R. C. Wallis, *Aust. J. Chem. 32* (1979) 1003; b) M. I. Bruce, T. W. Hambley, M. J. Liddell, A. G. Swincer, E. R. T. Tiekink, *Organometallics 9* (1990) 2886.

[3] a) E. Carmona, M. J. Marín, P. Palma, M. Paneque, M. L. Poveda, *Inorg.*

Chem. 28 (1989) 1985; b) G. López, G. García, J. Ruiz, G. Sánchez, J. García, C. Vicente, *J. Chem. Soc. Chem. Commun. 1989*, 1045; c) G. López, J. Ruiz, G. García, C. Vicente, J. M. Martí, M. D. Santana, *J. Organomet. Chem. 393* (1990) C53.
[4] H. E. Bryndza, W. Tam, *Chem. Rev. 88* (1988) 1163.
[5] Unpublished X-ray diffraction data have established the binuclear nature of $[(C_6F_5)_2Ni(\mu\text{-}OH)_2Ni(C_6F_5)_2]^{2\ominus}$, with an average Ni–O bond length of 1.91 Å.
[6] $[NBu_4)_2[\{(C_6F_5)_2Ni(\mu\text{-}OH)\}_2]$ (0.150 g, 0.115 mmol), was added to a solution of malononitrile (0.759 g, 11.5 mmol) in benzene (50 mL) and the mixture was refluxed for 2 h. The benzene was evaporated under vacuum and the resulting sticky material was treated with ethanol and vigorously stirred to give a beige solid, which was isolated (55% yield) and identified as 4,6-diamino-2-cyanomethyl-3,5-pyridinedicarbonitrile (Trimer I). Correct C,H,N elemental analysis. M.p. 330 °C. MS: *m/z* 198 ($M^{\oplus}$, 100%); IR (Nujol): $\tilde{\nu}$ [cm^{-1}] = 3400–3200, 1600, 1560, 1500; VIS-UV (in MeOH): λ_{max} [nm] = 313, 245 (sh), 237. ^{1}H-NMR (80 MHz, [D_6]acetone, TMS): δ = 4.15 (s, 2H), 7.45 (s, 2H), 7.65 (s, 2H).
[7] H. Inoue, K. Hara, J. Osugi, *Rev. Phys. Chem. Jpn. 46* (1976) 64.
[8] A. J. Fatiadi, *Synthesis 1978*, 165.
[9] W. J. Geary, *Coord. Chem. Rev. 7* (1971) 81.
[10] It is interesting to note that in platinum complexes containing the [NC-CHCOOMe)$^{\ominus}$ ligand, the presence of a sharp, strong band at 2200 cm^{-1} was attributed to a Pt-CH(CN)COOMe) linkage, whereas a broad, strong band at 2150–2120 cm^{-1} was attributed to the N-bonded structure Pt-N=C=CHCOOMe: D. P. Arnold, M. A. Bennett, *J. Organomet Chem. 199*, (1980) 119.
[11] X-ray structure analysis of **1**: Philips PW 1100 diffractometer, graphite monochromator, $Cu_{K\alpha}$ radiation; triclinic, space group $P\bar{1}$, a = 11.614(1), b = 13.836(1), c = 11.351(1) Å; α = 109.90(1), β = 100.85(1), γ = 93.66(1)°; Z = 1; ρ_{calcd} = 1.4301 g cm^{-3}. 5684 reflections were measured and the structure was refined, using 2600 data for which $I > 3.0\sigma(I)$, to converge with R = 0.087 und R_w = 0.078. Anisotropic thermal parameters were assigned to non-hydrogen atoms, while the H atoms were included as fixed contributors to the structure factors. Further details of the crystal structure investigation are available on request from the Fachinformationszentrum Karlsruhe, Gesellschaft für wissenschaftlich-technische Information mbH, W-7514 Eggenstein-Leopoldshafen 2 (FRG), on quoting the depository number CSD-55150, the names of the authors, and the journal citation.
[12] M. M. Brezinski, J. Schneider, L. J. Radonovich, K. J. Klabunde, *Inorg. Chem. 28* (1989) 2414.

BOOK REVIEWS

Book Reviews are written by invitation from the editor. Suggestions for books to be reviewed and for book reviewers are welcome. Publishers should send brochures or (better) books to the following address: Redaktion Angewandte Chemie, Postfach 101161, D-6940 Weinheim, Federal Republic of Germany. The editor reserves the right of selecting which books will be reviewed. Uninvited books not chosen for review will not be returned.

The Chemistry of Sulphenic Acids and their Derivatives. Edited by *S. Patai*. Wiley, Chichester 1990. xvi, 819 pp., hardcover, £ 190.00.—ISBN 0-471-92373-9

This volume of the *Patai* series sets out to provide a comprehensive account of the current state of knowledge concerning the chemistry of sulfenic acids and their derivatives. It can be said at the outset that this aim has, by and large, been fulfilled.

As the negative aspects of the book are in the minority, these will be mentioned first. Local patriotism in the choice of literature references can be justified in a publication intended for a local readership, even though it is of little value; however, an internationally orientated work should not concentrate almost exclusively on citations originating from the United Kingdom and the USA, as one finds in Chapters 1, 2 and 9. Nor should about 50% of the references be to the author's own publications, as is the case in Chapters 13 and 15. While on the subject of literature citations, it is remarkable that the name *H. Böhme* (Marburg) is only once cited (in Chapter 10), even though he could hardly be regarded as a minor contributor in the field of sulfenic acid derivatives! The only possible excuse for this is that many of the chapters contain references to earlier review articles. A further criticism is that there are few references to recent publications; for example, of the 70 references in Chapter 18 only eight are to publications after 1980.

In a monograph on sulfenic acids and their derivatives one can criticize the omission of the chemistry of sulfenyl carboxylates (mixed anhydrides of sulfenic and carboxylic acids); the only mentions of these are in the well-balanced contribution by *Horspool* (Chapter 11, pp. 539–540) in connection with their photochemistry, and in Table 15 (Chapter 10, p. 449) without further details. It seems strange that *D. R. Hogg* (Chapter 9) has not mentioned this class of compounds, which he has himself previously studied (see Ref. [7] in K. Schank et al., *J. Org. Chem. 48* (1983) 4580). It would also have been desirable to mention here the mixed anhydrides of sulfenic and sulfonic acids (K. Schank, F. Werner, *Phosphorus Sulfur 8* (1980) 335). Another puzzling question is that of the meaning of Table 1 (Chapter 1, p. 12) which lists bond lengths; this reviewer was unable, on the basis of the element symbols given, to relate these data to the formulas above and the compound classes to the left of them. Also the tables on pages 550–563 are only likely to be understood by readers familiar with the subject.

There are some excellent contributions that deserve a special mention, namely those by *A. R. Bassindale* and *I. Iley* (Chapter 4), *M. Mikolajczyk* et al. (Chapters 5 and 6), *S. Braverman* (Chapter 8), *G. Capozzi, G. Modena* and *L. Pasquato* (Chapter 10), *W. M. Horspool* (Chapter 11), *M. Zielinski* and *M. Kanska* (Chapter 14), *H. C. J. Ottenheijm* et al. (Chapter 16) and *P. K. Claus* (Chapter 17); these chapters are in themselves enough to make the book worth buying. Another good feature is the unusually small number of printing errors (examples of these few are Equation 17 on page 97,

where four methyl groups have unexpectedly become five, and formula **117** on page 455, which has a pentavalent carbon).

Lastly we come to the price. Books can be classified as cheap (rarely found), expensive (very common) or good value for the price. The reviewer places this one in the third category. It should be in every chemical library, and can be recommended to all chemists and biochemists other than those who associate sulfur compounds only with awful smells and keep well away from them.

The Chemistry of Sulphinic Acids, Esters and their Derivatives. Edited by *S. Patai*. Wiley, Chichester 1990. xvi, 728 pp., hardcover, £ 165.00.—ISBN 0-471-91918-7

In this further volume of the *Patai* series the aim was to give a comprehensive treatment, in 23 chapters, of sulfinic acids and their derivatives. It can be said at the outset that the conception of this volume is not nearly so successful as that of the volume on sulfenic acids. What should one expect of a work whose objective is that stated in the above title? 1) An attractive external presentation, an up-to-date and consistent nomenclature, and as few errors as possible in the typography and figures. 2) Contributions with a high level of scientific competence, with references to earlier review articles. The literature coverage should concentrate mainly on the period since the cutoff point of the previous review collection, bearing in mind, however, that in bringing out the most important features of a topic one must also refer (in an up-to-date context) to older publications. With regard to these two criteria, the *Patai* volume reviewed here has failed badly in some parts.

Although the external presentation is very attractive, the frequent switching between "sulphinyl" and "sulfinyl" is annoying. In the volume on sulfenic acids only one chapter was allowed to use the "f" spelling, but here this applies to seven of the chapters, with the additional complication that for Chapters 7 and 8 the contents list on the cover uses "ph" whereas the chapters themselves use "f".

With regard to errors in the text and figures, the following can be noted, without claiming the list to be complete: p. 89, what about stoichiometry in the equation given here?; p. 93, Section 11: elemental sulfur converts a sulfinate to a thiosulfonate, not to a thiosulfinate ArS(= O)SH; p. 133: in Figure 1 the assignment for H^4, which is cited at the top of page 135, is not shown; p. 193: electron distribution in Scheme 17?; p. 204: Equation (42) has kindly been credited to our group, but does not originate from here; p. 235, line 2: 1-damantyl; p. 376: in formula **117** a CH_2 group is missing; p. 433, Scheme 1: according to Equation (9) the reaction arrows go in the wrong direction (left side of the equation); p. 455: the "sulfonyl nitrites" referred to in Equation (4) contain neither a sulfonyl group nor a nitrite function; p. 462: in Equation (29) two negative charges appear from neutral molecules in the intermediate complex, then disappear again in the end products; p. 496, Scheme 6: hexavalent carbon; p. 498, Scheme 1: pentavalent nitrogen, Reference [25]: *Heesing* instead of *Hessing*; p. 534: the "dominant resonance structure" **18** seems questionable; p. 538, Equation (16): in the text the reaction is described as a photooxidation, whereas in the equation for the reaction the reaction conditions are given as H_2O_2/HOAc/60 °C; p. 542 discussing Ref. [87]: the oxidations are carried out using oxaziridines, not azyridines; p. 548, Figure 3: in ten formulas the positions of the ^{13}C NMR signals are not shown beside the correct carbon atoms; p. 552: Equation (47) indicates a baffling stoichiometry involving ethane; p. 597: diazomethane is given as CH_3N_2; p. 597, Scheme 4: the decomposition of sulfinyl peroxide must produce *tert*-butoxy, not *tert*-butyl radicals, especially in view of the fact that *tert*-butyl alcohol then appears as a reaction product; p. 611, Equation (27): $BF_2^{\ominus}$; Equation (28): the positive charge is missing from the ylid sulfur atom; Equation (32): according to the text the action of elemental sulfur gives sulfinamides, but the origin of the amide function is not explained; p. 612: formula **19** leads to an oxygen atom with an electron deficit; p. 615, Scheme 2, the second and third lines of the formula are barely understandable; p. 617, top line: "chain carrier ArN·" should probably read ArNH; p. 618, Equation (46): amyl nitrite is shown as the corresponding nitro compound; p. 619, Equation (48): here a phenyl group has become a phosphane; Equation (49): the nitrogen atom is missing from the educt, but then appears in the intermediate and end-product; p. 620, Equation (53): *m*-chloroperbenzoic acid is abbreviated as CPA; in Equation (55) a hydrogen transfer is shown (by the curved arrow) as taking place onto the group R^2 instead of onto the triple bond; p. 659, formula **14**: the OH group in the *ortho* position is missing. Of the entire volume Chapter 20 in particular is really annoying.

Also many of the chapters are less up-to-date than one would wish. For example, only seven of the 23 chapters include a reference to Volume E11 of Houben-Weyl, which was published in 1985 and contains the most recent comprehensive review to date of this class of compounds. In many of the chapters the proportion of literature references that relate to publications later than 1980 is about 10%; for certain chapters that may be justified, but for many it is not. This reviewer has some experience in the field of sulfinic acid chemistry, and has to disagree with many of the statements in the book. For example, it is claimed on page 3 that an *inter*molecular substitution of a sulfinate at the saturated carbon atom (p. 3) is not possible either for sulfones or for sulfinyloxy compounds. This is certainly true under normal circumstances, but is not an absolute rule (e.g. sulfones: D. T. Gibson, *J. Chem. Soc. 1937*, 1509; B. G. Boldyrev et al., *Zh. Org. Khim. 11* (1975) 455; sulfinyloxy compounds: K. Schank, *Houben-Weyl Bd. E11* (1985), p. 1148; pp. 1260, 1278 for sulfones). *Intra*molecular substitution of a sulfinate from a sulfone is cited (Ref. [14]) as occurring only under fairly brutal conditions; however, this must be compared with the synthesis of *trans*-chrysanthemum acid methyl ester (see L.-F. Tietze, Th. Eicher: *Reaktionen und Synthesen im organisch-chemischen Praktikum*, Thieme, Stuttgart 1981, p. 433), which was achieved in 72 h in DMF at room temperature. On page 318 mesomerism is confused with tautomerism, but it suffers this fate again and again, as it is often explained in terms of resonance. Nevertheless it always causes pain anew to a former student of *B. Eistert*, the author of the book "Tautomerie und Mesomerie". On page 456 the pioneering work of *Barnard* is mentioned (Ref. [11]), but without the important information that 1 mol of methylbenzenesulfenate requires only 0.7 mol of ozone to become quantitatively oxidized to methylbenzenesulfinate; $^3O_2$ is not capable of effecting the oxidation under these reaction conditions. On page 579 the reader is introduced to only two basically different methods for synthesizing sulfinyl chlorides: a) replacement of OH (or ONa) by Cl, and b) the chlorinating oxidation of sulfanes or disulfanes. One can excuse the fact that the citation given here ([Ref. 20]) only refers to *Herrmann*'s rediscovery of the method that we described using disulfide and sulfuryl chloride (W. Müller, K. Schank, *Chem. Ber. 111* (1978) 2870), since *Herrmann* also did not cite our work. However, the omission of the method for synthesizing sulfinyl chlorides by reacting thionyl chlo-

ride with suitable C-nucleophiles is unforgivable; this method has been applied by several research groups (e.g. trichloroethane sulfinyl chloride from 1,1-dichloroethene: B. M. Gladshtein et al., *Zh. Obshch. Khim. 41* (1971) 2580; CH-acid-ketones: J. Voss et al., *Angew. Chem. 92* (1980) 559; *Angew. Chem. Int. Ed. Engl. 19* (1980) 563; *Phosphorus Sulfur 10* (1981) 213; *Liebigs Ann. Chem. 1983*, 1116; K. Oda, *Synthesis 1981*, 661 (review!); M. Ohoka et al., *J. Org. Chem. 40* (1975) 3540; J. S. Pizey, K. Symeonides, *Phosphorus Sulfur 1* (1976) 41; *8* (1980) 1, and many others). It is also regrettable that the state of knowledge regarding the α-ketosulfones (p. 652) has apparently remained unchanged since 1949 (Ref. [68]). We first succeeded in synthesizing this class of compounds in 1977, and the fourth publication on the subject appeared in 1983 (K. Schank, H. Frisch, B. Zwanenburg, *J. Org. Chem. 48* (1983) 4580) not counting a correcting short communication (A. Senning, K. Schank, *Acta. Chem. Scand. Ser. B 32* (1978) 780. Unfortunately the book then goes on to mention in this connection the isolation of the mixed anhydride from benzoic acid and benzenesulfinic acid (Ref. [70]), which was subsequently corrected by us in the second publication on α-ketosulfones (K. Schank, F. Werner, *Liebigs. Ann. Chem. 1979*, 1977). Similarly the information concerning α-hydroxysulfones comes to an end in 1955, with no mention of our more recent publication on α-hydroxy-β-oxosulfones (*Chem. Ber. 99* (1966) 48; *103* (1970) 3087). However, this contribution includes an excellent discussion of the ambivalence of the sulfinate anions and its consequences.

Moreover, this volume of the *Patai* series contains some quite excellent contributions (those by *A. Nudelman, A. R. Bassindale* and *J. N. Iley*, by *U. Zoller, D. C. Dittmer* and *M. D. Hoey*, by *H. Fujihara* and *N. Furukawa*, by *S. Braverman, J. Drabowicz, P. Kielbasinski* and *M. Mikolajczyk*, and by *S. Oae, J. Shorter, T. Okuyama, A. Kalir* and *H. H. Kalir*). The only contribution that seems unsatisfactory is Chapter 20 in which, characteristically, the discussion of the *N*-sulfinylamines on page 605 does not once mention the name of *G. Kresze*, who pioneered this area. For readers who can live with the shortcomings mentioned above, the significant number of excellent articles in this volume, together with the aim of completing the series, are sufficient reasons to recommend it.

Kurt Schank [NB 1121/1125]
Institut für Organische Chemie
der Universität Saarbrücken (FRG)

New Solid Acids and Bases. By *K. Tanabe, M. Misono, Y. Ono* and *H. Hattori*. Elsevier, Amsterdam 1989. x, 365 pp., hardcover, HFl 375.00. – ISBN 0-444-98800-9

This well-organized monograph describes the present state of research in the field of solid acids and bases, and includes over 1300 literature references, most of them comparatively recent (up to 1988). The authors have taken great care to present the information concisely and accurately. Although the text is not easy reading because of its high information density, it is relieved by the many diagrams, tables and graphics. Since a large proportion of the carefully selected citations originate from Japan, one cannot escape the impression that Japanese research is at the forefront in this field.

After giving a definition of acid and base strengths on surfaces in Chapter 1, the whole question of "analysis" is treated in Chapter 2. The state of the art in determining acid and base strengths and their concentrations on solid surfaces is described. The importance of bifunctional surface sites and their determination is discussed in detail.

Chapter 3 is concerned with the surface acidities and basicities of metal oxides, mixed oxides, aluminas, zeolites, heteropolyacids, ion-exchange resins, metal sulfides, sulfates and phosphates, superacids and superbases. The metal oxides are treated in the order of the periodic table. Here the authors deal in great detail with the acidic and basic properties of the surfaces as influenced by the composition, pretreatment and mode of formation of the surfaces; in this connection they also discuss the catalytic properties and reactions of individual metal oxides. The importance of making a clear distinction between Brønsted and Lewis acidity, which seldom occur together, is emphasized. *Tanabe*'s theoretical model for mixed metal oxides is described; this allows one to predict the Lewis and Brønsted acidities of binary oxides. Special attention is given to mixed metal oxides based on SiO_2, Al_2O_3 and TiO_2. In the case of the aluminas the many different types of catalytic reactions in sheet silicates and other clays are discussed; the special properties of these sheet silicates as catalysts are clearly and concisely described. The discussion of zeolites is confined to a detailed consideration of the acidic properties as influenced by the Si/Al ratio, by pretreatment, and by metal exchange at the surface of the zeolite and in the skeletal structure. The newer aluminum phosphate zeolites are also briefly described. The section on heteropolyacids is mainly concerned with $H_3PW_{12}O_{40}$ and its metalated derivatives. Attention is here drawn to the differences between bulk and surface catalytic properties, and the relationship between catalytic activity and acidity.

Chapter 4 discusses the catalytic activity and selectivity of a wide variety of heterogeneously catalyzed reactions that are affected by the surface acidities and basicities of the catalysts used. The types of reactions considered are isomerizations, alkylations, acylations, the hydration of alkenes, methanol conversion, dehydrogenations, dehydrohalogenations, polymerizations, ester exchange, hydrolysis, catalytic cracking, hydrocracking and reforming, hydrogenations, oxidations, aldol condensations, NO reduction, and reactions of methanol and amines. It is impressive to learn how many homogeneous reactions have been successfully transformed into heterogeneous reactions of technological importance. This chapter gives a very concise, clear and informative summary of the knowledge about the catalysis of these reactions and the most effective catalysts. Much emphasis is placed on understanding the mechanisms of the reactions and their dependence on the surface acidities and basicities of the catalysts. With such a wide variety of reactions it is, of course, not possible to claim complete coverage; for example, in discussing the hydration of alkenes only that of ethylene is considered, and no reference is made to the problems of activity and selectivity that arise in the hydration of higher olefins.

The chapter on deactivation and regeneration of metal oxide catalysts is mainly confined to a discussion of the process of carbonation and the subsequent regeneration of the catalyst. The final chapter describes some advanced technological applications of solid acids and bases, such as gas sensors, sorbents and pressure-sensitive printing or copying papers.

This book, which deals with aspects of the chemistry of solids and surfaces, is a treasure of information, not only for everyone concerned with heterogeneous catalysis but also for all whose work is related to the chemistry of metal oxides. However, the text is difficult to read, since definite and in-

definite articles and prepositions are often missing or incorrectly used. Nevertheless, this book should be in the library of every scientist working in heterogeneous catalysis or related fields.

Wilhelm F. Maier [NB 1105 IE]
Fachbereich Chemie
der Universität-Gesamthochschule Essen (FRG)

Analytical NMR. Edited by *L. D. Field* and *S. Sternhell*. Wiley, Chichester 1989. viii, 250 pp., hardcover, £ 32.95.–ISBN 0-471-91714-1

Following the rapid developments that have occurred in NMR spectroscopy there is now a flood of monographs of widely different kinds. Just as one thinks that every corner of the potential readership must already have been covered, yet another publisher strikes out in a supposedly new direction. This book, containing a selection of review articles, is aimed at the (industrial) analytical chemist who is looking for up-to-date information on special applications. It seems to me that there is a real need here, as the NMR user frequently has problems in choosing between the many different experimental approaches.

Unfortunately in this case the disadvantages of a heterogeneous selection of articles are all too apparent. An illustration of this is the recommendation on page 44 that one should use 90° pulses for quantitative measurements, followed by the next author's recommendation (on page 73) to use pulses of 40° or less. Also there are annoying instances of repetition, for example in the discussion of quantitative NMR spectroscopy of solids on pages 52–56 and again on pages 95–98, and in the concept of cross-polarization which is explained by three different authors in a total of seven pages (fortunately they all agree).

The first article is an introduction entitled "Fundamental Aspects of NMR Spectroscopy". Such attempts to cover the fundamentals of NMR in just a few pages are apt to bring a tolerant smile. This article by *L. D. Field* (34 pp.) is, as expected, no better than previous attempts, and is unnecessary for an understanding of the articles that follow.

The second article by *J. R. Mooney* (22 pp.) is concerned with quantitative ^{13}C NMR spectroscopy. The emphasis is on experimental aspects; however, for the reader who starts off enthusiastically, it would have been useful and sobering to give some data on molar concentrations. The discussion of the mathematical treatment of the data, e.g. integration and corrections of baseline and of phase, is very superficial. Some important methods such as integration with interpolation, or the use of algorithms for the quantitative treatment of partially overlapping signals, are not mentioned.

However, tucked into the middle of the book are three articles which might lead one to consider buying it. The article "Analysis of Fossil Fuels" by *C. E. Snape* (48 pp.) gives an authoritative and comprehensive survey of the methods that should be used by the self-critical NMR spectroscopist, with the emphasis on analysis of solids and high-boiling fractions. This is followed by an article on "NMR of Zeolites, Silicates and Solid Catalysts" by *A. D. H. Clague* and *N. C. M. Alma* (41 pp.). Although the last of these topics is treated rather too briefly, the article offers the reader an excellent overview of the ^{29}Si and ^{27}Al NMR spectroscopy of zeolites and silicates, together with a wealth of references to original papers (240 citations) as a basis for studying these topics in more depth. The sixth chapter on "Biological Applications of NMR" by *P. W. Kuchel* (62 pp.) describes techniques for in vitro measurements on cell suspensions, organs and body fluids. This rapidly growing field of research could have a great future in view of the increasing restrictions on animal experiments. The emphasis in this review is on the experimental possibilities rather than on the biological interpretation of the results. This limitation is to be welcomed, as it enables the author to give an expert and complete review of the aspects related to analysis; some minor inaccuracies (e.g. on p. 160, where the correct expression is $160\Delta\nu_{1/2}$) can be excused.

The book ends with an article by *M. Spraul* and *R.-D. Reinhard* (25 pp.) on automation in the NMR laboratory. Unfortunately this is unlikely to help an experimentalist in his work. There are hardly any literature references for further reading (actually six altogether), although there is a section dealing with computerized interpretation of spectra. In view of the various data banks that are commercially available and the methods based on them (not a single mention here of the work of *W. Bremser*!), and the numerous algorithms for computerized analysis of two-dimensional NMR spectra that have come from groups such as those of *Ernst, Bodenhausen, Kalbitzer* and *Levy*, it is regrettable that so many opportunities have been missed here.

In summary: for practical work in the NMR laboratory some introductions that are more useful than this one already exist, and for obtaining a basic understanding of the experiments there are better books. The specialist already has access to comparable reviews in the usual journals. One can only hope that the needs of analysts will be met by other books that can be unreservedly recommended.

Herbert Kogler [NB 1095 IE]
Hoechst AG
Frankfurt/Main, FRG

Nomenclature of Inorganic Chemistry: Recommendations 1990. *International Union of Pure and Applied Chemistry*. Edited by *G. J. Leigh*. Blackwell Scientific Publications, Oxford 1990. xxiv, 289 pp., paperback, $ 27.50.–ISBN 0-632-02494-1. Hardcover version is no longer available.

Nomenclature has been an integral part of modern chemistry since its inception. The publication of Guyton de Morveau, Lavoisier, Berthollet, and de Fourcroy's *Méthode de nomenclature chimique* (1787) preceded by two years the publication of Lavoisier's *Traité élémentaire de chimie* (1789), which is universally regarded as marking the birth of modern chemistry. In 1913 the Council of the International Association of Chemical Societies appointed a commission on inorganic and organic nomenclature, and in 1921 its successor organization, the International Union of Pure and Applied Chemistry (IUPAC), appointed commissions on inorganic, organic, and biological chemistry.

The first report of the IUPAC's Commission on the Nomenclature of Inorganic Chemistry (CNIC) ("1940 Rules") was published in the leading journals of different countries. These rules, revised and rewritten, were published as a small book, *Nomenclature of Inorganic Chemistry 1957*, Butterworths, London 1959, ix, 93 pp., known as the "1957 Rules" or the "Red Book" from the color of its cover. A second revision, *Nomenclature of Inorganic Chemistry: Definitive Rules 1970*, Pergamon, Oxford 1971, xi, 110 pp., was supplemented by a 36-page IUPAC booklet, *How to Name an Inorganic Substance*, and by articles in various publications.

Since the appearance of the 1970 Rules, many new compounds have been prepared, some of which are difficult to name because they contain new types of bonding or structures. Trivial and local systems sprouted, especially for coordination and boron compounds, emphasizing the need for a systematic, widely comprehensible nomenclature. Consequently, in 1978 the IUPAC CNIC decided to replace the 1970 Red Book. The result is "not a revision... but a completely new version presented in a new way which it is hoped will be much more useful to the general reader." Because many of the new fields of chemistry are highly specialized and need complex names, the new edition will appear in several parts.

Part I, under review here, required 15 years to produce and is almost three times as long as its predecessor. It is concerned with the basic principles of nomenclature for the fundamental areas of inorganic chemistry. The principal authors, thirteen eminent chemists from the United States, the United Kingdom, France, the Netherlands and Hungary, hope that "its general principles will not be undermined, and that it should retain its currency for many years." Part II will deal with more specialized areas such as quasi-single strand inorganic polymers, organometallic and labeled compounds, and polyoxoanions; some of its contents have already been published in *Pure and Applied Chemistry*. Scheduled for publication in the near future, it will probably require more frequent revision because of its more specialized nature. Subsequent volumes are also planned.

The user-friendly 1990 edition contains more than 250 illustrations and is presented in an instructional format with numerous examples, rather than as a series of numbered rules as in previous editions. After two entirely new, concise chapters on the history and usages of inorganic nomenclature, the remaining nine chapters of Part I deal with elements, atoms, groups of atoms, formulas, names based on stoichiometry, solids, neutral molecular compounds, ions, substituent groups, radicals, salts, oxoacids and derived anions, coordination compounds, and boron hydrides (the "very thorough and useful" last two named sections are the longest in the book). Each chapter was written by nominated individuals, assisted by working parties, and was repeatedly reviewed and edited by about 15 CNIC members. British spelling is used consistently.

Because of the conflicting use of A and B notation for groups of elements in the periodic table, the unpopular 1-18 designation is presented as the preferred one, but the related controversy and other systems are discussed in an appendix, which concludes that "any ultimate recommendation... must be responsive to the broadest possible constituency." Another recommendation likely to be disputed or ignored by chemists is the use of "lanthanoid" and "actinoid," although "owing to wide current use, 'lanthanide' and 'actinide' are still allowed" even though "the ending -ide normally indicates a negative ion." Similarly, the system recommended for naming elements of atomic numbers greater than 103 not yet discovered or named by their discoverers, resulting in such awkward names as ununquadrium (element 114), will probably not find favor with most chemists, who are likely to continue referring to these species by atomic numbers. Other recommended changes include the avoidance of the term "radical" in anything other than the context of free radicals, the replacement of the terms "Stock number" and "Ewens-Bassett number" by the more readily comprehensible terms "oxidation number" and "charge number", the use of oxide names for anhydrides of fully dehydrated inorganic acids, and the use of configuration indexes for *fac* and *mer* isomers "for precise nomenclature purposes."

As expected for such a thoroughly reviewed and edited volume, the errors are few and minor, e.g., Gebieten for Gebiete, Jorisson for Jorissen, Damens for Damiens, and entitled for titled. A useful companion volume dealing with further types of species and providing additional examples has recently been published (Block, B. P.; Powell, W. H.; Fernelius, W. C. *Inorganic Chemical Nomenclature: Principles and Practice*, American Chemical Society, Washington, DC, 1990). CNIC Chairmen Joseph Chatt, Yves Jeannin and Daryle H. Busch and their dedicated band of collaborators, including editor G. J. Leigh, deserve our profound thanks for melding "established and traditional practices and systems of nomenclature" into a reference book that should be definitive for many years to come. I am pleased to recommend it highly not only to specialists concerned with problems of nomenclature but to all members of the international chemical community, who should find it invaluable in choosing correct and consistent names for inorganic and metalloorganic compounds dealt with in their research publications.

George B. Kauffman [NB 1151 IE]
California State University
Fresno, CA 93740 (USA)

Registered names, trademarks, etc. used in this journal, even when not marked as such, are not to be considered unprotected by law.

© VCH Verlagsgesellschaft mbH, W-6940 Weinheim, 1991. – Printed in the Federal Republic of Germany by Konrad Triltsch Druck- und Verlagsanstalt Würzburg.

All rights reserved (including those of translation into foreign languages). No part of this issue may be reproduced in any form — by photoprint, microfilm, or any other means — nor transmitted or translated into a machine language without written permission from the publishers. Only single copies of contributions, or parts thereof, may be made for personal use. This journal was carefully produced in all its parts. Nevertheless, authors, editors and publisher do not warrant the information contained therein to be free of errors. Readers are advised to keep in mind that statements, data, illustrations, procedural details or other items may inadvertently be inaccurate.

Valid for users in the USA: The appearance of the code at the bottom of the first page of an article (serial) indicates the copyright owner's consent that copies of the article may be made for personal or internal use, or for the personal or internal use of specific clients. This consent is given on the condition, however, that the copier pay stated per-copy fee through the Copyright Clearance Center, Inc. (CCC), for copying beyond that permitted by Sections 107 or 108 of the U.S. Copyright Law. This consent does not extend to other kinds of copying, such as copying, for general distribution, for advertising or promotional purposes, for creating new collective works, or for resale. For copying from back volumes of this journal see 'Permissions to Photo-Copy: Publisher's Fee List' of the CCC.

Editorial office: Postfach 10 11 61, W-6490 Weinheim, Federal Republic of Germany, Telephone (06201) 60 23 15, Telex 465 516 vchwh d, Telefax (06201) 602 328, E-Mail Z16@DHDURZ2 in Earn Bitnet.

Editor: *Peter Gölitz*

Associate editors: *D. I. Loewus, K. J. Schneider, A. Stimson.* **Editorial assistant:** *E. Schweikart*

Publishers: VCH Verlagsgesellschaft mbH. (Managing Directors: *Hans Dirk Köhler, Dr. Hardy G. Sehrt.*), Pappelallee 3, W-6940 Weinheim, Federal Republic of Germany.

Advertising office (Advertising Manager *R. J. Roth*): Postfach 10 11 61, W-6940 Weinheim, Federal Republic of Germany, Telephone (0 62 01) 60 61 36, Telex 4 67 155, Telefax (0 62 01) 606 156.

ANGEWANDTE CHEMIE
International Edition in English
Volume 30 · Number 7
July 1991
Pages 723–892

The Crystal Chemistry of Copper Oxometalates

By Hanskarl Müller-Buschbaum*

Dedicated to Professor Hans Georg von Schnering on the occasion of his 60th birthday

Up to three or four years ago oxocuprates were a class of chemical compounds no more remarkable than countless others. Then, as a result of the euphoria surrounding the high-temperature oxide superconductors and the discovery that copper plays an essential role in these materials, there was a world-wide awakening of interest in copper-containing oxide compounds. The number of scientists engaged in the synthesis and structure determination of copper oxometalates has grown from just a few to very many. As superconductivity is inseparably connected with the structure of the solid state, there has been a spontaneous awakening of interest in the role of copper in the crystal chemistry of solid materials, leading to new research projects on this aspect of oxocuprates. Most of the work published so far on the interesting chemistry of this group of compounds has related to individual compounds. New aids in describing complex solid state structures are now available through the development of methods that give three-dimensional displays of crystal structures using computer graphics terminals, as this review illustrates for the example of the oxocuprates.

1. Introduction

Since the discovery of the high-temperature oxide superconductors,[1, 2] oxocuprates have been at the focus of interest. As by-products of superconductivity research many new oxocuprates have been discovered, and there has been an intensification of research in the whole area of the crystal chemistry and coordination chemistry of copper in different oxidation states. In view of the large amount of published work on new copper-containing oxide compounds and phases, and the no less remarkable number of new investigations of oxocuprates that have long been known, a review of the crystal chemistry of copper oxometalates is now appropriate. The first review article on the crystal chemistry of copper appeared thirty years ago.[3] Nearly two decades later a series of oxocuprates with planar oxygen coordination were described in a report on planar coordinated ions in oxometalates.[4] At about the same time a review article appeared discussing the plasticity of Cu^{2+} coordination spheres in complex compounds.[5] However, up to now there have been no reviews of the crystal chemistry of oxocuprate(I) compounds or of mixed-valence oxocuprates, nor has there been a comprehensive account of the newly reported copper oxometalates and the valence-specific anomalous properties of copper in these substances. The present article surveys this latest chapter in the crystal chemistry of oxometalates, grouped in order of the valence of the copper atom; within each group the various compounds are described according to principles that emerge with respect to the coordination of oxygen to the copper atom. All the oxide superconductors are intentionally excluded, as their structures have already been reviewed in a recent article.[6] Also excluded are those phases that belong to one of the known high-temperature superconductors, even though they do not themselves exhibit superconducting properties.

In order for the crystal chemistry of copper to be more clearly understood, the structures of some selected compounds have been displayed using a graphic workstation and

[*] Prof. Dr. Hk. Müller-Buschbaum
Institut für Anorganische Chemie der Universität
Olshausenstrasse 40–60, W-2300 Kiel (FRG)

 © VCH Verlagsgesellschaft mbH, W-6940 Weinheim, 1991 0570-0833/91/0707-0723 $ 3.50+.25/0

are reproduced here in color. Such images produced by a scanning graphics VDU represent the latest technology for displaying the structures of three-dimensional solids. For reasons of cost it has been necessary to reduce the number of images of copper oxometalate structures with octahedral or tetrahedral coordination to a minimum. However, this is an acceptable limitation since, as will appear later, most of these compounds do not belong to the oxocuprates group. The clarity of the color images also makes it possible to limit the descriptions of the structures to the basic essentials.

2. The Crystal Chemistry of Oxocuprate(I) Compounds

2.1. Isolated O–Cu–O Dumbbell Structures

2.1.1. O–Cu–O Dumbbells in Irregular Formations

The crystal chemistry of copper-containing oxometalates is determined not only by the proportions of the different elements appearing in the empirical formula, but also by the specific properties of the ions present in the compound. A good example of this is Rb_3CuO_2,[7] whose structure is representative of a particular type found in oxocuprate(I) compounds. In the crystal structure of Rb_3CuO_2 the O–Cu–O dumbbell coordination usually found for Cu^+ ions is partly obscured by an excess of Rb^+ ions which alters the structure, so that only isolated O–Cu–O dumbbells occur. In Figure 1 the violet-colored bonds represent the coordination of the Cu^+ ions (yellow spheres) by the O^{2-} ions (blue spheres).[*] These dumbbell formations are shown extending beyond the region of the polyhedra around the rubidium atoms, so as to show the presence of isolated O–Cu–O units in the crystal structure. Although in this article on oxocuprates the main focus of attention is the coordination of copper, one cannot ignore the no less interesting crystal chemistry of the large alkali metal ions in these metal-rich compounds. From the published studies on Rb_3CuO_2 it is seen, when considering the primary structure, that each of the three alkali metal ion sites has a tetrahedral oxygen environment. Such a low coordination number is unusual for ions of large volume, and is a direct consequence of the extreme shortage of anionic coordination partners. The secondary structure shows that Rb(1) (red polyhedra) forms a two-dimensional arrangement of polyhedra. The polyhedra around Rb(2) (green spheres) and Rb(3) (orange polyhedra) are each joined together by one side to form a network. As Figure 1 shows, the Cu^+ ions are enclosed within this loose coordination of the alkali metal ions, which gives them a nearly linear dumbbell environment.

The crystal structure of $Cu_5Ta_{11}O_{30}$ shown in Figure 2[8] is of a completely different type; however, it also contains isolated O–Cu–O units. Ta^{5+} has the octahedral oxygen coordination that is typical of oxometalates. The octahedra occupied by the non-equivalent tantalum ions are distinguished by different colors (Ta(1): red, Ta(2): yellow, Ta(3): green). In the region of the octahedra shown in yellow one can recognize a perovskite-type structure. It is also interesting that each of the inner regions of the perovskite blocks contains no Cu^+. The rather irregularly arranged O–Cu–O dumbbells are mainly in positions linking the green and red TaO_6 octahedra.

2.1.2. O–Cu–O Dumbbells in Planar Configurations

An interesting feature of the alkali metal oxocuprate(I) compounds is the change in crystal chemistry from Rb_3CuO_2 to K_3CuO_2.[9] Whereas rubidium and potassium behave similarly in many areas of chemistry, this is not the case for the oxocuprates, and this leads to different structural types. Figure 3 shows the structure of K_3CuO_2. Here the potassium ions occupy four non-equivalent sites, three of which again have a tetrahedral oxygen environment, as shown by the orange, green and white polyhedra, corresponding to K(1) to K(3) respectively. To provide a better insight into the crystal structure, K(4) is here shown in spherical form (red spheres). Also, to make it clear that the coordination of the large K^+ ions does not completely enclose them in a shell of O^{2-} ions, the radii chosen for three of the potassium sites were approximately 80% of that of the K^+ ion. Even with an alkali metal ion of this size, Figure 3 clearly shows that it is not fully coordinated. The lattice formed by the K/O polyhedra contains within it nearly linear O–Cu–O dumbbells, and these lie in parallel planes in the crystal structure.

[*] Apart from a few exceptions, which are clearly pointed out, copper ions are shown as yellow spheres, regardless of oxidation state, and oxygen ions by blue spheres. All Cu–O bonds are shown in violet. For other elements and polyhedra the colors are explained in each case.

Hanskarl Müller-Buschbaum was born in 1931 in Wallendorf in the Thüringer Wald. He studied chemistry and physics at the University of Greifswald, finally gaining his doctorate in 1960 under the supervision of H. Witzmann for research on UV-excited borate luminophores. He then joined the research staff at Siemens in Munich, where he carried out research work on hard superconductors. In 1962 he continued his academic career at the University of Münster with Wilhelm Klemm and in 1965 he joined Rudolf Hoppe at the University of Giessen where he gained his habilitation in 1966 for work on the generation of high temperatures with the low-pressure/high-frequency plasma burner and its application in high-temperature solid-state reactions. In 1969 he accepted the offer of a professorial chair for inorganic chemistry at the University of Kiel. His main research interests focus on solid-state chemical reactions at high temperatures using high frequency plasma discharges and the synthesis of metastable materials with the CO_2 laser technique.

2.1.3. O–Cu–O Dumbbells Forming Links Between Layers

A particularly interesting alkali metal oxocuprate(I) compound is KNa_2CuO_2,[10] which has exactly linear O–Cu–O dumbbells. Figure 4 shows that the alkali metal and oxygen ions are arranged in layers, which are linked by Cu^+ ions to form the three-dimensional structure. This compound, which has a marked deficiency of non-metallic ions, again shows the unusual coordination of Na^+ and K^+. If one limits the radii of these ions to the center of electron density radii as determined crystallographically, it can be seen that Na^+ has tetrahedral coordination to four O^{2-} ions (red polyhedra and spheres), and K^+ has tetragonal pyramidal coordination to five O^{2-} ions (green polyhedra and spheres). One can also see from Figure 4 how these polyhedra are arranged and linked together. However, if the radii assumed for the alkali metal ions are increased to 80% of the ionic radii found in the tables, one obtains a better understanding of the unusual coordination of these large ions. This applies especially to the remarkably asymmetrical environment of the K^+ ions. The K^+ ion lies outside the basal plane of the square pyramid, but despite this its distance from the apex of the pyramid is appreciably less than that from the four O^{2-} coordination partners in the basal plane of the pyramid. All of the O^{2-} ions lying on the opposite side of the tetragonal pyramids are very far distant. If one assumes the radius of the Cu^+ ion to be increased from 0.3 Å to values between 0.6 and 1.0 Å, the KNa_2CuO_2 structure is found to contain layers of potassium and copper resembling those of a metal. This can be regarded as a filled variant of the $XeFe_2$ structure.[10]

Other examples in which O–Cu–O dumbbell units act as links between layers are $CuMnO_2$,[11] compounds with delafossite-type structures, $CuAlO_2$,[12–15] and the halogenooxocuprates Ba_2CuO_2Cl,[16] Sr_2CuO_2Cl,[17] Sr_2CuO_2Br,[18] and Ba_2CuO_2Br.[19] Figure 5 shows the structure of the mineral krednerite, $CuMnO_2$, and Figure 6 that of the delafossites. The $CuMnO_2$ structure consists of layers of MnO_6 octahedra (green) joined together by Cu^+ ions. This results in the Cu^+ ion adopting a linear dumbbell coordination to O^{2-} ions. The delafossite structure has more closely packed adjacent layers of MO_6 octahedra (red octahedra in Fig. 6). Both these classes of compounds show a well-defined layer structure, including planes that contain only Cu^+ ions.

In the halogenooxocuprates, M_2CuO_2X (M = alkaline-earth metal, X = halogen), the region containing the layers of octahedra is expanded compared to that in the delafossite structure, having in this case a double layer of edge-sharing MO_6 octahedra. In addition to the dumbbell-type coordination of Cu^+, which is important for the crystal chemistry of oxocuprate(I) compounds, these compounds are also interesting with regard to the arrangement of the Cl^- ions in the double layers of octahedra and the geometry of the MO_3Cl_3 octahedra. Figure 7 shows the structure of Sr_2CuO_2Cl. Here the Cl^- ions (orange spheres) are shown as having a radius of half the actual ionic radius (0.9 Å). It can be seen that they are always in the middle plane of the double layers of octahedra. The Cu^+ ions are thus screened from Cl^-, which is necessary for energetic reasons. If the Cl^- ions were at the outer faces of the layers of octahedra and were at the same time coordination partners of Cu^+, the coulomb part of the lattice energy compared to the lattice energy of the copper would be greatly reduced. A closer examination of the SrO_3Cl_3 octahedra shows that one of the triangular faces is formed by three Cl^- ions, whereas the opposite face is formed by three O^{2-} ions. For reasons of symmetry the centers of the Cl^- or O^{2-} ions in each triangular face are all separated by the same distance. This means that the distances between the oxygen ions are the same as the X–X separations, and are therefore much greater than normal, especially in compounds for which $X = Br^-$. The equality of the O_3 and Cl_3 triangular faces in the SrO_3Cl_3 octahedra, which is required by symmetry, makes it apparent why a corresponding iodine compound can no longer form a structure of the Ba_2CuO_2Cl type.[16] The compound Ba_2CuO_2I also exists, but the classification adopted here, according to the types of O–Cu–O dumbbells in the crystal structure, means that it must be dealt with in the next section. To conclude the discussion of the present group of compounds, it should be noted that the Sr^{2+} or Ba^{2+} ions occupy off-center positions within the MO_3X_3 octahedra which are shown in a filled representation in Figure 7, being shifted in the direction of the oversized O^{2-} triangular faces.

2.1.4. O–Cu–O Dumbbells as Tunnel Units

Within the last few years, a number of compounds have been reported as having structures in which O–Cu–O dumbbells are held within a closed network of polyhedra. Compounds of the general formula $CuLnW_2O_8$, in which Ln is a lanthanoid metal or yttrium, have been especially thoroughly studied. An earlier publication[20] reported that $CuLnW_2O_8$ crystallizes in two structural types. For Ln = La to Dy the α-$LiPrW_2O_8$ type is formed,[21] whereas for the smaller lanthanoid ions (Ln = Ho to Lu) and yttrium the β-$LiYbW_2O_8$ type is formed.[22] It should be noted that according to the latest convention for describing compounds of the general formula $M^ILnW_2O_8$, the low-temperature form of $CuNdW_2O_8$ must be described as α-$CuNdW_2O_8$. The authors expressed the view that no polymorphism occurred, but this later proved to be incorrect. Neither structure (α-$LiPrW_2O_8$ or β-$LiYbW_2O_8$) is identical to the structure of $CuNdW_2O_8$ which is shown in Figure 8. This recent discovery indicates that a third type of structure exists, and appears to be a consequence of the conditions of preparation.[23] The publication[23] reports a structure determination carried out on single crystals of $CuNdW_2O_8$. In Figure 8 one can clearly recognize the double octahedra of WO_6 (green polyhedra) joined at their edges; these are linked through Nd^{3+} ions (red spheres) to form a three-dimensional framework. The coordination polyhedra around the Nd^{3+} ions, which are here shown unfilled, can be regarded as trigonal prisms. Here again the radius of the Nd^{3+} ion has been reduced slightly from that given in tables[24] to a value of 0.9 Å in order to give a better insight into the crystal structure. The tunnels which are left in the $[NdW_2O_8]^-$ part of the lattice contain Cu^+ ions spaced at equal intervals. These have a coordination number of two due to the nearest oxygen neighbors. In this case, however, the O–Cu–O dumbbells are markedly non-linear, with an angle of 167°. The existence of this structural type has been further confirmed by an independen

study[25] on single crystals of β-$CuYW_2O_8$, which also showed that small Ln^{3+} ions can form structures of this type.

Another oxocuprate(I) compound with Cu^+ ions in a tunnel structure is $Sr_9Zn_4Cu_2O_{14}$.[26] This forms a unique structural type whose main feature is an Sr/O lattice. In Figure 9 the SrO_6 octahedra, which are appreciably deformed, are shown in red, together with trigonal prisms capped at one end. In the direction of the long a-axis the sequence of the layers is prism—octahedron—octahedron—prism. In Figure 9 the triples formed by Sr_3O_{12} octahedra joined by their faces, which can be recognized in the middle of the unit cell and at $x = 0$ (left and right edges) are an interesting feature. The zinc polyhedra, shown here in green, partly fill the Sr/O lattice. Owing to the fact that Figure 9 shows only the polyhedra within the region of one unit cell, it is not apparent here that the ZnO_4 tetrahedra are joined to form Zn_2O_7 units whose bond angle Zn—O—Zn differs markedly from 180°. Further details can be found in the literature.[26] The role of the Cu^+ ion in the crystal chemistry is here that of a tunnel unit. The tunnels in the $[Sr_9Zn_4O_{14}]^{2-}$ framework are so severely distorted that for Cu^+ there are only two O^{2-} ions that can act as coordination partners across the shortest dimension of the tunnel.

The last example of Cu^+ as a tunnel unit that will be described here is Ba_2CuO_2I.[19] From the standpoint of its empirical formula this halogenooxocuprate(I) compound belongs to the M_2CuO_2X group (X = halogen) described in Section 2.1.3. There it was explained that opposite triangular faces of the octahedra contain O^{2-} and X^- ions, with the result that, owing to symmetry requirements, the O—O distances are abnormally large. On going from $X = Br^-$ to $X = I^-$ it is found that a completely new type of structure is formed, as shown in Figure 10. Each of the four barium sites (green, red and yellow polyhedra) is surrounded by O^{2-} and I^- ions (orange spheres) in a severely distorted octahedral structure. The three-dimensional linking of these octahedra gives a lattice structure containing small rectangular tunnels and large hexagonal tunnels. The Ba(1) site is not involved in the formation of the hexagonal tunnel, and similarly Ba(2) does not form part of the small rectangular tunnel. It can be seen from Figure 10 that Cu(1), which is in the rectangular tunnel, has a nearly linear dumbbell type coordination, with an O—Cu—O bond angle of 178°. The larger hexagonal tunnel contains two $Cu^+(2)$ ions; despite the fact that in this case the dumbbells are considerably bent (165.6°), the distance between the ions (1.80 Å) is shorter than that for Cu(1).

2.2. O—Cu—O Dumbbells in Linked Formations

2.2.1. *Linking of O—Cu—O Dumbbells to Form Rings*

The compound KAgO, which has been known for a long time,[27] has a crystal chemistry which is also shared by some oxocuprate(I) compounds, including KCuO,[28] NaCuO, RbCuO,[29, 30] and LiCuO.[31, 32] The KAgO type structure adopted by these compounds is a remarkable one, which will be described with the help of two figures. First let us consider the coordination of the alkali metal ions (red spheres with a radius of 0.5 Å). Owing to the limited availability of oxygen ions relative to the cations, the alkali metal ions Li^+ to Rb^+ have only a fourfold coordination to O^{2-} in this type of structure. The resulting polyhedron can be regarded as being formed from an octahedron by removing two *cis* oxygen ions from the base plane. The abnormally large molar volume is explained by the existence of relatively large channels along the [001] direction. Cu^+ ions are built into this alkali metal-oxygen lattice, which again results in a dumbbell type O—Cu—O coordination. A novel, and so far unique, feature of this class of compounds is the formation of closed Cu_4O_4 four-membered rings. In Figure 12, the bonds between the alkali metal and oxygen ions have been omitted so as to show more clearly the closed polyhedra made up of dumbbells (violet bond lines). A more recent study[31] has shown that the Cu_4O_4 rings are exactly planar.

2.2.2. *Linking of O—Cu—O Dumbbells to Form Chains*

The compounds MCuO (M = Li to Rb) described above have a structure into which the larger Cs^+ ion does not fit. CsCuO represents a new structural type within the alkali metal oxocuprate(I) class.[28, 33] In this type of crystal structure the O—Cu—O units are linked to form zig-zag chains. In Figure 13, the coordination around the Cs^+ ions is shown by closed polyhedra (red), linked by dumbbells formed by the coordination of O^{2-} to Cu^+. Here again, as in compounds described in Section 2.1.3, there is a layer-like structure. Layers of fourfold coordinated Cs^+ ions are joined together through Cu^+ ions. The CsCuO structure shows some similarities to the KAgO type insofar as here also the polyhedron around the Cs^+ ion can be regarded as a portion of an octahedron. Here again, two of the *cis* sites of the octahedron are not occupied by O^{2-} ions. Features of interest are the O—Cu—O angle of 178°, departing slightly from the ideal value of 180°, and the fact that, as can be seen from Figure 13, all the O—Cu—O dumbbells that are linked together to form infinite one-dimensional chains are bent in the same direction.

Infinite one-dimensional zig-zag chains have also been found for oxocuprate(I) compounds of alkaline-earth metals, namely for $SrCu_2O_2$[34] and $BaCu_2O_2$.[35] The basis of these strutures is shown in Figures 14 and 15. It can be seen that the SrO_6 or BaO_6 octahedra are joined at their edges in a space-filling structure, with the Sr^{2+} or Ba^{2+} ions shown as red spheres in Figure 14 and as red polyhedra in Figure 15. The lattice of the octahedra contains spaces along two directions for infinite one-dimensional O—Cu—O chains which extend throughout the structure in the same way as in CsCuO.

2.2.3. *Linking of O—Cu—O Dumbbells to Form Layers*

In $K_3Cu_5O_4$, $Rb_3Cu_5O_4$, $Cs_3Cu_5O_4$ and $Rb_2KCu_5O_4$ the O—Cu—O dumbbells are linked together in a much more complicated fashion,[31, 36, 37] as shown in Figure 16. We start by considering the coordination spheres of the alkali metal ions, with Rb^+ as an example. In Figure 16 the three metal sites occupied by rubidium are shown by red polyhedra and by red spheres whose radius is 80% of the tabulated ionic radius.[24] The fourfold coordination of Rb^+ which is

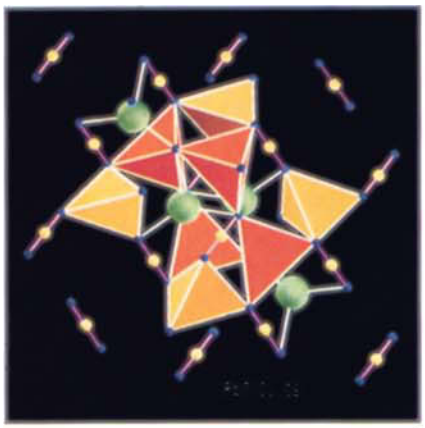

1

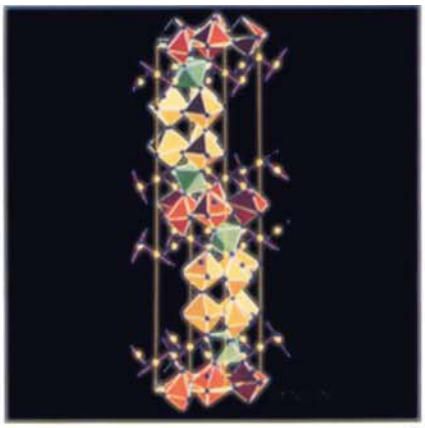

2

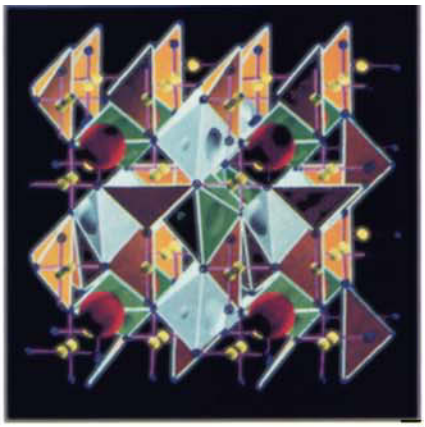

3

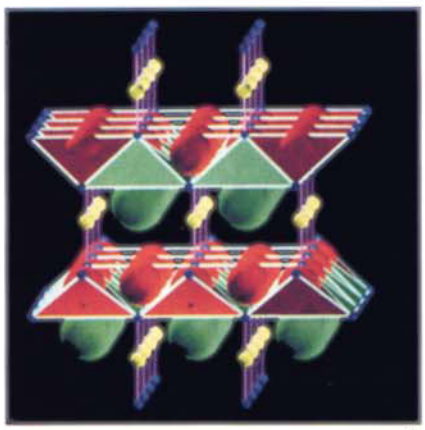

4

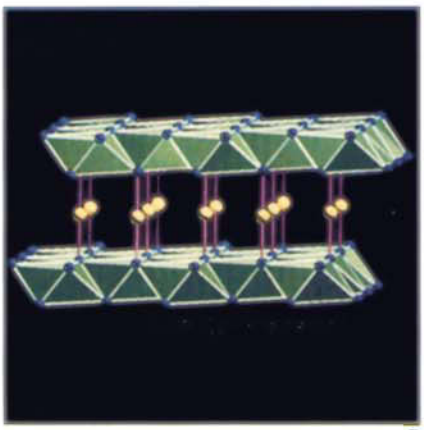

5

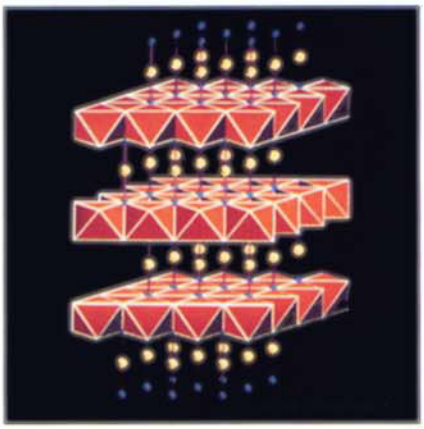

6

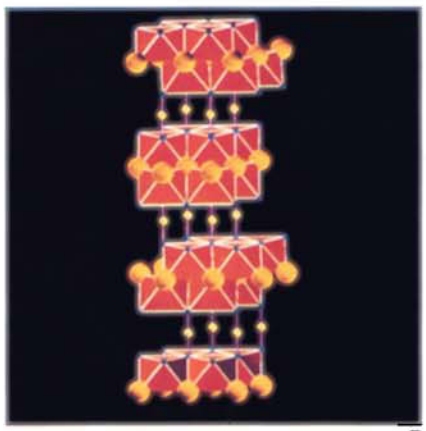

7

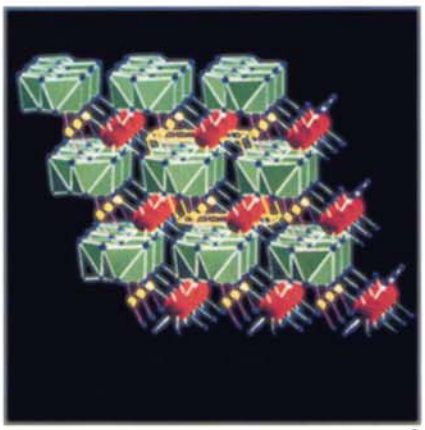

8

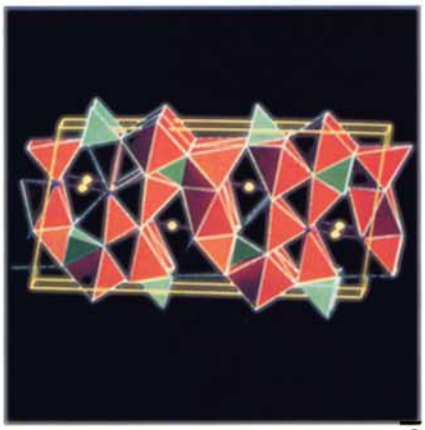

9

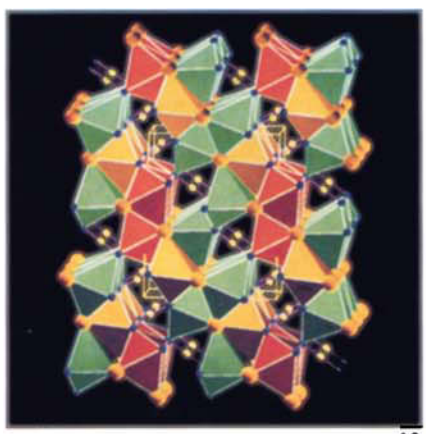

10

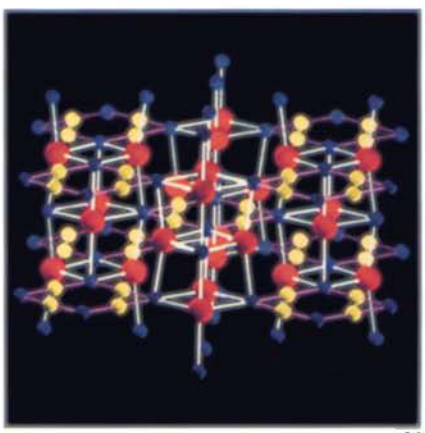

11

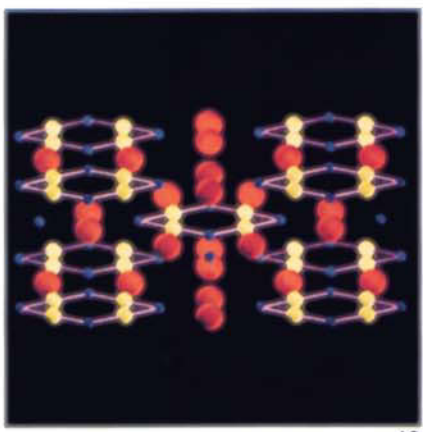

12

evident from the figure can again be deduced from the valence angles of an octahedron. Two of the *cis* sites of each octahedron are not occupied by O^{2-} ions. The resulting distortion of the portion of the octahedron gives a shape which is almost a tetrahedron. The asymmetric and open coordination of all the Rb sites, which is comparable with the situation in KNa_2CuO_2, can be clearly seen. The alkali metal ions together with a proportion of the O^{2-} ions form a layer structure which is again linked by O–Cu–O dumbbells. Helical chains with the structure –O–Cu–O–Cu– extend along the [010] direction, and are linked along the direction of the *a*-axis by other Cu^+ ions to form an open Cu/O network, $^2_\infty[Cu_5O_4]$. Evidently this class of compounds represents a step towards a three-dimensional network of O–Cu–O units, but so far no further examples of this have been found in oxocuprate(I) compounds.

2.3. Departures from the Dumbbell Type O–Cu–O Coordination

In Section 2.1.4 compounds with the β-$CuLnW_2O_8$ structure were described. It was also mentioned there that an older publication[38] had indicated, on the basis of the lattice constants of compounds with the general formula $CuLnW_2O_8$, that these were isotypes of the α-$KNdW_2O_8$ structure. The papers already cited[20, 21] also indicate the existence of triclinic compounds with the α-$LiPrW_2O_8$ structure in which Li^+ is replaced by Cu^+. Recently, single crystals of $CuLaW_2O_8$ and $CuSmW_2O_8$ were synthesized for the first time,[39] and these revealed that the structure and the coordination behavior of Cu^+ towards O^{2-} involves further subtleties. The crystal structure of $CuLnW_2O_8$ (Ln = La or Sm), as shown in Figure 17, contains blocks of four WO_6 octahedra (green) which are joined together by their edges. The $[W_4O_{16}]^{8-}$ groups are held together in a three-dimensional structure by the lanthanoid ions (red spheres) and Cu^+ ions. Up to now it has appeared that the crystal chemistry of oxocuprate(I) compounds always involves dumbbell units of a more or less linear type. However, the compound $CuLaW_2O_8$ shows a departure from this structural feature. On the basis of the Cu–O interionic distances (1.89 Å; 1.95 Å; 2.36 Å; 2.70 Å), it must be assumed that here Cu^+ has a [2 + 1] coordination. This can be clearly seen at the lower edge of Figure 17, despite the foreshortening in the perspective view. Thus the dominance in the oxocuprate(I) compounds described so far of the dumbbell type O–Cu–O coordination is broken in the case of $CuLaW_2O_8$, and the range of types must be extended to include a rare planar trigonal coordination. In $CuSmW_2O_8$ the Cu–O distances give a stronger indication of a deformed octahedron, which is ultimately derived from the coordination around Li^+ in α-$LiPrW_2O_8$.

The structure of Cu_2WO_4, which was finally clarified recently,[40, 41] fits well into this picture of the transition from a Cu^+ environment of the dumbbell type to others with higher coordination numbers. The structure is shown in Figure 18. The non-equivalent tungsten sites (W(1): red, W(2): green, W(3): orange, W(4): white) have octahedral coordination to O^{2-}. It can be seen from Figure 18 that the crystal lattice contains isolated blocks of four octahedra, each formed by the joining together of two pairs. However, the most interesting aspect in the context of the oxocuprate(I) compounds is the coordination of the Cu^+ ions. The Cu–O distances indicate the presence of copper ions with a dumbbell-type coordination, shown here by the violet colored bonds to O^{2-}. However, there are also sites that can be described by a [2 + 1] coordination, and others with threefold coordination. In Figure 18, the [2 + 1]-coordinated groups have also been shown as O–Cu–O dumbbells for simplicity. The departure from linearity is apparent even in the color graphics images. The Cu^+ sites that have unambiguous threefold coordination to O^{2-} are shown with a yellow background to emphasize the near-planarity of the CuO_3 polygons. The Cu^+ ion is in fact slightly shifted out of the plane of the three oxygen ions.

For compounds in which Cu^+ ions are present in a tetrahedral oxygen environment, the departure from the dumbbell formation is beyond dispute. An example of this type is $Cu_6Mo_5O_{18}$,[42, 43] whose crystal structure is shown in Figure 19. The polyhedra shown in green are those around Mo^{6+}, while those around Cu^+ are distinguished by yellow. The details of the linking between the polyhedra can be found in the original papers. If the empirical formula is changed somewhat to $Cu_4Mo_5O_{17}$, we obtain a compound[44, 45] in which the majority of the Cu^+ sites have a tetrahedral coordination. In this copper oxomolybdate one of the sites, Cu(2), already has octahedral coordination to O^{2-}, and a consideration of the overall picture for all the cuprates reported up to now shows an almost continuous transition from C. N. = 2 to C. N. = 6 (C. N. = coordination number). The study of $CuNb_3O_8$[46] cited here as additional evidence also contains tetrahedrally coordinated Cu^+. The oxomolybdates mentioned above and the oxoniobate $CuNb_3O_8$ should not be regarded as oxocuprate(I) compounds. This point will be considered further in the summary (Section 7). In these compounds Cu^+ acts as a cation in the anionic partial lattice formed by $[Mo_5O_{18}]^{6-}$, $[Mo_5O_{17}]^{4-}$ or $[Nb_3O_8]^-$, and thus the specific crystal chemical behavior typified by the dumbbell type O–Cu–O coordination is here replaced by a different behavior like that of the cations in salt-like compounds.

3. The Crystal Chemistry of Mixed-Valence Oxocuprates(I)/(II)

Mixed-valence oxocuprates formed by the Cu^+ and Cu^{2+} oxidation states were of no real importance until the discovery of the lead superconductor $Pb_2Sr_{2.24}Nd_{0.76}Cu_2O_{8+x}$,[47] and were ignored in research on oxocuprates. The compound Cu_2TiO_4[48] was known, and the mineral paramelaconite, Cu_4O_3, had been known for many years,[49] and was studied in greater detail in the 1940s.[50] It was not until 38 years later that the complicated structure of this compound, whose constitution is expressed in terms of the different copper valence states as $Cu^I_2Cu^{II}_2O_3$, was finally determined.[51] The remarkably complicated crystal structure of Cu_4O_3 will be shown here, even though this involves an appreciable sacrifice in relation to other compounds because of the necessary limit on the number of colored illustrations. Figures 20 and 21 show the coordination in the partial lat-

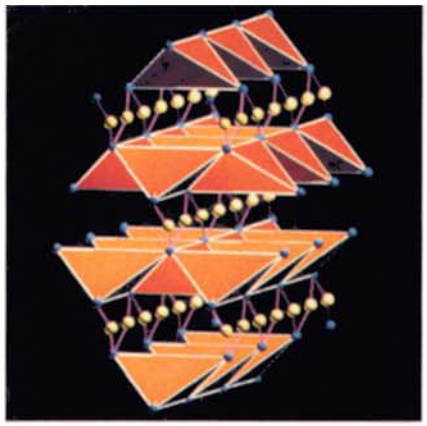

13

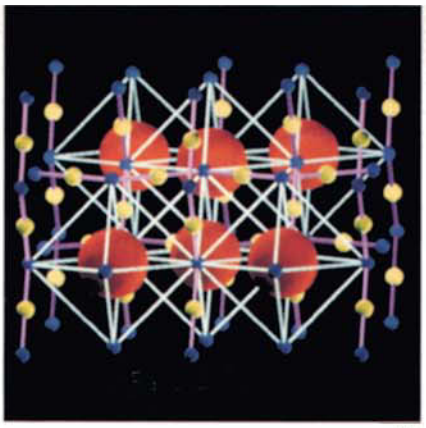

14

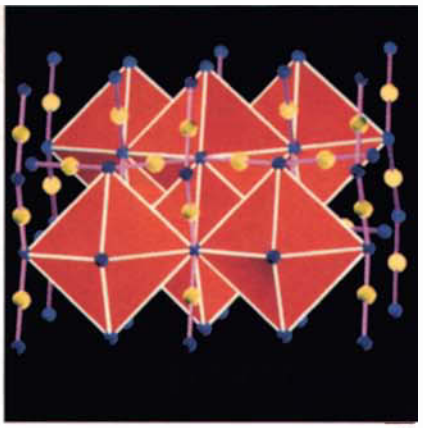

15

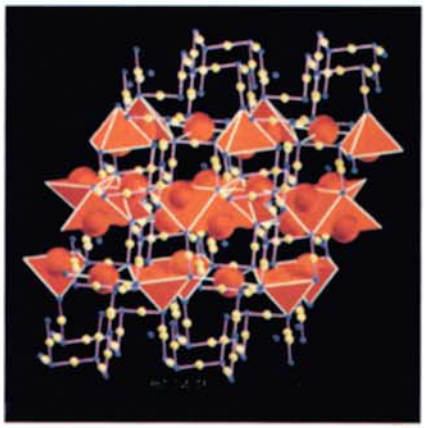

16

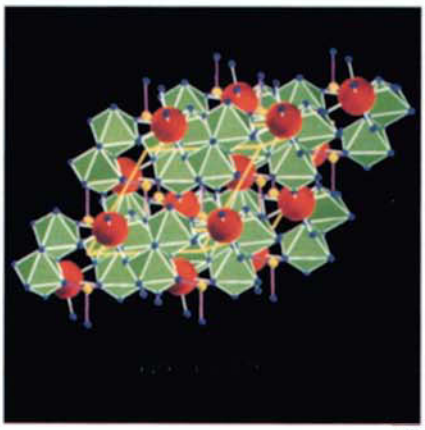

17

18

19

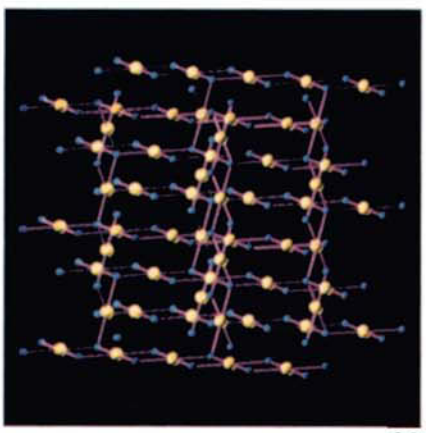

20

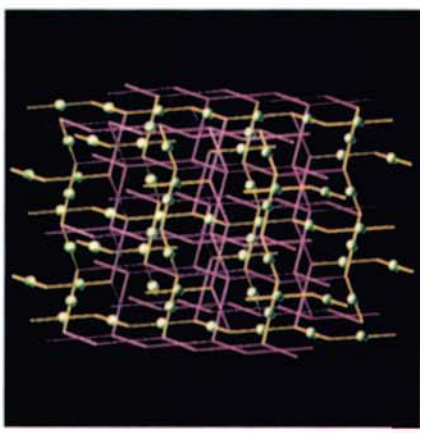

21

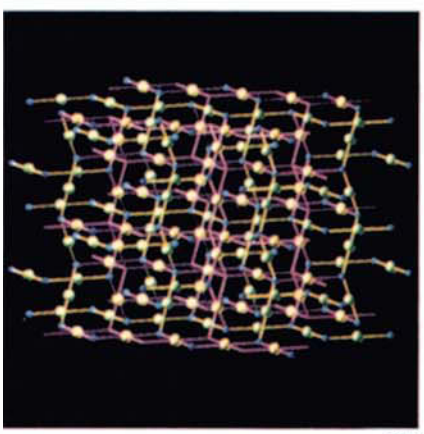

22

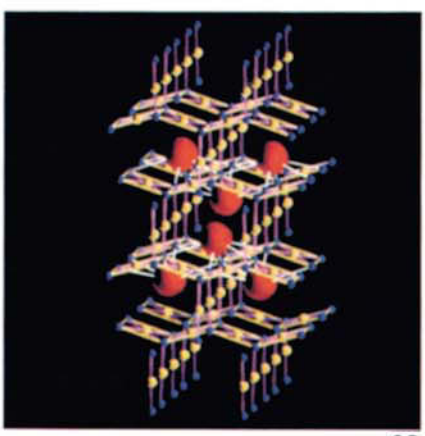

23

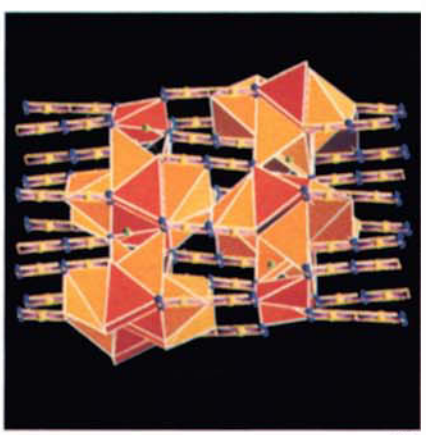

24

tices formed by the Cu^{2+} and Cu^{+} ions. It can be seen from Figure 20 that the Cu^{2+} ions have a square planar coordination to O^{2-}. Infinite one-dimensional chains of CuO_4 squares joined by their edges run in the vertical and horizontal directions, and are linked at each crossing point by a common oxygen ion partner to form a loose three-dimensional lattice. In Figure 21 this three-dimensional network is reduced to only the Cu^{2+}–O^{2-} bonds, which are shown in violet. The figure also shows the positions of the Cu^{+} ions (green) and their dumbbell-type coordination (yellow bonds). It can be seen that the open-structured $[Cu^{II}_2O_3]^{2-}$ part of the lattice is filled by one-dimensional zig-zag chains of $O-Cu^{I}-O$ dumbbell units. The essential feature of this binary oxide structure is the crystallochemical separation of two oxidation states, apparently without the valency fluctuations that often occur with other transition metals. Figure 22 shows the positions of all the ions in the complex structure of this oxide (Cu_4O_3), which has so far not been possible to produce synthetically.

In the course of experiments aimed at preparing thallium-containing superconductors the compound $TlCu_2O_2$ was discovered.[52] This is in fact $Tl^{I}Cu^{I}Cu^{II}O_2$, containing the Tl^{+} ion which has interesting crystallographic properties. In $TlCu_2O_2$ the Tl^{+} ion shows the expected lone pair effect.[53] Figure 23 shows the structure and the coordination of all the metal ions involved. In the form of presentation chosen here it can be clearly seen that undulating chains made up of planar Cu/O polyhedra (joined by their edges) run in the horizontal direction. The square polygons are shown with a yellow border. This is the coordination sphere of Cu^{2+}. These isolated $^{1}_{\infty}[CuO_2]$ chains are joined transversely (i.e. in the vertical direction) by Cu^{+} ions in a dumbbell-type coordination. Finally, the spacing in the third dimension is fixed by the Tl^{+} ions (shown here with a radius of 1.0 Å). Figure 23 gives the impression that the Tl^{+} ions are held in a tunnel structure. This is not the case, however; instead these ions are active partners in the formation of the three-dimensional network. It can be seen that the Tl^{+} ions lie close to the planar CuO_4 chains, thereby leaving sufficient space for the s^2 electron pairs. It should also be noted that Figure 23 shows only the Tl^{+} ions within one unit cell, whereas the Cu/O coordination is shown well beyond the limits of the cell.

During the preparation of this article, but after the figures had already been completed, I became aware of a report[54] describing two new mixed-valence oxocuprates of lithium, $LiCu_2O_2$ (A) and $LiCu_3O_3$ (B). The structures of both these compounds show close similarities to $TlCu_2O_2$. The Cu^{+} ions have a dumbbell-type coordination, and both (A) and (B) have $O-Cu-O$ units arranged in a square network. The Cu^{2+} ion has a planar coordination to four O^{2-} ions, and in compound (B) one of the copper ions, Cu(2), is in the plane of the oxygen ions while the other one, Cu(3), is outside the plane. A fifth O^{2-} neighbor, which should also be included on the basis of its distance (2.41 Å), extends the coordination of Cu(2) to form a tetragonal pyramid. This polyhedron will appear repeatedly in Section 5 on the oxocuprate(II) compounds. The essential difference between (A) and (B) is in the occupancy of the sites by lithium and copper. In (A) the Li^{+} and Cu^{+}/Cu^{2+} ions occupy clearly defined sites, whereas in (B) the Cu(2) and Cu(3) copper ion sites are partially occupied by randomly distributed Li^{+} ions. Finally, it may be mentioned that a mixed-valence Cu^{2+}/Cu^{3+} compound with the formula $Li_2Cu_2O_4$ has long been known to exist,[55] although its structure is not known.

4. The Crystal Chemistry of Oxocuprate(III) Compounds

It would appear logical to treat the oxocuprates in order of increasing oxidation states, but instead this section will describe the few known examples of oxocuprate(III) compounds. The justification for this is that Cu^{3+} (a d^8 ion) is the only one which, due to its electron configuration, consistently follows a square planar coordination to oxygen. It is therefore easier to first consider the CuO_4 units that are invariably planar in the solid state, before moving on to the less consistent crystal chemistry of the oxocuprate(II) compounds.

4.1. Isolated Double Square Structures Formed from Planar Units

The only known example of an oxocuprate with isolated Cu_2O_6 double squares is $Na_6Cu_2O_6$.[56] In Figure 24 the coordination around Na(1), Na(2), Na(5) and Na(6) is indicated by filled red and yellow polyhedra. As it was not yet possible at the time of writing to use transparent colors on the graphic workstation, Na(3) and Na(4) were shown as spheres (green, radius 0.2 Å) to give a clearer impression of the crystal structure. The polyhedra around Na^{+} can be described as distorted tetrahedra in the cases of Na(2) and Na(6), octahedra for Na(1), Na(3) and Na(4), and a trigonal prism for Na(5). An important feature of the crystal chemistry of oxocuprate(III) compounds is the isolated Cu_2O_6 unit that is held within the Na/O lattice. This is exactly the configuration found in electron-deficient compounds such as $AuCl_3$, which is commonly used as a teaching example to illustrate how the electron deficiency is rectified by dimerization to Au_2Cl_6. It should be noted that the deviations from planarity in $Na_6Cu_2O_6$ are only slight, and in Figure 24 the Cu/O coordination spheres have been continued beyond the region of the Na/O polyhedra for greater clarity.

4.2. Isolated Chains of Planar Units

Up to now oxocuperate(III) compounds with $^{1}_{\infty}[CuO_2]$ chains have only been observed for alkali metal cuprates. $NaCuO_2$[55] and $KCuO_2$[57] were prepared as long ago as the 1950s, but their structures were not determined until more than a decade later. As an example, the structure of $NaCuO_2$[58] will first be described. In Figure 25 the NaO_6 octahedra are shown as red octahedra, which are joined by their edges to form two-dimensional layers as in the delafossites. Cu^{3+} ions are located between the layers in such a way that they are in a square planar environment of O^{2-} ions. The linking of planar units by their edges leads to one-dimensional chains (Fig. 25). It can be seen that the $^{1}_{\infty}[CuO_2]$ chains are rigidly coupled to the NaO_6 octahedra, which

means that the Cu–Cu distance of 2.75 Å is equal to the Na–Na distance within the layers of octahedra. This coupling between chains and octahedra evidently explains why $KCuO_2$, $RbCuO_2$ and $CsCuO_2$ cannot form this structure.

In $KCuO_2$[59] the requirement for equal Cu–Cu and K–K distances is avoided by the formation of the crystal structure shown in Figure 26. Here K^+ has a trigonal prismatic coordination to O^{2-} as shown by the red polyhedra. However, the essential feature of the linking of the KO_6 prisms is a sequence in which prisms containing K^+ ions alternate with empty prisms. If the Cu–O distances were the same as in $NaCuO_2$, the same chain structure would result, but in $KCuO_2$, $RbCuO_2$, and $CsCuO_2$ the distances between the alkali metal ions are considerably greater due to the presence of the empty trigonal prisms. A recent neutron diffraction study[60] on $NaCuO_2$ and $KCuO_2$ indicated the same crystal chemistry. These authors also cite results on $NaCoO_2$[61] for comparison; its structure is of the α-$NaFeO_2$ type, which is understandable if one assumes that the planar CuO_4 polygon (4×1.85 Å) is extended by adding two very distant O^{2-} neighbors to form an octahedron.

Na_3CuO_3[62] is another cation-rich oxocuprate. However, the recent finding[56] that it has a monoclinic β form has reopened the discussion regarding its crystal chemistry. Another possibility to be considered[56] is a mixed-valence cuprate(II)/(III) with the formula $Na_{12}Cu^{II}_2Cu^{III}_2O_{11}$.

The last compound to be mentioned in this section is $TlSr_2CuO_6$.[63] Here the Cu–O distances (4×1.88 Å; 2×2.49 Å) indicate a stretched octahedron. However, this seems unlikely for copper in the oxidation state Cu^{3+}. Confirmation of this structure would prove that Cu^{3+} can show deviations from strict planarity and from its valence-specific crystal chemistry.

5. The Crystal Chemistry of Oxocuprate(II) Compounds

This section, which has deliberately been delayed until now, describes the many different coordination forms of Cu^{2+}. The discussion will be structured by taking as a common thread the coordination polyhedra around the copper ion. For reasons of space and cost the numerous examples of compounds with Cu^{2+} ions in closed polyhedra will be reduced to a basic minimum.

5.1. Isolated Planar Units

One of the earliest oxocuprate(II) compounds with isolated square planar units to be investigated was Bi_2CuO_4.[64, 65] Figure 27 shows that CuO_4 square units with their planes parallel to the *a*/*a* plane of the tetragonal unit cell are stacked up along the [001] direction. Here again the borders of the CuO_4 squares are shown in yellow. As in the columnar structures of the planar coordinated ions Ni^{2+}, Pt^{2+} and Pd^{2+}, successive CuO_4 squares are rotated by 45° relative to each other about the stacking axis. The Bi^{3+} ions, shown in red, link the isolated planar CuO_4 units to form the three-dimensional crystal lattice. Figure 28 shows the coordination of the Bi^{3+} ions. Owing to the presence of the s^2 electron lone pair, the coordination sphere of the bismuth ion is open on one side; each of the electron lone pairs extends to the middle of a tunnel formed by four stacks of CuO_4 polygons.

Another group of compounds with isolated square planar units are those of the general formula $BaCuLn_2O_5$ (Ln = La to Nd).[66–68] Their structure consists of a lattice of trigonal prisms formed by O^{2-} ions around Ln^{3+} (capped at two of the rectangular faces) and a cubic coordination around the Ba^{2+} ion. The complete crystal structure is shown in Figures 29 and 30. In Figure 29, the BaO_{8+2} polyhedra are shown in open form, with the Ba^{2+} ions represented by red spheres whose radius is about 80% of the tabulated value[24] for this ion. Figure 30 shows the Ba/O polyhedra (red) in a closed representation, whereas the trigonal prisms around the Ln^{3+} ions (green spheres) have been left open. Both figures show that the yellow-bordered CuO_4 squares are isolated from one another in the crystal lattice. It will be shown later (in Section 6.1) that in other compounds with the formula $BaCuLn_2O_5$, as one progresses from Ln = Sm towards the heavier lanthanoid elements a new structure without planar coordinated Cu^{2+} ions appears.

A third example with isolated planar units is $CuTa_2O_6$;[69, 70] its structure is shown in Figure 31. So that the arrangement of the planar units formed by O^{2-} ions around Cu^{2+} can be clearly seen, the Cu/O partial lattice has been extended well beyond the limits of one unit cell. Despite the distortion introduced by the perspective view, it can be seen that the CuO_4 squares are arranged with their planes perpendicular to the directions of the three cartesian axes. Considering these in conjunction with the TaO_6 octahedra, which are shown in red and form a distorted perovskite-type partial structure, the structure in Figure 31 can be understood as one in which each CuO_4 square links the corners of two octahedra in the severely deformed octahedral lattice. The distortion from the ideal perovskite structure results in the presence of large and small holes in the structure. The large holes are usually unoccupied, and the fact that an ion is missing from the perovskite structure is indicated in the empirical formula $Cu\square Ta_2O_6$, where $\square$ represents a hole.

The last compound with isolated CuO_4 squares that will be described is $CaCu_3Ge_4O_{12}$,[71] which shows a puzzling structural resemblance to $CuTa_2O_6$. The similarity between the crystal chemistries of the two compounds can be understood from considerations based on their molecular formulas. If we double the formula $Cu\square Ta_2O_6$, which indicates the unoccupied large holes ($\square$) in the perovskite lattice, we obtain $Cu_2\square_2Ta_4O_{12}$. If four Ta^{5+} ions are replaced by four Ge^{4+} ions, the deficit of four positive charges must be compensated for. This is achieved by introducing one Ca^{2+} ion and one Cu^{2+} ion. The chemical constitution, with the holes in the perovskite lattice now filled, is given by $Cu_2(Ca,Cu)Ge_4O_{12}$. If we now look at Figure 32, we see that it depicts the above situation. $CaCu_3Ge_4O_{12}$ contains all the crystal chemical structural units of $CuTa_2O_6$, and in addition the holes in the perovskite lattice are now filled. The tilting of the GeO_6 octahedra (shown in green in Fig. 32) causes deformation holes at the center and corners of the unit cell, which are occupied by the Ca^{2+} ions shown in red. The holes of the second type in the empirical formula $Cu_2\square_2Ta_4O_{12}$ are occupied by Cu^{2+} ions in such a way that

the corners of the octahedra which are tilted towards each other form the corners of the planar CuO_4 groups.

5.2. Single Chains Formed by Isolated Planar Units

The first, and up to now the only, known oxocuprate(II) of an alkali metal is Li_2CuO_2. It was first mentioned in 1943, and was later reported as a light brown powder.[55, 73] Almost ten years after the first suggested structure had been put forward, single crystals were obtained,[74] allowing a full X-ray structure determination. It turned out that the earlier suggested structure, based on powder diffraction data, was in principle correct, and the structure of the compound is shown in Figure 33. The LiO_4 tetrahedra, shown in red, are arranged in layers which are joined together by isolated chains of CuO_4. The planar polygons around the Cu^{2+} ions are joined by their edges, as in $NaCuO_2$ and $KCuO_2$ (Figs. 25, 26). The most recent study of Li_2CuO_2 by neutron diffraction[75, 76] is concerned with the magnetic structure. Below 10 K an antiferromagnetic structure is observed, which means that the Cu^{2+} magnetic dipoles have an antiparallel orientation along the 0,0,0 and $1/2,1/2,1/2$ directions perpendicular to the *c*-axis.

This topic is concluded by noting that isolated chains of edge-linked CuO_4 squares have also been observed in phases with the constitution $M_{14}Cu_{24}O_{38-x}$;[179] this has been discussed in more detail in a previous article.[6]

Investigations of two oxocuprate(II) compounds of alkaline-earth metals, namely Ca_2CuO_3[77] and Sr_2CuO_3,[78] led to the first observations of isolated chains of corner-linked CuO_4 squares. In the course of attempts to prepare bismuth-type superconductors, single crystals of Ca_2CuO_3 were obtained by accident, and were used in a later reinvestigation of the crystal structure of this compound.[79] Figure 34 shows the characteristic arrangement in this type of structure. Trigonal prisms (shown in red) are formed by the coordination of O^{2-} ions around Ca^{2+} or Sr^{2+}. One of the rectangular faces of each prism is capped by a seventh O^{2-} ion. Four MO_6 prisms are joined by their long edges of rectangular faces to form a square tunnel, which is occupied by Cu^{2+} ions positioned at the points corresponding to the triangular faces of the prisms. The seventh coordination partner of the alkaline-earth ion forms transverse links to adjacent double chains of prisms running parallel to the first. In Figure 34 the CuO_4 squares are again shown with yellow borders for clarity.

Compounds with the general formula $Ln_2Cu_2O_5$ show a structure which goes beyond the isolated straight chains of CuO_4 squares of the kind described above, in that two types of linkage patterns (by corners and by edges) are combined. This structural type was first observed for $In_2Cu_2O_5$.[80; 81] Subsequently it was confirmed by single crystal studies on the compounds with Ln = Ho to Lu,[82] Sc[83] and Y[84], and the coordination of the copper ion was determined more precisely. Figure 35 shows how the LnO_6 octahedra (yellow) are linked together to form a lattice. Rods formed by edge-linked octahedra are joined by their corners to form a framework with wide tunnels whose cross-section is an elongated hexagon. The tunnel diameter is large enough to accomodate two Cu^{2+} ions which, with their nearest oxygen neighbors, form an edge-linked Cu_2O_6 pair of squares. These pairs of squares, which resemble those in $Na_6Cu_2O_6$ (Fig. 24), are joined by two diagonally opposite corners to form one-dimensional ribbons (see Fig. 35). Here again the CuO_4 squares are shown with a yellow border. However, the view of the $^1_\infty[Cu_2O_5]$ chains chosen here does not make it clear that the individual CuO_4 polygons are twisted. This not only makes them markedly non-planar, but also alters the coordination polyhedra of the Cu^{2+} ions, a point that will be discussed later in Section 5.7.

5.3. Double Chains of Planar Units

In the double chains of the $SrCuO_2$ structure[85] the degree of cross-linking between the square planar CuO_4 polygons is greater than in the compounds discussed up to now, as Figure 36 illustrates. In a direct comparison with Figure 34, it is seen that the linking between the polyhedra around the Sr^{2+} ions (singly capped trigonal prisms shown in red) is very similar. However, in Figure 36 there is a gap at one of the longitudinal edges, bridged by a double Cu/O chain (shown by the yellow borders around the CuO_4 squares). The isolated planar double chains can be regarded as consisting of Cu_2O_4 units joined at two of their edges. However, there are a number of other structural relationships between Sr_2CuO_3 and $SrCuO_2$, which have been discussed in detail in a previous article.[6]

Attempts in our laboratory to prepare the compound $CaCuO_2$, which should be an isotype of $SrCuO_2$, have invariably failed. Reports of the preparation of $CaCuO_2$ at 850 °C[86] appear to have later been refuted.[87] Again in the course of research on superconductors, while investigating systems containing the oxides of copper and alkaline-earth metals, a phase $Ca_{0.86}Sr_{0.14}CuO_2$ with a unique crystal structure was discovered.[88] Independently of this, other investigators[87] discovered the phase $Ca_{0.91}Sr_{0.09}CuO_2$, containing very little strontium, which comes closest in its constitution to the pure compound $CaCuO_2$. The surprising results reported by these two groups remind us yet again of the remarkable inventiveness of nature. To understand the structure of $Ca_{0.91}Sr_{0.09}CuO_2$ we must imagine a perovskite $CaM^{IV}O_3$ in which the tetravalent ion M is replaced by Cu^{2+}. This automatically involves the loss of one oxygen ion per formula unit. If we remove an oxygen ion from one, and only one edge of the cubic perovskite structure, this means that the Cu^{2+} ion occupying the former M^{4+} site is in a planar environment. This leads to planar networks of CuO_4 squares, as described in the next section.

5.4. Networks of Planar Units

As was shown at the end of the previous section, $Ca_{1-x}Sr_xCuO_2$ ($x \simeq 0.09-0.14$) crystallizes in a distorted perovskite structure forming networks of the type $^2_\infty[CuO_2]$ arranged in parallel planes. One of the oxocuprate(II) compounds with a network structure (square planar CuO_4 polygons joined at all corners) that has been known for quite a long time is Nd_2CuO_2.[89] It was at first assumed that the oxometalates with the general formula Ln_2CuO_4 (Ln = La to Gd) belonged to the K_2NiF_4 structural

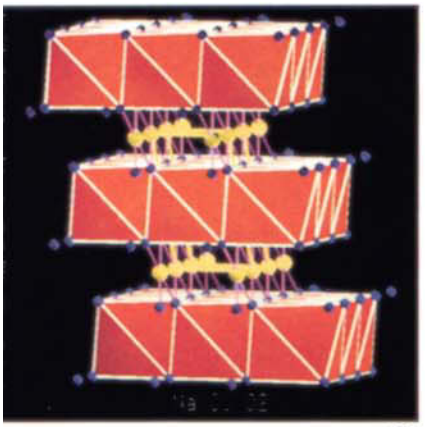

25

26

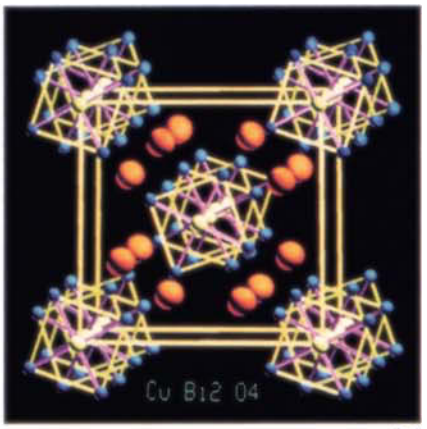

27

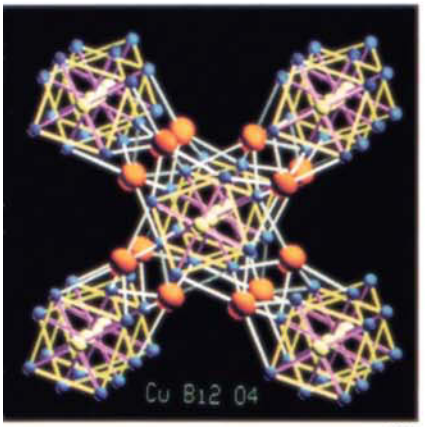

28

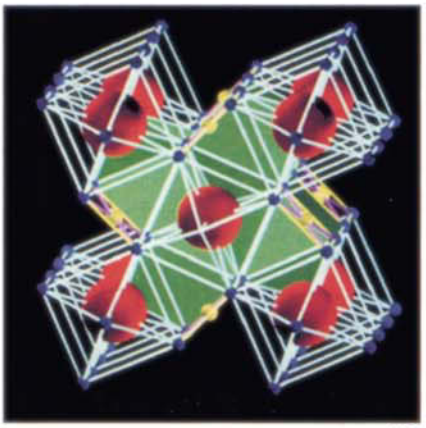

29

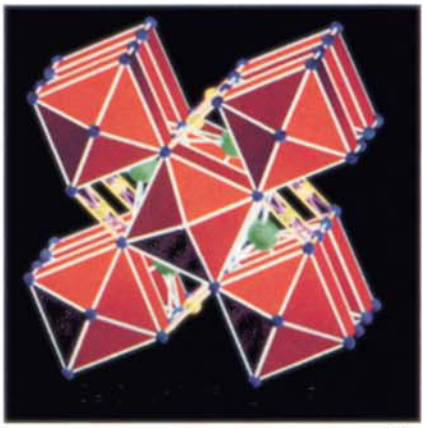

30

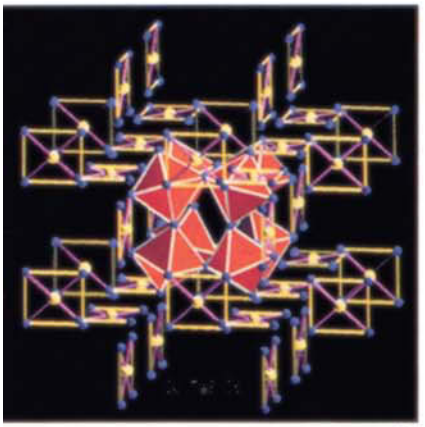

31

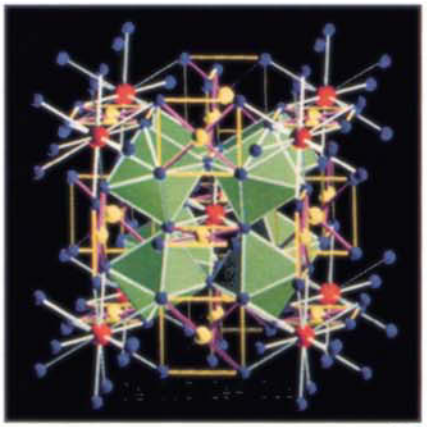

32

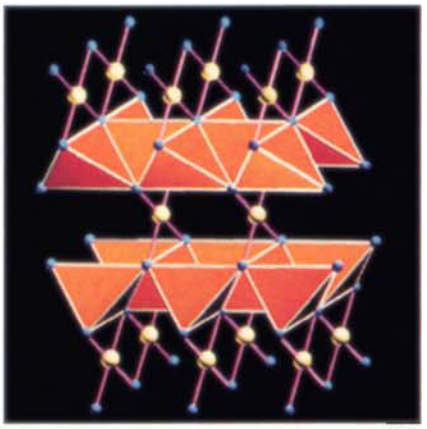

33

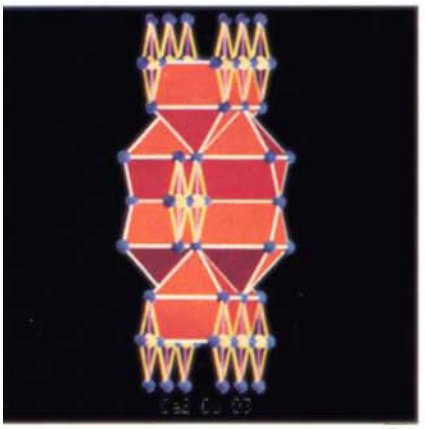

34

35

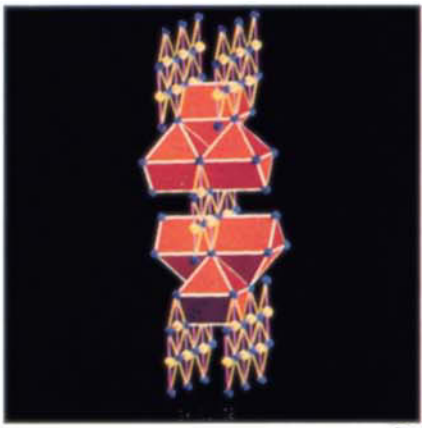

36

type,[90-92] and thus crystallized with octahedrally coordinated Cu^{2+}. In fact, however, the structure that is now accepted for this group of compounds is that shown in Figures 37 and 38, which is only distantly related to the K_2NiF_4 structure. A notable characteristic of this structure is the infinite two-dimensional Cu/O network, which can be seen especially clearly at the center of Figure 37. The CuO_4 squares are shown with a yellow border. It can be seen that alternate sites within the square grid of oxygen ions are unoccupied. The Nd^{3+} ions (red spheres) are positioned centrally above these unoccupied squares. The change from the K_2NiF_4 type structure to the Nd_2CuO_4 type also involves an alteration to the coordination polyhedra of the large ions (Nd^{3+} in this case). Whereas in the K_2NiF_4 structure these can be described as singly capped square antiprisms, they are practically cubic in the Nd_2CuO_4 structure. It can be seen from Figure 38 that the planar Cu/O networks are linked together by double cubes joined by their faces. The Nd^{3+} ions are shifted away from the centers of the cubes, which increases the Nd–Nd distance. It is also evident from Figure 38 that in the direction of the long axis, above and below each planar CuO_4 polyhedron, there is an empty cube formed by eight O^{2-} ions. More recent studies on the transition between the La_2CuO_4 structure with non-planar copper coordination and the Nd_2CuO_4 type have shown that for the range of ionic radii from that of Ce^{3+} up to Gd^{3+} the crystal structure shown in Figures 37 and 38 with planar coordinated copper is formed.[93,94] It is also interesting that in $Nd_2(Cu,Ni)O_4$ the Cu^{2+} and Ni^{2+} ions again have octahedral coordination,[95] despite the fact that Ni^{2+}, with a d^8 configuration, would be expected to show planar coordination. However, as it was found that compounds with the formula $Nd_{2-x}Ce_xCuO_4$ also have superconducting properties,[96] the crystal structures of numerous phases with the constitution $Nd_{2-x}M_xCuO_4$ were studied in detail, in the course of which another structure (described in the literature as the T″ or T* phase) was discovered.[97] These studies led to the interesting conclusion that the T″ or T* phase contains structural units that are a modified version of those in the crystal structures of La_2CuO_4 and Nd_2CuO_4. The octahedral or planar copper coordination is partially transformed into a square pyramidal type. The T* phase has been investigated by neutron diffraction,[98,99] and results on this have been summarized and discussed together with the already known compounds La_2CuO_4 (T phase) and Nd_2CuO_4 (T′ phase).[100]

Networks formed by planar units are common, but they do not always have a planar structure. A good example of an undulating network made up of planar CuO_4 polygons is seen in the compounds $CaCu_2O_3$,[101] $MgCu_2O_3$[102] and the recently newly prepared $CoCu_2O_3$.[103] In the case of $CaCu_2O_3$, the electrical conductivity and magnetic properties have also been measured recently.[104] Figure 39 shows its structure, with CaO_6 octahedra (red) held between undulating Cu/O networks. It can be seen in the upper part of this figure that each of the unoccupied O_4 squares in the Cu/O network is bridged by a face of an octahedron. When Ca^{2+} is replaced by smaller ions (Mg^{2+}, Co^{2+}), the distortion of the Cu/O network becomes more severe.[103] Surprisingly, it has not been possible to prepare mixed crystals of $CaCu_2O_3$ and $MgCu_2O_3$. These would be important as a means of studying how the coordination sphere of the Cu^{2+} ion changes with the nature of the M^{2+} ion. The interatomic distances of the pure compounds show that the two O^{2-} neighbors of the Cu^{2+} ions, which are quite large distances in $CaCu_2O_3$, move closer in $MgCu_2O_3$ when Ca^{2+} is replaced by Mg^{2+}. On the evidence of the Cu–O distances in $MgCu_2O_3$ and $CoCu_2O_3$ it must be concluded that here the Cu^{2+} ions have an octahedral [4 + 2] coordination. Surprisingly, it has recently been found that mixed crystals with the constitution $Ca_{1-x}Co_xCu_2O_3$[103] can be formed, from which it emerges that the deformation of the Cu/O network does not change in a linear manner with the radius of the M^{2+} ion. From this it appears that for compounds of the type $Ca_{1-x}M_xCu_2O_3$ a planar copper–oxygen lattice, which is of interest with regard to superconductors, is only to be expected as one moves to larger ions ($M = Sr^{2+}$, Ba^{2+}). Unfortunately, however, replacing Ca^{2+} by these ions is difficult owing to the tendency for preferential formation of the compounds $SrCuO_2$, Sr_2CuO_3 and $BaCuO_2$.

The phase $Bi_{0.31}Ca_{5.64}Sr_{4.05}Cu_{17}O_{29}$,[105] which will here be referred to for brevity as $M_{10}Cu_{17}O_{29}$, is a classic example of a continuous transition in the manner of formation of the Cu^{2+} coordination polyhedra. In Figure 40, the complicated structure of this phase has been reduced to show only the Cu/O coordination. To give a clearer impression the planar units are shown with a yellow border. The structure of $M_{10}Cu_{17}O_{29}$ contains planar networks of square-coordinated Cu^{2+} ions, like those described earlier in this section, and isolated chains as described in Section 5.2. However, the most interesting aspect is the twisting of some of the CuO_4 squares which occurs at regular intervals along the chains. This twisting results in a gradual transition form planar to tetrahedral coordination.

5.5. Planar Units Extended to Form Polyhedra

The description of the crystal chemistry of copper in its twofold oxidation state has up to this point been confined to situations where the Cu^{2+} ion has a planar coordination to O^{2-}. However, this is not the only type of copper coordination occurring in oxocuprate(II) compounds, as is shown by the following examples.

In the course of experiments aimed at preparing Sr_2CuO_2 from $SrCO_3$ and CuO, the compound $Sr_2CuO_2(CO_3)$ was obtained.[106] The features of particular interest in its crystal chemistry are shown in Figure 41. First, one again notices the square network of O^{2-} ions, with Cu^{2+} ions occupying alternate squares. Also, here again the Sr^{2+} ions, shown in red, are positioned above the unoccupied squares. In addition one sees, in the middle of Figure 41, a grouping of O^{2-} ions around a carbon atom (green), which forms the CO_3^{2-} group lying between the layers. This at first sight very unusual coordination of carbon can only be understood by assuming that the CO_3^{2-} groups are randomly orientated in space. Here the spheres representing the O^{2-} ions in the CO_3 groups are drawn significantly smaller than normal, so as to indicate that these oxygen sites are under-occupied in a random way. Furthermore, it can be seen that the oxygen ion at one of the sites in the middle is shown somewhat larger, to indicate that this site has a higher occupancy than the other

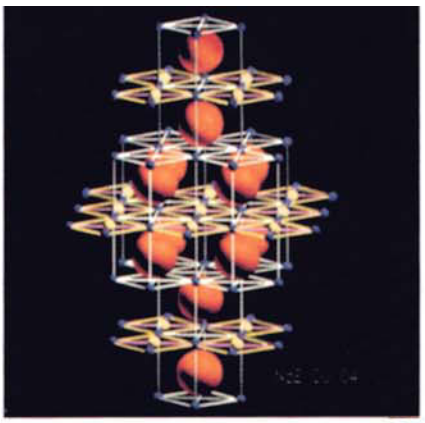

37

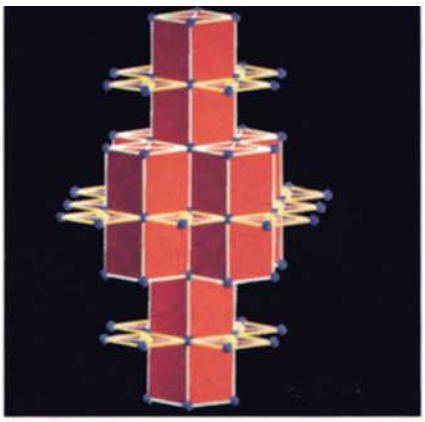

38

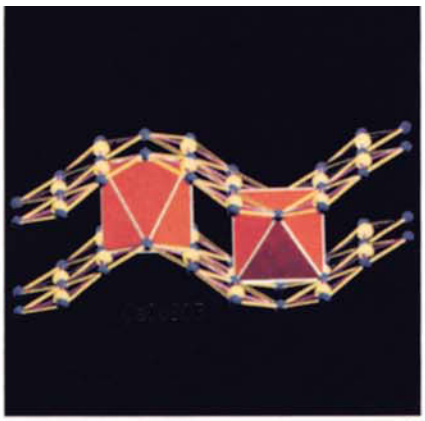

39

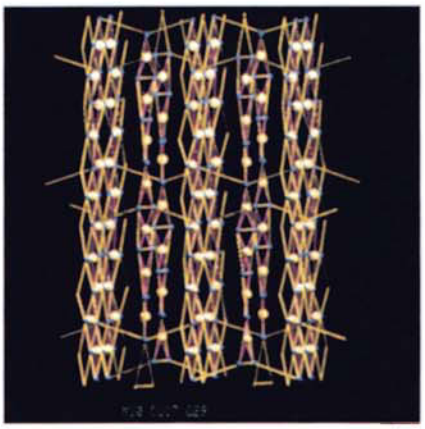

40

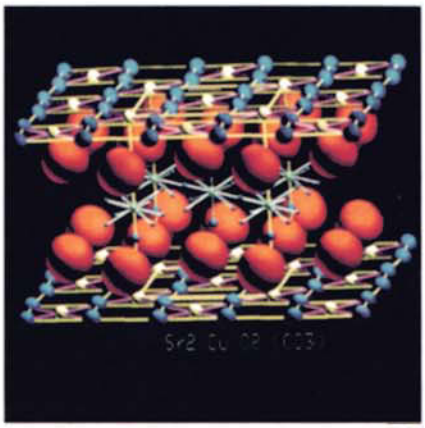

41

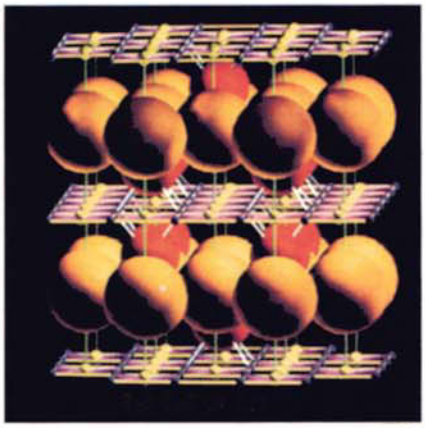

42

43

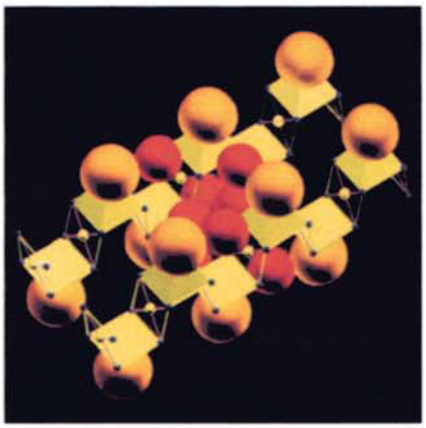

44

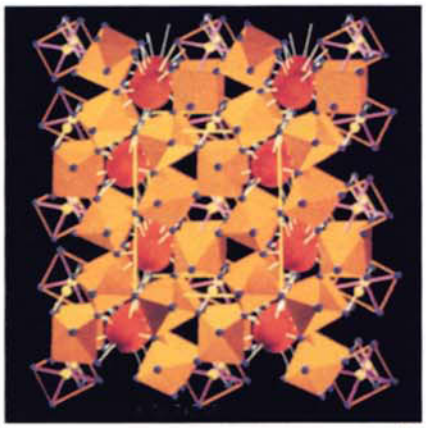

45

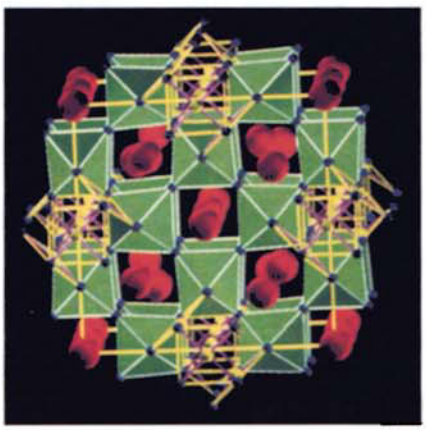

46

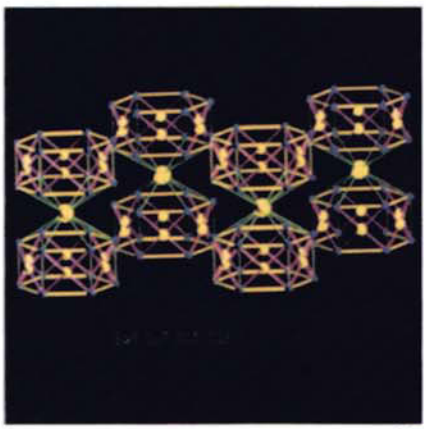

47

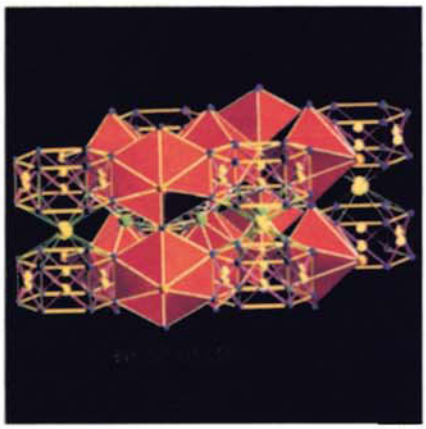

48

eight. It is this site that forms the extension of the planar CuO_4 polygon to give a stretched octahedron. It must therefore be assumed that in microregions octahedral CuO_6 polyhedra can occur in addition to the usual planar CuO_4 polygons.

Cu^{2+} also exhibits a crystal chemistry similar to that described above in the halogenooxocuprate(II) compounds. For example we consider here $Ba_2Cu_3O_4X_2$ with $X = Cl^-$ and Br^-,[107,108] and $Sr_2Cu_3O_4X_2$ with $X = Cl^-$ and Br^-.[109,110] Figure 42 shows the structure of $Ba_2Cu_3O_4Cl_2$, with planar Cu/O networks, as already described in many previous examples. Here each Ba^{2+} ion (red) is held in a position above an unoccupied square of four O^{2-} ions. The halogen ions, shown as orange spheres whose radius is 80% of the actual ionic radius, form bridges between the Cu/O networks, with the result that the Cu^{2+} ion gains two X^- ions as extra neighbors, giving rise to a stretched CuO_4X_2 octahedron. However, it can be seen, with the help of the green lines shown between Cu^{2+} and X^-, that only alternate CuO_4 squares are extended by X^- to form octahedra.

If the molecular formula of the above barium compound is modified in the direction of more Ba^{2+} and less Cu^{2+}, we obtain $Ba_3Cu_2O_4Cl_2$,[111] which belongs to a new class of compounds in which copper shows an unusual crystal chemistry. Figures 43 and 44 give an insight into the crystal structure of this compound. In the first figure one can see zig-zag chains of square planar CuO_4 polygons together with five-fold coordinated copper in square CuO_4Cl pyramids. The latter polyhedra, shown in yellow, each have a Cu^{2+} ion within. A Cl^- ion at a further site (orange sphere) forms the only coordination partner of the Ba^{2+} ion (red sphere). Figure 44 shows how the space is filled by the large Ba^{2+} and Cl^- ions. Here the Ba^{2+} ions (red) and the Cl^- ions (orange) are shown with 80% radii. The Cl(2) site, which is the only one belonging to the Ba^{2+} ion, has been omitted from Figure 44. It is interesting that the already relatively short Cu–Cu distance observed in a linear chain of edge-linked squares ($\simeq 2.69$ Å) is here further shortened to 2.45 Å by the zig-zag creasing (in accordance with the representation in Figures 34 and 44). The Cu–Cu distances would be even shorter if it were not for the displacement of the Cu^{2+} ions towards the interiors of the tetragonal CuO_4Cl pyramids. Partial oxidation of the copper in $Ba_3Cu_2O_4Cl_2$ might be expected to result in one-dimensional metallic conductivity along the direction of the alternating sequence of polyhedra (square—tetragonal pyramid—square...). The structure of $Ba_3Cu_2O_4Cl_2$ shows that in the crystal chemistry of oxocuprate(II) compounds, planar CuO_4 polyhedra can be extended by halogen ions to form square pyramids.

As our final example of a transition from a planar Cu^{2+} environment to three-dimensional polyhedra we consider $KCuTa_3O_9$.[112] As Figure 45 shows, the $[Ta_3O_9]^{3-}$ framework can be regarded as a tetragonal bronze structure. Here it must be mentioned, by way of explanation, that the tetragonal bronzes, such as $Pb_5Nb_{10}O_{30}$,[113,114] $Ba_6CoNb_9O_{30}$[115] and $Ba_6Ti_2Nb_8O_{30}$,[116] have an octahedral structure with tunnels of triangular, rectangular and pentagonal shape, which are small, medium-sized and large respectively. The large Pb^{2+} and Ba^{2+} ions are present only within the two larger types of tunnels (square- and pentagonal-shaped). The Nb^{5+} ion can be partly replaced by smaller ions, as the above examples show. The electrical neutrality is then maintained by the occupation of the tunnels. In the case of $Ba_4CoTa_{10}O_{30}$[117] it has been shown that this bronze structure belongs to the $Na_2Nb_{12}O_3F_2$ type.[118,119] This means that the pattern of the linking in the octahedral lattice is slightly altered,[117] which results in a distortion of the rectangular tunnels, enabling these also to accept small ions such as Co^{2+}. This alteration in the linkage pattern of the MO_6 octahedra in the bronze structure also occurs in $KCuTa_3O_9$.[112] The structure of this compound is shown in Figure 45. The TaO_6 octahedra are shown in yellow, and the large K^+ ions in the large pentagonal tunnels are shown as red spheres. However, a more interesting point is that the distorted rectangular tunnels are occupied by Cu^{2+} ions. It can be seen that the two crystallographic sites of copper, Cu(1) (orange border) and Cu(2) (yellow border), are both shown with only a square planar environment. The way in which the planar units are arranged perpendicular to each other in the rectangular tunnel sites can be seen most clearly at the top edge of Figure 45. However, the representation chosen here does not quite give a true impression of the coordination of the copper ions, as the Cu(1) environment (orange-colored squares) is extended by two O^{2-} neighbors at a distance of 2.4 Å to form a [4 + 2] coordination (a distorted trigonal prism). Also the ion at Cu(2) "sees" more distant oxygen neighbors; the distance of 2.7 Å is exceptionally large, and these are therefore not regarded as bonding O^{2-} ions.

5.6. Planar Units Linked to Form Giant Polyhedra

It has been shown so far that CuO_4 polygons can join together in chains, ribbons and planes. These examples show only small departures from two-dimensionality, in the form of undulating networks and zig-zag chains. This is not the case, however, for $Ba_3Cu_3In_4O_{12}$,[120] which has the unusual crystal structure shown in Figure 46. It consists of a lattice of InO_6 octahedra (green) linked by their corners forming a structure of square tunnels. Some of the tunnels are occupied by Ba^{2+} ions, shown here in red, whereas others contain Cu^{2+} ions, which are coordinated with the neighboring oxygen ions of the tunnel walls to form a skeleton consisting of CuO_4 squares. The viewing angle in the figure reveals a succession of planar CuO_4 squares spaced at equal intervals with their planes perpendicular to the viewing direction. These are joined together by other CuO_4 squares orientated with their planes along the direction of the tunnel axis. These latter CuO_4 squares are arranged in opposing pairs, and with increasing distance from the observer the orientations of their planes alternate through 90°. This results in a giant polyhedron which is infinite along one dimension, and consists entirely of CuO_4 squares (Fig. 46).

A second example of an oxocuprate with giant polyhedra, although closed ones in this case, is $Ba_9Cu_7O_{15}Cl_2$.[121] In this halogenooxocuprate(II) compound Cu^{2+} behaves in an unusual way. It can be seen from Figure 47 that the hexagonal rings are formed by six planar CuO_4 units (with yellow borders) linked together, with copper in the Cu(1) sites, and these in turn are joined together through Cu(2) (large yellow spheres). Here Cu(2) has the unusual coordination number

C.N. = 12. In the crystal lattice, therefore, Cu(2) lies at the center of a hexagonal prism formed by O^{2-} ions. These chains of polyhedra formed by infinite linking along one dimension are further linked together in the third dimension through Ba^{2+} ions (Fig. 48, red polyhedra). Here Ba^{2+} has a [6 + 2] coordination (six O^{2-} and two Cl^- ions) in the form of a hexagonal bipyramid. The peaks of the pyramids are formed by the Cl^- ions (orange-colored). This coordination of Ba^{2+} can be understood if one regards it as arising from a spherical close packing arrangement (regular cuboctahedron), in which three O^{2-} ions on each side of the sixfold planar coordination are replaced by one Cl^- ion.

Probably the most complicated crystal structure found is that of an oxocuprate which appeared to have the very simple empirical formula "$BaCuO_2$".[122] This very easily prepared compound was later reinvestigated, and it was found that the true constitution is $Ba_{44}Cu_{45}O_{90}$.[123-125] The cubic unit cell contains two such formula units, and thus has a total of 358 atoms. Of these, Figure 49 shows only the 88 Ba^{2+} ions and the 180 O^{2-} ions. The reader may like to try to envisage how the additional 90 Cu^{2+} ions can be fitted into this abundance of atomic sites and bonds in such a way that each Cu^{2+} ion has the correct coordination. Nature has solved this problem in a masterly fashion. The incorporation of the Cu^{2+} ions and the resulting coordination can be thought of as occurring in a stepwise manner. In Figure 50, tetragonal pyramids (yellow) formed by O^{2-} ions around Cu^{2+} are shown along the edges of the unit cell and on the normals to the large faces. The crystallographic sites Cu(4) and O(6) are not all fully occupied. This means that where the adjacent square base faces of the tetragonal pyramids are packed too closely together in Figure 50, therefore only alternate ones are in fact present. The same also applies to the corresponding Cu^{2+} ions of these pyramidal fragments. Another publication on "$BaCuO_2$" proposes, on the basis of Fourier synthesis calculations, that further randomly unoccupied O^{2-} and Cu^{2+} sites exist.[126] However, for some of the Fourier peaks this calculation gives Cu–O distances that are hardly credible (1.75 Å, 1.71 Å, 1.25 Å and 1.22 Å), unless sites that are too close together are assumed to be alternately unoccupied. To summarize, the hypothesis that Cu(4) is coordinated by randomly occupied sites is ambiguous and can only be understood in a vague way according to plausibility considerations. Figure 50 also shows that on the diagonals of the unit cell there are large gaps in the partial lattice. As can be seen from Figure 51, these are occupied by ring-shaped Cu_6O_{12} units. Thus we find here the same structural principles as in $Ba_9Cu_7O_{15}Cl_2$ (Fig. 47). However, in contrast to the compound described earlier, the six-membered rings are internally twisted in this case, and as a result the CuO_4 polygons are no longer exactly planar. Also in "$BaCuO_2$" the corners and the center of the cubic unit cell are occupied by another giant polyhedron of a special kind. This is shown in Figure 52 in open form (with yellow borders to the CuO_4 squares), and in Figure 53 with the planar CuO_4 units filled in yellow. Three mutually orthogonal rings, each made up of eight CuO_4 squares, are fused together to form a roughly spherical giant polyhedron with a diameter of about 6.5 A. Figure 53 clearly shows that those Cu^{2+} ions that are shown in Figure 50 with tetragonal pyramidal coordination are pushed out of the plane of the square towards the inside of the square pyramid. Thus, of the eighteen Cu^{2+} ions in the giant polyhedron, six are not in a planar oxygen environment. The discovery that the formula "$BaCuO_2$" must be corrected corresponds to an empty giant polyhedron. From each unit cell volume, which would otherwise have the constitution 90 $BaCuO_2 = Ba_{90}Cu_{90}O_{180}$, two Ba^{2+} ions are missing (from the center and a corner of the unit cell), so that the formula corresponding to this volume is $2 \times Ba_{44}Cu_{45}O_{90}$. Figure 54 illustrates how this comes about. Here one is looking into the interior of the large polyhedron and sees a portion of its inner surface. The spherical cavity, with a diameter of more than 6 Å, has 18 Cu^{2+} ions and 24 O^{2-} ions distributed over its surface, with the result that a charged particle in the interior of this giant polyhedron is surrounded by a roughly spherical shell with alternating positive and negative surface charges, and the coulomb attraction and coulomb repulsion forces are approximately balanced.

5.7. The Transition from Planar to Three-Dimensional Coordination

It was mentioned in Section 5.2, in connection with the example of $HoCu_2O_5$ (Fig. 35), that Cu^{2+} ions can certainly also have a distorted square coordination. This was also the case for parts of the $M_{10}Cu_{17}O_{29}$ crystal structure (Fig. 40). For oxocuprate(II) compounds of the $Ln_2Cu_2O_5$ series, it has been found[127] that the distortion of the CuO_4 squares is a function of the size of the Ln^{3+} ion. For large ions one obtains the [4 + 1] coordination of Cu^{2+} that is shown in Figure 55. At the ends of the Cu/O double chains that run parallel to each other it can be seen that one corner of the CuO_4 square is bent away. As a result, each Cu^{2+} ion acquires a fifth O^{2-} neighbor, forming a polyhedron in the form of a severely distorted tetragonal pyramid.

Transitions from planar units to polyhedra can be seen more clearly in the novel phases $La_{8-x}Sr_xCu_8O_{20-x/2}$.[128-131] The situation is illustrated by Figure 56, where the lanthanoid ions are shown in green. The coordination polygons of copper are shown in yellow, as in previous examples where copper ions were shown as spheres. It is immediately apparent that the Cu^{2+} ions are present in three different types of coordination: first, in isolated chains of square planar units; second, in an octahedral coordination; and third, in a tetragonal pyramid, with the positions interchanging cyclically between 0.25, 0.75 and 0.0. It should be noted that the Cu^{2+} ion shown in orange is in the base plane of the square pyramid.

The crystal structure of $La_{8-x}Sr_xCu_8O_{20-x/2}$ (Fig. 56) is related to that of $La_4BaCu_5O_{13+x}$,[132] as is evident from Figure 57. In this compound the chains of planar CuO_4 polyhedra are absent. To facilitate comparison with Figure 56, the lanthanoid ions in $La_4BaCu_5O_{13+x}$ (Fig. 57) are again shown in green, while the Ba^{2+} ion is shown as a red sphere. In this phase also the Cu^{2+} ions that are shown in orange do not lie inside the CuO_5 pyramids (yellow) but in their base planes. These structural features are not exceptional cases, as they are also found in other crystal structures, for example that of $Ba_3Y_2PtCu_2O_{10}$ (Fig. 58).[133] In Figure 58, the Ba^{2+} ions are shown in red, both as spheres and in a cubic coordi-

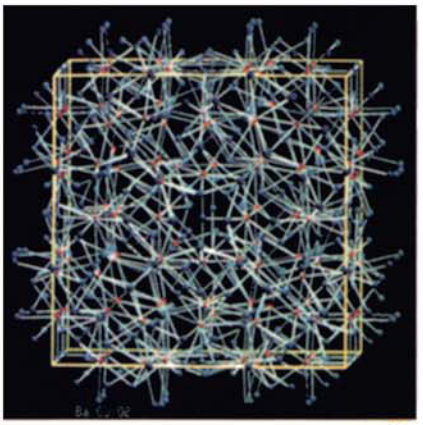

49

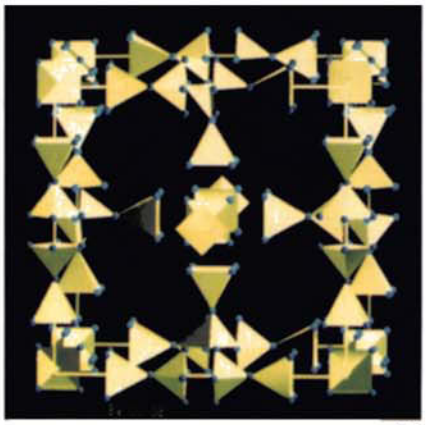

50

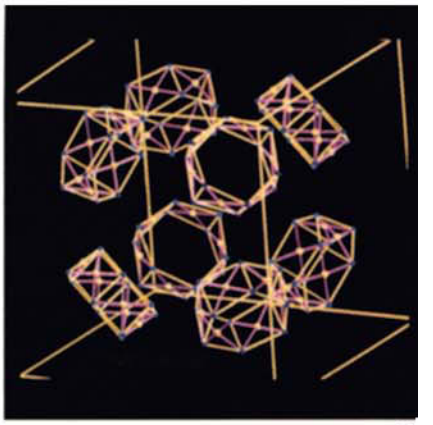

51

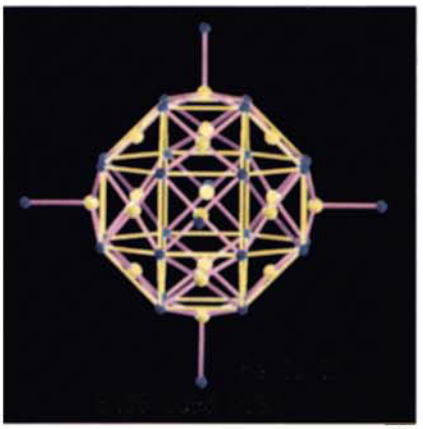

52

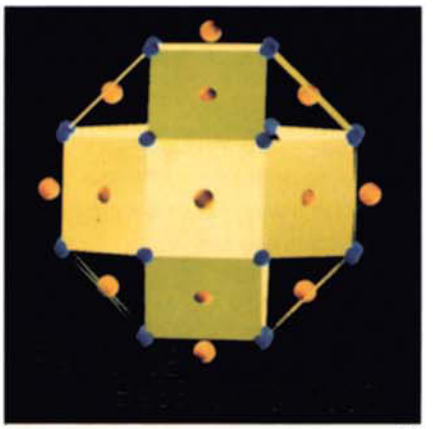

53

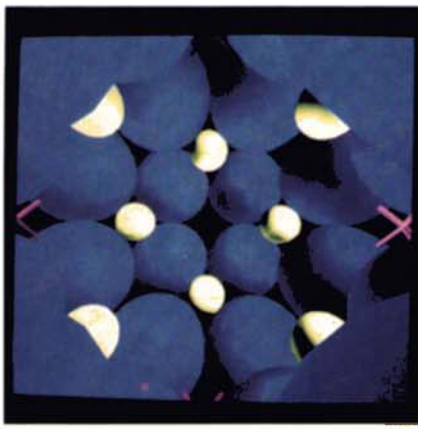

54

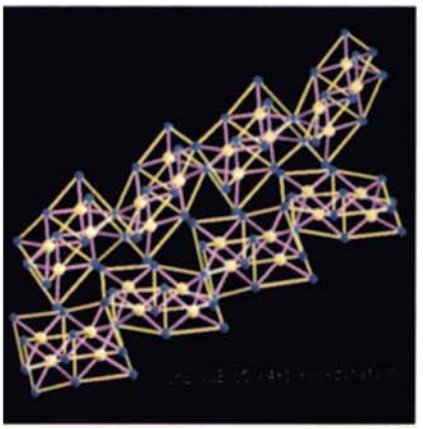

55

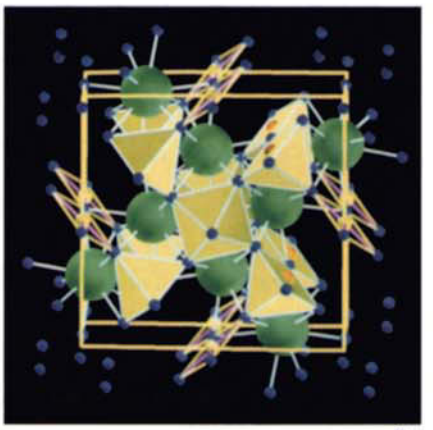

56

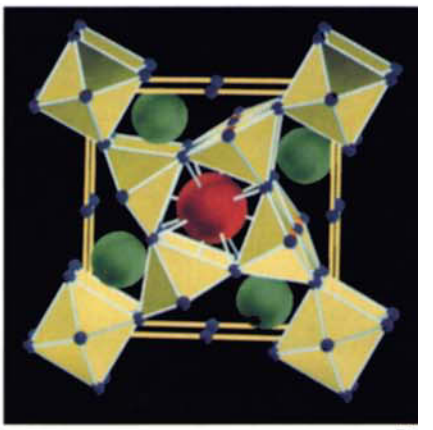

57

58

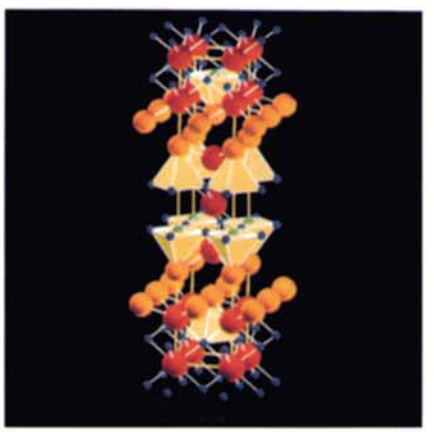

59

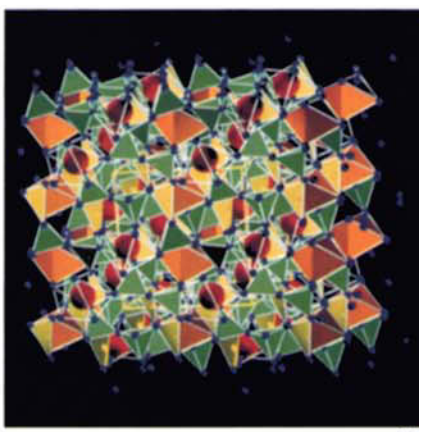

60

nation. The PtO_6 octahedra are orange-colored, and the tetragonal pyramids around the Cu^{2+} ions are shown in yellow, while the Y^{3+} ions are shown as green spheres. It can be clearly seen that in this compound also the copper ions do not lie inside the tetragonal pyramids formed by the oxygen ions. The same is found for the halogenooxocuprate $Ca_3Cu_2O_4Cl_2$ whose structure has recently been published.[134] Its structure is derived from the $Sr_3Ti_2O_7$ type;[125] other isotypes of $Ca_3Cu_2O_4Cl_2$ are the phases $Ln_{2-x}A_{1+x}Cu_2O_{6-x/2}$[136,137] and $Ba_3In_2O_6$[138] and related compounds.[139,140] The removal of one oxygen ion from the $Sr_3Ti_2O_7$ type results in compounds with the general formula $M_3A_2X_6$, whose structure is shown in Figure 59 for the case of $Ca_3Cu_2O_4Cl_2$. The double layer of octahedra in the $Sr_3Ti_2O_7$ type structure is replaced here by a double layer of tetragonal CuO_4Cl pyramids (yellow polyhedra), each with a Cl^- ion (orange-colored sphere) at its apex. The Ca^{2+} ions are shown in red. Those Cu^{2+} ions that are here shown in green can be clearly seen projecting out of the faces of the pyramids.

A particularly good example of the transition from planar to three-dimensional coordination is seen in the severely distorted CuO_4 squares in $CaCuV_2O_7$.[141] The complete structure of this compound is shown in Figure 60. The polyhedra around the vanadium ions are shown in green and those around Ca(2) in orange, while the Ca(1) ions are shown as red spheres in open polyhedra. However, from the standpoint of the coordination of the Cu^{2+} ions, the main point of interest here concerns the severely twisted CuO_4 squares, which are shown in yellow. The twisting is, however, not so severe as to produce a regular tetrahedron; instead the CuO_4 coordination in $CaCuV_2O_7$ can be regarded as comparable with the twisted squares in $M_{10}Cu_{17}O_{29}$ (Fig. 40).

6. Cu^{2+} Ions in Closed Polyhedra

6.1. Tetrahedra, Square Pyramids, and Small Distorted Polyhedra

We have already encountered in the previous section some crystal structures (those of $La_{8-x}Sr_xCu_8O_{20-x/2}$ and $La_4BaCu_5O_{13+x}$, Figs. 56 and 57) in which a proportion of the Cu^{2+} ions have an octahedral coordination to O^{2-}. The following examples show that Cu^{2+} ions in oxometalates can also occur exclusively in closed polyhedra. Figure 61 shows that $Cu_2V_2O_7$ has perfectly formed CuO_4 tetrahedra (yellow) and VO_4 tetrahedra (red).[142] Tetrahedrally coordinated Cu^{2+} ions are also found in, for example, α-$CuVO_3$,[143] $Cu_xV_4O_{11}$[144] and the β-alumina (Ba,Sr)-$CuAl_{10}O_{17}$.[145]

Figure 62 shows the essential features of the structure of a group of compounds with the general formula $BaCuLn_2O_5$.[68,84,146,147] This group of copper-containing oxometalates constitutes a further structural type with the same empirical formula as those in Section 5.1, but having Cu^{2+} in a square pyramidal instead of a planar coordination. The green polyhedra are trigonal prisms formed by O^{2-} ions around Ln^{3+} ions, while the red polyhedra show the oxygen environment of the Ba^{2+} ions, and the yellow square pyramids with a noticeably stretched apex have Cu^{2+} ions within them.

Identical Cu^{2+} coordination polyhedra are found for $SrCuV_2O_7$,[148] whose structure is shown in Figures 63 and 64. The Sr^{2+} ions and the polyhedra around Sr^{2+} are shown in red, while those around V^{5+} are green and around Cu^{2+} are yellow. It is clearly seen that the V_2O_7 double tetrahedra, which are not linked in a straight line, are joined to form a network with the yellow CuO_5 polyhedra. Further details of the coordination spheres can be found in the original publication.[148] In $SrCuV_2O_7$ the Cu^{2+} ions are again unambiguously found to occupy the interior of a tetragonal pyramid formed by their coordination to oxygen. Other examples of structures in which Cu^{2+} ions have a square pyramidal coordination are those of α-$Cu_2V_2O_7$[149] and β-$Cu_2V_2O_7$.[142,150]

When we move on to the barium copper oxovanadate $BaCu_2V_2O_8$,[151] which contains a higher proportion of copper, we obtain a new insight into the crystal chemistry of the Cu^{2+} ion. The Cu–O distances found for this compound (4×1.94 to 1.98 Å; 1×2.31 Å; 1×2.65 Å) indicate that here we have a transition from a tetragonal pyramid to an octahedron. Figure 65 shows the complete structure of $BaCu_2V_2O_8$. The polyhedra around Ba(1) are shown in red, while the Ba(2) sites are shown by orange-colored spheres and the tetrahedra around the V^{5+} ions are shown in green. In constructing the polyhedra around the Cu^{2+} ions (yellow), the value assumed for the Cu–O distance was 2.31 Å. However, the sixth O^{2-} neighbor, whose distance is 43% greater than those for the base of the octahedron (1.94 to 1.98 Å), is not shown. If one were to ignore the sixth O^{2-} neighbor, this would, of course, result in the Cu^{2+} ion lying in the plane of the tetragonal pyramid, and this indicates that the more distant coordination partner (2.65 Å) cannot be totally ignored. Examples of structures with a combination of tetragonal pyramids and octahedra are those of $Cu_3Mo_2O_9$,[152] $Cu_{4-x}Mo_3O_{12}$ ($x = 0.15$)[153] and $CuMoO_4$.[154]

6.2. Cu^{2+} Ions with Octahedral Coordination

The best known example of the group of oxometalates with copper in a stretched octahedral coordination, following the discovery of the superconductor $La_{2-x}Sr_xCuO_4$, is the lanthanum oxocuprate La_2CuO_4.[93,155] Of all the compounds with the general formula Ln_2CuO_4 (Ln = lanthanoid), La_2CuO_4 is the only one with octahedrally coordinated Cu^{2+}; this is surprising, and remains unexplained. In all the other compounds (Ln = Pr to Gd), Cu^{2+} has a planar oxygen environment (see Section 5.4). Despite its orthorhombic symmetry and the slight tilting of the base faces of the CuO_6 octahedra relative to each other, the structure of La_2CuO_4 is of the same type as K_2NiF_4. Figure 66 shows the crystal structure of La_2CuO_4. A noticeable feature is the position of the La^{3+} ions, shown as red spheres, which are quite close to the large faces of the square antiprisms formed by the O^{2-} ions. It is less obvious from the figure that the CuO_6 octahedra (yellow) are considerably elongated in the direction of the long c-axis. The oxygen partners orientated along the [001] axis, i.e. at the upper and lower vertices, are

61

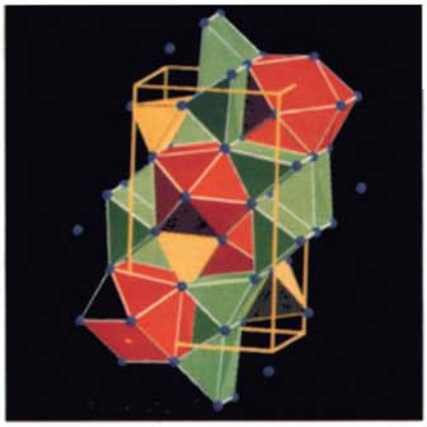

62

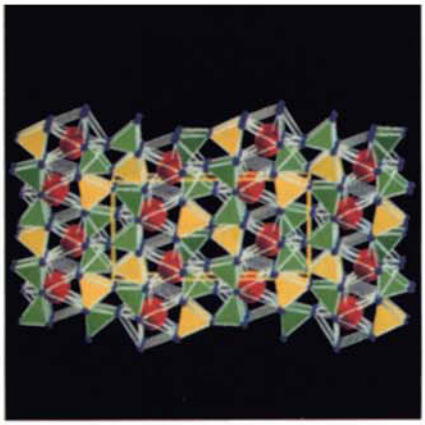

63

64

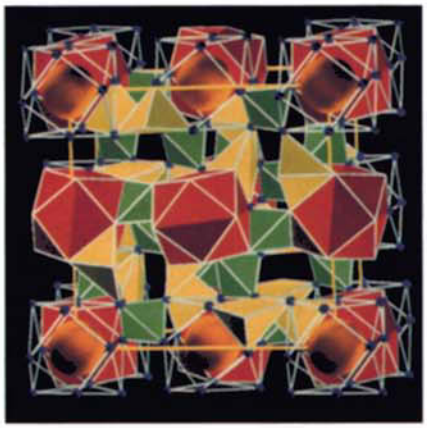

65

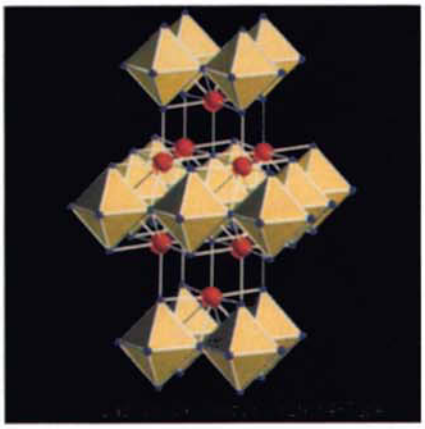

66

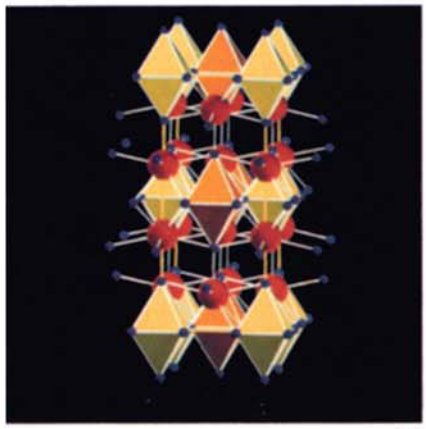

67

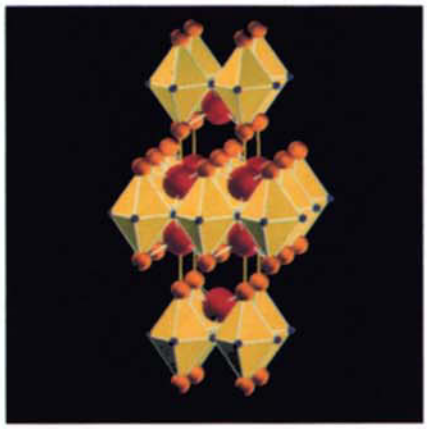

68

69

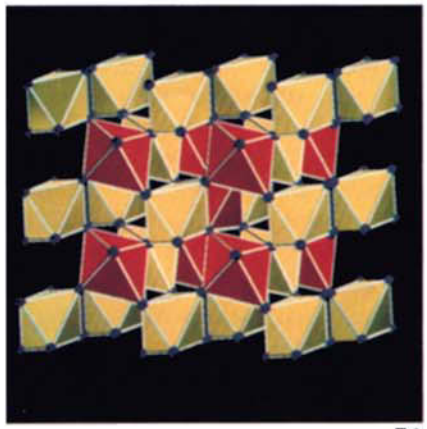

70

71

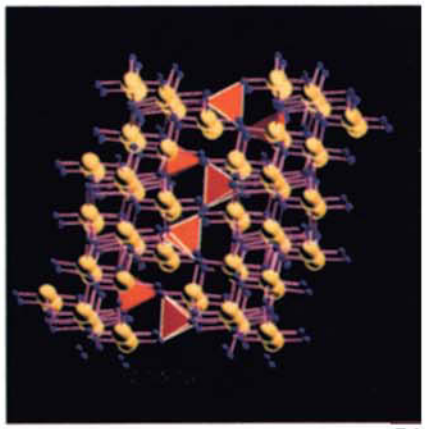

72

about 30% further away from the Cu^{2+} ion than are those in the basal plane of the octahedron.

The compound $La_2Li_{0.5}Cu_{0.5}O_4$, whose structure has recently been published,[156] is closely related to La_2CuO_4. It can be seen from Figure 67 that the layers of octahedra, resembling those of La_2CuO_4, are here made up of orderly arrays of octahedra occupied by Cu^{2+} (yellow) and Li^+ (orange). As before, the lanthanum ions are shown in red, and their arrangement corresponds to that in La_2CuO_4.

The halogenooxocuprates with the constitution $M_2CuO_2X_2$ are also variants of the K_2NiF_4 type structure, as shown by the results for the cases where $M = Sr^{2+}$, $X = Cl^-$[157] or Br^-,[158] and $M = Ca$, $X = Cl^-$ or Br^-.[159] The relationship of their crystal chemistry to that of La_2CuO_4 can be seen from Figure 68. Comparing this with Figure 66, it is evident that here the apexes of the octahedra orientated along the [001] direction are occupied by halogen ions (orange-colored spheres). The noticeably greater Cu–X distances lead to an enlargement of the square antiprism coordination around the Sr^{2+} or Ca^{2+} ions (red spheres), with the result that these cations are now within the MO_4X_5 polyhedra (M = Ca, Sr; X = Cl, Br).

Recently there has been increased activity in the measuring of the physical properties of halogenooxocuprates. As an example we may take the compound $Sr_2CuO_2Cl_2$, whose electrical conductivity, band gaps and magnetic properties have been investigated.[160]

Ba_2CuWO_6 also has considerably stretched octahedra (shown in yellow Fig. 69).[161] However, a more interesting feature in this compound is the [6 + 2] coordination of O^{2-} ions around Ba^{2+}, shown here by red polyhedra. It is shown here in filled surface form, together with the elongated CuO_6 octahedra (yellow) and the WO_6 octahedra (green). This structure should be compared with that in Figure 48, where we saw that in $Ba_9Cu_7O_{15}Cl_2$, the Ba^{2+} ion is surrounded by six O^{2-} ions and two Cl^- ions forming a hexagonal bipyramid. It was noted that there one had a spherical close packing arrangement in which three O^{2-} ions were replaced by a Cl^- ion, which is understandable in view of the size of the Cl^- ion. In the compound Ba_2CuWO_6 that is under discussion here, the Cl^- ions of Figure 48 have been formally replaced by O^{2-} ions in a one-for-one exchange, which means that the space occupied by three O^{2-} ions in the regular cuboctahedron of the spherical close packing shrinks to the volume of a single O^{2-} ion. This results in a BaO_{6+2} bipyramid.

To finish these examples of octahedrally coordinated Cu^{2+} ions we consider Figures 70, 71 and 72. Figure 70 shows the crystal structure of $CuUO_4$[162, 163] and Figure 71 that of $CuVO_3$.[164, 165] Both structures contain isolated CuO_6 octahedra, shown in yellow. Figure 72 shows the structure of $V_2Cu_5O_{10}$,[166] consisting of a tightly knit lattice made up of CuO_6 octahedra and trigonal bipyramids, within which lie isolated VO_4 tetrahedra. The "ball and stick" representation chosen here gives a better indication of the dense network formed by the Cu/O polyhedra in $V_2Cu_5O_{10}$. Other compounds with octahedrally coordinated Cu^{2+} ions are $CuSb_2O_6$,[167, 168] $CuGeO_3$,[169, 170] $LiVCuO_4$,[171, 172] CuV_2O_6,[173] $Cu_xV_2O_5$,[174] $Cu_3V_2O_6$[175] and $Ba_4CaCu_3O_{8.61}$.[176]

Finally, it must be mentioned that Cu^{2+} can also have a trigonal bipyramidal coordination,[166, 167] and in the phase $Cu_{0.64}V_2O_6$ it lies within a doubly capped trigonal prism of O^{2-} ions.[178] The very large Cu–O distances found in $Cu_{0.64}V_2O_5$ (2.45 Å, 2.55 Å and 2.65 Å) lead one to suspect that there is a valence exchange with the vanadium ions and that the large CuO_{6+2} prisms are occupied by Cu^+ as the cation.

7. Summary

The crystal chemistry of copper in oxometalates, as presented through the examples that have been discussed in Sections 2 to 6, conveys an impression of the many different types of coordination adopted by copper in solids, depending on its oxidation state and on its role in the crystal structure. Of the oxidation states of copper, the Cu^{3+} ion is the only one that at present appears to behave consistently, apart from an isolated exception. The oxocuprate(III) compounds discussed here all have Cu^{3+} in a square planar environment of oxygen ions, the observed planar coordination conforming to what is expected for the d^8 electron configuration. Unfortunately, the number of oxocuprate(III) compounds that have been studied thoroughly is very small, and consequently the question of possible departures from planarity cannot yet be answered with certainty.

Although a sweeping generalization cannot be made, the Cu^+ oxidation state is typically found to result in an O–Cu–O coordination with a more or less well-defined dumbbell shape. This structure is found for all compounds with alkali metals, and for all compounds containing bulky and strongly basic ions such as Ca^{2+}, Sr^{2+}, Ba^{2+}, Nd^{3+} or La^{3+}. Thus, when large cations are present, the Cu^+ ions and the associated oxygen ions take on the role of a kind of anionic partial lattice whose main crystal chemical characteristic is the dumbbell-shaped O–Cu–O coordination. Compounds of this type are referred to as oxocuprate(I) compounds. One can also include in this class compounds in which the anionic role of the copper is not so obvious in their constitution, for example as in $CuAlO_2$ (Fig. 6), $Sr_9Zn_4Cu_2O_{14}$ (Fig. 9) and β-$CuNdW_2O_8$ (Fig. 8). In addition to these oxocuprate(I) compounds there are other examples, such as α-$LaCuW_2O_8$ (Fig. 17) and Cu_2WO_4 (Fig. 18), that contain structures other than the dumbbell-shaped coordination (e.g. those containing planar CuO_3 groups), through to the more radically different types with tetrahedral coordination ($Cu_6Mo_5O_{18}$, Fig. 19) and octahedral coordination ($Cu_4Mo_5O_{17}$). In the latter two compounds Cu^+ has the role of a cation in a situation comparable with salt-type compounds of non-metals, and it thus loses the dumbbell-shaped coordination typical of oxocuprate(I) compounds.

The crystal chemistry of oxocuprate(II) compounds is by far the most interesting, as it encompasses a wide variety of types of coordination ranging from isolated planar CuO_4 units to closed polyhedra. The results from studies during the last ten years, especially those that have given rise to research programs on superconductors, lead one to seriously question whether the planar Cu^{2+} coordination that has in

the past been regarded as characteristic of oxocuprate(II) compounds is truly typical for this oxidation state. Unfortunately the situation on this point is confused owing to the existence of a pronounced Jahn–Teller effect for the Cu^{2+} ion with its d^9 configuration. Where Cu^{2+} is in a truly planar environment of O^{2-} ions this is, after all, just a limiting case of a severely stretched octahedron. Some examples of compounds in which the planarity of the polygons formed by O^{2-} ions around Cu^{2+} is only apparent are $CaCu_3Ge_4O_{12}$ (Fig. 32), $CaCu_2O_3$ (Fig. 39) and $KCuTa_3O_9$ (Fig. 45), since there is a degree of arbitrariness in ignoring the coordination to distant O^{2-} neighbors in these oxocuprate(II) compounds; in most cases these have the effect of extending the planar polygons to form stretched octahedra. On the other hand there are other examples, such as $La_{8-x}Sr_xCu_8O_{20-x/2}$ (Fig. 56), $La_4BaCu_5O_{13+x}$ (Fig. 57), $Ba_3Y_2PtCu_2O_{10}$ (Fig. 58) and $Ca_3Cu_2O_4Cl_2$ (Fig. 59), and also many oxide superconductors that are not covered in this article, whose structures indicate quite different preferences with regard to the arrangement of coordination partners. In the examples mentioned, Cu^{2+} is regarded as having a square pyramidal coordination, but this does not take into account the fact that the Cu^{2+} ion "ignores" the fifth (more distant) coordination partner, insofar as it lies exactly in the base plane of the square pyramid. Is the apex of the square pyramid really a normal coordination site, despite its relatively close proximity to the Cu^{2+} ion? There is less ambiguity regarding the other compounds, directly comparable with the above, in which the apex of the tetragonal pyramid is formed by a halogen ion (examples: $Ca_3Cu_2O_4Cl_2$, Fig. 59, and $Ba_3Cu_2O_4Cl_2$, Figs. 43 and 44); this ion must be regarded as a normal coordination partner in view of its size in relation to the Cu–Cl distance.

It has also been shown here that for the oxometalates of divalent copper one can recognize transitions from a planar to a closed (three-dimensional) coordination, for example in $Ho_2Cu_2O_5$ (Fig. 55) and $CaCuV_2O_7$ (Fig. 60). Copper in the divalent oxidation state can also exhibit well-formed coordination polyhedra of the tetragonal pyramidal, bipyramidal, tetrahedral and octahedral types. Thus it can be concluded that the Cu^{2+} ion, like the Cu^+ ion, adapts its crystal chemical role according to the nature of the cations present in the compound concerned.

From the above we can arrive at the following statement concerning the crystal chemical role of divalent copper in oxo compounds: if the Cu^{2+} ions together with oxygen form an anionic partial lattice, then they assume a planar coordination. This also applies to compounds with extremely stretched octahedra that cannot be accounted for by a Jahn–Teller distortion. The neighboring ions that extend the polyhedra to form an apparently octahedral [4 + 2] coordination make a negligible contribution as coordination partners, and under these circumstances it seems justifiable to regard the coordination as being reduced to planar polygons. Coordination in the form of square pyramids with Cu^{2+} in their basal planes can also be regarded as evidence that the copper forms part of an anionic partial lattice. In either of these cases one has an oxocuprate(II) compound. If, on the other hand, Cu^{2+} acts as a cation, as in the numerous oxovanadates (or in salts of non-metals), one finds closed polyhedra such as tetrahedra, octahedra, bipyramids or trigonal prisms. Compounds of this kind should be described as copper oxometalates.

The crystal chemical function of Cu^{2+} in compounds with square pyramids or moderately stretched octahedra, such as $BaCuLn_2O_6$ (Fig. 62), La_2CuO_4 (Fig. 66) or $M_2CuO_2X_2$ (Fig. 68), remains unclear. In La_2CuO_4 chemical considerations indicate that the strongly basic La^{3+} ion is the cation, so that the Cu^{2+} ion is compelled to become a constituent of the anionic partial lattice. However, this view is contradicted by the fact that one cannot ignore the two distant O^{2-} neighbors which extend the planar coordination to form a stretched octahedron. A good example of how the crystal chemical role of Cu^{2+} is adapted according to the basicity of the ions involved is provided by structures of the $CaCu_2O_3$ type. The Cu^{2+} ion is only rather weakly basic compared with Ca^{2+}, which means that for practical purposes it has an anionic role in the crystal structure and is planar coordinated. In the analogous compounds $MgCu_2O_3$ and $CoCu_2O_3$, Cu^{2+} is similar in basicity to Mg^{2+} or Co^{2+}. Consequently two further O^{2-} ions are drawn into the coordination, thereby unambiguously extending it to form a stretched octahedron (cf. Section 5.4). This shows that for the divalent oxidation state of copper also the transition from oxocuprate to copper oxometalate is gradual rather than abrupt.

The ability of Cu^{2+} to form giant polyhedra within the three-dimensional crystal lattice is a unique phenomenon in copper–oxygen chemistry. The beauty of the shapes of these and the elegant simplicity that frequently emerges in the way they are formed from planar units comes as a reward for the often very laborious work of structure determination.

In conclusion one is left with the impression that, despite the fact that many oxo compounds of copper have been studied in great detail in the intervening years, the crystal chemistry of these compounds certainly does not present a simpler and clearer picture today than it did thirty years ago, when the first review article on the subject appeared.[3]

I thank the Fonds der Chemischen Industrie and the Bundesministerium für Forschung und Technologie for providing funds to purchase a computer graphics workstation. My colleagues Dr. Bluhm and Herr Voss wrote the computer programs for the scanning method used to display the crystal structures in color. Herr Gressling helped in the preparation of a series of ORTEP files used in preparing the 3D graphics. I thank them all for their help.

Received: November 5, 1990 [A 820 IE]
German version: *Angew. Chem. 103* (1991) 741
Translated by Dr. *J. K. Becconsall*, Pwlleli (UK).

[1] J. G. Bednorz, K. A. Müller, *Z. Phys. B64* (1986) 189.
[2] J. G. Bednorz, K. A. Müller, *Angew. Chem. 100* (1988) 757; *Angew. Chem. Int. Ed. Engl. 27* (1988) 735.
[3] J. Zemann, *Fortschr. Mineral. 39* (1961) 59.
[4] Hk. Müller-Buschbaum, *Angew. Chem. 89* (1977) 704; *Angew. Chem. Int. Ed. Engl. 16* (1977) 674.
[5] J. Gazo, I. B. Bersuker, J. Garaj, M. Kabesova, J. Kohout, H. Langenfelderova, M. Melnik, M. Serator, F. Valach, *Coordin. Chem. Rev. 19* (1976) 253.
[6] Hk. Müller-Buschbaum, *Angew. Chem. 101* (1989) 69, *Angew. Chem. Int. Ed. Engl. 28* (1989) 1472.
[7] W. Carl, R. Hoppe, *Z. Anorg. Allg. Chem. 574* (1989) 79.
[8] L. Jahnberg, *J. Solid State Chem. 41* (1982) 286.
[9] W. Losert, R. Hoppe, *Z. Anorg. Allg. Chem. 521* (1985) 69.
[10] W. Losert, R. Hoppe, *Z. Anorg. Allg. Chem. 515* (1984) 87.

[11] Y. D. Kondrashev, *Kristallografiya 3* (1958) 696.
[12] H. Hahn, C. de Lorent, *Z. Anorg. Allg. Chem. 279* (1955) 281.
[13] B. U. Köhler, M. Jansen, *Z. Kristallogr. 165* (1983) 213.
[14] T. Ishiguro, A. Kitazawa, M. Mizulani, M. Kato, *J. Solid State Chem. 40* (1981) 170.
[15] J. Darriet, A. Ammar, A. Wichainehai, J. P. Doumere, *Rev. Chim. Miner. 23* (1986) 318.
[16] R. Kipka, Hk. Müller-Buschbaum, *Z. Anorg. Allg. Chem. 430* (1977) 250.
[17] Hk. Müller-Buschbaum, W. Leib, *Monatsh. f. Chem. 116* (1985) 1.
[18] A. Boehlke, Hk. Müller-Buschbaum, *Z. Anorg. Allg. Chem. 574* (1989) 177.
[19] A. Boehlke, Hk. Müller-Buschbaum, *J. Less-Comm. Met. 150* (1990) 311.
[20] P. V. Klevtsov, A. P. Perepelitsa, A. V. Sinkevich, *Sov. Phys. Cristallogr. 25* (1980) 624.
[21] R. F. Klevtsova, K. Yu. Kharchenko, S. V. Borisov, V. A. Efremov, P. V. Klevtsov, *Sov. Phys. Cristallogr. (Engl. Transl.) 24* (1979) 258.
[22] R. F. Klevtsova, N. V. Belov, *Kristallografiya 15* (1979) 43.
[23] H. C. Mumm, Hk. Müller-Buschbaum, *Z. Anorg. Allg. Chem. 566* (1988) 25.
[24] R. D. Shannon, *Acta Crystallogr. A 32* (1976) 751.
[25] Hk. Müller-Buschbaum, T. Krüger, *Z. Anorg. Allg. Chem.*, in press.
[26] A. Boehlke, Hk. Müller-Buschbaum, *Z. Anorg. Allg. Chem. 583* (1990) 17.
[27] H. Sabrowsky, R. Hoppe, *Z. Anorg. Allg. Chem. 358* (1968) 241.
[28] K. Hestermann, R. Hoppe, *Z. Anorg. Allg. Chem. 360* (1968) 113.
[29] R. Hoppe, K. Hestermann, F. Schenk, *Z. Anorg. Allg. Chem. 367* (1969) 275.
[30] D. Fischer, W. Carl, H. Glaum, R. Hoppe, *Z. Anorg. Allg. Chem. 585* (1990) 75.
[31] W. Karl, D. Kissel, R. Hoppe, *Europ. J. Solid State Inorg. Chem. 27* (1990) 5.
[32] H.-N. Migeon, M. Zanne, C. Gleitzer, *J. Solid State Chem. 16* (1976) 325.
[33] H. Klassen, R. Hoppe, *Z. Anorg. Allg. Chem. 497* (1983) 70.
[34] C. L. Teske, Hk. Müller-Buschbaum, *Z. Anorg. Allg. Chem. 379* (1970) 113.
[35] C. L. Teske, Hk. Müller-Buschbaum, *Z. Naturforsch. 27 B* (1972) 296.
[36] R. Hoppe, W. Losert, *Z. Anorg. Allg. Chem. 504* (1983) 60.
[37] H. Klassen, R. Hoppe, *Z. Anorg. Allg. Chem. 494* (1982) 20.
[38] A. P. Perepelitsa, A. V. Sinkevich, *Ukrain. Khim. Zh. 44* (1978) 1241.
[39] A. Boehlke, Hk. Müller-Buschbaum, *J. Less-Comm. Met. 162* (1990) 141.
[40] B. O. Marinder, P. L. Wang, P. E. Werner, M. Westdahl, A. F. Andresen, D. Louer, *Acta Chem. Scand. 41* (1987) 152.
[41] H.-C. Mumm, Hk. Müller-Buschbaum, *J. Less-Comm. Met. 142* (1988) 85.
[42] M. Koop, Hk. Müller-Buschbaum, *Z. Anorg. Allg. Chem. 531* (1985) 140.
[43] E. M. McCarron III, J. C. Calabrese, *J. Solid State Chem. 62* (1986) 64.
[44] M. Koop, Hk. Müller-Buschbaum, *Z. Anorg. Allg. Chem. 530* (1985) 7.
[45] E. M. McCarron III, J. C. Calabrese, *J. Solid State Chem. 65* (1986) 215.
[46] B. O. Marinder, P. E. Werner, E. Wahlstrom, G. Malmros. *Acta Chem. Scand. A 34* (1980) 51.
[47] R. J. Cava, B. Batlogg, J. J. Krajenski, L. W. Rupp, L. F. Schneemeyer, T. Siegrist, R. B. van Dover, P. Marsh, W. F. Beck, Jr., P. K. Gallagher, S. H. Glarum, J. H. Marshall, R. C. Farrow, J. V. Waszczak, R. Hull, P. Trevor. *Nature (London) 336* (1988) 211.
[48] K. J. Range, F. Ketterl, *Z. Naturforsch. B 32* (1977) 1356.
[49] G. A. Koenig, *Proc. Acad. Nat. Sci. Philadelphia* (1891) 284.
[50] C. Frondel, *Am. Mineral. 26* (1941) 657.
[51] M. O'Keeffe, J.-O. Bovin, *Amer. Mineral. 63* (1978) 180.
[52] A. Adam, C. Felser-Wenz, H.-U. Schuster, R. Hoppe, *Z. Anorg. Allg. Chem.*, in press.
[53] G. B. Hyde, St. Andersson, *Inorganic Crystal Structures*, Wiley, Chichester 1989, pp. 257–271.
[54] S. J. Hibble, J. Köhler, A. Simon, S. Paider, *J. Solid State Chem. 88* (1990) 534.
[55] W. Klemm, G. Wehrmeyer, K. Bade, *Z. Elektrochem. 63* (1959) 56.
[56] N. Bukovec, J. Leban, R. Hoppe, *Z. Anorg. Allg. Chem. 563* (1988) 79.
[57] K. Wahl, W. Klemm, *Z. Anorg. Allg. Chem. 270* (1952) 69.
[58] K. Hestermann, R. Hoppe, *Z. Anorg. Allg. Chem. 367* (1969) 261.
[59] K. Hestermann, R. Hoppe, *Z. Anorg. Allg. Chem. 367* (1969) 249.
[60] E. N. Brese, M. O'Keefe, R. B. von Dreele, V. G. Young, Jr., *Solid State Chem. 83* (1989) 1.
[61] M. Jansen, R. Hoppe, *Z. Anorg. Allg. Chem. 408* (1974) 97.
[62] K. Hestermann, R. Hoppe, *Z. Anorg. Allg. Chem. 367* (1969) 270.
[63] J. S. Kim, J. S. Swinnea, H. Steinfink, *J. Less-Comm. Met. 156* (1989) 347.
[64] R. Arpe, Hk. Müller-Buschbaum, *Z. Anorg. Allg. Chem. 426* (1976) 1.
[65] J. C. Bovin, J. Trehoux, D. Thomas, *Bull. Soc. Franc. Min. Cristallogr. 99* (1976) 193.
[66] C. Michel, L. Er-Rakho, B. Raveau, *Rev. Chim. Miner. 21* (1984) 85.
[67] S. Schiffler, Hk. Müller-Buschbaum, *Monatsh. Chem. 117* (1986) 465.
[68] Hk. Müller-Buschbaum, P. Sonne, *J. Less-Comm. Met.* in press.
[69] V. Propach, *Z. Anorg. Allg. Chem. 435* (1977) 161.
[70] H. Vincent, B. Bochu, J. J. Aubert, J. C. Joubert, M. Marezio, *J. Solid State Chem. 24* (1978) 245.
[71] Y. Ozaki, M. Ghedira, J. Chenevas, J. C. Joubert, M. Marezio. *Acta Crystallogr. B33* (1977) 3615.
[72] G. Woltersdorf, *Z. Anorg. Allg. Chem. 252* (1943) 126.
[73] D. P. Den Os, *Dissertation*, Leiden (1962).
[74] H. Rieck, R. Hoppe, *Z. Anorg. Allg. Chem. 379* (1979) 157.
[75] F. Sapina, J. Rodrigues-Carvajal, M. J. Sanchis, R. Ibanes, A. Beltram, D. Beltram, *Solid State Commun. 74* (1990) 779.
[76] R. Hoffmann, R. Hoppe, W. Schäfer, *Z. Anorg. Allg. Chem.*, in press.
[77] C. L. Teske, Hk. Müller-Buschbaum. *Z. Anorg. Allg. Chem. 379* (1970) 234.
[78] C. L. Teske, Hk. Müller-Buschbaum, *Z. Anorg. Allg. Chem. 371* (1969) 325.
[79] M. Hjorth, J. Hyldtoft, *Acta Chem. Scand. 44* (1990) 516.
[80] G. Bergerhoff, H. Kasper, *Acta Crystallogr. 24* (1968) 388.
[81] H.-R. Freund, Hk. Müller-Buschbaum, *Z. Anorg. Allg. Chem. 441* (1978) 103.
[82] H.-R. Freund, Hk. Müller-Buschbaum, *Z. Naturforsch. B 32* (1977) 609.
[83] H.-R. Freund, Hk. Müller-Buschbaum, *Z. Naturforsch. B 32* (1977) 1123.
[84] C. Michel, B. Raveau, *J. Solid State Chem. 43* (1982) 73.
[85] C. L. Teske, Hk. Müller-Buschbaum, *Z. Anorg. Allg. Chem. 379* (1970) 234.
[86] M. Arjomand, D. J. Machin, *J. Chem. Soc. Dalton Trans.* (1975) 1061.
[87] H. Yamane, Y. Miyazaki, T. Hirai, *J. Ceram. Soc. Jpn. Inter. Ed. 97* (1989) 140.
[88] T. Siegrist, S. M. Zahurak, D. W. Murphy, R. S. Roth, *Nature (London) 334* (1988) 231.
[89] Hk. Müller-Buschbaum, W. Wollschläger, *Z. Anorg. Allg. Chem. 414* (1975) 76.
[90] M. Foex, A. Nancheron, M. Line, *C. R. Hebd. Seances Acad. Sci. 250* (1960) 3028.
[91] R. Fruhour, K. Vorres, *A. E. C. Accession No. 46–246 Rept. Bo. TID 220-207*, Paper E (1965)
[92] V. F. Savshenko, Ya. S. Rubinshik, *Vestni Akad. Nauk Beloruss. SSR Ser. Khim. 6* (1969) 44.
[93] B. Grande, Hk. Müller-Buschbaum, M. Schweizer, *Z. Anorg. Allg. Chem. 428* (1977) 120.
[94] B. Knieriemen, *Diplomarbeit*, Universität Kiel (1987).
[95] Hk. Müller-Buschbaum, O. Harneit, *Z. Anorg. Allg. Chem. 573* (1989) 7.
[96] Y. Tokura, H. Takagi, S. Uchida, *Nature (London) 337* (1989) 345.
[97] E. Takayama-Muromachi, Y. Matsui, Y. Uchida, F. Izumi, M. Onoda, K. Kato, *Jpn. J. Appl. Phys. Part 2 27* (1988) L 2283.
[98] F. Izumi, E. Takayama-Muromachi, A. Fujumori, T. Kamiyama, H. Asano, J. Akimitsu, H. Sawa. *Physica C (Amsterdam) 158* (1989) 440.
[99] E. Takayama-Muromachi, Y. Uchida, M. Koboyashi, M. Kato, *Physica C (Amsterdam) 158* (1989) 449.
[100] J. F. Bringley, S. S. Trail, B. A. Scott, *J. Solid State Chem. 88* (1990) 590.
[101] C. L. Teske, Hk. Müller-Buschbaum, *Z. Anorg. Allg. Chem. 370* (1969) 134.
[102] H. Drenkhahn, Hk. Müller-Buschbaum, *Z. Anorg. Allg. Chem. 418* (1975) 116.
[103] Hk. Müller-Buschbaum, A. Tomaszewska, *Z. Kristallogr.*, in press.
[104] Th. Zeiske, H. A. Graf, H. Dachs, K. N. Clausen, *J. Solid State Commun. 71* (1989) 501.
[105] T. Siegrist, L. F. Schneemeyer, S. A. Sunshine, J. Y. Waszczak. *Mater. Res. Bull. 23* (1988) 1429.
[106] H.-G. von Schnering, M. Hartweg, L. Walz, T. Popp, M. Becker, M. Schwarz, *Forschungsbericht MPI Stuttgart* (1988).
[107] R. Kipka, Hk. Müller-Buschbaum, *Z. Anorg. Allg. Chem. 419* (1976) 588.
[108] R. Kipka, Hk. Müller-Buschbaum, *Z. Anorg. Allg. Chem. 424* (1976) 1.
[109] B. Grande, Hk. Müller-Buschbaum, *Z. Naturforsch. B 31* (1975) 405.
[110] B. Grande, Hk. Müller-Buschbaum, *Z. Naturforsch. B 31* (1976) 1183.
[111] R. Kipka, Hk. Müller-Buschbaum, *Z. Anorg. Allg. Chem. 422* (1976) 231.
[112] D. Groult, M. Hervieu, B. Raveau, *J. Solid State Chem. 53* (1984) 184.
[113] W. M. Francombe, B. Lewis, *Acta Crystallogr. 11* (1958) 696.
[114] H. Brusset, H. Giller-Pandrant, S. D. Voliotis, *Mater. Res. Bull. 6* (1971) 5.
[115] U. Lehmann, Hk. Müller-Buschbaum, *Z. Anorg. Allg. Chem. 480* (1981) 149.
[116] P. B. Jamieson, S. C. Abrahams, *Acta Crystallogr. Sect. B 24* (1986) 984.
[117] B. Jasper-Tönnies, Hk. Müller-Buschbaum. *Monatsh. Chem. 115* (1984) 1151.
[118] S. Andersson, *Acty Chem. Scand. 19* (1965) 2285.
[119] M. Lundberg, *Acta Chem. Scand. 19* (1965) 2274.
[120] H.-G. von Schnering. L. Aleandri, *J. Less-Common Met.* in press.
[121] R. Kipka, Hk. Müller-Buschbaum, *Z. Naturforsch. B 31* (1976) 1067.
[122] R. Kipka, Hk. Müller-Buschbaum, *Z. Naturforsch. B 32* (1977) 121.
[123] W. Leib, *Diplomarbeit*, Universität Kiel (1983).
[124] W. Gutau, Hk. Müller-Buschbaum, *J. Less-Common. Met. 152* (1989) L 11.
[125] M. T. Weller, D. R. Lines, *J. Chem. Soc. Commun. 1989*, 484.
[126] E. F. Paulus, G. Miehl, H. Fueß, I. Yehia, U. Löchner. *J. Solid State Chem.* in press.
[127] C. Müller, *Diplomarbeit*, Universität Kiel (1989)

[128] L. Er-Rakho, C. Michel, B. Raveau, *J. Solid State Chem. 73* (1988) 514.
[129] Y. Tokura, J. B. Torrance, A. I. Nazal, T. C. Huang, C. Ortiz, *J. Am. Chem. Soc. 109* (1987) 7555.
[130] N. Murayama, S. Sagakuchi, R. Wakai, E. Sudo, A. Tsuzuki, Y. Torii. *Jpn. J. Appl. Phys. Part 2 27* (1988) L 55.
[131] J. Y. Lee, J. S. Kim, J. S. Swinnea, H. Steinfink, *J. Solid State Chem. 84* (1990) 335.
[132] C. Michel, L. Er-Rakho, M. Hervieu, J. Pannetier, B. Raveau, *J. Solid State Chem. 68* (1987) 143.
[133] U. Geiser, L. C. Porter, H. H. Wang, T. A. Allen, J. M. Williams. *J. Solid State Chem. 73* (1988) 243.
[134] T. Sowa, M. Hiratani, K. Miyauchi, *J. Solid State Chem. 84* (1990) 178.
[135] S. N. Ruddlesden, P. Popper. *Acta Crystallogr. 11* (1958) 54.
[136] N. Nguyen, L. Er-Rakho, C. Michel, J. Choisnet, B. Raveau, *Mater. Res. Bull. 15* (1980) 891.
[137] N. Nguyen, J. Choisnet, B. Raveau, *Mater. Res. Bull. 17* (1982) 567.
[138] K. Mader, Hk. Müller-Buschbaum. *Z. Anorg. Allg. Chem. 559* (1988) 89.
[139] A. Lalla, Hk. Müller-Buschbaum, *Rev. Chim Miner. 24* (1987) 605.
[140] A. Lalla, Hk. Müller-Buschbaum, *Z. Anorg. Allg. Chem.*, in press.
[141] R. Vogt, Hk. Müller-Buschbaum, *Z. Anorg. Allg. Chem.*, in press.
[142] D. Mercurio-Lavaud, B. Frit, *Acta Crystallogr. B29* (1973) 2737.
[143] J. R. Rea, E. Kostiner, *J. Solid State Chem. 7* (1973) 17.
[144] J. Galy, D. Lavaud, *Acta Crystallogr. B27* (1971) 1005.
[145] W. Gutasu, Hk. Müller-Buschbaum, *Z. Anorg. Allg. Chem. 582* (1990) 21.
[146] St. Schiffler, Hk. Müller-Buschbaum, *Z. Anorg. Allg. Chem. 540/541* (1986) 243.
[147] J. Aride, S. Flandroise, M. Taibi, M. Boukhari, M. Drillon, J. L. Soubeyroux, *Solid State Commun. 72* (1989) 459.
[148] R. Vogt, Hk. Müller-Buschbaum, *Z. Anorg. Allg. Chem.*, in press.
[149] C. Calvo, R. Faggiani, *Acta Crystallogr. B31* (1975) 603.
[150] D. Mercurio-Lavaud, B. Frit, *C. R. Acad. Sci. Ser. C 277* (1973) 1101.
[151] R. Vogt, Hk. Müller-Buschbaum, *Z. Anorg. Allg. Chem.*, in press.
[152] L. Kihlborg, R. Norresham, B. Olivecrona, *Acta Crystallogr. Sect. B27* (1971) 2066.
[153] L. Katz, A. Kasenally, L. Kihlborg, *Acta Crystallogr. Sect. B27* (1971) 2071.
[154] S. C. Abrahams, J. L. Bernstein, P. B. Jamieson, *J. Chem. Pys. 48* (1968) 2619.
[155] J. M. Longo, P. M. Raccah. *J. Solid State Chem. 6* (1973) 526.
[156] J. P. Attfield, G. Ferey, *J. Solid State Chem. 80* (1989) 112.
[157] B. Grande, Hk. Müller-Buschbaum, *Z. Anorg. Allg. Chem. 417* (1975) 68.
[158] B. Grande, Hk. Müller-Buschbaum, *Z. Anorg. Allg. Chem. 433* (1977) 152.
[159] B. Grande, Hk. Müller-Buschbaum, *Z. Anorg. Allg. Chem. 429* (1977) 88.
[160] L. L. Miller, X. L. Wang, S. X. Wang, C. Stassis, D. C. Johnston, J. Faber Jr., C.-K. Loong, *Phys. Rev. B41* (1990) 1921.
[161] D. Reinen, H. Weitzel, *Z. Anorg. Allg. Chem. 424* (1976) 31.
[162] S. Siegel, H. R. Hoekstra, *Acta Crystallogr. B24* (1968) 967.
[163] W. Gutau, *Dissertation*, Univ. Kiel (1990).
[164] J. R. Rea, P. W. Bless, E. Kostiner. *J. Solid State Chem. 5* (1972) 446.
[165] B. Chamberland, *J. Solid State Chem. 1* (1970) 138.
[166] R. D. Shannon, C. Calvo, *Acta Crystallogr. B29* (1973) 1338.
[167] A. Bystroem, G. Hoek, B. Mason. *Arkiv Kemi Min. Geolog. B15* (1942) 1.
[168] Noureddin-Habibi, *Bull. Soc. Chim. Fr. 1976* (1976) 77.
[169] Y. Grinetti, *Bull. Soc. Chim. Belg. 63* (1954) 209.
[170] H. Voellenkle, A. Wittmann, H. Nowotny, *Monatsh. Chem. 98* (1967) 1352.
[171] J. C. Joubert, J. C. Grenier, A. Durif, *C. R. Hebd. Seances Acad. Sci. 260* (1965) 2472.
[172] A. Durif, J. C. Grenier, J. C. Joubert, Duc-Tran-Qui, *Bull. Soc. Fr. Mineral Cristallogr. 89* (1966) 407.
[173] C. Calvo, D. Manolescu, *Acta Crystallogr. B29* (1973) 1743.
[174] J. Galy, D. Lavaud, A. Casalot, P. Hagenmuller, *J. Solid State Chem. 2* (1970) 531.
[175] R. D. Shannon, C. Calvo, *Canad. J. Chem. 50* (1972) 3944.
[176] C. Greaves, P. R. Slater, *Solid State Commun. 73* (1990) 629.
[177] E. Gebert, L. Kihlborg, *Acta Chem. Scand. 23* (1969) 221.
[178] H.-P. Christian, Hk. Müller-Buschbaum, *Z. Naturforsch B29* (1974) 713.
[179] T. Popp, M. Hartweg, H.-G. von Schnering, *Z. Kristallogr. 286* (1988) 238.

Chemical Reactions in the Manufacture of Waveguides for Long Distance Optical Data Transmission

By Michael Binnewies,* Marion Jerzembeck, and Andreas Kornick

Dedicated to Professor Hans Georg von Schnering on the occasion of his 60th birthday

One of the modern high technologies which has advanced enormously in the last few years is glass fiber technology. This is used in the manufacture of glass fibers for lighting purposes and for the optical transfer of analog and digital data with a high transfer density. The technical demands made on the glass fibers required for data transfer, the optical waveguides, are extremely high and are already fulfilled to a large extent by industry. At present about four million kilometers of fiber, worth ca. 800 million DM are produced worldwide (10% in the Federal Republic of Germany). Numerous chemical processes take place during the manufacture of optical waveguides. However, in contrast both to the high and constantly growing demands on the quality and to the increasing production volume of such fibers, little is in fact known about the reactions involved. The present article will attempt to develop a picture of the multifarious reactions occurring in the course of this technical process on the basis of literature data and our own studies.

1. Introduction

The transmission of analog, and in particular digital signals at a high spatial and temporal information density has been of rapidly growing importance in the past few years. Classical metallic conductors are subject to physical limits as far as the maximum information density which can be transmitted is concerned. Much higher information densities should in principle be achievable when optical communication media are used. The prerequisites for an effective transfer of information with the aid of light are:

1. Powerful transmitters.
2. Materials which are capable of fast modulation of the light waves.
3. Transfer media which permit the transmission of the modulated light waves across long distances with as low a degree of attenuation as possible.
4. Sensitive and fast light detectors.

Scientific progress in solid-state chemistry and physics during the last 20 years has played a decisive role in the development, manufacture and in particular in the *understanding* of the materials referred to under 1, 2 and 4. However, the transfer medium, the optical waveguide, has been brought to an exemplary state of technical perfection in a manner which is basically empirical (though by no means less effective!); the term "empirical" refers not to the well-known *physical* basis of this technology but to the extremely complex *chemical* reactions occurring during the manufacturing processes. It is however by no means unknown in history for technologies to undergo purely empirical development. The best-known example is the history of metallurgy, in the beginnings of which our ancestors were able to obtain metals from oxide minerals and coal without knowing anything of the chemistry involved (to say nothing of the Boudouard equilibrium!). The heretical postulate which could be put forward at this juncture is: *research is not necessary*. In the case of many technically manufactured materials the scientist is justifiably still interested even today in the material itself, while the processes by which it is formed are of only minor interest. The relationships between the properties and the genesis of a material are often studied only empirically in the absence of parallel studies which can lead to an understanding of the chemical mechanisms involved in their formation.

[*] Prof. Dr. M. Binnewies, Dipl.-Chem. M. Jerzembeck, Dipl.-Chem. A. Kornick
Institut für Anorganische Chemie und Analytische Chemie der Universität Albertstrasse 21, W-7800 Freiburg (FRG)

1.1. The Physical Principle of the Optical Waveguide

The purpose of the present article is not to present the physical background of light propagation in optical waveguides in detail but to investigate the chemical processes involved in their manufacture. However, a brief look at the physical principle[1] appears imperative in order that we can understand why "chemistry" is in fact necessary here at all.

When a ray of light passing through a medium of refractive index n_1 is incident on a medium of lower refractive index n_2 ($n_1 > n_2$) at an angle of incidence below a certain limiting value it will undergo total reflection, i.e. it cannot leave the medium. Thus if it is possible to produce a transparent rod consisting of a core of refractive index n_1 and a coating of refractive index n_2, light entering the core of the rod at one end will exit at the other end without being able to leave the rod sideways at any stage; this will be the case even when the rod is bent. Such a rod can be easily prepared by fusing a glass tube (n_2) on to a glass rod (n_1) and readily be drawn out to give a thin filament without any appreciable change in the refractive index profile, so that the optical properties remain unchanged. A so-called step-index fiber in which the refractive index changes in a stepwise manner over the fiber cross-section (Fig. 1a) does however have one principle disadvantage which makes a high transmission density impossible; this is the dispersion (for details see Ref. [2]). One of the important points here is that light pulses which enter an optical waveguide can have differing transit times: a pulse which enters exactly parallel to the fiber axis will in an ideal case be able to exit the fiber without undergoing

reflection (assuming the fiber to be linear). However, a pulse which is subject to repeated reflection will traverse a longer path and will thus exit the fiber with a certain small time delay. This leads to a broadening of the output signal with respect to the input signal and thus a priori to a lower transmission density. These differences in the transit time can be considerably reduced if the refractive index does not vary in a stepwise manner across the fiber diameter but decreases from the fiber center to its boundary according to a certain predetermined parabolic function (Fig. 1 b). In this case the

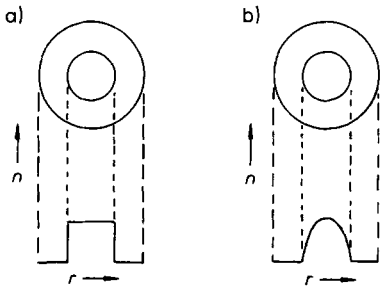

Fig. 1. Schematic representation of the variation of the refractive index across the fiber diameter in step index fibers (a) and gradient fibers (b).

light pulse which passes through the center of the fiber without undergoing reflection is slowed down by the higher refractive index (i.e. by the reduced light velocity) so that differences in transit time can be eliminated to a large extent. Such a fiber, known as a gradient fiber, can of course not be obtained simply by fusing a rod and a tube together.

2. The Internal Coating Process for the Manufacture of Gradient Fibers

Initial attempts to obtain gradient fibers involved the application of glass-forming powder layers of continually increasing refractive index to the inner surface of a quartz tube; the powder layers were subsequently fused to the quartz tube, and the blank thus prepared was then allowed to melt under controlled conditions to give a rod which could be pulled out to give a fiber. However, this process could not be developed to a stage suitable for commercial manufacture.

The much more successful processes used today involve the deposition from the gas phase of glass-forming oxides of higher refractive index.

The starting material is a tube made of high-purity quartz (external diameter ca. 3 cm, length ca. 2 m). A stream of oxygen containing $SiCl_4$ vapor is passed through the rotating tube. Dopant materials such as $GeCl_4$, BCl_3 and $P(O)Cl_3$ are added to this gas stream at concentrations which can be metered and varied exactly according to a predetermined program.[3] When the necessary energy of activation is applied, the reaction of the oxygen with the volatile halides or oxide halides of the elements silicon, germanium, boron and phosphorus leads to the formation of the oxides of these elements; these are deposited as solids on the inner surface of the quartz tube and fuse with it at high temperatures. Figure 2 shows the nature of the industrial process. The gas

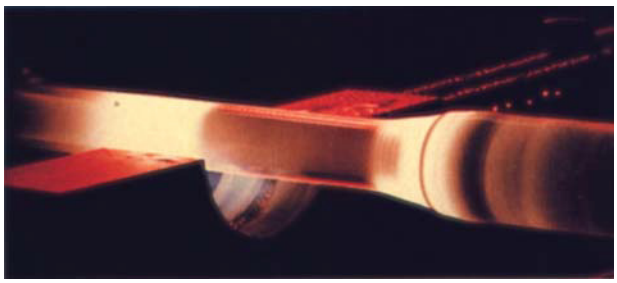

Fig. 2. Manufacture of the blanks for optical waveguides. The photograph shows a rotating glass tube through which the reaction mixture is passed. The tube is heated by oxyhydrogen burners which are slowly moved parallel to the axis of rotation of the tube during the process, which lasts several hours; an even deposition is thus achieved along the whole length of the tube.

mixture enters the quartz tube from the left and is heated by a battery of oxyhydrogen burners. The deposition of the solids occurs within and immediately subsequent to the zone of heating.

Variation of the concentrations of the added dopant substances permits the predetermination and continual variation of the refractive index of the deposited layers. Such a CVD (*C*hemical *V*apor *D*eposition) process makes it possible to obtain the required refractive index profile. When this goal has been achieved, the tube is fused at high temperatures to give a rod, from which a fiber can be drawn which has the originally constructed refractive index profile. Such a blank affords ca. 50 km of optical waveguide material.

Michael Binnewies, who was born in 1947 in Hagen/Westfalen (FRG), studied chemistry at the University of Münster, where he gained his Diploma and thereafter his doctorate in 1973 under the supervision of Harald Schäfer. He then spent a few years doing research into the development of mass spectrometric measuring techniques for the investigation of chemical transport reactions. His current research interests focus on high-temperature reactions, plasma chemistry, and halogen compounds of semi- and non-metals. After continuing his researches at the Max-Planck-Institut für Festkörperforschung, Stuttgart (1979), he returned to Münster, where he habilitated in 1985. In 1988 he accepted the offer of a professorial chair at the University of Freiburg.

Figure 3 shows a raster electron microscope picture of the end face of such a fiber. The deposited layers can be seen clearly within the higher-refracting core of the fiber. The activation of the required chemical reaction can be carried

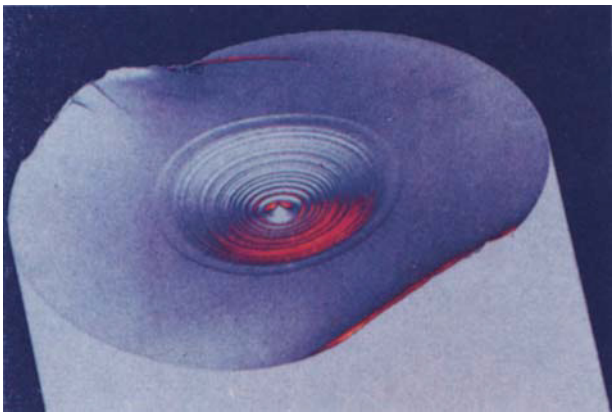

Fig. 3. Raster electron microscope picture of the end face of an optical waveguide. The external diameter of the fiber is ca. 120 μm.

out either thermally ($T > 1300$ K) or by means of the application of a non-isothermal plasma.

3. Chemical Reactions

The chemical reactions occurring in the course of the process described seem at a first glance to be simple [Eq. (a)–(d)]. All these reactions are exothermic, the equilibrium constants are larger than unity even at higher temperatures (except for (b)), ΔG^0 is negative (except for (b) above 1200 K). Some numerical values are collected in Table 1. The reactions (a)–(d), like all reactions involved in CVD processes,

$$SiCl_4 + O_2 \rightleftharpoons SiO_2 + 2Cl_2 \quad (a)$$

$$GeCl_4 + O_2 \rightleftharpoons GeO_2 + 2Cl_2 \quad (b)$$

$$2BCl_3 + 1.5O_2 \rightleftharpoons B_2O_3 + 3Cl_2 \quad (c)$$

$$4POCl_3 + 3O_2 \rightleftharpoons P_4O_{10} + 6Cl_2 \quad (d)$$

describe processes in which solids separate from a gaseous phase; thus molecular precursors undergo conversion into infinite three-dimensional lattices (the fact that the oxides are deposited as a glass rather than in a crystalline form is of no importance for the following discussion). Such processes cannot in fact be so simple as the equations (a)–(d) would lead one to expect. A number of very basic questions must be addressed when we consider how a solid is formed starting from a gas phase (or from a solution or melt): are detectable intermediates formed and what are their nature? What are the thermodynamic properties of the system? How does nucleation occur starting from such a gas phase? When can one already speak of the existence of a solid and when must one still speak of a molecule? Questions of this and similar types are presently being addressed and discussed by many groups working with "simpler" systems such as metal vapors (cluster formation in molecular beams).

In the following discussion we shall deal with the above reactions of the non-metal halides and oxide halides of silicon, germanium, and phosphorus, and attempt to find answers to some of the above questions.

Table 1. Selected thermodynamic data of the reactions (a)–(d).

Reaction	ΔH^0_{298} [kJ mol^{-1}]	ΔS^0_{298} [J K^{-1} mol^{-1}]	K_{1000}	K_{1500}	ΔG_{1200} [kJ mol^{-1}]
(a)	−242.7 [4]	−40.1 [4]	3.8×10^{10}	2.3×10^{6}	−194.6
(b)	−79.9 [4, 5]	−67.8 [4, 5]	4.3	0.17	1.5
(c)	−456.9 [4, 5]	−165.1 [4, 5]	1.7×10^{15}	1.9×10^{7}	−258.8
(d)	−770.7 [4]	−349.9 [4]	9.6×10^{21}	1.45	−350.8

3.1. The Reactions of $SiCl_4$ and $GeCl_4$ with O_2

The first studies of these apparently simple reactions were carried out long before their future technical importance could be imagined. In 1868 *Friedel* and *Ladenburg* reported the formation of Si_2OCl_6 during the reaction of $SiCl_4$ with O_2 in a porcelain tube heated by burning coke.[6] *Troost* and *Hautefeuille* obtained mixtures of higher molecular weight chlorosiloxanes in a similar manner a few years later.[7, 8] A series of further studies of the reaction followed in which the original results were confirmed and supplemented.[9, 10] A large number of related chlorosiloxanes have been described[11–13] and in part structurally characterized[11] in recent years. The common feature of all these reports is that the compounds described were prepared in the reaction between $SiCl_4$ and O_2 at high temperatures (around 1300 K) or in a gas discharge (plasma), i.e. in the same reaction and under similar conditions as those which are so important for the technology of the manufacture of optical waveguides. The chlorosiloxanes presently known are collected in Table 2. Thus, reaction (a) apparently does not by any means occur as formulated above via the formation and separation of solid SiO_2, but in a much more complex manner. How can we understand the formation of such a large number of compounds? Let us start by considering their structures. The plethora of siloxanes listed in Table 2 can be divided into four groups:

Table 2. Chlorosiloxanes observed in the plasmachemically and thermally activated reactions of $SiCl_4$ with O_2.

Formula	Plasma-chemical	Thermal	Formula	Plasma-chemical	Thermal
Si_2OCl_6	[12, 13]	[6], [9–13]	$Si_4O_5Cl_6$	[12, 13]	
$Si_3O_2Cl_8$	[12, 13]	[10–13]	$Si_5O_6Cl_8$	[12, 13]	[7, 8]
$Si_4O_3Cl_{10}$	[12, 13]	[10–13]	$Si_6O_8Cl_8$		[11, 13]
$Si_5O_4Cl_{12}$	[12, 13]	[10, 12]	$Si_6O_7Cl_{10}$	[13]	[11, 13]
$Si_6O_5Cl_{14}$	[12, 13]	[10]	$Si_7O_8Cl_{12}$		[13]
$Si_7O_6Cl_{16}$	[12]	[10]	$Si_7O_9Cl_{10}$		[13]
$Si_3O_3Cl_6$	[12, 13]	[11–13]	$Si_8O_{11}Cl_{10}$		[12]
$Si_4O_4Cl_8$	[12, 13]	[9–13]	Si_3OCl_8	[12]	
$Si_5O_5Cl_{10}$	[12, 13]	[11, 12]	Si_4OCl_{10}	[12]	
$Si_6O_6Cl_{12}$	[12, 13]	[12]	$Si_4O_2Cl_{10}$	[12]	
$Si_7O_7Cl_{14}$	[12]		$Si_5O_3Cl_{12}$	[12]	

Group 1: $Si_nO_{n-m}Cl_{2n+2}$ (n = 3–5, m = 2, 3)
Group 2: $Si_nO_{n-1}Cl_{2n+2}$ (n = 2–7)
Group 3: $Si_nO_nCl_{2n}$ (n = 3–7)
Group 4: $Si_nO_{n+m}Cl_{2n-2m}$ (n = 4–8, m = 1–3)

The siloxanes thus classified differ in their oxygen content, which increases on going from Group 1 to Group 4. This has consequences for the structure of the compounds:

Group 1. The composition indicates that Si–Si bonds must be present.[13] These siloxanes have only been observed in plasma-activated reactions, and they are of no importance for the following discussion.

Group 2. The compounds in this large group are built up from chains in which the Si atoms are bridged by oxygen atoms.[11, 14, 15]

Group 3. In most cases these molecules have closed monocyclic structures, although monocyclic arrangements with an exocyclic $SiCl_3$ group bonded via an oxygen bridge are known.[11] The molecular structure of $Si_4O_4Cl_8$ was determined by X-ray crystallography[16] (Fig. 4).

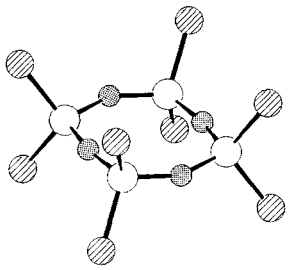

Fig. 4. Molecular structure of $Si_4O_4Cl_8$. Open circles are Si atoms, dotted are O atoms, and shaded are Cl atoms.

Group 4. Chlorosiloxanes which contain more oxygen than silicon atoms must be oligocyclic in nature. Bicyclic structures result for m = 1, tricyclic for m = 2,[11] etc. The limiting case in this series (n = m) is SiO_2. An initial relationship between the chlorosiloxanes and solid SiO_2 thus becomes clear.

An answer to the question as to the stability of the chlorosiloxanes is given by mass spectrometric studies of the reaction of $SiCl_4$ with O_2[12] and the thermolysis of Si_2OCl_6.[13] These have shown that the proportion of the siloxanes in the various groups changes greatly as a function of the reaction temperature (Fig. 5): the amount of chain-like siloxanes decreases very rapidly with increasing temperature, while the concentrations of the monocyclic and in particular of the oligocyclic siloxanes increase. Thus, an increase in the temperature accelerates reactions in which relatively oxygen-poor open chain siloxanes such as Si_2OCl_6 are converted into oxygen-richer compounds. This is shown by the representative reactions described by Equations (e) to (g).

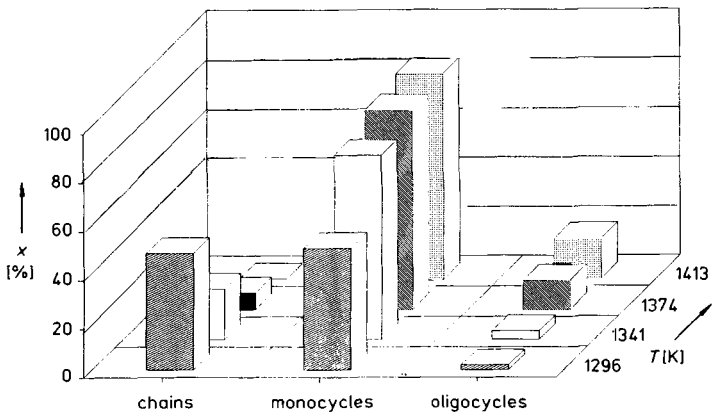

Fig. 5. Temperature dependence of the distribution of the chlorosiloxanes observed during the pyrolysis of Si_2OCl_6.

$$4\,Si_2OCl_6 \rightleftharpoons Si_4O_4Cl_8 + 4\,SiCl_4 \quad (e)$$

$$8\,Si_2OCl_6 \rightleftharpoons Si_6O_8Cl_8 + 10\,SiCl_4 \quad (f)$$

$$11\,Si_2OCl_6 \rightleftharpoons Si_8O_{11}Cl_{10} + 14\,SiCl_4 \quad (g)$$

The limiting case of such reactions is the decomposition of a siloxane to give the binary compounds $SiCl_4$ and SiO_2 [Eq. (h)]:

$$2\,Si_2OCl_6 \rightleftharpoons SiO_2 + 3\,SiCl_4 \quad (h)$$

What is the enthalpy and entropy balance of these reactions? Since the total number of Si–O and Si–Cl bonds remains unchanged, the reaction enthalpies are expected to be close to zero,[12, 13] as the bonding situation in the starting materials and products is very similar (see Section 3.2). However, increasing oxygen content and decreasing chlorine content in a siloxane corresponds to increasing stabilization. This can be demonstrated on the basis of the bond energies of the Si–O and Si–Cl bonds: Si–O bond 464.8 kJ/bond (in SiO_2, data from Ref. [4]), Si–Cl bond 399.5 kJ/bond (in $SiCl_4$, data from Ref. [4]). The reactions (e)–(h) thus involve the formation of a product with a lower enthalpy content (oxygen-richer siloxane and SiO_2 respectively) and a product with higher enthalpy content ($SiCl_4$), so that the energy balance will be around 0 kJ.

However, all four reactions involve an increase in the number of moles present, so that there is a gain in entropy. This entropy effect favors the formation of the oxygen-richer reaction products, and in particular that of the oxygen-richest compound SiO_2. It can thus be concluded that all the chlorosiloxanes must be metastable with respect to decomposition to give SiO_2 and $SiCl_4$. However, the formation of detectable amounts of SiO_2 is only observed above ca. 1500 K.[12] The origin of this reaction inhibition presumably lies in the fact that the formation of the SiO_2 structure must be a kinetically extremely complex process which requires a high energy of activation.

The increasing degree of formation of oxygen-rich siloxanes with increasing temperature signifies in several respects that these compounds are continually becoming more "SiO_2-like":

1. More and more Si–O bonds are formed.
2. The molecular structures become increasingly more complex (one-dimensional Si–O skeletons in the chain-like, two-dimensional in the monocyclic, and three-dimensional in the oligocyclic siloxanes).
3. The enthalpy content steadily approaches that of SiO_2.

Let us return to the technology of the optical waveguide manufacture (thermal activation of the reaction) and attempt to develop a picture of the reaction scheme on the basis of the above discussion: the gas mixture $SiCl_4/O_2$ (+ dopant materials) enters the glass tube at room temperature and is heated steadily as it approaches the heating zone. The formation of halosiloxanes, mainly Si_2OCl_6, starts at

around 1300 K. However, this cannot be the first step in the long reaction sequence which leads to solid SiO_2, as it would require a thermolecular reaction step in which two molecules of $SiCl_4$ and one molecule of oxygen combine with elimination of Cl_2. The primary formation of a reactive molecule appears much more likely, the most probable candidate being $Si(O)Cl_2$. Nothing is presently known with respect to the existence of this molecule in the gas phase; however, it has been detected in a helium-cooled argon matrix,[17] so that its intermediate formation in the gas phase also appears likely. The formation of cyclic siloxanes $Si_nO_nCl_{2n}$ in higher concentrations thus points to the formation of $Si(O)Cl_2$, since the former are oligomers of this reactive molecule and could be formed from it via oligomerization reactions. The formation of open-chain siloxanes such as Si_2OCl_6 from a reaction between $Si(O)Cl_2$ and excess $SiCl_4$ is also plausible. The formation of the oligocyclic siloxanes is most probably due to the entropically favored decomposition (see above) of the monocyclic compounds into oxygen-richer oligocycles and oxygen-poorer chain compounds or $SiCl_4$ (see above); other reaction pathways are of course possible. There are in principle two types of reaction which could in the final analysis be responsible for the deposition of SiO_2: either the decomposition of oligocyclic chlorosiloxanes which are presumably oxygen-rich and already contain several Si–O bonds to give the binary components SiO_2 and $SiCl_4$ (or oxygen-poorer siloxanes) or an exothermic reaction between chlorosiloxanes and oxygen via reactive intermediates which eventually leads to the formation of SiO_2 and Cl_2.

Figure 6 shows one of many possible routes from molecular $SiCl_4$ to solid SiO_2; this includes a number of the compounds listed in Table 2. Without any doubt the higher molecular weight siloxanes such as $Si_8O_{11}Cl_{10}$ are of particular interest in this connection; one of its many possible isomers is shown in Figure 6. A small detail of the SiO_2 structure, two SiO_4 tetrahedra joined via a common apex, is already preformed. The formation of solid SiO_2 from such molecules appears plausible and should be kinetically readily achievable. The formation of solid SiO_2 from $Si_8O_{11}Cl_{10}$ requires the formation of oxygen-poorer siloxanes (or $SiCl_4$) which can then re-enter the reaction cycle. The chlorosiloxanes formed in a stepwise manner can thus be regarded as intermediates in a chemical reaction between simple molecules ($SiCl_4$ and O_2) which eventually lead to the formation of a three-dimensional solid structure (including glasses). The formation of the Si–O bonds occurs in a stepwise manner: one or two Si–O bonds per Si atom in the chain molecules, two Si–O bonds in the monocycles and two, three (for the bridgehead Si atoms) or even four Si–O bonds ($Si_8O_{11}Cl_{10}$) in the oligocyclic siloxanes.

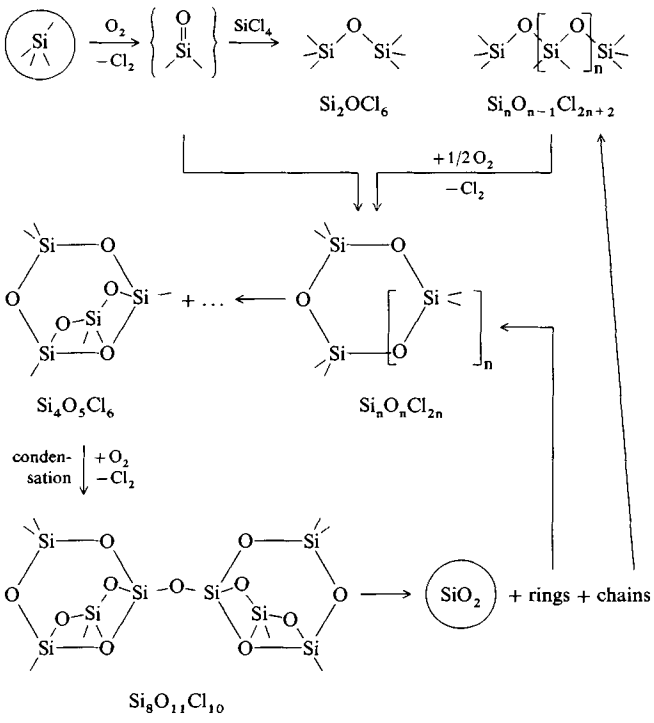

Fig. 6. Reaction scheme for a possible course of the reaction between $SiCl_4$ and O_2 to yield SiO_2.

Thus the system Si/Cl/O offers fascinating possibilities for studying the stepwise transition from molecular compounds to solids and thus for increasing our understanding of reactions of this type in which solids are deposited from the gas phase. The formation of this large variety of chlorosiloxanes (which are thermodynamically unstable with respect to SiO_2 and $SiCl_4$) is certainly not fortuitous; their stepwise formation is possibly a necessary prerequisite for the construction of an SiO_2 structure.

In contrast to the reaction pathways suggested here, other intermediates and mechanisms have been discussed in the literature. Thus in connection with optical waveguide technology *McAfee, Laudise* and *Hozack* have published a detailed paper dealing with the thermodynamics of gaseous species in the system Si/Ge/O/Cl; their discussion mainly involves the existence of lower (oxidation state + 2) halides and oxides of Si and Ge (i.e. molecules of very low molecular weight) in the temperature range 1400–4000 K.[18] However, the evidence presented above shows clearly that the deposition of SiO_2 is almost complete at temperatures of ca. 1500 K, so that a discussion of the composition of the gas phase at temperatures far above 1500 K does not appear particularly useful. In addition, thermodynamically unstable compounds such as the siloxanes discussed above are naturally not amenable to thermodynamic calculations.

In contrast to the reaction between silicon tetrachloride and oxygen, which has been studied in great detail, the literature contains very little information on the analogous reaction of germanium tetrachloride. Ge_2OCl_6 has been described as a reaction product.[19, 20] Our own studies of this reaction under the conditions of low-pressure gas discharge have also demonstrated the formation of the additional chlorogermoxanes $Ge_3O_2Cl_8$, $Ge_4O_3Cl_{10}$, $Ge_3O_3Cl_6$, $Ge_4O_4Cl_8$, $Ge_5O_5Cl_{10}$ and $Ge_4O_5Cl_6$.[21] This indicates that the system Ge/O/Cl is very similar to the system Si/O/Cl described above.

3.2. The Reaction of BCl_3 with O_2

Studies of the equilibrium between liquid B_2O_3 and BCl_3 vapor at temperatures above 500 K have demonstrated the existence of the cyclic chloroboroxines $B_3O_3Cl_3$ and $B_4O_4Cl_4$ as well as of BOCl, which is formed at measurable

concentrations at higher temperatures (> 1200 K).[22-24] The thermodynamic data determined indicate that at temperatures above 1000 K these compounds should be formed in a direct reaction between BCl_3 and O_2, i.e. during reactions of $SiCl_4/GeCl_4/BCl_3/P(O)Cl_3/O_2$-mixtures occurring during the manufacture of glass fibers. In contrast to the behavior of the siloxanes, the decomposition of (for example) $B_3O_3Cl_3$ into the binary compounds B_2O_3 (liquid) and BCl_3 (gas) is not expected. In agreement with this hypothesis the formation of $B_3O_3Cl_3$ has been detected spectroscopically in the course of the reaction of BCl_3 with O_2.[25] Studies of this reaction under plasmachemical conditions show that apart from the cyclic boroxines the linear molecules B_2OCl_4 and $B_3O_2Cl_5$ are also formed.[26] Oligocyclic analogues of the siloxanes are unknown in the system B/O/Cl. If the decomposition of the chloroboroxines cannot lead to the formation of B_2O_3, the deposition of which certainly occurs, the formation of the boroxide must occur via another reaction pathway. This can only involve the reaction of the initially formed boroxines with oxygen, which is present in excess. The thermodynamic data[4] for such reactions do indeed lead us to expect that the deposition of B_2O_3 will occur. Thus the reaction of $B_3O_3Cl_3$ with O_2 as shown in Equation (i) is strongly exothermic ($\Delta H^0_{298} = -551.7\ kJ\,mol^{-1}$,[4] though it is accompanied by an entropy loss ($\Delta S^0_{298} = -295.5\ J\,K^{-1}\,mol^{-1}$).[4]

$$2\ B_3O_3Cl_3\ (gaseous) + 1.5\ O_2 \rightleftharpoons 2\ B_2O_3\ (liquid) + 3\ Cl_2 \qquad (i)$$

These values lead to equilibrium constants much greater than unity even at high reaction temperatures.

Why is the thermal behavior of the gaseous chlorosiloxanes and chloroboroxines predicted on the basis of thermodynamics so different? To answer this question we shall take as an example the monocyclic compounds $Si_3O_3Cl_6$ and $B_3O_3Cl_3$ and their decomposition according to Equations (j) and (k) to give the binary compounds ($T > 1500$ K).

$$Si_3O_3Cl_6\ (gaseous) \rightleftharpoons 1.5\ SiO_2\ (solid) + 1.5\ SiCl_4\ (gaseous) \qquad (j)$$

$$B_3O_3Cl_3\ (gaseous) \rightleftharpoons B_2O_3\ (solid) + BCl_3\ (gaseous) \qquad (k)$$

Both reactions are expected to have low reaction enthalpies, since (with similar bonding conditions in starting materials and products) the number of element–oxygen and element–chlorine bonds remains unchanged (ΔH^0_{298} is unknown, $\Delta H^0_{298} = -42.9\ kJ\,mol^{-1}$[4]). The reason must thus lie in the entropy balance. Reaction (j) is expected to have a reaction entropy considerably larger than zero (see above), while for reaction (k), in which the number of moles is constant, there should be no great entropy change (experimental value: $\Delta S^0_{298} = -56.3\ J\,K^{-1}\,mol^{-1}$[4]). Thus, the different thermal behavior depends on the stoichiometry of the decomposition reactions of $B_3O_3Cl_3$ and $Si_3O_3Cl_6$ and the resulting difference in the entropy balance.

Attempts to obtain $B_3O_3Cl_3$ in the condensed phase have been unsuccessful; the main reason for this is also the change in the entropy balance of the decomposition reaction of hypothetical $B_3O_3Cl_3$ (solid, liquid) in favor of the decomposition products.

Since the thermodynamic data of several of the chloroboroxines formed in the system B/O/Cl are known, it is possible to discuss the relation between their stabilities and those of the starting material BCl_3 and the reaction product B_2O_3 [in the sense of Equation (c)]. The standard enthalpies of formation[4, 25, 26] of the compounds of interest here are plotted in Figure 7 against the quotients of the number of moles of B and O (as a measure of the composition of the compound). It is clear that the relationship between composition and energy content is almost linear. This shows that the bonding energies of the B–Cl bond in BCl_3 and of the B–O bond in B_2O_3 are almost the same as the corresponding bonding energies in the chloroboroxines. The replacement of

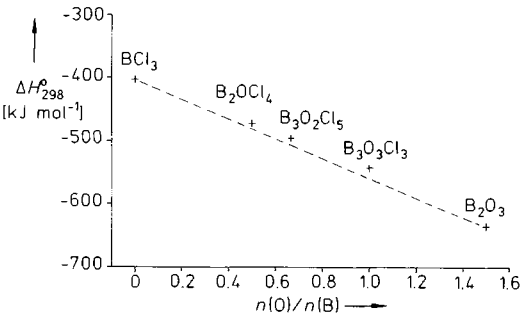

Fig. 7. Graphical representation of the enthalpy content of BCl_3, B_2O_3, B_2OCl_4, $B_3O_2Cl_5$ and $B_3O_3Cl_3$.

each B–Cl bond by a B–O bond corresponds to a stepwise approach to the thermodynamically stable final product B_2O_3 without any marked change in the bonding situation. Thus, from the thermodynamic point of view we can consider the formation of the chloroboroxines as initial steps towards the formation of B_2O_3. In this system the formation of a highly reactive molecule, here O=B–Cl, must also be considered as a possible first step; the oligomerization of this intermediate can lead to the formation of the cyclic boroxines,[24] while its reaction with excess BCl_3 makes possible the formation of B_2OCl_4 and longer chain analogues. Structural relationships between the molecular chloroboroxines and B_2O_3 are also evident, for example the tendency for the formation of chains and rings containing alternating O and B atoms which is also a feature of the structure of solid B_2O_3.

3.3. The Reaction between $POCl_3$ and O_2

Our own investigations into the plasma-activated reaction of PCl_3 with O_2[27] have demonstrated the formation of a

Table 3. Phosphorus oxychlorides observed in plasmachemically and thermally activated reactions.

Formula	Plasma-chemical	Thermal	Formula	Plasma-chemical	Thermal
$P_2O_3Cl_4$	[28]	[28–57]	$P_5O_6Cl_7$	[28]	[28, 36, 39]
$P_3O_6Cl_3$	[28]	[28, 36, 39, 40, 44, 46–48]	$P_6O_{13}Cl_4$	[28]	
			$P_6O_{12}Cl_6$	[28]	[28]
$P_3O_5Cl_5$	[28]	[28, 38, 39]	$P_6O_{11}Cl_8$	[28]	[28, 36]
$P_4O_9Cl_2$	[28]	[28]	$P_7O_{16}Cl_3$	[28]	
$P_4O_8Cl_4$	[28]	[28, 39]	$P_7O_{15}Cl_5$	[28]	[39]
$P_4O_7Cl_6$	[28]	[28, 36, 39]	$P_7O_{14}Cl_7$	[28]	
$P_5O_{11}Cl_3$	[28]	[39]	$P_8O_{17}Cl_6$	[28]	[39]
$P_5O_{10}Cl_5$	[28]	[28]			

large variety of phosphorus oxide chlorides.[28] The compounds detected in this reaction can also be obtained in the condensed phase from the reaction between P_4O_{10} and $POCl_3$ as well as from other reactions. They have been characterized by various spectroscopic (NMR, IR, Raman) and chromatographic techniques and in some cases structurally characterized. All the molecular oxide chlorides of phosphorus presently known which contain more than one P atom in the oxidation state + 5 are collected in Table 3. In analogy to the chlorosiloxanes these can be divided into several homologous series:

Group 1: $P_nO_{2n-1}Cl_{n+2}$ (n = 2–7)
Group 2: $P_nO_{2n}Cl_n$ (n = 3–7)
Group 3: $P_nO_{2n+1}Cl_{n-2}$ (n = 4–8)

In contrast to the situation in the siloxane series, the composition of the compounds does not permit us to draw unequivocal conclusions as to the structure of the compounds. Thus the members of Group 1 could be chain molecules, but there are also other possibilities: thus $P_4O_7Cl_6$ could also be an oligocyclic compound derived from P_4O_{10} by replacement of three terminal oxygen atoms by six chlorine atoms. Here we must refer to the experimental studies cited in Table 3. In analogy to the structural chemistry of the metaphosphates (the compounds discussed here correspond formally to the chlorides of the corresponding metaphosphates) we can expect the compounds in Group 2 to be monocyclic. However, oligocyclic compounds are also possible, at least in some cases. Thus while $P_4O_8Cl_4$ could be an eight-membered ring, a structure derived from P_4O_{10} by replacement of two terminal oxygen atoms by four chlorine atoms would also be in agreement with the structural chemistry of the phosphates. Group 3 must contain only oligocyclic compounds if we exclude structures in which a phosphorus atom is doubly bonded to two oxygen atoms. The literature contains no information regarding the thermodynamic stability of any of the compounds listed in Table 3. The most likely decomposition reaction involves the formation of P_4O_{10} and $POCl_3$, here demonstrated for the case of $P_5O_{10}Cl_5$ [Equation (l)]:

$$3\,P_5O_{10}Cl_5 \rightleftharpoons 2.5\,P_4O_{10} + 5\,POCl_3 \qquad (l)$$

Decomposition to give the binary components P_4O_{10} and PCl_5 (or PCl_3 and Cl_2) is not expected because of the extreme thermodynamic stability of $POCl_3$. The reaction enthalpy for the process described by (l) is unknown and cannot readily be estimated. The reaction entropy should however be clearly positive, so that we can assume that the decomposition products are thermodynamically favored. The compounds listed in Table 3 should thus be metastable. This is supported by reports[28, 44] in which the thermal instability of these oxide chlorides of phosphorus is described.

As in the system Si/O/Cl, metastable compounds are thus formed which can be regarded as intermediates in the reaction between $POCl_3$ and O_2 (the final product of this reaction in the manufacture of optical waveguides is certainly not molecular P_4O_{10} but compounds in which silicon atoms in SiO_2 are replaced by phosphorus, the excess positive charge being compensated by the incorporation of boron atoms at other positions in the lattice). The initial step in the long series of reactions leading to the deposition of the solid may well be the formation of PO_2Cl, which has been detected and characterized both in the gas phase by mass spectrometry[58] and by means of matrix spectroscopy[59] and photoelectron spectroscopy.[60] The formation of oligomers of this molecule ($P_nO_{2n}Cl_n$, n = 3–7) can be regarded as evidence for its primary formation.

3.4. Comments on the Incorporation of the Dopant Materials into the SiO_2 Matrix

In Sections 3.1–3.4 we have dealt separately with the chemical processes involved in the reactions between oxygen and the chlorides or oxide chlorides of silicon, germanium, boron and phosphorus. However, in the course of the technological application of these reactions in the manufacture of optical waveguides they will not occur in a spatially or temporally separated manner but simultaneously. The question thus arises as to the manner in which the dopants are incorporated into the SiO_2 glass occurs during the deposition of the solids are from the extremely complex gas phases present. Two basically different processes must be considered:

1. The oxides of the above elements are deposited in separate domains; the homogeneous distribution of the dopant substances occurs via diffusion processes.
2. The molecular "precursors" of the solids described above already contain the dopants in the form of "alien atoms".

It is of course not known whether these two possibilities are of any practical importance. However, since this is a question of scientific interest, we have carried out a series of experiments in which the plasma-activated reactions of oxygen with the mixtures $SiCl_4/GeCl_4$ and $SiCl_4/BCl_3$ were studied by mass spectrometry in order to clarify the situation regarding the possibility of the incorporation of "alien atoms" into the oxide halides of silicon. Since these gas phases naturally have enormously complex compositions, the analysis of the mass spectra obtained is difficult. It was however possible to identify the molecules $BSiOCl_5$, $BSi_2O_2Cl_7$, $SiGeOCl_6$, $Si_2GeO_2Cl_8$, $SiGe_2O_2Cl_8$ and $Si_2GeO_3Cl_6$ unequivocally.[21] This makes it clear that the incorporation of the alien atoms can in principle occur in the precursors of the solids. It can be assumed that both the above-mentioned possibilities for dopant incorporation will play a part in practice.

4. Summary and Future Prospects

The available information summarized above on the apparently very simple chemical reactions of elementary oxygen with the chlorides of silicon, germanium, boron and phosphorus which occur in the course of the manufacture of optical waveguides show clearly that the deposition of the solid oxides is preceded by the formation of a large number of oxide halides which can in several respects be regarded as precursor molecules of the oxides:

1. Their chemical compositions lie between those of the chlorides and the oxides, and are (in the case of the system $SiCl_4/O_2$ studied) strongly temperature-dependent in the

sense that the compounds become steadily oxygen-richer as the reaction proceeds (i.e. as the temperature increases).

2. The structural principles found in the oxides are already preformed in the oxide chloride molecules.
3. The thermodynamic stability of the oxide chlorides lies between those of the chlorides and the oxides.
4. Many of the oxide halides are formed even though they are thermodynamically unstable with respect to decomposition into the chloride and oxide. This can be explained on the basis that their intermediate formation is a necessary prerequisite for the construction of the solid oxide.
5. The primary formation of reactive, coordinatively unsaturated molecules ($SiOCl_2$, $GeOCl_2$, BOCl, PO_2Cl) is probable in all the cases discussed.

On the basis of the still very limited information presently available on the structures of the complex oxide chlorides it is possible to develop mechanisms which describe the transition from molecules to solids. These, although unconfirmed, appear reasonable in view of the establishment of the identities (and in many cases of the structures and stabilities) of the intermediately formed oxide chlorides. However, the enormously complex nature of the reactions involved makes it unlikely that it will become possible to obtain unequivocal evidence for the mechanisms discussed.

All the reactions described here lead to the deposition of oxides which are typical precursors of glasses. It should be noted that the information presently available indicates that the formation of polynuclear molecular oxide halides is limited to exactly these elements. This may be due to the fact that the latter have been the subject of particularly detailed studies, but it may also indicate that the prerequisites for the formation of such compounds are similar to those occurring during the formation of glasses (low coordination numbers, apical linking of the polyhedra).

The structural relationships between molecular compounds and "related" solids is by no means limited to the class of compounds described here. Thus for example we find details of the corresponding solid structures in many molecular cluster compounds.[61] A further impressive example is provided by the pyrolytic formation from $Si(CH_3)_4$ of a variety of carbosilanes, in which details of the lattice of the silicon carbide generated at high temperature are already preformed.[62]

Detectable unstable intermediates in which the final product of the reaction is already recognizable are also formed in other completely different reactions. Thus, *Goubeau* and *Keller* have demonstrated that the careful hydrolysis of BCl_3 leads to the formation of $B_3O_3Cl_3$,[63] i.e. exactly the same compound which is formed during the reaction between BCl_3 and O_2 in the gas phase at high temperatures. The formation of the siloxanes Si_2OCl_6, $Si_3O_2Cl_8$, $Si_4O_3Cl_{10}$, $Si_6O_2Cl_{14}$ and $Si_8O_3Cl_{18}$ was observed under analogous conditions during the hydrolysis of $SiCl_4$ and Si_2Cl_6 respectively.[64–66] It is thus clear that reactions can occur in a very similar manner even when they are carried out under such extremely different conditions. From this point of view it appears desirable to study the processes occurring during the hydrolysis of halides under the conditions described here as regards precursors (intermediates).

Numerous technical processes based on high-temperature reactions or on hydrolyses are carried out (successfully!) even though nothing is known about the course of the reactions involved. Monographs on industrial chemistry thus offer a rich source of impulses for scientific studies on the manner in which such reactions take place.

We thank the Deutsche Forschungsgemeinschaft and the Fonds der Chemischen Industrie for their support of our investigations. We also thank Kabelmetall Elektro, Stuttgart, for making available the photographs showing industrial processes and Dr. M. Wittmann of this company for valuable discussions and suggestions.

Received: December 3, 1990 [A 821 IE]
German version: *Angew. Chem. 103* (1991) 762
Translated by Professor *T. N. Mitchell*, Dortmund (FRG)

[1] Glass fibers used for the long distance optical data transmission are referred to as optical waveguides, while those used for lighting purposes are known as light-conducting fibers.
[2] P. Geittner, *Phys. Unserer Zeit 19* (1988) 37.
[3] BCl_3 has been replaced increasingly by Freon in recent years.
[4] M. W. Chase, C. A. Davies, J. R. Downey, D. J. Frurip, R. A. McDonald, A. N. Syverud, (JANAF Thermochemical Tables) *Phys. Chem. Ref. Data 14* (1985).
[5] I. Barin: *Thermochemical Data of Pure Substances*, VCH, Weinheim (1989).
[6] C. Friedel, A. Ladenburg, *Ann. Chem. Pharm. 147* (1868) 355.
[7] L. Troost, P. Hautefeuille, *Bull. Soc. Chim. Fr. 16* (1871) 240.
[8] L. Troost, P. Hautefeuille, *Ann. Chim. Phys. 7* (1887) 452.
[9] H. Reinboldt, W. Wisfeld, *Justus Liebigs Ann. Chem. 517* (1935) 198.
[10] W. C. Schumb, D. F. Holloway, *J. Am. Chem. Soc. 63* (1941) 2753.
[11] H. C. Marsmann, E. Meyer, *Z. Anorg. Allg. Chem. 548* (1987) 193.
[12] A. Kornick, M. Binnewies, *Z. Anorg. Allg. Chem. 587* (1990) 157.
[13] A. Kornick, M. Binnewies, *Z. Anorg. Allg. Chem. 587* (1990) 167.
[14] The relationships between the composition and the structure of the chlorosiloxanes described here are valid only if no Si–O double bonds are present.
[15] W. Arey, C. Glidewell, A. G. Robiette, G. M. Sheldrick, *J. Mol. Struct. 8* (1971) 413.
[16] D. Fenske, M. Jerzembeck, M. Binnewies, crystal structure analysis of $Si_4O_4Cl_8$, unpublished results.
[17] H. Schnöckel, *Z. Anorg. Allg. Chem. 460* (1980) 37.
[18] K. B. McAfee, R. A. Laudise, R. S. Hozack, *J. Lightwave Technol. 4* (1983) 555.
[19] R. Schwarz, P. W. Schenk, H. Giese, *Chem. Ber. 64* (1931) 362.
[20] P. Kleinert, D. Schmidt, H. J. Laukner, *Z. Anorg. Allg. Chem. 495* (1982) 157.
[21] A. Kornick, M. Binnewies, unpublished results.
[22] J. Blauer, M. Farber, *J. Chem. Phys. 39* (1963) 158.
[23] R. F. Porter, S. K. Gupta, *J. Phys. Chem. 68* (1964) 280.
[24] M. Farber, *Trans. Faraday Soc. 60* (1964) 301.
[25] D. J. Knowles, A. S. Buchanan, *Inorg. Chem. 4* (1965) 1799.
[26] M. Binnewies, *Z. Anorg. Allg. Chem. 571* (1989) 7.
[27] The reaction between PCl_3 and O_2 results in the formation of high concentrations of $P(O)Cl_3$ [28]. The products obtained from the reaction mixture PCl_3, $P(O)Cl_3$, O_2 should thus correspond to those of the reaction between $P(O)Cl_3$ and O_2.
[28] H. Bange, M. Binnewies, unpublished results.
[29] G. Müller-Schiedmayer, H. Harnisch, *Z. Anorg. Allg. Chem. 333* (1964) 260.
[30] R. Klement, K. H. Wolf, *Z. Anorg. Allg. Chem. 282* (1955) 149.
[31] A. Geuther, A. Michaelis, *Ber. Dtsch. Chem. Ges. 4* (1871) 766.
[32] R. Klement, O. Koch, K. H. Wolf, *Naturwissenschaften 41* (1954) 139.
[33] R. Klement, E. Rother, *Naturwissenschaften 45* (1958) 489.
[34] C. Oddo, *Gazz. Chim. Ital. 29* (1899) 330.
[35] P. C. Crofts, I. M. Downie, R. B. Heslop, *J. Chem. Soc.* (1960) 3673.
[36] H. Grunze, *Z. Anorg. Allg. Chem. 296* (1958) 63.
[37] G. N. Huntly, *J. Chem. Soc. 59* (1891) 202.
[38] L. C. D. Groenweghe, J. H. Payne, J. R. Van Wazer, *J. Am. Chem. Soc. 82* (1960) 5305.
[39] W. E. Morgan, T. Glonek, J. R. Van Wazer, *Inorg. Chem. 13* (1974) 1832.
[40] H. Grunze, *Z. Anorg. Allg. Chem. 298* (1959) 152.
[41] H. Grunze, *Z. Anorg. Allg. Chem. 324* (1963) 1.

[42] H. Grunze, *Z. Chem. 2* (1962) 313.
[43] M. Becke-Goehring, J. Sambeth, *Angew. Chem. 69* (1957) 640.
[44] M. Viscontini, K. Ehrhardt in: *Silicium, Schwefel, Phosphate*, (Colloq. Sekt. Anorg. Chem. Int. Union Reine Angew. Chemie, Münster 1954) Verlag Chemie, Weinheim 1955, p. 232.
[45] E. Fluck, *Angew. Chem. 72* (1960) 752.
[46] D. F. Toy, J. E. Blanche, US 3034826 (1962).
[47] R. Appel, G. Eisenhauer, *Chem. Ber. 95* (1962) 1756.
[48] K. H. Wolf, H. Grunze, *Z. Chem. 22* (1982) 211.
[49] A. Besson, *C. R. Hebd. Seances Acad. Sci. 124* (1897) 763.
[50] M. Baudler, R. Klement, E. Rother, *Chem. Ber. 93* (1960) 149.
[51] E. A. Robinson, *Can. J. Chem. 40* (1962) 1725.
[52] M. Becke-Goehring, A. Debo, E. Fluck, *Chem. Ber. 94* (1961) 1383.
[53] E. Fluck, *Chem. Ber. 94* (1961) 1388.
[54] R. A. Y. Jones, A. R. Katritzky, *Angew. Chem. 74* (1962) 60; *Angew. Chem. Int. Ed. Engl. 1* (1962) 32.
[55] G. S. Reddy, C. D. Weis, *J. Org. Chem. 28* (1963) 1822.
[56] H. Gerding, H. Gijben, B. Nieuwenhuijse, J. G. Van Raaphorst, *Recl. Trav. Chim. Pays-Bas 79* (1960) 41.
[57] E. A. Kravcenko, V. G. Morgunov, B. N. Kulikovsij, T. L. Novoderezkina, M. Meisel, *Z. Chem. 23* (1983) 143.
[58] M. Binnewies, *Z. Anorg. Allg. Chem. 507* (1983) 77.
[59] R. Ahlrichs, C. Ehrhardt, M. Lakenbrink, S. Schunck, H. Schnöckel, *J. Am. Chem. Soc. 108* (1986) 3596.
[60] M. Meisel, H. Bock, B. Solouki, M. Kremer, *Angew. Chem. 101* (1989) 1378; *Angew. Chem. Int. Ed. Engl. 28* (1989) 1381.
[61] S. C. Lee, R. H. Holm, *Angew. Chem. 102* (1990) 868; *Angew. Chem. Int. Ed. Engl. 29* (1990) 885.
[62] G. Fritz, *Angew. Chem. 99* (1987) 1150; *Angew. Chem. Int. Ed. Engl. 26* (1987) 1111.
[63] J. Goubeau, H. Keller, *Z. Anorg. Allg. Chem. 265* (1951) 73.
[64] J. Goubeau, R. Warncke, *Z. Anorg. Allg. Chem. 259* (1949) 109.
[65] W. C. Schumb, A. J. Stevens, *J. Am. Chem. Soc. 69* (1947) 726.
[66] W. C. Schumb, R. A. Lefever, *J. Am. Chem. Soc. 76* (1954) 2091.

On the Quasicrystalline State

By Sten Andersson,* Sven Lidin, Michael Jacob, and Osamu Terasaki

Dedicated to Professor Hans Georg von Schnering on the occasion of his 60th birthday

Zur Zeit ist zwar noch nicht ganz sicher, ob das durch unsere Brille Gesehene auch wirklich auf Dauer tragfähig sein wird, aber selbst wenn nur das Schöne in den Strukturen fester Stoffe bleiben sollte, es hätte sich allemal gelohnt.[**]

When we started to write the introduction to this article, we sought to describe *von Schnering*'s enormous contributions to solid-state science. Pages later we suddenly realized the introduction had become too long. As there was no way to shorten it, we gave up.

1. Introduction

In a little book by *Kowalewski*[3] published in 1921 there are some remarkable things we want to discuss. *Kowalewski* described the "Keplerschen Körper", a Kepler "Dreißigflach" that we now refer to as a rhombic triacontahedron or just triacontahedron. This polyhedron is built from what *Kowalewski* called Kepler rhombs, which have the property that the ratio of their diagonals is the golden mean, $\tau (= (\sqrt{5} + 1)/2)$. *Kepler* was interested in this polyhedron because it consists of two Platonic solids, the small diagonals forming the edges of a dodecahedron and the larger diagonals the edges of an icosahedron. Thirty such Kepler rhombs make up the triacontahedron, and *Kowalewski* showed how this solid can be built from two different building blocks (Bausteine), which he called "Flachblöcke" and "Steilblöcke" and we now call oblate and prolate rhombohedra. *Kowalewski* showed how ten of each kind make up the triacontahedron, and he was sure *Kepler* already knew this. Using a coloring scheme, *Kowalewski* derived our matching rules for filling space with such solids, in his case the triacontahedron. *Kowalewski* was not sure whether *Kepler* knew these rules.[4]

Kowalewski also found that, in a six-dimensional cube, 32 of the 64 corners constitute the six-dimensional *Urbild* of the triacontahedron. The other 32 corners also form an *Urform*, a *Komplement* of the first, which, in three dimensions, is a triacontahedron. He also showed that the 20 *Blöcke* (oblates and prolates) that make up the triacontahedron show up in the six-dimensional *Urbild* as equally sized three-dimensional cubes.

Kowalewski further described the rhombic dodecahedron as a compound of four oblates (Flachblöcke). Each such oblate is built of six rhombs, the diagonals having the ratio $1 : \sqrt{2}$ (Fig. 1). This fundamental Kowalewski oblate is the smallest unit that describes the body-centered cubic (bcc) structure and also is space-filling. Following Kowalewski, 14 of the 16 corners of a four-dimensional cube form the *Urbild* of the rhombic dodecahedron.

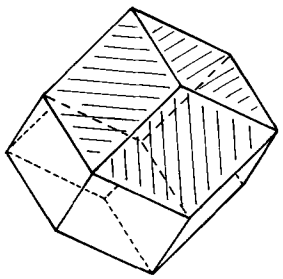

Fig. 1. The rhombic dodecahedron with one of the four Kowalewski "Flachblöcke" (oblates) that make up the solid.

2. Model for Quasicrystal Structures

Our first model was constructed from high-resolution electron microscopic (HREM) images of an AlCuFe alloy.[5, 6] It was clear it could be scaled down metrically by τ to four different structures. A recurrent theme in these structures is the principle of interpenetration. Polyhedra with icosahedral symmetry cannot fill space, but, if the polyhedra are allowed to interpenetrate, such packing can be achieved. The principle of interpenetration also explains the general features of

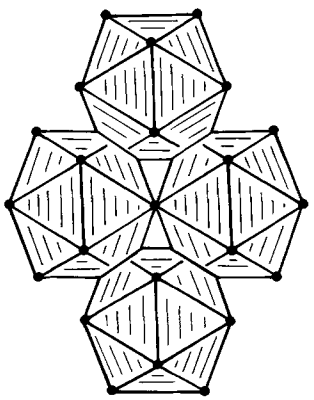

Fig. 2. Four icosahedra forming a Kepler rhomb.

[*] Prof. S. Andersson, S. Lidin, M. Jacob
Department of Inorganic Chemistry 2, Chemical Centre
P.O. Box 124
S-21100 Lund (Sweden)
O. Terasaki
Department of Physics, Tohoku University
Aramaki Aoba, Sendai 980 (Japan)

[**] It is not yet certain whether our way of seeing things will hold up in the long run. However, even if only the beauty in the structures of solids should remain, it will have been worth the effort [1, 2].

HREM images of quasicrystalline materials. These images invariably seem to be composed of intersecting polygons.

We can show the principle of interpenetration with our simplest structure ($n = 1$). Four icosahedra are organized so that their centers form a Kepler rhomb (Fig. 2). If the icosahedral edge length is set to unity, the short and long diagonals are τ and τ and $\tau + 1$, respectively. This arrangement forces the icosahedra to interpenetrate along the fivefold axis (Fig. 3), so that the rhomb edge (quasi cell constant) becomes $(\tau\sqrt{\tau^2 + 1})/2$.

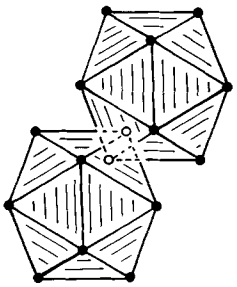

Fig. 3. The icosahedral interpenetration necessary to make the Kepler rhomb in Figure 2.

We have here the first fundamental building unit. We continue to fill space, with the important restriction that translation is forbidden, by adding icosahedra. A new type of interpenetration is created along the threefold axes of the icosahedron (Fig. 4). Having done this with a great number of icosahedra, we realize that prolates and oblates are created and they also appear to be joined together according to the matching rules. During the interpenetration most of the icosahedral corners are lost, but fivefold symmetry is imposed on the structure produced by the starting building block, the icosahedron.

In terms of prolates and oblates this is the same structure as reported before by *Elswijk* et al.[7] who also pointed out that the prolate structure is very close to a Laves phase structure. To this we want to add that two prolates joined via a mirror plane give a 36-atom unit of the hexagonal $MgZn_2$ structure, and also that the oblate contains an eight-atom bcc unit arranged as the Kowalewski oblate described in Figure 1. There is no need to use a special oblate structure—such units are always generated by the prolate arrangements. Another way to say this is that all the atoms of bcc units are created by prolates or $MgZn_2$ units or simply by the interpenetration principle.

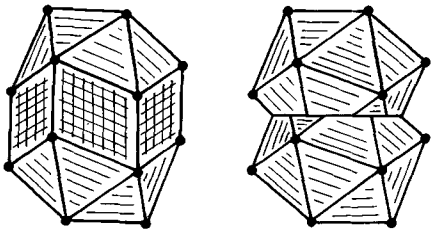

Fig. 4. Interpenetration along the icosahedral threefold axes.

The various steps in building a quasicrystal structure are shown with icosahedra in Figure 5. This algorithm, constructed[8] for deriving quasicrystal structures according to the interpenetration principle, will work equally well for the simulation of quasicrystal growth. This is of course general and applies also for members with $n = 2$–4. The expansion τ on $n = 1$ gives the structure shown in Figure 6 for the Kepler rhomb, which is the building unit for $n = 2$. The sequence along the fivefold axes is now as follows: interpenetration of icosahedra + interpenetration of pentagonal prisms and icosahedra. Along the twofold axes a part of the WAl_{12} structure is easily traced.

Complete icosahedral interpenetration on each corner of a central icosahedron gives the pentagonal dodecahedron, with edge lengths of unity. Complete pentagonal prism interpenetration on each corner of a central icosahedron gives the icosidocecahedron, with edge lengths of unity for $n = 1$ and 2. When further members are formed, the interpenetration around a central atom is interrupted along the twofold axis, that is, where parts of the Cr_3Si and WAl_{12} structures appear.

In the next member, $n = 3$, such icosidodecahedra are joined via icosahedra (Fig. 7); parts of the WAl_{12} structure form the threefold axis and the α-AlFeSi structure forms the twofold axis. We have earlier described the structures for $n = 4$.[5, 6] The structural and metric relationships for $n =$ 1–4 are given in Table 1.

Sten Andersson was born in 1931 on the island of Öland in Sweden. He studied at the University of Stockholm, where he received his Ph.D. in 1963. During his studies, he worked with the late A. D. Wadsley for one year (1960) in Melbourne. He was employed at the Research Institute of National Defense from 1962 to 1970 and was docent in Lund until 1983, when he became Professor of Inorganic Chemistry. He has published about 140 papers and one book, Inorganic Crystal Chemistry with B.G. Hyde. He has received an honorary doctorate from the University of Toulouse and was awarded the Humboldt research price in 1990. His present interest is the application of differential geometry and curvature to solid structures.

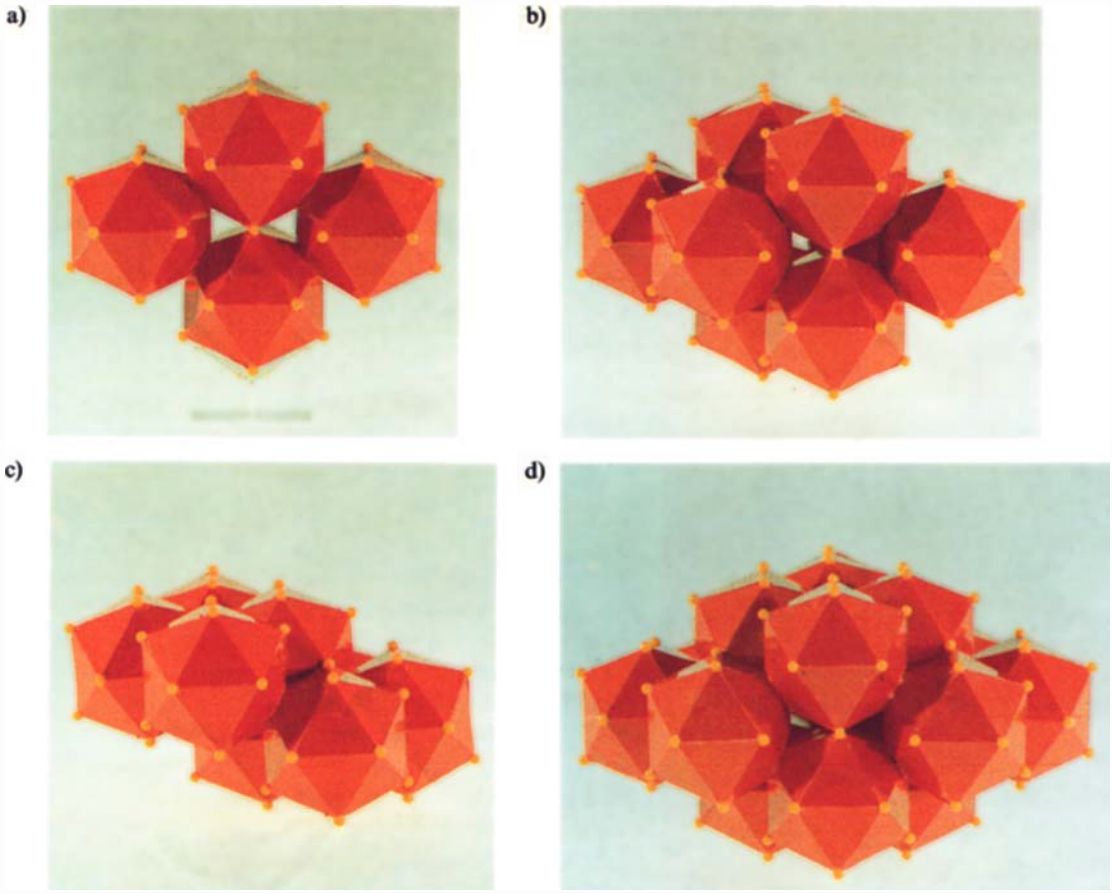

Fig. 5. *Icosahedra put together according to the interpenetration and nontranslational principle. Various well-known solids are formed directly:* a) a Kepler rhomb; b) two Kepler rhombs forming a prolate; c) two Kepler rhombs forming an oblate; d) two prolates and two oblates.

3. Relationships between the Model and the Structure of α-AlFeSi

The structures for $n = 3$ and 4 show strong similarities to the structure of the ternary alloy α-AlFeSi. In our description for $n = 4$,[5] we used the small rhombicosidodecahedron combined with the icosidodecahedron to build the structure. Later on we found that these two polyhedra also make up the α-AlFeSi structure, which we want to describe in more detail here.

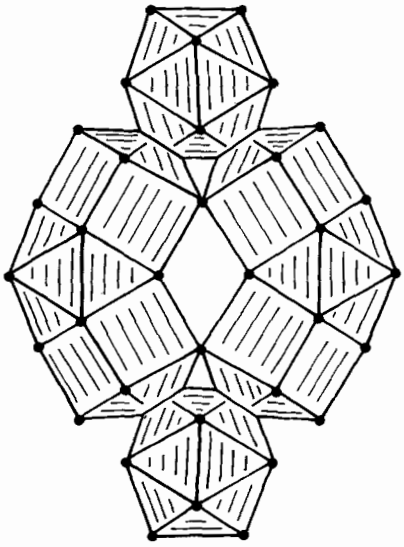

Fig. 6. Kepler rhomb for $n = 2$.

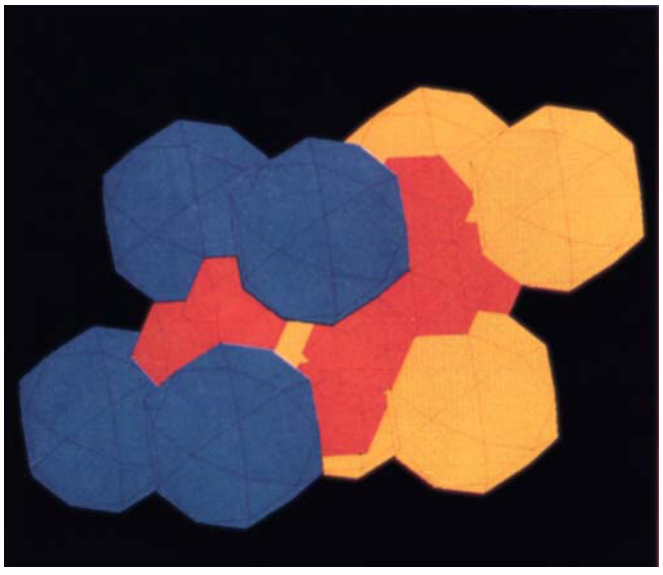

Fig. 7. Prolate for $n = 3$.

Table 1. Structural and metric relationships for $n = 1-4$.

n	Threefold quasi cell constant	Structure	Twofold quasi cell constant	Structure	Fivefold quasi cell constant
1	$\frac{\sqrt{3}}{2}$	bcc	τ	Cr_3Si	$\frac{\tau\sqrt{\tau^2+1}}{2}$
2	$\frac{\tau\sqrt{3}}{2}$	Cr_3Si	τ^2	WAl_{12}	$\frac{\tau^2\sqrt{\tau^2+1}}{2}$
3	$\frac{\tau^2\sqrt{3}}{2}$	WAl_{12}	τ^3	α-(AlFeSi)	$\frac{\tau^3\sqrt{\tau^2+1}}{2}$
4	$\frac{\tau^3\sqrt{3}}{2}$	α-AlFeSi	τ^4	–	$\frac{\tau^4\sqrt{\tau^2+1}}{2}$

In his structure determination of α-AlFeSi, *Cooper*[9] reports that in the cubic unit cell ($a = 12.56$ Å, space group $Im3$) certain sites are only partly occupied. He concludes that this is only an average structure, and that if space group $Pm3$ is used, with two different unit cells for a crystal, a chemically better model is obtained.

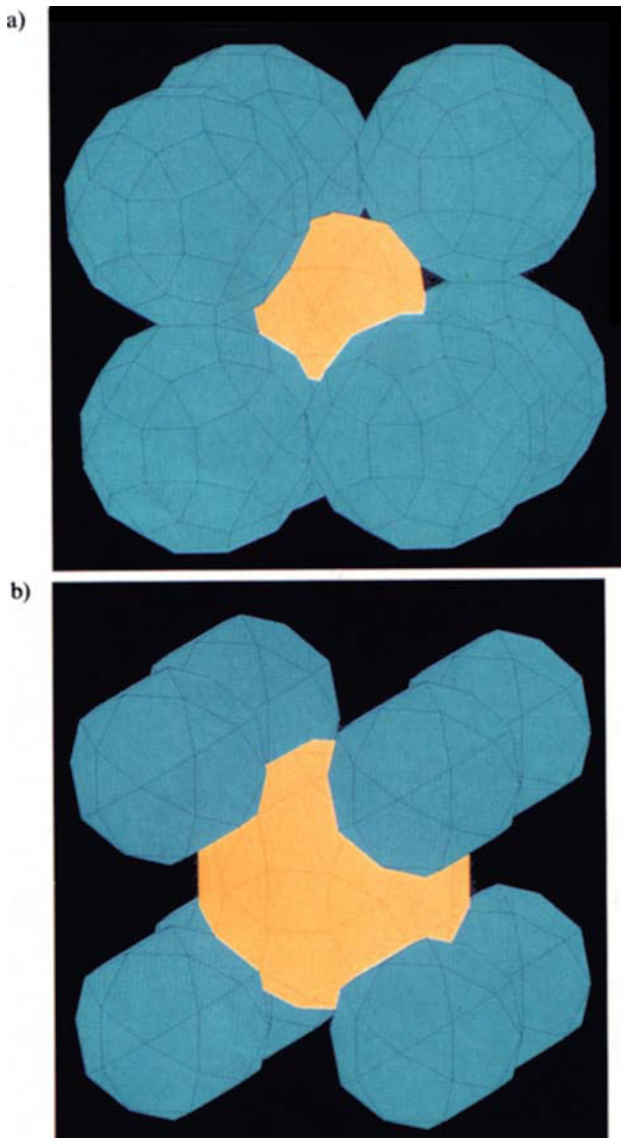

Fig. 8. The Cooper structures I (a) and II (b).

The Cooper structure is very accurately described with the small rhombicosidodecahedron sharing squares along the twofold axes and sharing triangles with an icosidodecahedron along the space diagonal. His two-unit-cell structures are then just related by a translation 1/2 1/2 1/2 (Fig. 8); his sets of coordinates for cell I and cell II were used in the calculation. The small rhombicosidodecahedron is built as follows: A central icosahedron is capped by pentagonal prisms to give the icosidodecahedron, which, in turn, is capped with pentagonal antiprisms to give the small rhombicosidodecahedron (Fig. 9).

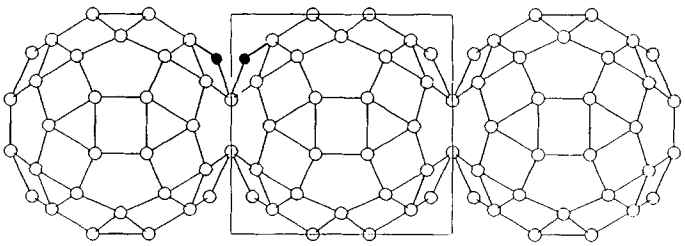

Fig. 9. The small rhombicosidodecahedron built of Al atoms in α-AlFeSi. The solid circles are undistorted polyhedral positions for Al(9).

Calculated and observed coordinates are given in Table 2. The major discrepancy is with atom Al(9). This atom has a distance to itself, via a mirror plane of 2.44 Å, and this is shortened for steric reasons. The square-face sharing of the small rhombicosidodecahedra forces neighboring atoms

Table 2. Comparison of observed [9] and calculated coordinates for α-AlFeSi.

Atom [a]	Observed x	y	z	Calculated x	y	z
Al(3)	0.165	0.101	0	$\frac{\tau^{-2}\sqrt{3}}{4} = 0.165$	$\frac{\tau^{-3}\sqrt{3}}{4} = 0.102$	0
Al(1)	0.378	0	0	$\tau^{-2} = 0.382$	0	0
Al(5)	0.115	0.187	0.300	$\frac{\tau^{-3}}{2} = 0.118$	$\frac{\tau^{-2}}{2} = 0.191$	$\frac{\tau^{-1}}{2} = 0.309$
Al(9)	0.327	0.403	0	$\frac{\tau^{-1}}{2} = 0.309$	$\frac{\tau^2+1}{2\tau^3} = 0.427$	0
Al(11)	0.128	0.117	0.5	$\frac{\tau^{-3}}{2} = 0.118$	$\frac{\tau^{-3}}{2} = 0.118$	0

[a] Al(2), Al(4), and Al(6) are obtained by translation $\frac{1}{2}\frac{1}{2}\frac{1}{2}$ from Al(1), Al(3), and Al(5), respectively. The Al(3) atoms are the corner atoms of the icosahedron centered in the icosidodecahedron. Al(1) and Al(5) are the corner atoms of the icosidodecahedron centered in the small rhombicosidodecahedron, but also "free". Al(9) and Al(11) are the corner atoms of the small rhombicosidodecahedron.

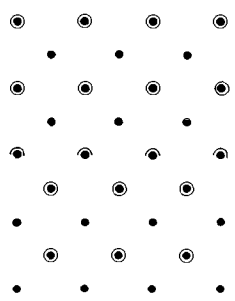

Fig. 10. Transition between two primitive structures—the average structure is body-centered. Small circles represent the icosidodecahedron, large the small rhombicosidodecahedron in *Cooper*'s structure.

from two polyhedra to come very close—after all, it is a large polyhedron—and the atoms are repelled from the polyhedral position. The standard deviation for this particular atom, $\sigma = 0.020$ Å, is also unique, since all other σ are less than 0.004 Å.

Alloy structures are often reported with certain sites partially occupied. *Cooper*'s solution to this problem using two unit cells is very elegant. We show in Figure 10 how domain regions could occur in a crystal.

Received: November 12, 1990 [A 822 IE]
German version: *Angew. Chem. 103* (1991) 771

[1] H. G. von Schnering, *Angew. Chem. 93* (1981) 44; *Angew. Chem. Int. Ed. Engl. 20* (1981) 33.
[2] H. G. von Schnering, R. Nesper, *Angew. Chem. 99* (1987) 1097; *Angew. Chem. Int. Ed. Engl. 26* (1987) 1059.
[3] G. Kowalewski: *Mathematica Delectans, Magische Quadrate und Magische Parkette. Der Keplersche Körper*, von Wilhelm Engelmann, Leipzig 1921.
[4] D. Levine, P. J. Steinhardt, *Phys. Rev. Lett. 53* (1984) 2477.
[5] S. Lidin, S. Andersson, J.-O- Bovin, J.-O. Malm, O. Terasaki, *Acta Crystallogr. Sect. A 45* (1989) FC33.
[6] S. Lidin, J.-O. Malm, S. Andersson, J.-O. Bovin, O. Terasaki in: *Colloque Quasicristaux, Orsay 1990*, p. 83.
[7] H. B. Elswijk, J. T. M. de Hosson, S. van Smaalen, J. L. de Boer, *Phys. Rev. B 38* (1988) 1681.
[8] S. Lidin, M. Jacob, unpublished.
[9] M. Cooper, *Acta Crystallogr. 23* (1967) 1106.

Complex Transition Metal Hydrides

By Welf Bronger*

Dedicated to Professor Hans Georg von Schnering on the occasion of his 60th birthday

Compounds having structural units formed by transition metals and hydrogen have only become known fairly recently. Only the synthesis and structural characterization of ternary metal hydrides $A_xM_yH_z$, in which A is an alkali or alkaline-earth metal and M is a transition metal, led to the discovery of anionic complex groups of the form $[MH_z]$. Although there are obvious structural similarities to the corresponding halides and oxides, the dynamic properties of the hydride ligand are somewhat unusual and are responsible for numerous phase transformations. Transitions throughout the range from saltlike to metallic behavior make us expect interesting physical properties and applications.

1. Introduction

Our knowledge concerning metal-hydrogen compounds is relatively meager. This is largely because the preparation of such compounds, which in many cases are unstable, is more laborious and complicated than for other compounds of metals with nonmetals, as also is the determination of their structures and properties. This explains the fact that already for the binary hydrides of many metals only incomplete or vague information is available regarding their existence and properties. So far as main-group metals are concerned this situation applies, for example, to the hydrides of gallium and indium, and to the corresponding compounds of the metallic elements in later groups of the Periodic System. A similar picture emerges for the transition metals. Here too there remain many unresolved questions, such as whether or not manganese hydrides exist that are compounds of unique structural types, what phases exist in the chromium–hydrogen system, and many more. However, even on the basis of the incomplete knowledge available one can already classify binary metal hydrides into three groups: saltlike hydrides, covalent hydrides and metallic hydrides. Typical representatives of the first group are the hydrides of the alkali metals and alkaline-earth metals. The second group includes the hydrides of the remaining main-group metals or semimetals, and the third group includes the transition metal hydrides. However, the boundaries between these three groups are not sharply defined; this is not surprising since already for the elements there is a gradual transition from metallic to nonmetallic behavior.

If we extend this method of classification from the binary to the ternary metal hydrides, we can expect to find that of the various possible combinations of binary components one will result in a further group of hydrides, in which one of the metals (A) belongs to the type that forms saltlike hydrides whereas the other (M) belongs to those that form metallic hydrides. Compounds of this group have the general formula $A_xM_yH_z$. These hydrides can have a range of properties varying from metallic to saltlike, depending mainly on the position of the metal A in the scale of electronegativities. Thus we can expect that hydrides in which the component A is a heavy alkali metal or alkaline-earth metal will have more saltlike properties, whereas those containing lithium or magnesium, for example, will have more metallic properties. One can also predict that these hydrides will have crystal structures containing complex $[H_yH_z]$ groups that are stabilized by accepting the valence electrons from the x atoms of element A to form $[M_yH_z]^{nx-}$ anions, where n = 1 for alkali metal compounds and n = 2 for compounds of alkaline-earth metals.

This article describes complex hydrides with the composition $A_xM_yH_z$ and attempts, on the basis of the knowledge so far established, to summarize the conclusions that emerge, both expected and unexpected, so as to build up an initial picture. This picture should then be looked at in a wider context, since research on metal hydride complexes in the field of molecular chemistry has recently experienced a notable increase in acitivity and has led to interesting discoveries. Furthermore, knowledge now being gained is likely to unite previously disparate points of view, since molecular chemistry and solid-state chemistry both stem from the same roots.[1]

2. Methods of Synthesis and Structure Determination

Methods for synthesizing ternary hydrides $A_xM_yH_z$ that have been investigated include both molecular reactions in solvents and solid-state reactions in gaseous atmospheres.

Reaction of metal-alkyl compounds with metal hydrides in suitable solvents is reported to give ternary hydrides; for example, it is claimed that $Zn(sec\text{-}C_4H_9)_2$ reacts with KH to give K_2ZnH_4,[2] and $LiCu(CH_3)_2$ reacts with $LiAlH_4$ to give $LiCuH_2$.[2] However, these findings have not been verified beyond any possible doubt; the structures of the compounds are not known, and thus no firm answer can be given to the question of whether or not solvent molecules are inserted to exercise a stabilizing role. In another reaction, which is reminiscent of alchemy, a perrhenate or a pertechnetate is allowed to react with elemental potassium in an aqueous solution of ethylenediamine, and after a work-up procedure one obtains the respective ternary hydrides K_2ReH_9[3] or K_2TcH_9.[4]

[*] Prof. Dr. W. Bronger
Institut für Anorganische Chemie der Technischen Hochschule
Professor-Pirlet-Str. 1, W-5100 Aachen (FRG)

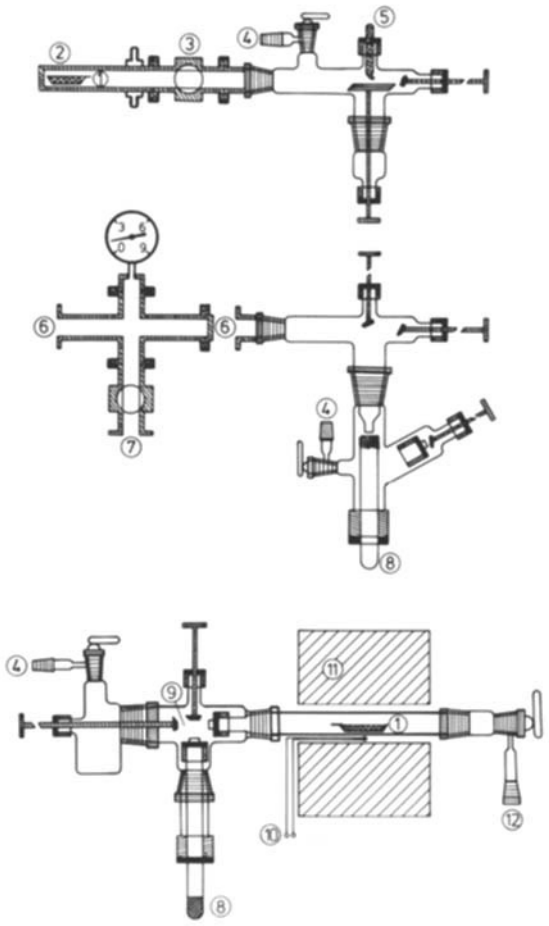

Fig. 1. Experimental arrangements for synthesizing binary and ternary metal hydrides. The upper two diagrams show types of apparatus for preparing binary alkali metal hydrides, while the bottom diagram illustrates the preparation of ternary hydrides: ① Reaction boats. ② Steel autoclave with cooling jacket. ③ Ball valve with flange connections. ④ Connection for vacuum/argon/hydrogen. ⑤ Ampoule containing alkali metal. ⑥ Connection for steel autoclave; ⑦ connection for vacuum/hydrogen. ⑧ Receiver tube for product. ⑨ Transfer chamber. ⑩ Thermocouple. ⑪ Reaction oven. ⑫ Connection for manometer.

In the solid-state reactions referred to, one either starts out from an intermetallic compound into which the hydrogen is directly inserted using suitable pressures and temperatures, or alternatively reacts a hydride of an alkali metal or alkaline-earth metal with a transition metal in an atmosphere of hydrogen or inert gas. These methods have been found useful especially during the last few years for synthesizing various ternary hydrides containing transition metals of subgroup eight. Examples are the hydrides Mg_2NiH_4,[5] obtained by reacting Mg_2Ni with hydrogen, and Na_2PtH_4,[6] obtained by reacting NaH with Pt in an atmosphere of hydrogen.

One of the reasons why there is as yet so little firmly established knowledge concerning complex metal hydrides is that many of them are extremely sensitive to air and moisture. However, the difficulties that otherwise occur in the synthesis and subsequent handling of these hydrides can be avoided by consistently working with closed apparatus systems. Figure 1 shows experimental arrangements that allow all the operations to be performed from outside the system using suitable manipulators.

In determining the crystal structures of metal hydrides one comes up against the problem that the positions of hydrogen atoms in an array of metal atoms can usually only be measured approximately, if indeed at all, by X-ray diffraction methods. The normal procedure based on measurements on single crystals is rarely successful here, especially in view of the fact that growing single crystals of hydrides is difficult. Consequently, the determination of the structure is usually approached by combining X-ray and neutron diffraction experiments on powdered samples; here the use of high resolution techniques is now becoming increasingly important.

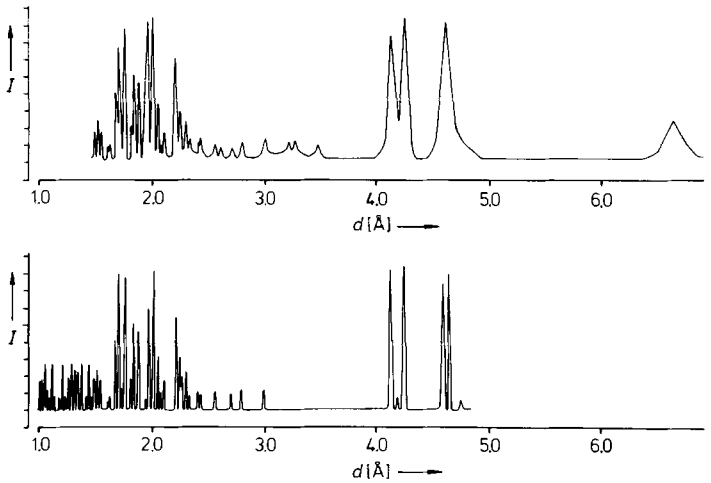

Fig. 2. Comparison of neutron diffraction patterns of Na_3RhD_6 measured using the TAS I and HRPD facilities (upper and lower traces respectively) at 295 K. The measurement times were 24 hours with TAS I and 12 hours with HRPD (the backgrounds were smoothed to produce the traces). The figure shows that some reflections which coincide in the TAS I trace are resolved when using the HRPD system. On the other hand, the neutron diffraction experiment using TAS I gives extra information at large *d*-values. For *d*-values greater than 3 Å the severe reduction in neutron flux with the HRPD system results in a progressive deterioration of the signal-to-noise ratio for a comparable measurement time, and consequently weak reflections cannot be detected in this region. *I* = intensity.

Welf Bronger, born in 1932 in Hamburg, studied chemistry at the universities of Innsbruck and Münster and gained his doctorate in 1961 under Wilhelm Klemm. After a short period working in industry for Degussa, he returned to the Universität Münster as an assistant, where he received his "Habilitation" in 1966. In 1969 he took up the chair of Inorganic and Analytical Chemistry at the Technische Hochschule, Aachen. His main research interests are concerned with intermetallic phases, metal chalcogenides and metal hydrides, with special emphasis on structural studies and magnetochemistry.

This is illustrated by Figure 2, in which two neutron diffraction patterns of Na_3RhD_6 are compared.[7] The upper one was recorded using a three-axis spectrometer (TAS I) with the cold neutron source of the DR3 reactor at the Risø National Laboratory (Denmark), whereas the lower one was recorded using a high-resolution time-of-flight spectrometer (HRPD) with the spallation source at the Rutherford Laboratory (Great Britain). In both these neutron diffraction experiments the deuterium compound was used because the scattering by ^1H atoms is not sufficiently coherent.

3. What Ternary Transition Metal Hydrides of Alkali Metals and Alkaline-Earth Metals are Known, and What are their Structures?

The structures of binary transition metal hydrides of the metallic type can be described as close-packed arrays of metal atoms containing interstitial hydrogen atoms. Isolated transition metal–hydrogen groups are only expected in compounds where they occur as anions stabilized in a matrix of cations. Thus, as has already been mentioned, ternary transition metal hydrides that satisfy the latter conditions will be obtained particularly for combinations with alkali or alkaline-earth metals.

Hydrides of this type will be described below; to begin with, compounds of alkaline-earth and alkali metals will be treated separately.

3.1. Ternary Hydrides of Transition Metals with Alkaline-Earth Metals

Our knowledge of complex hydrides of the type $A_xM_yH_z$, in which A is an alkaline-earth metal, is limited to those where M belongs to sub-group eight. Table 1 lists the compounds whose composition and crystal structure can be regarded as known with certainty.

Table 1. Transition metal hydrides of alkaline-earth metals whose structures are known with certainty [a].

Mg_2FeH_6 [8]	Mg_2CoH_5 [9]	Mg_2NiH_4 [5]
–	–	–
–	–	–
–	–	–
Mg_2RuH_6 [10]	–	–
Ca_2RuH_6 [11]	Ca_2RhH_5 [10, 11]	$CaPdH_2$ [15]
Sr_2RuH_6 [11]	Sr_2RhH_5 [11, 12]	–
Ba_2RuH_6 [12]	–	–
Mg_2OsH_6 [13]	–	–
–	Ca_2IrH_5 [11]	–
–	Sr_2IrH_5 [11, 14]	–
–	–	–

[a] Here, and in Tables 2 and 3, each field and symbolizes the region of a transition metal. Each box contains a family of hydrides of a specific transition metal. No entries indicate missing members.

The only iron compound so far known is Mg_2FeH_6, which is dark green and crystallizes with the K_2PtCl_6-type structure.[8] Its structure was determined by neutron diffraction measurements on Mg_2FeD_6. The arrangement of the atoms is shown in Figure 3. The magnesium and iron atoms occupy positions equal to those in fluorite, and the iron atoms are octahedrally coordinated by the hydrogen atoms. Mg_2CoH_5[9] and Mg_2NiH_4[5] both have high-temperature forms whose structures are analogous to that of the iron compound. In accordance with the different compositions

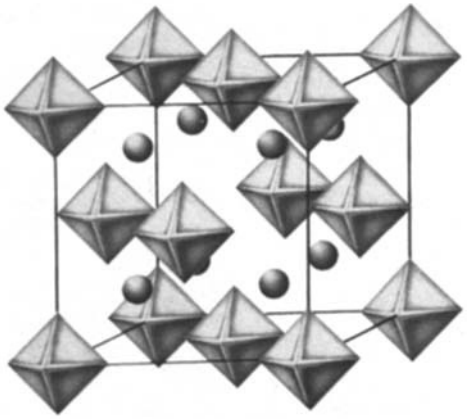

Fig. 3. Structure of Mg_2FeD_6 (K_2PtCl_6 type), showing the positions of the $[FeD_6]$ octahedra and the magnesium ions.

the hydrogen sites have occupancy factors of 5/6 for the cobalt hydride and 4/6 for the nickel hydride. It appears that in these cases there are dynamic processes occurring in the sphere of the hydrogen ligands, as it is found that these motions are frozen out at low temperatures; the cobalt and nickel atoms then adopt a tetragonal-pyramidal or a tetrahedral coordination by hydrogen respectively. Figure 4 shows selected regions of each of these structures.

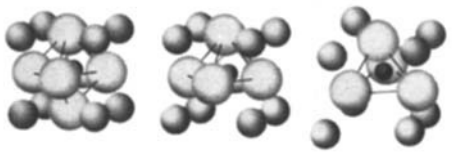

Fig. 4. Selected regions of the structures of Mg_2FeD_6 (left), Mg_2CoD_5 (middle) and Mg_2NiD_4 (right). The small dark spheres are the sites of the transition metal atoms, the medium-sized spheres those of the magnesium atoms, and the large pale spheres those of the hydrogen atoms.

An essentially analogous situation is found for hydrides of the 4d and 5d transition metals of sub-group eight. The ternary ruthenium hydrides[10–12] and Mg_2OsH_6[13] all crystallize with the K_2PtCl_2-type structure. The same is also true of the high-temperature forms of the rhodium and iridium hydrides A_2RhH_5 and A_2IrH_5 so far investigated, although here again the population parameters of the hydrogen positions are altered according to the composition.[11] Up to now exact structural data for a low-temperature form are only available for Sr_2IrH_5.[14] These indicate that the iridium atom has a hydrogen coordination that can be described as a tetragonal bipyramid, in which the four equatorial hydrogen sites are fully occupied. From the composition Sr_2IrH_5 one expects that the top and bottom apexes of the bipyramid should each have an occupancy of 0.5. The

value found experimentally was 0.7 (± 0.04), which may indicate a phase broadening.

$CaPdH_2$ crystallizes with an atomic arrangement similar to perovskite, as shown in Figure 5.[15] The occupancy factor for the hydrogen atom sites is 2/3. To investigate whether additional ordering occurs at low temperatures, neutron diffraction measurements were carried out at 10 K. The neutron diffraction pattern obtained was identical to that at room temperature. It seems possible that in this case, instead of a dynamic disordering of the hydrogen ligands, there is a statistical distribution of linear $[PdH_2]^{2-}$ units, which are distributed over the three directions in space without forming a superstructure. In the case of the corresponding sodium compound Na_2PdH_2 it has been possible to obtain direct evidence for such $[PdH_2]^{2-}$ groups (see Section 3.2).[16]

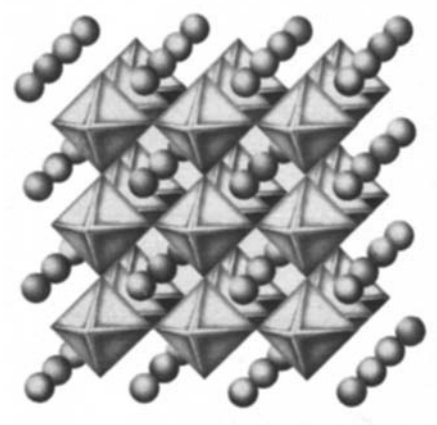

Fig. 5. The perovskite-like atomic arrangement of $CaPdD_2$. The hydrogen atoms occupy the vertices of the octahedra to the extent of 2/3 on average; the rest of the symbols correspond to those in Figure 3.

The results from measurements of electrical and magnetic properties that have so far been published show that ternary hydrides of transition metals with alkaline-earth metals do not have metallic properties. The observed electrical conductivities are at best in the semiconductor range, as is the case for the rhodium compounds, for example. These observations are supported by band structure calculations. Thus, for the series Mg_2FeH_6, Mg_2CoH_5 and Mg_2NiH_4, the calculated values for the energy gap between the valence and conduction bands are 1.8, 1.92 and 1.36 eV respectively. Magnetic susceptibility measurements show a very weak paramagnetism or diamagnetism.[17]

The compositions and structures of the above ternary hydrides suggest that the compounds should be described as complexes: in the $[MH_z]^{2x-}$ units—all of which are systems of 18 valence electrons except for the $[PdH_2]^{2-}$ anion—the hydrogen ligands form coordination polyhedra corresponding to the expected d-electron configurations of the transition metal atoms M. For Mg_2FeH_6 the magnetic susceptibility measurements and the Mössbauer spectrum indicate an iron(II) complex with a low-spin configuration.[17] In Mg_2CoH_5 it appears that the cobalt atoms have a spin-paired d^8 configuration; the tetragonal-pyramidal coordination shows four shorter Co–H distances and one somewhat longer distance to the apex of the pyramid (cf. Fig. 3).[9] In Mg_2NiH_4 the fourfold coordination leads, as expected, to a tetrahedral arrangement of ligands for Ni^0. The linear $[PdH_2]^{2-}$ group also fits into this picture, as it corresponds to the ligand arrangement in complexes of the isoelectronic Ag^+ ion.

To summarize, hydrides of the composition A_xMH_z (where A is an alkaline-earth metal) appear, on the basis of those known up to now, to have structures characterized by the presence of complex anions of the form $[MH_z]^{2x-}$. Here the M atoms evidently have oxidation numbers that are smaller than those in the corresponding halides, which appear to be their nearest structural relations. The treatment of the ternary hydrides of the alkali metals in the next section will still deepen our understanding.

3.2. Ternary Hydrides of Transition Metals with Alkali Metals

Table 2 lists all the complex hydrides of the type $A_xM_yH_z$ (where A is an alkali metal) whose structures are known with certainty. Among the ternary platinum hydrides the only one containing lithium known up to now is the phase $LiPtH_{0.66}$.[18] Its structure consists of an ordered hexagonal close-packed array of metal atoms, in which hydrogen atoms can reversibly enter or leave half of the tetrahedral sites up to an occupancy of 0.33. In the case of sodium the first complex platinum hydride was discovered, a colorless com-

Table 2. Transition metal hydrides of alkali metals whose structures are known with certainty [a].

–	–	–	–
–	–	–	–
–	–	–	–
–	–	–	Li_2PdH_2 [24]
–	–	Na_3RhH_6 [7]	Na_2PdH_2 [16]
K_2TcH_9 [4]	–	–	K_3PdH_3 [26]
–	–	Li_3IrH_6 [7]	A_2PtH_4 [b] [6, 19, 20]
–	–	Na_3IrH_6 [7]	A_3PtH_5 [c] [21]
K_2ReH_9 [3]	–	–	–

[a] See footnote in Table 1. [b] A ≙ Na, K, Rb, Cs. [c] A ≙ K, Rb, Cs.

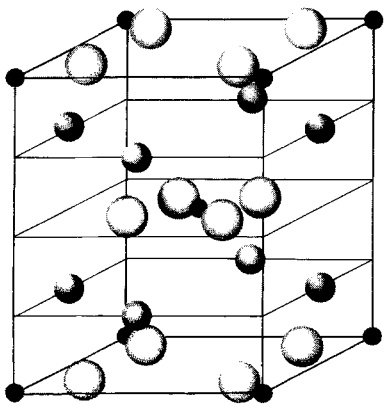

Fig. 6. Structure of Na_2PtD_4. The small dark spheres are the sites of the transition metal atoms, the medium-sized spheres those of the sodium atoms, and the large spheres those of the hydrogen atoms.

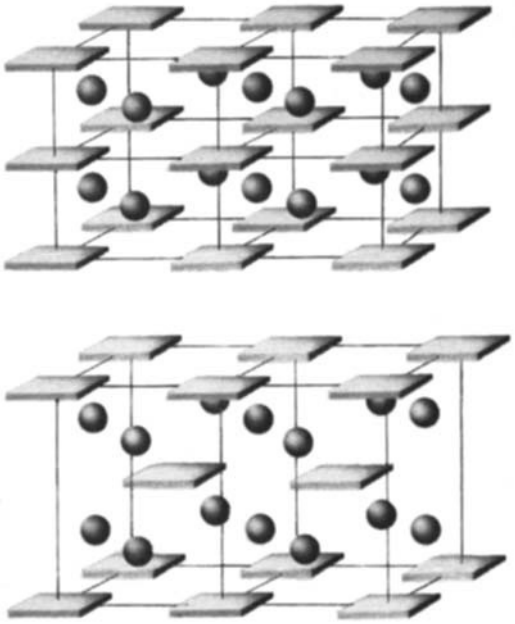

Fig. 7. Comparison of the structures of Na_2PtD_4 (lower diagram) and K_2PtCl_4 (upper diagram). The planar $[PtX_4]$ groups are shown by a single symbol in each case.

pound with the composition Na_2PtH_4.[6] Investigations of its structure revealed that it is of a hitherto unknown tetragonal type, which is shown in Figure 6. The characteristic structural units here are planar $[PtH_4]^{2-}$ groups. The structure is closely related to the K_2PtCl_4 type (see Fig. 7). Above 573 K it forms a second modification, in which the arrangement of the atoms corresponds to the K_2PtCl_6 type structure with the chlorine sites statistically occupied by hydrogen ligands with an occupancy factor of 2/3. Figure 8 shows how the crystal structures of the two modifications of Na_2PtH_4 are related.

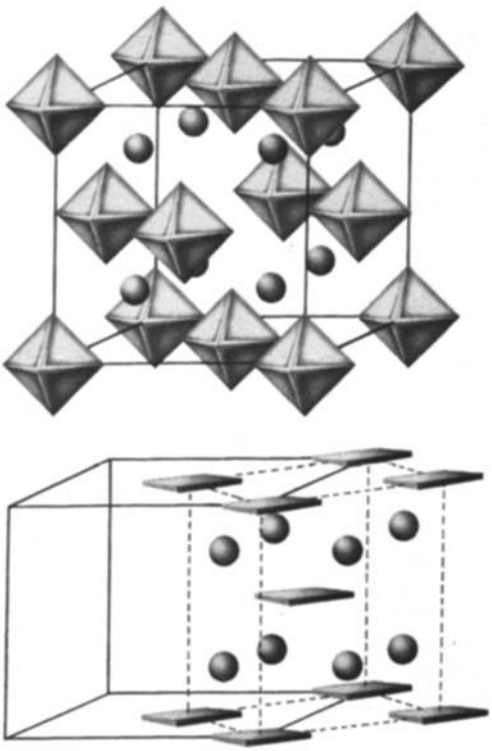

Fig. 8. The phase transformation in Na_2PtD_4. Lower diagram: low-temperature form; upper diagram: high-temperature form, in which hydrogen atoms occupy the vertices of the octahedra to the extent of 2/3 on average.

In the K/Pt/H system there again exists a colorless hydride with the composition K_2PtH_4.[19, 20] At room temperature its structure is already of the K_2PtCl_6 type. Neutron diffraction measurements on the deuterated compound K_2PtD_4 led to a complete structure determination, and showed that the deuterium sites have an occupancy factor of 2/3. Here again the statistical occupancy appears to involve a dynamic process (which will be discussed in more detail in Section 4), as is indicated by the appearance of a low-temperature form, in which the four hydrogen ligands attached to the platinum atom with its d^8 configuration result in the expected planar coordination (Fig. 9). Rb_2PtH_4 and Cs_2PtH_4 also each have two crystalline modifications, which are isotypes of the corresponding K_2PtH_4 structures.[20]

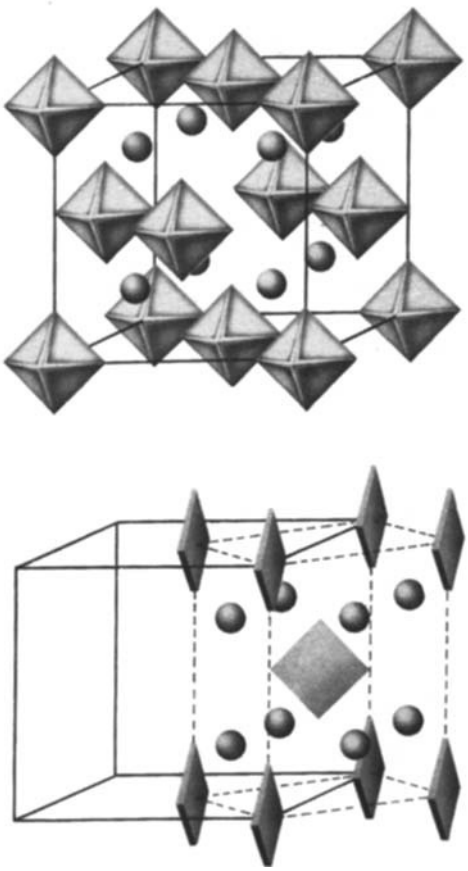

Fig. 9. Low-temperature and high-temperature modifications of K_2PtD_4. The arrangement of the diagrams and the symbols correspond to those in Figure 8.

In the preparation of K_2PtH_4, Rb_2PtH_4 and Cs_2PtH_4 it was found necessary to use an excess of the corresponding alkali metal hydride in each case. Closer investigation revealed that this is because hydrides containing a higher proportion of the alkali metal are formed initially, and these are then converted into the A_2PtH_4 compounds at higher temperatures. These novel hydrides have the formula A_3PtH_5,[21] with the atomic arrangement shown in Figure 10. This tetragonal structure contains two differently bonded types of hydrogen atoms. It is found that the first

type form the characteristic $[PtH_4]^{2-}$ units, whereas the second type are octahedrally coordinated by six alkali metal atoms, as in the binary alkali metal hydrides. The structural relationship of the complex hydrides to the corresponding halides, which has already been mentioned several times previously, is also found here, since the ternary fluorides A_3PdF_5, in which A is Rb or Cs, crystallize in the same structure type.[22] However, as is also commonly found in

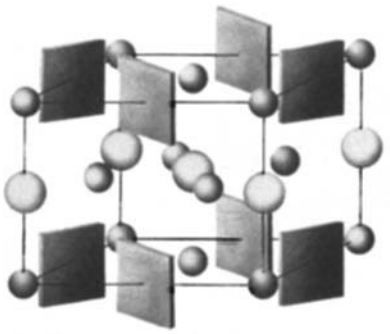

Fig. 10. Atomic arrangement of A_3PtD_5 with A ≙ K, Rb, Cs. The symbols correspond to those in the previous figures.

other cases, the hydrides differ from the halides in having a high degree of mobility in the coordination sphere of the transition metal atom. For example, studies of the structures of Rb_3PtH_5 and Cs_3PtH_5 and the corresponding deuterides as a function of temperature showed that at higher temperatures the structure changes from tetragonal to cubic, before the hydrides A_3PtH_5 decompose to A_2PtH_4 and AH (see Fig. 11). To describe this phase transition Figure 12 shows the arrangement of the atoms in the tetragonal (low temperature) form, projected along the *c*-axis. The alignment of the planar $[PtH_4]^{2-}$ groups results in different distances between the platinum and alkali metal atoms, the shorter distances being those perpendicular to the planar coordination of the ligands, while the longer distances are parallel to this plane. In the cubic (high-temperature) form all these distances are equal. Evidently motions occur within the $[PtH_4]^{2-}$ groups, such that the averaged structure corresponds again to an octahedral coordination of the hydrogen atoms around the platinum atoms with an occupancy factor of 2/3 (see Fig. 12).

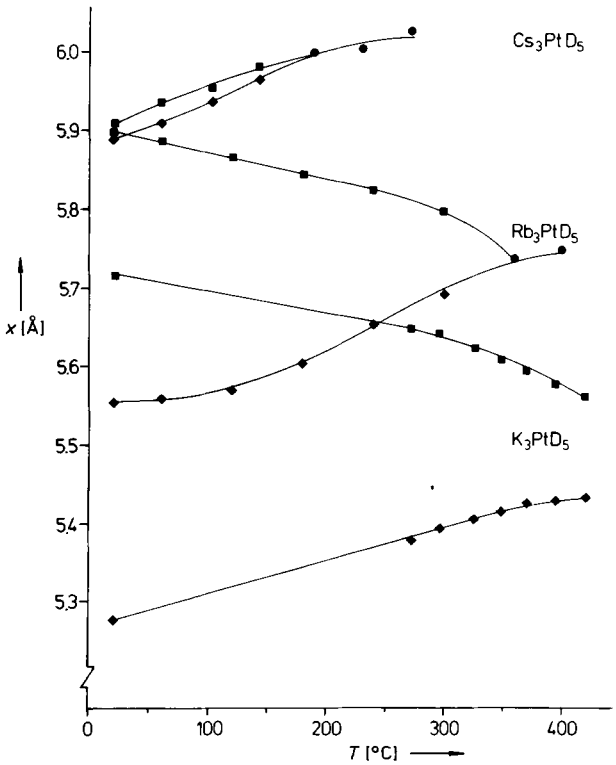

Fig. 11. Temperature dependence of the lattice constants in A_3PtD_5 (A ≙ K, Rb, Cs) from X-ray investigations. For the tetragonal (low-temperature) modification ♦ denotes values of $a/\sqrt{2}$ and ■ denotes values of *c*; for the cubic (high-temperature) modification ● denotes values of *a*. The transition temperatures *T* for the corresponding hydrogen compounds are the same within the limits of accuracy of the experiments.

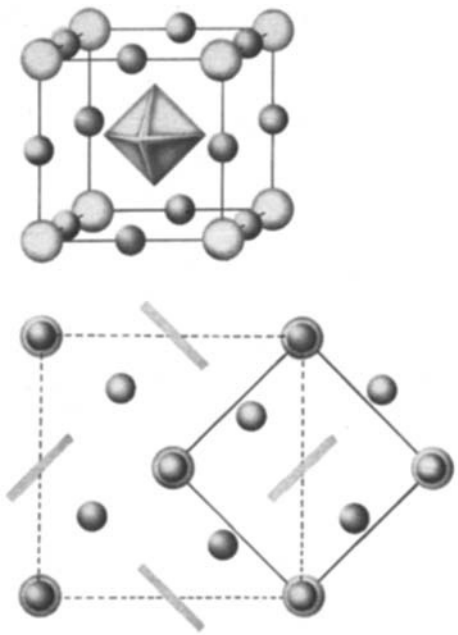

Fig. 12. The phase transformation in A_3PtD_5 (A ≙ Rb, Cs). Lower diagram: structure of the low-temperature modification shown as a projection along the *c*-axis (the $[PtD_4]$ groups are shown in an edge-on representation). Upper diagram: structure of the high-temperature phases; the D sites in the Pt/D octahedron are 2/3 occupied.

With regard to the palladium compounds, the hydride Na_2PdH_2 has already been mentioned earlier.[16] Its crystal structure is shown in Figure 13. The complex anions in this case are linear $[PdH_2]^{2-}$ groups. Assuming that the palladium atoms have an oxidation number of zero, the arrangement of the ligands here corresponds to that in analogous Ag^I complexes. Although there is no known halide whose crystal structure is an isotype of this, there is an oxide, Na_2HgO_2, in which the central atom has the same d^{10} configuration.[23] In the case of the Li/Pd/H system the isostructural compound Li_2PdH_2 has been reported.[24] Hydride phases with lower proportions of lithium also exist; as in the case of the platinum phases referred to earlier, their structures can be regarded as consisting of an ordered array of metal atoms in which the hydrogen atoms, enter octahedral sites in this case.[25]

Coming now to the K/Pd/H system, a yellow compound with the composition K_3PdH_3 has been synthesized.[26] Its

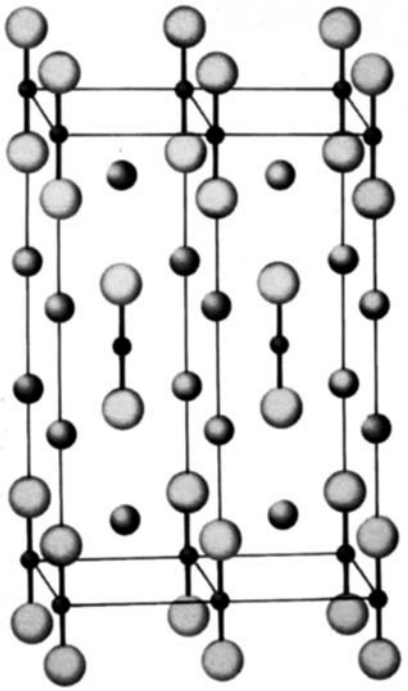

Fig. 13. Crystal structure of Na_2PdD_2; two tetragonal unit cells are shown. The symbols correspond to those in Figure 6.

structure is related to that of K_3PtH_5. Here again it is found that there are two differently bonded types of hydrogen atoms, firstly those in $[PdH_2]^{2-}$ groups that are characteristic of Pd^0, and secondly those that are octahedrally coordinated by potassium atoms, as in the potassium hydride. Owing to the space occupied by the linear groups the potassium octahedra are tilted relative to each other (see Fig. 14). A

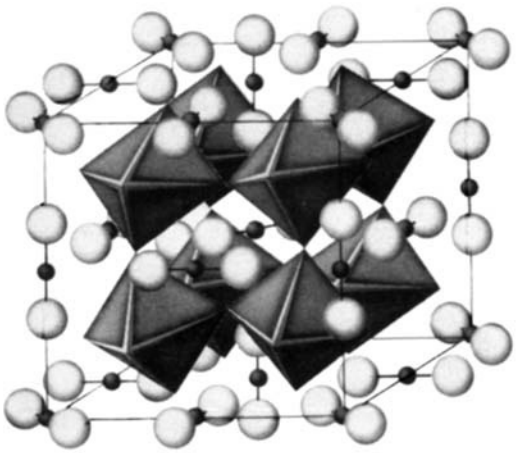

Fig. 14. Atomic arrangement of the tetragonal (low-temperature) modification of K_3PdD_3, showing the vertex-shared potassium octahedra, which have hydride ions at their centers, and the linear $[PdD_2]^{2-}$ groups.

phase transition is observed at 500 K, and this again appears to result from the dynamic behavior of the hydrogen atoms in the complex groups, so that the average arrangement of the ligands around the palladium atoms is of cubic symmetry. The tilting of the potassium octahedra thus disappears (see Fig. 15). This gives a cubic unit cell whose volume is one-eighth of that of the tetragonal cell in the low-temperature form. The arrangement of the potassium and palladium atoms corresponds to the Cu_3Au type structure, and is identical to that in the high-temperature modification of K_3PtH_5 (cf. Fig. 12).

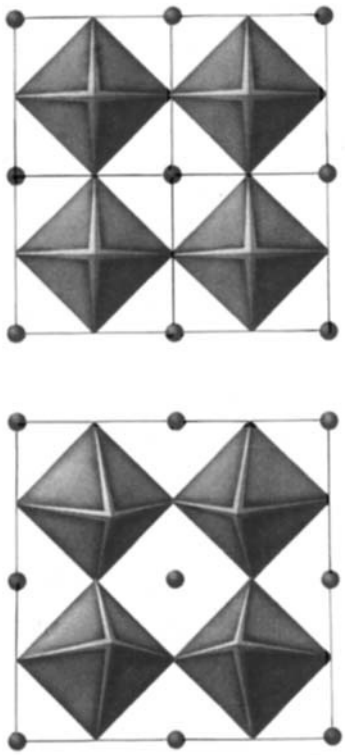

Fig. 15. Arrangement of the potassium octahedra and of the palladium atoms in the tetragonal, low-temperature modification of K_3PdD_3 (lower diagram) and in its cubic, high-temperature modification (upper diagram).

Up to now the only ternary alkali metal hydrides of the remaining platinum sub-group metals, whose structures are certainly known, are Li_3IrH_6, Na_3IrH_6 and Na_3RhH_6.[7] These are colorless compounds that crystallize in a rhombic structure. Here once more the structure-determining units are complex $[MH_z]^{x-}$ groups, in these cases almost regular octahedra consisting of $[IrH_6]^{3-}$ or $[RhH_6]^{3-}$ units (see Fig. 16).

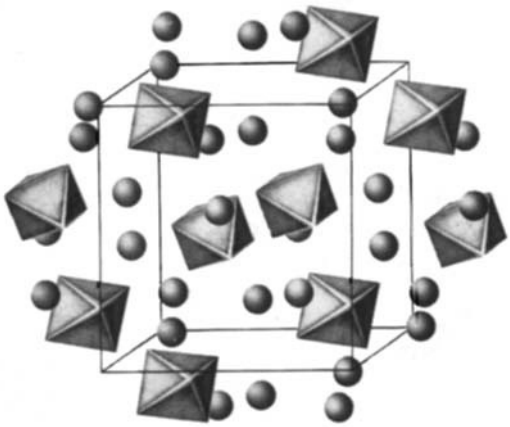

Fig. 16. Crystal structure of Na_3RhD_6, showing the $[RhD_6]$ octahedra and the positions of the sodium ions.

The ternary hydrides K_2ReH_9 and K_2TcH_9,[3,4] which, as mentioned earlier, were synthesized via molecular reactions in solvents, contain complex $[MH_9]^{2-}$ anions. The coordination polyhedron is a tricapped trigonal prism. A detailed structure determination has been carried out for K_2ReH_9, and shows that the Re–H distances are all equal within the threefold standard deviation. Figure 17 shows a selected region of the hexagonal atomic arrangement.

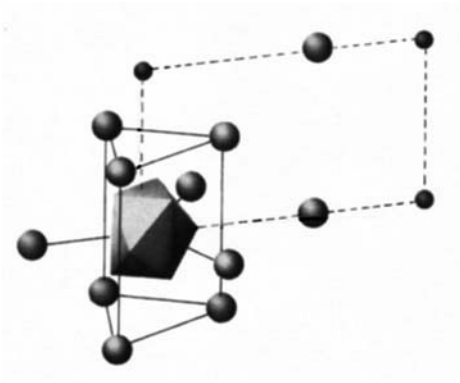

Fig. 17. A portion of the crystal structure of K_2ReH_9, showing the $[ReH_9]$ polyhedron, the positions of the adjacent potassium ions, and one *ac* plane of the hexagonal unit cell (dashed line).

Summarizing the results obtained up to now concerning the existence and structures of ternary transition metal hydrides with alkali metals, the picture already described for the compounds of the alkaline-earth metals in the previous section can now be extended to include these compounds. Here again, a characteristic feature of the structures is the presence of complex $[MH_z]^{x-}$ groups.

The heavy alkali metals are usually found to give colorless compounds, and transformations to phases with metallic properties are thus ruled out from the outset. Their structures show marked resemblances to those of the corresponding halides and chalcogenides. However, as in the ternary hydrides of the alkaline-earth metals, the higher oxidation states of the transition metals are not reached. Thus, the platinum compounds predominantly have planar $[PtH_4]^{2-}$ anions with platinum in the + 2 oxidation state. For palladium mainly Pd^0 complexes are known up to now; corresponding planar $[PdH_4]^{2-}$ or linear $[PtH_2]^{2-}$ units could so far only be stabilized as mixed crystals in the system Na/Pd/Pt/H.[20] The highest oxidation state found for rhodium and iridium is + 3. In this context the high oxidation state of + 7 in the hydrides K_2ReH_9 and K_2TcH_9 is surprising and difficult to understand. Some of the ternary hydrides containing lithium and sodium have interesting properties. For example, Na_2PdH_2 has a metallic gray appearance and shows semiconducting properties. The conductivity increases as the temperature is raised, and at 273 K was measured as $7.3 \times 10^{-2}\,cm^{-1}\Omega^{-1}$. In the Li/Pt/H and Li/Pd/H systems one already begins to find properties characteristic of metallic hydrides: there is considerable phase broadening, and dependent on the pressure or temperature the hydrogen undergoes a reversible uptake–release process, without a significant change in the arrangement of the metal atoms.

4. Hydrogen—an Anomalous Ligand?

The ternary hydrides $A_xM_yH_z$, in which A is an alkali metal or alkaline-earth metal and M is a transition metal, can be described as complex hydrides. Their crystal structures contain anionic $[MH_z]$ units. They have obvious similarities to the corresponding halides and oxides, but there are also some noticeable differences which clearly show that hydrogen is a special kind of ligand. Thus, one is struck by the fact that in all the crystal structures that have so far been determined—though these are admittedly few in number—isolated $[MH_z]$ complexes have always been found. Polynuclear complexes or framework structures, which are very common in ternary halides or chalcogenides, are not found here. It is even more surprising that the change in properties from those of isolated complexes to those of intermetallic phases is a direct transition, without any intermediate stages in which chain or layer structures are successively built up. This transition is illustrated by the following observations. The hydrides of the heavy alkali metals have essentially salt-like character, whereas Na_2PdH_2 is already a semiconductor, and the adjacent element, magnesium, forms a hydride, Mg_2NiH_4, in which the hydrogen can undergo a reversible uptake–release process as in typical metallic hydrides; finally, the Li/Pt/H and Li/Pd/H systems give compounds that show phase broadening and already have obvious metallic properties. These characteristic changes in the nature of the bonding could lead to interesting results especially concerning the magnetic and electrical properties, of which there have been few measurements up to now. One aspect worth mentioning here is that a number of binary and ternary hydrides of transition metals have been found to show superconductivity; for example, in the Pd/D system a maximum T_c value of 11 K has been reported.[27]

Another special feature of hydride ligands is their dynamic behavior. Thus the motional processes occurring in the sphere of the hydrogen ligands are responsible for the phase transitions that are observed in nearly all these systems. No corresponding behavior has ever been observed for the halides and chalcogenides with isotypic or closely related structures. In those complex hydrides that resemble metallic hydrides, such as Mg_2NiH_4, it is also found that at higher temperatures the hydrogen is released in a reversible process. Mg_2NiH_4 has potential applications as a hydrogen storage medium, especially as the hydrogen/metal mass ratio is more advantageous than for other transition metal hydrides. This compound has already been used by Daimler Benz for hydrogen-driven automobiles.[28]

An initial insight into the dynamic behavior of the hydrogen ligand is provided by NMR studies. Measurements have been made on K_2ReH_9 and K_2TcH_9 in solvents. A single line was found, which is explained by the fact that the hydrogen ligands are all equivalent as a result of rapid exchange.[3] In the case of K_2PtD_4, which undergoes a reversible crystallographic phase transition at 195 K (see Fig. 9), temperature-dependent ^{2}H-NMR measurements were performed on a powdered sample (see Fig. 18).[29] Below 180 K the width of the spectrum remains nearly constant, with a spin-lattice relaxation time T_1 of the order of minutes, indicating rigid lattice behavior. Between 180 and 210 K the shape of the spectrum changes radically. The experimental observations

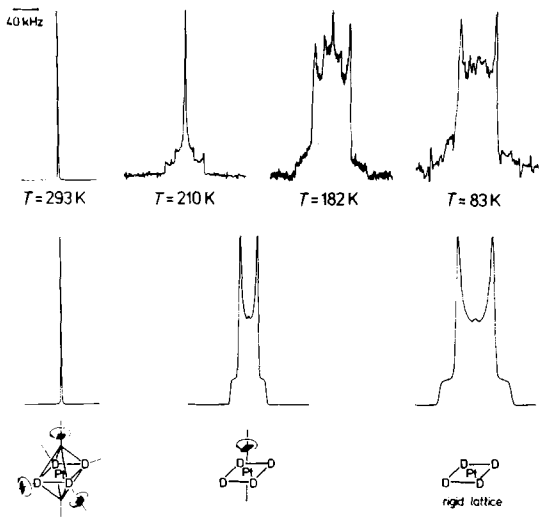

Fig. 18. ^{2}H-NMR spectra of K_2PtD_4 at different temperatures. Top: observed spectra. Bottom: calculated spectra for the dynamic processes described in the text.

are consistent with a model in which the square $[PtD_4]$ groups undergo rotational jumps in the plane of the square. Above the phase transition temperature the octahedral coordination of the platinum atoms results from rapid rotational jumps of the four deuterium atoms of each square planar unit around the fourfold axes. At 292 K, T_1 is 40 ms.

The different bonding situations in the hydrides cannot easily be explained in terms of the average metal–deuterium distances (Table 3). On the other hand, the volume increments give an indication of how wide a variation there is in the volume of the hydride ligands, especially when compared with the corresponding values for halides with analogous structures. In Figure 19 the volume increments for hydrogen in the complex hydrides $A_xM_yH_z$ are compared with the increments for fluorine and chlorine in the corresponding halide complexes $A_xM_yX_z$, in which X ≙ F or Cl. The plots give average volume increments as a function of the oxidation state of the transition metal M. The change in the volume increments for the fluoride and chloride ions are already known,[30] whereas this is the first time it has been possible to give values for the hydride ion. One is struck by the high "polarizability" of the hydride ion, which is indicated by the decrease of the volume increment with increasing oxidation number of the bonding partner. The volume contraction corresponds closely to that for the chloride ion, although the actual values are much closer to those for the fluoride ion, which shows scarcely and "polarizability". If we compare the alkali metal compounds with those of the alkaline-earth metals, the effect is seen even more clearly: in the latter compounds the increments for the fluoride ion show a slight increase with oxidation number, whereas for the chloride ion they are probably constant, and for the hydride ion there is again a marked contraction. This is greatest for the compounds in which one begins to observe a transition to metallic properties, and it is therefore not surprising that there are already appreciable deviations from the expected values in the cases of Na_2PdH_2 and $CaPdH_2$.

Table 3. Transition metal–deuterium distances [Å]. [a]

–	Mg_2FeD_6 1.56	Mg_2CoD_5 1.53	Mg_2NiD_4 1.54
–	–	–	–
–	–	–	–
–	Mg_2RuD_6 1.67	Na_3RhD_6 1.67	Li_2PdD_2 [b] 1.65
–	Sr_2RuD_6 1.69	Ca_2RhD_5 1.79	Na_2PdD_2 1.68
–	Ba_2RuD_6 1.74	Sr_2RhD_5 1.74	K_3PdD_3 1.68
K_2ReD_9 [b] 1.66	Mg_2OsD_6 1.68	Li_3IrD_6 1.65	$LiPtD_{0.66}$ 1.60
–	–	Na_3IrD_6 1.68	A_2PtD_4 [c] 1.63
–	–	Sr_2IrD_5 1.71	A_3PtD_5 [d] 1.62

[a] See footnote in Table 1. [b] In these cases the metal–deuterium distances were determined by extrapolation. [c] A ≙ Na, K, Rb, Cs. [d] A ≙ K, Rb, Cs.

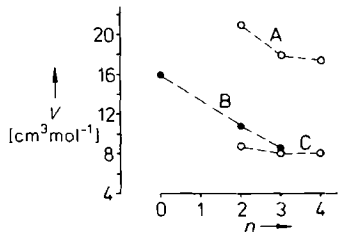

Fig. 19. Volume increments of X^- ions in compounds having the composition A_xMX_z, with X ≙ Cl (curve A), X ≙ H (curve B) and X ≙ F (curve C). In A_xMX_z, in all cases A represents K, Rb or Cs, and M is a transition metal of group eight.

Hydrogen—an anomalous ligand? Perhaps one should replace the question mark here by an exclamation mark!

5. Concluding Remarks

It has now become possible, through the use of specialized preparative techniques and by combining X-ray and neutron diffraction measurements over a wide range of temperatures, to begin to obtain a deeper insight into the relationships between structure and properties of complex transition metal hydrides. Only a few compounds have been studied in detail up to now, and those that are known at present nearly all belong to sub-group eight of the Periodic System. Thus there remains a great deal to be done. Indications regarding the existence of further hydrides which have not yet been properly characterized can be found in the literature. The study of this new group of compounds offers attractive prospects, since the position that they occupy between salts and metals is likely to result in interesting physical properties and applications.

I express sincere thanks to my present and former co-workers who have contributed to the investigations cited in this review. I expecially thank Dr. G. Auffermann and Dr. P. Müller. Thanks are also due to the Bundesministerium für Forschung und Technologie, the Deutsche Forschungsgemeinschaft, and the Fonds der Chemischen Industrie for financial support.

Received: December 21, 1990 [Z 825 IE]
German version: *Angew. Chem. 103* (1991) 776
Translated by Dr. *I. R. Beccansall*, Pwllheli (UK)

[1] a) R.G. Teller, R. Bau, *Struct. Bonding (Berlin) 44* (1981) 1; b) M. Brookhart, M.L.H. Green, L.-L. Wong, *Prog. Inorg. Chem. 36* (1988) 1; c) R.H. Crabtree, D.G. Hamilton, *Adv. Organomet. Chem. 28* (1988) 299.

[2] a) E.C. Ashby, R.G. Beach, *Inorg. Chem. 10* (1971) 2486; b) E.C. Ashby, J.J. Watkins, *ibid. 12* (1973) 2493; c) E.C. Ashby, T.F. Korenowski, R.D. Schwartz, *J. Chem. Soc. Chem. Commun. 1974*, 157.
[3] a) K. Knox, A.P. Ginsberg, *Inorg. Chem. 3* (1964) 555; b) C. Abrahams, A.P. Ginsberg, K. Knox, *ibid. 3* (1964) 558.
[4] A.P. Ginsberg, *Inorg. Chem. 6* (1964) 567.
[5] a) J.J. Reilly, R.H. Wiswall, *Inorg. Chem. 7* (1968) 2254; b) P. Zolliker, K. Yvon, J.D. Jorgensen, F.J. Rotella, *ibid. 25* (1986) 3590, and references cited therein.
[6] W. Bronger, P. Müller, D. Schmitz, H. Spittank, *Z. Anorg. Allg. Chem. 516* (1984) 35.
[7] W. Bronger, M. Gehlen, G. Auffermann, *Z. Kristallogr.*, in press.
[8] J.J. Didisheim, P. Zolliker, K. Yvon, P. Fischer, J. Schefer, M. Gubelmann, A.F. Williams, *Inorg. Chem. 23* (1984) 1953.
[9] a) P. Zolliker, K. Yvon, P. Fischer, J. Schefer, *Inorg. Chem. 24* (1985) 4177; b) E.J. Ivanov, I. Konstanchuk, A. Stepanov, Yan Jie, M. Pezat, B. Darriet, *ibid. 28* (1989) 613.
[10] W. Bronger, K. Jansen, unpublished.
[11] R.O. Moyer, C. Stanitski, J. Tanaka, M.I. Kay, R. Kleinberg, *J. Solid State Chem. 3* (1971) 541.
[12] W. Bronger, R.M. Beissmann, unpublished.
[13] M. Kritikos, D. Noréus, B. Bogdanovic, U. Wilczok, *J. Less Common Met. 161* (1990) 337.
[14] J. Zhuang, J.M. Hastings, L.M. Corliss, R. Bau, C.-Y. Wei, R.O. Moyer, *J. Solid State Chem. 40* (1981) 352.
[15] W. Bronger, K. Jansen, P. Müller, *J. Less Common Met. 161* (1990) 299.
[16] D. Noréus, K.W. Törnroos, A. Börje, T. Szabó, W. Bronger, H. Spittank, G. Auffermann, P. Müller, *J. Less Common Met. 139* (1988) 233.
[17] M. Gupta, L. Schlapbach, *Top. Appl. Phys. 63* (1988) 200.
[18] B. Nacken, W. Bronger, *Z. Anorg. Allg. Chem. 439* (1978) 29.
[19] W. Bronger, G. Auffermann, P. Müller, *J. Less Common Met. 116* (1986) 9.
[20] a) W. Bronger, G. Auffermann, P. Müller, *J. Less Common Met. 142* (1988) 243; b) W. Bronger, G. Auffermann, *ibid. 169* (1991) 173.
[21] W. Bronger, G. Auffermann, P. Müller, *Z. Anorg. Allg. Chem. 566* (1988) 31.
[22] B.G. Müller, *Z. Anorg. Allg. Chem. 491* (1982) 245.
[23] R. Hoppe, H.-J. Röhrborn, *Z. Anorg. Allg. Chem. 329* (1964) 110.
[24] K. Kadir, D. Noréus, *Z. Phys. Chem. N.F. 163* (1989) 231.
[25] B. Nacken, W. Bronger, *J. Less Common Met. 52* (1977) 323.
[26] W. Bronger, G. Auffermann, *J. Less Common Met. 158* (1990) 163.
[27] G. Wiesinger, G. Hilscher, *Top. Appl. Phys. 63* (1988) 329.
[28] H. Buchner, O. Bernauer, W. Staub, *Proc. 2nd World Hydrogen Energy Conf., Vol. 3*, Zürich, Switzerland 1988, p. 1677.
[29] W. Bronger, R.P. Jung, G. Neue, *Acta Crystallogr. Sect. A46* (1990) C366.
[30] W. Biltz: *Raumchemie der festen Stoffe*, Verlag von Leopold Voss, Leipzig 1934.

Transition-Metal Thiolates: From Molecular Fragments of Sulfidic Solids to Models for Active Centers in Biomolecules

By Bernt Krebs* and Gerald Henkel*

Dedicated to Professor Hans Georg von Schnering on the occasion of his 60th birthday

Thiolates are presently a subject of great interest in the chemistry of complexes involving transition-metal elements and soft ligands. The manifold electronic and steric capabilities offered by the monodentate ligands $RS^{\ominus}$ and the bidentate chelate ligands $^{\ominus}SRS^{\ominus}$ have been used to stabilize a broad spectrum of mononuclear, oligomeric, and polymeric complexes with new and remarkable structures and properties. Impetus has especially been provided by the synthesis of polynuclear cagelike homo- and heteroleptic metal–sulfur frameworks, which can often be regarded as "molecular fragments" of the structures of inorganic sulfides. Thiolates and mixed sulfide-thiolates of the late open- and closed-shell 3d metals (Fe, Co, Ni, Cu, Zn) and some of their homologues (Au, Cd, Hg), as well as of Mo, are of particular importance as model complexes for biologically important metal centers coordinated by sulfur. They have played an important role in increasing our understanding of the structure, bonding, and function of the reactive centers in ferredoxins, rubredoxins, nitrogenases, blue copper proteins, metallothioneins, and antiarthritic drugs.

1. Introduction

Transition-metal thiolates are an enormously rich class of compounds. As typical soft ligands (as defined by *Pearson*), the electron-rich thiolate groups $RS^{\ominus}$ and their multifunctional homologues have a great affinity for a large number of metals. They have been used as ligands since the very beginnings of coordination chemistry and were of importance for the development of this area of inorganic chemistry. Because of their chemical properties and their low solubilities, they have also found practical applications in, for example, analytical chemistry. However, many of the products synthesized have not been characterized precisely because of the lack of suitable physical techniques.

The thiolate ligands $RS^{\ominus}$ and $^{\ominus}SRS^{\ominus}$ are capable of extreme variations in their coordination and bonding to metals. While the monofunctional ligands can bond in a monodentate, μ_2-bridging or μ_3-bridging manner, the coordination possibilities offered by the difunctional thiolate anions are even greater. For various reasons the mono- and polynuclear complexes with a complete thiolate and/or sulfide coordination sphere are of special importance at present and are the subject of intensive studies. The polynuclear species in particular have multifarious and fascinating structural properties; in many cases they can be regarded as "molecular fragments" of the polymeric structures of solid sulfides.

Metal coordination centers with complete or partial sulfur coordination play an important part in the chemistry of life processes. Examples are provided by electron transferases such as the redox metalloproteins of iron (e.g., ferredoxins), oxidoreductases such as the nitrogenases (nitrogen-fixing enzymes), hydrolases such as the various zinc enzymes, nickel-containing hydrogenases, blue copper proteins such as plastocyanin, azurin, and ceruloplasmin, heterometalloenzymes such as cytochrome *c* oxidase, the group of nucleic acid binding proteins important in gene transcription, and the "metal-regulating" MerR proteins (mercury reductases), and, finally, the large group of metallothioneins, which are thought to have both a storage and transport function for metals and a detoxifying protective function against heavy metals. Thiolates are extremely useful as model ligands to simulate the bonding of the ligands present in biological systems (generally the thiolate function of cysteine) to active metals. Gold thiolates are of importance as drugs, particularly in arthritis therapy, and their use is likely to increase.

A new and interesting development is the use of volatile molecular thiolates as starting materials for the chemical vapor deposition (CVD) of metallic or sulfidic surface layers. In addition, the theoretical and practical interest in special 3d elements has been a major stimulus for the study of the chemistry of the polynuclear sulfur complexes of all the other transition metals; the spectacular development of this area promises to continue for some time.

Since the chemistry of metal–sulfur complexes is of such wide scope, this article will of necessity concentrate only on certain aspects of the very important class of homoleptic and heteroleptic polynuclear transition-metal complexes with thiolate or mixed sulfide-thiolate ligands. We shall limit our discussion to the chemistry of the important metals, Fe, Co, Ni, Cu, Ag, Au, Zn, Cd, and Hg. Complexes with 1,1-dithiolates and 1,2-dithiolenes, with other abiotic dithio ligands, or with pure sulfide and polysulfide coordination spheres, organometallic complexes with metal–carbon bonds and with π-acceptor ligands, complexes in which the metals have only a partial sulfur environment, and complexes with oxo ligands will not be included; here we refer the reader to detailed review articles.[1–14]

[*] Prof. Dr. B. Krebs
Anorganisch-Chemisches Institut der Universität
Wilhelm-Klemm-Strasse 8, W-4400 Münster (FRG)
Prof. Dr. G. Henkel
Fachgebiet Anorganische Chemie der Universität
Lotharstrasse 1, W-4100 Duisburg (FRG)

2. Iron Thiolate Complexes

2.1. The Homonuclear Centers of the "Simple" Iron–Sulfur Proteins

Iron is used by all known forms of life. The "simple" biomolecules with iron–sulfur centers include the rubredoxins, the ferredoxins, and the high-potential iron proteins (HIPIPs).[15] These molecules are known as iron–sulfur proteins. More complex metalloenzymes are also known; these contain additional prosthetic groups involving nickel (e.g., some hydrogenases and CO dehydrogenases)[16] and molybdenum or vanadium (e.g., nitrogenases).[17]

The mononuclear centers of the rubredoxins, the binuclear centers of the 2Fe-2S ferredoxins, and the tetranuclear centers of both the 8Fe-8S ferredoxins and the high-potential iron proteins (Fig. 1) were identified and completely characterized by about 1980.[18, 19]

Iron–sulfur proteins are characterized by distorted FeS_4 tetrahedra, which are linked in the polynuclear ferredoxin-like centers by common edges. The resulting short metal–metal distances allow for direct electronic interactions. The bridging ligands are always "naked" sulfide ions, and the terminally bonded sulfur atoms are provided by cysteine residues in the polypeptide chains.

The trinuclear iron–sulfur centers in ferredoxins from *Azotobacter vinelandii* (*Av* FdI) and *Desulfovibrio gigas* (*Dg* FdII)[20–22] were identified spectroscopically in 1980. Shortly thereafter, the structure of *Av* FdI was determined by protein crystallography.[23, 24] According to this study, the active center was discussed in terms of three vertex-linked FeX_4 tetrahedra, the distance between the iron atoms being about 4.1 Å. However, this structure did not agree with the results of resonance Raman studies of *Av* FdI in the native

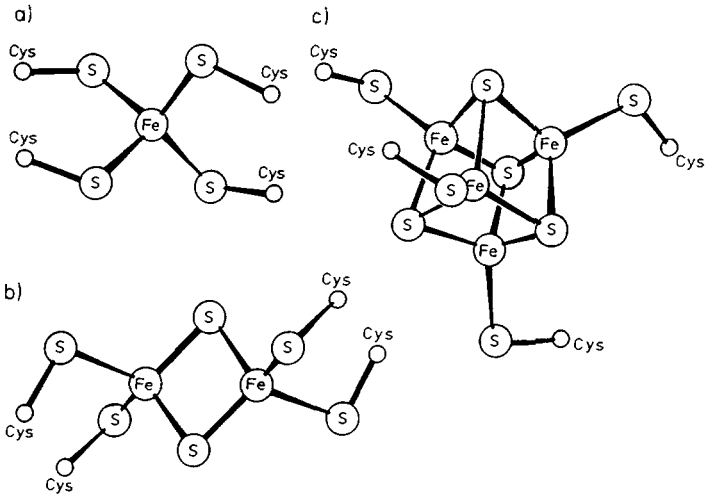

Fig. 1. Classical types of Fe–S centers in simple iron–sulfur proteins with cysteine ligands. a) 1Fe center in rubredoxins. b) 2Fe-2S center in chloroplast ferredoxins. c) 4Fe-4S center in bacterial and HIPIP ferredoxins.

state and of other proteins with 3Fe centers.[25] According to the resonance Raman studies and in agreement with EXAFS results on *Dg* FdII[26] and beef heart aconitase,[27] the iron atoms form an equilateral triangle with an edge length of about 2.7 Å.

Reinvestigations of the crystal structure of *Av* FdI[28–30] corrected the original results as far as the linking of the FeS_4 tetrahedra is concerned. The structure of the biological 3Fe centers corresponds to a model with an Fe_3S_7 framework, which we developed on the basis of the structural characteristics of the topologically related $[Fe_3S(SCH_2C_6H_2Me_2CH_2S)_3]^{2\ominus}$ (Fig. 2).[31, 32] According to protein structure analyses, trinuclear protein centers such

Gerald Henkel, born in 1948 in Burow (Mecklenburg), studied chemistry at the University of Kiel (1968–1973) and obtained his doctorate with B. Krebs at the University of Bielefeld in 1976. After work as a teaching and research assistant in Bielefeld (until 1977) and in Münster, he completed his habilitation (Münster, 1984) with work on coordination compounds of electron-rich transition metals with sulfur-containing ligands. Since 1988 he has been Professor of Inorganic Chemistry at the University of Duisburg, where he is Head of the Section Inorganic Chemistry/Solid State Chemistry. The main areas of his research are in the fields of structural and solid-state chemistry, of synthetic coordination chemistry (complexes with sulfur, selenium and tellurium ligands), and of bioinorganic chemistry.

Bernt Krebs, born in 1938 in Gotha (Thüringen), studied chemistry at the University of Göttingen, where he completed his doctorate with G. Gattow in 1965. From 1965 to 1966 he worked as a research assistant with W. C. Hamilton and D. F. Koenig at Brookhaven National Laboratory, Upton, N.Y. After returning to Göttingen, he completed his habilitation in 1969 in O. Glemser's laboratory with the synthesis and structure of Mo, Tc, and Re oxo compounds. In 1971 he took over an associate professorship at the University of Kiel, and in 1974 he became the first Professor of Inorganic Chemistry at the newly established University of Bielefeld. Since 1977 he has been Professor of Inorganic Chemistry at the University of Münster. His research interests include the synthesis and structural chemistry of polynuclear inorganic sulfur, selenium, and tellurium compounds, of polynuclear transition-metal oxo compounds, and of biologically relevant transition-metal complexes with sulfur ligands, as well as diffraction and other structural methods (EXAFS) in inorganic and bioinorganic chemistry.

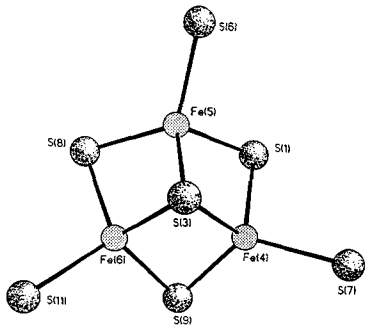

Fig. 2. Synthetic model of the 3Fe-4S center of 3Fe proteins [31].

as those in *Av* FdI are also present in *Dg* FdII[33] and in the (inactive) form of aconitase.[34-36]

In spite of the successful investigations in the area of "classical" protein centers, work closely associated with the name of *R. H. Holm*,[18, 19, 37] it has not yet been possible to synthesize any "good" models for the centers of the 3Fe ferredoxins. From the chemical point of view the 3Fe fragments of the complexes $[Fe_6S_9(SR)_2]^{4\ominus}$ (see Section 2.2.4) represent the best approximation presently available with respect to the oxidation state of the iron atoms and the chemical definition of the $[Fe_6S_{11}]$ framework.[38-42, 31]

2.2. Model Complexes

The class of homo- and heteroleptic iron thiolates comprises mono-, bi-, and tetranuclear species; the coordination number is generally 4 in all cases. Higher coordination numbers are apparently only achieved when the (mean) oxidation state of iron does not fall below + 3 and when, at the same time, the steric effects of the ligands would otherwise lead to too great a distortion of the FeS_4 tetrahedra. In the mixed sulfide-thiolate complexes, however, the coordination number is always 4; neighboring FeS_4 tetrahedra have common edges when the number of iron atoms is smaller than six. In other cases both vertex- and edge-linked FeS_4 tetrahedra occur simultaneously.

With respect to the manner in which the FeS_4 tetrahedra are linked, the binuclear sulfide-thiolate complexes are closely related to the binuclear iron thiolates. As in the 2Fe-2S ferredoxins themselves, their Fe_2S_6 frameworks form fragments of the infinite $[MS_2]_\infty$ chain of *trans*-edge-linked tetrahedra with the SiS_2 structure, as found in naturally occurring minerals such as erdite ($NaFeS_2 \cdot 2H_2O$)[43] or in synthetic inorganic solids such as the alkali-metal thioferrates(III).[43] The principle of linking FeS_4 tetrahedra via common vertices is also observed in the tetranuclear iron thiolates; in this case, however, no combination with edge-linking, as found in sulfide-thiolates, is observed.

2.2.1. *Binuclear Complexes*

The (formal) replacement of the cysteine residues in the 2Fe-2S ferredoxins by alkanethiolate ligands leads to binuclear mixed sulfide-thiolate complexes. The first compound of this class to be obtained was $[Fe_2S_2(SCH_2C_6H_4CH_2S)_2]^{2\ominus}$ (Fig. 3a).[45, 46] Since the iron atoms are trivalent, it was also the first model for (oxidized) 2Fe-2S ferredoxins.

Other binuclear iron sulfide-thiolates have since been described; these include complex ions with monofunctional thiolate ligands[39, 46] and analogous compounds with central Fe_2Se_2 centers[47, 48] or derivatives with terminally bonded halide ions.[49-52] An elegant route to binuclear iron sulfide-thiolate complexes involves the reduction of S_8 by ligands of the complex anion $[Fe(SR)_4]^{2\ominus}$, which are replaced in the course of the reaction by the sulfide ions formed.[53] Preparative and spectroscopic details can be found in review articles and the literature cited therein.[18, 19, 37, 54]

Purely inorganic derivatives of the binuclear sulfide-thiolate complexes with complete chalcogen ligand spheres have also been prepared: these include $[Fe_2S_2(S_5)_2]^{2\ominus}$[51, 55] and the interesting selenium analogue $[Fe_2Se_2(Se_5)_2]^{2\ominus}$[56] (Fig. 3b).

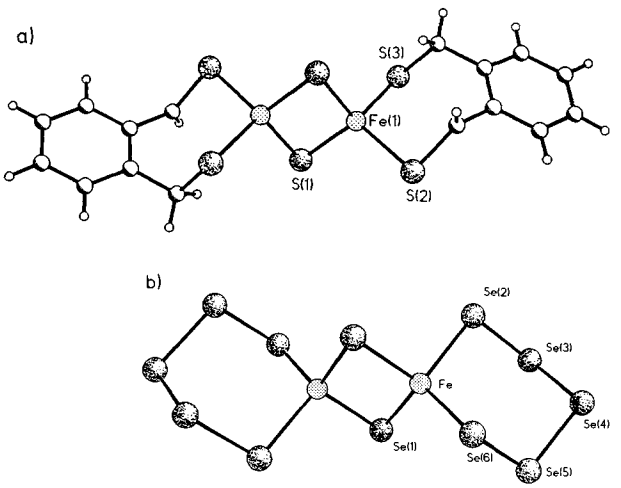

Fig. 3. Structural comparison of the anions $[Fe_2S_2(SCH_2C_6H_4CH_2S)_2]^{2\ominus}$ (a) [46] and $[Fe_2Se_2(Se_5)_2]^{2\ominus}$ (b) [56].

Homo- and heteroleptic iron thiolates form a further group of binuclear complexes with a complete sulfide ligand sphere. With the exception of the 1,2-dithiolate complexes, these compounds are characterized by a bi-tetrahedral Fe_2S_6 framework. In contrast to the sulfide-thiolates, these compounds contain thiolate bridges, which introduce only half as many negative charges into the complex as do the corresponding sulfide ions, so that in principle they favor lower oxidation states of iron. In these complexes the iron does indeed prefer the oxidation state + 2, and it has not so far been possible to isolate oxidized examples with tetrahedral metal coordination.

Binuclear thiolates of iron(III) can in principle be stabilized by the bonding of additional thiolate ligands, with a corresponding increase in the coordination number. However, the known examples are limited to complexes with bifunctional 1,2-dithiolate ligands such as $[Fe_2(SC_6H_3MeS)_4]^{2\ominus}$[57] (Fig. 4). The square-pyramidal coordination, which is unusual for iron thiolates, is due to the short S···S distances in the ligands; these do not permit a sufficiently undistorted tetrahedral sulfur coordination.[57-61]

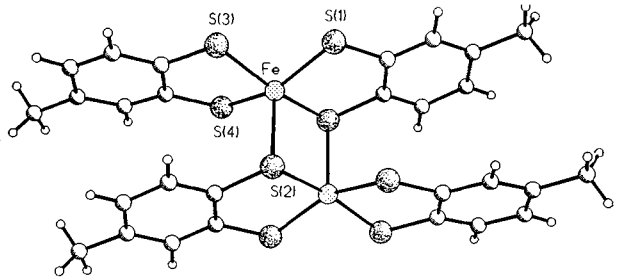

Fig. 4. Structure of $[Fe_2(S_2C_6H_3Me)_4]^{2\ominus}$ [57].

$[Fe_2(SCH_2C_6H_4CH_2S)_3]^{2\ominus}$, the first binuclear thiolate complex with tetrahedral FeS_4 centers to be isolated, was obtained as an unexpected product in the course of attempts to synthesize mononuclear compounds.[62, 63] Because of the bifunctionality of the ligands, the isomeric forms **IIa–c** shown in Figure 5 are theoretically possible. In addition to the frameworks with tetrahedral stereochemistry, Figure 5 also shows the corresponding frameworks for square-planar metal coordination (**Ia**, **Ib**). Isomer **IIa** was identified in

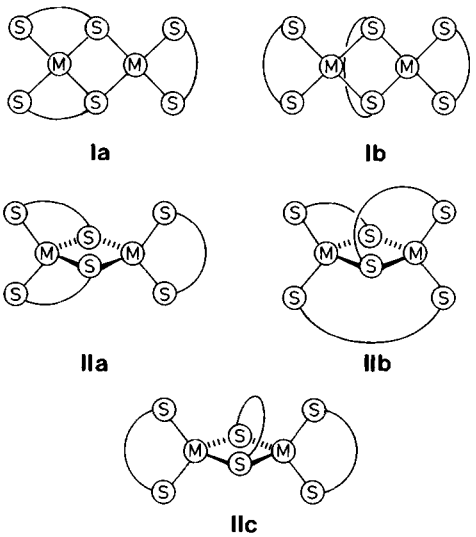

Fig. 5. Possible structural isomers of binuclear four-coordinated metal(II) dithiolates, $[M_2(SRS)_3]^{2\ominus}$. **Ia,b**: square planar. **IIa–c**: tetrahedral metal coordination [107].

$[Et_4N]_2[Fe_2(SCH_2C_6H_4CH_2S)_3]\cdot 2MeCN$; the alkyl groups are oriented *anti*, the Fe–Fe distance being 3.034 Å.[65, 66] The centrosymmetrical anion $[Fe_2(SEt)_6]^{2\ominus}$ has a similar configuration in the tetraethylammonium salt.[65] The synthesis of isomer **IIb** of the complex anion $[Fe_2(SCH_2C_6H_4CH_2S)_3]^{2\ominus}$ (Fig. 6, top) was also possible when other counterions were chosen.[66] In this case the coordination of one of the ligands is unusual: instead of acting as a chelating ligand, it occupies two terminal positions in the complex. Since the S–S distance in this ligand is only 4.25 Å, the complex is folded and the Fe–Fe distance is decreased to 2.88 Å. The unconventional bonding of the ligand also leads to the unusual *syn-exo* arrangement of the alkyl residues. Analogous complexes of cadmium,[67] cobalt,[68] and manganese[69] have also been described.

$[Fe_2(SCH_2C_6H_4CH_2S)_2(SPh)_2]^{2\ominus}$ (Fig. 6, bottom) is a heteroleptic iron thiolate with a centrosymmetric structure and terminal thiophenolate ligands.[66] The Fe–Fe distances in the planar $Fe_2(SR)_2$ units (*anti* configuration) are 2.98 Å; the complex is closely related to a derivative in which the thiophenolate ligands are replaced by dithiocarbamate groups.[57] The introduction of the bifunctional dithio ligands leads to an increase in the coordination number of iron and a lengthening of the Fe–Fe distance (3.16 Å). Heteroleptic complexes of this type are also formed by manganese.[69]

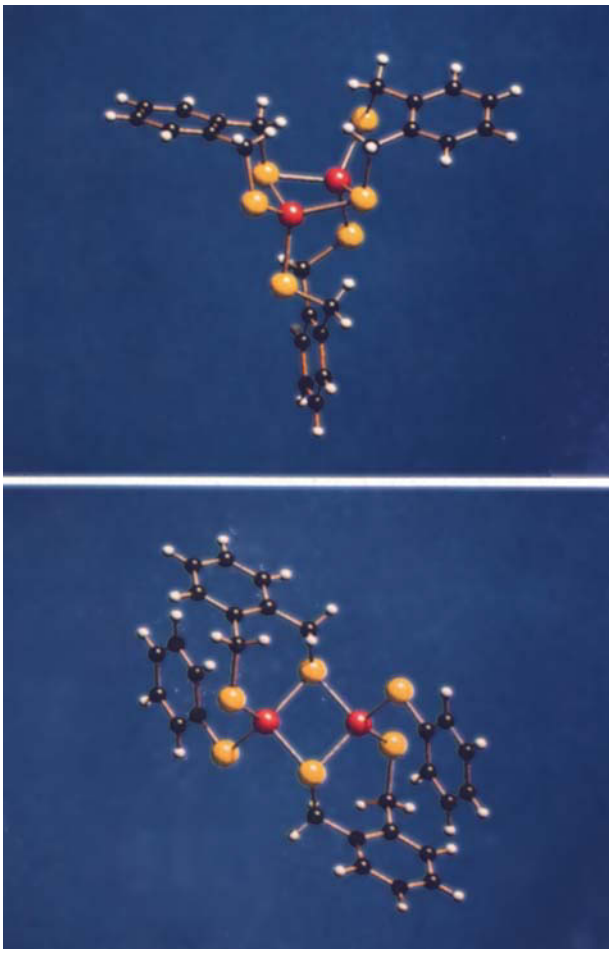

Fig. 6. Structures of the homologous anions $[Fe_2(SCH_2C_6H_4CH_2S)_3]^{2\ominus}$ (top) [66] and $[Fe_2(SCH_2C_6H_4CH_2S)_2(SPh)_2]^{2\ominus}$ (bottom) [66].

The magnetic behavior of the binuclear iron complexes is dominated by antiparallel spin couplings, which are due either to superexchange mechanisms with participation of orbitals from bridging sulfur atoms or to direct metal–metal interactions.

2.2.2. *Trinuclear Complexes*

Trinuclear thiolate complexes have not yet been described, although mixed iron sulfide-thiolate species are known, either as Fe^{III} complexes whose linear Fe_3S_8 frameworks correspond to fragments of the SiS_2 chain structure or as Fe^{II} complexes whose Fe_3S_7 frameworks have a defect cubane structure.

The first trinuclear iron sulfide-thiolate compound to be reported, $[Fe_3S(SCH_2C_6H_2Me_2CH_2S)_3]^{2\ominus}$ (Fig. 7, top), was initially obtained as an unexpected product of the reaction between 4,5-dimethyl-1,2-bis(methylthio)benzene, $FeCl_3$, *p*-thiocresol, and NaOMe in MeOH.[32] The synthesis proceeds in better yields when the reagents are mixed in stoichiometric ratios. When NaHS is used as the sulfide component and $(SCH_2C_6H_2R_2CH_2S)^{2\ominus}$ (R = Me or H) as the thiolate component, complexes of the general composition $[M_3S(SCH_2C_6H_2R_2CH_2S)_3]^{2\ominus}$ are formed; these are stable when M = Fe,[66] Co,[70] or Ni.[71] Similar reaction systems were studied in which the sulfide component was Li_2S, and analogous complexes with M = Fe and Co were isolated.[41] When NaHS is replaced by the corresponding selenium compound, the mixed selenide-thiolate complex $[Fe_3Se(SCH_2C_6H_4CH_2S)_3]^{2\ominus}$ is formed.[66]

According to the most recent protein structure analyses, the Fe_3S_7 framework of $[Fe_3S(SCH_2C_6H_2Me_2CH_2S)_3]^{2\ominus}$ described above (Fig. 2) is topologically closely related to the 3Fe-4S centers of ferredoxins and aconitase.[28–30, 33–36] Apart from the sulfide bridge, the complex also has three thiolate bridges; these probably stabilize the unusually low oxidation state, since Fe^{II} has so far not been observed in any other sulfide-thiolate complex. The thiolate character of the μ-S atoms and the low oxidation state of the iron are also responsible for the fact that chemical similarities to the 3Fe-4S protein centers are only small. The corresponding proteins contain only sulfide bridges; these stabilize a mixed-valent metal state with a mean oxidation state of + 2.67.[22] The search for model complexes for the biological 3Fe centers also led to the synthesis of the trinuclear complex $[Fe_3S_4(SEt)_4]^{3\ominus}$. The complex anion is formed in the reaction of $[Et_4N]_2[Fe(SEt)_4]$ with S_8; subsequent reaction with thiophenol leads to the formation of the analogous thiophenolate-substituted complex (Fig. 7, bottom).[39, 64] The Fe_3S_8 framework represents a trinuclear fragment of the SiS_2 structure and is thus an extension of the corresponding frameworks of binuclear compounds with edge-linked FeS_4 tetrahedra. Its magnetic behavior obeys the Curie–Weiss law with antiferromagnetically coupled iron atoms. The $S = 5/2$ ground state is commensurable with high-spin $Fe^{3\oplus}$ ions.[72]

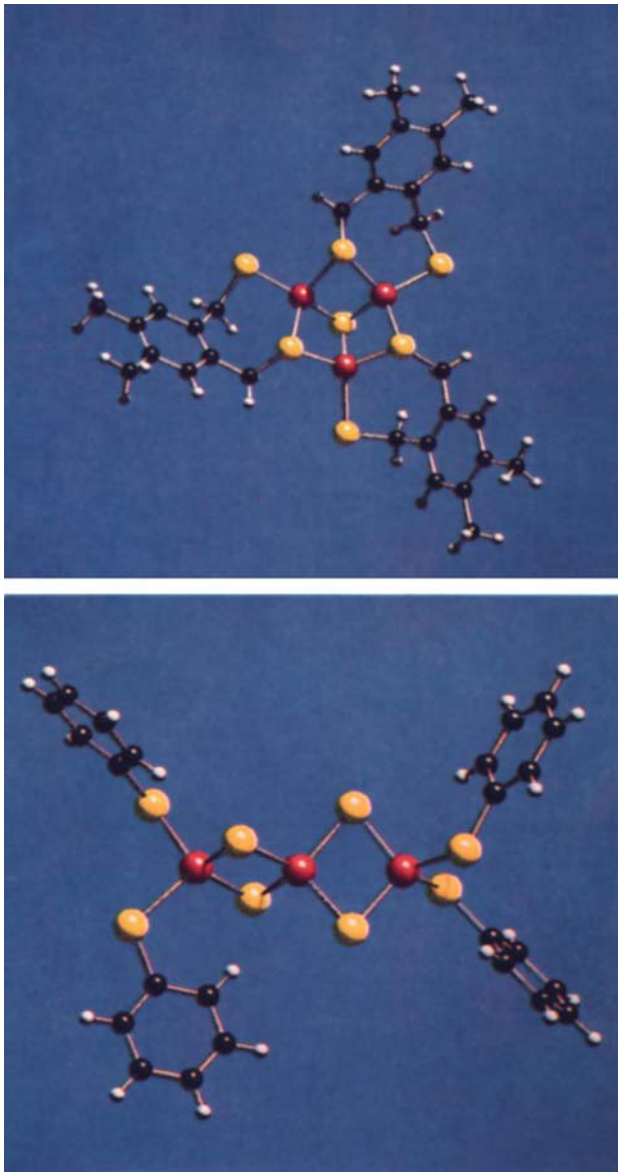

Fig. 7. Structures of the cyclic trinuclear $[Fe_3S(SCH_2C_6H_2Me_2CH_2S)_3]^{2\ominus}$ (top) [32] and the linear trinuclear $[Fe_3S_4(SPh)_4]^{3\ominus}$ (bottom) [64].

2.2.3. *Tetranuclear Complexes*

The synthesis of the first tetranuclear sulfide-thiolate complexes of iron has made electronic, chemical, and structural models for the active sites of 4Fe-4S proteins accessible. The preparation of $[Fe_4S_4(SCH_2Ph)_4]^{2\ominus}$ from $FeCl_3$, NaOMe, NaSH, and $PhCH_2SH$ in methanol was reported in 1972.[73, 74] Since that time, a large number of derivatives of the general composition $[Fe_4S_4(SR)_4]^{z\ominus}$ with $z = 1$, 2, and 3 have been prepared and studied; the extensive literature has been surveyed in several review articles.[18, 19, 37, 54]

A particularly important feature of these highly condensed compounds is the possibility of replacing sulfur by its homologues selenium and tellurium without any change in the mode of coordination. The structurally characterized derivatives in the series of mixed chalcogenide-chalcogenolate complexes $[Fe_4X_4(YR)_4]^{z\ominus}$ include the following anions:

X = S: $[Fe_4S_4(SePh)_4]^{2\ominus}$, $[Fe_4S_4(TePh)_4]^{2\ominus}$[75, 76]

X = Se: $[Fe_4Se_4(SPh)_4]^{2\ominus}$,[77] $[Fe_4Se_4(SPh)_4]^{3\ominus}$,[84] $[Fe_4Se_4(SePh)_4]^{2\ominus}$, $[Fe_4Se_4(SePh)_4]^{3\ominus}$, $[Fe_4Se_4(TePh)_4]^{3\ominus}$[75, 76]

X = Te: $[Fe_4Te_4(SPh)_4]^{3\ominus}$,[75, 76, 78, 79] $[Fe_4Te_4(SPh)_4]^{2\ominus}$, $[Fe_4Te_4(SePh)_4]^{3\ominus}$,[75, 76] $[Fe_4Te_4(TePh)_4]^{3\ominus}$[75, 76, 78, 80]

Compounds with a cubane-like Fe_4S_4 framework are as yet unknown in the chemistry of solid sulfides. Direct relationships between the structural principles of the tetranuclear chalcogenide-chalcogenolate complexes and crystalline nonmolecular solids do however exist in the system iron–tellurium; here the phase $Cs_7Fe_4Te_8$ is known to consist of defined $[Fe_4Te_8]^{7\ominus}$ units and $Cs^{\oplus}$ ions;[81] these units are closely related to the Fe_4Te_8 framework of the anion $[Fe_4Te_4(TePh)_4]^{3\ominus}$ (Fig. 8).

The central iron–sulfur framework of the tetranuclear sulfide-thiolate complexes consists of two interpenetrating tetrahedra, one formed by iron atoms, the other by sulfur

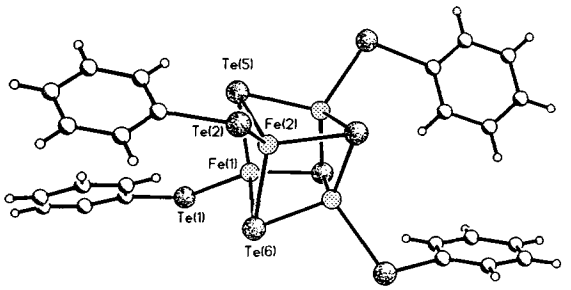

Fig. 8. The anion $[Fe_4Te_4(TePh)_4]^{3\ominus}$ in crystalline $[Et_4N]_3[Fe_4Te_4(TePh)_4] \cdot 2MeCN$ [80].

atoms. In the methanethiolate complex anion,[82] a typical example, the Fe–Fe distances are 2.7–2.8 Å, the S–S distances 3.7–3.8 Å (Fig. 9). The volumes of the tetrahedra in the redox system $[Fe_4S_4(SPh)_4]^{2\ominus}/[Fe_4S_4(SPh)_4]^{3\ominus}$ have been calculated as 2.41 and 2.40 Å^3 (Fe), respectively, and 5.54 and 5.75 Å^3 (S), respectively.[83, 84] The uptake of an additional electron thus leads to a significant increase in the volume of the (inner) S_4 tetrahedron, while the volume of the Fe_4 tetrahedron remains practically unchanged. Because of the short Fe···Fe distances, the magnetic behavior of the complexes is determined by antiparallel spin couplings, as in the bi- and trinuclear cases.

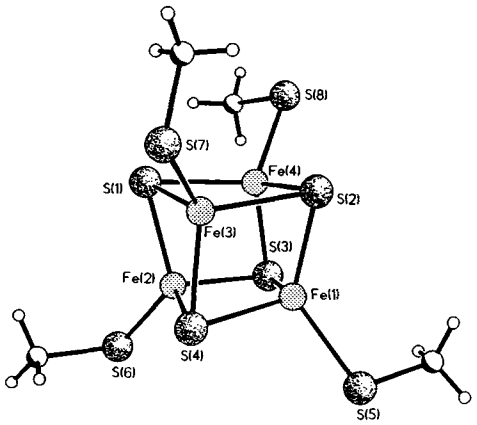

Fig. 9. Structure of $[Fe_4S_4(SMe)_4]^{2\ominus}$ [82] determined from neutron diffraction data.

Fe_4S_4 cubane frameworks in crystalline complexes deviate to a greater or lesser degree from an ideal T_d symmetry; this distortion and its possible origins have already been discussed in the literature.[85] It appears that the electronic ground state ($S = 0$) of the dianionic species $[Fe_4S_4(SR)_4]^{2\ominus}$ favors the tetragonal distortion of the Fe_4S_4 cubane unit. In the case of the more strongly reduced trianionic species $[Fe_4S_4(SR)_4]^{3\ominus}$ there is no uniform picture of distortion.[84–86]

A further group of tetranuclear complexes with complete sulfur ligand spheres is formed by the homoleptic thiolates $[Fe_4(SEt)_{10}]^{2\ominus}$[65] and $[Fe_4(SPh)_{10}]^{2\ominus}$ (Fig. 10),[87, 88] which, like the binuclear complexes, contain tetrahedrally coordinated Fe^{II}. In contrast to all other known complexes, the FeS_4 tetrahedra are linked here only via vertices. The metal–sulfur framework corresponds to a fragment of the zinc blende structure and contains an adamantane-like Fe_4S_6 cage with four terminally bonded thiolate sulfur atoms.

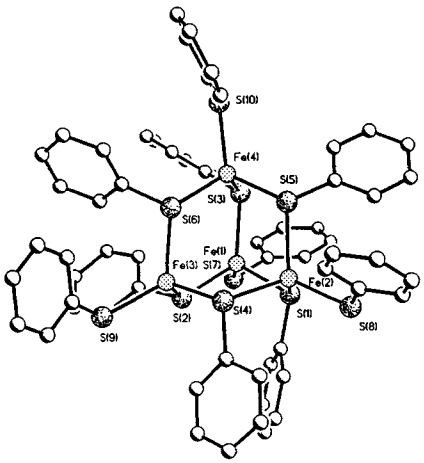

Fig. 10. Structure of the adamantane-like sulfide-thiolate anion $[Fe_4(SPh)_{10}]^{2\ominus}$ [88].

2.2.4. *Complexes Containing More than Four Iron Atoms*

Strenuous efforts have been made to prepare suitable models for the iron–sulfur centers of the 3Fe-4S proteins and the mixed iron–molybdenum–sulfur centers of the nitrogenases. In addition to the synthesis and characterization of trinuclear sulfide-thiolate complexes (see Section 2.2.2), a further milestone was the synthesis of hexanuclear sulfide-rich thiolates, which have played an important role in increasing our understanding of 3Fe-4S centers and the nitrogenases. The preparation of $[Fe_6S_9(SCH_2Ph)_2]^{4\ominus}$ (Fig. 11) was achieved via the reaction of $FeCl_3$ with $NaSCH_2Ph$ and Na_2S_2 in methanol.[31, 42, 89] The Fe_6S_{11} framework of this

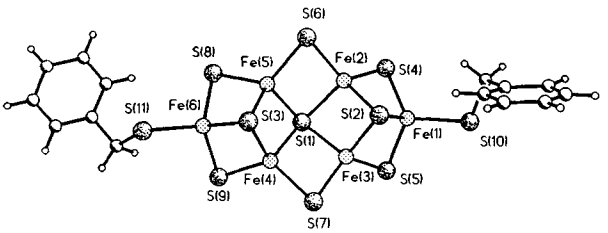

Fig. 11. The anion $[Fe_6S_9(SCH_2Ph)_2]^{4\ominus}$ in crystalline $[Et_4N]_4[Fe_6S_9(SCH_2Ph)_2] \cdot H_2O$ [42].

compound consists of six FeS_4 tetrahedra which are linked via common edges and vertices in such a way that all the iron atoms lie in a plane. The differing Fe–S distances, as well as the Mössbauer spectra, indicate that the four iron atoms in the center of the complex anion have an oxidation state of + 2.5, whereas the two terminal metal centers are Fe^{III}.

The sulfur atoms take up one of four different coordination states: in additon to a symmetrical μ_4-sulfide bridge there are two symmetrical μ_3-sulfide bridges, six μ_2-sulfide bridges, and two terminally bonded thiolate S atoms.

Comparably built complexes with ethanethiolate and *tert*-butanethiolate ligands were synthesized in a different man-

ner.[38, 39, 90] An interesting tetradecanuclear example is found in crystals of $[Et_4N]_6[\{Fe_6S_9(SMe)_2\}_2Na_2]$[31] (Fig. 12). It consists of two hexanuclear units which are linked via sodium. The sulfide ions in the subunits can be exchanged for selenide ions; in this way it was possible to obtain the hexanuclear selenide-thiolate complex $[Fe_6Se_9(SMe)_2]^{4\ominus}$,[40, 91] which was also structurally characterized.

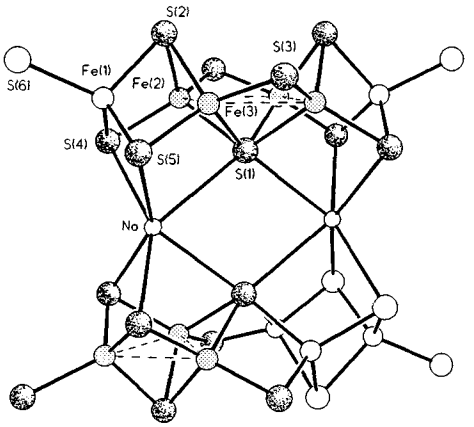

Fig. 12. $[(Fe_6S_{11})_2Na_2]$ framework of the $[\{(Fe_6S_9)(SMe)_2\}_2Na_2]^{6\ominus}$ structural unit in crystalline $[Et_4N]_6[\{(Fe_6S_9)(SMe)_2\}_2Na_2]$. The upper part shows an Fe_4S_9 unit as a part of a model for the M-Fe-S cluster (M = Mo, V) of nitrogenase, the lower part an Fe_3S_7 unit as a model for the 3Fe-4S centers of the 3Fe proteins [31].

Two important fragments of the metal–sulfur framework of the heteronuclear complex anion $[\{Fe_6S_9(SMe)_2\}_2Na_2]^{6\ominus}$ are emphasized in Figure 12: the Fe_4S_9 framework with the central square Fe_4 unit in the upper part of the molecule and the Fe_3S_7 framework of the trinuclear subunits at the lower left. Neighboring FeS_4 tetrahedra in the Fe_4S_9 unit are linked not only by common edges but also via common vertices. This interesting condensation principle, which is new in iron sulfide-thiolate chemistry, leads to the formation of square pyramids whose bases are occupied by iron atoms and whose vertices by sulfur atoms. In the parent compound, the structure of which is based on the Fe_4S_9 fragment, the bases of six of these (μ_4-S-Fe_4) pyramids are linked to form a cubic arrangement of iron atoms. In this model each of the eight iron atoms is surrounded by three sulfide ligands and bonded terminally to a thiolate group in such a way that a tetrahedral FeS_4 coordination is achieved.

On the basis of these considerations we developed a new structural hypothesis for the Fe–M–S centers of the molybdenum- (M = Mo) and vanadium-dependent (M = V) nitrogenases and the Mo–Fe and V–Fe cofactors isolated from them;[31, 42] a comparable suggestion based on the structural principles of a cobalt compound has also been made.[37, 92] The model (Fig. 13) contains a central cube formed by seven iron atoms and a heterometal. In the case of the vanadium-dependent enzymes this site is occupied by vanadium, in the biogenetically younger form by molybdenum. The heterometal cage is surrounded by an octahedron of sulfur atoms, which are located above the centers of the faces of the cube and therefore act as μ_4 bridges. The terminal ligands bonded to the iron atoms in the enzyme are thiolate residues

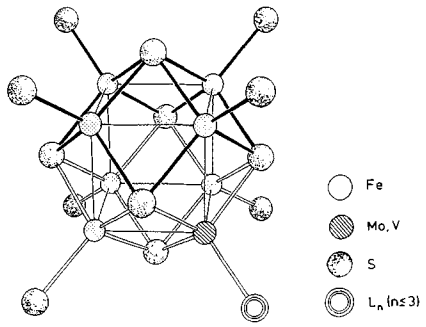

Fig. 13. $[Fe_7MS_{13}L_n]$ framework of the $[Fe_7MS_6(SR)_7L_n]^{z\ominus}$ cluster (M = Mo, V; n = 1, 2 or 3), which has been suggested as a model for the M–Fe–S center of nitrogenase. The atoms connected by bold lines correspond to the Fe_4S_9 unit in $[\{Fe_6S_9(SMe)_2\}_2Na_2]^{6\ominus}$ (compare Fig. 12 above) [31].

from cysteine groups. Molybdenum can most probably bond up to three exogenous ligands and thus has the necessary flexibility to coordinate both the N_2 molecule to be reduced and its activation products.

The Fe_3S_7 units of the hexanuclear complexes (Fig. 12) have a defect cubane structure, as in the trinuclear sulfide-thiolate complexes of Fe^{II}. Chemically they are closely related to the centers of the 3Fe-4S proteins, since all four μ-S atoms of this unit are simple sulfide ions and the iron atoms (mean oxidation state + 2.67) exist in corresponding states. It has not so far been possible to prevent the condensation of these units to form hexanuclear complexes.

An interesting extension of the condensation of these units was recently discovered in the complex salt $[n\mathrm{Pr}_4N]_6Na_4[Fe_{18}S_{30}] \cdot 14\,MeCN$,[93, 94] which contains only bridging sulfide ligands. The remarkable toroidal anion of this compound contains two Fe_6S_{11} units, the construction of which is similar to the metal-sulfur framework of the hexanuclear sulfide thiolate complexes; these Fe_6S_{11} units are linked via condensation with two three-membered chains of edge-linked FeS_4 tetrahedra in a cyclic manner.

3. Cobalt Thiolate Complexes

As in the case of iron, the coordination chemistry of cobalt with mono- and bifunctional thiolate ligands is dominated by the tendency to form tetrahedral MS_4 units, also in the presence of sulfide. However, in contrast to iron, cobalt avoids the formation of higher oxidation states than + 2 in its thiolate and sulfide-thiolate complexes. This probably prevents the formation of tetranuclear sulfide-thiolate complexes of cobalt with cubane-like M_4S_4 frameworks, although the latter are particularly stable in the case of iron.

The first cobalt complex with a mixed sulfide-thiolate ligand sphere was obtained in 1982 from the reaction of $CoCl_2$ with Li_2S and LiSPh in methanol solution in the presence of excess LiOMe.[92, 95] In the octanuclear anion $[Co_8S_6(SPh)_8]^{4\ominus}$ (Fig. 14) the cobalt atoms occupy the corners of a cube the lengths of whose sides lie between 2.63 and 2.68 Å; six sulfur atoms are arranged above the centers of the faces in the form of an octahedron. A second, much larger outer cube, whose faces are almost parallel to the faces of the inner Co cube, is formed by the eight S atoms of the thiophenolate ligands. The complex can be reduced to the

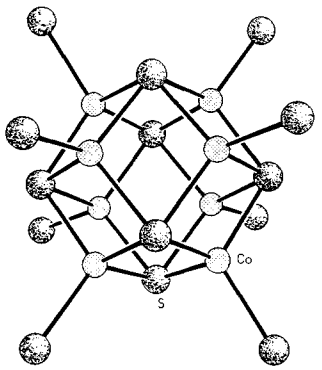

Fig. 14. Structure of the sulfide-thiolate anion $[Co_8S_6(SPh)_8]^{4\ominus}$. The phenyl groups have been omitted for the sake of clarity [92].

mixed-valent anion $[Co_8S_6(SPh)_8]^{5\ominus}$, with a slightly larger central Co_8S_6 cage.[92]

The cobalt compound $[Co_3S(SCH_2C_6H_4CH_2S)_3]^{2\ominus}$[41, 70] is an example of a trinuclear anion $[M_3S(SR)_6]^{2\ominus}$ with divalent metal atoms. Here, the bridging sulfide can be replaced not only by selenide but also by telluride when the homologous chalcogenides are used in the synthesis instead of NaHS. In this manner the novel complex anions $[Co_3Se(SCH_2C_6H_4CH_2S)_3]^{2\ominus}$ and $[Co_3Te(SCH_2C_6H_4CH_2S)_3]^{2\ominus}$ (Fig. 15) were obtained; these were the first mixed selenide-thiolate and telluride-thiolate complexes of cobalt[96] to be described. In addition, the bifunctional thiolate ligands can be replaced by the corresponding selenolates. Two members of the series of mixed cobalt chalcogenide-selenolate complexes are already known: $[Co_3S(SeCH_2C_6H_4CH_2Se)_3]^{2\ominus}$ and $[Co_3Se(SeCH_2C_6H_4CH_2Se)_3]^{2\ominus}$.[96]

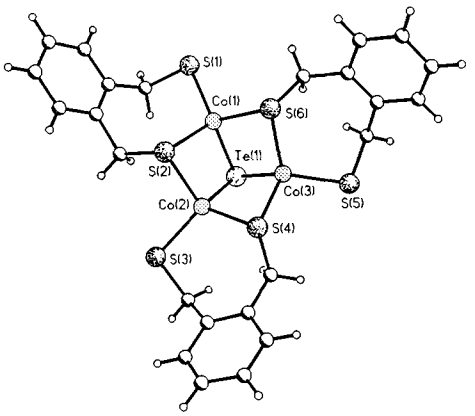

Fig. 15. The telluride-thiolate anion $[Co_3Te(SCH_2C_6H_4CH_2S)_3]^{2\ominus}$ [96].

Apart from these sulfide-thiolate complexes of cobalt and their Se- and Te-substituted derivatives, several multinuclear homoleptic cobalt thiolate complexes with complete sulfur ligand spheres have been prepared: $[Co_4(SPh)_{10}]^{2\ominus}$,[88, 97, 98] *syn*- and *anti*-$[Co_2(SEt)_6]^{2\ominus}$,[65] and *syn-exo*-$[Co_2(SCH_2C_6H_4CH_2S)_3]^{2\ominus}$ (isomer **IIb**, cf. Fig. 5).[68] With the exception of *syn*-$[Co_2(SEt)_6]^{2\ominus}$, they correspond to the analogous iron compounds. The general preparative and structural aspects of the iron thiolate complexes can thus in principle be transferred to the cobalt reaction system.

4. Nickel Thiolate Complexes

There has been extreme interest in nickel complexes with thiolate ligands ever since the discovery of nickel–sulfur interactions in hydrogenases from *Methanobacterium thermoautotrophicum*[99] and *Desulfovibrio gigas*[100] as well as in the CO dehydrogenase from *Clostridium thermoaceticum*.[101]

Both nickel complexes with ligands of the saturated thiolate type and with mixed sulfide-thiolate coordination generally contain divalent metal centers. In contrast to iron and cobalt, the divalent d^8 nickel in these compounds is characterized by square-planar MS_4 units which have a particularly strong tendency in both protic and aprotic solvents to form condensed species sharing common edges.[102] Heterocyclic Ni_2S_2 rings are thus formed; these are generally not completely planar, but are folded to a greater or lesser degreee along their S ··· S diagonals. Three structures are in principle possible for the Ni–S framework of the open-chain oligonuclear nickel thiolates with μ-S bridges:

1. fragments of the infinite one-dimensional zigzag-shaped $[NiS_2]_\infty$ chain (all-*trans* condensation of the NiS_4 units, Fig. 16a);
2. fragments of cyclic systems (Fig. 16b) such as the hexanuclear $[NiS_2]_6$ unit (all-*cis* condensation of the NiS_4 units);
3. fragments combining both types of condensation.

Examples of all three possibilities are in fact known. All open-chain nickel thiolates except for $[Ni_2(SEt)_6]^{2\ominus}$ and $[Ni_3(SEt)_8]^{2\ominus}$[103] are stabilized by bifunctional thiolate ligands.

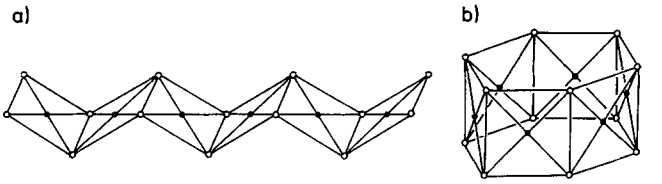

Fig. 16. Stereochemical possibilities for the arrangement of square-planar NiS_4 units: a) folded one-dimensional chain, *trans* condensation; b) cyclic arrangement, *cis* condensation [107].

The structural types found in the known metal(II) thiolates of coordination number 4 with bifunctional ligands are shown schematically in Figure 17. Several tetrahedrally coordinated species (structure types a, b, and d) are already known for iron and cobalt (see Sections 2 and 3), while the group with square-planar coordination (structure types c, e, f, and i) is limited to the nickel complexes (types g and h with tetrahedral sulfur coordination are found only for mercury).

Type c is found in $[Ni_2(SCH_2CH_2S)_3]^{2\ominus}$[104, 105] and also in $[Ni_2(SEt)_6]^{2\ominus}$,[103] which has monofunctional ligands. In contrast to the situation in all other known oligonuclear complexes, the central Ni_2S_2 unit in the latter complex is planar.

The extension of the metal–sulfur framework to include three coordination centers leads to structures of either type e or f, which are realized in $[Ni_3(SCH_2CH_2S)_4]^{2\ominus}$[106, 107] (type e, Fig. 18, top) and $[Ni_3(SCH_2C_6H_4CH_2S)_4]^{2\ominus}$[68, 107] (type f, Fig. 18, bottom). The trinuclear complexes differ in

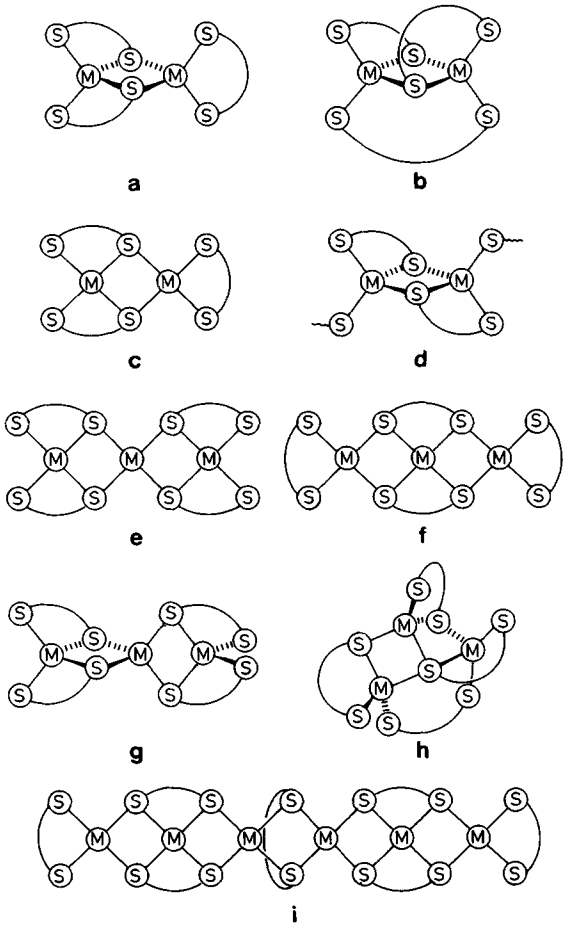

Fig. 17. Experimentally determined structures of tetracoordinated polynuclear metal(II) dithiolates. a) Fe, Zn; b) Mn, Fe, Co, Cd; c) Ni; d) Hg; e) Ni; f) Ni; g) Hg; h) Hg; i) Ni (see also [107]).

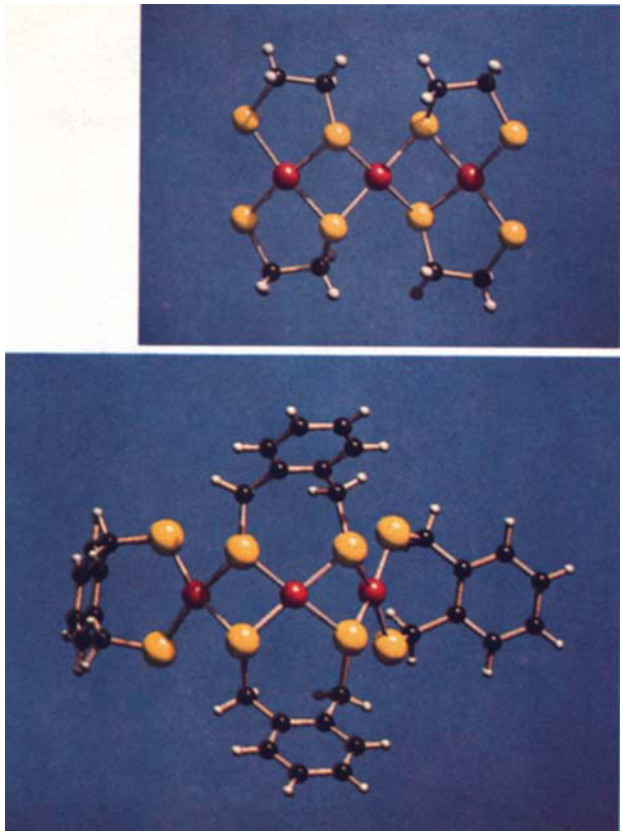

Fig. 18. Top: Structure of $[Ni_3(SCH_2CH_2S)_4]^{2\ominus}$ in crystalline $[Ph_4P]_2[Ni_3(SCH_2CH_2S)_4]$ (*trans* configuration). Bottom: Structure of the anion $[Ni_3(SCH_2C_6H_4CH_2S)_4]^{2\ominus}$ in crystals of $[Et_4N]_2[Ni_3(SCH_2C_6H_4CH_2S)_4] \cdot 2\,MeOH$ (*cis* configuration) [107].

the arrangement of the ligands and in the type of condensation (cf. Fig. 16): whereas *trans* linking is observed in the ethanedithiolate complex (Fig. 18a), *cis* linking is found in the *o*-xylene-α,α'-dithiolate complex (Fig. 18, bottom). Both types of linkage are observed in the hexanuclear complex anion $[Ni_6(SCH_2CH_2CH_2S)_7]^{2\ominus}$,[107] the unusual structure of which is shown in Figure 19 (structure type i). In the compound two trinuclear subunits with *cis* configuration are linked via a *trans* condensation step.

It is clear that hexanuclear nickel thiolates with all-*cis* condensed NiS_4 units can no longer form open-chain systems because the ends of the chain approach one another too closely. As a result, an additional condensation step occurs, which involves the two ends of the chain; this leads to the formation of cyclic complexes with a prismatic nickel–sulfur framework. Examples are provided by the hexanuclear species $[Ni_6(SR)_{12}]$ with R = Et[108–110] and R = C_2H_4OH[111] as well as $[Ni_6(SC_3H_6NHMe_2)_{12}]^{12\oplus}$.[112] The smallest stable cyclic complexes contain four nickel centers and thus have the general structure $[Ni_4(SR)_8]$. Compounds of this class exist with R = 4-(*N*-methylpiperidyl),[113] R = cyclohexyl (Fig. 20a),[114] and R = isopropyl;[115] the octanuclear $[Ni_8(SCH_2C(O)OEt)_{16}]$ is also known.[116] It is interesting that most cyclic thiolates have an even number of nickel centers. There are only two known cyclic compounds in which this number is odd, the novel pentanuclear complex $[Ni_5(SEt)_{10}]$ (Fig. 20b)[114] and the similarly constructed $[Ni_5(SCH_2SiMe_3)_{10}]$.[117]

The electrochemical behavior of the nickel thiolate complexes is of great interest because of the biological function of nickel in the hydrogenases and CO dehydrogenases. Whereas the open-chain nickel thiolates cannot be oxidized without their destruction, the cyclic neutral complexes are capable of electrochemical oxidation within the potential range of about 500–700 mV.[118] Chemical oxidation can be achieved by the use of elemental bromine or iodine in dichloromethane. For example, $[Ni_4(SC_3H_7)_8]$ can be oxi-

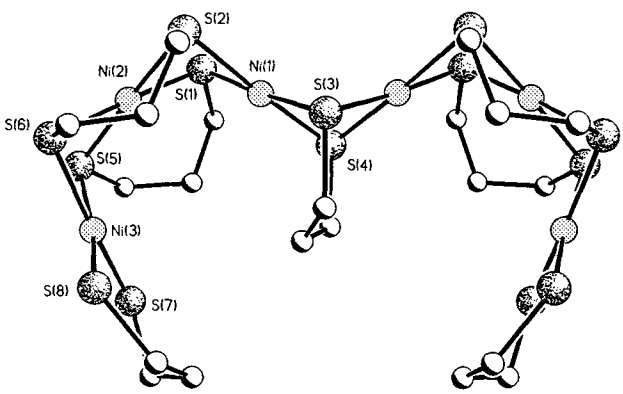

Fig. 19. The hexanuclear anion $[Ni_6(SCH_2CH_2CH_2S)_7]^{2\ominus}$ (mixed *cis*/*trans* configuration) [107].

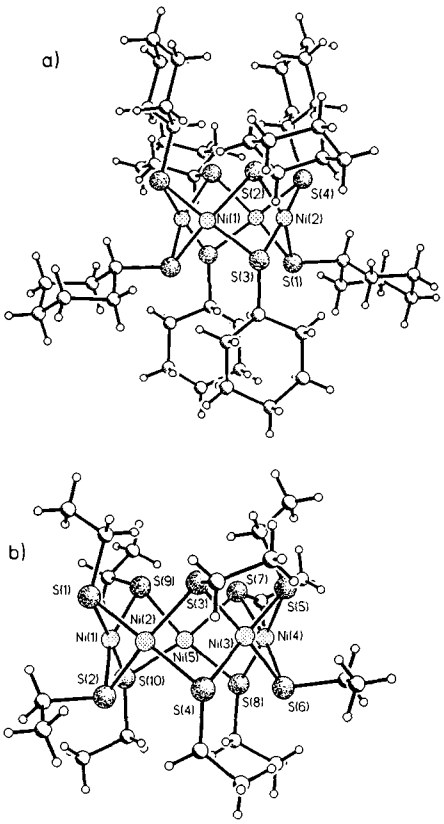

Fig. 20. Cyclic nickel thiolates with even and odd numbers of nickel centers. a) $[Ni_4(SC_6H_{11})_8]$; b) $[Ni_5(SEt)_{10}]$ [114].

dized by bromine to give black crystals of the novel complex $[Ni_4(SC_3H_7)_8Br]$, while oxidation with iodine leads to black $[Ni_4(SC_3H_7)_8I]$.[118] The crystals of $[Ni_4(SC_3H_7)_8Br]$ contain tetranuclear molecular complexes with one trivalent nickel atom each (Fig. 21). The nickel(II) centers have the

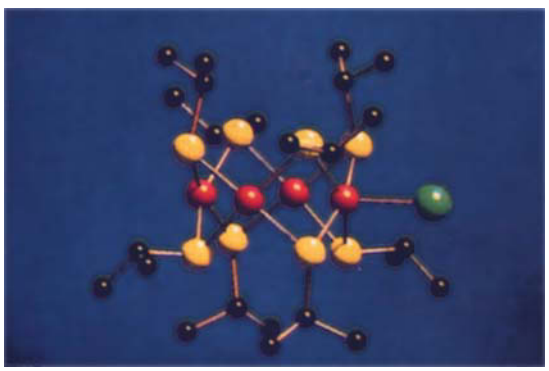

Fig. 21. Structure of the mixed-valent complex $[Ni_4(SC_3H_7)_8Br]$ [118].

usual sulfur environment with a mean Ni–S distance of 2.22 Å and the oxidized nickel atom binds a bromine in an axial position at a distance of 2.53 Å; the equatorial bonds to the S atoms are somewhat longer (mean value 2.26 Å). The molecules are arranged in the crystal along these axes in the form of infinite chains in such a way that the bromide ion is only 3.02 Å away from a (divalent) nickel atom of a neighboring molecule. The halogen atom in the iodo compound is bonded symmetrically between the Ni atoms within the chains; the Ni–I distances (2.82 and 2.88 Å) indicate almost complete bond-length equalization.

The condensation of square-planar NiS_4 units to give trinuclear systems is not limited to parallel edges of the central NiS_4 unit but can also take place at right angles. This type of sulfur linking leads to a sulfur atom which must be bonded to all three nickel atoms simultaneously. Trinuclear compounds of nickel with μ_3-S bridges are indeed known; however, these bridges are not formed by thiolate S atoms but only by sulfidic S atoms. An example with bifunctional thiolate ligands is $[Ni_3S(SCH_2C_6H_4CH_2S)_3]^{2\ominus}$.[71] Whereas the analogous Fe and Co compounds of the general type $[M_3S(SR)_6]^{2\ominus}$ exist in a defect cubane structure, the square-planar coordination observed here leads to a completely different structure. The seven sulfur atoms of the Ni_3S_7 unit occupy seven corners of a distorted cube, while the nickel atoms lie at the centers of three neighboring faces. In contrast to the situation for Fe^{II} and Co^{II}, trinuclear sulfide-thiolate complexes of nickel with monofunctional thiolate ligands have been obtained: $[Ni_3S(SMe)_6]^{2\ominus}$ (Fig. 22)[119] and $[Ni_3S(SPh)_6]^{2\ominus}$[120] are two further remarkable mixed sulfide-thiolate complexes of nickel.

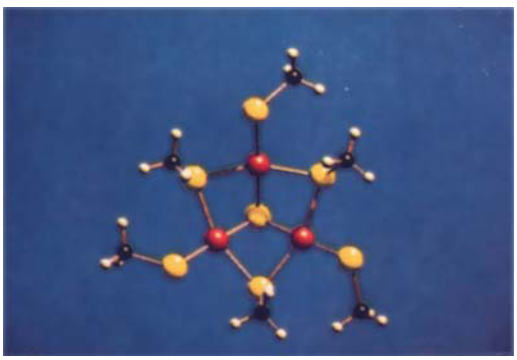

Fig. 22. Structure of the anion $[Ni_3S(SMe)_6]^{2\ominus}$ [119].

In addition to these "classical" sulfide-thiolate complexes, nickel also forms compounds which contain not only thiolate but also disulfide ions. The tetranuclear complex anion $[Ni_4(S_2)(SCH_2CH_2S)_4]^{2\ominus}$ (Fig. 23) can be obtained from the reaction of $NiCl_2$ with $NaSCH_2CH_2SNa$ and Na_2S_2 in MeOH.[106, 121] Complexes containing polysulfide and thio-

Fig. 23. Structure of the disulfide-thiolate anion $[Ni_4(S_2)(SCH_2CH_2S)_4]^{2\ominus}$ [121].

late ligands in the same molecule are unusual, since thiolates normally act as reducing agents towards S_8 and polysulfides, themselves being oxidized to organic disulfides. Apart from $[Ni_4(S_2)(SCH_2CH_2S)_4]^{2\ominus}$, only two further structurally characterized mixed polysulfide-thiolate complexes are known, namely, the trinuclear molybdenum compound $[Mo_3S(S_2)_3(SCH_2CH_2S)_3]^{2\ominus}$[69, 122] and the mononuclear vanadium complex $[V(S_2)S_2(SPh)]^{2\ominus}$.[123]

The first nickel thiolates in which the oxidation state of the metal is lower than two have recently been described. Reaction of $NiCl_2$ with *t*BuSNa in MeOH results in the formation of the octanuclear complex anion $[Ni_8S(SC_4H_9)_9]^{\ominus}$ (Fig. 24).[115] The reduction processes occurring in the

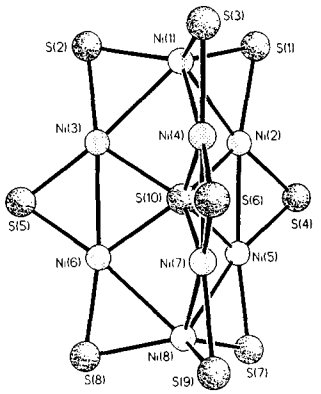

Fig. 24. The Ni_8S_{10} framework of the cluster anion $[Ni_8S(StBu)_9]^{\ominus}$ [115].

course of the reaction are not yet completely understood. In this novel mixed-valent sufide-thiolate complex six nickel atoms form a trigonal prism, the triangular faces of which are capped by two further nickel atoms; the mean oxidation state of the nickel is +1.25. The $[Ni_8S_{10}]$ unit has the first direct Ni–Ni bonds in a nickel thiolate complex, both between the capping nickel atoms and their metal neighbors and, within the prism, between atoms on opposing triangular faces. The presence of bonding interactions is shown by the short Ni ··· Ni distances of 2.47 and 2.44 Å; the Ni–Ni bonds are flanked by thiolate bridges. At the center of the Ni_6 prism there is a sulfide S atom which is bonded to all six nickel atoms at a (mean) distance of 2.18 Å. The trigonal-planar sulfur environment of the nickel atoms is just as unusual as their oxidation state.

5. Thiolate Complexes of the Metals of the Copper and Zinc Groups

The interest in the chemistry and the structural properties of the thiolates and sulfide-thiolates of the six metals in groups 11 and 12 has been stimulated by the great importance of completely or partially sulfur-coordinated biologically active copper, zinc, cadmium, and mercury centers; examples are provided by the blue copper proteins (plastocyanin, azurin, stellacyanin, ceruloplasmin, laccase), other important redox enzymes such as cytochrome *c* oxidase, and, in particular, the different types of metallothioneins (MT).[124–127] The latter are low-molecular-weight proteins (ca. 6 kD) characterized by a high cysteine content and a high metal:cysteine ratio, which ranges from 1:3 for the zinc and cadmium MTs to a value approaching 1:1 in the postulated $[Cu_6S_7]$, $[Cu_6S_9]$, and $[Cu_8S_{12}]$ units in copper MT (e.g., the copper MT from *Neurospora crassa*[125, 128]). The fascinating thiolates of the copper and zinc group are at present the subject of intensive investigation, and the synthesis of a series of remarkable new polynuclear complexes of Cu, Zn, Cd, and Hg has also stimulated the somewhat neglected chemistry of silver and gold. In addition, the chemistry of the gold thiolates is of interest because of the well-known antiarthritic properties of some members of this class of compounds (see, for example, Ref. [129]).

5.1. Copper Thiolates

Copper is normally monovalent in its thiolate complexes, and the coordination is generally trigonal planar, although a number of linearly coordinated examples are known. In the oligonuclear complexes, which are normally prepared from Cu^{I} or Cu^{II} salts and thiolates under various reaction conditions in solvents such as methanol, the ligands are normally bridging.

Copper forms characteristic tetranuclear complexes of the type $[Cu_4(SR)_6]^{2\ominus}$ with simple saturated or aromatic thiolates; these have a cagelike *tetrahedro*-Cu_4-*octahedro*-(μ-S) structure[130–136] (Fig. 25). As is

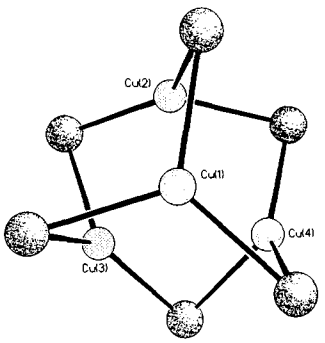

Fig. 25. The M_4S_6 framework of the complexes $[Cu_4(SR)_6]^{2\ominus}$.

shown by $[Cu_4(SMe)_6]^{2\ominus}$,[131] $[Cu_4(SEt)_6]^{2\ominus}$,[137] $[Cu_4(SPh)_6]^{2\ominus}$,[130–132] $[Cu_4(SCH_2CH_2S)_3]^{2\ominus}$,[133] and $[Cu_4(SCH_2C_6H_4CH_2S)_3]^{2\ominus}$,[134–136] the examples prepared so far, this structure is stabilized by both monofunctional and bifunctional thiolates. The compound $[Cu_3(SCH_2CH_2S)_3]^{3\ominus}$[60] in which the metal:ligand ratio is 1:1, contains a nonplanar $[Cu_3(\mu\text{-}S)_3]$ ring with trigonally coordinated copper. Under different reaction conditions the reaction with thiophenolate gives pentanuclear $[Cu_5(SPh)_7]^{2\ominus}$, the structure of which is derived from $[Cu_4(SPh)_6]^{2\ominus}$ by replacement of an $SPh^{\ominus}$ ligand by a linear PhS-Cu-SPh building block.[138, 139] When sterically demanding ligands such as $StBu^{\ominus}$ are used, steric hindrance leads to a ligand-poorer complex, the pentanuclear anion $[Cu_5(StBu)_6]^{\ominus}$, in which two copper centers are trigonally planar and three linearly coordinated. As for other thiolates of the d^{10} metals, there

are indications of weak bonding interactions between the metal atoms.

The heteroleptic complex $[Cu_7(SCH_2CH_2S)_4(SEt)]^{2\ominus}$ (Fig. 26) with mono- and bifunctional thiolate moieties contains a Cu_7 framework which consists of two vertex-linked Cu_4 tetrahedra.[134, 136, 143] If the central metal atom is removed, the remaining Cu_6S_9 framework, which has a trigonal-prismatic arrangement of the metal atoms, may serve as a model for the proposed metal–sulfur centers in copper metallothioneins.[125, 128] A compound of similar

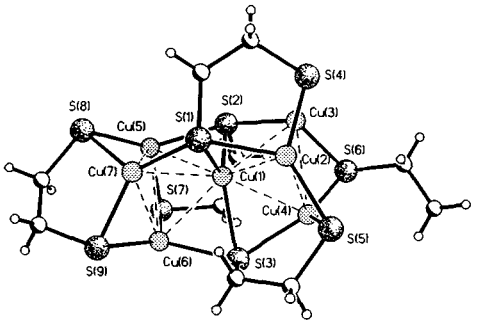

Fig. 26. Structure of the heteroleptic thiolate $[Cu_7(SCH_2CH_2S)_4(SEt)]^{2\ominus}$ [134, 136, 143].

composition with monodentate ligands, $[Cu_7(SEt)_8]^{\ominus}$, has a polymeric chain structure in which cagelike $[Cu_7(SEt)_{10}]$ structural units with trigonal-planar coordination of the Cu atoms are linked via four S atoms to give one-dimensional infinite polymers.[137, 144] A similar reaction system in which thioxanthate is present as a coligand affords the octanuclear $[Cu_8(SC_5H_{11})_4(S_2CSC_5H_{11})_4]$, in which the Cu_8S_{12} framework represents a new type of cage; Cu is coordinated in a trigonal-planar fashion and the cage consists of eight Cu_3S_3 rings in a boat form and two Cu_4S_4 rings.[145]

Two recently reported 1:1 complexes are worthy of particular attention, since they represent oligomers of the long-sought "simple" compound CuSR. The first of these is the octanuclear complex $[Cu_8\{SC_6H_2(iPr)_3\}_8]$ with a twisted 16-membered ring consisting of alternating linearly coordinated Cu and μ_2-bridged SR ligands;[146] the second is $[Cu_{12}\{SC_6H_4(o\text{-}SiMe_3)\}_{12}]$, in which the sterically demanding ligands cause the formation of a remarkable paddle-wheel-like $Cu_{12}S_{12}$ molecular skeleton[147, 148] (Fig. 27). Six

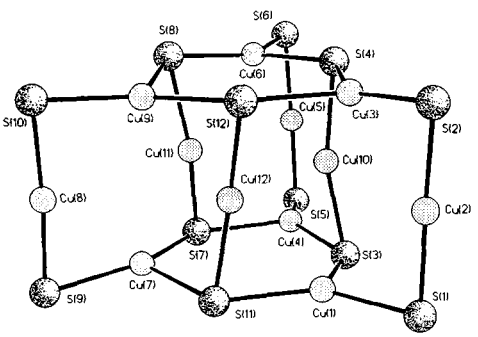

Fig. 27. $Cu_{12}S_{12}$ molecular framework of $[Cu_{12}\{SC_6H_4(o\text{-}SiMe_3)\}_{12}]$ [147, 148]. Only the thiolate S atoms of the 2-(trimethylsilyl)thiophenolate ligands are shown.

of the Cu^I atoms in the $[2_3](1,3,5)$-cyclophane-like structure are almost trigonal planar, the other six are linearly coordinated. The two parallel, "stacked" Cu_3S_3 rings are twisted with respect to one another by about 10°. The considerable contraction of the triangle Cu(10)-Cu(11)-Cu(12) in the direction of the center of the molecule (S–Cu–S angle 163.3°) possibly indicates the presence of weak attractive interactions between the metals.

There has also been great interest in the search for possible structural models for the copper centers in cytochrome *c* oxidase. The paramagnetic mixed-valent cluster complex $Cu^I_2Cu^{II}_3[\{SCH_2CH(CO_2CH_3)NHCH_2\text{-}\}_2]_3[ClO_4]_2 \cdot H_2O$ (Fig. 28)[149] can be regarded as a close approximation to the

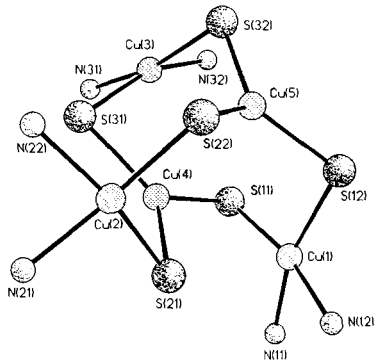

Fig. 28. $Cu^I_2Cu^{II}_3[\{SCH_2CH(CO_2CH_3)NHCH_2\text{-}\}_2]_3[ClO_4]_2 \cdot H_2O$: $Cu_5N_6S_6$ framework of the mixed-valent $[Cu^I_2Cu^{II}_3\{\{SCH_2CH(CO_2CH_3)NHCH_2\text{-}\}_2\}_3]^{2\oplus}$ cluster [149].

steric and electronic situation provided by the *cis*-$[CuN_2(his)S_2(cys)]$ ligand arrangement in Cu_A. There is a weak antiferromagnetic exchange coupling ($J = -0.26\ cm^{-1}$) between the three slightly distorted square-planar *cis*-$Cu^{II}N_2S_2$ units; the two Cu^IS_3 polygons are almost trigonal planar.

5.2. Silver and Gold Thiolates

The chemistry of the silver thiolates, their methods of preparation, and their stereochemistry (which tends

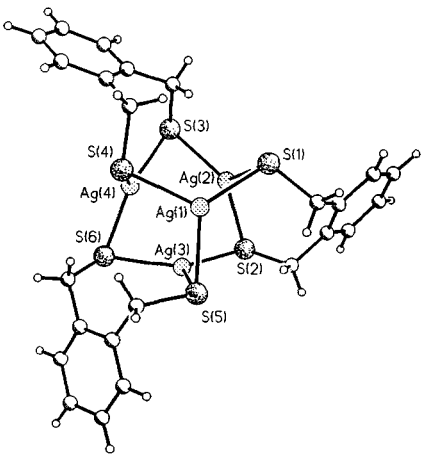

Fig. 29. Structure of the anion $[Ag_4(SCH_2C_6H_4CH_2S)_3]^{2\ominus}$ in crystals of $[Ph_4P]_2[Ag_4(SCH_2C_6H_4CH_2S)_3]$ [150].

Fig. 30. Structures of the polynuclear anions $[Au_2Cu_4(SCH_2CH_2S)_4]^{2\ominus}$ (left) and $[Ag_9(SCH_2CH_2S)_6]^{3\ominus}$ (right) [133].

towards the formation of cage structures) are all remarkably similar to those of copper. A series of polynuclear metal–sulfur frameworks has been reported in the recent literature. These range from the Ag_4S_6 cages in $[Ag_4(SCH_2C_6H_4CH_2S)_3]^{2\ominus}$[150] (Fig. 29) and in $[Ag_4\{SC_6H_3(Me)S\}_3]^{2\ominus}$[151, 152] to the pentanuclear Ag_5S_6 and Ag_5S_7 units in the (similarly anionic) complexes $[Ag_5(StBu)_6]^{\ominus}$ and $[Ag_5(SPh)_7]^{2\ominus}$[142, 139, 153] and to a large number of oligomeric or polymeric neutral $[AgSR]_n$ complexes. Their preparation is generally subject to steric control by the size and charge distribution of the ligands; important, and stereochemically extremely variable, structure elements are the (to a varying extent) undulating Ag_3S_3 and Ag_4S_4 metallacycles, which exhibit linear S–Ag–S coordination and can be associated via secondary Ag ··· S bonds. Examples are provided by the trinuclear $[Ag_3\{SC(SiPhMe_2)_3\}_3]$,[154] the tetranuclear $[Ag_4\{SC(SiMe_3)_3\}_4]$[154] and $[Ag_4\{SSi(OtBu)_3\}_4]$,[155] and the octanuclear complexes of the composition $[Ag_8\{SC_6H_4(o\text{-}SiMe_3)\}_8]$[148] and $[Ag_8\{SCH(SiMe_3)_2\}_8]$[154] with two ligand-bridged eight-membered Ag_4S_4 metallacycles.

Ligand-dependent oligomerization equilibria are observed in solution for 1:1 thiolates $[AgSR]$.[159] From these solutions it is possible to isolate ring oligomers and chain polymers with linear S–Ag–S coordination (and additional very weak secondary bonding interactions). The cyclohexyl derivative forms a 24-membered molecular metallacycle, $[Ag_{12}(SC_6H_{11})_{12}]$,[156, 157] while the 3-methylpentane derivative crystallizes as a chain polymer, $[AgSCMeEt_2]_n$.[160]

A series of remarkable mixed-metal complexes of the composition $[Au_{6-n}M_n(SCH_2CH_2S)_4]^{2\ominus}$ (with M = Ag, n = 4; M = Cu, n = 3,4), and $[Au_{9-n}Cu_n(SCH_2CH_2S)_6]^{3\ominus}$[133, 134, 136, 143, 150] (Fig. 30) are derived from the equally new anionic homoleptic cage complex $[Ag_9(SCH_2CH_2S)_6]^{3\ominus}$[133] or the postulated $[M_6(SPh)_8]^{2\ominus}$ (M = Cu, Ag).[158]

A stabilization of the polynuclear electroneutral silver thiolates $[AgSR]_n$ is apparently possible when additional phosphane ligands are present. Examples of a new heteroleptic polynuclear species of this type are provided by the octa- and tetradecanuclear tertiary alkanethiolates $[(AgSCMeEt_2)_8(PPh_3)_2]$ and $[(AgStBu)_{14}(PPh_3)_4]$.[161]

The chemistry of gold thiolate complexes is completely different from that of the homologous copper and silver complexes in that Au^I is only found in a linear two-coordinate form, which is observed in the above-mentioned mixed-metal complexes. In addition, gold is able to form stable thiolates of d^8 Au^{III}. Only complexes of low nuclearity have so far been obtained when aliphatic thiolates are used. Gold(III) forms a mononuclear anion, $[Au(SCH_2CH_2S)_2]^{\ominus}$, with square-planar coordination.[151, 152] The remarkable selenide-thiolate $[Au_2Se_2(SCH_2CH_2S)_2]^{2\ominus}$ (Fig. 31),[151, 152]

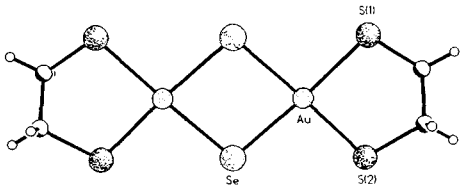

Fig. 31. Structures of $[Au_2Se_2(SCH_2CH_2S)_2]^{2\ominus}$ [151, 152].

the first member of a new class of heteroleptic mixed-ligand chalcogenide thiolates, was obtained from the system NaHSe/Se/$BH_4^{\ominus}$/$[Ph_4P][AuCl_3Br]$/ethane-1,2-dithiolate.

The anionic thiolatoaurates(I) $[Au_2(SCH_2CH_2CH_2S)_2]^{2\ominus}$ and $[Au_2(SCH_2C_6H_4CH_2S)_2]^{2\ominus}$[151, 152] (Fig. 32) are formed in the reaction between $[AuCl_4]^{\ominus}$ and propane-1,2-dithiolate or *o*-xylene-α,α′-dithiolate; the thiolates act as re-

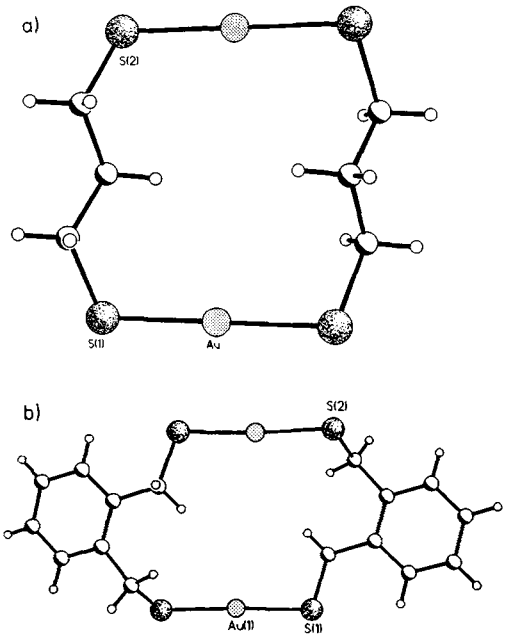

Fig. 32. Structures of $[Au_2(SCH_2CH_2CH_2S)_2]^{2\ominus}$ (a) and $[Au_2(SCH_2C_6H_4CH_2S)_2]^{2\ominus}$ (b) [151, 152].

ducing agents so that Au^I is formed. The complex anions contain interesting 12- and 14-membered metallacycles with linearly coordinated gold.

5.3. Zinc, Cadmium, Mercury

A chemistry with completely different reactive properties and individual structural principles is exhibited by the thiolates of the closed-shell d^{10} elements of group 12. Their reactive behavior is determined in a characteristic manner by their tendency to form polynuclear aggregates of tetrahedral building blocks; the interest in this class of compounds has been stimulated not only by their general chemistry but also by the necessity for the development of model systems for important classes of metal-centered bioactive molecules.

5.3.1. On the Bioinorganic Chemistry of Zn, Cd, and Hg

A large number of metalloenzymes of zinc are known; apart from the dominant coordination by imidazole and aquo ligands, partial or complete coordination by cysteine or methionine sulfur atoms is also important. Examples are provided by liver alcohol dehydrogenase (coordination at the catalytic center, $[ZnONS_2]$; "structural" zinc, $[ZnS_4]$), aspartate transcarbamylase ($[ZnS_4]$), β-lactamase ($[ZnN_3S]$), and 5-aminolevulinate dehydratase ($[ZnNS_3]$). As already mentioned, all three metals are found in metallothioneins; here again a predominantly tetrahedral coordination of the metals by sulfur must be assumed.[162-164] The metallothioneins of Zn, Cd, and Hg so far studied contain seven metal atoms, which, according to X-ray structural studies on Cd/Zn-thioneins, occur in two separate domains in the form of a trinuclear NH_2-terminal M_3S_9 and a tetranuclear COOH-terminal M_4S_{11} unit, each M (M = Zn, Cd) being bonded to four cysteine residues[124, 126, 162-164] (Fig. 33). At higher mercury concentrations the formation of Hg-richer metallothioneins (up to Hg_{18}) with lower coordination numbers and with higher degrees of condensation has been postulated.[165]

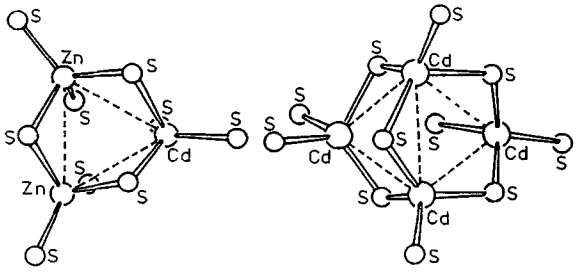

Fig. 33. The β and α domains of Zn/Cd metallothionein-2 from rat liver; in Cd metallothionein, the trinuclear center is closer to the amino terminal of the protein chain and the tetranuclear center is closer to the carboxyl terminal [163, 164].

The coordination of zinc (and other metals) by cysteine sulfur (and/or histidine nitrogen) atoms is also the most important structural principle of the nucleic acid binding proteins, which have only been recognized and intensively studied in the last few years. These transcription factors, in which zinc is an essential element, bond specifically to certain DNA sequences and thus modulate gene expression. The metal centers stabilize conserved partial sequences by complexation; these are folded to give the so-called "zinc fingers" (see, for example, Refs. [166-168]).

A further important role is played by HgS_x centers in the remarkable MerR proteins (mercury reductases). They provide the first example of "metal-regulating" proteins and may function as "genetic switches";[169] for example, bacteria can become resistant to the toxic effects of mercury. This is due to resistance genes, which cause the formation of MerR proteins and whose activation is controlled via these proteins as a function of the Hg concentration. The Hg-controlled self-regulating MerR proteins bond to heavy metals and are thus involved in signal transfer, so that they can, for example, act as sensitive biosensors for mercury in nanomolar and for cadmium in micromolar concentrations. The mercury in the protein is probably trigonally coordinated in a MerR dimer by three cysteine sulfur ligands[170, 171] (see also Ref. [199]).

Thiolates have long been used as selective drugs in the treatment of mercury (or As, Au, Sb, and Co) poisoning; they act by competing with the cysteine ligands of enzymes for coordination of these metals.[172] The commonly used reagents 2,3-dimercapto-1-propanol (BAL = British Anti-Lewisite) and penicillamine are being increasingly replaced by the water-soluble drugs sodium 2,3-dimercaptopropane-1-sulfonate and dimercaptosuccinic acid, which are administered orally.[173] Little is known about the structures of the insoluble polymeric mercury compounds.

5.3.2. Zinc and Cadmium Thiolates

The preparative methods for the synthesis of thiolates and sulfide thiolates of Zn, Cd, and Hg with a complete sulfur coordination sphere are similar to those used for the copper group; they typically involve the reaction between thiolate anions (or corresponding thiolate-sulfide mixtures) and the dihalides in solvents such as methanol, with subsequent precipitation as salts of large quaternary onium cations such as $[Ph_4P]^{\oplus}$, $[Ph_4As]^{\oplus}$, $[Ph_3PNPPh_3]^{\oplus}$, and $[nBu_4P]^{\oplus}$.

Mononuclear tetrahedral zinc and cadmium thiolates of the types $[Zn(SPh)_4]^{2\ominus}$, $[Cd(SPh)_4]^{2\ominus}$,[174] and $[Cd\{SC_6H_4(o\text{-}SiMe_3)\}_4]^{2\ominus}$[148] are stable and have been structurally characterized; species with trigonal-planar coordination of the metal are hardly known and can only be stabilized by sterically demanding ligands. The first examples, $[Zn(S\text{-}2,3,5,6\text{-}Me_4C_6H)_3]^{\ominus}$[175] and $[Cd(S\text{-}2,4,6\text{-}iPr_3C_6H_2)_3]^{\ominus}$,[176] have been described only recently. It has been suggested that this seldom encountered type of MS_3 coordination (M = Zn, Cd) may play a role in biologically important metal-cysteine systems.[168, 175]

Binuclear complexes of the type $[M_2(SR)_6]^{2\ominus}$ with R = Et or Me are known for all Zn, Cd, and Hg.[103, 177, 178] They contain an M_2S_6 unit formed by two edge-linked tetrahedra, which is also found in analogous Fe^{II} and Mn^{II} complexes and in other zinc and cadmium complexes containing aromatic and bidentate ligands; examples are $[M_2(SPh)_6]^{2\ominus}$[179] and $[M_2(SCH_2C_6H_4CH_2S)_3]^{2\ominus}$ with M = Zn, Cd.[177, 180]

A very characteristic structural feature of the polynuclear zinc and cadmium thiolates and sulfide-thiolates is their ten-

dency to form adamantane-like cage systems via parallel vertex-linked condensation of MS_4 tetrahedra; extension of these systems in three dimensions gives polymeric products.[10] The analogy to the zinc blende structure is clear: zinc blende is the final product of the condensation when all thiolate ligands are replaced by sulfide.

Examples of the first step in this condensation process involving parallel tetrahedra are the adamantane-like thiophenolate complexes $[M_4(SPh)_{10}]^{2\ominus}$ with M = Zn, Cd.[181-183] This adamantane framework is also found in the preparatively interesting heteroligand complexes $[M(EPh)_6X_4]$ (M = Zn, Cd; E = S, Se; X = Cl, Br, I), which can be prepared by direct halogenation (for example, using $PhICl_2$) of the anions $[M_4(EPh)_{10}]^{2\ominus}$.[184]

The next step is represented by the synthesis of decanuclear "macrotetrahedral" frameworks containing ten parallel tetrahedra; these contain 16 thiolate ligands, while the μ_3-bridging sulfur functions exist in the sulfide form. Examples are $[Zn_{10}S_4(SPh)_{16}]^{4\ominus}$,[185] $[Zn_{10}S_4(SCH_2C_6H_4CH_2S)_8]^{4\ominus}$[180] (Fig. 34), and $[Cd_{10}S_4(SPh)_{16}]^{4\ominus}$.[185] This framework, which resembles the zinc

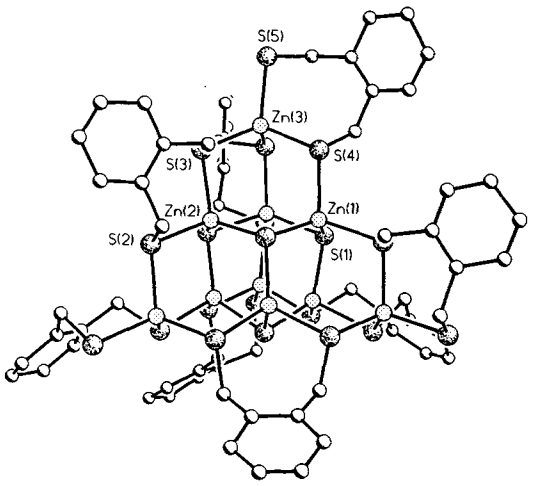

Fig. 34. Molecular structure of the polyanion $[Zn_{10}S_4(SCH_2C_6H_4CH_2S)_8]^{4\ominus}$ in crystals of $[nBu_4N]_4[Zn_{10}S_4(SCH_2C_6H_4CH_2S)_8] \cdot 8\,MeOH$ [180].

blende structure, is present in a modified form in the cation $[Cd_{10}(SCH_2CH_2OH)_{16}]^{4\oplus}$, in which the coordination of four of the Cd atoms is increased by the OH ligand functions to $[CdS_4O]$ (4x) or $[CdS_3O_3]$ (4x).[186, 187] An even higher degree of condensation in a molecular species has been achieved in the complex $[Cd_{17}S_4(SPh)_{28}]^{2\ominus}$[188] (Fig. 35). The Cd–S framework (T_d symmetry) contains a $Cd_{13}S_{28}$ core (zinc blende type) consisting of corner-sharing parallel CdS_4 tetrahedra; a central $Cd(\mu_4\text{-}S)_4$ tetrahedron is surrounded by a Cd_{12} cuboctahedron. Four of the eight triangular faces of the Cd_{12} cuboctahedron are capped by four additional outer $Cd(\mu\text{-}S)_3S$ tetrahedra in a wurtzite-like manner.

In the α-cristobalite-like structure of $[Cd(SPh)_2]_n$ the adamantane-like $[Cd_4(SPh)_{10}]$ units are three-dimensionally linked in the sense of polymeric $[(\mu\text{-}SPh)_6Cd_4(\mu\text{-}SPh)_{4/2}]$; the compound has a melting point of 340°C but dissolves readily with solvolysis in solvents such as DMF.[189, 190] The structure of the polymeric $[Cd(SC_6H_4pMe)_2]_n$, which is also composed of vertex-linked adamantane units, has interesting

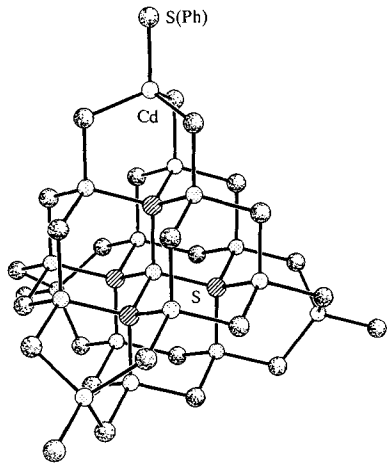

Fig. 35. Structure of $[Cd_{17}S_4(SPh)_{28}]^{2\ominus}$ [188].

analogies to the zeolite-like microporous aluminosilicate frameworks.[190] Furthermore, a polymer with the composition $[Cd_7(C_6H_4oMe)_{14}(DMF)_2]_n$ does not contain adamantane building blocks but consists of three-dimensionally cross-linked, spirocyclically linked Cd_3S_3 rings as well as macrocycles such as $[Cd_{24}S_{24}]$.[191]

The close chemical relationship between the d^{10} elements Zn^{II} and Cd^{II} and their isoelectronic neighbors in the periodic table, Ga^{III}, In^{III}, and Sn^{IV}, is shown clearly by the remarkable analogies between their oligomeric thiolate-sulfide species. Gallium, indium, and tin also form macrotetrahedral decameric thiolate-sulfide anions with $M_{10}S_{20}$ frameworks identical to those in $[M_{10}S_4(SPh)_{16}]^{4\ominus}$ (M = Zn, Cd). The anions $[M_{10}S_{16}(SPh)_4]^{6\ominus}$ (M = Ga, In) (Fig. 36),[192] as well as $[Sn_{10}O_4S_{20}]^{8\ominus}$,[193] have been prepared in solution. Even boron(III) compounds with analogous decameric $B_{10}S_{20}$ building blocks can be obtained via solid-state reactions: in

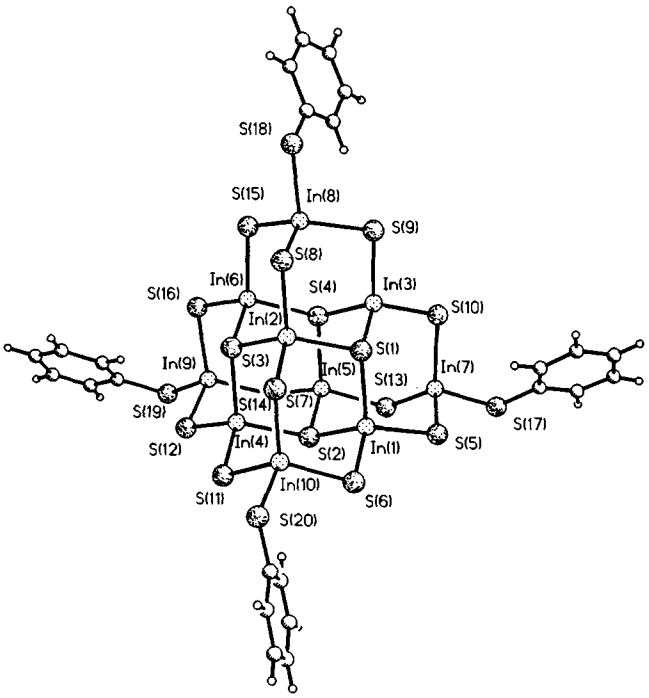

Fig. 36. Structure of $[In_{10}S_{16}(SPh)_4]^{6\ominus}$ in crystals of $[Et_4N]_6[In_{10}S_{16}(SPh)_4] \cdot MeOH$ [192].

$Ag_6[B_{10}S_{18}]$,[194,195] $Li_{6+2x}[B_{10}S_{18}]S_x$, $Li_5[B_7S_{13}]$, and $Na_6[B_{10}S_{18}]$,[196] these are linked in three dimensions via the four vertices of their macrotetrahedra.

The varying thiolate/sulfide ratios within the homologous series of decanuclear anions are in general caused by charge effects; an increase in the valency (formal charge) of the metals must lead to an increase in the amount of sulfide. Similar homologies exist for the tetranuclear adamantane-like species (see, for example, Ref. [195]).

A new series of topologically interesting molecular Cd chalcogenolates of the compositions $[Cd_8E(E'Ph)_{16}]^{2\ominus}$ with E, E' = S, Se, Te (including the complex $[Cd_8S(SPh)_{16}]^{2\ominus}$) form polycyclic cage systems of approximate *T* symmetry which can be described as *centro*-S-*tetrahedro*-Cd_4^i-*icosahedro*-(μ-SPh)$_{12}$-*tetrahedro*-Cd_4^0-*tetrahedro*-$(SPh)_4$ with tetrahedrally coordinated cadmium.[197] A similar icosahedral sulfur framework is found in the octanuclear thiolate halides $[Cd_8X(SCH_2CH_2OH)_{12}X_3]$ with X = Cl, Br, I; however, the tetrahedrally (5 x $[CdS_3X]$) or fivefold (3 x $[CdS_3O_2]$) coordinated cadmium atoms in these complexes form a compressed hexahedron.[198]

5.3.3. *Mercury Thiolates*

The flexible coordination properties of mercury make possible the formation of more or less distorted polyhedra $[HgS_n]$ (n = 2–4), depending on the electronic and steric requirements of the ligands. This has led to the synthesis of structurally very different mononuclear, oligomeric, and polymeric Hg^{II} thiolates (see also Ref. [199]). The mononuclear species include the following:

1. linear molecules $[Hg(SR)_2]$ which are associated to some extent in the solid state:

$[Hg(SEt)_2]$,[200] $[Hg(S\text{-}2,4,6\text{-}i\text{Pr}_3C_6H_2)_2]$,[176] $[Hg\{SC_6H_4(o\text{-}SiMe_3)\}_2]$,[201] $[Hg\{SCH_2CH(NH_3)COO\}\{SCH_2CH(NH_3)COOH\}]Cl \cdot 1/2H_2O$;[202]

2. anionic, trigonally coordinated complexes $[Hg(SR)_3]^{\ominus}$ with model character for important biomolecules:[170]

$[Hg(SPh)_3]^{\ominus}$,[203,204] $[Hg(S\text{-}2,4,6\text{-}i\text{Pr}_3C_6H_2)_3]^{\ominus}$,[176] $[Hg(S\text{t}Bu)_3]^{\ominus}$;[170]

3. species with tetrahedral coordination of the metal:

$[Hg(SPh)_4]^{2\ominus}$,[204] $[Hg(SC_6H_4Cl)_4]^{2\ominus}$,[205] $[Hg(SC_6F_5)_4]^{2\ominus}$,[206] $[Hg(C_6Cl_5)_4]^{2\ominus}$.[207]

Two types of binuclear Hg thiolates are known. Apart from $[Hg_2(SMe)_6]^{2\ominus}$,[178] which corresponds to the homologous Zn and Cd compounds, a neutral complex, $[Hg(2\text{-}SC_6H_4)_2SiMe_2]_2$, has also been obtained;[201] in this complex the linearly coordinated Hg atoms and the bridging bidentate ligands form a 16-membered heteronuclear [-Hg-S-C-C-Si-C-C-S]$_2$ ring. Other remarkable examples of oligomeric Hg^{II} thiolates are provided by the binuclear $[Hg_2(SPh)_4(PPh_3)_2]^{2\ominus}$[177] and the trinuclear anions $[Hg_3(SCH_2CH_2S)_4]^{2\ominus}$ and $[Hg_3(SCH_2C_6H_4CH_2S)_3]^{2\ominus}$[208,209] (Fig. 37). The structures of the anions, which are governed by the steric demands of the ligands, are completely different: ethane-1,2-dithiolate makes possible a linear Hg_3 arrangement (Fig. 37, left) with the coordination numbers 4 (tetrahedral, 1x) and 2 (quasi-linear, 2x), while the different "bite" of *o*-xylene-α,α'-dithiolate leads to a triangular arrangement of the metal atoms, resulting in HgS_4 tetrahedra with terminal (5x), μ_2-bridging (2x), and μ_3-bridging (1x) thiolate functions (Fig. 37, right).

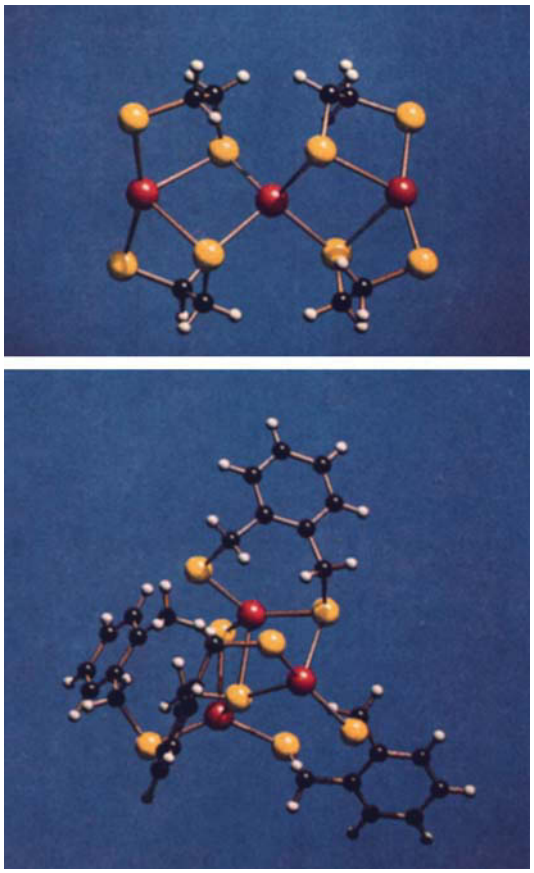

Fig. 37. Left: Structure of $[Hg_3(SCH_2CH_2S)_4]^{2\ominus}$ [208], Right: Structure of $[Hg_3(SCH_2C_6H_4CH_2S)_4]^{2\ominus}$ [209].

The novel pentanuclear anion $[Hg_5(SCH_2CH_2S)_4(SEt)_4]^{2\ominus}$[134,136] (Fig. 38) is the first mixed-ligand compound in the series of oligomeric Hg^{II} thiolates. The tetrahedrally coordinated central Hg in this anion is linked to the remaining Hg atoms via one of the thiolate sulfurs of the

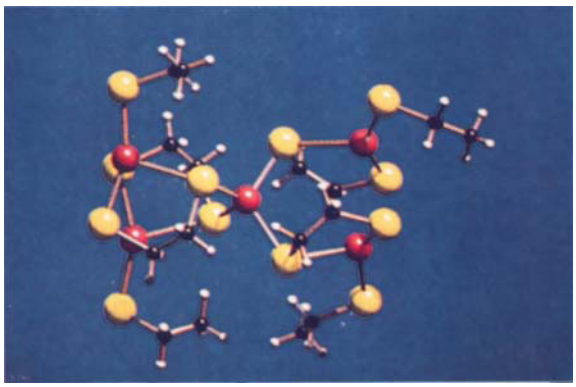

Fig. 38. Structure of $[Hg_5(SCH_2CH_2S)_4(SEt)_4]^{2\ominus}$ [134, 136].

four ethanedithiolate ligands, while the second thiolate sulfur and one $[SEt]^{\ominus}$ ligand complete the environment of the four outer Hg atoms to form a HgS_3 triangle which is considerably distorted from a trigonal symmetry.

The Hg thiolates show a pronounced tendency to undergo ligand-directed association with the formation of high-polymer aggregates by means of primary and/or secondary Hg–S bonds. As the series of polymeric phases so far characterized makes clear, a structurally rich area of new inorganic polymeric materials is in the process of development here; these may possibly be of importance as models for Hg-rich metallothioneins. $[Hg(StBu)_2]_n$[210] has a structure consisting of chains of edge-linked HgS_4 tetrahedra; this is analogous to the SiS_2 type of structure.

The three complexes $[\{Hg_2(SCH_2CH_2S)_3\}^{2\ominus}]_n$,[208] $[\{Hg_2(SCH_2CH_2CH_2S)_3\}^{2\ominus}]_n$,[134, 136] and $[\{Hg_2(SCH_2CH_2CH_2CH_2S)_3\}^{2\ominus}]_n$[211, 212] form a homologous series in which the surprisingly great influence of the ligands (and the cations and solvate molecules) on both structure and properties becomes clear. Tris(ethanedithiolato)dimercurate(2 −) (Fig. 39) exists in the form of infinite one-dimensional polymeric chains with centrosymmetric Hg_2S_6 subunits. The subunits, which consist of two edge-linked HgS_4 tetrahedra, contain two ethanedithiolate ligands and each subunit is linked to its neighbors through two $-CH_2-CH_2-$ chains.

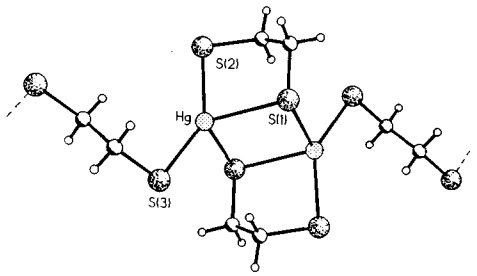

Fig. 39. Fragment of the polymeric chain structure of $[\{Hg_2(SCH_2CH_2S)_3\}^{2\ominus}]_n$ in crystals of $[Ph_4P]_2[Hg_2(SCH_2CH_2S)_3]$ [208].

In contrast, the propanedithiolato complex (Fig. 40) has a honeycomb-like two-dimensional polymeric structure with trigonal-planar coordination of the Hg atoms; the characteristic structural elements are unusually large undulating 36-membered $[Hg\text{-}S\text{-}CH_2\text{-}CH_2\text{-}CHg_2\text{-}S\text{-}]_6$ metallacycles. There are two isomeric butanedithiolate anions with completely different polymeric structures. Crystalline $[Ph_4P]_2[Hg_2\{SCH_2CH_2CH_2CH_2S\}_3] \cdot 3\,MeOH$ (Fig. 41a) forms a two-dimensional polymer with trigonal-planar coordination of the Hg atoms. The layer framework of the polyanions consists of condensed undulating 42-membered $[\text{-}Hg\text{-}S\text{-}CH_2\text{-}CH_2\text{-}CH_2\text{-}CH_2\text{-}S\text{-}]_6$ supermacrocycles. Crystalline $[Et_4N]_2[Hg_2\{SCH_2CH_2CH_2CH_2S\}_3] \cdot 2\,MeOH$ (Fig. 41b), however, contains Hg_2S_6 building blocks formed from two edge-linked HgS_4 tetrahedra, which are in turn linked with four neighboring units via butanedithiolate bridges to form a two-dimensional layer polymer. The layers contain fused four-membered [-Hg-S-Hg-S-] rings, 14-membered $[Hg\text{-}S\text{-}CH_2\text{-}CH_2\text{-}CH_2\text{-}CH_2\text{-}S\text{-}]_2$ rings and 28-membered $[Hg\text{-}S\text{-}CH_2\text{-}CH_2\text{-}CH_2\text{-}CH_2\text{-}S\text{-}]_4$ rings.[211, 212]

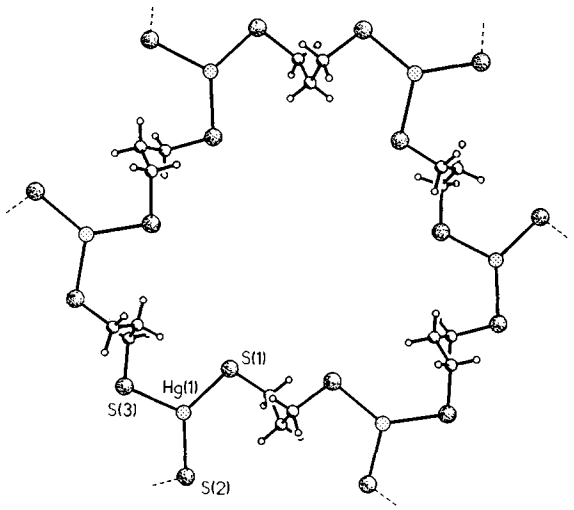

Fig. 40. Section of the polymeric layer structure of the anion $[\{Hg_2(SCH_2CH_2CH_2S)_3\}^{2\ominus}]_n$ in crystals of $[Ph_4P]_2[Hg_2(SCH_2CH_2CH_2S)_3] \cdot 2\,MeOH$ [134, 136].

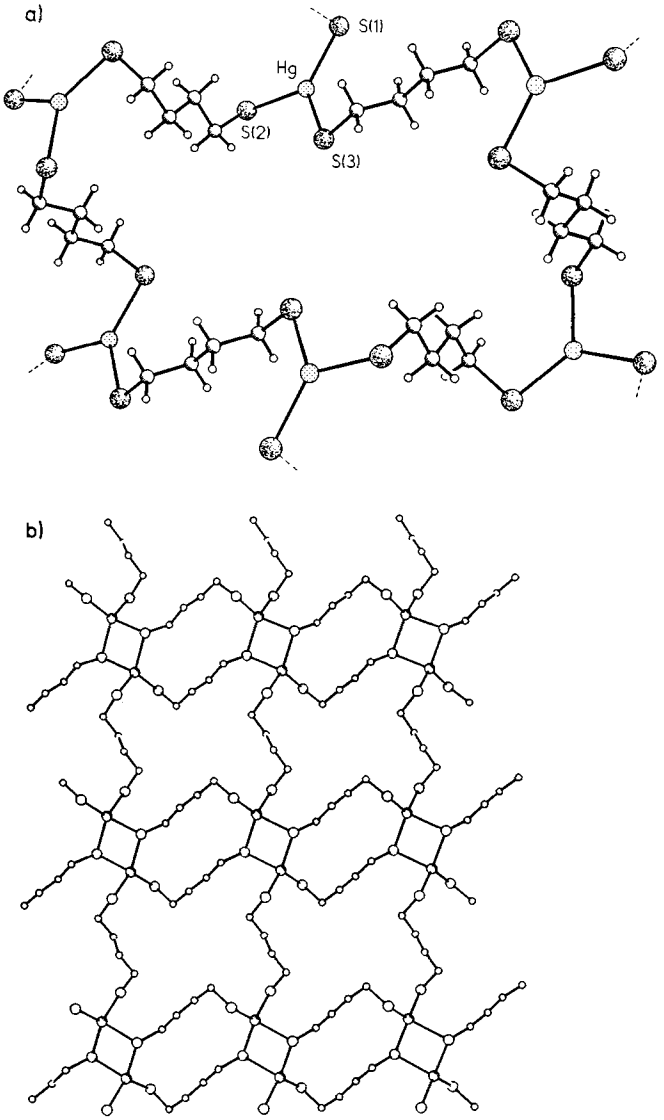

Fig. 41. Sections of the polymeric layer structures of the anion $[\{Hg_2(SCH_2CH_2CH_2CH_2S)_3\}^{2\ominus}]_n$ in crystals of $[Ph_4P]_2[Hg_2(SCH_2CH_2CH_2CH_2S)_3] \cdot 3\,MeOH$ (a) and in crystals of $[Et_4N]_2[Hg_2(SCH_2CH_2CH_2CH_2S)_3] \cdot 2\,MeOH$ [211, 212] (b).

6. Taking Stock and Looking Ahead: New Chances, Problems, and Applications

As the examples of metal thiolate chemistry discussed here make clear, this still expanding area of complex chemistry extends far into solid-state chemistry and materials science on the one hand and biology on the other. On the preparative side more emphasis needs to be placed on the synthesis of new thiolates of the early and late transition metals, which are not "fashionable" because of their lacking "biochemical relevance". In addition, the synthesis of cage and cluster systems of even higher nuclearity—with π acceptors as coligands, for example—must be pursued.

The solubility of the thiolate complexes in suitable polar protic and aprotic solvents, coupled with their thermal instability, suggests their potential use as precursor materials for the thermolytic preparation of chalcogenide and metal surface layers. This application will be particularly interesting for the metal-rich polynuclear cages and the thermally even more labile selenolate and tellurolate complexes; the generation of semiconductor layers is also conceivable.

The extremely important redox properties of the metal–sulfur systems, which could be treated only very briefly in this article, must also be systematically studied and preparatively applied for systems other than the classical metals (iron and copper) of redox enzymes. The remarkable stability of the cluster complexes $[Ni_8S(StBu)_9]^{\ominus}$[115] (Fig. 24) and $[Ni_4(SC_3H_7)_8X]$[118] (Fig. 21) leads us to expect that other transition metals will also provide a broad area of new and exciting thiolate complexes with metals in unusual oxidation states as well as new mixed-valence complexes. In the case of nickel, the much too neglected area of the hydrogenases is still awaiting the characterization of the active metal centers.

The redox properties of proteins with sulfur-coordinated metal centers promise to pave the way for the development of new specific sensors; the biosensor based on the Hg MerR proteins mentioned above provides a first example. It appears quite possible that similar sensor systems (possibly with reduced specificity, but increased stability) will be prepared with thiolate model systems; this could lead to a renaissance in the interest in thiolates, which have long been used in a conventional manner in chemical analysis.

Finally, it is also worthwhile for inorganic chemists to continue to work intensively on the development of thiolates which are of therapeutic (e.g., Au) and diagnostic use (e.g., ^{99m}Tc).

We thank all our present and past co-workers who were involved in the work cited here for their enthusiastic and zealous efforts. Thanks are due to B. Budde, Dipl.-Chem. S. Teipel, and Dipl.-Chem. D. Volkmer for their assistance. The Deutsche Forschungsgemeinschaft, the Fonds der Chemischen Industrie and the Bundesminister für Forschung und Technologie have all provided us with generous financial support.

Received: January 8, 1991 [A 824 IE]
German version: *Angew. Chem. 103* (1991) 785
Translated by Prof. Dr. *T. N. Mitchell*, Dortmund

[1] J. A. McCleverty, *Prog. Inorg. Chem. 10* (1969) 49.
[2] D. Coucouvanis, *Prog. Inorg. Chem. 11* (1970) 233; *ibid. 26* (1979) 301.
[3] R. Eisenberg, *Prog. Inorg. Chem. 12* (1970) 295.
[4] J. Willemse, J. A. Cras, J. J. Steggerda, C. P. Keijzers, *Struct. Bonding (Berlin) 28* (1976) 83.
[5] R. P. Burns, C. A. McAuliffe, *Adv. Inorg. Chem. Radiochem. 22* (1979) 303.
[6] A. Müller, B. Krebs (Eds.): *Sulfur—Its Significance for Chemistry, for the Geo-, Bio- and Cosmosphere and Technology*, Elsevier, Amsterdam 1984.
[7] R. P. Burns, F. P. McCullough, C. A. McAuliffe, *Adv. Inorg. Chem. Radiochem. 23* (1980) 211.
[8] D. Coucouvanis, *Acc. Chem. Res. 14* (1981) 201.
[9] M. Draganjac, T. B. Rauchfuss, *Angew. Chem. 97* (1985) 745; *Angew. Chem. Int. Ed. Engl. 24* (1985) 742.
[10] I. G. Dance, *Polyhedron 5* (1986) 1037.
[11] A. Müller, E. Diemann, *Adv. Inorg. Chem. 31* (1987) 89.
[12] P. J. Blower, J. R. Dilworth, *Coord. Chem. Rev. 76* (1987) 121.
[13] A. Müller, *Polyhedron 5* (1986) 323.
[14] D. Coucouvanis, A. Hadjikyriacou, M. Draganjac, M. G. Kanatzidis, O. Ileperuma, *Polyhedron 5* (1986) 349.
[15] W. Lovenberg (Ed.): *Iron-Sulfur Proteins, Vol. I, II, III*, Academic, New York 1973 and 1977, and references cited therein.
[16] J. R. Lancaster, Jr. (Ed.): *The Bioinorganic Chemistry of Nickel*, VCH, Weinheim 1988.
[17] A. Müller, W. Newton (Eds.): *Nitrogen Fixation – the Chemical-Biochemical-Genetic Interface*, Plenum, New York 1983, and references cited therein.
[18] R. H. Holm, J. A. Ibers in W. Lovenberg (Ed.): *Iron-Sulfur Proteins, Vol. III*, Academic, New York 1977, p. 205, and references cited therein.
[19] J. M. Berg, R. H. Holm in T. G. Spiro (Ed.): *Iron-Sulfur Proteins*, Wiley, New York 1982, p. 1, and references cited therein.
[20] M. H. Emptage, T. A. Kent, B. H. Huynh, J. Rawlings, W. H. Orme-Johnson, E. Münck, *J. Biol. Chem. 255* (1980) 1793.
[21] B. H. Huynh, J. J. G. Moura, I. Moura, T. G. Kent, J. LeGall, A. V. Xavier, E. Münck, *J. Biol. Chem. 255* (1980) 3242.
[22] H. Beinert, A. J. Thomson, *Arch. Biochem. Biophys. 222* (1983) 333.
[23] C. D. Stout, V. Pattabhi, A. H. Robins, *J. Biol. Chem. 255* (1980) 1797.
[24] D. Ghosh, W. Furey, Jr., S. O'Donnell, C. D. Stout, *J. Biol. Chem. 256* (1981) 4185.
[25] M. K. Johnson, R. S. Czernuszewicz, T. G. Spiro, J. A. Fee, M. V. Sweeney, *J. Am. Chem. Soc. 105* (1983) 6671.
[26] M. R. Antonio, B. A. Averill, I. Moura, J. J. G. Moura, W. H. Orme-Johnson, B.-K. Teo, A. V. Xavier, *J. Biol. Chem. 257* (1982) 6646.
[27] H. Beinert, M. H. Emptage, J.-L. Dreyer, R. A. Scott, J. E. Hahn, K. O. Hodgson, A. J. Thomson, *Proc. Natl. Acad. Sci. USA 80* (1983) 393.
[28] C. D. Stout, *J. Mol. Biol. 205* (1989) 545.
[29] C. D. Stout, *J. Biol. Chem. 263* (1988) 9256.
[30] G. H. Stout, S. Turley, L. C. Sieker, L. H. Jensen, *Proc. Natl. Acad. Sci. USA 85* (1988) 1020.
[31] H. Strasdeit, B. Krebs, G. Henkel, *Inorg. Chem. 23* (1984) 1816.
[32] G. Henkel, W. Tremel, B. Krebs, *Angew. Chem. 93* (1981) 1072; *Angew. Chem. Int. Ed. Engl. 20* (1981) 1033.
[33] C. R. Kissinger, E. T. Adman, L. C. Sieker, L. H. Jensen, J. LeGall, *FEBS Lett. 244* (1989) 447.
[34] A. H. Robbins, C. D. Stout, *J. Biol. Chem. 260* (1985) 2328.
[35] A. H. Robbins, C. D. Stout, *Proteins: Struct. Funct. Genet. 5* (1989) 289.
[36] A. E. Martin, B. K. Burgess, C. D. Stout, V. L. Cash, D. R. Dean, G. M. Jensen, P. J. Stephens, *Proc. Natl. Acad. Sci. USA 87* (1990) 598.
[37] R. H. Holm, *Chem. Soc. Rev. 10* (1981) 455, and references cited therein.
[38] G. Christou, M. Sabat, J. A. Ibers, R. H. Holm, *Inorg. Chem.* 21 (1982) 3518.
[39] K. S. Hagen, A. D. Watson, R. H. Holm, *J. Am. Chem. Soc. 105* (1983) 3905.
[40] H. Strasdeit, B. Krebs, G. Henkel, *Z. Naturforsch. B42* (1987) 565.
[41] K. S. Hagen, G. Christou, R. H. Holm, *Inorg. Chem. 22* (1983) 309.
[42] G. Henkel, H. Strasdeit, B. Krebs, *Angew. Chem. 94* (1982) 204; *Angew. Chem. Int. Ed. Engl. 21* (1982) 201; *Angew. Chem. Suppl. 1982*, 489.
[43] J. A. Konnert, H. T. Evans, Jr., *Am. Mineral. 65* (1980) 516.
[44] W. Bronger, A. Kyas, P. Müller, *J. Solid State Chem. 70* (1987) 262.
[45] J. J. Mayerle, R. B. Frankel, R. H. Holm, J. A. Ibers, W. D. Phillips, J. F. Weiher, *Proc. Natl. Acad. Sci. USA 70* (1973) 2429.
[46] J. J. Mayerle, S. E. Denmark, B. V. DePamphilis, J. A. Ibers, R. H. Holm, *J. Am. Chem. Soc. 97* (1975) 1032.
[47] J. G. Reynolds, R. H. Holm, *Inorg. Chem. 19* (1980) 3257.
[48] J. G. Reynolds, R. H. Holm, *Inorg. Chem. 20* (1981) 1873.
[49] G. B. Wong, M. A. Bobrik, R. H. Holm, *Inorg. Chem. 17* (1978) 578.
[50] Y. Do, E. D. Simhon, R. H. Holm, *Inorg. Chem. 22* (1983) 3809.
[51] A. Müller, N. H. Schladerbeck, E. Krickemeyer, H. Bögge, K. Schmitz, E. Bill, A. X. Trautwein, *Z. Anorg. Allg. Chem. 570* (1989) 7.
[52] W. Saak, S. Pohl, *Z. Naturforsch. B40* (1985) 1105.
[53] S. Han, R. S. Czernuszewicz, T. G. Spiro, *Inorg. Chem. 25* (1986) 2276.
[54] B. Krebs, G. Henkel in H. W. Roesky (Ed.): *Rings, Clusters and Polymers of Main Group and Transition Elements*, Elsevier, Amsterdam 1989, p. 439, and references cited therein.
[55] D. Coucouvanis, D. Swenson, P. Stremple, N. C. Baenziger, *J. Am. Chem. Soc. 101* (1979) 3392.
[56] H. Strasdeit, B. Krebs, G. Henkel, *Inorg. Chim. Acta 89* (1984) L11.
[57] G. Henkel, W. Tremel, U. Kuhlmann, B. Krebs, *Proc. Int. Conf. Coord. Chem. 21* (1980) 351.

[58] M. R. Snow, J. A. Ibers, *Inorg. Chem. 12* (1973) 249.
[59] T. Herskovitz, B. V. DePamphilis, W. O. Gillum, R. H. Holm, *Inorg. Chem. 14* (1975) 1426.
[60] C. P. Rao, J. R. Dorfman, R. H. Holm, *Inorg. Chem. 25* (1986) 428.
[61] D. T. Sawyer, G. S. Srivatsa, M. E. Bodini, W. P. Schaefer, R. M. Wing, *J. Am. Chem. Soc. 108* (1986) 936.
[62] R. W. Lane, J. A. Ibers, R. B. Frankel, R. H. Holm, *Proc. Natl. Acad. Sci. USA 72* (1975) 2868.
[63] R. W. Lane, J. A. Ibers, R. B. Frankel, G. C. Papaefthymiou, R. H. Holm, *J. Am. Chem. Soc. 99* (1977) 84.
[64] K. S. Hagen, R. H. Holm, *J. Am. Chem. Soc. 104* (1982) 5496.
[65] K. S. Hagen, R. H. Holm, *Inorg. Chem. 23* (1984) 418.
[66] G. Henkel, W. Tremel, B. Krebs, *Angew. Chem. 95* (1983) 317; *Angew. Chem. Int. Ed. Engl. 22* (1983) 319; *Angew. Chem. Suppl. 1983*, 323.
[67] W. Puls, *Diplomarbeit*, Universität Münster 1987.
[68] W. Tremel, B. Krebs, G. Henkel, *Angew. Chem. 96* (1984) 604; *Angew. Chem. Int. Ed. Engl. 23* (1984) 634.
[69] K. Greiwe, *Dissertation*, Universität Münster 1985.
[70] G. Henkel, W. Tremel, B. Krebs, *Angew. Chem. 95* (1983) 314; *Angew. Chem. Int. Ed. Engl. 22* (1983) 318; *Angew. Chem. Suppl. 1983*, 307.
[71] W. Tremel, B. Krebs, G. Henkel, *Inorg. Chim. Acta 80* (1983) L31.
[72] J. J. Girerd, G. C. Papaefthymiou, A. D. Watson, E. Gamp, K. S. Hagen, N. Edelstein, R. B. Frankel, R. H. Holm, *J. Am. Chem. Soc. 106* (1984) 5941.
[73] T. Herskovitz, B. A. Averill, R. H. Holm, J. A. Ibers, W. D. Phillips, J. F. Weiher, *Proc. Natl. Acad. Sci. USA 69* (1972) 2437.
[74] B. A. Averill, T. Herskovitz, R. H. Holm, J. A. Ibers, *J. Am. Chem. Soc. 95* (1973) 3523.
[75] G. Henkel, W. Simon, B. Krebs, *Z. Kristallogr. 186* (1989) 125.
[76] G. Henkel, A. Wilk, W. Simon, lecture at the Chemiedozententagung 1987.
[77] M. A. Bobrik, E. J. Laskowski, R. W. Johnson, W. O. Gillum, J. M. Berg, K. O. Hodgson, R. H. Holm, *Inorg. Chem. 17* (1978) 1402.
[78] G. Henkel, W. Simon, A. Wilk, B. Krebs, *Z. Kristallogr. 178* (1987) 921.
[79] P. Barbaro, A. Bencini, I. Bertini, F. Briganti, S. Midollini, *J. Am. Chem. Soc. 112* (1990) 7238.
[80] W. Simon, A. Wilk, B. Krebs, G. Henkel, *Angew. Chem. 99* (1987) 1039; *Angew. Chem. Int. Ed. Engl. 26* (1987) 1009.
[81] W. Bronger, M. Kimpel, D. Schmitz, *Angew. Chem. 94* (1982) 562; *Angew. Chem. Int. Ed. Engl. 21* (1982) 544; *Acta Crystallogr. Sect. B39* (1983) 235.
[82] G. Henkel, W. Tremel, B. Krebs, T. F. Koetzle, P. Coppens, *Proc. Eur. Crystallogr. Meeting 7* (1982) 223.
[83] L. Que, Jr., M. A. Bobrik, J. A. Ibers, R. H. Holm, *J. Am. Chem. Soc. 96* (1974) 4168.
[84] M. J. Carney, G. C. Papaefthymiou, M. A. Whitener, K. Spartalian, R. B. Frankel, R. H. Holm, *Inorg. Chem. 27* (1988) 346.
[85] M. J. Carney, G. C. Papaefthymiou, R. B. Frankel, R. H. Holm, *Inorg. Chem. 28* (1989) 1497, and references cited therein.
[86] M. J. Carney, G. C. Papaefthymiou, K. Spartalian, R. B. Frankel, R. H. Holm, *J. Am. Chem. Soc. 110* (1988) 6084.
[87] K. S. Hagen, J. M. Berg, R. H. Holm, *Inorg. Chim. Acta 45* (1980) L17.
[88] K. S. Hagen, D. W. Stephan, R. H. Holm, *Inorg. Chem. 21* (1982) 3928.
[89] G. Henkel, H. Strasdeit, B. Krebs, *Proc. Int. Conf. Coord. Chem. 22* (1982) 618.
[90] G. Christou, R. H. Holm, M. Sabat, J. A. Ibers, *J. Am. Chem. Soc. 103* (1981) 6269.
[91] H. Strasdeit, B. Krebs, G. Henkel, *Proc. Int. Conf. Coord. Chem. 23* (1984) 576.
[92] G. Christou, K. S. Hagen, R. H. Holm, *J. Am. Chem. Soc. 104* (1982) 1744.
[93] J. F. You, B. S. Snyder, G. C. Papaefthymiou, R. H. Holm, *J. Am. Chem. Soc. 112* (1990) 1067.
[94] J. F. You, B. S. Snyder, R. H. Holm, *J. Am. Chem. Soc. 110* (1988) 6589.
[95] G. Christou, K. S. Hagen, J. K. Bashkin, R. H. Holm, *Inorg. Chem. 24* (1985) 1010.
[96] F. Hardinghaus, *Dissertation*, Universität Münster 1989.
[97] I. G. Dance, J. C. Calabrese, *J. Chem. Soc. Chem. Commun. 1975*, 762.
[98] I. G. Dance, *J. Am. Chem. Soc. 101* (1979) 6264.
[99] P. A. Lindahl, N. Kojima, R. P. Hausinger, J. A. Fox, B. K. Teo, C. T. Walsh, W. H. Orme-Johnson, *J. Am. Chem. Soc. 106* (1984) 3062.
[100] R. A. Scott, S. A. Wallin, M. Czechowski, D. V. DerVartanian, J. LeGall, H. D. Peck, Jr., I. Moura, *J. Am. Chem. Soc. 106* (1984) 6864.
[101] S. P. Cramer, W.-H. Pan, M. K. Eidsness, T. Morton, S. W. Ragsdale, D. V. DerVartanian, L. G. Ljungdahl, R. A. Scott, *Inorg. Chem. 26* (1987) 2477.
[102] T. Yamamura, H. Miyamae, Y. Katayama, Y. Sasaki, *Chem. Lett. 1985*, 269.
[103] A. D. Watson, C. P. Rao, J. R. Dorfman, R. H. Holm, *Inorg. Chem. 24* (1985) 2820.
[104] B. S. Snyder, C. P. Rao, R. H. Holm, *Aust. J. Chem. 39* (1986) 963.
[105] J. R. Nicholson, G. Christou, J. C. Huffman, K. Folting, *Polyhedron 6* (1987) 863.
[106] W. Tremel, B. Krebs, G. Henkel, *J. Chem. Soc. Chem. Commun. 1986*, 1527.
[107] W. Tremel, M. Kriege, B. Krebs, G. Henkel, *Inorg. Chem. 27* (1988) 3886.
[108] P. Woodward, L. F. Dahl, E. W. Abel, B. C. Crosse, *J. Am. Chem. Soc. 87* (1965) 5251.
[109] H. Miyamae, T. Yamamura, *Acta Crystallogr. Sect. C44* (1988) 606.
[110] T. Yamamura, *Bull. Chem. Soc. Jpn. 61* (1988) 1975.
[111] R. O. Gould, M. M. Harding, *J. Chem. Soc. A1970*, 875.
[112] H. Barrera, J. C. Bayon, J. Suades, C. Germain, J. P. Declerq, *Polyhedron 3* (1984) 969.
[113] W. Gaete, J. Ros, X. Solans, M. Font-Altaba, J. L. Briansó, *Inorg. Chem. 23* (1984) 39.
[114] M. Kriege, G. Henkel, *Z. Naturforsch. B42* (1987) 1121.
[115] T. Krüger, B. Krebs, G. Henkel, *Angew. Chem. 101* (1989) 54; *Angew. Chem. Int. Ed. Engl. 28* (1989) 61.
[116] I. G. Dance, M. L. Scudder, R. Secomb, *Inorg. Chem. 24* (1985) 1201.
[117] B. K. Koo, E. Block, H. Kang, S. Liu, J. Zubieta, *Polyhedron 7* (1988) 1397.
[118] T. Krüger, *Dissertation*, Universität Münster 1991.
[119] G. Henkel, M. Kriege, K. Matsumoto, *J. Chem. Soc. Dalton Trans. 1988*, 657.
[120] K. Matsumoto, H. Nakano, S. Ooi, *Chem. Lett. 1988*, 823.
[121] W. Tremel, G. Henkel, *Inorg. Chem. 27* (1988) 3896.
[122] G. Henkel, K. Greiwe, W. Tremel, lecture at the Chemiedozententagung 1985.
[123] J. K. Money, J. R. Nicholson, J. C. Huffman, G. Christou, *Inorg. Chem. 25* (1986) 4072.
[124] J. H. R. Kägi, A. Schäffer, *Biochemistry 27* (1988) 8509, zit. Lit. and references cited therein.
[125] K. Lerch, in H. Sigel (Ed.): *Metal Ions in Biological Systems*, Vol. 13, Marcel Dekker, New York 1981, p. 299, and references cited therein.
[126] M. Vašák, J. H. R. Kägi in H. Sigel (Ed.): *Metal Ions in Biological Systems, Vol. 15*, Dekker, New York 1983, p. 213, and references cited therein.
[127] M. Margoshes, B. L. Vallee, *J. Am. Chem. Soc. 79* (1957) 4813; J. H. R. Kägi, B. L. Vallee, *J. Biol. Chem. 235* (1960) 3460; *ibid. 236* (1961) 2435; P. Pulido, J. H. R. Kägi, B. L. Vallee, *Biochemistry 5* (1966) 1768.
[128] G. N. George, J. Byrd, D. R. Winge, *J. Biol. Chem. 263* (1988) 8199; K. B. Nielson, C. L. Atkin, D. R. Winge, *ibid. 260* (1985) 5342.
[129] C. F. Shaw III, *Comments Inorg. Chem. 8* (1989) 233.
[130] D. Coucouvanis, C. N. Murphy, S. K. Kanodia, *Inorg. Chem. 19* (1980) 2993.
[131] I. G. Dance, G. A. Bowmaker, G. R. Clark, J. K. Seadon, *Polyhedron 2* (1983) 1031; I. G. Dance, J. C. Calabrese, *Inorg. Chim. Acta 19* (1976) L41.
[132] M. Baumgartner, W. Bensch, P. Hug, E. Dubler, *Inorg. Chim. Acta 136* (1987) 139.
[133] G. Henkel, B. Krebs, P. Betz, H. Fietz, K. Saatkamp, *Angew. Chem. 100* (1988) 1373; *Angew. Chem. Int. Ed. Engl. 27* (1988) 1326.
[134] P. Betz, *Dissertation*, Universität Münster 1986.
[135] J. R. Nicholson, I. L. Abrahams, W. Clegg, C. D. Garner, *Inorg. Chem. 24* (1985) 1092.
[136] G. Henkel, P. Betz, B. Krebs, unpublished results.
[137] M. Baumgartner, H. Schmalle, E. Dubler, *Polyhedron 9* (1990) 1155.
[138] I. G. Dance, *J. Chem. Soc. Chem. Commun. 1976*, 103.
[139] I. G. Dance, *Aust. J. Chem. 31* (1978) 2195.
[140] G. A. Bowmaker, G. R. Clark, J. K. Seadon, I. G. Dance, *Polyhedron 3* (1984) 535.
[141] I. G. Dance, *J. Chem. Soc. Chem. Commun. 1976*, 68.
[142] G. A. Bowmaker, L.-C. Tan, *Aust. J. Chem. 32* (1979) 1443.
[143] G. Henkel, P. Betz, B. Krebs, *Proc. Int. Conf. Coord. Chem. 24* (1986) 737 (*Chemika Chronika New Series, Special Issue*, August 1986).
[144] E. Dubler, M. Baumgartner, *Solid State Ionics 43* (1990) 193.
[145] R. Chadha, R. Kumar, D. G. Tuck, *J. Chem. Soc. Chem. Commun. 1986*, 188; *Polyhedron 7* (1988) 1121.
[146] Q. Yang, K. Tang, H. Liao, Y. Han, Z. Chen, Y. Tang, *J. Chem. Soc. Chem. Commun. 1987*, 1076.
[147] E. Block, M. Gernon, H. Kang, S. Lu, J. Zubieta, *J. Chem. Soc. Chem. Commun. 1988*, 1031.
[148] E. Block, M. Gernon, H. Kang, G. Ofori-Okai, J. Zubieta, *Inorg. Chem. 28* (1989) 1263.
[149] P. K. Bharadwaj, E. John, C.-L. Xie, D. Zhang, D. N. Hendrickson, J. A. Potenza, H. J. Schugar, *Inorg. Chem. 25* (1986) 4541.
[150] G. Henkel, P. Betz, B. Krebs, *Angew. Chem. 99* (1987) 131; *Angew. Chem. Int. Ed. Engl. 26* (1987) 145.
[151] K. Saatkamp, *Dissertation*, Universität Münster 1988.
[152] G. Henkel, K. Saatkamp, B. Krebs, unpublished results.
[153] I. G. Dance, L. J. Fitzpatrick, M. L. Scudder, *Inorg. Chem. 23* (1984) 2276.
[154] K. Tang, M. Aslam, E. Block, T. Nicholson, J. Zubieta, *Inorg. Chem. 26* (1987) 1488.
[155] W. Wojnowski, M. Wojnowski, K. Peters, E.-M. Peters, H. G. von Schnering, *Z. Anorg. Allg. Chem. 530* (1985) 79.

[156] S.-H. Hong, Å. Olin, R. Hesse, *Acta Chem. Scand. Ser. A 29* (1975) 583.
[157] I. G. Dance, *Inorg. Chim. Acta 25* (1977) L17.
[158] I. G. Dance, *Inorg. Chem. 20* (1981) 1487.
[159] S. Åkerström, *Acta Chem. Scand. 18* (1964) 1308; *Ark. Kemi 24* (1965) 505.
[160] I. G. Dance, L. J. Fitzpatrick, A: D. Rae, M. L. Scudder, *Inorg. Chem. 22* (1983) 3785.
[161] I. G. Dance, L. J. Fitzpatrick, D. C. Craig, M. L. Scudder, *Inorg. Chem. 28* (1989) 1853.
[162] I. L. Abrahams, I. Bremner, G. P. Diakun, C. D. Garner, S. S. Hasnain, I. Ross, M. Vašák, *Biochem. J. 236* (1986) 585; T. A. Smith, K. Lerch, K. O. Hodgson, *Inorg. Chem. 25* (1986) 4677.
[163] J. D. Otvos, I. M. Armitage, *Proc. Natl. Acad. Sci. USA 77* (1980) 7094; W. Braun, G. Wagner, E. Wörgötter, M. Vašák, J. H. R. Kägi, K. Wüthrich, *J. Mol. Biol. 187* (1986) 125; A. Arseniev, P. Schultze, E. Wörgötter, W. Braun, G. Wagner, M. Vašák, J. H. R. Kägi, K. Wüthrich, *J. Mol. Biol. 201* (1988) 637.
[164] W. F. Furey, A. H. Robbins, L. L. Clancy, D. R. Winge, B. C. Wang, C. D. Stout, *Science 231* (1986) 704.
[165] W. Cai, M. J. Stillman, *J. Am. Chem. Soc. 110* (1988) 7872.
[166] C.-W. Wu in I. Bertini, C. Luchinat, W. Maret, M. Zeppezauer (Hrsg.): *Zinc Enzymes*, Birkhäuser, Boston 1986, S. 563.
[167] J. M. Berg, *Science 232* (1986) 485; J. M. Berg in H. Sigel, A. Sigel (Eds.): *Metal Ions in Biological Systems, Vol. 25*, Dekker, New York 1989, p. 235, and references cited therein.
[168] T. Pan. J. E. Coleman, *Proc. Natl. Acad. Sci. USA 86* (1989) 3145.
[169] T. V. O'Halloran in H. Sigel, A. Sigel (Eds.): *Metal Ions in Biological Systems, Vol. 25*, Dekker, New York 1989, p. 105, and references cited therein.
[170] S. P. Watton, J. G. Wright, F. M. MacDonnell, J. W. Bryson, M. Sabat, T. V. O'Halloran, *J. Am. Chem. Soc. 112* (1990) 2824.
[171] J. G. Wright, H.-T. Tsang, J. E. Penner-Hahn, T. V. O'Halloran, *J. Am. Chem. Soc. 112* (1990) 2434.
[172] L. A. Stocken, *Biochem. J. 41* (1947) 358; W. T. Longcope, J. A. Luetscher, E. Calkins, D. Grob, S. W. Bush, H. Eisenberg, *J. Clin. Invest. 25* (1946) 557; A. Gilman, R. P. Allen, F. S. Philips, E. S. John, *ibid. 25* (1946) 549.
[173] H. V. Aposhion, *Annu. Rev. Pharmacol. Toxicol. 23* (1983) 193; L. Magos, *Br. J. Pharmacol. 6* (1976) 479.
[174] D. Swenson, N. C. Baenziger, D. Coucouvanis, *J. Am. Chem. Soc. 100* (1978) 1932.
[175] E. S. Gruff, S. A. Koch, *J. Am. Chem. Soc. 111* (1989) 8762.
[176] E. S. Gruff, S. A. Koch, *J. Am. Chem. Soc. 112* (1990) 1245.
[177] B. Krebs, W. Puls, G. Henkel, unpublished results.
[178] G. A. Bowmaker, I. G. Dance, B. C. Dobson, D. A. Rogers, *Aust. J. Chem. 37* (1984) 1607.
[179] I. L. Abrahams, C. D. Garner, W. Clegg, *J. Chem. Soc. Dalton Trans. 1987*, 1577.
[180] G. Henkel, J. Bremer, W. Tremel, B. Krebs, unpublished results.
[181] J. L. Hencher, M. A. Khan, F. F. Said, D. G. Tuck, *Inorg. Nucl. Chem. Lett. 17* (1981) 287.
[182] J. L. Hencher, M. A. Khan, F. F. Said, D. G. Tuck, *Polyhedron 4* (1985) 1263.
[183] K. S. Hagen, R. H. Holm, *Inorg. Chem. 22* (1983) 3171.
[184] P. A. W. Dean, J. J. Vittal, N. C. Payne, *Inorg. Chem. 26* (1987) 1683.
[185] A. Choy, D. Craig, I. Dance, M. Scudder, *J. Chem. Soc. Chem. Commun. 1982*, 1246; I. G. Dance, A. Choy, M. L. Scudder, *J. Am. Chem. Soc. 106* (1984) 6285.
[186] P. Strickler, *Chem. Commun. 1969*, 655.
[187] S. Lacelle, W. C. Stevens, D. M. Kurtz, J. W. Richardson, R. A. Jacobson, *Inorg. Chem. 23* (1984) 930.
[188] G. S. H. Lee, D. C. Craig, I. Ma, M. L. Scudder, T. D. Bailey, I. G. Dance, *J. Am. Chem. Soc. 110* (1988) 4863.
[189] D. Craig, I. G. Dance, R. Garbutt, *Angew. Chem. 98* (1986) 178; *Angew. Chem. Int. Ed. Engl. 25* (1986) 165.
[190] I. G. Dance, R. G. Garbutt, D. C. Craig, M. L. Scudder, *Inorg. Chem. 26* (1987) 4057.
[191] I. G. Dance, R. G. Garbutt, M. L. Scudder, *Inorg. Chem. 29* (1990) 1571.
[192] B. Krebs, K. Wiesmann, unpublished results; K. Wellmann, *Dissertation*, Universität Münster 1989.
[193] W. Schiwy, B. Krebs, *Angew. Chem. 87* (1975) 451; *Angew. Chem. Int. Ed. Engl. 14* (1975) 261.
[194] B. Krebs, H. Diercks, *Z. Anorg. Allg. Chem. 518* (1984) 101.
[195] B. Krebs, *Angew. Chem. 95* (1983) 113; *Angew. Chem. Int. Ed. Engl. 22* (1983) 113.
[196] P. zum Hebel, B. Krebs. M. Grüne, W. Müller-Warmuth, *Solid State Ionics 43* (1990) 133.
[197] G. S. H. Lee, K. J. Fisher, D. C. Craig, M. L. Scudder, I. G. Dance, *J. Am. Chem. Soc. 112* (1990) 6435.
[198] I. G. Dance, R. G. Garbutt, D. C. Craig, *Inorg. Chem. 26* (1987) 3732.
[199] J. G. Wright, M. J. Natan, F. M. MacDonnell, D. M. Ralston, T. V. O'Halloran, *Prog. Inorg. Chem. 38* (1990) 323.
[200] D. C. Bradley, N. R. Kunchur, *Can. J. Chem. 43* (1965) 2786.
[201] E. Block, M. Brito, M. Gernon, D. McGowty, H. Kang, J. Zubieta, *Inorg. Chem. 29* (1990) 3172.
[202] N. J. Taylor, A. J. Carty, *J. Am. Chem. Soc. 99* (1977) 6143.
[203] G. Christou, K. Folting, J. C. Huffman, *Polyhedron 3* (1984) 1247.
[204] J. Liesk, P. Schulz, G. Klar, *Z. Anorg. Allg. Chem. 435* (1977) 98; J. Liesk, G. Klar, *ibid. 435* (1977) 103.
[205] S. Choudhury, I. G. Dance, P. J. Guerney, A. D. Rae, *Inorg. Chim. Acta 70* (1983) 227.
[206] W. Beck, K. H. Stetter, S. Tadros, K. E. Schwarzhans, *Chem. Ber. 100* (1967) 3944.
[207] C. R. Lucas, M. E. Peach, *Inorg. Nucl. Chem. Lett. 5* (1969) 73.
[208] G. Henkel, P. Betz, B. Krebs, *J. Chem. Soc. Chem. Commun. 1985*, 1498.
[209] G. Henkel, P. Betz, B. Krebs, *Inorg. Chim. Acta 134* (1987) 195.
[210] N. R. Kunchur, *Nature (London) 204* (1964) 468.
[211] G. Henkel, W. Puls, W. Schmidt, B. Krebs, unpublished results.
[212] W. Puls, *Dissertation*, Universität Münster 1990.

Bonding Patterns in Intermetallic Compounds

By Reinhard Nesper*

Dedicated to Professor Hans Georg von Schnering on the occasion of his 60th birthday

Intermetallic phases have long been among the black sheep in the family of chemical compounds. Their chemical bonding has eluded description by the valence rules, which otherwise are extremely effective. As a result, understanding of the structure–bonding relationships in these phases to date has remained nebulous, even though they form the largest group of inorganic compounds. Their broad industrial applicability and richly varied structural chemistry call for new approaches for explaining their structures, electronic structures, and physical properties. A combination of new experimental and theoretical investigations has revealed interesting local aspects of chemical bonding in metals and thereby pointed to a route from the valence compounds, through the cluster and electron-deficient compounds, to the intermetallic phases.

*Die Zahl der bis jetzt bekannten einfachen wägbaren Stoffe beträgt 48; hiervon sind 38 metallischer Natur; die 10 übrigen erscheinen ohne metallisches Ansehen, theils gasförmig, theils in fester Gestalt. Sie sind die wichtigsten, welche durch die Mannigfaltigkeit ihrer Verbindungen die Einförmigkeit der Metalle aufheben.**

Leopold Gmelin 1817[1]

1. Introduction

Examination of modern chemical textbooks leads to the conclusion that *Gmelin*'s opinion, written 170 years ago as the introduction to his "Handbuch", is still valid today. Even at that time, the metallic elements possessed the greatest potential for chemical combination, since they formed by far the largest group. Nevertheless, we know much less about structure and chemical bonding in alloys and intermetallic compounds than in other classes of chemical compounds.

From the very beginning, the properties of metals and intermetallic compounds have been of use to man, so that these materials were always associated with cultures and civilizations. They occupied key positions as currency, tools, construction materials, and medical prostheses even in the earliest advanced civilizations. Mirrors made of δ-CuSn were apparently among the earliest metallic utensils.[2] The knowledge of better alloys often decided the outcome of wars and the weal and woe of nations in antiquity and the Middle Ages. Man has always known how to determine the properties of metals, to optimize them, and to exploit them—even without detailed knowledge of structures and chemical bonding. A listing of only the most important uses would exceed the scope of this article. Important research areas for traditional and future applications include refractory high-strength superalloys, magnetic compounds, superconductors, metallic glasses, and amorphous metals. Composite materials—combinations of intermetallic phases and nonconducting materials—are also expected to have a bright future in technology.

1.1. Intermetallic Compounds

In the last 20 years, a large number of inorganic compounds have been synthesized and their study has given much information about structure–property relationships. In particular the Zintl phases, which chemically are located between the insulators and the intermetallic phases, are worthy of mention here.[3, 4] The investigation of compounds with unusual electronic structures has broadened our knowledge and changed our viewpoint,[5–7] so that we can now confront intermetallic phases with new ideas and concepts.

The apparently uniform elements and their compounds have turned out to be enfants terribles in terms of chemical bonding. A major contribution to our better understanding of the complicated electronic structures of intermetallic phases has come from advanced theoretical methods, especially quantum mechanics.[10–12] The chemical bonding in these structures is complex, but, to an increasing extent, it is becoming quantitatively determinable and therefore clearer.[7–13] Today, it is impossible to give a comprehensive review of the great variety of intermetallic compounds within a single article. Therefore, the discussion here will focus on new and unusual attempts to understand intermetallic phases. That which is not understood can often be made more understandable through the use of analogies. Figure 1 gives an overview of the correlation between classes of chemical compounds, electron counts, and structural elements. Among the earliest systems to be understood electronically were the saltlike compounds, in which cationic and anionic components attain a complete octet or an 18-electron shell. Sulfates, phosphates, and derivatives of many other oxo acids showed that chemical units with varying strength of binding can exist side by side in a structure.

[*] Prof. Dr. Reinhard Nesper
Laboratorium für Anorganische Chemie
Eidgenössische Technische Hochschule
CH-8092 Zürich (Switzerland)

[*] The number of simple, weighable substances known to date is 48, 38 of which are of metallic nature; the remaining 10 seem to be without metallic appearance; some are gaseous, some solid. They are the most important, since they overcome the uniformity of the metals through the diversity of their compounds.

 © VCH Verlagsgesellschaft mbH, W-6940 Weinheim, 1991 0570-0833/91/0707-0789 $ 3.50+.25/0

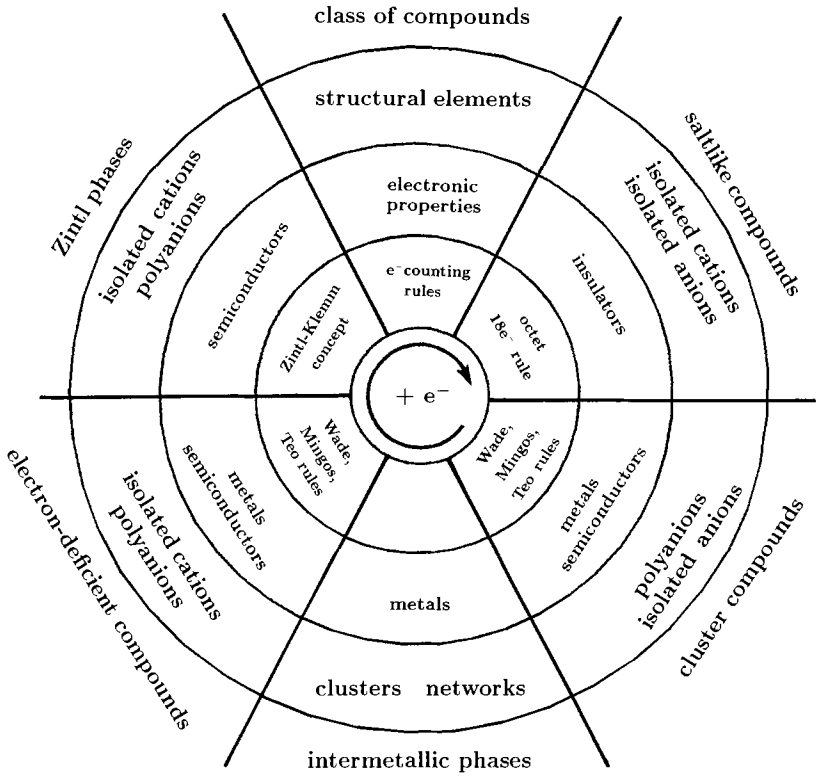

Fig. 1. Relations between classes of chemical compounds through the comparison of structural elements, electronic properties, and electron-counting rules. Note the exchange of anion and cation structures between the electron-deficient compounds and the cluster compounds.

The Zintl phases, with their various anion frameworks, now form a large family of compounds whose electronic structures mostly conform to the 8 − N rule.[5, 14, 15] Fundamentally speaking, they do not differ from the insulators. It is therefore not surprising that many insulator compounds have Zintl counterparts with similar chemical structures but different elements.

Borderline cases of Zintl phases, that is, those exhibiting "locally delocalized electrons" and not conforming to either the 8 − N rule or the Zintl–Klemm concept, mark the transition to the intermetallic phases. This transition can be investigated by systematic chemical combination. In the last twenty years, a large number of new intermetallic phases that, chemically speaking, must be located in the neighborhood of the Zintl phases have been synthesized in this way; however, we are only just beginning to understand the chemical bonding in their structures. The increasing knowledge of the bonding in intermetallic phases is leading to chemical structures whose overall chemical features make clear once again the unity of chemical materials.

If we leave the insulators and semiconductors in Figure 1, we can travel in two directions: to the electron-deficient compounds or to the cluster compounds. The former usually contain polyanions, and the latter, polycations. Both types of oligo- or polymeric building blocks belong to the so-called electron-deficient species. Often, however, they do not suffer from electron deficiency, but instead possess precisely adapted structures with well-defined electron counts. These so-called magic numbers of skeletal electrons are, as shown by *K. Wade*, *D. M. P. Mingos*, *B. K. Teo*, and many others, strongly dependent on the type of arrangement and less strongly on whether polycations or polyanions are present.[5] In many intermetallic compounds both cases occur, mostly well hidden in the jungle of high coordination numbers. Although their discovery will require the "right pair of spectacles",[*] theory and practice are correcting the optics to an increasing extent. *A. Simon* recently published a detailed re-

[*] *H. G. von Schnering* referred to this important instrument some time ago [4].

Reinhard Nesper, born in 1949 in Elze/Hannover, studied chemistry at the University of Münster and received his doctorate from the Max-Planck-Institut für Festkörperforschung in Stuttgart and the Universität Münster. From 1978 to 1990 he was a research fellow at the Max-Planck-Institut and, during this time, was also a guest researcher in Prof. R. Hoffmann's group at Cornell University (1984). He completed his Habilitation at the Universität Stuttgart in 1989, and in 1990 this was followed by his accepting a chair in inorganic chemistry at the ETH in Zürich. His research interests include solid-state chemistry, structure determination and electronic structures of solid materials, structure–property relationships, and general structural systematics.

view in this journal on clusters of valence-electron-poor metals.[33]

On going from the electron-deficient compounds to the cluster compounds, only the signs of the charges on the condensed units formally changes; the electronic structure of the cluster arrangement remains practically unchanged. Isoelectronic polyanionic and polycationic units often have the same structure.

The definition of the intermetallic compounds as a uniform family is not easy. A clear definition is almost impossible, in particular owing to the fluid transition to the semiconductors, the kaleidoscopic variety of chemical bonding, and the extremely diverse structural chemistry. *Pearson's Handbook of Crystallographic Data for Intermetallic Phases* by *P. Villars* and *L. D. Calvert*[17] contains crystallographic data for thousands of structures.[*] The simplest definition would be that intermetallic phases are (1) compounds between metals and (2) metallic conductors.

W. B. Pearson has distinguished five groups of intermetallic phases:[19]

1. Compounds with dense packing. These generally have molar volumes that are considerably smaller than the sum of the atomic volumes, and the interatomic distances are shorter than those calculated from *L. Pauling*'s formula for bond order n ($\triangleq$ valence/coordination number) in intermetallic phases with $d_n = d_1 - 0.6 \lg n$ (d_1 is the single-bond length).[20]
2. Compounds in which the band-structure energy accounts for a large part of the total energy (see Section 5.5). These include, among others, the Hume–Rothery phases (the so-called α, β, and γ phases), which occur only for certain valence-electron concentrations.[**][21–24]
3. Compounds with framework structures. In these compounds, all atoms form a common framework in which the distances to the nearest neighbors obey the Pauling formula (see above). They supposedly do not follow the valence and valence-electron-concentration rules.
4. Compounds with hybrid framework structures such as $BaAl_4$. These contain partial structures made up of one or more types of atom, which depend in certain ways on the number of valence electrons (see also Section 5.4).
5. *Pearson* named valence compounds, that is, compounds that follow the valence rules, as the fifth group. However, these are better classified as Zintl phases.

Numerous geometrical classifications have been given for groups of intermetallic compounds;[24–26] still, they do not clearly distinguish such compounds from other classes of compounds, such as Zintl phases.

1.2. Structure Maps

The first attempts to determine the range of existence of various structures were made in the 1920s for the structures of ionic crystals and were based on the ratios of the radii of rigid spheres.[20, 29–32] But even the separation of simple AB compounds in this way was not particularly successful. In the late 1970s chemical criteria were increasingly used to generate such structure maps. These criteria included the radii r_s and r_p for s and p orbitals,[36] which can be obtained from pseudopotential calculations, for example.[37] Radii for hybrid orbitals were developed for main-group and transition elements and used to discriminate between the structures.[38–40] In addition, *D. G. Pettifor* has empirically developed a new electronegativity scale which can be used to cleanly separate over 500 AB compounds (Fig. 2).[45] However, an atomic interpretation of his values remains to be found. On a much larger scale, *P. Villars* et al. have attempted to produce coordinates for the prediction of stable binary and ternary intermetallic compounds.[46, 47] Other recent attempts to derive chemical coordinates for the generation of structure maps can be found in a concise summary by *J. Hafner*.[12]

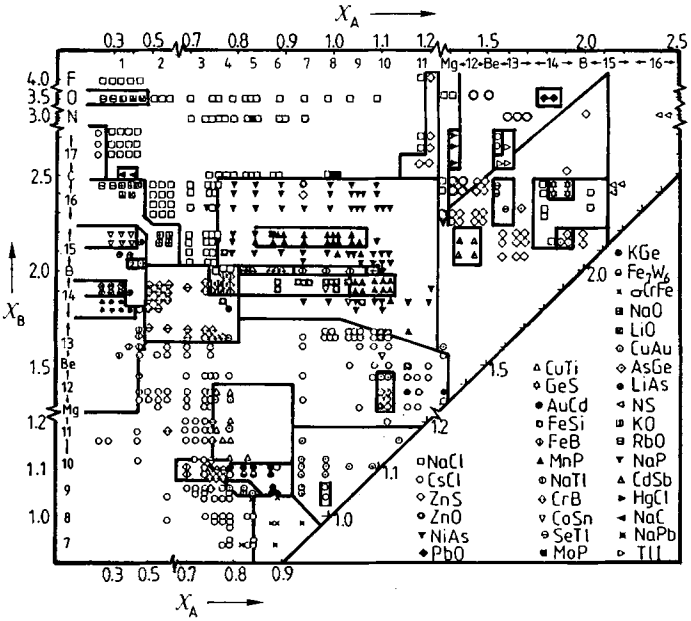

Fig. 2. Structural field after [45] with division of 574 AB compounds by means of a specially adjusted electronegativity.

2. Unusual Elemental Structures

2.1. α-Gallium: An Alternative to Boron Structures

Why does elemental gallium crystallize with a relatively complicated structure,[48] whereas aluminum has a simple face-centered cubic (fcc) structure? In fact, gallium does not evade the simple close packing very well. According to the latest ab initio SCF calculations of *M. Parrinello* et al., gallium has a choice between several structures that differ energetically by only a few $kJ\,mol^{-1}$.[49] The melting and boiling points of α-gallium (303 and 2510 K) differ considerably. The relatively high boiling temperature shows that the chemical bonds in gallium are by no means weak. Apparently, the melting point is so low because, above 303 K, gallium cannot

[*] About 21 000 publications from 1973 to 1982 (in part, up to 1984) were assessed. The *Binary Alloy Phase Systems* [18] comprise about 1800 binary phase diagrams.

[**] Valence-electron concentration (VEC) usually denotes the average number of valence electrons per atom.

decisively "choose" a particular crystal structure. Thus, continuous phase transformations are initiated, the result of which can only be a liquid phase.[51] Chemical real-time depictions of such processes are known from *J. O. Bovin*'s fantastic electron microscopic studies of small metal crystallites.[50]

The orthorhombic crystal structure of α-gallium shows two things (Fig. 3a):

1. A simple compromise is not the best solution. According to pseudopotential studies by *V. Heine* et al.,[11] it is energetically more favorable for gallium to form only five shorter contacts of differing length rather than twelve longer contacts of the same length: d(fcc Ga) = 3.03 Å (12×), d(α-Ga) = 2.48, 2.69 (2×), 2.79 Å (2×) for V(fcc Ga) = V(α-Ga). The difference in the distances allows a compromise between volume optimization and distance optimization (cf. Section 5.5). It is likely that many such competing effects are one reason for the difficulties we have in understanding intermetallic phases.
2. There are alternatives to boron structures. Figure 3b clearly reveals Ga_2 pairs with pronounced covalent bonding; this is why *M. Parrinello* et al. described α-Ga as a "molecular metal". However, the remaining partial structure is by no means a "typical metallic tangle" of long contacts. Instead, it turns out to be a two-dimensional polymer composed of semi-icosahedra. The optimum electron count for gallium, calculated by using the extended Hückel method due to *Hoffmann* et al.[8-10] is in fact three electrons per atom.[51] Thus, there is no electron deficiency; the structure is optimally adapted to a relatively low electron count. In this structure, with its semi-icosahedra oriented alternately upwards and downwards, the short Ga–Ga bonds are the terminal two-electron two-center bonds of the polyhedron fragments. It is indeed an alternative to boron structures, and it is certainly possible that a modification of boron with an α-Ga structure would have semiconducting properties.

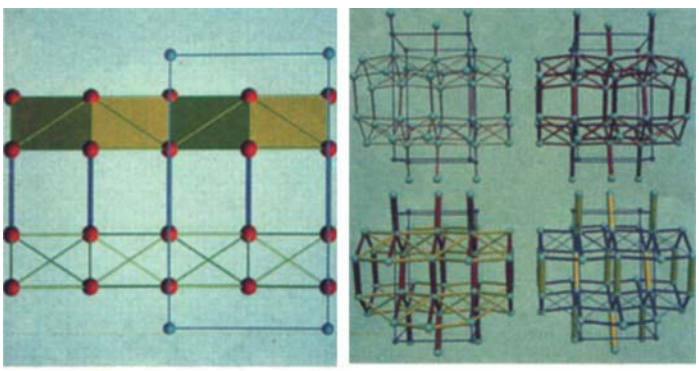

a b

Fig. 3. Structure (a) and probing of the chemical bonding (b) of α-Ga; (b) shows the change in the strength of chemical bonding (COOP) as the number of electrons increases from 1 to 2.5, 3.25 and 3.5 electrons per gallium (increasing, red; unchanged, yellow; decreasing blue) (top left, 1 electron per Ga; top right, 2.5 electrons per Ga; bottom left, 3.25 electrons per Ga; bottom right, 3.5 electrons per Ga).

Investigations of the variation of the chemical bonding with the number of electrons per atom show that, up to a value of three electrons per atom, the relative bond strength increases to approximately the same extent for all atoms. The relative strengths correspond more or less to the reciprocal distances (cf. Fig. 3b). The largest overlap population is attained at three electrons per Ga.[*] Above this value, the overlap population decreases, at first only for the bonds in the semi-icosahedra. However, up to about 3.25 electrons per Ga, the bonds in a graphitelike partial structure (Fig. 3b, bottom left), which contains the shortest Ga–Ga bonds, become increasingly strong. Hence, the graphite structure is implicitly contained in that of α-gallium and appropriate electron transfer to gallium could result in the corresponding changes in the distances!

If elemental aluminum is offered nucleation centers, a fantastic structural chemistry unfolds which barely resembles the dreary monotony of the elemental structure. Examples, from the many compounds of this type, include β-Mg_2Al_3, WAl_{12}, VAl_{10}, α-V_7Al_{45}, $LiMgAl_2$, Fe_3Al_{13}, Ni_4Mn_{60}, and, of course, the new quasicrystalline compounds such as $MnAl_6$.[60] From a chemical viewpoint, one would attribute to gallium a clear tendency to form few, but directed, bonds. But the same could be true of aluminum. However, this is not the case, because, as was mentioned earlier, aluminum has an fcc structure. The pseudopotential theory gives us interesting information here (see Section 5.5).

2.2. Manganese

Manganese does not adopt the simple arrangements of its neighboring elements either, namely, body-centered cubic (bcc: Cr, Fe) and hexagonal close-packed (hcp: Tc, Re). Manganese can apparently better do justice to its chemical bonding in a somewhat complex structure.[61] Manganese and aluminum are the crucial components in the quasicrystalline compounds known up to now. Both have a pronounced tendency to form directed chemical bonds (cf. Section 2.1). Manganese occurs in two complicated modifications: α-Mn with 58 atoms per unit cell and β-Mn with 20 atoms per unit cell and a chiral structure (space group $P4_132$).[48] In α-Mn, which is stable under normal conditions, four crystallographically distinct positions in the unit cell are occupied, the coordination polyhedra of which have 12, 13, and 16 neighbors. The large differences in the bond lengths and the differing magnetic moments[52] indicate that these positions have different crystallochemical functions. Conspicuous are the very short distances (between 2.24 and 2×2.38 Å) between Mn atoms joined to a fragment of a Friauf polyhedron, a truncated tetrahedron (T) (Fig. 4). It can be shown not only with the help of the cluster "spectacles" mentioned earlier,[4] but also by experimental and theoretical investigations, that these units are the centers of stability of the structure.

Decompositions of the α-Mn structure such as $Mg_{17}Al_{12}$ and $Li_xMg_{17-x}Al_{12}$, with partly ordered atomic distributions, have been found experimentally.[53-55] In both compounds, aluminum occupies exclusively one of the four crystallographically distinct Mn positions and forms isolated

[*] *R. Hoffmann*'s method of crystal orbital overlap populations (COOP) [8] allows the variation of the relative bond strength to be studied as a function of the number of valence electrons. This is also referred to as different degrees of filling in a rigid band model.

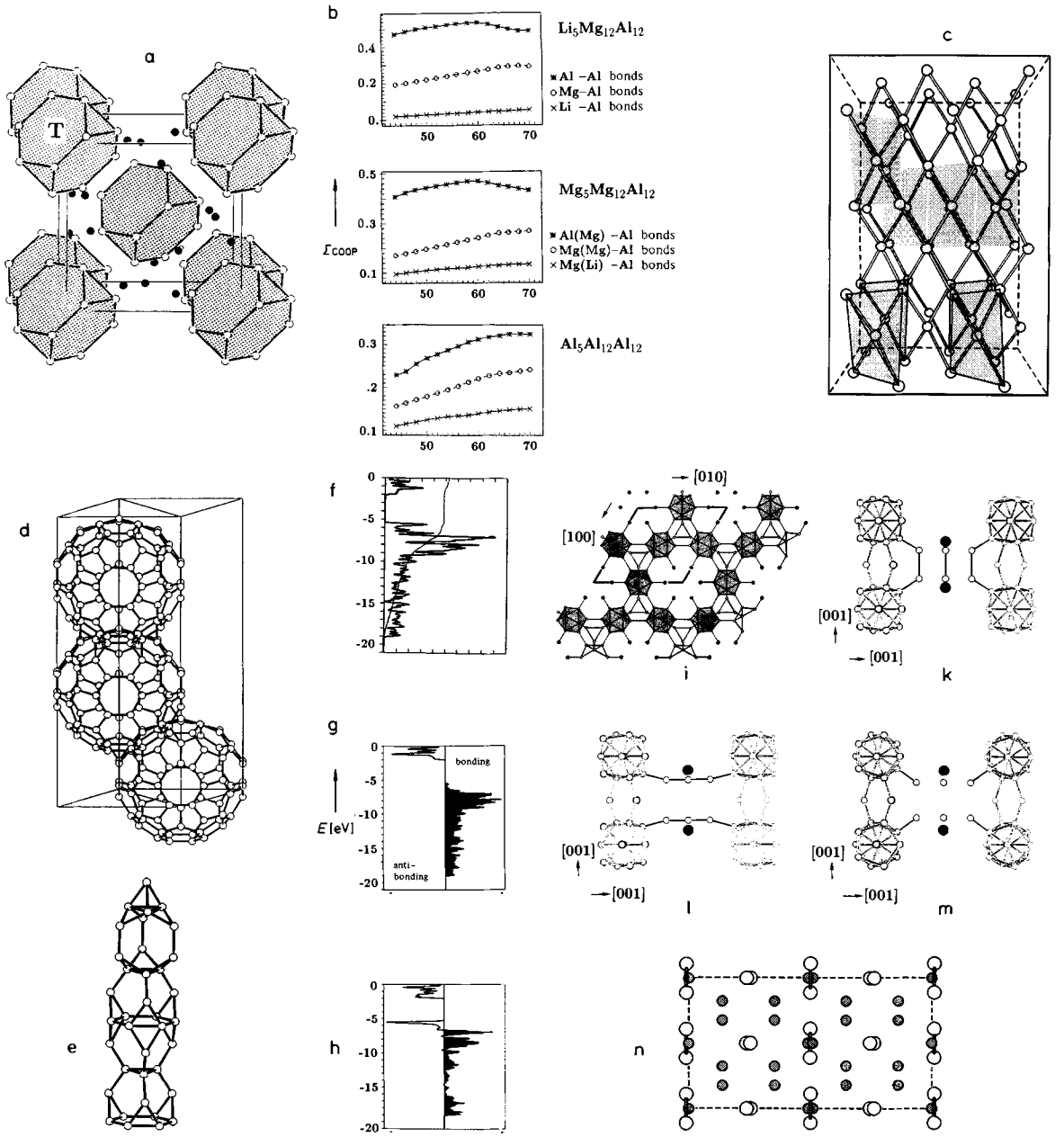

Fig. 4. Unusual elemental structures and intermetallic phases. a) Structure of the intermetallic phase $Li_5Mg_{12}Al_{12}$ as a model for α-Mn; the centers of the truncated tetrahedra (T) are occupied by Li; the coordinating atoms are Mg (solid circles) and Li (not visible). b) COOP sums for the model compounds $Li_5Mg_{12}Al_{12}$, $Mg_{17}Al_{12}$, and elemental Al in the α-Mn structure (electron counts apply to the primitive unit cell; high values of $\sum$ COOP correspond to strong bonding components. c) Structure of γ-Pu, with distorted tetrahedral coordination. d), e) Partial depiction of the Al framework in $LiMgAl_2$. f) Electronic density of states for the three-dimensional Al partial structure; weighted density of states (COOP) from (f), relative to the Al atoms with four (g) and with five and six neighbors (h). The highest bond strength (maximum overlap population) occurs at 4 electrons per Al for the former and at only about 3.5 electrons per Al for the latter. The more highly coordinated Al atoms apparently take part in "electron-saving" multicenter bonds. i) Structure of $Na_xMg_{5-x}Ga_6$ with three-dimensional Ga framework of icosahedra and truncated tetrahedra. k)–m) Part of the three-dimensional Ga framework in $Na_xMg_{5-x}Ga_6$ with different connections of the terminal Ga atoms (solid circles, Na and Mg atoms). The one- (m), two- (k), and three-bond (l) situations result in different electron requirements for the terminal Ga atoms. n) Structure of Mg_5Ga_3 with Ga–Ga double bonds.

Al_{12} clusters. In $Li_xMg_{17-x}Al_{12}$ a further position is reserved for Mg atoms. Two sites of higher symmetry exhibit mixed Li/Mg occupation. This natural partitioning of the structure can be understood by means of quantum-mechanical extended Hückel (EH) calculations (COOP[8, 9]), whereby the existence of compounds with main-group elements greatly simplifies the theoretical treatment because d orbitals need not be taken into account. For $Li_5Mg_{12}Al_{12}$, $Mg_{17}Al_{12}$ ($\triangleq Mg_5Mg_{12}Al_{12}$), and elemental aluminum with an α-Mn structure ($= Al_5Al_{12}Al_{12}$), one obtains, with increasing uncertainty, the following result (Fig. 4b):[55] The optimum electron count of 60 electrons for the truncated tetrahedron can be understood in terms of the 8 – N rule or the Zintl–Klemm concept. The Al atoms form three bonds, thus corresponding to pseudophosphorus atoms, and can be formally regarded as five-electron species, $(3b)Al^{2\ominus}$. The positions in $Li_5Mg_{12}Al_{12}$ occupied by Mg clearly participate in the 12 electron pairs (one per Al atom) which are directed outwards and which are not essentially involved in the bonding of the Al_{12} group. If it is assumed that there are 36 skeletal elec-

trons (18 topological bonds) in the Al_{12} unit, then this implies that the Friauf polyhedron strives to attain the electron count required for classical two-center two-electron bonds. At least for main-group elements such as gallium and aluminum, the truncated tetrahedron follows the Zintl–Klemm concept. α-Manganese, with its 58 instead of 60 electrons per truncated tetrahedron, also comes close to this description. However, significant electron transfer or charge disproportionation between the individual positions must occur (see above).

Many intermetallic phases, and particularly those with complex structures, contain Friauf polyhedra, whose stable framework is formed by truncated tetrahedra. Here, the simple valence-structure description might provide new insights until the theoretical methods become capable of treating structures with 200 or more atoms in the unit cell. However, it is not always easy to find the structural unit that is relevant to the chemical bonding in the structures of intermetallic phases. This requires knowledge of the particularly stable clusters. In this respect, the synthesis of polynary replacement structures will surely be of great help (see Section 3.3).

In the β-Mn structure, there are only two crystallographically distinct positions, but these behave towards each other analogously to those in α-Mn. The numerically superior Mn type (12 Mn) has 12 neighbors which are much more remote (d(Mn-Mn) ≈ 2.57 Å) than those of the other type (6 Mn), which once again exhibit three short distances of 2.36 Å and nine longer ones. This suggests that the majority components are cationic in nature and the minority components anionic.

2.3. Does Manganese Have Four Hands?

Interesting similarities between the structures of α-Mn, β-Mn, and γ-Pu as well as the two modifications of white phosphorus and P_4S_3 have been described by *H. G. von Schnering*[56] and *A. Simon*.[57]

White phosphorus, P_4, crystallizes at room temperature as a "stuffed" variant of α-Mn[56] in which each Mn atom is replaced by a P_4 molecule. As a 20-electron system, P_4 has four lone pairs, one on each P atom, which extend the vertices of the tetrahedron. These lone pairs avoid each other. The closest approaches of the P_4 groups should therefore occur in such a way that an optimum arrangement of tetrahedral faces and tetrahedral vertices is possible. If there is a correlation between the two structures in terms of chemical bonding, then the Mn atoms should also form directed bonds with tetrahedral character. Do the Mn atoms in α-Mn have sp^3-like bonds; that is, do they have "tetrahedrally oriented hands" that contribute to the formation of the α-Mn structure? This idea is not necessarily as eccentric as it might seem, given what was said in Section 2.2, but it must also explain why other structural solutions such as the diamond structure or, more so, the double diamond structure, namely, the body-centered cubic arrangement as in α-Fe, do not play a role. Apparently, the tetrahedron interacts more strongly in some directions and less strongly in others, completely in accordance with the geometry of the truncated tetrahedra Mn_{12} and $(P_4)_{12}$.

There is also a molecular analogue of the β-Mn structure. P_4S_3 crystallizes with a structure in which the centers of the molecules form the β-Mn arrangement.[58, 59] P_4S_3 molecules can undergo particularly dense packing with three neighboring molecules at specific positions, namely, in the direction of the fivefold surfaces. This requires that the other 12 neighbors be more remote.

Like almost all actinides, plutonium does not crystallize in a dense sphere packing; instead, it forms a distinctly distorted structure. This is attributed, among other things, to interactions between the f orbitals, which are more extended than those of the lanthanides. γ-Pu is the stable modification above 508 K.[48] The coordination number is ten, with four short distances of 3.026 Å and six longer distances of 3.16 to 3.29 Å. The four short distances correspond to the four possibilities of approaching a P_4 molecule in the direction of the faces. The structure can also be understood as a strongly distorted variation of the diamond structure. Figure 4c shows the unit cell, a larger section of the structure, and a polyhedra representation for the four nearest neighbors. Thus, the attractive interactions in γ-Pu and the closest approaches in P_4 are in the direction of the edges of these distorted tetrahedra. Interestingly, *W. B. Pearson* has categorized the elemental structures α-Pu, γ-Pu, α-Np, and α-U as unclassified structures.[24]

Even at room temperature, the molecular units P_4 and P_4S_3 tend to undergo librational and rotational movement. These excited states can best express themselves in different structures, such as those that are known for P_4. *Pauling* based his bonding theory for (transition) metals on the existence of different resonance structures. A large number of such valence states contribute to the average chemical bonding, to varying extents for each metal (cf. Section 5.3). It is certainly an unusual but interesting question whether there might be connections between these valence states and the librational movements in structurally related arrangements of molecules.

3. At the Zintl Border

The Zintl border between semiconducting and metallic elements, in its original form as given by *Zintl*, passed between groups 13 and 14 of the periodic table. Both as elements and in their compounds, boron, aluminum, indium, and thallium exhibit an extremely unconventional structural chemistry, whose complexity indicates the effect of directed chemical bonds. In addition, these elements often do not conform to the classical chemical bonding concepts. In its compounds, aluminum suddenly throws off the unprepossessing mask of its face-centered cubic (fcc) structure. Even before the discovery of quasicrystalline $MnAl_6$,[60] Al was known for the exceedingly complex structures of its intermetallic phases. Near the Zintl border, a particularly interesting entry into the structural chemistry of intermetallic compounds is possible. It is certainly no coincidence that in the last ten years so many preparative and theoretical investigations have been performed in precisely this region of the periodic table.

3.1. γ-Brass as a Borderline Case

The compounds $Li_{21}X_5$ (X = Si, Ge, Sn, Pb, Tl) crystallize in the γ-brass structure. It has been proved (up to now for

X = Si, Ge, Sn[64-66]) that earlier reports of the composition $Li_{22}X_5$ are erroneous. The central structural elements are $M_{20}X_6$ and $M_{22}X_4$ units, which geometrically are a combination of two tetrahedra, an octahedron, and a cuboctahedron and are thus a distorted section of a body-centered cubic parent structure.[64] *E. Parthé* et al. have described several such combinations of nested polyhedra as the fundamental building blocks of intermetallic phases.[69]

In spite of their high lithium contents, the silicides, germanides, and stannides are brittle materials with a silver metallic luster. As shown by the analysis of the formal charges $(Li_{21})^{20\oplus}$ $(Si^{4\ominus})_5$, they do not entirely conform to the Zintl–Klemm concept. Quantum-mechanical investigations have shown that, in the double formula unit, two electrons belong to an energetically low-lying, essentially Li-centered orbital.[70] This so-called cage orbital is symmetrically distributed over all 12 Li atoms of the outer cuboctahedron. Cage orbitals have also been found in other Li silicides and germanides with unusual electron counts.[7] All other valence electrons are in states which, as is typical of valence compounds (insulators and Zintl phases), can be assigned to the electronegative atoms. Thus, compounds such as $Li_{21}X_5$ behave like a cross between valence compounds and intermetallic phases. As γ-brass variants, they belong to the Hume–Rothery phases, while their properties (brittleness, semiconductivity) classify them as Zintl phases. Their electronic structure is similar to those of cluster compounds, which can be metallic or semiconducting. Most of the valence electrons are centered on the anions (X), but a small number remain on the cations and are available for cation–cation bonding.

The electronic structure of $Li_{21}Si_5$ shows a further feature: not only the atoms Li and Si, but also the larger structural elements $Li_{20}Si_6$ and $Li_{22}Si_4$, exchange electrons among themselves. This leads to donor–acceptor interactions between the groups $[Li_{20}Si_6]^{\delta\ominus}$ and $[Li_{22}Si_4]^{\delta\oplus}$ (cf. Section 2.2). The phases $M_{21}X_5$ can be used to demonstrate exemplarily the symbiotic relationship between classical valencies and metallic electronic states. Upon traveling further into the realm of intermetallic phases, the balance between the two changes: delocalization increases while charge separation decreases. Nevertheless, both types of chemical bonding are retained (cf. KNa_2, Section 3.4).

3.2. Aluminides and Gallides

Binary and ternary compounds of aluminum and gallium exhibit a particularly rich structural chemistry, in which nearly all features of chemical bonding that are known from boron compounds find a worthy counterpart. It is not only the aluminides of the transition metals that captivate us with their complex arrangements; even the long-known Mg-Al compounds have structures, of which until now only the simplest could be understood. Recently, *W. Uhl* et al. synthesized and characterized an isolated Al_{12} icosahedron surrounded by a sphere of ligand molecules.[67]

Experimental chemistry is particularly well suited for gaining insights into the chemical bonding in intermetallic phases. Since intermetallic phases allow far greater phase widths than semiconductors and insulators, the isomorphic replacement of components with the same or different valence makes possible an experimental probing of the chemical bonding. The partitioning of a structure AB_x by several components to give $(A,A')(B,B')_x$ has already been exemplified for α-Mn (Section 2.2). However, the question remains as to how the chemical bonding in the series of compounds $Li_xMg_{17-x}Al_{12}$ changes as x is varied. Increasing x means oxidation or removal of electrons. According to structural studies, this leaves the Al–Al distances in the truncated tetrahedron unchanged, but alters the distances to and between the coordinating Mg atoms. These changes can be understood in terms of the COOP formalism.[16, 55] The Mg-centered orbitals contain essentially surplus electrons (> 60) that are not required for the Al_{12} unit ($Li_5Mg_{12}Al_{12}$, 65 electrons per formula unit; $Mg_{17}Al_{12}$, 70 electrons per formula unit). Therefore, removal of electrons affects primarily these orbitals.

In the ternary system Li-Mg-Al a new ternary phase occurs near the composition $LiMgAl_2$.[55, 68] Although the numerous binary border phases of the system have metallic properties, they are not all able to accommodate well enough the variation of the valence electrons in ternary descendants of their structures. $LiMgAl_2$ has a novel, complex structure (see Fig. 9a, b).[55] The formation of complex structures is an indication of how close such phases are to the valence compounds. It seems reasonable to assume that most of the electrons are involved in local chemical bonding and that only a few mobile conduction electrons are present.

Quantum-mechanical treatment of the entire $LiMgAl_2$ structure is not yet feasible, although this is possible for the pure Al framework (Fig. 4d, e), which has "only" 46 atoms in its primitive rhombohedral cell. Its electronic density of states exhibits a band gap at 3.9 electrons per aluminum atom. Analysis of the COOP curves shows that the majority of the Al atoms, namely, those with four Al neighbors, attain their maximum relative valence at four electrons per atom.[*] The few Al atoms that are four- or fivefold coordinated by aluminum attain this maximum already at about 3.5 electrons per atom (see Fig. 4f–h). They are involved in multicenter bonding at condensation positions of the polyhedra. Unfortunately, a study of this type, which does not take the other atoms into account, suffices only for a highly qualitative understanding of the Al framework and is less relevant to the complete structure. Nevertheless, the isolated Al_{76} polyhedron could also be of interest for the chemistry of carbon—C_{76} as superball?

In the ternary system Na-Mg-Ga, a situation occurs similar to that observed in Li-Mg-Al. Here, the Na gallides $Na_{22}Ga_{39}$[74] and Na_7Ga_{13}[75], in particular, stand out owing to the complexity of their crystal structures. Apart from $NaGa_4$,[78, 79] the compounds Mg_2Ga_5,[80, 81] $MgGa_2$,[82] and MgGa[83] occur on the gallium-rich side of the ternary system. *J. Burdett* and *E. Canadell* have investigated the skeletal electron counts of a whole series of structurally complex gallides, especially those with large Ga polyhedra.[84] They found that the local chemical bonding in the polyhedral frameworks and their interconnections agreed well with the observed total electron count. The results are listed in Table 2. In principle, an extended Zintl–Klemm concept is

[*] This number refers to the COOP overlap populations.

used here, in which, in addition to the 8 − N rule, there are also other counting rules for special polyhedra.[85] After the electrons of the cations have been formally transferred to the anionic (gallium) partial structure, the geometry, electron counts, and electronic structures can be related to one another in a straightforward manner.

$Na_xMg_{5-x}Ga_9$[55,86] is a new ternary phase with its own structural type (see Fig. 4i). Ga_{12} icosahedra are condensed with truncated tetrahedra (see Section 2.2). A few terminal Ga atoms exhibit a site disorder with minor displacements (Fig. 4k–m). These are correlated with a disorder of the Na and Mg atoms in the immediate vicinity. Each of the three observed split positions of these terminal Ga atoms apparently belongs to a specific bonding state and to a corresponding electron requirement. Applying the Zintl–Klemm concept gives $(1b)Ga^{4\ominus}$, $(2b)Ga^{3\ominus}$, and $(3b)Ga^{2\ominus}$. Apparently, the compound can react locally to changes in the total electron count, without the basic framework of the Ga_{12} polyhedra being influenced.

A similar case has been reported by *Burdett* et al.[84] For the redox pair $Na_{21}Ga_{39}$ ($\triangleq Na_7Ga_{13}$)/$Na_{22}Ga_{39}$, the significant structural difference is the change in only one Ga–Ga bond from 2.43 to 2.54 Å. According to MO calculations by *Burdett* et al., the shorter distance corresponds to a double bond and supposedly represents the first of its type. The compound Ca_5Ga_3 apparently contains another case of a Ga–Ga multiple bond (see Fig. 4n). In terms of the Zintl–Klemm concept, Ca_5Ga_3 is formulated as $(Ca^{2\oplus})_5[(0b)Ga^{5\ominus}][Ga_2]^{5\ominus}$ with equal numbers of isolated Ga atoms and Ga_2 pairs per formula unit.[*] The bond length of 2.49 Å is not much longer than that in Na_7Ga_{13},[75] although both are considerably longer than would be expected for an uncharged Ga–Ga double bond. It is known, however, that the effective charge on the anion can lead to lengthening of the bonding even in the solid compound.[4,85–87] We ourselves have observed such local changes in bond length as a function of the valence electron count in the semiconducting phases $Li_{3-x}B_{14}$,[72,73] whereby the oxidized variants with $x \geq 0$ remain transparent, red semiconductors. Thus, in systems with phase widths, optimal electron counts can be attained by means of local geometrical changes.

There is still little known about how many of the disordered intermetallic phases in fact possess locally well-defined stable clusters whose variants are a result of differing local valence electron concentrations. The concepts of chemical twinning presented by *S. Andersson*[162] and by *E. Parthé* et al.[163–165] show that, for certain compositions, no optimal uniform structural solution exists in the sense that a local stoichiometry is maintained everywhere. Instead, it is often observed, also for intermetallic phases, that sections of stable structures with totally different compositions are bound together (chemically twinned). The result is a third composition, but one that only occurs globally and not locally (see Section 6.2).

3.3. Variants of the Th_6Mn_{23} Type

The Th_6Mn_{23} structure, with 116 atoms in the unit cell, is relatively complex (Figs. 5a, 9c[89]) and is built up from a large number of intermetallic phases M_6N_{23}.[*][41] The smaller, majority components are usually the electronegative atoms N. They form a partial structure, whose basic cluster is a so-called tetrahedral star—an arrangement of a central tetrahedron and four facially linked tetrahedra. All edges of the central tetrahedron are bridged by further N atoms (Fig. 5b), which are linked with the neighboring units to

[*] The atoms without homopolar bonds (0b) are given octet configurations (i.e., $(0b)Ga^{5\ominus}$). The remaining valence electrons are formally assigned to the Ga_2 pairs.

[*] Here, M and N are symbols for metal atoms [24]. N does not designate nitrogen.

Table 1. Structures, structure elements, and valence electron numbers for some aluminides and gallides.

Compound	Structure type	q [a]	Structure elements [b]	Z [c]	N_e [d]	$N_{e'}$ [d]	Ref.
K_3Ga_{13} [e]	K_3Ga_{13}	− 0.23	$\{12b)[Ga_{12}]^{2\ominus}\}_4$, $\{(11b)[Ga_{11}]^{2\ominus}\}_4$, $\{(3b)Ga^0\}_3$, $\{(4b)Ga^{\ominus}\}_8$	8	336 [f]	336	[99]
$NaGa_4$	$BaAl_4$	− 0.25	cf. Section 5.4				[100,101]
Li_2Ga_7 [e]	Li_2Ga_7	− 0.29	$\{(12b)[Ga_{12}]^{2\ominus}\}$, $\{(4b)Ga^{\ominus}\}$	6	360	360	[98]
KGa_3 [e]	KGa_3	− 0.33	$\{(8b)[Ga_8]^{2\ominus}\}$, $\{(4b)Ga^{\ominus}\}$	3	30	30	[110]
Na_7Ga_{13} [e]	Na_7Ga_{13}	− 0.54	$\{(9b)[Ga_{12}]^{5\ominus}\}_{12}$, $\{(18b)[Ga_{15}]^{11\ominus}\}_6$	18	828	828	[97]
$Na_{22}Ga_{39}$ [e]	$Na_{22}Ga_{39}$	− 0.55	$\{(11b)[Ga_{12}]^{4\ominus}\}_4$, $\{(10b)[Ga_{12}]^{6\ominus}\}_4$, $\{(13b)[Ga_{15}]^{11\ominus}\}_4$	4	552	556	[96]
Mg_2Ga_5	Mg_2Ga_5	− 0.80	$(4b)Ga^{\ominus}$	1	20	19	[103]
$(Ca,Mg)Ga_2$	$CaIn_2$	− 1.00	$(4b)Ga^{\ominus}$	1	8	8	[104]
LiAl	NaTl	− 1.00	$(4b)Al^{\ominus}$	1	4	4	[197]
$CaLi_xAl_{2-x}$	Laves phases	− 1.00	cf. Section 3.4	1	–	8 − 2x	[118]
Mg_2Al_3	Mg_2Al_3	− 1.33	complex structure	1	–	13	[122]
$LiMgAl_2$	$LiMgAl_2$	− 1.50	complex structure	1	–	9	[80]
Li_3Al_2	Li_3Al_2	− 1.50	$(3b)Al^{2\ominus}$	1	10	9	[198]
$Mg_{23}Al_{30}$	Mo	− 1.53	icosahedra, Friauf polyhedra	1	–	136	[213]
Mg_9Al_{11}	Mg_9Al_{11}	− 1.64					[208]
MgGa	MgGa	− 2.00	$(3b)Ga^{\ominus}$	1	4	4	[105]
$Li_4Mg_{13}Al_{12}$	α-Mn	− 2.50	$(3b)Al^{2\ominus}$	1	66	60	[80]
$Mg_{17}Al_{12}$	α-Mn	− 2.84	$(3b)Al^{2\ominus}$	1	60	70	[78]
Ca_5Ga_3	Cr_5B_3	− 3.33	$(0b)Ga^{5\ominus}$, $\{(2b)Ga^{3\ominus}\}_2$	1	17	16	[118]
Mg_2Ga	Li_2Sb	− 4.00	$(1b)Ga^{4\ominus}$	1	7	7	[214]
Mg_5Ga_2	Mg_5Ga_2	− 5.00	$(0b)Ga^{5\ominus}$	1	16	16	[215]

[a] Partial charge on Al or Ga for complete charge transfer from the cations. [b] (*n*b) gives the *n* binding partners of an atom in the unit. [c] Number of formula units in the counting. [d] Number of electrons (N_e) calculated by the counting rules or actual number of electrons ($N_{e'}$) based on *Z*. [e] After [84]. [f] Counting questionable.

form a three-dimensional cubic primitive array. The large M atoms form noncentered M_6 octahedra, which in turn make up a face-centered cubic partial structure. (In this respect, the M_6N_{23} structure is geometrically related to the fluorite type.) Finally, one type of N atom remains in an environment composed exclusively of M atoms if only the first coordination sphere is considered. Even without knowledge of the wide-ranging coordination chemistry of tetranuclear metal clusters, one would assume a versatile chemical behavior for the tetrahedral star. The complete unit $N_4[N_4]N_{6/2} \triangleq N_{11}$ combines virtually all possible coordinations of a tetrahedron. All edges and faces are coordinated in a μ_3 or μ_2 fashion by the larger M atoms, and the vertices are triply coordinated by M atoms. A glance at the literature confirms what was already suspected.[17] The structure provides a geometrical solution for widely differing structures such as Sr_6Li_{26}, with 35 electrons per formula unit, and $(Co_{16}Si_7)Ta_6$, with up to 90.[*] A valence compound, the Zintl phase $Mg_6(Cu_{16}Si_7) \triangleq (Mg^{2\oplus})_6(Cu^{\oplus})_{16}(Si^{4\ominus})_7$, is also found among the approximately 160 variants of this structure type. The ternary system Li-Ca-Al contains variants $Ca_6Li_xAl_{23-x}$ which exhibit characteristic partition patterns of the N partial structures (Fig. 5c–f; N = Li, Al). The (partially ordered) occupation of certain positions by Li gives rise to Al_{11-n} fragments. Since these generally do not

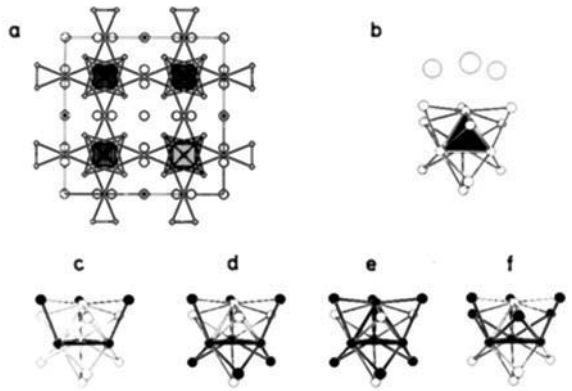

Fig. 5. The Th_6Mn_{23} type: a) Unit cell in the [001] direction (central Mn tetrahedra shaded; tetrahedral star, bottom right); b) Tetrahedral star with coordination of the edges of the central tetrahedron (black) by Mn atoms and the vertices by the large Th atoms (shown for one vertex). c)–f) Some possibilities of generating clusters as fragments of the tetrahedral star in the Th_6Mn_{23} type for $Ca_6Li_xAl_{23-x}$ variants. The solid circles are supposedly occupied by Al and the open circles by Li. According to COOP calculations, the following numbers of electrons per Al atom are assigned to these clusters for optimum bonding: 4.5 (c), 4.2 (d), 3.6 (e), and 3.2 (f) (*hypho*-icosahedron).

form isolated oligomeric units, but instead remain associated with other N atoms, their electron requirements can once again only be determined by means of band structure calculations (COOP). Indeed, initial investigations apparently show that a large number of differing fragments with specific electron requirements can readily be accommodated structurally.[71]

[*] Four valence electrons are taken into account for Si, five for Ta, and two for Co. Simple rules of how many of the d electrons contribute to the chemical bonding and how many remain essentially inert on the transition element could not be given up to now. Approaches to this problem, however, have been proposed by *Pauling* [20].

3.4. Laves Phases as Examples

Laves phases MN_2 belong to the typical intermetallic phases. The three classical types of Laves phases, with $MgCu_2$ (Fig. 6a, second top left, and Fig. 9a), $MgNi_2$ (Fig. 6a, third top left), or $MgZn_2$ structures (Fig. 6e, first top left), occur for different valence electron concentrations. *Laves* has himself stressed the importance of geometrical factors (highest possible symmetry, highest space filling, and highest number of neighbors), but only under the condition that no other factors are influential.[90] *Laves*'and *Parthé*'s corresponding model, based on rigid spheres, has already been criticized by *Pearson* as being inadequate.[24] Some intermetallic phases, even though they have a radius ratio r_M/r_N or 1.225, crystallize in other structures, like $ThAl_2$, which prefers the AlB_2 type. A general geometrical formulation, which relates the radii, coordination numbers, and the Vegard rule with one another, has been published recently by *A. Simon*.[91] Directed chemical bonding, however, gives rise to deviations from this concept. Thus, it would appear that a purely geometrical interpretation of the structural relationships in Laves phases leaves more questions open than it can satisfactorily answer.[24]

Pearson gives two alternative descriptions of Laves phases: (1) the large M atoms form 3^6 nets and the small N atoms form 3636 nets[*] (Kagomé nets) perpendicular to C_3 and C_6 axes, respectively (in hexagonal and rhombohedral structures, perpendicular to the [001] direction; in the cubic structure, perpendicular to the [*hhh*] directions with $h = \pm 1$). (2) The M and N atoms form 35^3 and 3535 nets (in the cubic structure, perpendicular to [*hh*0] directions with $h = \pm 1$). Regarded in this way, the Laves phases are related to Frank Kasper structures with predominantly icosahedral coordination.

As with the tetrahedral structures (e.g., the SiC variants[14]), a large number of polytypes can be generated by varying the stacking sequences in the Kagomé nets. Indeed, a whole series of these polytypes are now known (see Fig. 6 for examples) in addition to the simple types of Laves phases.

The study of these structures shows that Laves phases, as typical representatives of intermetallic phases, can also respond extremely sensitively to changes in composition and valence electron counts. In contrast to the polytypes for structures with tetrahedral structural units, the hexagonal sequence of the Kagomé nets results in a connection pattern of the N partial structure different from a cubic stacking. In the first case, vertex-sharing trigonal bipyramids N_5 are formed, in the second case vertex-sharing tetrahedra N_4. Even *Wade*'s electron-counting rules give different optimum numbers of valence electrons for the trigonal bipyramid and the tetrahedron. Having the formulas $N_5^{2\ominus}$ and $N_4^{4\ominus}$, the two are isoelectronic, but the electron requirement per N atom is greater for the tetrahedron.

This trend has also been found for the condensed polyhedra in the crystal structures of the ternary Laves phases $CaLi_xAl_{2-x}$.[96] In the ternary system Li-Ca-Al, $CaLi_2$ and $CaAl_2$ occur as border phases with hexagonal $MgZn_2$ and cubic $MgCu_2$ structures, respectively. The ternary mixed

[*] The Schäfli symbols denote the types and the numbers (small indices) of polygons around a net point: $3^6 \triangleq$ six triangles, $n^m \triangleq$ m n-gons.

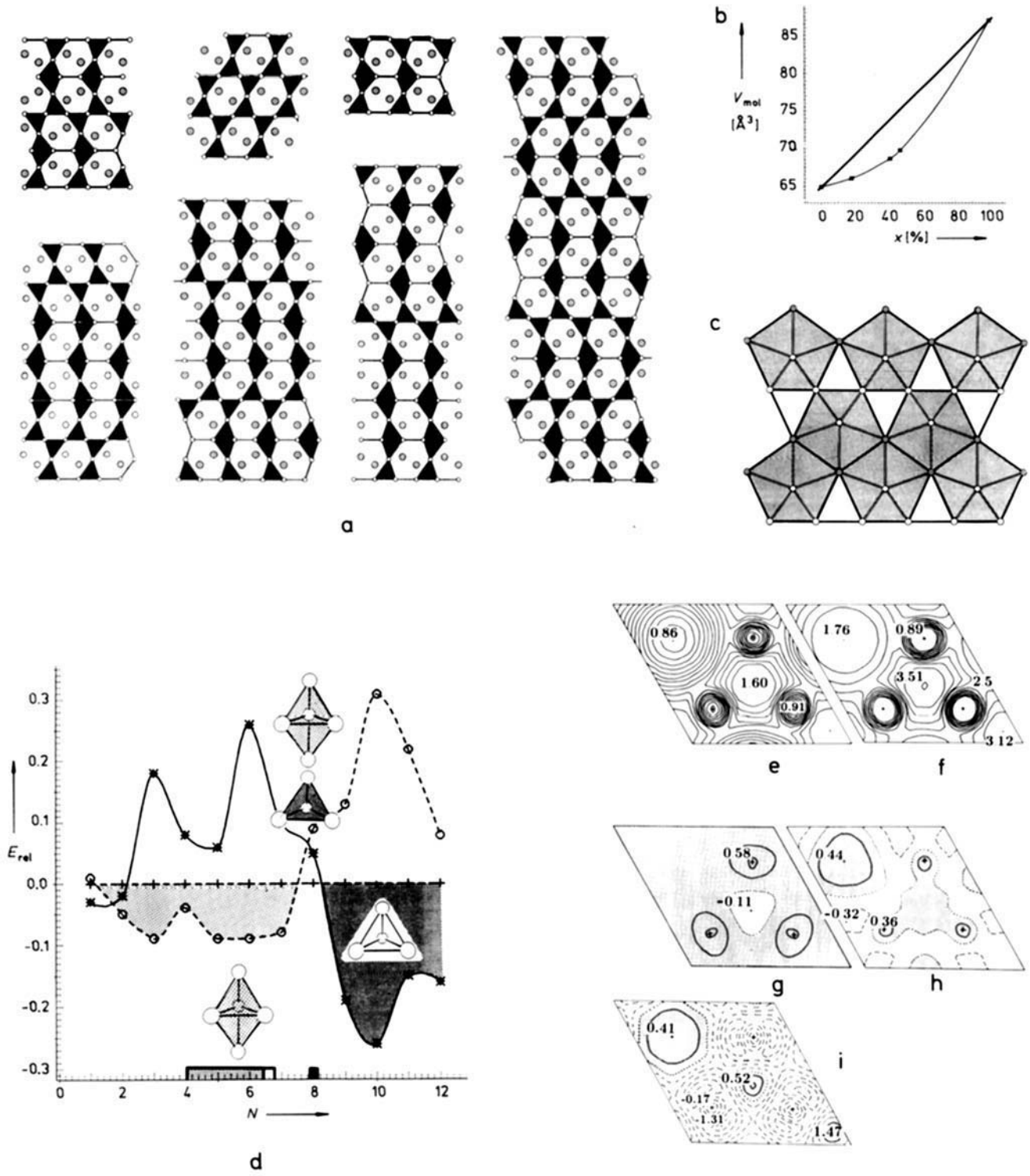

Fig. 6. Laves phases MN_2: a) Some stacking variants, with the polyhedra of the majority component N drawn in black. The hexagonal sequences are characterized by the linking of trigonal bipyramids N_5 (vertex-sharing bitriangular faces), and the cubic sequences by linking of tetrahedra N_4 (vertex-sharing triangular faces). b) Experimentally determined molar volumes for the ternary phases $CaLi_x Al_{2-x}$ as a function of composition. The deviation from the Vegard rule can clearly be seen. c) Nets of pentagons and triangles in the cubic Laves phase. d) Comparison of the relative energy values of the $MgCu_2$ (*), $MgZn_2$ (o), and MgN_2 (+) structures as a function of the valence electron count N from extended Hückel band-structure calculations [96]. The structures observed for the phases $CaLi_xAl_{2-x}$ are shown as blocks on the abscissa. e)–i) Calculated electron densities and electron density differences for the hexagonal Laves phase KNa_2 (e), $MgZn_2$ (f), $CaLi_2$ (g), $CaMg_2$ (h), and cubic $CaAl_2$ (i). Cross-sections through the basal plane of the trigonal bipyramid (for (i), through the center of the tetrahedron). The numbers are selected maxima and minima (reproduced from [12]).

phases $CaLi_xAl_{2-x}$ are found between them, but not over the entire range. With increasing Al content, they crystallize initially in the $MgZn_2$ type, then in the $MgNi_2$ structure with 50% hexagonal and 50% cubic stacking sequences, and finally in the $MgCu_2$ type. In this series, the number of valence electrons per formula unit increases from four to eight. In disagreement with the Vegard rule,[91] the changes in molar volume deviate significantly from a linear behavior (Fig. 6b). Comparative extended Hückel investigations are in good agreement with these observations. Figure 6 shows the cal-

culated relative stability ratios and the observed structures as a function of the number of valence electrons. For Laves phases that are composed of main-group elements, the determining factor for the choice of structure would appear to lie in the chemical bonding, which can adapt itself to different numbers of valence electrons through structural changes.[96]

Y. Komura et al. have found that with increasing valence electron concentration his ternary Laves phases containing copper, silver, and zinc exhibit first cubic, then hexagonal, and finally cubic structures again.[92-95] Thus, it is not clear whether this different sequence of structures is attributable to the influence of the d orbitals, or whether the cubic structure type is favored once again for valence electron concentrations less than four electrons per formula unit. The optimal valence electron concentrations for Laves phases with d metals have been calculated by *R. Haydock* and *R. L. Johannes* using a recursion method. The values obtained for the three classical Laves phases are listed in Table 2.

Table 2. Laves phases: comparison of structure types and preferred valence electron concentrations for main-group and transition-metal representatives [97].

Structure type	Valence electron concentration		
	Transition metal [a]		Main-group element
$MgCu_2$	≤ 3.4	≤ 7.7	≤ 6.4
$MgZn_2$	≤ 4.9		≤ 6.6
$MgNi_2$	6.5–6.9	≥ 7.7	≤ 8.0

[a] The values on the left are the optimal valence electron counts calculated for $CaAl_2$.

The local chemical bonding of the transition-metal compounds remains to be interpreted. In any case, the electron-poor alkali-metal compounds KNa_2, $CsNa_2$, and CsK_2 have hexagonal structures.

According to investigations by *J. Hafner*, the valence electron densities of binary intermetallic phases characteristically differ from those of the corresponding pure metals. Even in compounds such as KNa_2 (Fig. 6e) and CsK_2 he has found a density distribution with pronounced maxima that is considerably less homogeneous than those of the elemental structures. Thus, in $CaLi_2$ (Fig. 6g), maxima are observed at the Li positions, while in $CaMg_2$ (Fig. 6h) there is, in addition, electron density in the center of the Mg_5 polyhedron. Both compounds have the $MgZn_2$ structure (Fig. 6f). In the Al_4 tetrahedra of cubic $CaAl_2$ (Fig. 6i), the density reaches a particularly high value. Since the Al atoms do not lie in the same cross section as the centers of the tetrahedra shown in Figure 6i, the electron density around the Al atoms cannot be seen here. These interstitial maxima are entirely restricted to the interior of the N_4 tetrahedra ($MgCu_2$ type) or the N_5 trigonal bipyramids; polyhedra that involve M atoms are not affected.[12]

Such density redistributions are not only observed in Laves phases. Related alkali-metal compounds such as Cs_6K_7 exhibit similar effects. The M_6N_7 phases crystallize in a structure that contains two-dimensional sections of the cubic Laves phase, in which layers of vertex-sharing K_4 tetrahedra alternate with layers composed solely of Cs atoms. In the latter the electron density is uniform, whereas density maxima have been calculated for the centers of the K_4 polyhedra.[12]

The series of Laves phases demonstrates how the chemical bonding emerges stepwise from the original uniform electron density, starting from the pure alkali-metal compound, through calcium magneside,[*] to $CaAl_2$ with apparently quite strong chemical bonding (m.p. 1352 K). The wide variation in the Laves phases studied by *Komura* et al. also fits the concept of a stereoselective bonding.

4. How Are Structures Built Up?

Why do the compounds Cu_5Zn_8 and Cu_9Al_4 exist, since they have no similarity in chemical composition but are isomorphous, and have atomic arrangements of a ridiculous complexity?

W. Hume-Rothery 1926[21]

This question, posed by *W. Hume-Rothery* in 1926[21] and repeated by *F. Laves* in 1967,[90] has not yet been answered in a chemically satisfactory manner. On the contrary, in spite of the rapid development of theoretical methods for the description of the electronic structures of chemical compounds, the even faster advances in the determination of structures[98,99] have revealed new structures whose complexity is orders of magnitude greater than those of the older structures, which themselves have yet to be understood. Nowadays, quasicrystalline intermetallic phases are providing us with structures that are so large that even proteins and polymers are dwarfed in comparison. Each quasicrystal is effectively a giant molecule.

However, this example is not really necessary to demonstrate that intermetallic compounds, like classical valence compounds, are able to form extensive, complex structural patterns despite the forces of dense packing, which always favor the simplest geometrical solution.[11] *S. Samson*'s magnificent structure determinations on Mg_2Al_3, $NaCd_2$, and Cu_4Cd_3,[100-102] solved laboriously as early as 25 years ago, have been almost forgotten today owing to their great complexity. The compound Mg_2Al_3 serves us in many materials, even without our understanding its innermost chemical structure.

4.1. Polyhedra and Nets

The geometrical description of intermetallic phases is generally carried out in terms of the coordination polyhedra or of the arrangements of planar nets. These have been used, with different weightings, for the classification of the structures of these compounds in the monographs by *K. Schubert*,[23] *W. B. Pearson*,[24] *P. I. Kripyakewitsch*,[103] and *S. Andersson* and *B. G. Hyde*.[26] Some of the more commonly occurring polyhedra are depicted in Figure 7. Owing to the general trend towards dense packing, the larger poly-

[*] One automatically hesitates at this designation—a Mg polyanion is still too unusual. It is, however, fully consistent with the findings.

hedra are always centered. Hexagonal prisms (e.g., in VAl_{10}), square antiprisms (e.g., in VAl_{10}), and tetrahedra (e.g., in the Laves phases) can, like the pyramids, also occur without central atoms. Coordination with more than 12 neighbors arises especially if the atomic dimensions are markedly different. In the Frank–Kasper structures, to which the Laves phases are also assigned, coordination numbers of 12, 14, 15, and 16 are found. The Frank–Kasper polyhedra usually interpenetrate one another. They therefore give a confusing representation of the total structure, but can often be reduced to subunits that are relevant to the chemical structure. One such unit is the Friauf polyhedron, made up of 16 atoms, which can be divided into 12 + 4 and, in this form, is relevant to the chemical bonding (cf. Section 2.2).

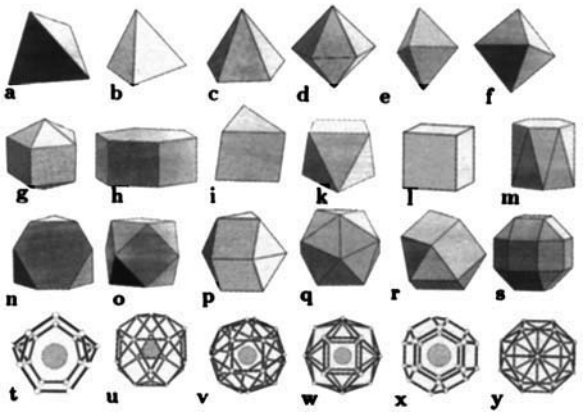

Fig. 7. Typical polyhedra in intermetallic phases (CN = coordination number): a) Tetrahedron (CN = 4); b) square pyramid (CN = 5); c) pentagonal pyramid (CN = 6); d) hexagonal bipyramid (CN = 8); e) trigonal bipyramid (CN = 5); f) octahedron (CN = 6); g) doubly capped pentagonal prisms (CN = 12); h) hexagonal prism (CN = 12), i) trigonal prism (CN = 6); k) Archimedian antiprism (square antiprism) (CN = 8); l) cube (CN = 8); m) hexagonal antiprism (CN = 12); n) truncated tetrahedron (core of the Friauf polyhedron, CN = 12); o) cuboctahedron (cubic dense packing, fcc, CN = 12); p) hexagonal counterpart of the cuboctahedron (anticuboctahedron, CN = 12); q) icosahedron (CN = 12); r) Edshammar polyhedron (CN = 11); s) coordination polyhedron (CP) around an Sr_6 octahedron in Sr_6Mg_{23} (CN = 44; 20 of the 32 faces are centered by Mg); t) B_{18} CP around Th in ThB_4 (CN = 18); u) Hg_{20} CP around Ba in $BaHg_{11}$ (CN = 20); v) Zn_{24} CP around Na in $NaZn_{13}$ (CN = 24); w) Mg_{20} CP around Ce in Ce_5Mg_{41} (CN = 20); x) B_{24} CP around U in UB_{12} (CN = 24); y) Cd_{22} CP around Ba in $BaCd_{11}$ (CN = 22). In t)–y), the central atom in the polyhedron is shown.

Even larger polyhedra that are centered by only one atom occur in, for example, Ce_5Mg_{41} as $CeMg_{18}$,[*] in $BaHg_{11}$ as $BaHg_{20}$, in $BaCd_{11}$ as $BaCd_{22}$, in $NaZn_{13}$ as $NaZn_{24}$, and in UB_{12} as UB_{24}.[24] In UB_{12}, boron forms a partial structure of uncentered cuboctahedra, from which in turn the B_{24} polyhedra are built up. A complete Sr_6 octahedron is surrounded by 44 Mg atoms in Sr_6Mg_{23}. Not all polyhedral descriptions are useful in terms of chemical bonding. Some polyhedra can be dissected or are only part of another stable unit. The condensation of clusters to give oligomeric and polymeric units and the increasing radial cluster size build bridges to the intermetallic phases. Studies of this topic are appearing in increasing numbers, indicating the importance attached to these links between "molecules" and the solid state.

[*] Eighteen Mg atoms surround one Ce atom.

The description of intermetallic phases by means of mostly planar nets of interconnected triangles, rectangles, pentagons, and hexagons has been reported in detail by *Pearson*,[24] by *O'Keeffe* and *Hyde*,[28] and in part by *Kripyakewitsch*.[103] All these authors concentrate on the geometrical relationships. Under the aspect of chemical bonding, these net descriptions must surely be revised; for instance, they contain widely differing interactions. An example is the description of the cubic Laves phase $MgCu_2$, in which nets of triangles and pentagons (Schläfli symbols: $3^5 + 3^5 3^5$,[24] see Fig. 6c) lie parallel to the ($hh0$) planes ($n = \pm 1$). The fact that both Mg and Cu atoms are involved in these nets is, however, somewhat misleading in terms of the chemical bonding, since the stronger interactions are those between the Cu atoms (see Section 3.4). Especially in the last five years, systematic theoretical investigations of the electron requirements of polyhedra and nets in intermetallic phases have been carried out (see Section 5.4 for further details).

4.2. Fractals and Quasicrystals

The reproduction of optimal building principles under differing boundary conditions is apparently one of the fundamental strategies of nature. In the real world, however, geometrical patterns can only be repeated with similarity and not with exact sameness because distances (d), surfaces ($\sim d^2$), and volumes ($\sim d^3$) are not simultaneously linearly scalable. Optimal patterns can, however, be repeated in similar form with a different scaling. This process is termed self-similarity, and it was *B. Mandelbrot* who first recognized it as the concept of fractal geometry and described it mathematically.[104] Not only have fractals opened up the comprehension of complex growth processes, they also present the possibility of establishing transitions between dimensions. For the mathematician a line is one-dimensional. Its chemical counterpart, a linear chain of atoms, however, is only a quasi-one-dimensional construction of three-dimensional objects (the atoms). Although a sufficiently long linear molecule may exhibit pronounced one-dimensional properties, it nevertheless has a two-dimensional surface (the van der Waals surface, for example) and a three dimensional distribution of electron density. The reactivity of a molecule is certainly a function of these and other properties and could depend on, among other things, a fractal dimension of $2 < n < 3$ between the surface and the volume based on its outer electrons.

The chemist must always single out those aspects that are fundamental to his purpose and use them to develop a strategy that fits his needs, especially when a complete theory is not available. I am sure that the use of fractal relationships has subconsciously long been a part of what is known as a "feel" for chemistry and chemical systems. It is therefore pleasing to see that Brownian motion is now known to have a fractal dimension $n > 1$.[105] Thus, a particle in motion presents, on time-average, something between a line and a surface for various interactions (e.g., chemical reactions), even if it possesses no extension of its own.

Fractal principles have been recognized for numerous growth processes. Apparently, only crystals, with their precisely defined order, are able to evade fractal behavior. Al-

though this may be true for the ideal crystal of a given structure, the number of favorable arrangements with a small translation period in three-dimensional space is not particularly large. The examination of suitable structures of varying complexity reveals indications of fractal building principles. That is, a favorable geometrical arrangement serves as a model for structures comprising individual atoms, clusters, molecules, or aggregates of clusters and molecules and will repeatedly reappear in a similar form but with different scalings.

As mentioned above, a single "orderly" crystal (just?) evades the fractal building principle. In contrast, quasicrystals embody precisely this principle in the form of the golden mean[60-62] as growth factor $[(\sqrt{5}+1)/2]$, which allows the formation of ordered structures, even without fulfillment of the translation symmetry. Models for quasicrystals such as $MnAl_4$ will now be briefly examined. There is much literature on this topic, including a contribution in this issue.[*] In quasicrystals, a complex structural pattern with wide-reaching order is maintained. All quasicrystals known up to now belong to the intermetallic phases. Therefore, long-range directed forces can also be highly effective in these compounds. However, the precise atomic positions have still to be determined and this is also an indication of the fractal character of these structures, since self-similarity does not reproduce precisely.

Figure 8f shows the growth of the cell edge of pseudo unit cells (Penrose cells, see below) according to the golden mean. In Figure 8d, radial growth according to the golden mean is shown for a tenfold point distribution. With increasing distance from the center, voids of ever-increasing size are inevitably formed, which, of course, in a real structure must be filled. As a simple approximation for the filling of the voids, one can begin the same construction at points lying further from the center. The diffraction pattern of such a distribution of only 550 points (Fig. 8e) is already remarkably similar to that obtained for fivefold projection directions in quasicrystals. Thus, the size of the voids increases with increasing distance from the center, but their shapes hardly differ from one another (Fig. 8d). Therefore, voids of various sizes must be filled with objects of similar geometry but with different numbers of atoms. This self-similarity—the similarity of differently sized parts of an object—is synonomous with the fractal concept.

Pauling has attempted to explain the structure of quasicrystalline $MnAl_4$ in terms of twinning of the translationally symmetrical structure of $Mg_{32}(Zn,Al)_{49}$ (see Fig. 9f).[106] Although controversial, his model comes quite close to the observations, even if it does not give us the best description of quasicrystals.[107] In any case, the relationship between large clusters in known translationally symmetrical structures and those in quasicrystals has become apparent through *Pauling*'s description.

Structures other than that of $Mg_{32}(Zn,Al)_{49}$ could possibly also be used to design models for the arrangements in quasicrystals. For instance, there is an interesting relationship between cubic dense packing and the pseudo unit cells of quasicrystals. *A. L. Mackay* defines these as three-dimensional representations of the two-dimensional Penrose patterns, which are composed of two different types of rhombohedra.[109] Today, it seems clear that quasicrystals possess something similar to a unit cell, namely, the two different pseudo cells (see Fig. 8f), both of which are rhombohedra but with differing angles.[111] Their space-filling arrangements are known as Penrose patterns.[108,109] The larger pseudo cell has a rhombohedral angle of $\alpha = 63.43°$, which is quite close to that of the primitive unit cell of the face-centered cubic lattice ($\alpha = 60°$) (Fig. 8b).[110] (The corresponding rhombohedron for the body-centered cubic lattice (Fig. 8a) has $\alpha = 70.46°$.) If an fcc structure is distorted to a rhombohedral angle of 63.43° and then subjected to a tripling operation, as shown in Figure 8c, the second pseudo cell is automatically generated in the remaining holes. Face-

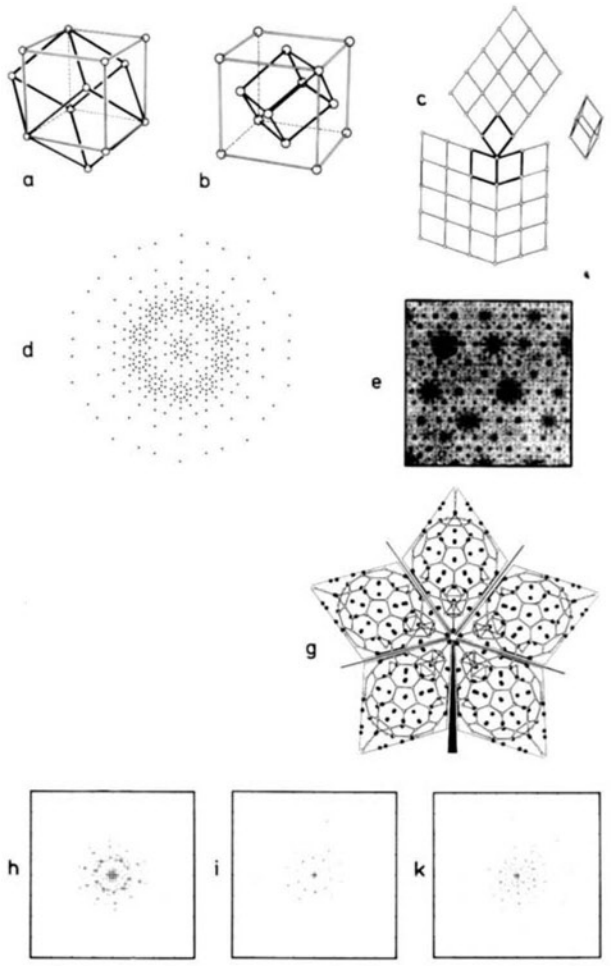

Fig. 8. Relationship between quasicrystalline arrangements and fcc structures: a), b) Primitive rhombohedral unit cells (solid lines) for the bcc and fcc lattice (rhombohedral angle $\alpha_{rh}^{bcc} = 70.46°$, $\alpha_{rh}^{fcc} = 60°$). c) Formal twinning of blocks of primitive fcc cells to give the nucleus of a Penrose pattern (central three unit cells). d) C_{10}-symmetrical model structure with the golden mean $[(\sqrt{5}+1)/2]$ as radial growth factor and the corresponding diffraction pattern. e) Diffraction pattern of (d). f) Section of a Penrose pattern with two types of "unit cells". The bold lines indicate Penrose cells with radial growth according to the golden mean. g) Smaller section of the Penrose pattern (f) with filling (decoration) of the unit cells by the $LiMgAl_2$ structure. The angular discrepancy between the primitive fcc cell and the large Penrose cell is emphasized. h)–k) Diffraction pattern of decorated Penrose cells such as (g) composed of 5, 20, and 55 cells [(h) inner, shaded part of (f); (i) inner, shaded and next lighter ring in (f); (k) all shaded cells in (f)]. Although the structural model was not optimized, increasingly quasicrystalline features are apparent in the diffraction patterns.

[*] S. Andersson, S. Lidin, M. Jacob, O. Terasaki, *Angew. Chem. 103* (1991) 771; *Angew. Chem. Int. Ed. Engl. 30* (1991) 754.

centered cubic structures can therefore be regarded as closely related to the arrangements of quasicrystals.

There is now little doubt that the quasicrystalline structures are built up according to Penrose patterns. However, as was mentioned earlier, very little is known about the so-called decoration (i.e., the structural content) of the pseudo cells. Should we, therefore, following in *Pauling*'s footsteps, search for decorations of the pseudo cells other than $Mg_{32}(Zn,Al)_{49}$? If so, then known aluminides and Mn compounds should be considered; for example, either those that exhibit an fcc arrangement or those which are related to it. Manganese and aluminum are the crucial components in the quasicrystals known up to now (Table 3). Both have a marked tendency to form directed chemical bonds (see Sections 2.1 and 2.2).

Table 3. Composition of some quasicrystalline compounds (minority components normalized to unity). One of the few quaternary quasicrystalline compounds known at present is $(Mn_{0.72}Fe_{0.28})Al_{85}Si_{14}$ [117].

Binary	Ref.	Ternary	Ref.	Ternary	Ref.
$PdAl_3$	[112]	Li_3CuAl_6	[118]	$FeCu_{1.33}Al_{4.33}$	[123]
$OsAl_{3.25}$	[112]	$Mn_{3.45}Al_{12.90}Si$	[114]	$OsCu_{1.33}Al_{4.33}$	[123]
$RhAl_{3.25}$	[112]	$Mn_{4.20}Al_{14.80}Si$	[116]	$CoCu_{1.33}Al_{4.33}$	[124]
$FeAl_{3.25}$	[112]	$Cr_{1.14}MnAl_{14.14}$	[117]	$NiCo_{1.33}Al_{4.33}$	[125]
$CoAl_{3.25}$	[112]	$Mn_{3.50}Al_{12.17}Si$	[113]	$MnPd_2Al_7$	[126]
$MnAl_{3.55}$	[113]	$Mn_{4.20}Al_{14.80}Si$	[113]	$RePd_2Al_7$	[126]
$MnAl_{4.00}$	[114]	$Mn_{2.75}Al_{14.11}Si$	[115]	$Mg(Al,Zn)_{1.53}$	[127]
$MnAl_{5.49}$	[115]	Mg_4CuAl_6	[119]		
$MnAl_{6.00}$	[114]	$Ni_{2.33}Al_{13.33}Si$	[120]		
$MnAl_{6.14}$	[116]	$V_{15}Ni_{10}Si$	[121]		
$CrAl_{6.14}$	[117]	$Cr_{2.5}Ni_{1.5}Si$	[122]		

"$LiMgAl_2$" is a new aluminide that has a complex rhombohedral structure and an almost fcc metric ($\alpha_{rh} = 59.7°$).[55] Its structure is composed of Al_{76} polyhedra, centered by $(Li,Mg)_{40}$ units (Fig. 9a), which are themselves filled by $(Li,Mg)_{7-9}Al_3$ polyhedra. The Al_{76} polyhedra form an fcc-like arrangement, which is, however, not cubic because the polyhedra exhibit only $3m$ symmetry (Fig. 9b). The polyhedra have 40 faces comprising 12 pentagons and 28 hexagons.[*] The pentagons are approximately oriented with the vertices of an icosahedron. However, fivefold symmetry applies only in the immediate environment of these rings. A symmetry center is also absent (icosahedral symmetry $5\bar{3}m$; symmetry of Al_{76}, approximately $\bar{4}3m$ and in reality $3m$). A projection of the rhombohedral unit cell along one of its axes clearly reveals elements of fivefold symmetry in the structure.

The formation of a fivefold twinning in this projection according to the Penrose pattern is now quite straightforward (cf. Fig. 8f). The result is a two-dimensional quasicrystalline structure. Such structures are already known and are termed pentagonal or decagonal phases.[113] Accordingly, a twinning to give an icosahedral quasicrystal must be performed in all six planes perpendicular to the six fivefold axes.[**]

[*] Such polyhedra are not usually found in the relevant literature, because, with their triply condensed hexagons, they should exhibit planar areas. The hexagons in this case are, however, neither regular nor planar.

[**] It can be shown that such structures possess translational symmetry in six-dimensional space.

In Figure 8h–k the calculated diffraction patterns in the direction of the fivefold axis for differently sized sections of the Penrose pattern (Fig. 8f) are shown. The sections contain 5(h), 20(i), and 55(k) unit cells of $LiMgAl_2$. The rapidly increasing resolution in the diffraction patterns can be seen clearly. This example is not intended to show that $LiMgAl_2$ could also form a quasicrystalline arrangement with exactly this observed structure, but is intended to demonstrate the close relationship between classical fcc arrangements and quasicrystalline structures.

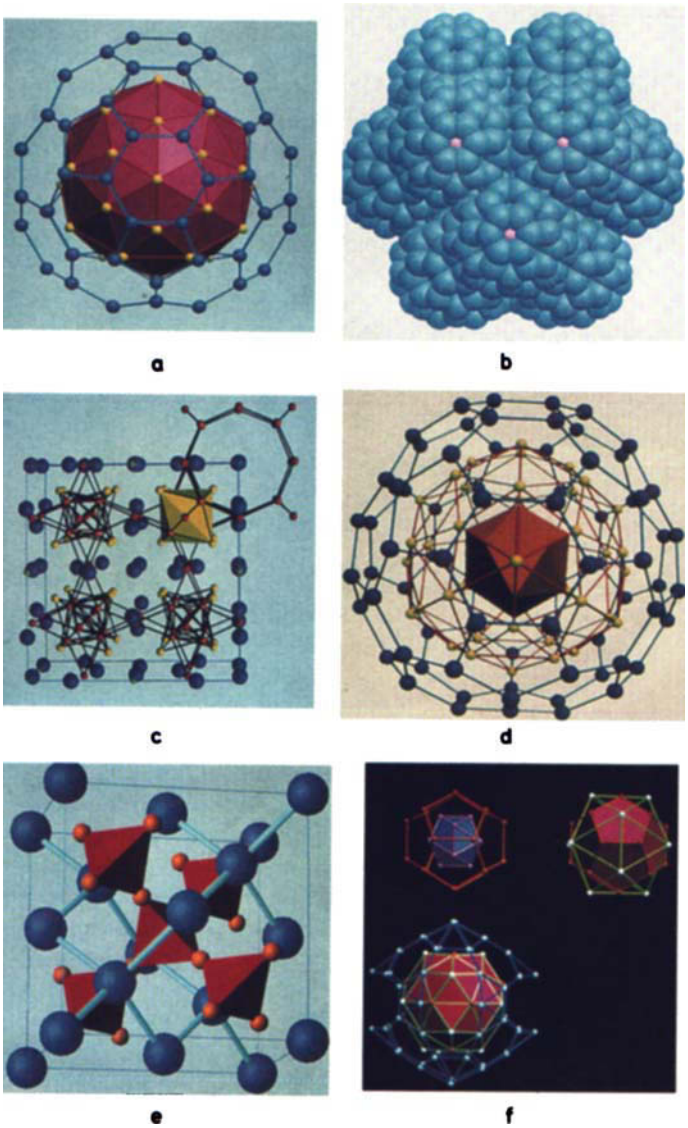

Fig. 9. Structures of intermetallic phases. $LiMgAl_2$: a) Al_{76} polyhedra (blue) with dual inner polyhedra (Li, $Mg)_{40}$ (red); b) space-filling model of 13 Al_{76} polyhedra (central + 12 outer polyhedra); c) structure of Th_6Mn_{23} with tetrahedral star (yellow) and Th atoms (blue); d) cation framework in $Bi_{22}Sr_{36}Al_{48}O_{141}$ [182] (Al, blue; Sr, yellow; Bi, central polyhedron; cf. Fig. 9a) (see Section 6.3); e) structure of the cubic Laves phase $MgCu_2$ (Mg, blue; Cu_4 tetrahedron, red); f) partial structure from $Mg_{32}(Zn,Al)_{49}$ [195], proposed by *Pauling* as model for crystallization centers in quasicrystals.

Who knows how many "poor crystals" that were discarded during their structural determination in fact exhibit quasicrystalline features. It will be interesting to see just how large the ever-growing number of such compounds will become in the future. Seek and ye shall find.

4.3. Structures, Holes, and Fractals

The atomic and molecular view of chemical species in particular has been enormously successful: just consider the formalism of the frontier orbitals in fragments, molecules, and clusters,[129] reaction mechanisms involving functional groups in organic chemistry,[130] or the study of active sites in enzymes. Today there are many incremental classifications in chemistry which allow important conclusions to be drawn without the need to analyze the total arrangement in each case.

Each granular description automatically has the consequence that there is something else between the grains or centers which is less stable: the holes or voids. Each structure possesses a priori holes, otherwise it would not be a structured object. At the same time this means that each structure can be filled to give a new variant, for example, by filling the holes according to their size.

The term homotypic is used for structural relationships in which the strict geometrical correspondence of isotypism is not fulfilled.[*] *K. Schubert*, in his book,[23] gives several examples of homostructural relationships, including replacement and inclusion structures. The description of replacement structures is based on dense packing (fcc, hcc). Either two or three neighboring atoms are replaced by a larger atom, giving rise to double or triple replacement structures. *Schubert* describes the $MgCu_2$ structure as a double-replacement variant of the fcc arrangement. If Mg is replaced appropriately by two smaller atoms, the fcc structure is obtained. Accordingly, $CaZn_5$ can be understood as a triple-replacement structure of a hexagonal-dense-packed arrangement.[23] Even in the very beginnings of structural chemistry, such connections were recognized and also found for intermetallic phases.

An example of such a real sequence of filled-up structures beginning with the diamond type is M_8(C, cF8) → M_8N_8 (NaTl, cF16) → M_8N_{16} ($MgCu_2$, cF24) → $M_{16}N_{16}$ (PtCu, cF32) → $M_8N_{16}O_{32}$ ($MgAl_2O_4$, cF56) → $M_{16}N_{160}$ (VAl_{10}, cF176) (see Fig. 16b).[63, 128] Possible correlations between stuffed intermetallic phases and ionic compounds are discussed in Section 6.3. In principle, the stuffing of the holes can be continued indefinitely because the filled-up structure itself has new holes.

Another series starts, for example, with the Cu structure, which has an fcc arrangement of Cu atoms (see Fig. 10d). Filling the tetrahedral holes generates the fluorite structure CaF_2. The replacement of the cations by $[PtCl_6]^{2\ominus}$ ions and of the anions by $K^{\oplus}$ ions leads to the K_2PtCl_6 structure, in which the octahedral holes of the original cubic dense packing are still unoccupied. Finally in Na_3AlF_6, they are occupied ($NaNa_2AlF_6$[25]). Such structural correlations appear to be quite natural, and they are known in various forms, although we are still a long way from having a comprehensive classification in this respect.

There are considerable problems in locating the holes in structures. Whereas this is simple for highly symmetrical structures, the search for the holes in complex structures can often only be performed by means of laborious model building. However, there is a well-known method that can be used for this purpose and which provides the required mathematical formalism. It is the partitioning of space into polyhedral regions, known as Voronoi polyhedra or Dirichlet domains (Fig. 10a–c).[133] Starting with a reference atom, one sets up

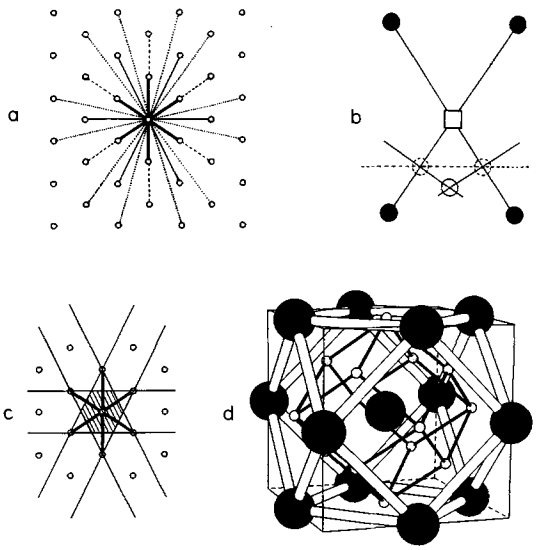

Fig. 10. Localization of holes in structures by construction of Voronoi polyhedra: a) Model structure with different coordination spheres (bold, thin, dashed, and dotted lines) around a central atom; b) construction of polyhedron faces perpendicular to the atomic bond lines; c) two-dimensional counterpart of the Voronoi polyhedron (the shaded region represents the interior of the polyhedron; its vertices define the first coordination by holes); d) fcc arrangement (large black circles) and corresponding holes (small circles; tetrahedral holes, shaded; octahedral holes, open). The corresponding Voronoi polyhedron is a rhombododecahedron (thin black lines).

planes on all interatomic vectors. These planes form a convex polyhedron around the starting point, whereby the faces of the polyhedron become smaller with increasing distance between the neighboring atoms. Thus, a distance range ≤ 6–7 Å is usually sufficient to obtain all the faces belonging to a polyhedron in a chemical structure. The more remote neighbors of the starting point generate planes which do not intersect with its (first) polyhedron. *F. L. Carter* proposed this method as a tool to determine effective coordination numbers.[134] The method always gives a limited number of neighbors in the first coordination sphere, whose contribution to the coordination number can be evaluated by means of the corresponding face of the polyhedron. Each of these contributions can be converted to a solid angle, which can be regarded as a measure of "how much room a neighbor is entitled to in the total panorama around an atom".

This purely geometrical viewpoint must be combined with physical quantities such as interaction functions if it is to be relevant to other than geometrical questions. Whether this method is superior to other attempts to calculate effective coordination numbers has up to now only been investigated to a limited extent. (A shelllike construction of structures, starting from one or more centers, has also not been treated in depth. This model has come under discussion again with the discovery of the quasicrystals; see Section 4.2.) *D. M. P.*

[*] Compounds are isostructural if they crystallize in the same structure type (e.g., $CaAl_2$ and $MgCu_2$). If the structure type contains positions with free parameters, then the (often controversial) question arises as to how large the differences in the free parameters may be. These cases are better referred to as isopointal structures [24], meaning the occupation of the same Wyckhoff positions in a space group.

Mingos has extended the analysis of solid-angle regions to the ligand distribution in multinuclear transition-metal clusters.[6] The construction of Voronoi polyhedra allows all coordination spheres around an atom to be successively determined. This will give us much information about dual relationships in structures.[*]

It must be emphasized that determination of holes is already contained in the rules for the construction of Voronoi polyhedra.[135] Owing to the dual relationship between Voronoi polyhedra and coordination polyhedra (see Fig. 10), the vertices of the Voronoi polyhedron are always the holes in a structure. Different compounds can even be taken into account in one structural type, since all distances are given by predetermined radii.[**]

The calculation of the holes for an fcc arrangement, for instance, can be performed as a "thought experiment". The coordination polyhedron is a cuboctahedron made up of the 12 nearest neighbors. The dual Voronoi polyhedron is a rhombododecahedron, whose vertices lie near to the centers of the faces of the coordination polyhedron, that is, exactly in all octahedral and tetrahedral holes.

There is no doubt that the positions of the inserted atoms in a stuffed structure need not be coincident with those of the biggest voids. Actually, covalent bonding avoids close-packed structures (cf. Section 5.5); the diamond structure is one example. The oxygen atoms in the β-cristobalite structure do not occupy the largest holes but those which have only twofold Si coordination. However, these smaller voids are part of the construction of Voronoi polyhedra as well. They fall near to the face centers of the polyhedra. It might be that the distribution of electrons in semiconducting or in intermetallic compounds, can be identified with the face centers or the vertices, respectively, of the corresponding Voronoi polyhedra (and of the anions in more covalent or more ionic salts; cf. Section 6.3).

The detection of holes and the analysis of their structural meaning is certainly an important contribution to the development of a comprehensive general structural chemistry.

4.4. Localized Electron Spaces?

In arrangements of atoms, are the positions that are unoccupied by atoms and relatively remote from all atoms really empty? Certainly not in all cases! Conspicuous empty spaces are found, for example, in structures with lone pairs. Here, it has long been known that the lone pairs are displaced into common structural regions, although there are no attractive interactions between them. Internal cavities and surfaces are formed like surfactant interfacial surfaces in liquids. Do intermetallic compounds also contain spatially discrete regions of weak and strong interactions? One is reluctant to carry out a classification of electrons and local spatial regions in intermetallic phases, because it is known that the valence electrons are hardly influenced by the positively charged atom cores, and because the latter are strongly shielded. Furthermore, the valence orbitals of metal atoms are very diffuse and extensive.

But these limitations should not be allowed to discourage us. The following questions must be posed: (1) Are the valence electrons sufficiently strongly influenced by the atom cores? Answer: probably, since for chemical bonding, these belong to the forbidden zone. Hence, chemical bonding between the cores must take place outside the so-called hard-core radii R_0, that is, in the interstitial region. (2) Do the electrons have a shortage of space? Yes, because they must avoid electron–electron repulsions as best they can. Although the location of optimal electron residences, for instance, by the so-called electron localization function (ELF), is still in its infancy,[137] the first results look promising. The ELF gives an interpretation of the electron density which allows the preferred locations of the electrons to be determined and displayed graphically. For instance, the space required for a lone pair can be seen clearly. Interesting results have already been obtained for selected molecules.[138]

5. Theory of Chemical Bonding in Intermetallic Phases

The literature on the theory of chemical bonding in intermetallic phases is very extensive. There are numerous interesting new contributions on methods and applications, for example, within the framework of the method of linear combination of muffin-tin orbitals, described by *O. K. Andersen* et al.[184] and by *N. E. Christensen*.[185, 186] In this article, therefore, emphasis is given to only a few of those works that deal in depth with the local picture of the chemical bonding in intermetallic phases.

5.1 *Pearson*'s Neighborhood Diagrams

W. P. Pearson has defined geometrical strain parameters which can be used to investigate series of compounds MN_x that crystallize in the same structural type.[24] The three different interactions M-M, M-N, and N-N are analyzed in terms of the observed distances d_M, d_N, and d_{MN} and the predicted values $D_M = 2r_M$, $D_N = 2r_N$, and $D_{MN} = 1/2(D_M + D_N)$. The strain parameter $(D_M - d_M)/D_N$ is plotted versus the ratio of the atomic diameters $D_M/D_N = r_M/r_N$ (= radius ratio). Figure 11 shows the values for a large number of cubic Laves phases with the $MgCu_2$ structure. The straight lines represent the corresponding expected values with $D_M - d_M = 0$, $D_N - d_N = 0$, and $D_{MN} - d_{MN} = 0$. *Pearson* differentiates three borderline cases:

1. The coordination-defined situation, in which the observed values lie close to an intersection. In this case, the expected values are obtained for the different coordinations (M-M, M-N, N-N).

[*] Two geometrical bodies exhibit a dual relationship if replacing the edges of one of them by faces generates the other. *Euler*'s formula for the number of edges (E), vertices (V), and faces (F) gives the relationship $E_{1,2} + 2 = V_1 + F_1 = F_2 + V_2$ with $E_1 = E_2$, $V_1 = F_2$, and $F_1 = V_2$. Dual polyhedron pairs are, for example, cube ($E_0 = 12$, $V_0 = 8$, $F_0 = 6$)/octahedron ($E_0 = 12$, $V_0 = 6$, $F_0 = 8$), and pentagonal dodecahedron ($E_{pd} = 30$, $V_{pd} = 20$, $F_{pd} = 12$)/icosahedron ($E_i = 30$, $V_i = 12$, $F_i = 20$).

[**] The best partition method has been developed by *F. Fischer* and *E. Koch* [136]. It is based on the so-called potential plane construction and always volume-filling if sufficient neighbors are included in the construction (see above [136]).

2. The "true" geometrically determined situation, in which the values lie between at least two straight lines over a wide range of D_M/D_N (cf. Fig. 11).

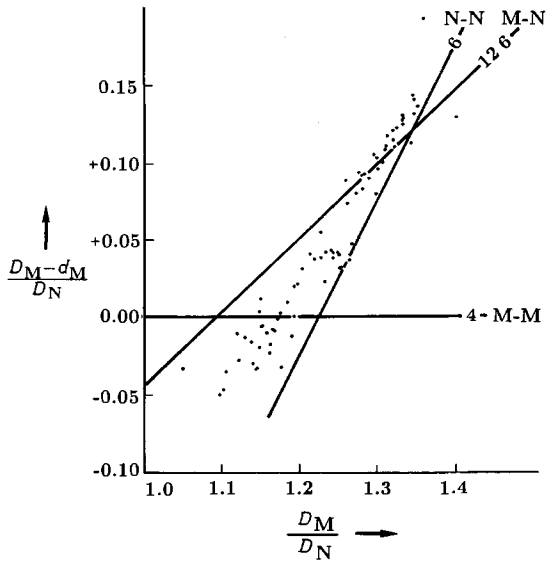

Fig. 11. Nearest-neighbor diagram [24] for the $MgZn_2$ structure type. The straight lines define the strain-free arrangements for M–M, M–N, and N–N interactions (normalized with respect to the M–M interactions). The most favorable number of neighbors is also given on the line.

3. Situations determined by chemical bonding, whereby the values run alongside a straight line that defines the dominant interaction. *Pearson* has shown in numerous examples that plots of this type can be used to identify the interaction that is most important for the chemical structure. More recent work on this topic has been published by *A. Simon*[91] and *W. B. Pearson*.[139]

This method is, however, unable to provide a deeper understanding of the accompanying chemical bonding. A combination with the basic pseudopotential theory of *Heine*, *Weaire*, and *Hafner*, which contains only the radial (distance) interaction, appears to be quite attractive (see Section 5.5).

5.2. *Schubert*'s Correlation Model

In the older literature, there are only a few references to the possibility that electrons in intermetallic phases can form correlation structures.[21, 187, 188] In a series of publications, *K. Schubert* has investigated a model in which the mutual evasion of electrons leads to correlation structures.[23, 140, 141] Instead of static structures, these are supposedly dynamic structures, which—and this is the most important point of the model—must be commensurable with the metric of the unit cell in at least two directions. According to his model, structures of intermetallic phases are only stable on this condition. *Schubert* starts from the assumption that the electrons are essentially free and concludes that their correlation structures must therefore be simple dense packings. Furthermore, he makes a distinction between valence and core electron correlations. In simple terms, this means that each structure of an intermetallic phase has two commensurate lattices, in the positions of which the respective valence or core electrons must be accommodated. The d electrons of the outer d shell of transition metals are usually counted as core electrons. Although *Schubert* has presented correlation structures for numerous compounds,[142–144] his model has met with little acceptance.

A legitimate reason for doubting the model is certainly the assumption of quasi-free electrons. In particular, the complex intermetallic phases exhibit a pronounced cluster-forming tendency and wide-range ordering, which indicates that electrons with varying strengths of binding are present.

However, it remains an open question whether the averaging of such effects will allow general trends to be determined by using the correlation lattices. The application of the ELF (see Section 4.4[138]) to intermetallic phases represents a further step towards an understanding of chemical bonding and, possibly, of the correlation structures of valence electrons in these compounds as well.

5.3. *Pauling*'s Theory of Asynchronous Resonance

Pauling has developed a modified valence bond theory to explain chemical bonding in metals, whereby resonance structures are postulated for the chemical bonds in insulators and semiconductors.[20, 146, 147] Since the coordination number in a metal is usually much larger than the number of available electron pairs, each possible bonding situation is assigned a resonance structure. *Pauling* regards this as a type of asynchronous resonance, in which, in contrast to insulators and semiconductors, resonance structures with charged atoms also occur (Scheme 1).[147]

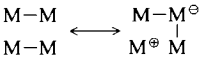

Scheme 1. Description of chemical bonding in metals by asynchronous resonance.

Two conditions must be fulfilled: unpaired electrons must be present and charge differences greater than ± 1 are not taken into account. *Pauling* has developed a statistical method for determining the number of resonance structures with covalent bonds per atom, v. According to this method, there are approximately as many synchronous as asynchronous resonance structures, and it is these additional valence structures which are responsible for the stabilization of metallic compounds. Specifically, the number of resonance structures depends on the valence v and the number of coordination or bonding partners L of the atoms involved. In addition, a distinction must be made between atoms in which the ratio of valence electrons N_e to valence orbitals N_0 is less than 1 (hypoelectronic) and those with a ratio greater than 1 (hyperelectronic) [Eqs. (1) and (2)].

$$v_{hypo} = \frac{v^{\frac{v}{2}}(L-v)^{\frac{L-v}{2}}L!}{L^{\frac{L}{2}}v!(L-v)!}\left(\frac{L-v}{L-v+1}+1+\frac{v}{v+1}\right) \quad (1)$$

$$v_{hyper} = \frac{\sqrt{2}L!v^{\frac{v-1}{2}}(L-v)^{\frac{L-v+1}{2}}}{L^{\frac{L}{2}}(v-\frac{1}{2})!\,(L-v+\frac{1}{2})!}\left(1+\frac{v(L-v+\frac{1}{2})}{(v+\frac{1}{2})(L-v)}\right) \quad (2)$$

The number of metal orbitals per atom, ω, that is, those orbitals subject to asynchronous resonance, is given by Equations (3) and (4), where $-z \leq v \leq +z$ defines a valence range, and e is defined in Equation (5).

$$\omega_{hypo} = \frac{4Lv - 4v^2 + 3L + 2}{6Lv - 6v^2 + 4L + 2} \tag{3}$$

$$\omega_{hyper} = \tfrac{1}{2}([e - \{e(e-1)\}^{\frac{1}{2}}] + 1) \tag{4}$$

$$e = \frac{(z+1)(L-z-1)}{L-2z-1} \tag{5}$$

A systematic study of the v and L values shows that the largest resonance stabilization in metals is possible when $v = L/2$, that is, when the number of resonance structures is half the number of bonding partners (Fig. 12). This result

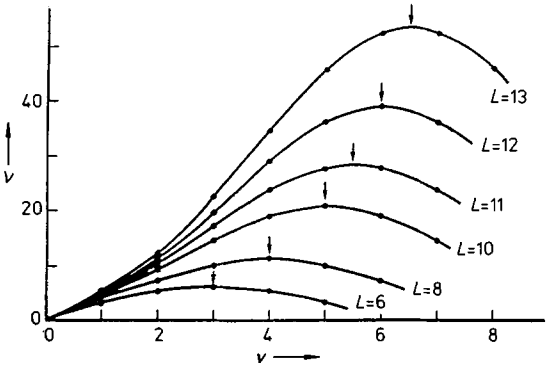

Fig. 12. Number of resonance structures, v, as a function of the number of ligands L and the valence v for intermetallic phases [145].

implies a statement, which *Pauling*, on account of his electron pair concept, has not formulated in his way: metals tend to form half-bonds.[*]

With transition metals such as tungsten, a valence is obtained which is indeed somewhat higher than six.[**] This is the highest valence expected for metals.[147] Using the theory of asynchronous resonance, *Pauling* et al. have determined a new set of single-bond radii.[147] At the same time, *Pauling* has improved his well-known relationship between distance d_n, single-bond length d_1, and bond order n by including the number of resonance structures [Eq. (6)].

$$d_n = d_1 - 0.700 \lg \{n[1 + 0.064(v-1)]\} \tag{6}$$

Two criticisms of the *Pauling* theory are encountered particularly often. First, an assumption about the valences must be made.[111] Second, a linear relationship is assumed to exist between the number of resonance structures and the energy.

[*] *Heine* and *Samson* [149], as well as *Bieber* and *Gautier* [150] have made the following interesting statement: Alloys of transition metals have ordered structures when the d bands are half-occupied. For almost empty or nearly filled d bands, cluster formation dominates. These conclusions are clearly related to the classical chemical rules of cluster formation for boranes as well as to the formation of nets for four-electron species.

[**] The number of neighbors in the W structure is 8 + 6 with distances of $\sqrt{3}/2$ a or a (a = lattice constant).

In a recently published article on the application of *Pauling*'s ideas to the improvement of proposed structures in structure–stability comparisons as well as the prediction of nonstoichiometry and the existence of intermetallic phases, *F. L. Carter* writes: "...we have found as a user (and not the originator) that the advantages of *Pauling*'s metallic radii scheme render it far superior to any other proposed approach... notwithstanding its limitations."[148] However, to this approval must be added the reservation that promising quantum-mechanical concepts are now available for problems such as the local chemical bonding in intermetallic phases (see Sections 5.4 and 5.5).

5.4. Extended Hückel Investigations

Since the early 1980s, *R. Hoffmann* has extended his work on molecules and coordination compounds to the study of the chemical bonding in typical solid-state structures and intermetallic phases. To this end, *M. H. Whangbo*, *R. Hoffmann*, and *T. Hughbanks* extended the EH method with formalisms which make it possible to compare fragments with a total structure and to investigate the local chemical bonding (COOP method[8]) in the solid state. In a series of studies, *R. H. Hoffmann* et al. and *J. Burdett* et al. obtained critical insights into the chemical bonding in intermetallic phases.[9,43] The method of moments developed by *J. Burdett* and *S. Lee* elegantly takes into consideration the differing neighborhood interactions.[41–44] It also gives promising and chemically comprehensible analyses in the study of nets of partial structures (see Fig. 13c), particularly those that have become known from the work of *W. B. Pearson*, *A. F. Wells*, *E. Hellner*, *M. O'Keeffe*, and *B. G. Hyde*.[24, 25, 27, 28]

One of the most commonly occurring structures of intermetallic phases is that of $BaAl_4$[169] or $ThCr_2Si_2$[170] as a ternary representative. More than 400 compounds crystallize in this structure type. Clearly, this arrangement must be capable of adapting to widely differing valence electron concentrations as the Th_6Mn_{23} structure does. In this connection, a series of interesting physical properties have been observed, including valence fluctuations, superconductivity with heavy fermions, and unusual magnetic properties.[171] As can be seen in Figure 13a, the AB_2X_2 type belongs to the framework structures in the Pearson classification (see Section 1.1). B_2X_2 layers are coordinated on both sides by the large A atoms. The B atoms form a square net, whose squares are coordinated by X atoms in such a way that the resulting square pyramids are alternately directed upwards and downwards. However, the crucial structural elements are the X–X contacts between the layers, which, through changes in the X–X distance, can adapt to changes in the valence electron concentration (Fig. 13b).[167, 168]

In a series of alkaline-earth transition-metal phosphides, reported by *A. Mewis*, P–P distances between 2.25 and 3.43 Å are found. Here, the entire range from a normal P–P single bond (2.20 Å) to a completely unbound state is found in a series of seven compounds AB_2P_2 (A = Ca, Sr; B = Fe, Co, Ni, Cu). The extended Hückel investigation clearly confirms that once again a bonding mechanism in accordance with the Zintl–Klemm concept is responsible for the adap-

tation. Depending on the filling of the electronic states, only bonding or bonding and antibonding P–P crystal orbitals are populated.[167] An understanding of the effect of the transition element B requires knowledge of some band-structure terminology. Electron-poor B atoms to the left of the periodic table populate the antibonding P–P states to a greater extent than the electron-richer atoms such as Ni and Cu. In the latter, the d states and the σ^* states fall into the same energy range owing to the higher effective nuclear charge. In other words, although Mn and Fe have fewer electrons than Ni and Cu, they transfer more electrons to the P atoms and are therefore more strongly oxidized.

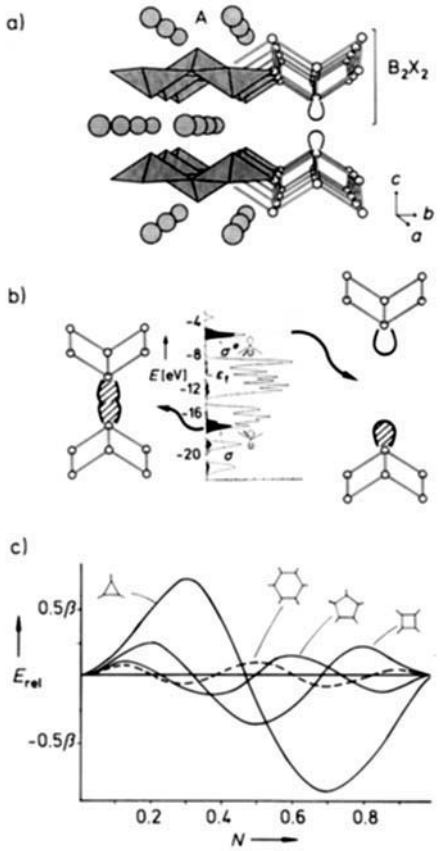

Fig. 13. Extended Hückel investigations [167]: a) $BaAl_4$ and $ThCr_2Si_2$ structure type: section of the crystal structure of $ThCr_2Si_2$. The B_2X_2 partial structure is shown on the left as a polyhedral depiction (square pyramid) and on the right as a framework. The X–X bond is shown by the hybrid orbitals (right-hand side, between the layers). b) X–X interactions as a function of the filling of the orbitals with electrons. Left: Short distance, bonding interaction, only the σ state is populated. Center: Density of states with contribution of σ and σ^* states [168]. Right: Large distance, nonbonding interaction, σ and σ^* states are populated (see text). c) Comparison of the relative energies for nets of triangles, squares, pentagons, and hexagons as a function of the number of electrons, calculated by the method of moments (reproducted from [13]).

W. Tremel and *R. Hoffmann* have elegantly studied the electronic structure of 4^4 networks in crystalline solids, which form either ideal or distorted arrangements, depending on the difference in electronegativity between the atoms and the number of valence electrons.[183] Some further studies of planar and puckered nets have been published by *Burdett* et al.[43] The quantum-mechanical study of polyhedra and nets has apparently turned out to be the fundamental starting point for the analysis of chemical bonding in intermetallic phases. These two merge in the borderline case in which the polyhedra become infinitely large (cf. footnote in Section 5.3).

5.5. Pseudopotential Theory

A remarkable theory of chemical bonding in metals was published about 20 years ago by *V. Heine*, *M. Cohen*, and *D. Weaire*.[111] In three detailed articles, they investigated pseudopotentials, their generation, and their application to metals as well as the relationships between pseudopotential theory and the formation of structures in metals and intermetallic phases. They split up the total energy of a crystal structure into several terms [Eq. (7)], of which only U_E and U_{BS}, the Coulomb or band-structure energy, are dependent on the structure (see also Section 6.1). U_0 is a function of the

$$U = U_0 + U_E + U_{BS} \tag{7}$$

atoms involved and contains no structure-specific information. The starting point for the work of *Heine* et al. is the statement that "the electronic band structure $E(\boldsymbol{k})$ for very many solids is recognizably a greater or smaller distortion from that of free electrons."[111] Of course, this does not imply that essentially free electrons are present in the compounds they have successfully studied. The perturbation of the free-electron gas may describe the real electron structure just as well or badly as a complementary theory based on the delocalization of a strongly localized electron structure (Fig. 14a).

First, a few definitions should be given. Figure 14b shows schematically the dependence of the energy $E(\boldsymbol{k})$ on the wave vector $\boldsymbol{k}$[*] for the free-electron gas (dotted line) and the perturbation by the periodic potential in a crystal structure (solid line). The function $E = f(\boldsymbol{k})$ is termed an electronic band. The parabolic relationship $E(\boldsymbol{k}) = 1/2k^2$ applies for the free-electron gas.

Between the energetically lowest unoccupied (LUMO in a molecule) and the highest occupied electronic state (HOMO in a molecule) is the Fermi level or Fermi energy E_F. In reciprocal $\boldsymbol{k}$ space, the corresponding value k_F is the radius of a sphere, the so-called Fermi sphere. However, this applies only for the free-electron gas. All real crystal structures have many bands, which can also cross one another if they have different symmetry. In metallic conductors the Fermi level is not a defined energy; it always intersects bands (see Fig. 14c, E_F^M); that is, the highest occupied and lowest unoccupied electronic states follow one another without an energy gap.

The intersection of the Fermi energy and an electronic band gives in one dimension a point, in two dimensions a line, and in three-dimensional $\boldsymbol{k}$ space a surface of intersection, which is termed the Fermi surface. This is the surface of the so-called Fermi body, which, in the case of a free-electron gas, includes the occupied electronic states. As mentioned previously, the Fermi surface is only spherical for a free-electron gas (see Fig. 14d). Each metal has its typical Fermi surface, which, depending on the structure and atomic proper-

[*] $\boldsymbol{k}$ represents vectors in reciprocal space and can also correspond to reciprocal lattice vectors in a crystal structure.

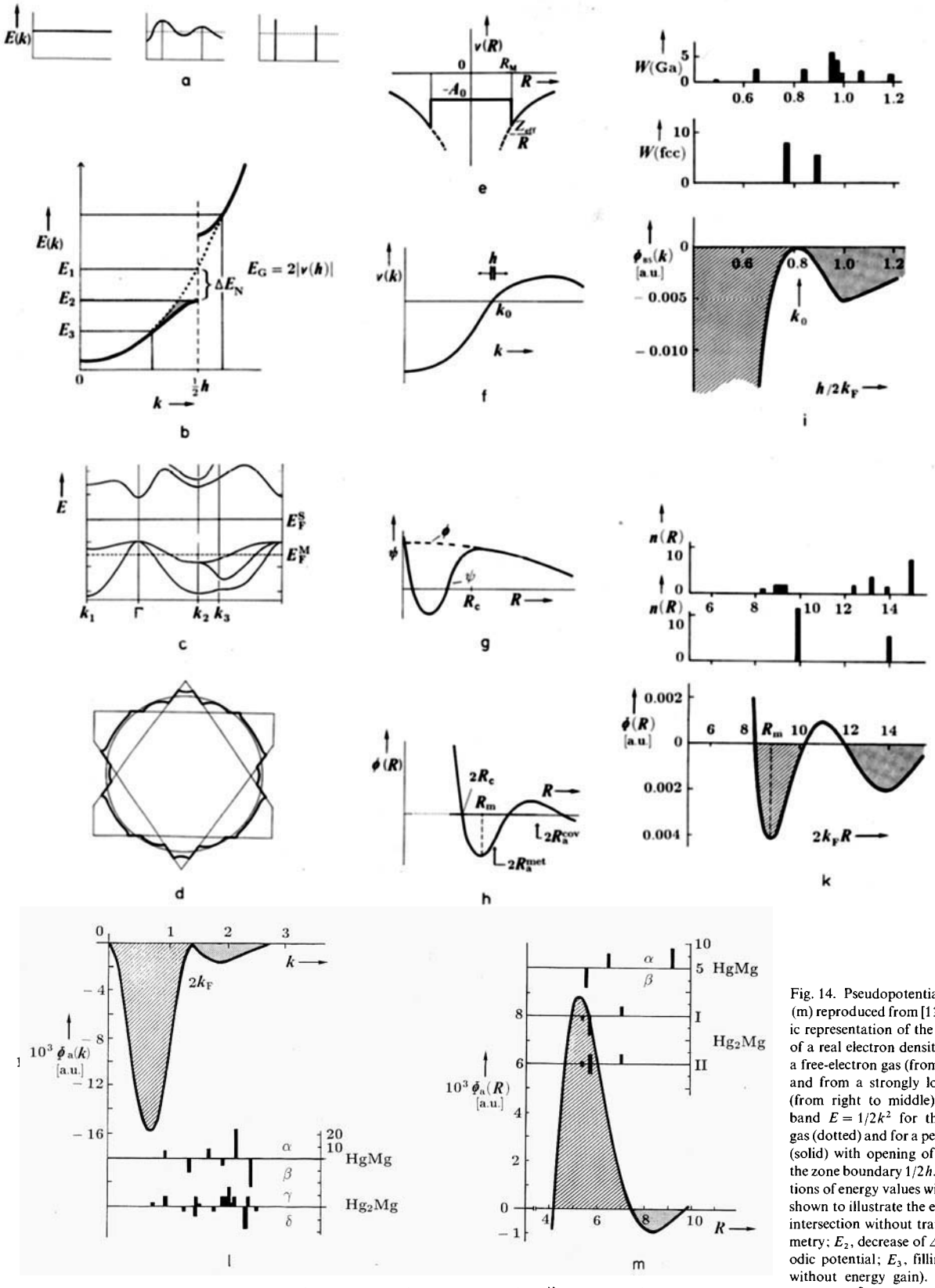

Fig. 14. Pseudopotential theory ((b)–(m) reproduced from [11]): a) Schematic representation of the approximation of a real electron density starting from a free-electron gas (from left to middle) and from a strongly localized picture (from right to middle). b) Electronic band $E = 1/2k^2$ for the free-electron gas (dotted) and for a periodic potential (solid) with opening of a band gap at the zone boundary $1/2h$. Three intersections of energy values with the band are shown to illustrate the energy gain (E_1, intersection without translational symmetry; E_2, decrease of ΔE_N by the periodic potential; E_3, filling of the band without energy gain). c) Part of the band structure of a metal (aluminum); the horizontal lines mark the Fermi energies E_F^M for a metal (dotted) and for a semiconductor "E_F^S" (solid). d) Intersection of the Fermi sphere (dotted) with a plane of $\boldsymbol{k}$ space. In the periodic potential, deformations of the Fermi surface arise at the zone boundaries (thin lines) with formation of band gaps. As an example, the experimentally determined [110] projection of the Fermi surface of lead is shown. e) Schematic depiction of an atomic pseudopotential v. Outside a limiting radius (model radius $\boldsymbol{R}_m$), the pseudopotential follows the Coulomb law $v(R) \sim Z_{eff}/R$. f) Fourier transformed pseudopotential $v(\boldsymbol{k})$. The position $v(\mathbf{k}_0) = 0$, which is as far as possible avoided by the important structure factors $\boldsymbol{h}$ of an energetically favorable structure, is marked. g) Schematic radial course of an orbital and a pseudo orbital (dotted). h) Schematic course of a pair correlation function $\Phi(\boldsymbol{R})$ and comparison of the relative positions of the atomic radii $\mathbf{R}_a$ to the hard-core radius $\mathbf{R}_c$ for electronegative elements with covalent semiconductor structures and for metals. Comparison of the pair correlation function $\Phi(\boldsymbol{k})$ (i) and $\Phi(\boldsymbol{R})$ (k) for gallium with the distribution of the structure factors, $\omega(h)$ and the histogram of distances, $n(\boldsymbol{R})$ for the α-Ga structure (top) and for the fcc arrangement (bottom). l) Comparison of the pair correlation function $\Phi_a(\boldsymbol{k})$ for Hg-Mg compounds and the structure factors for the observed structures of MgHg (CsCl type, α) and $MgHg_2$ ($MoSi_2$ type, γ) as well as for the structures given by a statistical distribution (MgHg, body-centered cubic, β; $MgHg_2$, body-centered tetragonal, δ). $\Phi_a(\boldsymbol{k})$ favors the ordered structures α, γ. m) Comparison of $\Phi_a(\boldsymbol{R})$ with the distance distribution for MgHg and $MgHg_2$ (α, Mg–Mg and Hg–Hg distances plotted downwards; β, Mg–Hg distances plotted downwards: I, distances around Mg; II, distances around Hg). Note the distance accumulation at the maximum of $\Phi_a(\boldsymbol{R})$.

ties, can adopt widely differing forms. Since the Fermi surfaces contain the least favorable, that is, the energetically highest lying, electronic states, a decrease in the surface always leads to an energy gain. The inclusion of a periodic potential, as is present in crystals, corresponds to the formation of zone boundaries in $\boldsymbol{k}$ space. For the electronic bands, the band gaps arising at these zone boundaries result in precisely such a decrease in the Fermi surface (Fig. 14d). It is therefore not surprising that periodic Fermi surfaces, like those of gold, resemble periodic minimal surfaces (see Section 6.1).

In insulators and semiconductors (Zintl phases), the Fermi level always lies in an energy gap which extends through the entire $\boldsymbol{k}$ space continuously but with varying width (Fig. 14c, E_F^S). The smallest gap between the highest occupied and the lowest unoccupied electronic state is the band gap E_G (Fig. 14b). This is called a direct band gap for a transition at the same $\boldsymbol{k}$ point and an indirect band gap for a transition between two different $\boldsymbol{k}$ points (Fig. 14c). Accordingly, there are also direct and indirect electronic transitions. The Fermi level lies in the middle of the band gap and therefore does not cross any bands, which means that insulators and semiconductors have no Fermi surface. The bands in these classes of substances are of course also subject to a stabilization by the periodic structure, which can be seen in the cross-sectional surface of constant energy $E(\boldsymbol{k}) < E_F$. As a rule, however, these cross-sectional surfaces become increasingly small as $E(\boldsymbol{k})$ approaches the highest energy of the highest occupied band, $E_m(\boldsymbol{k})$. Thus, in insulators and semiconductors, too, a minimization of the surface $E(\boldsymbol{k})$ occurs for the energetically unfavorable states with high energy, analogous to that discussed for metals. Indeed, the tendency to minimize the Fermi surfaces always corresponds to a tendency for the formation of valence compounds.[111]

Various approximations play an important role in the concept of *Heine* et al. First, the influence of the atomic-core regions is described by a pseudopotential $v(\boldsymbol{R})$ in real space (Fig. 14e) or $v(\boldsymbol{k})$ in reciprocal space (Fig. 14f). The effect of the pseudopotential approximation is shown in Figure 14g. In the valence region, the corresponding pseudoorbitals ϕ correspond to the valence orbitals ψ and can be chosen such that no nodes occur in the core region. For this, only the valence region need to be taken into account in the quantum-mechanical treatment. A further advantage is that the pseudopotential of an atom can be used for different valence states. The only structure-dependent quantities in Equation (7) are the Coulomb energy U_E and the so-called band-structure energy U_{BS}. The latter is largely determined by the lowering of the bands at the Brillouin zone planes. U_E is part of the electrostatic energy for pointlike cations in a uniform electron gas, most of which is also structure-independent, as shown by *F. Bertaut*[175,176] (see Section 6.1). U_E is only the structure-dependent correction term of the Coulomb energy.

Heine and *Weaire* emphasize in their studies that the Coulomb repulsion (or that of the charged atom cores) favors highly symmetrical structures. However, this means that only U_{BS} and related quantities are responsible for the formation of complex structures. In the following, some simple relationships will be developed on this basis. Figure 14b shows schematically the energy gain obtained for various Fermi energies when the bands split at the zone boundaries. The value of U_{BS} is proportional to the square of the band gap ($U_{BS} \sim -|v(\boldsymbol{h})|^2$) arising at the zone boundary $1/2h$. The lowering of the energy is large whenever $\mathbf{k}_F$ approaches a zone boundary as closely as possible and $v(\boldsymbol{h})$ adopts a high value.[*] Figures 14e and 14f show the radial pseudopotentials as a function of the real and reciprocal coordinates $\boldsymbol{R}$ and $\boldsymbol{k}$. The two representations $v(\boldsymbol{R})$ and $v(\boldsymbol{k})$ can be interconverted by Fourier transformation and are completely equivalent.

Of particular importance is the point $\mathbf{k}_0$ at which the pseudopotential has its root. If U_{BS} governs the formation of the structure, then, in the reciprocal representation, structure factors with high weight avoid the position $\mathbf{k}_0$. The lattice vectors $\boldsymbol{h}$ close to the origin are important here, because $v(\boldsymbol{k})$ decreases quite rapidly with increasing $\boldsymbol{k}$. A similar dependence occurs in the *Bertaut* "ansatz" of the Coulomb energy (see Section 6.1).

For the correlation of energetic and structural quantities, another function, the so-called band-structure characteristic Φ_{BS}, is more appropriate than the pure pseudopotentials. Φ_{BS} is a function of the product of two pseudopotentials and has the character of a pair potential. Since Φ_{BS} is also structure-independent, the only remaining structure-dependent terms in U_{BS} are the geometrical structure factors $S(\boldsymbol{h})$ in Equation (8).[**]

$$U_{BS} = \sum_h n_h |S(\boldsymbol{h})|^2 |v(\boldsymbol{h})|^2 \gamma(\boldsymbol{h}) = \sum_h W(\boldsymbol{h}) \Phi_{BS}(\boldsymbol{h}) \tag{8}$$

$W(\boldsymbol{h}) = n_h |S(\boldsymbol{h})|^2$ is termed the structural weight.[111] Exclusively this quantity contains the structural information and it corresponds to the sum of the squares of symmetry-equivalent normalized structure factors (n = multiplicity of $S(\boldsymbol{h})$). For $\Phi_{BS}(\boldsymbol{k})$, too, the following applies: structure factors $S(\boldsymbol{h})$ with large weight $W(\boldsymbol{h})$ should avoid the first root $\mathbf{k}_0$ and should lie in the region of the minima of $\Phi_{BS}(\boldsymbol{k})$.

$\Phi(\boldsymbol{R})$ is a corresponding pair potential in real space (Fig. 14h) and is made up of a Coulomb term and the Fourier transform of $\Phi_{BS}(\boldsymbol{k})$ [Eq. (9)]. This function is directly

$$\Phi(\boldsymbol{R}) = \frac{q^2}{|\boldsymbol{R}|} + \frac{2\Omega}{(2\pi)^3} \int \Phi_{BS}(\boldsymbol{k}) \exp(i\boldsymbol{k}\boldsymbol{r})\, d^3k \tag{9}$$

relevant to the distances between two atoms. The distances should avoid the maxima, especially the first maximum, of the pair correlation function. However, $\Phi(\boldsymbol{R})$ is not a complete interatomic potential; it is a reorganization potential for constant volume. The radial course of $\Phi_{BS}(\boldsymbol{k})$ and $\Phi(\boldsymbol{R})$ is shown in the lower part of Figures 14i and 14k. For aluminum, the fcc arrangement best fulfills these conditions. The set of cubic structure factors $S(\boldsymbol{h})$ with $|\boldsymbol{h}| < 2\mathbf{k}_F$ can make significant contributions to U_{BS}.

[*] In some cases, this can occur through formation of superstructures; that is, through small changes in the translation lattice, corresponding zone boundaries can optimally approach the Fermi surface. In other cases, two very different structure types with different Fermi surfaces may compete with one another, whereby, depending on the number of valence electrons, one of them is favored energetically. This idea is the basis of the Hume-Rothery rules [177-179].

[**] $\varepsilon(\boldsymbol{k})$ is a shielding function, the dielectric function of the free-electron gas. $\chi(\boldsymbol{h})$ is termed the polarization operator or perturbation characteristic [11, 12]. These two quantities introduce correlation and exchange interactions for the nonuniform electron gas. $\gamma(\boldsymbol{h}) = \chi(\boldsymbol{h})\varepsilon(\boldsymbol{k})$ is structure-independent in this approximation.

Heine and *Weaire* showed that gallium, in contrast to aluminum, cannot crystallize well with an fcc structure, because the cubic structure factors F (111) lie to close to $\mathbf{k}_0$ with $\Phi_{BS}(\mathbf{k}_0) = 0$. The observed structure (α-gallium) has a significantly better $W(\boldsymbol{h})$ distribution. Accordingly, distances with large weight (higher abundance, $n(\boldsymbol{R})$) in the distance spectrum of the α-gallium structure can far better avoid the maximum of $\Phi(\boldsymbol{R})$ than those of the fcc arrangement with the same volume (Fig. 14k).

According to *Heine*, distortion of structures arises as a result of the difficulty of simultaneously achieving volume and distance optimization in a highly symmetrical structure. The volume requirement in intermetallic phases is usually not structure-dependent, but is instead a function of the atomic electron density.[11] A corresponding observation, made more than 60 years ago, was the basis for a compilation of volume increments by *W. Biltz* and *W. Klemm*.[151] Typical examples of simple distorted structures are those of Zn, Cd, and Hg, with their unusual c/a ratios of 1.8562, 1.8856, and 1.936, as well as the structures of Ga and In.

Figure 14h shows the relationship between the more open structures in covalent semiconductor arrangements and the dense packings of the intermetallic phases through the curve $\Phi(\boldsymbol{R})$. Elements with high effective nuclear charges have a hard-core radius R_0 that is small compared with the atomic radius R_A. Given the volume requirement $4/3\,\pi R_a$, only a few neighbors can have the particularly favorable distance R_m (diamond structure: $R_m/R_a \approx 0.70$). For intermetallic phases R_m/R_a is about 0.9.[11]

After a few modifications, *Heine*'s approach can also be used to investigate the stability of alloys and intermetallic phases. In a compound $A_{1-c}B_c$, the different interactions A-A, A-B, and B-B must be taken into account. After splitting up the pseudopotential in the crystal, $V(\boldsymbol{k})$, one obtains an expression for the potential that contains two terms [Eq. (10)]. The first term is the sum of the structure factors

$$V(\boldsymbol{k}) = S_{AB}(\boldsymbol{k})\,\bar{v}(\boldsymbol{k}) + [c\,S_A(\boldsymbol{k}) - (1-c)\,S_B(\boldsymbol{k})]\,v_{diff} \qquad (10)$$

with

$$S_{AB}(\boldsymbol{k}) = S_A(\boldsymbol{k}) + S_B(\boldsymbol{k})$$
$$\bar{v}(\boldsymbol{k}) = c\,v_B(\boldsymbol{k}) + (1-c)\,v_A(\boldsymbol{k})$$
$$v_{diff}(\boldsymbol{k}) = v_A(\boldsymbol{k}) - v_B(\boldsymbol{k})$$

for the atoms, namely, S_A and S_B, multiplied by an average atomic pseudopotential $\bar{v}$. The second term is a weighted correction which involves the difference potential v_{diff}. For the band structure energy per ion one then obtains Equation (11). The first term contributes to the reciprocal lattice

$$\begin{aligned} U_{BS} &= \sum_{\boldsymbol{h}} |S_{AB}(\boldsymbol{h})|^2 \bar{v}(\boldsymbol{h})^2\,\gamma(\boldsymbol{h}) + \sum_{\boldsymbol{k}} [c\,S_A(\boldsymbol{k}) - (1-c)\,S_B(\boldsymbol{k})] \\ &\quad [c\,S_A^*(\boldsymbol{k}) - (1-c)\,S_B^*(\boldsymbol{k})]\,v_{diff}(\boldsymbol{k})^2\,\gamma(\boldsymbol{h}) \\ &= \sum_{\boldsymbol{h}} |S_{AB}(\boldsymbol{h})|^2\,\Phi_{BS}\,v(\boldsymbol{h}) + \sum_{\boldsymbol{k}} [c\,S_A(\boldsymbol{k}) \\ &\quad - (1-c) S_B(\boldsymbol{k})]\,\Phi_{BS}^{diff}(\boldsymbol{k}) \end{aligned} \qquad (11)$$

vectors, which correspond to the Bragg points, while at these points the second term is zero. For $\boldsymbol{k} \neq \boldsymbol{h}$ only the second term, which takes into account the degree of ordering in the structure, is present. The splitting into two terms corresponds to the concept of coherent and incoherent scattering in diffraction experiments. For ordered structures, the structure factors $S_{AB}(\boldsymbol{h})$ belong to a subcell—which must be chosen appropriately—in the true unit cell. The remaining Bragg points form the group $S_{AB}(\boldsymbol{k})$ of the superstructure cell. Once again, the first strong structure factors have considerable influence on U_{BS} and therefore on the formation of the structure. Large values of $S_{AB}(\boldsymbol{h})$ should coincide with the minima of $\Phi_{BS}(\boldsymbol{k})$, and those of type $S_A(\boldsymbol{k})$ and $S_B(\boldsymbol{k})$ with the minima of $\Phi_{BS}^{diff}(\boldsymbol{k})$. The second term in Equation (11) is also known as the reorganization term or as the energy of alloy formation. The expression for the structure-dependent component of the total energy in real space, obtained by Fourier transformation of U_{BS} and adding the Coulomb energies of the atom cores U_E, contains corresponding summations over all pair interactions A-A, A-B, and B-B for a phase $A_{1-c}B_c$. Equations (12), (13) and (14) are the general form of this pseudopotential theory for alloys and intermetallic phases. The first term in Equation (13) and (14) is in each case the corresponding Coulomb component.

$$\begin{aligned} U_E + U_{BS} &= \frac{N}{2} \sum_{i \neq j} \Phi_M(\boldsymbol{R}_{ij}) + c^2 \sum_{i \neq j}^{AA} \Phi_a(\boldsymbol{R}_{ij}) \\ &\quad + (1-c)^2 \sum_{i \neq j}^{BB} \Phi_a(\boldsymbol{R}_{ij}) \\ &\quad - 2c(1-c) \sum_{i \neq j}^{AB} \Phi_a(\boldsymbol{R}_{ij}) \end{aligned} \qquad (12)$$

$$\Phi_M = \frac{(q_A + q_B)^2}{4|\boldsymbol{R}|} + \frac{2\Omega}{(2\pi)^3} \int \Phi_{BS}(\boldsymbol{k}) \exp(i\,\boldsymbol{k}\boldsymbol{r})\,d^3k \qquad (13)$$

$$\Phi_a = \frac{(q_A - q_B)^2}{4|\boldsymbol{R}|} + \frac{2\Omega}{(2\pi)^3} \int \Phi_{BS}^{diff}(\boldsymbol{k}) \exp(i\,\boldsymbol{k}\boldsymbol{r})\,d^3k \qquad (14)$$

Figure 14l shows the course of Φ_a and the correlation for the Hg-Mg pair with the structure factors $S(\boldsymbol{k})$ of the compounds HgMg (CsCl structure) and Hg_2Mg ($MoSi_2$ structure).[11] The structure factors of the ordered structures (plotted upwards) are closer to the minimum of $\Phi(\boldsymbol{k})$ than those of the disordered arrangements (plotted downwards). Accordingly, for the ordered structures, the distances between different types of atoms, $\Phi_a(\boldsymbol{R})$, lie at large values of the function, and those between like atoms at the smallest values (Fig. 14m). The result is that the structural part of the total energy is decreased.[11]

Heine's and *Weaire*'s theory has been derived from first principles and presented in an extended form in a recently published monograph by *Hafner*, which describes the consequences of extending the theory to perturbations of higher than second order as well as the treatment of compounds with transition metals.[12]

The pseudopotential theory of metals and intermetallic phases can be of great use to the chemist, because it elegantly simplifies the complex interplay of difficultly definable pair interactions—especially in intermetallic compounds—and restricts them in the basic form to radial interactions. In contrast to *Pauling*'s relationship between distance and bond order,[20] $\Phi(\boldsymbol{R})$ is not a monotonously ascending or descending function. It is precisely the radial sequence of minima and maxima of $\Phi(\boldsymbol{R})$ which is of crucial importance for the formation of the structure.

The energetical gradation resulting from perturbation theory treatment leads to a total energy composed of the increments U_0, U_E, and U_{BS}, which is in accordance with the chemist's conception. This is also true of U_{BS} and the pair interaction Φ_{BS}, which, by taking into account the partial structure factors, can be related to the partial structures. Because the localized pseudopotentials and the band-structure character are not dependent on the direction, the preceding analysis can also be applied to metallic melts and amorphous metals. According to *Hafner*, the metals Zn, Cd, Hg, In, and Tl exhibit asymmetric coordination even in the molten state. *Nagel* and *Tauc* postulate that the average interatomic distance is so large that the maxima of the distance spectrum coincide with the minima of the pair potential function $\Phi(\boldsymbol{R})$.[152] Although there are no bands, Brillouin zones, or well-defined reciprocal lattice vectors for such a system, this hypothesis has provided remarkably good results.[12] This indicates that smaller, noncrystalline units can also be approximately described in this way and confirms the idea that the band-structure description contains a large amount of information on local bonding.

5.6. The Density of Alloys

The rules, which are a priori incompatible, are often used to derive densities and related quantities. The Vegard rule assumes a linear dependence of the unit-cell dimensions and interatomic distances upon the atomic radii r_A and r_B.[154] The so-called Zen law postulates the additivity of the volumes.[155] However, a comprehensive review of volume additivity, treated in terms of ionic and intermetallic phases, was published much earlier by *Biltz* and *Klemm*.[151] According to *Hafner*, these rules "are perhaps the only laws in physics for which it is much harder to find a system to agree with, than to disagree with".[12] Owing to their different dimensions, $\sum r_i$ and $\sum v_i$ ($\sim\sum r_i^3$) cannot simultaneously show a linear dependence. However, both quantities are optimized as well as possible in each structure, and it therefore seems only natural that complications arise which lead to the formation of distorted, complex or open, voluminous structures.

Hafner gives a quadratic relation for the change in density in an intermetallic compound whose components A and B have the same valence [Eq. (15)]. The values R_s are the radii of one-electron spheres $4/3\pi R_s^3 = V(e)$, which thus represent the electron density.[*]

$$\begin{aligned} \bar{R}_S^2 &= c_a^2 \bar{R}_{S_A} + c_B^2 \bar{R}_{S_B} \\ \bar{R}_S &= -1 + 1.229\, R_S \\ \bar{R}_{S_{A/B}} &= -1 + 1.229\, R_{S_{A/B}} \end{aligned} \tag{15}$$

Deviations $\Delta R < 0.1\%$ occur for the alkali-metal alloys K/Rb, K/Cs, and Rb/Cs and for Ca/Sr phases.[12] Interestingly, the optimized quantity is apparently a surface ($\bar{R}_s^2$). Whether this surface is related to geometrical surfaces such as periodic nodal surfaces (see Section 6.1) has not yet been investigated.

[*] Variational methods performed as a function of the electron density are termed density functional methods. They are used in various forms for calculating the electronic structures of chemical compounds.

6. Structural Principles and Similarity Relationships

6.1. Inner Surfaces

We are just beginning to learn about the principles according to which gaps or chemically weak interactions are arranged in crystal structures, or rather how they are arranged by the stronger interactions. The surfaces of all stable solid or liquid materials strive for the formation of a minimal surface. The energetical situation on the surface is always less favorable than that in the interior of a solid or liquid substance. But in the interior, too, the distribution of the interactions is structured rather than uniform. In the interior of each structure there are forces of differing strength, and it is a logical consequence that the weaker interactions are grouped around the stronger interactions in an ensemble of the smallest possible size. This tendency leads to the formation of inner surfaces, which in the crystal apparently strive for the form of a symmetry-adapted minimal surface.[174]

It was recently recognized that the symmetry-adapted minimal surfaces in crystals can be replaced by periodic nodal suraces (PNS). The PNS can easily be derived by Fourier transformation of the shortest symmetry-consistent structure factors.[*] In many cases the general root distributions in space groups with translational symmetry form curved periodic surfaces in three-dimensional space. Upon inclusion of physical quantities, the density amplitudes (potential distribution or electron densities) are rescaled, but the PNS's are essentially retained. The general equation for the generation of the PNS is (16), where $\boldsymbol{R}$ and $\boldsymbol{h}$ are the vectors in real and reciprocal space, α_h is the phase angle, and $S(\boldsymbol{h}) = 1/N \sum_j \exp(i\boldsymbol{R}_j\boldsymbol{h})$ is the so-called geometrical structure factor, calculated by summation over all atom positions of each unit cell. In *Bertaut*'s equation for the Coulomb

$$0 = \rho(\boldsymbol{R}) = \sum_{\boldsymbol{h}} S(\boldsymbol{h}) \cos(\boldsymbol{R}\boldsymbol{h} - \alpha_h) \tag{16}$$

potential, $S(\boldsymbol{h})$ is replaced by a corresponding expression $F(\boldsymbol{h})$, which is summed over the charges q_j ($F(\boldsymbol{h}) = 1/N \sum_j q_j \exp(i\boldsymbol{R}_j\boldsymbol{h})$).[175, 176] Owing to spreading of the charges over a large region, only a few of the coefficients near the origin $F(\boldsymbol{h})$ have a significant weight. The corresponding nodal surfaces $\rho(\boldsymbol{R}) = 0$ are identical to those of Equation (16). The Coulomb components of the lattice energy after *Bertaut* is made up of two terms [Eq. (17)]. The second

$$U_{Coul} = \frac{1}{2\Omega} \sum_{\boldsymbol{h}} S(\boldsymbol{h})^2 \frac{|\Phi(\boldsymbol{h})|^2}{|\boldsymbol{h}|^2} - \frac{3}{5R} \sum_i q_i^2 \tag{17}$$

term is a constant for each compound and is structure-independent (cf. pseudopotential theory, Section 5.5). It contains only a normalized sum of the squares of the charges. The first term contains the required structural information,

[*] The six reciprocal points $hkl = \pm 100$, 0 ± 10, and 00 ± 1 with $|F_{hkl}| = 1$ and phase angle $\alpha_{hkl} = 0$, for example, belong to the symmetry group $Pm3m$. Their Fourier transform gives a density space with artificial density amplitudes. However, the roots are determined by the symmetry!

which, according to *Bertaut*, is already contained with high accuracy in a few structure factors $F(\boldsymbol{h})$.[176]

As we have already shown, a few structure factors very close to the origin afford periodic nodal surfaces which have a fundamental influence on the structure of the total ensemble.[173, 174] Up to now it was unclear which of the structure factors further removed from the origin of reciprocal space still make an appreciable contribution to the formation of the structure. This relationship can be explained in terms of the pseudopotential theory. In the framework of the pseudopotential theory (Section 5.5), those structure factors that contribute significantly to the Coulomb component of the total energy lie close to the origin in a strongly negative region of the pair interaction Φ_{BS} (Fig. 14i). These can, however, also simultaneously contain contributions from the heteroatomic pair interaction Φ_a. These are precisely the structure factors that *Bertaut* uses to calculate the Coulomb component of the lattice energy and which we have used in the derivation of the structure-determining PNS. Other structure factors with significant influence on the total energy lie to both sides of the root of Φ_{BS}. In principle, both these and the former are suitable for the generation of the PNS, the general geometrical organizer of the structures. The PNS should be independent of fine adjustment of the potential functions because they determine the general geometrical pattern, whereas the latter depend on individual atomic properties.

A publication by *V. N. Novikow* is of particular interest in connection with our concept of structure formation by means of the PNS.[153] He describes melting as a transition from a Euclidean space to a curved space, whereby the two states, crystal and liquid, are treated as crystalline forms in appropriately chosen space groups. The curvature of the corresponding space is the ordering parameter for the transition crystal → liquid. While the formation of structures for crystals can be generalized in terms of the curved two-dimensional PNS, there are apparently related three- and higher-dimensional descriptions for noncrystalline states. This concept is also of interest in connection with the six-dimensional description of the structures of quasicrystals.

6.2. Chemical Twinning

For Laves phases (Section 3.4), the formation of stacking variants, some of which have considerable translation periods, has already been referred to. They form a link to a family of structures in which simpler basic motifs are combined to give a more complex arrangement. *S. Andersson* has named such arrangements chemical twinning.[162] *E. Parthé* et al. have also studied numerous cases of this type, which they calls intergrowth structures.[163–166] Typical examples are shown in Figure 15. The structure of $CeNiSi_2$, for instance, consists of an alternating stacking of two-dimensional sections of the $BaAl_4$ structure—or rather the $ThCr_2Si_2$ type—and the AlB_2 structure (Fig. 15b).[163] Although the composition $Ce(NiSi_2)$ is not formed locally and would apparently be less stable, the composition AB_3 finds an optimal energetical solution in the stacking of AB_4 ($\triangleq CeNi_2Si_2$) and AB_2 ($\triangleq CeSi_2$) layers.[*] Actually, this type of structure formation is simply a logical extension of structures with isolated heteroatomic clusters to one and two dimensions. The relevance to Zintl phases, in which one-, two-, and three-dimensional polyanions form their own partial structures, is clearly evident. The two layers $CeSi_2$ and $CeNi_2Si_2$ will most likely exhibit an acceptor–donor behavior with correspond-

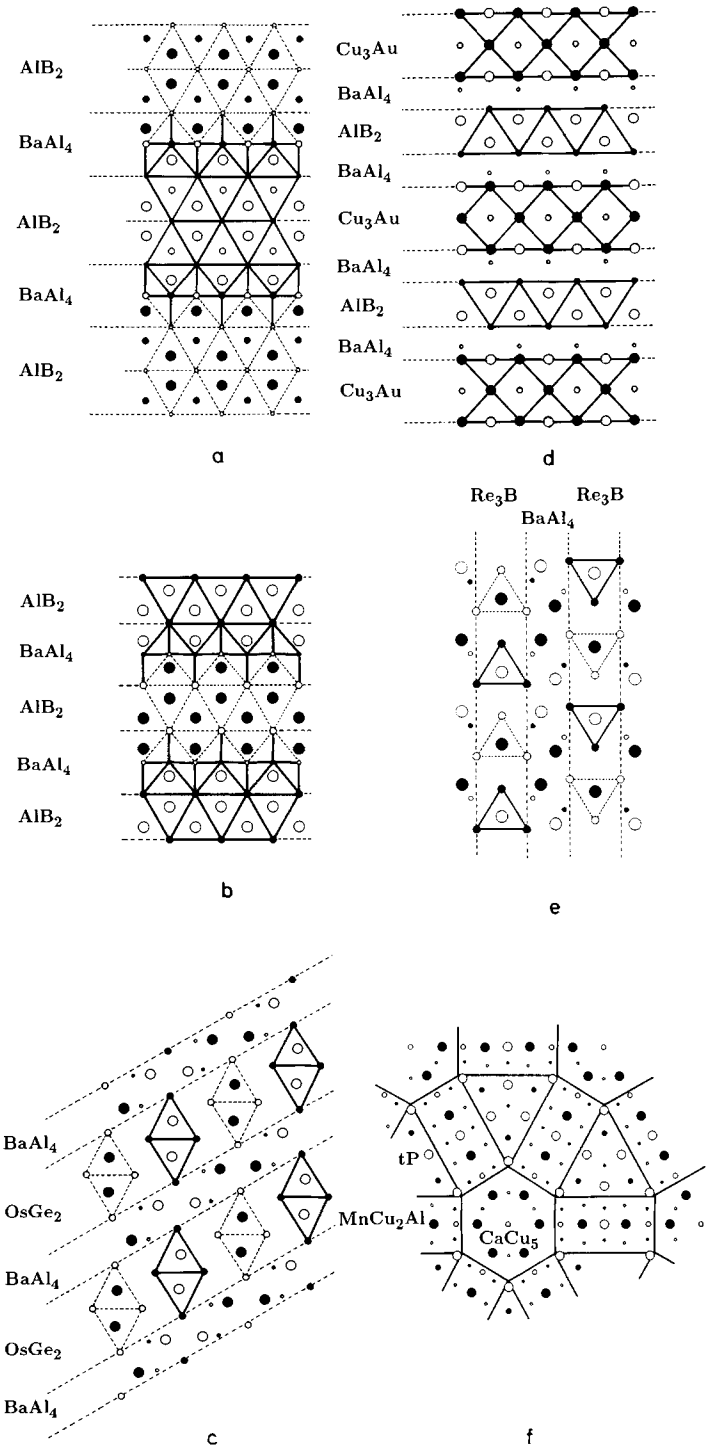

Fig. 15. Examples of chemical twinning [163, 164]. Compounds and structure types of the blocks making up the structure: a) $Ca_3Rh_4Ge_4$ and b) $CeNiSi_2$, respectively, consisting of $BaAl_4$ and AlB_2 blocks; c) $ScCoSi_2$, consisting of $BaAl_4$ and $OsGe_2$ blocks; d) $Ca_3Co_2Sn_7$ consisting of $BaAl_4$ and Cu_3Au blocks; e) $Sc_3Co_2Si_3$ consisting of $BaAl_4$ and Re_3B blocks; f) $Y_{13}Pd_{40}Sn_{31}$ cyclically consisting of $CaCu_5$, $MnCu_2Al$ (Heusler phase [199]), and primitive tetragonal (tP) blocks.

[*] The A_6B_7 variant Cs_6K_7 of the Laves phase $MgCu_2$ also belongs to this family of structures (see Section 6.3).

ing charge transfer. *R. Hoffmann* et al. have recently described similar cases of pure variants of the $ThCr_2Si$ type.[167, 168]

Further examples are shown in Figure 15. In a remarkable manner whole blocks of simple structures are used as building elements for complex arrangements. The connection with inner surfaces as boundary surfaces between the individual structural blocks also becomes clear.

Can we go any further at this point? Do structures not arising from translationally symmetrical layer formation and multiple twinning in accordance with a given point symmetry exist? The answer is yes. Why should interpenetration structures not exist, in which one-, two-, or three-dimensional partial structures interpenetrate without intersecting one another, roughly like the strands of a rope or the links of a chain, with intermediate curved boundary surfaces. These boundary surfaces are once again the periodic nodal surfaces described in Section 6.1.

At this point, a new challenge for the theoretical methods arises: If clusters, chains, and frameworks are relatively stable units, then they must have unfavorable electronic surface states. These should essentially be the energetically unfavorable orbitals, corresponding to the HOMOs and LUMOs in molecules. Will it now be possible to describe theoretically the building of complex structures with two approximations? One of these must determine the chemical bonding in the actual interior of the partial structures, while the other must consider the chemical bonding at the surfaces by means of appropriate frontier orbitals (i.e., according to *Hoffmann*[129]). Such an incremental approach would have great advantage over any total calculation of the band structure, first because it could greatly reduce the amount of calculation needed, and second because the general building principles of structures would be taken into account. Preliminary approaches of this kind have been used in recent theoretical treatments of structures.

6.3. Are Intermetallic Phases Electrides?

A few years ago *von Schnering* himself used the term electride for a metal in connection with quantum-mechanical calculations on a high-pressure modification of cesium, namely, Cs IV.[156, 173] The reason for this was that in Cs IV the 6s electrons are "compressed" into free d states. These d states have their highest probability at the centers of trigonal prisms in a sixfold coordination of the neighboring Cs cores. In a structure-chemical sense the electrons behave like anions.[*]

In this sense the existing knowledge of structural chemistry could perhaps be useful in locating favored electron spaces. Could anion distributions in ionic structures give, for instance, indications of the electron density in structurally related intermetallic phases? Only to a limited extent, of course; since anions cannot be orthogonal to one another, they cannot avoid mutual repulsion in this way. However, they are affected by repulsions similar to those between electrons. They may also be subject to a directional dependence if particular bond angles are favored by the covalent component of the bonding. Ligand or crystal field theory provides the bridging link that describes the interaction between anionic ligands and the electrons remaining on the central atom. It also gives very clear explanations for the distribution of the valence electrons in multinuclear clusters such as those in $MoCl_2$[158] and Nb_3Cl_7[159]. In $MoCl_2$ ($\triangleq Mo_6Cl_8Cl_4$), the Mo_6 octahedron is coordinated by eight $Cl^{\ominus}$ ions, which occupy μ_3 positions over the faces, leaving the 12 edges (= 24 skeletal electrons) as the only remaining available electron spaces. In contrast, the Nb_6 octahedron in Nb_3Cl_7 ($\triangleq [Nb_6Cl_{12}]Cl_2$) is surrounded by $Cl^{\ominus}$ ions over the 12 edges, leaving space for at most eight electron pairs over the faces of the octahedron (= 16 skeletal electrons).[160] Can insulators and semiconductors therefore serve as models for possible electron distributions in structurally related intermetallic phases?

"Oxides as stuffed alloys"—the concept of the structures of oxides as stuffed intermetallic compounds is discussed in an article by *M. O'Keeffe* and *B. G. Hyde* in which the authors present a number of structural relationships between the two classes of compounds.[161] The basis of this relationship is the fact that the pure cation distribution in oxides is often isotypic with the complex structure of an intermetallic phase. Can we invert this concept: "intermetallic phases as electrides"? It is hardly surprising when electronegative ligands occupy precisely those positions in a structure which are also the preferred locations of electrons. In other words, could the electrons find good residence regions at those points in the structure where the favored anion positions are found?

Agreement of the number of oxygen atoms in oxides AB_xO_y with the number of valence electrons in the corresponding intermetallic phases AB_x is not surprising because the cations must provide one electron pair per $O^{2\ominus}$ ion. The structural correlations are nevertheless striking, since there is no reason to form the same or similar AB_x pattern in both cases, unless the distributions of the negative particles ($O^{2\ominus}$ in AB_xO_y and $(e)_2$ in AB_x structures) are similar.

It has long been known for instance, that Si atoms in α-Si (diamond structure) and those in β-cristobalite exhibit isotypic structures and partial structures. Inserting an oxygen atom in the middle of each Si–Si bond of α-Si gives, with a corresponding increase in volume, the cristobalite structure (d(Si-Si, α-Si) = 236 pm, d(Si-O-Si, β-cristobalite) = 340 pm). A similar relationship exists between the structure of Cu and that of cuprite Cu_2O, a doubly interpenetrating β-cristobalite structure.[25]

There is of course a series of elements with different electron counts and, therefore, differing electron distributions, but *O'Keeffe* and *Hyde* have also given a number of different examples for stuffing the Cu structure, namely, Cu_2O, MgO, Cu_3O_4, Y_2O_3, and ThO_2. It is not difficult to find metals with the Cu structure and a number of anions corresponding to the number of electrons.

Another example is the cubic Laves phase $MgCu_2$. In its variant $CaAl_2$, eight valence electrons per formula unit are present. The corresponding oxide $MgAl_2O_4$ has the spinel structure, in which the Mg and Al atoms, as partial structure, form the structure of the Laves phase. The oxygen atoms form an fcc arrangement in spinel. This might not be a bad correlation structure for the electrons in $CaAl_2$ according to

[*] This conjecture had been formulated before the result of the quantum-mechanical treatment was known.

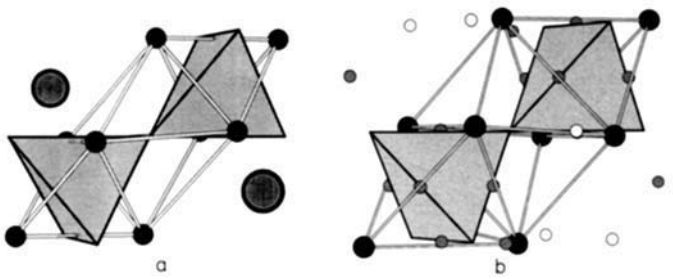

Fig. 16. Comparison of the spinel and VAl_{10} structures: a) An octahedral hole (open framework) and two tetrahedral holes (shaded) in spinel ($MgAl_2O_4$; O atoms, solid circles). In the cubic Laves phase $MgCu_2$, the Mg atoms occupy tetrahedral and the Cu atoms octahedral holes (vertices of the shaded tetrahedra). b) Similar section of the VAl_{10} structure (small circles: Al atoms, open and hatched circles indicate different crystallographic positions; V atoms center the octahedra (open sticks) ≅ vertices of the shaded Al tetrahedra). The solid circles correspond to the O positions in (a) and are not occupied by atoms in VAl_{10}.

Table 4. Comparison of the structures of intermetallic compounds and oxides as well as of valence electron pairs and oxide anions. The numbers of valence electrons given can vary because the number of sterically active pairs is not known before hand.

Structure type	Intermetallic phase/metal	Filling variant	Electron pairs per formula unit	Anions formula unit
Cu	Cu	Cu_2O	0.5	0.5
	Cu	MgO	0.5	1
	$CaAl_2$	Cu_3O_4	4.0	4
	Al_2	Y_2O_3	3.0	3
	Pb	ThO_2, CaF_2	2.0	2
Cu_3Au	Cu_3Au	$TlPd_3O_4$	2.0–4.5	4
CuPt	CuPt	$NaFeO_2$	1.5–2.0	2
$MoPt_2$	$MoPt_2$	Li_2CuO_2	2.0	2
WAl_5	WAl_5	Li_5ReO_6	7.5–10.5	6
$TiAl_3$	$TiAl_3$	Na_3PaF_8	6.5	8
Mg	Mg	ZnO	1.0	1
	Sc_2	La_2O_3	3.0	3
	Re	YF_3	3.5	3
Sm	Sm_3	Th_3N_4	4.5	4
$BaPb_3$	$BaPb_3$	Ca_3SiO_5	4.0–7.0	5
Ni_3Sn	Ni_3Sn	Li_3PO_4	4.0–5.0	4
W	W	χ-La_2O_3	3.0	3
β-Hg	β-Hg	TiO_2	1.0	2
NaTl	NaTl	$KFeO_2$	2.0	2
CuZn	$(CuZn)_2$	$Ca_2Fe_2O_5$	3.0–4.0	5
$MoSi_2$	$MoSi_2$	Sr_2TiO_4	2.0	2
Fe_3Al	Fe_3Al	BaW_2O_6	4.5–6.0	6
UCo	UCo	$K_2Pb_2O_3$	3.0	3
Cu_2MnAl	Cu_2MnAl	K_2NaAlF_6	3.5–5.0	6
$MgCu_2$	$CaAl_2$	Mg_2AlO_4	4.0	4
CrB	CrB	β-Ga_2O_3	3.0	3
FeB	FeB	$BaSO_4$	3.0	4
Mn_5Si_3		$Ca_5P_3O_{12}OH$	11	13
NiAs	NiAs	$BaNiO_3$	3.0–3.5	3
MnP	MnP	$CuSO_4$	3.0–4.0	4
A_2B_5	Mg_5Ga_2	$Na_5Zr_2F_{13}$	8.0	13
Th_3P_4	Th_3P_4	$Bu_4Si_3O_{12}$	12.0–16.0	12
W_2CoB_2	W_2CoB_2	$Mg_3(BO_3)_2$	6.0	6
U_3Si_2	U_3Si_2	$CaZnSi_2O_7$	8.0	7
$PbCl_2$	Ni_2Si	Ca_2SiO_4	4.0	4
FeS_2	FeS_2	ZrP_2O_7	7.0	7
SiP_2	SiP_2	SiP_2O_7	7.0	7
$CuAl_2$	$CaAl_2$	$Ca_2CO_3F_2$	3.5–4.0	5
Cr_3Si	Cr_3Si	$NaPt_3O_4$	4.0–5.0	4
Re_3B	Re_3B	Fe_3BO_6	3.0–5.0	6
$PtPb_4$	$PtPb_4$	$BaMn_4O_8$	5.0–9.0	8
Th_3Pd_5	Th_3Pd_5	$K_3V_5O_{14}$	8.0–11.0	14
diamond	Si, Ge, Sn	SiO_2 (cristobalite)	2.0	2
γ-Ge	γ-Ge	SiO_2 (keatite)	2.0	2
AlP	AlP	$AlPO_4$	4.0	4
LiAlSi	LiAlSi	$NaAlSiO_4$	4.0	4
LiGaGe	LiGaGe	$KAlSiO_4$	4.0	4
CrB_4	CrB_4	$CaAl_4Si_2O_8$	7.0–7.5	8

Schubert. However, this would require that the electrons be present as pairs. In the local picture there are four bonding skeletal electron pairs per Al_4 tetrahedron which can be combined to hybrids with bonding interactions over the four faces. The $O^{2\ominus}$ ions in the spinel structure are found precisely at these positions and thus form an electrostatically favorable (distorted) hetercubane Al_4O_4 (Fig. 16a). This coincidence may also be purely accidental; in all stuffing variants of the $MgCu_2$ structures, however, the positions of the $O^{2\ominus}$ ions or of the bonding electrons of the Al_4 tetrahedron are not occupied by the additional atoms. These regions are apparently reserved for the skeletal electrons.

The structure of the cubic Laves phase $MgCu_2$ can also be understood as a bonding model for Zintl phases of the NaTl type. In the middle of each bond of the diamondlike partial structure of Tl atoms, $MgCu_2$ has a Cu atom. The Mg atoms are located at the Na positions of NaTl.

In Figures 9a and 9d, two remarkably similar patterns are depicted. The former is the Al_{76} unit with dual inner $(Li,Mg)_{40}$ polyhedra in $LiMgAl_2$, in whose interior an icosahedron and an Edshammar polyhedron exhibit disordered interpenetration.[16, 55] This description could also (approximately) apply for Figure 9d. This is a new ternary oxide, $Bi_{22}Sr_{36}Al_{48}O_{141}$[182] (only the cation positions are shown!). One can find many correlations of this type (cf. Table 4), even though these were collected according to other criteria,[161] and on closer examination even more will be found. However, the stage of qualitative correlation will only be overcome through quantitative experimental and theoretical investigations.

7. Summary and Future Prospects

The family of intermetallic phases is an exciting class of chemical compounds with a wealth of geometric forms and chemical bonding. New concepts and methods make tangible their electronic structures even in the chemist's language.

The chemist is used to "seeing the chemical bonding". A pure ensemble of points representing the atomic positions, as given by the structure determination, will inevitably result in his drawing in lines. But which lines are superior to other connections? Which are important?[*] Through the spectacles of individual authors (e.g., von Schnering's cluster spectacles[4]) many different aggregations have been revealed in one and the same structure. In some cases, arrangements and correlations are found which had already been surmised in the early days of structural chemistry.[**] Recently, the theoretical methods have, with good approaches and results, made inroads into the problems of phase stabilities and phase diagrams of intermetallic phases. With the pseudopotential theory and COOP[8] we have the means to analyze locally even slight differences in chemical bonding and thereby calculate the strength of our auxiliary lines in the structural picture. The pseudopotential theory makes it possible to weight the relative importance of the interatomic interac-

[*] "Nothing but the bonds are shown here, and no longer the atoms!" (*H. G. von Schnering* in a lecture on the occasion of the 50th anniversary of *E. Zintl*'s death).

[**] "As an older person, it is easy for me to admit that there are even older persons who also have had good ideas" (*H. G. von Schnering*).

tions by means of the pair correlation function $\Phi(R)$. $\Phi(R)$ is ideally suited to calculating nearest neighbor diagrams and determining the dominant correlations. A more precise analysis of these diagrams would seem to be of interest from the viewpoint of structural chemistry.

However, it seems to me that too little attention has been paid to the local, or at least semilocal, aspect of the chemical bonding. At a time of an enthusiastic "clustering" of chemistry, accompanied by the continual discovery of magic numbers of electrons and in which the universal character of chemical bonding principles is expanding to cover all classes of chemical substances, *Dalton* appears once again to have won territory from the regime of *Berthollet*. The experimental chemist is, in any case, like the first pioneer in a new land. His results provide new impulses for changes in and improvement of the theory. It is to be hoped that the experimental chemists and the theoreticians find ever more common ground—at least the omens for this are good. It is certain that in the field of intermetallic phases, deeper knowledge can only be attained through the interaction of both of them.

I wish to thank my co-workers for their help and advice, and for energetically making up for miscellaneous research opportunities that were unavailable during the move to Zürich. Special thanks is owed to my family for their patience and support.

Received: February 4, 1991 [A 823 IE]
German version: *Angew. Chem. 103* (1991) 806

[1] L. Gmelin: *Handbuch der theoretischen Chemie*, F. Varrentrapp, Frankfurt am Main 1817, reprint: Springer, Berlin 1988.
[2] J. H. Westbrook, *Metall. Trans. A 8* (1977) 1327.
[3] Basic contributions: E. Zintl, G. Brauer, *Z. Phys. Chem. B 20* (1933) 245; E. Zintl, *Angew. Chem. 52* (1939) 1; W. Klemm: *FIAT-Review of German Science, Naturforschung and Medizin in Deutschland 1939–1946, Anorganische Chemie Teil IV 26*, p. 103; W. Klemm, E. Hohmann: *Alkalisilizide, Alkaligermanide, ihre Darstellung und einige wichtige Eigenschaften, interner Bericht*, Universität Münster, Januar 1947; recent reviews: H. Schäfer, B. Eisenmann, *Rev. Inorg. Chem. 3* (1981) 29; H. G. von Schnering, *Nova Acta Leopold, n. 264 59* (1985) 165, and references cited therein; H. G. von Schnering in A. L. Rheingold (Ed.): *Homoatomic Rings, Chains and Macromolecules of Main Group Elements*, Elsevier, Amsterdam 1977, Chapter 14; H. G. von Schnering, *Vortr. Rheinisch-Estfäl. Akad. Wiss. Nat.-Ing.-Wirtschaftswiss. 325* (1984) 7; H. Schäfer, *Annu. Rev. Mater. Sci. 15* (1985) 1, and references cited therein.
[4] H. G. von Schnering, *Angew. Chem. 93* (1981) 44; *Angew. Chem. Int. Ed. Engl. 20* (1981) 33, and references cited therein.
[5] The 8 – N rule, in contrast to the octet rule, takes into consideration the number of bonds; see W. Klemm, *Trab. Reun. Int. React. Solidos 3rd 1956 1* (1957) 447; E. Mooser, W. B. Pearson, *Phys. Rev. 101* (1956) 1608; W. Klemm, *Proc. Chem. Soc. London 1959*, 329; E. Mooser, W. B. Pearson, *Prog. Semicond. 5* (1960) 103; E. Busmann, *Z. Anorg. Allg. Chem. 313* (1961) 90; W. Klemm: *Festkörperprobleme*, Vieweg, Braunschweig, 1963; electron counting rules for polyhedra: K. Wade, *Adv. Inorg. Chem. Radiochem. 18* (1976) 1, 67; B. K. Teo, *J. Chem. Soc. Chem. Commun. 1983*, 1362; *Inorg. Chem. 23* (1984) 1251; B. K. Teo, N. J. A. Sloane, *ibid. 24* (1985) 4545; N. J. A. Sloane, B. K. Teo, *J. Chem. Phys. 83* (1985) 6520; B. K. Teo, H. Zhang, *Inorg. Chem. 27* (1988) 414; *Inorg. Chim. Acta 144* (1988) 173; D. M. P. Mingos, J. Hawes, *Struct. Bonding (Berlin) 63* (1985) 1; D. M. P. Mingos, R. L. Johnston, *ibid. 68* (1987) 29; D. M. P. Mingos, L. Zhenyang, *ibid. 71* (1989) 1.
[6] D. M. P. Mingos, *Inorg. Chem. 21* (1982) 464.
[7] R. Ramirez, R. Nesper, H. G. von Schnering, M. C. Böhm, *J. Phys. Chem. Solids 48* (1987) 51.
[8] T. Hughbanks, R. Hoffmann, *J. Am. Chem. Soc. 105* (1983) 3528.
[9] R. Hoffmann: *Solids and Surfaces. A Chemist's View of Bonding in Extended Structures*, VCH Publishers, New York 1989; *Angew. Chem. 99* (1987) 871; *Angew. Chem. Int. Ed. Engl. 26* (1987) 846.
[10] M.-H. Whangbo, R. Hoffmann, R. B. Woodward, *Proc. R. Soc. London A 366* (1979) 23; M.-H. Whangbo, *Acc. Chem. Res. 16* (1983) 95.
[11] V. Heine, D. Weaire, *Solid State Phys. 24* (1970) 247.
[12] J. Hafner: "*From Hamiltonian to Phase Diagrams*", *Solid State Sciences 70*, Springer, Berlin 1987, and references cited therein.
[13] J. K. Burdett, S. Lee, T. J. McLarnan, *J. Am. Chem. Soc. 107* (1985) 3083.
[14] E. Parthé: *Cristallochimie des Strucutres Tétraédriques*, Gordon and Breach, Paris 1972.
[15] R. Nesper, H. G. von Schnering, *TMPM Tschermaks Mineral. Petrogr. Mitt. 32* (1983) 195.
[16] R. Nesper, *Jahrb. Akad. Wiss. Göttingen 1989*, 15.
[17] P. Villars, L. D. Calvert: *Pearson's Handbook of Crystallographic Data for Intermetallic Phases*, American Society for Metals, Metals Park, OH 44073, USA 1985.
[18] T. B. Massalski, J. L. Murray, L. H. Bennett, H. Baker: *Binary Alloy Phase systems*, American Society for Metals, Metals Park, OH 44073, USA 1986.
[19] W. B. Pearson, *J. Less-Common Met. 109* (1985) L 3.
[20] L. Pauling: *The Nature of the Chemical Bond*, Cornell Univerity Press, Ithaca, New York 1960. *Die Natur der chemischen Bindung*, Verlag Chemie, Weinheim 1976.
[21] W. Hume-Rothery, *J. Inst. Met. 35* (1926) 313.
[22] W. Ekman, *Z. Phys. Chem. B 12* (1931) 57.
[23] K. Schubert: *Kristallstrukturen zweikomponentiger Phasen*, Springer, Berlin 1964.
[24] W. B. Pearson: *The Crystal Chemistry and Physics of Metals and Alloys*, Wiley, New York 1972.
[25] A. F. Wells: *Strucutral Inorganic Chemistry*, Clarendon Press, Oxford 1990.
[26] S. Andersson, B. G. Hyde: *Inorganic Crystal Structures*, Wiley, New York 1989.
[27] E. Hellner, *Neues Jahrb. Mineral. Monatsh. 1971*, 227.
[28] M. O'Keeffe, B. G. Hyde, *Philos. Trans. R. Soc. London A 295* (1980) 553.
[29] A. Landé, *Z. Phys. 191* (1920) 1.
[30] J. A. Wasastjerna, *Commentat. Phys.-Math. II* (1924) No. 7, p. 1
[31] V. M. Goldschmidt, *Skr. Nor. Vidensk. Akad. Kl. 1, Mat.-Naturvidensk. Kl. 2* (1926).
[32] V. M. Goldschmidt, *Ber. Dtsch. Chem. Ges. 60* (1927) 1294.
[33] A. Simon, *Angew. Chem. 100* (1988) 164; *Angew. Chem. Int. Ed. Engl. 27* (1988) 159.
[34] T. P. Martin, *Angew. Chem. 98* (1986) 197; *Angew. Chem. Int. Ed. Engl. 25* (1986) 197.
[35] T. P. Martin, *Chem. Phys. Lett. 172* (1990) 209; *ibid. 176* (1991) 343.
[36] J. St. John, A. N. Bloch, *Phys. Rev. Lett. 33* (1974) 1095.
[37] A. Zunger, M. L. Cohen, *Phys. Rev. Lett. 41* (1978) 53.
[38] A. Zunger, *Phys. Rev. B 22* (1980) 5839.
[39] J. C. Phillips, *Solid State Commun. 22* (1977) 549.
[40] J. K. Burdett, G. D. Price, S. L. Price, *Phys. Rev. B 24* (1981) 2903.
[41] J. K. Burdett, *J. Am. Chem. Soc. 102* (1980) 450.
[42] J. K. Burdett, S. Lee, W. C. Sha, *Croat. Chem. Acta 57* (1984) 1193.
[43] J. K. Burdett, *Prog. Solid State Chem. 15* (1984) 173.
[44] J. K. Burdett, *Chem. Rev. 88* (1988) 3.
[45] D. G. Pettifor, *Solid State Commun. 51* (1984) 37.
[46] P. Villars, *J. Less-Common Met. 119* (1986) 175.
[47] P. Villars, K. Girgis, F. Hulliger, *Solid State Commun. 42* (1982) 89.
[48] J. Donohue: *The Structures of the Elements*, Wiley, New York 1972.
[49] X. G. Gong, G. L. Chiarotti, M. Parrinello, E. Tosatti, unpublished.
[50] J.-O. Bovin, *Angew. Chem. 100* (1988) 580; *Angew. Chem. Int. Ed. Engl. 27* (1988) 555.
[51] H. G. von Schnering, R. Nesper, unpublished.
[52] J. S. Kasper, B. W. Roberts, *Phys. Rev. 101* (1956) 537.
[53] P. Schobinger-Papamantellos, P. Fischer, *Naturwissenschaften 57* (1970) 128.
[54] E. Schürmann, *Gießereiforschung 32* (1980) 167.
[55] R. Nesper, *Habilitationsschrift*, Universität Stuttgart 1988.
[56] H. G. von Schnering, unpublished.
[57] A. Simon, H. Borrmann, H. Craubner, *Phosphorus Sulfur 30* (1987) 507.
[58] W. May, *Dissertation*, Universität Münster 1978.
[59] H. G. von Schnering, W. May, T. Chattopadhyay, unpublished.
[60] D. Shechtman, I. Blech, D. Gratias, J. W. Cahn, *Phys. Rev. Lett. 53* (1984) 183.
[61] A. J. Bradley, J. Thewlis, *proc. R. Soc. London A 115* (1927) 25.
[62] O. Greis, *Nachr. Chem. Tech. Lab. 38* (1990) 1346.
[63] E. Hellner, *Acta Crystallogr. 19* (1965) 703.
[64] R. Nesper, H. G. von Schnering, *J. Solid State Chem. 70* (1987) 48.
[65] R. Nesper, H. G. von Schnering, unpublished.
[66] A. Grüttner, *Dissertation*, Universität Stuttgart 1982.
[67] W. Uhl, M. Layh, A. Vester, J. Wagner, lecture at the *Chemiedozententagung* Duisburg 1991.
[68] E. Schürmann, H.-J. Voss, *Gießereiforschung 33* (1981) 47.
[69] B. Chabot, K. Cenzual, E. Parthé, *Acta Crystallogr. Sect. A 37* (1980) 6.
[70] R. Ramirez, R. Nesper, H. G. von Schnering, M. C. Böhm, *Z. Naturforsch. A 41* (1986) 1267; R. Ramirez, *Dissertation*, Universität Stuttgart 1986.

[71] R. Nesper, unpublished.
[72] G. Mair, *Dissertation*, Universität Stuttgart 1984.
[73] G. Mair, R. Nesper, H.G. von Schnering, *J. Solid State Chem. 75* (1987) 30.
[74] R.G. Ling, C. Belin, *Acta Crystallogr. Sect. B38* (1982) 1101.
[75] U. Frank-Cordier, G. Cordier, H. Schäfer, *Z. Naturforsch. B37* (1982) 119.
[76] M. Tillard-Charbonel, C. Belin, *C. R. Acad. Sci. Ser. 2 306* (1988) 1161.
[77] C. Belin, *Acta Crystallogr. Sect. B36* (1980) 1339.
[78] K. Frank, *Z. Naturforsch. B37* (1982) 119.
[79] G. Bruzzone, *Acta Crystallogr. Sect. B25* (1969) 1206.
[80] G.S. Smith, Q. Johnson, D.H. Wood, *Acta Crystallogr. Sect. B25* (1969) 554.
[81] B. Predel, D.W. Stein, *J. Less-Common Met. 18* (1969) 203.
[82] G.S. Smith, K.F. Mucker, Q. Johnson, D.H. Wood, *Acta Crystallogr. Sect. B25* (1969) 549.
[83] K. Schubert, F. Gauzzi, K. Frank, *Z. Metallkd. 54* (1963) 422.
[84] J.K. Burdett, E. Canadell, *J. Am. Chem. Soc. 112* (1990) 7207.
[85] R. Nesper, *Prog. Solid State Chem. 20* (1990) 1.
[86] R. Nesper, *Angew. Chem. 101* (1989) 99; *Angew. Chem. Int. Ed. Engl. 28* (1989) 58.
[87] K.H. Vogel, *Dissertation*, Universität Stuttgart 1990.
[88] C. Belin, R.G. Ling, *C. R. Seances Acad. Sci. Ser. 2 294* (1982) 1083.
[89] J.V. Florio, R.E. Rundle, A.I. Snow, *Acta Crystallogr. 5* (1952) 449.
[90] F. Laves in J.H. Westbrook (Eds.): Intermetallic Compounds, Wiley, New York 1967 (reprint: Krieger, New York 1977), p. 129.
[91] A. Simon, *Angew. Chem. 95* (1983) 94; *Angew. Chem. Int. Ed. Engl. 22* (1983) 96.
[92] Y. Komura, *Acta Crystallogr. 15* (1962) 770.
[93] Y. Komura, Y. Kitano, *Acta Crystallogr. Sect. B33* (1977) 2496.
[94] Y. Komura, K. Tokunaga, *Acta Crystallogr. Sect. B36* (1980) 1548.
[95] Y. Komura, Y. Kitano, *XVth Congr. Int. Union Crystallogr.* (Bordeaux 1990), Abstr. PS 11.01.09.
[96] R. Nesper, G.J. Miller, unpublished.
[97] R. Haydock, R.L. Johannes, *J. Phys. F5* (1975) 2055.
[98] J. Karle, *Angew. Chem. 98* (1986) 611; *Angew. Chem. Int. Ed. Engl. 25* (1986) 614.
[99] H. Hauptmann, *Angew. Chem. 98* (1986) 601; *Angew. Chem. Int. Ed. Engl. 25* (1986) 603.
[100] S. Samson, *Acta Crystallogr. 19* (1965) 401.
[101] S. Samson, *Nature (London) 195* (1962) 259.
[102] S. Samson, *Acta Crystallogr. 23* (1967) 526.
[103] P.I. Kripyakewitsch: *structuretypen der Intermetallischen Phasen*, Verlag Nauka, Moskau 1977.
[104] B. Mandelbrot: *The Fractal Geometry of Nature*, Freeman, New York 1982.
[105] H. Genz: *Symmetrie – Bauplan der Natur*, Piper 1987.
[106] L. Pauling in M.V. Jarić, D. Gratias (Eds.): *A periodicity and Order*, Academic Press, San Diego 1989, p. 137.
[107] Just like a powder sample, a multiply twinned crystal generates not more and not fewer Bragg reflections than the corresponding single crystal. For quasicrystals one observes a large and increasing number of sharp reflections with increasing resolution. This can only be result of a nontranslational symmetry in three dimensions. However, all these reflections can be indexed on the basis of a six-dimensional reciprocal lattice with six integral numbers. It is not clear yet whether an icosahedral chemical twinning of twelve or more very small crystallites could yield an adequate description of quasicrystalline structures. Translational symmetry, however, would then be lost again.
[108] R. Penrose, *Bull. Inst. Math. Appl. 10* (1974) 266.
[109] A.L. Mackay, *Physica A114* (1982) 609, and references cited therein..
[110] S. Andersson, R. Nesper, H.G. von Schnering: *Seminar über Quasikristalle*, Öland, Schweden 1989, unpublished.
[111] A.L. Mackay, *J. Microsc. (Oxford) 146* (1987) 233.
[112] K.H. Kuo, *J. Less-Common Met. 163* (1990) 9, and references cited therein.
[113] W. Steurer, *Phase Transitions 16/17* (1989) 181.
[114] P. Guyot, M. Audier, R. Lequette, *J. Phys. (Les Ulis Fr.) 47* (1986) C3-389.
[115] E.A. Stern, Y. Ma, C.E. Bouldin, *J. Phys. (Les Ulis Fr.) 47* (1986) C3-371.
[116] J.M. Dubois, C. Janot, M. de Boissieu, *Quasicryst. Mater. Proc. I.L.L./CODEST Workshop 1988*, 97.
[117] R. Belissent, F. Bouree-Vigneron, P. Sainfort, *J. Phys. (Les Ulis Fr.) 47* (1986) C3-361.
[118] P. Sainfort, B. Dubost, *J. Phys. (Les Ulis Fr.), 47* (1986) C3-321.
[119] V.V. Rao, T.R. Anantharaman, *Phase Transitions 16/17* (1989) 609.
[120] L.X. He, X.Z. Li, Z. Zhang, K.H. Kuo, *Phys. Rev. Lett. 61* (1988) 1116.
[121] H. Chen, D. Li, K.H. Kuo, *Phys. Rev. Lett. 60* (1988) 1645.
[122] N. Wang, H. Chen, K.H. Kuo, *Phys. Rev. Lett. 59* (1987) 1010.
[123] A.P. Tsai, A. Inoue, Y. Yokoyama, T. Masumoto, *J. Mater. Sci. Lett. 7* (1988) 322.
[124] L.X. He, Y.K. Wu, K.H. Kuo, *J. Mater. Sci. 7* (1988) 1284.
[125] A.P. Tsai, A. Inoue, T. Masumoto, *Mater. Trans. JIM Jpn 30* (1989) 463.
[126] A.P. Tsai, A. Inoue, Y. Yokoyama, T. Masumoto, *Philos. Mag. Lett. 61* (1990) 9.
[127] C.L. Henley, V. Elser, *Philos. Mag. B53* (1986) L 59.
[128] The Pearson symbolism for the classification of crystal structures uses the three quantities (l, M, n) l denotes the crystal system (c = cubic; h = hexagonal, trigonal; t = tetragonal; o = orthorhombic; m = monoclinic; a = anorthic), M stands for the Bravais type (P = primitive; I = body-centered; F = face-centered; R = rhombohedral; A, B, C = singly face-centered), and *n* is the number of atoms per unit cell.
[129] R. Hoffmann, *Angew. Chem. 94* (1982) 725; *Angew. Chem. Int. Ed. Engl. 21* (1982) 711.
[130] J.B. Hendrickson, *Angew. Chem. 102* (1990) 1328; *Angew. Chem. Int. Ed. Engl. 29* (1990) 1286.
[131] T. Hahn (Ed.): *International Tables of Crystallography, Vol. A*, Reidel, Dordrecht, Holland 1983.
[132] G. Voronoi, *Crelle's Journal 98* (1908) 134, 138.
[133] P.G.L. Dirichlet, *Crelle's Journal 40* (1850) 209.
[134] F.L. Carter, *Acta Crystallogr. 34* (1978) 2962.
[135] R. Nesper, H.G. von Schnering, unpublished.
[136] W. Fischer, E. Koch, *Z. Kristallogr. 153* (1980) 255.
[137] A.D. Becke, K.E. Edgecombe, *J. Chem. Phys. 92* (1990) 5397.
[138] A. Savin, A.D. Becke, J. Flad, R. Nesper, H. Preuss, H.G. von Schnering, *Angew. Chem. 103* (1991) 421; *Angew. Chem. Int. Ed. Engl. 30* (1991) 409.
[139] W.B. Pearson, *Philos./Trans. R. Soc. London 298* (1980) 39.
[140] K. Schubert, *J. Less-Common Met. 18* (1969) 203.
[141] K. Schubert, *MATCH 13* (1982) 75, 113.
[142] K. Schubert, *Z. Kristallogr. 165* (1983) 23.
[143] K. Schubert, *Z. Metallkd. 77* (1986) 721.
[144] K. Schubert, *Z. Metallkd. 80* (1989) 783.
[145] L. Pauling, *Proc. Natl. Akad. Sci. USA 72* (1975) 4200.
[146] L. Pauling, *J. Solid State Chem. 54* (1984) 297.
[147] L. Pauling, Z.S. Herman: *Modelling of Structure and Properties of Molecules*, Horwood, New York 1987, p. 5.
[148] F.L. Carter, *NBS Spec. Publ. 496* (1978) 763 ("A valence bond test for the validity of intermetallic and semiconducting structures").
[149] V. Heine, J. Samson, *J. Phys. F13* (1983) 2155.
[150] A. Bieber, F. Gautier, *Acta Metall. 34* (1986) 2291.
[151] W. Biltz: *Raumchemie der festen Stoffe*, L. Voss, Leipzig 1934.
[152] S.R. Nagel, J. Tauc, *Phys. Rev. Lett. 35* (1975) 380.
[153] V.N. Novikow, *Phys. Lett. A104* (1984) 103.
[154] L. Vegard, *Z. Phys. 5* (1921) 17.
[155] E-an Zen, *Am. Mineral. 41* (1956) 523.
[156] N.E. Christensen, S. Sathpathy, unpublished.
[157] H.G. von Schnering, private communication.
[158] A. Simon, H.G. von Schnering, H. Schäfer, *Z. Anorg. Allg. Chem. 355* (1967) 295.
[159] A. Simon, H.G. von Schnering, H. Wöhrle, H. Schäfer, *Z. Anorg. Allg. Chem. 339* (1965) 155.
[160] H. Nohl, O.K. Andersen, *Supercond. d- f-Band Met. Proc. Conf. 4th 1982*, 161.
[161] M. O'Keeffe, B.G. Hyde, *Struct. Bonding (Berlin) 61* (1985) 77.
[162] S. Andersson, *Angew. Chem. 95* (1983) 67; *Angew. Chem. Int. Ed. Engl. 22* (1983) 69.
[163] E. Parthé, B. Chabot, in K. A. Gschneidner, Jr., L. Eyring (Eds.): *Handbook on the Physics and Chemistry of Rare Earths, Vol. 6*, North-Holland, Amsterdam 1984, p. 113.
[164] K. Cenzual, E. Parthé, *Acta Crystallogr. Sect. C40* (1984) 1127.
[165] E. Parthé, B. Chabot, K. Cenzual, *Chimia 39* (1985) 164.
[166] E. Parthé: *Elements of Inorganic Structural Chemistry*, Pöge, Leipzig 1990.
[167] R. Hoffmann, C. Zheng, *J. Phys. Chem. 89* (1985) 4175.
[168] C. Zheng, R. Hoffmann, *Z. Naturforsch. B41* (1986) 292.
[169] K.R. Andress, E. Albertini, *Z. Metallkd. 27* (1935) 126.
[170] Z. Ban, M. Sikirica, *Acta Crystallogr. 18* (1965) 594.
[171] W. Assmus, M. Herrmann, U. Rauchschwalbe, S. Regel, W. Lieke, H. Spille, S. Horn, G. Weber, F. Steglich, G. Cordier, *Phys. Rev. Lett. 52* (1984) 469.
[172] A. Mewis, *Z. Naturforsch. B35* (1980) 141.
[173] H.G. von Schnering, R. Nesper, *Angew. Chem. 99* (1987) 1097; *Angew. Chem. Int. Ed. Engl. 26* (1987) 1059.
[174] R. Nesper, H.G. von Schnering, unpublished.
[175] F. Bertaut, *J. Phys. Radium 13* (1952) 499.
[176] F. Bertaut, *J. Phys. Chem. Solids 39* (1978) 97.
[177] J.H. Westbrook (Ed.): *Intermetallic Compounds*, Wiley, New York 1967; reprint: Krieger, New York 1977.
[178] A.F. Westgren, *Angew. Chem. 45* (1932) 33.
[179] W. Hume-Rothery, *J. Inst. Met. 35* (1926) 295, 303.
[180] K. Kisho, J.O. Brittain, *J. Phys. Chem. Solids 40* (1979) 933.
[181] K.-F. Tebbe, H.G. von Schnering, B. Rüter, G. Rabeneck, *Z. Naturforsch. B28* (1973) 600.
[182] A. Popp, H.G. von Schnering, *Jahresb. Max-Planck-Inst. Festkörperforschung 1989*, I-88; A. Popp, *Dissertation*, Universität Stuttgart 1990.

[183] W. Tremel, R. Hoffmann, *J. Am. Chem. Soc. 109* (1987) 124.
[184] O. K. Andersen, O. Jepsen, D. Glötzel, „Highlights in Condensed Matter Theory", *Proc. Int. Sch. Phys. Enrico Fermi 89th 1985* (1985) 59.
[185] N. E. Christensen, *Phys. Rev. B32* (1985) 6145.
[186] N. E. Christensen, *Phys. Rev. B32* (1985) 207.
[187] F. Haber, *Verh. Dtsch. Phys. Ges. 13* (1911) 1117, 1128.
[188] E. Wigner, F. Seitz, *Phys. Rev. 43* (1933) 804.
[189] E. D. Levine, E. J. Rapperport, *Trans. Metalll. Soc. AIME 227* (1963) 1204.
[190] E. Schürmann, H.-J. Voss, *Gießereiforschung 33* (1981) 47.
[191] B. Predel, K. Hülse, *Z. Metallkd. 69* (1978) 690.
[192] E. Schürmann, *Gießereiforschung 29* (1977) 107.
[193] C. Suryanarayana, S. K. Tiwari, T. R. Anantharaman, *Z. Metallkd. 69* (1978) 155.
[194] K. Taketoshi, *Jpn. J. Appl. Phys. 10* (1971) 1311.
[195] G. Bergmann, J. L. T. Waugh, L. Pauling, *Acta Crystallogr. 10* (1957) 254.
[196] S. Samson, K. Gordon, *Acta Crystallogr. Sect. B24* (1968) 1004.
[197] K. Frank, K. Schubert, *J. Less-Common Met. 20* (1970) 215.
[198] K. Schubert, K. Frank, R. Gohle, A. Maldonado, H. G. Meissner, A. Raman, W. Rossteutscher, *Naturwissenschaften 50* (1963) 41.
[199] F. Heusler, *Verh. Dtsch. Phys. Ges. 5* (1903) 219; *Angew. Chem. 17* (1904) 260.

Between Stars and Metals: Phosphorus Monoxide, PO

By *Wolfgang A. Herrmann**

Sodium nitroprusside,[1a] red or black Roussin salt[1b]—this is how the beginning student encounters nitrogen monoxide as complex ligand in his basic labcourse training, whilst his more advanced fellow student has to know about "π-acid ligands" in organometallic complexes such as **1**–**3**.[2, 3]

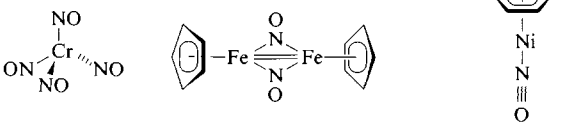

1 **2** **3**

The old "*Emeléus and Andersen*" (first published in 1940) already enthused about the great future of nitrosyl-complex compounds.[4] And, indeed, this area of chemistry has impressively developed parallel to the metal carbonyl research initiated by *Hieber* and his school in Munich.[5] Common features establish the isovalent relationship between carbon monoxide and the nitrosyl cation ("nitrosonium" ion), as manifested in stable salts such as [NO] [BF_4]:

1) CO and (to an even greater extent) $NO^{\oplus}$ act as π-acceptor ligands *par excellence* towards low-valent metals. The NO valence vibration frequencies decrease more markedly (300–500 cm^{-1}) than those of CO (100–300 cm^{-1}) upon complexation with metals.

2) CO and $NO^{\oplus}$ are normally two-electron ligands with linear M–C–O and M–N–O atomic sequences of similar dimensions. Accordingly, isoelectronic series of complexes exist, e.g. in the case of tetrahedrally configurated complexes of the type $[M(CO)_n(NO)_{4-n}]$ (n = 0–4) (Table 1), within

Table 1. Melting points [°C] and NO vibration frequencies [cm^{-1}] of an isovalent electronic series of CO/NO-metal complexes.

	$[Cr(NO)_4]$	$[Mn(CO)(NO)_3]$	$[Fe(CO)_2(NO)_2]$	$[Co(CO)_3NO]$	$[Ni(CO)_4]$
M.p.	39	27	18	−1	−19
ν(NO)	1721	1823, 1734	1810, 1766	1806	–

which there is a regular gradation of properties. The "nitrosyl shift rule" formulated by *Seel* in the early years of this chemistry (1942) groups together complexes of this type[3a] and enables a certain degree of reaction designing. μ_2- (cf. **2**) and μ_3-coordination are known for the nitrosyl ligand, but occur more rarily than in the case of carbon monoxide. (Neutral NO is a three-electron ligand.)

3) In contrast to carbon monoxide, there are also complexes with bent M–N–O arrangement (one-electron ligand), namely in the sense of the isomeric equilibrium **A** (linear) ↔ **B** (bent).

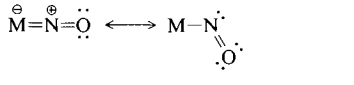

A; d^n-M^z/$[NO]^{\oplus}$ **B**; d^{n-2}-M^{z+2}/$[NO]^{\ominus}$

An example for arrangement **B** is the square-pyramidally structured cation $[\{P(C_6H_5)_3\}_2Ir(CO)Cl(NO)]^{\oplus}$.[6] Arrangement **B** occurs when the π* acceptor orbital of the $NO^{\oplus}$ ligand is energetically lowered to such an extent relative to the metal d-orbitals that a d-electron pair can be transferred to the ligand and become stereochemically active. **A** and **B** are not reliably distinguishable by IR spectroscopy.

4) NO ligands are far less readily displaced from metals than carbon monoxide. Most NO reactions are accompanied by redox processes, which complicate this chemistry considerably.

Applications of nitrosyl complexes are first met with only recently in catalysis, e.g. in olefin metathesis with the system $[Mo(NO)_2Cl_2\{P(C_6H_5)_3\}_2]/[(C_2H_5)AlCl_2]$, though the importance of the respective class of substances here lags far behind that of the metal carbonyls. Of academic interest are the novel thionitrosyl (NS) complexes, which are best prepared from trithiazyl trichloride (*cyclo*-$N_3S_3Cl_3$) or thionitrosyl salts [NS] [Y].[7]

This brief survey of the nitrosyl-metal complexes should highlight possible perspectives which are conceivable in the case of the likewise recently initiated class of *phosphorus monoxide* complexes: *Otto J. Scherer* at al. report a first metal complex of the PO molecule, hitherto only detected (spectroscopically) "between the stars" i.e. in interstellar space (see communication on p. 852). Oxidation of the square pyramidal $[WNi_2P_2]$complex **4** to give the (structurally analogous) $[WNi_2(P{=}O)_2]$ derivative **5** of the *nido* type is elegantly achieved in 60% yield by means of bis(trimethylsilyl)-

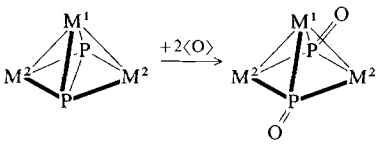

4 $M^1 = W(CO)_4$ **5**
$M^2 = (\eta^5\text{-}C_5H_5)Ni$

peroxide.[8] The P–P bond is cleaved, and both PO groups assume bridge positions (μ_3-coordination). The P–O distances (146–148 pm) are very long. However, they do not deviate from those calculated and experimentally found for *free* PO. The IR data are surprising: ν(PO) = 1218 cm^{-1} (free) and 1260 cm^{-1} in the complex **5**. For CO and NO, as well as the homologous ligands CS and NS, respectively,

[*] Prof. Dr. W. A. Herrmann
Anorganisch-chemisches Institut der Technischen Universität München
Lichtenbergstrasse 4, W-8046 Garching (FRG)

the differences are greater, especially in the bridged form: $\nu(NO^{\oplus}) = 2376\ cm^{-1}$; $\nu(NO) = 2250\ cm^{-1}$ (free), ca. $1350\ cm^{-1}$ in μ_3-coordination.

A comparison with the higher homologues of carbon monoxide—thio-, seleno-, and tellurocarbonyl[9]—reveals that the significance of the IR data decreases in the quoted sequence. Nevertheless, in the case of bridge coordination, the differences between the free ligands, as far as data are available, and their metal-fixed form remain the same (Table 2). One must, of course, be particularly careful when

Table 2. Characteristic vibration frequencies [cm^{-1}] and bond lengths [pm] of metal complexes of higher chalcogen derivatives of carbon monoxide [a].

	M–CO	M–CS	M–CSe	M–CTe
ν(CX)	2000–1800	1450–1150	1130–1060	ca. 1050
d(CX)	113–118	143–178	ca. 160	190–195
d(MC)	170–190	ca. 188	ca. 191	ca. 180

[a] X = chalcogen atom. Data for neutral metal complexes (η^1-coordination), the values of the lowest series apply for M = Os.

interpreting the IR data when vibrational couplings can be expected due to more complex structures. However, the bonding of all these diatomic ligands is weakened upon metal complexation. The readiness of the ligands to undergo additional intermolecular metal complexation increases with increasing basicity (O < S < Se < Te). The *trans* influence increases in the series CO < CS < CSe < CTe.[9c] CS and NS are better σ-donors and stronger π-acceptors than their oxygen analogues, and they adapt far better than the latter to the conditions of the complex fragment.

And what about PO's neighbors? Whereas SiO and $BO^{\ominus}$—both carbonyl analogues?—have thus far defied all attempts at their metal complexation, SO complexes are very well known.[10] Bridge-bonding sulfur monoxide is encountered in the complexes **6** (from thiirane 1-oxide) and **7** (from

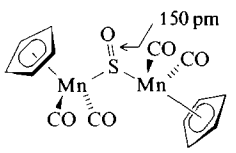

6

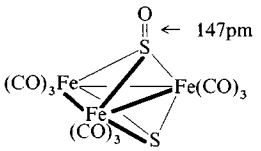

7

the μ_3-disulfido complex with H_2O_2), in which SO acts as four-electron ligand. The Lewis basicity of P_x- and S_x-ligand ensembles attached to the metal facilitates their comparatively easy oxidation, whereas nitrido- and carbido-complexes are mostly inert in this respect, even though the N and C atoms, respectively, are not shielded. As shown by IR and X-ray diffraction data, the SO ligand has a weaker bond in the complexed state than in the free state, irrespective of its type of coordination: $\nu(SO) = 1137\ cm^{-1}$ (free), 1050–$1130\ cm^{-1}$ (complexed).[10] A frontier orbital situation similar to that in CO is found for SO, only that the two additional electrons occupy the antibonding 3π-orbital and enforce bending of the atomic sequence MSO towards themselves (η^1-coordination, e.g. $[IrCl(SO)\{P(i\text{-}C_3H_7)_3\}_2]$). Ready cleavage ($\rightarrow$ SO) and oxidation ($\rightarrow L_xM\text{-}SO_2$) appear typical for terminally bound sulfur monoxide, which indeed disproportionates extremely rapidly according to Equation (a).

$$3SO \longrightarrow S_2O + SO_2 \qquad (a)$$

If one considers *Scherer*'s PO complex **5** in the context of the nearest relatives (NO, NS, SO) a wide variety of structures can be expected. Despite little prospects of a terminally metal-bound phosphorus monoxide, an interesting synthetic chemistry is expected to develop by way of PO functionalization reactions. If M^1 in **5** is replaced by a less reactive group (isolobal principle!), then, for example, the reduction P=O → P or olefinations P=O → P=CH_2 (with Tebbe reagent?) would be conceivable. Also cluster couplings via P–P bonds (with low-valent titanium or samarium reagents) and "metathesis" reactions in the sense P=O → P=S can be envisaged.

German version: *Angew. Chem. 103* (1991) 835

[1] To remind the reader: a) "disodium nitrosylprussiate" = $Na_2[Fe(NO)(CN)_5]$, isoelectronic with $Na_4[Fe(CN)_6]$ and $Na_3[Fe(CO)(CN)_5]$; b) preparation by passage of nitrogen monoxide through an aqueous suspension of iron(II) sulfide in dilute alkali-metal sulfide; $M_2[Fe_2(NO)_4S_2]$ (red) and $M[Fe_4(NO)_7S_4]$ (black).

[2] Reviews: a) B. F. G. Johnson, J. A. McCleverty, *Prog. Inorg. Chem. 7* (1966) 277; b) W. P. Griffith, *Adv. Organomet. Chem. 7* (1968) 211; c) R. Eisenberg, C. D. Meyer, *Acc. Chem. Res. 8* (1975) 26; d) D. M. P. Mingos, D. J. Sherman, *Adv. Inorg. Chem. 34* (1989) 293.

[3] a) The homoleptic $[Cr(NO)_4]$ **1** was first described in 1972: M. Herberhold, A. Razavi, *Angew. Chem. 84* (1972) 1150; *Angew. Chem. Int. Ed. Engl. 11* (1972) 1092; b) **2**: H. Brunner, *J. Organomet. Chem. 14* (1968) 173; J. L. Calderon, S. Fontana, E. Frauendorfer, V. W. Day, D. A. Iske, *ibid. 64* (1974) C16; c) **3**: cf. G. Brauer (Ed.): *Handbuch der Präparativen Anorganischen Chemie, Vol.* 3, 3rd Edit, Enke-Verlag, Stuttgart 1981, p. 1989ff.

[4] H. J. Emeléus, J. S. Andersen: *Ergebnisse und Probleme der modernen Anorganischen Chemie*, Julius Springer, Berlin 1940.

[5] W. A. Herrmann, *J. Organomet. Chem. 383* (1990) 21; cf. also *Chem. Unserer Zeit 22* (1988) 113.

[6] D. J. Hodgson, J. A. Ibers, *Inorg. Chem. 7* (1968) 2349.

[7] M. Herberhold, *Nachr. Chem. Tech. Lab. 29* (1981) 365.

[8] O. J. Scherer, J. Braun, P. Walther, G. Heckmann, G. Wolmershäuser, *Angew. Chem. 103* (1991) 861; *Angew. Chem. Int. Ed. Engl. 30* (1991) 852.

[9] a) I. S. Butler, *Acc. Chem. Res. 10* (1977) 359; b) W. R. Roper, *J. Organomet. Chem. 300* (1986) 167; c) G. R. Clark, K. Marsden, C. E. F. Rickard, W. R. Roper, L. J. Wright, *ibid. 338* (1988) 393; d) review: H. Werner, *Angew. Chem. 102* (1990) 1109; *Angew. Chem. Int. Ed. Engl. 29* (1990) 1077.

[10] a) G. Schmid, G. Ritter, T. Debaerdemaker, *Chem. Ber. 108* (1975) 3008; b) review: W. A. Schenk, *Angew. Chem. 99* (1987) 101; *Angew. Chem. Int. Ed. Engl. 26* (1987) 98; c) A. Neher, I.-P. Lorenz, *ibid. 101* (1989) 1389 and *28* (1989) 1342; d) I.-P. Lorenz, J. Messelhäuser, W. Hiller and K. Haug, *ibid. 97* (1985) 234 and. *24* (1985) 228.

Activation of Methane

By Helmut Schwarz *

The selective functionalization of alkanes[1] has been called "the search for the chemist's Holy Grail" by *Barton*[2] and the most important of all C–H bond activation reactions is the metal-mediated activation of methane. On the one hand, this is due to the great economic interest in the direct transformation of methane to more "valuable" products such as methanol[3] or its oligomerization to higher hydrocarbons (Fischer–Tropsch synthesis[4]). On the other hand, this transformation poses a scientific challenge that has been met piecemeal at best. In recent years, many research groups have attempted to elucidate at least the principal aspects of methane activation and there have been many reports of success.[5] The work discussed here involves reaction of naked transition-metal ions $M^{\oplus}$ or coordinatively unsaturated metal fragments $ML^{\oplus}$ in the gas phase in molecular-beam-type experiments.

Earlier attempts to carry out oxidative additions of CH_4, as shown in Equation (a), failed for the simple reason that the insertion is endothermic for most metal ions $M^{\oplus}$ (M = Sc, Y, lanthanides, U, Ti, V, Nb, Cr, Fe, Co, Rh, Ni, Zn). Only electronically or translationally excited species

$$CH_4 + M^{\oplus} \longrightarrow [H\text{-}M\text{-}CH_3]^{\oplus} \longrightarrow \text{product} \qquad (a)$$

brought about insertion. Moreover, dehydrogenation [Eq. (b)], which proceeds readily for higher alkanes with many $M^{\oplus}$,[6] causes problems in the case of methane, since the reaction is only exothermic for metals with $D^0(M^{\oplus}\text{-}CH_2) \geqq 111$ kcal mol^{-1}. Transition-metal ions $M^{\oplus}$ of the first and second period do not fulfill the prerequisite.[7]

$$CH_4 + M^{\oplus} \longrightarrow [M{=}CH_2]^{\oplus} + H_2 \qquad (b)$$

Dehydrogenation does take place for metal ions of the third row, as shown by experiments with $Ta^{\oplus}$[8] and $Os^{\oplus}$.[9] In a recent paper,[10] *Irikura* and *Beauchamp* not only reported the reaction of all 5d elements from $Hf^{\oplus}$ to $Au^{\oplus}$ with CH_4,[11] but also showed that, for some metals, slow ligand condensation reactions, in which several CH_2 units are linked [Eq. (c)], follow the rapid dehydrogenation. For example, $W^{\oplus}$ reacts with CH_4 to give ions as large as $WC_8H_{16}^{\oplus}$ (Fig. 1 shows the first condensation steps). The exothermicity of the dehydrogenative CH_2 coupling [Eq. (c)] implies

$$M^{\oplus} + n\,CH_4 \longrightarrow [MC_nH_{2n}]^{\oplus} + n\,H_2 \qquad (c)$$

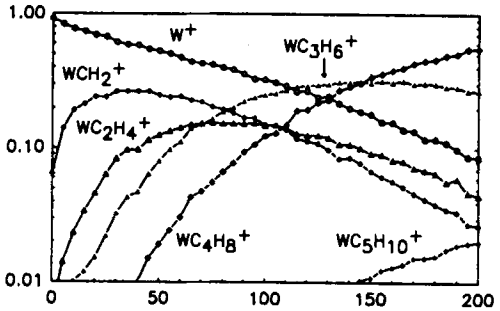

Fig. 1. Reaction of labeled $^{186}W^{\oplus}$ with methane (3.5×10^{-6} Torr). The relative intensity I is plotted against the reaction time t.

unusually strong bonding of the C_nH_{2n} fragment to the metal ion. Thermochemical considerations reveal that, for n = 4, for example, each of the two metal–carbon bonds in the resulting metallacyclopentane has a bond energy of at least 69 kcal mol^{-1}.

Beauchamp's observation may be of fundamental importance for the understanding of elementary processes in C_1 chemistry, since this is the first time that the coupling of CH_2 units, which is so characteristic of Fischer–Tropsch synthesis, does *not* have to take place at several metal centers.

It should be mentioned that doubly charged transition-metal cations $M^{2\oplus}$ (M = Nb, Ta, Zr) are also capable of inducing dehydrogenation and Fischer–Tropsch-like coupling of CH_4 [Eq. (d)],[12] in addition to hydride- and charge-transfer reactions. Owing to competition with hydride and electron transfer [Eqs. (e) and (f)], however, this variant is only of interest in special cases.

$$M^{2\oplus} + CH_4 \longrightarrow [MCH_2]^{2\oplus} \longrightarrow [MC_nH_{2n}]^{2\oplus}, [MC_nH_{2n-2}]^{2\oplus} \qquad (d)$$
(Nb, Ta, $n \leq 6$; Zr, $n \leq 5$)

$$M^{2\oplus} + CH_4 \longrightarrow MH^{\oplus} + CH_3^{\oplus} \qquad (e)$$

$$M^{2\oplus} + CH_4 \longrightarrow M^{\oplus} + CH_4^{\oplus\cdot} \qquad (f)$$

Of particular interest is the direct oxidation of methane to methanol by oxometal fragments [Eq. (g)], which is very important for the mechanism of the σ-metathesis reaction described by Equation (h) and, in the area of enzyme-mediated processes, for the mechanism of methane monooxygenase.[1] The investigation of these processes with isolated metal ions can justifiably be regarded as providing models for the complicated processes of heterogeneous or enzymatic catalysis. If entropic effects are ignored to a first approximation, since

$$[M{=}O]^{\oplus} + CH_4 \longrightarrow M^{\oplus} + CH_3OH \qquad (g)$$
$$(\Delta H_r^{\circ} = D(M^{\oplus}\text{-}O) = -90.0 \text{ kcal mol}^{-1})$$

$$[M{=}O]^{\oplus} + CH_4 \longrightarrow [M{=}CH_2]^{\oplus} + H_2O \qquad (h)$$
$$(\Delta H_r^{\circ} = D(M^{\oplus}\text{-}O) - D(M^{\oplus}\text{-}CH_2) = -6.6 \text{ kcal mol}^{-1})$$

[*] Prof. Dr. H. Schwarz
Institut für Organische Chemie der Technischen Universität
Strasse des 17. Juni 135, W-1000 Berlin 12 (FRG)

they are presumably small for gas-phase reactions, then the reactions described by Equations (g) and (h) will only proceed if they are exothermic.

Straightforward thermochemical considerations lead to the values given below the equations; for example, both processes are favored for those metals whose $D(M^{\oplus}\text{-}O)$ value is relatively small.

Whereas initial attempts to carry out reactions analogous to Equations (g) and (h) failed, the groups of *Beauchamp*[9] and *Schwarz*[14] have recently shown that both $OsO^{\oplus}$ and $FeO^{\oplus}$ [Eq. (i)] are able to activate CH_4. The most recent investigations[15] have provided further evidence on the intermediates involved along the $[Fe,C,H_4,O]^{\oplus}$ hypersurface, for example, $CH_4 \cdot FeO^{\oplus}$, $FeOH^{\oplus} \cdot CH_3$, $CH_3Fe(H)O^{\oplus}$, and $H_2C{=}Fe(H)OH^{\oplus}$.

$$FeO^{\oplus} + CH_4 \xrightarrow{\begin{array}{l}(57\%)\\(2\%)\\(41\%)\end{array}} \begin{array}{l}[FeOH]^{\oplus} + CH_3^{\bullet}\\ [FeCH_2]^{\oplus} + H_2O\\ Fe^{\oplus} + CH_3OH\end{array} \quad (i)$$

Although $Fe^{\oplus}$ was used in equimolar amounts in the experiments described so far [Eq. (i)], the possibility of a *catalytic* activation of CH_4 with $FeO^{\oplus}$ remains, since the $Fe^{\oplus}$ generated in the course of reductive elimination of CH_3OH can be reoxidized with N_2O, for example, and can thereby reenter the cycle (Scheme 1).[16]

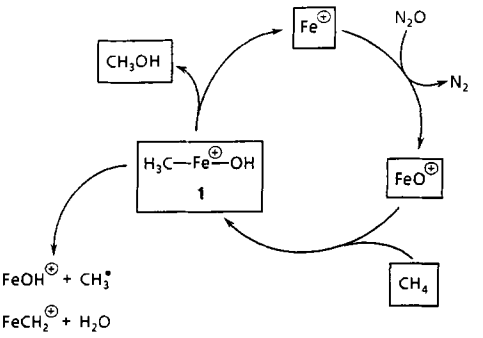

Scheme 1.

Presumably, the metal centers in enzyme-catalyzed and in enzyme-free processes of alkane oxidation are high-valent ionic iron oxides in systems containing iron.[1, 2, 13, 17] The exact oxidation state of iron and the precise composition of the active centers are still matters of speculation. Recently, gas-phase experiments in which the stoichiometry and oxidation states were perfectly controlled showed[18] that the Fe^{IV} oxide $[O{=}Fe{-}OH]^{\oplus}$ is also capable of oxidizing CH_4 [Eq. (j)].

Noteworthy is the finding that $[O{=}Fe{-}OH]^{\oplus}$, a 12-electron complex, yields no products of radical nature, in contrast to $FeO^{\oplus}$ (an 11-electron complex). This result is presumably of importance for understanding the mechanism of enzyme-mediated oxygenations.

$$[O{=}Fe{-}OH]^{\oplus} + CH_4 \xrightarrow{\begin{array}{l}(25\%)\\(10\%)\\(65\%)\end{array}} \begin{array}{l}[FeOCH_3]^{\oplus} + H_2O\\ [HFeOH_2]^{\oplus} + CH_2O\\ [FeOH]^{\oplus} + CH_3OH\end{array} \quad (j)$$

Irikura and *Beauchamp*[19] recently reported on their attempts to generate porphyrin complexes, $[MP]^{\oplus}$, in the gas phase and to use these—after oxidation to the corresponding oxo complexes—as enzyme-like models for the C–H oxygenation mediated, for example, by cytochrome P-450. Although both the preparation of $[MP]^{\oplus}$ and its oxidation to $[Fe(P)OH]^{\oplus}$ were accomplished, $[Fe(P)O]^{\oplus}$ has not yet been synthesized, but perhaps this is only a matter of time.

German version: *Angew. Chem. 103* (1991) 837

[1] a) A. E. Shilov: *Activation of Saturated Hydrocarbons by Transition Metal Complexes*, Reidel, Boston 1984; b) C. L. Hill (Ed.): *Activation and Functionalization of Alkanes*, Wiley Interscience, New York 1989; c) J. A. Davies, P. L. Watson, J. F. Liebman, A. Greenberg: *Selective Hydrocarbon Activation; Principles and Progress*, VCH Publishers, New York 1990.

[2] D. H. R. Barton, *Aldrichimia Acta 23* (1990) 3.

[3] H. D. Gesser, N. R. Hunter, C. B. Prakash, *Chem. Rev. 85* (1985) 235.

[4] R. B. Anderson: *The Fischer-Tropsch Synthesis*, Academic, Orlando 1984.

[5] For other key work, see: a) low-temperature, palladium(II)-mediated oxidation of methane to methanol derivatives: L.-C. Kao, A. C. Hutson, A. Sen, *J. Am. Chem. Soc. 113* (1991) 700; b) molecular-beam experiments on dissociative association of CH_4 on Ni surfaces: S. T. Ceyer, *Science 249* (1990) 133; c) matrix experiments with (1) transition-metal fragments: R. N. Perutz, *Pure Appl. Chem. 62* (1990) 1103 and (2) photochemically excited metal atoms: R. H. Hauge, J. L. Margrave, Z. Kafafi in L. Andrews, M. Moskovits (Eds.): *Chemistry and Physics of Matrix-Isolated Species*, Elsevier, Amsterdam 1989, Chapter 10; d) methane activation by "free" Pt_x clusters (x = 2–5): D. J. Trevor, D. M. Cox, A. Kalder, *J. Am. Chem. Soc. 112* (1990) 3742; e) advances in the controlled doping of traditional catalysts with (1) Cu^{I}/Fe^{III} (to ZnO): Z. Sojka, R. G. Herman, K. Kler, *J. Chem. Soc. Chem. Commun. 1991*, 185 and (2) lanthanide/ruthenium oxide catalysts: A. T. Ashcraft, A. K. Cheetham, J. S. Foord, M. L. H. Green, C. P. Grey, A. J. Murrell, P. D. F. Vernon, *Nature 344* (1990) 319.

[6] Review: K. Eller, H. Schwarz, *Chem. Rev.*, in press.

[7] J. A. Martinho Simoes, J. L. Beauchamp, *Chem. Rev. 90* (1990) 629.

[8] S. W. Buckner, T. J. MacMahon, G. D. Byrd, B. S. Freiser, *Inorg. Chem. 28* (1989) 3511.

[9] K. K. Irikura, J. L. Beauchamp, *J. Am. Chem. Soc. 111* (1989) 75.

[10] K. K. Irikura, J. L. Beauchamp, *J. Am. Chem. Soc. 113* (1991) 2769.

[11] A detailed analysis of the electronic structure of these metal ions and their role in CH_4 activation will appear soon. The promotion and exchange energies, as well as the relative and absolute sizes of the s and d orbitals of $M^{\oplus}$, govern the reactivity: K. K. Irikura, J. L. Beauchamp, *J. Phys. Chem.*, in press.

[12] a) J. R. Gord, B. S. Freiser, S. W. Buckner, *J. Chem. Phys. 91* (1989) 7530; b) T. J. MacMahon, Y. A. Ranasinghe, B. S. Freiser, *J. Phys. Chem.*, in press.

[13] Review: P. A. Frey, *Chem. Rev. 90* (1990) 1343.

[14] D. Schröder, H. Schwarz, *Angew. Chem. 102* (1990) 1468; *Angew. Chem. Int. Ed. Engl. 29* (1990) 1433.

[15] D. Schröder, H. Schwarz, unpublished results.

[16] For the $Fe^{\oplus}$-mediated *catalytic* oxidation of, for example, C_2H_6 with N_2O, see D. Schröder, H. Schwarz, *Angew. Chem. 102* (1990) 1466; *Angew. Chem. Int. Ed. Engl. 29* (1990) 1431.

[17] a) P. R. Ortiz de Montellano (Ed.): *Cytochrome P-450: Structure, Mechanism and Biochemistry*, Plenum, New York 1986; b) D. Mansay, *Pure Appl. Chem. 62* (1990) 741; c) D. H. R. Barton, E. Csuhai, D. Doller, N. Ozbalik, G. Balavoine, *Proc. Natl. Acad. Sci. USA 87* (1990) 3401.

[18] D. Schröder, H. Schwarz, *Angew. Chem.*, in press.

[19] K. K. Irikura, J. L. Beauchamp, *J. Am. Chem. Soc. 113* (1991) 2767.

Light-Directed Parallel Synthesis of Up to 250000 Different Oligopeptides and Oligonucleotides**

By *Günter von Kiederowski**

The development of enzyme inhibitors based on oligopeptides makes it imperative to prepare a daunting number of oligopeptides with different sequences and to test their binding properties in order to find an optimally binding ligand. Even if we restrict ourselves to the twenty naturally occurring amino acids, $20^2 = 400$ dipeptides, $20^3 = 8000$ tripeptides, and in general 20^N oligopeptides of length N are possible. A systematic testing of all sequence alternatives with conventional techniques is already out of the question with tetrapeptides (160000 compounds). Molecular modeling and quantitative structure–activity relationships rule out many sequence alternatives based on a known guide sequence, but for a "rational drug design"[1] in the true sense, a three-dimensional structure of the receptor must be known. The prerequisite for "irrational drug design"[2] (i.e., the filtering out of binding sequencer from the pool of statistical sequences) is the ability to isolate the best ligand in pure form and in high enough quantities for a structure determination—or it must be possible to raise the concentration to the required level. This last criterion restricts irrational drug design largely to biopolymers that can be cloned (e.g., antibodies) or replicated in vitro (nucleic acids). Such attempts to select and amplify biomolecules possessing the desired binding properties have already been honored in a Highlight in this journal.[3]

Recently *Fodor* et al. described a chemical method for irrational drug design.[4] A combination of three processes—solid-phase synthesis, photolithography, and affinity labeling—makes it possible to lay down next to each other up to 250000 different oligopeptides or oligonucleotides per square centimeter on a glass slide and to test their binding to a given receptor molecule. The principle of photolithographic solid-phase synthesis is shown in Figure 1 for the example of the parallel construction of two dipeptides from two amino acids.

The glass surface is first treated with 3-(aminopropyl)triethoxysilane and then the free amino groups, now bound the the glass surface by a C_3 spacer, are protected with a nitroveratryloxycarbonyl (NVOC) group (Step **I**), which can be photochemically removed. On illumination (Step **II**) only those NVOC groups that are not covered by an opaque mask are removed. The irradiated amino groups on the surface (field **A**) are now acylated with the first amino acid, which is protected by NVOC and is activated as its 1-hydroxybenzotriazol (HOBt) ester (Step **III**). Field A is now masked, and field B exposed to light and thereafter acylated with the second amino acid, thus completing the first phase of the synthesis (Step **IV**). Further analogous irradiation and coupling steps construct the dipeptides in the second phase (Step **V**).

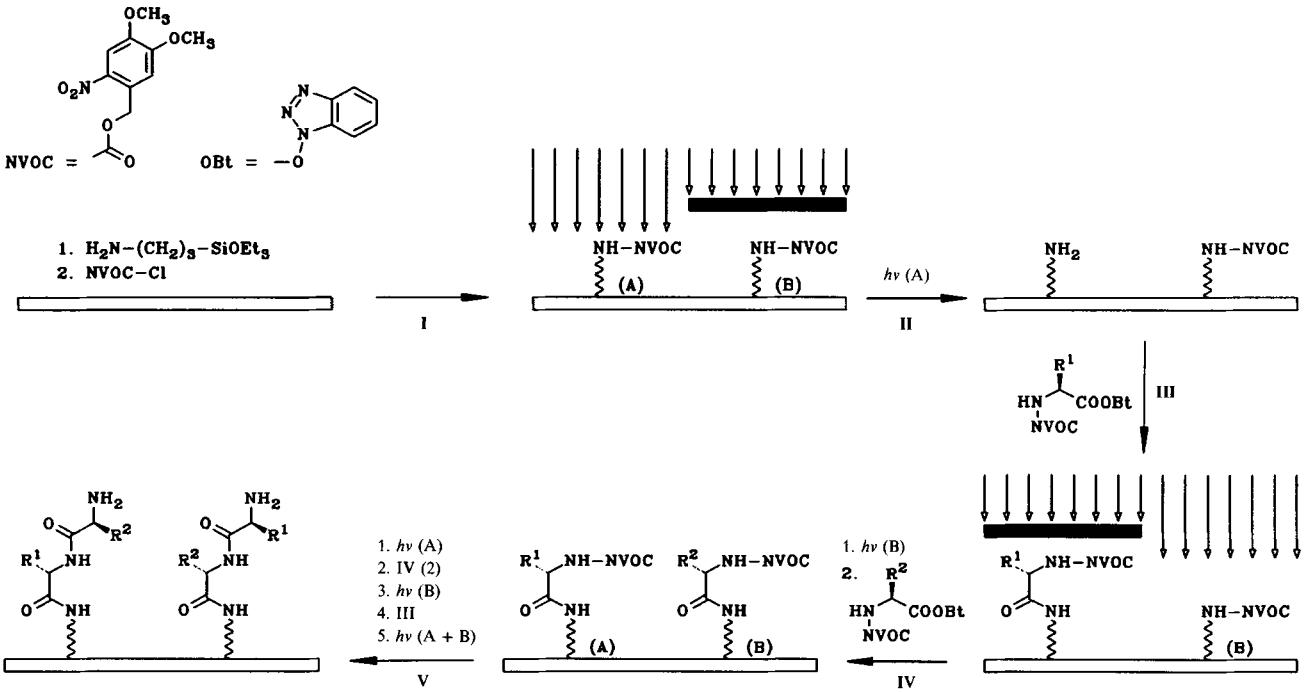

Fig. 1. Light-directed parallel synthesis of two dipetides from two amino acids in two irradiation fields.

In practice strips of the surface are exposed in each photolysis and coupling round of the synthesis. The strips irradiated in the next round lie perpendicular to those of the preced-

[*] Dr. G. von Kiedrowski
Institut für Organische Chemie der Universität
Tammannstrasse 2, W-3400 Göttingen (FRG)

ing round. This corresponds to oligopeptide construction in the rows and columns of a square matrix and enables a considerably shorter synthesis than were possible with successive illumination of each field. The shortest synthesis is achieved with the binary masking technique, in which the direction of the strip is changed in every cycle and its width is reduced to half every second cycle, while the number of strips in the mask is doubled. In this way, with n synthesis cycles 2^n different oligomers can be constructed, whose lengths are described by a binomial distribution (combinatorial synthesis). Ten synthesis cycles, for example, yield 1024 (minus 1) different peptides with "1 of length 0", and successively 10, 45, 120, 210, 252, 210, 120, 45, and 1 with lengths 1–10. Each peptide sequence is situated at one field of the (32 × 32) matrix.

The last irradiation step removes the *N*-terminal NVOC groups of all peptides; other deprotecting steps may be necessary to free the functional groups in side chains. For the affinity test the glass slide is simply held in a solution of the fluorescence-labeled receptor, rinsed, and scanned under the fluoresence microscope. The affinity of a peptide for a given receptor is determined from the fluorescence intensity of the corresponding field in the array. The authors demonstrated the whole process on a combinatorial synthesis of 1024 peptides, whose binding to the antibody 3E7 was to be tested. The 15 peptides with clearly recognizable affinity all begin with the sequence 5′-H_2N-Tyr-Gly. This result agrees with those by *Cwirla* et al., who claim an *N*-terminal tyrosine residue as the key determinant in the binding to 3E7.[5]

As light source, the authors used a mercury arc lamp, that required an exposure of 20 min at $\lambda = 365$ nm and 12 mW cm^{-2}. Shorter exposure times should be possible with an argon laser. To prevent excitation at aromatic side chains and, in particular, a photochemical decomposition of tryptophan, shorter wavelengths are not recommended. The total yield per synthesis cycle (irradiation and coupling) lies between 85 and 95%, so that for oligopeptides with more than ten amino acids the process only makes sense in exceptional cases. With mask technology a resolution of $> 20\ \mu m^2$ per synthesis field can be achieved; thus with $50\ \mu m^2$ elements, 250000 syntheses can be addressed on a glass cover slide for microscopy. The authors show that their process is not only restricted to oligopeptides, but can also be applied to light-directed oligonucleotide syntheses, in which case 5′-NVOC-protected nucleoside-3′-cyanoethylphosphoamidites are suitable monomeric building blocks.

Three critical questions must, however, be answered experimentally before a general application to affinity studies is recommended:

1. Does the carrier-bound oligopeptide have the same conformation as in solution?
2. Which spacer can be used as alternative to a C_3-chain, so that a large proportion of biological receptors can bind unhindered?
3. Can the yields of the synthesis cycles be improved, for instance, by the use of other protecting groups?

We wait in suspense for a report in the near future that the authors can suggest a solution to these problems. If this is the case it is foreseeable that light-driven parallel synthesizer machines, similar to the present peptide and DNA synthesis machines with soon revolutionize many university and pharmaceutical research laboratories. The site of the Affymax Research Institute of the authors in "Silicon Valley" will, of course, not hinder the the development of the first prototype of the commercial machines.

German version: *Angew. Chem. 103* (1991) 839

[1] H. Frühbeis, R. Klein, H. Wallmeier, *Angew. Chem. 99* (1987) 413; *Angew. Chem. Int. Ed. Engl. 26* (1987) 403.

[2] The term "irrational drug design" was recently proposed by *S. Brenner* at a symposium on natural and artificial selection processes (Max-Planck-Institut für Biophysikalische Chemie, Göttingen, 17th–19th April 1991). In contrast to "rational drug design", in which more or less detailed knowledge about the receptor, the ligands, and their interaction is available and does influence the development of better ligands, "irrational drug design" embodies attempts in the face of a void of knowledge in which a large repertoire of ligands are tested blindly.

[3] A. Plückthun, L. Ge, *Angew. Chem. 103* (1991) 301; *Angew. Chem. Int. Ed. Engl. 30* (1991) 296.

[4] S. P. A. Fodor, J. L. Read, M. C. Pirrung, L. Stryer, A. T. Lu, D. Solas, *Science 251* (1991) 767.

[5] S. E. Cwirla, E. A. Peters, R. W. Barrett, W. J. Dower, *Proc. Natl. Acad. Sci. USA 87* (1990) 6378.

Communications may be submitted in English *or* in German. Further details regarding the submission of communications can be found in the "Notice to Authors" reproduced in the January issue of the journal. Copies thereof may be obtained from the editorial office upon request.

In_7Cl_9—A New "Old" Compound in the System In-Cl**

By *Horst Philipp Beck** and *Doris Wilhelm*

Dedicated to Professor Hans Georg von Schnering on the occasion of his 60th birthday

The compounds In^ICl,[1,2] In_2Cl_3 ($In^I_3In^{III}Cl_6$),[3] In_5Cl_9 ($In^I_3In^{III}_2Cl_9$),[4] and $InCl_3$[5,6] have been unambiguously characterized in the system In-Cl. The phase diagram of the quasi-binary system InCl-$InCl_3$ has been investigated repeatedly by thermoanalytical methods.[7-10] The results indicated that, besides the above-mentioned compounds, a compound of composition In_3Cl_4 ($InCl_{1.33}$) or In_4Cl_5 ($InCl_{1.25}$) exists. However, this phase has still not been unambiguously characterized chemically or structurally. During our investigations of the system InCl-$SnCl_2$,[11] we discovered a new binary mixed-valent phase of the In-Cl system, since, surprisingly, the redox reaction between $In^{\oplus}$ and $Sn^{2\oplus}$ led to the formation of In^{III} according to the reaction equation $In^{\oplus} + Sn^{2\oplus} \rightarrow In^{3\oplus} + Sn^0$. This phase of composition In_7Cl_9 ($InCl_{1.29}$) can also be prepared directly from stoichiometric amounts of InCl and $InCl_3$ by sintering (14 d, 220–250 °C) or by sublimation from $InCl/In_2Cl_3$ mixtures. We believe that this phase is in fact the insufficiently characterized phase mentioned above.

The structure of In_7Cl_9 ($In^I_6In^{III}Cl_9$),[12] like that of the low-temperature phase of InCl, can be derived from the NaCl type. In both cases, relatively small displacements of the cations from their ideal positions result in aggregates of cations with ns^2 configuration: triangles and tetrahedra for InCl (with In^I–In^I distances of 3.61 to 3.68 Å) and only triangles for In_7Cl_9 ($d(In^I\text{-}In^I) = 3.87$ Å). In InCl, In^I_3 triangles are linked through bridging In^I cations to form a complex three-dimensional network with isolated In^I_4 tetrahedra in its cavities (Fig. 1, left). The transition from the InCl structure to that of In_7Cl_9 occurs formally by replacement of the bridging In^I cation by a $Cl^{\ominus}$ anion and of one corner of the tetrahedron by the higher-valent In^{III} cation. This change results in disruption of the network into individual triangles and, after displacement of the In^{III} corners of the tetrahedra, only the base triangles remain (Fig. 1, right).

This aspect of the structural relationship is particularly emphasized in the left and right side of Figure 1, which shows a comparable section of the cation partial lattice of the two compounds. For the sake of clarity, only the cations are shown in the picture of the α-InCl structure and, besides the cations, only the $Cl^{\ominus}$ ions (large circles) that replace In ions in the picture of In_7Cl_9. To clarify further the relationship to the tetrahedra in InCl, narrow lines are drawn from the In^{III} cations of In_7Cl_9 to the In^I triangles despite the relatively large separations. Replacement of the In^I cation by a halogen anion leads to a rotation of the surrounding In^I_3 aggregates in In_7Cl_9. As a result, the $Cl^{\ominus}$ ion is drawn closer to one of its cations (from about 3.6 to 3.2 Å) owing to Coulomb interaction. All In^I_3 triangles are now symmetrically equivalent.

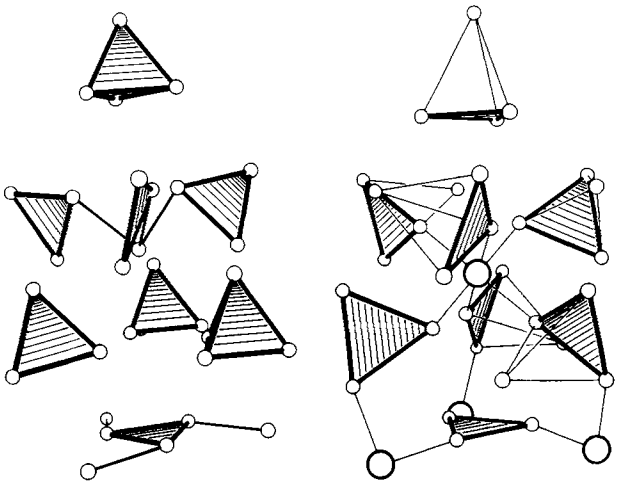

Fig. 1. Left: Cation structure in α-InCl. Right: Partial structure of In_7Cl_9 (see text). Small circles, In^I and In^{III}; large circles, $Cl^{\ominus}$. The separations are inversely proportional to the thickness of the lines drawn.

The In–In distances in InCl are about 10% longer than those in In metal. In In_7Cl_9 they are markedly longer, so that an interaction involving electron-pair bonding may be ruled out with certainty. In our view, the special aggregation to In_3 triangles best satisfies the steric requirements of a lone pair on indium (cf. Ref. [13]). Figure 2 shows the distorted anion coordination. The anion polyhedra, one of which is highlighted in bold lines, are open in the direction of neighboring cations. The repulsion between the ns^2 centers and the anions (noble-gas configuration) is thereby minimized (see also Refs. [14, 15]), in that lone pairs with strong excentricity[16]

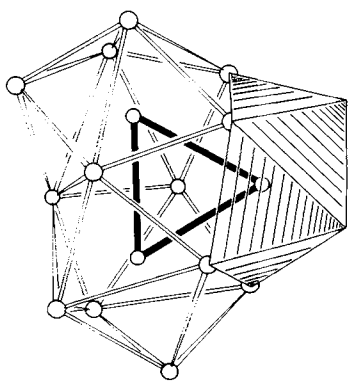

Fig. 2. Coordination of anions around an In_3 group. The In atoms are joined by bold dashed lines. One of the anion polyhedra is highlighted by bold lines.

[*] Prof. Dr. H. P. Beck, Dipl.-Chem. D. Wilhelm
FR 11.4 Anorganische und Analytische Chemie und
Radiochemie der Universität
Im Stadtwald, W-6600 Saarbrücken 11 (FRG)

[**] This work was supported by the Deutsche Forschungsgemeinschaft.

are oriented toward the same region. The lowering of the ionicity by the smaller electronegativity of the ns^2-configurated cations[17] and the "mutual shielding" of the positive charge centers by the s^2 electrons[13] contribute to the stabilization of these unusual structures.

Received: January 25, 1991 [Z 4403 IE]
German version: *Angew. Chem. 103* (1991) 897

CAS Registry numbers:
In_7Cl_9, 134131-31-0; InCl, 13465-10-6; $InCl_3$, 10025-82-8; In_2Cl_3, 107102-51-2.

[1] J. M. van den Berg, *Acta Crystallogr. 20* (1966) 905.
[2] C. P. J. M. van der Vorst, G. C. Verschoor, W. J. A. Maaskant, *Acta Crystallogr. Sect. B 34* (1978) 3333.
[3] G. Meyer, *Z. Anorg. Allg. Chem. 478* (1981) 39.
[4] G. Meyer, *Z. Anorg. Allg. Chem. 445* (1978) 140.
[5] D. H. Templeton, G. F. Carter: *J. Phys. Chem. 58* (1954) 940.
[6] M. A. Seyed Sadjadi, P. Vitse, *J. Appl. Crystallogr. 11* (1978) 292.
[7] R. J. Clark, E. Griswold, J. Kleinberg, *J. Am. Chem. Soc. 80* (1958) 4764.
[8] A. P. Palkin, N. V. Ostrikova, T. N. Vigutova, *Russ. J. Inorg. Chem. (Engl. Transl.) 8* (1963) 1344.
[9] P. I. Fedorov, N. S. Malova, *Russ. J. Inorg. Chem. (Engl. Transl.) 13* (1968) 1309.
[10] G. Meyer, R. Blachnik, *Z. Anorg. Allg. Chem. 503* (1983) 126.
[11] H. P. Beck, D. Wilhelm, A. Hartl-Gunselmann, *Z. Anorg. Allg. Chem.*, in press.
[12] Crystallographic data for In_7Cl_9: bright yellow crystals; m.p 250 °C, cubic, space group *Pa*3 (No. 205), $a = 12.218(3)$ Å, $V = 1823.9$ Å^3, $Z = 4$, $\varrho_{calcd} = 4.09\,g\,cm^{-3}$, $\lambda(Mo_{K\alpha}) = 0.71069$ Å, $\mu(Mo_{K\alpha}) = 99\,cm^{-1}$, 10810 reflections measured at room temperature with a Huber diffractometer, 546 unique reflections; all were considered as observed ($I > 3.0\sigma(I)$). After data reduction with CRYSTAN [18], the structure was solved by direct methods and, after application of absorption correction (DIFABS [21]), refined by the least-squares method (full matrix) SHELX. $R = 0.046$. Further details of the crystal structure investigation may be obtained from the Fachinformationszentrum Karlsruhe, Gesellschaft für wissenschaftlich-technische Information mbH, W-7514 Eggenstein-Leopoldshafen 2 (FRG), on quoting the depository number CSD-55290, the names of the authors, and the journal citation.
[13] H. P. Beck, W. Milius, *Z. Anorg. Allg. Chem. 562* (1988) 105.
[14] C. P. J. M. van der Vorst, *J. Phys. Chem. Solids 42* (1981) 655.
[15] C. P. J. M. van der Vorst, W. J. A. Maaskant, *J. Solid State Chem. 34* (1980) 301.
[16] J. Galy, R. Enjalbert, *J. Solid State Chem. 44* (1982) 1.
[17] R. T. Sandersen, *Inorg. Chem. 25* (1986) 1856.
[18] H. Burzlaff, R. Böhme, M. Gomm: *CRYSTAN, A Crystallographic Program System for Minicomputers*, Universität Erlangen-Nürnberg 1978.
[19] W. C. Hamilton, *Acta Crystallogr. 12* (1959) 609.
[20] G. M. Sheldrick: *SHELX-76, Program for Crystal Structure Determination*, Cambridge 1976; *SHELXS-86, FORTRAN-77 Program for the Solution of Crystal Structures from Diffraction Data*, Göttingen 1986.
[21] N. Walker, D. Stuart: *DIFABS, A Program for Correcting Diffractometer Data for Absorption Effects*, Chemistry Department, Queen Mary College, London 1983.

Phenylsodium Compounds with η^3-Allyl or η^6-Phenyl Coordination**

By *Siegfried Corbelin, Jürgen Kopf, Nis Peter Lorenzen*, and *Erwin Weiss**

Dedicated to Professor Hans Georg von Schnering on the occasion of his 60th birthday

After a phase of intensive structural investigation of organolithium compounds, interest is turning increasingly toward organosodium compounds.[2] The latter are accessible by metalation of hydrocarbons[3] with *n*-butylsodium, although the applicability of this method of synthesis is limited.[1]

Reaction of allylbenzene with *n*-butylsodium gave bright yellow 1-phenylallylsodium, which, on addition of the chelator PMDTA (pentamethyldiethylenetriamine) or directly in

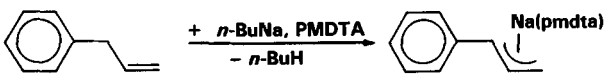

1

a one-pot reaction, afforded the solvate [Na(1-PhC_3H_4-(pmdta)] (**1**). The X-ray structure analysis of **1** shows a contact ion pair with η^3 coordination of the allyl system (Fig. 1).

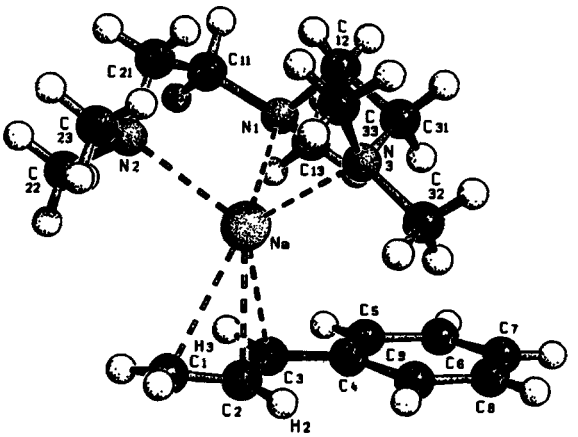

Fig. 1. Molecular structure of **1** [5]. Important distances [pm] and angles [°]: Na-C1 279.1(9), Na-C2 257.7(7), Na-C3 267.6(3), Na-N1 243.1(5), Na-N2 242.8(5), Na-N3 245.6(5), C1-C2 130.9(14), C2-C3 146.9(9), C3-C4 141.8(6), C4-C5 142.0(9), C5-C6 139.6(10), C6-C7 137.5(10), C7-C8 137.8(13), C8-C9 137.4(11), C9-C4 141.2(9); C1-C2-C3 127.2(8), C5-C4-C9 115.8(6), C4-C5-C6 121.4(6), C5-C6-C7 120.4(7), C6-C7-C8 119.2(7), C7-C8-C9 121.4(7), C8-C9-C4 121.5(7).

Only a few allyllithium compounds have been investigated so far by X-ray methods, although allyl anions are of special interest as simple resonance-stabilized systems. Examples include [Li(η^2-C_3H_5)(pmdta)],[8] [Li(η^3-1,3-$Ph_2C_3H_3$)-(Et_2O)]$_n$,[9a] and [Li{η^3-1,3-$(SiMe_3)_2C_3H_3$}(tmeda)].[9b] For allyllithium, ab initio calculations correctly predicted the deformations in the allyl anion caused by the metal[10] and, moreover, favored a Li site on the mirror plane of the allyl anion. Only for [Li(η^2-C_3H_5)(pmdta)] did the X-ray structure analysis reveal a strongly asymmetric site with η^2 coordination, due largely to the bulky PMDTA ligand.

NMR investigations and MO calculations indicate that allylsodium should also be symmetric (C_s).[11] In agreement with these findings, the allyl system in **1** is η^3-coordinated as in other metalated allyl systems. However, the middle C atom, C2, exhibits the shortest Na–C contact (258 pm). The distances to the outer C atoms, C1 and C3 (279 and 268 pm, respectively), differ, although this is expected owing to the different substitution of the terminal C atoms. The C–C distances within the allyl system differ by an unexpectedly large amount (131 and 147 pm). On the other hand, the increase in the angle of the allyl group (127°) and the decrease in the angle (116°) at the *ipso*-C atom of the phenyl group, C4, appear normal; the latter, for example, is observed for [NaPh(pmdta)]$_2$ as well.[12]

We obtained 1-phenylcyclohexenylsodium, a further carbanion with a phenyl-substituted allyl system, in the same

[*] Prof. Dr. E. Weiss, Dr. S. Corbelin, Priv.-Doz. Dr. J. Kopf, Dr. N. P. Lorenzen
Institut für Anorganische und Angewandte Chemie der Universität Martin-Luther-King-Platz 6, W-2000 Hamburg 13 (FRG)
[**] Metal-Alkyl and Metal-Aryl Compounds, Part 46. This work was supported by the Deutsche Forschungsgemeinschaft and the Fonds der Chemischen Industrie. Part 45: [1].

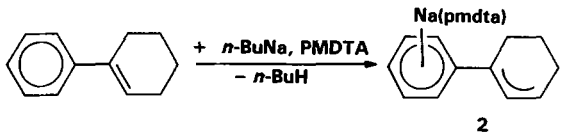

2

way by metalation of 1-phenylcyclohexene and isolated it as the PMDTA solvate **2**.

Because of the close analogy to **1**, we also expected an η^3 coordination of the allyl moiety here. Surprisingly, however, the X-ray structure analysis (Fig. 2) showed an η^6 coordination of the phenyl moiety, whereby the Na ion is sandwiched between the chelating ligand and the carbanion.

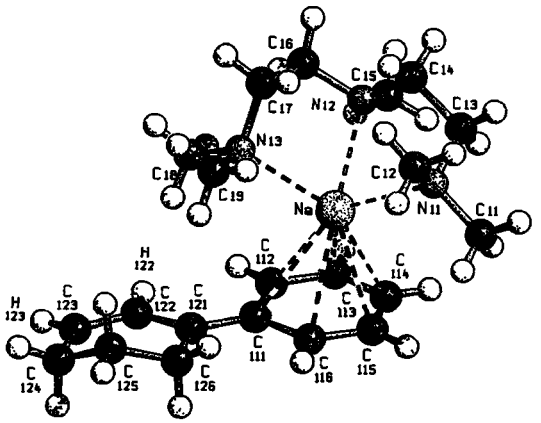

Fig. 2. Molecular structure of **2** [13]. Important distances [pm] and angles [°]: Na-C111 295.8(2), Na-C112 294.5(2), Na-C113 286.6(3), Na-C114 275.2(3), Na-C115 270.1(2), Na-C116 277.4(2), Na-N11 254.0(2), Na-N12 244.3(2), Na-N13 244.5(2), C111-C112 144.0(3), C112-C113 138.1(3), C113-C114 139.5(3), C114-C115 138.9(4), C115-C116 138.5(3), C111-C116 143.7(3), C111-C121 141.1(3), C121-C122 143.1(3), C122-C123 135.9(4), C123-C124 148.2(4), C124-C125 151.4(4), C125-C126 151.2(4), C126-C121 149.2(3); C112-C111-C116 113.4(2), C111-C112-C113 123.0(2), C112-C113-C114 121.4(2), C113-C114-C115 117.7(2), C114-C115-C116 121.8(2), C115-C116-C111 122.7(3), C121-C122-C123 124.3(2).

What is the reason for the different coordination of the two anions? The $[Na(pmdta)]^{\oplus}$ ion has a nearly hemispherical shape; that is, the metal ion is shielded on one side. In **2**, a close approach of $[Na(pmdta)]^{\oplus}$ to the allyl system is prevented by steric interaction between the H atoms of the methyl groups of PMDTA and the neighboring CH_2 groups (C124–126). The negative charge of the planar, conjugated carbanion is also delocalized over the phenyl moiety, however. For steric and electrostatic reasons, therefore, the solvated cation prefers to shift along this negatively charged hypersurface to the phenyl group, where it is optimally coordinated.

The six Na–C distances are not identical (270 pm (C115) to 296 pm (C112)); thus, the η^6 coordination is not symmetrical. According to all previous experience,[14, 16] the metal–C interactions in organosodium compounds are more flexible than in their lithium analogues. The deformation of the coordination geometry in **2** can therefore be explained in terms of packing effects in the lattice. In any case, the Na ion interacts with only one carbanion; all other Na–C distances to symmetry-related carbanions are larger than 460 pm and therefore meaningless.

The angles in the phenyl group are not identical; they are significantly smaller than 120° at the opposite-lying C atoms C111 and C114. The C–C distances in the phenyl group correlate with the corresponding Na–C distances: short C–C distances are associated with short Na–C distances. In the allyl system, the C–C distances are significantly shorter than those between the sp^3-hybridized C atoms C124 to C126 (151 pm).

Important in this context is tetraphenylallylsodium–diethyl ether, recently characterized by X-ray analysis.[15] In this case, too, the Na ion cannot approach the allyl system for steric reasons and is therefore sandwiched between two phenyl rings. An additional ether molecule coordinated to the Na ion closes the cage formed by the phenyl groups.

Experimental Procedures

1: a) 1-Phenylallylsodium: *n*-Butylsodium [3,4] (1.8 g, 23 mmol) was suspended in a mixture consisting of 70 mL of benzene and 30 mL of *n*-hexane and the stirred solution was treated dropwise with allylbenzene (3 mL, 23 mmol). The reaction mixture was stirred for 3 h and the precipitated, finely crystalline 1-phenylallylsodium was then collected by filtration, washed with a mixture of 50 mL of hexane and 20 mL of benzene, and dried under reduced pressure. The product was obtained as a deep yellow, pyrophoric crystalline powder (needles), which is sparingly soluble in hexane and benzene; under inert gas, it is stable from some time in the dark. Yield 2.84 g (90%) (contains some *n*-butylsodium). b) 1-Phenylallylsodium (0.6 g, 4.3 mmol) was suspended in a mixture of 10 mL of hexane and 2 mL of benzene and then largely dissolved by addition of PMDTA (10 mL, 5 mmol) with stirring. The solution was cooled to 10 °C, filtered, and allowed to stand at 7 °C; after a long period of time, intense yellow, very pyrophoric needles of **1** formed. Yield 0.5 g (38%); soluble in hexane, readily soluble in benzene. Correct analyses for Na, C, H, N. Compound **1** was also obtained directly from *n*-butylsodium, allylbenzene, and PMDTA in 28% yield, in analogy to the synthesis of **2**.

2: *n*-Butylsodium (2.6 g, 32 mmol) was suspended in 50 mL of hexane and dissolved by addition of PMDTA (6.3 mL, 30 mmol, dried over CaH_2). A solution of 1-phenylcyclohexene (5 g, 32 mmol) in 100 mL of benzene was then added in a single portion to the yellow, turbid solution. The solution immediately turned red and violet **2** (8.7 g) precipitated. Compound **2** was collected by filtration and dried under oil-pump vacuum. When the filtrate was allowed to stand at 7 °C, an additional 0.9 g of **2** was obtained, including single crystals suitable for X-ray structure analysis. Air-sensitive, but not pyrophoric. Total yield 9.6 g (90%, based on *n*-BuNa); correct analyses for Na, C, H, N.

Received: February 4, 1991 [Z 4420 IE]
German version: *Angew. Chem. 103* (1991) 875

CAS Registry numbers:
1, 133778-91-3; **2**, 133778-92-4; PMDTA, 3030-47-5; 1-phenylallylsodium, 114599-77-8; allylbenzene, 300-57-2; 1-phenylcyclohexene, 771-98-2; *n*-butylsodium, 3525-44-8.

[1] N. P. Lorenzen, J. Kopf, F. Olbrich, U. Schümann, E. Weiss, *Angew. Chem. 102* (1990) 1481; *Angew. Chem. Int. Ed. Engl. 29* (1990) 1441.
[2] Review: C. Schade, P. von R. Schleyer, *Adv. Organomet. Chem. 27* (1987) 169.
[3] a) H. Köster, E. Weiss, *J. Organomet. Chem. 168* (1979) 273; b) C. Schade, W. Bauer, P. von R. Schleyer, *ibid. 295* (1985) C25.
[4] L. Lochmann, J. Pospisil, D. Lim, *Tetrahedron Lett. 22* (1966) 257.
[5] Crystal structure analysis of **1**: $NaC_{18}H_{32}N_3$, $P2_1/n$, $a = 867.8(4)$, $b = 1453.4(8)$, $c = 1564.9(6)$ pm, $\beta = 99.10(3)°$, $V = 1949(2) \times 10^6$ pm^3, $\rho_{calcd} = 1.068$ g cm^{-3}, $Z = 4$, crystal size $0.3 \times 0.3 \times 0.7$ mm^3, 153 K, $Cu_{K\alpha 1}$ radiation, Enraf-Nonius CAD4, scan width $2.25 < \theta < 67°$, 2273 symmetry-independent and significant reflections [$|F| > 6\sigma(F)$]. Structure solution by direct methods supplemented by difference Fourier and LSQ calculations, 237 refined parameters, $R = 0.127$, $R_w = 0.101$ ($w = 1/\sigma^2|F|$), all non-hydrogen atoms refined with anisotropic temperature factors; the positions of H2 and H3 were determined directly, those of the remaining H atoms were placed at calculated positions in the refinement [6, 7].
[6] G. M. Sheldrick, *SHELXS-86, Programs for Crystal Structure Solution*, Universität Göttingen 1986. G. M. Sheldrick, *SHELX-76, Programs for Crystal Structure Determination*, University of Cambridge 1975. Structure drawings with *SCHAKAL88. E. Keller, J. Appl. Crystallogr. 22* (1989) 19.
[7] Further details of the crystal structure investigation may be obtained from the Fachinformationszentrum Karlsruhe, Gesellschaft für wissenschaftlich-technische Information mbH, W-7514 Eggenstein-Leopoldshafen 2 (FRG), on quoting the depository number CSD-55141 the names of the authors, and the journal citation.
[8] U. Schümann, E. Weiss, H. Dietrich, W. Mahdi, *J. Organomet. Chem. 322* (1987) 299.
[9] a) G. Boche, H. Etzrodt, M. Marsch, W. Massa, G. Baum, H. Dietrich, W. Mahdi, *Angew. Chem. 98* (1986) 84; *Angew. Chem. Int. Ed. Engl. 25* (1986) 104; b) G. Boche, personal communication.
[10] Compare the references cited in [8].

[11] T. Clark, C. Rhode, P. von R. Schleyer, *Organometallics 2* (1983) 1344, and references cited therein.
[12] U. Schümann, U. Behrens, E. Weiss, *Angew. Chem. 101* (1989) 481; *Angew. Chem. Int. Ed. Engl. 28* (1989) 476.
[13] Crystal structure analysis of **2**: $NaC_{21}H_{36}N_3$, $P\bar{1}$, $a = 876.9(2)$, $b = 988.8(4)$, $c = 1274.1(3)$ pm, $\alpha = 100.52(2)$, $\beta = 94.66(2)$, $\gamma = 94.13(2)°$, $V = 1078.3(5) \times 10^6$ pm^3, $\rho_{calcd} = 1.089$ g cm^{-3}, $Z = 2$, crystal size $0.3 \times 0.3 \times 0.9$ mm^3, 173 K, $Cu_{K\alpha 1}$ radiation, Enraf-Nonius CAD4, scan width $2.25 < \theta < 76.5°$, 4202 symmetry-independent and significant reflections [$|F| > 3\sigma(F)$] structure solution by direct methods (SHELXS-86 [6]) supplemented by difference Fourier and LSQ calculations (SHELX-76) [6], 288 refined parameters, $R = 0.0610$, $R_w = 0.0608$ ($w = 1/\sigma^2(F)$), all non-hydrogen atoms were refined with anisotropic temperature factors; the positions of H122 and H123 were determined directly, those of the remaining H atoms were place at calculated positions in the refinement [6, 7].
[14] S. Corbelin, N. P. Lorenzen, J. Kopf, E. Weiss, *J. Organomet. Chem.*, in press.
[15] H. Bock, K. Ruppert, Z. Havlas, D. Fenske, *Angew. Chem. 102* (1990) 1095; *Angew. Chem. Int. Ed. Engl. 29* (1990) 1042. Cf. also tetraphenylethylenedisodium–bis(diethylether). H. Bock, K. Ruppert, D. Fenske, *Angew. Chem. 101* (1989) 1717; *Angew. Chem. Int. Ed. Engl. 28* (1989) 1685.

Enzymatic Two-Step Synthesis of *N*-Acetylneuraminic Acid in the Enzyme Membrane Reactor

By *Udo Kragl, Daniel Gygax, Oreste Ghisalba,* and *Christian Wandrey**

N-Acetylneuraminic acid (Neu5Ac, **4**) is the best-known member of a special class of amino sugars, the sialic acids. These compounds are incorporated at the terminal positions of glycoproteins and glycolipids, which play an important role in biological recognition processes.[1, 2] Derivatives of Neu5Ac have found use as inhibitors of sialidases.[3] Neu5Ac activated with cytidine 5'-monophosphate has been used in the in vitro synthesis of sialyloligosaccharides.[4] Since this class of substances has attracted increasing interest owing to its biological function, increasing amounts of Neu5Ac are required. The compound is isolated from natural sources at present. Its accessibility is therefore limited and its price relatively high.

In recent years several enzymatic syntheses of Neu5Ac (**4**) starting from *N*-acetylmannosamine (ManNAc, **2**) and pyruvic acid (**3**), have been described with *N*-acetylneuraminic acid aldolase (E.C. 4.1.3.3) as catalyst.[5] A seven- to tenfold excess of **3** was usually used in order to attain high yields. Compound **2** was prepared chemically by base-catalyzed epimerization of *N*-acetylglucosamine (GlcNAc, **1**).[6] The reaction product contains the two epimers in a ratio of about 1:1. Compound **1** is not a substrate for the aldolase.[5]

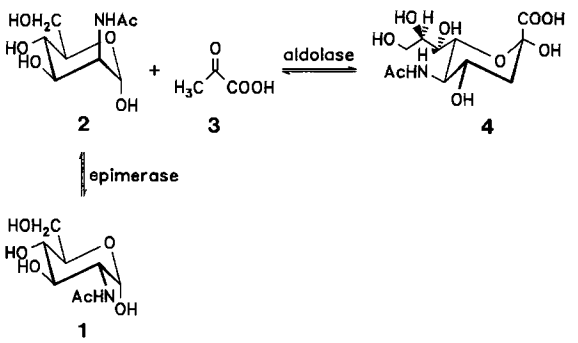

Here we describe a procedure in which the epimerization is accomplished enzymatically with *N*-acetylglucosamine 2-epimerase (E.C. 5.1.3.8).[7] Coupling this reaction with the enzyme reaction mentioned above allows **2** to be converted directly into **4** without isolation. The synthesis of Neu5Ac (**4**) can be achieved in a particularly economic way by using the two enzymes in dissolved form in the enzyme membrane reactor (EMR).

The use of purified enzymes in the EMR is an established procedure.[8] The principle behind the EMR is shown schematically in Figure 1. The substrates are pumped into the reactor through a sterile filter at a constant rate corresponding to a constant residence time. The enzymes, in homogeneous solution, are retained in the reactor by an ultrafiltration membrane that is permeable only to the substrates and products. The setup is sterilized before use, so that the addition of antibacterial agents, which would have to be separated from the products, is unnecessary.

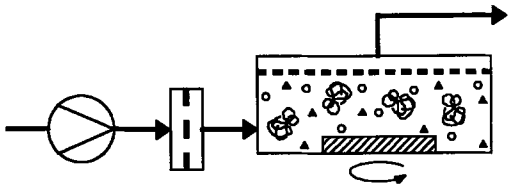

Fig. 1. Principle of the enzyme membrane reactor with pump and sterile filter.

Batch experiments and kinetic investigations were carried out to determine the conditions for continuous use of the two enzymes. Both enzymes can be used in a pH range of 7.0 to 8.0 without loss of activity or stability. Since the EMR operates as a continuously stirred tank reactor with constant discharge, the pH in the reactor can be held constant at 7.5 by controlling the pH of the substrate solution. Buffers are completely unnecessary, so that the workup is simplified. Based on the equilibrium position of the reaction of **2** and **3** to give **4**, the temperature was set at 25 °C ($K_{25} = 28.7$ L mol^{-1}).[9] Lower temperatures shift the equilibrium to the product side; K was found to be 83.1 L mol^{-1} at 10 °C. However, the activity of the aldolase at this temperature is only 20% of that at 25 °C, so that high conversion can only be achieved by increasing the residence time. The enzyme concentration cannot be raised arbitrarily to compensate for the lower activity, since, at high concentrations, only part of the protein is in the active conformation.

The epimerase requires ATP and $Mg^{2\oplus}$ for activation, so that these substances must be added to the substrate solution.[7] The aldolase is inhibited only very weakly by **1** (19% loss of activity when 200 mM **1** is used in the synthesis) and not at all by $MgCl_2$ and ATP. Since the epimerase is inhibited by **3**, a multiple excess of **3** cannot be employed. On the other hand, high concentrations of **1** lead to higher intermediate concentrations of **2**, which shift the equilibrium position of the second reaction toward Neu5Ac. This is also advantageous in view of the chromatographic isolation of the product with anion exchangers, since **3** and **4** exhibit similar pK_a values in the region around 2.2. Compounds **1** and **2** are not bound and can easily be recovered. The concentration–time curve for the continuous synthesis of **4** is shown in Figure 2. After an initial phase, all compounds attain a constant concentration.

[*] Prof. Dr. C. Wandrey, Dipl.-Chem. U. Kragl
Forschungszentrum Jülich, Institut für Biotechnologie
Postfach 19 13, W-5170 Jülich (FRG)
Dr. D. Gygax, Dr. O. Ghisalba
Ciba Geigy AG, Zentrale Forschungslaboratorien
Basel (Switzerland)

In this way, 15 g of Neu5Ac was synthesized and isolated with a space–time yield of 109 $g L^{-1} d^{-1}$ (based on the reactor volume). A decrease in the conversion, which would have indicated deactivation of the enzyme, was not observed. Moreover, by-products, which would have indicated lowered enzyme selectivity, were not found. In the reaction, 28% of **1** was converted and 35% of **3**; 64% of **2**, formed as an intermediate, was converted. When an epimeric mixture

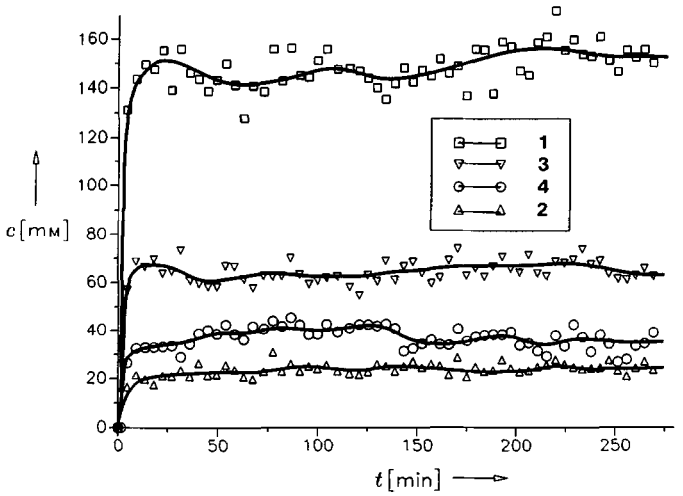

Fig. 2. Concentration–time curve for the continuous synthesis of *N*-acetylneuraminic acid (**4**) in the enzyme membrane reactor. Starting concentrations: 200 mM **1**, 100 mM **3**, 5 mM ATP, 5 mM $MgCl_2 \cdot 6H_2O$; pH 7.5; 25°C; 11.9 $mg mL^{-1}$ epimerase; 4.0 $mg mL^{-1}$ aldolase; residence time 171 min.

of **1** and **2** was used, conversions of between 80 and 90% in 4–5 days were reported, whereby **4** was isolated in yields of up to 67%.[5] In order to achieve the higher conversion, an eightfold excess of **3** was employed. The ratio of excess **3** to the product formed, **4**, has a large effect on the isolation of product, however. This value is about 1.9 in our work, whereas it was about 8 in earlier studies.[5] The smaller this value, the easier it is to isolate the products by chromatography. At the same time, the required volume of exchanger is reduced, resulting in savings in both time and cost.

The procedure described here, which can be scaled up, allows Neu5Ac (**4**) to be prepared in large amounts directly from inexpensive GlcNAc (**1**).

Experimental Procedure

The EMR (volume 14.3 mL) was sterilized with 0.1 percent peracetic acid. The ultrafiltration membrane (YM-5, Amicon, Witten) was pretreated with 1 $mg mL^{-1}$ of bovine serum albumin. After addition of 11.9 $mg mL^{-1}$ of epimerase (0.1 $U mg^{-1}$) and 4.0 $mg mL^{-1}$ of aldolase (8.5 $U mg^{-1}$) (both enzymes from Toyobo, Osaka, Japan), the substrate solution (1400 mL, 200 mM **1**, 100 mM **3**, 5 mM ATP, 5 mM $MgCl_2 \cdot 6H_2O$, ph 7.5, no buffer) was pumped through the reactor with a residence time of 171 min. The pH was controlled by taking samples from the reactor outlet, and the amounts of the various components were determined by HPLC. HPLC conditions: BioRad Aminex HPX-87H column, 6 mM sulfuric acid eluent, 0.9 $mL min^{-1}$ flow rate at 65°C; photometric detection at 205 nm. Isolation of the product was carried out in analogy to the described procedure by anion-exchange chromatography on Dowex 1X2, 200–400 mesh, formate form, using gradient elution with formic acid (0 to 0.5 M) [2]. The neuraminic acid fractions were lyophilized. Yield 15 g (35%). The 200-MHz ^1H NMR spectrum in D_2O is in agreement with the literature data [5, 10]; purity according to HPLC > 99%; $[\alpha]_{25\,°C}^{D} = -28.8°$ ($c = 1$ in H_2O), identical with commercially available **4**; correct elemental analysis.

Received: January 30, 1991 [Z 4412 IE]
German version: *Angew. Chem. 103* (1991) 854

CAS Registry numbers:
1, 10036-64-3; **2**, 14131-64-7; **3**, 127-17-3; **4**, 21646-00-4; *N*-acylglucosamine-2-epimerase (E.C.5.1.3.8), 37318-34-6; aldolase, 9027-60-5.

[1] R. Schauer: *Sialic Acids—Chemistry, Metabolism and Function*, Springer, Wien 1982, and references cited therein.
[2] R. Schauer, *Adv. Carbohydr. Chem. Biochem. 40* (1982) 131–234; *Methods Enzymol. 138* (1987) 132–161.
[3] P. Meindl, G. Bodo, P. Palese, J. Schulman, H. Tuppy, *Virology 58* (1974) 457; E. Zbiral, H. Brandstetter, R. Christian, R. Schauer, *Liebigs Ann. Chem. 1987*, 781–786.
[4] K.G. Nilsson, *Carbohydr. Res. 188* (1989) 9–17; C. Augé, R. Fernandez-Fernandez, C. Gautheron, *ibid. 200* (1990) 257–268, and references cited therein.
[5] C. Augé, C. Gautheron, S. David, A. Malleron, B. Cavayé, B. Bouxom, *Tetrahedron 46* (1990) 201–214; D. Comb, S. Roseman, *J. Am. Chem. Soc. 80* (1958) 497–499; M.-J. Kim, W.J. Hennen, M. Sweers, C.-H. Wong, *ibid. 110* (1988) 6481–6486; E.S. Simon, M.D. Bednarski, G.M. Whitesides, *ibid. 110* (1988) 7159–7163, and references cited therein.
[6] C.T. Spivak, S. Roseman, *J. Am. Chem. Soc. 81* (1959) 2403–2404.
[7] A. Datta, *Biochemistry 9* (1970) 3363–3370; S. Gosh, S. Roseman, *J. Biol. Chem. 240* (1965) 1531–1536.
[8] M.-R. Kula, C. Wandrey, *Methods Enzymol. 136* (1987) 9–21; D. Vasic-Racki, M. Jonas, C. Wandrey, W. Hummel, M.-R. Kula, *Appl. Microbiol. Biotechnol. 31* (1989) 215–222.
[9] $K = [N\text{-acetylneuraminic acid}] \times [N\text{-acetylmannosamine}]^{-1} \times [\text{pyruvate}]^{-1}$.
[10] E.B. Browm, W.S. Brey, W. Weltner, *Biochim. Biophys. Acta 399* (1975) 124–130.

Do Partial Charges Alone Govern the Relative Stability of the Isomeric Heptaheteronortricyclane Anions $[P_{7-x}As_x]^{3\ominus}$?**

By *Armin Burkhardt, Wolfgang Hönle,** and *Ulrich Wedig*

Dedicated to Professor Hans Georg von Schnering on the occasion of his 60th birthday

Mixed crystals with the composition $Rb_3[P_{7-x}As_x]$ ($O \leq x \leq 7$) can be synthesized from stoichiometric amounts of the elements at 900 K. The dark red mixed crystals with $x \approx 3$ dissolve completely in ethylenediamine. The ^{31}P NMR spectrum shows that, as in the polyphosphides M_3P_7 (M = Li–Cs), trianions with heteronortricyclane structure (cf. Fig. 1) are present and show valence tautomerism at room temperature. According to the intensities of the ^{31} P NMR signals, a particular P/As ratio is not favored in the cluster.[1]

Böhm and *Gleiter*[2] employed MINDO/3 calculations to investigate the valence tautomerism of $P_7^{3\ominus}$. They analyzed the charge distribution in the trianion and the structure of the transition state and calculated an activation energy of 59.12 $kJ mol^{-1}$ for the tautomerism. This value is in good agreement with the results of the variable-temperature ^{31}P NMR investigations of *Baudler* et al.[3, 4]

Gimarc and *Joseph* applied the concept of "topological charge stabilization" to mixed nortricyclane clusters.[5] They thereby interpreted the experimental findings of *Blachnik* and *Wickel*, who showed that mainly PA_3S_3 was present in a mixture of P_4S_3 and As_4S_3 in a 1 : 3 molar ratio.[6] According to their concept, particularly stable structures are formed when, in a homoatomic isoelectronic reference system, the positions of greatest charge density are occupied by those heteroatoms with the largest electronegativity. They determined the charge density at each position by population analysis starting from an extended Hückel wave function for

[*] Dr. W. Hönle, Dipl.-Chem. A. Burkhardt, Dr. U. Wedig
Max-Planck-Institut für Festkörperforschung
Heisenbergstrasse 1, W-7000 Stuttgart 80 (FRG)

[**] This work was supported by the Bundesministerium für Forschung und Technologie and by the Hoechst AG.

$P_7^{3\ominus}$. In later work, *Gimarc* and *Ott* used the same approach to make, for example, predictions about the relative stability of clusters with the composition $[P_{7-x}As_x]^{3\ominus}$.[7]

Prompted by discrepancies between predictions made in this way and our NMR investigations,[1] we carried out restricted Hartree–Fock calculations[8] on clusters with the composition $[P_{7-x}As_x]^{3\ominus}$ ($x = 0,1,2,3,7$). To ensure reliable ab initio treatment of the valence shell on the one hand and to limit the required calculations on the other, we used pseudopotentials adjusted to ionization and excitation energies.[9] A double zeta basis set with polarization functions (DZP), which was optimized for these pseudopotentials, was used.[10] Expansion of the basis set to include diffuse s and p functions (DZPD)—as usually carried out for anions—led to no significant changes in the structural parameters (Table 1). Moreover, because of the structural interrelationship of the clusters discussed, the valence electron correlation was not expected to affect significantly the properties observed. All cluster structures, as well as the transition state postulated in Ref. [2], were optimized in the highest point group symmetry possible.

Table 1. Comparison of the independent structure parameters ($C_{3v} - 3m$) of $P_7^{3\ominus}$ and Li_3P_7, obtained in HF calculations using different basis sets, with the experimental values for Li_3P_7, (energies in Hartrees, distances in $a_0 = 5.29 \times 10^{-11}$ m, angles in °). For the structure of $P_7^{3\ominus}$ see Figure 1, *top left*.

	Isolated $P_7^{3\ominus}$			Li_3P_7
	DZP	DZPD	exp. [13]	DZP [10]
E_{val}	−44.664092	−44.695588	–	−67.466587
ε_{homo}	+0.196383	+0.169834	–	−0.283442
r_{bb} [a]	4.25	4.24	4.26	4.19
r_{be} [a]	4.09	4.09	4.05	4.16
r_{ae} [a]	4.18	4.18	4.17	4.15
ω_{eae} [a]	102.6	102.4	101.7	101.0

[a] r_{bb}, distance between the basal atoms; r_{ae}, distance between the equatorial and the apical atoms; r_{be}, distance between the equatorial and basal atoms; ω_{eae}, equatorial-apical-equatorial angle.

Ab initio calculations on isolated anionic systems are problematic, because orbitals with positive orbital energies can be occupied. This indicates that such systems are not stable in the context of the Hartree–Fock approximation. These orbital energies can be reduced to zero by including continuum functions.[11] Work of *Pyykkö* et al. shows, however, that the structures of anionic systems optimized at the Hartree–Fock level are in good agreement with the experimental structures.[12] This is ascribed to the use of a restricted basis set, which is optimized for binding states, and to stabilization of these systems by counterions in the solid state or in solution.

We, too, have found that our calculations for the free ion $P_7^{3\ominus}$ and for Li_3P_7 are in good agreement with the experimental structure data (Table 1).[13] The deviations for Li_3P_7 are due to the omission of the solvent molecules and to the small Li–P distances. Nonetheless, the agreement is good enough to justify the use of the method and to obviate the calculation of the normal frequencies.

The structures and partial charges of $P_7^{3\ominus}$, the postulated transition state (TS) involved in valence tautomerism, and the most stable isomers of $[P_5As_2]^{3\ominus}$ and $[P_4As_3]^{3\ominus}$ are shown in Figure 1. To name these isomers, we use the number of the apical, equatorial, and basal As atoms (cf. Fig. 1). If this approach does not result in an unambiguous classification, a descriptor Z is added when an equatorial and a basal As atom are neighboring, and a descriptor E when this is not the case.

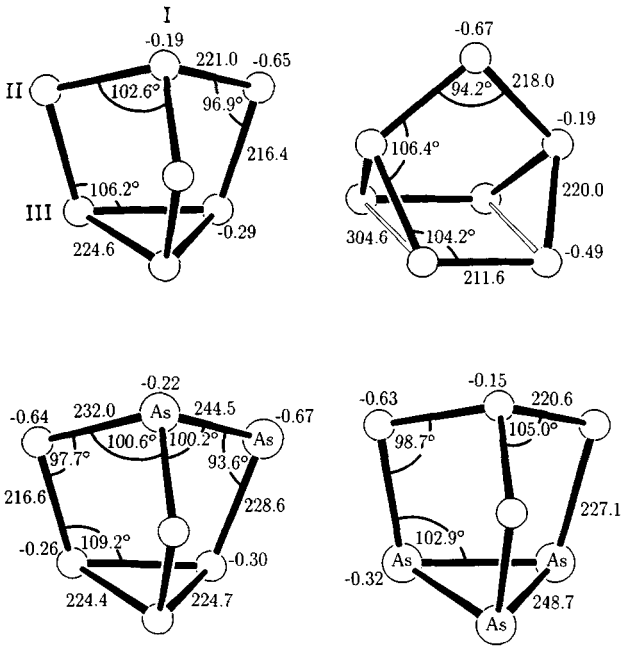

Fig. 1. Optimized structures of selected heteronortricyclane anions. The Mulliken partial charges, as well as important bond lengths [pm] and bond angles, are given. The arsenic atoms are specially labeled. Top left: $P_7^{3\ominus}$, ground state ($C_{3v} - 3m$). Top right: transition state (TS) ($C_{2v} - 2m$). Bottom left: $[P_5As_2]^{3\ominus}$, isomer 110 ($C_s - m$). Bottom right: $[P_4As_3]^{3-}$, isomer 003 ($C_{3v} - 3m$). *I* = apical, *II* = equatorial, *III* = basal position.

The partial charges for $P_7^{3\ominus}$ and its postulated transition state are more balanced than those determined by *Böhm* and *Gleiter*[2] and the interatomic distances are slightly larger. We found an activation energy of 65.6 kJ mol^{-1} for the valence tautomerism of this ion, a value also in good agreement with Ref. [2]. For $As_7^{3\ominus}$—in which valence tautomerism has not yet been experimentally observed—we calculated an activation energy of 63.5 kJ mol^{-1}. Replacement of a P atom by an As atom in the mixed clusters led to an increase in the corresponding bond lengths by 12–24 pm and to considerable deformation of the cluster. The Mulliken partial charges

Table 2. Valence energies in Hartrees for selected heteronortricyclanes $[P_{7-x}As_x]^{3\ominus}$ obtained by Hartree–Fock calculations. Energies are given in kJ mol^{-1} of the energetically favored isomer in each case. See text for the nomenclature of the isomers.

Isomer	Symmetry	E_{val} [Hartree]	ΔE_{rel} [kJ mol^{-1}]
$P_7^{3\ominus}$			
000	C_{3v}	−44.6640925	0.00
TS	C_{2v}	−44.6391043	65.61
$[P_6As]^{3\ominus}$			
100	C_{3v}	−44.3151544	0.00
010	C_s	−44.3148276	0.86
001	C_s	−44.3137626	3.65
$[P_5As_2]^{3\ominus}$			
110	C_s	−43.9673387	0.00
011Z	C_s	−43.9664889	2.23
020	C_s	−43.9655599	4.67
002	C_s	−43.9649991	6.14
101	C_s	−43.9649839	6.18
011E	C_1	−43.9645376	7.35
$[P_4As_3]^{3\ominus}$			
003	C_{3v}	−43.6178362	0.00
030	C_{3v}	−43.6163156	3.99
$As_7^{3\ominus}$			
133	C_{3v}	−42.2323509	0.00
TS	C_{2v}	−42.2081733	63.48

on the As atoms are only slightly larger than those on the corresponding P atoms, in agreement with recent electronegativity values.[14]

A glance at Table 2 shows that the difference in energy between the individual isomers is less than 7.4 kJ mol^{-1}, which corresponds to only about 10% of the activation energy of valence tautomerism. Thus, the valence tautomerism is not expected to favor specific isomers and a classification of the isomers as stable, metastable, and unstable is inappropriate. In view of the method used, the small differences between the isomers do not allow far-reaching conclusions to be drawn.

These results contradict the predictions of *Gimarc* and *Ott*,[7] who assumed in their work that the relative energy differences were considerably larger than the rotational barrier found. It is therefore unsatisfactory to consider relative cluster stability only in terms of its dependence on partial charges, since this ignores a number of important factors such as bond energy, polarizability, and, above all, framework strain, which is undoubtedly present in the clusters examined. Here we use $[P_4As_3]^{3\ominus}$ to discuss the effect of substitution by arsenic on framework strain.

The bond angle of 60° necessary for formation of the basal three-membered ring—without consideration of the bent bonds present—requires less angle deformation energy for an element with larger atomic radius. Furthermore, the bonds in the ring are thereby considerably lengthened, resulting in less angle deformation at the equatorial and apical atoms. This explains not only the stability of PAs_3S_3[6] but also a series of experimental findings which show that phosphorus can readily be replaced by arsenic if the strain in the pure phosphorus framework is thereby reduced. Examples are arsenic-substituted Hittorf phosphorus with the composition $P_{20}As$, helical structures of the type $M(P_{1-x}As_x)_7$ with M = Li,Na and $x \leq 0.50$, and $P_2As_2S_7$. In the first case, exclusively one position is occupied by 0.5 As[15] and, in the second case, the substitution is governed by the decreasing strain on going from the periphery to the axis of the helix.[16] In the third case, a long P–P bond in P_4S_7 is substituted in such a way that the framework strain decreases.[7]

Received: December 27, 1990;
revised: April 8, 1991 [Z 4362 IE]
German version: *Angew. Chem. 103* (1991) 850

CAS Registry numbers:
$P_7^{3\ominus}$ (isomer 1), 39040-22-7; $P_7^{3\ominus}$ (isomer 2), 133931-98-3; $[P_6As]^{3\ominus}$ (isomer 1), 121158-17-6; $[P_6As]^{3\ominus}$ (isomer 2), 121158-18-7; $[P_6As]^{3\ominus}$ (isomer 3), 121158-19-8; $[P_5As_2]^{3\ominus}$ (isomer 1), 121158-22-3; $[P_5As_2]^{3\ominus}$ (isomer 2), 121158-23-4; $[P_5As_2]^{3\ominus}$ (isomer 3), 121158-24-5; $[P_5As_2]^{3\ominus}$ (isomer 4), 121158-25-6; $[P_5As_2]^{3\ominus}$ (isomer 5), 121158-26-7; $[P_5As_2]^{3\ominus}$ (isomer 6), 121158-27-8; $[P_4As_3]^{3\ominus}$ (isomer 1), 121158-43-8; $[P_4As_3]^{3\ominus}$ (isomer 2), 121158-38-1; $As_7^{3\ominus}$ (isomer 1), 102330-30-3; $As_7^{3\ominus}$ (isomer 2), 133931-99-4.

[1] W. Hönle, H. G. von Schnering, *Angew. Chem. 98* (1986) 370; *Angew. Chem. Int. Ed. Engl. 25* (1986) 352.
[2] M. C. Böhm, R. Gleiter, *Z. Naturforsch. B 36* (1981) 498.
[3] M. Baudler, H. Ternberger, W. Faber, J. Hahn, *Z. Naturforsch. B 34* (1979) 1690.
[4] M. Baudler, *Angew. Chem. 94* (1982) 590; *Angew. Chem. Int. Ed. Engl. 21* (1982) 492.
[5] B. M. Gimarc, P. J. Joseph, *Angew. Chem. 96* (1984) 518; *Angew. Chem. Int. Ed. Engl. 23* (1984) 506.
[6] R. Blachnik, U. Wickel, *Angew. Chem. 95* (1983) 313; *Angew. Chem. Int. Ed. Engl. 22* (1983) 317.
[7] B. M. Gimarc, J. J. Ott, *Inorg. Chem. 28* (1989) 2560.
[8] R. Ahlrichs, M. Häser: *Programm TURBOMOLE (J. Comput. Chem. 10* (1989) 104).
[9] G. Igel-Mann, H. Stoll, H. Preuß, *Mol. Phys. 65* (1988) 1321.
[10] A. Burkhardt, U. Wedig, W. Hönle, H. Preuß, H. G. von Schnering, unpublished; A. Burkhardt, *Diplomarbeit*, Max-Planck-Institut für Festkörperforschung 1989; A. Burkhardt, W. Hönle, H. G. von Schnering, U. Wedig, H. Preuß, *25. Symp. Theor. Chem. Collect. Abstr. 1989*, 33.
[11] R. Ahlrichs, *Chem. Phys. Lett. 34* (1975) 570.
[12] P. Pyykkö, Y. Zao, *J. Phys. Chem. 94* (1990) 7753.
[13] V. Manriquez, W. Hönle, H. G. von Schnering, *Z. Anorg. Allg. Chem. 539* (1986) 95.
[14] A. L. Allred, E. G. Rochow, *J. Inorg. Nucl. Chem. 5* (1958) 264; R. T. Sanderson: *Polar Covalence*, Academic Press, New York 1983.
[15] W. Hönle, H. G. von Schnering, unpublished.
[16] W. Hönle, H. G. von Schnering, *IVth Eur. Crystallogr. Meet. Oxford Collect. Abstr. B 1977*, 552.
[17] W. Hönle, C. Wibbelmann, W. Brockner, *Z. Naturforsch. B 39* (1984) 1088.

$Li_{10}P_4N_{10}$—A Lithium Phosphorus(v) Nitride Containing the New Complex Anion $P_4N_{10}^{10\ominus}$**

By *Wolfgang Schnick** and *Ute Berger*

Dedicated to Professor Hans Georg von Schnering on the occasion of his 60th birthday

Phosphorus(v) nitrides, like the nitrides of other light main-group elements (boron, aluminum, silicon), are potential starting compounds for the development of new ceramic materials with special properties.[1] However, a systematic entry to the class of compounds comprising binary phosphorus(v) nitrides and their ternary compounds with electropositive elements has been hindered in the past, because the methods used to prepare these compounds did not lead to defined, pure or monocrystalline products. Recently, we employed a new method to prepare defined and finely crystalline P_3N_5.[2] We obtained pure Li_7PN_4, as well as $LiPN_2$, by reaction of the binary nitrides P_3N_5 and Li_3N. Exact structural characterization of these ternary nitrides led to the first detailed knowledge of the structure of phosphorus(v) nitrides in the solid state.[3, 4] "Isolated" $PN_4^{7\ominus}$ ions were found in Li_7PN_4, whereas, in $LiPN_2$, which has a P–N partial structure analogous to β-cristobalite, PN_4 tetrahedra are vertex-linked on all sides to produce the highest conceivable degree of interconnection. Both compounds show a noticeable cation mobility in the solid state and are therefore novel lithium ion conductors.[5]

We have now discovered $Li_{10}P_4N_{10}$, a new lithium phosphorus(v) nitride whose composition lies between those of Li_7PN_4 and $LiPN_2$ and which therefore represents the first example of a phosphorus(v) nitride with an intermediate degree of condensation of PN_4 tetrahedra. $Li_{10}P_4N_{10}$ can be prepared by solid-state reaction of the binary nitrides Li_3N and P_3N_5 [Eq. (a)] as well as by reaction of $LiPN_2$ with Li_3N [Eq. (b)] or of Li_7PN_4 with P_3N_5 [Eq. (c)]. The title compound is obtained as a colorless powder and as transparent octahedral single crystals.[6]

$$10\,Li_3N + 4\,P_3N_5 \xrightarrow[W\ crucible,\ N_2]{720\,^\circ C,\ 5d} 3\,Li_{10}P_4N_{10} \quad (a)$$

$$2\,Li_3N + 4\,LiPN_2 \xrightarrow[W\ crucible,\ N_2]{700\,^\circ C,\ 5d} Li_{10}P_4N_{10} \quad (b)$$

$$10\,Li_7PN_4 + 6\,P_3N_5 \xrightarrow[W\ crucible,\ N_2]{630\,^\circ C,\ 10d} 7\,Li_{10}P_4N_{10} \quad (c)$$

[*] Dr. W. Schnick, Dipl.-Chem. U. Berger
Institut für Anorganische Chemie der Universität
Gerhard-Domagk-Strasse 1
W-5300 Bonn 1 (FRG)

[**] This work was supported by the Minister für Wissenschaft und Forschung des Landes Nordrhein-Westfalen and by the Fonds der Chemischen Industrie.

Single-crystal X-ray structure analysis[7] revealed that $Li_{10}P_4N_{10}$ has an ionic structure and contains the new complex anion $P_4N_{10}^{10\ominus}$, which is isoelectronic to molecular phosphorus(V) oxide, P_4O_{10} (Fig. 1). The anion shows ideal T_d symmetry in the solid. As expected, the IR spectrum of $Li_{10}P_4N_{10}$ displays six vibrational bands for the complex anion between 540 und 1070 cm^{-1}.[8] The P–N bonds to the terminal nitrogen atoms of the $P_4N_{10}^{10\ominus}$ ion are significantly shorter than those to the bridging N atoms (P-N2 158.1(3), P-N1 167.6(3) pm). This is presumably due to a greater degree of polar-bond character in the bonds between phosphorus and terminal nitrogen.

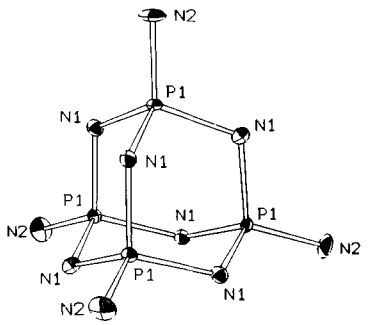

Fig. 1. Structure of the $P_4N_{10}^{10\ominus}$ ion in the solid state (ellipsoids drawn at 50% probability). Selected distances [pm] and angles [°] (standard deviations in parentheses): P-N2 158.1(3), P-N1 167.6(3); N1-P-N2 112.7(1), N1-P-N1 105.9(1), P-N1-P 116.0(2).

Surprisingly, the packing of the $P_4N_{10}^{10\ominus}$ ions in the solid corresponds to that of molecular As_4O_6 in the cubic high-temperature phase arsenolite, despite the differing compositions.[9, 10] Thus, the $P_4N_{10}^{10\ominus}$ ions in the solid are arranged in a zinc blende fashion, resulting in an appreciably more favorable packing of the complex anions compared with, for example, molecular phosphorus(V) oxide, P_4O_{10} (distorted body-centered arrangement).[11] It is this ionic structure formed by lithium cations and $P_4N_{10}^{10\ominus}$ anions which renders possible the space-saving packing, which cannot be achieved for the topologically comparable and isoelectronic, but uncharged, P_4O_{10}.

The arsenolite-like packing of the $P_4O_{10}^{10\ominus}$ ions in the solid forces the $Li^{\oplus}$ ions in $Li_{10}P_4N_{10}$ to occupy markedly different positions. In addition to trigonal-planar coordination of $Li^{\oplus}$ ions, tetrahedral and even near-octahedral coordination by nitrogen are found. Finally, one-tenth of the $Li^{\oplus}$ ions in $Li_{10}P_4N_{10}$ are distributed with disorder over positions with a multiplicity higher than the actual number of atoms. The Li–N contact distances (193–220 pm) correspond roughly to the sum of the ionic radii[12, 13] and they increase, as expected, with the coordination number of the cations.

The close packing of the complex anions realized here is apparently caused by the tendency toward coordinative saturation of the $Li^{\oplus}$ ions. Owing to the topology of the complex $P_4N_{10}^{10\ominus}$ ions, however, it is not possible to coordinate the relatively large number of $Li^{\oplus}$ ions ($Li^{\oplus}$: $P_4N_{10}^{10\ominus}$ = 10:1) in the same way. For this reason the $Li^{\oplus}$ ions are distributed over positions that, from the viewpoint of crystal chemistry, are surrounded by nitrogen in an unusual number of different ways. Analogously to Li_7PN_4 and $LiPN_2$, we expect $Li_{10}P_4N_{10}$ to exhibit a significant lithium ion conductivity.

Received: January 15, 1991 [Z 4387 IE]
Publication delayed at authors' request
German version: *Angew. Chem. 103* (1991) 857

CAS Registry numbers:
Li_3N, 26134-62-3; P_3N_5, 12136-91-3; $LiPN_2$, 60883-88-7; Li_7PN_4, 11118-04-0; $Li_{10}P_4N_{10}$, 133670-95-8.

[1] E. V. Borisov, E. E. Nifant'ev, *Russ. Chem. Rev. 46* (1977) 842.
[2] W. Schnick, J. Lücke, unpublished.
[3] W. Schnick, J. Lücke, *J. Solid State Chem. 87* (1990) 101.
[4] W. Schnick, J. Lücke, *Z. Anorg. Allg. Chem. 588* (1990) 19.
[5] W. Schnick, J. Lücke, *Solid State Ionics 38* (1990) 271.
[6] The composition of $Li_{10}P_4N_{10}$ was determined by elemental analysis (lithium by flame photometry, phosphorus as molybdovanadatophosphate by photometry, and nitrogen as indophenol by photometry). The absence of hydrogen (N–H) was checked by IR spectroscopy.
[7] $Li_{10}P_4N_{10}$: $Fd\bar{3}m$, a = 1230.9(1) pm, Z = 8, Enraf-Nonius CAD4 diffractometer, $Mo_{K\alpha}$ radiation, graphite monochromator, scan width 2°, ω scan, 958 measured reflections with $2° \le \theta \le 32°$, 166 symmetry-independent reflections with $F_0 \ge 3\sigma(F_0)$, R_{int} = 0.047, anisotropic refinement. R = 0.074, R_w = 0.042 with $w = 10.8/(\sigma^2(F_0))$. Further details of the crystal structure investigation may be obtained from the Fachinformationszentrum Karlsruhe, Gesellschaft für wissenschaftlich-technische Information mbH, W-7514 Eggenstein-Leopoldshafen 2 (FRG), on quoting the depository number CSD-55175, the names of the authors, and the journal citation.
[8] In the IR spectrum (KBr and PE discs, range 4000 to 150 cm^{-1}) the only vibrational bands observed were those expected on the basis of the site symmetry (T_d) of the complex $P_4N_{10}^{10\ominus}$ anion in the solid state: $\upsilon_{as}(P{=}N_{exo})$, 1067 cm^{-1}; $\delta(P{=}N_{exo})$, 541 cm^{-1}; cage vibrations, 1000, 839, 778, and 660 cm^{-1}.
[9] K. E. Almin, A. Westgren, *Ark. Kemi B15* (1942) 1.
[10] Temperature-dependent Guinier photographs revealed no phase transitions between −100 and +120 °C for $Li_{10}P_4N_{10}$.
[11] M. Jansen, M. Möbs, *Z. Kristallogr. 159* (1982) 283.
[12] A. Rabenau, *Solid State Ionics 6* (1982) 277.
[13] W. H. Baur, *Crystallogr. Rev. 1* (1987) 59.

$Sr_2Li[Fe_2N_3]$ and $Ba_2Li[Fe_2N_3]$: Nitridoferrate(II) Isotypes with $^1_\infty[(FeN_{3/2})_2^{5\ominus}]$ Anions**

By *Peter Höhn, Sabine Haag, Wolfgang Milius,* and *Rüdiger Kniep**

Dedicated to Professor Hans Georg von Schnering on the occasion of his 60th birthday

$Li_4[FeN_2]$, the only nitridoferrate(II) known so far, contains $[FeN_2]^{4\ominus}$ units isostructural to CO_2.[1] Trigonal-planar $[FeN_3]^{6\ominus}$ anions, isostructural to $[CO_3]^{2\ominus}$, have been found in the nitridoferrates(III) $Ba_3[FeN_3]$[2] and $(Ca_3N)_2[FeN_3]$.[3] We have now succeeded in synthesizing $Sr_2Li[Fe_2N_3]$ and $Ba_2Li[Fe_2N_3]$,[4] nitridoferrate(II) isotypes containing the polymeric anions $^1_\infty[(FeN_{3/2})_2^{5\ominus}]$ (Fig. 1), whose structure is closely related to that of the formally isoelectronic B_2S_3[5] (Fig. 2). Fe^{II} is coordinated in a distorted trigonal-planar fashion. The Fe^{II}–N bonds in the crystal structures of $Sr_2Li[Fe_2N_3]$ (187.2(3), 190.0(3), and 193.1(4) pm) and $Ba_2Li[Fe_2N_3]$ (186.6(8), 190.9(7), and 191.7(3) pm) are longer than Fe^{III}–N bonds in the trigonal-planar anions $[FeN_3]^{6\ominus}$ ($Ba_3[FeN_3]$, 173(1) pm;[2] $(Ca_3N)_2[FeN_3]$, 177(2) pm[3]), but they are in very good agreement with the lengths of the Fe^{II}–N bonds (186(1) pm) in the linear anions

[*] Prof. Dr. R. Kniep[+], Dipl.-Ing. P. Höhn, Dipl.-Ing. (FH) S. Haag, Dr. W. Milius
Max-Planck-Institut für Festkörperforschung,
Heisenbergstraße 1, W-7000 Stuttgart 80 (FRG)
[+] Permanent address:
Eduard-Zintl-Institut der Technischen Hochschule,
Hochschulstraße 10, W-6100 Darmstadt (FRG)

[**] This work was supported by the Deutsche Forschungsgemeinschaft, the Fonds der Chemischen Industrie, and the Vereinigung von Freunden der TH-Darmstadt.

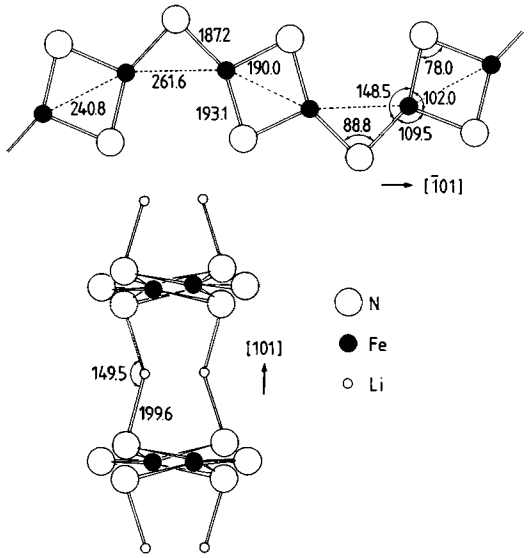

Fig. 1. $Sr_2Li[Fe_2N_3]$: Section of the anion chain $^1_\infty[(FeN_{3/2})_2^{5\ominus}]$ (top) and linking to give the layers $^2_\infty\{Li_{2/2}[(FeN_{3/2})_2]^{4\ominus}\}$ (bottom). Bond lengths in pm, bond angles in °; maximum standard deviations for distances (7), for angles (9), referred in each case to the last digit given.

$[FeN_2]^{4\ominus}$ of $Li_4[FeN_2]$.[1] The polymeric anions $[(FeN_{3/2})_2^{5\ominus}]$ are formed by linking of FeN_3 groups through two common nitrogen atoms, thereby giving planar Fe_2N_4 groups with central Fe_2N_2 four-membered rings and short transannular $Fe^{II}\cdots Fe^{II}$ contacts (240.8(2) pm (243.5(2) pm)).[6] Linking of the Fe_2N_4 groups through common exocyclic nitrogen atoms results in the $^1_\infty[(FeN_{3/2})_2^{5\ominus}]$ chains. Figure 2 shows the close relationship of the $^1_\infty[(FeN_{3/2})_2^{5\ominus}]$ anion partial structure to the formally isoelectronic B_2S_3[5] (24-electron systems: two electrons are counted for each Fe^{II} and the d^6 system is ignored).

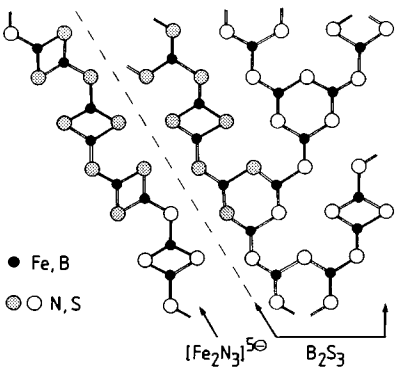

Fig. 2. Comparison of the B_2S_3 layer structure[5] with the formally isoelectronic chain anion $[Fe_2N_3]^{5\ominus}$. Identical linking patterns are indicated by dashed lines.

The discussion of further structural details will be restricted to the strontium compound: The $^1_\infty[(FeN_{3/2})_2^{5\ominus}]$ chains are joined through Li–N bonds along [101] to form layers, $^2_\infty\{Li_{2/2}[(FeN_{3/2})_2]^{4\ominus}\}$ (Fig. 1., bottom), in which the Li–N bond lengths are 199.6(7) pm and the N–Li–N bond angles 149.5(9)°. For comparison, the Li–N bonds in the crystal structure of Li_3N[7] are 193.8(1) pm (twofold coordinated Li) and 210.6(1) pm (threefold coordinated Li). The strontium ions lie between the $^2_\infty\{Li_{2/2}[(FeN_{3/2})_2]^{4\ominus}\}$ layers and are coordinated in a distorted trigonal-bipyramidal fashion by nitrogen. The Sr–N distances (257.8(5) to 277.6(1) pm) are in the range of the sums of the effective ionic radii (260 to 275 pm[8]).

Experimental Procedure

For the synthesis of $Sr_2Li[Fe_2N_3]$ ($Ba_2Li[Fe_2N_3]$), Li_3FeN_2[9], Sr_2N[10], and Fe (Li_3N[7], Ba_3N_2[11], and Fe) were used in a molar ratio of 1 : 3 : 5 (4 : 2 : 1). The powders were mixed and pressed into pellets under inert atmosphere, heated (100 °C h^{-1}) in iron crucibles to 750 °C, and kept at this temperature for 36 h under a stream of nitrogen (1 atm, about 5 L h^{-1}). Cooling was carried out at a rate of 20 °C per hour (10 °C per hour). The shiny black reaction products, thin layers of which appear red when viewed against the light, contained small amounts of unreacted iron besides the quaternary compounds. Single crystals (tetragonal prisms) suitable for structure analyses were isolated under paraffin and placed in sealed Lindemann capillaries.

Received: February 6, 1991 [Z 4429 IE]
German version: *Angew. Chem. 103* (1991) 874

CAS Registry numbers:
$Sr_2Li[Fe_2N_3]$, 133870-39-0; $Ba_2Li[Fe_2N_3]$, 133840-38-9; $Li_3[FeN_2]$, 12332-29-5; Sr_2N, 37194-83-5; Fe, 7439-89-6; Li_3N, 26134-62-3; Ba_3N_2, 12047-79-9.

[1] A. Gudat, R. Kniep, A. Rabenau, *Angew. Chem. 103* (1991) 217; *Angew. Chem. Int. Ed. Engl. 30* (1991) 199.
[2] P. Höhn, R. Kniep, A. Rabenau, *Z. Kristallogr.*, in press.
[3] G. Cordier, P. Höhn, R. Kniep, A. Rabenau, *Z. Anorg. Allg. Chem. 591* (1990) 58.
[4] $Sr_2Li[Fe_2N_3]$ ($Ba_2Li[Fe_2N_3]$): Structure determination and crystallographic data: monoclinic, $C2/c$; $a = 655.9(1)$ (687.5(2)), $b = 1141.4(2)$ (1178.1(4)), $c = 659.3(1)$ (680.9(2)) pm, $\beta = 93.28(5)$ (92.39(2))°; $Z = 4$; $\rho_{calcd.} = 4.53$ (4.53) g cm^{-3} 1548 (713) measured, 637 (595) unique reflections; $R = 0.027$ (0.037), $R_w = 0.021$ (0.038). STOE-STADI-4 single-crystal diffractometer, $Mo_{K\alpha}$, graphite monochromator, $T = 300$ K. – Further details of the crystal structure investigation are available on request from the Fachinformationszentrum Karlsruhe, Gesellschaft für wissenschaftlich-technische Information mbH, W-7514 Eggenstein-Leopoldshafen 2 (FRG), on quoting the depository number CSD 55249, the names of the authors, and the journal citation.
[5] H. Diercks, B. Krebs, *Angew. Chem. 89* (1977) 327; *Angew. Chem. Int. Ed. Engl. 16* (1977) 313.
[6] Recently, we also found isolated, planar $[Fe_2N_4]^{8\ominus}$ units in the crystal structures of $Ca_2[FeN_2]$ and $Sr_2[FeN_2]$: *P. Höhn*, Dissertation in progress, TH-Darmstadt.
[7] A. Rabenau, H. Schulz, *J. Less Common Met. 50* (1976) 155.
[8] W. Baur, *Cryst. Rev. 1* (1987) 59.
[9] A. Gudat, R. Kniep, A. Rabenau, W. Bronger, U. Ruschewitz, *J. Less Common Met. 161* (1990) 31.
[10] N. E. Brese, M. O'Keeffe, *J. Solid State Chem. 87* (1990) 134.
[11] R. Künzel, *Dissertation*, Universität Stuttgart 1980.

$[Cu(\eta^2\text{-}H_2)Cl]$, a Model Compound for H_2 Complexes. Ab Initio Calculations and Identification by IR Spectroscopy**

By *Harald S. Plitt, Michael R. Bär, Reinhart Ahlrichs,** and *Hansgeorg Schnöckel**

Dedicated to Professor Hans Georg von Schnering on the occasion of his 60th birthday

In 1984, *Kubas* et al. synthesized $[W(CO)_3(PCy_3)_2(H_2)]$ (Cy = cyclohexyl), the first complex in which molecular hy-

[*] Prof. Dr. H. Schnöckel, H. S. Plitt
Institut für Anorganische Chemie der Universität
Meiserstrasse 1, W-8000 München 2 (FRG)
Prof. Dr. R. Ahlrichs, M. R. Bär
Institut für Physikalische Chemie und Elektrochemie der Universität
Kaiserstrasse 12, W-7500 Karlsruhe (FRG)

[**] This work was supported by the Deutsche Forschungsgemeinschaft and the Fonds der Chemischen Industrie. We wish to thank the Leibniz-Rechenzentrum der Bayerischen Akademie der Wissenschaften for its support of the theoretical investigations.

drogen is coordinated to a metal center in an η^2 fashion.[1] Subsequently, further compounds of this kind were characterized as stable solids,[2] in argon matrixes,[3] and in liquid xenon.[4] As in the case of the tungsten complex, however, the stability of these complexes was increased by additional ligands. Simpler hydrogen complexes, which could serve as model compounds for this class of substances, are still unknown.[5] Here we report the preparation of [Cu(η^2-H_2)Cl], a copper complex that represents the first compound of this kind accessible to both experimental and theoretical investigation.

Cocondensation of copper(I) chloride[6] and elemental hydrogen[7] in an argon matrix results in the immediate appearance of new IR absorption bands,[8, 9] which must be assigned to a CuCl complex with hydrogen coordinated in a side-on fashion (see Table 1 and Ref. [10]). These absorption

Table 1. Absorption frequencies [a] of matrix-isolated [Cu(η^2-H_2)Cl] and of the corresponding mono- and dideuterated complexes.

Assignment	[Cu(η^2-H_2)Cl]	[Cu(η^2-$^1H^2H$)Cl]	[Cu(η^2-$^2H_2$)Cl]
ν(CuCl)	410.7	$\approx$409	407.8
$\nu(CuH)_{as}$	934.8	765.6	696.6
$\nu(CuH)_s$	1538.9	1353.7	1077.0
ν(HH)	3222.0 [b]	2900.4	2394.6

[a] All frequencies in cm^{-1}. [b] Besides these bands, an absorption band at 3425.95 cm^{-1} was observed in all spectra obtained in experiments with CuCl and $^1H_2$. The assignment of this band is still questionable [14].

bands were not observed in control experiments involving either CuCl and argon or a mixture of hydrogen and argon. The positions of the bands of the metal–hydrogen stretching vibrations of [Cu(η^2-H_2)Cl] are in good agreement with those found by *Kubas* et al. for solid [$W(CO)_3$-$(PCy_3)_2(H_2)$].[11] However, those authors appear to have mistakenly reversed the assignments of the antisymmetric and symmetric absorption bands.[11]

Ab initio calculations[15] on free CuCl and H_2 as well as on [Cu(η^2-H_2)Cl] with C_{2v} symmetry and on the corresponding complex with hydrogen coordinated in an end-on fashion ($C_{\infty v}$ symmetry) gave geometries and IR absorption frequencies[16] for the free species in good agreement with those already reported.[20]

The calculated H–H distance in [Cu(η^2-H_2)Cl] is 80.7 pm (MP2) or 79.4 pm (CPF) and therefore lengthened by 6.9 pm

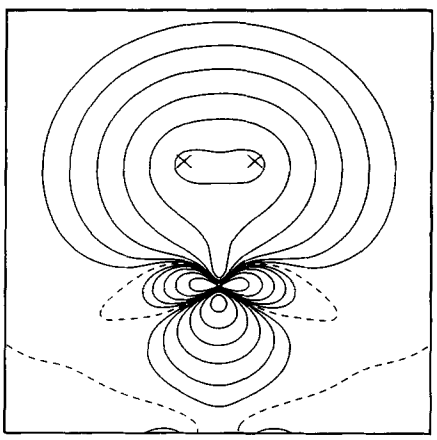

Fig. 1. Contour diagram of the 10_{a_1} MO of [Cu(η^2-H_2)Cl]. Values of the wave function: 0.0 (nodal plane, dashed line), $\pm$ 0.02, $\pm$ 0.04, $\pm$ 0.08, $\pm$ 0.16, $\pm$ 0.32, $\pm$ 0.64.

or 4.9 pm, respectively, compared with that in H_2.[16] The Cu–H distance in [Cu(η^2-H_2)Cl] is 157.2 pm (MP2) or 161.1 pm (CPF) and thus significantly longer than that in CuH (146.2 pm).[20] By contrast, the Cu–Cl distance in [Cu(η^2-H_2)Cl] is 204.7 pm (MP2) or 207.5 pm (CPF), values hardly different from the value for free CuCl.[16]

A cross-section through the electron density of the H–H–Cu bond in the molecular plane is shown in Figure 1. According to a population analysis[21] of the SCF wave function, the MO shown forms a strong three-center bond (shared electron number (SEN) = 1.1). This three-center bond is largely responsible for both the bonding H–H interaction and the bonding Cu–H interactions. Other MOs do not make significant contributions to the H–H or Cu–H bonds. A comparison of the experimentally determined and calculated positions of the IR bands, together with their scaled intensities, is shown in Figure 2. The harmonic fre-

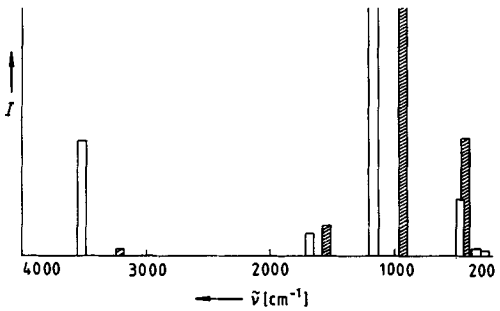

Fig. 2. Schematic drawing of the experimentally determined (hatched) and calculated (MP2) IR spectrum (frequencies and intensities *I*, the latter normalized to that of the most intense band) for [Cu(η^2-H_2)Cl].

quencies calculated for [Cu(η^2-H_2)Cl] on the MP2 level (Table 2) deviate from the experimental values by the amounts expected when anharmonicity of the vibrations is not taken into consideration. On the other hand, the IR frequencies obtained by ab initio calculation and their isotopic shifts are in good agreement with the corresponding results of normal coordinate analysis; both procedures assume a harmonic approximation.

Table 2. Frequencies [a] calculated for [Cu(η^2-H_2)Cl] and for the corresponding mono- and dideuterated complexes on the MP2 level.

Assignment	[Cu(η^2-$^1H_2$)Cl]	[Cu(η^2-$^1H^2H$)Cl]	[Cu(η^2-$^2H_2$)Cl]
"rocking"	285.6	239.6	213.2
"out of plane"	308.3	272.1	230.2
ν(CuCl)	445.7	443.7	441.9
$\nu(CuH)_{as}$	1170.1	936.9	842.0
$\nu(CuH)_s$	1681.9	1496.2	1191.5
ν(HH)	3517.0	3055.1	2488.5

[a] All frequencies in cm^{-1}.

The harmonic frequencies were also calculated for the complex with H_2 coordinated in an end-on fashion. The two negative eigenvalues in the force constant matrix of this molecule show that the calculated geometry does not correspond to a local minimum on the potential hypersurface.

Energy optimization did not give a potential minimum for a copper complex with a bent H_2 ligand (C_s symmetry); these calculations converged to the geometry of [Cu(η^2-H_2)Cl].

The energies of formation for the side-on and end-on complexes were also determined by ab initio calculations

(Scheme 1).[17] The calculated values show that both complexes are stable toward decomposition to the starting compounds. The end-on complex is appreciably less stable than

$$CuCl + H_2 \rightarrow [Cu(\eta^2\text{-}H_2)Cl] + 93\,kJ\,mol^{-1}(84\,kJ\,mol^{-1})$$

$$CuCl + H_2 \rightarrow [Cu(\eta^1\text{-}H_2)Cl] + 19\,kJ\,mol^{-1}(23\,kJ\,mol^{-1})$$

Scheme 1.

$[Cu(\eta^2\text{-}H_2)Cl]$. The bond energies of $[Cu(\eta^2\text{-}H_2)Cl]$ correspond in magnitude to those for the first coordination of a CO ligand to a nickel center.[22]

The surprisingly large energies of formation and the strong CuH_2 three-center bond in $[Cu(\eta^2\text{-}H_2)Cl]$ indicate that attempts to stabilize complexes of composition $[(CuCl)_n(H_2)_m]$ and related compounds at low temperatures should be promising. Also of interest would be an investigation of the properties of monomeric copper(I) chloride with respect to catalytic hydrogenation.

Received: January 11, 1991 [Z 4378 IE]
German version: *Angew. Chem. 103* (1991) 848

CAS Registry numbers:
$[Cu(\eta^2\text{-}^1H_2)Cl]$, 133870-40-3; $[Cu(\eta^2\text{-}^1H^2H)Cl]$, 133870-41-4; $[Cu(\eta^2\text{-}^2H_2)Cl]$, 133870-42-5; $[^{65}Cu(\eta^2\text{-}^1H_2)^{35}Cl]$, 133870-43-6; $[^{63}Cu(\eta^2\text{-}^1H_2)^{37}Cl]$, 133870-44-7; $[^{65}Cu(\eta^2\text{-}^1H_2)^{37}Cl]$, 133870-45-8; $[^{65}Cu(\eta^2\text{-}^2H_2)^{35}Cl]$, 133870-46-9; $[^{63}Cu(\eta^2\text{-}^2H_2)^{37}Cl]$, 133870-47-0; $[^{65}Cu(\eta^2\text{-}^2H_2)^{37}Cl]$, 133870-48-1; Ar, 7440-37-1; D_2, 7782-39-0; ^{35}Cl, 13981-72-1; ^{37}Cl, 13981-73-2; ^{63}Cu, 14191-84-5; ^{65}Cu, 14119-06-3.

[1] G. J. Kubas, R. R. Ryan, B. L. Swanson, P. J. Vergamini, H. J. Wasserman, *J. Am. Chem. Soc. 106* (1984) 451–452.
[2] R. H. Crabtree, *Acc. Chem. Res. 23* (1990) 95–101.
[3] R. L. Sweany, *J. Am. Chem. Soc. 107* (1985) 2374–2379; R. L. Sweany, A. Moroz, *ibid. 111* (1989) 3577–3583.
[4] G. E. Gadd, R. K. Upmacis, M. Poliakoff, J. J. Turner, *J. Am. Chem. Soc. 108* (1986) 2547–2552; R. K. Upmacis, M. Poliakoff, J. J. Turner, *ibid. 108* (1986) 3645–3651.
[5] Cocondensation of metal atoms and hydrogen in noble gas matrixes resulted in cleavage of the H_2 bond and formation of hydride bonds to the metal center: G. A. Ozin, C. Gracie, *J. Phys. Chem. 88* (1984) 643–645; G. A. Ozin, J. G. McCaffrey, *ibid. 88* (1984) 645–648.
[6] Monomeric copper(I) chloride was synthesized by reaction of copper turnings with elemental chlorine at about 1300 K in a Knudsen cell.
[7] The usual conditions of matrix isolation allow condensation of hydrogen and its isotopes in concentrations of up to 10% in argon matrixes: G. R. Smith, J. A. Warren, W. A. Guillory, *J. Chem. Phys. 65* (1976) 1591–1593; J. A. Warren, G. R. Smith, W. A. Guillory, *ibid. 72* (1980) 4901–4908.
[8] We have already described the cryostats and the vaporization conditions: R. Ahlrichs, R. Becherer, M. Binnewies, H. Borrmann, M. Lakenbrink, S. Schunck, H. Schnöckel, *J. Am. Chem. Soc. 108* (1986) 7905. The IR investigations were carried out with an FT IR instrument (Bruker IFS66v). Above 500 cm^{-1} the spectra were recorded with a resolution of one wave number; below 500 cm^{-1}, the resolution was two wave numbers.
[9] If, instead of $^1H_2$, deuterium or mixtures of $^1H_2$, $^2H_2$, and $^1H^2H$ were used, the bands were shifted (Table 1). These isotope shifts confirm the presence of a single H_2 ligand in the species investigated.
[10] In addition to the frequencies in Table 1, bands in the region of the CuCl stretching vibration were also observed. We assign these to CuCl stretching modes (νCuCl) of the following isotopomers of $[Cu(\eta^2\text{-}H_2)Cl]$: $(^1H_2)^{65}Cu^{35}Cl$, 408.84 cm^{-1}; $(^1H_2)^{63}Cu^{37}Cl$, 404.02 cm^{-1}; $(^1H_2)^{65}Cu^{37}Cl$, 401.12 cm^{-1} and $(^2H_2)^{65}Cu^{35}Cl$, $\approx$ 406 cm^{-1}; $(^2H_2)^{63}Cu^{37}Cl$, 401.12 cm^{-1}; $(^2H_2)^{65}Cu^{37}Cl$, 398.23 cm^{-1}. The relative intensities of these bands in the spectra correspond to those of unperturbed CuCl with its four natural isotopomers: $^{63}Cu^{35}Cl$, 420.41 cm^{-1}; $^{65}Cu^{35}Cl$, 418.00 cm^{-1}; $^{63}Cu^{37}Cl$, 413.66 cm^{-1}; $^{65}Cu^{37}Cl$, 411.25 cm^{-1}. T. P. Martin, H. Schaber, *J. Chem. Phys. 73* (1980) 3541–3546. These findings, together with the observed $^1H/^2H$ shifts for the symmetric and antisymmetric CuH stretching vibration [9] confirm the composition of the investigated species as consisting of an H_2 ligand and a CuCl unit.
[11] For $[Cu(\eta^2\text{-}H_2)Cl]$, force constant calculations were carried out for the five A_1 and B_1 vibrational modes [12]. Owing to the large anharmonicity of the vibrational modes involving hydrogen [13], the harmonic frequencies and their corresponding isotopic shifts are not comparable with the experimental data. These model calculations (normal coordinate analysis and ab initio calculations for $[Cu(\eta^2\text{-}H_2)Cl]$) show that, due to the small bond angle at the metal atom (α = 29.7° (MP2), 28.5° (CPF)), a strong coupling for the metal–hydrogen bonds and, in addition, a high CuH/CuH interaction force constant are expected for the coordination of an H_2 ligand to a metal center. This also means, however, that the antisymmetric CuH stretching vibration will lie at lower wave numbers than the antisymmetric. This assignment is generalizable, since the comparable band positions and isotopic shifts of the MH vibrational modes in $[Cu(\eta^2\text{-}H_2)Cl]$ and the hydrogen complexes so far known indicates similar vibrational motions.
[12] For the model calculations on the force field of $[Cu(\eta^2\text{-}H_2)Cl]$ (A_1 and B_1 symmetry), the following force constants were estimated: f(CuCl) = 230, f(CuH) = 100, f(HH) = 300, f(ClCuH) = 10, f(CuH/CuH) = 45, f(CuH/HH) = 5, f(CuCl/CuH) = 10 Nm^{-1}.
[13] H. J. Becher, *Fortschr. Chem. Forsch. 10* (1968) 156–205.
[14] We assume that the band at 3425.95 cm^{-1} is assignable to a combination mode ($2 \cdot \nu(CuH)_{as} + \nu(CuH)_s$) shifted by Fermi resonance. The intensity of this absorption band would then be due almost solely to the HH stretching vibration. In experiments with $^1H_2$, $^1H^2H$ and $^2H_2$, additional but only poorly resolved, absorptions were observed at higher wave numbers (4122.14, 3731.13, and 2965.44 cm^{-1}). They do not correspond to the previously observed vibrations of matrix-isolated hydrogen. Moreover, they only appear when CuCl is also present in the matrix. We therefore assign these bands to a weak interaction of molecular hydrogen with monomeric copper(I) chloride. This assignment is supported by the small deviation of the measured HH absorption frequencies compared with those in hydrogen, as well as the corresponding relation in the $^2H_2$ complexes.
[15] Both CI calculations with the CPF method [18] (only geometry optimization) and MP2 calculations with the program package CADPAC [19] (geometry optimization and harmonic frequencies) were carried out. Basis sets for the CI calculations: copper-relativistic pseudopotential (Ne core) 8s7p6d2f/[6,5,3,2]; chlorine 12s9p2d1f/[7,5,2,1]; hydrogen 6s2p1d/[4,2,1]. Basis sets for the MP2 calculations: copper 14s11p6d3f/[8,6,4,2]; chlorine 12s9p2d/[7,5,2]; hydrogen 5s1p/[3,1].
[16] The following results were obtained for the free molecules CuCl and H_2 (MP2/CPF/Exp. [20]): d(CuCl) = 205.8/207.7/205.1 pm; ω(CuCl) = 420.3/412.5/415.3 cm^{-1}; d(HH) = 73.8/74.5/74.1 pm; ω(HH) = 4545.3/4351.5/4401.2 cm^{-1}.
[17] The energies calculated on the MP2 level are given. The corresponding values for the CPF method are given in parentheses.
[18] R. Ahlrichs, P. Scharf, C. Ehrhardt, *J. Chem. Phys. 82* (1985) 890.
[19] R. D. Amos, J. E. Rice, *CADPAC: The Cambridge Analytic Derivatives Package*, Issue 4.0, Cambridge 1987.
[20] K. P. Huber, G. Herzberg: *Molecular Spectra and Molecular Structure IV. Constants of Diatomic Molecules*, Van Nostrand, Toronto 1979.
[21] A Roby-Davidson population analysis was performed: E. R. Davidson, *J. Chem. Phys. 46* (1967) 3320; K. R. Roby, *Mol. Phys. 27* (1974) 81; R. Heinzmann, R. Ahlrichs, *Theor. Chim. Acta 41* (1976) 33. The occupation numbers (SEN – shared electron number) thereby obtained are a reliable measure for the strength of covalent bonding. Typical values are SEN = 2.94 for N_2, SEN = 2.28 for a C=C double bond, and SEN = 1.46 for a hydrogen molecule. R. Ahlrichs, C. Ehrhardt, *Chem. Unserer Zeit 19* (1985) 120.
[22] In A. E. Stevens, C. S. Feigerle, W. C. Lineberger, *J. Am. Chem. Soc. 104* (1982) 5026–5031: Ni + CO → Ni(CO) + $\approx$ 140 $kJ\,mol^{-1}$.

A Telluradistannirane and a 1,3-Ditelluradistannetane by Stepwise Addition of Tellurium to a Distannene**

By *Annemarie Schäfer, Manfred Weidenbruch,* Wolfgang Saak, Siegfried Pohl,** and *Heinrich Marsmann*

Dedicated to Professor Hans Georg von Schnering on the occasion of his 60th birthday

The presence of element–element double bonds in disilenes **1**[1] and digermenes **2**,[2–8] but not in distannenes, has

[*] Prof. Dr. M. Weidenbruch, Dr. A. Schäfer, Prof. Dr. S. Pohl, Dipl.-Chem. W. Saak
Fachbereich Chemie der Universität
Carl-von-Ossietzky-Straße 9–11, W-2900 Oldenburg (FRG)
Prof. Dr. H. Marsmann, Fachbereich Chemie der Universität (GH), Paderborn

[**] Compounds of Germanium and Tin, Part 6. This work was supported by the Deutsche Forschungsgemeinschaft and the Fonds der Chemischen Industrie. Part 5: M. Weidenbruch, K. Schäfers, K. Peters, H. G. von Schnering, *J. Organomet. Chem. 381* (1990) 173.

been established unambiguously. Thus, *Lappert*'s distannene **3**,[9] the only structurally characterized compound of this kind, is better regarded as a double donor–acceptor adduct of the two stannylenes (stannanediyls) **4**. This description is

$R_2E{=}ER_2$ — **1**, E = Si; **2**, E = Ge — R = alkyl, aryl

$R_2SnSnR_2 \rightleftharpoons 2\,R_2Sn$: — **3** — **4** — R = $(Me_3Si)_2CH$

consistent with the tin–tin bond length, which is only slightly shorter than that of a tin–tin single bond,[9, 10] the results of quantum-mechanical calculations,[10] the solid-state ^{119}Sn NMR data,[11] and, finally, the reversible decomposition to two stannylenes **4** in solution.[12]

On the other hand, the distannene **7**, synthesized by *Masamune* and *Sita*,[13] probably does have a tin–tin multiple bond according to spectroscopic evidence. Compound **7** is accessible by photolysis or thermolysis of the cyclotristannane **6**, with which it is in thermal equilibrium over a broad temperature range. A more detailed characterization of **7** has been hindered so far by the laborious synthesis of **6**, which is obtained in only 12% overall yield starting from tin tetrabromide.[13]

$$6\,\mathrm{ArylMgBr} + 3\,SnCl_2 \longrightarrow \underset{\mathbf{6}}{\overset{\mathrm{Aryl_2Sn}}{\overset{\mathrm{Sn}}{\overset{\mathrm{Aryl_2Sn{-}SnAryl_2}}{}}}} \rightleftharpoons 3/2\,Aryl_2Sn{=}SnAryl_2$$

5 — **7**

Aryl = 2,4,6-iPr$_3$C$_6$H$_2$

We have now found that treatment of tin(II) chloride with the aryl Grignard **5** provides a high-yield and extremely simple synthetic route to **6** and therefore **7**. This synthesis makes it possible to study the chemical behavior of **7**. Thus, **7** undergoes smooth [2 + 1] cycloaddition with tellurium to give the telluradistannirane **8**, the first compound with an Sn_2X framework.[14] Crystals of **8** are stable to light and to temperatures below their melting point. The X-ray structure analysis of **8**[15] (Fig. 1) reveals a nearly equilateral triangle consisting of one tellurium atom and two tin atoms. The tin–tin and tin–tellurium bonds are somewhat longer than those usually found. Especially interesting is the environment of the tin atoms; it is formed by the two *ipso*-carbon atoms of the aryl groups and the other tin atoms as nearest neighbors. The sums of the bond angles at Sn1 and Sn2, 355° and 357°, respectively, indicate a nearly planar bonding geometry, in remarkable agreement with that found for the silicon and germanium atoms in recently prepared telluradisiliranes[16] and telluradigermiranes,[17] respectively. These comparable structures indicate that the bonding is similar in all three three-membered ring compounds. Further treatment of **8** with tellurium, as well as reaction of **7** with tellurium in excess, leads exclusively to the 1,3-ditelluradistannetane **9**, whose constitution was established mainly by ^{119}Sn and ^{125}Te NMR spectroscopy. It remains an open question whether this known ring system[18] is formed here by insertion of tellurium into the tin–tin bond, which is shielded by substituents, or whether insertion of tellurium into the comparatively easily accessible tin–tellurium bond first leads to formation of a 1,2-ditelluradistannetane, which then rearranges to the constitutional isomer **9**.

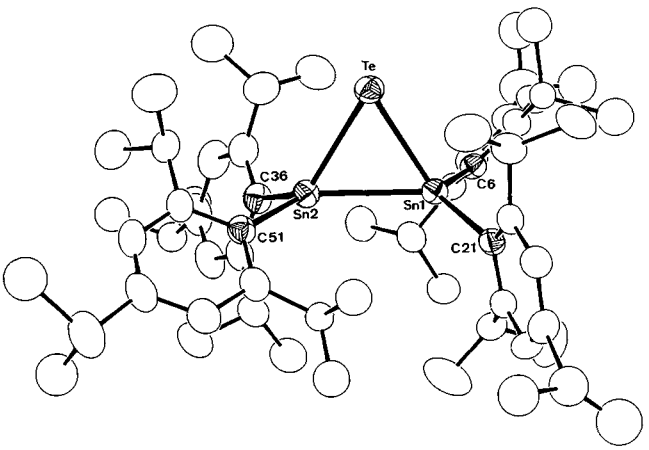

Fig. 1. Molecular structure of **8** (ORTEP, thermal ellipsoids at 30% probability, hydrogen atoms omitted). Selected bond lengths [pm] and angles [°]: Sn1-Sn2 282.7(1), Sn1-Te 280.0(1), Sn2-Te 277.9(1), Sn1-C6 217.7(7), Sn1-C21 219.1(6), Sn2-C36 217.0(6), Sn2-C51 215.9(8); Sn1-Te-Sn2 60.9(1), Te-Sn2-Sn1 59.9(1), Sn2-Sn1-Te 59.2(1); torsion angle (average of the angles between the opposite planes defined by C21-Sn1-Sn2/C51-Sn2-Sn1 and by C6-Sn1-Sn2/C36-Sn2-Sn1) 13.5°.

The lighter chalcogens sulfur and selenium react analogously with **7** to give the corresponding three- and four-membered ring compounds. However, these products are always formed simultaneously, their relative amounts depending on the ratio of the starting materials, and their separation is difficult. We will report later on their isolation.

Experimental Procedure

8: Compound **6** (2.00 g, 1.27 mmol) was allowed to react with tellurium (0.25 g, 1.96 mmol) in refluxing toluene (40 mL) until the red color of **7** had vanished (about 2 h). After separation of unreacted tellurium and removal of toluene by distillation under vacuum, the residue was crystallized twice from *n*-pentane to give 1.60 g (71%) of **8** as yellow-orange cubes (m.p. 175°C, turns dark red above 163°C). ^1H NMR (300 MHz, C_6D_6): δ = 1.27 (m, 72H), 2.83 (sept, 4H), 3.96 (very broad, 8H), 7.15 (s, 8H, $^4J(^{119}Sn\text{-}^1H)$ = 21.7 Hz). ^{13}C NMR (75.44 MHz, C_6D_6): δ = 14.21; 22.66, 24.10, 24.39, 24.66, 25.96, 34.46; 40.05 (broad), 122.95, 150.47, 155.29 (broad). ^{119}Sn NMR (93.23 MHz, C_6D_6, versus Me_4Sn): δ = −594, $^1J(^{119}Sn\text{-}^{117}Sn)$ = 3382 Hz. ^{125}Te NMR (78.87 MHz, C_6D_6, versus Me_2Te): δ = −903, $^1J(^{125}Te\text{-}^{119}Sn/^{117}Sn)$ = 844/806 Hz. UV/VIS: λ_{max} [nm] (ε) = 378 (3060). Correct C,H,Te analysis.

9: a) Similarly, **6** (2.00 g, 1.27 mmol) and tellurium (0.50 g, 3.92 mmol) were allowed to react in 40 mL of refluxing toluene for 15 h. Corresponding workup afforded 1.80 g (73%) of **9** as orange needles (m.p. 229–231°C). ^1H NMR (300 MHz, C_6D_6): δ = 1.33 (d, 24H, ^3J = 6.9 Hz), 1.40 (d, 48H, ^3J = 7.0 Hz), 2.89 (sept, 4H), 4.16 (sept, 8H), 7.15 (s, 8H, $^4J(^{119}Sn\text{-}^1H)$ = 25.2 Hz). ^{13}C NMR (75.44 MHz, C_6D_6): δ = 24.10, 25.35, 34.49, 37.31, 122.41, 134.67, 150.56, 154.45. ^{119}Sn NMR (93.23 MHz, C_6D_6, versus Me_4Sn): δ = −752, $^2J(^{119}Sn\text{-}^{117}Sn)$ = 417 Hz. ^{125}Te NMR: (78.87 MHz, C_6D_6, versus Me_2Te): δ = 171, $^1J(^{125}Te\text{-}^{119}Sn/^{117}Sn)$ = 1975/1894 Hz. UV/VIS: λ_{max} [nm] (ε) = 460 (320). Correct C,H,Te analysis. b) Likewise, reaction of **8** (0.50 g, 0.42 mmol) and tellurium (70 mg, 0.55 mmol) for 15 h in refluxing toluene) gave **9** in quantitative yield (NMR).

Received: December 17, 1990 [Z 4330 IE]
German version: *Angew. Chem. 103* (1991) 873

CAS Registry numbers:
6, 98526-67-1; **7**, 98526-68-2; **8**, 133777-55-6; **8**·0.5 pentane, 133777-57-8; **9**, 133777-56-7.

[1] Review: R. West, *Angew. Chem. 99* (1987) 1231; *Angew. Chem. Int. Ed. Engl. 26* (1987) 1201.
[2] S. Masamune, Y. Hanzawa, D.J. Williams, *J. Am. Chem. Soc. 104* (1982) 6137.
[3] J.T. Snow, S. Murakami, S. Masamune, D.J. Williams, *Tetrahedron Lett. 25* (1984) 4191.
[4] P.B. Hitchcock, M.F. Lappert, S.J. Miles, A.J. Thorne, *J. Chem. Soc. Chem. Commun. 1984*, 480.
[5] S.A. Batcheller, S. Masamune, *Tetrahedron Lett. 29* (1988) 3383.
[6] W. Ando, T. Tsumuraya, *Organometallics 7* (1988) 1882; T. Tsumuraya, S. Sato, W. Ando, *ibid. 9* (1990) 2061.
[7] T. Tsumuraya, S. Sato, W. Ando, *Organometallics 7* (1988) 2015.
[8] S. Masamune, S.A. Batcheller, J. Park, W.S. Davies, O. Yamashita, Y. Ohta, Y. Kabe, *J. Am. Chem. Soc. 111* (1989) 1988.
[9] D.E. Goldberg, D.H. Harris, M.F. Lappert, K.M. Thomas, *J. Chem. Soc. Chem. Commun. 1976*, 261.
[10] D.E. Goldberg, P.B. Hitchcock, M.F. Lappert, K.M. Thomas, A.J. Thorne, T. Fjeldberg, A. Haaland, B.E.R. Schilling, *J. Chem. Soc. Dalton Trans. 1986*, 2387.
[11] K.W. Zilm, G.A. Lawless, R.M. Merrill, J.M. Millar, G.G. Webb, *J. Am. Chem. Soc. 109* (1987) 7236.
[12] P.J. Davidson, D.H. Harris, M.F. Lappert, *J. Chem. Soc. Dalton Trans. 1976*, 2228; T. Fjeldberg, A. Haaland, M.F. Lappert, B.E.R. Schilling, R. Seip, A.J. Thorne, *J. Chem. Soc. Chem. Commun. 1982*, 1407.
[13] S. Masamune, L.R. Sita, *J. Am. Chem. Soc. 107* (1985) 6390 and Suplementary Material.
[14] P. Brown, M.F. Malon, K.C. Molloy, *J. Chem. Soc. Chem. Commun. 1989*, 1621.
[15] **8** · 0.5 *n*-pentane: triclinic, space group $P\bar{1}$, $a = 1358.1(2)$, $b = 1555.9(3)$, $c = 1730.3(4)$ pm; $\alpha = 101.40(1)$, $\beta = 91.77(2)$, $\gamma = 144.40(1)°$, $V = 3237.8 \times 10^6$ pm^3, $Z = 2$, $\rho_{calcd} = 1.246$ g cm^{-3}. 9673 unique reflections, 8420 observed ($I > 2\sigma(I)$), 568 variables, $R = 0.042$, $R_w = 0.044$. Further details of the crystal structure investigation may be obtained from the Fachinformationszentrum Karlsruhe, Gesellschaft für wissenschaftlich-technische Information mbH, W-7514 Eggenstein-Leopoldshafen 2 (FRG), on quoting the depository number CSD-55174, the names of the authors, and the journal citation.
[16] R.P.-K. Tan, G.R. Gillette, D.R. Powell, R. West, *Organometallics 10* (1991) 546.
[17] T. Tsumuraya, Y. Kabe, W. Ando, *J. Chem. Soc. Chem. Commun. 1990*, 1159.
[18] H. Puff, R. Gattermayer, R. Hundt, R. Zimmer, *Angew. Chem. 89* (1977) 556; *Angew. Chem. Int. Ed. Engl. 16* (1977) 547; H. Puff, G. Bertram, B. Ebeling, M. Franken, R. Gattermayer, R. Hundt, W. Schuh, R. Zimmer, *J. Organomet. Chem. 379* (1989) 235.

On the Electrochemical Oxidation of $Cs^{\oplus}$ and Other Alkali-Metal Ions in Liquid Sulfur Dioxide and Acetonitrile **

By *Christophe Jehoulet* and *Allen J. Bard**

A recent paper suggested that $Cs^{\oplus}$ (as the $OTeF_5^{\ominus}$ salt) could be oxidized electrochemically at a Pt electrode in acetonitrile solutions containing $Et_4N^{\oplus}PF_6^{\ominus}$ at ca. + 3 V vs. SCE (near the background oxidation limit of MeCN).[1] The addition of cryptand decreased the potential for the observed oxidation to 2.7 V vs. SCE. Similar oxidation waves were not seen with $K^{\oplus}$, $Rb^{\oplus}$, and $nBu_4N^{\oplus}$ salts of $OTeF_5^{\ominus}$. However, the oxidation of $Cs^{\oplus}$ at such a relatively low potential appears to be at variance with our studies of electrochemical oxidations in liquid SO_2, which has been shown to have a background oxidation limit of > +5 V vs. SCE, considerably beyond that of MeCN.[2-4] Indeed, in a recent paper[4] it was shown that a $CsAsF_6$ supporting electrolyte in liquid SO_2 allowed studies to + 5 V without apparent oxidation of the $Cs^{\oplus}$. We report here cyclic voltammetric studies of $Cs^{\oplus}$ and other alkali-metal ions in liquid SO_2 which suggest that oxidation of these ions may be possible, but only at considerably more positive potentials than those suggested from the MeCN studies.[1] These studies were carried out with an ultramicroelectrode[5] (UME) (10- or 25-μm diameter) to minimize effects of solution resistance and allow studies of the salts to be carried out in the absence of supporting electrolyte.[3,4] The possibility of hydration of these salts and its influence on the electrochemical response was also examined. Finally, we reexamined the behavior of these compounds in MeCN.

Experiments in SO_2 with $CsAsF_6$ as a supporting electrolyte in the study of other compounds have been reported.[4] However, we have not been able to reproduce some aspects of this earlier work. For example, we found the maximum solubility of $CsAsF_6$ at −70 °C to be about 4 mM and oxidation of $Cs^{\oplus}$ to occur at less positive potentials. Figure 1 A shows a cyclic voltammogram (CV) of a 4 mM solution at a 10-μm UME in SO_2 without added supporting electrolyte. Figure 1 A was obtained for a saturated solution; the solubility of $CsAsF_6$ and the other alkali salts in liquid SO_2 was very low (≈4 mM for $CsAsF_6$ and even lower for the other alkali-metal salts). The CV recorded with an UME (10- or 25-μm diameter) did not show a reverse cathodic wave, even for higher scan rates (up to 20 Vs^{-1}), suggesting low stability of the oxidation product. The half-wave potential $E_{1/2}$, was 4.75 V vs. SCE for $CsAsF_6$. The other alkali salts, $KAsF_6$ or $RbAsF_6$, were also studied in the absence of supporting electrolyte and displayed similar electrochemical behavior ($E_{1/2}$ values of 4.64 and 4.66 V vs. SCE for $K^{\oplus}$ and $Rb^{\oplus}$, respectively). However, SO_2 is a resistive solvent and in order to get more quantitative information, it was necessary

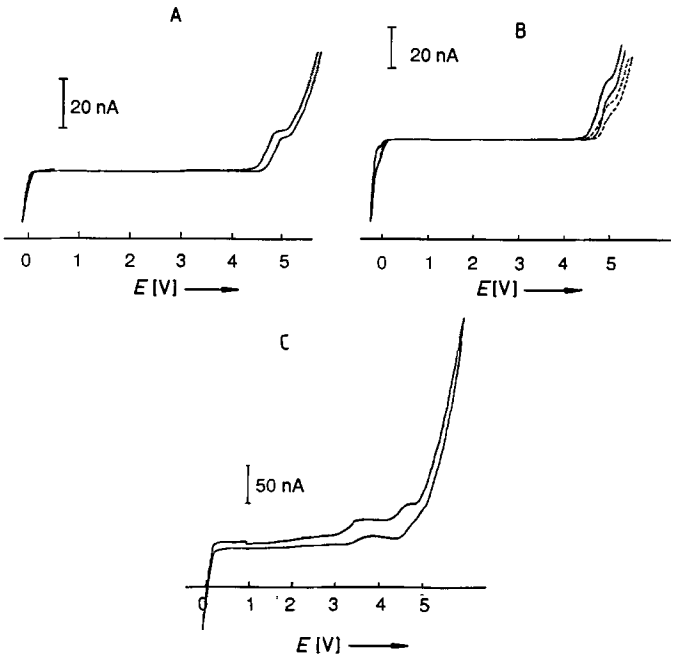

Fig. 1. Cyclic voltammogram of solutions of $Cs^{\oplus}$ at 203 K in liquid SO_2. Scan rate, 1 Vs^{-1}; working electrode, platinum disk, 10-μm diameter (A and B), 50-μm diameter (C). A) Saturated solution of $CsAsF_6$ (≈4 mM) without supporting electrolyte. B) $CsAsF_6$ (3.5 mM) with nBu_4NAsF_6 (5.2 mM). Solid curve: compound in presence of supporting electrolyte. Dashed curve: supporting electrolyte alone. C) Saturated solution of $CsClO_4$ without supporting electrolyte.

[*] Prof. A. J. Bard, Dr. C. Jehoulet
Department of Chemistry, The University of Texas at Austin
Austin, TX 78712 (USA)

[**] Electrochemistry in Liquid SO_2, Part 10. This work was supported by the National Science Foundation (CHE8901450). Part 9: [4]

to compensate for the effect of ohmic drop and migration. Therefore, experiments were performed with nBu$_4$NAsF$_6$ as a supporting electrolyte. We found this electrolyte to be oxidized at slightly more positive potentials than $Cs^{\oplus}$ ($E_{1/2} = 4.9 \pm 0.1$ V vs. SCE). Electrolytes with shorter alkyl chains[4] oxidize at more positive potentials, but their lower solubilities and rates of dissolution made them less convenient than nBu$_4$NAsF$_6$. A CV for the oxidation of $Cs^{\oplus}$ is shown in Figure 1B. The oxidation wave did not display a reverse wave and occurred at about the same potential as that for the oxidation of nBu$_4$N$^{\oplus}$, as expected from the $E_{1/2}$ values of the alkali salts found in the preliminary experiments. The other alkali salts displayed the same electrochemical behavior.

The $E_{1/2}$ values for the oxidation of various alkali cations are given in Table 1. These correspond to those found for the experiments without supporting electrolyte. The $E_{1/2}$ found for $Cs^{\oplus}$ is much more positive than the one reported previously.[1] The experiments were also conducted as a function of salt concentration. The limiting current (i_l) varied with concentration (Fig. 2), in the absence and presence of supporting electrolyte. The linear variation observed shows that the oxidation wave is effectively due to the oxidation of the added salt. Unfortunately, we could not determine the number of electrons, n, involved in the electrode reaction by coulometry. However, a rough estimate of the diffusion coefficient, D, was made assuming a one- or a two-electron charge-transfer reaction and using the expression of the steady-state current for a micro-disk.[5] The values obtained at $-70\,^{\circ}C$ are given in Table 1. Those values can be used together with the Stokes–Einstein equation to estimate the diameter of the solvated ion. The values obtained in the case of a one-electron transfer seem more compatible with the value of the crystalline radius, even in the case of solvation by molecules of solvent.

Table 1. Electrochemical parameters of alkali salts.

Salt	$E_{1/2}$ [V] vs SCE	D [10^{-5} cm^{2}s^{-1}]		d [Å] [a]		r [Å] [9]
		$n = 1$	$n = 2$	$n = 1$	$n = 2$	
$CsAsF_6$	4.73 ± 0.07	1.68	0.84	5.9	11	1.65
$RbAsF_6$	4.67 ± 0.07	2.10	1.05	4.75	9.5	1.49
$KAsF_6$	4.64 ± 0.1	2.38	1.19	4.1	8	1.33
$NaPF_6$	4.8	–	–	–	–	–

[a] Calculated from the Stokes–Einstein relationship.

Several other experiments were undertaken to demonstrate that the oxidation was due to the alkali-metal ion rather than the anion ($AsF_6^{\ominus}$) or adventitious water. For example, alkali-metal salts are easily hydrated and this can affect their electrochemical behavior. Therefore, alkali salts were dried in a vacuum oven at 150 °C for 48 h and stored in a dry box under a helium atmosphere. To determine the amount of water in the compounds and its possible effect on the voltammograms, the salts were titrated by the Karl Fischer method. The reagent (Fluka) was standardized with sodium tartrate dihydrate salt as described by *Neuss* et al.[6] Titrations were performed with both visual and amperometric end-point detection. To prevent any contamination of the reagents, titrations were conducted[7] in the dry box under a helium atmosphere. All reagents were opened and used only in the dry box. This should exclude all contamination by external moisture.

After the standardization of the reagent, the salts were added in MeOH solution. There was no change in the color of the solution or in the amperometric current, even after stirring for more than 30 min. Thus, the water in the salt was less than 0.05%. This implies that, in each experiment, the concentration of water in the cell from the compound was less than 10 μM. This low concentration is not compatible with the waves seen in the voltammograms. Moreover, when water was intentionally added to the solutions to observe its effect on the electrochemical behavior, it catalyzed the limiting oxidation process and produced sharp peaks totally different from the waves attributed to the alkali metals; the same behavior was observed with imperfectly dried compound. Sometimes the compounds also displayed a small wave at about 3.8 V vs. SCE, which can be assigned to the moisture from the salt. This wave was also observed when a small amount of water was added to the solution. These observations suggest that the alkali-metal wave in the voltammograms cannot be attributed to free water or that bound to ions.

Finally, to demonstrate that the wave was not due to $AsF_6^{\ominus}$ oxidation, $CsClO_4$ was examined in SO_2 in the absence of supporting electrolyte. The voltammogram (Fig. 1C) displayed two oxidation waves. The first one is assigned to the oxidation of the perchlorate anion, as observed in previous studies.[2, 8] The other $E_{1/2}$ was the same as that observed with $CsAsF_6$ solutions.

This study suggests that the alkali-metal cations might be oxidized, but only at high potentials in SO_2. This oxidation cannot be observed in MeCN. The electrochemical behavior of $CsAsF_6$ in MeCN was studied in our laboratory and Fig-

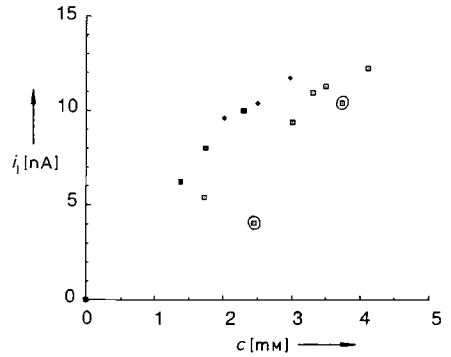

Fig. 2. Steady-state current as a function of concentration for various salts. ◆ = $RbAsF_6$; ■ = $KAsF_6$; ⊡ = $CsAsF_6$. Circled values were recorded without supporting electrolyte; these currents are lower because of electrorepulsion (migration) effects on the cation at these very positive potentials. The current was determined after subtraction of the nBu$_4$N$^{\oplus}$ background. The reduction of the solvent was chosen as a reference potential. This procedure does not allow the use of a large amount of supporting electrolyte (1–10 mM) and therefore requires measurement with UMEs. (Working electrode: platinum disk, 10-μm diameter).

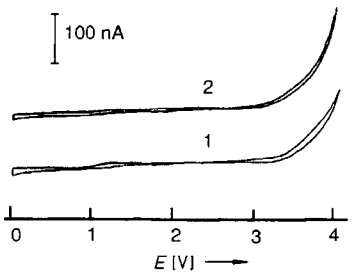

Fig. 3. Cyclic voltammograms of $CsAsF_6$ in acetonitrile at 298 K. 1) nBu$_4$NPF$_6$ (0.1 M) and [2.2.2]cryptand (5.9 mM) in acetonitrile. 2) In the presence of $CsAsF_6$ (6 mM). Acetonitrile was dried on Woelm neutral activated alumina before use. Scan rate, 0.2 Vs^{-1}; working electrode, platinum disk, 25 μm diameter.

ure 3 shows that the voltammogram does not display any oxidation wave before background, even in the presence of cryptand, introduced to stabilize the oxidized form of the alkali cation.

The oxidation of $Cs^{\oplus}$ and the other alkali-metal ions in SO_2 is not unambiguous. It is surprising that $Cs^{\oplus}$, $Na^{\oplus}$, and $K^{\oplus}$ are oxidized at the same potential, given their very different ionization potentials in the gas phase. However, salts from different origins show the same behavior, suggesting that a common impurity is unlikely. Water, the most likely candidate impurity, does not show this CV behavior, and the effect of added electrolyte suggests the oxidation wave can be attributed to a positive species.

Experimental Procedure

The measurements, the purification of SO_2, and the preparation of the supporting electrolyte, nBu$_4$NAsF$_6$ and the alkali salts (CsAsF$_6$, RbAsF$_6$, KAsF$_6$) followed the procedure described previously[3, 4]. NaPF$_6$ (Aldrich) was used after recrystallization from Me$_2$SO/CH$_2$Cl$_2$ and drying in a vacuum oven under the same conditions as above.

Experiments in MeCN were performed in a dry box (Vacuum Atmospheres) under a helium atmosphere using high-purity MeCN with a low concentration of water (0.003%) (Burdick & Jackson). Kryptofix (Aldrich) and Woelm neutral activated alumina (ICN Biomedicals) were used as received. The supporting electrolyte, nBu$_4$NPF$_6$, was thrice recrystallized from EtOH/THF (1:1), then dried in a vacuum oven and stored in the dry box.

Received: December 11, 1990 [Z 4318 IE]
German version: *Angew. Chem. 103* (1991) 882

[1] K. Moock, K. Seppelt, *Angew. Chem. 101* (1989) 1713; *Angew. Chem. Int. Ed. Engl. 28* (1989) 1676.
[2] L. A. Tinker, A. J. Bard, *J. Am. Chem. Soc. 101* (1979) 2316.
[3] E. Garcia, J. Kwak, A. J. Bard, *Inorg. Chem. 27* (1988) 4377.
[4] E. Garcia, A. J. Bard, *J. Electrochem. Soc. 137* (1990) 2752.
[5] R. M. Wightman, D. O. Wipf in A. J. Bard (Ed.): *Electroanalytical Chemistry*, Dekker, New York 1989, p. 267, and references cited therein.
[6] J. D. Neuss, M. G. O'Brien, H. A. Frediani, *Anal. Chem. 23* (1951) 1332.
[7] J. Mitchell, Jr., D. M. Smith: *Aquametry, Vol. 3*, Wiley, New York 1980.
[8] P. Castellonese, G. Launay, *Bull. Soc. Chim. Fr. 7–8* (1978) I-317.
[9] L. Pauling: *The Nature of the Chemical Bond*, 3rd ed., Cornell University Press, Ithaca, NY, USA 1960; *Die Natur der chemischen Bindung*, Verlag Chemie, Weinheim 1976.

Cryptatium: A Species of Expanded Atom/Radical Ion Pair Type from Electroreductive Crystallization of the Macrobicyclic Sodium Tris(Bipyridine) Cryptate**

By *Luis Echegoyen, André DeCian, Jean Fischer,* and *Jean-Marie Lehn**

The inclusion of a metal cation into a macropolycyclic ligand results in the formation of a very large, charge-diffuse cryptate cation.[1, 2] The spherically shaped cryptates of alkali-metal cations[1] are expected to have very low surface charge density and to interact very weakly with anions or solvent molecules. They represent an extrapolation of the $Cs^{\oplus}$ cation (1.65 Å radius) to very large size (about 5 Å radius) and might formally be considered as "super-heavy" alkali-metal cations.[2] If the anion associated with such a cation is an electron, the resulting species could be considered as a very large alkali-metal atom of extremely low ionization potential (which in the isolated state would have analogies with a Rydberg atom) or as a salt containing an electron as anion, an electride,[3, 4] such as that derived from the $K^{\oplus}$ cryptate of the ligand [2.2.2], $\{[K^{\oplus} \subset$cryptand 2.2.2$], e^{\ominus}\}$. Between the two extremes, the atom and the electride, one may envisage (as suggested earlier by Lehn[5]) a species in which the electron would be located on acceptor sites incorporated into the ligand shell surrounding the metal cation bound in the molecular cavity of a spheroidal cryptate, thus yielding a self-contained neutral entity. Such a unit represents a way of expanding the atom by stabilizing the electron on a ligand orbital rather than on a metal-centered one. It may be described either as a radical contact ion pair, containing a more or less delocalized electron, or, more intriguingly, as a sort of molecular "expanded atom".[6, 7]

We now report the generation and some physical and structural properties of such a species formed by electroreductive crystallization of the sodium cryptate $[Na^{\oplus} \subset \mathbf{1}]$ of the macrobicyclic tris(bipyridine) ligand **1** [tris(bpy)].[8]

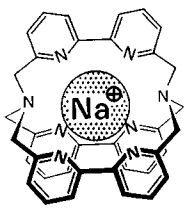

$[Na^{\oplus} \subset \mathbf{1}]$

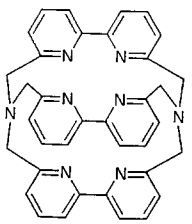

1

Electrochemical reduction of a solution of $[Na^{\oplus} \subset \mathbf{1}]\,Br^{\ominus}$ in dimethylformamide (DMF) gave three clearly resolved, quasi-reversible reductions at $E_{1/2} = -2.40$, -2.51, and -2.68 V versus $Fc^{\oplus}/Fc$ (Fc = ferrocene), with anodic and cathodic peak potentials $E_p^a = -2.36$, -2.44, -2.61 and $E_p^a = -2.44$, -2.57, -2.73 V vs $Fc^{\oplus}/Fc$.[9] They correspond respectively to the monoreduced (neutral), direduced (monoanionic), and trireduced (dianionic) derivatives of the starting cryptate. The species formed may be considered to result from the successive reduction of the three bipyridyl groups of the tris(bpy) cryptand. Multiple electron reduction has been reported for other bpy complexes such as $[Ru(bpy)_3]^{2\oplus}$.[10]

Cyclic voltammetry in acetonitrile gave the same results as in DMF, but coulometric reduction at -2.50 V led to the deposition of a deep blue solid from the beginning of the experiment. No color developed in the bulk of the stirred solution during the electrolysis; only a faint and transitory purplish color was seen in the vicinity of the working Pt coil electrode, while the deeply colored solid accumulated on its surface. This solid did not have the usual "fluffy" appearance of most electrodeposited materials; it appeared fairly crystalline from the beginning. As soon as the Ar atmosphere was removed, the solid faded to a colorless-yellowish precipitate. Based on these results, a controlled-current electrocrystallization was attempted, using high-vacuum condi-

[*] Prof. Dr. J.-M. Lehn, Prof. Dr. L. Echegoyen[+]
Laboratoire de Chimie Supramoléculaire, Institut Le Bel
Université Louis Pasteur
4, rue Blaise Pascal, 67000 Strasbourg (France).
Dr. A. DeCian, Prof. Dr. J. Fischer
Laboratoire de Cristallochimie, Institut Le Bel
Université Louis Pasteur
[+] Permanent address: Chemistry Department, University of Miami
Coral Gables, Florida 33124 (USA)

[**] This work was performed during a sabbactical leave of *L.E.* from the University of Miami. *L.E.* wishes to thank the Fogarty International Center of the National Institutes of Health for a Senior International Fellowship (1 F06 TW 01 551-01). Support from the CNRS (URA 422 and URA 424) is gratefully acknowledged.

tions.[11] It led to the formation on the cathode, of good deep blue-violet, air-sensitive crystals of pyramidal shape (Fig. 1), which were subjected to X-ray crystallographic analysis.[12]

Fig. 1. Crystals formed on a Pt wire cathode by electroreduction of the sodium cryptate $[Na^{\oplus} \subset \mathbf{1}]Br^{\ominus}$.

Two views of the crystal structure determined are shown in Figure 2 together with the packing. The species is a cryptate complex in which the sodium cation is contained in the cavity of the tris(bpy) macrobicyclic ligand, as in the case of the sodium bromide cryptate of the related tris(phenanthroline) [tris(phen)] macrobicycle.[13]

Comparison of the structural data of the latter complex[13] with the present one is especially instructive. Whereas bromide ions are located in the crystal lattice of $[Na^{\oplus} \subset$ tris(phen)$]Br^{\ominus}$, no anions are found in the present structure, in which the molecules of complex are tightly packed (Fig. 2) together with one acetonitrile molecule of crystallization for each complex. The shortest $Na^{\oplus} \cdots Na^{\oplus}$ distance is 8.21 Å. In addition, this close packing leaves no "empty" space that could contain electrons as in the case of the electrides.[3,4] Consequently, the present species is electroneutral, and the electron must be located on the tris(bpy) ligand.

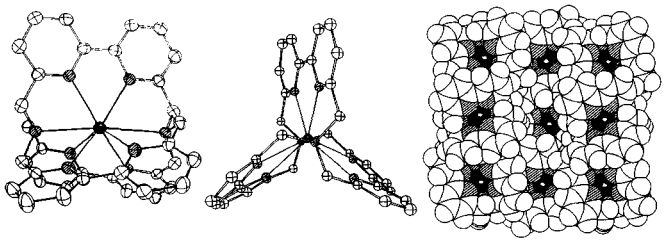

Fig. 2. Crystal structure of the sodio-cryptatium species $\{[Na^{\oplus} \subset \mathbf{1}]e^{\ominus}\} \cdot CH_3CN$ formed by electroreduction. Left: ORTEP side-view into the cavity showing the coordination of $Na^{\oplus}$ to the eight N sites; the bpy′ unit is at the top; center: ORTEP view along the bridgehead axis N, $Na^{\oplus}$, N; right: space filling presentation of the crystal packing showing the absence of any significant void.

The tris(phen) $Na^{\oplus}$ complex showed an approximate $\mathbf{C}_3$ symmetry axis. In contrast, the $[Na^{\oplus} \subset \mathbf{1}]$ cryptate cation presents a $\mathbf{C}_2$ axis, through the $Na^{\oplus}$ cation and the middle of the 2,2′-connecting bond of the uppermost bpy in Figure 2 (left) (designated by bpy′).

The $Na^{\oplus} \cdots$ N distances to the bridgehead nitrogens are 2.780 Å, very close to those in the tris(phen) complex (2.79 Å).[13] The $Na^{\oplus} \cdots$ N distances to the heterocyclic nitrogens display striking features: they are much shorter for the bpy′ nitrogens (2.589 Å) than for the other two, identical bipyridines (2.82–283 Å), whereas in the tris(phen)-$Na^{\oplus}$ complex they fall between these two values (2.70 Å).[13] Thus in the present complex, the $Na^{\oplus}$ cation is pulled towards the unique bpy′ group, suggesting that the unpaired electron is located on this bpy′ unit. Further support comes from the C2–C2′ distances; this distance is appreciably shorter for bpy′ (1.418 Å) than for the other two bpy groups (1.482 Å). In addition, whereas bpy′ is almost flat, the two other bpy units are not (dihedral angles of 0.7(5)° and 15.9(4)° between the two pyridine groups respectively). These features are consistent with the generation of the anion radical $bpy^{\bullet\ominus}$, where the additional electron is introduced into the lowest unoccupied molecular orbital of bpy which is bonding between the two pyridine rings.[14] The bpy′ groups do not overlap in the crystal.

The anion radical $bpy^{\bullet\ominus}$, obtained by electrochemical reduction, forms paramagnetic ion pairs whose ESR features have been described.[15]. The neutral species $[M(bpy)_3]^{\circ}$ (with M = Ru, Fe, or Os) have been generated via coulometric reduction of the dicationic parent complexes.[16] On the other hand, the electrochemical reduction of macrocyclic complexes incorporating an electron acceptor site has been studied in solution.[17]

Additional information comes from spectroscopie data. Allowing some of the crystals to decompose in air afforded a yellowish material. FAB mass spectrometry showed the peak corresponding to $[\mathbf{1}, Na^{\oplus}]$ at 597 *m/z*; the spectrum was identical to that of an authentic sample of the starting material, $[Na^{\oplus} \subset \mathbf{1}]Br^{\ominus}$. The 200-MHz ^1H NMR spectrum of this air-decomposed material was also the same as that of the starting complex.

All the above data agree with the formulation of the species obtained by electrocrystallization of $[Na^{\oplus} \subset \mathbf{1}]Br^{\ominus}$ as a neutral entity, which one may consider to be an expanded alkali-metal atom or a radical contact ion pair $\{[Na^{\oplus} \subset \mathbf{1}]e^{\ominus}\}$, and term *sodio-cryptatium*, the first member of the cryptatium family. The crystal structure indicates that, in the solid, the electron is localized on one of the bpy units, $[Na^{\oplus} \subset (bpy^{\ominus})(bpy)_2]^{\bullet}$.[18] Such a species is also of interest by its analogy with the monoreduced and the excited states, respectively $[Ru^{II}(bpy^{\ominus})(bpy)_2]^{\oplus}$ and $[Ru^{III}(bpy^{\ominus})(bpy)_2]^{2\oplus *}$, of the very intensively studied $[Ru(bpy)_3]^{2\oplus}$ complex,[19] providing structural data for the $(bpy^{\ominus})$ unit in these states. The sequence: metal atom, cryptatium, electride,[3,4] may be depicted as shown in Figure 3, representing for instance the cases: Na, $\{[Na^{\oplus} \subset \mathbf{1}]e^{\ominus}\}$, $\{[K^{\oplus} \subset$ cryptand-2.2.2$]e^{\ominus}\}$, where the electron is progressively "removed" from the atom.

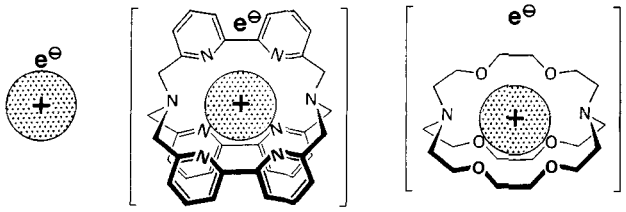

Fig. 3. Schematic representation of the series: (from the left to right) alkali-metal atom, cryptatium (expanded atom or radical contact ion pair $\{[Na^{\oplus} \subset \mathbf{1}]e^{\ominus}\}$), electride (Rydberg atom or electron salt) $\{[K^{\oplus} \subset$ cryptand-2.2.2$]e^{\ominus}\}$.

Numerous extensions of these results may be envisaged. The ESR spectra of the substance in the solid state and in

solution should provide information about electron delocalization within a given bpy unit and over the three bpy groups of the ligand, a feature of special significance for an expanded atom description.[20] Conductivity and magnetic properties are also of much interest. Furthermore, it might be possible to extend the list of such molecular "elements" from sodio-cryptatium to doubly reduced calcio-cryptatium and to triply reduced lanthano-cryptatium, for instance.

Received: February, 4, 1991 [Z 4422 IE]
German version: *Angew. Chem. 103* (1991) 884

CAS Registry numbers:
$[Na^{\oplus} \subset \mathbf{1}]Br^{\ominus}$, 134055-00-8; $[Na^{\oplus} \subset \mathbf{1}]e^{\ominus}$, 134055-01-9; $[Na^{\oplus} \subset \mathbf{1}]e^{\ominus} \cdot CH_3CN$, 134055-02-0.

[1] J. M. Lehn, *Acc. Chem. Res. 11* (1978) 49.
[2] J.-M. Lehn, *Pure Appl. Chem. 52* (1980) 2303.
[3] R. H. Huang, M. K. Faber, K. J. Moeggenborg, D. L. Ward, J. L. Dye, *Nature (London) 331)* (1988), 599.
[4] J. L. Dye, *Science (Washington D.C.) 247* (1990) 663; *Pure Appl. Chem. 61* (1989) 1555.
[5] See ref. [2], footnote on page 2310.
[6] Note also the species $Li(NH_3)_4$ described as $[Li^{\oplus}(NH_3)_4e^{\ominus}]$ [6a] and $N(CH_3)_4$ [6b] formed by electrochemical reduction of the corresponding cation.
[7] a) N. Mammano, M. J. Sienko, *J. Am. Chem. Soc. 90* (1968) 6322; b) R. K. Quinn, J. J. Lagowski, *J. Phys. Chem. 72* (1968) 1374; J. O. Littlehailes, B. J. Woodhall, *Discuss. Faraday Soc. 45* (1968) 187.
[8] J.-C. Rodriguez-Ubis, B. Alpha, D. Plancherel, J.-M. Lehn, *Helv. Chim. Acta 67* (1984) 2264.
[9] The electrochemical reduction of a colorless 1 mM solution of $[Na^{\oplus} \subset \mathbf{1}]Br^{\ominus}$ containing 0.1 M tetrabutylammonium hexafluorophosphate (Bu_4NPF_6) in DMF was conducted on a glassy carbon working electrode using a Pt coil as counter electrode and an $Ag^{\circ}/AgBr$ reference electrode. Fc was added as an internal reference to measure the potentials; the sweep rate was 100 $mVsec^{-1}$. Potentials versus saturated calomel electrode (SCE) are obtained by subtracting 0.4 V; see R. R. Gagne, C. A. Koval, G. C. Lisensky, *Inorg. Chem. 19* (1980) 2854; G. Gritzner, J. Kuta, *Pure Appl. Chem. 56* (1984) 461.
[10] Y. Ohsawa, M. K. De Armond, K. W. Hanck, D. E. Morris, D. G. Whitten, P. E. Neveux, Jr., *J. Am. Chem. Soc. 105* (1983) 6522.
[11] The electrocrystallization cell was made by our own glassblower and consisted of an H-type arrangement with a glass frit (porosity no. 5) separating the two compartments. The compartments were coupled to the high vacuum independently, in order to be able to distill the solvent through the vacuum line directly into them, without going through the glass frit. In this fashion, it was possible to save complex by placing typically, 7 mg in only one of the compartments along with enough supporting electrolyte (Bu_4NPF_6) for a 0.1 M solution, while using only electrolyte in the other compartment. The typical vacuum obtained was ca. 10^{-5}–10^{-6} mm. The current was controlled with a current source made in the institute. In this two-electrode configuration, both electrodes were Pt wires, 0.7 mm in diameter and ca. 3 cm long. The optimal current was 10 μA and a typical run was complete in 15 hours. After this period deep blue-violet crystals of pyramidal shape had formed on the cathode (Fig. 1); they were of optimal size and qualitity for X-ray analysis. For removal from the cell, the vacuum was broken with purified Ar, and the electrode removed and placed in a Schlenck tube. After selection under the microsope of several crystals for X-ray analysis, the electrode was taken out of the Schlenck tube under a strong nitrogen flow, the highly air-sensititve crystals were removed from the Pt surface, and one was quickly selected and mounted for X-ray analysis all under a constant cold nitrogen stream.
[12] a) Crystal data: $C_{38}H_{33}N_9Na$, $M_r = 638.74$, tetragonal, space group $I4_1$, $a = 14.685(4)$, $c = 14.731(4)$ Å, $V = 3176.7$ Å^3, $\varrho_{calcd} = 1.335$ gcm^{-1}, $Z = 4$, $\mu(Cu_{K\alpha}) = 7.392$ cm^{-1} (graphite monochromator). A total of 1021 reflections were collected using a Philips PW1100/16 automatic diffractometer. Quantitative data were obtained at -100 °C using a locally built gas flow device. The resulting data set was analyzed using an Enraf-Nonius SDP/VAX package [12b]. Three standard reflections measured every hour during the data collection period showed no significant trend. The raw step-scan data were converted to intensities using the Lehmann–Larsen method [12c] and corrected for Lorentz, polarization, and absorption factors. The structure was then solved with SIR [12d] and refined to $R = 0.036$ using 897 reflections with $I > 3\sigma^*(I)$. b) B. A. Frenz: *The Enraf-Nonius CAD4-SDP* in H. Schenk, R. Olthof-Hazekamp, H. Van Koningveld, G. C. Bassi (Eds.): *Computing in Crystallography* Delft University press 1978, 64–71; c) M. S. Lehmann, F. K. Larsen, *Acta Crystallogr. Sect. A30* (1974) 580; d) M. C. Burla, G. Cascarano, G. Giacovazzo, A. Nunzi, G. Polidori, *Acta Crystallogr. A43* (1987) 370. e) Further details of the crystal structure investigations are available on request from the Director of the Cambridge Crystallographic Data Centre, University Chemical Laboratory, Lensfield Road, GB-Cambridge CB21EW (UK), on quoting the full journal citation.
[13] A. Caron, J. Guilhem, C. Riche, C. Pascard, B. Alpha, J.-M. Lehn, J.-C. Rodriguez-Ubis, *Helv. Chim. Acta 68* (1985) 1577.
[14] Y. Ohsawa, M.-H. Wangbo, K. W. Hanck, M. K. De Armond, *Inorg. Chem. 23*(1984) 3426.
[15] W. Kaim, *Chem. Ber. 114* (1981) 3789 and references therein; T. Takeshita, N. Hirota, *J. Am. Chem. Soc. 93* (1971) 6421.
[16] The neutral species precipitated after two-electron reduction of the parent complexes $[M(bipy)_3]^{2\oplus}$ in CH_3CN; they have been studied by ESR in the solid state and in DMF solution; see A. G. Motten, K. W. Hanck, M. K. De Armond, *Chem. Phys. Lett. 79* (1981) 541; D. E. Morris, K. W. Hanck, M. K. De Armond, *J. Am. Chem. Soc. 105* (1983) 3032; D. E. Morris, K. W. Hanck, M. K. De Armond, *Inorg. Chem. 24* (1985) 977.
[17] A. Kaifer, L. Echegoyen, D. A. Gutowski, D. Goli, G. W. Gokel, *J. Am. Chem. Soc. 105* (1983) 7168; H. Bock, B. Hierholzer, F. Vögtle, G. Hollmann, *Angew. chem. 96* (1984) 74; *Angew. Chem. Int. Ed. Engl. 23* (1984) 57; R. E. Wolf, Jr., S. Cooper, *J. Am. Chem. Soc. 106* (1984) 4646; D. A. Gutowski, M. Delgado, V. J. Gatto, L. Echegoyen, G. W. Gokel, *ibid. 108* (1986) 7553; H. Bock, H.-F. Herrmann, *ibid. 111* (1989) 7622.
[18] The crystal structure of the dimer of a fluorenone radical contact ion pair has been reported earlier: H. Bock, H.-F. Herrmann, D. Fenske, H. Goesmann, *Angew. Chem. 100* (1988) 1125; *Angew. Chem. Int. Ed. Engl. 27* (1988) 1067.
[19] M. K. De Armond, M. L. Myrick, *Acc. Chem. Res. 22* (1989) 364 and references therein.
[20] An intriguing case of spherical delocalization would be represented by a "fullerium" species derived from a fullerene such as C_{60}, containing a metal ion $M^{n\oplus}$ in the internal cavity and n electrons on the carbon framework, $\{[M^{n\oplus} \subset C_{60}]ne^{\ominus}\}$. For the redox behaviour of C_{60} see: P.-M. Allemand, G. Srdanov, A. Koch, K. Khemani, F. Wudl, Y. Rubin, F. Diederich, M. M. Alvarez, S. J. Anz, R. L. Whetten, *J. Am. Chem. Soc. 113* (1991) 2780 and references therein.

Isolated and Condensed Ta_2Ni_2 Clusters in the Layered Tellurides $Ta_2Ni_2Te_4$ and $Ta_2Ni_3Te_5$**

By *Wolfgang Tremel**

Dedicated to Professor Hans Georg von Schnering on the occasion of his 60th birthday

Chalcogenides of the early transition metals have been intensively investigated in recent years owing to their physical properties (e.g., anisotropic optical and electrical properties, superconductivity, charge density waves).[1] However, nearly all preparative investigations have been limited to sulfides and selenides.[2] Until very recently, tellurides were ignored,[3] even though their chemical uniqueness is already indicated by a comparison of simple binary compounds with analogous formulas: $NbSe_3$[4]—one of the best-studied inorganic compounds—has no counterpart among the tellurides; $HfTe_5$[5] and $TaTe_4$,[6] in turn, have no counterpart among the sulfides and selenides. Although the trichalcogenides MQ_3 (M = Ti, Zr, Hf; Q = S, Se, Te) are similar in terms of formula and structure for the sulfides, selenides, and tellurides,[7] the compounds exhibit significant differences in their properties.[8]

The starting point of our work was an investigation of the electronic structures of the layer compounds MTe_2 (M = Hf, Ta, W, Re).[9] The crystal structures of these compounds are derived from the CdI_2 structure. The $HfTe_2$ structure (d^0 system) corresponds to the CdI_2 aristotype.[10, 11] $TaTe_2$

[*] Dr. W. Tremel
Anorganisch-chemisches Institut der Universität
Wilhelm-Klemm-Strasse 8, W-4400 Münster (FRG)

[**] This work was supported by the Bundesministerium für Forschung und Technologie (grant number 05439 GXB3).

(d^1),[12] WTe_2 (d^2),[13] and $ReSe_2$ (d^3),[14] on the other hand, represent structural variants whose metal partial structures are distorted in a way characteristic of the respective band occupation. Analysis of the band structure in this series of compounds showed that the changes in structure are induced electronically.[9] An interesting partial result of this investigation was the finding that, in $TaTe_2$ the Ta–Ta bonding orbitals are not completely occupied; therefore, modification of the structure should be possible by, for example, inclusion of cations.

Surprisingly, the reaction of Ta, Te, and Ni did not lead to inclusion of Ni in the interlayer regions, but instead to the novel layer compounds $Ta_2Ni_2Te_4$[15–17] and $Ta_2Ni_3Te_5$,[18,19] which contain isolated and condensed Ta_2Ni_2 cluster units, respectively. In both compounds, the layers are held together by van der Waals interactions only ($d_{Te-Te} \geq 3.846(2)$ Å).

The structure of $Ta_2Ni_2Te_4$ can be described starting from a hexagonal close packing of Te atoms; one-half of the octahedral holes in this packing are occupied by Ta atoms and one-quarter of the tetrahedral holes are occupied by Ni atoms. As illustrated in Figure 1, this description reveals the structural relationship to the NiAs and CdI_2 structure. Figure 1a shows a projection of the NiAs structure along *c*. Removal of every second layer of metal atoms in planes parallel to *bc* (open circles) results in formation of a (fictitious) $TaTe_2$ layer structure. The distortion of the $TaTe_2$ partial structure by movement of the Ta atoms in the directions shown by the arrows and the partial occupation of the tetrahedral holes (marked by black points in Fig. 1a) leads to the structure of $Ta_2Ni_2Te_4$. Pairwise shift of the Ta atoms away from the centers of the octahedral holes of one layer results in a coordination of the Ta atoms by 4+2 Te atoms (d_{Ta-Te}: 2.789 and 3.235 Å).

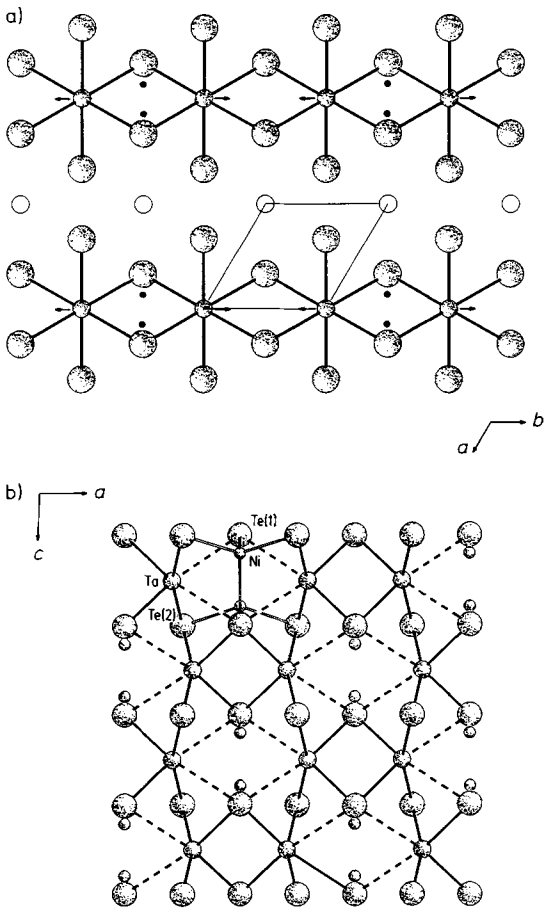

Fig. 1. a) Derivation of the $Ta_2Ni_2Te_4$ structure from the NiAs structure; parallel projection along [001] (large circles, Te; medium-sized circles, Ta). For explanation see text. b) Parallel projection of the $Ta_2Ni_2Te_4$ structure on a layer along [010] (large circles, Te; medium-sized circles, Ta; small circles, Ni). The different Ta-Te distances are symbolized by differing lines joining the atoms (solid line, $d_{Ta-Te} = 2.789$ Å; dashed line $d_{Ta-Te} = 3.235$ Å).

Noteworthy are the following points: (1) The known CdI_2 structure type is derived from the NiAs structure by removal of every second layer of metal atoms in planes parallel to *ab*. The two structures thus differ only in the arrangement of the metal layers. This gives rise to the question why only the CdI_2 structure type is observed. (2) In the (fictitious) $TaTe_2$ structure, tetrahedral holes exist between the layers and within the layers, but only the latter are occupied. Presumably, therefore, this "alternative" structural variant is stabilized by inclusion of Ni atoms within the layers.[20] The occupation of the octahedral and tetrahedral holes within a layer results in rhombuslike Ta_2Ni_2 clusters[21] ($d_{Ni-Ni} = 2.503(6)$, $d_{Ta-Ni} = 2.646(2)$ Å), which are linked through longer Ta–Ni and Ta–Ta contacts ($d_{Ni-Ta} = 2.873(3)$, $d_{Ta-Ta} = 3.196(1)$, 3.236(2) Å) to form a two-dimensional network (Fig. 2).

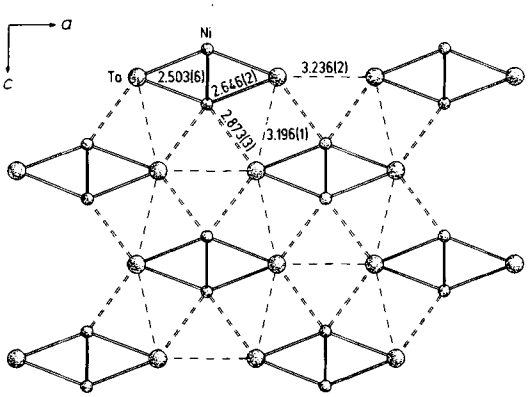

Fig. 2. $Ta_2Ni_2Te_4$, parallel projection of the metal lattice along [010] (large circles, Ta; small circles, Ni).

The Ni–Ni distance in the Ni_2Ta_2 clusters is nearly identical with the Ni–Ni distance in Ni metal ($d_{Ni-Ni} = 2.492$ Å);[22] an assessment of the Ni–Ta distance of 2.646 Å is possible by comparison with the metal-rich sulfidic phase $Ta_9Ni_2S_6$[23] ($d_{Ta-Ni} = 2.495$ Å).

The second compound obtained upon reaction of $TaTe_2$ with nickel, $Ta_2Ni_3Te_5$, like $Ta_2Ni_2Te_4$, has a layer structure. Figure 3 shows projections of the structure along *b* (Fig. 3a) and *a* (Fig. 3b). Each unit cell contains two $Ta_2Ni_3Te_5$ layers, which are stacked along *a*, and each layer has two chemically distinguishable Ni positions. Ni atoms of type A display short distances to two other Ni(A) atoms and Ni atoms of type B exhibit no Ni–Ni contacts.

A possible structural description is based on the hierarchy of interatomic distances. All Ni atoms are coordinated in a (distorted) tetrahedral fashion by Te ($\bar{d}_{Ni(A)-Te} = 2.562$ Å (3×), 2.744 Å (1×); $\bar{d}_{Ni(B)-Te} = 2.553$ Å (4×)), and the Ta atoms are surrounded in a square-pyramidal fashion by five Te atoms ($d_{Ta-Te} = 2.757$ Å (1×), 2.785 Å (2×), 2.869 Å (2×)). Furthermore, each metal atom displays other metal–metal contacts. The Ni(A) atoms have two further Ni(A) neighbors ($d_{Ni-Ni} = 2.502$ Å) and three Ta neighbors ($\bar{d}_{Ta-Ni} = 2.648$ Å (1×), 2.717 Å (2×)) and the Ta atoms possess five Ni neighbors ($\bar{d}_{Ta-Ni(A)} = 2.648$ Å (1×), 2.717 Å

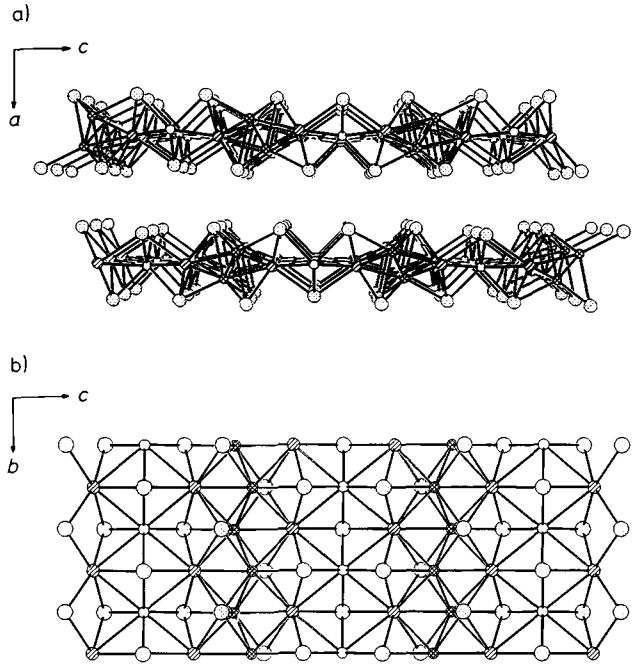

Fig. 3. $Ta_2Ni_3Te_5$: a) Perspective view of a section of the layer structure along [010]. b) Parallel projection of a layer along [100] (dotted circles, Te; hatched circles, Ta; cross-hatched circles, Ni(A); open circles, Ni(B)).

(2×); $\bar{d}_{Ta-Ni(B)} = 2.922$ Å (2×)); Ni atoms of type B have only four neighboring Ta atoms ($\bar{d}_{Ta-Ni(B)} = 2.922$ Å).

A structural description in terms of polyhedra starts from a chain of $NiTe_4$ tetrahedra. Ni(A) atoms are part of a chain of edge-linked $NiTe_4$ tetrahedra and Ni(B) atoms part of a chain of vertex-linked tetrahedra. Finally, the pyramidal $TaTe_5$ building blocks are linked through five common edges with five neighboring $NiTe_4$ tetrahedra.

More instructive for understanding the structure and for elucidating the structural relationship of $Ta_2Ni_2Te_4$ and $Ta_2Ni_3Te_5$ is to consider the partial "naked-metal" structure of one layer (Fig. 4). The $Ta_2Ni_3Te_5$ structure also contains

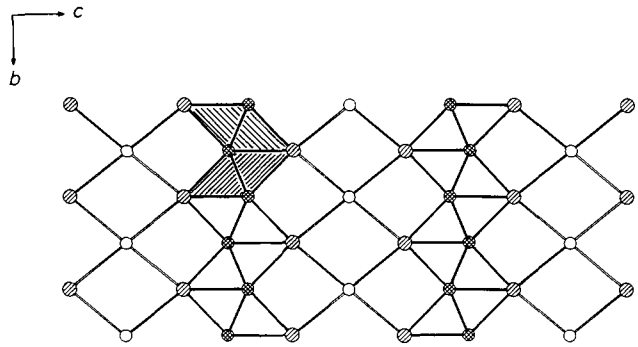

Fig. 4. $Ta_2Ni_3Te_5$: Projection of the metal lattice along [100] (hatched circles, Ta; cross-hatched circles, Ni(A); open circles, Ni(B)). Two of the rhombus-shaped Na_2Ni_2 clusters are highlighted by shading.

rhombuslike Ta_2Ni_2 clusters, but, in this case, they are linked through common Ta–Ni edges to give $^1_\infty[Ta_2Ni_2]$ chains; that is, cluster condensation through *trans* edges results in one-dimensional infinite chains. These chains are joined through the Ni(B) atoms to form a two-dimensional metal layer.

This structural description has mnemonic advantages. In principle, the occurrence of clusters in compounds of electron-deficient 4d and 5d metals is not surprising[24]—remarkable, however, is the occurrence of condensed clusters in typical layer compounds. Some of the few known examples are ZrCl,[25] $TbClH_{1-x}$,[26] and $Gd_2Cl_2C_2$,[27] where octahedral metal clusters are condensed to form two-dimensional layers. Also remarkable is the occurrence of layer compounds for nonmetal/metal ratios of 1/1. Here, too, the low-valent zirconium halides (e.g., ZrCl) are a prime example. Presumably, therefore, the "isoelectronic correlation" Zr-Cl and Ta-Te is not a mere coincidence.

Metallic properties are expected for both compounds, $Ta_2Ni_2Te_4$ and $Ta_2Ni_3Te_5$,[28] as shown by an attempt to assign formal oxidation numbers on the basis of electronegativity considerations (e.g., $(Ta^{2\oplus})_2(Ni^{2\oplus})_2(Te^{2\ominus})_4$ or $(Ta^{3\oplus})_2(Ni^{1\oplus})_2(Te^{2\ominus})_4$ for the former and $(Ta^{2\oplus})_2(Ni^{2\oplus})_3(Te^{2\ominus})_5$ for the latter). Band-structure calculations of the LCAO type (EH approximation)[29] confirm that this approach is basically correct. The calculated density of states for $Ta_2Ni_2Te_4$ with the contributions of Ta and Ni (Fig. 5a) shows the metallic character of the compound. The calculated Ta–Ta, Ta–Ni, and Ni–Ni overlap populations (COOP diagram, Fig. 5b) indicate the relative strength of the respective metal–metal interactions. The numerical values of 0.040, 0.155, and 0.156/0.078 ($d_{Ta-Ni} = 2.646(2)/2.873(3)$ Å) for the Ni–Ni, Ta–Ta, and Ta–Ni overlap populations reveal the importance of Ta–Ta and Ta–Ni interactions in comparison to Ni–Ni interactions.

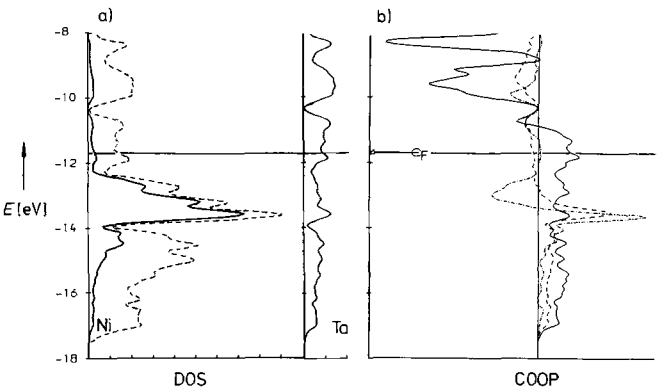

Fig. 5. a) Density of states (DOS) for $Na_2Ni_4Te_4$. Left: Total density (dashed line) and Ni partial density. Right: Ta partial density. b) COOP diagram (left, antibonding; right, bonding): solid line, Ta-Ta; dashed line, Ta-Ni (average); dashed and dotted line, Ni-Ni. The Fermi level is marked by a horizontal line.

The high formation tendency of the title compounds and the preferred formation of clusters instead of inclusion of the 3d metal in the interlayer region may be ascribed to the large affinity between electron-deficient and electron-rich metals (according to the generalized Lewis acid-base concept of *Brewer* et al.[30]). This fact is also documented by the synthesis of other related compounds such as M_2FeTe_4 (M = Nb, Ta), $M_2M'_2Te_4$ (M' = Fe, Co; M = Nb, Ta), TaM'_2Te_2 (M' = Co, Ni) $Ta_4M'Te_4$ (M' = Fe, Co),[31], and $TaFe_{1+x}Te_3$ ($x \approx 0.07$).[32]

Received: February 15, 1991 [Z 4442 IE]
German version: *Angew. Chem. 103* (1991) 900

[1] See, for example, a) J. A. Wilson, A. D. Yoffe, *Adv. Phys. 18* (1969) 193; b) J. A. Wilson, F. J. DiSalvo, S. Mahajan, *ibid. 24* (1975) 117; c) P. Monceau (Ed.): *Electronic Properties of Inorganic Quasi One-Dimensional Compounds, Part 1 and 2*, Reidel, Dordrecht 1985; d) J. Rouxel (Ed.): *Crystal Chemistry and Properties of Materials with Quasi One-Dimensional Structures*, Reidel, Dordrecht 1986; e) H. Kimamura (Ed.): *Theoretical Aspects*

of Band Structures and Electronic Properties of Pseudo One-Dimensional Solids, Reidel, Dordrecht 1985; f) M. S. Whittingham, A. J. Jacobson (Eds.): *Intercalation Chemistry*, Academic Press, New York 1982; g) R. H. Friend, A. D. Yoffe, *Adv. Phys. 36* (1987) 1.

[2] a) S. A. Sunshine, D. A. Keszler, J. A. Ibers, *Acc. Chem. Res. 20* (1987) 395; b) A. Meerschaut, P. Grenouilleau, R. Brec, M. Evain, J. Rouxel, *J. Less-Common Met. 116* (1986) 229; c) J. Rouxel, R. Brec, *Annu. Rev. Mater. Sci. 16* (1986) 137.

[3] a) $NbNiTe_5$: E. Liimatta, J. A. Ibers, *J. Solid State Chem. 71* (1987) 384; $NbPdTe_5$: E. Liimatta, J. A. Ibers, *ibid. 77* (1988) 141; $TaNiTe_5$ and $Ta_3Pd_3Te_{14}$: E. Liimatta, J. A. Ibers, *ibid. 78* (1989) 7; b) $TaTe_2$: S. Lee, N. Nagasundaram, *Chem. Mater. 1* (1989) 597; c) Ta_4SiTe_4: M. E. Badding, F. J. DiSalvo, *Inorg. Chem. 29* (1990) 3952; d) An excellent review on tellurium-rich tellurides: P. Böttcher, *Angew. Chem. 100* (1988) 781; *Angew. Chem. Int. Ed. Engl. 27* (1988) 759.

[4] a) A. Meerschaut, J. Rouxel, *J. Less-Common Met. 24* (1975) 117; b) J. L. Hodeau, M. Marezio, C. Rouceau, R. Ayroles, A. Meerschaut, J. Rouxel, P. Monceau, *J. Phys. C 11* (1978) 4117; c) for a short review see S. Kagoshima, H. Nagasawa, T. Sambongi: *One-Dimensional Conductors*, Springer, Berlin 1988, Chapter 4.

[5] S. Furuseth, L. Brattås, A. Kjekshus, *Acta Chem. Scand. 27* (1973) 2367.

[6] E. Bjerkelund, A. Kjekshus, *J. Less-Common Met. 7* (1964) 231.

[7] W. Krönert, K. Plieth, *Z. Anorg. Allg. Chem. 336* (1963) 207; L. Bråttas, A. Kjekshus, *Acta Chem. Scand. 26* (1972) 3441; *Acta Chem. Scand A 29* (1975) 623.

[8] See, for example, E. Canadell, Y. Mathey, M.-H. Whangbo, *J. Am. Chem. Soc. 110* (1988) 104, and references cited therein.

[9] J. G. Smeggil, S. Bartram, *J. Solid State Chem. 5* (1972) 391.

[10] H. D. Megaw: *Crystal Structures: A Working Approach*, Saunders, Philadelphia 1973, p. 216.

[11] B. E. Brown, *Acta Crystallogr. 20* (1966) 264.

[12] B. E. Brown, *Acta Crystallogr. 20* (1966) 268.

[13] N. W. Alcock, A. Kjekshus, *Acta Chem. Scand. 19* (1965) 79.

[14] W. Tremel, *Inorg. Chem. 30* (1991), in press.

[15] In order to synthesize $Ta_2Ni_2Te_4$, the corresponding stoichiometric amounts of the elements, together with I_2 as mineralizer, were heated in a sealed quartz glass tube for 14 d at 1000 °C. The product (EDAX (energy dispersive X-ray spectroscopy): Ta, Ni, Te) consists of platelets with a metallic luster and is a single phase according to the Guinier diagram.

[16] Space group *Pmna* (No. 53), $Z = 2$ (based on $Ta_2Ni_2Te_4$), $a = 7.897(1)$, $b = 7.228(1)$, $c = 6.230(1)$ Å (Siemens R3), $Mo_{K\alpha}$ ($\mu = 51.60\ mm^{-1}$); crystal size, $0.04 \times 0.035 \times 0.035\ mm^3$; ω-2θ scan, $2\theta_{max} = 75$ °C, 1734 reflections $(h, k, +l)$, empirical absorption correction, 807 symmetry-independent reflections, $R(F_0)/R_w = 0.0646/0.0693$. b) Further details in the crystal structure investigations are available on request from Fachinformationszentrum Karlsruhe, Gesellschaft für wissenschaftlich-technische Information mbH, W-7514 Eggenstein-Leopoldshafen 2 (FRG), by quoting the depository number CSD-55272, the names of the authors, and the journal citation.

[17] An independent structure determination of $Ta_2Ni_2Te_4$ was recently reported: J. L. Huang, B. G. Huang. *Acta Crystallogr. Sect. A 46 (Suppl.)* (1990) C-287.

[18] $Ta_2Ni_3Te_5$ was synthesized from the corresponding stoichiometric amounts of the elements at 900 °C in a sealed quartz glass tube (10 d) with addition of $TeCl_4$ as mineralizer. The product (EDAX: Ta, Ni, Te) consists of needles with metallic luster which are up to 1 cm long. The Pd analogue $Ta_2Pd_3Te_5$ was synthesized under analogous conditions ($T = 850$ °C). Lattice constants $a = 13.989(3)$, $b = 3.713(1)$, $c = 18.630(4)$ Å, space group *Pnma* (Nr. 62), $Z = 4$.

[19] Space group *Pnma* (No. 62), $Z = 4$, $a = 13.897(4)$, $b = 3.695(1)$, $c = 17.729(6)$ Å (Siemens R3), $Mo_{K\alpha}$ (μ) $= 45.49\ mm^{-1}$); crystal size, $0.006 \times 0.03 \times 0.15\ mm^3$; ω-2θ scan, $2\theta_{max} = 80°$, 3321 reflections (h, k, l), empirical absorption correction, 3158 symmetry-independent reflections, 2353 with $I > 2\sigma(I)$, $R(F_0)/R_w = 0.043/0.044$ [16b].

[20] The preferential occurrence of the CdI_2 structure type can be understood on the basis of LCAO band-structure calculations (extended Hückel (EH) approximation) and on the basis of symmetry arguments. The incorporation of nickel (and, in general, of elements of the iron group) in the tetrahedral holes of a layer of the $TaTe_2$ structure leads to their electronic stabilization due to interaction of unoccupied t_{2g} levels of tantalum with the corresponding occupied levels of nickel: W. Tremel, unpublished results.

[21] The formulation $Ta_2Ni_2Te_4$ (instead of $TaNiTe_2$) was chosen in order to give the cluster formal recognition as well.

[22] *CRC Handbook of Chemistry and Physics*, 60th ed., CRC Press, Boca Raton, FL (USA) 1980

[23] B. Harbrecht, H. F. Franzen, *J. Less-Common Met. 113* (1985) 349.

[24] A. Simon, *Angew. Chem. 93* (1981) 23; *Angew. Chem. Int. Ed. Engl. 20* (1981) 1.

[25] A. W. Struss, J. D. Corbett, *Inorg. Chem. 9* (1970) 1373.

[26] H. Mattausch, A. Simon, K. Ziebeck, *J. Less-Common Met. 113* (1985) 149.

[27] U. Schwanitz-Müller, A. Simon, *Z. Naturforsch. B40* (1985) 710.

[28] W. Tremel, unpublished results.

[29] Extended Hückel approximation: R. Hoffmann, *J. Chem. Phys. 39* (1963) 1397. H_{ij} matrix elements: J. H. Ammeter, H.-B. Bürgi, J. C. Thibeault, R. Hoffmann, *J. Am. Chem. Soc. 100* (1978) 3686. Tight-binding approximations: M.-H. Whangbo, R. Hoffmann, *ibid. 100* (1978) 6093; M.-H. Whangbo, R. Hoffmann, R. B. Woodward, *Proc. R. Soc. London A 366* (1979) 23. Parameters for Ta: J. Li, R. Hoffmann, M. E. Badding, F. J. DiSalvo, *Inorg. Chem. 29* (1990) 3943; parameters for Ni and Te: J.-F. Halet, R. Hoffmann, W. Tremel, E. Liimatta, J. A. Ibers, *Chem. Mater. 1* (1989) 351. Special k points: R. Ramirez, M. C. Böhm, *Int. J. Quantum Chem. 30* (1986) 391.

[30] L. Brewer, P. R. Wengert, *Metal. Trans. 4* (1973) 83.

[31] W. Tremel, *Habilitationsschrift*, Münster 1991.

[32] E. Potthoff, W. Tremel, unpublished results.

$[Cp_2Fe_2(CO)_3(\mu\text{-Si}t\text{Bu} \cdot \text{NMI})]I$: The First Silanetriyldiiron Complex**

By *Yasuro Kawano*, *Hiromi Tobita*, and *Hiroshi Ogino**

The chemistry of mononuclear[1] and dinuclear[2] carbyne complexes is well established. However, there are no reports on the analogous silanetriyl complexes. Here we wish to report the synthesis and crystal structure of the first donor-stabilized cationic silanetriyl diiron complex, **1** (NMI = *N*-methylimidazole), which was isolated as **1**-I.

$[Cp_2Fe_2(CO)_3(\mu\text{-Si}t\text{Bu} \cdot \text{NMI})]^{\oplus}$

The synthesis of **1**-I was achieved by exchanging an iodide on the silanediyl bridge of the μ-silanediyl complex **2**[3] with a strong Lewis base, NMI.

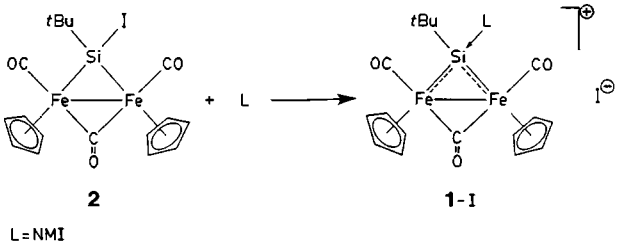

2 **1**-I

L = NMI

The unprecedented silanetriyl-bridged structure of **1**-I was determined unequivocally by an X-ray crystal structure analysis (Fig. 1).[4] Coordination of the lone pair on the nitrogen atom of NMI to the Si atom in the *tert*-butylsilanetriyl ligand causes pyramidalization of the silicon atom (the angle between the Fe_2Si plane and Si–C8 is 143.2°). The two Cp rings, which are mutually *cis*, and the *tert*-butyl group are located on the same side of the Fe_2SiC bicyclic ring. The distance between the Si and I atoms (5.388(2) Å) is substantially longer than the sum of the effective van der Waals radii of Si and I (4.08 Å).[5] This clearly indicates that there is no chemical bond between Si and I. The plane of the five-membered ring of NMI is parallel to the Fe–Fe bond and the NMI ligand is disordered between the two possible orientations related by a crystallographic mirror plane. The Fe–Si

[*] Prof. Dr. H. Ogino, Y. Kawano, Dr. H. Tobita
Department of Chemistry, Faculty of Science
Tohoku University
Aoba-ku, Sendai 980 (Japan)

[**] This work was supported by the Nissan Science Foundation and by the Ministry of Education, Science and Culture (Grant-in-Aid for International Scientific Research Program). NMI = *N*-methylimidazole.

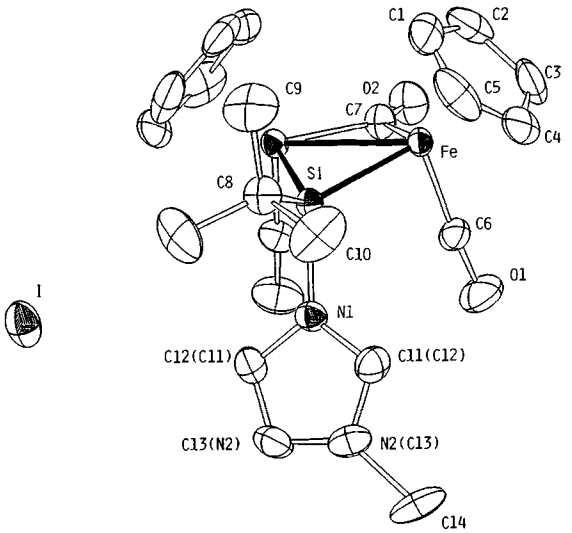

Fig. 1. Crystal structure of **1**-I (ORTEP, thermal ellipsoids at the 30% probability level, H atoms omitted). Selected interatomic dictances [Å] and angles [°]: Si···I 5.388(2), Si–Fe 2.262(2), Si–N1 1.885(7), Si–C8 1.910(9), Fe–Fe' 2.626(2), Fe–C6 1.745(6), Fe–C7 1.913(8), C6–O1 1.137(8), C7–O2 1.185(12); Fe–Si–Fe' 70.96(7), C8–Si–N1 96.2(4); $SiFe_2$ plane and Si–C8 vector 143.2, $SiFe_2$ plane and Si–N1 vector 120.7.

bond length (2.262(2) Å) is shorter than the known values for neutral silanediyl-bridged diiron complexes, **3**

$[Cp_2Fe_2(CO)_3(\mu\text{-SiH}t\text{Bu})]$ **3**

(2.270(1) and 2.272(1) Å)[6] and $[Cp_2Fe_2(CO)_3\{\mu\text{-SiMe(SiMe}_3)\}]$ (2.294(1) and 2.301(1) Å).[7, 8] Also, the Si–N bond length is 1.885(7) Å, which is significantly longer than the usual value for Si–N covalent bonds (ca. 1.75 Å).

When NMI was added to a CD_3CN solution of **2**, two new singlets, assignable to the Cp and *tert*-butyl groups of **1** appeared at lower field than the corresponding signals of **2**. Even when the bromo derivative of **2**, $[Cp_2Fe_2(CO)_3(\mu\text{-SiBr}t\text{Bu})]$, was used instead of **2**, the formation of **1** could be confirmed by ^{1}H NMR spectroscopy. The ^{29}Si NMR signal of **1** in CD_3CN appears at remarkably low field ($\delta = 251.5$), which is consistent with the existence of a "silanetriyl" ligand.

The FAB mass spectrum of **1**-I in a sulfolane matrix clearly shows the peak of the cation **1** at $m/z = 493$. Interestingly, the spectrum also shows a peak assignable to the base-free silanetriyl complex $[Cp_2Fe_2(CO)_3(\mu\text{-Si}t\text{Bu})]^{\oplus}$ at $m/z = 411$.

In the IR spectrum of **1**-I, ν_{CO} bands of carbonyl ligands appear at 1980, 1932, and 1766 cm^{-1}, which are higher in wavenumber than those of **3** by about 30 cm^{-1} on average. This is attributable to the decrease in back-donation from Fe atoms to carbonyl ligands caused by back-donation from Fe atoms to the electron-deficient Si atom in **1**.

Cation **1** is readily reduced by $NaBH_4$ to give **3** in fair yield, whereas **2** does not react with $NaBH_4$ under the same experimental conditions. This result also demonstrates the electron deficiency of the Si atom in **1**. The activation of a silicon-containing group by a Lewis base promises to be of synthetic importance.[12]

Experimental Procedure

N-Methylimidazole (14 μL, 0.18 mmol) was added to a stirred solution of **2** (88 mg, 0.16 mmol) in 1 mL of CH_3CN. The mixture was allowed to stand at 40 °C for 30 min, then gradually cooled to room temperature. Et_2O (2 mL) was added and the reaction mixture was cooled to − 48 °C. After 2 h, the supernatant fluid was removed by syringe. The red crystals thus obtained, **1**-I · CH_3CN, were washed with Et_2O (2.5 mL) three times and dried under vacuum. Yield 65 mg (0.10 mmol, 66%). Correct elemental analysis. ^{1}H NMR (200 MHz, CD_3CN): $\delta = 1.40$ (s, 9H; *t*Bu), 3.83 (s, 3H; NCH_3), 5.10 (s, 10H; Cp), 7.29, 7.46, 8.82 (m, 3 × 1H; $CH_3C_3H_3N_2$). ^{13}C NMR (75.5 MHz, CD_3CN): $\delta = 29.1$ (NCH_3), 29.9 ($C(CH_3)_3$), 36.3 ($C(CH_3)_3$), 86.4 (Cp), 123.3, 128.6, 141.4 ($CH_3C_3H_3N_2$), 213.6 (*CO*). The μ-CO signal was not observed because of the low solubility of **1**-I in CD_3CN. IR (KBr): $\tilde{\nu}$[cm^{-1}] = 1980, 1932, 1766 (ν CO). FAB-MS (sulfolane matrix): *m/z* 493 ($M^{\oplus}$, 38%), 411 ([*M* − NMI]$^{\oplus}$, 53), 203 ([CpFeNMI]$^{\oplus}$, 100), 83 ([NMI + H]$^{\oplus}$, 74).

Received: January 31, 1991 [Z 4416 IE]
German version: *Angew. Chem. 103* (1991) 877

CAS Registry numbers:
1-I, 134080-09-4; **1**-I · CD_3CN, 134174-84-8; **2**, 126778-51-6; *N*-methylimidazole, 616-47-7.

[1] a) W. A. Nugent, J. M. Mayer: *Metal-Ligand Multiple Bonds*, Wiley, New York 1988; b) H. Fischer, P. Hofmann, F. R. Kreissl, R. R. Schrock, U. Schubert, K. Weiss: *Carbyne Complexes*, VCH, Weinheim 1988.
[2] C. P. Casey, M. Crocker, G. P. Niccolai, P. J. Fagan, M. S. Konings, J. Am. Chem. Soc. 110 (1988) 6070, and references cited therein.
[3] H. Tobita, Y. Kawano, H. Ogino, *Chem. Lett. 1989*, 2155.
[4] Crystal data for **1**-I · CH_3CN: orthorhombic, space group *Pbnm* (variant of No. 62), $a = 16.371(4)$, $b = 17.043(3)$, $c = 9.975(2)$ Å, $V = 2783(1)$ Å^3, $Z = 4$. The structure was solved by the heavy atom method and refined by block diagonal least-squares methods using UNICS-III. All atoms except for hydrogen were refined anisotropically. Some of the hydrogen atoms were found by difference synthesis and refined isotropically. The positions of the other hydrogen atoms were calculated and fixed. The final reliability factors were $R = 0.056$ and $R_w = 0.065$ for 2125 reflections with $|F_o| > 3\sigma(F_o)$. Further details of the crystal structure investigation are available on request from the Director of the Cambridge Crystallographic Data Centre, University Chemical Laboratory, Lensfield Road, GB-Cambridge CB2 1EW (UK), on quoting the full journal citation.
[5] A. Bondi, *J. Phys. Chem. 68* (1964) 441.
[6] H. Tobita, Y. Kawano, M. Shimoi, H. Ogino, *Chem. Lett. 1987*, 2247.
[7] K. Ueno, N. Hamashima, M. Shimoi, H. Ogino, *Organometallics 10* (1991) 959.
[8] For mononuclear complexes, there are some shorter Fe–Si distances, e.g., [Cp'Fe(CO){$SiMe_2$···O(Me)···SiMe(OMe)}] (2.207(3) and 2.222(3) Å) [9], [$(CO)_4Fe{=}SiCl_2$ · HMPA] (2.214(1) Å) [10], and [PPN][$Fe(CO)_3$-(PPh_3)($SiCl_3$)] (2.197(3) Å) [11].
[9] K. Ueno, H. Tobita, M. Shimoi, H. Ogino, *J. Am. Chem. Soc. 110* (1988) 4092.
[10] C. Zybill, *Nachr. Chem. Tech. Lab. 37* (1989) 248.
[11] J. W. Connolly, A. H. Cowley, C. M. Nunn, *Polyhedron 9* (1990) 1337.
[12] G. A. Olah, S. C. Narang, *Tetrahedron 38* (1982) 2225.

Photocatalysis of the Homogeneous Water-Gas Shift Reaction under Ambient Conditions by Cationic Iridium(III) Complexes**

By *Raymond Ziessel**

The reaction of CO with H_2O to form CO_2 and H_2 [Eq. (a), $\Delta H^{\circ}_{298} = -41$ kJ mol^{-1}] is an important industrial reaction, the so-called water-gas shift reaction (WGSR). It is

$$CO(g) + H_2O(g) \rightleftharpoons CO_2(g) + H_2(g) \qquad (a)$$

a practical method for the production of H_2 and for the elimination of CO, which contaminates industrial gases in-

[*] Dr. R. Ziessel
Ecole Européenne des Hautes Etudes des Industries Chimiques de Strasbourg, IPCMS/GMI
1, rue Blaise Pascal, F-67008 Strasbourg (France)

[**] We wish to thank Professor *V. Balzani* and *K. J. Watson* for helpful and stimulating discussions and Dr. *C. de Bellefon* for measuring FT-IR spectra. This work was supported by the Centre National de la Recherche Scientifique.

volved in catalytic processes (e.g., Haber–Bosch synthesis of NH_3).[1] Conventional heterogeneous catalysts,[2] based on chromium-activated iron oxide or cobalt-molybdenum oxides are only active at high temperatures and pressures ($T > 400\,°C$, $p > 200$ atm CO). Homogeneous catalysts based on metal carbonyls, $M(CO)_6$,[3] work under milder conditions (180 °C, 35 atm) in alkaline or acidic medium. Recently, Ir^{I}[4] and Ru^{II}[5-6] complexes have been shown to efficiently catalyze the *thermal WGSR* at 100 °C/1 atm and at 20–80 °C/1–35 atm, respectively. Examples of the *photoassisted WGSR* have been reported using heterogeneous TiO_2[7] or ZnS.[8] A true homogeneous *photochemical WGSR* has not as yet been found, despite many attempts using bipyridine complexes of Ru^{II}.[9]

The thermodynamics of the WGSR make it important to find catalytic systems that are active at low temperatures. The negative entropic term, $S^{\circ}_{298} = -42\,J\,K^{-1}$, of reaction (a) disfavor it as the temperature is increased, in spite of its exergonic character at room temperature ($\Delta G^{\circ}_{298} = -28\,kJ\,mol^{-1}$). In addition, efficient room-temperature catalysts would allow large energy savings, since liquid water could be used instead of steam. We describe here our results and mechanistic analysis of the first highly efficient light-assisted WGSR, which takes place under extremely mild conditions (room temperature, ambient pressure, neutral pH, visible light) and is catalyzed by novel Ir^{III} pentamethylcyclopentadienyl (Cp*) complexes containing novel 4,4′-substituted bipyridine ligands (L).

The complexes of type $[Cp^*Ir(L)Cl]^{\oplus}Cl^{\ominus}$ (**2**, Scheme 1) were prepared, almost quantitatively, by reaction of a dimethylformamide solution of $[\{Cp^*IrCl(\mu\text{-}Cl)\}_2]$[10] with

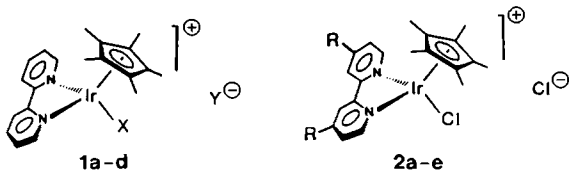

Scheme 1. Ir^{III} catalysts for the water-gas shift reaction. **1a**, X = Y = Cl; **1b**, X = Y = CF_3SO_3; **1c**, X = H, Y = $B(C_6H_5)_4$; **1d**, X = OH, Y = CF_3SO_3; **2a**, R = COOH; **2b**, R = COO*i*Pr; **2c**, R = Br; **2d**, R = NO_2; **2e**, R = NMe_2.

Table 1. Selected NMR spectroscopic data (in CD_3CN at 200.1 MHz (^1H) and 50.3 MHz (^{13}C)) and mass-spectrometric data (FAB^+) for complexes **1a–b** and **2a–e**

Complex	$\delta(^1H)$ [a]	$\delta(^{13}C\{^1H\})$ [a]	*m/z* [b]
1a	1.67	90.35 8.68	519.0
1b	1.69	89.52 9.36	633.1
1c	1.93	91.44 9.52	484.0
1d	1.70	90.89 9.11	501.1
2a	1.72	89.49 9.42	607.1
2b	1.68	91.45 8.89	691.2
2c	1.64	90.77 8.74	676.8
2d	1.70	92.29 8.90	609.0
2e	1.61	88.03 8.67	605.3

[a] Chemical shifts of the Cp* ligand. [b] *m*-Nitrobenzyl alcohol as matrix. All species display a molecular ion peak with the expected isotopic distribution (ca. 35% ^{191}Ir and 65% ^{193}Ir) and a peak corresponding to the loss of the coordinated chloride (**1a**, **2a–e**), triflate (**1b**), or hydroxide (**1d**).

two equivalents of the 4,4′-substituted, ligand (substituents: R = COOH,[11] COO*i*Pr,[12] Br,[13] NO_2,[14] NMe_2[13,15]). The complexes were recrystallized by slow diffusion of diethyl ether into an acetonitrile solution of the crude material. Compound **1b** was quantitatively synthesized by allowing **1a** to react with two equivalents of silver trifluoromethanesulfonate in acetonitrile. Their compositions have been established by ^1H and ^{13}C NMR spectroscopy, positive fast atom bombardment (FAB^+) mass spectroscopy (Table 1), and elemental analysis. When complexes **1a–d** and **2a–c**, **e** were irradiated with visible light in the presence of CO (1 atm) and H_2O at 25 °C, CO_2 and H_2 were detected by gas chromatography (Table 2). All complexes showed a marked

Table 2. Photochemical WGSR catalyzed by complexes **1a–d** and **2a–e** under CO (1 atm) at room temperature and for various pH values [a]

Complex	pH [b]	V_{H_2} [mL]	*n* [c]
1a, **1c**, or **2a** [d]	7.0	–	–
1a	5.0	0.6	3
	7.0	1.1	6
	9.0	0.6	3
1b	7.0	1.1	6
1c	7.0	0.4	3
1d	7.0	1.1	6
2a	5.0	3.3	16
	7.0	12.3	58
	9.0	11.0	52
	11.0	7.6	36
2b	2.0	1.5	8
	5.0	4.2	22
	7.0	–	–
2c	2.6	0.3	1
	5.0	1.2	6
	7.0	0.6	3
2d [e]	5.0	traces	–
	7.0		–
	9.0		–
2e	5.0	–	–
	7.0	0.5	3
	9.0	1.2	6

[a] Irradiation for 2 h with white light ($\lambda > 400$ nm). [b] Adjusted using a 0.01 M phosphate buffer. [c] Calculated by dividing the number of moles of H_2 by the number of moles of the starting complexes. [d] Dark reaction with a 15-h contact time. [e] Bleaching of the solution after a few minutes of irradiation.

pH effect on catalytic activity (Fig. 1, left) which proved that both CO oxidation (favored in basic media) and H_2 formation (accelerated in acid media) are two kinetically important reactions. Figure 1, right, shows that the rate of H_2 formation increases with increasing catalyst concentration. In the concentration range of 0.045–0.20 mM of catalyst **2a**, the reaction showed a first-order rate dependence on catalyst concentration, with a calculated rate constant of $0.34\,h^{-1}$.

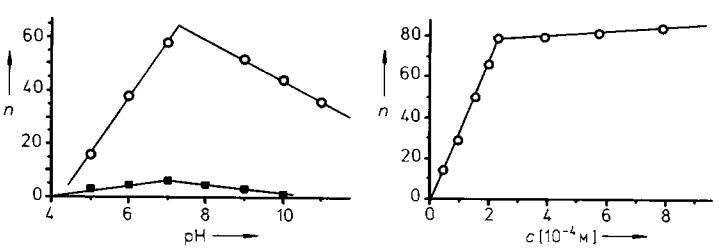

Fig. 1. Left: Effect of pH on the turnover number *n* of the photochemical WGSR (2.3×10^{-4} M **2a** (o) and **1a** (■), 1 atm CO, 15 °C, irradiation time 2 h). Right: Effect of catalyst concentration (**2a**) on *n* (15 °C, 1 atm CO, pH 7.0, irradiation time 2 h).

A remarkable increase in catalytic activity was observed when the nonsubstituted ligand **1a** was substituted with electron-withdrawing groups such as COOH (**2a**) or COO*i*Pr (**2b**). However, a dramatic decrease in activity was observed when an electron-donating substituent such as NMe_2 (**2e**) was used. This suggests that the substitution pattern in the 4,4′-position of the bipyridine strongly affects the rate-limiting step of this process, via an electronic effect. The absence of catalytic activity of the NO_2-substituted complex (**2d**) is due to a light-assisted hydrolysis of the NO_2 group, followed by loss of the ligand, as shown by the disappearance of the metal–ligand charge-transfer absorption band in the UV/VIS absorption spectra. It is also of interest to note that the thermal displacement of $Cl^{\ominus}$ by CO appears not to limit the efficiency of the process. The use of a more labile ligand ($CF_3SO_3^{\ominus}$ in complex **1b**) had no effect on the rate of reaction (Table 2).

The effect of temperature on the rate of H_2 formation was studied between 15 and 45 °C with two different complexes (**1a** and **2a**), as shown in the plot of ln *r* versus $1/T$ in Figure 2. Activation energies, E_a, of 29.6 kJ mol^{-1} and

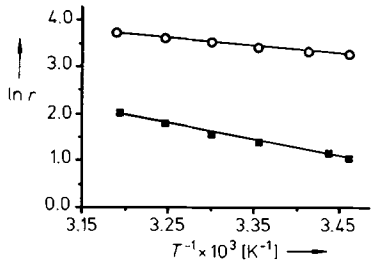

Fig. 2. Effect of temperature on the rate *r* [M min^{-1}] of the photochemical WGSR (2.3×10^{-4} M **2a** (o) and **1a** (■), 1 atm CO, Ph 7.0, irradiation time 1 h).

14.6 kJ mol^{-1} were found for complexes **1a** and **2a**, respectively. Assuming that the photochemical step has a very low activation energy,[16] these values indicate, by comparison with similar values obtained in thermal WGS processes described in the literature,[17] that decarboxylation of intermediate **B** (Scheme 2) is the rate-limiting step. Other studies on systems with higher activation energies (96–100 kJ mole^{-1}) show that the rate-limiting step is no longer decarboxylation but the reductive elimination of H_2.[4, 18] The presence of an electron-withdrawing group on the bpy-chelate halves the E_a and thus favors the decarboxylation of the intermediate. This is in good agreement with the observation that classical organic acids are much easier to decarboxylate when an electron-withdrawing group is present in the molecule.[19, 20]

From the above observations, along with further ^1H and ^{13}C NMR experiments carried out in sealed NMR tubes with labeled ^{13}CO, a proposed mechanism for the overall WGSR catalyzed by $[Cp^*Ir(L)Cl]^{\oplus}$ is shown in Scheme 2. It involves the formation of a highly reactive Ir^{III}-CO complex (intermediate **A** in Scheme 2) by CO displacement of $Cl^{\ominus}$. These species could not be isolated but have been characterized by ^{13}C NMR ($\delta = 178.2$ for precursor **1a** and 163.1 for precursor **2a** with CD_3CN as internal standard), FT-IR ($\nu_{CO} = 2069$ cm^{-1} for precursor **1a** and 2095 cm^{-1} for precursor **2a** in D_2O), and UV/VIS absorption spectroscopy (broad bands centered at 402 nm for precursor **1a** and 410 nm for precursor **2a**). Nucleophilic attack of water at this carbonyl gives the hydroxycarbonyl intermediate **B**, whose formation might also strongly be favored by the pres-

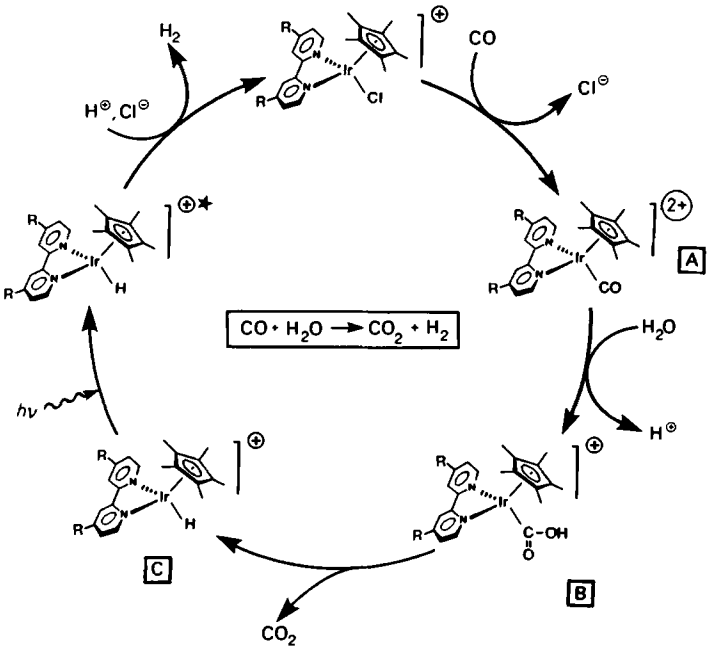

Scheme 2. Proposed reaction mechanism for the homogeneous catalysis of the photochemical WGSR by Ir^{III} complexes.

ence of an electron-withdrawing group on the bpy ligand. Preparation of related carboxylato-bpy Ir^{III} derivatives[21] and exchange reactions of water oxygen with cationic carbonyl oxygen[22] have previously been described. Decarboxylation of intermediate **B** (the rate-limiting step) gives a hydrido-Ir^{III} species[23, 24] (intermediate **C**), which, under photolysis and protonation, liberates H_2 and the starting complex. The photochemical nature of this last step was established as follows: (1) no H_2 was produced in the dark; (2) when complexes **1a**, **2a**, **b** were kept in the dark under CO (1 atm) in a sealed NMR tube, the ^1H NMR spectrum of the solution shows peaks at $\delta = -11.4$, -11.8, and -12.09, respectively, for hydride intermediates **C** in Scheme 2. These signals disappear after short photolysis; (3) dissolution of $[Cp^*Ir(bpy)(H)]^{\oplus}$,[23, 24] under vacuum in the dark, in phosphate buffer at pH = 7.0 results in no H_2 formation. Upon irradiation, however, stoichiometric amounts of H_2 are generated. All these observations corroborate the fact that the formation of H_2 is a fast reaction under irradiation.

The possibility that intermediate **B** could be formed by insertion of CO into Ir^{III}-OH was ruled out by the absence of thermal or photochemical reactivity of complex **1d** with carbon monoxide.

Experimental Procedure

The water-gas shift reaction was carried out in a 30-mL thermostated Schlenk flask containing 10 mL of 0.01 M phosphate buffer (pH 2 to 13) and 0.45×10^{-4} to 7.9×10^{-4} M **1a–d** and **2a–e**. Thermal equilibrium (in the range of 5–60 °C) was ensured by a water/ethyleneglycol circulation in a double-walled Schlenk flask. The flask and contents were degassed by three freeze–pump–thaw cycles and the internal pressure was adjusted to 1 atm with CO (99.94% purity). Irradiation was conducted with a 250-W halogen lamp (slide projector) focused on the solution. Gaseous samples were analyzed by gas chromatography. The sealed NMR tubes (5 or 10 mm) were prepared as previously described,[25] under a 90.5% ^{13}C-enriched CO atmosphere. The 200-MHz (^1H NMR) and 50-MHz (^{13}C NMR) spectra of the solution were recorded in aqueous phosphate buffer using 20% CD_3CN as internal standard. A homonuclear presaturation program (solvent suppression) was used to record the ^1H NMR spectrum.

Received: December 13, 1990 [Z 4325 IE]
German version: *Angew. Chem. 103* (1991) 863

[1] R. M. Laine, E. J. Crawford, *J. Mol. Catal. 44* (1988) 357.
[2] R. P. A. Sneeden in G. Wilkinson, F. G. A. Stone, E. W. Abel (Eds.): *Comprehensive Organometallic Chemistry*, Pergamon, Oxford 1982, p. 9 and references cited therein.
[3] A. D. King, Jr., R. B. King, D. B. Yang, *J. Am. Chem. Soc. 102* (1980) 1028; *J. Chem. Soc. Chem. Commun. 1980*, 529; *J. Am. Chem. Soc. 103* (1981) 2699.
[4] J. P. Collin, R. Ruppert, J. P. Sauvage, *Nouv. J. Chim. 9* (1985) 395.
[5] H. Ishida, K. Tanaka, M. Morimoto, T. Tanaka, *Organometallics 5* (1986) 724.
[6] M. M. Taqui Khan, S. B. Halligudi, S. Skukla, *Angew. Chem. 100* (1988) 1803; *Angew. Chem. Int. Ed. Engl. 27* (1988) 1735.
[7] S. Sato, J. M. White, *J. Am. Chem. Soc. 102* (1980) 7206; *J. Catal. 69* (1981) 128.
[8] H. Kisch, W. Schlamann, *Chem. Ber. 119* (1986) 3483.
[9] D. Choudhury, D. J. Cole-Hamilton, *J. Chem. Soc. Dalton Trans. 1982*, 1885; K. Tanaka, M. Morimoto, T. Tanaka, *Chem. Lett. 1983*, 901.
[10] J. W. Kang, K. Moseley, P. M. Maitlis, *J. Am. Chem. Soc. 91* (1969) 5970.
[11] A. Launikonis, P. A. Lay, A. W.-H. Mau, A. M. Sargeson, W. H. F. Sasse, *Aust. J. Chem. 39* (1986) 1053.
[12] K. D. Bos, J. G. Kraaijkamp, J. G. Noltes, *Synth. Commun. 9* (1979) 497.
[13] G. Maerker, F. H. Case, *J. Am. Chem. Soc. 80* (1958) 2745.
[14] D. Wenkert, R. B. Woodward, *J. Org. Chem. 48* (1983) 283.
[15] R. A. Jones, B. D. Roney, W. H. F. Sasse, K. O. Wade, *J. Chem. Soc. B* (1967) 106.
[16] V. Balzani, V. Carassiti *Photochemistry of Coordination Compounds*, Academic, New York, 1970; V. Balzani, F. Bolletta, M. T. Gandolfi, M. Maestri, *Top. Curr. Chem. 75* (1978) 1–64.
[17] E. C. Baker, D. E. Hendriksen, R. Eisenberg, *J. Am. Chem. Soc. 102* (1980) 1020.
[18] C.-H. Cheng, D. E. Hendriksen, R. Eisenberg, *J. Am. Chem. Soc. 99* (1977) 2891.
[19] S. Oae, W. Tagaki, K. Uneyama, I. Minomida, *Tetrahedron 24* (1968) 5283.
[20] E. Buncel, T. K. Venkatachalam, B. C. Menon, *J. Org. Chem. 49* (1984) 413.
[21] V. Albano, P. L. Bellon, M. Sansoni, *Inorg. Chem. 8* (1969) 298.
[22] O. J. Darensbourg, Isr. *J. Chem. 15* (1977) 247.
[23] R. Ziessel, *J. Chem. Soc. Chem. Commun.* (1988) 16.
[24] M-T. Youinou, R. Ziessel, *J. Organometal. Chem. 363* (1989) 197.
[25] J.-M. Lehn, R. Ziessel, *J. Organometal. Chem. 382* (1990) 157.

complexes. Therefore, it has been possible to synthesize a broad variety of new substituted μ-alkylidene and μ-isocyanide diiron complexes (Scheme 1).

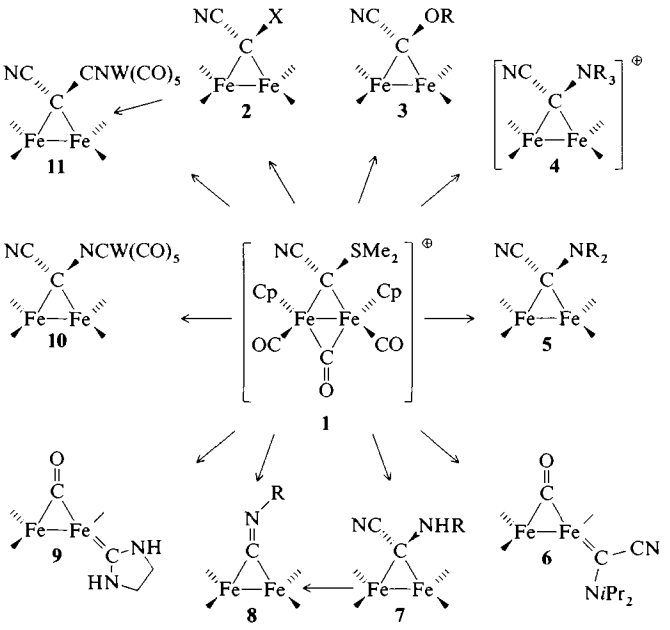

Scheme 1. For clarity's sake three CO and two Cp ligands are omitted for compounds **2**–**11**. Products and reaction conditions (MeCN solvent, room temperature, under inert atmosphere). **2:** See text (X=H, CN, SMe, Me, OC(O)Me). **3:** With HOR in excess (R=Me, Et, *i*Pr, CH_2Ph, allyl, $CH_2CH_2NMe_2$). **4:** With NMe_3 or diazabicyclooctane (DABCO) in excess. **5:** With HNR_2 in excess ($HNMe_2$, HNMeEt, $HNEt_2$, $HN(CH_2)_4CH_2$, $HN(CH_2)_5CH_2$). **6** (*cis* or *trans*): With $NHiPr_2$. **7:** With NH_2Ph. **8:** With excess of NH_2R (R=Me, Et, *i*Pr, cyclohexyl, CH_2CH_2OH, $CH_2CH_2NMe_2$). **9** (*cis* or *trans*): With excess of $H_2N(CH_2)_2NH_2$. **10:** With excess of $[W(CO)_5CN]^{\ominus}$. **11:** From **2** (X=CN) and $[W(CO)_5(thf)]$.

Dinuclear Cyanoalkylidene Complexes of Iron**

By *Vincenzo G. Albano, Silvia Bordoni, Dario Braga, Luigi Busetto,* Antonio Palazzi,* and *Valerio Zanotti*

Compounds containing a cyanoalkylidene, C(CN)X, as bridging ligand are not very common, in spite of the vast literature on μ-alkylidene bimetallic complexes.[1] In fact, prior to our synthesis of $[Fe_2Cp_2(CO)_2(\mu\text{-}CO)\{\mu\text{-}C(CN)SMe\}]$,[2] only two such complexes had been reported. Both contained the μ-$C(CN)_2$ group.[3] Very recently, we succeeded in preparing the complex sulfonium salt **1** via *S*-

$[Fe_2Cp_2(CO)_2(\mu\text{-}CO)\{\mu\text{-}C(CN)SMe_2\}]SO_3CF_3$ **1**

methylation of the μ-(methylthio)cyano complex.[4] The chemistry of the cation in **1** has now revealed a surprising versatility. The concomitant presence of the electron-withdrawing CN and the nucleofugal Me_2S substituents at the bridging carbon atom confers on **1** the properties of both cationic μ-alkylidyne[5] and terminal dichloroalkylidene[6]

Reaction of **1** with $NaBH_4$, nBu_4NCN, LiMe/CuCN, NaAc, or NaSMe results in elimination of Me_2S to form complexes of type **2**. These reactions clearly demonstrate the pseudo-cyanoalkylidyne nature of the sulfonium salt. This behavior is even more evident in the reactions with alcohols, which spontaneously produce high yields of a variety of alkylidene complexes **3**, including those containing functionalized or sterically demanding alkoxy groups. Although the configuration of **1** is *cis* according to X-ray analysis,[7] the μ-cyanoalkylidenes **2** and **3** exist as a mixture of *cis* and *trans* isomers, which could not be separated by column chromatography or fractional crystallization (Table 1). We assume that the *cis-syn* form with the smaller CN substituent of the alkylidene moiety on the Cp side is the main isomer. In complex **2** (X=H), however, the small difference in steric hindrance of the substituents on the alkylidene unit favors a comparable distribution of the three isomers in CD_2Cl_2 as solvent (*cis-syn*:*cis-anti*:*trans* $\approx$ 3.3:1.6:1). These isomer ratios were estimated from NMR data by analogy with recent findings on the related $[Fe_2Cp_2(CO)_2(\mu\text{-}CO)\{\mu\text{-}C(H)SR\}]$[8] complexes in which the lowest-field ^1H NMR methylidene proton signal was attributed to the isomer bearing H on the Cp side (*cis-anti*).

Reactions with a variety of primary amines cause degradation of the metal-bound μ-$C(CN)SMe_2$ fragment; only the bridging atom is retained in the resulting isocyanide complexes **8**. These reactions, similar to those already reported for mononuclear dichloro-[6] and dithiocarbene[9] complexes, have been now successfully extended to the preparation

[*] Prof. L. Busetto, Dr. S. Bordoni, Prof. A. Palazzi, Dr. V. Zanotti
Dipartimento di Chimica Fisica ed Inorganica dell'Università
Viale Risorgimento 4, I-40136 Bologna (Italy)
Prof. V. G. Albano, Prof. D. Braga
Dipartimento di Chimica G. Ciamician, Università di Bologna.

[**] This work was supported by the Ministero Università e Ricerca Scientifica e Tecnologica (MURST) and the Consiglio Nazionale Ricerche (CNR).

Table 1. Relevant physical data for the compounds **2**–**11** [a].

2 (X=H): red crystals (m.p., 195–197 °C). IR (CH_2Cl_2): $\tilde{\nu}$[cm^{-1}] = 2158 (CN), 2002, 1965, 1804 (CO). ^{1}H NMR: δ = 4.87 (s, Cp, *cis* + *trans*), 6.81 (s, μ-C*H*, *cis-syn* = isomer which bears CN on the Cp side), 7.94 (s, μ-C*H*, *trans*), 8.86 (s, μ-C*H*, *cis-anti*). ^{13}C NMR: *cis-syn*, δ = 266.6 (μ-CO), 211.9 (CO), 136.3 (br, CN *cis* + *trans*), 97.5 (μ-C), 90.7 (Cp); *cis-anti* = 266.3 (μ-CO), 211.1 (CO), 95.0 (μ-C), 88.5 (Cp); *trans* = 267.1 (μ-CO), 212.2, 211.3 (CO), 97.3 (μ-C), 92.2, 90.2 (Cp).

2 (X=CN): deep-violet crystals (80%; m.p., 160 °C). IR (CH_2Cl_2): $\tilde{\nu}$[cm^{-1}] = 2183 (CN), 2019, 1989, 1822 (CO). ^{1}H NMR: δ = 5.00 (s, Cp, *cis* + *trans*). ^{13}C NMR (CD_3NO_2): *cis*, δ = 255.5 (μ-CO), 205.4 (CO), 125.7, 125.2 (CN), 87.1 (Cp), 62.5 (μ-C); *trans* = 204.4 (CO), 88.6 (Cp). *cis*/*trans* = 10/1.

3 (R=Et): bright red crystals (90%; m.p., 164 °C). IR (CH_2Cl_2): $\tilde{\nu}$[cm^{-1}] = 2162 (CN), 2007, 1970, 1798 (CO). ^{1}H NMR: *cis-syn*, δ = 4.80 (s, Cp), 4.16 (q, 2H, OCH_2), 1.24 (t, 3H, CH_3). ^{13}C NMR: *cis-syn*, δ = 268.9 (μ-CO), 210.9 (CO), 129.3 (CN), 175.1 (μ-C), 90.8 (Cp), 70.8 (OCH_2CH_3), 15.4 (OCH_2CH_3); *trans* = 92.2, 91.9 (Cp). *cis-syn*/*trans* = 8/1.

4 (R=Me): IR (MeCN): $\tilde{\nu}$[cm^{-1}] = 2165 (CN), 2003, 1980, 1821 (CO).

5 (R=Me): red crystals (69%; m.p., 132–133 °C). IR (CH_2Cl_2): $\tilde{\nu}$[cm^{-1}] = 2148 (CN), 2004, 1970, 1799 (CO). ^{1}H NMR ($CDCl_3$): *cis-syn*, δ = 4.79 (s, Cp), 2.84 (s, Me). ^{13}C NMR: *cis-syn*, δ = 267.6 (μ-CO), 211.0 (CO), 161.6 (μ-C), 127.5 (CN), 91.0 (Cp), 49.6 (Me); *trans*: 87.5, 87.2 (Cp).

6: red-violet crystals (64%; m.p., 124 °C). IR (CH_2Cl_2): $\tilde{\nu}$[cm^{-1}] = 2177 (CN), 1949, 1742 (CO). ^{1}H NMR: δ = 4.4 (s, br, Cp), 3.9 (m, br, C*H*(Me)$_2$), 1.5 (s, br, Me).

7 (R=Ph): dark red crystals (m.p., 147–149 °C). IR (CH_2Cl_2): $\tilde{\nu}$[cm^{-1}] = 2166 (CN), 1992, 1954, 1798 (CO). ^{1}H NMR ($CDCl_3$): δ = 4.9 (s, Cp), 5.4 (s, NH), 6.9–7.3 (m, Ph). ^{13}C NMR: δ = 267.0 (μ-CO), 211.8 (CO), 91.8 (Cp), 147.0, 117.1, 130.3, 121.0, 124.9 (Ph); 89.2 (Cp) [b].

8 (R=$(CH_2)_2OH$): dark red crystals (55%; m.p., 130 °C). IR (CH_2Cl_2) $\tilde{\nu}$[cm^{-1}] = 2133 (CNR), 1990, 1949, 1786, 1748 (CO). ^{1}H NMR: δ = 4.7, 4.5 (s, br, Cp), 4.0–3.8 (m, br, CH_2CH_2OH), 3.4–3.3 (m, br, CH_2CH_2OH), 2.2 (s, br, OH).

9: red crystals (43%; m.p., 189–190 °C). IR (CH_2Cl_2): $\tilde{\nu}$[cm^{-1}] = 1934, 1714 (CO). ^{1}H NMR ($CDCl_3$): δ = 4.62, 4.38 (s, Cp), 3.25 (s, 4H, N–CH_2), 6.24 (s, 2H, N–H). ^{13}C NMR: δ = 290.8 (μ-CO), 224.0 (CO), 88.8, 87.3 (Cp), 46.0 (CH_2).

10: red-violet crystals (95%, m.p., 149–150 °C. IR (CH_2Cl_2): $\tilde{\nu}$[cm^{-1}] = 2188 (CN), 2125 (NCW), 2015, 1987, 1822 (FeCO), 2053, 1947 (WCO). ^{1}H NMR: δ = 4.99 (s, Cp). ^{13}C NMR: *cis-syn*, δ = 260.3 (μ-CO), 209.4 (FeCO), 198.6 (WCO), 195.3 (W(CO)$_4$), 91.7 (Cp); *trans*, δ = 93.1, 93.0 (Cp).

11: red-violet crystals (m.p., 177–179 °C). IR (CH_2Cl_2): $\tilde{\nu}$[cm^{-1}] = 2198 (CNW), 2187 (CN), 2020, 1992, 1828 (FeCO), 2074, 1936, 1897 (WCO). ^{1}H NMR: δ = 5.10 (s, Cp). ^{13}C NMR [$(CD_3)_2CO$]: *cis-syn*, δ = 257.8 (μ-CO), 210.1 (FeCO), 202.2 (WCO), 197.8 (W(CO)$_4$), 136.9 (CNW), 128.6 (CN), 92.9 (Cp), 60.0 (μ-C); *trans* = 258.2 (μ-CO), 210.0, 209.7 (FeCO), 202.0 (WCO), 198.1 (W(CO)$_4$), 92.6, 92.2 (Cp), 59.3 (μ-C).

[a] 200-MHz ^{1}H and ^{13}C{^{1}H} NMR spectra recorded in CD_2Cl_2 at 25 °C with TMS as standard, unless stated otherwise. [b] Due to **8** (R=Ph); see text.

of a variety of dinuclear species, including those containing functionalized μ-isocyanide ligands. The isolation of **4** and **5** from the reaction of **1** with tertiary and secondary amines suggests that formation of **8** proceeds via ammonium (type **4**) and aminoalkylidene complexes (type **7**), which subsequently lose HCN. In the reaction with the weakly basic aniline, the supposed intermediate has been isolated and structurally characterized by an X-ray diffraction study (Fig. 1). This intermediate shows the same *cis-syn* arrangement of the substituents as **1**. The retained *syn* arrangement observed for **7** and suggested for the major isomer in **3**–**5**, **10**, and **11** may be due to an attack of the nucleophile from the less hindered CO face of the μ-cyanoalkylidyne intermediate formed from **1** after loss of Me_2S. Complex **7**,[10] which is slowly transformed into the μ-phenylisocyanide complex in solution, represents the first structurally characterized dinuclear μ-aminoalkylidene complex in which no stabilization due to additional coordination to one of the metals through the amino N atom or the functionalized end of the amino group is present.[11] It may therefore be assumed that the electron-withdrawing CN group stabilizes the dimetallacyclopropane ring even when a π-donating N atom is present on the μ-C atom. The crystal structure of *cis*-**7** (R = Ph) (Fig. 1) indicates that the lone pair on the aniline nitrogen atom is not parallel to the π orbital on the carbene atom (C4) nor to the π orbitals of the phenyl ring. The torsion angles C5-C4-N2-C6 (42°) and C4-N2-C6-C7 (17°) indicate a better interaction with the phenyl ring, as confirmed by the bond distances N2-C4 (1.429(3) Å) and N2-C6 (1.397(3) Å). The reactions of **1** with the bulky diisopropylamine or with ethylenediamine, which, respectively, afford the terminal aminocarbene complexes **6** and **9**, indicate that steric as well as electronic effects play a role in the position of the alkylidene group. Either sterically demanding or π-donating N-substituents at the bridging carbon may ultimately cause the alkylidene ligand to shift from the expected bridging to the terminally coordinated position.

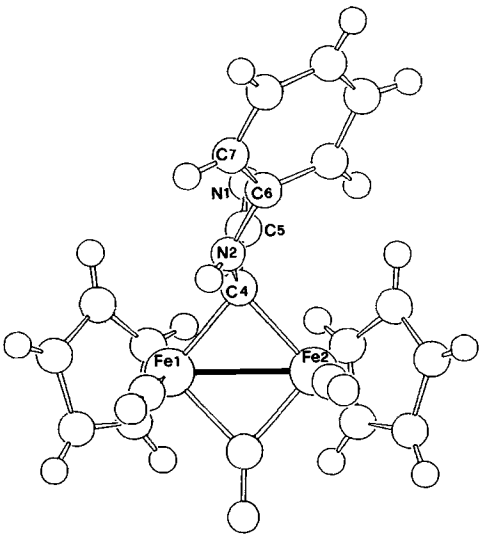

Fig. 1. Molecular structure of *cis*-**7** (R = Ph). The molecule adopts an asymmetric conformation but is present as a racemic mixture in the crystal. Space group $P2_1/c$, a = 9.711(2), b = 11.910(2), c = 16.426(1) Å, β = 89.91(1)°, Z = 4, V = 1899.8 Å^3, $2\theta \leq 56°$, 3664 measured reflections, 3607 observed ($I > 2\sigma(I)$), 317 refined parameters, anisotropic temperature factors for non-hydrogen atoms, R = 0.029. Selected bond lengths [Å] and angles [°]: Fe1-Fe2 2.533(1), C4-Fe1 2.004(2), C4-Fe2 2.028(2), C4-C5 1.450(3), C5-N1 1.155(3), C4-N2 1.429(3), N2-C6 1.397(3); C5-C4-N2 108.7(2), C4-N2-C6 127.9(2).

The strong electrophilic properties of the μ-C atom in **1** are also evident from its reaction with the nitrogen end of the metalate $[W(CO)_5CN]^{\ominus}$, which yields complex **10**. In **10**, the unusual (cyano)isocyanoalkylidene group, C(CN)NC, is bonded to three metal centers. Complex **10** is isomeric to **11**, which has been obtained by reaction of the dicyanoalkylidene complex **2** (X=CN) with [W(CO)$_5$(thf)]. Whereas the isomer **11** reacts with pyridine (Py) to form quantitatively **1** and [M(CO)$_5$Py], the isocyano form **10** does not react with pyridine or CO up to 100 atm. This observation is in line with the predicted ability of the isocyano function to stabilize carbenes,[12] which has recently been confirmed through the preparation of the somehow related terminal alkylidene complex $[(CO)_5CrC(NCCl_2)(NCMnCp(CO)_2]$.[13]

Experimental Procedure

2 (X=H): Complex **1** (370 mg, 0.64 mmol) was dissolved in MeCN (10 mL) and the resulting solution was treated with $NaBH_4$ (35 mg, 0.93 mmol); the color of the solution turned immediately from red brown to red and the solvent was removed under vacuum. The residue was dissolved in dichloromethane and filtered on an alumina column (5 × 3 cm). The red solution was evaporated to dryness under vacuum and the residue crystallized from CH_2Cl_2 layered with *n*-pentane at − 20 °C to yield 168 mg (72%) of **2** (X=H).

3 (R=CH_2-CH=CH_2): In a typical experiment, **1** (300 mg, 0.52 mmol) was dissolved in MeCN (15 mL) and an excess of $HOCH_2$-CH=CH_2 (4 mL) was added after stirring. The resulting solution was filtered on an alumina column (10 × 3 cm; eluent, CH_2Cl_2). The collected solution was evaporated to dryness and the residue recrystallized from CH_2Cl_2 layered with *n*-pentane at − 20 °C to afford 162 mg (74%) of **3** (m.p. 124–126 °C, dec.).

5 (R=Me): Gaseous dimethylamine was bubbled into an MeCN solution (10 mL) of **1** (91 mg, 0.16 mmol); the color of the solution turned immediately bright-red and the mixture was dried under vacuum. The residue, worked up as described for **2**, was crystallized from CH_2Cl_2 layered with *n*-pentane to yield 45 mg (69%) of **3**.

6: Complex **1** (108 mg, 0.19 mmol) in MeCN (10 mL) was treated with $NHiPr_2$ (40 mg, 0.4 mmol). The reaction mixture immediately turned from red-brown to violet and the solvent was evaporated to dryness. After dissolving the residue in CH_2Cl_2, the solution was chromatographed on an alumina column (15 × 3 cm) by using CH_2Cl_2/petroleum ether (1/2, v/v) as eluent. After eluting the first fraction containing $[Fe_2(Cp)_2(CO)_4]$, the second fraction was collected and the solvent evaporated to dryness. Crystallization from CH_2Cl_2 layered with *n*-hexane at − 20 °C afforded 56 mg (64%) of **6**.

7 (R=Ph): Complex **1** (160 mg, 0.28 mmol) was dissolved in MeCN (10 mL) and treated with aniline (0.54 mmol). After 10 min the mixture was worked up as described for **5**, yielding 40 mg (32%) of **7**. When the same reaction was carried out with a fivefold excess of aniline,, complex **8** (R=Ph) was obtained in 60% yield. This latter complex was also obtained (90%) by stirring a CH_2Cl_2 solution of **7** for 24 h.

11: Complex **2** (X=CN) (100 mg, 0.26 mmol) was dissolved in THF (10 mL) and treated with $[W(CO)_5(thf)]$, which was obtained from photolysis of $[W(CO)_6]$ (275 mg, 0.78 mmol) in THF (20 mL). The reaction mixture was stirred overnight and dried under vacuum. The residue, dissolved in CH_2Cl_2 (≈3 mL) was chromatographed on an alumina column (15 × 3 cm). Elution with CH_2Cl_2/petroleum ether (1/1, v/v) gave four fractions containing: (1) $[W(CO)_6]$, (2) a small amount of the complex bearing the fragment μ-[C{CN-$W(CO)_5$}$_2$] (15 mg), (3) **11**, and (4) the starting complex **2**. The third fraction was concentrated (3 mL) and layered with *n*-pentane. On cooling to − 20 °C, 130 mg (70% yield) of **11** was obtained.

Received: December 18, 1990 [Z 4336 IE]
German version: *Angew. Chem. 103* (1991) 895

CAS Registry numbers:
1, 125894-70-4; *cis-syn*-**2** (H), 125894-82-8; *cis-anti*-**2** (H), 126059-68-5; *trans*-**2** (H), 133962-76-2; *cis*-**2** (CN), 36180-80-0; *trans*-**2** (CN), 133962-77-3; *cis-syn*-**3** (R = Et), 125894-74-8; *trans*-**3** (R = Et), 133962-78-4; *cis-syn*-**3** (R = $CH_2CH=CH_2$), 133887-38-4; **4** (R = Me), 133887-31-7; *cis-syn*-**5** (R = Me), 125894-71-5; *trans*-**5** (R = Me), 133962-79-5; **6**, 133887-32-8; **7** (R = Ph), 133887-37-3; **8** (R = $(CH_2)_2OH$), 133887-33-9; **9**, 133887-34-0; *cis-syn*-**10**, 133887-35-1; *trans*-**10**, 133962-80-8; *cis-syn*-**11**, 133887-36-2; *trans*-**11**, 133962-81-9; $HOCH_2CH=CH_2$, 107-18-6; $NHMe_2$, 124-40-3; $NHiPr_2$, 108-18-9; NH_2Ph, 62-53-3; $W(CO)_6$, 14040-11-0.

[1] W. A. Herrmann, *Adv. Organomet. Chem. 20* (1982) 159; J. Holton, M. F. Lappert, R. Pearce, P. I. W. Yarrow, *Chem. Rev. 83* (1983) 135.
[2] L. Busetto, S. Bordoni, V. Zanotti, V. G. Albano, D. Braga, *Gazz. Chim. Ital. 118* (1988) 667.
[3] R. B. King, M. S. Saran, *J. Am. Chem. Soc. 95* (1973) 1811; E. I. Smyslova, E. G. Perevalova, V. P. Dyadchenko, K. I. Grandberg, Yu. L. Slovokhotov, Yu. T. Struchkov, *J. Organomet. Chem. 215* (1981) 269.
[4] L. Busetto, S. Bordoni, V. Zanotti, V. G. Albano, D. Braga, U. Schubert (Eds.): *Advances in Metal Carbene Chemistry*, Kluwer, Dordrecht 1989, p. 141.
[5] C. P. Casey, M. Crocker, P. C. Vosejpka, P. J. Fagan, S. R. Marder, M. A. Gohdes, *Organometallics 7* (1988) 670.
[6] M. A. Gallop, W. R. Roper, *Adv. Organomet. Chem. 25* (1986) 121.
[7] V. G. Albano, S. Bordoni, D. Braga, L. Busetto, V. Zanotti, *Coll. Abstr. 12th European Crystallogr. Meet.*, Moscow 1989, S. 191.
[8] N. C. Schroeder, R. Funchess, R. A. Jacobson, R. J. Angelici, *Organometallics 8* (1989) 521.
[9] F. B. McCormick, R. J. Angelici, *Inorg. Chem. 18* (1979) 1231; L. Busetto, V. Zanotti, V. G. Albano, D. Braga, M. Monari, *J. Chem. Soc. Dalton Trans. 1988*, 1067.
[10] Crystal structure analysis: CAD-4 diffractometer, $Mo_{K\alpha}$ radiation, room temperature, $\omega/2\theta$-scan method. Further details of the crystal structure investigation may be obtained from the Director of the Cambridge Crystallographic Data Centre, University Chemical Laboratory, Lensfield Road, GB-Cambridge CB2 1EW (UK), on quoting the full journal citation.
[11] J. H. Davis, Jr., C. M. Lukehart, L. Sacksteder, *Organometallics 6* (1987) 50; R. D. Adams, D. F. Chodosh, N. M. Golembeski, *J. Organomet. Chem. 139* (1977) C39.
[12] J. B. Moffat, *Int. J. Quantum Chem. 19* (1981) 771.
[13] G. Beck, W. P. Fehlhammer, *Angew. Chem. 100* (1988) 1391; *Angew. Chem. Int. Ed. Engl. 27* (1988) 1344.

Optically Active "Stereocomplexes" of Isotactic Poly(methyl methacrylates) with Main-Chain Chirality **

By *Günter Wulff** and *Joachim Petzoldt*

Dedicated to Professor Leonhard Birkofer on the occasion of his 80th birthday

The possible occurrence of optical activity in linear vinyl- and vinylidene polymers due to the configuration or conformation of the main chain has long been discussed.[1] Isotactic chains such as **1** pose an interesting problem in this respect. In principle, such chains can be chiral if the end groups differ. However, this difference is negligible for long chains, so that such chains should behave as *meso* forms. Depending on their molar mass, they should thus exhibit only very small optical activity or practically none. They can therefore be called "cryptochiral".[2]

Anionic polymerization of trityl methacrylate in the presence of chiral catalysts, first introduced by *Okamoto* et al.,[3] gives isotactic polymers that exhibit high optical activity and are present as stable, one-handed (atropisomeric) helices. After replacement of the trityl group by the very much smaller methyl group, the polymer adopts a random-coil conformation and the optical activity almost vanishes (residual rotation $[\alpha]^{20}_{546} < 1.2°$).[3] However, investigations of the oligomers obtained in this polymerization reaction show that the stereogenic centers in the main chain are formed with high asymmetric induction and with uniform absolute configuration.[4] These kinds of compounds thus offer the first models for the investigation of enantiomerically pure, cryptochiral isotactic chains.

We have now varied the chain ends R^1 and R^2 in such enantiomerically pure or enriched isotactic poly(methyl methacrylates) (PMMA) in order to study their effect on the optical activity. In addition, we have attempted to investigate not only the effect of configuration but also that of conformation on the optical activity. Isotactic PMMA can undergo a transition to helical conformations; for identical chain ends (*meso* form), the (+) and (−) helices should be formed with equal probability. However, if helix formation from one chain end is favored owing to differing chain ends, then diastereomeric (+) and (−) helices should be formed from an enantiomerically pure chain and one screw sense of the helix should be preferred.

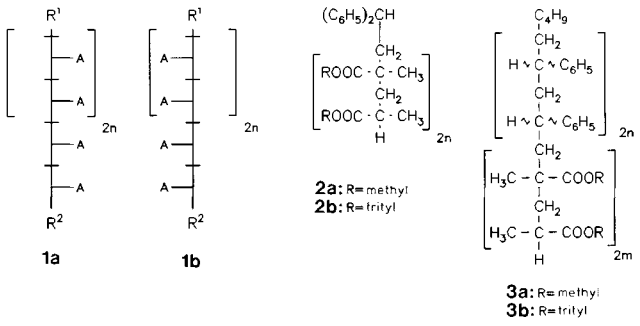

[*] Prof. Dr. G. Wulff, Dipl. Chem. J. Petzoldt
Institut für Organische Chemie und Makromolekulare Chemie der Universität
Universitätsstrasse 1, W-4000 Düsseldorf (FRG)

[**] On the Chirality of Polyvinyl Compounds, Part 14. This work was supported by the Ministerium für Wissenschaft und Forschung des Landes Nordrhein-Westfalen and by the Fonds der Chemischen Industrie. We thank Prof. Dr. *G. Challa*, Groningen, Netherlands, for valuable suggestions. Part 13: G. Wulff, Y. Wu, *Makromol. Chem. 191* (1990) 3005.

Table 1. Molar masses and optical rotation of the newly prepared polymers.

Polymer[a]	No.	M_n[b] R=trityl PTMA part	M_n[b] R=methyl PMMA part	Styrene part	$[\alpha]_{546}^{20}$[°] R=trityl[c]	$[\alpha]_{546}^{20}$[°] R=methyl[c]	R=methyl as stereocomplex[d]
(+)**2**	1	15000	4700	–	+422	0.9 ± 0.2	−3.0 ± 0.1
(−)**2**	2	17800	5600	–	−412	−0.7 ± 0.2	+1.6 ± 0.2
(+)**2**	3	20000	6300	–	+429	+0.6 ± 0.2	−2.7 ± 0.2
(+)**2**	4	24300	7600	–	+439	+0.6 ± 0.2	−2.5 ± 0.2
(+)**2**	5	26800	8300	–	+422	+0.4 ± 0.2	−1.7 ± 0.1
3	1	19400	5900	5800	0	0 ± 0.2	0 ± 0.2
(−)**3**	2	12500	3800	7500	−402	−1.4 ± 0.4	−7.4 ± 0.3
(+)**3**	3	14800	4500	6800	+438	+1.4 ± 0.2	+9.9 ± 0.3
(+)**3**	4	15700	4800	6800	+453	+0.7 ± 0.3	+9.9 ± 0.3
(−)**3**	5	16100	4900	8300	−389	−1.9 ± 0.4	− 11.6 ± 0.3

[a] In the table and in the text, polymers **2** and **3** with R = methyl are indicated by the letter **a**, those with R = trityl by the letter **b**. Polymer **2b** was prepared by anionic polymerization of trityl methacrylate with diphenylmethyllithium/(+)- or (−)-2,3-dimethoxy-1,4-bis(dimethylamino)butane ((+)- or (−)-DDB) in toluene at −78 °C. The block copolymers **3** [7] were obtained by anionic polymerization of styrene with *n*-butyllithium/(+)- or (−)-DDB in toluene at −20 °C followed by further polymerization at −78 °C after addition of trityl methacrylate[7]. In the case of **3** (No. 1), the reaction was initiated with *n*-butyllithium/tetramethylethylenediamine. [b] The molar masses refer to the poly(trityl methycrylate) (PTMA), the poly(methyl methacrylate) (PMMA), and the polystyrene moieties. The values were determined for the methyl esters by NMR investigation and gel permeation chromatography (versus polystyrene as standard). [c] The values given are the specific optical rotations based on the weight percent of PTMA or PMMA. **2b** and **3b** in THF, $c = 0.4-0.6$; **2a** in benzene, $c = 0.33$; **3a** in benzene, $c = 0.15$. The limits of error refer to the accuracy of the polarimeter. [d] The stereocomplexes were prepared with syndiotactic PMMA ($M_n = 35000$) according to [6]. Weight ratio of syndiotactic PMMA to **2a** or to **3a** 4:1. Total concentration in benzene 2 wt %.

Poly(methyl methacrylates) (PMMA) (see Table 1) with diphenylmethyl and hydrogen (**2a**) as well as with atactic polystyrene and hydrogen (block copolymer **3a**) as end groups were prepared from the corresponding optically active poly(trityl methacrylates) (PTMA). In both cases, the tritylated polymers **2b** and **3b** exhibited strong optical rotations ($[\alpha]_{546}^{20}$ 389–453°), whereas the methyl esters **2a** and **3a** showed only residual rotations of 0.4–1.9°. These rotations are in part near the limits of detection and are due to the configuration of the chains. By appropriate choice of the catalyst (+)- and (−)-2,3-dimethoxy-1,4-bis(dimethylamino)butane ((+)- and (−)-DDB), polymers **2** and **3** with either positive or negative rotation could be obtained.

In order to transform the chains into helices to an appreciable extent, "stereocomplexes" with achiral syndiotactic PMMA chains were prepared. In such stereocomplexes, the isotactic PMMA chain is present as a tightly folded inner helix in a 9/1 double helix with syndiotactic PMMA.[5] The complex formation in benzene or toluene could be detected by NMR spectroscopy[6] (about 40% of isotactic PMMA complexed) and showed the expected temperature dependence. The optical activity due to complex formation gradually disappears as the temperature is raised to about 70 °C, leaving only the residual rotation due to the configuration.

Table 1 shows the optical rotations obtained by complex formation. For polymers **2a** (R = methyl), the absolute values are a factor of 2.3 to 4.5 larger than for the uncomplexed polymers, whereas they are enhanced up to tenfold for the block copolymer **3a**. Noteworthy is the fact that, for the same absolute configuration in the chains of **2a** and **3a** (R = methyl) as well as for the same sign of optical rotation of **2b** and **3b** and of the uncomplexed polymers **2a** and **3a**, the sign of the rotation reverses only for the homopolymers **2a** on complexation. This means that the complexed polymers **2a** and **3a** must exist as helices of opposite screw sense; for example, helix formation might begin at the diphenyl end in **2a** and at the H end in **3a**.

The investigations show, therefore, that even a large difference in the chain ends of isotactic polymers is not sufficient to cause significant optical activity due to the configuration of the main chain. However, the chirality inherently present in the polymer structure (cryptochirality) can be revealed by complexing the polymer with a chiral superstructure. Unfortunately, the method described here does not allow the preparation of polymers with appreciably higher molar masses, which would allow more detailed study of the dependence of the optical activity on molar mass.

Received: February 11, 1991 [Z 4436 IE]
German version: *Angew. Chem. 103* (1991) 870

[1] M. Farina, *Top. Stereochem. 17* (1987) 1; G. Wulff, *Angew. Chem. 101* (1989) 22; *Angew. Chem. Int. Ed. Engl. 28* (1989) 21.
[2] K. Mislow, P. Bickart, *Isr. J. Chem. 15* (1976/77) 1.
[3] Y. Okamoto, K Suzuki, K. Ohta, K. Hatada, H. Yuki, *J. Am. Chem. Soc. 101* (1979) 4763.
[4] G. Wulff, R. Sczepan, A. Steigel, *Tetrahedron Lett. 27* (1986) 1991; Y. Okamoto, E. Yashima, T. Nakano, K. Hatada, *Chem. Lett. 1987*, 759.
[5] G. Challa, E. Schomaker, *Macromolecules 22* (1989) 3337.
[6] J. Spevacek, B. Schneider, *Makromol. Chem. 175* (1974) 2939.
[7] R. Sczepan, *Dissertation*, Universität Düsseldorf 1985.

cyclo-As_8 as Complex Ligand**

By *Otto J. Scherer,* Rainer Winter, Gert Heckmann,* and *Gotthelf Wolmershäuser*

Dedicated to Professor Hans Georg von Schnering on the occasion of his 60th birthday

In the complex chemistry of substituent-free E_n units (E = P, As, Sb, Bi), the following arsenic species have been stabilized by coordination: *cyclo*-As_3, *cyclo*-As_4, *cyclo*-$As_5^{\ominus}$, and *cyclo*-As_6.[1] The largest rings found for the polyarsenides are the $As_7^{\ominus}$ unit, a norbornadiene analogue, and the crown-shaped *cyclo*-$As_8^{8\ominus}$ unit in the ionic compounds $[As_7\{Cr(CO)_3\}]^{3\ominus}$ (**1**)[2] and $^1_\infty[Rb\{NbAs_8\}]^{2\ominus}$ (**2**), respectively.[3] In analogy to cyclooctatetraene (**A**), structure **B** can formally be postulated for a *cyclo*-As_8 unit.

[*] Prof. Dr. O. J. Scherer, Dipl.-Chem. R. Winter,
Dipl.-Chem. G. Heckmann[+], Dr. G. Wolmershäuser[+]
Fachbereich Chemie der Universität
Erwin-Schrödinger-Strasse, W-6750 Kaiserslautern (FRG)
[+] X-ray structure analyses

[**] This work was supported by the Fonds der Chemischen Industrie (doctoral fellowship for *R. W.*).

Reaction of the tetracarbonylniobium compound **3** with yellow arsenic (As_4) in excess results in formation of the binuclear niobium complex **5** in about 17% yield together

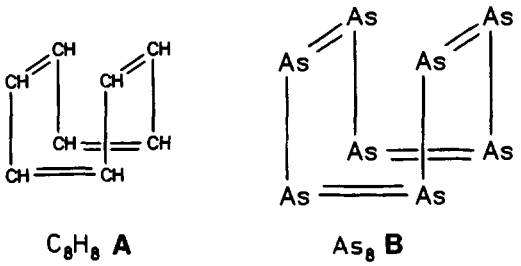

C_8H_8 **A** As_8 **B**

with small amounts of the trinuclear complex **4**,[4] whose structure has not yet been established. Complex **5** reacts with $[Cr(CO)_5(thf)]$ to give **6**.

$$[Cp''Nb(CO)_4] \xrightarrow[170\,^\circ C,\ 2\ h]{As_4,\ decalin} [(Cp''Nb)_3As_6] + [(Cp''Nb)_2(\mu,\eta^{4:4}\text{-}As_8)]$$
3 **4** **5**

$$\mathbf{5} \xrightarrow[THF,\ 20\,^\circ C,\ 1.5\ h]{[Cr(CO)_5(thf)]} [(Cp''Nb)_2\{As_8Cr(CO)_5\}]$$
6

$Cp'' = \eta^5\text{-}1,3\text{-}t\mathrm{Bu}_2C_5H_3$

Complex **4** forms a brown, microcrystalline powder, **5** mahogany-colored crystalline needles with metallic luster, and **6** red crystals, which are sparingly soluble in petroleum ether, moderately soluble in benzene, and readily soluble in dichloromethane; **4** exhibits the best solubility.

The ^1H NMR spectrum[4] of **4** reveals only one kind of Cp″ ligand even at low temperatures. For **5** and **6**, the signal pattern expected on the basis of symmetry[4] is observed.

X-ray crystal structure analyses[5] show that, for both **5** and **6**, the arsenic analogue **B** of cyclooctatetraene forms a puckered, strongly distorted eight-membered ring (Figs. 1 and 2, respectively). To our knowledge, such a coordination geometry has not yet been observed for cyclooctatetraene complexes.[6] Possibly, the two ten-valence-electron fragments Cp″Nb are largely responsible for this *cyclo*-As_8 distortion. Together with the two sets of four arsenic atoms As1, As2′, As4, As3 and As1′, As2, As4′, As3′ in **5** (Fig. 1) as well as As3, As5, As7, As8 and As1, As2, As4, As6 in **6** (Fig. 2), they define two distorted tetragonal pyramids. The corresponding bond lengths and angles in the Nb_2As_8 framework, which consists of annelated three-, four-, and five-membered rings, differ only slightly in **5** and **6**. The average

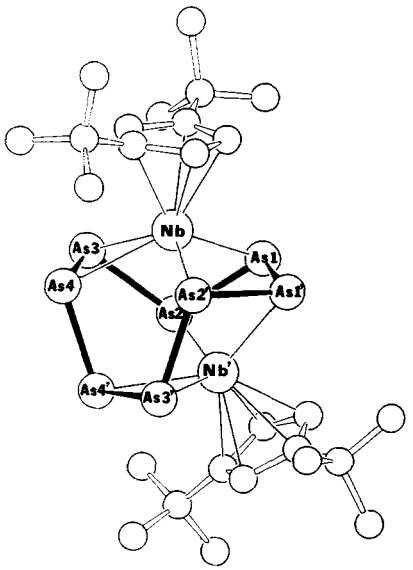

Fig. 1. Molecular structure of **5**. Selected bond lengths [Å] and angles [°]: Nb-As1 2.585(2), Nb-As2′ 2.545(2), Nb-As3 2.642(2), Nb-As4 2.744(2), As1-As1′ 2.530(3), As1-As2 2.402(2), As2-As3 2.422(2), As3-As4 2.355(3), As4-As4′ 2.429(3), Nb-$Cp''_{(center)}$ 2.13; As1′-As1-As2 106.3(3), As1-As2-As3 107.9(1), As2-As3-As4 96.9(1), As3-As4-As4′ 99.9(1), $Cp''_{(center)}$Nb-Nb′ 158.3.

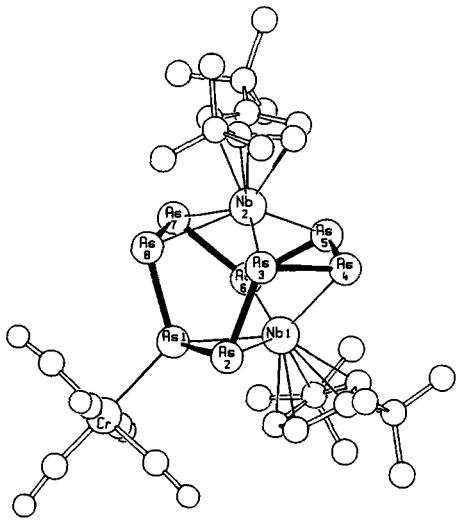

Fig. 2. Molecular structure of **6**. Selected bond lengths [Å] and angles [°]: Nb2-As5 2.573(6), Nb2-As3 2.533(5), Nb2-As7 2.637(6), Nb2-As8 2.735(6), Nb1-As4 2.576(6), Nb1-As6 2.539(5), Nb1-As2 2.669(5), Nb1-As1 2.714(5), As5-As4 2.546(6), As4-As3 2.393(6), As3-As2 2.380(6), As2-As1 2.361(6), As1-As8 2.432(6), As8-As7 2.360(7), As7-As6 2.390(6), As6-As5 2.380(6), As1-Cr 2.508(8), Nb1-$Cp''_{(center)}$ 2.09, Nb2-$Cp''_{(center)}$ 2.08; As5-As4-As3 106.1(2), As4-As3-As2 107.1(2), As3-As2-As1 94.6(2), As2-As1-As8 102.6(2), As1-As8-As7 98.0(2), As8-As7-As6 99.1(2), As7-As6-As5 108.0(2), As6-As5-As4 106.6(2), $Cp''_{(center)}$Nb1-Nb2 162.4, $Cp''_{(center)}$Nb2-Nb1 156.3.

values of the very different As–As and Nb–As distances are 2.415 and 2.629 Å, respectively, for **5** and 2.405 and 2.622 Å, respectively, for **6**; these bond lengths are 2.405 Å for **1**[2] and 2.434 as well as 2.619 Å for **2**[3] and are also comparable to $\bar{d}$(As-As) in complexes with $(RAs)_n$ ligands.[7] The average value of the As–As–As angle is 102.8° in **5** and **6**. Noteworthy are the following transannular distances, some of them very short: Nb···As1′ = 3.022(2) and Nb···As2 = 2.861(2) Å in **5**; Nb1···As3 = 2.882(5), Nb1···As5 = 2.999(5), Nb2···As4 = 3.010(5), and Nb2···As6 = 2.854(5) Å in **6**. The Nb···Nb distance in **5** (3.326(2) Å) and **6** (3.311(5) Å) lies at the limits of bonding interactions.[8]

Experimental Procedure

4, **5**: Complex **3**[9] (765 mg, 2.00 mmol), dissolved in 10 mL of decalin, and 150 mL of a freshly prepared decalin solution of As_4 (ca. 862 mg = 2.9 mmol) were stirred at about 170 °C and the reaction was monitored by IR (after ca. 2 h, CO bands were no longer observed). After removal of the solvent under oil-pump vacuum (ca. 50 °C bath temperature), the black-brown, oily residue was treated with 3 mL of CH_2Cl_2 and about 2.5 g of Al_2O_3 (basic, 3% H_2O) and the mixture was then dried under oil-pump vacuum until it was free-flowing. Unreacted, red **3** (20 mg, 2.6%) was eluted with petroleum ether (column: 30 × 2.5 cm, Al_2O_3). Complex **4** (106 mg, 4.3% based on reacted **3**) was eluted with petroleum ether–toluene (20:1). Recrystallization from toluene–hexane (1:2) afforded 88 mg (3.6%) of brown, microcrystalline **4**. Complex **5** was eluted as a mahogany-colored fraction with petroleum ether–toluene (10:1). Concentration of the solution to about 5 mL followed by two-day crystallization gave 196 mg (8.8% based on reacted **3**) of **5**. An additional 177 mg (8.0%) could be isolated from the mother liquor. Suitable single crystals were obtained

by dissolving **5** in diethyl ether, adding petroleum ether, gently concentrating the solution until the onset of crystallization, and allowing the solution to stand for two days at room temperature. Complex **5** forms mahogany-colored crystalline needles.

6: A solution of [Cr(CO)$_5$(thf)], prepared photochemically from freshly sublimed [Cr(CO)$_6$] (11.7 mg, 0.053 mmol), in 50 mL of THF was added to **5** (61 mg, 0.053 mmol). The reaction mixture was stirred for about 1.5 h at room temperature (IR monitoring showed no further increase in the newly appeared CO bands) and then worked up as described for **5**. Unreacted **5** (8 mg, 13.1%) was eluted as a mahogany-colored fraction with petroleum ether–diethyl ether (15:1), followed by a red-brown fraction of **6**. The fraction of **6** was concentrated to about 10 mL and allowed to stand at room temperature. Ruby-red, cube-shaped crystals of **6** (48 mg, 71% based on reacted **5**) formed within 20 h. An additional 3 mg of product was isolated from the mother liquor (total yield 51 mg (76%)).

Received: February 11, 1991 [Z 4437 IE]
German version: *Angew. Chem. 103* (1991) 860

CAS Registry numbers:
3, 133887-27-1; **4**, 133887-28-2; **5**, 133887-29-3; **6**, 133887-30-6; As$_4$, 12187-08-5; [Cr(CO)$_5$(thf)], 15038-41-2.

[1] Recent review: O. J. Scherer, *Angew. Chem. 102* (1990) 1137; *Angew. Chem. Int. Ed. Engl. 29* (1990) 1104.
[2] B. W. Eichhorn, R. C. Haushalter, J. C. Huffman, *Angew. Chem. 101* (1989) 1081; *Angew. Chem. Int. Ed. Engl. 28* (1989) 1032.
[3] H. G. von Schnering, J. Wolf, D. Weber, R. Ramirez, T. Meyer, *Angew. Chem. 98* (1986) 372; *Angew. Chem. Int. Ed. Engl. 25* (1986) 353.
[4] ^{1}H NMR (400 MHz for **4** and **5**, 298 K), **4** (C_6D_6): δ = 5.87(br, 2H), 4.76(br, 1H), 1.29(s, 18H), ^{13}C NMR (400 MHz, CD_2Cl_2, 298 K): δ = 123.1(s), 91.9(d, ^1J(CH) = 165 Hz), 88.0(d,^1J(CH) = 172 Hz), 32.7(q, ^1J(CH)=126 Hz), 32.1(s). **5** (CD_2Cl_2): δ = 4.78(t, 1H), 4.74(t, 1H), 4.24(t, 1H), each ^3J(HH) = ^4J(HH) = 2.4 Hz, 1.14(s, 9H), 0.97(s, 9H). **6** (200 MHz, C_6D_6, 298 K): δ = 4.97(t, ^4J(HH) = 2.20 Hz), 4.73(dd, ^3J(HH) = 3.08, ^4J(HH) = 2.20 Hz), 4.48(dd, ^3J(HH) = 2.94, ^4J(HH) = 2.35 Hz), 4.30(dd,^3J(HH) = 2.94, ^4J(HH) = 2.35 Hz), 4.20(dd,^3J(HH) = 3.08, ^4J(HH) = 2.20 Hz), 4.17(t, ^4J(HH) = 2.35 Hz), 1.33(s, 9H), 1.16(s, 9H), 0.99(s, 9H), 0.90(s, 9H). IR(hexane): $\tilde{\nu}$(CO) [cm^{-1}] = 2049(s), 1977(m), 1938(vs), 1928(vs), 1919(s). MS (70 eV), **4**: *m/z* 1259.4 ($M^{\oplus}$, 100%), 630.0 ($M^{2\oplus}$, 31%), and further fragments. Correct C,H analyses.
[5] a) Complex **5** forms monoclinic crystals, *C2/c*; *a* = 25.103(3), *b* = 8.067(3), *c* = 17.699(3) Å, β = 99.53(1)°, *Z* = 4, 3099 unique reflections (Mo$_{K\alpha}$: $1.5 \le \theta \le 25°$), 1748 observed with $I \ge 2\,\sigma(I)$; 183 parameters, *R* = 0.053, R_w = 0.049[5c]; b) Complex **6** forms orthorhombic crystals, p_{ccn}; *a* = 17.319(3), *b* = 20.027(2), *c* = 24.343(17), *Z* = 8, 3946 unique reflections (Mo$_{K\alpha}$: $1.5° \le \theta \le 25°$), 1711 observed with $I \ge 2\,\sigma(I)$; 221 parameters, *R* = 0.068, R_w = 0.0635[5c]; c) The structures were solved and refined using the programs SHELXS-76, SHELX-86. Further details of the crystal structure investigation may be obtained from the Fachinformationszentrum Karlsruhe, Gesellschaft für wissenschaftlich-technische Information mbH, W-7514 Eggenstein-Leopoldshafen 2 (FRG), on quoting the depository number CSD-55255, the names of the authors, and the journal citation.
[6] J. H. Bieri, T. Egolf, W. von Philipsborn, U. Piantini, R. Prewo, U. Ruppli, A. Salzer, *Organometallics 5* (1986) 2413; W. E. Geiger, A. Salzer, J. Edwin, W. von Philipsborn, U. Piantini, A. L. Rheingold, *J. Am. Chem. Soc. 112* (1990) 7113, zit. Lit.
[7] Recent review: A.-J. Di Maio, A. L. Rheingold, *Chem. Rev. 90* (1990) 169.
[8] L. Messerle, *Chem. Rev. 88* (1988) 1225.
[9] R. Winter, O. J. Scherer, unpublished

Phosphorus Monoxide (PO) as Complex Ligand**

By *Otto J. Scherer*, Jürgen Braun, Peter Walther, Gert Heckmann,* and *Gotthelf Wolmershäuser*

In contrast to the ubiquitous nitrogen monoxide (NO), whose ligand properties also have been investigated in detail,[1] only a few spectroscopic data[3] have thus far been reported for the phosphorus analogue PO, probably the most abundant phosphorus-containing molecule occurring in interstellar clouds.[2]

Reaction of diphospha-dinickela-tetrahedrane with [W(CO)$_5$(thf)] leads to formation of the Ni_2WP_2-complex **2**, which can be oxidized with bis(trimethylsilyl) peroxide to give **3**, the first complex with a PO ligand. **1**, **2** and **3** form,

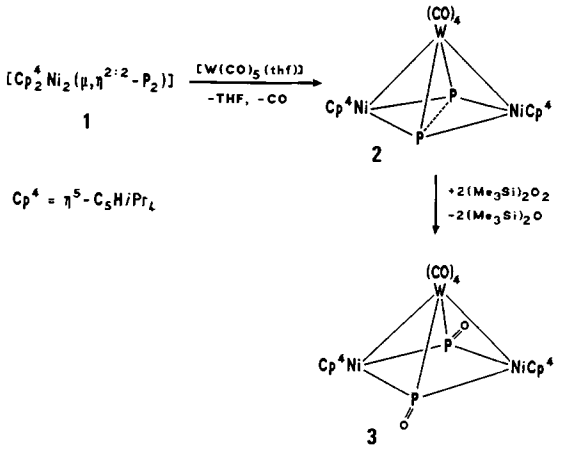

respectively, black, dark green, and black crystals, which are briefly stable in air, readily to moderately soluble in pentane, and very readily to readily soluble in benzene and dichloromethane. Solutions of **2** are extremely sensitive to traces of oxygen. Table 1 lists the most important X-ray structure data[4] and IR ($\tilde{\nu}$(CO), $\tilde{\nu}$(PO)) and ^{31}P-NMR[5] spectroscopic data of the complexes **1**–**3**.

Table 1. Selected bond lenghts [Å] and angles [°] as well as $\tilde{\nu}$(CO), $\tilde{\nu}$(PO) [cm^{-1}] and ^{31}P-NMR data of the complexes **1**–**3**.

	1	**2**	**3**
P1-P2	2.053(5)	2.304(4)	2.624(5)
Ni1-P1	2.186(3)	2.178(4)	2.148(4)
Ni2-P1	2.185(3)	2.176(3)	2.135(4)
Ni1-P2	2.182(3)	2.161(3)	2.141(4)
Ni2-P2	2.186(3)	2.174(4)	2.134(4)
Ni1-Cp$^4_{(center)}$	1.72	1.74	1.735
Ni2-Cp$^4_{(center)}$	1.73	1.73	1.715
W-P1		2.507(3)	2.524(5)
W-P2		2.512(3)	2.516(4)
Ni1-W		2.849(1)	2.847(2)
Ni2-W		2.848(1)	2.847(2)
Ni1-Ni2	2.571(1)	3.66	3.37
P1-O1			1.480(10)
P2-O2			1.462(9)
P1-Ni1-P2	56.1(1)	64.1(1)	75.4(2)
P1-Ni2-P2	56.0(1)	63.9(1)	75.8(2)
Ni1-P1-Ni2	72.1(1)	115.5(1)	103.7(2)
Ni1-P2-Ni2	72.1(1)	116.2(1)	104.0(2)
Dihedral angle Ni1, P1, P2 / Ni2, P1, P2	96.4	176.5	189.6
δ(^{31}P{^{1}H}) [a]	288.2 (s)	403.5 (s)	354.0 ("s") ^1J(WP) 68 Hz
$\tilde{\nu}$(CO) [b]		2029 (s), 1958 (s) 1946 (m), 1905 (s)	2043 (s), 1975 (s) 1962 (w), 1925 (s)
$\tilde{\nu}$(PO) [b]			1260 (s)

[a] In C_6D_6, 162 MHz, 85% H_3PO_4 ext. [b] In hexane.

If one compares the bond distances and angles in the complexes **1**–**3** one sees that $\bar{d}$(N–P) decreases in the transition from the symmetrical diphospha-dinickela-tetrahedrane **1**

[*] Prof. Dr. O. J. Scherer, Dr. J. Braun, Dipl.-Chem. P. Walther, Dipl.-Chem. G. Heckmann [+], Dr. G. Wolmershäuser [+]
Fachbereich der Chemie der Universität
Erwin-Schrödinger-Strasse, W-6750 Kaiserslautern (FRG)
[+] X-ray structure analyses.

[**] This work was supported by the Fonds der Chemischen Industrie.

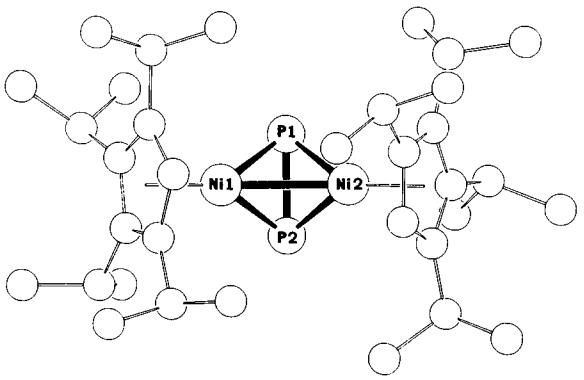

Fig. 1. Structure of **1** in the crystal [4a].

(Fig. 1) to the tetragonal-pyramidally structured complexes **2** (Fig. 2) and **3** (Fig. 3) with rhomboidal Ni_2P_2 pyramid base, from 2.185 Å in the case of **1** through 2.17 Å (**2**) to 2.14 Å in the case of **3**.

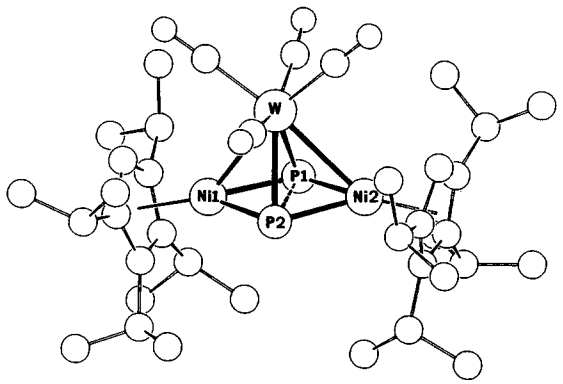

Fig. 2. Structure of **2** in the crystal [4b].

The P–P distance in **1** (2.053(5) Å) lies in the expected range,[6] whereas an extremely short P–P distance [7] of 2.304(4) Å is found in the Ni_2P_2 pyramid base in the case of **2**. Indeed, the P–P bond here is even shorter than in the

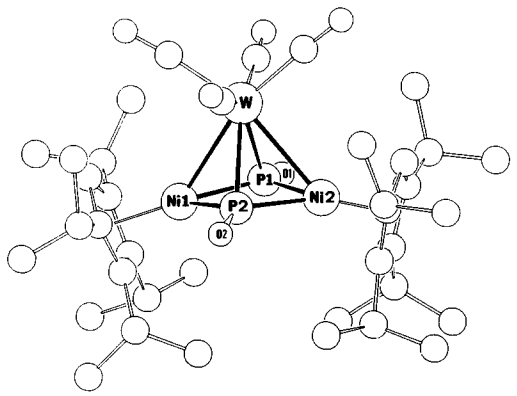

Fig. 3. Structure of **3** in the crystal [4c].

molecules $(RB)_2P_2$ (2.349(2) Å[8a]) and $[(R_2Si)_2P_2\{W(CO)_5\}_2]$ (2.342(2) Å[8b]) with E_2P_2-butterfly framework.

The complexes **1**–**3** are further illustrative examples for the isolobal principle.[9] If one imagines that two P atoms in white phosphorus (P_4) are each replaced by an isolobal Cp^4Ni fragment, then one finds an average length of 2.23 Å for the six bonds in **1** (in the case of P_4 2.21 Å); a similarly good agreement is found in the case of **2** ($\bar{d}$(Ni–P) = 2.17 Å) and $[Cp^*(CO)_2Nb(\eta^4\text{-}P_4)]$ ($\bar{d}$(P–P) = 2.16 Å[10]).

The most remarkable structural moiety in **3** are the μ_3-PO ligands, whose P–O bond lengths of 1.46 and 1.48 Å agree completely with the calculated (1.46 Å[3a]) and experimental values (1.48 Å[3b]) for the PO molecule. $\tilde{\nu}$(PO), with a value of 1260 cm^{-1} in the case of **3** compared to 1218 cm^{-1} in the uncomplexed PO[3c] and 1240 cm^{-1} for the terminal P=O group of the P_4O,[3c] is slightly shifted to higher wave numbers.

Whereas a very slight out-of-plane folding of ca. 3° about the P–P axis and towards the W atom is observed for the rhomboidal Ni_2P_2 structural moiety in **2**, in the case of **3** one finds a folding of ca. 10° in the opposite direction (Table 1). In **2** and **3** the four CO ligands are arranged almost ecliptically to the Ni_2P_2 pyramid base.

According to the Wade-Mingos electron-counting rules[11] **1** has six and **2** and **3** have seven skeletal electron pairs, and thus a *nido* framework structure. Extended Hückel MO calculations on the star-shaped $[\{(OC)_5W\}_3As_2]$[12] with three 16-valence electron (VE) $W(CO)_5$-fragments show that in this case :As≡As: functions as 6e donor ($4\times\pi$, $2\times\sigma$). If one extends this bond description to **2**, the 14VE-$W(CO)_4$ fragment and two 15VE-Cp^4Ni fragments would be formally bound to one :P≡P: unit; to achieve 18VE per metal atom, the linking of two Ni–W bonds would then be required for the formation of the tetragonal pyramid in **2**.

Experimental

2: A solution of **1** (87 mg, 0.135 mmol) [13] in ca. 5 mL of freshly distilled THF was treated with a solution of $[W(CO)_5(thf)]$, prepared by irradiation (30 min; 150 W mercury high-pressure lamp) of 71 mg (0.202 mmol) of $W(CO)_6$ in 70 mL of freshly distilled THF, and the mixture stirred at room temperature. After ca. 10–15 min the initially deep-brown solution turned brilliant neon green (weak evolution of CO!). After 20 min the solvent was removed in a high vacuum and the residue scraped from the walls of the glass vessel and transferred to a silica gel/petroleum ether column (30 × 2 cm). The remainder of the residue was removed from the vessel with a little petroleum ether and also transferred to the column. Upon elution with petroleum ether/toluene (20:1) a brilliant green fraction was obtained, from which, after removal of the solvent, we recovered 114 mg (90% referred to **1**) of **2** (dark green powder). Subsequent recrystallization from a little hot heptane (80 °C) by slow cooling to room temperature afforded **2** in the form of glittering green needle-like crystals.

3: A solution of $(Me_3Si)_2O_2$ (34 μL, 0.152 mmol) in diethyl ether (10 mL) was added dropwise within 10 min to a solution of **2** (36 mg 0.038 mmol) in diethyl ether (15 mL). The mixture was then stirred for 20 h at room temperature, whereupon a gradual change in color from brilliant green through dark green to red was observed. After removal of solvent in an oil-pump vacuum the residue remaining was transferred with a little petroleum ether to a column (30 × 1.5 cm) packed with silica gel (activity grade II). Upon chromatographic separation, elution with petroleum ether/ether (7:1) initially afforded traces (< 1 mg) of a pale green fraction (monooxidized **2**), then **3** as a dark-red fraction. After removal of solvent from the latter in an oil-pump vacuum there remained 22 mg (60% based on reacted **2**) of **3**, which formed blackish, block-shaped crystals upon recrystallization from a little hexane.

Received: March 11, 1991 [Z 4487 IE]
German version: *Angew. Chem. 103* (1991) 861

CAS Registry numbers:
1, 133966-85-5; **2**, 133966-86-6; **3**, 133983-39-8; $[W(CO)_5(thf)]$, 36477-75-5; $(Me_3Si)_2O_2$, 5796-98-5.

[1] D. M. P. Mingos, D. J. Sherman, *Adv. Inorg. Chem. 34* (1989) 293.
[2] H. E. Matthews, P. A. Feldman, P. F. Bernath, *Astrophys. J. 312* (1987) 358.
[3] a) L. L. Lohr, *J. Phys. Chem. 88* (1984) 5569; b) J. E. Butler, K. Kawaguchi, E. Hirota, *J. Mol. Spectrosc. 101* (1983) 161; c) L. Andrews, M. Mc. Cluskey, Z. Mielke, R. Withnall, *J. Mol. Struct. 222* (1990) 95, and references cited therein.

[4] a) **1** crystallizes monoclinically, $P2_1/c$; $a = 12.465(1)$, $b = 15.786(1)$, $c = 17.629(2)$ Å, $\beta = 96.62(1)°$, $Z = 4$, 5039 independent reflections ($Mo_{K\alpha}$: $1.5° \leq \theta \leq 25.0°$), 3651 observed with $I \geq 2\sigma(I)$; 343 parameters, $R = 0.064$, $R_w = 0.078$ [4d]; b) **2**: $P2_1/n$; $a = 13.019(2)$, $b = 17.586(3)$, $c = 18.557(3)$ Å, $\beta = 106.62(1)°$, $Z = 4$, 4751 independent reflections ($Mo_{K\alpha}$ $0.5° \leq \theta \leq 22.5°$), 3981 observed with $I \geq 2\sigma(I)$; 424 parameters, $R = 0.045$, $R_w = 0.055$ [4d]; c) **3**: triclinic, $P\bar{1}$; $a = 12.724(8)$, $b = 17.996(10)$, $c = 10.412(9)$ Å, $\alpha = 98.87(5)$, $\beta = 111.34(5)$, $\gamma = 90.61(5)°$, $Z = 2$, 5690 independent reflections ($Mo_{K\alpha}$: $1.5° \leq \theta \leq 22.5°$), 3649 observed with $I \geq 2\sigma(I)$; 383 parameters, $R = 0.058$, $R_w = 0.060$ [4d]. d) Solution and refinement of structures with the program systems SHELXS-86, SHELX-76. Further details of the crystal structure investigations are available on request from the Fachinformationszentrum Karlsruhe, Gesellschaft für wissenschaftlich-technische Information mbH, W-7514 Eggenstein-Leopoldshafen 2 (FRG), on quoting the depository number CSD-55342, the names of the authors, and the journal citation.

[5] ^{1}H NMR (400 MHz, C_6D_6, C_6D_5H as int. standard): δ(CH) = 5.19 (s, 2H) **1**, 4.93 (s, 2H) **2**, 4.80 (s, 2H) **3**; δ ($CHMe_2$) = 2.98 (sept., 4H; ^3J(HH) = 6.8 Hz), 2.65 (sept., 4H; ^3J(HH) = 7.2) **1**, 2.81 (sept., 4H; ^3J(HH) = 6.8), 2.71 (sept., 4H; ^3J(HH) = 7.2) **2**, 3.15 (sept., 4H; ^3J(HH) = 7.1), 3.00 (sept., 4H; ^3J(HH) = 6.8) **3**; δ($CHMe_2$) = 1.53, 1.15 (each d, 12H; ^3J(HH) = 6.8), 1.48, 1.26 (each d, 12H; ^3J(HH) = 7.2) **1**; 1.42, 1.20 (each d, 12H; ^3J(HH) = 7.2), 1.21, 1.13 (each d, 12H; ^3J(HH) = 6.8) **2**; 1.54, 1.45 (each d, 12H; ^3J(HH) = 7.1), 1.48, 0.83 (each d, 12H; ^3J(HH) = 6.8) **3**.

[6] Recent review: O. J. Scherer, *Angew. Chem. 102* (1990) 1137; *Angew. Chem. Int. Ed. Engl. 29* (1990) 1104.

[7] Cf. the short Si···Si distance of 2.31 Å in tetramesitylcyclodisiloxane (M. J. Michalczyk, M. J. Fink, K. J. Haller, R. West, J. Michl, *Organometallics 5* (1986) 531) and its theoretical importance (R. S. Grev, H. F. Schaefer III, *J. Am. Chem. Soc. 109* (1987) 6577; C. Liang, L. C. Allen, *ibid. 113* (1991) 1878).

[8] a) P. Kölle, G. Linti, H. Nöth, K. Polborn, *J. Organomet. Chem. 355* (1988) 7; b) M. Driess, A. D. Fanta, D. Powell, R. West, *Angew. Chem. 101* (1989) 1087; *Angew. Chem. Int. Ed. Engl. 28* (1989) 1038.

[9] R. Hoffmann, *Angew. Chem. 94* (1982) 725; *Angew. Chem. Int. Ed. Engl. 21* (1982) 711.

[10] O. J. Scherer, J. Vondung, G. Wolmershäuser, *Angew. Chem. 101* (1989) 1395; *Angew. Chem. Int. Ed. Engl. 28* (1989) 1355.

[11] See for example: K. Wade, *Adv. Inorg. Chem. Radiochem. 18* (1976) 1; D. M. P. Mingos, *Acc. Chem. Res. 17* (1984) 311.

[12] B. Sigwarth, L. Zsolnai, H. Berke, G. Huttner, *J. Organomet. Chem. 226* (1982) C5.

[13] J. Braun, *Dissertation*, Universität Kaiserslautern 1990.

Triple Inclusion by a Calixarene: the Crystal Structure of the Europium(III) Complex of Bis(homooxa)-*p-tert*-butylcalix[4]arene **

By *Zouhair Asfari, Jack M. Harrowfield,* Mark I. Ogden, Jacques Vicens,* and *Allan H. White*

The inclusion chemistry of the calixarenes[1] is remarkably varied. Both neutral and cationic guests are numerous.[1-3] A particular form of cation inclusion is the direct coordination of a metal ion, and in seeking to characterize the coordination chemistry of the calixarenes with lanthanide and actinide elements,[4-9] we have also been interested in establishing the influence of metal-ion binding on other forms of inclusion. As has been noted by others,[10] the dissymmetric conformation adopted by *p-tert*-butylcalix[8]arene in several of its metal-ion complexes even raises the prospect of selective inclusion of chiral species.

The crystal structure of the europium(III) complex of *p-tert*-butylcalix[4]arene (**L1**)[7] shows a form of "double inclusion" in which the metal ion is bound by phenoxide coordination and a molecule of dimethylformamide (DMF) solvent is included within the ligand "cup" possibly as a result of Van der Waals interactions between the solvent methyl groups and the ligand *t*Bu substituents. The polar carbonyl moiety of DMF is directed out of the cup and away from the metal. In contrast, the two included DMF molecules of $[Eu_2$(*p-tert*-butylcalix[8]arene−6 H)$(dmf)_5]$[4,6] are bound to the metal atom through carbonyl O atoms. As a result, these DMF molecules are oriented in such a way that the carbonyl moieties are directed *into* the calixarene cavity. A similar orientation of dimethylsulfoxide (DMSO) is seen in its inclusion complex with "free" **L1**,[7] however, suggesting that factors other than binding to a coordinated metal ion can favor insertion of a polar moiety deep within the calixarene.

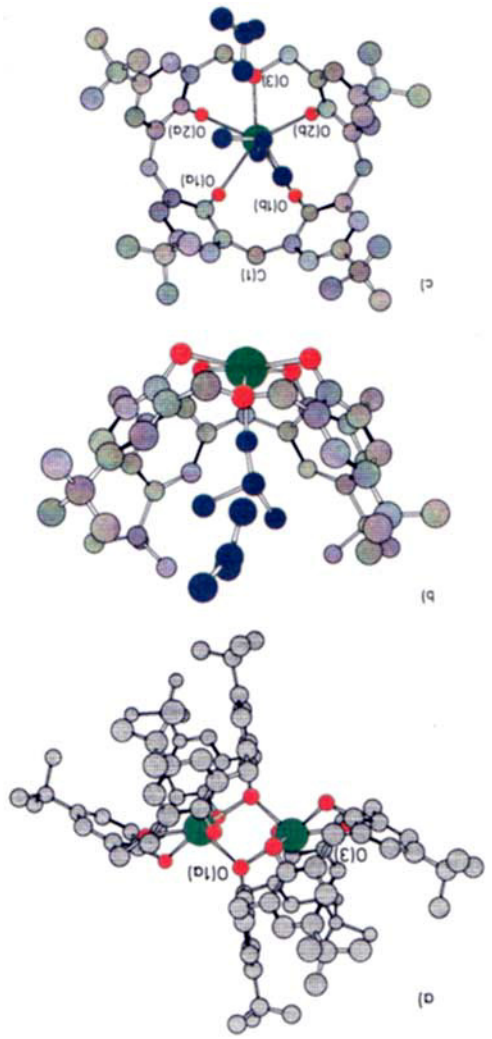

Figure 1. a) A view of the centrosymmetric dimer, normal to the Eu_2O_2 plane, obtained using the atomic coordinates and the molecular modeling program "Chem 3D+" from Cambridge Scientific Computing. The coordinated DMSO and the included acetone molecule are omitted for clarity. Eu(green), O(red). b) A single Eu/L2 aggregate, showing the disposition of the major components of the coordinated DMSO and acetone molecules (blue). Eu–O (DMSO) 2.28(1) Å; Eu–O1a 2.46(1), Eu–O1b 2.47(1), Eu–O2a 2.28(1), Eu–O2b 2.23(1), Eu–O3 2.67(1) and Eu($\bar{x},\bar{y},\bar{z}$)-O1a 2.29 Å. Eu and O3 lie 0.26 and 1.51 Å out of the O1a-O1b-O2a-O2b plane ($\chi^2 = 6$), respectively. c) As b), projected normal to the O1a-O1b-O2a-O2b plane; DMSO and the disordered *t*Bu group without H atoms. The inversion related O1a···Eu line lies beneath the Eu···O1a line; i.e., it is unsymmetrically disposed relative to the median C1···Eu···O(3) line vertical to the page with consequent loss of perfect *m* symmetry in respect to such parameters as phenyl/O_4 dihedral angles (Table 1).

[*] Prof. Dr. J. M. Harrowfield, Dr. M. I. Ogden, Prof. Dr. A. H. White
Department of Chemistry
University of Western Australia
Nedlands, 6009 (Australia)
Dr. Z. Asfari, Prof. Dr. J. Vicens,
Ecole Européene des Hautes Etudes des Industries Chimiques
Strasbourg (France)

[**] We acknowledge support of this work by the Australian Research Council

In this regard, it is notable that the position of the methyl group of these included solvent molecules is similar, relative to the calix rim, in all these complexes.

The crystal structure of the present europium(III) complex of bis(homooxa)-*p*-*tert*-butylcalix[4]arene (**L2**)[11] shows the presence of a binuclear species (Fig. 1) similar to that found with **L1**. There are, however, several significant differences. Most obvious is the fact that, seemingly as a result of the increase in the size of the ligand and a strong coordinative interaction with the ether-oxygen donor atom (Scheme 1), the metal ion is drawn further into the ligand cup of **L2**, thereby leaving no room for any unincluded solvent binding as found with the Eu complex with **L1**. Seven-coordination

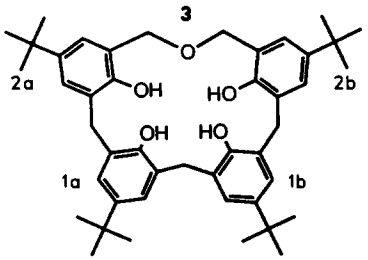

Scheme 1. The structure of the fully protonated ligand, bis(homooxa)-*p*-*tert*-butylcalix[4]arene, **L2**. Component numbering as applied in the complex ion structure (and used in the text) is indicated.

of the metal ion is retained by *O*-coordination of a DMSO molecule which also has its methyl groups positioned close to the *t*Bu rim of the calixarene and which therefore can be considered coordinatively included. Nonetheless, this does not, in this system at least, mean that further inclusion is impossible, and perhaps the most interesting feature of this structure determination is the inclusion of a second neutral molecule, the solvent acetone,[12] selectively included from an acetone/acetonitrile mixture.

One of the principal reasons for the investigation of calixarenes has been their potential as "enzyme mimics",[1] and certainly this structure demonstrates that it is entirely reasonable to regard the calixarenes as molecules wherein a substrate, possibly activated by metal ion coordination, may be held in a weakly solvating environment in close proximity to a reactant species.

Chiefly in respect of the pitch of the 2a/2b phenyl rings (Table 1), the ligand conformation in the europium complex of **L2** defines a considerably steeper cup than is found in either the fully protonated ligand or the uranyl-ion complex.[9] The remoteness of the ether-oxygen donor O3 from the uranium atom implies that **L2** is essentially quadridentate in the latter, and hence the rather different conformation observed in the europium complex may be due to the distortions resulting from the strong interaction of all five donor atoms with the metal ion. The fact that **L2** is fully deprotonated in the uranyl-ion complex but only triply deprotonated in the europium species must also give rise to some differences; the locations of the phenoxide protons in the Eu complex are somewhat uncertain, and Eu–O(na,b) distances are remarkably symmetrical, although O1a has a very close interaction with Eu($\bar{x}$,$\bar{y}$,$\bar{z}$). Of particular relevance, however, may be the close contact between O1b of one ligand and O2a of its inversion image, with the possible implication of a hydrogen bond. Whatever the cause of conformational differences, the simply included molecules, (a triethylammonium cation for the uranyl-ion complex, acetone for the europium-ion complex, and dimethylformamide in the free

Table 1. Metal and ligand parameters. Distances are in [Å]; δ is the deviation of the metal from the phenoxide plane; φ is the dihedral angle [°] between the plane of the benzene rings and that defined by O1a, O1b, O2a and O2b; **L1** = *p*-*tert*-butylcalix[4]arene, **L2** = bis(homooxa)-*p*-*tert*-butylcalix[4]arene [a].

	Ligand		Complexes		
	L1	L2	Eu/L1	Eu/L2	UO_2/L2
M-O1a	–	–	2.395(6)	2.46(1)	2.247(6)
M-O1b	–	–	2.143(6)	2.47(1)	2.249(8)
M-O2a	–	–	2.150(7)	2.28(1)	2.261(7)
M-O2b	–	–	2.558(6)	2.23(1)	2.275(6)
M···O3	–	–	–	2.67(1)	3.534(8)
O1a···O1b	2.635(8)	2.746(5)	2.951(8)	2.83(2)	2.941(8)
O2a···O2b		3.057(5)	2.953(9)	4.06(2)	3.678(8)
O1···O2		2.753(4)	3.001(9)	2.98(2)	3.05(1)
			2.903(9)	3.03(3)	3.05(1)
O1···O2b	3.727(8)	3.995(5)	4.685(8)	4.51(2)	4.49(1)
			3.473(9)	4.54(2)	4.48(1)
O2···O3		2.810(5)		2.91(2)	3.02(1)
				2.89(2)	3.07(1)
δM(1a)			1.51(2)	2.35(3)	1.92(2)
δM(1b)			0.23(2)	2.06(4)	2.01(2)
δM(2a)			0.59(2)	1.88(3)	1.47(2)
δM(2b)			1.83(2)	2.06(3)	1.47(2)
Φ(1a)	54.6(2)	67.4(1)	68.3(2)	60.3(6)	60.0(3)
Φ(1b)			42.8(3)	49.7(6)	62.9(3)
Φ(2a)		31.8(1)	51.8(3)	54.9(6)	45.4(3)
Φ(2b)			68.7(2)	62.8(5)	46.6(3)

[a] Eu···Eu, O···O of the central Eu_2O_2 plane are 3.9067(7), 2.661(6) Å in Eu/L1; in Eu/L2, 3.772(2) and 2.88(1) Å. In Eu/L1, the O1a-O1b-O2a-O2b array is puckered (χ^2 = 2978; δO: 0.19, −0.25, −0.24, 0.23, δEu 1.01 Å), whereas in Eu/L2 it is planar (χ^2 = 6.1; δO < 0.02 Å; δEu, O3: 0.26, 1.51 Å). O1a, O1b, O2a, and O2b correspond to O1–O4 of ref. [8]).

ligand) occupy a similar position above the CH_2OCH_2 chain in all.

We have not as yet fully characterized complexes with all the rare earths, but the yttrium(III) complex with **L2**, for example, appears, on the basis of microanalytical results and its solution ^{1}H NMR spectrum (Fig. 2; Table 2), to adopt the

Table 2. Resonances in the 300-MHz ^{1}H NMR spectrum of $[Y_2(L-3H)_2(dmso)_2]\cdot 2$ acetone [a].

δ = 0.29, 0.32 (s, CH_3 of DMSO), 1.24, 1.25, 1.30, 1.31 (s, $C(CH_3)_3$), 1.54 (s, acetone), 3.36, 3.40, 5.45, 5.49, 3.62, 3.66, 5.90, 5.94, 3.64, 3.68 [c], 6.40, 6.44 (d, pairs, $ArCH_2Ar$ [b]), 3.68 [c], 3.71, 5.12, 5.15, 3.78, 3.81, 5.41, 5.44 (d, pairs, $ArCH_2O$ [b]), 6.76–7.45 (d, 8 pairs, aromat. H), 15.08 (s, phenol. OH).

[a] The weak signals at δ = 1.15, ca. 4.0, 6.61, and 7.21 vary in intensity depending upon the age of the sample and appear to be due to small amounts of free ligand, possibly produced by dissociation or hydrolysis due to adventitious water. [b] Assignments based on decoupling experiments. [c] Overlapping peaks.

same binuclear structure in solution as found for europium in the solid state. Thus, all five methylene groups are nonequivalent, as are the four *t*Bu groups and the eight aromatic protons.[13, 14] For the mononuclear uranyl-ion complex,[9] the solution ^{1}H NMR spectrum demonstrates retention of the effective plane of symmetry through the ligand seen in the solid state. As noted previously, however, the europium and yttrium complexes do retain one phenolic proton which could reduce the symmetry of any mononuclear solution species. A special feature of the yttrium spectrum is the upfield shift of the DMSO methyl group resonances, consistent with coordinative inclusion of the DMSO molecule where the methyl groups are placed in close proximity to the calixarene phenyl rings. The nonequivalence of the two methyl groups suggests that any rotation of the DMSO mol-

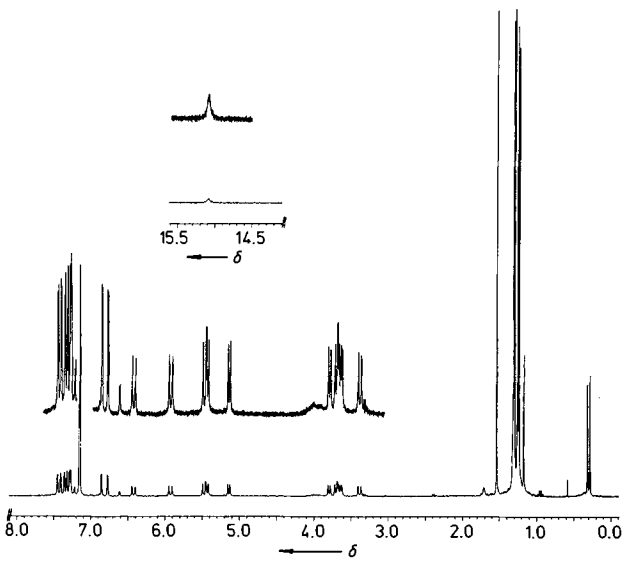

Figure 2. The 300-MHz ^{1}H NMR spectrum of $[Y_2(L2-3H)_2(dmso)_2]\cdot 2$ acetone in C_6D_6 at 298 K.

ecule in the ligand cavity is slow on the time scale of the NMR experiment. The resonance due to the acetone molecule does not exhibit any significant change from the chemical shift expected for acetone in benzene, suggesting that this molecule is easily displaced from the ligand cavity, at least in benzene solution.

Experimental

Synthesis of $[Eu_2(L2-3H)_2(dmso)_2]\cdot 2$ acetone: L2·acetone [9] (0.25 g, 0.34 mmol) was dissolved in acetone (10 mL), and triethylamine (0.5 mL) was added giving a clear, colorless solution. A solution of $[Eu(dmso)_7](ClO_4)_3$ (0.38 g, 0.38 mmol) in CH_3CN (10 mL) was then added at room temperature forming a clear orange solution. $[Eu_2(L2-3H)_2(dmso)_2]\cdot 2$ acetone was deposited overnight as orange plates, and was collected by filtration (0.17 g, 52%). Correct elemental analysis.

Synthesis of $[Y_2(L2-3H)_2(dmso)_2]\cdot 2$ acetone: The procedure was essentially as described for the europium derivative, substituting $[Y(dmso)_7](ClO_4)_3$ for $[Eu(dmso)_7](ClO_4)_3$. The compound was deposited as colorless plates (0.17 g, 55%). Correct elemental analysis.

Received: December 13, 1990 [Z 4326 IE]
German version: *Angew. Chem. 103* (1991) 887

CAS Registry numbers:
$[Eu_2(L2-3H)_2(dmso)_2]\cdot 2$ acetone, 134078-27-6; $[Y_2(L2-3H_2(dmso)_2]$, 134078-28-7.

[1] C. D. Gutsche: *Calixarenes*, The Royal Soc. Chem., Cambridge 1989.
[2] I. Alam and C. D. Gutsche, *J. Org. Chem. 55* (1990) 4487 and references cited therein.
[3] A good illustration of the sometimes unexpectedly complicated nature of calixarene inclusion is provided by F. Corazza, C. Floriani, A. Chiesi nilbersC. Guastini, *J. Chem. Soc. Chem. Commun. 1990*, 640.
[4] B. M. Furphy, J. M. Harrowfield, D. L. Kepert, B. W. Skelton, A. H. White, F. R. Wilner, *Inorg. Chem. 26* (1987) 4231.
[5] L. M. Engelhardt, B. M. Furphy, J. M. Harrowfield, D. L. Kepert, A. H. White, F. R. Wilner, *Aust. J. Chem. 41* (1988) 1465.
[6] J. M. Harrowfield, M. I. Ogden, A. H. White, F. R. Wilner, *Aust. J. Chem. 42* (1989) 949.
[7] B. M. Furphy, J. M. Harrowfield, M. I. Ogden, B. W. Skelton, A. H. White, F. R. Wilner, *J. Chem. Soc. Dalton Trans.* 1989, 2217.
[8] J.-C. G. Bünzli, J. M. Harrowfield in J. Vicens, V. Böhmer (Eds.): *Calixarenes: A Versatile Class of Macrocyclic Compounds*, Kluwer, Dordrecht, The Netherlands 979.
[9] J. M. Harrowfield, M. I. Ogden, A. H. White, *J. Chem. Soc. Dalton Trans.* 1991, 979.
[10] G. E. Hofmeister, F. E. Hahn, S. F. Pedersen, *J. Am. Chem. Soc. 111* (1989), 2318.
[11] X-ray crystallography data: $[Eu_2(L2-3H)_2(dmso)_2]\cdot 2$ acetone, $C_{94}H_{122}Eu_2O_{12}S_2\cdot 2C_3H_6O$, $M_r = 1928$. Monoclinic, $P2_1/c$, $a = 17.306(7)$, $b = 14.258(9)$, $c = 23.33(1)$ Å, $\beta = 117.25(3)°$, $V = 5117$ Å^3. ϱ_{calcd} ($Z = 1$ dimer) = 1.25 g mL^{-1}. $F(000) = 2008$. Enraf-Nonius (CAD-4 diffractometer, monochromatic $Mo_{K\alpha}$ radiation, $\lambda = 0.71069$ Å, $\mu_{Mo} = 12.2$ cm^{-1}; specimen: $0.35\times 0.20\times 0.10$ mm (capillary) (twinned; data measured on the major reciprocal lattice component), $A^*_{min,max}$ (Gaussian correction), 1.10, 1.27. $2\theta_{max} = 45°$, 6461 independent reflections, 3267 with $I > 3\sigma(I)$ (nonoverlapping). Full matrix least-squares refinement, anisotropic thermal parameter refinement confined to Eu, O, nondisordered *t*Bu groups, and major DMSO component; $R = 0.076$, $R_w = 0.072$, $n_v = 385$. Within the ligand one *t*Bu group was disordered over two sites, populations 0.56(4), 1 − 0.56(4). The DMSO is disordered with single envelopes for O, C, and two for S, populations: 0.77(2), 1 − 0.77(2). Thermal motion is high at the molecular periphery and on the acetone solvent. Further details of the crystal structure investigation may be obtained from the Fachinformationszentrum Karlsruhe, Gesellschaft für wissenschaftlich-technische Information mbH, W-7514 Eggenstein-Leopoldshafen 2 (FRG), on quoting the depository number CSD-55149, the names of the authors, and the journal citation.
[12] Simple inclusion of acetone has been observed with various calixarenes, see ref. [2] and A. W. Coleman, S. G. Bott, S. D. Morley, C. M. Means, K. D. Robinson, H. Zhang, J. L. Atwood, *Angew. Chem. 100* (1988) 1412; *Angew. Chem. Int. Ed. Engl. 27* (1988) 1361.
[13] The complex appears to be considerably more rigid in solution than the ligand itself; uncomplexed **L2** in chloroform shows a coalescence temperature of −2 °C for the CH_2OCH_2 resonances and −8 °C for the $ArCH_2Ar$ resonances; see C. D. Gutsche, L. J. Bauer, *J. Am. Chem. Soc. 107* (1985) 6052.
[14] The ^{1}H NMR spectrum of the europium(III) complex, which will be one of the subjects of a later publication concerned more generally with the spectroscopy of lanthanide complexes of the calixarenes, is more complicated to interpret because of the shifting and appreciable broadening effects of europium. It is, however, possible to identify eight aromatic proton resonances at $\delta = 19.25$, 17.41, 12.99, 5.16, 4.03, 3.57, 2.95, and −3.35, confirming that at least the symmetry of the complex in solution is the same as that in the solid.

A Novel Oligomer of Condensed Metal Atom Clusters in $[Y_{16}Ru_4I_{20}]$**

By *Martin W. Payne*, *Masahiro Ebihara*, and *John D. Corbett**

Dedicated to Professor Hans Georg von Schnering on the occasion of his 60th birthday

Heterometal atoms (Z) bound within M_6X_{12}-type metal halide clusters are relatively recent discoveries. The first examples involved 3d elements in the phases $[Zr_6(Z)I_{12}]$, $[Zr_6(Z)I_{12}]I_2$,[1] and $[Zr_6(Z)Cl_{12}]Cl_3$.[2, 3] Transition metals encapsulated in the rare-earth-metal (R) iodide clusters $[R_6(Z)I_{10}]$ and $R[R_6(Z)I_{12}]$ were subsequently established among R = Y, Pr, Gd for a much larger range of Z, namely Mn–Cu, Ru–Pd, and Re–Au.[4, 5] Newer products from the condensation of such clusters through shared metal edges (and halogens) into infinite chains, first discovered with centered nonmetals in compounds like $[Sc_7(C_2)Cl_{10}]$[6] and $[Y_4(C)I_5]$,[7] have recently been found in the form of single chains for $[La_4(Ru)I_5]$ and $[Pr_4(Z)I_5]$, Z = Co, Ru, Os,[8] and double chains for $[Pr_6(Ru_2)I_6]$, $[Y_6(Ir_2)I_6]$, etc.[9] To date all structures have exhibited either isolated clusters or those condensed into infinite chains or sheets, regardless of the interstitial type. (A few cluster dimers like $[Gd_{10}C_4Cl_{18}]$[10] are exceptions.) We report here a remarkable oligomeric example of condensed halide clusters, in this

[*] Professor J. D. Corbett, Dr. M. W. Payne, Dr. M. Ebihara
Department of Chemistry, Iowa State University
Ames, IA 50011 (USA)

[**] This research was supported by the National Science Foundation, Solid State Chemistry, grant DMR-8902954, and was carried out in facilities of the Ames Laboratory, DOE.

case with the same composition as single chain compounds of other R elements, such as $[La_4(Ru)I_5]$.

The metal portion of the remarkable $[Y_{16}(Ru_4)I_{20}]$ consists of a 16-membered Friauf polyhedron of yttrium centered by a tetrahedron of Ru.[11] As shown in Figure 1 A, this polyhedron can be generated by truncation of every apex of a larger tetrahedron (open circles, included for clarity) followed by capping the approximately hexagonal faces of the resulting unit Y_{12} with a Y_4 tetrahedron (outlined by open connections). In this case, Y1 and Y3 define the truncated unit and Y2 caps the faces (Fig. 1 B). Finally, the Y_{16} unit encapsulates four Ru atoms that form an ideal tetrahedron within experimental error ($d = 3.572(3)$ Å) and are, in fact, the inner image of the starting, outer tetrahedron. The $[Y_{16}Ru_4]$ polycluster has $\bar{4}2m(D_{2d})$ symmetry and is completely separated from other similar clusters by iodine bridges (see below). Polyhedra like that found here with yttrium are well-known in Laves phases where they are condensed with other polyhedra and are usually centered by a single atom.[13] On the other hand, the untruncated polyhedron in Figure 1 A, but without interstitials, has recently been found as $[Os_{20}CO_{40}]^{2-}$.[14]

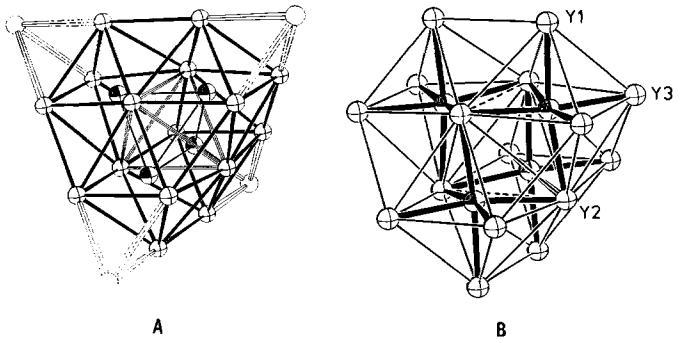

Fig. 1. The $Y_{16}Ru_4$ cluster in $[Y_{16}Ru_4I_{20}]$ ($\bar{4}2m(D_{2d})$ symmetry, major axis vertical). A) The generation of a Y_{16} cluster by consecutive truncation of larger tetrahedron (open spheres), introduction of tetrahedron of Y2 atoms on hexagonal faces (open outline), and encapsulation of Ru_4 tetrahedron (shaded spheres). B) The same cluster as generated by pairwise condensation of four centered Y_6Ru clusters (with shared edges in the dimers dashed) and the numbering of the yttrium atoms.

It is easy to see (without special glasses[15]) that the new cluster can also be viewed as the condensation product of four $[Y_6(Ru)I_{12}]$-type octahedral clusters—as emphasized in Figure 1 B—in a two-by-two manner starting with pairs of clusters joined by shared Y2–Y2 edges (dashed lines); the same process forms the infinite chain structures. The Ru atoms in the oligomer are somewhat displaced toward each other; *trans* angles in the Y_6Ru octahedra are 168.5° (×2) and 169.6(1)°; however, the Ru–Ru separations still correspond to negligible bonding (Pauling bond order ca. 0.02). The geometry of the $Y_{16}Ru_4$ metal core is analogous to that found in the cubanelike $[Cl_{16}Te_4]$,[16] except that the displacements are in the opposite sense, reflecting the very different types of interactions between Y–Y and Cl···Cl. Distortions in $[Y_{16}(Ru_4)I_{20}]$ appear to be largely the result of the rather diverse surroundings for the three types of yttrium atoms, through their proximity to other metals and iodine as follows: Y1 (top and bottom atoms, Fig. 1) is surrounded by 5 Y, 1 Ru, and 4 + 1(exo) I atoms; Y2 (capping hexagonal faces) by 6 Y, 3 Ru, and 3 I; Y3 (unshared waist atoms) by 5 Y, 1 Ru, and 4 + 1 I. The Y–Y and Y–Ru distances are in the ranges of 3.581(2) Å to 3.920(3) Å and 2.684(3) to 2.837(3) Å, respectively. Long, shared Y2–Y2 edges not counted in the foregoing are 4.284(2) Å in the dimers (dashed) and 4.337(3) Å (×2) between pairs of condensed octahedra with a vertical component to the distance.

Four unique iodine functionalities serve to cap triangular faces or bridge edges on the yttrium polyhedron as well as to interconnect each cluster to eight others in a three-dimensional network. One example of each type is illustrated in Figure 2. Four pseudotetrahedral connections arise from I2 and I4 bridging between clusters, as shown for the pair centered at $\frac{3}{4}, \frac{1}{4}, \frac{1}{4}$ and $\frac{1}{4}, \frac{3}{4}, \frac{3}{4}$; the $I4^{i-i}$ arrangement is reminiscent of that in $[Y_6(Ru)I_{10}]$.[4] A second group of four clusters lie along $\pm \boldsymbol{a}$ and $\pm \boldsymbol{b}$ from each cluster. These are interlinked

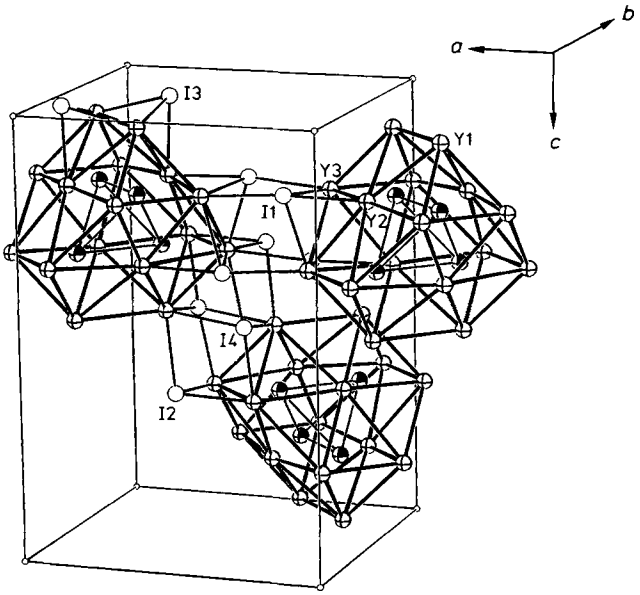

Fig. 2. The two modes of intercluster bonding through shared iodine atoms (open spheres); see text.

by I1 atoms that cap Y3–Y3–Y2 faces and are also exo to Y3 atoms in an adjoining cluster and vice versa. One such connection is shown at the top center of Figure 2. Finally, I3 atoms, two of which are shown at the top left, cap Y1–Y2–Y1 faces and are not involved in intercluster bridging. The structure can also be described in terms of cubic-close-packed I and Ru layers that lie parallel to $(2\bar{2}3)$, the yttrium ordering in octahedral holes clustered about the ruthenium sites.

Extended Hückel calculations indicate that the $[Y_{16}(Ru_4)I_{20}]$ cluster with its 60 cluster-based electrons has a closed shell configuration and a calculated band gap of ca. 0.3 eV.[17] The splitting of T_d orbital symmetries on descent to D_{2d} is small, so the labels of the former can be used for simplification. The Y(d)–I(5p) bonding and iodine nonbonding 5p levels lie in a group below −10.8 eV, while a narrow band of ten MOs between −8.5 and −9.0 eV are principally Y–Ru bonding, the lowest four being s- and t_{2g}-like on Ru. A group of three MOs ($t_2 + a_1 + e$ (HOMO)) above this between −7.9 and −7.5 eV are basically only Y–Y bonding. The energy disposition of these three classes of bond types is quite similar to that calculated for the chain compound $[Pr_4(Ru)I_5]$,[8] basically reflecting intrinsic characteristics of centered $[R_6(Ru)I_{12}]$ clusters. The six lowest antibonding MOs, with a t_1 LUMO, lie between −7.2 and −6.6 eV and are all Y–Ru-"t_{2g}" in character except

for the next to the lowest (a_1), which resembles the a_{2u} of many $[M_6(Z)X_{12}]$ clusters.[1] Bonding within the cluster appears to be dominated by Y–Ru interactions; overlap populations are from 1.7 to 2.8 times those for the majority of the Y–Y bonds. The long Y2–Y2 separations discounted earlier are only about half as large. More striking are the low populations for Y3–Y3 between dimers (3.920 Å) and the Y1–Y1 separation at the top and bottom of the clusters (3.870 Å). These values are only 25–30% of those of the principal Y–Y interactions.

The discovery of this surprising macrocluster of centered octahedral clusters is a forecast of still more novel chemistry and structures. Further considerations of the structure and bonding suggest that smaller rare-earth elements may be more favorable for such aggregates.

Experimental Procedure

The high purity of the reagents, the synthetic and sublimation techniques for YI_3, and the reaction procedures utilizing welded Nb tubing have been described [5, 6]. Reactions with Y:Ru:I ratios between 4:1:5 and 1:1:1 at temperatures from 800 °C to 975 °C and reaction times of three to four weeks were explored in a search for condensed cluster systems. The main products were only $[Y_{16}(Ru_4)I_{20}]$ and the double chain $[Y_6(Ru_2)I_6]$ [9]; no clear boundary exists between the two. Ratios for Y:I of less than 4:5 gave only the known $[Y_7(Ru)I_{12}]$ and $[Y_6(Ru)I_{10}]$ [4, 5], and for Y:Ru:I of 1:<1:1, $[Y_6(Ru_2)I_6]$. The black $[Y_{16}(Ru_4)I_{20}]$ grew as small cubes and octahedra that were fused together on faces and edges. Reactions run at higher temperatures (950–975 °C) favored the formation of $[Y_6(Ru_2)I_6]$, while those at lower temperatures gave 90–100% yields of $[Y_{16}(Ru_4)I_{20}]$. Analogous reactions with Pr and Gd yielded only the infinite chain polymorph $[Pr_4(Ru)I_5]$ [8] and other phase types noted above. Extended Hückel calculations were performed on an isolated cluster with the experimental distances and the composition $[(Y_{16}(Ru_4)I_{20})I_{16}]^{16-}$, the extra iodine atoms representing those with intercluster bridging functions. Charge-self-consistent valence energies derived for $[Y_6(Ru)I_{10}]$ [4] were utilized.

Received: January 30, 1991 [Z 4415 IE]
German version: *Angew. Chem. 103* (1991) 842

CAS Registry numbers:
$[Y_{16}(Ru_4)I_{20}]$, 133070-92-5; $[Y_6(Ru_2)I_6]$, 134131-21-8.

[1] T. Hughbanks, G. Rosenthal, J. D. Corbett, *J. Am. Chem. Soc. 110* (1988) 1511.
[2] F. Rogel, J. Zhang, M. W. Payne, J. D. Corbett, *Adv. Chem. Ser. 226* (1990) 369.
[3] J. Zhang, J. D. Corbett, *Inorg. Chem. 30* (1991) 431.
[4] T. Hughbanks, J. D. Corbett, *Inorg. Chem. 28* (1989) 631.
[5] M. W. Payne, J. D. Corbett, *Inorg. Chem. 29* (1990) 2246.
[6] S.-J. Hwu, J. D. Corbett, K. R. Poeppelmeier, *J. Solid State Chem. 57* (1985) 43.
[7] S. M. Kauzlarich, T. Hughbanks, J. D. Corbett, P. Klavins, R. N. Shelton, *Inorg. Chem. 27* (1988) 1791.
[8] M. W. Payne, P. K. Dorhout, J. D. Corbett, *Inorg. Chem. 30* (1991), 1467.
[9] M. W. Payne, J. D. Corbett, unpublished research.
[10] E. Warkentin, R. Maase, A. Simon, *Z. Anorg. Allg. Chem. 491* (1982) 323.
[11] The crystal structure was determined at 25 °C by direct methods with the aid of a CAD 4 diffractometer, $Mo_{K\alpha}$-radiation ($\mu = 497.3\ cm^{-1}$), a $0.32 \times 0.32 \times 0.34\ mm^3$ crystal, and two octants of data with a 2θ limit of 65°. Tetragonal, $P4_2/nnm$ (no. 134), $Z = 8$ (based on $[Y_4RuI_5]$), $a = 12.1650(4)$, $c = 18.085(1)$ Å (Guinier data), $R(R_w) = 0.033(0.043)$; empirical absorption correction [12]. Further details on the structural investigation and results may be obtained from an author (*J. D. C*) or from the Fachinformationszentrum Karlsruhe, Gesellschaft für wissenschaftlich-technische Information mbH, W-7514 Eggenstein-Leopoldshafen 2, FRG, quoting the depository number CSD-55256, the names of the authors and the journal citation.
[12] N. Walker, D. Stuart, *Acta Crystallogr. Sect. A 17* (1983) 192.
[13] B. G. Hyde, S. Andersson: *Inorganic Crystal Structures*, Wiley, New York 1989, p. 375.
[14] A. J. Amoroso, L. H. Gade, B. F. G. Johnson, J. Lewis, P. R. Raithby, W.-T. Wong, *Angew. Chem. 103* (1991) 102; *Angew. Chem. Int. Ed. Engl. 30* (1991) 107.
[15] H.-G. von Schnering, *Angew. Chem. 93* (1981) 44; *Angew. Chem. Int. Ed. Engl. 20* (1981) 50.
[16] B. Buss, B. Krebs, *Inorg. Chem. 10* (1971) 2795.
[17] The compound exhibits a small temperature-independent paramagnetism of ca. 4.9×10^{-4} emu mol^{-1} $[Y_4RuI_5]$ between 310 and ca. 60 K, with a presumed Curie tail. The former may represent an intrinsic van Vleck (field-induced) behavior.

Enantioselective Complexation of Flexible and Rigid Substrates through Molecular Recognition**

By *Michael Famulok, Kyu-Sung Jeong, Ghislain Deslongchamps,* and *Julius Rebek, Jr.**

The interaction of chiral drugs with their target receptors involves highly enantioselective recognition mechanisms. In order to get a better understanding of such processes, a current thrust in molecular recognition research concerns the synthesis of abiotic low molecular weight receptors capable of enantioselective complexation of neutral substrates.[1] A well-known example of this is found in nature in the form of the antibiotic, vancomycin. This macrocycle disrupts the synthesis of bacterial cell walls by its highly enantioselective binding to the carboxy terminal sequence D-alanyl–D-alanine of the peptidoglycan precursors.[2]

Recently we introduced a synthetic receptor molecule **1a** whose two enantiomers bind the cyclic dipeptide diketo-

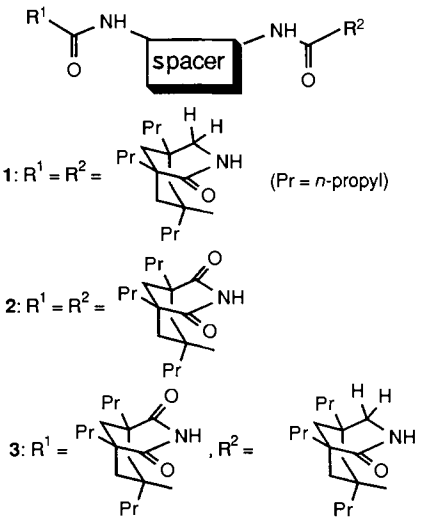

a: spacer = 2,6-naphthyl
b: spacer = 2,7-naphthyl
c: spacer = *p*-phenylenediamine

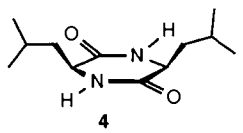

4

piperazine **4** with considerable enantioselectivity, corresponding to a difference in relative binding affinities of more than 2.5 kcal mol^{-1}.[3]

[*] Prof. J. Rebek, Jr., Dr. M. Famulok[+], Dr. K.-S. Jeong, Dr. G. Deslongchamps[++]
Department of Chemistry
Massachusetts Institute of Technology
Cambridge, MA 02139 (USA)
[+] Current address: Department of Molecular Biology
Wellman-9, Massachusetts General Hospital
Boston, MA 02114 (USA)
[++] Current address: Département de Chimie
Université Laval
Québec, QC, G1K 7P4 (Canada)

[**] We thank the National Institutes if Health and Hoechst Celanese for support of this work. *M. F.* is grateful to the Deutscher Akademischer Austauschdienst for a NATO Science Foundation fellowship, and *G. D.* to the Natural Sciences and Engineering Research Council of Canada for a postdoctoral fellowship.

Here we extend our studies to other neutral substrates including the cyclic L-hydantoins **5–8**, L-hydroorotic acid methyl ester (**9**) and linear molecules such as the dipeptides **10–15**.

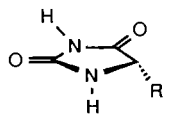

5: R = CH_2Ph
6: R = CH_2-$CH(CH_3)_2$
7: R = $CH(CH_3)_2$
8: R = $CH(CH_3)CH_2CH_3$

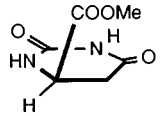

9

N-CBz-A1-A2-NHBn (N-CBz = *N*-carbobenzoxy, Bn = benzyl)

10: A1 = glycine; A2 = L-leucine
11: A1 = L-leucine; A2 = glycine
12: A1 = L-isoleucine; A2 = glycine
13: A1 = A2 = L-isoleucine
14: A1 = A2 = glycine
15: A1 = A2 = L-alanine

The hydantoins (**5–8**) and hydroorotic acid methyl ester (**9**) are complexed by the (+)- and (−)-enantiomers of the dilactam **1b**. For the complexation of dipeptides we investigated the achiral diimides **2** and the chiral imide lactam **3c**. The enantiomers of **3c** and **1b** were seperated on a chiral Pirkle column.[4] The absolute stereochemistry of the receptor enantiomers (+)-**1b**, (−)-**1b**, (+)-**3c**, and (−)-**3c** was not determined. Association constants were measured by ^1H NMR titrations.[5] The results of the binding studies are shown in Table 1.

Table 1. Association constants [M^{-1}] and $\Delta\Delta G$ values [$\Delta\Delta G$ = ΔG (−)-enantiomer − ΔG (+)-enantiomer] of the chiral receptor **1b** with substrates **5–9** and **14** [a], the achiral receptors **2b** with **14**, **2c** with **12** and **14** [a], and the chiral receptor **3c** with **10–15**.

Substrate	Association constants K_a[M^{-1}] of (−)-**1b**	(+)-**1b**	**2b**	**2c**	(−)-**3c**	(+)-**3c**	$\Delta\Delta G$ [kcal mol^{-1}]
5	4800	1720					−0.6
6 [b]	1050	390					−0.6
7	7080	705					−1.4
8	7070	650					−1.4
9	380	*2110*					*1.0*
10					1672	1003	−0.3
11					4736	2340	−0.4
12				9000	4250	2320	−0.4
13					62	134	0.5
14	186 [a]		900	5900	2920 [a]		
15					320	405	0.2

[a] With the achiral **14** racemic chiral receptors **1b** and **3c** were used. [b] The low K_a's are due to the fact that the $CDCl_3$ solution contained 10% [D_8]THF.

The phenylalanine- and leucine-derived hydantoins **5** and **6** bind to **1b** with differences in the relative binding affinities of -0.6 kcal mol^{-1} in favor of (−)-**1b**. Branching at the β-carbon of the substrate, as found in the valine- and isoleucine-derived hydantoins **7** and **8**, greatly increases the enantiomeric differentiation ($\Delta\Delta G = -1.4$ kcal mol^{-1}). The L-hydroorotic acid methyl ester (**9**) binds with lower binding constants than the hydantoins (see Table 1). With $\Delta\Delta G = 1.0$ kcal mol^{-1}, the relative binding affinities of **1b** to **9** are in the order of values observed for enantioselective recognition of other neutral substrates.[1]

These results are in accordance with the proposed binding mode shown in Scheme 1. In **16α**, up to four hydrogen bonds can form between substrates **5–8** and receptor **1b**. Molecular modeling studies of complex **16β** show that the β-CH_2 group of the substrates **5** and **6** allows the γ-branched side chain to rotate out of unfavorable steric interactions to the receptor. Such a rotation is impossible with the $-CH(CH_3)_2$ and the

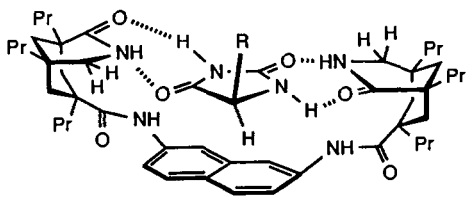

16α

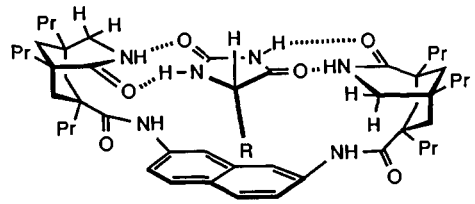

16β

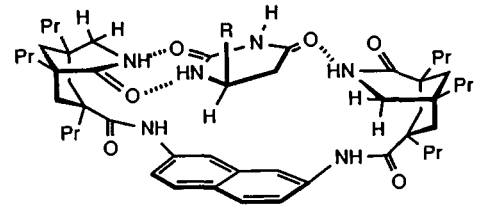

17

Scheme 1. Proposed binding modes for the enantiomers of **1b** to the hydantoins **5–8** (**16**) and the hydroorotic acid methyl ester **9** (**17**).

$-CH(CH_3)CH_2CH_3$ group of substrates **7** and **8** respectively. The six-membered ring of the hydroorotic acid methyl ester (**9**) is too large for optimal fit into the cleft. Therefore three hydrogen bonds can at best be formed with **1b**, which accounts for the lower binding constants. The direction of the $\Delta\Delta G$ values for **9** changes with respect to the $\Delta\Delta G$ values for the hydantoins **5–8**. The proposed structures of complexes **16** and **17** give an excellent rationale for this difference. The enantioselectivity of these receptors for L-hydantoins and for the L-hydroorotic acid methyl ester (**9**) are among the highest observed with neutral substrates.

Enantioselectivity in the binding of the chiral, non-C_2-symmetric **3c**[6] to the flexible dipeptide substrates **10–13** is detectable ($\Delta\Delta G = -0.3$ to 0.5 kcal mol^{-1}), but much lower than that with the rigid **7–9**. A chiral, C_2-symmetric macrocycle recently presented by *Still* et al.[7] shows considerable enantioselective binding to acetyl-L-alanine derivatives, including the dipeptides $CH_3C(O)$-L-ala-L-ala-OBn/$CH_3C(O)$-D-ala-D-ala-OBn ($\Delta\Delta G \approx 1.1$ kcal mol^{-1}).

The achiral diimide **2c** binds to the nonchiral dipeptide **14** with a binding constant of 5900 M^{-1}. The corresponding *rac*-**3c** complexes **14** with half the K_a ($K_a = 2920$ M^{-1}, see Table 1). These results are in accordance with the two binding modes **18α, β**, shown in Scheme 2.

In the diimide receptor **2c**, the peptide has four possibilities of fitting into the cleft, whereas in **3c**, only two binding

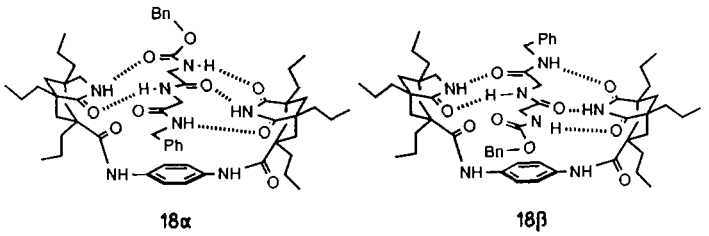

18α 18β

Scheme 2. Proposed binding modes for the complexation of N-CBz-gly-gly-NHBn (**14**) by **3c**.

permutations are possible (Scheme 2). This results in a statistical factor of 2 in the observed relative affinities of **2c** and **3c** for dipeptide **14**. We observe the same trend with the chiral peptide **12**, which binds to the achiral diimide **2c** with $K_a = 9000\ M^{-1}$ and to (−)-**3c** with $K_a = 4250\ M^{-1}$ (see Table 1).[8]

The five hydrogen bonds depicted in **18α, β** do not necessarily have to correspond to a binding constant higher than that observed in **16**. Rigid, cyclic molecules show binding constants ranging from ca. $7000\ M^{-1}$ (**7**, **8**) to more than $70000\ M^{-1}$ (**4**),[2a, b] although only four hydrogen bonds are present in the complexes. In the binding mode proposed by *Still* et al. for dipeptide complexes,[6] three hydrogen bonds are present. The binding constants observed in $CDCl_3$, however, are in the order of 10 to $100\ M^{-1}$. Whether the lower binding constants in these linear (presumably very flexible) molecules with respect to rigid substrates are due to less optimal fit into the cleft or to changes in the peptide tertiary structure upon complexation ("induced fit"; perhaps involving intramolecular H-bonds), remains to be investigated. We are currently studying the binding mode of **18** and the tertiary structure of the uncomplexed peptides by NMR spectroscopy.

The binding of linear dipeptides by **3c** is sensitive to steric effects. The (−)-enantiomer of **3c** binds N-CBz-L-leu-gly-NHBn (**11**) and N-CBz-L-ile-gly-NHBn (**12**) much better than N-CBz-L-ile-L-ile-NHBn (**13**) (K_a: **11** $4736\ M^{-1}$, **12** $4250\ M^{-1}$, **13** $62\ M^{-1}$, see Table 1). With the bulky side chain at the carboxy terminal end (**10**, $K_a = 1672\ M^{-1}$) the K_a is nearly thirty times higher than with **13**. Small side chains in both amino acid residues, as in N-CBz-L-ala-L-ala-NHBn (**15**) gave comparatively low binding constants (K_a: **15** $320\ M^{-1}$). These results suggest that **3c** displays selectivity towards the glycine-containing dipeptides.

The dilactam **1b** expands the spectrum of receptors for the enantioselective complexation of neutral substrates. The structural features provided by these compounds are very convenient for the rational design of enantioselective receptors for rigid cyclic guest molecules. The enantioselectivity of the asymmetric chiral imide lactams **3c** in binding studies with flexible dipeptides, is comparatively low, even though relatively high binding constants were obtained. We are currently developing clefts which contain chiral spacers for enantioselective dipeptide recognition.

Received: January 14, 1991 [Z 4381 IE]
German version: *Angew. Chem. 103* (1991) 880

CAS Registry numbers:
(−)-**1b**, 124001-78-8; (+)-**1b**, 134001-79-9; **2b**, 134001-81-3; **2c**, 133931-79-0; (−)-**3c**, 133931-74-5; (+)-**3c**, 134001-80-2; **5**, 40857-14-5; **6**, 40856-75-5; **7**, 40856-74-4; **8**, 40856-76-6; **9**, 39681-15-7; **10**, 133931-75-6; **11**, 133931-76-7; **12**, 133931-77-8; **13**, 133931-78-9; **14**, 40847-10-7; **15**, 133947-28-1.

[1] a) P. D. Castro, T. M. Georgiadis, F. Diederich, *J. Org. Chem. 54* (1989) 5835; b) W. C. Still in S. M. Roberts (Ed.): *Molecular Recognition—Chemical and Biochemical Problems*, Royal Soc. Chem., London 1989, S. 197; c) P. E. J. Sanderson, J. D. Kilburn, W. C. Still, *J. Am. Chem. Soc. 111* (1989) 8314; d) For a more general contribution see: Y. Dobashi, A. Dobashi, H. Ochiai, S. Hara, *J. Am. Chem. Soc. 112* (1990) 6121, and literature cited therein.

[2] a) J. P. Waltho, D. H. Williams, D. J. M. Stone, N. J. Skelton, *J. Am. Chem. Soc. 110* (1988) 5638; b) N. Pant, A. D. Hamilton, *ibid. 110* (1988) 2002; c) Y. Suzuki, S. Nishiyama, S. Yamamura, *Tetrahedron Lett. 30* (1989) 6043.

[3] a) K.-S. Jeong, A. V. Muehldorf, J. Rebek, Jr., *J. Am. Chem. Soc. 112* (1990) 6144; b) K.-S. Jeong, T. Tjivikua, A. V. Muehldorf, G. Deslongchamps, M. Famulok, J. Rebek, Jr., *ibid. 113* (1990) 201.

[4] W. H. Pirkle, T. Pochapsky, *Chem. Rev. 89* (1989) 347. Separation conditions: **3c**: isocratic elution on a "Pirkle Pilot Prep" column (L-3,5-dinitrophenylglycine) with ethyl acetate/hexane (70/30). (+)-Enantiomer $[\alpha]_D^{20} = +37.8°$; (−)-enantiomer $[\alpha]_D^{20} = -37.0°$. **1b**: isocratic elution with chloroform/isopropyl alcohol (95/5). (+)-Enantiomer $[\alpha]_D^{23} = +64°$; (−)-enantiomer $[\alpha]_D^{23} = -63°$.

[5] The association constants were determined in $CDCl_3$ from the ^1H NMR titration data by nonlinear least-squares fit of the saturation curves; errors are estimated as ± 10%. The observed ^1H NMR signals were due to the lactam-NH in **1b**, the imide NH in **2**, and the aromatic protons in **3c**. Titrations were carried out at 295 K (± 1 K). In the peptide complexation studies with **2**, clearly the strongest binding constants were obtained in combination with the *p*-phenylenediamine spacer **c**. Therefore, **3c** was the only imide lactam receptor that was synthesized for this study. We also synthesized the (racemic) dilactam receptor **1c**, but this compound was insoluble in $CDCl_3$.

[6] The synthesis of **3c** will be described in the forthcoming full paper.

[7] R. Liu, P. E. J. Sanderson, W. C. Still, *J. Org. Chem. 55* (1990) 5189.

[8] Compound **14** binds to the diimide **2b** with a 5-fold higher K_a than to the related dilactam **1b** (see Table 1). That indicates that all three binding points of at least one imide function in the receptors are required for strong binding to the aminobenzyl-protected dipeptides. N-CBz-gly-gly-methyl ester, a dipeptide that lacks the additional amide group provided by the aminobenzyl-protecting group in **14**, binds to the diimides **2b** and **2c** with 10 to 15 times lower K_a's than does **14**. These results give further support for the binding mode **19**, in which the carboxy terminal NH-group in **14** forms a hydrogen bond to the imide moiety in receptor **3c**

Synthesis and Structure of an N_2Sb_2 Ring with Different Types of Coordination for Antimony Atoms**

By *Herbert W. Roesky,* Kay Hübner, Mathias Noltemeyer,* and *Michael Schäfer*

Dedicated to Professor Hans Georg von Schnering on the occasion of his 60th birthday

$Me_3Si–N=PPh_3$ reacted with $TeCl_4$ to yield a four-membered Te_2N_2 ring and not, as we expected, a chloro-bridged heterocycle.[1] Thus the question arose how $SbCl_3$, the corresponding compound of the neighboring element antimony, would react on treatment with a $Me_3SiN=S$ system. The reaction of *N,N'*-bis(trimethylsilyl)dimethylsulfodiimide (**1**)[2] with $SbCl_3$ in trichloromethane in the mole ratio 1:1 led to the Sb_2N_2 system (**2**).

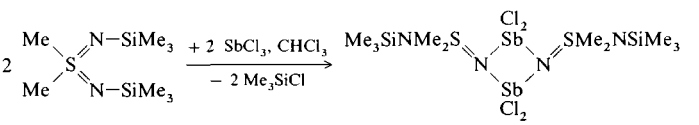

1 **2**

[*] Dr. H. W. Roesky, Dipl.-Chem. K. Hübner, Dr. M. Noltemeyer
Institut für Anorganische Chemie der Universität
Tammannstrasse 4, W-3400 Göttingen (FRG)
Dipl.-Chem. M. Schäfer
Fachbereich Chemie der Philipps-Universität

[**] This work was supported by the Deutsche Forschungsgemeinschaft, the Volkswagen-Stiftung, and the Fonds der Chemischen Industrie.

Compound **2** is a colorless, air-stable solid, and good quality crystals can be obtained on crystallization from MeCN. The molecular structure of **2** (Fig. 1, top) was surprising. As in the above-mentioned reaction with tellurium, a four-membered nitrogen–metal ring had formed, whose chemically equivalent antimony atoms Sb1 and Sb2 were differently coordinated. Both antimony atoms are, to a first approximation, in a pseudo-trigonal-bipyramidal environment. In the case of Sb1, N1 and N2 occupy equatorial positions (Sb1–N1 209.6(2), Sb1–N2 212.7(2) pm), while Cl1 and Cl2 are axially bound (Sb1–Cl1 261.8(1), Sb1–Cl2 259.0(1) pm). At Sb2, N2 and Cl3 are in equatorial (Sb2–N2 206.4(2), Sb2–Cl3 239.3(1) pm) and N1 and Cl4 in axial positions (Sb2–N1 223.3(2), Sb2–Cl4 258.0(1) pm). The different Sb–N and Sb–Cl bond lengths are thus adequately accounted for.

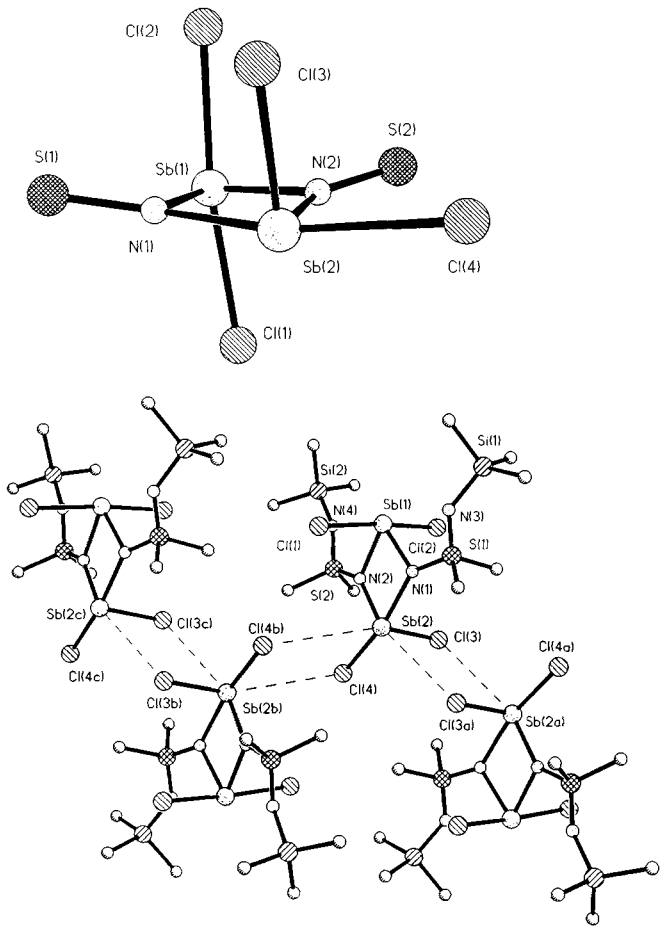

Fig. 1. Top: Structure of the Sb_2N_2 rings of **2**, surrounded by their immediate neighbors; bottom: arrangement of four molecules of **2** in the crystal structure. Selected bond lengths [pm] and angles [°]: Sb1-Cl1 261.8(1), Sb1-Cl2 259.0(1), Sb1-N1 209.6(2), Sb1-N2 212.7(2), Sb2-Cl3 239.3(1), Sb2-Cl4 258.0(1), Sb2-N1 223.3(2), Sb2-N2 206.4(2), S1-N1 155.7(3), S1-N3 149.5(3), S2-N2 157.1(3), S2-N4 149.1(3); Sb1-N1-Sb2 105.1(1), Sb1-N2-Sb2 110.2(1), N1-Sb1-N2 72.9(1), N1-Sb2-N2 71.3(1), Cl1-Sb1-N1 91.4(1), Cl3-Sb2-Cl4 87.0(1), Cl2-Sb1-N1 90.1(1), N2-Sb2-Cl3 98.0(1).

In the crystal **2** associates to form chains (Fig. 1, bottom). The Cl–Sb distances within the chain are 375 pm (Sb2···Cl3a, Cl3···Sb2a) and 411 pm (Sb2···Cl4b···Sb2b). If one includes neighboring atoms arising from the association in the consideration of the geometry, Sb2 has distorted octahedral environment. Furthermore, we assume that mainly the *cis* $Me_3SiNSMe_2$ residues determine the coordination sphere of the antimony atoms. The four-membered ring is not planar, but folded (ca. 10° along the Sb1–Sb2 axis). The deviations from the best plane are approximately 50 pm.[3] The mean Sb–N distance (213.0 pm) is comparable to that in known four-membered Sb_2N_2 rings.[4–6]

The ^1H NMR spectrum at room temperature shows two singlets at $\delta = 3.6$ ($S–Me_2$) and $\delta = 0.5$ (Si–Me). The peak with the highest m/z ratio in the mass spectrum (341) corresponds to the fragment ion $[M/2 - Me]^+$. The ^{121}Sb Mössbauer spectrum also conforms to these findings (Fig. 2).[7] From the least-squares fit two antimony positions

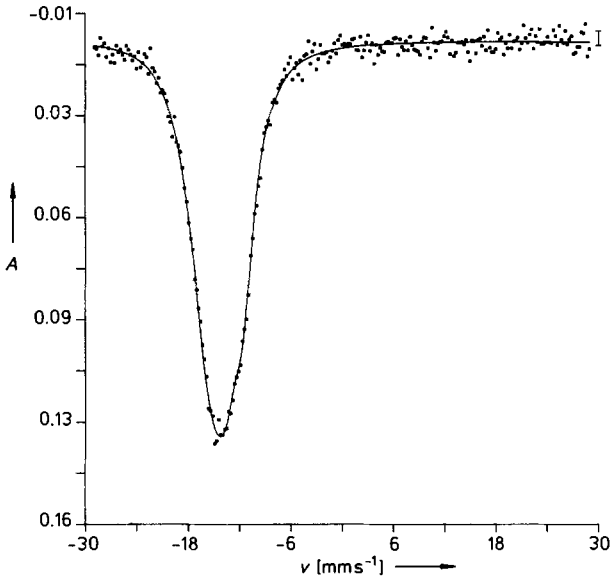

Fig. 2. ^{121}Sb Mössbauer spectrum of **2**. A = resonance absorption, v = relative velocity.

are observed with typical isomer shifts for Sb^{III} compounds of $-13.5(1)$ (Sb1) and $-14.9\ mm\,s^{-1}$ (Sb2). The 24 overlapping lines of the spectrum make it difficult to determine the quadrupole splitting with certainty. The best fit gave values for ΔE^Q of 21.0(1.0) (Sb1) and $-13.4(1.5)\ mm\,s^{-1}$ (Sb2). The negative quadrupole splitting at Sb2 (trigonal-bipyramidal mononuclear compounds of Sb^{III} generally show positive quadrupole splittings[9]) is probably due to the almost perendicular arrangement of the lone pairs on the Sb atoms. If it is assumed that the gradient of the electrical field is determined only by the position of the lone pairs,[10] this arrangement leads to a ratio of 2:−1 for the quadrupole splittings, according to the point charge model[11] for ideal trigonal-bypramidal Sb atoms. When one considers the approximations involved (influence of the other ligands on the electric field, deviations from ideal trigonal-bipyramidal structure, errors in fit due to the two superimposed Sb sites), the agreement between model and experiment is surprisingly good.

In conclusion, we could show that **2** is the first four-membered ring system which in the solid state has two chemically equivalent elements in different environments in the ring.

Experimental Procedure

2: A solution of **1** (1.2 g, 4.9 mmol) in $CHCl_3$ (40 mL) was added dropwise to a solution of $SbCl_3$ (1.1 g, 4.9 mmol) in $CHCl_3$ (100 mL) within 1 h at room temperature. With the addition of the first drops, the initially clear solution became cloudy. Thereafter the reaction was stirred at room temperature for a further 12 h, and the white, flocculent solid which formed was separated by

filtration. The filtrate was allowed to stand at room temperature for a day, whereupon more solid precipitated and was removed by filtration, before the filtrate was evaporated to dryness. The solid, yellow, granular residue was dissolved in MeCN and the solution allowed to stand for 12 h. Single crystals of **2** suitable for an X-ray structure analysis were obtained. Yield: 0.3 g, m.p. 165°C (dec.). IR: $\tilde{\nu}$ [cm^{-1}] = 1260 vs, 1094 vs, 975 vs, 842 vs, 758 vs, 636 vs, 535 s, 415 m, 313 s. Correct elemental analysis (Cl, N).

Received: March 12, 1990
Supplemented version: June 12, 1990 [Z 3849 IE]
German version: *Angew. Chem. 103* (1991) 856
Publication delayed on authors' request

CAS Registry numbers:
1, 19923-46-7; **2**, 134109-79-8; $SbCl_3$, 10025-91-9; ^{121}Sb, 14265-72-6.

[1] J. Münzenberg, H. W. Roesky, M. Noltemeyer, *Chem. Ber. 122* (1989) 1915.
[2] R. Appel, I. Ruppert, F. Knoll, *Chem. Ber. 105* (1972) 2492.
[3] **2** (M_r = 712.0): space group $P2_1/c$, a = 942.9(1), b = 1608.3(2), c = 1700.1(2) pm, β = 93.63(1)°, V = 2.5730 nm^3, Z = **4**, $\varrho_{ber.}$ = 1.84 $g\,cm^{-3}$, dimensions of the crystal: 0.4 × 0.4 × 0.7 mm^3, Siemens-Stoe AED2 four-circle diffractometer, 4986 reflections from 7.0 to 2θ = 45° ($Mo_{K\alpha}$; λ = 71.069 pm), 3339 symmetry-independent reflections and 3025 with $F > 3\sigma(F)$ for the refinement (SHELXTL Plus): R = 0.0207, R_w = 0.0261, $w^{-1} = \sigma^2(F) + 0.0001\,F^2$. Further details of the crystal structure investigation may be obtained from the Fachinformationszentrum Karlsruhe, Gesellschaft für wissenschaftlich-technische Information mbH, W-7514 Eggenstein-Leopoldshafen 2 (FRG) on quoting the depository number CSD-54657, the names of the authors and the journal citation.
[4] U. Müller, *Z. Anorg. Allg. Chem. 388* (1972) 207.
[5] G. Rajca, W. Schwarz, J. Weidlein, *Z. Naturforsch. B39* (1984) 1219.
[6] W. Neubert, H. Pritzkow, H. P. Latscha, *Angew. Chem. 100* (1988) 298; *Angew. Chem., Int. Ed. Engl. 27* (1988) 287.
[7] Source ($Ba^{121}SnO_3$) and absorber were cooled to 4.2 K in a cryostat bath with liquid helium. A NaI(Tl) scintillation detector was used. Both the 37.2 keV Mössbauer transition and the escape peak of the NaI crystal (ca. 8 keV) were used. The spectrum was recorded in time mode with a 512-channel analyzer. The curve was fitted using the least-squares method, in which the intensity ratios of the 12 transitions were parameters [8]. Shifts are given relative to $BaSnO_3$.
[8] G. K. Shenoy, B. P. Dunlap, *Nucl. Instrum. Methods 71* (1969) 285.
[9] M. Alamgio, P. W. C. Barnard, J. D. Donaldson, *J. Chem. Soc. Dalton Trans. 1980*, 1542.
[10] M. Schäfer, J. Pebler, B. Borgsen, F. Weller, K. Dehnicke, *Z. Naturforsch. B45* (1990) 1243.
[11] G. M. Bancroft, R. H. Platt, *Adv. Inorg. Chem. Radiochem. 15* (1972) 59.

Mo–Mo Quadruple Bonds Bridged by 1,8-Naphthyridinyl-2,7-Dioxide: an Insight into the Nature of a Parallel-Linked Stiff-Chain Polymer: $+M^nM\sim\sim\sim M^nM+_x$**

By *Roger H. Cayton, Malcolm H. Chisholm,* John C. Huffman*, and *Emil B. Lobkovsky*

Dedicated to Professor Hans Georg von Schnering on the occasion of his 60th birthday

The reactions between 1,8-anthracene dicarboxylic acid and $[Mo_2(O_2CR)_4]$ compounds lead to materials that we formulate as stiff-chain polymers[1] as depicted by **1** below. These materials tend to be insoluble in THF once the degree of polymerization x approaches 10. We are exploring the use

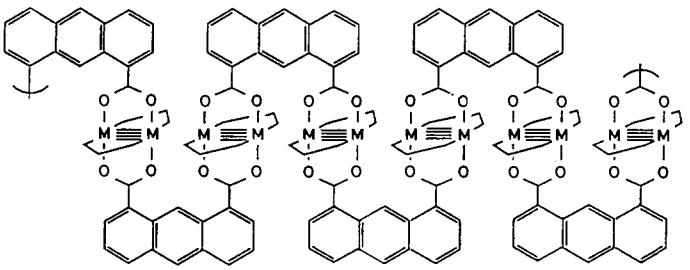

1

of long chain carboxylates (soaps) as attendant ligands with the hope of obtaining more soluble polymers.

The dimer $[\{Mo_2(O_2CtBu)_3\}_2(\mu\text{-}C_{16}H_8O_4)]$, **2**, has been prepared and studied in some detail[2] but regrettably no single crystals have been obtained that were suitable for X-ray analysis.

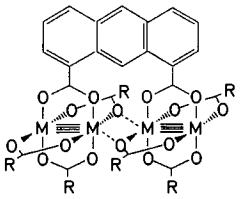

2, R = *t*Bu, M = Mo

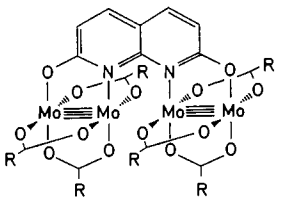

3, R = *t*Bu

We have, however, been able to prepare a dimer bridged by 1,8-naphthyridinyl-2,7-dioxide (**3**) which in turn provides a model for a tetranuclear subunit of a naphthyridinyl dioxide-bridged polymer, **4**.

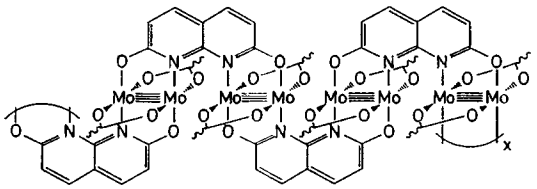

4

The synthesis of the dimer **3** is outlined by the reaction shown in equations a to c.[3]

$$[Mo_2(O_2CtBu)_4] + Me_3O^{\oplus}BF_4^{\ominus} \xrightarrow[CH_2Cl_2/CH_3CN]{22\,^\circ C} [Mo_2(O_2CtBu)_2(CH_3CN)_6](BF_4)_2 \quad (a)$$

5 → **6**

$$\mathbf{6} + \mathbf{5} \underset{CH_3CN}{\rightleftharpoons} 2\,[Mo_2(O_2CtBu)_3(CH_3CN)_2]BF_4 \quad (b)$$

7

$$\mathbf{7} + Na_2O_2N_2C_8H_4 \xrightarrow[THF/MeOH]{0\,^\circ C} [\{Mo_2(O_2CtBu)_3\}_2(\mu\text{-}O_2N_2C_8H_4)] \quad (c)$$

3

Orange crystals of **3** were obtained from THF, and the molecular structure determined by X-ray crystallography[4] is shown in Figure 1. The metal–metal distances alternate along the Mo_4 chain (short, 2.12 Å; long, 3.17 Å; short, 2.09 Å) consistent with the view of two localized Mo–Mo quadruple bonds brought together by the 1,8-naphthyridinyl-2,7-dioxide bridge. There is a twisting of the dimer

[*] Professor M. H. Chisholm, Dr. R. H. Cayton, Dr. J. C. Huffman, and Dr. E. B. Lobkovsky
Department of Chemistry and Molecular Structure Center
Indiana University
Bloomington, IN 47405 (USA)

[**] We thank the National Science Foundation for support and for a postdoctoral fellowship (R. H. C.). n represents the number of the bonds between the metal centers.

(Mo–Mo–Mo angle 149°) brought about by the desire of each Mo atom to coordinate to an oxygen atom along the Mo–Mo axis. The twisting allows a μ-carboxylate ligand of one Mo_2 unit to bind to a Mo atom of its neighboring Mo_2 unit as indeed occurs in the solid-state and liquid-crystalline phases of the $[Mo_2(O_2CR)_4]$ compounds.[5] This interaction is relatively weak as judged by the long Mo···O distances of 2.81 and 2.84 Å.

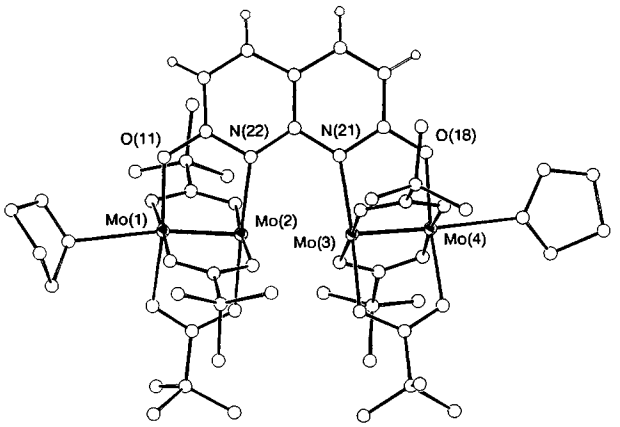

Fig. 1. A ball-and-stick drawing of the 2,7-naphthyridinyl dioxide-bridged tetranuclear complex **3**·2THF. Selected bond distances [Å]: Mo1–Mo2 = 2.0960(3), Mo2–Mo3 = 3.171(1), Mo3–Mo4 = 2.0963(4), Mo1–O(THF) = 2.5596(4), Mo4–O(THF) = 2.4943(4), Mo1–O11 = 2.0626(4), Mo4–O18 = 2.0662(4), Mo2–N22 = 2.1871(4), Mo3–N21 = 2.1682(5), Mo–O(pivalate) = 2.11(1).

In solution the temperature-dependent NMR behavior of **2** and **3** is very similar. At room temperature there are, in addition to the signals of the anthracene and naphthyridinyl dioxide ligands, only two types of *t*Bu resonances (2:1 ratio) indicating a time-averaged structure of C_{2v} symmetry. At low temperatures (**2**, −80 °C, $[D_8]$THF; **3**, −50 °C, CD_3OD/CD_2Cl_2) the signal of intensity 2 splits into two signals to give a 1:1:1 pattern as expected for a molecule displaying only C_2 symmetry due to the axial $(Mo_2\cdots O)_2$ interactions noted above. Evidently these weak $(Mo_2\cdots O)_2$ bonds are easily broken ($\Delta G^{\neq}$ = ca. 9–10 kcal mol^{-1}) leading to the time-averaged structure with a mirror plane and presumably a linear (or at least nearly linear) Mo_4 chain. It should be noted that in the C_{2v} structure the rigid nature of the spanning ligands constrains the "inner" Mo atoms to be separated by only 2.4–2.7 Å.

The 1,8-anthracene dicarboxylate and 1,8-naphthyridinyl-2,7-dioxide ligands are stereochemically correspondent as shown in Scheme 1, and we believe the Mo_4 chains in **2** and **3** must be very similar. However, the extent of electronic coupling in these molecules is remarkably different.

Compound **3** exhibits two successive oxidation waves (representing the removal of electrons from the Mo–Mo δ orbitals) in THF separated by 373 mV, whereas the analogous oxidations of **2** are estimated to be separated by only ca. 100 mV. The exact $\Delta E_{1/2}$ value of **2** cannot be determined due to competitive oxidation of the electrons from the anthracene ligand; however the analogous tungsten complex displays a $\Delta E_{1/2}$ of only 156 mV. (The tungsten compounds are invariably more strongly coupled than their molybdenum analogues.[2]) The coupling in **3** is similar to that of the Creutz–Taube ion (**8**, $\Delta E_{1/2}$ = 390 mV):[6]

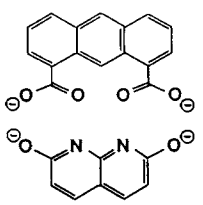

Scheme 1. Stereochemical equivalence of the ligands anthracene dicarboxylate and naphthyridinyl dioxide.

$[(H_3N)_5Ru(\mu\text{-pyrazine})Ru(NH_3)_5]^{n+}$ **8**, n = 4–6

Because of the vastly different degrees of electronic communication between the Mo_2 centers in **2** and **3** we suggest that the coupling in **3** occurs through the naphthyridine bridge. This is supported by Fenske–Hall MO calculations[7] that reveal strong interactions between the Mo–Mo δ and the naphthyridine π orbitals as shown in Scheme 2, **A**. By contrast two Mo–Mo quadruple bonds separated by 2.4 Å in a parallel alignment show little orbital mixing for their in- and out-of-phase combinations.

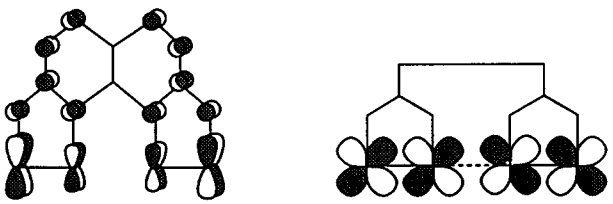

Scheme 2. **A** = HOMO of **3** from Fenske–Hall MO calculations; Mo–Mo δ orbitals form 60%. **B** = HOMO of a Ru_2 dimer, whose structure is analogous to that of **3**.

The situation could be very different for parallel-linked Ru_2 dimers where the HOMO would contain both M–M π* and M···M π interactions as shown schematically in Scheme 2 B. Therefore by the appropriate choice of either metal or ligand bridge we believe that stiff chain polymers of the type schematically represented by **1** or **4** will show insulating, semi-conducting, or metallic properties.

Experimental Procedure

All syntheses were carried out under an inert atmosphere (N_2) and using dry and degassed solvents.

Compound **6** was prepared in a manner directly analogous to that reported in Ref. [3a] for $Mo_2(O_2CCH_3)_2(CH_3CN)_6(BF_4)_2$.

Compound **7** was prepared by combining **5** (0.524 g, 0.88 mmol) and **6** (0.716 g, 0.88 mmol) in CH_3CN and heating to 70 °C for 24 hours. Removal of the volatiles under vacuum afforded a peach-colored powder which, after repeated washings with toluene, was 89 mol % pure (^{1}H NMR). The tetranuclear complex, **3**, was prepared by adding a 0 °C methanol solution of $Na_2O_2N_2C_8H_4$ (0.138 g, 0.67 mmol) (see Ref. [3b]) to a 0 °C THF solution of **7** (0.800 g, 1.28 mmol) and warming to room temperature. The volatiles were removed under vacuum and the residue extracted with THF. The extracts were filtered through celite, concentrated, then cooled to −20 °C to yield orange crystals (0.520 g, 70%). Satisfactory elemental analyses were obtained for all compounds.

The polymer shown in **4** could be prepared by the treatment of a THF solution of $[Mo_2(O_2C\text{-}n\text{-}C_{11}H_{23})_2(CH_3CN)_6](BF_4)_2$ (0.485 g, 0.48 mmol) with a methanol solution of $Na_2O_2N_2C_8H_4$ (0.099 g, 0.48 mmol), removal of the volatiles under vacuum, and extraction of the residue with toluene. Elemental analysis of the polymer indicates the average general formula, $Na[Mo_2(O_2C\text{-}n\text{-}C_{11}H_{23})_2(O_2N_2C_8H_4)]_{20}(CH_3CN)_2(BF_4)$.

Received: February 15, 1991 [Z 4448 IE]
German version: *Angew. Chem. 103* (1991) 893

CAS Registry numbers:
3, 134078-46-9; **5**, 55946-68-4; **6**, 134078-47-0; **7**, 134078-49-2; Mo, 7439-98-7.

[1] M. Ballauff, *Angew. Chem. 101* (1989) 261; *Angew. Chem. Int. Ed. Engl. 28* (1989) 253.

[2] R. H. Cayton, M. H. Chisholm, *J. Am. Chem. Soc. 111* (1989) 8921; and results to be published.

[3] a) F. A. Cotton, A. H. Reid, Jr., W. Schwotzer, *Inorg. Chem. 24* (1985) 3965; C. D. Garner, W. Clegg, G. Pimblett, *J. Chem. Soc., Dalton Trans.* (1986) 1257; b) G. R. Newkome, S. J. Gartis, V. K. Majestic, F. R. Fronczek, G. Chiari, *J. Org. Chem. 46* (1981) 833.

[4] Crystal data at $-169\,^{\circ}C$: $a = 15.714(3)$, $b = 15.923(2)$, $c = 15.109(2)$ Å, $\alpha = 113.37(1)$, $\beta = 104.50(1)$, $\gamma = 66.51(1)^{\circ}$, $Z = 2$, $\rho_{calcd} = 1.494\ g\,cm^{-3}$ and space group $P\bar{1}$. Of the 10939 reflections collected ($Mo_{K\alpha}$, $6^{\circ} \leq 2\theta \leq 45^{\circ}$), the number with $F > 3\sigma(F)$ was 6656. The structure was solved by the usual combination of direct methods (MULTAN78) and Fourier synthesis. All hydrogen-atom positions were calculated by using idealized geometries and $d(C-H) = 0.95$ Å. These calculated positions were fixed for the final cycles of refinement leading to $R = 0.0612$ and $R_w = 0.0641$. Further details of the crystal structure investigation may be obtained from the Fachinformationszentrum Karlsruhe, Gesellschaft für wissenschaftlich-technische Information mbH, W-7514 Eggenstein-Leopoldshafen 2 (FRG) on quoting the depository number CSD-55257, the names of the authors and the journal citation.

[5] R H. Cayton, M. H. Chisholm, F. D. Darrington, *Angew. Chem. 102* (1990) 1490; *Angew. Chem. Int. Ed. Engl. 29* (1990) 1481.

[6] D. E. Richardson, H. Taube, *Coord. Chem. Rev. 60* (1984) 114; H. S. Lim, J. Barclay, F. C. Anson, *Inorg. Chem. 11* (1972) 1460.

[7] M. B. Hall, R. F. Fenske, *Inorg. Chem. 11* (1972) 768.

New Intermediate Phases of the Composition $La_{2n+2}Cu_{n+4}O_{4n+7}$ in the La–Cu–O System: the Crystal Structure and Thermal Stability of $La_2Cu_2O_5$ **

By *Rolf Norrestam,* Mats Nygren,* and *Jan-Olov Bovin*

Dedicated to Professor Hans Georg von Schnering on the occasion of his 60th birthday

In the lanthanum oxide–copper(II) oxide system, La_2CuO_4 has been considered to be the only existing intermediate phase.[1, 2] La_2CuO_4 is of particular interest, as compounds such as $La_{2-x}M_xCuO_4$, M = Sr and Ba, which have the La_2CuO_4 structure type are superconducting[3] with transition temperatures exceeding 30 K. We now describe a new phase obtained when growing single crystals of La_2CuO_4 according to the preparation scheme suggested by *Chen* et al.[4] for the growth of crystals of the composition $(La,Sr)_2CuO_4$ from CuO flux. The X-ray powder photographs of the obtained specimen showed extra intense lines of an unknown phase. Needle-shaped crystals were selected from the specimen and examined by single crystal X-ray diffraction techniques.[5] These proved to be $La_2Cu_2O_5$ and all the extra lines in the powder photograph belong to this phase.

Powder samples of $La_2Cu_2O_5$ and $La_8Cu_7O_{19}$ were obtained by heat treatment of carefully mixed La_2O_3 (dried) and CuO mixtures pressed into tablets. The tablets were placed in Pt crucibles, heat-treated in air or in oxygen at various temperatures between 1050 and 1125 °C for 15–20 hours, and then quenched by allowing them to cool outside the furnace. Almost monophasic samples were obtained in the temperature range 1075–1100 °C. A slight excess of CuO seems to favor the formation of $La_2Cu_2O_5$. Outside this temperature range La_2CuO_4 is the dominant phase. Partial replacement of La^{3+} in $La_2Cu_2O_5$ by divalent ions, such as Mg^{2+}, Ca^{2+}, Sr^{2+}, and Ba^{2+} or tetravalent ions such as Ce^{4+} and Th^{4+} has been attempted. Crystals large enough for electrical measurements were grown in a flux of CuO. All the powder specimens prepared have been characterized by means of their X-ray powder patterns, obtained in a Guinier-Hägg focusing camera.

From single crystal X-ray diffraction data,[5] the probable space groups (as deduced from systematic absences in the reflection data) are *Cn* or *C2/n*. The choice of the centrosymmetric space group *C2/n* is supported by the observed distributions of normalized structure factors[6] and by the outcome of the structural refinements. The structure was solved by heavy atom techniques. Refining the occupancies of the oxygen atomic positions did not reveal any substantial deviation from 100%. The atomic coordinates and thermal parameters are listed in Table 1 and selected interatomic distances in Table 2.

Table 1. Fractional atomic coordinates ($\times 10^4$) and thermal parameters ($\times 10^4$ Å^2) for the structure of $La_2Cu_2O_5$.

Atom	*x*	*y*	*z*	*U*
La1	1133.5(2)	5206(1)	2317.2(1)	62(1)
La2	4023.5(2)	5345(1)	1347.3(1)	64(1)
La3	1265.8(2)	4934(1)	981.9(1)	65(1)
Cu1	2572.4(4)	158(2)	1808.0(2)	61(1)
Cu2	4356.7(5)	3761(2)	287.4(2)	102(2)
Cu3	2635.3(5)	−52(2)	391.5(2)	84(1)
O1	2621(3)	54(11)	1100(1)	92(5)
O2	2583(3)	5165(10)	1810(1)	102(5)
O3	790(3)	−277(11)	385(1)	102(6)
O4	787(3)	387(11)	1620(1)	115(6)
O5	4358(3)	283(12)	2081(1)	130(6)
O6	2910(3)	4913(11)	351(1)	114(6)
O7	4517(3)	531(11)	852(1)	95(6)
O8	2500	164(15)	2500	87(7)

Table 2. Copper–oxygen bond distances in $La_2Cu_2O_5$.

Cu1–O1	1.971(4)	Cu2–O3	1.982(4)	Cu3–O1	1.959(4)
Cu1–O2	1.875(4)	Cu2–O3	1.909(4)	Cu3–O3	2.562(4)
Cu1–O2	1.880(4)	Cu2–O6	2.102(5)	Cu3–O6	1.937(5)
Cu1–O4	2.421(5)	Cu2–O7	1.947(4)	Cu3–O6	1.911(5)
Cu1–O5	2.428(5)	Cu2–O7	2.963(4)	Cu3–O6	2.022(5)
Cu1–O8	1.934(4)			Cu3–O7	2.649(4)

A sketch of the $La_2Cu_2O_5$ structure is given in Figure 1. A characteristic pattern is the occurrence of slabs of La_2CuO_4, which are the width of two octahedra, each centered around Cu1[7, 8] (Fig. 1). The walls separating the La_2CuO_4 slabs consist of the oxygen coordination polyhedra formed around the Cu2 and Cu3 atoms. These polyhedra are connected to the La_2CuO_4 slabs by corner-sharing. The irregular coordination geometries around Cu2 and Cu3 show some slight resemblance to those found in the $M'_2Cu_2O_5$ phases, where M′ are smaller trivalent rare-earth ions.[9]

The polyhedron of O atoms within 2.96 Å from Cu2 in the $La_2Cu_2O_5$ structure can be considered as a flattened tetrahedron with Cu–O bond distances ranging from 1.91 to

[*] Prof. Dr. R. Norrestam, Prof. Dr. M. Nygren
Departments of Inorganic and Structural Chemistry
Arrhenius Laboratory, Stockholm University
S-10691 Stockholm (Sweden)
Dozent J.-O. Bovin
National Center for HREM, Chemical Center
University of Lund, P. O. Box 124, S-22100 Lund (Sweden)

[**] This work was financially supported by the Swedish Natural Science Research Council. We are grateful for the assistance of *A. Sjödin* and *M. Ekelund* with parts of the synthetic work.

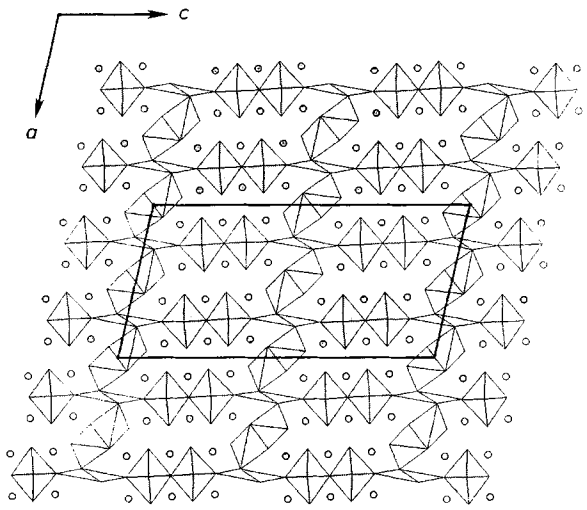

Fig. 1. Polyhedral representation of the structure of $La_2Cu_2O_5$, projected along [0 1 0]. For clarity, only the coordination polyhedra around the Cu atoms are shown: the positions of La atoms are indicated by circles.

2.10 Å. Two such tetrahedra share an edge. These entities are linked to infinite bands of edge-sharing polyhedra around the Cu3 atoms extending in the *b* direction (Fig. 2). The coordination geometry around Cu3 may be considered as an elongated octahedron, where bond lengths of the four approximately equatorial Cu–O bonds range from 1.91 to 2.02 Å and the two axial ones are about 2.6 Å. The average bond distances for the Cu and La atoms agree with expected bond distances.[10]

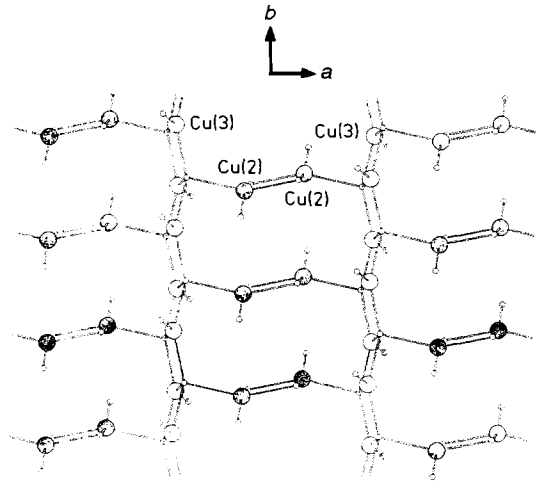

Fig. 2. Ball-and-stick representation, viewed perpendicular to (0 0 1), of the atomic arrangement in the walls separating the La_2CuO_4 slabs in the $La_2Cu_2O_5$ structure.

The structural features within the La_2CuO_4 slabs agree with those found for La_2CuO_4 itself[7, 8] (Table 2), namely, elongated octahedra around Cu1 and nine-coordinated La^{3+} ions (i.e., all atoms within 3.2 Å). Thus, it seems reasonable to expect that phases related to $La_2Cu_2O_5$, but with other widths of the La_2CuO_4 slabs, might exist. Such predicted phases would have the general compositions $La_{2n+2}Cu_{n+4}O_{4n+7}$ ($La_4Cu_5O_{11}$, $La_6Cu_6O_{15}$ ($=La_2Cu_2O_5$), $La_8Cu_7O_{19}$, $La_{10}Cu_8O_{23}$, ..., La_2CuO_4, where $n = 1-\infty$ is the number of edge-sharing CuO_6 octahedra between La_2CuO_4 slabs). The phase compositions can alternatively be written $mLa_2CuO_4 \cdot 3\,CuO$ ($m = 2,3,\ldots$), emphasizing the occurrence of La_2CuO_4 building blocks. The unit cell parameters would ideally only show an increment in the *c* axis of 7.5 Å for each additional La_2CuO_4 unit.

High resolution transmission electron microscopy (HREM) on $La_2Cu_2O_5$ and $La_8Cu_7O_{19}$ crystals show that some crystals are rich in structural defects.[11] The first three members of the series can sometimes exist together in the same crystal, but there are also crystals of $La_2Cu_2O_5$ fairly free from defects. The HREM images (Fig. 3a) agree with the structure of the n = 2 member as determined by X-ray diffraction methods. From HREM pictures of crystals of $La_8Cu_7O_{19}$ (Fig. 3b), the predicted structure of the n = 3 member was verified.

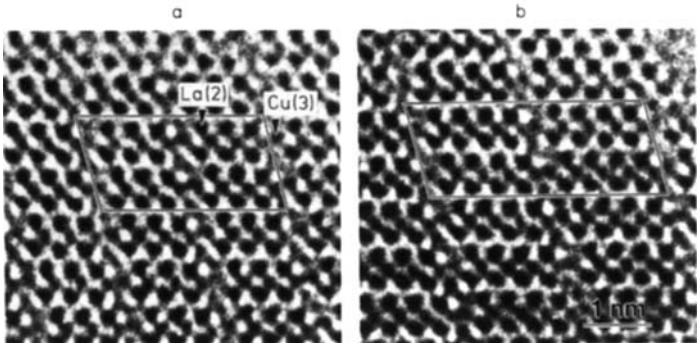

Fig. 3. HREM (JEM-4000EX) images of thin crystal fragments of a) $La_2Cu_2O_5$ and b) $La_8Cu_7O_{19}$, imaged with the electron beam down [0 1 0]. The metal positions are imaged as black spots and the La2 and Cu3 positions are marked with arrows.

HREM studies show that the structures of the members in the present homologous series are different from those of the series $La_{n+1}Cu_nO_{3n+1}$ (n = 1,2,...), stable below ca. 900 °C, observed by *Davies* and *Tilley*.[12] For this series no samples with n > 1 as a major constituent has been prepared. While the present series can be written $mLa_2CuO_4 \cdot 3\,CuO$, the *Davies* and *Tilley* series can be written $mLaCuO_3 \cdot La_2CuO_4$, emphasizing the different types of building blocks forming the structures. The latter series thus contains both Cu^{2+} and Cu^{3+}, while the former contains only Cu^{2+}.

The unit cell parameters of $La_2Cu_2O_5$ ($a = 13.877(2)$, $b = 3.750(1)$, $c = 27.571(3)$ Å and $\beta = 102.87(1)°$, calculated from 46 uniquely indexed powder pattern line positions) agree well with those obtained for the selected single crystal. Annealing of samples of the nominal composition $La_8Cu_7O_{19}$, at 1075 °C, yielded samples containing $La_8Cu_7O_{19}$ as the major phase. The expected powder pattern for $La_8Cu_7O_{19}$ was calculated,[13] using geometrically predicted atomic coordinates. The cell parameters for $La_8Cu_7O_{19}$ ($a = 13.833(3)$, $b = 3.761(1)$, $c = 35.128(8)$ Å and $\beta = 103.59(3)°$) refined from the powder photographs agree well with those predicted.

The electrical properties of $La_2Cu_2O_5$ have been investigated using four-probe conductivity measurements on single crystals of sizes up to 1 mm in length[14] and on powder pellets containing $La_2Cu_2O_5$ as major phase. These studies showed that $La_2Cu_2O_5$ exhibited insulating properties. The narrow temperature range of stability (1075–1100 °C) seems to prevent the preparation of $La_2Cu_2O_5$ samples where part of the La^{3+} ions have been replaced by M^{2+} or M^{4+} ions. Thus, all samples were found to contain La_2CuO_4, $La_{2-x}M_xCuO_4$ and CuO, but no $La_2Cu_2O_5$. In an attempt to

incorporate excess oxygen into the structure, powder pellets with $La_2Cu_2O_5$ as major phase were annealed at an oxygen pressure of 150 atm at 800, 400, and 200 °C during 24 h, 48 h, and 1 week, respectively. The oxygen content of the samples was determined by thermogravimetric methods and shown to be the same before and after the annealing ($La_2Cu_2O_{5\pm0.01}$). The electrical measurements revealed them still to be insulators. $La_2Cu_2O_5$ samples annealed at 900 °C in nitrogen atmosphere decomposed into La_2CuO_4 and CuO.

Received: January 30, 1991 [Z 4413 IE]
German version: *Angew. Chem. 103* (1991) 891

CAS Registry numbers:
$La_2Cu_2O_5$; 87138-88-3; $La_8Cu_7O_{19}$, 134131-22-9; La_2O_3, 1312-81-8; CuO, 1317-38-0.

[1] D. Klibanow, K. Sujata, T. O. Mason, *J. Am. Ceram. Soc. 71* (1988) C267–C269.
[2] W. Wong-Ng, B. Paretzkin, E. R. Fuller, Jr., *J. Solid State Chem. 85* (1990) 117–132.
[3] J. G. Bednorz, K. A. Müller, *Z. Phys. B 64* (1986) 189–193.
[4] C. Chen, B. E. Watts, B. M. Wanklyn, P. Thomas, *Solid State Commun. 66* (1988) 611–612.
[5] $La_2Cu_2O_5$, $M_r = 484.9$, monoclinic, space group $C2/n$, $Z = 12$, $a = 13.893(9)$, $b = 3.754(2)$, $c = 27.587(11)$ Å, $\beta = 102.84(7)°$, $V = 1403(1)$ Å^3, $\varrho_{ber.} = 6.89(1)$ g · cm^{-3}, $Mo_{K\alpha}$ ($\lambda = 0.71069$ Å, $\mu = 623$ cm^{-1}), Stoe AED 2 ($\omega/2\theta$ Scan), $T = 291(1)$ K, crystal size $0.036 \times 0.040 \times 0.32$ mm^3, $\sin\theta_{max}/\lambda = 1.0$ Å^{-1}. 5208 observed, 5075 unique, and 2965 significant [$I > 5 \cdot \sigma(I)$] reflections. Lorentz, polarization, and numerical absorption corrections (transmission factor range 0.07–0.20). $R_{int} = 0.026$ after corrections. Heavy atom techniques. Anisotropic La and Cu, isotropic O atoms; 85 refined parameters. $R = 0.028$ and $R_w = 0.032$ for significant reflections with $w = (\sigma|F|^2 + 0.0002\,|F|^2)^{-1}$. $R_w = 0.042$ for all 5075 reflections. Residual electron density (max.) = 1.0 eÅ^{-3}. Further details of the crystal structure investigation may be obtained from the Fachinformationszentrum Karlsruhe, Gesellschaft für wissenschaftlich-technische Information mbH, W-7514 Eggenstein-Leopoldshafen 2 (FRG), on quoting the depository number CSD-55288, the names of the authors, and the journal citation.
[6] T. Srikrishan, S. Partasarathy, *Z. Kristallogr. 131* (1970) 186–195.
[7] J. M. Longo, P. M. Raccah, *J. Solid State Chem. 6* (1973) 526–531.
[8] B. Grande, H. Müller-Buschbaum, M. Schweizer, *Z. Anorg. Allg. Chem. 428* (1977) 120–124.
[9] H.-R. Freund, H. Müller-Buschbaum, *Z. Anorg. Allg. Chem. 441* (1978) 103–106.
[10] R. D. Shannon, *Acta Crystallogr. Sect. A 32* (1975) 751–767.
[11] J.-O. Bovin, R. Norrestam, M. Nygren, G. Svensson, unpublished.
[12] A. H. Davies, R. J. D. Tilley, *Nature (London) 326* (1987) 859–861.
[13] K. Yvon, W. Jeitscho, E. Parthé, *J. Appl. Crystallogr. 10* (1977) 73–74.
[14] T. Hörlin, T. Niklewski, M. Nygren, *Chem. Scr. 13* (1978) 201.

2,2′-(Ethynediyl)bis(4-alkoxy-1-naphthols) and Dinaphthofuro[3,2-*b*]furans—Substances with Unusual Photoreactivity and Photochromic Behavior

By *Andreas Johann Schmidt*, *Hartmut Laatsch** and *Mathias Noltemeyer*

Colorless dialkoxydinaphthofuro[3,2-*b*]furans of type **1**[1a] become momentarily blue and then violet in UV light ($\lambda_{max} = 604$ nm, dimethyl sulfoxide (DMSO)), whereby a dimeric *trans*-quinonemethide[1b] of type 2 is formed as sole end product. A short-lived intermediate, which we interpret as the *cis*-configurated **4**, is detectable by UV spectroscopy ($\lambda_{max} = 608$ nm) during the reaction; **4** can thermally recyclize to the starting compound **1**, most likely in an antarafacial [$4_s + 4_a$] cycloaddition. Furofurans and bismethides thus form a novel photochromic system, which is remarkable because of the unusual mechanism, the intensity of the color change, and the large difference in the absorption maxima of starting material and product.[2]

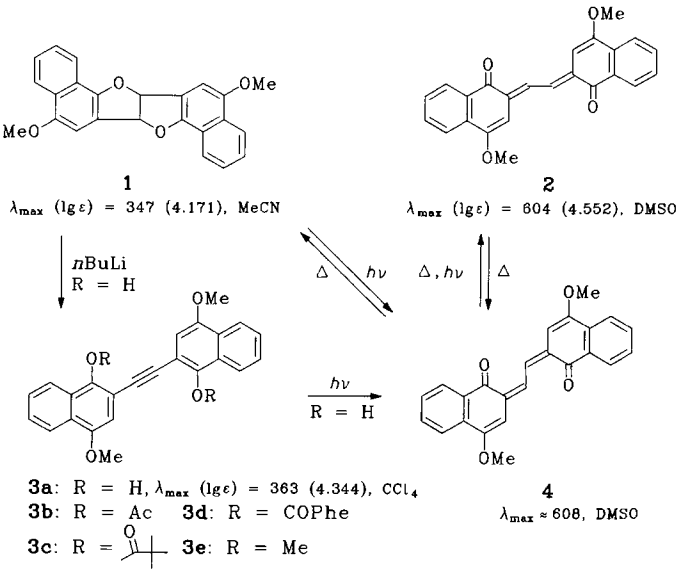

Scheme 1. Photochromic transformation of the furofuran **1**.

Unfavorable, however, is the rapid isomerization of the initially formed (*Z*,*Z*)-methide **4** into the (*E*,*E*)-form **2**, whose cyclization to **1** requires activation energies around 100 kJ mol^{-1}. We therefore decided to investigate the influence of bridgehead substituents on the stability of **4** and the photochromic behavior of **1**.

Lithiation of **1** and subsequent reaction with alkyl halides, however, did not lead to bridgehead-substituted furofuran, but to the alkyne **3a**. Apparently the anion **5** is not stable, even at low temperatures, as trapping experiments with deuterium oxide always revealed the presence of only unchanged starting compound **1** besides **3**. Presumably the ring-opening proceeds in two steps, since the furylnaphthalene **6** postulated as intermediate also reacts in the form of its anion with *n*-butyllithium to give the alkyne **3a**. Similarly, 3-bromobenzofuran reacts with *n*-butyllithium to give *o*-hydroxyphenylacetylene.[3]

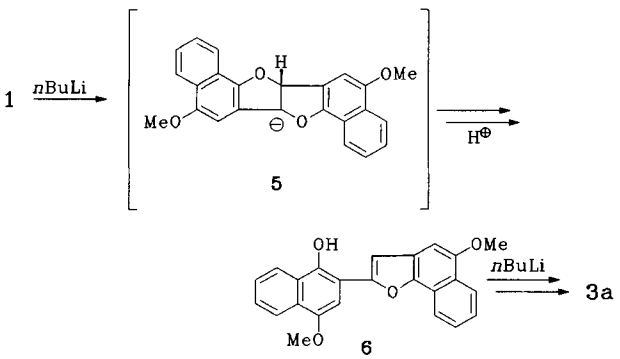

Scheme 2. Anionic rearrangement of **1** to **3a**.

[*] Prof. Dr. H. Laatsch, A. J. Schmidt
Institut für Organische Chemie der Universität
Tammannstrasse 2, W-3400 Göttingen (FRG)
Dr. M. Noltemeyer
Institut für Anorganische Chemie der Universität Göttingen (FRG)

In contrast, reactions with acid chlorides at room temperature led to the *O*-acylated alkyne derivatives **3b**–**3d** in yields of between 75 and 90%. The naphthol **3a** could easily be liberated from these by hydrolysis with methanolic sodium hydroxide; **3a** reacts with dimethyl sulfate via phase transfer catalysis to give the tetramethyl ether **3e** in high yields; upon treatment with trifluoroacetic acid or also on heating in boiling 1,2-dichlorobenzene, **3a** cyclizes to **6** in high yields.

The naphthol **3a** and its derivatives **3b**, **3c** and **3e** fluoresce remarkably strongly (Φ_f(**3a**) = 0.223). An X-ray structure analysis of **3b** revealed that the planes of the two naphthalene units are rotated through ca. 40° with respect to each other in the crystal, whereby the acetate moieties assume a synperiplanar arrangement referred to the triple bond;[4] bond lengths and angles lie in the expected range.

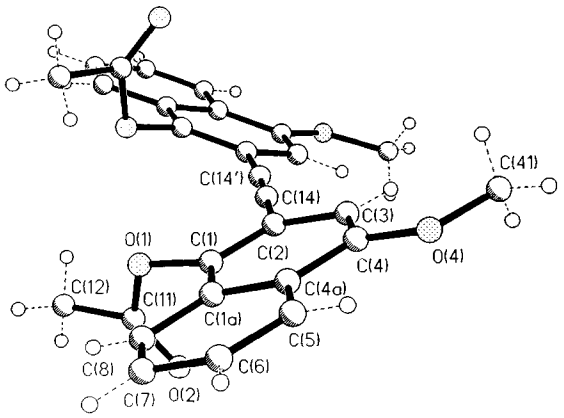

Fig. 1. Structure of **3b** in the crystal [4].

Of the numerous known diarylalkynes only the di-(2-hydroxyphenyl)acetylene[5] is hydroxylated in the *o*,*o*'-position to the triple bond; no unusual properties have been reported. Quite unexpected, therefore, was the extreme photolability of **3a**, which rearranges in less than 20 ns into the dimeric (*Z*/*Z*)-methide **4** under UV light, even at 120 K.[6] Also as solid or molecular dispersion in a polymer matrix, the dimethyl ether **3a** is momentarily tinted blue in light (long wavelength UV or photoflash). No parallel for this photoreaction has thus far been observed in the acetylene series.

Acetylene is present in the first excited state in a configuration corresponding to the *trans*-butene.[7] If **3a** is appropriately bent in the electronically excited state, the unusual photoreaction of the alkyne **3a** is best explained in terms of a double [1,5]-sigmatropic hydrogen shift to give the (*Z*/*Z*)-configurated, dimeric quinomethide **4**. Indeed, preliminary measurements show that **4** is formed from **3a**; apparently side reactions and secondary reactions are concealed by the rearrangement.

The anionic ring opening of **1** promises wide application for the synthesis of hydroxylated aryl- and diarylalkynes. And conversely, an alternative synthesis of the latter opens up the possibility of a photochemical access to novel, substituted furofurans and also the opportunity to investigate their photochemical behavior.

Experimental

2,2'-(Ethynediyl)bis(4-methoxy-1-naphthol) **3a**: a) a suspension of furofuran (1.0 g, 2.7 mmol) in anhydrous THF (50 mL) was treated with 6.7 mL (10.8 mmol) of *n*BuLi (1.6 M in hexane) at room temperature under N_2. After 6 hours' stirring 10 mL of MeOH were pipetted into the green fluorescing solution, and stirring continued for 10 minutes. The reaction mixture was then filtered with CH_2Cl_2 through silica gel (10 × 3 cm) and the residue obtained on evaporating the filtrate recrystallized from toluene/petroleum ether. **3a** (672 mg; 67%) was obtained in the form of colorless needles which decomposed on melting at 174°C and exhibited a blue fluorescence in solution. b) An analogous reaction of 640 mg (1.73 mmol) of **6** in 30 mL of anhydrous THF with 2.16 mL (3.46 mmol) of *n*BuLi (1.6 M in hexane) yielded 493 mg (76%) of **3a**. c) A suspension of **3b** (160 mg, 35.2 mmol) in MeOH (30 mL) and 10 mL of 2 N NaOH was heated under reflux in an atmosphere of N_2 for 10 min. The reaction mixture was neutralized with acetic acid and extracted with CH_2Cl_2. The organic phase, after evaporation and drying over magnesium sulfate, gave a polymeric material at the start, and then two major zones on column chromatography (CH_2Cl_2) through silica gel. Fraction 1 contained 18 mg (11%) of educt (R_f = 0.9, CH_2Cl_2), fraction 2 88 mg (76% based on conversion) of **3a** (R_f = 0.75, CH_2Cl_2).—UV (CCl_4): λ_{max} (lg ε) = 264 (4.811), 287 (4.549), 363 nm (4.344); ^{1}H NMR (200 MHz, $CDCl_3$): δ = 8.27 (m, 4H), 7.62 (m, 4H), 6.80 (s, 2H; 3-, 3'-H), 6.18 (s, 2H; 1-, 1'-OH), 4.02 (s, 6H; 4-, 4'-OMe); ^{13}C NMR ($CDCl_3$, 50.3 MHz, 50°C): δ = 149.4 (C-4,4'), 148.6 (C-1,1'), 127.3 (C-8a,8a'), 127.1 (C-6,6'), 126.7 (C-7,7'), 124.5 (C-4a,4a'), 122.3 (C-5,5'), 122.2 (C-8,8'), 104.5 (C-3,3'), 101.3 (C-2,2'), 91.5 (C-alkyne), 55.9 (CH_3).

2,2'-(Ethyndiyl)bis(1-acetoxy-4-methoxynaphthalene) **3b**: A suspension of **1** (1.0 g, 2.7 mmol) in anhydrous THF (50 mL) was treated with 6.7 mL (10.8 mmol) of *n*BuLi (1.6 M in hexane) under N_2. After 12 h stirring 0.77 mL (10.8 mmol) of acetyl chloride was pipetted into the mixture and stirring continued for 12 h. The mixture was transferred to a silica gel column (10 × 3 cm), eluted with CH_2Cl_2 and the pale yellow residue obtained on evaporation of the eluate purified by crystallization from toluene/petroleum ether. 1.09 g (89%) of **3b** was obtained as colorless monoclinic needles, which melted with decomposition at 224°C and fluoresced intense blue in solution.—^{1}H NMR (200 MHz, $CDCl_3$): δ = 8.32 (m, 2H), 7.86 (m, 2H), 7.60 (m, 4H; 6-, 6'-H, 7-, 7'-H), 6.96 (s, 2H; 3-, 3'-H), 4.02 (s, 6H; 4-, 4'-OMe), 2.52 (s, 6H; Ac-H).

3c [8] and **3d** [9] were formed analogously by trapping reactions of the anion with pivaloyl and benzoyl chloride, respectively; **3e** [10] was obtained by reaction of **3a** with dimethyl sulfate.

Received: October 23, 1990;
revised: March 19, 1991 [Z 4248 IE]
German version: *Angew. Chem. 103* (1991) 858

CAS Registry numbers:
1, 133870-93-6; **3a**, 133870-94-7; **3b**, 133870-95-8; **3c**, 133870-96-9; **3d**, 133870-97-0; **3e**, 133870-98-1; **6**, 84101-79-1.

[1] a) The signals of the bridgehead H atoms in **1** showed no splitting upon addition of chiral shift reagents. The ^{13}C-^{1}H coupling of 7.5 Hz points, however, to a *cis* coupling of the rings; for measurements on analogous benzene derivatives see: B. Cardillo, M. Cornia, L. Merlini, *Gazz. Chim. Ital. 105* (1975) 1151. b) We deduced the *trans-trans* structure from the configurational stability in the presence of iodine and from the anisotropy-determined downfield shift of the olefin signals in the ^{1}H-NMR spectrum.
[2] H. Laatsch, *Liebigs Ann. Chem. 1982*, 1808.
[3] H. Gilman, D.S. Melstrom, *J. Am. Chem. Soc. 70* (1948) 1655.
[4] **3b** crystallizes in the space group *C*2/*c* with the cell constants *a* = 2794.6(9), *b* = 767.6(9), *c* = 2296.3(9) pm; β = 92.30°; *V* = 4.922 nm^3, *Z* = 8, ϱ_{calcd} = 1.34 Mg m^{-3}; μ(Mo$_{K\alpha}$) = 0.19 mm^{-1}. 5140 (3215 independent) reflections measured on a STOE four-circle diffractometer, 2472 with $|F| > 3\sigma(|F|)$ used for all calculations: R = 0.069; R_w = 0.068; $w^{-1} = \delta^2(|F_0|) + g|F_0|^2$. Further details of the crystal structure investigation are available on request from the Fachinformationszentrum Karlsruhe, Gesellschaft für wissenschaftlich-technische Information mbH, W-7514 Eggenstein-Leopoldshafen 2, (FRG) on quoting the depository number CSD-55057, the names of the authors, and the journal citation.
[5] R. L. Letsinger, J. R. Nazy, *J. Am. Chem. Soc. 81* (1959) 3013.
[6] We thank Dr. *K. H. Grellmann*, Max-Planck-Institut für Biophysikalische Chemie, Göttingen (FRG), for the measurement. Irradiation was carried out with an Excimer laser (λ = 308 nm); absorption measurement at λ = 600 nm, *T* = 120 K, *d* = 1 cm. The increase in absorption took place within the pulse width of the laser of 15 ns and could not be resolved.
[7] C.K. Ingold, G.W. King, *J. Chem. Soc. 1953*, 2702.
[8] M.p. 262°C; ^{1}H NMR (200 MHz, $CDCl_3$): δ = 8.24 (m, 2H; 8-, 8'-H), 7.7 (m, 2H; 5-, 5'-H), 7.54 (m, 4H; 6-, 6'-H, 7-, 7'-H), 6.85 (s, 2H; 3-, 3'-H), 4.00 (s, 6H; 4-, 4'-OMe), 1.48 (s, 18H, 6C-Me).
[9] M.p. 302°C (decomp.), ^{1}H NMR (200 MHz, [D$_6$]DMSO, 100°C): δ = 8.38 (d, *J* = 8 Hz, 4H; *o*,*o*'-Phe), 8.24 (m, 2H), 7.92–7.82 (m, 4H), 7.80–7.62 (m, 8H), 6.46 (s, 2H; 3-, 3'-H), 3.76 (s, 6H; O-Me).
[10] M.p. 139°C; ^{1}H NMR (200 MHz, $CDCl_3$): δ = 8.25 (m, 4H; 5-, 5'-H, 8-, 8'-H), 7.60 (m, 4H; 6-, 6'-H, 7-, 7'-H), 6.94 (s, 2H, 3-, 3'-H), 4.24 (s, 6H; 1-, 1'-OMe), 4.06 (s, 6H; 4-, 4'-OMe).

Stereoselective Synthesis of Acetal-β,β-diglucosides, a Novel Class of Glycosides and Chiral Acetals**

By *Lutz F. Tietze** and *Matthias Beller*

Dedicated to Professor Horst Prinzbach

Owing to their chemical properties and physiological functions, glycosides are of outstanding importance in chemistry and biology.[1] For the chemical industry they are of interest as potential raw material for the synthesis of novel products.[2] A possibility of gaining access to novel useful sugar derivatives involves the development of previously unknown glycoside structures. We describe here the synthesis of acetal diglycosides, a novel class of substances.

The carbohydrate derivatives occurring in Nature are predominantly *O*-glycosides in which a sugar is linked with an alcohol at an anomeric center. In addition there are also compounds, such as, e.g. secologanin, the parent compound of the secoiridoid glycosides and precursor of many alkaloids which are characterized by linkage of a cyclic hemiacetal with the anomeric center of a sugar.[3] Thus far unknown, however, are glycosides **4**–**7**, in which two sugars are

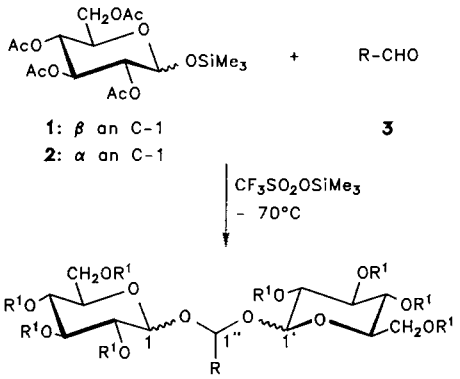

4: R^1 = Ac, β an C-1 und C-1'

5: R^1 = Ac, α an C-1, β an C-1'

6: R^1 = Ac, α an C-1 und C-1'

7: R^1 = H, β an C-1 und C-1'

	R = *n*-C_5H_{11}	CH_3	$(CH_3)_2CH$	$(CH_3)_3C$	$Ph(CH_2)_2$	Ph
3–**8**,**11**	**a**	**b**	**c**	**d**	**e**	**f**

bound via an aldehyde. Such substances are of interest because of their unusual trisacetal structure, their synthetic potential as chiral acetals,[4] and because of their potentially special material properties, e.g. as emulsifiers.

The synthesis of acetal-diglycosides,[5] e.g. of the acetyl-protected acetyl-β,β-diglucosides **4a**–**f** can be accomplished very easily by reaction of trimethylsilyl-2,3,4,6-tetra-*O*-acetyl-β-D-glucopyranoside **1** with aldehydes **3a**–**f** in the presence of trimethylsilyl trifluoromethanesulfonate (trimethylsilyl triflate) as catalyst (Table 1).[6] Subsequent removal of the protecting groups (e.g. from **4a**) by solvolysis with potassium carbonate in methanol affords the deprotected compounds (e.g. **7a** in 83% yield). The products **4a**–**f** are

Table 1. Synthesis of acetal-β,β-diglucosides **4**.

Educts	Products	1:3 [mmol]	Yield [%]
1 + **3a**	**4a**	1:0.6	83
1 + **3b**	**4b**	1:2	80
1 + **3c**	**4c**	1:2	70
1 + **3d**	**4d**	1:1	18
		1:2	22
		1:3	26
1 + **3e**	**4e**	1:0.6	38
		1:2.5	48
1 + **3f**	**4f**	1:1.2	14
		1:3	36
		1:5	46
		1:9	54

formed stereoselectively at −78 °C with retention at the anomeric center of the trimethylsilyl-β-D-glucopyranoside **1** employed. At higher temperatures however, the reaction leads to a mixture of acetal-β,β- **4**, -α,β- **5** and -α,α-diglucosides **6**, which are very difficult to separate chromatographically. The yield of acetal-β,β-diglucosides **4** largely depends, as expected, on the reactivity of the aldehyde **3** employed. Simple aldehydes such as **3a** or **3b**, which are not deactivated by steric and electronic effects afford the acetyl-protected acetal-β,β-diglucosides **4a** and **4b** respectively in very good yields already on using a slight excess of the aldehyde. The yield of **4** decreases with increasing steric bulkiness of the aldehydes (**3b** < **3e** < **3d**); however, this effect can be partially compensated by using an excess of the aldehyde (Table 1). The poor yields in the reaction of benzaldehyde **3f** with **1** are presumably due to the low carbonyl activity of **3f**. In analogy to the synthesis of **4**, the acetal-α,α-diglucoside **6a** could be obtained in 26% yield by in situ anomerization[7] of **1** to **2** (0 °C, 10 mol-% trimethylsilyl triflate) and subsequent reaction with two equivalents of hexanal **3a** at −70 °C in the presence of trimethylsilyl triflate. The acid stability of **4a**–**4f** is greater than that of corresponding acetals of aliphatic alcohols.

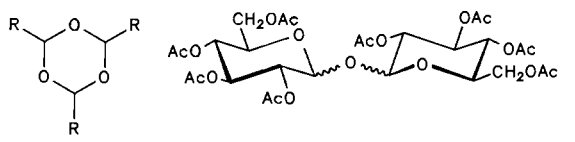

8 **9**

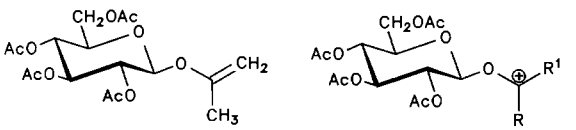

10 **11**

The aldehyde trimers **8** and the trehaloses **9** are formed as by-products in the synthesis of **4**–**6**. The chromatographic separation of the trehaloses **9** from the acetal-diglycosides **4** and **6** was difficult in some cases (**4b**,**e**), but could be achieved by repeated column chromatography.

Attempts to prepare acetal-diglucosides by reaction of **1** and **2** with ketones under the same conditions have thus far failed. With acetone, the vinyl-β-glucoside **10** is formed in 16% yield as well as **9**. We attribute this to the fact that the carbocation **11** postulated by us as intermediate is not reactive enough towards **1** and **2** because of steric interactions when $R^1 \neq H$. This explanation is consistent with the strong

[*] Prof. Dr. L. F. Tietze, Dr. M. Beller
Institut für Organische Chemie der Universität
Tammannstrasse 2, W-3400 Göttingen (FRG)

[**] Glycoside Syntheses, Part 19. This work was supported by the Fonds der Chemischen Industrie.—Part 18: L. F. Tietze, C. Schröter, S. Gabius, U. Brinck, A. Goerlach, H.-J. Gabius, *Bioconjug. Chem.*, in press.

dependence of the yields on steric requirements in the reaction of **1** with the aldehydes **3**.

The ^{1}H- and ^{13}C-NMR spectra of the acetal-diglucosides **4**–**7** are complex, since the two pyranose rings are magnetically non-equivalent. Surprising is the relatively large difference in the chemical shifts for C-1 and C-1′ in **4** and **7** ($\Delta\delta \leq 3.83$). Comparable differences are also observed for the signals of 1-H and 1′-H ($\Delta\delta \leq 0.59$). The presence of two β-glucosidic bonds in **4** and **7** follows from the doublet at $\delta = 4.6-5.1$ with $J = 7.5-8$ Hz for 1-H and 1′-H. In the ^{1}H-NMR spectrum of the acetal-α,α-diglucoside **6** 1-H and 1′-H give rise to signals at $\delta = 5.41-5.52$ with $J = 3.5$ Hz. The signal of 1″-H appears in the spectra of **4**–**7** as a triplet at $\delta = 4.64-5.05$ with $J = 5.5-7.5$ Hz.

Received: February 15, 1991 [Z 4445 IE]
German version: *Angew. Chem. 103* (1991) 879

CAS Registry numbers:
1, 19126-95-5; **3a**, 66-25-1; **3b**, 75-07-0; **3c**, 78-84-2; **3d**, 630-19-3; **3e**, 104-53-0; **3f**, 100-52-7; **4a**, 133851-55-5; **4b**, 133851-56-6; **4c**, 133851-57-7; **4d**, 133851-58-8; **4e**, 133851-59-9; **4f**, 133851-60-2; **6a**, 133851-61-3; **7a**, 133851-62-4; **10**, 114828-10-3; acetone, 67-64-1.

[1] N. Sharon (Ed.): *Complex Carbohydrates, their Biochemistry, Biosynthesis and Functions*, Addison Wesley, Reading, MA, USA 1975; R.R. Schmidt, *Angew. Chem. 98* (1986) 213; *Angew. Chem. Int. Ed. Engl. 25* (1986) 212; H. Paulsen, *ibid. 94* (1982) 184 and *21* (1982) 155.

[2] J. Schurz, *Nachr. Chem. Tech. Lab. 36* (1988) 388; J. Daub, *ibid. 36* (1988) 896.

[3] L.F. Tietze, *Angew. Chem. 95* (1983) 840; *Angew. Chem. Int. Ed. Engl. 22* (1983) 828.

[4] T. Sato, J. Otera, H. Nozaki, *J. Am. Chem. Soc. 112* (1990) 901; D. Schinzer, *Synthesis 1988*, 263; J. Zimmermann, D. Seebach, *Helv. Chim. Acta 70* (1987) 1104; T. Mukaijama, M. Murakami, *Synthesis 1987*, 1043; A. Ghribi, A. Alexakis, J.F. Normant, *Tetrahedron Lett. 25* (1984) 3075; A. Mori, K. Ishihara, H. Yamamoto, *ibid. 27* (1986) 987; K. Maruoka, S. Nakai, M. Sakurai, H. Yamamoto, *Synthesis 1986*, 130; K.A. Nelson, E.A. Mash, *J. Org. Chem. 51* (1986) 2721; W.S. Johnson, C.A. Harbert, B.E. Ratcliffe, R.D. Stipanovic, *J. Am. Chem. Soc. 98* (1976) 6188.

[5] *Experimental procedure:* A stirred solution of **1** (315 mg, 0.75 mmol) and **3a** (108 μL, 0.90 mmol) in dichloromethane (10 mL) was treated under an inert gas and in the absence of moisture at −78 °C with trimethylsilyl triflate (28 μL, 0.15 mmol). After 3d at −78 °C the reaction was terminated by addition of 0.20 μmL of a 1:1 mixture of ethanol/triethylamine. Chromatography on silica gel (*tert*-butylmethyl ether/petroleum ether 3:1) afforded 239 mg (83%) of **4a** as a colorless foam. ^{1}H NMR ($CDCl_3$): $\delta = 0.88$ (t, $J = 6$ Hz, 3H; CH_3), 1.20–1.42 (m, 6H; 3″-H_2, 4″-H_2, 5″-H_2), 1.56–1.70 (m, 2H; 2″-H_2), 1.99, 2.00, 2.01, 2.03, 2.06, 2.09, 2.13 (7s, 24H; CH_3CO), 3.62–3.78 (m_c, 2H; 5-H, 5′-H), 4.08–4.34 (m, 4H, 6-H_2, 6′-H_2), 4.62 (d, $J = 8$ Hz, 1H; 1-H), 4.82 (d, $J = 8$ Hz, 1H; 1′-H), 4.92–5.30 (m, 7H; 2-H, 2′-H, 1″-H, 3-H, 3′-H, 4-H, 4′-H).

[6] For analogous glycosidations which lead to acyclic acetal-monoglycosides see: L.F. Tietze, R. Fischer, *Angew. Chem. 93* (1981) 1002; *Angew. Chem. Int. Ed. Engl. 20* (1981) 696; *Tetrahedron Lett. 22* (1981) 3239. Compounds of this type are employed in the development of antitumor agents: L.F. Tietze in E. Borowski, D. Shugar (Eds.): *Molecular Aspects of Chemotherapy*, Pergamon, Oxford 1990, p. 55.

[7] L.F. Tietze, R. Fischer, H.-J. Guder, *Synthesis 1982*, 946.

Circular Dichroism of a Chiral Cyanine Dye Dimer Trapped in γ-Cyclodextrin**

By *Volker Buss**

Aggregation of cyanine dyes in polar solvents or on solid matrices is a phenomenon of considerable theoretical and practical interest. The characteristic spectral changes accompanying dye aggregation[1] are easily understood at least on a qualitative level. Thus, the appearance in the UV of a new high-intensity band blueshifted relative to the monomer is generally assumed to indicate the formation of a sandwich-type dimer (or oligomer) aggregate. Recently, it was shown that β- and γ-cyclodextrin greatly enhance dimerization of certain cyanine dyes presumably by stabilization of the sandwich inside the cyclodextrin cavity.[2] We have now observed what appears to be the first example of a chiral cyanine dye dimer trapped within the channel of two γ-cyclodextrin molecules.

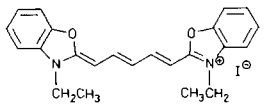

1

The temperature-dependent UV spectra of 3,3′-diethyloxadicarbocyanine iodide (DODC iodide, **1**) in a moderately concentrated (10^{-2} M) aqueous solution of γ-cyclodextrin, with 15% ethylene glycol added to allow cooling below 0 °C, are shown in Figure 1, left. The spectra change little with temperature because, under these conditions, most of the dye molecules are present already as dimers. This behavior is in contrast to what is observed in the circular dichroism (CD) spectra obtained under identical conditions (Fig. 1, right): the positive band at 534 nm, which must be attributed to dimer absorption, is gradually replaced by another band with negative amplitude, while the weak positive band at 589 nm increases in amplitude. There is a negative band at 635 nm (also manifest as a broad baseline absorption in the UV) whose origin we are not able to explain fully at the moment.

The changes brought about in the CD spectra by cooling the sample can be enhanced considerably by increasing the cyclodextrin concentration. Figure 2 shows the UV and CD spectra of DODC in a 50/50 (v/v) mixture of ethylene glycol and water in the presence of 0.125 M γ-cyclodextrin. The monomer absorption is markedly higher at room temperature owing to the high diol content. However, lowering the temperature increases the dimer concentration, and from about −50 °C on an equilibrium is reached comparable to the one in Figure 1, left.[3]

In the corresponding CD spectra the positive dimer absorption at 534 nm is observed only in passing while the spectra at lower temperature are dominated by the features which started to develop in Figure 1, namely, two strong

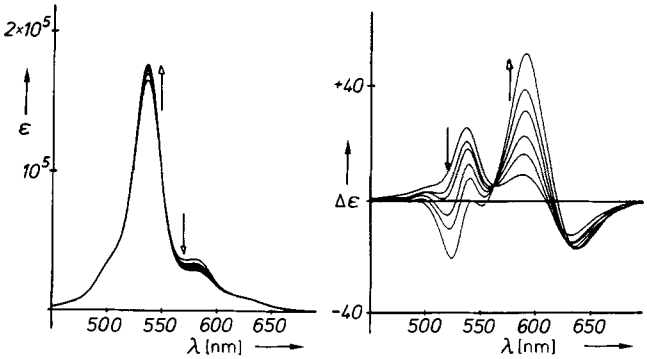

Fig. 1. Temperature-dependent UV (left) and CD spectra (right) of a solution of **1** (8.8×10^{-4} M) and γ-cyclodextrin (0.01 M) in 15% (v/v) ethylene glycol/water. Curves correspond to measurements at +10, 0, −5, −10, −15, and −20 °C. Arrows indicate direction of spectral changes as the temperature is lowered.

[*] Prof. Dr. V. Buss
Fachgebiet Theoretische Chemie der Universität
Lotharstrasse 1, W-4000 Duisburg (FRG)

[**] This work was supported by the Fonds der Chemischen Industrie and by KaliChemie. *R. Knierim* provided excellent technical help.

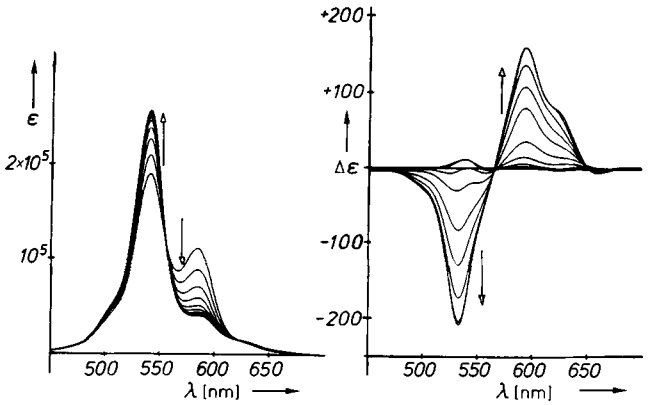

Fig. 2. Temperature-dependent UV (left) and CD spectra (right) of a solution of **1** (6×10^{-4} M) and γ-cyclodextrin (0.125 M) in 50% (v/v) ethylene glycol/water. Curves correspond to measurements at +25, +5, −10, −25, −40, −50, −60, −70, and −80 °C. UV maxima are at 539 and 583 nm, CD maxima at 533 and 594 nm.

oppositely signed, almost symmetrical bands with maxima at 533 and 594 nm and rotatory strengths, at −80 °C, of, respectively, -33.6×10^{-39} and $+31.5\times10^{-39}$ cgs units. Sufficient concentrations of both dye and cyclodextrin are necessary for the formation of what looks very much like an exciton coupling effect. In solutions with either a low γ-cyclodextrin concentration (e.g., 10^{-3} M in the presence of 6×10^{-4} M DODC) or dye concentration (10^{-5} M with 10^{-2} M γ-cyclodextrin) couplet formation is almost negligible even at −80 °C.

Since neither temperature changes nor changes in the dye or cyclodextrin concentration affect the position of the dimer band in the UV at 539 nm, we are dealing with basically the same dimer geometry throughout the experiment. On the other hand, the strong absorptions observed in the CD spectra indicate a chiral distortion of the dimer brought about by the interaction with γ-cyclodextrin. A structural model that explains all the observed phenomena and is in line with what is known about cyclodextrin host–guest complexes is depicted schematically in Figure 3. According to this model γ-cyclodextrin and DODC form a 2:2 inclusion complex with the dye dimer being trapped inside the channel formed by two cyclodextrin molecules. Chiral interaction between host and guest results in a twist of the dye monomers against each other, whose magnitude cannot be ascertained without much more work (according to the UV data it is rather small) but whose absolute sense is that shown in Figure 3.

X-ray analyses of several α-cyclodextrin complexes have revealed the existence of hydrogen-bridged dimers with the relative orientation of the cyclodextrin monomers being dependent on the guest molecules: head-to-tail dimers are found in the complex formed with methyl orange,[4] while, in complexes with metal iodides[5] or, recently, in a mixed-sandwich iron complex,[6] the cyclodextrin monomers are bridged head-to-head.

The difference between these two types of dimers is fundamental: following the oligosaccharide chain (e.g., in the 1 → 4 direction of the glycosidic bonds) the sense of rotation with respect to the symmetry axis is inverted when passing through the channel of the head-to-head dimer, a consequence of the dihedral symmetry of the host (D_8 in the case of γ-cyclodextrin). In the head-to-tail dimer, on the other hand, (C_8 symmetry), it stays the same. It follows that a guest molecule inside a cyclodextrin dimer of the first kind will experience opposite chiral forces, such as twists in opposite directions, in the two halves of the host. It is reasonable to assume, therefore, that the DODC dimer **1** observed through its chiroptic properties is of the twisted geometry shown in Figure 3 and that the reason for this is the head-to-head dimerization of the two cyclodextrin monomers.

Correlation between the absolute chirality of the DODC dimer in Figure 3 and the shape of the CD couplet is straightforward. A preliminary calculation on the basis of an extended dipole model[7] and using a distance between the planes of the dye molecules of 400 pm gave an exciton splitting of 2500 cm^{-1}. This value should be compared to the energy difference of 1900 cm^{-1} between the two excited states leading to CD bands at 533 and 594 nm.[8] For twist angles of 3 and 5° the calculated rotatory strengths for the two exciton states are ±11 and $\pm20\times10^{-39}$ cgs units, respectively. These values are an indication that the proposed model is able to account for the observed spectral properties. More elaborate calculations are in progress.

Received: January 11, 1991 [Z 4377 IE]
German version: *Angew. Chem. 103* (1991) 889

[1] F. P. Schäfer in F. P. Schäfer (Ed.): *Dye Lasers*, Springer, Berlin 1976, p. 1.
[2] K. Kasatani, M. Ohashi, M. Kawasaki, H. Sato, *Chem. Lett.* 1987, 1633; K. Kasatani, M. Ohashi, H. Sato, *Carbohydr. Res. 192* (1989) 197; M. Ohashi, K. Kasatani, H. Shinohara, H. Sato, *J. Am. Chem. Soc. 112* (1990) 5824.
[3] The slight increase of the extinction coefficient compared to that of Figure 1 ($lg\varepsilon_{539} = 5.4$ vs. 5.25) is probably due to the better solubility of the dye in ethylene glycol, which influences specimen preparation.
[4] K. Harata, *Bull. Chem. Soc. Jpn. 49* (1976) 1493.
[5] M. Noltemeyer, W. Saenger, *J. Am. Chem. Soc. 102* (1980) 2710.
[6] B. Klingert, G. Rihs, *Organometallics 9* (1990) 1135.
[7] The transition moment was approximated by two opposite charges, of 0.21 *e* each, located at a distance of 1000 pm in the long axis of the dye monomer.
[8] Actually, the two states will be closer in energy because the oppositely signed CD bands tend to shift the maxima apart.

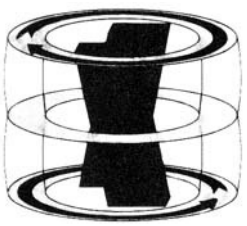

Fig. 3. Schematic drawing of the host–guest complex formed between two γ-cyclodextrin molecules and **1**. It shows the twisted dye aggregate inside the channel formed by the two γ-cyclodextrin monomers. The arrows indicate the torque exerted on the dye dimer by the two cyclodextrin monomers. They are opposite, leading to the observed chirality of the dye aggregate, if the two host monomers are joined head-to-head.

Tricarbonyl-η^6-(3,4-dimethylenecyclobutene)chromium(0), a Second Isomer of [(Benzene)Cr(CO)$_3$]

By *Doris Rau* and *Ulrich Behrens**

Dedicated to Professor Erwin Weiss on the occasion of his 65th birthday

Dimethylenecyclobutene **1**, like fulvene **2**, is a monocyclic isomer of benzene with three conjugated double bonds. **1**

[*] Prof. Dr. U. Behrens, Dipl.-Chem. D. Rau
Institut für Anorganische und Angewandte Chemie der Universität
Martin-Luther-King-Platz 6, W-2000 Hamburg 13 (FRG)

and **2**, which have found considerable theoretical interest in the past,[1-3] are, according to MO calculations, polar compounds.[4]

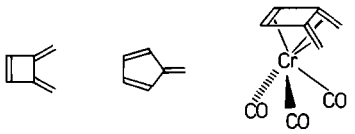

1 **2** **3**

By reaction of **1** with $[Cr(CH_3CN)_3(CO)_3]$ in pentane we have now been able to obtain the first transition metal complex of **1**, namely complex **3**, in which, as confirmed by an X-ray structure analysis (Fig. 1),[6] all six C atoms of the ligand are coordinated.[5] As in [(fulvene)$Cr(CO)_3$],[7] the two exocyclic C–C bonds are bent strongly (32°) from the ring plane, thus enabling a good interaction of the exocyclic π bonds with the chromium atom. The $Cr(CO)_3$ group is so

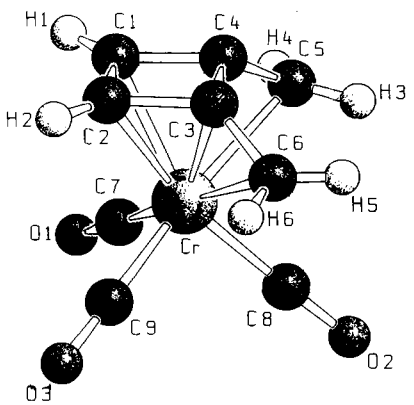

Fig. 1. Structure of **3** in the crystal. Clearly recognizable is the bending of the two exocyclic bonds (32°). Important bond lengths [Å] and angles [°]: Cr–Cl 2.186(2), Cr–C2 2.188(2), Cr–C3 2.041(2), Cr–C4 2.036(2), Cr–C5 2.318(2), Cr–C6 2.323(3), Cr–C7 1.848(2), Cr–C8 1.871(2), Cr–C9 1.864(2), C1–C2 1.394(4), C1–C4 1.459(3), C2–C3 1.469(3), C3–C4 1.490(3), C4–C5 1.372(3), C3–C6 1.371(3); C7–Cr–C8 91.7(1), C7–Cr–C9 88.1(1), C8–Cr–C9 (92.3(1), C2–C1–C4 91.9(2), C1–C2–C3 91.9(2), C2–C3–C4 87.8(2), C3–C4–C1 88.5(2), C2–C3–C6 129.7(2), C1–C4–C5 129.7(2), C4–C3–C6 125.3(2), C3–C4–C5 125.1(2); angle between the planes C1/2/3/4 and C3/4/5/6 40.6(1).

arranged that a CO ligand lies in the projection between the two exocyclic C–C bonds. A rotation of the $Cr(CO)_3$ group through 180°—this conformation is realized in [(fulvene)$Cr(CO)_3$][7]—would lead to superposition of two CO ligands and the two exocyclic C–C bonds. The C–C distances in the ligand are only slightly influenced by the coordination of the $Cr(CO)_3$ group (compare: dimethylenecyclobutene[3]). The three double bonds are found to be only about 3 pm longer, the three single bonds about 1 pm shorter. Thus, the interaction between chromium atom and ligand is apparently not very strong. The $Cr(CO)_3$ group has C_s symmetry. Two OC–Cr–CO angles are 92°, the other 88°.

That the dimethylenecyclobutene ligand is in fact not bound tightly is demonstrated by the reaction of **3** with trimethylphosphane, which results in cleavage of **1** and formation of $[Cr(CO)_3(PMe_3)_3]$. The [(fulvene)$Cr(CO)_3$] complex reacts differently, namely with addition of the phosphane to the exocyclic C atom.[7]

Experimental

All operations were carried out under nitrogen. A suspension of tris(acetonitrile)tricarbonylchromium (1.35 g, 5.2 mmol) in pentane (30 mL) was treated with ca. 1 g (13 mmol) of dimethylenecyclobutene [8] and the resulting mixture boiled under reflux for 4 h. After removal of the solvent in a vacuum, the residue was taken up in 20 mL of pentane and filtered. On cooling to 0 °C the complex **3** crystallized in the form of orange colored platelets. Yield 400 mg (36%). Spectroscopic data: IR (KBr): $\tilde{\nu}$[cm^{-1}] = 1994, 1950, 1883 (CO); ^{1}H NMR (400 MHz, C_6D_6, TMS): δ = 4.58 (s, 2H; CH), 2.58, 1.96 (d, ^2J = 2.3 Hz, each 2H; CH_2); MS (70 eV): *m/z* 214 ($M^{\oplus}$, 14%), 186 ($M^{\oplus}$ − CO, 10), 158 ($M^{\oplus}$ − 2CO, 12), 130 ($M^{\oplus}$ − 3CO, 40), 52 ($Cr^{\oplus}$, 100).

Received: October 25, 1990 [Z 4251 IE]
German version: *Angew. Chem. 103* (1991) 847
Publication delayed at authors' request

CAS Registry numbers:
1, 5291-90-7; **3**, 133777-09-0; $[Cr(CH_3CN)_3(CO)_3]$, 16800-46-7.

[1] B. A. W. Coller, M. L. Heffernan, A. J. Jones, *Austr. J. Chem. 21* (1968) 1807.
[2] J. Waite, M. G. Papadopoulos, *Z. Naturforsch. A 40* (1985) 142.
[3] R. D. Brown, P. D. Godfrey, B. T. Hart, A. L. Ottrey, M. Onda, M. Woodruff, *Austr. J. Chem. 36* (1983) 639.
[4] R. D. Brown, F. R. Burden, *Chem. Commun. 1966*, 448.
[5] An η^2-coordinated complex of **1** is known: R. B. King, C. A. Harmon, *J. Am. Chem. Soc. 98* (1976) 2409. Also known are $Cr(CO)_3$ complexes of a higher homologue, a substituted *ortho*-quinodimethane. Here, two cyclic and one exocyclic double bond are coordinated: M. Yalpani, R. Benn, R. Goddard, G. Wilke, *J. Organomet. Chem. 240* (1982) 49. *ortho*-Quinodimethane-chromium complexes are also discussed as important intermediates: E. P. Kündig, G. Bernardinelli, J. Leresche, P. Romanens, *Angew. Chem. 102* (1990) 421; *Angew. Chem. Int. Ed. Engl. 29* (1990) 407.
[6] Single crystals from pentane: a = 6.355(1), b = 7.255(1), c = 9.940(2) Å; α = 86.74(1), β = 81.40(1), γ = 79.66(1)°; V = 445.6(2) Å^3; Z = 2; ϱ_{calcd} = 1.596 g cm^{-3}; $P\bar{1}$ (No. 2); crystal dimensions 0.8 × 0.3 × 0.2 mm; measuring range 5° < 2θ < 55°; 2008 independent reflections, 1760 observed with $F > 6\sigma(F)$; anisotropic temperature factors for the non-hydrogen atoms, H atoms isotropic with d(C–H) = 96 pm; 142 refined parameters; R = 0.032, R_w = 0.033. Further details of the crystal structure determination are available on request from the Fachinformationszentrum Karlsruhe, Gesellschaft für wissenschaftlich-technische Information mbH, W-7514 Eggenstein-Leopoldshafen 2 (FRG), on quoting the depository number CSD-55146, the names of the authors, and the journal citation.
[7] O. Koch, F. Edelmann, U. Behrens, *Chem. Ber. 115* (1982) 1313.
[8] W. D. Hustman, H. J. Wristers, *J. Am. Chem. Soc. 89* (1967) 342.

A Tetrathiotrimethylenemethane Derivative**

By *Martin R. Bryce,* Malcolm A. Coffin, Michael B. Hursthouse* and *Mohammed Mazid*

A major contemporary challenge facing the organic chemist is the synthesis of high-spin or ferromagnetic systems. Many theoretical models have been proposed for obtaining ferromagnetically interacting spins in organic solids,[1-7] and in this context the study of trimethylenemethane (TMM) derivatives is of considerable interest.[8-14] TMM is a triplet diradical which is relatively stable, considering it is a "Y-antiaromatic", 4π-electron structure.[15] It is known that the thermal stability of TMM is enhanced by its incorporation into a five-membered ring (i.e. a 2-alkylidene-1,3-cyclopentadiyl derivative)[9, 16] and theoretical calcula-

[*] Dr. M. R. Bryce, M. A. Coffin
Department of Chemistry, University of Durham
Durham DH1 3LE (UK)
Professor M. B. Hursthouse, Dr. M. Mazid
Department of Chemistry
Queen Mary and Westfield College
Mile End Road, London E1 4NS (UK)

[**] This work was supported by the Science and Engineering Research Council. We thank *Y.-L. Chang* and *L. H. Sutcliffe* for the ESR spectra.

tions show that alkylthio- and dialkylamino-substituents stabilize triplet TMM relative to both singlet TMM and singlet methylenecyclopropane.[11]

In this communication we describe the synthesis, X-ray structure and reactions of the novel heterocycle **2** in which the TMM framework is both incorporated into a five-membered ring and is tetrathio-substituted. **2** is, in some ways,

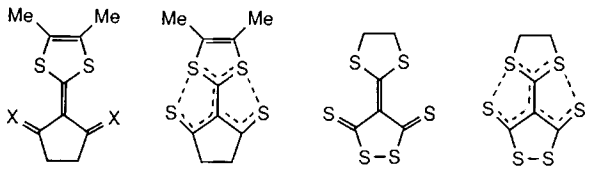

1, X=O
2, X=S

2' **3** **3'**

structurally related to compound **3**, which has recently been synthesized using a completely different methodology by *Wudl* and co-workers.[12] However, there are striking differences in the reactivity of **2** and **3**.

The reaction of 4,5-dimethyl-2-methylthio-1,3-dithiolium iodide[17] and the anion of 1,3-cyclopentanedione, under conditions described previously for analogous reactions,[18] yielded the diketone **1** (48% yield, m.p. 216–218 °C), which on thionation with phosphorus pentasulfide (anhydrous benzene, 50 °C, 2 h) afforded the title compound **2** as orange crystals (58% yield, m.p. > 340 °C; λ_{max} (CH_2Cl_2) = 262, 370, 464 nm; δ_H ($CDCl_3$) = 3.31 (s, 4H) and 2.49 (s, 6H); δ_C ($CDCl_3$) = 205.0, 171.7, 143.2, 131.4, 47.8 and 13.3).

values; (iii) the S···S distances (S1–S3 and S2–S4) are considerably shorter (by ca. 0.7 Å) than the sum of the van der Waals radii of two S atoms; (iv) the C7–C9 bond length of 1.328 Å is normal for a C=C double bond, which implies that the two π electrons of this bond are not involved to any extent in the delocalized system in **2'**. Molecule **2** is essentially planar but with a small amount of puckering at the ethylene bridge of the dithione ring. A packing diagram reveals that molecule **2** forms overlapping dimers in the solid state within which there are two relatively short intermolecular non-bonding S···S contacts (viz. S3–S4' = 3.912 Å and S1–S4' = 3.960 Å) (Fig. 1, right).

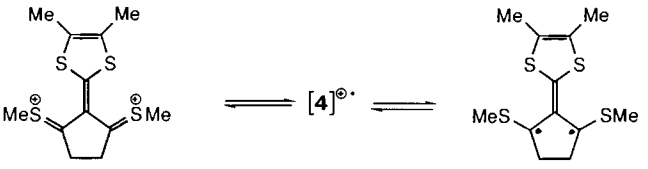

4 **5**

Wudl et al. observed that compound **3** did not react with methyl iodide, either neat at room temperature or in refluxing acetone.[12] In marked contrast to this, both thioxo sulfur atoms of compound **2** are readily methylated by methyl iodide in dichloromethane at 20 °C to yield the air-stable dication salt **4** (black powder, 90% yield, m.p. 119–125 °C (decomp.); λ_{max} (CH_2Cl_2) = 295 and 461 nm). This observation is entirely consistent with the X-ray data which imply that compound **2** is less aromatic than compound **3**.

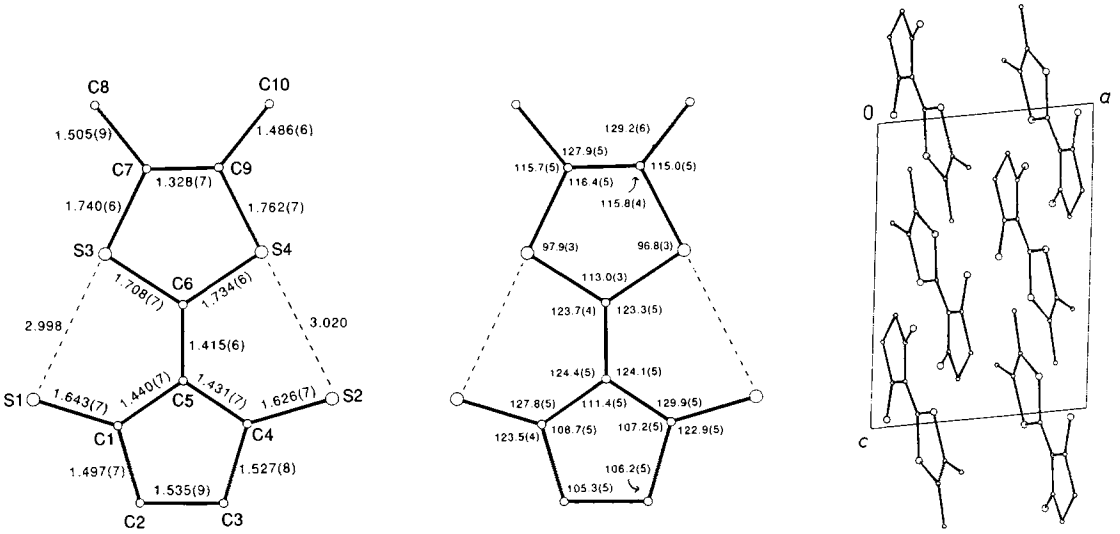

Fig. 1. Structure of **2** in the crystal with bond lengths (left) and angles (middle). Typical bond lengths are: C=S 1.55 Å [21], C–S 1.82 Å [21], S···S (van-der-Waals distance) 3.7 Å [21, 22]. Right: Unit cell of **2** viewed along the *b* axis.

The X-ray crystal structure[19] of **2** (Fig. 1) establishes that the molecule is best represented as a hybrid of dithione structure **2** and the heteroaromatic 10π-electron 1,2-dithiolo-1,2-dithiole structure **2'**. *Wudl*'s compound **3** exhibits more pronounced 10π-electron delocalization (**3'**).[12] Intramolecular bond distances and angles for **2** are shown in Figure 1. Notable features are as follows: (i) while there is considerable shortening of both the C1–C5 and C4–C5 bonds, they are significantly longer than the C5–C6 bond; (ii) the C=S bond lengths are longer (by ca. 0.07 Å) than the accepted literature

Cyclic voltammetry of dication **4** revealed two reversible one electron reductions at $E_1^{1/2} = +0.34$ and $E_2^{1/2} = +0.61$ V vs Ag/AgCl.[20] These data clearly point to the formation in solution of the tetrathiotrimethylenemethane diradical **5**, for which delocalized structures comprising a 1,3-dithiolyl radical can be drawn. Attempts to detect diradical **5** by ESR spectroscopy have, to date, been unsuccessful. The strong ESR signal obtained in dichloromethane solution from reduction of dication **4** is assigned to the radical cation $4^{\bullet\oplus}$. The spectra at 293 K and 153 K are

featureless and the g value of 2.0059 is consistent with spins partially localized at the sulfur atoms.

Received: January 2, 1991 [Z 4369 IE]
German version: *Angew. Chem. 103* (1991) 867

CAS Registry numbers:
1, 134177-77-8; **2**, 134177-78-9; **4**, 134177-79-0; **5**, 134177-80-3; 1,3-cyclopentanedione, 3859-41-4; 4,5-dimethyl-2-methylthio-1,3-dithiolium iodide, 105580-73-2.

[1] H. M. McConnell, *J. Phys. Chem. 39* (1963) 1910.
[2] N. Mataga, *Theor. Chim. Acta 10* (1968) 372.
[3] A. A. Ovchinnikov, *Theor. Chim. Acta 47* (1978) 297.
[4] T. J. LePage, R. Breslow, *J. Am. Chem. Soc. 109* (1978) 6412.
[5] J. S. Miller, A. J. Epstein, W. A. Reiff, *Chem. Rev. 88* (1988) 201.
[6] E. Dormann, M. J. Nowak, K. A. Williams, R. O. Angus, Jr., F. Wudl, *J. Am. Chem. Soc. 109* (1987) 2594.
[7] Proceedings of The Symposium on Ferromagnetic and High Spin Molecular Based Materials, Dallas, April 1989: *Mol. Cryst. Liq. Cryst. 176* (1989).
[8] J. E Berson, *Acc. Chem. Res. 11* (1978) 446.
[9] J. A. Novak, R. Jain, D. A. Dougherty, *J. Am. Chem. Soc. 111* (1990) 7618.
[10] M. Keshavarz n.,bersD. Cox, R. O. Angus, F. Wudl, *Synthesis 1988*, 641.
[11] F. Closs, W. Breimaier, W. Frank, R. Gompper, A. Hohenester, *Synth. Met. 29* (1989) E 537.
[12] F. Wudl, G. Srdanov, B. Rosenau, D. Wellman, K. Williams, S. D. Cox, *J. Am. Chem. Soc. 110* (1988) 1316.
[13] F. Adams, R. Gompper, A. Hohenester, H.-U. Wagner, *Tetrahedron Lett. 29* (1988) 6921.
[14] R. Bushby, C. Jarecki, *J. Chem. Soc. Perkin Trans. 1 1990*, 2335.
[15] P. Dowd, *Acc. Chem. Res. 5* (1972) 242.
[16] J. A. Berson, *Acc. Chem. Res. 11* (1978) 446.
[17] A. J. Moore, M. R. Bryce, *J. Chem. Soc. Perkin Trans. 1 1991*, 157.
[18] R. Gompper, E. Kutter, *Chem. Ber. 98* (1965) 1365.
[19] a) X-ray structure analysis of **2**: $C_{10}H_8S_4$; $M_r = 258.45$; monoclinic space group $P2_1/n$; $a = 7.634(3)$, $b = 14.018(3)$ Å; $c = 10.561(3)$ Å; $\beta = 96.53(3)°$, $V = 1122.84$ Å^3; $Z = 4$; $\mu = 7.7$ cm^{-1}; $\varrho_{calcd} = 1.53$ g cm^{-3}; $T = 297$ K; $\lambda(Mo_{K\alpha}) = 0.71069$; $R = 0.056$; $R_w = 0.048$ for 3665 unique observed reflections. b) Further details of the crystal structure investigations are available on request from the Director of the Cambridge Crystallography Data Centre, University Chemical Laboratory, Lensfield Road, Cambridge, CB2 1EW (UK), on quoting the full journal citation.
[20] Data are relative to Ag/AgCl, platinum electrode, compound **4** (ca. 1×10^{-5} M) with electrolyte tetraethylammonium hexafluorophosphate (0.01 M) in dry dichlormethane under argon, 20°C, initial reductive scan, rate 100 mVs^{-1}, using a BAS 100 Electrochemical Analyser. The C.V. was unchanged after continuous cycling for 0.5 h between 1.0 and 0.0 V. We note that the redox potentials of compound **4** are similar to those of tetrathiafulvalene ($E_1^{1/2} = +0.34$, $E_2^{1/2} = +0.78$ V measured under identical conditions) and we are, therefore, pursuing the possibility of forming organic conductors based on system **4**.
[21] J. Emsley: *The Elements*, Oxford University Press, Oxford 1989, p. 180.
[22] See also: S. C. Nyburg, C. H. Faerman, *Acta Crystallogr. B41* (1985) 274 and references cited therein.

Synthesis and Stereoselective Reactions of (*R*)-α-Sulfonyloxynitriles**

By *Franz Effenberger** and *Uwe Stelzer*

Dedicated to Professor Hans Georg von Schnering on the occasion of his 60th birthday

(*R*)- and (*S*)-cyanohydrins are accessible via the enzyme-catalyzed addition of hydrocyanic acid to aldehydes.[1] They are useful, inter alia, for the production of enantiomerically pure α-hydroxycarboxylic acids[1c, 2] and β-aminoalcohols.[1a, 2] We report here on an important extension of the synthetic potential of optically active cyanohydrins by conversion of the hydroxy group into a good leaving group. Of particular interest are reactions of the cyanohydrin derivatives in which the nitrogen of the cyano group remains in the molecule, since compounds of this type are not directly accessible via α-amino- or α-hydroxycarboxylic acids.

Whereas stereoselective nucleophilic substitution in the α-position of carboxylic acids and carboxylates presents few difficulties,[3] very little is known about a corresponding reaction of α-substituted nitriles.[4] Starting from optically active nitriles with a leaving group in the α-position, only α-halonitriles have so far been prepared,[4] but these readily racemize in the presence of halide ions liberated in substitution reactions.[4a] Optically active α-sulfonyloxynitriles, which should be considerably more stable configurationally on account of the less nucleophilic sulfonate leaving groups,[3] have so far not been described. By reaction of the optically active cyanohydrins (*R*)-**1** as starting compounds with the sulfonyl halides and anhydrides **2**, we have now been able to synthesize aliphatic and aromatic (*R*)-α-sulfonyloxynitriles (*R*)-**3** free of racemization and in good yields.

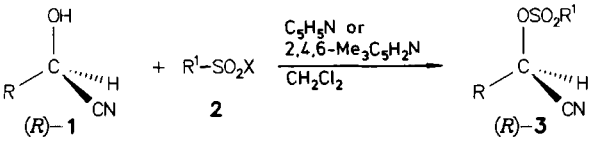

X = Hal, OSO_2R^1

R	R^1
Alkyl, Cyclohexyl	4-$CH_3C_6H_4$, CH_3, CF_3
Aryl	CH_3, CF_3

With aliphatic cyanohydrins the tosylates and methane- and trifluoromethanesulfonates were synthesized in pure form. In the case of aromatic cyanohydrins, however, the preparation of mesylates is possible, but trifluoromethanesulfonates could only be synthesized and allowed to react in situ. These findings are consistent with data given in the literature on racemic cyanohydrin sulfonates, according to which the aliphatic compounds can be distilled without decomposition, whereas, e.g., the tosylate of mandelic nitrile already decomposes at room temperature.[5]

So far, it has not been possible to develop a suitable method for the direct determination of the optical purity of the compounds (*R*)-**3**. No information about the enantiomeric excesses can be gleaned from the experimentally determined rotation values, which lie between + 20° and + 60°, because of a lack of data for comparison. That the sulfonylations of (*R*)-**1** leading to (*R*)-**3** proceed without racemization could be demonstrated by the reactions of the α-sulfonyloxynitriles (*R*)-**3** with nucleophiles outlined in Scheme 1. According to Scheme 1, the cyanohydrin derivatives (*S*)-**4**, α-(phthaloylamino)nitriles (*S*)-**5**, α-azidonitriles (*S*)-**6**, and aziridines (*S*)-**7** are readily accessible in optically active form from the compounds (*R*)-**3**.

The reactions (b) and (c) have so far only been carried out with the aliphatic α-sulfonyloxynitriles (*R*)-**3**, the reactions (a) and (d) with both aliphatic as well as aromatic α-sulfonyloxynitriles (*R*)-**3**. Already at room temperature the reaction of (*R*)-**3a** with potassium acetate leads in very good yields to the cyanohydrin acetate (*S*)-**4a**, the enantiomeric purity of which was estimated by comparative investigations[6] to be 96.1% *ee*. Since the (*R*)-**1a** employed had an enantiomeric

[*] Prof. Dr. F. Effenberger, Dipl.-Chem. U. Stelzer
Institut für Organische Chemie der Universität
Pfaffenwaldring 55, W-7000 Stuttgart 80 (FRG)

[**] Enzyme-Catalyzed Reactions, Part 11. This work was supported by the Bundesministerium für Forschung und Technologie and by the Fonds der Chemischen Industrie.—Part 10: F. Effenberger, M. Hopf, T. Ziegler, J. Hudelmayer, *Chem. Ber.*, in press.

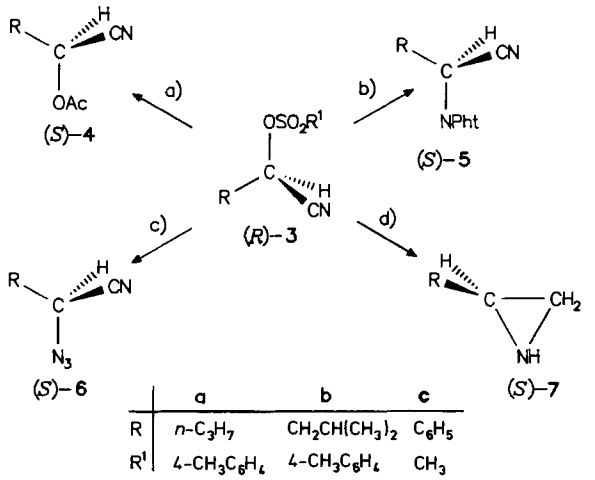

Scheme 1. a) (*R*)-**3a** + 1.5 mol CH_3CO_2K in dimethylformamide (DMF), 79 h, 20 °C; 84% (*S*)-**4a** (*ee* = 96%). b) (*R*)-**3a** + 1.5 mol potassium phthalimide in DMF, 6 d, 20 °C; 70% (*S*)-**5a** (*ee* = 93%). Pht = phthaloyl. c) (*R*)-**3b** + 1.5 mol KN_3 in DMF, 3 d, 20 °C; 78% (*S*)-**6b** ($[\alpha]_D^{20} = -36.1°$ (*c* = 0.77, CH_2Cl_2)). d) A solution of (*R*)-**3b** in Et_2O was added dropwise to a solution of $LiAlH_4$ in Et_2O at −80 °C; after warming to room temperature within 2 h the mixture was neutralized at −70 °C with K_2HPO_4/KH_2PO_4 buffer (pH 7); 64% (*S*)-**7b** ($[\alpha]_D^{20} = -16.8°$ (*c* = 5.39, EtOH)). (*R*)-**3c** was allowed to react under the same conditions; 56% (*S*)-**7c** ($[\alpha]_D^{20} = +31.7°$ (*c* = 2.59, $CHCl_3$)).

purity of 96.3% *ee*, it must be concluded that the conversion of (*R*)-**1a** into (*R*)-**3a** proceeds almost free of racemization and the nucleophilic substitution of (*R*)-**3a** leading to (*S*)-**4a** solely involves an S_N2-mechanism. Since aliphatic (*S*)-cyanohydrins, in contrast to the (*R*)-cyanohydrins, are not accessible via the enzyme-catalyzed addition of hydrocyanic acid to aldehydes,[1c] this route provides a valuable extension to the synthesis of aliphatic (*S*)-cyanohydrins.

The reactions with potassium phthalimide leading to *N*-phthaloyl-protected α-aminonitriles (*S*)-**5**[7] and with potassium azide leading to the α-azidonitriles (*S*)-**6** also take place at room temperature. α-Azidonitriles have thus far not yet been described in the literature, neither as (*R*)- nor as (*S*)-enantiomers. That the substitutions of (*R*)-**3b** to give (*S*)-**6b** also proceed stereoselectively, was confirmed by hydrogenation of (*S*)-**6b** in the known (2*S*)-1,2-diamino-4-methylpentane.[8] The enantiomeric excess in (*S*)-**5a** was determined with NMR-shift reagents to be 93% *ee*.

Aziridines[9] are of equally great importance as intermediates in synthesis as oxiranes. The ready accessibility of the compounds (*R*)-**3** opened up the possibility of preparing optically active aziridines (*S*)-**7** in a simple way by the method of *Ohta* et al.,[4b] via hydrogenation of the cyano group with $LiAlH_4$, followed by intramolecular substitution. The optical purity of the compounds (*S*)-**7b** and (*S*)-**7c** obtained were determined by comparison of their rotation values with data quoted in the literature,[10] though in the hydrogenation of (*R*)-**3c** there arises the problem that difficultly separable 2-phenylethylamine is formed as by-product.

α-Sulfonyloxynitriles (*R*)-**3** show a pronounced dependence on structure in nucleophilic substitutions: the aliphatic compounds react with potassium acetate and other nucleophiles exclusively with inversion of configuration, the aromatic compounds, on the other hand, generally with racemization. Partial Walden inversion is found also upon reaction of the aromatic compounds with cesium acetate but only when trifluoromethanesulfonates are employed. A favoring of the S_N2-reaction is also observed in the case of the aromatic compounds by way of an intramolecular reaction with formation of a three-membered ring, as follows from the reaction of (*R*)-**3c**, which gives (*S*)-**7c** in good optical yields. An explanation for this reaction behavior of the α-sulfonyloxynitriles of aromatic cyanohydrins could possibly be the additional stabilization of the benzyl cations by the nitrile group in the α-position.[11]

Received: February 8, 1991 [Z 4433 IE]
German version: *Angew. Chem. 103* (1991) 866

CAS Registry numbers:
1a, 10021-63-3; **1b**, 110905-95-8; **1c**, 10020-96-9; **3a**, 133870-86-7; **3b**, 133870-87-8; **3c**, 133870-88-9; **4a**, 129313-21-9; **5a**, 133908-38-0; **6b**, 133870-89-0; **7b**, 23852-57-5; **7c**, 25260-42-8.

[1] a) W. Becker, H. Freund, E. Pfeil, *Angew. Chem. 77* (1965) 1139; *Angew. Chem. Int. Ed. Engl. 4* (1965) 1079; b) F. Effenberger, T. Ziegler, S. Förster, *ibid. 99* (1987) 491 and *26* (1987) 458; c) F. Effenberger, B. Hörsch, S. Förster, T. Ziegler, *Tetrahedron Lett. 31* (1990) 1249; d) U. Niedermeyer, M.-R. Kula, *Angew. Chem. 102* (1990) 423; *Angew. Chem. Int. Ed. Engl. 29* (1990) 386; e) U. Niedermeyer, M.-R. Kula, DE-A 3823866 (July 14, 1988); E. Wehtje, P. Adlercreutz, Bo Mattiasson, *Biotechnol. Bioeng. 36* (1990) 39.

[2] T. Ziegler, B. Hörsch, F. Effenberger, *Synthesis 1990*, 575.

[3] a) F. Effenberger, U. Burkard, J. Willfahrt, *Liebigs Ann. Chem. 1986*, 314, and references cited therein; b) U. Burkard, F. Effenberger, *Chem. Ber. 119* (1986) 1594.

[4] a) I. A. Smith, *Ber. Dtsch. Chem. Ges. 71* (1938) 634; b) K. Ichimura, M. Ohta, *Bull. Chem. Soc. Jpn. 43* (1970) 1443.

[5] a) R. M. Dodson, H. W. Turner, *J. Am. Chem. Soc. 73* (1951) 4517; b) J. D. London, I. Wellings, *J. Chem. Soc. (London) 1959*, 1780.

[6] F. Effenberger, B. Gutterer, T. Ziegler, E. Eckhardt, R. Aichholz, *Liebigs Ann. Chem. 1991*, 47.

[7] a) Yu M. Shafran, V. A. Bakulev, V. S. Mokrushin, *Usp. Khim. 58* (1989) 250; b) J. Jenni, H. Kühne, B. Prijs, *Helv. Chim. Acta 45* (1962) 1163.

[8] a) S. Schnell, P. Karrer, *Helv. Chim. Acta 38* (1955) 2036; b) H. Brunner, M. Schmidt, G. Unger, *Eur. J. Med. Chem. 20* (1985) 509.

[9] J. A. Deyrup in A. Hassner (Ed.): *Heterocyclic Compounds, Vol. 42, Part 1*, Wiley, New York 1983, p. 1 ff..

[10] a) (*S*)-**7b**: H. Rubinstein, B. Feibush, E. Gil-Av, *J. Chem. Soc. Perkin Trans. 2 1973*, 2094; see also [4b]; b) (*S*)-**7c**: S. Fujita, K. Imamura, H. Nozaki, *Bull. Chem. Soc. Jpn. 44* (1971) 1975.

[11] a) P. G. Gassman, T. T. Tidwell, *Acc. Chem. Res. 16* (1983) 279; b) P. G. Gassman, J. J. Talley, K. Saito, T. L. Guggenheim, M. M. Doherty, D. A. Dixon, *Prepr. Am. Chem. Soc. Div. Pet. Chem. 28* (1983) 334.

Ligand-Stabilized Bimetallic Colloids Identified by HRTEM and EDX**

By *Günter Schmid*,* *Andreas Lehnert*, *Jan-Olle Malm*, and *Jan-Olov Bovin*

Dedicated to Professor Hans-Georg von Schnering on the occasion of his 60th birthday

Bimetallic clusters and colloids are of special interest for two reasons. Firstly, they may serve as models for studying the formation of different alloys. Secondly, it is possible to save precious metal, like Pt, by optimizing the synthetic conditions so that only very thin surface layers occur.

Miner et al.[1] described the synthesis of gold–platinum and palladium–platinum alloys as monodisperse sols by

[*] Prof. Dr. G. Schmid, Dipl.-Chem. A. Lehnert
Institut für Anorganische Chemie der Universität
Universitätsstrasse 5–7, W-4300 Essen 1 (FRG)
Dr. J. O. Bovin, M. Sc. J.-O. Malm
National Center for HREM, Inorganic Chemistry 2
Chemical Center, P.O. Box 124, S-22100 Lund (Sweden)

[**] *G. S.* and *A. L.* are grateful to the Fonds der Chemischen Industrie for financial support. *J.-O. B* and *J.-O. M.* thank the Swedish Natural Science Research Council and the Swedish National Energy Administration. HRTEM = high-resolution transmission electron microscopy; EDX = energy disperse X-ray microanalysis.

simultaneous reduction of corresponding salt mixtures in various molar ratios. They asserted that formation of gold–platinum alloys occurs at any atomic ratio, even if the two metals show a broad miscibility gap between 2 and 85 wt.-% Au.[2] The homogeneous character of the various Au/Pt alloys was suggested to be proven by means of optical spectra, sedimentation measurements, and electron microscopy investigations. The particle sizes used in the relevant investigations varied between 3–6 nm. The variations in the d_{111}-spacing could not be determined accurately enough by transmission electron microscopy (TEM) to confirm the homogeneity of the particles being as claimed in the paper by *Miner* et al.

This paper describes the synthesis of ligand-stabilized bimetallic colloids and will identify the shell structure of such particles by high-resolution transmission electron microscopy (HRTEM) and energy dispersive X-ray (EDX) microanalysis.

Gold colloids with a diameter of 18 nm[3, 4] can be covered by platinum or palladium shells, if an aqueous solution of the colloids is added to a solution of H_2PtCl_6 or H_2PdCl_4 and H_3NOHCl. The original red color of the gold colloid then changes to brown-black. Addition of *p*-$H_2NC_6H_4SO_3Na$ stabilizes the generated particles in the same manner as P(*m*-$C_6H_4SO_3Na)_3$ the gold colloids,[3] so they can be isolated in the solid state. This kind of stabilization differs characteristically from former methods in the literature when colloids were more or less embedded into various polymers. The ligands used here behave like in complexes and clusters and impart the colloids "molecular" character. The colloid shows a metallic luster. The HRTEM studies of the gold–platinum and gold–palladium particles show that there are considerable differences between their structures even if the size is uniform (ca. 35 nm) in both cases.

In the case of the Au/Pt particles we observe uniform heterogeneous agglomerates, which have an average gold content of around 15 atomic%. These agglomerates are built up by a gold core surrounded by platinum crystals of about 5 nm. They are connected together in a rather "open" way, as can be seen in Figure 1 (left). The EDX microanalysis shows clearly that the outer layer of small crystals consists of platinum (cf. Fig. 1, right). This is demonstrated by comparing the spectrum obtained by focusing the electron beam (diameter 30 nm) over the whole particle (lower left circle in Fig. 1, left), which affords information about both Au and Pt, with the one recorded when the beam only covers the outer 5 nm of the particle (the circle to the right in Fig. 1, left). The latter spectrum includes only signals from Pt, as presented in the Au and $Pt_{L\alpha}$ spectra compared in Figure 1 (right). The beam broadening (0.8 nm at 200 kV and 10 nm crystal thickness) is negligible in small particles of this thickness.

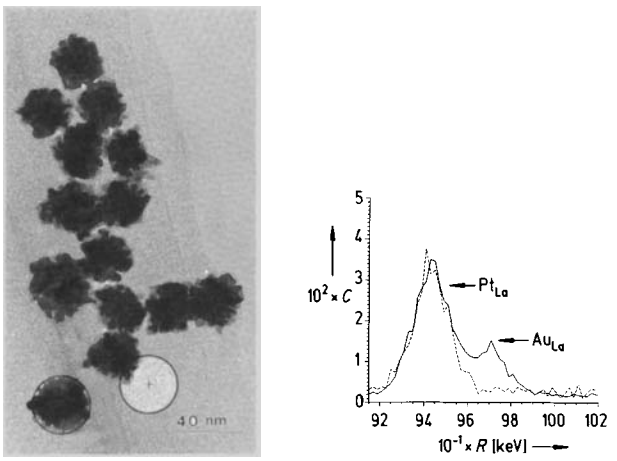

Fig. 1. Left: HRTEM image of gold/platinum particles supported on an amorphous carbon film. The selected EDX spectra (right) are recorded with the electron beam positioned as the circles indicate in the picture on the left. The counting time of the EDX spectrum recorded with the beam touching the edge of the particle is ten times longer than in the case of the centered beam. – – – edge of particle, — center of particle. C = count rate, R = measuring range, L_α signifies the electron transition from the M shell into the L shell.

The HRTEM images of the Au/Pt particles indicate that the growth of the outer Pt layer is preceded by a pregrowth of 5 nm small crystals of Pt. These small crystals are then added to the surface of the 18 nm large Au particles.

Laser-optical diffractograms of images of the 35 nm large particles show that the crystals constituting the whole particle can in principle be oriented in two different ways with respect to each other (Fig. 2, left). The particle marked **A** has almost all the small crystals oriented in the same crystallographic direction, as shown by the optical diffractogram of **A**.

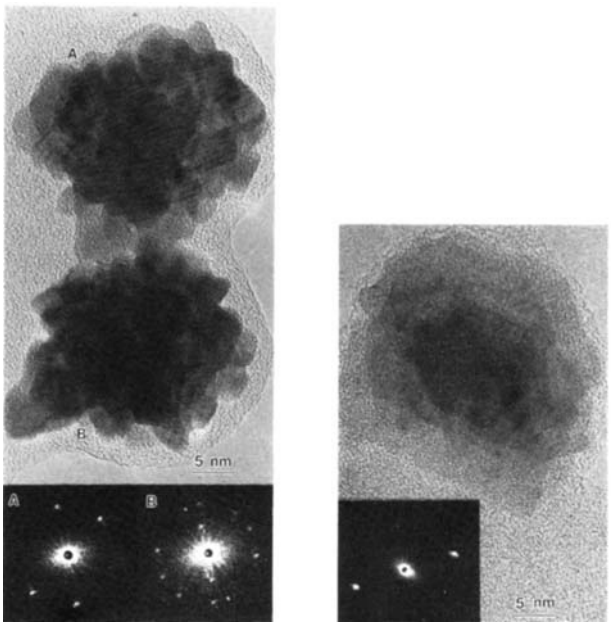

Fig. 2. Left: Two different types of Au/Pt particles imaged with HRTEM at 400 kV. The optical diffractogram of the whole particle **A** is shown below on the left and the corresponding one of **B** below on the right. Right: a structurally well-ordered Au/Pd particle imaged with HRTEM at 400 kV. The optical diffractogram of the whole particle is inserted.

On the other hand, the optical diffractogram of **B** shows a random orientation for the small Pt crystals making up the outer layer of the particle. The reason for the two kinds of intergranular structures is not fully understood but it may well depend on the structure of the 18-nm Au core. Earlier investigations[5] of the structure of gold colloids show that the structure can either be single crystal without defects or a multiply twinned structure. A single crystal structure of the core may well give rise to the particle type **A** if the Pt crystals add on epitaxial to the Au core, while the multiply twinned structure gives several possibilities to different orientations of the added-on Pt crystals.

In contrast to the gold platinum alloy, gold and palladium form a continuous series of solid solutions.[2] If an aqueous solution of H_2PdCl_4 is reduced by hydoxylamine in the presence of 18-nm gold colloids, followed by a complexation

with p-$H_2NC_6H_4SO_3Na$, gold/palladium colloids can be isolated as a silver grey, metallic looking precipitate. Such colloids are soluble in water giving a brown color.

HRTEM investigations of these colloids show different intergranular structural images than the Au/Pt combinations. Two different types of particles can be distinguished. In Figure 2, right, one particle with the whole structure ordered is shown, as indicated by the optical diffractogram inserted. A comparison of this particle with the Au/Pd particle **A** in Figure 2, left, shows that the Au/Pd particle has a smoother surface—most likely resulting in a smaller surface area. The dark nucleus of the Au/Pd particle can be interpreted as the gold core, which is surrounded by the lighter shell of well-ordered palladium atoms. This will turn up more clearly for the lighter Pd shell compared to Pt.

The second type of structure for the Au/Pd case is similar to the type **B** of Au/Pt in Figure 2 in such a way that the particle also gives an optical diffractogram of "polycrystalline" type (Fig. 3, left). The intergranular structure has also in this case a smoother surface compared to the Au/Pt case. The HRTEM image of the approximately spherical specimen also shows a darker core.

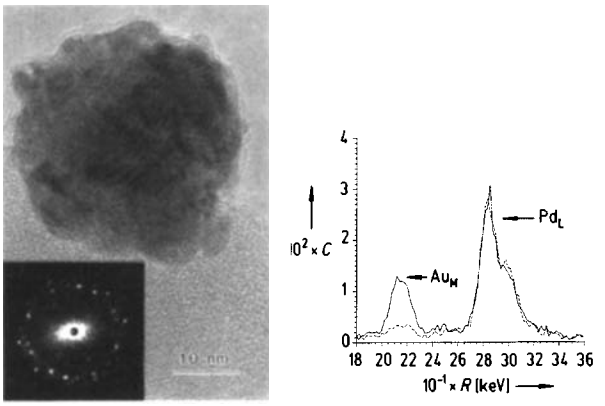

Fig. 3. Left: HRTEM image of a "polycrystalline" Au/Pd particle recorded at 400 kV and with the corresponding optical diffractogram inserted. Right: A comparison of EDX spectra recorded from a Au/Pd particle, with the electron beam positioned as the circles indicate in Figure 1. The counting time of the EDX spectrum recorded with the beam touching the edge of the particle is ten times longer than the centered case. --- particle edge, — particle center. C = count rate, R = measuring range, L and M signify electron transitions into the L and M shells, respectively, from higher states, not distinguishable if α or β.

The EDX spectrum of such a single particle shows a composition of about 17 atomic% of gold and 83 atomic% of palladium. Analyses of peripheral parts of the particle (cf. in Fig. 1) give a spectrum of almost pure palladium (cf. Fig. 3). The composition of the colloids varies only a little. The colloid shown in Figure 3 has a diameter of about 36 nm. As the nucleate gold colloids have an average diameter of 18.5 nm, the Au:Pd ratio is calculated to be between 1:5 and 1:6. This is in good agreement with analytical results, giving an average atomic ratio of about 1:5 for Au/Pd particles.

During the observation, using a beam current intensity of 20–40 Acm^{-2}, the particles were stable apart from some surface rearrangements, which can always be seen on metallic surfaces. The X-ray microanalyses were performed with a little less intense electron beam ($\sim 5\ Acm^{-2}$). In no case could any structural changes in the particles be observed.

The sequence of the metals can also be reversed in this kind of particles. For example, 15-nm palladium colloids can be prepared by treatment of $PdCl_2$ in hydrochloric acid solution with trisodium citrate. Tetrachloroauric acid is added to the colloidal solution and is then reduced by hydroxylamine to generate the outer shell of gold. The stabilization of such Pd/Au colloids by P(m-$C_6H_4SO_3Na)_3$ yields isolable colloids. Their color is like that of pure ligand-stabilized gold colloids.

From these investigations it can be assumed that bimetallic colloids can easily be prepared and stabilized. HRTEM and EDX have proven to be useful methods for establishing the structure of the layered colloids.

Experimental

Gold–platinum colloids: 1600 mL of completely demineralized water was heated to boiling in a 2 L beaker. 16 mL of a 1 per cent solution of $HAuCl_4$ (5.00 g Au/L) and 80 mL of a 1 per cent solution of trisodium citrate was added gradually with vigorous stirring. The solution was then kept boiling for another hour. Approximately 1500 mL of a ruby red gold sol containing particles of 18–19 nm in diameter, was obtained, as observed in many electron microscopic investigations. This gold colloid solution was stirred into a mixture of 116 mL of a 1 per cent solution of H_2PtCl_6 (5.00 g Pt/L) and 100 mL of 1 per cent solution of H_3NOHCl in 8 L of water and was then heated to 60 °C. In the course of 3 h the red color of the gold sol changed to the dark brown color of platinum colloids. To stabilize the particles, 50 mg of $H_2NC_6H_4SO_3Na$ was added to the solution. Concentration in a water-jet pump vacuum followed until coagulation began (decolorizing of the solution). The precipitate was separated by centrifugation (5000 revolutions per minute) and dried under vacuum.

Gold–palladium colloids: The gold sol, prepared by the procedure above, was diluted to 8 L in a 10 L beaker. In the course of 8 h 83 mL of a 0.037 molar solution of H_2PdCl_4 (6.6 g $PdCl_2$ and 7.5 mL of a 1 n HCl in 1 L of H_2O) and 100 mL of a 1 per cent solution of H_3NOHCl were simultaneously added dropwise. After 48 hours' stirring at room temperature 2 g of p-$H_2NC_6H_4SO_3Na$ was added, and an isolation procedure carried out as described above. The product consisted of silver-grey gold–palladium colloids, completely soluble in water.

Microanalysis and microscopy: The colloid was dispersed in methanol and transferred onto a holey carbon support film. The sample was then loaded into the microscope while still wet with methanol, and the high vacuum inside the microscope column was used to evaporate the solvent. The ligands stabilizing the colloids can be removed when the electron beam irradiates the area of observation. High resolution electron microscopy was performed with a JEM-4000EX, which was operated at an accelerating voltage of 400 kV and able to achieve a structural resolution of 0.16 nm. The energy dispersive X-ray (EDX) microanalysis was performed with a Link AN 10000 system coupled to a JEM-2000FX STEM-microscope with a beam focusing ability of 30 nm. The EDX spectra were evaluated with a software for thin foil analysis, Link RTS 2/FLS.

Received: Dezember 27, 1990 [Z 4356 IE]
German version: *Angew. Chem. 103* (1991) 852

[1] R. S. Miner, Jr., Namba, J. Turkevich, *Proc. VII. Intern. Congr. Catal.*, Elsevier, New York 1981.
[2] M. Hansen, *Consitutions of binary Alloys*, McGraw Hill, New York 1958.
[3] G. Schmid, A. Lehnert, *Angew. Chem. 101* (1989) 773; *Angew. Chem. Int. Ed. Engl. 28* (1989) 780.
[4] J. Turkevich, P. C. Stevenson, J. Hillier, *Discuss. Faraday Soc. 11* (1951) 55.
[5] J.-O. Bovin et al., unpublished.

The Structure of $IF_8^{\ominus}$**

By *Ali-Reza Mahjoub* and *Konrad Seppelt**

Dedicated to Professor Hans Georg von Schnering on the occasion of his 60th birthday

The only main group element heptafluoride reported so far, IF_7, forms an adduct with NOF which has been formulated as $NO^{\oplus}IF_8^{\ominus}$.[1] However, vibrational spectroscopic studies permitted no unequivocal conclusions to be drawn

[*] Prof. Dr. K. Seppelt, Dipl.-Chem. A.-R. Mahjoub
Institut für Anorganische und Analytische Chemie der Freien Universität Fabeckstrasse 34–36, W-1000 Berlin 33 (FRG)

[**] This work was supported by the Deutsche Forschungsgemeinschaft and the Fonds der Chemischen Industrie.

regarding the structure of the adduct. Coordination numbers greater than six are of interest since usually several structures are conceivable, and we are not always able to predict the correct one with our current model concepts. Thus, a pentagonal bipyramidal structure has been established for IF_7, but *nothing exact is known* about deviations from the ideal geometry (pseudorotation).[2] For the coordination number eight, generally two structures are discussed, the Archimedean square antiprism and the dodecahedron. The elucidation of the structure of salts with the anion $IF_8^{\ominus}$ is thus of fundamental importance, as this ion contains eight equal ligands, and non-bonding electron pairs or a d-orbital participation (as in the case of subgroup elements) do not need to be taken into consideration.

Other than previously described,[1] reaction of NOF and IF_7 takes place in the ratio 3:1 [Eq. (a)].

$$3\,NOF + IF_7 \longrightarrow \underset{\mathbf{1}}{[NO(NOF)_2]IF_8} \qquad (a)$$

Compound **1** can be recovered in the form of large colorless crystals by sublimation at $-20\,^{\circ}C$. However, the crystals still have a measurable vapor pressure at $-100\,^{\circ}C$, so that the X-ray diffraction had to be carried out at the lowest temperature achievable with our equipment ($-163\,^{\circ}C$).

The cation and anion moieties are significantly separated from each other. The shortest distances between the iodine atom and oxygen atoms are 380, 384, 394 and 398 pm. The cation moiety is a polymer of $NO^{\oplus}$ and NOF, in which the fluorine atoms are bridging (Fig. 1). Noteworthy is that the

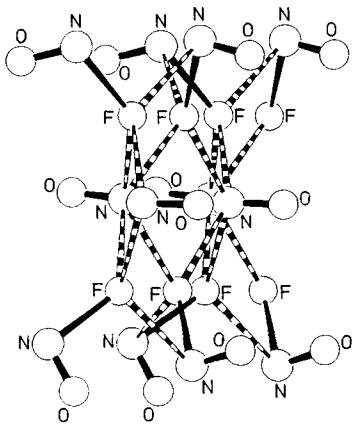

Fig. 1. Section of the cation moiety of **1**, Schakal plot. The structure consists of a layer of square-pyramidally surrounded nitrogen atoms (N–O 105.2–106.4(8), N···F 228.0–241.1 pm) and a double layer of pyramidal NX_3 units (N–O 102.3–17.5(8), N–F 184.2–203.0(8), N···F 241.0–260.5(8) pm).

nitrogen atoms bearing formal charges have a square-pyramidal geometry with apical oxygen atoms and four basal fluorine atoms.

Interestingly, the two crystallographically independent $IF_8^{\ominus}$ ions have square antiprismatic geometries (Fig. 2a), whose bond lengths and angles differ only very slightly. Apparently a regular antiprism is formed, i.e. all distances and all respective angles are of almost equal size. A regular antiprism is described by one distance and by only one angle, the latter determining the elongation or the flatness of the antiprism. The important angle here is the F–I–F angle between two neighboring fluorine atoms within one hemisphere; it is 73.3° (average of 16 values, Fig. 2b). This angle leads to an angle of 78.1° (average of 16 values) between neighboring fluorine atoms of different hemispheres. The similarity of the two angles indicates that the square $IF_8^{\ominus}$ antiprism is neither mentionably elongated nor flattened along the S_8 axis.

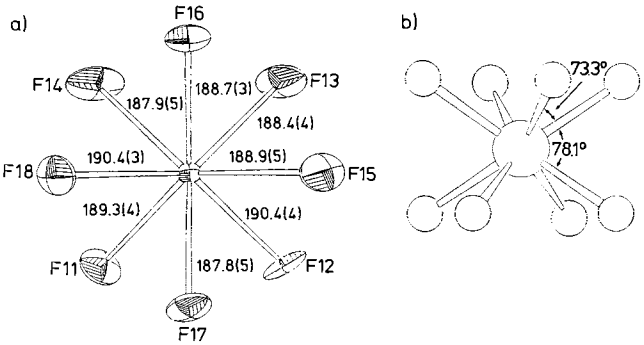

Fig. 2. a) The anion $IF_8^{\ominus}$(I) in **1**, ORTEP plot, vibration ellipsoids at the 50% probability level. The crystallographically different anion (II) is almost identical. b) Side view of the $IF_8^{\ominus}$ ion (I), Schakal plot. The angle F–I–F between neighboring fluorine atoms within a hemisphere (73.1, 73.5, 73.7, 74.7, 73.0, 73.1, 73.3, 72.0(2)°) are only slightly smaller than those between neighboring fluorine atoms between two hemispheres (77.0, 78.6, 78.2, 77.8, 76.2, 76.3, 78.5, 77.5(2–3)°).

$IF_8^{\ominus}$ also has square-antiprismatic geometry in the compound $[(CH_3)_4N]IF_8$ **2**. However, owing to a fourfold disorder or twinning, which involves only the anion, the bond lengths and angles in this structure determination must be regarded as very inaccurate (Fig. 3).

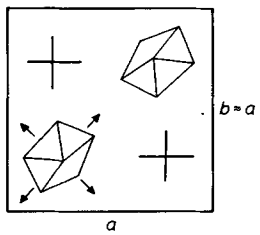

Fig. 3. Structure of **2** in the crystal, projection on (001) of the pseudotetragonal cell, $a \approx b$. The square antiprism is inclined to [001]. As indicated by the four arrows, the anion has four possible orientations, which arise from the four fold disorder or—more likely—from the twinning. The crosses denote cations.

In the compound $(NO^{\oplus})_2XeF_8^{2\ominus}$,[3] the anion $XeF_8^{2\ominus}$, which has an additional non-bonding electron pair, likewise has a square-antiprismatic geometry. The angles, as shown in Figure 2b, are extraordinarily similar to those in $IF_8^{\ominus}$ (73.1–75.8° within the hemispheres, 76.2–77.7° between the hemispheres). Only the lengths of the bonds to the four fluorine atoms in one hemisphere are somewhat longer. Nevertheless, no apparent space for accomodation of the nonbonding pair of electrons is made available by this small deviation from the ideal structure. Rather, the deviations are attributed to different contacts to the cations. It can be assumed that the small $NO^{\oplus}$ ion interacts electrostatically much more strongly than the larger cations in **1** and **2**.

The pair of ions $IF_8^{\ominus}/XeF_8^{2\ominus}$ provide the second example demonstrating that a structural principle remains unchanged on introducing a non-bonding electron pair, but that merely all the bond lengths are enlarged. The first example is the pair $BrF_6^{\oplus}/BrF_6^{\ominus}$.[4] The likely explanation for the failure of the electron-pair repulsion model[5] is that the bromine atom with six fluorine atoms and the iodine or xenon atom with eight fluorine atoms as ligands are sterically already so crowded that the non-bonding electron pair must reside in a centrosymmetric orbital, which, however, leads to a bond lengthening.

Experimental

1: In a metal vacuum apparatus NOF and IF_7 were condensed in the molar ratio 3:1 into a Teflon FEP tube, which was then sealed. Upon storage at $-20\,^{\circ}C$, colorless crystals separated out. A suitable crystal ($0.6 \times 0.6 \times 0.2\,mm^3$) was transferred with a special apparatus [6] to a CAD4 diffractometer ($Mo_{K\alpha}$, $-163\,^{\circ}C$, ω-θ scan). $a = 618.92(7)$, $b = 1039.43(17)$, $c = 2842.14(15)$ pm, $P2_12_12_1$ (No. 19). 4475 measured reflections in the range $2^{\circ} < \theta < 35^{\circ}$, $+h$, $+k$, $+l$, 4445 unique reflections, 4070 reflections with $I \geq 3\sigma(I)$, $\mu = 19.5\,cm^{-1}$, full matrix. SHELXTL plus, all atoms anisotropic, $R = 0.038$, $R_w = 0.032$.

2: Anhydrous $(CH_3)_4N^{\oplus}F^{\ominus}$ [7] was suspended in CH_3CN in a Teflon FEP tube; a slight excess of IF_7 was then condensed into the suspension. The fluoride dissolved with formation of a complex, which upon cooling crystallized out in the form of needle shaped crystals. Diffraction photographs showed that all reflections are slightly split. $a = 866.9(3)$, $b = 866.9(2)$, $c = 683.6(3)$ pm, $\alpha = \beta = \gamma = 90^{\circ}$ ($-153\,^{\circ}C$). 927 measured reflections in the range $2^{\circ} < \theta < 30^{\circ}$, $\pm h$, $+k$, $+l$, 460 unique reflections, 431 reflections with $I \geq 3\sigma(I)$, $\mu = 31.8\,cm^{-1}$, full matrix. Calculation with SHELXTL plus in space group $P4/nmm$ (No. 129); C, N and I anisotropic, H in isotropically fixed calculated positions, F fourfold disordered, isotropic: $R = 0.049$, $R_w = 0.043$. Calculation with the program SFLS [8] in the space group $Pmmn$ (No. 59) according to the twinning law (010)(−100)(001) gave $R = 0.051$, $R_w = 0.045$ for C, N, I anisotropic, F isotropic, twofold disordered, without H. For a non-disordered anion the space group $P2_1mn$ (No. 31) would suffice. Refinement in this space group however generates four positions again for each fluorine atom.

Further details of the crystal structure determinations are available on request from the Fachinformationszentrum Karlsruhe, Gesellschaft für wissenschaftlich-technische Information mbH, W-7514 Eggenstein-Leopoldshafen (FRG), on quoting the depository number CSD-55274, the names of the authors, and the journal citation.

Received: January 30, 1991 [Z 4410 IE]
German version: *Angew. Chem. 103* (1991) 844

CAS Registry numbers:
$IF_8^{\ominus}$, 53568-65-3; $(NOF)_2 \cdot NO^{\oplus}IF_8^{\ominus}$, 134152-23-1; $[(CH_3)_4N]IF_8$, 134131-34-3.

[1] C.J. Adams, *Inorg. Nucl. Chem. Lett. 10* (1974) 831.
[2] W.J. Adams, H.B. Thompson, L.S. Bartell, *J. Chem. Phys. 53* (1970) 4040.
[3] S.W. Peterson, J.H. Holloway, B.A. Coyle, J.M. Williams, *Science 173* (1971) 1238.
[4] A.R. Mahjoub, A. Hoser, J. Fuchs, K. Seppelt, *Angew. Chem. 101* (1989) 1528; *Angew. Chem. Int. Ed. Engl. 28* (1989) 1526; K.O. Christe, W.W. Wilson, *Inorg. Chem. 28* (1989) 3275; W.W. Wilson, K.O. Christe, *ibid. 28* (1989) 4172. In this sense, even the anions of the type $[TeX_6]^{2\ominus}$ (X = Cl, Br, I) and $[SeX_6]^{2\ominus}$ (X = Cl, Br) and similar antimony and bismuth anions represent no exception from the electron-pair repulsion model. High crystal symmetry (at least the presence of one symmetry center for the central atom) generates dynamically distorted structures. With lower symmetry the structures are even statically distorted: W. Abriel, C. Friedrich, *Z. Naturforsch. B40* (1985) 1691; W. Abriel, *ibid. B42* (1987) 415; W. Abriel, E.-J. Zehnder, *ibid. B42* (1987) 1273; *Acta Crystallogr. Sect. B42* (1986) 449; W. Abriel, H. Ehrhardt, *Angew. Chem. 96* (1984) 965; *Angew. Chem. Int. Ed. Engl. 23* (1984) 963.
[5] R.J. Gillespie, R.S. Nyholm, *Q. Rev. Chem. Soc. 11* (1957) 339; R.J. Gillespie, *Angew. Chem. 79* (1967) 885; *Angew. Chem. Int. Ed. Engl. 6* (1967) 819.
[6] M. Veith, H. Bärnighausen, *Acta Crystallogr. Sect B30* (1974) 1806; H. Schumann, W. Genthe, E. Hahn, M.B. Hossein, D. von der Helm, *J. Organomet. Chem. 299* (1986) 67.
[7] W.W. Wilson, K.O. Christe, J. Feng, R. Bau, *J. Am. Chem. Soc. 112* (1990) 7621.
[8] Program for the calculation of twinned crystals: H. Bärninghausen, *Z. Kristallogr. 170* (1985) 5; M. Eitel, *Dissertation*, Universität Karlsruhe 1985.

Different Reaction Behavior of Lead Bis(tri-*tert*-butoxygermanate) and Lead Bis(tri-*tert*-butoxystannate) towards Nonacarbonyldiiron**

By *Michael Veith** and *Johannes Hans*

Dedicated to Professor Hans Georg von Schnering on the occasion of his 60th birthday

In the course of our comparative studies on molecular compounds of elements of the fourth main group in their lower oxidation state II (cf. Refs. [1–3]) we have now carried out reactions of the homologues lead bis(tri-*tert*-butoxygermanate) **1** and the corresponding stannate **2** with nonacarbonyldiiron in order to investigate the stereochemical activity of the lone pair of electrons on the metallic element. Whereas **1** at room temperature contains a linear arrangement of the metallic elements (Ge, Pb and Ge are connected to each other via *tert*-butoxy groups, whereby the lead atom forms the center of the $\bar{3}(S_6)$ symmetric arrangement and thus possesses no stereochemically effective electron pair), the Sn ··· Pb ··· Sn array in **2** is bent.[3] We had expected that it would be possible to influence the coordination sphere of the central lead atom by coupling $Fe(CO)_4$ units to the Lewis basic germanium and tin atoms in **1** and **2**, respectively, and by the concomitant withdrawal of electron density. As can be seen in Equations (a) and (b) the products **3** and **4** are

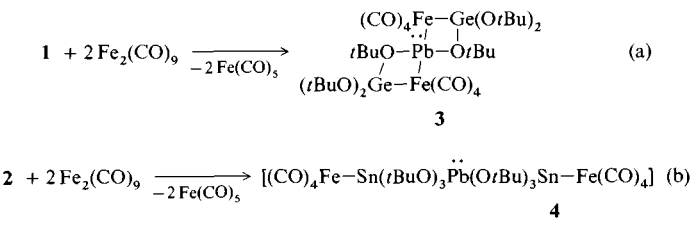

$[M(OtBu)_3Pb(OtBu)_3M]$ **1**, M = Ge; **2**, M = Sn

$$\mathbf{1} + 2\,Fe_2(CO)_9 \xrightarrow[-2\,Fe(CO)_5]{} \underset{\mathbf{3}}{(CO)_4Fe{-}Ge(OtBu)_2 \cdots Pb(OtBu)_2 \cdots Ge{-}Fe(CO)_4} \quad (a)$$

$$\mathbf{2} + 2\,Fe_2(CO)_9 \xrightarrow[-2\,Fe(CO)_5]{} \underset{\mathbf{4}}{[(CO)_4Fe{-}Sn(tBuO)_3Pb(OtBu)_3Sn{-}Fe(CO)_4]} \quad (b)$$

formed, which are similar in their composition, behave similarly spectroscopically, and differ noticeably only in their color.[4]

Single-crystal X-ray structure analyses of **3** and **4** (Fig. 1 and 2) show that **3** has a pseudocrystallographic twofold axis, **4** a crystallographic twofold axis, in each case passing through the lead atom. In **4** the metal atoms are, as expected, coupled one-dimensionally, whereas **3** is spirocyclic, with the lead atom as spirocenter of two four-membered PbFeGeO rings. In the slightly folded, trapezoidal oxametallacycles the lead atom (smallest angle), as expected, takes over the main burden of the ring strain. Whereas all five metal atoms in **3** are coupled via σ bonds, in **4** only the tin atoms are bound directly to the iron atom.

Due to replacement of four *tert*-butoxy groups by two $Fe(CO)_4$ moieties the environment of the lead atom in **3** is completely different from that in the starting compound **1**.

[*] Prof. Dr. M. Veith, Dr. J. Hans
Institut für Anorganische Chemie der Universität
Im Stadtwald 1, W-6600 Saarbrücken (FRG)

[**] Chemistry of Alkoxystannates, Part 7. This work was supported by the Deutsche Forschungsgemeinschaft and the Fonds der Chemischen Industry.—Part 6: M. Veith, K. Kunze, *Angew. Chem. 103* (1991) 92; *Angew. Chem. Int. Ed. Engl. 30* (1991) 95.

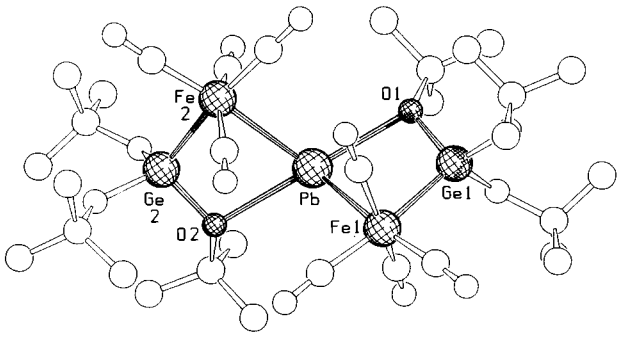

Fig. 1. Molecular structure of **3** [4, 5]. The unmarked spheres are carbon atoms or oxygen atoms. Hydrogen atoms have been omitted. Important bond lengths [Å] and angles [°] (see also text): Ge1–Fe1 2.395(3), Ge2–Fe2 2.396(3), Ge1–O1 1.80(1), Ge1–O5 1.75(1), Ge1–O6 1.782(8), Ge2–O3 1.78(1), Ge2–O4 1.789(9); Fe1–Pb–Fe2 112.9(1), O1–Pb–Fe2 108.5(2), O2–Pb–Fe1 109.1(2), Pb–Fe1–Ge1 80.0(1), Pb–Fe2–Ge2 80.4(1), O1–Ge1–Fe1 102.9(3), O2–Ge2–Fe2 103.0(3), Ge1–O1–Pb 100.5(4), Ge2–O2–Pb 100.6(4).

The lead atom is ψ-trigonal-pyramidally coordinated with two long[3] Pb–O bonds (2.64(1) Å), which run axially (O1–Pb–O2 = 177.7(2)°) and two likewise long Fe–Pb distances (Pb–Fe1 = 2.939(2), Pb–Fe2 = 2.934(2) Å) in the equatorial plane, which is inclined to the O1–Pb–O2 axis (O1–Pb–Fe = 72.5(2)°, O2–Pb–Fe2 = 72.6(2)°). It can be concluded from the observed geometry and the long distances that the central lead atom is, furthermore, divalent, but in contrast to

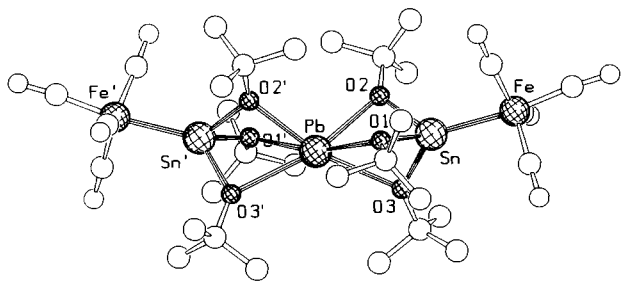

Fig. 2. Molecular structure of **4** [4, 5] (see also caption to Fig. 1). Selected bond lengths [Å] and angles [°]: Pb–O1 2.566(7), Pb–O2 2.482(7), Pb–O3 2.730(7), Fe–Sn 2.476(1), Sn–O1 2.027(6), Sn–O2 2.031(6), Sn–O3 1.992(7), Sn···Pb 3.327(1); C(axial)–Fe–Sn 171.6(5), Fe···Sn···Pb 172.6(1), mean values: O–Pb–O 63.2(1), 113.5 (6.0), 164.6(8), O–Sn–O 84.9(2.0), O–Sn–Fe 128.6(2.0).

that in **1** has a stereochemically effective electron pair (for related and similar coordination spheres of Si^{II}, Ge^{II} and Sn^{II} with ligands such as $C(PMe_2)_3^{\ominus}$ cf. Ref. [6]). The unusually long Pb–Fe contacts in **3** are unmistakable when compared with the Pb–Fe distances in $[Pb\{Fe(CO)_4\}_4]$ (2.62(1) Å)[7] or in the dianion $[Pb\{Fe(CO)_4\}_2Fe_2(CO)_8]^{2\ominus}$ (2.62(1)–2.83(1) Å).[8] The bonds from the distorted tetrahedrally coordinated germanium atoms can be regarded as simple σ bonds (in $[Ge\{Fe(CO)_4\}_4]$: Ge–Fe = 2.41(2) Å[9] and in the $[GeFe_4(CO)_{14}]^{2\ominus}$ dianion 2.38(2) Å[7]), the bonds to the two-coordinate oxygen atoms being expectedly shorter than those to the three-coordinate atoms.[3] Accordingly, on the basis of the structure and simple bonding models, **3** can be formally described in terms of a $Pb^{2\oplus}$ ion and two $[Ge(OtBu)_3Fe(CO)_4]^{\ominus}$ ions which coordinate the lead atom chelate-like via an oxygen atom and a "nucleophilic" iron atom. This description is naturally to be regarded as only *one* of many possibilities, since other resonance structures can be arrived at with other electron assignments. Also worth mentioning is that **3** can be converted, at least purely formally (but reasonably from a structural point of view), into a structure **5** which is analogous to **4**, by rotation about the Ge–O axes of the four-membered rings **3** remaining after opening of the Fe–Pb bonds [Eq. (c)].

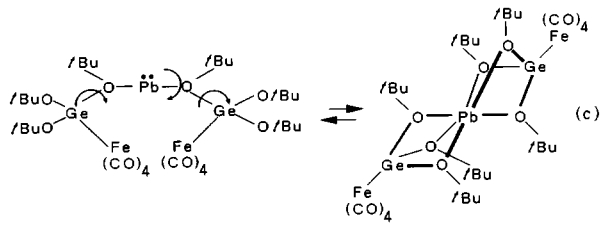

3 **5**

How far such a rearrangement in the reverse direction plays a role in the formation of **3** is still unclear. Remarkably, however, only one ^{1}H-NMR signal is observed for the *tert*-butyl groups of **3** in solution,[4] which at least indicates intramolecular mobility (also the CO vibration frequencies of **3** hardly differ from those of **4**).

The most important difference between **2**[3] and **4** is the enhanced distortion of the coordination sphere of the lead atom; thus, for example, the Sn···Pb···Sn angle decreases from 173.5° to 165.0(0)°, and the angle of intersection of the O_3-planes of the tris(*tert*-butoxy) moieties increases from 10.8° to 24.3°. The overall striking feature is that the whole molecule is *curved*, with the curvature extending to the axial carbonyl groups (concerning curved structures in chemistry see Ref. [10]).

It follows from these results that a withdrawal of electron density at the germanium or tin atom in compounds such as **1** and **2** not only has a local effect, but affects the whole molecule, and the stereochemical activity of the lone electron pair at the central lead atom is manifested more strongly. In analogy to the definition presented in Ref. [3], the ligands at the lead atom (tri(*tert*-butoxy)germanate and -stannate) appear to become inflexible in the transition from **1** and **2** to **3** and **4**, respectively. However, as the different structures of **3** and **4** show, the withdrawal of electron density can be so strong that rearrangements occur. Referred to the metal atoms, we have here the "transition" from a structure with bonding oxygen atoms between the metals (**4**) to a metal cluster (**3**).

Experimental

A solution of 0.7 mmol of **1** [3] or **2** [3] in 25 mL of toluene was added dropwise to a suspension of 0.51 g (1.40 mmol) of nonacarbonyldiiron in 15 mL of toluene. After 2 h and 12 h stirring, respectively, the reaction is complete; the solution of **1** turned ruby red, that of **2** yellow. After filtration and removal of solvent in a vacuum there remained a solid residue, which was recrystallized from 5 mL of cyclohexane (**3**) or toluene (**4**); yields: **3**, 0.72 g (84%); **4**, 0.79 g (95%) [4].

Received: January 27, 1991 [Z 4396 IE]
German version: *Angew. Chem. 103* (1991) 846

CAS Registry numbers:
1, 133778-93-5; **2**, 133778-94-6; **3**, 133798-04-6; **4**, 133798-05-7; $Fe_2(CO)_9$, 15321-51-4.

[1] M. Veith, *Angew. Chem. 99* (1987) 1; *Angew. Chem. Int. Ed. Engl. 26* (1987) 1.
[2] M. Veith, R. Lisowsky, *Angew. Chem. 100* (1988) 1124; *Angew. Chem. Int. Ed. Engl. 27* (1988) 1087.
[3] M. Veith, J. Hans, L. Stahl, P. May, V. Huch, A. Sebald, *Z. Naturforsch. B46* (1991) 403.

[4] **3**: m.p. 180 °C (decomp.); ruby-red to black crystals; ^{1}H NMR (80 MHz, benzene, 25 °C, TMS): δ = 1.49; IR (THF): ν(CO) = 2048(s), 1965(vs), 1925(vs) cm^{-1}; MS (70 eV): m/z 1114 ($M^{\oplus}$ − CH_3 with ^{56}Fe, ^{74}Ge, ^{207}Pb, 60%), 668 ([Pb(O*t*Bu)$_3$GeFe(CO)$_4$]$^{\oplus}$, 100). Monoclinic, space group: $C2/c$, a = 33.57(2), b = 9.329(9), c = 29.19(2) Å, β = 103.1(1)°; Z = 8; 3478 reflections with 548 $F_o < 2\sigma$, 281 parameters, R = 0.051, R_w = 0.049 [5].—**4**: m.p. 190 °C (decomp.); golden yellow crystals; ^{1}H NMR (80 MHz, benzene, 25 °C, TMS): δ = 1.42; IR (THF): ν(CO) = 2040(m), 1962(vs), 1936(vs) cm^{-1}; MS (70 eV): m/z 1217 ($M^{\oplus}$ with ^{56}Fe, ^{116}Sn, ^{207}Pb, 10%), 712 ([Pb(O*t*Bu)$_3$SnFe(CO)$_4$]$^{\oplus}$, 100). Monoclinic, space group $C2/c$, a = 14.273(8), b = 16.278(9), c = 20.158(9) Å, β = 102.1(1)°; Z = 4; 3789 reflections with 553 $F_o < 2\sigma$, 259 parameters, empirical absorption correction, R = 0.044, R_w = 0.053 [5].

[5] Further details of the crystal structure investigations are available on request from the Fachinformationszentrum Karlsruhe, Gesellschaft für wissenschaftlich-technische Information mbH, W-7514 Eggenstein-Leopoldshafen 2 (FRG), on quoting the depository number CSD-55254, the names of the authors, and the journal citation.

[6] H. H. Karsch, M. Hollstein, G. Müller, *Z. Naturforsch. B45* (1990) 775, and references cited therein.

[7] K. H. Whitmire, C. B. Lagrone, M. R. Churchill, J. C. Fettinger, *Inorg. Chem. 26* (1987) 3491.

[8] C. B. Lagrone, K. H. Whitmire, M. R. Churchill, J. C. Fettinger, *Inorg. Chem. 25* (1986) 2080.

[9] D. Melzer, E. Weiss, *J. Organomet. Chem. 255* (1983) 335.

[10] H. G. von Schnering, R. Nesper, *Angew. Chem. 99* (1987) 1097; *Angew. Chem. Int. Ed. Engl. 26* (1987) 1059.

Ring Opening of a Cyclobutabenzene Complex under Very Mild Conditions**

By *Hans G. Wey* and *Holger Butenschön**

Dedicated to Professor Paul Binger on the occasion of his 60th birthday

Cyclopentadienyl and arene complexes with annelated four-membered ring moieties are of special interest because of their ring-opening reactions leading to non-planar di-*exo*-methylene compounds and successive stereoselective cycloadditions with dienophiles. So far only two such reaction sequences are known: an η^5-(bicyclo[3.2.0]hepta-1,3-dienyl)-cobalt(I) complex reacts at 200 °C in 13 h with several dienophiles to give the corresponding [4 + 2] cycloadducts.[1] Reaction of η^6-(1-ethoxycyclobutabenzene)tricarbonylchromium(0) with the unusual dienophile *trans*-bis(trimethylsilyl)ethene at 160° leads in 6 h to formation of the corresponding tetralin complex.[2] We report here on the

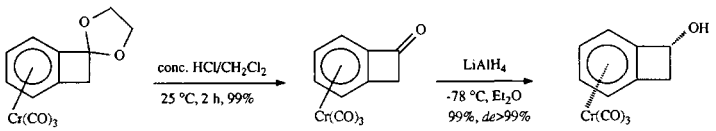

1 **2** **3**

preparation of the tricarbonylchromium(0) complexes **2** and **3** of the 1-oxo and the 1-hydroxycyclobutabenzenes, respectively, as well as on the ready ring-opening of the alkoxide **5** obtainable from **3** and the trapping of the intermediate with conventional dienophiles.

[*] Dr. H. Butenschön, Dr. H. G. Wey
Max-Planck-Institut für Kohlenforschung
Kaiser-Wilhelm-Platz 1, W-4330 Mülheim an der Ruhr 1 (FRG)

[**] *H. G. W.* thanks the Max-Planck-Gesellschaft for a doctoral fellowship and *H. B.* thanks the Verband der Chemischen Industrie for a Liebig fellowship. We thank Herr *M. Brands* for help with the purification of **6** and Prof. Dr. *G. Wilke* for supporting interest.

The reaction of 1-oxocyclobutabenzene with [Cr(CO)$_6$] affords **2** in only 4% yield. In contrast, **2** is readily accessible in 99% yield as an orange-red powder (m.p. 70.9 °C) by hydrolysis of **1**[3] in a two-phase mixture of dichloromethane and concentrated hydrochloric acid. The identity of **2**, with its three sp^2-C centers in the four-membered ring one of the most strained arene complexes known to date, follows unequivocally from the spectroscopic data (IR, ^{13}C NMR; ^{1}H NMR see Table 1), the mass spectrum, and the correct elemental analysis. Like **2**, the tricarbonylchromium(0) complex **3** of the 1-hydroxycyclobutabenzene is also not obtainable by direct reaction of the ligand with [Cr(CO)$_6$] or [Cr(CO)$_3$(NH$_3$)$_3$].[3b] Therefore **2** was reduced with lithium aluminum hydride to **3**. The withdrawal of electrons by the tricarbonylchromium(0) moiety leads to a noticeable increase in reactivity of the keto group: whereas 1-oxocyclobutabenzene is reduced to the extent of 83% in 30 min in boiling diethyl ether,[4] the reduction of the corresponding tricarbonylchromium(0) complex **2** proceeds immediately at −78 °C, as can be seen by the immediate color change from orange-red to pale yellow upon dropwise addition of **2** to the reducing agent. The yield of **3** of 99%—under considerably milder conditions and shorter reaction time—is also significantly higher than that in the reduction of the tricarbonylchromium(0) complexes of indan-1-one (36 °C, 8 h, 84%) and tetralin-1-one (36 °C, 8 h, 72%).[5] Moreover, the reduction of **2** to **3** proceeds diastereoselectively to the *endo*-1-hydroxy compound: the ^{1}H- and ^{13}C-NMR spectra show only the signals of one diastereomer. Also only one diastereomer is detectable by analytical HPLC (de > 99%). That **3** is, in analogy to the products of the reductions of the higher homologues,[5] in fact the *endo*-1-hydroxy compound could be demonstrated by an NOE experiment. A CO ligand in **3** was replaced by a PPh_3 ligand by irradiation in the presence of PPh_3; this led to formation of **4** in 49% yield.

Table 1. ^{1}H-NMR data of **2**–**4** and **6**.

2: (200 MHz, [D$_8$]THF): δ = 3.81 (d, 1 H, *exo*-2-H or *endo*-2-H, ^2J(*exo*-2, *endo*-2) = −16.4 Hz), 4.02 (d, 1 H, *exo*-2-H or *endo*-2-H), 5.27 (dd, 1 H, 4-H, ^3J(4,5) = 6.2 Hz, ^3J(4,3) = 6.4 Hz), 5.82 (dd, 1 H, 5-H, ^3J(5,6) = 6.2 Hz), 5.89 (d, 1 H, 6-H), 6.02 (d, 1 H, 3-H)

3: (200 MHz, [D$_8$]THF): δ = 2.87 (dd, 1 H, *endo*-2-H, ^2J(*endo*-2, *exo*-2) = −13.9 Hz, ^3J(*endo*-2, *exo*-1) = 2.2 Hz), 3.35 (dd, 1 H, *exo*-2-H, ^3J(*exo*-2, *exo*-1) = 5.2 Hz), 4.72 (br, 1 H, OH), 5.04 (ddd, 1 H, 4-H, ^3J(3,4) = 6.2 Hz, ^3J(4,5) = 5.9 Hz, ^4J(4,6) = 1.3 Hz), 5.06 (dd, 1 H, 1-H) 5.39 (ddd, 1 H, 5-H, ^3J(5,6) = 6.2 Hz, ^4J(3,5) = 0.7 Hz), 5.45 (dd, 1 H, 6-H, ^5J(1,6) = 0.9 Hz), 5.68 (dd, 1 H, 3-H)

4: (200 MHz, [D$_8$]THF): δ = 3.04 (dd, 1 H, *endo*-2-H, ^2J(*exo*-2, *endo*-2) = −13.5 Hz, ^3J(*endo*-2, *exo*-1) = 2.3 Hz), 3.34 (dd, 1 H, *exo*-2-H, ^3J(*exo*-2, *exo*-1) = 5.4 Hz), 3.56 (d, 1 H, OH, ^3J(OH, *exo*-1) = 9.4 Hz), 3.87 (m, 1 H, 5-H, ^3J(5,6) = 6.5 Hz, ^3J(4,5) = 5.9 Hz, J(3,P) = 6.0 Hz), 4.33 (ddd, 1 H, 4-H, ^3J(3,4) = 6.1 Hz, J(4,P) = 3.4 Hz), 4.76 (d, 1 H, 3-H), 5.05 (m, 1 H, *exo*-1-H), 5.25 (d, 1 H, 6-H), 7.3 (m, 9 H, 8-H, 9-H), 7.52 (m, 6 H, 7-H)

6: (400 MHz, [D$_8$]THF): δ = 2.73 (dd, 1 H, 4-H, ^2J(4α, 4β) = −17.0 Hz, ^3J(4β,3) = 11.9 Hz), 3.04 (dd, 1 H, 4-H, ^3J(4α,3) = 6.3 Hz), 3.12 (dd, 1 H, 2-H, ^3J(3,2) = 12.0 Hz, ^3J(2,1) = 3.4 Hz), 3.24 (ddd, 1 H, 3-H), 3.65 (s, 3 H, 12-H), 3.68 (s, 3 H, 11-H), 4.79 (dd, 1 H, ^3J(1,OH) = 3.4 Hz), 5.16 (d,OH), 5.36 (dd, 1 H, 6-H or 7-H), 5.43 (d, 1 H, 8-H or 5-H), 5.58 (dd, 1 H, 7-H or 6-H), 5.63 (d, 1 H, 5-H or 8-H)

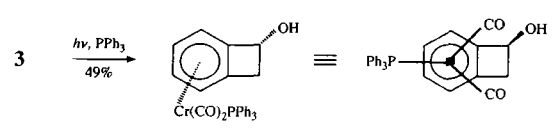

4 ■ = Cr

Instead of a NOE between the *ortho* protons of the PPh_3 ligand and the protons of the four-membered ring, however, a NOE at the protons of the benzene ring in the bicyclic ligand was observed. Apparently that conformation is preferred in which the PPh_3 ligand is oppositely disposed to the four-membered ring. The reason for this could be the *endo*-1-hydroxy group, as the conformation found for **4** was not preferred in the case of the *exo*-1-trimethylsilyl compound.[3]

The DSC (differential scanning calorimetry) analysis of **3** shows a reaction above 101 °C, from which we presume, in analogy to other results, that it involves a thermal opening of the four-membered ring to give an *ortho*-quinodimethane complex. Attempts to trap such a complex as a [4 + 2] cycloadduct with dimethyl fumarate, however, afforded only decomposition products. On the basis of the results reported by *Choy* et al.[6] we considered it possible that the four-membered ring of the alkoxide **5** opens at lower temperatures than that of the alcohol **3**. Therefore, **3** was allowed to react with 1.1 equivalents of *n*-butyllithium at −78 °C in THF, whereupon an immediate color change from bright yellow to brown-red occurred. After 1 h the clear solution was treated with 1.1 equivalents of dimethyl fumarate. After hydrolysis at 0 °C a slightly contaminated cycloadduct **6** was obtained in a total yield of 89% and was characterized on the basis of the spectroscopic data (IR, ^{13}C NMR; ^1H NMR see Table 1) and the mass spectrum.[7] In analogy to the findings of *Kündig* et al.[2] we assume that the hydroxy group in **6** is *exo*. The complex **6** is likewise obtained as the main product when the reaction is carried out with dimethyl maleate as dienophile. Whether this follows as a result of an isomerization of the dienophile at the transition metal[11] or a radical reaction is currently under investigation. No statement can yet be made regarding the structure of the intermediary *ortho*-quinodimethane complex; a complex with an η^6-coordinated ligand[2, 8] is as equally conceivable as one with an η^4-coordinated *ortho*-quinodimethane ligand as a result of an $\eta^6 \rightarrow \eta^4$ ring slippage reaction.[9]

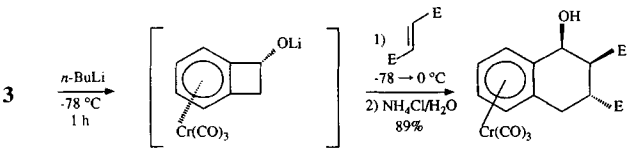

We have shown that the ketone complex **2** and the alcohol complex **3**, which are not obtainable by a direct route, can be prepared in very high yields almost diastereoselectively. Compared to the two hitherto known ring-opening reactions of cyclopentadienyl and arene complexes containing four-membered annelated rings, the reaction starting from **3** offers considerable advantages. The lower reaction temperature of more than 160 °C, markedly shorter reaction time, and higher yield, as well as accessibility of various educts[10] from the 1-oxocyclobutabenzene complex **2** and the use of commercially available dienophiles make the reaction not only mechanistically but also preparatively interesting. The resolution of chiral **2** should enable the formation of enantiomerically pure *ortho*-quinodimethane complexes, which are of importance for the enantioselective synthesis of polycyclic natural products.[11, 12]

Received: February 5, 1991 [Z 4427 IE]
German version: *Angew. Chem. 103* (1991) 871

CAS Registry numbers:
1, 122114-03-8; **2**, 122114-02-7; **3**, 134110-48-8; **4**, 134110-49-9; **6**, 134110-50-2; dimethyl fumarate, 624-49-7.

[1] H. Butenschön, *Angew. Chem. 102* (1990) 1058; *Angew. Chem. Int. Ed. Engl. 29* (1990) 1057.
[2] E. P. Kündig, G. Bernardinelli, J. Leresche, P. Romanens, *Angew. Chem. 102* (1990) 421; *Angew. Chem. Int. Ed. Engl. 29* (1990) 407.
[3] a) H. G. Wey, H. Butenschön, *J. Organomet. Chem. 350* (1988) C8; b) H. G. Wey, P. Betz, H. Butenschön, *Chem. Ber. 124* (1991) 465.
[4] L. Horner, P. V. Subramaniam, K. Eiben, *Justus Liebigs Ann. Chem. 714* (1968) 91, and references cited therein.
[5] W. R. Jackson, T. R. B. Mitchell, *J. Chem. Soc. B 1969*, 1228.
[6] W. Choy, H. Yang, *J. Org. Chem. 53* (1988) 5796.
[7] By repeated dissolution in THF and subsequent trapping by addition of pentane a sample was obtained which gave a satisfactory elemental analysis. The ^1H NMR spectrum of the crude product showed signals of very low intensity which indicated a diastereomer of **6**. The relative configuration in the ligand of **6** follows from the ^1H-NMR data. The question as to which side of the ligand the $Cr(CO)_3$ unit is coordinated is presently under investigation.
[8] M. Yalpani, R. Benn, R. Goddard, G. Wilke, *J. Organomet. Chem. 240* (1982) 49.
[9] J. M. O'Connor, C. P. Casey, *Chem. Rev. 87* (1987) 307.
[10] Grignard additions of **2** likewise proceed in very good yield with high diastereoselectivity: H. G. Wey, *Dissertation*, Ruhr-Universität Bochum 1990; M. Brands, H. Butenschön, unpublished.
[11] K. P. C. Vollhardt, *Acc. Chem. Res. 10* (1977) 1.
[12] W. Oppolzer, *Synthesis 1978*, 793.

Spontaneous Self Assembly of an Octanuclear Iron-Nickel Cluster by Reaction of $[Fe_6S_6I_6]^{2\ominus}$ with $[NiI_4]^{2\ominus}$ **

By *Wolfgang Saak* and *Siegfried Pohl**

Dedicated to Hans Georg von Schnering on the occasion of his 60th birthday

Numerous metalloproteins contain clusters of transition metals in their active sites. In many cases, however, not even the structure of these centers is known. Thus, the structures proposed for the active site of the FeMo cofactor of nitrogenase are based only on spectroscopic and analytical data,[1] according to which the central unit is formed from an $[M_8S_6]$ cluster. Remarkably, with $[Fe_8S_6I_8]^{3\ominus}$[2] so far only one cluster corresponding at least structurally with this model, for example in the "Fe-only" nitrogenase,[3] has been synthesized. In contrast, electron-richer clusters of this type, i.e. with cobalt and nickel, have not only been prepared synthetically,[4, 5] but are also found in minerals such as the pentlandites,[6] bartonite,[7] or djerfisherite[8] (see also Ref. [9]). This would suggest that $[Fe_8S_6]$ clusters can be stabilized by incorporation of nickel. Calculations of the electronic structures of clusters in pentlandites point in the same direction.[10]

By reaction of Fe–S clusters with nickel complexes we have found a novel route to Fe–Ni clusters and have been able to isolate such a cluster with cubic arrangement of the metals (regarding an $[Fe_3NiS_4]$ cluster, see Ref. [11]), which is of interest in connection with cluster transformations in the active site of nitrogenase.

Reaction of $[Fe_4S_4I_4]^{2\ominus}$ with iodine and $[NiI_4]^{2\ominus}$ leads to formation of a $[Fe_3Ni_5S_6I_8]^{4\ominus}$ cluster anion which can be isolated as the ammonium salt in ca. 70% yield.

[*] Prof. Dr. S. Pohl, Dipl. Chem. W. Saak
Fachbereich Chemie der Universität
Postfach 2503, W-2900 Oldenburg (FRG)

[**] This work was supported by the Deutsche Forschungsgemeinschaft and the Fonds der Chemischen Industrie.

Initially, $[Fe_6S_6I_6]^{2\ominus}$ is formed quantitatively according to Equation (a) by oxidation of the tetranuclear cluster (see also

$$2[Fe_4S_4I_4]^{2\ominus} + 3I_2 \longrightarrow [Fe_6S_6I_6]^{2\ominus} + 2[FeI_4]^{\ominus} + 2S \qquad (a)$$

Ref. [12]). In the second step the hexanuclear iron cluster reacts according to Equation (b) with tetraiodoniccolate(II) to give $[Fe_3Ni_5S_6I_8]^{4\ominus}$, which can be isolated as the salt $(PhCH_2NEt_3)_4[Fe_3Ni_5S_6I_8]$ **1** in the form of black crystals.

$$[Fe_6S_6I_6]^{2\ominus} \xrightarrow{[NiI_4]^{2\ominus}} [Fe_3Ni_5S_6I_8]^{4\ominus} \qquad (b)$$

Upon evaporation of the solution an $[Fe_2S_2I_4]^{2\ominus}$ anion with the same cation can be crystallized in pure form. Whereas $[Fe_2S_2I_4]^{2\ominus}$ and $[FeI_4]^{\ominus}$, which is also formed, contain only iron(III), the M_8 cluster is made up exclusively of divalent metal ions and contains almost the total nickel employed. This mode of reaction suggests a great tendency for formation of an electron-rich cluster.

1 was characterized by an X-ray structure analysis.[13] The cluster anion (Fig. 1) with approximate O_h symmetry has crystallographic C_{4h} symmetry. The eight cubically arranged metal atoms together with the circumscribing S_6 octahedron form a rhombododecahedron. A differentiation between iron and nickel is already impossible because of the symmetry of the cluster. The metal–metal distances (mean value: 268.1 pm) are significantly shorter than the corresponding values in $[Fe_8S_6I_8]^{3\ominus}$ (mean value: 272.3[2] and 274.0 pm[14]), but are comparable with those in $[Co_8S_6(SPh)_8]^{4\ominus}$ [4] and $[Ni_8S_6Cl_2(PPh_3)_6]$.[5]

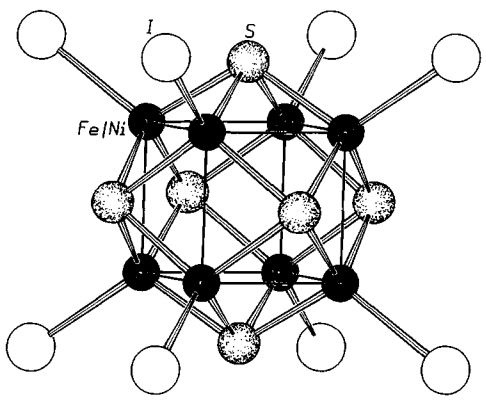

Fig. 1. Cluster anion of **1** in the crystal (C_{4h} symmetry). Important bond lengths [pm] and angles [°] (M ≙ Fe/Ni): M–M 267.7(2) and 268.5(3), M–I 254.6(1), M–S 223.8(3); M–S–M 106.3(1) and 73.6(1); M–S–I 112.2(1) and 112.9(1).

Differences and similarities, respectively, are also found in the number of skeletal electrons. For $[M_8S_6]$ clusters with π-donors *Burdett* and *Miller*[10] determined an optimal electron number of 110, a value which is reached exactly by $[Fe_3Ni_5S_6I_8]^{4\ominus}$ and almost by $[Co_8S_6(SPh)_8]^{4\ominus}$ with 108 electrons. Corresponding clusters with π-acceptor ligands, e.g. $[Ni_8(PPh)_6(CO)_8]$[15] or $[Ni_8(PPh)_6(CO)_4(PPh_3)_4]$[16] contain 120 skeletal electrons (see also Ref. [17]).

In contrast $[Fe_8S_6I_8]^{3\ominus}$ contains only 99 skeletal electrons. This unusually low number perhaps explains the high reactivity of this cluster anion (see Ref. [2]). A comparable $[Fe_8S_6]$ cluster fragment in the nitrogenase should, however, also show a high reactivity rather than high stability. Particularly effective are redox reactions by cluster transformations, since a larger number of electrons can be "reacted" in this way.

$$[Fe_8S_6]^{4\oplus} \rightleftharpoons [Fe_6S_6]^{4\oplus} + 2Fe^{3\oplus} + 6e \qquad (c)$$

Thus, in analogy to the reversal of the formation of $[Fe_3Ni_5S_6I_8]^{4\ominus}$ according to Equation (c), six electrons, as are required for the N_2 reduction, could be "set free" by a cluster transformation. The apparently essential homocitrate[18] could favor this transformation by complexing the iron(III) ions formed. An N_2 reduction in such a dinuclear complex is not inconsistent with the previously synthesized model complexes (see, in particular, Ref. [19] and, concerning bridged clusters, Ref. [20]).

Experimental

All operations were carried out under N_2 in anhydrous N_2-saturated solvents. BTEA: benzyltriethylammonium BTBA: benzyltri-*n*-butyl-ammonium.
1: A solution of $(BTEA)_2[Fe_4S_4I_4]$ (0.933 g, 0.75 mmol), $(BTBA)_2[Fe_4S_4I_4]$ (0.353 mg, 0.25 mmol) and I_2 (0.381 g, 1.5 mmol) in CH_2Cl_2 (150 mL) was heated for 15 min under its own pressure at ca. 50 °C. After cooling and addition of a solution of 1.119 g (1 mmol) of $(BTBA)_2[NiI_4]$ in 60 mL of CH_2Cl_2 this process was repeated. Crystallization commenced after 3–4 h and was complete after ca. 12 h. A small amount of finely powdered precipitate was removed by washing on a coarse frit. 0.35 g (72%) of **1** was obtained (satisfactory analyses of all elements). The use of different cations is necessary for the crystallization of pure **1**.

Received: February 19, 1991 [Z 4452 IE]
German version: *Angew. Chem. 13* (1991) 869

CAS Registry numbers:
$(BTEA)_2[Fe_4S_4I_4]$, 133870-49-2; $(BTBA)_2[Fe_4S_4I_4]$, 133870-50-5; $(BTBA)_2[NiI_4]$, 133870-51-6.

[1] G. Henkel, H. Strasdeit, B. Krebs, *Angew. Chem. 94* (1982) 204; *Angew. Chem. Int. Ed. Engl. 21* (1982) 201; *Angew. Chem. Suppl. 1982*, 489; R. H. Holm, *Chem. Soc. Rev. 10* (1981) 455; H. Strasdeit, B. Krebs, G. Henkel, *Inorg. Chem. 23* (1984) 1816.
[2] S. Pohl, W. Saak, *Angew. Chem. 96* (1984) 886; *Angew. Chem. Int. Ed. Engl. 23* (1984) 907.
[3] P. E. Bishop, D. M. L. Jarlenski, D. R. Hetherington, *Proc. Natl. Acad. Sci. USA. 77* (1980) 7342; R. N. Pau, L. A. Mitchenell, R. L. Robson, *J. Am. Chem. Soc. 171* (1989) 124; J. R. Chisnell, R. Premakumar, P. E. Bishop, *J. Bacteriol. 170* (1988) 27; B. K. Burgess, *Chem. Rev. 90* (1990) 1377.
[4] G. Christou, K. S. Hagen, R. H. Holm, *J. Am. Chem. Soc. 104* (1982) 1744; G. Christou, K. S. Hagen, J. K. Bashkin, R. H. Hom, *Inorg. Chem. 24* (1985) 1010.
[5] D. Fenske, J. Hachgenei, J. Ohmer, *Angew. Chem. 97* (1985) 684; *Angew. Chem. Int. Ed. Engl. 24* (1985) 706.
[6] V. Rajamani, C. T. Prewitt, *Can. Mineral. 12* (1973) 178.
[7] H. T. Evans, Jr., J. R. Clark, *Am. Mineral. 66* (1981) 376.
[8] S. C. Lee, R. H. Holm, *Angew. Chem. 102* (1990) 868; *Angew. Chem. Int. Ed. Engl. 29* (1990) 840.
[9] B. S. Tani, *Am. Mineral. 62* (1977) 819, and references cited therein.
[10] J. K. Burdett, G. J. Miller, *J. Am. Chem. Soc. 109* (1987) 4081; see also: G. G. Hoffman, J. K. Bashkin, M. Karplus, *ibid. 112* (1990) 8705.
[11] S. Ciurli, S. Yu, R. H. Holm, *J. Am. Chem. Soc. 112* (1990) 8169.
[12] W. Saak, S. Pohl, *Z. Naturforsch. B 40* (1985) 1105; W. Saak, G. Henkel, S. Pohl, *Angew. Chem. 96* (1984) 153; *Angew. Chem. Int. Ed. Engl. 23* (1984) 150.
[13] **1** crystallizes tetragonal, *I4/m*, $a = 1632.7(1)$, $c = 1458.0(1)$ pm, $V = 3886.6 \times 10^6$ pm^3, $Z = 2$, $\rho_{calcd} = 2.081$ g cm^{-3}, $Mo_{K\alpha}$ radiation, $2\theta_{max} = 48°$, 1460 independent reflections, 1100 observed ($I > 2\sigma(I)$), number of variables 95, empirical absorption correction (ψ scan), $R = 0.045$, $R_w = 0.040$ – Program: G. M. Sheldrick, SHELX-76 (Program for Crystal Structure Determination), Cambridge, England 1976; SHELXS-86, Göttingen 1986; drawing: E. Keller SCHAKAL 86, Freiburg 1986. Refinement of the Fe/Ni position carried out with the occupation factors 0.375 (Fe) and 0.625 (Ni). Further details of the crystal structure investiga-

tion are available on request from the Fachinformationszentrum Karlsruhe, Gesellschaft für wissenschaftlich-technische Information mbH, W-7514 Eggenstein-Leopoldshafen 2 (FRG), on quoting the depository number CSD-55273, the names of the authors, and the journal citation.
[14] Values from structure determinations with different cations, see: S. Pohl, W. Saak, *Z. Naturforsch. B43* (1988) 457.
[15] L. D. Lower, L. F. Dahl, *J. Am. Chem. Soc. 98* (1976) 5046.
[16] D. Fenske, R. Basoglu, J. Hachgenei, F. Rogel, *Angew. Chem. 96* (1984) 160; *Angew. Chem. Int. Ed. Engl. 23* (1984) 160.
[17] J. W. Lauher, *J. Am. Chem. Soc. 100* (1978) 5305.
[18] J. Imperial, T. R. Hoover, M. S. Madden, P. W. Ludden, V. K. Shah, *Biochemistry 28* (1989) 7796, and references cited therein.
[19] D. Sellmann, W. Soglowek, F. Knock, M. Moll, *Angew. Chem. 101* (1989) 1244; *Angew. Chem. Int. Ed. Engl. 28* (1989) 1271.
[20] D. Coucouvanis, *Acc. Chem. Res. 24* (1991) 1.

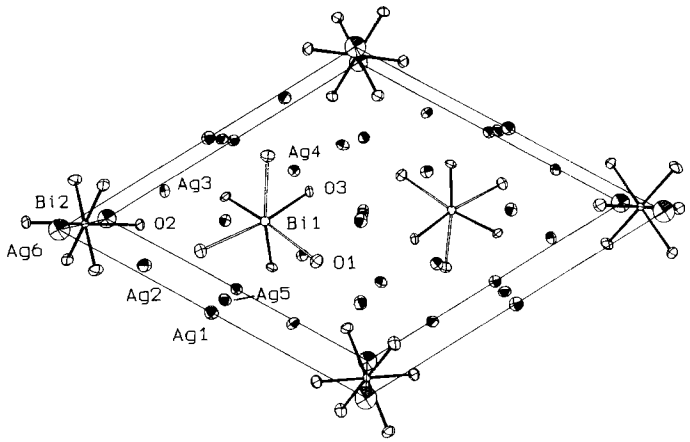

Fig. 1. Structure of $Ag_{25}Bi_3O_8$. View in the *c*-direction. Important bond lengths [pm] and angles [°]: Bi 1-O1 250.7(7) 3×, Bi 1-O3 220.7(5) 3×, Bi 2-O2 213.0(6) 6×, Ag 1-O1 208(1) 2×, Ag 2-O1 212.4(7), Ag 2-O2 214(1) Ag 3-O2 214.0(7), Ag 3-O3 217.4(6), Ag 4-O1 210.5(8), Ag 4-O3 210.3(8), Ag 5-O3 209.9(7) 2×, Ag 6-O2 254.7(6) 6×; O1-Ag 1-O1' 179.9(9), O1-Ag 2-O2 166.5(3), O2-Ag 3-O3 168.8(2), O1-Ag 4-O3 174.2(6) O3-Ag 5-O3' 179.8(8).

$Ag_{25}Bi_3O_{18}$, a Potentially Valence-Unstable Bi^{III}/Bi^{V} Compound **

By *Manfred Bortz* and *Martin Jansen**

Dedicated to Professor Hans Georg von Schnering on the occasion of his 60th birthday

As demonstrated for example by $BaBiO_3$[1] and its variants generated by incorporation of potassium[2] or lead,[3] mixed valence Bi^{III}/Bi^{V} oxides are suitable candidates for semiconductor/metal transitions or even for phase transformations in the superconducting state.[4] There are plausible concepts, according to which a conceivable mechanism for the formation of Cooper pairs in the sense of the Bardeen-Cooper-Schrieffer (BCS) theory is seen in the periodic localization of two electrons to the non-bonding pair at Bi^{III} and their delocalization (transition to Bi^{V}), and the accompanying atomic shifts corresponding to a normal vibration.[5] This concept together with the meanwhile largely confirmed knowledge that monovalent silver in silver-rich oxides also tends to form cluster-like partial structures corresponding to the arrangement in silver metal with an unoccupied s-band,[6] would lead one to expect interesting electronic effects. In the case of silver-rich bismuth(III/V) oxides, the aforementioned semiconductor/metal transitions might result.

With $Ag_{25}Bi_3O_{18}$ we present one of the first compounds with these structural properties, which at the same time is the most rich in silver of the hitherto known ternary silver(I) oxides. One difficulty encountered in its synthesis from the binary components Ag_2O and "Bi_2O_5" or from Ag_2O and $AgBiO_3$ was in choosing the correct reaction temperature and oxygen pressure; too high a temperature (too low an O_2 pressure) led to silver(III) bismuthates; conversely, bismuth in the oxidation state + V was preferred. Crystal growth required the addition of water as mineralizer.[7] The new silver bismuthate was first obtained in the form of single crystals admixed with other phases. After determination of the composition of the single crystals by energy dispersive microanalysis[10] and X-ray structure analysis[11] it was possible to prepare single-phase powders on a gram scale.

$Ag_{25}Bi_3O_{18}$ forms shiny black crystals and is not air-sensitive. Thermal decomposition[13] takes place between 410 and 480 °C, leading to metallic silver and Bi_2O_3.

According to the X-ray structure analysis (Fig. 1) the compound undoubtedly contains both trivalent (Bi 1) and pentavalent (Bi 2) bismuth. Bi 1 has characteristic trigonal-pyramidal coordination with three proximal (3 × 221 pm) and three more distant (3 × 251 pm) oxygen neighbors, while Bi 2 is surrounded by an almost regular octahedral array of six oxygen atoms at a distance of 213 pm; thus, in each case, the assigned valence is consistent with that in other comparable bismuth oxides as regards the distances and the type of coordination polyhedron. The crystallographically independent silver atoms Ag 1 to Ag 5 are each twofold coordinated by oxygen atoms, whereby the angles at silver lie between 167 and 180°. Measurement of the electrical conductivity by the four-point method[14] showed a temperature dependence typical for semiconductors at relatively high specific resistances ($\rho = 7.9\ \Omega$cm, $T = 273$ K). This is to be expected, since, according to the results of the structural analysis, the valence electrons are localized.

According to the structural geometry a simple process is now conceivable by which the Bi^{III} is converted into Bi^{V} and at the same time the electron pair delocalized: by shifting the oxygen atoms into the coordination sphere of Bi 1 by less than 40 pm the unsymmetrical 3 + 3 coordination (characteristic for Bi^{III}) can convert into a regular octahedral coordination (Bi^{V}). Of the various possible ways of experimentally determining this process we first selected measurement of the reflection in the infrared spectral region under pressure.[15] Indeed above 1.9 GPa at 300 K a Drude-like optical behavior with a sharp plasma reflection edge at 0.5 eV is observed. With increasing pressure this reflection edge shifts to higher energies, thus indicating a steady increase in the density of free charge carriers. This process is reversible, i.e., the metallic behavior cannot be kept metastable under normal pressure. All further exploratory investigations of this interesting semiconductor/metal transition must therefore be carried out under permanent pressure.

Received: January 27, 1991 [Z 4406 IE]
German version: *Angew. Chem. 103* (1991) 841

CAS Registry numbers:
Ag_2O, 20067-12-3; Bi_2O_5, 35984-07-7; $Ag_{25}Bi_3O_{18}$, 133832-28-7.

[*] Prof. Dr. M. Jansen, Dipl.-Chem. M. Bortz
Institut für Anorganische Chemie der Universität
Gerhard-Domagk-Strasse 1, W-5300 Bonn 1 (FRG)

[**] This work was supported by the Deutsche Forschungsgemeinschaft (Gottfried-Wilhelm-Leibniz Programm), the Bundesministerium für Forschung und Technologie, and the Fonds der Chemischen Industrie.

[1] D. E. Cox, A. W. Sleight, *Acta Crystallogr. B24* (1982) 1968.
[2] R. J. Cava, B. Batlogg, J. J. Krajewski, R. C. Farrow, L. W. Rupp, Jr., A. E. White, K. T. Short, W. F. Peck, T. Y. Kometani, *Nature 332* (1988) 814.

[3] A. W. Sleight, J. L. Gillson, P. E. Bierstedt, *Solid State Commun. 17* (1975) 27.
[4] H. G. von Schnering, L. Walz, M. Schwarz, W. Becker, M. Hartweg, T. Popp, B. Hettich, P. Müller, G. Kämpf, *Angew. Chem. 100* (1988) 604; *Angew. Chem. Int. Ed. Engl. 27* (1988) 574.
[5] A. Simon, *Chem. Unserer Zeit 22* (1988) 1; A. Simon, *Angew. Chem. 99* (1987) 602; *Angew. Chem. Int. Ed. Engl. 26* (1987) 579.
[6] M. Jansen, *Angew. Chem. 99* (1987) 1136; *Angew. Chem. Int. Ed. Engl. 26* (1987) 1098.
[7] *Synthesis*: Intimate mixtures of Ag_2O (prepared according to Ref. [8]) and "Bi_2O_5" (prepared according to Ref. [9]) in the ratio Ag:Bi 25:3 were allowed to react with H_2O (2 mL) in silver crucibles in a stainless steel autoclave at an O_2-pressure of 10 MPa. After a reaction time of 1–2d, black crystals are formed.
[8] G. Brauer (Ed.): *Handbuch der Präparativen Anorganischen Chemie*, Enke, Stuttgart 1962, p. 912.
[9] G. Gattow, W. Klippel, *Z. Anorg. Allg. Chem. 470* (1980) 25.
[10] The ratio of the metals was determined by energy dispersive microanalysis (EDX PV9800) (calcd. Ag. 89.3 Bi 10.7%, obs. Ag. 90.1, Bi 9.9%).
[11] Crystal data: $Ag_{25}Bi_3O_{18}$ crystallizes trigonally. Space group $P\bar{3}$ (No. 147) with $a = 1158.9(1)$, $c = 623.9(1)$ pm (Guinier data, standard α-quartz; $a = 491.3$, $c = 540.5$ pm), $Z = 1$, $\mu(Mo_{K\alpha}) = 344.16\ cm^{-1}$. 8430 reflections measured (four-circle diffractometer Enraf-Nonius CAD-4 with $Mo_{K\alpha}$ graphite monochromator), $\omega/2\theta$ scan, 1409 independent reflections ($2\theta_{max} = 60°$). Absorption and extinction corrections. Solution of structure by direct methods and subsequent difference Fourier syntheses (SHELX-76 and SHELXS-86) [12]. Refinement of the parameters with anisotropic temperature factors (least squares method) gave for 1369 reflections with $I > 2\sigma(I)$ $R = 3.9\%$, $R_w = 3.4\%$ ($w = 3.857/\sigma^2(F)_o$). Further details of the crystal structure investigation are available on request from the Fachinformationszentrum Karlsruhe, Gesellschaft für wissenschaftlich-technische Information mbH, W-7514 Eggenstein-Leopoldshafen 2 (FRG), on quoting the depository number CSD-55253, the names of authors, and the journal citation.
[12] G. Sheldrick: *SHELX-76/SHELXS-86-Programmsystem*, Cambridge (UK) and Göttingen (FRG) universities.
[13] The decomposition was monitored by simultaneous thermal analysis (STA 429, Pt/Rh crucible, purged with Ar, heating rate 5 K min^{-1}) between 20 and 550°C.
[14] The measurement was carried out on a pellet (silver contact) of 9 mm diameter and 1 mm thickness in the temperature range 10–298 K.
[15] M. Bortz, M. Jansen, K. Syassen, H. Wilhelm, unpublished.

Endohedral Cluster Compounds: Inclusion of Helium within $C_{60}^{\bullet\oplus}$ and $C_{70}^{\bullet\oplus}$ through Collision Experiments **

By *Thomas Weiske, Diethard K. Böhme, Jan Hrušák, Wolfgang Krätschmer*, and *Helmut Schwarz**

Dedicated to Dr. Curt Brunnée

Of all the C_x carbon clusters,[1] the fullerene C_{60} (the "third allotropic form of carbon"[2]) is currently of greatest interest, largely because it can be produced in macroscopic quantities with the convenient method developed by *Krätschmer, Huffman*, et al.[3] Not long thereafter sufficient experimental evidence had been reported[1–3] to verify the visionary suggestion[4, 5] that C_{60} was the celebrated icosahedron of the I_h-point group.

What are the physico-chemical properties of C_{60}? Early results suggest, for example, that doped C_{60} can be regarded as a three-dimensional organic superconductor,[6] that it can be hydrogenated by the Birch-reduction to produce $C_{60}H_{36}$,[7] and that up to 24 methyl groups can be added to the polyanions of C_{60} as has just been reported.[8] Is an "endohedral chemistry", i.e. a chemistry which proceeds inside the cage of C_{60} or its radical cation, $C_{60}^{\bullet\oplus}$ also possible? While theory has postulated a variety of endohedral cluster compounds for C_{60} with interesting properties,[9] experimental findings for the production of C_xM-clusters ($x \geq 60$; M = La, Cu, Ba, Sr) from the laser-induced vaporization of a mixture of salt and graphite have been interpreted more diversely: *Smalley* et al.[10] indicate that their experimental results point to the production of a spherically-constructed C_x cluster with a metal atom inside it; on the other hand, *Kaldor* et al.[11] are of the opinion that $C_{60}La$, for example, is an empty C_{60} cluster which has "custody" of the metal on its outside surface.

Here we report results of a molecular-beam experiment in which mass-selected ions of $C_{60}^{\bullet\oplus}$ and $C_{70}^{\bullet\oplus}$ produced by electron-impact ionization at 70 eV collide with a stationary neutral gas N; products are observed which are dependent on the nature of the collision gas and which leave no doubt about the incorporation of N.[12]

Earlier experiments have already shown[13] that highly accelerated $C_{60}^{\bullet\oplus}$ and $C_{70}^{\bullet\oplus}$ ions lose C_2 unimolecularly and even-numbered C_n units ($n = 2, 4, 6$ etc.) upon collisional activation (CA);[14] however, nothing has been reported about the incorporation of N. Perhaps this is a consequence of the limited performance parameters of the mass spectrometers which have been employed, which do not allow certain experiments to be performed. The four-sector machine used by us (Scheme 1) records measurements which demonstrate

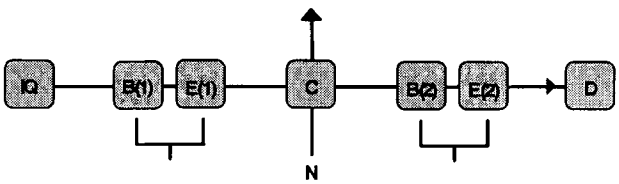

Scheme 1. Sketch of the tandem mass spectrometers used in this study: IQ = ion source, B = magnetic sector, C = collision chamber, E = electric sector, D = ion detector, N = neutral gas. For a complete description of the machine see Ref. [15].

the incorporation of N according to the collision-induced reaction [Eq. (a)].

$$C_x^{\bullet\oplus}\ (8\ keV) + N \longrightarrow [C_{x-n} + N]^{\bullet\oplus} + C_n \qquad (a)$$

$x = 60, 70$ $n = 2, 4, 6, \ldots$

For this purpose $C_x^{\bullet\oplus}$ ions ($x = 60$ or 70) were accelerated up to 8 keV, were mass-selected in the B(1)E(1) sector (resolution $m/\Delta m = 1500$), and then were allowed to react with various gases N in the collision cell C with ca. 75% reduction of the primary ion beam. The products of this high-energy

[*] Prof. Dr. H. Schwarz, Dr. T. Weiske
Institut für Organische Chemie der Technischen Universität
Strasse des 17. Juni 135, W-1000 Berlin 12 (FRG)
Prof. D. K. Böhme
Department of Chemistry and Centre of Research
in Earth and Space Science
York University
North York, Ontario M3J 1P3 (Canada)
Dr. J. Hrušák
Institut of Macromolecular Chemistry
Czechoslovak Academy of Sciences
Heyrovsky Square 2, CS-16202 Prague (Czechoslovakia)
Dr. W. Krätschmer
Max-Planck-Institut für Kernphysik
Postfach 103980, W-6900 Heidelberg

[**] This research was supported by the Deutsche Forschungsgemeinschaft and the Fonds der Chemischen Industrie. *D. K. B.* is grateful to the Alexander von Humboldt Foundation for a Senior Scientist Award.

reaction were detected and identified with a combined momentum and energy analysis ("linked scan": B(2)/E(2) = constant[16]). With H_2, D_2, Ar, and SF_6, the experiments show exclusive production of fragments in which C_n (n = 2, 4, 6, 8) or, less likely,[13b] multiple units of C_2 have been splitt off. A typical example is shown in Figure 1 for N = D_2. The same processes were observed for the other gases, but the relative intensities are somewhat different because of differences in "center-of-mass" energy, E_{cm}.[17]

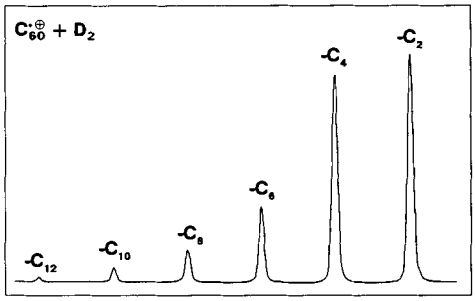

Fig. 1. CA mass spectrum for $C_{60}^{\bullet\oplus}/D_2$; E_{cm} = 44.2 eV.

A fundamentally different result is obtained when helium is used as a collision gas (Fig. 2). New signals appear at *higher* masses at all signals, corresponding to the loss of C_n; the mass difference Δm is equal to 4 when ^{4}He is used (Fig. 2, top) and 3 when ^{3}He is used (Fig. 2, bottom). The differences

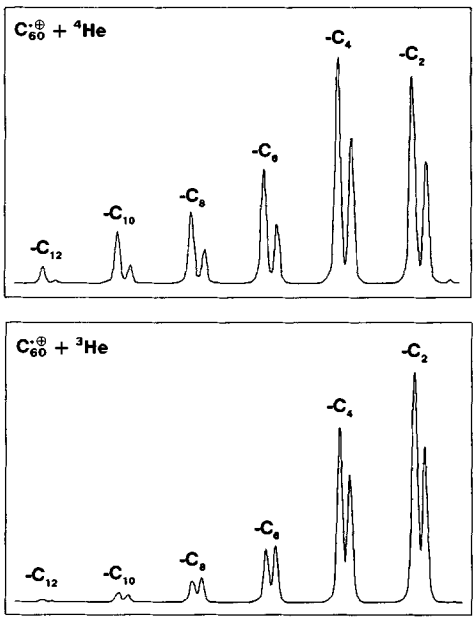

Fig. 2. CA mass spectra for $C_{60}^{\bullet\oplus}$ with ^{4}He(E_{cm} = 44.2 eV) (top) and ^{3}He(E_{cm} = 33.2 eV) (bottom).

which appear with D_2 and He cannot be accounted for by energy since E_{cm} is identical for these two gases; other factors (presumably size and shape of N) must be responsible. Totally analogous results are obtained with $C_{70}^{\bullet\oplus}$: while helium is incorporated (appearance of $[C_{70-n}He]^{\bullet\oplus}$), the other collision partners only lead to collision-induced elimination (loss of C_n). The observation that the $C_{60}^{\bullet\oplus}$/He fragment arises from $C_{70}^{\bullet\oplus}$/He (Fig. 4) is particularly noteworthy. If *Smalley*'s argument[5d] that loss of C_2 units is accompanied by a "repair" of the cluster-cage applies, this $C_{60}^{\bullet\oplus}$/He is the fullerene-noble gas complex which has been sought for a long time.[18]

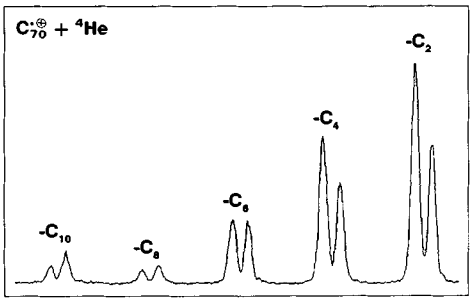

Fig. 3. CA mass spectrum for $C_{70}^{\bullet\oplus}$ with ^{4}He (E_{cm} = 37.9 eV).

The location of the helium atom in the $[C_{x-n}He]^{\bullet\oplus}$ clusters of course cannot be determined with the experiments described here, but there are indirect indications that we are almost certainly dealing with intra-cavity bonding rather than with cluster ions in which helium is fixed to the outer wall. The process $C_{60}^{\bullet\oplus} \rightarrow C_{58}^{\bullet\oplus} + C_2$ requires at least 4–5 eV according to *Lifshitz* et al.[13e] and *Smalley* et al.,[19] while the binding energy of He to $C_6H_6^{\bullet\oplus}$, for example, is less than 0.2 eV accoding to ab initio MO calculations.[20] If the helium was not incorporated by the cage during the collision process, it would have had to leave the complex on energetic and kinetic grounds before a C_2 unit splits off. Accordingly an increase in mass, Δm = 3 and 4, would not have appeared. Furthermore mass-selected $[C_xHe]^{\bullet\oplus}$ ions lose not He, but C_2 unimolecularly.

How much energy is required to bring a helium atom inside the $C_x^{\bullet\oplus}$ cages (x = 60, 70)? We have obtained an upper limit of less than 10 eV in model calculations in which He is forced through a C_6H_6 or $C_6H_6^{\bullet\oplus}$ plane.[20] This energy barrier,[21] whose accuracy should not be overemphasized, is clearly smaller than the kinetic energy of greater than 30 eV which is available to the collision complexes $C_x^{\bullet\oplus}$/He (x = 60, 70). Consequently, the inclusion of a helium atom into the cluster is energetically possible. *There is no doubt that a He atom is incorporated into the $C_x^{\bullet\oplus}$ (x = 60, 70) cluster in the course of the collision.*

The experiments and thoughts presented here provide a first item in the cornucopia of endohedral bonded (ionized) C_x fullerenes.[2, 9, 22]

Received: May 23, 1991
German version: *Angew. Chem. 103* (1991) 898

[1] Review: W. Weltner, Jr., R. J. Van Zee, *Chem. Rev. 89* (1989) 1713.
[2] a) J. F. Stoddart, *Angew. Chem. 103* (1991) 71; *Angew. Chem. Int. Ed. Engl. 30* (1991) 70, and references cited therein; b) F. Diederich, R. L. Whetten, *ibid. 103* (1991) 695 and *30* (1991) 678.
[3] W. Krätschmer, L. D. Lamb, K.Fostiropoulos, D. R. Huffman, *Nature (London) 347* (1990) 354.
[4] E. Osawa, *Kagaku* (Kyoto) **25** (1970) 85.
[5] a) H. W. Kroto, J. R. Heath, S. C. O'Brien, R. F. Curl, R. E. Smalley, *Nature (London) 318* (1985) 162; c) For "the story of buckminsterfullerenes" see: R. E. Smalley, *The Sciences (N.Y.) 31* (1991), No. 2, p. 22.
[6] A. F. Hebard, M. J. Rosseinsky, R. C. Haddon, D. W. Murphy, S. H. Glarum, T. T. M. Palstra, A. P. Ramirez, A. R. Kortan, *Nature (London) 350* (1991) 600.
[7] R. E. Haufler, J. Conceicao, L. P. F. Chibante, Y. Chai, N. E. Byrne, S. Flanangan, M. M. Haley, S. C. O'Brien, C. Pan, Z. Xiao, W. E. Billups, M. A. Cinfolini, R. H. Hauge, J. L. Margrave, L. J. Wilson, R. F. Curl, R. E. Smalley, *J. Phys. Chem. 94* (1990) 8634.

[8] J. W. Bausch, G. K. Surya Prakash, G. A. Olah, D. S. Tse, D. C. Lorents, Y. K. Bae, R. Malkotra, *J. Am. Chem. Soc. 113* (1991) 3205.
[9] a) J. Cioslowski, *J. Am. Chem. Soc. 113* (1991) 4139; b) J. Cioslowski, E. D. Fleischmann, *J. Chem. Phys. 94* (1991) 3730; c) A. H. H. Chang, W. C. Ermler, R. M. Pitzer, *ibid. 94* (1991) 5004.
[10] a) J. R. Heath, S. C. O'Brien, Q. Zhang, Y. Lin, R. F. Curl, H. W. Kroto, F. K. Tittel, R. E. Smalley, *J. Am. Chem. Soc. 107* (1985) 7779; b) F. D. Weiss, J. L. Elkind, S. C. O'Brien, R. F. Curl, R. E. Smalley, *J. Am. Chem. Soc. 110* (1988) 4464.
[11] a) D. M. Cox, D. J. Trevor, K. C. Reichmann, A. Kaldor, *J. Am. Chem. Soc. 108* (1986) 2457; b) D. M. Cox, K. C. Reichmann, A. Kaldor, *J. Chem. Phys. 88* (1988) 1588; c) A. Rosén, B. Wästberg, *J. Am. Chem. Soc. 110* (1988) 8701.
[12] Presented for the first time: D. K. Böhme, T. Weiske, J. Hrušák, W. Krätschmer, H. Schwarz, *37th Annu. Conference on Mass Spectrom. and Allied Top. (ASMS)*, Nashville, TN, USA, May 21, 1991.—We have heard from Dr. M. M. Ross, Naval Research Laboratories, Washington, D.C., that he has repeated our experiment after the ASMS conference and obtained the same results.
[13] a) P. P. Radi, M. T. Hsu, J. Brodbelt-Lustig, M. Kincon, M. T. Bowers, *J. Chem. Phys. 92* (1990) 4817; b) A. B. Young, L. M. Cousins, A. G. Harrsion, *Rapid Commun. Mass Spectrom. 5* (1991) 226; c) D. R. Luffer, K. H. Schram, *ibid. 4* (1990) 552; d) P. P. Radi, M.-T. Hsu, M. E. Rincon, P. R. Kemper, M. T. Bowers, *Chem. Phys. Lett. 174* (1990) 223; e) C. Lifshitz, M. Iraqi, T. Peres, J. E. Fischer, *Int. J. Mass Spectrom. Ion Processes*, in press; f) C. Lifshitz, M. Iraqi, T. Peres, J. E. Fischer, *Rapid Commun. Mass Spectrom. 5* (1991) 238; g) D. Schröder, D. Sülzle, *J. Chem. Phys. 94* (1991), 6933; h) R. J. Doyle, Jr., M. M. Ross, *J. Phys. Chem.*, in press.
[14] Reviews: a) R. G. Cooks (Ed.): *Collision Spectroscopy*, Plenum, New York 1978; b) K. Levsen, H. Schwarz, *Mass Spectrom. Rev. 2* (1983) 77; c) J. Bordas-Nagy, K. R. Jennings, *Inst. J. Mass Spectrom. Ion Processes 100* (1990) 105.
[15] a) R. Srinivas, D. Sülzle, T. Weiske, H. Schwarz, *Int. J. Mass Spectrom. Ion Processes*, in press; b) R. Srinivas, D. Sülzle, W. Koch, C. H. DePuy, H. Schwarz, *J. Am. Chem. Soc.*, in press.
[16] J. R. Chapman: *Practical Organic Mass Spectrometry*, Wiley, Chichester, England 1985, Chapter 6.
[17] The "center of mass"-energy (E_{cm}) determines the maximum energy which can be transferred in a collision of a projectile A with a stationary particle N. The following relationship holds: $E_{cm} = E_A[m_N/(m_N + m_A)]$, where E_A = kinetic energy of A (corresponding to 8000 eV in the experiments described here) and m_i the masses of A and N.
[18] Direct production of $C_{60}^{\oplus\bullet}$/He or $C_{70}^{\oplus\bullet}$/He according to Equation (a) in a high-energy collision experiment is fundamentally impossible on kinematic grounds. However, we are planning experiments with "slow" $C_x^{\oplus\bullet}$ ions. Furthermore, we intend to expose the $C_x^{\oplus\bullet}$/He species to a neutralization–reionization (NRMS) experiment. The experiment (which has not yet been performed because of insufficient intensities) will answer the question about the existence of neutral C_xHe clusters.
[19] S. C. O'Brien, J. R. Heath, R. F. Curl, R. E. Smalley, *J. Chem. Phys. 88* (1988) 220.
[20] The ab initio MO calculations were performed at the MP2/6-31G**// MP2/3-21G* level of theory. We expect that calculations with larger basis sets will lead to *smaller* values for the binding energy of $C_6H_6^{\oplus\bullet}$/He as well as for the energy required to pass He through a C_6H_6 or $C_6H_6^{\oplus\bullet}$ plane.
[21] For MNDO calculations of the barrier for the *endo* → *exo* migration of $Li^{\oplus}$ in C_x clusters see: D. Bakowies, W. Thiel, *J. Am. Chem. Soc. 113* (1991) 3704.
[22] Note added in proof (12 June 1991): First experiments with $C_{60}^{\oplus\bullet}$ and Ne (E_{CM} = 216 eV) show that this noble gas can also be incorporated into the cavity (appearance of $[C_{60-n}Ne]^{\oplus\bullet}$, $n = 2 - 10$), but the "yield" is a factor 10 smaller than in the case of He.

BOOK REVIEWS

Book Reviews are written by invitation from the editor. Suggestions for books to be reviewed and for book reviewers are welcome. Publishers should send brochures or (better) books to the following address: Redaktion Angewandte Chemie, Postfach 101161, D-6940 Weinheim, Federal Republic of Germany. The editor reserves the right of selecting which books will be reviewed. Uninvited books not chosen for review will not be returned.

Comprehensive Medicinal Chemistry. The Rational Design, Mechanistic Study and Therapeutic Application of Chemical Compounds. Six volumes. Edited by *C. Hansch, P. G. Sammes* and *J. B. Taylor*. Pergamon, Oxford 1990. Hardcover \$ 1995.00. (Individual volume: \$ 350.00 each).—ISBN 0-08-032530-0 (complete work)

Volume 1: General Principles. Volume Editor: *P. D. Kennewell*. xv, 811 pp.—ISBN 0-08-037057-8

The first section of this volume is very heterogeneous in content; it sets out to describe the development of medicinal chemistry by giving a chronology of drug introductions and tracing the history of the pharmaceutical industry. It shows how the different initial conditions and environments existing in German-speaking countries, in Great Britain and in the USA have led to the industry developing in different ways. The important role of legislation and of public regulatory agencies such as the FDA in imposing quality standards is emphasized, and it is shown how this led to a strengthening of the German and North American pharmaceutical companies even before the First World War.

The account of drug introductions is not in chronological order, nor is it complete. Admittedly it would not be possible to cover this subject exhaustively within the space allowed, but it is surprising that some important milestones such as the introduction of antihyperlipidemic aryloxycarboxylic acids ("Fibrates"), HMG-CoA-reductase inhibitors ("Lovastatin") and calcium antagonists of the dihydropyridine type are not included. On the other hand the space devoted to compounds such as LSD, tetrahydrocannabinol and chloramin-T is disproportionately large in relation to their importance. Antibacterial agents and their development are discussed in detail, but only penicillins and cephaalosporins are covered. Neither quinolones nor carbapenemes are mentioned. The important contribution of the azoles in antifungal therapy is also ignored. This not entirely successful historical introduction ends with brief accounts of Egyptian, Greek and Arabic medicine, plus two separate chapters on traditional Chinese and Indian medicine.

The second section on "Targets of Biological Active Molecules" follows a logical sequence, starting with the essentials of anatomy and physiology and proceeding via cell architecture to the identification of specific macromolecular targets. Principles of general pharmacology, such as the receptor theory, are derived in the course of the discussion.

Although the introduction to anatomy and physiology is pleasingly concise, this means that the non-biologists for whom this chapter is mainly intended will find that their needs are not fully satisfied here; it would have been useful to include references to suitable books covering these topics.

It is difficult to understand why a topic so important to pharmacology as the smooth muscular system is given such little emphasis, hidden away under the headings "Musculoskeletal System" and "The Neuromuscular Junction". The otherwise good introduction to renal physiology lacks a clear and full explanation of the renin–angiotensin–aldosterone system. The physiology of the central nervous system is treated systematically from an anatomical standpoint. The same also applies to the discussion of endocrine glands and of hormones, although here some new findings such as those concerning ANP, EDRF and endothelin are not mentioned. As the treatment is so concise, one expects that it should be clear and unambiguous, and should not conflict at any point with the textbooks (as, for example, in the cases of the Hagen-Poiseuille equation or of renal autoregulation). The chapter provides good basic information in the simplified account of the complex relationships in the immune system. However, only a relatively small amount of space is devoted to the AIDS problem. Basic concepts of general pharmacology and their quantitative aspects are explained with the help of examples. The contents of the articles entitled "The Concept of Bioselectivity" and "Bioselectivity" could have been presented more concisely by either combining them or relating them more effectively.

The third section, "Bioactive Materials", begins with an excellent discussion of structure–activity relationships, their importance for classifying active substances, and the problems that this entails. The two following chapters illustrate, for the benefit of outsiders, the complex nature of the search for new structural types with pharmaceutical activity. However, the expert too will undoubtedly discover here stimulating viewpoints for example the discussion of the advantages and disadvantages of different types of organizational structures for finding and evaluating new active agents in an interdisciplinary way. Two chapters deal with natural products, but these are devoted exclusively to hormones. In some parts the discussion becomes lost in experimental details that are of little interest to the outsider. On the other hand the chapter on analytical methods is clearly presented. Unfortunately, however, the great advances made possible by the use of molecular biological techniques in this field are only touched on briefly. This is followed by a rewarding chapter in which the many problems that nowadays confront a chemist engaged in process development are described. Even readers unfamiliar with this field will gain a clear impression of the factors that often force one to adopt a synthetic strategy far removed from the laboratory method.

The field of gene molecular biology, gene structure and cloning techniques is only covered in a very patchy fashion, as is evident from the fact that there are only 40 literature references altogether. It would have been better to save this space by referring the reader to appropriate textbooks, and to devote it instead to gene expression and manipulation, which is only treated very briefly in the following chapter. Although many topics are touched on, the information content remains rather meager. The final chapter ("Genetic Engineering: Commercial Applications") deals with the therapeutic applications of recombinant proteins and fits very well into the subject area of this series. However, it does not make any reference to antibodies produced by genetic engineering.

The last section, "Socio-Economic Factors of Drug Development", is again very heterogeneous. The topics covered are regulatory authorities, the organization and funding of pharmaceutical research, health care systems, clinical pharmacology, animal experiments, and patenting. Nearly all the material on the first four subjects named above relates to the situations in Great Britain and the USA. For an international standard source it would have been desirable to also discuss the situation in the European Community, which will become an increasingly important factor in the future, and also to describe, at least briefly, the special features of the Japanese licensing mechanisms for pharmaceuticals. Apart from these reservations most of the chapters provide good concise reviews of their subjects. There are special sections devoted to the now highly interesting topics of "Good Clinical Practice" (GCP), "Good Manufacturing Practice" (GMP) and "Postmarketing Surveillance" (PMS).

To summarize, in aiming to present a comprehensive account of this broad area the authors have in general given basic information, but the chapters vary greatly in their provision of references to literature covering the topics in greater depth. One would have liked to find more cross-references to more detailed discussions to be found in other chapters or in other volumes of this series, and this would undoubtedly have added greatly to the usefulness of the volume.

John E. Butler, Rainer Groß
Gert Gruenewaldt, Peter Rounding,
Axel Unterbeck, Thomas Weihrauch

Volume 2: Enzymes and other Molecular Targets. Volume Editor: *P. G. Sammes*. xvii, 887 pp.—ISBN 0-08-037058-6

Volume 2 deals with enzymic processes, and also describes agents that interfere with the synthesis of the bacterial cell wall or produce changes in nucleic acids. It begins with a general introduction describing the structures, nomenclature and classification of enzymes, the mechanisms of catalysis and inhibition, and the development of resistance and tolerance towards antimicrobial agents. This is followed by descriptions of particular enzymes and enzyme systems of importance. It is, of course, not possible within this relatively limited space (a little over 500 pages) to give an exhaustive survey of this complex field. The criteria used in making the selection have clearly been based mainly on pathophysiological importance and on the ability to influence systems by pharmacological means. In the following commentary several chapters will be picked out as examples.

The article on protease inhibitors (*D. H. Rich*, University of Wisconsin) is confined to inhibitors of low molecular mass, with the main emphasis on renin and ACE inhibitors. Unfortunately there is not much discussion of the relationship to biology and medicine. Good features are the inclusion of X-ray structural data and the discussion of "molecular mechanics" calculations. The chapter on enzyme cascades, coagulation, fibrinolysis and hemostasis agents (*M. P. Taylor*, Warner Lambert Company) gives a very good overall description of the processes of hemostasis, fibrinolysis and coagulation. Less satisfactory, however, are the formula schemes and diagrams, which could have been set out more clearly, and are too small relative to the typeset formulas. Whereas the account of fibrinolysis therapy includes references to the latest developments in molecular biology (e.g. the use of rTPA), the discussion of blood coagulation does not give enough information about developments of this kind (e.g. the treatment of hemophilia using rFVIII as an alternative to plasma concentrates). In general molecular biological aspects are underrepresented; for example, the cloning of blood factors and the techniques that have grown from it are not adequately covered. In contrast the chapters on the arachidonic acid cascades (*G. A. Higgs, E. A. Higgs* and *B. Moncada*, Wellcome Research Laboratories), on phosphodiesterase inhibitors (*R. E. Weishaar* and *J. A Bristol*, Warner Lambert Company), on phospholipase-A_2

(*H. van den Bosch*, Utrecht), and especially that on protein kinases (*K. J. Murray* and *B. A. Warrington*, Smith, Kline and French) contain comprehensive information, presented concisely with clear tables and diagrams. In the last-named chapter especially, a wealth of information on all the known protein kinase inhibitors, including structure–activity relationships and a discussion of the biological effects, is clearly and concisely presented. This chapter is of equal interest to the chemist and the biologist. However, it would have been useful, especially from the standpoint of up-to-dateness, to include here a discussion of the protein phosphatases and their inhibitors; this would undoubtedly have contributed to giving a more complete picture of cellular regulatory mechanisms.

The clearly set out and succinct chapter on agents that affect nucleic acids provides the reader with a soundly-based insight into the various molecular mechanisms involved. Suggestions are put forward for setting up selective therapeutic strategies to counteract tumor cells and pathogens. The chapters that follow discuss other aspects of antimicrobial agents: the development of resistance and tolerance to antibiotics, substances that intervene in metabolic processes, and agents that affect cell walls. The discussions of these include details on a wealth of chemical structures and pharmacological effects. However, this inevitably means that some aspects are treated too briefly and without sufficient attention to the latest state of knowledge. The disjointed treatment is especially noticeable in the fact that there are two chapters on β-lactams by different groups of authors.

There is no doubt that Volume 2 of this work again illustrates the general rule that length and up-to-dateness are inversely related, despite the fact that quite a number of the chapters contain references to recent literature (1986 to 1988). This, and the non-uniformity in the treatment due to the large number of authors, are penalties that the reader must incur along with the benefits of comprehensive books of this kind. Nevertheless, the book is of considerable value because of the wealth of information that it contains. The biologist working in the pharmaceuticals area who needs to find ways of controlling cellular or molecular processes will find here many pointers to active compounds that are already known. Looked at from this standpoint, as a reference source, the book is undoubtedly a valuable addition to the literature.

Stefan Wohlfeil, Erwin Bischoff,
Rüdiger W. Braun, Axel Dalhoff,
Detlef Schmidt

Volume 3: Membranes and Receptors. Volume Editor: *J. C. Emmett*. xvii, 1280 pp.—ISBN 0-08-037059-4

The third volume of the handbook deals with the pharmacology of the cell membrane and of membrane receptors. The arrangement of the contents according to types of mechanisms is sensible and makes it easy to find the subject areas one is seeking; unfortunately, though, sufficient cross-references are not provided to enable one to gather information on processes that fall into several mechanistic categories (as in the case of the "receptor operated ion channel", for example). Also one searches in vain for membrane processes of such central importance as active and passive ion transport. These are in fact treated in Volume 2 with its vague title "Enzymes and other Molecular Targets".

The explanatory sections on methods and mechanisms that introduce the volume as a whole and some individual chapters are very useful, especially for readers new to the field. For example, the introductory section on the structure and function of cell membranes gives a comprehensive and very clearly set out overview of the current state of knowledge in this area. As well as indicating some general principles of membrane biochemistry with the help of examples, the techniques used to study these systems are introduced in an easily understandable way. These topics include the quantitative analysis of ligand–receptor interactions and a brief review of methods for isolating and purifying membrane receptors and investigating their molecular biology.

The chapter on transduction of signals and "second messenger" analogues unfortunately fails to live up to its promise to introduce the reader to the mechanisms of signal transduction. It seems that the adenylate cyclase, guanylate cyclase and phospholipase C systems are only mentioned here as a vehicle for including a few literature citations. The discussion that follows deals only with "second messenger" analogues, and here reference is continually made to "inositol 1,4,5-triphosphate" instead of the correct name inositol 1,4,5-trisphosphate.

The authors of the chapters on neurotransmitters and their receptors have succeeded in providing an excellent and informative review of this field, which has now become very complex. A pleasing feature here is the use of a standard structure for each of the chapters. Starting with a description of neuroanatomy and of the neurotransmitter pathways in the brain and/or its periphery, the authors proceed to discuss the biosynthesis and metabolism of each type of neurotransmitter. This is followed by the mode of action of the neurotransmitters and the ways in which they are influenced by agonists and antagonists.

The traditional classification of receptors according to their response to synthetic transmitter analogues is nowadays being replaced increasingly by one based on molecular biological criteria. It has not been possible to cover this aspect adequately here, in view of the rapid developments that have occurred in the last few years.

Most of the authors conclude their discussion of the receptors concerned by describing the potential or already practised therapeutic applications of agents with specific activity towards the neurotransmitter–receptor system. This means that each chapter is a very useful and informative reference source, not only for chemists, biochemists and pharmacologists but also for medical scientists, providing a clear description of the sequence from the chemical synthesis of a receptor-specific substance to a practical therapeutic agent.

The treatment of peptide receptors is very clear and informative, and the division of this complex subject into ten chapters is appropriate. These describe the characterization of the receptors, their biosynthesis and metabolism, the ways in which they are affected by the endogeneous peptides and by peptide and non-peptide ligands, and, where appropriate, the therapeutic applications of these substances. Structure–activity relationships are treated at considerable length.

In the chapter on angiotensin receptors one would have liked to be given a rather more balanced treatment by the inclusion of important research results from other groups. Moreover, the non-peptide angiotensin-II antagonists are underrepresented, being only mentioned in a single sentence. One also searches in vain for a description of endothelin receptors.

In the treatment of ionic channels the pharmacology of the sodium and calcium channels in particular is covered very well and in great detail. However, the discussion of the potassium channels fails to come up to standard because of recent developments that are not included. Chloride channels are not treated at all.

The lymphokins and cytokins of the immune system are treated separately. Although this makes for a clear division of topics, it means that the complex interaction between these mediators is not sufficiently brought out. Some of the sub-chapters, such as the account of the physiological and clinical importance of interleukins, are very informative. On the other hand the importance of the role of TNF is understated; in the account of analytical techniques there is not enough discussion of the advantages and disadvantages of the various methods, and some of the literature references are not mentioned in the text. The bibliographies are in many cases more than five years out of date, and thereby fail to live up to expectations in this respect, especially in the discussion of pharamacological agents that affect the immune system.

The final chapter of this volume is devoted to the molecular structure, regulation and ligand chemistry of the most important intracellular receptor systems, namely vitamin D, thyroid hormone and steroid hormone. The treatment is for the most part of an impressively high standard. An exception to this is the physiology and pathophysiology of the steroid receptors, which unfortunately has been subdivided and placed in different parts of the chapter in a confusing way. The literature references here are up-to-date and comprehensive, making it easy for the reader to refer to the original papers when special questions arise.

To summarize, this volume is a substantial collection of good review articles dealing with specific topics, but cannot be regarded as a self-contained textbook or comprehensive work of reference.

Martin Bechem, Arno Friedl, Siegbert Hebisch, Gabriele Hecker, Henning Sommermeyer, Hans-Peter Stasch

Volume 4: Quantitative Drug Design. Volume Editor: *C. A. Ramsden*. xvi, 766 pp.—ISBN 0-08-037060-8

Volume 4 of this work contains 24 articles by well-known authors. The main emphasis is on the "classical" methods of investigating structure–activity relationships and on molecular modeling methods.

Methods for quantifying the physicochemical properties of chemical structures and their interactions are treated in detail. The discussion is concentrated mainly on computer-aided theoretical methods, ranging from molecular fragment approaches to predicting lipophilic behavior (*A. J. Leo*), through to molecular dynamics methods for calculating relative free energies of ligand–receptor complexes (*J. A. McCammon*).

The quantitative description of biological data and the transport of substances to the target site are each covered in only one chapter, these being by *Y. C. Martin* et al. and *J. C. Dearden* respectively.

Several further articles are devoted to the models and mathematical techniques used in correlating structure with activity; for example, the *Hansch* approach and the *Free–Wilson* method are described in detail with many examples by *T. Fujita* and *H. Kubinyi* respectively. Other articles are concerned with the design of testing programs and methods of pattern recognition. This group of articles is completed by an account of some further methods, including the application of substructure analysis for predicting toxicity and choosing suitable test compounds for screening tests (*P. N. Craig*), followed by a description of the distance-geometry method (*A. K. Ghose* and *G. M. Crippen*).

The use of models and molecular graphics techniques in drug design is described in three articles by *R. Langridge* and *T. E. Klein*, by *G. R. Marshall* and *C. B. Naylor*, and by *J. M. Blaney* and *C. Hansch*. The relationship between these and the quantitative methods is also discussed.

The editors do not appear to have set out to present a balanced and comprehensive account of all the models and methods that are in use in this field. In some cases the authors of the contributions seek to justify the omissions, as, for example, in the case of the unduly brief treatment of connectivity indices. In other topics, such as the treatment of QSAR parameters for peptides or the study of structure-pharmacokinetic relationships, the omissions are less easy to understand.

The unavoidable instances of overlapping between the contributions have mainly been kept to a reasonable minimum. However, this is not always the case in the introductory articles; for example, the information on chemical data banks could have been shortened, as these were already listed in Volume 1.

The layout of the volume is excellent. However, the long period required to prepare it has meant that only developments up to about 1988 are included. For this reason some topics of current importance, such as 3D data banks, computer methods for designing ligands to match known receptor structures, and methods of quantifying chemical similarity, are unfortunately not included.

Despite the high price and the fact that some good monographs on this field already exist, especially in the QSAR area, the eminence of the contributing authors ensures that the book is of a high standard and will be successful.

Eike Möller, Martin Blunck

Volume 5: Biopharmaceutics. Volume Editor: *J. B. Taylor*. xvii, 756 pp.—ISBN 0-08-037061-6

Volume 5 is concerned with "Biopharmaceutics" and embraces a wide range of topics, from "Principles of Pharmacokinetics and Metabolism" through "Analytical Methodology" to matters of pharmacy and formulation in "Chemistry and Pharmacy in Drug Development".

The first part deals with the fundamentals of pharmacokinetics, beginning with general chapters on absorption, distribution and metabolism. These chapters provide the scientist involved in pharmaceuticals development with a good overview of the basic principles underlying pharmacokinetics. Especially useful is the concisely written chapter by *T. N. Tozer*, which forms an excellent introduction for the beginner. The emphasis that is placed on the physiological basis of pharmacokinetic processes in these introductory chapters, for example that on absorption (*Dennis*), is commendable. However, it would have been desirable to include here a more detailed treatment of bioavailability and bioequivalence, which has become a highly interesting theme in recent years. The chapter on "Distribution and Clearance Concepts" by *Gaillot* et al. contains an excellent summary of current knowledge concerning the physiological basis and importance of distribution processes, but clearance concepts deserved to be treated at considerably greater length.

The section on "Sites of Drug Metabolism, Prodrugs and Bioactivation" contains a well organized discussion of aims and approaches in the design of prodrugs. The comprehensive bibliography and the tables listing details of review articles are useful for readers from other disciplines. The very large field of bioactivation of chemicals to form reactive intermediates, and the toxicological problems that this causes, is only treated in the form of a concise summary, which is understandable.

These general review articles are followed by discussions of some special areas, some of which are very up-to-date.

These short reviews also serve to provide the specialist with a quick overview. Readers interested in following these up in greater depth are helped by the mainly well selected bibliographies, which extend up to about 1988.

In the very informative chapter by *Juchau* on "Species Differences in Drug Metabolism" the benefits and problems arising in the use of various animal species as models for predicting effects on humans are discussed. In drawing attention to the effects of extrahepatic biotransformation and to differences in the isoenzyme patterns of different species, and discussing enzyme systems that have received little study, the authors make it clear that present knowledge still leaves many gaps. Equally informative and interesting are the chapters on "Developmental Drug Metabolism" (*Juchau*) and "Stereoselectivity..." (*Lennard* et al.). There are further specialized chapters on highly topical matters, such as that on "Chronokinetics" (*Reinberg* et al.). The remarkable variations observed in pharmacokinetic processes according to the time of day are described with many examples, and the relative importance of endogenic factors (biorhythms) and exogenic factors (e.g. food intake) is examined. To complete the picture, some of the methodology used to investigate these problems is described. It is pointed out that the regular, and therefore predictable, cyclic changes that are observed in chronokinetics studies are of practical importance in the development of programmed delivery devices, and the possible therapeutic implications are also discussed.

The chapter by *Paalzow* on "Pharmacodynamics" discusses concentration–activity relationships by considering numerous examples. The detailed description of the mathematical models used is sufficient to enable the reader to become thoroughly involved in the theories of this area of research; the comprehensive and up-to-date bibliography offers further new ideas in this field.

The second part, entitled "Analytical Methodology", suffers to a noticeable extent from the problems caused by the complexity of this subject. The growth that has occurred in analytical chemistry in recent years is such that there is a danger of parts of this chapter being reduced to a mere collection of technical terms. For example, under the title "Isolation and Identification of Metabolites" the book covers, in only 18 pages, not only enzymic but also chromatographic and spectroscopic methods. Such a sketchy summary can at best only be of interest to beginners. The introduction to biological analytical techniques by *Chamberlain* is excellent from a learning standpoint. However, one would have preferred this chapter to be more up-to-date; for example, the use of monoclonal antibodies only receives a brief mention. *Boobis* et al. review techniques for in vitro investigations of the metabolization of foreign substances, including a detailed evaluation of alternative experimental procedures. This chapter also includes a very comprehensive bibliography. *Vaughan* describes the mathematical aspects of pharmacokinetics from a strongly theoretically-orientated standpoint. In view of the intended readership it would have been desirable here to relate the discussion more closely to the physiological background and the application of the theoretical model to practical situations.

The final part, entitled "Chemistry and Pharmacy in Drug Development", covers a variety of topics, ranging from the properties of pharmaceutical substances, and their consequences for the formulation of products by conventional methods, also taking physiological factors into account, to new approaches such as drug targeting.

The first article, by *Curry* and *Thakker*, is entitled "Physicochemical Principles", and is mainly concerned with the crystallinity and particle size distribution of pharmaceutical compounds and their consequences for the method of formulation. Here it would have been useful to include a more detailed description of other important variables and techniques for adjusting them at the pre-formulating stage. In the chapter on "Formulation" *Florence* and *Halbert* emphasize the importance of in vitro tests on drug release for arriving at the best formulation. This is followed in logical sequence by a description of in vitro and in vivo correlation methods, including a useful table listing many published studies on this theme.

In their contribution on "Routes of Administration and Dosage Regimens" *Johnson* and *Lewis* provide the newcomer to the subject of formulation with a comparative review of the advantages and disadvantages of various alternative routes of administration in pharmaceutical therapy. Newer therapeutic routes such as the nasal administration of peptides, buccal administration, and transdermal absorption are described. The second part of this article, which deals with devising dosage regimens, seems out of place in the part of the book concerned with pharmacy, especially as it has already been treated in the first part, "Principles of Pharmacokinetics and Metabolism".

The article on "Delivery System Technology" discusses various methods of retarding drug release and ways of achieving improved absorption with peroral formulations. Transdermal therapeutic systems are also discussed as a modern formulation principle, together with the requirements that must be satisfied by the substances to be administered because of the structure of the skin; here the principles are related to practical situations by describing a number of commercial products.

In the noteworthy review of "Drug Targeting" by *Crommelin* and *Storm* the authors provide a comprehensive overview of the current situation in this very active field of research, including much information that is useful not only for newcomers but for those already working in this area. A commendable feature is the comprehensive and up-to-date bibliography.

This volume must be evaluated in relation to the ambitious claim that the collection of articles represents "a milestone ... in terms of coverage, clarity, and a sustained high level of presentation". In view of the wide range of topics covered, it is understandable that it has not been possible to treat all of these with equal thoroughness, although there has clearly been an effort to achieve complete coverage. Taken as a whole this collection, despite some weaknesses, offers a good overall survey of the current state of knowledge in biopharmaceutics, and it provides easy access to more advanced reading. It can therefore be recommended for all scientists interested in the development of pharmaceuticals.

Hans-Peter Krause, Hans-Jürgen Ahr, Michael Boberg, Jürgen Günther

Volume 6: Cumulative Subject Index and Drug Compendium. Volume Editor: *C. J. Drayton.* xv, 991 pp.—ISBN 0-08-037062-4

This is a useful book.

The first 236 pages consist of a detailed subject index to Volumes 1–5. This is followed by a "Drug Compendium" of over 700 pages, compiled by *P. N. Craig* in a remarkably laborious achievement. This lists over 5500 compounds (established and potential pharmaceuticals, pharmacological agents, etc.) with their generic names and their structural formulas produced by the ChemBase program. The principal sources that have been drawn on are *USAN* and the *USP Dictionary of Drug Names*, while additional data have come

from the *Merck Index (10th edition), The National Formulary, Annual Reports in Medical Chemistry, The American Drug Index,* and *Martindale: The Extra Pharmacopoeia.* Besides structure and generic name (from *USAN* or *INN*) further entries are given: the CAS Registry Number, the molecular mass, molecular formula, partition coefficients and indications of the physiological effects and therapeutic uses.

It is evident that identifying the first manufacturer has been problematic, and has led to numerous incorrect statements. In the author's favor it must be admitted that outsiders can easily lose their way in the jungle of licensing, cross-licensing, subsidiary companies, franchises, etc., but more care should have been taken in this area. It is evident that other authors should be warned against using the book as their primary source with regard to first manufacturers—it could lead to regrettable mistakes.

The entry *classification* is also not very clearly presented. Insufficient attention has been given to consistently listing not only the activities but also the mechanisms. It would have been worthwhile to go into this matter thoroughly, since the mechanism of action is particularly important to the medicinal chemist involved in drug design; this is especially the case when making a search in the 3(D)-Database (Molecular Design Ltd.), which is identical in content.

Despite the above teething troubles, which one hopes will be overcome in the next edition, the verdict still remains: this is a useful book.

Wolfgang Hartwig [NB 1129 IE]
Address of all the reviewers of this work:
Bayer AG
Pharmaforschungszentrum Wuppertal (FRG)

Adolf Butenandt. Biochemiker, Hormonforscher, Wissenschaftspolitiker. By *P. Karlson.* Wissenschaftliche Verlagsgesellschaft, Stuttgart 1990. 336 pp., hardcover DM 78.00. – ISBN 3-8047-0830-7

It is risky enough to write the biography of an eminent scientist and individual during his lifetime, and even more so when it comes from one of his closest students. Is it not essential to stand at some distance to write a biography? Can a student and close friend such as *Peter Karlson* write a biography of his "boss" and teacher, without falling into the traps of either excessive praise or resentment? This book proves that such doubts are unfounded.

Karlson spent 24 years close to *Butenandt*, years that witnessed many changes in *Butenandt*'s many-sided life, including the beginnings of research into viruses, insect biochemistry, and hormones and the introduction of the gene-product hypothesis. It was in the latter studies that *Karlson* was most closely involved. However, the lively and absorbing account is not confined to these years; the author has carried out scholarly study into *Butenandt*'s childhood and youth, his hometown, and his student days, and he has continued this into *Butenandt*'s later years with devoted interest. His factual and impressive account of the life of this great researcher contains not only a wealth of scientific history and factual information, but also much personal detail and historical background.

I first came to know *Adolf Butenandt* personally during my work in the Max-Planck-Gesellschaft from 1962 onwards, although of course I was already familiar with his work before this. For me an important criterion in assessing any one of the older generation is how he behaved during the Hitler regime, and therefore I will quote from *Karlson*'s book the passage describing how *Butenandt* was forced to turn down the Nobel Prize: "Butenandt was summoned to the Reichskultursministerium. At the door stood a towering SS man, who remained there silently on guard duty. On the desk lay a very harshly worded letter of refusal. Menzel said: 'This draft has been on the Führer's desk and he has approved it, and therefore none of its text can be altered.' Butenandt read the letter, found it unacceptable, and said that he was unable to sign it immediately. He was given three days to think it over. Menzel dismissed him with the words: 'But please consider carefully what consequences it will have for you and your family if you fail to obey an order of the Führer in wartime!' Adolf Butenandt went home with this moral dilemma and discussed it with his wife. After much thought they decided together that Butenandt would not sign this letter, but would instead send a courteous and factual letter to Stockholm. Shortly afterwards Alfred Kühn and Fritz von Wettstein arrived. They too were aware of the text of the letter that Butenandt was supposed to sign. They both urged him not to put up any foolish resistance in view of the menacing political situation. Kühn's exact words were 'I shall not leave your house until you promise us that you will not do anything foolish. You would achieve nothing by refusing to sign, and you would risk bringing ruin on your family and your academic institute. That would be stupid.' These conversations, especially those with his friends Kühn and Wettstein, finally persuaded Butenandt to sign the letter... it still remains a painful recollection for Butenandt that he yielded to the President's [the President of the Kaiser-Wilhelm-Gesellschaft] request and to his friends' entreaties. He said this was the only time that he had ever signed anything that was untrue!" Can any scientist of the younger generation fully appreciate what was going on at that time in the country and in the minds of many of its people? It is good to find such matters treated so openly in this biography.

Reviewing this comprehensive and, at the same time, highly readable account of the life's work of *Adolf Butenandt* has again evoked my admiration of the remarkable versatility of this researcher. After earning a Nobel Prize for the discovery and structure determination of sex hormones, he went on to achieve at least two or three further scientific successes of comparable importance, in his research on viruses, in the isolation and structure determination of insect hormones, and finally in his research on gene products which was stimulated by his association with *Kühn*. However, it is unfortunate from the standpoint of scientific history that the scientific community has apparently forgotten that *Butenandt* proposed the "one gene one enzyme" theory as early as 1940, at least five years before *George Beadle*.

I experienced firsthand *Butenandt*'s activities in the organizational aspects of science, especially his work as president of the Max-Planck-Gesellschaft. *Karlson* describes this period of *Butenandt*'s life from a thorough knowledge of the facts, telling how for twelve years *Butenandt* guided the fortunes of the Max-Planck-Gesellschaft in a way that was both well-informed and personally honest—one can even say in a noble and dignified way.

This discussion has now become not only a favorable book review but also a eulogy of *Butenandt* himself—I hope he will forgive me.

The book can be recommended to everyone with an interest in scientific history, from the student to the emeritus professor. Their scientific knowledge will benefit from reading it, and it will extend their knowledge of scientific history and of the turbulent period covered by *Butenandt*'s life from

1903 onwards. Thus, *Peter Karlson*'s biography of *Adolf Butenandt* is an important book from many points of view.

Friedrich Cramer [NB1135IE]
Max-Planck-Institut für experimentelle Medizin
Göttingen (FRG)

Countercurrent Chromatography. By *W. D. Conway*. VCH Verlagsgesellschaft, Weinheim 1990. 475 pp., hardcover DM 138.00. – ISBN 3-527-26527-9

Liquid-liquid distribution, the partition of a mixture of substances between two incompletely miscible liquid phases, is an effective method for separating mixtures of involatile soluble compounds. It became important as Craig distribution and partition chromatography, and nowadays it is still the basis of many technical separation processes. Regrettably it has now been almost entirely replaced in the laboratory by modern chromatographic methods. Even today it still has potential uses in the laboratory by virtue of its excellent capabilities, especially for isolating and purifying involatile compounds on a preparative scale. Particular advantages are the ability to simply and accurately calculate the efficiency of separation, and the ease with which the method can be scaled up.

Therefore the appearance of this comprehensive review of recent developments in the field of liquid-liquid chromatography is very welcome. The main chapters of the book describe the development of countercurrent chromatography, methods for producing the flow of the phases and the centrifugal forces, liquid partition and mixing of the phases, chromatography theory, solvent systems and applications. A comprehensive and well arranged bibliography follows the main text.

The book describes the techniques and equipment for achieving chromatographic separation, usually in a helical column made of glass or plastic, without the need for a solid porous membrane between the two liquid phases. Relative motion between the phases is obtained using either gravitational or centrifugal forces. The centrifugal forces are produced by rotating the separating apparatus in various ways. The fact that so many different arrangements are described illustrates that the development of the technique is still far from finished, and it will probably be some time yet before there is a routine system that is versatile enough for general use. The systems described here are capable of separating up to 1 g of a mixture with a separation efficiency of 350 to 1000 theoretical plates. The time required to achieve separation is of the order of hours.

Although countercurrent chromatography will undoubtedly always remain a specialized technique, it is nevertheless desirable that it should become widely used. In view of the continually growing importance of methods for isolating and purifying compounds, one needs to have access to as wide a variety of efficient separation techniques as possible. The book reviewed here is a comprehensive introduction to this subject, and can be recommended.

Herbert Feltkamp [NB1133IE]
Bayer AG
Pharma Analytik und Qualitätskontrolle
Leverkusen (FRG)

Corrigendum

The communication entitled "Parabolic Growth of a Self-Replicating Hexadeoxynucleotide Bearing a 3′–5′-Phosphonamidate Linkage" by *G. von Kiedrowski, B. Wlotzka, J. Helbing, M. Matzen*, and *S. Jordan* (*Angew. Chem. 103* (1991) 456; *Angew. Chem. Int. Ed. Engl. 30* (1991) 423) contained an error. The values of k_a and k_b calculated for *Rebek*'s system (T. Tjivikua, P. Ballister, J. Rebek, Jr., *J. Am. Chem. Soc. 112* (1990) 1249–1250) are wrong. The following values are correct: $k_a = (4.26 \pm 0.09) \times 10^{-2}\ \mathrm{M}^{-3/2}\ \mathrm{s}^{-1}$, $k_b = (1.94 \pm 0.04) \times 10^{-3}\ \mathrm{M}^{-1}\ \mathrm{s}^{-1}$. These values are in agreement within the limits of error with those caluclated by *Rebek* on the basis of Equation (a) given in our communication (J. Rebek, private communication). The value for ε is therefore not 80—as given in the text—but 22. For the exponential model (note [9] in our communication), the regression coefficients are $k_a = (5.20 \pm 0.24) \times 10^{-1}\ \mathrm{M}^{-2}\ \mathrm{s}^{-1}$ and $k_b = (2.56 \pm 0.07) \times 10^{-3}\ \mathrm{M}^{-1}\ \mathrm{s}^{-1}$; the sum of least squares exceeds that of the square-root model by a factor of 4.6. The other information in this communication is not affected.

Registered names, trademarks, etc. used in this journal, even when not marked as such, are not to be considered unprotected by law.

© VCH Verlagsgesellschaft mbH, W-6940 Weinheim, 1991. – Printed in the Federal Republic of Germany by Konrad Triltsch Druck- und Verlagsanstalt Würzburg.

All rights reserved (including those of translation into foreign languages). No part of this issue may be reproduced in any form — by photoprint, microfilm, or any other means — nor transmitted or translated into a machine language without written permission from the publishers. Only single copies of contributions, or parts thereof, may be made for personal use. This journal was carefully produced in all its parts. Nevertheless, authors, editors and publisher do not warrant the information contained therein to be free of errors. Readers are advised to keep in mind that statements, data, illustrations, procedural details or other items may inadvertently be inaccurate.

Valid for users in the USA: The appearance of the code at the bottom of the first page of an article (serial) indicates the copyright owner's consent that copies of the article may be made for personal or internal use, or for the personal or internal use of specific clients. This consent is given on the condition, however, that the copier pay stated per-copy fee through the Coypright Clearance Center, Inc. (CCC), for copying beyond that permitted by Sections 107 or 108 of the U.S. Copyright Law. This consent does not extend to other kinds of copying, such as copying, for general distribution, for advertising or promotional purposes, for creating new collective works, or for resale. For copying from back volumes of this journal see 'Permissions to Photo-Copy: Publisher's Fee List' of the CCC.

Editorial office: Postfach 10 11 61, W-6490 Weinheim, Federal Republic of Germany, Telephone (06201) 60 23 15, Telex 465 516 vchwh d, Telefax (06201) 602 328, E-Mail Z16@DHDURZ2 in Earn Bitnet.

Editor: *Peter Gölitz*

Associate editors: *D. I. Loewus, K. J. Schneider, A. Stimson.* **Editorial assistant:** *E. Schweikart*

Publishers: VCH Verlagsgesellschaft mbH. (Managing Director: *Hans Dirk Köhler.*), Pappelallee 3, W-6940 Weinheim, Federal Republic of Germany.

Advertising office (Advertising Manager *R. J. Roth*): Postfach 10 11 61, W-6940 Weinheim, Federal Republic of Germany, Telephone (0 62 01) 60 61 36, Telex 4 67 155, Telefax (0 62 01) 606 156.

ANGEWANDTE CHEMIE
International Edition in English
Volume 30 · Number 8
August 1991
Pages 893–1050

The Isocyanide–Cyanide Rearrangement; Mechanism and Preparative Applications**

By Christoph Rüchardt,* Michael Meier, Klaus Haaf, Joachim Pakusch, Erwin K. A. Wolber and Barbara Müller

Dedicated to Professor Horst Prinzbach on the occasion of his 60th birthday

Until recently the isocyanide–cyanide rearrangement was of interest almost solely as an example of a unimolecular gas-phase reaction, and kinetic studies had been carried out in only a few simple cases. Kinetic measurements in solution were made possible only by the discovery and suppression of a parallel free-radical chain process which leads to the same products. The rate of the isomerization is almost independent of the structure of the starting material and of the substituents present. An exception is provided by extreme steric hindrance in three dimensions which, as in tris-α-substituted triptycyl isocyanides, leads to a considerable increase in the activation energy. The results can be interpreted in terms of a purely sigmatropic mechanism, as predicted by ab initio calculations. The preparative application of this rearrangement reaction requires the suppression of side reactions and can best be carried out by flash pyrolysis; yields are then almost quantitative. Allyl isocyanides react without allyl isomerization, optically active isocyanides with complete retention of configuration. New, economically interesting syntheses for the known nonsteroidal anti-inflammatory drugs ibuprofen and (*S*)-naproxene are described. The application of the useful synthetic building blocks, the optically active β-acyloxy cyanides, which are formed from optically active α-amino acids, will be demonstrated.

1. Introduction

Organic isocyanides **1** were known as early as the middle of the last century,[1] mainly because their characteristic and obnoxious smell demonstrated their formation in the course of unsuccessful attempts to form cyanides **2** from alkyl halides and silver cyanide. However, their exact structure[1] could only be determined when modern spectroscopic methods were introduced. Hückel, MNDO, and finally ab initio MO calculations[2] led to a clarification of the bonding situation. Results obtained for methyl isocyanide are given in

R–NC R–CN
1 **2**

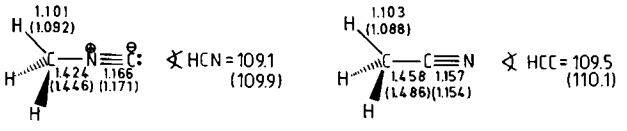

Fig. 1. Bond lengths (in Å) and angles for methyl isocyanide [3a] and acetonitrile [3b] determined from microwave spectroscopy [3] or MINDO and ab initio calculations [2] (values in brackets).

[*] Prof. Dr. C. Rüchardt, Dr. M. Meier, Dr. K. Haaf, Dr. J. Pakusch, Dipl.-Chem. E. K. A. Wolber, Dipl.-Chem. B. Müller
Institut für Organische Chemie und Biochemie der Universität
Albertstrasse 21, W-7800 Freiburg (FRG)

[**] Besides this IUPAC name, the rearrangement is often referred to as the isonitrile–nitrile rearrangement in the literature. Nomenclature example: acetonitrile ≡ methyl cyanide ≡ ethanenitrile.

 © VCH Verlagsgesellschaft mbH, W-6940 Weinheim, 1991 0570-0833/91/0808-0893 $ 3.50+.25/0

Figure 1; they correspond formally to an iminocarbene resonance hybrid **3**.

While the chemistry of the isocyanides has received fresh impetus since the introduction of practicable synthetic meth-

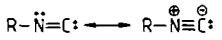

3

ods such as the dehydration of formamides as described by *Ugi* et al.,[4] the history of the isocyanide–cyanide rearrangement goes back to the last century;[5] preparative applications of the reaction were, however, almost unknown at that time.[7] *Weith*[8] showed in 1873 that the evil-smelling phenyl isocyanide **4** formed in the reaction of aniline with $CHCl_3$ and KOH was transformed by heating into the much less odorous phenyl cyanide **5**.

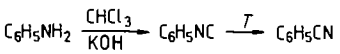

4 **5**

At an early stage this reaction was grouped together with the known 1,2-rearrangements such as the Wagner–Meerwein, Beckmann, Curtius, or Criegee rearrangements;[9, 10] it has more recently been compared to the Lewis–Zollinger isotopomerization of the aromatic diazonium ions (isoelectronic to the isocyanides) which occurs during hydrolysis to phenols[5] [Eq. (a)] and the corresponding thermal rearrangement of acetylenic anions[5] [Eq. (b)].

(a)

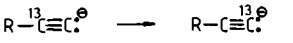

(b)

2. Reaction Mechanism and Transition State

Formulations of the transition state for the isocyanide–cyanide rearrangement were considered at an early stage, particularly for comparison with the known 1,2-sextet rearrangements; they can be discussed in terms of the two alternative extreme formulations **6** and **7** (Fig. 2).

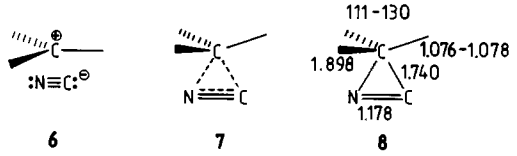

6 **7** **8**

Fig. 2. Suggested structures for the transition state in the rearrangement of methyl isocyanide to acetonitrile. **6**: π-complex with hypovalent, carbenium-like, migrating C atom; **7**: sigmatropic transition state with hypervalent five-bonded (carbonium-like) migrating C atom; **8**: results of ab initio calculations [11]. Bond lengths in Å and angles in degrees.

Detailed studies carried out by the group of *B. S. Rabinowitch* in the 1960's[5] used the thermal rearrangement of methyl isocyanide, and later ethyl isocyanide, to check the RRKM theory[6] of the chemical kinetics of unimolecular gas-phase reactions. The rearrangement is ideal for this purpose; it is a quantitative, uncatalyzed, and homogeneous first-order gas-phase reaction. Kinetic measurements were carried out across a wide range of pressure and temperature, and the typical decrease of the reaction rate and the corresponding increase of the activation energy with increasing pressure were verified by the RRKM theory. It was necessary to assume a three-membered transition state **7** with defined geometric parameters. The agreement between experiment and theory was confirmed by the measurement of kinetic isotope effects,[5] kinetic shock tube experiments[5] and studies of thermal explosions.[12] Without recourse to the assumptions of the kinetic gas theory, *H. F. Schaeffer III* et al. calculated the transition state for the methyl isocyanide rearrangement using ab initio methods and the gradient technique for geometry optimization.[11] The calculated transition state is compatible with the findings of *Rabinovitch* et al., although the bond lengths and angles differ considerably.

The structural parameters for methyl isocyanide and methyl cyanide (see Fig. 1) and for the transition state **8** for the rearrangement predicted by ab initio calculations[2, 11] are striking in that the migrating methyl group maintains its H–C–H bond angle of 109° throughout the reaction, while the N–C triple bond is elongated by only 1% in the transition state. The activation energy calculated by *Schaeffer III* et al. (E_a = 40.9 kcal mol^{-1})[11] agrees relatively well with the experimental value of 38.4 kcal mol^{-1}.[13] The calculations[11] also predict that there will be no charge separation in the transition state, which thus corresponds much more closely to **7** than to **6**.

Christoph Rüchardt was born in Munich in 1929. He studied chemistry at the Ludwig-Maximilian University in Munich and the University of Georgia in Athens, gaining the degrees of M.Sc. (1952), Dipl.-Chem. (1954), and Dr. rer. nat. (1956), the latter under the supervision of R. Huisgen. From 1957–1959 he worked as a postdoctoral fellow at Harvard University with P. D. Bartlett and at the California Institute of Technology with J. D. Roberts. After his habilitation in Munich (1963) he accepted a chair of organic chemistry at the University of Münster in 1968. In 1972 he moved to the University of Freiburg, where he has been Rector since 1987. Rüchardt is a member of the Heidelberger Akademie der Wissenschaften. His main research interests involve reaction mechanisms, free radical chemistry, questions involving bond dissociation, and stereochemistry.

Attempts to verify these predictions by a kinetic determination of the dependence of the reactivity on the structure of the isocyanide were initially subject to difficulties.[14] The results obtained when the reaction was carried out *in solution* in glass ampules were often not reproducible and were dependent on the concentration, the solvent, and the degree of care taken in degassing the solution. The activation entropy was strongly negative, the reaction order higher than unity, and additional reaction products were formed in a side reaction. Under these conditions the sigmatropic reaction was accompanied by a free radical chain process leading to the same reaction products;[5, 15] this process is probably initiated by autoxidation steps, as indicated by the fact that extremely careful degassing can eliminate the unwanted side effects [Eq. (c)]. The two chain steps, free radical addition to the isocyanide and subsequent β scission, led to the formation of the cyanide.

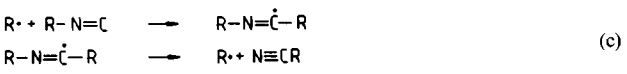

(c)

The free radical reaction was also eliminated by the addition of 1,1-diphenylethene or 3-pyridyl cyanide as inhibitors.[15, 16] Under these conditions at 200–220 °C the rearrangement generally occurs almost quantitatively, so kinetic measurements in solution are possible. A side reaction which occurs in certain cases was observed during the isomerization of triphenyl isocyanide **9** to triphenylacetonitrile **10** [Eq. (d)].[17] This cationic chain reaction[18] can also lead to an extreme acceleration of the reaction, particularly when catalyzed by Lewis acids. The addition of ethanol as a cation trap thus leads to the stabilization of these isocyanides.[18]

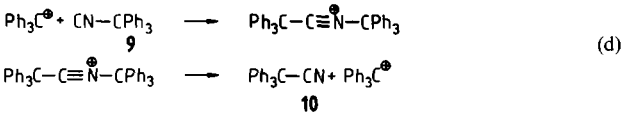

(d)

The isomerization of cumyl isocyanide and the highly sterically congested aliphatic *tert*-alkyl isocyanides is apparently also perturbed by this cationic side reaction. In contrast β elimination appears to occur only very seldom, since the yields of cyanide are generally almost quantitative.[7, 10]

The first kinetic studies were carried out by *Casanova* et al.,[19] in diglyme as solvent but without the addition of a radical inhibitor; as for the Curtius rearrangement,[10] almost no difference in reactivity between methyl, ethyl, isopropyl, and *tert*-butyl isocyanide was observed (see Table 1). However, the reaction rate increases greatly within this series for both the Beckmann and Criegee rearrangements, since in these reactions there is a charge separation in the transition state (as in **6**).[10] The slight fall in reactivity exhibited by secondary and tertiary alkyl isocyanides could be due to a steric effect which inhibits the formation of the three-membered transition state (**7**).

Table 1. Relative reactivities of various isocyanides R–NC in diglyme at 200 °C [19].

R	Me	Et	*i*Pr	*t*Bu	C_6H_5	*p*-ClC_6H_4	*p*-$CH_3C_6H_4$
k_{rel}	5.6	7.8	2.6	≡ 1.0	20.6	18.2	23.8

The absence of charge separation in the transition state was also demonstrated by the absence of a polar substituent effect on the isomerization of aryl isocyanides (Table 1).

The ready isomerization of cyclobutyl isocyanide (without any formation of cyclopropylcarbinyl or homoallyl cyanide) has been considered a further argument against the transition state **6**.[19] This is, however, by no means conclusive, since the cyclobutyl residue also remains unchanged during the 1,2-shift of the Beckmann and Criegee rearrangements. The observation of *partial* retention of the stereochemistry of optically active 2-butyl isocyanide during the isomerization to the cyanide[19] is also a poor mechanistic criterion for

Table 2. Free activation energies $\Delta G^{\neq}$(250 °C) [kcal mol^{-1}] and reaction rates $10^4\,k_1$ [s^{-1}] at 210 °C of the isocyanide-cyanide rearrangement in hexadecane, dodecane or mesitylene [10]; % yield denotes the preparative results of flash pyrolysis experiments [7].

Compound		$\Delta G^{\neq}$(250 °C)	$10^4\,k_1$	Yield [%]
α Branching				
11	*n*-C_7H_{15}–CH_2–NC	36.4	2.95	98
12	*n*-C_6H_{12}–$CH(CH_3)$–NC	37.6	0.97	100 [a]
13	*n*-C_5H_{11}–$C(CH_3)_2$–NC	39.2	0.18	92
β Branching				
14	C_6H_5–$C(CH_3)_2$–CH_2–NC	37.8	0.86	96
15	$[(CH_3)_2CH]_2CH$–NC	38.3	0.51	99
α Substitution				
16	C_6H_5–CH_2–NC	36.3	4.16	99
17	C_6H_5–$CH(CH_3)$–NC	37.4	1.25	95
18	*p*-CH_3O–C_6H_4–CH_2–NC	35.7	7.33	98
19	*p*-NO_2–C_6H_4–CH_2–NC	36.5	3.04	96 [a]
9	$(C_6H_5)_3C$–NC	38.1	0.64	90
20	CH_3OOC–CH_2–NC	36.9	2.22	97
Cyclic structures				
21	Cyclopropyl-NC	38.1	0.66	92
22	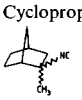	*exo*: 39.5 *endo*: 39.8	0.11 0.12	97 95
Bridgehead structures [10]				
23	1-adamantyl-NC	39.0	0.22	98
24	1-bicyclo[2.2.2]octyl-NC	39.6	0.13	97
25	1-bicyclo[2.2.1]heptyl-NC	38.8	0.27	101 [a]
26	3-homoadamantyl-NC	38.8	0.23	100
27	9,10-dihydro-9-isocyano-9,10-[1′,2′]-benzenoanthracene [b]	44.1	0.001	96
28	9,10-dihydro-9-isocyano-1,4,5,8,13,16-hexamethyl-9,10-[1′,2′]-benzenoanthracene [b]	48.6	4.11×10^{-7}	91 [a]
Aromatic isocyanides				
29	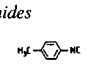	35.3	10.3	99 [a]
30		35.0	14.3	99 [a]
31		36.6	2.59	98 [a]
32	[20, 21]	38.4	0.28	98 [a]
33	[20]	35.2	11.8	91 [a]
34	[20]	36.0	6.48	96 [a]

[a] In solution under kinetic conditions. [b] Triptycene derivatives are named as in Chemical Abstracts.

the structure of the transition state, since the migration occurs with *complete* retention during the Beckmann and Criegee rearrangements. Possibly the conditions used by *Casanova*[19] did not completely suppress the free radical chain reaction leading to racemization [Eq. (c)].

A more recent, wide-ranging kinetic study[10, 20, 21] of the electronic and steric effects on the reactivity of aliphatic and aromatic isocyanides presents reliable experimental criteria for the definition of the structure of the transition state of the isocyanide-cyanide rearrangement (Table 2). The separation of $\Delta G^{\neq}$ into $\Delta H^{\neq}$ and $\Delta S^{\neq}$ is not taken into account in Table 2 (see refs. [10, 20, 21]), since in all cases $\Delta S^{\neq}$ lies close to zero ($0 \pm 3\,J\,K^{-1}\,mol^{-1}$).

As expected, α branching slows the reaction rate though only by a factor of 16 (see entries **11**–**13**). The small effect of the β branching, particularly in **15**, indicates that in the transition state the presence of two bulky α substituents does not lead to additional steric interactions because one is situated in front of and the other behind the plane of the ring (see Fig. 2). It was unfortunately not possible to measure the kinetics of isomerization of $(t\mathrm{BuCH_2})_2\mathrm{C(CH_3)NC}$ (**56**), because product analysis showed that under these conditions β elimination and/or ionic chain decomposition has a disturbing effect.[22] The small influence of branching on the reaction rate supports transition state **7** rather than **6**, since in the latter the bond angles at the migrating C-atom should increase, thus leading to back-strain effects (i.e., an increase in rate due to release of steric compression at the back side of the reaction center by an increase in the bond angles). The behavior of the cyclic isocyanides **21** and **22** agree with this hypothesis.

A particularly significant argument against charge separation in the transition state is provided by the lack of influence of α-aryl and α-carbomethoxy groups on the reactivity (cf. **9**, **18**–**20**). The small increase in reactivity of the triphenylmethyl isocyanide **9** compared with *tert*-octyl isocyanide **13** (less than a factor of 4) and the lack of a substituent effect (**18**, **19**) can only be interpreted in terms of the hypervalent transition state **7** with a pentacoordinate carbon atom which is incapable of further conjugation.

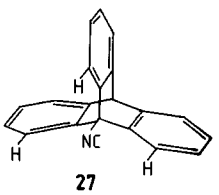

27

The lack of change of the H–C–H angle at the migrating C atom becomes clear from the reactivity of the bridgehead isocyanides **23**–**27**. Apart from 9-triptycyl isocyanide (**27**), these rearrange at rates which do not differ significantly from that of the open-chain *tert*-octyl isocyanide **13**; virtually no other reactions are known which do not exhibit a bridgehead effect.

The unusual behavior of **27**, which reacts 200 times more slowly than the other bridgehead isocyanides, but only 600 times more slowly than triphenylmethyl isocyanide **9**, cannot be due to an electronic aryl effect. Instead an explanation was sought in the steric congestion in three dimensions caused by the hydrogen atoms in β positions to the NC group. This hypothesis was confirmed by the investigation of the rearrangement of the hexamethyl derivative, **28**.

The hexamethyltriptycyl isocyanide (**28**) was prepared, though only in poor yield, from 1,4,5,8-tetramethyl-9-anthryl isocyanide (**34**). On heating to 250–300 °C this isocyanide, which is strongly sterically hindered in *three* dimensions, isomerizes quantitatively to the corresponding cyanide.[23] The activation energy required to form the transition state is 4.5 kcal mol^{-1} higher than for **27**.[23b] The temperature at which the half-life is 1 h, differs by almost 60 °C for the two isocyanides (303 and 361 °C), which emphasizes that the three-membered ring of the transition state can no longer avoid strong steric repulsions due to the β-methyl groups. Thermochemical calculations show that the C–NC bond dissociation energy for aliphatic isocyanides is about 100 kcal mol^{-1},[20, 23b] so that even in the case of **28**, the most stable of all known isocyanides, an alternative dissociation–recombination reaction mechanism is out of the question.

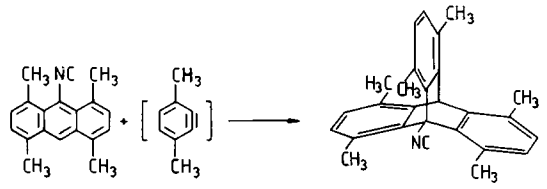

34 **28**

It is amazing that aromatic isocyanides are only slightly more reactive than their aliphatic counterparts (cf. **29** and **11**), that polar substituent effects are small (see Tables 1 and 2), and that the introduction of bulky groups into *ortho* positions of phenyl isocyanide (**4**) or in positions 1 and 8 of 9-anthryl isocyanide (**33**) lowers the reactivity only minimally (cf. **30**–**32** and **34**). The phenonium-like transition state (**35**) postulated for most electron sextet rearrangements requires charge separation and can therefore be excluded. Thus, both the aliphatic and the aromatic rearrangements pass through a hypervalent three-center transition state (**36** or **37**). One of the resulting advantages is the avoidance of charge separation.

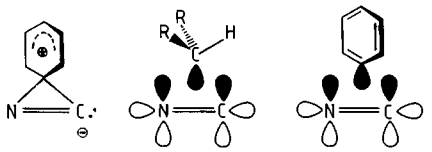

35 **36** **37**

In the aliphatic case (**36**) a gauche arrangement of the two groups R leads to minimal steric interactions with the NC group; in the aromatic case (**37**) the preferred conformation involves an orthogonal arrangement of the three-membered ring and the aromatic ring. Otherwise *ortho* substituents would give rise to a more pronounced decrease in reactivity due to steric effects, as is shown by hexamethyltriptycyl isocyanide **28**. The effect of two *ortho tert*-butyl groups in **32** is, in contrast, surprisingly small. The greater reactivity of the aromatic isocyanides compared with that of the aliphatic

compounds, in spite of the loss of conjugation energy in the transition state, is probably explained by the smaller steric interactions in the transition state of the aromatic isocyanide. A further advantage of the sigmatropic reaction pathway via **37** is that the aromatic π system remains almost unperturbed.

Aliphatic and aromatic isocyanides also differ only very little in their heats of isomerization. More recent experimental results[24] for mesityl isocyanide (**30**, $\Delta H_{isom} = -19.8\ kcal\,mol^{-1}$), 1-adamantyl isocyanide (**23**, $-19.3\ kcal\,mol^{-1}$), and 1-norbornyl isocyanide (**25**, $-21.7\ kcal\,mol^{-1}$) are in agreement with older values for methyl isocyanide ($-23.7\ kcal\,mol^{-1}$) and ethyl isocyanide ($-21.5\ kcal\,mol^{-1}$); the latter were obtained from controlled thermal explosion experiments.[25] The conjugation energy of the cyanide and isocyanide groups with the aromatic ring is apparently very similar.

The isocyanide–cyanide rearrangement of aliphatic and aromatic isocyanides is thus characterized by an amazingly small dependence of the reactivity on the structure of the substrate. Almost all the compounds in Table 2 react in virtually quantitative yields at between 210 °C and 250 °C with $\tau_{1/2} = 1$ h under the special conditions of the kinetic measurements in solution (addition of inhibitor, degassed solution). This is, however, apparently not the case for isocyanide groups attached to heteroatoms, such as trimethylsilyl isocyanide **38**; this compound is reported to be in equilibrium with the cyanide **39** at room temperature.[26]

$$(CH_3)_3Si{-}NC \rightleftharpoons (CH_3)_3Si{-}CN$$
38 **39**

Isocyanide groups attached to carbanionic or free radical C atoms also appear to isomerize more rapidly. The isomerization energies of the isocyanomethyl anion and the α-isocyanomethyl radical were estimated from thermochemical data (-25.5 and $-14.3\ kcal\,mol^{-1}$ respectively).[20, 27] α-Lithiated isocyanides are important organometallic intermediates which can be handled at room temperature.[1, 28] However, the phosphorus ylide anion **40**, which has a structural element similar to an α-metalated isocyanide, isomerizes to **41** at 70 °C.[29]

$$(C_6H_5)_3\overset{\oplus}{P}{-}\overset{\ominus}{C}H{-}NC \longrightarrow (C_6H_5)_3\overset{\oplus}{P}{-}\overset{\ominus}{C}H{-}CN$$
40 **41**

The isomerization of α-isocyanoalkyl radicals was studied recently in a kinetic competition system.[20] Evidence for their isomerization had previously been observed by *U. Schöllkopf* and co-workers,[30] who were, however, not able to provide a reliable mechanistic interpretation.

Heating the diisocyanide **42** to 60 °C led to the formation of 38% 1,2-dicyanotetraphenylethane as well as four uncharacterized by-products (thin-layer chromatography). Since the isocyanide–cyanide rearrangement normally occurs at or above 200 °C, independent of the structure of the starting material, these results indicate an isomerization pathway involving primary homolysis of the C–C bond in **42** to give α-isocyanodiphenylmethyl radicals **43**, which isomerize at 60 °C to α-cyanodiphenylmethyl radicals **44**. The latter are known to be in equilibrium with **45** under the reaction conditions.[31] Since isocyano groups stabilize alkyl radicals less well than cyano groups (resonance energy $H_r = 2.5 \pm 0.7$ and $4.1 \pm 0.5\ kcal\,mol^{-1}$),[20] the isomerization should occur in the direction **43** → **44**. When **42** was heated in an ESR spectrometer, the primary spectrum observed was that attributable to **43**, which was then completely transformed into one corresponding to **44**.

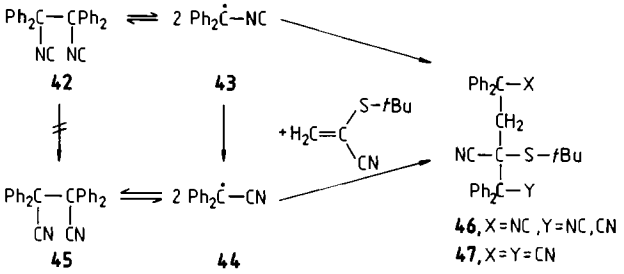

The thermolysis of **42** in the presence of a 25-fold excess of α-(*tert*-butylmercapto)acrylonitrile led to the formation of the adducts **46** and **47** in 97% yield. In the presence of 9,10-dihydroanthracene as an H donor the 1,2-diisocyanides **48a–c** similarly yielded the nonisomerized and isomerized products **49** and **50** derived from the radicals **51** and **52**; in the absence of the H donor **53** is formed. Although the system for $R = CH_3$ (**48a**) could unfortunately not be analyzed quantitatively since **49a** also rearranged slowly to **50a** under the reaction conditions, it has the advantage of being least affected by side reactions. The differing yield ratios of **50**:**49**

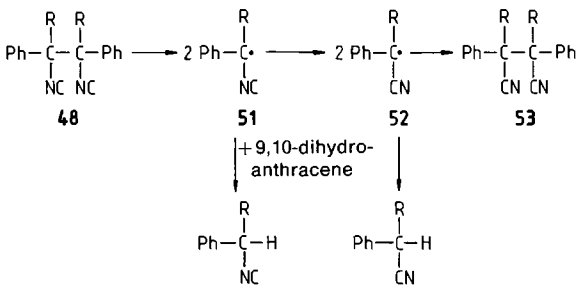

a, R = CH_3 (196 °C)	23%	50%
b, R = C_2H_5 (171 °C)	26%	35%
c, R = iC_4H_9 (138 °C)	3%	14%

can be understood in part when the longer lifetime of the radicals **51** at lower temperatures (where trapping is slower) is taken into account: the ratio **52**:**51** increases while the side reactions of **51** which decrease its yield also become more important. Independent experiments reveal that the radicals **52** are less prone to side reactions. On the other hand, these trapping experiments demonstrate that free radicals **51** can isomerize at relatively low temperatures during their short lifetime in this system. The rate of the isomerization is thus considerably higher than that of saturated isocyanides.

More difficult to understand is the observation that the synthesis of the isocyanides **48** via oxidation of the lithiated

isocyanides **49** at −70 °C by 2,3-dibromo-2,3-dimethylbutane gives the corresponding cyanide **53** as well as the required isocyanide **49**. The dimerization possibly occurs within the organometallic aggregates and involves complex mechanisms which open new avenues for isomerization, for example, through formal recombination of radicals and "carbanions" to give dimeric radical anions.[32] *Kehne*[30] has, however, suggested that the radical dimerization of **51** could also be accompanied by rearrangement (Scheme 1).

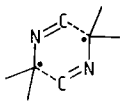

Scheme 1. Possible explanation for the formation of **53** in the synthesis of **48** from **49**.

This could explain why the synthesis of the isocyanides **48** only yielded 1,2-dicyanoethanes **53**, but no mixed dimers.

3. Preparative Application

Why did (until very recently) the isocyanide–cyanide rearrangement fail to find a place in the synthetic chemist's arsenal of preparative methods?[7] The reaction offers an additional method for chain extension and is in principle the reverse of the well-known degradation reactions of the Curtius, Hoffmann, and Lossen types (Scheme 2).

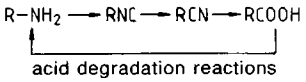

Scheme 2. Isocyanide–cyanide rearrangement as reverse of common degradation reactions.

One reason is no doubt the formerly difficult preparation of isocyanides;[4] a second lies in the high reaction temperatures (>200 °C). These require the use of high-boiling solvents, which often lead to separation problems during workup. In addition, *Yamada* et al. have shown[33] that under these conditions the formation of cyanides from optically active amines is accompanied by extensive loss of the optical activity. This is not due solely to a base-catalyzed racemiza-

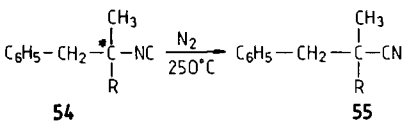

54 **55**

	% retention in diphenylether	% retention no solvent
a, R = $COOC_2H_5$	9	0
b, R = C_2H_5	90	47

tion of the cyanides, since *tert*-isocyanides such as **54** also react to give partially racemized **55**. Thus the rearrangement of the isocyanides **54a** and **54b** gave **55a** and **55b** in over 75% yield, but with considerably lower optical activity.[33]

The key to understanding and overcoming this preparative disadvantage was provided by our observation that the optical yields were always higher when working in solution than in the absence of solvent. This led to the suggestion that the free radical chain reaction (c) competes under these conditions with the stereospecific rearrangement and that the racemization occurs at the free radical stage. Because of its higher reaction order, the chain reaction dominates to a greater degree at higher concentrations than in more dilute systems. This hypothesis agreed with the results of stereospecific isocyanide rearrangements at very high temperatures (270–310 °C).[34] Either these reactions took place in the gas phase, or an increase of the reaction temperature accelerated the first-order reaction more than it did the radical chain process. Our hopes of overcoming these disadvantages for the application of the isocyanide rearrangement in synthesis by recourse to flash pyrolysis were indeed realized, as shown by the yields documented in Table 2:[7] in all cases they are ca. 90% or higher. The unwanted chain reaction is suppressed by working in the gas phase at 10^{-2} torr, while at the high reaction temperatures (520–550 °C) the unimolecular rearrangement is favored over potential side reactions such as β elimination because its activation entropy is very close to zero. Since all isocyanides react at comparable rates the standard conditions described above apply to a wide range of substrates. The required equipment is readily available[7, 35] and can be dimensioned to convert 20 g isocyanide to the cyanide in ca. 30 min[36] with ease. Extremely sterically hindered compounds also react very readily, as is demonstrated by the simple synthesis of 2,4,6-tri(*tert*-butyl)phenyl cyanide.[21] Yields of the cyanide are high even in those cases which were shown to be accompanied by large amounts of by-products under the conditions used in the kinetic studies, for example, isocyanides **56** (93% cyanide),[22] **57** (77%), and **58** (85%).[20]

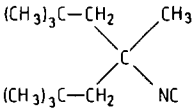

56

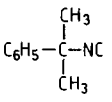

57

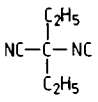

58

However, the isomerization of 2-phenylcyclopropyl isocyanide[7] and of 1-homocubyl isocyanide[7] was accompanied by ring opening reactions. Some examples of preparative applications for chain extension are shown in Scheme 3.[37]

A new simple approach to α-alkylphenylacetic acids, which are important as antipyretics and insecticides of the pyrethroid type,[38] is particularly attractive. Examples are the high-yield syntheses of ibuprofen **59a** and naproxene **59b**.[39]

For less volatile isocyanides, flash pyrolysis can be replaced by short contact flow thermolysis, although the yields are lower.[7, 35]

Under these novel reaction conditions the isocyanide–cyanide rearrangement has two additional important synthetic advantages: allyl and propargyl isocyanides react without allyl isomerization (see examples in Scheme 3); this

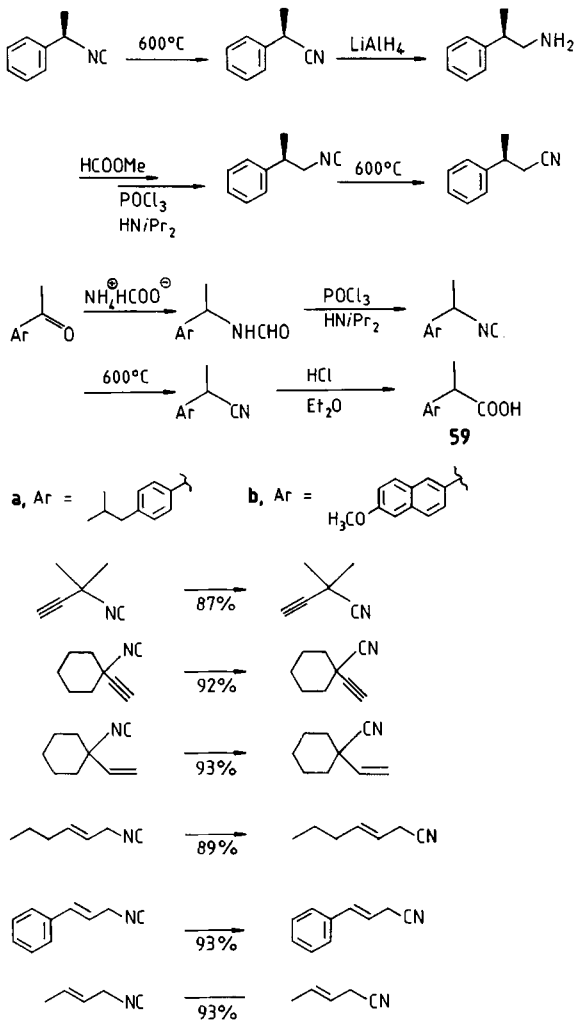

Scheme 3. Examples for the use of the isocyanide–cyanide rearrangement for chain extension.

is an advantage offered by only few reactions, in particular sextet rearrangements.

The second advantage is the ability to convert optically active amines into cyanides, and thus to carboxylic acids, without racemization. Amines can in general be readily separated into their enantiomers by classical racemate separation methods, while the "wrong" enantiomer can probably be racemized under the conditions of a Leuckart–Wallach reaction. Interesting applications are thus possible, independent of the modern methods for the synthesis of enantiomerically pure amines. An example of potential industrial importance is the preparation of the important nonstereoidal anti-inflammatory drug naproxene (**59b**) in the form of the pure (*S*)-enantiomer (Scheme 4);[39] a technical stereo-

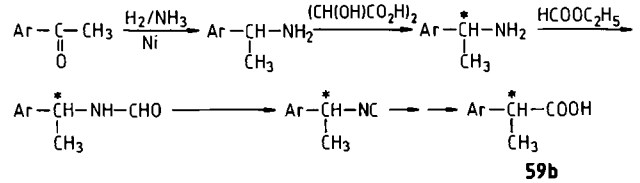

Scheme 4. Synthesis of (*S*)-naproxene (**59b**) by using the isocyanide–cyanide rearrangement.

specific synthesis for the latter has been described only very recently.[38]

Finally the next step was to develop new synthetic building blocks and new syntheses starting from naturally available optically active amines, in particular from α-amino acids (**60**). Since isocyanides derived from esters of α-amino acids cannot be handled without racemization because of the high acidity of the α-hydrogen atoms,[7, 36] we prepared optically active β-amino alcohols (**62**) by reduction of the amino acids

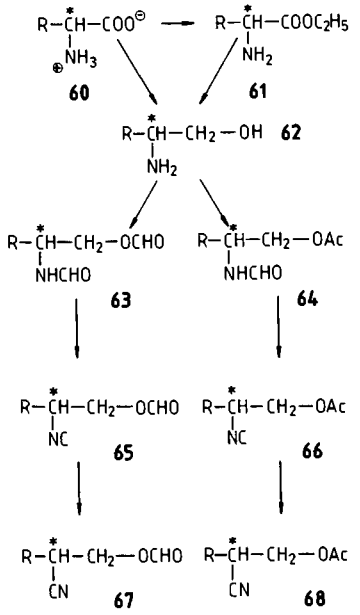

or their esters (**61**); these were either diformylated in one step to give **63** or successively formylated and acetylated to give **64**.[36, 40] These compounds can be converted by standard

Table 3. Preparation of β-acyloxy cyanides **67** and **68** from optically active α-amino acids **60** by flash pyrolysis of the β-acyloxy isocyanides **65** and **66** [36].

Amino acid	Reaction steps	β-Acyloxy-cyanide	Yield for rearrangement [%]	Total yield [%]
(*S*)-phenylalanine	4	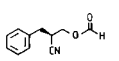	83	54
(*S*)-leucine	6	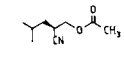	90	61
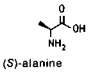 (*S*)-alanine	6	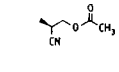	91	50
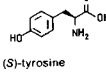 (*S*)-tyrosine	7	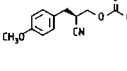	93	47
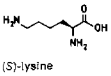 (*S*)-lysine	5	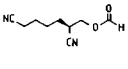	83	55
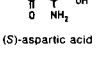 (*S*)-aspartic acid	8	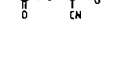	93	52

methods into the isocyanides **65** and **66**, flash pyrolysis of which gives the cyanides **67** and **68** in 70–93% yield; ester pyrolysis was observed as a side reaction. The yields obtained for various types of amino acid are shown in Table 3. The techniques used for the protection of the functional groups and the reaction conditions optimized for each particular amino acid[43] will not be discussed here. The overall yields of the optically pure β-acyloxy cyanides **67** and **68** of 47–61% indicate the considerable potential of this synthetic sequence.

The use of **67** (R = benzyl) will be given here as an example of the application of these new synthetic building blocks in further chemical transformations.

1. Reduction of **67** with H_2/Pd and subsequent hydrolysis to give the aminoalcohol **69** (92%) can be followed by cyclization either with formaldehyde to give (*R*)-5-benzyl-1,3-oxazinane **70** (87%) or with carbonyl diimidazole (di-1-imidazolyl ketone) to give (*R*)-5-benzyl-1,3-oxazinan-2-one **71** (63%); both products are optically pure.

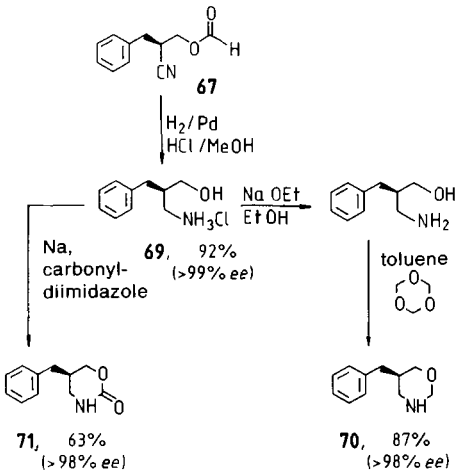

2. Cyanide **67** can be converted by a Pinner reaction into the β-hydroxymethyl ester **72**,[40] which in turn was treated with I_2/PPh_3/imidazole to give the β-iodomethyl ester **73**.[36] Iodine can be removed by the tributyltin hydride reduction,[41] giving the optically active α-methyl-β-phenylpropionate **74**. The iodide **73** can also undergo reductive addition

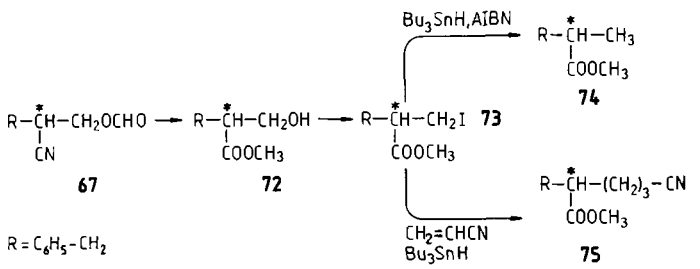

to acrylonitrile in the presence of tributyltin hydride according to *Giese*'s procedure,[42] affording an enantiomerically pure product **75**.[36]

3. Finally, we were also able to transform the acyloxycyanide **67** (from phenylalanine) through a well-developed synthetic sequence[40] into the optically pure 3-benzyl β-lactam. Corresponding β-lactams were also prepared from alanine and leucine.[36]

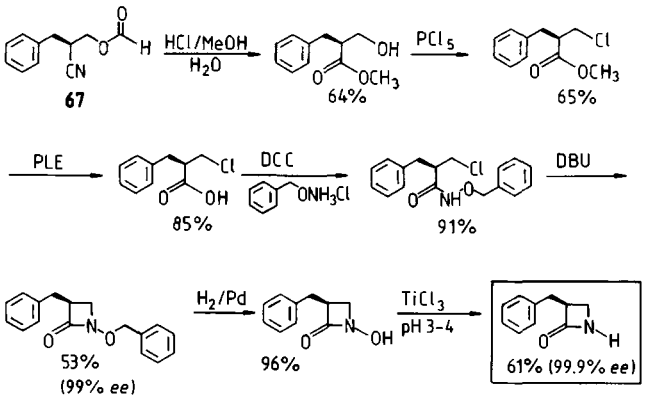

Scheme 5. Synthesis of β-lactams starting, in effect, from phenylalanine. PLE = pig liver esterase, DCC = dicyclohexyl carbodiimide, DBU = 1,8-diazabicyclo[5.4.0]undec-7-ene.

4. Summary and Future Prospects

The development of the methodology for the preparative application of the isocyanide–cyanide rearrangement provides a process for chain extension of amines and ketones (subsequent to Wallach-Leuckart reduction) to give cyanides and carboxylic acids; this process takes place in the opposite direction to the well-known Curtius and Hofmann degradation reactions. The wide variety of applications demonstrated here for selected examples leads us to expect that this rearrangement will soon be included in the chemist's standard repertoire of synthetic reactions.

Studies of the rearrangement for isocyanides in exceptional valence states, such as radicals, anions, α-metalated isocyanides or radical ions are still at a preliminary stage (Scheme 6).

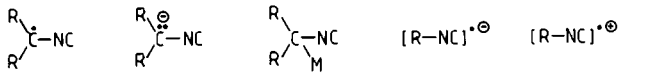

Scheme 6. Isocyanides in exceptional valence states. M = metal.

Substantial reactivity differences are expected in this series. The isomerization of isocyanide functions bonded to atoms other than carbon has also hardly been studied as yet. The investigation of such reactions is not only of theoretical interest, but could also lead to the discovery of milder reaction conditions for the isomerization, for example, under the influence of one-electron redox catalysts.[44]

We thank Dr. Günter Range, Dr. Ingrid Mergelsberg, and Dipl.-Chem. Constantin von Kessel for important preliminary investigations, Dr. M. Schmittel for useful discussions, and the Fonds der Chemischen Industrie and the Deutsche Forschungsgemeinschaft for their support of our own work in this area of chemistry.

Received: January 16, 1991 [A 828 IE]
Translated by Dr. T. Mitchell, Dortmund
German version: *Angew. Chem. 103* (1991) 907

[1] a) I. Ugi (Ed.).: *Isocyanide Chemistry*, Academic Press, New York 1971; b) J. A. Green, P. T. Hoffmann in [1a]; p. 1; c) H. M. Walborsky, M. P. Periasamy in S. Patai, Z. Rappoport (Eds.): *The Chemistry of Triple Bonded Functional Groups, Part 2, Supplement*, Wiley-Interscience, New York 1983, p. 835.
[2] J. B. Moffat, *Chem. Phys. Lett. 55* (1978) 125.
[3] a) M. Kessler, H. Ring, R. Trambornio, W. Gordy, *Phys. Rev. 79* (1950) 54; b) C. C. Costain, *J. Chem. Phys. 29* (1958) 864.
[4] a) P. Hoffmann, G. Gokel, D. Marquarding, I. Ugi in [1a], p. 9; b) R. Obrecht, R. Herrmann, I. Ugi, *Synthesis 1985*, 400.
[5] K. M. Maloney, B. S. Rabinovitch in [1a], p. 41.
[6] For the Rice-Ramsperger-Kassel-Marcus theory, see for example, P. J. Robinson, K. A. Holbrook: *Unimolecular Reactions*, Wiley-Interscience, New York 1972.
[7] M. Meier, C. Rüchardt, *Chem. Ber. 120* (1987) 1.
[8] W. Weith, *Ber. Dtsch. Chem. Ges. 6* (1873) 210.
[9] a) J. March: *Advanced Organic Chemistry*, Wiley-Interscience, New York 1985, p. 942; b) G. W. Wheland: *Advanced Organic Chemistry*, 2nd ed., Wiley, New York 1949, Chapter 12; c) T. H. Lowry, R. K. Schueller: *Mechanismen und Theorie in der Organischen Chemie*, Verlag Chemie, Weinheim 1980, Chapter 5.
[10] M. Meier, B. Müller, C. Rüchardt, *J. Org. Chem. 52* (1987) 648.
[11] P. Saxe, Y. Yamaguchi, P. Pulay, H. F. Schaeffer III, *J. Am. Chem. Soc. 102* (1980) 3719.
[12] P. Q. E. Clothier, M. T. G. Glionna, H. O. Pritchard, *J. Phys. Chem. 89* (1985) 2992.
[13] F. W. Schneider, B. S. Rabinovitch, *J. Am. Chem. Soc. 84* (1962) 4215.
[14] G. Range, *Dissertation*, Universität Freiburg 1979.
[15] M. Meier, C. Rüchardt, *Tetrahedron Lett. 24* (1983) 4671.
[16] The extreme reactivity of isocyanides in free radical additions is well known (see Ref. 27 in [10]) and has been applied for preparative purposes by various authors; see e.g. D. H. R. Barton, W. B. Motherwell in B. M. Trost, C. R. Hutchinson (Eds.): *Organic Synthesis Today and Tomorrow*, Pergamon, Oxford 1981; p. 19; S. S. Kim, *Tetrahedron Lett. 1977*, 2741; G. Stork, P. M. Sher, *J. Am. Chem. Soc. 105* (1983) 6765.
[17] T. Austad, J. Songstad, *Acta Chem. Scand. 26* (1972) 3141.
[18] M. Meier, C. Rüchardt, *Chimia 40* (1986) 228.
[19] J. Casanova, Jr., N. D. Werner, R. E. Schuster, *J. Org. Chem. 31* (1966) 3473.
[20] J. Pakusch, *Dissertation*, Universität Freiburg 1990.
[21] J. Pakusch, C. Rüchardt, *Chem. Ber. 122* (1989) 1593.
[22] The preparative isomerization of **56** to the corresponding cyanide in 93% yield by flash pyrolysis at 570 °C, which contradicts these observations, is possibly due to the strongly negative activation entropies of the side reactions; $\Delta G^{\neq}$ values are thereby increased significantly at high temperatures.
[23] a) J. Pakusch, C. Rüchardt, *Chem. Ber. 123* (1990) 2147; b) unpublished results.
[24] M. Meier, B. Dogan, H.-D. Beckhaus, C. Rüchardt, *New J. Chem. 11* (1987) 2.
[25] H. O. Pritchard, *Can. J. Chem. 57* (1979) 2677, and references cited therein.
[26] a) D. E. J. Arnold, S. Cradock, E. A. V. Ebsworth, J. D. Murdoch, D. W. H. Rankin, D. C. J. Skea, R. K. Harris, B. J. Kimber, *J. Chem. Soc. Dalton Trans. 1981*, 1349; b) K. Georgiou, A. C. Legon, *J. Mol. Struct. 78* (1982) 257.
[27] a) S. Moran, H. B. Ellis, Jr., D. J. DeFrees, A. D. McLean, S. E. Paulson, G. B. Ellison, *J. Am. Chem. Soc. 109* (1987) 6004; b) S. Moran, H. B. Ellis, Jr., D. J. DeFrees, A. D. McLean, G. B. Ellison, *ibid. 109* (1987) 5996.
[28] W. A. Böll, F. Gerhart, A. Nürrenbach, U. Schöllkopf, *Angew. Chem. 82* (1970) 482; *Angew. Chem. Int. Ed. Engl. 9* (1970) 458.
[29] G. Zinner, W. P. Fehlhammer, *Angew. Chem. 97* (1985) 990; *Angew. Chem. Int. Ed. Engl. 24* (1985) 979.
[30] a) U. Schöllkopf, D. Stafforst, R. Jentsch, *Liebigs Ann. Chem. 1977*, 1167; b) D. Stafforst, *Dissertation*, Universität Göttingen 1975; c) H. Kehne, *Diplomarbeit*, Universität Göttingen 1978.
[31] C. Rüchardt, H.-D. Beckhaus, *Top. Curr. Chem. 130* (1986) 1.
[32] G. Russell, R. K. Khanna, *Adv. Chem. Ser. 215* (1987) 355.
[33] a) S.-I. Yamada, K. Takashima, T. Sato, S. Terashima, *Chem. Commun. 1969*, 811; b) S.-I. Yamada, M. Shibasaki, S. Terashima, *ibid. 1971*, 1008; c) M. Shibasaki, S. Terashima, S.-I. Yamada, *Chem. Pharm. Bull. 21* (1973) 552; d) M. Shibasaki, T. Sato, N. Ohasi, S. Terashima, S.-I. Yamada, *ibid. 21* (1973) 1868.
[34] a) F. Lautenschlager, G. F. Wright, *Can. J. Chem. 41* (1963) 863; b) R. W. Horobin, N. R. Kahn, Y. McKenna, B. G. Hutley, *Tetrahedron Lett. 1966*, 5087.
[35] R. F. C. Brown: *Pyrolytic Methods in Organic Chemistry*, Academic Press, New York 1980.
[36] K. Haaf, *Dissertation*, Universität Freiburg 1990.
[37] E. K. A. Wolber, *Dissertation*, Freiburg 1991.
[38] a) C. Giordano, G. Castaldi, F. Uggeri, *Angew. Chem. 96* (1984) 413; *Angew. Chem. Int. Ed. Engl. 23* (1984) 413; b) C. Giordano, G. Castaldi, S. Cavicchioli, M. Willa, *Tetrahedron 45* (1989) 4243; c) H. Gärtner, U. Salz, C. Rüchardt, *Angew. Chem. 96* (1984) 166; *Angew. Chem. Int. Ed. Engl. 23* (1984) 162.
[39] E. K. A. Wolber, C. Rüchardt, unpublished results.
[40] K. Haaf, C. Rüchardt, *Chem. Ber. 123* (1990) 635.
[41] D. P. Curran, *Synthesis 1988*, 417, 489.
[42] B. Giese: *Radicals in Organic Synthesis*, Pergamon, Oxford 1986, p. 56.
[43] K. Haaf, C. Rüchardt, unpublished results.
[44] See for example, J. P. Dinnocenzo, M. Schmittel, *J. Org. Chem. 53* (1988) 4147.

Strained-Ring and Double-Bond Systems Consisting of the Group 14 Elements Si, Ge, and Sn**

By Takeshi Tsumuraya, Scott A. Batcheller, and Satoru Masamune*

Dedicated to Professor Dr. Emanuel Vogel

The organometallic chemistry of the Group 14 elements E = Si, Ge, Sn in the 1980's is highlighted by the successful construction and thorough characterization of three systems previously thought to be too reactive to exist: 1) three-membered ring compounds including cyclotrisilane, cyclotrigermane, and cyclotristannane, 2) molecules containing E–E double bonds including disilene, digermene, and distannene, and 3) strained polycycles containing a skeleton of Group 14 elements, such as bicyclo[1.1.0]tetrasilane, hexagermaprismane, and octasilacubane. The majority of these numerous compounds now available are fully substituted with bulky ligands to suppress the reactivity intrinsic to the systems. These compounds permit examinations of 1) the variation of physical and chemical properties of a system with these elements and also with the ligands and 2) how two systems are interrelated thermally and photochemically with the intermediacy of the divalent (carbene-like) species. Theoretical calculations on virtually all of the parent compounds discussed in this review are evaluated alongside the experimental results. Some polycycles may constitute a stepping-stone on the way to compounds with a triple bond.

1. Introduction

Over the past decade significant and exciting progress has been made in the organometallic chemistry of Group 14 elements (E = Si, Ge, Sn). Species once thought to exist only as reactive intermediates such as divalent (carbene-like) species have been thoroughly characterized,[1] and molecules containing double bonds to Group 14 atoms (including $R_2E{=}ER_2$) have yielded to synthesis.[2] Furthermore, numerous compounds with these elements embedded in small and highly strained rings are now available.[3] Perhaps most importantly, these accomplishments have greatly enhanced our understanding of the bonding in these systems.

Our research in Group 14 chemistry was initiated in 1980 as an extension of the prior work on strained carbocyclic skeletons such as cyclobutadiene.[4] The accumulated results obtained in our and other laboratories since then clearly demonstrate that 1) the chemistry of the three-membered rings $(R_2E)_3$ is intimately related to that of the corresponding double-bond systems ($R_2E{=}ER_2$) and carbene analogues (R_2E), 2) the physical and chemical properties of these systems with Si, Ge, and Sn vary systematically with the elements in a manner consistent with theory, and 3) strained polycyclic molecules can be constructed with these elements and exhibit unique properties often unexpected from their carbogenic analogues. This review outlines the framework of this Si, Ge, and Sn chemistry, minimizing overlap in content with recent review articles on 1) E–E double-bond systems as reactive intermediates,[1d, 2d, e, 5] 2) compounds containing Si and Ge doubly bonded to other elements,[2d–f] and 3) theoretical aspects of disilenes and small ring organosilicon compounds.[6]

2. The Chemistry Known Prior to 1980

2.1. Cyclopolysilanes and Disilenes

The first attempted preparation of a disilene ($R_2Si{=}SiR_2$) was made by *Kipping* in 1911.[7] Treatment of dichloroethylphenylsilane (**1a**) with sodium metal in the manner of a Wurtz coupling reaction provided a compound which was thought to be 1,2-diethyl-1,2-diphenyldisilene (**2a**). In 1921 *Kipping* and *Sands* recorded a similar reaction of dichlorodiphenylsilane (**1b**), only to report that the product expected to be tetraphenyldisilene (**2b**) was actually a cyclopolysilane derivative according to quantitative analyses of iodine absorption.[8] The reaction product from **1b** and sodium was eventually shown to be a mixture of $(Ph_2Si)_n$ with n = 4–6

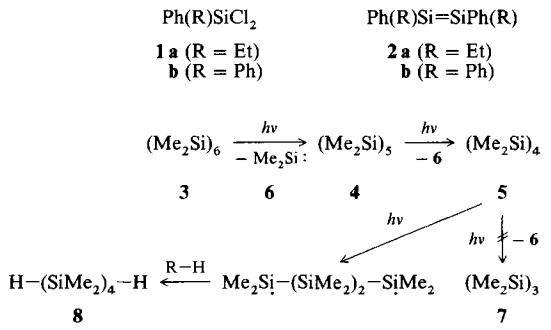

Scheme 1.

[*] Prof. Dr. S. Masamune, Dr. T. Tsumuraya, Dr. S. A. Batcheller
Department of Chemistry, Massachusetts Institute of Technology
Cambridge, MA 02139 (USA)

[**] Abbreviations used in the text: Solvents and reagents: *m*-CPBA = *meta*chloroperbenzoic acid; DCA = 9,10-dicyanoanthracene; DME = dimethoxyethane; TCNE = tetracyanoethylene. Substituent groups: 1-Ad = 1-adamantyl; Cy = cyclohexyl; Dep = 2,6-diethylphenyl; Dip = 2,6-diisopropylphenyl; Dis = bis(trimethylsilyl)methyl; Dit = 4-*tert*-butyl-2,6-diisopropylphenyl; Dmp = 2,6-dimethylphenyl; Dmt = 4-*tert*-butyl-2,6-dimethylphenyl; Mes = mesityl (2,4,6-trimethylphenyl); Nep = neopentyl; Np = naphthalenide; Phen = 9-phenanthryl; Tip = 2,4,6-triisopropylphenyl; TMS = trimethylsilyl; *p*-Tol = *p*-tolyl; Tsi = tris(trimethylsilyl)methyl.

by *Gilman* et al. in the 1960's.[9] This result was consistent with *Burkhard*'s 1949 report that described the isolation of dodecamethylcyclohexasilane (**3**), the first identified peralkylcyclopolysilane, on treatment of dichlorodimethylsilane with sodium metal.[10] Such results raised serious doubt as to whether stable disilenes could exist.

Later *Kumada* and *Ishikawa* discovered that photolysis of **3** with a low-pressure mercury lamp afforded two of the lower homologues, cyclopentasilane **4** and cyclotetrasilane **5**, with the successive extrusions of dimethylsilylene **6** (Scheme 1).[11] However, hexamethylcyclotrisilane **7**, expected from the ring contraction of **5**, was not observed in this photolysis. Instead, the cyclotetrasilane underwent homolytic scission of the Si–Si bond to give a diradical which abstracted hydrogen atoms from the solvent to produce linear tetrasilane **8**.

A large number of cyclopolysilanes $(R^1R^2Si)_n$ with R^1,R^2 = alkyl or aryl and $n \geq 4$ have subsequently been constructed by the reaction of the corresponding dichlorosilanes (or, less frequently, α,ω-dihalopolysilanes) with alkali or alkaline-earth metals.[12] The ring size of the cyclopolysilanes obtained varies with the type of substituent. For instance, the reductive coupling of dichlorodimethylsilane provides mainly $(Me_2Si)_6$ as the thermodynamically controlled product,[13] while the analogous reactions of diisopropyl- or *tert*-butylmethyldichlorosilanes afford cyclotetrasilanes.[12a,d]

Thus, by 1980 numerous derivatives of the type $(R_2Si)_n$ with R = alkyl, aryl, halogen[14] and $n \geq 4$, and several parent compounds $(H_2Si)_n$ with $n \geq 5$ had been synthesized and characterized.[15] Cyclopolysilanes show characteristic properties which are consistent with the interpretation that 1) the energy of the Si–Si σ bond is high (as compared with C–C σ bonds) and 2) contiguous Si–Si bonds (as in Si–Si–Si) experience electron delocalization.[12e–h] This latter effect is manifested in the electronic and photoelectron (PE) spectra of compounds such as $(Me_2Si)n$ with n = 4, 5, and 6 and in ESR spectra of the anion- and cation-radicals derived from $(Me_2Si)_n$ with n = 5 and 6.[12e–h, 16]

In 1969, *Peddle* et al. provided evidence for the existence of tetramethyldisilene as a transient species in the thermolysis of the compounds **9** and **10** with anthracene, isolating the Diels–Alder adduct **11**.[17] This pioneering work rekindled the investigation of disilenes, and several publications quickly appeared which supported the existence of disilenes as reactive intermediates.[18, 19] In 1979 *Sakurai* et al. reported that thermolysis of disilene precursors **12a** and **b** with anthracene provided adducts which retained the original configurations of **12a** and **b** to 95%.[19] This indicated that rotation about the Si–Si double bond was slow compared to

Satoru Masamune was born in Fukuoka, Japan in 1928. As one of the first Fulbright exchange students he pursued, and completed in 1957, Ph.D. work at the University of California, Berkeley. After temporary research appointments at the University of Wisconsin and Mellon Institute he joined, in 1964, the Faculty of the University of Alberta, Canada and stayed there until he moved in 1978 to his present location, Massachusetts Institute of Technology. He now holds the chair of the Arthur C. Cope Professorship His major honors include election to Fellow of the Royal Society of Canada (1975) and Fellow of the American Academy of Arts and Sciences (1987), The American Chemical Society Awards for Creative Work in Synthetic Chemistry (1978), the A. C. Cope Scholar Award from the American Chemical Society (1987), and selection as Centenary Lecturer of the Chemical Society, London (1980). His research interests lie in the synthesis and characterization of π-electron systems and natural products synthesis. His major accomplishments in the first area concern cyclobutadiene, [10]annulenes, the $(CH)_5^+$ pyramidal cation, and the subject discussed in this Article. Masamune's work in natural product chemistry included syntheses of diterpenes, indole alkaloids, and macrolide chemistry. The latter has led to the development of a powerful strategy in asymmetric syntheses which directed him into the field of abiotic and biotic catalysts.

Takeshi Tsumuraya was born in Ibaraki, Japan in 1962, and studied group 14 organometallic chemistry at University of Tsukuba where he completed his doctoral work in 1990 under the direction of Professor W. Ando. Since 1990 he has been a postdoctoral associate in the Chemistry Department at Massachusetts Institute of Technology and investigating germanium chemistry and then catalytic antibodies with Professor S. Masamune.

Scott A. Batcheller, born on November 1, 1961 in Cincinnati, Ohio, completed his undergraduate work at the University of Miami (Florida) in 1983 and his Ph.D. under Prof. S. Masamune at Massachusetts Institute of Technology in 1989. His thesis work primarily concerned studies on the three-membered and double-bond systems consisting of silicon and germanium. In 1989, he held a brief post-doctoral position with Cambridge Isotope Laboratories, where he synthesized organic compounds labeled with stable isotopes. Batcheller now works as a Product Development Chemist for EM Science in Cincinnati, an associate of E. Merck, Darmstadt.

the rate of cycloaddition (Scheme 2), thus demonstrating the typical π character of that bond.

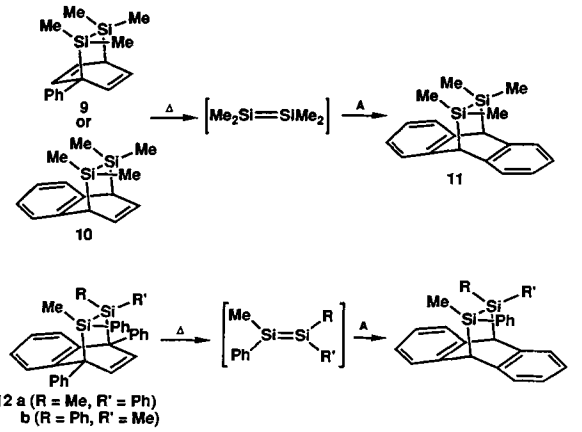

Scheme 2. A = anthracene

2.2. Cyclopolygermanes and Digermenes

In 1930 *Kraus* and *Brown* first investigated the reaction of dichlorodiphenylgermane with sodium in xylene,[20] but the main product, octaphenylcyclotetragermane, was not identified until *Neumann* and *Kühlein*'s reinvestigation, carried out in 1963.[21] Many cyclopolygermanes $(R_2Ge)_n$ with $n \geq 4$ were subsequently synthesized.[22]

Evidence seemingly consistent with the intermediacy of a digermene was presented in 1973 by *Satgé* et al. and *Mazerolles* et al.[23] Photochemical decomposition of digermylmercury compounds **13a,b** could possibly have provided digermenes or equivalent species, which were trapped by 2,3-butadione or dienes (Scheme 3). In 1976 *Lappert* et al.

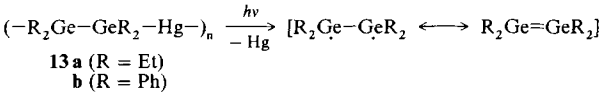

Scheme 3.

reported the preparation of bis[bis(trimethylsilyl)methyl]germanium(II) (**14a**), a stable dialkylgermylene, which dimerizes to digermene **14b** in crystalline form as confirmed in 1984 by X-ray crystal analysis (Scheme 4).[24]

2.3. Cyclopolystannanes and Distannenes

In 1852 *Löwig* prepared what was initially considered to be a divalent organotin compound by treatment of ethyl iodide with a sodium–tin alloy.[25] This product (so-called "diethyl tin") and "diphenyl tin" have since been obtained by a variety of methods. Later, *Neumann* et al. established that these compounds were mixtures of polymers which contained both straight and branched chains, including $(Et_2Sn)_5$ and $(Ph_2Sn)_n$ with $n = 5$ and 6.[26] By 1980 several cyclopolystannanes $(R_2Sn)_n$ with $n \geq 4$ had been characterized.[27]

In 1973 *Lappert* et al. isolated a dialkyltin(II) compound, bis[bis(trimethylsilyl)methyl]tin(II) (**15a**) and showed by X-ray analysis that this compound exists as a dimer, distannene **15b**, in crystalline form.[24a, b, d, e, 28] Compound **15b** was the first verified example of an E–E double-bond system for the heavier elements of Group 14. However, interest in this compound was tempered because it dissociates to the monomer in solution or in the gas phase (Scheme 4). It is therefore regarded as a formal dimer of stannylene, not an authentic doubly bonded species. These compounds will be discussed in Section 5.

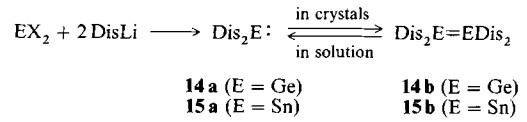

Scheme 4. X = Cl or $N(TMS)_2$

3. An Approach to the Construction of Reactive Systems

Prior to 1980, cyclotrisilanes such as **16** were thought to be synthetically inaccessible due to the reactivity intrinsic to this strained system. During the course of our investigation of cyclobutadienes during the 1970's we encountered a similar situation. The synthesis and characterization of cyclobutadiene derivatives were eventually achieved by attaching bulky substituents to the ring, as shown in **17**, in order to block dimerization and suppress attack by external reagents.[4, 29]

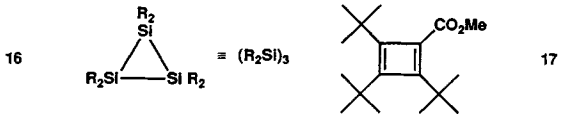

The adoption of this simple concept in Group 14 chemistry, coupled with fortuitous discovery of the photochemical conversion of **16** into the corresponding disilenes, laid the foundation for the many subsequent discoveries presented in this review.

4. Cyclotrisilanes, Cyclotrigermanes, and Cyclotristannanes

4.1. Synthesis

4.1.1. Cyclotrisilanes

The employment of 2,6-dimethylphenyl groups as substituents on silicon and judicious selection of reaction conditions led to the first isolation of a cyclotrisilane derivative in our laboratories in the fall of 1981.[30] Thus, the reduction of dichlorobis(2,6-dimethylphenyl)silane with lithium naphthalenide (LiNp) provides hexakis(2,6-dimethylphenyl)cyclotrisilane (**16a**) in 10% yield. This compound displays long

Si–Si bond distances, a general inertness to moisture and oxygen, and temperature-dependent ^{1}H NMR spectra, all giving testimony to the high degree of steric congestion around the cyclotrisilane framework in **16a**. (Compare with the cyclotetrasilanes $(R_2Si)_4$ which react readily with oxygen if the substituents are small, e.g., R = CH_3[11].) Various other hexaaryl- and trialkyltriaryl-substituted cyclotrisilanes (**16b–g**) have since been synthesized in a similar manner (Scheme 5).[31]

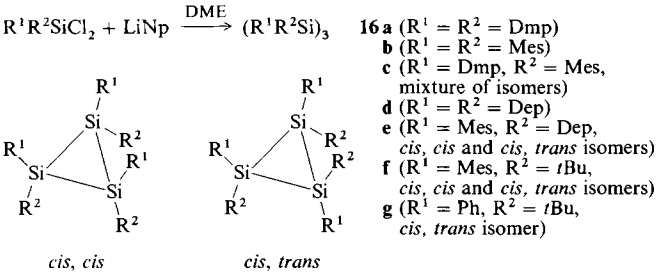

Scheme 5.

The aryl substitution of **16a** was expected to cause significant perturbation of the electronic structure intrinsic to the cyclotrisilane system. In order to eliminate this complication, the synthesis of peralkyl derivatives was undertaken. Thus, the reductive cyclization of 1,3-dichlorohexaalkyl trisilanes **18a,b** was found to proceed effectively to provide **19a,b** in 80–90% yield using a particular combination of reductants and solvents, different from that used for the synthesis of **16a** (Scheme 6).[32] In 1983 *Nagai* et al.

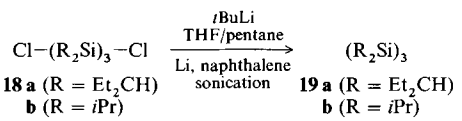

Scheme 6.

independently succeeded in the synthesis of **20**, through the reaction of dichlorodineopentylsilane with lithium (Scheme 7).[33] *Weidenbruch* et al. achieved the synthesis of the much sought hexa-*tert*-butylcyclotrisilane **21** in 1984 from the treatment of di-*tert*-butyldiiodosilane or 1,2-dibromotetra-*tert*-butyldisilane with lithium naphthalenide.[34] Interestingly, this reaction proceeds very efficiently despite the extreme steric congestion of the substituents, evidenced by extraordinarily long Si–Si and Si–C bond lengths in **21** (X-ray analysis). Replacement of one *tert*-butyl group on each silicon atom by less encumbering isopropyl or cyclohexyl groups leads to the formation of either cyclotrisilanes **22a,b** or cyclotetrasilanes depending on the reaction conditions employed.[35] A persilyl cyclotrisilane **23** has also been recently prepared by the reduction of 2,2-dibromohexaethyltrisilane with sodium.[36]

Irradiation of octaisopropylcyclotetrasilane (**24**) also reportedly provided hexaisopropylcyclotrisilane (**19b**),

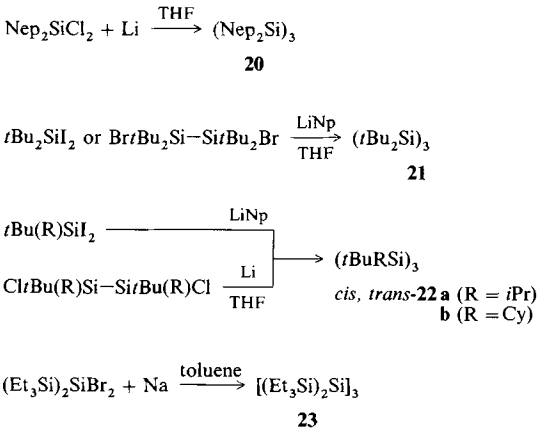

Scheme 7.

which was characterized only by UV spectroscopy (λ_{max} = 310 nm).[37] Prolonged photolysis of **24** apparently afforded disilene **25** (Scheme 8).

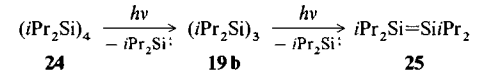

Scheme 8.

4.1.2. Cyclotrigermanes

In 1982 we isolated the first cyclotrigermane, hexakis(2,6-dimethylphenyl)cyclotrigermane **26a** in 17% yield, using much the same synthetic methodology developed for cyclotrisilane **16a**.[38] Similarly, cyclotrigermanes $(R^1R^2Ge)_3$ with $R^1 = R^2$ = 2,6-diethylphenyl (**26b**); R^1 = *tert*-butyl, R^2 = mesityl (*cis,trans*-**26d**); R^1 = mesityl, R^2 = 2,6-diethylphenyl (*cis,cis*- and *cis,trans*-**26e**) have also yielded to synthesis (Scheme 9).[31c,39] *Ando* and *Tsumuraya*[40] have since

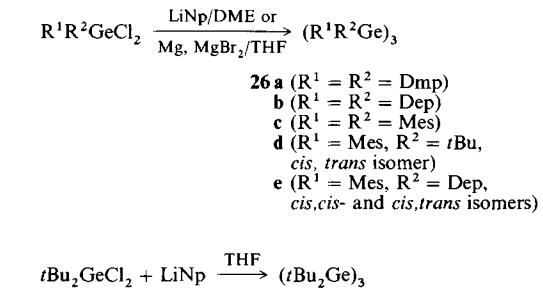

Scheme 9.

improved the synthesis of cyclotrigermanes of the type $(R^1R^2Ge)_3$ (**26a**, **26b**, and **26d**, as well as **26c**, $R_1 = R_2$ = mesityl), using Mg as a reductant. In 1988 *Weidenbruch* et al. succeeded in isolating hexa-*tert*-butylcyclotrigermane **27**, the only peralkylcyclotrigermane reported to date, by the reduction of di-*tert*-butyldichlorogermane with lithium naphthalenide.[41]

4.1.3. Cyclotristannanes

In 1983, the first cyclotristannane derivative **28a** yielded to synthesis through the same general strategy successful for the first cyclotrisilane and cyclotrigermane (Scheme 10).[42] This product can also be prepared by the reaction of 2,6-diethylphenyllithium with tin dichloride.[43] However, an interesting observation was made in the synthesis of hexakis(2,4,6-triisopropylphenyl)cyclotristannane (**28b**).[44] As shown in Scheme 10, the reaction of dichlorobis(2,4,6-triisopropylphenyl)stannane (**29**) with lithium naphthalenide provided distannane **30**, which upon further treatment with the same reductant at 60 °C (in the absence of the dichloride **29**) led to the formation of **28b**. The mechanism of this latter reaction apparently involves an equilibration between **28b** and the corresponding distannene, and is discussed in Section 5.1.3.

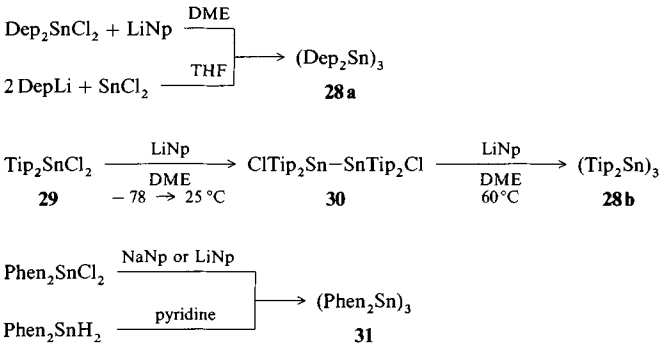

Scheme 10.

In 1984 *Neumann* and *Fu* reported the preparation of hexa-9-phenanthrylcyclotristannane (**31**) from either $Phen_2SnCl_2$ or $Phen_2SnH_2$.[45a] The so-called "di-(9-phenanthryl)tin" products prepared much earlier from 9-phenanthrylmagnesium bromide and tin dichloride[45b] were found to contain **31** also.[45c]

4.2. Molecular Structures

4.2.1. Theoretical Studies

Since the successful synthesis of cyclotrisilane **16a**, a number of theoretical calculations on the parent compound $(H_2Si)_3$ have appeared.[6,46] The predicted Si–Si bond distance of 2.33–2.34 Å is slightly shorter than that of cyclotetrasilane $(H_2Si)_4$ (2.37–2.38 Å) or disilane ($H_3Si-SiH_3$, 2.35 Å).[6,46,47] The calculated strain energy (SE) of $(H_2Si)_3$ is 36–41 kcal mol^{-1}, significantly larger than the 16–17 kcal mol^{-1} strain energy of $(H_2Si)_4$. This result contrasts with the observation that the analogous three- and four-membered rings are almost equally strained (ca. 27 kcal mol^{-1}) in the carbon series.[48] Similar results have been obtained for the cyclotrigermane and -stannane. The expected Ge–Ge bond distance of 2.448 Å in $(H_2Ge)_3$ is shorter than that expected in $(H_2Ge)_4$ (2.462 Å); the SE of $(H_2Ge)_3$ is calculated to be 44.6 kcal mol^{-1}, which is considerably larger than that of $(H_2Ge)_4$ (13.5 kcal mol^{-1}).[49] The Sn–Sn bond distance in $(H_2Sn)_3$ is predicted to be 2.80 Å, while that in $(H_2Sn)_4$ is estimated at 2.81 Å.[46a]

4.2.2. Observed Structures

To date the X-ray crystal structures of six cyclotrisilanes (**16a**, *cis,trans*-**16f**, *cis,cis*-**16f**, **20**, **21**, and *cis,trans*-**22b**), four cyclotrigermanes (**26a**, **26b**, *cis,cis*-**26e**, **27**), and a cyclotristannane (**28a**) have been determined. Selected data pertinent to the structures are summarized in Table 1, including bond lengths computed for the three parent compounds.

All of the crystal structures of these ring compounds show equilateral or nearly equilateral triangular Si, Ge, and Sn skeletons with E–E bonds longer than predicted for the parent compounds (see 4.2.1). The observed large bond lengths are likely due to steric congestion caused by a high degree of substitution.

Table 1. Selected structural parameters of the three-membered ring compounds $(R^1R^2E)_3$.

Cpd.	R^1	R^2	E	*d*(E-E) [Å]	*d*(E-C) [Å]	Ref.
16a	Dmp	Dmp	Si	2.375, 2.442, 2.425	1.90–1.93	[30]
cis,cis-**16f**	Mes	*t*Bu	Si	2.425, 2.428, 2.431	1.92–1.93 for Si–C_{Aryl} 1.97 for Si–*t*Bu	[50]
cis,trans-**16f**	Mes	*t*Bu	Si	2.395, 2.413, 2.441	1.92–1.94 for Si–C_{Aryl} 1.93–1.97 for Si–*t*Bu	[50]
20	Nep	Nep	Si	2.386, 2.367, 2.386 (A) [a] 2.414, 2.378, 2.414 (B) [a]	1.89–1.92 1.91–1.93	[33b]
21	*t*Bu	*t*Bu	Si	2.551, 2.551, 2.551	1.970	[34a]
cis,trans-**22b**	Cy	*t*Bu	Si	2.442, 2.419, 2.442	1.905–1.926	[35b]
	(H	H	Si	2.33–2.34) [b]		
26a	Dmp	Dmp	Ge	2.543, 2.543, 2.537	1.977-2.015	[38]
26b	Dep	Dep	Ge	2.590, 2.590, 2.590	2.00	[31c]
cis,cis-**26e**	Dep	Mes	Ge	2.531, 2.534, 2.564	1.982–2.006	[31c]
27	*t*Bu	*t*Bu	Ge	2.563, 2.563, 2.563	2.056	[41]
	(H	H	Ge	2.45) [b]		
28a	Dep	Dep	Sn	2.870, 2.856, 2.854	2.167–2.203	[42]
	(H	H	Sn	2.80) [b]		

[a] The asymmetric unit contains two crystallographically independent molecules (A and B). [b] Computed values.

4.3. Physical Properties

4.3.1. Electronic Absorption Spectra

The absorption maxima of peralkylcyclotrisilanes are located above 300 nm (Table 2). By comparison, the maxima of similar linear trisilanes, for example **18a,b** and their dihydrides, and even the long linear peralkylpolysilanes, $Me(Me_2Si)_nMe$ (n = 10–24), which exhibit more red-shifted absorptions than their shorter analogues, are all under 300 nm.[12e–h, 51] The absorbances of **19b** and **20** exhibit bathochromic shifts from those of cyclotetrasilanes with the same substituents.[12a, 52] This tendency is consistent with the finding that the absorption maxima move to longer wavelengths with a decrease of the ring size (nine- to four-membered) in other series of cyclopolysilanes.[3d, 12e–h]

Table 2. Electronic absorptions of cyclotrisilanes $(R^1R^2Si)_3$.

Cpd.	R^1	R^2	λ_{max} [nm] (log ε)	Ref.
19a	Et_2CH	Et_2CH	304 (2.4), 328 (2.5)	[32]
19b	*i*Pr	*i*Pr	299 (sh, 2.5), 323 (sh, 2.4)	[31d]
21	*t*Bu	*t*Bu	340, 390	[34a]
20	Nep	Nep	310 (2.5)	[33a]
16a	Dmp	Dmp	260 (4.6), 344 (sh, 3.0)	[30]
16b	Mes	Mes	262 (4.7), 348 (sh, 3.0)	[31d]
16c	Mes	Dmp	265 (4.6), 342 (sh, 3.0)	[31d]
16d	Dep	Dep	267 (4.6), 353 (2.6), 387 (2.5)	[31a]
cis,cis-**16e**	Mes	Dep	267 (4.9), 290 (4.6), 351 (2.9), 380 (2.8)	[31c]
cis,trans-**16e**	Mes	Dep	267 (4.6), 290 (4.3), 329 (2.6), 382 (2.4)	[31c]
cis,cis-**16f**	Mes	*t*Bu	263 (4.3), 379 (2.7), 412 (2.7)	[31b]
cis,trans-**16f**	Mes	*t*Bu	261 (4.5), 334 (3.0), 363 (3.0)	[31b]
23	Et_3Si	Et_3Si	335 (3.1)	[36]

The bathochromic shift observed for peralkylcyclotrisilanes is in all likelihood caused by the weaker σ bond of the strained ring and the delocalization over the σ orbitals. In addition, the steric repulsion created by the bulky substituents results in long, weak Si–Si bonds. As the bulk of the substituents increases, the absorption maxima of the cyclotrisilanes shift to red in the order of **19b** < **19a** < **21**.

Table 3. Electronic absorptions of cyclotrigermanes and cyclotristannanes $(R^1R^2E)_3$.

Cpd.	R^1	R^2	E	λ_{max} (log ε) [nm]	Ref.
26a	Dmp	Dmp	Ge	265 (4.7)	[38]
26b	Dep	Dep	Ge	272 (4.7), 309 (sh)	[39]
26c	Mes	Mes	Ge	268 (4.7), 310 (sh)	[40]
cis,trans-**26d**	Mes	*t*Bu	Ge	247 (4.6), 339 (3.3)	[39b]
cis,cis-**26e**	Mes	Dep	Ge	270 (4.6), 308 (4.1)	[31c]
cis,trans-**26e**	Mes	Dep	Ge	270 (4.6), 308 (4.1)	[31c]
28a	Dep	Dep	Sn	295 (4.7) [a]	[42]
28b	Tip	Tip	Sn	300 (4.7) [a]	[44]

[a] The absorptions tail off into the visible region.

The arylated cyclotrisilanes also show absorptions beyond 330 nm (Table 2). Similarly, cyclotrigermanes and cyclotristannanes have intense absorptions above 300 nm (Table 3).

4.3.2. Mass Spectra

The electron impact mass fragmentation patterns of peralkyl and peraryl cyclotrisilanes are characteristic and distinct.[31d] The molecular ion peaks ($M^{\oplus}$) of peraryl cyclotrisilanes are either very weak or absent; predominating is the tetraaryl disilene cation-radical **32a** produced by extrusion of a diarylsilylene from $M^{\oplus}$.[30] Other characteristic fragments are the 1,1,2-triaryldisilenyl cation **32b**, the triarylsilyl cation **32c**, the diarylsilylene cation-radical **32d**, and the monoarylsilylenyl cation **32e** (Scheme 11). By contrast, the $M^{\oplus}$ peaks of peralkylcyclotrisilanes are typically strong.[32] The dominant mode of fragmentation in this case

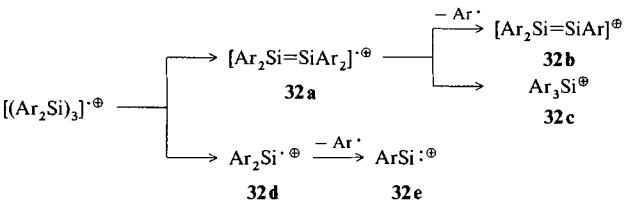

Scheme 11. Fragmentation of perarylcyclotrisilanes in the mass spectrometer.

appears to be the loss of a substituent as the corresponding alkene; the three-membered ring apparently remains intact upon electron impact (Scheme 12). The mass spectra of the trialkyltriarylcyclotrisilanes show both of the fragmentation patterns mentioned above.[31b]

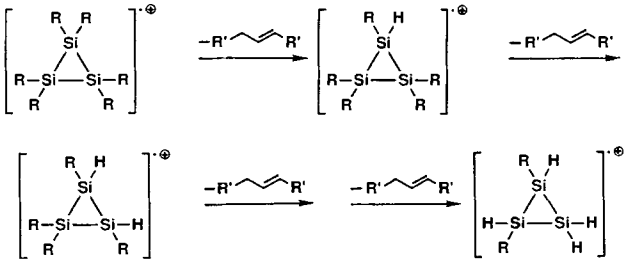

Scheme 12. Fragmentation of peralkylcyclotrisilanes **19a** and **19b** in the mass spectrometer. **19a**: R = Et_2CH, R′ = CH_3; **19b**: R = *i*Pr, R′ = H.

Cyclotrigermanes and -stannanes exhibit similar tendencies in their electron impact mass spectra.[38, 42]

4.3.3. NMR Spectroscopy

Most of the known aryl-substituted three-membered ring compounds show temperature-dependent ^1H NMR signals, indicating hindered rotation of the aromatic rings around the axis of the $M–C_{Ar}$ bond.[30, 38, 42]

As shown in Table 4, ^{29}Si nuclei in cyclotrisilanes are relatively shielded. Chemical shift values fall between $\delta = -30$ and -80 for alkyl-[33a] and aryl-substituted[53] cyclotrisilanes and $\delta = -174.38$ for persilylated cyclotrisilane **23**.[36] The $^1J_{^{29}Si-^{29}Si}$ coupling constant in cyclotrisilanes can be as small as 24.1 Hz,[54] compared to typical ^1J values of 55–70 Hz in unstrained Si–Si bonds.[54, 55] These observations

Table 4. ^{29}Si chemical shifts of cyclotrisilanes $(R^1R^2Si)_3$.

Cpd.	R^1	R^2	$\delta(^{29}Si)$	Ref.
16d	Dep	Dep	−50.8	[53]
cis,cis-**16e**	Mes	Dep	−52.69	[31c]
20	Nep	Nep	−81.68	[53]
cis,trans-**16g**	Ph	*t*Bu	−33.42, −37.33	[54]
23	Et_3Si	Et_3Si	−174.38	[36]

are consistent with the view that the magnitude of ^1J is correlated to the amount of s character of the silicon ring orbitals. This will be discussed further in Sections 5.3.2 and 9.1.

^{119}Sn NMR chemical shift values for cyclotristannanes **28a** and **28b**, $\delta = -416.5$ and -378.9, respectively, are also indicative of shielded tin nuclei.[42, 44] The spectra of both **28a** and **28b** exhibit ^{117}Sn–^{119}Sn satellites ca. 7–8% as intense as the parent signal (Fig. 1), which is consistent only

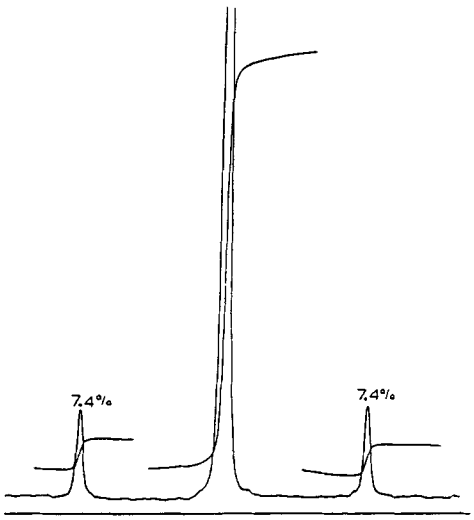

Fig. 1. The ^{1}H-decoupled ^{119}Sn NMR spectrum (100.74 MHz) of cyclotristannane **28b** in [D_{14}]methylcyclohexane.

with formulations as cyclotristannanes (see Section 9.2 for an elaboration of the technique).[44]

4.3.4. Electrochemical Properties

Peralkylcyclotrisilanes **20** and **21** have been shown by cyclic voltammetry to possess unusually low oxidation potentials (0.44 V (vs. SCE) in CH_3CN and 0.84 V (vs. SCE) in DME compared to 0.94–1.48 V vs. SCE in CH_3CN for cyclopolysilanes $(R_2Si)_n$ with $n \geq 4$[3c, 57]). Cyclotrigermanes **26b** and **26c** also show relatively low oxidation potentials of 0.80 V (vs. SCE) and 0.72 V (vs. SCE), respectively.[58]

Similar to other cyclopolysilanes, cyclotrisilane **21** is easily converted into the anion-radical, which can be detected by ESR spectroscopy (<200 K).[3c] *Nagai* et al. showed that electron-transfer reagents promoted ring-opening of **20**, producing a linear product (**33**) upon trapping with ethanol (Scheme 13).[59]

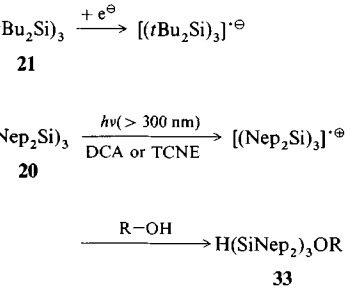

Scheme 13. DCA = 9,10-dicyanoanthracene, TCNE = tetracyanoethylene.

4.4. Chemical Properties

4.4.1. Oxygenation and Related Reactions

Although most of the cyclotrisilanes and cyclotrigermanes are inert to atmospheric oxygen, the relatively less hindered cyclotrisilane **19a** is slowly converted into the corresponding oxa compound **34a** on standing in air for several days at room temperature (Scheme 14).[32] Compound **19b** is instantly converted into monoxa and dioxa derivatives (Si_3O and Si_3O_2) under similar conditions.

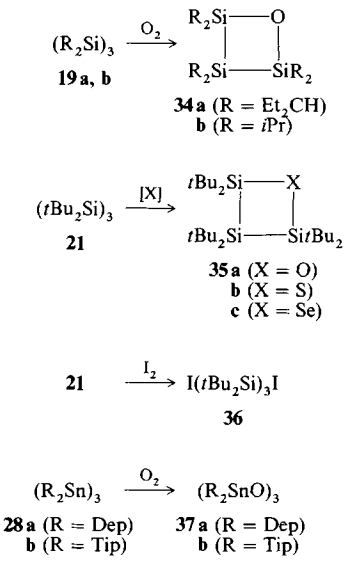

Scheme 14. [X] = O_2, DMSO, *m*-CPBA, S_8, and Se.

Compound **21** is inert to atmospheric oxygen in the crystalline form, but in solution it reacts with oxygen, DMSO, or *m*CPBA to yield the oxa compound **35a**.[60] Sulfur and selenium also react with **21** to provide the corresponding four-membered heterocycles. Treatment of **21** with iodine leads to the efficient formation of the 1,3-diiodotrisilane **36**, which has unusually long Si–Si bonds of 2.581 and 2.644 Å;[61] the longest Si–Si bond length reported thus far is ca. 2.70 Å found in hexa-*tert*-butyldisilane.[62] Cyclotristannanes **28a** and **28b** are air-stable in crystalline form, but in solution are converted by air into the corresponding cyclotristannoxanes **37a** and **37b**, respectively.[42, 44]

4.4.2. Cleavage of Three-Membered Rings into Double-Bond and Divalent Species

Of the many reactions **38** undergo, photoinduced cleavage of these three-membered rings is undoubtedly the most exciting, giving rise to the double-bond systems **39** and the corresponding carbene-like species **40**, which dimerize to **39** in solution (Scheme 15).[3a] In the case of cyclotrigermanes and

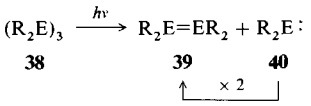

Scheme 15. E = Si, Ge, Sn.

cyclotristannanes, thermal conversion to $R_2E{=}ER_2$ has also been observed.[31c, 44, 63] Decomposition of cyclotrisilane catalyzed by a palladium complex also gives disilene and silylene.[64] *Weidenbruch* et al. reported many reactions of di-*tert*-butylsilylene (**40a**) and tetra-*tert*-butyldisilene (**39a**), both of which were generated by the photolysis or the palladium-catalyzed decomposition of **21** (Scheme 16; see also Section 5.6.1).[3c, 64–67] The conversion (and interconver-

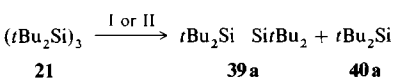

Scheme 16. I: *hν*; II: $[Pd(PPh_3)_2Cl_2]$, Δ.

sion) of **38** into **39** has turned out to be a reaction of central importance, and this chemistry is elaborated in the following section.

5. Disilenes, Digermenes, and Distannenes

Three recent review articles on disilene chemistry are now available.[2a, d, e] As noted in the introduction, this section attempts to minimize overlap and summarizes the significant accomplishments with different emphasis.

5.1. Synthesis

Syntheses of stable disilenes, digermenes, and distannenes for the most part have involved the same reactions, the most common being 1) dimerization of carbene analogues, 2) photochemical transformation of the strained rings (**38**), and 3) reductive coupling reactions that presumably involve a β elimination. For the purpose of cohesiveness, the following discussion of these syntheses will be grouped according to synthetic method.

5.1.1. Dimerization of Silylenes, Germylenes, and Stannylenes

In 1981 *West*, *Fink*, and *Michl* succeeded in isolating the first disilene derivative, tetramesityldisilene (**41**), by photolysis of linear trisilane **42** and consequent dimerization of the divalent intermediate, dimesitylsilylene (**43**) (Scheme 17).[68] The blue silylene **43** has itself been observed (λ_{max} at 577 nm) by photolysis of the trisilane in a 3-methylpentane glass at −196 °C and can be trapped with reagents such as

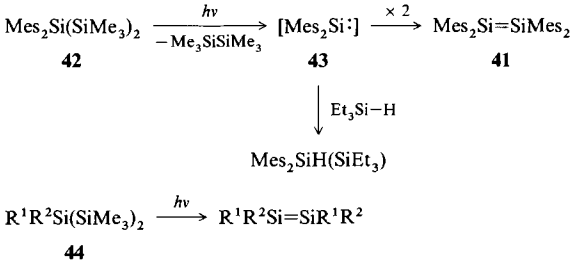

Scheme 17. At least one of R^1 or R^2 is an aryl group.

triethylsilane upon annealing the glass. In the absence of a trapping reagent **43** dimerizes to form disilene **41** upon annealing. The photolysis of linear trisilanes represented by **44** has since become a general method for the preparation of stable disilenes.[2a, 69]

In 1973 and 1976 (before the disilene synthesis described above) *Lappert* et al. reported the syntheses of dialkylstannylene **15a** and dialkylgermylene **14a**, respectively, by the reactions of $(Me_3Si)_2CHLi$ with divalent tin and germanium compounds (Scheme 4).[24, 28] Both compounds **15a** and **14a** form the corresponding centrosymmetric dimers (**15b** and **14b**) in crystalline form with the E atoms well within bonding distance (see Section 5.2.2).[24a–c, e] However, both **15b** and **14b** easily dissociate extensively, if not entirely, to their monomers **15a** and **14a** in solution, as demonstrated by their solution reactivity (see Sections 5.6.2.1 and 5.6.3).[1g, 24c]

The method used by *West* for the synthesis of stable disilene derivatives is also applicable to some digermenes.[70–72] Irradiation of the bis(trimethylsilyl) germanes **45** with a low-pressure mercury lamp yielded the corresponding germylene derivatives (**46**) which dimerized to digermenes **47a–f** as shown in Scheme 18.

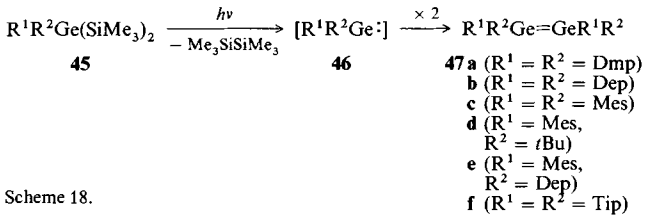

Scheme 18.

5.1.2. Photochemical Cleavage of Cyclotrisilanes, Cyclotrigermanes, and Cyclotristannanes

In 1981, our synthesis of the first cyclotrisilane derivative **16a** led us to discover that its photolysis produces the corresponding disilene, tetrakis (2,6-dimethylphenyl)disilene (**48**),

almost quantitatively as shown in Scheme 19.*[30] The cyclotrisilane **16a** (1 equiv) initially provides on photolysis disilene **48** (1 equiv) and silylene **49** (1 equiv), the latter species providing additional disilene **48** (0.5 equiv) by dimerization. The formation of silylene **49** in the photolysis of **16a** is confirmed by trapping with 2,3-dimethyl-1,3-butadiene, yielding the cycloadduct **50**.[73] The photolysis of cyclotrisilanes has been adapted for the synthesis of a variety of stable and marginally stable disilenes.[31-34,36]

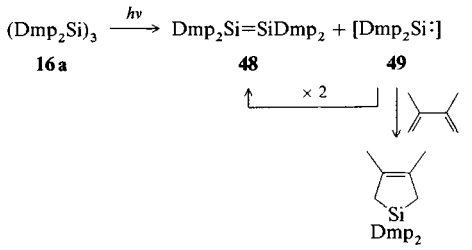

Scheme 19.

In 1984 we reported that different ratios of isomeric disilenes (*Z*)-**51** and (*E*)-**51** were obtained from separate photolyses of the 1,2,3-tri-*tert*-butyl-1,2,3-trimesitylcyclotrisilanes (*cis,cis*-**16f** and *cis,trans*-**16f**).[31b] This suggests that cyclotrisilanes undergo photofragmentation with retention of configuration at silicon in the disilene fragment. Furthermore, in the case of *cis,trans*-**16f**, it has been demonstrated that one of the two possible modes of cleavage of the three-membered ring (mode A, Scheme 20) is favored over the other (mode B) by a factor of 4.** Preference of mode A over mode B may reflect the fact that the Si–Si bond between the two *cis*-oriented mesityl groups (2.441 Å) in *cis,trans*-**16f** is

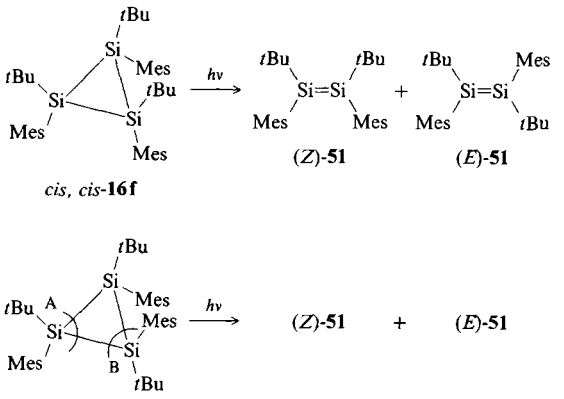

Scheme 20. Top: (*Z*)-**51**:(*E*)-**51** = 7.1:1; bottom: (*Z*)-**51**:(*E*)-**51** = 0.38:1

[*] When the synthesis of disilene **48** was accomplished, the disilene system was unknown (the submission date of the communication describing **48** was December 7, 1981 [30]). We, as newcomer to this field, were not aware that *West*'s communication [68] on the synthesis of tetramesityldisilene (**41**) was in press at that time.

[**] The observed *Z* to *E* ratio of 7.1:1 for *cis,cis*-**16f** agrees well with the calculated ratio of 6.9:1, which is calculated on the basis of the kinetic product *Z* to *E* distribution ratio of 1.6:1 observed for silylene dimerization. For *cis,trans*-**16f**, if mode A is favored over mode B by a factor of 4 the ratio can be calculated to be 0.39:1, which also agrees very well with the observed ratio of 0.38:1. The *Z* to *E* ratio calculated for random cleavage is 0.75:1; for mode A only it is 0.26:1.

longer (and weaker) than the other two Si–Si bonds (2.395 Å and 2.413 Å).[50]

In 1982 solution spectra were first recorded for a digermene derivative, tetrakis(2,6-dimethylphenyl)digermene (**47a**), formed upon photolysis of cyclotrigermane **26a**.[38] Digermene **47a** could not be isolated due to the slow conversion of **26a** into **47a** and eventual photodecomposition of **47a**. It is now clear that **26a** and **47a** constitute a photoequilibrated mixture and the cyclotrigermane/digermene ratio is subtly affected by the structure of substituents. In contrast to **26a**, hexakis(2,6-diethylphenyl)cyclotrigermane **26b** undergoes exceptionally clean photolytic conversion into digermene **47b** in > 90% yield.[39] Thus, **47b** was the first isolated digermene that retains its structural integrity in solution (Scheme 21), as substantiated by both its physical properties and solution reaction products (see below).[39,58,74,75] Other cyclotrigermanes similarly provide the corresponding digermenes, but only the photolysis of **26b** is clean enough to permit facile isolation of a digermene of 100% purity. This contrasts with the highly efficient photochemical conversions of arylated cyclotrisilanes into disilenes (see above).[3a]

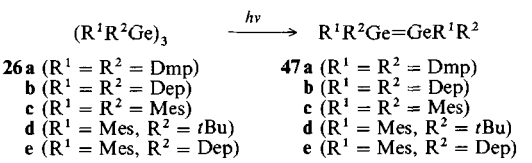

Scheme 21.

Irradiation of 1,2,3-trimesityl-1,2,3-tris(2,6-diethylphenyl)-cyclotrigermanes (*cis,cis*- and *cis,trans*-**26e**) provides a mixture of isomeric digermenes (*Z*)- and (*E*)-**47e**, the ratio of which is dependent upon which cyclotrigermane is used.[31c] The stereochemical courses of the photolyses appear to be much the same as those observed for the analogous disilenes described above.

This photolyis strategy was successfully extended to the synthesis of tin analogues in 1985 (Scheme 22).[44] Although conversion of **28a** into the corresponding distannene was not effected, irradiation of **28b** at −78 °C provided a 100% yield of distannene **52**, whose structure has been established by ^{119}Sn NMR spectroscopy (see Section 9.2). Thermal reversion of **52** to **28b** is sufficiently slow at −78 °C to permit the isolation and characterization of **52** (see the following section).

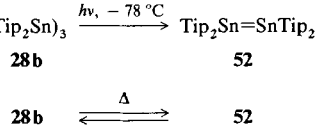

Scheme 22.

As noted above, the yield of the photoconversion of three-membered ring compounds **38** (1.0 equiv) to tetraaryl double-bond systems **39** (1.5 equiv, Scheme 15) is highly dependent on the nature of E and its ligand.[3a] The steric demand for the high-yield photoconversion (**38** → **39**) in-

creases in the order of E = Si < Ge < Sn: the tetrakis(2,6-dimethylphenyl), tetrakis(2,6-diethylphenyl), and tetrakis(2,6-diisopropylphenyl) substituents on E are needed for the series Si, Ge, and Sn, respectively.

5.1.3. *Thermal Cleavage of the Three-Membered Rings*

No example of thermal conversion of a cyclotrisilane into a disilene is known, but such reactions have been identified for cyclotrigermanes and -stannanes.[31c, 44, 63] For example, cyclotrigermanes **26b, c** and **e** have all been found to produce low concentrations of digermenes in solution at or above 80 °C.[31c, 63] Thermolysis of **26c** in the presence of various trapping reagents generates products resulting from the reaction of both the digermene and/or the germylene in high yield.[63] Equilibrium constants have been recently established between the cyclotrigermanes and digermenes at these temperatures.[76]

Cyclotristannane **28b** and distannene **52** are cleanly interconvertible.[44] This interconversion proceeds very slowly at low temperature (−78 °C), but rapidly at higher temperatures (90 °C). The equilibrium favors **28b** (> 99.9%) at or below 0 °C, but a substantial amount of **52** exists at 90 °C (Scheme 22).

5.1.4. *Reductive Coupling and Elimination Reactions*

The syntheses of disilenes and digermenes by reductive coupling exactly complement their syntheses by ring photolysis. In this way, double-bond systems possessing larger substituents than can be tolerated upon the corresponding three-membered ring systems are generally constructed.[77] In 1987 we synthesized tetrakis[bis(trimethylsilyl)methyl]disilene **53** by the reductive coupling of diiodosilane derivative **54** with lithium naphthalenide in THF (Scheme 23), representing the first isolation of a stable tetraalkyldisilene.[78] *Nagai* et al. found independently that either the reductive coupling of dichlorobis(2,4,6-triisopropylphenyl)silane or the reductive elimination of the corresponding 1,2-dichlorodisilane **55** using lithium naphthalenide provided stable disilene **56**.[79] Similarly, isomeric disilenes (*Z*)- and (*E*)-**57** have been prepared by us in good yield.[80]

$$\underset{\mathbf{54}}{Dis_2SiI_2} + LiNp \xrightarrow{THF} \underset{\mathbf{53}}{Dis_2Si{=}SiDis_2}$$

$$Tip_2SiCl_2 \text{ oder } ClTip_2Si{-}SiTip_2Cl \xrightarrow[DME]{LiNp} \underset{\mathbf{56}}{Tip_2Si{=}SiTip_2}$$
$$\mathbf{55}$$

$$Dip(Mes)SiCl_2 + LiNp \xrightarrow{DME} \underset{\mathbf{57}}{Dip(Mes)Si{=}SiDip(Mes)}$$

Scheme 23.

Treatment of the 2,6-diisopropylphenyl-substituted dichlorogermane derivatives **58** and **59** with lithium naphthalenide directly produces the corresponding digermenes (Scheme 24).[80, 81] The synthesis of **61** is significant as it represents the first and only digermene of type $R^1R^2Ge{=}GeR^1R^2$ ($R^1 \neq R^2$) to be isolated, which has permitted the measurement of the activation energy required for $Z \rightleftharpoons E$ isomerization in a digermene (see Section 5.4).[80]

$$\underset{\mathbf{58}}{Dip_2GeCl_2} + LiNp \xrightarrow{DME} \underset{\mathbf{60}}{Dip_2Ge{=}GeDip_2}$$

$$\underset{\mathbf{59}}{Dip(Mes)GeCl_2} + LiNp \xrightarrow{DME} \underset{\mathbf{61}}{Dip(Mes)Ge{=}GeDip(Mes)}$$

Scheme 24.

5.1.5. *Photochemical Retro Diels–Alder Reaction*

Sterically crowded tetra-*tert*-butyldisilene **39a** is obtained by low-temperature photolysis of 2,3-benzo-7,7,8,8-tetra-*tert*-butyl-7,8-disilabicyclo[2.2.2]octa-2,5-diene (**62**), which is prepared by the reaction of di-*tert*-butyldichlorosilane with lithium naphthalenide (Scheme 25).[82] Disilene **39a** is rather unstable thermally. It has a half-life of only several hours at room temperature and has been purified to an extent of approximately 40%.

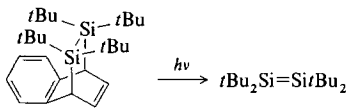

62 **39a**

Scheme 25.

5.2. Molecular Structures

5.2.1. *Theoretical Studies*

An extensive theoretical investigation of the ground-state geometry of parent disilene $H_2Si{=}SiH_2$ (**63**) has been carried out in recent years.[83] As shown in Table 5, calculations at various levels lead to different results with regard to the ground-state conformation of **63**, especially the fold (or bent) angle α. This marked basis-set dependence may reflect a flat potential surface for varying α in disilene **63**. The most sophisticated calculation provides a very large fold angle of 36°.[83n]

In contrast to disilene, the calculated geometries of parent digermene, $H_2Ge{=}GeH_2$ (**64**), and distannene, $H_2Sn{=}SnH_2$ (**65**), have been found to be nearly independent of the basis set or the method of calculation (Table 6). Theoretical studies on **64** using various basis sets predict a *trans*-bent geometry with a relatively short Ge=Ge bond length of 2.27–

Table 5. Calculated structural parameters of disilene ($H_2Si=SiH_2$ **63**).

d(Si=Si) [Å]	α[°]	Method	Basis set	Ref.
2.1575	0.0	SCF	TZ	[83a]
2.15	0.0	SCF	d(Si)	[83b]
2.102	12.9	SCF	4-31G	[83c]
2.150	[a]	CI/SCF	3-21G	[83d]
2.127	0.0	SCF	DZP	[83e]
2.165	25.7	MP2	6-31G**	[83f]
2.171	0.0	CEPA	DZP	[83g]
2.134	11.2	SCF	6-31G*	[83h]
2.127	15.6	MCSCF	DZP	[83i]
2.108	1.1	SCF	TZP	[83j]
2.116	0.0	MP4/SCF	6-31G*	[83k]
2.192	38.5	SCF	TZP	[83l]
2.164	17	MP2	PZ + 2P	[83m]
2.236	36.3	CASSCF	6-31G**	[83n]
2.125	11.4	SCF	DZP	[83o]

[a] Not given. Angle α as in I.

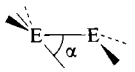

I

2.33 Å and a significant fold angle of 34–40°. Likewise, parent distannene **65** is calculated to have a Sn=Sn bond of ca. 2.7 Å and a wider fold angle of 41–49°.

In summary, both the calculated stability of the *trans*-bent form relative to the planar form* and the predicted fold angle α in $H_2E=EH_2$ increase with the atomic number of E (E=Si, Ge, Sn). In the *trans*-bent conformation for Ge and Sn, stabilization of the homo $\pi(b_u)$ orbital which is mixed with the E–E σ^* orbital predominates over destabilization of E–E $\sigma(a_g)$ bonding.[24e] The degree of orbital mixing and hence the degree of bending, α, depends on the energy difference between the $\pi(b_u)$ orbital and the E–E σ^* orbital; this energy difference decreases with increasing atomic number of E.

Table 6. Calculated geometries of $H_2E=EH_2$, **64** (E = Ge) and **65** (E = Sn).

E	d(E=E) [Å]	α [°] [a]	Method	Basis set	Ref.
Ge	2.325	38.9	CI	ECP + DZP	[84a]
Ge	2.272	36.2	RHF	DZ	[84b]
Ge	2.30	40	RHF		[24e]
Ge	2.307	38.1	HF	ECP + 21G	[84e]
Ge	2.270	34.6	SCF	DZP	[83o]
Ge	2.315	36.5	SCF	DZP	[84f]
Sn	2.71	46	RHF		[24e]
Sn	2.6866	48.2	SCF/MP2		[84d]
Sn	2.702	41.0	HF(SCF)	DZP	[84e]
Sn	2.717	48.9	SCF	DZP	[84f]

[a] For definition of α, see Table 5.

5.2.2. *Observed Structures*

To date five disilene derivatives, three digermene derivatives, and a distannene derivative have been subjected to crystallographic analysis; pertinent data are summarized in Table 7.

[*] This correlates with the increasing energy difference between the singlet and triplet states of EH_2. Although the ground state of CH_2 is a triplet of $^3B_1$ symmetry [85], EH_2 where E=Si [86], Ge [86c, 87], and Sn [86c, 87, 88] have singlet ground states of $^1A_1$ symmetry; the energy gap (ΔE_{ST}) between the $^1A_1$ and $^3B_1$ states increases in the order Si < Ge < Sn. A simple rule has been proposed that links the occurrence of a *trans*-bent distortion to a function of ΔE_{ST} of carbene and its analogues and the double-bond energy $E_{\sigma+\pi}$ [89].

Disilenes have the following structural characteristics: 1) shortened Si=Si bond distances of 2.14–2.16 Å relative to known, unstrained Si–Si single bonds (ca. 2.35 Å) and 2) generally planar disilene moieties (fold angles ca. 0°) with a small or no twist angle. Only disilene **41** exhibits sizable fold angles of 10° and 13°.[90b] The small differences found between **41** and other disilenes may reflect a shallow potential energy surface for the out-of-plane *trans* bending.

All three digermenes apparently have *trans*-bent double bonds and fold angles increase with steric congestion. The Ge=Ge bond lengths also increase as the pyramidalization at Ge becomes more pronounced. The relatively large ligands in (*Z*)-**61**[80] and **14b**[24e] compared with those in **47b**[39] apparently force the Ge=Ge bonds in the former compounds to elongate to where mixing of the homo $\pi(b_u)$ orbital and the Ge–Ge σ^* orbital becomes important. As a result (*Z*)-**61** and **14b** favor markedly *trans*-bent conformations. Although the crystal structure of (*Z*)-**61** is very similar to that of *Lappert*'s digermene **14b**, the latter exists as a dimer only in crystalline form and dissociates to the corresponding germylene **14a** in solution,[24c] whereas (*Z*)-**61** retains its structural integrity.[80] Therefore, the observed small bond dissociation energy of **14b** is apparently not directly related to its conformation.

Table 7. Selected structural parameters of double-bond systems ($R^1R^2E=ER^1R^2$).

Cpd.	E	R^1	R^2	Comments	d(E=E) [Å]	Fold angle α [°]	Twist angle [°]	Ref.
41	Si	Mes	Mes	[a]	2.16 (0.92) [c]	18	12	[90b]
41	Si	Mes	Mes		2.14 (0.91)	10, 13	3	[90b]
(*E*)-**51**	Si	Mes	*t*Bu	*E* isomer	2.14 (0.91)	0	0	[69a]
	Si	Mes	1-Ad	*E* isomer	2.14 (0.91)	3	0	[69d]
	Si	Dep	Dep		2.14 (0.91)	0	10	[69a]
	Si	Tip	Tip		2.14 (0.91)	0	3	[79a]
47b	Ge	Dep	Dep		2.21 (0.90)	12	10	[39, 80]
(*Z*)-**61**	Ge	Mes	Dip	*Z* isomer [b]	2.30 (0.93)	36	7	[80]
14b	Ge	Dis	Dis		2.35 (0.96)	32	0	[24e]
15b	Sn	Dis	Dis		2.77 (1.00)	41	0	[24e]

[a] The crystal contains toluene. [b] The crystal contains THF. [c] The value in parentheses is the ratio of double bond length to a single bond length of 2.35 (Si), 2.46 (Ge), or 2.78 Å (Sn).

In distannene **15b**,[24e] the Sn=Sn bond has a fold angle of 41° and its length is comparable to that of an average Sn–Sn single bond, therefore representing a further enhancement of the effects discussed above. Table 7 shows that the fold angles increase in the order Si, Ge, Sn and that the shortening of the E–E double bonds compared to E–E single bonds decreases in this sequence.[3a]

5.3. Physical Properties

5.3.1. *Electronic Absorptions*

All stable double-bond systems color yellow to red. The electronic absorption maxima lie between 390 and 500 nm (Table 8). The longest-wavelength absorptions have been attributed to electron transitions between the modified π and π* orbitals as described in the previous section. These ab-

Table 8. Electronic absorptions of double-bond systems ($R^1R^2E{=}ER^1R^2$).

Cpd.	E	R^1	R^2	Comments	λ_{max} [nm] (log ε)	Ref.
	Si	Nep	Nep		400	[33a]
	Si	Et_2CH	Et_2CH		390	[32]
39a	Si	*t*Bu	*t*Bu		305(3.7), 433(3.4)	[82]
53	Si	Dis	Dis		357(3.9), 393(4.1)	[78]
(*E*)-**51**	Si	Mes	*t*Bu	*E* isomer	400sh, 338	[69b]
48	Si	Dmp	Dmp		340(3.4), 422(3.8)	[30]
41	Si	Mes	Mes		343(3.8), 420(4.0)	[68]
	Si	Mes	Dep	mixture of *E,Z*	345(4.0), 426(4.3)	[31c]
	Si	Dep	Dep		354(4.0), 426(4.2)	[31a]
(*Z*)-**57**	Si	Dip	Mes	presumed *Z*	336(4.0), 430(4.3)	[80]
56	Si	Tip	Tip		347(4.0), 432(4.2)	[79a]
	Si	Mes	1-Ad	*E* isomer	338, 394sh	[69d]
	Si	Mes	*N*-TMS_2	*E* isomer	351(3.7), 483(3.7)	[69c]
	Si	Mes	*N*-TMS_2	*Z* isomer	372(3.9), 468(3.5)	[69c]
	Si	Et_3Si	Et_3Si		430	[36]
47a	Ge	Dmp	Dmp		408(3.9)	[38]
47c	Ge	Mes	Mes		406	[71]
47d	Ge	Mes	*t*Bu	mixture of *Z,E*	378	[39b]
47e	Ge	Mes	Dep	mixture of *Z,E*	412(3.6–4.0)	[31c]
(*Z*)-**61**	Ge	Dip	Mes	*Z* isomer	412(4.6)	[80]
47b	Ge	Dep	Dep		412(3.9)	[39]
47f	Ge	Tip	Tip		305(4.0), 418(4.5)	[81]
60	Ge	Dip	Dip		418(4.6)	[81]
14b	Ge	Dis	Dis	[a]	302(3.2), 414(3.0)	[24b]
52	Sn	Tip	Tip		494(4.6)	[44]
15b	Sn	Dis	Dis	[a]	332(3.0), 495(2.8)	[24b]

[a] These compounds dissociate to the corresponding carbene analogues in solution.

sorbances are considerably red-shifted from those of ethenes.

While tetraalkyldisilenes (except tetra-*tert*-butyl derivative **39a**) have absorption maxima at about 400 nm, the absorptions of tetraaryldisilenes are red-shifted by 20–30 nm, perhaps due to a weak conjugation effect. Dialkyldiaryldisilenes and tetraalkyldisilenes have essentially equal absorption maxima even though only the former carry aryl groups, possibly because these aryl rings are oriented in such a manner as to prohibit conjugation.[69a,d] The unexpectedly high λ_{max} (433 nm) of disilene **39a** is possibly caused by significant twisting of the Si=Si bond due to steric repulsion.[82]

The absorptions of digermenes are slightly blue-shifted compared to those of disilenes, while those of distannenes are largely red-shifted. The wavelengths of the lowest energy absorptions of digermenes are not significantly affected by their conformations.

The extinction coefficients (ε) of *Lappert*'s distannene **15b** are dependent on concentration and temperature; the value of ε for the absorption at 332 nm increases upon dilution while that for the 495 nm absorption decreases.[56,78] This suggests that two different species give rise to these absorptions. Based on the proximity of the two lowest energy absorptions observed for compounds **15b** and **52** and also on the results of low-temperature ^{119}Sn NMR spectroscopy (see the following section), the absorption at 495 nm can probably be assigned to the dimeric form. These spectroscopic data can, however, be interpreted differently.

5.3.2. NMR Spectroscopy

Similar to the deshielding observed in the ^{13}C chemical shifts of doubly bonded carbons compared to those of saturated hydrocarbons, the ^{29}Si nuclei of disilenes are strongly deshielded. Chemical shifts range from $\delta = 49$ to 95 (vs. TMS).[2a,68,69,79a] The solid state ^{29}Si NMR spectrum of tetramesityldisilene (**41**) has been reported to exhibit anisotropy comparable to that in the solid state ^{13}C NMR spectrum of ethene, indicating that the electronic structures of the Si=Si and C=C bonds are similar.[91] The ^{29}Si NMR coupling constants, $^1J_{Si=Si}$, observed for disilenes of 155–158 Hz represent an almost twofold increase over the $^1J_{Si-Si}$ values typically seen in unstrained Si–Si single bonds.[92] (Ab initio calculations on the parent disilene predicted a slightly higher $^1J_{Si=Si}$ value of 183.6 Hz.[93]) This indicates a greater s character for the orbitals involved in disilene bonding, which is consistent with sp^2 hybridization of Si atoms in disilenes.

The ^{119}Sn signal of distannene **52** also appears in a strongly deshielded region ($\delta = 427.3$ vs. Me_4Sn) and is accompanied by two tin–tin coupling satellites ($^1J_{^{119}Sn-^{117}Sn} = 2930$ Hz; relative peak intensities, 3.8% of the parent peak) which are expected only for a structure possessing two directly bonded tin atoms (see section 9.2).[44] The $^{119}Sn\{^1H\}$ NMR spectrum of *Lappert*'s distannene **15b** taken at −90.7 °C features two signals at $\delta = 735$ and 750, each with its own pair of $^{119}Sn-^{117}Sn$ coupling satellites ($^1J_{^{119}Sn-^{117}Sn} = 3317$ Hz for $\delta = 735$ and $^1J_{^{119}Sn-^{117}Sn} = 1784$ Hz for $\delta = 750$; intensities, ca. 3.5% of the main resonance).[56,78,94] These results suggest that **15b** exists, at least partially, in a dimeric form in solution at low temperatures. A large magnitude of anisotropy has also been observed in the ^{119}Sn cross polarization/magic angle spinning NMR (CPMAS) spectrum of **15b**.[94]

5.3.3. IR and Raman Spectroscopy

The Si=Si stretching vibrations of disilenes **41** and (*Z*)-**51** have been observed by Raman spectroscopy at 529 and 525 cm^{-1}, respectively.[2a,68] These frequencies are about 30% higher than those of Si–Si stretching vibrations, reflecting the (at least partial) double-bond character of disilenes.

Tetramethyldigermene has been isolated in an argon and a nitrogen matrix at 5 K, and its IR and Raman spectra have been recorded.[95] The observed frequencies are in good agreement with the calculated values for the *trans*-bent (C_{2h}) digermene with d(Ge=Ge) = 2.30 Å and a fold angle α of 37°. The ν_{Ge-Ge} Raman band of 404 cm^{-1} is definitely higher than that of $Me_3Ge-GeMe_3$, indicating some double-bond character in this digermene.

5.3.4. Electrochemical Properties

The electrochemical behavior of tetraaryldisilenes and dialkyldiaryldisilenes has been investigated by cyclic voltammetry, and all compounds apparently undergo irreversible oxidation and reduction.[96] The oxidation potentials are very similar for both types of disilenes (0.38–0.54 V vs. SCE), while the reduction potentials for the tetraaryldisilenes (−2.03– −2.20 V vs. SCE) are much lower than those for the arylalkyldisilenes (−2.66 and −2.64 V vs. SCE).

This may be due to a lowering of the LUMO energy by interaction of disilene "π^*" and aromatic π^* orbitals in tetraaryldisilenes; such an interaction is apparently minimized in diaryldialkyldisilenes as deduced from X-ray analysis.[69a, d]

5.4. Energy of the E=E π Bond in Si, Ge, and Sn Double-Bond Systems

The synthesis of an *E* or *Z* stereoisomer of type $R^1R^2E{=}ER^1R^2$ ($R^1 \neq R^2$) provides a means of measuring the activation energy required for thermal $E \rightleftharpoons Z$ isomerization which is normally equated to the so-called π-bond energy of the E=E bond. To date, several such disilene derivatives and a digermene derivative have been isolated, and the rates for their $E \rightleftharpoons Z$ thermal interconversions have been measured in standard fashion.[31b, c, 69c, d, 80] These compounds containing E–E double bonds exhibit first-order isomerization kinetics, and the kinetic parameters pertinent to these first-order processes are summarized in Table 9. The more stable isomers of all known disilenes of type $R^1R^2Si{=}SiR^1R^2$ have an *E* configuration. By contrast, the *Z* isomer of digermene **61** has been found to be more stable than the corresponding *E* isomer.[80]

The mechanism of these isomerizations exclusively involves rotation about the E=E bond, instead of a thermal dissociation–recombination. Thus, the presence of 2,3-dimethylbutadiene, an efficient silylene and germylene trapping agent, did not affect the rates of isomerization or produce trapping products even after prolonged exposure at temperatures where the isomerization is completed within a few hours. Interestingly, digermene **47e** has been found to show non-first-order kinetics in the $E \rightleftharpoons Z$ isomerization, suggesting the existence of a mechanism other than simple rotation about the Ge=Ge bond for less hindered digermenes.[31c]

The enthalpies of activation for the disilene $E \rightleftharpoons Z$ isomerizations fall between 25 and 28 kcal mol^{-1} (except for disilene **51**).* The π-bond energy for PhMeSi=SiPhMe (**66**) is estimated at greater than 26 ± 5 kcal mol^{-1} from a thermochemical analysis of $E \rightleftharpoons Z$ isomerization of **66**,[98] which has been generated as an intermediate by *Sakurai* et al.[19] (see Section 2.1). This is in good agreement with the $E \rightleftharpoons Z$ thermal isomerization kinetics data described above (Table 9). The enthalpy of activation for the Ge=Ge bond isomerization is somewhat lower than that of the disilene isomerization. Most recent calculations arrive at an estimate of about 25 kcal mol^{-1} for the double bonds of both parent disilene and digermene.[83o, 99] Considering the sizable ligands employed in the derivatives used in the experiment, theory and experiment are in reasonable agreement.

The dissociation energy of the Sn=Sn bond is apparently very small, and experimental attempts to measure the kinetic parameters for $E \rightleftharpoons Z$ isomerization of a distannene have not yet appeared.

Table 9. Kinetic parameters for $E \rightleftharpoons Z$ isomerizations for $R^1R^2E{=}ER^1R^2$.

Cpd.	E	R^1	R^2	$\Delta H^{\ddagger}_{Z-E}$ [kcal·mol^{-1}]	$\Delta S^{\ddagger}_{Z-E}$ [cal K^{-1}·mol^{-1}]	$\Delta H^{\ddagger}_{E-Z}$ [kcal·mol^{-1}]	$\Delta S^{\ddagger}_{E-Z}$ [cal K^{-1}·mol^{-1}]	Ref.
51	Si	Mes	*t*Bu	23	−8 to −12	28	−13 to −17	[31b]
51	Si	Mes	*t*Bu	31	+11			[69c]
				(33) [a]	(+19) [a]			
	Si	Mes	Dep	26	−4	27	−2	[80]
57	Si	Mes	Dip	26	−5	27	−2	[80]
	Si	Mes	1-Ad	28	+5	27	−4	[69d]
				(27) [a]	(+3) [a]	(27) [a]	(−4) [a]	
	Si	Mes	$NTMS_2$	25	0			[69c]
61	Ge	Mes	Dip	22	−5	20	−10	[80]

[a] Data from *West* recalculated according to the Eyring formula, using the rate constants measured at the highest and lowest temperatures.

5.5. Dissociation Energy

Ab initio molecular orbital calculations on the parent $H_2E{=}EH_2$ systems predict E=E dissociation energies near 52–58 kcal mol^{-1} for E = Si,[83h, o] 30–45 kcal mol^{-1} for E = Ge,[24e, 83o, 84a] and 22–28 kcal mol^{-1} for E = Sn.[24e, 84d] These energies contrast with the high stability of C–C double bonds and are much lower than the E–E single bond dissociation energies.[24e, 100] Recently, several experiments which support the above computed data have appeared.

Although disilenes are stable to 170 °C for a prolonged period of time, digermene **47b** and distannene **52** undergo facile thermal transformation (Scheme 26).[31c, 44] Thus, digermene **47b**, which is stable at or below room temperature, is slowly converted into cyclotrigermane **26b** above 80 °C. Similar conversion of distannene **52** into cyclotristannane **28b** has been observed at even lower temperatures. The distannene **52** is kinetically stable at −78 °C, but is cleanly converted into **28b** at 0 °C (Scheme 22), as noted earlier.

$$\underset{\textbf{47b, 52}}{R_2E{=}ER_2} \rightleftharpoons 2\,R_2E{:}$$

$$R_2E{:} + R_2E{=}ER_2 \rightleftharpoons \underset{\textbf{26b, 28b}}{(R_2E)_3}$$

Scheme 26. **47b**, **26b**: E = Ge, R = Dep; **52**, **28b**: E = Sn, R = Tip.

The simplest mechanism for the direct conversion of a double-bond system into the corresponding three-membered ring involves the initial rate-determining, first-order dissociation of $R_2E{=}ER_2$ into two R_2E species, each of which then reacts with a second molecule of $R_2E{=}ER_2$ to form the cyclotrimer. Preliminary kinetic investigation of this reaction suggests that an upper limit to the dissociation energy of **47b** is about 30 kcal mol^{-1}.[76] The enthalpy of dissociation

[*] Table 9 shows that we [31b] and West et al. [69c] reported two sets of kinetic parameters which show a nonnegligible discrepancy for the isomerization of disilene **51**. While we used the Eyring equation to obtain $\Delta H^{\ddagger}$ and $\Delta S^{\ddagger}$ from two rate constants measured at temperatures that are sufficiently different (>20 °C), the other group measured rates at several different temperatures and analyzed the data using an Arrhenius plot. The solvents used were also different: [D_{14}]methylcyclohexane (*Masamune*) and [D_6]benzene (*West*). It was stated that our data "may be less accurate since it (our data) is based on rate measurement at only two temperatures" [2a]. This statement is unacceptable. The errors in securing the kinetic parameters are minimized by the use of a large difference ΔT between the extreme temperatures *T* and *T'*, but not by addition of rate constants measured at temperatures between *T* and *T'* [97]. Moreover, our data are reproducible [39b]. We only offer the explanation that this discrepancy may be due to a solvent effect.

of the Sn=Sn bond is definitely lower than that of digermene dissociation (estimated near 20 kcal mol^{-1}), although we have not obtained accurate kinetic parameters.

The low dissociation energies associated with *Lappert*'s digermene **14b** and distannene **15b** appear to be due largely to the unique stabilization of the monomers by the $CH(SiMe_3)_2$ group (β effect). The enthalpy for the dissociation of **15b** to **15a** has been reported as 12.8 kcal mol^{-1}.[94] Unlike its Ge and Sn counterparts **14b** and **15b**, disilene **53** does not dissociate in solution to a detectable extent.[78] This obviously reflects the expected high thermodynamic stability of the Si–Si double bond relative to those for the Ge–Ge and Sn–Sn double bonds.

5.6. Chemical Properties

5.6.1. Disilenes

The reactions of aryl-substituted disilenes, as summarized in *West*'s 1987 review,[2a] are diagrammed in Scheme 27.[68, 73, 101, 102] More recently, *Weidenbruch* has investigated the reactions of tetra-*tert*-butyldisilene (**39a**) (Scheme 28).[3c, 64, 65c, 66, 103, 104] These schemes show that disilenes undergo addition of protic acids (HX), halogens (X_2), and chalcogens, as well as complexation with transition metals, cycloadditions, and oxidation (see the next section).

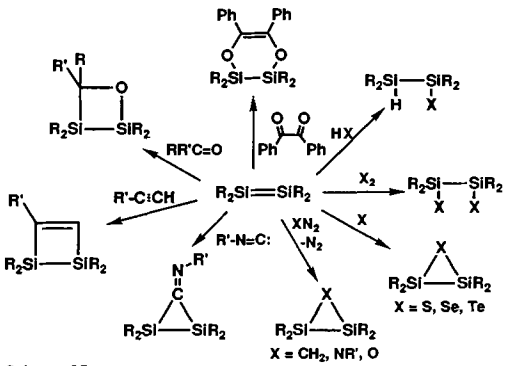

Scheme 27.

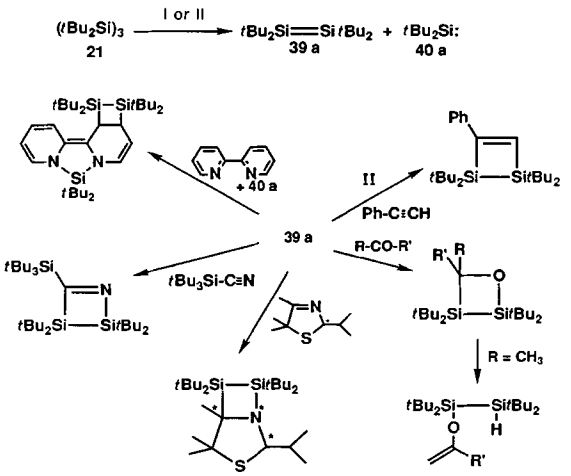

Scheme 28. I: *hv*; II: $[Pd(PPh_3)_2Cl_2]$, Δ.

In addition to these bimolecular reactions, disilenes undergo several isomerization reactions in the absence of external reagents, as exemplified by $E \rightleftharpoons Z$ isomerization (see Section 5.4),[31b, 69c, d] thermal rearrangement,[103a] and 1,2-migration of aryl substituents (Scheme 29).[105] Many new ring

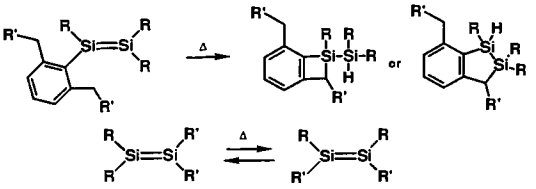

Scheme 29.

systems have been constructed from disilenes.[2a, 3c, 66, 102b] The following reactions deserve further discussion.

5.6.1.1. Oxidation

Disilenes are highly reactive toward oxygen. Many solid disilenes react with atmospheric oxygen to provide 1,3-cyclodisiloxanes **67** with retention of configuration (Scheme 30).[92, 101b, c, f, 102] When disilenes are oxidized in solution two products form: 1,2-dioxadisiletanes **68** and oxadisiliranes **69**.[101c, 102] The former (**68**) slowly rearranges

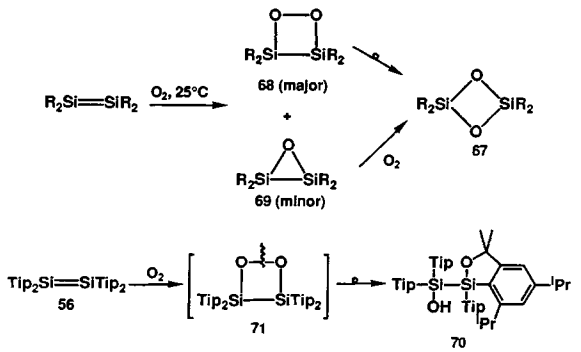

Scheme 30.

to cyclodisiloxane **67**, and the latter (**69**) undergoes further oxidation also to **67**. The oxidation of tetrakis(2,4,6-triisopropylphenyl)disilene (**56**) has been found to provide a novel rearrangement product **70**, very likely through 1,2-dioxadisiletane **71**.[79b]

5.6.1.2. Formation of η^2-Disilene Complexes

Very recently, η^2-disilene complexes **72** have been synthesized by the reaction of tetramesityldisilene (**41**) with platinum complexes (Scheme 31).[106a] Several stable η^2-disilene complexes have also been isolated by different routes.[106, 107] Furthermore, less sterically encumbered disilenes (such as tetramethyldisilene) can be stabilized as η^2-disilene–metal complexes. The significantly short Si–Si bond of **73a** (2.260 Å) reflects the partial double-bond character of its Si–Si bond.[107]

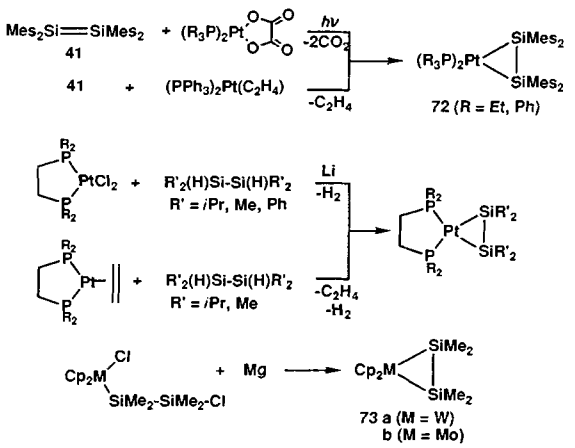

Scheme 31.

5.6.1.3. *Additional Bimolecular Reactions*

Although disilene **48** reacts smoothly with diazomethane to yield a disilirane,[73] the reaction of tetramesityldisilene (**41**) with *p*-tolyldiazomethane has been found to provide azadisiliridine **74** (Scheme 32).[108] Disilene **41** also reacts with nitrosobenzene and nitrobenzene to provide 1,2-oxazadisiletidine **75** and 1,3,2-dioxazadisilolidine **76**, respectively.[109]

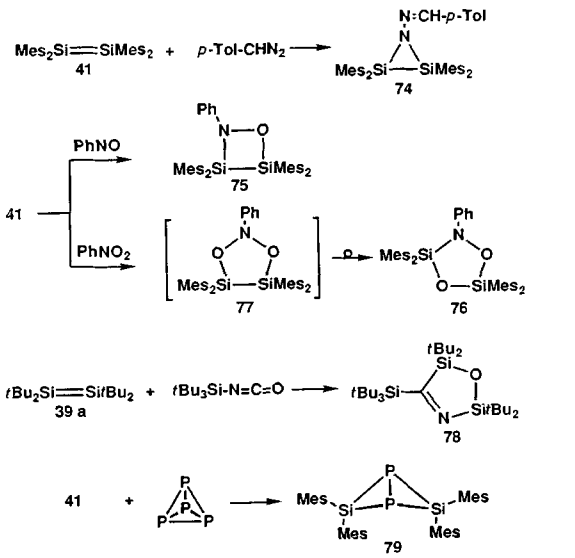

Scheme 32.

The latter compound may be produced by an interesting rearrangement of the initially formed [3+2]-cycloaddition product **77**. A similar type of rearrangement has been observed in the addition of isocyanate to tetra-*tert*-butyldisilene (**39a**), providing a similar five-membered heterocyclic product **78**.[102] Disilene **41** also reacts with white phosphorus to give the bicyclic compound **79** in good yield.[110]

5.6.1.4. *Chemical Properties of Tetrakis[bis(trimethylsilyl)-methyl]disilene (53)*

The chemistry of disilene **53** is worthy of special attention because its Ge and Sn counterparts **14b** and **15b** both predominantly dissociate to the corresponding monomers in solution as already noted above. Disilene **53** shows no indication of dissociation into the corresponding bis(disyl)silylene (**80**) in solution; its chemical properties are fully consistent with the disilene formulation.[78] It reacts with water to provide the corresponding hydrate **81**. Rather unexpectedly, **53** is inert to methanol even in a refluxing THF solution over 24 h. However, photolysis rapidly cleaves **53** into

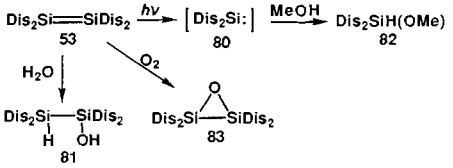

Scheme 33.

silylene **80**, which subsequently reacts with methanol to afford the methoxysilane **82**. Bubbling O_2 through a solution of **53** provides the oxadisilirane **83** as the major product (Scheme 33).

5.6.2. *Digermenes*

The known digermenes are divided into two separate groups: 1) the readily dissociating digermene **14b** of *Lappert* and 2) tetraaryldigermenes that retain their structural integrity in solution. The reactions of the former are probably more accurately regarded as reactions of germylenes, and those of the latter are much the same as the corresponding disilenes.

5.6.2.1. *Lappert's Digermene (14b)*

The monomer **14a** derived from **14b** 1) behaves as a Lewis base, 2) undergoes oxidative addition to form a tetravalent germanium compound, and 3) yields a germyl radical (Scheme 34).[24c] The products derived from these processes are generally monogermanium compounds. Recently, a novel three-membered heterocycle **84** has been prepared by the addition of **14a/14b** to phosphaalkyne **85**.[111]

5.6.2.2. *Tetraaryldigermenes*

1,2-Additions and Cycloadditions

Tetraaryldigermenes readily react with protic species to provide 1,2-addition products and also undergo

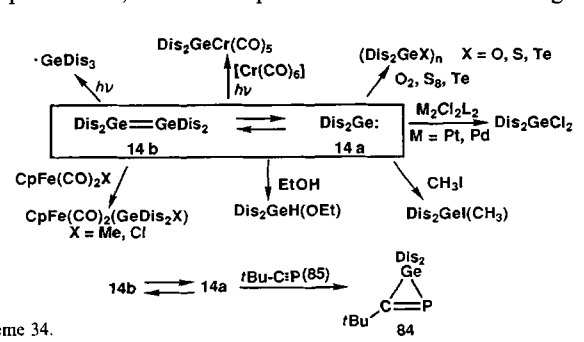

Scheme 34.

smooth cycloadditions with a variety of reagents to provide new three- or four-membered ring systems (Scheme 35).[38–40a, 58, 70, 74, 75, 81, 112] Reactions of digermenes with sulfur, selenium, and tellurium provide three-membered rings consisting of two germanium atoms and the chalcogen atom. Digermenes apparently undergo [2+3]-cy-

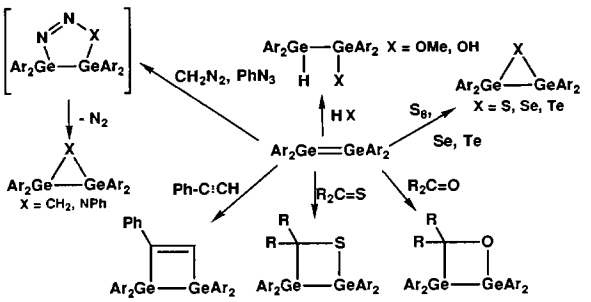

Scheme 35.

cloadditions with diazomethane or phenyl azide, in each case generating three-membered ring products following loss of N_2. Digermenes also react with phenylacetylene as well as carbonyl and thiocarbonyl compounds to provide the formal [2+2]-cycloadducts in good yield.

Oxidation

Tetrakis(2,6-diethylphenyl)digermene (**47b**) and tetrakis(2,6-diisopropylphenyl)digermene (**60**) undergo oxidation in a manner generally analogous to, but subtly different from, that observed for the disilene series (Scheme 36).[74b]

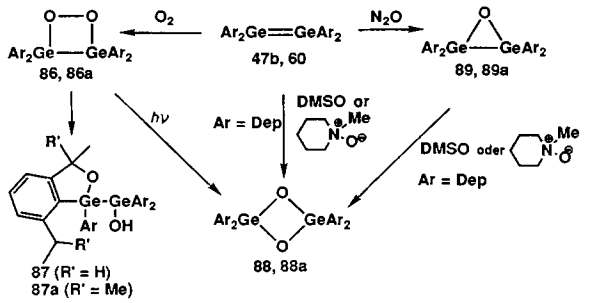

Scheme 36. **86**–**89**, Ar = Dep. **86a**–**89a**, Ar = Dip.

Thus, exposure of digermene **47b** in toluene to O_2 provides 1,2-dioxadigermetane derivative **86** quantitatively, which upon heating at 90 °C rearranges to **87**. The 1,2-dioxadigermetane **86** is photochemically converted into cyclodigermoxane **88**. This thermal and photochemical behavior of **86** contrasts with that of silicon analogue **68**, which undergoes thermal rearrangement to provide **67**.[101c, 102] However, the thermal rearrangement of **86** to **87** is analogous to the oxygenation behavior of disilene **56**.[79b] Digermene **60** behaves similarly and provides **86a**, **87a**, and **88a**.

Cyclodigermoxane **88** has also been obtained directly and quantitatively from **47b** upon treatment with excess DMSO or *N*-methylmorpholine-*N*-oxide. Treatment of digermenes **47b** and **60** with nitrous oxide produces oxadigermiranes **89** and **89a**, respectively, via [2+3]-cycloadditions followed by loss of N_2. Conversion of **89** into **88** with DMSO or *N*-methylmorpholine-*N*-oxide proceeds very rapidly compared to the conversion of digermene **47b** into **88** by the same reagent; therefore, **89** appears to be a likely intermediate in this latter conversion.

Reductive Cleavage

Rather unexpectedly, treatment of digermene **60** with an excess of lithium naphthalenide leads to Ge–C_{Ar} bond cleavage to provide the isolable digermenyllithium **90** (germanium analogue of a vinyllithium), a species hitherto unknown in Si, Ge, and Sn double-bond chemistry (Scheme 37).[81] Compound **90** is an extremely air-sensitive, red crystalline compound which reacts readily with methanol to give digermane **91**. In contrast, the reduction of digermene **47b** with lithium naphthalenide under the same conditions provides products which are converted upon protonation into diarylgermane, tetraaryldigermane, and unidentified polymers. 1,3-Diethylbenzene was not obtained; therefore, cleavage of a Ge–C_{Ar} bond apparently does not occur in this case.

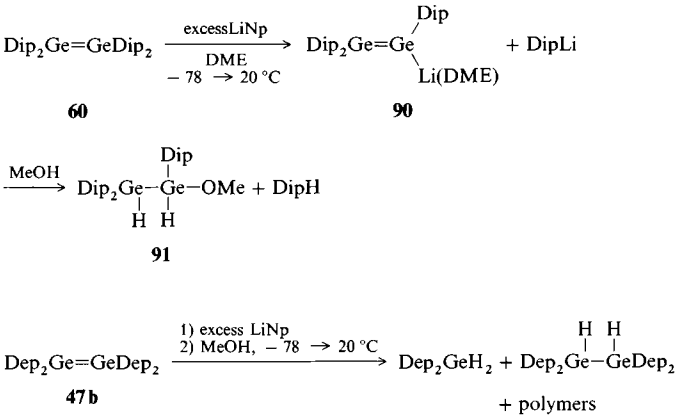

Scheme 37.

5.6.3. Distannenes

In a manner similar to *Lappert*'s digermene **14b**, **15b** behaves as the corresponding monomer **15a** as summarized in Scheme 38.[1g] Several other reactions have been recorded

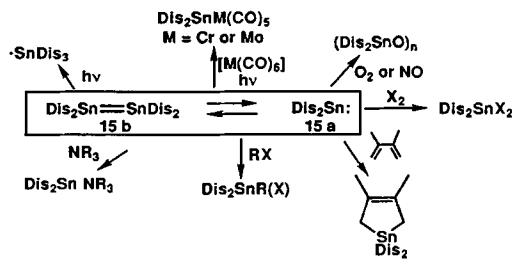

Scheme 38. X = Halogen

recently. Addition of distannene **15b**/**15a** to boranediylborirane **92**, which behaves as carbene **92a** in the presence of suitable reagents, leads to the formation of the stable stannaethene **93** (Scheme 39).[113a] Distannene **15b**/**15a** also re-

acts smoothly with cyclic acetylene **94** to afford pale yellow crystalline stannacyclopropene derivative **95**.[113b] Although **95** is stable in crystalline form or in solution below $-25\,^{\circ}C$, it readily reverts to **15a/15b** and acetylene **94** in solution at room temperature. This behavior is reminiscent of the thermal equilibrium between a cyclotristannane and a distannene.[44]

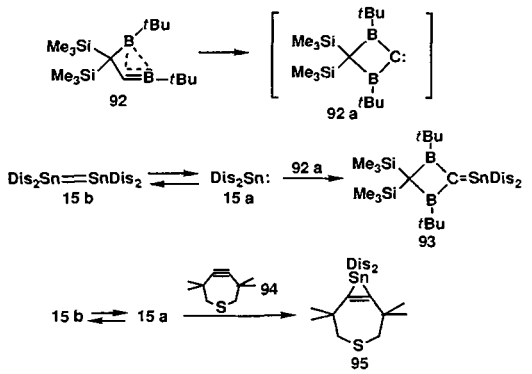

Scheme 39.

The above reactions provide products containing only one tin atom per molecule. However, more recent investigations show that some reactions provide products in which the Sn–Sn moiety may have been preserved. Phosphaalkyne **85** reacts with distannene **15b/15a** to afford a derivative of the 1,2,3-phosphadistannetene **96** (Scheme 40).[114] Direct reaction of distannene **15b** with **85** has been proposed for the formation of **96**, although successive additions of stannylene **15a** to **85** cannot be ruled out (see below). In contrast to the reaction with the alkyne **94**, **15b/15a** reacts only slowly with cyclooctyne **97** to provide the stable 1,2-distannetene **98** quantitatively.[115] Successive insertion of stannylene **15a**

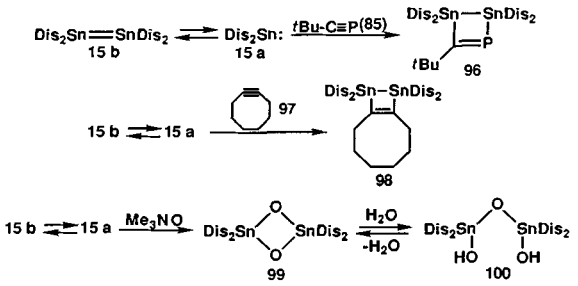

Scheme 40.

into the alkyne has been proposed for this reaction. Very recently, *Lappert* et al. reported the synthesis of the first cyclodistannoxane derivative **99** obtained by the oxidation of distannene **15b/15a** using Me_3NO.[116] Compound **99** easily hydrolyzes to yield **100**, which is converted back to **99** by dehydration. The structures of both **99** and **100** have been established by X-ray analysis.

In contrast with **15b**, tetraaryldistannene **52** retains its double bond at $-78\,^{\circ}C$, as noted above. Thus, bubbling dioxygen through a solution of **52** at $-78\,^{\circ}C$ leads to the quantitative formation of cyclodistannoxane **101**, which is thermally unstable and eventually forms cyclotristannoxane **37b** (>90% conversion within 24 h at room temperature).[117] Compound **101** is easily hydrolyzed to **102** (Scheme 41). Whether the observed products arise from oxidation of the distannene **52** or reactive intermediate stannylene **103** has not been determined.

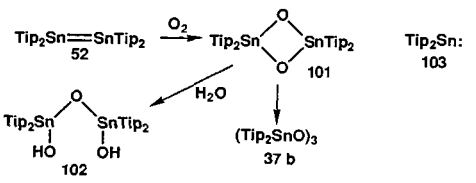

Scheme 41.

6. Small-Ring Compounds Derived from Disilenes, Digermenes, and Distannenes

The reaction products of the unsaturated compounds produced several new small-ring systems, some of which merit further elaboration.

6.1. Cyclodisiloxanes, Cyclodigermoxanes, and Cyclodistannoxanes

The structures of four cyclodisiloxanes (**67a–d**), one cyclodigermoxane (**88**), and one cyclodistannoxane (**99**) have been established by X-ray crystal analysis, and selected structural parameters are summarized in Table 10. These four-membered rings have abnormally small E–O–E bond angles, ranging from 86° to 98°. Even more surprising are the presumably nonbonded E···E distances across the ring, ranging from 2.31 to 2.45 Å for E = Si, 2.617 Å for E = Ge, and 2.94 Å for E = Sn. These values represent 98–106% of the corresponding E–E single bond distances (Si–Si: 2.35 Å, Ge–Ge: 2.46 Å, Sn–Sn: 2.78 Å).

Table 10. Selected structural parameters for the cyclodisiloxanes, cyclodigermoxanes, and cyclodistannoxanes, **II**.

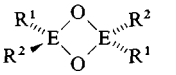

Cpd.	E	R^1	R^2	<E-O-E [°]	d(E···E) [Å] [a]	Ref.
67a	Si	Mes	Mes	86.2	2.306 (0.98)	[101f]
67b	Si	Mes	*t*Bu	91.1	2.396 (1.02)	[101f]
67c	Si	Mes	*N*-TMS_2	89.7, 89.4	2.349 (1.00)	[101f]
67d	Si	*t*Bu	*t*Bu	95.8	2.453 (1.04)	[102b]
88	Ge	Dep	Dep	92.1	2.617 (1.06)	[74b]
99	Sn	Dis	Dis	97.5	2.94 (1.06)	[116]

[a] The value in parentheses is the ratio of d(E···E)/d(E–E).

These characteristic features have raised questions concerning bonding in cyclodisiloxanes.[101b,f,102] Different models suggest that either 1) there is a σ bond between the silicon atoms, making the Si–O bonds necessarily electron-deficient (structure $\mathbf{B}_1$) or 2) there is a localized σ-bond

framework in which oxygen–oxygen repulsion dominates the structure, thus forcing the two silicon atoms together (structure $\mathbf{B}_2$). Several theoretical investigations support structure $\mathbf{B}_2$ for the parent cyclodisiloxane $(H_2SiO)_2$.[118a–e]

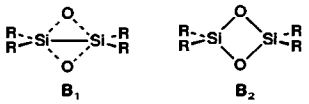

$\mathbf{B}_1$ $\mathbf{B}_2$

The small $^1J_{^{29}Si-^{29}Si}$ coupling constants of ca. 4.0 Hz observed for cyclodisiloxanes are consistent with this theoretical result,[92, 118f] since in structure B_1 $^1J_{^{29}Si-^{29}Si}$ should be within the range of 55–70 Hz obtained for directly bonded Si–Si bonds. Apparently 1) the shortening of the Si···Si distance in disiloxanes is due mainly to the short Si–O bond (1.66 Å) compared to other bond lengths and 2) the "effective" van der Waals radius of the Si atom along the direction toward the other Si atom is smaller than that normally established for this atom.[119] Structural homology for the ring system is further discussed in Section 9.3.

6.2. Disiliranes and Digermiranes

To date, the crystal structures of four disiliranes **104a–e**[120] and six digermiranes **105a–f** have been determined (see Table 11 for selected parameters). A surprising feature

Table 11. Selected structural parameters for the three-membered rings of type **III**.

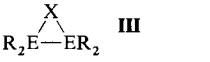

III

Cpd.	E	R	X	ΣE [°] [a]	d(E–E) [Å]	Ref.
104a	Si	Dmp	CH_2	357.4, 357.7	2.272	[73]
104b	Si	Mes	S	357.4	2.289	[101d]
104c	Si	Mes	O	359.9	2.227	[101i]
104d	Si	Mes	*N*-TMS	357, 358	2.230	[102b, 101j]
105a	Ge	Mes	S	357.3, 356.7	2.376	[112]
105b	Ge	Dep	S	357.3	2.387	[31c]
105c	Ge	Dep	Se	356.7	2.398	[31c]
105d	Ge	Dep	Te	355.4, 355.5	2.435	[75b]
105e	Ge	Dep	CH_2	356.9	2.379	[58]
105f	Ge	Dep	*N*-Ph	358.2	2.379	[58]

[a] ΣE = <R-E-E′ + <R′-E-E′ + <R′-E-R

of these systems except for telluradigermirane **105d** are the relatively short E–E distances, which are not characteristic of other known three-membered ring compounds of $(R_2E)_3$ type: cyclotrisilanes and cyclotrigermanes have longer-than-normal bond lengths, as shown in Section 4.2.2. (Note that the replacement of R_2E in $(R_2E)_3$ rings with X relieves the steric congestion in the $(R_2E)_3$ rings.) Table 11 shows that, as the electronegativity of X increases, the Si–Si bonds are shortened and the deviation of the C_2Si–Si unit (where C represents the *ipso* C atom of the aryl substituent) from coplanarity becomes less pronounced. Similar tendencies have been observed for the analogous germanium compounds, although to a lesser extent.

In the most extreme case, oxadisilirane **104c**, the Si–Si bond distance is actually closer to those for Si–Si double

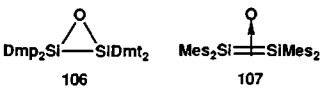

106 **107**

bonds (2.13–2.16 Å) than Si–Si single bonds (ca. 2.35 Å). Furthermore, the C_2Si–Si framework is planar.[101i] *West* has proposed a bonding model in which a significant amount of the double-bond character of the disilene is retained in **104c**. The large $^1J_{^{29}Si-^{29}Si}$ coupling constant of 99 Hz measured for **106**, which is intermediate between that of disilenes (155 Hz) and disilanes (55–70 Hz), indicates that the oxadisilirane **104c** may be described as a π complex **107**.[101i, 121] (The $^1J_{^{29}Si-^{29}Si}$ of cyclotrisilane is small—24 Hz; see Section 4.3.3.)

7. Comments on Reductive Coupling of Dihalosilanes and Their Germanium and Tin Analogues

In summarizing the construction of ring systems and double-bond systems by reductive coupling of various dihalosilanes, -germanes and -stannanes, one notes that there exist distinct parallels in the silicon and germanium series. Upon treatment with lithium naphthalenide, bis(2,6-dimethylphenyl)- and bis(2,6-diethylphenyl)dichlorosilane and the corresponding dichlorogermanes provide three-membered ring compounds,[30, 31a, 38, 39] whereas the unsaturated compounds $(R_2E{=}ER_2)$ are obtained as the major products from dichlorobis(2,4,6-triisopropylphenyl)silane and dichlorobis(2,6-diisopropylphenyl)germane under similar conditions.[79a, 81] In the tin series, reductive coupling of both dichlorobis(2,6-diethylphenyl)- and dichlorobis(2,4,6-triisopropylphenyl)stannanes leads to the corresponding cyclotristannanes, respectively.[42, 44] That these results are apparently inconsistent with those of the Si and Ge series is only superficial; reductive coupling of dichlorobis(2,4,6-triisopropylphenyl)stannane proceeds via the initial formation of the corresponding distannene, which is rapidly converted into cyclotristannane under the reaction conditions.[44]

These cyclotrimerizations may be proceeding through routes such as those outlined in Scheme 42. This mechanism involves the stepwise building of the polysilane, -germane or -stannane backbone until the steric congestion of the substituents "forces" the ends of the chain so close together that the chain is likely to cyclize (known as the Thorpe-Ingold effect). With 2,6-dimethylphenyl or 2,6-diethylphenyl groups on dichlorosilanes or dichlorogermanes, the cyclization occurs when the chain reaches the trimeric stage **108**. Indeed, for E = Si and Ge the compounds **109** undergo reductive cyclization with lithium naphthalenide in good yields, rather than further chain elongation, even in the presence of excess starting material R_2EX_2.[3a] When the substituents on E become even larger, the intermediate **110** may be too congested to permit chain elongation and prefers to undergo β elimination to form a double bond. This apparently occurs in the silicon and germanium series and even in the tin series (see above) when the substituents are 2,6-di- or 2,4,6-triisopropylphenyl groups. The involvement of a β elimination is supported by the alternative synthesis of disilene **56** by the reductive treatment of the 1,2-dichlorodisilane **55**.[79b] Con-

ceivably, the attempted reductive coupling of R_2EX_2 where the substituents R are sufficiently large to prohibit the first coupling could result in the generation of a stable carbene analogue (R_2E:).[122]

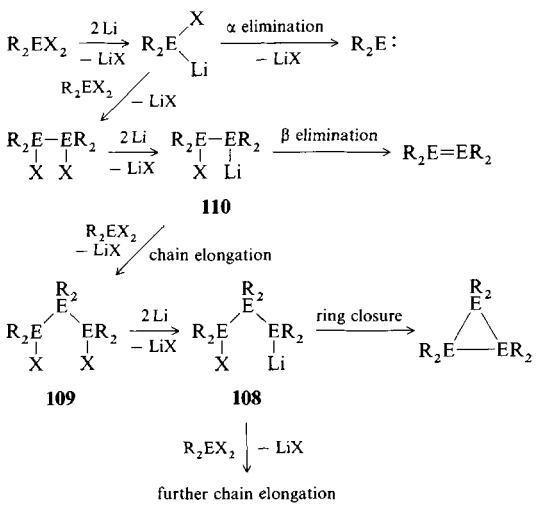

Scheme 42. Reductive coupling of dihalosilane, -germane, and stannane.

Cyclotrisilanes, -germanes, and -stannanes could possibly result from the addition of a carbene analogue (R_2E:) to an E–E double-bond system in a manner similar to the reaction between carbenes and olefins. This process has been postulated in situations where a rapid equilibration between three-membered rings and double bonds is feasible.[31c, 44, 76] The formation of cyclotristannane **28b** from dichlorodistannane **30**,[44] and **28a** from tin dichloride and the aryllithium[43] constitute examples. In contrast, the above equilibration for Ge is attainable only at high temperatures and is not possible for Si, and therefore the R_2E: addition reaction is unlikely to be involved in the reductive coupling of dihalogermanes and -silanes. However, definite proof to endorse this interpretation is yet to be secured.

8. Strained Polycyclic Systems

Our work with the three-membered rings of Si, Ge, and Sn, was extended to strained polycyclic systems. The successful construction of a bicyclo[1.1.0]tetrasilane derivative in 1985 stimulated the work in this field.[123] Numerous stable polycyclic compounds of theoretical interest have recently been prepared by either stepwise or "one-shot" synthetic schemes.

8.1. Bicyclic Compounds

8.1.1. Bicyclo[1.1.0]tetrasilanes

Scheme 43 outlines the synthesis of 1,3-di-*tert*-butyl-2, 2, 4, 4-tetrakis(2, 6-diethylphenyl)bicyclo[1.1.0]tetrasilane (**111**).[123, 124] Treatment of the trichlorodisilane **112** with lithium naphthalenide gives rise to the cyclotetrasilane **113**, which after purification is subjected to a second reductive

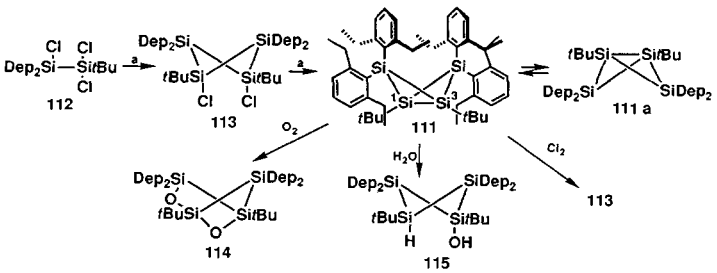

Scheme 43. a: 2 equiv LiNp

cyclization with the same reductant at 0 °C to provide **111** quantitatively. Compound **111** is extremely reactive and its exposure to air, water (atmospheric moisture), and chlorine immediately converts **111** into **114**, **115**, and **113**, respectively. A notable feature of the bicyclic ring is its facile inversion (**111** ⇌ **111a**). Thus, while three distinct ethyl signals appear in the ^{1}H NMR spectrum taken at −30 °C or below, these signals are replaced by a single quartet–triplet pair at 115 °C, indicating that all the aryl groups have attained equivalence on the NMR time scale. The barrier to this inversion is estimated to be ca. 15 kcal mol^{-1}.

The crystal structure (Fig. 2) of **111** shows the crucial Si1–Si3 bond to be relatively (and unexpectedly) short (2.373(3) Å).[123b] This bond is believed to be highly bent and rich in p character.

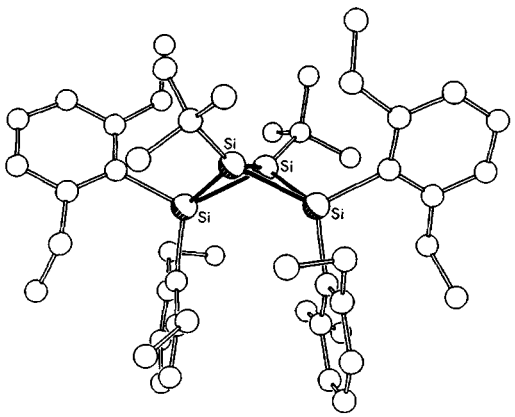

Fig. 2. Structure of the bicyclo[1.1.0]tetrasilane **111** in the crystal.

Several ab initio calculations on the parent compound **116** show two distinctly different energy minima, namely **116a** (central Si1–Si3 distance of ca. 2.3–2.4 Å) and **116b** (the corresponding bond length is 2.7–2.8 Å).[46g, 125] The former is 17 kcal mol^{-1} less stable than the latter (MC–SCF level). Other geometrical differences between these two minima are the dihedral angles between the three-membered rings (ca. 120° for **116a** vs. 140° for **116b**) and the Si–Si–H angles at the bridgehead positions (ca. 140° for **116a** vs. 90° for **116b**). That the observed short central Si1–Si3 bond in **111** corresponds to that of the less stable **116a** rather than

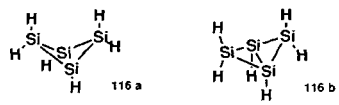

116b is possibly due to the steric requirements of the bulky bridgehead substituents.

The reactivity of the Si1–Si3 bond in a bicyclo[1.1.0]tetrasilane is further enhanced by placing aryl groups on the bridgehead positions. Reductive cyclization of trichlorodisilane **117** under similar conditions to those applied to **112** leads to products which result from the reductive cleavage of the Si1–Si3 bond of the bicyclic system.[126] Thus, treatment of **117** with 5 equiv of lithium naphthalenide provides, after hydrolysis, **118** as the sole isolable product (Scheme 44). The use of 3.5 equiv of reductant leads to a 4:1

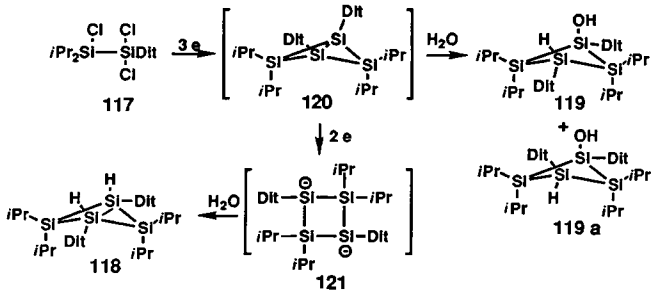

Scheme 44.

mixture of **119** and **119a** after hydrolysis. By analogy to the hydrolysis of **111**, the precursor of **119** is in all likelihood **120**. The Si1–Si3 bond in **120** appears to be further reduced to yield **121** with the excess reductant, a reaction not observed for **111** even at room temperature.

Reductive coupling of trichlorodisilane **122** with excess reductant appears to proceed in a manner similar to that described for **117**.[126] Thus, reaction of **122** with 5 equiv of lithium powder at −78 °C provides a mixture of three cyclotetrasilane derivatives **123a, b**, and **c** (Scheme 45). All

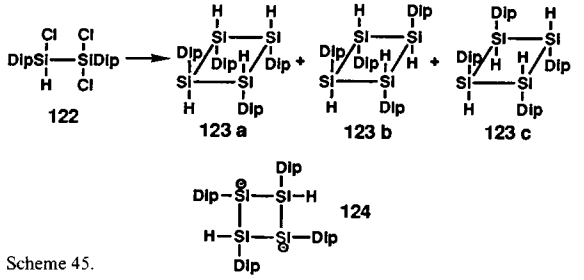

Scheme 45.

of these products apparently form from the corresponding dianion **124** and represent the first cyclotetrasilane derivatives of the $(RHSi)_4$ type.

8.1.2. Bicyclo[1.1.1]pentasilanes

The dianion **121**, which is formed as shown in Scheme 44, reacts with excess dichlorosilanes **125a–c** to provide **126a–c** (Scheme 46).[119] The crystal structure of **126a** dicloses the following interesting structural features. As expected, the three cyclotetrasilane rings are highly puckered with an average dihedral angle of 60°, which contrasts with the 0–37°

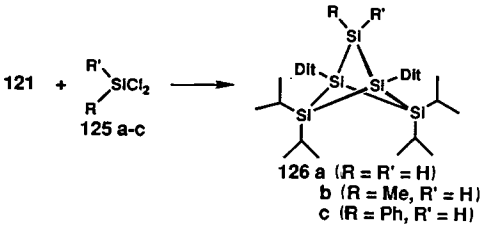

Scheme 46.

angle normally found in monocyclic systems.[3b, d] The Si-Si-Si angles in **126a** are very close to the C-C-C angles found in bicyclo[1.1.1]pentanes **127**,[127] showing a high degree of structural homology between the carbon and silicon systems, a feature also seen in other similar Group 14 ring systems (see Section 9.3).

8.1.3. Bicyclo[2.2.0]hexasilanes and Tin Analogues

In 1987 *Nagai* et al. isolated in 3% yield the first bicyclo[2.2.0]hexasilane derivative **128** from the reaction products obtained from the cocondensation of 1,1,2,2-tetrachlorodiisopropyldisilane and 1,2-dichlorotetraisopropyldisilane with lithium (Scheme 47).[128a] The X-ray analysis of **128** discloses a *cis*-fused structure with a central Si–Si bond distance of 2.394 Å, which is comparable to those for the peripheral Si–Si bonds (2.385–2.426 Å).[128b] This structure is consistent with the computed structure of the parent compound **129**.[125d]

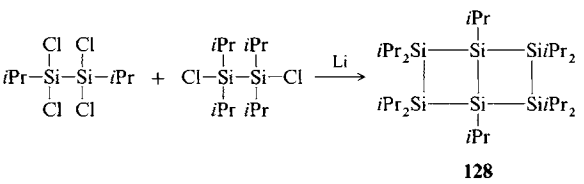

128

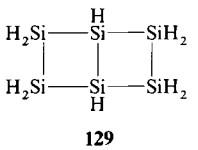

129

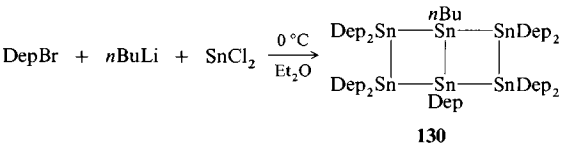

130

In 1989, *Sita* and *Bickerstaff* isolated in 1.5% yield bicyclo[2.2.0]hexastannane derivative **130**, from the reaction product of 2,6-diethylphenyllithium with tin dichloride in ether at 0 °C.[43] The selection of reaction conditions is critical, as a similar reaction in a different solvent (THF) at 0 °C provides the corresponding cyclotristannane **28a**. The crystal structure of **130** shows tin–tin bond lengths of 2.82–2.93 Å, which fall in the range commonly found for cyclopolystannanes possessing bulky ligands. The mechanism of formation of **130** is not obvious.

In contrast to the high reactivity of bicyclo[1.1.0]tetrasilanes toward a variety of reagents, bicyclo[2.2.0]hexasilane

(**128**) and -stannane (**130**) are air-stable. This may reflect the fact that Si, Ge, and Sn four-membered rings become significantly less strained. The computed strain energy (SE) of parent bicyclo[2.2.0]hexasilane **129** (ca. 30 kcal mol^{-1}) is much lower than that of parent bicyclo[1.1.0]tetrasilane **116** (ca. 65 kcal mol^{-1}).[46g, j, 125d]

8.2. Polycyclic $(RE)_{2n}$ Systems with E=Si, Ge, and Sn

The successful construction of the strained rings discussed above naturally aroused intense interest in the tetrahedrane, prismane, and cubane systems consisting of Group 14 elements. Not only are the physical properties of these new systems interesting in their own right, but they are also potential precursors to the corresponding triple-bond systems (RE≡ER). Calculations on singlet disilyne tend to agree that the relative stabilities increase in the order of linear disilyne (**131a**, $D_{\infty h}$), *trans*-bent disilyne (**131b**, C_{2h}), silasilene (**131c**, C_{2v}), and bridged disilyne (**131d**, C_{2v}).[6, 129] Recently, the

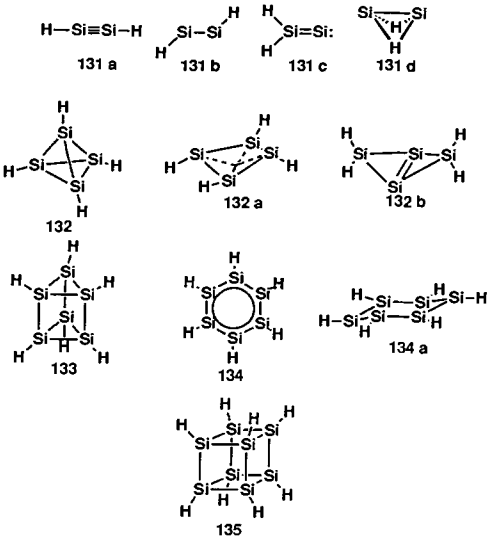

possible generation and trapping of dimethyldisilyne has been claimed.[130]

8.2.1. Theoretical Aspects

For the $(SiH)_4$ energy surface *Schaefer* and *Clabo* predict the isomer (**132**) of T_d symmetry to be, at least, a kinetically stable species which is connected by a large barrier to other $(SiH)_4$ isomers.[131] The local minimum of **132** is also identified by *Sax* and *Kalcher*.[132] In contrast to these results *Nagase* and *Nakano* contend that **132** is unlikely to be a minimum on the potential energy surface and isomerizes without a barrier.[133] Relative stabilities increase in the order of tetrasilatetrahedrane **132**, cyclotetrasilabutadiene **132a**, and bicyclo[1.1.0]tetrasilabut-1(3)-ene **132b**.[134]

For the $(SiH)_6$ species *Nagase* and *Sax* have found that hexasilaprismane (**133**) is the most stable of the Si_6H_6 isomers,[135a, b] consistent with the reluctance of silicon to form double bonds. Hexasilabenzene, unstable relative to **133**, was initially predicted by *Nagase*, *Sax*, and *Schaefer* to have a planar D_{6h} symmetry (**134**),[135] which was later replaced by *Nagase* and *Sax* with a chairlike puckered structure of D_{3d} symmetry (**134a**).[136] This dependence of the results on the method of computation may reflect a flat potential energy surface on which **134** and **134a** are located.

An interesting comparison of **132**, **133**, and **135** (octasilacubane) has been carried out by *Nagase* et al.[46e] The calculated Si–Si bond lengths increase in the order **132** (2.314 Å), **133** (2.359, 2.375 Å), and **135** (2.396 Å). Therefore, the Si–Si bond lengths in the three-membered rings are shorter than the typical bond length, while those in the four-membered rings are longer (see Section 4.2.1 for the structures of $(H_2Si)_3$ and $(H_2Si)_4$). Moreover, the SE decreases in the order of **132** (140.9 kcal mol^{-1}), **133** (113.8), and **135** (93.5). The octasilacubane **135** contains markedly less strain than the carbocyclic analogue, cubane (SE = 154.7 kcal mol^{-1}).[48] This result generally holds for silicon four-membered rings relative to cyclobutanes, which is probably due to an increasing tendency to keep the $(ns)^2(np)^2$ valence electron configuration in compounds with the heavier atoms. As a result, 90° bond angles with a low strain are made favorable.[137] Similarly, the germanium, tin, and lead counterparts are calculated to show low strain energies compared to that of cubane.[137]

8.2.2. Preparation and Structures of $(RE)_{2n}$

The successful construction of bicyclo[1.1.0]tetrasilane from 1,1,2-trichlorodisilane ($RCl_2Si-SiClR'_2$) suggests that 1,1,2,2-tetrachlorodisilanes ($RCl_2Si-SiCl_2R$) could serve, with the judicious selection of R, as precursors of hitherto unknown polycyclic systems including those represented by the molecular formula $(RSi)_{2n}$. Thus, reductive coupling of the tetrachlorodisilane **136** leads to the formation of several products from which **137** is isolated as a minor product after hydrolytic workup (Scheme 48).[3a] Compound **137** proba-

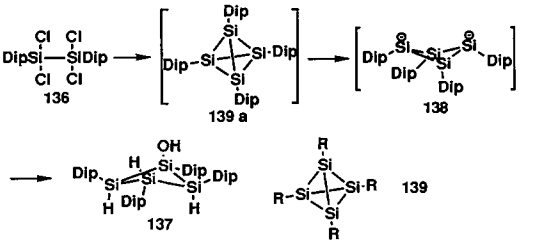

Scheme 48.

bly arises from intermediate **138**, which may have formed by the reductive cleavage of one of the Si–Si bonds of tetrasilatetrahedrane **139a**. From this result and the results outlined in Schemes 44 and 45 it becomes clear that a tetrasilatetrahedrane derivative **139** or other $(RSi)_{2n}$ derivatives would have to be "loaded" with bulky alkyl (rather than aryl) substituents in order to be synthesized.

The reductive oligomerization of 1,2-di-*tert*-butyl-1,1,2,2-tetrachlorodisilane (**140**) proceeds in a unique and somewhat unexpected manner to provide tricyclo[2.2.0.0^{2,5}]hexasilanes **141** and **142**, and tetracyclo[3.3.0.0^{2,7}.0^{3,6}]octasilane **143** as

outlined in Scheme 49.[138] The reaction course is sensitive to the reductant/**140** molar ratio. Typically, use of 2.5 equiv of lithium naphthalenide in the reduction followed by fractional recrystallization gives rise to compounds **144** (8–20% yield), **141a** (4%), **142** (6%), and **143a** (6%). In contrast, an

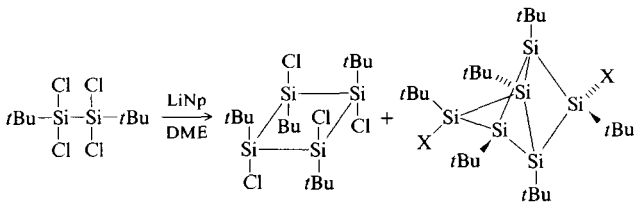

140 **144** **141a** (X = Cl)
b (X = CH_3)

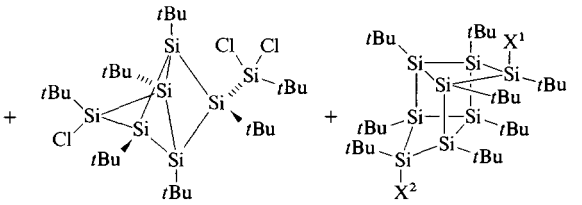

142 **143a** ($X^1 = X^2 = Cl$)
b ($X^1 = CH_3$, $X^2 = Cl$)
c ($X^1 = X^2 = CH_3$)

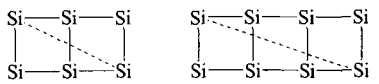

141 **143**

Scheme 49.

increase in the amount of reductant to 5 equiv leads to the formation of **141b**, **143b**, and **143c**. All spectral data including 2D-INEPT-INADEQUATE $^{29}Si-^{29}Si$ coupling data (INEPT = *I*nsensitive *N*uclei *E*nhanced by *P*olarization *T*ransfer, INADEQUATE = *I*ncredible *N*atural *A*bundance *D*ouble *Qua*ntum *T*ransfer *E*xperiment; see Section 9.1) are fully consistent with the structures shown in Scheme 49, and the molecular structures of **142** and **143a** have been established by X-ray analysis. The anion derived from **141a** appears to react with DME and **140** to provide **141b** and **142**, respectively, and **143b**, **143c** are derived from the anion or dianion formed by the reduction of **143a**. Since the structures of the products have been established, the likely pathways leading to these interesting products can be suggested. The dotted lines in the two skeletons **141** and **143** indicate the modes of intramolecular ring closure that are involved in the formation of these tri- and tetracyclic systems. No traces of octasilacubane and hexasilaprismane derivatives were found among the reduction products of **140**.

Syntheses analogous to that of **143a** have been reported recently. Thus, *Weidenbruch* et al. and *Sakurai* et al. have described the synthesis of [3.3.0.$0^{2,7}$.$0^{3,6}$]octagermane derivatives **145a** and **b** by the reduction of tetrahalodigermanes **146a** and **b** (Scheme 50).[139]

In addition to many precursors of type $RX_2Si-SiX_2R$ (R = Tsi, X=Br; R = Dis, X=Cl; R = Et_3Si, X=Cl; R = 1-Ad, X=Cl[53]) used for the construction of the $(RE)_{2n}$ system, a number of REX_3 compounds have been subjected to reductive coupling, often failing to generate in-

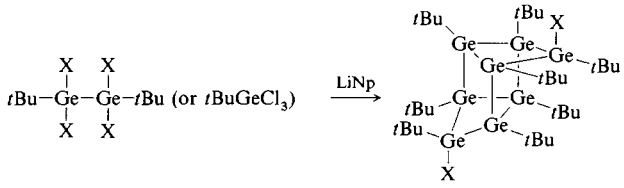

146a (X = Br)
b (X = Cl)

145a (X = Br)
b (X = Cl)

Scheme 50.

teresting ring systems such as tetrahedranes, prismanes, and cubanes.[140] The exceptions are two "one-shot" syntheses of a cubane and a prismane which are detailed below.

In 1988 *Nagai* et al. reported the successful synthesis of the first octasilacubane, **147**, obtained by condensation of 2,2,3,3-tetrabromo-1,4-di-*tert*-butyl-1,1,4,4-tetramethyltetrasilane (**148**) or 1,1,1-tribromo-2-*tert*-butyl-2,2-dimethyldisilane (**149**) with sodium (Scheme 51).[141] Octasilacubane **147** is an air-sensitive yellow compound. The structural assignment is based on its simple ^1H, ^{13}C, and ^{29}Si NMR spectra, consistent with the highly symmetrical structure. The crystal structure of **147** has not been reported.

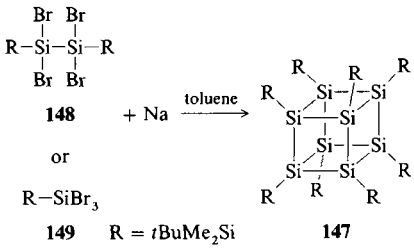

148 + Na → **147**
or
$R-SiBr_3$
149 R = $tBuMe_2Si$

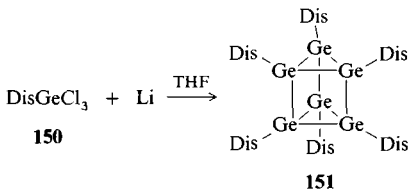

150 → **151**

Scheme 51.

Sakurai et al. have found that reductive coupling of bis(trimethylsilyl)methyltrichlorogermane (**150**) by lithium provides hexagermaprismane **151** as a yellow crystalline compound.[142] This compound is unexpectedly stable toward atmospheric oxygen and moisture. The prismane structure has been established by X-ray analysis. Notably, the Ge–Ge bond lengths in the triangles (2.578–2.584 Å) are longer than those in the rectangles (2.516–2.526 Å). This relationship lies in marked contrast with theoretical results (2.502 Å for the triangles and 2.507 Å for the rectangles of the parent hexagermaprismane which is free from steric congestion of the substituents).[137]

8.3. [1.1.1]Propellane System

[1.1.1]Propellane **152a** is an intriguing species that has received considerable experimental[143] and theoretical interest,[144] which focuses on the nature of the interbridgehead C–C bond. Recently, several theoretical investigations on the parent compound of the silicon analogue of **152a**, **152b**, have been reported.[46j, 125c, 145] The computed Si–Si

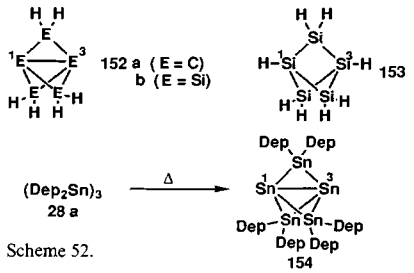

Scheme 52.

bond length of the central bridgehead bond Si1–Si3 is considerably stretched to ca. 2.72 Å, while the peripheral Si–Si bond length of 2.35 Å is normal. This central bond length of 2.72 Å is rather close to the nonbonding Si1 ··· Si3 distance of bicyclo[1.1.1]pentasilane **153** (2.92 Å, see Section 8.1.2).[146] These structural features show that the molecule possesses significant singlet diradical character. The calculated strain energy of **152b** is 62–70 kcal mol^{-1},[46j, 145] which is relatively low, particularly in comparison with the strain energy of **152a** (98 kcal mol^{-1}).[48]

In 1989 *Sita* and *Bickerstaff* succeeded in the isolation of a pentastanna[1.1.1]propellane derivative **154** in 13% yield by the thermolysis of cyclotristannane **28a** in xylene at 200 °C (Scheme 52).[147] Compound **154** is an air-sensitive, dark blue-violet crystalline compound and shows temperature-dependent ^{1}H NMR spectra. The propellane structure of **154** is verified by X-ray crystallography. The length of the pivotal Sn1–Sn3 bond is 3.367 Å, which falls well outside the normal range of Sn–Sn bonds (2.93–3.05 Å). This feature and the ^{119}Sn NMR spectrum are consistent with a significant singlet diradical character for the structure of **154**.

8.4. Spiropentasilane

In 1984 *Boudjouk* reported the synthesis of spiropentasilane **155** by the reductive ring closure of tetrakis(dimethylhalosilyl)silanes **156** with lithium (Scheme 53) in good

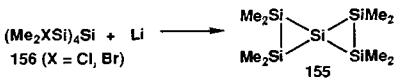

Scheme 53.

yield.[148] The assignment of the structure to **155** is based on the ^{1}H NMR spectrum and the products obtained from several chemical reactions. The stability of **155** is surprising, since this strained ring is "protected" only by the small methyl groups (see Section 4.1.1).

9. Instrumental and Interpretational Techniques Specially Adapted to This Research

9.1. 2D INEPT-INADEQUATE ^{29}Si NMR Spectroscopy for Determination of ^{29}Si–^{29}Si Long-Range Couplings in Strained Cyclic Polysilanes

^{13}C 2D-INADEQUATE spectroscopy has seen widespread use in the convenient disclosure of connectivity of carbon atoms in complex organic molecules.[149] This technique is extremely powerful when the size of ^{13}C–^{13}C one bond coupling (^1J) is much larger than that of long-range coupling (^nJ, n ≥ 2), which is usually the case in acyclic and unstrained systems.[150] Use of the INEPT-INADEQUATE technique specifically modified for ^{29}Si nuclei to obtain ^{29}Si–^{29}Si couplings can similarly reveal the connectivity of complex polysilane frameworks.[54]

Table 12. ^{29}Si–^{29}Si coupling constants in several acyclic or monocyclic polysilanes.

Cpd.	δ [a]	^1J [Hz]	^nJ (n ≥ 2) [Hz]
157	−1.55 (1) [b]	68.4 (3–4)	4.9 (2–4)
	−3.92 (4)	65.4 (1–2)	2.9 (1–3)
	−37.54 (3)	57.6 (2–3)	2.9 (1–4)
	−63.78 (2)		
158	−22.90 (1)	62.1 (3–4 or 3′–4)	9.4 (2–4 or 2′–4)
	−40.33 (3 and 3′)	57.4 (1–2 or 1–2′)	8.2 (1–3 or 1–3′)
	−42.21 (2 and 2′)	[c] (2–3, 2′–3′)	
	−42.59 (4)		
159	−18.50 (1)	57.6 (1–2 or 1–2′)	9.8 (1–3 or 1–3′)
	−41.73 (2 and 2′)	[c] (2–3, 2′–3′)	9.8 (2–3′, 3–2′)
	−43.22 (3 and 3′)		
160	9.11 (1 or 3)	46.9 (1–2 or 1–2′)	27.3 (1–3)
	1.40 (3 or 1)	46.9 (2–3 or 2′–3)	
	−8.02 (2 and 2′)		
16g	−33.42 (2 and 2′)	24.1 (1–2 or 1–2′)	
	−37.33 (1)		

[a] ^{29}Si chemical shifts and coupling constants of **157**–**160** and **16g** in C_6D_6 (25 °C) at 53.7 MHz; standard Me_4Si. [b] The numbers in parentheses refer to the silicon atom numbering scheme shown in the structures of **157**–**160** and **16g**. [c] The chemical shifts of these ^{29}Si nuclei were too close to permit accurate measurement of the coupling constant between them.

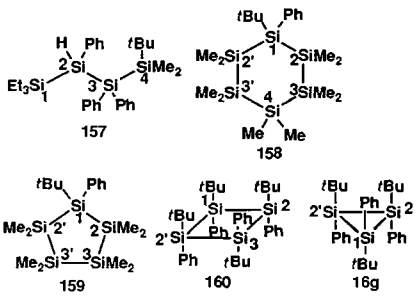

Information on the size of ^{29}Si–^{29}Si coupling constants has been extended.[55] Table 12 and 13 list ^1J and ^nJ of **157**–**160**, **16g**, **143a,b**, and **142**. Acyclic compounds, represented by **157**, show ^1J values in the range 55–70 Hz, while the ^2J and ^3J values are an order of magnitude smaller (2.5–5.0 Hz). In the (relatively) strain-free six- and five-membered ring compounds **158** and **159**, the ^1J values are slightly decreased, but a sizable increase in ^2J values is observed. In the strained systems **160** and **16g**, ^1J values are still approximately twice as large as ^2J values in **160**, but the observed ^1J for **16g** is only 24.1 Hz. This increase in the magnitude of ^1J with an increase in ring size is consistent with the view that the magnitude of ^1J reflects the amount of s character of the Si ring orbitals.

The 2D-NMR spectrum of polycyclic compound **143b** reveals the presence of fifteen ^{29}Si–^{29}Si couplings of approximately 20 to 40 Hz as shown in Figure 3. Since this system has eleven Si–Si bonds, four of the fifteen couplings

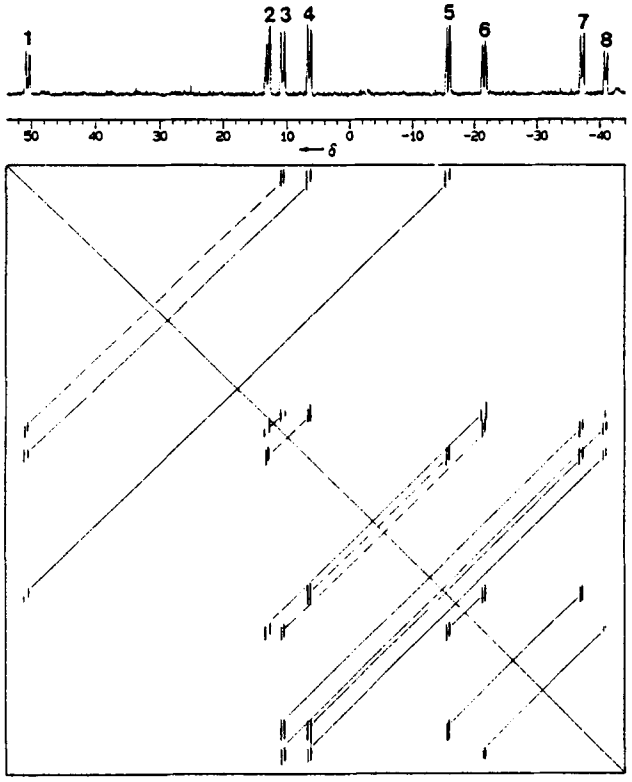

Fig. 3. 53.7 MHz $^{29}Si-^{29}Si$ 2D-INEPT-INADEQUATE spectrum of the tetracycle **143b** in C_6D_6 and projection of the 2D spectrum onto the F_2 axis (top). Signals connected by solid lines correspond to one-bond interactions (^1J); those connected by dotted lines denote long-range couplings (^nJ).

must be long-range (^nJ, $n \geq 2$). Through somewhat lengthy but logical arguments, ^{29}Si signals 1–8 are assigned to the Si nuclei of compound **143b** in the manner shown in Table 13. With the completion of the spectral assignment of **143b**, that of **143a** follows. In **143a** there are three pairs of observable,

Table 13. $^{29}Si-^{29}Si$ coupling constants for the polycyclic polysilanes **143a**, **b** and **142**.

Cpd. [a]	^1J [Hz]		^nJ ($n \geq 2$) [Hz]
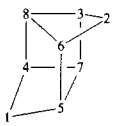 **143b**	42.2 (2–6)	41.8 (1–5)	24.1 (1–3)
	41.0 (2–3)	33.4 (1–4)	23.1 (4–5)
	30.8 (4–7)	28.9 (3–8)	22.5 (3–6)
	28.3 (3–7)	25.7 (4–8)	19.9 (2–4)
	25.7 (5–6)	18.0 (5–7)	
	17.3 (6–8)		
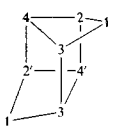 **143a**	41.0 (1–3, 1′–3′)		23.5 (1–2′, 1′–2)
	35.1 (1–2, 1′–2′)		23.5 (2–3, 2′–3′)
	29.3 (2–4, 2′–4, 2′–4′)		5.8 (1–4, 1′–4′)
	17.5 (3–4, 3′–4′)		
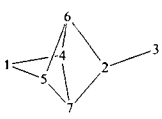 **142**	43.0 (2–3)	36.1 (1–4)	13.7 (1–3)
	34.1 (2–6)	32.2 (2–7)	16.6 (3–4)
	29.3 (1–5)	27.4 (5–7)	
	24.5 (4–6)	23.4 (4–7)	
	[b] (5–6)		

[a] The silicon nuclei of each molecule are numbered according to the order of their chemical shifts as shown in Figure 3. [b] The chemical shifts of these ^{29}Si nuclei were too close to permit accurate measurement of the coupling constant between them.

significant long-range couplings of which one is rather small (5.8 Hz). Compound **142** also exhibits two sizable long-range couplings, and the most appropriate chemical shift assignments of **142** are given in Table 13.

West and *Hengge* independently reported 2D ^{29}Si NMR spectroscopy of five- and six-membered rings, showing that this is an efficient method for the structure determination of silicon frameworks.[151] In these systems ^1J couplings can be easily distinguished from long-range ones ^nJ ($n \geq 2$). However, in strained systems such as **143** and **142**, ^1J and ^nJ couplings cannot be distinguished merely through the inspection of their magnitudes.

A considerable amount of information has been accumulated pertaining to long-range $^{13}C-^{13}C$ couplings in both unstrained and strained systems. In comparison with the data in Tables 12 and 13, long-range $^{13}C-^{13}C$ and $^{29}Si-^{29}Si$ interactions show more or less similar trends, although the latter are more pronounced in strained systems. The ^4J value in **142** is particularly noteworthy.

9.2. Determination of *n* for Cyclopolystannanes $(R_2Sn)_n$ by ^{119}Sn NMR Spectroscopy

Due to the natural abundance of ^{117}Sn (7.67%, $I = 1/2$), cyclopolystannanes ($[R_2Sn]_n$, $n \geq 1$) theoretically produce a unique set of $^{119}Sn-^{117}Sn$ coupling satellites with the upper limit of ^mJ and the intensities of the satellites governed by n as shown in Table 14.[56]

Table 14. Calculated intensities of the satellite signals arising from $^mJ(^{119}Sn-^{117}Sn)$ coupling in the ^{119}Sn NMR spectra of cyclopolystannanes $(R_2Sn)_n$. The intensities of the satellites are relative to the main resonance.

n	Intensities [%] ^1J	^2J	^3J
1	0	0	0
2	4.1	0	0
3	8.2	0	0
4	8.2	4.1	0
5	8.2	8.2	0
6	8.2	8.2	4.1
7	8.2	8.2	8.2

For comparison of these calculated intensities Table 15 lists experimental values for various cyclopolystannanes. Of primary interest is the ^{119}Sn NMR spectrum of the cyclotristannane **28a** whose structure has been determined by X-ray analysis.[42] The main resonance should be accompanied by

Table 15. Observed ^{119}Sn chemical shifts, $^mJ(^{119}Sn-^{117}Sn)$ coupling constants, and intensities of satellites relative to the main resonance in the ^{119}Sn NMR spectra of cyclopolystannanes $(R_2Sn)_n$.

Cpd.	n	δ	^mJ [Hz]	Intensities [%]
28a	3	−416.5	$^1J = 2285$	8.2
161 [a]	4	−76.8	$^1J = 624$	8.2
			$^2J = 3850$	4.2
162 [b]	2	−108.7	$^1J = 4211$	3.7
28b	3	−378.9	$^1J = 3017$	7.4
52	2	427.3	$^1J = 2930$	3.8

[a] **161**: $[(Me_3SiCH_2)_2Sn]_4$; [b] **162**: $Me_3Sn-SnMe_3$.

only two satellites with relative intensities of 8.2% of the main resonance. The actual spectrum fits this prediction; the satellite intensities are measured at 8.2% of the parent peak.[44] The ^{119}Sn NMR spectrum of cyclotetrastannane **161**, whose structure has also been confirmed by X-ray analysis,[152] also generates two sets of coupling constants that are in close agreement with the predictions.[44] However, **161** unexpectedly exhibits a ^{2}J coupling constant larger than that of the ^{1}J coupling.[153] Finally, the ^{119}Sn NMR spectrum of hexamethyldistannane **162** shows the expected satellite intensities (3.7% of the main resonance).[44, 56]

The general applicability of the above technique permitted the structures of cyclotristannane **28b** and distannene **52** to be easily determined without recourse to X-ray crystal analysis.[44] ^{119}Sn NMR splitting patterns should henceforth serve as a powerful tool for the structural determination of other cyclopolystannanes.

Caution must be taken in interpreting spectral data, however. For example, accurately determining whether a cyclopolystannane is five- or six-membered relies on the ability to unequivocally determine the presence of a ^{3}J value, and experimentally, this is not always easy to do, especially when ^{3}J may be smaller than the experimental linewidth of the main resonance. For some polycyclic structures, ^{3}J is near zero due to the 90° dihedral angles in certain structures. The power of the technique still remains, however, in its ability to determine the symmetry of a polystannane and relative intensities can be used to distinguish between the $(R_2Sn)_n$ and $(RSn)_n$ series.

9.3. Comments on Structural Homology

Comparison of the two molecular structures **126a** and **127** in Scheme 54 reveals a high degree of structural homology.[119] Thus, in **126a** the ratio of the nonbonding Si1 ··· Si3 distance (NBD) to the averaged length of the Si–Si bonds (BL) is 1.27, a ratio close to that observed for carbocycle **127**. Two other examples having the same framework are **142** and the unknown trioxo analogue **163** whose geometry was computed recently. Both **142** and **163** exhibit NBD/BL ratios of ca. 1.21.

The validity of this approximate homology rule is not confined to the compounds of the above series I but also applies to those of four other series. Thus, a nearly constant NBL/BL ratio was obtained for each series II (cyclobutane system), III (bicyclo[2.2.1]heptane system), IV (bicyclo-[3.3.1]nonane system), and even V ([1.1.1]propellane system where the E1 and E3 are uniquely bonded).

The oxygen-bridged compounds **163** in series I, **67** in series II, and **164** in series V are of particular interest. The finding that the Si ··· Si distance in compound **67** falls within the normal Si–Si BL has aroused much discussion on the nature of the bonding between those Si atoms (Section 6.1).[101b, f, 102, 118] Compound **163** is calculated to have an Si ··· Si NBD of 2.06 Å, a distance well below the normal Si–Si bond distance;[146, 154] similarly **164** has a very short bridgehead Si–Si bond distance of 2.089 Å.[145b] The remarkable consistency observed for each of series I, II, and V implies that the shortening of the Si ··· Si distance of **163**, **67**, and **164** is due mainly to the short Si–O (ca. 1.66 Å) bond distance compared to others in these ring systems. The approximate homology rule appears to provide an instant, good estimate on the NBD of unknown and known compounds.

10. Final Remarks

Approximately 10 years have passed since the synthesis of the first cyclotrisilane derivative and subsequent generation of the corresponding disilene. The silicon project has been extended to include Ge and Sn and also to the synthesis of strained polycyclic systems. Its pursuit has been extremely rewarding, and the synthesis of each new compound has been accompanied by excitement. At this moment several immediate synthetic targets are obvious: 1) a pentasila-[1.1.1]propellane derivative (from the bicyclo[1.1.1]pentasilane derivative), 2) a tetrasilatetrahedrane, and 3) a disilyne, the challenge increasing in this order. Additionally,

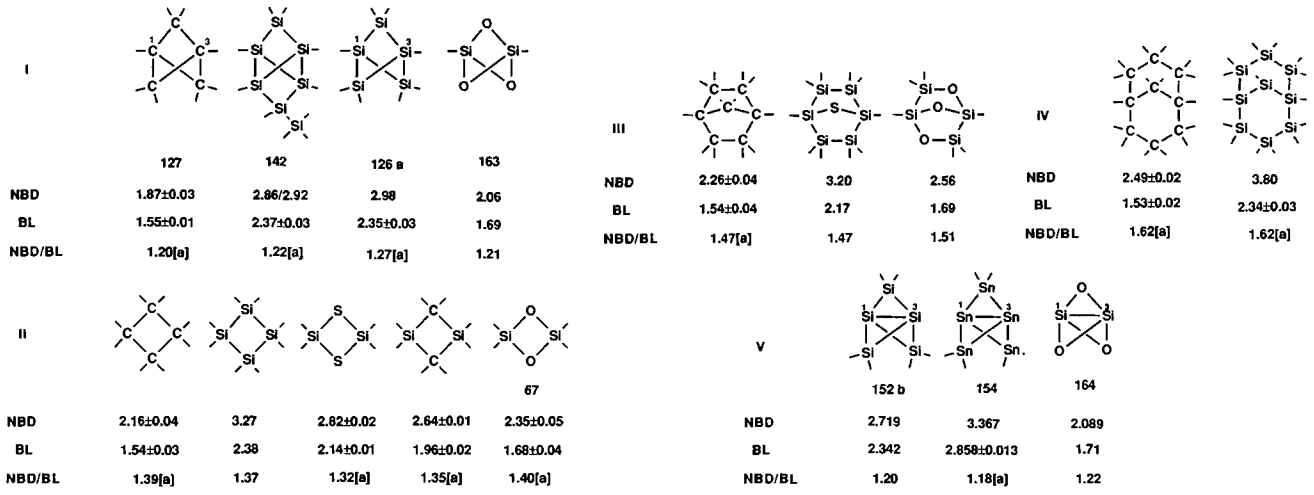

Scheme 54. The NBD/BL ratio in bi- and monocycles; NBD and BL are given in [Å]. The analogous carbacyclic and tin systems are also shown for comparison. [a] NBD/BL from averaged distances.

the project will not be complete without the generation and spectral characterization of the parent cyclotrisilane, -germane, and -stannane as well as disilene, -germene, and -stannene, following the approach of our previous work on cyclobutadiene.

In addition to the above relatively short range prospects, two fundamental problems of Group 14 element chemistry concern 1) the meager understanding of the reaction mechanisms involving organometallic compounds (even for the oxygenation of Si–Si to Si–O–Si with O_2) and 2) the almost complete lack of synthetic methodology for E–E bond formation except for the Kipping reaction. This is in sharp contrast with the enriched knowledge of carbon chemistry, and it is not obvious how to explore these unknown fields. Here exists a real challenge; the discovery of a new E–E bond-forming reaction will herald a new generation of this chemistry and may also be needed for the synthesis of a triple bond between these elements.

Addendum (May 6, 1991)

After submission of the original manuscript several articles pertinent to this review have appeared; also, those who read our manuscript have kindly called to our attention references which we had overlooked. These additional references[155–166] are tabulated below with reference numbers, titles, and the locations where they should be inserted.

Ref.	Title	Location
[155]	Germylenes and Stannylenes	[1]
[156]	Di-, Poly- and Cyclostannanes	[27]
[157]	Low-Temperature Photochemistry of Oxy-Substituted Trisilanes	4.1.1
[158]	Heavy Atom Main Group 4 Analogues of Carbenes, Radicals, and Alkenes: The Use of Bulky Trimethylsilyl-Substituted Ligands	[94] and Scheme 38
[159]	Photochemistry of a Matrix-Isolated Geminal Diazide. Dimethylgermylene	5.3.3
[160]	Determination of the Intensities of Raman-Active Vibrations in Molecules and Crystal Lattice	5.3.3
[161]	Disilaselenirane and Disilatellurirane: Synthesis and Crystal Structures	5.6.1.3 and 6.2
[162]	Thiadistannirane, 1,2-Dithiadistannetane, and Selenadistannirane: Small Rings with Tin–Tin Bonds	5.6.3 and 6.2
[163]	Octakis(2,6-diethylphenyl)octastannacubane	8.2.2
[164]	Decakis(2,6-diethylphenyl)decastanna[5]prismane: Characterization and Molecular Structure	8.2.2
[165]	Chemical Reduction of a Pentastanna[1.1.1]propellane Derivative and the Synthesis and Molecular Structure of a Bicyclo[1.1.1]pentastannane	8.3
[166] a)	Transition Metal–Tin Chemistry	9.2
b)	Naked-Metal Clusters in Solution. 4. Indications of the Variety of Cluster Species Obtainable by Extraction of Zintl Phases: Sn_4^{2-}, $TlSn_8^{5-}$, $Sn_{9-x}Ge_x^{4-}$ (x = 0–9), and $SbTe_4^{4-}$	9.2
c)	Organotin Compounds. 31. Dodecamethylcyclohexastannane and Dodecaperdeuteriomethylcyclohexastannane	9.2
d)	Bindungsabstände zwischen Organylsubstitierten Zinnatomen II. Cyclo-Tetrastannane	9.2

We wish to thank with great pleasure the many collaborators who are listed in the references. They have contributed experimentally as well as conceptually to the development of the Group 14 metal chemistry summarized in this review. We would like to acknowledge the careful examination and criticisms of the manuscript kindly offered by Orin Tempkin of our laboratories as well as many of the experts in this field including Michael Lappert, Wilhelm Neumann, Jacques Satgé, Larry Sita, and Manfred Weidenbruch. Many of the improvements are a direct result of their efforts but errors remain ours. The work quoted in the review has been supported by grants from the National Science Foundation (USA) as well as from the Kao Corporation (Japan).

Received: December 11, 1990 [A 827]
German version: *Angew. Chem. 103* (1991) 916

[1] Silylenes: a) P. P. Gaspar in M. Jones, Jr., R. Moss (Eds.): *Reactive Intermediates, Vol. 1* (1978) p. 229; *Vol. 2* (1981) p. 335; *Vol. 3* (1985) p. 333, Wiley, New York, b) P. P. Gaspar, D. Holten, S. Konieczny, *Acc. Chem. Res. 20* (1987) 329; germylenes: c) J. Satgé, M. Massol, P. Rivière, *J. Organomet. Chem. 56* (1973) 1; d) P. Rivière, M. Rivière-Baudet, J. Satgé, in G. Wilkinson, F. G. A. Stone, E. W. Abel (Eds.): *Comprehensive Organometallic Chemistry, Vol. 2*, Pergamon, Oxford 1982, p. 399; e) J. Satgé, *Pure Appl. Chem. 56* (1984) 137; stannylenes: f) R. Marx, W. P. Neumann, K. Hillner, *Tetrahedron Lett. 25* (1984) 625; g) J. D. Cotton, P. J. Davidson, M. F. Lappert, *J. Chem. Soc. Dalton Trans. 1976*, 2275; h) W. P. Neumann, *Rev. Silicon, Germanium, Tin, Lead Compd.* (1978) 81; i) A. G. Davis, P. J. Smith in G. Wilkinson, F. G. A. Stone, E. W. Abel (Eds.): *Comprehensive Organometallic Chemistry*, Pergamon, Oxford 1982, Chapter 11, p. 519.

[2] Disilenes: a) R. West, *Angew. Chem. 99* (1987) 1231; *Angew. Chem. Int. Ed. Engl. 26* (1987) 1201; b) R. West, *Pure Appl. Chem. 56* (1984) 163; c) R. West, *Science (Washington DC) 225* (1984) 1109; Si=X: d) G. Raabe, J. Michl, *Chem. Rev. 85* (1985) 419; e) G. Raabe, J. Michl in S. Patai, Z. Rappoport (Eds.): *The Chemistry of Organic Silicon Compounds*, Wiley, New York 1989, Chapter 17, p. 1015; Ge=X: f) J. Barrau, J. Escudié, J. Satgé, *Chem. Rev. 90* (1990) 283.

[3] a) S. Masamune in E. R. Corey, J. Y. Corey, P. P. Gaspar (Eds.): *Silicon Chemistry*, Ellis Horwood, New York 1988, Chapter 25, p. 257; b) Y. Nagai, H. Wantanabe, H. Matsumoto in E. R. Corey, J. Y. Corey, P. P. Gaspar (Eds.): *Silicon Chemistry*, Ellis Horwood, New York 1988, Chapter 24, p. 247; c) M. Weidenbruch, *Comments Inorg. Chem. 5* (1986) 247; d) H. Watanabe, Y. Nagai in H. Sakurai (Ed.): *Organosilicon and Bioorganosilicon Chemistry*, Ellis Horwood, Chichester 1985, Chapter 9, p. 107.

[4] T. Bally, S. Masamune, *Tetrahedron 36* (1980) 343.

[5] a) J. Satgé, *Adv. Organomet. Chem. 21* (1982) 241; b) J. Satgé, *Rev. Silicon Germanium Tin Lead Compds. 8* (1983) 291.

[6] Y. Apeloig in S. Patai, Z. Rappoport (Eds.): *The Chemistry of Organic Silicon Compounds*, Wiley, New York 1989, Chapter 2, p. 57.

[7] F. S. Kipping, *Proc. Chem. Soc. London 27* (1911) 143.

[8] a) F. S. Kipping, J. E. Sands, *J. Chem. Soc. Trans. 119* (1921) 830; b) *ibid. 119* (1921) 848; c) F. S. Kipping, *J. Chem. Soc.* (1927) 2719.

[9] H. Gilman, G. L. Schwebke, *J. Am. Chem. Soc. 86* (1964) 2693, and references cited therein.

[10] C. A. Burkhard, *J. Am. Chem. Soc. 71* (1949) 963.

[11] a) M. Ishikawa, M. Kumada, *J. Chem. Soc. Chem. Commun. 1970*, 612; b) *J. Organomet. Chem. 42* (1972) 325; c) *Adv. Organomet. Chem. 19* (1981) 51.

[12] a) H. Wantanabe, T. Muraoka, M. Kageyama, Y. Nagai, *J. Organomet. Chem. 216* (1981) C45; b) H. Wantanabe, T. Muraoka, Y. Kohhara, Y. Nagai, *Chem. Lett. 1980*, 735; c) C. W. Carlson, K. Matsumura, R. West, *J. Organomet. Chem. 194* (1980) C5; d) M. Bierbaum, R. West, *ibid. 131* (1977) 179; for reviews of cyclopolysilanes: e) R. West in G. Wilkinson, F. G. A. Stone, E. W. Abel (Eds.): *Comprehensive Organometallic Chemistry, Vol. 2*, Pergamon, Oxford 1982, Vol. 2, Chapter 9.4, p. 365; f) R. West, E. Carberry, *Science (Washington DC) 189* (1975) 179; g) R. West, *Pure Appl. Chem. 54* (1982) 1041; h) E. Hengge, H. Stüger in H. W. Roesky (Ed.): *Rings, Clusters, and Polymers of Main Group and Transition Elements*, Elsevier, Amsterdam 1989, p. 107.

[13] a) L. F. Brough, R. West, *J. Organomet. Chem. 194* (1980) 139; b) S.-M. Chen, A. Katti, T. A. Blinka, R. West, *Synthesis 1985*, 684.

[14] a) E. Hengge, D. Kovar, *J. Organomet. Chem. 125* (1977) C29; b) E. Hengge, D. Kovar, *Z. Anorg. Allg. Chem. 458* (1979) 163; c) E. Hengge, D. Kovar, *Angew. Chem. 93* (1981) 698; *Angew. Chem. Int. Ed. Engl. 20* (1981) 678.

[15] a) E. Hengge, G. Bauer, *Angew. Chem. 85* (1973) 304; *Angew. Chem. Int. Ed. Engl. 12* (1973) 316; b) E. Hengge, G. Bauer, *Monatsh. Chem. 106* (1975) 503; c) E. Hengge, D. Kovar, *Z. Anorg. Allg. Chem. 459* (1979) 123.

[16] a) C. Pitt in A. L. Rheingold (Ed.): *Homoatomic Rings, Chains, and Macromolecules of Main Group Elements*, Elsevier, Amsterdam 1977, p. 203; b) H. Bock, W. Ensslin, *Angew. Chem. 83* (1971) 435; *Angew. Chem. Int. Ed. Engl. 10* (1971) 404; c) H. Bock, E. Ensslin, F. Fehér, R. Freund, *J. Am. Chem. Soc. 98* (1976) 668; d) E. Carberry, R. West, G. E.

Glass, *ibid. 91* (1969) 5446; e) H. Bock, W. Kaim, M. Kira, R. West, *ibid. 101* (1979) 7667.
[17] a) G. J. D. Peddle, D. N. Roark, A. M. Good, S. G. McGeachin, *J. Am. Chem. Soc. 91* (1969) 2807; b) D. N. Roark, G. J. D. Peddle, *ibid. 94* (1972) 5837.
[18] a) C. L. Smith, J. Pounds, *J. Chem. Soc. Chem. Commun. 1975*, 910; b) R. T. Conlin, P. P. Gaspar, *J. Am. Chem. Soc. 98* (1976) 868; c) T. J. Barton, J. A. Kilgour, *ibid. 98* (1976) 7231; d) *ibid. 98* (1976) 7746; e) W. D. Wulff, W. T. Goure, T. J. Barton, *ibid. 100* (1978) 6236; f) H. Sakurai, T. Kobayashi, Y. Nakadaira, *J. Organomet. Chem. 162* (1978) C43; g) Y. Nakadaira, T. Kobayashi, T. Otsuka, H. Sakurai, *J. Am. Chem. Soc. 101* (1979) 486.
[19] H. Sakurai, Y. Nakadaira, T. Kobayashi, *J. Am. Chem. Soc. 101* (1979) 487.
[20] C. A. Kraus, C. L. Brown, *J. Am. Chem. Soc. 52* (1930) 4031.
[21] a) W. P. Neumann, K. Kühlein, *Tetrahedron Lett. 1963*, 1541; b) W. P. Neumann, K. Kühlein, *Justus Liebigs Ann. Chem. 683* (1965) 1; see also: c) O. M. Nefedov, M. N. Manakov, A. D. Petrov, *Dokl. Akad. Nauk SSSR 147* (1962) 1376.
[22] a) M. Richter, W. P. Neumann, *J. Organomet. Chem. 20* (1969) 81; b) E. Carberry, B. D. Dombek, S. C. Cohen, *ibid. 36* (1972) 61; for a review, see: c) M. Lesbre, P. Mazerolles, J. Satgé, *The Organic Compounds of Germanium*, Wiley, New York 1971.
[23] a) P. Mazerolles, M. Joanny, G. Tourrou, *J. Organomet. Chem. 60* (1973) C3; b) P. Rivière, J. Satgé, D. Soula, *C. R. Seances Acad. Sci. Ser. C. 277* (1973) 895.
[24] a) D. E. Goldberg, D. H. Harris, M. F. Lappert, K. M. Thomas, *J. Chem. Soc. Chem. Commun. 1976*, 261; b) P. J. Davidson, D. H. Harris, M. F. Lappert, *J. Chem. Soc. Dalton Trans. 1976*, 2268; c) P. B. Hitchcock, M. F. Lappert, S. J. Miles, A. J. Thorne, *J. Chem. Soc. Chem. Commun. 1984*, 480; d) T. Fjeldberg, A. Haaland, B. E. R. Schilling, M. F. Lappert, A. J. Thorne, *J. Chem. Soc. Dalton Trans. 1986*, 1551; e) D. E. Goldberg, P. B. Hitchcock, M. E. Lappert, K. M. Thomas, A. J. Thorne, T. Fjeldberg, A. Haaland, B. E. R. Schilling, *ibid. 1986*, 2387.
[25] C. Löwig, *Justus Liebigs Ann. Chem. 84* (1852) 308.
[26] a) W. P. Neumann, K. König, *Angew. Chem. 74* (1962) 215; *Angew. Chem. Int. Ed. Engl. 1* (1962) 212; b) W. P. Neumann, *Angew. Chem. 75* (1963) 225; *Angew. Chem. Int. Ed. Engl. 2* (1963) 165.
[27] a) W. V. Farrar, H. A. Skinner, *J. Organomet. Chem. 1* (1964) 434; W. P. Neumann, J. Pedain, R. Sommer, *Justus Liebigs Ann. Chem. 694* (1966) 9 and references cited therein; for reviews, see: c) W. P. Neumann, *Nachr. Chem. Tech. Lab. 30* (1982) 191; d) W. P. Neumann: *The Organic Chemistry of Tin*, Wiley, New York 1970.
[28] a) J. Davidson, M. F. Lappert, *J. Chem. Soc. Chem. Commun. 1973*, 317, see also: b) T. Fjeldberg, A. Haaland, M. F. Lappert, B. F. R. Schilling, R. Seip, A. J. Thorne, *ibid. 1982*, 1407.
[29] a) S. Masamune, N. Nakamura, M. Suda, H. Ona, *J. Am. Chem. Soc. 95* (1973) 8481; b) L. T. J. Delbaere, M. N. G. James, N. Nakamura, S. Masamune, *ibid. 97* (1975) 1973.
[30] S. Masamune, Y. Hanzawa, S. Murakami, T. Bally, J. F. Blount, *J. Am. Chem. Soc. 104* (1982) 1150.
[31] a) S. Masamune, S. Murakami, J. T. Snow, H. Tobita, D. J. Williams, *Organometallics 3* (1984) 333; b) S. Murakami, S. Collins, S. Masamune, *Tetrahedron Lett. 25* (1984) 2131; c) S. A. Batcheller, Ph. D. dissertation, Massachusetts Institute of Technology 1989; d) S. Murakami, Ph.D dissertation, University of Tokyo 1985; e) S. Masamune, unpublished results.
[32] S. Masamune, H. Tobita, S. Murakami, *J. Am. Chem. Soc. 105* (1983) 6524.
[33] a) H. Watanabe, T. Okawa, M. Kato, Y. Nagai, *J. Chem. Soc. Chem. Commun. 1983*, 781; b) H. Watanabe, M. Kato, T. Okawa, Y. Nagai, M. Goto, *J. Organomet. Chem. 271* (1984) 225.
[34] a) A. Schäfer, M. Weidenbruch, K. Peters, H.-G. von Schnering, *Angew. Chem. 96* (1984) 311; *Angew. Chem. Int. Ed. Engl. 23* (1984) 302; see also: b) P. Boudjouk, U. Samaraweera, R. Sooriyakumaran, J. Chrusciel, K. R. Anderson, *ibid. 100* (1988) 1406; and *27* (1988) 1355.
[35] a) M. Weidenbruch, K.-L. Thom, *J. Organomet. Chem. 308* (1986) 177; b) M. Weidenbruch, K.-L. Thom, S. Pohl, W. Saak, *ibid. 329* (1987) 151.
[36] H. Matsumoto, A. Sakamoto, Y. Nagai, *J. Chem. Soc. Chem. Commun. 1986*, 1768.
[37] a) H. Watanabe, Y. Kougo, Y. Nagai, *J. Chem. Soc. Chem. Commun. 1984*, 66; see also: b) H. Watanabe, Y. Kougo, M. Kato, H. Kuwabara, T. Okawa, Y. Nagai, *Bull. Chem. Soc. Jpn. 57* (1984) 3019.
[38] S. Masamune, Y. Hanzawa, D. J. Williams, *J. Am. Chem. Soc. 22* (1982) 6137.
[39] a) J. T. Snow, S. Murakami, S. Masamune, D. J. Williams, *Tetrahedron Lett. 25* (1984) 4191; b) J. T. Snow, Ph.D. dissertation, Massachusetts Institute of Technology 1987.
[40] a) W. Ando, T. Tsumuraya, *Tetrahedron Lett. 27* (1986) 3251; b) *J. Chem. Soc. Chem. Commun. 1987*, 1514.
[41] M. Weidenbruch, F.-T. Grimm, M. Herrndorf, A. Schäfer, K. Peters, H. G. von Schnering, *J. Organomet. Chem. 341* (1988) 335.
[42] S. Masamune, L. R. Sita, D. J. Williams, *J. Am. Chem. Soc. 105* (1983) 630.
[43] L. R. Sita, R. D. Bickerstaff, *J. Am. Chem. Soc. 111* (1989) 3769.
[44] S. Masamune, L. R. Sita, *J. Am. Chem. Soc. 107* (1985) 6390.
[45] a) J. Fu, W. P. Neumann, *J. Organomet. Chem. 272* (1984) C5; b) G. Bähr, R. Gelius, *Chem. Ber. 91* (1958) 829; c) W. P. Neumann, J. Fu, *J. Organomet. Chem. 273* (1984) 295.
[46] a) J. Rubio, F. Illas, *J. Mol. Struct: THEOCHEM 110* (1984) 131; b) W. W. Schoeller, T. Dabisch, *J. Chem. Soc. Chem. Commun. 1985*, 1706; c) A. F. Sax, *Chem. Phys. Lett. 129* (1986) 66; d) R. S. Grev, H. F. Schaefer III, *J. Am. Chem. Soc. 109* (1987) 6569; e) S. Nagase, M. Nakano, T. Kudo, *J. Chem. Soc. Chem. Commun. 1987*, 60; f) M. S. Gordon, D. Bartol, *J. Am. Chem. Soc. 109* (1987) 5948; g) P. von R. Schleyer, A. F. Sax, J. Kalcher, R. Janoschek, *Angew. Chem. 99* (1987) 374; *Angew. Chem. Int. Ed. Engl. 26* (1987) 364; h) D. Cremer, J. Gauss, F. Cremer, *J. Mol. Struct: THEOCHEM 169* (1988) 531; i) W. W. Schoeller, T. Dabisch, *Inorg. Chem. 26* (1987) 1081; j) D. B. Kitchen, J. E. Jackson, L. C. Allen, *J. Am. Chem. Soc. 112* (1990) 3408.
[47] A. F. Sax, *Chem. Phys. Lett. 127* (1986) 163.
[48] K. B. Wiberg, *Angew. Chem. 96* (1986) 312; *Angew. Chem. Int. Ed. Engl. 25* (1986) 312.
[49] S. Nagase, M. Nakano, *J. Chem. Soc. Chem. Commun. 1988*, 1077.
[50] J. C. Dewan, S. Murakami, J. T. Snow, S. Collins, S. Masamune, *J. Chem. Soc. Chem. Commun. 1985*, 892.
[51] a) H. Gilman, W. H. Atwell, E. L. Schwebke, *J. Organomet. Chem. 2* (1964) 369; b) W. G. Boberski, A. J. Allred, *ibid. 88* (1975) 65.
[52] H. Matsumoto, M. Minemura, K. Takatsuna, Y. Nagai, M. Goto, *Chem. Lett. 1985*, 1005.
[53] S. Masamune, Y. Kabe, unpublished results.
[54] M. Kuroda, Y. Kabe, M. Hashimoto, S. Masamune, *Angew. Chem. 100* (1988) 1795; *Angew. Chem. Int. Ed. Engl. 27* (1988) 1727.
[55] E. A. Williams in S. Patai, Z. Rappoport (Eds.): *The Chemistry of Organic Silicon Compounds*, Wiley, New York 1989, Chapter 8, p. 511.
[56] L. R. Sita, Ph.D. dissertation, Massachusetts Institute of Technology 1985.
[57] H. Watanabe, K. Yoshizumi, T. Muraoka, M. Kato, Y. Nagai, T. Sato, *Chem. Lett. 1985*, 1683.
[58] T. Tsumuraya, S. Sato, W. Ando, *Organometallics 9* (1990) 2061.
[59] H. Watanabe, M. Kato, E. Tabei, H. Kuwabara, N. Hirai, T. Sato, Y. Nagai, *J. Chem. Soc. Chem. Commun. 1986*, 1662.
[60] M. Weidenbruch, A. Schäfer, *J. Organomet. Chem. 269* (1984) 231.
[61] M. Weidenburch, B. Blintjer, K. Peters, H. G. von Schnering, *Angew. Chem. 98* (1986) 1090; *Angew. Chem. Int. Ed. Engl. 25* (1986) 1129.
[62] N. Wiberg, H. Schuster, A. Simon, K. Peters, *Angew. Chem. 98* (1986) 100; *Angew. Chem. Int. Ed. Engl. 25* (1986) 79.
[63] W. Ando, T. Tsumuraya, *J. Chem. Soc. Chem. Commun. 1989*, 770.
[64] A. Schäfer, M. Weidenbruch, S. Pohl, *J. Organomet. Chem. 282* (1985) 305.
[65] a) M. Weidenbruch, A. Schäfer, K. Peters, H. G. von Schnering, *J. Organomet. Chem. 314* (1986) 25; b) A. Schäfer, M. Weidenbruch, W. Saak, S. Pohl, *Angew. Chem. 99* (1987) 806; *Angew. Chem. Int. Ed. Engl. 26* (1987) 776; c) M. Weidenbruch, A. Schäfer, H. Marsmann, *J. Organomet. Chem. 354* (1988) C12.
[66] For a review, see: M. Weidenbruch, A. Schäfer, F. Grimm, K.-L. Thom, *Phosphorus Sulfur Silicon Relat. Elem. 41* (1989) 229.
[67] See also a) T. Tsumuraya, S. Sato, W. Ando, *Organometallics 8* (1989) 161; b) W. Ando, T. Tsumuraya, *ibid. 8* (1989) 1467.
[68] R. West, M. J. Fink, J. Michl, *Science (Washington DC) 214* (1981) 1343.
[69] a) M. J. Fink, M. J. Michalczyk, K. J. Haller, R. West, J. Michl, *Organometallics 3* (1984) 793; b) M. J. Michalczyk, R. West, J. Michl, *J. Am. Chem. Soc. 106* (1984) 821; c) M. J. Michalczyk, R. West, J. Michl, *Organometallics 4* (1985) 826; d) B. D. Shepherd, D. R. Powell, R. West, *ibid. 8* (1989) 2664.
[70] S. Collins, S. Murakami, J. T. Snow, S. Masamune, *Tetrahedron Lett. 26* (1985) 1281.
[71] a) W. Ando, H. Itoh, T. Tsumuraya, H. Yoshida, *Organometallics 7* (1988) 1880; b) W. Ando, H. Itoh, T. Tsumuraya, *ibid. 8* (1989) 2759.
[72] W. Ando, T. Tsumuraya, A. Sekiguchi, *Chem. Lett. 1987*, 317.
[73] S. Masamune, S. Murakami, H. Tobita, D. J. Williams, *J. Am. Chem. Soc. 105* (1983) 7776.
[74] a) S. A. Batcheller, S. Masamune, *Tetrahedron Lett. 29* (1988) 3383; b) S. Masamune, S. A. Batcheller, J. Park, W. M. Davis, O. Yamaguchi, Y. Ohta, Y. Kabe, *J. Am. Chem. Soc. 111* (1989) 1888.
[75] a) W. Ando, T. Tsumuraya, *Organometallics 7* (1988) 1882; b) T. Tsumuraya, Y. Kabe, W. Ando, *J. Chem. Soc. Chem. Commun. 1990*, 1159.
[76] S. A. Batcheller, S. Masamune, unpublished results.
[77] See, however, P. Boudjouk, B.-H. Han, K. R. Anderson, *J. Am. Chem. Soc. 104* (1982) 4992. *Boudjouk*'s synthesis of **41** has been found to be irreproducible.
[78] S. Masamune, Y. Eriyama, T. Kawase, *Angew. Chem. 99* (1987) 601; *Angew. Chem. Int. Ed. Engl. 26* (1987) 584.
[79] a) H. Watanabe, K. Takeuchi, N. Fukawa, M. Kato, M. Goto, Y. Nagai, *Chem. Lett. 1987*, 1341; b) H. Watanabe, K. Takeuchi, K. Nakajima, Y. Nagai, M. Goto, *ibid. 1988*, 1343.

[80] S. A. Batcheller, T. Tsumuraya, O. Tempkin, W. M. Davis, S. Masamune, *J. Am. Chem. Soc. 112* (1990) 9394.
[81] J. Park, S. A. Batcheller, S. Masamune, *J. Organomet. Chem. 367* (1989) 39.
[82] S. Masamune, S. Murakami, H. Tobita, *Organometallics 2* (1983) 1464.
[83] a) R. Daudel, R. E. Kari, R. A. Poirier, J. D. Goddard, I. G. Csizmadia, *J. Mol. Struct. 50* (1978) 115; b) F. F. Roelandt, D. F. van de Vondel, G. P. van der Kelen, *J. Organomet. Chem. 165* (1979) 151; c) L. C. Snyder, Z. R. Wasserman, *J. Am. Chem. Soc. 101* (1979) 5222; d) R. A. Poirier, J. D. Goddard, *Chem. Phys. Lett. 80* (1981) 37; e) H. Lischka, H.-J. Köhler, *ibid. 85* (1982) 467; f) K. Krogh-Jespersen, *J. Phys. Chem. 86* (1982) 1492; g) H. J. Köhler, H. Lischka, *J. Am. Chem. Soc. 104* (1982) 5884; h) K. Krogh-Jespersen, *ibid. 107* (1985) 537; i) K. Ohta, E. R. Davidson, K. Morokuma, *ibid. 107* (1985) 3466; j) A. F. Sax, *J. Comput. Chem. 6* (1985) 419; k) B. T. Luke, J. A. Pople, M.-B. Krogh-Jespersen, Y. Apeloig, M. Karni, J. Chandrasekhar, P. von R. Schleyer, *J. Am. Chem. Soc. 108* (1986) 270; l) G. Olbrich, *Chem. Phys. Lett. 130* (1986) 115; m) K. Somasundram, D. A. Amos, N. C. Handy, *Theor. Chim. Acta 70* (1986) 393; n) H. Teramae, *J. Am. Chem. Soc. 109* (1987) 4140; o) R. S. Grev, H. F. Schaefer III, K. M. Baines, *ibid. 112* (1990) 9458.
[84] a) G. Trinquier, J.-P. Malrieu, P. Rivière, *J. Am. Chem. Soc. 104* (1982) 4529; b) S. Nagase, T. Kudo, *J. Mol. Struct: THEOCHEM 103* (1983) 35; c) T. Fjeldberg, A. Haaland, M. F. Lappert, B. E. R. Schilling, R. Seip, A. J. Thorne, *J. Chem. Soc. Chem. Commun. 1982*, 1407; d) A. Márquez, G. G. Gonzàlez, J. F. Sanz, *Chem. Phys. 138* (1989) 99; e) C. Liang, L. C. Allen, *J. Am. Chem. Soc. 112* (1990) 1039; f) G. Trinquier, *ibid. 112* (1990) 2130.
[85] a) I. Shavitt, *Tetrahedron 41* (1985) 1531; b) P. R. Bunker, P. Jensen, W. P. Kraemer, R. Beardsworth, *J. Chem. Phys. 85* (1986) 3724; c) H. F. Schaefer III, *Science (Washington DC) 231* (1986) 1100.
[86] a) M. S. Gordon, *Chem. Phys. Lett. 114* (1985) 348; b) K. Balasubramanian, A. D. McLean, *J. Chem. Phys. 85* (1986) 5117; c) A. Selmani, D. R. Salahub, *ibid. 89* (1988) 1529.
[87] R. A. Phillips, R. J. Buenker, R. Beardsworth, P. R. Bunker, P. Jensen, W. P. Kraemer, *Chem. Phys. Lett. 118* (1985) 60.
[88] K. Balasubramanian, *J. Chem. Phys. 89* (1988) 5731.
[89] J.-P. Malrieu, G. Trinquier, *J. Am. Chem. Soc. 111* (1989) 5916; see also [84f].
[90] a) M. J. Fink, M. J. Michalczyk, K. J. Haller, R. West, J. Michl, *J. Chem. Soc. Chem. Commun. 1983*, 1010; b) B. D. Shepherd, C. F. Campana, R. West, *Heteroat. Chem. 1* (1990) 1.
[91] K. Z. Zilm, D. M. Grant, J. Michl, M. J. Fink, R. West, *Organometallics 2* (1983) 193.
[92] H. B. Yokelson, A. J. Millevolte, B. R. Adams, R. West, *J. Am. Chem. Soc. 109* (1987) 4116.
[93] V. Galasso, G. Fronzoni, *Chem. Phys. 103* (1986) 29.
[94] K. W. Zilm, G. A. Lawless, R. M. Merrill, J. M. Millar, G. G. Webb, *J. Am. Chem. Soc. 109* (1987) 7236.
[95] P. Bleckmann, R. Minkwitz, W. P. Neumann, M. Schriewer, M. Thibud, B. Watta, *Tetrahedron Lett. 25* (1984) 2467.
[96] B. D. Shepherd, R. West, *Chem. Lett. 1988*, 183.
[97] K. B. Wiberg in *Physical Organic Chemistry*, Wiley, New York 1964, p. 374.
[98] G. Olbrich, P. Potzinger, B. Reimann, R. Walsh, *Organometallics 3* (1984) 1267.
[99] a) M. W. Schmidt, P. N. Truong, M. S. Gordon, *J. Am. Chem. Soc. 109* (1987) 5217; b) P. von R. Schleyer, D. Kost, *ibid. 110* (1988) 2105; c) D. A. Hrovat, H. Sun, W. T. Borden, *J. Mol. Struct: THEOCHEM 163* (1988) 51.
[100] R. Walsh, *Acc. Chem. Res. 14* (1981) 246.
[101] a) M. J. Fink, D. J. DeYoung, R. West, J. Michl, *J. Am. Chem. Soc. 105* (1983) 1070; b) M. J. Fink, K. J. Haller, R. West, J. Michl, *ibid. 106* (1984) 822; c) M. J. Michalczyk, R. West, J. Michl, *J. Chem. Soc. Chem. Commun. 1984*, 1525; d) R. West, D. J. DeYoung, K. J. Haller, *J. Am. Chem. Soc. 107* (1985) 4943; e) D. J. DeYoung, R. West, *Chem. Lett. 1986*, 883; f) M. J. Michalczyk, M. J. Fink, K. J. Haller, R. West, J. Michl, *Organometallics 5* (1986) 531; g) C. Zybill, R. West, *J. Chem. Soc. Chem. Commun. 1986*, 857; h) H. B. Yokelson, A. J. Millevolte, K. J. Haller, R. West, *ibid. 1987*, 1605; i) H. B. Yokelson, A. J. Millevolte, G. R. Gillette, R. West, *J. Am. Chem. Soc. 109* (1987) 6865; j) G. R. Gillette, R. West, *J. Organomet. Chem. 394* (1990) 44.
[102] Reviews: a) R. West, H. B. Yokelson, G. R. Gillette, A. J. Millevolte in E. R. Corey, J. Y. Corey, P. P. Gaspar (Eds.): *Silicon Chemistry*, Ellis Horwood, New York 1988, Chapter 26, p. 270; b) R. West, G. R. Gillette, H. B. Yokelson, A. J. Millevolte, *Phosphorus Sulfur Silicon Relat. Elem. 41* (1989) 3.
[103] a) M. Weidenbruch, B. Flintjer, S. Pohl, D. Haase, J. Martens, *J. Organomet. Chem. 338* (1988) C1; b) M. Weidenbruch, A. Lesch, K. Peters, H. G. von Schnering, *Chem. Ber. 123* (1990) 1795.
[104] M. Weidenbruch, B. Flintjer, S. Pohl, W. Saak, *Angew. Chem. 101* (1989) 89; *Angew. Chem. Int. Ed. Engl. 28* (1989) 95.
[105] a) H. B. Yokelson, J. Maxka, D. A. Siegel, R. West, *J. Am. Chem. Soc. 108* (1986) 4239; b) H. B. Yokelson, D. A. Siegel, A. J. Millevolte, J. Maxka, R. West, *Organometallics 9* (1990) 1005.
[106] a) E. K. Pham, R. West, *Organometallics 9* (1990) 1517; b) *J. Am. Chem. Soc. 111* (1989) 7667.
[107] D. H. Berry, J. Chey, H. S. Zipin, P. J. Carroll, *J. Am. Chem. Soc. 112* (1990) 452.
[108] H. Piana, U. Schubert, *J. Organomet. Chem. 348* (1988) C19; see also [103j].
[109] G. R. Gillette, J. Maxka, R. West, *Angew. Chem. 101* (1989) 90; *Angew. Chem. Int. Ed. Engl. 28* (1989) 54.
[110] M. Driess, A. D. Fanta, D. R. Powell, R. West, *Angew. Chem. 101* (1989) 1087; *Angew. Chem. Int. Ed. Engl. 28* (1989) 1038.
[111] A. H. Cowley, S. W. Hall, C. M. Nunn, J. M. Power, *J. Chem. Soc. Chem. Commun. 1988*, 753.
[112] T. Tsumuraya, S. Sato, W. Ando, *Organometallics 7* (1988) 2015.
[113] a) H. Meyer, G. Baum, W. Massa, S. Berger, A. Berndt, *Angew. Chem. 99* (1987) 559; *Angew. Chem. Int. Ed. Engl. 26* (1987) 546; b) L. R. Sita, R. D. Bickerstaff, *J. Am. Chem. Soc. 110* (1988) 5208.
[114] A. H. Cowley, S. W. Hall, C. M. Nunn, J. M. Power, *Angew. Chem. 100* (1988) 874; *Angew. Chem. Int. Ed. Engl. 27* (1988) 838.
[115] L. R. Sita, I. Kinoshita, S. P. Lee, *Organometallics 9* (1990) 1644.
[116] M. A. Edelman, P. B. Hitchcock, M. F. Lappert, *J. Chem. Soc. Chem. Commun. 1990*, 1116.
[117] J. Park, S. Masamune, unpublished results.
[118] a) M. O'Keefe, G. V. Gibbs, *J. Chem. Phys. 81* (1984) 876; b) T. Kudo, S. Nagase, *J. Am. Chem. Soc. 107* (1985) 2589; c) S. M. Bachrach, A. Streitweiser, *ibid. 107* (1985) 1186; d) M. O'keefe, G. V. Gibbs, *J. Phys. Chem. 89* (1985) 4574; e) R. J. Berenstein, S. Scheiner, *Int. J. Quantum Chem. 29* (1986) 1191; for another interpretation of the structure of cyclodisiloxane: f) R. S. Grev, H. F. Schaefer III, *J. Am. Chem. Soc. 109* (1987) 6577.
[119] Y. Kabe, T. Kawase, J. Okada, O. Yamashita, M. Goto, S. Masamune, *Angew. Chem. 102* (1990) 823; *Angew. Chem. Int. Ed. Engl. 29* (1990) 794.
[120] For 3-methylenedisiliranes: a) M. Ishikawa, H. Sugisawa, M. Kumada, T. Higuchi, K. Matsui, K. Hirotsu, J. Iyoda, *Organometallics 2* (1983) 174; for a disilacyclopropanimine derivative: [101h].
[121] Theoretical calulations on disiliranes: J. A. Boatz, M. S. Gordon, *J. Phys. Chem. 93* (1989) 3025; see also [118f] and [46h].
[122] a) L. Lange, B. Meyer, W.-W. du Mont, *J. Organomet. Chem. 329* (1987) C17; b) K. Mochida, A. Fujii, N. Tsuchiya, K. Tohji, Y. Udagawa, *Organometallics 6* (1987) 1811.
[123] a) S. Masamune, Y. Kabe, S. Collins, D. J. Williams, R. Jones, *J. Am. Chem. Soc. 107* (1985) 5552; b) R. Jones, D. J. Williams, Y. Kabe, S. Masamune, *Angew. Chem. 98* (1986) 176; *Angew. Chem. Int. Ed. Engl. 25* (1986) 173; see also: c) S. Collins, J. A. Duncan, Y. Kabe, S. Murakami, S. Masamune, *Tetrahedron Lett. 26* (1985) 2837.
[124] For the $Si_4^{6\ominus}$ cluster anion in Ba_3Si_4: a) B. Eisenmann, K. H. Janzen, M. Schäfer, A. Weiss, *Z. Naturforsch. B24* (1969) 457; b) H. G. von Schnering, *Angew. Chem. 93* (1981) 44; *Angew. Chem. Int. Ed. Engl. 20* (1981) 33; for the 2,4-disilabicyclobutane system: c) G. Fritz, S. Wartanessian, E. Matern, W. Höule, H. G. von Schnering, *Z. Anorg. Allg. Chem. 475* (1981) 87.
[125] a) T. Dabisch, W. W. Schoeller, *J. Chem. Soc. Chem. Commun. 1986*, 896; b) S. Collins, R. Dutler, A. Rauk, *J. Am. Chem. Soc. 109* (1987) 2564; c) W. W. Schoeller, T. Dabisch, T. Busch, *Inorg. Chem. 26* (1987) 4383; d) S. Nagase, T. Kudo, *J. Chem. Soc. Chem. Commun. 1988*, 54; e) J. A. Boatz, M. S. Gordon, *J. Phys. Chem. 92* (1988) 3037; for bicyclo[1.1.0]-tetragermane: [49].
[126] T. Kawase, S. A. Batcheller, S. Masamune, *Chem. Lett. 1987*, 227.
[127] a) A. Padwa, E. Shefter, E. Alexander, *J. Am. Chem. Soc. 90* (1968) 3717; b) J.-F. Chiang, S. H. Bauer, *ibid. 92* (1970) 1614; c) A. Almenningen, B. Andersen, B. A. Nyhus, *Acta. Chem. Scand. 25* (1971) 1217.
[128] a) H. Matsumoto, H. Miyamoto, N. Kojima, Y. Nagai, *J. Chem. Soc. Chem. Commun. 1987*, 1316; b) H. Matsumoto, H. Miyamoto, N. Kojima, Y. Nagai, M. Goto, *Chem. Lett. 1988*, 629.
[129] a) J. S. Binkley, *J. Am. Chem. Soc. 106* (1984) 603; b) B. T. Colegrove, H. F. Schaefer III, *J. Phys. Chem. 94* (1990) 5593 and references cited therein.
[130] a) A. Sekiguchi, S. S. Zigler, R. West, J. Michl, *J. Am. Chem. Soc. 108* (1986) 4241; b) A. Sekiguchi, S. S. Zigler, K. J. Haller, R. West, *Recl. Trav. Chim. Pays-Bas 107* (1988) 197; c) A. Sekiguchi, G. R. Gillete, R. West, *Organometallics 7* (1988) 1226.
[131] D. A. Clabo, Jr., H. F. Schaefer III, *J. Am. Chem. Soc. 108* (1986) 4344.
[132] A. F. Sax, J. Kalcher, *J. Chem. Soc. Chem. Commun. 1987*, 809.
[133] S. Nagase, M. Nakano, *Angew. Chem. 100* (1988) 1098; *Angew. Chem. Int. Ed. Engl. 27* (1988) 1081.
[134] A. F. Sax, J. Kalcher, *J. Comput. Chem. 10* (1989) 309.
[135] a) S. Nagase, T. Kudo, M. Aoki, *J. Chem. Soc. Chem. Commun. 1985*, 1121; b) A. F. Sax, R. Janoschek, *Angew. Chem. 98* (1986) 634; *Angew. Chem. Int. Ed. Engl. 25* (1986) 651; c) D. A. Clabo, Jr., H. F. Schaefer III, *J. Chem. Phys. 84* (1986) 1664.
[136] a) S. Nagase, H. Teramae, T. Kudo, *J. Chem. Phys. 86* (1987) 4513; b) A. F. Sax, J. Kalcher, R. Janoschek, *J. Comput. Chem. 9* (1988) 564.
[137] S. Nagase, *Angew. Chem. 101* (1989) 340; *Angew. Chem. Int. Ed. Engl. 28* (1989) 329.

[138] Y. Kabe, M. Kuroda, Y. Honda, O. Yamashita, T. Kawase, S. Masamune, *Angew. Chem. 100* (1988) 1793; *Angew. Chem. Int. Ed. Engl. 27* (1988) 1725.
[139] a) M. Weidenbruch, F.-T. Grimm, S. Pohl, W. Saak, *Angew. Chem. 101* (1989) 201; *Angew. Chem. Int. Ed. Engl. 28* (1989) 198; b) A. Sekiguchi, H. Naito, H. Nameki, K. Ebata, C. Kabuto, H. Sakurai, *J. Organomet. Chem. 369* (1989) C1.
[140] Formation of $(RSi)_n$ (R = *n*-hexyl) from the reductive coupling of $RSiCl_3$: P. A. Bianconi, T. W. Weidman, *J. Am. Chem. Soc. 110* (1988) 2342.
[141] H. Matsumoto, K. Higuchi, Y. Hoshino, H. Koike, Y. Naoi, Y. Nagai, *J. Chem. Soc. Chem. Commun. 1988*, 1083.
[142] A. Sekiguchi, C. Kabuto, H. Sakurai, *Angew. Chem. 101* (1989) 97; *Angew. Chem. Int. Ed. Engl. 28* (1989) 55.
[143] a) K. B. Wiberg, F. H. Walker, *J. Am. Chem. Soc. 104* (1982) 5239; for a review: b) K. B. Wiberg, *Chem. Rev. 89* (1989) 975.
[144] a) K. B. Wiberg, *J. Am. Chem. Soc. 105* (1983) 1227; b) J. E. Jackson, L. C. Allen, *ibid. 106* (1984) 591; c) K. B. Wiberg, R. F. W. Bader, C. D. H. Lau, *ibid. 109* (1987) 985.
[145] a) P. von R. Schleyer, R. Janoschek, *Angew. Chem. 99* (1987) 1312; *Angew. Chem. Int. Ed. Engl. 26* (1987) 1267; b) S. Nagase, T. Kudo, *Organometallics 6* (1987) 2456; for pentagerma[1.1.1]propellane: c) S. Nagase, T. Kudo, *ibid. 7* (1988) 2534.
[146] S. Nagase, T. Kudo, T. Kuratake, *J. Chem. Soc. Chem. Commun. 1988*, 1063.
[147] L. R. Sita, R. D. Bickerstaff, *J. Am. Chem. Soc. 111* (1989) 6454.
[148] a) P. Boudjouk, R. Sooriyakumaran, *J. Chem. Soc. Chem. Commun. 1984*, 777; for a theoretical calculation on the parent spiropentasilane: b) M. S. Gordon, P. Boudjouk, *J. Am. Chem. Soc. 107* (1985) 1439.
[149] a) A. Bax: *Two-Dimensional Nuclear Magnetic Resonance in Liquids*, Delft University Press, Delft 1982, Chapter 5; b) W. E. Hull in W. R. Croasmun, R. M. K. Carlson (Eds.): *Two-Dimensional NMR Spectroscopy. Applications for Chemists and Biochemists*, VCH Publishers, New York 1987, Chapter 2.
[150] For example: a) A. Bax, S. P. Kempsell, R. Freeman, *J. Magn. Reson. 41* (1980) 349; b) M. A. Phillipi, R. J. Wiersema, J. R. Brainard, R. E. London, *J. Am. Chem. Soc. 104* (1982) 7333; c) R. Freeman, T. Frenkiel, M. B. Rubin, *ibid. 104* (1982) 5545.
[151] a) J. Maxka, B. R. Adams, R. West, *J. Am. Chem. Soc. 111* (1989) 3447; b) E. Hengge, F. Schrank, *J. Organomet. Chem. 362* (1989) 11.
[152] V. K. Belsky, N. N. Zemlyansky, N. D. Kolosova, I. V. Borisova, *J. Organomet. Chem. 215* (1981) 41.
[153] a) T. N. Mitchell, G. Walter, *J. Chem. Soc. Perkin. Trans. 2 1977*, 1842; b) T. N. Mitchell, M. El-Behairy, *J. Organomet. Chem. 141* (1977) 43.
[154] A. Streitwieser, *J. Chem. Soc. Chem. Commun. 1989*, 1261.
[155] W. P. Neumann, *Chem. Rev. 91* (1991) 311.
[156] W. P. Neumann in A. L. Rheingold (Ed.): *Homoatomic Rings, Chains and Macromolecules of Main Group Elements*, Elsevier, Amsterdam 1977, p. 227.
[157] G. R. Gillette, G. Noren, R. West, *Organometallics 9* (1990) 2925.
[158] M. F. Lappert, *Silicon Germanium Tin Compd. 9* (1986) 129.
[159] J. Barrau, D. L. Bean, K. M. Welsh, R. West, J. Michl, *Organometallics 8* (1989) 2606.
[160] P. Bleckmann, M. Thibud, H.-D. Trippe, *J. Mol. Struct. 142* (1986) 303.
[161] R. P. Tan, G. R. Gillete, D. R. Powell, R. West, *Organometallics 10* (1991) 546.
[162] A. Schäfer, M. Weidenbruch, W. Saak, S. Pohl, H. Marsmannn, *Angew. Chem. 103* (1991) 873; *Angew. Chem. Int. Ed. Engl. 30* (1991) 834.
[163] L. R. Sita, I. Kinoshita, *Organometallics 9* (1990) 2865.
[164] L. R. Sita, I. Kinoshita, *J. Am. Chem. Soc. 113* (1991) 1856.
[165] L. R. Sita, I. Kinoshita, *J. Am. Chem. Soc. 112* (1990) 8839.
[166] a) M. S. Holt, W. L. Wilson, J. H. Nelson, *Chem. Rev. 89* (1989) 11; b) R. W. Rudolph, W. L. Wilson, R. C. Taylor, *J. Am. Chem. Soc. 103* (1981) 2480; c) B. Watta, W. P. Neumann, J. Sauer, *Organometallics 4* (1985) 1954; d) H. Puff, C. Bach, W. Schuh, P. Zimmer, *J. Organomet. Chem. 312* (1986) 313.

The Biochemical Reactions of Organometallics with Enzymes and Proteins

By Alexander D. Ryabov*

Most specialists doing organometallic chemistry have little understanding of what modern biochemistry is. On the other hand, most biochemists believe that organometallic chemistry stands much apart from the problems they study. But the real distance, if any, between these magnificent pyramids of modern science is progressively decreasing. Their interaction has given birth to a new branch of science, organometallic biochemistry, the general aspects of which are discussed here.

1. Introduction

This article will not deal with the chemistry of vitamin B_{12}, a natural organometallic molecule with a cobalt–carbon bond,[1] which has long served as a firm, but the only, bridge between organometallic chemistry and biochemistry, two very active areas of modern science. Instead, the article will focus on a newborn branch of science, organometallic biochemistry. This area no longer centers around the chemistry of vitamin B_{12} itself and its numerous models,[2–7] but has spread out to encompass many organometallic compounds which can undergo various biochemical transformations in the presence of enzymes or microorganisms. At present, biocatalysts are not sufficiently "educated" to carry out the direct synthesis of organometallics from metals, ions, or complexes and organic structures, but they are able to modify organometallics and, in some cases, to cleave selectively a carbon–metal bond. Moreover, organometallics have been "taught" to be substrates of biocatalysts and, therefore, to undergo enzyme-catalyzed transformations. The biochemical reactions of organometallic reagents, mostly in the presence of enzymes and microorganisms, will be discussed here in three sections. Section 2 shows the use of biocatalysts in selective conversions of organometallics. Section 3 describes systems in which redox-active organometallics behave as substrates in reactions catalyzed by oxidases and peroxidases. Section 5 deals with enzymes that destroy environmentally damaging organometallic species, organomercurials in particular, in the biosphere. These enzymes are in fact unique, since they catalyze the cleavage of the "heart" of organometallic molecules, the metal–carbon bond.

2. Selective Conversions of Organometallics by Biocatalysts

2.1. General Remarks

The impressive achievements in the use of enzymes[8–13] and microorganisms[14] in organic synthesis, a general understanding that they can function both in binary mixtures of organic solvents and water and in pure organic solvents,[15–19] and the demonstration that the specific catalytic activity of enzymes entrapped in reversed micelles is preserved or even increased without any loss in stability[20] were compelling reasons for the use of biocatalysts in organometallic synthesis as well. In fact, many organic syntheses realized in the presence of biocatalysts proved that enzymes display much broader substrate specificity than once assumed.[11] Therefore, it was reasonable to expect that organometallics would also be accepted as substrates by enzymes. On the other hand, since organometallics are usually water-insoluble, their reactions with enzymes have to be carried out in nonaqueous media. This is indeed a challenging problem for both chemists and biochemists. Moreover, the catalytic activity and specificity of an enzyme can be tuned by properly varying its environment, for example, in the inner cavity of reversed micelles[21] and, probably, by changing the composition of the organic medium. Therefore, there are ways to adjust the enzyme specificity with respect to a particular organometallic substrate.

2.2. From Carbon to Silicon and Germanium

Organometallic biosynthesis has not yet reached the state where detailed critical analysis is possible. But there are two basic approaches. The first is aimed at metallocene compounds, in particular ferrocene derivatives. We will see later that, at present, ferrocene derivatives are undoubtedly the most "biological" materials in the ocean of organometallic compounds. The second approach, which is being developed by the group of *Tacke*, may seem trivial at a first glance, but, in fact, it is a very balanced, well-reasoned, and fruitful concept. The idea is simple: since enzymes carry out enantiomeric synthesis of many, not necessarily natural, organic compounds, why should not these enzymes convert a compound with one or several silicons replacing carbons. Indeed, some enzymes of microorganisms do! Further, if silicon, why not germanium? Again, such enzymes have been found! The virtue of this "simple" approach cannot be overestimated, since optically active organosilicon compounds are already used as so-called siladrugs.[22–24] The corresponding germanium species may appear even more advantageous, since even now they are considered as possible alternatives to platinum complexes in cancer chemotherapy.[22, 25, 26]

The first report by *Tacke* et al.[27] dealt with the microbiological enantioselective reduction of trimethylsilylalkyl acetoacetates **1b, d** to the corresponding (+)-3(*S*)-hydroxybutanoates **2** in the presence of *Kloeckera corticis* (ATCC 20109) [Eq. (a)]. The enantiomeric purity was found to be

[*] Prof. A. D. Ryabov
Division for Chemistry
G. V. Plekhanov Institute of National Economy
Stremyanny per. 28, 113054 Moscow (USSR)

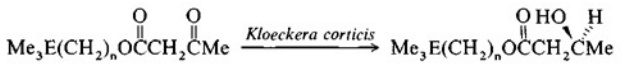

80% for **2a**, **b**, **d** and 65% for **2c**. Remarkably, replacement of carbon by silicon increases the enantiomeric purity of the products formed.

Trigonopsis variabilis (DSM 70714) appeared to be the best yeast among one hundred tested for the enantioselective reduction of acetyldimethylphenylsilane (**3**) to (*R*)-(1-hydroxyethyl)dimethylphenylsilane (**4**) [Eq. (b)]. *Trigonopsis*

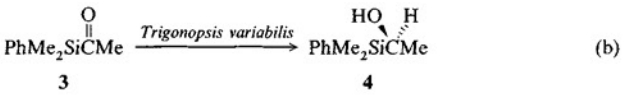

3 4

variabilis showed the best results concerning the reaction rate, the isolation of **4**, and its purity with respect to the formation of biogenic by-products.[28] When resting cells were used under optimal conditions (37 °C, pH 6–8, 0.25 g L^{-1} of **3**), product **4** was isolated in 70% yield with an enantiomeric purity of 86%. Preliminary studies have shown that acetyldimethylphenylgermane is also accepted as a substrate by *Trigonopsis variabilis* to give the reduction product as the *R* enantiomer. Interestingly, the activity of the yeast decreases on going from the silicon compound **3** to the germanium compound to the carbon compound (21:12:1). Unexpectedly, the activity of the carbon analogue of **3** was substantially lower than that of the silicon and germanium derivatives. The enantioselective microbial reductions of RR′R″SiC(O)Me (R = Me, R′ = Ph, R″ = Me_3C, Me_3Si) to the corresponding alcohols can be performed in the presence of *Trigonopsis variabilis*.[29]

Silacyclohexanones also undergo enantioselective reduction. In particular, growing cells of the yeast *Kloeckera corticis* reduce 1,1-dimethyl-1-silacyclohexan-2-one (**5**) to afford the corresponding enantiomeric alcohol **6** in 60% yield (92% *ee*) [Eq. (c)]. Recrystallization from *n*-hexane increases the optical purity up to 99% *ee*.[30] A similar route to opti-

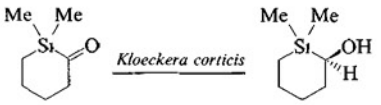

5 6

cally active (1*R*,2*S*)-1-methyl-1-phenyl-1-silacyclohexan-2-ol, starting from racemic 1-methyl-1-phenyl-1-silacyclohexan-2-one (**7**), was reported.[31] The diastereomerically pure product could be obtained by two biotransformation steps and one chemical step (Scheme 1).Diastereoselective reduction of **7** by *Kloeckera corticis* gave a 1:1 mixture of (1*S*,2*R*)- and (1*R*,2*S*)-1-methyl-1-phenyl-1-silacyclohexan-2-ol in 97% yield with a diastereomeric excess of about 90%. The quantitative esterification of the mixture with acetyl chloride in pyridine afforded again a 1:1 mixture of the corresponding acetates. This mixture was then converted into optically active alcohol **8** with *R* configuration at silicon and *S* configuration at carbon by a highly enantioselective hydrolysis with *Puchia pijperi* (ATCC 20127). After separation from the unreacted 1*S*,2*R* acetate by chromatography on silica gel, the desired product was isolated in a very pure form (*ee* > 96%).

The examples discussed above convincingly show clear perspectives of this field of organometallic biochemistry. One may expect that organometallic molecules with tetrahedral metal centers will also be involved in such biotransformations. Undoubtedly, these studies will be stimulated by the tremendous need for new drugs.

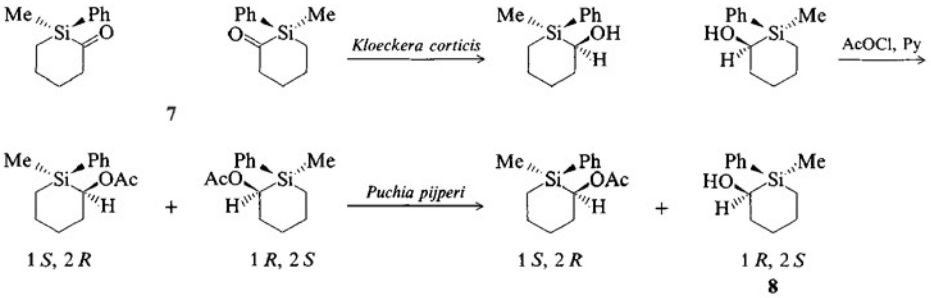

Scheme 1. Two biotransformations and one chemical step afford diastereomerically pure **8**.

Professor Alexander D. Ryabov was born in Moscow in 1953 and educated at Moscow State University. He graduated in 1976, obtained a Ph.D. degree in 1979 and a Doctor of Science degree in 1987. Since 1989 he has been Professor of Chemistry at the Division for Chemistry, G. V. Plekhanov Institute of National Economy. His present interests are aimed at enzymes and organometallics.

2.3. Ferrocene and Cymantrene Derivatization

The history of biotransformations of ferrocene probably started in 1971 when *Johnson* and *Murray* reported on microbial hydroxylation of 1,2-(α-oxotetramethylene)ferrocene (**9**) in the presence of the mold *Sporotrichum sulfurescens* (ATCC 7169) to afford hydroxyketone **10**.[32] The best results were obtained at low substrate levels. Compound **10** was the optically active, *exo* product, thus suggesting the enzymatic nature of the oxidation [Eq. (d)].

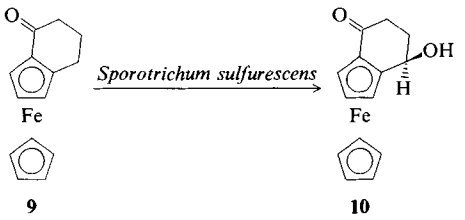

9 **10** (d)

A detailed investigation of the asymmetric reduction of carbonyl ferrocene derivatives has been launched by *Ratajczak* and *Misterkiewicz*,[33] who reported that formylferrocene, ferrocenyl trifluoromethyl ketone (**11**), and [3]ferrocenophan-1-one (**12**) are effectively reduced by baker's yeast in the presence of D-glucose, (Table 1, entries 1, 2, 5). Formylferrocene, in particular, is quantitatively reduced at 33 °C in a matter of 20–40 min to hydroxymethylferrocene. Prochiral molecules **11** and **12** are transformed into (−)-1-ferrocenyl-2,2,2-trifluoroethanol and (−)-[3]ferrocenophan-1-ol in 50 and 10% yield, respectively. Acetyl-, propionyl-, isobutyryl-, benzoyl-, and 1,1′-diacetylferrocene, as well as **9**, did not undergo the reduction by baker's yeast. The product of reduction of **11** initially has an optical rotation of − 6.4,[33] which was finally increased to − 27.7, the yield being 90.5%.[34] Use of other microorganisms extends the substrate specificity of the reduction. In particular, although acetylferrocene (Table 1, entry 3) is resistant to baker's yeast, other microorganisms, such as *Candida tropicalis* (IFO 199), *Pichia quercuum* (IFO 949), and *Saccharomyces cerevisiae* (IFO 305), reduce this compound to the corresponding *S* alcohol.[35] The yield is low, but the reduction gives a high enantiomeric excess (96% *ee*). Additional examples of microbiological or enzymatic redox transformations aimed at the -CO-⇌-CH(OH)- couple are summarized in Table 1. Entries 6 and 7 need special comment. 1,2-Bis(hydroxymethyl)ferrocene (**13**) was oxidized with horse liver alcohol dehydrogenase (HLADH) at 30 °C, pH 8.3, in the presence of $NAD^{\oplus}$ and glutamate dehydrogenase for cofactor recycling.[36] The product isolated has the same properties, except for the sign of optical rotation, as the material obtained by the HLADH-catalyzed reduction of 1,2-diformylferrocene (**14**) in the presence of NADH and ethanol at 5 °C and pH 7.5. The fact that HLADH oxidizes *meso*-diol **13** to the 1*R*,2*S* semialdehyde and reduces *meso*-dialdehyde **14** to the 1*S*,2*R* antipode indicates that the enantiotopic discrimination of HLADH for the *meso* compounds is the same for both oxidation and reduction reactions. Such a phenomenon had not been previously observed,[36] although

Table 1. Redox transformations of ferrocene derivatives (Fc-R).

Entry	Starting material	Product	Microorganism or enzyme	Yield [%] (*ee* [%])	Ref.
1	Fc-CHO	Fc-CH_2OH	baker's yeast	100	[33]
2	Fc-$COCF_3$ **11**	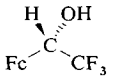	baker's yeast	50 90.5	[33] [34]
3	Fc-$COCH_3$	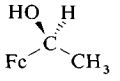	*Candida tropicalis* *Saccharomyces cerevisiae*	7 (96)	[35]
4	Fc-COD	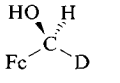 *S*	baker's yeast	90.8	[38]
5	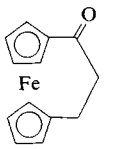 **12**	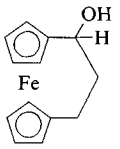 (−)	baker's yeast	10	[33]
6	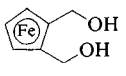 **13**	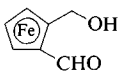 (1*R*, 2*S*)	HLADH, $NAD^{\oplus}$	81 (86)	[36]
7	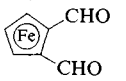 **14**	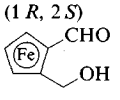 (1*S*, 2*R*)	HLADH, NADH	80(94)	[36]
8	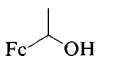 **15**	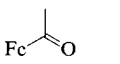	HLADH, $NAD^{\oplus}$, FMN	44(100)	[37]

a large number of HLADH-catalyzed asymmetric syntheses involving *meso* diols or diketones had been carried out. The organometallic nature of substrates **13** and **14** thus reveals some features of HLADH catalysis which are hidden in the case of purely carbon substrates.

Entry 8 presents an example of kinetic resolution of racemic alcohols. Notably, the corresponding ruthenocene and osmocene derivatives behave in a similar way.[37]

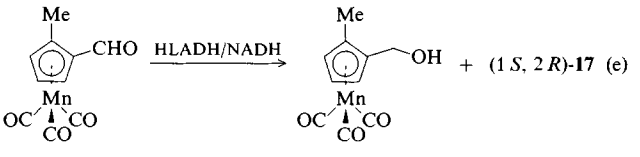

17 (1*R*, 2*S*)-**18** + (1*S*, 2*R*)-**17** (e)

Alcohol dehydrogenase was also used for kinetic resolution of chiral aldehydes in the cymantrene series. Enantioselective reduction of (±)-tricarbonyl(η^5-1-formyl-2-methylcyclopentadienyl)manganese (**17**) with HLADH and NADH at 4 °C and pH 7 afforded (1*R*,2*S*)-**18** in 35% yield together with unreacted (1*S*,2*R*)-**17** (31%) [Eq. (e)]. Remarkably, (1*R*,2*S*)-**17** can be easily obtained from (1*R*,2*S*)-**18** by oxidation with manganese dioxide.[37]

Lipases are another class of enzymes that readily accept the ferrocene functionality. In particular, reaction of 1-hydroxyethylferrocene (**15**) with vinyl propionate in toluene in the presence of porcine pancreas lipase yielded (*R*)-**16** [Eq. (f)]. The reaction is irreversible since the acylating agent affords a volatile product, acetaldehyde.[39] The enantiomeric purity of the (*S*)-**15** and (*R*)-**16** thus obtained is 84%. Similar transformations have also been carried out using lipase from *Pseudomonas fluorescens* in *tert*-butyl alcohol as solvent with $MeCOOCH{=}CH_2$ as an acylating agent.[40]

$$\mathbf{15} + EtCOOCH{=}CH_2 \xrightarrow{PPL} \textit{S}\text{-}\mathbf{15} + Fc(H)(OCOEt) + H_3CCHO \qquad (f)$$

R-**16**

2.4. Other Examples

Therisod[41] has recently reported on lipase-catalyzed transesterification in benzene or cyclohexane via *O*-stannyl ethers [Eq. (g)]. Lipases from porcine pancreas (PPL), *Chromobacterium viscosum*, and *Candida cylindracea* were tested. Only lipase from the latter source was indifferent to organometallic substrates. The highest rate of PPL-catalyzed reaction was achieved for reaction of ethyl butanoate with $Me(CH_2)_5OSnBu_3$. Interestingly, stannyl ethers were found to be much more active than the corresponding alcohols.

$$R^2{-}C(=O){-}O{-}Et + R^1OSnR_3 \rightleftharpoons R^2{-}C(=O){-}O{-}R^1 + EtOSnR_3 \qquad (g)$$

R = Me, *n*-Bu; R^1 = *n*-C_6H_{13}, cyclohexyl; R^2CO = acetyl, *n*-butyryl, capryloyl, lauryl

Organic chemists widely use the chromium tricarbonyl moiety, a powerful electron-releasing group, which, on complexation, strongly affects the reactivity of arenes.[42] An intriguing question is how such complexation affects the enzymatic reactivity of arenes. Additionally, such a complexation with asymmetrically 1,2-disubstituted arenes gives rise to a pair of enantiomers, which might be kinetically resolved by enzymes or microorganisms.

In the presence of D-glucose, (η^6-acetophenone)tricarbonylchromium (**19a**) can be converted into (*S*)-(η^6-1-phenylethanol)tricarbonylchromium (**20a**) by baker's yeast[43] and by *Saccharomyces cerevisiae*[35] in 96% (99% *ee*) and 94% (74% *ee*) yield, respectively [Eq. (h)]. Remarkably, baker's yeast reduces uncomplexed acetophenone under the same conditions to (*S*)-1-phenylethanol in only 69% yield, with an optical purity of only 92%.[43] With the more bulky propionate complex **19b**, the reduction was very slow; after two weeks, only a 20% yield of **20b** was obtained. In

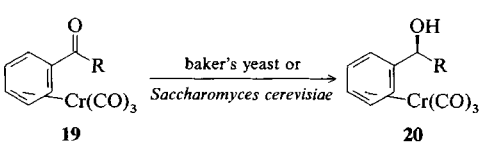

(h)

19 **20**

19a, R = Me; **19b**, R = Et

contrast, free propiophenone is 50% reduced in six days. In both cases, the enantiomeric excess of *S* alcohol was 87%. The analogue of **19a** in which one CO ligand is replaced by PPh_3 is not reduced either. Thus, the steric bulk in this part of the molecule also affects drastically the reaction course. The effect of bulky groups has two possible explanations. First, the size of the organometallic substrate may be too large for the enzyme active site. Second, a change in the steric bulk may cause a change in the permeability of cell walls to organometallic substrates; that is, the hydrophobicity of the organometallic substrate is changed. It is difficult to assess which contribution is larger until studies with individual enzymes are carried out.

In general, the reduction follows the so-called Prelog rule illustrated by Equation (i).[43] As would be expected, more complex substrates give several products. For example, reduction of (±)-(η^6-indanone)tricarbonylchromium by baker's yeast affords the (−)-(*S*)-*endo* alcohol **21** and the (−)-(*S*)-*exo* alcohol **22** in 47% (55% *ee*) and 5% (71% *ee*) yield,

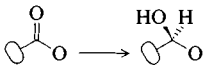

(i)

respectively, together with unreacted material, which was chemically reduced by $NaBH_4$ to the (+)-(*R*)-*endo* alcohol **23** (48%, 25% *ee*)[44] (Scheme 2). Similarly, the tetralone complex **24** is reduced without the formation of the *exo* product. A 52% yield of the 1*S* *endo* alcohol (92% *ee*) was achieved in a buffered solution at pH 7. Use of unbuffered media decreases the optical purity of the product to 83% *ee*.

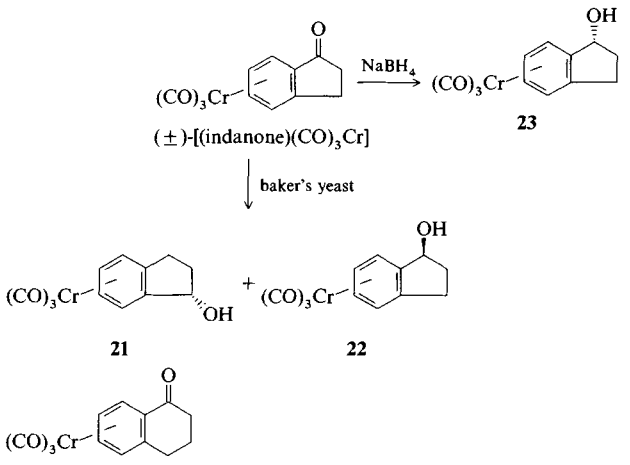

Scheme 2. Reduction of (±)-[(η^6-indanone)$(CO)_3$Cr] with baker's yeast.

Several examples of enantioselective microbiological kinetic resolution of chiral organometallics are shown below. Enantioselective reduction of (±)-(η^6-1-formyl-2-methoxybenzene)tricarbonylchromium (**25**) by baker's yeast at 22 °C in water, in the presence of D-glucose, afforded (+)-(*R*)-(η^6-1-hydroxymethyl-2-methoxybenzene)tricarbonylchromium (**26**) with 66% *ee* and optically active, unchanged (+)-(1*S*)-(η^6-1-formyl-2-methoxybenzene)tricarbonylchromium (**27**) with 81% *ee*[45] (Scheme 3). Even better resolution of **25** was

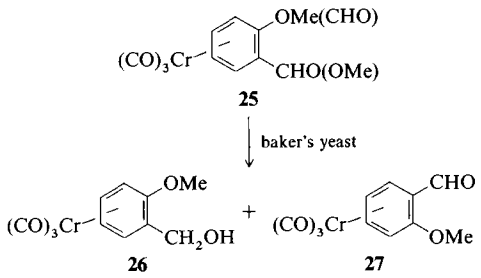

Scheme 3. Kinetic resolution of a racemate by enantioselective reduction with baker's yeast.

achieved in the presence of HLADH and NADH.[37] The optical purity of the compound was as high as 100%.

Another enzyme successfully used for resolution of a racemic organometallic compound is pig liver esterase (PLE)[46] (Scheme 4). The PLE-catalyzed reaction of the

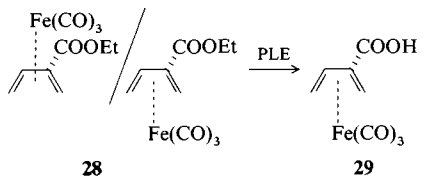

Scheme 4. Resolution of enantiomers with pig liver esterase (PLE).

racemic 2-ethoxycarbonyl-substituted butadieneiron complex **28** in aqueous methanol (pH 7, room temperature, 30 h) affords acid **29** in 40% yield. The unhydrolyzed ester was recovered and hydrolyzed (LiOH) to give the antipode of **29** in 38% yield. Both the enzymatic hydrolysis product (**29**) and the acid obtained from the unhydrolyzed ester were found to be of 85% *ee*. The optical purity of both the acids was raised to > 98% *ee* by one recrystallization.

2.5. Organometallics in NADH/NAD$^{\oplus}$ Recycling

The conversion of NAD$^{\oplus}$ to NADH requires a transfer of two electrons and one proton, and, obviously, it is not easy to carry out such a process concertedly. A stepwise transfer should be avoided since it may lead to the enzymatically inactive NAD$^{\oplus}$ dimer.[47] Indeed, the NADH recycling in dehydrogenase reactions is still a barrier that prevents a decrease in the cost of dehydrogenase-promoted asymmetric syntheses.[48] The recognition that a two-electron, one-proton transfer is the same as a hydride transfer may be the key to a solution of this problem. The hydride is transferred in one step, and, undoubtedly, the best hydride carriers are transition-metal complexes.[49] Such a transfer was first realized by *Steckhan* and co-workers.[50] On the basis of results reported earlier by *Kölle* and *Grätzel*,[51] they demonstrated that the complex [Cp*(bpy)ClRh]Cl can be electrochemically[50] or chemically reduced by formate[52, 53] to give, presumably, the hydride complex [Cp*(bpy)HRh]$^{\oplus}$, which, in turn, can reduce NAD$^{\oplus}$ to NADH. As a result, the electrochemically driven enzymatic reduction of pyruvate to D-lactate catalyzed by D-lactate dehydrogenase became possible at a rate of five turnovers per hour.[50] The yield of D-lactate was 67% with an enantiomeric excess of 93.5%.

This approach is obviously promising in view of the vast possibilities of transition-metal complexes as oxidants or reductants of the corresponding forms of nicotinamide cofactors. The species involved need not necessarily be organometallic in nature. A detailed discussion of this area is beyond the scope of this review, but a few examples can be mentioned. In particular, a tris(2,2'-bipyridyl) complex of rhodium(III) was reported to carry out the electrochemical regeneration of NADH from NAD$^{\oplus}$.[54] Photochemical reduction of NAD(P)$^{\oplus}$ to NAD(P)H was also described.[55, 56] The reverse reaction, that is, regeneration of NAD$^{\oplus}$ and NAD(P)$^{\oplus}$, occurs in the presence of $[FeL_3]^{2\oplus}$[57] and $[RuL_3]^{2\oplus}$[58] complexes, where L is a 2,2'-bipyridine- or 1,10-phenanthroline-type ligand.

3. The Reactions of Oxidases and Peroxidases in the Presence of Organometallics

This is undoubtedly the most advanced area of organometallic biochemistry and was relaunched in 1984 by *Cass* et al.,[59] who reported on the extremely advantageous mediator abilities of ferrocene derivatives in glucose-oxidase-catalyzed oxidation of β-D-glucose. Of course, many other examples of redox processes involving proteins and coordination compounds or organometallic species had been known and reviewed,[60–62] but none is as appropriate to the present discussion as the above-mentioned results. The work of *Cass* et al. has stimulated both rapid production of novel amperometric biosensors and intensive research in this field (see Section 3.1).

3.1. Ferrocenes as Substrates of Oxidases

Enzymes using flavin adenine dinucleotide as cofactor can catalyze oxidation of various molecules by O_2 to yield hydrogen peroxide together with the corresponding oxidation product [Eq. (j)]. An example is the oxidation of β-D-glucose catalyzed by glucose oxidase (GOD)[59] [Eq. (k)]. Remarkably, ferricenium ions have also been found to be substrates of glucose oxidase (GOD);[59] the organometallic ions replace O_2.

$$\text{Red-H}_2 + \text{O}_2 \longrightarrow \text{Ox} + \text{H}_2\text{O}_2 \qquad \text{(j)}$$

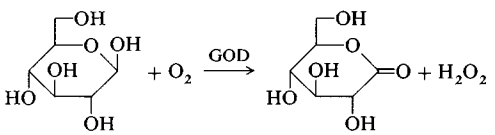

(k)

Cyclic voltammetry is the best technique for monitoring this catalysis. It is nicely seen in Figure 1 that practically the limiting currents are achieved in the system ferrocene–D-glucose–GOD, while the absence of either of the latter two components restores the trace typical of ferrocene alone. The electrocatalysis in the presence of the organometallic media-

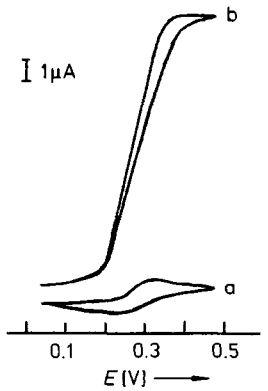

Fig. 1. a) The dc cyclic voltammogram of hydroxycarbonylferrocene (0.05 mM) at pH 7 and 25°C, in the presence of D-glucose (50 nM) at a scan rate of 1 mVs^{-1}. b) As for (a), but with addition of GOD (10.9 μM) [59].

tor can be accounted for in terms of Equations (l)–(n),[59] where E(ox) and E(red) are oxidized and reduced forms of

$$E(ox) + \beta\text{-D-glucose} \longrightarrow E(red) + \text{D-gluconolactone} \quad (l)$$

$$E(red) + 2\,Fc^{\oplus} \longrightarrow E(ox) + 2\,Fc + 2\,H^{\oplus} \quad (m)$$

$$2\,Fc - 2e^{-} \longrightarrow 2\,Fc^{\oplus} \quad (n)$$

GOD, respectively, and Fc is a ferrocene derivative. Other oxidases that function in a similar way, ferrocenes

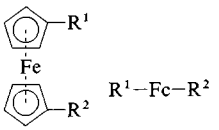

R^1–Fc–R^2

Table 2. Oxidases accepting ferricenium ions as substrates and the corresponding rate constants k for oxidation of reduced enzymes..

Enzyme	Substrate	R^1–Fc–R^2 R^1	R^2	E_0 [mV] vs. SCE	$10^{-5}\,k$ [$M^{-1}s^{-1}$]	Ref.
glucose oxidase	D-glucose	CH_3	CH_3	100	0.77	[59]
glucose oxidase	D-glucose	H	H	165	0.26	[59]
glucose oxidase	D-glucose	$H_2C{=}CH$	H	250	0.30	[59]
glucose oxidase	D-glucose	COOH	H	275	2.01	[59]
glucose oxidase	D-glucose	COOH	COOH	285	0.26	[59]
glucose oxidase	D-glucose	Me_2NCH_2	H	400	5.25	[59]
pyruvate oxidase	pyruvate	COOH	H	275	0.2	[63]
xanthine oxidase	xanthine	COOH	H	275	4.0	[63]
sarcosine oxidase	sarcosine	COOH	H	275	0.1	[63]
diaphorase	NADH	COOH	H	275	0.2	[63]
glutathione reductase	NAD(P)H	COOH	H	275	2.0	[63]
CO oxidase	CO	COOH	H	275	4.0	[63]
flavocytochrome b_2	L-lactate	COOH	H	275	67.0	[63]
alcohol dehydrogenase	MeOH	COOH	H	275	2.0	[63]
L-lysine oxidase	L-lysine	COOH	H	275	[a]	[67]
L-lysine oxidase	L-lysine	Me_2NCH_2	H	275	[a]	[67]

[a] Not measured.

(R^1–Fc–R^2), and the corresponding rate constants for the oxidation of reduced enzymes evaluated from the electrochemical data are shown in Table 2. Two similar enzymes tried, oxalate oxidase and choline oxidase, did not couple with ferrocenes.[63] The rather large values of the second-order rate constants in Table 2 show that oxidases readily accept ferrocenes, which therefore appear to be true substrates of the enzymes. Octacyanomolybdate(IV) and octacyanotungstate(IV) are also accepted by lactate and sarcosine oxidase in the same way.[64] The rate constants for the oxidation of the reduced enzymes by $W(CN)_8^{3\ominus}$ or $Mo(CN)_8^{3\ominus}$ are almost as high as those for ferricenium ions [$(3-4)\times 10^4\ M^{-1}s^{-1}$]. Glucose oxidase and D-amino acid oxidase react with a poly(vinylpyridine) complex of $[OsL_2Cl]^{\oplus/2\oplus}$ (L = 2,2′-bipyridyl) similarly.[65,66]

The principle of enzymatic enhancement of the electrochemical response of organometallic mediators described above has already been realized in many amperometric biosensors, including that for the monitoring of D-glucose[59] and carbon monoxide.[68] This promising approach to designing biosensors[69–71] has stimulated further studies in the field of organometallic biochemistry. Although organometallic mediators are indeed very effective, bioelectrocatalytic systems without mediators are thought to be more advantageous.[72–77] Therefore, an attempt was undertaken to make the oxidase–ferrocene systems pseudo-mediatorless by covalent attachment of ferrocenes to the enzyme.[78–80] When GOD was modified by $Fc(CH_2)_nCOOH$ (n = 0, 1, and 3) using water-soluble carbodiimides, it appeared to be electrocatalytically active without added ferrocenes. It is tempting to conclude that there is direct electrical communication between chemically modified GOD and electrodes, but a subsequent report[81] that ferrocene-modified bovine serum albumin is also a mediator of the electron transport between the active site of GOD and an electrode indicated that ferrocene-modified GOD may function intermolecularly. In any case, oxidoreductases modified by organometallic species are a challenging object for research.[82] In this respect, one purely organometallic approach to ferrocene-modified enzymes should be mentioned.[83] It is based on the high activity of organomercurials toward free cysteine residues of proteins.[84] Reaction of chloroferrocenylmercury, for example, with cytochrome c from baker's yeast results in attachment of the ferrocenylmercury group to the Cys-102 residue [Eq. (o)]. The product obtained is electrochemically active with a wave at 450 mV versus the normal hydrogen electrode (NHE). Apparently, this approach can be successfully applied to oxidoreductases, if the catalytically important SH groups remain intact.

$$\text{CYT(Cys 102)-SH} + \text{ClHgFc} \longrightarrow \text{CYT(Cys 102)-SHgFc} + H^{\oplus} + Cl^{\ominus} \quad (o)$$

Interestingly, while flavoproteins couple with oxidized ferrocenes, peroxidase catalyzes the oxidation of ferrocenes by hydrogen peroxide.[85] Unmodified ferrocene, together with $FcCH_2OH$, FcCHMeOH, $FcCMe_2OH$, $FcCH_2COOH$, $FcB(OH)_2$, and $FcCH_2N^+Me_3I^{\ominus}$, were involved. This observation has led to the development of an amperometric biosensor for hydrogen peroxide where ferrocenes shuttle between an electrode and the active site of peroxidase[86] and of cytochrome c peroxidase.[87]

3.2. Ferrocenes in Immunoassay

Ferrocenes as hydrophobic molecules are perfect guests for cyclodextrins in aqueous media.[88,89] It has been recently reported[90] that ferricenium ions also form inclusion com-

plexes with cyclodextrins [Eq. (p)]. The complexed species are no longer substrates of glucose oxidase and do not give rise to catalytic currents in the system ferrocene–D-glucose–GOD. Thus, the incorporation of ferrocenes into the host cavities or their shielding by the fragments of large molecules may dramatically affect the mediator abilities of ferrocenes.

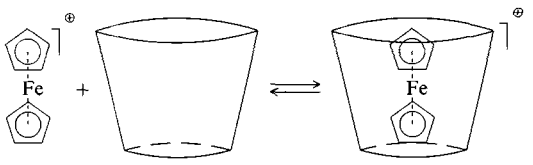

(p)

This effect is evidently disadvantageous in the case of simple ferrocene-based sensors, since host molecules will interfere with the oxidase response. But it is very advantageous if immunoanalysis is concerned. Consider a molecule in which a hapten is covalently bound to ferrocene. If this conjugate does not lose its affinity for the corresponding antibodies, the antigen–antibody interaction can result in the shielding of the organometallic moiety and, hence, the conjugate may become bioelectrocatalytically inactive. If free antigen is now added to the system, it will replace the conjugate, since the affinity of the free antigen is at least as high as that of the conjugate. The conjugate liberated will now be accepted by an oxidase and the resulting increase in current will be a function of the concentration of the free antigen. This approach has been realized in analyses for thyroxine[91, 92] and lidocaine.[93] The corresponding conjugates **30** and **31** were prepared. A closely related procedure for quantification of human chorionic gonadotrophin was also described.[94, 95] The coupling of ferrocene conjugates with oxidases is a

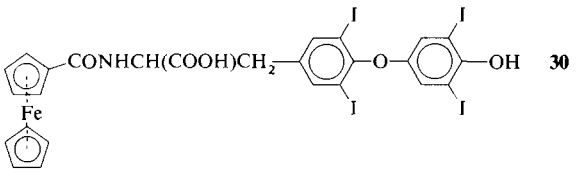

30

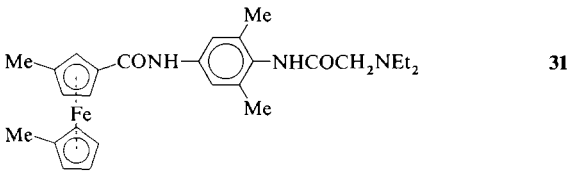

31

breakthrough in the metalloimmunoassay concept put forward by *Cais* et al.[96, 97] in the late 1970s. Many ferrocene, cobaltocene, and cymantrene derivatives of estriol, morphine, barbiturates, amphetamine, and cocaine were then prepared, but the necessity of using atomic absorption spectrometry as analytical routine precluded the general acceptance of this approach.

It should be emphasized that even simple binding of ferrocene conjugates to the corresponding antibodies decreases the electrochemical response of a ferrocene label. This was first shown for ferrocenecarboxylic acid conjugated with morphine.[98] The effect is low, however, and does not meet the requirements of current immunoassays.[99] The use of the oxidase enhancement improves the situation considerably, making it appropriate for analyses.

The ability to change the redox potentials of functionalized ferrocenes by varying their side chains offers a way to use various proteases in bioelectroanalysis. For example, compound **32** was prepared for assaying alkaline phosphatase and estriol.[100] The key point here is that the substrate of alkaline phosphatase, compound **32**, has a quasi-reversible peak at 390 mV. Product **33** has two irreversible peaks, corresponding to oxidation of the phenol and ferrocene moieties, at 590 and 180 mV, respectively, versus the saturated calomel electrode (SCE). Remarkably, the oxidation of the product of enzymatically driven reaction (q) occurs at a potential 210 mV lower than that of the starting substrate. The product thus can be detected in an excess of the substrate, thereby allowing the assay of alkaline phosphatase. In fact, the enzyme was monitored at a level of 1.2×10^{-12} M. The procedure was also found suitable for the enzyme-linked immunoassay using alkaline phosphatase as a marker enzyme. Three criteria have been put forward[100] for achieving further enzyme amplification:

1. The product must have a lower oxidation potential than the substrate.
2. The difference in oxidation potential must be of the order of 100–200 mV.
3. The product in its oxidized form must be accepted by an enzyme of the glucose-oxidizing type.

4. Receptors That Bind Organometallic Species

Of course, there are no receptors yet that are specific for organometallics. However, attachment of organometallics to biomolecules need not eliminate their ability to be accepted by receptors. This strategy has been worked out in a very elegant procedure for assaying hormone receptors by FT-IR spectroscopy.[101] Its general principles have already been reviewed twice by the authors[102, 103] and, therefore, only a brief outline will be given here for the sake of demonstrating what unexpected and hence exciting results organometallic biochemistry can provide.

Most proteins have an IR "window" around 2000 cm^{-1}. Metal carbonyls, on the contrary, have a strong absorption in this region. Further, $[Cr(CO)_3]$, $[Cr(CO)_2CS]$, or related

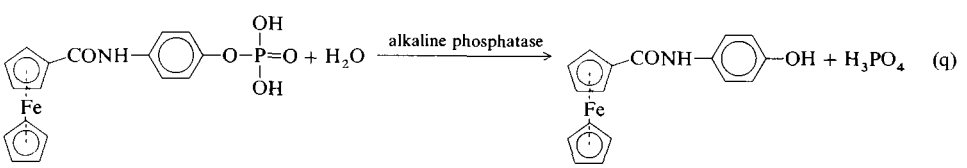

(q)

32 ($E_{1/2}$ = 390 mV) **33** ($E_{1/2}$ = 180 mV)

fragments can be attached to a variety of biologically relevant molecules[104-106] including estradiol derivatives.[101] The organochromium-labeled steroids **34** are stable in aqueous methanol, and their relative binding affinities to estrogen receptor vary in the range 0.4–28%, the highest value being achieved when R = $HO(CH_2)_3$. The latter com-

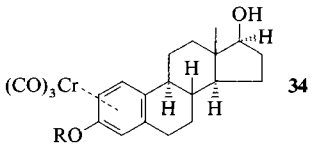

34

pound has been prepared in a tritiated form with a high specific activity. It binds reversibly to the estradiol receptor in lamb uterine cytosol with a dissociation constant (K_D = 0.85 nM) and a number of binding sites close to the values observed for estradiol itself. The level of nonspecific binding is low, and the hormone is not bound significantly to other nontarget tissues. The tricarbonylchromium-labeled molecules are good markers for detection of hormone receptors by FT-IR at 1880 and 1957 cm^{-1} in the case of **34**. This and other related examples[107] show how advantageous organometallic derivatization of biomolecules can be. Not only novel drugs[108] but also convenient markers may be prepared in this way.

5. Organometallic Lyases

One of the environmental hazards brought about by civilization is pollution by heavy metals. Particularly dangerous is organomercury poisoning. The total oceanic reservoir of mercury is estimated at 200 million tons. The reservoir of the volatile forms (Hg^0 and MeHgX) in the atmosphere is about 4 million tons with an annual flux between these reservoirs of roughly 15000 tons.[109] Mercuric salts are biomethylated with methyl coenzyme B_{12} to give methyl mercuric salts and this organomercurial is a potent human neurotoxin. To survive, nature has had to develop a mechanism for resisting the invasion of organometallics.[110] Bacteria chose a two-step two-enzyme detoxification strategy for recycling organomercurials back to nontoxic, volatile, elemental Hg^0.[111-115] The first enzyme, organomercury lyase,[116,117] catalyzes a protonolytic cleavage of a carbon–mercury bond [Eq. (r)]. The second, mercuric ion reductase,[118-124] reduces Hg^{II} to Hg^0 in an NADPH-dependent process [Eq. (s)].

$$H_3C{-}HgX + H_2O \longrightarrow CH_4 + Hg(OH)X \quad (r)$$

$$Hg(OH)X + NADPH \longrightarrow Hg^0 + NADP^{\oplus} + H_2O + X^{\ominus} \quad (s)$$

To this end, nature has created an enzyme whose natural substrate is an organometallic molecule and which attacks at the carbon–metal bond.

5.1. Organomercury Lyase: Structure and General Properties

Organomercury lyase is a simple monomeric polypeptide with a molecular weight of 22400 Da.[116] Qualitative neutron activation analysis indicated the absence of metal ions in the pure enzyme. It should be pointed out, however, that the absence of Pb, Mg, Ca, Mo, Ir, and Sn cannot be unequivocally established by this method. The amino acid composition and the amino-terminal sequence of the enzyme have also been reported. Remarkably, there are four cysteine residues. The Lineweaver–Burk plot for organomercury lyase activity with MeHgCl shows a strong substrate inhibition above 1 mM for reasons as yet undetermined. The same effect is also observed for *t*BuHgCl but not for other mercurials. The rate of enzymatic protonolysis is dependent on both the structure and the concentration of the buffer thiol. Indeed, the rate for cysteine (5 mM) is eight times the rate for 2-mercaptoethanol (5 mM), and no protonolysis occurs with 2-aminoethanethiol. In the case of cysteine, no protonolysis of EtHgCl takes place at concentrations less than 2 mM. At concentrations greater than 2 mM, the rate increases with increasing cysteine concentration and finally levels off above 15 mM.

The enzyme catalyzes the protonolysis of a wide range of organomercurials of type RHgX but does not accept those of type RHgR (Table 3). This is rather curious in view of the fact that the former are much more labile to acidic cleavage.[125]

Table 3. Substrate specificity and kinetic parameters of organomercurials in the lyase-catalyzed reaction [116].

Substrate	V_{max} [nmol $mg^{-1} min^{-1}$]	K_m [mM]	Turnover [min^{-1}]
MeHgCl	31	0.5	0.7
*n*BuHgCl	880	0.9	20
*s*BuHgCl	110	0.8	2.5
*t*BuHgCl	40	0.8	2.5
PhHgCl	670	0.9	15.0
(crotyl)HgCl	2600	1.3	58
$H_2C{=}CHHgCl$	530	1.0	12
(*cis*-2-butenyl)HgCl	10700	3.3	240
MeHgMe	0		0

Another remarkable feature of the enzyme is the pH profiles for V_{max} and $V_{max}K_m^{-1}$ determined with EtHgCl. The rate increases up to pH 10.2, where denaturation of the enzyme occurs, the apparent pK_a being 9.0. Again, there is a dramatic discrepancy with the protonolytic cleavage of organomercurials, where the rate is first-order in the acid.[125] Much work has been done on elucidating the detailed mechanism of the enzymatic C–Hg bond cleavage.[117] The discrimination between S_N1, radical, S_E1, and S_E2 pathways in favor of the latter has been made on the basis of mechanistic study of the reactivity patterns of organomercurials **35**–**38**.

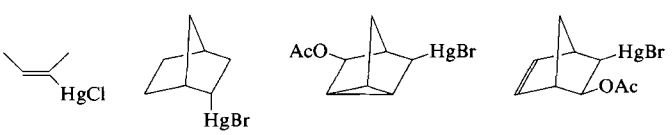

35 **36** **37** **38**

The conversion of **35** and **36** demonstrates the retention of stereochemical configuration. The former affords exclusively *cis*-2-butene, while the latter transforms into the *endo* deuterio product. The enzymatic protonolysis of **37** and **38**, which are very diagnostic for probing radical steps,[126] occurs without skeletal rearrangements and radical intermediates, thus ruling out a radical pathway.

The substrate specificity of the lyase has been also studied.[117] Various organomercurials of the type RHgCl are converted, including alkyl, alkenyl, allyl, and phenyl derivatives (Table 3). Among these, compound **35** and MeHgCl turned to be the most and the least reactive, respectively. The significant solvent deuterium isotope effect at pH 7.4 of $V_{max}(H_2O)/V_{max}(D_2O)$ is equal to 2.1 and 4.9 for turnover of **35** and EtHgCl, respectively, suggesting a kinetically important proton delivery. Finally, the stoichiometric formation of 2-butene and Hg^{II} from **35** and of methane and Hg^{II} from MeHgCl eliminates the possibility of an S_N1 solvolytic mechanism.

Concerning the fate of organomercurials in the active site of the lyase, the following suggestions, depicted in Scheme 5,

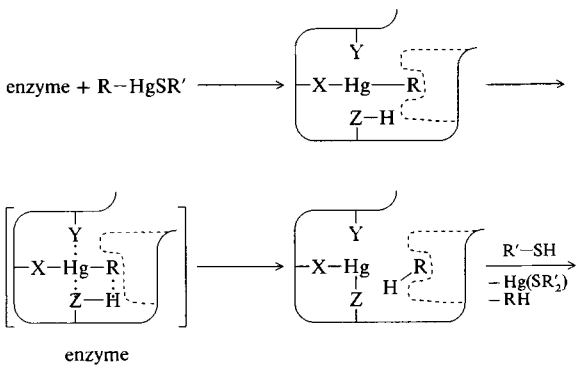

Scheme 5. Proposal for the interaction of organomercurials with the active site of the lyase.

have been put forward.[117] The substrates undergo initial binding to the enzyme via coordination to group X to give an enzyme–substrate complex (saturation kinetics are observed for all substrates). Coordination of another nucleophilic moiety, Y, to the organomercurial would then activate the C–Hg bond toward protonolysis. This conclusion was made in view of the well-documented nucleophilic assistance of the electrophilic cleavage of carbon–metal bonds.[125, 127] The carbon–mercury bond rupture would then occur via the indicated S_E2 transition state, although the present state of knowledge does not allow a discrimination between three- and four-centered pathways. It is believed, however, that the latter pathway is more likely. Finally, exchange of Hg^{II} with thiols in the solvent leads to free enzyme ready for another catalytic cycle. Without excess thiols in the buffer for removing Hg^{II} from the enzyme active site, the enzyme accumulates as an inhibited enzyme–Hg^{II} complex.

Organostannanes were the next organometallics subjected to catalysis by organomercury lyase.[128] Of the compounds tested, tetravinyltin is turned over with the highest specific activity, yielding ethene as the organic product. Similarly, triethylvinyltin undergoes turnover by the lyase to yield ethene and ethane in a 97:3 ratio, at 1/60 the rate of tetravinyltin turnover. Finally, Me_4Sn and Me_3SnF yield small amounts of methane prior to eventual loss of enzyme activity. The loss is consistent with the observed inhibition by Me_2SnBr_2. Interestingly, silicon and germanium counterparts of stannanes accepted by the lyase do not undergo the enzymatic cleavage, nor do Et_4Sn, Bu_4Sn, Et_3SnOAc, and $BuSnCl_3$. Hence, the enzymatic activity may be very specific to the nature of the metal center.

Organomercury lyase attracted the attention of many workers involved in various fields, and a model system was soon provided by chemists.[129] It threw light on both the assistance by thiol ligation and the nature of nucleophilic catalysis. Compound **39** was prepared and its protonolysis rates were measured under various conditions. At pH 6.6

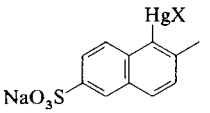

39a, X = S(SH)CH2SO3Na

39b, X = Cl

with 0.3 M phosphate buffer, k_{obsd} is $10^{-7}\ s^{-1}$. In the presence of 100 equivalents of 2,3-dimercaptopropanesulfonate, k_{obsd} is $10^{-4}\ s^{-1}$. Most (90%) of this rate acceleration is observed on adding only two equivalents of dithiol. Ligation of **39** is therefore completed and the substrate is **39a**. The reaction is catalyzed by buffer since $k_{obsd} = (k + k_{BT}[B]_t)$, where $[B]_t$ is the total buffer concentration. In formate, acetate, or phosphate buffers the plots of $\lg k_{BT}$ versus pH are bell-shaped, the maximal rates being observed at pH values of about 4, 5, and 6, respectively. The bell-shaped profile of the reaction points to the importance of both the buffer acid and the buffer base and this finds explanation in a sequential two-step mechanism with a pH-dependent change in the rate-determining step [Eq. (t)]. This study suggests that ligation

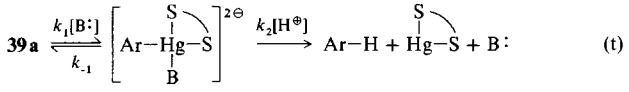

(t)

by two thiols is necessary not only for removing Hg^{II} from the active site of the lyase but for creation of the actual substrate as well.

6. Summary and Outlook

Organometallic biochemistry will undoubtedly develop extensively in the near future. There is a great variety of objects for research, especially in the field of organometallic biosynthesis and biosensoring. Both university and industrial chemists and biochemists will be involved. Environmental and health problems associated with increasing use of organometallics in industry and medicine will probably stimulate further studies in this field.

I thank Dr. Vadim V. Mozhaev for critical reading of the manuscript and stimulating criticism.

Received: June 6, 1990 [A 826 IE]
German version: *Angew. Chem. 103* (1991) 945

[1] D. Dolphin (Ed.): *B_{12}, Vol. 1, 2*, Wiley Interscience, New York 1982.
[2] D. Lexa, J.-M. Saveant, *Acc. Chem. Res. 16* (1983) 235–243.
[3] R. G. Finke, D. A. Shiraldi, B. J. Mayer, *Coord. Chem. Rev. 54* (1984) 1–22.
[4] P. Dowd, M. Shapiro, *Tetrahedron 40* (1984) 3063–3067.
[5] P. Dowd, M. Shapiro, *Tetrahedron 40* (1984) 3069–3086.
[6] P. J. Toscano, L. G. Marzilli, *Prog. Inorg. Chem. 31* (1984) 105–204.
[7] L. Randaccio, N. Bresciani Pahor, E. Zangrando, L. G. Marzilli, *Chem. Soc. Rev. 18* (1989) 225–250.
[8] G. M. Whitesides, C. H. Wong, *Angew. Chem. 97* (1985) 617–638; *Angew. Chem. Int. Ed. Engl. 24* (1985) 617–638.
[9] J. B. Jones, *Tetrahedron 42* (1986) 3351-3403.
[10] A. Akiyama, M. Bednarsky, M.-J. Kim, E. S. Simon, H. Waldman, G. M. Whitesides, *CHEMTECH. 1988*, 627.
[11] E. J. Toone, E. S. Simon, M. D. Bednarski, G. M. Whitesides, *Tetrahedron 45* (1989) 5365–5422.
[12] F. S. Sariaslani, *CRC Crit. Rev. Biotechnol. 9* (1989) 171–257.
[13] W. Hummel, M.-R. Kula, *Eur. J. Biochem. 184* (1989) 1–13.
[14] S. Servi, *Synthesis 1990*, 1–25.
[15] A. M. Klibanov, *CHEMTECH. 1986*, 354–359.
[16] A. M. Klibanov, *Acc. Chem. Res. 23* (1990) 114–120.
[17] Yu. L. Khmelnitsky, A. V. Levashov, N. L. Klyachko, K. Martinek, *Enzyme Microb. Technol. 10* (1988) 710–724.
[18] D. S. Dordick, *Enzyme Microb. Technol. 11* (1989) 194–211.
[19] A. Tanaka, K. Sonomoto, *CHEMTECH. 1990*, 112–117.
[20] K. Martinek, A. V. Levashov, N. L. Klyachko, Yu. L. Khmelnitsky, I. V. Berezin, *Eur. J. Biochem. 155* (1986) 453–468.
[21] Yu. L. Khmelnitsky, A. V. Kabanov, N. L. Klyachko, A. V. Levashov, K. Martinek in M.-P. Pileni (Ed.): *Structure and Reactivity in Reverse Micelles*, Elsevier, Amsterdam 1989, pp. 230–261.
[22] A. J. Crowe, *Chem. Ind. (London) 1983*, 304–310.
[23] R. Tacke, H. Zilch, *Endeavour 10* (1986) 191-197.
[24] R. Tacke, H. Zilch, *Actual Chim. 1986*, 75–82.
[25] J. S. Thayer, *Appl. Organomet. Chem. 1* (1987) 227–234.
[26] B. K. Keppler, *New J. Chem. 14* (1990) 389–403.
[27] R. Tacke, H. Lynoh, B. Stumpf, W. Rainer, A. K. Kieslich, L. Ernst, *Z. Naturforsch. B38* (1983) 616–620.
[28] C. Syldatk, H. Andree, A. Stoffregen, F. Wagner, B. Stumpf, L. Ernst, H. Zilch, R. Tacke, *Appl. Microbiol. Biotechnol. 27* (1987) 152–158.
[29] R. Tacke, K. Fritsche, A. Tafel, F. Wuttke, *J. Organomet. Chem. 388* (1990) 47–55.
[30] R. Tacke, H. Hengelsberg, H. Zilch, B. Stumpf, *J. Organomet. Chem. 379* (1989) 211–216.
[31] R. Tacke in H. Sakurai (Ed.): *Organosilicon and Bioorganosilicon Chemistry. Structure, Bonding, Reactivity and Synthetic Application*, Ellis Horwood, Chichester 1985, pp. 251–262.
[32] R. A. Johnson, H. C. Murray, *J. Chem. Soc. Chem. Commun. 1971*, 989–990.
[33] A. Ratajczak. B. Misterkiewicz, *Chem. Ind. (London) 1976*, 902–903.
[34] V. I. Sokolov, L. L. Troitskaya, T. I. Rozhkova, *Gazz. Chim. Ital. 117* (1987) 525–527.
[35] Y. Yamazaki, K. Hosono, *Agric. Biol. Chem. 52* (1988) 3239–3239.
[36] Y. Yamazaki, K. Hosono, *Tetrahedron Lett. 29* (1988) 5769–5770.
[37] Y. Yamazaki, K. Hosono, *Tetrahedron Lett. 30* (1989) 5313–5314.
[38] V. I. Sokolov, L. L. Troitskaya, O. A. Reutov, *Dokl. Akad. Nauk. SSSR 237* (1977) 1376–1379.
[39] Y.-F. Wang, J. J. Lalonde, M. Momongan, D. E. Bergbreiter, C.-H. Wong, *J. Am. Chem. Soc. 110* (1988) 7200–7205.
[40] N. W. Boaz, *Tetrahedron Lett. 30* (1989) 2061–2064.
[41] M. Therisod, *J. Organomet. Chem. 361* (1989) C8–C10.
[42] V. N. Kalinin, *Usp. Khim. 56* (1987) 1190–1227.
[43] J. Gillois, D. Buisson, R. Azerad, G. Jaouen, *J. Chem. Soc. Chem. Commun. 1988*, 1224–1225.
[44] J. Gillois, G. Jaouen, D. Buisson, R. Azerad, *J. Organomet. Chem. 367* (1989) 85–93.
[45] S. Top, G. Jaouen, J. Gillois, C. Baldoli, S. Maiorana, *J. Chem. Soc. Chem. Commun. 1988*, 1284–1285.
[46] N. W. Alcock, D. H. G. Crout, C. M. Henderson, S. E. Thomas, *J. Chem. Soc. Chem. Commun. 1988*, 746–747.
[47] R. W. Burnett, A. L. Underwood, *Biochemistry 7* (1968) 3328–3333.
[48] C. H. Keith, G. M. Whitesides, *Appl. Biochem. Biotechnol. 14* (1987) 147–197.
[49] J. P. Collman, L. S. Hegedus, J. R. Norton, R. G. Finke: *Principles and Applications of Organotransition Metal Chemistry*, University Science Books, Mill Valley, CA, USA 1987, Chapter 13.
[50] R. Ruppert, S. Herrmann, E. Steckhan, *Tetrahedron Lett. 28* (1987) 6583–6586.
[51] U. Kölle, M. Grätzel, *Angew. Chem. 99* (1987) 572–575; *Angew. Chem. Int. Ed. Engl. 26* (1987) 567–570.
[52] R. Ruppert, S. Herrmann, E. Steckhan, *J. Chem. Soc. Chem. Commun. 1988*, 1150–1151.
[53] E. Steckhan, S. Herrmann, R. Ruppert, J. Thömmes, C. Wandrey, *Angew. Chem. 102* (1990) 445–447; *Angew. Chem. Int. Ed. Engl. 29* (1990) 388–390.
[54] S. Grammenudi, M. Franke, F. Vogtle, E. Steckhan, *J. Inclusion Phenom. 5* (1987) 695–707.
[55] S. Aono, I. Okura, *Inorg. Chim. Acta 152* (1988) 55–59.
[56] I. Willner, R. Maidan, M. Shapira, *J. Chem. Soc. Perkin Trans. 2 1990*, 559–564.
[57] J. Komoschinski, E. Steckhan, *Tetrahedron Lett. 29* (1988) 3299–3300.
[58] R. Ruppert, E. Steckhan, *J. Chem. Soc. Perkin Trans. 2 1989*, 811–814.
[59] A. E. G. Cass, G. Davis, G. D. Francis, H. A. O. Hill, W. J. Aston, I. J. Higgins, E. O. Plotkin, L. D. L. Scott, A. P. F. Turner, *Anal. Chem. 56* (1984) 667–671.
[60] R. Szentrimay, P. Yeh, T. Kuwana in D. Sawyer (Ed.): *Electrochemical Studies of Biological Systems*, ACS, Washington, DC, USA 1977, pp. 143–183.
[61] M. L. Fultz, R. A. Durst, *Anal. Chim. Acta 140* (1982) 1–18.
[62] Y. Kulis, V. Razumas: *Biocatalysis in Electrochemistry of Organic Compounds*, Vilnius, Mokslas 1983, pp. 52–74.
[63] M. J. Green, H. A. O. Hill, *J. Chem. Soc. Faraday Trans. 1 82* (1986) 1237–1243.
[64] I. Taniguchi, S. Miyamoto, S. Tomimura, F. M. Hawkridge, *J. Electroanal. Chem. Interfacial Electrochem. 240* (1988) 333–339.
[65] Y. Degani, A. Heller, *J. Am. Chem. Soc. 111* (1989) 2357–2358.
[66] B. A. Gregg, A. Heller, *Anal. Chem. 62* (1990) 258–263.
[67] A. D. Ryabov, E. M. Tyapochkin, E. S. Ryabova, M. D. Reshetova, A. A. Karyakin, *Metalloorg. Khim. 3* (1990) 1384–1390.
[68] A. P. F. Turner, W. J. Aston, I. J. Higgins, J. M. Bell, G. Davis, H. A. O. Hill, *Anal. Chim. Acta 163* (1984) 161–174.
[69] P. N. Bartlett, R. G. Whitaker, *Biosensors 3* (1987/1988) 359–379.
[70] J. E. Brew, H. A. O. Hill *Eur. J. Biochem. 172* (1988) 261–269.
[71] D. C. Johnson, M. D. Ryan, G. S. Wilson, *Anal. Chem. 60* (1988) 147R–162R.
[72] S. D. Varfolomeev, *Methods Enzymol. 137* (1988) 430–440.
[73] R. M. Paddock, E. F. Bowden, *Electroanal. Chem. Interfacial Electrochem. 260* (1989) 487–494.
[74] L. H. Guo, H. A. O. Hill, G. A. Lowrance, *J. Electroanal. Chem. 266* (1989) 379–396.
[75] A. Szues, G. D. Hitchens, J. O. M. Bockvis, *Bioelectrochem. Bioenerg. 21* (1989) 133-148.
[76] S.-I. Yabuki, H. Shinohara, M. Aizawa, *J. Chem. Soc. Chem. Commun. 1989*, 945–946.
[77] P. de Taxis Du Poet, S. Miyamoto, T. Murakami, J. Kimura, I. Karube, *Anal. Chim. Acta 235* (1990) 255–263.
[78] Y. Degani, A. Heller, *J. Phys. Chem. 91* (1987) 1285–1289.
[79] Y. Degani, A. Heller, *J. Am. Chem. Soc. 110* (1988) 2615–2620.
[80] P. N. Bartlett, R. G. Whitaker, M. J. Green, J. Frew, *J. Chem. Soc. Chem. Commun. 1987*, 1603–1604.
[81] F. Mizutani, M. Asai, *Denki Kagakuoyobi Kogyo Butsuri Kagaku 56* (1988) 1100–1101.
[82] A. Heller, *Acc. Chem. Res. 23* (1990) 128–134.
[83] N. M. Kostić, *Comments Inorg. Chem. 8* (1989) 137–162.
[84] Yu. M. Torchinsky: *Sulfur in Proteins*, Nauka, Moscow 1977.
[85] R. Epton, M. E. Hobson, G. Marr, *J. Organomet. Chem. 149* (1978) 231–244.
[86] J. E. Frew, M. A. Harmer, H. A. O. Hill, S. I. Libor, *J. Electroanal. Chem. 201* (1986) 1–10.
[87] J. M. Cooper, M. Alvarez-Icaza, C. J. McNeil, P. N. Bartlett, *J. Electroanal. Chem. 272* (1989) 57-70.
[88] J. F. Stoddart, R. Zarzycki, *Recl. Trav. Chim. Pays-Bas 107* (1988) 515–528.
[89] V. I. Sokolov, *Metalloorg. Khim. 1* (1988) 25–33.
[90] A. D. Ryabov, E. M. Tyapochkin, S. D. Varfolomeev, A. A. Karyakin, *Bioelectrochem. Bioenerg. 24* (1990) 257–262.
[91] G. A. Robinson, G. Marinazzo, G. C. Forrest, *J. Immunoassay 7* (1986) 1–15.
[92] T. Yao, G. A. Rechnitz, *Biosensors 3* (1987/1988) 307–312.
[93] K. D. Gleria, H. A. O. Hill, C. J. McNeil, M. J. Green, *Anal. Chem. 58* (1986) 1203–1205.
[94] G. A. Robinson, G. Martinazzo, G. C. Forrest, *Biosensors 2* (1986) 45–57.
[95] G. A. Robinson, V. M. Cole, G. C. Forrest, *Biosensors 3* (1987/1988) 147–160.
[96] M. Cais, S. Dani, Y. Eden, O. Gandolfi, M. Horn, E. E. Isaacs, Y. Josephi, Y. Saar, E. Slovin, L. Snarski, *Nature 270* (1977) 534–535.
[97] M. Cais, *Methods Enzymol. 92* (1982) 445–448.
[98] S. Weber, W. Purdy, *Anal. Lett. 12* (1979) 1–9.
[99] P. Tijssen: *Practice and Theory of Enzyme Immunoassays*, Elsevier, Amsterdam 1985.
[100] C. J. Neil, I. J. Higgins, J. V. Bannister, *Biosensors 3* (1987/1988) 199–209.
[101] A. Vessieres, S. Top, A. Ismail, I. S. Butler, M. Louer, G. Jaouen, *Biochemistry 27* (1988) 6659–6666.
[102] I. S. Butler, A. Vessieres, G. Jaouen, *Comments Inorg. Chem. 8* (1989) 269–286.
[103] G. Jaouen, A. Vessieres, *Pure Appl. Chem. 61* (1989) 565–572.
[104] N. A. Sasaki, P. Potier, M. Savignac, G. Jaouen, *Tetrahedron Lett. 29* (1988) 5759–5762.

[105] M. Gruselle, P. Deprez, S. Greenfield, G. Jaouen, J.-P. Larue, D. Thouvenot, *J. Organomet. Chem. 359* (1989) C 53–C 56.
[106] L. L. Troitskaya, V. I. Sokolov, V. J. Bakhmutov, O. A. Reutov, M. Gruselle, C. Cordier, G. Jaouen, *J. Organomet. Chem. 364* (1989) 195–206.
[107] A. Vessieres, S. Tondu, G. Jaouen, S. Top, A. A. Ismail, G. Teutsch, M. Moguilewsky, *Inorg. Chem. 27* (1988) 1850–1852.
[108] I. Haiduc, C. Silvestru, *Coord. Chem. Rev. 99* (1990) 253–296.
[109] C. Walsh, T. Begley, A. Walts, *Pure Appl. Chem. 59* (1987) 295–298.
[110] M. J. Moore, M. D. Distefano, L. D. Zydowsky, R. T. Cummings. C. T. Walsh, *Acc. Chem. Res. 23* (1990) 301–308.
[111] T. Tesuka, K. Tonomura, *J. Biochem. 80* (1976) 79–87.
[112] T. Tesuka, K. Tonomura, *J. Bacteriol. 135* (1978) 138–143.
[113] T. Tesuka, Y. Takahashi, *Agric. Biol. Chem. 52* (1988) 3183–3185.
[114] J. B. Robinson, O. H. Tuovinen, *Microbiol. Rev. 48* (1984) 95–124.
[115] B. H. Belliveau, J. T. Trevors, *Appl. Organomet. Chem. 3* (1989) 283–294.
[116] T. P. Begley, A. E. Walts, C. T. Walsh, *Biochemistry 25* (1986) 7186–7192.
[117] T. P. Begley, A. E. Walts, C. T. Walsh, *Biochemistry 25* (1986) 7192–7200.
[118] B. S. Fox, C. T. Walsh, *J. Biol. Chem. 257* (1982) 2498–2503.
[119] B. S. Fox, C. T. Walsh, *Biochemistry 22* (1983) 4082–4088.
[120] R. G. Schultz, K. G. Au, C. T. Walsh, *Biochemistry 24* (1985) 6840–6848.
[121] M. D. Distefano, K. G. Au, C. T. Walsh, *Biochemistry 28* (1989) 1168–1183.
[122] M. J. Moore, C. T. Walsh, *Biochemistry 28* (1989) 1183–1194.
[123] M. D. Distefano, M. D. Moore, C. T. Walsh, *Biochemistry 29* (1990) 2703–2713.
[124] E. Gopinath, T. W. Kaaret, T. C. Bruice, *Proc. Natl. Acad. Sci. USA 86* (1989) 3041–3044.
[125] O. A. Reutov, I. P. Beletskaya, V. I. Sokolov: *Mechanisms of Reactions of Organometallic Compounds*, Khimia, Moscow 1972.
[126] G. M. Whitesides, J. San-Filippo, Jr., *J. Am. Chem. Soc. 92* (1970) 6611–6624.
[127] A. D. Ryabov, *Chem. Rev. 90* (1990) 403–424.
[128] A. E. Walts, C. T. Walsh, *J. Am. Chem. Soc. 110* (1988) 1950–1953.
[129] E. Gopinath, T. C. Bruice, *J. Am. Chem. Soc. 109* (1987) 7903–7905.

Lise Meitner and Fission: Fallout from the Discovery

By Ruth Lewin Sime*

Much has been written about *Lise Meitner*, but she remains on the periphery. Of her pioneering work in nuclear physics, little is said; she is remembered primarily for nuclear fission, a discovery in which she did not share. Especially in Germany the staging seldom varies: *Otto Hahn* in the spotlight, *Fritz Straßmann* in his shadow, *Lise Meitner* in the wings, dimly outlined in reflected light. Her role is open to speculation. One writer sees her work "crowned by the Nobel Prize for Otto Hahn";[1] another, once director of an institute that bears her name, portrays her as the physicist who obstructed the discovery from the start.[2] Often she is cast as *Hahn*'s *Mitarbeiterin*;[3] sometimes she is completely invisible, as in one of the world's great science museums, which for 30 years displayed[4] the fission apparatus–equipment assembled by *Lise Meitner* on a table in *her* laboratory in *her* physics section of the Kaiser-Wilhelm-Institut für Chemie—without ever mentioning her name.[**] The principals themselves do not agree. In his memoirs, *Hahn* has remarkably little to say of his closest colleague and friend. Only over a glass of wine, we are told, "konnte ihm die Äusserung entschlüpfen: 'Ich weiss nicht; ich fürchte, Lischen hätte mir die Uranspaltung verboten.'"[5] ("he might let slip: 'I don't know; I'm afraid Lischen would have forbidden me to discover fission.'") *Straßmann* insists: "Lise Meitner war die geistig Führende in unserem Team gewesen"![6] ("Lise Meitner was the intellectual leader of our team"!) From *Lise Meitner* herself we have no autobiography. Available, however, is the large collection of letters and documents she has left behind, and these make it possible for us to learn much more.

1. Introduction

The historian *Fritz Stern* has written of this century's most famous scientist, "Einstein and Germany: they illuminate each other."[7] The same can be said of *Lise Meitner*, only more so—because she was more attached to Germany, because she stayed longer and never cut her ties to it, because her best years of work and the bitter consequences of her exile could not be separated from the science, culture, and politics of her German experience.

She came to Berlin from her native Vienna in 1907. Women were still excluded from Prussian universities, yet she found a place of work and a chance to prove herself. Before long Germany was her professional home, the sanctuary that rescued her, as she believed, from a wasted life in Austria.[8] In time the milestones of her career became markers for the inclusion of women into German science; she flourished in Germany's brilliant physics community and became one the great nuclear physicists of her day.

After 1933 her very success in Germany made her cling to what she had and stay too long, and when she was driven out, finally, exile shattered her career and clouded her scientific reputation. In December 1938, five months after *Meitner* fled Berlin, *Hahn* and *Straßmann* identified barium as a product of the neutron irradiation of uranium. This was, as *Meitner* herself put it, "wirklich ein Meisterstück radioaktiver Chemie"[9] ("truly a masterpiece of radiochemistry"); it was also an intrinsic part and the direct result of a team investigation which *Meitner* brought to Berlin, led for four years, and to which she made crucial contributions until the end. There can be no doubt that had *Meitner* been anything other than a "non-Aryan" in exile, she would have fully shared in the discovery.[10] Instead, she—and physics—were eventually blamed for the failure to make the discovery sooner.

In this article I intend to show that *Lise Meitner*'s exclusion arose not from science but from the racial policies and political aberrations of National Socialist Germany, and to show further that her exclusion was unjustly perpetuated—indeed, deliberately reinforced—long after the Third Reich was over. This article is not a comprehensive review of the fission discovery: it is, instead, an alternative perspective, a focus upon *Lise Meitner* and her work. By documenting her leadership of the uranium investigation in Berlin, I wish to emphasize the importance of physics and its essential interplay with chemistry; by showing that *Meitner* remained a de facto member of the Berlin team until the discovery and beyond, I intend to make clear that political, not scientific, considerations kept her from being acknowledged. Finally, I wish to examine the aftermath of the discovery, during which *Meitner*'s exclusion was codified, physics blamed, and history distorted. For this I shall turn primarily to *Otto Hahn*, who claimed the discovery for chemistry alone, and whose singular prominence in postwar Germany ensured that his version would dominate. Fifty years have passed: there is a need for balance. With this article I seek to reintegrate *Meitner* with the discovery, physics with chemistry, science into its historical and political context.

[*] Dr. R. L. Sime
Department of Chemistry
Sacramento City College
Sacramento, CA 95822 (USA)

[**] On 4 July 1991 the Deutsches Museum placed a bust of Lise Meitner in the *Ehrensaal*, where busts, reliefs, and portraits of 38 renowned scientists, discoverers, and inventers are displayed, including Nikolaus Copernicus, Johannes Gutenberg, Carl Benz, Conrad Röntgen, Max Planck, Albert Einstein, and Otto Hahn.

2. The Beginnings of the Uranium Project

Although the discovery of fission is certainly an important chapter in the history of chemistry,[11] it was driven by fundamental questions of nuclear physics. The physicist who originated the investigation was *Enrico Fermi*; the physicist who brought it to Berlin and framed it at every step was *Lise Meitner*. Some years later, in 1944, she described the beginnings to *Max von Laue*. She was in Stockholm by then, unhappy with her working conditions; *von Laue* had suggested that her dissatisfaction was due to the absence of *Otto Hahn*:

> ... so ist Ihre strikte Erklärung, es fehle mir die Zusammenarbeit mit Otto, so irrig, dass ich, verzeihen Sie, lieber Freund, etwas lächeln musste. Otto und ich haben von 1920–1935 auf ganz getrennten Gebieten gearbeitet, er hat sich sogar nach eigenem Geständnis gar nicht für meine physikalischen Probleme interessiert und wir sind dabei sehr gute Freunde geblieben. Dass wir dann nach so langer Zeit wieder gemeinsam gearbeitet haben, lag daran, dass mich die Fermi'schen Untersuchungen brennend interessiert haben und es mir zugleich klar war, dass man mit Physik allein auf diesem Gebiet nicht weiter kommen konnte. Es musste ein so ausgezeichneter Chemiker wie Otto mithelfen, wenn es Erfolg haben sollte. Ich habe mehrere Wochen gebraucht, bis ich Otto dafür interessiert hatte, er wird es Ihnen gern bestätigen, dass es sich so verhält.[12][*]

2.1. Neutron Irradiations

The investigations which so interested *Lise Meitner* began in Rome in March 1934[13, 14] when Fermi and his co-workers sought to induce nuclear reactions and create new radioactive isotopes by irradiating elements with neutrons. Proceeding systematically through the periodic table, they succeeded first with fluorine and then aluminum;[15] two weeks later they reached lanthanum and reported nearly 20 more.[16, 17] The Italian scientists sent their results to *Ricerca Scientifica*, and mailed preprints a few days later to 40 or so of the most prominent and active nuclear physicists worldwide.[18, 19] *Lise Meitner* was thus among the first to learn of the work in Rome; by May she had verified[20] their neutron irradiations of Al, Si, P, Cu, and Zn, observing the first three in a cloud chamber and measuring the half-lives of the activities formed.

2.1.1. Lise Meitner's Background[21–26]

Expert in radioactivity and familar with neutron reactions, *Meitner* was in a perfect position to pursue these experiments. Her work in radioactivity went back to 1906 in Vienna; from 1907 in Berlin she and *Otto Hahn* identified several new radioisotopes, developed techniques of radioactive recoil, pioneered in magnetic beta spectra, and in 1918 discovered protactinium ($Z = 91$).[27] By then they were in the Kaiser-Wilhelm-Institut für Chemie in Berlin-Dahlem, each heading their own section. About 1920, when radioactivity no longer seemed to promise fundamental new insights,[28] *Meitner* turned to the infant field of nuclear physics, while *Hahn* stayed with the refinement and development of radiochemical techniques.

Always close to theory, *Meitner* explored nearly every aspect of experimental nuclear physics: the sequence of radioactive decay, the continuous beta spectrum, nuclear scattering experiments, high-energy gamma radiation. She was quick to use and adapt new instruments, among them the Wilson cloud chamber for nuclear reactions and Geiger-Müller counters for studies of gamma absorption. After the discovery of the neutron and positron in 1932, she used the cloud chamber to determine neutron mass, and she was the first to observe electron–positron pair formation. *Otto Hahn* would later remember this as a period when her work, far more than his, brought international recognition to their institute.[29] In addition to her own students and assistants, *Meitner* frequently welcomed foreign visitors to the institute. One of them was *Franco Rasetti*, an associate of *Fermi*, who spent most of the year 1932 in Dahlem learning the nuclear techniques—radioactivity, neutron sources, cloud chamber—needed for the new experimental program in Rome.[30]

[*] Your assertion that what is missing for me is the collaboration with Otto is so much in error that—forgive me, dear friend—I had to smile a little. Otto and I worked from 1920 to 1935 in completely separate fields; he in fact admitted that he was not at all interested in my physics problems and still we remained good friends. That we worked together once again after such a long time was due to the fact that Fermi's investigations were of consuming interest to me, and it was at once clear to me that one could make no progress in this field with physics alone. The help of an outstanding chemist such as Otto was needed to get results. It took me several weeks to get Otto interested; he will gladly verify for you that it went that way.

Ruth Lewin Sime was born in New York City in 1939, graduated from Barnard College in 1960, and obtained her doctorate in chemistry from Harvard University under William Lipscomb in 1964 for X-ray diffraction studies of molecular structures. Since then she has been engaged primarily in teaching chemistry; she is involved with programs designed to increase the representation of women and minority students in math-based sciences. Her interest in Lise Meitner began some 15 years ago when she taught a women's studies course on "Women in Science" and discovered, to her surprise, that little scholarly attention had been paid to Meitner's life and work. She is currently completing a scientific and personal biography of Lise Meitner.

Fig. 1. *Lise Meitner*, ca. 1937 (Source: Archives of Churchill College, Cambridge, England)

2.2. Elements beyond Uranium: "Ich fand diese Versuche so faszinierend..." ("I found these experiments so fascinating...")

As *Fermi* and his group worked their way through the periodic table, some generalizations became evident: (n, α) and (n, p) reactions were observed only for lighter elements; heavy elements favored neutron capture (n, γ); the new artificial radioactivities in every case decayed by beta emission to the next higher element. Thus, when the neutron irradiation of uranium yielded several new beta emitters, Fermi suggested "the spontaneous hypothesis that the active substance of U might have atomic number 93."[31] This appeared in *Ricerca Scientifica* in May; in *Nature* in June, *Fermi* cautiously proposed the possible formation of elements 94 and 95, although he considered it "premature to form any definite hypothesis on the chain of disintegrations involved."[32, 33] It was at this point that *Lise Meitner* spoke to *Otto Hahn*:

> Ich fand diese Versuche so faszinierend, daß ich sofort nach deren Erscheinen im Nuovo Cimento und in der Nature[34] Otto Hahn überredete, unsere... direkte Zusammenarbeit wieder aufzunehmen, um uns diesen Problemen zu widmen.[9][*]

It took several weeks, *Meitner* remembered, to get *Otto* interested.

2.2.1. Otto Hahn

Hahn remembered it differently. In his memoirs there is no mention of *Meitner*'s initiative; instead *Hahn* always traced the impetus for the Berlin investigation to *Aristide von Grosse*, a former student who had embroiled *Hahn* in an unpleasant public dispute over the discovery and properties of protactinium:[35]

> Nach dem Erscheinen dieser Arbeiten durch Fermi etc. kam eine Arbeit von v. Grosse und Agruss, nach der es durchaus nicht sicher sei, daß die Fermischen Körper El. 93 oder ähnliches seien, sondern es sei durchaus mit dem El. 91: Ekatantal [Protactinium] zu rechnen. Nach diesen Arbeiten beschlossen L. Meitner und ich, die Fermischen Arbeiten zu wiederholen und die Grossesche Annahme zu prüfen.[*]

Hahn wrote this in 1945[36] and used almost the same words in 1946, 1950, 1959, 1962, and 1968,[37-41] among others. But the note by *von Grosse* and *Agruss* did not appear in *Physical Review*[42] until 1 August 1934, and it would not have arrived in Germany before the end of August, many weeks after *Lise Meitner* first approached *Otto Hahn*.[43] *Hahn*'s repeated failure to credit *Meitner* for initiating their collaboration cannot be attributed entirely to memory lapse, because a published record exists: in their first joint uranium publication[44] *Hahn* and *Meitner* clearly state: "Wir haben im Laufe einiger anderer Versuche—here they cite two earlier neutron studies[20, 46] done by *Meitner* on her own—"jetzt eine eingehende Untersuchung dieser Uranprozesse in Angriff genommen..." ("In the course of several other experiments we have now undertaken a thorough investigation of these uranium processes...")

2.3. Formation of the Berlin Team

In August 1934 the institute was closed for vacation; in September *Meitner* and *Hahn* traveled to Leningrad for the centenary of *Mendeleev*'s birth. Although *Fermi*'s experiments were very much on *Meitner*'s mind,[46] they could not begin work in earnest until their return.

In a comparison of neutron sources, *Meitner* found[45] that fast neutrons are required for the (n, α) and (n, p) reactions typical of light elements, while slower neutrons are more readily captured by heavy elements. This mirrored the discovery[47] by *Fermi* and his group a few weeks later that neutrons slowed by hydrogenous materials enhance the efficacy of neutron-capture reactions.

For their first joint work[44] *Meitner* and *Hahn* verified four beta activities found in Rome. Two had half-lives of 10 s and 40 s, too short for chemical identification, but two others, with half-lives of 13 min and 90 min, could be distinguished chemically from every element from Hg to U. Assisted by *Fritz Straßmann*, a young analytical chemist in the institute, *Hahn* and *Meitner* developed an improved procedure for coprecipitating these with platinum and rhenium sulfides, took special pains to prove that none of the activities were isotopes of protactinium, and concluded, as *Fermi*

[*] I found these experiments so fascinating that, as soon as they appeared in Nuovo Cimento and Nature, I talked to Otto Hahn about resuming our direct collaboration once again... in order to resolve these problems.

[*] After the appearance of the articles by Fermi, etc. came an article by v. Grosse and Agruss, according to which it was not at all certain that the Fermi activities were element 93 or so, but that it most likely was element 91: Ekatantal [Protactinium]. After these articles L. Meitner and I resolved to repeat the Fermi experiments and test Grosse's assumptions.

had, that the 13-min and 90-min activities might well be elements 93 and 94.

Meitner and *Hahn* soon realized that the 13-min and 90-min activities were themselves mixtures[48] and in mid-1935 asked *Straßmann* to join them full-time. Their team was bound by political affinity as well: *Meitner*, "non-Aryan"; *Hahn*, anti-Nazi; *Straßmann*, the exceptionally principled younger man whose aversion to National Socialism and refusal to join the NS-associated *Verein Deutscher Chemiker* isolated him within the institute and made him unemployable outside.[49]

3. "Wege und Irrwege"—Roads and Mistaken Roads

Later, *Lise Meitner* would describe the road to the discovery of fission as "astonishingly long and in part a mistaken road" ("erstaunlich lang und zum Teil ein Irrweg".[9] *Fermi*, *Meitner*, indeed all who worked on the uranium investigation were misled by two false premises, one from physics—that only small changes would occur in nuclear processes—and the other from chemistry—that elements beyond uranium would be higher homologues of the third-row transition elements Re, Os, Ir, Pt, etc. When neutron irradiation of uranium yielded new beta activities which coprecipitated with platinum and rhenium sulfides, the two assumptions unluckily dovetailed—and even after the discovery of fission proved the first one wrong, scientists still did not suspect that the second was wrong as well.[50]

However mistaken, these false premises do not entirely account for the failure to explore alternatives. *Ida Noddack*'s suggestion[51] of a major nuclear breakup was never seriously considered;[52] *Noddack* herself did not pursue it; *Max Delbrück*, *Meitner*'s *Haustheoretiker* for a time, remembered with chagrin how he helped in the "Holzweg der zahllosen 'Transuran'-Isomere" (the "bog of countless 'transurane' isomers") instead of finding a way out.[53]

There was something dazzling about elements beyond uranium.[54] That, coupled with the great difficulty of identifying weak new activities in the presence of the strong natural radioactivity of uranium, led the Berlin team to investigate only the platinum sulfide precipitate, which, they presumed, contained the "transuranes". For the most part they ignored the filtrate, assuming it contained nothing more than uranium and its natural decay products. This was a mistake, *Meitner* remembered:

> Unsere Fällungen bei Bestrahlung mit schnellen Neutronen wurden immer so ausgeführt, daß U, Pa und Th im Filtrat bleiben mußten, wodurch wir meinten eine gewisse Stütze für die Transurannatur der gefällten Elemente zu gewinnen. Darum haben wir – und das war unser Irrtum – zunächst niemals, auch nicht bei den Versuchen mit verlangsamten Neutronen, die Filtrate unserer Fällungen untersucht.[91][*]

[*] During irradiation with fast neutrons our precipitations were always conducted so as to keep U, Pa and Th in the filtrate, from which we drew a certain support for the transurane nature of the precipitated elements. Thus we—and this was our mistake—for a time never examined the filtrate, not even in the experiments with slowed neutrons.

The oversight was remarkable, because the Berlin group did discover that an important activity, a 23-min U, was produced only when slowed neutrons were used.[55]

> Also ich glaube wirklich unser Unglück war, dass wir die Filtrate nicht untersuchten. Wir konnten sich nicht untersuchen, weil wir das Uran drin gehabt haben, nicht wahr, da konnten wir nichts sehen. Wir hatten zu schwache Bestrahlungsquellen... [D]ie Chemiker wollten absolut nicht, ich habe sie geplagt, sie sollen es machen wie ich dort war, weil ich so unruhig war. Gerade weil ich zu wenig von Chemie verstehe, war ich natürlich immer unruhig über das was nicht gemacht worden ist, aber dann haben es ja Hahn und Strassmann so wunderbar gemacht, also zu der Zeit hat es wirklich keine Chemiker gegeben, die das hätten machen können.[56][*]

Later *Hahn* and his associates would claim the discovery for chemistry alone, blaming the "Irrwege" solely upon physics and its assumption of small nuclear changes. This was not done in a spirit of scientific objectivity—it ignored the mistakes of chemistry and the guidance of physics. Physics did not predict fission, to be sure, but it detected errors chemistry could not; without physics, chemists would not have begun the investigation; without physics they would have had no reason to sustain it.

3.1. Chemistry: Certainty

The scientific literature of the period[57] makes clear that the investigation was fed by chemical data but interpreted by nuclear physics. The dual roles are particularly evident in parallel reports by *Hahn*, the senior author for chemistry, and by *Meitner* for physics. In 1936 and 1937, the Berlin chemists listed three U activities and two parallel "transurane" sequences including two EkaRe (the presumed element 93), two EkaOs (94), one EkaIr (95), and one EkaPt (96), all beta emitters. Of the uranium activities, just one, 23-min U, was chemically certain; the 10-s and 40-s activities, too short-lived for chemical identification, were attributed to U because genetic sequences obtained from radioactivity data indicated they preceded the two EkaRe. Altogether, the fit between the chemistry expected for transuranium elements and the genetic sequences seemed too good not to be true. In 1936: "[D]ie Zuordnung des 2.2-Min- und des 16-Min-Körpers zum Eka-Rhenium ist frei von Willkür; sowohl die genetischen Beziehungen als auch die chemischen Eigenschaften lassen wohl keinen Zweifel über ihre Zugehörigkeit zum Element 93."[58] ("The assignment of the 2.2-min and 16-min activities of EkaRe is unquestionable; not only the genetic relationships but also the chemical properties really leave no doubt they belong to element 93.") And for EkaOs, EkaIr, and EkaPt, "sind wir nach ihrem allge-

[*] I really think our misfortune was that we didn't search the filtrate. We couldn't search it because uranium was in it, we couldn't see anything. Our neutron sources were too weak... The chemists absolutely didn't want to, I begged them to do it while I was there because I was so disturbed by it. Because I understood too little chemistry I was naturally always worried about what wasn't done, but then Hahn and Straßmann did such a wonderful job; surely at the time no other chemists could have done it.

meinen chemischen Verhalten sicher bezüglich ihrer Gruppen-Zugehörigkeit" ("we are certain from their general chemical properties to which group they belong").[58] In 1937: "Vor allem steht ihre chemische Verschiedenheit von allen bisher bekannten Elementen ausserhalb jeder Diskussion."[59] ("Above all, their chemical distinction from all previously known elements needs no further discussion.")

3.2. Physics: Doubt

As the chemists grew more confident with each new link in the chain of transuranes, the physical interpretation was buckling under a profusion of data. It was *Meitner*'s task to integrate chemistry, radiochemistry, and her own physical experiments into nuclear reactions that made sense. Her recognition that this could not be done sustained the investigation.

To account for three uranium activities, *Meitner* first proposed[60] three different neutron–uranium reactions, but after an exhaustive series of physical experiments she concluded that all three reaction mechanisms appeared the same. She correctly identified the 23-min U as U-239,[61] formed by a typical resonance capture of fairly slow neutrons by U-238. But the 10-s and 40-s U, which headed the two parallel series of "transuranes", also appeared to be U-239: both series varied identically with neutron energy, were produced by fast neutrons and enhanced by thermal neutrons. Together the results were incomprehensible: the triple isomerism of U-239 was problematic, *inherited* triple isomerism persisting for several generations virtually impossible. In 1937 she concluded: "Dieses Ergebnis ist mit den Kernvorstellungen sehr schwer in Übereinstimmung zu bringen."[55] ("This result is very difficult to reconcile with current ideas of nuclear structure.") And in 1938, after thorium showed similar multiple isomerism: "Dieser Erklärungsversuch stößt auf erhebliche Schwierigkeiten..."[62] ("This attempt at an explanation runs into considerable difficulty...") In addition, *Meitner* was always particularly disturbed by the long chain of beta decays EkaRe, EkaOs, EkaIr, EkaPt, and beyond: capture of just one neutron by U-238 should not have produced instability so great that five or more beta decays were required to relieve it:

> [I]ch war immer unglücklich darüber weil ich nicht verstehen konnte, 'wie kann eigentlich die Kernladung steigen bei derselben Masse?' Das war immer, was ich [C. F. von] Weizsäcker gefragt habe: Wie ist das möglich? Also ich war nie glücklich über unsere Versuche vor der fission.[63][*]

In Paris, meanwhile, *Irène Curie* and *Paul Savitch* had examined the entire uranium mixture without chemical separation and reported a strong new 3.5-h beta emitter with unexplained chemical properties.[64] In Berlin they ascribed it to contamination and named it "Curiosum".[65]

[*] I was always unhappy about it because I couldn't understand 'How can the nuclear charge increase [so much] with the same mass?' That's what I always asked Weizsäcker: How can that be? You see, I was never satisfied with our experiments before fission.

4. Escape from Germany

In 1938 came the *Anschluß* and then whispers: "Die Jüdin gefährdet das Institut".[66] ("The Jewess endangers the Institute.") *Hahn* grew nervous, mindful that Prof. *Kurt Heß*, a "fanatic Nazi" ("fanatischer Nationalsozialist")[67] who worked in the *Gastabteilung* (guest section) upstairs in the Kaiser-Wilhelm-Institut für Chemie, was eager for his position. Her dismissal imminent, *Meitner* learned that technical and academic people would be forbidden to leave Germany; she fled secretly on 13 July 1938. Dutch friends, physicists *Dirk Coster* and *Adriaan Fokker*, got her into Holland; *Niels Bohr* and Swedish friends arranged a place for her in *Manne Siegbahn*'s Nobel Institute for Experimental Physics in Stockholm.[68]

4.1. "Radium" Isomers

Meitner and *Hahn* had worked under the same roof for 31 years; their separation was a shock to them both. Intellectually, however, she was not immediately cut off from Berlin. *Meitner* and *Hahn* wrote to each other[69, 70] constantly; she was still very much a member of the team.

On 23 October *Meitner* was inquiring[71] about the Curie–Savitch 3.5-h substance just as a new report[72] by the Paris scientists reached Berlin. Suspecting that the 3.5-h substance might contain radium, *Straßmann* proposed his own cleaner method of separation.[73] "Vielleicht hat sogar ein Ra-Isotop was dabei zu tun" ("Perhaps a Ra isotope has something to do with it"), *Hahn* wrote *Meitner* on 25 October,[74] and a week later;

> Wir sind jetzt *fast* überzeugt, daß es sich um einige – 2 oder 3 – Radiumisotope handelt, die sich in Ac etc. umwandeln... Es wäre uns natürlich sehr lieb, Du würdest Dir den Fall einmal überlegen, wie eine α-Strahlenumwandlung [U(n, α) → Th → Ra] mit wahrscheinlich auch langsamen Neutronen zu Stande kommen kann, und dabei gleich auch wieder mehrere Isomere...[75][*] (text highlighted in the original is here printed in italics)

Meitner responded instantly:

> Ich will mir brennend gern überlegen, wie Ra od[er] Ac Isotope entstehen können, wenn Du mir nur tatsächlicher schreiben wolltest... Warum glaubt Ihr daß mehrere Körper da sind, habt Ihre mehrere Halbwertszeiten? Warum glaubt Ihr daß es verstärkbar ist? Habt Ihr mit langsamen Neutronen erheblich mehr bekommen? Und wie stark ist denn die Aktivität... verglichen mit dem 16 Min K[örper (Eka-Re)]?... Bitte sei lieb und beantworte alle Fragen. Auch wenn es noch nicht so definitiv ist...[76][**]

[*] We are now *almost* convinced that we are dealing with several—2 or 3—radium isotopes which decay to actinium, etc... Naturally, we would like it very much if you could think about the situation, how an α-transformation [U(n,α) → Th → Ra] can come about, probably also with slow neutrons, and at the same time produce several isomers...

[**] I am extremely eager to think over how Ra or Ac isotopes could be produced, if you would only write more factual details. Why do you think it is several substances, do you have several half-lives? Why do you think it can be enhanced? Did you get considerably more with slow neutrons? How strong is the activity... compared to the 16-min [EkaRe]?... Please be nice and answer all these questions. Even if it's not yet so definite...

The reaction conditions, *Otto Hahn* replied,[77] were essentially the same as for the transuranes. In *Naturwissenschaften* he and *Straßmann* listed three Ra and three Ac isomers and emphasized, "Hier liegt also wohl zum ersten Male der Fall einer *α-Strahlenabspaltung mit verlangsamten Neutronen vor*"[78] ("Here surely for the first time is a case of *α-particles being split off by slow neutrons.*")

4.2. Meeting in Copenhagen

A week later *Lise Meitner* and *Otto Hahn* met in Copenhagen, both invited to *Bohr*'s Institute for Theoretical Physics. There, face-to-face, *Meitner* could make clear to *Hahn* that something was terribly wrong with the new Ra-Ac isomers: an (n, α) reaction induced by slow neutrons was truly impossible.

Their meeting took place three days after the *Kristallnacht*; it was a secret outside Copenhagen. And years later in his memoirs, *Hahn* never mentioned it, although he did recall *Bohr* being "skeptical" and "quite unhappy"[79, 80] ("ziemlich unglücklich") about the radium isomers, and he even remembered talking to *Meitner*'s nephew *Otto Robert Frisch*.[65] But we know from the guest book in *Bohr*'s institute that *Lise Meitner* was there from November 10 to 17,[81] and we know from *Hahn*'s own pocket calendar[82, 83] that she met his train at 6:48 on the morning of November 13, that they had breakfast together and talked for hours, that the next day, after breakfast with *Niels* and *Margrethe Bohr*, *Lise Meitner* and her nephew took *Hahn* to the station and saw him off on the 11:13 train to Berlin. There is also no doubt that *Lise Meitner* forcefully urged *Otto Hahn* to examine the radium isomers more thoroughly than before: this was the message *Hahn* brought back to Berlin. *Straßmann* remembered clearly:

> Jedenfalls hat sie (laut einer Äußerung von O. Hahn) dringend darum gebeten, diese Experimente noch einmal sehr sorgfältig und intensiv zu überprüfen... Zum Glück hatte L. Meitners Ansicht und Urteil bei uns in Berlin ein so großes Gewicht, daß die erforderlichen Kontrollversuche sofort unternommen wurden.[84][*]

4.3. *Barium: "Eine Art Arbeit zu Dreien"*

A few days later *Hahn* and *Straßmann* began the fractional crystallization experiments which led directly to the discovery of barium.[85, 86] From their own statements, we know they still regarded *Meitner* as a member of their team. *Straßmann* wrote later:

> Was bedeutet es, daß Lise Meitner nicht *direkt* teilhatte an der 'Entdeckung'?? Ihrem Impulse ist der Beginn des gemeinsamen Weges mit Hahn, ab 1934, zuzuschreiben – *4 Jahre danach gehörte sie zu unserem Team* –, anschließend war sie von Schweden aus gedanklich mit uns verbunden... Hahn hatte gründliche radiochemische, nur übliche analytische Kenntnisse—bei mir war es umgekehrt, und die Analytik gab den Ausschlag! Aber es ist meine Überzeugung: Lise Meitner war die geistig Führende in unserem Team gewesen, und darum gehörte sie zu uns – auch wenn sie bei der "Entdeckung der Kernspaltung" nicht gegenwärtig war.[6][*]

At the time *Hahn* felt the same. He informed *Meitner* about barium on December 19, without speaking to any of the institute physicists:[87] "Ich habe mit Straßmann verabredet, dass wir vorerst nur Dir dies sagen wollen." ("Strassmann and I have agreed that for now we shall tell only you.") The barium finding was a "schreckliche[r] Schluß" ("frightful conclusion"); he pleaded for interpretation:

> Vielleicht kannst du irgend eine phantastische Erklärung vorschlagen... Falls Du irgendetwas vorschlagen könntest, das Du publizieren könntest, dann wäre es doch noch eine Art Arbeit zu Dreien![88][**]

Anxious to publish quickly, *Hahn* did not wait for *Meitner*'s reply before submitting the article to *Naturwissenschaften* on 22 December. He[89] mentioned the barium results only at the end, after pages of radium data, and then "with hesitation" ("zögernd"). His report expresses the chemistry-physics duality that had characterized the entire investigation. From the chemistry he drew confidence—"Als Chemiker müßten wir... statt Ra, Ac, Th die Symbole Ba, La, Ce einsetzen"[***]—and from physics, doubt: "Als der Physik in gewisser Weise nahestehende 'Kernchemiker' können wir uns zu diesem, allen bisherigen Erfahrungen der Kernphysik widersprechenden, Sprung noch nicht entschließen..."[90][***] To *Lise Meitner* he wrote:[88] "Wir wissen dabei selbst, dass es eigentlich nicht in Ba zerplatzen *kann*!... Also überleg Dir noch, ob sich nicht irgendeine Möglichkeit ausdenken liesse; so etwa Ba-Isotope mit viel höheren A.G. [Atomgewicht] als 137?"[****] *Hahn* had not yet realized that uranium had split in two.[91]

Lise Meitner received *Hahn*'s letter on December 21, her first news of the barium finding. She answered by return mail:

> Mir scheint vorläufig die Annahme eines so weitgehenden Zerplatzens sehr schwierig, aber wir haben in der

[*] In any case (according to what O. Hahn said) she urgently requested that these experiments be very carefully and intensively scrutinized one more time... Fortunately, L. Meitner's opinion and judgement carried such weight with us in Berlin that we immediately undertook the necessary control experiments.

[*] What did it matter that Lise Meitner did not *directly* participate in the "discovery"?? Her impulse was the beginning of the work with Hahn from 1934, *4 years later she belonged to our team*; in addition she was in close contact with us from Sweden... Hahn was thoroughly versed in radiochemistry, only the usual analytical knowledge—with me it was the reverse, and analytical chemistry achieved the result! But I am convinced, L. Meitner was the intellectual leader of our team, therefore she was one of us, even if she was not actually present for the "discovery of fission".

[**] If there is anything you could propose which you could publish, then after all it would still in a way be work by the three of us!

[***] As chemists we should substitute the symbols Ba, La, Ce for Ra, Ac, Th... As "nuclear chemists" fairly close to physics we can not yet resolve to take this step which goes against all previous experience in nuclear physics.

[****] We ourselves know that it cannot really break apart to Ba!... You should reconsider whether there isn't some other possibility; for example, Ba isotopes with much higher atomic weights than 137?

Kernphysik so viele Überraschungen erlebt, dass man auf nichts ohne weiteres sagen kann: es ist unmöglich.[92][*]

Hahn must have been surprised and relieved. In November *Meitner* had vehemently objected to the radium isomers; now she was puzzled but not opposed, intuitively ready to consider the barium result an expansion rather than a contradiction of previous experience in nuclear physics.

Years later, *Hahn* was known to say that had *Lise Meitner* remained in Berlin, she might have talked him out of the discovery, might have "forbidden" him to make it.[93] Clearly, *Meitner*'s letter of 21 December says just the opposite—and at the time *Hahn* must have found it most reassuring, because only after he received it on 23 December did he add to the *Naturwissenschaften* galley proofs a paragraph suggesting that the uranium nucleus has split in two.[94] This strengthened the article, showing that *Hahn* and *Straßmann* had not just identified barium, but understood that fission had taken place. Meanwhile, during their holiday together between Christmas and New Year's Day, *Meitner* and her nephew *Otto Robert Frisch* did propose and prepared to publish the first theoretical interpretation of the fission process.[95]

Meitner's contributions to the discovery thus formed a continuum from the first work in Berlin to the discovery of barium and beyond. At the end only her physical presence was missing. *Meitner* and *Hahn*'s own experience shows that physical presence is not required at all times for every member of a team: in 1917 and 1918 when *Hahn* was in the army, *Meitner* did nearly all the work, and both, without question, were credited with the discovery of protactinium.[27, 96] In 1938 *Lise Meitner* was excluded only because the same racial policies that had driven her from Germany made it impossible for her to be part of the barium publication, made it uncomfortable, as we shall see, for *Hahn* to even admit his ongoing collaboration with a "non-Aryan" in exile.

4.4. Transmutation: "Wir haben die Physik absolut nicht berührt..."

Meitner knew nothing could be done;[97] congratulating *Hahn* and *Straßmann* for their "beautiful finding" ("wunderschönes Ergebnis") she could not help but add; "I stand here with very empty hands." ("wenn ich jetzt auch mit sehr leeren Händen dastehe."[98]) It was worse, for while her name was missing from the discovery of barium, it was still firmly associated with the false "transuranes", which *Meitner* now understood to be fission fragments, not elements beyond uranium at all.

The timing was bad: *Meitner* was struggling to make a new start in Stockholm. She feared for her reputation, worried that people might say: "[D]ie Drei haben also Unsinn gemacht, und jetzt nach dem Weggang des einen haben die zwei andern das in Ordnung gebracht."[99] ("The three must have done nonsense, and now that one is gone the other two made it right.") She hoped[100] *Hahn* would say in his next paper that the discovery of barium was based upon techniques and results they had developed together. She could not imagine that *Hahn* himself would soon suppress and deny not only her ongoing collaboration, but the value of nearly everything she had done before.

On 16 January 1939 *Meitner* and *Frisch* sent their theoretical explanation of the fission process to *Nature*.[101] They described the nucleus as a classical liquid drop, its surface tension diminishing under increasing charge, dividing in two, converting mass into 200-MeV energy, forming neutron-heavy fission fragments whose long chain of beta decays finally made sense. It was a good piece of work, *Meitner* knew. Although it could not compensate for being excluded from the discovery itself, it tied her to it, permitted her to be the first to lay inherited isomerism and the "transuranes" to rest, and allowed her to salvage one earlier result: the 23-minute U-239 was still valid and the precursor of the first true element 93.

Meanwhile in Berlin the barium report appeared in *Naturwissenschaften* on 6 January 1939—and physicists in the institute were most upset that they had not been told before. *Hahn* was vulnerable, surrounded by Party members of all degrees of enthusiasm and opportunism, worried about the ambitious and dangerous Prof. *Heß* in the *Gastabteilung* upstairs.[102] When he wrote the next Hahn–Straßmann paper[103] at the end of January, *Hahn* gave only the briefest mention to *Meitner*'s earlier contributions and barely acknowledged the theoretical interpretation of *Meitner* and *Frisch*.[104]

Meitner reacted with despair. To her brother she wrote:

> Hahn hat jetzt in Fortsetzung unserer letzten gemeinsamen Arbeiten ganz wunderbare Dinge gefunden... Und so sehr mich diese Resultate wissenschaftlich und persönlich für Hahn freuen – so denken hier jetzt manche Menschen, dass ich überhaupt nichts gemacht habe.[105][*]

In Stockholm, she wrote to *Hahn*, she had a room in *Siegbahn*'s institute but no equipment, no help, no rights; she had ideas for experiments but could not do them, and she did not get along with *Manne Siegbahn*:

> Jetzt wird Siegbahn allmählich glauben – besonders nach Euern so schönen Ergebnissen, dass ich überhaupt nichts gemacht habe und Du auch die ganze Physik in Dahlem gemacht hast. Ich verliere allmählich allen Mut. Verzeih diesen unfrohen Brief. Ich weiss manchmal nicht mehr, was ich mit meinen Leben anfangen soll. Wahrscheinlich geht es vielen, die weggegangen sind, so wie mir, aber darum ist es doch sehr schwer.[106][**]

[*] To me at the moment the assumption of such a large-scale breakup appears very difficult, but we have experienced so many surprises in nuclear physics that one can not unconditionally say: it is impossible.

[*] Hahn has just published absolutely wonderful things based on our work together... And much as this makes me happy for Hahn, personally and scientifically, many people here must think I contributed nothing to it.

[**] Now Siegbahn will gradually believe, especially after your beautiful results, that I never did anything and you also did all the physics in Dahlem. I am gradually losing all my courage. Forgive this unhappy letter. Sometimes I don't know what to do with my life. Most probably there are many who emigrated who feel as I do, but still it is very hard.

Hahn responded with a list of physicists and their complaints:

> Ich fürchte, es wird mir auch etwas übel genommen, daß wir strikte nichts über unsere Versuche erzählten... [Ich] möchte den Herren [Physikern im Institut] aber doch nicht beichten, daß Du der Einzige warst, der sofort alles erfahren hat... Wie Du glauben kannst, Siegbahn denkt, Straßmann und ich machten auch die Physik, verstehe ich nicht. Wir haben bei der ganzen Arbeiterei die Physik absolut nicht berührt, sondern immer und immer wieder nur chemische Trennungen gemacht. Wir kennen doch unsere Grenzen und wissen natürlich auch, daß in diesem besonderen Falle es zweckmäßig war, nur Chemie zu machen... [D]ie Arbeit über das Uran [ist mir] ein vom Himmel gesandtes Geschenk. Ich fürchte nämlich manchmal, daß Dr. K.[107] dem Herrn... allmählich Teile des Instituts geben will...[108][*]

In this letter *Hahn* reveals the fear that drove him, in just two months, to transmute "eine Art Arbeit zu Dreien" into a work that "absolutely did not touch upon physics". By redefining the discovery to be just those chemical separations he and *Straßmann* had done in December, he divorced fission from physics—and himself from *Lise Meitner*.

5. Priorities

Hahn never retreated from this view. Throughout the spring of 1939 he was in a state of constant anxiety, fearful of losing priority for his "heaven-sent gift". As physicists worldwide rushed into print, they occasionally failed to cite *Hahn* and *Straßmann* fully. *Hahn* was defensive and irritable: he quarrelled with *Meitner*, with *Bohr*, with English colleagues; when *Lise Meitner* suggested he might have been more generous to *Curie* and *Savitch* he was annoyed;[109] when *Ida Noddack* chastised him for failing to mention her 1934 paper, he refused to answer.[110] As a non-Nazi he was feeling isolated in Germany; as a German, estranged from scientists abroad. Even as a chemist he felt left out. Having convinced himself the discovery owed nothing to physics, he was irritated to see the development of fission so throughly dominated by physicists, the more so because he had trouble understanding what they were doing. He never developed a close relationship with physicists in his institute; it was *Lise Meitner* who patiently explained things to him.[111] Finally, by the summer of 1939, his institute seemed secure, his position safe: "Die 'Uranspaltung' hat da die ganze Situation gerettet."[66] ("Fission saved the entire situation.")

[*] I fear it is held against me that we said nothing to anyone about our findings... I do not want to confess to these gentlemen that you were the only one who learned of everything immediately... I don't understand how you can believe that Siegbahn thinks Straßmann and I also did physics. In all our work we absolutely did not touch upon physics, but instead we did chemical separations over and over again. We know our limits and also know of course that in this case it was useful to do only chemistry... [For me] the uranium work [fission] is a heaven-sent gift. Namely, I was fearful sometimes that... Dr. K. wants gradually to turn over parts of the institute to Herr...

6. The Bomb

During the war *Lise Meitner* and *Otto Hahn* corresponded cautiously, avoiding politics, the war, fission. In Sweden *Meitner* felt forever homeless,[112] unwelcome in *Siegbahn*'s institute, isolated from nuclear physics. To her distress she saw herself become a nonperson in Germany, her work either ignored entirely[113] or cited using an "Auswahlprinzip bei Zitieren"[114] ("selection principle for citation")—that is, with her name omitted. She tried not to dwell on her troubles; much as she wished for the defeat of Germany, she agonized over the war casualties on both sides.[115] In 1943 she was asked to join the British scientists bound for Los Alamos. It would have meant escape from Sweden, interesting physics, valued colleagues. But she could not do it: "I will not work on a bomb!"[116] She knew very little of the corresponding German effort, only that it existed, that *Werner Heisenberg* was in charge and *Hahn* involved—enough to be anxious whenever reports came in of powerful new German weapons.[117]

When the war in Europe ended without an atomic bomb, she was greatly relieved; the news of Hiroshima came as an enormous shock.[118] For weeks the press swarmed around her, made up interviews when she refused to talk to them, got the facts wrong when she did.

Otto Hahn meanwhile was interned in Farm Hall, a country estate near Cambridge, England. He, too, was shocked by the bomb, then upset that the scientist of the day was not he, but *Lise Meitner*. In his memoirs, he noted: "Zum Teil unwahre Angaben über die Entdeckung; besonders am Anfang spielt Lise Meitner dabei eine große Rolle, ich selbst werde nicht genannt."[119] ("Partly untrue articles about the discovery; especially in the beginning Lise Meitner played a large role. I myself was not mentioned.") On 8 August 1945, two days after President *Truman*'s announcement of the first bomb, *Hahn* prepared a press release:

> So lange Prof. Meitner in Deutschland war, war von einer Spaltung des Urans keinerlei Rede. Sie wurde für unmöglich gehalten. Auf Grund von ausführlichen, chem. Untersuchungen über die bei der Bestrahlung des Urans mit Neutronen auftretenden chemischen Elemente wurden Ende des Jahres 1938 Hahn und Strassmann zu der Annahme gezwungen, dass bei diesen Vorgängen das Uran in zwei Teile zerplatzt, von denen ein Teil, das chem. Element Barium, sicher nachgewiesen wurde... Mit ihrem Neffen, Dr. O. R. Frisch gab [Prof. Meitner] eine Erklärung für diese von Hahn und Strassmann experimentell gefundene, bisher für unmöglich gehaltene "Atomspaltung".[120][*]

This was the summer of 1945; it could have been a new beginning, a time to set the record straight, to recall *Meitner*'s part in the Berlin team and the discovery of fission.

[*] ... As long as Prof. Meitner was in Germany, there was no discussion of the fission of uranium. It was considered impossible. Based on extensive chemical investigations of the chemical elements resulting from neutron irradiation, Hahn and Strassmann were forced to assume at the end of 1938 that uranium splits into two parts... of which one part, the element barium, was identified with certainty... With her nephew, Dr. O. R. Frisch, [Prof. Meitner] explained these experimental findings of Hahn and Strassmann, the 'atom-splitting' which until then had been considered impossible...

Instead, *Hahn* was taking care to create the impression that *Meitner* had done nothing for fission except "consider it impossible" and prevent it from being discoverd earlier.

7. Suppressing the Past

Hahn was calling upon fission to serve again—not himself this time, but his defeated country. He had already been awarded the 1944 Chemistry Nobel Prize—in secret, but he knew. He would use his personal prestige and the importance of the discovery to call attention to Germany's misery, to rebuild German science. To do this, he felt it necessary to make the discovery his, and his alone. He saw no purpose in looking back to the injustices of the Nazi period; he felt no personal necessity to make amends. With the Third Reich gone, the old nationalism resurged. *Hahn* was concerned for Germany—and only Germany.

Meitner had sensed this attitude even before the end of the war. In March 1945 she wrote to a Swedish friend:

> Die Briefe der deutschen Freunde klingen sehr gedrückt und doch glaube ich nicht, dass sie ganz erfasst haben, welchem Schicksal sie Deutschland durch ihre Passivität ausgeliefert haben. Und noch weniger scheinen sie sich bewusst, dass sie ein Stück Mitverantwortung haben für die schrecklichen Verbrechen, die Deutschland begangen hat. Dieser Gedanke macht mich richtig unglücklich. Wie soll die Welt Vertrauen zu einem neuen Deutschland haben, wenn seine besten und geistig höchst stehenden Vertreter nicht diese Einsicht haben und nicht den brennenden Wunsch haben, gut zu machen, was gut zu machen ist. Sie müssten das nicht nur stark fühlen, sondern sich zur gegebenen Zeit offen dazu bekennen. Aber ich fürchte, davon sind sie noch sehr weit entfernt. Darum glaube ich auch nicht an einen Widerstand "en masse" von innen heraus.[121][*]

Otto Hahn was released from Farm Hall in January 1946 and returned to a Germany that was hungry, cold, utterly destitute. His letters to *Lise Meitner* were a litany of hardships. *Meitner* sympathized, she sent packages—more than she could afford—but she could not stand *Hahn*'s nationalistic self-absorption. When *Otto Hahn* complained about food shortages, demeaning travel restrictions, and requisitioned apartments, *Lise Meitner* responded sharply that Germany had inflicted suffering and death upon millions;[122] when he wrote," [O]b das Verhalten der Besatzungsmächte heute so sehr großzügiger ist als das der Deutschen in Teilen der besetzten Länder, möchte ich fast bezweifeln"[123] ("I almost doubt that the behavior of the current occupation forces is so much nobler than that of the Germans in the occupied countries"), *Meitner* was aghast and reminded him of the millions murdered by Germans in occupied Poland.[124] They fought continuously until December 1946, when *Otto Hahn* and his wife *Edith* came to Stockholm for his Nobel Prize. *Meitner* expected their visit to be an "Eiertanz"[125]—like walking on eggs—but she was determined to be friendly.

Hahn came to Stockholm not only to claim his Prize, but to plead for Germany.[126] *Lise Meitner* was prepared for that, but she did not fully realize until then that she no longer had a place in *Hahn*'s life, or even his memory. In his many press interviews, he never spoke of their work together; not once did he even mention her name. In his Nobel lecture[37] he could not omit her entirely, but he gave no sense of their teamwork and emphasized instead that the discovery had been made in opposition to the experience of nuclear physics.

After the *Hahns* left, *Lise Meitner* tried to sort things out in letters to friends:

> Dass [Hahn] mit keinen Wort mich in seinen Inverviews erwähnt hat, geschweige von unserer mehr als 30jährigen Zusammenarbeit etwas gesagt hat, fand ich etwas schmerzhaft. Was ihn dazu veranlasst haben mag, ist komplizierter Natur. Er ist überzeugt, dass den Deutschen Unrecht geschieht und das umso mehr als er die Vergangenheit einfach verdrängt. Daher war sein einziger Gedanke hier für Deutschland zu sprechen. Ich bin ein Teil der zu verdrängenden Vergangenheit und das umso mehr als ich bevor er hierher kam... versuchte, ihn darauf aufmerksam zu machen, dass die anständigen Deutschen Deutschland nur helfen können, wenn sie die Geschehnisse objectiv sehen...[127][*]

> In seinem... Interview, sagte er... er sei glücklich, dass sich Deutschland nicht mit der Schuld der Konstruktion einer Atombombe und dem sinnlosen Töten von so vielen tausend Menschen belastet hätte. Ich versuchte ihm klar zu machen, dass er das wohl hätte sagen dürfen, wenn er dazu gefügt hätte, er sei darum darüber froh, weil die Deutschen ja so viel Schreckliches getan hätten. Aber darauf ging er wieder nicht ein... [E]r verdrängt die Vergangenheit mit aller Macht, obwohl er die Nazi wirklich immer gehasst und verachtet hat. Aber da sein zweites Hauptmotiv ist, Deutschland wieder zu internationalem Ansehen zu bringen und er weder ein starker Charakter, noch ein sehr nachdenklicher Mensch ist, leugnet er einfach das Geschehene oder bagatellisiert es...[128][**]

[*] The letters from German friends sound very depressed, yet I don't think they comprehend just what fate has befallen Germany through their passivity. And they understand even less that they bear some responsibility for the horrible crimes Germany has committed. These thoughts make me terribly unhappy. How shall the world trust a new Germany when its best and intellectually most prominent people do not have the insight to understand this and do not have a burning desire to make whatever amends are possible? They must not only feel this strongly, but at the proper time state it openly. But I fear they are still far from it. For this reason I do not believe that for the most part they had a strong inner resistance.

[*] I found it quite painful in his interviews Otto didn't say one word about me, let alone our 30 years of work together. His motivation is somewhat complicated. He is convinced that Germans are being treated unjustly, the more so in that he simply suppresses the past. Therefore his only thought here was to speak for Germany. I am part of that suppressed past, the more so since before he came... I tried to tell him that decent Germans can help Germany only by seeing things objectively...

[**] In one interview he said... he was glad that Germany was not burdened with the guilt of constructing an atomic bomb and causing the needless deaths of so many thousands. I tried to tell him that he certainly might say that, but only if he also said that Germany had done so many terrible things. But he did not respond to that... He suppresses the past with all his might, even though he always truly hated and despised the Nazis. One of his motives is to gain international respect for Germany once again, and since he does not have a very strong character, nor is he a very thoughtful person, he deceives himself about the facts, or belittles their importance.

In 1947 *Fritz Straßmann* asked *Lise Meitner* to come to Mainz as head of physics and director of the newly relocated Kaiser-Wilhelm-Institut (soon-to-be Max-Planck-Institut) für Chemie.[129] She considered the offer, but only because she valued *Straßmann*; then she refused.[130] To a Swedish friend she wrote:

> [D]ie Deutschen [haben] noch immer nicht begriffen, was geschehen ist und alle Greuel, die nicht ihnen persönlich widerfahren sind, völlig vergessen. Ich glaube, ich würde in dieser Atmosphäre nicht atmen können.[131][*]

Ten years after fleeing Germany, *Meitner* finally understood she could not return.

8. Postscript: "die *Mitarbeiterin*"[3]

Meitner did not continue her battles with *Hahn*. A nostalgic warmth gradually returned to their friendship, and she often visited Germany for lectures and conferences. Underneath, nothing was resolved. *Hahn* became postwar Germany's major scientific hero: Nobel laureate, president of the Max-Planck-Gesellschaft, prototype of the "decent German", lionized at every turn. *Meitner*, in every sense the outsider, was witnessing the disappearance of her scientific past. In 1953 she wrote to *Hahn*:

> Jetzt möchte ich etwas Persönliches schreiben, das mich bedrückt und das ich Dich bitte in Erinnerung an unsere mehr als 40-jährige Freundschaft und mit dem Wunsch, mich zu verstehen, zu lesen. In dem Bericht der Max-Planck-Gesellschaft wird der Vortrag, den ich in Berlin gehalten habe (ein rein physikalischer Vortrag) angeführt und ich werde genannt als "langjährige Mitarbeiterin unseres Präsidenten." Gleichzeitig habe ich in der Naturwissenschaftlichen Rundschau einen Artikel von Heisenberg gelesen über die Beziehungen zwischen Physik und Chemie in den letzten 75 Jahren, wo die einzige Erwähnung von mir... lautet: "Die langjährige Mitarbeiterin Hahns, Frl. Meitner."[132] Ich bin im Jahr 1917 vom Verwaltungsrat des K.W. für Chemie offiziell mit der Einrichtung der Physikalischen Abteilung betraut worden und habe sie 21 Jahre geleitet. Versuche Dich einmal in meine Lage hineinzudenken! Was würdest Du dazu sagen, wenn Du nur charakterisiert würdest als der langjährige Mitarbeiter von mir? Soll mir nach den letzten 15 Jahren, die ich keinem guten Freund durchlebt zu haben wünsche, auch noch meine wissenschaftliche Vergangenheit genommen werden? Ist das fair? Und warum geschieht-es?[133][**]

It is unlikely that *Hahn* understood; certainly he never spoke out on *Meitner*'s behalf. On the contrary, in his autobiographies[40, 41] his treatment of *Lise Meitner* the person was utterly perfunctory—except for a few coarse anecdotes[134] she appears more a ghost than a real human being. His protrayal of *Lise Meitner* the scientist gives little sense of their early collaboration or her independent work, no mention of her initiative in 1934, her leadership of the Berlin team, their crucial meeting in Copenhagen, her encouragement later. Apparently written without consulting scientific literature, correspondence, or his own personal diaries, *Hahn*'s autobiographies reveal a memory so faulty, superficial, selective, and self-serving that his character and motives must be called into question. It may be that *Hahn*'s self-deception and absence of feeling, which served as a survival tactic under a terror regime, congealed so irreversibly in the post-war period that it became impossible for him to examine the past. *Lise Meitner*, in her Viennese way, simply said: "Man kann wahrscheinlich nicht ein so charmanter Mensch sein und daneben sehr tief sein."[135] ("Probably one can not be such a charming person and also very deep.")

Meitner's public reaction was muted; she had no desire to battle the phenomenon of *Otto Hahn*.[136] Indeed, *Hahn*'s unparallelled celebrity status spawned an enormous quantitiy of derivative biographical material. A chorus of former associates, none close, echoed his contention that fission had nothing to do with physics or *Meitner*. Fission, they insisted, was discovered by the chemists in spite of the physicist.[137] In Germany only *Fritz Straßmann* and *Max von Laue* cared to recognize the obvious: if *Lise Meitner* had not been forced to emigrate, "sie wäre sonst zweifellos in der einen oder anderen Form an der Entdeckung der Uranspaltung mitbeteiligt..."[6, 138] ("she would undoubtedly, in one form or other, have participated in the discovery of fission.")

Had *Lise Meitner* been in Germany in December 1938, the discovery would have been hailed as the brilliant work of an interdisciplinary team. Instead, the politics of race demanded her exclusion. Rather than recognizing this as an injustice, *Hahn* and his followers invented spurious scientific explanations for it: they blamed the victim. Arrogantly, with misplaced national pride, they denied the injustice, created new injustice, perpetuated it—and implicated themselves.

9. Future

Primo Levi has written, "[T]he entire history of the [Third] Reich can be re-read as a war against memory, an Orwellian falsification of memory, falsification of reality, negation of reality."[139] *Lise Meitner*'s experience shows how memory and reality came to be falsified, even by those who were nominally anti-Nazi, even by scientists who were trained to pursue the truth. But for *Meitner*, at least, it appears that a

[*] The Germans have still not grasped what has happened and have completely forgotten all atrocities that did not personally happen to them. I think I could not breathe in such an atmosphere.

[**] Now I want to write something personal, which bothers me, and which I ask you to read with our more than 40-year friendship in mind and with the desire to understand me. In the report of the Max-Planck-Gesellschaft there is reference to a lecture I gave in Berlin (a purely physics lecture), and I am named as the long-time *Mitarbeiterin* of our President. At the same time I read an article by Heisenberg in Naturwissenschaftliche Rundschau about the relationship between physics and chemistry in the last 75 years, where the only mention of me... is: "Hahn's long-time *Mitarbeiterin*, Frl. Meitner." In 1917 I was given official responsibility by the board of the K.W. für Chemie to set up the Physics Section, and I led it for 21 years. Try to put yourself in my place. What would you say, if you were only characterized as the "long-time *Mitarbeiter*" of mine? After the last 15 years, which I wouldn't wish on any friend, shall my scientific past also be taken from me? Is that fair? And why is it happening?

genuine rehabilitation is underway: a new generation has begun to illuminate *Lise Meitner*'s scientific past, her life, and the world in which she lived.[140]

I am grateful to Irmgard Straßmann and the late Professor Fritz Straßmann for valuable discussions, to Ulla Frisch and the late Professor Otto Frisch for access to the Meitner Collection in Churchill College, to the late Marie-Luise Rehder for untold help, and to Dr. Marion Kazemi and the Archiv zur Geschichte der Max-Planck-Gesellschaft for access to the archives. I wish to thank Joan Bromberg, Stanley Goldberg, and Pieter Van Assche for critically reading this article. Support by the (U.S.) National Science Foundation and the National Endowment for the Humanities is gratefully acknowledged.

Received: April 5, 1990 [A 829 IE]
German version: *Angew. Chem. 103* (1991) 956

[1] R. Feyl: "Lise Meitner 1878–1968" in *Der lautlose Aufbruch – Frauen in der Wissenschaft*, Luchterhand, Darmstadt 1983, p. 162.
[2] K.-E. Zimen, *Atomwirtsch. Atomtech. 33* (1988) 588; *Zimen* was director of the Hahn-Meitner-Institut in Berlin.
[3] *Mitarbeiterin* translates as "co-worker", but the German has more connotation of subordinate. For a recent example: H. Rechenberg, *Phys. Bl. 44* (1988) 453; also see [4].
[4] The Deutsches Museum's display of the so-called "Arbeitstisch von *Otto Hahn*" mentioned *Straßmann* only at the side and *Meitner* not at all until early 1989, when a small sign was added denoting *Meitner* as *Hahn*'s *Mitarbeiterin*. Recently, the display has been altered to include *Hahn*, *Meitner*, and *Straßmann*, with appropriate changes in the audiotape and written material.
[5] W. Heisenberg, *Orden pour le mérite für Wissenschaft und Künste, Reden und Gedenkworte 9* (1968/1969) 111.
[6] F. Straßmann: *Kernspaltung – Berlin Dezember 1938*, Privatdruck, Mainz 1978, p. 23; reprinted in [22], p. 211.
[7] F. Stern: *Dreams and Delusions: National Socialism in the Drama of the German Past*, Vintage, New York 1989, p. 27.
[8] Letter from *Lise Meitner* to *Elisabeth Schiemann*, 31 December 1913; unless otherwise specified, all correspondence is from the Meitner Collection, Churchill College, Cambridge (England).
[9] L. Meitner, *Naturwiss. Rundsch. 16* (1963) 167.
[10] *Max von Laue* expressed this in 1957; see Section 8 and [6, 22].
[11] a) G. Herrmann, *Angew. Chem. 102* (1990) 469; *Angew. Chem. Int. Ed. Engl. 29* (1990) 481; b) G. Herrmann, *Nucl. Phys. A 502* (1989) 141c.
[12] *Meitner* to *Max von Laue*, 4 September 1944.
[13] E. Segrè: *Enrico Fermi: Physicist*, University of Chicago Press, Chicago 1970, p. 73.
[14] E. Segrè (Ed.): *Enrico Fermi: Collected Papers (Note e Memorie)*, University of Chicago Press, Chicago (Accademia Nazionale dei Lincei, Roma) 1962, Vol. 1, p. 640.
[15] E. Fermi, *Ric. Sci. 5(1)* (1934) 283; 25 March 1934; Engl. transl. in [14], pp. 674–675.
[16] E. Fermi, *Ric. Sci. 5(1)* (1934) 330; Engl. transl. in [14], p. 676.
[17] E. Fermi, *Nature (London) 133* (1934) 757; submitted on 10 April 1934.
[18] Ref. [13], p. 74.
[19] *Meitner* to *Enrico Fermi*, 16 May 1934.
[20] L. Meitner, *Naturwissenschaften 22* (1934) 420.
[21] O. R. Frisch, *Biogr. Mem. Fellows R. Soc. 16* (1970) 405.
[22] F. Krafft: *Im Schatten der Sensation: Leben und Wirken von Fritz Straßmann*, Verlag Chemie, Weinheim 1981, Chap. 2.
[23] F. Krafft, *Angew. Chem. 90* (1978) 876; *Angew. Chem. Int. Ed. Engl. 17* (1978) 826.
[24] C. Kerner: *Lise, Atomphysikerin*, Beltz, Weinheim 1986.
[25] S. A. Watkins, *Am. J. Phys. 51* (1983) 551.
[26] R. L. Sime, *J. Radioanal. Nucl. Chem. 142* (1990) 13.
[27] R. L. Sime, *J. Chem. Educ. 63* (1986) 653.
[28] L. Badash: *Radioactivity in America*, Johns Hopkins University Press, Baltimore 1979, p. 213. *Badash* speaks of radiochemistry's "suicidal success... the field effectively ceased to exist."
[29] D. Hahn (Ed.): *Otto Hahn, Erlebnisse und Erkenntnisse*, Econ Verlag, Düsseldorf 1975, p. 43.
[30] Ref. [14], p. 548.
[31] E. Fermi, E. Amaldi, O. D'Agostino, F. Rasetti, E. Segrè, *Ric. Sci. 5(1)* (1934) 452; Engl. transl. in [14], p. 677.
[32] E. Fermi, F. Rasetti, O. D'Agostino, *Ric. Sci. 5(1)* (1934) 536; submitted on 6 June 1934.
[33] E. Fermi, *Nature (London) 133* (1934) 898; appeared on 16 June 1934.
[34] The *Nature* reference is undoubtedly [33], published on 16 June 1934; *Meitner* may have meant *Ricerca Scientifica*, (Refs. [31] or [32]) rather than the *Nuovo Cimento* review articles (E. Fermi, *Nuovo Cimento 11* (1934) 429 and E. Amaldi, E. Fermi, F. Rasetti, E. Segrè, *ibid. 11* (1934) 442) published in July, which included no results not previously reported in *Ricerca Scientifica* and *Nature*. In any event, it is evident that *Meitner* knew of *Fermi*'s uranium results by June.
[35] See [29], pp. 40–41; O. Hahn, L. Meitner, *Naturwissenschaften 19* (1931) 738; A. von Grosse, O. Hahn, L. Meitner, *ibid 20* (1932) 362.
[36] Ref. [29], p. 47.
[37] *Nobel Lectures Chemistry* 1942–1962, Elsevier, Amsterdam 1964, p. 172; also see in [41], p. 253.
[38] O. Hahn: *New Atoms*, Elsevier, New York 1950, p. 17.
[39] O. Hahn, *Naturwissenschaften 46* (1959) 158.
[40] a) O. Hahn: *Vom Radiothor zur Uranspaltung: Eine wissenschaftliche Selbstbiographie*, Vieweg, Braunschweig 1962, p. 116; b) O. Hahn: *A Scientific Autobiography* (transl. by W. Ley), MacGibbon & Kee, London 1967, p. 141.
[41] a) O. Hahn: *Mein Leben*, Bruckmann, München 1968, p. 148; b) O. Hahn: *My Life* (transl. by E. Kaiser and E. Wilkins), Herder and Herder, New York 1970, pp. 147–148.
[42] A. von Grosse, M. Agruss, *Phys. Rev. 46* (1934) 241.
[43] In [41a] (p. 148) and [41b] (p. 147) *Hahn* even "remembers" that he and *Meitner* did not learn of *Fermi*'s experiments until they returned from a conference in the Soviet Union in *September* 1934 and were prodded by *Max Delbrück* to repeat them.
[44] O. Hahn, L. Meitner, *Naturwissenschaften 23* (1935) 37.
[45] L. Meitner, *Naturwissenschaften 22* (1934) 759.
[46] L. Meitner, *Naturwissenschaften 22* (1934) 733.
[47] E. Fermi, E. Amaldi, B. Pontecorvo, F. Rasetti, E. Segrè, *Ric. Sci. 5(2)* (1934) 282–283; Engl. transl. in [14], p. 761.
[48] O. Hahn, L. Meitner, *Naturwissenschaften 23* (1935) 230.
[49] Ref. [22], pp. 40–47; in 1986 *Straßmann* was posthumously honored by the Israeli Holocaust Memorial (Yad Vashem) for hiding a Jewish friend during the war.
[50] E. Segrè, *Phys. Rev. 55* (1939) 1104; also [64].
[51] I. Noddack, *Z. Angew. Chem. 47* (1934) 653.
[52] *E. Amaldi*, a member of *Fermi*'s group, remembers a bias against *Noddack* (Ref. [22], p. 316); this was also true in Berlin. For further discussion, see P. Van Assche, *Nucl. Phys. A 480* (1988) 205.
[53] Ref. [22], pp. 103–104.
[54] P. R. Weart in W. R. Shea (Ed.): *Otto Hahn and the Rise of Nuclear Physics*, Reidel, Dordrecht 1983, p. 105. In Berlin it was hoped that the international attention for the "transuranes" might somehow protect the three political undesirables and their institute.
[55] L. Meitner, O. Hahn, F. Straßmann, *Z. Phys. 106* (1937) 249.
[56] L. Meitner, interview on 12 May 1963, American Institute of Physics (New York) Oral History Project.
[57] Contemporary reviews include L. Quill, *Chem. Rev. 23* (1938) 87; L. A. Turner, *Rev. Mod. Phys. 12* (1940) 1; see also [11a].
[58] O. Hahn, L. Meitner, F. Straßmann, *Ber. Dtsch. Chem. Ges. 69* (1936) 905.
[59] O. Hahn, L. Meitner, F. Straßmann, *Ber. Dtsch. Chem. Ges. 70* (1937) 1374.
[60] L. Meitner, O. Hahn, *Naturwissenschaften 24* (1936) 158.
[61] 23-m U-239 necessarily decays to element 93, but the Berlin team, hampered by weak neutron sources and distracted by the other "transuranes", did not detect it; see [11a].
[62] L. Meitner, F. Straßmann, O. Hahn, *Z. Phys. 109* (1938) 538.
[63] Ref. [56]; also in [101], *Meitner* wrote: "The long chain of beta decays has always puzzled us."
[64] H. G. Graetzer, D. J. Anderson: *The Discovery of Fission, A Documentary History*, Van Nostrand, New York 1971, p. 34-37.
[65] Ref. [29], p. 58.
[66] Ref. [29], p. 54.
[67] Ref. [22], p. 43.
[68] R. L. Sime, *Am. J. Phys. 58* (1990) 262.
[69] Ref. [22], pp. 234ff.
[70] J. Lemmerich: *Die Geschichte der Entdeckung der Kernspaltung*, Katalog zur Ausstellung in der TU Berlin und im Deutschen Museum München; Universitätsbibliothek Technische Universität Berlin, Berlin 1988, pp. 157ff.
[71] *Meitner* to *Hahn*, 23 October 1938.
[72] I. Curie, P. Savitch, *J. Phys. Radium 9* (1938) 355.
[73] Ref. [22], p. 207.
[74] *Hahn* to *Meitner*, 25 October 1938.
[75] *Hahn* to *Meitner*, 2 November 1938.
[76] *Meitner* to *Hahn*, 4 November (incorrectly dated 4 October) 1938.
[77] *Hahn* to *Meitner*, 5/6 November 1938; O. Hahn, F. Straßmann, *Naturwissenschaften 26* (1938) 755; submitted on 8 November 1938.
[78] In the same year (1938), when neutron irradiation of thorium produced what appeared to be similar Ra-Ac isomers, *Meitner* calculated (in [62]) that an (n,α) process was possible only with *fast* neutrons.

[79] Refs. [41a] and [41b], p. 150.
[80] O. Hahn, *Naturwiss. Rundsch. 15* (2) (1962) 43; *Hahn* writes: "Ihm [Bohr] war die Abspaltung von zwei α-Strahlen aus dem Uran unheimlich. Er konnte sie nicht für möglich halten..." ("For him [Bohr] the splitting off of two α-particles from uranium was unimaginable. He considered it impossible.") Surely this came from *Meitner* (perhaps *Bohr* also).
[81] Ref. [22], p. 208, note 17.
[82] O. Hahn, 1938 Siemens-Taschenkalender, 13 and 14 November 1938 (Archiv zur Geschichte der Max-Planck-Gesellschaft, Berlin-Dahlem); quoted in [83].
[83] P. Brix, *Phys. Bl. 45* (1989) 1.
[84] Ref. [6], p. 18; [22], p. 208.
[85] Ref. [22], pp. 247ff.
[86] In 1945 (Ref. [29], p. 58) *Hahn* does not give a reason for the fractionation experiment: "Aus irgendwelchen Gründen wollten wir unsere Ra-Isotope etwas anreichern" ("For some reason or other we wanted to enrich our Ra-isotopes somewhat"); later, in Ref. [41a], pp. 255–256, Ref. [38], p. 20, Ref. [80], etc., he says only that fractionations were needed to detect the weak radiation of a long-lived Ra isomer, a reason *G. Hermann* in Ref. [11a,b] regards as "rather trivial". More likely, *Hahn* and *Straßmann* were responding to *Meitner*'s request they look for thorium, since if $Ra \rightarrow Ac \rightarrow Th$ were true, the resulting Th-231 would be identical or isomeric to the known UY. See *Meitner* to *Hahn*, 26 November and 5 December 1938, abridged in Ref. [22], pp. 250–251.
[87] Ref. [22], pp. 104–105.
[88] *Hahn* to *Meitner*, 19 December 1938; facsimile in Ref. [70], pp. 166–167.
[89] The *Hahn/Straßmann* articles were written by *Hahn* alone. See [6], p. 19, [22], p. 209.
[90] O. Hahn, F. Straßmann, *Naturwissenschaften 27* (1939) 11.
[91] W. Gerlach: *Ein Forscherleben unserer Zeit*, Oldenbourg, München 1969, p. 53.
[92] *Meitner* to *Hahn*, 21 December 1938; facsimile in Ref. [70], p. 171.
[93] According to *E. Bagge*, *Hahn* said in 1945: "Wenn Frl. Meitner im Dezember 1938 noch im Institut gewesen wäre, hätte sie uns das Barium ausgeredet." ("If Frl. Meitner had still been in the institute in December 1938, she would have talked us out of barium.") [Private communication, *R. Fleischmann* to *P. Van Assche*, 1982]; also see *Heisenberg* in [5]. Although such second- and third-hand reports require evaluation of the sources, they are consistent with *Hahn*'s later refusal to include *Meitner* in the discovery.
[94] *Hahn* to *Eva von Bahr-Bergius*, 23 December 1938; in [22], p. 267.
[95] O. R. Frisch: *What Little I Remember*, Cambridge University Press, Cambridge 1979; pp. 115–117.
[96] According to *Fritz Krafft*: "Eine entsprechende Loyalität hätte sie dann eigentlich auch 1938 erwarten können." ("She certainly could have expected a corresponding loyalty in 1938.") See F. Krafft: *Lise Meitner*, Hahn-Meitner-Institut HMI-B448, January 1988 (talk given 2 December 1987.) In their 1918 protactinium paper *Hahn* was even *first* author: O. Hahn, L. Meitner, *Phys. Z. 19* (1918) 257.
[97] Even a joint retraction of the transuranes was "vermutlich undurchführbar" because it was politically impossible (perhaps illegal?) for *Meitner* to publish in Germany (*Meitner* to *Hahn*, 1 January 1939); she did not tell *Hahn* details of the Meitner–Frisch interpretation until it was accepted by *Nature* "weil Du ja nicht in der Lage bist, sie unveröffentlicht zu zitieren und weil sie allerlei prüfbare Behauptungen enthält." ("because you are not in a position to cite it before publication, and because it contains a number of (experimentally) provable statements.") (*Meitner* to *Hahn*, 18 January 1939). See also [104].
[98] *Meitner* to *Hahn*, 3 January 1939.
[99] *O. R. Frisch* to *Hahn*, 4 January 1939 in [22], p. 271.
[100] *Meitner* to *Hahn*, 18 January 1939.
[101] L. Meitner, O. R. Frisch, *Nature (London) 143* (1939) 239.
[102] Ref. [29], pp. 64–66.
[103] O. Hahn, F. Straßmann, *Naturwissenschaften 27* (1939) 89.
[104] *Hahn* also did not acknowledge the suggestion by *Meitner* and *Frisch* of the second fission fragment Kr and its decay products, even though the search for these in Berlin began concurrently or just after receipt of the Meitner–Frisch manuscript. See [22], p. 282–284, and R. L. Sime, *J. Chem. Educ. 66* (1989) 373.
[105] *Meitner* to *Walter Meitner*, 6 February 1939.
[106] *Meitner* to *Hahn*, 5 February 1939; see *Krafft* in [23] for more on *Meitner*'s conditions in Sweden.
[107] Possibly a certain Prof. Krauch (see [29], pp. 64–65) who was pressuring the "politisch belastet" ("politically tainted") Hahn.
[108] *Hahn* to *Meitner*, 7 February 1939.
[109] *Meitner* to *Hahn*, 2 June 1939; *Hahn* to *Meitner*, 5 June 1939.
[110] Ref. [22], pp. 315ff.
[111] *Meitner* to *Hahn*, 12 and 15 July 1939.
[112] *Meitner to Max von Laue*, 12 November 1946.
[113] In a 1941 review of fission theory, *Meitner*'s once-close associate *C. F. von Weizsäcker* cited everyone except *Meitner* and *Frisch*; see C. F. von Weizsäcker, *Forsch. Fortschr. 17* (1941) 10; for *Meitner*'s reaction, see *Meitner* to *Hahn*, 20 January 1941. Also F. Krafft, *Mitt. Österr. Ges. Geschichte Naturwiss. 4* (1984) 1, note 15. The practice of not citing the work of Jewish authors, omitting their names, or attributing their work to others was nearly universal; to my knowledge no attempt has been made since 1945 to correct the record.
[114] *Meitner* to *Hahn*, 15 April 1943: citing publications of *Hahn* and *Meitner*, *Fritz Houtermans*, in 1943, substituted *Straßmann*'s name for hers.
[115] *Meitner* to *Eva von Bahr-Bergius*, 27 May 1941.
[116] O. R. Frisch: "Lise Meitner" in *Dictionary of Scientific Biography, Vol. 9*, Scribners, New York 1974, p. 260; Margaret Gowing: *Britain and Atomic Energy 1939–1945*, MacMillan, London 1964, pp. 261ff.; L. Eppstein, Sweden 1988, private communication.
[117] *Meitner* to *Eva von Bahr-Bergius*, 21 June 1944.
[118] Meitner Diaries: August, September 1945; Churchill College Archives, Cambridge (England).
[119] Ref. [29], p. 72.
[120] "Prof. L. Meitner and the splitting of uranium," *Hahn* to Major *Rittner*, Farm Hall, 8 August 1945. *Meitner*'s response, as given in a 1963 interview (Ref. [56], p. 18): "...die Chemiker behaupten... [daß] wir Physiker solche Prozesse (Fission) für unmöglich erklärt haben, aber wir haben sie ja nie diskutiert..." ("The chemists claim that we physicists declared such processes (fission) to be impossible, but we in fact never discussed it...")
[121] *Meitner* to *Eva von Bahr-Bergius*, 30 March 1945.
[122] *Meitner* to *Hahn*, 1 April 1946.
[123] *Hahn* to *Meitner*, 17 September 1946.
[124] *Meitner* to *Hahn*, 20 October 1946.
[125] *Meitner* to *Frisch*, 28 November 1946.
[126] *Hahn*, [41a], pp. 208–210; [41b], pp. 201–203.
[127] *Meitner* to *Eva von Bahr-Bergius*, 24 December 1946.
[128] *Meitner* to *James Franck*, 16 January 1947 (incorrectly dated 1946).
[129] *Straßmann* to *Meitner*, 11 November 1947.
[130] *Meitner* to *Straßmann*, 21 December 1947, and *Meitner to Hahn*, 6 June 1948.
[131] *Meitner* to *Eva von Bahr-Bergius*, 10 January 1948.
[132] Space does not here permit a discussion of the effect of gender inequity upon *Meitner*, but it is unlikely that a male scientist of *Meitner*'s status would be remembered as anyone's *Mitarbeiter*. That *Heisenberg*, who knew *Meitner* very well when she was still in Germany, would refer to her as *Hahn*'s *Mitarbeiterin* and ignore her work probably indicates chauvinism of more than one variety.
[133] *Meitner* to *Hahn*, 22 June 1953.
[134] *Hahn*, [40a], p. 86, pp. 147–148.
[135] *Meitner* to *Lola Allers*, 29 December 1946.
[136] In a very mild response to *Hahn*'s 1962 scientific biography, *Meitner* in 1963 ("Wege und Irrwege zur Kernenergie" [9]) described for the first time her own initiative and noted mistakes in both physics and chemistry; much the same in a 1963 taped interview: Ref. [56].
[137] So stated by *Zimen* in [2]. For "proof" *Zimen* suggests that physicist *Manne Siegbahn* knew *Meitner* personally and would have nominated her for a Nobel Prize had her work deserved it. The suggestion is disingenuous and mean: *Zimen*, who lived in Sweden at the time, surely knows that it was precisely the poor relationship between *Meitner* and *Siegbahn* that *prevented* her from being considered for a Prize. *K. Starke* (*J. Chem. Educ. 56* (1979) 771) is less strident but also ties the discovery to *Meitner*'s absence (which he attributes to her loss of Austrian citizenship!).
[138] In the U.S.A. this was understood; according to *Glenn Seaborg* (personal communication, 1988), *Meitner* was included with *Hahn* and *Straßmann* in the 1966 Enrico Fermi Prize for this reason.
[139] P. Levi: *The Drowned and the Saved* (R. Rosenthal, transl.), Vintage International, New York 1989, p. 31.
[140] An abbreviated list of recent German contributions: The work of *Fritz Krafft* (Refs. [22, 23, 96]) has had significant influence; *Charlotte Kerners*'s book [24] received the (West) German prize for *Jugendliteratur* in 1987; the comments of *Renate Feyl* [1] have struck a resonant chord, so also the work by *H. Königsdorfer*: *Respektloser Umgang*, Luchterhand, Darmstadt 1986; *Lemmerich*'s 1988–1989 "Ausstellung zur Geschichte der Kernspaltung" [70] included *Meitner* equitably; ceremonies in 1988 and 1989 for the Lise-Meitner-Gymnasium in Böblingen included contributions by *Peter Brix* (Heidelberg) (P. Brix, *MPG-Spiegel* 1/90, p. 29), *Paul Kienle* (GSI Darmstadt) und *Evelies Mayer* (TH Darmstadt).

Toward the Understanding of Immunosuppression

By *Horst Kessler,* Dale F. Mierke, David Donald,* and *Mark Furber*

Slowly the fog is lifting: the elucidation of the three-dimensional molecular structure of the immunosuppressive compounds cyclosporin A (CsA) **1**,[1,2] FK506 **2**,[3] and rapamycin **3**, as well as biochemical observations are illuminating the mechanisms of immunosuppression.[4] A cascade of events take place (Fig. 1): the antigen is presented to the T-cell receptor (TCR) on the surface of the T-lymphocyte with the major histocompatability protein (MHC) and induces a signal which is transmitted through the cytoplasm to the nucleus by an unknown mechanism leading to the production of interleukin-2 (IL-2). CsA and FK506 inhibit this process. Rapamycin, on the other hand, acts later on in the cascade inhibiting the differentiation and proliferation of T-cells normally stimulated via IL-2.

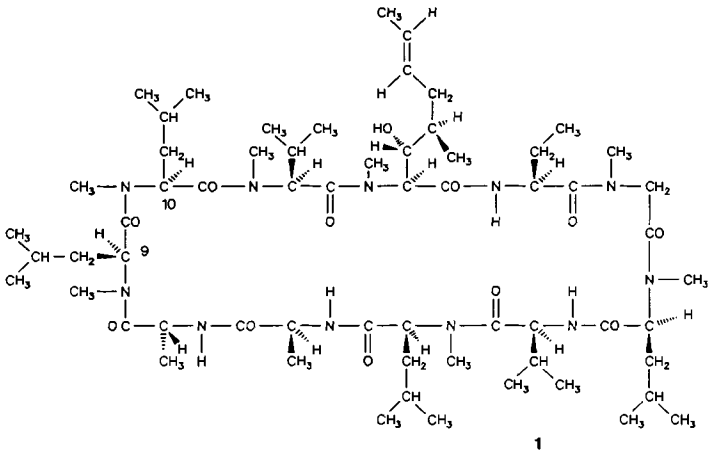

1

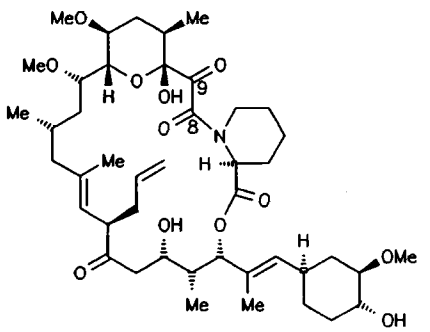

2

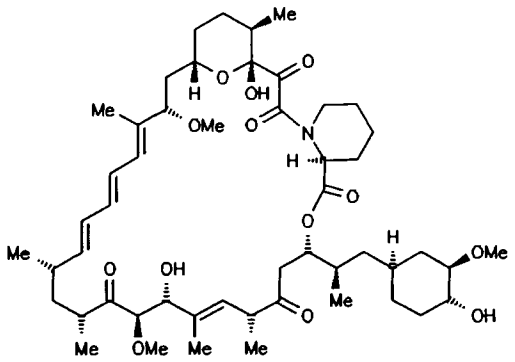

3

Cell surface	Cytoplasm	Nucleus	Inhibitor
Antigen + MHC molecule reacts with T-cell receptor	Signal →	Production of interleukin-2	FK506 Cyclosporin A
Interleukin-2 and receptor	Signal →	Proliferation and differentiation of T-cells	Rapamycin

Fig. 1. The cascade of events leading to differentiation and proliferation of T-lymphocytes.

The medical relevance of immunosuppression is large: many illnesses are caused by unwanted reactions of the immunosystem. The success of transplantation surgery is to a large extent based on the "miracle" drug cyclosporin.[5] With the use of cyclosporin we can now transverse the fine line between graft rejection and infection of the patient due to a necessary suppression of the immune system.

Cyclosporin is a water-insoluble, lipophilic undecapeptide, whose spatial structure is well known in solid state and solution.[6] Recently a peptidomacrolide, FK506,[7] approximately 100-fold more active, was isolated and is currently undergoing clinical testing. The structure of FK506 is also well known.[7,8]

A first breakthrough in the understanding of the biology of immunosuppression came from the discovery of the cytosolic binding proteins cyclophilin (for cyclosporin) and FK506 binding protein (FKBP).[9] These proteins are ubiquitous rotamases (i.e. enzymes that catalyze the already fast *cis-trans* isomerism of peptide bonds).[10] Whether this property is directly connected with immunosuppressive activity is not yet clear. However, while bound to the protein the immunosuppressive is transported from the cell wall to the nucleus through the cytosol of the T-lymphocyte.[4] The structure of the cyclosporin–cyclophilin complex in solution was studied independently by the groups of *K. Wüthrich* at the ETH Zürich, Switzerland[2] and *S. Fesik* from Abbott laboratories, USA.[1] The results, which are in press, have been shrouded in secrecy. Until now it is only known that the *cis* peptide bond between MeLeu^9 and MeLeu^{10} of free cyclosporin is changed to *trans* when it is bound.[1] Is this an effect of the rotamase?

Recently a preliminary publication of the structure of the FK506–FKBP complex by the group of *M. Karplus* and *S. Schreiber* from Harvard appeared.[3] For this complex a characteristic high-field shift of all proton signals of the piperidine ring of FK506 was observed and explained as an

[*] Prof. Dr. H. Kessler, Dr. D. F. Mierke
Organisch-chemisches Institut der Technischen Universität München
Lichtenbergstrasse 4, W-8046 Garching (FRG)
Dr. D. Donald, Dr. M. Furber
Fisons Pharmaceutical
Bakewell Road, Loughborough LE10OH (UK)

 © VCH Verlagsgesellschaft mbH, W-6940 Weinheim, 1991 0570-0833/91/0808-0954 $ 3.50+.25/0

effect of the close proximity of the indole ring of the only tryptophan residue in FKBP. An NOE (*N*uclear *O*verhauser *E*nhancement) from substrate to receptor is direct proof of this assumption. The basis for all of the described studies is the use of isotope-labeled substrates and/or receptors. Labeling with ^{13}C, ^{15}N, and ^{2}H allow a filtering of the interesting information and an unambiguous identification and localization of the interacting species.

Which rotamer of the amide bond of FK506 corresponds to the bioactive form (while bound)?[11] In the crystal there is a *cis* orientation,[7] which also dominates (2:1) in $CDCl_3$ solution.[8] However, the structurally related rapamycin is *trans* in the crystal.[12] The knowledge of the conformation in the bound state is important for the design of therapeutically interesting analogues. In our opinion, the above-mentioned article[3] yields clear hints for a *trans* conformation in the FK506–FKBP complex: a comparison of the proton chemical shifts of the piperidine ring in the complex[3] and of both rotamers in solution[8] exhibits a high-field shift in the complex for all protons. There is only one exception: the equatorial proton at C2 is essentially not shifted if a *cis* peptide bond is assumed (Fig. 2). This makes no sense. If a

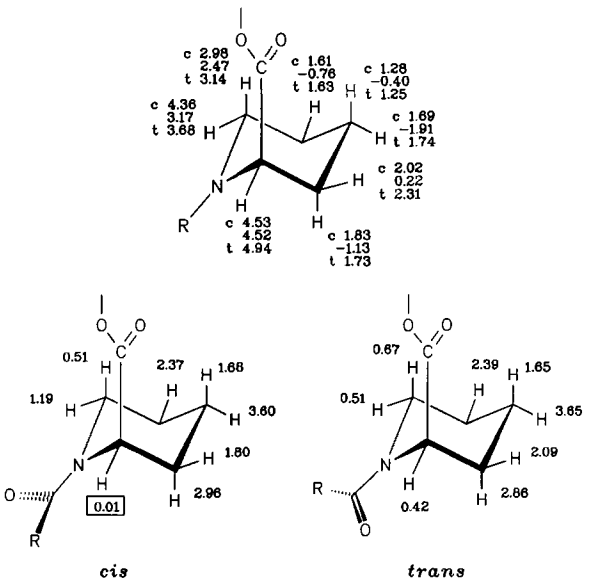

Fig. 2. Top: Comparison of the ^1H NMR chemical shifts of the piperidine ring of FK506 in the complex (number in the middle) with both rotamers of the amide bond of the free molecules in $CDCl_3$ (c = *cis*, t = *trans*). Bottom: the induced negative shift values caused by complexation are shown for both rotamers (see text).

trans rotamer is assumed, a reasonable high-field shift for all signals is observed. Also, the direct coupling of the carbonyl carbons 8 and 9 (see structural formula **2**) in the complex (61 Hz)[11] corresponds to that of the *trans* FK506 in solution (61 Hz) and not the *cis* rotamer (64 Hz).[13]

We look forward with great interest to the refined structures of the immunosuppressants and their receptors. In any case it is already clear that in spite of the very similar binding region of FK506 and rapamycin, which indicate a similar structure in the complex, the pure compounds exhibit different conformations of this region in the crystal. Hence, the structure at least one of the immunosuppressants differs in the crystal and in the complex. Cyclosporin also changes the backbone conformation from solution or crystal to the bound molecules.

Schreiber et al. have proposed that FK506 is an analogue of the transition state.[11] The carbonyl group $C^9{=}O$ is perpendicular to the amide plane ($O{=}C^8{-}N$) and therefore corresponds to a 90° twisted amide bond. Similar to statine, an inhibitor and the transition-state analogue of the aspartic proteases,[14] where the number of atoms in the chain does not exactly correspond to the peptide chain, the additional carbonyl group $C^8{=}O$ of FK506 does not disturb the inhibiting function. An acyl residue with a carbonyl group in the plane of the piperidine ring of FK506 is necessary to ensure the axial position of the ester group at C2. Hence, FK506 exhibits a delicate balance of a spatial structure, which certainly creates headaches for pharmaceutical chemists.[15]

German version: *Angew. Chem. 103* (1991) 968

[1] S. W. Fesik, R. T. Gampe, H. L. Eaton, G. Gemmecker, E. T. Olejniczak, P. Neri, T. F. Holzman, D. A. Egan, R. Edalji, R. Simmer, R. Helfrich, J. Hochlowski, M. Jackson, *Biochemistry, 30* (1991) 6574–6583. A preliminary report of this work has appeared: R. T. Gampe, T. F. Holzmann, D. A. Egan, R. Edalji, J. R. Simmer, R. Helfrich, V. Kishore, D. H. Rich, *Science (Washington, D. C.) 250* (1990) 1406.

[2] C. Weber, G. Wider, B. von Freyberg, R. Traber, W. Braun, H. Widmer, K. Wüthrich, *Biochemistry, 30* (1991) 6563–6574.

[3] T. J. Wandless, S. W. Mischnick, M. K. Rosen, M. Karplus, S. L. Schreiber, *J. Am. Chem. Soc. 113* (1991) 2339.

[4] S. L. Schreiber, *Science (Washington, D. C.) 251* (1991) 283.

[5] R. M. Wenger, *Angew. Chem. 97* (1985) 88; *Angew. Chem. Int. Ed. Engl. 24* (1985) 77.

[6] a) H.-R. Loosli, H. Kessler, H. Oschkinat, H.-P. Weber, T. J. Petcher, A. Widmer, *Helv. Chim. Acta 68* (1985) 682; b) H. Kessler, M. Köck, T. Wein, M. Gehrke, *Helv. Chim. Acta 73* (1990) 1818.

[7] H. Tanaka, A. Kuroda, H. Marusawa, H. Hatanaka, T. Kino, T. Gudo, M. Hashimoto, T. Taga, *J. Am. Chem. Soc. 109* (1987) 5031.

[8] a) P. Karuso, H. Kessler, D. F. Mierke, *J. Am. Chem. Soc. 112* (1990) 9434; b) P. Karuso, P. Schmieder, H. Kessler, D. F. Mierke, *Helv. Chim. Acta*, in press.

[9] a) G. Fischer, H. Bang, C. Mech, *Biomed. Biochem. Acta 43* (1984) 1101; b) N. Takahashi, T. Hayano, M. Suzuki, *Nature (London) 337* (1989) 473; c) G. Fischer, B. Liebold-Wittmann, K. Lang, T. Kiefhaber, F. X. Schmid, *ibid. 337* (1989) 476.

[10] a) J. J. Siekierka, S. H. Y. Hung, M. Poe, C. S. Lin, N. H. Sigal, *Nature (London) 341* (1989) 755; b) M. W. Harding, A. Galat, D. E. Uehling, S. L. Schreiber, *ibid. 341* (1989) 758; c) R. B. Freedman, *ibid. 341* (1989) 692; d) R. F. Standaert, A. Galat, G. L. Verdine, S. L. Schreiber, *ibid. 346* (1990) 671; e) M. Tropschug, E. Wachter, S. Mayer, E. R. Schönbrunner, F. X. Schmid, *ibid. 346* (1990) 674.

[11] M. K. Rosen, R. F. Standaert, A. Galat, M. Nakatsuka, S. L. Schreiber, *Science (Washington, D. C.)248* (1990) 863.

[12] J. A. Findlay, L. Radics, *Can. J. Chem. 58* (1980) 579.

[13] Naturally this argument alone is weak since the coupling can change when bound, but the work of *Schreiber* et al. has clearly shown that FK506 is not covalently bound.

[14] D. H. Rich in A. J. Barrett, G. Salvesen (Eds.): *Proteinase Inhibitors*, Elsevier, Amsterdam 1986, p. 179.

[15] Note Added in Proof: Recently three articles appeared describing the structure of FKBP [16, 17] and the FK506–FKBP complex.[18] The structure of FK506 in the complex in fact shows a *trans* amide and also differs from the structure of pure FK506 in solution.

[16] J. M. Moore, D. A. Peattie, M. J. Fitzgibbon, J. A. Thomson, *Nature (London) 351* (1991) 248.

[17] S. W. Mischnick, M. K. Rosen, T. J. Wandless, M. Karplus, S. L. Schreiber, *Science (Washington, D. C.) 252* (1991) 836.

[18] G. D. Van Duyne, R. F. Standaert, P. A. Karplus, S. L. Schreiber, J. Clardy, *Science (Washington, D. C.) 252* (1991) 839.

Energetic and Constitutional Hysteresis in Bistable Molecules

By *Ulrich Kölle**

Bistable or multistable systems, so-called flip-flops, which remain in a state Z_1 until they are converted by a trigger signal into a second state Z_2, are the key building blocks of all digital electronic devices. *Taube* and *Sano*[1] have recently realized such a system at the molecular level in an elegant way in the form of a dinuclear Ru-sulfide/Ru-sulfoxide complex.

In principle, any isomeric pair whose isomers are separated by a sufficiently high activation energy barrier constitutes such a bistable chemical system. However, the interconversion of the isomers can involve complicated chemical operations, including even chemical degradation and synthesis with the breaking and making of bonds; such conversions can no longer be considered as being equivalent to electrical triggering.

Molecules which photochemically isomerize and undergo thermal reconversion approach more closely the ideal of a triggerable multistable molecular system; like the norbornadiene/quadricyclene system [Eq. (a)], which, together with similar compounds, has been studied intensively as a converter of light energy into storable thermal energy.[2] A conversion catalyst, for example a suitable transition metal complex, can be used as trigger for the thermal reconversion.

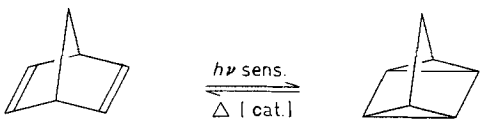

(a)

Systems in which the conversion in both directions is triggered photochemically by light of suitable wavelengths already show a high degree of reversibility. In a series of Fe^{II} complexes[3] with relatively weak ligands which have been investigated by *Gütlich* et al., the thermal conversion barrier between a ^1A- and a ^5T-term is large enough in both directions to prevent a spontaneous conversion, at least at temperatures < 60 K. The reason for this is the considerably larger ionic radius of a high-spin Fe^{II} ion compared to the low-spin form. On the other hand, high-spin and low-spin forms can be intentionally interconverted by selective light excitation [Eq. (b)].

$$^1A_{1g}\,[Fe(mtz)_6]^{2+} \underset{h\nu\,(700\ nm)}{\overset{h\nu\,(350-650\ nm)}{\rightleftharpoons}} {}^5T_{2g}\,[Fe(mtz)_6]^{2+} \qquad \text{(b)}$$

mtz = 1-methyl-1*H*-tetrazole

At present, most examples of triggerable isomerizations involve transition metal complexes in which the triggering is brought about by an electrochemical oxidation or reduction at the electrode. In some cases the process is not only completely reversible, but also selectively and specifically triggerable by applying a suitable potential.

[*] Prof. Dr. U. Kölle
Institut für Anorganische Chemie der Technischen Hochschule
Templergraben 55, W-5100 Aachen (FRG)

For a bistable system in the above sense, however, not only the comparatively trivial recharging is necessary but also a concomitant chemical reaction, often an isomerization. Such a system (Scheme 1) is characterized by (at

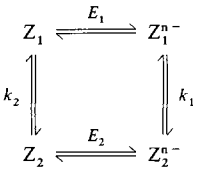

Scheme 1.

least) two redox potentials E_1 and E_2 and, in each case, two chemical reactions with the rate constants k_1 and k_2. The redox pairs $Z_{1(2)}/Z_{1(2)}^{n-}$ are in principle reversibly interconvertible; however, if the subsequent chemical reaction is sufficiently rapid, the electron transfer appears irreversible. Since Z_1 and Z_2^{n-} differ in chemical constitution, E_1 and E_2 can differ. In electroanalytical terminology this is designated an ECEC system. In the cyclic voltammogram such a system is characterized by a more or less strong displacement of the reduction peak compared to the oxidation speak.

These systems are bistable in the above sense when the chemical reaction can be separated from the electron transfer; i.e. the energy minima Z_1^{n-} and Z_2, which are reached after the electron transfer, must be separated by a small activation barrier from the stable configuration Z_2^{n-} or Z_1 for each charge state (see Scheme 2). In organotransition-

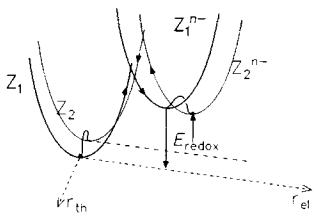

Scheme 2. r_{el} = electrochemical reaction coordinate, r_{th} = thermal reaction coordinate.

metal complexes which obey the 18-electron rule, the constitution often changes upon varying the charge of the complex. As long as this process is reproducible and reversible a chemical bistable system can exist.

Many compounds in which reversible bond rearrangements take place during a charge transfer have long been known, and redox isomerizations have recently been reviewed in detail.[4] However, the possibility of isomerization does not appear to suffice for separate redox potentials in reduction and oxidation; rather, examples are known in which the redox transition takes place reversibly electrochemically despite drastic changes in the molecular structure.[5]

Examples of compounds in which the reduction potential and oxidation potential differ greatly, and in which reversible bond breaking and bond formation take place dur-

 © VCH Verlagsgesellschaft mbH, W-6940 Weinheim, 1991 0570-0833/91/0808-0956 $ 3.50+.25/0

ing the course of the charge transfer are dinuclear carbonyl derivatives with metal–metal bonding ([{Mn(CO)$_5$}$_2$], [{Co(CO)$_4$}$_2$], [{CpFe(CO)$_2$}$_2$] etc.[6]), for which reductive cleavage and oxidative coupling of the metal–metal bond are characteristic reactions. Closed cycles in the ECEC scheme are realized in particular when the metal centers are linked by suitable substituents (e.g. fulvalenes).[7] In sandwich complexes, the formation and breakage of peripheral C–C bonds, concomitantly in some cases with isomerization of the π-cyclic ring ligands during the charge transfer, is a frequently observed reaction.[8] But also purely intramolecular redox isomerizations with closed cycles have in the meantime been well documented. Examples are the *cis-trans-* and *fac-mer*-isomerizations of octahedral carbonyls [ML$_4$(CO)$_2$] and [ML$_2$L$'_2$(CO)$_2$], respectively, of the chromium and manganese groups, the cleavage of a metal–metal bond in dinuclear, anionically bridged transition metal complexes during a two-electron reduction, and the opening of clusters by the uptake of electrons.

In some sandwich complexes which can change their oxidation states in two-electron steps, a change in the hapticity and thus an isomerization occurs in accord with the equivalence of one double bond to two complex electrons in the valence electron count,[9] for example by bending of an η^6-arene to give an η^4-cyclohexatriene ligand. So-called pseudo-triple-decker complexes alter the conformation of the cyclic π-bridge ligand during the charge transfer.[4]

The reversible rearrangement of bonds in the redox isomerization of the diruthenium complex [(CpRu)$_2$(cot)] (Scheme 3) is *one* of the examples that has been studied in detail.[10] Two [CpRu] units are linked via a cyclooctatetraene unit to give a neutral molecule in which two C-atoms are pentacoordinated. Upon oxidation to the dication a C–C bond is opened and a so-called flyover complex is formed. A detailed insight into the reaction mechanism is

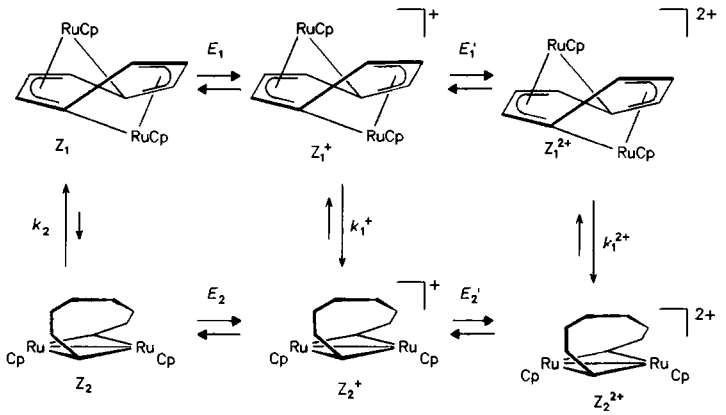

Scheme 3.

provided in this case by cyclic voltammetry. Firstly, the system is characterized by a chemically irreversible two-electron oxidation and reduction with potentials of 0.02 and − 0.26 V (glassy carbon electrode), due to the fact that $E_2' < E_1$ and $E_2 \approx E_2'$. Below room temperature the isomerization $Z_1^+ \rightarrow Z_2^+$ is slow. The oxidation of Z_1 gradually becomes a reversible one-electron oxidation and a second oxidation step can be observed at 0.4 V ($Z_1^{+/2+}$). This clearly shows that the isomerization takes place at the stage of the monocation at room temperature (indeed the generation of Z_1^{2+} at low temperature leads to another product). A similar sequence is found for the reduction of the stable and likewise structurally characterized dication Z_2^{2+}, with the exception, that here, reduction to the flyover neutral complex must take place first in order to trigger the isomerization to Z_1.

Finally, in the area of classical complex chemistry, redox isomerization can be expected wherever an ambident ligand changes its coordination site with changing oxidation state of the central metal. The few well-known examples are all from the coordination chemistry of Ru, since both Ru^{II} as well as Ru^{III} are coordinated exclusively octahedrally, and in addition, both oxidation states are inert to substitution.

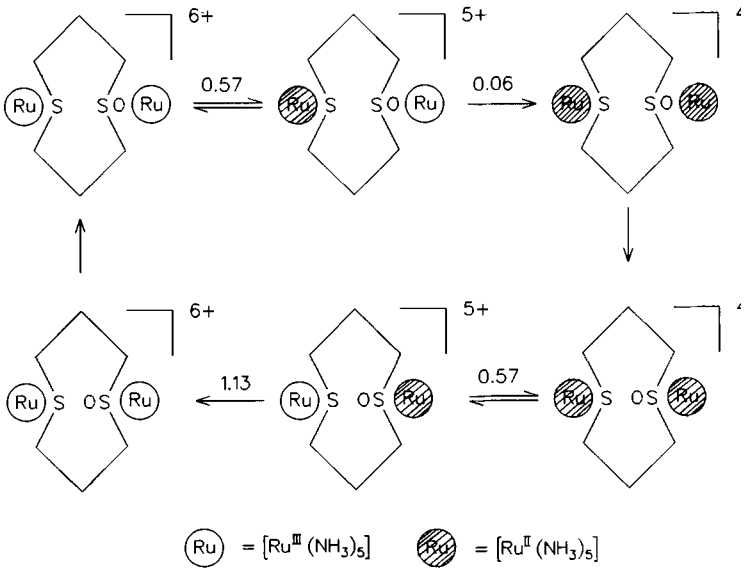

Scheme 4.

In sulfoxide complexes the transition Ru^{II} → Ru^{III} can lead to a bond isomerization from Ru–SO to Ru–OS. This fact is exploited by *Taube* et al.[11] The authors have incorporated an S-function and an SO-function into a macrocycle and complexed both groups to a [Ru(NH$_3$)$_5$]-unit (Scheme 4). Starting from a complex in which both Ru atoms have the oxidation state + II, firstly the Ru–S group and subsequently, at a more positive potential, the Ru–SO function is oxidized. The isomerization to the Ru–OS isomer takes place during the second oxidation step. The Ru$^{3+/2+}$ potential of the Ru–OS group now lies at a more negative value than that of the Ru–S function, so that Ru^{III}–S is reduced prior to Ru^{III}–OS during the back-reduction. Thus, by selective redox triggering both the Ru–OS as well as the Ru–SO isomer can be generated, depending upon whether one starts from the completely oxidized or reduced complex with Ru–S as Ru^{II} or Ru^{III} center. As the authors remark, similar cases can be expected in coordination chemistry in the case of ambident ligands capable of bond isomerization (NO_2^-, NCS^-, CN^-, R_2SO).

A broad spectrum of applications are conceivable for molecules which can be triggered selectively between different states: from micro- and macroscopic display systems to

molecular information storage devices. The results obtained by *Taube* et al. disclose, in particular, a strategy for the planned search for novel systems with molecular hysteresis, which could satisfactorily meet practical requirements.

German versions: *Angew. Chem. 103* (1991) 970

[1] M. Sano, H. Taube, *J. Am. Chem. Soc. 113* (1991) 2327.
[2] P. S. Mariano, T. L. Rose, A. A. Leone, L. Fisher in R. R. Hautala, R. B. King, C. Kutal (Eds.): *Solar Energy*, Clifton, New York 1979, p. 299 ff.
[3] P. Poganiuch, S. Decurtins, P. Gütlich, *J. Am. Chem. Soc. 112* (1990) 3270, P. Gütlich, P. Poganiuch, *Angew. Chem. 103* (1991) 1015; *Angew. Chem. 30* (1991) 975.
[4] W. E. Geiger, (Stuctural Consequences of Electron Transfer) *Prog. Inorg. Chem. 33* (1985) 275.
[5] See, for example, $[\{(C_5H_4)Rh(CO)(PPh_3)\}_2]$: N. G. Connelly, A. R. Lucy, J. D. Payne, A. M. R. Galas, W. E. Geiger, *J. Chem. Soc. Dalton Trans. 1983*, 1879.
[6] N. G. Connelly, W. E. Geiger, *Adv. Organomet. Chem. 23* (1983) 18.
[7] R. Moulton, T. W. Weidman, K. P. C. Vollhardt, A. J. Bard, *Inorg. Chem. 25* (1986) 1846.
[8] N. El Murr, J. E. Sheats, W. E. Geiger, J. D. L. Holloway, *Inorg. Chem. 18* (1979) 1443; U. Kölle, T.-Z. Ding, H. Keller, B. L. Ramakrishna, E. Raabe, C. Krüger, G. Raabe, J. Fleischhauer, *Chem. Ber. 123* (1990) 227, and references cited therein.
[9] R. G. Finke, R. H. Voegeli, E. D. Laganis, V. Boekelheide, *Organometallics 2* (1983) 347; W. J. Bowyer, W. E. Geiger in [4], p. 321; U. Kölle, B. Fuss, *Chem. Ber. 119* (1986) 116.
[10] W. E. Geiger, A. Salzer, J. Edwin, W. von Philipsborn, U. Piantini, A. L. Rheingold, *J. Am. Chem. Soc. 112* (1990) 7113.

Dyes for Visual Distinction between Enantiomers: Crown Ethers as Optical Sensors for Chiral Compounds**

By *Fritz Vögtle** and *Peter Knops*

The discovery of crown ethers by *Pedersen* and the study of their complexation properties heralded the blossoming of the supramolecular chemistry which deals with host–guest interactions.[1] Crown ethers enable not only the selective complexation of cations and neutral organic molecules; with chiral crown ethers as host compounds, the (enantio)selective complexation of optically active guests can be achieved.[2]

By combining a crown ether with chromophoric units a "chromoionophore" is created. With these crown-dyes the selective cation complexation is made visible by a color change in the same molecule.[3] Figure 1 gives an idea of the significant effects which can be achieved with a crown ether coupled to a quinonimine.

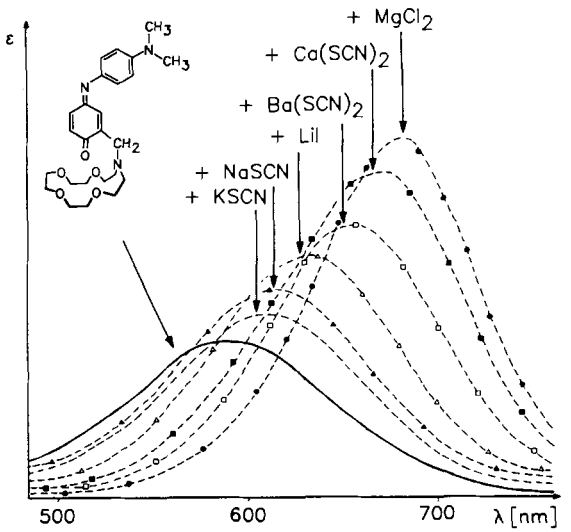

Fig. 1. Selective ion detection by a chromoionophore of the neutral quinonimine type as a result of cation-selective absorption of light.

Now the fascinating challenge of making the enantioselective complexation of chiral guests visible through a color change was recognized, i.e. of being able to see the enantiomeric differentiation of chiral guests by an optically active host molecule in order to draw conclusions about the absolute configuration of the guest molecule. Figure 2 illustrates the concept: through complexation of the chiral guest **1** with the enantiomerically pure chromoionophore **2**, different shifts for the absorption maximum are induced for the resulting complexes depending on the absolute configuration of the guest **1**. In the ideal case, these can be observed with the naked eye.

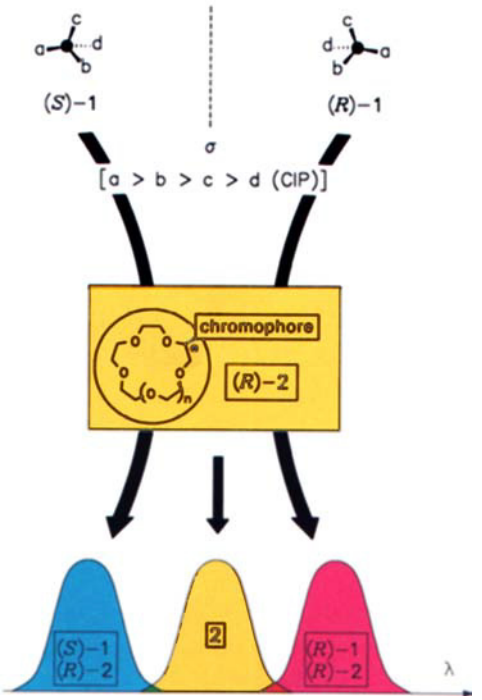

Fig. 2. Mode of action of chiral chromoionophores (schematic) for the visual recognition and differentiation of enantiomeric guest compounds.

[*] Prof. Dr. F. Vögtle, Dr. P. Knops
Institut für Organische Chemie und Biochemie der Universität
Gerhard Domagk-Strasse 1, W-5300 Bonn 1 (FRG)

However, the first attempts to make the structural difference between the enantiomers of optically active ammonium ions visible through color effects with the chiral crown-dye **3** based on tartaric acid ("chiroselective halochromism") failed:[4, 5] neither ^{1}H NMR nor CD and UV/VIS spectra of solutions of **3** showed the anticipated changes on addition of chiral guests, and also extraction experiments were without success.

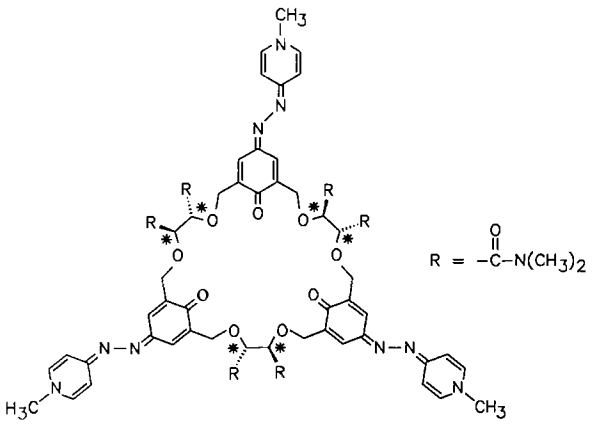

3

The color-giving azamerocyanin unit proved to be the problem in these studies, since it was protonated on addition of the ammonium ions $RNH_3^{\oplus}$, and furthermore, the ionophore periphery of **3** seemed too flexible, and lacked other coordination sites, to provide sufficiently strong interactions with the guest molecules. Consideration of models also revealed that the D_3 symmetry of the potential host was unfavorable for enantioselective complexation.

The breakthrough in distinguishing primary, secondary, and tertiary amines from one another, and in differentiating between the enantiomers of chiral amines by UV/VIS spectroscopy was finally achieved in 1985 by *Misumi* et al.:[6, 7] the chiral hosts **4**–**6** could be prepared through a combination of the long-known *acid* (phenolic) crown ethers with 2,4-dinitroazobenzene units as color-giving component. Addition of amines to ethanolic solutions of **4**–**6** afforded violet solutions of the ammonium phenolates, and distinct shifts of the absorption maxima in the UV/VIS spectra (up to 11 nm) were observed between complexes with the enantiomeric forms of the guest. (See also the review by *Misumi*.[7]) The visual differentiation between the enantiomers of a guest with host molecules **4**–**6** is, however, not possible because the difference in wavelength of the absorption maxima of the diastereomeric complexes is too slight.

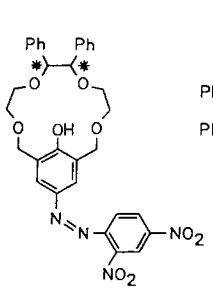

4

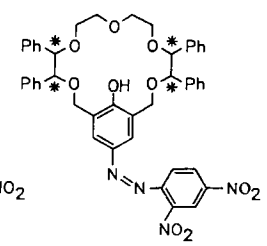

5

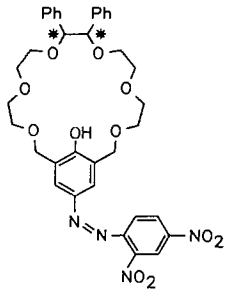

6

Recently *Shinkai* et al.[8] were able to intensify the effects for the chiral recognition of optically active ammonium ions by chiral crown ethers. They utilized the property that the wavelength of reflection for incident light in cholesteric liquid crystals depends on the pitch of the helical structures in the liquid crystalline phase: introduction of complexes of steroid crown ether **7** with chiral ammonium compounds

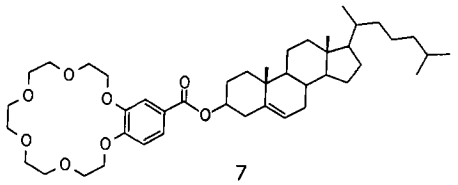

7

into a cholesteric liquid-crystal matrix gave visible color changes. The difference in wavelength of reflection between the diastereomeric complexes was up to 65 nm and thus capable of observation with the naked eye.[8] The conventional chromophoric group is no longer required, as here the whole system of crown-ether complex and liquid crystal functions as (supramolecular) chromophore.

The visual chiral recognition of not only optically active ammonium salts, but also alkali-metal salts of chiral compounds is possible. Alkali-metal salts of (*R*)- and (*S*)-mandelic acid similarly form complexes with steroid crown ether **7**; introduction of these complexes into a cholesteric liquid-crystal matrix changes the pitch of the helical structure depending on the chirality of the anion used, and (*R*) and (*S*) isomers can be distinguished by the observed color of the liquid crystal.[9] The complexation recognition process is thereby transferred through the chiral crown-ether to the overall structure of the liquid crystal and, in general, an only slight color difference in the diastereomeric host–guest complexes is significantly intensified and can be detected by the naked eye.

The liquid-crystal system used by *Shinkai* et al. can therefore be considered the first direct (visual) optical sensor for chirality. Particularly important for the optical differentiation of enantiomers in these studies appears to be the extension of the chromoionophore concept: the self-aggregation and -organization of liquid crystals is exploited to intensify the slight color effect markedly—a lesson in the logical application of knowledge from supramolecular chemistry.

Thus by using chiral host compounds it is possible today to distinguish the enantiomers of an optically active compound alone on the grounds of the color of their complexes. The progress in this area of chiral chromoionophores has, however, by no means reached an end; most recent reports describe halochromic and "chirosolvatochromic" betaine dyes,[11] and research on chiral large-cavity compounds[12] with color-giving units are under way.

German version: *Angew. Chem. 103* (1991) 972

[1] Cf. F. Vögtle: *Supramolecular Chemistry*, Wiley, Chichester 1991, p. 27ff.
[2] a) M. Newcomb, R. C. Helgeson, D. J. Cram, *J. Am. Chem. Soc. 96* (1974) 7367; b) G. Dotsevi, Y. Sogah, D. J. Cram, *ibid. 98* (1976) 3038; c) R. C.

Helgeson, K. Koga, J. M. Timko, D. J. Cram, *ibid. 95* (1973) 3021; d) R. C. Helgeson, J. M. Timko, D. J. Cram, *ibid. 95* (1973) 3023; e) R. C. Helgeson, J. M. Timko, P. Moreau, S. C. Peacock, J. M. Mayer, D. J. Cram, *ibid. 96* (1974) 6762; f) L. R. Sousa, D. H. Hoffman, L. Kaplan, D. J. Cram, *ibid. 96* (1974) 7100.

[3] F. Vögtle, *Pure Appl. Chem. 52* (1980) 2405; see also: M. Takagi in Y. Inoue, G. W. Gokel (Eds.): *Cation Binding by Macrocycles*, Dekker, New York 1990, p. 465.

[4] G. Hollmann, F. Vögtle, *Chem. Ber. 117* (1984) 1355; cf. J. P. Dix, F. Vögtle, *Angew. Chem. 90* (1978) 893; *Angew. Chem. Int. Ed. Engl. 17* (1978) 857.

[5] H. G. Löhr, F. Vögtle, *Acc. Chem. Res. 18* (1985) 65.

[6] T. Kaneda, K. Hirose, S. Misumi, *J. Am. Chem. Soc. 111* (1989) 742.

[7] S. Misumi, *Pure Appl. Chem. 62* (1990) 493.

[8] T. Nishi, A. Ikeda, T. Matsuda, S. Shinkai, *J. Chem. Soc. Chem. Commun. 1991*, 339.

[9] S. Shinkai, T. Nishi, T. Matsuda, *Chem. Lett. 1991*, 437.

[10] See [1], p. 231 ff.

[11] C. Reichardt, M. Wilk, *Liebigs Ann. Chem. 1990*, 189; see also: C. Reichardt, S. Asharin-Fard, *Angew. Chem. 103* (1991) 614; *Angew. Chem. Int. Ed. Engl. 30* (1991) 558.

[12] F. Vögtle, R. Berscheid, W. M. Müller, unpublished results.

VCH Index Library

The electronic index comes with the search module of the literature-management program, VCH Biblio. You can use this index on all PCs running with MS-DOS.

ANGEWANDTE CHEMIE
International Edition in English

Soon available

At the press of a button

The annual index of "Angewandte" is soon available on 5 1/4" and 3 1/2" diskettes.

Yearly updates will keep this invaluable electronic library complete. You can search the cumulative contents in mere seconds.

Price: ca. DM 34.00 plus shipping and handling.

Special news! In honor of the 30th anniversary of "Angewandte Chemie I.E." the cumulative index will also be available on diskette.

VCH
Software
P.O. Box 101161
D-6940 Weinheim

VCH

Communications may be submitted in English *or* in German. Further details regarding the submission of communications can be found in the "Notice to Authors" reproduced in the January issue of the journal. Copies thereof may be obtained from the editorial office upon request.

Polyacetylene in Polyacrylonitrile Matrix: Novel Soluble Matrix Polyacetylenes by Ylide-Nickel Catalysis**

By *K. Alexander Ostoja Starzewski** and *Günter M. Bayer*

Dedicated to Professor Karl Heinz Büchel

The bis(ylide)nickel catalysts **1**, which we described in 1985,[1] are characterized by one rearranged and one structurally intact ylide ligand. They exhibit high activity and offer good possibilities for control of selectivity (molecular mass, degree of branching) in ethene polymerization.[1-4] Their likewise remarkable suitability for the synthesis of polyacetylene,[5] especially in highly polar solvents, prompted us to carry out polymerization experiments in polyacrylonitrile/dimethylformamide (PAN/DMF) solutions. A better stability, for example, is expected for polyacetylene in a highly polar polymer matrix, since the matrix should serve as a barrier to oxygen. However, such a material has not yet been prepared, perhaps because of the sensitivity of the Ziegler–Natta catalysts often used.[6] Our strongly polar bis(ylide)nickel catalysts have now proved to be doubly interesting in this respect.

$[NiPh(Ph_2PCHCPhO)(Me_3PCH_2)]$ **1a**

When acetylene is admitted to a solution of catalyst **1a** in PAN/DMF at 60 °C, an exothermic reaction occurs and the solution almost immediately turns black-violet; the catalyst is active and polymerizes acetylene. However, no polyacetylene can be filtered out and even highly dilute solutions, that is, low-viscosity solutions, show no evidence of sediment formation, even after standing for long periods. The polyacetylene is soluble and can be precipitated with, for example, toluene as a black polymer—referred to as PANPAC in the following discussion. The FT-IR spectrum of the solid shows, besides the polyacrylonitrile bands, the characteristic absorptions of a polyacetylene with a high *trans/cis* ratio ($\geq 80:20$). In order to determine the polyacetylene content of PANPAC, a calibration curve was obtained by grinding PAN with differing amounts of insoluble PAC. To characterize such reaction products spectroscopically, we used the quantitative UV/VIS spectrum of the homogeneous reaction solution in addition to the FT-IR spectrum of the solid. The UV/VIS spectrum shows a broad absorption band (halfwidth: 300–400 nm) with a maximum near 545 nm, corresponding to an average conjugation length of about 20 double bonds.[7] By correlation of IR and UV data, we calculated a mean specific extinction coefficient of 108 $L g^{-1} cm^{-1}$ (1.24×10^5 cm^{-1} based on pure polyacetylene with a density of 1.15 $g cm^{-3}$[8]) for the absorption maximum of the solubilized polyacetylene in the visible region. This value is in good agreement with the literature values for "classical" cross-linked, insoluble polyacetylene (1×10^5 to 4×10^5 cm^{-1}[9]). Thus, measurement of the UV extinction allows determination of the respective PAC content of the solution and, for known PAN concentration, that of PANPAC.

The solubility properties and spectroscopic features of the novel matrix polyacetylenes indicate that they are graft copolymers in which polyacetylene branches are attached to a polyacrylonitrile backbone.[10] The examples in Tables 1 and 2 show the scope of variation for the composition of such polymers as well as the corresponding reaction conditions. Particularly noteworthy are the easy attainment of high PAC contents and the solubilization present in all cases.

Table 1. Acetylene content x_{PAC} in PANPAC and UV/VIS absorption maximum λ_{max} of soluble PANPAC for different concentrations of catalyst, c_{cat} [a].

$c_{cat.}$ [mmol per g PAN]	λ_{max} [nm]	x_{PAC} [mol %] UV	IR
0.2	540	28	28
0.3	545	42	46
0.4	550	53	55
0.5	545	60	59
0.6	545	68	67

[a] After 15 min of acetylene polymerization in 1% PAN/DMF solution at 60 °C with **1a**.

Table 2. Acetylene content x_{PAC} in PANPAC and UV/VIS absorption maximum λ_{max} of soluble PANPAC for different polymerization times t [a].

t [min]	λ_{max} [nm]	x_{PAC} [mol %] UV	IR
5	510	18	18
15	550	53	55
30	535	63	62
60	540	70	69

[a] Acetylene polymerization with 0.4 mmol of **1a** per gram of polyacrylonitrile in 1% PAN/DMF solution at 60 °C.

Decisive for the efficiency *and* selectivity is again the presence of the structurally intact ylide ligand.[1] If this ligand is replaced by triphenylphosphane, for example, as in **2**, only a small amount of acetylene reacts. The reaction solution is yellow and the UV/VIS spectrum shows no absorption maximum between 400 and 800 nm. Use of the active bis(ylide)nickel catalysts, on the other hand, allows the absorption maximum for visible light to be shifted to shorter or

[*] Dr. K. A. Ostoja Starzewski, Dr. G. M. Bayer
Bayer AG, Zentrale Forschung und Entwicklung
Wissenschaftliches Hauptlaboratorium
W-5090 Leverkusen 1 (FRG)

[**] Electronic Structure and Reactivity of Ylide Systems, Part 17. Part 16: [5].

[NiPh(Ph_2PCHCMeO)(Me_3PCH_2)] **1b**

[NiPh(Ph_2PCHCPhO)(iPr_3PCHPh)] **1c**

[NiPh(Ph_2PCHCPhO)(Ph_3P)] **2**

longer wavelengths by variation of the ligand, in accordance with different average degrees of polyene conjugation. When **1b** is used, for example, the absorption maximum is around 450 nm and the product contains about 85% *trans* double bonds. With the more active catalyst **1c**, the PANPAC is deep blue with an absorption maximum near 670 nm and more than 90% *trans* double bonds (Fig. 1). With respect to

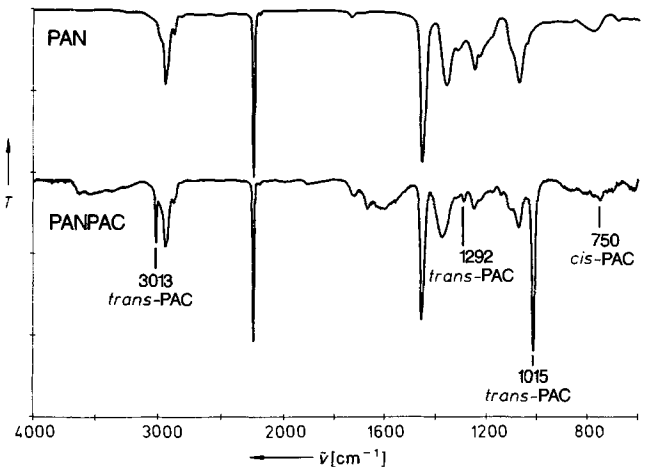

Fig. 1. FT-IR spectrum of PANPAC with 32 mol% acetylene; the polyacetylene segments have about 95% *trans* configuration [11] (bottom). For comparison: polyacrylonitrile (top). T = transmittance.

their conjugation length, the *trans* polyacetylene segments are no longer distinguishable from classical *trans*-PAC by UV spectroscopy. For comparison, the absorption maximum of classical cross-linked and correspondingly high-molecular-mass *trans*-PAC lies at 645–670 nm, whereas the corresponding isomer with mainly *cis* configuration absorbs most strongly at about 540 nm.[9]

The ability to control the percentage content of polyacetylene in PANPAC by varying the amount of catalyst and the polymerization time allows novel, soluble, and processable PAC-containing polymers to be prepared directly. The key prerequisites are thereby fulfilled to develop polyacetylene into an "advanced material".[12]

Received: February 22, 1991 [Z 4459 IE]
German version: *Angew. Chem. 103* (1991) 1012

[1] K. A. Ostoja Starzewski, J. Witte, *Angew. Chem. 97* (1985) 610; *Angew. Chem. Int. Ed. Engl. 24* (1985) 599.

[2] K. A. Ostoja Starzewski, J. Witte, K. H. Reichert, G. Vasiliou in W. Kaminsky, H. Sinn (Eds.): *Proc. Int. Symp. Transition Metals and Organometallics as Catalysts for Olefin Polymerization (Hamburg 1987)*; Springer, Heidelberg 1988, pp. 349–360.

[3] K. A. Ostoja Starzewski, J. Witte in R. Quirk (Ed.): *Proc. Int. Symp. Transition Metal Catalyzed Polymerizations (Akron, OH, USA 1986)*, Cambridge Univ. Press, New York 1988, pp. 472–496.

[4] K. A. Ostoja Starzewski, J. Witte, *Angew. Chem. 99*, (1987) 76; *Angew. Chem. Int. Ed. Engl. 26* (1987) 63.

[5] K. A. Ostoja Starzewski, J. Witte, *Angew. Chem. 100* (1988) 861; *Angew. Chem. Int. Ed. Engl. 27* (1988) 839.

[6] The current state of this direction of research encompasses block and graft copolymers and is surveyed in: a) C. Kröhnke, G. Wegner in H. Bartl, J. Falbe (Eds.): *Houben-Weyl, Methoden der organischen Chemie, Vol. E20/2*, Thieme, Stuttgart 1987, p. 1312–1365; b) J. A. Stowell, A. J. Amass, M. S. Beevers, T. R. Farren, *Polymer 30* (1989) 195; important work on, for example, c) poly(pentenylene-*b*-acetylene): T. R. Farren, A. J. Amass, M. S. Beevers, J. A. Stowell, *ibid. 30* (1989) 1008; d) poly(styrene-*b*-acetylene): M. Aldissi, A. R. Bishop, *ibid. 26* (1985) 622; e) polyisoprene-polyacetylene: F. R. Bates, G. L. Baker, *Macromolecules 16* (1983) 704; f) polybutadiene-polyacetylene: S. Destri, M. Catellani, A. Bolognesi, *Macromol. Chem., Rapid Commun. 5* (1984) 353.

[7] Cf., e.g., K. Knoll, R. R. Schrock, *J. Am. Chem. Soc. 111* (1989) 7989 and references cited therein.

[8] G. Perego, G. Lugli, U. Predetti, M. Cesari, *Makromol. Chem. 189* (1988) 2657 and references cited therein.

[9] H. Fujimoto, K. Kamiya, J. Tanaka, M. Tanaka, *Synth. Met. 10* (1985) 367 and references cited therein.

[10] In the formation of a poly(acrylonitrile-*g*-acetylene) graft copolymer, an organometallic reaction involving CH activation is also conceivable in addition to a reaction at the nitrile groups; cf., e.g., G. Czekay, T. Drewello, H. Schwarz, *J. Am. Chem. Soc. 111* (1989) 4561 and references cited therein.

[11] The assignment of the PAC bands as well as the calculation of the *trans* content [% *trans* = $100\ A_{1015}/(1.3\ A_{750} + A_{1015})$] was carried out as described by a) H. Shirakawa, T. Ito, S. Ikeda, *Polymer J. 4* (1971) 231; b) T. Ito, H. Shirakawa, S. Ikeda, *J. Polym. Sci. Polym. Chem. Ed. 12* (1974) 11; cf. also c) Z. Chen, Z. Shen, M. Liu, M. Shi, D. O. Hummel, *Makromol. Chem. 188* (1987) 2687, 2697.

[12] K. A. Ostoja Starzewski, unpublished.

Thiadistannirane, 1,2-Dithiadistannetane, and Selenadistannirane: Small Rings with Tin–Tin Bonds**

By *Annemarie Schäfer, Manfred Weidenbruch,* Wolfgang Saak, Siegfried Pohl*, and *Heinrich Marsmann*

Dedicated to Professor Peter Sartori on the occasion of his 60th birthday

A number of molecules with multiple bonds between heavy main-group elements have been isolated in recent years and have proven to be excellent building blocks for otherwise hardly accessible compounds. For example, disilenes, $R_2Si{=}SiR_2$, and digermenes, $R_2Ge{=}GeR_2$, react smoothly with heavy chalcogens to give three-membered ring systems, namely, the thia-,[1] selena-, and telluradisiliranes[2] and the thia-,[3] selena-,[3,4] and telluradigermiranes.[5]

Surprisingly, no additions to tin–tin double bonds have been reported, even though the formally reverse reaction was observed in 1985 by *Masamune* and *Sita*.[6] On heating hexakis(2,4,6-triisopropylphenyl)cyclotristannane (**1**), they obtained distannene **2**, which is stable in solution. However, **1** was only accessible in low yield via a multistep synthesis.[6] Recently, we showed that treatment of tin(II) chloride with 2,4,6-triisopropylphenylmagnesium bromide gives **1** in a single step and in high yield. Moreover, reaction of **2** with tellurium afforded a telluradistannirane, the first three-membered ring with a Sn_2X framework.[7]

[*] Prof. Dr. M. Weidenbruch, Dr. A. Schäfer, Dipl.-Chem. W. Saak, Prof. Dr. S. Pohl
Fachbereich Chemie der Universität
Carl-von-Ossietzky-Strasse 9–11, W-2900 Oldenburg (FRG)
Prof. Dr. H. Marsmann
Fachbereich Chemie der Universität-Gesamthochschule, Paderborn (FRG)

[**] Compounds of Germanium and Tin, Part 8. This work was supported by the Deutsche Forschungsgemeinschaft and the Fonds der Chemischen Industrie. Part 7: M. Weidenbruch, J. Schlaefke, K. Peters, H. G. von Schnering, *J. Organomet. Chem.*, in press.

The reaction of **2** with sulfur proceeds differently, since the reaction is complete—as revealed by disappearance of the deep red color of **2**—only when the ratio of starting materials is one to two (Scheme 1). Two products are isolated. Their elemental analyses and mass spectra indicate the presence of isomeric dithiadistannetanes. The colorless isomer was identified as the known 1,3-dithiadistannetane **4**,[8] the yellow isomer as the 1,2-dithiadistannetane **3**. The constitution of **3** is supported, for example, by the ^{119}Sn NMR spectrum, which shows a $^1J(^{119}Sn,^{117}Sn)$ coupling of 4667 Hz, typical for molecules with a tin–tin bond.

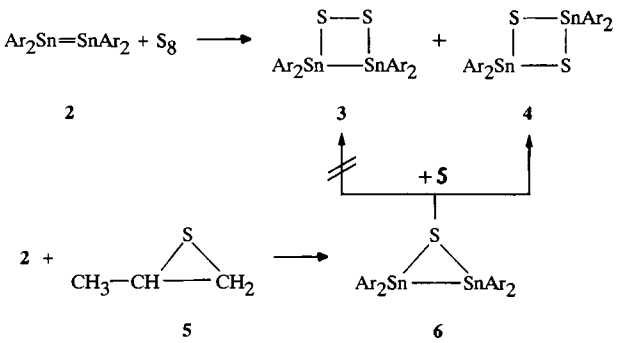

Scheme 1. Ar = 2,4,6-iPr$_3$C$_6$H$_2$.

The X-ray structure analysis of **3**[9] (Fig. 1) confirms this proposal and also shows several unexpected features. The Sn_2S_2 four-membered ring is folded with an interplanar an-

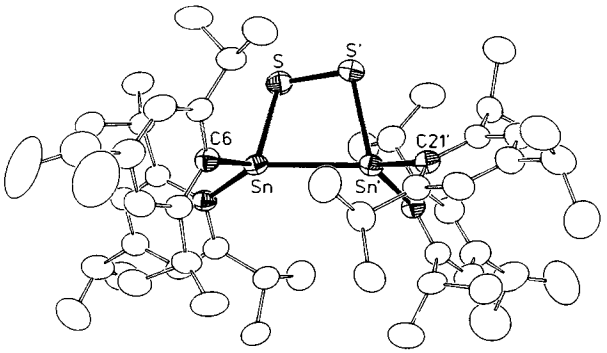

Fig. 1. Molecular structure of **3** (ORTEP, thermal ellipsoids at 30% probability, hydrogen atoms omitted). Symmetry-equivalent atoms are indicated by primes. Selected bond lengths [pm] and angles [°]: Sn–Sn' 288.9(1), Sn–S 248.0(1), S–S' 209.1(3), Sn–C6 218.9(4), Sn–C21 217.9(4); Sn–S–S' 95.8(1), S–Sn–Sn' 78.2(1); torsion angle (average of the angles between the opposite-lying planes C6–Sn–Sn'/C21'–Sn'–Sn and C6'–Sn'–Sn/C21–Sn–Sn') 0.7.

gle of 22° between the Sn–Sn'–S and Sn–Sn'–S' planes. The molecule possesses crystallographic C_2 symmetry, the C_2 axis passing through the midpoints of the S–S and Sn–Sn bonds. Especially interesting is the coordination sphere of the tin atoms; the two C atoms of the aryl groups together with the other tin atom form a nearly planar ligand environment (the sum of angles at each tin atom is 354°). A similar phenomenon was observed for oxa-,[10] thia-,[1] and selenadisiliranes,[2] for example, and was discussed, in connection with the short Si–Si distances, as evidence for π complexes between the disilene and the chalcogen atoms. A similar model of bonding is ruled out for **3**, however, since all bonds within the ring are lengthened relative to those usually found.

The ready formation of **3** is surprising, because the analogous ring systems with heavy elements of the 4th main group were previously unknown. In organic chemistry, too, 1,2-dithietanes were long regarded as only reactive intermediates, until, a few years ago, the first four-membered ring of this kind was isolated as part of a polycyclic system.[11]

The thiadistannirane **6**, which is not accessible by treatment of **2** with sulfur, is smoothly obtained by reaction of **2** with methylthiirane **5** (see Scheme 1). The constitution of **6** was established from the elemental analysis, the mass spectrum, and the ^{119}Sn NMR spectrum, in which the $^1J(^{119}Sn,^{117}Sn)$ coupling of 5745 Hz indicates, as in the case of **3**, the presence of a tin–tin bond. Moreover, further reaction of **5** with **6** results in insertion of sulfur into the tin–tin bond to give exclusively **4**.

The latter reaction, together with other findings, makes plausible the following proposal for the formation of **3** and **4**. Addition of an S_2 fragment to **2** results in direct formation of **3**; any **6** formed during the heterogeneous reaction reacts spontaneously with sulfur to give **4**. The possibility that **4** might be formed from **3** by a sequence of cycloreversion and cycloaddition reactions could not be verified experimentally, since **3** remained unchanged after heating for several days. Likewise, the assumption that stannylenes (stannanediyls), initially formed by fragmentation of **2**, might react with sulfur to afford rings **3** and **4** via stannathiones, Ar_2SnS, can probably be excluded. In this case, in analogy to the reaction of **5** with **6**, only the thermodynamically favored ring **4** should form.

The reactivity of selenium lies between that of sulfur and tellurium, as is evident in its reaction with **2** (Scheme 2). Even for a less than stoichiometric amount of selenium, only a mixture of the selenadistannirane **7** and the 1,3-diselenadis-

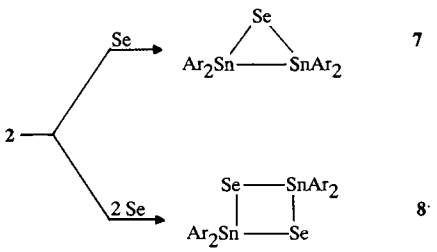

Scheme 2. Ar = 2,4,6-iPr$_3$C$_6$H$_2$.

tannetane **8** is formed. The constitution of both rings was established by elemental analyses and spectroscopic data. Characteristic of **7** is again the ^{119}Sn NMR spectrum, which shows a $^1J(^{119}Sn,^{117}Sn)$ coupling of 4873 Hz and thus supports the presence of the tin–tin bond in **7**.

Experimental Procedure

3 and **4**: Sulfur (0.15 g, 4.70 mmol) was added to **1** (2.00 g, 1.27 mmol) in 50 mL of toluene at 90 °C and the mixture was kept at this temperature for 0.5 h, its color turning from red to yellow. Toluene was replaced by n-pentane and unreacted sulfur was filtered off. HPLC of this solution showed that quantitative conversion had occurred to give a mixture of **3** (55%) and **4** (45%). Fractional crystallization from n-pentane gave initially 0.75 g (35%) of **3** as yellow crystals, m.p. 232–234 °C, ^{1}H NMR (300 MHz, C_6D_6): δ = 1.16 (m, 72H), 2.71 (sept, 4H), 3.52 (very broad, 8H), 7.06 (s, $^4J(^{119}Sn,^1H)$ = 20 Hz, 8H). ^{13}C NMR (75.44 MHz, C_6D_6): δ = 14.23, 22.67, 24.06, 25.44, 34.53, 38.70, 122.78, 150.76, 154.43. ^{119}Sn NMR (93.23 MHz, C_6D_6, versus Me_4Sn): δ =

121.5 $^1J(^{119}Sn,^{117}Sn)$ = 4666 Hz). MS (CI, isobutane): *m/z* 1115 ($M^{\oplus}$ + 1, 23%). UV/VIS: λ_{max} [nm] (ε) = 391 (756).

Subsequently, 0.40 g (19%) of colorless **4** was obtained from a small amount of *n*-pentane: m.p. 234–236 °C, ^{1}H NMR: δ = 1.14 (d, 24H), 1.22 (d, ^3J(H,H) = 7 Hz, 48H), 2.69 (sept, ^3J(H,H) = 7 Hz, 4H), 3.92 (m, broad, 8H), 7.06 (s, $^4J(^{119}Sn,^1H)$ = 28.3 Hz, 8H). ^{13}C NMR: δ = 24.02, 25.17, 34.55, 37.05, 122.57, 142.56, 150.96, 155.06. ^{119}Sn NMR: δ = −46.9 ($^2J(^{119}Sn,^{117}Sn)$ = 174 Hz).

6: Addition of **5** (0.14 g, 1.90 mmol) in 7 mL of toluene to **1** (2.00 g, 1.27 mmol) in 50 mL of toluene at 90 °C resulted in a spontaneous color change from red to yellow. Toluene was replaced by *n*-pentane and the sparingly soluble products were removed by filtration. Crystallization from about 5 mL of *n*-pentane gave 1.2 g (58%) of **6** as bright yellow crystals, m.p. 169–172 °C. ^{1}H NMR (300 MHz, C_6D_6): δ = 1.22 (m, 72H), 2.72 (sept, 4H), 3.77 (very broad, 4H), 3.90 (very broad, 4H), 7.06 (s, $^4J(^{119}Sn,^1H)$ = 24.4 Hz, 8H). ^{13}C NMR (75.44 MHz, C_6D_6): δ = 24.08, 24.57, 25.18, 25.64, 34.55, 37.04, 39.13 (broad), 122.35, 150.62, 155.08 (broad), 155.30 (broad). ^{119}Sn NMR (93.23 MHz, C_6D_6, versus Me_4Sn): δ = −309 ($^1J(^{119}Sn,^{117}Sn)$ = 5745 Hz). UV/VIS: λ_{max} [nm] (ε) = 340 (12320).

Further treatment of **6** with **5** under the same conditions gave exclusively **4** and no **3** (HPLC, NMR analysis).

7: Compound **1** (2.00 g, 1.27 mmol) and selenium (0.20 g, 2.53 mmol) were heated in 50 mL of toluene for about 1 h at 90 °C until the deep red color of **2** had vanished. Toluene was replaced by *n*-pentane and unreacted selenium was filtered off. Fractional crystallization from *n*-pentane resulted initially in a mixture of **7** and **8**, followed by precipitation of 0.50 g (23%) of **7** as light yellow crystals, m.p. 158–162 °C. ^{1}H NMR (300 MHz, C_6D_6): δ = 1.17 (m, 72H), 2.72 (sept, 4H), 3.69 (very broad, 8H), 7.06 (s, $^4J(^{119}Sn,^1H)$ = 21.9 Hz, 8H). ^{13}C NMR (75.44 MHz, C_6D_6): δ = 24.09, 24.58, 25.19, 25.77, 34.53, 39.83 (broad), 122.33, 150.56, 155.34. ^{119}Sn NMR (93.23 MHz, C_6D_6, versus Me_4Sn): δ = −393, ($^1J(^{119}Sn,^{117}Sn)$ = 4873 Hz). ^{77}Se NMR (47.67 MHz, C_6D_6, versus Me_2Se) δ = −378 ($^1J(^{119/117}Sn,^{77}Se)$ = 432/413 Hz). UV/VIS: λ_{max} [nm] (ε) 0345 (6790).

8: Compound **1** (2.00 g, 1.27 mmol) and selenium (0.31 g, 3.90 mmol) were refluxed in 40 mL of toluene for 15 h. The workup was analogous to that of **7**. Crystallization from *n*-pentane gave 2.1 g (91%) of colorless **8**, m.p. 243–245 °C. ^{1}H NMR: δ = 1.15 (d, ^3J(H,H) = 6 Hz, 24 H), 1.22 (d, ^3J(H,H): = 6 Hz, 48H), 2.71 (sept, 4H), 3.97 (m, 8H), 7.04 (s, $^4J(^{119}Sn,^1H)$ = 28 Hz, 8H). ^{13}C NMR: δ = 24.06, 25.20, 34.56, 37.01, 122.56, 140.16, 150.87, 154.89. ^{119}Sn NMR: δ = −253 ($^2J(^{119}Sn,^{117}Sn)$ = 318 Hz). ^{77}Se NMR: δ = 84 ($^1J(^{119/117}Sn,^{77}Se)$ = 868/831 Hz).

All new compounds gave correct C,H,S(Se) elemental analyses.

Received: March 25, 1991 [Z 4533 IE]
German version: *Angew. Chem. 103* (1991) 978

CAS Registry numbers:
1, 98526-67-1; **3**, 134391-62-1; **3** · 0.5 pentane, 134391-63-2; **4**, 126857-71-4; **5**, 1072-43-1; **6**, 126857-72-5; **7**, 134391-64-3; **8**, 134391-65-4.

[1] R. West, D. J. De Young, K. J. Haller, *J. Am. Chem. Soc. 107* (1985) 4942.
[2] R. P.-K. Tan, G. R. Gillette, D. R. Powell, R. West, *Organometallics 10* (1991) 546.
[3] T. Tsumuraya, S. Sato, W. Ando, *Organometallics 7* (1988) 2015.
[4] S. Batcheller, S. Masamune, *Tetrahedron Lett. 29* (1988) 3383.
[5] T. Tsumuraya, Y. Kabe, W. Ando, *J. Chem. Soc. Chem. Commun. 1990*, 1159.
[6] S. Masamune, L. R. Sita, *J. Am. Chem. Soc. 107* (1985) 6390.
[7] A. Schäfer, M. Weidenbruch, W. Saak, S. Pohl, H. Marsmann, *Angew. Chem. 103* (1991) 873; *Angew. Chem. Int. Ed. Engl. 30* (1991) 834.
[8] P. Brown, M. F. Mahon, K. C. Molloy, *J. Chem. Soc. Chem. Commun. 1989*, 1621.
[9] **3** · 0.5 pentane: monoclinic, space group $C2/c,a$ = 1542.0(1), b = 2715.8(2), c = 1675.4(1) pm; β = 104.93(2)°, V = 6779 × 10^6 pm^3, Z = 4, ϱ_{calcd} = 1.163 g cm^{-3}. 5563 unique reflections, 4596 observed ($I > 2\sigma(I)$) 305 parameters, R = 0.046, R_w = 0.045. Programs: G. M. Sheldrick, SHELX-76, Program for Crystal Structure Determination, University of Cambridge, Cambridge 1976; G. M. Sheldrick, SHELX-86, Göttingen 1986; Drawing: C. K. Johnson, ORTEP II, Report ORNL-5138; Oak Ridge National Laboratory, Oak Ridge, TN, 1976. Further information on the crystal structure determination is available on request from the Fachinformationszentrum Karlsruhe, Gesellschaft für wissenschaftlich-technische Information mbH, W-7514 Eggenstein-Leopoldshafen 2 (FRG), by quoting the depository number CSD-55363, the names of the authors, and the journal citation.
[10] H. B. Yokelson, A. J. Millevolte, G. R. Gillette, R. West, *J. Am. Chem. Soc. 109* (1987) 6865.
[11] K. C. Nicolaou, C.-K. Kwang, M. E. Duggan, P. J. Carroll, *J. Am. Chem. Soc. 109* (1987) 3801.

Light Absorption as well as Crystal and Molecular Structure of *N,N'*-Dimethylindigo: An Example of the Use of Synchrotron Radiation**

By *Gerhard Miehe,* Peter Süsse,* Vladimir Kupcik,† Ernst Egert, Martin Nieger, Gerold Kunz, Ralf Gerke, Burkhard Knieriem, Matthias Niemeyer,* and *Wolfgang Lüttke**

Dedicated to Professor Horst Prinzbach on the occasion of his 60th birthday

N,N'-Dialkylindigos (**1**) absorb at considerably longer wavelengths than the parent compound **2**[1–4] (Table 1); their solutions in organic solvents appear green to the eye, whereas those of indigo appear blue. This phenomenon was first recognized by *K. J. Braakman*,[3] who ascribed it to the inductive effect of the *N*-alkyl groups. His finding that the color band shifts to longer wavelengths as the steric bulk of the *N*-alkyl groups increases indicated, however, that the bathochromism is due less to their inductive effects than to their steric interaction with the carbonyl groups.[2, 5–8] Bathochromism due to steric hindrance was first observed in 1942 by *K. J. Brunings* and *A. H. Corvin*[9] for cyanine dyes and was interpreted theoretically in 1956 by *E. Heilbronner* and *R. Gerdil*.[10] According to their studies, such an effect is expected when the degree of double bonding in the central bond undergoing twisting is greater in the electronic ground state than in the excited state. In this case, the loss of resonance energy due to sterically induced torsion around the central bond and the resulting decrease in overlap of the π orbitals is greater in the ground state than in the excited state, assuming the torsion angles are the same; the energy of the ground state is thereby increased more than that of the excited state and the excitation energy is correspondingly decreased. An important argument favoring this model in the case of the *N,N'*-dialkylindigos **1** has been provided by *M. Klessinger* on the basis of HMO and PPP calculations:[6, 7] Indeed, the π bond order of the central bond of indigo (**2**) is substantially higher in the ground state (HMO, 0.628; PPP, 0.688) than in the first excited state (HMO, 0.453; PPP 0.494).

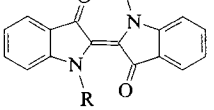

1 R = alkyl
2 R = H
3 R = CH_3

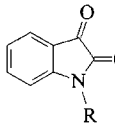

4 R = CH_3
5 R = H

However, experimental proof has been lacking so far; it should provide information on whether, for example, *N,N'*-

[*] Dr. G. Miehe
Institut für Kristallographie und Mineralogie der Universität
Senckenberganlage 30, W-6000 Frankfurt am Main 1 (FRG)
Prof. Dr. P. Süsse, Prof. Dr. V. Kupcik †
Mineralogisches Institut der Universität
Goldschmidtstrasse 1, W-3400 Göttingen (FRG)
Prof. Dr. E. Egert, M. Nieger
Institut für Organische Chemie der Universität
Niederurseler Hang, W-6000 Frankfurt am Main 50 (FRG)
Prof. Dr. W. Lüttke, Dipl.-Chem. G. Kunz, R. Gerke, Dr. B. Knieriem, Dr. M. Niemeyer
Institut für Organische Chemie der Universität
Tammannstrasse 2, W-3400 Göttingen (FRG)

[**] Theoretical and Spectroscopic Investigations of Indigo Dyes, Part. 23. This work was supported by the Bundesministerium für Forschung und Technologie (Project: Structure Analysis with Synchrotron Radiation 05320 IAB 8). Part 22: H. Meier, W. Lüttke, *Liebigs Ann. Chem. 1981*, 1303.

Table 1. Wavelengths λ [nm] of the longest-wavelength absorption band of indigo dyes. The values measured in *n*-hexane were taken from [3], the others were measured.

	In solution					Solid
	n-Hexane	*p*-Xylene	CH_2Cl_2	$CHCl_3$	CH_3CN	KBr
indigo **2**	–	597	598.5	604	596	654
N-methylindigo	–	631.5	631	636.5	622	658
N,N'-dimethylindigo **3**	647	641	649	654.5	643	678.5
N,N'-diethylindigo	683	–	–	653	–	–
N,N'-diisopropylindigo	708	–	–	–	–	–

dimethylindigo (**3**)—like indigo (**2**)[11–15]—is planar or twisted. An X-ray structure analysis of **3** was therefore carried out;[16, 17] in addition, its structure was calculated using the π-SCF force-field program PIMM.[18, 19] Furthermore, the crystal structure of *N*-methylisatin (**4**) was determined.[20, 21] In **4**, which may be regarded as a "half-molecule" of *N,N'*-dimethylindigo (**3**), the inductive effect of the methyl groups is retained, but their steric effects are eliminated.

The first structure determination of **3**, carried out with $Mo_{K\alpha}$ radiation, yielded correct results,[17] but was inadequate owing to the low scattering ability of the small crystals, which were free of a multidomain texture. We therefore used synchrotron radiation (five-circle diffractometer in the HASYLAB[22]) to determine the structure once again. A total of 2055 unique reflections (97% of which were significant) were measured for a crystal with the dimensions $0.05 \times 0.08 \times 0.18$ mm^3 at a wavelength of $\lambda = 1.2127$ Å. The available intensity of the primary beam was about 40 times greater than that of a conventional X-ray tube. These data were easily refined and led to an *R* value of 0.032 ($R_w = 0.027$). The standard deviations of the distances of the "heavy" atoms were 0.003 Å on average, those of the C–H distances 0.015 Å (C-ring-H). The statistical variance of the individual values is on the order of magnitude of the experimental standard deviations. A reasonable determination of the anisotropic temperature factors of the hydrogen atoms was accomplished in addition to the refinement of their site parameters. Their physical relevance is immediately evident when the H atoms bonded to the aromatic ring are compared with those of the *N*-CH_3 groups. It is clearly revealed that the *N*-CH_3 groups do not rotate freely, but merely undergo a torsional vibration with a relatively large amplitude (Fig. 1). To our knowledge, this work represents the first physically meaningful determination of the hydrogen vibrational ellipsoids from X-ray diffraction data.

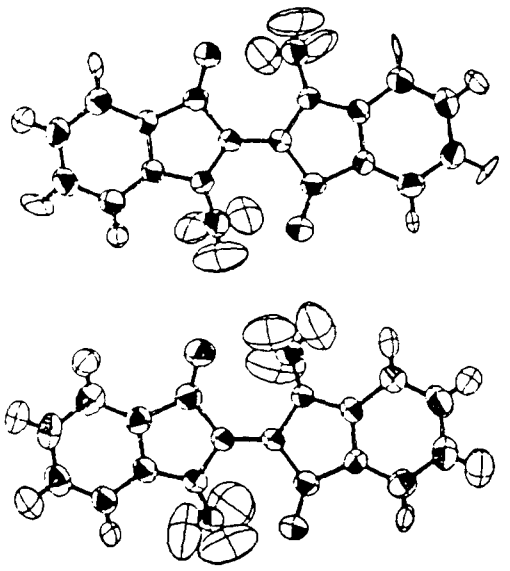

Fig. 1. The molecular shapes and thermal vibrations of **3** (top, molecule **I**; bottom, molecule **II**). The large amplitudes of the torsional vibrations of the *N*-methyl groups are clearly evident.

Although the two molecules in the asymmetric unit of the unit cell of **3** are crystallographically independent, their molecular shapes are practically identical. They have *trans* configuration; their C_2-symmetric shape is best described as that of a "bent" propeller (Fig. 2). The six carbon atoms of each benzene ring and all six atoms directly bonded to each ring are exactly coplanar within the standard deviations; only the C atoms of the central bond (C2 and C2') deviate slightly from this plane (<0.1 Å). The two planar halves of the molecule are twisted by $\beta = 26°$ with respect to each other; moreover, they are tilted in the same direction by an average of $\alpha = 9.5°$ with respect to the central C–C bond. The two C atoms of the central bond thereby adopt a slightly pyramidal bonding geometry and undergo a hybridization change from sp^2 toward sp^3. This is revealed in the fact that the length of the C=C bond of **3** (1.376 Å) considerably exceeds the value for indigo (**2**; 1.342 Å)[15] and the standard value for a C=C bond (1.337 Å) (cf. Table 2). The two *N*-

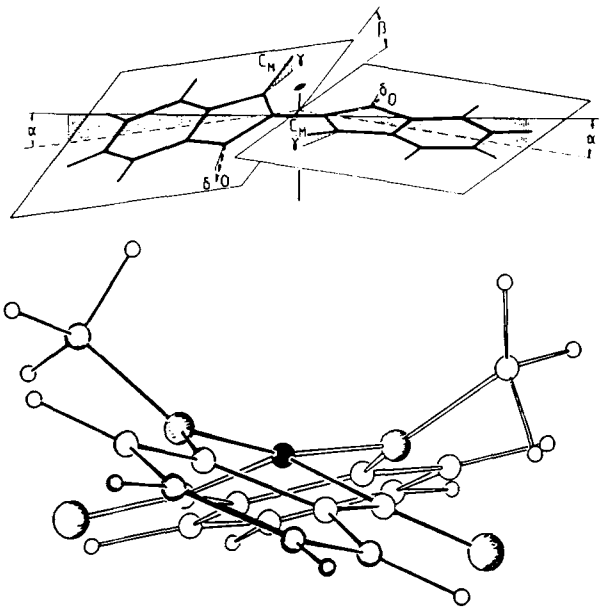

Fig. 2. Molecular shape of **3**: a) schematic; b) viewed along the C=C bond.

Table 2. Comparison of the average interatomic distances [Å] in **3** and **4** [a].

Bond	*N,N'*-Dimethylindigo **3**		Standard distances [23]	*N*-Methylisatin **4**	
	Crystal structure analysis	PIMM calculation [18, 19]		Crystal structure analysis	PIMM calculation [18, 19]
C–C (ring)	1.383(5)	1.401	1.395	1.381(7)	1.402
C=C (central)	1.376(2)	1.379	1.337	1.219 [b]	1.206 [b]
C–N (ring)	1.386	1.415	1.426	1.380	1.407
C–N (methyl)	1.443	1.477	1.472	1.452	1.488
C–H (ring)	0.97	1.079	1.084	-	-
C–H (methyl)	0.93	1.079	1.091	-	-

[a] The bond lengths [Å] of **3** were obtained by averaging over the four crystallographically independent "half-molecules". [b] This value corresponds to the C2–O2 bond length of **4**.

CH_3 groups are bent away from the planes of the five-membered rings; the N-CH_3 bending angles are 14 and 19.5°. Analogously, but in an opposite direction to the bending of the CH_3 groups, the two carbonyl oxygen atoms lie at an angle of $\delta = 4.5°$ on average with respect to the planes. Noticeably, the interatomic distances in **3** (Fig. 3 and Table 2)

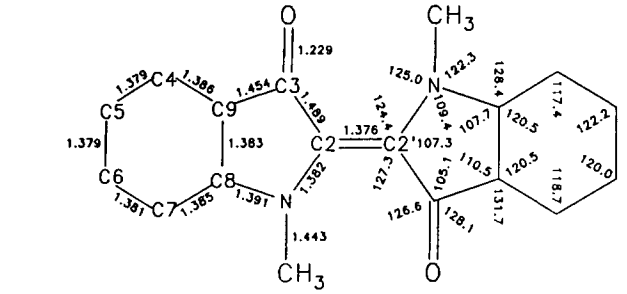

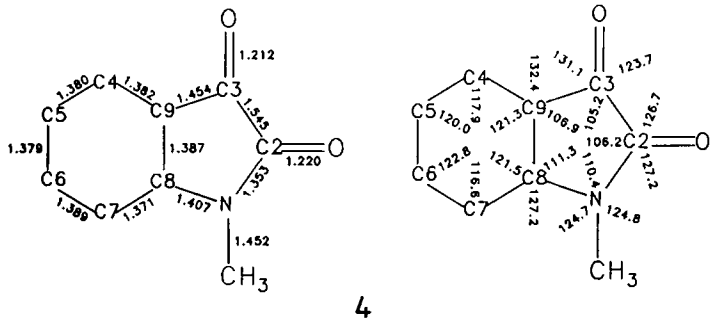

Fig. 3. Bond lengths [Å] and angles [°] of **3** (top) and **4** (bottom). The values for **3** correspond to a structure averaged from four half-molecules.

are systematically shorter than those calculated using the force-field PIMM[18,19] and than the standard distances found in tables,[23] because none of the distances have been corrected for vibrations.

N-Methylisatin (**4**; Table 2),[21] like isatin (**5**),[24] is completely planar. The C–C bonds in the benzene ring of **4** are practically just as long as those in **3**. There are differences in the five-membered rings, however, especially for C2–C3 and C2–N, as well as for N–CH_3 and the C=O bond. These differences are explained by the planar structure of **4** and probably also by the differing polarity of the C2–O bond of **4** compared to the C=C bond of **3**.

The high accuracy of the structure determination made possible by synchrotron radiation allows a detailed analysis of the effect of stacking of the molecules in the lattice on the molecular structure of **3**. The molecular shape is not significantly influenced by the intermolecular interactions in the lattice. This is also indicated by the observation that the IR spectra of the solid and of solutions of **3** in nonpolar solvents are very similar and that, on going from the solid to nonpolar solution, only a small frequency shift of 420 cm^{-1} is found for the longest-wavelength band in the visible spectrum. Thus, the twisted shape of the free molecule **3**, due to steric hindrance, is responsible for the complicated lattice structure (Fig. 4). The structure strives to achieve the greatest possible planarity of the packed layers, like that realized in the lattices of most planar indigo dyes. Although not possible for the entire *N*,*N*′-dimethylindigo molecule owing to its sterically induced nonplanarity, planar stacking is realized for its mutually twisted halves. As shown in Figure 4,

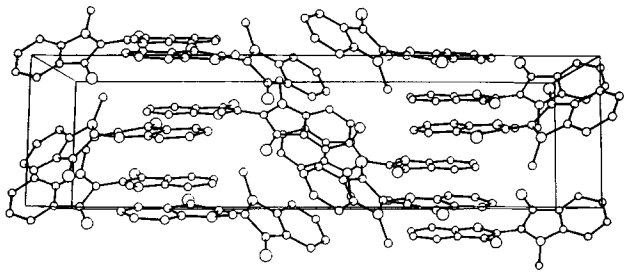

Fig. 4. Schematic representation of the crystal structure of **3**. The molecules **I** are stacked along the edges of the unit cell, the molecules **II** in between.

each molecule of **3** is involved in two stacking systems which are tilted toward each other. In contrast to biphenyl, for example, which is strongly twisted in the gas phase,[25] but is planar in the crystal,[26] the lattice energy is not sufficient in **3** to achieve a planar shape in the face of strong intramolecular steric hindrance. It may be assumed with certainty that **3** possesses the same twisted shape in solution as in the crystal.

The crystal structure of **3** is characterized by a large unit cell ($V = 2806$ Å^3; indigo (**2**), $V = 580.5$ Å^3[15]) and by different stacking of the two crystallographically independent molecules **I** and **II**. They each form separate layers; in the case of molecules **I**—arranged along the edges of the unit cells—this feature is expressed in a somewhat stronger twisting and a smaller aplanarity of the N-CH_3 groups as well as in a stronger vibrational motion compared to **II**.

Thus, *N*,*N*′-dimethylindigo (**3**) is deformed in a very complex way; therefore, the bathochromism of **3** and of its alkyl homologues[3] in comparison to indigo (**2**) is in fact a consequence of the steric interaction of the C=O groups with the N-CH_3 groups, in the sense proposed by *E. Heilbronner* and *R. Gerdil*.[10] This conclusion is confirmed by PPP CI calculations,[2] which we undertook in order to determine separately the effect of torsion around the central C=C bond and of pyramidalization at the N and CO groups on the excitation energy ΔE (S_0-S_1) and on the oscillator strength of the longest-wavelength band of **1**. As shown by the data in Table 3, each of these molecular deformations causes roughly the same bathochromism and the effects are additive.

Table 3. Effect of molecular deformation on the light absorption of **1** according to PPP calculations.

Molecular shape	Excitation energy ΔE (S_0-S_1) [nm]	[cm^{-1}]	Oscillator strength	lg ε
planar	529.5	18886	0.701	4.35
central torsion 26°	541.4	18470	0.723	4.36
N and CO pyramidalization	540.1	18515	0.619	4.29
central torsion 26° and pyramidalization	550.1	18178	0.644	4.31

According to the theory of deformation of C=C bonds,[28–33] their torsion is necessarily associated with a pyramidalization of the two C atoms, which leads to a local increase in the electron density and to a decrease in the C=C π bond order. The C=C pyramidalization found in the structure analysis of **3** ($\alpha = 9.5°$) and the analogous deformation of the N-CH_3 groups ($\gamma = 14$ and 19.5°) explain the higher reactivity of *N*,*N*′-dimethylindigo (**3**) relative to planar indigo (**2**):

(1) On irradiation with visible light, **3**—but not indigo (**2**)—is transformed into its *cis* form;[5, 34–36] the latter, in turn, transforms back into the *trans* isomer in the dark. In comparison to planar photoisomerizable indigoids, such as thioindigo,[34, 35] both processes are appreciably facilitated in **3** by the sterically caused torsion of the molecule. Since, in the photoisomerization of **3**, in contrast to that of other indigo dyes, no short-lived triplet intermediate has been observed, the *trans-cis* rearrangement presumably occurs via a singlet mechanism in the case of **3**.[37, 38]

(2) The high electron density at the central C atoms of **3** makes it readily oxidizable in solution.[39] Apparently, this oxidation occurs via a [2 + 2] cycloaddition of singlet oxygen to form a dioxetane, since we have found that *N*-methylisatin (**4**) is ultimately formed by cleavage of the C=C bond of **3**.

(3) Because of the pyramidalization of the N atoms, *N,N'*-dimethylindigo (**3**) is more basic than planar indigo (**2**). This explains why **3**, unlike **2**, reacts with mineral acids to form soluble salts.[5, 33]

(4) The twisted structure of **3**, together with its inability to form hydrogen bridges, explains why **3** possesses a much lower melting point (182 °C) and a lower density (1.31 $g\,cm^{-3}$) than indigo (**2**: 392 °C and 1.518 $g\,cm^{-3}$). Furthermore, it is responsible for the fact that **3**, in contrast to the planar indigo dyes, is soluble even in nonpolar solvents and that **3**, in contrast to planar thioindigo, has no affinity for cotton fibers.

Received: March 7, 1991 [Z 4477 IE]
German version: *Angew. Chem. 103* (1991) 1008

[1] L. Ettinger, P. Friedländer, *Ber. Dtsch. Chem. Ges. 45* (1912) 2074.
[2] E. B. Knott, *J. Soc. Dyers Colour. 67* (1951) 302.
[3] K. J. Braakmann, *Dissertation*, Universität Amsterdam 1943.
[4] The UV bands of **3** are also shifted to longer wavelengths to varying extents in comparison of those of **2**.
[5] J. Weinstein, G. M. Wyman, *J. Am. Chem. Soc. 78* (1956) 4007.
[6] M. Klessinger, *Diplomarbeit*, Universität Freiburg 1959.
[7] W. Lüttke, M. Klessinger, *Chem. Ber. 97* (1964) 2352.
[8] This interpretation is also supported by the largely identical group electronegativities of alkyl groups with different volumes: J. Mullay, *J. Am. Chem. Soc. 107* (1985) 7271.
[9] K. J. Brunings, A. H. Corvin, *J. Am. Chem. Soc. 64* (1942) 593.
[10] E. Heilbronner, R. Gerdil, *Helv. Chim. Acta 39* (1956) 1966.
[11] A. Reis, W. Schneider, *Z. Kristallogr., Kristallgeom., Kristallphys., Kristallchem. 68* (1928) 543.
[12] H. von Eller, *Bull. Soc. Chim. Fr. 106* (1955) 1444.
[13] E. A. Gribowa, *Kristallografiya 1* (1956) 53.
[14] G. Miehe, V. Kupcik, P. Süsse, *Z. Kristallogr. 149* (1979) 149.
[15] P. Süsse, M. Steins, V. Kupcik, *Z. Kristallogr. 184* (1988) 269.
[16] Synthesis of **3**: P. Friedländer, L. Ettinger, *Ber. Dtsch. Chem. Ges. 45* (1912) 2074.
[17] Crystal structure determination of **3**: space group $P2_1/c$ (needlelike crystals along *c*), $a = 13.99$, $b = 27.54$, $c = 7.35$ Å, $\beta = 97.75°$; $V = 2806$ Å^3, $\varrho = 1.31\ g\,cm^{-3}$. The asymmetric unit contains two molecules $C_{18}H_{14}N_2O_2$ ($Z = 8$). Additional information on the probable molecular shape and a stacking vector revealed by the Patterson function afforded normalized structure factors, which were used successfully with MULTAN 77 ($Mo_{K\alpha}$: 2624 unique reflections, 1774 of which were observed $R_w = 0.064$). See also [21].
[18] H. J. Lindner, *Tetrahedron 30* (1974) 1127.
[19] H. Beck, *Staatsexamensarbeit*, Universität Göttingen 1985.
[20] Synthesis of **4**: G. Heller, *Ber. Dtsch. Chem. Ges. 40* (1907) 1291.
[21] Structure determination of **4**: space group $P2_1/c$, $a = 8.327(1)$, $b = 10.802(2)$, $c = 17.609(3)$ Å, $\beta = 103.26(1)°$, $V = 1542$ Å^3, $Z = 8$; crystal dimensions: $0.2 \times 0.3 \times 0.7$ mm^3; 4868 measured dimensions $2\theta_{max} = 50°$ ($Mo_{K\alpha}$), 1690 symmetry-independent reflections with $|F| > 3\sigma(F)$ used in the structure solution (direct methods) and refinement (223 parameters); C, N and O atoms were refined anisotropically, H atoms were located by difference electron density determination and refined with the riding model $R = 0.081$ ($R_w = 0.068$, $w^{-1} = \sigma(F)^2 + 0.0004 \times F^2$) [17]. Further details on the crystal structure determination are available on request from the Fachinformationszentrum Karlsruhe, Gesellschaft für wissenschaftlich-technische Information mbH, W-7514 Eggenstein-Leopoldshafen 2 (FRG), on quoting the depository number CSD-52827, the names of the authors, and the journal citation.
[22] V. Kupcik, M. Wendschuh-Josties, A. Wolf, R. Wulf, *Nucl. Instrum. Methods Phys. Res. Sect. A 246* (1986) 624.
[23] Taken from: *International Tables for X-ray Crystallography*, Kynoch Press, Birmingham 1969.
[24] G. H. Goldschmidt, F. J. Llewellyn, *Acta Crystallogr. 3* (1950) 291.
[25] A. Almenningen, O. Bastiansen, L. Fernholt, B. N. Cyvin, S. J. Cyvin, S. Samdal, *J. Mol. Struct. 128* (1985) 59.
[26] G. P. Charbonneau, Y. Delugeard, *Acta Crystallogr. B 33* (1977) 1586.
[27] The CI calculations take into account the 45 lowest-energy singly excited configurations. The deviations of the molecule from planarity have been accounted for by the angle dependence of the β integrals of the respective bonds according to the equation $\beta(\theta) = \beta(0)\cos\theta$.
[28] O. Ermer: *Aspekte von Kraftfeldrechnungen*, W.-Baur-Verlag, München 1981, p. 62 ff.
[29] W. L. Mock, *Tetrahedron Lett. 1972*, 475.
[30] L. Radom, J. A. Pople, W. L. Mock, *Tetrahedron Lett. 1972*, 479.
[31] K. N. Houk in W. H. Watson (Ed.): *Stereochemistry and Reactivity of Systems Containing π-Electrons*, Verlag Chemie International, Deerfield Beach, FL, USA 1983, p. 1 ff.
[32] N. G. Rondan, M. N. Paddon-Row, P. Caramella, K. N. Houk, *J. Am. Chem. Soc. 103* (1981) 2436.
[33] R. C. Haddon, *Acc. Chem. Res. 21* (1988) 243.
[34] R. Pummerer, G. Marondel, *Justus Liebigs Ann. Chem. 602* (1957) 228; *Chem. Ber. 93* (1960) 2384.
[35] G. M. Wyman, A. Zenhäusern, *Ber. Bunsenges. 72 Phys. Chem.* (1968) 326.
[36] C. R. Giuliano, L. D. Hess, J. D. Margerum, *J. Am. Chem. Soc. 90* (1968) 587.
[37] D. Schulte-Frohlinde, H. Hermann, G. M. Wyman, *Z. Phys. Chem. N. F. 101* (1976) 115.
[38] H. Görner, J. Pouliquen, J. Kossanyi, *Can. J. Chem. 65* (1987) 708.
[39] G. A. Russell, G. Kaupp, *J. Am. Chem. Soc. 91* (1969) 3851.

d-Electron Density in Formal d^0 Systems from Multiplet Splitting in the Photoelectron Spectrum of Permanganates**

By *Michael Schmalz, Robert Schöllhorn,* and *Robert Schlögl**

An important aspect of current ideas on the bonding in high-temperature superconductors of the oxocuprate type is electron transfer from the 2p band of the oxygen ions to the copper d band. The resulting holes in the anion band lead to a mixed-valence state. This can be formulated according to the ionic model as shown in Equation (a).[1, 2]

$$Cu^{2+/3+}/O^{2-} \rightleftharpoons Cu^{2+}/O^{2-/1-} \qquad \text{(a)}$$

In order to assess how real the differences in charge density are in Equation (a), it is necessary to quantify the difference between formal oxidation state and real charge density. The magnitude of this difference allows an assessment of the relevance of the ionic model, which is used throughout structural chemistry, to a discussion of bonding.

A proven method for the spectroscopic analysis of charge density distribution is photoelectron spectroscopy (PES). It has been applied, for example, to transition-metal chalcogenides of the type $CuCr_2X_4$, which were shown to have

[*] Prof. Dr. R. Schlögl
Institut für Anorganische Chemie der Universität
Niederurseler Hang, W-6000 Frankfurt am Main 50 (FRG)
Dipl.-Chem. M. Schmalz, Prof. Dr. R. Schöllhorn
Institut für Anorganische und Analytische Chemie
der Technischen Universität
Strasse des 17. Juni 135, W-1000 Berlin 12 (FRG)

[**] This work was supported by the Fonds der Chemischen Industrie and by the Bundesministerium für Forschung und Technologie. We thank the Fritz-Haber-Institut, Berlin, für allowing us to use their Leybold EA11 photoelectron spectrometer.

holes in the p band.[3] This charge transfer was found by analysis of the Se 3d spectra. An analogous procedure is not possible for oxidic solids, since the apparently unavoidable presence of OH^- ions makes it very difficult to distinguish between the O 1s binding energy of formal oxide ions (O^{2-}) and that of less shielded oxygen species (O^-), which are possibly also present [Eq. (a)].[2, 4, 5] Nonetheless, permanganates may be used as suitable model substances for an investigation of the difference between formal oxidation state and real charge density in oxides, since the color of these salts cannot be explained in terms of an ionic model with the formal oxidation states Mn^{7+} (d^0 system) and O^{2-} (s^2p^6). Moreover, the MnO_4^- compounds ($AgMnO_4$, $KMnO_4$) are solids that, owing to their molecular-ion lattice, exhibit only small band-structure contributions to the total electron structure, so that the charge distribution can be studied locally.

PES is a surface-sensitive method (information depth ca. 1000 pm); for the application discussed here, therefore, the surface of the sample must be an exact representation of the bulk. This condition can be fulfilled by cleaving the permanganate single crystals under ultrahigh vacuum. Owing to its molecular-ion character, moreover, this system tolerates only small oxygen disorder, in contrast to binary or polynary copper oxides, so that the uncertainty in the valence of the transition metal is much reduced. Furthermore, numerous quantum-mechanical calculations have already been carried out for the MnO_4^- ion, which has long had the same importance in theoretical inorganic chemistry as benzene has had in theoretical organic chemistry.[6]

PES allows the charge density distribution to be determined on the basis of the chemical shifts. However, the system discussed here poses difficulties, since, on the one hand, electrostatic charging—due to the insulator properties of the compounds—and, on the other hand, different lattice energies—due to the differing crystal structures of the compounds required as reference systems—perturb the chemical shifts.[7]

Therefore, the analysis of the d-electron population was performed on the basis of a quantum-mechanical effect seldom used in PES, namely, multiplet splitting. Multiplet splitting, which is caused by the exchange interaction between an unpaired core electron arising through photoionization and the total spin of the d electrons of the valence shell, leads to two final states. The very observation of multiplet splitting, therefore, shows the presence of d electrons in the valence shell.[8] Multiplet splitting is unambiguously observable for photoemission from s states, since intense additional structures appear in the spectra of p and d shells, resulting primarily from a very large number of possible final states. However, a disadvantage is the low intensity of the s bands. In practice, the interpretation of all photoemission structures is further hindered by additional characteristic energy losses.[7]

The samples were first characterized by X-ray diffraction[9] and their composition was established by atomic absorption spectrometry (AAS). The lattice constants of the compounds $AgMnO_4$, $KMnO_4$, and MnF_2 were found to be in good agreement with the reported values.[10] Older publications reported that the Mn 3s spectrum of $KMnO_4$ was not measurable.[11, 12] This may have been due to features of the instruments used, which resulted in a low intensity, or, alternatively, to sample surfaces that did not consist of MnO_4^- ions.

That the substances we investigated contained authentic MnO_4^- was revealed by the composition of the surfaces measured using theoretically determined effective cross-sections[13] (Table 1). The somewhat larger surface values for the cations in the MnO_4^- compounds are probably due to small contamination with KOH, as indicated by the results of the AAS analysis and the form of the O 1s peak in the photoelectron spectrum.[14] The slightly too large content of oxygen is due to the incorporation of OH^- groups into the crystal; these groups are also revealed by a shoulder at about 531.5 eV in the O 1s PE spectra. Under our experimental conditions (surfaces cleaved in situ, ultrahigh vacuum), the Mn 3s spectra of the permanganates exhibited a splitting that was smaller than that of the other manganese compounds; this finding is in agreement with the highest formal oxidation state Mn^{7+}. The Mn 3s spectrum of $KMnO_4$, as an example of the permanganates, is compared with that of MnF_2 in Figure 1. The contribution of the splitting, ΔE_A, is given in Table 1 for all compounds investigated.

Table 1. Binding energies E_B and mulitplet splitting ΔE_A (determined by PE spectroscopy) as well as surface and volume composition of the manganese compounds investigated.

Compound	E_B Mn $2p_{3/2}$ [eV]	ΔE_A [eV] Mn 3s	Composition Surface	Volume
$KMnO_4$	643.1	4.18	$K_{1.23}MnO_{4.24}$	$K_{0.99}MnO_{3.76}$
$AgMnO_4$	642.3	4.2	$Ag_{1.28}MnO_{4.1}$	–
MnO_2 (pyrolusite)	642.9	4.69	$MnO_{2.99}$	$MnO_{2.1}$ $MnO_{1.997}$
MnO_2 (manganite)	642.9	–	$MnO_{4.35}$	$MnO_{2.38}$
MnF_2	643.7	6.5	$MnF_{2.19}$	–

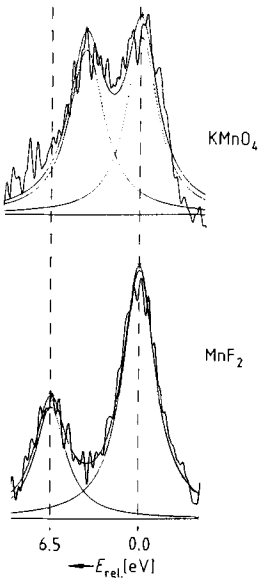

Fig. 1. Mn 3s PE spectra of $KMnO_4$ and MnF_2. The origin of the binding-energy scale in both cases was taken to be the maximum of the lower-energy peak [8, 15].

Further evidence for the presence of MnO_4^- is provided by a comparison with the Mn 2p spectra. These spectra display the same line profile for the two compounds ($AgMnO_4$, $KMnO_4$). The binding energies of the Mn 2p electrons are higher relative to the oxygen 1s electrons than in the reference compounds; the relatively small difference between these energies and that in the formally only tetravalent manganese ion in MnO_2 shows, however, that the permanganate ion cannot be identified by its chemical shift alone. The exact

position of a photoemission line is not only influenced by the electron density at the atom under consideration in its ground state, but also by a number of intra- and interatomic effects (see above). The difference in the values for the two permanganates results from the differing polarizability of the counterion (K^+ is harder than Ag^+) and confirms the effect of the spectroscopic ground state (extraatomic electrostatic shielding[7]) on the binding energies; an actual difference in the Mn charge density is ruled out by the identical geometries of the MnO_4 tetrahedra.[16–18]

The multiplet splittings for $AgMnO_4$ and $KMnO_4$ (4.2 and 4.18 eV, respectively) can now be converted into the corresponding d-electron populations by using theoretical data adjusted for the binary transition-metal compounds.[19] For $\Delta E_A = 4.2$ eV, 3.5 d electrons were calculated for MnO_4^-. This value is in general agreement with the calculated electron densities, which predict an electron deficit in the Mn 3d orbitals of 0.1–1.5 charges relative to the free atom.[20] The charge on manganese, which is small compared to the formal oxidation state, indicates that the real charge on oxygen is not -2, but rather much smaller, so that the binding energy usually given for O^{2-} in transition-metal oxides (-530.5 eV) in reality always includes a considerable covalent interaction. An attempt[21] to identify occupied Mn 3d levels in $KMnO_4$ directly through valence-band photoemission gave results that were qualitatively in agreement with the data presented here. Since valence-band spectroscopy is not state-selective, however, the data from Ref. [21] provide only evidence and not proof.

A value of -0.5 resulted for the charge on the oxygen atoms in the permanganate ion. Presumably, however, there is also an interaction between the Mn 4s/4p orbitals and the O 2p orbital.[20] The spectroscopically determined d-electron population should only be regarded as a lower limit. This uncertainty results from the fact that PES, as a typical high-energy spectroscopy, does not measure the pure electronic ground state of a system.

The results obtained here for the molecular species MnO_4^- cast doubt on an analysis of bonding that assumes formal oxidation states, at least in oxidic solids. Thus, the high-temperature superconductors that show metal-like conduction at room temperature, should exhibit considerable orbital interaction between the "cations" and "anions" owing to the formation of bands (overlap between O 2p and Cu 3d orbitals). Clearly, therefore, Equation (a) does not reflect the actual bonding, since neither ionic formula in Equation (a) is correct. Owing to covalent interactions, oxygen always has an appreciably smaller net charge than would have been expected according to the ionic formula. The differentiation of oxygen ions with differing charge (O^{2-} and O^{-}), attempted on the basis of PE O 1s data,[4] should be viewed very critically. The nonequivalence of the oxygen atoms might be due to differing geometric surroundings and *not* to different oxidation states.

Thus, the *valence problems* in inorganic solids are actually a problem of describing chemical interactions, which do not appear in the context of the multicenter orbital interaction long assumed in the theory of molecules. The description of solids in terms of ions with integral charges, which is very common in structural chemistry, is only a very crude model for the analysis of chemical bonding in extended periodic solids.

Received: December 17, 1990;
revised: March 8, 1991 [Z 4334 IE]
German version: *Angew. Chem. 103* (1991) 983

[1] R. J. Cavam *Spektrum Wiss. 1990*, No. 10, p. 118; *Sci. Am. 263* (1990), No. 8, p. 24.
[2] R. Schlögl, H. Eickenbusch, W. Paulus, R. Schöllhorn, *Mater. Res. Bull. 24* (1989) 181.
[3] A. Payer, M. Schmalz, W. Paulus, R. Schöllhorn, R. Schlögl, *Mater. Res. Bull. 25* (1990) 515.
[4] C. N. R. Rao, P. Ganguly, J. Gopalakrishnan, D. D. Sarma, *Mater. Res. Bull. 22* (1987) 1159.
[5] S. L. Qiu, M. W. Ruckman, N. B. Brookes, P. D. Johnson, J. Chen, C. L. Lin, M. Strongin, B. Sinkovic, J. E. Crow, C. Lee, *Phys. Rev. B37* (1988) 3747.
[6] J. P. Dahl, C. J. Dahlhausen in P. Löwdin (Ed.): *Advances in Quantum Chemistry*, Academic Press, New York 1968, pp. 170–226.
[7] M. Cardona, L. Ley, *Top. Appl. Phys. 17* (1978) 60–84.
[8] P. S. Bagus, A. J. Freeman, F. Sasaki, *Phys. Rev. Lett. 30* (1973) 850.
[9] Measured lattice constants [Å] [°] for the compounds investigated: $KMnO_4$: $a = 9.109(6)$, $b = 5.720(3)$, $c = 7.426(3)$; $AgMnO_4$: $a = 5.6250(7)$, $b = 8.3378(9)$, $\beta = 92.49(1)$; MnO_2(pyrolusite): $a = b = 4.390(5)$, $c = 2.880(10)$; MnO_2(maganite): $a = b = 4.403(2)$, $c = 2.869(4)$; MnF_2: $a = b = 4.8653(6)$, $c = 3.3030(6)$.
[10] JCPDS powder diffraction file 12-716, 24-735 (MnO_2), 24-727 A (MnF_2), 20-487 ($AgMnO_4$), and 7-23 ($KMnO_4$).
[11] J. C. Carver, G. K. Schweitzer, T. A. Carlson, *J. Chem. Phys. 57* (1972) 973.
[12] J. S. Ford, R. B. Jackman, G. C. Allen, *Philos. Mag. A 49* (1984) 657.
[13] J. H. Scofield, *J. Electron Spectosc. Relat. Phenom. 8* (1976) 129.
[14] R. D. W. Kemmit in A. F. Trotman-Dickenson (Eds.): *Comprehensive Inorganic Chemistry*, Pergamon, Oxford 1973, pp. 798–812.
[15] Owing to electron-correlation effects, the intensity ratio in MnF_2 deviates from 1:1 and has an idealized value of 7:5.
[16] E. G. Boonstra, *Acta Crystallogr. 24* (1968) 1053.
[17] J. Palenik, *Inorg. Chem. 6* (1967) 503.
[18] F. M. Chang, J. Jansen, *Z. Kristallogr. 169* (1984) 295.
[19] D. A. Shirley, *Phys. Scri.* (1975) 177.
[20] A review is given by *E. Schleitzer-Steinkopf* in *Gmelin: Handbuch der Anorganischen Chemie, Mangan Teil C 2*, Springer, Berlin 1975, pp. 28–30.
[21] R. Prins, T. Novakov, *Chem. Phys. Lett. 16* (1972) 86.

The *cyclo*-P_4 Ligand as 12-Electron Donor**

By *Manfred Scheer,** *Eckhard Herrmann,** *Joachim Sieler,* and *Matthias Oehme*

A P_4 unit can be present in complexes as the *tetrahedro*-P_4 ligand **A** as in **1**[1] and **2**[2] and as planar *cyclo*-P_4 ligands **B** (rectangular) and **C** (square) as nearly realized in **3**[3] and **4**,[4] respectively. Complexes in which the four lone pairs of a *cyclo*-P_4 ligand are each bonded to a metal atom were previously unknown.[5]

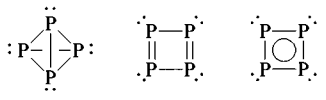

A **B** **C**

$[Ni(np_3)(\eta^1\text{-}P_4)]$ **1**
$[Rh(Ph_3P)_2Cl(\eta^2\text{-}P_4)]$ **2**
$[\{Co(\eta^5\text{-}C_5Me_4Et)\}_2(\eta^4\text{-}P_4)]$ **3**
$[Nb(\eta^5\text{-}C_5Me_5)(CO)_2(\eta^4\text{-}P_4)]$ **4**

Reaction of white phosphorus with $[M(CO)_5(thf)]$, M = Cr or W [Eq. (a)], has now afforded complexes in which a square-planar P_4 unit serves as a 12-electron donor.

[*] Dr. M. Scheer, Prof. Dr. E. Herrmann
Institut für Allgemeine und Anorganische Chemie der Universität
Weinbergweg 16, O-4050 Halle (Saale) (FRG)
Doz. Dr. J. Sieler[+], Dipl.-Chem. M. Oehme[+]
Institut für Anorganische Chemie der Universität Leipzig
[+] X-ray structure analysis

[**] This work was supported by the Fonds der Chemischen Industrie.

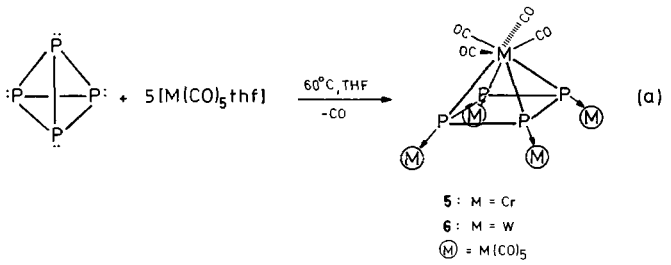

The position of the ^{31}P NMR signal recorded for a solution of white phosphorus in THF ($\delta = -527.5$) hardly shifts at all ($\delta = -528.4$[6]) on addition of [(M(CO)$_5$(thf)], M = Cr or W, at room temperature; that is, no reaction is evident. On warming the solution to 60 °C, the multiplets of an AM_2X spin system appear in the ^{31}P NMR spectrum and complexes **5** and **6** can be isolated from solution. Apparently, the transformation of white phosphorus to the square-planar P_4 ligand of type **C** occurs only at higher temperature and is accompanied by decarbonylation of an [M(CO)$_5$] unit to an [M(CO)$_4$] unit.

Complex **5** forms brown crystals and complex **6** forms red, light-sensitive crystals, which are readily soluble in CH_2Cl_2, THF, acetone, and pyridine, moderately soluble in diethyl ether and toluene, and sparingly soluble in *n*-pentane. They are stable for short periods on exposure to air.

Under the conditions of EI mass spectrometry (70 eV, 100 °C), **5** and **6** cannot be ionized without decomposition. In addition to a weak-intensity peak (5%) for $P_4^{\oplus}$ (*m/z* 124), primarily peaks for the fragment ions $[M(CO)_n]^{\oplus}$ (n = 6 ··· 1) are found. In the ^{31}P NMR spectra of **5** and **6** in CD_2Cl_2 in the temperature range of 198–301 K, only one signal is observed in each case; for **6**, this signal displays a complex ^{183}W satellite pattern.[7] When **5** or **6** is dissolved in THF, on the other hand, the above-mentioned multiplet of an AM_2X spin system appears in both cases owing to an as yet unexplained interaction with the solvent.[8] In the temperature range of 215–301 K, the ^{13}C NMR spectrum of each of the two compounds in CD_2Cl_2 reveals two signals, a sharp singlet for the *cis* CO groups and, at somewhat lower field, a very broad signal for the other CO groups. In the region of CO stretching modes, the IR spectra of **5** and **6** in the solid state[7] show the band pattern expected for local C_{4v} symmetry of the [M(CO)$_5$] complex fragments.[9]

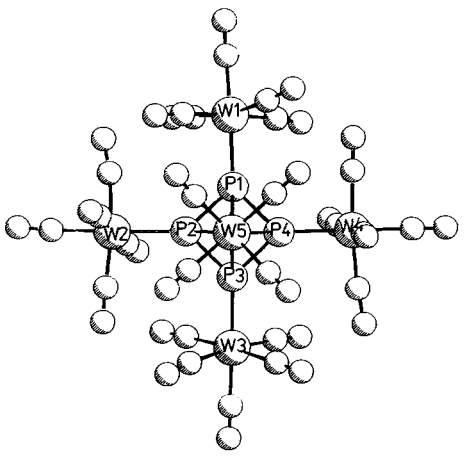

Fig. 1. Molecular structure of **6**. The atoms are drawn as spheres with arbitrary radii. Selected distances [Å] and angles [°]: P1-P2 2.148(9), P1-P4 2.155(9), P2-P3 2.161(9), P3-P4 2.147(9), P1-W1 2.451(7), P2-W2 2.445(7), P3-W3 2.457(6), P4-W4 2.428(7), P1-W5 2.620(7), P2-W5 2.592(6), P3-W5 2.602(6), P4-W5 2.601(7); P1-P2-P3 90.3(3), P2-P3-P4 89.6(3), P3-P4-P1 90.5(3), P4-P1-P2 89.7(3), W5-P1-W1 133.9(2), W5-P2-W2 135.6(2), W5-P3-W3 137.5(2), W5-P4-W4 134.5(2).

The crystal structure analysis of **6**[10] (Fig. 1) shows that a complex with higher pseudosymmetry is formed. The central unit is a square-planar P_4 group (deviations of the phosphorus atoms from the best plane: 0.006(7) Å), which formally arises from the P_4 tetrahedron by homolytic cleavage of two P–P bonds. The four valence electrons (VE) thereby made available augment the 14 VE of a [W(CO)$_4$] unit to give 18 VE, corresponding to the noble-gas rule. The tungsten atom of the [W(CO)$_4$] unit lies above the center of the P_4 ring, so that a square WP_4 pyramid is formed (distance W-P_4 (center) = 2.111(1) Å). The four CO groups are in eclipsing positions with respect to the four phosphorus atoms. The lone pair of each phosphorus atom is involved in further bonding to a [W(CO)$_5$] unit. Thus, the central *cyclo*-P_4 ligand of the entire complex provides 12 VE, the maximum number expected for a structure of type **C**.

The P–P bond lengths (average 2.153(9) Å) are shorter than that of a P–P single bond (2.21(2) Å[12]) and correspond roughly to the P–P distance calculated for the energetically most favorable "antiaromatic" structure **C** of tetraphosphacyclobutadiene (2.143 Å[13]).

Similar distances were also found for **4** (average 2.16 Å[4]) and for the pseudotetrahedral [W_2(O*i*Pr)$_6$(py)P_2], which contains a μ-P_2 ligand (2.154(4) Å[14]). The slight rhomboidal distortion of the P_4 ring in **4** might be due to the different substituents on the metal in the 14-VE complex fragment [Nb(η^5-C_5Me_5)(CO)$_2$]. In **6**, which contains the highly symmetrical [W(CO)$_4$] cap, all P–P distances are identical within the limits of error.

The plane of the four terminal tungsten atoms lies 0.408(1) Å below the P_4 square. The nearly identical $P–W_{terminal}$ bond lengths (average 2.445(7) Å) are comparable to those in [{W(CO)$_5$}(μ_4-P){Co_3(CO)$_9$}] (2.427 Å[15]), in which a lone pair of a "naked" phosphorus atom stabilizes a [W(CO)$_5$] complex fragment. As expected, the P–W bond lengths to the capping tungsten atom are somewhat longer (average 2.604(7) Å).[16]

Experimental Procedure

A solution of [M(CO)$_6$] (5.6 mmol), M = Cr or W, in 250 mL of THF was irradiated at room temperature with UV light (medium-pressure Hg lamp) until 5.6 mmol of CO had evolved. The resulting solution was concentrated under vacuum to 50 mL and then treated with P_4 (124 mg, 1 mmol), dissolved in 15 mL of THF. The solution was stirred for 30 min at room temperature, then warmed to 60 °C and immediately evaporated to dryness at this temperature under vacuum. The residue was suspended in 20 mL of *n*-pentane, filtered off, and then extracted several times with hot *n*-pentane. (In the case of M = W, 150 mg of **6** (8%) crystallized from the extracts.) The washed residue was dissolved in 10 mL of CH_2Cl_2. The resulting solution was concentrated under vacuum to about 5 mL, treated with 1 mL of a mixture of Et_2O and *n*-pentane (1:1), and allowed to stand at −40 °C. The crystals thereby formed were recrystallized several times from CH_2Cl_2/Et_2O/*n*-pentane (4:1:1, ca. −40 °C) to give, for M = Cr, 0.3 g (28%) of **5** (dec. 150 °C) and, for M = W, 0.7 g (40%) of **6** (dec. 175 °C).

Received: March 9, 1991 [Z 4483 IE]
German version: *Angew. Chem. 103* (1991) 1023

[1] np$_3$ = tris(2-diphenylphosphinoethyl)amine; P. Dapporto, S. Midollini, L. Sacconi, *Angew. Chem. 91* (1979) 510; *Angew. Chem. Int. Ed. Engl. 18* (1979) 469.
[2] A. P. Ginsberg, W. E. Lindsell, K. J. McCullough, C. R. Sprinkle, A. J. Welch, *J. Am. Chem. Soc. 108* (1986) 403–416.
[3] O. J. Scherer, M. Swarowsky, G. Wolmershäuser, *Angew. Chem. 100* (1988) 423–424; *Angew. Chem. Int. Ed. Engl. 27* (1988) 405; O. J. Scherer, *Nachr. Chem. Techn. Lab. 35* (1987) 1140–1144.
[4] O. J. Scherer, J. Vondung, G. Wolmershäuser, *Angew. Chem. 101* (1989) 1395–1397; *Angew. Chem. Int. Ed. Engl. 28* (1989) 1355.

[5] Reviews: M. Scheer, E. Herrmann, *Z. Chem. 30* (1990) 41–55; O. J. Scherer, *Angew. Chem. 102* (1990) 1137–1155; *Angew. Chem. Int. Ed. Engl. 29* (1990) 1104; M. Di Vaira, P. Stoppioni, M. Peruzzini, *Polyhedron 6* (1987) 351–382.
[6] $^{31}P\{^1H\}$ NMR (32.438 MHz, 85% H_3PO_4 (ext.)), ca. 0.1 M solutions.
[7] ^{31}P NMR (81.026 MHz, CD_2Cl_2, 85%. H_3PO_4 (ext.)): **5**: $\delta = 158.2$ (301 K), 152.3 (198 K); **6**: $\delta = 19.2$ (301 K), 13.9 (198 K); ^{13}C NMR (50.327 MHz, CD_2Cl_2, TMS). **5** (301 K): $\delta = 212.1$ (s), 213.8 (br, $W_{1/2} = 60$ Hz); **5** (215 K): $\delta = 211.4$ (s), 212.7 (br, $W_{1/2} = 80$ Hz); **6** (301 K): $\delta = 193.1$ (s), 194.8 (br, $W_{1/2} = 90$ Hz); **6** (215 K): $\delta = 191.7$ (s), 194.1 (br, $W_{1/2} = 80$ Hz). The complex crystallizes below 215 K. IR (KBr): **5**: $\tilde{\nu} = 2070$ (s), 1936 (vs); **6**: $\tilde{\nu} = 2072$ (vs), 1942 (vs) cm^{-1}; IR (CH_2Cl_2): **5**: $\tilde{\nu} = 2062$ (m), 2017 (w), 1980 (vs), 1954 (sh); **6**: $\tilde{\nu} = 2064$ (m), 2035 (w), 1958 (vs), 1932 (sh) cm^{-1}.
[8] M. Scheer, M. Dargatz, E. Herrmann, unpublished.
[9] J. Weidlein, U. Müller, K. Dehnicke: *Schwingungsspektroskopie*, Thieme, Stuttgart 1982, p. 114.
[10] Crystal structure analysis of **6**: red platelets, $0.1 \times 0.08 \times 0.12$ mm^3, space group $P1$, $Z = 2$, $a = 11.945(3)$, $b = 12.604(3)$, $c = 14.446(4)$ Å, $\alpha = 100.54(1)$, $\beta = 106.64(1)$, $\gamma = 94.60(1)°$, $V = 2028.2$ Å^3 ($T = 291$ K). Data collection: Huber four-circle diffractometer $Mo_{K\alpha}$ radiation ($\gamma = 0.7107$ Å), $\theta/2\theta$ scan, $2° \leq 2\theta \leq 52°$, 7304 measured reflections. 7201 symmetry-independent. The structure was solved by direct methods using 5255 reflections with $F > 3\sigma F$ [11]. The anisotropic refinement (514 parameters) converged at $R = 0.065$, $R_w = 0.068$. Further details on the crystal structure investigation are available on request from the Fachinformationszentrum Karlsruhe, Gesellschaft für wissenschaftlich-technische Information mbH, W-7514 Eggenstein-Leopoldshafen 2 (FRG), on quoting the depository number CSD-55344, the names of the authors, and the journal citation.
[11] G. M. Sheldrick: *SHELX-86*, Programm zur Strukturlösung und Verfeinerung, Göttingen 1986.
[12] L. R. Maxwell, S. B. Hendrichs, V. M. Mosley, *J. Chem. Phys. 3* (1935) 699.
[13] G. Ohanessian, P. C. Hiberty, J.-M. Lefour, J.-P. Flament, S. S. Shaik, *Inorg. Chem. 27* (1988) 2219–2224.
[14] M. H. Chisholm, K. Folting, J. C. Huffmann, J. J. Koh, *Polyhedron 4* (1985) 893–895.
[15] R. Lal De, H. Vahrenkamp, *Z. Naturforsch. B40* (1985) 1250–1257. Cf. also $[W(CO)_5PMe_3]$ (d(P-W) = 2.516 Å): F. A. Cotton, D. J. Darensbourg, B. W. S. Kolthammer, *Inorg. Chem. 20* (1981) 4440–4442.
[16] Cf. $[\{\mu\text{-}W(CO)_4\}(MeP)]$ (d(P-W) = 2.502 Å): P. S. Elmes, B. M. Gatehouse, B. O. West, *J. Organomet. Chem. 82* (1974) 235–241.

Synthesis and Structure of the Pentaisopropylcyclopentadienyl Radical**

By *Helmut Sitzmann** and *Roland Boese*

Carbon radicals constitute an important and extensive area of organic chemistry. However, surprisingly little is known about cyclopentadienyl radicals.[1] Except for the pentaaryl derivatives,[2a–d] the C_5R_5 radicals are very unstable and those with R = halogen,[2e] CH_3,[2f] H, D,[1,2g] and COOMe[1] have only been characterized by ESR,[2b,d,e,f] electron-nucleus double resonance (ENDOR),[2c] UV,[2b,d] and laser-induced fluorescence spectroscopy (LIF)[2g] in solution,[2c,d,f] in the gas phase,[2g] or in a matrix.[2e]

Pentaisopropylcyclopentadienylsodium[3] and $FeCl_2$ react in THF at −75 °C (16 h) and at − 35 °C (12 h) to form the pentaisopropylcyclopentadienyl radical **1**. The yellow-green, extremely air-sensitive crystals of **1** sublime at about 75 °C/10^{-3} mbar, are stable to at least 130 °C, and dissolve in, for example, pentane, toluene, diethyl ether, and THF. The ^1H NMR spectrum[4] of a solution of **1** saturated at 60 °C shows two broad signals for the methyl and methine protons in an intensity ratio of 6:1. When the solution is warmed to 100 °C, the methyl signal shifts from $\delta = 22.0$ to $\delta = 19.4$, its half-width decreasing from 1700 to 1400 Hz, and the methine signal shifts from $\delta = 13.5$ to $\delta = 14.5$ Hz, its half-width increasing from 850 to over 1100 Hz. On cooling the solution to room temperature, **1** crystallizes unchanged from solution.

In the ESR spectrum (Bruker ESP 300) of a toluene solution of **1**, a broad singlet is observed at room temperature. At 190 K, it is split by hyperfine coupling to a multiplet with 20 observed lines. The coupling constants of 0.16 G (methine H) and 0.32 G (methyl H) were determined by spectral simulation. The g value of 2.0025 does not differ from that of the electron ($g = 2.0027$) within the limits of error. The hyperfine coupling constants of the methine protons of **1** are small compared with those of the methyl protons of the C_5Me_5 radical (6.4 G), presumably because, at 190 K, the methine proton lies in the plane of the five-membered ring and, therefore, the angle θ between the π-electron system of the ring C atoms and the methine C–H bond is 90°. Since, apart from an additive increment, this coupling is proportional to $\cos^2\theta$,[5] its small contribution is in accordance with expectation.

The EI mass spectrum of **1** displays, in addition to the molecular ion peak (m/z 275.3), which is observed in neither the mass spectrum of 1,2,3,4,5-pentaisopropylcyclopentadiene nor in that of tetraisopropylcyclopentadienone (**2**), oxygen-containing fragments,[6] including the molecular ion peak of **2**. Spectroscopic data[17] and the crystal structure of **2**[18] were obtained.

Radical **1** is the first cyclopentadienyl radical to be characterized by X-ray structure analysis.[7] As already known from dynamic NMR investigations on $[(C_5iPr_5)Mo(CO)_3(CH_3)]$[8] and $[(C_5iPr_5)CoCp]$[9] and from the crystal structure of hexaisopropylbenzene,[10] the isopropyl groups are arranged around the five- and six-membered rings in a paddlewheel-like fashion. In the crystal, half of the lattice sites are occupied by radicals with an opposite arrangement of the isopropyl groups, as confirmed by structure determinations on three different crystals, in part at

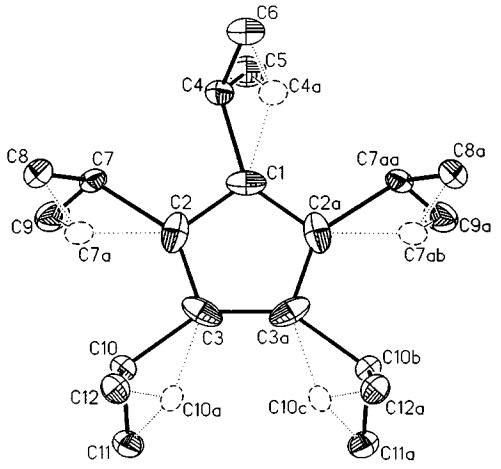

Fig. 1. Molecular structure of **1**. For important bond lengths and angles, see text. Two sets of methine C atoms (C7, C4a, C7ab, C10c, C10, and C7a, C4, C7aa, C10b, C10a) appear owing to the disorder of radicals with opposite orientation of the isopropyl groups; see Fig. 2.

[*] Dr. H. Sitzmann
Fachbereich Chemie der Universität
Erwin-Schrödinger-Strasse, W-6750 Kaiserslautern (FRG)
Dr. R. Boese
Institut für Anorganische Chemie der Universität-Gesamthochschule Essen

[**] We thank Dipl.-Chem. *H. Slodzyk* for the mass spectra and Dipl.-Chem. *G. Heckmann* for the ESR spectra. Our special thanks are owed to Prof. Dr. *O. J. Scherer* for his active interest and for his valuable suggestions in carrying out this work.

higher temperatures. Superstructure reflections were not observed. The crystallographic mirror plane through C1, C5, and C6 perpendicular to the five-membered ring (Fig. 1) is obtained by averaging over this disorder (cf. Ref. [10]). The anisotropic displacement parameters (ADPs), especially of the ring C atoms, result from the overlap of oppositely oriented rings (Fig. 2). A comparable disorder in the crystal has been discussed in detail for hexaisopropylbenzene.[10]

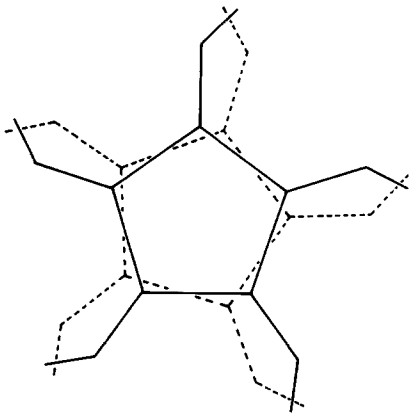

Fig. 2. Overlapping of the two possible orientations of **1** in the crystal.

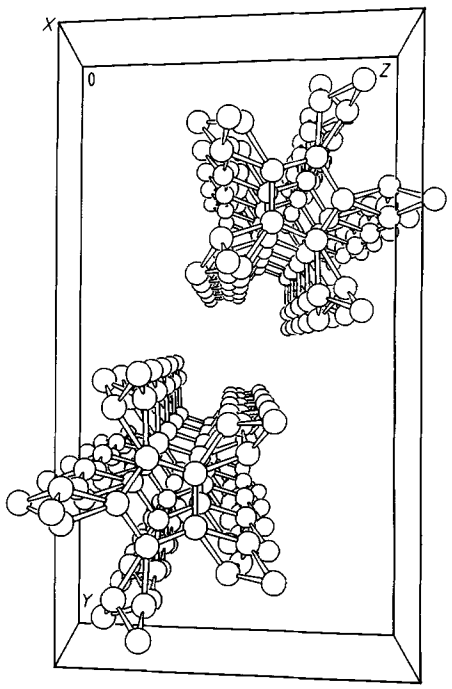

Fig. 3. Stacking of **1** in the crystal. See text for explanation.

Assuming that the differently oriented radicals differ little in their geometry, the C–C bond lengths in the ring are not affected by the disorder and are somewhat larger (C1-C2 1.412(2) Å, C2-C3 1.401(1) Å) than the C–C distance in the cyclopentadienyl anion (calculated value, 1.393 Å;[11] average value in $NaC_5Me_5 \cdot$ TMEDA, 1.377 Å[12]) and are in good agreement with the values of coordinated C_5H_5 ligands (average value in ferrocene, 1.406 Å[13]). The five-membered ring is planar, as shown by the internal ring angles at C1, C2, and C3 (107.5(2)°, 108.1(2)°, and 108.1(1)°, respectively) and the sum of the angles (529.9°). According to the Jahn–Teller theorem, stabilization of the cyclopentadienyl radical is expected to occur through distortion of the D_{5h} geometry; ab initio calculations predict a stabilization of 7–8 kcal mol^{-1}.[14] ESR spectroscopic investigations of the pentafluorocyclopentadienyl radical in a hexafluorobenzene single-crystal matrix indicate that a permanent Jahn–Teller distortion is present only below 8 K.[2e] For neither the unsubstituted nor the deuterated cyclopentadienyl radical did LIF down to 0.6 K reveal evidence of a permanent distortion.[2g] The slight distortions from the ideal geometry of a five-membered ring cannot be interpreted as a Jahn–Teller distortion in the case of **1**. A possible distortion at lower temperatures, however, cannot be ruled out for **1**. Along the crystallographic *x* axis, **1** forms stacks of eclipsing, equally spaced, planar five-membered rings, whereby the ring planes adopt an angle of 23° with respect to the stack axis (Fig. 3) (compare the stacking of $Si_5^{6\ominus}$ rings in the silicides $Li_{12}Si_7$[15a] and Li_8MgSi_6[15b]) and the rings are 5.82 Å apart owing to the bulky isopropyl substituents. This interplanar distance is apparently too large for a stable coordination of two pentaisopropylcyclopentadienyl ligands to an iron center. Possibly, other sterically encumbered cyclopentadiene ligands will also fail to form ferrocenes, but instead afford cyclopentadienyl radicals, if their dimerization or disproportionation is hindered by steric or electronic effects. In the absence of a central atom, the pentaisopropylcyclopentadienyl radical also forms the polymeric sandwich structure of a metal-free polydecker in the crystal. On the other hand, the use of lead as central atom recently gave the first decaisopropylmetallocene.[16]

Experimental Procedure

A solution of pentaisopropylcyclopentadienylsodium (1.49 g, 5.0 mmol) in 60 mL of THF was cooled to −75 °C and anhydrous iron(II) chloride (0.318 g, 2.5 mmol) was added. The reaction mixture was stirred for 16 h at the same temperature, allowed to warm to −50 °C over 3–4 h, and, finally, stirred for 3 h at this temperature and for 12 h at −30 °C, during which time the initially gray-white precipitate gradually turned dark. The black-brown suspension was concentrated at 0 °C and suspended in 80 mL of petroleum ether. The brownish solution obtained by centrifugation was concentrated in a 100-mL round-bottom flask and **1** was sublimed into a surmounting glass tube at 10^{-3} mbar and about 75 °C. The impurities caused by traces of air and moisture were more volatile and collected in the upper part of the tube. Yield 500 mg (1.8 mmol, 36%) of yellow-green crystals.

Received: March 7, 1991 [Z 4479 IE]
German version: *Angew. Chem. 103* (1991) 1027

CAS Registry numbers:
1, 134484-82-5; **2**, 99458-90-9; pentaisopropylcyclopentadienylsodium, 129943-90-4.

[1] M. Regitz, B. Giese (Eds.): *Methoden der Organischen Chemie (Houben-Weyl), Bd. E19a (C-Radikale)*, Thieme, Stuttgart 1989.
[2] a) K. Ziegler, B. Schnell, *Justus Liebigs Ann. Chem. 445* (1925) 266; b) A. A. Kuznetsov, S. N. Novikov, A. N. Pravednikov, *Izv. Akad. Nauk SSSR Ser. Khim. 2* (1979) 297; c) W. Kieslich, H. Kurreck, *J. Am. Chem. Soc. 106* (1984) 4328; d) W. Broser, P. Siegel, H. Kurreck, *Chem. Ber. 101* (1968) 69; e) T. Chen, Hs. H. Günthard, *Chem. Phys. 97* (1985) 187; f) A. G. Davies, J. Lusztyk, *J. Chem. Soc. Perkin Trans. 2 1981*, 692; g) L. Yu, J. M. Williamson, T. A. Miller, *Chem. Phys. Lett. 162* (1989) 431.
[3] H. Sitzmann, *Z. Naturforsch. B44* (1989) 1293.
[4] Bruker AM 400, 400 MHz, C_6D_6, $\delta(C_6D_5H) = 7.159$ as internal standard.
[5] N. M. Atherton: *Electron Spin Resonance*, Wiley, New York 1973, p. 105.
[6] EI-MS (30 eV): *m/z* 334.3 ($[M + OC_3H_7]^{\oplus}$, 6%); 318.4 ($[M + C_3H_7]^{\oplus}$, 12); 291.3 ($[M + O]^{\oplus}$, 31); 276.3 ($[M + H]^{\oplus}$, 59); 275.3 ($M^{\oplus}$, 35); 249.2 ($C_5iPr_4OH^{\oplus}$, 60); 248.2 ($C_5iPr_4O^{\oplus}$, 100); 233.1 ($C_5iPr_4H^{\oplus}$, 61); 191.0 ($C_5iPr_3H_2^{\oplus}$, 39); 148.9 ($C_5iPr_2H_3^{\oplus}$, 85); 106.8 ($C_5iPrH_4^{\oplus}$, 26). Striking here, in contrast to previously recorded EI mass spectra of isopropyl-substituted cyclopentadienes and their derivatives, is the absence of a C_3H_7 fragment. Possibly, a cation of mass 318.4 is formed from **1** and $C_3H_7^{\oplus}$, the latter arising by fragmentation. Exposure of **1** to O_2 results in formation of tetraisopropylcyclopentadienone (**2**) [17, 18] as stable end product. The fate of the fifth isopropyl group was not investigated; it is presumably lost from the initially formed oxidation product "$C_5iPr_5O_2$" as isopropoxy radical. Evidence for this is provided by the peak at *m/z* 334.4, which might

have arisen by combination of this product with **1**. A 2:1 product of **1** and O_2 might be bis(pentaisopropylcyclopentadienyl) peroxide, whose asymmetric cleavage product would be expected to give rise to the signal at m/z at 291.3.

[7] A single crystal with dimensions of 0.41 × 0.30 × 0.28 mm³, obtained by vacuum sublimation in a sealed ampoule, was used for structure determination. A total of 1263 unique reflections were collected at 110 K on a Nicolet R3m/V X-ray four-circle diffractometer with $Mo_{K\alpha}$ radiation and graphite monochromator in the angle range $3 \leq 2\theta \leq 45°$ according to the method of *Wyckoff*; 1040 with $F_0 \leq 4\sigma(F)$ were observed reflections. On the basis of the diffractometer angles of 26 reflections, the cell was determined to be monoclinic in the space group $P2_1/m$, $a = 6.337(2)$, $b = 16.225(5)$, $c = 9.257(3)$ Å, $\beta = 101.94(2)°$, $V = 931.2(5)$ Å³, $Z = 2$. The structure was solved using the program SHELXTL-PLUS; all atoms except for hydrogen atoms were refined anisotropically and the hydrogen atoms were refined isotropically as rigid groups (C-H = 0.96 Å, C-C-H and H-C-H 109.5°); 118 parameters; $R = 0.044$, $R_w = 0.054$. Further details of the crystal structure determination are available on request from the Fachinformationszentrum Karlsruhe, Gesellschaft für wissenschaftlich-technische Information mbH, W-7514 Eggenstein-Leopoldshafen 2 (FRG), on quoting the depository number CSD-320 289, the names of the authors and the journal citation.

[8] H. Sitzmann, *Chem. Ber. 123* (1990) 2311.

[9] B. Gloaguen, D. Astruc, *J. Am. Chem. Soc. 112* (1990) 4607.

[10] J. Siegel, A. Gutièrrez, W. B. Schweizer, O. Ermer, K. Mislow, *J. Am. Chem. Soc. 108* (1986) 1569.

[11] E. D. Jemmis, P. von R. Schleyer, *J. Am. Chem. Soc. 104* (1982) 4781.

[12] T. Aoyagi, H. M. M. Shearer, K. Wade, G. Whitehead, *J. Organomet. Chem. 175* (1979) 21.

[13] J. D. Dunitz, L. E. Orgel, A. Rich, *Acta Crystallogr. 9* (1956) 373.

[14] a) W. T. Borden, E. R. Davidson, *J. Am. Chem. Soc. 101* (1979) 3771; b) T.-K. Ha, R. Meyer, Hs. H. Günthard, *Chem. Phys. Lett. 69* (1980) 510.

[15] a) M. C. Böhm, R. Ramirez, R. Nesper, H. G. von Schnering, *Phys. Rev. B30* (1984) 4870; b) R. Ramirez, R. Nesper, H. G. von Schnering, *Chem. Phys. 95* (1985) 17.

[16] H. Sitzmann, unpublished results.

[17] **2**: IR (cyclohexane): $\tilde{\nu}$[cm⁻¹] = 1708 (C=O). ^{1}H NMR (200 MHz, C_6D_6, C_6D_5H as internal standard): $\delta = 2.78$ (sept, ^3J(H,H) = 7.0 Hz, 2H; CH), 2.69 (sept, ^3J(H,H) = 7.2 Hz, 2H; CH), 1.28 (d, ^3J(H,H) = 7.0 Hz, 12H; CH_3), 1.06 (d, ^3J(H,H) = 7.2 Hz, 12H; CH_3). Correct C,H,O analysis, ^{13}C NMR spectrum, and X-ray structure analysis [18].

[18] X-ray structure analysis of **2**: A single crystal with dimensions of 0.38 × 0.25 × 0.19 mm³ was used to obtain 2041 unique reflections at 103 K on a Nicolet R3m/V X-ray four-circle diffractometer with $Mo_{K\alpha}$ radiation and graphite monochromator in the angle range $3 \leq 2\theta \leq 45°$ according to the method of *Wyckoff*; 1718 with $F_0 \geq 4\sigma(F)$ were observed reflections. On the basis of the diffractometer angles of 50 reflections, the cell was determined to be monoclinic in the space group. $P1$, $a = 6.000(1)$, $b = 8.192(1)$, $c = 17.003(2)$ Å, $\alpha = 95.32(2)$, $\beta = 90.22(1)$, $\gamma = 110.37(1)°$, $V = 779.5(2)$ Å³, $Z = 2$. The structure was solved using the program SHELXTL-PLUS; all atoms except the hydrogen atoms were refined anisotropically and the hydrogen atoms were refined isotropically as rigid groups (C-H 0.96 Å, C-C-H and H-C-H 109.5°; 191 parameters; $R = 0.045$, $R_w = 0.056$. Further details of the crystal structure determination are available on request from the Fachinformationszentrum Karlsruhe, Gesellschaft für wissenschaftlich-technische Information mbH, W-7514 Eggenstein-Leopoldshafen 2 (FRG), on quoting the depository number CSD-320290, the names of the authors, and the journal citation.

Synthesis of Sterically Hindered Tellurophenols and the Structure of $[Cd(\mu\text{-}TeC_6H_2Me_3)_2]_\infty$ **

By *Manfred Bochmann,* Andrew P. Coleman, Kevin J. Webb, Michael B. Hursthouse,* and *Muhammed Mazid*

We have recently shown that sterically hindered thiolato and selenolato complexes of cadmium show unusually low coordination numbers and possess sufficient volatility to be useful as one-component precursors for the deposition of II/VI semiconductor films from the vapor phase.[1] We now report the synthesis and isolation of related tellurols and the first structurally characterized cadmium tellurolato complex, $[Cd(\mu\text{-}TeC_6H_2Me_3\text{-}2,4,6)_2]_\infty$.

Protonation of a slurry of ArTeLi (**1**) in petroleum ether by $HBF_4 \cdot Et_2O$ at −78 °C leads to the formation of the corresponding tellurols (**2**) in almost quantitative yield (Scheme 1). Removal of the solvent at low temperature allows the isolation of the compounds as colorless crystalline low-melting solids, which are thermally unstable and light-sensitive. Whereas the high solubility of **2b** precludes crystallization from petroleum ether solutions even at −100 °C, **2a,c** may be recrystallized from petroleum ether at −70 °C. Contrary to expectation, there is no increase in thermal stability with increasing steric hindrance of the compounds; in fact, **2a** is noticeably more stable than **2c**. The instability of aryl tellurols has previously precluded their isolation;[2] for example, PhTeH was only identified in solution as a hydrolysis product of $PhTeSiMe_3$.[3]

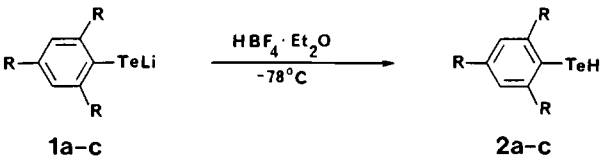

Scheme 1. **a**, R=Me; **b**, R=*i*Pr; **c**, R=*t*Bu.

The ^{125}Te NMR data for **2** are given in Table 1; the data for the anions **1**[4] have been included for comparison. The

Table 1. ^{125}Te NMR data of [2,4,6-$R_3C_6H_2$TeM][a].

R	M=Li	$\Delta\nu_{1/2}$ [Hz]	M=H	J(Te, H) [Hz]
Me	−383.7	140	−91.41	63
*i*Pr	−478.5	38	−134.77	48.6
*t*Bu	9.2	11	153.77	51.9

[a] M = Li measured in THF, 28 °C; M = H in $CDCl_3$, −20 °C, using a 2 M solution of Ph_2Te_2 in $CDCl_3$ as external standard ($\delta = 434.24$), referenced against neat Me_2Te ($\delta = 0$).

^1J(Te,H) coupling constants are comparable to those of PhTeH,[3] H_2Te, and H_3MTeH (M = Si, Ge)[5] deduced from proton spectra, whereas for $[(C_5Me_5)Re(CO)_2H(TeH)]$ significantly higher coupling constants were found.[6]

The addition of $[Cd\{N(SiMe_3)_2\}_2]$[7] to solutions of **2a** leads to the instantaneous precipitation of $[Cd(TeC_6H_2Me_3\text{-}2,4,6)_2]$ (**3a**) as a fine-crystalline solid [Eq. (a)]. An identical

$$2\,\mathbf{2a} + [Cd\{N(SiMe_3)_2\}_2] \longrightarrow \underset{\mathbf{3a}}{[Cd(TeC_6H_2Me_3\text{-}2,4,6)_2]_\infty} + 2\,HN(SiMe_3)_2 \quad \text{(a)}$$

product is obtained from $CdCl_2$ and $C_6H_2Me_3TeSnnBu_3$.[8] Compound **3a** is almost insoluble in nonpolar solvents but is more soluble in DMF, DMSO, or pyridine than its sulfur and selenium analogues[9] and is obtained from DMF as yellow cubic crystals. It shows a very simple ^{1}H NMR spectrum in $[^2H]_5$-pyridine and presumably exists as a four-coordinate monomer, $[(py)_2Cd(TeAr)_2]$. Attempts to isolate this adduct failed, however, whereas the analogous thiolato com-

[*] Dr. M. Bochmann, Dr. A. P. Coleman, K. J. Webb
School of Chemical Sciences, University of East Anglia
GB-Norwich NR4 7TJ (UK)
Prof. M. B. Hursthouse, Dr. M. Mazid [+]
Department of Chemistry, Queen Mary and Westfield College
Mile End Road, GB-London E1 4NS (UK)

[+] X-ray crystallography

[**] This work was supported by the Science and Engineering Research Council (UK) and the Royal Signals and Radar Establishment.

plex $[(py)_2Cd(SAr)_2]$ is easily obtained.[9] Compound **3a** decomposes in refluxing mesitylene to give polycrystalline CdTe.

In spite of the importance of CdTe-based solid-state materials, the chemistry of related molecular telluride complexes is poorly developed. Surprisingly few examples of cadmium tellurolates are known,[10] and to our knowledge none have been structurally characterized. The structure of **3a** was therefore determined.[11]

Complex **3a** exists in the solid state as a one-dimensional coordination polymer, with almost symmetrically bridging mesityltellurolato ligands and tetrahedrally coordinated cadmium (Fig. 1, left). The average Cd–Te distance of

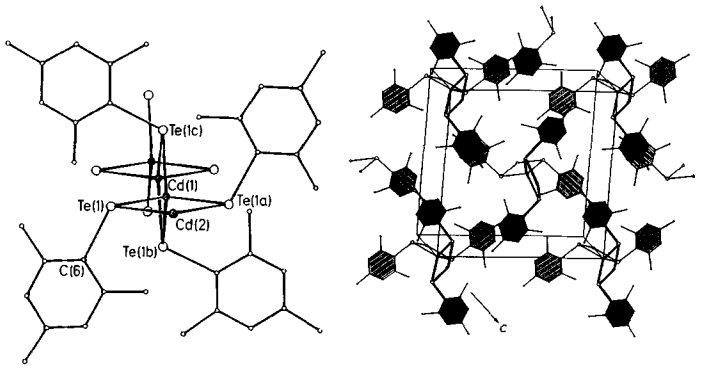

Fig. 1. Structure of $[Cd(TeCH_2Me_3)_2]_\infty$ (**3a**). Left: Part of an individual chain, showing the atomic numbering scheme. All but four of the mesityl substituents have been omitted for clarity. Right: Crystal-packing diagram, illustrating the separation of the one-dimensional polymeric units as a consequence of the spatial requirements of the mesityl substituents. Selected bond lengths [Å] and angles [°]: Cd(1)-Te(1) 2.838(8), Cd(2)-Te(1) 2.835(9), C(6)-Te(1) 2.164(12). Cd(1)-Te(1)-Cd(2) 84.0(1), Te(1)-Cd(1)-Te(1a) 95.9(1), Te(1)-Cd(1)-Te(1b) 116.7(1), Te(1)-Cd(2)-Te(1a) 96.0(1), C(6)-Te(1)-Cd(1) 107.0(10).

2.837 Å is very close to the distance of 2.80 Å of cubic (zinc blende type) CdTe. The relatively open structure is formed as a result of the spatially demanding mesityl substituents, which separate the individual $[Cd(\mu\text{-}Te)_2]_\infty$ chains (Fig. 1, right). As has been demonstrated recently, the structures of cadmium aryl thiolates, $Cd(SAr)_2$, depend on the steric requirements of the aryl groups and can range from a three-dimensional arrangement of adamantanoid cages (Ar = Ph[14]) in a macrocyclic network if an *ortho* substituent is present (Ar = $2\text{-}MeC_6H_4$[15]) to the complete disruption of the polymeric lattice, with formation of molecular dimers in the case of extreme steric hindrance.[1, 9] Compound **3a** occupies an intermediate position in this sequence.[16]

Experimental Procedure

2a: All experiments were carried out under argon with anhydrous deoxygenated solvents. To a stirred solution of dimesitylditelluride[17] (0.543 g, 1.10 mmol) in 10 mL of THF at −78 °C was added via syringe a solution of 1 M $LiBHEt_3$ in THF (2.4 mL, 2.4 mmol). The color turned from deep-red to pale yellow within a minute. After stirring the mixture for 15 min the solvent was removed in vacuo at room temperature. The residue was suspended in 40 mL of petroleum ether (b.p. 40–60 °C) and cooled to −78 °C. $HBF_4 \cdot Et_2O$ (0.80 g, 4.97 mmol) was injected via syringe and the mixture was allowed to slowly warm to −20 °C. It was stirred at this temperature until the lithium tellurolate had dissolved. After filtration the solution was concentrated in vacuo at −20 °C and cooled to −78 °C to obtain the product as a colorless solid which began to turn pink above −30 °C and decomposed above 0 °C with gas evolution and precipitation of elemental tellurium. The crude yield was essentially quantitative. ^1H NMR (90 MHz, $CDCl_3$, 0 °C): $\delta = -2.68$ (s, Te–H), 2.16 (s, 3H, *p*-Me), 2.26 (s, 6H, *o*-Me), 6.80 (s, 2H). ^{13}C NMR ($CDCl_3$, −40 °C): $\delta = 20.6$ (*p*-Me), 28.8 (*o*-Me), 126.7 (Te-*C*), 127.7 (*m*-C), 136.5 (*p*-C), 141.6 (*o*-C). If the addition of $HBF_4 \cdot Et_2O$ was carried out in THF as solvent, extensive decomposition took place even at −78 °C.

2b: $[(2,4,6\text{-}i\text{Pr}_3C_6H_2Te)_2]$: To $[2,4,6\text{-}i\text{Pr}_3C_6H_2MgBr]$, prepared from $[2,4,6\text{-}i\text{Pr}_3C_6H_2Br]$ (20 g, 70.6 mmol) in 100 mL of THF (100% yield after 2-h reflux), was added finely powdered tellurium (9.0 g, 70 mmol) at −50 °C with rapid stirring. The mixture was allowed to warm slowly to room temperature and stirred until the tellurium had reacted completely. The pale-green solution was oxidized by treatment with O_2, poured onto 2 M HCl (200 mL), and extracted with petroleum ether (3 × 200 mL). After evaporation of the solvent the red-purple product was recrystallized from ethanol, m.p. 91–93 °C (18.5 g, 80%).The tellurol **2b** was obtained from $[(2,4,6\text{-}i\text{Pr}_3C_6H_2Te)_2]$ as described for **2a**. Its high solubility prevented recrystallization. The compound turns brown slowly at −30 °C and rapidly at 5 °C. ^1H NMR ($CDCl_3$, −20 °C): $\delta = -2.95$ (s, Te–H), 1.60 (d, 18H, *o*- and *p*-$CHMe_2$), 2.80 (septet, 1H, *p*-$CHMe_2$), 3.28 (septet, 2H, *o*-$CHMe_2$), 6.95 (s, 2H). ^{13}C NMR ($CDCl_3$, −40 °C): $\delta = 23.8$ (*o*-$CHMe_2$), 24.1 (*p*-$CHMe_2$), 34.0 (p-$CHMe_2$), 39.5 (*o*-$CHMe_2$), 113.2 (Te–*C*), 121.3 (*m*-C), 148.8 (p-C), 152.6 (*o*-C).

2c: Obtained from $[(2,4,6\text{-}t\text{Bu}_3C_6H_2Te)_2]$[18] as described for **2a** as a crystalline solid. The compound begins to turn pale-pink at −40 °C and decomposes on warming to room temperature. ^1H NMR ($CDCl_3$, −20 °C): $\delta = -1.25$ (s, 1H, Te-H), 1.24 (s, 9H, *p*-*t*Bu), 1.58 (s, 18H, *o*-*t*Bu), 7.40 (s, 2H). ^{13}C NMR ($CDCl_3$, −40 °C): $\delta = 31.5$ (p-CMe_3), 32.6 (*o*-CMe_3), 34.8 (*p*-CMe_3), 39.0 (*o*-CMe_3), 119.6 (Te-*C*), 122.7 (*m*-C), 149.1 (*p*-C), 154.4 (*o*-C).

3a: To a solution of **2a** (0.545 g, 2.20 mmol) in 20 mL of petroleum ether (b.p. 40–60 °C) at −20 °C was added via syringe a solution of $[Cd\{N(SiMe_3)_2\}_2]$ (0.47 g, 1.08 mmol) in 40 mL of petroleum ether. After stirring for 20 min the residue was allowed to warm to room temperature, filtered off, washed with 20 mL of petroleum ether and recrystallized from DMF to give yellow crystals (0.372 g, 0.54 mmol, 50%). Correct elemental analysis. ^1H NMR (C_5D_5N): $\delta = 2.13$ (s, 3H, *p*-Me), 2.30 (s, 6H, *o*-Me), 6.72 (s, 2H).

Received: February 15, 1991 [Z 4444 IE]
German version: *Angew. Chem. 103* (1991) 975

CAS Registry numbers:
1a, 92720-47-3; **1b**, 134848-01-4; **1c**, 99334-76-6; **2a**, 134847-97-5; **2b**, 134847-98-6; **2c**, 134847-99-7; **3a**, 134848-02-5; $[(2,4,6\text{-}Me_3C_6H_2Te)_2]$, 92720-46-2; $[(2,4,6\text{-}i\text{Pr}_3C_6H_2Te)_2]$, 131922-65-1; $[(2,4,6\text{-}t\text{Bu}_3C_6H_2Te)_2]$, 99354-18-4; $[Cd\{N(SiMe_3)_2\}_2]$, 3323-04-4; $[(py)_2Cd(2,4,6\text{-}Me_3C_6H_2Te)_2]$, 134848-00-3; $2,4,6\text{-}i\text{Pr}_3C_6H_2Br$, 21524-34-5; Te, 13494-80-9.

[1] M. Bochmann, K. Webb, M. Harman, M. B. Hursthouse, *Angew. Chem. 102* (1990) 703; *Angew. Chem. Int. Ed. Engl. 29* (1990) 638; M. Bochmann, K. J. Webb, *Abstr. 5th Int. Conf. Metalorg. Vapour Phase Epitaxy*, Aachen 1990, S. 205; M. Bochmann, K. J. Webb in L. V. Interrante, K. F. Jensen, L. H. Dubois, M. E. Gross (Eds.): *Mat. Res. Soc. Symp. Proc. 204: Chemical Perspectives of Microelectronic Materials II* (Material Research Society, 1991), p. 149.
[2] H. Gysling in S. Patai, Z. Rappoport, *The Chemistry of Organic Selenium and Tellurium Compounds, Vol. 1*, Wiley, Chichester 1986, p. 650.
[3] J. E. Drake, R. T. Hemmings, *Inorg. Chem. 19* (1980) 1879.
[4] $[C_6H_2tBu_3TeLi(thf)_3]$ is known: W. W. Du Mont, R. Hensel, S. Kubiniok, L. Lange, T. Severengiz, *Phosphorus Sulfur 38* (1988) 85. The structures of $[C_6H_2Me_3TeNa(tmeda)_2]$ and $[C_6H_2i\text{Pr}_3TeK(18\text{-crown-}6)]$ have recently been determined: P. J. Bonasia, J. Arnold, *J. Chem. Soc. Chem. Commun. (1990)* 1299.
[5] C. Glidewell, D. W. H. Rankin, G. M. Sheldrick, *Trans. Farad. Soc. (1969)* 1409.
[6] W. A. Herrmann, C. Hecht, E. Herdtweck, H. J. Kneuper, *Angew. Chem. 99* (1987) 158; *Angew. Chem. Int. Ed. Engl. 26* (1987) 132.
[7] H. Bürger, W. Sawodny, U. Wannagat, *J. Organomet. Chem. 3* (1965) 113.
[8] $[C_6H_2Me_3TeSnnBu_3]$ is obtained from ArTeLi and nBu_3SnCl in THF as a yellow oil, ca. 100%. ^1H NMR MHz, C_6D_6): $\delta = 0.3–1.5$ (m, 27H, Bu), 1.90 (s, 3H, *p*-Me), 2.43 (s, 6H, *o*-Me), 6.73 (s, 2H).
[9] M. Bochmann, K. J. Webb, M. Mazid, M. B. Hursthouse, *J. Chem. Soc. Dalton Trans.*, in press.
[10] I. D. Sadekov, G. M. Abakarov, S. G. Kuren, A. D. Garnovski, V. I. Minkin, *Zh. Obshch. Khim. 56* (1986) 2168 (*Chem. Abstr. 106*, 60224t); M. L. Steigerwald, C. R. Sprinkle, *J. Am. Chem. Soc. 109* (1987) 7200; S. M. Stuczynski, J. G. Brennan, M. L. Steigerwald, *Inorg. Chem. 28* (1989) 4431; J. Kischkewitz, D. Naumann, *Z. Allg. Anorg. Chem. 547* (1987) 167.
[11] **3a**: Crystals from dimethylformamide. X-ray measurements were made using an Enraf-Nonius FAST TV area detector diffractometer and graphite-monochromated $Mo_{K\alpha}$ radiation. Unit cell parameters and intensity data were obtained using the relevant procedures in the "small molecule" version of the SADONL software[12]. Approximately one hemisphere of data was scanned up to $(\sin\theta/\lambda)_{max} = 0.65$, leading to a total of 4772 data, of which 1632 were unique ($R_{int} = 0.069$). The structure was solved via the heavy atom method and refined by full-matrix least squares. An absorption correction based on the DIFABS procedure[13] was applied. Tetragonal, space group $P\bar{4}b2$, $a = b = 15.945$, $c = 7.594$ Å, $Z = 4$, $\varrho_{calcd} = 2.085$ g cm^{-3}. $R = 0.057$. Further details on the crystal structure analysis are available from the Director of the Cambridge Crystallograph-

ic Data Centre, University Chemical Laboratory, Lensfield Road, GB-Cambridge CB2 1EW (UK), on quoting the full journal citation.
[12] J. W. Pflugrath, A. Messerschmidt, *The MADNES System*, Version 11.9 (1989), modified for small-molecule work by B. Schierbeck, Enraf-Nonius, Delft.
[13] N. Walker, D. Stuart, *Acta Crystallogr. Sect. A 39* (1983) 158.
[14] D. C. Craig, I. G. Dance, R. G. Garbutt, *Angew. Chem. 98* (1986) 178; *Angew. Chem. Int. Ed. Engl. 25* (1986) 165; I. G. Dance, R. G. Garbutt, D. C. Craig, M. L. Scudder, T. D. Bailey, *J. Chem. Soc. Chem. Commun. 1987*, 1164; I. G. Dance, R. G. Garbutt, D. C. Craig, M. L. Scudder, *Inorg. Chem. 26* (1987) 4057.
[15] I. G. Dance, R. G. Garbutt, M. L. Scudder, *Inorg. Chem. 29* (1990) 1571.
[16] Previous examples of one-dimensional polymeric cadmium thiolates involve octahedral or dodecahedral coordination of the metal: I. G. Dance, M. L. Scudder, R. Secomb, *Inorg. Chem. 22* (1983) 1794; E. Dubler, E. Gyr, *ibid. 27* (1988) 1466; M. B. Hursthouse, O. Z. F. Khan, M. Mazid, M. Motevalli, P. O'Brien, *Polyhedron 9* (1990) 541.
[17] M. Akiba, M. V. Lakshmikantham, K. Y. Jen, M. P. Cava, *J. Org. Chem. 49* (1984) 4819.
[18] L. Lange, W. W. Du Mont, *J. Organomet. Chem. 286* (1985) C1; W. W. Du Mont, L. Lange, H. H. Karsch, K. Peters, E. M. Peters, H. G. von Schnering, *Chem. Ber. 121* (1988) 11.

Thermal and Light-Induced Spin Crossover to a Metastable Low-Spin State in $[Fe(mtz)_6](CF_3SO_3)_2$ **

By *Philipp Gütlich** and *Peter Poganiuch*

Dedicated to Professor Hans Georg von Schnering on the occasion of his 60th birthday

Thermal spin crossover in coordination compounds of 3d transition metals has been well known for many years. The high-spin (HS) $\leftrightarrow$ low spin (LS) crossover[1] has been well investigated by a number of physical methods.[2, 3] In our investigations of the spin-crossover system $[Fe(ptz)_6](BF_4)_2$ (ptz = 1-propyltetrazole), we discovered a fascinating novel photophysical phenomenon, which we called "light-induced excited spin state trapping" (LIESST):[4, 5] Irradiation with green light ($\lambda \approx 550$ nm) into the $^1A_1 \rightarrow {}^1T_1$ absorption band at sufficiently low temperatures ($T \leq 50$ K) results in quantitative transformation of the LS state of this complex to a metastable HS state, the lifetime of which can be practically infinite. The mechanism was elucidated.[5] It is crucial that the $^3T_1$ state lie lower in energy than the $^1T_1$ state, since this allows double intersystem crossing, which leads finally to the $^5T_2$ state: $^1A_1 \rightarrow {}^1T_1 \rightarrow {}^3T_1 \rightarrow {}^5T_2$. LIESST has meanwhile been achieved for several spin-crossover systems,[6-9] even when these were embedded in polymer film.[10] It was also shown that, on irradiation with red light ($\lambda \approx 750$ nm) into the $^5T_2 \rightarrow {}^5E$ band, the metastable HS($^5T_2$) state can be pumped back to the stable LS state, again via double intersystem crossing, $^5E \rightarrow {}^3T_1 \rightarrow {}^1A_1$.[11]

Recently, we also reported that irradiation of an iron(II) complex with HS ground state, $[Fe(mtz)_6](BF_4)_2$, with red light at low temperatures causes a transition to a metastable LS state with an extremely long lifetime (weeks).[12] We referred to this process as LIESST(H $\rightarrow$ L) in order to distinguish it from the original LIESST, which now is referred to as LIESST(L $\rightarrow$ H). The metastable LS state can also be pumped back to the stable HS state in the case of LIESST(H $\rightarrow$ L) by irradiation with green light.[12] The mechanism of the formation and the conditions required for a long lifetime of the metastable LS($^1A_1$) state are given in Figure 1: Red light excites the $^5T_{2g}$ state to the ^5E_g state,

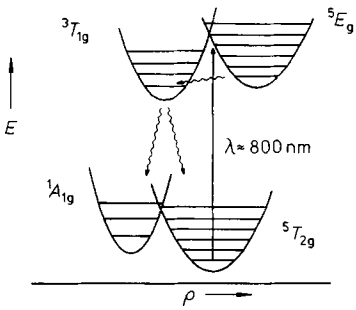

Fig. 1. The mechanism of the LIESST(H $\rightarrow$ L) process. $\rho = A_1$ vibrational coordinate.

which then undergoes intersystem crossing to the $^3T_{1g}$ state owing to favorable spin-orbit coupling. Within nanoseconds this intermediate state once again undergoes intersystem crossing to the metastable $^1A_{1g}$ state. The $^3T_{1g}$ state could also relax back to the $^5T_{2g}$ ground state with equal probability. However, continuous irradiation of the $^5T_2 \rightarrow {}^5E$ transition (the lamp is turned on for a time that is several orders of magnitude longer than the lifetimes of the excited states involved) pumps the system completely into the LS($^1A_1$) state. Decisive for very long lifetimes of the metastable $^1A_1$ state is the highest possible barrier between the $^1A_1$ and $^5T_2$ states, which can be achieved for the smallest possible difference in energy between the lowest vibrational levels and the largest possible difference in the metal–ligand distances in the $^5T_2$ and $^1A_1$ states.

Here we discuss the complex compound $[Fe(mtz)_6](CF_3SO_3)_2$ (**1**, mtz = 1-methyl-1*H*-tetrazole), which exhibits a second example of LIESST(H $\rightarrow$ L). Compound **1** shows a complex magnetic behavior, governed by a thermal spin crossover with hysteresis ($T_c\downarrow = 158$ K, $T_c\uparrow = 174$ K) and a phase transition that is independent of the spin crossover. Variable-temperature ^{57}Fe Mössbauer spectroscopic measurements confirmed the results of the magnetic measurements and, in addition, provided information on the two, apparently different iron(II) environments in this system (Fig. 2). From 295 to about 190 K, the Mössbauer spectra show only one asymmetric (texture!) quadrupole doublet, which has parameters typical for iron(II)-HS. Below 190 K, a transition (with hysteresis of only about 8 K width) takes place to another iron(II)-HS (HS1 $\rightarrow$ HS2) and is complete at about 175 K. At still lower temperatures, the above-mentioned thermal spin crossover occurs at this lattice site and, at about 140 K, is complete with an HS fraction of 65% (Fig. 3). On heating, hysteresis is observed in the conversion curve $\gamma_{HS}(T)$ of the doublet assigned to HS2; this hysteresis has the same width (16 K) and occurs in the same temperature range as for the susceptibility measurements. It is presumably due to a crystallographic phase transition that accompanies the thermal spin crossover. For LIESST investigations, we recorded a Mössbauer spectrum of **1** at 20 K (Fig. 4, top). The two outer resonance signals belong to the HS2($^5T_2$) state and the inner signal belongs to the LS($^1A_1$) state. After irradiation of **1** with green light ($\lambda \approx 350-$

[*] Prof. Dr. P. Gütlich
Institut für Anorganische und Analytische Chemie der Universität
Staudinger Weg 9, W-6500 Mainz (FRG)
Dr. P. Poganiuch
Ammoniaklaboratorium-ZAA/I
BASF AG
W-6700 Ludwigshafen (FRG)

[**] This work was supported by the Bundesministerium für Forschung und Technologie and by the Fonds der Chemischen Industrie. mtz = 1-methyl-1*H*-tetrazole.

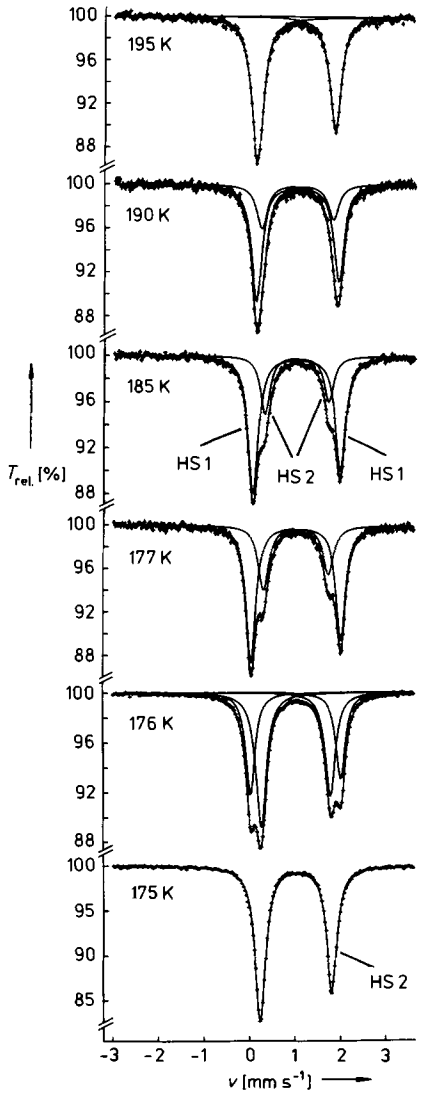

Fig. 2. ^{57}Fe Mössbauer spectra of **1** in the range $T = 195-175$ K, in which a change in the lattice and an accompanying HS1 → HS2 transition occurs. T_{rel} = relative transmission, ν = rate.

650 nm, xenon lamp and filter) at 20 K, the Mössbauer spectrum was unchanged; that is, LIESST(L → H) does not take place under these conditions. The reason is that the lifetime of the metastable HS state is less than one minute and thus too short to be detected in the Mössbauer experiment.

In a further experiment, again at 20 K, we irradiated the sample with red light ($\lambda \leq 700$ nm). The subsequently recorded Mössbauer spectrum (Fig. 1, middle) clearly shows that the intensity of the HS2 doublet has decreased and that of the singlet has increased. Unquestionably, a light-induced transition from the stable $^5T_2$ state to a metastable $^1A_1$ state has taken place, corresponding to the mechanism depicted in Figure 1. The fact that, in the experiment described here, the fraction of the HS2 state has decreased from 65% (fraction of the resonance area) to only 27% is merely due to the broadband irradiation. Wavelength ranges of $\lambda \geq 700$ nm cause the transition $^5T_2 \rightarrow {}^5E$, which requires an energy of 12200 cm^{-1},[5, 11, 12] but, at the same time, excite the very weak and broad $^1A_1 \rightarrow {}^3T_1$ band at about 10300 cm^{-1}; LIESST(L → H) can also occur via this path, namely, $^1A_1 \rightarrow {}^3T_1 \rightarrow {}^5T_2$, as recently shown by *A. Hauser* in our group.[13]

The lifetime of the metastable LS state generated by LIESST(H → L) is on the order of days at $T = 20$ K. At

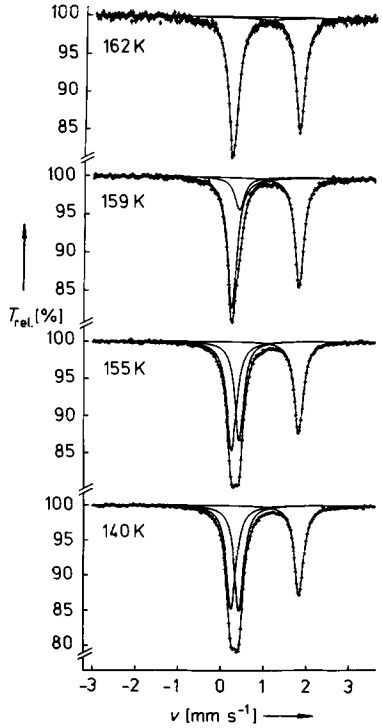

Fig. 3. ^{57}Fe Mössbauer spectra of **1** in the temperature range where the thermal spin crossover $^5T_2$(HS) ↔ $^1A_1$(LS) occurs, with a remaining HS fraction of about 65% at 140 K.

$T \approx 40$ K, noticeable decay to the stable HS2 state occurs (increase from 27% to 45% in the fraction of the HS2 doublet in the Mössbauer spectrum over 24 h). A Mössbauer spectrum recorded after warming the sample to 60 K (Fig. 4, bottom) is again nearly identical with that recorded before irradiation at 20 K. The radiationless back-relaxation to the ground state proceeds via a nonadiabatic multiphoton process.[14, 15]

Athough both complexes, **1** and $[Fe(mtz)_6](BF_4)_2$, for which a light-induced spin crossover from the stable HS($^5T_2$) state to a long-lived metastable LS($^1A_1$) state has been

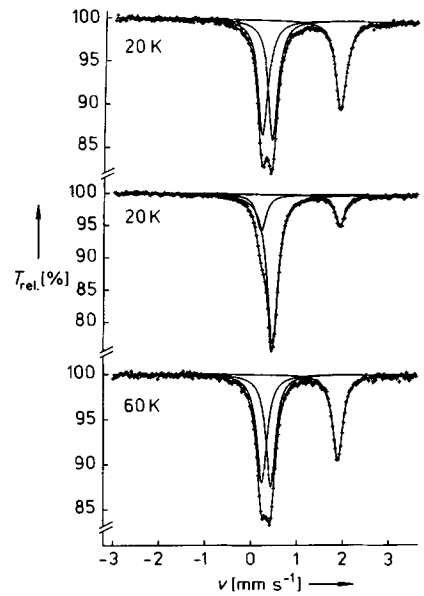

Fig. 4. ^{57}Fe Mössbauer spectra at 20 K before irradiation (top) and after irradiation with red light (middle), as well as after subsequent warming to 60 K (bottom). LIESST(H → L) is clearly revealed by the decrease in the intensity of the HS2 doublet (outer signals) and the increase in the intensity of the LS singlet.

achieved, differ only in the anion, their thermal spin-crossover behavior differs considerably; on the other hand, the LIESST(L → H) behavior is similar in the two cases.

Experimental Procedure

The ligand mtz was prepared as described in the literature [16]. In order to synthesize **1**, iron powder was first dissolved in aqueous 2 M trifluoromethanesulfonic acid (Aldrich). The excess iron powder was then filtered off and the solution was gently concentrated under nitrogen until $[Fe(H_2O)_6](CF_3SO_3)_2$ began to crystallize. The product was collected by filtration and washed with a small amount of cold water and ether. Complex **1** was obtained from a concentrated aqueous solution of $[Fe(H_2O)_6](CF_3SO_3)_2$ and mtz in a molar ratio of 1:6 under nitrogen; the solution was further concentrated by applying a stream of oxygen-free nitrogen until **1** began to crystallize. After filtration and washing, **1** was recrystallized from nitromethane. The values of the elemental analyses are in good agreement with the theoretical values.

The magnetic susceptibility χ was measured with a Foner magnetometer in the range $20 \leq T \leq 270$ K (He-flow cryostat) in a magnetic field of 1 T. The diamagnetic correction for **1** was determined by χ measurement at room temperature on an analogously prepared zinc complex ($\chi = -648 \times 10^{-6}$ cm^{3}mol^{-1}). The value of the magnetic moment was calculated from the equation $\mu_{eff} = 2.828\,(\chi_m T)^{1/2}$ (χ_m = corrected molar susceptibility).

^{57}Fe Mössbauer spectra were recorded with a conventional spectrometer. The ^{57}Co/Rh source was kept at room temperature, while the absorber (enclosed in a Plexiglass container, 3 cm^2 area, with ca. 7 mg cm^{-2} Fe) was mounted in a flow cryostat (CF506, Oxford Instruments). The cryostat was equipped with windows of transparent Mylar film. The temperature at the absorber was measured with a carbon/glass resistor mounted directly on the sample holder. The Mössbauer signals were fitted to Lorentzian curves.

Received: February 15, 1991 [Z 4443 IE]
German version: *Angew. Chem. 103* (1991) 1015

CAS Registry numbers:
$[Fe(mtz)_6](CF_3SO_3)_2$, 134565-01-8; $[Zn(mtz)_6](CF_3SO_3)_2$, 134565-02-9.

[1] In the context of ligand field theory, this is referred to as the $^5T_2(O_h) \leftrightarrow {}^1A_1(O_h)$ transition in the approximation of regular octahedral symmetry.
[2] H. A. Goodwin, *Coord. Chem. Rev. 18* (1976) 293.
[3] P. Gütlich, *Struct. Bonding (Berlin) 44* (1981) 83.
[4] S. Decurtins, P. Gütlich, C. P. Köhler, H. Spiering, A. Hauser, *Chem. Phys. Lett. 105* (1984) 1.
[5] S. Decurtins, P. Gütlich, K. M. Hasselbach, A. Hauser, H. Spiering, *Inorg. Chem. 24* (1985) 2174.
[6] S. Decurtins, P. Gütlich, C. P. Köhler, H. Spiering, *J. Chem. Soc. Chem. Commun. 1985*, 430.
[7] P. Poganiuch, P. Gütlich, *Inorg. Chem. 26* (1987) 455.
[8] R. Herber, *Inorg. Chem. 26* (1987) 173.
[9] A. W. Addison, S. Burman, C. G. Wahlgren, O. A. Rajan, T. M. Rowe, E. Sinn, *J. Chem. Soc. Dalton Trans. 1987*, 2621.
[10] A. Hauser, J. Adler, P. Gütlich, *Chem. Phys. Lett. 152* (1988) 468.
[11] A. Hauser, *Chem. Phys. Lett. 124* (1986) 543.
[12] P. Poganiuch, S. Decurtins, P. Gütlich, *J. Am. Chem. Soc. 112* (1990) 3270.
[13] A. Hauser, *J. Chem. Phys.*, in press.
[14] E. Buhks, G. Navon, M. Bixon, J. Jortner, *J. Am. Chem. Soc. 102* (1980) 2918.
[15] A. Hauser, P. Gütlich, *Coord. Chem. Rev. 97* (1990) 1.
[16] T. Kamiya, Y. Saito, DE-A P2147023.5 (1971).

Rubyrin: A New Hexapyrrolic Expanded Porphyrin**

By *Jonathan L. Sessler,* Takashi Morishima,* and *Vincent Lynch*

Although, a number of "expanded porphyrins", large pyrrole-containing macrocyclic analogues of the porphyrins (e.g. porphine, **1**), are now known,[1-9] only a few aromatic examples have been reported which contain more than four pyrrolic subunits.[1-3] Unfortunately, for the most part the chemistry of these latter systems has been communicated in only the briefest fashion and structural information is available only for derivatives of sapphyrin (e.g. **2**)[1c-1e] in the all-pyrrole series.[3] Thus, the preparation and study of new polypyrrolic systems remains of interest. Such studies could provide important information on the fundamental and interrelated questions of ring size, aromaticity, and effective macrocycle stability, as well as providing an important entry into the development of improved photosensitizers for photodynamic applications[10] or new chelating receptors for the complexation of anions[1c,1e] and cations.[1,3,7,8] In this communication, we report the synthesis and structural characterization of an alkyl-substituted derivative of the diprotonated form of a new class of hexapyrrolic expanded porphyrins, **3**. To the best of our knowledge, this latter compound, to which we have assigned the trivial name "rubyrin" (from the Latin *rubeus*),[11] based on the intense bright red color of the diprotonated derivatives, represents the parent form of the largest structurally characterized expanded porphyrin system prepared to date.

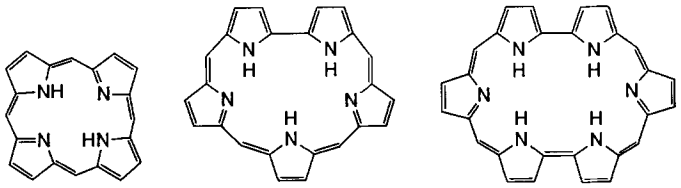

1 **2** **3**

The synthesis of the diprotonated form of 4,8,13,18,23,27-hexaethyl-3,9,14,17,22,28-hexamethylrubyrin (**4**) contains two key steps. The first involves the acid-catalyzed condensation between the bis-α-free bipyrrole **5**[1c] and the acetoxy-activated pyrrole **6**.[12] This reaction, which was carried out in analogy to earlier syntheses of symmetric tripyrranes,[9] gave the protected tetrapyrrole derivative **7** in roughly 66% yield. Standard nearly quantitative debenzylation then gave the diacid **8**. This, in turn, was used without delay in the next step, an acid-catalyzed [4] + [2] MacDonald-type[13] oxidative condensation with the readily available[1c] diformyl bipyrrole, **9**. This second critical step of condensation and accompanying air oxidation taken together provided, following workup and chromatographic purification, the diprotonated rubyrin derivative (**4a**) in roughly 20% yield.[14] Washing either this purified ditosylate salt or the crude reaction mixture with aqueous 10% hydrochloric acid then produced the more crystalline dihydrochloride derivative, **4b** in yields of 63% (based on **4a**) and 40% (based on **8**), respectively.

Formally, rubyrin (**3**) and its derivatives may be considered as 26π-electron annulenes. Thus, the diprotonated salts **4a** and **4b** were expected to be aromatic. The spectroscopic data is consistent with this formulation. For instance, low-field *meso*-like methine signals and high-field internal NH resonances were observed in the ^{1}H NMR spectra as would be expected for a large aromatic expanded porphyrin system. In the specific case of **4b** in $CDCl_3$ these signals were observed at $\delta = 11.58$ and 11.60 (in a 1:1 ratio), and at -4.97 and -5.30 (in a 2:1 ratio), respectively, values which compare closely to those observed for the dihydrochloride salt of 3,8,12,13,17,22-hexaethyl-2,7,18,23-tetramethylsapphyrin

[*] Prof. J. L. Sessler, Dr. V. Lynch, T. Morishima
Department of Chemistry and Biochemistry
University of Texas
Austin, TX 78712 (USA)

[**] This work was supported by the National Institutes of Health grant AI 28845 to *J. L. S.*, who also thanks the NSF for a Presidential Young Investigator Award (1986), the Alfred P. Sloan Foundation for a Research Fellowship (1989–1991), and the Camille and Henry Dreyfus Foundation for a Teacher-Scholar Award (1988–1992). *T. M.* is grateful to Mitsubishi Kasei Co. for supporting an academic research leave (1989–1991).

([H_2-Sap]$^{2\oplus}$) measured under the same experimental conditions.[1c] In addition, both **4a** and **4b** display Soret-like and Q-type transitions in their UV-VIS spectra, which, as would be expected for a large aromatic expanded porphyrin, are considerably red-shifted as compared to those of smaller porphyrin-like systems. In fact, relative to [H_2-Sap]$^{2\oplus}$ and [H_2-OEP]$^{2\oplus}$ (the diprotonated derivative of 2,3,7,8,12,13,17,18-octaethylporphyrin) measured under similar experimental conditions, the Soret band of **4b** is shifted by ca. 50 and 100 nm, respectively (cf. Fig. 1),[15] and the lowest energy Q-type band by about 180 and 270 nm, respectively.

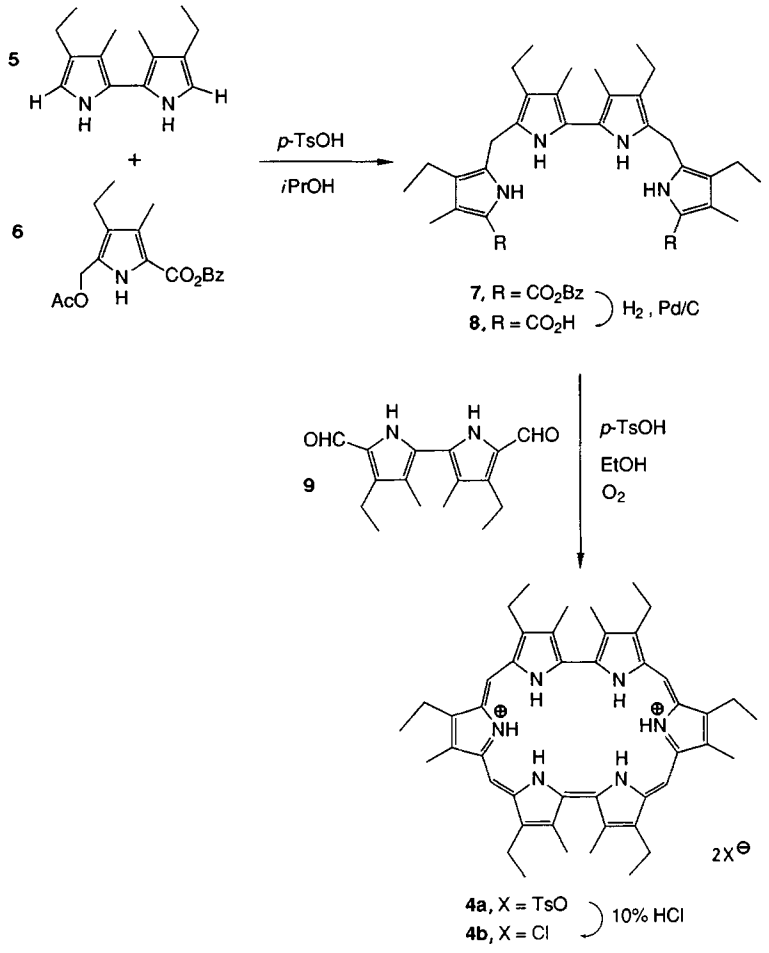

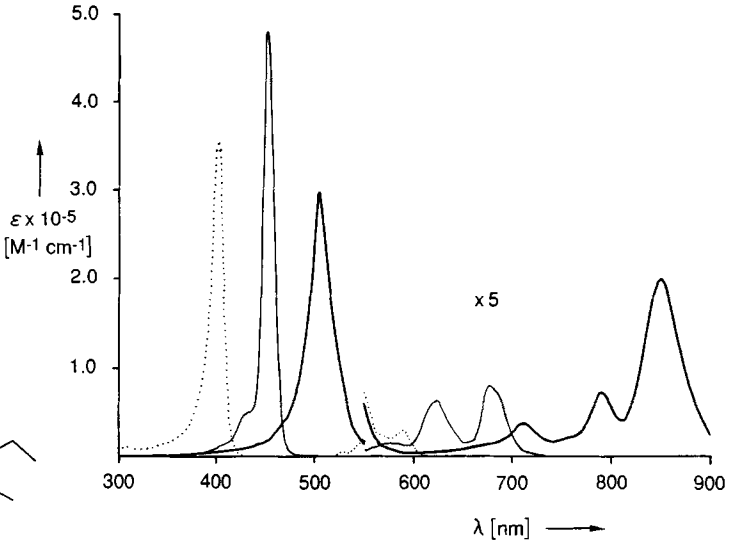

Fig. 1. The UV-VIS absorption spectra of **4b** (——) and the diprotonated derivatives of 2,3,7,8,12,13,17,18-octaethylporphyrin (recorded in the presence of excess trifluoroacetic acid (·····) and 3,8,12,13,17,22-hexaethyl-2,7,18,23-tetramethylsapphyrin (recorded as the dihydrochloride salt) [15] (——) in dilute CH_2Cl_2.

Further evidence for the aromatic nature of rubyrin was obtained from the X-ray diffraction structure analysis of **4b**.[17] As illustrated in Figure 2, this revealed a nearly planar conformation for the core macrocycle that is only slightly waffled by virtue of interactions with the hydrogen-bound chloride counter anions (the maximum deviation (for C2) of the C and N macrocycle atoms from the mean plane is 0.509(4) Å). In fact, this lack of distortion is reminiscent of that seen in the X-ray structure of [H_2-OEP]$^{2\oplus}$[18a] and several recently reported diprotonated bisvinylogous expanded porphyrins,[5d, 5e] suggesting a significant through-cycle π-electron conjugation in **4b**. Consistent with this conclusion is the finding that the average C–C and C–N bond distances within the formal 26π-electron periphery (1.394 Å and 1.375 Å, respectively) are close in value to those observed in the corresponding diprotonated OEP structure (1.390 Å and 1.375 Å, respectively).[18a] Interestingly, however, the interpyrrole angles at the bridging methines (137.0 and 137.6°) are considerably greater than those found in protonated porphyrins (ca. 127°).[18] Thus, the expanded porphyrin **4b** displays a more open inner core than is expected for a directly appended "three-quarter porphyrines" linked by two sets of interpyrrole bonds. Nonetheless, it is clear that from a structural point of view, compound **4b** displays all properties expected of an aromatic system.

In spite of the evident aromatic nature of **4b**, efforts to obtain the free-base form (corresponding to **3**), or metal complexes derived from it, have so far proved unsuccessful.[19] However, as for the diprotonated form of sapphyrin[1c, 1e] and possibly other cationic expanded porphyrins,[5, 6] the diprotonated rubyrin system acts as an effective anion receptor. For instance, preliminary spectroscopic studies indicate that diprotonated rubyrin can bind both fluoride and phosphate anions in a strong and nonlabile manner.[20] These results lead us to suggest that protonated rubyrins could prove useful in the recognition and

Table 1. Characterization data for new compounds.

4a: decomp. above 220°C; ^{1}H NMR (300 MHz, $CDCl_3$): δ = −4.14 (s, 2H, NH), −3.68 (s, 4H, NH), 1.50 (s, 6H; PhCH_3), 1.90 (d, J_{HH} = 7 Hz, 4H, phenyl H), 2.30 (m, 18H, CH_2CH_3), 3.90 (s, 12H, CH_3), 4.10 (m, 8H, CH_2CH_3), 4.30 (s, 6H, CH_3), 4.70 (q, 4H, CH_2CH_3), 4.90 (d, J_{HH} = 7 Hz, 4H, phenyl H), 11.18 (m, 4H, *meso-H*); HRMS (FAB): *m/z* 694.4707 ($M^{\oplus}$ − 2TsO$^{\ominus}$), calcd for $C_{46}H_{58}N_6$ 694.4723 (±0.0016).

4b: decomp. above 230°C; ^{1}H NMR (300 MHz, $CDCl_3$): δ = −5.30 (s, 2H, NH), −4.97 (s, 4H, NH), 2.09 (m, 12H, CH_2CH_3), 2.34 (t, J_{HH} = 7 Hz, 6H, CH_2CH_3), 4.06 (s, 12H, CH_3), 4.40 (s, 6H, CH_3), 4.43 (m, 8H, CH_2CH_3), 4.82 (q, J_{HH} = 7 Hz, 4H, CH_2CH_3), 11.58 (s, 2H, *meso-H*) 11.60 (s, 2H, *meso-H*); ^{13}C NMR (75.5 MHz, $CDCl_3$): δ = 12.98, 15.73, 17.50, 17.99, 21.05, 21.29, 92.74, 92.88, 126.47, 127.30, 129.03, 129.65, 130.73, 136.38, 139.32, 143.31; UV/VIS (CH_2Cl_2): λ_{max} [nm] (ε) = 505 (302 000), 711 (11 000), 791 (15 500), 850 (38 000); HRMS (FAB): *m/z* 694.4660 ($M^{\oplus}-Cl_2$), calcd for $C_{46}H_{58}N_6$ 694.4723 (±0.0063).

7: m.p. 163–166°C; ^{1}H NMR (300 MHz, $CDCl_3$): δ = 0.83 (t, 6H, CH_2CH_3), 1.10 (t, 6H, CH_2CH_3), 2.02 (s, 10H, CH_3 and CH_2CH_3), 2.12 (s, 6H, CH_3), 2.46 (m, 4H, CH_2CH_3), 3.70 (br. s, 6H, pyrrole-CH_2 and CH_2Ph), 4.55 (br. s, 2H, CH_2Ph), 6.85 (m, 4H, aromatic), 7.21 (m, 6H, aromatic), 9.89 (br. s, 2H, NH), 10.98 (br. s, 2H, NH); ^{13}C NMR (75.5 MHz, $CDCl_3$): δ = 11.20, 11.30, 15.21, 15.61, 16.86, 18.20, 22.34, 65.91, 113.97, 117.12, 120.76, 121.29, 123.36, 123.51, 126.53, 126.88, 127.64, 127.82, 133.80, 135.97, 164.48; HRMS (CI): *m/z* 726.4142 ($M^{\oplus}$), calcd for $C_{46}H_{54}N_4O_4$ 726.4145 (±0.0003).

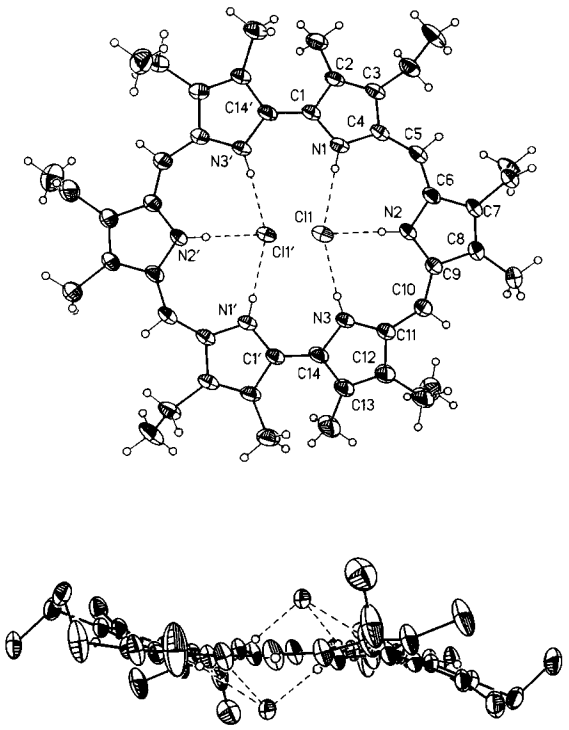

Fig. 2. Molecular structure of **4b** in the crystal showing partial atom labeling scheme and the H-bonding interactions of the chloride counterions with the macrocycle (dashed lines). Top: View perpendicular to the plane through the nitrogen atoms. Below: Side view showing the nearly planar conformation of the core macrocycle. The macrocycle has an inversion center. Atoms labeled with a′ are related by $-x,1-y,1-z$. Thermal ellipsoids are scaled to the 30% probability level. H atoms represented as spheres of arbitrary size, disordered atoms and the chloroform molecules not shown. Selected bond distances [Å] and angles [°]: N1–C1, 1.373(5); N1–C4, 1.394(6); C1–C2, 1.437(7); C2–C3, 1.362(5); C3–C4, 1.429(6); C4–C5, 1.381(5); C5–C6, 1.379(6); C6–C7, 1.421(5); C7–C8, 1.377(9); C8–C9, 1.449(8); N2–C6, 1.383(7); N2–C9, 1.367(5); N1–N2, 3.483(5); N1–N3, 5.559(5); N1–N1′, 6.352(7); N1–N2′, 5.836(5); N1–N3′, 3.078(5); N2–N2′, 7.213(7); N3–N3′, 6.354(7); N1–C11, 3.265(4); N2–C11, 3.158(4); N1–C4–C5, 130.1(4); C3–C4–C5, 123.4(4); C4–C5–C6, 137.6(5); C5–C6–C7, 122.9(5); C5–C6–N2, 129.5(4).

through-membrane transport of biologically active substrates, including for example nucleotide analogues.[21]

Experimental Procedure

7: Compounds **5** (3.72 g, 17.2 mmol), **6** (10.9 g, 34.5 mmol), and dry isopropyl alcohol (140 mL) were combined and heated at 80 °C to effect complete dissolution. *p*-Toluenesulfonic acid monohydrate (30 mg) was then added and the resulting green solution heated at reflux for 10 hours under nitrogen. The resulting suspension was then cooled and kept at 0 °C for one hour. Filtration, washing with cold ethanol, and drying in vacuo afforded **7** as a fine, off-white powder (8.24 g, 66%), which could be further purified by recrystallization from CH_2Cl_2/MeOH.

8: The dibenzyl ester **7** (0.24 g, 0.33 mmol) was dissolved in dry THF (100 mL) and subjected to hydrogenation over 10% palladium-charcoal (40 mg) at 1 atm H_2. The catalyst was then separated by filtration, the solvent reduced in volume on a rotary evaporator, and the product precipitated by trituration with hexanes. The pale blue precipitate was collected by filtration, dried in vacuo (yield 0.16 g (90%) of **8**), and used directly in the synthesis of **4a**.

4a and **4b:** Compounds **9** (136 mg, 0.5 mmol) and **8** (273 mg, 0.5 mmol) were dissolved with warming in 1.0 L of dry ethanol. The mixture was then allowed to cool to room temperature and 2.0 g of *p*-toluenesulfonic acid monohydrate added all at once. Oxygen was then bubbled through the stirred mixture for 18 h. The ethanol was then removed on a rotary evaporator and the dark purple residue taken up in $CHCl_3$ and purified by column chromatography (Merck type 60 (230–400 mesh) Silica gels; first $CHCl_3$ and then $CHCl_3$/MeOH (98/2) as eluents). Collection of the dark red fraction and removal of the solvent gave 105 mg (20%) of **4a** which could be purified further by recrystallizing from $CHCl_3$/hexane. Dissolving compound **4a** in dichloromethane and washing with a 10% aqueous solution of HCl for 2 h at room temperature then afforded, after workup, product **4b** in ca. 63% yield. This same material could also be obtained in roughly 40% net yield by treating the crude condensation product (from **8** and **9**) with a 10% aqueous solution of HCl prior to workup and chromatography. Single crystals of **4b** were obtained by vapor diffusion recrystallization from $CHCl_3$/pentane.

Received: March 8, 1991 [Z 4486IE]
German version: *Angew. Chem. 103* (1991) 1018

[1] Sapphyrins and samaragdyrins: a) M. J. Broadhurst, R. Grigg, A. W. Johnson, *J. Chem. Soc. Perkin Trans. 1 1972*, 2111–2116; b) V. J. Bauer, D. L. J. Clive, D. Dolphin, J. B. Paine, III, F. L. Harris, M. M. King, J. Loder, S.-W. C. Wang, R. B. Woodward, *J. Am. Chem. Soc. 105* (1983) 6429–6436; c) J. L. Sessler, M. J. Cyr, V. Lynch, E. McGhee, J. A. Ibers, *ibid. 112* (1990) 2810–2813; d) A. K. Burrell, J. L. Sessler, M. J. Cyr, E. McGhee, J. A. Ibers, *Angew. Chem. 103* (1991) 83–85; *Angew. Chem. Int. Ed. Engl. 30* (1991) 91–93; e) J. L. Sessler, M. J. Cyr, A. K. Burrell, *Synlett 1991* 127–133.

[2] Pentaphyrins and hexaphyrins: a) H. Rexhausen, A. Gossauer, *J. Chem. Soc. Chem. Commun. 1983*, 275; b) A. Gossauer, *Bull. Soc. Chim. Belg. 92* (1983) 793–795.

[3] Structurally characterized "expanded phthalocyanines", the superphthalocyanines, are known: V. W. Day, T. J. Marks, W. A. Wachter, *J. Am. Chem. Soc. 97* (1975) 4519–4527.

[4] Platyrins: a) R. A. Berger, E. LeGoff, *Tetrahedron Lett. 1978*, 4225–4228; b) E. LeGoff, O. G. Weaver, *J. Org. Chem. 52* (1987) 710–711.

[5] Vinylogous porphyrins: a) M. Gosmann, B. Franck, *Angew. Chem. 98* (1986) 1107–1108; *Angew. Chem. Int. Ed. Engl. 25* (1986) 1100–1101; b) G. Knübel, B. Franck, *ibid. 100* (1988) 1203–1211 and *27* (1988) 1170–1172; c) M. Gosmann, A. Vogt, B. Franck, *Liebigs Ann. Chem. 1990*, 163–168; d) H. König, C. Eickemeier, M. Möller, U. Rodewald, B. Franck, *Angew. Chem. 102* (1990) 1437–1439; *Angew. Chem. Int. Ed. Engl. 29* (1990) 1393–1395; e) S. Beckmann, T. Wessel, B. Franck, W. Hönle, H. Borrmann, H. G. von Schnering, *ibid. 102* (1990) 1439–1441 bzw. *29* (1990) 1395–1397.

[6] Stretched porphycenes: a) N. Jux, P. Koch, H. Schmickler, J. Lex, E. Vogel, *Angew. Chem. 102* (1990) 1429–1431; *Angew. Chem. Int. Ed. Engl. 29* (1990) 1385–1387; b) E. Vogel, N. Jux, E. Rodriguez-Val, J. Lex, H. Schmicker, *ibid. 102* (1990) 1431–1434 and *29* (1990) 1387–1390.

[7] Texaphyrins: a) J. L. Sessler, T. Murai, V. Lynch, M. Cyr, *J. Am. Chem. Soc. 110* (1988) 5586–5588; b) J. L. Sessler, T. Murai, G. Hemmi, *Inorg. Chem. 28* (1989) 3390–3393; c) B. G. Maiya, T. E. Mallouk, G. Hemmi, J. L. Sessler, *ibid. 29* (1990) 3738–3745.

[8] For examples of nonaromatic large pyrrole-containing macrocycles see: a) F. V. Acholla, K. B. Mertes, *Tetrahedron Lett. 25* (1984) 3269–3270; b) F. V. Acholla, F. Takusagawa, K. B. Mertes, *J. Am. Chem. Soc. 107* (1985) 6902–6908; c) H. Adams, N. A. Bailey, D. A. Fenton, S. Moss, C. O. Rodriguez de Barbarin, *J. Chem. Soc. Dalton Trans. 1986*, 693–699; d) D. E. Fenton, R. Moody, *ibid. 1987*, 219–220; e) K.-H. Schumacher, B. L. Franck, *Angew. Chem. 101* (1989) 1292–1294; *Angew. Chem. Int. Ed. Engl. 28* (1989) 1243–1245. See also refs. [5b] and [9].

[9] J. L. Sessler, V. Lynch, M. R. Johnson, *J. Org. Chem. 52* (1987) 4394–4397.

[10] For discussions of this point see: J. L. Sessler, M. Cyr, B. G. Maiya, M. L. Judy, J. T. Newman, H. Skiles, R. Boriack, J. L. Matthews, T. C. Chanh, *Proc. SPIE Int. Opt. Eng. 1203 (Photodynamic Therapy: Mechanisms II)* (1990) 233–245, and references therein. See also ref. [5e].

[11] The systematic name for **3** is: 29,30,31,32,33,34-hexaazaheptacyclo-[24.2.1.$1^{2,5}$.$1^{7,10}$.$1^{12,15}$.$1^{16,19}$.$1^{21,24}$]tetratriaconta-1,3,5,7(31),8,10,12,14,16,18,20,22,24(34),25,27-pentadecaene.

[12] A. W. Johnson, I. T. Kay, E. Markham, P. Price, K. B. Shaw, *J. Chem. Soc. 1959*, 3416–3424.

[13] G. P. Arsenault, E. Bullock, S. F. MacDonald, *J. Am. Chem. Soc. 82* (1960) 4384–4389.

[14] Interestingly, in additon to **4a**, several other macrocyclic products, including 3,7,12,18,22-pentaethyl-2,8,13,17,23-pentamethylsapphyrin and a partially reduced, rubyrin-like system, 4,8,13,18,23,27-hexaethyl-3,9,14,17,22,28-hexamethyl-29,30,31,32,33,34-hexaazaheptacyclo-[24.2.1.$1^{2,5}$.$1^{7,10}$.$1^{12,15}$.$1^{16,19}$.$1^{21,24}$]tetratriaconta-1,3,5,7,9,11,13,15,17,19,21,23,25,27-tetradecaene, were also isolated in low yields in the course of this critical [4] + [2] condensation. In light of its bright violet color, this latter material is assigned the trivial name of iodyrin. ^{1}H NMR (300 MHz, $CDCl_3$): $\delta = 0.98$ (m, 9H; CH_2CH_3), 1.09 (m, 9H; CH_2CH_3), 2.06 (m, 18H; CH_3), 2.37 (m, 6H; CH_2CH_3), 2.57 (m, 6H; CH_2CH_3), 6.78 (m, 4H; „*meso*"-H), 11.85 (s, 1H; NH), 12.32 (s, 1H; NH), 12.51 (s, 1H; NH), 12.60 (s, 1H; NH), 12.62 (s, 1H; NH), 12.74 (s, 1H; NH); MS (FAB): *m/z* 696 ($M^{\oplus}$ + 1, 4%), 695 ($M^{\oplus}$, 5), 307 (22), 154 (100); UV/VIS (CH_2Cl_2): $\lambda_{max} = 538$ nm.

[15] Here, the sapphyrin dihydrochloride salt was used so as to allow a direct comparison to the rubyrin system **4b**. Adding excess TFA, however, served to increase the intensity of the sapphyrin Soret band (by ca. 15%), but not that of **4b**, suggesting that either conversion to the diprotonated form may not be complete in the former case or that the spectrum of $[H_2\text{-Sap}]^{2\oplus}$ is highly anion-dependent. On the basis of independent evidence [1e, 16] we currently favor the latter explanation.

[16] B. G. Maiya, M. Cyr, A. Harriman, J. L. Sessler, *J. Phys. Chem. 94* (1990) 3597–3601.

[17] **4b**: $[C_{46}H_{56}N_6H_2]\ Cl_2 \cdot 2\ CHCl_3$, triclinic, space group P1 (No. 2), $Z = 1$, $a = 10.196(8)$, $b = 11.141(8)$, $c = 13.476(9)$ Å, $\alpha = 67.18(5)$, $\beta = 72.97(6)$, $\gamma = 68.56(6)°$, $V = 1293(2)$ Å^3, $\varrho_{calc} = 1.29\ g\,cm^{-3}$ (173 K) $F(000) = 526$. Data collected at 173 K on a Nicolet R3 diffractometer, graphite monochromator, $Mo_{K\alpha}$ radiation ($\lambda = 0.7107$ Å), ω scan, $2\theta = 50°$, 4573 unique reflections, 2871 with $F_o^2 > 3\sigma(F_o^2)$. The structure was solved by direct methods and refined by full-matrix least-squares (SHELXTL-Plus, Nicolet XRD, Madison, WI, USA) with anisotropic thermal parameters for the non-hydrogen atoms. Hydrogen atoms on C18, C19, C19A, C20, C21, C22, C22A, and C23 were idealized (C-H 0.96 Å), while all others were taken from a ΔF map. All were refined isotropically. Inversion center at 0,1/2,1/2 resulting in the occupational disorder of the ethyl and methyl groups of the pyrrole ring containing N2. The $Cl^{\ominus}$ ions are H-bonded to the pyrrolic hydrogens and to the $CHCl_3$ solvate molecules. $R = 0.0529$, $R_w = 0.0678$, goodness of fit = 2.284 for 361 parameters. The minimum and maximum peaks in the final ΔF map were -0.30 and $0.38\ e^-$ Å^{-3}, respectively. Further details of the crystal structure are available on request from the Director of the Cambridge Crystallographic Data Centre, University Chemical Laboratory, Lensfield Road, GB-Cambridge CB21 1EW (UK), on quoting the full journal citation.

[18] a) E. Cetinkaya, A. W. Johnson, M. F. Lappert, G. M. MacLaughlin, K. W. Muir, *J. Chem. Soc. Dalton Trans 1 1974*, 1236–1243; b) A. Stone, E. B. Fleischer, *J. Am. Chem. Soc. 90* (1968) 2735–2748.

[19] Subsequent to the submission of this manuscript, an analogue of **4b**, derived from **8** and 5,5′-diformyl-4,4′-dipropyl-2,2′-bipyrrole, was prepared in our laboratory. This system (λ_{max} (CH_2Cl_2) = 501, 692, 771, 817 nm), which presumably allows for more rotational freedom about one of the bipyrrolic bonds (and hence a flatter macrocyclic array), was found to be stable in its free-base form. Interestingly, this new free-base material is also ruby red in CH_2Cl_2 solution (λ_{max} (CH_2Cl_2) = 513, 711, 789, 844 nm).

[20] We thank Dr. *A. K. Burrell* of this department for his help in carrying out these experiments

[21] For a discussion of alternative approaches to these problems see: H. Furuta, D. Magda, J. L. Sessler, *J. Am. Chem. Soc. 113* (1991) 978–985, and references therein.

The Synthesis and Structure of the Yellow and Green Forms of $[Nb(O)Cl_3(PMe_3)_3]$ and the Orange and Green Forms of $[Nb(S)Cl_3(PMe_3)_3]$; Examples of Perfectly Matched Bond-Stretch Isomers?**

By *Alan Bashall, Vernon C. Gibson,* Terence P. Kee, Mary McPartlin,* Oliver B. Robinson*, and *Alan Shaw*

We report the syntheses of two pairs of seven-coordinate niobium isomers, yellow and green $[Nb(O)Cl_3(PMe_3)_3]$ (**1**) and orange and green $[Nb(S)Cl_3(PMe_3)_3]$ (**2**). These pairs of compounds appear to be perfectly matched bond-stretch isomers; there has been no previous report of this type of isomerism for a thiometal complex. The full X-ray structure analysis of the two pairs of isomers and the persistence of the thio isomers in solution (by IR spectroscopy) provide the best evidence so far for the reality of the phenomenon of bond-stretch isomerism. All four complexes are isostructural and isomorphous and have distorted mono-capped octahedral coordination geometries, with the significant differences between the isomeric pairs lying mainly in the bond lengths to the metal and the observed Nb=O and Nb=S stretches.

The first experimental evidence of the phenomenon of bond-stretch isomerism came from a series of green and blue octahedral oxomolybdenum complexes synthesized twenty years ago and thought originally to be geometric isomers.[1] X-ray structure analyses of the only suitable crystals that could be obtained, those of blue $[Mo(O)Cl_2(PMe_2Ph)_3]$ and green $[Mo(O)Cl_2(PEt_2Ph)_3]$, showed identical *cis-mer* coordinations with the only differences in the overall structures being the relative orientations of the phosphane organo groups and unexpected discrepancies in the Mo=O bonds, which were very much shorter in the more stable blue compound (1.676(7) Å)[2] than in the less stable green compound (1.803(11) Å).[3] It was deduced that the blue ($\tilde{\nu}$(Mo=O) 954 cm^{-1}) and green ($\tilde{\nu}$(Mo=O) 943 cm^{-1}) forms of the complex $[Mo(O)Cl_2(PMe_2Ph)_3]$ were the first examples of a new type of isomerism, named *distortion* isomerism at that time.[4]

Unambiguous examples of this class of isomerism have proved extremely elusive despite widespread interest,[5] and until now there has only been one case of full characterization of a perfectly matched, isostructural and isomorphous pair. They are the blue and green isomers of the cationic complex $[LW(O)Cl_2]^+$ (L = *N,N′,N″*-trimethyl-1,4,7-triazacyclononane), in which, despite relatively high errors in the parameters due to disorder of the PF_6^- counterion, significant W=O bond-length differences (1.719(18) and 1.893(20) Å, respectively) were established.[6] This has prompted a recent theoretical treatment of this phenomenon in transition-metal complexes and its reclassification as bond-stretch isomerism,[7] a term originally proposed for hypothetical organic species with double energy minima on simple bond stretching.[8]

In the present work we find that a mixture of the two isomers of compounds **1** and **2** are generated from reactions of trimethylphosphane with either base-free $[Nb(E)Cl_3]_n$ or the acetonitrile adducts $[Nb(E)Cl_3(CH_3CN)_2]$ (E = O, S) (Scheme 1). The proportions of the isomers arising in the

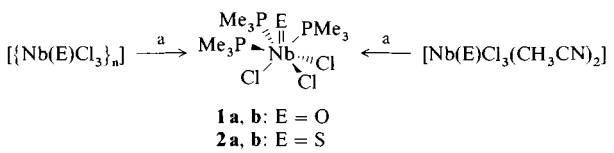

1a, b: E = O
2a, b: E = S

Scheme 1. a: + 3 PMe_3, in CH_2Cl_2. **a**, **b** refer to the bond-stretch isomers; **a** is the isomer with the shorter Nb–E bond, **b** the isomer with the longer Nb–E bond. For details on the crystallizations, see the text. For the ratio of reaction products and the reaction times, see Table 1.

crude product mixtures are dependent on which of these two starting materials is employed and the length of time the reaction mixture is allowed to stir (approximate ratios, determined by IR spectroscopy for specified reaction times, are shown in Table 1). However, pure batches of each isomer may be obtained by straightforward crystallization proce-

Table 1. Dependence of product ratios of isomers **1** and **2** on the starting compound and the reaction time *t*.

	$[\{Nb(O)Cl_3\}_n]$	$[Nb(O)Cl_3(CH_3CN)_2]$	$[\{Nb(S)Cl_3\}_n]$	$[Nb(S)Cl_3(CH_3CN)_2]$
a:**b**	90:10	40:60	20:80	45:55
t	5 h	12 h	12 h	2 d

[*] Dr. V. C. Gibson, T. P. Kee, O. B. Robinson, A. Shaw
Department of Chemistry, University Science Laboratory
South Road, GB-Durham DH1 3LE (UK)
Prof. M. McPartlin, A. Bashall
School of Chemistry, The Polytechnic of North London
Holloway Road, GB-London N7 8DB (UK)

[**] We thank the Scientific and Engineering Research Council (UK) for studentships (*T. P. K., O. B. R.*, and *A. S.*) and Courtaulds plc for financial support (*O. B. R.*). We are grateful to Dr. *C. K. Prout* and Prof. *K. Wieghardt* for valuable discussions.

dures. For example, a batch of crystals consisting solely of **1a** may be obtained either by concentration and cooling (to ca. $-50°$ C) of the CH_2Cl_2 reaction solution generated from $[\{Nb(O)Cl_3\}_n]$ or by removal of the CH_2Cl_2 solvent followed by extraction of the dried residue with toluene and cooling to $-20°$ C overnight. Complex **1b** may be obtained by a similar low-temperature toluene crystallization of the mixture arising from $[Nb(O)Cl_3(CH_3CN)_2]$ or, alternatively, by allowing a solution of **1a** in toluene to stand at $-20°$ C for several days. Analogous procedures are employed to isolate single-component batches of **2a** and **2b**; **2a** is obtained by low-temperature toluene crystallization of the crude mixture arising from $[Nb(S)Cl_3(CH_3CN)_2]$ and **2b** from the mixture generated from $[\{Nb(S)Cl_3\}_n]$.

The first isomer to be isolated was yellow $[Nb(O)Cl_3(PMe_3)_2]$ (**1a**) and a Nb=O distance of 1.781(6) Å and mean Nb–Cl distance of 2.518(3) Å were established.[9] Later, the green form **1b** was obtained and, although the IR spectra of the individual isomers have a strikingly similar appearance (Fig. 1), they are readily distinguished by the

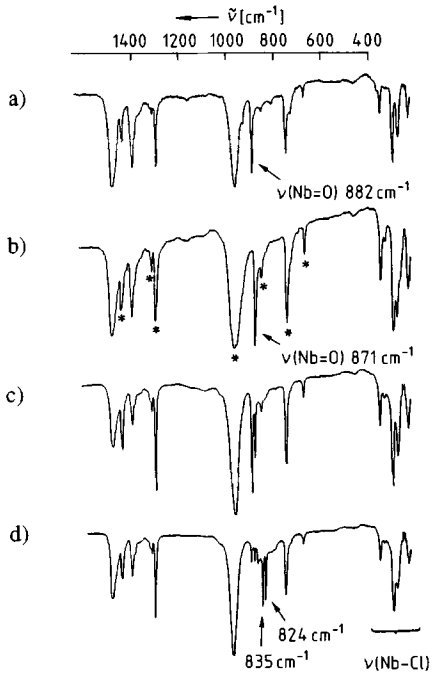

Fig. 1. Comparison of the IR spectra (Nujol mull, CsI $\tilde{\nu}$[cm^{-1}]) of the bond-stretch isomers of $[Nb(O)Cl_3(PMe_3)_2]$: a) pure **1a**; b) pure **1b**; c) a mixture of **1a** and **1b**; d) a mixture of ^{18}O-labeled **1a** and **1b**. The asterisk denotes bands attributed to Nb-PMe_3 stretching and bending modes.

observation of $\tilde{\nu}$(Nb=O) for **1a** at 882 cm^{-1} ($\tilde{\nu}$(Nb=^{18}O): found 835 cm^{-1}; calcd 833 cm^{-1}) compared to that for **1b** at 871 cm^{-1} ($\tilde{\nu}$(Nb=^{18}O): found 824 cm^{-1}; calcd 821 cm^{-1}). Although **1b** was initially thought to be a geometric isomer of **1a**, X-ray structure analysis[10] of **1b** has shown that the two structures are virtually identical in all respects except for the bond lengths to the metal (Fig. 2) and, although there are slight changes in O–Nb–Cl angles, the mean values are not significantly different in the two isomers. In the green isomer **1b** the Nb=O bond (1.929(6) Å)[11] is 0.148 Å (ca. 25σ) longer than that observed earlier[9] in the yellow isomer **1a**, and this lengthening is accompanied by a relatively small but significant contraction in the Nb–Cl distances (mean 0.023 Å, ca. 10σ). The solid-state evidence of the nature of

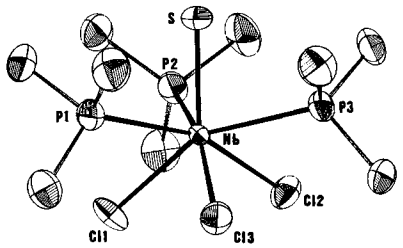

Fig. 2. The monocapped octahedral coordination geometry observed for **1** and **2** illustrated using a perspective view of **2b** with thermal ellipsoids plotted at the 50% probability level. Selected bond lengths [Å] and angles [°] with, in each case, the first parameter referring to the **a** isomer and that for the **b** isomer in square brackets (those for **1a** are from [9]): $[Nb(O)Cl_3(PMe_3)_2]$ (**1a**) [**1b**]: Nb-O 1.781(6) [1.929(6)], Nb-Cl(1) 2.516(3) [2.486(2)], Nb-Cl(2) 2.533(3) [2.508(2)], Nb-Cl(3) 2.505(3) [2.491(2)], Nb-P(1) 2.642(3) [2.645(2)], Nb-P(2) 2.633(3) [2.638(2)], Nb-P(3) 2.645(3) [2.643(2)]; O-Nb-Cl 121.2–127.8(2) [119.7–128.6(3)], O-Nb-P 73.3–76.9(2) [75.0–77.2(2)] · $[Nb(S)Cl_3(PMe_3)_2]$: (**2a**) [**2b**]: Nb-S 2.196(2) [2.296(2)], Nb-Cl(1) 2.487(2) [2.475(1)], Nb-Cl(2) 2.518(2) [2.501(1)], Nb-Cl(3) 2.490(2) [2.483(1)], Nb-P(1), 2.640(2) [2.647(1)], Nb-P(2) 2.640(2) [2.654(1)], Nb-P(3) 2.635(2) [2.647(1)]; S-Nb-Cl 123.4–128.9(1) [121.8–131.2(1)], S-Nb-P 77.4–77.6(1)–[75.8–76.9(1)].

the isomers appears unambiguous, but some caution in its interpretation is required due to a slight disorder in the crystals of **1b**;[12] fortunately, this problem does not occur for the thio analogues.

From reactions with thioniobium starting materials (Scheme 1) pure crystals of the orange (**2a**) and green (**2b**) forms of $[Nb(S)Cl_3(PMe_3)_2]$ were obtained and readily distinguished not only by their color but also by a marked difference in their IR spectra, $\tilde{\nu}$(Nb=S) occurring at 455 cm^{-1} for **2a** compared to 489 cm^{-1} for **2b** (Fig. 3a, b).

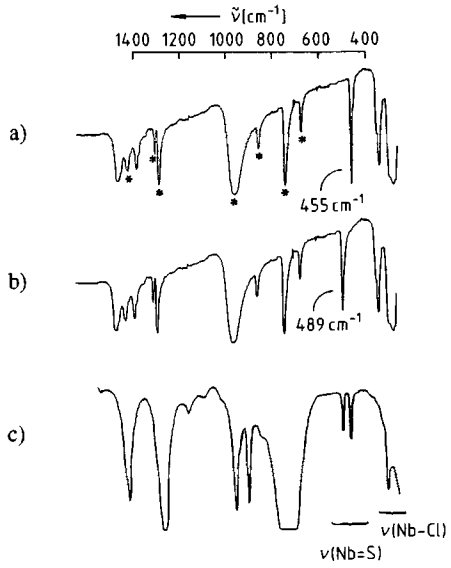

Fig. 3. Comparison of the solid-state and solution IR spectra, $\tilde{\nu}$[cm^{-1}], of the bond-stretch isomers of $[Nb(S)Cl_3(PMe_3)_2]$: a) pure **2a** (Nujol mull, CsI); b) pure **2b** (Nujol mull, CsI); c) **2a**/**2b** mixture (CH_2Cl_2 solution). The asterisk denotes bands attributed to Nb-PMe_3 stretching and bending modes.

Shifts identical to these solid-state values are obtained for **2a** and **2b** in CH_2Cl_2 solution (Fig. 3c). The X-ray structure analyses[10] of **2a** and **2b** reveal a very similar coordination geometry (Fig. 2) to that of their oxygen analogues and show that the main difference in the two isomers is in the respective Nb=S distances of 2.196(2) and 2.296(1) Å, respectively.[13]

The Nb=S length in the green isomer **2b** is thus 0.100 Å (ca. 70σ) longer than in the isomorphous orange form **2a** and there is also a slight but significant contraction in the Nb–Cl bond lengths (mean 0.012 Å, ca. 8σ) in **2b**. The large observed change in $\tilde{\nu}$(Nb=S) is in the opposite direction from that expected from the relative bond lengths of **2a** and **2b**; the origin of this anomaly is not clear.

The bromo analogues of **1** and **2** may be obtained by essentially analogous procedures, but so far only the **b** isomers have been isolated in a pure form. Interestingly, the bands due to Nb–E stretches in the IR spectra of the bromo isomers are coincident with their chloro analogues, indicating that the halide ligand apparently exerts little or no influence on $\tilde{\nu}$(Nb=E).

Our results for seven-coordinate sytems appear to provide further evidence for bond-stretch isomerism; the clear identification of the characteristic Nb=S stretches of isomers **2a** and **2b** both in Nujol mull and in CH_2Cl_2 solution seems to rule out any explanation of the phenomenon as a solid-state artifact.

Received: September 27, 1990;
supplemented: April 24, 1991 [Z 4212 IE]
German version: *Angew. Chem. 103* (1991) 1021

CAS Registry numbers:
1, 119174-67-3; **2**, 134735-29-8; [Nb(O)Cl_3], 13597-20-1; [Nb(S)Cl_3], 60994-00-5; [Nb(O)$Cl_3(CH_3CN)_2$], 64681-95-4; [Nb(S)$Cl_3(CH_3CN)_2$], 63510-32-7.

[1] A. V. Butcher, J. Chatt, *J. Chem. Soc. A 1970*, 2652.
[2] Lj. Manojlovic nuibers*hem. Commun. 1971*, 147; *J. Chem. Soc. A 1971*, 2496.
[3] J. Chatt, Lj. Manojlovic-Muir, K. W. Muir, *Chem. Commun. 1971*, 655; Lj. Manojlovic-Muir, K. W. Muir, *J. Chem. Soc. Dalton Trans. 1972*, 686.
[4] A recent reexamination of oxomolybdenum complexes [K. Yoon, G. Parkin, A. L. Rheingold, *J. Am. Chem. Soc. 113* (1991) 1437] shows that a continuum of apparent Mo=O bond lengthening in the solid state may be achieved when pure blue [Mo(O)$Cl_2(PMe_2Ph)_3$] is contaminated with the yellow trichloride [$MoCl_3(PMe_2Ph)_3$]. Such results for crystals with unresolved disorder of oxo and chloro ligands at equivalent sites could provide an explanation of the reported bond lengthening and the observed blue/green color differences, but the observation of different Mo=O stretches for blue and green [Mo(O)$Cl_2(PMe_2Ph)_3$] [1] is less readily explained as a result of low-level contamination with the trichloride.
[5] F. A. Cotton, M. P. Diebold, W. J. Roth, *Inorg. Chem. 26* (1987) 2848 and references therein.
[6] K. Wieghardt, G. Backes-Dahmann, B. Nuber, J. Weiss, *Angew. Chem. 97* (1985) 773; *Angew. Chem. Int. Ed. Engl. 24* (1985) 777.
[7] Y. Jean, A. Lledos, J. K. Burdett, R. Hoffmann, *J. Am. Chem. Soc. 110* (1988) 4506.
[8] W.-D. Stohrer, R. Hoffmann, *J. Am. Chem. Soc. 94* (1972) 1661.
[9] V. C. Gibson, T. P. Kee, R. M. Sorrell, A. Bashall, M. McPartlin, *Polyhedron 7* (1988) 2221.
[10] Crystal data: All crystals were monoclinic, space group $P2_1/c$, $Z = 4$. **1b**: [$C_9H_{27}P_3ONbCl_3$], $a = 15.149(3)$, $b = 11.344(3)$, $c = 11.652(3)$ Å, $\beta = 93.53(2)°$, $M = 443.50$, $V = 1996.83$ Å^3, $\rho_{calcd} = 1.475$ g cm^{-3}, $F(000) = 904$, $R = 0.0426$ for 2303 data, $\mu(Mo_{K\alpha}) = 11.21$ cm^{-1}, green crystal of size $0.48 \times 0.39 \times 0.11$ mm^3. **2a**: [$C_9H_{27}P_3SNbCl_3$] $a = 15.190(3)$, $b = 11.415(3)$, $c = 11.690(3)$ Å, $\beta = 93.76(2)°$, $M = 459.56$, $V = 2024.63$ Å^3, $\rho_{calcd} = 1.507$ g cm^{-3}, $F(000) = 936$, $R = 0.0553$ for 2652 data, $\mu(Mo_{K\alpha}) = 11.99$ cm^{-1}, orange crystal of size $0.35 \times 0.28 \times 0.26$ mm^3. **2b**: [$C_9H_{27}P_3SNbCl_3$], $a = 15.151(3)$, $b = 11.565(3)$, $c = 11.668(3)$ Å, $\beta = 92.34(2)°$, $M = 459.56$, $V = 2042.78$ Å^3, $\rho_{calcd} = 1.494$ g cm^{-3}, $F(000) = 936$, $R = 0.0429$ for 2888 data, $\mu(Mo_{K\alpha}) = 11.88$ cm^{-1}, green crystal of size $0.34 \times 0.37 \times 0.26$ mm^3. Crystals were mounted in Lindemann tubes under inert atmosphere and absorption-corrected diffractometer data with $I/\sigma(I) \geq 3.0$ were used in all determinations. Further details on the crystal structure determination are available from the Director of the Cambridge Crystallographic Data Centre, University Chemical Laboratory, Lensfield Road, Cambridge CB2 1EW (England), on quoting the full literature citation.
[11] It was not possible to be certain from the X-ray results alone that the O atom was not from a hydroxo ligand, but this possibility has been ruled out; there is no evidence for a hydroxyl group from IR and ^{1}H NMR spectroscopy and vibrating sample magnetometry shows **1b** to be diamagnetic; [Nb(OH)$Cl_3(PMe_3)_3$] would be a d^1 complex and therefore paramagnetic.
[12] In the initial refinement an extremely long Nb=O bond of 2.087(5) Å was observed and the oxygen-atom anisotropic thermal ellipsoid showed marked elongation in the Nb–O direction. Furthermore, there was residual electron density (ca. 1.5 e) in this direction at a distance of 0.51 Å beyond the oxygen atom. This has been interpreted as due to a small component of a second virtually isostructural molecule, with an axial chlorine atom, disordered in the crystal. Satisfactory refinement was obtained with 80% occupancy of axial positions by an oxygen atom and 20% by a chlorine atom. This gave a Nb–Cl(4) bond length of 2.33(2) Å, a value close to that observed [F. A. Cotton, M. P. Diebold, W. J. Roth, *Polyhedron 4* (1985) 1103] for the axial Nb–Cl bond of 2.409(4) Å in the green tetrachloride [$NbCl_4(PMe_3)_3$], which has crystals isomorphous with those of **1b**. It seems probable that the disorder is due to the presence of a small amount of this virtually isostructural compound in the crystal (possibly originating in the slight decomposition that occurs during the formation of **1b** from **1a**); the possibility that the 20% component is a *geometric* isomer of the oxo compound (i.e., that the 80% component is in fact residual **1a** with the apparent bond lengthening being an artifact of the disorder) was also considered, but this was ruled out by the absence of a second $\tilde{\nu}$(Nb=O) stretch corresponding to **1a** in the IR spectrum of **1b**.
[13] As Cl and S have similar numbers of electrons, the possibility that **2b** is a geometric isomer, with an "equatorial" Nb=S disordered over the three chlorine sites was also considered. However, this model may be ruled out because it would require occupancy of the axial site by a chloro ligand and consequently a very much longer bond of ca. 2.4 Å would have been observed; the thermal ellipsoid of this atom shows no evidence of any disorder that might produce apparent bond *shortening*. Furthermore, a mixture of **2a** plus a geometric isomer accounting for the bond parameters in **2b** is not consistent with the IR spectra (see Fig. 3), which show that both **2a** and **2b** are single-component species. The thermal ellipsoids of the sulfur atom in **2b** (see Fig. 2) show no elongation in the Nb–S direction and there is no evidence of any disorder of the type seen in the solid-state structure of **1b**.

trans-[Mo(η^2-*O,C*-PhNCO)(η^2-*C,N*-PhNCO)(*syn*-Me_8[16]aneS$_4$)]; Novel Discrimination of the C=O and C=N Bonds of PhNCO at Stereochemically Different Axial Sites**

By *Toshikatsu Yoshida,* Tomohiro Adachi, Kenji Kawazu, Akira Yamamoto,* and *Nobuyoshi Sasaki*

Recently we have shown that the [Mo(*syn*-Me_8[16]aneS$_4$)] moiety in the complexes *trans*-[ML_2(syn-Me_8[16]aneS$_4$)] (L=N_2, PhNC) exerts different electronic perturbation upon the two axial η^1-coordinated π-acid ligands.[1] This has been proved theoretically to arise from the stereoelectronic effect due to the pyramidal distortion of the MoS_4 frame in the [Mo(*syn*-Me_8[16]aneS$_4$)] moiety. For example, *trans*-[Mo(PhNC)$_2$(*syn*-Me_8[16]aneS$_4$)] contains both a severely bent and an essentially linear isocyanide ligand.[1c] In addition, the two axial sites of the [Mo(*syn*-Me_8[16]aneS$_4$)] moiety are in stereochemically different environments; the site surrounded by the macrocyclic carbon atoms is congested while the opposite site is uncongested.[2] Therefore, the [Mo(*syn*-Me_8[16]aneS$_4$)] moiety is expected to discriminate two π-acidic ligands possessing different electronic and steric properties at the axial sites. Indeed, this has been achieved by the bis(phenylisocyanate) complex **1**, where the η^2-*O,C*-PhNCO ligand, which is sterically less demanding than η^2-*C,N*-PhNCO, occupies specifically the congested axial site. The novel recognition of the C=O and C=N bonds of PhNCO was proved to be steric in origin by theoretical calculations on **1** and its possible isomers such as **1′**.

[*] Prof. Dr. T. Yoshida, T. Adachi, K. Kawazu, A. Yamamoto, S. Sasaki
Department of Chemistry, Faculty of Integrated Arts and Sciences
University of Osaka Prefecture
Sakai, Osaka 591 (Japan)

[**] This work was supported by a Grant-in-Aid for Scientific Research (No. 02804050) from the Japanese Ministry of Education, Science, and Culture. Me_8[16]aneS$_4$ = 3,3,7,7,11,11,15,15-octamethyl-1,5,9,13-tetrathiacyclohexadecane.

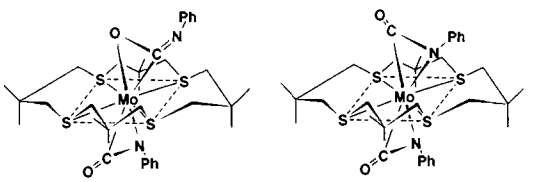

1 1'

trans-[Mo(η^2-*O,C*-PhNCO)(η^2-*C,N*-PhNCO)(*syn*-Me_8[16]aneS$_4$)] **1**

trans-[Mo(η^2-*C,N*-PhNCO)$_2$(*syn*-Me_8[16]aneS$_4$)] **1'**

Treatment of *trans*-[Mo$(N_2)_2$(*syn*-Me_8[16]aneS$_4$)][1b] with a 2.5 molar amount of PhNCO in toluene at room temperature for 5 h gave **1** as thermally stable crystals (35%).[3] Observation of both C=O (1702 cm^{-1}) and C=N (1570 cm^{-1}) stretching bands in the IR spectrum indicates that one PhNCO molecule coordinates through the C=N bond, the other through the C=O bond. This is shown unequivocally by its crystal structure (Fig. 1).[4]

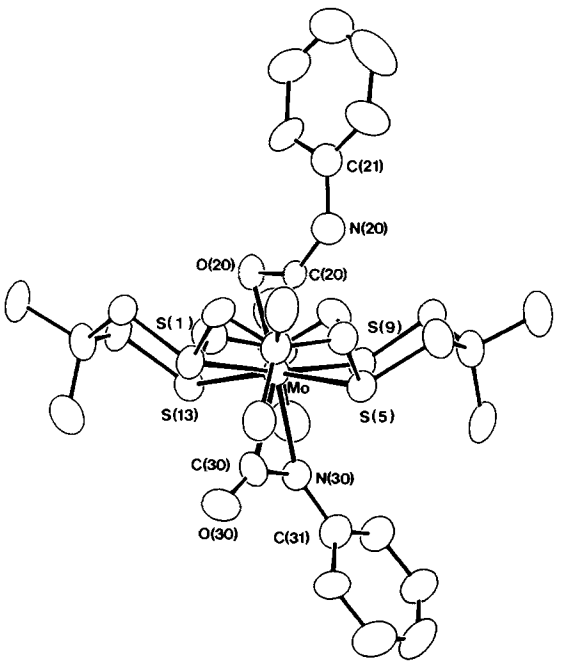

Fig. 1. Crystal structure of **1**. Selected bond lengths [Å] and angles [°]: Mo-S(1) 2.471(3), Mo-S(5) 2.472(4), Mo-S(9) 2.448(3), Mo-S(13) 2.491(4), C(20)-N(20) 1.279(11), C(30)-O(30) 1.243(14); S(1)-Mo-S(5) 89.9(1), S(5)-Mo-S(9) 90.4(1), S(9)-Mo-S(13) 91.1(1), S(1)-Mo-S(13) 90.6(1), C(30)-Mo-N(30) 34.9(4), C(20)-N(20)-C(21) 124.9(12), N(30)-C(30)-O(30) 138.8(10), C(30)-N(30)-C(31) 124.9(10).

Complex **1** crystallizes as a discrete monomer with the Mo atom in a slightly distorted octahedral environment. The η^2-C=O and η^2-C=N bonds are mutually staggered and each eclipses a *trans* S–Mo–S vector. This conformation has also been observed in *trans*-[Mo$(CH_2{=}CH_2)_2(PMe_3)_4$][5] and *trans*-[Mo$(CO_2)_2$(*i*PrNC)$(PMe_3)_3$][6] and has been confirmed theoretically to be most stable one.[7] The strong coordination of both PhNCO ligands may be deduced from the short Mo–C(20) and Mo–C(30) bond lengths (2.075(8) and 2.118(11) Å, respectively), which are evidently shorter than the Mo–C distances in *trans*-[Mo$(CH_2{=}CH_2)_2(PMe_3)_4$] (2.270(5) Å)[5] and *trans*-[Mo$(HC{\equiv}CH)_2$(*syn*-Me_8[16]aneS$_4$)] (2.166(12) Å).[8] The [Mo(η^2-*O,C*-PhNCO)] moiety is structurally similar to the [Mo(η^2-CO_2)] unit in *trans*-[Mo(η^2-$CO_2)_2$(*i*PrNC)$(PMe_3)_3$].[6] Thus, the Mo–C(20), Mo–O(20) (2.147(8) Å), and C(20)–O(20) distances (1.295(15) Å), as well as the O(20)–Mo–C(20) (35.7(4)°) and O(20)–C(20)–N(20) angles (131.8(10)°) are comparable to the corresponding values for the CO_2 complex cited above (2.105(10), 2.147(7), and 1.26(2) Å; 34.5(10) and 133.5(10)°). The Mo–C(30), Mo–N(30) (2.157(8) Å), and C(30)–N(30) distances (1.282(14) Å) of the [Mo(η^2-*C,N*-PhNCO)] moiety may be compared with the respective lengths of the η^2-iminoacyl complex [Mo(η^2-PhN=CMe)(η^5-C_5H_5)$(CO)_2$] (2.106(5), 2.143(4), and 1.233(6) Å, respectively).[9]

Although the Me_8[16]aneS$_4$ ligand adopts *syn* conformation as observed for the complexes *trans*-[ML_2(syn-Me_8[16]aneS$_4$)] (L=N_2,[1b] PhNC,[1c] CO[10]), their geometries about the Mo atom differ significantly. Thus, the MoS_4 framework of **1** deforms slightly toward tetrahedral geometry with S(1)–Mo–S(9) and S(5)–Mo–S(13) angles of 171.4(1) and 166.9(1)°, respectively. By contrast, a pyramidal distortion with *trans* S–Mo–S angles of 173.8(1)–175.7(1)° was found for the η^1-coordinated π-acid complexes, where the Mo atom deviates from the plane of the four S atoms toward the ring C atoms. Such a tetrahedral deformation may enhance the d_π–p_{π^*} interaction between the Mo atom and the C=N bond of PhNCO located at the uncongested axial site. In fact, extended Hückel MO calculations indicate that the model compound **A**, with the observed

trans-[Mo(η^2-*O,C*-HNCO)(η^2-*C,N*-HNCO){*syn*-$(SH_2)_4$}] **A**

trans S–Mo–S angles of **1**, is 13.3 kcal mol^{-1} more stable in total energy than the pyramidally distorted structure with *trans* S–Mo–S angles of 175°.[11]

Transition-metal complexes of organoisocyanates have received extensive interest as intermediates in metal-mediated transformations of isocyanates.[13a] However, only polynuclear complexes with bridging isocyanates,[13a] such as [{U(η^5-$C_5H_4Me)_3$}$_2$(μ-η^1-*O*-,η^2-*C,N*-PhNCO)][13b] and [W_2(OCCMe$_3)_6$(μ-η^2-*O,C*-, η^2-*C,N*-PhNCO)], have been characterized so far by X-ray structural study.[13c] Furthermore, the η^2-C=O coordination has only two precedents, [Mo(η^2-PhNCO)$_2$(dppe)$_2$] (dppe = 1,2-bis(diphenylphosphino)ethane)[13d] and the ditungsten complex cited above, where the bonding mode in the former complex was based only on the IR spectral data. Therefore, complex **1** represents the first example of a well-characterized mononuclear bis(organoisocyanate) complex with both η^2-C=O and η^2-C=N coordinations.

What are the origins for the novel discrimination of the C=O and C=N bonds of PhNCO at the sterochemically different axial sites in **1**? In view of the slight distortion of the MoS_4 framework toward tetrahedral geometry, electronic factors may not be crucial in determining the coordination modes at the axial sites. This is supported by extended Hückel MO calculations on four possible isomers of the model compound of **1**, **A**–**D**, where the HNCO ligand at the congested axial site of **A** and **B** is shown in the first parenthe-

trans-[Mo(η^2-*C,N*-HNCO)(η^2-*O,C*-HNCO)L_4] **B**

trans-[Mo(η^2-*O,C*-HNCO)$_2L_4$] **C**

trans-[Mo(η^2-*C,N*-HNCO)$_2L_4$] **D**

L_4 = *syn*-$(SH_2)_4$

ses. Their relative total energies are 0, 0.4, 4.4 and -3.6 kcal mol^{-1}, respectively.[11] Although the difference in energy between the (η^2-*O,C*-HNCO)(η^2-*C,N*-HNCO) and (η^2-*C,N*-HNCO)$_2$ isomers is small, the calculations are inconsistent with the observed structure.

Next, we used molecular mechanics calculations to examine the steric factor responsible for discriminating the two functionalities of PhNCO.[14] The energy-minimized structure found for **1**, which agrees well with the X-ray structure,[17] is 12.3 kcal mol^{-1} lower in total strain energy than that calculated for **1'**. The high strain energy of the latter seems to stem mainly form stereochemical repulsion between the axial hydrogen atoms of ring CH_2 groups and the η^2-*C,N*-PhNCO ligand at the congested axial site. To reduce these steric repulsions as much as possible, both of the *trans* S–Mo–S vectors should bend toward the uncongested axial site. In fact, the S(5)–Mo–S(13) angle (161.7°) in **1'** is more acute and the S(1)–Mo–S(9) angle (175.0°) more obtuse than the corresponding angles of **1** discussed above. Thus, the novel discrimination of the C=O and C=N bonds of PhNCO at the axial sites can be explained in terms of steric control rather than electronic effects.

Since the space available for an axial ligand at the congested site can be adjusted by the ring size of *syn*-crown thioethers,[2] the present result may provide a basis for further development of crown thioether complexes as hosts in molecular recognition through coordination at the metal center.

Received: February 28, 1991 [Z 4464 IE]
German version: *Angew. Chem. 103* (1991) 1025

[1] a) T. Yoshida, T. Adachi, T. Ueda, *Pure Appl. Chem. 62* (1990) 112. b) T. Yoshida, T. Adachi, M. Kaminaka, T. Ueda, T. Higuchi, *J. Am. Chem. Soc. 110* (1988) 4872. c) T. Adachi, N. Sasaki, T. Ueda, M. Kaminaka, T. Yoshida, *J. Chem. Soc. Chem. Commun. 1989*, 1320.

[2] T. Toshida, T. Adachi, T. Ueda, T. Tanaka, F. Goto, *J. Chem. Soc. Chem. Commun. 1990*, 342.

[3] Yellow crystals (from Me_2CO), m.p. 160–168 °C (dec.). Correct C, H, N analysis for **1** · Me_2CO. IR (Nujol): $\tilde{\nu}$[cm^{-1}] = 1702 s (C=O), 1570 vs (C=N); the ν(C=O) bands due to η^2-*C,N*-PhNCO and Me_2CO appear coincidentally at the same wave number since the unrecrystallized crude complex also showed the same band at 1702 cm^{-1}. ^{1}H NMR ([D$_8$] toluene, 30 °C): δ = 0.78 (s, 6H, Me), 1.01 (s, 6H, Me), 1.93 (b, 4H, CH_2), 3.0 (b, 4H, CH_2), 7.28 (t, J = 7.5 Hz, 1H, *m*-Ph), 7.38 (t, J = 7.5 Hz, 1H, *m*-Ph), 7.81 (d, J = 7.5 Hz, 1H, *o*-Ph), 8.17 (d, J = 7.5 Hz, 1H, *o*-Ph); the signals of the *p*-phenly proton overlap with those of [D$_8$]toluene.

[4] Crystal data of **1**: $C_{34}H_{50}N_2O_2S_4Mo$ · Me_2CO, monoclinic, space group $P2_1/c$, a = 14.214(6), b = 13.727(4), c = 23.080(15) Å, β = 119.33(4), V = 3926(4) Å^3, Z = 4, ρ_{calcd} = 1.335 g cm^{-3}, $\mu(Mo_{K\alpha})$ = 5.7 cm^{-1}. 6861 unique reflections ($3 \le 2\theta \le 50°$) collected on a Rigaku AFC-6 diffractometer; 3182 reflections with $F_0 \ge 4\sigma(F_0)$ were used in the structure refinement: $R(R_w)$ = 0.069(0.064) ($w^{-1} = \sigma^2(F_0) + 0.0002\ (F_0^2)$), GOF = 1.51. Further details of the crystal structure investigation may be obtained from the Fachinformationszentrum Karlsruhe, Gesellschaft für wissenschaftlich-technische Information mbH, W-7514 Eggenstein-Leopoldshafen 2 (FRG), on quoting the depository number CSD-55338, the names of the authors, and the journal citation.

[5] E. Carmona, J. M. Marine, M. L. Poveda, J. L. Atwood, R. D. Rogers, *J. Am. Chem. Soc. 105* (1983) 3014.

[6] R. Alvarez, E. Carmona, J. M. Marin, M. L. Poveda, E. G.-Puebla, A. Monge, *J. Am. Chem. Soc. 108* (1986) 2286.

[7] a) C. Bachmann, J. Demuynck, A. Veillard, *J. Am. Chem. Soc. 100* (1978) 2366. b) E. S. Marcos, R. Caballol, G. Triquier, J.-C. Barthelat, *J. Chem. Soc. Dalton Trans. 1987*, 2373.

[8] T. Yoshida et al., unpublished data.

[9] R. D. Adams, D. F. Chodosh, *Inorg. Chem. 17* (1978) 41.

[10] T. Yoshida, T. Adachi, T. Ueda, M. Watanabe, M. Kaminaka, T. Higuchi, *Angew. Chem. 99* (1987) 1182; *Angew. Chem. Int. Ed. Engl. 26* (1987) 1171.

[11] The H_{ij} values and the orbital exponents for the Mo atom were taken from [12], while those of the H, N, O, and S atoms are standard ones. The bond parameters of the [Mo(η^2-*O,C*-HNCO)] and [Mo(η^2-*C,N*-HNCO)] moieties, as well as the [Mo{*syn*-(SH$_2$)$_4$}] unit, were those found in **1**. The effect of deformation of the MoS_4 framework on the total energy was examined by preserving the above bond parameters except for the *trans* S–Mo–S angles.

[12] P. Kubacek, R. Hoffmann, *J. Am. Chem. Soc. 103* (1981) 4320.

[13] a) P. Braunstein, D. Nobel, *Chem. Rev. 89* (1989) 1927 and references cited therein. b) J. G. Brennan, R. A. Andersen, *J. Am. Chem. Soc. 107* (1985) 514. c) F. A. Cotton, E. S. Shamshoum, *ibid. 107* (1985) 4662. d) F. Minzoi, C. Pelizzi, G. Predieri, *J. Organomet. Chem. 231* (1982) C6.

[14] Molecular mechanics calculations were carried out employing MOLBD3 *by Boyd* [15]. Stretching, bending, and torsional parameters involving the Mo atom and NCO fragments were determined by fitting the energy-minimized structure of **1** to the X-ray structure. Nonbonded parameters for the Mo atom were estimated by *Allinger*'s method [16]. The other interaction parameters were based on the values published by *Allinger* [16]. Initial coordinates for the refinement were taken from the crystal structure coordinates of **1** except for those of η^2-*C,N*-PhNCO located at the congested side in **1'**, which were derived from those of **1** by application of the S_4 symmetry operation. The total strain energies of **1** and **1'** are 61.7 and 74.0 kcal mol^{-1}, respectively. The energy-minimized structures assessed for **1** and **1'** and their selected bond lengths and angles are deposited as the supplementary material.

[15] R. H. Boyd, *J. Chem. Phys. 49* (1968) 2573.

[16] N. L. Allinger, *Adv. Phys. Org. Chem. 13* (1976) 1.

[17] The average bond length and angle deviations, δ, estimated from Equations [18] are 0.025 Å and 1.4°, respectively.

$$\delta = 1/N\left\{\sum_{i=1}^{N} |r_i(\text{obs}) - r_i(\text{calc})|\right\} \quad \text{(a)}$$

$$\delta = 1/N\left\{\sum_{i=1}^{N} |\theta_i(\text{obs}) - \theta_i(\text{calc})|\right\} \quad \text{(b)}$$

[18] J. A. Deiters, J. C. Gallucci, T. E. Clark, R. R. Holmes, *J. Am. Chem. Soc. 99* (1977) 5461.

Unusual Mode of Addition of 1,2-Alkadienylidene Carbenes to 1,3-Dienes: 1,4 Addition to Rigid and Flexible 1,3-Dienes

By *Hikaru Sugita, Kazuhiko Mizuno,* Toshiki Mori, Kakuzo Isagawa,** and *Yoshio Otsuji**

Electrophilic carbenes, such as dihalocarbenes, add to 1,3-dienes usually in a 1,2 manner to produce cyclopropane derivatives.[1] The 1,4 addition of carbenes and carbene analogues is very rare, and it is in fact essentially limited to enforced cisoid dienes.[2–6] Earlier, we found that 1,2-alkadienylidene carbenes can be generated efficiently from 2,2-disubstituted-1,1-dibromocyclopropanes via double dehydrobromination under phase-transfer conditions and that the 1,2-alkadienylidene carbenes thus generated add to alkenes to afford alkenylidenecyclopropanes [Eq. (a)].[6–8] We now report that 1,2-alkadienylidene carbenes add to 1,3-dienes in both 1,2 and 1,4 manner. To the best of our knowledge, this is the first example in which the 1,4 addition of such carbenes becomes one of the major paths even for stereochemically flexible 1,3-dienes.

Treatment of 1,1-dibromo-2,2-diphenylcyclopropane (**1a**) with an aqueous 50% NaOH solution under phase-transfer conditions in the presence of an excess of 2-methyl-1,3-butadiene (**2b**) afforded the 1,2-adduct **3b** and the 1,4-adduct **4b** in a 78:22 ratio in 37% yield [Eq. (b)]. The 1,2-adduct **3b** was stable under the reaction conditions and no indication of isomerization of **3b** to **4b** was observed. Therefore, **4b** is probably produced directly via a 1,4 addition of 3,3-diphenylpropadienylidene to **2b**. In a similar manner, the propadienylidenes generated from **1a–c** also added to 1,3-dienes **2a–e** to afford 1,2 and 1,4 adducts in 5–87% yield

[*] Dr. K. Mizuno, Dr. K. Isagawa, Prof. Dr. Y. Otsuji, H. Sugita, T. Mori
Department of Applied Chemistry, College of Engineering
University of Osaka Prefecture
Sakai, Osaka 591 (Japan)

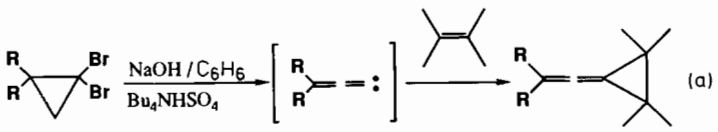

(a)

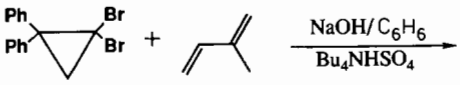

1a 2b

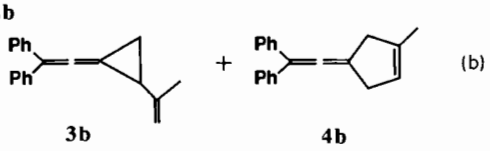

(b)

3b 4b

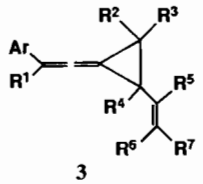

3

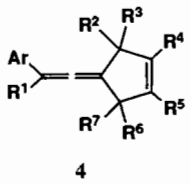

4

a, R^1=Ar=Ph, $R^2 \sim R^7$=H

b, R^1=Ar=Ph, R^2=R^3=R^4=R^6=R^7=H, R^5=Me

c, R^1=Ar=Ph, R^2=R^3=R^6=R^7=H R^4=R^5=Me

d, R^1=Ar=Ph, R^3=R^4=R^5=R^6=H R^2=R^7=Me

e, R^1=Ar=Ph, R^4=R^5=H R^2=R^3=R^6=R^7=Me

f, R^1=Ar=4-MeOC_6H_4, $R^2 \sim R^7$=H

g, R^1=Me, Ar=Ph, $R^2 \sim R^7$=H

h, R^1=Me, Ar=Ph, R^2=R^3=R^4=R^6=R^7=H, R^5=Me

h', R^1=Me, Ar=Ph, R^2=R^3=R^5=R^6=R^7=H, R^4=Me

Table 1. Reaction of 1,2-alkadienylidene carbenes (generated from **1**) with 1,3-dienes **2**.

Cyclopropane		Diene	1,2 Adduct (product ratio [a])		1,4 Adduct	Total yield [%]
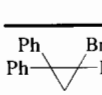	**1a**	**2a**	**3a**	(86:14)	**4a**	87
1a		**2b**	**3b**	(78:22)	**4b**	37
1a		**2c**	**3c**	(60:40)	**4c**	48
1a		**2d**	**3d**	(95: 5)	**4d**	58
1a		**2e**	**3e**	(100: 0)	**4e**	72
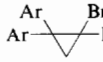	**1b** [b]	**2b**	**3f**	(26:74)	**4f**	30
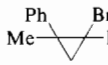	**1c**	**2a**	**3g** [c]	(100: 0)	**4g**	46
1c		**2b**	**3h** + **3h'** [d]	(70:30)	**4h**	5

[a] The ratios were determined from the 270-MHZ ^{1}H NMR spectra. [b] Ar- = 4-Me-OC_6H_4. [c] Two stereoisomers were obtained in a 1:1 ratio. [d] The two regioisomers **3h** und **3h'** were obtained in a 1:1 ratio. However, the ratios of the stereoisomers were not determined.

(Table 1; spectroscopic data for **2** and **4** are given in Table 2). In the case of the reaction of 1,1-dibromo-2,2-bis(4-methoxyphenyl)cyclopropane (**1b**) with **2b**, the 1,4-adduct **4f** was obtained more selectively, although the yield was not high.

Table 2. Relevant ^{1}H NMR (67 MHz, $CDCl_3$; δ values[a]), ^{13}C NMR, and IR spectroscopic data for the adducts **3**, **4**, **6**, and **8**.

Compound	^{1}H NMR [b]	^{13}C NMR [c]	IR (neat) [cm^{-1}] [d]
3a	1.72 (dd, 1H), 2.08 (dd, 1H), 2.69 (dt, 1H), 5.05 (d, 1H, J = 8.7 Hz), 5.23 (d, 1H, J = 14.7 Hz), 5.67 (ddd, 1H, J = 8.1, 8.7, 14.7 Hz)	190.1	1999
4a	3.38 (br.s, 4H), 5.78 (br s, 2H)	[e]	[e]
3c	1.53 (s, 3H), 1.76 (s, 3H), 1.99 (d, 1H, J = 6.9 Hz), 1.77 (d, 1H, J = 6.9 Hz), 4.84 (s, 1H), 4.93 (s, 1H)	188.7	1997
4c	1.66 (s, 6H), 3.31 (s, 4H)	199.7	[e]
3d	1.37 (d, 3H, J = 6.1 Hz), 1.69 (dd, 3H, J = 1.6, 6.5 Hz), 1.94 (m, 1H), 2.31 (dd, 1H, 5.1, 7.8 Hz), 5.35 (ddq, 1H, J = 13.6 Hz), 5.63 (m, 1H)	189.4	1992
4d	1.24 (d, 6H, J = 7.1 Hz), 3.63 (q, 2H), 5.68 (br s, 2H)	[e]	[e]
3e	1.32 (s, 3H), 1.42 (s, 3H), 1.74 (d, 3H), 1.76 (s, 3H), 2.57 (d, 1H, J = 7.9 Hz), 5.12 (dd, 1H), 5.12 (d, 1H)	187.9	1984
3f	1.70 (s, 3H), 1.92 (m, 2H), 2.71 (dd, 1H, J = 6.1, 7.4 Hz), 4.83 (s, 1H), 4.93 (s, 1H)	[e]	1997
4f	1.76 (s, 3H), 3.86 (s, 2H), 3.87 (s, 2H), 5.36 (s, 1H)	194.4	[e]
6	1.65 (s, 4H), 2.25 (s, 4H), 3.28 (s, 4H)	200.1	1949
8	1.48 (m, 1H), 1.76 (m, 1H), 2.38 (m, 2H), 2.56 (s, 1H), 2.57 (s, 1H), 5.68 (m, 1H), 6.11 (m, 1H)	189.2	1990

[a] Tetramethylsilane as internal standard. [b] Aliphatic and olefinic protons. [c] Chemical shifts of central carbon of 1,2-diene moiety. [d] Absorption maximum of 1,2-diene moiety. [e] Not determined.

The reaction of 3-methyl-1,2-butadienylidene (generated by 1,3 elimination from 3-chloro-3-methyl-1-butyne) with **2b** was reported by *Sasaki* et al. in 1974.[3] In that case however, only the 1,2 adduct was obtained and the regioselectivity was in sharp contrast with our results.

From **1a** and 1,2-dimethylenecyclohexane (**5**), the 1,4-adduct **6** was obtained as the sole isolable product. However, the reaction of **1a** with 1,3-cyclohexadiene (**7**) and 2,5-dimethyl-2,4-hexadiene (**2e**) gave only the 1,2-adducts **8** and **3e**, respectively. Spectroscopic data for **6** and **8** are given in Table 2.

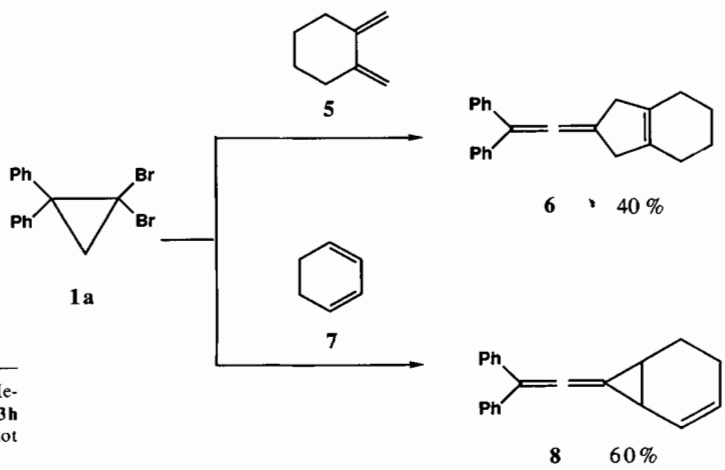

Although we do not have unequivocal evidence, it is quite reasonable to assume that the 1,2-alkadienylidene carbenes are involved as common key intermediates in the above reactions.[6-9] They add to 1,3-dienes in both 1,2 and 1,4 manner and selectively undergo 1,4 addition to an enforced cisoid 1,3-diene such as **5**.

Experimental Procedure

3b/4b: A mixture of nBu$_4$NHSO$_4$ (2 mmol) and aqueous 50% NaOH (100 mL) was added to a benzene solution containing 1,1-dibromo-2,2-diphenylcyclopropane (**1a**, 1 mmol) and an excess of 2-methyl-1,3-butadiene (**2b**, 5 mmol). The mixture was vigorously stirred at room temperature for 24 h. Flash column chromatography on silica gel with hexane gave the 1,2-adduct **3b** and the 1,4-adduct **4b** in a 78:22 ratio in 37% yield.

Control experiment: A mixture of nBu$_4$NHSO$_4$ (0.8 mmol) and an aqueous 50% NaOH (25 mL) was added to a benzene solution containing **3b** (0.4 mmol) and the resulting mixture was vigorously stirred at room temperature for 22 h. Compound **3b** remained unchanged (270-MHz ^{1}H NMR spectrum) and was quantitatively recovered.

3b (oil): ^{1}H NMR (270 MHz, CDCl$_3$): δ = 1.69 (s, 3H), 1.79 (dd, 1H, J = 6.0, 7.0 Hz), 1.95 (dd, 1H, J = 7.0, 8.7 Hz), 2.71 (dd, 1H, J = 6.0, 8.7 Hz), 4.82 (s, 1H), 4.92 (s, 1H), 7.18–7.40 (m, 10H). ^{13}C NMR (67 MHz, CDCl$_3$): δ = 15.0, 19.2, 28.8, 83.1, 111.4, 112.2, 127.0, 126.9, 127.9, 128.3, 128.4, 128.4, 128.6, 137.7, 143.0, 189.2. IR: $\tilde{\nu}$[cm^{-1}] = 3060, 2978, 1999, (C=C=C), 1638, 1599, 1493, 1473, 1444, 1031, 888, 768, 692.

4b (oil): ^{1}H NMR (270 MHz, CDCl$_3$): δ = 1.75 (s, 3H), 3.28 (s, 2H), 3.34 (s, 2H), 5.36 (s, 1H), 7.16–7.37 (m, 10H). ^{13}C NMR (67 MHz, CDCl$_3$): δ = 16.5, 37.8, 41.5, 122.8, 126.9, 128.2, 128.4, 128.5, 128.6, 138.8, 143.0, 199.9. IR: $\tilde{\nu}$[cm^{-1}] = 3060, 3030, 2892, 1949 (C=C=C), 1659, 1601, 1493, 1454, 1444, 770, 696.

Received: January 24, 1991 [Z 4401 IE]
German version: *Angew. Chem. 103* (1991) 1000

[1] Review articles on carbenes and carbene analogues: a) W. E. Keller: *Phase Transfer Reactions, Vol. 1, 2*, Thieme, Stuttgart 1986 and 1987; b) M. Regitz (Ed.): *Houben-Weyl: Methoden der Organischen Chemie, Band E19b*, Thieme, Stuttgart 1989; c) P. J. Stang, *Chem. Rev. 78* (1978) 383.
[2] a) P. D. Bartlett, A. S. Wingrove, R. Owyang, *J. Am. Chem. Soc. 90* (1968) 6067; b) A. G. Anastassiou, *ibid. 90* (1968) 1527; c) L. A. M. Turkenburg, W. H. de Wolf, F. Bickelhaupt, *Tetrahedron Lett. 23* (1982) 769; d) H. Mayr, U. W. Heigl, *Angew. Chem. 97* (1985) 567; *Angew. Chem. Int. Ed. Engl. 24* (1985) 579; e) L. W. Jenneskens, W. H. de Wolf, F. Bickelhaupt, *ibid. 97* (1985) 568 and *24* (1985) 585; f) N. A. Le, M. Jones, Jr., F. Bickelhaupt, W. H. de Wolf, *J. Am. Chem. Soc. 111* (1989) 8491; g) J. B. Lambert, B. T. Ziemnicka-Merchant, *J. Org. Chem. 55* (1990) 3460.
[3] T. Sasaki, S. Eguchi, T. Ogawa, *J. Org. Chem. 39* (1974) 1927.
[4] T. B. Patrick, D. J. Schmidt, *J. Org. Chem. 42* (1977) 3354.
[5] H. Fujimoto, R. Hoffmann, *J. Phys. Chem. 78* (1974) 1167.
[6] Recent review article on 1,2-alkadienylidene carbenes: P. J. Stang, in M. Regitz (Eds.): *Houben-Weyl: Methoden der Organischen Chemie, Band E19b*, Thieme, Stuttgart 1989, p. 136.
[7] L. Crombie, P. J. Griffiths, B. J. Walker, *Chem. Commun. 1969*, 1206.
[8] K. Isagawa, Y. Kimura, Y. Tomita, K. Mizuno, Y. Otsuji, *1989 Int. Symp. Carbene-Type Reactive Intermediates, Kyoto, Japan* (Abstract P-18).
[9] M. S. Baird, *Top. Curr. Chem. 144* (1988) 137.

An Imide Radical Anion which Assembles into π-Stacks in Solution**

By *Jean-François Penneau* and *Larry L. Miller**

Partially oxidized or reduced π-stacks are the most common structural elements in conducting organic charge transfer salts of the broad class typified by tetracyanoquinodimethane/tetrathiafulvalene (TCNQ/TTF).[1] We have observed unusual spectral effects which lead to the conclusion that the radical anion $\mathbf{1}^{\bullet\ominus}$ assembles into similar π-stacks in solution. In particular the NIR, and ESR of $\mathbf{1}^{\bullet\ominus}$ in aqueous NaCl are extremely similar to the spectra of the conducting solid complex salt of $\mathbf{1}^{\bullet\ominus}$ and provide a spectral signature for π-stacks. Although π-dimers of radical anions are well known,[2] we know of no examples of radical ion π-stacks in solution.[3] Such entities are interesting as models for conducting solids and the solutions have potential utility as infrared dyes.[5]

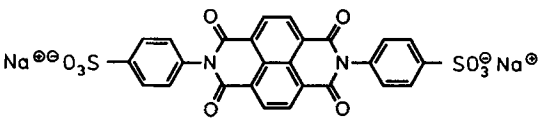

1

$\mathbf{1}^{\bullet\ominus}$, formed by electrochemical reduction in DMF,[6] shows absorption in the visible spectral region, with the most intense band at λ = 473 nm (ε = 31 000), and a 13-line ESR spectrum well simulated by a_H(4H) = 1.90 G, a_N(2N) = 0.95 G. The spectra were essentially identical to those of similar naphthalene diimide radical anions[6] and a_H conformed to expectations based on a Hückel MO calculation and solution of the McConnell equation. It is concluded that the monomeric radical anion is present.

In aqueous media it was convenient to generate the radical anion by reduction of **1** with one equivalent of sodium dithionite. In the absence of oxygen the solutions were stable for weeks. In water or in 80% H_2O/20% DMF the optical spectrum of $\mathbf{1}^{\bullet\ominus}$ was quite different from the spectrum in neat DMF. There was a new NIR band at 1140 nm (ε = 3900) and the VIS band was shifted to 453 nm. This observation is consistent with the literature on radical ion dimers in aqueous media.[2] Such dimers, e.g. $(TCNQ^{\bullet\ominus})_2$, give NIR bands due to charge transfer between the π-electron systems in the stacks, and a Davidov blue shift of the VIS absorption. Since the room-temperature spectrum in water follows Beers law over the range 0.02–2 mM, we conclude that essentially all the radical anions are dimerized under these conditions. Raising the temperature to 90 °C caused the spectrum of $\mathbf{1}^{\bullet\ominus}$ in aqueous DMF to revert to that of the monomer in DMF. The ESR spectrum underwent corresponding changes. In water or aqueous DMF a weak, 25-line spectrum (a_H = 1.93, a_N = 1.08 G) was observed at room temperature. Raising the temperature of the aqueous DMF solution to 100 °C did not change the shape, but by using a nitroxyl standard it was shown that the spin concentration increased from 7% to 94% of the $\mathbf{1}^{\bullet\ominus}$ concentration. The weak signal at room temperature is consistent with literature reports which indicate that radical ion π-dimers have diamagnetic ground states.[2]

In aqueous NaCl solutions there was an unexpected evolution of the NIR absorption. As the concentration of $\mathbf{1}^{\bullet\ominus}$ or NaCl was increased the absorption moved to much longer wavelengths. This is illustrated in Figure 1 for 0.43–4.3 mM $\mathbf{1}^{\bullet\ominus}$ in 0.5 M NaCl. As a further example, the spectrum of $\mathbf{1}^{\bullet\ominus}$ (4.8 mM) in 5 M NaCl had a maximum at 1740 nm and extended far into the IR region. Such very long-wavelength absorptions are characteristic of charge transfer along the delocalized π-stacks of solid, conducting, charge transfer salts.[2, 7] The ESR spectrum underwent an unexpected change as well. In dilute solutions the weak, 25-line spectrum was observed, but in concentrated solutions the signal was asymmetric (Fig. 2).

[*] Prof. L. Miller, Dr. J.-F. Penneau
Department of Chemistry, University of Minnesota
Minneapolis, MN 55455 (USA)

[**] This work was supported by the Office of Naval Research and the National Science Foundation. We thank *B. Stallman* for the synthesis of **1**.

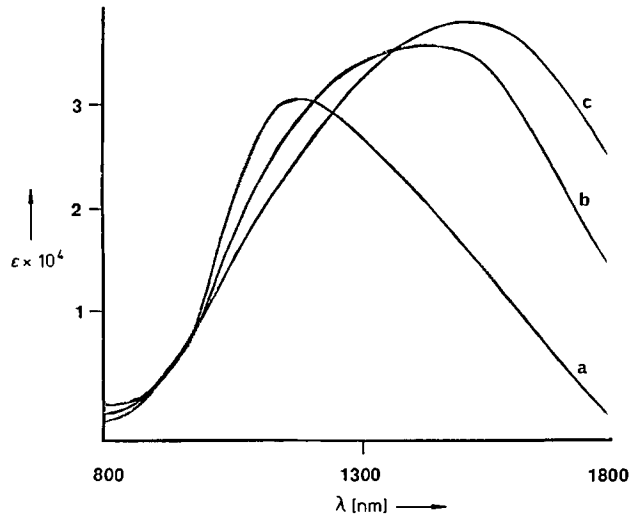

Fig. 1. NIR spectra of $1^{\cdot\ominus}$ in 0.5 M aqueous NaCl solution. Concentration of $1^{\cdot\ominus}$. a) 0.43 mM. b) 2.1 mM. c) 4.3 mM.

When a solution of $1^{\cdot\ominus}$ in water was slowly evaporated under vacuum a shiny black film resulted. The ESR spectrum of the film was anisotropic and the line shape depended on the orientation of the film in the magnetic field (Fig. 2).

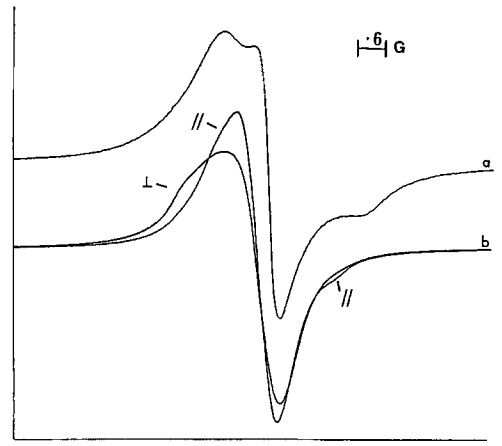

Fig. 2. ESR spectra of $1^{\cdot\ominus}$. a) 8 mM in 0.5 M aqueous NaCl at 280 K. b) Thin film, (⊥) with thin dimension perpendicular to magnetic field; (∥) with one long dimension parallel to magnetic field at 300 K. Scale bar corresponds to 0.6 Gauss.

These spectra suggest that the asymmetric solution spectrum results from unoriented, slowly tumbling aggregated radicals, that are similar to the oriented radicals immobilized in the film.[8] A KBr pellet of the film, like the NaCl solutions of $1^{\cdot\ominus}$, showed an NIR absorption extending into the IR. The 4-probe conductivity of a pure pressed pellet was 0.1 S cm^{-1}.

Thus, it has been demonstrated that $1^{\cdot\ominus}$ assembles into an aggregate in aqueous NaCl which has similar optical and magnetic resonance properties as the conducting solid. These spectral qualities are characteristic of radical anion stacks. Indeed, an X-ray crystal structure of a conducting naphthalene dianhydride salt has shown π-stacks of radical anions.[9] Whether the stacks in solution are composed of only $1^{\cdot\ominus}$ or are doped with another redox state is not known. It does seem important, however, that $1^{\cdot\ominus}$ is actually a tri-anion. This increases the water solubility and gives a propensity for ion aggregation.[4]

Received: March 13, 1991 [Z 4493 IE]
German version: *Angew. Chem. 103* (1991) 1002

[1] J. R. Ferraro, J. M. Williams: *Introduction to Synthetic Electrical Conductors*, Academic Press, New York, 1987.
[2] R. H. Boyd, W. D. Phillips, *J Chem. Phys. 43* (1965) 2927; Z. G. Soos, S. R. Bondeson in J. S. Miller (Ed.): *Extended Linear Chain Compounds*, Plenum Press, New York 1983, 193–257; S. Nakayama, K. Suzuki, *Bull Chem. Soc Jpn. 46* (1973) 3694; M. de Sorgo, B. Wasserman, M. Szwarc, *J. Phys. Chem. 76* (1972) 3468; N. Sakai, I. Shirotani, S. Minomura, *Bull. Chem. Soc. Jpn. 44* (1971) 675.
[3] This phenomenon is somewhat analogous to the aggregation of certain dyes [4], which form stacks and give excitonic bands. Because the dyes are closed shell molecules the bonding between molecules in the stack, the electronic structure of the stack, and the nature of the optical transition are somewhat different. There appear to be no examples of dye aggregates that absorb at such long wavelengths. There are no long-wavelength bands in aqueous NaCl solutions of neutral **1**.
[4] D. G. Duff, C. H. Giles in F. Franks (Eds.): *Water: A Comprehensive Treatise, Vol. 4*, Plenum Press, New York, 1975, Chap. 3.
[5] J. Fabian, R. Zahradnik, *Angew. Chem. 101* (1989) 693; *Angew. Chem. Int. Ed. Engl. 28* (1989) 677.
[6] T. M. Dietz, B. J. Stallman, W. S. V. Kwan, J. F. Penneau, L. L. Miller, *Chem. Commun. 1990*, 367.
[7] J. B. Torrance, B. A. Scott, B. Welber, F. B. Kaufman, P. E. Seiden, *Phys. Rev. B19* (1979) 730.
[8] J. E. Wertz, J. R. Bolton: *Electron Spin Resonance*, Chapman and Hall, New York, 1986, Chap. 7, 8.
[9] G. Heywang, L. Born, H. G. Fitzky, T. Hassel, J. Hocker, H.-K. Müller, B. Pittel, S. Roth, *Angew. Chem. 101* (1989) 462; *Angew. Chem. Int. Ed. Engl. 28* (1989) 483.

Enantiomer Separation on Immobilized Chirasil-Metal and Chirasil-Dex by Gas Chromatography and Supercritical Fluid Chromatography **

By *Volker Schurig*,* *Dieter Schmalzing*, and *Michael Schleimer*

Dedicated to Professor Michael Hanack

The development of surface-bonded stationary phases by cross-linking and/or chemical binding ("immobilization") represented a breakthrough in high-resolution capillary chromatography.[1] The resulting merits are stable films, low bleeding of the stationary phase, high washout stability, and hence use in splitless and on-column sampling. To achieve universal physico-, chemo-, and enantioselective stationary phases based on chemically modified chiral polysiloxanes, e.g. Chirasil-Val,[2] Chirasil-Metal[3] and Chirasil-Dex,[4, 5] an immobilization on the glass surface is desirable.

We describe here the immobilization of *enantioselective* metal chelate and cyclodextrin phases. Chiral polysiloxanes can be immobilized thermally or radically.[6–9] The nickel(II) Chirasil-Metal **1** prepared by us according to Scheme 1 and the octanyl Chirasil-Dex **2c** obtained according to Scheme 2 can be immobilized thermally on the fused silica surface with binding rates of up to 75%.[12] The thermal immobilization does not lead to any decomposition and/or epimerization,

[*] Prof. Dr. V. Schurig, Dipl.-Chem. D. Schmalzing
Dipl.-Chem. M. Schleimer
Institut für Organische Chemie der Universität
Auf der Morgenstelle 18, W-7400 Tübingen (FRG)

[**] This work was supported by the Deutsche Forschungsgemeinschaft, the Fonds der Chemischen Industrie und Chrompack International, Middelburg (The Netherlands) (supply of fused-silica capillary columns). We thank *G. J. Nicholson*, *U. Mühleck* and Professor *E. Bayer*, Tübingen, for valuable discussions.

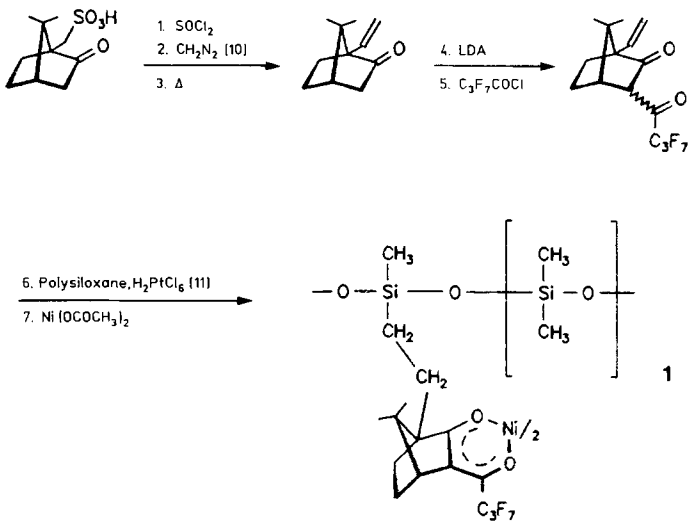

Scheme 1. Synthesis of the chemically modified chiral polysiloxanes Ni^{II}/Chirasil-Metal **1** [12]. LDA = lithium diisopropylamide. The polysiloxane used in step 6 was a 10–13:90–87 mixture of methylhydro/dimethylpolysiloxane.

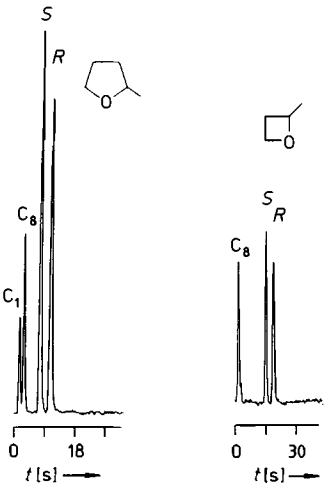

Fig. 1. Enantiomer separation by complexation GC (1.5 m × 0.05 mm (I. D.) fused silica capillary column, coated with immobilized **1** [12]). Left: 2-methyltetrahydrofuran, 115 °C, 2.0 bar N_2. Right 2-methyloxetane, 140 °C, 2.0 bar N_2.

either in the case of the metal chelates or in the case of the cyclodextrin derivatives; this is confirmed by the decrease in the separation factor α, which does not exceed 5 to 10% (depending upon the racemate checked). Typical gas-chromatographic enantiomer separations are shown in Figures 1 (immobilized **1**) and 2 (immobilized **2c**). As can be seen from Figure 1, in particular, the use of shorter columns having small internal diameters (I. D.) enables very short analysis times. The capillary column immobilized with chemically bonded Chirasil-Metal **1** exhibits a markedly higher temperature stability than the previously described physical mixtures of Chirasil-Metal phases and polysiloxanes,[13] and thus extends the scope of complexation gas chromatography considerably.

The capillary columns immobilized with chemically bound Chirasil-Dex **2c** show none of the disadvantages of

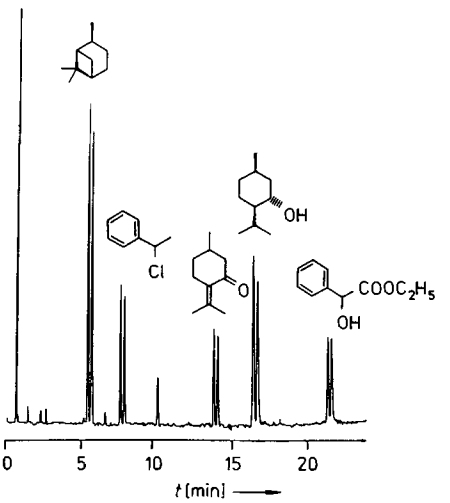

Fig. 2. Enantiomer separation of *cis*-pinane, (1-chloroethyl)benzene, pulegone, isomenthol, and ethyl mandelate by inclusion GC (10 m × 0.1 mm (I. D.) fused silica capillary column, coated with immobilized **2c** [12]). 1 min isothermally at 80 °C, then with 3 K min^{-1} up to 140 °C, 1 bar H_2.

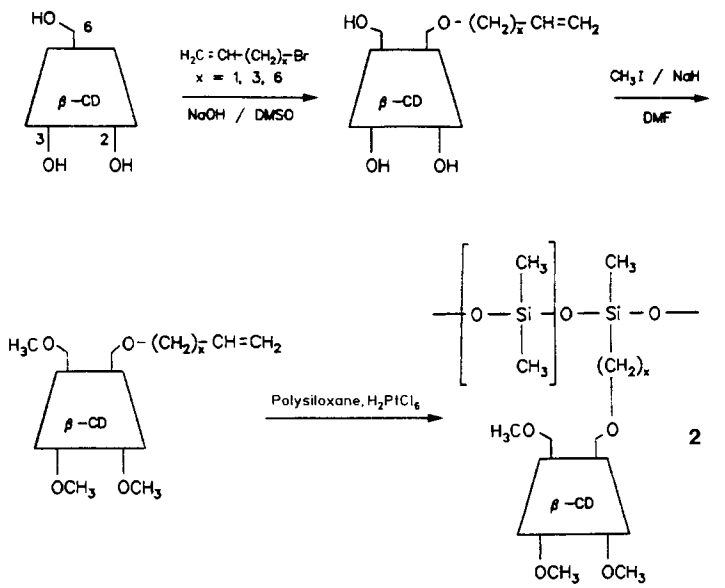

Scheme 2. Synthesis of the chemically modified chiral polysiloxanes Chirasil-Dex **2a–c** [4]. DMSO = dimethyl sulfoxide, DMF = dimethylformamide, polysiloxane = methylhydro/dimethylpolysiloxane 5/95. **2a**, $x = 3$ (Dex 1); **2b**, $x = 5$ (Dex 2); **2c**, $x = 8$ (Dex 3).

the columns coated with neat (pentylated/acylated) cyclodextrin derivatives, such as tendency to formation of droplets, sensitivity towards thermal shock, long conditioning times, low tolerance towards solvent introduction upon direct injection (splitless, on-column),[14] and limited lifetime.[15]

By quantitative immobilization of **1** in a capillary column with small internal diameter (1.5 m × 0.05 mm) it was possible for the first time to extend complexation chromatography to supercritical fluid chromatography. The enantiomers of 1-(2-naphthyl)ethanol and 1-phenylethanol could already be separated quantitatively in a 1.5-m column in less than 10 minutes at 80 °C with carbon dioxide as supercritical mobile phase (α in each case 1.4, R_s in each case 1.65; Fig. 3). Remarkably, the mobile phase carbon dioxide apparently has too low a Lewis basicity to block free coordination sites on the metal ion for enantioselective complexation of the alcohols. Together with immobilized octanyl Chirasil-Dex **2c**, which is also suitable for the separation of enantiomers in

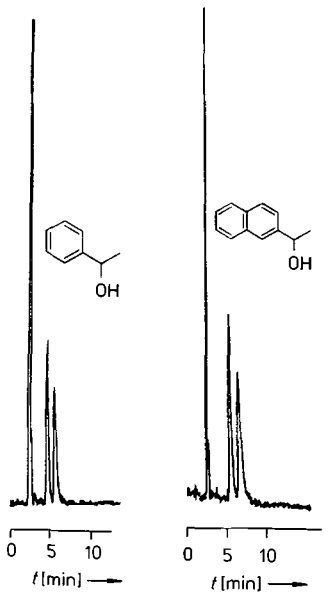

Fig. 3. Enantiomer separation by complexation SFC (1.5 m × 0.05 mm (I. D.) fused silica capillary column, coated with immobilized **1**). Left: 1-phenylethanol, 80 °C, 100 atm CO_2. Right: 1-(2-naphthyl) ethanol, 80 °C, 130 atm CO_2.

SFC,[16] two further systems, based on complementary methods are now available for the separation of enantiomers with supercritical gases. These systems combine the advantages of capillary GC (high efficiency and speed, universal detection) and high-pressure liquid chromatography (no limitation to volatile and thermally stable components). The supercritical mobile phase used, carbon dioxide, is compatible with the universal flame ionization detector and with mass spectrometric coupling. Because of the good solvating properties of the supercritical gases, SFC enantiomer separations are achieved already at low temperature. Since the separation factors α increase with decreasing temperature in the region of enthalpy-control of the enantiomer separation,[17] the lower efficiency of SFC compared to GC can thus be largely compensated.

Received: March 25, 1991 [Z 4545 IE]
German version: *Angew. Chem. 103* (1991) 994

[1] K. Grob: *Making and Manipulating Capillary Columns for Gas Chromatography*, Hüthig, Heidelberg 1986.
[2] H. Frank, G. J. Nicholson, E. Bayer, *J. Chromatogr. Sci. 15* (1977) 174; *Angew. Chem. 90* (1978) 396; *Angew. Chem. Int. Ed. Engl. 17* (1978) 363.
[3] V. Schurig, R. Link in D. Stevenson, I. D. Wilson (Eds.): *Chiral Separations*, Proceedings *of the International Meeting on Chromatography 1987*, Plenum, New York 1988, p. 91.
[4] V. Schurig, D. Schmalzing, U. Mühleck, M. Jung, M. Schleimer, P. Mussche, C. Duvekot, J. C. Buyten, *J. High Resolut. Chromatogr. 13* (1990) 713.
[5] P. Fischer, R. Aichholz, U. Bölz, M. Juza, S. Krimmer, *Angew. Chem. 102* (1990) 439; *Angew. Chem. Int. Ed. Engl. 29* (1990) 427.
[6] G. Lai, G. Nicholson, E. Bayer, *Chromatographia 26* (1988) 229; G. Lai, U. Mühleck, G. Nicholson, E. Bayer, *J. Chromatogr. 540* (1991) 217.
[7] X. Lou, Y. Sheng, L. Zhou, *J. Chromatogr. 514* (1990) 253.
[8] W. Röder, F.-J. Ruffing, G. Schomburg, W. H. Pirkle, HRC & CC *J. High Resolut. Chromatogr. Chromatogr. Commun. 10* (1987) 665.
[9] J. S. Bradshaw, S. K. Aggarwal, C. A. Rouse, B. J. Tarbet, K. E. Markides, M. L. Lee, *J. Chromatogr. 405* (1987) 169.
[10] G. Opitz, N. Fischer, *Angew. Chem. 77* (1965) 41; *Angew. Chem. Int. Ed. Engl. 4* (1965) 70.
[11] S. A. Matlin, W. J. Lough, L. Chan, D. M. H. Abram, Z. Zhou, *J. Chem. Soc. Chem. Commun. 1984*, 1038.
[12] Immobilization conditions: capillary columns coated statically with **1** were conditioned for 100 h at 180 °C in a weak stream of nitrogen (no hydrogen!). Capillary columns coated statically with **2** were conditioned for 36 h at 230 °C in a weak stream of hydrogen. In all cases the columns were washed with ten column volumes each of methanol followed by methanol/dichloromethane and dichloromethane. The binding rate was determined as 75% by comparison of the capacity factor for *n*-tridecane before and after the washing at 130 °C.
[13] V. Schurig, *J. Chromatogr. 441* (1988) 135.
[14] W.-Y. Li, H. L. Jin, D. W. Armstrong, *J. Chromatogr. 509* (1990) 303.
[15] W. Meltzow, lecture note at the *Int. Symp. Instrum. Anal. Chem. Comput. Technol.*, InCom 1991, Düsseldorf, 22 February 1991.
[16] V. Schurig, Z. Juvancz, G. J. Nicholson, D. Schmalzing, *J. High Resolut. Chromatogr. 14* (1991) 58.
[17] V. Schurig, J. Ossig, R. Link, *Angew. Chem. 101* (1989) 197; *Angew. Chem. Int. Ed. Engl. 28* (1989) 194.

Syndiotactic Poly(1-oxo-2-phenyltrimethylene): On the Mode of the Chain Growth under Palladium Catalysis

By *Marco Barsacchi, Giambattista Consiglio,* Lorenzo Medici, Giorgio Petrucci,* and *Ulrich W. Suter*

Palladium-containing catalytic systems modified by phosphorus or nitrogen ligands and having anions that coordinate weakly or not at all display different chemoselectivity in carbonylation reactions of olefins, depending on the nature of the ligand or the anion or both. Thus, when styrene is the substrate and methanol the solvent, the catalytic system formed in situ from $Pd(CH_3COO)_2$/1,10-phenanthroline(phen)/p-$CH_3C_6H_4SO_3H$ in the absence of hydrogen and in the presence of an oxidant such as 1,4-benzoquinone catalyzes the chemo- and regioselective formation of a new interesting polymeric material, poly(1-oxo-2-phenyltrimethylene),[1] which is the strictly alternating copolymer of carbon monoxide and styrene (Scheme 1). The preformed complex

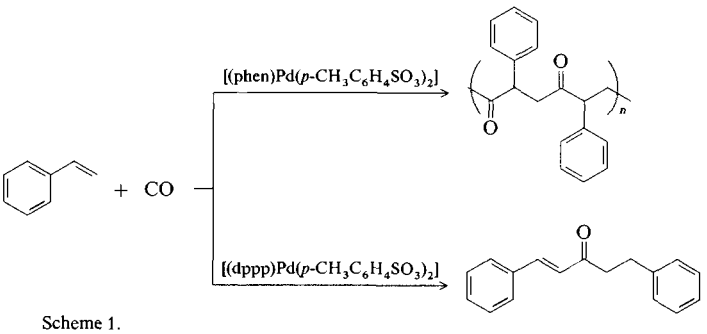

Scheme 1.

[(1,10-phen)Pd(p-$CH_3C_6H_4SO_3$)$_2$] behaves similarly.[2] By contrast, in nonprotic solvents [(dppp)Pd(p-$CH_3C_6H_4SO_3$)$_2$] (dppp = 1,3-bis(diphenylphosphino)propane) brings about selective carbonylation to *E*-1,5-diphenylpent-1-en-3-one even under high hydrogen partial pressure.[3] Steric discrimination is evident for these reactions. The formation of diastereomerically pure *E*-1,5-diphenylpent-1-en-3-one implies a complete discrimination between the two diastereotopic hydrogen atoms during β elimination from the inter-

[*] Prof. Dr. G. Consiglio, L. Medici
Eidgenössische Technische Hochschule
Technisch-Chemisches Laboratorium
ETH-Zentrum, Universitätsstrasse 6, CH-8092 Zürich (Switzerland)
Prof. Dr. U. W. Suter, Dr. M. Barsacchi, Dr. G. Petrucci
Eidgenössische Technische Hochschule, Institut für Polymere
Zürich (Switzerland)

mediate complex **1**. A remarkable enantioface selection takes place instead in the formation of poly(1-oxo-2-phenyltrimethylene). In fact, previous studies have shown that this

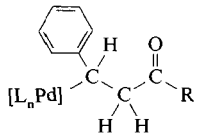

1, $R=CH_2CH_2\text{-}C_6H_5$
2, $R=[CH(C_6H_5)CH_2CO]_nR'$

polymer is obtained with a highly stereoregular structure (ca. 80% syndiotactic triads *rr* and ca. 10% of each of the two different atactic triads *rm* and *mr*).[4]

The absence of the isotactic triad *mm* is an indication that the stereochemistry of the growing chain is chain-end-controlled.[4, 5] This type of steric control is normally considered more effective when the regioselectivity of the monomer insertion leads to intermediates that have a secondary carbon atom bound to the metal (compare **2**).[6] This mode of insertion was observed in the syndiospecific polymerization of styrene by the homogeneous $Ti(PhCH_2)_4$/methylalumoxanes catalytic system[7] or in the isospecific oligomerization of styrene using the [(η^3-methallyl)(η^4-cycloocta-1,5-diene)-nickel(II)] hexafluorophosphate/P(*cyclo*-$C_6H_{11})_3$ catalyst precursor.[8] In the case of poly(1-oxo-2-phenyltrimethylene), however, no information on how the polymeric chain grows, i.e., on the regioselectivity of the insertion of the olefinic monomer exists.[9]

We report here on the identification of the end groups in the poly(1-oxo-2-phenyltrimethylene) copolymer, from which a secondary regioselectivity for the insertion of styrene into the growing chain may be inferred. ^1H and ^{13}CNMR spectroscopy[4] gave no clear indication of possible end groups for the copolymer prepared according to *Drent*,[1] even though carbomethoxy end groups appeared probable.[1] Attempts to reduce the chain length by working in the presence of hydrogen[10] caused almost complete suppression of copolymer formation even at low hydrogen partial pressure. By increasing the amount of the oxidant (1,4-benzoquinone) the selectivity of the reaction is shifted towards the formation of low molecular weight products. Dimethyl 2-phenylbutanedioate (**3**)[11] and dimethyl 2,5-diphenyl-4-oxopimelate (**4**) (probably present as a single diastereomer) were isolated and identified by MS and ^1H

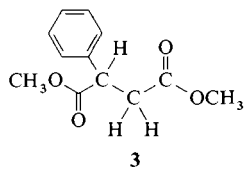

3

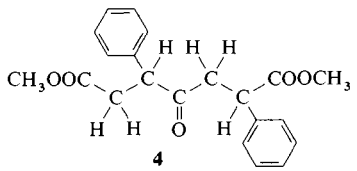

4

and ^{13}CNMR spectroscopy. Both compounds present two different carbomethoxy groups in the ^{13}CNMR spectrum (**3**: δ = 54.5, 54.0, 177.1, and 178.5; **4**: δ = 54.7, 54.1, 177.5, and 178.8 in hexafluoro-2-propanol.

A copolymerization reaction using [(1,10-phen)Pd(*p*-$CH_3C_6H_4SO_3)_2$] as the catalyst precursor allowed us to obtain a small amount of a highly stereoregular, low molecular weight copolymer ($M_n \approx 2000$) through fractional crystallization. The ^{13}CNMR spectrum also showed two different carbomethoxy groups (δ = 54.5, 54.1, 177.5 and 178.9). Similar signals at δ = 54.2 and 54.0 were recognized in the high molecular weight copolymer prepared from labeled $^{13}CH_3OH$. Studies on different copolymer samples show that quite often only one carbomethoxy group can be recognized and when two signals are present, the one at higher magnetic field has the larger intensity. These results imply that the polymer chain begins by insertion of a styrene unit into a metal–carbomethoxy bond and terminates by alcoholysis of a metal–acyl bond. The preparation of a copolymer using labeled $C_6H_5CH=^{13}CH_2$ allowed us to identify a new end group, $C_6H_5CH=^{13}CHCO$ (δ = 125.2 ppm). This end group shows that β-hydrogen elimination from an intermediate of type **2** can be responsible for chain termination, in a way similar to that observed in the synthesis of *E*-1,5-diphenylpent-1-en-3-one. At the moment we cannot specify the geometry of the double bond. We found no signals attributable to the alternative unsaturated termination $^{13}CH_2=C(C_6H_5)CO$ ($\delta \approx 118$ ppm[12]) or to the corresponding saturated end groups [$C_6H_5CH_2\text{-}^{13}CH_2$ and $^{13}CH_3CH(C_6H_5)$]. Unfortunately, due to the relatively high molecular weight, the signals corresponding to the two different carbomethoxy terminations could not be clearly identified. However, a signal at δ = 38.1 could safely be attributed to a CH_2 group in a structure of type **5**, based on DEPT experiments and the ^{13}CNMR data obtained for **4**. In all stereoregular samples of the copolymer in which only one carbomethoxy termination is observed, this signal is also always present. Since this group must correspond to the initiation of the polymeric chain, the signal at $\delta \approx 38$ identifies the regioselectivity of the first entering olefinic unit as a secondary insertion. Therefore, on the basis of the high regularity of the copolymer, the regioselectivity of the chain growth is also identified. This conclusion is also in keeping with the higher intensity (which should indicate the initiation of the chain) of the methoxy signal at higher field (54.0 as against 54.2 ppm), which can be assigned[12] to structure **5** rather than **6**.

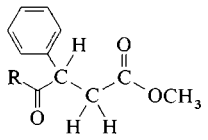

5

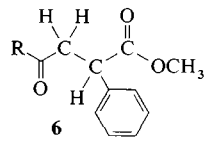

6

On the basis of the secondary regioselectivity of the insertion, the presence of $C_6H_5CH=CHCO$ end groups shows that the termination of the chain is not a consequence of an inversion in the regioselectivity of insertion of the monomer. This seemed possible because of the selective synthesis of *E*-1,5-diphenylpent-1-en-3-one with [(dppp)Pd(*p*-$CH_3C_6H_4SO_3)_2$] (Scheme 1) as the catalyst precursor. The inversion of the regioselectivity was, indeed, recognized as a reason for termination for the polymerization of propylene with soluble Ziegler–Natta catalysts[13] and for the aforementioned isospecific oligomerization of styrene.[8]

To summarize, [(1,10-phen)Pd(*p*-$CH_3C_6H_4SO_3)_2$] gives rise to a carbomethoxypalladium species which catalyzes the strictly alternating copolymerization of carbon monoxide and styrene through secondary insertion of consecutive *ul* enantiofaces[14] of styrene units; chain termination is due either to a β-hydrogen elimination step or to alcoholysis of an acyl intermediate. The reasons for the high diastereoselectivity of the process, which appears to be chain-end-controlled, are not clear at the moment. It has been reported recently that complexes of the type [(Chelate ligand)Pd(COCH$_3$)(Solvent)]BF_4 coordinate styrene before under-

going olefin insertion and β-hydrogen elimination to *E*-1-phenylbut-1-en-3-one.[15] It should thus be possible to synthesize similar compounds of the type [(Chelate ligand)Pd(COR*)(Styrene)]BF_4 (R* = Chiral group related to the growing chain of the copolymer) in which enantioface discrimination can be investigated.

Received: March 18, 1990 [Z 4510 IE]
German version: *Angew. Chem. 103* (1991) 992

[1] E. Drent, *Eur. Pat. Appl.* 229408 (1986) (*Chem. Abstr. 108* (1988) 6617).
[2] L. Medici, *Diplomarbeit*, ETH Zürich (1990).
[3] C. Pisano, G. Consiglio, A. Sironi, M. Moret, *J. Chem. Soc. Chem. Commun. 1991*, 421–423.
[4] P. Corradini, C. De Rosa, A. Panunzi, G. Petrucci, P. Pino, *Chimia 44* (1990) 52–54.
[5] J. A. Ewen, *J. Am. Chem. Soc. 106* (1984) 6355–6364.
[6] For an alternative explanation see: J. A. Ewen, R. L. Jones, A. Razavi, J. D. Ferrara, *J. Am. Chem. Soc. 110* (1988) 6255–6256.
[7] a) A. Zambelli, P. Longo, P. Longo, C. Pellecchia, A. Grassi, *Macromolecules 20* (1987) 2035–2037; b) C. Pellecchia, P. Longo, A. Grassi, P. Ammendola, A. Zambelli, *Makromol. Chem. Rapid Commun. 8* (1987) 277–279.
[8] a) J. R. Ascenso, A. R. Dias, P. T. Gomes, C. C. Romao, Q.-T. Pham, D. Neibecker, I. Tkatchenko, *Macromolecules 22* (1989) 998–1000; b) P. Longo, A. Grassi, L. Oliva, P. Ammendola, *Makromol. Chem. 191* (1990) 237–242.
[9] T.-W. Lai, A. Sen, *Organometallics 3* (1984) 866–870.
[10] H. Wittwer, P. Pino, U. W. Suter, *Macromolecules 21* (1988) 1262–1269.
[11] D. E. James, J. K. Stille, *J. Am. Chem. Soc. 98* (1976) 1810–1823.
[12] E. Pretsch, T. Clerc, J. Seibl, W. Simon: *Strukturaufklärung organischer Verbindungen*, 3rd ed., Springer, Berlin 1986.
[13] P. Pino, P. Cioni, J. Wei, *J. Am. Chem. Soc. 109* (1987) 6189–6191.
[14] D. Seebach, V. Prelog, *Angew. Chem. 94* (1982) 696–702; *Angew. Chem. Int. Ed. Engl. 94* (1982) 654–660.
[15] a) K. Vrieze, G. P. C. M. Dekker, C. J. Elsevier, I. M. Han, P. W. N. M. van Leeuven, R. Rulke, *VII Int. Symp. Homogeneous Catal.*, Lyon, France 1990, Abstracts p. 59; b) G. P. C. M. Dekker, K. Vrieze, P. W. N. M. van Leeuven, C. J. Elsevier, *ibid.*, p. 137.

Oxidation of Alkanes by $[Fe(O)OH]^{\oplus}$ in the Gas Phase—the Role of Iron Oxidation State in C–H Activations**

By *Detlef Schröder* and *Helmut Schwarz**

Dedicated to Professor Horst Prinzbach on the occasion of his 60th birthday

Despite all progress our understanding of the mechanistic details of the metal-mediated functionalization of non-activated C–H bonds[1] is at best rudimentary. The role played by the iron complexes in some of these reactions has, however, been explained: high valence ionic iron oxides are present at the reaction center both in enzymatic and enzyme-free processes.[1, 2] However, the exact oxidation state of the iron as well as the exact composition of the active centers are still a matter of speculation.

On the other hand, a control of the stoichiometry and the oxidation states of the metal oxides has been realized in experiments in the gas phase; mass selected cations of metal oxides of well-defined composition are allowed to react with organic substrates. With this method it was recently possible to elucidate the details of the activation of CH_4[3] and C_2H_6[4] and the mechanisms of the dehydrogenation of alkanones[5] with naked $FeO^{\oplus}$. We report here on reactions of $[O=Fe-OH]^{\oplus}$ (formally an Fe^{IV} oxide) with selected alkanes under the conditions of Fourier Transform Ion Cyclotrotron Resonance (FTICR).[6, 7]

In the system $[Fe(O)OH]^{\oplus}/CH_4$ the processes described in Equation (a) take place.[14] Two findings are remarkable: 1) the rate constant k_1 of the overall reaction (ca. 10^{-10} $cm^3 s^{-1}$ per molecule) is only about half the value of that of the reaction of $FeO^{\oplus}$ with CH_4;[3] 2) the 12e-complex $[Fe(O)OH]^{\oplus}$ affords exclusively closed-shell neutral molecules (H_2O, CH_2O, and CH_3OH). On the other hand, in the case of the Fe^{III} compound $FeO^{\oplus}$, an 11e-complex, the $H^{\bullet}$ abstraction (generation of $CH_3^{\bullet}$) predominates.[3]

$$[O=Fe-OH]^{\oplus} + CH_4 \xrightarrow{k_1} \begin{cases} 25\% \rightarrow [FeOCH_3]^{\oplus} + H_2O \\ 10\% \rightarrow [HFeOH_2]^{\oplus} + CH_2O \\ 65\% \rightarrow [FeOH]^{\oplus} + CH_3OH \end{cases} \quad (a)$$

An insight into the mechanism is provided by the reaction of $[Fe(O)OH]^{\oplus}$ with CD_4 [Eq. (b)];[15] k_2 is one tenth of k_1.

$$[O=Fe-OH]^{\oplus} + CD_4 \xrightarrow{k_2} \begin{cases} 30\% \rightarrow [FeOCD_3]^{\oplus} + HDO \\ 25\% \rightarrow [FeOD]^{\oplus} + CD_3OH \\ 45\% \rightarrow [FeOH]^{\oplus} + CD_3OD \end{cases} \quad (b)$$

The abundance difference in generating $[FeOD]^{\oplus}$ or $[FeOH]^{\oplus}$ is not explainable by an isotope effect alone, since a C–D bond must be cleaved in both cases. All findings can however be described by Scheme 1: route ⓐ can, due to the symmetry of **2**, explain the formation of $[FeOH]^{\oplus}$ and $[FeOD]^{\oplus}$, but it cannot explain the specific loss of HDO. The latter presumably, arises from **4** (route ⓑ) in competition with the reductive elimination of CD_3OD. If one ignores kinetic isotope effects then it follows from the percentage ratio given in Equation (b) that ⓐ and ⓑ are almost equally probable.

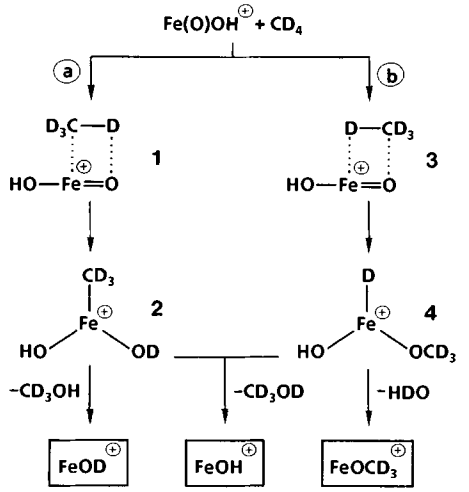

Scheme 1. Mechanism of the reaction of $[Fe(O)OH]^{\oplus}$ with CD_4.

[*] Prof. Dr. H. Schwarz, Dipl.-Chem. D. Schröder
Institut für Organische Chemie der Technischen Universität
Strasse des 17. Juni 135, W-1000 Berlin 12 (FRG)

[**] This work was supported by the Deutsche Forschungsgemeinschaft, the Fonds der Chemischen Industrie, and the Volkswagen-Stiftung. We thank our colleagues Sir *D. H. R. Barton* (College Station), *H. Vorbrüggen* (Berlin), and *M. H. Zenk* (Munich) for literature citations.

In the system $[Fe(O)OH]^{\oplus}/C_2H_6$ the generation of C_2H_4 (50%) and of $[FeOH]^{\oplus}/C_2H_6O$ (45%) predominates; formation of H_2O (5%) is a side reaction (Scheme 2). An in-

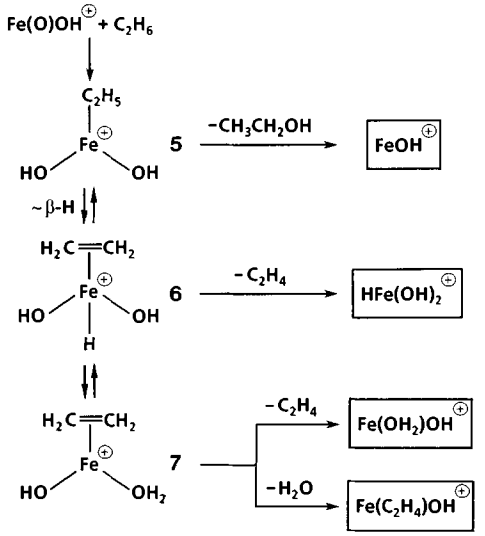

Scheme 2. Mechanism of the reaction of $[Fe(O)OH]^{\oplus}$ with C_2H_6.

sight into the course of the reaction in both processes is provided by the use of CH_3CD_3. Instead of unlabeled ethene, both $C_2H_2D_2$ and C_2HD_3 (2.3:1) are then found to be generated; we therefore conclude that the β-hydrogen transfer must be reversible.[16] Whether the generation of ethene from **6** or from **7** takes place is still unclear. Compound **7** is presumably the precursor for the dehydration. The product distribution $[FeOH]^{\oplus}/[FeOD]^{\oplus}$ (8:1) in the reaction of $[Fe(O)OH]^{\oplus}$ with CH_3CD_3 permitted the estimation of the isotope effect in the generation of **5**. If no secondary isotope effect occurs in the reductive elimination of ROD or ROH (R = ethyl), a value of $k_H/k_D \approx 3.5$ is obtained for the oxidative addition of the C–H and C–D bonds.[17]

In order to investigate the reactivity of $[Fe(O)OH]^{\oplus}$ with higher alkanes, reactions were carried out with *n*-butane and isobutane (Scheme 3). Besides the processes already ob-

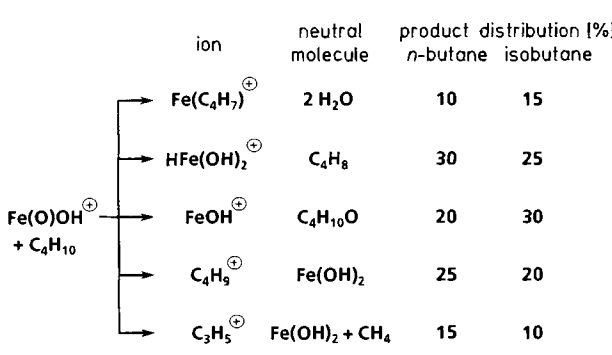

Scheme 3. Reaction of $[Fe(O)OH]^{\oplus}$ with *n*-butane and isobutane.

served in the reaction with ethane, a double dehydration as well as hydride transfer to the iron oxide (generation of $C_4H_9^{\oplus}$ and $C_3H_5^{\oplus}$) is observed here for the first time.

The chemistry of $FeO^{\oplus}$[3] and of $[Fe(O)OH]^{\oplus}$ with simple alkanes is thus quite different; $FeO^{\oplus}$ is not only significantly more reactive than $[Fe(O)OH]^{\oplus}$, but also the product distribution is different, insofar as no radicals are detected in the case of the Fe^{IV} oxide. This result is possibly not without importance for an understanding of the mechanisms of enzyme-initiated oxygenations.

Received: January 18, 1991 [Z 4394 IE]
German version: *Angew. Chem. 103* (1991) 987

CAS Registry numbers:
$[Fe(O)OH]^{\oplus}$, 134180-34-0; CH_4, 74-82-8; C_2H_6, 74-84-0; *n*-butane, 106-97-8; isobutane, 75-28-5; D_2, 7782-39-0.

[1] a) R. A. Sheldon, J. K. Kochi: *Metal-Catalysed Oxidation of Organic Compounds*, Academic, New York 1981; b) A. E. Shilov: *Activation of Saturated Hydrocarbons by Transition Metal Complexes*, Reidel, Boston 1984; c) H. D. Gesser, N. R. Hunter, C. B. Prakush, *Chem. Rev. 85* (1985) 235; d) C. L. Hill: *Activation and Functionalization of Alkanes*, Wiley, New York 1989; e) see also special issue (October/November) von *New J. Chem. 13* (1989); f) J. A. Davies, P. L. Watson, J. F. Liebman, A. Greenberg (Eds.): *Selective Hydrocarbon Activation. Principles and Progress*, VCH Publishers, New York 1990; g) D. H. R. Barton, *Aldrichimica Acta 23* (1990) 3, refers to the problem as "the search for the chemists' Holy Grail".

[2] Ausgewählte Literatur: a) V. Ullrich, *Top. Curr. Chem. 83* (1979) 67; b) F. P. Guengerich, T. L. Macdonald, *Acc. Chem. Res. 17* (1984) 9; c) G. M. Whitesides, C.-H. Wong, *Angew. Chem. 97* (1985) 617; *Angew. Chem. Int. Ed. Engl. 24* (1985) 617; d) P. R. Ortiz de Montellano (Ed.): *Cytochrome P-450: Structure, Mechanism and Biochemistry*, Plenum, New York 1986; e) B. Meunier, *Bull. Soc. Chim. Fr. 1986*, 578; f) P. A. Frey, *Chem. Rev. 90* (1990) 1343; g) D. H. R. Barton, E. Csuhai, D. Doller, N. Ozbalik, G. Balavoine, *Proc. Natl. Acad. Sci. USA 87* (1990) 3401; h) J. E. Baldwin, M. Bradley, *Chem. Rev. 90* (1990) 1079; i) D. Mansay, *Pure Appl. Chem. 62* (1990) 741; j) R. A. Leisung, B. A. Brennan, L. Que, Jr., B. G. Fox, E. Münck, *J. Am. Chem. Soc. 113* (1991) 3988, and references cited therein.

[3] a) D. Schröder, H. Schwarz, *Angew. Chem. 102* (1990) 1468; *Angew. Chem. Int. Ed. Engl. 29* (1990) 1433; b) H. Schwarz, *ibid. 103* (1991) 837 and *30* (1991) 820.

[4] a) D. Schröder, H. Schwarz, *Angew. Chem. 102* (1990) 1466; *Angew. Chem. Int. Ed. Engl. 29* (1990) 1431; b) T. C. Jackson, D. B. Jacobson, B. S. Freiser, *J. Am. Chem. Soc. 106* (1984) 1252; c) M. M. Kappes, R. H. Staley, *ibid. 103* (1981) 1286.

[5] D. Schröder, K. Eller, H. Schwarz, *Helv. Chim. Acta 73* (1990) 380.

[6] For other examples of gas-phase reactions of hydrocarbons with high-valence, ionic metal oxides such as $[ClCrO_2]^{\oplus}$ or $OsO_x^{\oplus}$ (x = 0 – 4) see a) D. M. Walba, C. H. DePuy, J. J. Grabowski, V. M. Bierbaum, *Organometallics 3* (1984) 498; b) K. K. Irikura, J. L. Beauchamp, *J. Am. Chem. Soc. 111* (1989) 75.

[7] Conditions: $Fe^{\oplus}$ ions were generated from a stainless steel target with the aid of a ND-YAG laser (Spectron system, λ = 1064 nm) by laser desorption/laser ionization [9] in the external ion-source of a Spectrospin CMS-47X mass spectrometer [8]. The metal ions were transferred to the actual ICR cell by a system of electrical potentials and lenses. After deceleration they were stored in a magnetic field of a superconducting magnet (Oxford Instruments) (maximum field strength 7.05 T). The $^{56}Fe^{\oplus}$ isotope, as also all other ions in the reactions to be described, were isolated by FERETS[10] and allowed to react with N_2O to give $FeO^{\oplus}$ [4c, 11]. Since this reaction is strongly exothermic (1.8 eV) [12], excited products are formed which are subsequently quenched by collision with the buffer gas (argon). $FeO^{\oplus}$ was isolated and allowed to react with CH_4 according to the procedure described in [3] to give $FeOH^{\oplus}$. After renewed isolation the latter was oxidized with N_2O to $[Fe(O)OH]^{\oplus}$. In order to generate a sufficient amount of $[Fe(O)OH]^{\oplus}$ for the reaction with alkanes, the sequence $Fe^{\oplus} \rightarrow FeO^{\oplus} \rightarrow FeOH^{\oplus}$ was carried out twice without isolation of the intermediates. The total cycle time (including reaction with the substrates and detection of the products) was ca. 20 s. This pulse sequence could only be realized, by using a total of four valves: pulse valve 1 for the injection of N_2O ($p \approx 10^{-5}$ mbar), pulse valve 2 for the injection of CH_4 (generation of $FeOH^{\oplus}$) with $p_{max} \approx 5 \times 10^{-6}$ mbar, leak valve 2 serves for the introduction of the alkanes, which react with $Fe(O)OH^{\oplus}$ ($p = 0.5-5 \times 10^{-9}$ mbar). Of the three conceivable connectivities for $[Fe(O)OH]^{\oplus}$ ($[O{=}Fe{-}OH]^{\oplus}$, $[O{=}Fe(O)H]^{\oplus}$, and $[FeOOH]^{\oplus}$) only $[O{=}FeOH]^{\oplus}$ is likely according to CID experiments and H/D exchange reaction with D_2O. Under CID conditions we obtained the ions $[FeOH]^{\oplus}$ (35%), $FeO^{\oplus}$ (30%) and $Fe^{\oplus}$ (35%); exchange with D_2O afforded $[OFeOD]^{\oplus}$[13].

[8] Detailed description: a) K. Eller, H. Schwarz, *Int. J. Mass. Spectrom. Ion Processes 93* (1989) 243; b) K. Eller, W. Zummack, H. Schwarz, *J. Am. Chem. Soc. 112* (1990) 621.

[9] a) B. S. Freiser, *Talanta 32* (1985) 697; b) *Anal. Chim. Acta 178* (1985) 137.

[10] R. A. Forbes, F. H. Laukien, J. Wronka, *Int. J. Mass Spectrom. Ion Processes 83* (1988) 23.

[11] M. M. Kappes, R. H. Staley, *J. Phys. Chem. 85* (1981) 942.

[12] S. K. Loh, E. R. Fisher, L. Lian, R. H. Schultz, P. B. Armentrout, *J. Phys. Chem. 93* (1989) 3159.
[13] For the characterization of $[M-H]^{\oplus}$ (M = transition metal) and $[M-OH]^{\oplus}$ ions see also a) T. J. Carlin, L. Sallans, C: J. Cassady, D. B. Jacobson, B. S. Freiser, *J. Am. Chem. Soc. 105* (1983) 6320; b) L. F. Halle, F. S. Klein, J. L. Beauchamp, *ibid. 106* (1984) 2543; c) C. J. Cassady, B. S. Freiser, *ibid. 106* (1984) 6176; d) D. B. Jacobson, B. S. Freiser, *ibid. 107* (1985) 72; e) C. J. Cassady, B. S. Freiser, *ibid. 108* (1986) 5690.
[14] Other processes, such as charge transfer ($[Fe(O)OH]^{\oplus} + CH_4 \rightarrow CH_4^{\oplus} + [Fe(O)OH]$) or hydride abstraction ($[Fe(OH)_2]^{\oplus} + CH_4 \rightarrow CH_3^{\oplus} + [Fe(OH)_2]$ do not take place.
[15] The loss of formaldehyde in the system $[Fe(O)OH]^{\oplus}/CD_4$ is slowed down by a considerable isotope effect. The product $[DFe(OHD)]^{\oplus}$ formed by loss of formaldehyde exchanges its deuterium atoms rapidly with the "residual water" present in the ICR cell; a quantitative description of this process is not possible.
[16] The signal corresponding to the elimination of C_2H_3D is too weak for quantitative evaluation. This holds true also for the cleavage of D_2O from the complex $[Fe(O)OH]^{\oplus}/CH_3CD_3$. H_2O and HDO are formed in the ratio 1:1.
[17] This value is based on the assumption that the pathway ⓑ for the activation of methane (Scheme 1) does not occur.

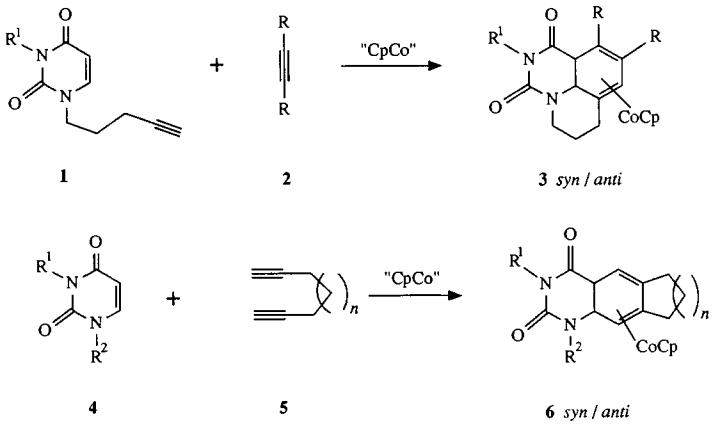

Scheme 1. The designation *syn* and *anti* indicates the position of the Co atom relative to the tertiary hydrogen atoms of the cyclohexadiene ring.

Chemo- and Stereoselective Cobalt-Mediated [2+2+2]Cycloaddition of Alkynes with Uracil Derivatives. A Novel Synthetic Entry to Modified Nucleosides**

By *Roland Boese,** *Jean Rodriguez*, and *K. Peter C. Vollhardt**

The uracil nucleus is present in a multitude of biologically important molecules, including the nucleic acids, and its selective modification has been a challenge in the quest for the development of new medicinal agents, particularly those effective for the treatment of cancer and viral infections, such as herpes and AIDS.[1] In this effort, the 5,6-double bond has played a limited role as a target for synthetic elaboration.[2] We report that $[CpCoL_2](L=CO, C_2H_4)$[3] activates this unit to undergo [2+2+2] cycloadditions to alkynes, generating novel fused 5,6-dihydropyrimidine-2,4-dione complexes, in most cases with remarkable chemo- and stereoselectivity (Scheme 1, Table 1).[4]

The starting materials **1** and **4** were prepared in high yields by adaptation or application of standard literature procedures.[5] The results summarized in Table 1 deserve several comments:

1) While systematic optimization has not been carried out, the efficiency of the cyclization is strongly affected by changes in the reaction conditions, as noted earlier in analogous cases.[6] Thus, the yields for **6a–c** are deceptively low, because of incomplete conversions of starting materials (the yields based on recovered **4a** are 96, 89, and 94%, respectively). Indeed, simply changing the solvent to boiling xylene increases the yield of isolated **6b** to 76%.

2) The reaction is remarkably chemoselective; especially noteworthy is the synthesis of **6**, in which the heterocyclic double bond is engaged in an entirely intermolecular fashion, a synthetic variant that has failed in the cases of the indole, pyrrole, and imidazole nuclei.[6]

3) As expected,[6] products **3** emerge mainly in the *anti*-configuration. Interestingly, however, the *syn*-isomers of **6a–c** are formed exclusively.

Table 1. Results of the respective cyclizations of **1** and **4** with **2** and **5** mediated by CpCo [4] [a].

Uracil derivatives **1/4**		Cocyclizing alkyne	Products (yield [%]) [b]
1a	$R^1 = C_6H_5CO$	**2a** $R = Si(CH_3)_3$	**3a** (28)[*anti:syn* = 5]
1a		**2b** $R = COOCH_3$	**3b** (61)[*anti*]
1b	$R^1 = H$	**2a**	**3c** (35)[*anti:syn* = 10]
		2b	**3d** (73)[*anti*]
4a	$R^1 = R^2 = CH_3$	**5a** ($n = 1$)	**6a** (53)[*syn*]
		5b ($n = 2$)	**6b** (57)[*syn*]
		5c ($n = 3$)	**6c** (22)[*syn*]
4b	$R^1 = CH_3$, R^2 = 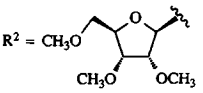	**5b**	**6d** (71) [7.5:4:1:1]
4c	$R^1 = CH_3$, R^2 = 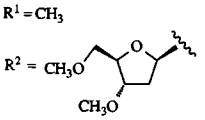	**5b**	**6e** (94) [45:4:1:1]
4d	$R^1 = H$, R^2 = 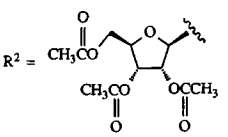	**5b**	**6f** (37) [1:1:1:1]

[a] Conditions: **3**: To **1** (1 equiv.) and **2a** (co-solvent) or **2b** (5 equiv.) in THF is added $[CpCo(CO)_2]$ (1.5–1.8 equiv.) in THF at room temperature under N_2 over a period of 17–21 h (syringe pump) while irradiating the reaction mixture with a slide projector lamp (Sylvania ELH 300 W). **6a–d**: To irradiated **4a** (1 equiv.) in boiling toluene (or **4b** in xylene) is added under N_2 a mixture of **5** (2 equiv.) and $[CpCo(CO)_2]$ (2 equiv.) in toluene over a period of 18–22 h (syringe pump). **6e,f**: To irradiated **4** (1 equiv.) in boiling THF is added under argon simultaneously via two syringes **5b** (2 equiv.) and $[CpCo(CH_2CH_2)_2]$ in THF. [b] The diastereomeric ratios were determined ^{1}H-NMR spectroscopically on the crude products after flash chromatography on SiO_2 and before further chromatographic purification.

[*] Prof. Dr. K. P. C. Vollhardt, Dr. J. Rodriguez
Department of Chemistry
University of California at Berkeley
and
The Chemical Sciences Division,
Lawrence Berkeley Laboratory, Berkeley, CA 94720 (USA)
Dr. R. Boese
Institut für Anorganische Chemie der Universität-Gesamthochschule
Universitätstr. 5–7, Postfach 10 37 64, W-4300 Essen 1 (FRG)

[**] This work was supported by the National Institutes of Health (GM 22479), *J. R.* acknowledges the award of a postdoctoral fellowship by the Fonds de Bourse de Recherche Scientifique et Technique de l'OTAN (1987/1988).

4) Most promising for future exploration are the cocyclizations of the enantiomerically pure nucleoside models **4b–d**, bearing what might be considered chiral auxiliary sugar substituents. Their potential utility is demonstrated in the *highly diastereoselective* construction of **6e**.

5) As discussed previously,[3, 6] the position of the cobalt atom relative to those of the adjacent cyclohexadiene tertiary hydrogens is readily ascertained exploiting the metal's distinctive magnetic anisotropy. In this way, the major diastereomer of **6d** and **6e** was assigned the *syn*-configuration. To corroborate these conclusions and perhaps obtain some clues with respect to the selectivity of the addition of **4c** to **5b**, an X-ray structural analysis of **6e** (major isomer) was performed (Fig. 1).[7]

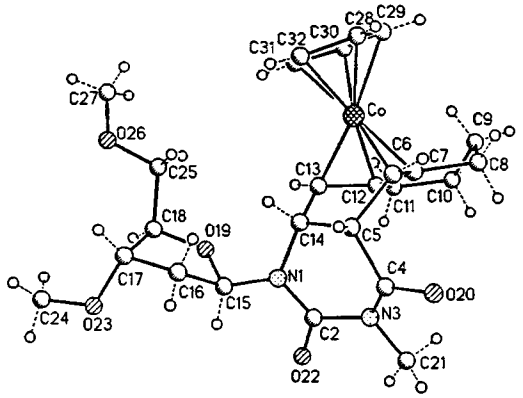

Fig. 1. Structure of **6e** (major isomer) in the crystal (SHELXTL). Selected distances [Å] and angles [°]: Co-C6 2.014(3), Co-C7 1.960(3), Co-C12 1.991(3), Co-C13 2.001(3), Co-Cp (ring centroid) 1.675, N1-C2 1.357(3), N1-C14 1.476(3), C2-N3 1.405(3), N3-C4 1.401(4), C4-C5 1.506(4), C5-C6 1.529(4), C5-C14 1.527(4), C6-C7 1.428(4), C7-C12 1.410(4), C12-C13 1.439(4), C13-C14 1.530(4), C6-C7-C12-C13 5.3, C6-C5-C14-C13 25.9, C4-C5-C14-N1 34.5.

While it is probably premature to speculate on the origin of the diastereoselectivity observed in the formation of **6e** (and the lack thereof on route to **6d** and **6f**), it is nevertheless presumed that the conformation of the sugar substituents in the starting materials is decisive.[9]

6) As noted previously,[3, 6] the [CpCo(diene)] complexes are subject to oxidative degradation, liberating hitherto unavailable heterocyclic ligands [e.g. CpCo-free **6b**, $CuCl_2$ (4 equiv.), Et_3N (12 equiv.), THF/H_2O 0 °C, 2 min, 91 %)].[4]

Extension of this methodology to other nucleic acid bases, and to the "tagging" of the nucleic acids themselves, are currently under investigation.

Received: March 22, 1991 [Z 4527 IE]
German version: *Angew. Chem. 103* (1991) 1032

[1] a) For selected recent references, see: D. M. Coe, P. L. Myers, D. M. Parry, S. M. Roberts, R. Storer, *J. Chem. Soc. Chem. Commun. 1990*, 151; b) K. Hirota, H. Sajiki, Y. Maki, H. Inoue, T. Ueda, *ibid. 1989*, 1659; c) R. W. Armstrong, S. Gupta, F. Whelihan, *Tetrahedron Lett. 30* (1989) 2057; d) N. Bischofsberger, *ibid. 30* (1989) 1621; e) J. C. Martin (Ed.): *Nucleotide Analogues as Antiviral Agents (ACS Symp. Ser. 401) Am. Chem. Soc.* Washington, DC, USA 1989.

[2] a) D. J. Brown in A. R. Katritzky, C. W. Reese (Eds.): *Comprehensive Heterocyclic Chemistry, Vol. 3*, Pergamon, New York 1984, p. 57; b) S. T. Reid, *Adv. Heterocycl. Chem. 30* (1980) 239.

[3] K. P. C. Vollhardt, *Angew. Chem. 96* (1984) 525; *Angew. Chem. Int. Ed. Engl. 23* (1984) 539.

[4] All new compounds gave satisfactory analytical and/or spectral data. For example: **3d**: orange-red crystals, m.p. = 210 °C (decomp.); IR ($CHCl_3$): $\tilde{\nu}$ = 3390, 2950, 1710, 1485, 1450, 1430, 1265 cm^{-1}; ^1H NMR (300 MHz, $CDCl_3$): δ = 1.83 (m, 4H), 2.70 (d, J = 8 Hz, 1H), 2.78 (m, 1H), 2.94 (d, J = 8 Hz, 1H), 3.74 (s, 3H), 3.81 (s, 3H), 4.51 (m, 1H), 4.90 (s, 5H), 5.56 (s, 1H), 7.49 (s, 1H); ^{13}C NMR (75 MHz, CD_2Cl_2): δ = 23.9, 34.2, 43.6, 45.9, 52.1, 52.8, 55.0, 61.2, 72.3, 78.2, 78.9, 83.5, 151.6, 168.5, 170.9, 172.2; MS (70 eV): m/z 445 ($M^{\oplus}$, 6%), 444(28), 442(2), 383(2), 378(4), 318(42), 288(34), 287(100). **6b** (free ligand): colorless crystals, m.p. 112–114 °C; IR (C_6H_6) $\tilde{\nu}$ = 2940, 2860, 1715, 1675, 1480, 1415, 1280, 1100 cm^{-1}; ^1H NMR (300 MHz, C_6D_6): δ = 1.16 (m, 2H), 1.33 (m, 2H), 1.91 (m, 3H), 2.17 (m, 1H), 2.54 (dd, J = 7.6, 6.6 Hz, 1H), 2.69 (s, 3H), 3.24 (s, 3H), 3.33 (m, 1H), 5.83 (bd, J = 1.7 Hz, 1H), 5.50 (d, J = 6 Hz, 1H); ^{13}C NMR (75 MHz, C_6D_6): δ = 24.4, 27.7, 30.8, 30.9, 33.5, 39.7, 52.9, 117.7, 118.4, 136.2, 138.3, 153.2, 170.0; MS (70 eV): m/z 247 ($M^{\oplus}$, 18%). 246(100), 245(95), 217(40), 104(76), 91(69). **6e** (major isomer): yellow crystals, m.p. 156–158 °C; IR (C_6H_6): $\tilde{\nu}$ = 3090, 3035, 2980, 2930, 2820, 1705, 1670, 1460, 1355, 1285, 1205, 1200, 1130, 1110, 1100, 1060 cm^{-1}; ^1H NMR (400 MHz, CD_2Cl_2): δ = 1.67 (m, 1H), 1.76 (m, 1H), 2.03 (m, 5H), 2.24 (m, 1H), 2.28 (m, 1H), 2.33 (m, 1H), 2.69 (dd, J = 10, 5.7 Hz, 1H), 2.88 (s, 3H), 3.03 (d, J = 5.7 Hz, 1H), 3.29 (m, 1H), 3.33 (s, 1H), 3.46 (s, 1H), 3.59 (m, 2H), 3.92 (dt, J = 6.1, 3.2 Hz, 1H), 3.98 (m, 2H), 4.71 (s, 5H), 5.89 (dd, J = 8.3, 6.1 Hz, 1H); ^{13}C NMR (75 MHz, C_6D_6): δ = 23.5, 23.7, 27.6, 28.8, 29.2, 35.2, 39.8, 44.5, 52.5, 53.5, 56.5, 58.9, 73.6, 81.1, 81.7, 82.3, 87.0, 92.2, 95.0, 151.7, 171.8; MS (70 eV): m/z 501 ($M^{\oplus}$, 4%), 500(15), 356(15), 354(20), 256(9), 159(33), 124(25), 113(35), 87(20), 45(100).

[5] a) K. A. Cruickshank, J. Jiricny, C. B. Reese, *Tetrahedron Lett. 25* (1984) 681; b) R. W. Chambers, *Biochemistry 4* (1965) 219; c) R. B. Baker, G. B. Chheda, *J. Pharm. Sci. 54* (1965) 25; d) E. Wittenburg, *Chem. Ber. 99* (1966) 2380; e) J. Žemlička, J. Smrt, F. Sörm, *Coll. Czech. Chem. Commun. 29* (1964) 635; f) I. Ciucanu, F. Kerek, *Carbohydr. Res. 131* (1984) 209.

[6] K. P. C. Vollhardt, *Lect. Heterocycl. Chem. 9* (1987) 59.

[7] Crystal size: 0.36 × 0.26 × 0.25 mm^3, orthorhombic, space group $P2_12_12_1$, $2\theta_{max}$ = 50°, a = 8.913(1), b = 11.269(1), c = 23.791(3) Å, $\alpha = \beta = \gamma$ = 90°, V = 2389.7(5) $Å^3$, Z = 4, ρ_{calcd} = 1.391 $g\,cm^{-3}$, μ = 0.75 mm^{-1}, Nicolet-R3m/V diffractometer with $Mo_{K\alpha}$ radiation at 125 K; 4240 reflections collected, 3856 treated as observed [$F_o \geq 4\sigma(F)$]; structure solved by direct methods and refinement with full matrix least squares, 324 parameters, rigid groups for hydrogen atoms; common isotropic U values for each group and anisotropic U values for all other atoms, except O26 and O26A which are disordered and calulated with site occupation factors of 0.5; the absolute structure was established by refinement of η = 1.033(23) [8], R = 0.035, R_w = 0.033, $w^{-1} = [\sigma^2(F_o) + 1.5 \times 10^{-4} F_o^2]$. Maximum residual electron density 0.43 e $Å^{-3}$. Further details of the crystal structure investigation may be obtained from the Fachinformationszentrum Karlsruhe, Gesellschaft für wissenschaftlich-technische Information mbH, W-7514 Eggenstein-Leopoldshafen 2 (FRG), on quoting the depository number CSD-320197, the names of the authors, and the journal citation.

[8] D. Rogers, *Acta Crystallogr. Sect. A 37* (1981) 734.

[9] See, for example, J. H. Prestegard, S. I. Chan, *J. Am. Chem. Soc. 91* (1969) 2843; M. P. Schweizer, J. T. Witkowski, R. K. Robins, *ibid. 93* (1971) 277; H. Dugas, B. J. Blackburn, R. K. Robins, R. Deslauriers, I. C. P. Smith, *ibid. 93* (1971) 3468; T. C. Thurber, L. B. Townsend, *J. Heterocycl. Chem. 9* (1972) 629; M. P. Schweizer, E. B. Banta, J. T. Witkowski, R. K. Robins, *J. Am. Chem. Soc. 95* (1973) 3770; G. I. Birnbaum, G. A. Gentry, *ibid. 105* (1983) 5398; G. W. M. Visser, R. E. Herder, P. Noordhuis, O. Zwaagstra, J. D. M. Herscheid, F. J. J. de Kanter, *J. Chem. Soc. Perkin Trans. 1 1988* 2547; P. C. Kline, A. Serianni, *J. Am. Chem. Soc. 112* (1990) 7373.

Arsenic Compounds in Organic Synthesis: Pentamethinium Salts from Aminoarsanes and Pyrylium Salts

By *Yves Madaule, Myriam Ramarohetra, Jean-Gérard Wolf,* Jean-Paul Declercq,* and *Antoine Dubourg*

Compared to the well known arsenic ylides, *Wittig* reagents frequently used in natural products synthesis,[1] other organoarsenic compounds are seldom used as synthetic intermediates in preparative organic chemistry. Examples

[*] Dr. J. G. Wolf, Dr. Y. Madaule, M. Ramarohetra,
University Paul Sabatier, URA CNRS 471
F-31062 Toulouse Cedex (France)
Prof. Dr. J. P. Declercq
University of Louvain-la-Neuve (Belgium)
Dr. A. Dubourg
University of Montpellier (France)

of such compounds that have been used are the very reactive *tris*(dialkylamino)arsanes[2] which react with ketones to give enamines.[3]

We describe here a novel reaction of aminoarsanes with pyrylium salts, which leads to formation of pentamethinium salts. Pyrylium salts[4] are important and versatile reagents, and methods have already been developed for the synthesis of some highly substituted derivatives.[5] In solution, oxonium and carbonium forms of the pyrylium salts are in equilibrium with each other. Our interest was thus compellingly turned to studying the electrophilic attack of aminoarsanes on this system. Due to the high reactivity of the starting compounds and the good "leaving-group" ability of As_4O_6, pure pentamethinium salts **1**–**5** are formed in high yields (≥90% in all cases in CH_3CN) in the reaction with 2,6-diarylpyrylium perchlorates (Scheme 1).

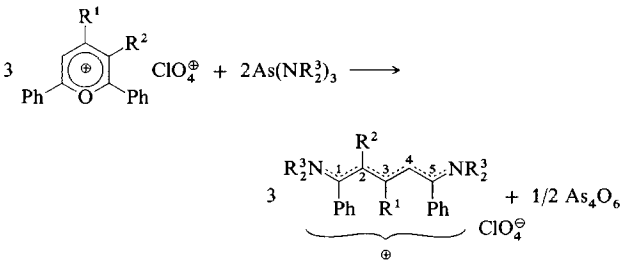

1, R^1 = Ph, R^2 = H, R^3 = Me
2, R^1 = R^2 = H, R^3 = Me
3, R^1 = Ph, R^2 = R^3 = Me
4, R^1 = Ph, R^2 = H, R^3_2 = $(CH_2)_4$
5, R^1 = Ph, R^2 = H, R^3_2 = $(CH_2)_2O(CH_2)_2$

Scheme 1. Synthesis of **1**–**5** from corresponding substituted pyrylium salts and dialkylaminoarsanes.

A closely related reaction of pyrylium salts with masked arsanes such as $As(SiMe_3)_3$ was previously attempted by *G. Märkl* et al., who hoped to obtain doubly substituted arsinines in this way. This Dilthey-like reaction (synthesis of pyridines) succeeded in the case of the synthesis of phosphinines from $P(SiMe_3)_3$ and pyrylium salts,[6] but in the case of the arsenic compounds only 3-azapyrylium salts were sufficiently electrophilic to lead to azaarsinines.[7]

All the compounds **1**–**5** were fully characterized spectroscopically (IR, UV, ^{1}H- and ^{13}C-NMR), mass spectrometrically, and by elemental analyses.

Table 1 summarizes the most important ^{13}C-NMR and UV data of **1**–**5** and of the 1,5-bis(dimethylamino)-substituted parent compound DMP ((5-dimethylamino-2,4-dienylidene)dimethylammonium perchlorate). A comparison of these data and those in the literature[9] indicates an alternate charge distribution (positive for C1, C3 and C5, negative for C2 and C4) independent of substituents effects (which could be calculated in part from the $\Delta\delta_{^{13}C}$ contributions of DMP, **1** and **2**). In fact, if we consider that the steric hindrance in our compounds increases in the order **2**, **4**, **1**, **5** and **3**, the UV spectra of these compounds indeed show a continuous bathochromic shift of λ_{max} and a continuous decrease in the extinction thus indicating a progressively weaker conjugation. This fact is confirmed by the X-ray structure analysis of **1**,[10] one of the sterically most crowded compounds (Fig. 1).

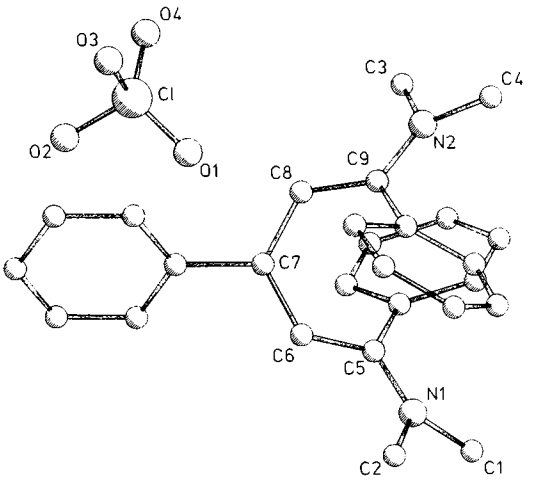

Fig. 1. Structure of **1** in the crystal. Selected bond lengths [Å] and angles [°]: N1-C1 1.488, N1-C2 1.466, N1-C5 1.305, C5-C6 1.417, C6-C7 1.385, C7-C8 1.412, C8-C9 1.422, N2-C3 1.437, N2-C4 1.470, N2-C9 1.361, C1-N1-C2 113.6, C1-N1-C5 125.7, C2-N1-C5 120.5, N1-C5-C6 120.3, C5-C6-C7 126.2, C6-C7-C8 124.2, C7-C8-C9 122.5, C8-C9-N2 119.2, C3-N2-C4 117.7, C3-N2-C9 120.4, C4-N2-C9 121.8. Deviations *D* from the mean plane (atom, *D* [Å]) N1-C5-C6-C7-C8-C9-N2 (N1, −0.14), (C5, 0.36), (C6, −0.16), (C7, 0.02), (C8, 0.16), (C9, −0.41), (N2, 0.17).

Unlike the well-known unsubstituted compound DMP,[11] compound **1** is a nonplanar, horseshoe-shaped, but still (*Z*)-conjugated system (average C–C bond length in the C_5-moiety ca. 1.41 Å). The terminal carbon atoms C5 and C9 are bent out respectively + 0.36 and − 0.41 Å from the mean N1–C5–C6–C7–C8–C9–N2 plane, which amounts to an almost symmetrical deformation. On the other hand, the ClO_4 anion rotates around Cl with two favored positions for O and O′, in each case with a structure occupation factor (SOF) equal to 77 and 23% respectively. The role of the substituents on C7 with respect to the structure of the carbon chain is presently being investigated.

We want to emphasize once again the characteristics of the reactions described here: 1) specificity: attempts to carry out

Table 1. Comparison of the most important ^{13}C-NMR (50.3 MHz, $CDCl_3$, 25°C, TMS) and UV data (CH_2Cl_2) of **1**–**5** and DMP [a].

	1	**2**	**3**	**4**	**5**	DMP [b]
^{13}C: (50.3 MHz, $CDCl_3$, 25°C, TMS)						
δC1; C5	169.29	170.16	165.75	165.16	168.77	161.62
δC2; C4	109.39	106.36	119.21, 108.80	108.52	111.52	102.77
δC3	169.03	161.66	163.75	168.81	170.71	162.52
UV: λ_{max} [nm], ε	500, 38000	442, 93300	521, 28500	498, 41000	517, 30000	416, 119500

[a] DMP is the only compound in this series for which numerous physical data are known. DMP crystallizes in two different forms, orange and yellow, which differ only in their arrangement in the lattice; in both cases the C_5-moieties and terminal amino groups are in a superimposable (*E*)-planar structure. The red form is obtained by crystallization with two molecules of H_2O. [b] ^{13}C-NMR spectrum in CD_3CN [8a], UV spectrum in EtOH [8b]. In the crystal λ_{max} = 412 nm and ε for the yellow modification 105600, for the orange modification 34600, and for the red modification 92700.

the same reaction with aminophosphanes led to addition compounds on the pyrylium moiety, analogously to the known addition of Ph_3P on pyrylium salts.[12] 2) Variation of the substitution pattern of pentamethinium salts which can be realized with both reagents: arsanes can easily introduce a large variety of amino groups; the pyrylium salt governs the substitution on the C_5-moiety. Using the method described here we were able to synthesize the first phenyl-substituted pentamethinium salts (and 1,5-disubstituted derivatives). Finally, it is important to underline the importance of developing new compounds in the pentamethinium series, which have proven useful in chemistry (dyes and intermediates in azulene synthesis[13], physics (laser, nonlinear optics in the crystal phase[14]) and biology (anthelmintics[15]).

Experimental procedure

1: A solution of 0.540 g (1.32 mmol) of 2,4,6-triphenylpyrylium perchlorate in 10 mL of acetonitrile was treated with 0.162 mL (0.88 mmol) of *tris*(dimethylamino)arsane. The mixture was stirred for two hours at room temperature. The fluorescence due to the pyrylium salt disappeared and the solution became deep red. As_4O_6 was then filtered off. After removal of the solvent, the precipitate was washed with pentane to yield a red powder (yield > 90%). Recrystallization from EtOH (100%) afforded bright red crystals, m.p. 195 °C, which were suitable for an X-ray structure analysis. **2**–**5** were obtained analogously.

Received: February 19, 1991 [Z 4456 IE]
German version: *Angew. Chem. 103* (1991) 1044

[1] Review Y. Z. Huang, Y. C. Shen, *Adv. Organomet. Chem. 20* (1982) 115–157; Y. Z. Huang, L. Shi, S. Li, *Synthesis 1988*, 975–977; P. Chabert, C. Mioskowski, J. R. Falk, *Tetrahedron Lett. 30* (1989) 2545–2548.
[2] Review: F. Kober, *Synthesis 1982*, 173–184.
[3] a) H. Weingarten, W. A. White, *J. Org. Chem. 31* (1966) 4041–4042; b) H. von Hirsch, *Chem. Ber. 100* (1967) 1289–1295; c) G. Manoussakis, *J. Inorg. Nucl. Chem. 30* (1968) 3100–3103.
[4] A. T. Balaban, *Org. Synth. Mod. Trends Proc. IUPAC Symp. 6th 1986* (1987), p. 263–274.
[5] Y. Maroni-Barnaud, P. Maroni, M. Simalty, Y. Madaule, *Bull. Soc. Chim. Fr. 1970*, 1398–1403; *ibid. 1971*, 546–551.
[6] G. Märkl, F. Lieb, A. Merz, *Angew. Chem. 79* (1967) 475; *Angew. Chem. Int. Ed. Engl. 6* (1967) 458.
[7] G. Märkl, S. Dielt, *Tetrahedron Lett. 29* (1988) 535–538.
[8] a) Yu. L. Slominskii, S. V. Popov, I. V. Repyakh, M. I. Povolotskii, A. D. Kachkovskii, G. G. Dyadyusha, *Teor. Eksp. Khim. 23* (1987) 687–692 and references cited therein; b) S. S. Malhotra, M. C. Whiting, *J. Chem. Soc. 1960*, 3812–3822; c) S. Dähne, B. Bornowski, B. Grimm, S. Kulpe, D. Leupold, M. Mäther, *J. Signalaufzeichnungsmater. 4* (1977) 277–284.
[9] a) R. Radeglia, *J. Prakt. Chem. 315* (1973) 1121–1130; R. Radeglia, E. Gey, Th. Steiger, S. Kulpe, R. Lück, M. Ruthenberg, M. Stierl, S. Dähne, *ibid. 316* (1974) 766–772; b) M. Honda, C. Katayama, J. Tanaka, *Acta Crystallogr. B42* (1986) 90–95.
[10] $C_{27}H_{29}N_2ClO_4$; space group: $Pca2_1$; unit cell dimensions: $a = 17.905(2)$, $b = 8.849(1)$, $c = 15.890(2)$ Å; $Z = 4$; $\rho_{calcd} = 1.27\ g cm^{-3}$; $Cu_{K\alpha}$ radiation; $2\theta_{max} = 135°$; 2501 independant reflections ($R_{Int} = 4.6\%$). Reflections observations: 1980 ($I > 2.5\sigma(I)$). Structure determination: SHELXS (Patterson) + DIRDIF; structure refinement: SHELX76 (using F): After last refinement: $R = 0.078$; $S = 1.44$. Further details of the crystal structure investigation are available on request from the Fachinformationszentrum Karlsruhe, Gesellschaft für wissenschaftlich-technische Information mbH, W-7514 Eggenstein-Leopoldshafen 2 (FRG), on quoting the depository number CSD-55339, the names of the authors, and the journal citation.
[11] a) Orange crystals, see [9b]; b) yellow crystals: J. O. Seltzer, W. Mathews, *J. Phys. Chem. 80* (1976) 631–635; F. Chentli-Benchikha, J. P. Declercq, G. Germain, M. Van Meerssche, *Cryst. Struct. Commun. 6* (1977) 421–424.
[12] V. T. Abaev, L. I. Kisarova, S. E. Emarmilidi, A. A. Bumber, I. E. Mikhailov, I. B. Blank, A. I. Yanovskii, Yu. T. Struchkov, O. Yu. Okhlobystin, *Zh. Obshch. Khim. 59* (1989) 1506–1515.
[13] W. Flitsch, J. R. Alan, M. Hohenhorst, *Tetrahedron Lett. 28* (1987) 4397–4398; K. Hafner, K. P. Meinhardt, *Org. Synth. 62* (1984) 134–139.
[14] J. Merski, C. J. Eckhardt, *J. Chem. Phys. 75* (1981) 3731–3742; S. H. Stevenson, D. S. Donald, G. R. Meredith, *Mater. Res. Symp. Proc., 109 (Nonlinear Opt. Prop. Polym)* (1988), 103–108.
[15] D. L. Garmaise, G. Y. Paris, CA–A C49222713 (1973), Abbott Lab. Ltd.

Effect of Intramolecular Coordination on Tantalum-Alkylidene-Centered Reactions: Synthesis and Structure of a Tantalum-Olefin Adduct and a Tantalum-Zinc-Alkylidene Complex**

By *Hendrikus C. L. Abbenhuis, Nantko Feiken, Henk F. Haarman, David M. Grove, Ernst Horn, Huub Kooijman, Anthony L. Spek,* and *Gerard van Koten**

Dedicated to Professor Hans-Georg von Schnering on the occasion of his 60th birthday

Recently, we started to explore the influence of intramolecular Lewis bases on tantalum-alkylidene reactivity. The potentially terdentate, monoanionic ligand $[2,6\text{-}(Me_2NCH_2)_2C_6H_3]^{\ominus}$ seemed well-suited for this research because of its demonstrated ability to stabilize high oxidation state transition metal centers [e.g. Fe^{III}[1] and Ni^{III}[2]] as well as unusual transition metal intermediates.[3] We have synthesized a tantalum-alkylidene complex $[TaCl_2\{2,6\text{-}(Me_2NCH_2)_2C_6H_3\}(CHtBu)]$ **1** that contains this spectator ligand.[4] Here we report the alkylidene-centered reactions of **1** with either an olefin (ethene) or a strong base (neopentylzinc chloride). These reactions (Scheme 1) lead to the formation of a tantalum-olefin adduct and a novel bimetallic tantalum zinc complex, respectively.

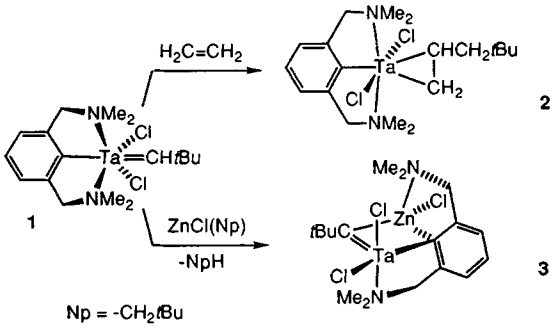

Scheme 1. Alkylidene-centered reactivity of **1**.

Treatment of the alkylidene complex **1** with an excess of ethene in pentane at 20 °C affords the neopentylethene adduct **2** which was characterized spectroscopically[5] and by X-ray structure analysis.[6] The structure determination (Fig. 1) shows **2** to be a mononuclear, distorted pentagonal bipyramidal tantalum complex. In this complex two chlorine atoms [Cl(1) and Cl(2)] occupy the axial *trans* positions. The equatorial plane contains the C(13) and C(14) atoms of the coordinated olefin together with the C(1), N(1) and N(2) atoms of the terdentate aryldiamine ligand. Both five-membered Ta–C–C–C–N chelate rings are puckered. The considerable lengthening of the olefinic bond (C(13)–C(14) = 1.436(10) Å) upon coordination to tantalum and the short distances between olefinic carbons C(13) and C(14) and tantalum (2.200(7) and 2.211(7) Å, respectively) make it more

[*] Prof. Dr. G. van Koten, H. C. L. Abbenhuis, N. Feiken, H. F. Haarman, Dr. D. M. Grove
Debye Research Institute, Department of Metal-Mediated Synthesis
University of Utrecht, Padualaan 8, 3584 CH Utrecht (The Netherlands)
Dr. E. Horn, H. Kooijman, Dr. A. L. Spek
Vakgroep Kristal- en Structuurchemie, University of Utrecht

[**] This work was supported in part (*H. C. L. A* and *A. L. S*) by the Netherlands Foundation for Chemical Research (SON) with financial aid from the Netherlands Organization for Scientific Research (NWO).

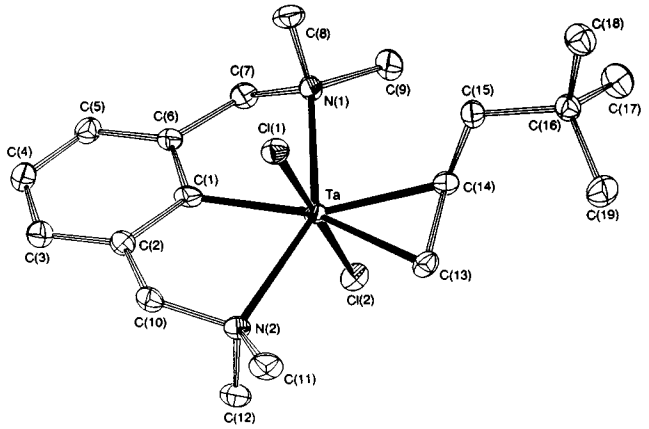

Fig. 1. Thermal motion ellipsoid plot (50% probability level) of **2** in the crystal. Selected bond lengths [Å] and bond angles [°]:Ta-Cl(1) 2.3702(18), Ta-Cl(2) 2.3608(18), Ta-C(1) 2.165(7), Ta-N(1) 2.353(6), Ta-N(2) 2.372(6), Ta-C(13) 2.200(7), Ta-C(14) 2.211(7); Cl(1)-Ta-Cl(2) 178.76(7), N(1)-Ta-N(2) 145.0(2), N(1)-Ta-C(14) 88.5(2), C(13)-Ta-C(14) 38.0(3).

acceptable to describe the structure as a tantalacyclopropane (with tantalum in oxidation state V).

The ^{1}H-NMR spectrum of **2**[5] is not temperature dependent to at least 80 °C, indicating a rigid structure of **2** also in solution. Characteristic for the terdentate coordination of the aryldiamine ligand are the four anisochronous NMe resonances at $\delta = 2.35$, 2.42, 3.27, and 3.45; olefinic multiplets shifted to high field at $\delta = 3.10$, 4.06, and 4.22 are indicative for the η^2-bonded neopentylethene function. In this function, the value of the olefinic $^1J_{^{13}C^{13}C}$ coupling is only 34 Hz (measured in an INADEQUATE $^{13}C\{^1H\}$-NMR experiment), which is more like the $^1J_{sp^3\text{-}C/sp^3\text{-}C}$ coupling in alkanes and cyclopropanes than the $^1J_{sp^2\text{-}C/sp^2\text{-}C}$ coupling in alkenes.[7] This finding again argues for the structure of **2** to be described as a tantalacyclopropane species.

Treatment of **1** with neopentylzinc chloride in Et_2O affords the bimetallic complex **3** which was characterized spectroscopically[5] and by X-ray structure analysis.[8] The structure determination (Fig. 2) shows **3** to be a tantalum-zinc-alkylidene complex that contains a bridging aryldiamine ligand that is nicely positioned to complete the coordination environment of both metal centers. The resulting coordination geometry around zinc is distorted tetrahedral, while the ligand array around tantalum is in between trigonal bipyramidal and square pyramidal (70% along the Berry pseudorotation coordinate towards the latter). The aryl ligand forms an unprecedented asymmetric bridge (via C(9)) between zinc and tantalum: the angle between the Ta–Zn vector and the least squares plane through the aryl carbon atoms is 65.2(2)° and deviates strongly from the expected 90° for a symmetrically bridging aryl unit. The structural data are such that it is possible to describe this bond as intermediate between either a two-electron three-center bond or a combination of a Ta–C σ-bond with a coordinative C → Zn bond involving electron donation from the filled p-orbital on C(9) to Zn. The latter description is equivalent to the type of bonding that would result from an electrophilic attack of a zinc cation at the *ipso*-carbon atom of the tantalum–aryl moiety.[10] The very short Ta=C alkylidene bond length (Ta–C(13) = 1.862(6) Å) together with the long Zn–C bond in the alkylidene unit (Zn–C(13) = 2.114(6)) also allow this complex to be described as a tantalum-alkylidyne species stabilized by a Lewis acid-base interaction with a zinc chloride cation. Similar arguments have been used to describe the structural characteristics of $[\{TaCl_2(\mu\text{-}C\textit{t}Bu)(MeOCH_2CH_2OMe)\}_2Zn(\mu\text{-}Cl)_2]$.[11]

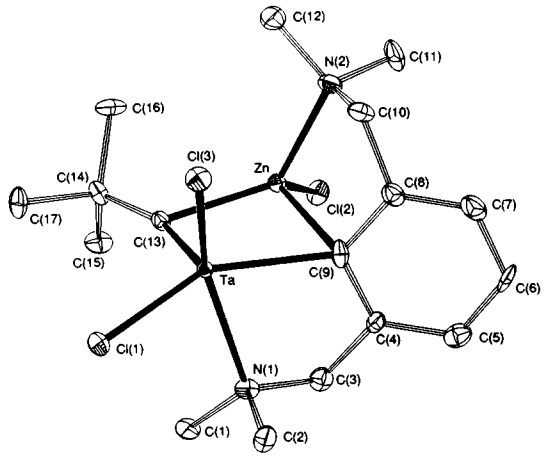

Fig. 2. Thermal motion ellipsoid plot (50% probability level) of **3** in the crystal. Selected bond lengths [Å] and bond angles [°]: Ta-Cl(1) 2.3830(15), Ta-Cl(3) 2.3628(16), Ta-C(9) 2.321(6), Ta-C(13) 1.862(6), Ta-N(1) 2.313(6), Ta-Zn 2.7286(9), Zn-Cl(2) 2.2143(16), Zn-C(9) 2.258(6), Zn-C(13) 2.114(6), Zn-N(2) 2.101(5); Cl(1)-Ta-Cl(3) 91.90(5), Cl(1)-Ta-C(13) 103.04(18), Cl(3)-Ta-C(9) 98.79(16), N(1)-Ta-C(9) 75.0(2), N(2)-Zn-Cl(2) 108.49(15), Cl(2)-Zn-C(9) 117.71(17), Cl(2)-Zn-C(13) 118.51(15).

Experimental Procedure

2: A purple suspension of 4.03 mmol of **1** [4] in pentane (100 mL) saturated with ethene at 20 °C was stirred for 24 h. The resulting green turbid solution was filtered, and the solvent removed from the filtrate in vacuo to give 3.23 mmol of emerald green **2** (80%). The complex can be crystallized from a minimum of pentane. Correct C,H,N analysis.

3: A purple suspension of 12.3 mmol of **1** [4], 7.12 mmol of $ZnCl_2$, and 6.16 mmol of $[Zn(CH_2\textit{t}Bu)_2]$ in Et_2O (100 mL) was stirred at 20 °C for five days. The solvent was removed in vacuo and the sticky residue triturated with hexane. The resulting red powder was extracted with 150 mL of warm (50 °C) benzene. The extract was concentrated in vacuo to ca. 50 mL and layered with pentane (200 mL). After storage of the extract at 20 °C for three days, large red crystals of **3** (9.70 mmol, 79%) were isolated. Correct C,H,N analysis.

Received: January 29, 1991 [Z 4409 IE]
German version: *Angew. Chem. 103* (1991) 1046

[1] A. de Koster, J. A. Kanters, A. L. Spek, A. A. H. van der Zeijden, G. van Koten, K. Vrieze, *Acta Crystallogr. C41* (1985) 893.
[2] D. M. Grove, G. van Koten, R. Zoet, N. W. Murrall, A. J. Welch, *J. Am. Chem. Soc. 105* (1983) 1379.
[3] G. van Koten, J. Terheijden, J. A. M. van Beek, I. C. M. Wehman-Ooyevaar, F. Muller, C. H. Stam, *Organometallics 9* (1990) 903.
[4] H. C. L. Abbenhuis, D. M. Grove, P. van der Sluis, A. L. Spek, G. van Koten, *Recl. Trav. Chim. Pays-Bas 109* (1990) 446.
[5] ^{1}H NMR (200.13 MHz, C_6D_6, 25 °C, TMS): **2**: $\delta = 1.33$ (s, 9H; *t*Bu), 2.12 and 2.97 (dd, 2H; $CH_2\textit{t}Bu$), 2.35, 2.42, 3.27, and 3.45 (s, 12H; NCH_3), 3.10 and 4.06 (m, 2H; H_2C=CH-), 4.22 (m, 1H; H_2C=C*H*-), 3.64, 3.68, 4.49, and 4.61 (d, ^2J(H,H) = 12 Hz, 4H; CH_2N), 7.10 (dd, 2H; *o*-C_6H_3), 7.27 (t, 1H, *p*-C_6H_3). **3**: $\delta = 1.55$ (s, 9H; *t*Bu), 1.75, 1.94, 2.42, and 2.71 (each s, 12H; NCH_3), 2.26, 2.33, 4.43, and 5.03 (d, ^2J(H,H) = 13 Hz, 4H; CH_2N), 6.62 (dd, 2H; *o*-C_6H_3), 6.97 (t, 1H; *p*-C_6H_3). $^{13}C\{^1H\}$ NMR (50.32 MHz, C_6D_6, 25 °C, TMS): **2**: $\delta = 30.5$ ($C(CH_3)_3$), 40.7 ($C(CH_3)_3$), 52.6, 52.8, 54.5, and 55.8 (NCH_3), 58.6 ($CH_2C(CH_3)_3$), 78.3, and 78.8 (CH_2N), 87.8 (H_2C=CH-), 95.2 (H_2C=CH-), 204.7 (Ar, *ipso*-C); **3**: $\delta = 35.2$ ($C(CH_3)_3$), 51.2 ($C(CH_3)_3$), 47.4, 47.9, 48.1, and 54.0 (NCH_3), 67.0, and 71.6 (CH_2N), 175.2 (Ar, *ipso*-C), 295.4 (C*t*Bu).
[6] Crystal structure data for **2**: $C_{19}H_{33}Cl_2N_2Ta$, $M = 541.34$, triclinic space group $P\bar{1}$, $a = 8.3199(14)$, $b = 9.041(2)$, $c = 14.054(3)$ Å, $\alpha = 94.531(19)$, $\beta = 90.748(15)$, $\gamma = 92.856(17)°$, $V = 1052.4(4)$ Å^3, $Z = 2$, $\rho_{calcd} = 1.708$ g cm^{-3}, $\mu(Mo_{K\alpha}) = 54.2$ cm^{-1}. A block-shaped crystal (ca. 0.6 × 0.2 × 0.1 mm) of **2**, mounted on a glass fibre, was used for data collection on an Enraf-Nonius CAD-4 diffractometer at 100 K with Zr-filtered $Mo_{K\alpha}$ radiation ($\theta_{max} = 30.26°$). The structure was solved with automated Patterson methods followed by peak optimalization (SHELXS-86). H-atoms were introduced at calculated positions (C-H = 0.98 Å). An absorption correction was applied (Gaussian integration correction factors range

from 1.69 to 4.51). Full-matrix least-squares refinement of positional and anisotropic thermal parameters of all non-H atoms and an overall isotropic thermal parameter for H atoms converged at a final R value: 0.043 $wR = 0.051$; $w^{-1} = \sigma^2(F)$ for 5267 unique reflections with $I \geq 2.5\sigma(I)$ [9].

[7] H. O. Kalinowski, S. Berger, S. Braun in: *Carbon-13 NMR Spectroscopy*, Wiley, Chichester 1988, p. 549.

[8] Crystal structure data for **3**: $C_{17}H_{28}Cl_3N_2TaZn$, $M = 613.11$, orthorhombic space group $P2_12_12_1$, $a = 9.725(2)$, $b = 10.436(2)$, $c = 20.766(3)$ Å, $V = 2107.5(7)$ Å^3, $Z = 4$, $\rho_{calcd} = 1.932$ g cm^{-3}, $\mu(Mo_{K\alpha}) = 66.8$ cm^{-1}. A red-brown block-shaped crystal (ca. 0.37 × 0.63 × 0.80 mm) of **3**, mounted on a glass fiber, was used for data collection on an Enraf-Nonius CAD-4-diffractometer at 100 K with Zr-filtered $Mo_{K\alpha}$ radiation ($\theta_{max} = 29.4°$) The structure was solved with Patterson and Fourier techniques (SHELXS-86). H-atoms were introduced at calculated positions (C-H = 0.98 Å). An empirical absorption correction was applied (DIFABS). Full-matrix least-squares refinement converged at a final R value: 0.034 $wR = 0.054$; $w^{-1} = \sigma^2(F) + 0.0017(F)^2$ for 4746 unique reflections with $I \geq 2.5\sigma(I)$ [9].

[9] Further details of the crystal structure investigation are available on request from the Director of the Cambridge Crystallographic Data Centre, University Chemical Laboratory, Lensfield Road, GB-Cambridge CB2 1EW (UK), on quoting the full journal citation.

[10] For recent examples of bridging aryl functions see: G. van Koten, *J. Organomet. Chem. 400* (1990) 283; P. R. Markies, G. Schat, O. S. Akkerman, F. Bickelhaupt, W. J. J. Smeets, P. van der Sluis, A. L. Spek, *ibid. 393* (1990) 315.

[11] A. W. Gal, H. van der Heijden, *J. Chem. Soc. Chem. Commun. 1983*, 420.

Coupling of Alkynes with Carbene Ligands to Tungsten-coordinated Cyclopropenes and Their Stereoselective Isomerization to Vinylcarbene Complexes**

By *Helmut Fischer,* Josef Hofmann*, and *Elvira Mauz*

Dedicated to Professor Paul Binger on the occasion of his 60th birthday

Reactions of cyclopropenes with transition metals find many uses in organic synthesis.[1] For some of the transition metal-catalyzed reactions the sequence cyclopropene → cyclopropene complex → vinylcarbene complex (or metallacyclobutene) → organic product has been postulated.[2] Both cyclopropene complexes[3, 4] as well as vinylcarbene complexes[4, 5] and metallacyclobutenes[6] have been prepared from transition metal complexes and cyclopropenes. So far however, it has not been possible to verify the step cyclopropene complex → vinylcarbene complex.

Cyclopropene complexes are generally prepared by ligand substitution. Their synthesis from carbene complexes and alkynes has thus far never been reported, though the intermediary formation of a cyclopropene in the reaction of 2-butyne with a cationic benzylidenedicarbonyl(cyclopentadienyl)iron complex has been postulated on the basis of the reaction products.[7] We now report the synthesis of isolable cyclopropene complexes by addition of alkynes to carbene complexes and the demonstration of stereoselective intramolecular ring opening to give vinylcarbene complexes.

The benzylidene complex **1a**[8] reacts at −80 °C in one to two hours with an equimolar amount of phenylacetylene to give the cyclopropene complex **2a**. This is stable only below ca. −40 °C. Above −30 °C, **2a** rapidly isomerizes in solution to the vinylcarbene complex **3a**. Upon reaction of **1a** with

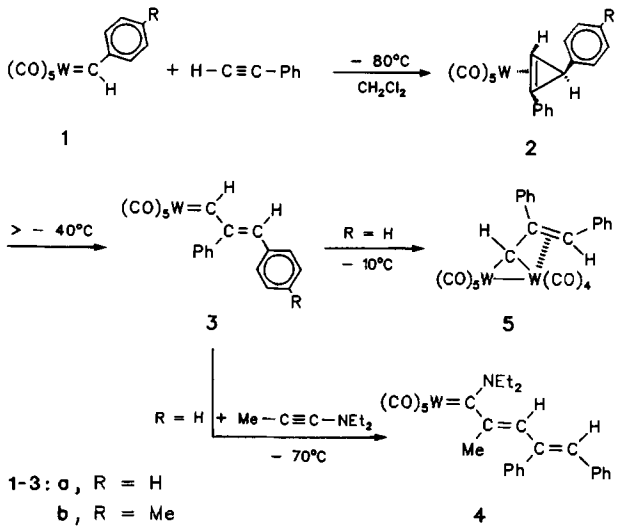

phenylacetylene on a preparative scale, mixtures of **2a** (major product) and **3a** are generally obtained which are difficult to separate. In contrast to **2a** however, **3a** already reacts rapidly at −70 °C with diethylpropynylamine to give **4**. The compounds **2a** and **4** can be separated chromatographically at −70 °C, hence **2a** is obtainable in pure form in this way.

The structure of the cyclopropene complex **2a** could be confirmed spectroscopically. The IR spectrum indicated a pentacarbonyl complex. The benzylidene-H NMR signal is shifted upfield by more than 14 ppm compared to that in **1a**, while the signal of the original sp-CH atom of phenylacetylene is shifted ca. 2 ppm downfield. The assignments are supported by the spectrum of [D]**2a** (obtained from **1a** and Ph–C≡C–D). The ^{13}C-NMR spectrum of **2a** shows, in addition to the signals for the CO substituents and the two phenyl groups, signals for three further carbon atoms between $\delta = 34$ and 65, of which two couple with the tungsten atom (J(W,C) = 16 and 19 Hz). Signals at low field ($\delta > 210$), characteristic for carbene complexes, are absent.

According to the NMR spectra the rearrangement of **2a** to **3a** is stereoselective; carbene complexes isomeric with **3a** could not be detected. The structure of **3a** follows unequivocally from the characteristic downfield position of the carbene-H and carbene-C NMR signals ($\delta = 16.64$ and 331.1, resp.). Above ca. −10 °C, **3a** reacts further to give **5** (major product) and two other, so far not fully characterized complexes. The formation of carbene-bridged dinuclear complexes such as **5** is typical for the thermolysis of strongly electrophilic carbene complexes in inert solvents.[8b, 10] X-ray structure analyses were carried out on the complexes **4**, **5** (Fig. 1)[9] and **6** (see below). In all compounds the two phenyl groups are *cis* oriented.

When a solution of **2a** in the presence of triphenylphosphane is warmed from −70 °C to −10 °C, the ylide complex **6** is formed. It follows, therefore, that the rearrangement **2a** → **3a** most likely proceeds intramolecularly. In the case of a dissociative process (cleavage of the cyclopropene and attack of the resulting pentacarbonyltungsten fragment at a C–C σ-bond of the cyclopropene with ring opening to give

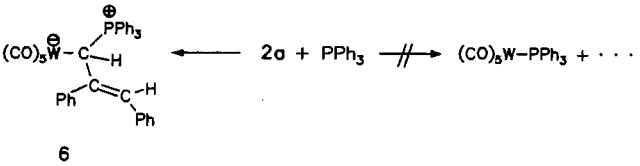

[*] Prof. Dr. H. Fischer, Dr. J. Hofmann, Dipl.-Chem. E. Mauz
Fakultät für Chemie der Universität
Postfach 55 60, W-7750 Konstanz 1 (FRG)

[**] This work was supported by the Stiftung Volkswagenwerk, the Fonds der Chemischen Industrie, and the Land Baden-Württemberg (Project: Metal-Centered Substrate Transformations).

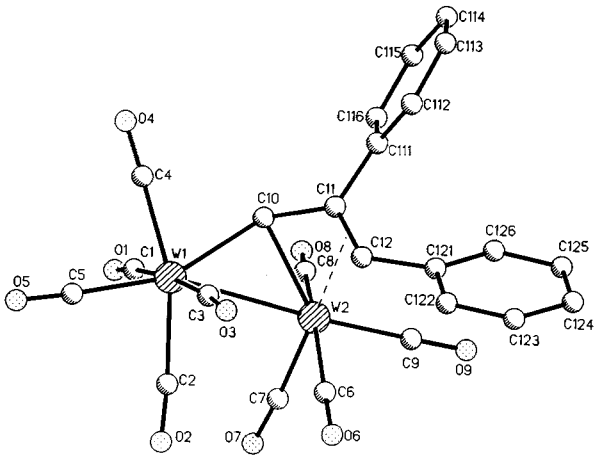

Fig. 1. Structure of **5** in the crystal (H atoms omitted). Important distances [Å], angles and torsion angles [°], standard deviations in brackets: W1–W2 3.119(1), W1–C10 2.238(8), W2–C10 2.216(8), W2–C11 2.417(9), W2–C12 2.459(8), C10–C11 1.458(10), C11–C12 1.421(10); W1–C10–W2 88.9(3), W1–W2–C10 45.9(2), W2–C10–C11 79.3(5), C10–C11–C12 116.4(7); W1–W2–C10–C11 135.6(5), W2–C10–C11–C12 −55.6(7), C10–C11–C12–C121 164.3(8).

3a) the formation of pentacarbonyl(triphenylphosphane)-tungsten would be expected. This, however, could not be detected. **6** is apparently formed by nucleophilic addition of PPh_3 to **3a**. (Phosphanes are frequently used to trap unstable carbene complexes.[11]).

Also the *p*-Me-substituted complex **1b** reacts analogously to **1a** with phenylacetylene. **2b** is slightly more stable than **2a** and rearranges somewhat more slowly to **3b**. Considerably more rapid, however, is the ring opening in the cyclopropene complex formed by addition of *p*-methylphenylacetylene to **1a**; this complex has been detected NMR spectroscopically only.

Formally, **3** is formed by insertion of the C≡C bond of the alkyne into the W=C bond of **1**. Insertion of electron-rich alkynes into metal–carbene carbon bonds have long been known[11, 12] and have been studied in detail.[13] However, the regioselectivity of these insertions and that of those described here are inverse. This shows that insertions of triple bonds into metal–carbene carbon bonds in coordinatively saturated complexes can proceed via several associative mechanisms.

Experimental

The reactions can be carried out both in CH_2Cl_2 as well as in CH_2Cl_2/pentane. The structures of all the complexes, with the exception of **3a**, were confirmed spectroscopically (IR, ^1H, ^{13}C-NMR) and by elemental analyses. **3a** was characterized only spectroscopically. X-ray structural analyses were carried out on complexes **4**–**6**.

2a: ^1H NMR (CD_2Cl_2, −70 °C): δ = 2.81 (s, sp^3-CH), 5.20 (s, =CH), 6.9–7.5 (m, Ph); ^{13}C NMR (CD_2Cl_2, −70 °C): δ = 34.0 (sp^3-C), 46.4 (J(W,C) = 19 Hz, =CH), 64.7 (J(W,C) = 16 Hz, =CPh), 125.5, 126.1, 127.7, 128.4, 131.9, 142.6 (Ph), 195.3 (J(W,C) = 127 Hz, *cis*-CO), 205.1 (J(W,C) = 135 Hz, *trans*-CO); IR (hexane): $\tilde{\nu}$(CO) [cm^{-1}] = 2089 m, 1995 s, 1967 s, 1956 vs.

3a: ^1H NMR (CD_2Cl_2, −40 °C): δ = 7.78 (s, $C_\beta H$), 6.9–7.7 (m, Ph), 16.64 (s, W=CH); ^{13}C NMR (CD_2Cl_2, −40 °C): δ = 149.2 (C_α), 165.7 (C_β), 196.7 (*cis*-CO), 216.1 (*trans*-CO), 331.1 (W=C); IR (hexane): $\tilde{\nu}$(CO) [cm^{-1}] = 2072 s, 1964 vs.

4: Yield 60%; m.p. 102 °C; ^1H NMR ($CDCl_3$): δ = 1.33, 1.40 (each t, J = 7.2 Hz, CH_2CH_3), 1.52 (s, =CCH_3), 3.63 (dq, J = 7.0, 3.1 Hz, 2H, CH_2), 4.02 (dq, J = 13.2, 6.7 Hz, 1H, NCH_2), 4.17 (dq, J = 13.2, 7.3 Hz, 1H NCH_2), 5.57 (s, =CH), 6.56 (s, benzylidene-H), 6.9–7.5 (m, Ph); ^{13}C NMR ($CDCl_3$, room temperature): δ = 14.0, 14.9, 16.2 (CH_3), 47.0, 55.6 (CH_2), 127.4, 127.8, 128.8, 129.2, 129.3, 131.5, 136.8, 140.4 (Ph), 121.9, 126.7, 138.6, 148.2 (=C), 198.6 (J(W,C) = 128 Hz, *cis*-CO), 202.9 (J(W,C) = 126 Hz, *trans*-CO), 257.0 (J(W,C) = 90 Hz, W=C): IR (hexane): $\tilde{\nu}$(CO) [cm^{-1}] = 2063 m, 1969 w, 1934 vs, 1917 s.

5: Yield 25%; m.p. 129 °C; ^1H NMR ($CDCl_3$, 30 °C): δ = 4.27 (s, μ-CH), 6.9–7.4 (m, Ph), 9.85 (s, =CH); ^{13}C NMR ($CDCl_3$, 0 °C): δ = 93.2 (=C), 126.0 (=C), 128.3, 128.7, 128.9, 129.1, 130.0, 130.5, 134.8, 140.8 (Ph), 161.3 (μ-C), 195.1 (J(W,C) = 122 Hz, CO), 200.0 (CO), 206.6 (br, CO); IR (hexane): $\tilde{\nu}$(CO) [cm^{-1}] = 2087 s, 2049 vs, 2008 s, 2000 s, 1982 vs, 1952 s, 1930 m.

6: Yield 65%; decomp. above 80 °C; ^1H NMR (CD_2Cl_2, −70 °C): δ = 3.28 (d, ^2J(P,H) = 12.5 Hz, WCH), 6.51 (d, J(P,H) = 4.0 Hz), 6.6–8.0 (m, Ph); IR (hexane): $\tilde{\nu}$(CO) [cm^{-1}] = 2059 m, 1962 w, 1915 vs, 1900 s.

Received: February 19 (1991) [Z 4553 IE]
German version: *Angew. Chem. 103* (1991) 1013

[1] a) P. Binger, H. M. Büch, *Top. Curr. Chem. 135* (1987) 77; b) M. S. Baird, *ibid. 144* (1988) 137; c) B. Halton, M. G. Banwell in Z. Rappoport (Ed.): *The Chemistry of the Cyclopropyl Group*, Wiley, Chichester 1987, p. 1223–1339.
[2] Cf., for example, P. Binger, B. Biedenbach, *Chem. Ber. 120* (1987) 601.
[3] a) J. P. Visser, A. J. Schipperijn, J. Lukas, D. Bright, J. J. deBoer, *Chem. Commun. 1971*, 1266; b) S. Fredericks, J. L. Thomas, *J. Am. Chem. Soc. 100* (1978) 350; c) H. Lehmkuhl, R. Paul, C. Krüger, Y.-H. Tsay, R. Benn, R. Mynott, *Liebigs Ann. Chem. 1981*, 1147.
[4] P. Binger, P. Müller, R. Benn, R. Mynott, *Angew. Chem. 101* (1989) 647; *Angew. Chem. Int. Ed. Engl. 28* (1989) 610.
[5] a) J. Klimes, E. Weiss, *Angew. Chem. 94* (1982) 207; *Angew. Chem. Int. Ed. Engl. 21* (1982) 205; b) T. Valeri, F. Meier, E. Weiss, *Chem. Ber. 121* (1988) 1093.
[6] a) R. C. Hemond, R. P. Hughes, D. J. Robinson, A. L. Rheingold, *Organometallics 7* (1988) 2239; b) R. P. Hughes, M. E. King, D. J. Robinson, J. M. Spotts, *J. Am. Chem. Soc. 111* (1989) 8919.
[7] M. Brookhart, M. B. Humphrey, H. J. Kratzer, G. O. Nelson, *J. Am. Chem. Soc. 102* (1980) 7802.
[8] a) C. P. Casey, S. W. Polichnowski, A. J. Shusterman, C. R. Jones, *J. Am. Chem. Soc. 101* (1979) 7282; b) H. Fischer, S. Zeuner, K. Ackermann, *J. Chem. Soc. Chem. Commun. 1984*, 684.
[9] **5**: monoclinic, $P2_1/c$, a = 15.288(3), b = 10.004(3), c = 16.559(4) Å, β = 107.94(2)°, V = 2409(1) Å^3, Z = 4, $\mu(Mo_{K\alpha})$, ϱ_{calcd} = 2.24 g cm^{-3}, Nicolet R3m Four-circle diffractometer. Data collection: T = 300 K, Wykoff scan, ω = 1.5–29.3° min^{-1}, 4517 independent reflections with 4.0 < 2θ < 51.0°, 3586 with $|F_0| > 6\sigma(F_0)$. Solution of structure by direct methods (SHELXTL PLUS). R = 0.036, R_w = 0.049. Residual electron density 1.8 eÅ^{-3}. Further details of the crystal structure investigation are available on request from the Fachinformationszentrum Karlsruhe, Gesellschaft für wissenschaftlich-technische Information mbH, W-7514 Eggenstein-Leopoldshafen 2 (FRG) on quoting the depository number CSD-55336, the names of the authors, and the journal citation.
[10] H. Fischer, S. Zeuner, K. Ackermann, J. Schmid, *Chem. Ber. 119* (1986) 1546.
[11] Cf. K. H. Dötz, H. Fischer, P. Hofmann, F. R. Kreissl, U. Schubert, K. Weiss (Eds.): *Transition Metal Carbene Complexes*, Verlag Chemie, Weinheim 1983.
[12] K. H. Dötz, C. G. Kreiter, *J. Organomet. Chem. 99* (1975) 309.
[13] H. Fischer, K. H. Dötz, *Chem. Ber. 113* (1980) 193.

Ammoniumyl Salt-Induced Diels-Alder Reaction of Ketenes—Control of [2 + 2] vs. [4 + 2] Selectivity **

By *Michael Schmittel** and *Heinke von Seggern*

Dedicated to Professor Horst Prinzbach on the occasion of his 60th birthday

[2 + 2]-Cycloaddition products are formed exclusively with a remarkable periselectivity in the thermal reaction of ketenes with dienes.[1] Although the Diels-Alder products

[*] Dr. M. Schmittel, Dipl.-Chem. H. von Seggern
Institut für Organische Chemie und Biochemie der Universität
Albertstrasse 21, W-7800 Freiburg (FRG)

[**] Electron Transfer Catalyzed Reactions, Part 1. This work was supported by the Deutsche Forschungsgemeinschaft, the Land Baden-Württemberg, the Wissenschaftliche Gesellschaft Freiburg, and the Fonds der Chemischen Industrie (*H.v.S.*). We thank Prof. Dr. *C. Rüchardt* for continued support of our studies and *R. Burth* and *C. Wöhrle* for help with the preparative work. Thanks are also due to Prof. *Dr. H. Fritz* and Dr. *D. Hunkler* for recording the ^1H-NMR-NOE difference spectra and for help with their interpretation.

are as a rule thermodynamically more stable they are obtained only in very few special cases.[2] An explanation for this periselectivity has been given by *Woodward* and *Hoffmann*:[3] with the *antara,supra* [2 + 2] cycloaddition, a route with low activation energy is available for ketenes and dienes. Studies by *Bauld*[4] in particular have recently shown that both symmetry-allowed as well as symmetry-forbidden cycloadditions can be accelerated considerably by radical-cation catalysis. We now describe the application of this method to ketene cycloadditions so as to realize activation of electron-rich and hence thermally unreactive ketenes and to steer the selectivity in the direction of the [4 + 2] cycloadducts.

The electron-rich arylmethylketenes **1** (E_p = 0.91 V) and **2** (E_p = 1.11 V) were chosen as model compounds.[5] Both ketenes are sufficiently stable towards homodimerization

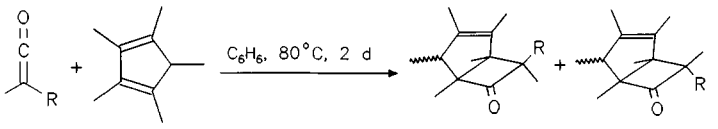

1 2 3 4a 4b 5a 5b

1, 4 : R = *p*-$MeOC_6H_4$; 2, 5 : R = *p*-MeC_6H_4

under suitable conditions and can therefore be obtained in high purity. Since the oxidation potentials of the reactants have to be matched for radical-cation catalyzed, crossed cycloadditions,[6] pentamethylcyclopentadiene **3** (E_p = 0.87 V) was chosen as diene. As electron-transfer catalyst we chose tris(*p*-tolyl)ammoniumyl hexafluoroantimonate **S1** ($E_{1/2}$ = 0.76 V).[7]

$(p\text{-}MeC_6H_4)_3N^{\bullet\oplus}\ SbF_6^{\ominus}$

S1

The slow thermal reaction (2 d, 80 °C) of **1** or **2** with **3** to give the cyclobutanones **4** (54%)[8] and **5** (37%) confirms the low reactivity of the ketenes. As in related systems, the *endo* isomers (**4a**:**4b** = 53:1; **5a**:**5b** = 27:10) are preferentially formed.

The ammoniumyl-salt induced reactions of **1** or **2** with **3** proceed orders of magnitude more rapidly, and are complete within a few minutes at 0 °C[9] (Table 1, Scheme 1). The Diels-Alder adducts **6** and **7**, respectively, are formed selectively as main products;[10] not even trace amounts of the cyclobutanones **4** and **5** can be detected. Surprisingly, additional dimers are formed in small yields as by-products

Table 1. Cycloaddition products in the ammoniumyl salt **S1** induced reaction of the ketenes **1** and **2** with the diene **3** in the molar ratio 1:1.

Ketene	Mol-% S1	*t* [min]	Products [a]
1	25	5	**6a** (31%), **6b** (11%), **8** (11%)
1	25	2	**6a** (24%), **6b** (10%), **8** (8%)
1	25	0.5	**6a** (18%), **6b** (6%), **8** (4%)
1	25 [b]	10	**6a** (21%), **6b** (8%), **8** (18%)
1	50 [c]	20	**6a** (18%), **6b** (5%), **8** (n.d.)
2	50 [d]	5	**7a** (30%), **7b** (9%), **9** (<1%)
2	50	5	**7a** (14%), **7b** (6%), **9** (6%)

[a] Only unchanged ketene, trapped as methyl ester, could be identified as sole non-polymeric product (>5%); accuracy ± 2%; n.d.=not detected. [b] Addition of 250 mol-% tri-*p*-tolylamine. [c] Addition of 55 mol-% **10**. [d] Molar ratio ketene:diene=5:1.

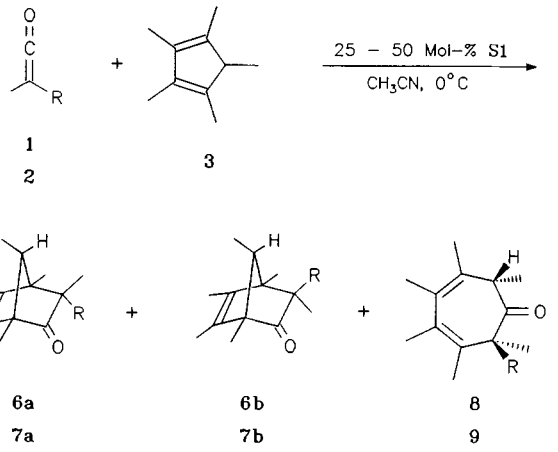

1 2 3 6a 7a 6b 7b 8 9

Scheme 1. **1**, **6**, **8**: R = *p*-$MeOC_6H_4$; **2**, **7**, **9**: R = *p*-MeC_6H_4.

which could be identified as cycloheptadienones **8** and **9**, respectively.[11]

To establish whether radical cation or acid catalysis is involved in this reaction we investigated the influence of 2,6-di-*tert*-butyl pyridine **10** on the product formation.[12, 13] The addition of **10** to the reaction of **1** with **3** completely suppresses the formation of **8**, whereas in the case of **6** only the yield is somewhat lower. This rules out acid catalysis for the formation of **6** and **7**, whereas **8** and **9** are apparently formed via acid catalysis, as could be additionally documented by control experiments.[14]

In analogy to related reactions,[4] this cycloaddition could be explained in terms of a radical cation catalyzed chain mechanism. However, here, the chains must be very short. A problem of this reaction is apparently the high acidity[13] of the radical cations occurring as intermediates, so that in end effect acid catalyzed reactions are always taking place at the same time. Naturally these side reactions can be prevented by addition of **10**; however, added base also favors deprotonation of the radical cations and removes them from the cycloaddition.

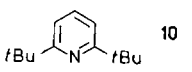

10

The Diels-Alder adducts **6** and **7** obtained selectively in the presence of **S1** are formed with marked preference for the *endo*-isomers (**6a**:**6b** = 3:1; **7a**:**7b** = 3:1), as is also observed in other radical cation catalyzed Diels-Alder reactions.[4] Remarkably, the reaction is extremely facioselective: in each case only the *anti*-isomer could be detected NMR spectroscopically. This demonstrates once again that radical cation catalyzed reactions can proceed very selectively despite low activation energies.

Investigations by *Bauld* et al. have shown that radical cation catalyzed Diels-Alder reactions are not necessarily concerted, but often proceed stepwise.[15] Radical catalyzed cyclobutanation and 1,3-sigmatropic ring expansion take place consecutively. This raises the question of whether cyclobutanones also occur as intermediates in the formation of **6** and **7**. A detailed study by *Schwarz* et al.[16] of the reaction of the ethenone radical cation with ethylene in the gas phase clearly indicates, in contrast to results of a study by *Gross* et al.,[17] that the cyclobutanone radical cation is no minimum on the energy hypersurface along the reaction coordinate. Consequently, a concerted mechanism is plausible for the cycloaddition step leading to formation of **6** and **7**.

To answer the question concerted/stepwise the *endo*- and *exo*-vinylcyclobutanones **4a** and **4b** were allowed to react

under the conditions of the ammoniumyl salt-initiated cycloaddition. In order to avoid acid-catalyzed reactions of the vinylcyclobutanones, as have been described by *Lee-Ruff* et al.,[18] the reaction was carried out in the presence of 50 mol-% **S1** and 55 mol-% **10**. After 5 min the unchanged reactants **4** were recovered quantitatively. Hence, the cyclobutanones **4** cannot be intermediates of the ammoniumyl salt-initiated Diels-Alder reaction of **1** or **2** and **3**.

The results reported here show that Diels-Alder adducts can be obtained selectively via the ammoniumyl salt-initiated cycloaddition of ketenes and dienes. This mode of reaction ideally complements the thermal chemistry of the ketenes. Further studies are in progress concerning the reaction mechanism and the preparative scope of the reaction as well as the control of selectivity.

Received: February 19, 1991 [Z 4455 IE]
German version: *Angew. Chem. 103* (1991) 981

CAS Registry numbers:
1, 134419-96-8; **2**, 134419-97-9; **3**, 4045-44-7; **4**, 134419-98-0; **5**, 134419-99-1; **6a**, 134420-00-1; **6b**, 134420-04-5; **7a**, 134420-01-2; **7b**, 134420-05-6; **8**, 134420-02-3; **9**, 134420-03-4; **10**, 585-48-8; **S1**, 78090-05-8.

[1] R. Huisgen, P. Otto, *Chem. Ber. 102* (1969) 3475.
[2] H. Mayr, U. W. Heigl, *J. Chem. Soc. Chem. Commun. 1987*, 1804.
[3] R. B. Woodward, R. Hoffmann, *Angew. Chem. 81* (1969) 797; *Angew. Chem. Int. Ed. Engl. 8* (1969) 781.
[4] N. L. Bauld, *Tetrahedron 45* (1989) 5307, and references cited therein.
[5] The oxidation potentials E_p (versus SCE) were determined by cyclic voltammetry in acetonitrile at 100 mVs^{-1}: 1 mM substrate, 0.1 M tetra-*n*-butylammonium hexafluorophosphate, ferrocene as reference.
[6] J. Mlcoch, E. Steckhan, *Tetrahedron Lett. 28* (1987) 1081.
[7] E. Steckhan, *Top. Curr. Chem. 142* (1987) 1.
[8] The cyclobutanones were identified on the basis of the spectroscopic (^{1}H-NMR difference-NOE, ^{13}C NMR, IR, MS) and elemental analysis data. The characteristic bands at 1763–1765 cm^{-1} in the IR spectra confirm the cyclobutanone structures.
[9] A solution of **1** or **2** and **3** in acetonitrile (in each case 0.5 M) was treated within a maximum of 2 min at 0° C under argon with a 0.05–0.25 M solution of **S1** in acetonitrile. After expiration of the reaction time the mixture was quenched with methanolate solution.
[10] The stereochemistry of the products was made plausible on the basis of ^{1}H-NMR difference NOE spectra: ^{1}H NMR (250 MHz, $CDCl_3$): **6a**: δ = 0.76 (q, J = 1.3 Hz, 3H), 0.82 (d, J = 6.5 Hz, 3H), 1.08 (s, 3H), 1.14 (s, 3H), 1.40 (s, 3H), 1.54 (q, J = 1.3 Hz, 3H), 2.26 (q, J = 6.5 Hz, 1H), 3.75 (s, 3H), 6.72 (d, J = 9.1 Hz, 2H), 6.83 (d, J = 9.1 Hz, 2H); **6b**: δ = 0.74 (d, J = 6.5 Hz, 3H), 0.98 (s, 3H), 1.14 (s, 3H), 1.35 (s, 3H), 1.52 (q, J = 1.3 Hz, 3H), 1.72 (q, J = 1.3 Hz, 3H), 2.25 (q, J = 6.5 Hz, 1H), 3.78 (s, 3H), 6.79 (d, J = 9.1 Hz, 2H), 6.96 (d, J = 9.1 Hz, 2H); **7a**: δ = 0.70 (q, J = 1.3 Hz, 3H), 0.82 (d, J = 6.5 Hz, 3H), 1.08 (s, 3H), 1.13 (s, 3H), 1.40 (s, 3H), 1.51 (q, J = 1.3 Hz, 3H), 2.25 (s, 3H), 2.27 (q, J = 6.5 Hz, 1H), 6.78 (d, J = 9.1 Hz, 2H), 6.98 (d, J = 9.1 Hz, 2H); **7b**: δ = 0.70 (d, J = 6.5 Hz, 3H), 0.97 (s, 3H), 1.13 (s, 3H), 1.34 (s, 3H), 1.51 (q, J = 1.3 Hz, 3H), 1.70 (q, J = 1.3 Hz, 3H), 2.25 (q, J = 6.5 Hz, 1H), 2.25 (s, 3H), 6.72 (d, J = 9.1 Hz, 2H), 7.04 (d, J = 9.1 Hz, 2H); ^{13}C NMR (100 MHz): **6a**: δ = 7.6, 9.3, 10.0, 10.5, 12.1, 20.5, 55.0, 55.3, 56.7, 57.8, 64.8, 112.8, 126.9, 128.5, 136.2, 144.4, 157.8, 217.1; **6b**: δ = 7.1, 8.9, 10.2, 11.6, 13.3, 22.8, 55.3, 55.8, 56.9, 57.3, 64.1, 113.0, 129.4, 129.9, 134.9, 143.7, 157.8, 220.3; **7a**: δ = 7.5, 9.3, 10.0, 10.5, 12.2, 20.5, 22.7, 56.7, 56.8, 57.8, 64.9, 127.4, 128.4, 135.8, 137.0, 137.3, 144.2, 217.8; IR (CCl_4): **6a**: $\tilde{\nu}$ = 1733 cm^{-1}; **6b**: $\tilde{\nu}$ = 1733 cm^{-1}; **7a**: $\tilde{\nu}$ = 1734 cm^{-1}; **7b**: $\tilde{\nu}$ = 1734 cm^{-1}.
[11] The structures of the analytically pure cycloheptadienones **8** and **9** were elucidated by the usual spectroscopic methods and by reduction to the cycloheptadienols.
[12] D. W. Reynolds, K. T. Lorenz, H.-S. Chiou, D. J. Bellville, R. A. Pabon, N. L. Bauld, *J. Am. Chem. Soc. 109* (1987) 4960.
[13] P. G. Gassman, D. A. Singleton, *J. Am. Chem. Soc. 106* (1984) 7993.
[14] Reaction of **1** or **2** and **3** in the presence of 170 mol% CF_3SO_3H afforded **8** (58%) and **9** (59%) as sole cross dimers. This hitherto unknown reaction pathway opens an entry to highly substituted cycloheptadienones.
[15] T. Kim, R. J. Pye, N. L. Bauld, *J. Am. Chem. Soc. 112* (1990) 6285.
[16] N. Heinrich, W. Koch, J. C. Morrow, H. Schwarz, *J. Am. Chem. Soc. 110* (1988) 6332.
[17] C. Dass, M. L. Gross, *J. Am. Chem. Soc. 106* (1984) 5775.
[18] E. Lee-Ruff, A. C. Hopkinson, L. H. Dao, *Can. J. Chem. 59* (1981) 1675; V. P. Abegg, A. C. Hopkinson, E. Lee-Ruff, *ibid. 56* (1978) 99; L. H. Dao, A. C. Hopkinson, E. Lee-Ruff, *Tetrahedron Lett. 1978*, 1413.

The Structure of the Trimethylenemethane Dianion and the Question of Y-Aromaticity**

By *Alberto Gobbi, Preston J. MacDougall,* and *Gernot Frenking**

The facile formation of trimethylenemethane dianion **1** from isobutene and butyllithium[1] has been explained in terms of a novel type of conjugative stabilization ("Y-aromaticity")[2] which is supposedly exhibited in the D_{3h} form **1a**[2, 3] (Fig. 1).

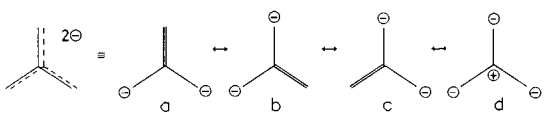

1a

Fig. 1. Resonance formulas for trimethylenemethane dianion **1a** (in the D_{3h} form).

Agranat and *Skancke*[3a] studied several isomers of $C_4H_6^{2\ominus}$ using ab initio methods and reported that **1a** was the most stable conformation. The stability of **1a** has also been attributed to favorable charge alternation.[4] Both explanations have been dismissed recently by *Wiberg*,[5] who studied the effect of replacing the terminal methylene groups in **1a** with oxygen.

We now report that all previous ab initio studies of **1**[2–5] have been concerned with a nonequilibrium geometry.[1,7] Dianion **1** has a nonplanar geometry with strongly pyramidal CH_2 groups. Ab initio calculations[6] show that the force-constant matrix of **1a** has three or four negative eigenvalues depending on the theoretical level![7] Thus, **1a** is a higher order saddle point on the $C_4H_6^{2\ominus}$ potential-energy surface and not "the most stable conformation".[3a] Relaxation of the symmetry constraint yields two conformations (**1b** and **1c**) which are true minima. The calculated structural data of **1a**, **1b**, and **1c** are shown in Table 1.

The methylene groups in the conformational minima **1b** and **1c** are strongly pyramidalized. The four carbon nuclei are nearly coplanar. The small deviation of the torsion angle C2-C1-C3-C4 from 180° is 2.9° in **1b** and 9.2° in **1c** (Table 1). The dihedral angle α between plane containing the CH_2

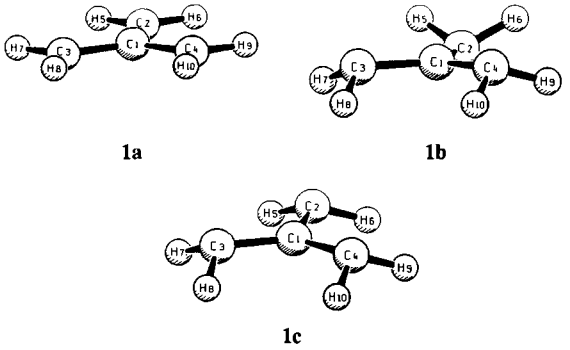

1a **1b**

1c

[*] Prof. Dr. Frenking, A. Gobbi
Fachbereich Chemie der Universität
Hans-Meerwein-Strasse, W-3550 Marburg (FRG)
Dr. P. J. MacDougall
Department of Chemistry, Texas A&M University
College Station, Texas 77843

[**] This work was supported by the Deutsche Forschungsgemeinschaft, the Fonds der Chemischen Industrie, and the computer companies Silicon Graphics and Convex.

Table 1. Calculated geometries for **1a**, **1b**, and **1c** at MP2/6-31G(d), showing bond lengths [Å] and angles [°]. Relative energies E_{rel} at MP2/6-31 + +G(d)//HF/6-31G(d) in kcal mol^{-1}. The values in parentheses are obtained at HF/6-31G(d). The partial charges q, obtained from an NBO analysis [8], are given at HF/6-31G(d).

	1a (D_{3h})	**1b** (C_s)	**1c** (C_{3v})
C1-C2	1.434 (1.431)	1.451 (1.451)	1.447 (1.445)
C1-C3	1.434 (1.431)	1.444 (1.442)	1.447 (1.445)
C2-C1-C3	120.0 (120.0)	119.8 (119.8)	119.8 (119.9)
H5-C2-H6	116.5 (116.6)	109.1 (109.0)	110.1 (110.3)
H7-C3-H8	116.5 (116.6)	110.0 (110.1)	110.1 (110.3)
C2-C1-C3-C4	180.0 (180.0)	177.1 (177.9)	170.8 (173.1)
α_1 [a]	0.0 (0.0)	48.5 (47.4)	42.1 (40.8)
α_2 [b]	0.0 (0.0)	44.5 (43.0)	42.1 (40.8)
E_{rel} [c]	4.3 (7.8)	0.0 (0.0)	2.0 (2.5)
i [d]	4 (3)	0 (0)	0 (0)
q(C1)	0.087	0.130	0.128
q(C2)	−0.923	−0.922	−0.913
q(C3)	−0.923	−0.911	−0.913
q(H5)	0.114	0.101	0.102
q(H7)	0.114	0.105	0.102
q(H9)	0.114	0.101	0.102

[a] Dihedral angle between the planes H5-C2-H6 and C2-C3-C4. [b] Dihedral angle between the planes H7-C3-H8 and C2-C3-C4. [c] Calculated total energy for **1b** is − 155.21544 Hartree at MP2/6-31 + +G(d)//HF/6-31G(d); at HF/6-31G(d) the total energy of **1b** is − 154.55975 Hartree. [d] Number of imaginary frequencies.

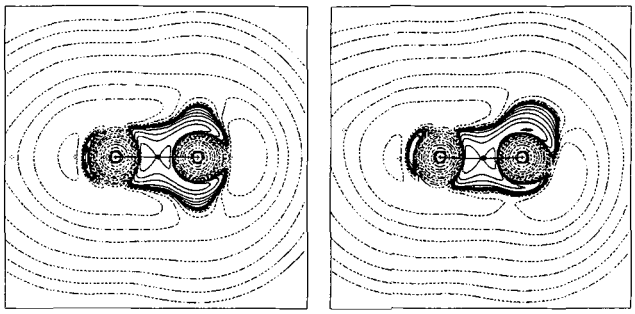

Fig. 2. Contour line diagrams of the Laplacian of the electronic charge distribution $-\nabla^2\rho(r)$ of **1a** and **1b** in the vertical (σ_v) plane. Dashed contour lines are in regions of charge depletion and solid lines in regions of charge concentration. The solid line connecting the atoms indicates the bond axis, filled circles denote bond critical points. In both plots, the central carbon C1 is on the left and C2 on the right.

groups and that defined by the terminal carbon atoms is 48.5° and 44.5° in **1b** and 42.1° in **1c**. The natural bond orbital (NBO) analysis[8] of the wave function shows the following hybridizations at carbon in the C–H bonds of **1b**: $sp^{2.93}$ (C2–H5), $sp^{2.83}$ (C3–H7), $sp^{2.84}$ (C3–H8). In **1c**, the carbon atoms are $sp^{2.46}$ hybridized in the C–H bonds. This indicates hybridization tending towards sp^3 at the terminal carbon atoms. In agreement with the change in hybridization from sp^2 towards sp^3, the C–C and C–H bonds are longer in **1b** and **1c** than in **1a**. The NBO analysis also suggests that the optimal Lewis-type structure for **1a** has nine bond orbitals (three C–C and six C–H bonds) and three lone-pair orbitals occupied by 1.75 electrons (C3, C4) and 1.77 electrons (C2). However, an occupation of 0.72 electrons is calculated for a non-Lewis type p(π) orbital at C1, which indicates strong π-electron donation from the lone-pair electrons into the formally empty p(π) orbital at C1. Thus, the "best" resonance form for **1** is *d* in Figure 1, but with pyramidal CH_2 groups.

Details of the C–C binding type and the electronic structure of **1a** and **1b** are revealed by the analysis of the one-electron density distribution $\rho(r)$ and its associated Laplacian $\nabla^2\rho(r)$.[12]

Figure 2 shows the contour lines of $\nabla^2\rho(r)$ for the C–C bonds of **1a** and **1b**.[13]

Inspection of the diagrams shown in Figure 2 clearly shows that the π-electron distribution of the C–C bond in **1a** and **1b** is shifted toward the terminal carbon atom. There is depletion ($\nabla^2\rho(r) > 0$, dashed lines) rather than charge concentration in the π-electron area at the central carbon atom. The Laplacian distribution for **1b** shows the existence of a nonbonded charge concentration, which is interpreted as a lone pair at the terminal carbon atom.[12] The shift in the charge distribution is also revealed by the location of the C–C-bond critical points r_b,[14] which are shown as dots in Figure 2.[12] In **1a**, r_b is located 0.755 Å from the central carbon atom and 0.679 Å from the terminal C. In **1b**, the corresponding values are 0.777 Å and 0.675 Å.[13] Thus, the C–C bonds in **1a** and **1b** are characterized by a strong shift of σ density towards the central carbon, with a concomitant counter-migration of the π density to the terminal carbons. This σ/π equilibrium has been observed and rationalized in allyl ions.[15]

The results of the geometry optimization indicate that **1** tries to adopt a structure in which the repulsion of electronic charge is minimized. In **1b**, two lone pairs are on one side of the plane spanned by the carbon atoms and one lone pair is one the other side.[11] In **1c**, all three lone pairs are on the same side of the plane. Consequently, **1b** is more stable than **1c** by 2.0 kcal mol^{-1} (Table 1). The minima are only 4.3 kcal mol^{-1} (**1b**) and 2.3 kcal mol^{-1} (**1c**) lower in energy than **1a**, which indicates a very low barrier for interconversion.

The trimethylenemethane dianion **1** is more stable than its isomeric forms, *cis*- and *trans*-butadiene dianions **2** and **3**, albeit much less than was previously reported.[3] Also, **2** and **3** adopt nonplanar geometries where the methylene groups are pyramidalized with the hydrogen atoms on the same (**2a**, **3a**) or on opposite (**2b**, **3b**) sides of the plane spanned by the carbon atoms (Table 2). Planar **2** is calculated with two (three in case of planar **3**) negative eigenvalues of the force-constant matrix (HF/6-31G(d)). The four conformational minima **2a**, **2b**, **3a**, and **3b** are 6.1–7.3 kcal mol^{-1} higher in energy than **1b** (Table 2). Previous studies, which considered

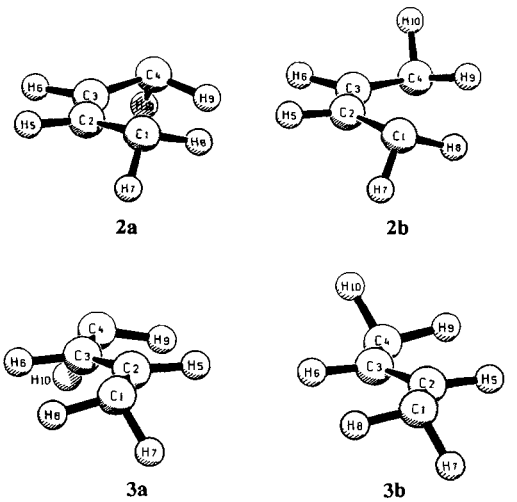

Table 2. Calculated structures for **2a**, **2b**, **3a**, **3b**. The structural data are given at HF/6-31G(d), the relative energies at MP2/6-31 + + G(d)//HF/6-31G(d). For details see Table 1.

	2a (C_s)	**2b** (C_2)	**3a** (C_2)	**3b** (C_i)
C1-C2	1.503	1.504	1.511	1.513
C2-C3	1.354	1.355	1.347	1.347
C1-C2-C3	135.1	135.4	132.7	132.8
H7-C1-H8	104.0	103.6	103.2	102.8
C1-C2-C3-C4	0.0	9.1	166.6	180.0
α_1 [a]	61.2	61.4	62.8	63.0
E_{rel} [b]	6.1 (9.9)	6.7 (10.3)	6.9 (5.3)	7.3 (5.6)
i	0	0	0	0
q(C1)	−0.976	−0.982	−0.972	−0.975
q(C2)	−0.289	−0.288	−0.285	−0.284
q(H5)	0.101	0.102	0.116	0.117
q(H7)	0.059	0.063	0.063	0.065
q(H8)	0.104	0.105	0.078	0.078

[a] Dihedral angle between the planes H7-C1-H8 and C1-C2-C3. [b] Relative to the energy of **1b** (see Table 1).

only planar **2** and **3**, reported energy differences of 26.4 and 30.6 kcal mol^{-1} relative to **1**.[3a] The slightly higher stability of the *cis* isomers **2a** and **2b** over the *trans* forms **3a** and **3b** may be explained by the better interactions between the n$_-$ combination of the terminal lone-pair orbitals with the C–C π^* bond, which is also found for isoelectronic difluoroethylene.[9] In agreement with this interpretation, the terminal C–C bonds are shorter and the central C–C bond is longer in **2a** and **2b** than in **3a** and **3b** (Table 2). In fact, the relative energies of the most stable conformations of **1**, **2**, and **3** are even quantitatively nearly the same as found for isoelectronic 1,1-, 1,2-*cis*, and 1,2-*trans* difluoroethylene.[9b]

Why are the Y-shaped dianions **1b** and **1c** more stable than the *cis* and *trans* isomers **2a**–**3b**? The comparison of the optimized structures which are true minima on the $C_4H_6^{2\ominus}$ potential-energy surface provides a reasonable answer. The negative charge is distributed over *three* carbon atoms in **1b** and **1c**, while it is concentrated mainly on *two* carbon atoms in the *cis* and *trans* forms. Moreover, the calculation of the charge distribution using the NBO analysis[8, 10] indicates a small positive charge at the central carbon atom of **1b** and **1c** indicating attractive interactions between C1 and the terminal carbon atoms (Table 1). Internal coulombic stabilization as the cause of the higher stability of **1** has already been suggested by *Klein*,[4] although he considered only the D_{3h} form **1a**. *Wiberg*[5] dismissed the idea of charge stabilization on the ground of the small size of the positive charge at C1. However, important is not the absolute size but the *difference* in charge interactions between **1b** and the isomeric forms **2a**–**3b**. In **1b**, there are small but *attractive* coulombic interactions between all carbon atoms directly bonded to each other. In **2a**, **2b**, **3a**, and **3b**, all carbon atoms are negatively charged and the coulombic interactions are purely repulsive. Although **2** and **3** have a π bond which is missing in **1**, the additional binding energy of the π bond is lower than the sum of the stabilizations of the three lone pairs in **1**, as a result of the adjacent π vacancy. We also refer to recent theoretical studies which show that π delocalization in benzene and other ring compounds is destabilizing, and that it is the energy of the σ bonds which enforces bond equalization.[16]

The analysis of the geometries and electronic structures of the conformational energy minima **1b**–**3b** clearly shows that the higher stability of the Y-shaped structures **1b** and **1c** relative to the *cis* and *trans* isomers **2a**–**3b** is caused by *maximally distant localization of the π electrons*, not delocalization or even aromaticity. All isomers adopt nonplanar geometries with strongly pyramidalized methylene groups to further separate the lone-pair electrons; this is achieved optimally in **1b**. There is no Y-aromaticity in the trimethylenemethane dianion!

Received: February 4, 1991 [Z 4423 IE]
German version: *Angew. Chem. 103* (1991) 1038

CAS Registry number: **1**, 41792-83-0.

[1] J. Klein, A. Medlik-Balan, *J. Chem. Soc. Chem. Commun.* (1973) 275.
[2] P. Gund, *J. Chem. Educ. 49* (1972) 100.
[3] a) I. Agranat, A. Skancke, *J. Am. Chem. Soc. 107* (1985) 867; b) S. Inagaki, Y. Hirabayashi, *Chem. Lett.* (1982) 709; c) S. Inagaki, H. Kawata, Y. Hirabayasi, *J. Org. Chem. 48* (1983) 2928.
[4] J. Klein, *Tetrahedron 39* (1983) 2733; ibid. *44* (1988) 503.
[5] K. B. Wiberg, *J. Am. Chem. Soc. 112* (1990) 4177.
[6] The Convex verrsions of the program packages CADPAC 4.0 and GAUSSIAN 90 have been used.
[7] The geometries and force-constant matrices of **1a**, **1b**, and **1c** have been calculated at the following levels of theory, and the number of imaginary frequencies for **1a** is given in parentheses: HF/3-21G (3), HF/6-31G(d) (3), HF/6-31 + + G(d) (4), MP2/6-31G(d) (4). Since the differences in the optimized geometries were found to be insignificant, the optimizations for isomeric forms of **2** and **3** have been carried out only at HF/6-31G(d).
[8] NBO 3.0—for a description of the method see: A. E. Reed, L. A. Curtiss, F. Weinhold, *Chem. Rev. 88* (1988) 899.
[9] a) N. D. Epiotis, *J. Am. Chem. Soc. 95* (1973) 3087; b) G. Frenking, W. Koch, M. Schaale, *J. Comput. Chem. 6* (1985) 189.
[10] The calculated result that **1b** and **1c** have small positive charges at the central carbon atom has been found at all levels of theory employed here. It has also been found for **1a** using a different technique for analyzing the molecular wave function (ref. [5]).
[11] In ref. [5], the optimized structure of a dilithio derivative of isobutene is shown, which exhibits a nonplanar C_4H_6 geometry with weakly pyramidalized CH_2 groups which is very similar to **1b**. This was interpreted [5] as resulting from a tendency to maximize the coulombic attraction between the lithium cations and the anion. Our results show that isolated **1** adopts an even more strongly pyramidalized structure.
[12] R. F. W. Bader, "Atoms in Molecules: A Quantum Theory", Oxford University Press, Oxford 1990.
[13] The $\nabla^2\rho(r)$ plot shown in Figure 2 for **1b** corresponds to the C1–C2 bond. The results for the C1–C3 and C1–C4 bonds are nearly identical.
[14] r_b denotes a point of minimum electron density $\rho(r)$ along the bond path, while $\rho(r)$ is a maximum in any direction perpendicular to the internuclear axis [12].
[15] T. S. Slee, P. J. MacDougall, *Can. J. Chem. 66* (1988) 2961.
[16] a) S. S. Shaik, P. C. Hiberty, J.-M. Lefour, G. Ohanessian, *J. Am. Chem. Soc. 109* (1987) 363; b) K. Jug, A. M. Köster, ibid. *112* (1990) 6772.
[17] A nonplanar geometry has been predicted for **1** using semi-empirical methods: M. N. Glukhovtsev, B. Ya. Simkin, *Izv. Sev.-Kavk. Nauchn. Tsentra Vyssh. Shk., Estestv. Nauki 2* (1989) 115; *Chem. Abstr. 113* (1990) 5348f.

Cyclooctatetraenylene Vinylenes**

By Petra Auchter-Krummel and *Klaus Müllen**

Dedicated to Professor Heinz A. Staab on the occasion of his 65th birthday

The chemistry of stilbene, the higher oligo(*para*-phenylene vinylenes) (**1**),[1, 2] and the poly(phenylene vinylenes) (**2**)[3, 4] have been studied intensively from point of view of their synthesis, physical organic chemistry, and applications.[5] The outstanding redox and photochemical properties of the benzene homologue, cyclooctatetraene (COT),[6, 7] makes the successive replacement of the phenylene units in the linear π systems of **1** and **2** by cyclooctatetraene attractive. We

[*] Prof. Dr. K. Müllen, Dipl.-Chem. P. Auchter-Krummel
Max-Planck-Institut für Polymerforschung
Ackermannweg 10, W-6500 Mainz (FRG)

[**] Polyarylenes and Polyarylene Vinylenes, Part 6. This work was supported by the Deutsche Forschungsgemeinschaft and the Fonds der Chemischen Industrie. Part 5: K.-H. Koch, K. Müllen, *Chem. Ber. 124* (1991), No. 9.

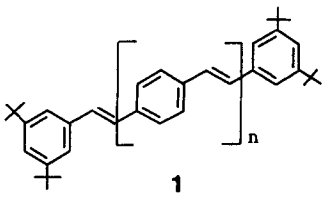

1

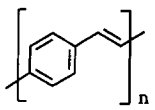

2

show that, starting from 1,5-difunctionalized cyclooctatetraene, derivatives of the type **3** and **4**, can be synthesized which exhibit extended π conjugation. Cyclic voltammetric and NMR spectroscopic investigations confirm the role of the title compounds as "charge storage" units and as substrates for thermally inducible charge transfer.

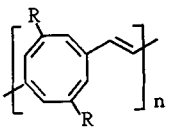

3, R = CH_3

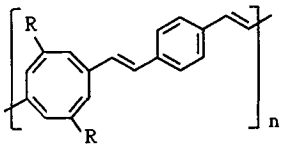

4, R = CH_3

The known cyclooctatetraene carbaldehyde **5a** and its easily accessible phosphonium salt **5b** serve as building blocks for olefination by Wittig or McMurry reactions.[8] Suitable 1,5-difunctionalized cyclooctatetraenes are not known. We therefore prepared the diester **6a** by thermolysis[9] of the semibullvalene **7**[10] and then transformed **6a** into the difunctional starting compounds **6b** and **6c**. The other starting compounds, **8** and **9a**, are easily accessible. The stepwise construction of a linear π system via the dialdehyde **13b**, also requires a compound in which one functionality has been protected, such as the ketal **9b**.

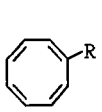

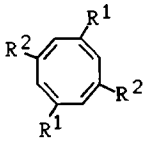

5a, R = CHO
5b, R = CH_2PPh_3Br

6a, $R^1 = CH_3$, $R^2 = COOCH_3$
6b, $R^1 = CH_3$, $R^2 = CH_2OH$
6c, $R^1 = CH_3$, $R^2 = CHO$

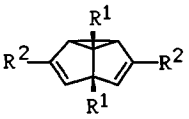

7, $R^1 = CH_3$, $R^2 = COOCH_3$

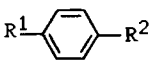

8, R^1 = H, $R^2 = CH_2PPh_3Br$
9a, $R^1 = R^2 = CH_2PPh_3Br$
9b, R^1 = , $R^2 = CH_2PPh_3Cl$

The following characteristics are typical for the construction of the chain:[11]
– The Wittig reaction gives better yields than McMurry coupling (**10a**[12] from **5a** and **5b** (KO*t*Bu, THF, 25°C, 65%; **10a** from 2 equiv of **5a** ($TiCl_4$), Zn/Cu, THF, 60°C) 19%).
– Chains with terminal phenyl units are distinctly more easily accessible than those with terminal cyclooctatetraene units (**13a** from **6c** and **8** 70%; **14** from **5a** and **9a** 12%).
– The "trimer" **11** and the monoaldehyde **10b** are both formed from **6c** and **5b**; **10b**, however, requires 2 equiv of **6b**.
– *E*/*Z* isomeric mixtures are formed; attempts at iodine-catalyzed formation of the all-*E* isomers (all structural formulas represent all-*E* isomers) led to decomposition, but separation of the isomers by chromatography is possible.
– The attempt to obtain a polymer from **6c** and **9a** affords the compound **4** with $n \approx 5$ as a THF-soluble fraction (30% w/w). According to the IR spectra, the higher molecular weight fractions have the same overall structure as the shorter chain products.

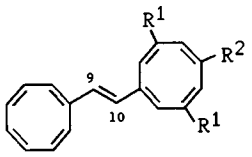

10a, $R^1 = R^2$ = H
10b, $R^1 = CH_3$, R^2 = CHO

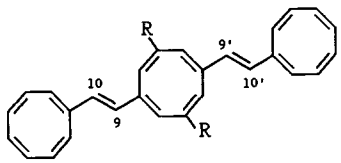

11, R = CH_3

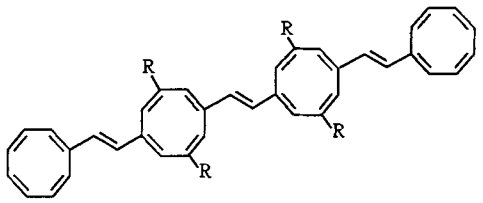

12, R = CH_3

The analogies to the benzene-like oligo(phenylene vinylenes) (**1**) are useful in the description of the chemical and physical properties of the compounds **10a**, **11**, and **12** (type **3**) and **13a**, **14**, and **15** (type **4**). As in the oligo(phenylene vinylenes),[14] (*E*/*Z*)-**13a** is slowly transformed into the (*E*/*E*) isomer (36 days, 32%) on irradiation with a mercury high pressure lamp (180 W, Q-600, Pyrex filter). Neither (*E*/*E*)-**13a** nor (*E*/*E*)-**14** are changed by irradiation at $\lambda \geq 300$ nm over the same period. The question whether photochemically initiated *Z*/*E* isomerizations of stilbene and **1a**[14] are diabatic or adiabatic makes a comparison of these compounds with the COT system **13a** desirable.

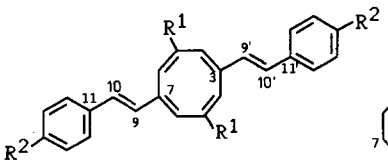

13a, $R^1 = CH_3$, R^2 = H
13b, $R^1 = CH_3$, R^2 = CHO

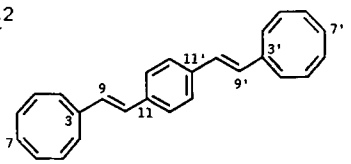

14

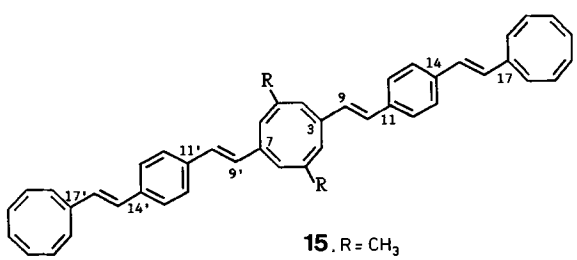

15, R = CH_3

Table 1. Selected physical and spectroscopic data for **6c**, **10a**, (*E*)-**10b**, **11**, **12**, (*E,E*)-**13a**, (*E,E*)-**13b**, (*E,E*)-**14**, (*E,E,E,E*)-**15**, (*E,E*)-**13a**$^{2\ominus}$/2K$^{\oplus}$, (*E,E*)-**14**$^{4\ominus}$/4K$^{\oplus}$ [a].

6c: m.p. = 140°C; MS (EI, 70 eV): *m/z* 188.0837 ($M^{\oplus}$).

10a: MS (EI, 70 eV) *m/z* = 232.1252 ($M^{\oplus}$); ^{1}H NMR: δ = 6.18 (s, H 9,10), .60–5.65 (m, 14H); ^{13}C NMR (75 MHz, $CDCl_3$): δ = 141.2, 132.6, 131.9, 131.7, 131.4, 130.8, 130,6.

(*E*)-**10b**: MS (FD, 4 kV): *m/z* 289.1 (24.5%), 288.2 (100%, $M^{\oplus}$); ^{1}H NMR ($CDCl_3$): δ = 9.49 (s, CHO), 6.69 (s, 1H), 6.2, 6.1 (AB, J_{AB} = 18.2 Hz), 5.98–5.7 (m, 10H), 1.92 (s, CH_3), 1.8 (s, CH_3).

11: MS (FD, 4 kV): *m/z* 389.2 (27%), 388.2 (100%, $M^{\oplus}$), 232.1 (9%); ^{1}H NMR ($CDCl_3$): δ = 6.2, 6.08 (AB, J_{AB} = 15.8 Hz), 5.98–5.78 (m, 18H), 1.84 (s, $2CH_3$); ^{13}C NMR ($CDCl_3$): δ = 141.3, 140.4, 139.3, 134.0, 132.5, 131.7, 131.1, 131.0, 130.6, 124.4, 23.7.

12: MS (FD, 4 kV): *m/z* 545.3 (51%), 544.3 (100%, $M^{\oplus}$).

(*E,E*)-**13a**: m.p. = 156°C; ^{1}H NMR: δ = 6.46, 6.85 (^3J = 16.0 Hz; H 9,9′,10,10′), 5.92 (s, 4H) [e], 1.93 (s, 6H; CH_3); ^{13}C NMR (50 MHz) [b]: δ = 139.5 (C 1,5), 140.5 (C 3,7), 124.7, 134.2 (C 2,4,6,8), 131.5 (C 9,9′), 128.8 (C 10,10′), 137.5 (C 11,11′), 23.3 (CH_3).

(*E,E*)-**13b**: m.p. = 132°C; MS: *m/z*: 392.1776 ($M^{\oplus}$). ^{1}H NMR: δ = 6.92, 6.47 (^3J = 15.2 Hz; H 9,10,9′,10′), 6.01 (s, 2H) [e], 5.94 (s, 2H) [e], 1.96 (s, 6H; CH_3), 9.95 (s, 2H; CHO).

(*E,E*)-**14**: m.p. = 178°C. ^{1}H NMR ($CDCl_3$): δ = 6.37, 6.85 (^3J = 16.2 Hz; H 9,10,9′,10′), 5.77–6.14 (m, 14H) [e]; ^{13}C NMR [d]: δ = 141.4 (C 3,3′), 131.5 (C 7,7′), 130.6, 131.6, 131.8, 132.1, 132.8 (C 1,2,4–6,8,1′,2′,4′–6′,8′), 130.7 (C 9,9′), 128.2 (C 10,10′), 136.5 (C 11,11′).

(*E,E,E,E*)-**15**: MS: *m/z* 592.3128; ^{1}H NMR ($CDCl_3$): δ = 6.78, 6.4 (AB, J_{AB} = 16.0 Hz, H 9,9′,10,10′), 6.86, 6.37 (AB, J_{AB} = 15.5 Hz, H 15,15′,16,16′), 6.1–5.7 (m, 18H), 1.95 (s, $2CH_3$).

(*E,E*)-**13a**$^{2\ominus}$/2K$^{\oplus}$: ^{1}H NMR: δ = 6.42, 7.3 (^3J = 15.5 Hz; H 9,10,9′,10′), 5.96 (s, 4H) [e], 2.84 (s, 6H; CH_3); ^{13}C NMR [c]: δ = 101.9 (C 1,5), 106.1 (C 3,7), 96.1 (C 2,4,6,8), 146.4 (C 9,9′), 109.2 (C 10,10′), 143.6 (C 11,11′), 34.8 (CH_3).

(*E,E*)-**14**$^{2\ominus}$/2K$^{\oplus}$: ^{1}H NMR: δ = 7.13, 7.08 (^3J = 11.0 Hz, 4H) [g], 6.29, 6.68 and 6.3, 7.41 (^3J = 16.4 and 14.6 Hz; H 9,10,9′,10′), 5.67–6.15 (m, 12H) [e], 5.5 (t, 2H) [e]; ^{13}C NMR: δ = 143.1 or 144.2 (C 3) [f], 101.6 (C 3′), 90.0, 94.0, 97.8, 101.0, 105.7, 123.0, 126.0, 127.2, 130.4, 132.0, 132.8, 147.2 C 1–10,1′–10) [f], 143.1 oder 144.2 (C 11) [f], 129.2 (C 11′).

(*E,E*)-**14**$^{4\ominus}$/4K$^{\oplus}$ [a]: ^{1}H NMR (400 MHz): δ = 7.06 (s, 4H) [g], 6.34, 7.29 (^3J = 15.2 Hz, 4H), 6.16 (d, J = 12 Hz; 4H) [e], 5.92 (t, J = 11 Hz; 4H) [e], 5.84 (t, J = 10 Hz; 4H) [e], 5.6 (t, J = 10 Hz; 4H) [e]; ^{13}C NMR: δ = 100.5 (C 3,3′), 90.2, 93.1, 95.1, 97.6 (C 1–8,1′–8′), 143.9 (C 9,9′), 108.2 (C 10,10′), 137.4 (C 11,11′).

[a] All NMR spectra, unless stated otherwise, are recorded in [D_8]THF, the neutral compounds at 25°C and ions at −30°C. [b] Assignment of the signals by H, C COSY NMR spectra (^{1}H: 300 Hz, ^{13}C: 75 MHz). [c] Assignment of the signals by correlation with chemical shifts with Hückel charge densities. [d] Assignment of the signals by selective ^{1}H decoupling. [e] Eight ring protons. [f] Assignment not possible. [g] Arene protons.

The electrochemical reduction of the title compounds by cyclic voltammetry convincingly documents their unusual redox systems (Table 2).

– In the homologous series of **1**, completely reversible one-electron transfers are observed. Increasing the chain length increases the number of redox steps, shifts the reduction potential to more negative values, and causes the potential difference between the first and second reduction, $\Delta E = E_1 - E_2$ to approach a minimum as a result of the decreasing Coulomb repulsions.[1]

– For the reduction of cyclooctatetraenylene vinylenes, the first wave corresponds to an electrochemically irreversible, but chemically reversible, two-electron transfer (see Table 2). This situation is similar to that of COT itself;[15–17] there the reason for the small potential difference ΔE is the electronic stabilization of the dianion, and the lack of electrochemical reversibility is due to the planarization of the ring at the radical anion stage. Thus as a first approximation, the first two-electron transfer in **10a**, **11**, **12**, **13a**, **14**, and **15** may be understood as a charging of the COT unit.

– The dominance of COT units as electrophores—in spite of potentially extended π conjugation—is also shown by the successive reductions. Finally each COT ring has taken up two electrons, and the "tetra-COT" system **12** is transformed into an octaanion!

– The difference in behavior between the "bis-COT" compounds **10a** and **14**, which are distinguished from one another by the length of the bridging group between two COT units, is characteristic. Compound **14** is reduced in two separate, irreversible, two-electron transfers, whereas in **10a** a reversible one-electron transfer follows an irreversible two-electron transfer. Evidently the addition of electrons to one of the COT units in **10a** leads at least to a partial planarization of the second ring. *Staley* et al. [18, 19] reached a similar conclusion for the dianion formation in a series of "bis COT" compounds.

The reduction with alkali metals allows a characterization of the resulting diamagnetic ions by spectroscopy.[20] A correlation of the ^{13}C NMR chemical shifts of (*E,E*)-**13a**$^{2\ominus}$/2K$^{\oplus}$ with the local π charge density (Table 1) suggests that the excess charge is localized mainly on the eight-membered ring and the olefinic centers C10(10′). No significant charging of the phenyl units is suggested by the ^{1}H NMR signals of the tetraanion salt (*E,E*)-**14**$^{4\ominus}$/4K$^{\oplus}$ (Table 1). Complete alkali-metal reduction of **10a** yields a tetraanion. The ^{1}H NMR signals of the olefinic protons occur at low field due to the diatropism (δ = 6.95, (s)) of the two eight-membered rings.

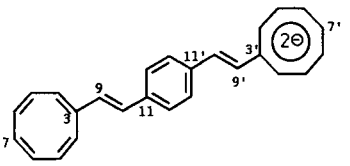

14$^{2\ominus}$

The occurrence of *two* AB systems for the olefinic protons in the ^{1}H NMR spectrum of the dianion salt (*E,E*)-**14**$^{2\ominus}$/2K$^{\oplus}$ (200 MHz, −30°C) suggests an "unsymmetric" charge distribution. The charge is localized on one COT ring. The spectra show no change at different temperatures, even up to 50°C (90 MHz), which excludes a thermally induced charge fluctuation below this temperature, although delocalization of charge should be the preferred electrostatic configuration. Such a charge redistribution in the anion implies that the second COT ring becomes coplanar in the intermediate stage, which results in an activation energy caused by geometric factors.[18, 19, 21]

That at low temperatures (−80°C) the charge in dianion **10a** is mainly localized on one ring may be deduced from the ^{1}H NMR spectrum ([D_8]THF, 200 MHz). Only one AB spin

Table 2. Cathodic peak potentials (E_{pc}) of cyclooctatetraenylene vinylenes as determined by cyclic voltammetry [a].

	T[°C]	E_{pc} [V] (No. of electrons transferred)
COT [b]	0	−2.12 [e] (2e)
10a [b]	0	−1.94 [e] (2e) −2.35 [d] (1e) −2.75 (1e)
12 [b]	−10	−2.01 [e] (4e) −2.17 [e] (2e) −2.52 [d] (1e) −2.67 (1e)
13a [c]	0	−2.18 [e] (2e)
14 [c]	0	−1.97 [e] (2e) −2.11 [e] (2e)
15[c]	0	−1.96 [e] (4e)

[a] 10^{-3} M solution in THF; electrolyte: Bu_4NPF_6. [b] Gold working electrode [c] Platinum working electrode [d] Reversible [e] Electrochemically reversible.

system is observed for the olefinic protons (H9 and H10), $\delta = 6.78$ and 6.57, $^3J = 14.8$ Hz). Due to an increase in temperature the shape of the lines changes. Coalescence occurs at $-15\,^{\circ}C$, and at temperatures $> 25\,^{\circ}C$ a sharp singlet is observed ($\delta = 6.67$). The Gibbs activation energy of this process that can be understood as an intramolecular charge redistribution, is estimated at $\Delta G^{\ddagger}_{(-15\,^{\circ}C)} = 12.8 \pm 0.3$ kcal mol^{-1}. In agreement with the cyclic voltammetry findings, the charge redistribution apparently occurs more easily in **10a**$^{2\ominus}$/2K$^{\oplus}$ than in **14**$^{2\ominus}$/2K$^{\oplus}$.

Whereas (*Z*)-stilbene is rapidly transformed into the *E* isomer on reduction with alkali metals,[22] at $-80\,^{\circ}C$ (*E,Z*)-**13a** can be converted into a dianion with its configuration intact, which isomerizes only very slowly into the *E,E* isomer (20% after 13 weeks at $-80\,^{\circ}C$).

Received: February 25, 1991 [Z4460 IE]
German version: *Angew. Chem. 103* (1991) 996

[1] J. Heinze, J. Mortensen, K. Müllen, R. Schenk, *J. Chem. Soc. Chem. Commun. 1987*, 701; R. Schenk, H. Gregorius, K. Mehrholz, J. Heinze, K. Müllen, *J. Am. Chem. Soc.*, in press.
[2] G. Drehfahl, R. Kühmstedt, H. Oswald, H.-H. Hörhold, *Makromol. Chem. 131* (1970) 89.
[3] R. A. Wessling, *J. Polym. Sci. Polym. Symp. 72* (1985) 55.
[4] H.-H. Hörhold, M. Helbig, D. Raabe, J. Opfermann, U. Scherf, R. Stockmann, D. Weiß, *Z. Chem. 27* (1987) 126.
[5] J. H. Burroughes, D. D. C. Bradley, A. R. Brown, R. N. Marks, M. MacKay, R. H. Friend, P. L. Burns, A. B. Holmes, *Nature 347* (1990) 539.
[6] G. I. Fray, R. G. Saxton: *The Chemistry of The Cyclooctatetraene and Its Derivatives*, University Press, Cambridge 1978.
[7] L. A. Paquette, *Tetrahedron 31* (1975) 2855.
[8] G. H. Harmann, A. Streitwieser, *J. Org. Chem. 38* (1973) 549.
[9] L. A. Paquette, S. V. Ley, R. H. Meisinger, R. K. Russel, M. Oku, *J. Am. Chem. Soc. 96* (1974) 5806.
[10] J. Sellner, H. Schuster, H. Sichert, J. Sauer, H. Nöth, *Chem. Ber. 116* (1983) 3751.
[11] All new compounds were characterized by elemental analysis and spectroscopic data. For typical examples see Table 1.
[12] The dianion of **10a** is already known [19], but the neutral compound and its electron transfer reactions have not been described.
[13] The electron absorption spectra of the compound types **3** and **4** are distinctly different. Compounds **10a**, **11**, and **12** have a broad poorly structured band at large wavelengths, which broadens further and undergoes a bathochromic shift on lengthening the chain (**10a**: $\lambda_{max} = 328$ nm ($\varepsilon = 3135$); **11**: 332 (5487); **12**: 431 (4298)), whereas **13**, **14**, and **15** are characterized by a narrow band at short wavelenths as well as an intensive, broad band at longer wavelengths (**13**: $\lambda_{max} = 293$ nm ($\varepsilon = 30799$); **14**: 365 (26483); **15**: 354 (91678)). On going from **14** to **15** the longer wavelength band increases in intensity, but, in complete contrast to the compound of the homologous series **1**, undergoes a slight hypsochromic shift.
[14] K. Sandros, M. Sundahl, O. Wennerström, U. Norinder, *J. Am. Chem. Soc. 112* (1990) 3082.
[15] A. J. Fry, C. S. Hutchins, *J. Am. Chem. Soc. 97* (1975) 591; R. D. Allendoerfer, R. H. Rieger, *ibid. 87* (1965) 2336; H. Kiesele, J. Heinze in H. Lund, M. Baizer (Ed.): *Organic Electrochemistry*, Dekker, New York 1991, p. 331.
[16] Since the first transfer of charge is irreversible in the case of COT, the cyclic voltammogram shows one wave, which does not imply a thermodynamically favored second transfer, because the second is shifted toward the negative by 120–150 mV with respect to the first.
[17] J. Heinze, M. Dietrich, K. Hinkelmann, K. Meerholz, F. Rashwan, *DECHEMA Monogr. 112* (1989) 61; *Chem. Abstr. 110* (1989) 221359r.
[18] B. Eliasson, S. W. Staley, *Prepr. Am. Chem. Soc. Div. Pet. Chem. 30* (1985) 620; *Chem. Abstr. 104* (1985) 50494a.
[19] S. W. Staley, C. K. Dustman, K. L. Facchine, G. E. Linkowsky, *J. Am. Chem. Soc. 107* (1985) 4003.
[20] The amount of charge on the anions can be shown chemically by trapping experiments. Thus the hexaanion **11**$^{6\ominus}$ (as potassium salt) forms a hexamethyl derivative on reaction with dimethyl sulfate, which can be detected by mass spectrometry.
[21] G. Krummel, W. Huber, K. Müllen, *Angew. Chem. 99* (1987) 1305; *Angew. Chem. Int. Ed. Engl. 26* (1987) 1290.
[22] F. Gerson, H. Ohya-Nishiguchi, M. Szwarc, G. Levin, *Chem. Phys. Lett. 53* (1977); T. A. Ward, G. Levin, M. Szwarc, *J. Am. Chem. Soc. 97* (1975) 258.

Formation of Doubly Vinyl-Bridged Binuclear Iridium Complexes by C-H Activation**

By *Angelika Nessel, Oliver Nürnberg, Justin Wolf,* and *Helmut Werner**

Dedicated to Professor Kurt Dehnicke on the occasion of his 60th birthday

Vinyl transition-metal complexes can be formed from nonactivated olefins in general only under drastic reaction conditions. *Bergman* and *Stoutland*[1] reported in 1985 that photolysis of [Cp*IrH$_2$(PMe$_3$)] (Cp* = C$_5$Me$_5$) in presence of ethene leads not only to the formation of the expected olefin compound [Cp*Ir(C$_2$H$_4$)(PMe$_3$)] (**1**), but also to the hydrido(vinyl) complex [Cp*IrH(HC=CH$_2$)(PMe$_3$)] (**2**), which on heating to ca. 180 °C isomerizes to give **1**. We now describe binuclear doubly vinyl-bridged iridium complexes that are obtained from well-known, easily accessible precursors and H$_2$C=CH*t*Bu in presence of base without photochemical activation.

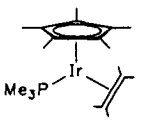

1

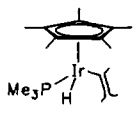

2

Previously, *Maitlis* et al. have shown[2] that [Cp*IrCl$_2$]$_2$ reacts with ethene and Na$_2$CO$_3$/EtOH to give [Cp*Ir(C$_2$H$_4$)$_2$]. The mesitylene osmium complex **3** behaves analogously and on treatment with C$_2$H$_4$ and Na$_2$CO$_3$/EtOH affords compound **4**.[3] If, however, ethene is replaced by 3,3-dimethyl-1-butene the carbonyl(hydrido)methyl complex **5** is formed.[4] Labeling experiments confirm that the ligands CO, CH$_3$, and H are really generated by stepwise fragmentation of ethanol in the coordination sphere of the metal.

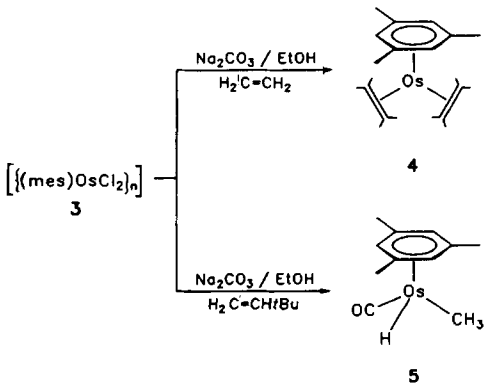

In contrast to our expectation, the reaction of [CpIrBr$_2$]$_2$ (**6**, Cp = C$_5$H$_5$) with H$_2$C=CH*t*Bu and Na$_2$CO$_3$/EtOH does not give [CpIrH(CH$_3$)(CO)],[5] but leads to a mixture of

[*] Prof. Dr. H. Werner, Dipl. Chem. A. Nessel, Dipl. Chem. O. Nürnberg, Dr. J. Wolf
Institut für Anorganische Chemie der Universität
Am Hubland, W-8700 Würzburg (FRG)

[**] This work was supported by the Deutsche Forschungsgemeinschaft (SFB347), the Fonds der Chemischen Industrie, and Degussa AG. We thank *M. Schulz* for his support in determining the X-ray crystal structure.

products in which, besides $[CpIr(H_2C{=}CHtBu)_2]$ (**7**),[6] also a small amount of the binuclear complex **8** is present. By using *i*PrOH instead of EtOH, compound **8** is isolated in 30% yield. The supposed structure of **8** is supported by the ^1H as well as the ^{13}C NMR data,[7] which unequivocally show the presence of a β-C-substituted vinylic ligand.

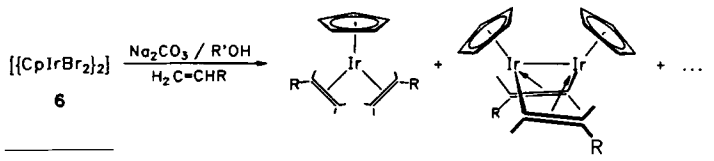

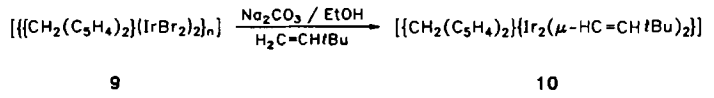

A clean reaction occurs between the polymeric dibromoiridium complex **9**,[8] prepared from $[\{CH_2(C_5H_4)_2\}\{Ir(C_2H_4)_2\}_2]$, and Na_2CO_3/EtOH in the presence of $H_2C{=}CHtBu$. The reaction mixture is warmed to 75–80 °C for 3 h, after which a red, moderately air-stable solid **10** is isolated. The NMR data of **10** are similar to those of **8**.[7] The structure of **10** is shown in Figure 1.[9] Each vinylic

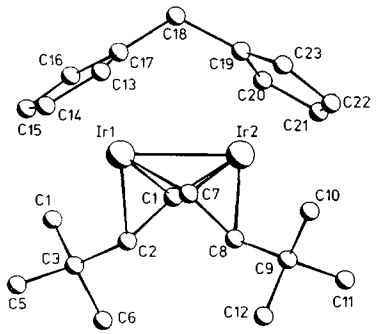

Fig. 1. Structure of **10** in the crystal. Selected bond distances [Å] and bond angles [°]: Ir1–Ir2 2.5495(5), Ir1–C1 2.098(9), Ir1–C2 2.212(9), Ir1–C7 2.037(9), Ir2–C1 2.010(9), Ir2–C7 2.137(9), Ir2–C8 2.204(9), C1–C2 1.40(1), C7–C8 1.42(1); Ir1-C1-Ir2 76.7(3), Ir1-C7-Ir2 75.2(3), Ir1-Ir2-C1 52.2(3), Ir2-Ir1-C7 54.2(3), Ir1-Ir2-C7 50.6(3), Ir2-Ir1-C1 50.1(3), C1-C2-C3 124(1), C7-C8-C9 123.1(8), C17-C18-C19 119.1(9).

group is coordinated to one metal atom via a σ and to the other metal atom via a π bond and thus behaves as a bridging unit. The Ir–Ir distance of 2.5495(5) Å is noteworthy because it is significantly shorter than a Ir–Ir single bond [2.70–2.75 Å][10] (which for electronic reasons would be expected for **10**) and comparable to that of a Ir–Ir double bond [2.554 Å].[11] We assume that the short metal–metal bond length is caused by the strain which is exerted by the bis(cyclopentadienyl)methane ligand on the rest of the molecule. An indication of this strain can be seen in the size of the C17-C18-C19 angle [119.1(9)°] which is ca. 10° wider than the tetrahedral angle.[12] The M–C and C–C distances in the $Ir_2(\mu\text{-}HC{=}CHtBu)_2$ unit correlate quite well with those of the binuclear rhodium complex $[(C_9H_6Me)_2Rh_2(\mu\text{-}HC{=}CH_2)(\mu\text{-}MeC{=}CHMe)]$ which has been prepared from $[(C_9H_6Me)Rh(C_2H_4)_2]$ and but-2-yne.[13]

To the best of our knowledge, compound **10** is the first example of a binuclear iridium complex in which two iridium atoms in the oxidation state +II are bridged by three organo groups and in which no terminal ligands such as CO, PR_3, or Cl are present. Particularly noteworthy in the synthesis of **10** are the mild conditions for the activation of a C–H bond in $H_2C{=}CHtBu$ with Na_2CO_3/EtOH which leads to the formation of a vinylic group. A similar conversion of an olefin $H_2C{=}CHR$ (R = *i*Pr, Ph) into a vinylic ligand HC=CHR in a mononuclear rhenium complex with *t*BuOK as base has recently been described by *Gladysz* et al.;[14] in that case the positive charge at the metal center is presumably crucial for the cleavage of the C–H bond.

Experimental Procedure

8: A suspension of **6** (121 mg, 0.15 mmol) in *i*PrOH (10 mL) was treated with Na_2CO_3 (500 mg, 4.72 mmol) and $H_2C{=}CHtBu$ (0.4 mL, 3.17 mmol) and warmed to 75 °C for 3 h. After cooling to room temperature, the solvent was removed, the residue was extracted with pentane (25 mL), and the extract was evaporated to dryness in vacuo. The red-brown oily residue was dissolved in hexane (4 mL), and the solution was chromatographed on Al_2O_3 (neutral, activity grade V, column length 20 cm). With hexane, first an orange and then a yellow fraction was eluted. The yellow fraction was evaporated to dryness in vacuo, and the residue was recrystallized from pentane (2 mL) at −78 °C. Yellow, moderately air-stable crystals were obtained: yield 30 mg (30%); m.p. 154 °C (dec.); correct elemental analysis. **10**: Prepared as described for **8**, using **9** [8] as starting material and ethanol as solvent; red crystals: yield 59%; m.p. 159 °C (dec.); correct elemental analysis.

Received: March 22, 1991 [Z 4521]
German version: *Angew. Chem. 103* (1991) 999

[1] a) P. O. Stoutland, R. G. Bergman, *J. Am. Chem. Soc. 107* (1985) 4581; b) J. Silvestre, M. J. Calhorda, R. Hoffmann, P. O. Stoutland, R. G. Bergman, *Organometallics 5* (1986) 1841; c) P. O. Stoutland, R. G. Bergman, *J. Am. Chem. Soc. 110* (1988) 5732. For reversed order of thermodynamic stability, i.e., $[\{Ir\}(H_2C{=}CHR)] < [\{Ir\}H(HC{=}CHR)]$ ($\{Ir\} = [IrCl(PiPr_3)_2]$) see: d) H. Werner, T. Dirnberger, M. Schulz, *Angew. Chem. 100* (1988) 993; *Angew. Chem. Int. Ed. Engl. 27* (1988) 948; e) C. K. Ghosh, J. K. Hoyano, R. Krentz, W. A. G. Graham, *J. Am. Chem. Soc. 111* (1989) 5480.

[2] K. Moseley, J. W. Kang, P. M. Maitlis, *J. Chem. Soc. A 1970*, 2875.

[3] S. Stahl, H. Werner, *Organometallics 9* (1990) 1876.

[4] S. Stahl, H. Werner, *J. Am. Chem. Soc. 113* (1991) 2944.

[5] Formation on photolysis of $[CpIr(CO)_2]$ in CH_4/C_6F_{14}: J. K. Hoyano, A. D. McMaster, W. A. G. Graham, *J. Am. Chem. Soc. 105* (1983) 7190.

[6] ^1H NMR (60 MHz, C_6D_6): δ = 4.98 (s, C_5H_5), 2.67 (d, J(H,H) = 10.6 Hz, H *cis* to *t*Bu), 1.56 (d, J(H,H)=8.3 Hz, H *trans* to *t*Bu), 0.97 (s, *t*Bu), 0.34 (dd, J(H,H) = 10.6 and 8.3 Hz, =C*H*tBu).

[7] **8**: ^1H NMR (90 MHz, C_6D_6): δ = 8.71 (d, J(H,H) = 9.6 Hz, *HC*=CH*t*Bu), 5.03 (s, C_5H_5), 2.42 (d, J(H,H) = 9.6 Hz, HC=C*Ht*Bu), 1.04 (s, *t*Bu); ^{13}C NMR (22.5 MHz, C_6D_6): δ = 97.2 (s, *HC*=CH*t*Bu), 78.8 (s, C_5H_5), 69.3 (s, HC=*C*H*t*Bu), 35.2 (s, *C*CH_3), 31.2 (s, C*CH*$_3$). **10**: ^1H NMR (90 MHz, $CDCl_3$): δ = 9.02 (d, J(H,H) = 9.8 Hz, *HC*=CH*t*Bu), 5.65, 5.04, 4.10, 3.91 (each s, *CH* of C_5H_4), 3.90 (m, CH_2), 2.77 (d, J(H,H) = 9.8 Hz, HC=C*Ht*Bu), 1.08 (s, *t*Bu); ^{13}C NMR (22.5 MHz, $CDCl_3$): δ = 98.75 (s, H*C*=CH*t*Bu), 85.8, 82.9, 78.9, 77.0 (each s, *C*H of C_5H_4), 69.7 (s, HC=*C*H*t*Bu), 66.0 (s, *C* of C_5H_4), 34.5 (s, *C*CH_3), 31.4 (s, C*C*H_3), 28.1 (s, *C*H_2).

[8] A. Nessel, *Dissertation*, Universität Würzburg 1991.

[9] Crystals from benzene; crystal dimensions 0.4 × 0.35 × 0.15 mm^3; monoclinic, space group $C2/c$; $Z = 8$; a = 20.050(8), b = 8.843(1), c = 24.25(1) Å; β = 99.53(2)°; V = 4241 Å^3; $\varrho_{exp.}$ = 2.16 g cm^{-3}; ϱ_{calcd} = 2.18 g cm^{-3}; max. $2\theta = 40°$ ($Mo_{K\alpha}$, λ = 0.70930 Å, graphite monochromator, zirconium filter, ω/θ scan); 4140 independent reflections, Lp and empirical absorption correction (μ = 62.5 cm^{-1}, ψ scan method, min. transmission 34%); direct methods (SHELXS-86), refinement with program packet SDP (Enraf-Nonius), hydrogen atoms calculated for ideal geometry, varied according to a riding method; R = 0.032, R_w = 0.041 for 1742 structure factors ($I_o > 3\sigma(I_o)$); reflex/parameter 6.55; residual electron density + 0.96/−1.16 eÅ^{-3}. Further details of the X-ray structure analysis are available on request from the Fachinformationszentrum Karlsruhe, Gesellschaft für wissenschaftlich-technische Information mbH, W-7514 Eggenstein-Leopoldshafen 2 (FRG), on quoting the depository number CSD-55 364, the names of the authors, and the journal citation.

[10] a) D. M. Heinekey, S. T. Michel, G. K. Schulte, *Organometallics 8* (1989) 1241; b) W. D. McGhee, R. G. Bergman, *J. Am. Chem. Soc. 110* (1988)

4246; c) M. D. Rausch, R. G. Gastinger, S. A. Gardner, R. K. Brown, J. S. Wood, *ibid. 99* (1977) 7870.
[11] R. G. Ball, W. A. G. Graham, D. M. Heinekey, J. K. Hoyano, A. D. McMaster, B. M. Mattson, S. T. Michel, *Inorg. Chem. 29* (1990) 2023.
[12] In the less strained binuclear rhodium complex $[\{CH_2(C_5H_4)_2\}\{Rh_2(CO)_2(\mu\text{-}CO)\}]$ the angle C-CH_2-C is 112.3(4)°: H. Werner, H. J. Scholz, R. Zolk, *Chem. Ber. 118* (1985) 4531.
[13] P. Caddy, M. Green, L. E. Smart, N. White, *J. Chem. Soc. Chem. Commun. 1978*, 839.
[14] T.-S. Peng, J. A. Gladysz, *Organometallics 9* (1990) 2884.
[15] Prepared from $[C_5H_5Ir(C_2H_4)_2]$ and Br_2 in hexane: J. Wolf, unpublished.

Titanate-Catalyzed Enantioselective Addition of Dialkylzinc Compounds—Generated in situ from Grignard Reagents in Ether—to Aldehydes**

By *Dieter Seebach,* Linda Behrendt,* and *Dorothee Felix*

Dedicated to Prof. Dr. Vlado Prelog on the occasion of his 85th birthday

Although zinc compounds are much older than Grignard reagents,[1] they play only a minor role in modern organic synthesis. Thus, the catalytic enantioselective addition of R_2Zn compounds[2] to aldehydes has been performed almost exclusively with commercially available solutions of diethylzinc in hexane or toluene.[3] Recently we discovered[4] that the reaction of diethylzinc with benzaldehyde, catalyzed by the spirotitanate **1**, gives enantioselectivities of 99:1 both

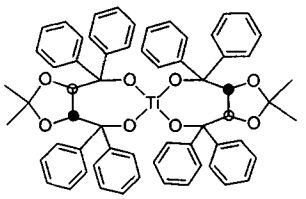

1

Scheme 1. Spirotitanate **1** synthesized from (*R,R*)-tartaric acid.

in ether and in toluene. This lead us to wonder if it would be possible to prepare MgX_2-free solutions of other dialkylzinc compounds[5a] directly from Grignard reagents,[5b] generated under the usual conditions according to Equation (a).

We took advantage of the well-known Schlenk equilibrium [Eq. (b)], which enables dialkylmagnesium compounds to be obtained pure after precipitation of MgX_2 with dioxane,[6] and treated Grignard solutions first with anhydrous $ZnCl_2$ [Eq. (c)], and then with dioxane. Separation of the precipitated $MgX_2 \cdot C_4H_8O_2$ complex, Equation (d),[2] gave clear solutions[7] which were used directly in the tetraisopropyltitanate-mediated addition to aldehydes, enantioselectively catalyzed by **1**. The whole one-pot procedure is shown in Equation (e); details about the conversions leading to alcohols **2**–**14** in > 90% *ee* are given in Table 1. Our initial concern that the longer chain alkylzinc and/or -titanium derivatives formed in solution would decompose by β-hydride abstraction[12] proved to be needless. Only primary alkylzinc reagents reacted with high enantioselectivities;[13] the conversion seems sensitive to steric congestion.[14]

In the course of determining the enantiomeric excess of the *sec*-alcohols produced—some of which have not yet been described in optically active form—we reached the limits of routine NMR methodology.[15] We therefore switched to GC analysis on chiral phases; details are given in Table 1.[16]

$$RCH_2X + Mg \xrightarrow{Et_2O} RCH_2MgX \quad (a)$$

$$2\,RCH_2MgX \rightleftharpoons (RCH_2)_2Mg + MgX_2 \quad (b)$$

$$2\,RCH_2MgX + ZnCl_2 \rightleftharpoons (RCH_2)_2Zn + MgX_2 + MgCl_2 \quad (c)$$

$$MgX_2 + \text{dioxane} \longrightarrow X_2Mg \cdot \text{dioxane} \downarrow \quad (d)$$

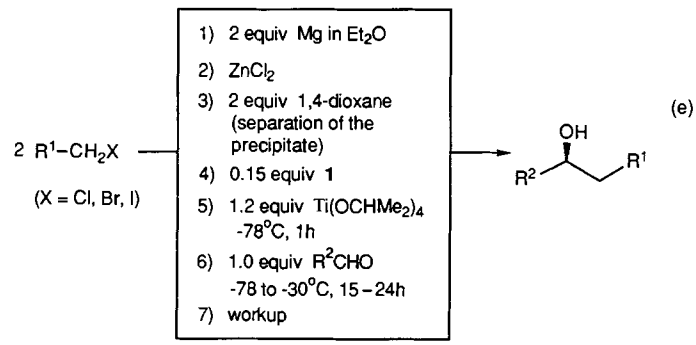

(e)

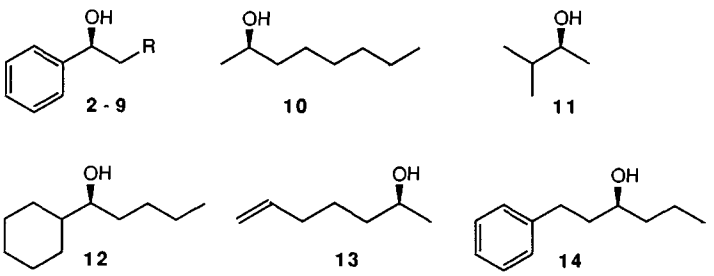

Table 1. Reaction of several primary Grignard reagents with aldehydes under the conditions given in Eq. (e) and in the experimental procedure [8a]. *R/S* ratios determined by gas chromatography [8–11].

Grignard reagent	aldehyde	product	yield [%]	*S/R*
CH_3MgI	C_6H_5CHO	**2**	55	97:3
C_2H_5MgBr	C_6H_5CHO	**3**	40	99:1
C_3H_7MgBr	C_6H_5CHO	**4**	52	99:1
C_4H_9MgBr	C_6H_5CHO	**5**	82	98:2
C_4H_9MgCl	C_6H_5CHO	**5**	70	99:1
$C_8H_{17}MgBr$	C_6H_5CHO	**6**	31[a]	98:2
$(CH_3)_2CHCH_2MgBr$	C_6H_5CHO	**7**	30[b]	97.5:2.5
$(CH_3)_2CH(CH_2)_2MgBr$	C_6H_5CHO	**8**	82	98.5:1.5[e]
$CH_2{=}CH(CH_2)_2MgBr$	C_6H_5CHO	**9**	83	95:5[e]
$C_6H_{13}MgI$	CH_3CHO	**10**	> 98	15:85[f]
CH_3MgBr	$(CH_3)_2CHCHO$	**11**	40[c]	> 95:5
C_4H_9MgBr	*cyclo*-$C_6H_{11}CHO$	**12**	35[d]	95:5
CH_3MgI	$CH_2{=}CH(CH_2)_3CHO$	**13**	69	97.5:2.5
C_3H_7MgBr	$C_6H_5(CH_2)_2CHO$	**14**	60	> 95:5[e, f]

[a] The zinc reagent was used in insufficient amounts. [b] Conversion occurred very slowly; reaction time 60 h. [c] Isolation made difficult by low b.p. of **11**. [d] Reaction was quenched too early. [e] Determination of the absolute configuration of the main enantiomer is based on the assumption that the alkyl group is transferred to the *Si* face of the aldehyde. [f] GC separation was not successful; *S/R* ratio determined by $[\alpha]_D$.

[*] Prof. Dr. D. Seebach, Dipl.-Chem. L. Behrendt, Dr. D. Felix
Laboratorium für Organische Chemie der Eidgenössischen Technischen Hochschule
ETH-Zentrum, Universitätstrasse 16, CH-8092 Zürich (Switzerland)

[**] The results described herein are part of the proposed dissertation of *L. Behrendt*. This research was generously supported by Firmenich SA (Geneva) and Sandoz AG (Basel).

The results in this communication are progress toward development of enantioselective and catalytic variants of classical reactions in organic synthesis.[3, 17]

Typical procedure

8: A 1.0 M zinc chloride solution in Et_2O (Aldrich) [20 mL, 0.02 mol] was diluted with 10 mL Et_2O and isopentyl magnesium bromide (0.04 mol in ether, ca. 2.2 M) was added. The resulting suspension was stirred at room temperature for 2 h, then treated with 12 mL 1,4-dioxane, and stirred for an additional 45 min. Subsequent filtration under an inert atmosphere yielded a clear solution of zinc reagent. This was added at −78 °C to a previously prepared solution of spiro compound **1** (1.38 g, 1.4 mmol) and $Ti(OCHMe_2)_4$ (3.57 mL, 12 mmol) in 20 mL of Et_2O. The mixture was stirred at −78 °C for 1 h, PhCHO (1.0 mL, 10 mmol) was added, and the reaction temperature was raised to − 30 °C. After complete conversion (TLC assay) the reaction was quenched at − 30 °C with saturated NH_4Cl solution (20 mL), ether added (50 mL), and the mixture filtered through Celite. The organic layer was washed with water and brine, dried over Na_2SO_4, filtered, and evaporated in vacuo. Pentane was added to the resulting oil, which initiated the crystallization of the diol ligand originating from spiro compound **1**. The supernatant was again concentrated in vacuo and compound **8** isolated by bulb-to-bulb distillation. (For other conversions the product was additionally purified by flash chromatography through a short silica gel column.)

Received: March 8, 1991 [Z 4482 IE]
German version: *Angew. Chem. 103* (1991) 991

CAS Registry numbers:
1, 131213-82-6; **2**, 1445-91-6; **3**, 613-87-6; **4**, 22135-49-5; **5**, 33652-83-4; **6**, 131320-85-9; **7**, 66283-21-4; **8**, 89537-67-7; **9**, 134679-60-0; **10**, 61925-50-6; **11**, 1517-66-4; **12**, 93548-33-5; **13**, 88980-13-6; **14**, 134627-14-8; CH_3MgI, 917-64-6; C_2H_5MgBr, 925-90-6; C_3H_7MgBr, 927-77-5; C_4H_9MgBr, 693-03-8; C_4H_9MgCl, 693-04-9; $C_8H_{17}MgBr$, 17049-49-9; $(CH_3)_2CHCH_2MgBr$, 926-62-5; $(CH_3)_2CH(CH_2)_2MgBr$, 4548-78-1; $CH_2=CH(CH_2)_2MgBr$, 7103-09-5; $C_6H_{13}MgI$, 89583-95-9; CH_3MgBr, 75-16-1; C_6H_5CHO, 100-52-7; $(CH_3)_2CHCHO$, 78-84-2; *cyclo*-$C_6H_{11}CHO$, 2043-61-0; $CH_2=CH(CH_2)_3CHO$, 764-59-0; $C_6H_5(CH_2)_2CHO$, 104-53-0; $ZnCl_2$, 7646-85-7; $Ti(OCHMe_2)_4$, 546-68-9.

[1] E. Frankland, *Ann. Chem. Pharm. 71* (1849) 171–213; P. Barbier, *C. R. Hebd. Seances Acad. Sci. 128* (1899) 110; V. Grignard, *ibid. 130* (1900) 1322.

[2] K. Nützel, *Methoden der Organischen Chemie (Houben-Weyl) 4th ed.*, Vol. XIII/2a, 570–634; see especially pp. 598 and 599.

[3] Of nearly 100 cited examples in the newest review article, about 85 are performed with diethylzinc and nearly all of them in toluene or hexane: R. Noyori, M. Kitamura, *Angew. Chem. 103* (1991) 34–55; *Angew. Chem. Int. Ed. Engl. 30* (1991) 49–69.

[4] B. Schmidt, D. Seebach, *Angew. Chem. 103* (1991) 100; *Angew. Chem. Int. Ed. Engl. 30* (1991) 99.

[5] a) By this procedure the handling of hazardous dialkyl zinc compounds is avoided. The principle of transmetalation from Mg to Zn derivatives has been known for quite a long time; see [1, 2]. b) The example of $Bu_2Mg + C_6H_5CHO$ showed that magnesium alkyl compounds do not themselves add enantioselectively to aldehydes with **1**/$Ti(OCHMe_2)_4$ (solvent: Et_2O/dioxan 10/1; − 100 to −78 °C, 53% **5**, 5% *ee*).

[6] W. Schlenk, W. Schlenk, *Ber. Dtsch. Chem. Ges. 62* (1929) 920; see also [2] p. 197.

[7] The transmetalation of Li compounds is also possible; a Bu_2Zn solution generated from BuLi and $ZnCl_2$ (2/1 in toluene) afforded, after steps 4–7 in Equation (e), **5** in a *S*/*R*-ratio of 99.5:0.5.

[8] a) All experiments have been carried out only once and are therefore not optimized. In contrast to most other catalysts used for enantioselective additions to carbonyl compounds to date, *both* enantiomeric forms of the one used in this case are easily accessible! The given configuration (*R*,*S*) of the enantiomer formed in excess was deduced by comparison of the measured $[\alpha]_D$ rotations with the literature values (*S* in the cases of **2**–**9** and **11**–**14**, *R* in the case of **10**) [8 b]. Unless otherwise noted, the enantiomeric excesses have been determined by gas chromatography: Alcohols **2**, **3**, **5**–**8**, **11**–**13** on heptakis(2,3,6-tri-*O*-methyl)-β-cyclodextrin in OV 1701 Vi [9, 11], 52 m × 0.27 mm (I.D.); **4**, **9** (TFA derivative) on octakis(3-*O*-butanoyl-2,6-di-*O*-*n*-pentyl)-γ-cyclodextrin in OV 1701 Vi (1:2) [10, 11], 50 m × 0.27 mm (I.D.). b) J. J. C. Gros, S. Bourcier in H. B. Kagan (Ed.): *Stereochemistry—Fundamentals and Methods, Vol. 4*, ("Absolute Configurations of 6000 Selected Compounds with One Asymmetric Carbon Atom") Thieme, Stuttgart 1977; S. H. Wilen in E. L. Eliel (Ed.): *Tables of Resolving Agents and Optical Resolutions*, University of Notre Dame Press, Notre Dame, IN, USA 1972; *Beilsteins Handbuch der Organischen Chemie, Bd. 1, 4, 1.–4. Ergänzungswerk*, Springer, Heidelberg; K. Mori, R. Bernotas, *Tetrahedron: Asymmetry 1* (1990) 87. The optical rotations of known compounds have in each case been measured in the solvent stated in the literature ($CHCl_3$, CCl_4, C_6H_6, C_2H_5OH, Et_2O, *n*-C_7H_{16}, or neat) and have been in reasonable agreement with the values given there.

[9] V. Schurig, H.-P. Nowotny, *J. Chromatogr. 441* (1988) 155–163; H.-P. Nowotny, D. Schmalzing, D. Wistuba, V. Schurig, *J. High Resolut. Chromatogr. 12* (1989) 383.

[10] W. A. König, R. Krebber, P. Mischnick, *J. High Resolut. Chromatogr. 12* (1989) 732.

[11] K. Grob: *Making and Manipulating Capillary Columns for Gas Chromatography*, Hüthig, Heidelberg 1986.

[12] D. Seebach, B. Weidmann, L. Widler in R. Scheffold (Ed.): *Modern Synthetic Methods, Vol. 3*, Salle & Sauerländer, (Aarau, Schweiz) and J. Wiley & Sons (New York, USA) 1983, pp. 217–353; H. G. Raubenheimer, D. Seebach, *Chimia 40* (1986) 12. The ate-complexes of **1** mentioned in [4] have only been stable with methyl or allyl; with butyl a green colour appeared [indicates Ti(III)derivatives].

[13] $(Me_2CH)_2Zn$ generated from $Me_2CHMgBr$ yielded after 55 h 88% of the adduct with PhCHO, *S*/*R* = 71/29. With $PhCH_2Cl$ and PhCHO 27% *rac*-$PhCH(OH)CH_2C_6H_5$ was obtained according to Equation (e).

[14] Cf. the slow formation of **7** (Table 1). With Me_3CCH_2Br and PhCHO, according to Equation (e) except at room temperature and for 72 h, we did not obtain any product. Me_3CCHO and Bu_2Zn gave 10% yield of $Me_3CCH(OH)Bu$ in 65% *ee* after 4 d.

[15] NMR shift reagents often cause a signal broadening unfavorable for determining extreme enantiomeric ratios. Derivatization, e.g. according to Mosher, may lead to changed isomeric ratios (kinetic resolution) and depends on the enantiomeric purity of the reagent, cf. W. A. König, K.-S. Nippe, P. Mischnick, *Tetrahedron Lett. 31* (1990) 6867.

[16] The diol used to prepare **1** has a great tendency to form inclusion compounds [K. Mori, F. Toda, *Tetrahedron: Asym. 1* (1990) 281; F. Toda, R. Toyotaka, H. Fukuda, *ibid. 1* (1990) 303]; we ensured in every case that the diol which separated during workup had no alcohol included—in which case the enantiomeric ratio could have been altered.

[17] D. Seebach, *Angew. Chem. 102* (1990) 1363; *Angew. Chem. Int. Ed. Engl. 29* (1990) 1320.

A Homogeneous Platinum Catalyst in the Stationary $BF_3 \cdot H_2O$ Phase for the Hydrogenation of Arenes**

By *István T. Horváth**

Although liquid-phase homogeneous catalysts generally have higher catalytic activity and selectivity than heterogeneous systems, product separation could be a major obstacle for industrial application.[1] An attractive solution to the separation problem is the immobilization of the liquid phase on solid carriers (Fig. 1).[2] The liquid phase can be the catalyst itself, or it may contain a dissolved catalyst. In order to maintain the catalytic performance of a supported liquid-phase (SLP) catalyst, the liquid phase must remain on the support throughout the reaction. An ideal SLP catalyst does not lose its liquid phase, which is therefore stationary, and the catalyst may be called a *stationary liquid-phase catalyst*.[3] Most of the SLP catalysts are used to catalyze reactions between gaseous reactants leading to gaseous products.[2g] SLP catalysts can also use a supported liquid phase with limited solubility in the reactants, products, and/or solvents. Water or aqueous acids are excellent choices for organic reactions performed in apolar media, and several such aqueous systems have been developed.[4]

Reduction of aromatic hydrocarbons has recently received much attention as a result of increased environmental

[*] Dr. István T. Horváth
Corporate Research Laboratories
Exxon Research and Engineering Company
Annandale, NJ 08801 (USA)

[**] The very careful technical work by *Raymond A. Cook* is gratefully acknowledged. Dr. *Michel Daage* and Dr. *John Robbins* (Exxon Research and Engineering Company) and Professor *John W. Larsen* (Lehigh University) are thanked for their helpful discussions.

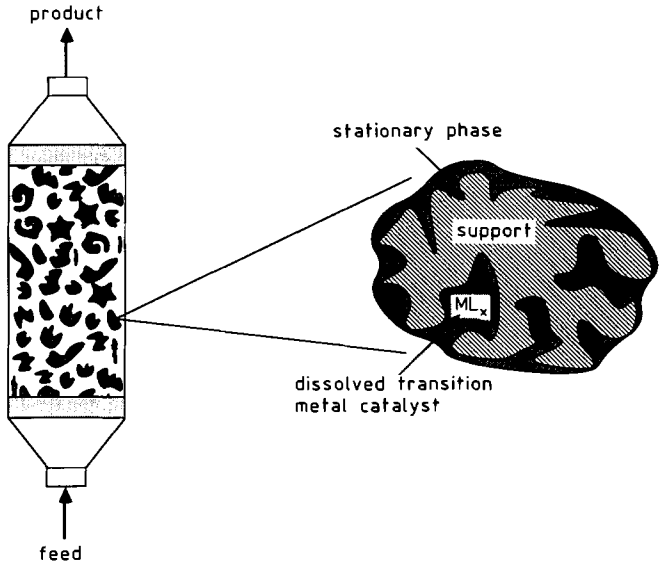

Fig. 1. Catalytic liquid phase immobilized on a solid support.

concern. Although heterogeneous transition-metal catalysts could be used for the hydrogenation of arenes, they generally require severe reaction conditions under which cracking and other undesirable side reactions could occur. In contrast, several homogeneous transition-metal catalysts are capable of selectively hydrogenating arenes at mild conditions.[5] Their application however, is limited by the difficult separation of the products from the catalysts. We wish to report the development of a stationary $BF_3 \cdot H_2O$ phase platinum catalyst for the hydrogenation of aromatic hydrocarbons at mild conditions.

A typical catalyst is prepared by impregnating 2 g of support[6] with a yellow solution of 0.2 mmol $PtCl_2(CH_3CN)_2$ in 1.4 g $BF_3 \cdot H_2O$ (an ionic platinum hydrogenation catalyst system developed by *Larsen* et al.[5i]) by the incipient wetness technique under N_2. The system is used without further treatment. The fresh catalyst is light yellow, and ^{195}Pt NMR spectroscopy of the liquid phase indicates the presence of two Pt^{II} species.[7] Hydrogenation of arenes occurs rapidly even at 25 °C under 2.76 MPa (400 psi) H_2 (Table 1), and the colorless products can be separated from the catalyst by filtration.[8] The hydrogenation of benzene leads to the quantitative formation of cyclohexane: no GC or NMR evidence was found for the presence of hydrogenolyzed, cracked, or partially reduced products. The benzene hydrogenation rate increases proportionally with increasing concentration of $[PtCl_2(CH_3CN)_2]$. Reduction of naphthalene results in the transient formation of tetralin, as expected, which is then hydrogenated to *cis*- and *trans*-decalin

Table 1. Hydrogenation of aromatic hydrocarbons with a homogeneous SLP $BF_3 \cdot H_2O$–platinum catalyst.

Arene	[C] [mmol]	[Pt] [mmol]	$BF_3 \cdot H_2O$ [g]	Support[a]	M[b] [g]	T [°C]	p[c] [MPa]	k[d] [mmol h^{-1}]
Benzene	385	0.10	1.4	CPG-240	2	25	2.76	20
Benzene	385	0.15	1.4	CPG-240	2	25	2.76	30
Benzene	385	0.20	1.4	CPG-240	2	25	2.76	40
Benzene	418	0.29	1.4	clay	2	25	5.52	52
Benzene	400	0.72	3.5	clay	5	40	5.52	435
Benzene	383	0.72	3.5	clay	5	75	5.52	958
Toluene	385	0.20	1.4	CPG-240	2	25	2.76	38
o-Xylene	385	0.20	1.4	CPG-240	2	25	2.76	35
Naphtalene	78	0.20	1.4	CPG-240	2	25	2.76	20

[a] See ref. [6]. [b] Amount of support. [c] H_2 partial pressure; 2.76 MPa = 400 psi. [d] Initial rate.

in a ratio of 9:1. During the course of the reactions the catalyst turns black, indicating slow reduction of some Pt^{II} species to metallic platinum. Treatment of the catalyst with H_2 prior to the addition of benzene also results in metallic platinum formation and catalyst deactivation.[9] In order to monitor the possible role of the chemical composition of the support, the hydrogenation of the 1:1:1:1 mixture of benzene, toluene, *o*-xylene, and 1,2,4-trimethylbenzene was investigated using different supports. The same catalytic system supported on CPG-240[6a] or on clay[6b] shows almost identical hydrogenation activities (Table 2). These data suggest that the support does not participate chemically in the hydrogenation, and the catalyst is operating in the aqueous acid phase.

Since SLP catalysts could lose catalytically active species into the organic phase, a leaching test was performed by using two autoclaves connected through a 7 μm filter. In the first autoclave toluene was hydrogenated at 2.76 MPa (400 psi) H_2 partial pressure and 25 °C to methylcyclohexane up to 68% conversion.[8] The solution was then pumped through the filter at 2.76 MPa and 25 °C into the second autoclave, leaving the SLP $BF_3 \cdot H_2O$–platinum catalyst in the former. The second autoclave also contained benzene. No further reaction was found for toluene and no reaction at all for benzene in the next 24 hours. These results unambiguously show that no catalytically active platinum species is leached from the stationary $BF_3 \cdot H_2O$ phase under hydrogenation conditions.

The continuous performance of the $BF_3 \cdot H_2O$–platinum catalyst was investigated in a tubular trickle-bed reactor (∅ 12.5 mm).[10] Benzene and solvents were neither dried nor saturated with $BF_3 \cdot H_2O$. The hydrogenation of benzene was performed at 25 °C and 2.76 MPa H_2 using 0.1 g $[PtCl_2(CH_3CN)_2]$ in 1.4 g $BF_3 \cdot H_2O$ on 2.0 g SiO_2[6c] as catalyst. During the first four hours the catalyst reached its steady-state (10% conversion of benzene to cyclohexane)

Table 2. Selectivities for the reduction of a 1:1:1:1 mixture of benzene, toluene, *o*-xylene, and 1,2,4-trimethylbenzene with a homogeneous SLP $BF_3 \cdot H_2O$–platinum catalyst at 22 °C under 2.76 MPa H_2.

Time [h]	Support	C_6H_6	C_6H_{12}	MeC_6H_5	MeC_6H_{11}	$Me_2C_6H_4$	$Me_2C_6H_{10}$	$Me_3C_6H_3$	$Me_3C_6H_9$
2	CPG	89.8	10.1	93.5	6.5	97.4	2.6	99.3	0.7
2	Clay	90.1	9.9	93.3	6.6	97.2	2.7	99.1	0.9
4	CPG	78.0	21.9	85.4	14.9	93.8	6.1	97.9	2.1
4	Clay	77.8	22.1	84.5	15.3	93.6	6.4	98.7	1.2
6	CPG	65.7	34.3	75.8	24.2	89.3	11.7	97.2	2.9
6	Clay	66.2	33.8	76.1	23.9	89.6	10.6	98.0	1.9
8	CPG	54.3	45.7	66.2	33.8	84.6	15.4	95.1	4.8
8	Clay	53.5	46.6	65.7	34.4	85.0	15.1	96.3	4.6

and retained this activity over the next 48 hours. After this period the conversion gradually decreased indicating slow catalyst deactivation. The reaction was stopped after 75 hours, while the catalyst was still active, for catalyst characterization. The used catalyst again contained some metallic platinum. Elemental and water analyses revealed that the amount of water on the catalyst had increased slightly and that some BF_3 had leached from the $BF_3 \cdot H_2O$ phase.[11] These results implied that the BF_3/H_2O ratio decreased during the reaction, leading to a weaker and less active acid system. Indeed, when $BF_3 \cdot 1.3\,H_2O$ was used as a liquid phase for the hydrogenation of benzene, the catalytic activity dropped by 30%.

The effect of the lower acidity suggests that the reaction is initiated by the protonation of the arene ring either by $H[BF_3OH]$ or by a cationic platinum species formed by the reaction of $[PtCl_2(MeCN)_2]$ and $BF_3 \cdot H_2O$ under hydrogen. In the first case the formed arenium ion is then hydrogenated by a platinum species able to activate and transfer three moles of molecular hydrogen. In contrast, in the second mechanism the initially formed platinum complex activates and transfers the H_2 to the already coordinated arene ring. To gain further insight into how the catalytic system operates, we are currently investigating the hydrogenation of $[D_6]$benzene at 25 °C and a H_2 pressure of 2.76 MPa.[5b,h] Preliminary GC–MS and NMR analysis of samples taken periodically showed less than 0.5% D/H exchange for $[D_6]$benzene and the formation of 99.5% pure $[D_6]$cyclohexane.[12] While the formation of platinum colloids cannot be ruled out at present, the results are consistent with a homogeneous platinum complex system operating in the liquid phase.

Received: February 1, 1991 [Z 4418IE]
German version: *Angew. Chem. 103* (1991) 1042

CAS Registry numbers:
$[PtCl_2(CH_3CN)_2]$, 13869-38-0; $BF_3 \cdot H_2O$, 15799-89-0; C_6H_{12}, 110-82-7; MeC_6H_{11}, 108-87-2; $Me_2C_6H_{10}$, 583-57-3; $Me_3C_6H_9$, 2234-75-5; benzene, 71-43-2; toluene, 108-88-3; *o*-xylene, 95-47-6; naphthalene, 91-20-3; 1,2,4-trimethylbenzene, 95-63-6; *cis*-decalin, 493-01-6; *trans*-decalin, 493-02-7.

[1] a) G. W. Parshall: *Homogeneous Catalysis*, Wiley, New York 1980; b) J. P. Collman, L. S. Hegedus, J. R. Norton, R. G. Finke: *Principles and Applications of Organometallic Chemistry*, University Science Books, Mill Valley, CA, USA 1987.

[2] a) R. Z. Moravec, W. T. Schelling, C. F. Oldershaw, GB-B 511 556; b) R. Z. Moravec, W. T. Schelling, C. F. Oldershaw, CA-B 396994; c) G. J. K. Acres, D. C. Bond, B. J. Cooper, J. A. Dawson, *J. Catal. 6* (1966) 139; d) P. R. Rony, *Chem. Eng. Sci. 23* (1968) 1021; e) P. R. Rony, *J. Catal. 14* (1969) 142; f) P. R. Rony, J. M. Roth, *J. Mol. Catal. 1* (1975/76) 13; g) J. Villadsen, H. Livbjerg, *Catal. Rev. Sci. Eng. 17* (1978) 203.

[3] While the letter S in the abbreviation of SLP catalyst can stand either for supported or stationary liquid phase, the latter is perhaps a more accurate and precise description for a catalyst of constant performance.

[4] a) G. E. Langlois, J. E. Walkey, *Pet. Refiner 31* (1952) 79; b) R. E. Robinson, US-A 3190912; c) K. Fujimoto, Y. Negami, T. Takahashi, T. Kunugi, *Ind. Eng. Chem. Prod. Res. Dev. 11* (1972) 303; *ibid. 13* (1972) 237; d) I. S. Shaw, J. S. Dranoff, J. B. Butt, *Ind. Eng. Chem. Res. 27* (1988) 935; e) J. P. Arhancet, M. E. Davis, J. S. Merola, B. E. Hanson, *Nature (London) 339* (1989) 454; *J. Catal. 121* (1990) 327; f) I. T. Horváth, *Catal. Lett. 6* (1990) 43.

[5] a) E. L. Muetterties, F. J. Hirsekorn, *J. Am. Chem. Soc. 96* (1974) 4063; b) E. L. Muetterties, M. C. Rakowski, F. J. Hirsekorn, W. D. Larson, V. J. Basus, F. A. L. Anet *ibid. 97* (1975) 751; c) M. J. Russell, C. White, P. M. Maitlis, *J. Chem. Soc. Chem. Commun. 1977*, 427; d) P. M. Maitlis, *Acc. Chem. Res. 11* (1978) 301; e) E. L. Muetterties, J. R. Bleeke, *ibid. 12* (1979) 324; f) M. A. Bennett, *CHEMTECH 1980*, 444; g) R. H. Fish, *Ann. N. Y. Acad. Sci. 415* (1983) 292; h) J. Blum, I. Amer, K. P. C. Vollhardt, H. Schwartz, G. Hohne, *J. Org. Chem. 52* (1987) 2804; i) J. C. Cheng, J. Maioriello, J. W. Larsen, *Energy Fuels 3* (1989) 321; j) R. H. Fish, *Aspects Homogeneous Catal. 7* (1990) 65.

[6] a) CPG-240: silica, pore diameter 237 Å; pore volume 0.95 mL g^{-1}; surface area 77.5 m^2 g^{-1}; b) clay (attapulgite): pore volume 0.5 mL g^{-1}; surface area 110 m^2 g^{-1}; c) Shell Silica Spheres (S980 G): pore diameter 50 Å, pore volume 1.0 mL g^{-1}, surface area 80 m^2 g^{-1}.

[7] The ^{195}Pt NMR spectrum of 0.28 g $[PtCl_2(MeCN)_2]$ in 5.6 g D_2O shows two signals at $\delta = -2048$ and -2070, both in the typcial chemical shift region for Pt^{II} metal complexes. The identification of this species is in progress.

[8] The hydrogenation reactions were performed at constant pressures in a 300 mL-Hastelloy (H) autoclave equipped with a 7 μm filter attached to the dip-leg for sample removal. In a typcial procedure the reactor was charged with the catalyst and 70 g *n*-heptane as solvent under N_2 at 25 °C. The arenes were added at reaction pressure, and the progress of the reactions were followed by GC analysis of samples taken periodically.

[9] Pretreatment of the catalyst with 2.76 MPa (400 psi) H_2 for 18 and 89 hours decreases the rate of the hydrogenation of benzene by a factor 0.75 and 0.4 respectively.

[10] A solution of 30% benzene in *n*-heptane was used at 0.25 mL min^{-1} feed rate and 75 mL min^{-1} H_2 flow rate.

[11] Addition of 0.5% $BF_3 \cdot OEt_2$ to the feed did not stabilize the catalyst, suggesting a complicated deactivation mechanism.

[12] ^{13}C NMR spectroscopy of the CS_2 solution of $[D_6]$cyclohexane revealed the presence of two species in a ratio of 92 to 8. The elucidation of the stereochemistry of $C_6H_6D_6$ is in progress.

Mixed-Anion Aggregates of Metalated Organics: Preparation and Structure of the Mixed-Anion Tetramer $(PhO^{\ominus}Li^{\oplus} \cdot HMPA)_3(\mu_3\text{-}HMPA \cdot Li^{\oplus})NCS^{\ominus}$ **

By *Paul R. Raithby, David Reed, Ronald Snaith,** and *Dominic S. Wright*

We report the planned syntheses and structures of two unusual lithium compounds. The lithium phenoxide complex **1** [HMPA = $OP(NMe_2)_3$] is *moisture-stable*, and molecular mass measurements and ^{7}Li, ^{31}P NMR spectroscopy show it to be a tetramer ($n = 4$) in arene solutions. Complex **1** has been used as a template in the course of developing a route to *mixed-anion* metalated species. Thus, reaction of phenol *and* an inorganic-anion source, ammonium thiocyanate (NH_4NCS), with butyllithium (3:1:4 molar ratios) in toluene containing HMPA affords **2**. The crystal structure of **2** shows that it also is a cubane-like tetramer; however, the $NCS^{\ominus}$ anion does not bridge $Li^{\oplus}$ cations in a μ_3 manner (as the $PhO^{\ominus}$ anions do), but rather one HMPA so bridges and $NCS^{\ominus}$ is terminal on one $Li^{\oplus}$.

$(PhO^{\ominus}Li^{\oplus} \cdot HMPA)_n$ **1** $(PhO^{\ominus}Li^{\oplus} \cdot HMPA)_3(\mu_3\text{-}HMPA \cdot Li^{\oplus})NCS^{\ominus}$ **2**

Complex **1** aroused our interest in view of our recent findings that water can be a ligand within lithiated organics $R^{\ominus}Li^{\oplus}$ ($R^{\ominus}$ = alkyl, aryl, alkynyl, amido, enolato, alkoxy etc.). Such species are notoriously moisture-sensitive, i.e., equilibrium (a) lies to the right, yet in complexes such as $OxLi \cdot TMEDA \cdot H_2O$ ($Ox^{\ominus}$ = 2-mercaptobenzoxazoyl, $C_6H_4O(C{=}S)N^{\ominus}$, TMEDA = $Me_2N(CH_2)_2NMe_2$),[1a]

[*] Dr. R. Snaith, Dr. P. R. Raithby, Dr. D. S. Wright
University Chemical Laboratory
Lensfield Road, Cambridge CB2 1EW (UK)
Dr. D. Reed
Department of Chemistry
West Mains Road, Edinburgh EH9 3JJ (UK)

[**] This work was supported by Gonville and Caius College, Cambridge (Research Fellowship for *D. S. W.*) and by the Associated Octel Co. Ltd. (*R. S.*). We thank also the Science and Engineering Research Council (S.E.R.C.) for the provision of high-field NMR facilities.

$(OxLi \cdot HMPA \cdot H_2O)_2$, and $(OxLi \cdot HMPA)_2 \cdot H_2O$,[1b] equation (b) is valid.

$$R^{\ominus}Li^{\oplus} + H_2O \rightleftharpoons RH + Li^{\oplus}OH^{\ominus} \quad (a)$$

$$R^{\ominus}Li^{\oplus} + H_2O \longrightarrow R^{\ominus}Li^{\oplus} \cdot OH_2 \quad (b)$$

These aqua complexes are stable because the pK_a of OxH is slightly less than that of H_2O, and H_2O insertion displaces the $S^{\delta-}$ centers of the (NCS)Li chelate ring found in the anhydrous complexes, resulting in stabilizing $S^{\delta-} \cdots H_2O$ hydrogen bonding. We reasoned, therefore, that an $R^{\ominus}Li^{\oplus}$ whose precursor RH is substantially more acidic than H_2O, and which has no displaceable functionality to engage in hydrogen bonding with inserted H_2O, should be moisture-stable, i.e., the left-hand side of equilibrium (a) should dominate. Phenol is one obvious candidate. We found that reaction of PhOH with *n*BuLi (1:1) in toluene yielded an amorphous white solid, $(PhO^{\ominus}Li^{\oplus})_n$. However, a similar reaction in the presence of HMPA (1 equiv) afforded a solution, which gave crystals of **1** on refrigeration. As anticipated, these crystals were indefinitely air-stable: the IR and ^1H NMR spectra of samples exposed to air are identical to those of mulls and solutions made up under dry nitrogen. Indeed, **1** was recrystallized, unchanged, from aqueous toluene.

The crystal structure of **1** has not been resolved due to disorder among HMPA ligands, but it is probably a cubane-like tetramer (see Fig. 1). Such tetramers are the norm for 1:1

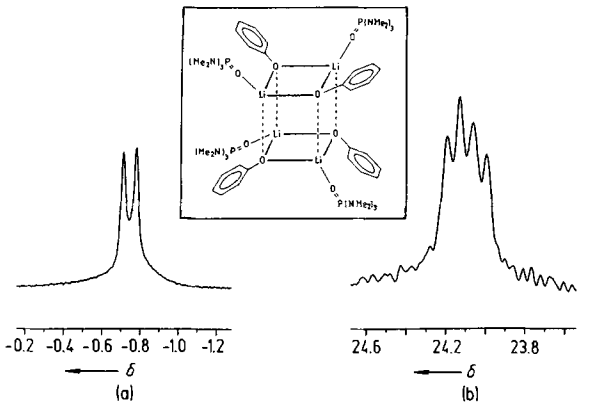

Fig. 1. NMR spectra of **1** in $C_6D_5CD_3$ at $-90\,^{\circ}C$. a) ^7Li b) ^{31}P. Inset: proposed tetrameric structure of **1**.

complexes of lithiated organics containing monodentate Lewis bases (L), such as lithium alkyls R_3CLi, aryls ArylLi, alkynyls $RC{\equiv}CLi$, imides $R_2C{=}NLi$, and enolates $R(=CH_2)COLi$.[2] This widespread occurrence has been rationalized using ring-stacking ideas.[2d, 3] A tetrameric structure is certainly evident from studies on **1** in solution. Cryoscopic relative molecular mass measurements give association state (n) values of 3.7 ± 0.2 (0.05 M benzene solution, relative to $n = 1$) to 4.0 ± 0.1 (0.20 M). The ^7Li NMR (139.96 MHz) spectrum of **1** in $C_6D_5CD_3$ (0.40 M) at $-90\,^{\circ}C$ consists of a doublet [Fig. 1(a)] corresponding to the coupling of each ^7Li nucleus to the ^{31}P atom of just one (i.e., a terminal) HMPA ligand [$^2J_{^7Li^{31}P} = 9.5$ Hz]. Such coupling through (O=P) bonds has been seen before, in the ^7Li NMR solution spectrum of $(LiBr)_2 \cdot 3\,HMPA$;[4] three μ_2-HMPA ligands link the LiBr units, giving a 1:3:3:1 quartet ($^2J = 3.8$ Hz; note the stronger coupling for terminal HMPA ligation in **1**). However, for the first time, such coupling is also observable in the ^{31}P NMR (145.79 MHz) spectrum [Fig. 1(b)]: recorded on the same solution of **1** at $-90\,^{\circ}C$, this consists of the expected 1:1:1:1 quartet (I of $^7Li = 3/2$), $^2J = 9.5$ Hz.

The stability and structure of **1** made it an ideal template for testing a synthetic strategy towards mixed-anion metalated species. Specifically, the recently described "ammonium salt route", which involves reacting solid NH_4X salts with a metal source (metal, hydride, or organometallic) and a Lewis base (L), has afforded many complexes of type $(M_aX_b \cdot xL)_n$, e.g., with M = Li, Na, K,[5a-f] Sr, Ba,[5g] La, Eu, Mn;[5h] X = an inorganic anion like Hal, NCS, BF_4; and L = HMPA, TMEDA etc.

Integration of this route with a usual metalation procedure (RH + metal source) should assemble *mixed-anion* complexes ($X^{\ominus}$ from NH_4X, $R^{\ominus}$ from RH), e.g., equation (c).

$$NH_4X_{(s)} + RH + 2n\text{BuLi} \xrightarrow[\text{toluene}]{x\,L} (Li^{\oplus}X^{\ominus}) \cdot (R^{\ominus}Li^{\oplus}) \cdot xL + NH_3 + 2n\text{BuH} \quad (c)$$

This idea works. It is easy to substitute just one $PhO^{\ominus}Li^{\oplus}$ unit by $Li^{\oplus}NCS^{\ominus}$ in **1**, $n = 4$. Thus, addition of *n*BuLi solution (4 equiv) to NH_4NCS (1 equiv) suspended in a toluene solution of PhOH and HMPA (3 and 4 equiv, respectively) caused a vigorous reaction accompanied by gas evolution. Chilling of the resulting solution afforded crystals of **2** in good yield. In contrast to **1**, **2** is air-sensitive. The solid-state structure of **2**[6] (Fig. 2) is a tetrameric array with four $Li^{\oplus}$

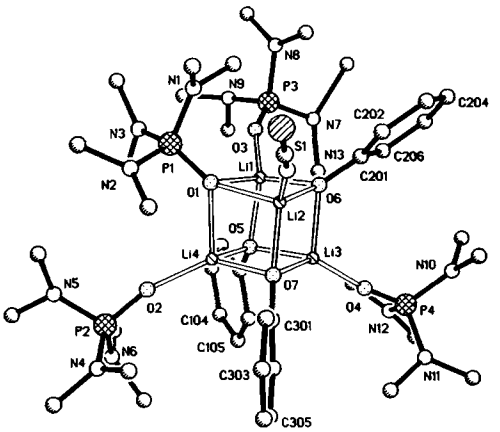

Fig. 2. Molecular structure of **2** in the crystal.

ions, three of which bear terminal HMPA ligands (mean Li–O distance, 1.88(2) Å). The three $PhO^{\ominus}$ anions form μ_3 bridges across the metal cations (mean Li–O distance, 1.98(2) Å). However, the fourth bridging position is taken up not by $NCS^{\ominus}$, which is terminal (Li–N distance, 2.04(2) Å), but by the fourth HMPA molecule (mean Li–O distance, 2.11(2) Å). Such a μ_3 mode for HMPA has been observed once before, in the structure of $(KNCS)_3 \cdot 5\,HMPA$ where two of the HMPA ligands cap a triangle of $K^{\oplus}$ ions.[5e]

Two sets of earlier results are pertinent to our studies on **2**. Firstly, IR spectroscopic investigations into the state of aggregation of LiNCS in ether solvents have shown that the CN stretching frequency is sensitive to structural changes: the monomeric ion pair $Li^{\oplus}NCS^{\ominus}$ (so with a terminal anion) has this band at ca. 2060–2070 cm^{-1},[7a] the $(Li^{\oplus}NCS^{\ominus})_2$ dimer (a μ_2-$NCS^{\ominus}$) at ca. 2030–2040 cm^{-1},[7b] and the

$(Li^{\oplus}NCS^{\ominus})_4$ cubane tetramer (a μ_3-$NCS^{\ominus}$) at ca. 1990–2000 cm^{-1}.[7c] Mixed halide–thiocyanate cubanes, e.g., $(LiBr)_3 \cdot LiNCS$ in Et_2O [$\tilde{\nu}$(CN), 2003 cm^{-1}] have also been detected.[7d] In the Nujol mull IR spectrum of **2** the major band occurs at 2072 cm^{-1}, in accord with the presence of terminal (rather than μ_3-) $NCS^{\ominus}$ ligands. Secondly, two mixed organolithium–lithium bromide tetramers have been isolated: $(PhLi \cdot OEt_2)_3 \cdot LiBr$[8a] and $[(cyclo\text{-}C_3H_5Li)_2 \cdot (LiBr)_2] \cdot 4Et_2O$.[8b] In both, the anions occupy corners of the cube, and all the Et_2O ligands are terminal (cf, the behavior of HMPA in **2**). These complexes were isolated from reactions of excess Li metal with PhBr and with *cyclo*-C_3H_5Br, respectively (yields: unspecified and ca. 30%). Presumably in each case the major product is the complexed "pure" organolithium, $(PhLi \cdot OEt_2)_4$[8a] and (*cyclo*-$C_3H_5Li \cdot OEt_2)_4$. Indeed, the major impetus of such work was the fact that commercially supplied organolithium solutions (e.g., MeLi, PhLi), synthesized from Li + RHal (2:1), are often catalogued as containing lithium halide. The results imply that specific mixed-anion aggregates are present in such solutions, which possess different (often enhanced) reactivity from that of the "pure" reagent. However, the isolation of these RLi–LiBr species can be contrasted with the currently described planned assembly of mixed-anion aggregates as the only product, as exemplified in the synthesis of **2**.

We are exploring the implications of the syntheses and properties of **1** and **2**. Complex **1** establishes likely thermodynamic ground rules for preparing moisture-stable metalated organics. The synthetic strategy leading to **2** promises particularly wide scope. R in RH, X in NH_4X, the metal M, and the donor L of equation (c) could all be varied, as could the $R^{\ominus}$:$X^{\ominus}$ stoichiometry (3:1 $PhO^{\ominus}$:$NCS^{\ominus}$ in **2**). Most importantly, the metal aggregate need not be a tetramer: even restricting M to Li, $(RLi)_n$ aggregates are known[2] with n = 2 and 3 (rings), 4 (rings and cubanes), 5 (trigonal bipyramid), 6 (pseudooctahedron), 8 (stacked dimeric rings), and higher.

Experimental Procedure

1: *n*-Butyllithium (6.3 mL, 1.60 M solution in hexane, 10 mmol) was added at 20 °C to a solution of phenol (0.94 g, 10 mmol) and HMPA (1.79 g, 10 mmol) in toluene (10 mL). A vigorous exothermic reaction ensued, producing a colorless solution. Refrigeration at 0 °C for two days gave an initial crop of colorless cubic crystals of **1**. First batch yield 0.91 g, 33%; further cooling afforded more of **1**; no other product was isolated. M.p. > 260 °C (decomp.); correct C, H, Li, N, P analyses; ^1H NMR (C_6D_6, 250 MHz, 25 °C) δ = 7.33 (m, 4H, *o*- and *m*-H of $PhO^{\ominus}$), 6.79 (t of t, 1H, *p*-H of $PhO^{\ominus}$), 2.35 (d, 18H of HMPA, J = 9.3 Hz). Cryoscopic relative molecular mass measurements on **1** were carried out using previously described procedures [9].

2: *n*-Butyllithium (6.3 mL, 1.60 M solution in hexane, 10 mmol) was added at 20 °C to a stirred suspension of NH_4NCS (0.19 g, 2.5 mmol) in toluene (10 mL) containing dissolved PhOH (0.71 g, 7.5 mmol) and HMPA (1.79 g, 10 mmol). A vigorous exothermic reaction and gas evolution ensued, during which all of the solid NH_4NCS reacted. The resulting solution was cooled to room temperature, giving colorless cubic crystals of **2**. First batch yield 1.51 g, 60%; further cooling afforded more of **2**; no other product was isolated. M.p. 240 °C (decomp.); correct C, H, N, P analyses; IR: (Nujol mull) $\tilde{\nu}$(CN) of $NCS^{\ominus}$ at 2072 cm^{-1} (vs), 2031 cm^{-1} (m); ^1H NMR (C_6D_6, 250 MHz, 20 °C) δ centered at 7.29 (m, 15H of 3 $PhO^{\ominus}$), 2.38 (d, 72H of 4 HMPA, J = 9.1 Hz).

Received: February 28, 1991 [Z 4462/4463]
German version: *Angew. Chem. 103* (1991) 1040

CAS Registry numbers: **1**, 134940-44-6; **2**, 134940-45-7.

[1] a) D. Barr, P. R. Raithby, P. von R. Schleyer, R. Snaith, D. S. Wright, *J. Chem. Soc. Chem. Commun. 1990*, 643; b) D. R. Armstrong, D. Barr, P. R. Raithby, P. von R. Schleyer, R. Snaith, D. S. Wright, *Inorg. Chim. Acta*, in press.

[2] For reviews describing the crystal structures of lithiated organics see: a) W. Setzer, P. von R. Schleyer, *Adv. Organomet. Chem. 24* (1985) 353; b) D. Seebach, *Angew. Chem. 100* (1988) 1685; *Angew. Chem. Int. Ed. Engl. 27* (1988) 1624; c) G. Boche, *ibid. 101* (1989) 286 and *28* (1989) 277; d) K. Gregory, P. von R. Schleyer, R. Snaith, *Adv. Inorg. Chem.*, in press.

[3] a) D. Barr, W. Clegg, R. E. Mulvey, R. Snaith, K. Wade, *J. Chem. Soc. Chem. Commun. 1986*, 295; b) D. R. Armstrong, D. Barr, R. Snaith, W. Clegg, R. E. Mulvey, K. Wade, D. Reed, *J. Chem. Soc. Dalton Trans. 1987*, 1071; c) D. Barr, R. Snaith, W. Clegg, R. E. Mulvey, K. Wade, *ibid. 1987*, 2141.

[4] D. Barr, M. J. Doyle, P. R. Raithby, R. Snaith, D. S. Wright, R. E. Mulvey, D. Reed, *J. Chem. Soc. Chem. Commun. 1989*, 318.

[5] a) D. Barr, R. Snaith, D. S. Wright, R. E. Mulvey, K. Wade, *J. Am. Chem. Soc. 109* (1987) 7891; b) D. Barr, M. J. Doyle, R. E. Mulvey, P. R. Raithby, R. Snaith, D. S. Wright, *J. Chem. Soc. Chem. Commun. 1988*, 145; c) D. Barr, M. J. Doyle, S. R. Drake, P. R. Raithby, R. Snaith, D. S. Wright, *ibid. 1988*, 1415; d) *Polyhedron 8* (1989) 215; e) *Inorg. Chem. 28* (1989) 1767; f) D. Barr, M. J. Doyle, P. R. Raithby, R. Snaith, D. S. Wright, R. E. Mulvey, D. Reed, *J. Chem. Soc. Chem. Commun. 1989*, 318; g) D. Barr, A. T. Brooker, M. J. Doyle, S. R. Drake, P. R. Raithby, R. Snaith, D. S. Wright, *ibid. 1989*, 893; h) *Angew. Chem. 102* (1990) 300; *Angew. Chem. Int. Ed. Engl. 29* (1990) 285.

[6] Crystal data for **2**: $C_{43}H_{87}N_{13}O_7P_4SLi_4$, monoclinic, $P2_1/a$ (alternative setting $P2_1/c$, No. 14), a = 15.165(2), b = 18.189(2), c = 23.314(4) Å, β = 108.27(1)°, M = 1322.16, V = 6106(2) Å^3, Z = 4, ϱ_{calcd} = 1.438 g cm^{-3}, $F(000)$ = 2320, $Mo_{K\alpha}$-radiation, λ = 0.71069 Å, $\mu(Mo_{K\alpha})$ = 1.71 cm^{-1}. The structure was solved by a combination of direct methods and Fourier difference techniques and refined by blocked-matrix least-squares. Some of the HMPA ligands show considerable disorder. P, O, Li, the NCS ligand, and the ordered N atoms from the HMPA ligands refined anisotropically. Phenyl and methyl-H atoms on ordered HMPA ligands placed in idealized positions, allowed to ride on the relevant carbon atoms, and refined with a common isotropic thermal parameter. One HMPA ligand severely disordered; two sites of disordered N and C atoms refined with partial occupancies. 8663 reflections measured ($5 < 2\theta < 45°$), corrected for absorption and decay. 4453 unique observed with $F > 5\sigma(F)$. R = 0.100, R_w = 0.109. Further details of the crystal structure investigation may be obtained from the Director of the Cambridge Crystallographic Data Centre, University Chemical Laboratory, Lensfield Road, Cambridge CB2 1EW (U.K.). Any request should be accompanied by the full literature citation for this communication.

[7] a) D. Paoli, M. Luçon, M. Chabanel, *Spectrochim. Acta Part 34* (1978) 1087; b) *ibid. 35* (1979) 593; c) M. Chabanel, M. Luçon, D. Paoli, *J. Phys. Chem. 85* (1981) 1058; d) P. Goralski, M. Chabanel, *Inorg. Chem. 26* (1987) 2169.

[8] a) H. Hope, P. P. Power, *J. Am. Chem. Soc. 105* (1983) 5320; b) H. Schmidbaur, A. Schier, U. Schubert, *Chem. Ber. 116* (1983) 1938, and references therein.

[9] D. Reed, D. Barr, R. E. Mulvey, R. Snaith, *J. Chem. Soc. Dalton Trans. 1986*, 557.

Conversion of a Diatropic Bridged Annulene into a Paratropic Species on Metal Complexation**

By *Reginald H. Mitchell** and *Pengzu Zhou*

Very little is known about metal-complexed large ring annulenes. A recently prepared[1] tris-(μ-acetylene)dicobalt complex containing the *cyclo*-C_{18} ligand grossly distorts the acetylenic bond so that comparison with the as yet unknown ligand will be difficult. Tricarbonylchromium complexes of two bridged [10]annulenes, 1,6-methano[10]annulene, and 2,7-methanoaza[10]annulene, have been described by *Günther* et al.[2] and *Vogel* et al.[3] respectively, as having delocalized 10π-electron systems. The complexation of a [14]annulene such as **1** interested us since it does not have a conveniently arranged set of six p orbitals to complex to chromium in contrast to the [10]annulenes above. Moreover, the chemical shift of the internal methyl protons in **1** and its derivatives is an excellent probe for the delocalization pres-

[*] Prof. R. H. Mitchell, Dr. P. Zhou
Department of Chemistry, University of Victoria
Box 3055, Victoria, B.C. V8W 3P6 (Canada)

[**] We thank the Natural Sciences and Engineering Research Council of Canada and the University of Victoria for the support of this work.

ent in the periphery.[4–6] We therefore thought that preparation of metal complexes of **1** would bring further insight into annulene complexation.

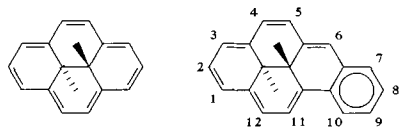

1 **2**

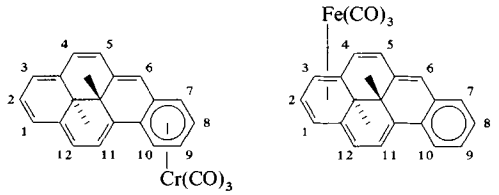

3 **4**

Thus far however, we have not been able to prepare any metal complex of **1**. The attempted reactions of **1** with $[Cr(CO)_6]$, $[Cr(CO)_3(CH_3CN)_3]$, $[Cr(CO)_3(naphthalene)]$, and $[Fe_2(CO)_9]$ failed. Treatment of **1** with $Cp_2Fe/Al/AlCl_3$, or of the dianion of **1** with $FeCl_2$, or irradiation of **1** in the presence of $[CpFe(p\text{-xylene})]PF_6$ all failed to give isolable products. To test whether the strong delocalization present in **1** was in part inhibiting complex formation, we investigated the benzannulene **2**, in which alternation of π and σ bonds in both the benzene and annulene rings is strong (bond fixation). Not surprisingly, the commonly η^6-bonded tricarbonylchromium moiety coordinated only to the benzene ring to give **3**.[3] The commonly η^4-bonded tricarbonyliron moiety, however, formally has a choice and could coordinate either to the partially bond-fixed benzene ring or to the annulene ring of **2**. Complexation of the annulene ring should be preferred, since the resulting bond fixation then permits the formation of a fully delocalized benzene ring, and as a consequence minimal ring current is anticipated in the macro-ring of such a complex. In fact, reaction of **2** with $[Fe_2(CO)_9]$ in refluxing benzene did give a single product (**4**) in 40% yield. The chemical shifts of the internal methyl protons appeared at $\delta = 2.00$ and 1.71, immediately ruling out complexation of the benzenoid ring, since a value close to that of **1** ($\delta = -4.2$) would have been expected. The position of complexation shown for **4** is evident from the shielded chemical shift ($\delta = 3.78$) of proton H1 (at the end of the complexed diene), which together with the small coupling constant between H2 and H3, suggests that **4** is a nonfluxional molecule. The fact that the internal methyl protons of **4** are more deshielded than those of the nonaromatic model **5** ($\delta = 0.97$) is exceptionally interesting. An anisotropic effect of the $Fe(CO)_3$ moiety cannot be the cause, since the chemical shift of both methyl groups in *both* **6** and **7** (which can be considered good model compounds for **2** and **4**) is $\delta = 1.0$. Similarly any deshielding effect from the now full benzene ring in **4**, is easily calculated using *Memory*'s equation[7] to be about $\Delta\delta = 0.05$ ppm, which is again negligible. We therefore propose that a paratropic ring current is present in **4**. This would rationalize the $\Delta\delta = 1$ downfield shifts of the internal methyl protons of **4** relative to **5**, since the chemical shifts of the known,[8] geometrically very similar, paratropic [12]annulene **8** are at $\delta = 2.58$. Moreover *Günther*'s Q value[9] can be calculated for the benzene unit of **2** as 0.99 and 1.02. These are less than the limiting value of 1.04 and thus clearly suggest that the large ring of **4** is paratropic (a delocalized 4n π-electron system). This can be accounted for by assuming a contribution of a resonance structure in which back-donation of two electrons by iron into the π system occurs. The resulting 16π-electron system would be expected to be paratropic. Indeed, the chemical shifts of the benzene-ring protons in **4** (H7–10) are all shielded with respect to those in benzene itself, which would not be expected if the macrocyclic ring were atropic (bond-fixed). Furthermore, the coupling constants of this benzene-like ring are almost equal and not strongly alternating as they would be if **4** were a 20π system, rather than the proposed benzo-fused 16π system. The downfield shifts of the internal methyl groups of **4**, however, are small relative to those observed when two real charges are added to such systems,[10] suggesting only a small degree of charge transfer between metal and the ligand.

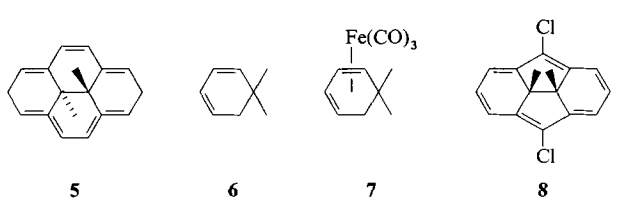

5 **6** **7** **8**

Whilst the stability of tricarbonylcyclobutadiene iron is well known,[11] and is consistent with the idea of metalloaromaticity proposed by Fenske,[12] donation to a $(4n + 2)\pi$ system to give what is formally an antiaromatic product, is very remarkable.

Experimental

A mixture of $[Fe_2(CO)_9]$ (262 mg, 0.72 mmol)[13] and benzodihydropyrene **2** (50 mg, 0.18 mmol)[14] in benzene (1 mL) was refluxed with stirring under N_2 for 1 h. After cooling, the residue was chromatographed over silica gel (eluant: petroleum ether). The third fraction contained the complex **4**, (30 mg, 40%), which was recrystallized from chloroform and heptane. Deep red crystals, m.p. 156°C (decomp.); ^1H NMR (360 MHz, $CDCl_3$, 25°C, standard $CHCl_3$ at $\delta = 7.240$); $\delta = 7.24$ (m, $J(7,8) = 7.5$ Hz, $J(7,9) = 1.5$ Hz, $J(7,10) = 0.3$ Hz, 1H; H7), 6.92 and 6.93 (m, $J(8,9) = 7.4$ Hz, $J(8,10) = 1.2$ Hz, 2H; H8,9), 6.77 (m, $J(9,10) = 7.6$ Hz, 1H; H10), 5.96 (d, $J(11,12) = 5.8$ Hz, 1H; H11), 5.90 (d, $J(5,4) = 9.4$ Hz, 1H; H5), 5.85 (s, 1H; H6), 5.43 (dd, $J(1,2) = 6.2(5)$ Hz, $J(2,3) = 4.4$ Hz, 1H; H2), 5.38 (d, 1H; H4), 5.30 (dd, $J(1,3) = 1.3$ Hz, 1H; H), 5.29 (d, 1H; H12), 3.78 (dd, 1H; H1), 2.00, 1.71 (s, 3H; each CH_3); ^{13}C NMR (62.9 MHz, $CDCl_3$): δ = 211.30 (carbonyl C), 143.67, 140.96, 138.37, 134.26, 131.79 (quaternary aryl C), 130.84, 128.52, 127.97, 127.76, 127.40, 123.94, 122.52, 117.26, 112.23 (aryl CH), 81.17 (quarternary aryl C, coordinated to Fe), 79.61, 77.49, 67.25 (aryl CH, coordinated to Fe), 43.04, 42.80 (bridged quaternary C), 25.89, 25.16 (internal $-CH_3$); IR (KBr) $\tilde{\nu}$ [cm^{-1}] = 2040, 1960, 1345, 880, 820, 740, 600, 550; UV/VIS (cyclohexane): λ_{max} [nm](ε) = 348(8750); MS (70 eV): m/z 422 ($M^{\oplus}$, 20%), 394(35), 366(25), 323(100). Correct elemental analysis (C, H).

Received: February 19, 1991 [Z 4454 IE]
German version: *Angew. Chem. 103* (1991) 1031

CAS Registry numbers:
2, 66093-76-3; **4**, 134627-15-9.

[1] Y. Rubin, C. B. Knobler, F. Diederich, *J. Am. Chem. Soc. 112* (1990) 4966–4968.
[2] H. Günther, W. Grimme, *Angew. Chem. 78* (1966) 1063; *Angew. Chem. Int. Ed. Engl. 5* (1966) 1043–1044.
[3] G. Hilken, T. Kinkel, M. Schwamborn, J. Lex, H. Schmickler, E. Vogel, *Angew. Chem. 94* (1982) 790; *Angew. Chem. Int. Ed. Engl. 21* (1982) 784.
[4] R. H. Mitchell, P. Zhou, S. Venugopalan, T. W. Dingle, *J. Am. Chem. Soc. 112* (1990) 7812–7813.
[5] R. H. Mitchell, *Adv. in Theoret. Interesting Molec. 1* (1989) 135–199.
[6] R. H. Mitchell, S. Venugopalan, P. Zhou, T. W. Dingle, *Tetrahedron Lett. 31* (1990) 5281–5284.
[7] J. D. Memory, *J. Magn. Reson. 73* (1977) 241–244.
[8] H. Kohnz, B. Dull, K. Müllen, *Angew. Chem. 101* (1989) 1375; *Angew. Chem. Int. Ed. Engl. 28* (1989) 1343–1345.

[9] D. Cremer, H. Günther, *Justus Liebigs Ann. Chem. 763* (1972) 87–108.
[10] R. H. Mitchell, C. E. Klopfenstein, V. Boekelheide, *J. Am. Chem. Soc. 91* (1969) 4931–4932; K. Müllen, T. Meul, P. Schade, H. Schmickler, E. Vogel, *ibid. 109* (1987) 4992–5003.
[11] G. F. Emerson, L. Watts, R. Pettit, *J. Am. Chem. Soc. 87* (1965) 131–133.
[12] B. E. Bursten, R. F. Fenske, *Inorg. Chem. 18* (1979) 1760–1765.
[13] R. B. King: *Organometallic Syntheses, Vol. 1*, Academic, New York 1965, p. 93–94.
[14] R. H. Mitchell, P. Zhou, *Tetrahedron Lett. 37* (1990) 5277–5280.

Synthesis and Structure of the Potassium Salts of 1,3,2-Diazaboroles**

By *Günter Schmid,* Jürgen Lehr, Michael Polk,* and *Roland Boese*

Recently we reported the synthesis and properties of a series of 2,3-dihydro-1*H*-1,3,2-diazaboroles **1**.[1] They are formally derived from pyrrole by substitution of C=C– by an isoelectronic BN group.

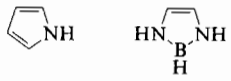

Diazaboroles have already been used in complexes as 6π electron systems.[1] Like pyrrole, dihydro-1,3,2-diazaboroles can also be converted into their anions, which offer interesting possibilities for preparative chemistry. Thus, in a reaction with potassium *tert*-butyl alcoholate, *N*-trimethylsilyl-substituted diazaboroles **1a–d** can be transformed into the potassium salts **2a–d** in good yields (60–70%) [Eq.(a)] and isolated as colorless to beige pyrophoric powders which are very soluble in THF.

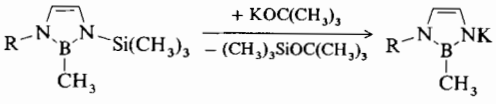

(a)

1 **2**

a, R = CH_3; **b**, R = C_2H_5; **c**, R = $CH(CH_3)_2$; **d**, R = $C(CH_3)_3$

The ^{1}H NMR signals of these anions are hardly shifted with respect to those of the neutral dihydro-1,3,2-diazaboroles, which means that the negative charge is localized mainly on the metalized nitrogen atom. The ^{13}C NMR spectra show that, with the exception of the adjacent carbon atom (for which $\Delta\delta = 10$ to lower field), the transformation from neutral ring into anion leaves the electronic environment of the carbon atoms virtually unchanged. A slight shift of $\Delta\delta \approx 2$ to higher field for the ^{11}B NMR signal on transformation of **1a–d** into the anions **2a–d** is caused by the loss of the trimethylsilyl group, which markedly withdraws the electron density from the nitrogen atom in **1a–d**. In the anion the electron density is distributed across the acidic boron atom to a greater extent (Table 1).

Only in the case of the anion **2d** could crystals suitable for X-ray crystallography be obtained. However, these crystals also contain potassium *tert*-butyl alcoholate and, surprisingly, dipotassium dimethylsilanediolate, $(CH_3)_2SiO_2K_2$, an as yet unknown compound, which we shall discuss later. Anion **2d** is arranged in the crystal in a characteristic way around a threefold rotatory inversion axis (Fig. 1): Twelve diazaborolyl anions (green) are so arranged that six "parallel" rings form an inner circle and a further six an outer circle. The 18 *tert*-butyl alcoholate anions (red) occupy positions on the outer periphery of the circle, with the oxygen atoms directed inwards and the $C(CH_3)_3$ groups outwards. Six

Table 1. NMR data for the compounds **1a–d** and **2a–d** [a].

1a: ^{1}H NMR: $\delta = 0.20$ (s, 9H, $Si(CH_3)_3$), 0.54 (s, 3H, BCH_3), 2.87 (s, 3H, NCH_3), 6.10 (d, 1H, H4, $J = 1.7$ Hz), 6.15 (d, 1H, H5, $J = 1.7$ Hz); $^{13}C\{^1H\}$ NMR: $\delta = -4.7$ (BCH_3, $J(^{11}B, ^{13}C) = 90$ Hz); 0.7 ($Si(CH_3)_3$), 32.2 (NCH_3), 115.2 (C4), 121.1 (C5); ^{11}B NMR: $\delta = 29.4$

1b: ^{1}H NMR: $\delta = 0.20$ (s, 9H, $Si(CH_3)_3$), 0.59 (s, 3H, BCH_3), 1.0 (t, 3H, CH_2-CH_3, $J = 7.3$ Hz), 3.23 (q, 2H, CH_2-CH_3, $J = 7.3$ Hz), 6.19 (br. s, 2H, H4, H5); $^{13}C\{^1H\}$ NMR: $\delta = -4.7$ (BCH_3, $J(^{11}B, ^{13}C) = 80$ Hz), 0.7 ($Si(CH_3)_3$), 18.0 (CH_2-CH_3), 40.2 (CH_2-CH_3), 115.4 (C4), 119.1 (C5); ^{11}B NMR: $\delta = 29.1$

1c: ^{1}H NMR: $\delta = 0.21$ (s, 9H, $Si(CH_3)_3$), 0.65 (s, 3H, BCH_3), 1.10 (d, 6H, $CH(CH_3)_2$, $J = 6.7$ Hz), 6.23 (d, 1H, H4, $J = 2.2$ Hz), 6.34 (sept, 1H, $CH(CH_3)_2$, $J = 6.7$ Hz), 6.77 (d, 1H, H5, $J = 2.2$ Hz); $^{13}C\{^1H\}$ NMR: $\delta = -4.7$ (BCH_3, $J(B^{11}, ^{13}C) = 88$ Hz), 0.8 ($Si(CH_3)_3$), 24.5 ($CH(CH_3)_2$), 45.6 ($CH(CH_3)_2$), 115.2 (C4), 115.6 (C5); ^{11}B NMR: $\delta = 28.9$

1d: ^{1}H NMR: $\delta = 0.22$ (s, 9H, $Si(CH_3)_3$), 0.81 (s, 3H, BCH_3), 1.33 (s, 9H, $C(CH_3)_3$), 6.19 (d, 1H, H4, $J = 2.2$ Hz), 6.43 (d, 1H, H5, $J = 2.2$ Hz)

2a: ^{1}H NMR: $\delta = 0.39$ (s, 3H, BCH_3), 3.14 (s, 3H, NCH_3), 6.09 (d, 1H, H4, $J = 1.8$ Hz), 6.16 (d, 1H, H5, $J = 1.8$ Hz); $^{13}C\{^1H\}$ NMR: $\delta = -4.4$ (BCH_3), 32.6 (NCH_3), 117.9 (C5), 124.1 (C4); ^{11}B NMR: $\delta = 26.8$

2b: ^{1}H NMR: $\delta = 0.38$ (s, 3H, BCH_3), 1.15 (t, 3H, CH_2-CH_3, $J = 7.2$ Hz), 3.45 (q, 2H, CH_2-CH_3, $J = 7.2$ Hz), 6.10 (d, 1H, H4, $J = 1.7$ Hz), 6.17 (d, 1H, H5, $J = 1.7$); $^{13}C\{^1H\}$ NMR: $\delta = -4.1$ (BCH_3), 19.1 (CH_2-CH_3), 40.7 (CH_2-CH_3), 115.5 (C5), 124.4 (C4); ^{11}B NMR: $\delta = 27.5$

2c: ^{1}H NMR: $\delta = 0.44$ (s, 3H, BCH_3), 1.22 (d, 6H, $CH(CH_3)_2$, $J = 6.7$ Hz), 3.89 (sept, 1H, $CH(CH_3)_2$, $J = 6.7$ Hz), 6.26 (br.s, 2H, H4, H5); $^{13}C\{^1H\}$ NMR: $\delta = -4.8$ (BCH_3), 23.2 ($CH(CH_3)_2$), 46.3 ($CH(CH_3)_2$), 112.0 (C5), 120.1 (C4); ^{11}B NMR: $\delta = 28.9$

2d: ^{1}H NMR: $\delta = 0.54$ (s, 3H, BCH_3), 1.37 (s, 9H, $C(CH_3)_3$), 6.11 (d, 1H, H4, $J = 2.0$), 6.26 (d, 1H, H5, $J = 2.0$ Hz); $^{13}C\{^1H\}$ NMR: $\delta = 1.2$ (BCH_3), 32.7 ($C(CH_3)_3$), 52.2 ($C(CH_3)_3$), 114.0 (C5), 121.5 (C4); ^{11}B NMR: $\delta = 29.8$

[a] ^{1}H and ^{13}C NMR values for **1a–d** in C_6D_6, for **2a–d** in [D_8]THF, ^{11}B NMR values for all compounds in THF.

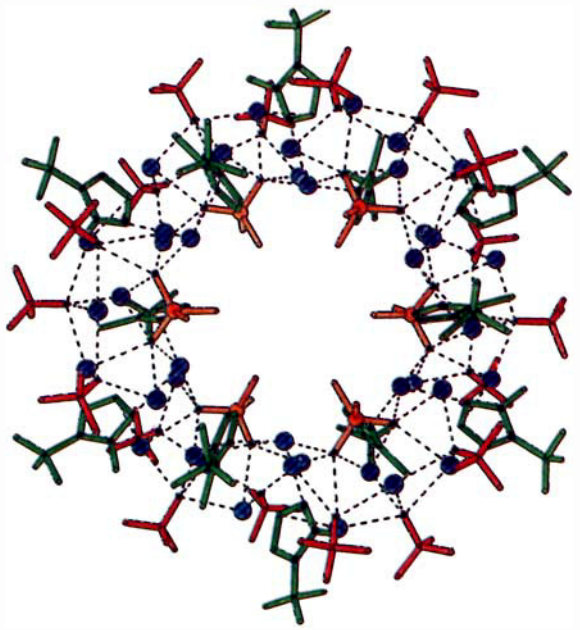

Fig. 1. Section of the unit cell of **2d** showing the contacts to the potassium ions (blue), diazaborolyl rings (green), *tert*-butyl alcoholate (red) and dimethylsilanediolate (orange).

[*] Prof. Dr. G. Schmid, Dipl.-Chem. J. Lehr, Dr. M. Polk, Dr. R. Boese
Institut für Anorganische Chemie der Universität
Universitätsstrasse 5–7, W-4300 Essen 1 (FRG)
[**] This work was supported by the Fonds der Chemischen Industrie.

$(CH_3)_2SiO_2^{2-}$ dianions (orange) occupy the innermost sites of the tirelike construction, which together with the methyl groups define the point group $\bar{3}$. Thus, a highly symmetrical ring arises, which has 42 K^+ ions (blue) corresponding to the 12 diazaborolyl, 18 *tert*-butyl alcoholate and 6 silanediolate anions.

The residual electron density above the center of the tire indicates that a disordered THF molecule, which cannot be located precisely, is situated there. The similarly disordered *tert*-butyl groups of the diazaborolyl ring and the *tert*-butanolate anions had to be calculated as rigid groups with fixed bond lengths and bond angles. With the exception of potassium, all atoms were refined isotropically.

Figure 2 shows the asymetric unit in which the environment of the diazaborolyl anions is best recognized. All five atoms of the ring N1′B2′N3′C4′C5′ have contacts to both potassium ions, K2 and K7, and the corresponding bond lengths [pm] are in good agreement: K2–N1′ 329/K7–N1′ 346, K2–B2′ 322/K7–B2′ 343, K2–N3′ 300/K7–N3′ 304, K2–C4′ 315/K7–C4′ 323, and K2–C5′ 294/K7–C5′ 290. K1 has bonding contacts with this ring through N3′ (K1–N3′ 284 pm) and C4′ (K1–C4′ 297 pm), and with the other ring within this asymmetric unit through N3 and C5. The function of K4 corresponds to that of K7. If K4 and K7 are arbitrarily defined as those belonging to the diazaborolyl anions, the cations K1, K2, K3, and K5 compensate for the negative charge of the two *tert*-butyl alcoholate ions and the silanediolate ion.

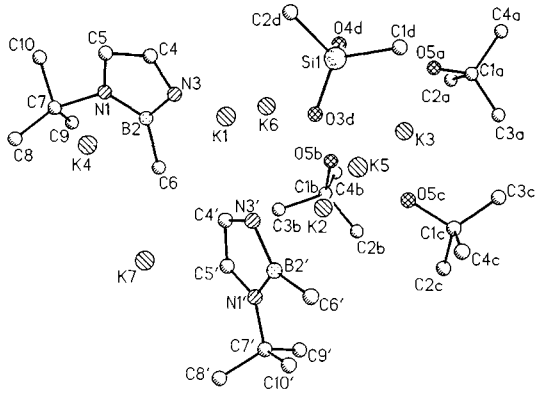

Fig. 2. Environment about the diazaborolyl rings in the asymmetric unit (contacts of potassium ions not shown; atoms have arbitrary radii).

The bond lengths and angles within the two *tert*-butyl-2-methyl-1*H*-1,3,2-diazaborolyl anions in this asymmetric unit agree to a large extent within experimental error. Only the bond between N1′ and B2′ (150 pm) appears significantly longer than the B2′–N2′ bond (143 pm); nevertheless, the corresponding distances in the other ring (146 and 141 pm) suggest that the longer N1′–B2′ distance is due to the inaccuracy of the structure determination resulting from crystal quality. The other B–N bond lengths of between 141 and 146 pm lie within the expected range. A significant difference in distance between the boron atom and the substituted and unsubstituted nitrogen atom is not observed.

The formation of the dimethylsilanediolate, initially detected by X-ray crystallography, is interesting. Till now only the unstable free dimethylsilanediol has been described. The possible utilization of the dipotassium salt formed here in exceptionally small concentrations could be of interest in preparative silicon chemistry. We attribute the formation of $(CH_3)_2SiO_2K_2$ to traces of KOH in the K-*tert*-butyl alcoholate. *R. Köster* et al.[3] showed that $(CH_3)_3Si$ groups in the vicinity of boryl substituents react with KOH by loss of methane. Such a reaction sequence applied twice to **1d** is a plausible explanation for the formation of $(CH_3)_2SiO_2K_2$. Indeed, mass spectrometry shows that more methane is released on increasing the KOH concentration. The formation of 1-*tert*-butyl-2,3-dihydro-2-methyl-1*H*-1,3,2-diazaborole is detected by ^{11}B NMR spectroscopy ($\delta = 26.5$). $(CH_3)_2SiO_2K_2$ has not as yet been isolated.

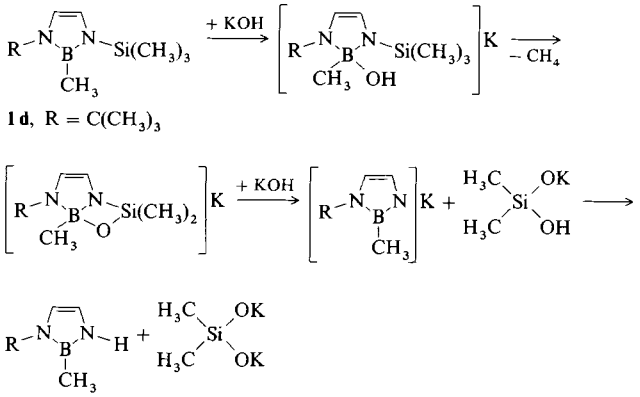

Experimental Procedure

1d: A solution of *n*BuLi in hexane (580 mmol, 365 mL, 1.6 M) was added dropwise to a solution of *N*-*tert*-butyl-N′-trimethylsilylethylenediamine in pentane (54.6 g, 290 mmol, 500 mL) at −78 °C over 2 h. The mixture was then heated under reflux for 1 h, again cooled to −78 °, and a solution of dibromomethylboron in pentane (53.8 g, 290 mmol, 100 mL) is added dropwise within 2 h. The solution was stirred for 10 h at room temperature, whereupon the solvent was removed under vacuum. **1d** was removed from the nonvolatile components by condensation. Fractional distillation at 107 °C/30 Torr yields pure **1d** (42.4 g, 69 %).

2d: A freshly prepared and titrated solution of K-*tert*-butanolate (6.5 mmol) in THF was added to a THF solution of **1d** (1.8 g, 8.6 mmol, 50 mL). The solution was heated for 1 h under reflux and then evaporated to dryness. The residue was suspended in pentane (50 mL) and the white, pyrophoric **2d** was filtered off (0.68 g, 68 %).

Received: March 18, 1991 [Z4511 IE]
German version: Angew. Chem. 103 (1991) 1029

CAS Registry numbers:
1a, 134879-68-8; **1b**, 134879-69-9; **1c**, 134879-70-2; **1d**, 134879-71-3; **2a**, 134904-71-5; **2b**, 134879-72-4; **2c**, 134879-73-5; **2d**, 134879-74-6; $K_7(\overline{NtBuBMeNCHCH})_2(OtBu)_3(Me_2SiO_2)$, 134879-75-7; $Me_3SiNHCH{=}CHNHMe$, 134879-64-4; $Me_3SiNHCH{=}CHNHEt$, 134879-65-5; $Me_3SiNHCH{=}CHNHiPr$, 134879-66-6; $Me_3SiNHCH{=}CHNHtBu$, 134879-67-7; $MeBBr_2$, 17933-16-3.

[1] G. Schmid, M. Polk, R. Boese, *Inorg. Chem. 29* (1990) 4421.

[2] Structure determination of $K_{42}[\overline{NtBuBMeNCHCH}]_{12}[OtBu]_{18}[Me_2SiO_2]_6$: Crystal dimensions 0.26 × 0.24 × 0.15 mm³; measured at 220 K on a R3m/V Nicolet four-circle diffractometer with $Mo_{K\alpha}$ radiation (graphite monochromator); further degradation of the crystal quality prevented stronger cooling; rhombohedral, a, b = 3911.4(10), c = 1659.5(7) pm, α, β = 90, γ = 120°, V = 21 988(12) × 10⁶ pm³, space group $R\bar{3}$ (no. 148), Z = 3, ϱ_{calc} = 1.314 g cm⁻³, μ = 0.76 mm⁻¹, $2\theta_{max}$ = 40°, 3954 independent reflections, of which 2287 observed ($F_0 \geq 4\sigma(F)$), 216 parameters for the refinement without hydrogen atoms, only potassium atoms with anisotropic shift factors, angle restrictions for the *tert*-butyl groups, whose shift factors indicate strong disorder. R = 0.109, R_w = 0.104, w^{-1} ($\sigma^2(F_0) + 0.005F_0^2$), maximal residual electron density 10⁶ × 0.93 e pm⁻³ in 0/0/0.758, one disordered THF molecule expected in this position could not be refined. Further details of the crystal structure investigation may be obtained from the Fachinformationszentrum Karlsruhe, Gesellschaft für wissenschaftlich-technische Information mbH, W-7514 Eggenstein-Leopoldshafen 2 (FRG) on quoting the depository number CSD-320 251, the names of the authors and the journal citation.

A New Economical Process for the Preparation of Silver(I,III) Oxide, AgO

By *Sabine Kielhorn, Dieter H. Buß, Oskar Glemser,* Roland Gerner,* and *Gerald Jeske*

Silver(I,III) oxide (AgO), a strong oxidizing agent, is used in chemical technology and has become increasingly important in batteries.[1] It is prepared from weakly acidic solutions of silver salts through oxidation by ozone and more often from alkaline silver nitrate solutions at temperatures between 80 and 90 °C through oxidation with peroxodisulfate.[2] Both these preparations are uneconomical.[3, 4]

We now report that AgO can be prepared through oxidation of an aqueous, alkaline silver nitrate solution with mixtures of sulfur dioxide and oxygen or air, or with mixtures of sulfite solutions and oxygen or air in up to 98% yield. Both the pH of the solution (10.5–10.6) and the redox potential (480–600 mV, referred to an Ag/AgCl electrode) are kept constant at temperatures between 70 and 90 °C.

The reaction suspension always requires a small sulfite concentration, but an excess of sulfite or SO_2 must be avoided. Under these conditions the sulfurous acid is formed by a chain reaction of peroxo compounds, as one suspected from reports by *Taube* et al.[5] These intermediates have a higher oxidation potential than oxygen in alkaline solution. The net reaction is formulated in Equation (a).

$$[O_2SOO]^{2\ominus} + 2Ag^{\oplus} + 2OH^{\ominus} \longrightarrow 2AgO + SO_3^{2\ominus} + H_2O \qquad (a)$$

The silver(I,III) oxides prepared by the new process have high charging capacities of between 408 and 426 $mAh\,g^{-1}$; the theoretical value is 497 $mAh\,g^{-1}$.[9]

Experimental Procedure[6]

Two examples are given: 1. The pH of distilled water (1.5 L in a 4-L round-bottomed flask, 70 °C) was adjusted to 10.55 by addition of CO_2-free sodium hydroxide solution (4 mL) and was kept constant within ± 0.05 during the precipitation. A redox potential of 545–555 mV was attained by passing a stream of SO_2 (1 $L\,h^{-1}$) and O_2 (500 $L\,h^{-1}$) through the solution. A solution of silver nitrate (2M) was added dropwise and care was taken that the reduction potential did not change. Yield: 93.3% black powder [7], which showed only those lines of AgO in the X-ray diffraction pattern. [8].

2. To an aqueous alkaline solution prepared as in 1 (pH 10.53 ± 0.03) is added a sodium sulfite solution (0.1 M, 1800 $mL\,h^{-1}$) to attain a redox potential of 600 mV. A solution of $AgNO_3$ is then added dropwise without changing the redox potential. Yield: 97% AgO; the X-ray diffraction pattern is identical to that obtained in method 1 [9].

Received: March 11, 1991 [Z 4488 IE]
German version: *Angew. Chem. 103* (1991) 1017

CAS Registry numbers:
AgO, 1301-96-8; $AgNO_3$, 7761-88-8.

[1] *Ullmann's Encycl. Ind. Chem. 5th ed.*, Verlag Chemie, Weinheim, *Vol. A3*, p. 343; *Ullmann's Encykl. Tech. Chem., 4. Aufl.*, Verlag Chemie, Weinheim, *Band 21*, 1982, p. 340.

[2] Varta-Batterie AG, DT 2430910 (1974); G. Brauer: *Handbuch der präparativen anorganischen Chemie, Band III*, Enke, Stuttgart 1978, S. 998.

[3] Other possibilities for the synthesis of AgO from silver(I) salts through reaction with potassium permanganate, hypochlorite, or through electrochemical routes are less important.

[4] Cf. *Gmelin Handbuch der anorganischen Chemie, Silber B1*, Verlag Chemie, Weinheim 1971, p. 106.

[5] Z. Halperin, H. Taube, *J. Am. Chem. Soc. 74* (1952) 380.

[*] Prof. Dr. O. Glemser, Dr. S. Kielhorn, Dr. D. H. Buß
Institut für Anorganische Chemie der Universität
Tammannstrasse 4, W-3400 Göttingen (FRG)
Dr. R. Gerner, Dr. G. Jeske
Degussa, W-6450 Hanau 1 (FRG)

[6] Precipitation in a 4-L six-necked, round-bottomed flask; pH measurement: Ingold pH measuring chain (HA-265); measurement of potential: silver rod covered with spongy silver, reference electrode Ag/AgCl on Luggin capillaries. Computer-controlled addition of solutions by electric diaphragm pumps (CFG), computer Rockwell AIM65. Solutions (p.a. quality chemicals): 2 M $AgNO_3$, 4 M NaOH, 0.1 M Na_2SO_3. After precipitation the products were washed till free of alkali and nitrate, filtered by suction, and dried in a rotary evaporator at 1580 Pa and 70 °C. For a complete description see ref. [9].

[7] Determination of the AgO content with iodide in a solution acidified with acetic acid; iodine was released and titrated with thiosulfate (see ref. [4]).

[8] The X-ray diffraction patterns were recorded with $Co_{K\alpha}$ radiation on a STADI-P diffractometer (company Stoe). The θ values and intensities agreed with the data in the ASTM library. Values for AgO (oxidation with SO_2/O_2): [*d*[pm] (I/I_0 [%])]: 279(100.0), 262(38.5), 241(75.1), 228(33.0), 174(7.7), 170(16.0), 167(8.7), 162(21.2), 148(9.0), 146(7.1), 145(10.6), 140(9.7).

[9] Further examples and descriptions of the electrochemical measurements in S. Kielhorn, *Dissertation*, Universität Göttingen 1989.

Synthesis and Structure of an Azadistanniridine**

By *Hansjörg Grützmacher** and *Hans Pritzkow*

Three-membered rings containing two silicon or germanium atoms and a heteroatom Y in the ring are known and have remarkable structures.[1] We report now the synthesis and structure of the first azadistanniridine.

The reaction of bis[2,4,6-tris(trifluoromethyl)phenyl]stannylene (**1**), which is also monomeric in the solid state,[2] with mesityl azide (**2**)[3] in the molar ratio 2.5:1 leads to spontaneous nitrogen evolution and the formation of azadistanniridine (**3**) in good yield.[4] This compound crystallizes from the reaction solution in the form of large, red crystals which cannot be dissolved in organic solvents without decomposition (Scheme 1).

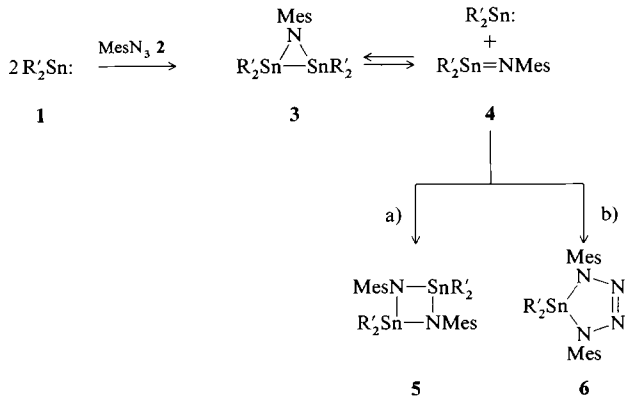

Scheme 1. R' = 2,4,6-$(CF_3)_3C_6H_2$, Mes = mesityl; a) Reaction of **1** with **2** in a molar ratio of 2.5:1 or of warmed toluene with **3**; b) reaction of **1** with **2** in a molar ratio of 1:3.5.

If the reaction of **1** with **2** in C_6D_6 is monitored by ^{119}Sn NMR spectroscopy, initially only one signal (**3**, $\delta = -194$) can be detected besides that of **1** ($\delta = 682$). After several hours at room temperature the intensity of the signal of **1**

[*] Dr. H. Grützmacher, Dr. H. Pritzkow
Anorganisch-chemisches Institut der Universität
Im Neuenheimer Feld 270, W-6900 Heidelberg (FRG)

[**] This work was supported by Prof. *G. Huttner* and Prof. *W. Sundermeyer*. The Deutsche Forschungsgemeinschaft, the Fonds der Chemischen Industrie, and the Dr. Otto Röhm Gedächtnisstiftung provided financial support. We thank one of the referees for valuable comments.

again increases relative to **3** and as second product of the cycloreversion, the diazadistannetidine **5** begins to crystallize.

On treatment of crystals of **3** with warmed toluene (ca. 60 °C) a color change from red to yellow takes place and again a [2 + 1] cycloreversion[5] yields stannylene **1** and stannanimine **4**, which in agreement with the results of *Wiberg* and *Vasisht*[6] dimerizes to **5**. On reaction of **1** with **2** in the ratio 1:3.5 the stannanimine is trapped almost quantitatively by **2** in a [2 + 3] cycloaddition to form **6**.[6]

The result of the X-ray structure analysis[7] of **3** is shown in Figure 1. Although the tin–nitrogen bond lengths lie within the typical range for sterically hindered cyclic tin–nitrogen compounds,[8] the tin–tin bond in **3** (2.709 Å) is very short:[9] the difference between this distance and that in distannene **7**[10] (2.768 Å, formal Sn–Sn double bond) is significant; in comparison with tetrahedrally surrounded elemental tin (2.81 Å) this bond is 0.1 Å shorter. The sum of the basal exocyclic bonding angles about the tin atoms is 356°, corresponding with that found in three-membered rings containing two Si or Ge atoms and one heteroatom.[1] The trigonal-planar configuration of the nitrogen atom N1 is remarkable. This is not typical for stannaazanes [R_2SnNR'][8] and cannot be attributed to steric influences. The nitrogen atom in **5** is clearly pyramidal (sum of the bond angles 353° and the carbon–nitrogen bond is twisted 21.5° out of the ring plane), although in the four-membered ring the geometry causes crowding of the substituents not present in the three-membered ring.[11] These structural characteristics can be explained if the three-membered rings are understood in terms of π-donor complexes of the Dewar–Chatt–Duncanson model,[12] or if a bent-bond molecular description is used.[13]

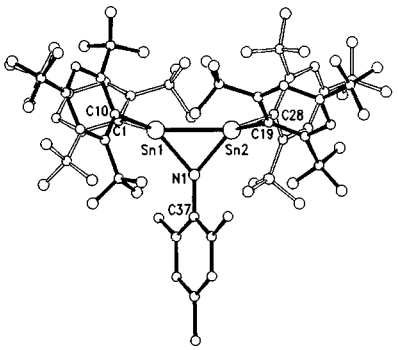

Fig. 1. Structure of **3** in the crystal. Important bond lengths [Å] and angles [°]: Sn1–Sn2 2.709(2), Sn1–N1 2.079(11), Sn2–N1 2.074(16), Sn1–C1 2.305(8), Sn1–C10 2.316(9), Sn2–C19 2.301(10), Sn2–C28 2.306(12); Sn1–N1–Sn2 81.4(4), Sn1–N1–C37 138.9(12), Sn2–N1–C37 139.7(10), Sn2–Sn1–N1 49.2(4), Sn2–Sn1–C1 125.3(3), Sn2–Sn1–C10 128.9(3), C1–Sn1–C10 101.6(3), Sn1–Sn2–N1 49.4(3), Sn1–Sn2–C19 125.2(3), Sn1–Sn2–C28 129.6(3), C19–Sn2–C28 101.3(4).

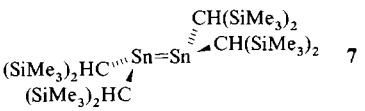

7

Received: March 15, 1991 [Z 4504 IE]
German version: *Angew. Chem. 103* (1991) 976

CAS Registry numbers:
1, 131079-28-2; **2**, 14213-00-4; **3**, 134311-22-1.

[1] a) Si–Si–C: S. Masamune, S. Murakami, H. Tobita, D. J. Williams, *J. Am. Chem. Soc. 105* (1983) 7776; b) Si–Si–N: G. R. Gillette, R. West, *J. Organomet. Chem. 394* (1990) 45; c) Si–Si–O: H. B. Yokelson, A. J. Millevolte, G. R. Gillette, R. West, *J. Am. Chem. Soc. 109* (1987) 6865; d) Si–Si–S: R. West, D. J. De Young, K. J. Haller, *ibid. 107* (1985) 4942; e) Si–Si–Se and Si–Si–Te: R. Peng-Koon Tan, G. R. Gillette, D. R. Powell, R. West, *Organometallics 10* (1991) 546; f) Ge–Ge–C and Ge–Ge–N: T. Tsumuraya, S. Sato, W. Ando, *ibid. 9* (1990) 2061; g) Ge–Ge–S: T. Tsumuraya, S. Sato, W. Ando, *ibid. 7* (1988) 2015; h) Ge–Ge–Te: T. Tsumuraya, Y. Kabe, W. Ando, *J. Chem. Soc. Chem. Commun. 1990*, 1159.

[2] H. Grützmacher, H. Pritzkow, *Organometallics 10* (1991) 23.

[3] I. Ugi, H. Perlinger, L. Behringer, *Chem. Ber. 91* (1958) 2330.

[4] *Experimental*: All reactions were conducted in carefully dried solvents and equipment. Compound **1** (2 g, 3 mmol) was dissolved in *n*-hexane (10 mL) and **2** (0.19 g, 1.2 mmol) added by syringe. The reaction solution turned red and nitrogen evolution was observed. After ca. 1 h **3** began to crystallize and was filtered after 24 h; yield: 75–80%. **3**: M.p. 137 °C, the melt decolorizes. ^{19}F NMR (C_6D_6, 84.25 MHz): $\delta = -57.4$ (broad, 24 F, *ortho*-CF_3), -63.3 (s, 12 F, *para*-CF_3); ^{1}H NMR (C_6D_6, 89.55 MHz): $\delta =$ 1.79 – 2.21 (m, 9 H, CH_3), 7.53 – 8.25 (m, 10 H, aromat. H); MS (70 eV): *m/z*(%) 815 ($R'_2Sn{=}NMes$, 2.4), 682 (R'_2Sn, 6), 663 ($R'_2Sn{-}F$, 3), 401 ($R'Sn$, 36), 262 ($C_9H_2F_8$, 6), 243 ($C_9H_2F_7$, 100).

[5] J. Barrau, J. Escudié, J. Satgé, *Chem. Rev. 90* (1990) 283, and references cited therein.

[6] N. Wiberg, S.-K. Vasisht, *Angew. Chem. 103* (1991) 105; *Angew. Chem. Int. Ed. Engl. 30* (1991) 93.

[7] Compound **3**: Twinned crystals, space group $P\bar{1}$, $a = 13.981(13)$, $b = 14.170(13)$, $c = 15.032(13)$ Å, $\alpha = 73.26(7)$, $\beta = 80.54(7)$, $\gamma = 64.85(6)°$, $V = 2578$ Å^3, $Z = 2$. 11214 measured reflections of which 5850 observed [$I > 2\sigma(I)$, four-circle diffractometer, $Mo_{K\alpha}$ radiation, ω scan]. Because of the twinning, only 2867 reflections could be used in the structure determination. Refinement: Sn and some F atoms anisotropically; C, N isotropically. The *para*-CF_3 groups are disordered and were each approximated by two rigid groups (isotropically); the phenyl rings were refined isotropically as rigid groups. R=0.074, R_w=0.083 (407 parameters). Further details of the crystal structure investigation may be obtained from the Fachinformationszentrum Karlsruhe, Gesellschaft für wissenschaftlich-technische Information mbH, W-7514 Eggenstein-Leopoldshafen 2 (FRG) on quoting the depository number CSD-55337, the names of the authors and the journal citation.

[8] H. Puff, D. Hänsgen, N. Beckermann, A. Roloff, W. Schuh, *J. Organomet. Chem. 373* (1989) 37.

[9] Somewhat shorter tin–tin bonds occur in five-coordinate acetate-bridged stannanes. A comparative review is found in H. Puff, B. Breuer, G. Gehrke-Brinkmann, P. Kind, H. Reuter, W. Schuh, W. Wald, G. Weidenbrück, *J. Organomet. Chem. 363* (1989) 265.

[10] D. E. Goldberg, P. B. Hitchcock, M. F. Lappert, K. M. Thomas, A. J. Thorne, T. Fjeldberg, A. Haaland, B. E. R. Schilling, *J. Chem. Soc. Dalton Trans. 1986*, 2387.

[11] Particulars of the structure of **5** and a detailed discussion on the reactivity of **3**, **5**, and **6** and the wider significance follows.

[12] R. S. Grev, H. F. Schaefer III, *J. Am. Chem. Soc. 109* (1987) 6577; D. Cremer, E. Kraka, *ibid. 107* (1985) 3800; D. Cremer, J. Gauss, E. Cremer, *THEOCHEM. 46* (1988) 531.

[13] J. A. Boatz, M. S. Gordon, *J. Phys. Chem. 93* (1989) 3025.

Recombination of Carbocation–Sulfinate Ion Pairs**

By *Wolfgang Kirmse** and *Ekkehard Herpers*

Dedicated to Professor Horst Prinzbach on the occasion of his 60th birthday

The study of ion pairs gives an insight into the short-range orientation of charged molecules.[1] Since the pioneering work of *Winstein*[2] on the heterolysis of C–X bonds, the behavior of carbocations in ion pairs has been thoroughly investigated. Most often the counterions chosen were carboxylates[3] and sulfonates.[4] Sulfinates aroused little interest, although the chirality of the sulfur atom in alkyl sulfi-

[*] Prof. Dr. W. Kirmse, Dipl.-Chem. E. Herpers
Fakultät für Chemie der Ruhr-Universität
Universitätsstrasse 150, W-4630 Bochum 1 (FRG)

nates and the ambident character of the sulfinate ion promises additional information. The rearrangement of alkyl sulfinates to alkyl sulfones is known,[5, 6] but we are aware of only one report on the recombination of a carbocation with the oxygen atom of a sulfinate ion: *Fava* et al. observed that the racemization of optically active benzhydryl-*p*-toluenesulfinate competes with the rearrangement to sulfone.[7] We have utilized the chirality of the ^{18}O-labeled *p*-toluenesulfinate ion to analyze such reactions in more detail.

First we considered a system in which the dissociation and recombination are practically irreversible. The reaction of 2-norpinanol (bicyclo[3.1.1]heptan-2-ol) with *p*-toluenesulfinyl chloride afforded a mixture (1:1) of the diastereomeric norpinyl-*p*-toluenesulfinates (**2A, B**, 95%). Only one of these could be obtained in pure form, through chromatography.[8] Heating of **2A**[9] in formamide (130°C, 2 h) caused a rearrangement to *endo*-2-norbornyl *p*-tolyl sulfone (**1**)[10] (10%), *endo*-2-norbornyl-*p*-toluenesulfinate (**4**) [12] (two diastereoisomers, 66.7 and 11.4%), *exo*-2-norbornyl-*p*-toluenesulfinate (**5**)[13] (two diastereomers, 5.1 and 5.0%), and *exo*-norbornyl *p*-tolyl sulfone (**7**)[14] (1.2%). In the analogous rearrangement of 2-norpinyl sulfonates and carboxylates to 2-norbornyl derivatives,[15] the norbornyl cation **3** was formed initially and reacted further with nucleophiles at C2 to afford less strained *endo*-2-norbornyl products (**4**). The rearrangement of **3** to the 2-norbornyl cation **6**, from which the *exo*-norbornyl products **5** are formed, competed with nucleophilic capture (Scheme 1).

Besides the product distribution, the following findings are important: 1) Compound **2B** did not form during the rearrangement of **2A**. The isomerizations of **4A** into **4B**, and vice versa, did not occur at 130°C, and those of **5A** and **5B** only very slowly. 2) Labeling of the ester oxygen atom of **2A** with ^{18}O[16] afforded the following distribution of ^{18}O in the products:[17] In the more abundant diastereomer (66.7%) of **4** only the ester oxygen atom was labeled. The less abundant diastereomer (11.4%) bore the label only at the doubly bonded oxygen atom (**4B**). In the diastereomers of **5** the ^{18}O was equally distributed over both oxygen functionalities.[17]

The following conclusions may be drawn from these findings: 1) Under these reaction conditions, thermally induced inversion of the sulfur occurs neither in the *p*-toluenesulfinic acid esters nor in the *p*-toluenesulfinate ion. 2) On recombination of the ion pairs **3** and **6**, the oxygen atom of the sulfinate ion is favored over the sulfur atom as binding partner (**4**:**1** = 7.4; **5**:**7** = 8.4). On **2** → **4** rearrangement (the anion remains on the *endo* side), the carbocation returns preferentially to the oxygen atom of the *p*-toluenesulfinate ion from which it dissociated (**4A**:**4B** = 5.9). 3) The **2** → **5** rearrangement (the anion migrates to the *exo* side) takes place with recombination at both O atoms of the *p*-toluenesulfinate ion, as well as at C1 and C2 of the 2-norbornyl cation;

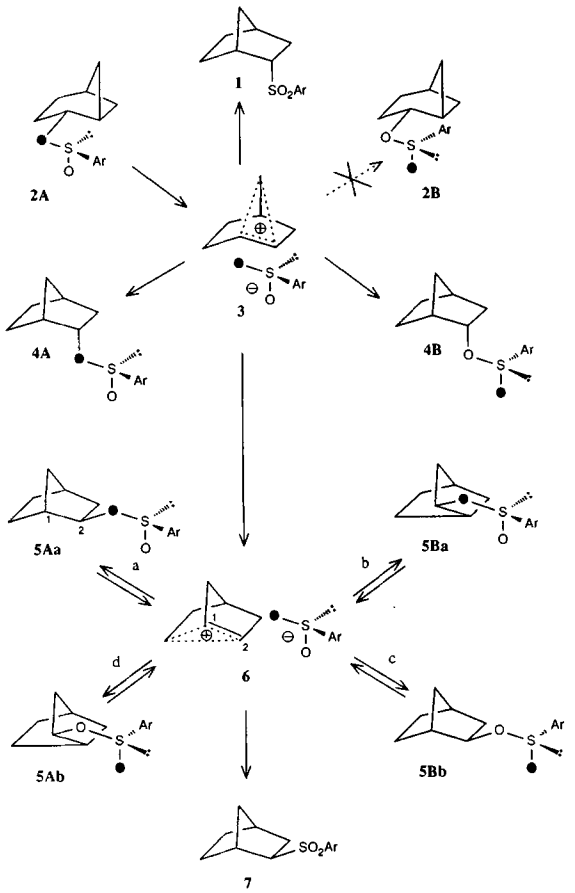

Scheme 1. • = ^{18}O, Ar = *p*-$CH_3C_6H_4$, a = $^{18}O \rightarrow C2$, b = $^{18}O \rightarrow C1$, c = $^{16}O \rightarrow C2$, d = $^{16}O \rightarrow C1$.

we find equal amounts of **5Aa**, **5Ab**, **5Ba**, and **5Bb** (the upper case letters represent diastereomers and lower case letters isotopomers; see Scheme 1).

Bearing these principles in mind, we turned our attention to the reversible dissociation–recombination of *exo*-2-norbornyl-*p*-toluenesulfinate (**5**). The reaction proceeded at a convenient rate in formamide at 150°C and in trifluoroacetic acid at room temperature. The results of the labeling experiments in these solvents hardly differed (Table 1).[18] The ion pair **6** may recombine in four ways: a) $^{18}O \rightarrow C2$, b) $^{18}O \rightarrow C1$, c) $^{16}O \rightarrow C2$, d) $^{16}O \rightarrow C1$. With **5Aa** as starting material,[19] path a) was not measurable (regeneration of **5Aa**) and b) was favored by a factor 3–4 over c). This preference was confirmed by labeling the norbornyl residue: deuterium from the 2-position of **5A** appeared predominantly in the 1-position of **5B**.[20] The distributions of ^{18}O and D agreed well (nos. 1 and 3, and 4 and 6 of Table 1). As in the

Table 1. Product and isotope distributions for the dissociation/recombination of *exo*-2-norbornyl-*p*-toluenesulfinate **5**.

No.	Starting material, conditions	Diastereomers[a]	Isotope distribution[b]		Proportion [%] as isomer			
		5A:**5B**	**5Aa**:**5Ab**	**5Ba**:**5Bb**	**5Aa**	**5Ba**	**5Bb**	**5Ab**
1	^{18}O-**5A**, $HCONH_2$, 150°C, 2 h	77.3:22.7	98.2: 1.8	76.4:23.6	75.9	17.3	5.4	1.4
2	^{18}O-**5A**, $HCONH_2$, 150°C, 5 h	58.2:41.8	85.8:14.2	72.6:27.4	49.9	30.3	11.5	8.3
3	2-D-**5A**, $HCONH_2$, 150°C, 2 h	81.3:18.7	97.4: 2.6	76.5:23.5	79.2	14.3	4.4	2.1
4	^{18}O-**5A**, TFA[c], 25°C, 30 min	84.3:15.7	98.1: 1.9	80.0:20.0	82.7	12.6	3.1	1.6
5	^{18}O-**5A**, TFA, 25°C, 2 h 59.0:41.0	59.0:41.0	89.0:11.0	72.5:27.5	52.5	29.7	11.3	6.5
6	2-D-**5A**, TFA, 25°C, 30 min	75.1:24.9	97.7: 2.3	79.7:20.3	73.4	19.8	5.1	1.7
7	^{18}O-**5B**, $HCONH_2$, 150°C, 2 h	21.1:78.9	77.7:22.3	97.4: 2.6	16.4	76.8	2.1	4.7
8	^{18}O-**5B**, TFA, 25°C, 30 min	15.2:84.8	80.8:19.2	98.3: 1.7	12.3	83.4	1.4	2.9

[a] Determined by gas chromatography [12]; (±0.2%). [b] Determined by ^{13}C or ^{2}H NMR spectroscopy [17, 20]; (±0.5%). [c] Trifluoroacetic acid.

2 → **4** rearrangement, the 2-norbornyl cation returned mainly to the oxygen atom of the *p*-toluenesulfinate ion from which it dissociated. Furthermore, the results in Table 1 show that C1 and C2 of the 2-norbornyl cation are not equivalent in ion pair recombination. For **5Aa** the recombination path c) was favored by a factor 2–3 over d). This finding was supported by experiments with **5Ba** (no. 7 and 8 in Table 1): recombination b) was not measurable; the ratio of paths a), d), and c) was about 8:2:1. The complementary results for **5Aa** and **5Ba** preclude the predominant formation of one diastereomer on recombination of **6**.[21] Instead the *p*-toluenesulfinate ion returned, *after* the exchange of the oxygen atom, preferentially to the carbon atom of the 2-norbornyl cation from which it dissociated (C2). A corresponding preference must also be valid *before* oxygen exchange.

The symmetric, bridged structure of the 2-norbornyl cation has been established by several spectroscopic and theoretical studies.[22] As a rule, nucleophiles do not discriminate between C1 and C2. Exceptions are known, however: for example, the addition of HX to norbornene[23a] or the decomposition of 2-norbornanediazonium ions,[23b] where the norbornyl cation is trapped in unsymmetric form. The dependence of such processes on the solvent[24] suggests the intervention of ion pairs in which the counterion is found closer to C2 than to C1 depending on the history of its formation. In contrast to this interpretation, no regioselective recombination has been observed on heterolysis of 2-norbornyl derivatives.[25] Our results close this gap: they confirm that the close-range order in ion pairs can lead to discrimination between C1 and C2 of the 2-norbornyl cation.

Received: February 5, 1991 [Z4428 IE]
German version: *Angew. Chem. 103* (1991) 989

CAS Registry numbers:
2A, 134334-51-3; **4A**(^{18}O), 134334-54-6; **5Aa**, 134334-52-4; **5Bb**, 134334-53-5; 2-norpinol, 38102-34-0; *p*-toluenesulfinyl chloride, 10439-23-3; *exo*-2-norbornanol, 497-37-0.

[1] Summaries: a) M. Szwarc: *Ions and Ion Pairs in Organic Reactions*, Wiley, New York 1972; b) J. M. Harris, *Prog. Phys. Org. Chem. 11* (1974) 89; c) T. E. Hogen-Esch, *Adv. Phys. Org. Chem. 15* (1977) 153; d) H. Kessler, M. Feigel, *Acc. Chem. Res. 15* (1982) 2.

[2] S. Winstein, E. Clippinger, A. H. Fainberg, R. Heck, G. C. Robinson, *J. Am. Chem. Soc. 78* (1956) 328.

[3] a) H. L. Goering, *Rec. Chem. Prog. 21* (1960) 109; b) H. L. Goering, J. T. Doi, *J. Am. Chem. Soc. 82* (1960) 5850; c) H. L. Goering, J. L. Levy, *ibid. 86* (1964) 120; d) H. L. Goering, J. T. Doi, K. D. McMichael, *ibid. 86*(1964) 1951; e) H. L. Goering, R. G. Briody, G. Sandrock, *ibid. 92* (1970) 7401; f) H. L. Goering, H. Hopf, *ibid. 93* (1971) 1224; g) H. L. Goering, G. S. Koerner, E. C. Linsay, *ibid. 93* (1971) 1230.

[4] a) S. Winstein, P. E. Klinedinst, G. C. Robinson, *J. Am. Chem. Soc. 832* (1961) 885; b) S. Winstein, P. E. Klinedinst, E. Clippinger, *ibid. 83* (1961) 4986; c) A. F. Diaz, I. Ladzins, S. Winstein, *ibid. 90* (1968) 1904; d) H. L. Goering, R. W. Thies, *ibid. 90* (1968) 2967, 2968; e) H. L. Goering, B. E. Jones, *ibid. 102* (1980) 1628; f) C. Paradisi, J. F. Bunnett, *ibid 103* (1981) 946; g) Y. Yukawa, H. Morisaki, K. Tsuji, S.-G. Kim, T. Ando, *Tetrahedron Lett. 1981*, 5187; h) C. Paradisi, J. F. Bunnett, *J. Am. Chem. Soc. 107* (1985) 8223; i) M. Fujio, F. Sanematsu, Y. Tsuno, M. Sawada, Y. Takai, *Tetrahedron Lett. 29* (1988) 93; j) P. Dietze, M. Wojciechowski, *J. Am. Chem. Soc. 112* (1990) 5240.

[5] S. Braverman in S. Patai, Z. Rappoport, C. J. M. Stirling (Ed.): *The Chemistry of Sulfones and Sulfoxides*, Wiley, Chichester 1988, Chap. 13.

[6] Some allyl and propargyl sulfinates undergo concerted [2,3]-sigmatropic rearrangements, e.g., a) S. Braverman, *Int. J. Sulfur Chem. Part C6* (1971) 149; b) S. Braverman, H. Mechoulam, *Tetrahedron 30* (1974) 3883; c) S. Braverman, D. Segev, *J. Am. Chem. Soc. 96* (1974) 1245; d) P. A. Grieco, D. Boxler, *Synth. Commun. 5* (1975) 315; e) J. E. Baldwin, O. W. Lever, N. R. Tzodikov, *J. Org. Chem. 41* (1976) 2312; f) K. Hiroi, R. Kitayama, S. Sato, *J. Chem. Soc. Chem. Commun. 1983*, 1740; *Chem. Pharm. Bull. 32* (1984) 2628; g) D. J. Knight, G. H. Whitham, J. G. Williams, *J. Chem. Soc. Perkin Trans. 1 1987*, 2149.

[7] E. Ciuffarin, M. Isola, A. Fava, *J. Am. Chem. Soc. 90* (1968) 3594.

[8] HPLC: 25 × 2.5 cm Polygosil 60-10 C_{18}, methanol:water = 7:3. Although many "cuts" of the overlapping peaks were made, only the first fraction could be obtained pure (monitored by GC). ^{13}C NMR ($CDCl_3$, 100.6 MHz) [p = primary, s = secondary, t = tertiary, q = quarternary carbon atom (DEPT): δ = 21.46 (p), 25.16 (s), 26.15 (s), 26.45 (s), 33.11 (t), 33.60 (s), 40.16 (t), 79.76 (t), 125.03 (t), 129.53 (t), 142.33 (q), 142.33 (q), 142.78 (q).

[9] The structural analysis has not yet been completed; the assignment of the diastereomers is arbitrary. Racemates were used; only one enantiomer is shown in Scheme 1.

[10] Prepared by a Diels–Alder reaction from cyclopentadiene and ethynyl *p*-tolyl sulfone [11] and subsequent hydrogenation (Pd–C, ethyl acetate) for comparison; yield 94%, m.p. 62 °C.

[11] T. J. Chow, T. H. Lin, *Bull. Inst. Chem. Acad. Sin. 33* (1986) 47; *Chem. Abstr. 107* (1987) 39256.

[12] Prepared from *endo*-2-norbornanol and *p*-toluenesulfinyl chloride (pyridine, 0 °C, 48 h, 98%) for comparison. The isomers were separated by gas chromatography (32 m capillary column, Carbowax + KOH, 165 °C), but not on a preparative scale (HPLC). The mixture showed clearly separated ^{13}C NMR signals for C2 of the diastereomers, δ = 78.40 and 78.56.

[13] Prepared from *exo*-2-norbornanol and *p*-toluenesulfinyl chloride (pyridine, 28 °C, 48 h, 92%); separation of the diastereomers by HPLC [8]. ^{13}C NMR($CDCl_3$): **A**: δ = 21.49 (p), 24.24 (s), 28.08 (s), 34.99 (s), 35.40 (t), 40.87 (s), 42.91 (t), 81.69 (t), 124.99 (t), 129.55 (t), 142.36 (q), 142.95 (q); **B**: δ = 21.48 (p), 24.13 (s), 28.03 (s), 34.90 (s), 35.34 (t), 430.36 (s), 42.88 (t), 80.49 (t), 125.10 (t), 129.58 (t), 142.32 (q), 142.67 (q).

[14] S. Cristol, G. D. Brindell, *J. Am. Chem. Soc. 76* (1954) 5699.

[15] Review: W. Kirmse, *Acc. Chem. Res. 19* (1986) 36.

[16] The incorporation of ^{18}O was achieved by exchange between 2-norpinanone and $H_2{}^{18}O$, followed by reduction ($NaBH_4$), esterification, and separation by HPLC [8]. The sample of **4A** used contained 32% ^{18}O.

[17] The ester ^{18}O atom caused a shift of $\Delta\delta$=0.04 to higher field for the ^{13}C NMR signal of C2. The quantitative analysis was performed by integration of the ^{16}O-^{13}C and ^{18}O-^{13}C signals (**4**: ± 2%; **5**: ± 10% because of the small quantities). For the method, see [4i].

[18] With increasing reaction times, the ratio of the diastereomers and the ^{18}O label approached an equal distribution (cf. no. 1 and 2, 4 and 5 in Table 1); moreover the concentration of **5** decreased as a result of rearrangement to sulfone 7 and solvolysis (formation of 2-norbornyl formate or trifluoroacetate. Theoretically the preferences of the ion-pair recombination are clearest at small turnovers. In practice the experimental error is then large. We chose a compromise between these divergent requirements in our 15–30% turnovers.

[19] ^{18}O-*exo*-2-norbornanol was prepared by hydroxymercuration of norbornene in $H_2{}^{18}O$/THF and treated further to give **5Aa** and **5Ba** [13](53.6% ^{18}O).

[20] Preparation of [2-^{2}H]-*exo*-2-norbornanol: N. H. Werstiuk, D. Dhanoa, G. Timmins, *Can. J. Chem. 61* (1983) 2403. ^{2}H NMR ($CHCl_3$, 61.4 MHz): [^{2}H]-**5A**: δ = 4.28, 2.26; [^{2}H]-**5B**: δ = 4.28, 2.48.

[21] The solvolysis of a 1:1 mixture of **5A** and **5B** also gave no indication of diastereoselective recombination. No significant change in the **5A**:**5B** ratio was observed during the decrease in concentration of **5**.

[22] More recent summaries: a) D. Lenoir, Y. Apeloig, D. Arad, P. von R. Schleyer, *J. Org. Chem. 53* (1988) 312; b) G. A. Olah, G. K. S. Prakash, R. E. Williams, L. D. Field, K. Wade: *Hypercarbon Chemistry*, Wiley, New York 1987, p. 157; c) P. Vogel: *Carbocation Chemistry*, Elsevier, Amsterdam 1985, p. 281.

[23] Review: a) H. C. Brown: *The Nonclassical Ion Problem* (with comments by P. von R. Schleyer), Plenum, New York 1977, p. 225; b) [23a], p. 219.

[24] a) Dediazotization: W. Kirmse, R. Siegfried, *J. Am. Chem. Soc. 105* (1983) 950; b) HX addition: W. Kirmse, S. Brandt, *Chem. Ber. 117* (1983) 2524.

[25] a) E. J. Corey, J. Casanova, Jr., P. A. Vatakencherry, R. Winter, *J. Am. Chem. Soc. 85* (1963) 169; b) S. G. Smith, J. P. Petrovich, *J. Org. Chem. 30* (1965) 2882; c) L. A. Spurlock, T. E. Parks, *J. Am. Chem. Soc. 92* (1970) 1279.

Synthesis and Interconversion of New $(CH)_{14}$ Isomers**

By *Wolf-Dieter Fessner,** and *Maria Rodriguez*

Dedicated to Professor Horst Prinzbach on the occasion of his 60th birthday

The homologous series of $(CH)_{2n}$ hydrocarbons—valence isomers of [2n]annulenes—continue to be the subject of the

[*] Dr. W.-D. Fessner, M. Rodriguez
Institut für Organische Chemie und Biochemie der Universität
Albertstrasse 21, W-7800 Freiburg (FRG)

[**] This work was supported by the Fonds der Chemischen Industrie. We thank BASF AG for a gift of cyclooctatetraene.

most varied studies because of their theoretical importance and their unusual propensity towards photochemical, thermal, and catalytic conversions. In connection with studies to differentiate between through-space (e.g. in isodrines **A**[1] or homohypostrophenes **D**[2]) and through-bond electronic interactions (e.g. in triblattenes **B**[3] or *hemi*-pagodanes **C**[4]),

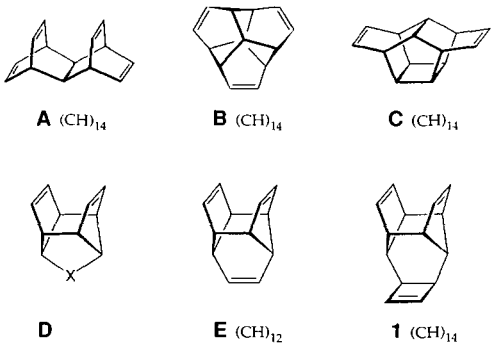

we were interested in the properties of the polycycle **1**, a new unsaturated member of the $(CH)_{14}$ family, and in its potential as precursor for the C_{2v}-symmetric $(CH)_{12}$ triene **E**. Here we report on two high-yield routes to **1**, starting from the known COT–*p*-benzoquinone cycloadduct **2**, and on first results for its thermal and photochemical transformations into further $(CH)_{14}$ isomers.

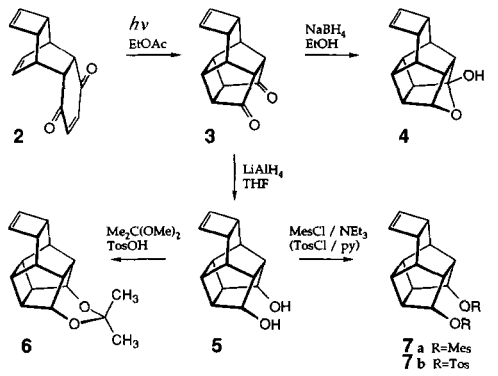

We chose the structurally related diketone **3** as starting material for the cyclobutene-bridged diene **1**, based on the analogous syntheses of hypostrophene and C_{2v}-symmetric homologues **D**.[2, 5, 6] Compound **3** is obtained efficiently by intramolecular [2+2] photocycloaddition from the tetracycle **2**, which is in turn accessible through the Diels–Alder reaction of COT and *p*-benzoquinone (literature yield[7]: 25%); by improving the [4+2] cycloaddition to a 65–70% yield (sealed tube, THF, 24h at 125°C; or diglyme, 24h at 140°C), the valuable diene component could be used effectively. In contrast to the known synthesis routes for dienes of type **D**—obtained mainly through an acid catalyzed skeletal isomerization with participation by the photochemically formed four-membered ring[2, 6]—the reactivity of the cyclobutene unit required a modified strategy. Therefore, we selected as primary target the *exo,exo*-diiodide **8**, which appeared accessible through nucleophilic substitution from suitable precursors and able to undergo a subsequent 1,4 elimination to **1**.

Whereas the reduction of diketone **3** with $NaBH_4$ stops at the hemiacetal (**4**) stage, with $LiAlH_4$ it proceeds smoothly

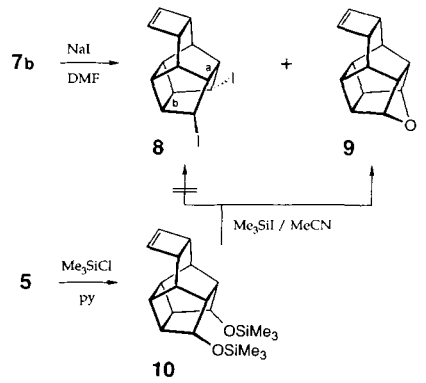

to form a sparingly soluble diol (70%, m.p. 202°C). The simplicity of the NMR spectra and the coupling pattern suggested high molecular symmetry and an *endo,endo* configuration for the alcohol functions in **5**, which was confirmed by transformation into the acetonide **6** (76%, m.p. 108°C). As the bis(mesyl) ester **7a** (91%, m.p. 102°C) proved to be unstable on storage, we used the bis(tosylate) **7b** (86%, m.p. 134°C) for reaction with NaI. Although the workup yielded the desired inversely configurated compound **8**, the amounts were not satisfactory (18%, m.p. 156°C), and the ether **9** was the major component (36%, m.p. 92°C). The latter is probably formed by a competitive attack of the nucleophile at the sulfonate and subsequent intramolecular substitution. In an attempt to prepare the diiodide **8** from the bis(silyl) ether **10** by treatment with iodotrimethylsilane, only **9** was isolated instead (65%), which must be attributed on one hand to steric hindrance and on the other to anchimeric stabilization of electrophilic intermediates.

After the treatment of **8** with Na/K alloy in ether, the ^1H NMR spectrum of the crude product showed signals due to olefinic compounds. Separation of the components into the heptacycle **12** (9%) and the trienes **11** (5%) and **1** (74%, m.p. 88°C) was achieved by chromatography on $AgNO_3$-impregnated aluminum oxide with pentane/ether mixtures.[8] The ratio of the trienes, which can be attributed to competing 1,4 cleavage of the comparably oriented relay bonds **a** and **b**, may be interpreted as a reflection of the relative bond strain. The formation of a pentaprismane homologue (**12**), however, is without precedent;[5] one can only speculate on the character of the homo- or heterolytic impulse which triggers the transannular bond formation.

The unsatisfactory total yield of **1** and the effort required for its chromatographic separation made us look for an alternative synthesis. And indeed, on treatment with Zn/HOAc[2, 9] the diketone **3** forms the enone **13** surprisingly

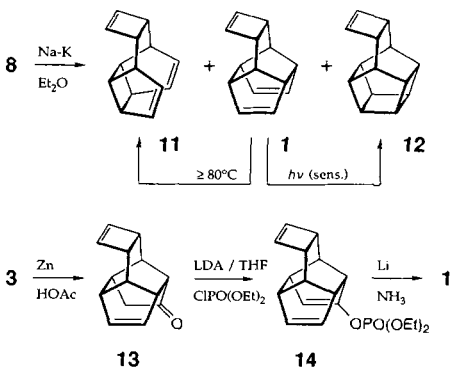

smoothly (59%, m.p. 87 °C[8] ; in addition 27% of **4**) without attack on the cyclobutene unit. Esterification of the corresponding enolate to afford the phosphate **14** (91%, oil) and its subsequent reduction with lithium in ammonia yields exclusively the triene **1** (75%) in economical total yield.

The reactions of **1** are noteworthy. Moreover, they serve to confirm its structure: Triplet-sensitized photolysis (acetone, Hg medium pressure lamp, Duran filter) initiates [2+2] cycloaddition to **12** typical for dienes **D**, while heating in solution to ≥ 80 °C induces a quantitative, regiospecific [3,3] shift to **11**. No indication is found in the ^{1}H NMR spectrum for the participation of isomer **15** (≤ 1%, Fig. 1) in

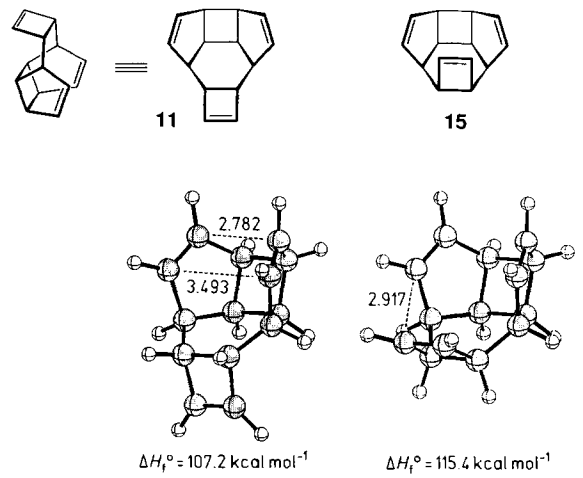

Fig. 1. Comparison of the calculated minimum geometries of the potential Cope isomers of **1**; heat of formation and intramolecular distances from MM2 calculations [11].

an equilibrium. In contrast, attempts to induce the thermal isomerization of the enolate of **13** or of the enol ester **14** were dominated by unspecific decomposition.

The exclusive formation of the *anti* isomer **11** is in agreement with force-field calculations, which estimate an energy higher by ca. 8 kcal mol^{-1} for the *syn* isomer **15** (both higher homologous unsaturated *tris*-[3.2.2]-σ-homobenzenes[10]) as a result of steric compression and unfavorable torsional interactions (Fig. 1). However, the heat of formation of the experimentally less stable structural isomer **1** ($d_{\pi-\pi} = 2.651$ Å) is strongly underestimated (ca. 0.8 kcal mol^{-1} *lower* than **11**),[11] which has to be ascribed in part to destabilizing π–π interactions neglected by the computational method (MM2).

Received: January 14, 1991 [Z4383 IE]
Publication delayed on authors' request.
German version: *Angew. Chem. 103* (1991) 985

CAS Registry numbers:
1, 134208-60-9; **2**, 86471-43-4; **3**, 3037-86-3; **4**, 134208-61-0; **5**, 134208-62-1; **6**, 134208-63-2; **7a**, 134208-64-3; **7b**, 134208-70-1; **8**, 134208-65-4; **9**, 134208-66-5; **10**, 134208-67-6; **11**, 134208-68-7; **12**, 134237-88-0; **13**, 134208-69-8; **14**, 134237-89-1.

[1] a) J.-P. Melder, F. Wahl, H. Fritz, H. Prinzbach, *Chimia 41* (1987) 426–428; b) H. Prinzbach, G. Sedelmeier, H.-D. Martin, *Angew. Chem. 89* (1977) 111-112; *Angew. Chem. Int. Ed. Engl. 16* (1977) 103–104.

[2] a) W.-D. Fessner, G. Sedelmeier, L. Knothe, H. Prinzbach, G. Rihs, Z.-Z. Yang, B. Kovac, E. Heilbronner, *Helv. Chim. Acta 70* (1987) 1816–1842; b) G. Sedelmeier, H. Prinzbach, H.-D. Martin, *Chimia 33* (1979) 329–332, and references cited therein.

[3] a) W.-D. Fessner, H. Prinzbach, *Tetrahedron 42* (1986) 1797–1803; b) H. Müller, J.-P. Melder, W.-D. Fessner, D. Hunkler, H. Fritz, H. Prinzbach, *Angew. Chem. 100* (1988) 1140–1143; *Angew. Chem. Int. Ed. Engl. 27* (1988) 1103–1106.

[4] G. Sedelmeier, W.-D. Fessner, R. Pinkos, C. Grund, B. A. R. C. Murty, D. Hunkler, G. Rihs, H. Fritz, C. Krüger, H. Prinzbach, *Chem. Ber. 119* (1986) 3442–3472.

[5] G. R. Underwood, B. Ramamoorthy, *Chem. Commun. 1970*, 12–13; Erratum: *ibid. 1971*, 600.

[6] a) E. C. Smith, J. C. Barborak, *J. Org. Chem. 41* (1976) 1433–1437; b) A. P. Marchand, T.-C. Chou, J. D. Ekstrand, D. van der Helm, *ibid. 41* (1976) 1438–1444; c) P. E. Eaton, L. Cassar, R. A. Hudson, D. R. Hwang, *ibid. 41* (1976) 1445–1448; d) D. C. Dong, J. T. Edward, *Can. J. Chem. 58* (1980) 1324–1326.

[7] J. C. Barborak, D. Khoury, W. F. Maier, P. von R. Schleyer, E. C. Smith, W. F. Smith, C. Wyrick, *J. Org. Chem. 44* (1979) 4761–4766.

[8] Selected ^{1}H NMR data (250 MHz, $CDCl_3$): pentacyclo[6.6.0.0^{2,12}.0^{3,6}.0^{7,11}]tetradeca-4,9,13-triene **1**: $\delta = 2.19$ (m, 2H), 2.25 (m, 2H), 2.64 (m, 2H), 2.99 (m, 2H), 6.07 (dd, 2H), 6.16 (dd, 2H), 6.32 (s, 2H). – (1α,2α,3α,6α,7β,10β,11α,14α)-Pentacyclo[9.3.0.0^{2,6}.0^{3,14}.0^{7,10}]tetradeca-4,8,12-triene **11**: $\delta = 2.94$ (m, 4H), 3.14 (s, 2H), 4.65 (m, 2H), 5.32 (d, 2H), 5.71 (d, 2H), 6.05 (s, 2H). – Heptacyclo[6.6.0.0^{2,7}.0^{3,6}.0^{4,14}.0^{5,9}.0^{10,13}]-tetradec-11-ene **12**: $\delta = 2.01$ (m, 2H), 2.78–2.90 (m, 6H), 3.03 (m, 2H), 3.10 (m, 2H), 6.30 (s, 2H). – (±)-*anti*-Pentacyclo[6.6.0.0^{2,12}.0^{3,6}.0^{7,11}]-tetradeca-4,13-dien-9-one **13**: $\delta = 1.92$ (dd, 1H), 2.11 (d, 1H), 2.24–2.37 (m, 2H), 2.46 (m, 3H), 2.66 (m, 1H), 2.97 (m, 2H), 6.17 (m, 1H), 6.31 (m, 1H), 6.36 (s, 2H).

[9] E. Wenkert, J. E. Yoder, *J. Org. Chem. 35* (1970) 2986–2989.

[10] M. Maas, M. Lutterbeck, D. Hunkler, H. Prinzbach, *Tetrahedron Lett. 24* (1983) 2143–2146.

[11] As this trend persists for diverse structural variants of type **D**, the order of magnitude of the error (≥ 5 kcal mol^{-1}) also implies an unsatisfactorily balanced parameterization of the MM2 force field (N. L. Allinger, *J. Am. Chem. Soc. 99* (1977) 8127–8134) for cyclopentene compounds. W.-D. Fessner, W. R. Roth, unpublished results.

1,2,3-Triphospha-4-silabicyclo[1.1.0]butanes from Activated, Stable Phosphasilenes and White Phosphorus**

By *Matthias Drieß**

Bicyclo[1.1.0]butanes in which the ring-C atoms are completely replaced by silicon and/or elements of Group 15 are interesting because of their unusual bonding.[1] Comparative experimental and theoretical studies of bicyclo[1.1.0]butane derivatives with P_4 (**A**) and Si_4 (**B**) frameworks[2] indicate that the bonds between the bridgehead atoms are substantially weakened in the silicon skeleton, but both systems possess remarkable ring dynamics.

Recently the first bicyclo[1.1.0]butane with a Si_2P_2 framework, a 1,3-diphospha-2,4-disilabicyclo[1.1.0]butane derivative (**C**) was reported.[3] The P–P bond in **C** has a diradical nature; this system therefore resembles compounds of type **A** more than type **B**.[4] Type **C** compounds were prepared by treatment of tetraorganodisilenes ($R_2Si{=}SiR_2$) with white phosphorus[3] and lately also by dehydrogenation of 2,2,4,4-tetraorgano-1,3-diphospha-2,4-disiletanes.[5] The smooth access to **C** from disilenes and P_4 raised the question whether this synthesis principle would not also be effective for the as yet unknown SiP_3 systems, **D**. Kinetically stable phosphasilenes ($R_2Si{=}PR$) which must be thermally stable yet reactive enough to react with P_4 are required as starting compounds. The only phosphasilene stable at 60 °C which could be obtained pure (spectroscopic criteria), Is(*t*Bu)Si=PMes*[6] (Is = 2,4,6-triisopropylphenyl (isityl), Mes* = 2,4,6-tri-*tert*-

[*] Dr. M. Drieß
Anorganisch-chemisches Institut der Universität
Im Neuenheimer Feld 270, W-6900 Heidelberg (FRG)

[**] This work was supported by the Fonds der Chemischen Industrie and the Deutsche Forschungsgemeinschaft.

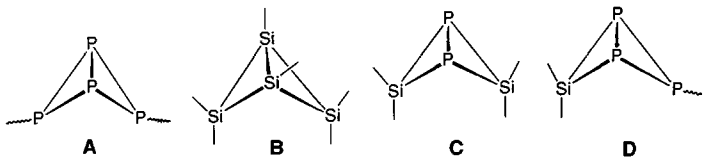

butylphenyl), seemed unsuitable as it reacts only slowly with relatively strong oxidizing agents like sulfur and selenium. Appropriate precursors appeared to be the phosphasilenes **2a** and **b**, which have a triorganylsilyl group attached to the $\lambda^3\sigma^2$-coordinated P atom. Compounds **2a** and **b** were obtained by elimination of LiF from the corresponding lithiophosphanes **1a** and **b**.[7]

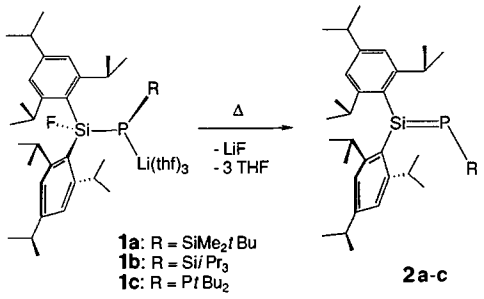

Furthermore, **2c**, a phosphasilene with a phosphanyl substitutent at P is accessible by this route. The derivatives **2** are stable under the conditions of the synthesis, in contrast to other analogously prepared compounds such as $t\mathrm{Bu_2Si{=}P{-}Si}t\mathrm{Bu_3}$ and $t\mathrm{Bu_2Si{=}P}t\mathrm{Bu}$.[8] The thermal stability of **2** (**a**, **b** 2 h in toluene at 90 °C and **c** 12h in toluene at 110 °C without change) is attributed in the first instance to the bulky aryl groups on silicon. Compounds **2** were obtained as orange oils and shown by NMR spectroscopy to be pure when the precursors were the analytically pure **1**,[9] but crystals of **2** have not yet been obtained.

The data from ^{31}P and ^{29}Si NMR spectroscopy (Table 1) reflects the unusual bonding mode in the strongly polarized

Table 1. ^{31}P and ^{29}Si NMR data of compounds **2a–c**. Coupling constants J in Hz.

	$\delta(^{31}P)$	$^1J(PP)$	$\delta(^{29}Si)$	$^1J(P{=}Si)$	$^1J(P{-}Si)$
2a	17.7	–	178.4 (d, Si=P)	149	–
	–	–	14.2 (d, Si–P)	–	72
2b	11.1	–	167.8 (d, Si=P)	160	–
	–	–	20.8 (d, Si–P)	–	78
2c	72.2 (d, P=Si)	214	184.6 (dd)[a]	158	–
	26.6 (d, $Pt\mathrm{Bu_2}$)	214	–	–	–

[a] ^2J(Si, P) = 43.

P–Si (p–p)π systems **2**, which are activated by the σ-donor groups on phosphorus. In comparison with the known phosphasilenes of *Bickelhaupt* et al.,[6] which have only aryl substituents on the phosphorus and silicon atoms ($\delta(^{31}P)$ = 136–93.5),[6] the resonance signals of the $\lambda^3\sigma^2$ P atoms in **2** are shifted to higher field by up to $\Delta\delta$ = 124.9 (!). The position of the ^{29}Si signals at extremely low field and the characteristically large $^1J_{P-Si}$ coupling constants leave no doubt that the Si atoms have threefold coordination and Si–P π bonds.[6] The unusual position of the ^{31}P and ^{29}Si NMR signals is attributed to the strong σ-donor influence of the triorganosilyl- and di-*tert*-butylphosphanyl groups on phosphorus. This influence decreases, as anticipated, along the series $\mathrm{SiiPr_3} > \mathrm{SiMe_2}t\mathrm{Bu} > \mathrm{P}t\mathrm{Bu_2}$.

The treatment of **2a, b** with white phosphorus in the molar ratio 2:1 at 60–70 °C does yield the 1,2,3-triphospha-4-silabicyclo[1.1.0]butanes (**3a, b**),[10] whose composition has been

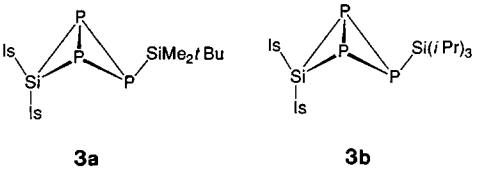

3a **3b**

established by EI mass spectra and correct elemental analysis.[10] Their structure can be unambiguously deduced from NMR data: in the ^{31}P NMR spectrum a doublet is observed for the bridgehead phosphorus atoms at very high field as expected (**3a**: δ = – 331.5, $^1J_{PP}$ = 163 Hz; **3b**: δ = – 328.3, $^1J_{PP}$ = 173 Hz) and a triplet for the peripheral P atom (**3a**: δ = – 257.5; **3b**: δ = – 247.2). The ^{29}Si skeletal atoms in **3a, b** give a doublet of triplets in the ^{29}Si NMR spectrum (INEPT pulse sequence; X part of an A_2MX spin system where A, M = ^{31}P, X = ^{29}Si; **3a**: δ = – 34.4, $^1J_{SiP}$ = 74 Hz, $^2J_{SiP}$ = 27 Hz; **3b**: δ = – 37.1, $^1J_{SiP}$ = 72 Hz, $^2J_{SiP}$ = 23 Hz). The $^1J_{SiP}$ coupling constants are in the same region as those of 1,3-diphospha-2,4-disilabicyclo[1.1.0]butanes (76–78 Hz) and thus typical for silicon atoms in three-membered rings.[11]

Since the isityl groups on silicon are bulky and since in each case only one configuration of **3a, b** is formed, it appears that the triorganosilyl substituent favors the *exo* position.

Besides the disilenes, these phosphasilenes are the only known compounds with (p–p)π bonds between main-group elements which degrade P_4 under relatively mild conditions. This route leads formally to the breaking of the π and the σ bonds of the heteroalkene group.

Experimental Procedure

2a: A solution of analytically pure **1a**[7] (1.25 g, 1.52 mmol) in toluene (20 mL) was heated for 6 h at 60–70 °C, during which the initially colorless solution becomes deep orange. The clear solution was cooled and after the ^{31}P NMR spectrum confirmed that the reaction was complete, an excess of Me_3SiCl (0.82 g, 7.6 mmol) was added and the mixture stirred for a further 12 h at room temperature. The resulting orange suspension was evaporated to dryness at 10^{-2} Torr, and the residue was taken up in pentane (10 mL) and filtered over a G-IV frit. Removal of the pentane yielded **2a** (pure according to the NMR spectrum). Yield: 802 mg (91 %), deep orange oil. **2b, c** were prepared similarly: **2b** (yield 796 mg, 1.28 mmol, 94 %) from **1b** (1.18 g, 1.36 mmol); **2c** (yield 638 mg, 0.84 mmol, 91 %) from **1c** (810 mg, 0.92 mmol).

3a: Freshly sublimed white phosphorus (46.5 mg, 0.37 mmol) was added to a solution of **2a** (400 mg, 0.75 mmol) in toluene (20mL) and heated for 12 h at 70 °C. The initially deep orange solution paled to light yellow. The solvent was removed at 25 °C and 10^{-2} Torr, and the residue taken up in pentane, the volume reduced to ca. 5 mL, and the resulting solution left to stand at – 30 °C to crystallize. Yield: 142.9 mg (0.24 mmol, 32 %); pale yellow, microcrystalline powder. M.p. 214–216 °C. **3b**: Analogous to **3a** from **2b** (492 g, 0.86 mmol). Yield: 223 mg (0.35 mmol, 41 %) of a light yellow solid. M.p. 231–232 °C.

Received: March 22, 1991 [Z 4519 IE]
German version: *Angew. Chem. 103* (1991) 979

[1] P. von R. Schleyer, F. A. Sax, J. Kalcher, R. Janoschek, *Angew. Chem. 99* (1987) 375; *Angew. Chem. Int. Ed. Engl. 26* (1987) 364; T. Dabisch, W. W. Schoeller, *J. Chem. Soc. Chem. Commun. 1986*, 896; W. W. Schoeller, C. Lerch, *Inorg. Chem. 22* (1983) 2992; S. Collins, R. Dutler, R. Rauk, *J. Am. Chem. Soc. 109* (1987) 2567; P. Jutzi, U. Meyer, S. Opiela, M. M. Olmstead, P. P. Power, *Organometallics 9* (1990) 1459.

[2] P_4: R. Riedel, H.-D. Hausen, E. Fluck, *Angew. Chem. 97* (1985) 1050; *Angew. Chem. Int. Ed. Engl. 24* (1985) 1056; E. Niecke, R. Rüger, B. Krebs, *ibid. 94* (1982) 553 bzw. **21** (1982) 544; Si_4: S. Masamune, Y. Kabe, S. Collins, D. J. Williams, R. Jones, *J. Am. Chem. Soc. 107* (1985) 5552; R. Jones, D. J. Williams, Y. Kabe, S. Masamune, *Angew. Chem. 98* (1986) 176; *Angew. Chem. Int. Ed. Engl. 26* (1986) 173.

[3] M. Drieß, A. D. Fanta, D. Powell, R. West, *Angew. Chem. 101* (1989) 1087; *Angew. Chem. Int. Ed. Engl. 29* (1989) 1038.

[4] This finding is new. Ab initio MO calculations were done on the parent system $(H_2Si)_2P_2$, which confirm the singlet–diradical character of the P–P bond: R. Janoschek, unpublished results. This explains the relatively large P–P bond length of 2.38 Å in **C** (ca. 0.15 Å longer than a P–P single bond). See also refs. [3], [5].

[5] M. Drieß, H. Pritzkow, M. Reisgys, *Chem. Ber. 124* (1991), No. 9.

[6] C. N. Smit, F. Bickelhaupt, *Organometallics 6* (1987) 1156; H. M. M. Bastiaans, F. Bickelhaupt, Y. van den Winkel, *Phosphorus, Sulfur, Silicon and Rel. Elem. 49/50* (1990) 333; H. M. M. Bastiaans, F. Bickelhaupt, *J. Organomet. Chem. 405* (1991) 183.

[7] **1a–c** were prepared from diisityl(phosphanyl)fluorosilane [5] by lithiation with *n*BuLi at −78 °C in THF, followed by reaction with $Me_2SitBuCl$, $iPr_3Si{-}O{-}SO_2CF_3$ or tBu_2PCl, and further litiation with *n*BuLi. The compounds are recrystallized several times from hexane at −10 °C; they are each analytically pure and contain three molecules of THF per lithium atom.

[8] $tBu_2Si{=}PtBu$: U. Klingebiel, R. Boese, D. Bläser, M. Andrianarison, *Z. Naturforsch. B44* (1989) 265; $tBu_2Si{=}PSitBu_3$: N. Wiberg, H. Schuster, *Chem. Ber. 124* (1991) 93.

[9] **2a**: ^{1}H NMR (200 MHz, 295 K, [D$_8$]Toluol): δ = 0.184 (d, 6H, $SiMe_2tBu$, ^3J(PH) = 2 Hz), 1.090 (s, 9H, $SiMe_2tBu$), 1.167–1.305 (br.m, 36H, *o*-CHMe_2 and *p*-CHMe_2), 2.757 (sept, 2H, *p*-C*H*Me$_2$, *J*(HH) = 6.7 Hz), 3.686 (br., 2H, *o*-C*H*Me$_2$), 3.989 (br., 2H, *o*-C*H*Me$_2$), 7.016 (s, 2H, *arom.* H), 7.027 (s, 2H, *arom.* H). – MS (EI, 70 eV): *m/z* (%) 530 (M$^\oplus$, 14), 515 ((M − Me)$^\oplus$, 3), 327 ((M − Is)$^\oplus$, 15), 203 (Is$^\oplus$, 100). **2b**: ^{1}H NMR (200 MHz, 295 K, [D$_8$]Toluol): δ = 1.119–1.233 (m, 33H, CHMe_2 and SiCHMe_2), 1.361 (d, 24H, CHMe_2), *J*(HH) = 6.8 Hz), 2.775 (sept, 2H, C*H*Me$_2$, *J*(HH) = 6.8 Hz), 3.442 (br., 2H, C*H*Me$_2$), 3.644 (br., 2H, C*H*Me$_2$), 7.021 (s, 2H, *arom.* H), 7.074 (s, 2H, *arom.* H). – MS (EI, 70 eV): *m/z* (%) 572 (M$^\oplus$, 7), 529 ((M − *i*Pr)$^\oplus$, 3), 486 ((M − 2*i*Pr)$^\oplus$, 12), 354 ((M − Is − *i*Pr)$^\oplus$, 8), 43 (*i*Pr$^\oplus$, 100). **2c**: ^{1}H NMR (200 MHz, 295 K, [D$_8$]Toluol): δ = 1.265 (br., 36H, CHMe_2), 1.376 (d, 18H, *t*Bu, ^3J(PH) = 11.1 Hz), 2.814 (br., 2H, *p*-C*H*Me$_2$), 3.630 (br., 2H, *o*-C*H*Me$_2$), 3.837 (br., 2H, *p*-C*H*Me$_2$), 7.093 (s, 4H, *arom.* H). – MS (EI, 70 eV): *m/z* (%) 560 (M$^\oplus$, 31), 503 ((M − *t*Bu)$^\oplus$, 8), 460 ((M − *t*Bu − *i*Pr)$^\oplus$, 15), 301 ((M − Is − *t*Bu − *i*Pr + 1)$^\oplus$, 12) 57 (*t*Bu$^\oplus$, 100).

[10] **3a**: ^{1}H NMR (200 MHz, C_6D_6, 295 K): δ = 0.214 (d, 3H, Si*Me*, *J*(PH) = 1.8 Hz), 0.353 (d, 3H, Si*Me*, *J*(PH) = 1.8 Hz), 1.107 (s, 9H, *t*Bu), 1.207 (br., 18H, CHMe_2), 1.247 (br., 18H, CHMe_2), 2.768 (br.m, 2H, *p*-C*H*Me$_2$), 3.588 (br.m, 2H, *o*-C*H*Me$_2$), 3.811 (br.m, 2H, *o*-C*H*Me$_2$), 6.382 (s, 2H, *arom.* H), 6.884 (s, 2H, *arom.* H). – MS (EI, 70 eV): *m/z* (%) 592 (M$^\oplus$, 24); **3b**: ^{1}H NMR (200 MHz, 295 K, C_6D_6): δ = 1.127 (br., 21H, Si*i*Pr), 1.217–1.221 (br., 36H, CHMe_2), 2.773 (br., 2H, *p*-C*H*Me$_2$), 3.571 (br., 2H, *o*-C*H*Me$_2$), 3.661 (br., 2H, *o*-C*H*Me$_2$), 6.372 (s, 2H, *arom.* H), 6.892 (s, 2H, *arom.* H). – MS (EI, 70 eV): *m/z* (%) 634 (M$^\oplus$, 22).

[11] M. Baudler, H. Jongebloed, *Z. Anorg. Allg. Chem. 458* (1979) 9; M. Weidenbruch, M. Herrendorf, A. Schaefer, K. Peters, H. G. von Schnering, *J. Organomet. Chem. 295* (1985) 7; M. Baudler, T. Pontzen, *Z. Anorg. Allg. Chem. 491* (1982) 27; see also [4], [5].

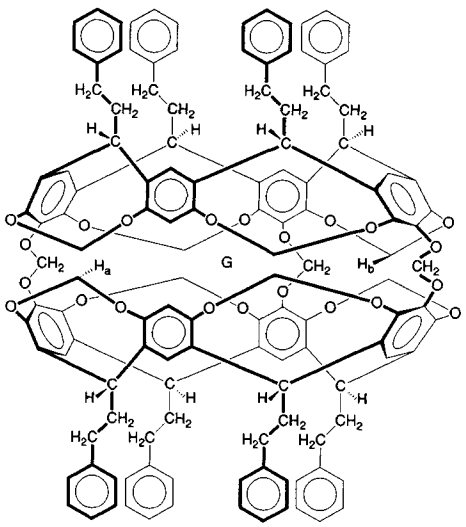

The Taming of Cyclobutadiene**

By *Donald J. Cram,* Martin E. Tanner,* and *Robert Thomas*

Cyclobutadiene, $(CH)_4$, is the Mona Lisa of organic chemistry in its ability to elicit wonder, stimulate the imagination, and challenge interpretive instincts. No other organic compound combines such a fleeting existence and so many different syntheses, with such a propensity for different chemical reactions, and with the variety of calculations of its structure.[1–3]

We report here the synthesis and reactions of cyclobutadiene lodged in the cavity (inner phase) of the hemicarceplex **1** · $(CH)_4$. Hemicarcerand **1** combines an enforced inner phase large enough to accommodate small guest molecules such as dimethylacetamide, benzene, or tetrahydrofuran (THF) with a portal which allows guest entry and exit at temperatures above 100 °C. The eight $C_6H_5CH_2CH_2$ appendages of **1** · G serve as solubilizing groups.[4, 5] In **1** · $(CH)_4$, the shell of the host protects the guest $(CH)_4$ from dimerization[2, 3] and from reactants too large to pass through the portal of **1**, rendering **1** · $(CH)_4$ stable at ordinary temperatures. The synthesis and reactions of $(CH)_4$ are the first that have been carried out in the confined *inner phase* of a hemicarcerand.[4] Scheme 1 formulates these reactions, and identifies them by their enclosure in the rectangular box outlined by the heavy lines. Reactions previously run by *Corey* et al.[6, 7] in ordinary solutions (**2** → **3** → **4**) and by *Maier* et al. and *Schweig* et al.[8] (**4** → **2**, flash pyrolysis) are enclosed by dashed lines. Prior reactions carried out by

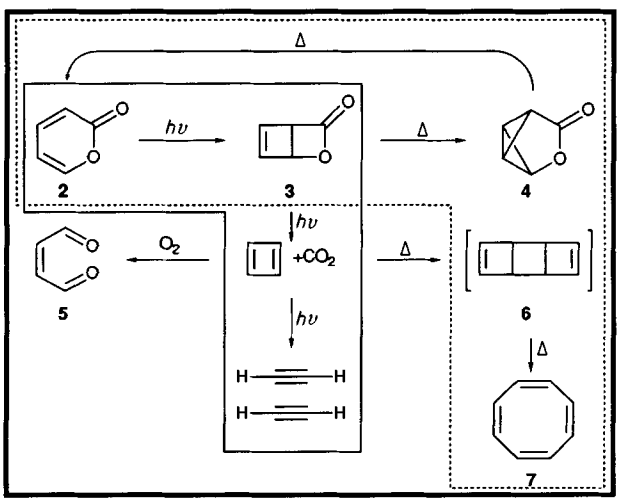

Scheme 1. Thermal and photochemical transformations of α-pyrone. The three frames contain reactions carried out: ---- historically in solution and gas phase; —— historically in an argon matrix at 8 K; —— in the inner phase of the hemicarcerand **1**, and reported here (except cyclooctatetraene formation, which occurs outside).

[*] Prof. D. J. Cram, Dr. M. E. Tanner, Dr. R. Thomas
Department of Chemistry and Biochemistry
University of California at Los Angeles
Los Angeles, CA 90024 (USA)

[**] We warmly thank the National Science Foundation for Grant NSF CHE 8802800, the U.S. Public Health Service for Grant GM-12640, and S.E.R.C./N.A.T.O. for support for *R. T.*

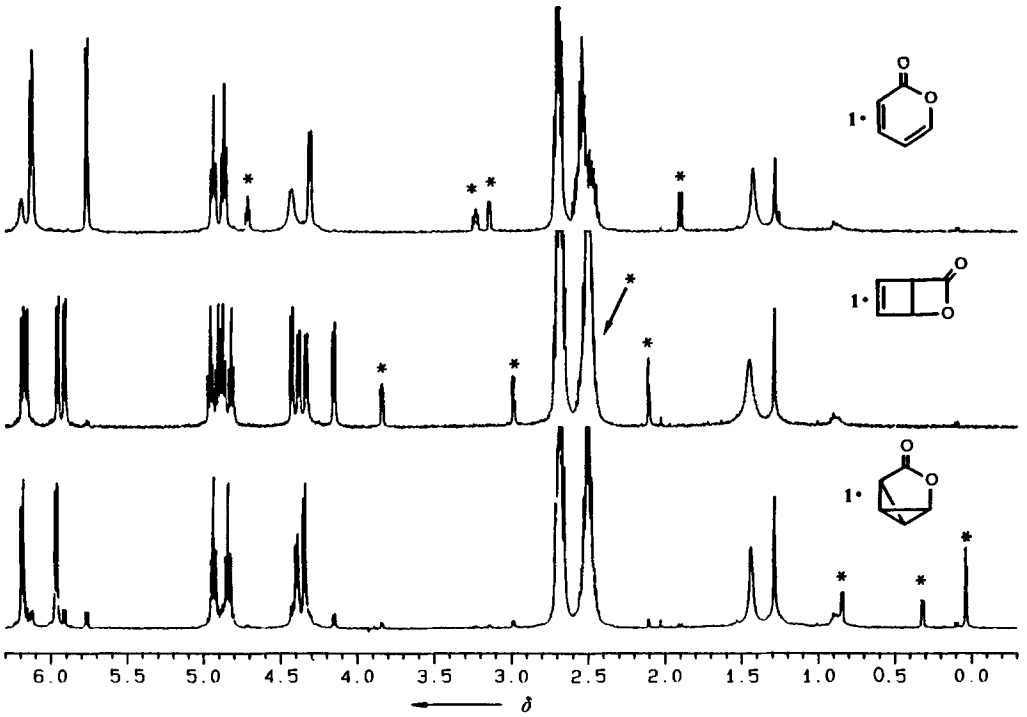

Fig. 1. ^{1}H NMR spectra (500 MHz, $CDCl_3$, 60°C) of hemicarceplexes **1** · **2**, **1** · **3**, and **1** · **4**. Signals marked by stars are due to guests.

Chapman et al.[9] and *Kranz* et al.[10] in an argon matrix at 8 K are enclosed by solid lines. *Maier* et al. have prepared and characterized the stable cyclobutadiene derivatives **8**[11] and **9**,[12a] the latter concurrently with *Masamune* et al.,[12b]

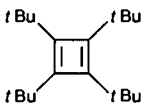

8

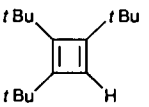

9

in which $(CH_3)_3C$ groups sterically stabilize the cyclobutadiene system.

Hemicarceplex **1** · α-pyrone (**1** · **2**) was prepared by refluxing empty **1**[4, 5] in 3:1 C_6H_5Cl/α-pyrone, then precipitating the cooled complex with hexanes. The host-to-guest ratio of **1** · α-pyrone was established by elemental analysis[13] and its ^{1}H NMR spectrum (Fig. 1). Solutions of **1** · α-pyrone in degassed $CDCl_3$ (ca. 3 mM) or [D_8]THF (ca. 1 mM) were sealed in standard borosilicate-glass NMR tubes, which were irradiated at 25°C with a 75 W xenon arc lamp for 30 min. The 500 MHz ^{1}H NMR spectra of the resulting $CDCl_3$ and [D_8]THF solutions (Fig. 2) each gave a sharp singlet for incarcerated $(CH)_4$ at $\delta = 2.27$ and 2.35 respectively. The latter signal is $\Delta\delta = 3.03$ upfield from that of the ring proton of **9** in [D_8]THF at $\delta = 5.38$[2] due to the shielding effects of the host in **1** · $(CH)_4$. Similarly the proton singlet of **1** · C_6H_6 is $\Delta\delta = 3.49$ upfield of free C_6H_6 dissolved in $CDCl_3$ at 22°C.[5] The host's inward-pointing H_a and H_b protons (see **1** · G) gave sharp doublets in the ^{1}H NMR spectrum of **1** · $(CH)_4$ at $\delta = 4.27$ and 4.36, providing direct evidence that cyclobutadiene possesses a singlet ground state (Fig. 2). Triplet $(CH)_4$ would dramatically broaden and shift the host signals, as did triplet O_2 in the spectrum of **1** · O_2.[4]

The sharpness of these H_a and H_b signals shows that in **1** · $(CH)_4$ the guest is rotating rapidly on the ^{1}H NMR time scale about all its axes with respect to the host. This fact strongly suggests that the CO_2 molecule generated as a companion reaction product was expelled through the portal during the photolysis. Other studies demonstrated that CO_2 rapidly enters and leaves the interior of free **1** dissolved in $CDCl_3$ at 25°C.[5] Examination of Corey–Pauling–Koltun (CPK) molecular models of **1** · $(CH)_4$ · CO_2 suggests that shuffling of the two guests in the cavity should be too slow to randomize their positions rapidly enough on the ^{1}H NMR time scale to provide sharp doublets for the host's H_a and H_b signals. Analogy for the CO_2 ejection is found in the loss by heating, of *only one* of two CH_3CN guests from a termolecular complex similar to **1** · $(CH)_4$ · CO_2.[14]

Changes in the irradiation times pointed to both precursers for, and products of **1** · $(CH)_4$. Shorter times provided up to 60% conversion of **1** · **2** into bound photopyrone (**1** · **3**, ^{1}H NMR), which on further irradiation gave **1** · $(CH)_4$. Longer times enhanced the ^{1}H NMR signal at $\delta = 1.91$, barely visible in Figure 2, which is due to free acetylene. This peak was absent in the starting solution of **1** · α-pyrone. Authentic acetylene dissolved in $CDCl_3$ also gave a signal at $\delta = 1.91$ in its ^{1}H NMR spectrum. When the **1** · $(CH)_4$ solution produced by irradiation was purged with xenon gas, the 1.91 peak disappeared from its ^{1}H NMR spectrum, as did the peak for authentic acetylene on similar treatment. Addition of aqueous ammoniacal cuprous chloride to a post-irradiation solution which contains **1** · $(CH)_4$ and C_2H_2 produced the deep red color of cuprous acetylide.[15] Solutions of **1** · α-pyrone before irradiation or of free **1** in $CDCl_3$ before or after irradiation did not test positively for acetylene. Thus incarcerated cyclobutadiene upon photolysis gave acetylene, just as did cyclobutadiene in an argon matrix at 8 K.

An FTIR spectrum of **1** · α-pyrone in $CDCl_3$ exhibits bands at 1733, 1719, 1539, and 1246 cm^{-1} due to the incarcerated **2**, which compare with bands at 1737, 1719, 1546, and 1247 cm^{-1} for free **2** in $CDCl_3$. These bands disappeared in the spectrum of **1** · $(CH)_4$, which gave no carbonyl

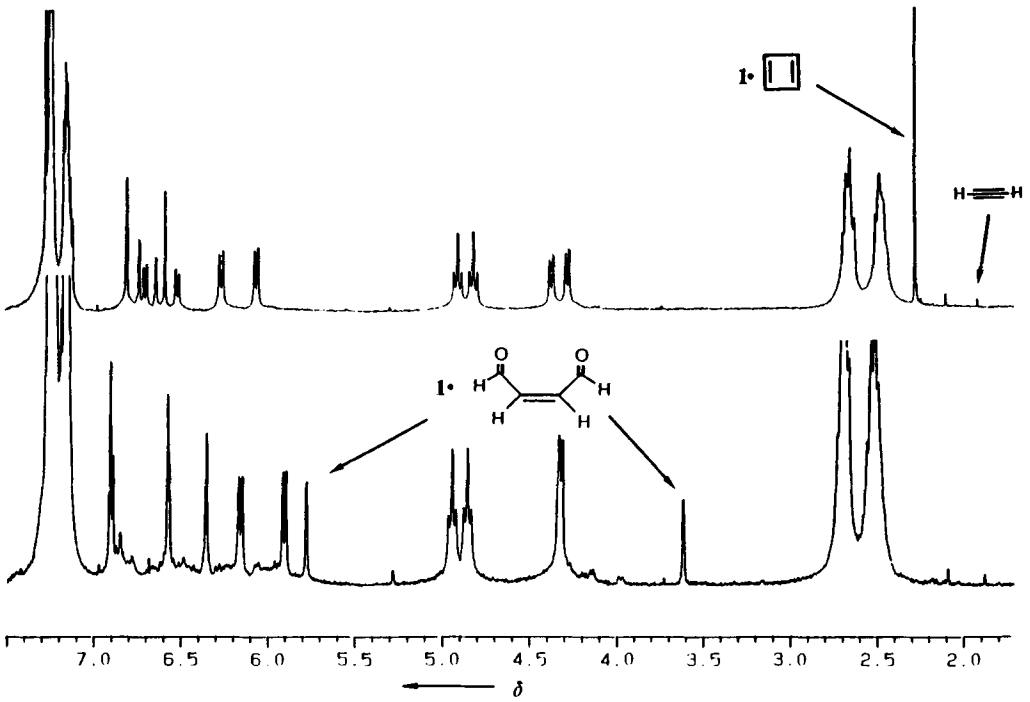

Fig. 2. ^{1}H NMR spectra (500 MHz, $CDCl_3$, 60°C) of hemicarceplexes **1** · $(CH)_4$ and **1** · (*Z*)-OHCCH=CHCHO.

signals in the 1650–1850 cm^{-1} region. The appearance of a signal at 1233 cm^{-1} provides additional evidence for the formation of cyclobutadiene. This band is assigned to the carbon–carbon stretching frequency which appeared at 1240 cm^{-1} in the argon-matrix experiment.[9] Host bands obscured the other signals of $(CH)_4$.

When heated at 220°C for 5 min in an NMR tube sealed under vacuum, **1** · $(CH)_4$ dissolved in [D_8]THF underwent complete guest exchange to give **1** · $(CD_2)_4O$, whose ^{1}H NMR *host* signals corresponded to **1** · THF prepared previously.[5] A new singlet appeared in the spectrum at $\delta = 5.71$, which is due to free cyclooctatetra-1,3,5,7-ene (**7**). The contents of the tube when opened exuded the pungent and characteristic odor of **7**. Addition of authentic **7** to the solution intensified the 5.71 peak. Thus the freed cyclobutadiene must have dimerized to give **6**, which thermally rearranged to give **7**. The intermediacy of cyclobutadiene dimers, though not demonstrated, is hardly in question. They rearrange to give **7**, a reaction whose half-life is ca. 20 min at 140°C.[16]

The cyclobutadiene guest of a **1** · $(CH)_4$ solution in $CDCl_3$ reacts readily with O_2 to give what is probably **1** · (*Z*)-OHCCH=CHCHO. When a stream of O_2 was bubbled vigorously through a solution of **1** · $(CH)_4$ in $CDCl_3$ at 25°C for 10 min, a 50% conversion to a new complex was observed (change in ^{1}H NMR spectrum). The conversion was complete after the resulting solution had stood 30 min under an atmosphere of O_2. The 500 MHz ^{1}H NMR spectrum taken at 60°C of the malealdehyde[17] complex (Fig. 2) provided guest signals as broad singlets at $\delta = 5.77$ and 3.61. These were shown by selective irradiation to be coupled. The signal at $\delta = 5.77$ is good evidence for the aldehydic protons being shifted upfield by $\Delta\delta \approx 4$ from their usual positions. An examination of CPK models of **1** · (*Z*)-OHCCH=CHCHO indicates that these protons are located in the high-shielding polar regions of the host. The position of the signal at $\delta = 3.61$ is typical for a bound alkene proton.[5] Like the guest's signals, several of the host's signals are broad at 25°C (no loss of symmetry), but unlike the former, these sharpened when the spectral solution was warmed. The increased size and somewhat restricted motion of the malealdehyde over cyclobutadiene in the complex accounts for this broadening in the spectrum of **1** · (malealdehyde).

The FTIR spectrum of this new complex exhibited a broad band at 1696 cm^{-1}, indicative of the presence of an unsaturated aldehyde. The formation of **1** · (*E*)-OHCCH=CHCHO instead of the *Z* complex cannot be ruled out based on the spectral data. Precedence for the reaction, **1** · $(CH)_4 + O_2 \rightarrow$ **1** · (*Z*)-OHCCH=CHCHO, is found in the reaction of tetra-*tert*-butylcyclobutadiene (**8**) with O_2 to give (*Z*)-*t*BuCOC(*t*Bu)=C(*t*Bu)CO*t*Bu.[18] The formation of malealdehyde (**5**) from the reaction of gaseous $(CH)_4$ with O_2 has been suggested by *Hedaya* et al., who detected an adduct of $m/z = 84$ by mass spectrometry.[19]

A comparison of the UV spectra of **1** and **1** · α-pyrone (**1** · **2**) in $CDCl_3$ shows no electronic interaction between host and guest. The strong absorbance due to the aromatic rings of the host ends abruptly at 300 nm, leaving a small UV window for the selective photolysis of α-pyrone in **1** · **2**. Irradiation of 2–4 mM solutions of **1** · **2** in $CDCl_3$ at 25°C with a 75 W xenon arc lamp fitted with a filter for $\lambda < 300$ nm ($SnCl_2$/HCl aqueous solution) caused the gradual, quantitative conversion of **1** · **2** to **1** · photopyrone (**1** · **3**, see Scheme 1). The reaction was followed by changes in the 500 MHz ^{1}H NMR spectrum. It required 1 h for completion. Figure 1 shows the spectra of **1** · **2** and **1** · **3** at 60°C. Several of the host signals are broad in **1** · **2** at 25°C due to restricted motion of the guest (relative to host) on the ^{1}H NMR time scale. In the spectrum of **1** · **3**, the host's global signals are fairly sharp at 25°C, but are doubled, indicating that the long axes of **3** and **1** are roughly coincident in **1** · **3**, and that **3** is not rapidly rotating about its short axis on the ^{1}H NMR time scale. These signals are still sharp at 60°C, and three of the signals of bound **3** appeared at $\delta = 3.84$, 2.98, and 2.10 (one proton each). The fourth was located

using ^{1}H-^{1}H COSY spectroscopy ($CDCl_3$, 22 °C). It appeared at $\delta = 2.46$, coupled to the guest signals at $\delta = 2.98$ and 2.10. The δ values for **3** of **1** · **3** are consonant with those of free **3** in CCl_4[6] ($\delta = 6.73$, 6.59, 5.30, and 4.40) after allowing for the shielding effects of the host.

Further evidence for the existence of **1** · **3** was obtained by FTIR spectroscopy ($CDCl_3$). The lactone carbonyl stretch of free **2** appears as a doublet at 1719 and 1737 cm^{-1}. Incarcerated **2** also gives a doublet at 1719 and 1733 cm^{-1}, indicating that residence within the host does not dramatically change the absorption frequency from that in a $CHCl_3$ solution. After irradiation these signals were replaced by a strong absorption at 1847 cm^{-1}, and a weak one at 1823 cm^{-1}. This is consistent with the reported carbonyl absorption of free **3** as a double peak at 1848 and 1818 cm^{-1} (CCl_4).[6] Thin-layer chromatography (silica, 3:7 hexanes/$CHCl_3$) shows that the photoproduct has a higher R_f value than **1** · **2**. The most likely reason for this difference is that the carbonyl group of **1** · **2** can interact with the exterior (through the shell opening), whereas that of the bicyclic lactone cannot. Complex **1** · **3** remained unchanged when stored in the solid state for 2 weeks, and no signs of decomplexation or rearrangement were observed in a $CDCl_3$ solution at 25 °C over a 24 h period.

After **1** · **3** was heated as a solid for 17 h at 90 °C, 80% of the complex existed as **1** · **4**, 13% remained as **1** · **3**, and 7% had reverted to **1** · **2**. The 500 MHz ^{1}H NMR spectrum ($CDCl_3$, 60 °C) of **1** · **4** (Fig. 1) gave guest signals at $\delta = 0.84$ (1H), 0.31 (1H), and 0.03 (2H), and their relationships were positively identified by decoupling experiments. These signals were somewhat broadened at 25 °C. The upfield position of these signals indicates that none are due to C=CH protons. Their chemical shifts are consistent with signals reported for free **4** in $CDCl_3$ of $\delta = 4.72$ (1H), 3.50 (2H), and 2.45 (1H),[7] if allowances are made for the shielding effects of the host in the spectrum of **1** · **4**. The coupling constants for **4** in **1** · **4** were also in agreement with those reported for **4** in $CDCl_3$. Notably, the long range coupling between the protons on either side of the carboxy bridge in **4** of **1** · **4** was 5.0 Hz, compared to 5.2 Hz for **4** in $CDCl_3$ at room temperature.[7] Even though the H_a signals of **1** · **4** were broadened at 25 °C, the north–south hemispheric symmetry of the host is evident. The FTIR spectrum of **1** · **4** in $CDCl_3$ gave a strong peak at 1821 cm^{-1}, not far from the absorptions at 1818 and 1795 cm^{-1} for **4** in $CDCl_3$.[7] The thin-layer chromatographic behavior of **1** · **4** was identical to that of **1** · **2**.

Strong evidence for proposed structures, **1** · **2**, **1** · **3**, and **1** · **4**, was provided by the conversion of **1** · **4** into **1** · **2** by heating solid **1** · **4** at 140 °C for 20 h. Thus the elemental composition of all three complexes was maintained throughout the interconversions of the three complexes. The conversion, **4** → **2**, has been reported to occur during flash vacuum pyrolysis of **4** at 600 °C.[8]

We have illustrated here the following new phenomena: 1) A starting material (e.g. α-pyrone) can be introduced (mass law and heat) into the inner phase of an empty hemicarcerand of complementary dimensions (**1**) to form a hemicarceplex (**1** · **2**) in which constrictive binding[5] contributes substantially to its stability as a complex. 2) Three photochemical reactions have been run in the inner phase, **2** → **3** → $(CH)_4$, $(CH)_4 \rightarrow 2(CH)_2$, and **2** → **3**. Interesting questions arise as to how the lower wavelength light (200–250 nm) required for the formation of cyclobutadiene (and its reaction to give acetylene) is transmitted through the aryl shell of the host (a photosensitization process?). 3) The cyclobutadiene is thermally stable in the inner phase at ordinary temperatures, and exists as a singlet. 4) When heated to 220 °C in [D_8]THF, the following thermal transformations occur: **1** · $(CH)_4 \rightarrow$ **1** + $(CH)_4$, $2(CH)_4 \rightarrow$ [dimer] → $(CH)_8$ (cyclooctatetraene) and **1** + $(CD_2)_4O \rightarrow$ **1** · $(CD_2)_4O$. 5) When oxygen and **1** · $(CH)_4$ are both dissolved in the same $CDCl_3$ solution the oxygen enters the inner phase to produce the bimolecular reaction, O_2 + **1** · $(CH)_4 \rightarrow$ **1** · (*Z*)-OHCCH=CHCHO. 6) Two thermal reactions have been run in the inner phase with the hemicarceplexes themselves being in the solid state: **1** · **3** → **1** · **4** (at 90 °C) and **1** · **4** → **1** · **2** (at 120 °C). Within the limits of ^{1}H NMR spectral criteria, these transformations that occur in the inner phase are quantitative. We anticipate that many highly reactive species containing bent acetylene, allenic, or aromatic rings, radicals, carbenes, etc. can be prepared and examined in the inner phases of appropriate hemicarcerands.

We believe it to be both realistic and useful to regard the "inner phase" of carcerands and hemicarcerands to be a *new phase of matter*.[20] It differs in principle from the inside phases of clathrates and zeolites in its unique molecular composition: *one host molecule provides one discrete molecular inner phase*. Experimentally, hemicarcerands and hemicarceplexes can exist in the solid, solution, or even gaseous phases (inside a mass spectrometer)[5] and therefore their inner phases are not dependent on the bulk phase. Inner-phase reactions have been reported here which occur when the complex is in the solid or bulk-liquid phases. Clathrate inner phases disappear on dissolution of the solvates, and zeolites are insoluble, polymeric solids.

Received: May 3, 1991 [Z 4609]
German version: *Angew. Chem. 103* (1991) 1048

[1] M. P. Cava, M. J. Mitchell: *Cyclobutadiene and Related Compounds*, Academic, New York 1967.
[2] T. Bally, S. Masamune, *Tetrahedron 36* (1980) 343.
[3] G. Maier, *Angew. Chem. 100* (1988) 317; *Angew. Chem. Int. Ed. Engl. 27* (1988) 309.
[4] M. E. Tanner, C. B. Knobler, D. J. Cram, *J. Am. Chem. Soc. 112* (1990) 1659.
[5] D. J. Cram, M. E. Tanner, C. B. Knobler, *J. Am. Chem. Soc. 113* (1991), in press.
[6] E. J. Corey, J. Streith, *J. Am. Chem. Soc. 86* (1964) 950.
[7] E. J. Corey, W. H. Pirkle, *Tetrahedron Lett. 1967*, 5255.
[8] G. Maier, M. Hoppe, K. Lanz, H. P. Reisenauer, *Tetrahedron Lett. 25* (1984) 5645; J. Kreile, N. Münzel, A. Schweig, H. Specht, *Chem. Phys. Lett. 124* (1986) 140.
[9] O. L. Chapman, C. L. McIntosh, J. Pacansky, *J. Am. Chem. Soc. 95* (1973) 614.
[10] C. Y. Lin, A. Krantz, *J. Chem. Soc. Chem. Commun. 1972*, 1111.
[11] G. Maier, S. Pfriem, U. Schäfer, R. Matusch, *Angew. Chem. 90* (1978) 552; *Angew. Chem. Int. Ed. Engl. 17* (1978) 520.
[12] a) G. Maier, A. Alzérreca, *Angew. Chem. 85* (1973) 1056; *Angew. Chem. Int. Ed. Engl. 12* (1973) 1015; b) S. Masamune, N. Nakamura; M. Suda, H. Ona, *J. Am. Chem. Soc. 95* (1973) 8481.
[13] Elemental analysis calculated for $C_{136}H_{116}O_{24}$: C 76.53, H 5.48; Found: C 76.48, H 5.48.
[14] J. A. Bryant, M. T. Blanda, M. Vincenti, D. J. Cram, *J. Am. Chem. Soc. 113* (1991) 113.
[15] F. Feigl: *Spot Tests in Organic Analysis*, 7th ed., Elsevier, Amsterdam 1966, p. 404.
[16] M. Avram, I. G. Dinulescu, E. Marica, G. Mateescu, E. Sliam, C. D. Nenitzescu, *Chem. Ber. 97* (1964) 382.
[17] D. L. Hufford, D. S. Tarbell, T. R. Koszalka, *J. Am. Chem. Soc. 74* (1952) 3014.
[18] H. Irngartinger, N. Riegler, K.-D. Malsch, K.-A. Schneider, G. Maier, *Angew. Chem. 92* (1980) 214; *Angew. Chem. Int. Ed. Engl. 19* (1980) 211.
[19] E. Hedaya, R. D. Miller, D. W. McNeil, P. F. D'Angelo, P. Schissel, *J. Am. Chem. Soc. 91* (1969) 1875.
[20] "Every closed surface which lies wholly within a phase contains a region of space which may itself be regarded as a phase." P. T. Landsberg: *Monographs in Statistical Physics, Vol. 2*, Interscience Publ., New York 1961, p. 153.

1,4,5,8-Tetrakis(dimethylamino)naphthalene: Synthesis, Structure, "Proton Sponge" and Electron Donor Properties**

By *Thomas Barth, Claus Krieger, Franz A. Neugebauer,* and *Heinz A. Staab**

In the context of our studies on relatives of 1,8-bis(dimethylamino)naphthalene **1** ("proton sponge"),[1,2] the comparison with 1,4,5,8-tetrakis(dimethylamino)naphthalene **2** was of interest, which contains twice the pairwise *peri*-arrangement of dimethylamino groups associated with "proton sponge" properties. This posed the question of the mutual influence of these two structural units, which should be evident from the pK_a values for the first and second protonation steps of **2**. Moreover, being a structural isomer of the recently prepared 2,3,6,7-tetrakis(dimethylamino)naphthalene **3**,[3] **2** was of interest as an electron donor in which formally two structural units corresponding to the 1,4-bis(dimethylamino)benzene ("tetramethyl-*para*-phenylenediamine," TMPD) are coupled together.

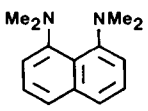

1

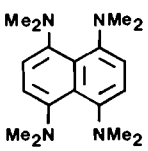

2

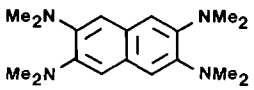

3

For the synthesis of **2**, 1,3-dimethyl-1*H*-perimidin-2(3*H*)-one **4**[4] was nitrated in glacial acetic acid to give the 6,7-dinitro compound **5**[5] (m.p. ≈ 310 °C, decomp.; 33% yield), which upon ring-opening (potassium hydroxide, methanol) yielded 1,8-bis(methylamino)-4,5-dinitronaphthalene **6** (m.p. ≈ 235 °C (decomp.); 66%).[5] Subsequent *N*-methylation (methyliodide, potassium carbonate, dimethylformamide) afforded the bis(dimethylamino) compound **7** (dark red crystals, m.p. 280 °C (decomp.); 32%).[5] Catalytic hydrogenation (Pd/C, ethyl acetate) of **7** gave the rather unstable compound **8**, which was converted according to the procedure described by *Quast* et al.[6] (sodium hydride, dimethyl sulfate, tetrahydrofuran) into **2** (yellow crystals, m.p. 193.5 °C; 31% referred to **7**).[5] The ^{1}H-NMR spectrum of **2**, consisting of only two singlets [δ = 2.65 (s, 24H), 6.75 (s, 4H); 500 MHz, [D_6] dimethyl sulfoxide], reflects the high molecular symmetry of **2**.

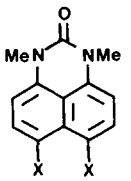

4: X = H
5: X = NO_2

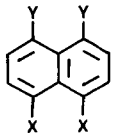

6: X = NO_2, Y = $NHMe_2$
7: X = NO_2, Y = NMe_2
8: X = NH_2, Y = NMe_2

[*] Prof. Dr. H. A. Staab, Dipl.-Chem. T. Barth, C. Krieger, Prof. Dr. F. A. Neugebauer
Abteilung Organische Chemie
Max-Planck-Institut für medizinische Forschung
Jahnstrasse 29, W-6900 Heidelberg (FRG)

[**] Novel "Proton Sponge" Compounds, Part 10.—Part 9: H. A. Staab, M. A. Zirnstein, C. Krieger, *Angew. Chem. 101* (1989) 73; *Angew. Chem. Int. Ed. Engl. 28* (1989) 86.

The steric interaction within the two pairs of *peri* dimethylamino groups is a major factor determining the structure of **2**. Figure 1 shows a top view of the naphthalene skeleton of this structure[7] (above) as well as a side view along the central C(4a)–C(8a) bond (middle) and a view perpendicular to the C_2-axis (below). Compared to the situation in **1**[8] the stronger steric strain by the four *peri* substituents leads to a particularly marked twisting of the naphthalene system about the central C(4a)–C(8a) bond (torsion angle C(1)–C(8a)–C(4a)–C(4): 18.8°); as a consequence the N ··· N distances are expanded to 274.5(1) pm.[9] The neighboring dimethylamino groups in the *peri* positions evade steric contacts by rotation about the C(1)–N(1') and

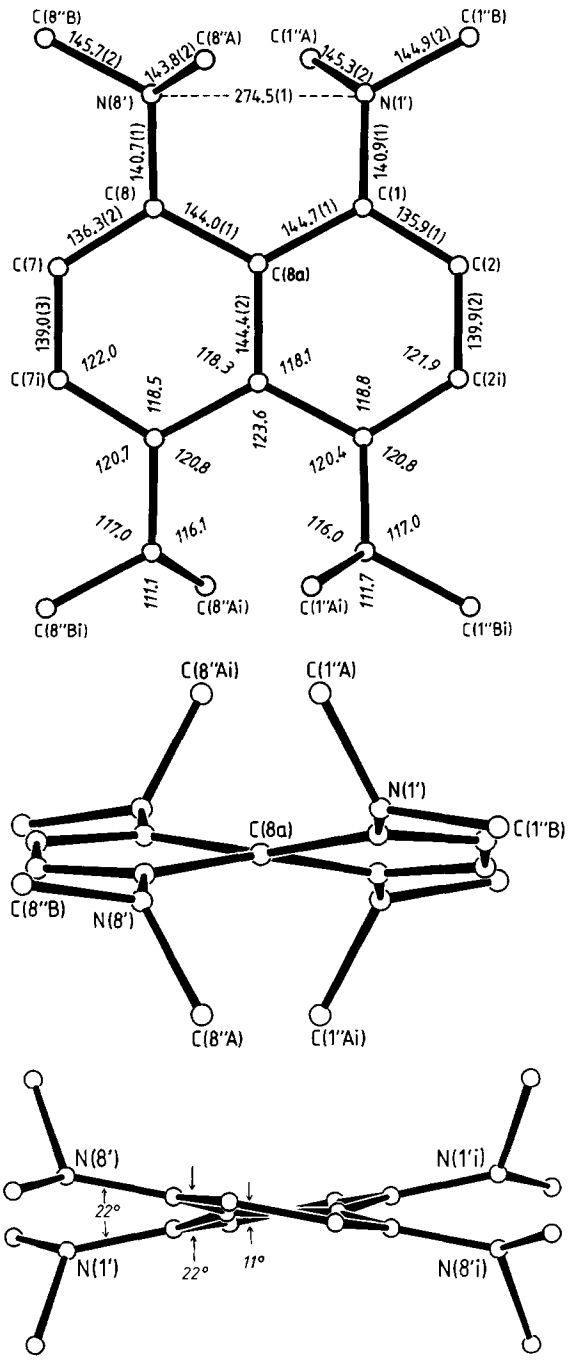

Fig. 1. Structure of **2** in the crystal. Above: Top view of the naphthalene skeleton with bond lengths [pm] and angles [°] (standard deviations for the last place in brackets); middle: side view along the C(4a)–C(8a) bond; below: side view a long the twofold axis perpendicular to the other views with interplanar angles: 11° [angle between C(2)–C(2i)–C(8ai)-C(8a) and C(7)–C(7i)–C((8ai)–C(8a)]; 22° [C(1)–C(2)–C(8a) and C(7)–C(8)–C(8a)] [7].

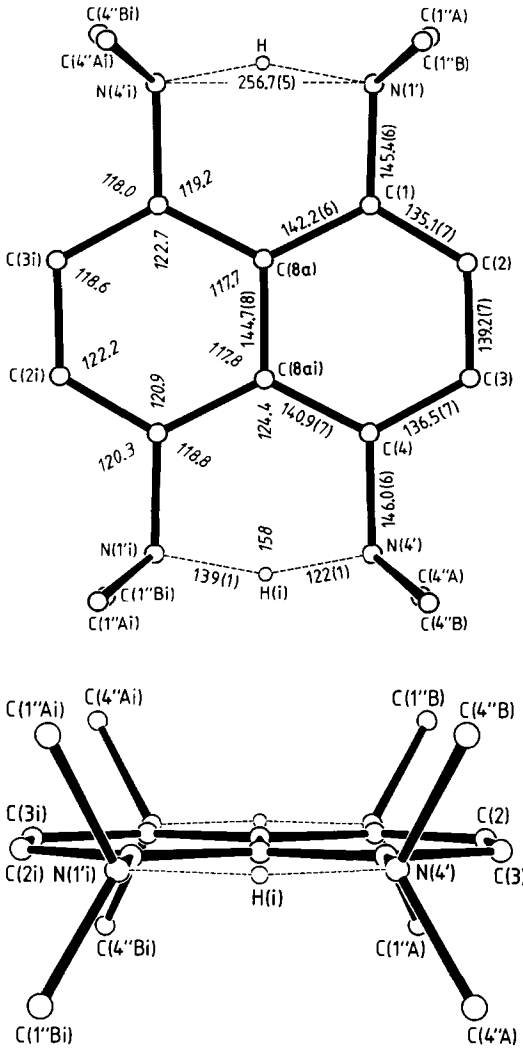

Fig. 2. Structure of the dication of $2 \cdot (HBr)_2$ in the crystal. Above: Top view of the naphthalene plane with bond lengths [pm] and angles [°] (standard deviations in units for the last given place); below: side view along the C(4a)–C(8a) bond [14].

C(8)–N(8') bonds (Fig. 1, middle). This conformation, as also peculiarities in bond lengths and angles, display similar trends as those in **1** and other naphthalene "proton sponges".[10]

The "double proton sponge" **2** is diprotonated by excess strong acid; reaction with tetrafluoroboric acid-etherate in diethyl ether leads to the formation of $2 \cdot (HBF_4)_2$.[5] By deprotonation with an equivalent amount of **2**, also the monoprotonated $2 \cdot HBF_4$ can be detected ^{1}H-NMR spectroscopically in [D$_6$]dimethyl sulfoxide.[11] The ^{1}H-NMR spectra of both salts show the expected downfield shift [$2 \cdot H^{\oplus}$: $\delta = 18.75$; $2 \cdot (2H)^{2\oplus}$: $\delta = 18.80$] for the signals of the protons in the N···H···N bridge. By NMR spectroscopic determination of the protonation-deprotonation equilibria in [D$_6$]dimethyl sulfoxide[12] a first protonation

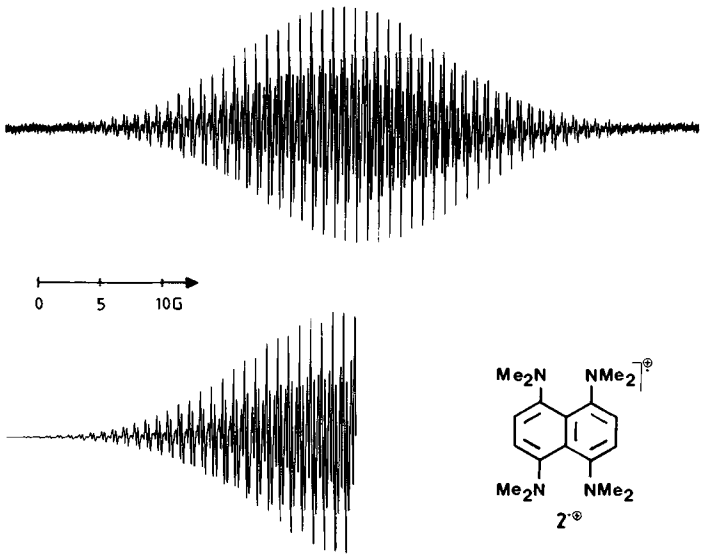

Fig. 3. ESR spectrum of $2^{\cdot\oplus}$ in dichloromethane at 220 K (above) and spectra simulation (below) with the data given in text (line width 0.11 G).

step with $pK_{a(1)} = 9.8 \pm 0.5$ and a second with $pK_{a(2)} = 4.9 \pm 0.2$ (referred to **1** with $pK_a = 7.5$[13]) are obtained for **2** on the dimethyl sulfoxide pK_a scale.[13] **2** is thus a significantly stronger base than **1** in the first protonation step. We attribute this not only to the + M effect of each of the *para* dimethylamino groups but also to an indirect steric ("buttressing") effect, which has also been observed in other 1,8-bis(dimethylamino)naphthalenes with substituents in the two other *peri* positions C(4) and C(5).[10]

A salt of diprotonated **2** suitable for the X-ray structure analysis, namely **2**-dihydrobromide-pentahydrate (m.p. 247 °C (decomp.), from water),[5] was obtained by reaction of **2** with hydrogen bromide. Figure 2 shows the structure of the $2 \cdot (2H)^{2\oplus}$ moiety viewed perpendicularly onto the naphthalene system (top) and from the side along the central C(4a)–C(8a) bond (bottom).[14] Particularly striking is that **2** is almost completely planarized by the diprotonation and the accompanying formation of two strong N···H···H hydrogen bridges. Accordingly, the N···N distances are shortened to 256.7(5) pm. The N···H···N hydrogen bridge forms an angle of about 158° and is unsymmetrical with regard to the N···H bond lengths.

1,4,5,8-Tetrakis(dimethylamino)naphthalene **2** is a much stronger electron-donor than the 2,3,6,7-substituted isomer **3**. Whereas two oxidation steps, each corresponding to a one-electron transition were determined cyclovoltammetrically at $E_{ox} = -0.01$ V and $+0.07$ V (Fc/Fc$^{\oplus}$ = 0.0 V, Fc = ferrocene) for **3**,[3] in the case of **2** under the same conditions[15] the cyclovoltammogram shows a reversible two-electron transition at $E_{ox} = -0.50(1)$ V, which consists of two superposed one-electron steps and leads to the formation of the dication $2^{2\oplus}$. The stability of this dication could be associated with a favorable charge and bond delocalization in which all four dimethylamino groups participate (Scheme 1).

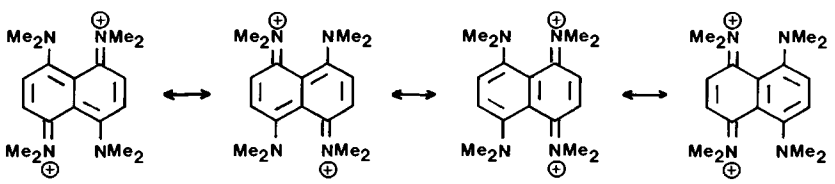

Scheme 1.

By electron transfer to tris(4-bromophenyl)amminium hexachloroantimonate or by oxidation with iodine also the radical cation $2^{\bullet\oplus}$ can be generated, whose ESR spectrum in dichloromethane at 220 K is shown in Figure 3. The analysis was achieved with the aid of the ^{1}H-hyperfine structure coupling constants determined by ENDOR and general triple resonance spectroscopy:[16] a(H) = + 3.55, a(H) = + 1.78, and a(H) = − 1.51 G. Simulation of the ESR spectrum (Fig. 3, bottom) gave a(N) = 2.65 (4 N), a(H) = 3.54 (12 H), a(H) = 1.77 (12 H) and a(H) = 1.53 (4 H) G. The g factor (2.0029) lies in the expected range.[17] The appearance of different N-methyl proton signals in the ESR spectrum of $2^{\bullet\oplus}$ at 220 K indicates a restricted rotation about the C_{aryl}–N bond with two different arrangements of the methyl groups. This effect was also observed in the case of the radical cation of 1,2,4,5-tetrakis(dimethylamino)benzene but not in the case of the radical cation $3^{\bullet\oplus}$ isomeric with $2^{\bullet\oplus}$.[17]

Received: February 8, 1991 [Z 4432 IE]
German version: *Angew. Chem. 103* (1991) 1006

CAS Registry numbers:
2, 134180-29-3; **2** · HBF_4, 134208-55-2; **2** · $(HBF_4)_2$, 134180-30-6; **2** · $(HBr)_2$, 134180-31-7; $2^{2\oplus}$, 134180-32-8; $2^{\bullet\oplus}$, 134180-33-9; **4**, 2306-08-3; **5**, 134180-25-9; **6**, 134180-26-0; **7**, 134180-27-1; **8**, 134180-28-2.

[1] R. W. Alder, M. R. Bryce, N. C. Goode, N. Miller, J. Owen, *J. Chem. Soc. Perkin Trans. 1 1981*, 2840.
[2] Recent review on "proton sponge" compounds: H. A. Staab, T. Saupe, *Angew. Chem. 100* (1988) 895; *Angew. Chem. Int. Ed. Engl. 27* (1988) 865.
[3] K. Elbl-Weiser, C. Krieger, H. A. Staab, *Angew. Chem. 102* (1990) 183; *Angew. Chem. Int. Ed. Engl. 29* (1990) 211; cf. also K. Elbl, C. Krieger, H. A. Staab, *ibid. 98* (1986) 1024 and *25* (1986) 1023.
[4] O. Christmann, *Chem. Ber. 98* (1965) 1282; cf. also A. F. Pozharskii, I. S. Kashparov, *Khim. Geterotsikl. Soedin. 1972*, 860.
[5] Elemental analyses and spectroscopic data are consistent with the given structures.
[6] H. Quast, W. Risler, G. Döllscher, *Synthesis 1972*, 558.
[7] Crystal structure data of **2**: orthorhombic crystals (from pentane), space group *Pbcn* (No. 60, Int. Tables), a = 1007.1(1), b = 1746.3(2), c = 1018.5(1) pm; Z = 4, ϱ_{calcd} = 1.114 g cm^{-3}; 2158 symmetry independent, measured reflections, 1300 with $I \geq 3.0\sigma(I)$ classed as observed; solution of structure by direct methods (MULTAN 82); R = 0.042 [18].
[8] H. Einspahr, J. B. Robert, R. E. Marsh, J. D. Roberts, *Acta Crystallogr. Sect. B29* (1973) 1611.
[9] An even stronger twisting of the naphthalene skeleton resulting in even longer N···N distances were revealed in an X-ray structure analysis of 1,8-bis(dimethylamino)-4,5-dinitronaphthalene **7**: C. Krieger, unpublished.
[10] Cf. also H. A. Staab, K. Oberdorf, C. Krieger, unpublished.
[11] ^{1}H NMR (500 MHz, [D$_6$]dimethyl sulfoxide) of **2** · HBF_4: δ = 2.76 (s, 12 H), 3.04 (d, ^3J = 1.8 Hz, 12 H), 7.02 (d, ^3J = 8.5 Hz, 2 H), 7.79 (d, ^3J = 8.5 Hz, 2 H), 18.75 (br. s, 1 H); of **2** · $(HBF_4)_2$: δ = 3.14 (s, 24 H), 8.39 (s, 4 H), 18.80 (br. s, 2 H).
[12] T. Barth, *Diplomarbeit*, Universität Heidelberg 1990.
[13] Cf. R. L. Benoit, D. Lefebvre, M. Fréchette, *Can. J. Chem. 65* (1987) 996.
[14] Crystal structure data of **2** · $(HBr)_2$ · $(H_2O)_5$: tetragonal crystals, space group *P4/n* (No. 85, Int. Tables), a = 1814.2(2), c = 793.2(1) pm, Z = 4; ϱ_{calcd} = 1.406 g cm^{-3}; 3329 symmetry independent, measured reflections, 1579 classed as observed with $I \geq 3.0\sigma(I)$; solution of structure by direct methods (MULTAN 82); R = 0.046 [18].
[15] Cyclic voltammetry in acetonitrile/0.1 M tetrabutylammonium perchlorate, glassy carbon electrode versus Ag/AgCl; ferrocene standard $Fc/Fc^{\oplus}$ = 0.0 V.
[16] H. Kurreck, B. Kirste, W. Lubitz, *Angew. Chem. 96* (1984) 171; *Angew. Chem. Int. Ed. Engl. 23* (1984) 173, and references cited therein.
[17] K. Elbl-Weiser, F. A. Neugebauer, H. A. Staab, *Tetrahedron Lett. 30* (1989) 6161.
[18] Further details of the crystal structure analyses are available on request from the Fachinformationszentrum Karlsruhe, Gesellschaft für wissenschaftlich-technische Information mbH, W-7514 Eggenstein-Leopoldshafen 2, on quoting the depository number CSD-55233, the names of the authors, and the journal citation.

Aromatic Systems with Polymethine-like Structures: A Structural Comparison of Bis- and Tris(dimethylamino)phenalenium Ions**

By *Heinz A. Staab,* Jörg Hofmeister*, and *Claus Krieger*

The structure analysis of the dication of 1,2,4,5-tetrakis-(dimethylamino)benzene[1] showed quite clearly that the cyclic delocalization of aromatic π-systems can be largely removed as a result of the formation of only weakly coupled polymethine-like partial structures. From absorption spectroscopic studies *Dähne* et al.[2] have been able to classify conjugated π-electron systems into aromatic, olefinic, and polymethine-like partial structures; *Fabian*[3] has supported such a "building-block model" by quantum chemical calculations. However, the validity and limits of this heuristic concept require further experimental verification.

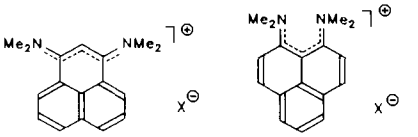

1 2

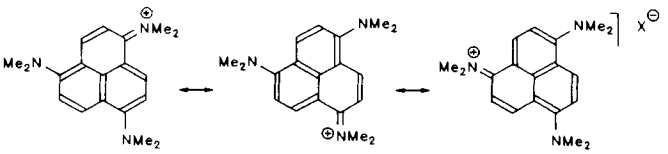

3

In this connection our interest focussed on a comparison of the structures of the 1,3- and 1,9-bis(dimethylamino)phenalenium salts **1** and **2**. In both cases trimethinecyanine partial substructures can be formulated, of which that in the case of **1** has the all-*trans* arrangement, whereas in the case of **2** the *peri* position of the dimethylamino substituents enforce an all-*cis* arrangement. More important in connection with the problem outlined above is, however, that **1** and **2** differ with respect to the part of the π-electron system *not* incorporated in the polymethine moiety: in **1** this would be a naphthalene system, in **2** a benzene system; the benzene system would be bound to the polymethine fragment via double bonds and the central single bond.

In contrast to **1** and **2**, in the case of the 1,4,7-tris(dimethylamino)phenalenium ion **3** polymethine substructures with only weak coupling to the remaining π-electron system were not to be expected since, here, three equivalent mesomeric structures should prevail.

The syntheses of **1**–**3** are based on previous work of other authors,[5, 6] especially of *Hünig* and *Wolff*.[4] **1** (X = BF_4) (red needles, m.p. 201 °C; 91% yield) was formed upon reaction of 1,3-dimethoxyphenalenium tetrafluoroborate[4] with dimethylamine in dichloromethane.[7] For X-ray structure analysis the tetrafluoroborate was converted by bromide ion-exchange (QAE-Sephadex A-25, water) into **1** (X = Br), which crystallized from dichloromethane/ethyl acetate as the

[*] Prof. Dr. H. A. Staab, Dr. J. Hofmeister, C. Krieger
Abteilung Organische Chemie
Max-Planck-Institut für medizinische Forschung
Jahnstrasse 29, W-6900 Heidelberg (FRG)

[**] Electron Donor Acceptor Compounds, Part 48. Part 47: K. Elbl-Weiser, C. Krieger, H. A. Staab, *Angew. Chem. 102* (1990) 183; *Angew. Chem. Int. Ed. Engl. 29* (1990) 211.

hemihydrate (red prisms, m.p. 230–231 °C (decomp.); 82% yield).[7]

For the synthesis of **2**, 9-dimethylaminophenalenone was allowed to react with trimethyloxonium tetrafluoroborate (dichloromethane, 20 °C) to give 1-dimethylamino-9-methoxyphenalenium tetrafluoroborate (m.p. 192–194 °C (decomp.); 79% yield),[7] from which **2** (X = BF_4) was obtained (m.p. 172 °C; 63% yield) by reaction with dimethylamine.[7] The halogenides **2** (X = Cl, Br, I) can be obtained by ion-exchange; in contrast to the chloride and bromide, which are very hygroscopic, **2** (X = I) can be obtained pure (m.p. 214 °C, from dichloromethane/ethyl acetate).[7] 1,4,7-Tris(dimethylamino)phenalenium salts **3** were synthesized from 4,7-dihydroxyphenalenone,[6] which was methylated with diazomethane (ether/dichloromethane, − 10 °C; 46% yield) to give 4,7-dimethoxyphenalenone (m.p. 180 °C).[7] Upon treatment with trimethyloxonium tetrafluoroborate (dichloromethane, 20 °C) 1,4,7-trimethoxyphenalenium tetrafluoroborate was formed (m.p. 300–310 °C (decomp.); 83%),[7] whose reaction with dimethylamine in acetonitrile gave **3** (X = BF_4) (m.p. 300–303 °C (decomp.); 93% yield).[7] Subsequent anion-exchange reactions furnished **3** (X = I), which crystallized from dichloromethane/diethyl ether with dichloromethane in the ratio 1:1 (dark red crystals, m.p. 289 °C (decomp.)), and **3** (X = Br) (dark red prisms, m.p. 272 °C, from dichloromethane/ethyl acetate).[7]

According to the structure analysis of **1** (X = Br),[8] the bond lengths (Fig. 1 A) for the N(1′)-C(1)–C(3)–N(3′) region are consistent with a symmetrical polymethine structure: the C(1)–C(2) and C(2)–C(3) bonds show the characteristic bond equalization of such a mesomeric system; the C(1)–N(1′) and C(3)–N(3′) distances are consistent with a partial double bond character of these bonds. This polymethine structural unit is coupled via two single bonds with the second substructure of the π-electron system, whose bond lengths correspond to a naphthalene unit. Figure 1 B shows that this naphthalene subunit is almost planar, whereas the polymethine moiety is twisted from this plane so that it can assume an essentially planar arrangement with inclusion of the dimethylamino groups.

In the case of **2** (X = I), an X-ray structure analysis revealed a polymethine substructure, two nearly isolated double bonds and a benzenoid six-membered ring.[9] Due to high vibration amplitudes in the region C(3a)–C(4)–C(5)–C(6)–C(6a) the exact determination of bond lengths and angles was limited. The structure analysis of a mixed crystal of **2** (X = Cl, Br)[10] (measured in a sealed capillary because of the hygroscopicity) led, however, to a confirmation of these results. Characteristic features of this structure are the polymethine moiety with mesomeric bond equalization in the region N(1′)–C(1)–C(9a)–C(9)–N(9′), the high double bond character with bond lengths of 133.9(4) and 134.3(4) pm for C(2)–C(3) and C(7)–C(8), respectively, and the benzenoid character of the remaining six-membered ring (Fig. 2 A). The side view (viewed along the central C(9a) ··· C(5) axis) shows that the polymethine system of **2**, in contrast to that of **1**, is not completely planar due to the *peri*-arrangement, but that the steric interaction between the dimethylamino groups leads to a stronger torsion about the C–N bonds (torsion angle C(9a)–C(1)–N(1′)–C(1″B) 19.5° and C(9a)–C(9)–N(9′)–C(9″B) 25° (Fig. 2 B).

Whereas X-ray structure analyses confirmed the "building block model" of polymethine-like, olefinic and aromatic structural units in the case of **1** and **2**, the results of the structure analyses of the salts of **3** are consistent with expectation that no such substructures are definable in these cases. In the case of **3** (X = I) an approximate C_3 symmetry of the

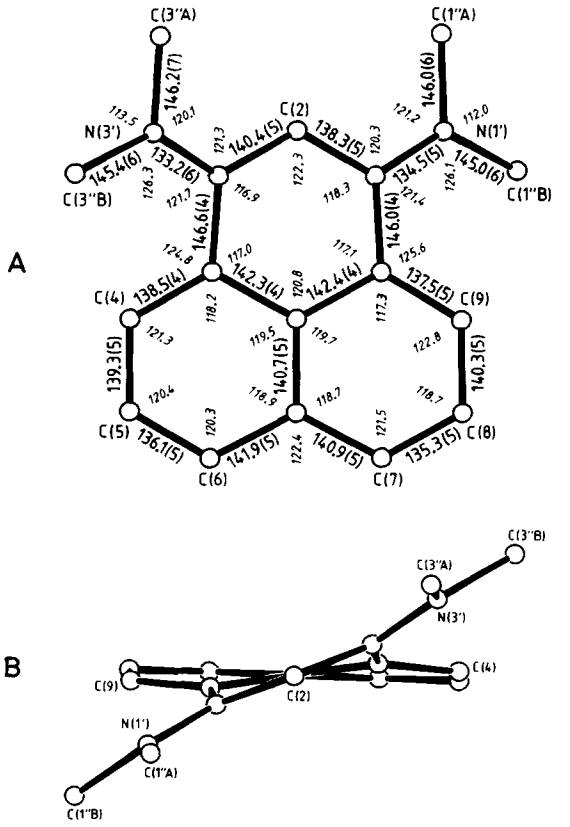

Fig. 1. Structure of the phenalenium ion of **1** (X = Br) viewed perpendicular to the "naphthalene" plane (A) with bond lengths [pm] and angles [°] (in brackets standard deviations in units of the last decimal place) and side view along the C(2) ··· C(6A) axis (B) [8].

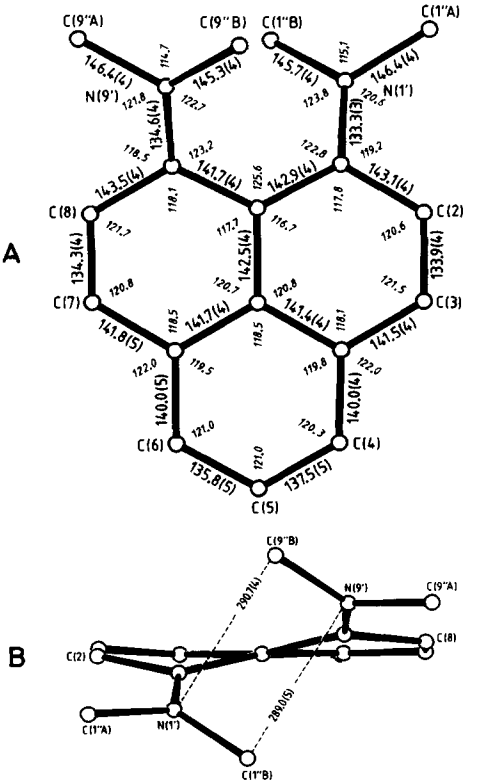

Fig. 2. Structure of the phenalenium ion of **2** (X = Cl, Br) viewed perpendicular to the phenalenium plane (A) with bond lengths [pm] and angles [°] (in brackets standard deviations in units of the last decimal given) and side view along the C(9a) ··· C(5) axis (B) [10].

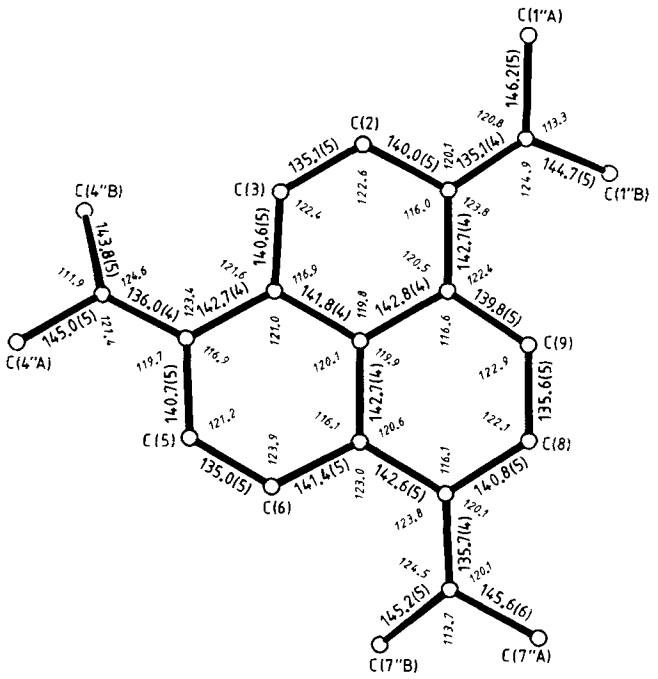

Fig. 3. Structure of the phenalenium ion of $3 \cdot CH_2Cl_2$ (X = I) viewed perpendicular to the phenalenium plane with bond lengths [pm] and angles [°] (in brackets, standard deviations in units of the last decimal given) [11].

cation was found for the phenalenium moiety, and individual polymethine units could not be identified. Remarkable, however, is the high bond order, which can be deduced from the short C(2)–C(3), C(5)–C(6), and C(8)–C(9) distances (Fig. 3).[11]

3 (X = Br), which has the same structure as the iodide with respect to the phenalenium ion, exhibits a particularly interesting lattice packing: the cations of **3** are stacked with an ecliptical arrangement of the phenalene skeletal frameworks along the *c*-axis, whereby the dimethylamino groups of neighboring cations are in exactly staggered positions. The interplanar distances alternate between 376 and 396 pm; the shorter distance is apparently linked to the hexagonal network of bromide ions, which surround the pair of phenalenium ions with the shorter interplanar distance (Fig. 4).[12]

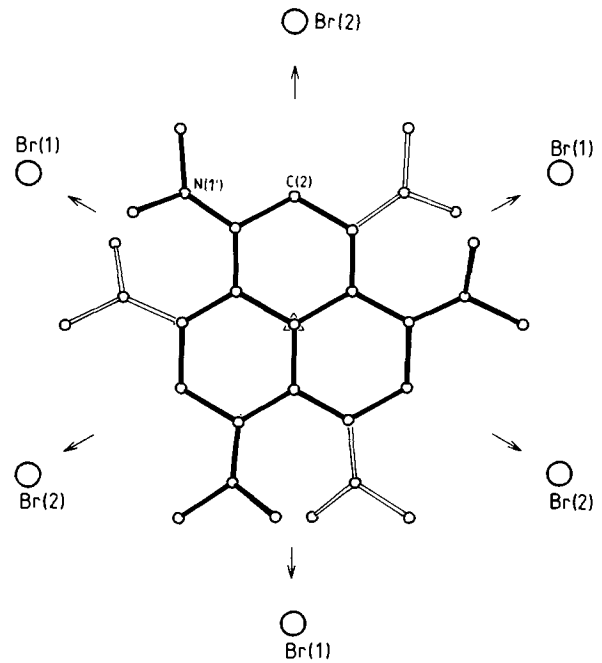

Fig. 4. Structure of **3** (X = Br): view of a pair of phenalenium ions along the stacking axis (*c*-axis) [12].

Received: February 8, 1991 [Z 4431 IE]
German version: *Angew. Chem. 103* (1991) 1003

[1] K. Elbl, C. Krieger, H. A. Staab, *Angew. Chem. 98* (1986) 1024; *Angew. Chem. Int. Ed. Engl. 25* (1986) 1023.
[2] S. Dähne, D. Leupold, *Angew. Chem. 78* (1966) 1029; *Angew. Chem. Int. Ed. Engl. 5* (1966) 984; S. Dähne, F. Moldenhauer *Prog. Phys. Org. Chem. 15* (1985) 1, and references cited therein.
[3] J. Fabian, *J. Prakt. Chem. 320* (1978) 361, and references cited therein.
[4] S. Hünig, E. Wolff, *Justus Liebigs Ann. Chem. 732* (1970) 26.
[5] K. D. Franz, R. L. Martin, *Tetrahedron 34* (1978) 2147; cf. also K. D. Franz, *J. Org. Chem. 44* (1979) 1704; R. Neidlein, Z. Behzadi, *Chem. Ztg. 102* (1978) 199.
[6] M. Jarcho, *J. Am. Chem. Soc. 90* (1968) 4644; J. K. Elwood, *J. Org. Chem. 38* (1973) 2425, 2430.
[7] Elemental analysis and spectroscopic data are consistent with the assumed structures.
[8] Crystal structure data of **1** (X = Br)-hemihydrate: monoclinic, space group $I2/a$; $a = 2016.3(4)$, $b = 745.6(2)$, $c = 2115.0(4)$ pm, $\beta = 107.72(2)°$; $Z = 8$, $\varrho_{calcd} = 1.492\ g\,cm^{-3}$; 2923 measured reflections, 1768 classed as observed with $I \geq 3.0\sigma(I)$. Solution of structure by direct methods (MULTAN), $R = 0.038$ [13].
[9] Crystal structure data of **2** (X = I): monoclinic, space group $C2/c$; $a = 874.6(2)$, $b = 2543.8(3)$, $c = 745.5(2)$ pm, $\beta = 109.26(2)°$; $Z = 4$, $\varrho_{calcd} = 1.6024\ g\,cm^{-3}$; 1899 measured reflections, 1175 classed as observed with $I \geq 3.0\sigma(I)$. Solution of structure by direct methods (MULTAN), $R = 0.031$ [13].
[10] Crystal structure data of **2** (X = Cl, Br): monoclinic, space group $P2_1/a$; $a = 826.6(2)$, $b = 1805.7(4)$, $c = 1096.4(2)$ pm, $\beta = 107.49(2)°$; $Z = 4$, $\varrho_{calcd} = 1.315\ g\,cm^{-3}$; 2730 measured reflections, 1633 classed as observed with $I \geq 3.0\sigma(I)$, solution of structure by direct methods (MULTAN), $R = 0.053$ [13].
[11] Crystal structure data of **3** (X = I): monoclinic, space group $P2_1/a$; $a = 769.0(2)$, $b = 1265.7(3)$, $c = 2197.4(4)$ pm, $\beta = 93.34(2)°$; $Z = 4$, $\varrho_{calcd} = 1.575\ g\,cm^{-3}$; 2208 measured reflections, 1814 classed as observed with $I \geq 3.0\sigma(I)$. Solution of structure by Patterson synthesis (heavy atom method); difference Fourier synthesis for the establishment and solution of the structure of the cation; after usual refinement $R = 0.025$ [13].
[12] Crystal structure data of **3** (X = Br): trigonal, space group $P312$; $a = 1143.0(1)$, $c = 772.4(1)$ ppm; $Z = 2$, $\varrho_{calcd} = 1.422\ g\,cm^{-3}$; 769 measured reflections, 514 classed as observed with $I \geq 3.0\sigma(I)$. Solution of structure by Patterson synthesis with the help of detailed symmetry considerations; $R = 0.056$ [13].
[13] Further details of the crystal structure investigations are available on request from the Fachinformationszentrum Karlsruhe, Gesellschaft für wissenschaftlich-technische Information mbH, W-7514 Eggenstein-Leopoldshafen 2 (FRG), on quoting the depository number CSD-55232, the names of the authors, and the journal citation.

Enediyne Compounds Equipped with Acid-, Base- and Photo-Sensitive Triggering Devices. Chemical Simulation of the Dynemicin A Reaction Cascade**

By *K. C. Nicolaou,* W.-M. Dai, S. V. Wendeborn, A. L. Smith, Y. Torisawa, P. Maligres,* and *C.-K. Hwang*

The recent isolation of the novel anticancer agent dynemicin A (**1**)[1] and the proposed cascade of reactions

[*] Prof. K. C. Nicolaou, Dr. W.-M. Dai, S. V. Wendeborn, Dr. A. L. Smith, Dr. Y. Torisawa, P. Maligres, and Dr. C.-K. Hwang
Department of Chemistry, Research Institute of Scripps Clinic
10666 N. Torrey Pines Road, La Jolla, CA 92037 (USA)
and
Department of Chemistry
University of California, San Diego
La Jolla, CA 92037 (USA)

[**] This work was supported by the National Institutes of Health (USA) and the National Science Foundation (USA). *A. L. S.* thanks the Science and Engineering Research Council (SERC) for the award of a NATO fellowship.

(Scheme 1)[2] for its mode of action generated considerable excitement in the chemical and biological communities.[3] In this communication we report (a) the design, synthesis and chemistry of a number of model systems equipped with acid-, base-, and photo-sensitive triggering devices; (b) the simulation of the dynemicin A cascade; and (c) the observation of a number of labile intermediates along this reaction cascade.

The hypothesized mechanism of action of dynemicin A (**1**) postulates intercalation, bioreduction, epoxide opening, trapping of the generated intermediates with nucleophiles, and electroaromatization to form benzenoid diradicals[4] which damage DNA. Scheme 1 outlines these reactions and

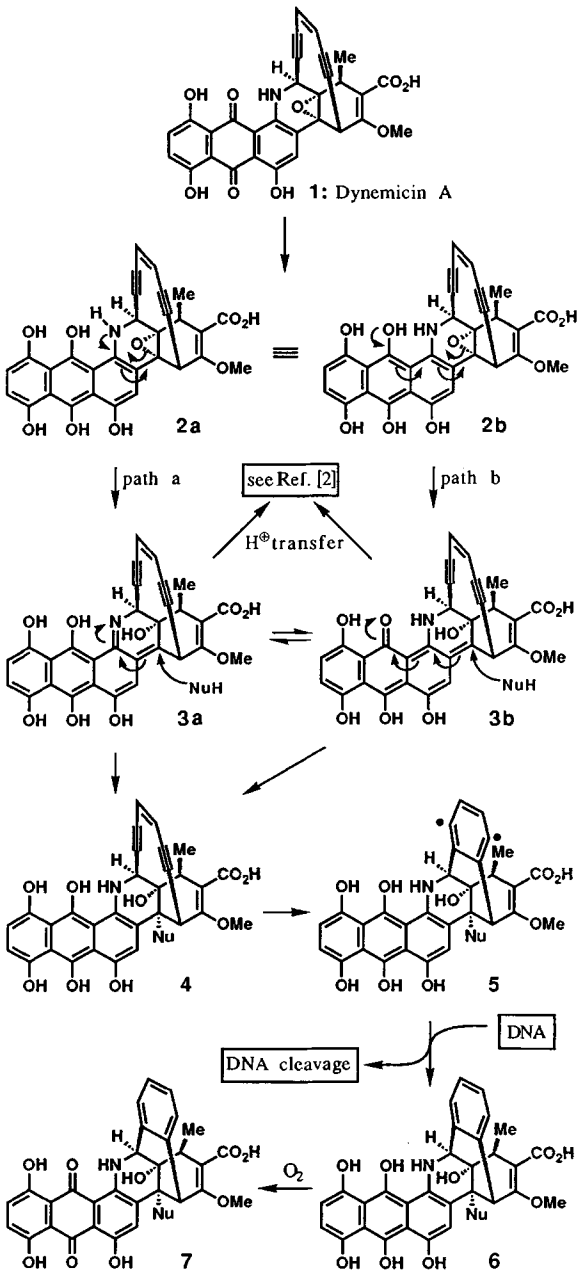

Scheme 1. Proposed mechanism of action of dynemicin A (**1**).

shows the postulated intermediates.[1, 2] Questions, however, remain as to the relevance of the two scenarios, originating from **2a** or **2b** (tautomeric structures), the existence and lifetime of the various intermediates, the timing of bioreduction in relation to intercalation, and the nature of the nucleophiles involved. Of particular interest was the generation of compounds with free amino or hydroxy groups on the aromatic moiety capable of donating their electrons into the epoxide side forming quinone or iminoquinone methide species corresponding to structures **3b** or **3a**, respectively (Scheme 1).

In order to allow for the generation of the parent enediyne system **12**, compound **10** was designed and synthesized from the previously reported **8**[3a, b] as shown in Scheme 2. Thus,

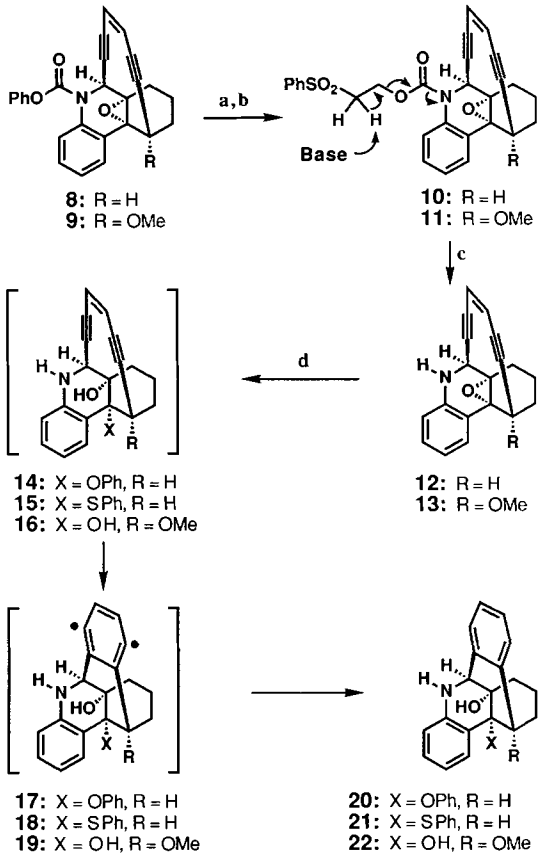

Scheme 2. a) 3.0 equiv. of $CsCO_3$, 0.5 equiv. of [18]crown-6, 10 equiv. of $PhS(CH_2)_2OH$, CH_3CN, 25°C, 12 h; b) 2.5 equiv. of MCPBA, CH_2Cl_2, 0–25°C, 85% overall (**10**), 82% overall (**11**); c) [for **10** → **12**] $CsCO_3$ (excess), 0.5 equiv. of [18]crown-6, dioxane, 25°C, 1 h, high yield based on TLC; [for **11** → **13**] 1.2 equiv. of diazabicycloundecene (DBU), C_6H_6, 5°C, 0.5 h, 97%; d) [for **12** → **20**] 2.0 equiv. of PhOH, 1,4-cyclohexadiene, 25°C, 2 h, 25%; [for **12** → **21**] 2.0 equiv. of PhSH, 1,4-cyclohexadiene, 25°C, 2 h, 33%; [for **13** → **22**] 0.5 equiv. of TsOH · H_2O, dioxane/H_2O/1,4-cyclohexadiene (4:1:1), 60°C, 2 h, 20%.

reaction of **8** with $PhSCH_2CH_2OH$ followed by oxidation with *meta*-chlorobenzoic acid (MCPBA) led to the formation of **10**[5] in 85% overall yield. Indeed, compound **10** served as an excellent precursor to **12**, although the latter proved to be too labile for isolation. The reactivity of **12** and its ability to cleave DNA (*vide infra* and Ref. [3a]) add credibility to the notion of the involvement of pathway **2a** → **3a** → **4** → **5** (Scheme 1) and the intermediacy of an iminoquinone methide as a significantly contributing species in the mode of action of dynemicin A **1**—at least as a partial scenario. Freshly generated **12** was successfully trapped in dioxane/1,4-cyclohexadiene solutions with phenol and thiophenol leading to compounds **20** (25%) and **21**[5] (33%) respectively. Interestingly, the methoxy compound **13**, pre-

pared from **9**[3, a, b] via a similar sequence (**9** → **11** → **13**, Scheme 2) in 97% yield, proved to be quite stable under basic or neutral conditions.[6] Treatment of **13**, however, with $TsOH \cdot H_2O$ in the presence of 1,4-cyclohexadiene resulted in triggering of the cycloaromatization furnishing compound **22** (20% yield). These transformations are assumed to proceed via intermediates **14**–**19**. An X-ray crystallographic analysis of **13**[7] confirmed its molecular structure (Fig. 1) and revealed a number of interesting parameters, e.g. a *cd* distance of 3.63 Å (calcd. 3.61 Å, MMX) and the nonlinearity of the acetylenic groupings.

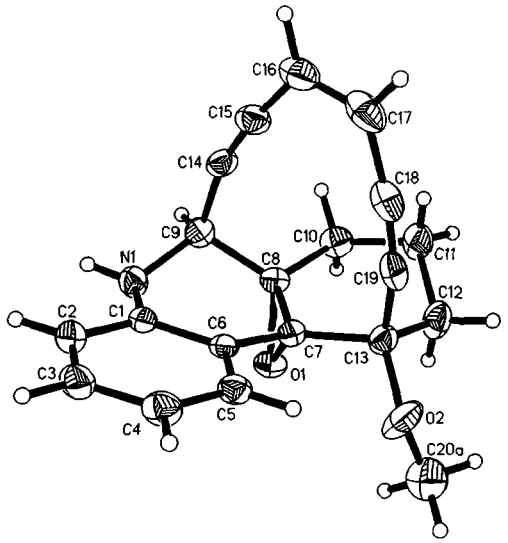

Fig. 1. ORTEP drawing of dynemicin A model compound **13**. *cd* distance [*r*(C14–C19)]: 3.63 Å. Angles at acetylenic carbons: C14, 163.2°; C15, 173.0°; C18, 169.3°; C19, 160.5°.

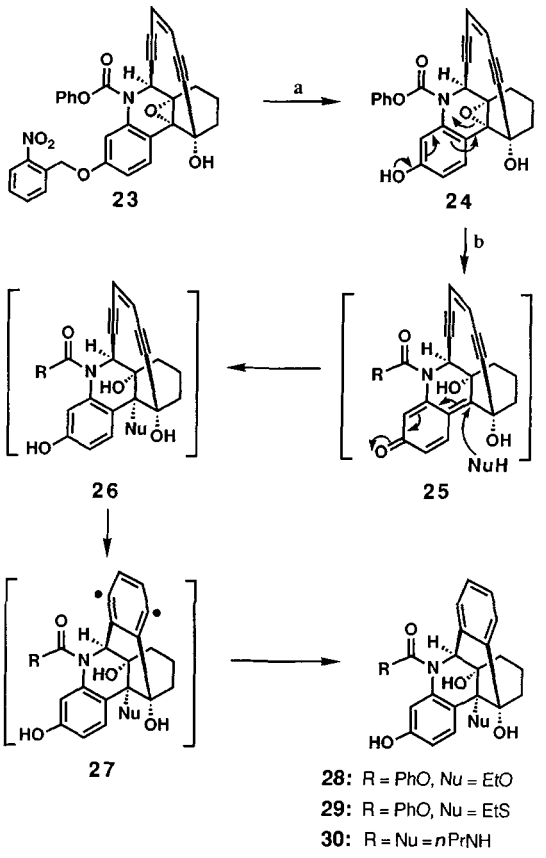

Scheme 3. a) *hv*, THF-H_2O (10:1), argon, 0°C, 40 min; b) EtOH-THF-phosphate buffer (pH 8.0) (1:1:1), argon, 25°C, 1.5 h, **28**, 31% from **23**; or EtSH-THF-phosphate buffer (pH 8.0) (1:1:1), argon, 25°C, 1.5 h, **29**, 34% from **23**; or $nPrNH_2$-THF-phosphate buffer (pH 8.0) (1:1:1), argon, 25°C, 1.5 h, **30**, 46% from **23**.

Enediyne model system **23** (Scheme 3) was designed for its potential to generate species **24** under photolytic, neutral conditions.[8] Following the strategy developed earlier for the synthesis of **8**,[3 a, b] compound **23**[5] was constructed in good overall yield. Irradiation of **23** in aqueous THF (Hanover mercury lamp, pyrex filter) at ice-cooling temperature resulted in clean conversion to **24**[5] as observed by TLC and ^{1}H-NMR spectroscopy ([D_8]THF: D_2O = 10:1, 300 MHz).[5] Attempted isolation of **24** led to decomposition, whereas treatment of crude **24** in a pH 8.0 buffer/THF solution containing the nucleophiles EtOH, EtSH, or $nPrNH_2$ under argon furnished aromatized products **28** (31%), **29** (34%), or **30** (46%) respectively, presumably via intermediates **25**–**27** (Scheme 3). These observations implicate quinone methide intermediate **25**[9] in this cascade formed from **24** under the basic conditions as shown in Scheme 3. Quinone methide intermediates have been implicated in the mode of action of anthracycline antibiotics[10] and dynemicin A **1** (Scheme 1).[2] Noteworthy was the isolation of the novel enediyne compound **31**[11] (Scheme 4) in ~ 10% yield from the reaction of **24** with EtOH (along with **28**) in air as a sensitive but stable molecule under neutral conditions. Remarkably, treatment of the isolable phenol **33**[5] (Scheme 4) under similar conditions (THF/pH 9.0 buffer, air) resulted in the isolation of **34** (35%) and **35** (25%) as stable molecules. Compound **31** represents a novel molecular architecture with DNA cleaving properties (*vide infra*).

The pivaloate esters **36** and **37** (Scheme 5) were also synthesized according to the previously discussed general strate-

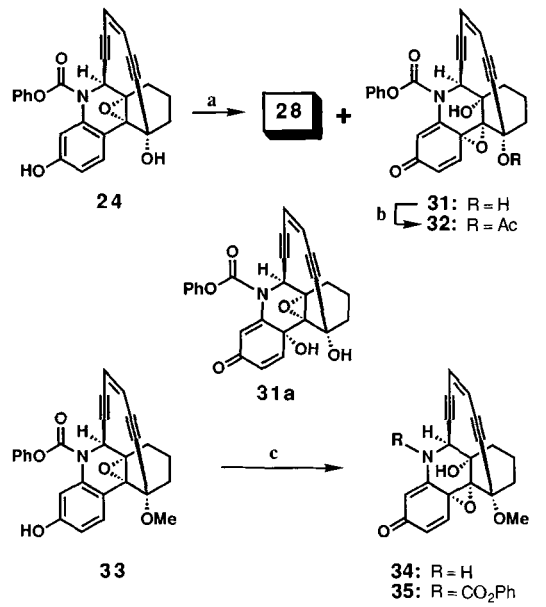

Scheme 4. a) EtOH-THF-phosphate buffer (pH 8.0) (1:1:1), air, 25°C, 1.5 h, **28**, 33% plus **31**, 9%; b) Ac_2O-pyridine, dimethylaminopyridine (DMAP) (cat.), 25°C, 1 h, 84%; c) THF-pH 9.0 buffer [boric acid/potassium chloride/sodium hydroxide] (1:1), air, 25°C, 48 h, **34**, 35% plus **35**, 25%.

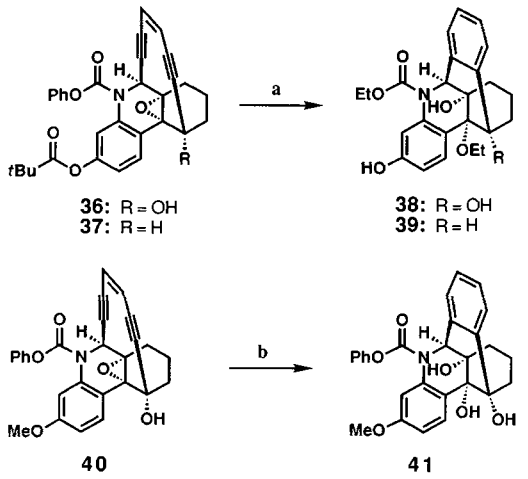

Scheme 5. a) 4 equiv. of LiOH, EtOH-H_2O (3:1), 25 °C, 4–6 h, **38**, 56% from **36**, or **39**, 42% form **37**; b) 1 equiv. of TsOH · H_2O, C_6H_6-1,4-cyclohexadiene (1:1), 25 °C, 1.5 h, 32%.

gy[3a,b] for their potential to liberate phenolic species of type **24** (Scheme 3), thus presenting yet another triggering mechanism to initiate the dynemicin A cascade. Indeed, upon exposure to LiOH in aqueous EtOH at ambient temperatures, compounds **36** and **37** were smoothly converted into products **38** (56%) and **39** (42%) respectively, presumably via a sequence involving intermediates similar to **24**–**27** and with concomitant carbamate exchange (EtO for PhO). The methoxy compound **40** was also synthesized and exhibited reasonable stability under neutral and basic conditions. As expected, however, this compound cyclized rapidly under acidic conditions. For example, upon treatment with TsOH · H_2O in the presence of 1,4-cyclohexadiene, **40** afforded the aromatized product **41** (32%). Presumably, these reactions proceed via intermediates similar to those shown in Scheme 2.

Compounds **12**, **24**, and **31** were found to cause significant DNA cleavage when incubated with supercoiled ΦX174 DNA (Fig. 2, lanes 2, 4 and 5). Noteworthy in these experiments is the observation of double strand cuts as well as single strand cuts, as is the case with dynemicin A (**1**).[2] As expected from their chemical profiles, the methoxy derivatives **13**, **33**, **34** and **35** exhibited diminished activity against DNA. The potency of these compounds is expected to increase by tethering them to suitable DNA-binding molecules.

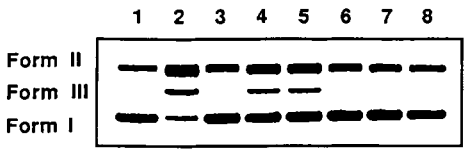

Fig. 2. Supercoiled DNA interaction with selected model compounds. ΦX174 DNA was incubated for 24 h at 37 °C with compounds **12**, **13**, **24**, **31**, **33**, **34** and **35** in buffer (50 mM Tris-HCl, pH 8.0) and analyzed by electrophoresis (1% agarose gel, ethidium bromide stain). Lane 1: DNA control; Lane 2: **12** (5 mM); Lane 3: **13** (5 mM); Lane 4: **24** (5 mM); Lane 5: **31** (5 mM); Lane 6: **33** (5 mM); Lane 7: **34** (5 mM); Lane 8: **35** (5 mM).

The chemistry described here supports the viability of both paths a and b of Scheme 1 as triggering mechanisms for the dynemicin A cascade by showing that a lone pair of electrons on a heteroatom (N or O) strategically positioned on the aromatic ring in relation to the epoxide moiety serves to initiate the cycloaromatization reaction. Such reactive species may be generated within the cell by enzymatic reactions or, as shown above, be released from suitable precursors under mild conditions in the laboratory. In addition, the described observations are interesting in that they allow for the scenario of bioreduction prior to intercalation as well as for the possibility of DNA interacting nucleophilically against quinone methide species such as **3a** or **3b** (Scheme 1).[2b] Thus the proposition that dynemicin A (**1**) may be interacting with DNA by a dual mechanism (nucleophilic and radical) appears attractive, not only because of the observed preference for cleavage at adenine and guanine,[2a] but also in view of the chemistry of **24**.

The foundation is now in place for the development of potent and sequence-specific DNA cleaving molecules by attaching enediyne systems such as the ones described herein to DNA binding moieties, allowing them to bind to their target regions, and then triggering them to initiate cleavage. Analogous applications in the area of drug design, particularly in cancer chemotherapy, may be envisioned.

Received: March 8, 1991 [Z 4485 IE]
German version: *Angew. Chem. 103* (1991) 1034

[1] a) M. Konishi, H. Ohkuma, K. Matsumoto, T. Tsuno, H. Kamei, T. Miyaki, T. Oki, H. Kawaguchi, G. D. VanDuyne, J. Clardy, *J. Antibiot. 42* (1989) 1449; b) M. Konishi, H. Ohkuma, T. Tsuno, T. Oki, G. D. VanDuyne, J. Clardy, *J. Am. Chem. Soc. 112* (1990) 3715.

[2] Protonation of quinone methide **3b** in path b (Scheme 1) provides a second mode of triggering the Bergman cyclization, see: a) Y. Sugiura, T. Shiraki, M. Konishi, T. Oki, *Proc. Natl. Acad. Sci. USA 87* (1990) 3831; b) Y. Sugiura, T. Arakawa, M. Uesugi, T. Shiraki, H. Ohkuma, M. Konishi, *Biochemistry 30* (1991) 2989; c) T. Shiraki, Y. Sugiura, *ibid. 29* (1990) 9795.

[3] a) K. C. Nicolaou, A. L. Smith, S. V. Wendeborn, C.-K. Hwang, *J. Am. Chem. Soc. 113* (1991) 3106; b) K. C. Nicolaou, C.-K. Hwang, A. L. Smith, S. V. Wendeborn, *ibid. 112* (1990) 7416; c) J. A. Porco, Jr., F. J. Schoener, T. J. Stout, J. Clardy, S. L. Schreiber, *ibid. 112* (1990) 7410; d) P. Magnus, S. M. Fortt, *J. Chem. Soc. Chem. Commun. 1991*, 544; e) J. P. Snyder, G. E. Tipsword, *J. Am. Chem. Soc. 112* (1990) 4040; f) M. F. Semmelhack, J. Gallagher, D. Cohen, *Tetrahedron Lett. 31* (1990) 1521; g) P. A. Wender, C. K. Zercher, *J. Am. Chem. Soc. 113* (1991) 2311.

[4] a) R. G. Bergman, *Acc. Chem. Res. 6* (1973) 25; b) R. R. Jones, R. G. Bergman, *J. Am. Chem. Soc. 94* (1972) 660; c) T. P. Lockhart, P. B. Gonita, R. G. Bergman, *ibid. 103* (1981) 4091; d) N. Darby, C. V. Kim, J. A. Salaun, K. W. Shelton, S. Takadar, S. Masamune, *J. Chem. Soc. Chem. Commun. 1971*, 1516; e) H. N. C. Wong, F. Sondheimer, *Tetrahedron Lett. 21* (1980) 217.

[5] Selected physical data for compounds **10**, **13**, **21**, **23**, **24** and **30**–**34**: **10**: R_f = 0.22 (silica, 70% diethyl ether in petroleum ether); ^{1}H NMR (500 MHz, $CDCl_3$): δ = 7.92–7.10 (m, 9H, aromatic), 5.73 (d, J = 10.1 Hz, 1H, olefinic), 5.63 (d, J = 10.1 Hz, 1H, olefinic), 5.37 (br.s, 1H, NC*H*), 4.65–4.22 (m, 2H, $SO_2CH_2CH_2$), 3.73 (s, 1H, $CHCH_2$), 3.48 (m, 2H, $SO_2CH_2CH_2$), 2.43–1.52 (m, 6H, CH_2); ^{13}C NMR (125 MHz, $CDCl_3$): δ = 134.01, 129.3, 128.5,128.1, 127.9, 127.1, 125.2, 124.8, 121.9, 101.7, 93.7, 91.2, 88.6, 70.1, 60.9, 59.3, 55.0, 49.4, 29.3, 23.1, 22.3, 15.6; IR ($CDCl_3$): $\tilde{\nu}_{max}$ = 2975, 2950, 1715, 1360, 1300, 1150 cm^{-1}; HRMS: calcd. for $C_{28}H_{23}SNCs$ ($M^{\oplus}$ + Cs): 618.0351, found: 618.0352. – **13**: R_f = 0.61 (silica, 70% diethyl ether in petroleum ether); ^{1}H NMR (500 MHz, $CDCl_3$): δ = 8.32 (d, J = 7.34 Hz, 1H, aromatic), 7.11 (t, J = 7.34 Hz, 1H, aromatic), 6.82 (t, J = 7.34 Hz, 1H, aromatic), 6.55 (d, J = 7.34 Hz, 1H, aromatic), 5.83 (d, J = 8.8 Hz, 1H, olefinic), 5.73 (dd, J = 8.8, 1.74 Hz, 1H, olefinic), 4.32 (d, J = 1.74 Hz, 1H, NCH), 4.00 (br.s, 1H, NH), 3.50 (s, 3H, OCH_3), 2.36–1.68 (m, 6H, CH_2); ^{13}C NMR (125 MHz, $CDCl_3$): δ = 142.2, 131.0, 128.3, 123.1, 122.5, 122.0, 119.3, 115.9, 100.2, 96.9, 94.6, 87.3, 79.6, 72.9, 62.9, 29.0, 24.6, 19.0; IR ($CDCl_3$): $\tilde{\nu}_{max}$ = 3400, 2950, 2850, 1100, 1080 cm^{-1}; HRMS: calcd for $C_{20}H_{17}O_2N$ ($M^{\oplus}$): 303.1337, found 303.1348. – **21**: R_f = 0.40 (silica, 70% diethyl ether in petroleum ether); ^{1}H NMR (500 MHz, $CDCl_3$): δ = 7.63 (d, J = 7.5 Hz, 1H, aromatic), 7.35 (m, 2H, aromatic), 7.18 (d, J = 7.0 Hz, 1H, aromatic), 7.14 (t, J = 7.0 Hz, 1H, aromatic), 7.09 (t, J = 7.0 Hz, 1H, aromatic), 7.03 (m, 3H, aromatic), 6.87 (d, J = 7.0 Hz, 1H, aromatic), 6.80 (t, J = 7.0 Hz, 1H, aromatic), 6.61 (t, J = 7.0 Hz, 1H, aromatic), 6.31 (d, J = 7.5 Hz, 1H, aromatic), 4.12 (2s, 2H, NH and NCH), 3.73 (s, 1H, O*H*), 3.62 (t, J = 2.82 Hz, 1H, $CHCH_2$), 2.80 (ddd, J = 12.8, 12.8, 5.6 Hz, 1H, CH_2), 2.41 (ddt, J = 12.8, 12.8, 4.5 Hz, 1H, CH_2), 1.75 (dd, J = 13.16, 4.88 Hz, 1H, CH_2), 1.54 (m, 1H, CH_2), 1.39 (br.d, J = 13.16 Hz, 1H, CH_2), 0.9 (m, 1H, CH_2); ^{13}C NMR (125 MHz, $CDCl_3$): δ = 141.6, 139.2, 137.1, 135.1,

133.7, 130.6, 128.1, 127.8, 127.4, 127.0, 126.8, 126.4, 119.9, 115.8, 70.4, 62.1, 55.6, 33.3, 29.8, 28.0, 18.8; IR ($CDCl_3$): $\tilde{\nu}_{max}$ = 3450, 3390, 3070, 2930, 2870, 1490, 1470 cm^{-1}; HRMS: calcd. for $C_{25}H_{23}OSN$ ($M^{\oplus}$): 385.1500, found 385.1500. – **23**: R_f = 0.78 (silica, 50% diethyl ether in benzene); ^1H NMR (300 MHz, C_6D_6): δ=8.97 (d, J = 9.0 Hz, 1H, aromatic), 7.72 (d, J = 8.3 Hz, 1H, aromatic), 7.52 (d, J = 7.7 Hz, 1H, aromatic), 7.13–7.01 (m, 5H, aromatic), 6.97–6.87 (m, 2H, aromatic), 6.81 (br.d, J = 8.9 Hz, 1H, aromatic), 6.66 (t, J = 7.9 Hz, 1H, aromatic), 5.90 (br.s, 1H, CHN), 5.31 (d, J = 10.1 Hz, 1H, olefinic), 5.17 (dd, J = 10.1, 1.7 Hz, 1H, olefinic), 5.13 and 5.04 (AB, J = 16.0 Hz, 2H, ArylCH$_2$O), 2.29 (br.s, 1H, OH), 2.15–1.85 (m, 4H, CH$_2$), 1.70–1.60 (m, 1H, CH$_2$), 1.37–1.29 (m, 1H, CH$_2$); IR ($CHCl_3$): $\tilde{\nu}_{max}$ = 3690, 3600, 2952, 2868, 1720, 1615, 1528, 1381, 1344, 1303 cm^{-1}; HRMS; calcd for $C_{33}H_{25}N_2O_7$ ($M^{\oplus}$ + H): 561.1162, found 561.1162. – **24**: R_f = 0.63 (silica, 50% diethyl ether in benzene); ^1H NMR (300 MHz, [D$_8$]THF:D$_2$O, 10:1): δ = 8.53 (d, J = 8.8 Hz, 1H, aromatic), 7.45–7.10 (m, 5H, aromatic), 6.88 (d, J = 2.5 Hz, 1H, aromatic), 6.63 (dd, J = 8.8, 2.5 Hz, 1H, aromatic), 5.97 (d, J = 10.0 Hz, 1H, olefinic), 5.78 (dd, J = 10.0, 1.6 Hz, 1H, olefinic), 5.46 (br.s, 1H, CHN), 2.35–1.55 (m, 6H, CH$_2$). – **30**: R_f = 0.33 (5% methanol in methylene chloride); ^1H NMR (300 MHz, $CDCl_3$): δ = 7.43 (dd, J = 5.3, 3.5 Hz, 1H, aromatic), 7.25–7.10 (m, 4H, aromatic), 6.56 (dd, J = 8.4, 2.2 Hz, 1H, aromatic), 6.53 (d, J = 2.2 Hz, 1H, aromatic), 5.58 (s, 1H, CHN), 5.46 (t, J = 5.6 Hz, 1H, CH$_2$N*H*CON), 3.19–2.95 (m, 2H, C*H*$_2$NHCON), 2.80 (dt, J = 11.3, 6.3 Hz, 1H, CH$_2$C*H*$_2$NH), 2.53–2.26 (m, 5H, CH$_2$C*H*$_2$N*H*, C*H*$_2$, O*H*), 1.84 (s, 1H, O*H*), 1.68 (dd, J = 12.4, 4.7 Hz, 1H, CH$_2$), 1.61–1.36 (m, 5H, C*H*$_2$CH$_2$NHCON, C*H*$_2$CH$_2$NH, CH$_2$), 0.94 (t, J = 7.3 Hz, 3H, C*H*$_3$CH$_2$CH$_2$NHCON), 0.89 (dd, J = 4.8, 2.4 Hz, 1H, C*H*$_2$), 0.83 (t, J = 7.3 Hz, 3H, C*H*$_3$CH$_2$CH$_2$NH), 0.78–0.59 (m, 1H, CH$_2$); IR ($CHCl_3$): $\tilde{\nu}_{max}$ = 3591, 3439, 3270, 2964, 2935, 1645, 1613, 1500, 1459, 1416, 1252, 1188 cm^{-1}; HRMS: calcd. for $C_{26}H_{34}N_3O_4$ ($M^{\oplus}$ + H): 452.2549, found: 452.2549. – **31**: R_f = 0.41 (silica, 50% diethyl ether in benzene); 1H NMR (300 MHz, $CDCl_3$): δ = 7.87 (d, J = 10.4 Hz, 1H, olefinic), 7.44–7.35 (m, 3H, aromatic), 7.20–7.14 (m, 2H, aromatic), 6.76 (d, J = 2.2 Hz, 1H, olefinic), 6.51 (dd, J = 10.4, 2.2 Hz, 1H, olefinic), 5.92 (d, J = 9.9 Hz, 1H, olefinic), 5.86 (dd, J = 9.9, 1.7 Hz, 1H, olefinic), 5.21 (d, J = 1.7 Hz, 1H, CHN), 3.74 (d, J = 2.3 Hz, 1H, O*H*, exchangeable with D_2O), 3.23 (dddd, J = 14.7, 9.7, 9.7, 2.3 Hz, 1H, C*H*$_2$), 2.34–2.15 (m, 2H, CH$_2$), 2.29 (s, 1H, OH, exchangeable with D_2O), 2.15–1.95 (m, 2H, CH$_2$), 1.88 (ddd, J = 14.7, 8.3, 1.8 Hz, 1H, C*H*$_2$); ^{13}C NMR (125 MHz, $CDCl_3$): δ = 185.5, 151.8, 150.4, 147.6, 138.9, 134.2, 129.7, 129.7, 127.9, 126.3, 123.8, 123.3, 121.3, 121.3, 98.3, 93.9, 90.5, 89.1, 79.3, 74.9, 68.3, 59.8, 59.5, 33.6, 26.4, 14.2; IR ($CHCl_3$): $\tilde{\nu}_{max}$ = 3545, 2958, 2927, 2856, 1733, 1666, 1608, 1403, 1296, 1285, 1198 cm^{-1}; UV ($CHCl_3$, $c = 2.7 \times 10^{-4}$ M): λ_{max} (lg ε) = 310 (3.65, sh), 290 (3.96, sh), 258 (4.16) nm; HRMS: calcd. for $C_{26}H_{19}NO_6Cs$ ($M^{\oplus}$ + Cs): 574.0267, found 574.0284. – **32**: R_f = 0.61 (silica, 50% diethyl ether in benzene); ^1H NMR (300 MHz, $CDCl_3$): δ = 7.44–7.37 (m, 3H, aromatic), 7.30 (d, J = 10.4 Hz, 1H, olefinic), 7.20–7.15 (m, 2H, aromatic), 6.76 (d, J = 2.0 Hz, 1H, olefinic), 6.53 (dd, J = 10.4, 2.0 Hz, 1H, olefinic), 5.94 (d, J = 9.8 Hz, 1H, olefinic), 5.84 (dd, J = 9.8, 1.8 Hz, 1H, olefinic), 5.20 (d, J = 1.8 Hz, 1H, CHN), 3.87 (d, J = 2.6 Hz, 1H, OH, exchangeable with D_2O), 3.18 (dddd, J = 14.5, 9.3, 9.3, 2.6 Hz, 1H, CH$_2$), 2.81 (ddd, J = 13.1, 8.7, 3.0 Hz, 1H, CH$_2$), 2.30–2.23 (m, 1H, CH$_2$), 2.18 (s, 3H, COCH$_3$), 2.12–2.01 (m, 2H, CH$_2$), 1.93 (ddd, J = 14.5, 8.3, 2.2 Hz, 1H, CH$_2$); ^{13}C NMR (125 MHz, $CDCl_3$): δ = 185.1, 167.8, 151.9, 150.4, 147.9, 138.1, 134.4, 129.7, 129.7, 128.2, 126.3, 124.0, 123.9, 121.3, 121.3, 96.1, 94.0, 91.7, 89.3, 78.8, 75.2, 72.5, 59.5, 59.5, 28.5, 26.3, 14.0; IR ($CHCl_3$): $\tilde{\nu}_{max}$ = 3552, 1738, 1667, 1639, 1608, 1403, 1296, 1287 cm^{-1}; HRMS: calcd. for $C_{28}H_{21}NO_7Cs$ ($M^{\oplus}$ + Cs): 616.0372, found. 616.0398. – **33**: R_f = 0.3 (silica, 50% diethyl ether in petroleum ether); ^1H NMR (500 MHz, $CDCl_3$): δ = 8.22 (d, J = 8.8 Hz, 1H, aromatic), 7.32 (t, J = 7.6 Hz, 2H, aromatic), 7.18 (t, J = 7.3 Hz, 1H, aromatic), 7.10 (bd, J = 6.9 Hz, 2H, aromatic), 6.89 (br.s, 1H, aromatic), 6.65 (dd, J = 8.8, 2.7 Hz, 1H, aromatic), 5.82 (d, J = 10.0 Hz, 1H, olefinic), 5.67 (dd, J = 10.0, 1.7 Hz, 1H, olefinic), 5.48 (s, 1H, OH), 5.28 (br.s, 1H, CHN), 3.47 (s, 3H, OCH$_3$), 2.28 (dd, J = 15.1, 8.2 Hz, 1H, CH$_2$), 2.15 (m, 2H, CH$_2$), 1.92 (m, 2H, CH$_2$), 1.75 (m, 1H, CH$_2$); ^{13}C NMR (125 MHz, $CDCl_3$): δ = 155.1, 150.9, 136.8, 133.2, 131.9, 130.1, 129.3, 129.3, 125.8, 124.2, 124.1, 122.2, 121.6, 120.5, 113.0, 99.5, 94.9, 88.4, 79.3, 72.1, 63.2, 52.1, 50.5, 28.5, 23.2, 18.9; IR ($CHCl_3$): $\tilde{\nu}_{max}$ = 3400, 3004, 2979, 2935, 2875, 1720, 1384, 1111 cm^{-1}; HRMS: calcd for $C_{27}H_{21}NO_5Cs$ ($M^{\oplus}$ + Cs): 572.0474, found 572.0429. – **34**: R_f = 0.31 (silica, diethyl ether); ^1H NMR (500 MHz, $CDCl_3$): δ = 7.37 (d, J = 10.3 Hz, 1H, olefinic), 6.36 (dd, J = 10.4, 2.0 Hz, 1H, olefinic), 5.85 (d, J = 9.8 Hz, 1H, olefinic), 5.81 (dd, J = 9.8, 1.7 Hz, 1H, olefinic), 5.10 (d, J = 2.0 Hz, 1H, olefinic), 4.13 (d, J = 4.0 Hz, 1H, O*H*), 4.07 (d, J = 3.0 Hz, 1H, olefinic), 3.72 (dd, J = 4.2, 1.7 Hz, 1H, CHN), 3.41 (s, 3H, OCH$_3$), 3.20 (m, 1H, CH$_2$), 2.36 (m, 1H, CH$_2$), 2.10 (m, 1H, CH$_2$), 1.88 (m, 1H, CH$_2$), 1.74 (m, 1H, CH$_2$); ^{13}C NMR (125 MHz, C_6D_6): δ = 184.4, 157.2, 137.7, 134.8, 123.3, 122.6, 113.3, 98.8, 98.4, 90.7, 87.2, 78.1, 74.8, 74.0, 58.4, 57.8, 51.5, 27.5, 27.4, 14.3; IR ($CHCl_3$: $\tilde{\nu}_{max}$ = 3527, 3385, 2956, 2929, 2856, 1656, 1597 cm^{-1}; UV ($CHCl_3$, $c = 2.2 \times 10^{-4}$ M): λ_{max} (lg ε) = 330 (3.09), 285 (3.38, sh), 256 (3.71), 244 (3.58, sh) nm; HRMS: calcd. for $C_{20}H_{17}O_4NCs$ ($M^{\oplus}$ + Cs): 468.0212, found 468.0254.

[6] The striking stability of compound **13** as compared to that of **12** may be attributed to the destabilization of the incipient benzylic carbenium ion by the methoxy group (electron withdrawal).

[7] We thank Dr. *Raj Chadha*, University of California, San Diego, for the X-ray crystallographic analysis. Further details of the crystal structure investigation are available on request from the Director of the Cambridge Crystallographic Data Centre, University Chemical Laboratory. Lensfield Road, GB-Cambridge CB21EW, on quoting the full journal citation.

[8] A hydroxy group at the the other *meta* position from the nitrogen atom on the aromatic ring is expected to show similar triggering capability.

[9] a) L. K. Dyall, S. Winston, *J. Am. Chem. Soc. 94* (1972) 2196; b) A. Zanarotti, *Tetrahedron Lett. 23* (1982) 3815; c) *J. Org. Chem. 50* (1985) 941; d) S. R. Angle, K. D. Turnball, *J. Am. Chem. Soc. 111* (1989) 1136; e) S. R. Angle, M. S. Louie, H. L. Mattson, W. Yang, *Tetrahedron Lett. 30* (1989) 1193; f) O. Crescenzi, C. Costantini, G. Prota, *ibid. 31* (1990) 6095; g) S. R. Angle, W. Yang, *ibid. 112* (1990) 4524.

[10] For recently postulated quinone methide intermediates in the area of anthracycline antibiotics, see: a) M. Boldt, G. Gaudiano, T. H. Koch, *J. Org. Chem. 52* (1987) 2146; b) G. Gaudiano, M. Egholar, M. J. Haddadin, T. H. Koch, *ibid. 54* (1989) 5090; c) M. Egholm, T. H. Koch, *J. Am. Chem. Soc. 111* (1989) 8291; d) K. Ramakrishnan, J. Fisher, *J. Med. Chem. 29* (1986) 1215; e) M. Boldt, G. Gaudiano, M. J. Haddadin, T. H. Koch, *J. Am. Chem. Soc. 111* (1989) 2283; f) G. Gaudiano, T. H. Koch, *J. Am. Chem. Soc. 112* (1990) 9423; g) K. Karabelas, H. W. Moore, *ibid. 112* (1990) 5372; h) G.Gaudiano, M. Frigerio, P. Bravo, T. H. Koch, *ibid. 112* (1990) 6704.

[11] Structure **31** was favored over **31a** (Scheme 4) on the basis of ^1H and ^{13}C NMR data of its monoacetate **32**[5]. Particularly revealing were chemical shift changes and NOE data which are in accord with structures **31** and **32**. Attempts to confirm this structure by X-ray crystallographic analysis are in progess.

Self-Assembling [2]Pseudorotaxanes**

By *Pier Lucio Anelli, Peter R. Ashton, Neil Spencer, Alexandra M. Z. Slawin, J. Fraser Stoddart,** and *David J. Williams*

The ability of the tetracationic cyclophane **1**[1] to form inclusion complexes[2] with π-donor aromatic substrates, e.g. 1,2- and 1,4-dimethoxybenzene, as a result of stabilizing dispersive forces that include (i) π/π-stacking and charge transfer interactions between the π-electron-rich hydroquinone rings and the π-electron-deficient bipyridinium units and (ii) electrostatic "T-type" edge-to-face interactions involving the hydroquinone rings and the *para*-phenylene units in the cyclophane has led us to examine the complexing behavior (Scheme 1) of some polytopic substrates such as **2**–**5** with **1**·4PF$_6$ (Fig. 1). Here, with reference to some fascinating X-ray crystallographic data, we describe the remarkable mutual ordering that occurs between the component molecular species in **1**·**2**·4PF$_6$ and **1**·**3**·4PF$_6$, compare their solid-state structures with that of the [2]catenane **1**·**6**·4PF$_6$ (Fig. 2) formed[3] between **1** and bisparaphenylene-34-crown-10 **6**,[4] and anticipate how the thermodynamically-driven ordered threading of substrates such as **2**–**5** through the centers of tetracations like **1** could be exploited in the construction of quite intricate molecular assemblies.

[*] Dr. J. F. Stoddart,[+] P. R. Ashton, Dr. N. Spencer
Department of Chemistry, The University
Sheffield S3 7HF (UK)

Dr. P. L. Anelli
Centro CNR "Sintesi e Stereochimica di Speciali Sistemi Organici"
20133 Milano (Italy)

A. M. Z. Slawin, Dr. D. J. Williams
Chemical Crystallography Laboratory
Department of Chemistry, Imperial College
London SW7 2AY (UK).

[+] Present address:
School of Chemistry, University of Birmingham
Edgbaston, Birmingham B15 2TT (UK)

[**] This work was supported by the Agricultural and Food, and Science and Engineering Research Councils in the United Kingdom and by Consiglio Nazionale delle Ricerche in Italy.

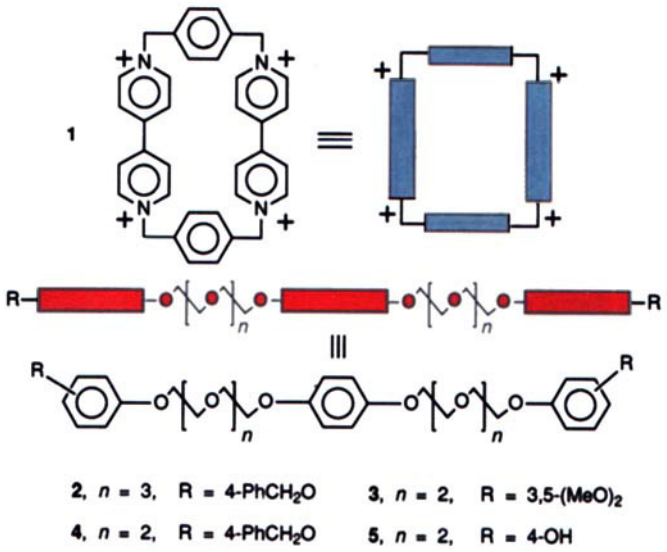

Fig. 1. The molecular components. The 'bead' is blue and the 'threads' are red.

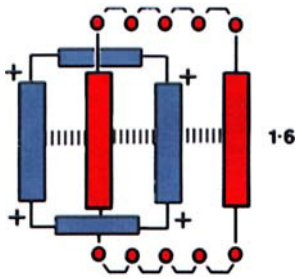

Fig. 2. The [2]catenane. The tetracationic cyclophane subunit **1** is blue and the bisparaphenylene-34-crown-10 **6** subunit is red.

When equimolar amounts of $\mathbf{1}\cdot 4PF_6$ were added, in turn (Scheme 1), to colorless solutions of **2**–**5** in MeCN, the latter immediately assumed a pronounced red color characteristic[2] of inclusion complex formation. In the cases of **2**, **3**, and **5**, vapor diffusion of $i Pr_2O$ into those solutions yielded gem quality crystals suitable for X-ray crystallography. Although the complex $\mathbf{1}\cdot\mathbf{4}\cdot 4PF_6$ did not afford single crystals that were good enough for X-ray crystal structure analysis, crystals of $\mathbf{1}\cdot\mathbf{5}\cdot 4PF_6\cdot 4MeCN$ were obtained of sufficient quality for X-ray crystallography.[5]

The X-ray structural analyses[5, 6] of $\mathbf{1}\cdot\mathbf{2}\cdot 4PF_6\cdot 2MeCN$ (Fig. 3) and $\mathbf{1}\cdot\mathbf{3}\cdot 4PF_6\cdot 2MeCN$ (Fig. 4) show that, in both cases, the polyether 'thread' is not only inserted through the center of the tetracationic 'bead' such that the middle hydroquinone ring is encircled, but its polyether

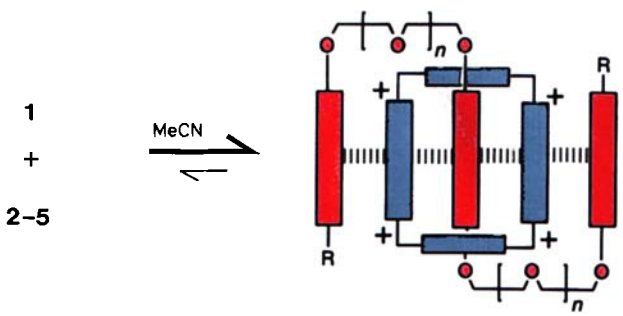

Scheme 1. Inclusion complexes of **1** and **2**–**5**.

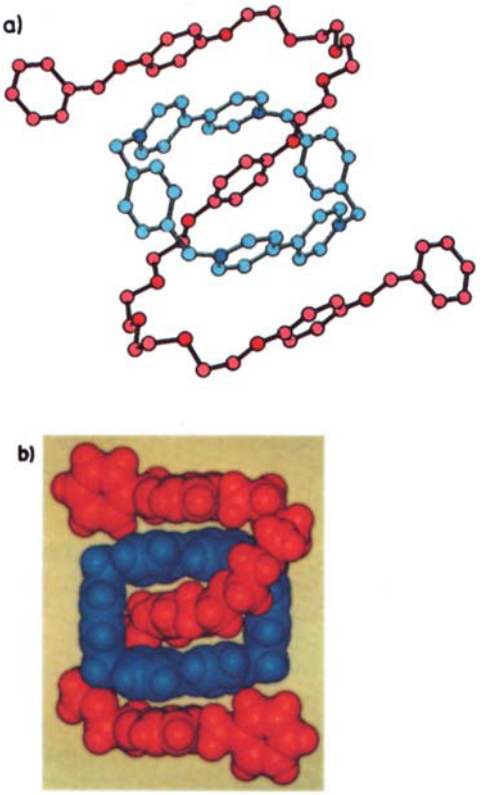

Fig. 3. a) Structure of $\mathbf{1}\cdot\mathbf{2}$ in the crystal. Crystal data for $C_{84}H_{90}N_4O_{12}\cdot P_4F_{24}\cdot 2MeCN$: triclinic, $a = 13.257(2)$, $b = 14.388(2)$, $c = 14.450(3)$ Å, $\alpha = 62.99(1)$, $\beta = 79.12(1)$, $\gamma = 69.03(1)°$, $V = 2292$ Å^3, space group $P\bar{1}$, $Z = 1$ (the molecule is disposed about a center of symmetry), $\rho = 1.46$ g cm^{-3}, $\mu(Cu_{K\alpha}) = 17$ cm^{-1}, 5005 independent observed reflections with $[|F_o| > 3\sigma(|F_o|), 2\theta \leq 116°]$, $R = 0.091$, $R_w = 0.110$. b) Space-filling representation. (The 'bead' is blue and the 'thread' is red.)

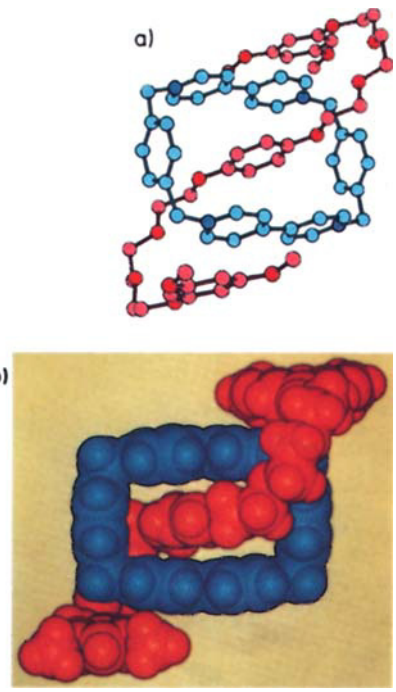

Fig. 4. a) Structure of $\mathbf{1}\cdot\mathbf{3}$ in the crystal. Crystal data for $C_{70}H_{78}N_4O_{12}\cdot P_4F_{24}\cdot 2MeCN\cdot X$ where X corresponds to unidentified solvent fragments of scattering approximately equal to C atoms: triclinic: $a = 11.863(3)$, $b = 13.834(2)$, $c = 13.857(3)$ Å, $\alpha = 77.79(1)$, $\beta = 79.75(2)$, $\gamma = 76.85(2)°$, $V = 2144$ Å^3, space group $P\bar{1}$, $Z = 1$ (the molecule is disposed about a center of symmetry), $\rho = 1.43$ g cm^{-3}, $\mu(Cu_{K\alpha}) = 18$ cm^{-1}, 3352 independent observed reflections with $[|F_o| > 3\sigma(|F_o|), 2\theta \leq 110°]$, $R = 0.113$, $R_w = 0.109$. b) Space-filling representation. (The 'bead' is blue and the 'thread' is red.)

chains also curl back on themselves around the 'bead' enabling the next aromatic donors in both directions to stack against the sides of the π-accepting bipyridinium units of **1**. The gross structure of the 'bead' **1** in both complexes resembles that of **1**[1] and its 1:1 complexes with 1,2- and 1,4-dimethoxybenzene.[2] The degrees of bowing of the sides of the 'beads' in **1·2** and **1·3** differ slightly: a) the $C-CH_2$ bonds, emanating from the *para*-phenylene units, subtend angles of 9° and 14°, respectively, and b) the $N^{\oplus}-CH_2$ bonds, associated with the bipyridinium moieties subtend angles of 28° and 21° respectively. Although there are marked differences in the twist angles between the pyridinium rings (19° for **1·2** and 4° for **1·3**), the separations between the bipyridinium units and the entrapped hydroquinone rings are ca. 3.5 Å in both cases. The angles of tilt[7] of the hydroquinone units within the 'beads' are 48° and 45° in **1·2** and **1·3**, respectively. The geometries adopted, which emphasize the symbiotic relationships between 'beads' and 'threads' capitalize upon stabilizing dispersive forces and associated charge transfer interactions that are enhanced further by electrostatic 'T-type' edge-to-face interactions.[8]

A striking feature of both polyether 'threads' in **1·2** and **1·3** is the presence of a common conformation for the first ten atoms emanating from the central hydroquinone rings. The sequence ($ag^-aag^+aag^-$) of the torsional angles is also present in one of the two polyether chains in the [2]catenane **1·6**. It is noteworthy that the inner surfaces of the polyether loops that pass over the junctions between the bipyridinium units and the *para*-phenylene rings of the 'beads' are lined with oxygen atoms in both cases. Such an arrangement satisfies the mutual electrostatic requirements of these portions of the 'beads' and 'threads'. The polyether chains in **1·2** linking the hydroquinone rings within the 'thread' are of an optimum length and geometry[9] enabling a π/π stacking interaction between these rings and their sandwiched bipyridinium units (interplanar separations, ca. 3.5 Å). This supramolecular arrangement is virtually identical with the molecular geometry present[3] within the [2]catenane **1·6**.

Whereas in **1·2** there is no formation of continuous stacks[10] within the crystals, in **1·3**, however, an interesting stacking arrangement (Fig. 5) is produced. The reduced length of the polyether chain in **1·3** compared to **1·2**, coupled with the retention of the chain conformation, does not permit the terminal 3,5-dimethoxyphenyl groups to approach (closest centroid-centroid distance, 4.4 Å) the center of the outer face of the bipyridinium units such that an optimum stacking interaction may occur. However, this requirement is satisfied by the approach of a lattice-translated and laterally-displaced complex. The resulting centroid-centroid separations between one of the translated bipyridinium rings and the virtually parallel (4° interplanar angle) 3,5-dimethoxyphenyl group is 3.6 Å.

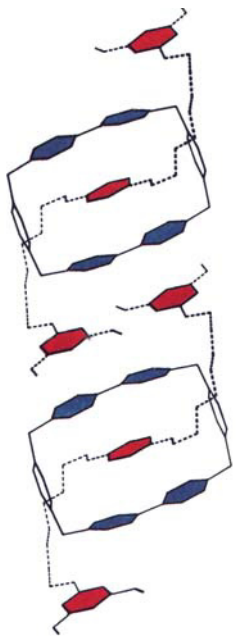

Fig. 5. Part of the continuous sequence of **1·3** in the crystal. The 'threads' are red and the 'beads' are blue.

In CD_3CN solutions, the ^{1}H-NMR spectra of **1·2**·4 PF_6 and **1·3**·4 PF_6 reveal considerable line broadening as well as chemical shift changes of up to 0.5 ppm commensurate with the formation of strong complexes in which slow intra-complex—and possibly also inter-complex—equilibria are clearly operative. Positive-ion FABMS[11] of these two 1:1 complexes afforded[12] peaks corresponding to the loss of *one* and *two* $PF_6^{\ominus}$ counterions respectively at $m/z = 1781$ and 1636 for **1·2**·4PF_6, and $m/z = 1601$ and 1456 for **1·3**·4PF_6.

The self-assembly[13] that functions between the tetracationic 'bead' **1** and the polyether 'threads' can now be exploited to template the synthesis of highly ordered rotaxanes and other prototypes of molecular devices.[14]

Experimental

2: Dialkylation (*t*BuOK/*t*BuOH/THF/reflux/65 h) of 1,4-dihydroxybenzene with 2-[2-[2-(benzyloxy)ethoxy]ethoxy]ethoxy]ethyl-4-methylbenzene sulfonate [15] gave (SiO_2:Et_2O) the dibenzyl ether (73%, oil). Hydrogenolysis (H_2/Pd on C/MeOH/CH_2Cl_2) afforded the diol (94%, oil) which was converted (TsCl/Et_3N/CH_2Cl_2/RT/15 h) into (SiO_2:$CHCl_3$/EtOAc) the ditosylate (78%, oil). Reaction (*t*BuOK/THF/reflux/15 h) with 4-(benzyloxy)phenol (2 mol. equiv.) gave **2** [52%, m.p. 91–93°C (Me_2CO); EI-MS: $m/z = 826$ ($M^{\oplus}$); ^{1}H NMR (CD_3CN): $\delta = 3.54-3.60$ (m, 16H), 3.69–3.72 (m, 8H), 3.97–4.01 (m, 8H), 5.00 (s, 4H), 6.80 (s, 4H), 6.80–6.90 (m, 8H), 7.28–7.43 (m, 10H)].

3 and **4**: Dialkylation (*t*BuOK/*t*BuOH/reflux/65 h) of 1,4-dihydroxybenzene with 2-[2-(2-chloroethoxy)ethoxy]ethanol afforded (SiO_2:EtOAc/MeOH) a diol (78%, m.p. 48–51°C) which was converted (TsCl/Et_3N/CH_2Cl_2/RT/15 h) into (SiO_2:$CHCl_3$/EtOAc) the corresponding ditosylate (94%, oil). Reaction (*t*BuOK/THF/reflux/20 h) with: (a) 3,5-dimethoxyphenol (2 mol. equiv.) yielded (SiO_2:light petroleum/EtoAc) **3** [74%, m.p. 64–66°C (MeOH/Et_2O); EI-MS: $m/z = 646$ ($M^{\oplus}$); ^{1}H NMR (CD_3CN): $\delta = 3.62$ (s, 8H), 3.72 (s, 12H), 3.72–3.75 (m, 8H), 3.99–4.05 (m, 8H), 6.06–6.09 (m, 6H), 6.81 (s, 4H)], (b) 4-benzyloxyphenol (2 mol. equiv.) yielded **4** [61%, m.p. 104–107°C (Me_2CO); EI-MS: m/z 738 ($M^{\oplus}$); ^{1}H NMR ($CDCl_3$): $\delta = 3.65-3.90$ (m, 16H), 3.96–4.15 (m, 8H), 5.00 (s, 4H), 6.80 (s, 4H), 6.78–6.87 (m, 8H), 7.28–7.44 (m, 10H)].

5: Hydrogenolysis (H_2/Pd on C/MeOH/CH_2Cl_2) of **4** afforded **5** [97%, m.p. 102–104°C (EtOH); EI-MS: m/z 558 ($M^{\oplus}$); ^{1}H NMR (CD_3CN): $\delta = 3.62$ (s, 8H), 3.70–3.74 (m, 8H), 3.97–4.02 (m, 8H), 6.52 (brs, 2H), 6.68–6.76 (m, 8H), 6.82 (s, 4H)].

Received: February 5, 1991 [Z 4424 IE]
German version: *Angew. Chem. 103* (1991) 1052

[1] B. Odell, M. V. Reddington, A. M. Z. Slawin, N. Spencer, J. F. Stoddart, D. J. Williams, *Angew. Chem. 100* (1988) 1605; *Angew. Chem. Int. Ed. Engl. 27* (1988) 1547.

[2] P. R. Ashton, B. Odell, M. V. Reddington, A. M. Z. Slawin, J. F. Stoddart, D. J. Williams, *Angew. Chem. 100* (1988) 1608; *Angew. Chem. Int. Ed. Engl. 27* (1988) 1550; see also M. V. Reddington, A. M. Z. Slawin, N. Spencer, J. F. Stoddart, C. Vicent, D. J. Williams, *J. Chem. Soc. Chem. Commun. 1991*, 630.

[3] P. R. Ashton, T. T. Goodnow, A. E. Kaifer, M. V. Reddington, A. M. Z. Slawin, N. Spencer, J. F. Stoddart, C. Vicent, D. J. Williams, *Angew. Chem. 101* (1989) 1404; *Angew. Chem. Int. Ed. Engl. 28* (1989) 1396; P. R. Ashton, C. L. Brown, E. J. T. Chrystal, T. T. Goodnow, A. E. Kaifer, K. P. Parry, D. Philp, A. M. Z. Slawin, N. Spencer, J. F. Stoddart, D. J. Williams, *J. Chem. Soc. Chem. Commun. 1991*, 634; C. L. Brown, D. Philp, J. F. Stoddart, *Synlett 1991*, 459, 462.

[4] B. L. Allwood, N. Spencer, H. Shahriari-Zavareh, J. F. Stoddart, D. J. Williams, *J. Chem. Soc. Chem. Commun. 1987*, 1061, 1064.

[5] Crystals of **1·5**·4PF_6·4MeCN had $C_{82}H_{52}F_{24}N_{12}O_{10}P_4$: triclinic, $a = 13.648(4)$, $b = 13.881(4)$, $c = 14.670(3)$ Å, $\alpha = 117.86(2)$, $\beta = 92.89(2)$, $\gamma = 103.11(2)°$, $V = 2353$ Å^3, space group $P\bar{1}$, $Z = 1$ (the molecule is disposed about a center of symmetry), $\rho = 1.40$ g cm^{-3}, $\mu(Cu_{K\alpha}) =$

17 cm^{-1}, 4161 independent observed reflections with [$|F_o| > 3\sigma(|F_o|)$, $2\theta \leq 110°$], $R = 0.078$, $R_w = 0.085$. The 'thread' in **1·5** is centrosymmetrically positioned within the 'bead' with the *para*-hydroxyphenyl groups layered between adjacent lattice-translated complexes producing a stacking mode analogous to that observed in **1·3**.

[6] Nicolet R3m diffractometer, ω-scans, $Cu_{K\alpha}$ radiation (graphite monochromator). The structures were solved by direct methods and refined anisotropically. Further details of the crystal structure investigations can be obtained from the Cambridge Crystallographic Data Centre, University Chemical Laboratory, Lensfield Road, Cambridge CB2 1EW (England). Any request should be accompanied by the full literature citation for this communication.

[7] The tilt angle is defined as the angle between the O···O vector within the hydroquinone rings and the N···N axis of the bipyridinium units.

[8] These edge-to-face interactions between the *para*-phenylene units in **1** and the hydroquinone rings in **2** and **3** have centroid-centroid separations of 5.1 and 5.2 Å, respectively, with corresponding interacting H···centroid distances of 2.9 and 2.8 Å. The C–H···centroid angles are 157 and 163°, respectively. For general discussions of these 'T-type' interactions, see R. O. Gould, A. M. Gray, P. Taylor, M. D. Walkinshaw, *J. Am. Chem. Soc. 107* (1985) 5921; S. K. Burley, G. A. Petsko, *Science (Washington, DC) 229* (1985) 23; *J. Am. Chem. Soc. 108* (1986) 7995; *Adv. Protein Chem. 39* (1988) 125; W. L. Jorgensen, D. L. Severance, *J. Am. Chem. Soc. 112* (1990) 4768; C. A. Hunter, J. K. M. Sanders, *ibid. 112* (1990) 5225.

[9] Within the hydroquinone units, there is present both *trans* geometries and coplanar dispositions for the associated oxymethylene functions. In common with the [2]catenane **1·6**, this coplanarity also extends to incorporate the next carbon atom in both directions. Similarly, the methoxy functions on the 3,5-dimethoxyphenyl group adopt characteristic coplanar conformations. See J. D. Mersh, J. K. M. Sanders, S. A. Matlin, *J. Chem. Soc. Chem. Commun. 1983*, 306 and references cited therein.

[10] There are, however, intermolecular 'T-type' edge-to-face interactions between adjacent benzyloxyphenoxy units in **1·2**, the terminal phenyl ring of one thread interacting in the crystallographic *b* direction with the hydroquinone ring of another and vice versa (centroid-centroid separation of 5.1 Å).

[11] FABMS were obtained using a Kratos MS80RF mass spectrometer and DS90 data system. Xenon was used to provide the primary beam of atoms and samples were mixed with a small amount of 3-nitrobenzyl alcohol matrix on a stainless steel probe. Spectra were recorded in the positive-ion mode at a scan speed of 30 s per decade.

[12] Similar fragmentation patterns were observed for **1·4·4PF$_6$** with m/z = 1693 [$(M - PF_6)^{\oplus}$] and 1548 [$(M - 2PF_6)^{\oplus}$] and **1·5·4PF$_6$** with m/z = 1513 [$(M - PF_6)^{\oplus}$] and 1368 [$(M - 2PF_6)^{\oplus}$]. However, with the exception of **1·3·4PF$_6$**, higher mass peaks were observed consistently for these 1:1 complexes at m/z = 2055 and 1910, which correspond to the loss of one and two $PF_6^{\ominus}$ counterions respectively from the dimeric species, $(\mathbf{1}\cdot 4PF_6)_2$. While the reason for this observation, when **2**, **4**, or **5** are initially threaded through **1**, is a subject for much speculation, the detection of cluster ions by FABMS is a well-established phenomenon. For a discussion of the behavior of cesium iodide cluster ions, see M. A. Baldwin, C. J. Proctor, I. J. Amster, F. W. McLafferty, *Int. J. Mass Spectrom. Ion Processes 54* (1983) 97.

[13] The strategy of self-assembly is not a new one. Some recent examples in chemical systems include the following: Catenanes and rotaxanes: C. O. Dietrich-Buchecker, J.-P. Sauvage, *Chem. Rev. 87* (1987) 795. Metallo-organic double helices: J.-M. Lehn, A. Rigault, J. Siegel, J. Harrowfield, B. Chevier, D. Moras, *Proc. Nat. Acad. Sci. USA 84* (1987) 2565; U. Koert, M. M. Harding, J.-M. Lehn, *Nature 349* (1990) 339. Surfaces: C. D. Bain, E. B. Troughton, Y. T. Tao, J. Evall, G. M. Whitesides, R. G. Nuzzo, *J. Am. Chem. Soc. 111* (1989) 321. Bibracchial lariat ethers carrying sidearms terminated by nucleic acid bases: G. W. Gokel, L. Echegoyen, M. Kim, J. C. Hernandez, M. de Jesus, *J. Incl. Phenom. 7* (1989) 73. Transition metal chelates: A. Schepartz, J. P. McDevitt, *J. Am. Chem. Soc. 111* (1989) 5976; R. W. Saalfrank, A. Stark, M. Bremer, H.-U. Hummel, *Angew. Chem. 102* (1990) 316; *Angew. Chem. Int. Ed. Engl. 29* (1990) 311. Superhelical strands: H. Yanagawa, Y. Ogawa, H. Furuta, K. Tsuho, *J. Am. Chem. Soc. 111* (1989) 4567. Ordered supramolecular strands: J.-M. Lehn, M. Mascal, A. DeCian, J. Fischer, *J. Chem. Soc. Chem. Commun. 1990*, 479. A self-replicating system: T. Tjivikua, P. Ballester, J. Rebek, Jr., *J. Am. Chem. Soc. 112* (1990) 1249. Threaded cyclodextrin molecular loop: T. V. S. Rao, D. S. Lawrence, *J. Am. Chem. Soc. 112* (1990) 3614; see also J. S. Manka, D. S. Lawrence, *ibid. 112* (1990) 3614; see also J. S. Manka, D. S. Lawrence, *ibid. 112* (1990) 2440. Hydrogen bonded molecular tapes: J. A. Zerkowski, C. T. Seto, D. W. Wierda, G. M. Whitesides, *ibid. 112* (1990) 9025; see also: C. T. Seto, G. M. Whitesides, *ibid. 112* (1990) 6409; *ibid. 113* (1991) 712.

[14] P. L. Anelli, P. R. Ashton, R. Ballardini, V. Balzani, M. Delgado, M. T. Gandolfi, T. T. Goodnow, A. E. Kaifer, D. Philp, M. Pietraszkiewicz, L. Prodi, M. V. Reddington, A. M. Z. Slawin, N. Spencer, J. F. Stoddart, C. Vicent, D. J. Williams, unpublished; P. L. Anelli, N. Spencer, J. F. Stoddart, *J. Am. Chem. Soc. 113* (1991) 5131.

[15] J. R. Beadle, S. H. Korzeniowski, D. E. Rosenberg, B. J. Garcia-Slanga, G. W. Gokel, *J. Org. Chem. 49* (1984) 1594.

Self-Assembling [3]Catenanes**

By *Peter R. Ashton, Christopher L. Brown, Ewan J. T. Chrystal, Timothy T. Goodnow, Angel E. Kaifer, Keith P. Parry, Alexandra M. Z. Slawin, Neil Spencer, J. Fraser Stoddart,** and *David J. Williams*

Recently, we reported the template-directed synthesis of the [2]catenane **4·4PF$_6$** in 70% yield as a result of reacting **1·2PF$_6$** with **2** in the presence of three molar equivalents of bisparaphenylene-34-crown-10 **3** (Scheme 1).[1, 2] The non-

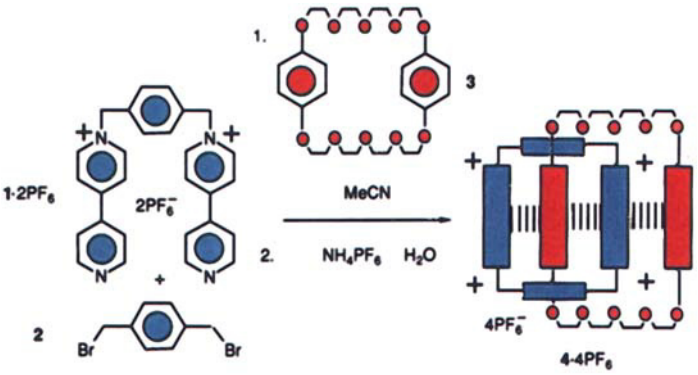

Scheme 1. The template-directed synthesis of the [2]catenane **4** [1, 2]. The chemical cartoons are defined in this scheme: *para*-phenylene rings ≡ small blue rectangles, bipyridinium units ≡ large blue rectangles, hydroquinone rings ≡ red rectangles.

covalent bonding interactions, which facilitate the highly efficient ring closure of the tetracationic cyclophane around the neutral macrocyclic polyether ring, 'live on' in both the solid- and solution-state structures of **4**. Molecular modeling indicates that, simply by replacing the phenylene rings in the tetracationic cyclophane by biphenylene units, it might be possible to thread two crown ether rings simultaneously through the interior portion of this 'expanded' tetracationic cyclophane.[3] Furthermore, and rather surprisingly, despite the requirement for the close approach of like entities, this objective has been achieved.

Here, we present results describing: (i) how the [3]catenanes[4] **8·4PF$_6$** and **9·4PF$_6$** can be prepared and isolated (Scheme 2) from MeCN solutions containing **3** and 1,5-dinaphtho-38-crown-10 **7** respectively in several-fold molar excesses whilst reacting **5·2PF$_6$** with almost equimolar amounts of **6** at room temperature; (ii) the FABMS of **8·4PF$_6$** and **9·4PF$_6$**; (iii) the X-ray crystal structure of **8·4PF$_6$**; (iv) the

[*] Dr. J. F. Stoddart,[+] P. R. Ashton, C. L. Brown, Dr. N. Spencer
Department of Chemistry, The University
Sheffield S3 7HF (UK)
Dr. E. J. T. Chrystal, Dr. K. P. Parry
Jealott's Hill Research Station, ICI Agrochemicals
Bracknell, Berkshire RG12 6EY (UK)
T. T. Goodnow, Prof. A. E. Kaifer
Department of Chemistry
University of Miami, Coral Gables, FL 33124 (USA)
A. M. Z. Slawin, Dr. D. J. Williams
Chemical Crystallography Laboratory
Department of Chemistry, Imperial College
London SW7 2AY (UK)
[+] Present address:
School of Chemistry, University of Birmingham
Edgbaston, Birmingham B15 2TT (UK)

[**] This work was supported by ICI Agrochemicals, the Agricultural and Food, and Science and Engineering Research Councils in the United Kingdom, and by the University of Miami in the United States.

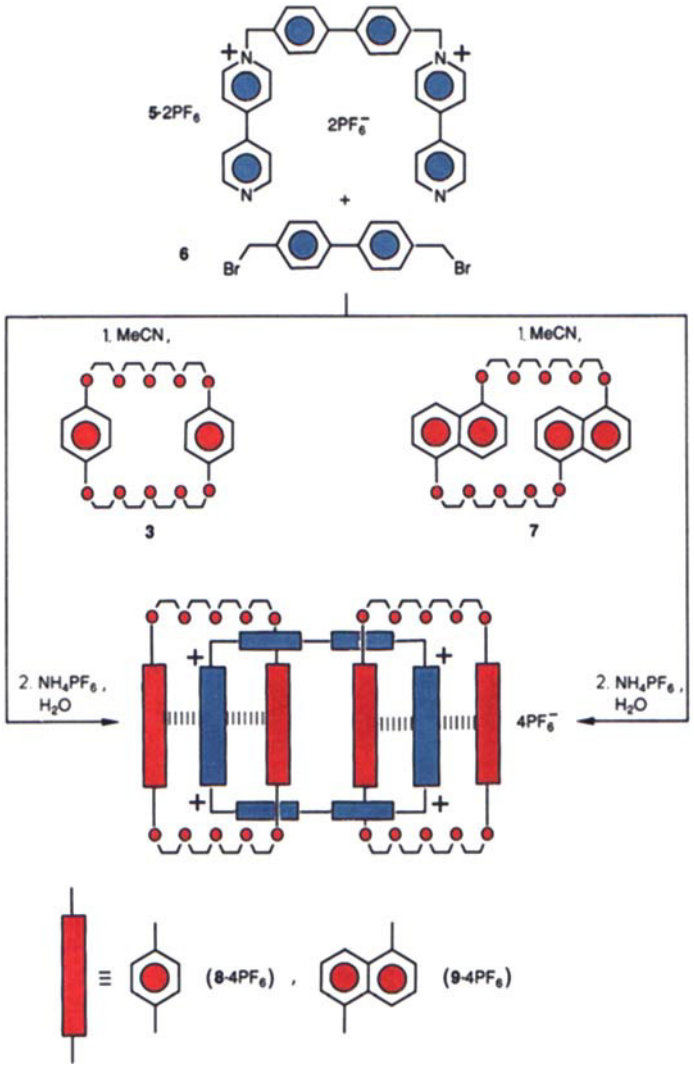

Scheme 2. The template-directed syntheses of the [3]catenanes **8** and **9**.

dynamic ^{1}H-NMR spectroscopic behavior of both **8**·4PF$_6$ and **9**·4PF$_6$; and (v) the electrochemical properties of **8**·4PF$_6$.

The [3]catenanes **8**·4PF$_6$ and **9**·4PF$_6$ were prepared[5] according to Scheme 2 in 20 and 31% yields, respectively. Positive-ion FABMS of **8**·4PF$_6$ and **9**·4PF$_6$ revealed[6] peaks respectively at m/z = 2183, 2038, and 1893, and m/z = 2381, 2236, and 2091 for loss, in each case, of one, two, and three $PF_6^{\ominus}$ counterions. Fragmentation peaks were also observed with the analogous counterion losses at m/z = 1647, 1502, and 1357, and m/z = 1745, 1600, and 1455 for the corresponding [2]catenanes, resulting from loss of a molecule of **3** and **7**, respectively from **8**·4PF$_6$ and **9**·4PF$_6$, respectively. In the former instance, the formation of a [3]catenane was confirmed by obtaining good quality single crystals which were subjected to X-ray crystallographic analysis.[7, 8] The solid-state structure (Fig. 1) of **8**·4PF$_6$ shows that the increase in the lengths of the neutral aromatic spacer groups (phenylene in the case of **1**, biphenylene in the case of **5**) between the two bipyridinium rings in the tetracationic cyclophane did not result in self-filling of the macrocycle. In accordance with the design strategy, the dimensions[9] of the macrocycle permit the simultaneous threading through its center of two molecules of **3** centrosymmetrically disposed with respect to each other. In addition to the sandwiching[10] of a bipyridinium group between approximately parallelly-aligned hydroquinone residues within each molecule of **3**, the inner pair of

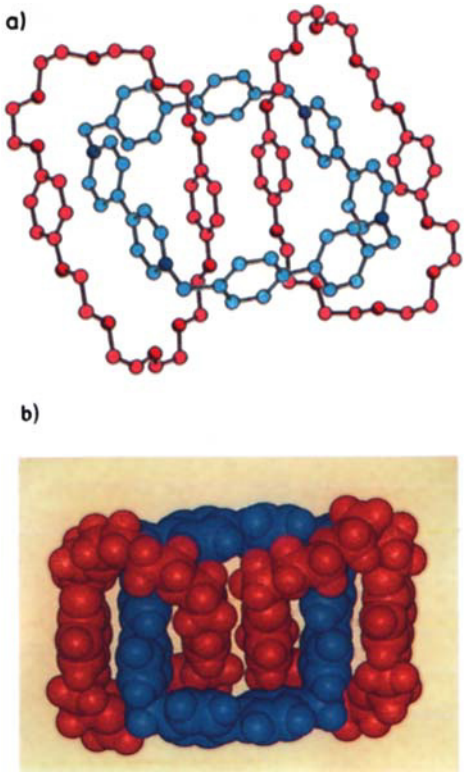

Fig. 1. a) Structure of **8** in the crystal with the donor and acceptor macrocycles shaded red and blue, respectively. O atoms are dark red and N atoms are dark blue. b) A computer-generated space-filling representation of the [3]catenane **8** based on the X-ray crystal structure data. The two polyether molecules are red and the tetracationic cyclophane unit is blue.

hydroquinone residues are positioned in a stacking arrangement (Fig. 2) with their mean planes only 3.63 Å apart. Each of these central hydroquinone units is displaced towards and inclined normal to one of the two phenylene rings within each biphenylene unit providing additional electrostatic edge-to-face stabilization.[10] An interesting feature of this ordering within the molecule is a loss of the alternating pattern

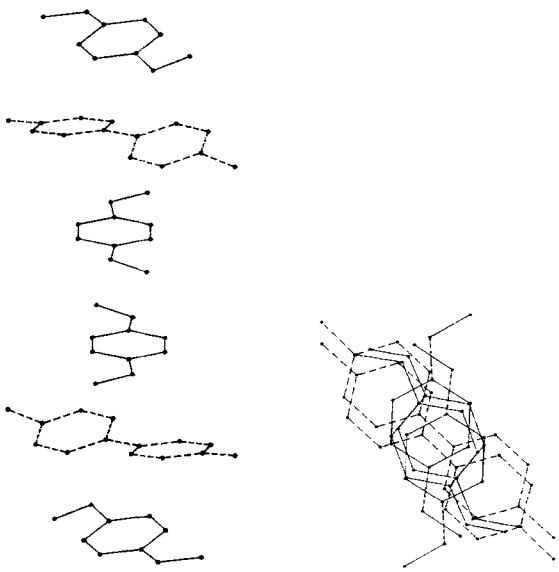

Fig. 2. The stacking arrangement of the 'inside' (green) and 'alongside' (red) donor hydroquinone rings in the solid-state structure of **8** with respect to the acceptor bipyridinium units (blue).

 © VCH Verlagsgesellschaft mbH, W-6940 Weinheim, 1991 0570-0833/91/0808-1040 $ 3.50+.25/0

of π-donors (D) and π-acceptors (A) that was observed[1, 2] in the case of the [2]catenane **4**·4PF$_6$. More suprisingly, however, this DADDAD sequence extends (Fig. 3) beyond the molecule throughout the crystal producing a continuously stacked array.[11]

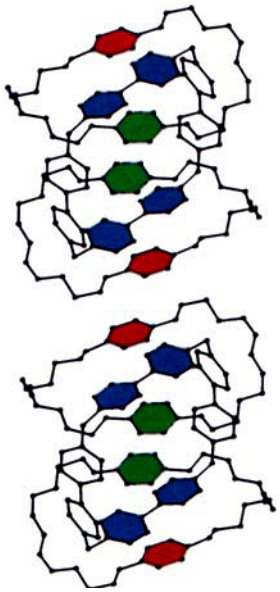

Fig. 3. Part of the continuous sequence of [3]catenanes **8** in the crystal. Donors are red or green and acceptors are blue.

As in the case of the [2]catenane **4**·4PF$_6$[1], both [3]catenanes **8**·4PF$_6$ and **9**·4PF$_6$ exhibit temperature dependencies in their ^{1}H-NMR spectra[12] recorded in CD_3COCD_3:CD_3CN (70:30) solutions. The averaged processes associated with the exchanges of the π-electron-rich *para*-phenylene and 1,5-naphtho units in **8** and **9** respectively, between 'inside' and 'alongside' environments with respect to the tetracationic cyclophane, have been probed by dynamic ^{1}H-NMR spectroscopy (Table 1). The $\Delta\Delta G_c^{\neq}$ of 2.6 kcal mol^{-1} between

Table 1. The parameters obtained from temperature dependent ^{1}H-NMR spectra recorded at 400 MHz in CD_3COCD_3:CD_3CN (70:30) for the [3]catenanes **8**·4PF$_6$ and **9**·4PF$_6$

[3]-Catenane	$\Delta\nu$ [Hz]	T_c [°C]	k_c [a] [s^{-1}]	$\Delta G_c^{\neq}$ [kcal mol^{-1}]
8·4PF$_6$	748 [b]	−25	1660	10.7
9·4PF$_6$	320 [c]	+20	710	13.3

[a] Values for k_c were obtained (I. O. Sutherland, *Annu. Rep. NMR Spectrosc. 4* (1971) 81) using the approximate expression $k_c = \pi(\Delta\nu)/(2)^{1/2}$, and the Eyring equation was then used to calculate $\Delta G_c^{\neq}$ at the coalescence temperature T_c. [b] $\Delta\nu$ value obtained from the limiting chemical shifts of $\delta = 4.32$ and $\delta = 6.19$ recorded at −70 °C, for the 'inside' and 'alongside' *para*-phenylene units, respectively, in **8**·4PF$_6$. [c] $\Delta\nu$ value obtained from the limiting chemical shifts of $\delta = 5.50$ and $\delta = 6.30$ recorded at −60 °C for the H2,H6 protons on the naphthalene units 'inside' and 'alongside', respectively, in **9**·4PF$_6$.

the $\Delta G_c^{\neq}$ values of 10.7 kcal mol^{-1} [13] for **8**·4PF$_6$ and 13.3 kcal mol^{-1} for **9**·4 PF$_6$[13] is a measure of just how much more demanding sterically and electronically it is for a pair of molecules of **7** than it is for a pair of molecules of **3** to revolve simultaneously around the tetracationic cyclophane. The observation of this process, irrespective of its precise mechanism, is a clear demonstration of the order which characterizes both **8**·4PF$_6$ and **9**·4PF$_6$ in the solution states.

Cyclic voltammetry[14] reveals the presence of only two redox couples at −455 and −879 mV vs SSCE for **8**·4PF$_6$, and at −559 and −898 mV vs SSCE for **9**·4PF$_6$. All of these redox couples correspond to reversible two-electron reduction processes, confirming the expected topological equivalence of the two bipyridinium units in both [3]catenanes. The aromatic π-electron donor moieties in **8** and **9** insulate and stabilize substantially the bipyridinium units, making their reduction more difficult. The values for the first reduction step are not dissimilar from those previously assigned[1, 15] to the 'inside' bipyridinium units of the [2]catenane **4**·4PF$_6$ and its analogue incorporating **7**.

The fact that **8**·4PF$_6$ and **9**·4PF$_6$ can be prepared (Scheme 2) with such relative ease is all the more remarkable when it is recognized that all attempts to obtain the tetracationic cyclophane, present in both **8** and **9**, as its tetrakis(hexafluorophosphate), have so far[16] been unsuccessful. *It is easier to construct the molecular assemblies than it is to create one of their components by itself. The message is a simple but exciting one—the prospects for self-assembly, as a synthetic paradigm, are extremely encouraging.*[17]

Experimental

8·4PF$_6$: **6** (208 mg, 0.6 mmol) was added as a solid during ca. 15 min to **5**·2PF$_6$ (400 mg, 0.5 mmol) and **3** (800 mg, 1.5 mmol) dissolved in dry MeCN (30 mL). The reaction mixture, which was stirred under nitrogen, turned deep red within 2 h and a red precipitate formed within 12 h. After continued stirring at room temperature for a further 9 days, the solvent was removed in vacuo to leave a bright red solid, which was extracted into $MeNO_2$. After filtration, an aqueous solution of NH_4PF_6 was added to the red solution until no further precipitation occurred. The precipitate was filtered off and extracted with $CHCl_3/MeNO_2$. Polymeric impurities were removed by filtration and the solvent was evaporated off to give a residue which crystallized from $MeNO_2$/EtOAc. The red product was collected by filtration, washed with H_2O, MeOH, and Et_2O, and then dried to give **8**·4PF$_6$ (240 mg, 20%) as a bright red solid, m.p. > 280 °C. Single crystals, suitable for X-ray crystallography, were grown by vapor diffusion of iPr_2O into a solution of **8**·4PF$_6$ in MeCN.

9·4PF$_6$: **4** (60 mg, 0.17 mmol), **5**·2PF$_6$ (122 mg, 0.15 mmol), and **7** (200 mg, 0.3 mmol) were dissolved in dry MeCN (5 mL)/$CHCl_3$ (1 mL) and the solution was stirred at room temperature for 60 h. The solvents were removed in vacuo to afford a bright purple solid, which was subjected to chromatography [SiO_2:MeOH/2 M $NH_4Cl/MeNO_2$ (7:2:1)]. A saturated aqueous NH_4PF_6 solution was added to the fraction of the eluant containing the crude product and the solvents were evaporated off. The solid residue was dissolved in $MeNO_2$ which was washed with H_2O to remove residual inorganic materials. Evaporation of the solvent gave a purple solid which was filtered as a slurry in H_2O, washed with MeOH and Et_2O, and then dried to give **9**·4PF$_6$ (100 mg, 31%), m.p. > 280 °C.

Received: February 5, 1991 [Z 4425 IE]
German Version: *Angew. Chem. 103* (1991) 1055

CAS Registry numbers:
5·2 PF$_6$, 134815-78-4; **6**, 20248-86-6; **8**·4 PF$_6$, 134815-81-9; **9**·4 PF$_6$, 134815-82-0.

[1] P. R. Ashton, T. T. Goodnow, A. E. Kaifer, M. V. Reddington, A. M. Z. Slawin, N. Spencer, J. F. Stoddart, C. Vicent, D. J. Williams, *Angew. Chem. 101* (1989) 1404; *Angew. Chem. Int. Ed. Engl. 28* (1989) 1396; P. R. Ashton, C. L. Brown, E. J. T. Chrystal, T. T. Goodnow, A. E. Kaifer, K. P. Parry, A. M. Z. Slawin, N. Spencer, J. F. Stoddart, D. J. Williams, *J. Chem. Soc. Chem. Commun. 1991*, 634; C. L. Brown, D. Philp, J. F. Stoddart, *Synlett 1991*, 459.

[2] P. L. Anelli, P. R. Ashton, R. Ballardini, V. Balzani, M. Delgado, M. T. Gandolfi, T. T. Goodnow, A. E. Kaifer, D. Philp, M. Pietraszkiewicz, L. Prodi, M. V. Reddington, A. M. Z. Slawin, N. Spencer, J. F. Stoddart, C. Vicent, D. J. Williams, *J. Am. Chem. Soc.*, in press.

[3] By employing a similar method to that described in the literature for the preparation of **1**·2PF$_6$ (W. Geuder, S. Hünig, A. Suchy, *Angew. Chem. 95* (1983) 501; *Angew. Chem. Int. Ed. Engl. 22* (1983) 489; *Tetrahedron 42* (1986) 1665), the dication **5**·2PF$_6$, m.p. 151–154 °C, was prepared in 37% yield by reaction of 4,4'-dibromomethylbiphenyl with an 8-fold molar excess of bipyridine in MeCN under reflux.

[4] [3]Catenanes have been obtained previously by multistep directed syntheses (G. Schill, C. Zürcher, *Angew. Chem. 81* (1969) 996; *Angew. Chem. Int. Ed. Engl. 8* (1969) 988; G. Schill, K. Murjahn, W. Vetter, *Justus Liebigs Ann. Chem. 740* (1970) 18; G. Schill, K. Rissler, H. Fritz, W. Vetter, *Angew. Chem. 93* (1981) 197; *Angew. Chem. Int. Ed. Eng. 20* (1981) 187; K. Rissler, G. Schill, H. Fritz, W. Vetter, *Chem. Ber. 119* (1986) 1374) and also, following demetalation, from Cu^{I}-templated syntheses of [3]catenates (J.-P. Sauvage, J. Weiss, *J. Am. Chem. Soc. 107* (1985) 6108; C. O. Dietrich-Buchecker, A. Khemiss, J.-P. Sauvage, *J. Chem. Soc. Chem. Commun. 1986*, 1376; C. O. Dietrich-Buchecker, J. Guilheim, A. K. Khemiss, J.-P. Kintzinger, C. Pascard, J.-P. Sauvage, *Angew. Chem. 99* (1987) 711; *Angew. Chem. Int. Ed. Engl. 26* (1987) 661; J. Guilheim, C. Pascard, J.-P. Sauvage, J. Weiss, *J. Am. Chem. Soc. 110* (1988) 8711); C. O. Dietrich-Buchecker, C. Hemmert, A. Khemiss, J.-P. Sauvage, *ibid. 112* (1990) 8002.

[5] The formation of **8**·4PF_6 and **9**·4PF_6 is quite remarkable given the fact that there is no evidence for complexation in MeCN between **5**·2PF_6 and either **3** or **7**. The mechanism of the reaction shown in Scheme 2—and indeed for the reaction shown in Scheme 1—is open to speculation at this stage. is conceivable that the dication **5**·2PF_6 reacts initially with two molar equivalents of 4,4′-dibromomethylbiphenyl to give an acyclic tetracation which then complexes with two molar equivalents of **3** or **7** before undergoing disproportionation with more of the dication **5**·2PF_6 rapidly and without the competitive unthreading of the macrocyclic polyether rings.

[6] FABMS was carried out on a Kratos MS80RF mass spectrometer (accelerating voltage, 3 kV; resolution, 1500) coupled to a DS 90 data system. The atom gun was an adapted saddle field source (Ion Tech Ltd) operated at ca. 7 keV and a tube current of ca. 2 mA. Xenon was used to provide a primary beam of atoms and the samples of **8**·4PF_6 and **9**·4PF_6 were dissolved in a small volume of 3-nitrobenzyl alcohol which had previously been coated onto a stainless steel probe tip. Spectra were recorded in the positive-ion mode at a scan speed of 30 s per decade.

[7] Crystal data for **8**·4PF_6:X (X represents unidentified partial occupancy solvent fragments): triclinic, $a = 13.462(3)$, $b = 15.002(4)$, $c = 16.180(4)$ Å, $\alpha = 72.40(2)$, $\beta = 83.46(2)$, $\gamma = 73.67(2)°$, $V = 2988$ Å^3, space group $P\bar{1}$, $Z = 1$ (the molecule is disposed about a center of symmetry) $\rho = 1.36$ g cm^{-3}, 3126 independent observed reflections with $[|F_o| > 3\sigma(|F_o|)$, $2\theta \leq 100°]$ refined to a current $R = 0.130$, $R_w = 0.143$.

[8] Nicolet R3m diffractometer, ω-scans, $Cu_{K\alpha}$ radiation (graphite monochromator). The structure was solved by direct methods and refined anisotropically. Further details of the crystal structure investigation can be obtained from the Cambridge Crystallographic Data Centre, University Chemical Laboratory, Lensfield Road, Cambridge CB2 1EW (England). Any request should be accompanied by the full literature citation of this communication.

[9] The tetracationic macrocycle adopts a rigid square box-like conformation with (i) an 18° twist angle between the two pyridinium rings of each bipyridinium unit and (ii) a 29° twist angle between the two phenylene rings of each biphenylene unit. The strain in the molecule is relieved by out-of-plane bending of the eight aromatic rings. Although the strain is distributed throughout the macrocycle, the maximum deviations are associated with the exocyclic N–CH_2 and C–CH_2 bonds emanating from the bipyridinium and biphenylene units respectively. In turn, these bonds subtend angles of 17° and 25° with respect to each other in the two different units. Distortions of this magnitude and more have been observed in the smaller tetracationic macrocycle (B. Odell, M. V. Reddington, A. M. Z. Slawin, N. Spencer, J. F. Stoddart, D. J. Williams, *Angew. Chem. 100* (1988) 1605; *Angew. Chem. Int. Ed. Engl. 27* (1988) 1547; P. R. Ashton, B. Odell, M. V. Reddington, A. M. Z. Slawin, J. F. Stoddart, D. J. Williams, *ibid. 100* (1988) 1608 and *27* (1988) 1550) present in the [2]catenane **4**·4PF_6 as well as in extremely strained macrocyclic biaryls (H. M. Colquhoun, C. C. Dudman, M. Thomas, C. A. O'Mahoney, D. J. Williams, *J. Chem. Soc. Chem. Commun. 1990*, 336) wherein the normally colinear C–CH_2 bonds emanating from the *para* positions subtend an angle of 65°!

[10] The mean planes (Fig. 2) of the inside (green) and alongside (red) hydroquinone rings are stacked 3.56 and 3.32 Å, respectively, from the mean plane of the bipyridinium ring system. There are also edge-to-face interactions (S. K. Burley, G. A. Petsko, *Science (Washington DC) 229* (1985) 23; *J. Am. Chem. Soc. 108* (1986) 7995; *FEBS Lett. 203* (1986) 139; *Adv. Protein Chem. 39* (1988) 125) between the inside (green) hydroquinone rings and the phenylene rings on the biphenylene units. The centroid-centroid distances for these T-type interactions are 5.03 and 5.93 Å, respectively, with the hydroquinone ring orthogonal to the nearer phenylene ring. For recent discussions on the nature of π-π interactions between aromatic molecules, see W. L. Jorgensen, D. L. Severance, *J. Am. Chem. Soc. 112* (1990) 4768 and C. A. Hunter, J. K. M. Sanders, *ibid. 112* (1990) 5525.

[11] The mean plane distance between 'alongside' (red) hydroquinone rings in neighboring [3]catenane molecules is 3.66 Å. It should be noted that all the O–CH_2 bonds are approximately planar (A. Makriyannis, S. Fesik, *J. Am. Chem. Soc. 104* (1982) 6462; L. I. Kruse, J. K. Cha, *J. Chem. Soc. Chem. Commun. 1982*, 1329; J. D. Mersh, J. K. M. Sanders, S. A. Matlin, *ibid. 1983*, 306) with respect to their hydroquinone rings, adopting, in relation to each other, *anti* geometries in the 'alongside' (red) hydroquinone rings and *syn* geometries in the 'inside' (green) hydroquinone rings.

[12] ^{1}H NMR for **8**·4PF_6 (400 MHz in CD_3COCD_3:CD_3CN, 70:30): at −70 °C, $\delta = 2.56$ (brs, 8H, CH_2O α to 'inside' OC_6H_4O), 3.41 (bs, 16H, β CH_2O), 3.61 (s, 8H, CH_2O α to 'alongside' OC_6H_4O), 3.77 (brs, 32H, γ and δ CH_2O), 4.32 (brs, 8H, 'inside' OC_6H_4O), 5.86 (s, 8H, $CH_2N^{\oplus}$), 6.19 (brs, 8H, 'alongside' OC_6H_4O), 7.79 (s, 16H, biphenylene-H), 7.84 (d, 8H, *m*-bpy-H), 9.09 (d, 8H, *o*-bpy-H) and at ambient temperature, $\delta = 3.13$ (brs, 16H, α-CH_2O), 3.60 (m, 16H, β-CH_2O), 3.81 (m, 16H, γ-CH_2O), 3.85 (m, 16H, δ-CH_2O), 5.25 (brs, 16H, OC_6H_4O), 5.88 (s, 8H, $CH_2N^{\oplus}$), 7.70–7.80 (m, 16H, biphenylene-H), 7.85 (d, 8H, *m*-bpy-H), 9.12 (d, 8H, *o*-bpy-H). ^{1}H NMR for **9**·4PF_6 (400 MHz in CD_3COCD_3:CD_3CN, 70:30) at −60 °C, $\delta = 3.49$–4.15 (m, 64H, α-CH_2O, β-CH_2O, γ-CH_2O, and δ-CH_2O), 3.72 (d, 4H, 'inside' H4,H8), 5.24 (t, 4H, 'inside' H3,H7), 5.50 (d, 'inside' H2,H6), 5.74 (d, 4H, $CH_2N^{\oplus}$), 6.02 (d, 4H, $CH_2N^{\oplus}$), 6.30 (d, 4H, 'alongside' H2,H6), 6.69 (d, 4H, *m*-bpy-H), 6.91 (d, 4H, *m*-bpy-H), 6.93 (t, 4H, 'alongside' H3,H7), 7.02 (d, 4H, 'alongside' H4,H8), 7.89 (d, 8H, α-biphenylene-H), 7.92–8.21 (m, 8H, β-biphenylene-H), 8.54 (d, 4H, *o*-bpy-H), 8.88 (d, 4H, *o*-bpy-H), and (400 MHz in CD_3CN) at + 60 °C, $\delta = 3.60$–3.95 (m, 64H, α-CH_2O, β-CH_2O, γ-CH_2O, and δ-CH_2O), 5.84 (brs, 8H, $CH_2N^{\oplus}$), 5.84 (brs, 8H, H2,H6), 6.12 (brm, 8H, H3,H7), 6.37 (d, 8H, *m*-bpy-H), 7.83 (d, 8H, α-biphenylene-H), 7.96 (d, 8H, β-biphenylene-H), 8.48 (brs, 8H, *o*-bpy-H). The signal for H4,H8 (8H) is too broad to be visible and merges into the baseline, presumably in the range $\delta = 5.50$–7.02.

[13] These $\Delta G_c^{\neq}$ values can be compared with those of 15.6 and 17.2 kcal mol^{-1}, both in CD_3CN, for the free energies of activation for the passage of **3** and **7**, respectively, through the smaller tetractionic macrocycle present in **4**·4PF_6 and in the analogous [2]catenane where naphtho units replace *para*-phenylene units. Clearly, it is easier for the two polyether rings to revolve simultaneously through the larger tetracationic macrocycle than it is for them to pass singly through the smaller one.

[14] Electrochemical experiments were performed with a Princeton Applied Research Model 175 universal programmer, a Model 173 potentiostat, and a Model 179 digital coulometer equipped with positive feedback circuitry for IR compensation. Voltammograms were recorded on a Soltec VP-6423S X-Y recorder. A glassy carbon disk electrode (0.080 cm^2), Pt flag, and sodium chloride saturated calomel (SSCE) were used as the working, auxiliary, and reference electrodes, respectively. All solutions for the voltammetric experiments were deoxygenated by sparging with nitrogen gas; a nitrogen atmosphere was maintained above the solution during the experiments.

[15] The *second* redox potential, measured for **4**·4PF_6 and its dinaphtho analogue, are − 438 and − 572 mV, respectively.

[16] So far, all attempts to prepare the large tetracationic macrocycle by template-directed methods, using, for example, bisparaphenylene-22-crown-6 as the template, have been unsuccessful.

[17] For examples of self-assembly in operation in chemical systems, see P. L. Anelli, P. R. Ashton, N. Spencer, A. M. Z. Slawin, J. F. Stoddart, D. J. Williams, *Angew. Chem. 103* (1991) 1052; *Angew. Chem. Int. Ed. Engl. 30* (1991) 1036, and references cited therein.

Molecular Trains: The Self-Assembly and Dynamic Properties of Two New Catenanes**

Peter R. Ashton, Christopher L. Brown, Ewan J. T. Chrystal, Keith P. Parry, Marek Pietraszkiewicz, Neil Spencer, and *J. Fraser Stoddart**

When the cyclobis(paraquat-*p*-phenylene) and cyclobis(paraquat-4,4′-biphenylene) tetracationic macrocycles were formed in the presence of an excess of bisparaphenylene-34-crown-10, a [2]catenane[1] and a [3]catenane[2] re-

[*] Dr. J. F. Stoddart,[+] P. R. Ashton, C. L. Brown, Dr. N. Spencer
Department of Chemistry
Sheffield S3 7HF (UK)

Dr. E. J. T. Chrystal, Dr. K. P. Parry
Jealott's Hill Research Station, ICI Agrochemicals
Bracknell, Berkshire RG12 6EY (UK)

Dr. M. Pietraszkiewicz
Institute of Physical Chemistry, Polish Academy of Sciences
01-224 Warsaw, Kasprzaka 44/52 (Poland)

[+] Present address:
School of Chemistry, University of Birmingham
Edgbaston, Birmingham B15 2TT (UK)

[**] This work was supported by the University of Sheffield, ICI Agrochemicals, and the Agricultural and Food, and Science and Engineering Research Councils in the United Kingdom, and the National Economic Development Organization in Japan.

spectively were obtained in good yields, i.e. increasing the size of the tetracationic macrocycle allowed[2] a [3]catenane to be made to order. With a view to extending the self-assembly protocol to the synthesis of [n]catenanes, we now decided to explore the consequences of increasing the size of the polyether macrocycle by a factor of two.

Here, we report: (i) the high-dilution, cesium-ion promoted,[3] phase transfer catalyzed[4] synthesis of tetrakisparaphenylene-68-crown-20 **3** in excellent yield[5] from its immediate precursors, the diphenol **1** and the ditosylate **2**; (ii) the preparation and isolation of the [2]catenane **6**·4PF_6 from a DMF solution containing **3**, whilst reacting **4**·2PF_6[6] with almost equimolar amounts of **5** at room temperature; (iii) the characterization of this new [2]catenane by FABMS,[7]; (iv) how, according to the temperature dependence of the ^{1}H-NMR spectra,[8] the cyclophane molecules appear to be behaving like a 'molecular train'.[9] We then demonstrate that a [3]catenane **7**·8PF_6 can be obtained when **3**, **4**·2PF_6 and **5** are allowed to react at 10 kbar. Finally, dynamic ^{1}H-NMR spectroscopy[10] shows how two 'molecular trains' in **7**·8PF_6 manage to travel together round the "circle line" formed by **3**.

We decided that the key to further progress in self-assembling catenanes was identifying an efficient synthesis[5] of **3** from readily-available starting materials, e.g. **1** and **2**. This objective was achieved by employing a unique combination of (i) a high-dilution reaction in DMF at high temperature (110 °C) using (ii) the "cesium effect"[3] (Cs_2CO_3/CsOTs) and (iii) phase-transfer catalysis[4] (Bu_4NI) in order to synthesize **3** in 62% yield[5] from **1** and **2** (Scheme 1). Although all our attempts to prepare catenanes incorporating **3** and the cyclobis(paraquat-4,4′-biphenylene) tetracation have been unsuccessful so far, reaction of **4**·2PF_6 in DMF at room temperature for 96 h with 1.1 molar equivalents of **5** in the presence of 0.7 molar equivalents of **3** led to a product (Scheme 1), which, after chromatographic purification and conversion to the tetrakis(hexafluorophosphate), was identified as the [2]catenane **6**·4PF_6. Positive-ion FABMS reveals peaks at m/z = 2028, 1884, and 1739 corresponding to the loss of one, two, and three $PF_6^{\ominus}$ counterions, respectively, from **6**·4PF_6.

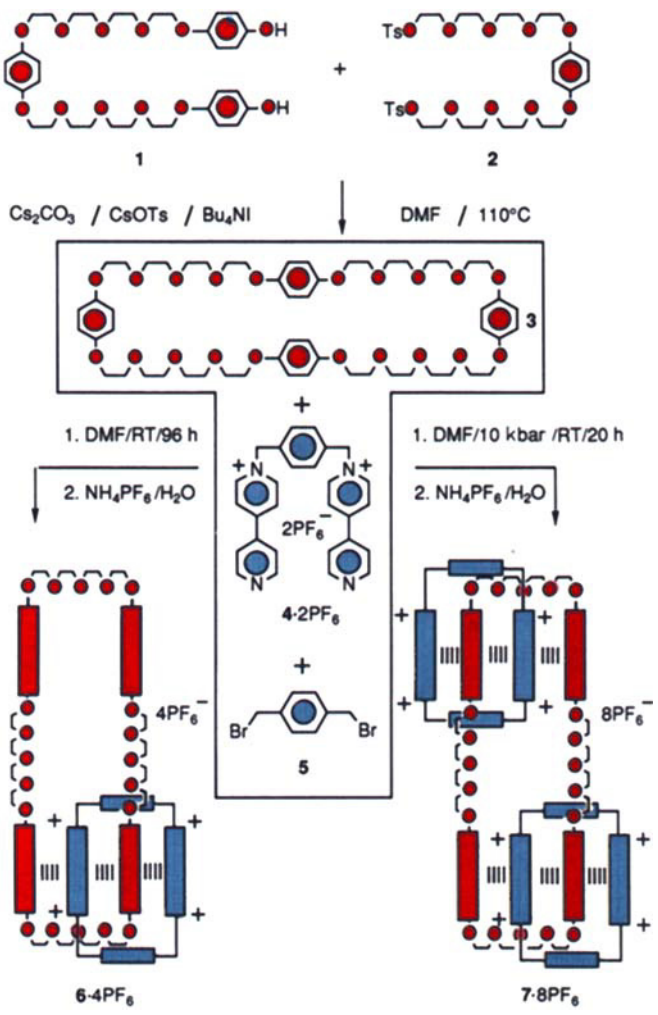

Scheme 1. The cesium template-directed synthesis of **3** from diphenol **1** and ditosylate **2** and the subsequent template-directed syntheses of the [2]catenane **6**·4PF_6 and the [3]catenane **7**·8PF_6 from **3**, **4**·2PF_6, and **5**. In the catenanes, **3** and the tetracationic cyclophane formed from **3** and **4** are represented by chemical cartoons: Hydroquinone rings ≡ red rectangles, *p*-phenylene rings ≡ small blue rectangles, bipyridinium units ≡ large blue rectangles, RT = room temperature.

The temperature dependence of the ^{1}H-NMR spectrum of the [2]catenane **6**·4PF_6, recorded in CD_3COCD_3,[8] reveals the presence of two different processes occurring simultaneously within the molecule (Table 1): (i) the macrocycle **3** (red) pirouettes about the OC_6H_4O axis of the "occupied" hydroquinone ring in the [2]catenane exchanging the 'inside' and 'alongside' bipyridinium rings of the tetracationic cyclophane (blue) while (ii) the tetracationic cyclophane moves along the polyether chains from one hydroquinone ring to the other around **3**. The first process, which is associated with a free energy barrier of 9.5 kcal mol^{-1}, is evident at −72 °C from the line broadening (60 Hz) experienced by the signal for the protons α to the nitrogen atoms on the bipyridinium rings in the tetracationic cyclophane (Table 1). Even-

Table 1. Kinetic and thermodynamic parameters [a] obtained from the temperature dependent ^{1}H-NMR spectra recorded at 400 MHz on the [2] catenane **6**·4PF_6 and on the [3]catenane **7**·8PF_6

Probe protons undergoing site exchange	$\Delta\nu$ [Hz]	k [s^{-1}]	T [°C]	ΔG^* [kcal mol^{-1}]
OC_6H_4O in **6**·4PF_6 [b]	32 [d]	101	13.5	14.1
o-bpy in **6**·4PF_6	60 [d]	189	−72	9.5
OC_6H_4O in **7**·8PF_6 [b] [c]	20 [e]	63	0	13.6

[a] Values of k were obtained by the exchange method (J. Sandström: *Dynamic NMR Spectroscopy*, Academic Press, London, 1982, Chapter 6) using the approximate expression $k = \pi(\delta\nu)$. The Eyring equation was used to calculate ΔG^* values at the coalescence temperature T. [b] The probe protons referred to are in the 'occupied' hydroquinone rings (black in Schemes 2 and 3–5). [c] The low-temperature behavior of **7**·8PF_6 is under investigation. However, we anticipate that it will be associated with a ΔG^* value of < 10 kcal mol^{-1}. [d] Recorded in a CD_3COCD_3 solution. [e] Recorded in a CD_3CN solution.

tually, below −80 °C, this signal separates into two signals arising from the 'inside' and 'alongside' bipyridinium units. Long before these low temperatures are reached (e.g. at −60 °C), the second process (Scheme 2) is 'frozen out' on the ^{1}H-NMR time scale in the form of (i) a high field singlet (4H) at ca. δ = 3.70, identified by a saturation transfer experiment, for the black hydroquinone ring 'station' at which the blue 'train' has 'stopped', (ii) an A_2B_2 system (8H) with δ = 6.25 and 6.36 for the hydroquinone rings (green) of the 'adjacent stations', and (iii) a low field singlet (4H) at δ = 6.91 for the hydroquinone ring (red) at the 'opposite station' across the **3** 'track' from the blue 'train'. By +13.5 °C, the signal for this red hydroquinone ring has broadened to 32 Hz, reflecting (Table 1) a free energy barrier of 14.1 kcal mol^{-1} resisting the 'running' of the blue 'train'

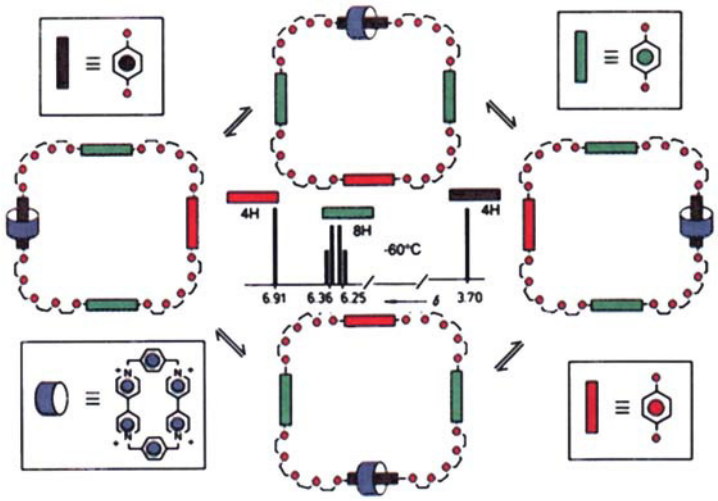

Scheme 2. The degenerate process, which involves movement of the blue tetracationic cyclophane from hydroquinone ring to hydroquinone ring around the red macrocycle **3** in the [2]catenane **6**·4PF$_6$. Bound hydroquinone rings are black. Unbound hydroquinone rings are green or red depending on whether they are, respectively, adjacent to or opposite the bound hydroquinone unit. The ^{1}H-NMR spectrum of the hydroquinone rings **6**·4PF$_6$ at $-60\,^\circ$C is represented by a stick diagram in the middle of the array of the scheme.

between stations. When the solvent is changed to CD_3CN and the temperature is raised to $+80\,^\circ$C, the hydroquinone rings at the black, green, and red 'stations' are averaged out on the ^{1}H-NMR time scale such that their protons resonate as a broad multiplet between $\delta = 5.76$ and 6.30. The blue 'molecular train' is now travelling round the red 'circle line' 14 thousand times a second while it rolls over on itself 9 million times a second!

During the preparation and isolation of the [2]catenane **6**·4PF$_6$, it was suspected that another product—namely the related [3]catenane in which **3** is encircled by two macrocyclic cyclobis(paraquat-*p*-phenylene) tetracations—might be a very minor product of the reaction. Recalling that the Menshutkin reaction[10] is promoted by ultra-high pressures,[11] we conducted the reaction of **4**·2PF$_6$ in DMF with **5** in the presence of approximately a sixth of a molar equivalent of **3** at room temperature under a pressure of 10 kbar for 20 h (Scheme 1). After treatment of the crude product with a saturated aqueous solution of NH_4PF_6 and fractional crystallization of the crude product from $MeNO_2/CHCl_3$ at $-18\,^\circ$C, the [3]catenane **7**·8PF$_6$ was identified by positive-ion FABMS, which revealed peaks at m/z = 3129, 2984, 2839, 2694, and 2549 corresponding to the loss of one, two, three, four, and five $PF_6^\ominus$ counterions, respectively, from **7**·8PF$_6$. Additional peaks at m/z = 2028 and 1884 which correspond (see above) to the loss of one and two $PF_6^\ominus$ counterions, respectively, from **6**·4PF$_6$, indicate that the [3]catenane fragments in the mass spectrometer to give the [2]catenane.

The temperature dependence of the ^{1}H-NMR spectrum[12] of the [3]catenane **7**·8PF$_6$, recorded in CD_3CN, reveals the presence of exchange processes analogous to those observed for the [2]catenane **6**·4PF$_6$. Although the low-temperature process, which occurs below $-40\,^\circ$C, is still under active investigation, a higher temperature one, which is associated with a free energy barrier of 13.6 kcal mol^{-1} (Table 1), relates to a site exchange process between diametrically opposite 'occupied stations', indicated by black hydroquinone rings (ca. $\delta = 3.39$, identified by a saturation transfer experiment at $-40\,^\circ$C), encircled by the blue tetracationic cyclophane and the diametrically opposite 'unoccupied stations', indicated by green hydroquinone rings ($\delta = 6.10$ at

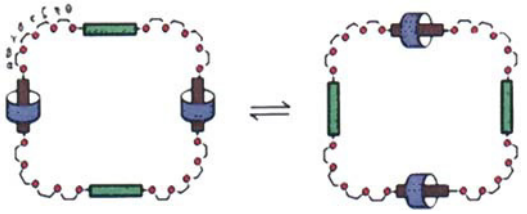

Scheme 3. The degenerate process that involves the simultaneous movement of the blue tetracationic cyclophane from one pair of diametrically opposed hydroquinone rings to the other pair of diametrically opposed hydroquinone rings. Bound hydroquinone rings are black, free hydroquinone rings are green.

$-40\,^\circ$C) (Scheme 3). Only one translational[13] isomer—the one shown in Scheme 3—is evident from an inspection of the ^{1}H-NMR spectrum at $-40\,^\circ$C, i.e. the two 'molecular trains' prefer to keep a free station between them in both directions as they do 'the loop'. Crashes do not happen!

It is really remarkable that such a highly positively-charged [3]catenane as **7**$^{8\oplus}$ can be self-assembled in a controlled, and stepwise manner starting from the 'red' macrocyclic polyether **3** and the components necessary to make the 'blue' tetracationic cyclophane via the intermediacy of the [2]catenane **6**$^{4\oplus}$. Encouragingly, dynamic ^{1}H-NMR spectroscopy reveals how, in both **6**$^{4\oplus}$ and **7**$^{8\oplus}$, the order that is associated with their template-directed syntheses 'lives on' in the highly ordered structural behavior they exhibit in solution.

Both the [2]catenane **6**$^{4\oplus}$ and the [3]catenane **7**$^{8\oplus}$ are reminiscent of 'trains' doing 'the loop' on a 'circle line'. One of the many challenges which remain is to show how a 'molecular train' can be driven in a highly controlled manner employing the appropriate signalling devices!

In particular, template-directed syntheses relying on (i) the "cesium effect" for the efficient production of a large neutral macrocycle and subsequently (ii) part, and then all, of this macrocycle acting as a template for the formation of one, and then two, linked tetracationic cyclophanes is a demonstration[14] of *how molecular recognition begets molecular recognition*. In practical terms, *this progressively cumulative aspect of self-assembly in synthesis is an appealing one.*

Experimental

1: Diphenol **1** was obtained in four steps starting from the commercially-available compounds, 4-benzyloxyphenol and 1,4-bis-(2-hydroxyethoxy)benzene. Alkylation (Bu_4NI, KOH, EtOH, 60°C, 15 h) of the former with 2-[2-(2-chloroethoxy)ethoxy]ethanol, followed by tosylation (TsCl, C_5H_5N) afforded the monotosylate, 1-benzyloxy-4-[2-[2-(2-hydroxyethoxy)ethoxy]ethoxy]benzene-4′-methylbenzene sulfonate, which was used to dialkylate (NaH, DMF) the latter. Catalytic hydrogenolysis (H_2, Pd/C, EtOH) of the dibenzyl ether, obtained from the dialkylation, gave **1** in 31% yield; m.p. 60–62°C; m/z (positive-ion FABMS) = 646 and 669 for $M^\oplus$ and $[M + Na]^\oplus$, respectively; δ_H (CD_3COCD_3) = 3.58–3.65 (m, 16H), 3.73–3.78 (m, 8H), 3.98–4.05 (m, 8H), 6.71–6.79 (m, 8H), 6.84 (s, 4H), 7.88 (s, 2H).

2: Hydroquinone was dialkylated (Bu_4NI, KOH, EtOH, 80°C, 20 h) with 2-[2-[2-(2-(chloroethoxy)ethoxy]ethoxy]ethanol to give a diol (73%), which on tosylation (TsCl, C_5H_5N) afforded the ditosylate **2** in 93% yield; oil; m/z (positive-ion FABMS) = 770 and 793 for $M^\oplus$ and $[M + Na]^\oplus$, respectively; δ_H (CD_3COCD_3) = 2.43 (s, 6H), 3.47–3.52 (m, 8H), 3.52–3.58 (m, 4H), 3.58–3.68 (m, 8H), 3.74–3.78 (m, 4H), 4.01–4.05 (m, 4H), 4.12–4.16 (m, 4H), 6.85 (s, 4H), 7.44–7.49 (m, 4H), 7.78–7.81 (m, 4H).

3: The diphenol **1** (323 mg, 0.5 mmol) and the ditosylate (385 mg, 0.5 mmol) were dissolved in DMF (20 mL) and the solution of these reactants in equimolar proportions was added dropwise during 3 h to a mixture of Cs_2CO_3 (1.63 g, 5 mmol), CsOTs (304 mg, 1 mmol), Bu_4NI (10 mg) in DMF (50 mL) which was heated to 110°C and stirred vigorously. Heating and stirring of the reaction mixture was continued for ca. 12 h. On cooling, the solution was filtered off, the residue was washed with $CHCl_3$, and the organic solvents were evaporated off under vacuum to give a residue which was partitioned between $CHCl_3$ (70 mL) and H_2O (5 mL). The $CHCl_3$ solution was concentrated to afford a crude

product which was subjected to chromatography [SiO_2: 3% MeOH in $CHCl_3$] to affort **3** (333 mg, 62%); m.p. 96–98 °C; *m/z* (positive-ion FABMS) = 1072 and 1095 for $M^{\oplus}$ and $[M + Na]^{\oplus}$ respectively; δ_H ($CDCl_3$) = 3.66–3.69 (m, 16H), 3.69–3.73 (m, 16H), 3.80–3.83 (m, 16H), 4.03–4.06 (m, 16H), 6.81 (s, 16H).

6·4PF_6: **5** (290 mg, 1.1 mmol), **4**·2PF_6 (772 mg, 1.0 mmol), and **3** (750 mg, 0.7 mmol) were dissolved in anhydrous DMF (40 mL) and the solution was stirred at room temperature for 96 h. The reaction mixture was added to a saturated aqueous solution of NH_4PF_6 and the temperature was raised to 90 °C, whereupon a highly colored precipitate formed. It was filtered off and washed successively with H_2O, MeOH, $CHCl_3$, and Et_2O. This solid residue was dissolved in $MeNO_2$ and polymeric material was removed by careful precipitation with $CHCl_3$. After further filtration, removal of the solvent from the filtrate by evaporation under reduced pressure furnished a red solid which was subjected to chromatography [SiO_2:MeOH/2M NH_4Cl/$MeNO_2$ (7:2:1)]. When the fractions containing the red product were mixed with a saturated aqueous solution of NH_4PF_6, the product precipitated out as an amorphous solid which was filtered, washed successively with H_2O, MeOH, and Et_2O, and then dried under vacuum to afford the pure [2]catenane **6**·4PF_6 (200 mg, 12%), as a red compound, m.p. > 280 °C. So far, all attempts to obtain single crystals suitable for X-ray crystallography have been unsuccessful.

7·8PF_6: **5** (180 mg, 0.68 mmol), **4**·2PF_6 (390 mg, 0.55 mmol) and **3** (100 mg, 0.09 mmol) were dissolved in dry DMF (10 mL) and the solution was subjected to ultra-high pressure (10 kbar) for 20 h at room temperature. The reaction was worked up as described above for **6**·4PF_6 prior to the point of chromatography to produce a mixture of this [2]catenane, along with the [3]catenane **7**·8PF_6 (34 mg, 11%), which was obtained by fractional crystallization following addition of $CHCl_3$ to a $MeNO_2$ solution and cooling it down to −18 °C before filtering off the dark red crystals, m.p. > 280 °C. Single crystals were obtained from vapor diffusion of BME (butyl methyl ether) into a MeCN solution (1 ml) of **7**·8PF_6 (5 mg). However, they suffer from severe crazing and rapid decomposition on removal from solution. Repeated attempts [15] with encapsulated small crystals have produced only barely discernible diffraction patterns in very long exposure photographs. These results indicate that the structure is either disordered or suffers from very high thermal vibrations. The photographic data obtained to date have not even been of adequate quality to discern either the unit cell or the space group. Further studies with better quality crystals, which are proving difficult to grow, are needed in order to solve this structural problem.

Received: February 5, 1991 [Z 4426 IE]
German Version: *Angew. Chem. 103* (1991) 1058

[1] P. R. Ashton, T. T. Goodnow, A. E. Kaifer, M. V. Reddington, A. M. Z. Slawin, N. Spencer, J. F. Stoddart, C. Vicent, D. J. Williams, *Angew. Chem. 101* (1989), 1404; *Angew. Chem. Int. Ed. Engl. 28* (1989) 1396; P. R. Ashton, C. L. Brown, E. J. T. Chrystal, T. T. Goodnow, A. E. Kaifer, K. P. Parry, D. Philp, A. M. Z. Slawin, N. Spencer, J. F. Stoddart, D. J. Williams, *J. Chem. Soc. Chem. Commun. 1991*, 634; C. L. Brown, D. Philp, J. F. Stoddart, *Synlett 1991* 459; P. L. Anelli, P. R. Ashton, R. Ballardini, V. Balzani, M. Delgado, M. T. Gandolfi, T. T. Goodnow, A. E. Kaifer, D. Philp, M. Pietraszkiewicz, L. Prodi, M. V. Reddington, A. M. Z. Slawin, N. Spencer, C. Vicent, D. J. Williams, *J. Am. Chem. Soc.*, in press.

[2] P. R. Ashton, C. L. Brown, E. J. T. Chrystal, T. T. Goodnow, A. E. Kaifer, K. P. Parry, A. M. Z. Slawin, N. Spencer, J. F. Stoddart, D. J. Williams, *Angew. Chem. 103* (1991) 1055; *Angew. Chem. Int. Ed. Engl. 30* (1991) 1039.

[3] It is well known that cesium salts (e.g. Cs_2CO_3 and CsOTs) of weak acids—particularly when they are dissolved in a dipolar aprotic solvent like DMF—exhibit some quite remarkable reactivity characteristics that render them extremely useful for synthetic purposes. Besides relating to the enhanced alkylation of nucleophiles, the "cesium effect", as it has been dubbed, refers to the rather spectacular observation that intermolecular substitutions are generally suppressed relative to intramolecular ones. For an assessment of the causes of the "cesium effect", see G. Dijkstra, W. H. Kruizinga, R. M. Kellogg, *J. Org. Chem. 52* (1987) 4230. For a recent critique on the 'cesium effect' see C. Galli, L. Mandolini, *J. Org. Chem. 56* (1991) 3045.

[4] It has been found (M. Pietraszkiewicz, unpublished results) that the alkylations of phenols with halogeno compounds, including chlorohydrins are accelerated significantly by the addition of phase-transfer catalysts, such as Bu_4NI, in basic media. The base-promoted dialkylation of diphenol **1** with ditosylate **2** is probably also subject to the same kind of phase-transfer catalysis.

[5] In the absence of the added cesium salts, the yield of **3** upon reaction of diphenol **1** with ditosylate **3** was very low indeed (< 5%). Other synthetic strategies were no more practical when they were put to the test. For example, after 1,11-bis[4-[2-(2-hydroxyethoxy)ethoxy]phenoxy]-3,6,9-trioxaundecane (3.1 g, 5.6 mmol) had been heated in THF (290 mL) under reflux in the presence of NaH (0.45 g, 18.7 mmol) for 7 days (N_2 atmosphere) with its derived ditosylate (5.0 g, 5.8 mmol) and the crude product was subjected to chromatography (SiO_2:MeOH/$CHCl_3$/Et_2O, 2/28/70), only 150 mg (2.5%) of **3** was isolated as a crystalline product, m.p. 96–98 °C.

[6] W. Geuder, S. Hünig, A. Suchy, *Angew. Chem. 95* (1983) 501; *Angew. Chem. Int. Ed. Engl. 22* (1983) 489; *Tetrahedron 42* (1986) 1665.

[7] FABMS was carried out on a Kratos MS80RF mass spectrometer (accelerating voltage, 3 kV; resolution, 1500) coupled to a DS90 data system. The atom gun was an adapted saddle field source (Ion Tech Ltd) operated at ca. 7 keV and a tube current of ca. 2 mA. Xenon was used to provide a primary beam of atoms and the samples of **6**·4PF_6 were dissolved in a small volume of 3-nitrobenzyl alcohol which had previously been coated on to a stainless steel probe tip. Spectra were recorded in the positive ion mode at a scan speed of 30 s per decade.

[8] ^{1}H NMR for **6**·4PF_6 (400 MHz): at −60 °C in CD_3COCD_3, δ = 3.29–4.15 (64H, m, OCH_2), 3.70 (4H, br s, 'occupied' OC_6H_4O), 5.97 (8H, br s, $CH_2N^{\oplus}$), 6.25 and 6.36 (2 × 4H, 2 × d, 'adjacent unoccupied' OC_6H_4O), 6.91 (4H, s, 'opposite unoccupied' OC_6H_4O), 8.00 (8H, bs, C_6H_4), 8.13 (8H, bd, *m*-bpy-H), 9.27 (8H, br d *o*-bpy-H), 9.27 (8H, br d *o*-bpy-H) and at +80 °C in CD_3CN, δ = 3.70–3.87 (64H, m, OCH_2), 5.72 (8H, s, $CH_2N^{\oplus}$), 5.76–6.30 (16H, br m, 'occupied' and 'unoccupied' OC_6H_4O), 7.74 (8H, d, *m*-bpy-H), 7.78 (8H, s, C_6H_4), 8.89 (8H, d, *o*-bpy-H).

[9] A [2]rotaxane composed of (i) a polyether chain intercepted by two hydroquinone rings and terminated by large triisopropylsilyl end groups and (ii) an encircling cyclobis(paraquat-*p*-phenylene) tetracationic macrocycle has been shown recently to behave like a molecular shuttle (P. L. Anelli, N. Spencer, J. F. Stoddart, *J. Am. Chem. Soc.*, in press).

[10] J. Jurczak, R. Ostaszewski, M. Pietraszkiewicz, P. Salanski, *J. Incl. Phenom. 5* (1987), 553.

[11] For a review of the use of ultra-high pressures in chemical synthesis, see N. S. Isaacs, A. V. George, *Chem. Brit. 23* (1987), 47.

[12] ^{1}H NMR for **7**·8PF_6 (400 MHz in CD_3CN): at −40 °C, δ = 3.30–3.35 (8H, m, α-OCH_2), 3.39 (8H, br s, 'occupied' OC_6H_4O), 3.46–3.52 (8H, m, θ-OCH_2), 3.54–3.60 (8H, m, β-OCH_2), 3.65–3.72 (8H, m, γ-OCH_2), 3.75–3.80 (8H, m, η-OCH_2), 3.80–3.83 (8H, m, δ-OCH_2), 3.83–3.90 (16H, br s, ε- and ζ-OCH_2), 5.61 (16H, br s, $CH_2N^{\oplus}$), 6.10 (8H, s, 'unoccupied' OC_6H_4O), 7.59 (16H, d, *m*-bpy-H), 7.70 (16H, s, C_6H_4), 8.80 (16H, d, *o*-bpy-H) and at +80 °C, δ = 3.66–3.70, 3.73–3.77, 3.80–3.84, 3.84–3.88 (4 × 16H, m, OCH_2), 5.05 (16H, br s, 'occupied' and 'unoccupied' OC_6H_4O), 5.71 (16H, s, $CH_2N^{\oplus}$), 7.78 (16H, d, *m*-bpy-H), 7.79 (16H, s, C_6H_4), 8.89 (16H, d, *o*-bpy-H).

[13] For a definition of translational isomerism, see G. Schill, K. Rissler, H. Fritz, W. Vetter, *Angew. Chem. 93* (1981) 197; *Angew. Chem. Int. Ed. Engl. 20* (1981) 187; G. Schill, N. Schweickert, H. Fritz, W. Vetter, *ibid. 95* (1983) 909 and *22* (1983) 889. We thank a referee for drawing our attention to the existence of this term. It is probable that the inversion process between the two degenerate species shown in Scheme 3 involves the intermediacy of the translational isomer where the blue tetracationic cyclophane occupies adjacent 'stations'. However, its concentration is clearly insufficient for it to be detected by ^{1}H-NMR spectroscopy.

[14] For a brief discussion of this concept, see J. F. Stoddart in C. Brown (Ed): *Chirality in Drug Design and Synthesis*, Academic Press, London, 1990, pp. 53–81.

[15] A. M. Z. Slawin, D. J. Williams, unpublished results.

Book Reviews are written by invitation from the editor. Suggestions for books to be reviewed and for book reviewers are welcome. Publishers should send brochures or (better) books to the following address: Redaktion Angewandte Chemie, Postfach 101161, D-6940 Weinheim, Federal Republic of Germany. The editor reserves the right of selecting which books will be reviewed. Uninvited books not chosen for review will not be returned.

Faszination Chemie. 7000 Jahre Kulturgeschichte der Stoffe und Prozesse. By *O. Krätz*. Callwey, Munich 1990. 331 pp., hardcover DM 148.00.—ISBN 3-7667-0984-4

When a book begins with a dedication "to the memory of Don Domenico Emanuele Cajetano, Count Ruggiero, Prince of Salerno... whose association with the mighty of this world, was to me, despite his sad end, a shining, though unfortunately never attainable, example. And remains such. Wherever the hangman at Küstrin in 1709 may have thrown his poor raven-gnawed remains, may God make the earth light for him!" you know that you are going to face neither a boring chemical text nor a pretentious art critical analysis.

Indeed, this dedication is an indicator of the wonderful style of the author of this book, *Otto Krätz*. In full command of the history of our science, he brings chemistry to life because it is a living enterprise to him. So within the book you will not only read *Cajetano Ruggiero*'s story, but also be faced with the wall paintings, on religious and alchemical themes, with which this alchemist, master of deceit and the politics of his time, decorated a cell in which he was once imprisoned. And you will see reproduced a broadside announcing *Ruggiero*'s demise.

To *Krätz* the history of chemistry is one with its present. He tells the story of the transformers of matter with style and wit—with an understated humor I will dare call British. And with a fantastic hoard of illustrations, drawn often from artifacts or books at the Deutsches Museum, where he has long worked (and obviously had fun...).

Espęcially strong is the extended discussion of alchemy, long a problem for chemists who would like to take the protochemistry, smile at the deceit, and forget the philosophy that powered this world view. *Krätz* does alchemy justice. He also has a wonderful, informed discussion of early synthetic materials. Here and nowhere else, you can learn about "Walosin", a synthetic fishbone for corsets, and the remarkably beautiful plastics from milk products. Hundreds of illustrations, some in the text, but most gathered in a section occupying over half the volume, grace this book.

My only disappointment is that Dr. *Krätz*'s story of our science by and large ignores the spiritual essence of the past century of chemistry. This is the molecule. It is true the external world still sees substances, too many of them, and their transformations. But in the mind of the chemist, even the most applied one, today roams freely the image, replete with distances, angles, bonds and functional groups, of the molecule. He or she, that imagined chemist, knows and thinks of matter transforming molecularly on the microscopic scale. The author of this book shows us *van't Hoff*'s models and a perfunctory α-helix. But nothing more of the way a chemist views the world today. It's a missed opportunity.

But this is a minor complaint about a truly beautiful book. It should be read by all, given as a prize to outstanding high school students the world over. It would make a lovely present by a chemist to her husband's non-chemist parents. "Faszination Chemie" makes wonderful episodic reading. With *Otto Krätz* as a witty, informed guide we see chemistry as an integral part of world culture, created by real people changing the stuff of this beautiful world.

Roald Hoffmann [NB 1176 IE]
Department of Chemistry
Cornell University
Ithaca, NY (USA)

The Chemistry of Organophosphorus Compounds. Vol. 1: Primary, Secondary, and Tertiary Phosphines, Polyphosphines, and Heterocyclic Organophosphorus(III) Compounds. Edited by *F. R. Hartley* (Series: The Chemistry of Functional Groups, Series Editor: *S. Patai*). Wiley, Chichester 1990. XIV, 739 pp., hardcover £ 185.00.–ISBN 0-471-92607-8.

This first volume of a four-volume series on "The Chemistry of Organophosphorus Compounds" was published in 1990 as part of the renowned series "The Chemistry of Functional Groups", edited by *S. Patai*. Many years have passed since the last major handbooks on the organic chemistry of phosphorus were published and, therefore, a new comprehensive work in the area of organophosphorus chemistry is certainly welcome. The seven-volume handbook "Organic Phosphorus Compounds", edited by *G. M. Kosolapoff* and *L. Maier*, appeared in the 1970s, and even the phosphorus supplements of the Houben-Weyl series are almost ten years old.

Primary, secondary, and tertiary phosphanes, as well as heterocyclic phosphorus(III) compounds, are treated in this first volume. The second volume, planned for 1992, will cover phosphane oxides, sulfides, and selenides. Phosphonium salts, ylides, and phosphoranes are the subject of the third volume, and phosphonous, phosphinous, phosphinic, and phosphonic acids, as well as their halogen derivatives, will be dealt with in the fourth and last volume.

It is difficult to judge the overall handbook just on the basis of the first volume, although certain tendencies are apparent and are bound to characterize the entire handbook. The first volume begins with an introductory chapter written by the editor, *F. R. Hartley*. The following chapters cover organophosphorus(III) compounds in terms of such general topics as structure and bonding, electrochemistry, free radical reactions, and thermochemistry (including here not only organophosphorus compounds). Phosphane complexes of transition metals and the biochemistry of phosphanes are also considered. These chapters, as well as those treating particular classes of compounds, are written by experts in the field.

The chapters are, in part, very detailed, clearly written, and well organized. Coverage of the literature is extensive but not exhaustive; even the recent literature is taken into account. Several chapters are almost monographs and are well suited to give an overview of a particular area.

 © VCH Verlagsgesellschaft mbH, W-6940 Weinheim, 1991 0570-0833/91/0808-1046 $ 3.50+.25/0

Noticeable in the first volume is the absence of several classes of compounds containing by phosphorus–carbon bonds: for example, P(III)–halogen compounds such as halophosphanes, R_nPX_{3-n} (R = alkyl, aryl, etc.; X = halogen; n = 1,2). These and related classes of compounds will presumably be covered in the last volume of the series. Whereas phosphaalkynes are discussed in detail in the first volume, no mention is made of phosphaalkenes or systems with P=P bonds. Furthermore, the subjects covered in Volume 1 and, eventually, in Volume 4 are closely related, although this is not stated explicitly. Perhaps Volume 4 should have been planned to directly follow the first volume.

This volume lacks a chapter on the NMR investigations of organophosphorus compounds, especially by ^{31}P NMR spectroscopy. However, several books that treat this subject have been published recently. On the other hand, the ESR spectra of free radicals derived from phosphanes are covered.

The author index is comprehensive, but the subject index leaves much to be desired. To locate specific information, therefore, a certain level of expertise is required. There are no serious typographical errors, apart from the apparently unavoidable misspellings of names.

The first volume of this series appears to have achieved its purpose, even though it is impossible to pass judgment on the entire series. Rapid publication of Volumes 2–4 is highly desirable, since the complete handbook promises to be very useful to phosphorus chemists. Although the very high price will limit wide availability of this first organophosphorus volume of the Patai series, no large chemistry library should be without it.

Reinhard Schmutzler [NB 1162 IE]
Institut für Anorganische und Analytische Chemie
der Technischen Universität Braunschweig (FRG)

Multiple Bonds and Low Coordination in Phosphorus Chemistry. Edited by *M. Regitz* and *O. J. Scherer*. Thieme, Stuttgart 1990. xviii, 478 pp., hardcover DM 468.00.—ISBN 3-13-752201-3

This volume entitled "Multiple Bonds and Low Coordination in Phosphorus Chemistry", edited by *M. Regitz* and *O. Scherer*, features numerous articles on a variety of topics which are comprehended by the title. The vast scope and interest of this fascinating field is emphasized by the large number of chapters (25) and the list of distinguished contributors. This research area, which originated in a number of laboratories in the 1960s, is a relatively young one. As the editors point out in their introduction, "hardly any other field of phosphorus chemistry has undergone such a brisk development in such a short time".

The opening chapter by the editors provides a brief overview of most, if not all, of the significant developments in the field. This is followed by an excellent chapter on "Bonding Properties of Low-Coordinated Phosphorus Compounds" by *W. Schoeller*. It begins by highlighting the reasons for the differences between the lighter main group elements and their heavier congeners. Many of the concepts discussed here should eventually be included in undergraduate inorganic textbooks. They will, one hopes, replace the often unsatisfactory "explanations" of such differences that are in current use. The emphasis is, of course, on phosphorus but the chapter should be of general interest to many chemists from a wide variety of areas. There is also much useful factual information on structures, bond strengths, molecular energy levels and computational work concerning phosphorus compounds.

The bulk of the remaining chapters are classified (not always accurately) according to whether the phosphorus coordination number is 1, 2 or 3.

Three chapters concern phosphorus coordination number 1. The first, dealing with phosphinidenes, is further divided into two parts which cover in situ generated phosphinidenes (by *F. Mathey*) and binuclear or bridging phosphinidenes (by *G. Huttner* and *H. Lang*). Owing to the extreme reactivity of the R-$\ddot{P}$: fragment, none of the stable compounds in this chapter involve singly coordinated phosphorus. The phosphinidenes are detected either spectroscopically or by trapping with transition metal–ligand fragments or organic and related substrates.

The second in the series of chapters on one-coordinate phosphorus (by *M. Regitz* and *P. Binger*) deals with the phosphaalkynes (P≡C-R). These are the phosphorus analogues of nitriles, and the existence of such species has been recognized for over 40 years. It was, however, the seminal discovery (by *Becker* in 1981) of a facile route to kinetically stabilized examples that has virtually created this field of investigation. The explosive growth in this area may be gauged from the fact that within 8 years (up to mid-1989) of the initial report about 200 papers have appeared on this subject. This chapter gives a comprehensive and well organized account of these developments.

The final chapter on one-coordinate phosphorus compounds (by *O. Scherer*) is concerned primarily with bonding and ligand properties of phosphorus units such as P≡N, P≡P and P_x. The two former units have no existence as stable separate entities under ambient conditions, although a related ionic species $[P{\equiv}N\text{-}R]^{\oplus}[AlCl_4]^{\ominus}$ has been structurally characterized recently. The vast majority of the work in this area has concerned P_x species as ligands in transition metal complexes. In almost all of these complexes the phosphorus is at least two- or even three-coordinate, so that the inclusion of these compounds in this particular section is somewhat surprising.

The second major part of this volume concerns phosphorus with coordination number 2. This section is the largest part of the book and comprises eleven chapters. Even so, not all types of two-coordinate phosphorus compounds are dealt with here, and there is virtually no coverage of two-coordinate phosphorus anions such as $[PR_2]^{\ominus}$ or of two-coordinate radical species such as $[:\dot{P}R_2]$, some of which are stable at room temperature. The largest chapters in this section are those by *R. Appel* dealing with the phosphaalkenes, phosphacarbaoligoenes and phosphaallenes, and by *G. Märkl* dealing with compounds that have phosphorus as part of an aromatic six-membered ring. There is also a chapter (by *A. Schmidpeter*) that deals with the delocalized five-membered rings involving phosphorus and a variety of heteroatoms. Acyclic delocalized two-coordinate phosphorus systems are covered by chapters on phosphenium cations (by *M. Sanchez, M. R. Mazieres, L. Lamandé, R. Wolf*) and on 2-phosphaallylic cations (by *A. Schmidpeter*). The remaining chapters in this section are concerned with various classes of two-coordinate phosphorus compounds. Included here are the landmark diphosphenes (*M. Yoshifuji*), the iminophosphenes (*E. Niecke*) and phosphorus compounds with multiple bonds to boron, silicon, germanium and tin (*F. Bickelhaupt*). Included also is a treatment of multiple bonds between two phosphorus atoms with different oxidation states and the closely related phosphinylidenesulfuranes (by *A. Schmidpeter*). The section is concluded by a chapter by *L. D. Quin* and *J. Szewczyk* on the oxophosphanes and their sulfur and selenium analogues.

The third major section of the book deals with phosphorus compounds with coordination number 3. While this is not normally regarded as a low coordination number for phosphorus, the compounds covered by this section certainly are unusual. There are eight chapters here, all of which concern pentavalent phosphorus involved in multiple bonding to either C, N, P, O, S or Se. The first three (by *R. Appel, H. Heydt, E. Niecke* and *D. Gudat*) deal with phosphoranes which have at least two multiple bonds to carbon, nitrogen, or a combination of these with bonds to O, S or Se. A chapter (by *M. Yoshifuji*) is devoted to phosphoranes involving double bonds to phosphorus in combination with double bonds to carbon, nitrogen, oxygen, sulfur or selenium. In addition, an article by *M. Meisel* deals with dioxo- and dithioxophosphoranes and the elusive metaphosphate anion. The two remaining chapters in this section by *G. Bertrand* and by *J.-P. Majoral* are concerned with pentavalent phosphorus compounds with triple bonds to carbon or nitrogen. The final chapter in the book (by *K. Karaghiosoff*) is an extremely useful summary of ^{31}P NMR data for low-coordinate and multiply bonded phosphorus compounds.

In summary, this volume covers most of the exciting developments in this field over the last 25 years or so. The list of contributors includes many of the leading figures who made much of this chemistry possible. The literature is scanned up to mid-1989 which, of necessity, means that many of the chapters are already out of date owing to the extremely rapid pace of development in these areas. Many readers will probably be aware that much, if not quite all, of the material within its covers has been previously reviewed in the literature—in some cases more than once. The main advantage with the present volume is that it saves you the trouble of searching for these reviews in the literature. Some of the chapters also serve to update the small number of areas that have not been reviewed within the last five years or so. The book is beautifully produced and is amply illustrated throughout. The standard of writing is, on the whole, excellent and there are only a few obvious typographical errors. Unfortunately, this attention to detail and presentation also exacts a price which, at around $ 300, few individuals can afford. In these days of budget restrictions, even many libraries will be forced to look askance at such an expenditure for a single volume. Having said that, I can think of few books that more effectively summarize so many of the most exciting developments in phosphorus chemistry over the last 25 years.

Philip P. Power [NB 1158 IE]
Department of Chemistry
University of California
Davis, CA (USA)

Cathodoluminescence. Theory and Applications. By *L. Ozawa*. VCH Verlagsgesellschaft, Weinheim/VCH Publishers, New York/Kodansha, Tokyo 1990. x, 308 pp., hardcover DM 196.00.—ISBN 3-527-27982-2/0-89573-936-4/4-06-204033-6

Cathodoluminescence is the physical process which is used in TV screens and Braun tubes of scientific instruments such as oscilloscopes to generate pictures by means of an electron beam. The electrons are accelerated in vacuum by a voltage of several kV and directed onto a screen containing small crystals of a material which emits visible luminescence when it is hit by the electron beam. *Lyuji Ozawa*'s book gives an introduction to the physics of cathodoluminescence, and contains detailed information on a large number of important luminescent crystals and their fields of application. It consists of three main parts.

The first part, which consists of Chapters 1 to 5, describes the fundamental principles of the generation of light by irradiating energetic particles into suitable luminescent materials. These materials, which are called "phosphors", are usually insulating or semiconducting inorganic crystals doped with a small amount of ions of a transition element. The latter emit the luminescence and are therefore called "activators". After a short introduction in Chapter 1, the author describes in Chapters 2 and 3 the basic effects of the irradiating electrons on crystals and activator ions. The important process which distributes the energy in the surface layer of the crystal is the excitation of secondary electrons by inelastic scattering of an incoming high-energy primary electron. The majority of the secondary electrons have rather low energies of only a few electron volts, and they give rise to the luminescence of the dopant ions, mainly via electron–hole recombination. Several possible mechanisms of the excitation of the ions are discussed. Since the energy is transferred from a primary electron to the luminescent centers via secondary electrons or electron–hole pairs, the motion and energy conversion of charge carriers play an important role in phosphor crystals. These topics are addressed in Chapters 4 and 5. It is shown how the motion can be investigated by varying the concentration of the activator ions, and by irradiating pulsed electron beams of different pulse durations into the samples. As a result of such measurements, an explicit model of the cathodoluminescence is proposed for the system Y_2O_2S:Eu.

After these general considerations, the second part of the book (Chapters 6 and 7) provides more detailed information on the optimization of cathodoluminescence phosphors for applications in picture tubes. Chapter 6 addresses some basic physical variables which should or should not be optimized in phosphor materials. It is shown, for instance, that the presence of a charge transfer band between activator ions and host crystal is not important for obtaining an efficient cathodoluminescence phosphor. On the other hand, the choice of the optimum activator concentration plays a much larger role. On the one hand, it is desirable to achieve an efficient radiative recombination of electron–hole pairs, but on the other hand, self-concentration quenching effects should be avoided as far as possible. The optimum concentrations are usually below one mole per cent. Other variables that can be adjusted are the crystal size and crystal structure of the phosphor. In Chapter 7 the author discusses some methods and engineering tricks to obtain bright cathodoluminescence picture tubes. He shows, for instance, how microcrystals of appropriate shape and uniform size can be grown. He also describes the best methods of measuring cathodoluminescence intensities on phosphor screens.

In the third part, which comprises Chapters 8 to 10 and occupies almost half the book, the author lists special properties of a large number of phosphorescent materials. Since it contains many luminescence spectra and other technical details, it will be useful for engineers working in this field. Chapter 8 describes the properties of rare-earth-activated phosphors. Because the visible part of their luminescence spectra consists mainly of relatively few sharp lines, they can be used in color TV screens. A different class of phosphor materials are semiconductor crystals of compounds of elements of Groups II and VI, which are the subject of Chapter 9. Their most important representatives are ZnSe and ZnS. They are characterized by broader luminescence bands, so that they can be used in monochrome screens. By adding

small amounts of metallic activators such as copper or silver, it is possible to change their color. In Chapter 10 characteristic properties of ZnO are described. Here the author does not limit the discussion to cathodoluminescence properties, but also comments on applications of this material in other fields including electrophotography, varistors, piezoelectricity and gas sensors.

In summary, the book is very useful both for the scientist who wants to understand the physical principles of cathodoluminescence and for the engineer who has to select or manufacture the right material for specific applications. The book collects together the research results of several decades, and for further information a number of references are given at the end of each chapter. Its only minor shortcoming is the relatively large number of typographic errors.

Lothar Kador [NB 1154 IE]
Lehrstuhl für Experimentalphysik IV
der Universität Bayreuth (FRG)

Electroanalysis of Biologically Important Compounds. (Series: Analytical Chemistry). By *J. P. Hart*. Ellis Horwood, Chichester 1990. 213 pp., hardcover $ 72.50.—ISBN 0-13-252107-5

Electroanalysis has been found to be widely applicable to many problems of clinical and biological significance. The subject presented by *J. Hart* is thus certainly timely. The objective of this book is to demonstrate the suitability of modern electroanalytical techniques for measuring biologically important compounds. The focus is on controlled-potential techniques, primarily classical voltammetry and liquid chromatography with electrochemical detection (LCEC). New trends such as biosensors, micro and modified electrodes, are also covered but in a limited depth. Detailed theory is not given and the approach is primarily experimental. In particular, the (clearly written) text offers various strategies for the determination of certain groups of biological compounds. The book is full of practical examples, including numerous (very recent) references. The material is divided into five chapters. The first is devoted to the basic principles and instrumentation of finite-current controlled-potential techniques. Chapters 2 and 3 deal with the electroanalysis of purine and pyrimidine derivatives, amino acids and proteins. Electrochemical methods for the determination of vitamins and coenzymes are discussed in Chapters 4 and 5. Overall, this book will be a very useful reference source for those involved in bioelectroanalysis and LCEC. The practical approach makes the book particularly appealing to industrial users.

Joseph Wang [NB 1169 IE]
Department of Chemistry
New Mexico State University
Las Cruces, NM (USA)

Robert Robinson—Chemist Extraordinary. By *T. I. Williams*. Clarendon Press, Oxford 1990, viii, 201 pp., hardcover £ 25.00.—ISBN 0-19-858180-7

Some sixteen years have passed since the death of *Robert Robinson* and this book is the first and, as yet, the only biography of one of the greatest figures in the history of organic chemistry. A master of natural product chemistry and an outstanding contributor to our understanding of organic chemical reactions, he dominated chemistry in Britain for half a century and at the same time played a vital part in the development of its chemical industry. That the appearance of a biography should have been so long delayed may seem extraordinary and yet it is understandable. *Robinson* never kept any records, apart from reprints of his published work and, although he repeatedly said that he would record everything in a detailed "scientific autobiography", he did not in fact make any serious attempt to do so until about 1970, by which time he was almost completely blind and unable to properly undertake such a demanding task. He did, nevertheless, set about it with astonishing vigor and, with the help of a few devoted young assistants, collected a vast amount of material so that, by the time of his death in 1975, he had put together a draft manuscript recording his work and career up to 1930, when he went to Oxford as Waynflete Professor. This manuscript was published posthumously by Elsevier in 1976 as Volume I of the planned autobiography *Memoirs of a Minor Prophet*. This volume showed all too clearly the effects of *Robinson*'s age and disabilities: liberally sprinkled with typographical errors which should have been eliminated at the proof stage, it contains recollections of individuals cheek by jowl with large and highly technical discussions of chemical problems, the whole book giving the clear impression of an ill-constructed draft which, had he been alive, would have been completely rewritten by its author before publication. In addition to the material which was published, he left a mass of manuscripts designed to be incorporated in a second volume but these were so incomplete and so preliminary in character that they could not be published and so no Volume 2 ever appeared.

As a result, apart from obituary notices and the long tribute by *Lord Todd* and *J. W. Cornforth* in *Biographical Memoirs of Fellows of the Royal Society* (1976, pp. 415–527), the entry in the *Dictionary of National Biography 1971–80*, and the *Proceedings of a special meeting of the Historical Group of the Royal Society of Chemistry* (1987), there has been no overall portrayal of *Robinson*'s genius and personality until the publication in 1990 of *Robert Robinson—Chemist Extraordinary* by *Trevor I. Williams*.

Overall, the volume gives a valuable and very fair account of *Robert Robinson*—a complex character if ever there was one! Dr. *Williams* has clearly put a great deal of work into collecting and sifting material from both professional and family sources and has produced an informative and well-balanced account of the life and work of an extraordinarily complex yet extremely human scientist. This he has done without getting lost in technicalities in those sections dealing with scientific work; in particular, he has included a chapter on the famous *Robinson–Ingold* quarrel which, I feel, will give the nonspecialist reader a clearer picture of that affair than he is likely to find elsewhere.

It is perhaps only natural that, as one who was closely associated with *Robert Robinson* from the autumn of 1931, when I joined his research group in Oxford, until his death in 1975, I should feel that, admirably comprehensive though it is, this book does not convey fully the warmth of *Robinson* the man, and his great love of children with whom he was always immensely popular. I shall always remember one occasion when, in the Swiss Alps, he and my younger daughter (she aged about 10 and he about 70) scrambled joyfully together on a rocky mountain top in such a way that one might have wondered whether they were not both about the same age.

Robert was completely shattered by the sudden death of his wife *Gertrude* in 1954 after 42 years of happy married life. His loneliness was, however, relieved by his second marriage

(in 1957) to *Stearn Hillstrom*, an American lady whom he first met during a visit to America on behalf of Shell. In his book Dr. *Williams* gives a very good account of *Robinson*'s first meeting with *Stearn* and of the, sometimes stormy, course of the marriage—indeed, as far as I know, it is the only account of that final phase of *Robinson*'s life in existence; *Stearn* had no scientific knowledge or interest but she cared deeply for *Robert* and greatly eased his latter days. Dr. *Williams* records also *Robinson*'s contacts with *Robert Maxwell* but, perhaps unavoidably, he does not seem to me to put quite enough weight on the connection and the friendship between them which had a great influence on *Robinson* in the post-war period.

To summarize: this is a comprehensive, well-written biography of a great scientist, and it will be a standard work of reference for any student of the rise of organic chemistry in the twentieth century and the imprint of *Robert Robinson* upon it.

Lord Todd [NB 1156IE]
Christ's College
Cambridge (United Kingdom)

Gas Chromatography—A Practical Course. By *G. Schomburg*. VCH Verlagsgesellschaft, Weinheim/VCH Publishers, New York 1990. xiv, 320 pp., paperback DM 76.00.—ISBN 3-527-27879-6/0-89573-889-9

Despite the spectacular advances in liquid chromatography during the last two decades, gas chromatography has retained its place as an important analytical technique for relatively volatile organic compounds. The modern gas chromatograph is often microprocessor-controlled and presents an impressive exterior festooned with dials, buttons and input keys, suggesting that the foremost requirement for operation is a high degree of virtuosity on the computer keyboard. It nevertheless remains true that successful gas chromatography depends on an appreciation of the theoretical factors controlling resolution, detection and quantitation, and the practical skill to translate these factors into optimum performance.

Designed as a practical guide, this book gives a detailed overview of the equipment, terminology and mathematical parameters in current use in GC, whilst avoiding unnecessarily elaborate theoretical treatments of the derivation of equations and terms. After presenting the conceptual framework, the author provides a series of chapters covering the techniques of packed and capillary column GC with flame ionization, thermal conductivity and electron capture detection, and the interfacing of GC to mass spectrometry, FT-IR and HPLC. There is a strong emphasis on practical aspects such as column evaluation, use of reference samples and standards for quantitation and for establishing retention parameters such as Kovats indices, and the selection and optimization of conditions for isothermal and temperature programmed separations of complex mixtures. The design and construction of key components of the equipment, such as split and splitless injectors for capillary columns, is examined at some length so that the influence of these factors on performance can be fully appreciated and practical errors resulting from their misuse avoided. Many of the recent developments and special methods in GC are covered, providing practical guidance on dealing with samples of low volatility and high polarity, trace analysis, coupling of capillary columns to one another and to chemical reactors for on-line reduction, pyrolysis and post-column reaction. There is an extensive series of examples of GC separations, demonstrating each of the major themes discussed in the text. The many examples of applications to real problems cover a wide range of compound classes, isothermal and temperature programmed separations of complex mixtures using different phases and detectors, multidimensional techniques and enantiomeric resolutions on chiral columns.

It is surprising that, in a book intended as a guide for the laboratory worker, there is an absence of some useful practical information, such as tables giving recommendations for the selection of appropriate stationary phases for different classes of compounds, and experimental details of standard derivatization procedures such as methylation, silylation and perfluoroacylation. In spite of this deficiency and some weaknesses in the English, punctuation and indexing, this text is highly recommended as a useful guide for those about to embark on the practice of gas chromatography.

Stephen A. Matlin [NB 1152 IE]
Chemistry Department
Warwick University
Coventry (United Kingdom)

Registered names, trademarks, etc. used in this journal, even when not marked as such, are not to be considered unprotected by law.

© VCH Verlagsgesellschaft mbH, W-6940 Weinheim, 1991. – Printed in the Federal Republic of Germany by Konrad Triltsch Druck- und Verlagsanstalt Würzburg.

All rights reserved (including those of translation into foreign languages). No part of this issue may be reproduced in any form — by photoprint, microfilm, or any other means — nor transmitted or translated into a machine language without written permission from the publishers. Only single copies of contributions, or parts thereof, may be made for personal use. This journal was carefully produced in all its parts. Nevertheless, authors, editors and publisher do not warrant the information contained therein to be free of errors. Readers are advised to keep in mind that statements, data, illustrations, procedural details or other items may inadvertently be inaccurate.

Valid for users in the USA: The appearance of the code at the bottom of the first page of an article (serial) indicates the copyright owner's consent that copies of the article may be made for personal or internal use, or for the personal or internal use of specific clients. This consent is given on the condition, however, that the copier pay stated per-copy fee through the Copyright Clearance Center, Inc. (CCC), for copying beyond that permitted by Sections 107 or 108 of the U.S. Copyright Law. This consent does not extend to other kinds of copying, such as copying, for general distribution, for advertising or promotional purposes, for creating new collective works, or for resale. For copying from back volumes of this journal see 'Permissions to Photo-Copy: Publisher's Fee List' of the CCC.

Editorial office: Postfach 10 11 61, W-6490 Weinheim, Federal Republic of Germany, Telephone (06201) 60 23 15, Telex 465 516 vchwh d, Telefax (06201) 602 328, E-Mail Z16@DHDURZ2 in Earn Bitnet.

Editor: *Peter Gölitz*

Associate editors: *D. I. Loewus, K. J. Schneider, A. Stimson.* **Editorial assistant:** *E. Schweikart*

Publishers: VCH Verlagsgesellschaft mbH. (Managing Director: *Hans Dirk Köhler.*), Pappelallee 3, W-6940 Weinheim, Federal Republic of Germany.

Advertising office (Advertising Manager *R. J. Roth*): Postfach 10 11 61, W-6940 Weinheim, Federal Republic of Germany, Telephone (0 62 01) 60 61 36, Telex 4 67 155, Telefax (0 62 01) 606 156.

ANGEWANDTE CHEMIE
International Edition in English
Volume 30 · Number 9
September 1991
Pages 1051–1192

Lantibiotics—Ribosomally Synthesized Biologically Active Polypeptides containing Sulfide Bridges and α,β-Didehydroamino Acids**

By Günther Jung*

Lantibiotics are polycyclic peptide antibiotics containing intrachain sulfide bridges, formed from the thioether groups of the amino acids lanthionine and β-methyllanthionine. They also contain α,β-unsaturated amino acids such as didehydroalanine and didehydroaminobutyric acid. A knowledge of the lantibiotic biosynthetic steps and the enzymes involved makes possible a gene technological construction of analogous highly modified polypeptides. To the family of lantibiotics belong nisin, an important food preservative, epidermin, a highly specific therapeutic agent against acne, a series of enzyme inhibitors, as well as immunologically interesting active peptides. Lantibiotics are produced by ribosomal synthesis, starting from inactive precursor proteins (prelantibiotics). The latter are post-translationally converted into the active peptide antibiotics through enzymic modifications. The modifying enzymes effect dehydrations at the serine and threonine residues and stereospecific additions of the cysteine thiol groups to the resulting α,β-unsaturated double bonds, which lead to the formation of several sulfide bridges. Upon subsequent proteolytic cleavage of the leader peptide, the biologically active lantibiotic is formed. Conformational analyses of the lantibiotics, as well as of their prepeptides, enables one to obtain information about the mechanism and steps of the biosynthesis. Antibodies against synthetic prepeptide sequences, and modern instrumental methods for the analysis of peptides, allow structural elucidation of the biosynthetic intermediates.

1. Introduction

Heterodet polycyclic *antibiotics* which contain thioether amino acids such as *lan*thionine as well as α,β-unsaturated amino acids are called *lantibiotics*.[1] To this class of natural products belong nisin, used as a preservative in the food industry,[2, 3] epidermin, a therapeutic agent against acne,[4] many enzyme inhibitors and immunologically active peptides such as ancovenin,[5] Ro 09–0198,[6] duramycin,[7] and the antibiotics mersacidin[8a] and actagardine.[8b] Some lantibiotics such as Pep5[9, 10] induce a voltage-dependent ion current in the lipid bilayer membranes.[10c]

The results of the structural elucidation of several new lantibiotics indicate that the biosynthesis of lantibiotics, with different sequence and secondary structure, proceeds according to a common principle. This differs fundamentally from the usual synthetic mechanism of most other peptide antibiotics. In contrast to the peptide antibiotics, which are synthesized via the multienzyme complexes (thiol esters) and enzyme systems, the biologically active, lanthionine-containing, secondary metabolites evolve from the ribosomally synthesized precursor proteins. These prelantibiotics consist of a leader sequence and a prolantibiotic, which post-translationally is enzymatically modified.[1] The serine and threonine residues are dehydrated to α,β-didehydroamino acids,

[*] Prof. Dr. G. Jung
Institut für Organische Chemie der Universität
Auf der Morgenstelle 18, W-7400 Tübingen (FRG)

[**] Based on a lecture delivered on the occasion of the Max Bergmann Medallion Award 1989, Wangen (Switzerland), October 15–18, 1989.

 © VCH Verlagsgesellschaft mbH, W-6940 Weinheim, 1991 0570-0833/91/0909-1051 $ 3.50+.25/0

and the thiol groups of the cysteine residues add to the resulting double bonds with formation of sulfide rings.

Depending on the variability and specificity of the modifying enzyme systems, one could incorporate analogous protein or peptide substrates into the lantibiotic biosynthesis systems, and thereby produce novel proteins, agonists, antagonists, inhibitors and enzymes which contain dehydroamino acids, sulfide bridges—instead of disulfide bridges—or lysinoalanine bridges. Therefore, lantibiotic biosynthesis is not only of interest in basic microbiological research, but also assumes a special role in the development of new methods in protein engineering.

The interdisciplinary microbiological and chemical research on lantibiotics began already in 1983 in Tübingen, starting with the fermentation, isolation and structural elucidation of the anti-acne therapeutic agent, epidermin. The structure of the tetracyclic, 21-peptide amide antibiotic epidermin was published in 1985.[4] The unusually intensive and well-coordinated collaboration between various research teams in microbiology and peptide chemistry led to the elucidation of additional new lantibiotics and substantial information was collected in a short time about their structural genes. Meanwhile, DNA sequences of several of the enzymes responsible for the biosynthesis have been determined. Therefore, complete elucidation of the biosynthetic steps, and the selective gene technological preparation of modified polypeptides and proteins with unusual building blocks is getting closer to a reality. Recent results of lantibiotic research are presented here for the first time in the form of a review.

2. Lantibiotics, Their Biological Activities and Possible Applications

Lantibiotics are produced by microorganisms of various genera, e.g. *Staphylococcus, Lactococcus, Bacillus*, and *Streptomyces*. It is specially useful to classify the lantibiotics on the basis of their different ring structure, into two sub-

Table 1. Composition of the lantibiotics and the strains producing them.

Lantibiotic	M_r	Amino [a] acids	Unusual amino acids [b] Lan	MeLan	Dha	Dhb	Others	Microorganisms
Type A								
Pep5	3488	34	2	1	–	3	–	*Staphylococcus epidermidis 5*
Nisin	3353	34	1	4	2	1	–	*Streptococcus lactis 6FS*, ATCC 11454; *Lancefield, group N*; *Lactococcus lactis*, DSM 20729
Subtilin	3317	32	1	4	2	1	–	*Bacillus subtilis*, ATCC 6633, DMS 347
Epidermin	2164	22	2	1	–	1	Cys(Avi)	*Staphylococcus epidermidis Tü 3298* (F16/P57)
Gallidermin	2164	22	2	1	–	1	Cys(Avi)	*Staphylococcus gallinarum Tü 3928*
Mersacidin	1825	20	–	4	1	–	Cys(Avi)	*Bacillus Y-85, 54728*
Actagardine	1890	19	1	3	–	–	–	*Actinoplanes*, ATCC 31048, ATCC 31049
Type B								
Cinnamycin = Ro 09-0198 = Lanthiopeptin	2041	19	1	2	–	–	HyAsp LysN-Ala	*Streptoverticillium cinnamoneum subsp. cinnamoneum*, DSM 40005; *Streptomyces longisporoflavus*, DSM 40165; *Streptomyces cinnamoneus Streptoverticillium griseoverticillatum Streptoverticillium cinnamoneum*
Duramycin = Leucopeptin	2012	19	1	2	–	–	HyAsp	*Streptoverticillium cinnamoneum subsp. cinnamoneum*, DSM 40646; *Streptoverticillium hachijoense* DSM 40144 *Streptomyces cinnamoneus forma azacoluta*
Duramycin B							LysN-Ala	*Streptoverticillim spec. R 2075*
C							LysN-Ala	*Streptomyces grieseoluteus R 2107*
Ancovenin	1959	19	1	2	1	–	–	*Streptomyces sp.*

[a] Total number of the precursor amino acids, e.g., in Pep5, a threonine was counted instead of the oxybutyryl residue. [b] For structural formulas see Scheme 1.

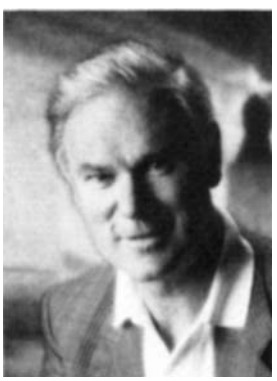

Günther Jung, who was born in Tübingen in 1937, studied chemistry at the Universität Tübingen, where he grained his doctorate in 1967 under the supervision of E. Bayer. After his habilitation 1971 in the natural products area he became professor of organic chemistry and biochemistry at the Universität Tübingen, after turning down numerous calls from other universities. He spent 1967/68 in the USA as an assistant professor at the University of Houston, Texas. In 1989 he was awarded the Max Bergmann Medal for his work on lantibiotics. His areas of research include the structural elucidation, mode of action and biosynthesis of larger polypeptide antibiotics and siderophores, structure-activity relationships of the neuropeptide Y, models for transmembrane channels, multiple peptide synthetic methods, B-, T-helper and T-killer cell epitope mapping and the development of synthetic peptide vaccines.

groups: Type A, lantibiotics of the nisin type, and type B, lantibiotics of the duramycin type (Table 1).

The actual composition of the structurally known lantibiotics is conceived through two recently elucidated representatives. These are the larger polypeptide Pep5[9] with a molecular mass of 3488 Da, and mersacidin[8a] with a molecular mass of 1825 (Table 1). These molecular masses correspond to peptides with 34 and 19 amino acids, respectively, in which the unusual building blocks that originate from the proteinogenic amino acids are also taken into account. Lantibiotics can contain between three and five sulfide rings made from *meso*-lanthionine (Lan) and (2*S*, 3*S*, 2*R*,)-3-methyllanthionine (MeLan). Moreover, they contain α,β-unsaturated amino acids such as α,β-didehydroalanine (Dha), α,β-didehydroaminobutyric acid (Dhb), *S*-aminovinyl-cysteine (Cys(Avi)), as well as *erythro*-3-hydroxyaspartic acid (HyAsp) and amine bridges from lysinoalanine (LysN–Ala) (Scheme 1). The antimicrobial effects of the lantibiotics

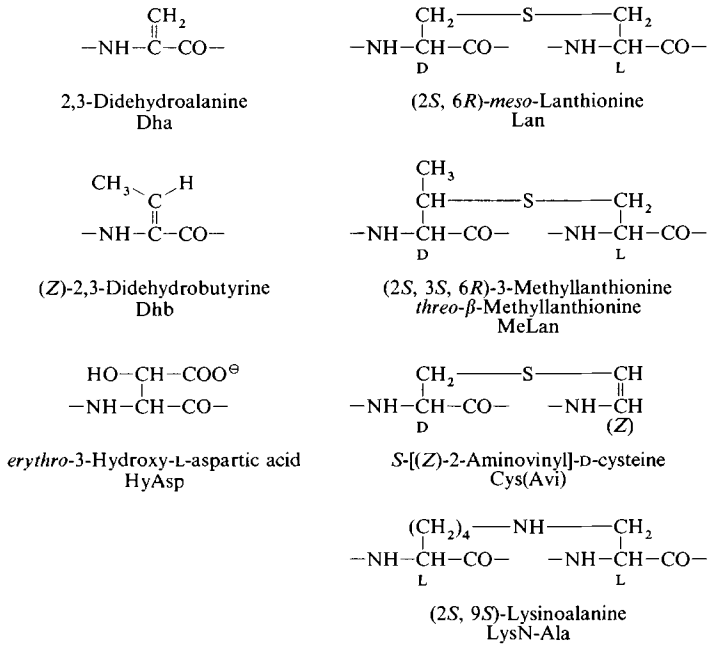

Scheme 1. Unusual amino acids in lantibiotics.

nisin,[2, 3] epidermin[4] and gallidermin[11] are predominantly directed against gram-positive bacteria (Table 2). There are a number of reasons why lantibiotics are classified more reasonably as *bacteriocins* and not as common antibiotics.

Nisin, a compound produced by *Streptococcus lactis* plays a very important role in food technology; since 1951 it has been produced by the tons as a natural preservative for vegetables, cheese, meat and cocoa.[3] Nisin has been known since 1928, and it poses no health hazards to humans, for it has presumably been consumed in dairy products for centuries. The proteases of the human stomach and intestinal tract hydrolyze it completely and it does not damage the gram-negative bacteria of intestinal flora. Thus, as a preservative in the cheese and meat industries, nisin has decisive advantages over the still used nitrates and nitrites, which produce carcinogenic nitrosamines.

Table 2. Effects and potential applications of lantibiotics.

Lantibiotic	Effect	Application
Type A		
Nisin [2, 3]	Batericide against gram-positive bacteria (*Clostridium botulinum, Streptococci, staphylococci*), cationic, lytic agent, inhibitor of peptidoglycan biosynthesis	Food preservative, antimalaria
Subtilin	similar to nisin	
Epidermin [4], Galli dermin [11]	against *Propionibacterium acne* (MIC < 0.125 mcg ml^{-1}) and staphylococci	Acne, eczema, folliculitis, impetigo
Pep5 [9, 10]	Autolysis of the gram-positive bacteria	Bacteriocin
Mersacidin [8a]	Bactericide against staphylococci	Antibiotic, Immune suppressor
Actagardine [8b]	Bactericide against streptococci, inhibitor of the peptidoglycan biosynthesis	Infections, septa
Type B		
Ancovenin [5]	Inhibitor of the angiotensin converting enzyme (ACE)	Blood pressure regulation
Cinnamycin [7] (= Ro 09-0198 [6], Lanthiopeptin [12])	Inhibitor of phospholipase A_2, ACE und HSV-1	Inflammations, blood pressure regulation, immune adjuvant, *Herpes simplex* virus
Duramycin [7] (= leucopeptin)	Inhibitor of phospholipase A_2	Antibiotic
Duramycin B, C [7d]	Inhibitor of phospholipase A_2	Inflammations

Interestingly, the strains producing the lantibiotics epidermin[4] and gallidermin,[11] which are biologically active against pathogenic skin germs such as *Propionibacterium acne*, staphylococci and streptococci, derive from human skin or chicken combs. Their effectiveness against acne is comparable to that of the macrolide antibiotic erythromycin. Upon therapeutic treatment with the macrolide antibiotics a resistance rapidly develops. However, no side effects have so far been observed when using epidermin and gallidermin. The highly effective epidermin and its structural analog gallidermin therefore constitute interesting alternatives to the vitamin A derivatives and erythromycin, specially for the therapeutic treatment of juvenile acne. Since Pep5 and epidermin producers are often found on the human skin,[10a] it is assumed that these belong to the healthy skin flora which function as natural protection against pathogenic microorganisms that could cause inflammation of the follicle ducts of the sebaceous glands.

Little is known about the location and mode of action of most of the lantibiotics on the molecular level. However, insights into the principle ("mechanism") of the antibacterial effect of Pep5,[10] nisin, subtilin, epidermin and gallidermin can be gained by biophysical experiments on lipid bilayer membranes, and by conformational analysis using 2D ^{1}H NMR and MDS (molecular dynamics simulations) and circular dichroism (CD). The high bactericidal activity of Pep5 could be attributed to a depolarization of the energized bacterial cytoplasm membrane[13] and induction of autolysis.[13g–j] In intact cells and artificial membranes, beginning with a trans-negative membrane potential of about 100 mV, voltage-dependent and short-lived pores with variable diameters up to 1 nm were induced.[13c] A similar effect could be demonstrated for nisin[13e] and subtilin,[13i] as well as for epidermin and gallidermin. Owing to the high

specificity of lantibiotics against certain bacteria, one may assume that besides the formation of the pores, still other mechanisms are involved in the biological activity. In particular, a distinct correlation could exist between the lipid composition of the membranes and the biological activity of the lantibiotics, as was demonstrated[7e-m] for duramycins,[7] which inhibit phospholipase A_2.[7d] Duramycins also increase membrane permeability.[7f] Resistance against duramycin can originate from a change of the lipid composition, e.g. by reduction of the content of diacylphosphatidylethanolamine (PE).[7e]

The gram-positive producing strains are sensitive towards the lantibiotics which they themselves produce. Hence, they develop a self-protecting principle which is secerned into the culture medium, and makes the bacteria immune (resistant) against their own products.[14]

3. Structural Elucidation of Lantibiotics

3.1. Nisin and Subtilin

The stereochemistry of lanthionine and related thioether amino acids was investigated by our group using chromatography and circular dichroism.[15] The unusual amino acid lanthionine, as well as lysinoalanine (Table 2) can cause cross-linking of the peptide chains with one another. These compounds are found in wool and food products if they are subjected to heat or alkali. The natural occurrence of lanthionine was demonstrated for the first time when it was found in the polypeptide antibiotic nisin discovered in 1928 (cf. Ref. [3]). The complicated structure of the polycyclic 34-peptide was elucidated by the pioneering work of *Erhard Gross* in 1971.[2] Shortly afterwards the structure of the related compound subtilin was published.[16] These two heterodet pentacyclic polypeptides possess five sulfide bridges at identical positions—formed by a lanthionine and four 3-methyllanthionine residues—as well as two dehydroalanines and one dehydrobutyrine (Fig. 1).

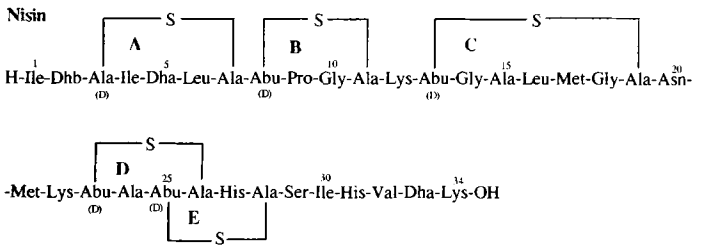

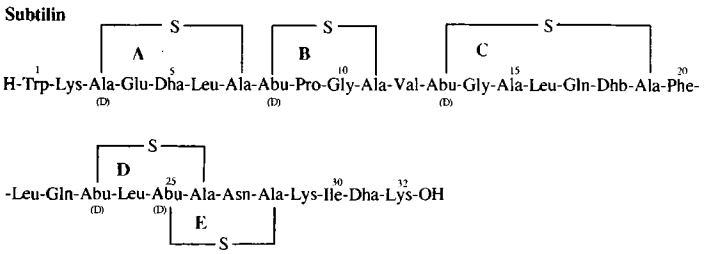

(2S, 6S)-Lanthionine (2S, 3S, 6R)-3-Methyllanthionine

Fig. 1. Structures of the heterodet pentacyclic lantibiotics nisin [2] and subtilin [17].

For the structural elucidation, *Gross* and collaborators employed two different methods to split off the sulfide bridges, before and after the enzymatic cleavage of nisin,[16] and subtilin.[17] One method was a special oxidative cleavage of the sulfide bridges, and the other, reductive ring cleavage by desulfurization with Raney nickel. The latter method led to the formation of one D- and one L-alanine residue from *meso*-Lan, whereas MeLan was converted into L-alanine and D-α-aminobutyric acid. The detection of α,β-didehydroamino acids is neither possible by amino acid analysis of the total hydrolyzate, nor by peptide sequencing using Edman degradation. This problem is due to the fact that Dha and Dhb are thereby decomposed and form a peptide acid amide and a ketoacyl residue. Figure 2 depicts the acid-catalyzed cleavage of nisin at Dha^{33}, which leads to the likewise active nisin (1–32) amide; an analogous cleavage also occurs at Dha^{5}, but not at Dha^{2}. *Gross* utilized this labile peptide bond in order to carry out an interesting solid phase synthesis of a peptide amide, whereby a resin bound dehydroalanine anchor functioned as an acid-labile intermediate and also furnished the nitrogen of the amide functional group.[16c,d] This reaction is reversible and the reactivity of the didehydroamino acids is responsible for the formation of nisin oligomers with molecular masses of up to 12000 Da.[16c] In the case of Pep5, dimers with molecular masses of up to 7000 Da have also been detected.

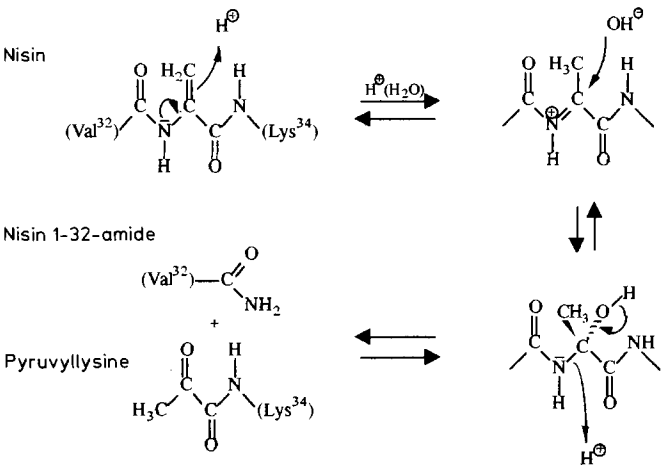

Fig. 2. Acidic cleavage of nisin at didehydroalanine (Dha) in position 33 [16c] leads to a peptide amide and pyruvyllysine [16d].

Besides the catalytic hydrogenation of the α,β-didehydroamino acids, *Gross* also carried out a further key reaction, namely the addition of benzylthiol and mercaptoethylamine to the double bonds of Dha and Dhb.[16,17]

According to our experience, neither desulfurization nor hydrogenation and addition of α-toluenethiol to lantibiotics

proceed quantitatively. Therefore, the accomplishment of the *Gross* team is to be respected all the more highly, for the structures of nisin and subtilin were correctly eludicated, without using HPLC, high-field NMR and FAB-MS. The correctness of these structures has now been proven by the sequencing of the structural genes.[18, 19]

After about 10 years of work, the total synthesis of nisin was achieved by the research group of *Shiba* in 1987.[20] The basic features of the method used are the dehydroalanine synthesis from 2,3-diaminopropionic acid by Hofmann degradation[20c] (Fig. 3), and the dehydrobutyrine synthesis by dehydration of threonine using soluble 1-ethyl-3(3-dimethylaminopropyl)carbodiimide and $Cu^{I}Cl$ catalysis.[20a] The sulfide bridges were prepared by partial desulfurization of the disulfide bridges of the sequence analogous cystine-containing peptides, using tris(diethylamino)phosphane[20d] (Fig. 3). Interestingly, this reaction can also be performed by employing polymer-bound peptides containing disulfide bridges.[20e]

was identical with the naturally occurring compound as regards antibacterial activity, HPLC chromatogram, FAB-mass spectrum and ^{1}H-NMR spectrum. On the basis of the enzymatic and synthetic fragments, it was established that the rings A and B are responsible for the antibiotic activity.

3.2. Epidermin and Gallidermin

One of the central problems in the structural elucidation of the lantibiotics is the sequence specific configurational assignment of the two C_α-atoms all *meso*-lanthionine and (2*S*, 3*S*, 6*R*)-3-methyllanthionine residues. This was resolved by us during investigation of the structure of epidermin, where we used comparative gas chromatographic studies on chiral glass capillaries with Chirasil-Val.[15a] Starting point for the structural elucidation was the preparation of many fragments by combination of enzymatic and chemical degradation steps. A crucial step involved the tryptic fragmenta-

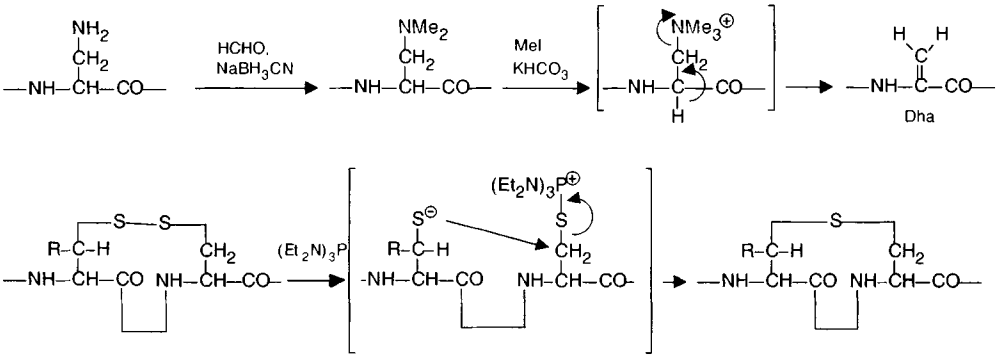

Fig. 3. Preparation of the didehydroalanine (Dha) from 2,3-diaminobutyric acid, and of the sulfide rings from disulfide bridges in the synthesis of nisin [20]; R = H (lanthionine); R = CH_3 (β-methyllanthionine).

The total synthesis of nisin was achieved by the condensation of five fragments (Fig. 4). The synthetic fragments 1–12 and 22–34 correspond to a tryptic and a BrCN cleavage fragment, respectively; therefore, their identification was possible by comparison with natural nisin. Synthetic nisin

tion of epidermin, by which a water soluble N-terminal fragment P1 and an insoluble C-terminal fragment P2 were produced. By using NMR, FAB-MS, and chemical derivatization, we found that as a result of the enzymatic cleavage of the Lys-Dhb peptide bond at the N-terminus of of the pre-

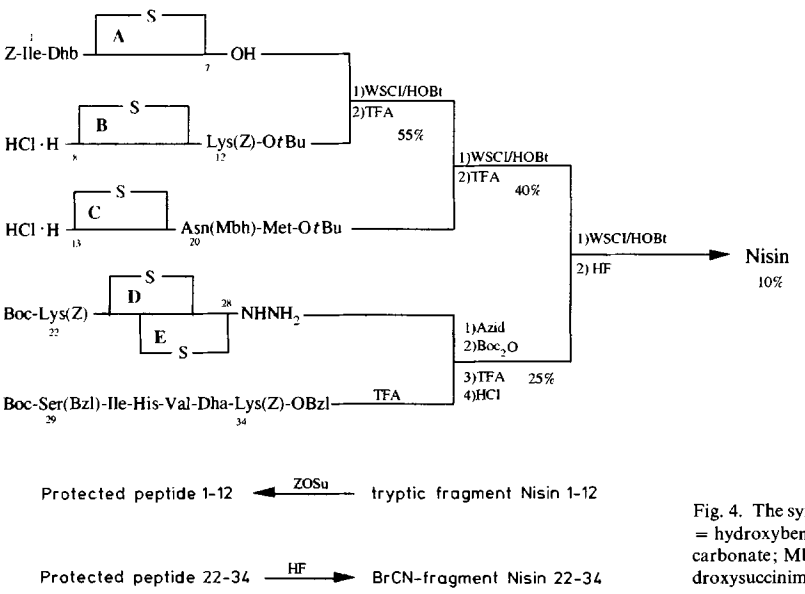

Fig. 4. The synthesis of nisin [20]. WSCI = water soluble carbodiimide; HOBt = hydroxybenzotriazole; TFA = trifluoroacetic acid; Boc_2O = di-*tert*-butyl carbonate; Mbh = methoxybenzhydryl; ZOSu = *O*-benzyloxycarbonyl-*N*-hydroxysuccinimide; Z = benzyloxycarbonyl.

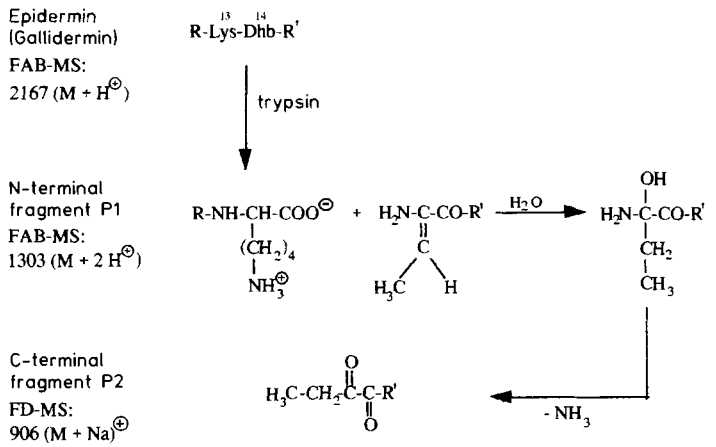

Fig. 5. Tryptic cleavage of epidermin [4] and gallidermin (= [Leu⁶]-epidermin) [11] to fragments **P1** and **P2** (cf. Figs. 6 and 7).

cursor of the fragment P2, a 2-oxobutyryl blocking group is produced (Fig. 5). N-Terminally bound α,β-didehydroamino acids Dha and Dhb are unstable, they add water and are deaminated to the α-ketoacyl residues. In contrast to the acid-catalyzed cleavage at Dha[5] and Dha[33] of nisin (Fig. 2), tryptic digestion produces no peptide amides, but peptides containing a carboxy C-terminus (Fig. 5).

The structural elucidation of the N-terminal fragment P1 (Fig. 6) could be carried out by FD-MS and FAB-MS—before and after desulfurization—as well as by automated Edman degradation of the desulfurized dodecapeptide 1–12. The sulfide bridges of the rings A and B of fragment P1 were assigned on the basis of FAB-MS spectrometry and by a Lys-C-endopeptidase cleavage of the ring 3–7.[4] For the structural elucidation of the N-acylated and C-terminally amidated fragment P2, NMR furnished useful information. Information was also gained by the desulfurization reaction using Raneynickel by which inhomogeneous products were obtained. This reaction afforded the important fragment with the C-terminal L-alanine-*N*-ethylamide (Fig. 6). The compound *S*-(2-aminoethyl)-D-cysteine (4-thialysine), which was identified in the above experiment, was also gas chromatographically detected in the hydrolyzate after hydrogenation of epidermin with Pd/C. Further information was obtained from the fragments of a wild partial hydrolysis using 0.1 N HCl at 93 °C. The structural investigation of

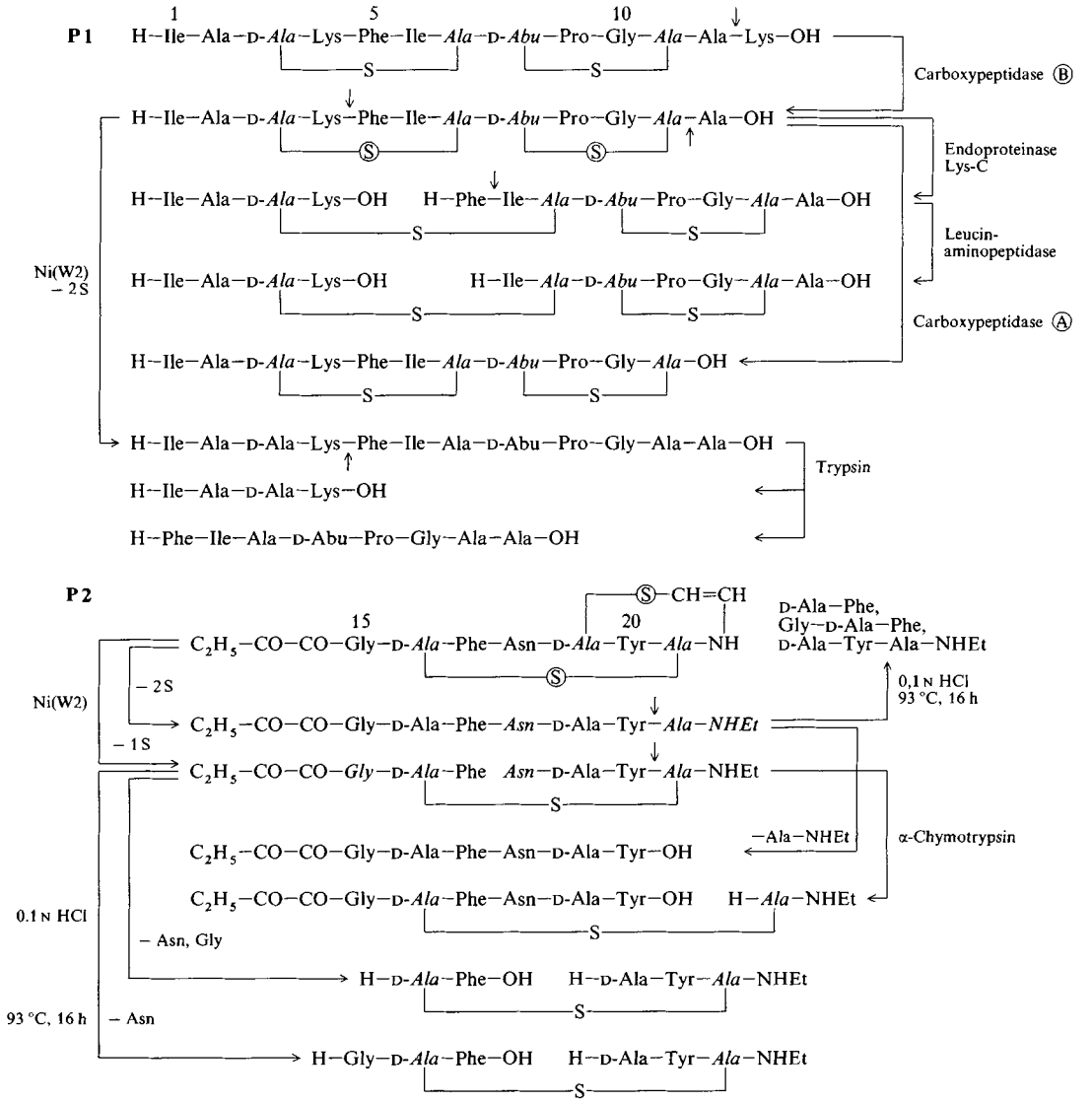

Fig. 6. Structural elucidation of epidermin by the preparative isolation of fragments **P1** and **P2** of the tetracyclic 21-peptide amide [4].

these fragments was achieved by means of mass spectrometry, end-group analysis and gas chromatography (GC) on chiral phases. Thus, for the first time in the case of epidermin, *S*-aminovinyl-D-cysteine could be determined as a building block in the C-terminal cycle of a peptide.[4]

The unequivocal elucidation of the structure of epidermin thus involved the use of many chemical, enzymatic and instrumental methods. For the structural elucidation of gallidermin, which is produced by *Staphylococcus gallinarum F16*,[111] we benefited from our experience with epidermin, but we used predominantly newer methods. The molecular mass of gallidermin was determined by FAB-MS. The sequence of the N-terminal segment up to Dhb^{14}, with the exception of the lanthionine bridge, could be determined by means of a gas-phase sequencer. The C-terminal fragment, obtained by tryptic digestion, could by characterized unambigously by the fragmentation pattern using thermospray LC-MS.[111] The complicated structure of the rings C and D could also be resolved on the basis of the thermospray mass spectrum. Finally, the connection of Lys^{13}-Dhb^{14} to the tryptic cleavage site could be deduced from the daughter ions of the FAB-MS.[111] Gallidermin was thus found to be [Leu^6]-epidermin (Fig. 7); it showed, despite this slight difference, a measurably increased antibiotic activity towards acne-producing germs.[11a]

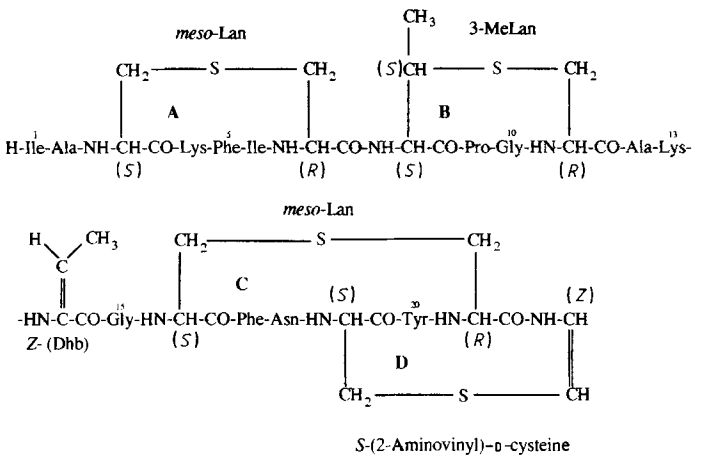

Fig. 7. Structures of the lantibiotics epidermin and gallidermin. The tryptic cleavage products **P1** and **P2** arise from proteolysis of the peptide bonds between residues 13 and 14 (cf. Fig. 5). Epidermin has Ile in position 6, gallidermin is [Leu^6]-epidermin.

The lantibiotics epidermin, gallidermin (Fig. 7) and Pep5 (Fig. 8) can be bound directly to the absorbing resin XAD-1180 from the culture medium.[21a-c] Pure epidermin and gallidermin are obtained by desorption and desalting on the ion exchanger IRC-50, and a final purification on RP-HPLC. Gallidermin can thus be prepared in an analyticaly pure enough form for clinical investigations.[21d]

3.3. The Lantibiotic Pep5

The lantibiotic Pep5 was isolated by *Sahl*,[10a] and, with a molecular mass of 3488 Da (FAB-MS), it is the largest representative of the lantibiotics known so far.[9] Owing to the presence of six Lys and two Arg residues, the tricyclic 34-peptide is extremely basic. Moreover, since it has a strong tendency to form dimers (cf. Section 3.1.), its structural elucidation was especially difficult. Pep5 contains three Dhb, two *meso*-Lan, and a (2*S*, 3*S*, 6*R*)-3-MeLan. In addition, the N-terminal residue is blocked by a 2-oxybutyryl group, which is derived from a Dhb residue, originating from a Thr in the prepeptide.

The key reactions in the structural elucidation of the strongly basic lantibiotic were enzymatic cleavage with chymotrypsin and endopeptidase Arg-C (Fig. 8).[9] Four pure

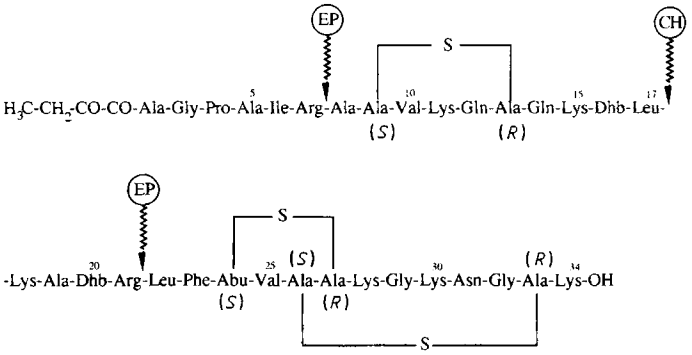

Fig. 8. Structure and main enzymic cleavage sites of the tricyclic, N-terminally blocked, 34-peptide antibiotic Pep5 [11]. Chymotrypsin (CH) cleaves the lantibiotic Pep5 into CH1 (1–17) and CH2 (18–34); endopeptidase Arg C (EP) cleaves CH1 into CA1 (1–7) and CA2 (8–17), CH2 is cleaved by EP to CA3 (18–21) and CA4 (22–34); besides one 2-methyllanthionine and two lanthionine bridges, there exist in position 1 one oxobutyryl (Oxb) and in positions 16 and 20 two dehydrobutyryl (Dhb) residues. Positions 1, 16, 20 and 24 in the precursor protein of Pep5 are occupied by four threonine residues (cf. Fig. 20).

fragments were obtained, which allowed the location of the sulfide bridges and the unsaturated amino acids. Mild acid hydrolysis effected preferentially peptide bond cleavage of Gly^3-Pro-Ala^5 from the N-terminal fragment CA1, which was also chemically synthesized for the comparative analysis. By means of the Edman degradation of enzymatic fragments, and above all, of the chemically derivatized fragments, a 34-peptide backbone could be deduced (Fig. 8). In this investigation, conversion of both Dhb residues into *S*-benzyl-3-methylcysteine by the addition of α-toluenethiol was useful. Interestingly, after this treatment with thiol, the blocked N-terminus becomes also accessible to the sequence determination. Therefore, using this addition product, the sequence 1–22 could be determined using a gas-phase sequencer. During this sequencing, no phenylthiohydantoin(Pth)-amino acids were detected at the sulfide bridges and the original Dhb residues.

3.4. Duramycins

In 1977 *Gross* published[7a], with reservation, the preliminary structures of cinnamycin[7b] and duramycin,[7c] which differed from each another by the Arg/Lys substitution at position 2. The structures published in the Refs. [2b, 7b, c] contain wrong amino acids and partly wrong rings. According to the newer investigations, these two lantibiotics fit into the general structural pattern of duramycins B and C,[7d] to

Table 3. Classification of the lantibiotics according to the charges, conformation and activity.

Lantibiotic	Charges positive	negative	net	Properties
Type A				
Pep5	8	1	7+	Long stretched, helical, cationic, amphiphilic polypeptide antibiotics; voltage dependent membrane channel formers
Nisin	4	1	3+	
Subtilin	4	2	2+	
Epidermin	3	0	3+	
Gallidermin	3	0	3+	
Mersacidin	3	1	0	
Actagardine	1	2	1−	hydrophobic
Type B				
Cinnamycin	3	2	1+	Compact, almost neutral amphiphilic polypeptides; enzyme inhibitors, immunologically active
Duramycin A	3	2	1+	
B	3	2	1+	
C	2	2	0	
Ancovenin	2	2	0	

which also belong the lantibiotics Ro 09-0189[6] (= cinnamycin[7], = lanthiopeptin[12], as well as leucopeptin[22] (= duramycin[7]) and ancovenin[5] (Table 3).

Reductive desulfurization (H_2/Pd, 10 Kp/cm^2, 50 °C) was employed for the structural elucidation of ancovenin[5] and lanthiopeptin.[12] By this ring opening and by using a proline specific endopeptidase, sequenceable fragments can be obtained. These fragments also enable establishment of the lysinoalanine ring position (Fig. 9). *Shiba*'s research group

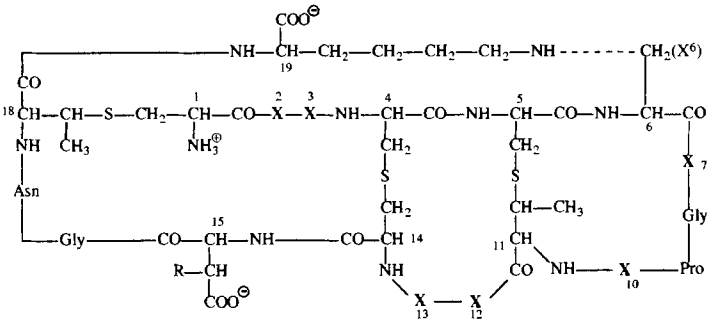

Fig. 9. General structure of the lantibiotics of subtype B (duramycins) according to *A. Fredenhagen* et al. [7d]. Amino acids X and residues R, see Table 4.

Table 4. Amino acids X of the general structure of subtype B (see Fig. 9).

	Duramycin = Leucopeptin	Cinnamycin = Ro 09-0198 = Lanthiopeptin	Duramycin B [d]	Duramycin C [d]	Ancovenin
X^2	Lys	Arg	Arg	Ala	Val
X^3	Gln	Gln	Gln	Asn	Gln
X^6	Ala [a]	Ala [a]	Ala [a]	Ala [a]	Dha [b]
X^7	Phe	Phe [c]	Phe	Tyr	Phe
X^{10}	Phe	Phe [c]	Leu	Leu	Leu
X^{12}	Phe	Phe [c]	Phe	Trp	Trp
X^{13}	Val	Val	Val	Ser	Ser
R	OH	OH	OH	OH	H

[a] Ala bridged with Lys^{19} as lysinoalanine; [b] α,β-didehydroalanine, not bridged with Lys^{19}; [c] L-Phe in cinnamycin; [d] proposed structures [7d].

ascertained the identity of the revised structure of Ro 09-0198[6] with lanthiopeptin.[12a] They pointed out[12c] its further possible identity with the known cinnamycin, and postulated that the lysine-containing duramycin is supposed to have the same ring system as Ro 09-1098 (= lanthiopeptin) (Ref. [10] in [12a]). The authors[12b] classified their lanthiopeptin producer L337-2 as *Streptoverticillium cinnamoneum*, whereas cinnamycin is produced by *Streptomyces cinnamoneus*.[7a] Therefore, cinnamycin has been twice more, duramycin one more rediscovered (cf. Tables 1 and 4).

3.5. Classification of the Lantibiotics according to Their Structural Features

The lantibiotics discussed so far, nisin, subtilin (Fig. 1), epidermin, gallidermin (Fig. 7) and Pep5 (Fig. 8), possess a series of common features which justify their classification in a subtype A, with nisin as a typical representative (Table 1). Lantibiotics of subtype A are strongly cationic peptides with two to seven positive charges and, with the exception of mersacidin and actagardine (Fig. 10), molecular masses of over 2100 Da, (Table 3). In spite of the different chain length, they show a clear structural relationship through sequence homology and similarity of the ring structure. In particular, the thioether amino acids are always N-terminal D- and C-terminal L-configurated, again with the exception of mersacidin and actagardine. Besides the unusual amino acids Lan and MeLan, only Dha and Dhb are to be found. Epidermin and gallidermin, whose C-terminal amino acids are altered through further modification to give Cys(Avi), are the exceptions here.[4, 11] The strains which produce the lantibiotics of subtype A are three *staphylococci*, one *streptococcus* and two *bacilli* (Table 1). Lantibiotics of the duramycin type (subtype B) are predominantly produced by *streptomyces* (Table 1). They have molecular masses of less than 2100 Da, and show markedly high ring homology (Fig. 9). In contrast to the lantibiotics of subtype A related to nisin, they contain at most one positive charge (Table 3).

Aside from the two sulfide bridges belonging to MeLan, and one belonging to Lan, which are always located at the same positions, another special feature of duramycins is the presence of a lysinoalanine bridge which binds the C-terminal Lys^{19} to position 6 (Fig. 9). In the case of ancovenin, this bridge is still not formed, therefore, ancovenin has another dehydroalanine residue at position 6. Not only the ring closure between positions 19 and 6, but also the sulfide bridges between positions 1 and 18 endow the lantibiotics of type B (duramycin) a more compact globular structure. This is in contrast with the more slender and screw-shaped lantibiotics of type A (nisin) (cf. Section 4.). All the duramycins show an *erythro*-3-hydroxyaspartic acid at position 15, with the exception of ancovenin in which this amino acid is not hydroxylated. Further common features within the subtypes A and B will be discussed in connection with the conformation, and above all, with the biosynthesis of lantibiotics.

3.6. Mersacidin and Actagardine

Nothing is known about the conformation or the biosynthesis of mersacidin,[8a] which was recently elucidated by means of 2D-^{1}H-NMR spectroscopy.[8a] It is difficult to classify this neutral lantibiotic (Fig. 10) to one of the sub-

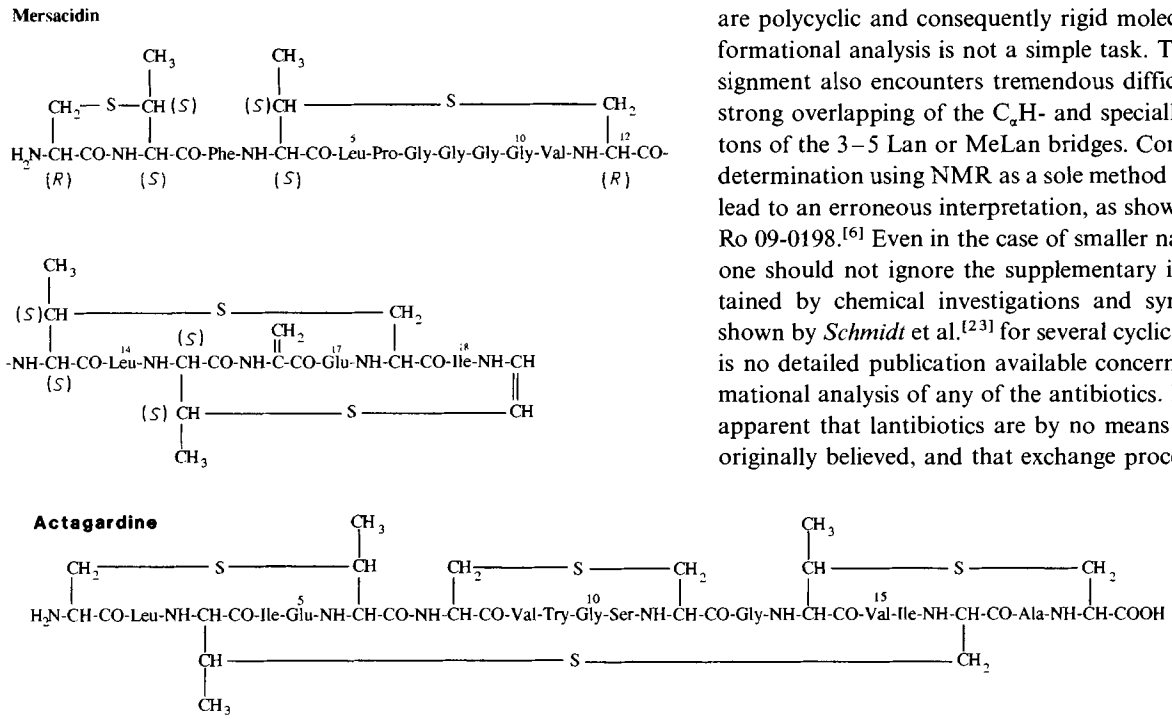

Fig. 10. Proposed structural formulas of the tetracyclic lantibiotics mersacidin [8a] and actagardine [8b] according to NMR studies.

types listed in Tables 1 and 3. On the one hand, like the duramycin type B it has a molecular mass of less than 2100 Da and no cationic properties, and on the other, it lacks the head-to-tail linking by sulfide and amine bridges, typical for duramycins. Since the C-terminus is amidated by a ring closure with the amino group of *S*-aminovinyl-L-cysteine with the *Z* configuration, it could more properly be compared with epidermin/gallidermin. To group A fits also the mersacidin producing bacillus, as well as the ring formation pattern with exception of the unusual MeLan bridge between positions 1 and 2.

The structural classification of actagardine is even more difficult; the proposed structure of this lantibiotic, which is effective against streptococci, was determined mainly by 2D ^{1}H NMR and was shown to be a heterodet tetracyclic 19-peptide.[8b] Actagardine is now the recommended name for an antibiotic family formerly called gardimycin.[8c-e] The published ring structure consists of one Lan and three MeLan bridges. In contrast to the type A lantibiotics, actagardine is an acidic and strongly hydrophilic molecule. Using actagardine as an example, it could be shown that chemical derivatization could convert a lantibiotic into an antibiotic with higher in vivo and in vitro activities.[8c]

4. Conformational Studies

Different research groups are currently investigating the conformation of the lantibiotics, mainly nisin, gallidermin/epidermin, Ro 09-0198, ancovenin and Pep5 by NMR spectroscopy. In this process, the structurally relevant parameters such as coupling constants, NOE-effects and temperature dependency are obtained from 1D and 2D experiments. These studies provide an experimental basis for the molecular geometry calculations. In spite of the fact that lantibiotics are polycyclic and consequently rigid molecules, their conformational analysis is not a simple task. The sequence assignment also encounters tremendous difficulty due to the strong overlapping of the $C_\alpha H$- and specially the $C_\beta H$-protons of the 3–5 Lan or MeLan bridges. Complete sequence determination using NMR as a sole method could especially lead to an erroneous interpretation, as shown in the case of Ro 09-0198.[6] Even in the case of smaller natural products, one should not ignore the supplementary information obtained by chemical investigations and syntheses, as was shown by *Schmidt* et al.[23] for several cyclic peptides. There is no detailed publication available concerning the conformational analysis of any of the antibiotics. It now becomes apparent that lantibiotics are by no means as rigid as was originally believed, and that exchange processes render determination of the solution conformation difficult. Nonetheless, the existing information makes it possible to draw several fundamental conclusions regarding the crude structure of the different lantibiotic types.

4.1. Conformation of Nisin

Several research groups are studying the conformation of nisin. Of these, three groups in the Netherlands, in the U.S.A., and in the UK have made similarly great progress. So far, the sequence specific assignments of the ^{1}H-NMR signals, deduced from the 400/600 MHz 2D experiments in H_2O/D_2O (DQF-COSY, TOCSY, NOESY), have been published.[24] An analysis of the NOE data showed a definite orientation of the rings A and B of the nisin N-terminal segment. Thus, proline 9 of ring B points towards ring A, and the side chains of methionine residues 17 and 21 are turned towards each other. Presumably the N-terminus of nisin forms an amphiphilic screw, similarly as in the case of epidermin and gallidermin (cf. Section 4.2.). A helix-like structure can also be expected on the basis of biophysical measurements on the ion channels[10c] which are induced by nisin, as will be shown in the following section.

Chan et al.[25] carried out further NMR experiments and was able to elucidate the structures of two acidic cleavage products of nisin, as well as a complete sequential signal assignment. Nisin 1–32 amide, which has lost two amino acids at the C-terminus, shows antibacterial activity similar to that of the native molecule (compare Fig. 2), whereas additional removal of Dha^5 or the ring A leads to a loss of activity.[25] *Palmer* et al.[26] report a comparative NMR and MDS conformational study of the separate rings A–E, as well as of the whole nisin molecule. The conformations of the separate rings are said to be very similar to the native nisin.

4.2. Conformation of Epidermins

Investigations on the conformation of the two lantibiotic analogues with Leu/Ile exchange in position 6 have been carried out by 2D ^{1}H NMR in water, dimethyl sulfoxide, and particularly in trifluoroethanol/water (9:1) at 500 MHz.[27] Preliminary results have briefly been described.[28]

Interproton distances from 190 NOEs (NOESY with different mixing times; cf. Fig. 11 and 12), dihedral angles from coupling constants (*J*-resolved 1D DQF COSY), and potential hydrogen bond donors from the temperature dependancy of the amide protons served as a basis for the MDS investigations to deduce the dominant conformation in a lipophilic medium (Fig. 13). For comparison, the conformations of the N-terminal fragment (1–13) and the whole molecule in DMSO and water were investigated. The C-terminus in particular shows a strong signal broadening in DMSO, which can be attributed to exchange processes with the traces of water present in DMSO. The screw-shape conformation is present in all the solvents (no regular helices). In the MDS study, based on the experimental data of the 2D-NMR measurements, the screw-like overall conformation remains surprisingly stable (Fig. 13). Solvent dependent NMR measurements, however, show local conformational changes corresponding to the behavior during the molecular dynamics simulation.

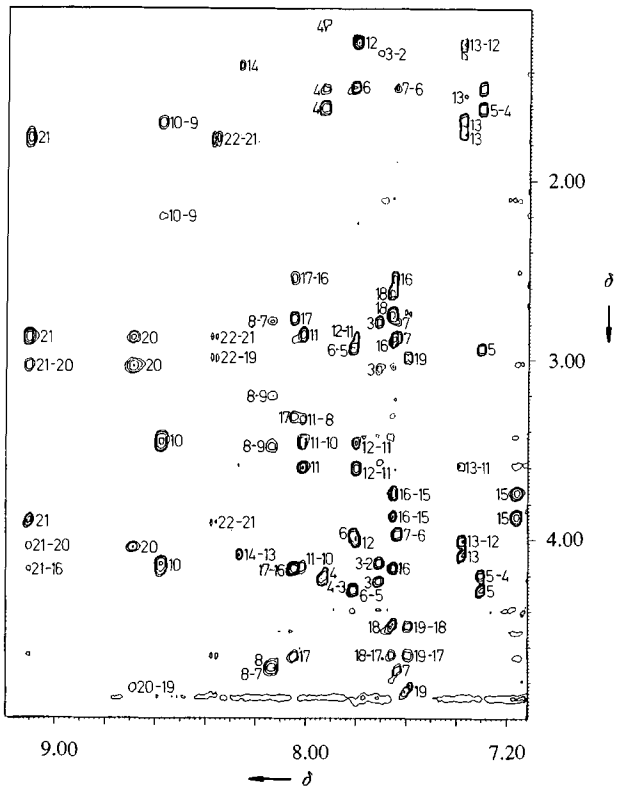

Fig. 12. ^{1}H-NMR NOESY (500 MHz) spectrum of gallidermin (T_M = 200 ms, TFE/H_2O (9:1)): The section shows conformational NOE-effects between the amide protons and CH_α, as well as the side chain protons.

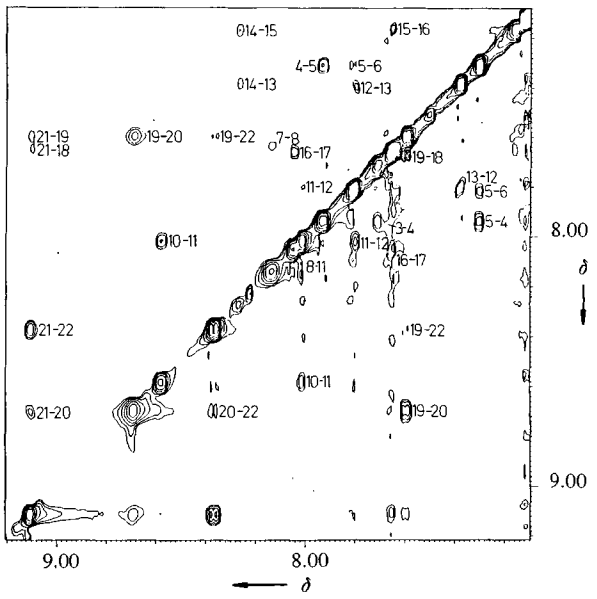

The results of the measurements in trifluoroethanol (Fig. 13) could serve as a clue to the behavior of the epidermins in lipid membranes. The stretching of the molecule to a total length of 30 Å, renders the bridging of the lipid bilayer membrane possible. Moreover, the helical arrangement causes the molecule to become amphiphilic with a lipophilic C-terminal segment, and a threefold positively charged hydrophilic side which is located at the N-terminal half of the helix (Fig. 13). Previous CD measurements on epidermin in different solvents also indicate the existence of a uniform conformation. On the basis of our conformational investigations, the epidermins exhibit a dipole moment of about 54 Debye in DMSO, which increases to 75 Debye through transition to a long stretched helix in the more lipophilic solvent trifluoroethanol. The structure of gallidermin in water is used by us in MDS studies as a guide for developing trypsin stable analogs (Fig. 14).

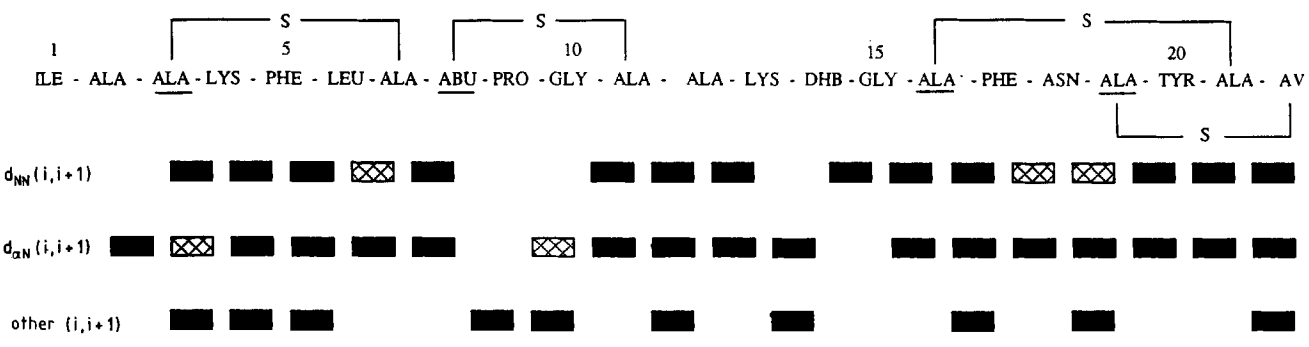

Fig. 11. Top: ^{1}H-NMR NOESY (500 MHz) spectrum of gallidermin (= [Leu^6]-epidermin) in trifluoroethanol/water; mixing time t_M = 200 ms. The segment shows NH_i-NH_{i+1} contacts, which occur typically in the helical parts. Bottom: Summary of all the sequential contacts.

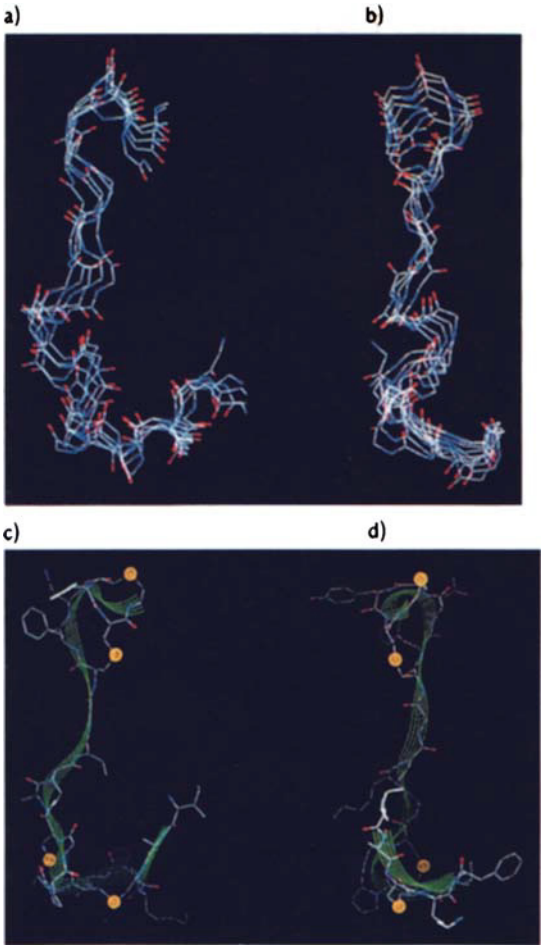

Fig. 13. Representation of the conformation of gallidermin as deduced from an MDS investigation on the basis of the conformational parameters derived from 2D-NMR measurements. a) and b) orthogonal depiction of five convergent structures (only backbone atoms: red = O, blue = N, white = C, light blue = H); c) and d) backbone as ribbon (green) with sulfide rings (yellow = S) and side chains.

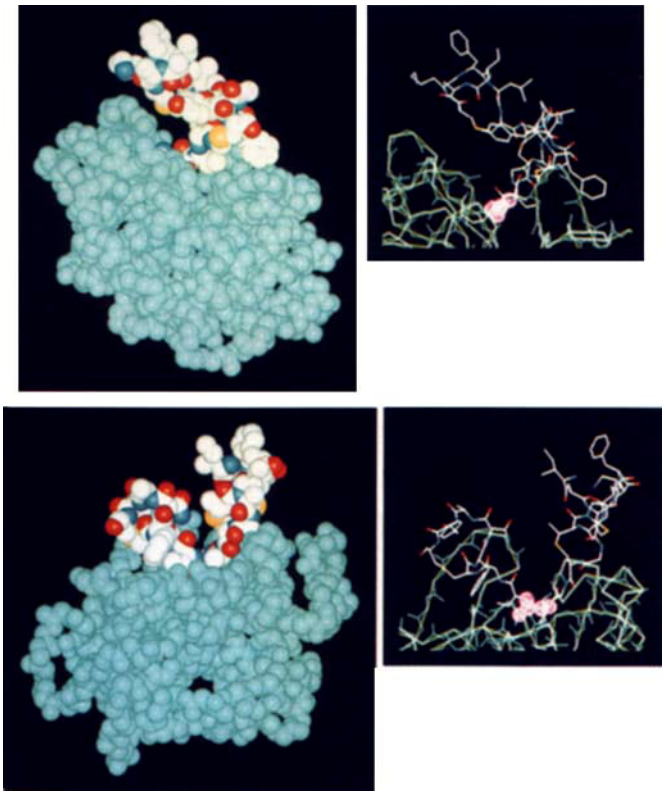

Fig. 14. Model of the gallidermin-trypsin interaction. Trypsin cleaves gallidermin at Lys^{13}-Dhb^{14} (purple atoms; cf. Figs. 5, 6). The model was calculated using distance geometry molecular dynamics simulations (DGEOM, Amber). Gallidermin assumes a bent conformation upon fitting to the enzyme cleft, thus it shows similarity to the trypsin inhibitor BPTI (bovine pancreatic trypsin inhibitor). On the basis of this structural model, it is possible to construct stable analogs against trypsin.

4.3. Conformation of Pep5

For the tricyclic lantibiotic Pep5 with two α,β-didehydroamino acids, we could prove the existence of a helical structure in a lipophilic surrounding by CD measurements. This is formed, e.g., in trifluoroethanol or other alcohols and in water after the addition of sodium dodecylsulfate. According to our preliminary NMR investigations in trifluoroethanol and water, the linear region 14–22 in particular (Fig. 8) is helical ($\alpha/3_{10}$) in the former solvent, as shown by the strong NH–NH-contacts in this segment. We are currently investigating the conformation of Pep5 in trifluoroethanol and water using NMR and MDS methods.

4.4. Conformation of the Duramycin Type B

The conformation of the tetracyclic 19-peptide antibiotic Ro 09-0198 (= cinnamycin = lanthiopeptin) in solution[6] can serve as a model structure for MDS investigations of all the lantibiotics of the duramycin type B (Tables 1 and 3). The cinnamycin molecule has a compact, almost globular structure in DMSO.[6] In this molecule, the hydrophilic amino acids are located on one side, the lipophilic ones, including the three phenylalanines, on the other half of the molecule. The natural exchanges within the lantibiotic series of type B (Fig. 9) such as, e.g., Lys^3/Arg, Gln^3/Asn, Phe^7/Tyr, Phe^{10}/Leu, Phe^{12}/Trp could hardly change the overall conformation; however, they cause pronounced differences in the biological properties.[7] The jump from duramycin C[7d] to ancovenin[5] is considerably larger, which is due to the fact that the lysinoalanine bridge is missing and the position 6 is occupied by dehydroalanine with its conformationally restricting properties.

Interestingly, cinnamycin shows analogous inhibitory properties on the angiotensin converting enzyme (ACE),[6b] as has been reported for ancovenin.[5] Apparently, the fourth ring of cinnamycin does not destroy the binding to the enzyme; but unfortunately no data are available for comparison. Therefore, it is not clear which structural elements are responsible for the ACE inhibitory action. Only a short note has appeared about the ancovenin conformation in DMSO.[5b] Accordingly, ancovenin in DMSO shows, similarly to cinnamycin, a compact conformation with the amphiphilic character.

The antibiotic activity of the duramycins could be due to interactions with the membrane components, as has been shown by studies on duramycin resistant bacilli.[7e–m] Duramycins and cinnamycin are potent inhibitors of human phospholipase A_2 which show activity in the micromolar region.[7d] Also in the enzyme/inhibitor interaction, the am-

phiphilicity and presumably the membrane accessibility of duramycins certainly play a decisive role.

5. Biosynthesis of Lantibiotics

5.1. Lantibiotics Evolve from Precursor Proteins

The most exciting aspect of lantibiotic research is undoubtedly the biosynthesis of these molecules. *Hurst*[3] and *Ingram*[30] found that inhibitors of protein synthesis hinder nisin production in the *Streptococcus lactis* suspension. *Hurst* could demonstrate the plausibility that when basic peptide extracts from a nonproducing strain are added to a cell extract of the wild type, nisin will be produced. These were the first experimental hints that nisin, unlike other peptide antibiotics, is not biosynthesized by a multienzyme thiotemplate mechanism,[31] but by ribosomally synthesized precursor proteins.[3, 31] By employing radioactively labeled cysteine, threonine and serine, *Ingram* showed that these amino acids are precursors of lanthionine and 3-methyllanthionine. By using [^{35}S]-labeled cysteine, it could be shown that the inactive precursor proteins of subtilin could be converted into subtilin.[32] A subtilin precursor was immune-precipitated with the antisubtilin antiserum,[32, 33] however, it was not characterized in detail. Hints about a plasmid controlled biosynthesis of nisin were first reported by *Kazak* et al.[33]

Apart from the structural elucidation of epidermin,[4] we were interested in its biosynthesis. In the case of epidermin, it was likewise possible to prove its ribosomal biosynthesis and to block production of the antibody by addition of inhibitors of the protein and RNA synthesis.[34] At that time, it was not clear whether lantibiotics are built by the cleavage of larger proteins, or whether they are produced by a very special biosynthetic system via independent structural genes, e.g., in the same way as hormones from prepeptides. As long ago as 1985 we first explicitly postulated the amino acid sequence of the precursor peptides of the lantibiotics nisin, subtilin, and epidermin, and we attempted to isolate a precursor peptide of epidermin.[4, 29]

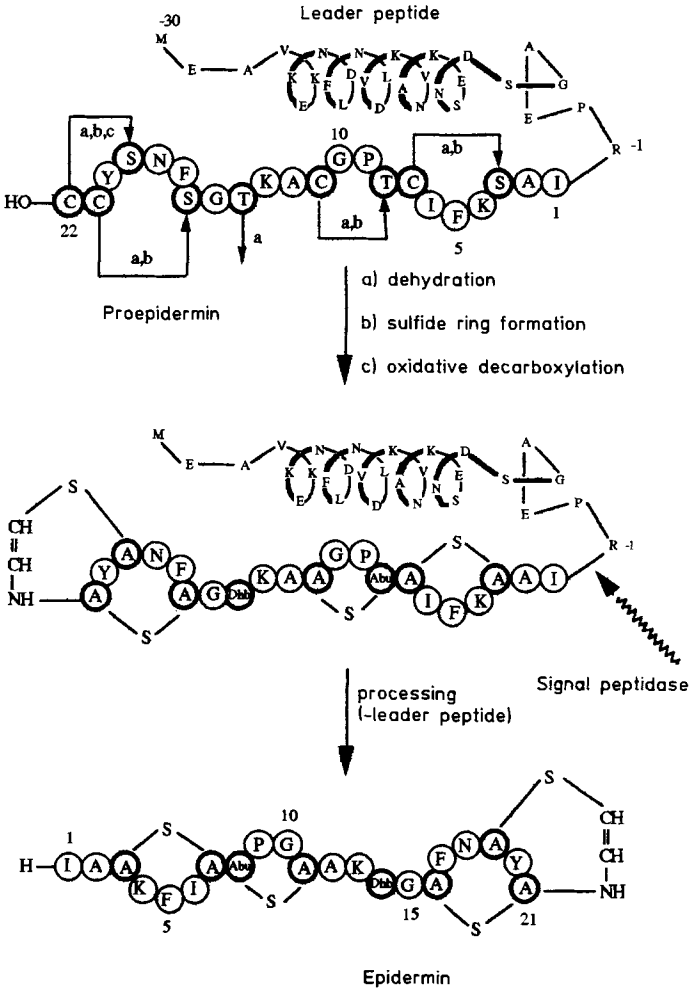

Fig. 15. Postulated [4, 29] and proven [1] events of the epidermin biosynthesis by modification of the precursor protein, preepidermin (amino acids in the single letter codes).

5.2. Prelantibiotics and Their Structural Genes

We assumed a ribosomal synthesis of a proepidermin which is enzymatically dehydrated at the serine and threonine residues in the modification steps (Fig. 15).[4] Subsequently, four cysteine thiol groups are supposed to add stereospecifically to the four α,β-didehydroamino acids to build the sulfide rings.

Assuming this order of events and the sequence-specific proof of the C_α-configurations of the Lan and MeLan residues, we postulated a proepidermin which carries at the resulting lanthionine half with D configuration (= *S*) the precursor amino acid—L-serine for *meso*-lanthionine, and L-threonine for (2*S*, 3*S*, 6*R*)-3-methyllanthionine. The C-terminal half of the sulfide bridges with the L-configuration (= *R*) must then originate from L-cysteine. Consequently, the configuration of the C_α-atoms of the L-Ser and L-Thr residues in the prolantibiotics are inverted during conversion into lantibiotics. In the case of epidermin in particular, an α,β-(*Z*)-didehydrobutyrine residue (from threonine) remains in the middle of the molecule which does not encounter a further cysteine residue for the addition. Furthermore, we postulated an additional enzymatic modification during epidermin synthesis in which the unusual cyclic vinylamide develops at the C-terminus (Figs. 6 and 7). The appearance of the Nδ-amide linked building block *S*-(2-aminovinyl)-D-cysteine in the position 19 can be explained by assuming that a further C-terminal Cys^{22} exists whose thiol group adds to Dha^{16} and is subsequently decarboxylated[4, 29] (cf. Fig. 17).

It was completely unclear in which form such a prelantibiotic could be found: bound to a signal sequence, as a segment of a protein, as a free or membrane bound peptide, unmodified or partially modified. Therefore, several strategies have been used for studying lantibiotic biosynthesis. In the case of epidermin—two experimental attempts—the direct isolation of the basic precursor protein, as well as proof of the prelantibiotic by means of the antipeptide antibodies have long been unsuccessful. In the case of Pep5, however, both methods recently led to success in collaboratory studies with *Sahl*.[38]

In cooperation with the microbiologists *Entian* and *Götz*, gene technological methods have been employed as a third and rapidly successful method.[1] Using a mixed DNA probe derived from the pentapeptide sequence Lys-Phe-Ile-Cys-Thr of proepidermin,[4, 29] the structural gene of epidermin was searched for. This synthetic oligonucleotide 5'-GTG(A)-CAT(G,A)ATG(A)AAT(C)TT-3' gave a hybridization signal with the 54 kilobase (Kb) plasmid *pEpi 32* of *Staphylococcus epidermis Tü 3298*. With restriction analyses, subcloning and rehybridization, the structural gene of epidermin *epi* A could be localized on a 2.2 Kb *Eco* IR/*Bg* III fragment.[1]

The sequencing of *epi* A according to the dideoxy method of *Sanger* yielded an open reading for the epidermin with 52 amino acids (Fig. 16).[1] The beginning of the reading frame

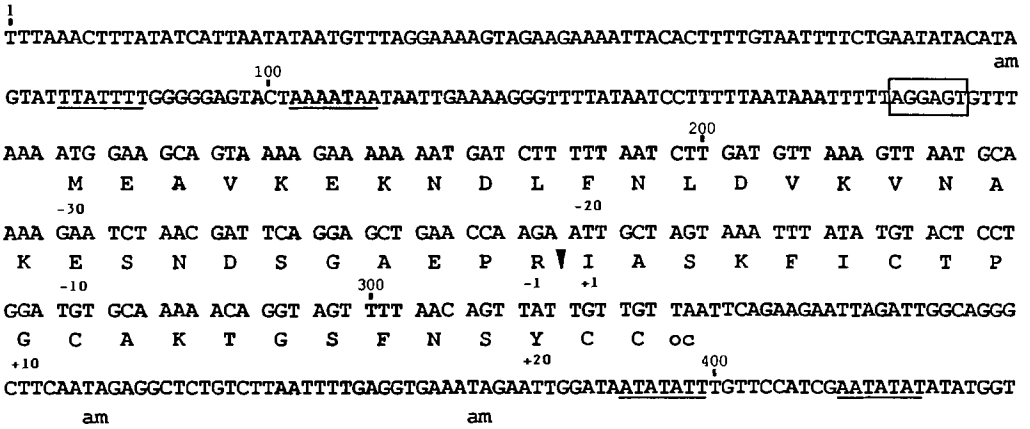

Fig. 16. Preepidermin structural gene: Open reading frame of 237 base pairs is defined by the codons TAG (amber) and TAA (ocher); Shine-Dalgarno sequence is framed; inverted repeats (underlined); proteolytic cleavage point of the signal peptidase (arrow) between leader peptide and proepidermin segment [1]. Amino acids in one letter codes: Leader peptide − 30 to − 1, proepidermin + 1 to + 22.

is marked by a single methionine codon ATG, which localized seven base pairs after a Shine-Dalgarno sequence AGGAGT; a TAA stop codon terminates the structural gene, directly after the two base triplets TGT which code two consecutive cysteine residues. In front of the structural gene of the prolantibiotic there is a leader sequence of 30 amino acids in length. The processing site for epidermin lies between Arg^{-1} and Ile^{+1}. The sequencing of the epidermin structural gene[1] demonstrated for the first time that lantibiotics evolve from ribosomally synthesized precursor proteins (Fig. 16).

Following this breakthrough, further research activities progressed rapidly. After epidermin, the structures of the complex antibiotics gallidermin,[11] Pep5[9] and, in collaboration with *Kessler*, cinnamycin[6] could be elucidated. The research team of *Entian* determined—on the DNA level—the sequences of the structural genes of the prelantibiotics pregallidermin[35] and pre-Pep5,[36] whose structures have been postulated by us, and finally, precinnamycin as a representative of lantibiotics of the type B.[37] The research team of *Götz* succeeded in characterizing the gallidermin-producing gene completely. The sequences of many of the participating enzymes in the biosynthesis of epidermin could be determined—on the DNA level—by *Entian* and his co-workers. At the same time *Hansen* and associates,[18b] and simultaneously *Entian* et al.[18a] determined the sequence of the structural gene of nisin. *Banerjee* and *Hansen* determined the precursor gene of subtilin.[19] In conclusion, it must be emphasized that the chemical structure of the lantibiotics which have been elucidated by us, could also be confirmed in detail by the sequencing of the structural genes. Finally, we could determine the sequences of the precursor proteins of the Pep5 biosynthesis which recently have been isolated by *Sahl*.[38] Some of these results will be discussed in the following section.

5.3. Comparison of the Lantibiotics

A comparison of the prediction profiles of the secondary structure, flexibility, hydropathy and hydrophilicity, which have been plotted with the help of our program EPICON 89,[39] as well as the helix-wheel plots of the six prelantibiotics known so far (Table 5) show surprisingly great similarities (Fig. 17).

Table 5. Lantibiotic precursors: Sequence length and localization of the structural gene (cf. Table 1).

	Leader peptide	Prolantibiotic	Prelantibiotic	Structural gene
Type A				
Epidermin [1]	− 30 → − 1	+ 1 → 22	52	Plasmid
Gallidermin [35]	− 30 → − 1	+ 1 → 22	52	Chrom. DNA
Pep5 [36]	− 26 → − 1	+ 1 → 34	60	Plasmid
Nisin [18]	− 23 → − 1	+ 1 → 34	57	Plasmid/DNA
Subtilin	− 24 → − 1	+ 1 → 32	56	Chrom. DNA
Type B				
Cinnamycin [37]	− 58 → − 1	+ 1 → 19	77	Chrom. DNA

Particularly striking is that all the leader sequences are very hydrophilic and strongly charged, do not contain cysteine, and most probably are folded to an amphiphilic α-helix in a lipophilic environment. In contrast, the prolantibiotic sequence is more lipophilic and its secondary structure is characterized by the preferential β-turn and lack of α-helices. It contains Ser, Thr and Cys, which become mod-

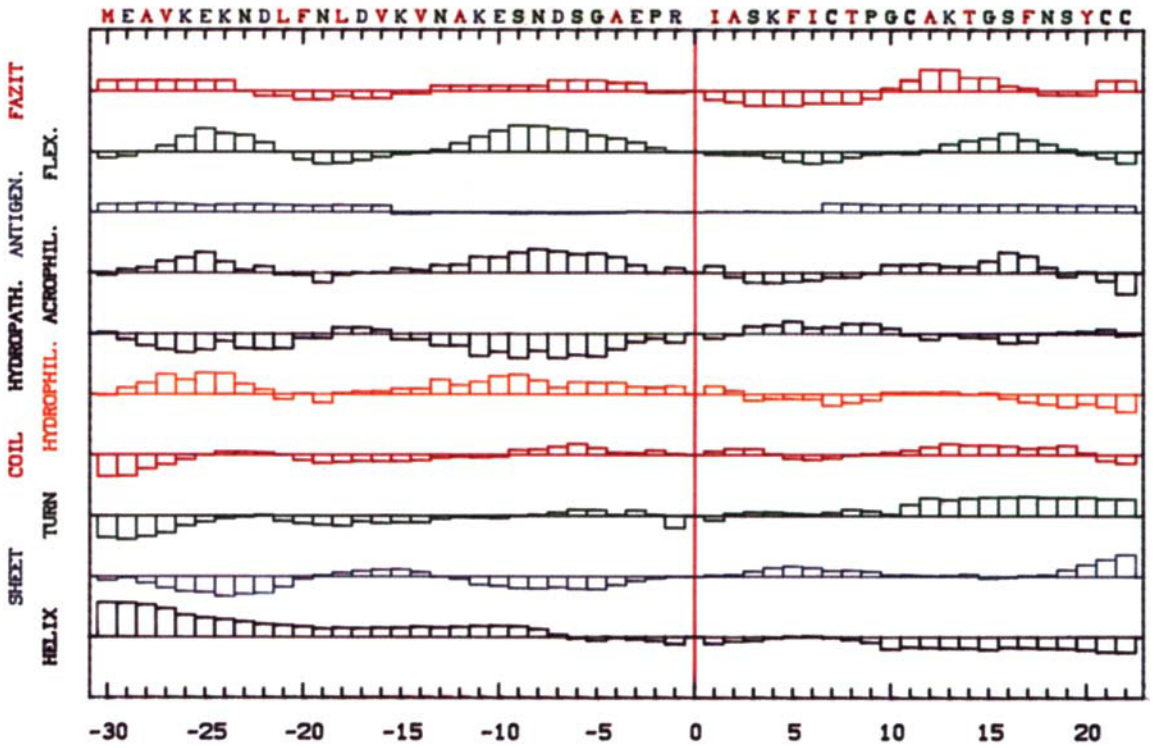

Fig. 17. Prediction profile of the epidermin precursor with the leader sequence − 30 to − 1, and prolantibiotic segment 1–22 [1], as determined by the program EPICON 89 [39]. "Fazit" is the sum of the following differently weighted predictions, and indicates the positions of the possible continuous B-cell epitopes. Flexibility (Flex.) shows flexible surface areas; antigenicity (antigen.) is calculated from the parameters derived from a comparison of the known sequential epitopes for different protein types; acrophilicity (acrophil.) shows the surface probability; hydropathy (hydropath.) predicts hydrophobicity, and hydrophilicity (hydrophil.) hydrophilic region. The prediction of the secondary structure is illustrated by the coil, turn, β-sheet and α-helix probabilities.

Type A Prolantibiotics*:

Nisin (a), **Subtilin** (b)

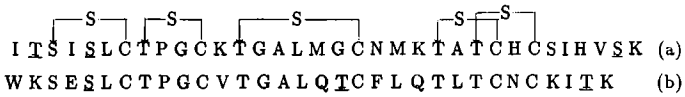

Epidermin (c), **Gallidermin** (d)

Pep5 (e)

Mersacidin (f)

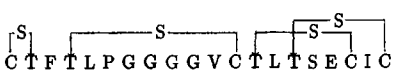

Actagardine (g)

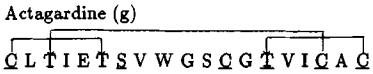

Type B Prolantibiotics*:

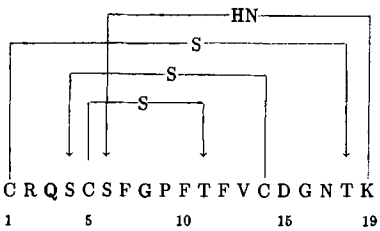

Fig. 18. Formation of the sulfide rings and α,β-didehydroamino acids in the prolantibiotic segment of prelantibiotics of type A (a–e) with the known structural genes (upper half). The prolantibiotic sequences of (f) and (g) are still not confirmed on the basis of their DNA; in the case of (g), configurational assignments of the C_α-carbon atoms are lacking. The sulfide ring formation in prelantibiotics of type B is shown in the lower half of the Figure. From the type B prolantibiotics, so far only the sequence of the structural gene of precinnamycin has been determined. * The arrows indicate direction of the sulfide bridge formation, starting from L-cysteine. Half of the *meso*-Lan and (2*S*, *S*, 6*R*)-3-MeLan molecules with the D-configuration are formed by the addition of L-cysteine thiol groups to Dha (from L-Ser) and Dhb (from L-Thr) residues, respectively. Underlined Ser and Thr residues remain Dha and Dhb in the processed lantibiotic (valid only for the type A). ** No lysinoalanine bridge 19 → 6 in ancovenin; however, with the exception of ancovenin, all the type B lantibiotics possess HyAsp in the position 15.

ified to α,β-didehydroamino acids and build sulfide bridges (Fig. 18).

The atypical leader sequences possess no lipophilic segment containing more than four amino acids; moreover, they contain many bonds accessible to endopeptidase cleavage. In contrast, the prolantibiotic part seems to be more resistant towards proteases. In the mature lantibiotics, such as, e.g., the epidermins and duramycins, there exist mostly only a few typical cleavage sites.

It is interesting to compare the processing site of the prelantibiotics (Table 6). Evidently the signal peptidases, which cleave the mature lantibiotic from the leader sequence, can attack a well-accessible and hydrophilic turn. Table 6 underscores the strong conservation of this site in the prelantibiotics of subtype A: The residues (+ 2) and (+ 1) are mainly hydrophobic, (− 1) is positively charged or polar, (− 2) always Pro, (− 3) negatively charged or polar, (− 4) always hydrophobic. With the help of fluorophor-labeled substrates of the signal peptidase, we are currently searching for the processing enzymes in the cell extracts.

Table 6. Signal peptidase cleavage sites (−) of prelantibiotics and prehormones (for comparison).

Prelantibiotics (cf. Table 5) [a]	− 5	− 1 +1
Nisin	Gly-Ala-Ser-	Pro -Arg—Ile-Thr-Ser-Ile
Subtilin	Lys-Ile-Thr-	Pro -Gln—Trp-Lys-Ser-Glu
Epidermin	Gly-Ala-Glu-	Pro -Arg—Ile-Ala-Ser-Lys
Gallidermin	Gly-Ala-Glu-	Pro -Arg—Ile-Ala-Ser-Lys
Pep5	Glu-Leu-Glu-	Pro -Gln—Thr-Ala-Gly-Pro
Cinnamycin	Thr-Glu-Ala-Phe-Ala—	Cys-Arg-Gln-Ser
Prehormones (for comparison)		
ANP	Ala-Gly-	Pro -Arg—Ser-Leu-Arg
Substance P	Ile-Ala-Arg—Arg-	Pro -Lys-Pro

[a] Modified amino acid residues in the lantibiotic are marked

In comparison to the precursor proteins of the lantibiotic type A (e.g. nisin), the only known prelantibiotic of type B differs considerably. This is precinnamycin (= pre-Ro 09-0198, prelanthiopeptin), whose structural gene sequence was recently determined by *Kaletta* and *Entian*.[37] Remarkably, the leader sequence of this prelantibiotic of subtype B is about twice as long, i.e., it consists of 58 amino acids (Table 5). It is predicted that the part which immediately follows N-terminally to the processing site, has a high α-helix probability. Similarly as in the other lantibiotics, one finds here high lipophilicity and β-turn probability in the 19 amino acid segment which C-terminally follows the leader peptide, and in which the ring formation takes place. The completely different processing site of procinnamycin (Table 6), which by no means shows homology to the prelantibiotics of subtype A, likewise points to different signal peptidases for these two subtypes.

5.4. Synthesis and Conformation of Leader Peptides

In order to obtain experimental data about the α-helix in the leader region of the prelantibiotics, as shown by the prediction plot, we synthesized all the leader peptides by the Merrifield method, using the Fmoc/*t*Bu strategy and maximum side-chain protection.[40] The amino acids were activated by the new coupling reagent TBTU (2-(1*H*-benzotriazol-1-yl)-1,1,3,3-tetramethyluronium tetrafluoroborate). After purification on Sephadex G25 and RP18-HPLC, very pure products were obtained whose identification was achieved by amino acid analysis, racemization test, Edman degradation, and ion-spray mass spectrometry.

Circular dichroism spectra were recorded in trifluoroethanol/water mixtures. Two negative Cotton effects at 207 and 220 nm as well as a positive ellipticity at 194 nm indicated an α-helical conformation in all the leader peptides (Fig. 19). The α-helical content increased as expected with increasing lipophilicity of the solvents. By comparing these peptides with peptides of similar size and known α-helix content, an α-helix content of 70 ± 15% in trifluoroethanol/water (9:1) could be estimated. Therefore, the extremely hydrophilic prelantibiotic leader peptides possess a very high α-helix content in a lipophilic medium. Before discussing the results of these studies concerning the biosynthesis, I would like to outline the exciting results obtained on isolation and characterization of the intermediates in the biosynthesis of the lantibiotic Pep5.

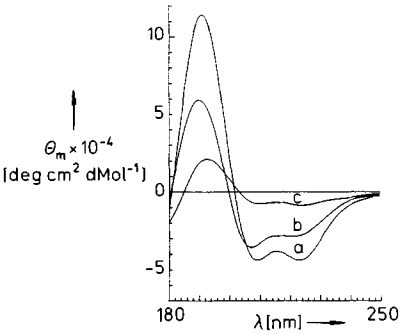

Fig. 19. CD-Spectra of the isolated natural precursor protein pre-Pep5 (sequence −26 to +34) of lantibiotic Pep5 (a), synthetic α-helical leader peptide −26 to −21 of Pep5 (b), and isolated naturally occurring lantibiotic Pep5 (c) in trifluoroethanol/water (9:1).

5.5. Isolation and Structural Elucidation of Modified and Unmodified Prelantibiotics

In collaboration with *Sahl*, we attempted to characterize the precursor protein of pre-Pep5, as a primary translational product in the biosynthesis of the tricyclic lantibiotic Pep5.[9, 10] A 60 amino acids long pre-Pep5 could be deduced from the sequencing of the structural gene.[36] The synthetic helical leader peptide with 26 amino acids was used as an immunogen to produce polyclonal antibodies. In the crude extracts of the Pep5-producing strain *Staphylococcus epidermidis 5*, several similar proteins with molecular masses of 6000 to 7000 Da have been identified. These proteins were subjected to RP-HPLC for a rapid isolation and characterization.[38] For the isolation, a high concentration of the serine protease inhibitor, phenylmethylsulfonyl fluoride (PMSF), had to be added.

One of the two isolated proteins reacted likewise with the polyclonal serum, which was obtained after immunization with a C-terminal Pep5 fragment containing two sulfide bridges. Neither lanthionine nor 3-methyllanthionine have been detected by amino acid analysis of this isolate. We were able to carry out an automated Edman degradation using a gas-phase sequencer and on line PTH detection with about 800 pmol material. The amino acid sequence obtained was comparable to the Edman degradation of 400 pmol of the synthetic leader peptide[40] (Fig. 20). Edman degradation, however, stopped at the first threonine residue of the prolantibiotic region. We considered this an indication of the post-translational modification that had already occurred at this position.[38]

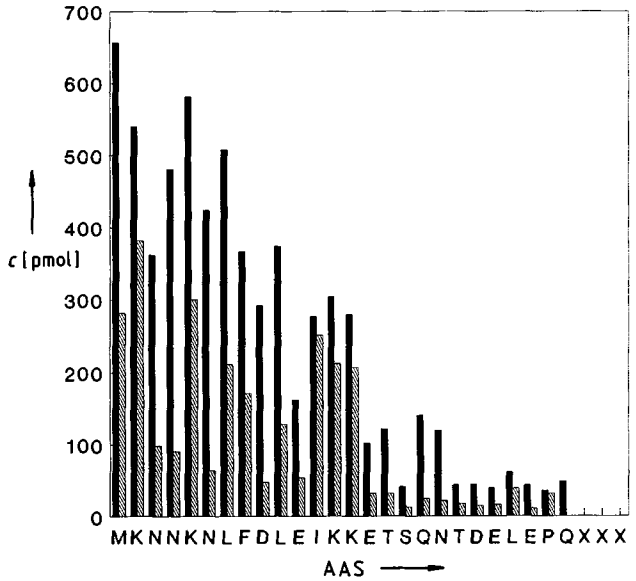

Fig. 20. Yields of the Edman degradation steps of the isolated pre-Pep5 (black columns) compared with the degradation of the synthetic leader peptide −26 to −1 (shaded columns). c = concentration of PTH-amino acid in pmol per degradation step, AAS = amino acid sequence.

With the modest amount of peptide solution which remained available after the Edman degradation, we could carry out a mass spectrometric investigation using the new method of ion-spray mass spectrometry with the API-III spectrometer. The solution was fed to the spectrometer via a glass capillary at the rate of 5 μL/min for 10 min. From the resulting mass spectra of the multiply charged prelantibiotic ions, a molecular mass of 6575 ± 1.7 Da was determined (Fig. 21). This agreed with a pre-Pep5 molecule which is dehydrated at the four threonine and two serine residues of the prelantibiotic region. This sixfold dehydrated protein has a calculated molecular mass of 6576.7 Da.

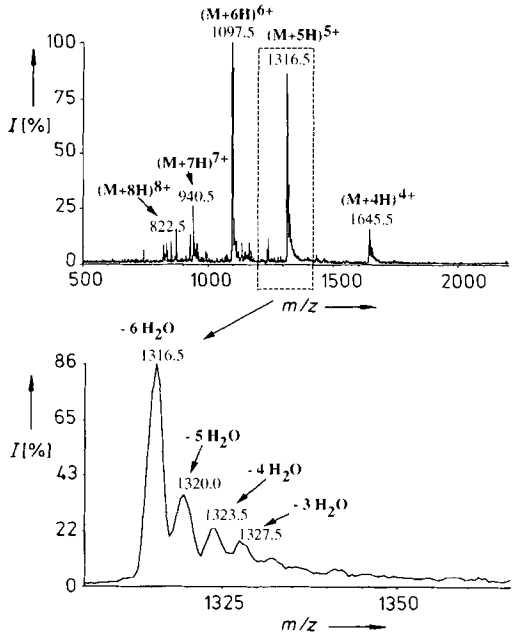

Fig. 21. Ionspray API-III mass spectrum of the isolated and 6-fold dehydrated pre-Pep5. The peaks correspond to each molecular ion with the same molecular mass of 6575 ± 1.7 Da, but with different charges (4+ to 8+). The extra peaks which are visible on the background are due to the masses of the partially dehydrated precursor proteins.

The sixfold dehydrated pre-Pep5 (Fig. 22) is so far the first isolated and characterized precursor protein of a ribosomally synthesized and post-translationally modified peptide antibiotic. Our results show that lantibiotic biosynthesis is initiated by a selective dehydration of the hydroxyamino acids at the prolantibiotic part of the primary translational product. The sulfide ring formation is, therefore, not directly

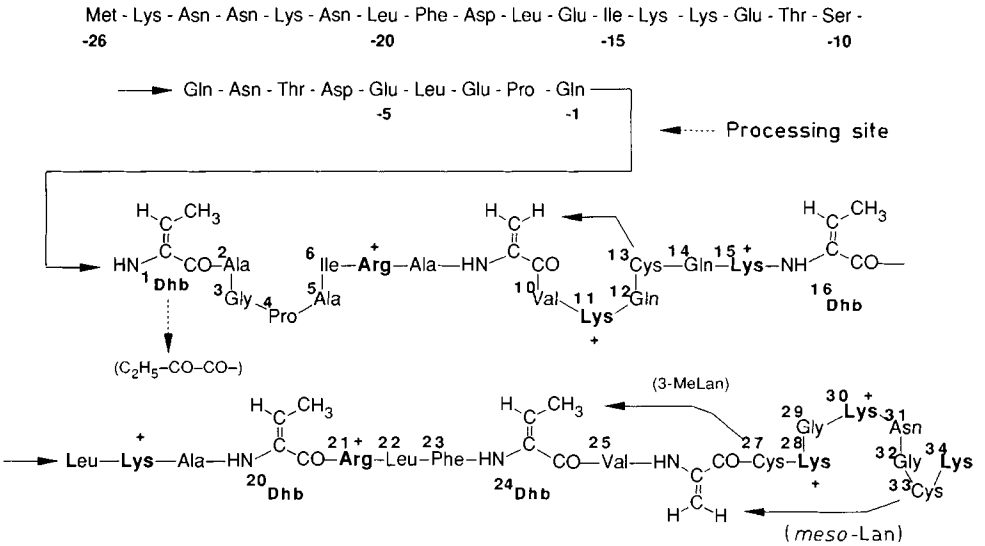

Fig. 22. Structure of the isolated precursor protein of Pep5 (pre-Pep5) with the sixfold dehydrated prolantibiotic region (1 to 34). − 26 to − 1 is the α-helical leader region.

connected with the dehydration step. Consequently, in the biosynthetic scheme of a lantibiotic (Fig. 15), the dehydrated prelantibiotic must be classified as an isolable intermediate. Shortly afterwards, the completely unmodified pre-Pep5 and a pre-Pep5 with sulfide rings and dehydroamino acids could similarly be isolated and characterized by sequencing and mass spectrometry. Thus, all of the intermediates of the modified precursor protein of a lantibiotic postulated so far have been experimentally determined for the first time.

6. Outlook

With the isolation of unmodified, up to sixfold dehydrated and also sulfide ring-containing pre-Pep5 biosynthetic intermediates, it has been possible to make a decisive step towards an unambiguous elucidation of the lantibiotic biosynthesis. The enzymes required for the post-translational modification and processing could so far be localized on the DNA level, but could not be isolated. At the moment, the following areas are being investigated by the research groups of *Entian*, *Götz*, *Sahl* and by us. The mechanism of the enzymatic dehydration is being studied to find out, e.g., whether the hydroxy group is converted into a better leaving group through phosphorylation by cyclic AMP dependent kinases, as happens in the dehydration of free serine and threonine, or whether another activation takes place.

We still do not know how the stereospecific addition of the cysteinyl SH-groups to the double bonds of the α,β-didehydroamino acids is catalyzed. An originally discussed, spontaneous ring formation can be ruled out, although in experimental chemistry these thiol additions are possible. However, for the occurrence of this reaction at room temperature, a thousandfold excess of thiol and many days of reaction time are required. The order of the ring formation, from C-terminal to N-terminal, or vice versa, is also not known. The discovery of the natural intermediates,[38] and the chemical synthesis of unmodified prelantibiotics[40] demonstrate, however, the experimental possibilities of studying the mechanism of the ring formation.

The enzyme which takes part in the modification of the preepidermins and premersacidin, and catalyzes the oxidative decarboxylation to the aminovinyl group, could gain special interest in connection with the findings concerning the biosynthesis of scents from flowers and insects which also contain vinylic structures derived from carboxylic acid precursors.[41]

Finally, we do not know how the signal peptidase functions, and whether at the same time it is a protein involved in an export function. Does this reaction partly occur on a multifunctional enzyme complex, or successively on the isolated localized enzymes?

Especially interesting is also the question of how the producing cells protect themselves against toxic lantibiotics. To clarify the principle of this self-protection,[14] different investigations are presently being carried out in the fields of protein analysis and genetics. In principle, a protecting effect of the leader peptide would be conceivable. As long as the hydrophilic leader peptide is covalently bound to the modified lantibiotic, or when it is bound—by intermolecular interaction—to the already cleaved lantibiotic, the latter cannot exert its toxic effect on the cell wall.

An active participation of the leader region during the modification steps is very probable, this is based on the high content of charged amino acids, the negative net charge, a very similar processing site and the α-helical content. On the basis of the conservation of these properties by all the known prelantibiotics, the leader peptide is at least supposed to have the functional role of stabilizing a definite conformation of the prolantibiotic segment. The leader peptide could also actively participate in the enzymatic modification steps. Finally, the leader peptide could carry the recognition region for the attachment to the modifying enzymes, signal peptidase or exporting protein.

Interestingly, the half-life of the primary translational product is very short, as it is evidently dehydrated immediately in the native producing cells.[38] We use, therefore, totally synthesized pre- and prolantibiotics as substrates for the dehydrating enzymes. The total synthesis of preepidermin with 52 residues has already been carried out successfully by segment condensation of protected purified fragments.[40] Provided that the formation of the double bond does not proceed immediately after the protein synthesis, one could quickly determine the specificity and possible application of these enzymes with the help of a large number of synthetic substrates.

In microbial genetics, sequence modified lantibiotics are already produced by the use of synthetic structural genes. For this purpose, plasmids with mutated structural genes are employed for the transformation of the producing strains. Thus, the resulting altered lantibiotics are investigated for their antimicrobial activity, sequence, and conformation. The first analogue prepared by this procedure through base exchange ("site directed mutagenesis") could already be isolated and tested by *Götz* and his group in Tübingen.[42]

The author is grateful for the intensive and exciting cooperation of the microbiological and gene technological research teams of K.-D. Entian, P. Fiedler, F. Götz, H.-G. Sahl, R. G. Werner, and especially H. Zähner, the coordinator of the Sonderforschungsbereich 323. The structural elucidations, conformational analyses, and peptide syntheses were carried out by my highly motivated co-workers H. Allgaier, R. Kellner, S. Freund, S. Stevanovic and A. Beck-Sickinger. I thank A. Bayer for critically reviewing the manuscript. The molecular dynamics simulation was performed in cooperation with O. Gutbrod and G. Folkers. Thanks are also due to W. A. Gibbons for the work which was carried out by S. Freund in his research laboratory in London and for the unproblematical access to his 500 MHz NMR spectrometer. I also thank the Deutsche Forschungsgemeinschaft for financially supporting the groups of SFB 323.

Received: July 10, 1990;
revised: March 20, 1991 [A 833 IE]
German version: *Angew. Chem. 109* (1991) 1067
Translated by Dr. *B. Hemmasi*, Tübingen (FRG)

[1] N. Schnell, K.-D. Entian, U. Schneider, F. Götz, H. Zähner, R. Kellner, G. Jung, *Nature 333* (1988) 276.

[2] a) E. Gross, J. L. Morell, *J. Am. Chem. Soc. 93* (1971) 4634; b) E. Gross in L. Fox (Ed.): *Thirty years of protein structure elucidation*, Dekker, New York 1976; c) E. Gross, J. H. Brown in A. Loffet (Ed.): *Peptides 1976*, Editions de l'Université de Bruxelles, Brüssel 1976, p. 183.

[3] a) A. Hurst, *Adv. Appl. Microbiol. 27* (1981) 85; b) K. Rayman, A. Hurst in E. J. Vandamme (Ed.): *Biotechnology of industrial antibiotics*, Dekker, New York 1984, p. 607, and references cited therein.

[4] a) H. Allgaier, G. Jung, R.-G. Werner, U. Schneider, H. Zähner, *Angew. Chem. 97* (1985) 1052; *Angew. Chem. Int. Ed. Engl. 24* (1985) 1051; b) *Eur. J. Biochem. 160* (1986) 9.

[5] a) T. Wakamiya, Y. Ueki, T. Shiba, Y. Kido, Y. Motoki, *Tetrahedron Lett. 26* (1985) 665; b) M. Nishikawa, T. Teshima, T. Wakamiya, T. Shiba, Y. Kobayashi, T. Ohkubo, Y. Kyogoku, Y. Kido in T. Shiba, S. Sakakibara (Eds.): *Peptide Chemistry*, Protein Research Foundation, Osaka 1988, p. 71; c) T. Shiba, T. Wakamiya, K. Fukase, A. Sano, K. Shimbo, Y. Ueki, *Biopolymers 25 (Suppl.)* (1986) S11–S19.

[6] a) H. Kessler, S. Steuernagel, M. Will, G. Jung, R. Kellner, D. Gillessen, T. Kamiyama, *Helv. Chim. Acta 71* (1988) 1924; b) S. Steuernagel, *Dissertation*, Universität Frankfurt 1989.

[7] a) E. Gross, *Adv. Exp. Med. Biol. B86* (1977) 131; b) W. Dworidi, O. L. Shotwell, R. G. Benedict, T. G. Pridham, L. A. Lindenfelser, *Antibiot. Chemother. 4* (1954) 1135; c) O. L. Shotwell, F. H. Stodola, W. R. Michael, L. A. Lindenfelser, R. G. Dworschack, T. G. Pridham, *J. Am. Chem. Soc. 80* (1958) 3912; d) A. Fredenhagen, G. Fendrich, F. Märki, W. Märki, J. Gruner, F. Raschdorf, H. H. Peter, *J. Antibiot. 43* (1990) 1403; e) S. Clejan, A. A. Guffanti, M. A. Cohen, T. A. Krulwick, *J. Bacteriol. 171* (1989) 1744; f) P. M. Sokolove, P. A. Westphal, M. B. Kester, R. Wierwille, K. Sikora-Van Meter, *Biochim. Biophys. Acta 983* (1989) 15; g) E. A. Dunkley, S. Clejan, A. A. Guffanti, T. A. Krulwick, *ibid. 943* (1988) 13; h) L. Chen, P. C. Tai, *J. Bacteriol. 169* (1987) 2373; i) G. Lindblom, M. Sjoelund, L. Rilfors, *Liq. Cryst. 3* (1988) 783; j) E. Kinne-Saffran, R. Kinne, *Pfluegers Arch. 407 (Suppl. 2)* (1986) 180; k) J. Navorro, J. Chabot, K. Sherill, R. Aneja, S. A. Zahler, E. Racker, *Biochemistry 24* (1985) 4645; l) S. Choung, T. Kobayashi, K. Takemoto, H. Ishitsuka, K. Inoue, *Biochim. Biophys. Acta 940* (1988) 180; m) S. Choung, T. Kobayashi, J. Inoue, K. Takemoto, H. Ishitsuka, K. Inoue, *ibid. 940* (1988) 171.

[8] a) Ger. offen. DE 38 27 868 A1 of February 22, 1990, German Patentoffice; b) J. K. Kettenring, A. Malabarba, K. Vĕkey, B. Cavalleri, *J. Antibiot. 53* (1990) 1082; c) A. Malabarba, R. Pallanza, M. Berti, B. Cavalleri, *ibid. 53* (1990) 1089; d) F. Parenti, H. Pagani, G. Beretta, *ibid. 29* (1976) 501; e) C. Coronelli, G. Tamoni, G. C. Lancini, *ibid. 38* (1985) 1506.

[9] a) R. Kellner, G. Jung, M. Josten, C. Kaletta, K.-D. Entian, H.-G. Sahl, *Angew. Chem. 101* (1989) 618; *Angew. Chem. Int. Ed. Engl. 28* (1989) 616; b) R. Kellner, G. Jung, C. Kaletta, K.-D. Entian, H. G. Sahl, *Pept. Proc. Eur. Pept. Symp. 20th 1989*, 369.

[10] a) H.-G. Sahl, H. Brandis, *J. Gen. Microbiol. 127* (1981) 377; b) H.-G. Sahl, M. Grossgarten, W. R. Widger, W. A. Cramer, H. Brandis, *Antimicrob. Agents Chemother. 27* (1985) 836; c) G. Bierbaum, H.-G. Sahl, *Arch. Microbiol. 141* (1985) 249.

[11] a) R. Kellner, G. Jung, T. Hörner, H. Zähner, N. Schnell, K.-D. Entian, F. Götz, *Eur. J. Biochem. 177* (1988) 53; b) R. Kellner, G. Jung, *Pept. Proc. Eur. Pept. Symp. 20th 1989*, 366.

[12] a) T. Wakamiya, K. Fukase, N. Naruse, M. Konishi, T. Shiba, *Tetrahedron Lett. 29* (1988) 4771; b) N. Naruse, O. Tenmyo, K. Tomita, M. Konishi, T. Miyaki, H. Kawaguchi, K. Fukase, T. Wakamiya, T. Shiba, *J. Antibiot. 42* (1989) 837; c) K. Fukase, T. Wakamiya, N. Naruse, M. Konishi, T. Shiba in M. Ueki (Ed.): *Peptide Chemistry 1988*, Protein Research Foundation, Osaka 1989, p. 221.

[13] a) H.-G. Sahl, H. Brandis, *FEMS Microbiol. Lett. 1* (1983) 75; b) H.-G. Sahl, *J. Bacteriol. 162* (1985) 833; c) M. Kordel, R. Benz, H.-G. Sahl, *ibid. 170* (1988) 84; d) E. Ruhr, H.-G. Sahl, *Antimicrob. Agents Chemother. 27* (1985) 841; e) H.-G. Sahl, M. Kordel, R. Benz, *Arch. Microbiol. 149* (1987) 120; f) H.-G. Sahl, *Forum Microbiol. 10* (1987) 330; *ibid. 10* (1987) 337; g) G. Bierbaum, H.-G. Sahl, *Arch. Microbiol. 141* (1985) 249; h) *FEMS Microbiol. Lett. 58* (1988) 223; i) M. Kordel, F. Schüller, H.-G. Sahl, *FEBS Lett. 244* (1989) 99; j) G. Bierbaum, H.-G. Sahl, *J. Bacteriol. 169* (1987) 5452.

[14] H.-G. Sahl, H. Erssfeld-Dressen, G. Bierbaum, M. Josten, M. Kordel, M. Reis, F. Schüller, *Zentralbl. Bacteriol. Microbiol. Hyg. Abt. 1 Orig. A 267* (1987) 173.

[15] a) E. Küsters, H. Allgaier, G. Jung, E. Bayer, *Chromatographia 18* (1984) 287; b) G. Jung, M. Ottnad, M. Rimpler, *Eur. J. Biochem. 35* (1973) 436; c) G. Jung, M. Ottnad, *Chem. Ztg. 98* (1974) 147; d) G. Jung, M. Ottnad, in K. Maas (Ed.): *Themen zur Chemie des Schwefels*, Hüthig, Heidelberg 1975, p. 167, and references cited therein.

[16] a) E. Gross, J. L. Morell, *J. Am. Chem. Soc. 89* (1967) 2791; b) *ibid. 92* (1970) 2919; c) E. Gross in R. Walter, J. Meienhofer (Eds.): *Pept. Proc. Am. Pept. Symp. 4th 1975*, 31; d) E. Gross, K. Noda, B. Nisula, *Angew. Chem. 85* (1973) 672; *Angew. Chem. Int. Ed. Engl. 12* (1973) 664; e) E. Gross in J. L. Fox, Z. Deyl, A. Blazej (Eds.): *Protein Structure Evolution*, Dekker, New York 1976, p. 69.

[17] a) E. Gross, H. H. Kiltz, L. C. Craig, *Hoppe-Seyler's Z. Physiol. Chem. 354* (1973) 799; b) H. H. Kiltz, E. Gross, *ibid. 354* (1973) 802; c) *ibid. 354* (1973) 805; d) E. Nebelin, E. Gross, *ibid. 354* (1973) 807; e) E. Gross, H. H. Kiltz, E. Nebelin, *ibid. 354* (1973) 810.

[18] a) C. Kaletta, K.-D. Entian, *J. Bacteriol. 171* (1989) 1597; b) G. W. Buchman, S. Banerjee, J. N. Hansen, *J. Biol. Chem. 263* (1988) 16260; c) H. M. Dodd, N. Horn, M. J. Gasson, *J. Gen. Microbiol. 136* (1990) 555.

[19] S. Banerjee, J. N. Hansen, *J. Biol. Chem. 263* (1988) 9508.

[20] a) K. Fukase, M. Kitazawa, A. Sano, K. Shimbo, H. Fujita, S. Horimoto, T. Wakamiya, T. Thiba, *Tetrahedron Lett. 29* (1988) 795; b) K. Fukase, M. Kitazawa, H. Sano, K. Shimbo, H. Fujita, S. Horimoto, T. Wakamiya, T. Shiba in T. Shiba, S. Sakakibara (Eds.): *Peptide Chemistry 1987*, Protein Research Foundation, Osaka 1988, p. 337; c) S. Nomoto, A. Sano, T. Shiba in N. Izumiya (Ed.): *Peptide Chemistry 1978*, Protein Research Foundation, Osaka 1979, p. 35; d) T. Wakamiya, Y. Oda, K. Fukase, T. Shiba, *Bull. Chem. Soc. Jpn. 58* (1985) 536, and references cited therein; e) M. Kitazawa, K. Fukase, T. Wakamiya, T. Shiba in T. Miyazawa (Ed.): *Peptide Chemistry 1986*, Protein Research Foundation, Osaka 1987, p. 317.

[21] a) T. Hörner, H. Zähner, R. Kellner, G. Jung, *Appl. Microbiol. Biotechnol. 30* (1989) 219; b) T. Hörner, V. Ungermann, H. P. Fiedler, H. Zähner, R. Utz, R. Kellner, G. Jung, *ibid. 32* (1990) 511; c) G. Jung, H. Allgaier, R. Kellner, U. Schneider, T. Hörner, H. Zähner, R.-G. Werner, in H. Chmiel, W. P. Hammes, J. E. Bailey (Eds.): *Biochemical Engineering*, Fischer, Stuttgart 1987, p. 494; d) H. Allgaier, private communication.

[22] S. Kondo, M. Sezaki, M. Shimura, K. Sato, T. Hara, *J. Antibiot. 17* (1964) 262.

[23] a) U. Schmidt, A. Lieberknecht, U. Kazmaier, E. Haslinger, *Angew. Chem. 102* (1990) 562; *Angew. Chem. Int. Ed. Engl. 29* (1990) 514; b) U. Schmidt, R. Utz, P. Gleich, *Tetrahedron Lett. 26* (1985) 4367; c) U. Schmidt, R. Utz, *Angew. Chem. 96* (1984) 723; *Angew. Chem. Int. Ed. Engl. 23* (1984) 725; d) A. Lieberknecht, H. Griesser, *Tetrahedron Lett. 28* (1987) 4275.

[24] M. Slijper, C. W. Hilbers, R. N. H. Konings, F. J. M. van de Ven, *FEBS Lett. 252* (1989) 22.

[25] a) W. C. Chan, B. W. Bycroft, L.-Y. Lian, G. C. K. Roberts, *FEBS Lett. 252* (1989) 29; b) W. C. Chan, L.-Y. Lian, B. W. Bycroft, G. C. K. Roberts, *J. Chem. Soc. Perkin Trans. 1 1989*, 2359.

[26] a) D. E. Palmer, D. F. Mierke, C. Pattaroni, K. Nunami, S. Ro, Z. Huang, T. Wakamiya, K. Fukase, M. Kitazawa, H. Fujita, T. Shiba, M. Goodman, *Pept. Chem. Struct. Biol. Funct. Proc. Am. Pept. Symp. 11th 1990*, 616; b) D. E. Palmer, D. F. Mierke, C. Pattaroni, M. Goodman, T. Wakamiya, V. Fukase, M. Kitazawa, H. Fujita, T. Shiba, *Biopolymers 28* (1989) 397.

[27] a) S. Freund, O. Gutbrod, G. Folkers, W. A. Gibbons, G. Jung, *Biopolymers 31* (1991) 803; b) S. Freund, G. Jung, O. Gutbrod, G. Folkers, W. A. Gibbons, *Pept. Proc. Eur. Pept. Symp. 21th 1991*, 538.

[28] G. Jung, *Pept. Synth. Struct. Biol. Funct. Proc. Am. Pept. Symp. 11th 1990*, 865. (Note: This publication contains the wrong duramycin sequence after E. Gross [7a, 2c].)

[29] a) H. Allgaier, *Dissertation*, Universität Tübingen 1985; b) G. Jung, H. Allgaier, R. G. Werner, U. Schneider, H. Zähner in D. Theodoropoulos (Ed.): *Peptides 1986*, de Gruyter, Berlin 1987, p. 241.

[30] a) L. Ingram, *Biochim. Biophys. Acta 224* (1970) 263; b) *ibid. 184* (1969) 216.

[31] F. Lipman, W. Gevers, H. Kleinkauf, R. Roskowski, *Adv. Enzymol. Relat. Areas Mol. Biol. 35* (1971) 64.

[32] C. Nishio, S. Komura, K. Kurahashi, *Biochem. Biophys. Res. Commun. 16* (1983) 751.

[33] W. Kazak, M. Rajchert-Trzpil, W. T. Dobrzanski, *J. Gen. Microbiol. 83* (1974) 295.

[34] U. Schneider, *Dissertation*, Universität Tübingen 1985.

[35] a) N. Schnell, K.-D. Entian, F. Götz, T. Hörner, R. Kellner, G. Jung, *FEMS Microbiol. Lett. 58* (1989) 263; b) F. Götz, K.-D. Entian, G. Jung, H. Zähner in T. Wadström, I. Eliasson, I. Holder, A. Ljungh (Eds.): *Pathogenesis of Wound and Biomaterial-Associated Infections*, Springer, Heidelberg 1990, p. 285.

[36] C. Kaletta, K.-D. Entian, R. Kellner, G. Jung, M. Reis, H. G. Sahl, *Arch. Microbiol. 152* (1989) 16.

[37] C. Kaletta, K.-D. Entian, G. Jung, *Eur. J. Biochem. 199* (1991) 411.

[38] H. P. Weil, A. G. Beck-Sickinger, J. Metzger, S. Stevanovic, G. Jung, M. Josten, H.-G. Sahl, *Eur. J. Biochem. 194* (1990) 217.

[39] a) W. Tröger, *Dissertation*, Universität Tübingen 1990; b) W. Tröger, G. Jung, unpublished results.

[40] A. G. Beck-Sickinger, G. Jung, unpublished results.

[41] G. Görger, W. Boland, *Eur. J. Biochem. 185* (1989) 237.

[42] Note: "The First International Workshop on Lantibiotics" was held in Bad Honnef (FRG) on April 15–18, 1991. All reports will be published as original papers in G. Jung and H.-G. Sahl (Eds): *Nisin and Novel Lantibiotics*, Escom. Publ., Leiden, 1991.

Cyclopentadienyl–Actinide Complexes: Bonding and Electronic Structure

By Bruce E. Bursten* and Richard J. Strittmatter

Shortly after the discovery of ferrocene, *Reynolds* and *Wilkinson* demonstrated that actinide elements are capable of forming organometallic compounds containing the cyclopentadienyl (Cp) ligand. The compound they reported, $[Cp_3UCl]$, was the first of a host of organoactinide complexes that contain Cp and substituted Cp ligands. In 1968, *Streitwieser* and *Müller-Westerhoff* synthesized uranocene, $[(C_8H_8)_2U]$, a molecule whose existence had been predicted five years earlier by *R. D. Fischer*. Because uranocene has no analogue in transition-metal chemistry, its synthesis stimulated new interest in organoactinide chemistry and in comparisons with organotransition-metal chemistry. Since that time, Cp and substituted Cp ligands, such as pentamethylcyclopentadienyl (Cp*), have become the most important and flexible ligands in actinide organometallic chemistry. In the past 15 years especially, the bonding of Cp ligands to actinide elements has been extensively probed by both experiment and theory. There are both significant similarities and equally significant differences in the bonding of the Cp ligand to the f-element metals compared to the d-element metals.

1. Introduction

Since the discovery of the remarkable structure of ferrocene, $[(\eta^5\text{-}C_5H_5)_2Fe]$ (**1**), in 1952,[1] the cyclopentadienyl (Cp) ligand has played a central role in organometallic chemistry. In the flurry of activity that followed the synthesis of **1**, alkali cyclopentadienides were allowed to react with a wide variety of metal halides in an effort to synthesize new organometallics with π-bonded Cp ligands. The birth of the organometallic chemistry of the actinide elements came in 1956, with the report by *Reynolds* and *Wilkinson* of $[Cp_3UCl]$ (**2**), which contains three Cp ligands π-bonded to uranium.[2] In the early 1960s, *E. O. Fischer* and co-workers reported the preparation of $[Cp_4An]$ complexes (**3**; An = Th, U);[3] the presence of four π-bonded Cp ligands is without precedent among the transition elements.

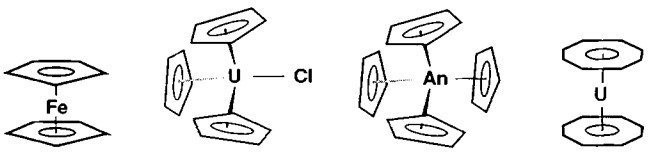

1 **2** **3** **4**

The distinct nature of organoactinide chemistry compared to organotransition-metal chemistry was boldly underscored in 1968 with the synthesis of uranocene $[(\eta^8\text{-}C_8H_8)_2U]$ (**4**) by *Streitwieser* and *Müller-Westerhoff*.[4] This beautiful molecule, whose existence had been considered theoretically five years earlier by *R. D. Fischer*,[5] consists of two planar C_8 rings sandwiching a uranium atom[6] and has no analogue among the transition elements. Actinocenes of many of the other actinide elements were subsequently synthesized[7] and studied both spectroscopically[8] and theoretically.[9] The electronic structure of uranocene is still a matter of intense experimental and theoretical interest; in 1989, for example, state-of-the-art photoelectron spectroscopic[10] and ab initio theoretical[11] studies of the molecule were reported. The synthesis of uranocene is often considered the beginning of modern organoactinide chemistry, and many excellent review articles and monographs on this field have appeared in recent years.[12]

In the past two decades organoactinide chemistry has fluorished with the synthesis of the first isolable compounds containing uranium–carbon σ bonds in 1973,[13] the discovery of facile activation of CO by thorium and uranium alkyls in 1978,[14] the synthesis of the first uranium–carbon multiple bond in 1981,[15] the synthesis of the first compounds containing supported[16] and unsupported[17] metal–metal bonds involving an actinide element in 1985, the synthesis of the first molecular actinide carbonyl complex that is stable at room temperature in 1986,[18] and the synthesis of both the first mixed C_8H_8-Cp complex of an actinide metal[19] and the first neutral homoleptic uranium alkyl complex in 1989.[20] All but the last of these significant developments have involved organoactinide complexes with Cp or substituted Cp ligands.

In this review, we will present the development of bonding models for Cp–actinide complexes, a topic that has been studied in detail only in the last decade. We will focus particularly on the use of molecular orbital (MO) theory as an electronic structural probe of these systems. When possible, we will discuss the relationship of the MO results to experimental studies, particularly those involving photoelectron spectroscopy (PES), which has been the most widely used experimental probe of bonding in organoactinide chemistry.[21] We begin with a brief historical discussion of the challenges posed by the presence of valence f orbitals. The remainder of the discussion is separated, somewhat arbitrarily, into a focus on Cp-to-actinide bonding and the bonding of Cp–actinide complexes to other ligands.

2. The Electronic Structural Challenge of the 5f Elements

Although the development of organoactinide chemistry came shortly after the birth of modern organotransition-

[*] Prof. B. E. Bursten, Dr. R. J. Strittmatter
Department of Chemistry
The Ohio State University
Columbus, OH 43210 (USA)

metal chemistry, the level of understanding of the former has lagged well behind that of the latter. For example, in transition-metal organometallics, the effective-atomic-number (or eighteen-electron) rule allows one to predict, a priori, the existence and inherent stability of many compounds. No such rule exists in organoactinide chemistry: compounds have been reported with formal electron counts as low as nine, $[U\{CH(SiMe_3)_2\}_3]$,[20] and as high as twenty-eight, $[Cp_3Np \cdot 3thf]$.[22] The reasons for the comparatively low level of understanding of the bonding in organoactinide complexes are manifold: (1) There is a paucity of experimental results in organoactinide chemistry relative to organotransition-metal chemistry. The high radioactivity and transient existence of most actinide elements preclude systematic studies of organoactinide complexes in which the metal atom is varied. Thorium and uranium are the only actinide elements that are relatively easy to study in the laboratory. (2) The large sizes of actinide atoms lead to highly variable and unpredictable coordination numbers. (3) The number of electrons in organoactinide complexes is large enough to make rigorous quantum-chemical calculations exceptionally demanding computationally. (4) Relativistic effects are profound for the actinide elements. Although there have been numerous studies demonstrating the importance of relativistic effects in the heavy elements,[23] these phenomena remain poorly understood by many chemists, hindering the understanding of electronic-structure results on the actinide elements. (5) Actinide metals contain valence f orbitals, with which many chemists are uneasy.[24] Furthermore, the computer codes for many quantum-chemical methods are not able to accommodate valence f orbitals.

Even before the emergence of organoactinide chemistry, the relative importance of the valence 5f orbitals in describing the bonding and electronic structure in actinide compounds had been, and continues to be, a question of considerable debate among theoretical and experimental chemists. In one of the earliest references to f orbitals, *Van Vleck* pointed out that they are essential for describing the bonding in complexes with high coordination numbers (as are commonly found in organoactinide complexes).[25] *Eisenstein* used a group-theoretical approach to argue for the involvement of 5f orbitals in covalent bonding in $[UO_2]^{2+}$, $[UCl_6]$, and $[UCl_4]$.[26] *Kettle* and co-workers presented stereochemical arguments for f-orbital involvement in bonding,[27] but later concluded that f-orbital bonding is usually weak because of the small size and energetic inaccessibility of the f orbitals.[28]

The first chemical evidence that 5f orbitals are involved in bonding was presented by *Glueckauf* and *McKay* in 1950 in connection with their work on uranyl nitrate.[29] These conclusions were challenged less than five months later by *Katzin*,[30] starting the persistent controversy over the bonding in the uranyl ion.[31] Further work in the 1950s on uranyl and uranyl-like ions also focused on the question of f-orbital participation in bonding.[32] *Coulson* and *Lester* surveyed this early work and concluded that f-orbital covalency is significant, although they suggested that the important orbitals are the 6f rather than the 5f orbitals.[33] Differences in the complexing behaviors of the lanthanide and actinide halides led *Seaborg* and co-workers to invoke hybridization of the 5f, 6d, and 7s orbitals in order to account for the greater tendency of the actinides to form covalent complex ions.[34]

The question of f-orbital participation has also been at the fore of organoactinide chemistry. *Moffitt* reported a qualitative discussion of the orbital interactions in $[Cp_3U]^+$ in the report of the synthesis of **2**.[35] An early review on bonding in f-element organometallics concluded that the properties of these materials, both chemical and physical, are intermediate between the covalent organotransition-metal complexes and the ionic carbocyclic salts of the alkali metals.[36] It further noted that evidence exists for some appreciable f-orbital contribution to the bonding in the early An^{IV} complexes. Later empirical studies of the bonding have concentrated on trends in molecular geometry and steric factors. One such

Bruce E. Bursten was born in Chicago, Illinois, in 1954. He received his S. B. degree with honors in chemistry from the University of Chicago (1974) and his Ph.D. degree (with R. F. Fenske) form the University of Wisconsin (1978). Following two years as an NSF Postdoctoral Fellow at Texas A & M University (with F. A. Cotton), he joined the faculty of The Ohio State University, where he is currently Professor of Chemistry. He has been a Fellow of the Alfred P. Sloan Foundation and a Camille and Henry Dreyfus Foundation Teacher-Scholar and he has received both the Distinguished Teaching Award and the Distinguished Scholar Award at his university. His research interests include the electronic structure of transition-metal and actinide complexes, organometallic photochemistry, metal–metal bonding, and applied quantum chemistry.

Richard J. Strittmatter was born in Washington, DC, in 1963. He received his B. S. degree in chemistry from Wake Forest University (1985) and his Ph.D. degree in inorganic chemistry (with B. E. Bursten) from The Ohio State University (1990). He spent six months of his graduate studies at Los Alamos National Laboratory under the supervision of Dr. A. P. Sattelberger. His dissertation research involved computational and experimental investigations of the bonding and electronic structure of organoactinide and related transition-metal compounds. He is currently a Senior Chemist at Nalco Chemical Company in Naperville, Illinois, where he is a member of the Advanced Recycling Technologies Department in the Water and Waste Treatment Division.

study, based on the limited number of structures available at the time, concluded that the bonding in organoactinides is predominantly ionic.[37] A cone-packing model based on steric effects has been developed and used to explain molecular geometry, reaction pathways, ligand rearrangement, and disproportionation.[38] One very recent study defines a "steric coordination number" that can be used for molecular structure comparison and bond-length prediction,[39] while another uses statistical analysis of structural data to seek evidence for covalency in Cp complexes of the alkaline earths and f elements.[40] The debate over metal–ligand covalency in organoactinide complexes is clearly an unresolved issue.[41]

3. Cyclopentadienyl–Actinide Bonding

Because the Cp ligand has such a dominant role in organotransition-metal chemistry, actinide cyclopentadienyls lend themselves more readily to comparison with transition-metal systems than do the actinocenes. A major theme of this section will be the similarities and differences in the bonding of Cp ligands to actinides and transition metals. In one of the first direct theoretical comparisons of the bonding of a Cp ligand to an actinide and a transition metal, *Tatsumi* and *Hoffmann* used quasi-relativistic extended Hückel (EH) molecular orbital theory[42] to compare the interaction of a Cp^- ligand with a U^{6+} ($5f^0$) and an Fe^{2+} ($3d^6$) ion.[43] They found a vanishingly small U–Cp overlap population for $[CpU]^{5+}$ in contrast to a sizable one for $[CpFe]^+$. This report suggests that the interaction between Cp and U^{VI} is largely ionic, consistent with the fact that only a very small number of organoactinide complexes contain neutral π-donor ligands. It is apparent, however, that covalency could become more important for lower oxidation states of uranium; most known actinide cyclopentadienyls involve metals in a formal +3 or +4 oxidation state, and we will focus on these systems in the ensuing discussion.

3.1. Tetrakis(cyclopentadienyl) Complexes

$[Cp_4An]$ compounds (**3**) have been synthesized for An = Th,[3b] Pa,[44] U,[3a] and Np.[45] The crystal structure of $[Cp_4U]$ shows that it is pseudotetrahedral with all four Cp ligands bound in an η^5 fashion.[46] From the isotropic ^1H NMR shift in $[Cp_4U]$, a total spin delocalization of 24% was estimated over the four Cp ligands,[47] a result that seemed incompatible with the rather long U–C distance and the generally contracted radial distribution of 5f orbitals. Although aspects of this work were questioned,[48] the temperature dependence of the paramagnetic shift between 165 and 428 K confirms the original indication of a remarkably large indirect electron-spin transfer.[49]

The ^{237}Np Mössbauer spectrum of $[Cp_4Np]$ shows an isomer shift of $+0.72\ cm\ s^{-1}$,[22] appreciably different from those of ionic Np^{IV} compounds. This observation suggests a significant electron contribution from the Cp ligands to the metal orbitals in $[Cp_4Np]$, although not as great as that found for $[(\eta^8\text{-}C_8H_8)_2Np]$. This spectroscopic evidence for covalent contributions to the bonding in $[Cp_4Np]$ agrees with chemical evidence for covalent contributions to the bonding in $[Cp_3UCl]$, which does not react with $FeCl_2$ to form ferrocene.[2]

Many theoretical studies of the electronic structure of $[Cp_4An]$ systems have been undertaken. In an effort to interpret the temperature dependence of the magnetic susceptibility of $[Cp_4U]$, calculations were performed on the model tetrahedral system $[(\eta^6\text{-}C_6H_6)_4An]$.[50] Three different semiempirical approaches were used, all of which led to essentially the same results and successfully simulate the temperature dependence of the magnetic susceptibility. In a related study, the bands of the room-temperature absorption spectrum of $[Cp_4U]$ have been identified, with good agreement between observed and calculated values.[51]

Quasi-relativistic EH and Xα-SW molecular orbital calculations on $[Cp_4Th]$ and $[Cp_4U]$ have been reported.[52] In both the EH and Xα-SW results, the calculated molecular orbitals are energetically grouped in a fashion well described by tetrahedral symmetry (Fig. 1). Apart from a small An 7s

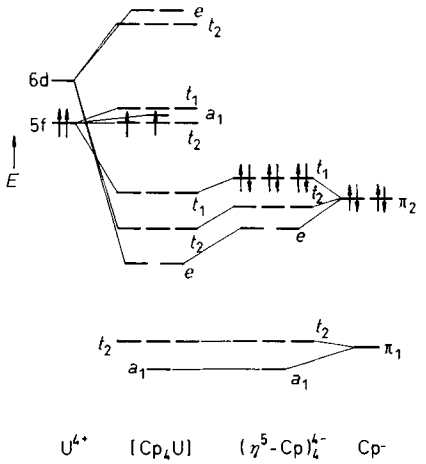

Fig. 1. Qualitative MO diagram of $[Cp_4U]$ under pseudotetrahedral symmetry.

contribution, the Xα-SW results show no important metal contributions to the Cp π_1 orbitals. The Cp π_2 orbitals donate significantly into both the An 5f and 6d orbitals; the ligand donation into the metal 6d orbitals is comparable to or even greater than the donation into the metal 5f orbitals. It was shown further that donation into the 6d orbitals is a more stabilizing interaction than donation into the 5f orbitals.[53] Under tetrahedral symmetry, the energetic ordering of these Cp π_2-based orbitals was calculated to be $t_1 > t_2 > e$. The HOMO of the uranium complex is essentially a pure 5f atomic orbital, in which the two unpaired metal-based electrons reside. In general, the EH calculations show much less metal 5f and 6d involvement in the metal–ligand bonding orbitals than do the Xα-SW calculations.

Prior to these calculations, the valence PE spectra of $[Cp_4Th]$ and $[Cp_4U]$ were reported.[54] Four ionization bands are evident in the 6–10-eV ionization energy (IE) region of $[Cp_4U]$ (Fig. 2). As is the case for uranocene,[10] the first ionization band is readily assigned to ionization of the U-based 5f electrons. The other three bands are due to the ligand-based π_2 MOs. On the basis of relative band intensities under both He(I) and He(II) ionization sources, the authors assigned the Cp π_2 ionization energies in the order

$t_1 < e < t_2$. In conjunction with the above EH and Xα-SW calculations, the He(I) and He(II) PE spectra of the methyl-substituted cyclopentadienyl complexes, [Cp′$_4$Th] and [Cp′$_4$U] (Cp′ = η^5-$C_5H_4CH_3$), were also reported.[52] A satisfactory agreement was found between the calculated Xα-SW transition-state IEs and the experimental ones, although the calculated values are uniformly too low by about 0.3 eV. The calculations support an assignment for the Cp π_2 ionizations of $t_1 < t_2 < e$, in disagreement with the earlier assignment made by *Green* et al.[54] The authors therefore questioned the assumption that the increase in the He(II) PE cross section is greater for the 5f orbitals than for the 6d orbitals.[52]

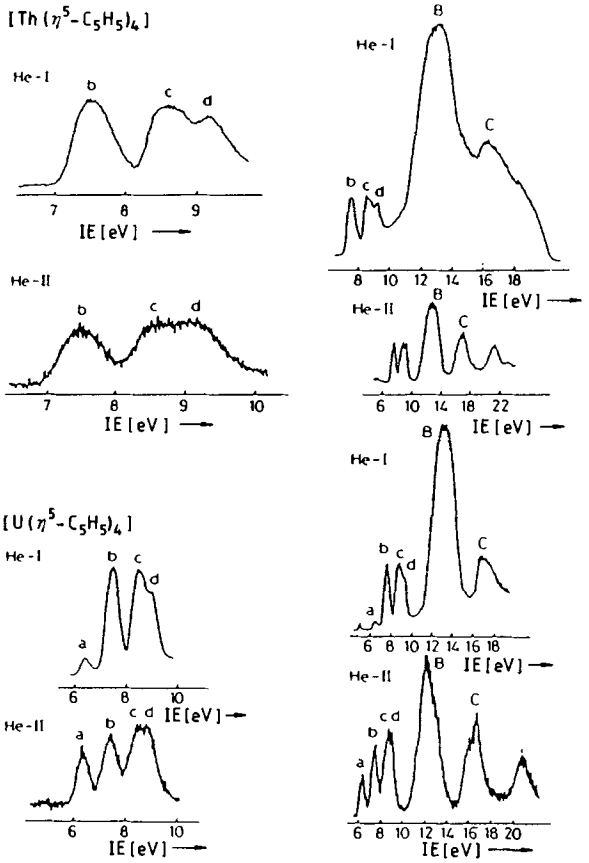

Fig. 2. He(I) and He(II) photoelectron spectra of [Cp$_4$Th] and [Cp$_4$U] [54].

Because the coordination of four η^5-Cp ligands is unique to the 5f elements, the preference of actinides for η^5- over η^1-Cp bonding has been studied. *Tatsumi* and *Nakamura* have used EH calculations to compare [(η^5-Cp)$_4$U] and [(η^5-Cp)$_3$(η^1-Cp)U], the latter being similar to the well-known [Cp$_3$UR] (R = alkyl) complexes. They find [(η^5-Cp)$_4$U] to be more stable than [(η^5-Cp)$_3$(η^1-Cp)U], in agreement with experiment.[55] Similar calculations on the allyl derivatives [Cp$_3$U(η^3-allyl)] and [Cp$_3$U(η^1-allyl)] predict the latter to be more stable than the former, again in agreement with experiment. The authors propose that the preference for monohapto over polyhapto coordination is a consequence of several delicately balanced factors, including the fact that η^1-allyl is a stronger σ donor than η^1-Cp.

3.2. Tris(cyclopentadienyl) Complexes

The binding of three η^5-Cp ligands is arguably the most common coordination sphere found in organoactinide complexes. For actinides in the +3 oxidation state, both the "base-free" [Cp$_3$An] complexes (**5**) and those with an additional bound Lewis base, [Cp$_3$AnL] (**6**), are commonly known. The tetravalent actinides often form neutral complexes of the type [Cp$_3$AnX] (**7**), where X is a formally anionic ligand such as halide or alkyl. In this section we will focus on the bonding of the three Cp ligands to the actinide center; the discussion of the An–L and An–X σ bonds is deferred to Section 4.

Compounds **5** are known for the actinide elements from Th to Cf, and the Cm and Cf adducts represent the only well-characterized organometallic compounds of those elements. Two such compounds have been structurally characterized: both [Cp″$_3$Th][56] (Cp″ = η^5-1,3-(Me$_3$Si)$_2$C$_5$H$_3$) and [Cp‴$_3$U][57] (Cp‴ = η^5-Me$_3$SiC$_5$H$_4$) exhibit planar, pseudo-D_{3h} structures with respect to the metal–Cp(centroid) vectors. Compounds of type **6** or **7** are pseudotetrahedral molecules in which the centroids of the Cp rings occupy three vertices.[58–60] These molecules have actual or near C_{3v} point symmetry.

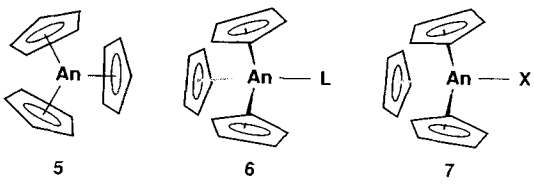

Placing Cp ligands in threefold symmetry about a metal center imposes interesting symmetry restrictions on the metal–ligand interactions. This fact was first recognized by *Moffitt*, who presented a qualitative treatment of the orbital interactions in [Cp$_3$U]$^+$ as part of the paper on the synthesis of [Cp$_3$UCl].[35] Under C_{3v} symmetry, the π_2 orbitals of the Cp ligands are bases for the $a_1 + a_2 + 2e$ representations. The symmetry-allowed metal–ligand orbital interactions are given in Table 1. It is particularly notable that the ligand-based a_2 orbital cannot interact with s, p, or d orbitals on the central metal, but is allowed to interact with one of the f orbitals. This observation has been used to explain how the seemingly 20-electron transition-metal complex [(η^5-

Table 1. Metal orbital interactions with Cp_3^{3-} under C_{3v} symmetry.

Cp_3^{3-} orbital	Metal	
	s, p, d orbitals	f orbitals
	s	f_{z^3} (fσ)
a_1	p_z (pσ) d_{z^2} (dσ)	$f_{x(x^2-3y^2)}$ (fφ)
	p_x, p_y (pπ)	f_{xz^2}, f_{yz^2} (fπ)
e	d_{xz}, d_{yz} (dπ) $d_{x^2-y^2}$, d_{xy} (dδ)	f_{xyz}, $f_{z(x^2-y^2)}$ (fδ)
a_2	-	$f_{y(3x^2-y^2)}$ (fφ)

$Cp)_3(\eta^1$-Cp)Zr] is, in actuality, an 18-electron complex that satisfies the effective-atomic-number rule.[61] The allowed interaction of the a_2 ligand-based orbital with an f orbital has been proposed as a reason for the abundance of $[Cp_3An]$ complexes vis-à-vis the scarcity of $[Cp_3M]$ complexes among the transition metals.[62]

Quantitative MO calculations on $[Cp_3An]$ systems corroborate *Moffitt*'s symmetry analysis. EH calculations on $[Cp_3U]^+$ indicate 8% U 5f contribution to the ligand-based a_2 orbital.[55] Quasi-relativistic Xα-SW calculations on $[Cp_3U]$ put the U 5f contribution at 29%.[62] These latter calculations were also used to analyze the other donations from the π_2 orbitals of the Cp_3^{3-} ligand fragment to the U^{3+} center. The ligand *e* orbitals, which can donate to the U 5f, 6d, or 7p orbitals, preferentially interact with the 6d orbitals, as was found for the $[Cp_4An]$ complexes. Thus, only the 5f orbital of a_2 symmetry is significantly affected by the ligand field. The ligand a_1 orbital, which is spatially less favorable for interaction with the $6d_{z^2}$ orbital, interacts more weakly with the U atom than the other ligand orbitals. The overall result of these interactions is depicted in Figure 3.

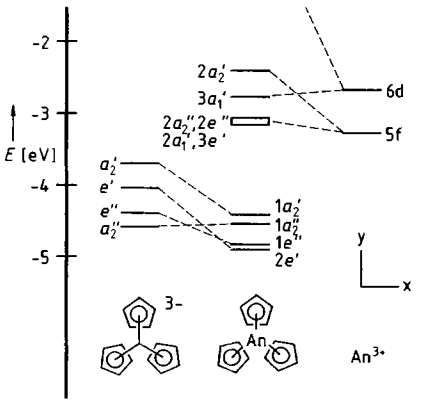

Fig. 3. MO diagram showing the interaction of Cp_3^{3-} with U^{3+} to form $[Cp_3U]$ [69].

A molecular orbital comparison of the bonding in $[Cp_3U]$ and $[UCl_3]$ indicates significantly greater ligand-to-metal donation in the former than in the latter.[62] Similar conclusions were drawn in a comparison of $[Cp_4U]$ and $[UCl_4]$.[53] The greater donation by Cp was taken as evidence of greater covalency in U–Cp bonding than in U–Cl bonding.

EPR spectra of powdered samples and solutions of $[Cp''_3Th]$ were obtained in the temperature range 10–300 K.[63] Using a simplified crystal field model, the authors found that the data are only consistent with a $5f^0 6d^1$ ground electron configuration for the Th^{III} compound. This conclusion was corroborated by quasi-relativistic Xα-SW calculations on $[Cp_3Th]$,[64] which showed a single 6d orbital lower in energy than the Th 5f block of orbitals. These authors also investigated $[Cp_3An]$ compounds where An = Pa to Pu, and found that the 5f block of orbitals was lowered in energy across the series, while the energy of the 6d-based a_1 orbital increased slightly. These results led to the predictions that $[Cp_3Pa]$ should have a $5f^1 6d^1$ ground electron configuration and that the transuranium compounds should have a $5f^n 6d^0$ ground electron configuration. The Xα-SW calculations showed an exceedingly small energy difference between the $5f^2 6d^1$ and the $5f^3 6d^0$ ground electron configurations for $[Cp_3U]$, although more rigorous calculations that include spin–orbit coupling favor the $5f^3 6d^0$ configuration.[65]

The nature of the An^{III}–Cp bonding has been investigated spectroscopically and chemically. An early study involved estimation of the nephelauxetic parameters of $[Cp_3Am]$ and $[Cp_3Cm]$ by a comparison of their visible absorption and emission spectra with those of the aqueous ions.[66] Although the parameters are greater than those of $[Cp_3M]$ compounds of the lanthanide series, the covalency relative to the aqueous +3 ions of 2.8% and 2.5% for $[Cp_3Am]$ and $[Cp_3Cm]$, respectively, is indicative of highly ionic organometallic bonding. The Mössbauer isomer shift of $[Cp_3Np \cdot thf]$ ($+3.64\ cm\ s^{-1}$) is very close to that of $[NpCl_3]$ ($+3.54\ cm\ s^{-1}$), suggesting very little difference in the bonding of the Cp and Cl ligands.[22] Protolysis of the metal–Cp bonds in $[Cp_3U]$ [Eq. (a)] has been taken as chemical evidence for significant ionic character in the metal–ligand bonding.[67]

$$[Cp_3U] + HCN \rightarrow [Cp_2(CN)U] + C_5H_6 \qquad (a)$$

A preliminary account of the bonding in the transuranium $[Cp_3An]$ compounds compares the $[Cp_3An]$ series to the corresponding $[AnCl_3]$ compounds.[68] Proceeding from Th to Cf, the 5f orbitals drop dramatically in energy for $[AnCl_3]$ compounds. Although the same qualitative trends are followed in the $[Cp_3An]$ series, the Cp ligand is a much better donor to the actinide metal than the Cl ligand and consequently buffers the charge on the metal, resulting in a much less dramatic 5f orbital energy drop.[69]

$[Cp_3ThX]$ and $[Cp_3UX]$ compounds (**7**), including Th^{IV} and U^{IV} compounds with the modified Cp ligands Cp′ and indenyl, have been extensively investigated by PES.[54, 70–72] The lowest ionization band in the U^{IV} complexes, at 6.5 to 7.0 eV, is not present in the Th^{IV} compounds and is therefore assigned to the $5f^2$ electrons of U^{IV}. This assignment has been corroborated by He(II) spectroscopic studies. As expected with a change in oxidation state of the metal, the first ionization band in the U^{III} complex $[Cp_3U \cdot thf]$ occurs at lower IE than in the U^{IV} complexes.[54]

The ionizations due to the Cp π_2 orbitals in both $[Cp_3ThX]$ and $[Cp_3UX]$ complexes appear as three bands in their PE spectra. The ionization energies vary with the nature of the Cp ligand in the order indenyl < Cp′ < Cp. Comparison of the He(I) spectra with the He(II) spectra indicates much greater 5f-orbital participation in the metal–ring bonding in the uranium compounds than in the thorium compounds (Fig. 4). Moreover, the spectra indicate that the 5f covalency in the indenyl compounds is much greater than in the unsubstituted Cp compounds.[70]

All $[Cp_3AnX]$ compounds with X = Cl exhibit one ionization band slightly above the Cp π_2 bands, which is assigned to ionization from a lone pair of the chloride ligand (band d, Fig. 4).[71] This assignment is supported by a shift of this band to lower energy when X = Br or OCH_3, and by its complete absence when X = BH_4 or CH_3.

Nonrelativistic DV-Xα calculations on $[Cp_3UX]$ (X = F, Cl, Br) have been performed in conjunction with a PES in-

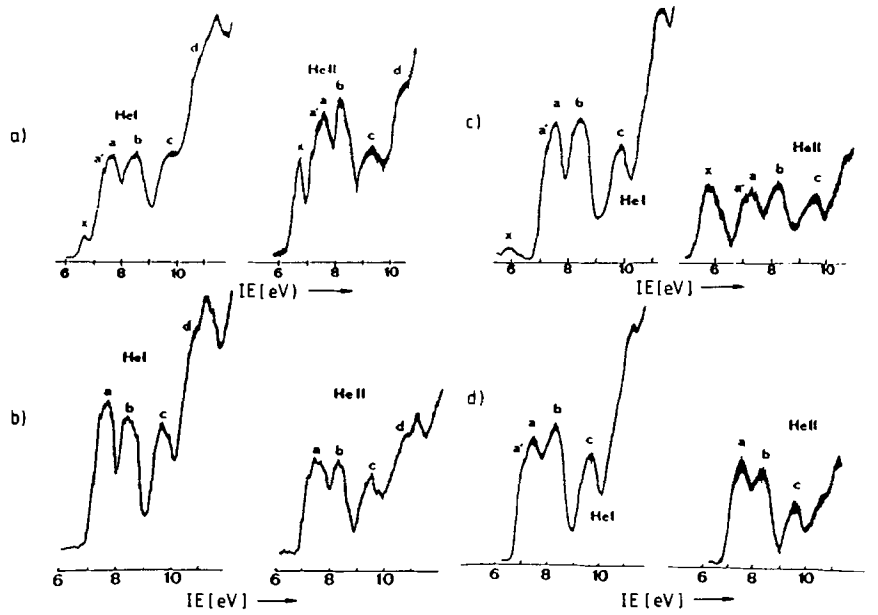

Fig. 4. Low-energy region of He(I) and He(II) spectra of a) [U(indenyl)$_3$Cl], b) [Th(indenyl)$_3$Cl], c) [U(indenyl)$_3$CH$_3$], and d) [Th(indenyl)$_3$CH$_3$] [70].

vestigation.[72] The above general assignments agree quite well with the calculations. Transition-state ionization energies were calculated for [Cp_3UCl] and are in good agreement with experiment, including the correlation between the relative intensities of the He(I) spectra and orbital population analysis. The uranium 6d contribution to the metal–ligand bonding orbitals appears to be underestimated in the calculations owing to the nonrelativistic approach.

3.3. Bis(cylcopentadienyl)actinide Complexes

A multitude of early-transition-metal [Cp_2MX_2] compounds are known, and their chemistry has been studied extensively. The corresponding An^{IV} complexes with unsubstituted cyclopentadienyl ligands, [Cp_2AnX_2], are a relatively uncommon class of compounds, largely because of the high affinity of the actinide centers for Cp ligands. Thus, the reactions of [$AnCl_4$] with cyclopentadienide salts generally yield either [Cp_3AnCl] or [Cp_4An];[2, 3] it is not possible to "stop" the reaction at [Cp_2AnCl_2].[73] Some [Cp_2AnX_2] complexes have been isolated when X is a strong π-donor or chelating bidentate ligand.[74]

Sterically hindered cyclopentadienyl ligands, especially pentamethylcyclopentadienyl (Cp*), have been used to generate bis(cyclopentadienyl)actinide complexes. For example, the reaction between [$AnCl_4$] and [Cp*MgCl] leads to the replacement of two Cl ligands by Cp* ligands, yielding [$Cp^*_2AnCl_2$] (**8**; An = Th, U).[75] Complexes **8** are structurally analogous to transition-metal [Cp_2MX_2] and [$Cp^*_2MX_2$] systems, with a pseudotetrahedral geometry about the actinide center.[76, 77] Because the ligand array in **8** is identical to that of well-characterized transition-metal systems, the direct comparison of homologous actinide and transition-metal complexes is facilitated.

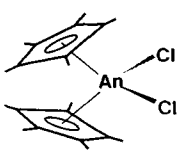

8

The valence PE spectra of [$Cp^*_2ThCl_2$] and [$Cp^*_2UCl_2$] are quite similar to those of analogous Zr and Hf compounds.[54, 78] The first ionization band of the uranium complex is due to the 5f electrons of this f^2 complex. The ionization bands due to the Cp π_2 orbitals are lower in energy than the bands due to the chloride lone pairs in [$Cp^*_2MCl_2$] (M = Zr, Th, U); this ordering is reversed in [Cp_2WCl_2]. Furthermore, the bands assigned to the Cp π_2 orbitals are essentially isoenergetic for the [$Cp^*_2MCl_2$] complexes, suggesting that either the metal–ring bonding is similar for the three compounds or that metal–ring interactions are of little importance in determining the relative energies of these ring molecular orbitals. Comparison of these compounds with several Cp-containing organometallic compounds indicates that the metal–ring bonding in these organoactinides tends to be much more ionic than the bonding in [$Cp^*_2MoCl_2$] and [Cp_2VCl], although it is less ionic than in lanthanide compounds such as [(Cp_2GdCl)$_2$] and [(Cp_2YCl)$_2$].[54]

Comparison of the PE spectra of [$Cp^*_2AnMe_2$] compounds with those of the dichlorides reveals the greater electron-releasing ability of the two methyl ligands.[78] The 5f ionization in [$Cp^*_2UMe_2$] is at lower IE than that in [$Cp^*_2UCl_2$] although the energy difference is much smaller than would have been expected in a similar d^2 system. The Cp π_2 bands, which are also at lower IE than in the chloride complexes, show greater energetic dispersion in the actinide spectra than in the spectrum of [$Cp^*_2ZrMe_2$], probably due to enhanced metal–ring interaction involving the 5f orbitals.

PES investigations of [Cp_2UX_2] compounds with unsubstituted Cp ligands and chelating or π-donating X ligands have been reported.[79] The lowest-energy ionization band in each of these compounds is due to the $5f^2$ electrons of the U^{IV} metal center, with the energetic ordering inversely related to the electron-donating ability of the ligand X: S_2CNEt_2 (6.19 eV) < NEt_2 (6.24 eV) < $O_2CC(CH_3)_3$ (6.73 eV) <

BH_4 (7.97 eV). For $[Cp_2U(BH_4)_2]$, which has no low-energy bands due to ionization from the BH_4 ligands, the next three lowest bands have a 1:2:1 ratio and are due to ionizations from the Cp π_2 orbitals. The splitting between the extremes of these bands is comparable to that of other $[Cp_2^*UX_2]$ complexes; as expected, the splitting is smaller than that of the Cp π_2 bands in $[Cp_3UX]$ compounds or Cp_4U. The large energy dispersion of the π_2 ionization bands and their variable He(I)/He(II) intensity ratios indicate that the splitting is not solely due to interligand repulsion, and it was concluded that there is a sizable interaction between Cp π_2 molecular orbitals and uranium 5f and 6d orbitals. The pivalate complex $[Cp_2U\{O_2CC(CH_3)_3\}_2]$, which is dimeric in solution,[74c] possesses a pseudooctahedral geometry and is more sterically crowded than other $[Cp_2UX_2]$ systems. The greater repulsion within the Cp_2 framework results in a broad featureless band for the Cp π_2 ionizations of this complex. The spectra of the NEt_2 and S_2CNEt_2 complexes are complicated by the overlap of bands due to ionizations from nitrogen 2p lone pairs and from sulfur 3p lone pairs, respectively, with the Cp π_2 bands. Nevertheless, in the case of the amido complex, the authors assigned the lowest of these bands to be nitrogen lone-pair orbitals, whereas for the dithiocarbamate complex the lowest-energy band is assigned to the Cp π_2 orbitals.

The PES results have been used to rationalize the reactivity of these complexes.[79] The IEs of the Cp π_2 orbitals in $[Cp_2U(BH_4)_2]$ are the highest yet observed for $[Cp_2UX_2]$ and $[Cp_2^*UX_2]$ complexes, consistent with the high stability and, hence, the low reactivity of the complex. With the exception of the $5f^2$ electrons, the highest occupied orbital of $[Cp_2U(NEt_2)_2]$ is an almost pure nitrogen 2p lone pair, consistent with the higher reactivity of the complex toward molecules containing dipolar double bonds and acidic hydrogens. In $[Cp_2U(O_2CCMe_3)_2]$ and $[Cp_2U(S_2CNEt_2)_2]$, the orbital immediately below the $5f^2$ electrons is localized on the Cp ligands, but is energetically close to molecular orbitals centered on the X ligands. These relative orbital energetics could be responsible for the greater lability of the U–Cp bonds in these complexes relative to $[Cp_2U(NEt_2)_2]$, in which the U–N bond is more labile.

The bonding in $[Cp_2^*UX_2]$ (X = Cl, Me) has been studied via quasi-relativistic Xα-SW calculations on the corresponding Cp complexes.[80] Although the calculated IEs are uniformly too low, the calculated band splittings are in excellent accord with the experimental PES data, indicating that the extent of the uranium–ligand interaction is properly estimated by the quasi-relativistic calculations. The bonding of the Cp rings is similar in the two compounds, with sizable contributions from the metal 6d and 5f orbitals. The CH_3^- ligand is a stronger σ donor than the Cl^- ligand, as evidenced by the higher energy of the 5f orbitals in $[Cp_2UMe_2]$ than in $[Cp_2UCl_2]$. The calculations show no evidence that Cl^- acts as a π donor to uranium. Support for this conclusion comes from a comparison of $[Cp_2UCl_2]$ with $[Cp_4U]$ and $[UCl_4]$.[53] The 5f block of orbitals in $[Cp_2UCl_2]$ is much closer in energy to the corresponding block in $[Cp_4U]$ than in $[UCl_4]$; the energy of the 5f orbitals is principally governed by interaction with the Cp ligands. The remaining two U^{IV} electrons are in essentially pure uranium 5f atomic orbitals that are clustered in a narrow band, consistent with the paramagnetism of the molecules. By contrast, analogous calculations on $[Cp_2MoCl_2]$ predict it to be diamagnetic, again consistent with experiment.

4. Cyclopentadienyl–Actinide Complexes with σ-Bonded Ligands

In addition to An–Cp bonds, the $[Cp_3AnL]$, $[Cp_3AnX]$, and $[Cp_2AnX_2]$ complexes discussed in the preceding section also contain σ bonds between one or more ligands and the actinide atom. The nature of these actinide–ligand σ bonds and their similarities to and differences from actinide–ligand π bonds are the focus of this section.

The differences between σ and π bonds involving the actinide atoms was first addressed theoretically by *Tatsumi* and *Hoffmann*.[43] Using extended Hückel theory, they found a far more substantial interaction between a CH_3^- ligand and a U^{6+} ion than between a Cp^- ligand and the same ion. The U–C overlap population in U–CH_3^{5+} is large and comparable to that found for Fe-CH_3^-. The U $5f_{z^3}$, $6d_{z^2}$, 7s, and $7p_z$ orbitals all contribute to the U–C σ bond.

4.1. Tris(cyclopentadienyl)actinide Complexes

4.1.1. The Nature of An–X σ Bonding

As mentioned in Section 3.2, when a fourth ligand binds to a $[Cp_3An]$ fragment, the Cp ligands pyramidalize to open a coordination site for the ligand to approach. Quasi-relativistic EH calculations on $[Cp_3U]^+$ show that, upon pyramidalization, orbitals possessing primarily uranium 6d character are stabilized owing to increased 6d–7p mixing.[55] This effect is most pronounced for the $6d_{z^2}$ orbital and the $7p_z$ orbital, resulting in an energetically low-lying, hybridized σ-bonding orbital situated to accept electron charge from an incoming fourth ligand. This orbital, which is primarily uranium $6d_{z^2}$, is approximately 4 eV above the 5f block of orbitals in the EH calculations.

Xα-SW results also indicate a low-energy σ-bonding orbital;[64] however, this orbital is approximately isoenergetic with the 5f block of orbitals in $[Cp_3U]$ and is actually lower in energy than the 5f block of orbitals in $[Cp_3Th]$ (cf. Section 3.2). The different oxidation states of uranium in $[Cp_3U]^+$ and $[Cp_3U]$ could account for some of the energetic discrepancy between the EH and Xα-SW results, and the two methods differ in the energetic placement of the 5f orbitals relative to the 6d orbitals. As was the case in the EH calculations, the Xα-SW results also show hybridization of this orbital upon pyramidalization of the Cp ligands.

Ziegler et al. have used local density functional (LDF) theory to study the An–R σ-bond energies in $[Cl_3AnR]$ (An = Th, U; R = H, CH_3) complexes.[81] Their methodology employed *Becke*'s density functional[82] and the Hartree–Fock–Slater LCAO program of *Baerends* et al.[83] In addition to nonrelativistic calculations on the molecules, two levels of relativistic correction were studied: a first-order relativistic method based on perturbation theory, and a quasi-relativistic method based on optimization of the valence density with respect to the first-order relativistic

Hamiltonian. The authors found that the bond energies calculated by the latter method were in excellent accord with the experimental An–R bond energies for $[Cp^*_2An(R)(Cl)]$ complexes.[84] Interestingly, the nonrelativistic calculations, which give very poor calculated bond energies, indicate that the An $5f_{z^3}$ orbital is the most important one in the formation of the An–R bond. When the quasi-relativistic method is used, the energy of the 5f orbitals increases; as a result, the $6d_{z^2}$ orbital becomes the dominant An orbital in the bond.

It is clear from all of the above studies that a hybridized σ-bonding orbital possessing primarily $6d_{z^2}$ character is responsible for the high Lewis acidity of $[Cp_3U]$. An Xα-SW investigation of the interaction of $[Cp_3U]$ with a hydride ligand, to form the hypothetical "σ-only" compound $[Cp_3UH]$, indicates that the metal participation in the U–H bond is indeed dominated by the $6d_{z^2}$ orbital with minor contributions from the $5f_{z^3}$, $7p_z$, and 7s orbitals.[62] Also, the 5f block of orbitals in $[Cp_3U]$ shows no increased splitting upon interaction with the hydrogen atom, further supporting the minor role of the 5f orbitals in σ bonding. The authors note that this σ-bonding interaction is typical for all Cp_3U–X or Cp_3U–L σ bonds. It is interesting to note here a suggestion, based on thermochemical data, as to why $[Cp_3UH]$ has never been isolated despite numerous synthetic attempts.[85] If the bond disruption energy D(U-H) is assumed to be 10 kcal mol^{-1} greater than D(U-CH_3), then bimolecular H_2 elimination from $[Cp_3UH]$ may be sufficiently close to thermoneutrality to be entropically driven. Support for this notion comes from the results of LDF calculations on $[Cl_3AnR]$ systems,[81] which indicate that actinides, like the early transition metals,[86] form bonds of nearly equal strength to hydrogen and alkyls.

4.1.2. An–X Bond Energies

Marks and co-workers have reported extensive thermochemical studies of the nature of actinide–ligand σ bonding. A thermochemical study of alkyl adducts of $[Cp_3U]$ reveals that the U–R bond energies, $D(Cp_3U\text{–}R)$, span a wide range of about 58 kcal mol^{-1}.[85] These values are roughly 20 kcal mol^{-1} lower than the analogous $D(Cp_2UR\text{-}R)$ values; this difference is attributed to the greater steric congestion in the $[Cp_3UR]$ systems. The experimental bond energies indicate that severe nonbonded interligand repulsions destabilize the U–R bond in $[Cp_3UR]$. The bond enthalpies for $[Cp_2UR_2]$ and $[Cp_3UR]$ follow qualitatively similar trends with U-Me ≥ U-$CH_2CH_2CH_2$Me > U-CH_2Ph. Consistent with the calculations of *Ziegler* et al.,[81] the actinide–alkyl bond enthalpies parallel those of the group 4 transition-metal complexes. A plot of $D(Cp_3U\text{-}R)$ versus D(R-H) shows a roughly linear correlation (Fig. 5). The greatest deviations are observed for R = *n*Bu and R = CH_2Ph, for which the D(U-R) values are lower and higher than anticipated, respectively. The deviation in the former may reflect the steric demands of the *n*Bu ligand, while the deviation in the benzyl complex may be indicative of inductive effects in the benzyl ligand. Both R = vinyl and R = C≡CPh fall on the linear plot, evidence that U–R π bonding is not a major effect.

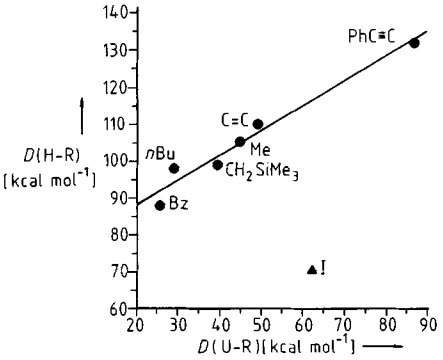

Fig. 5. A plot of U–R bond energies in $[Cp^*_3UR]$ versus R–H bond energies [85].

Among the alkyl groups studied thermochemically, the U–C≡CPh bond is the strongest, consistent with the relative shortness of the U–C bond in $[Cp_3UC{\equiv}CPh]$.[87] EH studies of $[Cp_3UR]$ complexes indicate a significant increase in the U–C overlap population of the model complex $[Cp_3UC{\equiv}CH]$ relative to $[Cp_3UCH_3]$.[55] Interestingly, σ interactions in $[Cp_3UC{\equiv}CH]$ account for half of the increase in the overlap population, indicating that π interactions are less important than might be inferred from the short U–C bond. Thus, the calculated results are in good accord with the conclusions of the thermochemical studies.

4.1.3. An–X Multiple Bonds and π Bonding

Cramer, Gilje et al. have explored multiple U–C bonding in $[Cp_3UR]$ systems where R is a phosphoylide.[15] The U–C bond in $[Cp_3UCH\{P(CH_3)_2(C_6H_5)\}]$ (**9**) is the shortest yet

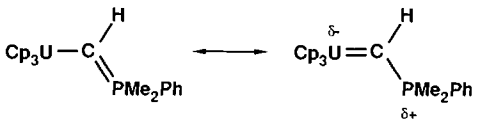

9

observed (2.29 Å); even after correcting for the difference in hybridization of the carbon atom, the U–CH(PR_3) bond is still 0.11 Å shorter than the uranium–carbon bond in $[Cp_3U(n\text{Bu})]$.[88] As was the case for $[Cp_3UC{\equiv}CH]$, EH calculations on the model complex $[Cp_3UCHPH_3]$ show a significant increase in the U–C overlap populations relative to $[Cp_3UCH_3]$.[55] In contrast to the acetylide complex, however, this increase is almost entirely due to a π interaction between the C pπ orbital of $CHPH_3$ and the uranium $5f_{yz^2}$ (7%), $6d_{yz}$ (2%), and $7p_y$ (1%) orbitals.

The π-bonding effects have been found to be important in $[Cp_3UL]$ compounds where the fourth ligand is not an alkyl. For example, phosphite ($P(OR)_3$) and isocyanide (CNR) ligands, which are generally classified as π-acceptor ligands, bind more strongly to $[Cp_3U]$ than do pyridine, THF, or nitriles, which are σ-only ligands.[89] *Andersen* and *Brennan* demonstrated that exposure of carbon monoxide to a hydrocarbon solution of $[Cp^*_3U]$ leads to quantitative evidence for

U–L π bonding.[18] The carbonyl adduct, [Cp‴UCO] (**10**), exhibits a carbonyl stretch in the IR spectrum at ν_{CO} = 1976 cm^{-1}, about 170 cm^{-1} lower than ν_{CO} for free carbon monoxide. This lowering of the C–O stretching frequency is indicative of metal-to-carbonyl π back-bonding.

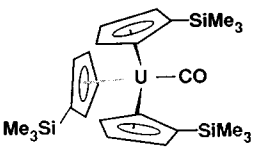

10

The electronic structure of **10** has been investigated via quasi-relativistic Xα-SW calculations on the model complex [Cp_3UCO].[90] The U–CO σ bond is similar to the U–H σ bond discussed above, with the CO carbon "lone-pair" orbital donating into the predominantly U $6d_{z^2}$ σ-acceptor orbital. A significant π interaction occurs between the CO π* orbitals and the U 5fπ orbitals. The resultant doubly-degenerate U–CO π-bonding molecular orbital is stabilized below the remaining 5f block of orbitals. As such, it is the HOMO of the complex, and, consistent with the experimental findings, it represents significant metal-to-carbonyl π back-bonding (Fig. 6). The interaction of [Cp_3U] with the even stronger π acid NO to give the hypothetical [Cp_3UNO] complex results in greater π back-bonding, which would stabilize the HOMO more than in [Cp_3UCO].[62] Because NO has one more electron than CO, it is predicted that this still unknown molecule could be the first diamagnetic U^{IV} compound.

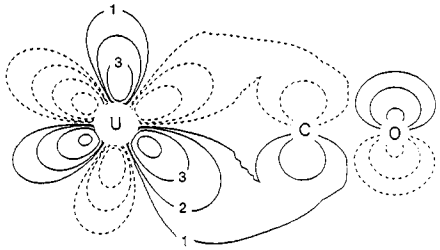

Fig. 6. Contour plot of the HOMO of [Cp_3UCO] in a plane containing the U, C, and O atoms [90].

The U–CO bond disruption enthalpy for **10** is about 10 kcal mol^{-1}.[85] Compared to the typical disruption enthalpies of about 40 kcal mol^{-1} for early transition-metal carbonyls, the U–CO value is quite low, comparable to $D(Cp_3U\text{-thf})$. Because the C–O stretching frequency of **10** suggests bonding similar to that in typical transition-metal complexes, the low bond enthalpy is attributed to severe interligand nonbonded repulsions.

Because the molecular structure of **10** has not been determined conclusively and uranium is known to be highly oxophilic, the possibility of an oxygen-bound isocarbonyl adduct, [Cp_3UOC], was considered.[90] The π* orbitals of CO are localized on the carbon atom, which is not adjacent to the uranium atom in the isocarbonyl complex, precluding any significant π back-bonding. The probable reason that the isocarbonyl complex is unstable relative to the carbonyl complex is that the U–OC σ bond involves the oxygen "lone-pair" orbital of carbon monoxide, which is at too low an energy to interact with the empty σ-acceptor orbital of uranium. Instead, the isocarbonyl interacts with the filled "semi-core" 6p orbitals of uranium, resulting in a "filled–filled" interaction and no net bonding.

Crystallographic studies also provide support for uranium-to-fourth-ligand π back-bonding.[91] A comparison of isostructural uranium and cerium compounds reveals that the M–N distances are comparable in [Cp'_3U(quin)] (quin = [$N(CH_2CH_2)_3CH$]) and [Cp'_3Ce(quin)], whereas the M–P distances in [Cp'_3UPMe_3] and [$Cp'_3U\{P(OCH_2)_3CEt\}$] are significantly shorter than those in the corresponding cerium complexes. The authors conclude that there is π back-bonding from [Cp'_3U] to the phosphine and phosphite ligands, whereas the lanthanide compound, [Cp'_3Ce], can only interact with the Lewis bases in a σ-only or purely electrostatic manner. Similarly, the M–O distances in [Cp_3Pr(thf)] and [Cp_3U(thf)] are comparable, while the M–C distance in [Cp‴UCNEt] is considerably shorter than that in [$Cp_3PrCNEt$], giving evidence for uranium-to-isocyanide π back-bonding.

Further evidence for the different bonding interactions of lanthanides and early actinides with isocyanide ligands comes from an IR spectroscopic investigation of [Cp_3MCNEt] compounds.[92] The C–N stretching frequencies for the lanthanide compounds are all at about 2200 cm^{-1}, approximately 50 cm^{-1} higher than ν_{CN} in free CNEt. The increase in ν_{CN} is common for CNR ligands bound to higher-valent transition-metal atoms and is indicative of little or no π back-bonding.[93] By contrast, the C–N stretching frequencies of the early actinide (Th to Am) compounds span a range of 60 cm^{-1}, with [$Cp_3ThCNEt$] exhibiting the lowest ν_{CN} (2140 cm^{-1}) and [$Cp_3AmCNEt$] the highest (2202 cm^{-1}). The greater sensitivity of ν_{CN} to the metal atom in the actinide series relative to the lanthanide series, while not conclusive evidence of significant π back-bonding, does portend different bonding in the organoactinide complexes from that in the organolanthanide complexes.

Multiple bonding between the [Cp_3U] fragment and nitrogen- and oxygen-containing donor ligands has been extensively investigated both experimentally[94, 95] and theoretically.[96] A variety of different N-donor complexes, spanning a broad range of U–N bond lengths, have been made and structurally characterized: [Cp_3UNPh_2], 2.29 Å; [Cp_3UNPPh_3], 2.07 Å; [$Cp_3UNC(Me)CHPMePh_2$], 2.06 Å; [Cp_3UNPh], 2.02 Å. All of these U–N bonds are significantly shorter than those generally observed in complexes that contain neutral N-donor ligands bound to uranium, which are typically 2.4–2.8 Å.[91, 95]

The great variations observed in U–N bond length and the difficulties in describing the above structures with single resonance forms have prompted EH calculations on the model complexes $[Cp_3UNH_3]^+$ and [Cp_3UL] (L = NH_2, NPH_3, NHCHCHPH, NPh).[96] The calculations indicate significant N 2pπ-to-U π donation, primarily into the 6dπ orbitals, for the latter three complexes. The authors propose that the strongest U–N π bonding should be observed in a uranium nitride complex such as $[Cp_3UN]^{q-}$. No such organoactinide

nitride complexes are yet known. The σ donation from nitrogen to uranium is much greater for the formally anionic nitrogen ligands than for the neutral NH_3 ligand. The authors demonstrate an excellent correlation between the total U–N overlap population (calculated at a constant U–N bond length of 2.06 Å for all compounds) and the crystallographically observed U–N bond length for this series of five compounds (Fig. 7). The positive charge on U is largest for $[Cp_3UNPh]$, consistent with its formulation as a $5f^1$ U^V complex.

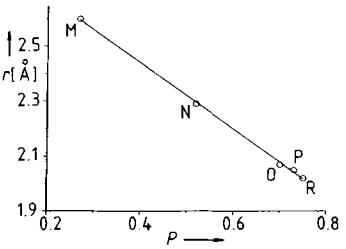

Fig. 7. Plot of observed U–N distances r, versus, U–N overlap populations P calculated at U-N = 2.06 Å for a series of $[Cp_3UX]$ systems: M = $[Cp_3UNH_3]$; N = $[Cp_3UNH_2]$; O = $[Cp_3UNPH_3]$; P = $[Cp_3UNCHCHPH_3]$; R = $[Cp_3UNPh]$ [96].

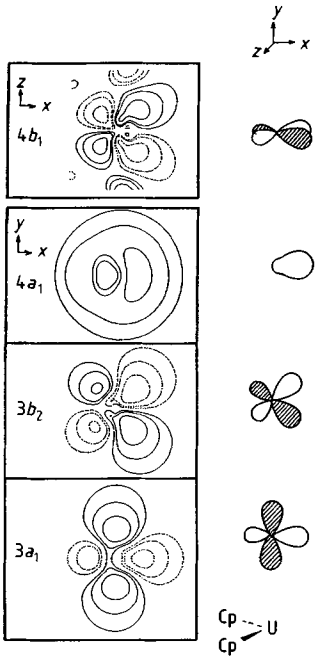

Fig. 8. Contour plots of the important valence orbitals in a $[Cp_2U]^{2+}$ fragment [99].

The same authors also performed calculations on the series of model complexes $[Cp_3UOH_2]$, $[Cp_3UOPH_3]$, $[Cp_3UOCHCHPH_3]^+$, and $[Cp_3UOCH_3]$ in order to investigate variations in U–O bonding.[96] Again, an excellent correlation between calculated U–O overlap population and observed U–O bond length (over a range of > 0.4 Å) was obtained. On comparing homologous compounds containing U–N and U–O bonds, the authors conclude that the nitrogen donors are better able to form multiple bonds to uranium.

Xα-SW calculations on $[Cp_3UOH]$ corroborate the conclusions of the EH studies.[62] Significant donation from the O 2pπ orbitals into the U 6d and, to a lesser extent, the 5f orbitals was observed. The π donation from alkoxide ligands to actinide atoms has been used to rationalize the unusually large U–O–R bond angles observed in actinide alkoxide complexes.[97, 98]

4.2. Bis(cyclopentadienyl)actinide Complexes

4.2.1. The An–X σ Bond

Among the most extensively studied actinide–ligand σ bonds are those in the host of $[Cp_2^*AnX_2]$ (An = Th, U] systems. The An–X bonds in these complexes exhibit a remarkably diverse chemistry, which often parallels that observed in $[Cp_2MX_2]$ complexes of the transition metals. The unoccupied frontier orbitals of a $[Cp_2U]^{2+}$ fragment as obtained from EH calculations are shown in Figure 8.[99] These orbitals, which are primarily 6d in character, closely resemble those of $[Cp_2Ti]^{2+}$,[61] although the $[Cp_2U]^{2+}$ orbitals are somewhat higher in energy and more diffuse. In both the actinide and transition-metal systems, the frontier orbitals are able to accept charge from formally anionic σ-donor ligands, leading to metal–ligand bonds of a_1, b_2, and, for the actinide systems only, b_1 symmetry.

The donor ability of the X ligands in $[Cp_2^*AnX_2]$ systems directly affects the valence orbital energies of the complexes. A comparison of the PE spectra of $[Cp_2^*AnMe_2]$ and $[Cp_2^*AnCl_2]$ reveals that the Cp π_2 ionization bands are at lower IE in the former than in the latter.[78] Similarly, the $5f^2$ ionization in $[Cp_2^*UMe_2]$ occurs at lower IE than that in $[Cp_2^*UCl_2]$, although the difference between the two (0.21 eV) is significantly less than that observed in d^2 transition-metal systems (e.g., a difference of 0.7 eV between the first IEs of $[Cp_2'MoCl_2]$[100] and $[Cp_2MoMe_2]$[101]). It seems surprising that, in spite of strong An–Me σ-bond formation, the decrease in $5f^2$ IE for $[Cp_2^*UMe_2]$ relative to $[Cp_2^*UCl_2]$ is so much less than that for $[Cp_2^*UCl_2]$ relative to $[UCl_4]$. Xα-SW calculations on $[Cp_2AnX_2]$ (X = Cl, Me) also indicate that CH_3^- is a stronger σ donor than Cl^-, and that Cl^- is not a significant π donor to uranium.[80]

Marks et al. have done detailed studies on the structures, reactivities, and bond energies of $[Cp_2^*AnR_2]$ (R = hydride or alkyl) systems.[102] The bis(neopentyl) complex $[Cp_2^*Th(CH_2CMe_3)_2]$ (**11**) exhibits an unusual geometry in which the two neopentyl groups are significantly inequivalent: one has a much shorter Th–C bond and shows a very obtuse Th–C–C angle[103] (Fig. 9). This behavior is attributed to an agostic interaction[104] between the α C–H bonds and the Th center. An EH analysis of the model complex $[Cp_2Th(C_2H_5)_2]$ indeed indicates a significant agostic interaction at large Th–C–C angles.[99, 105] The calculated potential energy curve as a function of one Th–C–C angle is at a minimum near the experimentally observed angle of 158°. The potential curve is quite shallow, consistent with the observed stereochemical nonrigidity of the alkyl groups in **11**.

The apparent affinity of Th^{IV} for additional electron density, as evidenced in the agostic behavior described above,

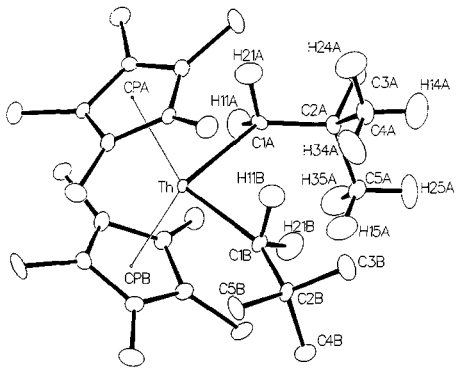

Fig. 9. The 50 K neutron diffraction structure of **11**. Significant bond angles and distances: Th-C1A-C2A = 132.1°; Th-C1A = 2.543 Å, Th-C1B-C2B = 158.2°; Th-C1B = 2.456 Å [103].

has been used to explain the remarkable ability of such compounds to activate C–H and H–H bonds.[106] For example, **11** can be entropically driven to strained thoracyclobutane **12**, which undergoes facile ring-opening C–H activation reactions [Eq. (b)].[107, 108] Oxidative addition of R–H to **12**

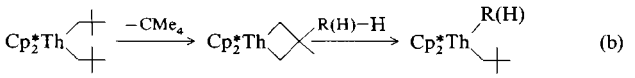

(b)

11 **12** **13**

can be ruled out as a possible step in the transformation of **12** to **13**; such a step would require the formal oxidation of d^0f^0 Th^{IV}. The kinetic data on reactions such as **12** → **13** are consistent with a concerned, four-center heterolytic C(H)–H activation pathway, involving precoordinaton of the activated bond (Scheme 1).[108] This mechanism parallels those that

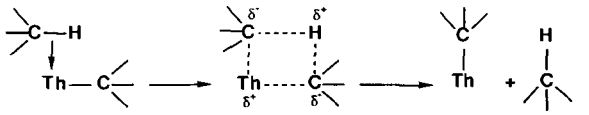

Scheme 1. Four-center C(H)–H activation mechanism.

have been proposed[109, 110] and studied theoretically[111] for C–H bond activation by d^0 transition-metal and lanthanide organometallics. In both of these latter types of systems, the metal d orbitals are the most important ones with respect to precoordination, suggesting a similar role of the 6d orbitals in the actinide systems.

4.2.2. An–X Bond Energies

Thermochemical studies of $[Cp_2^*AnR_2]$ and $[Cp_2MR_2]$ have yielded experimental values for the An–R and M–R bond disruption enthalpies.[112–114] Representative values of the bond disruption enthalpies for Equations (c) and (d)

$$Cp_2^*AnR_2(g) \longrightarrow Cp_2^*AnR(g) + R^{\cdot}(g) \quad (c)$$

$$Cp_2MR_2(g) \longrightarrow Cp_2MR(g) + R^{\cdot}(g) \quad (d)$$

are listed in Table 2. The Th–R bonds are generally about 5–10 kcal mol^{-1} stronger than the analogous U–R bonds. The An–R bonds are generally stronger than the corresponding M–R bonds, where M is a middle or late transition metal,[113] and slightly stronger than, or comparable to, M–R bonds of the early transition metals.[114] As mentioned earlier, the trends in bond disruption enthalpies have been successfully modeled theoretically, and the greater strength of the M–R bonds of the early transition metals is attributed to the repulsive interactions between the filled d orbitals of the late transition metals and the occupied ligand orbitals.[115]

Table 2. Bond disruption enthalpies D(M-R) [kcal mol^{-1}] for selected M–R bonds.

Compound	D(M-R)	Ref.
$[Cp_2^*ThMe_2]$	77.2	[111]
$[Cp_2^*Th(C_6H_5)Cl]$	90.5	[112]
$[Cp_2^*UMe_2]$	67.8	[112]
$[Cp_2^*U(C_6H_5)Cl]$	86.7	[112]
$[Cp_2^*ZrMe_2]$	67.0	[113]
$[Cp_2ZrMe_2]$	67.2	[113]
$[Cp_2^*HfMe_2]$	72.0	[113]

Interestingly, the Th–R bond disruption enthalpies in $[Cp_3ThR]$ complexes are significantly larger (by about 5 kcal mol^{-1}) than those in the corresponding $[Cp_2^*ThR_2]$ complexes.[116] These results were somewhat surprising in that the presence of three Cp ligands should increase the steric congestion about the Th center. The authors propose that the bond-strength difference in the two systems might be due to differences in the Th–R orbital overlap, although significant differences in the bonding are not evident in the PE spectra.[78]

4.2.3. CO Insertion Products and Other Adducts

Marks et al. have demonstrated that, like the early transition-metal metallocene alkyls, $[Cp_2^*An(R)(X)]$ and $[Cp_2^*AnR_2]$ systems readily insert CO and other small molecules into their An–R bonds [Eq. (e)].[117]

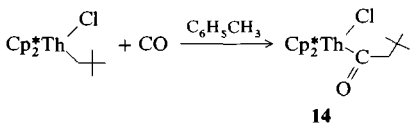

(e)

14

The crystal structure of **14** (Fig. 10) reveals an unusually short Th–O distance, 0.07 Å shorter than the Th–C(acyl) bond. In contrast, the M–O distances observed in most transition-metal acyls are invariably longer than the M–C distances. These observations led the authors to favor formulation of the actinide-acyl moiety as a carbene-like dihapto acyl (**15**) rather than as a "normal" metal acyl group (**16**). Similar observations have been made for the insertion of CO into An–NR_2 bonds, yielding η^2-carbamoyl complexes[118] and for the insertion of isocyanides into An–R bonds.[119] The carbene-like description (**15**) of the bonding in actinide-

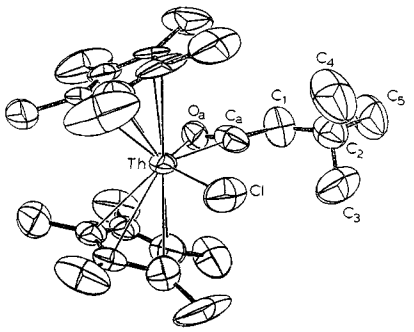

Fig. 10. ORTEP drawing of the nonhydrogen atoms for the $[Th\{(CH_3)_5C_5\}_2\{\eta^2\text{-}COCH_2C(CH_3)_3\}]Cl$ molecule [117].

acyl and related complexes is in accord with the remarkable C–C coupling reactions that they exhibit.[14a, 117]

15 16

A notable difference in the structures of actinide acyls and those of transition metals is the orientation of the η^2-acyl C–O bond relative to the other σ-bonded ligand. Actinide acyls exhibit both the "O-outside" (**17**) and "O-inside" (**18**) structures; in the carbamoyl complexes $[Cp^*_2An(CONMe_2)Cl]$, for example, both isomers exist in equilibrium in solution.[120] By contrast, all structurally characterized acyl complexes of the group 4 metals show only the O-inside structure **18**.[121, 122] *Tatsumi, Hofmann,*

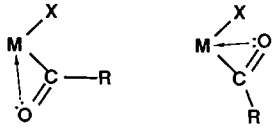

17 18

Hoffmann et al. have used EH calculations to investigate the preference for η^1- versus η^2-acyls and, for the latter, the preference for O-outside versus O-inside coordination.[123] The question of η^1 versus η^2 coordination was addressed by comparison of the interactions of a $COCH_3^-$ ligand with the $[Mn(CO)_5]^+$, $[Cp_2ZrMe]^+$, and $[Cp_2UCl]^{3+}$ metal fragments. Each fragment has a frontier orbital appropriate for the formation of a M–C σ bond with the acyl ligand. The latter two fragments also contain an unoccupied orbital that is capable of accepting density from the acyl oxygen lone pair, thus favoring the η^2-acyl geometry. In the more electron-rich $[Mn(CO)_5]^+$ fragment, the 3d orbital that would be appropriate to accept charge from the acyl oxygen is occupied, precluding a Mn–O(acyl) interaction and leading to an η^1-acyl structure. The shape of the U-based hybrid orbital in $[Cp_2UCl]^{3+}$ that fosters the η^2-acyl bonding stabilizes the O-outside structure **17** in the actinide-acyl relative to that in the transition-metal complex: for $[Cp_2Zr(COMe)Me]$, structure **17** is calculated to be about 5 kcal mol^{-1} less stable than structure **18**; for $[Cp_2U(COMe)Cl]^{2+}$, the two structures are essentially isoenergetic, in accord with the experimental observations.

The electronic structure of the 1,3-diene compounds of $[Cp^*_2Th]$ and $[Cp^*_2U]$ has also been investigated. The 1,3-diene complexes of zirconium, $[Cp_2Zr(1,3\text{-diene})]$, can exhibit either s-*cis* (**19**) or s-*trans* (**20**) structures.[124] On the other

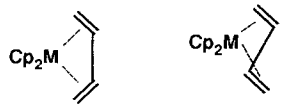

19 20

hand, $[Cp^*_2Th(C_4H_6)]$ shows only the s-*cis* structure.[125] EH calculations show a sizable energy gap between the minima of the s-*cis* and the s-*trans* isomers for both $[Cp_2Th(C_4H_6)]$ (0.74 eV) and $[Cp_2U(C_4H_6)]$ (0.42 eV), favoring the s-*cis* geometry in each case.[99] Similar calculations on $[Cp_2Zr(C_4H_6)]$ show that the s-*cis* and the s-*trans* geometries are well balanced (0.07 eV in favor of s-*cis*). The difference between the actinide and the zirconium results stems from the $3a_1$ frontier orbital of the $[Cp_2M]$ fragment (Fig. 8). For zirconium this a_1 orbital interacts with the π_3^* orbital of butadiene equally well in either the s-*cis* or the s-*trans* geometry, but for the actinide compounds the $3a_1$–π_3^* interaction is much greater in the s-*cis* geometry. The butadiene terminal carbon atoms in the actinide compounds have a large negative charge. The high polarity in the Th–C(terminal) bonds is consistent with the violent reactivity of the complex with organic carbonyls and with the facile insertion of pyridine into the Th–C bond.

Tatsumi and *Nakamura* have also compared two isomers of $[Cp_2U(C_4H_4)]$, namely, the actinacyclopentadiene complex, $[Cp_2UCH{=}CHCH{=}CH]$, and the cyclobutadiene complex, $[Cp_2U(\eta^4\text{-}C_4H_4)]$.[99] While no examples of actinide cyclobutadiene compounds exist, there is a known actinacyclopentadiene complex, $[Cp^*_2U(C_4Ph_4)]$.[126] The metallacyclopentadiene complex is calculated to be 2.5 eV more stable than the hypothetical cyclobutadiene complex. However, the authors note that $[Cp_2U(\eta^4\text{-}C_4H_4)]$ would be kinetically stable because (1) the U-to-η^4-C_4H_4 bonding is reasonably strong (actually stronger than U-to-Cp bonding) and (2) a C–C bond cleavage of $[Cp_2U(\eta^4\text{-}C_4H_4)]$ with simultaneous formation of two U–C σ bonds is symmetry forbidden.

The bonding in the bis-pyrazolate complexes $[Cp_2Mo(pz)_2]$, $[Cp_2Mo(pz)_2]^{2+}$, and $[Cp_2U(pz)_2]$ (pz = $C_3H_3N_2^-$) has been investigated via EH calculations.[127] The pz ligand can adopt either an η^1 (two-electron donor) or an η^2 (four-electron donor) coordination geometry, as it does in the case of $[Cp_3U(pz)]$.[128] The electronically favored structures for the molybdenum complexes are those predicted by the effective-atomic-number rule, that is η^1,η^1 for the neutral complex and η^2,η^2 for the dicationic complex. In contrast, $[Cp_2U(pz)_2]$ exhibits an η^2,η^2 minimum with the calculated U–N–N angles in close agreement with the crystal structure of $[Cp^*_2U(pz)_2]$.[129] The choice of η^1 versus η^2 coordination is similar to that of the acyl complexes and can be explained in terms of the same frontier orbitals.

There have been several studies of the mechanism of CO insertion into the actinide–alkyl bonds of $[Cp^*_2AnR_2]$ sys-

tems. EH calculations have been used to investigate the pathway by which a CO molecule approaches $[Cp_2U(CH_3)_2]^{2+}$ prior to insertion into the M–R bond.[123] Approach of the CO ligand along a path perpendicular to the plane containing the two Cp centroids and the metal atom is found to have no appreciable barrier, consistent with the experimental result that CO insertion is extremely facile.

$[Cp^*_2AnR_2]$ and $[Cp^*_2AnRX]$ have been shown to undergo facile carbonylation with subsequent C=C bond formation to yield monomeric or dimeric products such as **21** and **22**.[130] A possible mechanism for the formation of **21** via

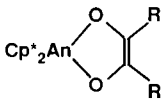

21

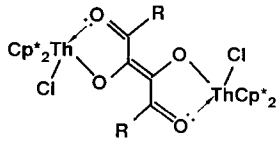

22

stepwise CO insertion to yield the bis(η^2-acyl) complex, with subsequent coupling of the two acyl ligands, has been considered.[131] The bis-acyl complex $[Cp_2U(COR)_2]^{2+}$ is predicted to have a bis-η^2 structure, in contrast to early-transition-metal complexes in which the η^1,η^2 structure is found to be the most stable. The HOMO of $[Cp_2Ti(COR)_2]$ is destabilized on proceeding from the η^1,η^2 structure to the η^2,η^2 structure by an unfavorable out-of-phase interaction of the acyl lone pairs. For $[Cp_2U(COR)_2]$, the HOMO also has out-of-phase acyl lone-pair orbitals in the η^2,η^2 structure; now, however, these can interact favorably with a U 5f orbital. The HOMO is therefore stabilized on going from η^1,η^2 to η^2,η^2. These results are consistent with the observed η^2,η^2 structure of $[Cp^*_2U(CONMe_2)_2]$.[132]

The least-motion pathway for acyl coupling (C=C bond formation) in $[Cp_2U(COR)_2]^{2+}$ is a symmetry-forbidden process with a calculated barrier as high as 1.6 eV. The optimum reaction path is one in which the two acyl groups rotate up to 30° out of planarity on the approach to the transition state, which then collapses to the planar enediolate product **21**. The barrier for this pathway is 0.7 eV. The resulting enediolate compound is 2.9 eV more stable than the $(\eta^2\text{-COR})_2$ structure, indicating that the coupling is highly exothermic. The twisting of the η^2-COR groups out of the equatorial plane costs surprisingly little energy (0.1 eV), and support for this motion comes from the structure of the complex $[Cp^*_2U(CONMe_2)_2]$, which has twisted cabamoyl groups.[132] The absence of carbamoyl coupling is due to the electronic influence of the NR_2 groups, which results in a "more-forbidden" least-motion pathway with a barrier of 2.9 eV and a non-least-motion pathway having a barrier of 1.1 eV. A completely different pathway has been proposed for acyl coupling to enediolates at a $[Cp_2Zr]$ center.[133]

Polysulfide ligands such as S_5^{2-} form metallacycles with both actinide and transition-metal atoms. In contrast to transition-metal MS_5-containing complexes, which all exhibit chair conformations of the MS_5 ring, $[Cp^*_2ThS_5]$ shows an unprecedented twist-boat conformation (Fig. 11).[134] This compound has unusually short Th–β-S distances, indicative of some interaction between the metal and the terminal S–S bonds (S_1-S_2 and S_4-S_5) of the S_5^{2-} ligand. EH calcu-

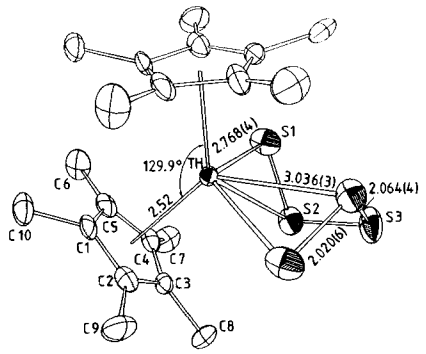

Fig. 11. Crystal structure of $[Cp^*_2ThS_5]$ [134].

lations on $[Cp_2ThS_5]$ indicate donation from the two highest occupied MOs of S_5^{2-} into empty orbitals (predominantly 6d) on the $[Cp_2Th]^{2+}$ fragment. While the Th–α-S bonding dominates, significant Th–β-S bonding is also indicated.

4.3. Mono(cyclopentadienyl)actinide Complexes

$[CpU\{(CH_2)(CH_2)P(C_6H_5)_2\}_3]$ (**23**) has the longest U–C σ bonds yet reported (2.66 Å). EH calculations on this compound give an average U–C σ-bond overlap population of 0.26 compared with an overlap population of −0.03 for U–C(Cp), indicating covalency in the U–C σ bonds.[135] However, the overlap populations for the U–C σ bonds in this compound are much smaller than that found for the U–C σ bond in $[Cp_3UCH_3]$. That the difference is not a result of the long U–C bonds in **23** was supported by calcu-

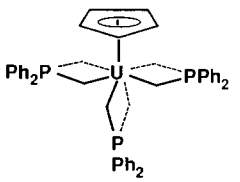

23

lations on the compound with U–C distances of 2.4 Å (the same as in $[Cp_3UCH_3]$. At this distance the overlap population increases only slightly to 0.27. The small overlap populations (and, hence, the long U–C distance) are due to the outward deformation of the ylide-carbon lone pairs along a direct line to the uranium atom. In addition, the coplanarity of the five carbon atoms and slight repulsive interactions between the lone pairs on adjacent ylides will further reduce the size of the inward-pointing orbital lobes.

5. Actinide–Cyclopentadienyl Complexes Containing Metal–Metal Bonds

To date, no bonds between two actinide centers have been observed in organoactinide chemistry. The possibility of 5f-based metal–metal bonds in the naked uranium and neptunium dimers have been investigated via nonrelativistic Xα-SW molecular orbital calculations.[136] These results suggest a

$\sigma^2\pi^4\delta^4\phi^2$ configuration for U_2, leading to a sextuple bond, and a $\sigma^2\pi^4\delta^4\phi^4$ configuration for Np_2, yielding a septuple bond. The separation between the ϕ_u and the ϕ_g orbitals is only 0.3 eV in Np_2, which might lead to a high-spin configuration and a pentuple bond. A recent ab initio calculation of the electronic structure of U_2, including relativistic effective core potentials and electron correlation, casts doubt on the simple f-orbital overlap model for U–U bonding.[137]

Two systems that contain phosphido-bridged bonds between Th and a transition metal have recently been reported. Reaction of $[Cp^*_2Th(PPh_2)_2]$ with $[Pt(cod)_2]$ in the presence of PMe_3 yields complex **24a**, which has a Th–Pt distance of 2.98 Å, 0.2 Å shorter than the sum of the covalent radii of the metal atoms.[138] On the basis of this structural information, along with ^{31}P NMR data and comparisons with other heterobimetallics, the authors conclude that **24a** contains a direct Th–Pt bond. Their Hartree–Fock and generalized valence bond (GVB) ab initio calculations on the model compound $[Cl_2Th(\mu\text{-}PH_2)_2Pt(PH_3)]$ lead to qualitatively similar descriptions of the metal–metal bonding. The bond is formed between the $5d_{x^2-y^2}$ orbital on Pt and the $6d_{x^2-y^2}$ orbital on Th, with a larger fraction of electron density on the Pt center. A Mulliken population analysis reveals a charge of + 1.48 on the Th atom and a charge of 0.00 on the Pt atom. The authors conclude that the Th–Pt bond can be regarded as a formal donor–acceptor, or dative, bond from the "filled" $5d^{10}$ shell of Pt into the "empty" 6d shell of Th.

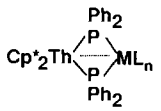

24 a: $ML_n = [PtPMe_3]$

b: $ML_n = [Ni(CO)_2]$

Complex **24b** has a Th–Ni distance of 3.206 Å, shorter than that expected from ionic model assumptions. EH calculations indicate that the Th–Ni overlap population, although negative at all distances investigated, is most favorable at the experimental distance of 3.2 Å and becomes increasingly more negative as the Th–Ni distance is lengthened to 3.7 Å.[139] Furthermore, of the major interactions among the metals and the bridging phosphido ligands, the Th–Ni interaction is the most sensitive to this geometrical change, indicating that the M–P bonds have some geometrical flexibility. When the molecule is divided into two fragments, two principal sources of Th–Ni interaction are discernible. The first is the filled–filled repulsion between the d levels of the Ni atom and the Th–PH_2 bonding orbitals resulting in a net antibonding interaction between Th and Ni. The second is the interaction between the filled d levels of $[Ni(CO)_2]$ and the frontier orbitals of $[Cp_2Th(PH_2)_2]$. The largest of these is a π interaction between the HOMO of $[Ni(CO)_2]$, which is a hybrid of d_{xz} and p_x that points toward the Th atom, and the $3b_2$ frontier orbital of Th. A σ interaction takes place between the SHOMO of $[Ni(CO)_2]$, a mixture of Ni $d_{x^2-y^2}$, d_{z^2}, p_z, and s orbitals, and the $3a_1$ frontier orbital of Th, a mixture of d_{z^2}, p_z, and s orbitals. Owing to the superior radial extension of the Th 6d orbitals, both the σ and the π interactions are dominated by the Th 6d orbitals rather than the Th 5f orbitals. Similar conclusions were reached on the basis of an Xα-SW calculation on compound **24b**.[140]

Marks et al. have prepared the first two complexes that contain a direct, unsupported bond between an actinide atom and a transition metal. The reaction of $[Cp^*_2ThX_2]$ with $[CpRu(CO)_2Na]$ yields compounds **25a** (X = Cl, I).[117] The iodo derivative has a Th–Ru bond length of 3.028 Å, comparable to the Zr–Ru bond length of 2.910 Å in compound **25b** ($X = OCMe_3$).[141] The nature of the metal–metal bonding in compounds **25** has been investigated using quasi-relativistic Xα–SW calculations on the model systems $[Cp_2(I)M\text{-}RuCp(CO)_2]$ (M = Zr, Th).[142] The M–Ru bonding is virtually the same in these two systems and consists of donation from the filled $4d_{z^2}$ orbital of Ru into the empty d_{z^2} orbital of Th or Zr. The result is a slightly "bent" M–Ru σ bond (Fig. 12) that is highly polarized (ca. 70%) toward the Ru atom. Thus, the bond is best described as a dative donor–acceptor bond formed by donation from $[CpRu(CO)_2]^-$ to a d^0 or d^0f^0 M^{IV} center. The authors note that $[CpRu(CO)_2]^-$ can be regarded as an "organometallic pseudohalide". This notion has been extended in the synthesis of several $[Cp_3AnMCp(CO)_2]$ (An = Th, U; M = Fe, Ru) derivatives.[143]

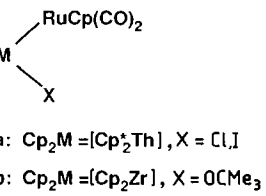

25 a: $Cp_2M = [Cp^*_2Th]$, X = Cl, I

b: $Cp_2M = [Cp_2Zr]$, $X = OCMe_3$

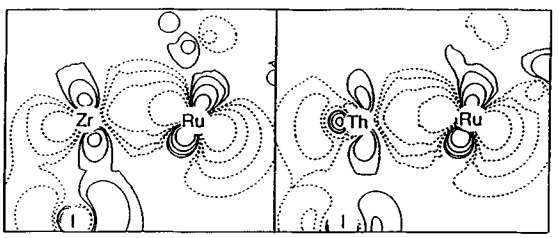

Fig. 12. Contour diagrams of the metal–metal bonding orbitals in the heterobimetallic complexes $[Cp_2(I)M\text{–}RuCp(CO)_2]$ (M = Zr, Th) [142].

6. Conclusion and Outlook

In this review, we have tried to emphasize the interplay between experimental and theoretical electronic structure investigations in the comparatively new and very exciting field of organoactinide chemistry. As is evident from the compounds discussed in this review, the lion's share of electronic structural study of organoactinide chemistry has involved complexes of the two most experimentally accessible actinide elements, namely, thorium and uranium. These studies point to some general conclusions concerning the qualitative description of the bonding in these systems:

1. The strong donor ability of formally anionic ligands leads to a generally high degree of covalency in organoactinide complexes, particularly compared to the actinide halides.

2. The actinide 6d orbitals are generally greater participants in the metal–ligand bonding than are the 5f orbitals, a notion first proposed by *Clark* and *Green* in their interpretation of the PE spectrum of uranocene.[144] As a result, the 6d orbitals are more affected by the organic "ligand field" than are the 5f orbitals.
3. The actinide 5f orbitals participate in metal–ligand bonding when symmetry dictates that no other actinide orbitals are available.
4. The metal-localized electrons in "non-f^0" complexes (such as those of U^{IV}) reside in nearly pure actinide 5f orbitals. Exceptions to this generalization can occur in coordinatively unsaturated early actinide complexes, such as $[Cp_3Th]$.

The picture that emerges is one in which there is a dichotomy in the roles of the actinide 5f and 6d orbitals, wherein the latter are used to bind the ligands and the former are used to house metal-based electrons. By contrast, in organotransition-metal complexes the valence nd orbitals serve as both the principal source of metal–ligand bonding and as the repository of metal-based electrons. This situation is shown schematically in Figure 13, wherein it can be seen how this simple description accounts for the paramagnetism of U^{IV} complexes vis-à-vis the diamagnetism usually observed in d^2 transition-metal organometallics, such as $[Cp_2MoCl_2]$.[80]

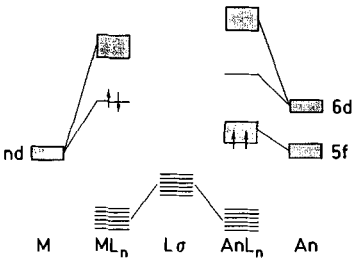

Fig. 13. Qualitative MO diagram comparing the roles of the metal-based orbitals in transition-metal complexes (left) and actinide complexes (right).

What is the future of organoactinide electronic structure investigations? The studies to date have focused primarily on the relative roles of the actinide orbitals in bonding and on the relationship of this bonding to that in transition-metal systems. From a quantum-chemical point of view, the electronic structure calculations on organoactinides have been comparatively crude; very little has been done with respect to electron correlation in these systems, and, although quasi-relativistic corrections have been employed, there has been scant consideration of the effects of spin–orbit coupling. This situation is changing rapidly as the speed and accessibility of supercomputers increases. The recent spin–orbit configuration interaction calculation on uranocene by *Chang* and *Pitzer*[111] is a portent of what may be expected in this field in the future.

Glossary: A Brief Outline of Electronic Structure Methods for Actinide Systems

As is apparent from the preceding discussion, a wide variety of electronic structure methods have been applied to large actinide-containing molecules. Each method employs certain approximations in the construction or solution of the electronic-structure problem, and each has inherent advantages and disadvantages. The following is a very brief summary (without references) of the methods cited in this review; for an in-depth discussion of the electronic structure methodologies, we refer the reader to our recent detailed review of these methods as well as their applications in organometallic and nonorganometallic actinide chemistry [145].

Nonrelativistic versus Quasi-relativistic versus Relativistic Methods: "Conventional" molecular electronic structure calculations, based on the Schrödinger wave equation, include no consequences of subjecting the system to the tenets of special relativity. These *nonrelativistic methods* assume that the mass of every electron in the system is equal to the rest mass of the electron and that the electron-spin coordinate can be treated completely independently of the spatial coordinates. For the heavier elements, such as the third-row transition metals and the actinide elements, these assumptions are invalid. The classical angular speeds of the core electrons in these elements are nonnegligible fractions of the speed of light and thus a relativistic mass correction is necessary. *Quasi-relativistic methods* are those that include such mass corrections (as well as more arcane effects, such as the Darwin correction) but still maintain separate spin and spatial coordinates. The results of quasi-relativistic molecular orbital methods resemble those of nonrelativistic methods in that spatial molecular orbitals, to which spin functions can be attached, are derived. The *quasi-relativistic extended Hückel* and *quasi-relativistic Xα-SW* methods are examples of quasi-relativistic molecular orbital methods.

In addition to the effects noted above, *relativistic methods* include the interaction of the spatial and spin properties of the electrons, that is, spin–orbit coupling. The Dirac equation, which merges quantum mechanics and special relativity, is the usual starting point for relativistic electronic structure methods. The application of the Dirac equation to molecules is far more complex than that of the nonrelativistic Schrödinger equation, and several calculational approaches to solving the equation have been used. The *relativistically parametrized extended Hückel (REX)* method of *Lohr* and *Pyykkö* is probably the simplest approach to a fully relativistic calculation. Because relativistic approaches explicitly include spin–orbit coupling, the states and orbitals that result are bases for the double group of the molecule rather than the more familiar single group. Owing to the computational complexity of fully relativistic methods, relatively few such calculations have been performed to date on organoactinide systems.

Molecular Orbital Methods: Most of the electronic structure calculations reported here employ the molecular orbital approximation, in which it is assumed that each electron experiences the average field of all the other electrons in the molecule. The molecular orbitals are usually expanded as a linear combination of atomic orbitals (LCAO), which can be either analytical or numerical functions. In the *Hartree–Fock* method, which has been used sparingly for heavy element systems, all of the relevant integrals are solved exactly. In order to make such calculations computationally feasible, *relativistic effective core potentials* (ECPs or RCPs) are generally used. ECPs, which are based on relativistic atomic calculations, replace the core atomic orbitals and thus greatly reduce the number of molecular integrals while preserving the relativistic effects on the core electrons. Approximate LCAO-MO methods, such as the *extended Hückel method*, use either empirical or semiempirical approximations to some of the molecular integrals.

A family of molecular orbital methods that has moved to the fore in recent years is that based on *local density functional (LDF)* methods. These methods replace the nonclassical, nonlocal exchange interaction inherent to the Hartree–Fock method with a local exchange operator, which is dependent on the electron density raised to a fractional power. Because the equations involving the local exchange operator cannot be solved readily using analytical methods, the application of LDF methods depends on several numerical methodologies. The earliest LDF method, the *Xα scattered-wave (Xα-SW)* or *multiple-scattering Xα (MS-Xα)* method, uses a model Hamiltonian based on surrounding each atom of the molecule with a sphere. Scattering theory techniques are used to satisfy the boundary equations at the sphere surfaces. The orbitals ob-

tained are hybrid numerical/analytical functions that are based in part on a multicenter scattering wave function. Quasi-relativistic corrections can be easily added to Xα-SW calculations, and a fully relativistic version of the method has also been implemented.

The newer LDF methods use an atomic orbital basis in which to expand the molecular orbitals. The necessary molecular integrals are calculated by using numerical integration techniques. The *discrete-variational Xα (DV-Xα)* method uses numerical atomic orbitals that are obtained from atomic calculations. A fully relativistic implementation of this method, called the *Dirac–Slater discrete variational (DS-DV)* method, provides a relatively inexpensive means of performing relativistic calculations on large molecules. The *Hartree–Fock–Slater (HFS)* method is very similar to the DV-Xα method, except that analytical functions are used to represent the atomic orbitals. Quasi-relativistic and relativistic effects have also been incorporated into the HFS method.

Electron Correlation Methods: The importance of including electron correlation in electronic structure calculations has been well established for light-atom systems. Using a molecular orbital solution as a starting point, correlation is generally included via additional *configuration interaction (CI)* or *multiconfiguration self-consistent-field (MCSCF)* calculations. Because these techniques are extremely computationally demanding, only recently have they seen application to organoactinide complexes. ECPs are used to replace core electrons in such calculations, and spin–orbit effects can be included explicitly. The *generalized valence bond (GVB)* method, which includes electron correlation relative to a molecular orbital description, has also seen limited application to organoactinide systems. The GVB method uses a different form of the wave function than do molecular-orbital-based methods.

It is a great pleasure to acknowledge our co-workers at The Ohio State University, especially Anne Fang, Kevin Novo-Gradac, Melanie Pepper, Larry Rhodes, and Bill Schneider, who have made significant contributions to our understanding of organoactinide chemistry. We are also grateful to many colleagues elsewhere for stimulating discussions and to the Isotope and Nuclear Chemistry Division of Los Alamos National Laboratory for generously hosting both of us. We wish to thank the U.S. Department of Energy, the Petroleum Research Fund (administered by the American Chemical Society), the Ohio Supercomputer Center, the Associated Western Universities, and the Ohio State University Graduate School for their generous support of our research in actinide chemistry.

Received: September 12, 1990 [A 830 IE]
German version: *Angew. Chem. 103* (1991) 1085

[1] a) T. J. Kealy, P. L. Pauson, *Nature 168* (1951) 1039; b) S. A. Miller, J. A. Tebboth, J. F. Tremaine, *J. Chem. Soc. 1952*, 632; c) G. Wilkinson, M. Rosenblum, M. C. Whiting, R. B. Woodward, *J. Am. Chem. Soc. 74* (1952) 2125; d) E. O. Fischer, W. Pfab, *Z. Naturforsch. 7B* (1952) 377.
[2] L. T. Reynolds, G. Wilkinson, *J. Inorg. Nucl. Chem. 2* (1956) 246.
[3] a) E. O. Fischer, A. Treibner, *Z. Naturforsch. B 17* (1962) 276; b) E. O. Fischer, Y. Hristidu, *ibid. 17* (1962) 275.
[4] A. Streitwieser, Jr., U. Müller-Westerhoff, *J. Am. Chem. Soc. 90* (1968) 7364.
[5] R. D. Fischer, *Theor. Chim. Acta 1* (1963) 418.
[6] a) A. Zalkin, K. N. Raymond, *J. Am. Chem. Soc. 91* (1969) 5667; b) A. Avdeef, K. N. Raymond, K. O. Hodgson, A. Zalkin, *Inorg. Chem. 11* (1972) 1083.
[7] Th: A. Streitwieser, Jr., N. Yoshida, *J. Am. Chem. Soc. 91* (1969) 7528; Pa: J. Goffart, J. Fuger, D. Brown, G. Duyckaerts, *Inorg. Nucl. Chem. Lett. 10* (1974) 413; Np, Pu: D. G. Karraker, J. A. Stone, E. R. Jones, Jr., N. Edelstein, *J. Am. Chem. Soc. 92* (1970) 4841.
[8] See, for example: a) R. F. Dallinger, P. Stein, T. G. Spiro, *J. Am. Chem. Soc. 100* (1978) 7865; b) W. D. Luke, A. Streitwieser, Jr., (Lanthanide and Actinide Chemistry and Spectroscopy) *ACS Symp. Ser. 131* (1980) 93.
[9] See, for example: a) K. D. Warren, *Struct. Bonding (Berlin) 33* (1977) 97; b) N. Rösch, A. Streitwieser, Jr., *J. Organomet. Chem. 145* (1978) 195; c) P. Pyykkö, L. L. Lohr, Jr., *Inorg. Chem. 20* (1981) 1950; d) N. Rösch, A. Streitwieser, Jr., *J. Am. Chem. Soc. 105* (1983) 7237; e) N. Rösch, *Inorg. Chim. Actra 94* (1984) 297; f) P. M. Boerrigter, E. J. Baerends, J. G. Snidjers, *Chem. Phys. 122* (1988) 357.
[10] J. G. Brennan, J. C. Green, C. M. Redfern, *J. Am. Chem. Soc. 111* (1989) 2373.
[11] A. H. H. Chang, R. M. Pitzer, *J. Am. Chem. Soc. 111* (1989) 2500.
[12] a) T. J. Marks, A. Streitwieser, Jr., in J. J. Katz, L. R. Morss, G. T. Seaborg (Eds.): *The Chemistry of the Actinide Elements*, Chapman and Hall, New York 1986, Chap. 22; b) T. J. Marks in [12a], Chap. 23; c) T. J. Marks, R. D. Ernst in G. Wilkinson, F. G. A. Stone, E. W. Abel (Eds.): *Comprehensive Organometallic Chemistry*, Pergamon, Oxford, Chap. 21; d) T. J. Marks, *Science 217* (1982) 989; e) T. J. Marks, *Prog. Inorg. Chem. 25* (1979) 223; f) T. J. Marks, I. L. Fragalà (Eds.): *Fundamental and Technological Aspects of Organo-f-Element Chemistry*, Reidel, Dordrecht 1985; g) T. J. Marks, R. D. Fischer (Eds.): *Organometallics of the f-Elements*, Reidel, Dordrecht 1979.
[13] a) G. Brandi, M. Brunelli, G. Lugli, A. Mazzei, *Inorg. Chim. Acta 7* (1973) 319; b) A. E. Gebala, M. Tsustui, *J. Am. Chem. Soc. 95* (1973) 91; c) T. J. Marks, A. M. Seyam, J. R. Kolb, *ibid.* (1973) 5529.
[14] a) J. M. Manriquez, P. J. Fagan, T. J. Marks, C. S. Day, V. W. Day, *J. Am. Chem. Soc. 100* (1978) 7112; b) K. Tatsumi, A. Nakamura, P. Hofmann, R. Hoffmann, K. G. Moloy, T. J. Marks, *ibid. 108* (1986) 4467, and references therein; c) This first report of migratory insertion of CO by actinide alkyls was followed by the first report of CO insertion into metal–hydride bonds to form metal formyls: P. J. Fagan, K. G. Moloy, T. J. Marks, *ibid. 103* (1981) 6959.
[15] R. E. Cramer, R. B. Maynard, J. C. Paw, J. W. Gilje, *J. Am. Chem. Soc. 103* (1981) 3589.
[16] J. M. Ritchey, A. J. Zozulin, D. A. Wrobleski, R. R. Ryan, H. J. Wasserman, D. C. Moody, R. T. Paine, *J. Am. Chem. Soc. 107* (1985) 501.
[17] R. S. Sternal, C. P. Brock, T. J. Marks, *J. Am. Chem. Soc. 107* (1985) 8270.
[18] J. G. Brennan, R. A. Andersen, J. L. Robbins, *J. Am. Chem. Soc. 108* (1986) 335.
[19] T. M. Gilbert, R. R. Ryan, A. P. Sattelberger, *Organometallics 8* (1989) 857.
[20] W. G. Van Der Sluys, C. J. Burns, A. P. Sattelberger, *Organometallics 8* (1989) 855.
[21] See, for example: a) I. L. Fragalà in T. J. Marks, R. D. Fischer (Eds.): *Organometallics of the f-Elements*, Reidel, Dordrecht 1979, p. 421; b) J. C. Green, *Struct. Bonding (Berlin) 43* (1981) 37.
[22] D. G. Karraker, J. A. Stone, *Inorg. Chem. 11* (1972) 1742.
[23] a) P. Pyykkö, *Chem. Rev. 88* (1988) 563, and references therein; b) P. Pyykkö, J. P. Desclaux, *Acc. Chem. Res. 12* (1979) 276; c) K. S. Pitzer, *ibid. 12* (1979) 271.
[24] For a discussion of f orbitals see: a) H. G. Friedman, G. R. Choppin, D. G. Feuerbacher, *J. Chem. Educ. 41* (1964) 354; b) E. A. Orgryzlo, *ibid. 42* (1965) 150.
[25] J. H. Van Vleck, *J. Chem. Phys. 3* (1935) 803.
[26] J. C. Eisenstein, *J. Chem. Phys. 25* (1956) 142.
[27] S. F. A. Kettle, A. J. Smith, *J. Chem. Soc. A 1967*, 688.
[28] S. F. A. Kettle, A. J. P. Pioli, *J. Chem. Soc. A 1968*, 122.
[29] E. Glueckauf, H. A. C. McKay, *Nature 165* (1950) 594.
[30] L. I. Katzin, *Nature 166* (1950) 605.
[31] K. Tatsumi, R. Hoffmann, *Inorg. Chem. 19* (1980) 2656.
[32] a) R. E. Connick, Z. Z. Hugus, Jr., *J. Am. Chem. Soc. 74* (1952) 6012; b) R. J. Elliott, *Phys. Rev. 89* (1953) 659; c) J. C. Eisenstein, M. H. L. Pryce, *Proc. R. Soc. (London) A 229* (1955) 20.
[33] C. A. Coulson, G. R. Lester, *J. Chem. Soc. 1956*, 3650.
[34] a) K. Street, Jr., G. T. Seaborg, *J. Am. Chem. Soc. 72* (1950) 2790; b) R. M. Diamond, K. Street, Jr., G. T. Seaborg, *ibid. 76* (1954) 1461.
[35] W. Moffitt in [2].
[36] E. C. Baker, G. W. Halstead, K. N. Raymond, *Struct. Bonding (Berlin) 25* (1976) 23.
[37] K. N. Raymond, C. W. Eigenbrot, Jr., *Acc. Chem. Res. 13* (1980) 276.
[38] L. Xing-Fu, F. Xi-Zhang, X. Ying-Ting, W. Hai-Tung, S. Jie, L. Li, S. Peng-Nian, *Inorg. Chim. Acta 116* (1986) 85.
[39] J. Marcalo, A. Pires De Matos, *Polyhedron 8* (1989) 2431.
[40] P. C. Sockwell, T. P. Hanusa, *Inorg. Chem. 29* (1990) 76.
[41] C. J. Burns, B. E. Bursten, *Comments Inorg. Chem. 2* (1989) 61.
[42] P. Pyykkö in S. Wilson (Ed.): *Methods in Computational Chemistry, Vol. 2*, Plenum, New York 1980, p. 136.
[43] K. Tatsumi, R. Hoffmann, *Inorg. Chem. 23* (1984) 1633.
[44] F. Baumgärtner, E. O. Fischer, B. Kanellakopulos, P. Laubereau, *Angew. Chem. 81* (1969) 182; *Angew. Chem. Int. Ed. Engl. 8* (1969) 202.
[45] F. Baumgärtner, E. O. Fischer, B. Kanellakopulos, P. Laubereau, *Angew. Chem. 80* (1968) 661; *Angew. Chem. Int. Ed. Engl. 7* (1968) 634.
[46] J. H. Burns, *J. Am. Chem. Soc. 95* (1973) 3815.
[47] R. von Ammon, B. Kanellakopulos, R. D. Fischer, *Chem. Phys. Letters 2* (1968) 513.
[48] T. H. Siddall, III, W. E. Stewart, D. G. Karraker, *Chem. Phys. Letters 3* (1969) 498.
[49] R. von Ammon, B. Kannellakopulos, R. D. Fischer, *Chem. Phys. Letters 4* (1970) 553.
[50] H.-D. Amberger, R. D. Fischer, B. Kanellakopulos, *Z. Naturforsch. B 31* (1976) 12.
[51] H.-D. Amberger, *J. Organomet. Chem. 110* (1976) 59.

[52] B. E. Bursten, M. Casarin, S. DiBella, A. Fang, I. L. Fragalà, *Inorg. Chem. 24* (1985) 2169.
[53] B. E. Bursten, A. Fang, *Inorg. Chim. Acta 110* (1985) 153.
[54] J. C. Green, M. R. Kelly, J. A. Long, B. Kanellakopulos, P. I. W. Yarrow, *J. Organomet. Chem. 212* (1981) 329.
[55] K. Tatsumi, A. Nakamura, *J. Organomet. Chem. 272* (1984) 141.
[56] P. C. Blake, M. F. Lappert, J. L. Atwood, H. Zhang, *J. Chem. Soc. Chem. Commun. 1986*, 1148.
[57] a) J. G. Brennan, *Ph.D. Dissertation*, University of California, Berkeley (1985); b) A. Zalkin, J. G. Brennan, R. A. Andersen, *Acta Crystallogr. Sect. C 44* (1988) 2104.
[58] H. J. Wasserman, A. J. Zozulin, D. C. Moody, R. R. Ryan, K. V. Salazar, *J. Organomet. Chem. 254* (1983) 305.
[59] C. Wong, T. Yen, T. Lee, *Acta Crystallogr. 18* (1965) 340.
[60] J. Leong, O. Hodgson, K. N. Raymond, *Inorg. Chem. 12* (1973) 1329.
[61] J. W. Lauher, R. Hoffmann, *J. Am. Chem. Soc. 98* (1976) 1729.
[62] B. E. Bursten, L. F. Rhodes, R. J. Strittmatter, *J. Am. Chem. Soc. 111* (1989) 2758.
[63] W. K. Kot, G. V. Shalimoff, N. M. Edelstein, M. A. Edelman, M. F. Lappert, *J. Am. Chem. Soc. 110* (1988) 986.
[64] B. E. Bursten, L. F. Rhodes, R. J. Strittmatter, *J. Am. Chem. Soc. 111* (1989) 2756.
[65] R. J. Strittmatter, *Ph.D. Dissertation*, The Ohio State University, Columbus, OH, USA 1990.
[66] L. J. Nugent, P. G. Laubereau, G. K. Werner, K. L. Vander Sluis, *J. Organomet. Chem. 27* (1971) 365.
[67] B. Kanellakopulos, E. Dornberger, H. Billich, *J. Organomet. Chem. 76* (1974) C42.
[68] B. E. Bursten, L. F. Rhodes, R. J. Strittmatter, *J. Less-Common Met. 149* (1989) 207.
[69] R. J. Strittmatter, B. E. Bursten, *J. Am. Chem. Soc. 113* (1991) 552.
[70] I. L. Fragalà, J. Goffart, G. Granozzi, E. Ciliberto, *Inorg. Chem. 22* (1983) 216.
[71] I. Fragalà, E. Ciliberto, R. D. Fischer, G. R. Sienel, P. Zanella, *J. Organomet. Chem. 120* (1976) C9.
[72] A. Vittadini, M. Casarin, D. Ajò, M. Bertoncello, E. Ciliberto, A. Gulino, I. Fragalà, *Inorg. Chem. Acta 121* (1986) L23.
[73] a) L. Doretti, P. Zanella, G. Faraglia, I. Faleschini, *J. Organomet. Chem. 43* (1972) 339; b) B. Kanellakopulos, C. Aderhold, E. Dornberger, *ibid. 66* (1974) 447; c) K. Bagnall, J. Edward, A. C. Tempest, *J. Chem. Soc. Dalton Trans. 1978*, 295; d) R. D. Ernst, W. J. Kennelly, C. Secaur-Day, V. W. Day, T. J. Marks, *J. Am. Chem. Soc. 101* (1979) 2656.
[74] a) A. L. Arduini, N. M. Edelstein, J. E. Jamerson, J. G. Reynolds, K. Schmid, J. Takats, *Inorg. Chem. 20* (1981) 2470; b) A. L. Arduini, J. G. Jamerson, J. Takats, *ibid. 20* (1981) 2474; c) A. L. Arduini, J. Takats, *ibid. 20* (1981) 2480.
[75] J. M. Manriquez, P. J. Fagan, T. J. Marks, *J. Am. Chem. Soc. 100* (1978) 3939.
[76] V. W. Day, T. J. Marks, unpublished results cited in [12a].
[77] C. W. Eigenbrot, Jr., K. N. Raymond, *Inorg. Chem. 21* (1982) 2653.
[78] E. Ciliberto, G. Condorelli, P. J. Fagan, J. M. Manriquez, I. Fragalà, T. J. Marks, *J. Am. Chem. Soc. 103* (1981) 4755.
[79] A. L. Arduini, J. Malito, J. Takats, E. Ciliberto, I. Fragalà, P. Zanella, *J. Organomet. Chem. 326* (1987) 49.
[80] B. E. Bursten, A. Fang, *J. Am. Chem. Soc. 105* (1983) 6495.
[81] T. Ziegler, V. Tschinke, E. J. Baerends, J. G. Snijder, W. Ravenek, *J. Phys. Chem. 93* (1989) 3050.
[82] A. Becke, *J. Chem. Phys. 84* (1986) 4524.
[83] E. J. Baerends, D. E. Ellis, P. Ros, *Chem. Phys. 2* (1973) 71.
[84] J. W. Bruno, H. A. Stecher, L. R. Morss, D. C. Sonnenberger, T. J. Marks, *J. Am. Chem. Soc. 108* (1986) 7275.
[85] L. E. Schock, A. M. Seyam, M. Sabat, T. J. Marks, *Polyhedron 7* (1988) 1517.
[86] T. Ziegler, W. Cheng, E. J. Baerends, W. Ravenek, *Inorg. Chem. 27* (1988) 3458.
[87] J. L. Atwood, C. J. Haines, M. Tsutsui, A. E. Gebala, *J. Chem. Soc. Chem. Commun. 1973*, 452.
[88] G. Perego, M. Cesari, F. Farina, G. Lugli, *Acta Crystallogr., Sect. B B32* (1976) 3034.
[89] J. G. Brennan, S. D. Stults, R. A. Andersen, A. Zalkin, *Inorg. Chim. Acta 139* (1987) 201.
[90] B. E. Bursten, R. J. Strittmatter, *J. Am. Chem. Soc. 109* (1987) 6606.
[91] J. G. Brennan, S. D. Stults, R. A. Andersen, A. Zalkin, *Organometallics 7* (1988) 1329, and references therein.
[92] B. Kanellakopulos in T. J. Marks, R. D. Fischer (Eds.): *Organometallics of the f-Elements*, Reidel, Dordrecht 1978.
[93] L. Malatesta, F. Bonati: *Isocyanide Complexes of Metals*, Wiley, New York 1969.
[94] J. G. Brennan, R. A. Andersen, *J. Am. Chem. Soc. 107* (1985) 514.
[95] R. E. Cramer, U. Engelhardt, K. T. Higa, J. W. Gilje, *Organometallics 6* (1987) 41, and references therein.
[96] R. E. Cramer, F. Edelmann, A. L. Mori, S. Roth, J. W. Gilje, K. Tatsumi, A. Nakamura, *Organometallics 7* (1988) 841.
[97] B. E. Bursten, M. Casarin, D. E. Ellis, I. Fragalà, T. J. Marks, *Inorg. Chem. 25* (1986) 1257.
[98] A. P. Sattelberger, W. G. Van Der Sluys, *Chem. Rev. 90* (1990) 1027.
[99] K. Tatsumi, A. Nakamura, *J. Am. Chem. Soc. 109* (1987) 3195.
[100] C. Cauletti, J. P. Clark, J. C. Green, P. E. Jackson, I. L. Fragala, E. Ciliberto, A. W. Coleman, *J. Electron Spectrosc. Relat. Phenom. 18* (1980) 61.
[101] J. C. Green, S. Jackson, B. Higginson, *J. Chem. Soc., Dalton Trans. 1975*, 403.
[102] P. J. Fagan, J. M. Manriquez, E. A. Maatta, A. M. Seyam, T. J. Marks, *J. Am. Chem. Soc. 103* (1981) 6650.
[103] J. W. Bruno, G. M. Smith, T. J. Marks, C. K. Fair, A. J. Schultz, J. M. Williams, *J. Am. Chem. Soc. 108* (1986) 40.
[104] M. Brookhart, M. L. H. Green, L.-L. Wong, *Prog. Inorg. Chem. 36* (1988) 1.
[105] K. Tatsumi, A. Nakamura, *Organometallics 6* (1987) 427.
[106] Z. Lin, T. J. Marks, *J. Am. Chem. Soc. 109* (1987) 7979.
[107] J. W. Bruno, T. J. Marks, V. W. Day, *J. Am. Chem. Soc. 104* (1982) 7357.
[108] C. M. Fendrick, T. J. Marks, *J. Am. Chem. Soc. 108* (1986) 425.
[109] P. L. Watson, G. W. Parshall, *Acc. Chem. Res. 18* (1985) 51.
[110] H. H. Brintzinger, *J. Organomet. Chem. 171* (1979) 337.
[111] H. Rabaa, J.-Y. Saillard, R. Hoffmann, *J. Am. Chem. Soc. 108* (1986) 4327.
[112] J. W. Bruno, T. J. Marks, L. R. Morss, *J. Am. Chem. Soc. 105* (1983) 6824.
[113] J. W. Bruno, H. A. Stecher, L. R. Morss, D. C. Sonnenberger, T. J. Marks, *J. Am. Chem. Soc. 108* (1986) 7275.
[114] L. E. Schock, T. J. Marks, *J. Am. Chem. Soc. 110* (1988) 7701.
[115] T. Ziegler, V. Tschinke, L. Versluis, E. J. Baerends, W. Ravenek, *Polyhedron 7* (1988) 1625.
[116] D. C. Sonnenberger, L. R. Morss, T. J. Marks, *Organometallics 4* (1985) 352.
[117] P. J. Fagan, J. M. Manriquez, T. J. Marks, V. W. Day, S. H. Vollmer, C. S. Day, *J. Am. Chem. Soc. 102* (1980) 5393.
[118] P. J. Fagan, J. M. Manriquez, S. H. Vollmer, C. S. Day, V. W. Day, T. J. Marks, *J. Am. Chem. Soc. 103* (1981) 2206.
[119] A. Dormond, A. A. Elbouadili, C. Moïse, *J. Chem. Soc. Chem. Commun. 1984*, 749.
[120] P. Hofmann, P. Stauffert, K. Tatsumi, A. Nakamura, R. Hoffmann, *Organometallics 4* (1985) 404.
[121] P. T. Wolczanski, J. E. Bercaw, *Acc. Chem. Res. 13* (1980) 121.
[122] G. Erker, *Acc. Chem. Res. 17* (1984) 103, and references therein.
[123] K. Tatsumi, A. Nakamura, P. Hofmann, P. Stauffert, R. Hoffmann, *J. Am. Chem. Soc. 107* (1985) 4440.
[124] G. Erker, J. Wicher, K. Engel, F. Rosenfeldt, W. Dietrich, C. Krüger, *J. Am. Chem. Soc. 102* (1980) 6346.
[125] G. M. Smith, H. Suzuki, D. C. Sonnenberger, V. W. Day, T. J. Marks, *Organometallics 5* (1986) 549.
[126] J. M. Manriquez, P. J. Fagan, T. J. Marks, S. H. Vollmer, C. S. Day, V. W. Day, *J. Am. Chem. Soc. 101* (1979) 5075.
[127] K. Tatsumi, A. Nakamura, *Inorg. Chim. Acta 139* (1987) 247.
[128] C. W. Eigenbrot, Jr., K. N. Raymond, *Inorg. Chem. 20* (1981) 1553.
[129] C. W. Eigenbrot, Jr., K. N. Raymond, *Inorg. Chem. 21* (1982) 2653.
[130] a) T. J. Marks, V. W. Day, in [12f], pp. 115–157; b) T. J. Marks, J. M. Manriquez, P. J. Fagan, V. W. Day, C. S. Day, S. H. Vollmer, (Lanthanide and Actinide Chemistry and Spectroscopy) *ACS Symp. Ser. 131* (1980) 3.
[131] K. Tatsumi, A. Nakamura, P. Hofmann, R. Hoffmann, K. G. Moloy, T. J. Marks, *J. Am. Chem. Soc. 108* (1986) 4467.
[132] P. J. Fagan, J. M. Manriquez, T. J. Marks, V. W. Day, S. H. Vollmer, C. S. Day, *J. Am. Chem. Soc. 103* (1981) 2206.
[133] a) P. Hofmann, P. Sauffert, M. Frede, K. Tatsumi, *Chem. Ber. 122* (1989) 1559; b) D. M. Roddick, J. E. Bercaw, *ibid. 122* (1989) 1579.
[134] D. A. Wrobleski, D. T. Cromer, J. V. Ortiz, T. B. Rauchfuss, R. R. Ryan, A. P. Sattelberger, *J. Am. Chem. Soc. 108* (1986) 174.
[135] R. E. Cramer, A. L. Mori, R. B. Maynard, J. W. Gilje, K. Tatsumi, A. Nakamura, *J. Am. Chem. Soc. 106* (1984) 5920.
[136] B. E. Bursten, G. A. Ozin, *Inorg. Chem. 23* (1984) 2910.
[137] M. Pepper, B. E. Bursten, *J. Am. Chem. Soc. 112* (1990) 7803.
[138] P. J. Hay, R. R. Ryan, K. V. Salazar, D. A. Wrobleski, A. P. Sattelberger, *J. Am. Chem. Soc. 108* (1986) 313.
[139] J. V. Ortiz, *J. Am. Chem. Soc. 108* (1986) 550.
[140] M. A. Makhyoun, B. D. El-Issa, B. A. Salsa, *J. Mol. Struct. 153* (1987) 241.
[141] C. P. Casey, R. F. Jordan, A. L. Rheingold, *J. Am. Chem. Soc. 105* (1983) 665.
[142] B. E. Bursten, K. J. Novo-Gradac, *J. Am. Chem. Soc. 109* (1987) 904.
[143] R. S. Sternal, T. J. Marks, *Organometallics 6* (1987) 2621.
[144] J. P. Clark, J. C. Green, *J. Chem. Soc. Dalton Trans. 1977*, 505. The assignment of the ionization bands of uranocene has been a matter of some controversy: J. P. Clark, J. C. Green, *J. Organomet. Chem. 112* (1976) C14; I. Fragalà, G. Condorelli, P. Zanella, E. Tondello, *ibid. 122* (1976) 357; [10].
[145] M. Pepper, B. E. Bursten, *Chem. Rev. 91* (1991) 719.

Groups of Organic Molecules That Operate Collectively

By Fredric M. Menger*

A "chemical system" is defined as an assemblage of molecules that collectively does something interesting or useful. The key word here is "collectively", a word that implies an interdependency and a group behavior that can be quite different from that of individual molecules. Batteries, computer chips, concrete, mayonnaise, shampoo, paint, liquid crystal displays, composites, and viruses are all examples of commonly encountered systems. A host–guest or "supramolecular" complex, on the other hand, would not be considered a system (as defined here), because only two species are involved. A chemical system is multimolecular, a collection of molecules interlocked in a tangle of dependencies. The review delves into a variety of chemical systems investigated by the author, including micelles, water pools, films, vesicles, and polymers. All of them can be categorized as "self-assembling" or "self-organizing" in the sense that defined structures arise spontaneously owing to noncovalent forces among the component molecules. Such chemical systems are useful for many purposes, including decontamination of environmentally dangerous substances, drug delivery, and separation of organic compounds.

1. Introduction

This review deals with "chemical collectivism": the chemistry of molecules that operate within organized assemblies called "systems". A living cell is the most remarkable example of a chemical system. Through a poorly understood cooperation and interdependence among the cellular components, an entity is created that exceeds the sum of the parts. Groups of molecules, properly assembled, can obviously accomplish much more than an equal number of molecules functioning separately. In this article, I will describe organic systems that play on that principle.

H. Ringsdorf et al.[1] wrote recently, "macromolecular chemistry... has become a classical discipline... with all the advantages and handicaps of maturity. Harvest is plentiful, the results are abundant—but one has to ask: where is the future, where are the adventures?" It seems likely that a major path for future organic research will course its way through communities of molecules. As with human communities, the individual molecular species dictates the behavior of the group, while, concurrently, the group imposes constraints upon the individuals. One would wish to understand this interrelationship in greater detail.

Tens of thousands of organic reactions, generally carried out one at a time in a nonaggregated mode, are now in hand. Although no one can deny the value of adding further to this wealth, one can likewise not ignore the need to incorporate into organic chemical thought many relatively unfamiliar forms of matter such as the coacervate, microemulsion, polyaphron,[39] vesicle, and film. These aggregated systems are, after all, composed of simple organic molecules, and they provide unique capabilities (to be described) for performing tasks such as running reactions, delivering drugs, and separating compounds. It is the goal of this article to promote research into organic molecules that self-assemble and do interesting things as a consequence.

In the biological world, self-assembly is a built-in tendency. Amino acid chains, for example, fold spontaneously into enzymes of precise shape. Raw flagellin from bacteria will, when placed in a petri dish, rapidly transform itself into isolated flagella. Ribosomes, membranes, and (at the highest level) developing embryos exemplify the wondrous ability to self-organize into complex structures. It is this capacity to create "form" that prompted *E. Schrödinger* to call living material "aperiodic crystals". Chemists will no doubt contribute substantially to future research into biological "form" just as they have to our current understanding of biological "substance". Progress in the subject is already evident from the growing number of publications on organic "forms" such as micelles, vesicles, films, and emulsions. Although these self-assembling systems are pitifully simple compared to biological structures, they represent a necessary first step in the evolving field.

Our past research has focused heavily on self-assembling systems, a wide variety of which are covered in this article. Since each topic is discussed herein via experiments carried out at Emory, the article is more a personalized "lecture in print" than a review. By including an assortment of self-assembling systems, I illustrate the richness of "chemical collectivism", but, unfortunately, I also make a thorough literature coverage impractical. To counter this problem, general references, containing comprehensive lists of relevant citations, are given at the beginning of each section. Thus, the reader can quickly locate work from a worldwide body of scientists who are also involved in chemical systems and who have provided key insights and inspirations in the area.

It will be noted that this article contains few tables, equations, and graphs. Perhaps, I have been unduly influenced by a quote from *R. J. Waller*:[2] "Excessive focus on detail and procedure at the expense of vision, of dreams, of reflection, is a good way to get rid of romance. We in the academic world have mastered this approach." Missing details (including all the synthetic sequences) can be obtained from the original literature.

2. Acidity at a Micelle Surface[3]

A "surfactant" is a compound possessing an ionic or polar head group attached to a long hydrocarbon tail (Scheme 1).

[*] Prof. F. M. Menger
Department of Chemistry, Emory University
Atlanta, GA 30322 (USA)

Upon exposure to water, 20–150 surfactant molecules assemble into a roughly spherical aggregate called a "micelle".

$CH_3(CH_2)_{11}OSO_3^{\ominus}Na^{\oplus}$ $\quad$ $CH_3(CH_2)_{15}\overset{\oplus}{N}(CH_3)_3Br^{\ominus}$

Scheme 1. Two examples of surfactants with ionic head groups.

The chains point inward, while the ionic head groups reside at the micelle surface near the bulk water. Surfactants, and their micellar systems, have found their way into almost every major commercial industry (food, cosmetic, pharmaceutical, petroleum, metal, and paper, to name a few). Being so useful and relatively simple, micelles seemed ideally suited for our initial entry into the chemical systems field. Since surfactants assemble only above a critical micelle concentration (cmc), we could compare directly monomer and aggregate properties by operating both below and above the cmc.

One of the first questions we asked was, "What is the pK_a of an ionizable head group at the micelle surface?"[4] This question brings up two notable points: (1) Even the most basic information on molecular aggregates was unavailable just a few years ago. (2) Securing such information (which would require only an afternoon with single-molecule chemistry) can extend to many months when an aggregate is involved. Chemical systems do not confess their secrets without arduous prodding.

Micellar dodecyldimethylammonium ion (Scheme 2) was selected for the pK_a studies. Now determining the pK_a of a monomeric amine, such as $C_6H_{13}NH_3^{\oplus}$, is trivial—one

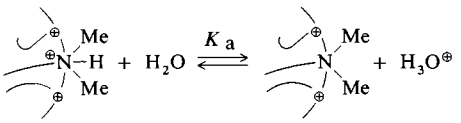

Scheme 2. Acid-base reaction of a micellar ammonium surfactant, n-$C_{12}H_{25}NMe_2$.

merely titrates. Unfortunately, this is not possible with an aggregated amine salt, because titration with base generates free amine and destroys the micelle. There appeared only one way to obtain the pK_a: determine the forward and reverse rate constants and calculate K_a from the quotient of the two values. Dynamic NMR (a technique that provides rate data on species at equilibrium) was called upon for the purpose. Thus, if the proton remains on the nitrogen for a long time relative to the NMR time scale, one observes a methyl signal that is split into a doublet. If, on the other hand, the proton departs and returns rapidly, the splitting is washed out, and one sees only a singlet. Intermediate cases give line shapes that, with the aid of a computer, allow calculation of proton-transfer rates. The main experimental requirement is that the pH be adjusted to low values where the proton exit/entry process is neither too fast nor too slow for the NMR measurement.

It was found that the pK_a of the micellized amine is 1.4 units more acidic than the equivalent monomeric form. Positive charge accumulated on the micelle surface drives proton loss to the right relative to that of monomeric amine. A pK_a differential of 1.4 between aggregate and monomer was, historically, an important number because it constituted our first evidence that the micelle periphery is "rough". If the cationic head groups had been confined to a smooth spherical surface, then electrostatic effects among the proximate head groups would have produced discrepancies even greater than 1.4 pK_a units.

Acid-base properties at the interface of a molecular assembly can, in principle, be determined by adsorbing a pH-sensitive dye onto the aggregate. (Cationic dyes, for example, bind strongly to anionic micelles and vice versa.) Two problems plague this widely employed "probe" approach:[5] (1) Since dyes are often large, multifunctional molecules, they easily modify the fragile environment on which they are asked to report. (2) Since the location(s) of the dye in or on the aggregate is (are) difficult to establish, uncertainty exists over exactly what portion of the micelle is represented by the observed pK_a values. These problems, common to most probe studies, are avoided in our kinetically determined pK_a method because no potentially damaging probe is involved and the "site of action" necessarily corresponds to the head-group region.

Defining the structure and behavior of "single" organic compounds can often be a simple task owing to the power of modern instrumentation. Such is not the case, as we have just seen, for molecular aggregates where a higher dimension of complexity pervades the experiments. Thus, a chemical system requires an in-depth evaluation of numerous attributes that are irrelevant to single-molecule chemistry: aggregation number, shape, exit/entry rates of components, internal viscosity, water content, chain conformation, heats of aggregation, ion binding, solubilizing power, interfacial acidity, etc.

Fredric M. Menger's biographical data are omitted because, he claims, "they are of doubtful general interest". Suffice it to say that the unusual collage of ideas assembled in the accompanying article reflects his philosophy that "life, though short, is wide enough for a multitude of adventures if only the love of comfort and habit do not entomb the soul."

Characterization is burdened further by the fact that many properties (e.g., water content) are almost certainly not uniform throughout the assembly. Yet technical difficulties should not discourage research into chemical systems; their inherent interest, their prevalence in nature, and their considerable commercial potential more than compensate for the problems.

3. Chain Conformation within Assemblages[6]

Chemical systems in water are frequently stabilized by hydrophobic interactions among hydrocarbon chains of the component molecules. Chain conformation becomes a central issue in such cases. Are the chains linear or bent? If bends are present, where along the chains do they predominate? Are the kinks transient or permanent? How does chain-bending affect behavior (such as ion permeability through a membrane assembly)? The following sections describe three entirely different approaches (spectrometric, kinetic, and double ^{13}C-labeling) which our laboratory has used to deduce conformational properties within molecular assemblies. Although the examples are taken from the micelle area, the methodologies can be applied to additional chemical systems such as membranes and microemulsions.

3.1. Spectrometric Approach[7]

The acetylenic proton of RC≡CH has a solvent-dependent chemical shift. For example, the δ value for 1-hexyne increases from 1.66 in cyclohexane to 2.04 in acetone to 2.19 in 2:1 methanol/water. An acetylenic unit buried within an aggregate can, therefore, be used to sense and monitor micropolarity. If the terminal acetylenic unit in surfactants **1** and **2** encounters only an "oil droplet" within the micelle

$HC{\equiv}CCD_2(CH_2)_{10}OSO_3^{\ominus}$ **1** $HC{\equiv}CCD_2(CH_2)_{10}\overset{\oplus}{N}(CH_3)_3$ **2**

interior, then the chemical shift should be similar to that in cyclohexane. To the extent that the acetylenic proton "sees" water, the chemical shift will increase. Since motion within a micelle is rapid relative to the NMR time scale, the observed shift will simply be a weighted average from the nonpolar and aqueous environments. We found that micellar **1** and **2** possess δ values of 2.10 and 2.16, respectively, proving that the chain termini come into contact with water a surprisingly high percentage of the time. Note that monomeric molecules, in equilibrium with aggregated material, cannot be affecting the results; under our conditions (i.e., concentrations 25 times above the cmc) the monomer levels were far too low to contribute significantly to the weighted average. The conclusion is inescapable: chain termini are definitely not buried in a dry "oil droplet".

In order to grasp the import of the results with **1** and **2**, it is necessary to understand how micellar structure was perceived prior to the time that our experiments were carried out. For decades, both journal articles and texts discussed micellar organization in terms of the so-called Hartley model (Fig. 1 A).[8] Two features in particular were widely accepted, namely, linear chains and a dry interior. In fact, a micelle was often referred to as "an oil droplet with an ionic coat" and analyzed in terms of a "two-state" Hartley model. Our experiments with **1** and **2** (buttressed by theoretical work of others[9]) forces one to abandon the classical picture. Either water penetrates into the aggregate, wherein lie the acetylenic reporter groups, or else the chains loop around so as to expose the chain termini to the aqueous surface. In actual fact, we now believe that both phenomena occur,[10] and that micelles are far more disorganized than was believed in the past (Fig. 1 B). At first, chemists clung tenaciously to the Hartley model despite accumulating evidence, such as given above, that would seem to demand a revision. Only slowly did the idea of "wet" chain termini and other manifestations of micellar disorder diffuse into colloid literature. One sees here how difficult it is to define indisputably the structure of even a "simple" chemical system such as a micelle.

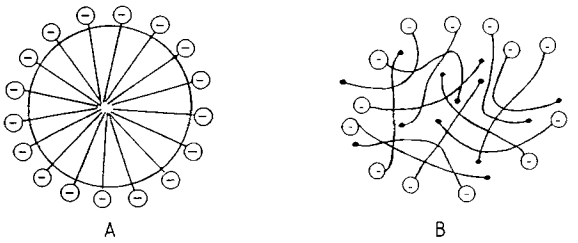

Fig. 1. A) The Hartley "two-state" model showing a dry oil droplet surrounded by an ionic coat. Terminal methyl groups are buried in the center of the system. B) Schematic of a revised micelle model [10] embodying many features absent in the Hartley model: rough surface, water-filled pockets, chain looping, nonradial distribution of chains, and contact of terminal methyls (indicated by heavy dots) with water.

Could it be that acetylenic surfactants **1** and **2** behave differently from their totally saturated counterparts? Or, rephrased, could the acetylene moieties of **1** and **2** be perturbing the "normal" micelle structure? We had, of course, specifically selected the acetylenic probe because of its relatively innocuous properties. Thus, the acetylene group has spatial requirements similar to the ethyl group (19.6 and 23.9 $cm^3 mol^{-1}$, respectively) and a positive Hansch hydrophobicity of + 0.40 (compared to −0.67 for OH and +0.56 for CH_3).[11] Relative to conventional fluorescent, ESR, and NMR probes, the acetylenic unit seemed to us fairly harmless. Perhaps the best evidence that the acetylenic probe was nonperturbing came from an observed similarity between cmc values for **1** and **2** and their saturated counterparts. Since looping halves the chain length, one would have expected unusually large cmc values had the triple bond actually induced looping in **1** and **2** over and above what occurs "normally".

3.2. Kinetic Approach[12]

The basic plan was to incorporate double bonds into the surfactant chains and then measure their rates of oxidation

by $KMnO_4$ present in the water external to the micelles.[13] Rates of $KMnO_4$ consumption were easily monitored via its intense absorption at 545 nm. If the olefinic units were confined to a close-packed hydrocarbon core, such as portrayed in classical micelle models,[8] then the permanganate (being ionic) would be unable to reach the double bonds and convert them into diols.

Two olefinic surfactants, **3** and **4**, suffice to illustrate the main conclusions from a more extensive kinetic study. Micellar **3** oxidized at a rate similar to simple monomeric olefins (both terminal and internal). But it reacted 156 times faster than micellar **4**. The fast oxidation of micellar **3**, and the

$H_2C{=}CH(CH_2)_8CO_2^{\ominus}$ **3** $CH_3(CH_2)_7CH{=}CH(CH_2)_7CO_2^{\ominus}$ **4**

unexpected difference between terminal and internal olefins within the aggregates, can be explained only in terms of looping and molecular disorder that place chain termini of **3** at the water-rich micellar periphery. Double bonds in the middle of **4** remain effectively buried despite nonlinear conformations imposed on the surfactant molecules. These simple but revealing experiments once again point to a nonradial organization within micelles. Chain termini, once thought to congregate permanently near the center of the system,[8] must "sample" the micelle surface frequently.

The double bond is a small, apolar functionality prevalent in naturally occurring lipids. Consequently, we felt it unlikely that surfactant **3** loops abnormally (owing, perhaps, to a "hydrophilicity" of the double bond relative to fully saturated chains). But the possibility cannot definitely be ruled out. In the next section, I discuss another method for investigating chain conformation where uncertainty is totally eliminated.

3.3. Double ^{13}C-Labeling[14]

Long-range coupling (^3J) between two ^{13}C atoms through three bonds obeys a typical Karplus-type function. Thus, $^3J_{anti} = 3.5-4.0$ Hz, whereas $^3J_{gauche} = 1.5$ Hz. By synthesizing chains bearing two ^{13}C atoms at known locations, we can deduce the time-averaged conformation at a particular linkage. The method is nondisruptive and works equally well for single compounds or multimolecular systems.

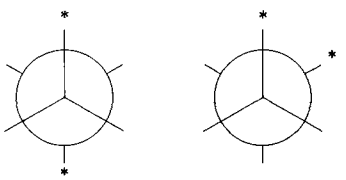

$^3J_a = 3.5-4.0$ Hz $^3J_g = 1.5$ Hz

Scheme 3. ^3J coupling between ^{13}C atoms.

Monomeric [3,6-$^{13}C_2$]tridecylamine (Scheme 4) in chloroform has $^3J = 3.8$ Hz. However, in acidic water (pH = 2) at concentrations manyfold higher than the cmc, the corresponding amine salt has $^3J = 2.0$ Hz. As seen from the limiting values of $^3J_{anti}$ and $^3J_{gauche}$ (Scheme 3), the monomeric state is essentially linear, whereas the majority of the C4–C5 linkages in the micelle are *gauche*. Aggregation clearly imposes severe bending at the C4–C5 site. Information of this type is almost impossible to achieve by any other current method.

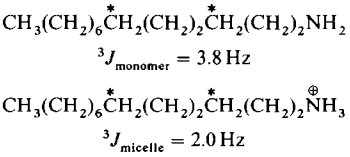

Scheme 4. Effect of the degree of aggregation on the J value. Top: In chloroform. Bottom: In aqueous acid.

The nonaggregating diamine in Scheme 5 has $^3J = 3.8$ Hz in ethanol and in acidic water, once again demonstrating a preferred linearity in the monomeric state. When the diamine was adsorbed into or onto a sodium dodecyl sulfate micelle, the coupling constant changed only slightly to 3.5 Hz. Adsorbed diamine clearly maintains its transoid character within the aggregate owing, very likely, to a tangential orientation (Scheme 6). Such an orientation allows both ammonium groups to reside near the bulk water. In contrast to the micelle behavior, diamine bound to an enzyme, trypsin, gives a ^3J value characteristic of 100% *gauche* (Scheme 6). Double ^{13}C-labeling requires a tedious synthetic effort, and at present we appear to be the only ones using it (not only with micelles but with DNA complexes, single-molecule chemistry, etc.). But the method would seem to have a promising future, particularly in characterizing fragile chemical and biological systems that are easily perturbed by conventional probes. In fact, double ^{13}C-labeling would be an excellent way of determining exactly how probes or additives modify chain conformation when they enter molecular aggregates. Data are currently unavailable on the subject. Systems research is a field in its infancy!

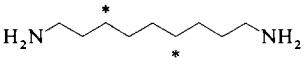

Scheme 5. A nonaggregating diamine.

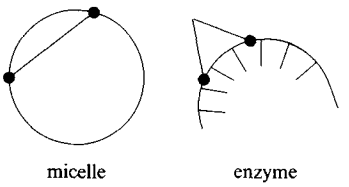

Scheme 6. Conformation of a diamine bound to a micelle or to an enzyme.

4. Self-Assembling Systems as Catalysts[12]

We have for many years been interested in developing catalysts based on molecular assemblages. But before providing specifics, it is worthwhile to define the word "catalyst". First and foremost, a catalyst must significantly accelerate a reaction. The question then arises, "What constitutes a significant acceleration?" Ten percent increase? One-hundred-fold? A million? As discused in a publication entitled "An Essay on Significance", a newly encountered effect should, if possible, be related to a carefully defined "expectation".[15] In some cases, even a ten percent increase might be considered significant (e.g., a 10% pay raise relative to a 3% inflation). In our work with catalytic systems, it was easy to "frame" the data: we desired accelerations of $\geq 10^5$, similar to those found with enzymes. Such large accelerations were necessary because (1) we wanted (as a challenge) to imitate enzymes as closely as possible and (2) we wanted to destroy certain chemical warfare agents at a rate that would be useful from a practical standpoint. According to this definition of significance, a 10- to 100-fold catalysis would be considered a failure for us.

Catalysis also incorporates the concept of "turnover". A single catalyst molecule must operate on a substrate molecule, finish the job, and then go on to operate on additional substrate molecules. This somewhat obvious point is mentioned here because stoichiometric reactions have at times been incorrectly termed "catalytic". The most common example involves a nucleophilic attack on a carboxylic acid derivative (Scheme 7). Only if the intermediate, RCOB, is

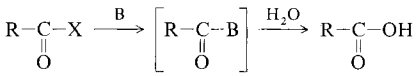

Scheme 7. An example of a stoichiometric reaction when RCOB is stable.

hydrolytically reactive can one accurately claim that B is a catalyst; otherwise, the reaction is stoichiometric in B. Stoichiometric reactivity in our work on chemical systems was unacceptable because we were interested in destroying environmentally dangerous compounds at reasonable cost. This required devising true catalysts that are not irreversibly consumed during the reactions. The use of three quite different molecular assemblies in catalytic processes is summarized in the next section.

4.1. Atlanta-1 ("A-1")[16]

In 1985, we synthesized and examined a micellar catalyst, dubbed A-1, that hydrolyzed phosphate esters. As will be shown, the aggregated catalyst functions by (1) noncovalently binding the phosphate ester, (2) splitting the ester while

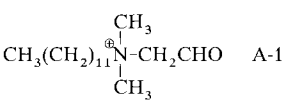

A-1

covalently retaining the phosphoryl portion, and (3) dephosphorylating to regenerate the original catalytic entity. Thus, true catalysis was achieved.

Our interest in phosphate esters was related to the goal of destroying nerve agents, such as GD, which are among the most moathsome compounds known to man. We used the less toxic *p*-nitrophenyl diphenyl phosphate (PNPDPP) for

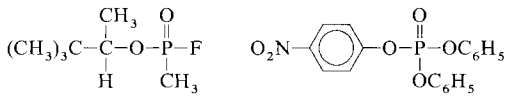

GD PNPDPP

our experiments because PNPDPP is not as reactive as GD; therefore, any catalyst that manages to hydrolyze PNPDPP is likely to be effective with the actual nerve agents.

A-1 forms micelles abruptly at its cmc of 8×10^{-4} M. Spectroscopic data proved that the catalyst exists as the aldehyde hydrate, which, under the reaction conditions (25°, pH = 9.0), forms a kinetically significant level of oxyanion [Eq. (a)]. The water-insoluble phosphate ester partitions to-

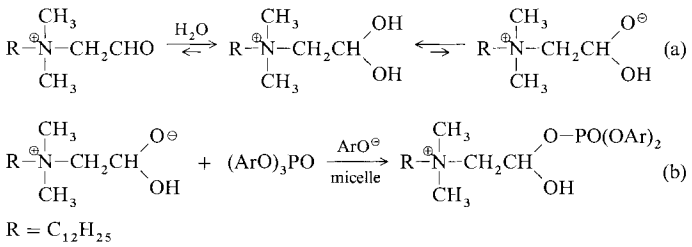

(a)

(b)

$R = C_{12}H_{25}$

tally from the buffer to the micelle where the phosphoryl group is transferred to an oxyanion [Eq. (b)]. Finally, and this is crucial for turnover, the presence of a second hydroxyl allows for a rapid dephosphorylation and, consequently, a regeneration of the original aldehyde catalyst [Eq. (c)].

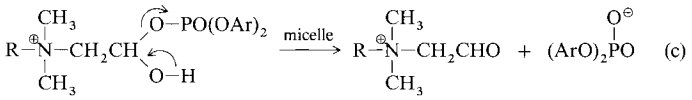

(c)

Proof that substrate preassociation to A-1 micelles is important consisted of showing that catalysis was lost with short-chain (nonmicellar) analogues of A-1. Proof that turnover is indeed taking place consisted of observing a 100% product yield even when the phosphate ester was in great excess over A-1. Preassociation and turnover are, of course, both reminiscent of enzymatic behavior.

Phosphate hydrolysis is 1800 times faster with 8 mM A-1 than in pure buffer without catalyst. Although reasonably fast by many standards, the rate is several orders of magnitude less than the $\geq 10^5$ we were seeking. Therefore, a second micellar catalyst, A-2, described in the next section, was developed to improve on this shortcoming.

4.2. Atlanta-2 ("A-2")[17]

A-2 is a copper-containing surfactant that forms "metallomicelles" above a cmc of 1.8×10^{-4} M. The copper-coated micelles bind PNPDPP with an enzymatic efficiency ($K_{assoc} = 2.6 \times 10^5$ M). Moreover, the micelles induce a 10^5 rate enhancement in the hydrolysis of PNPDPP (1 mM catalyst, 25 °C, pH = 8.0). Accelerations are even larger (10^6)

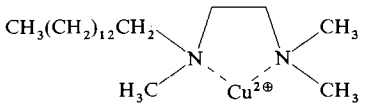

A-2

with a phosphodiester, bis(p-nitrophenyl) phosphate. There is no doubt that the aggregation process contributes substantially to the catalysis, because nearly 10^3 of the overall enhancement disappeared when A-2 was replaced by simple, nonmicellar copper complexes. Single-molecule chemistry is no match for systems chemistry!

The above results show that cupric ion is catalytically far more effective when confined to the micelle surface than when floating free in solution. High concentrations of cupric ion at the micelle surface create a large positive charge that enhances the electrophilicity of the metal. This was substantiated by polarographic studies in which we detected an unusual propensity of micellar cupric ion to accept electrons. The surface-activated copper is thought to polarize the P=O bond of the substrate and thus catalyze nucleophilic attack on the phosphorus (Fig. 2).

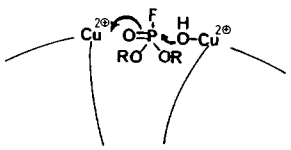

Fig. 2. Proposed mechanism for the 10^5–10^6-fold rate enhancement of nerve-agent hydrolysis by metallomicelles. $Cu^{2\oplus}$ ion confined to the cationic surface of the micellar system manifests an anhanced electrophilicity.

The half-life at 25 °C and pH = 7.0 of the nerve agent GD with 5.3 mM A-2 is only 50 s as opposed to 60 h at pH = 10.0 in the absence of A-2. Recall that this article began by defining a chemical system as "an assemblage of molecules that collectively do something interesting or useful". Self-assembling A-2 certainly complies with the definition.

4.3. Destruction of Mustards in Microemulsions[18]

No endeavor, however lofty, escapes exploitation, and chemistry is not an exception. The discipline that has given us antibiotics, nylon, and gasoline has also produced loathsome compounds such as chemical warfare agents. A solution to the problem, in the absence of restraint, is to develop chemical means to deactivate the compounds, that is, to combat chemistry with chemistry. Notable progress along these lines with regard to nerve agents was discussed in Section 4.2. Recently, our attention has turned toward mustard and related sulfides (Scheme 8). Mustards are environmentally persistent cytotoxic alkylating agents that can be manufactured with low technology and used in chemical weaponry. Their detoxification is hampered by an extreme insolubility in the solvent where they are potentially most reactive, water. We have oxidized mustard simulants (e.g., half-mustards) to nontoxic sulfoxides on a reasonable scale with a method that is simple, cheap, mild, and rapid.[19] The strategy (which could have general utility in organic chemistry) is based on an interesting type of multicomponent system, the microemulsion.

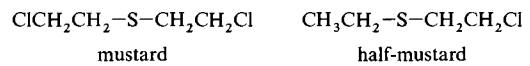

Scheme 8. Structure of mustard and half-mustard.

A microemulsion is an isotropic and optically transparent dispersion of oil in water (O/W) or water in oil (W/O) where "oil" is a hydrocarbon (Fig. 3). Such chemical systems form spontaneously when water, a hydrocarbon, a surfactant, and a "cosurfactant" (generally a low-molecular-weight alcohol) are mixed in specific proportions. Microemulsions, with dispersed droplets averaging 50–500 Å in diameter, remain clear indefinitely.

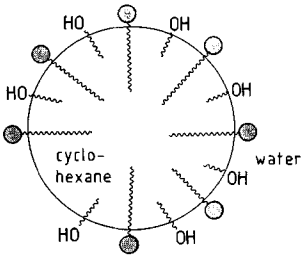

Fig. 3. Schematic representation of an O/W microemulsion stabilized by a long-chain surfactant and an alcoholic cosurfactant.

A favorite recipe of ours for an O/W microemulsion consists of (by weight) 3% cyclohexane in 82% water stabilized by 5% sodium dodecyl sulfate and 10% *n*-butanol. Although we have examined over two dozen additional microemulsions (both O/W and W/O of widely varying compositions), I will, for brevity, confine the discussion to this single preparation.

Half-mustard (Scheme 8, 0.18 mL) was dissolved in 15 mL of microemulsion. When 5% hypochlorite was then added to the system in a twofold excess over half-mustard, the half-mustard was, according to NMR spectroscopy, converted into sulfoxide extremely rapidly (i.e., in less than 15 s). Mustard present in the environment can, in contrast, persist for months.

Microemulsions formulated with nonalcoholic cosurfactants were not very active. We believe, therefore, that reactivity depends on an alkyl hypochlorite forming at the oil/water

interface where the alcohol is known to reside (Fig. 4). Subsequent oxidation of the half-mustard then proceeds either in or on the oil droplets.

Reaction capacity is excellent, 15 mL of microemulsion being capable of oxidizing as much as 1 mL of sulfide. Oil droplets in an O/W microemulsion can, obviously, solubilize large amounts of water-insoluble organic reactants. Since the reaction mixtures are homogeneous, no continuous stirring is necessary (a distinct advantage for applications in the real world).

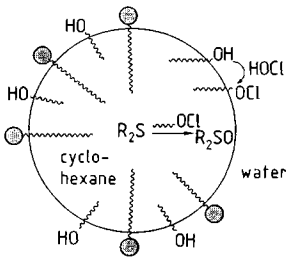

Fig. 4. Proposed mechanism for oxidation of mustard by hypochlorite in an O/W microemulsion. The speed of the reaction (see text) can be attributed to a large hydrocarbon/water contact area that permits "communication" between the water-soluble HOCl and the oil-soluble mustard with interfacial cosurfactant serving as an intermediary.

The speed and capacity of the oxidation are predicated on five components (water, cyclohexane, sodium dodecyl sulfate, *n*-butanol, and hypochlorite) all working in concert. Absence of any one of these components would impede or prevent reaction. Self-assembly converts what might have been a useless and intractable mixture into a system that can undo what mankind should not have wrought in the first place.

5. Monolayer Film Systems[20]

There ist a growing need for chemists, particularly those with biological leanings, to understand the principles governing noncovalent interactions. Host and guest, sensor and activator, channel and permeant, reactor and drug, enzyme and substrate, antibody and antigen, DNA and carcinogen: all partners recognize each other by noncovalent forces. Since noncovalent forces are involved in so many vital processes, and since (more to the point with regard to this article) intermolecular association holds together many chemical systems, we initiated a study of "molecular packing". A unique type of aggregate, the monolayer film, provided the experimental backdrop.[21, 22]

It should be stated forthwith that monolayer films have been an active branch of physical chemistry ever since the days of *Irving Langmuir*. No possibility exists of covering even a small portion of the vast literature on the subject in this article. Yet a sample of our recent experiments might be useful, particularly to illustrate the type of information made available by monolayer systems.

A monolayer film is a two-dimensional network one molecule thick. Most commonly, the film rests on a water "subphase". Monolayer films are often examined by means of a

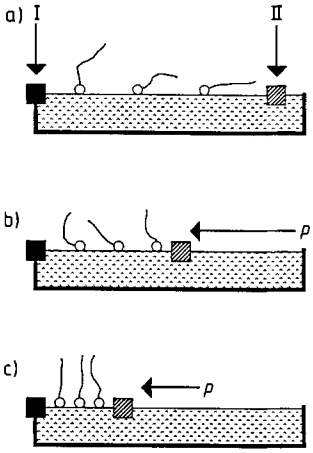

Fig. 5. Operation of a film balance with which, by means of a mobile barrier, it is possible to mechanically reorient molecules in the monolayer system. I = fixed barrier; p = pressure on the mobile barrier II. a) "Gaseous" phase; b) "liquid-expanded" phase; c) "condensed" phase.

simple and ingenious device: the film balance. Film balances measure the pressure exerted by a film while the area available to the component molecules is continuously reduced with a movable barrier (Fig. 5). As the film is compressed, molecules lying flat on the subphase are thereby forced into more vertical positions where they require less space. The ease of compressing the film, and the area per molecule at a given pressure, reveal how readily a film molecule tolerates the presence of its neighbors. Such information is, of course, crucial to the understanding of chemical systems.

Films were prepared from synthetic fatty acids and phospholipids composed of 18-carbon chains substituted at one of the four loci with groups of various sizes and polarities (methyl, *n*-butyl, phenyl, hydroxyl, and keto) (Scheme 9).

$$\underset{\substack{\uparrow\\16}}{CH_3CH_2CH_2}CH_2CH_2CH_2\underset{\substack{\uparrow\\12}}{CH_2}CH_2CH_2CH_2\underset{\substack{\uparrow\\8}}{CH_2}CH_2CH_2CH_2\underset{\substack{\uparrow\\4}}{CH_2}CH_2CH_2CO_2R$$

Scheme 9. C_{18} chains used to prepare films for film-balance studies. The positions substituted with Me, *n*Bu, Ph, OH, or O substituents are shown.

We were then able to pose, for example, the following questions: (1) How does film packing (i.e., the molecular area at a given pressure) vary with substituent size at a fixed location? (2) How does packing depend on where a particular substitutent is situated along the chain? (3) How does a mixed-film, composed of 50% 4-methyl and 50% 16-methyl fatty acid, differ in behavior from a film made from isomerically pure material? In effect, the film balance allowed us to ask questions about steric effects (*intermolecular* steric effects, not the more usual ones within a single molecule).

Having five substituents, four different locations, and the possibility of all sorts of mixture, we could obviously gather more data than can be described here. Brief examples suffice, however, to illustrate the utility of the method.

5.1. Butyl Substituents[21]

Figure 6 shows pressure–area isotherms (23.0 °C) for mixtures of unsubstituted stearic acid (SA) and 8-butylstearic

acid (8-BSA). As would be expected, the area per molecule decreases as the pressure on the film increases. The plots terminate when the film collapses (i.e., molecules in the monolayer pile up on one another). Two observations are of particular note: (1) An 8-butyl substituent caused a massive film expansion. At 5 dyn cm^{-1} pressure, the area occupied

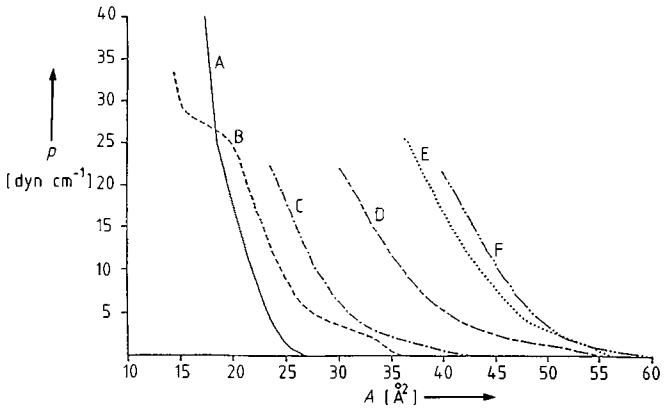

Fig. 6. Pressure–area isotherms (23.0 °C): A) stearic acid (SA); B) 10% 8-butylstearic acid (8-BSA) + SA; C) 25% 8-BSA + SA; D) 50% 8-BSA + SA; E) 75% 8-BSA + SA; F) 8-BSA. A = area per molecule.

per molecule increased from 23 Å^2 for 100% SA (plot A) to 48 Å^2 for 100% 8-BSA (plot F). It could be shown that alkyl substitution at position 8 has a far greater expansive effect than substitution at positions 4 or 16. (2) A mixture of 10% 8-BSA and 90% SA exhibited an anomalous pressure–area isotherm (plot B). Formation of "bulk" 8-BSA was observed at 25 dyn cm^{-1} where plot B forms a kink. Above 30 dyn cm^{-1} pressure, the SA film, separated from its 8-BSA, continued to compress more or less normally. Thus, the film balance can detect an extrusion of one phase from another within the two-dimensional array of mixed lipids.

5.2. Keto Substituents[22]

Film studies were performed on the keto-substituted phospholipid shown in Scheme 10. At 35 dyn cm^{-1} pressure, the lipid occupied 22 Å^2 per molecule. This is a surprisingly low value (similar to that of a single-chained surfactant and al-

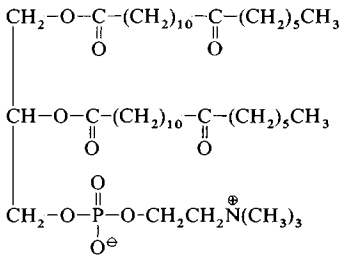

Scheme 10. Keto-substituted phospholipid used in film-balance studies.

most one-half that of the corresponding lipid without keto groups).

Apparently, at low pressures the keto lipid lies horizontally on the water surface (Fig. 7). High pressures force the reorientation of the molecules within the film such that one chain extends vertically into the air and the other vertically into the water. With the unsubstituted lipid, both chains point upward side-by-side and, consequently, require double the area. For reasons that are not understood, abnormally low packing areas were found for the 12-keto lipid but not for positional isomers having 6- or 8-keto substitution. These latter two lipids assume the usual side-by-side conformation.

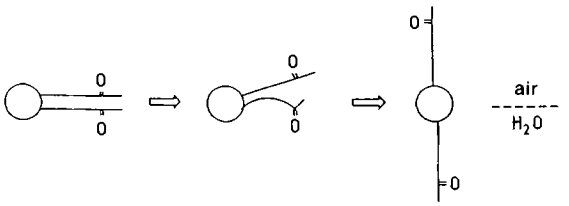

Fig. 7. Reorientation of a diketo lipid in a monolyer film system as pressure is exerted on the film. In the absence of keto groups, the lipid will reorient such that *both* chains extend upward into the air, and the area per molecule will be twice as great.

The point of citing these examples from more extensive studies is simply to draw attention to the power of the film balance in studying molecular packing. No other method allows such a controlled manipulation of molecular orientation. Information about molecular assemblages is obtained that cannot be secured by any other means.

6. Vesicles[23]

In Section 3.1, I mentioned how a surfactant with an ionic head group and a long hydrocarbon tail forms micelles. If, instead, the head group is attached to *two* tails, then the compound spontaneously aggregates into bilayers rather than micelles. This bilayer assumes the form of a closed sphere, called a vesicle, when the system is sonicated in water (Fig. 8).

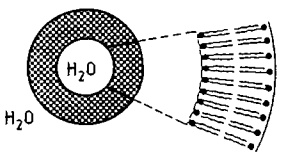

Fig. 8. Schematic of a vesicle composed of a bilayer of lipid molecules.

Vesicles represent an important and widely investigated type of chemical system. They give the investigator a feature unavailable in single-molecule chemistry: an inside and an outside separated by a physical barrier. It is a relatively simple matter to place compounds, such as dyes or drugs, within the vesicles, a capability that leads to a host of interesting experiments and potentially useful chemical devices.

6.1. Ion Channels[24]

The story begins with a remarkable biological compound called gramicidin. Gramicidin is a pentadecapeptide antibi-

otic which, in a dimeric form, enters membranes and creates a channel through which ions can flow (Fig. 9). So potent is gramicidin that a single channel carries a greater ion current than can an entire 1.0 × 1.0 mm gramicidin-free membrane. Our goal was to synthesize simple organic compounds that emulate the ion-channeling ability of gramicidin. As will be related, we succeeded in making a flux-promoting compound which is active in nanomole quantities and which actually surpasses gramicidin as a promoter of ion flux.

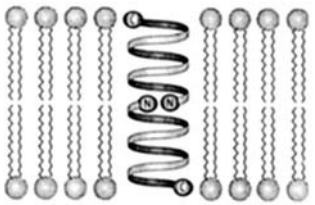

Fig. 9. Schematic of a gramicidin dimer embedded in a bilayer membrane. The interior of the coil provides a channel for ion flux across the membrane.

Before describing the channel compound, it is useful to describe the basic experiment (Fig. 10). Vesicles were prepared by sonicating a phospholipid mixed with an acid-responsive dye in a weak pH = 7.7 buffer. The vesicles enclosed a portion of the dye, the remainder residing outside. The latter was removed by gel permeation chromatography.

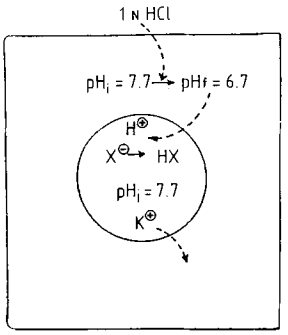

Fig. 10. Experimental scheme for detecting proton transport across a vesicle wall. Anionic dye (X^-) loses its fluorescence when protonated. Therefore, when the external pH is made more acidic than the internal pH with an aliquot of 1 N HCl, the fluorescence of internal dye will diminish according to how fast protons move through the membrane barrier.

When an aliquot of HCl was added, the external pH dropped immediately by a full pH unit. This created a "proton potential" with the proton concentration being greater on the outside than internally. Consequently, protons migrated inside in an attempt to equalize the pH. In so doing, encapsulated dye became protonated, thereby losing its fluorescence. The setup allowed us to follow the decrease of fluorescence as a function of time with and without the presence of a proton-conducting channel in the vesicle membrane.

It is interesting, but only from a historical point of view, that a certain compound we designed and synthesized to serve as a channel turned out to be inactive. As fortune would have it, however, intermediates in the preparation of the target molecule (and much simpler in structure than the target!) manifested an amazing ability to conduct ions at extremely low concentrations. The best of these is compound **5**. At nanomole levels, corresponding to only 45 molecules of

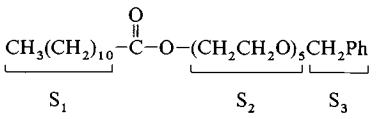

5

5 per 5000-lipid vesicle, the rates were measurably faster than with an equivalent amount of gramicidin.

Flux enhancement is structurally specific. Thus, all three sections of **5** (S_1, S_2, and S_3) are necessary. Activity is lost if both S_1 and S_3 are long chains, or if both S_1 and S_3 are benzyl groups. Activity also disappears when the S_1 tail or S_2 polyether is too short, or when the S_3 terminus is a hydroxyl. An investigation of over 25 analogues (both more and less hydrophobic than **5**) suggests strongly that precise alignment, rather than gross disruption, is required for ion conduction.

We surmise that a transport capability requires the benzyl group to anchor to the membrane surface (via an ion–dipole attraction known to occur between aromatic rings and the quaternary nitrogen of the lipid head group),[25] while the tail embeds itself in the membrane interior (Fig. 11). The

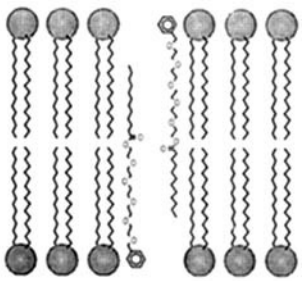

Fig. 11. Proposed orientation of **5** within a vesicle bilayer. A minimum of two molecules is required to span the entire membrane.

polyether moiety is thereby forced to span the leaflet where it, or its hydration shell, can conduct ions. A minimum of two molecules of **5** must become aligned to permit passage across the entire membrane.

There is no possibility that **5** acts merely as a "carrier" (i.e., a molecule that complexes with an ion and shuttles it dynamically through the membrane). Thus, **5** is useless in transmitting ions through a "liquid membrane" consisting of bulk chloroform. If **5** were a carrier, it would function well even in organic solvents.

We have just seen how a low ion flux can be converted into a high ion flux by trace quantities of a promoter. If a mechanism were available to rid the system of the promoter once the high ion flux has performed a particular function, then the components of a chemical switch would be at hand. Nature has already made wide use of such a process, and systems research will ultimately enable chemists to do likewise.

6.2. An Enzyme-Labile Vesicle[26]

Bone cancer cells produce and exude an inordinate amount of an enzyme, alkaline phosphatase, which catalyzes the hydrolysis of monophosphate esters [Eq. (d)]. Now consider the following scenario: (1) Vesicles loaded with an anti-

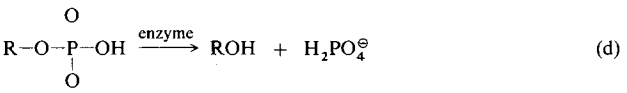

$$R{-}O{-}\overset{\overset{O}{|}}{\underset{\underset{O}{|}}{P}}{-}OH \xrightarrow{\text{enzyme}} ROH + H_2PO_4^{\ominus} \qquad \text{(d)}$$

tumor drug are prepared from a double-tailed surfactant having a phosphate head group. (2) When a vesicle comes into proximity of a bone cancer cell, the high local concentration of alkaline phosphatase removes the vesicular head groups (Fig. 12). (3) The destabilized vesicle "bursts" and

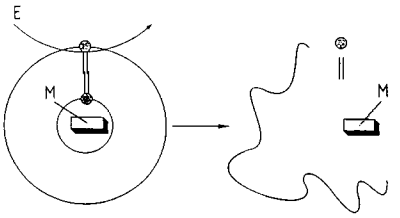

Fig. 12. Schematic of an enzyme-labile vesicle for use in drug release. M = drug, E = enzyme exuded by pathological cell.

releases its contents (the drug) thereby killing the cancer cell. Note that the scheme imparts specificity to the cancer therapy. Since the specificity derives not from the drug but from the shell around it, any cytotoxic drug may be used.

Although we have not yet developed a working system with alkaline phosphatase, we have made vesicles that are labile to another enzyme, acetylcholine esterase, which is produced in abnormal amounts by certain neuroblastoma cells. Acetylcholine esterase hydrolyzes acetylcholine as shown in Equation (e). Thus, it was expected that the double-tailed surfactant **6** could, by virtue of the acetylcholine-

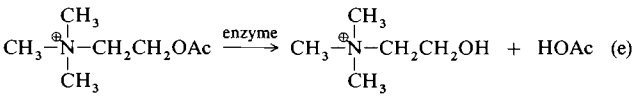

$$CH_3{-}\overset{\overset{CH_3}{|}}{\underset{\underset{CH_3}{|}}{\overset{\oplus}{N}}}{-}CH_2CH_2OAc \xrightarrow{\text{enzyme}} CH_3{-}\overset{\overset{CH_3}{|}}{\underset{\underset{CH_3}{|}}{\overset{\oplus}{N}}}{-}CH_2CH_2OH + HOAc \qquad \text{(e)}$$

like unit incorporated within it, act as a substrate for the enzyme. This in fact turned out to be the case.

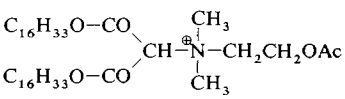

$$C_{16}H_{33}O{-}CO \quad \overset{\overset{CH_3}{|}}{CH{-}\overset{\oplus}{N}{-}CH_2CH_2OAc} \quad Br^{\ominus} \qquad \mathbf{6}$$
$$C_{16}H_{33}O{-}CO \quad \underset{\underset{CH_3}{|}}{}$$

Acetylcholine esterase removed the acetyl group of **6**, whereupon the resulting alcohol spontaneously cyclized to form a six-membered lactone plus hexadecanol. In other words, the vesicular surfactant loses one of its hydrocarbon tails subsequent to the enzyme action. Since surfactants with only one tail form micelles (not vesicles), the vesicles disintegrate in the presence of the enzyme.

Enzyme-induced vesicle destruction causes the release of guest molecules encapsulated within the vesicles. This was proven in the following manner. A water-soluble substrate of acetylcholine esterase, **7**, was placed inside vesicles composed of **6**. Hydrolysis of **7** was known to produce a highly

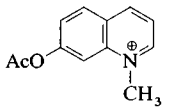

7

fluorescent product. Thus, when vesicles of **6**, loaded with **7**, were mixed with the enzyme, a burst of fluorescence appeared as the enzyme first chewed up the vesicles and then hydrolyzed **7** upon its escape from captivity. Heat-denatured acetylcholine esterase gave no such instantaneous emission of light, as would be expected with an enzyme-specific destructability.

6.3. Branched Lipids and Bilayer Membranes[27]

In Section 5, it was mentioned that we have synthesized a library of alkyl-substituted phospholipids. These materials were found to be potent inhibitors in multicomponent systems containing the enzyme phospholipase A_2[28] or protein kinase C.[29] Since it is preferable to confine the discussion here to chemical issues, I will relate only how branching affects the properties of bilayer membranes. Once again, extensive compilations of data, graphs, and details[27] are omitted for the sake of brevity and charm.

In 1884, it was written that phospholipids are the "centre, life, and chemical soul of all bioplasm. Amongst their properties, none are more deserving of further inquiry than those which may be described as their power of colloidation."[30] In modern terms, "colloidation" refers to the molecular bilayers that phospholipids spontaneously form when mixed with water. As already pointed out in Section 6, bilayers assume the shape of vesicles when the phospholipids are sonicated in water.

Bilayers undergo thermal transitions owing to changes in molecular packing within the hydrocarbon and head-group regions. These transitions are best detected by differential scanning calorimetry (DSC) in which excess heat capacity (corresponding to absorption of energy) is plotted versus temperature. DSC monitors the thermally induced transition of phospholipid bilayers from a relatively ordered state (below the transition temperature, T_c) to a more random state (above T_c). This process, not unlike that of melting, causes a sharp spike at T_c in the DSC graph.

Figure 13 shows a plot of T_c versus the methyl substitution site for six loci along the 18-carbon lipid chain. A striking "V-shaped" curve is observed. Methyls at position 10 clearly have a much greater effect on lowering T_c than do methyls at either end of the chain (i.e., at positions 4 or 16). We believe that this effect is due to a central kink in the lipids within the bilayers (as in a chevron on military uniforms). Arguments

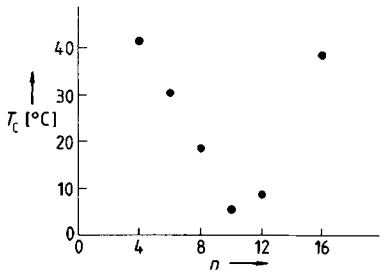

Fig. 13. Distearoyl phosphatidylcholines with methyl groups on both chains at position $n = 4, 6, 8, 10, 12$, or 16 show how the transition temperature of the lipid, T_c, varies with the methyl substitution site. Methyls in the center of the chain clearly perturb lipid packing more than methyls at either end. The same was shown to be true for ion transport through vesicle membranes prepared from the synthetic lipids.

in favor of such a packing mode are given elsewhere.[27] The main point worth making here is that we were able to exploit the observed disruptions to control membrane permeability, as described below.

We measured (by methods outlined in Section 6.1) ion permeability through vesicle walls made from our various chain-substituted phospholipids.[31] In essence, we carried out a "structure–activity" study where the focus of attention was the structure of a system rather than that of a single molecule. The fundamental discovery was that centrally located methyls promote transport of ions through the bilayer membranes more efficiently than do methyls at either end of the chains (similar to their effect on T_c). At a given location, an *n*-butyl group disrupts the membrane more than a methyl as measured by the efficiency of ion flux. Controlling membrane permeability via rational design of the component species would seem to be a highly promising and useful topic for future systems research.

6.4. Gemini Surfactants[32]

The final section on vesicles deals with a new type of double-chained compounds that we call "gemini surfactants". Although work is only partially completed, I mention it to drive home a point. Synthetic organic chemistry allows chemists access to a seemingly endless variety of new self-assembling molecules. These molecules are a scientific bonanza, allowing entry into a huge unfenced area where few people have staked claims and where the imagination can roam free. Take gemini surfactants for example. The molecules possess, in sequence, a long hydrocarbon chain, an ionic group, a rigid spacer, a second ionic group, and another hydrocarbon tail (Scheme 11). Geminis were synthesized as

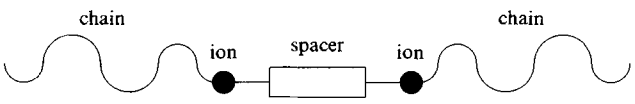

Scheme 11. Structure of a gemini surfactant.

the result of our asking a simple question that, to our surprise, had never before been addressed in the literature: How does a double-chained surfactant behave when the two chains within a molecule are prevented, by means of a large spacer such as stilbene, from lying side by side? We also wondered whether aggregation of geminis in water would superficially resemble polymer growth. In polymerizations, reactive end groups are always being generated, permitting continual elongation. The same is true for gemini aggregation except that the end groups are hydrophobically active rather than susceptible to covalent bonding.

According to surface tension measurements, geminis with 20 carbons per chain have a much *higher* cmc than geminis with 12 carbons per chain! This runs counter to all previously reported trends in surfactant chemistry. Normally, long-chained surfactants, with their greater propensity to aggregate in water, possess low cmc's. Dye-binding studies have shown that geminis with two 20-carbon chains form small clusters at extremely low concentrations ($<1 \times 10^{-5}$ M). Only at concentrations near 10 mM will these clusters cooperatively assemble into larger aggregates and, thereby, manifest a cmc. Geminis with 12 carbons, on the other hand, behave normally in that their cmc represents facile conversion into micelles from the *monomeric* state. Although geminis have just been synthesized, and we do not fully understand the structure of their aggregates, they exemplify how readily one can design and construct new self-assembling compounds that display unusual and potentially useful properties.

7. Of Pools and Polymers[33]

An entirely different type of chemical system will now be discussed: the water pool and porous polymers derived therefrom. Years ago, the term "water pool" was coined to depict aqueous microdroplets that can form in apolar solvents containing a surfactant, AOT.[34] So effective is AOT that one can readily dissolve 10–20% water in heptane to give optically clear solutions. The pools, on the order of 50 Å in diameter, are stable owing to the "molecular coating" of AOT at the water–heptane interface (see Fig. 14).

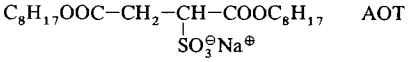

The central idea in our work was to use styrene/divinylbenzene instead of heptane for the apolar continuous phase.[35] This enabled us to photopolymerize the water-pool systems. The resulting solid was ground to a powder, leached with methanol to remove AOT, and dried (see Fig. 14) to produce porous polystyrene.

So-called BET measurements (based on N_2 adsorption data) proved that the polymers can achieve surface areas as high as 30 $m^2 g^{-1}$. Scanning electron micrographs confirmed the porous nature of the polymers. Preliminary results showed that the new materials have potential applications in controlled-release systems and in chromatographic separations.

7.1. Controlled Release[35]

As depicted in Figure 14, cupric ion can be dissolved in the water pools prior to photolysis. In this manner, it was possible to prepare copper-containing solid polymers that only slowly released the metal when stirred in water. Industrial testing of the materials for use as antifouling agents in marine paints is now in progress. A variety of water-soluble compounds should be amenable to controlled release by the same methodology.

Outwardly, the above chemical system appears complex: a mixture of styrene, divinylbenzene, water, AOT, and cupric ion. Molecular organization and compartmentalization, however, "derandomize" the system and convert it into something interesting and, perhaps, into something useful.

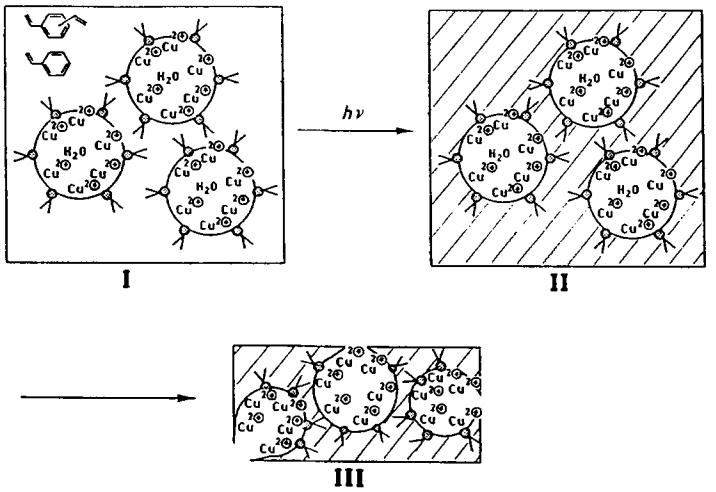

Fig. 14. Scheme for synthesizing porous polystyrene containing occluded copper ion. The darkened circle with two tails represent AOT surfactant. **I**: AOT-stabilized water pool in styrene/divinylbenzene. **II**: Pool in cross-linked polystyrene. **III**: Porous polystyrene obtained by grinding and drying.

7.2. Chromatography[35]

TLC plates were prepared from powdered porous polymer mixed with calcium sulfate as a binder. Using methanol as the developing solvent, we separated nitrobenzene, aniline, and phenol much more effectively on the polymer plates (R_f = 0.45, 0.65, and 0.92, respectively) than on silica plates (R_f = 0.94, 0.88, and 0.80, respectively). This was also true for the separation of the three nitrophenol isomers.

7.3. Porous Polystyrene with Chemically Active Surfaces[36]

Figure 15 presents a scheme, based on our water-pool method, for synthesizing porous polymers with high surface functionality. A monomer with the structure $XArCH{=}CH_2$, where X is a polar and chemically interesting moiety, orients at the water–hydrocarbon interface with X immersed in or near the pools. Since, as shown, the pool interface transforms into irregularities on the polymer surface, the X group becomes fixed to the polymer exterior rather than getting buried. The concept was tested with the diamine monomer **8**. It was demonstrated (by titration with $Cu^{2\oplus}$) that up to 89% of the diamine groups were fully exposed and available at the surface of the solid polymer. This compares with only 0.6% in copolymers formed without the surfactant-stabilized water pools.

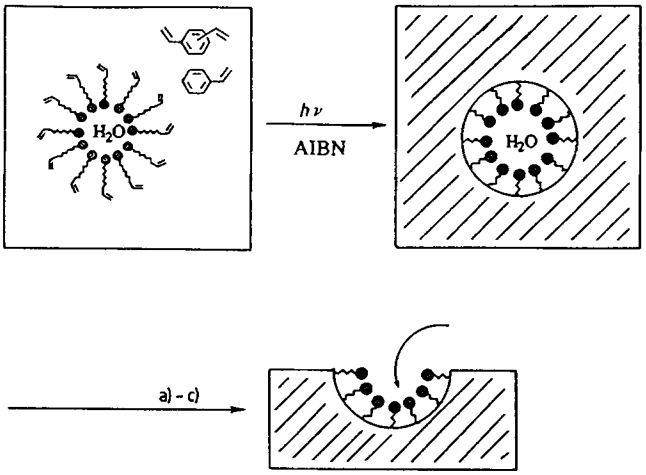

Fig. 15. Scheme for making polymers with high surface area plus high surface functionality. The heavy circles represent a functional group that is useful for catalytic, chromatographic, or other purpose where its existence on the polymer surface is required. The functional groups are polar and tend to assemble at the interface of the AOT-stabilized water pools. This is a multicomponent system containing initially styrene, divinylbenzene, water, AOT, functionalized monomer, and azodiisobutyronitrile (AIBN; a radical initiator). Organization and compartmentalization convert the complex mixture into a useful entity. a) Grind and sieve. b) Wash with MeOH and 20% aqueous NaOH. c) Dry. The arrow indicates the active surface.

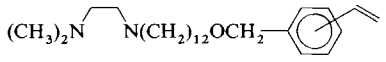

8

As a result of systems research, the potential now exists of creating new polymers that have (1) a high surface area and (2) a high surface functionalization. Applications of such materials in the field of catalysis and chiral separations are now being investigated.

8. Molecular Laminates[37]

Periodicity in crystalline solids leads to cooperative electronic effects and thus to useful properties of organic metals, semiconductors, ferromagnets, and optical devices. Yet the rational design of periodicity ("crystal engineering") remains a primitive art and an attractive subject for further pursuit. With this in mind, and with our ongoing affection for diverse organized assemblies (of which crystals are the most perfect), we set out to prepare crystals with alternating layers of metal and hydrocarbon.[38] Such "molecular laminates" were ultimately achieved via three new long-chain copper complexes (Fig. 16). The compounds assemble into layered arrays, each with its own peculiar packing mode.

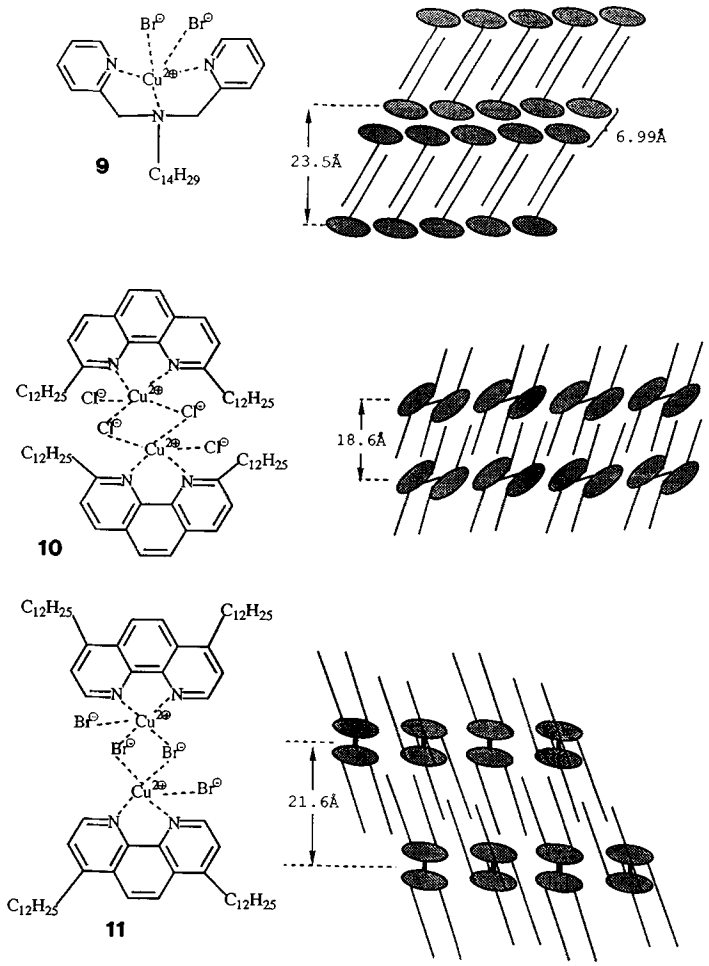

Fig. 16. Crystal packing differences among three long-chain copper complexes.

All three molecules crystallize with copper "sheets" separated by hydrocarbon. Compound **9** packs with heavily interdigitated chains that are fully extended except for one *gauche* linkage per chain. As indicated, the lattice is characterized by Cu–Cu distances of 6.99 Å and 23.5 Å. Compound **10** exists as a dimeric complex. Each aromatic ligand extends one of its chains upward and the other downward (again with a single *gauche* linkage per chain). The copper layers are only 18.6 Å apart. Compound **11** also exists as a dimeric complex, but (in contrast to **10**) chains from a given aromatic ring project in the same direction. Only one of the two side-by-side chains possess a *gauche* linkage. Copper layers are separated by 21.6 Å.

Layer-to-layer distances between sheets of heavy metals can obviously be affected by the number of chains, the length of the chains, and the location of the chains on the supporting scaffold. Information relating such parameters to crystal packing will ultimately allow a priori control of periodicity in solid systems.

9. Final Remark

Thus ends this personalized tour of "systems research". If the account is regarded as an interesting scientific tale, albeit a somewhat egocentric one, then I have fulfilled my objective. And if, perchance, somewhere a student happens to read this account, and is moved to pursue the field of chemistry, then this would be success in its purest, simplest, and most lasting form.

Three agencies (the Army Research Office, the National Institutes of Health, and the National Science Foundation) generously supported our research over the years. The Arakawa Chemical Co. and the Orient Chemical Co., both in Osaka, funded two fellowships. Dow Chemical Co. and LASPAU (Latin American Scholarship Program of American Universities) also provided fellowship support for our systems research. I am, of course, grateful to all the fine young chemists who did the actual experimentation; their names appear in the references. Professor Roald Hoffmann provided valuable comments about the original manuscript. I have also benefited considerably from regular visits with chemists at 3M Corp. (a company doing very well in the "systems research" business). Finally, I must mention my admiration of, and debt to, the diverse body of scientists from both hemispheres who have inspired my research group and who have given the field of self-assembling systems its key insights. There is something particularly egalitarian about systems research.

Received: November 13, 1990 [A 831 IE]
German version: *Angew. Chem. 101* (1991) 1104

[1] H. Ringsdorf, B. Schlarb, J. Venzmer, *Angew. Chem. 100* (1988) 117; *Angew. Chem. Int. Ed. Engl. 27* (1988) 113.
[2] R. J. Waller: *One Good Road is Enough: Stories and Essays*, Iowa State University Press, Ames, IA, USA 1990.
[3] For lead references on micelles see: a) J. H. Fendler: *Membrane Mimetic Chemistry*, Wiley, New York 1982; b) K. L. Mittal (Eds.): *Micellization, Solubilization and Microemulsions*, Plenum, New York 1977; c) K. L. Mittal, B. Lindman (Eds.): *Surfactants in Solution*, Plenum, New York 1984; d) K. L. Mittal (Eds.): *Surfactants in Solution*, Plenum, New York 1989; e) D. Myers: *Surfactant Science and Technology*, VCH, New York 1988.
[4] F. M. Menger, J. L. Lynn, *J. Am. Chem. Soc. 97* (1975) 948.
[5] F. M. Menger, J. M. Jerkunica, J. C. Johnston, *J. Am. Chem. Soc. 100* (1978) 4676.
[6] For lead references on chain conformation in micelles see: K. Watanabe, M. L. Klein, *J. Phys. Chem. 93* (1989) 6897; D. W. R. Gruen, *J. Colloid Interface Sci. 84* (1981) 281.
[7] F. M. Menger, J. F. Chow, *J. Am. Chem. Soc. 105* (1983) 5501.
[8] L. I. Osipow: *Surface Chemistry, Theory and Industrial Applications*, Reinhold, New York 1962, p. 175; L. R. Fisher, D. G. Oakenful, *Chem. Soc. Rev. 6* (1977) 25.
[9] D. W. R. Gruen, *Prog. Colloid Polym. Sci. 70* (1985) 6.
[10] F. M. Menger, *Acc. Chem. Res. 12* (1979) 111; *Nature 313* (1985) 603.
[11] C. Hansch, *Acc. Chem. Res. 2* (1969) 232.
[12] For lead references on micellar kinetics and catalysis see: J. H. Fendler, E. J. Fendler: *Catalysis in Micellar and Macromolecular systems*, Academic Press, New York 1975; b) H. Dugas, C. Penney: *Bioorganic Chemistry*, Springer, New York 1981, pp. 272–282; c) C. A. Bunton, *New Compr. Biochem. 6* (1984) 461; d) T. Kunitake, S. Shinkai, *Adv. Phys. Org. Chem. 17* (1980) 435.
[13] F. M. Menger, D. W. Doll, *J. Am. Chem. Soc. 106* (1984) 1109.
[14] F. M. Menger, D. W. Carnahan, *J. Am. Chem. Soc. 108* (1986) 1297; F. M. Menger, M. A. Dulany, D. W. Carnahan, L. H. Lee, *ibid. 109* (1987) 6899; F. M. Menger, L. L. D'Angelo, *ibid. 110* (1988) 8241.
[15] F. M. Menger, *J. Chem. Educ. 57* (1980) 351.
[16] F. M. Menger, L. G. Whitesell, *J. Am. Chem. Soc. 107* (1985) 707.
[17] F. M. Menger, L. H. Gan, E. Johnson, D. H. Durst, *J. Am. Chem. Soc. 109* (1987) 2800.
[18] For lead references on microemulsions and reactions in microemulsions see: a) L. M. Prince: *Microemulsions. Theory and Practice*, Academic Press, New York 1974; b) C. A. Bunton, F. de Buzzaccarini, *J. Phys. Chem. 86* (1982) 5010. c) R. A. Mackay, F. R. Longo, B. L. Knier, H. D. Durst, *ibid. 91* (1987) 861; d) D. G. Rance, S. Friberg, *J. Colloid Interface Sci. 60* (1977) 207; e) M. Almgren, F. Grieser, J. K. Thomas, *J. Am. Chem. Soc. 102* (1980) 3188.
[19] F. M. Menger, A. R. Elrington, *J. Am. Chem. Soc. 112* (1990) 8201.

[20] For lead references on monolayer films see: a) G. L. Gaines, Jr.: *Insoluble Monolayers at Liquid-Gas Interfaces*, Interscience, New York 1966; b) D. A. Cadenhead in J. F. Danielli, A. C. Riddiford, M. D. Rosenbery (Eds.): *Recent Progress in Surface Science, Vol. 3,* Academic Press, New York 1970, pp. 169–192; c) E. M. Arnett, J. Chao, B. J. Kinzig, M. V. Stewart, O. Thompson, R. J. Verbiar, *J. Am. Chem. Soc. 104* (1982) 389; d) R. Elbert, A. Laschewsky, H. Ringsdorf, *ibid. 107* (1985) 4134.
[21] F. M. Menger, M. G. Wood, Jr., S. Richardson, Q. Zhou, A. R. Elrington, M. J. Sherrod, *J. Am. Chem. Soc. 110* (1988) 6797.
[22] F. M. Menger, S. D. Richardson, M. G. Wood, Jr., M. J. Sherrod, *Langmuir 5* (1989) 833.
[23] For lead references on vesicles and membrane transport see: a) M. J. Ostro (Eds.): *Liposomes,* Dekker, New York 1983; b) J. H. Fendler: *Membrane Mimetic Chemistry,* Wiley, New York 1982, Chapter 6; c) J. Heller, R. W. Blake: *Controlled Release of Biomaterials*, Academic Press, New York 1980; d) D. W. Deamer, J. W. Nichols, *J. Membr. Biol. 107* (1989) 91; e) G. Gregoriadis: *Liposomes as Drug Carriers: Recent Trends and Progress*, Wiley, Chichester 1988.
[24] F. M. Menger, D. S. Davis, R. A. Persichetti, J.-J. Lee, *J. Am. Chem. Soc. 112* (1990) 2451.
[25] G. Gillberg, *Acta Chem. Scand. 20* (1966) 2019.
[26] F. M. Menger, D. E. Johnston, *J. Am. Chem. Soc. 113* (1991) 5467.
[27] F. M. Menger, M. G. Wood, Jr., Q. Z. Zhou, H. P. Hopkins, J. Fumero, *J. Am. Chem. Soc. 110* (1988) 6804.
[28] F. M. Menger, M. G. Wood, Jr., *Angew. Chem. 101*, (1989) 1277; *Angew. Chem. Int. Ed. Engl. 28* (1989) 1218.
[29] P. A. Charp, Q. Zhou, M. G. Wood, Jr., R. L. Raynor, F. M. Menger, J. F. Kuo, *Biochemistry 27* (1988) 4607.
[30] J. L. W. Thudichum: *A Treatise on the Chemical Constitution of the Brain*, Bailliere and Cox, London 1884.
[31] F. M. Menger, P. Aikens, unpublished results.
[32] F. M. Menger, C. A. Littau, *J. Am. Chem. Soc. 113* (1991) 1451.
[33] For lead references on pools and polymers see: a) M. Rosoff (Eds.): *Controlled Release of Drugs: Polymers and Aggregate systems*, VCH, New York 1989; b) J. M. Williams, A. J. Williams, A. J. Gray, M. H. Wilkerson, *Langmuir 6* (1990) 437; c) C. J. O'Connor, T. D. Lomax, R. E. Ramage, *Adv. Colloid Interface Sci. 20* (1984) 21; d) P. L. Luisi, B. E. Straub (Eds.): *Reverse Micelles*, Plenum, New York 1984.
[34] F. M. Menger, J. A. Donohue, R. F. Williams, *J. Am. Chem. Soc. 95* (1973) 286.
[35] F. M. Menger, T. Tsuno, G. S. Hammond, *J. Am. Chem. Soc. 112* (1990) 1263.
[36] F. M. Menger, T. Tsuno, *J. Am. Chem. Soc. 112* (1990) 6723.
[37] For lead references on crystal engineering see: a) T. E. Mallouk, H. Lee, *J. Chem. Educ. 67* (1990) 829; b) W. S. Durfee, M. Gurszecka, T. A. Olszak, W. Storck, H. Bradaczek, F. Willig, *J. Am. Chem. Soc. 111* (1989) 3699; c) K. Okuyama, Y. Soboi, K. Hirabayashi, A. Harada, A. Kumano, T. Kaziyama, M. Takayanagi, T. Kunitake, *Chem. Lett. 1984,* 2117; d) I. Pascher, S. Sundell, H. Hauser, *J. Mol. Biol. 153* (1981) 791; e) G. R. Desiraju: *Crystal Engineering: The Design of Organic Solids*, Elsevier, New York 1989.
[38] F. M. Menger, J. J. Lee, K. S. Hagen, *J. Am. Chem. Soc. 113* (1991) 4017.
[39] F. M. Menger, N. Balachander, E. van der Linden, G. S. Hammond, *J. Am. Chem. Soc. 113* (1991) 5119.

Lipoxins and Related Eicosanoids: Biosynthesis, Biological Properties, and Chemical Synthesis

By K. C. Nicolaou,* John Y. Ramphal, Nicos A. Petasis, and Charles N. Serhan**

Among the various enzymes found in human tissues that act on arachidonic acid, there are three major types of lipoxygenases (LO), operating at the 5-, 12-, and 15-positions. The 5-LO is a key enzyme and plays a central role in the biosynthesis of leukotrienes, which are potent arachidonate-derived mediators of allergy and inflammation. Because of the importance of the 5-LO-derived products in human pathophysiology, studies were initiated to examine the consequences of initial lipoxygenation at C15 of arachidonic acid as well as to probe interactions between the major LO pathways. These studies led to the identification of a new series of biologically active tetraene-containing eicosanoids termed lipoxins. This article summarizes the isolation, biosynthesis, and chemical synthesis of lipoxins and related systems, and reviews recent results concerning their formation and biological activities. The total synthesis of these molecules based on a new and general synthetic strategy involving palladium catalysis is reviewed. This synthetic approach has allowed the preparation of several types of acyclic eicosanoids in their naturally occurring forms which, in turn, allowed comparisons with naturally derived materials and enabled detailed studies of the biological actions of these biomolecules. Structure–activity relationships were also derived by combining chemical synthesis and biological investigations.

1. Introduction

The oxygenation of arachidonic acid (AA) by a wide range of human cell types results in the formation of several classes of biologically active products, termed eicosanoids because they contain twenty C atoms (Scheme 1). These metabolites have long been a focus of biomedical research due to their involvement in the regulation of inflammatory reactions,

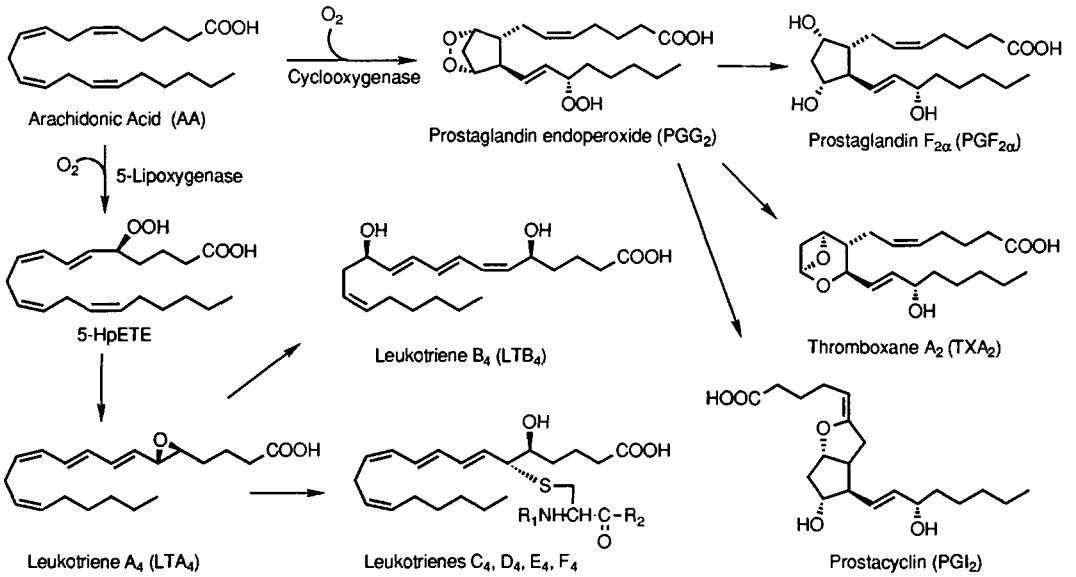

Scheme 1. Conversion of arachidonic acid (AA) to various eicosanoids.

[*] Prof. K. C. Nicolaou, J. Y. Ramphal
Department of Chemistry, Research Institute of Scripps Clinic
La Jolla, CA 92037 (USA)
and
Department of Chemistry, University of California, San Diego
La Jolla, CA 92093 (USA)
Prof. N. A. Petasis
Department of Chemistry, University of Southern California
Los Angeles, CA 90089 (USA)
[**] Prof. C. N. Serhan
Hematology Division, Department of Medicine
Brigham and Women's Hospital and Harvard Medical School
Boston, MA 02115 (USA)

smooth muscle tone, and hemodynamic events, allergy and asthma, as well as many other important physiological and pathophysiological phenomena.

The discoveries in the 60's and 70's by *S. Bergström*[1] and *B. Samuelsson*[2] on the structure and function of the prostaglandins (PG), the thromboxanes (TX), and the prostaglandin endoperoxides (PGH_2, PGG_2) have sparked extensive investigations in the eicosanoid field. Among the major findings that emanated from these efforts was the discovery of prostacyclin (PGI_2) by *J. Vane*,[3] who also

found that cyclooxygenase (PG endoperoxide synthetase), the central enzyme in the biosynthesis of both PG's and TX's, is inhibited by aspirin and other anti-inflammatory drugs, suggesting a mechanism of action for these molecules. Further studies by the *Samuelsson* group[4] on the metabolism of AA in leukocytes led to two other major pathways which are insensitive to treatment with aspirin. These involve the action of lipoxygenase enzymes (LO), one of which initiates oxygenation at C5 of AA (5-LO) and the other acting at C15 (15-LO). Additional work revealed that the 5-LO is a key enzyme in the biosynthesis of another major group of eicosanoids, the leukotrienes (LT), which were identified with the slow reacting substances of anaphylaxis. The LT's have generated considerable excitement because these compounds have proven to be important mediators of the cardinal signs of inflammation-eliciting vascular

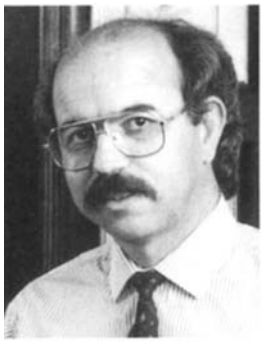

K. C. Nicolaou was born in Cyprus and received his Ph. D. degree from the University of London under Professors F. Sondheimer and P. Garratt. After postdoctoral work at Columbia University with Professor T. Katz and at Harvard University with Professor E. J. Corey, in 1976 he joined the faculty at the University of Pennsylvania, where he was promoted to Rhodes-Thompson Professor of Chemistry. He moved to La Jolla in 1989 to fill an unprecedented joint appointment as a Professor of Chemistry at the University of California San Diego and as the Darlene Shiley Professor of Chemistry and Chairman of the Department of Chemistry at the Research Institute of the Scripps Clinic. The recipient of numerous awards including the Alfred P. Sloan Award, a Guggenheim Fellowship, and a Humboldt Senior American Scientist Award, Nicolaou has been involved with the development of new ways of synthesizing complex organic molecules of natural or nonnatural origin. His research interests currently include the synthesis of molecules from the eicosanoid, macrolide, marine ionophore, and oligosaccharide areas, and the design, synthesis and study of biologically active molecules with DNA-cleaving and molecular-recognition properties.

John Y. Ramphal was born in 1963 in Georgetown, British Guiana. He studied at St. John Fisher University and Bucknell University where he completed his M. Sc. degree under Professor H. W. Heine, before joining Professor Nicolaou's group at the University of Pennsylvania. In 1989 he followed Professor Nicolaou to California, where he is currently in his final year of graduate studies. His research involves the synthesis of molecules from the eicosanoid and carbohydrate areas.

Nicos A. Petasis was born in Cyprus and received his undergraduate education at the Aristotelian University of Thessaloniki in Greece. In 1979 he joined the research group of Professor K. C. Nicolaou at the University of Pennsylvania and worked on the synthesis of endiandric acids and eicosanoids. After completing his Ph. D. in 1983, he stayed on as a postdoctoral fellow until 1987, when he joined the University of Southern California as an Assistant Professor of Chemistry. His current research interests include the development of new synthetic methods involving pericyclic reactions and organotitanium compounds, the development of bio-inspired strategies for the synthesis of natural products, and the design and synthesis of biomimetic systems.

Charles N. Serhan was born in New York and studied biochemistry at the State University of New York at Stony Brook. He received his Ph. D. degree in 1982 from New York University, where in the laboratory of G. Weissmann he first became interested in the biochemistry and cell biology of inflammatory responses. He spent the following years (1982–1986) as a visiting scientist at the Karolinska Institute in Stockholm, with Bengt Samuelsson. In 1987 he joined the faculty at Brigham and Women's Hospital and Harvard Medical School as Assistant Professor of Medicine (Biochemistry). Serhan has received several awards including the J. V. Satterfield Arthritis Investigator Award from the Arthritis Foundation, a Medical Foundation Research Fellowship from the Medical Foundation Inc., and an Established Investigatorship Award from the American Heart Association National Center. He was also named a Pew Scholar in the biomedical sciences. His current research interests include lipid and membrane biochemistry, signal transduction in human leukocytes and platelets, the biosynthesis and structural elucidation of biologically active lipids, and the role of lipid mediators in transcellular communication.

permeability, leukocyte influx, and contraction of smooth muscle. For their contributions, *Bergström*, *Samuelsson*, and *Vane* shared the 1982 Nobel Prize in Medicine.

Following the discovery of each of the major families of eicosanoids, there has been extensive work by synthetic chemists in academic and industrial laboratories aimed at the synthesis of the naturally occurring molecules as well as their structural analogues. This has led to the complete stereochemical assignment of these compounds and has prompted further studies on their biological actions. The chemistry and biology of eicosanoids, including the prostaglandins,[1, 5] the thromboxanes,[2, 5, 6] the prostacyclins,[3, 5, 6] and the leukotrienes,[4, 5] have been thoroughly reviewed.

A new class of LO-derived eicosanoids was recently discovered. The realization that the lipoxygenase enzymes (5-LO, 12-LO, 15-LO), previously found in plants, are also widely distributed in human tissues, has prompted investigations aimed at the interactions between these LO pathways. These studies led to the isolation of several new biologically active molecules, termed lipoxins (LX),[7–9] which can be generated by interactions between the human 5/15-LO's and 5/12-LO's (Scheme 2).

leukotrienes.[10–13] Also, recent results indicate that the LX's are formed in vivo and that they are associated with human disease.[14–16] Specifically, LXA_4 has been identified in bronchoalveolar lavage fluids[14] and LXA_4/LXB_4 in nasal polyps,[15] while a defect in LX production is observed with cells from patients with chronic myeloid leukemia.[16] Taken together, these findings suggest that the LX's are generated in vivo and may exhibit counterregulatory roles.

Below we review the isolation, biosynthesis, and biological actions of the lipoxins, and the total synthesis of these and related acyclic eicosanoids.

2. Isolation and Structural Elucidation of Lipoxins

While studying the transformation of [1-^{14}C]arachidonate (AA) in suspensions of mixed human leukocytes (e.g., neutrophils, eosinophils, basophils, etc.) with *Samuelsson* and *Hamberg* at the Karolinska Institute, *Serhan* observed that labeled AA was transformed into polar compounds that had not been previously described. Human leukocytes (e.g. A23187), without addition of other stimuli, rapidly oxygenate exogenous AA at the C15 position.[17, 18] Therefore,

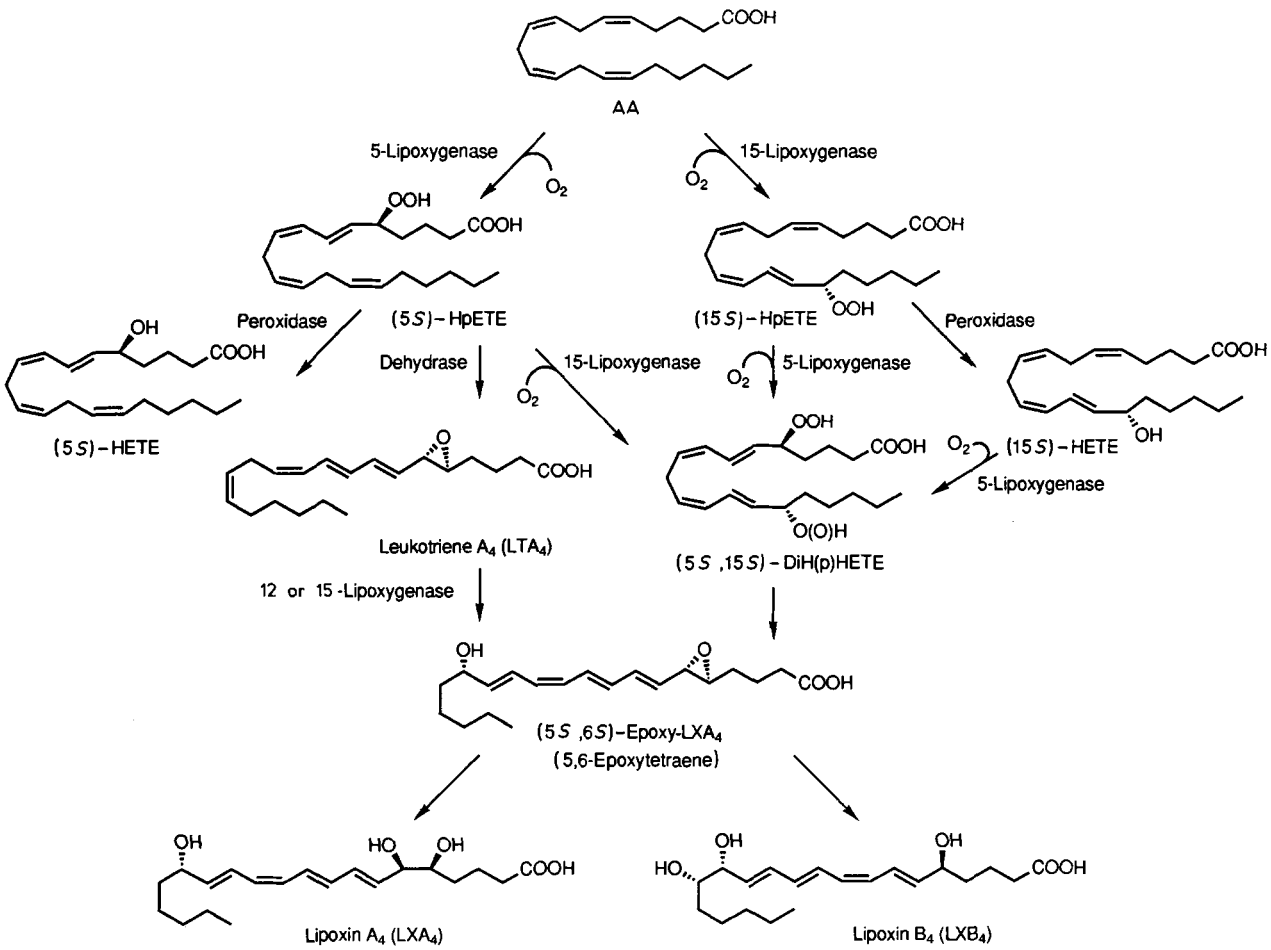

Scheme 2. Biosynthesis of the lipoxins in various systems.

The lipoxins display a unique spectrum of biological properties. For example, it was recently reported that LXA_4 can inhibit some of the "proinflammatory" actions of the

we investigated the products associated with 15-lipoxygenation of arachidonate. Results from several laboratories suggested that initial lipoxygenation at C15 could lead to the

formation of eicosanoids of biological interest.[17, 18] For example, (15*S*)-hydroxy-(5*Z*,8*Z*,11*Z*,13*E*)-icosatetraenoic acid, (15*S*)-HETE, had been identified as a major product of AA in both normal and asthmatic human lung tissue[19] and is found in microgram quantities in bronchoalveolar lavage fluids obtained from patients with chronic stable asthma after challenge.[20] Although 15-lipoxygenation of AA is a major route of its oxidation in a wide range of mammalian tissues and cell types,[21] receptor-mediated activation of 15-LO and the general physiological role of its products has remained an area of interest.

In order to mimic the cellular events that could have given rise to these novel polar compounds, as well as to prepare large amounts of the materials for both structural and biological studies, (15*S*)-HETE and the corresponding hydroperoxy derivative, (15*S*)-HpETE, were prepared, and the products formed upon their exposure to human leukocytes were monitored.[7, 8, 22–25] This approach facilitated the isolation and characterization of a new series of oxygenated products derived from AA that contain an unusual conjugated tetraene system (Scheme 2). These compounds arose through interactions between LO pathways and possess unique structures and novel biological properties. Therefore the trivial name lipoxin (*lipox*ygenase *in*teraction product) was proposed.[7, 8, 23]

Human leukocytes with an ionophore of divalent cations (A23187) gave an increased formation of these tetraene-containing eicosanoids, which facilitated their isolation in larger amounts.[7, 8, 22] The basic structures of the first two members of this series were determined by physical methods that included high-pressure liquid chromatography (HPLC), UV spectroscopy, gas chromatography–mass spectrometry (GC-MS), and oxidative ozonolysis. One compound was identified as 5,6,15-trihydroxy-7,9,11,13-icosatetraenoic acid,[7] and the other proved to be a positional isomer, 5,14,15-trihydroxy-6,8,10,12-icosatetraenoic acid.[8] When these biologically derived products were isolated following HPLC procedures and added to either human neutrophils, natural killer (NK) cells, or lung strips from guinea pigs, they elicited biological actions different from those previously observed with other eicosanoids. Therefore these new biologically active compounds were termed lipoxin A_4 (LXA_4) and lipoxin B_4 (LXB_4).[8, 24]

3. Biosynthesis and Stereochemistry of LXA_4 and LXB_4

It was important to determine next the complete stereochemistry of the biologically active LXA_4 and LXB_4, as well as identify the structures and actions of their naturally occurring isomers. Results obtained from isotopic oxygen investigations guided these studies: each of the tetraene-containing compounds generated by intact leukocytes carried an ^{18}O atom at C5 and the oxygen atoms of C6 of LXA_4 and C14 of LXB_4 and their isomers were not exclusively derived from molecular oxygen.[24] These findings and results of trapping studies with alcohol suggested that the formation of lipoxins in human leukocytes proceeds via an epoxide-containing intermediate.[22–26]

A synthetic approach was undertaken at this point to establish the stereochemistry of LXA_4 and LXB_4 (i.e., the geometry of the double bonds and the chirality of the C6 and C14 hydroxy groups). Both synthetic and biologically derived materials and several of their derivatives were subjected to analysis by UV spectroscopy, HPLC (cochromatography in several systems), and GC-MS, and, most importantly, they were assessed and compared for biological activities. LXA_4 proved to be (5*S*,6*R*,15*S*)-trihydroxy-(7*E*,9*E*,11*Z*,13*E*)-icosatetraenoic acid,[22] and LXB_4 (5*S*,14*R*,15*S*)-trihydroxy-(6*E*,8*Z*,10*E*,12*E*)-icosatetraenoic acid[25] (Scheme 2). A (6*S*) isomer of LXA_4, 6-epi-LXA_4, and two all-*trans* diastereomers, 11-*trans*-LXA_4 and 6-epi-11-*trans*-LXA_4, were also identified.[22, 24] These compounds are much less active than native LXA_4 in several bioassay systems.[22, 27]

Since multiple biosynthetic routes as well as cell–cell interaction can lead to formation of tetraene-containing eicosanoids, the finding that (15*S*)-HETE was rapidly transformed by activated leukocytes provided an important model for investigating one pathway in their formation.[22, 25] This route, the first to be documented, is outlined in Scheme 2.

(15*S*)-HETE is converted into (5*S*)-hydroperoxy-(15*S*)-hydroxy-(6*E*,8*Z*,11*Z*,13*E*)-icosatetraenoic acid ((5*S*,15*S*)-DiHpETE) by activated human leukocytes and further transformed into a 5,6-epoxytetraene, (5*S*,6*S*)-epoxy-LXA_4. This epoxide, or its equivalent, could be enzymatically transformed either into LXA_4 by the action of an epoxide hydrolase to yield the (5*S*,6*R*) diol moiety or into LXB_4 by attack at the C14 position with the generation of an 8*Z* double bond. Additional evidence for a 5,6-epoxytetraene intermediate in the biosynthesis was obtained with (15*S*)-hydroxy-(5*S*,6*S*)-epoxy-(7*E*,9*E*,11*Z*,13*E*)-icosatetraenoic acid prepared by chemical synthesis. This epoxide was quantitatively converted into LXA_4 (in vitro) by a purified cytosolic epoxide hydrolase.[26]

Other investigators have also postulated the role of epoxytetraenes in the formation of LXA_4, LXB_4, and their isomers[28–31] in model systems. *Kühn* et al.,[31] *Fitzsimmons* et al.,[28] and *Adams* et al.[29] have considered several hypothetical schemes to generate lipoxins. One involved an epoxide intermediate and another three consecutive oxygenations catalyzed by LO's which were not expected to involve oxygen not derived from molecular oxygen. It is clear from these results as well as results obtained from our biosynthetic studies with human leukocytes that the generation of 5,6-epoxytetraene from (15*S*)-HETE is an enzymatic event.[22, 24, 25]

Fitzsimmons et al.[28] suggested that, once formed, the 5,6-epoxytetraene could undergo nonenzymatic hydrolysis to yield a mixture of products including 14-epi-8-*trans*-LXB_4, 8-*trans*-LXB_4, and a racemic mixture of both LXA_4 and its (6*S*) isomer (6-epi-LXA_4), but not LXB_4. This notion was based upon the findings from experiments in which synthetic 5,6-epoxytetraene was added to leukocytes in suspension. However, those results did not clearly show whether the 5,6-epoxytetraene entered the cells when added exogenously, or whether it underwent hydrolysis in the extracellular medium before gaining access to cellular compartments. Moreover, the results of our time-course studies were not consis-

tent with this proposal. In particular, quantitatively higher amounts of LXA_4 were observed with cells that have not undergone lysis.[22, 32]

4. Enzymes Capable of Generating Lipoxins and Related Compounds

The initial proposal[7, 8] that tetraene-containing eicosanoids such as LXA_4 and LXB_4 are formed by several distinct biosynthetic routes has now been explored in several model systems using both purified and partially purified enzymes (Table 1). *Kühn* et al.[31] showed that a purified LO obtained from reticulocytes could convert the dihydroxy derivative, (5*S*,15*S*)-DiHETE, into trihydroxytetraenes. These transformations were blocked by inhibitors, heat denaturation, and anaerobic conditions. Thus, it was suggested that the products were enzymatically generated by LO reactions and two independent mechanisms were proposed.[31] One involves a 5,6-epoxide intermediate (vide supra), while the other implicates an intermediate generated by the action of LO on either the dihydroperoxy derivative, (5*S*,15*S*)-DiHpETE, or (5*S*,15*S*)-DiHETE. This second route can be considered a sequential triple lipoxygenation where a product of dioxygenation becomes a substrate for the third attack by an LO. Recently, these investigators[33, 34] have also demonstrated that the reticulocyte enzyme can convert 5,15-DiHETE into LXB_4, illustrating this triple lipoxygenation route. Along these lines, *Ueda* et al.[35] have shown that a 5-LO purified from porcine leukocytes can enzymatically generate a 5,6-epoxytetraene with either (15*S*)-HpETE or (15*S*)-HETE as substrate. Studies by this group, using a purified 12-LO from porcine leukocytes, indicate that LXB_4 can be generated by both the (14*R*)-oxygenase activity and the LXB_4 synthase activity of this enzyme with (5*S*,15*S*)-DiHETE.[36] Thus, the porcine enzyme can generate LXB_4 by both triple oxygenation and the formation of a putative 14(15)-epoxytetraene. However, unlike the porcine leukocyte, human neutrophils do not possess a 12-LO, and when 5,15-DiHpETE was added to intact human platelets, which contain 12-LO, LXB_4 was not generated.[25] Nevertheless, the results obtained with purified 12-LO from porcine leukocytes have suggested a potential enzymatic route to LXB_4 biosynthesis with intriguing mechanistic implications which may be of importance during cell–cell interactions.

In addition to utilizing hydroxy- and hydroperoxy-containing compounds as substrates, LO's can also utilize epoxide-containing compounds as substrates for the generation of lipoxin precursors. The soybean 15-LO, for example, rapidly transforms LTA_4 into a 5,6-epoxytetraene,[39] suggesting that 15-lipoxygenation of LTA_4 could give rise to lipoxins in various cells.

The role of initial oxygenation of AA by 5-LO, followed by interactions with either 12-LO or 15-LO, has been explored in studies with intact human platelets,[39, 41] rat mesangial cells,[42] and neutrophils.[40] Studies with human platelet-derived 100 000g supernatants, which display 12-LO activity, indicate that this 12-LO can react with LTA_4. These results exemplified the 12-LO's ($\omega - 6$) oxygenase activity and provide a role for this enzyme in lipoxin formation[40] (Scheme 2). Together, the results obtained with isolated enzymes have illustrated potential mechanisms for lipoxin production, some of which may be utilized by specific cell types. Whether two or more of these routes can operate simultaneously in a given cell system remains of interest.

Table 1. Generation of lipoxins and related compounds by cell-free and isolated enzyme systems.

Enzyme	Source	Substrates	Products	Ref.
15-/12-Lipoxygenase	Rabbit reticulocytes/Soybean	(5*S*,15*S*)-DiHETE	Trihydroxytetraenes	[31]
15-/12-Lipoxygenase	Reticulocyte	(15*S*)-HETE, AA	Lipoxin B_4	[33] [34]
5-Lipoxygenase	Porcine leukocytes	(15*S*)-HpETE, (5*S*,15*S*)-DiHETE	5,6-Epoxytetraene	[35]
12-Lipoxygenase	Porcine leukocytes	(15*S*)-HpETE, (5*S*,15*S*)-DiHpETE	Lipoxin B_4	[36]
5-Lipoxygenase	Potato tubers	(15*S*)-HpETE/AA	Lipoxin A_4/ Lipoxin B_4	[37] [38]
15-Lipoxygenase	Soybean	Leukotriene A_4	5,6-Epoxytetraene	[39]
12-Lipoxygenase	Human platelets (100 000g supernates)	Leukotriene A_4	Lipoxin A_4	[40]
Epoxide hydrolase (cytosolic)	Human liver	5,6-Epoxytetraene	Lipoxin A_4	[26]

5. Cell Types Which Generate Lipoxins

Several species have now been shown to generate lipoxins from endogenous and/or exogenous sources of substrates (Table 2). The first published reports of lipoxin formation from endogenous sources of either C20:4 (AA) or C20:5 were introduced by *Wong* et al.[44] and *Lam* et al.,[45] who demonstrate that addition of an isolated PLA_2 isoenzyme to porcine leukocytes generates LXB_4 and its isomers. Furthermore, eosinophil-rich granulocyte suspensions from humans form LXA_4, which correlates with the number of eosinophils in the incubation.[46] Eosinophils also generate peptidolipoxins via the 5,6-epoxytetraene intermediate.[47] The biological significance and role of these new products is under investigation.

Lipoxins were also recently found to be the major lipoxygenase products of macrophages isolated from Rainbow trout exposed to A23187.[48] This finding represents the first

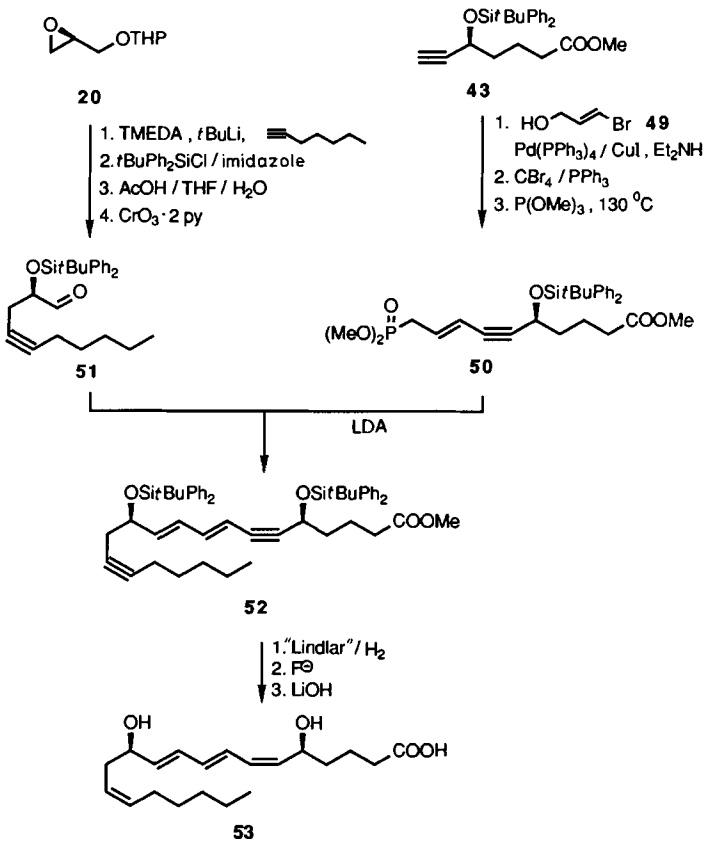

Scheme 11. Pd^0/Cu^I-catalyzed total synthesis of leukotriene B_4 (**53**). TMEDA = tetramethylethylendiamine, LDA = lithium diisopropylamide.

cidol THP ether **20** by epoxide opening with the lithio derivative of 1-heptyne, followed by silylation, removal of the THP group, and oxidation. Coupling of **50** and **51** under basic conditions furnished skeleton **52**, which was subjected to hydrogenation under Lindlar conditions to afford, after deprotection, leukotriene B_4 (**53**).

The acetylenic LTB_4 analogues **54** and **55** (Scheme 12) were also prepared from intermediate **52**. Similar chemistry

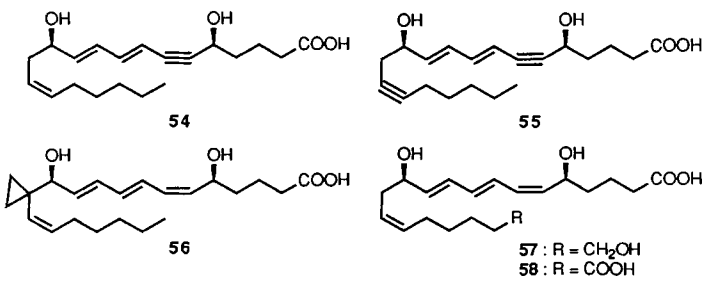

Scheme 12. Structures of synthesized leukotriene B_4 derivatives (**54–58**).

led to the ethano-substituted compound **56** and its dehydro analogues. These derivatives were targeted because replacing an allylic methylene group with a cyclopropyl moiety is a means of modulating the normal metabolism of arachidonic acid.[122]

The ω-oxidation products of LTB_4, 20-hydroxy- (**57**) and 20-carboxy- (**58**) leukotrienes B_4, are produced during the metabolism of LTB_4 (**53**) by human neutrophils. These molecules were also synthesized in enantiomerically pure forms following similar chemistry as described for LTB_4.[88]

A recent report from *Kobayashi*'s laboratories reported a highly practical route to LTB_4 by palladium-catalyzed coupling of vinyl iodide **59** with vinyl borane **60** (Scheme 13).[123]

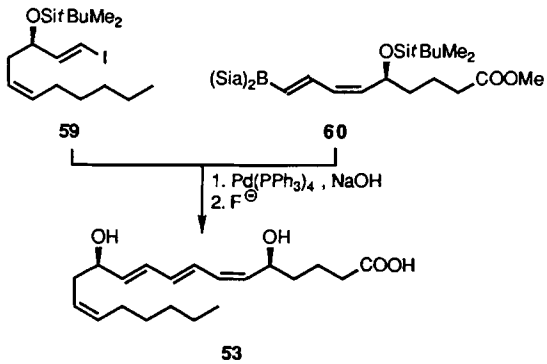

Scheme 13. Synthesis of LTB_4 (**53**) by *Kobayashi* et al. [123]. Sia = 1,2-dimethylpropyl (siamyl).

7.5. Synthesis of Lipoxins

As described in Sections 2 and 3, the basic structures assigned for the lipoxins were derived from biosynthetic considerations and degradation studies on isolated biological materials. These assignments were incomplete: configurations at C6 for lipoxin A_4 and C14 for lipoxin B_4 were not initially defined due to limited amounts of biologically derived materials. Moreover, the geometry of the double bonds at C11 of LXA_4 and C8 of LXB_4 needed to be confirmed.[7, 8] These stereochemical uncertainties, giving rise to several possible stereoisomers, dictated the design of a general and flexible strategy that would deliver each of these isomers stereoselectively and unambiguously for comparison and matching studies with natural samples and for biological evaluation. The Pd^0/Cu^I-based strategy that we had developed proved ideal for these targets. Indeed, we were able to synthesize a large number of isomeric lipoxin A[89–93] and lipoxin B[92–95] derivatives. With the availability of these compounds, and by the series of comparative studies with the natural materials discussed in Sections 2 and 3, we were able to assign the complete structures of both LXA_4 and LXB_4, as well as identify some additional naturally occurring isomers of this series.

Our syntheses of these compounds are outlined below. Other laboratories have also reported approaches to a number of these molecules.[28, 29, 78b, 124–127]

7.5.1. Synthesis of Lipoxin A_4 and Stereoisomers

Scheme 14 shows the retrosynthetic analysis of lipoxin A_4 (**61**) which led to intermediates **62**, **63**, and **64** as potential starting materials.[89] We anticipated that this strategy would generate sequentially a *cis* and a *trans* double bond

Lipoxins also exert unique actions on specific cell types (Table 5). LXA_4 elicits selective actions on human neutrophils,[8, 65–70] and recent results indicate that, in addition to inducing chemotaxis,[65] LXA_4 can also block both LTB_4- and FMLP-induced responses (i.e., LXA_4 blocks IP_3 generation and $Ca^{2\oplus}$ mobilization).[66, 67] Both LXA_4 and LXB_4 selectively stimulate lipid remodeling with neutrophils and release AA without stimulating LO activity.[68] LXA_4 and LXB_4 also display selective actions with natural killer cells blocking cytotoxicity,[71] while LXB_4 stimulates colony formation with human mononuclear cells.[61] In addition to its potential extracellular roles, LXA_4 may also have an intracellular role within its cell type of origin before its release to the extracellular environment. Thus, LXA_4 activates isolated protein kinase C (PKC) and is more potent than either diacylglyceride or native arachidonate.[73] The actions of LXA_4 appear to be more specific for the γ-subspecies of PKC, which is found in brain and spinal cord.[74] These events are of interest since PKC and its subspecies may play important roles in regulating cellular responses in a wide range of cell types including differentiation, cell proliferation, and hormone actions.

Table 5. Biological activities of lipoxins on individual cell types.

Bioassay	Compound	Response	Ref.
Human neutrophils	$LXA_4 > LXB_4$	Chemotaxis without aggregation	[65]
Human neutrophils	LXA_4	Inhibition of leukotriene and FMLP-induced chemotactic responses; i.e. blocks $Ca^{2\oplus}$ mobilization and IP_3 generation	[66, 67]
Human neutrophils	LXA_4 and LXB_4	Stimulation of lipid remodeling and release of AA without LO activation, $Ca^{2\oplus}$ mobilization or blocking of LTB_4 binding	[68]
Human neutrophils	5,6-epoxy-tetraene	Stimulation of mobilization of intracellular $Ca^{2\oplus}$	[70]
Human endothelial cells	LXA_4 and LXB_4	Stimulation of prostacyclin generation and release	[77]
Kidney mesangial cells	LXA_4	Inhibition of LTD_4-induced IP_3 generation and LTD_4 binding	[57]
Human mononuclear cells	LXB_4	Stimulation of colony formation in diffusion chambers	[72]
Human natural killer cells	LXA_4 and LXB_4	Blocking of cytotoxicity without altering target-cell binding	[71]
Protein kinase C (PKC) from human placenta	LXA_4	Activation of phosphorylation in the presence of $Ca^{2\oplus}$ and selection of substrate specificity	[73]
PKC-γ-subspecies bovine cerebellum	LXA_4	Selective activation	[74]

Results to date indicate that lipoxins can be generated by several biosynthetic routes, which can include lipoxygenase as well as cell–cell interactions. Both LXA_4 and LXB_4 carry selective biological activities in both in vivo and vitro systems, which suggests that they may be involved in regulating cellular responses of interest in inflammation and host defense. Future studies will clarify whether the lipoxins can inhibit or regulate the signs of inflammation in specific disease models.

7. Chemical Synthesis

Since the lipoxins, like other eicosanoids, were isolated from natural sources only in small quantities, the chemical synthesis of these molecules played a key role in the determination of their stereochemistry and allowed a systematic investigation of their biological properties and function. Because of the need to identify the naturally occurring stereoisomers and the desire to compare the biological activities of the various isomers, a flexible synthetic plan that would deliver a maximum number of isomers was sought.

The synthetic challenges posed by the lipoxins and other acyclic eicosanoids, such as the various mono- and dihydroxyeicosatetraenoic acids (HETE's, LTB_4, other DiHETE's) are twofold. Firstly, the eicosanoid skeleton with the correct double-bond geometries must be constructed, and secondly the proper stereochemistry of the hydroxyl-bearing stereocenters must be secured. The carbon skeleton of these polyunsaturated systems has often been assembled by Wittig-type C=C bond-forming reactions. We have designed an alternative general strategy based on a C–C bond-forming process involving palladium-catalyzed coupling of vinyl precursors. The stereochemical control at the various hydroxylated positions of these target molecules can be accomplished by using starting materials from the chiral pool, such as 2-deoxyribose or lactic acid. Our approach, however, relied heavily on the Sharpless asymmetric epoxidation reaction, which provides a highly flexible method for the preparation of a number of stereoisomers with high and predictable enantioselectivity. In this manner, we were able to synthesize a large number of frameworks with varying chirality.

In this section we review aspects of the inception, evolution, and application of our strategy to the total synthesis of a variety of natural and designed eicosanoids. Other approaches to these molecules developed elsewhere,[78] mainly by the groups of *E. J. Corey* and a group at Merck-Frosst, are not discussed.

7.1. The Palladium Catalysis Strategy

The evolution of our general strategy towards acyclic eicosanoids had its origin in the proposed biosynthetic mechanism involved in the formation of these naturally occurring molecules. According to this mechanism, an ($\alpha Z,\delta Z$)-pentadiene system (**1**) of arachidonic or related skeleton is converted by lipoxygenases and molecular oxygen via **2** into a conjugated (*Z,E*)-diene system (**3**) as shown in Scheme 3. It occurred to us, therefore, that focusing on a stereocontrolled and efficient construction of the framework of **3** may provide a general entry into this class of compounds.

The key retrosynthetic disconnection of our approach to **3** involved the formation of the middle C–C bond by Pd catalysis. Formation of **3** through selective hydrogenation of **4** allows the synthesis of this system by Pd^0/Cu^I coupling[79] of a terminal alkyne (**5**) and a vinyl bromide (**6**). Alternatively, direct construction of **3** is possible by using the Suzuki coupling reaction[80] of a vinyl iodide (**7**) and a vinyl boron derivative (**8**). For this purpose we utilized *Kishi*'s modification[81] of this process, involving Pd^0/TlOH catalysis. The central functionality in our construction of the polyunsaturated carbon frameworks was the alkyne moiety, which could be used as a precursor to a *Z*-olefin by serving as a coupling partner, or it could be converted stereoselectively

into the required vinyl derivatives **6**, **7**, or **8**. This feature of our strategy allowed the economical and expeditious preparation of a variety of desired intermediates. This synthetic planning had the flexibility to deliver a variety of skeletons by using a library of common intermediates and reactions. We have synthesized several types of acyclic eico-

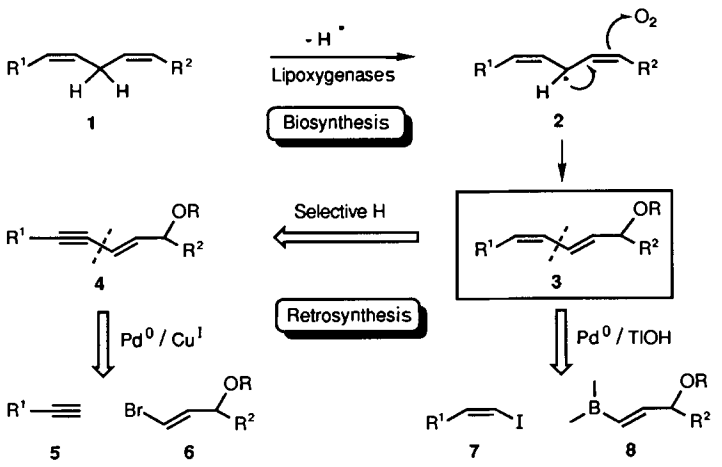

Scheme 3. Biosynthesis and retrosynthesis of acyclic eicosanoids. Here and in the following schemes, the R–C≡C–R′ units are often bent in order that the alkyne intermediates pictorially resemble the desired alkenes.

sanoids with this method, including monohydroxyicosatetraenoic acids (HETE's),[82–84] dihydroxy compounds (DiHETE's),[85, 86] leukotrienes B,[87, 88] lipoxins A,[89–93] and lipoxins B.[92–95]

7.2. Synthesis of Monohydroxyicosatetraenoic Acids (HETE's)

Several HETE's derived from the action of lipoxygenases on arachidonic acid have been identified. The main isomers are the 5-, 12- and 15-HETE's, while other isomers that have been isolated include the 8-, 9-, 11-, 19- and 20-HETE's. While a number of biological activities have been associated with these compounds, they also serve as precursors to a large number of other metabolites, such as several isomeric dihydroxy derivatives (DiHETE's), and some more highly oxygenated products. The isolation, structure elucidation, and biological properties of HETE's have recently been reviewed.[96] As outlined below, we have targeted a number of these acyclic eicosanoids.

(5*S*)-HETE: Several syntheses of 5-HETE (**15**) have been reported.[97–102] Our total synthesis of the (5*S*) enantiomer (Scheme 4)[82] involved the Pd^0/Cu^I strategy. The synthesis began with the diacetylene **9** which was coupled with allylic bromide **10**, and the resulting derivative **11** was selectively hydrogenated at the internal triple bond without interference from the silicon-bearing triple bond. After desilylation, the resulting alkyne with a terminal triple bond (**12**) was coupled with vinyl bromide (**13**, the synthesis analogous to that for the Ph_2tBuSi derivative is described in Scheme 9) under standard Pd^0/Cu^I conditions to afford skeleton **14**, which was again selectively reduced under Lindlar conditions leading,

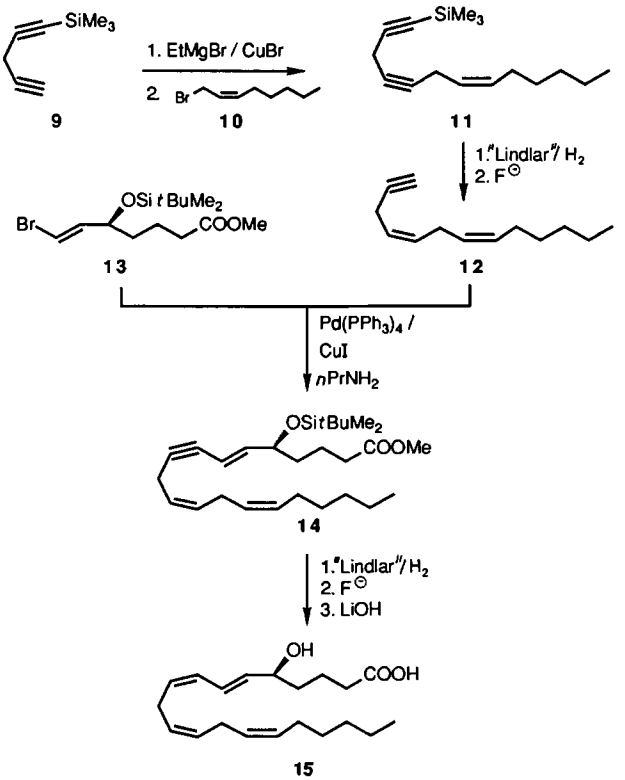

Scheme 4. Pd^0/Cu^I-catalyzed total synthesis of (5*S*)-HETE (**15**). "Lindlar" represents a palladium catalyst poisoned with lead as described by *Lindlar*.

after deprotection, to (5*S*)-HETE (**15**) in excellent overall yield (18%).

(12*S*)-HETE: A number of synthetic routes to both racemic and enantiomerically pure (12*S*)-HETE (**19**), the major product of 12-LO, have been accomplished.[103–109] We have devised stereocontrolled sequences to both enantiomers of this molecule. For the synthesis of (12*S*)-HETE (**19**) we utilized the standard strategy based on Pd^0/Cu^I coupling of vinyl bromide **16** and alkyne **17**, followed by mild hydrogenation of **18** and deprotection (Scheme 5).[82]

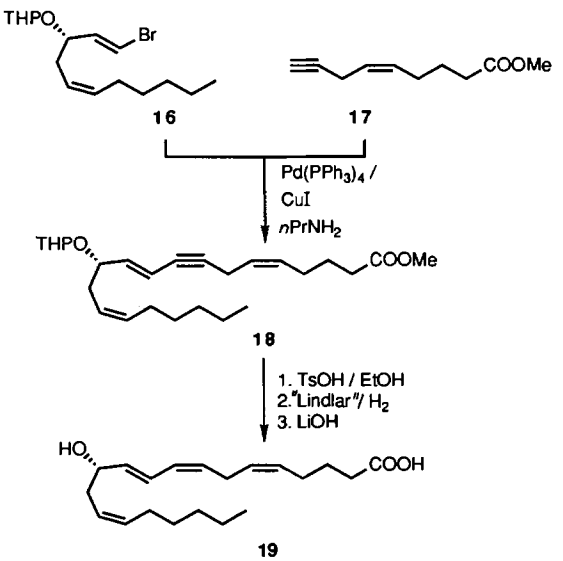

Scheme 5. Pd^0/Cu^I-catalyzed total synthesis of (12*S*)-HETE (**19**). THP = tetrahydropyranyl.

(12*R*)-HETE: This enantiomer (**25**), which can be generated by the action of the cytochrome P450 system on arachidonic acid, was also synthesized in these laboratories recently.[83] This synthesis was based on the Pd^0/TlOH-catalyzed coupling of vinyl boranes and vinyl halides. The strategy (Scheme 6) eliminates the need for selective reduction of C≡C bonds after the coupling step, and was also employed by us in the synthesis of (12*S*)-hydroxy-(5*Z*,8*E*,10*E*)-heptadecatrienoic acid (HHT),[110] a major metabolite of arachidonate. Thus, the enantiomerically pure epoxide **20**

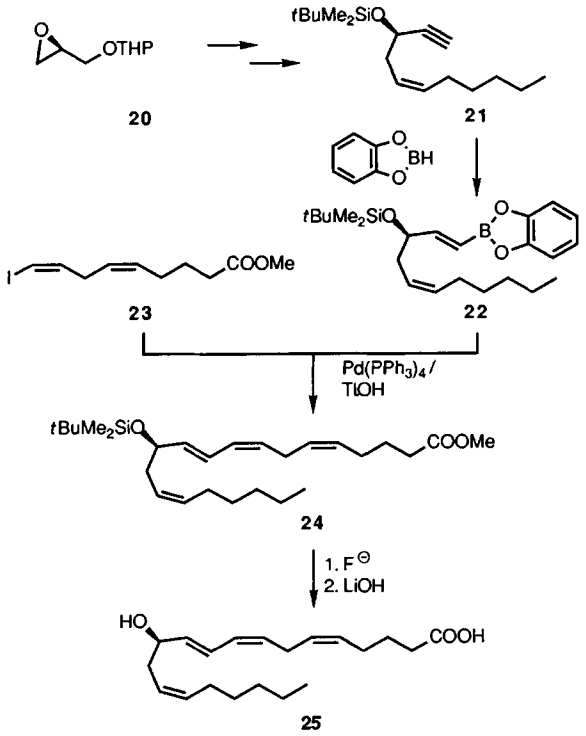

Scheme 6. Pd^0/Cu^I-catalyzed total synthesis of (12*R*)-HETE (**25**).

was converted into acetylenic derivative **21**, which was reacted with catechol borane to give the vinyl borane **22**. Coupling of **22** with vinyl iodide **23** using *Kishi*'s palladium(0)/thallium hydroxide method[81] directly afforded **24**. Finally, deprotection of **24** led to the targeted (12*R*)-HETE (**25**).

(15*S*)-HETE: The key step in our synthesis[84] of (15*S*)-HETE (**29**) (Scheme 7) was the coupling of acetylenic ester **26** with vinyl bromide **27** (for the synthesis see Scheme 9) under the Pd^0/Cu^I conditions to afford the desired skeleton **28**. Lindlar hydrogenation of **28** followed by deprotection led to (15*S*)-HETE (**29**) in high overall yield (63%). Other syntheses of this molecule have also been reported.[111, 112]

7.3. Synthesis of Dihydroxyicosatetraenoic Acids (DiHETE's)

Several naturally occurring DiHETE's have been identified which are formed either by the action of two lipoxygenases or by the hydrolysis of epoxide intermediates.

(5*S*,6*R*)-DiHETE: This is a biologically active metabolite of arachidonic acid derived from leukotriene A_4 (LTA_4,

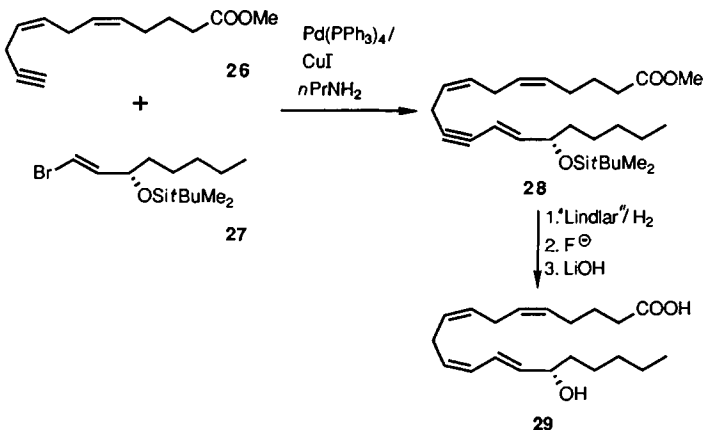

Scheme 7. Pd^0/Cu^I-catalyzed total synthesis of (15*S*)-HETE (**29**).

Scheme 1) by regio- and stereoselective enzymatic hydrolysis. Nonenzymatic hydrolysis of LTA_4 leads to a mixture of (5*S*,6*R*) and (5*S*,6*S*) isomers. In order to render these and other isomers readily available for biological studies and to compare their actions with those of lipoxin A_4, we synthesized all four 5,6-isomeric DiHETE methyl esters.[86] The synthesis of (5*S*,6*R*)-DiHETE methyl ester (**36**) is shown in Scheme 8.[86] Coupling of vinyl iodide **30** with (trimethylsilyl)acetylene assisted by $Pd(PPh_3)_4$/CuI catalysis, followed

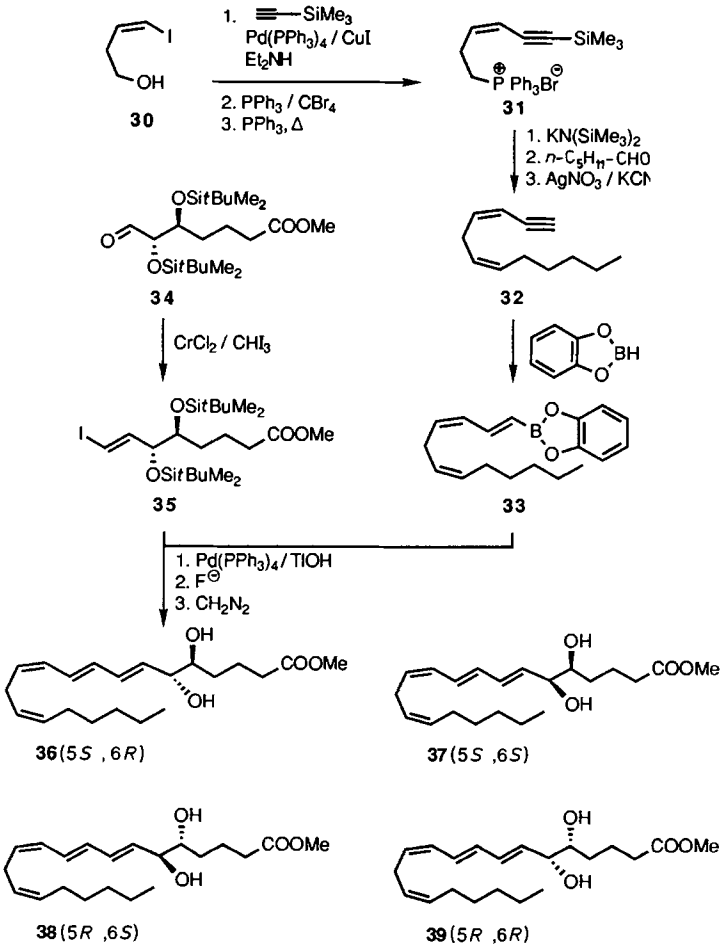

Scheme 8. Pd^0/Tl^IOH-catalyzed total synthesis of the (5*S*,6*R*)-diHETE methyl ester (**36**) and related compounds **37**–**39**.

by conversion of the alcohol into a bromide, and phosphonium salt formation, furnished compound **31** which was extended to acetylene **32** through a Wittig reaction. The vinyl borane **33** was then formed regioselectively and was coupled to vinyl iodide **35** under the usual conditions to afford, after functional group manipulation, the requisite (5*S*,6*R*)-DiHETE (**36**). The coupling partner **35** was prepared from aldehyde **34** (for synthesis see Scheme 14) by the action of $CrCl_2$ and CHI_3, according to the method of *Takai* et al.[113] Starting with the appropriate isomeric vinyl iodides and following similar chemistry as for **36**, (5*S*,6*S*)-**37**, (5*R*,6*S*)-**38**, and (5*R*,6*R*)-**39** DiHETE methyl esters were also prepared. A conceptually different synthesis of 5,6-DiHETE was reported by *Adams* et al.[29]

(5*S*,15*S*)-DiHETE: The interesting dihydroxylated arachidonic acid metabolite (5*S*,15*S*)-dihydroxy-(6*E*,8*Z*,11*Z*,13*E*)-icosatetraenoic acid (**45**) was the first linear eicosanoid to be synthesized by the Pd^0/Cu^I technology in these laboratories.[84] Its two *Z*,*E* diene systems provided two strategic disconnections that allowed its facile construction as summarized in Scheme 9. Thus, the key vinyl bromides **27** and **13′**, the Ph_2-substituted analogue of **13**, were synthesized from the protected acetylenic alcohols **40** and **43** (derived by enantioselective reduction of **42**) by tri-*n*-butyltin hydride addition and brominolysis. Coupling of **27** with the monoprotected α,ω-diyne **9** under the influence of Pd^0/Cu^I catalysis, followed by desilylation and a second coupling with vinyl bromide **13′** under the same conditions, led quickly to the desired skeleton **44** in high yield (62%). Lindlar hydrogenation of **44** followed by desilylation and ester hydrolysis afforded **45**, whereas deprotection of **44** allowed the formation of the novel 8,9,11,12-tetradehydro analogue of **45**.[84] *Fitzsimmons* and *Rokach*[114] have also reported the synthesis of **45**.

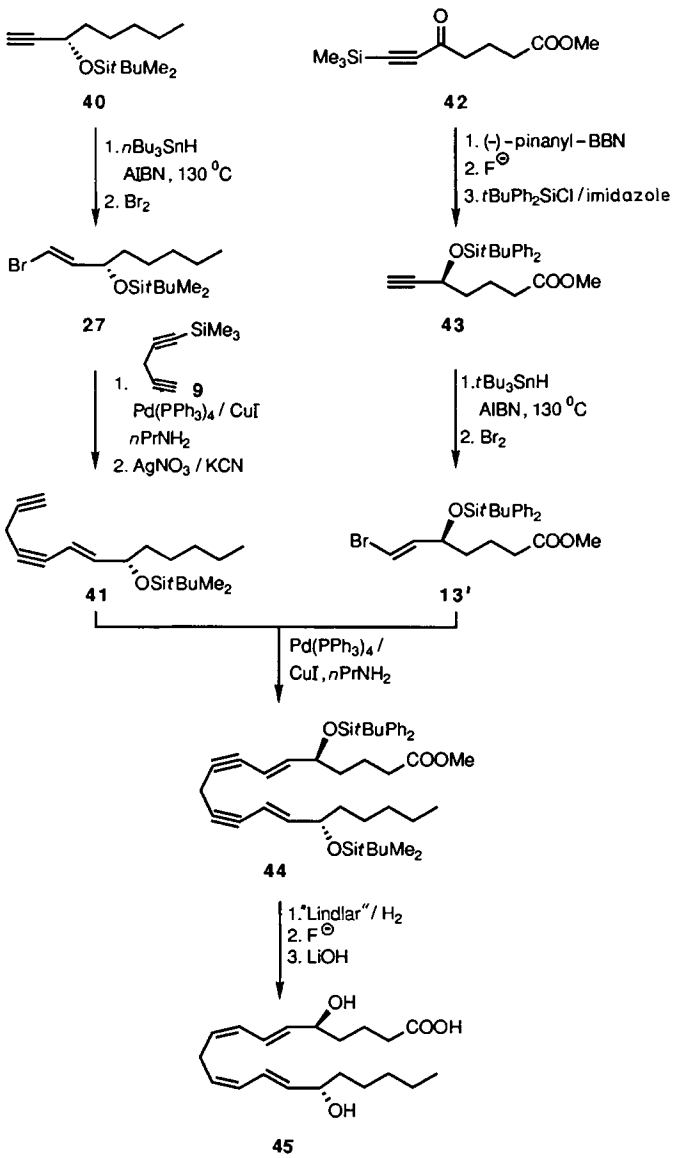

Scheme 9. Pd^0/Cu^I-catalyzed total synthesis of (5*S*,15*S*)-DiHETE (**45**). AIBN = azodiisobutyronitrile; BBN = 9-borabicyclononane.

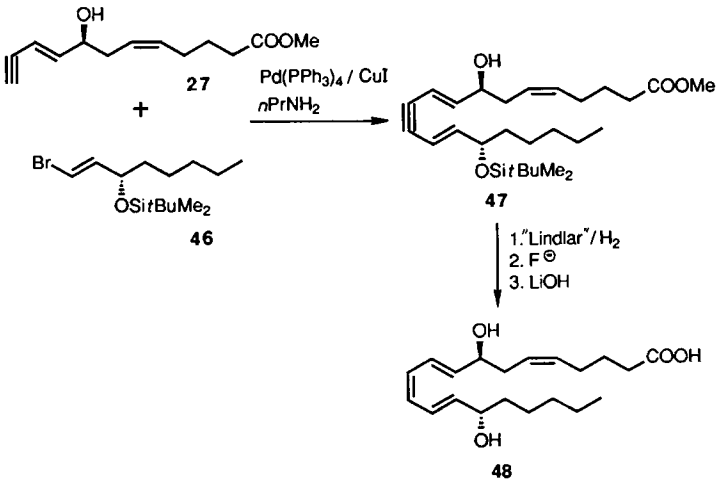

Scheme 10. Pd^0/Cu^I-catalyzed total synthesis of (8*S*,15*S*)-DiHETE (**48**).

(8*S*,15*S*)-DiHETE: The naturally occurring (8*S*,15*S*)-DiHETE (**48**) was synthesized in a stereocontrolled manner through the standard Pd^0/Cu^I coupling step between alkyne derivative **46** and vinyl bromide **27** as shown in Scheme 10.[85] Lindlar hydrogenation of the resulting **47** followed by desilylation and saponification gave **48** in high overall yield (66%). The 11,12-didehydro analogue of **48** was also generated from **47** by standard deprotection techniques.[85]

7.4. Synthesis of Leukotriene B_4 and Derivatives

One DiHETE of particular interest that has been studied extensively is leukotriene B_4 (LTB_4, **53**), derived from the enzymatic hydrolysis of the epoxide-bearing leukotriene A_4 (see Scheme 1). A number of synthetic approaches to this compound, an important chemotactic agent, have been developed at various laboratories.[78,115-121] Our synthesis of this molecule is indicated in Scheme 11.[87] Thus, Pd^0/Cu^I-catalyzed coupling of **43** (see Scheme 9) with vinyl bromide **49** followed by allylic bromide formation and Arbuzov reaction with trimethyl phosphite gave the key phosphonate **50**. This intermediate served as the C_1–C_{10} fragment for the synthesis of LTB_4 and several structural analogues. The other requisite key intermediate **51** was prepared from (*R*)-gly-

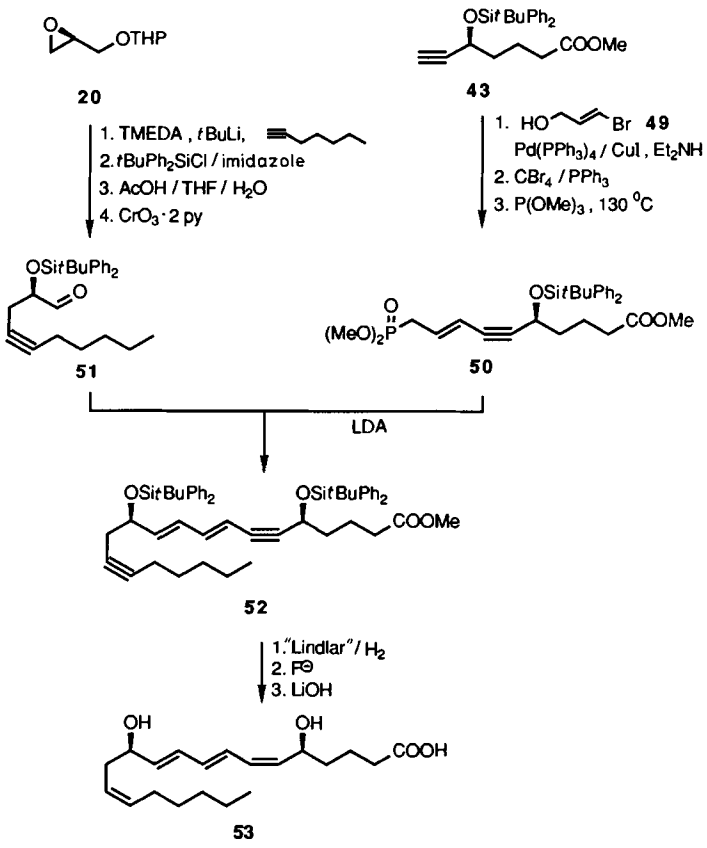

Scheme 11. Pd^0/Cu^I-catalyzed total synthesis of leukotriene B_4 (**53**). TMEDA = tetramethylethylendiamine, LDA = lithium diisopropylamide.

cidol THP ether **20** by epoxide opening with the lithio derivative of 1-heptyne, followed by silylation, removal of the THP group, and oxidation. Coupling of **50** and **51** under basic conditions furnished skeleton **52**, which was subjected to hydrogenation under Lindlar conditions to afford, after deprotection, leukotriene B_4 (**53**).

The acetylenic LTB_4 analogues **54** and **55** (Scheme 12) were also prepared from intermediate **52**. Similar chemistry

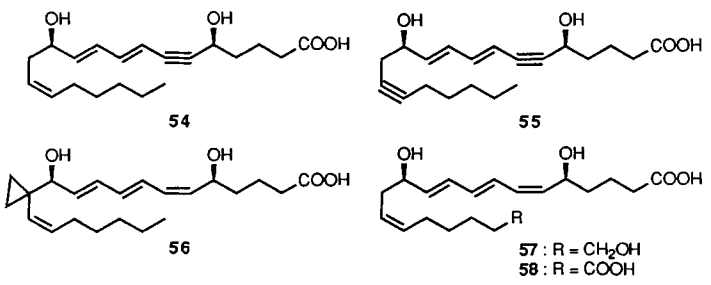

Scheme 12. Structures of synthesized leukotriene B_4 derivatives (**54–58**).

led to the ethano-substituted compound **56** and its dehydro analogues. These derivatives were targeted because replacing an allylic methylene group with a cyclopropyl moiety is a means of modulating the normal metabolism of arachidonic acid.[122]

The ω-oxidation products of LTB_4, 20-hydroxy- (**57**) and 20-carboxy- (**58**) leukotrienes B_4, are produced during the metabolism of LTB_4 (**53**) by human neutrophils. These molecules were also synthesized in enantiomerically pure forms following similar chemistry as described for LTB_4.[88]

A recent report from *Kobayashi*'s laboratories reported a highly practical route to LTB_4 by palladium-catalyzed coupling of vinyl iodide **59** with vinyl borane **60** (Scheme 13).[123]

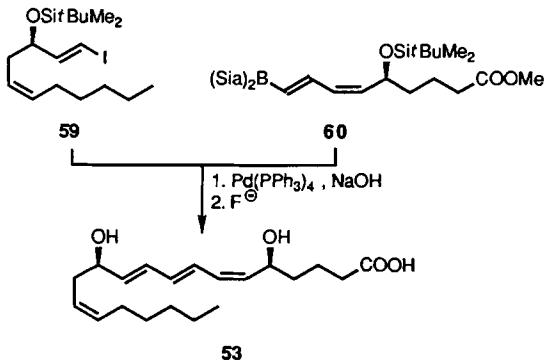

Scheme 13. Synthesis of LTB_4 (**53**) by *Kobayashi* et al. [123]. Sia = 1,2-dimethylpropyl (siamyl).

7.5. Synthesis of Lipoxins

As described in Sections 2 and 3, the basic structures assigned for the lipoxins were derived from biosynthetic considerations and degradation studies on isolated biological materials. These assignments were incomplete: configurations at C6 for lipoxin A_4 and C14 for lipoxin B_4 were not initially defined due to limited amounts of biologically derived materials. Moreover, the geometry of the double bonds at C11 of LXA_4 and C8 of LXB_4 needed to be confirmed.[7, 8] These stereochemical uncertainties, giving rise to several possible stereoisomers, dictated the design of a general and flexible strategy that would deliver each of these isomers stereoselectively and unambiguously for comparison and matching studies with natural samples and for biological evaluation. The Pd^0/Cu^I-based strategy that we had developed proved ideal for these targets. Indeed, we were able to synthesize a large number of isomeric lipoxin A[89–93] and lipoxin B[92–95] derivatives. With the availability of these compounds, and by the series of comparative studies with the natural materials discussed in Sections 2 and 3, we were able to assign the complete structures of both LXA_4 and LXB_4, as well as identify some additional naturally occurring isomers of this series.

Our syntheses of these compounds are outlined below. Other laboratories have also reported approaches to a number of these molecules.[28, 29, 78b, 124–127]

7.5.1. Synthesis of Lipoxin A_4 and Stereoisomers

Scheme 14 shows the retrosynthetic analysis of lipoxin A_4 (**61**) which led to intermediates **62**, **63**, and **64** as potential starting materials.[89] We anticipated that this strategy would generate sequentially a *cis* and a *trans* double bond

between C11 and C12 in the final structure. Furthermore the Sharpless asymmetric epoxidation procedure could be applied to obtain all four possible stereoisomers of fragment **64** by varying the double-bond geometry of the allylic alcohol precursor and the absolute configuration of the chiral auxiliary.

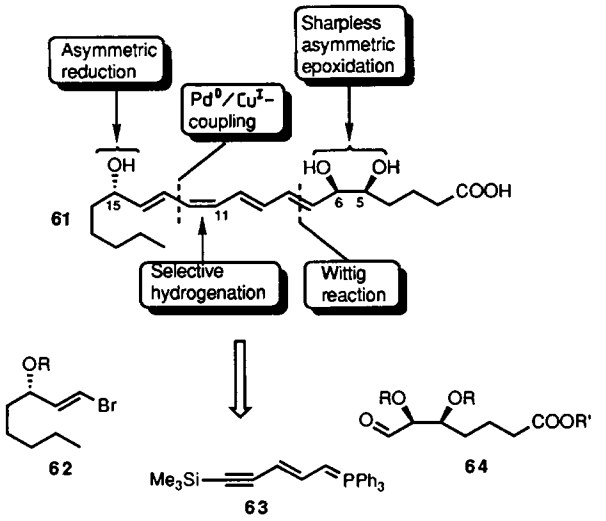

Scheme 14. Retrosynthetic analysis of lipoxin A_4 (**61**).

The total synthesis of (5*S*,6*R*,15*S*) lipoxin A_4 (**61**) and its all-*trans* isomer (**74**) summarized in Scheme 15 exemplifies the strategy for the synthesis of the lipoxin A_4 series.[89] Scheme 15 shows the construction of the requisite fragments **34** and **69** or **70** in pure forms by well-known methodology and depicts the key coupling reactions and final elaborations leading to the target molecules. Thus, coupling of the phosphorane derived from phosphonium salt **69** with aldehyde **34** led, in excellent yield (98%), to a mixture of *E* and *Z* products **71** and **72** (ca. 1:1 ratio), whereas coupling with the anion of the phosphonate **70** led to a lower *E*:*Z* ratio (ca. 1:3). The *Z* isomer **72** was, however, easily isomerized to the *E* compound (ca. 11:1 equilibrium mixture) with catalytic amounts of iodine. Pure **71** was then coupled with vinyl bromide **27** (see Scheme 9) under the standard Pd^0/Cu^I conditions to afford in excellent overall yield (80%) after desilylation, the basic lipoxin skeleton **73**. Although this compound was obtained as a 1:1 mixture with the δ-lactone formed by intramolecular transesterification, the latter could be converted into **73** upon hydrolysis and diazomethane treatment. Compound **73** was easily converted into lipoxin A_4 (**61**) by Lindlar hydrogenation and hydrolysis. The isomeric all-*trans* LXA_4 (**74**) was synthesized by hydrogenation of **73** followed by olefin isomerization with iodine and ester hydrolysis. In a similar manner we have also synthesized 19,19,20,20,20-pentadeuterio-LXA_4,[91] in an effort to aid the quantitative detection of eicosanoid **61** by GC-MS.

Biosynthetic studies using synthetic lipoxin epoxide (vide infra) and (15*S*)-HETE revealed the generation of additional compounds that contained the basic lipoxin structure (e.g. trihydroxytetraenes). In order to aid in the complete stereochemical assignment of these structures, as well as to make

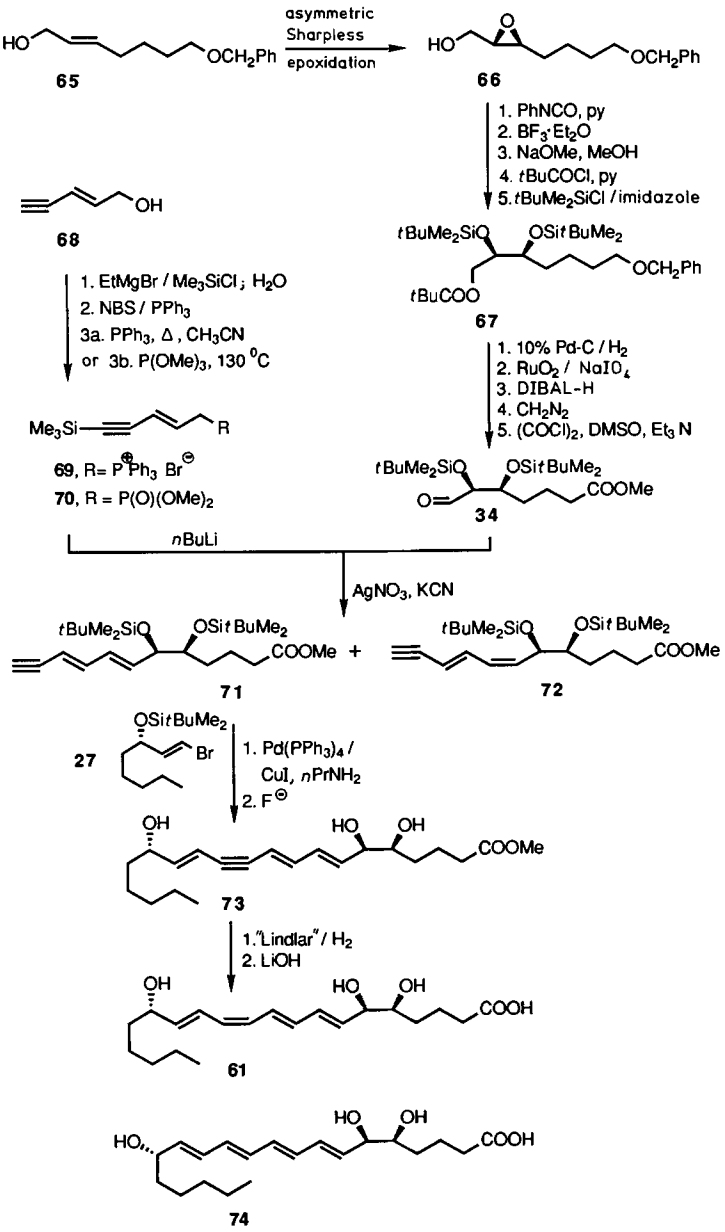

Scheme 15. Pd^0/Cu^I-catalyzed total synthesis of lipoxin A_4 (**61**) and 11-*trans*-LXA_4 (**74**). DIBAL-H = diisobutylaluminium hydride, DMSO = dimethyl sulfoxide.

them available for further biological studies, we targeted a number of stereoisomers of lipoxin A_4[92] which retain the (15*S*) stereochemistry of LXA_4 but differ from the original lipoxins in the geometry of the tetraene system and the stereochemistry at C5 or C6 or both. The construction of these new lipoxins was based on our general strategy towards linear eicosanoids described above, in which both the absolute stereochemistry of the stereogenic centers and the geometry of the double bonds is controlled. The powerful Pd^0/Cu^I-catalyzed coupling reaction between compounds with terminal triple bonds and vinyl halides features heavily in these syntheses. The Sharpless asymmetric epoxidation was also used to prepare, in optically active form, the diol moieties in these systems. The isomers synthesized (**75**–**80**) are shown in Scheme 16. Comparison of these synthetic compounds with biologically derived materials established[50] the complete

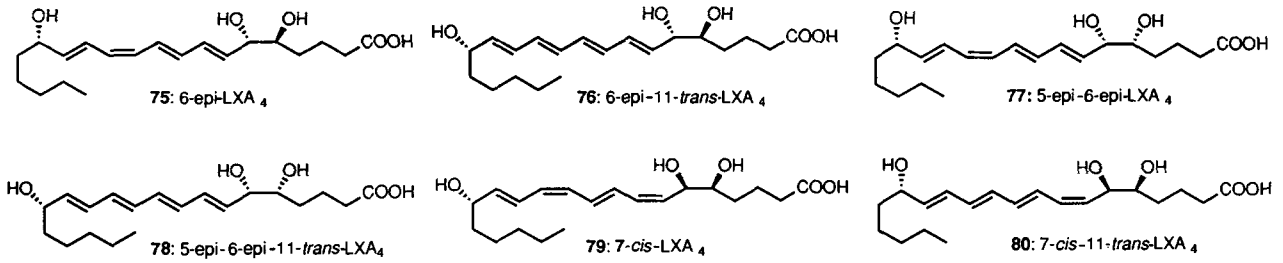

Scheme 16. Structures of synthesized lipoxin A_4 stereoisomers.

molecular structure of a new, naturally occurring lipoxin A_4, namely 7-*cis*-11-*trans*-lipoxin A_4, (**80**). Furthermore, the availability of these stereoisomers has already provided additional evidence for the high degree of stereospecificity involved in evoking biological responses by lipoxins.

7.5.2. *Total Synthesis of Lipoxin B_4 and Stereoisomers*

Biogenetic considerations and structural studies left the issues of geometry at C8 and of configuration at C14 of lipoxin B_4 (**81**) as the main stereochemical questions to be resolved. We therefore designed our strategy for the total synthesis of this molecule with the flexibility to vary these parameters.[94, 95] Scheme 17 presents the overall retrosynthetic analysis for this target and its isomers. The expectation

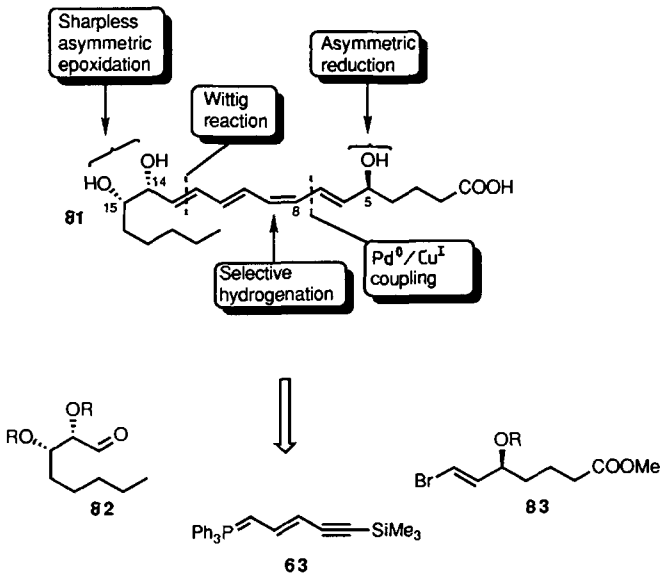

Scheme 17. Retrosynthetic analysis of lipoxin B_4 (**81**).

of a facile isomerization of an 8*Z* to an 8*E* double bond led us to target the 8*Z* isomers as the initial goals. Furthermore, the Sharpless asymmetric epoxidation reaction was expected to provide the necessary flexibility for preparing the requisite hydroxy compounds as well as other isomers for biological evaluation. The desired stereochemistry at C5 was to be secured by asymmetric reduction of a carbonyl function, whereas the 8*Z* geometry was expected from a selective Lindlar-type reduction. Finally, the key coupling reactions chosen to construct the lipoxin B skeleton were based on Wittig and Pd^0/Cu^I technologies as previously demonstrated in these laboratories.

The synthesis of the lipoxin B_4 and other members of this series[94, 95] (Scheme 18) began with the allylic alcohol **84** which, upon Sharpless asymmetric epoxidation, gave **85** which was in turn converted into triol **86** via urethane forma-

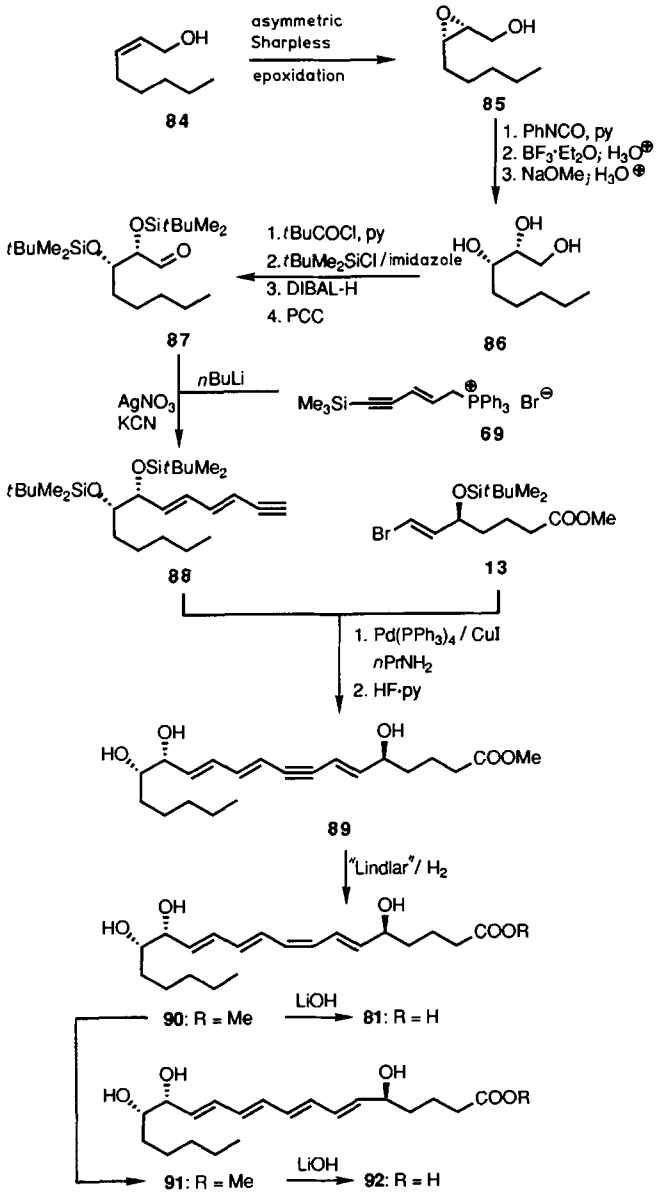

Scheme 18. Pd^0/Cu^I-catalyzed total synthesis of lipoxin B_4 (**81**) and 8-*trans*-LXB_4 (**92**). PCC = pyridinium chlorochromate.

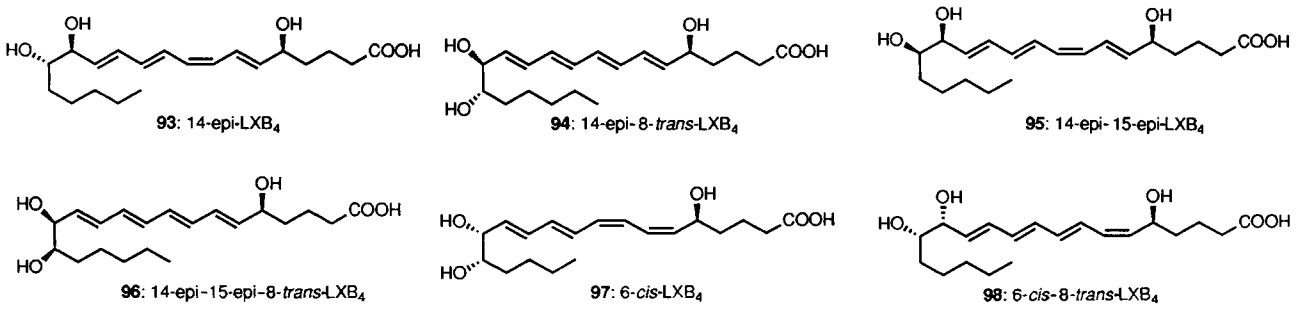

Scheme 19. Structures of the synthesized lipoxin B_4 stereoisomers.

tion and rearrangement. Standard chemical manipulations converted **86** into aldehyde **87**, which was condensed with the phosphorane derived from **69** to afford alkyne **88** together with its *cis* isomer (ca. 1:1 ratio). The *cis* isomer was isomerized by catalytic amounts of iodine to the *trans* compound (*trans*:*cis* ≈ 11:1 at equilibrium), and **88** coupled to the vinyl bromide **13** under the standard Pd^0/Cu^I conditions. Treatment of the resulting compound with HF · py gave a mixture of the LXB skeleton **89** and the corresponding δ-lactone (ca. 2:1 ratio), which was easily converted into **89** by saponification and methylation with diazomethane. Finally, Lindlar hydrogenation of **89** afforded lipoxin B_4 methyl ester (**90**) from which lipoxin B_4 itself (**81**) was generated in high yield (90%). In addition, **90** was isomerized to the all-*trans* lipoxin B_4 methyl ester **91**, which was hydrolyzed to the carboxylic acid **92**.

As discussed in Section 7.5.1 for LXA_4, it was desirable to obtain isomers of LXB_4 which retained the (5*S*) stereochemistry but varied the geometry of the olefinic bonds and the stereochemistry at the other hydroxyl-bearing stereocenters. Therefore, starting with the *E* isomer of alcohol **84** and utilizing (+)- or (−)-diethyl tartrate, we synthesized the LXB_4 isomers **93**–**98**, shown in Scheme 19, by modifications of the general strategy.[95]

7.5.3. *Total Synthesis of Lipoxins A_5 and B_5*

The isolation of lipoxins A_5 (LXA_5, 5,6,15-trihydroxy-7,9,11,13,17-icosapentaenoic acid) and B_5 (LXB_5, 5,14,15-trihydroxy-6,8,10,12,17-icosapentaenoic acid) by *Wong* et al.[128] prompted us to design and execute a stereocontrolled total synthesis of the suspected isomers (by analogy to LXA_4 and LXB_4). The targeted isomers were (5*S*,6*R*,15*S*)-trihydroxy-(7*E*,9*E*,11*Z*,13*E*,17*Z*)-icosapentaenoic acid and (5*S*,14*R*,15*S*)-trihydroxy-(6*E*,8*Z*,10*E*,12*E*,17*Z*)-icosapentaenoic acid.

The synthetic sequences were based upon the Pd^0/Cu^I-catalyzed strategy.[93] Scheme 20 summarizes the synthesis of LXA_5 starting with the readily available (*R*)-epoxyalcohol derivative **99**. Thus, 1-lithiobutyne reacted with **99** in the presence of TMEDA to afford, after Lindlar hydrogenation, silylation, and depyranylation, the *cis* olefin **100** in high overall yield (65%). Oxidation of **100**, followed by reaction with $CrCl_2/CHI_3$,[113] led to the vinyl iodide **101**. Coupling of **101** with the alkyne **71** (see Scheme 15) under the standard Pd^0/Cu^I conditions gave, after exposure to HF · py, a mixture of 11,12-didehydro lipoxin A_5 methyl ester **102**, and the corresponding δ-lactone. The latter compound was converted into **102** by treatment with methanol and triethylamine. Selective hydrogenation of **102** using Lindlar catalyst gave lipoxin A_5 methyl ester (**103**), together with small amounts of its 11-*trans* isomer (**105**). Compound **103** isomerized slowly at ambient temperatures to its *trans* isomer **105**, a process that was accelerated by catalytic amounts of iodine. Alkaline hydrolysis of **103** and **105** generated lipoxin A_5 (**104**) and its 11-*trans* isomer (**106**) respectively.

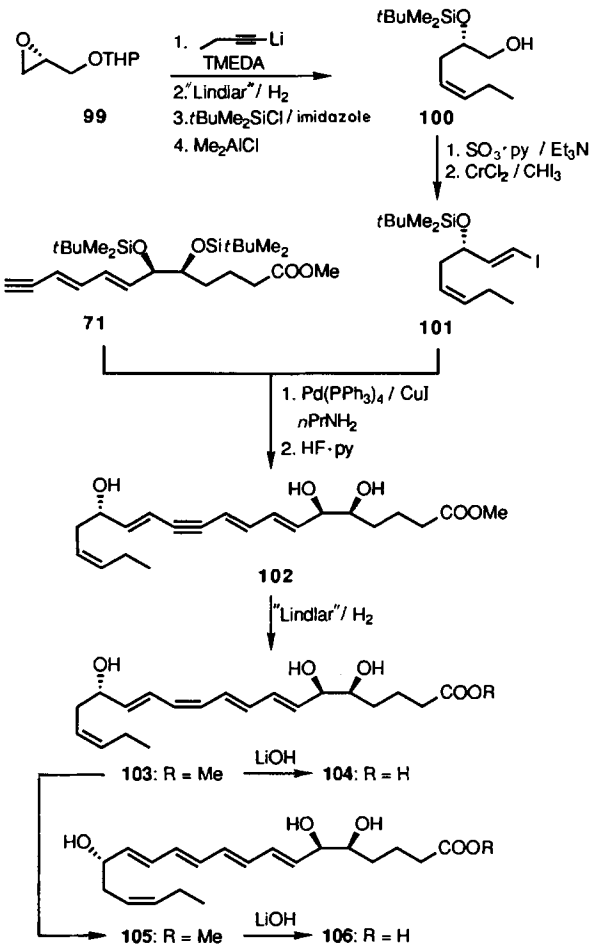

Scheme 20. Pd^0/Cu^I-catalyzed total synthesis of lipoxin A_5 (**104**) and 11-*trans*-LXA_5 (**106**).

The synthesis of lipoxin B_5 (**114**)[93] (Scheme 21) utilized the readily available epoxide **107**, phosphonate **70**, and vinyl bromide **13** as starting materials. The chemistry proceeded for the most part along similar lines as described for LXA_5 and LXB_4 with the three key coupling reactions: epoxide

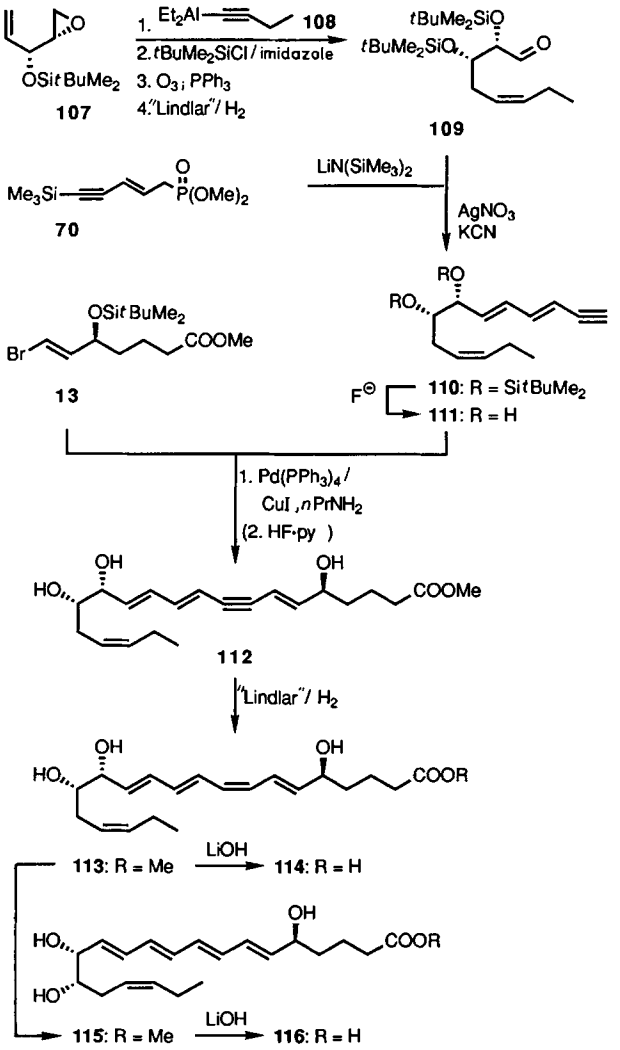

Scheme 21. Pd^0/Cu^I-catalyzed total synthesis of lipoxin (**114**) and 8-*trans*-LXB_5 (**116**).

opening of **107** with **108**, condensation of phosphonate **70** with **109**, and Pd^0/Cu^I-catalyzed coupling of **110** (or **111**) with **13** to give compound **112**. Ester **113** and then LXB_5 (**114**) were then formed as usual. The corresponding 8-*trans*-LXB_5 **116** was also generated from **113** through isomerization and alkaline hydrolysis of **115**.

7.5.4. Total Synthesis of the 5,6-Epoxytetraene, the Biosynthetic Precursor to Lipoxins A_4 and B_4, and Its 5,6-Methano Analogue

The early proposition of (15*S*)-hydroxy-(5*S*,6*S*)-epoxy-(7*E*,9*E*,11*Z*,13*E*)-icosatetraenoic acid as precursor to lipoxins A_4 and B_4 suggested this compound (see Scheme 2) as a synthetic target. Scheme 22 outlines the synthesis of the methyl ester of this epoxide (**122**) in enantiomerically pure form.[90] Thus, Pd^0/Cu^I-catalyzed coupling of the vinyl bromide **27** (see Scheme 9) with the alkynyl alcohol **68** proceeded smoothly to afford, after bromination and phosphonate formation, the key phosphonate intermediate **117**. Condensation of the lithio derivative of **117** with aldehyde **118** gave a 3:1 mixture of 7*E* and 7*Z* isomers of coupling product, which was converted into a 9:1 mixture by treatment with catalytic amounts of iodine. Difficulties with the reduction of the triple bond of this product necessitated the exchange of the silyl protecting group for an acetate to afford compound **120**. Purified **120** was successfully converted into the targeted compound **122** by Lindlar hydrogenation in the presence of quinoline, followed by deacetylation. Other groups have also reported syntheses of **122**.[30, 43] This labile epoxide could be stored with traces of triethylamine in benzene at $-40\,^{\circ}C$ for several days and used directly for biogenetic studies. It was indeed shown[26] that this compound could serve as a precursor to enzymatically generated LXA_4 and LXB_4.

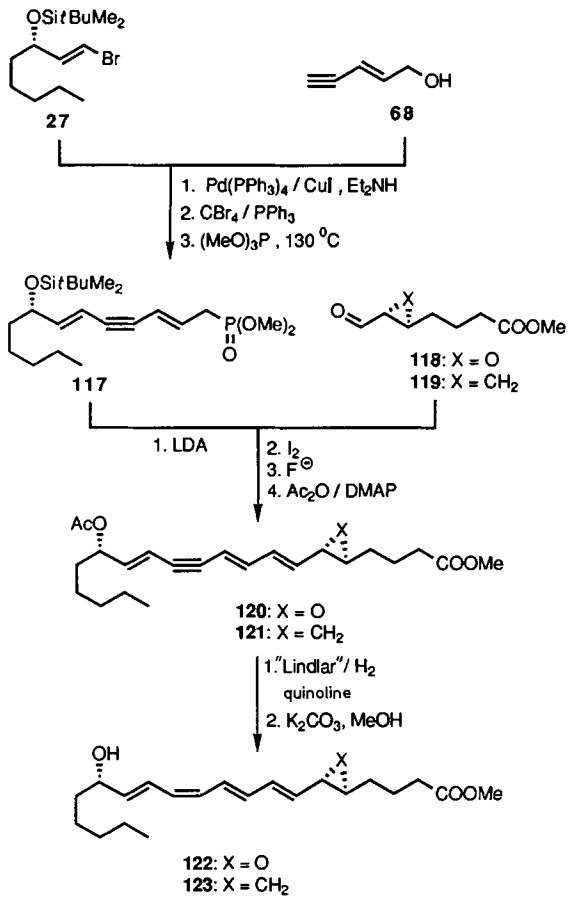

Scheme 22. Total synthesis of lipoxin epoxide methyl ester (**122**) and its 5,6-methano analogue (**123**). DMAP = 4-dimethylaminopyridine.

In order to selectively inhibit the enzymatic transformation of **122**, as we had earlier shown for leukotriene A_4,[129] we also targeted the methano analogue **123** (Scheme 22), which has a stable cyclopropyl group in the place of the labile epoxide moiety. This compound was prepared by similar chemistry from enantiomerically pure aldehyde **118** via intermediate **121** (Scheme 22).[90]

8. Summary and Future Outlook

The investigations on the combined effects of the major lipoxygenase pathways on arachidonic acid have resulted in the discovery of the lipoxins, a new class of biologically active eicosanoids. These trihydroxytetraene derivatives are

formed by initial lipoxygenation at either C15 or C5 and occur in two different substitution patterns termed lipoxins A_4 and lipoxins B_4, respectively. Many types of cells and enzyme systems were shown to produce these novel biomolecules. The stereochemical integrity (olefin geometry, chirality of hydroxy substituents) of the naturally derived lipoxins has been determined by comparisons with synthetically prepared materials.

To obtain all of the required compounds in isomerically pure form, a general synthetic strategy involving a key Pd^0/Cu^I-catalyzed coupling reaction between vinyl halides and terminal acetylenes was devised. Subsequent Lindlar hydrogenation affords the unique *E,Z*-diene system, common in a variety of acyclic eicosanoids. Since the labile conjugated *Z*-olefin moiety is generated during the final stages of the synthesis under neutral conditions, it becomes possible to form and maintain the desired conjugated olefin system in these acid- and base-sensitive molecules. An alternative strategy involving the Pd^0/Tl^I-catalyzed coupling of vinyl boronates with vinyl halides affords the conjugated systems directly.

We have demonstrated the powerful nature of this strategy by synthesizing not only the lipoxins and a large number of their isomers, but also several natural and nonnatural hydroxy (HETE) and dihydroxy (DiHETE) derivatives, including leukotriene B_4. Further applications of this synthetic approach to other acyclic eicosanoid systems, including a large number of structural analogues for biological evaluation, can be envisioned.

The discovery of the lipoxins and the availability of a variety of synthetic materials has prompted extensive studies on the biosynthesis and biological activities of these compounds. The lack of all the required enzymes in some cell types indicates the involvement of cell–cell interactions. Continuing work in this area has uncovered some distinct biological activities of the lipoxins, which suggest a regulatory role in the biosynthesis and action of other eicosanoids, including the leukotrienes and cyclooxygenase products. As such, the lipoxins may be involved in the cellular responses taking place during inflammation and other immunologically related conditions. These novel arachidonate-derived metabolites, therefore, constitute yet another self-regulating element of the remarkable eicosanoid cascade.

We are grateful to Professor B. Samuelsson and our many collaborators on this project, whose names appear in the references, for their valuable contributions. Financial support for this work by NIH, Merck Sharp & Dohme, Smith Kline & French and the Camille & Henry Dreyfus Foundation (K. C. N.), the PEW Scholar Program in the Biomedical Sciences, and American Heart Association (C. N. S.) is deeply appreciated.

Received: August 2, 1990 [A 832 IE]
German version: *Angew. Chem. 103* (1991) 1119

[1] S. Bergström, *Angew. Chem. 95* (1983) 865; *Angew. Chem. Int. Ed. Engl. 22* (1983) 858.
[2] B. Samuelsson, *Angew. Chem. 95* (1983) 854; *Angew. Chem. Int. Ed. Engl. 22* (1983) 805.
[3] J. R. Vane, *Angew. Chem. 95* (1983) 782; *Angew. Chem. Int. Ed. Engl. 22* (1983) 741.
[4] a) B. Samuelsson, *Angew. Chem. 94* (1982) 881; *Angew. Chem. Int. Ed. Engl. 21* (1982) 902; b) *Science 220* (1983) 568.
[5] Some recent reviews: a) A. L. Willis (Ed.): *Handbook of Eicosanoids: Prostaglandins and Related Lipids, Vols. 1A, 1B*, CRC Press, Boca Raton, FL, USA 1987; b) P. B. Curtis-Prior (Ed.): *Prostaglandins: Biology and Chemistry of Prostaglandins and Related Eicosanoids*, Churchill Livingstone, Edinburgh 1988; c) *Adv. Prostaglandin Thromboxane Leukotriene Res.*, New York (1976 to date).
[6] K. C. Nicolaou, G. P. Gasic, W. E. Barnette, *Angew. Chem. 90* (1978) 360; *Angew. Chem. Int. Ed. Engl. 17* (1978) 293.
[7] C. N. Serhan, M. Hamberg, B. Samuelsson, *Biochem. Biophys. Res. Commun. 118* (1984) 943.
[8] C. N. Serhan, M. Hamberg, B. Samuelsson, *Proc. Natl. Acad. Sci. USA 81* (1984) 5335.
[9] B. Samuelsson, S.-E. Dahlén, J. Lindgren, C. A. Rouzer, C. N. Serhan, *Science 237* (1987) 1171.
[10] K. F. Badr, D. K. DeBoer, M. Schwartzberg, C. N. Serhan, *Proc. Natl. Acad. Sci. USA 86* (1989) 3438.
[11] P. Hedqvist, J. Raud, U. Palmertz, J. Haeggström, K. C. Nicolaou, S. E. Dahlén, *Acta Physiol. Scand. 137* (1989) 571.
[12] T. H. Lee, C. E. Horton, A. U. Kyan, D. Haskard, A. E. G. Crea, B. W. Spur, *Clin. Sci. 77* (1989) 195.
[13] B. M. Grandordy, H. Lacroix, E. Mavoungou, S. Krilis, A. E. G. Crea, B. W. Spur, T. H. Lee, *Biochem. Biophys. Res. Commun. 167* (1990) 1022.
[14] T. H. Lee, A. E. G. Crea, V. Gant, B. W. Spur, B. E. Marron, K. C. Nicolaou, E. Reardon, M. Brezinski, C. N. Serhan, *Am. Rev. Respir. Dis. 141* (1990) 1453.
[15] J. A. Lindgren, C. Edenius, D. Steinhilber, A. Anggard, J. Palmblad, *Proc. 7th Int. Conf. Prostaglandins Relat. Compd.* (Florence 1990), p. 188.
[16] L. Stenke, B. Nasman-Glaser, J. A. Lindgren, *Proc. 7th Int. Conf. Prostaglandins Relat. Compd.* (Florence 1990), p. 7.
[17] P. Borgeat, L. de Fruteau, J. Maclouf, *Biochem. Pharmacol. 32* (1983) 381.
[18] C. N. Serhan, U. Lundberg, G. Weissmann, B. Samuelsson, *Prostaglandins 27* (1984) 563.
[19] M. Hamberg, P. Hedqvist, K. Radegen, *Acta Physiol. Scand. 110* (1980) 219.
[20] J. J. Murray, A. B. Tonnel, A. R. Brash, L. J. Roverts, P. Gosset, R. Workman, A. Capron, J. A. Oates, *N. Engl. J. Med. 315* (1986) 800.
[21] P. Needleman, J. Turk, B. A. Jakschik, A. R. Morrison, J. B. Lefkowith, *Annu. Rev. Biochem. 55* (1986) 69.
[22] C. N. Serhan, K. C. Nicolaou, S. E. Webber, C. A. Veale, S.-E. Dahlén, T. J. Puustinen, B. Samuelsson, *J. Biol. Chem. 261* (1986) 16340.
[23] C. N. Serhan, P. Y.-K. Wong, B. Samuelsson, *Prostaglandins 34* (1987) 201.
[24] C. N. Serhan, P. Fahlstadius, S.-E. Dahlén, M. Hamberg, B. Samuelsson, *Adv. Prostaglandin Thromboxane Leukotriene Res. 15* (1985) 163.
[25] C. N. Serhan, M. Hamberg, B. Samuelsson, J. Morris, D. G. Wishka, *Proc. Natl. Acad. Sci. USA 83* (1986) 1983.
[26] T. Puustinen, S. E. Webber, K. C. Nicolaou, J. Haeggström, C. N. Serhan, B. Samuelsson, *FEBS Lett. 207* (1986) 127.
[27] U. Ramstedt, C. N. Serhan, K. C. Nicolaou, S. E. Webber, H. Wigzell, B. Samuelsson, *J. Immunol. 138* (1987) 266.
[28] B. J. Fitzsimmons, J. Adams, J. F. Evans, Y. Leblanc, J. Rokach, *J. Biol. Chem. 260* (1985) 13008.
[29] J. Adams, B. J. Fitzsimmons, Y. Girard, Y. Leblanc, J. F. Evans, J. Rokach, *J. Am. Chem. Soc. 107* (1985) 464.
[30] E. J. Corey, M. M. Mehrotra, *Tetrahedron Lett. 27* (1986) 5173.
[31] H. Kühn, R. Weisner, H. Stender, *FEBS Lett. 177* (1984) 255.
[32] C. N. Serhan, *Biochim. Biophys. Acta 1004* (1987) 158.
[33] H. Kühn, R. Weisner, L. Alder, T. Schewe, H. Stender, *FEBS Lett. 208* (1986) 248.
[34] H. Kühn, R. Weisner, L. Alder, B. J. Fitzsimmons, J. Rokach, A. R. Brash, *Eur. J. Biochem. 169* (1987) 593.
[35] N. Ueda, S. Yamamoto, B. J. Fitzsimmons, J. Rokach, *Biochem. Biophys. Res. Commun. 144* (1987) 996.
[36] N. Ueda, C. Yokoyama, S. Yamamoto, B. J. Fitzsimmons, J. Rokach, J. A. Oates, A. R. Brash, *Biochem. Biophys. Res. Commun. 149* (1987) 1063.
[37] H.-Y. Ho, P. Y.-K. Wong, *Adv. Prostaglandin Thromboxane Leukotriene Res. 19* (1989) 137.
[38] C. C. Reddy, J. Whelan, M. K. Rao, P. Reddanna, *Adv. Prostaglandin Thromboxane Leukotriene Res. 19* (1989) 132.
[39] C. N. Serhan, K.-A. Sheppard, S. Fiore, *Adv. Prostaglandin Thromboxane Leukotriene Res. 20* (1990) 54.
[40] C. N. Serhan, K.-A. Sheppard, *J. Clin. Invest. 85* (1990) 772.
[41] C. Edenius, J. Haeggström, J. Å. Lindgren, *Biochem. Biophys. Res. Commun. 157* (1988) 801.
[42] R. Garrick, S.-Y. Shen, S. Ogunc, P. Y.-K. Wong, *Biochem. Biophys. Res. Commun. 162* (1989) 626.
[43] Y. Leblanc, B. J. Fitzsimmons, J. Rokach, N. Ueda, S. Yamamoto, *Tetrahedron Lett. 28* (1987) 3449.
[44] P. Y.-K. Wong, B. Spur, A. Hirai, Y. T. Yoshida, B. K. Lam, *Fed. Proc. 45* (1986) 927A.
[45] B. K. Lam, C. N. Serhan, B. Samuelsson, P. Y.-K. Wong, *Biochem. Biophys. Res. Commun. 144* (1987) 123.

[46] C. N. Serhan, U. Hirsch, J. Palmblad, B. Samuelsson, *FEBS Lett. 217* (1987) 242.
[47] D. Steinhilber, H. J. Roth, *FEBS Lett. 259* (1989) 168.
[48] T. R. Pettitt, A. F. Rowley, C. J. Secombes, *FEBS Lett. 1* (1989) 168.
[49] A. J. Marcus, M. J. Broekman, L. B. Safier, H. L. Ullman, N. Islam, C. N. Serhan, L. E. Rutherford, H. M. Korchak, G. Weissmann, *Biochem. Biophys. Res. Commun. 109* (1982) 130.
[50] K. C. Nicolaou, B. E. Marron, C. A. Veale, S. E. Webber, S.-E. Dahlén, B. Samuelsson, C. N. Serhan, *Biochim. Biophys. Acta 1003* (1989) 44.
[51] P. Walstra, J. Verhagen, M. A. Vermeer, J. P. M. Klerks, G. A. Veldink, J. F. G. Vliegenthart, *FEBS Lett. 228* (1988) 167.
[52] S. J. Kim, *Biochem. Biophys. Res. Commun. 150* (1988) 870.
[53] C. F. Ng, B. K. Lam, K. A. Pritchard, M. B. Stemerman, P. Hejny, P. Y.-K. Wong, *Biochim. Biophys. Acta 1004* (1989) 332.
[54] S. C. Lazarus, E. Zocca, *FASEB J. 2* (1988) A409.
[55] S.-E. Dahlén, J. Raud, C. N. Serhan, J. Björk, B. Samuelsson, *Acta Physiol. Scand. 130* (1987) 643.
[56] K. F. Badr, C. N. Serhan, K. C. Nicolaou, B. Samuelsson, *Biochem. Biophys. Res. Commun. 145* (1987) 408.
[57] K. F. Badr, D. K. DeBoer, M. Schwartzberg, C. N. Serhan, *Proc. Natl. Acad. Sci. USA 86* (1989) 3438.
[58] D. W. Busija, W. Armstead, C. W. Leffler, R. Mirro, *Am. J. Physiol. 256* (1989) 468.
[59] G. Feuerstein, A.-L. Siren, *FEBS Lett. 232* (1988) 51.
[60] P. Hedqvist, J. Raud, U. Palmertz, J. Haeggstroem, K. C. Nicolaou, S.-E. Dahlén, *Acta Physiol. Scand. 137* (1989) 571.
[61] S.-E. Dahlén, C. A. Veale, S. E. Webber, B. E. Marron, K. C. Nicolaou, C. N. Serhan, *Agents Actions 26* (1989) 93.
[62] C. A. J. Jacques, B. W. Spur, A. E. G. Crea, T. H. Lee, *Br. J. Pharmacol. 95* (1988) 562.
[63] J.-P. Cristol, P. Sirois, *Res. Commun. Chem. Pathol. Pharmacol. 59* (1988) 423.
[64] A. M. Lefer, G. L. Stahl, D. J. Lefer, M. E. Brezinski, K. C. Nicolaou, C. A. Veale, Y. Abe, J. B. Smith, *Proc. Natl. Acad. Sci. USA 85* (1988) 8340.
[65] J. Palmblad, H. Gyllenhammar, B. Ringertz, C. N. Serhan, B. Samuelsson, K. C. Nicolaou, *Biochem. Biophys. Res. Commun. 145* (1987) 168.
[66] T. H. Lee, C. E. Horton, U. Kyan-Aung, D. Haskard, A. E. G. Crea, B. W. Spur, *Clin. Sci. 77* (1989) 195.
[67] T. H. Lee, B. Grandordy, C. E. Horton, A. E. G. Crea, B. W. Spur, *FASEB J. 3* (1989) A1277.
[68] S. Nigam, S. Fiore, F. W. Luscinskas, C. N. Serhan, *J. Cell. Physiol. 143* (1990) 512.
[69] C. N. Serhan, E. Reardon, *Free Radical Res. Commun. 7* (1989) 341.
[70] F. W. Luscinskas, K. C. Nicolaou, S. E. Webber, C. A. Veale, M. A. Gimbrone, Jr., C. N. Serhan, *Biochem. Pharmacol. 39* (1990) 355.
[71] See [27].
[72] G. K. Popov, A. S. Nekrasov, A. L. Khshivo, A. G. Pochinskii, V. Z. Lankin, A. M. Vikhert, *Byull. Eksp. Biol. Med. 107* (1989) 80; *Chem. Abstr. 110* (1989) 13335j.
[73] A. Hansson, C. N. Serhan, J. Haeggström, M. Ingelman-Sundberg, B. Samuelsson, *Biochem. Biophys. Res. Commun. 134* (1986) 1215.
[74] M. S. Shearman, Z. Naor, K. Sekiguchi, A. Kishimoto, Y. Nishizuka, *FEBS Lett. 243* (1989) 177.
[75] T. L. Walden, Jr., *J. Radiat. Res. 29* (1988) 255.
[76] E. Wikström, P. Westlund, K. C. Nicolaou, S.-E. Dahlén, *Agents Actions 26* (1989) 90.
[77] M. E. Brezinski, M. A. Gimbrone, Jr., K. C. Nicolaou, C. N. Serhan, *FEBS Lett. 245* (1989) 167.
[78] a) E. J. Corey, D. A. Clark, A. Marfat in L. W. Chakrin, D. M. Bailey (Eds.): *The Leukotrienes: Chemistry and Biology*, Academic Press, Orlando, FL, USA 1984, p. 13; b) J. G. Atkinson, J. Rokach in A. L. Willis (Eds.): *Handbook of Eicosanoids: Prostaglandins and Related Lipids, Vol. 1B*, CRC Press, Boca Raton, FL, USA 1987, p. 175; c) J. Rokach, Y. Guindon, R. N. Young, J. Adams, J. G. Atkinson, *Total Synth. Nat. Prod. 7* (1988) 141.
[79] a) K. Sonogashira, Y. Tohda, N. Hogihira, *Tetrahedron Lett. 1975*, 4467; b) V. Ratovelomana, G. Linstrumelle, *Synth. Commun. 11* (1981) 917.
[80] a) N. Miyaura, Y. Yamada, A. Suzuki, *Tetrahedron Lett. 1979*, 3437; b) N. Miyaura, H. Suginome, A. Suzuki, *ibid. 22* (1981) 127; c) N. Miyaura, K. Yamada, H. Suginome, A. Suzuki, *J. Am. Chem. Soc. 107* (1985) 972.
[81] J. Uenishi, J.-M. Beau, R. W. Armstrong, Y. Kishi, *J. Am. Chem. Soc. 109* (1987) 4756.
[82] K. C. Nicolaou, T. Ladduwahetty, I. M. Taffer, R. E. Zipkin, *Synthesis 1986*, 344.
[83] K. C. Nicolaou, J. Y. Ramphal, Y. Abe, *Synthesis 1989*, 898.
[84] K. C. Nicolaou, T. Ladduwahetty, E. M. Elisseou, *J. Chem. Soc. Chem. Commun. 1985*, 1580.
[85] K. C. Nicolaou, S. E. Webber, *J. Am. Chem. Soc. 106* (1984) 5734.
[86] K. C. Nicolaou, J. Y. Ramphal, J. M. Palazon, R. A. Spanevello, *Angew. Chem. 101* (1989) 621; *Angew. Chem. Int. Ed. Engl. 28* (1989) 587.
[87] K. C. Nicolaou, R. E. Zipkin, R. E. Dolle, B. D. Harris, *J. Am. Chem. Soc. 106* (1984) 3548.
[88] K. C. Nicolaou, Y. S. Chung, P. Hernandez, I. M. Taffer, R. E. Zipkin, *Tetrahedron Lett. 27* (1986) 1881.
[89] K. C. Nicolaou, C. A. Veale, S. E. Webber, H. Katerinopoulos, *J. Am. Chem. Soc. 107* (1985) 7515.
[90] K. C. Nicolaou, S. E. Webber, *J. Chem. Soc. Chem. Commun. 1986*, 1816.
[91] B. E. Marron, R. A. Spanevello, M. E. Elisseou, C. N. Serhan, K. C. Nicolaou, *J. Org. Chem. 54* (1989) 5522.
[92] K. C. Nicolaou, B. E. Marron, C. A. Veale, S. E. Webber, C. N. Serhan, *J. Org. Chem. 54* (1989) 5527.
[93] K. C. Nicolaou, S. E. Webber, J. Y. Ramphal, Y. Abe, *Angew. Chem. 99* (1987) 1077; *Angew. Chem. Int. Ed. Engl. 26* (1987) 1019.
[94] K. C. Nicolaou, S. E. Webber, *J. Chem. Soc. Chem. Commun. 1985*, 297.
[95] K. C. Nicolaou, S. E. Webber, *Synthesis 1986*, 453.
[96] A. A. Spector, J. A. Gordon, S. A. Moore, *Prog. Lipid Res. 27* (1988) 271.
[97] J. E. Baldwin, N. V. Reed, E. J. Thomas, *Tetrahedron 7 (supplement 1)* (1981) 263.
[98] E. J. Corey, S. Hashimoto, *Tetrahedron Lett. 22* (1981) 299.
[99] J. Rokach, Y. Guindon, R. Zamboni, C. K. Lau, Y. Girard, M. Larue, R. A. Perry, J. G. Atkinson, *Tetrahedron Lett. 24* (1983) 999.
[100] B. P. Gunn, *Tetrahedron Lett. 26* (1985) 2869.
[101] E. J. Corey, J. O. Albright, A. E. Barton, S. Hashimoto, *J. Am. Chem. Soc. 102* (1980) 1433, 1435.
[102] J. Rokach, J. Adams, R. Perry, *Tetrahedron Lett. 24* (1983) 5185.
[103] Y. Leblanc, B. J. Fitzsimmons, J. Adams, F. Perez, J. Rokach, *J. Org. Chem. 51* (1986) 789.
[104] S. Manna, J. Viala, P. Yadagri, J. R. Falck, *Tetrahedron Lett. 27* (1986) 2679.
[105] T. Shimazaki, Y. Kobayashi, F. Sato, *Chem. Lett. 1988*, 1785.
[106] I. M. Taffer, R. E. Zipkin, *Tetrahedron Lett. 28* (1987) 6543.
[107] S. W. Djuric, J. M. Miyashiro, T. D. Penning, *Tetrahedron Lett. 29* (1988) 3459.
[108] a) E. J. Corey, H. Niwa, J. Knolle, *J. Am. Chem. Soc. 100* (1978) 1942; b) E. J. Corey, K. Kyler, N. Raju, *Tetrahedron Lett. 25* (1984) 5115.
[109] B. P. Gunn, D. W. Brooks, *J. Org. Chem. 50* (1985) 4417.
[110] K. C. Nicolaou, N. A. Stylianides, J. Y. Ramphal, *J. Chem. Soc. Perkin Trans. 1 1989*, 2131.
[111] J. Baldwin, D. I. Davies, L. Hughes, N. J. A. Gutteridge, *J. Chem. Soc. Perkin Trans. 1 1979*, 115.
[112] E. J. Corey, A. Marfat, J. R. Falck, J. O. Albright, *J. Am. Chem. Soc. 102* (1980) 1433.
[113] K. Takai, K. Nitta, K. Utimoto, *J. Am. Chem. Soc. 108* (1986) 7408.
[114] B. J. Fitzsimmons, J. Rokach, *Tetrahedron Lett. 25* (1984) 3043.
[115] a) E. J. Corey, A. Marfat, G. Gotto, F. Frion, *J. Am. Chem. Soc. 102* (1980) 7984; b) E. J. Corey, P. B. Hopkins, J. E. Munroe, A. Marfat, S. Hashimoto, *ibid. 102* (1980) 7986; c) E. J. Corey, A. Marfat, J. Munroe, K. S. Kim, P. B. Hopkins, F. Brion, *Tetrahedron Lett. 22* (1981) 1077; d) E. J. Corey, A. Marfat, D. J. Hoover, *ibid. 22* (1981) 1587.
[116] a) R. Zamboni, J. Rokach, *Tetrahedron Lett. 23* (1982) 2631; b) Y. Guindon, R. Zamboni, C. K. Lau, J. Rokach, *ibid. 23* (1982) 739; c) Y. Guindon, D. Delorme, C. K. Lau, R. Zamboni, *J. Org. Chem. 53* (1988) 267.
[117] a) Y. Le Merrer, C. Gravier, D. Micas-Languin, J. C. Despezay, *Tetrahedron Lett. 27* (1986) 4161; b) Y. Le Merrer, C. Gravier-Pelletier, D. Micas-Languin, F. Mestre, A. Dureault, J. C. Despezay, *J. Org. Chem. 54* (1989) 2409.
[118] L. S. Mills, P. C. North, *Tetrahedron Lett. 24* (1983) 409.
[119] C. Fuganti, S. Servi, C. Zirotti, *Tetrahedron Lett. 24* (1983) 5285.
[120] H. G. Davies, S. M. Roberts, B. J. Wakerfield, J. A. Winders, *J. Chem. Soc. Chem. Commun. 1985*, 1166.
[121] C. Q. Han, D. DiTullio, Y. F. Wang, C. J. Sih, *J. Org. Chem. 51* (1986) 1253.
[122] a) K. C. Nicolaou, N. A. Petasis, W. S. Li, T. Ladduwahetty, J. L. Randall, S. E. Webber, P. E. Hernandez, *J. Org. Chem. 48* (1983) 5400, 5403; b) J. B. Smith, D. M. Roth, A. M. Lefer, N. A. Petasis, K. C. Nicolaou, *Prostaglandins 29* (1985) 765.
[123] Y. Kobayashi, T. Shimazaki, F. Sato, *Tetrahedron Lett. 28* (1987) 5849.
[124] a) E. J. Corey, W. Su, M. B. Cleaver, *Tetrahedron Lett. 30* (1989) 4181; b) E. J. Corey, W. Su, *ibid. 26* (1985) 281; c) E. J. Corey, M. M. Mehrotra, W. Su, *ibid. 26* (1985) 1919.
[125] a) J. Adams, B. J. Fitzsimmons, J. Rokach, *Tetrahedron Lett. 25* (1984) 4713; b) Y. Leblanc, B. J. Fitzsimmons, J. Adams, J. Rokach, *ibid. 26* (1985) 1399; c) B. J. Fitzsimmons, J. Rokach, *ibid. 26* (1985) 3939.
[126] Y. Kobayashi, N. Kato, T. Shimazaki, F. Sato, *Tetrahedron Lett. 29* (1988) 6297.
[127] J. Morris, D. G. Wishka, *Adv. Prostaglandin Thromboxane Leukotriene Res. 16* (1986) 99; *Tetrahedron Lett. 27* (1986) 803.
[128] P. Y. K. Wong, R. Hughes, B. Lam, *Biochem. Biophys. Res. Commun. 126* (1985) 763.
[129] a) K. C. Nicolaou, N. A. Petasis, S. P. Seitz, *J. Chem. Soc. Chem. Commun. 1981*, 1195; b) Y. Koshishara, S. Murota, N. A. Petasis, K. C. Nicolaou, *FEBS Lett. 143* (1982) 13.

Incarcerated Atoms and Reactive Molecules

*By Henning Hopf**

The desire to "incarcerate" electrons, atoms, ions, and eventually complete molecules in compounds that are hollow in some way has been not only renewed again and again by the exceptionally rapid development of supramolecular chemistry, but also fulfilled in increasing measure. The attempts at encapsulation are older than host–guest chemistry itself, as such experiments with adamantane (which is, after all, also hollow) and related bi- and polycycles show. The source of this strong tendency to "conceal" species can possibly be explained only by psychology, but probably has something to do with the fact that compartmentalization is a characteristic of life itself: when the distinction between "inside" and "outside" disappears, life is snuffed out.

Whatever the underlying cause of this desire to hide things (which is also manifest in Art and Folklore as the innumerable examples from the artist *Christo* to the Russian Matrioschka doll-in-the-doll show), two papers will be discussed here in which spectacular incarcerations (Latin carcer = enclosure, prison, dungeon) are reported. In the first case a reactive molecule is stabilized by locking it into a molecular high security prison; in the second a (this time completely inert) atom is captured within a molecule never before proven to be a molecular trap.

To enable the direct or indirect observation of highly reactive compounds that have, under normal conditions, not the slightest chance of survival is a stimulating and important assignment, since such molecules are not only suitable for testing theoretical models, but always also challenge and incite the development of preparative and instrumental methodology.

Over the years several high-performance chemical procedures have been developed to tame "nonexistent" molecules; among them the protection of reactive species from external attack by bulky substituents, the decrease in reactivity by complexation with metal atoms or metal-containing fragments, and the freezing and isolation in low-temperature matrices are most prominent. The observation of exceptionally reactive compounds by ultrafast spectroscopic methods or in a mass spectrometer (lately also in the perfectly isolating conditions of interstellar space) has the disadvantage for the preparative chemist that no directly (that is, with the naked eye) visible quantities of the substance are produced. But the "chemical" techniques also have disadvantages: they can alter the properties of the object of observation drastically. Furthermore, the most powerful spectroscopic method of chemistry, NMR spectroscopy, is of limited value only, and sometimes not even applicable under the stabilizing conditions mentioned above.

There is probably no other molecule in organic chemistry that has been so thoroughly and successfully studied by the described stabilization methods than cyclobutadiene (**1**), a key compound besides benzene for testing all criteria and theories of aromaticity. A few years ago this led to the opinion of a leading researcher in this field that this chapter in organic chemistry could be closed, as "it is now secured textbook material".[1]

1

D. J. Cram, M. E. Tanner, and *R. Thomas* of the University of California in Los Angeles did not follow this advice and turned their attention to a long-known cyclobutadiene-forming process. They studied, *within* a cage molecule, the hemicarcerand **4**,[2] the photoisomerization/fragmentation of α-pyrone (**2**), originally proposed by *Corey* and studied by several research groups, which affords cyclobutadiene via the bicycle **3**.

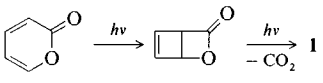

2 **3**

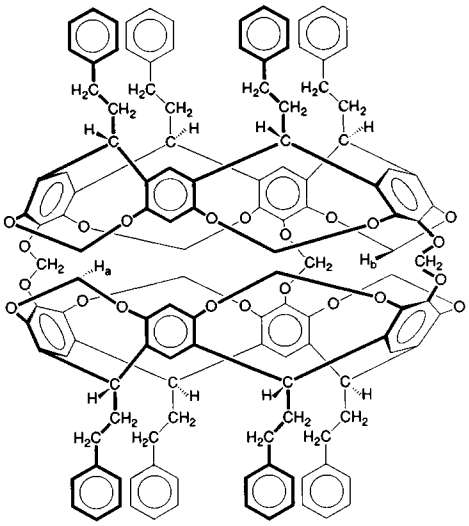

4

On irradiation of the **2** · **4** complex (formed from its components on boiling at reflux in chlorobenzene) in $CDCl_3$ or $(CD_2)_4O$ with light from a xenon lamp at room temperature in an NMR tube, a sharp new singlet is immediately observed in the 500 MHz ^1H NMR spectrum. This signal must be assigned to the complex between **1** and the host molecule **4**. The protons of the ligand which point inwards, H_a and H_b, also give rise to a sharp signal (doublet) in the ^1H NMR spectrum, which is interpreted as a clear indication of the singlet state of the **1** · **4** complex. A triplet state for **1** would cause drastically broadened and also shifted host signals, as for instance, a comparison with the (triplet) oxygen complex of **4** shows. Furthermore, the sharpness of these carcerand

[*] Prof. Dr. H. Hopf
Institut für Organische Chemie der Technischen Universität
Hagenring 30, W-3300 Braunschweig (FRG)

signals suggests that the cyclobutadiene guest is rapidly rotating in its cage and that the carbon dioxide that is also formed must have escaped its jail, which is too small for two inmates.

The mechanism of the formation of cyclobutadiene under these conditions of "complexation" and the subsequent chemistry of **1** was also studied. Among the interesting results is the observation that encapsulated **1** breaks down to acetylene on further irradiation, as does **1** prepared in an argon matrix at 8 K. Besides the ^{1}H NMR spectrum—unfortunately the authors have not yet reported further NMR studies such as the ^{13}C NMR spectrum and coupling constants—the FTIR spectra of the guest–host precursors **2** · **4** and **3** · **4** and finally the **1** · **2** complex were recorded.

Cram's paper is refreshingly "chemical": **1** reacts further by cyclobutadiene dimerization/valence tautomerization to afford cyclooctatetrene, which is (also) identified by its typical smell, and the scission product, acetylene, precipitates as copper salt. The question still remains unanswered how the exciting light penetrates the prison and reaches α-pyrone (**2**). The aryl substituents perhaps serve as photosensitizers.

At the end of this elegant paper, *Cram* presents a thought that will surely provoke exciting and possibly even controversial discussion. In his opinion the "inner phase" of carcerands and hemicarcerands form a new form of material or state of aggregation ("a new phase of matter"). In contrast to the hollow space inside clathrates and zeolites, for instance, the cages of these molecules are independent of the form and physical state: Hemicarcerands and related supramolecular systems and their complexes ("hemicarceplexes") exist in the solid, liquid, or gas phase. The characteristic peculiar to them—the hollow space, the inside surface—is maintained across all phase transitions. In other words, the inner surfaces and spaces of these systems are not bulk properties.

A second molecular container which was discussed from the beginning as a potential trap for a molecule, or at least an atom, is C_{60} fullerene (**5**). Already in their pioneer experiments (the simultaneous laser evaporation of salt/graphite mixtures), *Smalley* et al. maintained that they had obtained $C_x \cdot M$ clusters ($x \geq 60$, M = La, Cu, Ba, Sr) where the metal atoms were bound to the inside of the molecule. This interpretation was criticized by *Kaldor* et al. in whose opinion the metal ion of $C_{60} \cdot La$ is coordinated to the outer surface. As metal complexes of C_{60} fullerene (**5**) with externally bound metal atoms have since been found (structural evidence from X-ray crystallography!), *Kaldor*'s proposal has indeed some substance.

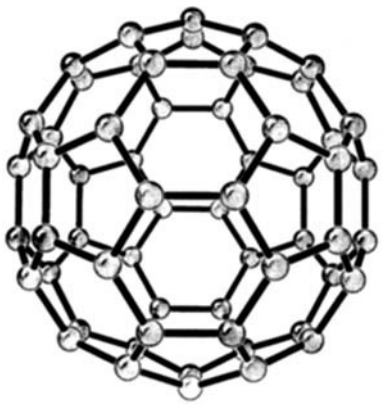

5

After the Krätschmer–Huffman method provided a convenient method of preparing macroscopic quantities of C_{60} (**5**) and C_{70}, the search for an "endohedral" chemistry of the fullerenes could be resumed. Now, the inclusion of helium atoms in $C_{60}^{\bullet\oplus}$ and $C_{70}^{\bullet\oplus}$ fullerene within a mass spectrometer, on collision of the preselected fullerene ions with a "stationary" noble gas, has been reported by four research groups in a common paper [*H. Schwarz* and *T. Weiske* (Technische Universität, Berlin), *K. Böhme* (York University, Ontario), *J. Hrušák* (Czechoslovakian Academy of Science, Prague) and *W. Krätschmer* (Max-Planck-Institut für Kernphysik, Heidelberg)].[3]

In a specialized tandem mass spectrometer accerelerated $C_x^{\bullet\oplus}$ ions were "stopped" by the collision gases H_2, D_2, Ar, and SF_6. In all cases the pattern obtained corresponded to the fragmentation of the $C_{60}^{\bullet\oplus}$ ion by expulsion of C_2, C_4, C_6, and C_8 units. A completely different pattern was recorded when helium was the collision partner. Under these conditions C_n fragments were also split off, but all signals showed an additional neighboring peak at higher mass (+ 4 for ^{4}He and + 3 for ^{3}He). This surprising observation at first said nothing about the site of coordination of the noble gas atom. Complexes with an exohedrally coordinated helium atom would probably give a similar fragmentation pattern.

Why then did the authors favor the inclusion structure? First, the $C_{70}^{\bullet\oplus}$ ion (which otherwise behaves similarly to **5** with the other collision gases) contains the fragment $C_{60}^{\bullet\oplus}$/He among others in the collision experiment with helium. That an externally bound helium atom can remain "glued" to the surface during this extreme fragmentation/cage repair process stretches the imagination—especially since ab initio MO calculations on model compounds without inside/outside discrimination (e.g. benzene) predict He bonding energies of ca. 0.2 eV, while for the process $C_{60}^{\bullet\oplus} \rightarrow C_{58}^{\bullet\oplus} + C_2$, for instance, at least 4–5 eV is required. The exohedral helium atom must therefore have long since disappeared before the C_n fragmentation begins—a direct contradiction of the experiment.

In the meantime collision experiments show that neon can also be captured by $C_{60}^{\bullet\oplus}$, but with a much reduced yield than in the case of the smaller helium.

The development of fullerene chemistry began on a "nonmeasurable" scale in outer space or within the mass spectrometer: only when visible quantities were obtained could one speak of a preparative breakthrough. Perhaps such a development will be repeated for endohedrally coordinated fullerene derivatives, now that the first atoms have been successfully enclosed within this molecular container.

German version: *Angew. Chem. 103* (1991) 1137

[1] G. Maier, *Angew. Chem. 100* (1988) 317; *Angew. Chem. Int. Ed. Engl. 27* (1988) 309.
[2] D. J. Cram, M. E. Tanner, R. Thomas, *Angew. Chem. 103* (1991) 1048; *Angew. Chem. Int. Ed. Engl. 30* (1991) 1024.
[3] T. Weiske, D. K. Böhme, J. Hrušák, W. Krätschmer, H. Schwarz, *Angew. Chem. 103* (1991) 898; *Angew. Chem. Int. Ed. Engl. 30* (1991) 884.

Designed Coupling of C_1 Ligands: Organometallic Model Reactions

By *Helmut G. Alt**

Carbon to carbon coupling is the most important step for the manufacture of organic fine and industrial chemicals. Metallic compounds, mostly catalysts, play an indispensible role in this process. Yet there is still a long way to go to understand the mechanism of metal-centered coupling of C_1 units such as in the Fischer–Tropsch synthesis. Now in this issue *Filippou* et al.[1] of the Technische Universität München reports astounding progress in this fundamentally important field. He not only achieved the planned synthesis of mononuclear bis(carbyne) metal complexes (**2**), but also the $C_1 + C_1$ coupling of the carbyne ligands to form an alkyne ligand (**2** → **3**/**4**, see Scheme 1).

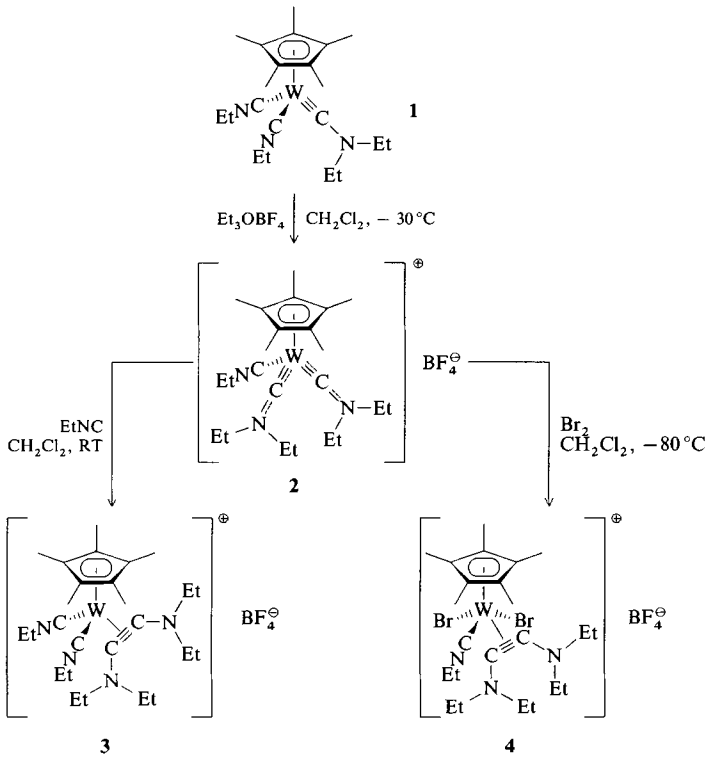

Scheme 1. Synthesis of the bis(carbyne) complex **2** by alkylation of **1** with Meerwein's reagent and $C_1 + C_1$ coupling in the ligand sphere of **2** to afford **3** and **4**.

How can two metal–carbon multiple bonds be opened simultaneously under mild conditions when thereby an electron deficiency arises at the metal center? *Filippou*'s concept is based on extended Hückel calculations, which predict that the coupling of two carbyne ligands is symmetry-allowed at a d^4 metal center and should proceed spontaneously, whereas a stabilization of the bis(carbyne) complexes is attained when the carbyne carbon atom is attached to π-donor substituents.[1–3] Exactly this is the case in *Filippou*'s complex: the limiting resonance formulas **A** and **B**, for which spectroscopic evidence exists,[1,4–6] show that in such bis(carbyne) complexes a "partially reduced" metal–carbon multiple bond is present.

The alkyne that results from the coupling reaction functions as a four-electron ligand, and the metal center thus must accommodate a deficit of only two electrons, which can be compensated by the entering isonitrile ligand or by the two bromine ligands.

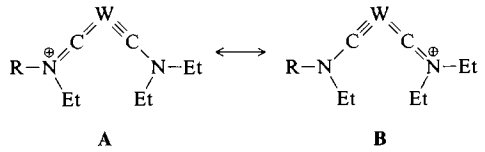

This classic coupling reaction was not coincidental, but the result of a well-planned strategy: previously *Filippou* et al. had assigned a key role to the ynamines in the acid-induced C–C coupling of carbyne and isocyanide ligands and to bis(carbyne) complexes in the reductive C–C coupling of two isocyanide ligands to yield ynediamines.[7]

In the light of *Filippou*'s findings,[1] it is logical to postulate the existence of bis(carbyne) intermediates for other metal-centered coupling reactions of C_1 units[8,9] as well, such as in the coupling of two carbonyl ligands to form bis(siloxy)acetylenes.[10] The exemplary results described here suggest a series of prospects: The designed construction of unsaturated C_2 ligands not capable of existence in unbound form opens new possibilities for the metal-centered synthesis of heterocycles. Furthermore, the transfer of this concept to transition-metal centers with other electron configurations gives a positive outlook for the directed cleavage of alkynes into unsaturated, metal-fixed C_1 fragments. The first successes have already been recorded.[7d]

German version: *Angew. Chem. 103* (1991) 1139

[*] Prof. Dr. H. G. Alt
Laboratorium für Anorganische Chemie
Universität Bayreuth
Universitätstrasse 30, W-8580 Bayreuth (FRG)

[1] A. C. Filippou, W. Grünleitner, C. Völkl, P. Kiprof, *Angew. Chem. 103* (1991) 1188; *Angew. Chem. Int. Ed. Engl. 31* (1991) 1167.
[2] H. Fischer, P. Hofmann, F. R. Kreißl, R. R. Schrock, U. Schubert, K. Weiss: *Carbyne Complexes*, VCH, Weinheim 1988.
[3] C. N. Wilker, R. Hoffmann, O. Eisenstein, *Nouv. J. Chim. 7* (1983) 535.
[4] J. Chatt, A. J. L. Pombeiro, R. L. Richards, *J. Chem. Soc. Dalton Trans. 1980*, 492.
[5] A. J. L. Pombeiro, R. L. Richards, *Transition Met. Chem. (Weinheim) 5* (1980) 55.
[6] A. C. Filippou, W. Grünleitner, *J. Organomet. Chem. 407* (1991) 61.
[7] a) A. C. Filippou, W. Grünleitner, *Z. Naturforsch. B44* (1989) 1023; b) A. C. Filippou, *Polyhedron 9* (1990) 727; c) A. C. Filippou, W. Grünleitner, *J. Organomet. Chem. 393* (1990) C10; d) A. C. Filippou, C. Völkl, W. Grünleitner, P. Kiprof, *Angew. Chem. 102* (1990) 224; *Angew. Chem. Int. Ed. Engl. 29* (1990) 207; e) A. C. Filippou, W. Grünleitner, *Z. Naturforsch. B46* (1991) 216.
[8] G. A. McDermott, A. Mayr, *J. Am. Chem. Soc. 109* (1987) 580.
[9] A. Mayr, C. M. Bastos, *J. Am. Chem. Soc. 112* (1990) 7797.
[10] R. N. Vrtis, S. J. Lippard, *Isr. J. Chem. 30* (1990) 331.

New Discoveries in the Realm of Metal–Metal Multiple Bonds: $[\eta^5\text{-}C_5Me_5)_2Co_2]$, the First Organometallic Multiple-Bond Complex without Bridging Ligands

By *Joachim Wachter**

Every advanced chemistry student should be clearly aware of the significance of the following experiment, which is relatively easy to perform, provided that it is carried out under inert gas atmosphere: If a light blue aqueous Cr^{II} solution is allowed to react with sodium acetate, red crystals of Cr^{II} acetate precipitate out. However, the path leading from the first synthesis of this compound in 1844 by *E. Peligot*[1] to the correct interpretation of its structure[2] (dimeric, extremely short Cr–Cr bonds) has been long. Only X-ray structure analysis was capable of revealing that the M–M distances in such compounds are much shorter than those in the corresponding metals. Hence, defined multiple-bond orders (2 for $[Re_3Cl_{12}]^{3\ominus}$[3] and 4 for $[Re_2Cl_8]^{2\ominus}$[4]) were first formulated in 1964.

Further examples were reported soon thereafter and led, in turn, to theoretical investigations and interpretations (for example, the involvement of d orbitals in the bonding system). An almost immediate consequence was the distinction between bridged and nonbridged systems, as exemplified by the two historical protagonists **1** and **2**, respectively.

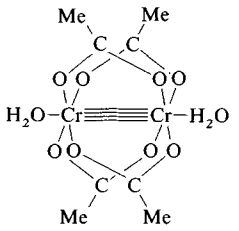

1

2

The significance of this classification only becomes clear when the chemistry of transition-metal carbonyl complexes and their derivatives is examined. It is immediately apparent that "... even today no unequivocal case of multiple M–M bonding (i.e., a bond without bridges) has ever been found in a metal carbonyl type system..."[5] This statement, made in 1982 by the grand master of the M–M bond, *F. A. Cotton*, is still valid today.

Numerous examples of double- and triple-bond systems involving π-acceptor ligands are known for elements of groups 3–8 of the periodic table. Although the diverse reactivity of these complexes has attracted much interest, the determination of defined bond orders has proven to be very problematic. For example, the distances in complexes **3** and **4** are equal despite differing bond orders.[6] Thus, bridging ligands complicate the matter. Similar relationships are found in the important class of compounds $[Cp_2M_2(CO)_4]$ (**5**; M = Cr, Mo, W).[7] On the basis of the 18-electron rule and the experimentally found M–M distances, an M–M triple bond has been postulated for these d^5–d^5 systems. In order to understand the overall system, however, it is necessary to consider the electronic situation of the CO bridges (σ + π bond, referred to as semi-bridging) and even that of the Cp ligands.

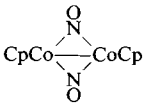

3

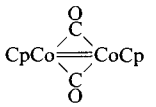

4

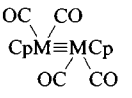

5

But how does one synthesize organometallic multiple-bond systems without bridging ligands? The answer, recently found by *J. J. Schneider* et al.,[9] is to cocondense a potential π ligand with cobalt atoms in a metal vaporization reactor. *G. A. Ozin* et al. have already had a similar idea, namely, the addition of naked metal atoms to benzene-derived ligands with the formation of bis(arene)metal complexes, but they were unable to isolate weighable amounts of a corresponding substance.[10]

Since the synthesis of dibenzenechromium from chromium vapor and benzene by *P. L. Timms* in 1969,[11] the cocondensation method has been continually developed in order to obtain organotransition-metal complexes.[12] For instance, the cocondensation of metal vapors with a wide range of substituted cyclopentadienes has usually afforded metallocene hydrides of the type $[Cp_2MoH_2]$ or $[Cp_2ReH]$.[13] Cobalt atoms, on the other hand, react with unsubstituted cyclopentadiene to give the mononuclear compound $[(\eta^5\text{-}C_5H_5)(\eta^4\text{-}C_5H_6)Co]$ (**6a**) as the sole isolable product.[14]

The decisive turn of events leading to a binuclear cobalt complex, as reported by *Schneider* et al., was brought about by increasing the proportion of metal to about 33% and using pentamethylcyclopentadiene (Cp*H). In this way, complex **7**, the first nonbridged organometallic multiple-bond complex, was obtained in 5–15% yield. At the same time, the permethylated sandwich complex **6b**, analogous to **6a**, and the complex **8** were formed; **8** is only the fifth structurally characterized homoleptic triple-decker complex and is thus a noteworthy rarity.

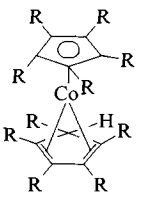

R = H: **6a**
R = Me: **6b**

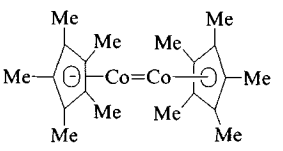

7

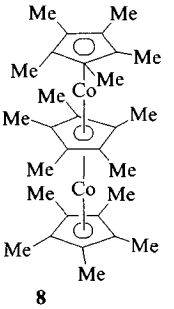

8

[*] Dr. J. Wachter
Institut für Anorganische Chemie der Universität
W-8400 Regensburg (FRG)

The structure of **7** is characterized by two parallel Cp* rings; the distance between the two Co atoms (2.253(1) Å) is 0.08 Å shorter than in $[Cp^*_2Co_2(\mu\text{-}CO)_2]$.[15] This finding and the effective atomic number (EAN) rule indicate the presence of a nonbridged M–M double bond, for which, on the whole, only one example has been established.[16] The relationship to **4** merely involves the addition of two CO bridges. These conclusions are contradicted, however, by the ^1H NMR spectrum of **7** ($\delta = 61.3$), which supports a marked paramagnetic component. Clearly, theoretical chemists have much to look into here! Similarly, a certain resistance of **7** toward C_2H_4 and Co (at least under the normal conditions used so far) seems not to support the presence of a Co–Co double bond.

The question now is whether relationships to the reactivity of **4'**, the pentamethylated derivative of **4**, can be established. A salient feature of ligand-bridged multiple-bond complexes

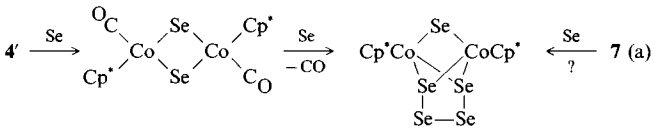

is that, usually, they readily undergo addition reactions involving opening of the bridge and only afterwards do they undergo substitution reactions [Eq. (a)]; the analogous transformation could occur directly from **7**, starting with addition.[17]

The prospect of being able to investigate the bonding and reactivity of nonbridged organometallic multiple-bond systems is why the successful synthesis of **7** is so significant. A sure goal will be to extend the preparation to other transition metals.

German version: *Angew. Chem. 103* (1991) 1140

[1] E. Peligot, *C. R. Hebd. Seances Acad. Sci. 19* (1844) 609; *Ann. Chim. Phys. 12* (1844) 528.
[2] F. A. Cotton, B. G. DeBoer, M. D. La Prada, J. R. Pipal, D. A. Ucko, *Acta Crystallogr. Sect. B 27* (1971) 1664.
[3] F. A. Cotton, T. E. Haas, *Inorg. Chem. 3* (1964) 10.
[4] F. A. Cotton, N. F. Curtis, C. B. Harris, B. F. G. Johnson, S. J. Lippard, J. T. Mague, W. R. Robinson, J. S. Wook, *Science 145* (1964) 1305.
[5] F. A. Cotton, R. A. Walton: *Multiple Bonds Between Metal Atoms*, Wiley, New York 1982, S. 4.
[6] I. Bernal, J. D. Korp, G. M. Reisner, W. A. Herrmann, *J. Organomet. Chem. 139* (1977) 321.
[7] A review on compounds of this type is given in [5], p. 245f.
[8] J.-S. Huang, L. F. Dahl, *J. Organomet. Chem. 243* (1983) 57; E. D. Jemmis, A. R. Pinhas, R. Hoffmann, *J. Am. Chem. Soc. 102* (1980) 2576.
[9] J. J. Schneider, R. Goddard, S. Werner, C. Krüger, *Angew. Chem. 103* (1991) 1145; *Angew. Chem. Int. Ed. Engl. 30* (1991) 1124.
[10] M. P. Andrews, G. A. Ozin, *J. Phys. Chem. 90* (1986) 1245.
[11] P. L. Timms, *Chem. Commun. 1969*, 1033.
[12] J. R. Blackborow, D. Young: *Metal Vapour Synthesis in Organometallic Chemistry*, Springer, Berlin 1979, p. 120f.
[13] G. N. Cloke, J. P. Day, J. C. Green, C. P. Morley, A. C. Swain, *J. Chem. Soc. Dalton Trans. 1991*, 789.
[14] P. L. Timms, *Adv. Inorg. Chem. Radiochem. 14* (1972) 121.
[15] L. M. Cirjak, R. E. Ginsburg, L. F. Dahl, *Inorg. Chem. 21* (1982) 940.
[16] The species here is the complex anion $[Re_3Cl_{12}]^{3\ominus}$ [3].
[17] H. Brunner, N. Janietz, W. Meier, J. Wachter, E. Herdtweck, W. A. Herrmann, O. Serhadli, M. L. Ziegler, *J. Organomet. Chem. 347* (1988) 237; H. Brunner, N. Janietz, J. Wachter, B. Nuber, M. L. Ziegler, *ibid. 367* (1989) 197.

Novel Building Blocks for the Synthesis of Organic Metals

By *Volker Enkelmann**

Organic crystals with special electrical, optical or magnetic properties are attracting increasing interest as "unconventional materials".[1] The special properties alluded to are not determined alone by the electronic structure of the individual molecule, but are only manifested upon interaction of many molecules in the solid state. It therefore does not suffice just to master the synthesis of suitable building blocks, an important step is obtaining the desired interactions in certain crystal structures. This has led to interest being always concentrated on a few model systems in which all steps, from the synthesis of the starting components up to and including reproducible crystallization, have been perfected.

High electrical conductivities in organic metals are, independently of the nature of the building blocks, always associated with certain structural principles. The crystal structure of the long known charge transfer (CT)-salt TTF/TCNQ (TTF = tetrathiafulvalene, TCNQ = tetracyanoquinodimethane, Fig. 1)[2] exhibits the most important features:[3] 1) crystallization of donor and acceptor molecules in segregated stacks with 2) uniform interstack distances; 3) formation of mixed valence states, i.e. only partial charge transfer between the stacks of the redox partners. The charge transport takes place along the stacks, whereby in TFF/TCNQ the two stacks contribute to the total conductivity independently of each other.

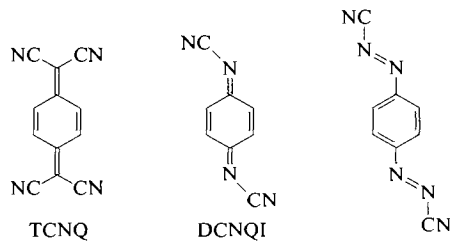

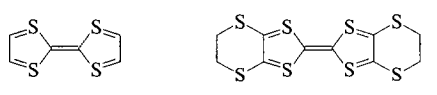

[*] Priv.-Doz. Dr. V. Enkelmann
Max Planck-Institut für Polymerforschung
Ackermannweg 10, W-6500 Mainz (FRG)

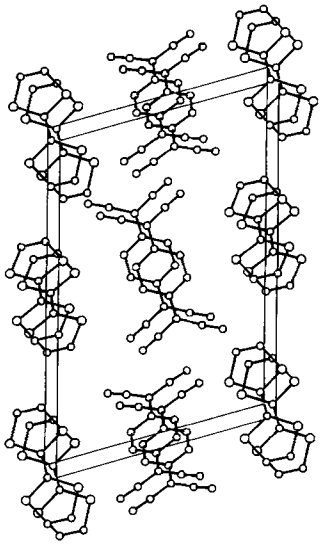

Fig. 1. Section of the crystal structure of TTF/TCNQ along the stack direction.

One could imagine that, by simple combination of many different electron donors and acceptors, a sort of building-block kit would be available with which one could construct almost any desired organic metal having tailor-made properties. Unfortunately this expectation is deceptive. In CT complexes of the type TTF/TCNQ, the redox potentials of the two partners must be carefully harmonized so as to guarantee the required partial charge exchange. In addition, there is the problem that the desired structures are not obtained during the crystallization step following the redox reaction. In many cases mixed stacks are formed in which donor and acceptor molecules interchange. These difficulties can be partly overcome if one of the two redox partners is replaced by stable counterions with formation of radical ion salts. However, crystal engineering, i.e. the selective growth of crystals with predetermined structure, is still an unachieved ideal.

A further reason for the number of building blocks being limited lies in the interdisciplinary nature of the work, which is necessary in this field. An overview of the organic metals so far investigated in detail—TTF/TCNQ, radical cation salts of TTF and analogously built fulvalenes such as, for example, tetramethyltetraselenafulvalene (TMTSF) or bis-(ethylenedithio)tetrathiafulvalene (BEDT-TTF), radical anion salts of TCNQ, aromatic radical cation salts[1]—shows that these systems have all been investigated and optimized over a long period of time by several working groups who have contributed their expertise and knowledge from the most diverse areas of organic synthesis, crystal growth through to special methods of solid-state spectroscopy and theory.

Whereas TTF has often been modified chemically (substitution, expansion of the π system, replacement of S by Se or Te), modification of the acceptor has so far been neglected, so that TCNQ is still used almost exclusively. *Hünig* and co-workers, however, have developed some valuable new acceptors, which can give new impetus in the field of organic metals.[4, 5]

For some time now, *N,N'*-dicyanoquinodiimine (DCNQI) and its derivatives have been readily accessible by a facile, one-step synthesis.[4] Like TCNQ they are two-step, reversible redox systems of the Wurster type which form stable radical anions. On the basis of the known analogy between the $=C(CN)_2$ and $=NCN$ groups it was expected that DCNQI would behave analogously to TCNQ. This has indeed been confirmed, since CT complexes such as, e.g., TTF/DCNQI can be obtained which behave similarly to the corresponding TCNQ salts. The special significance of DCNQI compounds lies in their ability to form metal salts having unusual properties.[6–9] Whereas the TCNQ salts are semiconductors, some DCNQI salts, e.g. [(2,5-dimethyl-DCNQI)$_2$Cu], exhibit typical metallic behavior. Figure 2 shows the temperature dependence of the specific conductivity and the crystal structure of this salt. The specific conductivity, which increases steadily to values of 500000 S cm^{-1} with decreasing temperature, underscores the metallic character of this salt, which counts among the most conductive organic metals (for comparison, the specific conductivity of copper at room temperature is 650000 S cm^{-1}).

Remarkable, and apparently essential for the resulting extraordinary properties, is the tight tetrahedral coordination of the copper ions by the C≡N groups of four neighboring

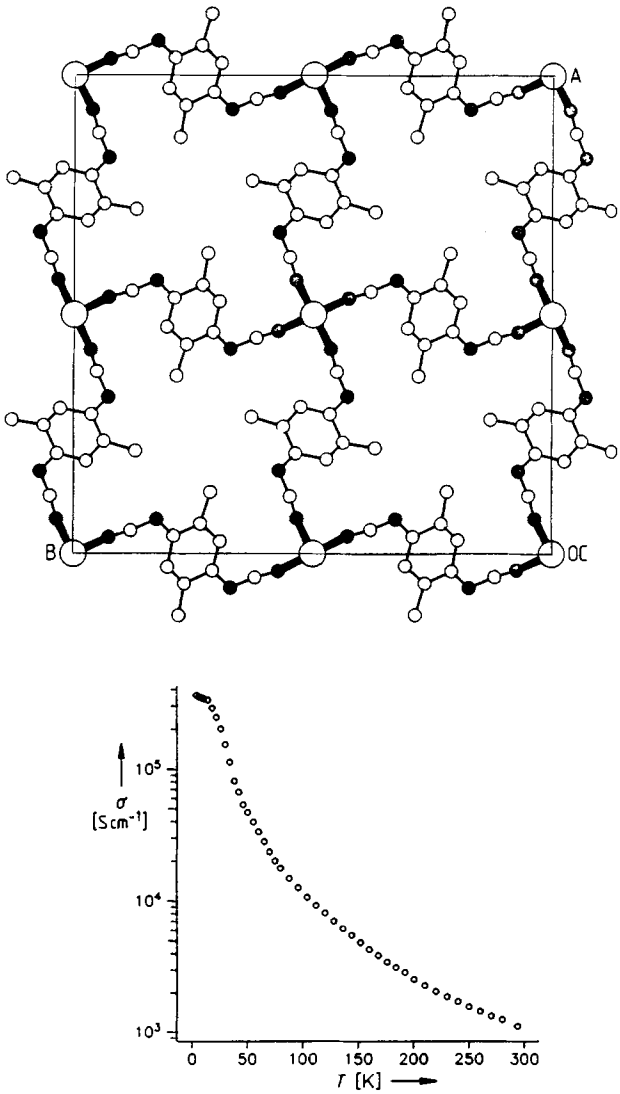

Fig. 2. Section of the crystal structure (top) and temperature dependence of the specific conductivity σ of [(2,5-DM-DCNQI)$_2$Cu] (bottom)[6].

stacks. This coupling of the DCNQI stacks increases the dimensionality and impairs Peierls transitions, which usually lead to semiconducting low-temperature phases in one-dimensional systems. Similar couplings by sulfur–sulfur interactions between one-dimensional molecular stacks are observed in many salts of TTF derivatives which form superconducting low-temperature phases. The particular importance of the DCNQI salts lies in the fact that the strength of the coupling can be varied by suitable choice of the counterion. When Cu is replaced by other metals isomorphic structures are obtained in which the C≡N···M distance increases in the sequence $Ag^{\oplus}$, $Tl^{\oplus}$, $Li^{\oplus}$. The conductivity decreases with decreasing coupling strength, and the transition temperature to superconducting low-temperature phases increases in the same sequence. The metal salts of DCNQI thus constitute ideal building blocks with which one can, within certain limits, selectively change macroscopic properties such as the conductivity, by suitable choice of molecular parameters (counterion, substitution).

Recently *Hünig* and co-workers have even gone one step further. TCNQ and DCNQI are acceptors of the Wurster type, whereas by means of a simple method for the synthesis of dicyanoazobenzenes (DCNABs) we now have access to acceptors of the inverse Wurster type (aromatic ground state and quinonoid oxidized form). Preliminary results obtained with CT complexes and salts of this new class of acceptors have shown that they have redox potentials similar to TCNQ and DCNQI and thus form radical anions of comparable stability. Moreover, they do not differ substantially from the well-known acceptors in their ability to form metal salts and conductive CT complexes.[10, 11] As an example, the crystal structure of 2,5-dimethyl-DCNAB/TFF is shown in Figure 3.

How are we to assess this new development? Since the concepts underlying the makeup of an organic metal have long been known, one cannot foresee any fundamentally new insights being gained in this area. It must be remembered, however, that the structural principles outlined here have been derived empirically from the common characteristics of many organic metals and are therefore of rather a qualitative nature. The new acceptors now readily accessible through the works of *Hünig* et al. improve the available set of building blocks considerably, and, within certain limits, make possible the fine tuning of molecular interactions by suitable choice of components. So there is hope that in the near future one will be able to make virtually quantitative predictions. The problems which could be solved with the help of new model structures include, in particular, the quantitative description of such macroscopic properties as the temperature dependence of specific conductivity and phase behavior (transition to semiconducting or superconducting low-temperature phases) on the basis of molecular interactions along the stack and between neighboring stacks of molecules.

One of the fundamental problems, however, remains unsolvable: the prediction of the crystal structure of organic molecules and the planned assembly of structures with predetermined properties is possible only within modest limits. Even with a much greater number of possible building blocks and a greater number of empirical structural rules it will depend upon the luck and skill of the experimenter as to whether a structure with the desired properties will be obtained.

In comparison to other properties which are only realized by the interaction of many molecules in larger units, the electrical conductivity in organic crystals is relatively well understood. Investigations on these systems therefore constitute ideal excercises for ambitious aims which are summarized under the concept molecular electronics. Here, one hopes that molecules which act as switches, energy transport media (molecular wires), logic units or storage systems can be used to construct larger functional units and actively participate in the processing, transmitting, and storage of information. The developments outlined here hint at the course that will have to be taken in the case of more complicated systems: 1) developing an improved building-block kit of suitable molecules; 2) synthesis of the simplest possible, well characterized models, e.g. single crystals; 3) empirical determination of structure-property relationships; 4) extension of these model concepts to the construction of more complicated structures.

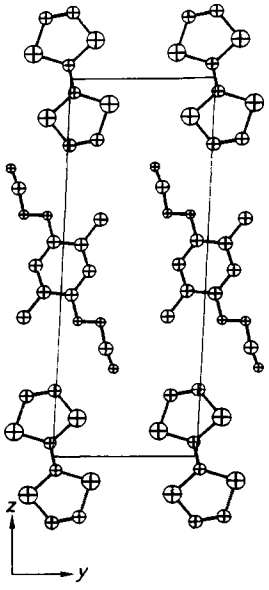

Fig. 3. Section of the crystal structure of 2,5-Me_2-DCNAB/TFF[11].

German version: *Angew. Chem. 103* (1991) 1142

[1] For an overview see *Synth. Met. 41–43* (1991).
[2] T. E. Phillips, T. J. Kistenmacher, J. P. Ferraris, D. O. Cowan, *J. Chem. Soc. Chem. Commun. 1973*, 471.
[3] A. F. Garito, A. J. Heeger, *Acc. Chem. Res. 7* (1974) 232.
[4] A. Aumüller, S. Hünig, *Angew. Chem. 96* (1984) 437; *Angew. Chem. Int. Ed. Engl. 23* (1984) 447; S. Hünig, P. Erk, *Adv. Mater. 3* (1991) 225.
[5] A. Aumüller, E. Hädicke, S. Hünig, A. Schätzle, J. U. von Schütz, *Angew. Chem. 96* (1984) 439; *Angew. Chem. Int. Ed. Engl. 23* (1984) 449.
[6] A. Aumüller, P. Erk, G. Klebe, S. Hünig, J. U. von Schütz, H.-P. Werner, *Angew. Chem. 98* (1986) 759; *Angew. Chem. Int. Ed. Engl. 25* (1986) 740.
[7] S. Hünig, A. Aumüller, P. Erk, H. Meixner, J. U. von Schütz, H.-J. Gross, U. Langohr, H.-P. Werner, H. C. Wolf, C. Burschka, G. Klebe, K. Peters, H. G. von Schnering, *Synth. Met. 27* (1988) B181.
[8] R. Kato, H. Kobayashi, A. Kobayashi, *Synth. Met. 27* (1988) B263.
[9] A. Kobayashi, T. Mori, H. Inokuchi, R. Kato, H. Kobayashi, *Synth. Met. 27* (1988) B275.
[10] S. Hünig, T. Metzenthin, *Angew. Chem. 103* (1991) 610; *Angew. Chem. Int. Ed. Engl. 30* (1991) 563.
[11] H. Almen, T. Bauer, S. Hünig, V. Kupčik, U. Langohr, T. Metzenthin, K. Meyer, H. Rieder, J. U. von Schütz, E. Tillmanns, H. C. Wolf, *Angew. Chem. 103* (1991) 608; *Angew. Chem. Int. Ed. Engl. 30* (1991) 561.

Communications may be submitted in English *or* in German. Further details regarding the submission of communications can be found in the "Notice to Authors" reproduced in the January issue of the journal. Copies thereof may be obtained from the editorial office upon request.

Reactivity of Cobalt Atoms towards 1,2,3,4,5-Pentamethylcyclopentadienyl: Synthesis and Structure of Bis(η^5-pentamethylcyclopentadienyl)-(μ_2-η^5:η^5-pentamethylcyclopentadienyl)dicobalt and Bis(η^5-pentamethylcyclopentadienyl)dicobalt **

By *Jörg J. Schneider,* Richard Goddard, Stefan Werner,* and *Carl Krüger*

Dedicated to Professor Kurt Schaffner

A directed synthesis of clusters with the help of "naked" metal atoms has so far only succeeded in a limited number of cases;[1] as a rule, clusters are formed only as by-products in metal atom reactions.[2] If cluster formation does not take place at all, this can be due to an unfavorable choice of stoichiometric ratios, temperature, or other more difficultly controllable reaction conditions (e.g. metal evaporation rate) during the metal atom reaction. We have now investigated the reaction of cobalt atoms with 1,2,3,4,5-pentamethylcyclopentadiene (Cp*H). Cp*H appeared to us to be especially suitable as ligand because of its unusual electronic properties and of the frequently excellent crystallization behavior of the resulting complexes.[3] Thereby we obtained, inter alia, a triple-decker complex and a novel Cp*Co dimer with an unusually short Co–Co bond. In the reaction of cobalt atoms with the unsubstituted ligand cyclopentadiene (CpH) only the sandwich complex (η^5-cyclopentadienyl)-(η^4-cyclopentadiene)cobalt **1** was formed.[4] As we have already been able to show in the case of reactions of nickel atoms with mono- and disubstituted cyclopentadienes, by skillful choice of the reaction conditions, not only the formation of mononuclear metal complexes but also the synthesis of clusters can be achieved.[5] We have now found that if cobalt atoms are allowed to react with Cp*H under comparable conditions, i.e. in a ligand/metal ratio of ca. 2:1 to 4:1, then, after column chromatographic work-up and subsequent crystallization of the crude product, the three cobalt complexes **2**, **3** and **4** can be isolated (Scheme 1). **2** is the permethylated 18-VE Co^I-sandwich complex analogous to **1**, and under the chosen conditions (ratio Cp^*H/Co_{atoms} ca. 3:1, $T = -120\,^\circ C$) is the main product (20%) of the reaction. **2** is characterized unequivocally by the spectroscopic data and the elemental analysis; the complexes **3** and **4** co-crystallize in varying yields (**3**: 0–5%, **4**: 5–15%) (see *Experimental*). So far, it has only been possible to isolate analytically pure **4** by repeated recrystallization. Despite careful crystallization from saturated hexane solutions we have always obtained single crystals of **3** grown in admixture with **4** which could only be separated by hand. Both compounds are deep black and are readily soluble in all the common solvents. **3** and **4** are more air-sensitive in solution than in the solid state. Crystals of **3** and **4** are stable for more than three months.

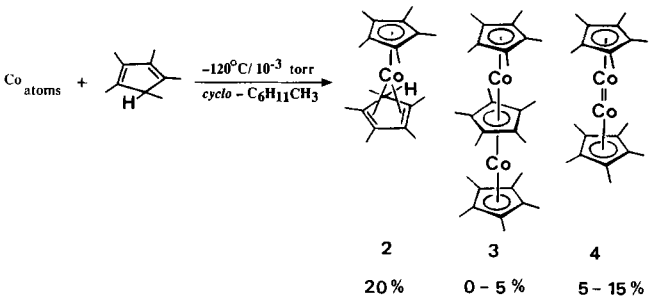

Scheme 1. Synthesis of **2**, **3** and **4** by metal atom reaction.

The molecular structure of **3** was elucidated by a crystal structure analysis[6] (Fig. 1). The disorder in the crystal structure of **3**, however, allows no detailed discussion of the individual bond lengths and angles. The Co atoms and the centroids of the Cp* rings are linear. The distance from the

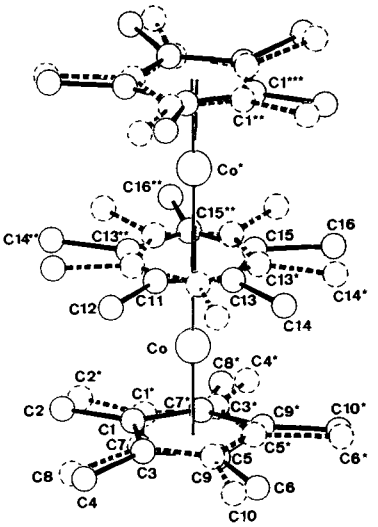

Fig. 1. Structure of **3** in the crystal. Important bond lengths, see text. The disorder is generated by the space group symmetry (2/*m*).

Co atom to the central Cp* ring is 1.770(2) Å, to the outer 1.724(1) Å. The Co–Co* distance is 3.539(1) Å, a direct metal–metal interaction can thus be ruled out. The compound is a further example of the previous group of structurally characterized homoleptic triple-decker complexes comprising only four complexes: the triple-decker cation $Cp_3Ni_2^{\oplus}$ **5** synthesized by *Werner* and *Salzer*,[7] the vanadium complex bis(η^5-cyclopentadienyl)(μ_2-η^6:η^6-benzene)divanadium **6** re-

[*] Dr. J. J. Schneider, Dr. R. Goddard, Dipl.-Chem. S. Werner, Prof. Dr. C. Krüger
Max-Planck-Institut für Kohlenforschung
Kaiser-Wilhelm-Platz 1, W-4330 Mülheim a.d. Ruhr 1 (FRG)

[**] Metal Atoms in the Synthesis of Metal Clusters, Part 4. *J. J. S.* thanks Prof. *Dr. G. Wilke* for supporting this work.—Part 3: J. J. Schneider, M. Nolte, C. Krüger, *J. Organomet. Chem. 403* (1991) C4.

ported by *Jonas* et al.,[8] the complex bis(η^6-mesitylene)-(μ_2-η^6:η^6-mesitylene)dichromium **7** recently prepared by *Lamanna* et al., likewise by a metal atom reaction,[9] and the triple-decker cation $Cp^*_3Ru_2^{\oplus}$ **8** synthesized by *Rybinskaya* et al.[10] In contrast to **5**, **7** and **8**, each of which fulfill the 30/34 valence electron (VE) rule of *Lauher* and *Hoffmann* for triple-decker complexes[11] (**5**: 34 VE; **7**, **8**: 30 VE), complex **3** with formally 33 VE—like **6** (26 VE)—is an exception to this rule. Accordingly, different paramagnetically induced shifts δ_{para} are observed in the ^{1}H-NMR spectrum for **3**. Thus, the signals for the two terminal Cp* rings are shifted downfield, whereas that for the bridging Cp* ring is shifted upfield relative to the solvent signal. This can be attributed to different spin transfer mechanisms. Surprisingly, **4** also exhibits paramagnetism in the ^{1}H-NMR spectrum. The presence of a triplet state is possibly an explanation for this observation. EPR investigations and calculations should prove informative here.[12] As expected a singlet ($\delta_{para} = 61$) is found for both Cp* rings. Preliminary investigations of the behavior of **4** on varying the temperature reveal a linear dependence between δ_{para} and the reciprocal temperature $1/T$.

Compound **4** is without precedence, as confirmed by a crystal structure analysis (Fig. 2).[6] A striking feature is the

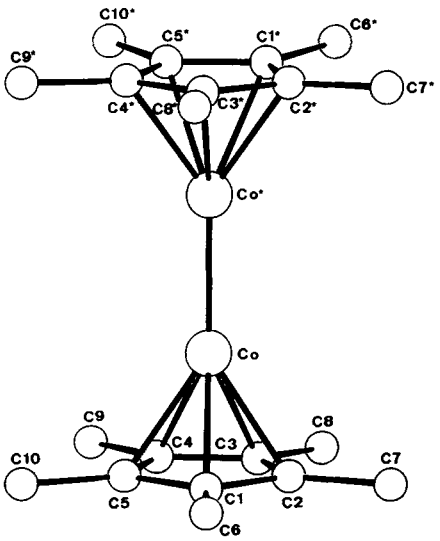

Fig. 2. Structure of **4** in the crystal. Important bond lengths, see text.

dumbbell-like, exactly linear arrangement of the two Cp*Co units. The Co—Co bond vector is perpendicular to a crystallographic twofold axis of rotation. The centroids of the Cp* rings are 1.689(1) Å distant from the Co atoms, while the corresponding distance in the triple-decker complex **3** is 1.724(1) Å. A possibly stronger interaction between the Cp* ligand and the Co atom in **4**, however, does not influence the arrangement of the methyl groups on the five-membered ring; the C atoms of the methyl groups lie approximately in the plane of the five-membered ring. The Co—Co bond length (2.253(1) Å) corresponds formally to a double bond, resulting in a 16 VE shell for each metal center in **4**. Other known compounds of similar structure contain either additional bridging ligands, in some cases resulting in a bending of the terminal rings,[13] or they exhibit far greater metal–metal distances, which then, despite additional bridging, still enable a linear arrangement of the metal-ligand units.[14]

According to preliminary investigations, **4** does not react with ethylene or even CO (1 bar, room temperature); it is recovered unchanged from the reaction mixture. We attribute the formation of the triple-decker complex **3** and the dimer **4** to the comparatively high metal atom concentrations in comparison to those usually used in metal atom reactions.[15] As the reaction progresses the reaction solution becomes largely depleted of the free ligand Cp*H, since this is consumed for the formation of **2** and Cp*Co units.[16] These Cp*Co units can then dimerize to **4** when present in sufficient concentration in the reaction solution. On the basis of matrix isolation experiments *Ozin* and *Andrews* already postulated a type of complex analogous to **4**[17] which should be formed upon addition of naked metal atoms to bis(arene)metal complexes.

The reaction of highly reactive Cp*Co units with the **2** already formed leads via cleavage of hydrogen to formation of **3**. Also conceivable, however, would be a reaction of Cp*Co units with previously formed decamethylcobaltocene leading to formation of **3**, similarly to the formation of **7** from mesitylene and chromium atoms.[18] By optimization of the reaction conditions (temperature, metal atom/ligand ratio, metal vaporization rate, etc) we hope to increase the yields of **3** and **4** in order to make these complexes accessible in larger amounts and with a view to possibly interesting secondary reactions.

Experimental

Cobalt metal (3 g, 50.9 mmol) was evaporated into 150 mL of a 5% solution of Cp*H in methylcyclohexane cooled to -120 °C by using a rotating metal vaporization reactor[19] (80 rpm). On completion of reaction a brownish-black solution had formed. This was siphoned out of the reactor, filtered, and the brownish-black filtrate evaporated down in a high vacuum. The oily residue was taken up in a little THF, treated with 20 g of Al_2O_3 (5% H_2O) and dried until flowable.

Chromatography on Al_2O_3 (5% H_2O) with pentane furnished, after subsequent crystallization, 3.3 g (10 mmol) of **2** (red crystals, -30 °C, ethanol/pentane); further elution with pentane/ether (1 : 1) afforded **3** and **4** as black zone (yield 2.5 g, black crystals, -20 °C, hexane).

2: ^{1}H NMR ([D$_8$]toluene, 200 MHz): $\delta = 1.62$ (s, 15H; CH_3), 0.38 (d, ^3J(H,H) = 6.1 Hz, 3H; CH_3), 0.92 (s, 6H; CH_3), 1.81 (s, 6H; CH_3), 2.15 (q, ^4J(H,H) = 0.3 Hz; 1H); ^{13}C NMR [D$_6$]benzene, 75.5 MHz): $\delta = 9.3$ (q, ^1J(C,H) = 125 Hz; CH_3(Cp*)), 10.6 (q, ^1J(C,H) = 124 Hz; CH_3), 11.8 (q, ^1J(C,H) = 124 Hz; CH_3), 19.3 (q, ^1J(C,H) = 125 Hz; CH), 54.4 (s, C_{diene}), 55.7 (d, ^1J(C,H) = 135 Hz; C_{sp^3}), 85.1 (s, C_{diene}), 87.6 (s, Cp* (C_{sp^2}), MS (70 eV): *m/z* 330 ($M^{\oplus}$, 10%), 315 ($M^{\oplus}$-CH_3, 100). Correct C, H, Co-analysis.

3: ^{1}H NMR ([D$_8$]) toluene, 200 MHz, 30 °C): $\delta = 38.8$ (s, 30H; CH_3), -41.0 (s, 15H; CH_3(μ-Cp*)), MS (70 eV): *m/z* 523 ($M^{\oplus}$, 21%), 329 ($M^{\oplus}$-Cp*-Co, 100).

4: ^{1}H NMR ([D$_8$])toluene, 200 MHz, 30 °C): $\delta = 61.3$ (s, br; CH_3), MS: decomposition. Correct C, H, Coanalysis.

Received: April 30, 1991 [Z 4599 IE]
German version: *Angew. Chem. 103* (1991) 1145

CAS Registry numbers:
2, 135075-04-6; **3**, 135075-05-7; **4**, 135075-06-8; Cp*H, 4045-44-7; Co, 7440-48-4.

[1] a) F. A. Vollenbroek, P. C. P. Bouton, J. P. van den Berg, J. J. Bour, *Inorg. Chem. 17* (1978) 1345; b) J. W. A. van Velden, J. J. Bour, F. A. Vollenbroek, P. T. Beurskens, J. M. Smits, *J. Chem. Soc. Chem. Commun. 1979*, 1162.

[2] a) L. Vasquez, H. Pritzkow, U. Zenneck, *Angew. Chem. 100* (1988) 705; *Angew. Chem. Int. Ed. Engl. 29* (1988) 706; b) G. J. Zimmermann, R. Wilozynski, L. G. Sneddon, *J. Organomet. Chem. 154* (1978) C29.

[3] E. J. Miller, S. J. Landon, T. B. Brill, *Organometallics 4* (1985) 533.

[4] P. L. Timms, *Adv. Inorg. Chem. Radiochem. 14* (1972) 121.

[5] J. J. Schneider, R. Goddard, C. Krüger, S. Werner, B. Metz, *Chem. Ber. 124* (1991) 301.

[6] Crystal data of **3**: *Cmca*, $a = 15.203(1)$, $b = 12.289(1)$, $c = 14.714(1)$ Å, $V = 2748.9$ Å^3, $Z = 4$, $\varrho_{calcd} = 1.26$ gcm^{-3}, $\lambda = 0.71069$ Å, $\mu = 12.19$ cm^{-1}, 8752 measured reflections ($\pm h$, $\pm k$, $+ l$), 2078 independent reflections, 1636 observed ($I > 2\sigma(I)$), $R = 0.085$, $R_w = 0.078$, 67 refined parameters, residual electron density 1.3 eÅ^{-3}, disorder (50 : 50) not removable even by refinement in the non-centrosymmetric space group *Aba2* (No. 41). No H-atomic positions were calculated. Crystal data of **4**: *P2/c*, $a = 9.533(1)$, $b = 8.514(2)$, $c = 12.376(2)$ Å, $\beta = 105.95(1)°$, $V = 965.8$ Å^3, $T = -173$ °C, $Z = 2$, $\varrho_{calcd} = 1.34$ gcm^{-3}, $\lambda = 0.71069$ Å, $\mu = 17.10$ cm^{-1}, 28569 measured reflections ($\pm h$, $\pm k$, $+ l$), analytical absorption correction (trans-

mission 0.5–0.9), 4973 independent reflections, 3863 observed ($I > 3\sigma(I)$), $R = 0.040$, $R_w = 0.062$, 100 refined parameters, residual electron density 2.5 eÅ^{-3} on the crystallographic twofold axis, 1.8 Å distant from both Co atoms. Further details of the crystal structure analyses are available on request from the Fachinformationszentrum Karlsruhe, Gesellschaft für wissenschaftlich-technische Information mbH, W-7514 Eggenstein-Leopoldshafen 2 (FRG), on quoting the depository number CSD-55400, the names of the authors, and the journal citation.

[7] H. Werner, A. Salzer, *Angew. Chem. 84* (1972) 949; *Angew. Chem. Int. Ed. Engl. 11* (1972) 930.

[8] A. W. Duff, K. Jonas, R. Goddard, H. J. Kraus, C. Krüger, *J. Am. Chem. Soc. 105* (1983) 5479.

[9] W. M. Lamanna, W. B. Gleason, D. Britton, *Organometallics 6* (1987) 1583.

[10] A. R. Kudinov, M. I. Rybinskaya, Y. T. Struchkov, A. I. Yanovskii, P. V. Petrovskii, *J. Organomet. Chem. 336* (1987) 187.

[11] J. W. Lauher, M. Elian, R. H. Summerville, R. Hoffmann, *J. Am. Chem. Soc. 98* (1976) 3219.

[12] F. Mark, MPI für Strahlenchemie, Mülheim a. d. Ruhr, unpublished.

[13] a) R. E. Ginsburg, L. M. Cirjak, L. F. Dahl, *J. Chem. Soc. Chem. Commun. 1979*, 468; *Inorg. Chem. 21* (1982) 940; b) M. Schulz, S. Stahl, H. Werner, *J. Organomet. Chem. 394* (1990) 469.

[14] a) P. Louca, J. A. K. Howard, *Acta Crystallogr. Sect. C43* (1987) 1908; b) I. Bernal, J. D. Korp, G. M. Reisner, W. A. Herrmann, *J. Organomet. Chem. 139* (1977) 321.

[15] J. R. Blackborrow, D. Young: *Metal Vapour Synthesis in Organometallic Chemistry*, Springer, Berlin 1979, Chap. 1.

[16] For the detection of reactive M-L fragments at low temperatures see: M. P. Andrews, S. M. Mattar, G. A. Ozin, *J. Phys. Chem. 90* (1986) 744.

[17] M. P. Andrews, G. A. Ozin, *J. Phys. Chem. 90* (1986) 1245.

[18] W. M. Lamanna, *J. Am. Chem. Soc. 108* (1986) 2096.

[19] P. L. Timms, *Angew. Chem. 87* (1975) 295; *Angew. Chem. Int. Ed. Engl. 14* (1975) 273.

The Cluster Anion $[Ru_6H(CO)_{15}S_3]^-$: A Planar Hexanuclear Metal Framework with Almost Perfect C_{3v} Symmetry

By *Ulf Bodensieck, Helen Stoeckli-Evans,* and *Georg Süss-Fink**

The structure analysis of the osmium complex $[Os_6(CO)_{17}\{P(OMe)_3\}_4]$ by *Lewis* et al.[1] showed that a hexanuclear cluster framework can be planar. Although several such "raft" clusters have been synthesized since then, the planar arrangement of the metal atoms in a hexanuclear cluster is more the exception than the rule.[2]

In an attempt to extend the activation of C_{sp^3}–H bonds observed in the rutheniumcarbonyl–alkylthiourea system[3] to methane, we were surprised to obtain the new cluster anion $[Ru_6H(CO)_{15}S_3]^-$ (**1**), which contains an approximately planar hexanuclear ruthenium skeleton with C_{3v} symmetry. Anion **1**, which has three outer Ru_3S tetrahedrons enclosing an inner Ru_3H tetrahedron, captures the imagination by the aesthetics of its molecular architecture.

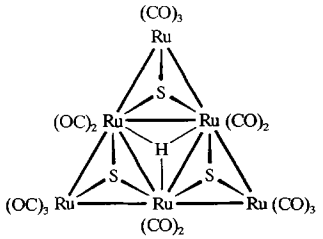

1

It is unclear how the cluster anion **1** arises on treatment of $[Ru_3(CO)_{12}]$ with tetramethylthiourea in an inert atmosphere (60 bar methane or nitrogen) in THF solution at 150 °C; during workup of the reaction mixture it precipitates as the tetramethylformamidinium salt from dichloromethane. It does not form under ambient pressure.

The single-crystal X-ray structure analysis of **1**[4] (Fig. 1) shows the almost planar metal framework in the form of a large triangle comprising four small triangles. The outer three small triangles are each capped by a μ_3-sulfido ligand, while the inner Ru_3 triangle is capped on the opposite side of the plane to the sulfido ligands by a μ_3-hydrido ligand. The ruthenium atoms Ru1, Ru3, and Ru5, situated at the corners of the large triangle, lie on average 0.55 Å out of the plane defined by Ru2, Ru4, and Ru6, on the side of the sulfido ligands.

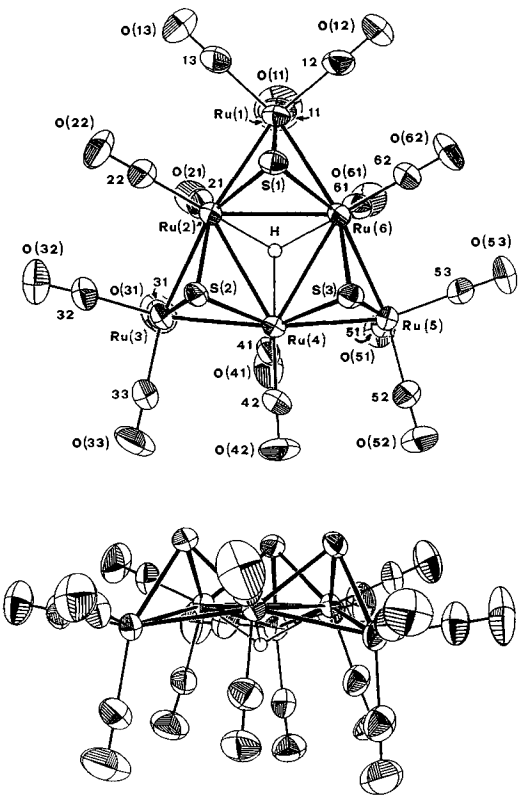

Fig. 1. View from above (top) and from the side (bottom) of the cluster anion $[Ru_6H(CO)_{15}S_3]^-$ (**1**) (ORTEP, 50% probability ellipsoids, C atoms of CO ligands are indicated by numbers only). Important atomic distances [Å] and angles [°]: Ru(1)-Ru(2) 2.779(1), Ru(1)-Ru(6) 2.767(1), Ru(2)-Ru(3) 2.776(1), Ru(2)-Ru(4) 3.027(1), Ru(2)-Ru(6) 3.003(1), Ru(3)-Ru(4) 2.790(1), Ru(4)-Ru(5) 2.763(1), Ru(4)-Ru(6) 3.034(1), Ru(5)-Ru(6) 2.772(1), Ru(1)-S(1) 2.302(1), Ru(2)-S(1) 2.384(1), Ru(2)-S(2) 2.370(1), Ru(3)-S(2) 2.303(1), Ru(4)-S(2) 2.375(1), Ru(4)-S(3) 2.372(1), Ru(5)-S(3) 2.308(1), Ru(6)-S(1) 2.379(1), Ru(6)-S(3) 2.371(1); Ru(2)-Ru(1)-Ru(6) 65.58(1), Ru(1)-Ru(2)-Ru(3) 157.92(2), Ru(1)-Ru(2)-Ru(6) 57.01(1), Ru(3)-Ru(2)-Ru(4) 57.27(1), Ru(4)-Ru(2)-Ru(6) 60.41(1), Ru(2)-Ru(3)-Ru(4) 65.89(1), Ru(2)-Ru(4)-Ru(3) 56.84(2), Ru(2)-Ru(4)-Ru(6) 59.40(1), Ru(3)-Ru(4)-Ru(5) 153.32(2), Ru(5)-Ru(4)-Ru(6) 56.92(1) Ru(4)-Ru(5)-Ru(6) 66.48(2), Ru(1)-Ru(6)-Ru(2) 57.40(2), Ru(1)-Ru(6)-Ru(5) 156.63(2), Ru(2)-Ru(6)-Ru(4) 60.19(1), Ru(4)-Ru(6)-Ru(5) 56.60(1).

The unusually high-field NMR signal ($\delta = -33.36$) for the hydrido ligand indicates that it is μ_3-bridging. In contrast, the anion $[Ru_6H(CO)_{18}(OCNMe_2)_2]^-$ (**2**) synthesized by *Kaesz* et al. contains a μ_2-hydrido ligand ($\delta = -17.08$), and the hexanuclear metal framework is folded.[5] In anion

[*] Prof. Dr. G. Süss-Fink, Prof. Dr. H Stoeckli-Evans, U. Bodensieck
Institut de Chimie, Université de Neuchâtel
Avenue de Bellevaux 51, CH-2000 Neuchâtel (Switzerland)

1 the distances between the ruthenium atoms which define the outer triangle are on average shorter (2.77 Å) than those of the inner triangle (3.02 Å). In the six-membered metal ring described for anion **2**, however, the Ru–Ru distances of the inner triangles (3.22 Å) are clearly longer. This is explained by only a partial transannular interaction in **2**.[5]

The hexanuclear ruthenium skeleton in **1** is stabilized by 15 CO ligands. Every Ru atom bears an axial CO ligand, while Ru2, Ru4, and Ru6 are each bonded to one and Ru1, Ru3, and Ru5 to two additional equatorial CO ligands. The three μ_3-sulfido ligands are situated on the same side of the plane of metal atoms. The μ_3-hydrido ligand must therefore lie on the other side for steric reasons, as the space-filling model shows (Fig. 2).

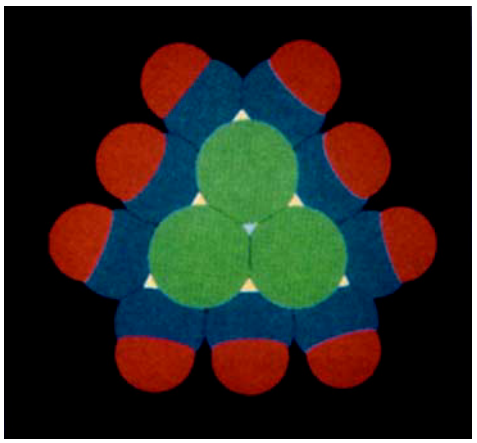

Fig. 2 SCHAKAL representation [6] of the cluster anion $[Ru_6H(CO)_{15}S_3]^-$ (**1**) (Ru yellow, S green, H gray, C blue, O red).

Experimental Procedure

All steps were performed under a N_2 atmosphere in dried, N_2-saturated solvents. $[Ru_3(CO)_{12}]$ (320 mg, 0.5 mmol) and $(Me_2N)_2CS$ (86 mg, 0.65 mmol) were dissolved in THF (20 mL) in a stainless steel autoclave (working volume 100 mL); the mixture was pressurized with methane (65 bar) and heated to 150 °C under constant stirring. After 2 h the reactor was cooled, the pressure released, and the red-brown solution evaporated to dryness. The residue was taken up in dichloromethane and anion **1** precipitated as the $[(Me_2N)_2CH]^+$ salt in the form of red-brown crystals. Yield: 38 mg (14%). IR(THF): $\tilde{\nu}$[cm^{-1}] = 2079w, 2051vs, 2001vs, 1987(sh)m, 1933vw (ν(CO)). ^{1}H NMR ($CDCl_3$, 200 MHz): δ = 8.04 (s, 1H; CH), 3.53 (s, br, 6H; Me), 3.38 (s, br, 6H; Me), − 33.36 (s, 1H; Ru_3H). Satisfactory C, H, N analyses.

Received: May 6, 1991 [Z 4613 IE]
German version: *Angew. Chem. 103* (1991) 1147

CAS Registry numbers:
$[(Me_2N)_2CH]$ [**1**], 135707-57-2; $[Ru_3(CO)_{12}]$, 15243-33-1; $(Me_2N)_2CS$, 2782-91-4.

[1] R. J. Goudsmit, B. F. G. Johnson, J. Lewis, P. R. Raithby, K. H. Whitmire, *J. Chem. Soc. Chem. Commun. 1982*, 640.

[2] D. M. P. Mingos, A. S. May in D. F. Shriver, H. D. Kaesz, R. D. Adams (Ed.): *The Chemistry of Metal Cluster Complexes*, VCH Publishers, New York 1990, p. 52.

[3] U. Bodensieck, H. Stoeckli-Evans, G. Süss-Fink, *J. Chem. Soc. Chem. Commun. 1990*, 267.

[4] X-ray data: Stoe-Siemens AED2 four circle diffractometer ($Mo_{K\alpha}$, graphite monochromator, λ = 0.71073 Å, ω/θ-techniques), solution and refinement with NRCVAX [7]. $[(Me_2N)_2CH]^+$ salt of **1**: space group $P2_1/n$, a = 11.580(1), b = 16.264(1), c = 18.174(3) Å, β = 93.45(1)°, V = 3416.6(7) Å^3, Z = 4, $\varrho_{calcd.}$ = 2.381 g cm^{-3}, μ = 18.6 cm^{-1}, Θ_{max} = 25°; 4803 independent reflections, numerical absorption by SHELX-76 [8] (transmission factors 0.643 (max) and 0.450 (min)), index limits h: − 13/13, k: 0/19, l: 0/21; 4685 reflections with $I > 3\,\sigma(I)$; although several hydrogen atoms could be determined from difference maps, all were placed in calculated sites (U_{iso} = $U_{eq(C)}$ + 0.01). The hydrido hydrogen atom was found in the last difference map. Its coordinates were fixed and only its U_{iso} value was refined (0.074 Å^2). Refinement with weighted anisotropic temperature factors for the non-hydrogen atoms, least-squares method, R = 0.029, R_w = 0.046, $w^{-1} = \sigma^2(F_0) + 0.0025\,(F_0^2)$; residual electron density in the last density difference map 0.57(max) close to a ruthenium atom and − 1.33 min Å^{-3}. Further details of the crystal structure investigation may be obtained from the Cambridge Crystallographic Data Centre, University Chemical Laboratory, Lensfield Road, GB-Cambridge CB2 1EW on quoting the names of the authors and the journal citation.

[5] N. M. Boag, C. B. Knobler, H. D. Kaesz, *Angew. Chem. 95* (1983) 243; *Angew. Chem. Int. Ed. Engl. 22* (1983) 249; *Angew. Chem. Suppl.* (1983) 198.

[6] E. Keller, *SCHAKAL 88, a FORTRAN Program for the Graphical Representation of Molecular and Crystallographic Models*, University Freiburg 1988.

[7] E. J. Gabe, Y. Le Page, J.-P. Charland, F. L. Lee, *NRCVAX, an Interactive Program system for Structure Analysis, J. Appl. Cryst. 22* (1989) 384.

[8] G. M. Sheldrick, *SHELX-76, Program for Crystal Structure Determination*, University of Cambridge 1976.

On a Metathesis Reaction of Tetrathiafulvalene (TTF)**

By *Henning Hopf*,* *Martin Kreutzer*, and *Peter George Jones**

Dedicated to Professor Horst Prinzbach on the occasion of his 60th birthday

We recently reported[1] an efficient method for the preparation of cyano(ethynyl)ethenes of type **1** and described their behavior as dienophiles in [2 + 4] cycloadditions. Because of the electron-withdrawing effect of the cyano substituents on the π-electron system, these compounds are potential acceptors for charge-transfer (CT) complexes, those with tetrathiafulvalene (**2**) and related compounds being of particular interest. Compound **2** is known to form electrically conducting "organic metals" with a large number of acceptor systems.[2, 3] We therefore allowed the enyne **1a** to react with **2**

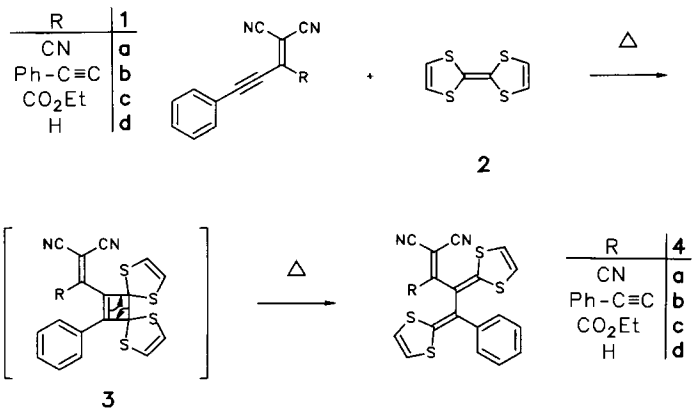

for two days in refluxing toluene and thereby obtained highly lustrous, black-violet crystals (77%). An X-ray structure analysis showed, however, that the product was not the expected CT complex but, surprisingly, the covalent compound **4a** (Fig. 1).[4] Its structure in the crystal is character-

[*] Prof. Dr. H. Hopf, Dipl.-Chem. M. Kreutzer
Institut für Organische Chemie der Universität
Hagenring 30, W-3300 Braunschweig (FRG)
Prof. Dr. P. G. Jones
Institut für Anorganische und Analytische Chemie der Universität
Hagenring 30, W-3300 Braunschweig (FRG)

[**] New Planar π Systems, Part 3. This work was supported by the Fonds der Chemischen Industrie and by BASF. Part 2: H. Hopf, M. Kreutzer, P. G. Jones, *Chem. Ber. 124* (1991) 1471.

ized by an almost orthogonal arrangement of the two nearly planar halves of the molecule (mean deviation 3 pm); the dihedral angle around the central C9–C10 bond is 96.79°. The spectroscopic and analytical data are also consistent with the proposed structure.[4] This reaction, in which tetrathiafulvalene is virtually cut in two, is not an isolated case. This was shown by further experiments with the acceptors **1b–d**, which afforded the cross-conjugated compounds **4b–d** (**4b**, 77; **4c**, 47; **4d**, 33% yield;[5] not optimized).

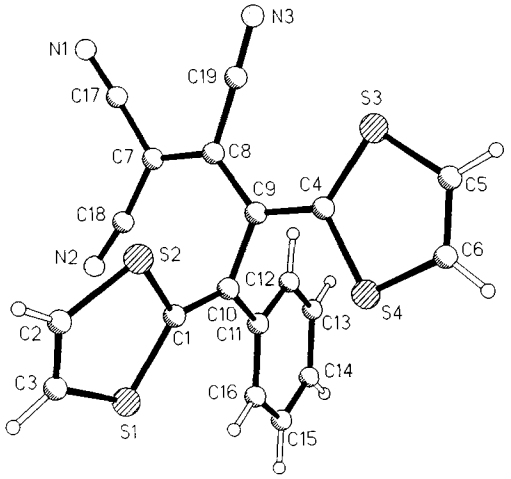

Fig. 1. Molecular structure of **4a**[9].

We assume that this reaction involves a metathesis process, which begins with the [2 + 2] cycloaddition of the triple bond of **1** to the central double bond of **2** to form the cyclobutene derivative **3**, which, in turn, is stabilized by electrocyclic ring opening to give **4**. Compounds of type **4** are not new. As early as 1970, *Hartzler* obtained adducts of type **4**, in addition to derivatives of tetrathiafulvalene, on reaction of electron-poor triple-bond dienophiles with carbon disulfide.[6] Control experiments showed, however, that the former reaction products are not transformed into the latter under the reaction conditions and that the formation of all reaction products can best be explained by the intermediacy of 1,3-dithiolium carbenes.[7] The above, simple route to **4** thus offers a new and variable approach to this class of substances. The success of the reaction is largely dependent on the structure of **1**, as is shown by addition experiments in which attempts were made in vain to add triple-bond dienophiles, such as diethyl acetylenedicarboxylate and ethyl phenylacetylenecarboxylate to **2**.

Compounds **4** are not only possible reaction partners for the preparation of novel donor/acceptor systems. The dicyanomethylene group also offers a broadly modifiable functionality.[8]

Received: April 5, 1991 [Z 4553 IE]
German version: *Angew. Chem. 103* (1991) 1148

CAS Registry numbers:
1a, 23225-88-9; **1b**, 18627-98-0; **1c**, 135513-88-1; **1d**, 13532-14-4; **2**, 31366-25-3; **4a**, 135513-89-2; **4b**, 135513-90-5; **4c**, 135513-91-6; **4d**, 135535-68-1.

[1] H. Hopf, M. Kreutzer, *Angew. Chem. 102* (1990) 425; *Angew. Chem. Int. Ed. Engl. 29* (1990) 393. The dicyano(ethynyl)ethene **1c** was prepared by Pd-catalyzed coupling of ethyl 3,3-dicyano-2-iodoacrylate with tri-*n*-butylstannylphenylacetylene.

[2] Review: see, for example A. F. Garito, A. J. Heeger, *Acc. Chem. Res. 7* (1974) 232.

[3] A. Aumüller, E. Hädicke, S. Hünig, A. Schätzle, J. U. von Schütz, *Angew. Chem. 96* (1984) 439; *Angew. Chem. Int. Ed. Engl. 23* (1984) 449.

[4] **4a**: ^{1}H NMR (400 MHz, [D$_6$]DMSO): δ = 6.90 (s, 2H), 7.20–7.25 (m, 1H), 7.35–7.45 (m, 4H), 7.50 (br. d, 1H), 7.55–7.65 (m, 3H), 7.66 (br. d, 1H), 7.79 (m, 2H). ^{13}C NMR (100 MHz), [D$_6$]DMSO): δ = 67.93 (s), 87.18 (s), 109.73 (s), 115.79(s), 117.86 (s), 118.47 (s), 120.08 (d), 120.15 (s), 120.76 (d), 121.45 (s), 125.52 (d), 125.82 (d), 126.52 (d), 128.90 (d), 129.12 (d), 129.44 (d), 131.60 (d), 132.14 (d), 136.37 (s), 139.74 (s), 147.62 (s), 175.09 (s). IR (KBr): $\tilde{\nu}$[cm^{-1}] = 2924 (m), 2204 (m), 2189 (m), 1501 (w), 1371 (m), 1322 (s), 660 (w). UV (acetonitrile): λ_{max} (lg ε) = 199 nm (4.71), 247 (4.41), 364 (4.35), 511 (4.44). MS (70 eV): *m/z* 482 (100%), 437 (58), 417 (10), 392 (10), 380 (15), 361 (18), 347 (19), 322 (15), 203 (24), 145 (20), 91 (11).

[5] The spectroscopic data for **4b–d** correspond largely to those for **4a** and are therefore omitted here.

[6] H. D. Hartzler, *J. Am. Chem. Soc. 92* (1970) 1412; vgl. C. G. Krespan, D. C. England, *J. Org. Chem. 33* (1968) 1850.

[7] H. D. Hartzler, *J. Am. Chem. Soc. 95* (1973) 4379.

[8] K. Wallenfels, K. Friedrich, J. Rieser, W. Ertel, H. K. Thieme, *Angew. Chem. 88* (1976) 311; *Angew. Chem. Int. Ed. Engl. 15* (1976) 261.

[9] Crystal structure analysis: space group $P2_1/n$, T = 178 K, a = 945.2(2), b = 1443.5(3), c = 1424.6(3) pm, β = 104.07(2)°, V = 1.8852(7) nm^3, Z = 4, ϱ_{calcd} = 1.436 Mg m^{-3}. $Mo_{K\alpha}$ radiation was used to collect 5214 intensities to 2θ = 50° (3308 unique, 2805 > $4\sigma(F)$). The *wR* value is 0.040; ω scans were used. The structure was refined anisotropically to R = 0.031. Further details of the crystal structure investigation are available on request from the Fachinformationszentrum Karlsruhe, Gesellschaft für wissenschaftlich-technische Information mbH, W-7514 Eggenstein-Leopoldshafen 2 (FRG), by quoting the depository number CSD-55362, the names of the authors, and the journal citation.

A Polymeric Tellurium Cation by Oxidation of Tellurium with Tungsten Bromides

By *Johannes Beck**

Transition-metal halides in which the metal is in a high oxidation state can oxidize tellurium to tellurium polycations. WCl_6 was used as oxidizing agent to synthesize $Te_8[WCl_6]_2$ (**1**), which contains the previously unknown $Te_8^{2\oplus}$ cation.[1] In the structure of **1**, an association of chalcogen cations was observed for the first time and the compound was formulated as the polymeric cation $[Te_n]^{n/4\oplus}$. The shortest interionic Te–Te distances in **1** (342.4 pm), however, are considerably longer than the intraionic distances of 270.4 to 299.3 pm.

A polymeric tellurium cation with largely equal Te–Te distances is present in Te_7WOBr_5 (**2**), which has now been prepared, likewise by oxidation of tellurium with tungsten halides. Reaction of seven equivalents of tellurium with one equivalent of a $WBr_5/WOBr_4$ mixture in an evacuated glass ampoule with a temperature gradient of 230 → 210 °C results in the formation of **2** as black, lustrous crystals, which are transported to the cooler end of the ampoule. This transport is made possible by the use of excess halide. Mixtures corresponding exactly to the composition Te_7WOBr_5, for example, $WOBr_4 + 5\,Te + Te_2Br$ or $WOBr_3 + 3\,Te + 2\,Te_2Br$ lead to the formation of **2** at 250 °C, though only as fine crystals; no transport is observed under these conditions. Above 300 °C, **2** decomposes to tellurium and volatile tungsten halides such as $WOBr_4$ and WO_2Br_2. When the temperature is decreased to 230 °C, **2** is formed once again. This thermal reversibility of formation and decomposition has already been observed for **1** and $Te_4[WCl_6]_2$[2] and is thus characteristic of polytellurium halotungstates.

The crystal structure analysis[3] shows that **2** is composed of one-dimensional polymeric tellurium cations, one-dimensional $[WOBr_4]_n$ chains, and free bromide ions. The poly-

[*] Dr. J. Beck
Institut für Anorganische Chemie der Universität
Engesserstrasse, W-7500 Karlsruhe (FRG)

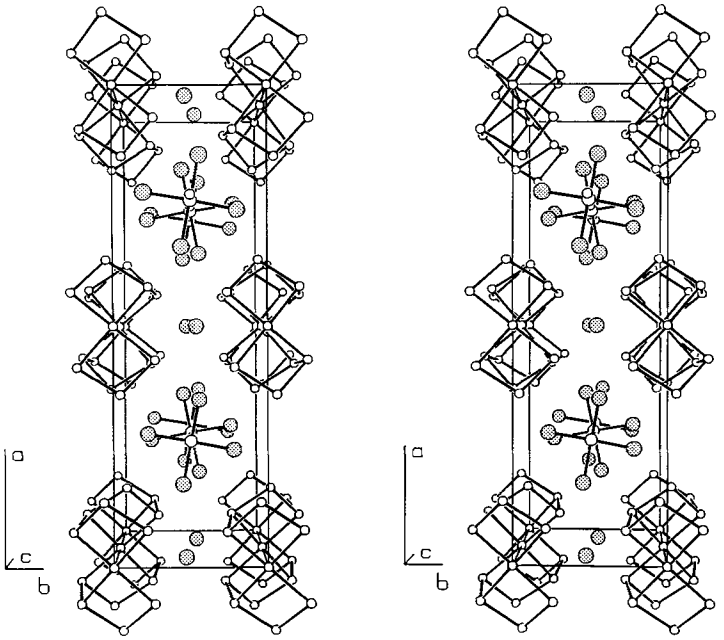

Fig. 1. Stereoscopic representation of the unit cell of **2**. Large dotted circles, Br atoms; small empty circles, Te atoms.

meric substructures extend along the crystallographic *c* axis (Fig. 1). In the $[WOBr_4]_n$ chains, square-pyramidal $WOBr_4$ monomers are present and are associated through asymmetric, linear $\cdots W{=}O \cdots W{=}O$ bridges (Fig. 2). This part of the structure is thus closely related to the structure of pure $WOBr_4$,[4] though the $WOBr_4$ groups in **2** are not arranged in an eclipsing fashion, but rather alternately twisted by 22° with respect to one another. The $[WOBr_4]_n$ substructure may be regarded either as a polymeric anion $[WOBr_4^{\ominus}]_n$ with W^V or as an uncharged chain with W^{VI}. There are thus two possi-

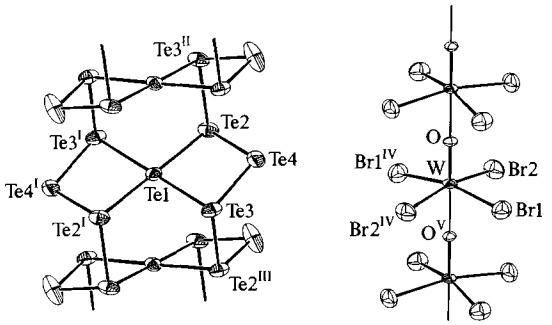

Fig. 2. Section of the polymeric chains composed of the ions $[Te_7^{2\oplus}]_n$ and $[WOBr_4^{\ominus}]_n$ in the structure of **2**. The ellipsoids of thermal vibration correspond to 70% probability. The superscripts refer to the symmetry operations that generate the symmetry-equivalent atoms. Selected bond lengths [pm] and angles [°]: Te1-Te2 297.6(1), Te1-Te3 293.9(1), Te2-Te4 274.7(1), Te3-Te4 277.4(1), Te2-Te3II 288.1(1), Te2-Te1-Te3 91.5(1), Te2-Te1-Te3I 88.5(1), Te1-Te2-Te4 83.4(1), Te1-Te3-Te4 83.6(1), Te2-Te4-Te3 100.2(1), W-O 172.8(7), W-OV 216.8(7), W-Br1 249.5(1), W-Br2 250.4(1), O-W-Br1 97.6(1), O-W-Br2 96.8(1).

bilities for an ionic formulation of **2**: $[Te_7^{\oplus}]_nBr^{\ominus} \cdot WOBr_4$ or $[Te_7^{2\oplus}]_n\,[WOBr_4^{\ominus}]_n\,Br^{\ominus}$. Both formulations include a paramagnetic center, $Te_7^{\oplus}$ in the former and W^V in $WOBr_4^{\ominus}$. The magnetic measurement on **2** shows the expected paramagnetism of one unpaired electron per formula unit. The reciprocal susceptibility is linear from 20 K to 320 K, the Curie–Weiss constant being −37 K and the magnetic moment 1.45 B.M. A decision on the oxidation state of the W atom can be made on the basis of the W–Br distances, which are 245 pm for W^V-Br[5] and between 250 and 260 pm for W^{VI}-Br.[6] The W–Br distances in **2** are 250.0 pm on average, favoring a formulation as the polymeric anion $[WOBr_4^{\ominus}]_n$. Analogous columnar arrangements of anions are known for $MoOCl_4^{\ominus}$[7] and $MoNCl_4^{\ominus}$.[8]

The polymeric tellurium cation in **2** consists of nearly planar centrosymmetric Te_7 units linked together to form a folded band (Fig. 2). The Te atoms show three different bonding capacities. Te1 is surrounded by four other Te atoms at a mean distance of 295.7 pm in a planar and nearly square fashion; Te2 and Te3 form three bonds and are joined to the neighboring Te_7 groups through bonds 288.1 pm long. Te4 forms two relatively short bonds to Te2 and Te3 (average 276.0 pm). In compounds with tellurium polyanions, structural motifs of the polymeric tellurium cation of **2** are realized in various ways.[9] The square-planar $Te_5^{6\ominus}$ anion in Ga_2Te_5 has 36 valence electrons.[10] A polymeric 32-electron anion, $[Te_5^{2\ominus}]_n$, is present in Rb_2Te_5[11] and Cs_2Te_5.[12] Because they have four valence electrons too few, the square Te_5 groups in these compounds are linked together through four Te–Te bonds to form polymeric bands. Re_2Te_5[13] contains discrete 44-electron anions, $Te_7^{2\ominus}$, which are isostructural to the central Te_7 unit of the polymeric cation in **2**. Assuming an ionic charge of +2 ($Te_7^{2\oplus}$) and 40 valence electrons and therefore four additional Te–Te bonds, the polymeric tellurium cation fits into this series. This is illustrated by the valence dash formulas in Scheme 1. Compound

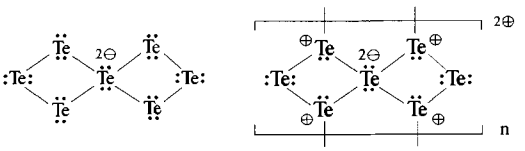

Scheme 1. Valence dash formulas for the ions $Te_7^{2\ominus}$ [13] und $[Te_7^{2\oplus}]_n$.

2 is thus best characterized by an ionic formula, $[Te_7^{2\oplus}]_n[WOBr_4^{\ominus}]_nBr^{\ominus}$. Extended Hückel band-structure calculations on the polymeric anions $[Te_5^{2\ominus}]_n$[14] show that the lengthening of the central four Te–Te bonds in the Te_5 unit is due to the additional occupation of antibonding states. The structural similarity to the $[Te_7^{2\oplus}]_n$ cation indicates that the bonding model for $[Te_5^{2\ominus}]_n$ may be extended to $[Te_7^{2\oplus}]_n$.

As in all compounds with chalcogen cations and halometalate anions, the structure of **2** reveals tellurium–bromine contacts that are considerably shorter than the sum of the van der Waals radii of 415 pm.[15] Figure 1 shows that the polymeric Te cations are completely surrounded by Br atoms. The shortest Te···Br distances of 333.7 and 343.7 pm occur between Te3 and the free $Br^{\ominus}$ ions.

Experimental Procedure

2: Te (2 g), WBr_5 (0.6 g), and $WOBr_4$ (0.6 g) were placed in a glass ampoule of 15-cm length and 1.5-cm diameter. The ampoule was evacuated and sealed and then put into a tube oven with a temperature gradient of 230 → 210 °C. Compound **2** separated out over several weeks at the cooler end of the tube as black, lustrous, needle- and plate-shaped crystals. The yield was about 80%. Small amounts of red WO_2Br_2 were always formed and precipitated along with the crystals of **2**, but they could be separated mechanically. The crystals of **2** hydrolyze slowly in moist air.

Received: April 19, 1991 [Z 4584 IE]
German version: *Angew. Chem.* *103* (1991) 1149

CAS Registry numbers:
2, 135108-07-5; Te, 13494-80-9; $WOBr_4$, 13520-77-9; WBr_5, 13470-11-6.

[1] J. Beck, *Angew. Chem. 102* (1990) 301; *Angew. Chem. Int. Ed. Engl. 29* (1990) 293.
[2] J. Beck, *Z. Naturforsch. B45* (1990) 413.
[3] Crystal structure analysis of **2**: Lattice contants $a = 2658.5(7)$, $b = 841.6(3)$, $c = 779.3(3)$ pm, orthorhombic space group *Pcca*, $Z = 4$, 1291 unique reflections with $I > \sigma(I)$ for 65 parameters, numerical absorption correction, $R = 0.027$. Further details on the crystal structure investigation are available on request from the Fachinformationszentrum Karlsruhe, Gesellschaft für wissenschaftlich-technische Information mbH, W-7514 Eggenstein-Leopoldshafen 2 (FRG), on quoting the depository number CSD-55574, the name of the author, and the journal citation.
[4] U. Müller, *Acta Crystallogr. Sect. C40* (1984) 915.
[5] W. Willing, U. Müller, *Acta Crystallogr. Sect. C43* (1987) 1425.
[6] P. Klingelhöfer, U. Müller, *Z. Anorg. Allg. Chem. 542* (1986) 7.
[7] U. Müller, E. Conradi, U. Patt-Siebel, M. Kersting, I. Schmidt, A. Khabou, K. Dehnicke, *Z. Anorg. Allg. Chem. 560* (1988) 95.
[8] U. Patt-Siebel, A. Khabou, U. Müller, K. Dehnicke, *Z. Anorg. Allg. Chem. 569* (1989) 91.
[9] P. Böttcher, *Angew. Chem. 100* (1988) 781; *Angew. Chem. Int. Ed. Engl. 27* (1988) 759.
[10] M. Julien-Pouzol, S. Jaulmes, F. Alapini, *Acta Crystallogr. Sect. B33* (1977) 2270.
[11] P. Böttcher, U. Kretschmann, *J. Less Common. Met. 95* (1983) 81.
[12] P. Böttcher, U. Kretschmann, *Z. Anorg. Allg. Chem. 491* (1982) 39.
[13] F. Klaiber, W. Petter, F. Hulliger, *J. Solid State Chem. 46* (1983) 112.
[14] J. Bernstein, R. Hoffmann, *Inorg. Chem. 24* (1985) 4100.
[15] L. Pauling: *Die Natur der chemischen Bindung*, Verlag Chemie, Weinheim 1968; *The Nature of the Chemical Bond*, Cornell University Press, Ithaca, NY, USA, 1960.

Intramolecular Base Stabilization of Si=N and Si=P Compounds and Related Transition-Metal Silanediyl Complexes

By *Robert Corriu,* Gérard Lanneau*, and *Christian Priou*

The efficiency of Lewis base coordination in stabilizing unsaturated species of silicon or germanium has been demonstrated.[1] For example, compound **1**, stabilized by intramolecular coordination of an amino naphthyl substituent, is a zwitterionic species.[2] Here we describe the analogous silicon derivatives **3** and **4**, which are stabilized by intramolecular coordination of the same amino aryl group and in which the silicon atom is directly bonded to nitrogen or phosphorus, as well as two transition-metal silanediyl complexes, **6** and **7**.

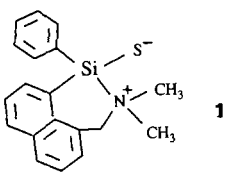

1

The silaphosphene **3** is obtained through the coupling reaction of aminonaphthyl(difluoro)phenylsilane, **2**, with $PhPLi_2$. In solution, the silaphosphene exists as an equilibrium mixture of two diastereomers, **3a** and **3b**, differing in the relative orientation of the *P* phenyl group, in the ratio 2/1 (observed by both ^{31}P and ^{29}Si NMR spectroscopy). Crystallization of the crude mixture from acetone affords isomer **3a**. In chloroform, equilibrium between the two isomers is reached in about one hour.

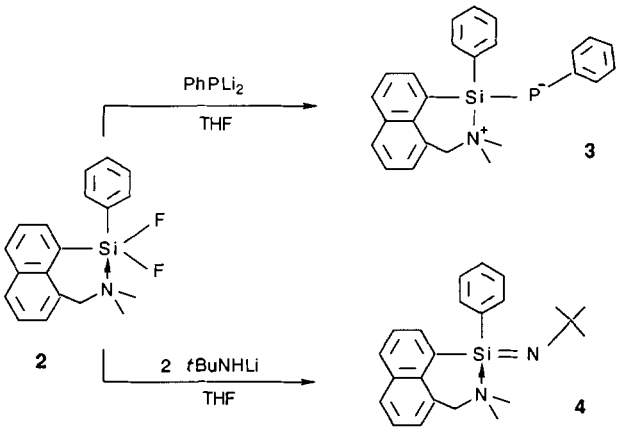

The NMR data of **3** reveal some interesting structural features (Table 1). For comparison, the values obtained by *Bickelhaupt* et al. for two sterically hindered base-free silaphosphenes have been also noted.[3] The ^{31}P and ^{29}Si NMR values reported by *Bickelhaupt* et al.[4] for base-free silaphosphenes correspond to strong deshielding: $\delta = +70$ to $+136$ (^{31}P NMR) and $+150$ to $+200$ (^{29}Si NMR) with high coupling constants ($^1J_{PSi} = 130-150$ Hz). The ^{29}Si NMR values for **3a**, **b** are $\delta = -2.7$ and -6.4, respectively, corresponding to an expected upfield shift due to the coordi-

Table 1. Selected NMR data for **1**–**7** [a] and related compounds.

Compd	$\delta(^1H)$ [b]	$\delta(^{13}C\{^1H\})$ [b]	$\delta(^{29}Si)$	$\delta(^{31}P)$ [J(Si,P)]	Ref.
1	2.50, 2.70 3.5–3.6 (m)	44.3, 46.0 64.3	21.5		[2]
2	1.95 4.10	39.3 (s) 57.6	−78.6 (t, J(Si,F) 253 Hz)		
3a	2.74 (s) 3.5–3.6 (m)	39.59 (d, J(C,P) = 5.4 Hz) [c] 26.45 (d, J(C,P) = 15.4 Hz) [c]	− 2.7	− 97.2 [9.2 Hz]	
3b	2.26 (s) 3.5–3.8 (m)	40.1 (br) 25.60 (d, J(C,P) 15.6 Hz) [c]	− 6.4	− 116.5 [24.1 Hz]	
4	2.10 4.10	44.3 62.5	− 9.6		
5	1.88 3.92	43.4 65.3	− 55.7 (t, J(Si,F) = 222 Hz)		[6]
6		50.3, 51.4 68.3	+101.1		
7		45.0, 48.0 65.9	+124.0		
$R^1R^2SiPR^3$ [d]			+198.8	+69.0 [153 Hz]	[3]
$R^3_2SiPR^4$ [e]			+151.2	136.0 [149 Hz]	[4]

[a] Solvent $CDCl_3$. [b] The $\delta(^1H)$ and $\delta(^{13}C)$ values for **1**–**7** refer to the NMe_2 group in the first line and to the CH_2N group in the second line. [c] Doublet tentatively assigned on the basis of a long-range C–P coupling constant. [d] R^1 = *t*Bu, R^2 = 2,4,6-*i*Pr$_3$ C_6H_2, R^3 = 2,4,6-$Me_3C_6H_2$. [e] R^4 = 2,4,6-*t*Bu$_3$ C_6H_2.

[*] Prof. Dr. R. Corriu, Dr. G. Lanneau, Dr. C. Priou
Laboratoire des Précurseurs Organométalliques de Matériaux URA 1097
Université des Sciences et Techniques du Languedoc-Case 007
Place E. Bataillon, F-34095 Montpellier Cedex 05 (France)

nation of nitrogen to silicon. The zwitterionic character of the diasteromeric silaphosphenes **3a** and **3b** is typified by two very high ^{31}P NMR chemical shifts ($\delta = -97.2$ and -116.5, $^1J_{PSi} = 9.2$ and 24.1 Hz, respectively), which are in accord with a "phosphoranide" structure. Also consistent with a partial Si–N bond are the observed $^3J_{PC}$ coupling constants (5–15 Hz) of the C-methyl atoms directly attached to nitrogen.

The silaimine **4** is similarly obtained in high yield upon reaction of **2** with two equivalents of *t*BuNHLi (Scheme 1 b). The second equivalent of *t*BuNHLi metalates the aminofluoro silyl intermediate, which cannot be detected by NMR spectroscopy. The by-product, *tert*-butylamine, is removed in vacuo, and the silaimine **4** (amine-free) is distilled off (b.p. 175 °C/0.05 Torr) without dimerization. Only one signal is detected at all temperatures by ^{29}Si NMR spectroscopy ($\delta = -9.6$). A priori, a plausible explanation would be that one diastereomer is favored.[3] Another possibility is that inversion of the imino N atom is too fast for NMR observation of both diastereomers, which is not true in the case of the Si–P derivatives **3a** and **3b**.

The silanediyl transition-metal complexes **6** and **7** are easily obtained by dehydrogenative coupling reaction of pentacoordinated silane **5**. With $[Fe(CO)_5]$, the reaction is performed by simply mixing the reactants in THF at room temperature for one hour, giving **6** in almost quantitative yield. With "methyl cymanthrene", $[(MeCp)Mn(CO)_3]$ (MeCp = η^5-C_5H_4Me), irradiation in THF or pentane is necessary to initiate the reaction; **7** is recrystallized from acetone.

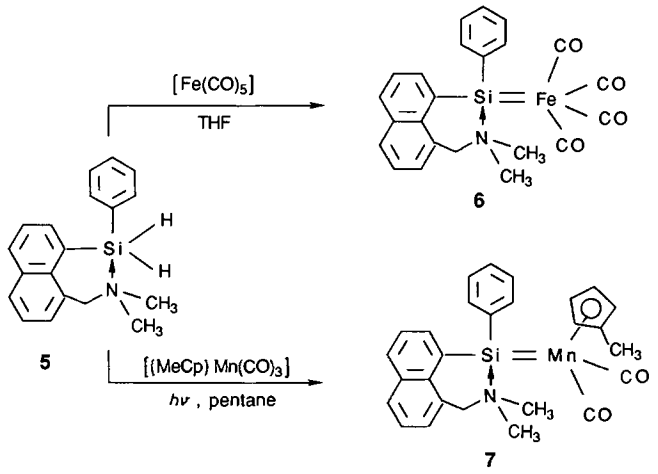

^1H NMR spectra of compounds **6** and **7** exhibit broad signals at all temperatures. As observed for the silanethione **1** ($\delta(^{13}C_{NMe_2}) = 46.0, 44.3$), ^{13}C NMR spectra of **6** and **7** show the presence of two diastereotopic methyl signals for the coordinatively bonded NMe_2 group. These signals ($\delta = 51.4$, 50.3 and 48.0, 45.0) are deshielded relative to the signals of the parent silane **5** ($\delta = 43.4$). Only one signal ($\delta = +217$) is observed for the fluxional CO ligands in the unhindered compound **6**. The more bulky MeCp ligand in **7** allows the two CO groups ($\delta = +234.1$, $+237.0$) to be differentiated. ^{29}Si NMR spectroscopy is a more appropriate analytical method to characterize these low-coordinated silicon species. The ^{29}Si NMR signals of the silanediyl complexes ($\delta = +101.1$ for **6**, 124.0 for **7**) are comparable with the values reported for similar base-stabilized dialkyl (aryl) silanediyl transition-metal complexes.[8] The absence of Si–H bonds in the complexes was demonstrated by using polarization transfer techniques (DEPT, INEPT).[9] A silanediyl complex with reversible intramolecular base stabilization is reported by *Zybill* et al. in the following communication.[10]

Like the silicon–sulfur double-bonded system **1**, stabilized by intramolecular coordination, compounds **3** and **4** are inert towards nucleophiles and electrophiles, Me_3SiCl, Ph_2SiH_2, S_8 and acetone. On the other hand, they are highly sensitive to oxygen or moisture, giving trimeric siloxane **8**.[2] Methanol in excess gives dimethoxysilane **9**.[2]

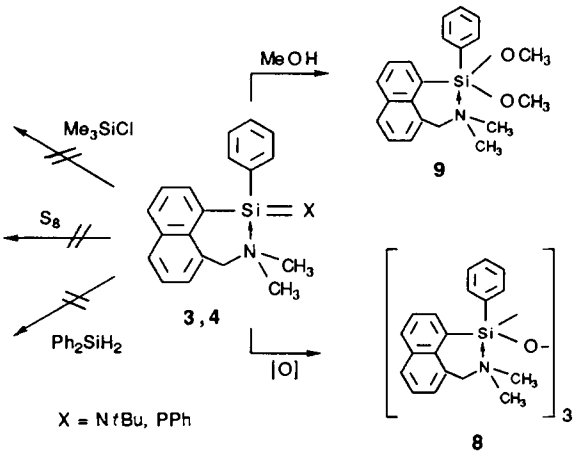

Preliminary studies have shown terminal silanediyl complex **6** to be unreactive towards alcohols and unsaturated hydrocarbons. A similar behavior has been observed with other transition-metal silanediyl species.[8] In the presence of air or moisture, **6** is immediately and quantitatively transformed into siloxane **8**. An attempt to obtain a disilene

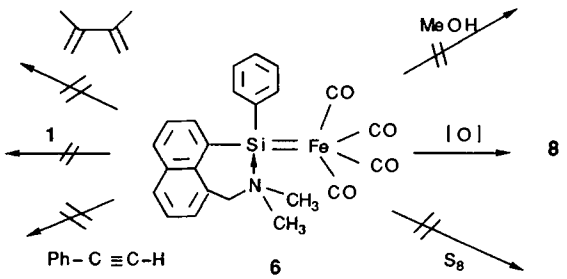

through exchange reaction with silanethione **1** was unsuccessful, despite the great affinity of iron for sulfur. We are currently investigating the use of these compounds as precursors of silanediyls for other reactions.

Experimental Procedure

Preparation of **2**: A solution of *n*-butyllithium (40 mL, 0.1 mol) in hexane (2.5 M) was added to 1-dimethylaminomethylnaphthalene (18.3 g, 0.098 mol) in Et_2O (100 mL). After stirring at room temperature for 24 h, the burgundy solution was added dropwise to phenyltrifluorosilane (16.4 g, 0.1 mol) over 1 h, giving a white precipitate. Compound **2** was isolated by filtration and recrystallization from $CHCl_3$. M.p. 108 °C; yield 16.3 g (50%).^1H NMR (60 MHz, $CDCl_3$, TMS int.): $\delta = 1.95$ (s, 6H, $N(CH_3)_2$), 4.10 (s, 2H; CH_2), 7–8.6 (m, 11H; Ar-H). ^{13}C NMR (62.9 MHz, $CDCl_3$, TMS int.): $\delta = 39.3$ ($N(CH_3)_2$), 57.6 (CH_2), 117–133 (Ar-C). ^{29}Si NMR (49.69 MHz, $CDCl_3$, TMS int.): $\delta = -78.6$ (t, J(Si, F) 253 Hz). ^{19}F NMR (60 MHz, $CDCl_3$, C_6F_6 int.): $\delta = +9.7$. MS (EI, 70 eV): m/z 326 ($M^+ - 1$, 7%). Correct elemental analysis for C, H, N, Si.

3: A yellow solution of dilithiophenylphosphide, prepared just prior to use from phenylphosphane (2.05 g, 18.6 mmol) and *n*-buthyllithium/hexane (2.0 M,

39 mmol) in THF (50 mL) was added dropwise to a solution of the difluorosilane **2** (6.99 g, 18.6 mmol) in THF (50 mL) at −18 °C with stirring. After 12 h at 25 °C, the filtrate was separated and the solvents removed in vacuo. Compound **3** was purified by sublimation at 220 °C/10^{-2} Torr. Yield 5.9 g (80%). Crystallization from acetone afforded 4.8 g (12 mmol) of isomer **3a**, m.p. 164 °C. Correct elemental analysis for C, H, N.

4: To an ice-cooled solution of *tert*-butylamine (0.582 g, 8 mmol) in THF (20 mL) was added dropwise a solution of *n*BuLi (10 mmol, 2.5 M in hexane). After 12 h at room temperature, the yellow solution was added dropwise with a canula to a stirred solution of **2** (1,5 g, 4 mmol) in THF (20 mL) at −18 °C. The dark red solution changed in 6 h to brown-yellow. The reaction mixture was stirred for a further 2 h, then filtered. The solvent was removed in vacuo and the waxy residue extracted with pentane/chloroform (60/40). The yellow oil was purified by kugelrohr distillation (b.p. 175 °C/0.02 Torr), giving **4**, yield 45%. NMR ($CDCl_3$): δ = 1.11 (s, 9H; *t*Bu), 2.10 (s, 6H; $N(CH_3)_2$), 4.10 (s, 2H; NCH_2), 6.9–8.1 (m, 11H; Ar-H). ^{13}C NMR ($CDCl_3$): δ = 34.3 ($C(CH_3)_3$, 44.3 ($N(CH_3)_2$, 50.7 (N-C), 62.5 (NCH_2), 125–145 (Ar-C). MS (EI, 70 eV): *m/z* 360 (M^+, 1%), 345 (60), 289 (15), 215 (10), 184 (18), 141 (40), 58 (100). Correct elemental analysis for C, H, N, Si.

6: **5** (0.52 g, 1.8 mmol) was added to a solution of $[Fe(CO)_5]$ (0.35 g, 1.8 mmol) in THF at 25 °C. The reaction mixture was stirred at that temperature for 1 h. Then, the brown-red solution was concentrated in vacuo, leaving **6** as a red solid (0.67 g, 82%). Recrystallization from acetone gave the analytically pure complex; m.p. 140 °C. ^{13}C NMR ($CDCl_3$): δ = 50.3, 51.4 (2s, N (CH_3)$_2$), 68.3 (s, CH_2), 125.1–139.6 (Ar-C), 217.0 (s, CO). IR (CCl_4): ν (CO) = 1977, 1956, 1916, 1898 cm^{-1}. MS (EI, 70 eV): *m/z* 457 (M^+, 5%) 429 (M^+ − CO, 9), 373 (M^+ − 3 CO, 20), 345 (M^+ − 4 CO, 30). Correct elemental analysis for C, H, N, Si.

7: **5** (2.21 g, 7.6 mmol), diluted in pentane (150 mL), was mixed with methylcymanthrene (1.6 g, 7.6 mmol) in a quartz reactor and irradiated at 20 °C for 5 h with a high-pressure Hg lamp. Removal of the solvent in vacuo left a brown solid, which was recrystallized from acetone. Yield: 1.6 g (44%); m.p. 230–231 °C. ^{13}C NMR ($CDCl_3$): δ = 14.6 (CH_3Cp), 82.8, 82.5 (2s, Cp), 103.1 (C-Me), 45.0, 48.0 (2s, $N(CH_3)_2$), 65.9 (s, CH_2), 121.6–136.2 (Ar-C), 234.1, 237.0 (2s, CO). IR ($CDCl_3$): ν (CO) = 1897, 1822 cm^{-1}. MS (EI, 70 eV): *m/z* 479 (M^+, 18%), 423 (M^+ − 2 CO, 81). Correct elemental analysis for C, H, N, Si.

Received: March 22, 1991 [Z 4526 IE]
German version: *Angew. Chem. 103* (1991) 1153

CAS Registry numbers:
2, 131032-19-4; **3**, 135366-47-1; **4**, 135366-48-2; **5**, 106586-06-5; **6**, 135366-49-3; **7**, 135366-50-6; **8**, 114410-94-5; $PhSiF_3$, 368-47-8; $[Fe(CO)_5]$, 13463-40-6; $[(\eta^5\text{-}C_5H_4Me)Mn(CO)_3]$, 12108-13-3; 1-dimethylaminomethylnaphthalene, 16413-71-1.

[1] N. Wiberg, *J. Organomet. Chem. 273* (1984) 141; for stabilized silaneimines, see, for example, N. Wiberg, G. Preiner, K. Schurz, *Chem. Ber. 121* (1988) 1407; N. Wiberg, K. Schurz, *J. Organomet. Chem. 341* (1988) 145 and references cited therein; R. Boese, U. Klingebiel, *ibid. 315* (1986) C17. Silenes: N. Wiberg, H. Kopf, *ibid. 315* (1986) 9; N. Wiberg, G. Wagner, G. Reber, J. Riede, G. Müller, *Organometallics 6* (1987) 35; M. Hesse, U. Klingebiel, *Angew. Chem. 98* (1986) 638; *Angew. Chem. Int. Ed. Engl. 25* (1986) 649. Silanediyls: K. P. Steele, W. P. Weber, *J. Am. Chem. Soc. 102* (1980) 6095; W. Ando, A. Sekiguchi, K. Hagiwara, A. Sakakibara, H. Yoshida, *Organometallics 7* (1988) 558; G. R. Gillette, G. H. Noren, R. West, *ibid. 6* (1987) 2617. For a related compound, see: P. Jutzi, D. Kanne, C. Kruger, *Angew. Chem. 98* (1986) 163; *Angew. Chem. Int. Ed. Engl. 25* (1986) 164. Stabilized silanediyl transition-metal complexes: C. Zybill, G. Müller, *Angew. Chem. 99* (1987) 683; *Angew. Chem. Int. Ed. Engl. 26* (1987) 669; *Organometallics 7* (1988) 1368; C. Zybill, D. L. Wilkinson, C. Leis, G. Müller, *Angew. Chem. 101* (1989) 206; *Angew. Chem. Int. Ed. Engl. 28* (1989) 203; D. A. Straus, T. D. Tilley, A. Rheingold, S. J. Geib, *J. Am. Chem. Soc. 109* (1987) 5872. For intramolecular stabilization, see: M. Veith, S. Becker, V. Huch, *Angew. Chem. 101* (1989) 1287; *Angew. Chem. Int. Ed. Engl. 28* (1989) 1237; *ibid. 102* (1990) 186 and *29* (1990) 216; H. H. Karsch, U. Keller, S. Gamper, G. Müller, *Angew. Chem. 102* (1990) 297; *Angew. Chem. Int. Ed. Engl. 29* (1990) 295; K. Keno, H. Tobita, M. Shimoi, H. Ogino, *J. Am. Chem. Soc. 110* (1988) 4092; G. Schmid, E. Welz, *Angew. Chem. 89* (1977) 823; *Angew. Chem. Int. Ed. Engl. 16* (1977) 785.

[2] P. Arya, J. Boyer, F. Carré, R. Corriu, G. Lanneau, J. Lapasset, M. Perrot, C. Priou, *Angew. Chem. 101* (1989) 1069; *Angew. Chem. Int. Ed. Engl. 28* (1989) 1016.

[3] Y. van der Winkel, H. M. M. Bastiaans, F. Bickelhaupt, *J. Organomet. Chem.*, in press; Y. van der Winkel, *Ph.D. Thesis*, Amsterdam University 1990.

[4] C. N. Smit, F. M. Lock, F. Bickelhaupt, *Tetrahedron Lett. 24* (1983) 3011; C. N. Smit, F. Bickelhaupt, *Organometallics 6* (1987) 1156.

[5] R. Boese, D. Bläser, *Z. Naturforsch B 44* (1989) 265; E. Niecke, E. Klein, M. Nieger, *Angew. Chem. 101* (1989) 792; *Angew. Chem. Int. Ed. Engl. 101* (1989) 751.

[6] J. Boyer, C. Brelière, F. Carré, R. Corriu, A. Kpoton, M. Poirier, G. Royo, J. Young, *J. Chem. Soc. Dalton Trans. 1989*, 43.

[7] R. Corriu, A. Kpoton, M. Poirier, G. Royo, A. de Saxce, J. Young, *J. Organomet. Chem. 395* (1990) 1.

[8] D. A. Straus, C. Zhang, G. E. Quimbita, S. D. Grumbine, R. H. Heyn, T. D. Tilley, A. I. Rheingold, S. J. Geib, *J. Am. Chem. Soc. 112* (1990) 2673. For a recent compilation on stabilized silanediyl–metal complexes, see T. D. Tilley in S. Patai, Z. Rappoport (Eds.): *The Chemistry of Organic Silicon Compounds*, Wiley, New York 1989, chapter 24, p. 1415.

[9] T. A. Blinka, B. J. Helmer, R. West, *Adv. Organomet. Chem. 23* (1984) 193.

[10] R. Probst, C. Leis, S. Gamper, E. Herdtweck, C. Zybill, N. Auner, *Angew. Chem. 103* (1991) 1155; *Angew. Chem. Int. Ed. Engl. 30* (1991) 1132

Reversible Intramolecular Base Stabilization of a Low-Coordinate Silicon Atom in the Silanediyl Complex $[(o\text{-}Me_2NCH_2C_6H_4)_2Si{=}Cr(CO)_5]$ **

By *Reiner Probst, Christian Leis, Siegfried Gamper, Eberhardt Herdtweck, Christian Zybill,** and *Norbert Auner**

Since the identification of base-stabilized silanediyl (silylene) complexes,[1, 2] the coordination chemistry of low-valent silicon ligands[3] has been developed rapidly. In addition to donor adducts of silanediyl complexes, also base adducts of cationic complex compounds,[4] metallasilaallenes,[5] and cyclic disilanediyl complexes[6] have become known. In many cases, these donor-stabilized complexes may be regarded as model compounds for reactive, base-free intermediates which play an important role in silanediyl-transfer reactions.[7]

Starting from the pentacoordinated silane **1**, *Corriu* et al. recently prepared the intramolecularly base-stabilized silanediyl complexes **2** and **3**, which are described in the preceding communication.[8] We have pursued this strategy

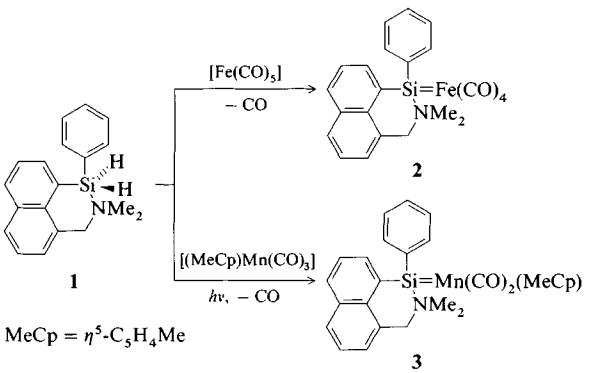

to obtain the title compound **7** by reaction of the dichlorosilane **6a** with $Na_2[Cr(CO)_5]$ and to prepare **8** from **6b**. Spectroscopic and structural investigations surprisingly indicated a reversible coordination of the "internal" base for both the pentacoordinated silane **6a** and the silanediyl complex **7**.

In solution the dichlorosilane **6a** contains a pentacoordinated silicon atom,[9] which is indicated by the ^{29}Si NMR

[*] Dr. C. Zybill, Prof. Dr. N. Auner, Dipl.-Chem. R. Probst, Dipl.-Chem. C. Leis, Dipl.-Chem. S. Gamper, Dr. E. Herdtweck Anorganisch-chemisches Institut der Technischen Universität München Lichtenbergstrasse 4, W-8046 Garching (FRG)

[**] This work was supported by the Fonds der Chemischen Industrie and the Deutsche Forschungsgemeinschaft. We thank the head of the department for financial support and *Jürgen Riede* for the measurement of crystallographic data set.

chemical shift ($\delta = -30.1$). The ^{1}H NMR spectra show that the two dimethylaminomethylphenyl substituents are equivalent at room temperature with the two phenyl rings rotating freely. This rotation can be frozen below $-13\,^\circ$C (coalescence temperature);[10] the estimated activation barrier for the process is $\Delta G^{\neq} = 56.3\ (\pm 5)\ \mathrm{kJ\,mol^{-1}}$.

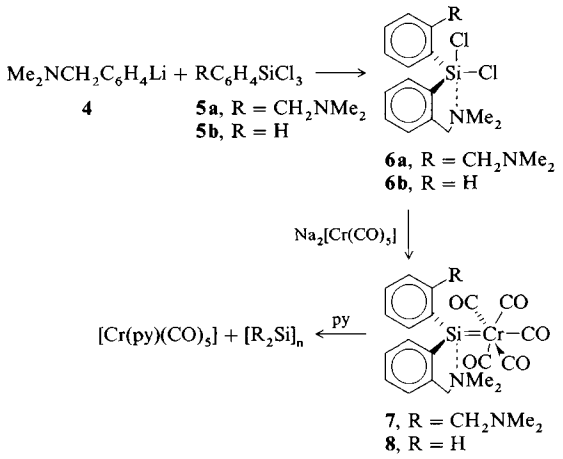

The spectroscopic results are confirmed by a single-crystal X-ray structure determination (Fig. 1).[11] The equatorial Si–Cl and Si–C distances (208.1(1), 186.9(1), and 187.0(1) pm) are similar to those in known pentacoordinated silanes. In accordance with the relatively weak Si–N2 bond (229.1(2) pm), the central silicon atom is slightly pyramidalized (sum of equatorial angles 356.9°).

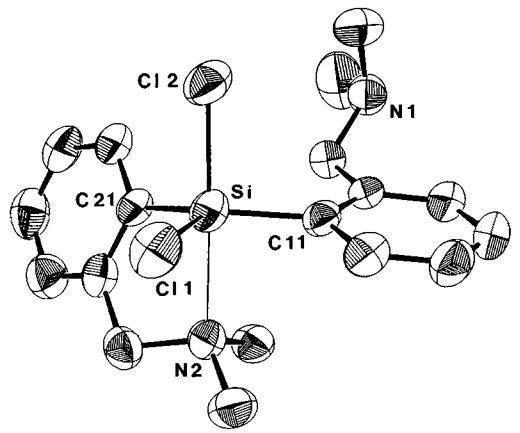

Fig. 1. Molecular structure of the dichlorosilane **6** (ORTEP, hydrogen atoms omitted). Selected distances [pm] and angles [°]: Si-Cl1 208.1(1), Si-Cl2 218.1(1), Si-N2 229.1(2), Si-C11 186.9(1), Si-C21 187.0(1), Si-N1 449.3(2); C11-Si-C21 132.16(6), Cl1-Si-C11 113.22(5), Cl1-Si-C21 111.53(4), Cl1-Si-Cl2 94.46(3), Cl1-Si-N2 86.72(3), Cl2-Si-N2 86.72(3).

Coupling of **6a** or **6b** with $Na_2[Cr(CO)_5]$ exclusively results in the formation of the complex compounds **7** and **8**. On the basis of the spectroscopic data, **7** and **8** are unequivocally silanediyl complexes; the extreme low-field shift of the ^{29}Si NMR signals (e.g., $\delta = 124.9$ for **7** at 22 °C), in particular, points to a relatively small donor → silicon interaction. The ^{29}Si NMR shifts are strongly temperature-dependent (e.g., $\delta = 138.8$ for **7** at 58.0 °C and 120.9 at $-40.0\,^\circ$C). This situation is reflected in the temperature dependence of the ^{1}H NMR spectra of **7**. At room temperature, the two dimethylamino groups are chemically equivalent; however, in contrast to **6a**, the signals of the methylene protons form an AB pattern ($\delta = 3.80$, 4.09, $^2J_{HH} = 12.2$ Hz). This is the result of hindered rotation of the phenyl substituents with simultaneous fixation of the two dimethylamino groups in the sense of an alternating, dynamical coordination of the nitrogen donor at a time to the silicon center (pentacoordination in the transition state).[12] Below $-21\,^\circ$C (coalescence, $\Delta G^{\neq} = 54.2\ (\pm 5)\ \mathrm{kJ\,mol^{-1}}$) this dynamical coordination does not occur and only one nitrogen donor is coordinated to silicon; the two dimethylaminomethylphenyl substituents are magnetically inequivalent. Above 58 °C, the two substituents on silicon show magnetic equivalence with coalescence of the AB system of the methylene protons to a singlet ($\delta = 3.90$). At temperatures above 58 °C, the "dynamical N–Si coordination" is lifted; the rotation of the phenyl substituents is now rapid on the ^{1}H NMR time scale and the nitrogen donors are no longer fixed to the silicon atom (structure **7a**). For **8**, a coalescence temperature of 95 °C ($\Delta G^{\neq} = 80.2\ (\pm 5)\ \mathrm{kJ\,mol^{-1}}$) was found; below this temperature, the dimethylamino substituent in **8** is rigidly coordinated to the silicon atom.[13]

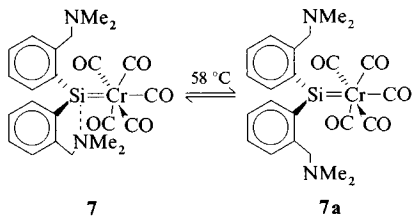

These findings were confirmed and supplemented by single-crystal X-ray structure analysis of **7** (Fig. 2). The silanediyl ligand in complex **7** is coordinated to the octahedral metal fragment. The Cr–Si bond length (240.8(1) pm) is noticeably short.[14] An ab initio calculation has predicted a Cr–Si distance of 240 pm in $[(OH)HSi{=}Cr(CO)_5]$;[15] a crude estimate based on covalent radii gives a value of 228 pm for a donor-free Cr–Si double bond and about 270 pm

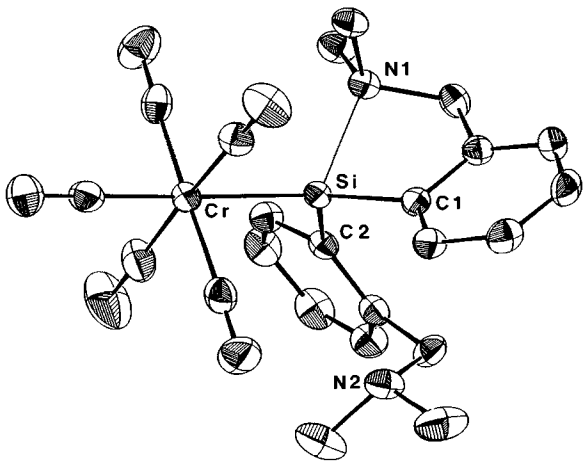

Fig. 2. Molecular structure of the silanediyl complex **7** (ORTEP, hydrogen atoms omitted). Selected distances [pm] and angles [°]: Cr-Si 240.8(1), Si-N1 204.6(2), Si-C1 189.8(2), Si-C2 190.8(2), Si-N2 330.9(2); Cr-Si-C1 120.3(1), Cr-Si-C2 116.9(1), C1-Si-C2 114.1(1), Cr-Si-N1 118.2(1), N1-Si-C1 83.6(1), N1-Si-C2 96.6(1).

for a Cr–Si single bond.[2b] The interaction of the two dimethylamino substituents with the silicon atom leads to a characteristic coordination geometry. The N1–Si distance (204.6(2) pm) is shorter than the N2–Si distance in the pentacoordinated compound **6a**; this underlines the high electrophilicity of the coordinated silanediyl ligand in **7**. On the other hand, this distance is considerably longer than those found in all structurally characterized compounds of this type[16] and is clearly outside the covalent range.[17] The only partially covalent character of the Si–N bond is confirmed by the activation barrier determined by NMR spectroscopy for exchange of the two dimethylamino units ($\Delta G^{\neq} = 67.1\ (\pm 5)$ kJ mol^{-1}). Furthermore, the extremely weak donor interactions (donor $\rightarrow \pi^*$ orbital) leads to $\lambda_{max} = 274$ nm (π–π^* transition of the Cr–Si double bond) in the UV spectrum; such a bathochromic shift has not been previously observed for similar compounds. The second dimethylamino group of **7** in the crystal is, in contrast to **6a**, also directed toward the silicon atom of the same molecule; the Si–N2 distance (330.9 pm) may be regarded as a van der Waals contact. Especially the increased Cr–Si–S1 and Cr–Si–C2 angles (116.9(1) and 120.3(1)°), which are characteristic of a donor adduct, as well as the C1–Si–C2 angle (114.1(1)° (sum of angles 351.3°) show a significant planarization of the coordination polyhedron at silicon formed by the three covalently bonded substituents.

The relatively loose donor bond implies a high reactivity of the complex. Base-induced silanediyl cleavage occurs in pyridine, trimethylphosphane, CO, or 2,3-dimethylbutadiene both thermally and photochemically. The resulting reaction mixtures are complex and contain mostly polymeric silanes.

Experimental Procedure

6: *o*-(*N*,*N*-dimethylaminomethyl)phenyllithium [19] (0.4 mol) was added in portions to a solution of $SiCl_4$ (22.9 mL, 0.2 mol) (distilled from K_2CO_3) and 50 mL of triethylamine in about 700 mL of diethyl ether. The reaction mixture turned pale yellow and began to reflux. After addition was completed, the reaction solution was refluxed for a further 2 h, followed by filtration and removal of all volatiles under vacuum. The crude product was recrystallized from diethyl ether. Yield: 50.5 g (68%). Compound **6b** was obtained analogously.

6a: ^{1}H NMR (270 MHz, $CDCl_3$, 22 °C, TMS): $\delta = 1.94$ (s, 6H; CH_3), 3.56 (s, 2H; CH_2), 7.32–7.36, 8.19 (m, 4H; C_6H_4). ^{1}H NMR (−28 °C, [D$_8$]toluene): $\delta = 3.46$, 3.66 (AB system, $^2J(^1H,^1H) = 12.0$ Hz, 2H; CH_2). ^{13}C NMR (67.8 MHz, $CDCl_3$, 22 °C): $\delta = 45.0$ (CH_3), 63.12 (CH_2), 126.60, 127.19, 130.11, 134.72, 134.85, 142.79 (C_6H_4). ^{29}Si NMR (53.5 MHz, $CDCl_3$): $\delta = -30.1$. CI-MS (70 eV): m/z 367 ($M^+ + 1$ for $C_{18}H_{24}Cl_2N_2Si$, 5%). M.p. 104 °C. Correct elemental analysis (C, H, N).

7: [$Na_2Cr(CO)_5$] (2.31 g, 9.71 mmol) was dissolved in 100 mL of THF with ultrasonication. The brown-yellow solution was cooled to about −40 °C and then dichlorosilane (3.55 g, 9.71 mmol), dissolved in 100 mL of THF, was slowly added dropwise to the stirred solution. After warming to room temperature, the reaction solution was stirred for a further 3 h. It was then decanted from precipitated NaCl by using a steel cannula and concentrated to about 10 mL under vacuum (5×10^{-2} Torr). At −20 °C, **7** crystallized as beige-yellow crystals. Yield: 1.5 g (32%). M.p. 170 °C. The compound is thermochromic (yellow → red). ^{1}H NMR (270 MHz, [D$_8$]toluene, 22 °C): $\delta = 2.57$ (s, 6H; CH_3), 3.80, 4.09 (dd, AB system, $^2J(^1H,^1H) = 12.2$ Hz, 2H; CH_2), 7.18–7.27, 7.61–7.71 (m, 4H; C_6H_4); (58 °C): 3.90 (s, 2H; CH_2). ^{13}C NMR (67.8 MHz, [D$_6$]acetone, 22 °C): $\delta = 43.44$ (CH_3), 64.68 (CH_2), 128.39, 128.69, 132.86, 137.06, 150.13 (C_6H_4), 212.82, 227.25 (CO). ^{29}Si NMR ([D$_8$]THF, 53.5 MHz, 22 °C): $\delta = 124.9$; (58 °C): 138.8; (−40.0 °C): 120.9. EI-MS (70 eV): m/z 488 (M^+ for $C_{23}H_{24}CrN_2O_5Si$ with correct isotopic pattern, 10%). IR (Nujol): ν(CO) = 2036 (m), 1916 (ss), 1884 (ss) cm^{-1}. UV/VIS (cyclohexane) $\lambda_{max} = 274$ nm, $\varepsilon_0 = 27000$. Correct elemental analysis (C, H, N).

8: The synthesis was carried out as described for **7**, 63% yield. M.p. 165–170 °C. ^{1}H NMR (270 MHz, [D$_8$]toluene, 22 °C): $\delta = 1.83$, 2.08 (s, 6H; NCH_3); 2.62, 3.04 (AB system, $^2J(^1H,^1H) = 14.0$ Hz, 2H; CH_2); 6.04 (d, $^3J(^1H,^1H) = 10.1$ Hz, 1H) 7.02 (t, $^3J(^1H,^1H) = 10.0$ Hz, 1H) 7.04 (d, $^3J(^1H^1H) = 10.1$ Hz, 1H) 8.08 (d, $^3J(^1H^1H) = 10.1$ Hz, 1H; $C_6H_4NMe_2$); 6.97 (s, 2H) 7.04 (d, $^3J(^1H,^1H) = 8.9$ Hz, 3H; C_6H_5). ^{29}Si NMR (53.5 MHz, [D$_8$]toluene, 22 °C) $\delta = 121.2$. EI-MS (70 ev): m/z 431 (M^+ for $C_{20}H_{17}CrO_5NSi$ with correct isotopic pattern, 100%). M.p. 165 °C. Correct elemental analysis (C, H, N).

Received: April 11, 1991 [Z 4564 IE]
German version: *Angew. Chem. 103* (1991) 1155

CAS Registry numbers:
4, 27171-81-9; **5a**, 135394-59-1; **5b**, 98-13-5; **6a**, 135394-60-4; **6b**, 135394-61-5; **7**, 135394-62-6; **8**, 135394-63-7; $Na_2[Cr(CO)_5]$, 51233-19-3.

[1] G. Schmid, E. Welz, *Angew. Chem. 89* (1977) 823; *Angew. Chem. Int. Ed. Engl. 16* (1977) 785.

[2] a) C. Zybill, G. Müller, *Angew. Chem. 99* (1987) 683; *Angew. Chem. Int. Ed. Engl. 26* (1987) 669; b) C. Zybill, G. Müller, *Organometallics 7* (1988) 1368; c) C. Zybill, D. L. Wilkinson, C. Leis, G. Müller, *Angew. Chem. 101* (1989) 206; *Angew. Chem. Int. Ed. Engl. 28* (1989) 203; d) C. Zybill, *Nachr. Chem. Tech. Lab. 37* (1989) 248; e) C. Leis, K. Lachmann, G. Müller, C. Zybill, *Polyhedron 10* (1991) 1163; f) C. Zybill, *Top. Curr. Chem. 160* (1991) 1.

[3] P. Jutzi, A. Möhrke, *Angew. Chem. 102* (1990) 913; *Angew. Chem. Int. Ed. Engl. 29* (1990) 893.

[4] a) D. A. Straus, T. D. Tilley, A. L. Rheingold, S. Geib, *J. Am. Chem. Soc. 109* (1987) 5872; b) D. A. Straus, C. Zhang, G. E. Quimbita, S. D. Grumbine, R. Heyn, T. D. Tilley, A. L. Rheingold, S. J. Geib, *ibid. 112* (1990) 2673; c) D. A. Straus, S. D. Grumbine, T. D. Tilley, *ibid. 112* (1990) 7801; d) T. D. Tilley in S. Patai, Z. Rappoport (Eds.): *The Chemistry of Organic Silicon Compounds*, Wiley, New York 1989.

[5] C. Zybill, D. L. Wilkinson, G. Müller, *Angew. Chem. 100* (1988) 574; *Angew. Chem. Int. Ed. Engl. 27* (1988) 583.

[6] a) K. Ueno, H. Tobita, M. Shimoi, H. Ogino, *J. Am. Chem. Soc. 110* (1988) 4092; b) H. Tobita, K. Ueno, M. Shimoi, H. Ogino, *ibid. 112* (1990) 3415.

[7] a) K. Yamamoto, H. Okinoshima, M. Kumada, *J. Organomet. Chem. 23* (1970) C7; b) K. Yamamoto, H. Okinoshima, M. Kumada, *ibid. 27* (1971) C31; c) H. Okinoshima, K. Yamamoto, M. Kumada, *J. Am. Chem. Soc. 94* (1972) 9263; d) K. H. Pannell, J. Cervantes, C. Hernandez, J. Cassias, S. Vincenti, *Organometallics 5* (1986) 1056; e) H. Tobita, K. Ueno, H. Ogino, *Chem. Lett. 1986*, 1777.

[8] a) R. Corriu, G. Lanneau, C. Priou, *Angew. Chem. 103* (1991) 1130; *Angew. Chem. Int. Ed. Engl. 30* (1991) b) N. Auner, W. Ziche, R. West, *Heteroatom. Chem. 2* (1991) 335.

[9] B. J. Helmer, R. West, R. J. P. Corriu, M. P. G. Royo, A. De. Saxce, *J. Organomet. Chem. 251* (1983) 295.

[10] The preliminary results of investigation by NMR spectroscopy indicate the presence, below −13 °C, of a rigidly pentacoordinated complex with diastereotopic methylene protons (AB system [12]), as found in the crystal structure.

[11] **6**: Crystal structure data: $C_{18}H_{24}Cl_2N_2Si$, colorless cubes (0.77 × 0.64 × 0.64 mm) $M_r = 367.4$, orthorhombic, *Pbca* (No. 61), $a = 1380.2(1)$, $b = 1790.8(2)$, $c = 1554.4(2)$ pm, $V = 3842 \times 10^6$ pm^{-3}, $Z = 8$, $\varrho_{calcd} = 1.270$ g cm^{-3}, μ[Mo$_{K\alpha}$] = 4.0 cm^{-1}, F(000) = 1552. Measurement parameters: Enraf-Nonius CAD4, $T = 294$ K, 3750 measured reflections ($\theta_{max} = 25°$; $+h, +k, +l$), 422 suppressed reflections and 312 reflections with negative intensity suppressed, 3016 unique reflections ($I > 0.0$) used for refinement. Decomposition correction (52.2 h, −14.9%), empirical absorption correction ($0.914 < T < 1.000$), extinction correction [$F_{c(corr.)} = F_c/(1 + \varepsilon F_c^2 Lp)$; $\varepsilon = 0.415 \times 10^{-7}$]. Structure solution: Direct methods (MULTAN 11/82, difference Fourier technique), 303 parameters; full-matrix least-squares refinement (STRUX-III; SDP), $R = 0.060$, $R_w = 0.039$, all heavy atoms refined anisotropically and all hydrogen atoms refined with isotropic displacement parameters (the hydrogen atoms at C17 and C18 included with only one collective value). Residual electron density + 0.39, −0.42 e$_0$Å^{-3}. **7**: Crystal data: $C_{23}H_{24}CrN_2O_5Si$, $M_r = 488.5$, triclinic, $P\bar{1}$ (No. 2), $a = 953.1(1)$, $b = 1033.9(1)$, $c = 1167.6(1)$ pm, $\alpha = 94.47(1)$, $\beta = 88.09(1)$, $\gamma = 96.68(1)°$, $V = 5115 \times 10^6$ pm^3, $Z = 2$, $\varrho_{calcd} = 1.42$ g cm^{-3}, μ[Mo$_{K\alpha}$] = 5.7 cm^{-1}, F(000) = 508. Measurement parameters: Syntex P2$_1$, $T = 218$ K, 4035 measured reflections ($\theta_{max} = 25°$; $\pm h, \pm k, +l$), 4035 unique reflections ($I > 0.0$) used for refinement, empirical absorption correction. Structure solution: Patterson (SHELX 86, difference Fourier technique), 385 parameters, full-matrix least-squares refinement (SHELX-76), $R = 0.040$, $R_w = 0.032$, all heavy atoms refined anisotropically and all hydrogen atoms refined with isotropic displacement parameters. Residual electron density + 0.27; −0.28 e$_0$Å^{-3}. Further details on the crystal structure investigation are available on request from the Fachinformationszentrum Karlsruhe, Gesellschaft für wissenschaftlich-technische Information mbH, W-7514 Eggenstein-Leopoldshafen 2 (FRG), on quoting the depository number CSD-55494, the names of the authors, and the journal citation.

[12] For exchange phenomena at silicon see: a) F. Carre, G. Cerveau, C. Chuit, R. J. P. Corriu, C. Reye, *Angew. Chem. 101* (1989) 474; *Angew. Chem. Int. Ed. Engl. 28* (1989) 489; b) D. Kummer, S. C. Chaudhry, J. Seifert, *J. Organomet. Chem. 382* (1990) 345; c) G. Klebe, *ibid. 332* (1987) 35; d) M. S. Gordon, L. P. Davis, L. W. Burggraf, *Chem. Phys. Lett. 163* (1989) 371.

[13] The dimethylamino substituent can be displaced from silicon by addition of stronger bases such as THF or acetone.
[14] Known Cr–Si bond lengths in donor-containing complexes: 243.1(1) pm for $[(CO)_5Cr{=}Si(OtBu)_2 \cdot HMPT]$, 240.9(1) pm in $[(CO)_5Cr{=}SiMe_2 \cdot HMPT]$, and 234.3(1) pm for $[(CO)_5Cr{=}SiCl_2 \cdot HMPT]$ ([2b, d]).
[15] H. Nakatsuji, J. Ushio, T. Yonezawa, *J. Organomet. Chem. 258* (1983) C1.
[16] For comparison: $[Cp^*(PMe_3)_2Ru{=}SiPh_2 \cdot CH_3CN]BF_4$ N-Si 193.2(8) pm ([4a]).
[17] Si–N covalent bond distances are in the range of 164–178 pm [8].
[18] Compare, for example, the pyramidalization at Si in $Mes_2Si{=}SiMes_2$: a) R. West, *Angew. Chem. 99* (1987) 1231; *Angew. Chem. Int. Ed. Engl. 26* (1987) 1201; b) M. J. Fink, M. J. Michalczyk, K. J. Haller, R. West, J. Michl, *Organometallics 3* (1984) 793.
[19] L. E. Manzer, *J. Am. Chem. Soc. 100* (1978) 8068.

Reduction of the Small Subunit of Ribonucleotide Reductase by Diimide: Evidence for the Formation of the Mixed-Valence Fe^{II}–Fe^{III} center**

By *Catherine Gerez, Jacques Gaillard, Jean-Marc Latour,* and *Marc Fontecave**

Binuclear non-heme iron centers are utilized in living organisms for reversible oxygen binding (hemerythrin, Hr), for oxygen activation (methane monoxygenase, MMO, and ribonucleotide reductase, RR), and for hydrolysis of organophosphate esters (purple acid phosphatase, PAP).[1]

Ribonucleotide reductase from *E. coli* consists of two nonidentical subunits, proteins R1 and R2.[2] Protein R2 is a homodimer, each polypeptide chain sequestering a binuclear ferric center, as recently confirmed by a three-dimensional X-ray analysis.[3] The function of the di-iron(III) center of R2 is to promote the specific one-electron oxidation of tyrosine 122 by dioxygen.[4] The generation of the tyrosyl radical is a prerequisite for an active enzyme.[2]

The presence of an oxo group bridging the two iron atoms is suggested from characteristic resonance Raman vibrations.[1] Moreover, the UV/VIS spectrum of R2 contains two bands at 370 and 325 nm, originating from a charge transfer from O^{2-} to Fe^{3+} and a sharp peak at 410 nm, contributed by the tyrosyl radical.[1] The metal cluster also exhibits a strong antiferromagnetic coupling of the two iron ions ($J = -110\ cm^{-1}$ for $\boldsymbol{H} = -2JS_1S_2$).[5] As a consequence, the di-iron(III) center is EPR-silent and the EPR spectrum of protein R2 only displays the characteristic signal of the tyrosyl radical at $g = 2.0047$.[6]

In general, binuclear iron clusters can also exist in two other redox states, the fully reduced $Fe^{II}Fe^{II}$ state and the EPR-active mixed-valence $Fe^{II}Fe^{III}$ state. However, only the first one has been observed and characterized in the case of protein R2.[4a, 7–9] In particular, its UV/VIS spectrum does not contain the bands at 325, 370, and 410 nm. Therefore, UV/VIS spectroscopy is a convenient method for monitoring the anaerobic reduction of protein R2 to the radical-free Fe^{II}–Fe^{II} state of the protein, called reduced R2.[4a, 7, 8]

In this paper, we report that 1) diimide is a very efficient reducing agent of the redox centers of protein R2, 2) the mixed-valence state of the binuclear center was detected by EPR spectroscopy during this reduction.

When protein R2 ($1\ mg\,mL^{-1}$)[10] was incubated in a spectrophotometric cuvette with diimide formed by in situ hydrolysis of 4 mM potassium azodicarboxylate[11] at pH 8.5 under anaerobic conditions, the spectrum of the solution slowly changed from that of the radical-containing Fe^{III}–Fe^{III} state to that of reduced R2,[4a, 5, 6] in approximately 2 h (data not shown). This clearly indicated that diimide was able to transfer electrons to the redox centers of protein R2, namely the di-iron(III) center and the tyrosyl radical. Probably, the low redox potential, the electric neutrality, and the small size of diimide molecules are responsible for the efficiency of the reaction. Actually, the active site is buried within the protein[3] and protected from negatively charged reducing agents.[7]

The reaction of 0.25 mM protein R2 with 6 mM potassium azodicarboxylate in 0.1 M deaerated Tris buffer, pH 8.5, was performed inside an argon-flushed EPR tube in a glove box to ensure anaerobic conditions. At intervals the tube was frozen in liquid nitrogen and the EPR spectrum was recorded at low temperatures (4–10 K). While the intensity of the characteristic EPR signal of the tyrosyl radical at $g = 2.00$ slowly decreased, a new weak signal appeared with all resonances below $g = 2$. On the other hand, no signal could be detected at $g \approx 16$ during the reaction. Such an EPR feature was recently observed during reduction of protein R2 by dithionite and assigned to reduced R2.[9]

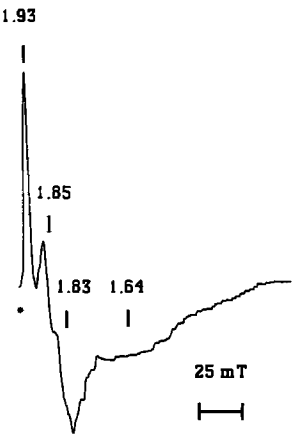

Fig. 1. EPR-spectrum of the R2 mixed-valence state. Experimental conditions: temperature, 5 K; power, 20 mW; amplitude modulation, 1.25 mT; frequency modulation, 100 kHz; resonance frequency, 9223 MHZ. The low field feature (marked with *) is partly caused by the saturated signal of the remaining tyrosyl radical.

Figure 1 shows the new EPR signal. This signal reached maximum intensity after approximately 1 h, when the reduction of the iron center and the tyrosyl radical was near completion, as indicated from the amplitude of the signal of the organic radical. It comprises a sharp resonance at $g_1 = 1.93$, two very close lines at $g_2 = 1.85$ and $g_{2'} = 1.83$, and a broad component at $g_3 \approx 1.64$, and probably originates from the superimposition of two rhombic signals with slightly different g values which causes the doubling of the central line and the broadening of the high-field component. As a consequence of this broadening and of the presence of a residual amount of unreduced tyrosyl radical, the intensity of the relevant $g < 2$ signal cannot be quantified accurately. However, from double integration of this signal, we estimated that the corresponding EPR-active species accounted for 2–

[*] Prof. M. Fontecave, C. Gerez
Université Joseph Fourier Chimie Recherche
301 rue de la chimie
Domaine Universitaire
Saint-Martin d'Hères, BP 53X, F-38041 Grenoble Cedex (France)
J. Gaillard, J.-M. Latour DSM/DRF, C.E.N.G.
25, avenue des Martyrs, BP 85X, F-38041 Grenoble Cedex (France)

[**] The financial support for this work has been provided by the Centre National de la Recherche Scientifique (research projects CNRS URA 332 and CNRS URA 1194).

5% of the total protein concentration. It is worth noting that no similar $g < 2$ signal could be detected when protein R2 was reduced by 1,4-dithio-L-threitol (DTT) at alkaline pH.[12] Dithionite in the presence of methyl viologen also failed to generate this signal.[7] This indicates that the corresponding species is extremely unstable.

Introduction of air resulted in the instantaneous increase of the $g = 2.00$ signal and disappearance of the $g < 2$ signal. The regeneration of the tyrosyl radical confirmed that reduced R2 was formed during the anaerobic step.[4a, b, 7-9] However, radical formation was not total (60% yield), probably because the diimide partly mobilized endogenous iron as suggested by the significant increase of the $g \approx 4.3$ signal. Instability of Fe^{II} in R2 is well-documented.[8] We checked that protein R2 was not irreversibly denatured by prolonged incubation with diimide. Actually, diimide-treated R2 could be fully reactivated through one cycle of iron chelation by 8-hydroxyqauinoline 5-sulfonate and reconstitution in the presence of Fe^{II} and ascorbate,[7] as monitoring by EPR spectroscopy shows.

The new signal resembles those previously reported for the two mixed-valence $Fe^{II}-Fe^{III}$ states of hemerythrin (g values of 1.95, 1.72, 1.57 and 1.96, 1.88, 1.66), methane monoxygenase ($g = 1.95$, 1.88, 1.78), and purple acid phosphatase ($g = 1.93$, 1.72, 1.56).[1, 13, 14] Also, a synthetic binuclear iron complex containing an $Fe^{II}-Fe^{III}$ cluster has similar $S = 1/2$ EPR characteristics arising from the antiferromagnetic interaction of a pair of high spin Fe^{II} and Fe^{III} ions.[15] Thus the $S = 1/2$ EPR spectrum of Figure 1 strongly suggests that a mixed-valence $Fe^{II}-Fe^{III}$ state was formed during reduction of R2 to reduced R2 by diimide.

Although the g values of the mixed-valance states of binuclear iron proteins fall in the same range, confirming that the clusters have a similar core structure, the observed differences are nevertheless significant. They reflect distortions at the Fe^{II} site as well as minor changes of the relative magnitudes of the exchange and zero-field splitting parameters.[16] It is therefore remarkable that the mixed-valence state of R2 gives an EPR spectrum which closely resembles that of $(\text{semi-metHr})_R$, the mixed-valence state produced by a one-electron reduction of methemerythrin.[1, 17] This suggests that the two iron atoms are only weakly antiferromagnetically coupled, which in turn suggests that the oxo bridge has been converted into a hydroxo bridge during reduction of R2.[16-19] Moreover, since Fe^{2+} in $(\text{semi-metHr})_R$ is six-coordinate, a similar geometry is likely to occur in the R2 mixed-valence state.

The doubling of the signal could originate from a dipolar interaction between the paramagnetic $Fe^{II}-Fe^{III}$ center and the residual tyrosyl radical, if present in the same polypeptide chain. However, this would also result in the splitting of the $g = 2.00$ signal. Since no change in the position or the width of this signal could be observed, this hypothesis must be excluded. Therefore, the doubling of the signal is probably related to the dissymmetry of the binuclear iron cluster. The presence of two structurally nonidentical iron ions[3] may explain the formation of two slightly different mixed-valent di-iron clusters, as found for the semimethemerythrins.[17, 18]

As mentioned above, reduced R2 obtained from reduction of R2 by dithionite exhibits an EPR signal at $g \sim 16$.[9] On the contrary, the $Fe^{II}-Fe^{II}$ center produced during reduction of R2 by diimide is EPR-silent. This situation is reminiscent of the one in deoxyhemerythrin, for which the generation of an analogous low field ($g \sim 13$) signal depends on the ligand bound at the free coordination site.[20] We therefore tentatively suggest that binding of diimide to the $Fe^{II}-Fe^{II}$ center of reduced R2 makes it EPR-silent. Such a binding would also explain the stabilization of the mixed-valence state. We are currently investigating the possibility for such coordination chemistry in ribonucleotide reductase.

Received: April 9, 1991 [Z 4560 IE]
German version: *Angew. Chem. 103* (1991) 1151

[1] J. Sanders-Loehr in T. M. Loehr (Ed.): *Iron Carriers and Iron Proteins*, VCH Publishers, New York 1989, p. 373.
[2] P. Reichard, *Annu. Rev. Biochem. 57* (1988) 349.
[3] P. Nordlund, H. Eklund, B. M. Sjöberg, *Nature (London) 345* (1990) 593.
[4] a) M. Fontecave, R. Eliasson, P. Reichard, *J. Biol. Chem. 264* (1989) 9164; b) M. Fontecave, C. Gerez, M. Atta, A. Jeunet, *Biochem. Biophys. Res. Commun. 168* (1990) 659.
[5] L. Petersson, A. Gräslund, A. Ehrenberg, B. M. Sjöberg, P. Reichard, *J. Biol. Chem. 255* (1980) 6706.
[6] Another weak signal is observed at $g = 4.3$ indicating the presence of adventitiously bound iron unavoidable in standard preparations of the protein.
[7] M. Sahlin, A. Gräslund, L. Petersson, A. Ehrenberg, B. M. Sjöberg, *Biochemistry 28* (1989) 2618.
[8] M. Fontecave, C. Gerez, D. Mansuy, P. Reichard, *J. Biol. Chem. 265* (1990) 10919.
[9] J. B. Lynch, C. Juarez-Garcia, E. Munck, L. Que, *J. Biol. Chem. 264* (1989) 8091.
[10] Protein R2 was prepared from an overproducing strain of *E. coli*: B. M. Sjöberg, S. Hahne, M. Karlsson, H. Jörnwall, M. Göransson, B. E. Uhlin, *J. Biol. Chem. 261* (1986) 5658.
[11] a) J. Thiele, *Justus Liebigs Ann. Chem. 271* (1892) 127; b) W. G. Hanstein, J. B. Lett, C. E. McKenna, T. G. Traylor, *Proc. Natl. Acad. Sci. USA. 58* (1967) 1314.
[12] The reaction was carried out as described for diimide but 1,4-L-dithiothreitol (10–20 mM) was used instead.
[13] L. Que, Jr., R. C. Scarrow: *Metal Clusters in Proteins 372 (ACS Symp. Ser.* (1988) 152).
[14] M. P. Woodland, D. S. Patil, R. Cammack, H. Dalton, *Biochim. Biophys. Acta. 873* (1986) 237.
[15] J. R. Hartman, R. L. Rardin, P. Chandhuri, K. Pohl, K. Wieghardt, B. Nuber, J. Weiss, G. C. Papaefthymiou, R. B. Frankel, S. J. Lippard, *J. Am. Chem. Soc. 109* (1987) 7387.
[16] P. Bertrand, B. Guigliarelli, C. More, *Nouv. J. Chim. 15* (1991), in press.
[17] L. L. Pearce, D. M. Kurtz, Jr., Y. M. Xia, P. G. Debrunner, *J. Am. Chem. Soc. 109* (1987) 7286.
[18] J. M. Mc Cormick, E. I. Solomon, *J. Am. Chem. Soc. 112* (1990) 2005.
[19] M. J. Maroney, D. M. Kurtz, Jr., J. M. Nocek, L. L. Pearce, L. Que, *J. Am. Chem. Soc. 108* (1986) 6871.
[20] R. C. Reem, E. I. Solomon, *J. Am. Chem. Soc. 109* (1987) 1216.

Synthesis, Structure, and Isomerization of the (*E*)- and (*Z*)-Isomers of a Diphosphene**

By *Edgar Niecke,** *Oliver Altmeyer*, and *Martin Nieger*

Dedicated to Professor Leopold Horner on the occasion of his 80th brithday

Aryl-substituted (*E*)-diazenes (E = N) **I** can be photochemically converted into the (*Z*)-form **II**, which, in turn, can be reconverted thermally into the (*E*)-form.[1] Since the isomerization **II** → **I** generally proceeds with release of energy, aryl-substituted diazenes have found lasting interest as storage systems for solar energy.[2]

[*] Prof. Dr. E. Niecke, Dr. O. Altmeyer, Dr. M. Nieger
Anorganisch-chemisches Institut der Universität
Gerhard-Domagk-Strasse 1, W-5300 Bonn (FRG)

[**] This work was supported by the Deutsche Forschungsgemeinschaft and the Fonds der Chemischen Industrie.—Partly based on a lecture delivered at the International Conference on Phosphorus Chemistry, Tallinn, USSR, September, 1989: E. Niecke, O. Altmeyer, D. Barion, R. Detsch, C. Gärtner, J. Hein, M. Nieger, F. Reichert, *Phosphorus Sulfur Silicon Relat. Elem.* 49/50 (1990) 321.

In contrast, very little has been reported about (*E*/*Z*)-isomerizations of the homologous diphosphenes (E = P);[3] an isomeric pair, from which the two forms could be isolated is thus far unknown.[4] We report here the synthesis and structure of such an isomeric pair, the isomeric interconversion, and a secondary reaction of the (*Z*)-isomer.

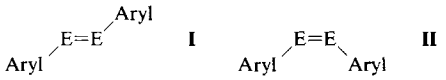

The hydrazinodihalogenophosphanes, **1a** and **1b**, which are accessible from phosphorus(III) chloride or bromide respectively and lithium tris(trimethylsilyl)hydrazide, react with 2,4,6-tri-*tert*-butylphenyl(trimethylsilyl)phosphide to give the thermostable diphosphanes **2a** and **2b**, respectively. Above −10 °C, these eliminate halosilane and form the P=P double-bond systems **3a** and **3b**, respectively (Scheme 1). Remarkable about this reaction is that, in the case of the chloro derivative **2a**, the (*E*)-isomer **3a** is formed selectively from the educts precipitating only in one diasteromeric form, whereas in the case of the bromo derivative **2b**, the *Z*-isomer **3b** is formed selectively.

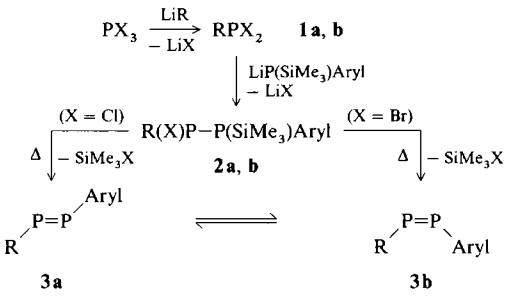

Scheme 1. **1a**, **2a**: X = Cl; **1b**, **2b**: X = Br; R = $(Me_3Si)_2NMe_3SiN$; aryl = 2,4,6-$tBu_3C_6H_2$.

If it is assumed that the thermally-induced cleavage of halosilane from the diphosphanes **2a**, **b** takes place via a *syn*-elimination and the rotameric equilibrium is controlled by steric effects, then the elimination must proceed from different diasteromeric pairs of enantiomers. On the basis of the very similar ^{31}P-NMR data of the educts (δ = 181, − 41, $J_{P,P}$ = 293 Hz (**2a**); 182, − 42, $J_{P,P}$ = 275 Hz (**2b**)) the (*E*)-isomer **3a** must be formed from the *S,R*-(*R,S*)-form with *trans* arrangement of the aryl and hydrazino substituents (g^1-rotamer), whereas the (*Z*)-isomer **3b** must be formed from the *S,S*-(*R,R*)-form with *trans* arrangement of the aryl and bromine substituents (g^2-rotamer).

In both isomers **3a**, **b** the phosphorus atom in the β-position to the hydrazino substituents is strongly shielded: ($\delta(^{31}P)$ = 311(PC) vs 481(PN) (**3a**); 190(PC) vs 358(PN) (**3b**)), which is consistent with the structure in the crystal (see below), and which can be interpreted in terms of the formation of a 4e-3c-NPP π-system. The relative shift differences between the (*E*)- and (*Z*)-form, $\Delta\delta(^{31}P)$, are of comparable magnitude for correspondingly substituted phosphorus atoms ($\Delta\delta$ = 123(PN), 121(PC)) and compare with those of the (*E*/*Z*) isomeric pair aryl–P=P–aryl ($\Delta\delta$ = 124, Aryl = 2,4,6-$tBu_3C_6H_2$[3]). The UV-VIS spectrum shows two absorption maxima above 300 nm, outside of the range of the π-π* transitions of the aryl substituent, which on the basis of their intensities should belong to the symmetry-forbidden n_+-π*-transition (λ_{max}[nm] = 318 (**3a**), 319 (**3b**)) and π_2-π*-transition of the NPP bond system (λ_{max}[nm] = 355 (**3a**), 365 (**3b**)), respectively.

The diphosphenes, which are storable almost indefinitely in the solid state, equilibrate in solution with formation of the isomeric form, whereby the establishment of equilibrium, with **3a**:**3b** = 11:6 (293 K), indicates a similar thermodynamic stability for both isomers ($\Delta\Delta G < 1$ kcal mol^{-1}). Spectroscopic analysis of the reversible transformation **3a** ⇌ **3b** ($k_{(293)Z/E} = 5.5(5) \times 10^{-7}$ s^{-1}; $k_{(293)E/Z} = 6.7(5) \times 10^{-7}$ s^{-1}) affords the free activation enthalpies $\Delta G^{\ddagger}_{(293)E/Z} = 25.5(5)$ and $\Delta G^{\ddagger}_{(293)E/Z} = 25.4(5)$ kcal mol^{-1}. These are significantly lower than the calculated rotational barrier for the parent compound HP=PH (34.0 kcal mol^{-1}[5]), which possibly can be attributed to the stabilization of the radical transition state.[6] The free activation enthalpy for the (*Z*/*E*)-isomerization, however, is markedly higher than that for the diphosphene aryl–P=P–aryl ($\Delta G^{\ddagger}_{(273)Z/E} = 20.3$ kcal mol^{-1}, aryl = 2,4,6-$tBu_3C_6H_2$[3]), whose (*Z*)-form could therefore not be isolated.

Figure 1 shows the structure of the diphosphenes **3a**, **b** in the crystal.[7] As in the already previously characterized aryl-

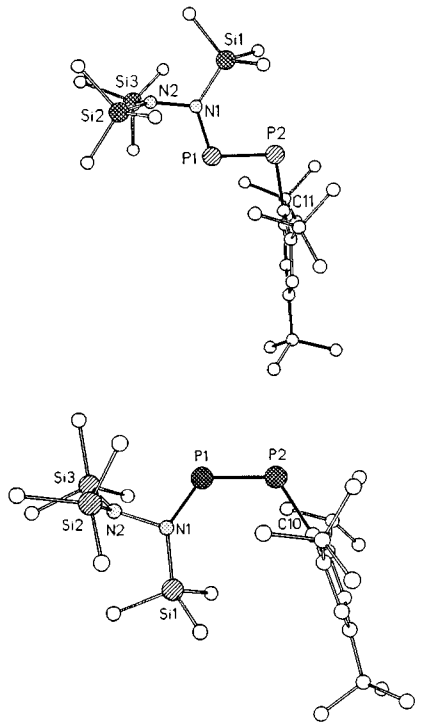

Fig. 1. Structure of the (*E*)-diphosphene **3a** in the crystal (top) and structure of the (*Z*)-diphosphene **3b** in the crystal (bottom). Important bond lengths [pm] and angles [°] of **3a** and **3b** (in square brackets): P-P 203.7(2) [202.7(3)], P-N 170.0(3) [168.6(7)], P-C 186.4(4) [187.8(9)], N-N 147.4(4) [150.6(8)]; P-P-N 106.1(1) [126.3(3)], P-P-C 97.6(1) [121.4(3)], P-N-N 112.5(2) [107.5(5)], P-N-Si 129.3(2) [136.4(4)], N-N-Si 118.1(2) [114.4(5)]; N-P-P-C 179.4(2) [1.5(6)].

substituted diphosphenes,[9] the aryl substituent is almost orthogonal to the central π-bond system (**3a**: 79; **3b**: 89°). The planar coordinated N atoms of the hydrazino substituents and the P atoms of the double bond system, on the other hand, lie in a plane, which enables formation of a 4e, 3c π-system. This is accompanied by a larger valence angle at P1 compared to P2, both in the (*E*)-form (106 vs 98°) as well as in the (*Z*)-form (126 vs 121°). In the latter, the P–P distance is also shorter (202.7(2) vs 203.7(3) pm in the (*E*)-form),

which can be explained in terms of the considerably greater angle at the phosphorus atoms and the associated greater s-part in the phosphorus bonds. This interpretation would also be consistent with the larger P–P coupling constants for the (*Z*)-isomer (554 compared to 516 Hz for the (*E*)-form). A comparison of the structural data of **3a** with those of the correspondingly substituted iminophosphane **4**[10] ((*E*/*Z*)-

(E)-$(Me_3Si)_2N(Me_3Si)N-P=N-2,4,6\text{-}tBu_3C_6H_2$ **4**

isomers in the iminophosphane system have thus far not been observed because of the energetically favored nitrogen inversion[11]) shows that the stereoelectronic influence of the silylated hydrazino substituents is comparable in both bond systems.

Similarly to the well-known isolable *E*-diphosphenes,[12] **3b** also slowly transforms in solution at room temperature[13] into the two symmetrically substituted diphosphenes **6** and **7**, which can be detected in the reaction solution after a few days.[14] It is assumed that their formation proceeds via the kinetically highly labile cyclotetraphosphane **5**, a head/head dimer of **3b** as intermediate.[12]

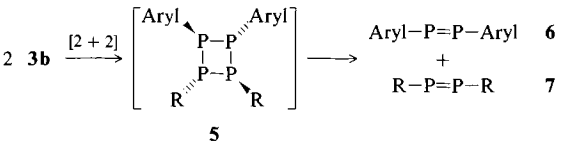

Experimental

1a [1b]: A solution of PCl_3 [PBr_3] (22 mmol) in ether (50 mL) was treated at -40 °C with an equimolar amount of $Li[N_2(SiMe_3)_3]$ dissolved in 100 mL of ether. The reaction mixture was warmed to room temperature, stirred for 12 h, and then the solvent was removed by evaporation. The residue was taken up in *n*-pentane, LiCl[LiBr] removed by filtration, and the crude product obtained on evaporation of the filtrate to dryness was recrystallized from a little *n*-pentane. Yield 94%, m.p. 115–116 °C [90%, 85–88 °C]. ^{31}P NMR (C_6D_6): $\delta = 165$ [168]; ^1H NMR (C_6D_6): $\delta = 0.23$ [0.30] (s, $NSiMe_3$) 0.40 [0.37] (s, $N(SiMe_3)_2$). **3a [3b]**: A solution of **1a [1b]** (5.0 mmol) in ether (20 mL) was cooled to -78 °C and treated dropwise with an equimolar amount of LiP($SiMe_3$)Mes* (Mes* = 2,4,6-$tBu_3C_6H_2$). The mixture, containing the NMR spectroscopically characterized phosphane **2a [2b]** was warmed to room temperature and stirred for 2 h. Halosilane cleavage and a deepening in color accompanied formation of the diphosphene **3a [3b]**. After removal of the volatile components, the residue was taken up in *n*-pentane and filtered to remove LiCl[LiBr]. The crude product obtained on evaporation was recrystallized from a little *n*-pentane. Yield: 2.1 g (79%), m.p. 158–160 °C [1.00 g (40%), 110–112 °C]. $^{31}P\{^1H\}$NMR (C_6D_6): $\delta = 481$, 311 (J(P,P) = 554 Hz) [358, 190 (J(P,P) = 516 Hz)]; ^1H NMR (C_6D_6): $\delta = 7.43$ [7.4] (t, J(H,P) = 1.24 Hz, [< 0.2 Hz], 2H (aryl), 1.55 [1.74] (d, J < 0.2 Hz [1.4 Hz], 18H, *o*-*t*Bu), 1.36 [1.30] (s, 9H, *p*-*t*Bu), 0.37 [0.25] (t, 9H, J(H,P) = 0.55 Hz [0.4 Hz], $PNSiMe_3$), 0.29 [0.06] (d, 18H, J(H,P) = 0.2 Hz [< 0.2 Hz], $NN(SiMe_3)_2$).—MS (70 eV): **3a**: *m*/*z* 554 ($M^{\oplus}$, 13%), 497 ($M^{\oplus}$ – *t*Bu, 2), 309 ($M^{\oplus}$ – Mes*, 14), 278 ($(SiMe_3)_3N_2P^{\oplus}$, 48), 276 (Mes*$P^{\oplus}$, 5), 73 ($SiMe_3^{\oplus}$, 100); **3b**: *m*/*z*: 554 ($M^{\oplus}$, 15%), 497 ($M^{\oplus}$ – *t*Bu, 4), 309 ($M^{\oplus}$ – Mes,* 25), 276 (Mes* $P^{\oplus}$, 3), 263 ($(SiMe_3)_3N_2P^{\oplus}$ – Me, 51), 245 (Mes,* 2.5), 205 ($(SiMe_3)_2NNP^{\oplus}$, 41), 160 ($(SiMe_3)_2N^{\oplus}$, 1), 73 ($SiMe_3^{\oplus}$, 100), 57 ($tBu^{\oplus}$, 81).

Received: April 11, 1991 [Z 4565 IE]
German version: *Angew. Chem. 103* (1991) 1158

CAS Registry numbers:
1a, 111437-98-0; **1b**, 135193-25-8; **2a**, 135193-22-5; **2b**, 135193-27-0; **3a**, 135193-23-6; **3b**, 135193-28-1; **4**, 135193-24-7; **6**, 83466-54-0; **7**, 135193-26-9; $Li[N_2(SiMe_3)_3]$, 22846-03-3; LiP($SiMe_3$)(2,4,6-$tBuC_6H_2$), 91443-42-4.

[1] G. S. Hartley, *Nature (London) 140* (1937) 281; E. R. Talaty, J. C. Fargo, *Chem. Commun. 1967*, 65.
[2] D. P. Fisher, V. Piermattie, J. C. Dabrowiak, *J. Am. Chem. Soc. 99* (1977) 284; A. W. Adamson, A. Vogler, H. Kunkely, R. Wachter, *ibid. 100* (1978) 1298.
[3] A.-M. Caminade, M. Verrier, C. Ades, N. Palilous, M. Koenig, *J. Chem. Soc. Chem. Commun. 1984*, 875; M. Yoshifuji, T. Sato, N. Inamoto, *Chem. Lett. 1988*, 1735.
[4] Stable (*E*)/(*Z*) isomers of metal complexed diphosphenes have already been reported: M. Yoshifuji, T. Hashida, N. Inamoto, K. Hirotsu, T. Horiuchi, T. Higuchi, K. Ito, S. Nagase, *Angew. Chem. 97* (1985) 230; *Angew. Chem. Int. Ed. Engl. 24* (1985) 211.
[5] "Bonding Properties of Low Coordinated Phosphorus Compounds", W. W. Schoeller in M. Regitz, O. J. Scherer (Ed.): *Multiple Bonds and Low Coordination in Phosphorus Chemistry*, Thieme, Stuttgart 1990, p. 5.
[6] In contrast to diazenes, the (*Z*/*E*)-isomerization in diphosphenes proceeds via a rotation of the double bond.
[7] X-ray structure analysis of **3a [3b]** ($C_{27}H_{56}N_2P_2Si_3$ [$C_{27}H_{56}N_2P_2Si_3$]) yellow crystals, crystal dimensions $0.4 \times 0.5 \times 0.6$ [$0.2 \times 0.8 \times 0.8$] mm; M_r = 554.9 [554.9]; space group $P2_1/n$ [$P2_1/n$] (No. 14), a = 990.9(2) [934.5(3)], b = 3551.9(9) [1592.8(8)], c = 1014.3(2) [2456.7(8)] pm, β = 97.52(2)° [100.16(3)°], V = 3.539 [3.600] nm^3, Z = 4 [4], ϱ_{calcd} = 1.04 [1.02] $g\,cm^{-3}$, $\mu(Mo_{K\alpha})$ = 0.24 [0.23] mm^{-1}; 6210 [5021] symmetry independent reflections ($2\theta_{max}$ = 50° [50°]), 3813 [2778] reflections with $|F| > 4\sigma(F)$ used for the structure solution (direct methods) and refinement (307 [307] parameters), non-hydrogen atoms anisotropic, H atoms refined with a "riding" model; R = 0.062 [0.100] (R_w = 0.059 [0.088], $w^{-1} = \sigma^2(F) + gF^2$, g = 0.0003 [0.0]. The relatively poor R value for the compound **3b** is attributed to the unfavorable crystal shape (platelets) and the poor diffraction by the crystals investigated. Therefore, in the case of **3b**, an empirical absorption correction was carried out with the program DIFABS [8]. See [10b].
[8] N. Walker, D. Stuart, *Acta Crystallogr. A 39* (1983) 158.
[9] "Diphosphenes" M. Yoshifuji in M. Regitz, O. J. Scherer (Eds.): *Multiple Bonds and Low Coordination in Phosphorus Chemistry*, Thieme, Stuttgart 1990, p. 321.
[10] a) Important bond lengths [pm] and angles [°] of **4**: P-N 167.2(4), 155.9(4), N-N 148.6(5), N-C 144.5(5); P-N-N 111.0(3), P-N-C 115.3(3), N-P-N 107.3(2); N-P-N-C -177.7(3). X-ray structure analysis of **4**: $C_{27}H_{56}N_3PSi_3$, yellow crystals, crystal dimensions $0.25 \times 0.5 \times 0.5$ mm; M_r = 538.0; space group $P2_1/n$ (No. 14), a = 991.3(3), b = 3462.0(19), c = 1010.7(4) pm, β = 99.33(3)°, V = 3.423 nm^3, Z = 4, ϱ_{calcd} = 1.04 $g\,cm^{-3}$, $\mu(Mo_{K\alpha})$ = 0.20 mm^{-1}; 4472 symmetry independent reflections ($2\theta_{max}$ = 45°), 2792 reflections with $F > 4\sigma(F)$ used for the structure solution (direct methods) and refinement (307 parameters), non-hydrogen atoms anisotropic, H atoms refined with "riding" model; R = 0.058 (R_w = 0.055, $w^{-1} = {}^2(F) + gF^2$, g = 0.0005). b) Further details of the crystal investigation are available on request from the Fachinformationszentrum Karlsruhe, Gesellschaft für wissenschaftlich-technische Information mbH, W-7514 Eggenstein-Leopoldshafen 2 (FRG), on quoting the depository number CSD-55424, the names of the authors, and the journal citation.
[11] E. Niecke, D. Gudat, *Angew. Chem. 103* (1991) 251; *Angew. Chem. Int. Ed. Engl. 30* (1991) 217.
[12] E. Niecke, B. Kramer, M. Nieger, *Angew. Chem. 101* (1989) 217; *Angew. Chem. Int. Ed. Engl. 28* (1989) 215.
[13] The decomposition is accelerated by the action of light.
[14] The compounds **6** and **7** were identified ^{31}P-NMR spectroscopically by addition of authentic samples, aryl–P=P–aryl (δ = 492 [15]) and RN–P=P–NR (δ = 325 [16]), respectively.
[15] M. Yoshifuji, I. Shima, N. Inamoto, K. Hirotsu, T. Higuchi, *J. Am. Chem. Soc. 104* (1982) 6167.
[16] O. Altmeyer, *Dissertation*, Universität Bonn 1990.

Methylating Reductive Dimerization of Aromatic Carbonyl Compounds, a Novel Organometallic Reaction**

By *Thomas Kauffmann,** *Jan Jordan*, and *Karl-Uwe Voss*

The reductive dimerization of carbonyl compounds with titanium[1] or tungsten reagents[2, 3] according to Equation (a) is already a well-established reaction in organic synthesis. We have now found a related reaction, according to

[*] Prof. Dr. T. Kauffmann, Dr. J. Jordan, Dipl.-Chem. K.-U. Voss
Organisch-chemisches Institut der Universität
Corrensstrasse 40, W-4400 Münster (FRG)

[**] Transition Metal Activated Organic Compounds, Part 35. This work was supported by the Deutsche Forschungsgemeinschaft and the Fonds der Chemischen Industrie. – Part 34. T. Kauffmann, A. Hülsdünker, D. Menges, H. Nienaber, L. Reithmeier, S. Robbe, D. Scherler, J. Schrickel, D. Wingbermühle, *Tetrahedron Lett. 31* (1990) 1553.

Equation (b), for which to our knowledge there is no known analogy.

$$R^1R^2C{=}O \longrightarrow R^1R^2C{=}CR^1R^2 \quad (a)$$

$$R^1R^2C{=}O \longrightarrow R^1R^2(Me)C{-}C(Me)R^1R^2 \quad (b)$$

Reaction of $[WOCl_3(thf)_2]$[4] as well as of the W^{VI} complexes $[WOCl_4]$,[4] $[(MeO)WOCl_3]$,[5] and $[(MeO)_4WCl_2]$[5] with, in each case, two molar equivalents of methyllithium in THF leads to μ-methylene complexes[6] which react as carbonyl olefinating reagents with aldehydes and ketones. In contrast, in the case of the W^V-complexes $[\{(nPrO)_3WCl_2\}_2]$ and $[\{(EtO)_3WCl_2\}_2]$, which were synthesized according to the method described in Refs. [7, 8] and which according to Refs. [8, 9] and some ^{1}H-NMR investigations[5] have the dimeric structures **1a** and **1b**, respectively, the corresponding reaction, with in each case 4 molar equivalents of MeLi and subsequently with *aromatic* aldehydes and ketones [Eq. (c)] led to methylating coupling (Table 1).[5, 10] The two

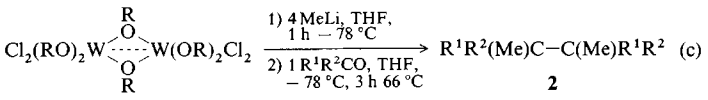

$$Cl_2(RO)_2W(\mu\text{-}O)_2W(OR)_2Cl_2 \longrightarrow R^1R^2(Me)C{-}C(Me)R^1R^2 \quad (c)$$

2

1a, R = *n*Pr; **1b**, R = Et

Table 1. Reactions according to Equation (c).

Reagent	Carbonyl compound	Product **2** Yield [%]	Isomeric ratio	Recovery Carbonyl cpd. [%]
1a	benzaldehyde	77	ca. 1:1	–
1a	4-methoxybenzaldehyde	76	ca. 1:1	–
1b	4-methoxybenzaldehyde	76	ca. 1:1	–
1a	heptanal	–	–	–
1a	acetophenone	83	–	–
1a	benzophenone	90 [a]	–	–
1a	cyclohexanone	–	–	ca. 100

[a] The disproportionation products 1,1-diphenylethane and 1,1-diphenylethene (each ca. 90% of theoretical) were isolated.

aliphatic carbonyl compounds listed in Table 1 did not undergo this reaction. The 2,2,3,3-tetraphenylbutane formed from benzophenone disproportionates to 1,1-diphenylethane and 1,1-diphenylethene;[11] accordingly only these disproportionation products could be isolated. All the products of the reactions listed in Table 1 are known.[12]

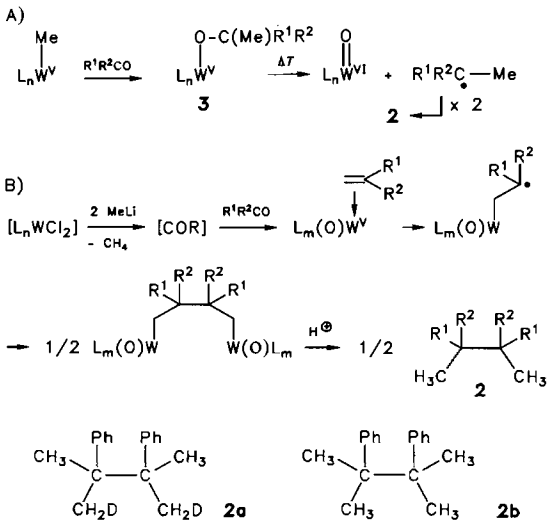

Scheme 1. A) Probable reaction mechanism. B) Rejected reaction mechanism. COR = carbonyl olefinating reagent.

For the reactions according to Equation (c) we postulated the mechanism formulated in Scheme 1 A, which probably takes place at the dimeric reagent. The homolysis of the O–C bond of **3** could be favored by the fact that the electron attracting oxo ligand formed enables an energy-decreasing mesomeric interaction with the electron repelling alkoxy ligands. The following observations in the reaction of **1a** with acetophenone rule out the alternative mechanism (Scheme 1 B):[5] a) no methane was liberated; b) on using D_2O instead of H_2O in the reaction the bisdeuterated product **2a** was not formed; c) **2a** was also not formed when $[D_8]$THF was used as solvent instead of THF; d) according to NMR investigations **2b** was already present before the hydrolysis.

Experimental

A solution of complex **1a** (4.32 g, 10 mmol) in tetrahydrofuran (25 mL) was treated under argon at −78 °C with a solution of four molar equivalents of methyllithium in ether (1.6 M). After stirring for 1 h at −78 °C (the negative Gilmann test with Michlers ketone [13] showed complete consumption of the methyllithium) one mol equivalent of the carbonyl compound was added to the mixture. The mixture was then warmed to room temperature within 1 h and heated under reflux for a further 3 hours. After cooling to room temperature the mixture was hydrolyzed with 25 mL of 2 N NaOH and worked up in the usual way.

Received: March 27, 1991 [Z 4541 IE]
German version: *Angew. Chem. 103* (1991) 1160

[1] J. E. McMurry, *Acc. Chem. Res. 7* (1974) 281; *16* (1983) 405.
[2] K. B. Sharpless, M. A. Umbreit, M. T. Nieh, T. C. Flood, *J. Am. Chem. Soc. 94* (1972) 6538.
[3] M. H. Chisholm, J. A. Klang, *J. Am. Chem. Soc. 111* (1989) 2324.
[4] T. Kauffmann, R. Abeln, S. Welke, D. Wingbermühle, *Angew. Chem. 98* (1986) 927; *Angew. Chem. Int. Ed. Engl. 98* (1986) 909.
[5] J. Jordan, *Dissertation*, Universität Münster 1990.
[6] T. Kauffmann in U. Schubert (Ed.): *Advances in Metal Carbene Chemistry*, Kluwer, Dordrecht, The Netherlands 1989, p. 359.
[7] W. J. Reagan, C. H. Brubaker, *Inorg. Chem. 9* (1970) 827.
[8] D. P. Rillema, C. H. Brubaker, *Inorg. Chem. 8* (1969) 1645.
[9] F. A. Cotton, L. R. Falvello, M. F. Fredrich, D. DeMarco, R. A. Walton, *J. Am. Chem. Soc. 105* (1983) 3088.
[10] K.-U. Voss, T. Kauffmann, unpublished results.
[11] K. Ziegler, W. Deparade, *Justus Liebigs Ann. Chem. 567* (1950) 123.
[12] 2,3-Diphenylbutane (two diastereomers): D. Y. Curtin, H. Gruen, B. A. Shoulders, *Chem. Ind (London) 1958*, 1205; 2,3-di-(4-methoxyphenyl)butane (two diastereomers): K. Sisido, H. Nozaki, *J. Am. Chem. Soc. 70* (1948) 778; 2,3-dimethyl-2,3-diphenylbutane: [11].
[13] H. Gilman, F. Schulze, *J. Am. Chem. Soc. 47* (1925) 2002.

Heterometallic Compounds Involving d- and f-Block Elements: Synthesis, Structure, and Magnetic Properties of Two New Ln_xCu_4 Complexes**

By *Alexander J. Blake, Paul E. Y. Milne, Peter Thornton*, and *Richard E. P. Winpenny**

Since the discovery of the unusual superconducting[1, 2] and magnetic[3, 4] properties of $ABa_2Cu_3O_{6+x}$ (A = Y, lan-

[*] Dr. R. E. P. Winpenny, Dr. A. J. Blake, P. E. Y. Milne
Department of Chemistry, University of Edinburgh
West Mains Road, GB-Edinburgh, EH9 3JJ (Scotland)
Dr. P. Thornton
Department of Chemistry
Queen Mary and Westfield College
University of London

[**] This work was supported by the Science and Engineering Research Council.

thanoids) perovskites, there have been surprisingly few model compounds reported which would enable magnetic interactions between copper and lanthanoids to be investigated within discrete molecules. The two exceptions to this are the Schiff base complexes of *Gatteschi* and co-workers,[5] and two Ln_2Cu_4 complexes synthesized by *Goodgame* et al.[6][*] Here we report the synthesis, characterization and preliminary magnetometry of two such compounds: an octanuclear La_4Cu_4 complex which contains unprecedented structural features, and a hexanuclear Gd_2Cu_4 complex in which the Gd and Cu atoms are ferromagnetically coupled.

Reaction of the anion of 2-hydroxypyridine (L) with copper nitrate and lanthanum perchlorate in methanol gives blue crystals. The structural analysis[7] reveals a salt (**1**) of ex-

$$[Cu_4La_4(L)_8(LH)_8(ClO_4)_2(NO_3)_2(OH)_4(CH_3O)_2](ClO_4)_2 \cdot 2H_2O \quad \mathbf{1}$$

tremely complicated stoichiometry. The octanuclear centrosymmetric dication is shown in Figure 1. The central region of the dication is dominated by a plane of four La atoms, with each La–La vector bridged by at least two oxygen atoms. The two pairs of Cu atoms are separated by this plane, and overall the eight metal atoms form a distorted hexagonal bipyramid.

La1 and its symmetry equivalent La1′ lie at the apices of the polyhedron (Fig. 1b), bridged by two μ_3-hydroxide ions (O9 and O9′) forming a centric La_2O_2 ring. O9 also bonds to La2, and La1 and La2 are further bridged by an oxygen (O4) from a deprotonated 2-hydroxypyridine. La1 and La2′ share three oxygen donors, O9′ and two oxygens (O2′ and O3) from deprotonated ligands. The La–La distances within these La_2O_2 rings vary from 3.8822(7) Å to 4.1416(7) Å, similar to those found in other Ln_2O_2 rings[8, 9] (allowing for the differing ionic radii of various lanthanoids).

La1 also shares a μ_3-hydroxide ion (O10) with both Cu1 and Cu2, and in addition the two copper atoms are bridged by O40 (an oxygen from a deprotonated methanol molecule) to form a Cu_2O_2 ring with a Cu–Cu distance of 3.0172(16) Å, again similar to those in related compounds.[10, 11] The La and Cu atoms are also linked by L units, which are in the main trinucleating: each oxygen atom bridges two La atoms and the nitrogen binds to Cu.

Each of the four crystallographically independent metal atoms has a different coordination geometry (Fig. 1b). La1 is nine-coordinate, bound to six shared oxygens as itemized above, a bidentate nitrate (O31 and O33) and an oxygen (O8) from a protonated ligand. The geometry is distorted monocapped square-antiprismatic. La2 is eight-coordinate, bound to four aforementioned bridging oxygens, an oxygen (O1) from a binucleating L unit, and three oxygens (O5, O6 and O7) from protonated ligands. The geometry corresponds to a square antiprism. Cu2 is square-pyramidal: the apical oxygen comes from a loosely associated ClO_4^- anion (Cu1–O11 2.508(8) Å); the basal donor atoms are two *cis* nitrogen atoms from L units (N1 and N3) and the two bridging oxygen atoms (O10 and O40) mentioned above. Cu2 has distorted square-planar geometry, again with two *cis* nitrogen atoms (N2 and N4) supplementing the shared oxygens. The bond lengths between metals and donor atoms are unexceptional; La–O varies from 2.37 to 2.69 Å, and Cu–O and Cu–N bonds between 1.93 and 2.00 Å (excepting the long bond to the apical perchlorate).

Several of these features are highly unusual. The plane of four La atoms, each vector bridged by oxygen atoms, is reminiscent of several multinuclear manganese complex-

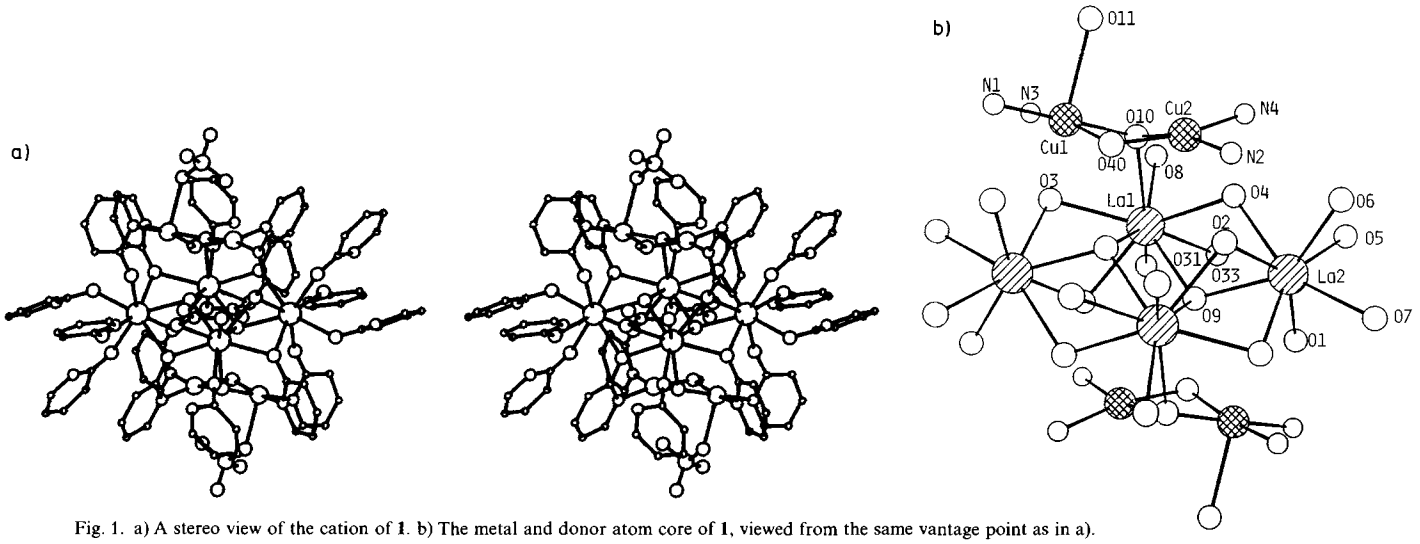

Fig. 1. a) A stereo view of the cation of **1**. b) The metal and donor atom core of **1**, viewed from the same vantage point as in a).

es[12] which have displayed interesting magnetic properties. Only once previously, in an octanuclear erbium complex,[13] has such a feature been observed for an f-block element. The interposing of such a plane between hetero metal atoms is unprecedented. The mean plane of the two Cu atoms and their six basal donor atoms is canted at 24.3° to the plane of four La atoms.

Attempts to make an analogous Gd_4Cu_4 complex have thus far failed. Instead a purple precipitate forms, which on treatment with HCl gives a green solution and, after one day, green crystals. The structure of the resulting compound (**2**) has been determined[7] (Fig. 2). The cation contains an octa-

$$[Cu_4Gd_2Cl_4L_8(LH)_4(H_2O)_4] \cdot 2Cl \cdot H_2O \quad \mathbf{2}$$

hedral metal core of four Cu and two Gd atoms. The arrangement of bridging atoms is similar to that found for other Ln_2Cu_4 complexes.[6] The 2-hydroxypyridine ligands

[*] Note added in proof (July 31, 1991): After this manuscript had been accepted, a paper appeared on the structure of a Y_2Cu_8–2-hydroxypyridine complex (S. Wang, *Inorg. Chem. 30* (1991) 2252). This complex was synthesized in virtually the same way as the Gd_2Cu_4– and Dy_2Cu_4–2-hydroxypyridine complexes described in [6].

act as trinucleating bridges, binding via the O atom to Gd and Cu atoms, and via the N to a second Cu atom. The Gd atoms are eight-coordinate with square antiprismatic geometry; the Cu atoms are five-coordinate with square-pyramidal geometry—two N and two O atoms in the basal plane (arranged *cis*), and a Cl atom in the axial position.

Magnetic measurements on both complexes[14] over the temperature range 310 K to 70 K show interesting behavior. In **1** there is strong antiferromagnetic coupling between pairs of Cu ions, presumably mediated by the μ_2-OMe and μ_3-OH ligands. This leads to a magnetic moment below the spin-only value at room temperature, and diamagnetic behavior below 100 K. In **2** the magnetic moment rises from 8.36 μ_B at 310 K to 8.78 μ_B at 170 K. Below this temperature the moment falls, reaching 8.16 μ_B at 70 K.

An explanation of this behavior in **2** is that there is ferromagnetic coupling between each Gd^{III} and the two Cu atoms with which it shares μ_2-carbonyl bridging oxygens (i.e., the labeled metals in Fig. 2). This accounts for the increase in magnetic moment between 310 K and 170 K. That the moment falls again below this temperature is probably due to anti-ferromagnetic coupling between the two Cu_2Gd "triangles" within each complete molecule of **2**. Thus, as observed previously,[5] copper and gadolinium ions appear to couple ferromagnetically.

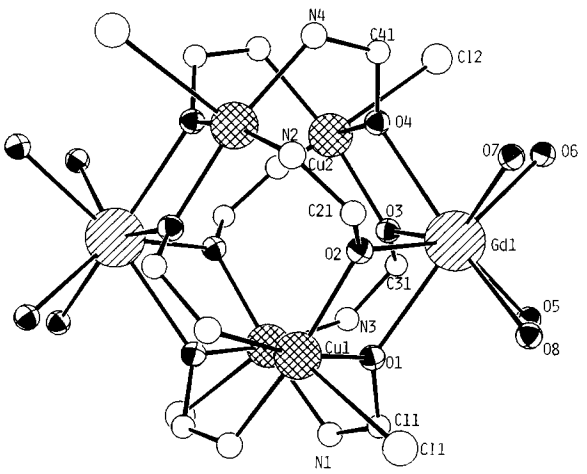

Fig. 2. The cation of **2**, with atoms not involved in metal-atom bridging omitted for clarity. Bond length ranges: Gd-O 2.283–2.507, Cu-O 1.965–2.008, Cu-N 1.969–1.997, Cu-Cl 2.640, 2.644 Å. Standard deviation 0.012 Å.

The straightforward synthetic procedures for **1** and **2** and the dependence of the resulting structure changes on reaction conditions suggest that a rich chemistry of mixed d-block and f-block complexes remains to be explored, and the observation of ferromagnetic coupling between d- and f-block elements confirms that this is a promising approach to new molecular magnets.[15]

Experimental procedure

1: deprotonated 2-hydroxypyridine (1 mmol, prepared from LH and KOH in water) was dissolved in methanol (5 ml) and copper nitrate (0.33 mmol) in methanol (2 ml) was added dropwise. The resulting green solution was filtered and lanthanum perchlorate (0.17 mmol) in methanol (1 ml) was added dropwise giving a purple solution, from which blue crystals grew after standing for 16 hours. IR: $\tilde{\nu}$(OH) = 3595 and 3510 cm^{-1}; $\tilde{\nu}$(CO) 1662, 1645, and 1605 cm^{-1}. No molecular ion observed by FABMS. Magnetic moment, solid state [(*T*/K) μ_{eff}/μ_B per Cu atom]: (309.8) 0.96, (288.6) 0.91, (268.5) 0.85, (247.6) 0.78, (227.7) 0.77, (207.2) 0.71, (187.2) 0.67, (165.5) 0.44, (145.8) 0.39, (125.9) 0.35, (106.0) 0.30. Diamagnetic within error below this temperature.

2: An analogous procedure using gadolinium perchlorate gave a purple precipitate. This was collected by centrifugation and suspended in fresh methanol (7 ml). Concentrated HCl (4 drops) was added, giving a green solution from which crystals formed after one day. IR: $\tilde{\nu}$(CO) 1652 and 1610 cm^{-1}. No molecular ion by FABMS. Magnetic moment, solid state [(*T*/K) μ_{eff}/μ_B per Cu_2Gd unit] (309.6) 8.36, (289.3) 8.49, (267.3) 8.43, (246.0) 8.45, (225.7) 8.68, (206.0) 8.68, (185.9) 8.75, (165.6) 8.78, (145.0) 8.66, (125.4) 8.43, (105.2) 8.13 (84.8) 8.34, (69.6) 8.16. Errors of ca. 1% in each measurement of μ_{eff}/μ_B.

Received: March 14, 1991 [Z 4496 IE]
German version: *Angew. Chem. 103* (1991) 1161

CAS Registry numbers:
1, 135426-09-4; **2**, 135393-32-7.

[1] J. G. Bednorz, K. A. Müller, *Z. Phys. B. 64* (1986) 189.
[2] P. H. Hor, R. L. Meng, Y. Q. Wang, L. Gao, Z. L. Huang, J. Bechtold, K. Forster, C. W. Chu, *Phys. Rev. Lett. 58* (1987) 1891.
[3] A. Poddar, P. Mandal, P. Choudhury, A. N. Das, B. Ghosh, *J. Phys. C. 21* (1988) 3323.
[4] J. W. Lynn, W.-H. Li, H. A. Mook, B. C. Sales, Z. Fisk, *Phys. Rev. Lett. 60* (1988) 2781.
[5] C. Benelli, A. Caneschi, D. Gatteschi, O. Guillou, L. Pardi, *Inorg. Chem. 29* (1990) 1750.
[6] D. M. L. Goodgame, D. J. Williams, R. E. P. Winpenny, *Polyhedron 8* (1989) 1531.
[7] Crystal data for $C_{82}H_{86}Cl_4Cu_4La_4N_{18}O_{46}$ **1**: orthorhombic, *Pccn*, with $a = 25.049(3)$, $b = 22.3211(14)$, $c = 19.5509(23)$ Å, $V = 10931$ Å^3, $M = 3011.0$, $Z = 4$, $\varrho_{calcd} = 1.828$ g cm^{-3}, $T = 298$ K, $\mu(Mo_{K\alpha}) = 2.491$ mm^{-1}. Crystal data for $C_{60}H_{62}Cl_6Cu_4Gd_2N_{12}O_{17}$ **2**: monoclinic, *C2/c*, $a = 19.206(3)$, $b = 18.096(4)$, $c = 24.090(9)$ Å, $\beta = 102.037(18)°$, $V = 8188$ Å^3, $M_r = 2004.5$, $Z = 4$, $\varrho_{calcd} = 1.626$ g cm^{-3}, $T = 298$ K, $\mu(Mo_{K\alpha}) = 2.89$ mm^{-1}. Stoë STADI-4 diffractometer, ω-2θ scans and learnt-profile method, (W. Clegg, *Acta. Crystallogr. Sect. A 37* (1981) 22), graphite-monochromated $Mo_{K\alpha}$ radiation. Both structures were solved by heavy atom methods, corrected for absorption, and refined anisotropically to give $R = 0.0393$ ($R_w = 0.0455$) and $R = 0.0619$ ($R_w = 0.0790$) respectively, for 4596 and 3174 independent observed reflections ($2\theta \leq 45°$, $F_o > 6\sigma(F)$]. Further details of the crystal structure investigations are available on request from the Director of the Cambridge Crystallographic Data Center, University Chemical Laboratory, Lensfield Road, GB-Cambridge CB3 1EW (UK) on quoting the full journal citation.
[8] H. J. Schugar, E. I. Solomon, W. L. Cleveland, L. Goodman, *J. Am. Chem. Soc. 97* (1975) 6442.
[9] I. A. Kahwa, S. Folkes, D. J. Williams, S. V. Ley, C. A. O'Mahoney, G. L. McPherson, *J. Chem. Soc. Chem. Commun. 1989*, 1531.
[10] D. M. L. Goodgame, D. J. Williams, R. E. P. Winpenny, *Polyhedron 8* (1989) 873.
[11] R. Willett, G. L. Breneman, *Inorg. Chem. 22* (1983) 326.
[12] G. Christou, *Acc. Chem. Res. 22* (1989) 328.
[13] J. C. A. Boeyens, J. P. R. de Villiers, *J. Cryst. Mol. Struct. 2* (1972) 197.
[14] Experimental procedures as in M. A. Laffey, P. Thornton, *J. Chem. Soc. Dalton Trans 1982*, 312.
[15] Note added in proof: Since acceptance of this manuscript the crystal structure of a Y_2Cu_8 complex of 2-hydoxypyridine has appeared [S. Wang, *Inorg. Chem. 30*, (1991), 2252]. This complex was prepared by an essentially identical route to that used to synthesize Gd_2Cu_4 and Dy_2Cu_4 complexes of 2-hydroxypyridine, as reported in [6].

A Novel Gallium–Phosphorus Cage Compound**

By *Alan H. Cowley,* Richard A. Jones,* Miguel A. Mardones, Jerry L. Atwood,** and *Simon G. Bott*

The revival of interest in "13–15" compounds of the heavier main-group elements is attributable in part to the potential utility of such species as semiconductor precursors. Thus far, much of the synthetic effort has focused on how the biligated R_2M (M = Al, Ga, In) and R'_2E (E = P, As, Sb)

[*] Prof. A. H. Cowley, Prof. R. A. Jones, M. A. Mardones
Department of Chemistry
The University of Texas at Austin
Austin, TX 78712 (USA)
Prof. J. L. Atwood, Dr. S. G. Bott
Department of Chemistry
University of Alabama
Tuscaloosa, AL 35486 (USA)

[**] This work was supported by the National Science Foundation, the Robert A. Welch Foundation, and the U.S. Army Research Office.

moieties are bonded together.[1] Significantly less emphasis has been placed on compounds that involve monoligated RM and R'E fragments.[*] In an effort to develop this area further, we treated $K_2[t\text{BuPP}t\text{Bu}]$[2] with $t\text{BuGaCl}_2$[3] in the expectation that a three-membered GaP_2 or six-membered Ga_2P_4 ring would be produced.[4] However, the reaction product is a novel Ga_3P_4 cage compound in which a $t\text{BuGaCl}_2$ unit behaves simultaneously as a Lewis acid and a Lewis base.

Addition of three equivalents of $t\text{BuGaCl}_2$ to two equivalents of $K_2[t\text{BuPP}t\text{Bu}]$ at $-78\,^\circ\text{C}$ in THF, followed by removal of the solvent and recrystallization of the residue from toluene, resulted in light yellow, crystalline **1**. The CI mass spectrum of **1** revealed a parent peak at m/z 804 (1.4%), followed by fragment ions at m/z 607 (59%) and 549 (100%), which correspond to $[M - t\text{BuGaCl}_2]^+$ and $[M - t\text{BuGaCl}_2 - t\text{Bu}]^+$, respectively. The loss of a $t\text{BuGaCl}_2$ fragment suggests a structure in which this molecule is attached to a $(t\text{Bu})_6Ga_2P_4$ ring system. Such a view is consistent with NMR spectroscopic data.[5] Thus, four tBuP groups and two different tBuGa units in 2:1 abundance are evident in the ^{1}H NMR spectrum. The $^{31}P\{^1H\}$ spectrum comprises two broad doublets of equal intensity with a coupling constant (284 Hz) that is indicative of a one-bond interaction. These data suggest that two of the phosphorus atoms are involved in coordination to the $t\text{BuGaCl}_2$ molecule. Further elucidation of the structure of **1** required an X-ray analysis (Fig. 1).[6] The solid state of **1** consists of

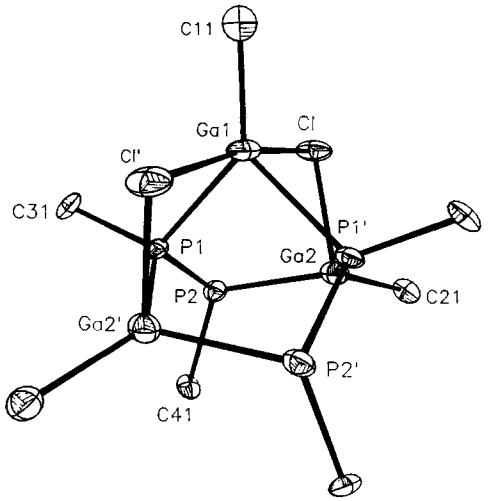

Fig. 1. View (ORTEP) of **1** showing the atom numbering scheme. The tBu methyl groups are omitted for clarity. Important bond distances [Å] and bond angles [°]: Ga1-P1 2.436(3), Ga1-C11 2.04(2), Ga1-Cl 2.681(3), Ga2-P2 2.363(3), Ga2-C21 2.01(1), Ga2-Cl 2.344(3), Ga2-P1' 2.416(3), P1-C31 1.895(9), P1-P2 2.182(3), P2-C41 1.91(1); P1'-Ga1-P1 90.55(8), P1'-Ga1-Cl 81.21(8), P1-Ga1-C11 134.66(6), P1-Ga1-Cl 92.14(8), Cl'-Ga1-Cl 170.47(8), Cl-Ga1-C11 94.78(6), P2-Ga2-Cl 89.8(1), P1'-Ga2-P2 107.8(1), P2-Ga2-C21 120.6(3), P1'-Ga2-Cl 88.7(1), P1'-Ga2-C21 129.6(3), Cl-Ga2-C21 103.4(2), Ga1-P1-Ga2' 87.56(7), Ga2'-P1-P2 122.0(1), Ga2'-P1-C31 117.5(3), Ga1-P1-P2 106.8(1), Ga1-P1-C31 113.6(3), P2-P1-C31 107.5(3), Ga2-P2-P1 97.3(1), P1-P2-C41 110.1(3), Ga2-P2-C41 116.3(3).

individual molecules and no short intermolecular contacts. Each molecule resides on a twofold axis that passes through Ga1 and C11. A convenient way to visualize the structure of **1** is to regard it as a complex of $t\text{BuGaCl}_2$ and ring system **2**.

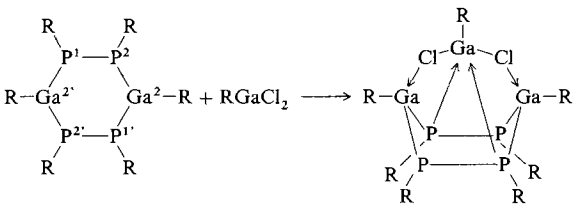

2 R = tBu **1**

Two of the phosphorus atoms of ring **2**, P1 and P1', are involved in electron-pair donation to the $t\text{BuGaCl}_2$ molecule and the bonding in the cluster is completed by the formation of Cl bridges between $t\text{BuGaCl}_2$ and the ring gallium atoms. In a formal sense, the $t\text{BuGaCl}_2$ molecule plays the role of both Lewis acid and Lewis base.[7] In this context, the geometry around Ga1 is best described as trigonal bipyramidal. Note, however, that the axial (Cl-Ga1-Cl' = 170.47(8)°) and equatorial (P1-Ga-P1' = 90.55(8)°) angles depart considerably from the ideal values as a consequence of the donor and acceptor interactions with the Ga_2P_4 ring. Note also that the Ga–Cl–Ga bridges are very unsymmetrical and that the Ga1–Cl distances (2.681(2) Å) are unusually long (cf. $[t\text{BuGa(Cl)P(H)Ar}']_2$, Ar' = 2,4,6-$t\text{Bu}_3C_6H_2$, Ga-Cl = 2.397(2) Å).[3] The Ga_2P_4 ring of **2** adopts a boat conformation, doubtless in large measure a response to maximizing the dative interactions between P1 and P1' and the $t\text{BuGaCl}_2$ molecule. Within the Ga_2P_4 ring, the bond lengths between Ga and the three-coordinate P atoms, P2 and P2', are somewhat shorter (2.363(3) Å) than those involving the four-coordinate P atoms, P1 and P1' (2.416(3) Å). Note, however, that the geometry at P2 and P2' is pyramidal (sum of angles = 323.7°); hence there is no evidence for dative P → Ga π bonding.

Attempts to isolate or detect ring system **2** by treatment of $K_2[t\text{BuPP}t\text{Bu}]$ with an equimolar quantity of $t\text{BuGaCl}_2$ were not successful. We therefore conclude that either compound **2** is unstable or the mechanism of formation of **1** does not involve **2**.

Experimental Procedure

A cold (−78 °C) solution of $t\text{BuGaCl}_2$ [3] (0.71 g, 3.61 mmol) in 20 mL of THF was added to a stirred suspension of $K_2[t\text{BuPP}t\text{Bu}] \cdot 0.5$ THF [2] (0.70 g, 2.40 mmol) in 20 mL of THF at −78 °C. The reaction mixture was allowed to attain ambient temperature over a 12 h period. Following this, the solvent and volatiles were removed under vacuum and the residue was extracted with toluene. After filtration and concentration of the filtrate, light yellow crystals of **1** were obtained in 44% yield (0.43 g) by cooling the solution to −20 °C. Compound **1** melts at 190–193 °C (dec.).

Received: March 7, 1991 [Z 4481 IE]
German version: *Angew. Chem. 103* (1991) 1163

CAS Registry numbers:
1, 135283-72-6; $K_2[t\text{BuPP}t\text{Bu}]$, 66874-44-0; $t\text{BuGaCl}_2$, 135257-35-1.

[*] Note added by the editorial staff: After the final version of this manuscript was received, this journal published a communication on a Ga_3P_3 compound consisting exclusively of RM and R'E fragments: H. Hope, D. C. Pestana, P. P. Power, *Angew. Chem. 103* (1991) 726; *Angew. Chem. Int. Ed. Engl. 30* (1991) 691.

[1] Review: A. H. Cowley, R. A. Jones, *Angew. Chem. 101* (1989) 1235; *Angew. Chem. Int. Ed. Engl. 28* (1989) 1208.
[2] M. Baudler, C. Gruner, G. Fürstenberg, F. Saykowski, V. Özer, *Z. Anorg. Allg. Chem. 446* (1978) 169.
[3] This compound exists as a dimer in the solid state: A. H. Cowley, R. A. Jones, M. A. Mardones, J. L. Atwood, S. G. Bott, *Heteroat. Chem. 2* (1991) 11.
[4] For seminal work on analogous boron rings, see: M. Baudler, A. Marx, J. Hahn, *Z. Naturforsch. B33* (1978) 355; M. Baudler, A. Marx, *Z. Anorg. Allg. Chem. 474* (1981) 18; M. Fehér, R. Fröhlich, K.-F. Tebbe, *ibid. 474* (1981) 31.

[5] **1**: ^{1}H NMR (300.15 MHz, 295 K, C_6D_6, TMS external standard): $\delta = 1.33$ (s, br, 36H; *t*BuP), 1.42 (s, 18H; *t*BuGa(ring)), 1.45 (s, 9H; *t*BuGaCl$_2$); ^{13}C{^{1}H} NMR (75.48 MHz, 295 K, C_6D_6, TMS external standard) $\delta = 29.7$ (s, C-P), 32.1 (s, br, C-Ga), 32.4 (s, $(H_3C)_3$CGa(ring)), 33.1 (s, br, (H_3C)CP); ^{31}P{^{1}H} NMR (121.5 MHz, 295 K, C_6D_6, 85% H_3PO_4 external standard): $\delta = -21.3$ (d, br, $^1J_{(P,P)} = 284$ Hz), -63.2 (d, br, $^1J_{(P,P)} = 284$ Hz).

[6] **1**: monoclinic, space group $C2/c$ (Nr. 15), $Z = 4$; $a = 17.569(2)$, $b = 12.112(1)$, $c = 18.775(2)$ Å, $\beta = 100.27(1)°$; $V = 3931$ Å^3 $\varrho_{ber.} = 1.363$ g cm^{-3}; $2° < 2\theta < 90°$ ($Mo_{K\alpha} = 0.71069$ Å, $\mu = 53.84$ cm^{-1}). A total of 3430 reflections were collected at 298 K using the $\theta/2\theta$ scan mode. Of these, 1430 reflections with $I > 6.0\ \sigma(I)$ were used to solve (Patterson) and refine (full-matrix least squares) the structure of **1**. $R = 0.0591$, $R_w = 0.0650$. There is some disorder in the *t*Bu groups. Further details of the crystal structure investigation can be obtained from the Fachinformationszentrum Karlsruhe, Gesellschaft für wissenschaftlich-technische Information mbH, W-7514 Eggenstein-Leopoldshafen 2 (FRG), by quoting the depository number CSD-55343, the names of the authors, and the journal citation.

[7] For a somewhat similar complex between a B_2N_2 ring and $TiCl_4$, see G. Schmid, D. Kampmann, W. Meyer, R. Boese, P. Paetzold, K. Delpy, *Chem. Ber. 118* (1985) 2418.

Tetrameric Gallium and Aluminum Chalcogenides, [*t*BuME]$_4$ (M = Al, Ga; E = S, Se, Te). A New Class of Heterocubanes**

By *Alan H. Cowley,* Richard A. Jones,* Paul R. Harris, David A. Atwood, Leopoldo Contreras*, and *Christof J. Burek*

Cubic chalcogenide clusters featuring transition-metal fragments, $[L_nM(\mu_3\text{-}E)]_4$ (E = S, Se, Te), constitute a well-known class of compounds.[1] However, the corresponding cubanes in which the organometallic moiety L_nM is replaced by a main-group fragment are nonexistent. The closest examples of main-group species with an M_4E_4 core possess the general formula $[RM(\mu_3\text{-}ER')]_4$ in which M = Mg[2] or Be,[3] E = O or S, and R and R′ are alkyl groups.[4] We were prompted to attempt the synthesis of group 13/16 cubanes of the type $[RM(\mu_3\text{-}E)]_4$ (M = Al, Ga; E = S, Se, Te) for two reasons. First, our recent synthesis of $[t\text{BuAl}(\mu_3\text{-}PSiPh_3)]_4$, the first aluminum–phosphorus cubane,[5] suggested the existence of isoelectronic group 13/16 analogues. Secondly, interest in group 13/16 cubanes stems both from their structures and bonding and also from their potential to function as precursors to layer compounds such as GaS, GaSe, and GaTe.[6]

The reaction of *t*Bu$_3$Ga with elemental sulfur, selenium, or tellurium in toluene at 25 °C affords cubanes $[t\text{BuGa}(\mu_3\text{-}E)]_4$ (**1**, E = S; **2**, E = Se; **3**, E = Te) in yields of 55 to 70%. In the cases of **1** and **2** the reaction mixtures also contain appreciable amounts of *t*Bu$_2$S and *t*Bu$_2$Se as well as other alkylated sulfur and selenium species (e.g., *t*Bu$_2$S$_2$ and *t*Bu$_2$Se$_2$) [Eq. (a)]. The reaction of *t*Bu$_3$Ga with H_2S represents an alternative high-yield route to **1** [Eq. (b)].

$$4\,t\text{Bu}_3\text{Ga} + 4\text{S} \longrightarrow \underset{\mathbf{1}}{[t\text{BuGa}(\mu_3\text{-S})]_4} + t\text{Bu}_2\text{S} + \text{other products} \quad \text{(a)}$$

$$4\,t\text{Bu}_3\text{Ga} + 4\,\text{H}_2\text{S} \longrightarrow \underset{\mathbf{1}}{[t\text{BuGa}(\mu_3\text{-S})]_4} + 4\,t\text{BuH} \quad \text{(b)}$$

After recrystallization or sublimation, compounds **1**–**3** were obtained as clear, colorless crystals. An X-ray diffraction study has been carried out on **1** (Fig. 1).[7] The molecule

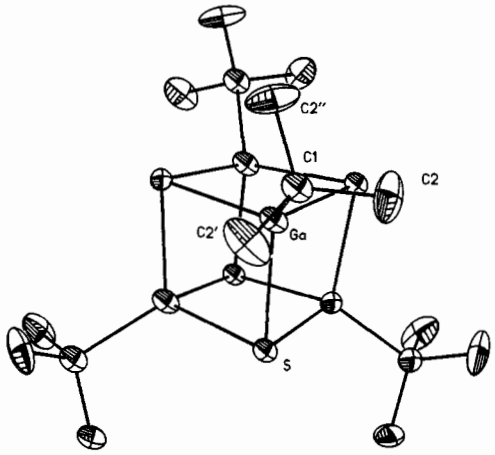

Fig. 1. View (ORTEP) of **1** showing the atom numbering scheme. Important bond distances [Å] and bond angles [°]: Ga-S 2.365(5), Ga-C1 2.00(4), C1-C2 1.48(3); S-Ga-S′ 87.0(3), Ga-S-Ga′ 92.3(3), S-Ga-C1 119.7(2). The atoms labeled with a prime are generated by reflection through a crystallographic center of symmetry.

contains only four unique atoms (Ga, S, C1, and C2) with each gallium atom lying on a fourfold symmetry site. The methyl groups of the *t*Bu units are perfectly disordered over six sites each with 50% occupancy. The angles of the cube

Table 1. Important physical data for **1**–**9**.

1: m.p. 208–216 °C (dec.). IR (KBr disk): $\tilde{\nu}$[cm^{-1}] = 2944 s, 2926 s, 2916 s, 2882 m, 2869 m, 2848 s, 2797 vw, 2741 vw, 2709 w, 1464 s, 1458, 1380 w, 1363 ssh, 1323 vw, 1310 w, 1261 w, 1170 m, 1079 w br, 1018 m, 1010 m, 943 w, 809 m sh, 711 m br. ^{1}H NMR (300.15 MHz, $CDCl_3$, 32 °C): $\delta = 1.09$ (s, *t*BuGa). ^{13}C{^{1}H} NMR (75.48 MHz): $\delta = 28.72$ ($(H_3C)_3C$Ga), 26.86 ($C(CH_3)_3$CGa). EI MS: *m/z* 635 ($C_{16}H_{36}Ga_4S_4$, $M^{\oplus}$)

2: m.p. 260–270 °C (dec.). IR (KBr disk): $\tilde{\nu}$[cm^{-1}] = 2945 s, 2926 s, 2913 s, 2878 m, 2868 m, 2845 s, 2708 w, 1463 s, 1456 s, 1387 w, 1362 ssh, 1164 s, 1007 m, 943 w, 908 vw, 805 m sh, 734 m br. ^{1}H NMR (300.15 MHz, $CDCl_3$, 27 °C): $\delta = 1.01$ (s, *t*BuGa). ^{13}C{^{1}H} NMR (75.48 MHz); $\delta = 26.68$ (s, $(CH_3)_3$CGa), ($(CH_3)_3C$Ga: quat. C atoms not observed). EI MS (^{69}Ga, ^{80}Se): *m/z* 824 ($C_{16}H_{36}Ga_4Se_4$, $M^{\oplus}$)

3: m.p. 92–98 °C (dec.). IR (KBr disk): $\tilde{\nu}$[cm^{-1}] = 2937 s, 2918 s, 2907 s, 2871 s, 2859 s, 2940 vs, 2758 w, 2729 w, 2701 w, 1460 s, 1451 s, 1435 w, 1384 m, 1360 ssh, 1206 w, 1154 s, 1003 s, 942 w, 801 m sh. ^{1}H NMR (300.15 MHz, $CDCl_3$, 27 °C): $\delta = 0.80$ (s, *t*BuGa); ^{13}C{^{1}H} NMR (75.48 MHz): $\delta = 26.64$ (CH_3)$_3$CGa) ($(CH_3)_3C$Ga: quat. C atoms not observed). EI MS (^{69}Ga, ^{128}Te): *m/z* 1016 ($C_{16}H_{36}Ga_4Te_4$, $M^{\oplus}$)

4: m.p. 285 ° (dec.). ^{1}H NMR (300 MHz, C_6D_6, 27 °C, TMS ext.): $\delta = 1.12$ (s, *t*BuAl); ^{13}C{^{1}H} NMR: $\delta = 26.78$ (s, $(CH_3)_3$CAl). EI MS: *m/z* 464 ($C_{16}H_{36}Al_4S_4$, $M^{\oplus}$)

5: m.p. 350 °C (dec.). ^{1}H NMR (C_6D_6): $\delta = 1.08$ (s, *t*BuAl); ^{13}C{^{1}H} NMR: $\delta = 26.70$ (s, $(H_3C)_3$CAl). EI MS: *m/z* 654 ($C_{16}H_{36}Al_4Se_4$, $M^{\oplus}$)

6: m.p. 400 °C (dec.). ^{1}H NMR (C_6D_6): $\delta = 1.05$ (s, *t*BuAl). ^{13}C{^{1}H} NMR: $\delta = 26.79$ (s, $(H_3C)_3$CAl). EI MS: *m/z* 847 ($C_{16}H_{36}Al_4Te_4$, $M^{\oplus}$)

7: m.p. 250–253 °C. ^{1}H NMR (C_6D_6): $\delta = 1.33$ (s, 18H; *t*BuAl), 1.35 (s, 9H; *t*BuS); ^{13}C{^{1}H} NMR: $\delta = 31.47$ (s, $(H_3C)_3$CAl), 35.88 (s, $(H_3C)_3$CS)

8: m.p. 336–340 °C. ^{1}H NMR: $\delta = 1.34$ (s, 18H; *t*BuAl), 1.48 (s, 9H, *t*BuSe). ^{13}C{^{1}H} NMR: $\delta = 31.12$ (s, $(H_3C)_3$CAl), 36.69 (s, $(H_3C)_3$CSe). EI MS: *m/z* 278 (This corresponds to a molecular ion for the monomeric unit) (*t*Bu$_2$AlSe*t*Bu)

9: m.p.: converts into **6** at 300 °C. ^{1}H NMR: $\delta = 1.36$ (s, 18H; *t*BuAl), 1.60 (s, 9H; *t*BuTe). ^{13}C{^{1}H} NMR: $\delta = 30.97$ (s, $(H_3C)_3$CAl), 39.23 (s, $(H_3C)_3$CTe)

[*] Prof. A. H. Cowley, Prof. R. A. Jones, Dr. P. R. Harris, D. A. Atwood, Dr. L. Contreras, C. J. Burek
Department of Chemistry
University of Texas at Austin
Austin, Texas 78712 (USA)

[**] This work was supported by the National Science Foundation, The Robert A. Welch Foundation, the Eastman Kodak Company, and the U.S. Army Research Office (DAAL 03-89-K-0164). Dr. *Contreras* is the recipient of a Fulbright Fellowship (1990/91). We thank Dr. *H. Gysling*, Eastman Kodak Company, for helpful discussions.

are close to the idealized values (Ga-S-Ga′ = 92.3(3) Å and S-Ga-S′ = 87.0(3) Å). The Ga–Ga distance (3.099(6) Å) indicates little or no metal–metal bonding within the cluster. The Ga–S distance of 2.365(5) Å is similar to the Ga–S single-bond distances found in $[Ph_2Ga(\mu\text{-}SEt)]_2$ (2.373(1) Å) and $[I_2Ga(\mu\text{-}SMe)]_2$ (2.398(5) Å).[8] Cubane structures for **1–3** are also consistent with analytical and spectroscopic data (Table 1). Thus, each compound exhibits a parent peak in the EI mass spectrum and the ^1H and $^{13}C\{^1H\}$ NMR spectra reveal that all four *t*Bu groups are equivalent. No ν_{E-H} peaks were detected in the IR spectra.

The corresponding reactions of tBu_3Al with sulfur, selenium, and tellurium also afford cubanes, $[t\text{BuAl}(\mu_3\text{-E})]_4$ (**4**, E = S; **5**, E = Se; **6**, E = Te). However, in these cases it is possible to isolate intermediate dimeric compounds of the type $[tBu_2Al(\mu_2\text{-E}t\text{Bu})]_2$ (**7**, E = S; **8**, E = Se; **9**, E = Te) as summarized in Equation (c). In these reactions no tBu_2E or other alkylated chalcogenide species have been detected.

$$2\,tBu_3Al + 2\,E \longrightarrow \underset{\mathbf{7-9}}{[tBu_2Al(\mu_2\text{-E}t\text{Bu})]_2} \qquad (c)$$

There is precedent[9] for the insertion of sulfur or selenium into aluminum–carbon bonds; however, this appears to be the first such insertion of tellurium. Compounds **4–9** were characterized spectroscopically (Table 1) and structural information for **9** was provided by an X-ray analysis.[7] The solid state of **9** consists of individual dimeric molecules with no short intermolecular contacts (Fig. 2). A twofold axis

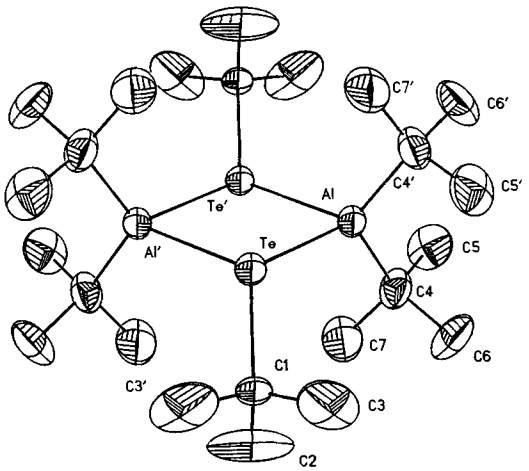

Fig. 2. View (ORTEP) of **9** showing the atom numbering scheme. Important bond distances [Å] and bond angles [°]: Te-Al 2.732(3), Te-C1 2.21(1), Al-C4 2.00(1); Te-Al-Te′ 86.1(4), Al-Te-Al′ 93.9(4), C1-Te-Al 107.1(5), C1-Te-Al′ 121.6(3), Te-Al-C4 121.1(3), Te-Al-C4′ 101.9(2), C4-Al-C4′ 120.8(2).

passes through the Al atoms and the Te, C1, and C2 atoms lie on a mirror plane; hence the Al_2Te_2 core is planar. The gallium–sulfur dimers $[Ph_2Ga(\mu_2\text{-SMe})]_2$ and $[I_2Ga(\mu_2\text{-SMe})]_2$ also have planar rings.[10] Interestingly, however, $[R_2Ga(\mu_2\text{-TePh})]_2$ ($R = Me_3CCH_2$)[11] and $[I_2Ga(\mu_2\text{-}Si\text{Pr})]_2$[12] adopt butterfly structures. The Al–Te bond distance of 2.732(3) Å in **9**, apparently the first such distance of a molecular compound, is 0.15 Å larger than the sum of tetrahedral covalent radii.[13]

Interestingly, the EI mass spectra for **7–9** exhibit molecular ions corresponding to the cubanes **4–6**. These implied dimer → cubane conversions also occur on the attempted sublimation of **7–9** [Eq. (d)]. The production of isobutene and

$$2[tBu_2Al(\mu_2\text{-E}t\text{Bu})]_2 \longrightarrow [t\text{BuAlE}]_4 + 2\,Me_2C{=}CH_2 + 2\,Me_3CH \qquad (d)$$

isobutane was detected by ^1H NMR spectroscopy. Heating toluene solutions of **7–9** at 100 °C for 48 h also results in quantitative conversion to the corresponding cubanes. The isolation of the intermediate dimeric compounds **7–9** and the absence of species such as tBu_2E and tBu_2E_2 in the tBu_3Al + E reaction mixtures suggest that the mechanistic pathway for the formation of the aluminum cubanes is different from those leading to gallium cubanes. Further studies which address this are in progress.

Experimental Procedure

1–3: Neat tBu_3Ga (0.6 mL, 2.5 mmol) was added dropwise to a stirred suspension of 5.0 mmol of elemental sulfur, selenium, or tellurium in toluene (25–30 mL) at room temperature. The suspensions were stirred (**1**, 1 h; **2**, 4 h) at room temperature; in the case of **3** it was necessary to heat the suspension to 60–70 °C for several hours. Toluene and other volatiles were then removed under reduced pressure. Waxy solid **1** was washed with 10 mL of cold (−78 °C) pentane. Mixtures of tBu_2E, tBu_2E_2, and other organochalcogenides were identified by ^1H NMR and mass spectroscopy in the washings. After one sublimation (150 °C, 10^{-2} Torr), the yield of colorless, microcrystalline **1** was 70%. Following filtration of the reaction solution from unreacted elemental Se or Te, pure **2** and **3** were obtained as colorless, crystalline solids in yields of 60 and 55%, respectively, by recrystallization from pentane solutions (−20 °C). Compound **1** can also be prepared by condensing an excess of H_2S (0.5 mL, 1.25 mmol) onto frozen, neat tBu_3Ga (0.3 mL, 1.25 mmol) at −78 °C. The mixture was allowed to warm until the H_2S exerted about 0.5 atm of pressure, as measured by a mercury manometer, before being cooled to −196 °C. This cycle was repeated two to three times to ensure completion of the reaction. Excess H_2S was allowed to boil off under a vigorous stream of nitrogen into a sodium hypochlorite bubbler solution (1%w/w) as the mixture was warmed to room temperature (15 min). The resulting white powder was extracted with warm (40 °C) toluene (15 mL). After filtration and concentration of the filtrate, colorless crystals of **1** formed in virtually quantitative yield (based on the tBu_3Ga consumed).

7–9: Neat tBu_3Al (0.5 mL, 2.5 mmol) was treated with 5.0 mmol of elemental sulfur, selenium, or tellurium as described above for **1–3**. The reaction times at 25 °C for **7** and **8** were 1 and 6 h, respectively; for **9**, the reaction mixture was heated for several hours at 60–70 °C. Following filtration from excess elemental S, Se, or Te and removal of the toluene and other volatiles, the resulting residues were recrystallized from pentane solution at −40 °C. Colorless **7** and **8** and yellow **9** were isolated as crystalline solids in yields of around 60%.

4–6: These cubanes can be produced quantitatively by heating toluene solutions of **7**, **8** and **9** to 100 °C for 48 h. Alternatively, these dimer → cubane conversions can be effected quantitatively by controlled pyrolysis of **7**, **8**, and **9** at 300 °C and 1 atm pressure. Partial conversion was also achieved under sublimation conditions (150 °C, 10^{-2} Torr). The gases evolved during the sublimation of **9** were shown to be an equimolar mixture of isobutene and isobutane by ^1H NMR spectroscopy.

Received: April 11, 1991 [Z 4566 IE]
German version: *Angew. Chem. 103* (1991) 1164

CAS Registry numbers:
1, 135283-83-9; **2**, 135283-84-0; **3**, 135258-40-1; **4**, 135258-41-2; **5**, 135258-42-3; **6**, 135258-43-4; **7**, 135283-85-1; **8**, 135258-44-5; **9**, 135258-45-6; tBu_3Ga, 55681-99-7; tBu_3Al, 4731-36-6.

[1] See, for example, G. L. Simon, L. F. Dahl, *J. Am. Chem. Soc. 95* (1973) 2164, and references therein.
[2] G. E. Coates, J. A. Heslop, *J. Chem. Soc. A 1968*, 631.
[3] G. E. Coates, A. H. Fishwick, *J. Chem. Soc. A 1968*, 635.
[4] For an excellent review of main-group cage compounds, see M. Veith, *Chem. Rev. 90* (1990) 3.
[5] A. H. Cowley, R. A. Jones, M. A. Mardones, S. G. Bott, J. L. Atwood, *Angew. Chem. 102* (1990) 1504; *Angew. Chem. Int. Ed. Engl. 29* (1990) 1409.
[6] See, for example, A. M. Mancini, G. Micocci, A. Rizzo, *Mater. Chem. Phys. 9* (1983) 29.

[7] **1**: cubic, space group $P\bar{4}3m$ (No. 215), $Z = 1$, $a = 8.68(1)$ Å, $V = 653(1)$ Å^3, $\varrho_{calcd} = 1.62$ g cm^{-3}, $2° < 2\theta < 30°$; ($Cu_{K\alpha}$, $\lambda = 1.5418$ Å, $\mu = 76.57$ cm^{-1}); $T = 24$ °C, 119 reflections, $\theta/2\theta$ scan mode, all 119 reflections had $I > 6\sigma(I)$ and were used to solve (Patterson and direct methods) and refine (full matrix, least squares) the structure of **1**. $R = 0.0454$, $R_w = 0.0569$. **9**: monoclinic, space group $C2/m$ (No. 12), $Z = 2$, $a = 17.36(1)$, $b = 11.97(1)$, $c = 8.52(1)$ Å, $\beta = 113.84(7)°$; $V = 1620(5)$ Å^3, $\varrho_{calcd} = 1.340$ g cm^{-3}; $2° < 2\theta < 40°$; ($Mo_{K\alpha}$, $\lambda = 0.71069$ Å, $\mu = 18.78$ cm^{-1}); $T = 24$ °C, 1440 reflections, $\theta/2\theta$ scan mode, of these 1234 reflections with $I > 6\sigma(I)$ were used to solve (Patterson and direct methods) and refine (full matrix, least squares) the structure of **9**. $R = 0.0533$, $R_w = 0.0668$. The Te atom was slightly disordered; however, the structure was refined successfully by assigning partial occupancies of 0.78 and 0.22 to the two positions. Futher details of the crystal structure investigations can be obtained from the Fachinformationszentrum Karlsruhe, Gesellschaft für wissenschaftlich-technische Information mbH, W-7514 Eggenstein-Leopoldshafen 2 (FRG), on quoting the depository number CSD-55575, the names of the authors, and the journal citation.

[8] G. G. Hoffmann, C. Burschka, *J. Organomet. Chem. 267* (1984) 229; A. Boardman, S. E. Feffs, R. W. H. Small, I. J. Worrall, *Inorg. Chim. Acta 99* (1985) L39.

[9] L. I. Zakharkin, V. V. Gavrilenko, *Iz. Akad. Nauk SSSR Ser. Khim. 1960*, 1391.

[10] G. G. Hoffmann, *Phosphorus Sulfur Relat. Elem. 28* (1986) 167.

[11] M. A. Banks, O. T. Beachley, Jr., H. J. Gysling, H. R. Luss, *Organometallics 9* (1990) 1979.

[12] G. G. Hoffman, C. Burschka, *Angew. Chem. 97* (1985) 965; *Angew. Chem. Int. Ed. Engl. 24* (1985) 970.

[13] L. Pauling, *The Nature of the Chemical Bond*, Cornell University Press, Ithaca, New York 1960; *Die Natur der chemischen Bindung*, Verlag Chemie, Weinheim 1976.

Bis(fluorocarbonyl) Peroxide; an Unusual Molecular Structure **

By *Hans-Georg Mack, Carlos O. Della Védova,* and *Heinz Oberhammer**

Dedicated to Professor Joseph Grobe

The most interesting feature in the structure of peroxides (X_2O_2) is the dihedral angle δ(XOOX). In the gas phase, this angle for the parent compound H_2O_2 is 120(5)°,[1a] but in most other peroxides it is larger: 123(4)° in $(CF_3)_2O_2$,[1b] 129(2)° in $(SF_5)_2O_2$,[1c] 135(5)° in $(CH_3)_2O_2$,[1d] 144(6)° in $(SiMe_3)_2O_2$,[1e] and 166(3)° in tBu_2O_2.[1e, 2] Two trends are evident from this rather limited number of experimental results: the dihedral angle increases with increasing steric requirements of the substituents and decreases with their increasing electron-withdrawing properties (cf. $(CF_3)_2O_2$ and $(CH_3)_2O_2$). Unusual structures that do not conform to these trends are found in difluoro- and dichloroperoxide.[3, 4] The dihedral angles for these compounds are smaller than 90° (88.1(4)° in F_2O_2 and 81.03(1)° in Cl_2O_2. Furthermore, the O–O bond in F_2O_2 is extremely short (121.9(2) pm) and the O–F bonds are very long (158.2(2) pm). Usually the qualitative explanation for the *gauche* orientation of substituents in peroxides is the interaction between the lone pairs on oxygen and the anomeric effect.[5] The latter describes a stabilizing overlap between the lone pairs of oxygen and the σ^* orbitals of the opposite O–X bond. The optimal dihedral angle thus depends on the form of the lone pairs, the size of the anomeric effect, and the steric demands of the substituents: according to this model the angle must be $\geq 90°$. From this point of view the structure of $(C(O)F)_2O_2$ promised to be interesting, since in this molecule a possible conjugation between the C=O π bonds might lead to a planar COOC framework, or at least to a pronounced opening of the dihedral angle.

In oxygen-rich $(C(O)F)_2O_2$ three conformers are possible, depending on the orientation of the two carbonyl groups, regardless of the dihedral angle δ(COOC): *syn-syn*, *syn-anti*, and *anti-anti*. Structures in which the carbonyl groups are

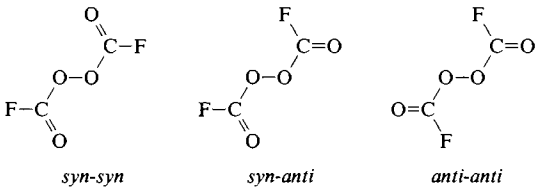

rotated around the O–C bond have not been considered. The C=O vibrational bands in the gas-phase and matrix IR spectra ($\nu_{as} = 1929$ and $\nu_s = 1902$ cm^{-1}) show that at room temperature only one conformer is present, and the shape of the symmetric band suggests a *syn-syn* structure.[6] This interpretation of the spectra is supported by ab initio calculations (HF/6-31G*). These calculations predict that the *syn-anti* conformer is 13.5 and the *anti-anti* conformer 26.9 kJ mol^{-1} higher in energy. The dihedral angle δ(COOC) and the other geometric parameters were determined by electron diffraction in the gas phase.

The analysis of the experimental radial distribution function calculated by Fourier transformation of the molecular scattering intensities (Fig. 1) confirmed the *syn-syn* configuration suggested by IR spectra and MO calculations. The

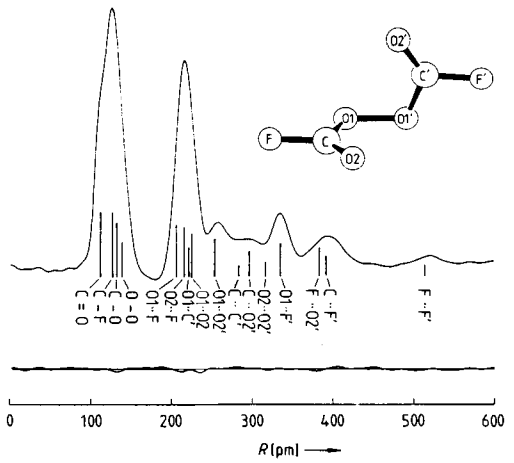

Fig. 1. Experimental radial distribution function for $(C(O)F)_2O_2$ and the difference curve. The positions of interatomic distances are indicated by vertical bars.

length of the interatomic distances between the two carbonyl groups corresponds to a dihedral angle δ(COOC) of ca. 85°. In the subsequent least-squares analysis of the scattering intensities, C_2 symmetry and nonrotated fluorocarbonyl groups (i.e., δ(O-O-C=O) = 0°) were assumed for this molecule. Optimization of the structure allowing for rotated carbonyl groups led to a value of $5 \pm 5°$ for this angle. The C–F

[*] Prof. Dr. H. Oberhammer, Dr. H.-G. Mack
Institut für Physikalische und Theoretische Chemie der Universität
Auf der Morgenstelle 8, W-7400 Tübingen (FRG)

Dr. C. O. Della Védova
Facultad de Ciencias Exactas
Universidad Nacional de La Plata
Departamento de Quimica, Quimica Inorganica
1900 La Plata (Argentina)

bond length could not be refined in the least-squares analysis because of high correlations.[7] The results of the electron diffraction study and the calculated parameters are given in Table 1.

Table 1. Experimental and calculated structural parameters for $(C(O)F)_2O_2$.

	E.B. [a]	HF/3-21G	HF/6-31G*
C=O	116.6(3)	117.2	116.0
C-F	132.0 [b]	132.0	129.0
O-C	135.5(4)	137.9	134.2
O-O	141.9(9)	144.5	136.9
O-C=O	128.8(10)	127.7	128.1
O-C-F	104.3(5)	105.6	105.6
F-C=O [c]	126.9(12)	126.7	126.3
O-O-C	109.4(9)	109.0	110.6
δ(C-O-O-C)	83.5(14)	87.3	89.5
δ(O-O-C=O)	0.0 [b]	6.4	4.1

[a] r_a distances [pm] and $\angle_a$ angles [°] from electron diffraction studies. Errors refer to the last digit and are 3σ values. [b] Not refined. [c] Dependent parameter.

Some of the calculated values, in particular the O–O distance, depend strongly on the basis set (3-21G or 6-31G*). In general, experimental bond lengths are better reproduced with the smaller basis set. The agreement in bond angles is excellent, and the small experimental dihedral angle is confirmed by these ab initio calculations. In other peroxides[8] the experimental dihedral angle is correctly predicted by calculations only when electron correlation is taken into account. The dihedral angle in bis(fluorocarbonyl) peroxide is extremely small (83.5(14)°), in contrast with the opening of the angle anticipated for conjugation between C=O π bonds. It is comparable with the corresponding angles in F_2O_2 and Cl_2O_2. These peroxides have strongly electron-withdrawing substituents and the dihedral angle of less than 90° can only be described by the above-mentioned model when an attractive interaction between the substituents is postulated. The overlap populations between the atoms of the fluorocarbonyl groups calculated by *Mulliken*'s method (HF/6-31G*) are indeed slightly *positive* in some cases (+ 0.002 a.u. for C···C', 0.007 a.u. for C···O2'), and the sum of all interactions (0.014 a.u.) corresponds to *attraction* between the substituents. This attraction between the C atom of each carbonyl group and the O atom of the other is responsible for the theoretically predicted twisting of the carbonyl groups about the O–C bond by 4–6°, which leads to a shortening of the C···O2' distances. This slight twisting was not observed in the electron diffraction study.

Experimental Procedure

$(C(O)F)_2O_2$ has been known for more than 20 years and was prepared here by the same method [9]. The scattering intensities were recorded with a Balzers Gas Diffractograph KD-G2 [10] using two camara distances (25 and 50 cm) and an accelerating voltage of ca. 60 kV. The electron wavelength was calibrated with ZnO powder. The temperature of the sample was − 45°C, of the inlet nozzle 10°C. Two photographic plates for each camera distance were evaluated by standard methods [11] and the scattering intensities in the s ranges of 20–180 nm^{-1} and 80–350 nm^{-1} were used for the structure analysis. Molecular scattering intensities were modified by a diagonal weighting matrix and known values [12] were used for the scattering amplitudes and phases. The ab initio calculations were performed using the GAUSSIAN 86 program [13] and 3-21G and 6-31G* basis sets on a Convex-C220 computer (ZDVAM, University of Tübingen).

Received: March 13, 1991 [Z4494 IE]
German version: *Angew. Chem. 103* (1991) 1166

CAS Registry number:
$(C(O)F)_2O_2$, 692-74-0.

[1] a) R. L. Redington, W. B. Olson, P. C. Cross, *J. Chem. Phys. 36* (1962) 1311; b) C. J. Marsden, L. S. Bartell, F. P. Diodati, *J. Mol. Struct. 39* (1977) 253; c) P. Zylka, H. Oberhammer, K. Seppelt, *ibid. 243* (1991) 411; d) B. Haas, H. Oberhammer, *J. Am. Chem. Soc. 106* (1984) 6146; e) D. Käss, H. Oberhammer, D. Brandes, A. Blaschette, *J. Mol. Struct. 40* (1977) 65.

[2] These dihedral angles are "effective" values as a result of the torsional vibration. The equilibrium value corresponding to the minimum of the O–O torsion potential, δ_e, can deviate substantially from them, e.g., δ_e = 111.8° in H_2O_2 and 119(4)° in $(CH_3)_2O_2$

[3] L. Hedberg, K. Hedberg, P. G. Eller, R. R. Ryan, *Inorg. Chem. 27* (1988) 232.

[4] M. Birk, R. A. Friedl, E. A. Cohen, H. M. Pickett, S. P. Sander, *J. Chem. Phys. 91* (1989) 6588.

[5] A. J. Kirby: *The Anomeric Effect and Related Stereoelectronic Effects at Oxygen*, Springer, Berlin 1983.

[6] C. O. Della Védova, *Dissertation*, Universität Bochum 1990.

[7] The C–F distance was set equal to the value calculated by the HF/3-21G method, which gives very good agreement with experimental C–F distances in FC(O)SCl (H.-G. Mack, H. Oberhammer, C. O. Della Védova, *J. Phys. Chem., 95* (1991) 4238) and $(C(O)F)_2S_2$ (unpublished).

[8] a) H.-G. Mack, D. Christen, H. Oberhammer, *Tetrahedron 44* (1988) 7363; b) D. Cremer, *J. Chem. Phys. 69* (1978) 4440.

[9] R. L. Talbott, *J. Org. Chem. 33* (1968) 2095.

[10] H. Oberhammer: *Molecular Structure by Diffraction Methods, Vol. 4*, The Chemical Society, London 1976, p. 24.

[11] H. Oberhammer, W. Gombler, H. Willner, *J. Mol. Struct. 70* (1981) 273.

[12] J. Haase, *Z. Naturforsch. A 25* (1970) 936.

[13] M. J. Frisch, J. S. Binkley, H. B. Schlegel, K. Raghavachari, C. F. Melius, R. L. Martin, J. J. P. Stewart, F. W. Bobrowicz, C. M. Rohlfing, L. R. Kahn, D. F. DeFrees, R. Seeger, R. A. Whiteside, D. J. Fox, E. M. Fleuder, J. A. Pople, *GAUSSIAN 86*, Carnegie-Mellon Quantum Chemistry Publishing Unit, Pittsburgh 1984.

On the Origin of π-Facial Diastereoselectivity in Addition Reactions of Cyclohexane-Based Systems**

By *Gernot Frenking,* Klaus F. Köhler*, and *Manfred T. Reetz*

The failure of the Felkin-Anh[1] model to explain the observed diastereoselectivity in nucleophilic additions to substituted cyclohexanones and related systems and the alternative rationale based on the "Cieplak model"[2] are currently topics of lively discussion in stereochemistry.[2, 3] The most detailed experimental study pertinent to the subject has been carried out by *Cieplak*, who could show that in 3-substituted cyclohexanones the relative proportion of axial attack of the nucleophile *increases* when the substituent becomes more electronegative.[2b] The same trend was also found for the addition of electrophiles to 3-substituted methylenecyclohexanes (Scheme 1).[2b]

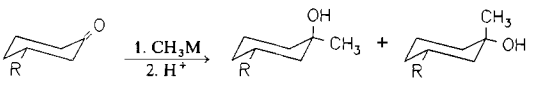

Scheme 1. Attack of a nucleophile CH_3M, for example CH_3Li, on a cyclohexanone.

The explanation given by *Cieplak* for the observed trend is based on a rather paradoxical assumption: Stereoelectronic control in cyclohexane-based systems is attributed to electron donation from the occupied orbitals of the cyclohexane

[*] Prof. Dr. G. Frenking, Dipl.-Chem. K. F. Köhler, Prof. Dr. M. T. Reetz
Fachbereich Chemie der Universität
Hans-Meerwein-Strasse, W-3550 Marburg (FRG)

[**] This work was supported by the Deutsche Forschungsgemeinschaft, the Fonds der Chemischen Industrie, and the computer companies Silicon Graphics and Convex.

ring into the vacent *antibonding* σ* orbital associated with the incipient bond (Fig. 1).

In our opinion the Cieplak model is dubious for several reasons. First, it is difficult to understand why such orbital interactions are operative only in cyclohexane-based systems, while in other molecules the Cieplak model fails.[4] Second, a model which favors one reaction course relative to others because of better electron donation into the *antibonding* orbital of the incipient bond is not consistent with the concept of "allowed" and "forbidden" reactions in terms of orbital interactions. It is a clear contradiction to the frontier orbital model (FMO).[5] Since the FMO model is one of the most successful qualitative models for organic reactions,[5] it is difficult to believe that in cyclohexane-based systems an "anti-FMO" mechanism such as the Cieplak model is operative.

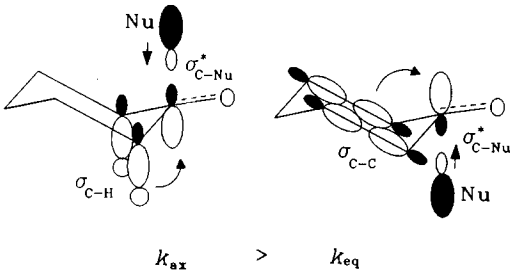

Fig. 1. Cieplak model [2] for the different interactions in the axial and equatorial attack of nucleophiles at cyclohexanones.

In this paper we show that the diastereoselectivity of nucleophilic additions to 3-substituted cyclohexanones observed by *Cieplak*[2b] can be explained without difficulties by the frontier-orbital model. To this end we calculated the transition state structures for the axial (a) and equatorial (e) addition of LiH to cylohexanone (1*(a), 1*(e)) and 3(e)-fluorocyclohexanone (2*(a), 2*(e)) using *ab initio* quantum chemical methods.[6] The optimized structures and relative energies are shown in Figure 2.

The rather long interatomic distances between the carbonyl C and the attacking hydride calculated for 1*(a), 1*(e), 2*(a), and 2*(e) indicate early transition states. Similar results have been found in earlier theoretical studies on the addition of LiH to carbonyl compounds.[4, 7] The axial attack of LiH at cyclohexanone is theoretically predicted to be favored by 1.4 kcal mol^{-1} relative to the equatorial attack (MP2/6-31G(d)//HF/3-21G). This is in agreement with experiments which show that in the reduction of 4-*tert*-butylcyclohexanone with $LiAlH_4$ a 92:8 ratio of equatorial:axial alcohol is obtained.[8] Substitution by fluorine in the (equatorial) 3(e)-position of cyclohexanone increases the calculated energy difference in favor of the axial attack, i.e. 2*(a) is 2.7 kcal mol^{-1} lower in energy than 2*(e) (Fig. 2). Thus, our calculated results for 1*(a), 1*(e), 2*(a), and 2*(e) agree with the observation[2b] that an electronegative substituent in the 3(e)-position of cyclohexanone favors axial attack.

Why are the transition states for axial attack 1*(a) and 2*(a) lower in energy than 1*(e) and 2*(e), respectively? *Houk* et al.[4a] suggested that the transition state for axial attack of a nucleophilic agent at cyclohexanone can be achieved without introducing significant ring strain, while the equatorial attack introduces torsional strain into the ring structure. We have recently shown[4c] that upon addition of LiH to 2-chloropropionaldehyde, the energy difference between the "Cram" and "anti-Cram" transition states is solely caused by the different energies of the substrate fragments in the transition state structures, and not by the interaction energies between the substrate and LiH. Figure 2 shows the relative energies of 1*(a), 1*(e), 2*(a), and 2*(e) calculated without LiH but with a frozen geometry of the substrate.

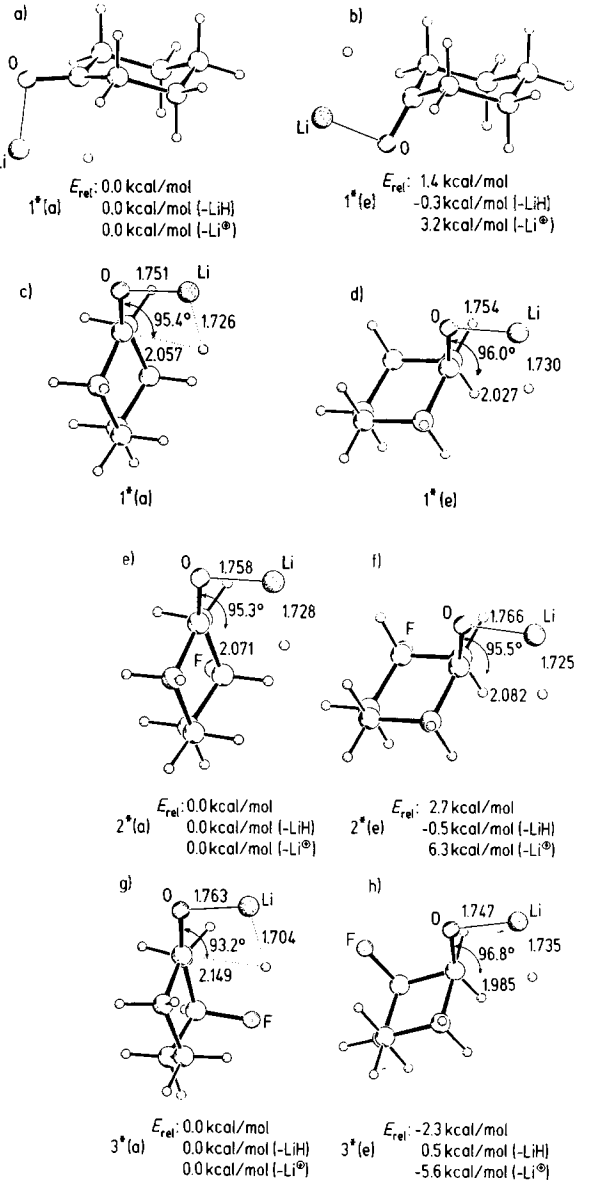

Fig. 2. Optimized transition state structures (HF/3-21G) for LiH attack at cyclohexanone systems. (a) Axial attack at cyclohexanone 1*(a); (b) equatorial attack at cyclohexanone 1*(e); (c) same as (a) but with different perspective which shows that the attacking nucleophile is *trans* to a C–H bond; (d) same as (b) but with a different perspective which shows that the attacking nucleophile is *trans* to a C–C bond; (e) axial attack to 3(e)-fluorocyclohexanone 2*(a); (f) equatorial attack to 3(e)-fluorocyclohexanone 2*(e); (g) axial attack at 3(a)-fluorocyclohexanone 3*(a); (h) equatorial attack at 3(a)-fluorocyclohexanone 3*(e). Interatomic distances are given in Å, relative energies in kcal mol^{-1} at MP2/6-31G(d)//HF/3-21G

The energy differences between the cyclohexanone fragments of the axial and equatorial transition states are very small, even favoring slightly the equatorial attack. This provides clear evidence against the hypothesis that the transition state for axial attack is favored because it needs less ring strain than the equatorial transition state.[4a] It follows that

the stability differences must be due to interactions between the substrate and LiH. Figure 2 also shows the energy differences of the transition states calculated without $Li^{\oplus}$, but with a frozen geometry of the anionic fragment. The data predict that 1*(a) is favored over 1*(e) because of the better interaction of the ketone with $H^{\ominus}$ (3.2 kcal mol^{-1}). The corresponding energy difference between 2*(a) and 2*(e) is 6.3 kcal mol^{-1}. The conclusion is that the higher rate of axial attack of LiH on 3(e)-fluorocyclohexanone is caused by the better electronic interactions of the ketone with the attacking nucleophilic agent, and not by the different deformations of the substrate in the transition states, as suggested for cyclohexanones[4a] and calculated for acyclic compounds.[4c]

What type of orbital interactions are responsible for the differences between axial and equatorial attack? Using FMO theory,[5] the reaction course for the addition of a nucleophile to a carbonyl group should be controlled by the orbital interactions between the HOMO of the nucleophile and the ($\pi^*_{C=O}$) LUMO of cyclohexanone. Then, the axial and equatorial attacks are different due to the nonequivalent distribution of the LUMO on the two faces of the carbonyl π bond. Figure 3 shows that the size of the LUMO of cyclohexanone is clearly larger on the axial side than on the equatorial side. The nonequivalence of the π^* LUMO is determined by the contribution of the 2s orbitals of the C and O atoms of the carbonyl group. Table 1 shows the coefficients of the 2s and 2p AOs[9] of the carbonyl C atom. The contribution of the 2s AO (0.26) is significant and indicates a clear preference for axial attack.[10]

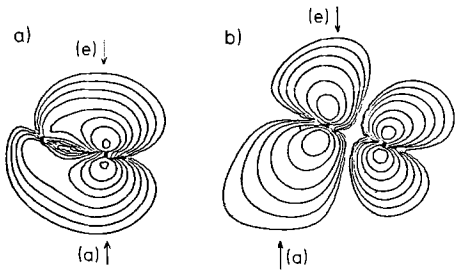

Fig. 3. Plot of the C=O π orbitals of cyclohexanone. The atoms are shown as dots, carbon at the left, oxygen at the right (6-31G(d)//3-21G). (a) $\pi_{C=O}$; b) $\pi^*_{C=O}$. The contour lines correspond to electron densities of 0.001, 0.002, 0.004, 0.008, 0.02, 0.04, 0.08, 0.2 atomic units.

The nonequivalence of the LUMO as the reason for preferential axial attack was originally suggested by *Klein*[11] who proposed that hyperconjugation of the ring C–C bonds with the carbonyl π bond causes unequal distribution of the LUMO, a greater extension being on the axial side (Fig. 4). However, *Klein*[11] also suggested that the occupied π orbital of exocyclic double bonds should be more extended on the equatorial side of the trigonal center, thus favoring equatorial attack for electrophilic addition, e.g. to methylenecyclohexane. This prediction, however, contradicts many experimental data.[2b, 8] Table 1 shows the AO coefficients of the occupied CO π orbital. The sign of the coefficients for the HOMO are the same for the LUMO! This means that both the CO π and π^* orbital are more extended to the axial side of the carbonyl bond. The same result is found for the π and π^* orbitals of the exocyclic double bond in methylenecyclohexane (Table 1). Thus, FMO theory predicts that orbital interactions during nucleophilic addition of small nucleophiles to cyclohexanone and electrophilic addition to methylenecyclohexane should for electronic reasons be preferred from the axial side, which is in agreement with experimental evidence.[2b, 8]

Table 1. Orbital coefficients [9] of the π and π^* orbitals of the exocyclic double bonds at the C_α atom for cyclohexanone and methylenecyclohexanone (Cy), 3(e)-fluorocyclohexanone and 3(e)-fluoromethylenecyclohexane (3F-Cy, e), and 3(a)-fluoromethylenecyclohexane (3F-Cy, a) at HF/6-31G(d)//HF/3-21G.

		Cyclohexanone		Methylenecyclohexane	
		$\pi_{C=O}$	$\pi^*_{C=O}$	$\pi_{C=C}$	$\pi^*_{C=C}$
Cy	2s(o)	−0.06	−0.26	−0.02	−0.16
	$2p_x$(o)	0.08	0.21	0.14	0.29
	$2p_y$(o)	−0.00	−0.00	−0.00	−0.00
	$2p_z$(o)	0.08	0.43	0.24	0.48
3F-Cy	2s(o)	−0.08	−0.28	−0.03	−0.17
e	$2p_x$(o)	−0.05	−0.14	−0.10	−0.24
	$2p_y$(o)	−0.03	−0.14	−0.06	−0.21
	$2p_z$(o)	0.09	0.47	0.25	0.50
3F-Cy	2s(o)	−0.04	−0.21		
a	$2p_x$(o)	−0.07	−0.23		
	$2p_y$(o)	0.01	0.07		
	$2p_z$(o)	0.10	0.41		

Klein[11] rationalized the axial preference for nucleophilic attack and the equatorial preference for electrophilic attack at the exocyclic double bond with hyperconjugation of the (C_α)p orbital with the (β)C–C σ orbital as shown in Figure 4. He assumed that hyperconjugation of the (C_α)p orbital with the (β)C–H σ orbital, which is also shown in Figure 4, is of secondary importance. However, the natural-bond-orbital (NBO) analysis[12] of cyclohexanone shows that the $\pi^*_{C=O}$ orbital interacts more *strongly* with the (β)C–H σ orbital than with the (β)C–C σ orbital. Since interactions between the $\pi_{C=O}$ and $\pi^*_{C=O}$ orbitals and the bonding and antibonding (β)C–H and (β)C–C orbitals are all symmetry allowed, it is difficult to predict a priori which interactions are dominant without carrying out quantum mechanical calculations.

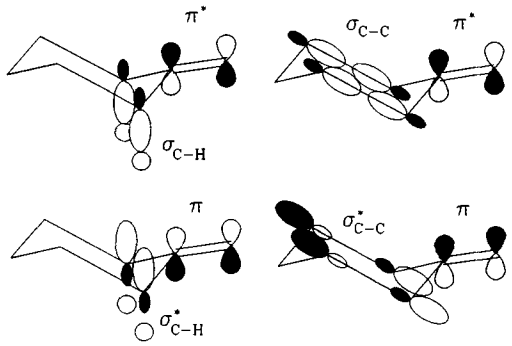

Fig. 4. Schematic representation of the hyperconjugation between the exocyclic π orbital and the (β)C–C and (β)C–H orbitals of cyclohexane systems.

What is the effect of the fluorine atom at the 3(e)-position of cyclohexanone on the relative size of the π orbitals on the axial and equatorial sides of the C–O bond? Table 1 shows the AO coefficients at the carbonyl C atom of the relevant orbitals. The contribution of the 2s(C) AO in the π orbitals is larger in the case of 3(e)-fluorocyclohexanone than in the case of cyclohexanone! Thus, FMO theory correctly predicts

that substitution at the equatorial 3-position of cyclohexanone by an electronegative substituent increases the preference for axial attack. Table 1 also shows that the contribution of the 2s(C) AO in the π orbitals in 3(a)-fluorocyclohexanone is smaller than in cyclohexanone. Indeed, our calculations predict a clear reversal towards equatorial attack for LiH addition to 3(a)-fluorocyclohexanone. This is in agreement with the calculated energies for the transition states 3*(a) and 3*(e) (Fig. 2). Equatorial attack is favored over axial attack by 2.3 kcal mol^{-1}, caused mainly by the better interactions between $H^{\ominus}$ and 3(a)-fluorocyclohexanone (5.6 kcal mol^{-1}). This is a further argument against the Cieplak model,[2] which predicts axial attack whether the electronegative substitutent is in the axial or in the equatorial position. The transition state for axial attack 3*(a) may additionally be disfavored by steric interactions between fluorine and the nucleophilic hydride ion. Our prediction that an electronegative substituent in the 3(a)-position of cyclohexanone enhances equatorial attack of a nucleophilic agent still has to be verified experimentally.

In conclusion, we have shown that symmetry-allowed frontier orbital interactions between the HOMO of the nucleophile and the LUMO of cyclohexanone favor axial over equatorial attack because the LUMO is more extended on the axial side of the carbonyl bond, and that the preference for axial attack is enhanced in 3(e)-fluorocyclohexanone. This inherent electronic preference can be overrided, however, by other factors such as steric interactions in the case of bulky nucleophiles.[13]

Received: April 19, 1991 [Z 4514 IE]
German version: *Angew. Chem. 103* (1991) 1167

CAS Registry numbers:
LiH, 7580-67-8; cyclohexanone, 108-94-1; 3-fluorocyclohexanone, 167409-00-7; methylenecyclohexane, 1192-37-6; 3-fluoromethylenecyclohexane, 135256-49-4.

[1] a) M. Chérest, H. Felkin, N. Prudent, *Tetrahedron Lett. 1968*, 2201, 2205; b) N. T. Anh, O. Eisenstein, *Nouv. J. Chim. 1* (1977) 62.
[2] a) A. S. Cieplak, *J. Am. Chem. Soc. 103* (1981) 4540; b) A. S. Cieplak, B. D. Tait, C. R. Johnson, Reetz, *ibid. 111* (1989) 8447.
[3] a) M.-H. Lin, J. E. Silver, W. J. le Noble, *J. Org. Chem. 53* (1988) 5155; b) G. Metha, F. A. Khan, *J. Am. Chem. Soc. 112* (1990) 6140; c) Y. Nagao, M. Goto, M. Ochiai, *Chem. Lett. 1990*, 1507.
[4] a) Y.-D. Wu, K. N. Houk, *J. Am. Chem. Soc. 109* (1987) 908; b) S. S. Wong, M. N. Paddon-Row, *J. Chem. Soc. Chem. Commun. 1990*, 456; c) G. Frenking, K. Köhler, M. T. Reetz, *J. Am. Chem. Soc.* unpublished results.
[5] a) K. Fukui, *Acc. Chem. Res. 4* (1971) 57; b) I. Fleming: *Frontier Orbitals and Organic Chemical Reactions*, Wiley, New York 1976.
[6] The geometries and vibrational frequencies were calculated at HF/3-21G. Improved total energies were computed at MP2/6-31G(d). The Convex versions of the program package GAUSSIAN 90 have been used: M. J. Frisch, M. Head-Gordon, G. W. Trucks, J. B. Foreman, H. B. Schlegel, K. Raghavachari, M. A. Robb, J. S. Binkley, C. Gonzales, D. J. DeFrees, D. J. Fox, R. A. Whiteside, R. Seeger, C. F. Melius, J. Baker, R. Martin, L. R. Kahn, J. J. P. Steward, S. Topiol, and J. A. Pople, Gaussian Inc., Pittsburgh, PA 1990.
[7] E. Kaufmann, P. v. R. Schleyer, K. N. Houk, Y.-D. Wu, *J. Am. Chem. Soc. 107* (1985) 5560.
[8] a) E. Eliel, R. S. Ro, *J. Am. Chem. Soc. 79* (1957) 5992; b) E. Eliel, S. R. Schroeter, *ibid. 87* (1965) 5031.
[9] We show the 2p(o) coefficients of the 6-31G(d) basis set, the 2p(i) coefficients are much smaller but show the same trends.
[10] The sign of the 2p-AO lobe on the axial side is the same as the 2s contribution in the HOMO and the LUMO. Therefore, the frontier orbitals are larger on the axial side and smaller on the equatorial side of the cyclohexanone ring.
[11] a) J. Klein, *Tetrahedron Lett. 1983*, 4307; b) J. Klein, *Tetrahedron 30* (1974) 3349.
[12] A. E. Reed, L. A. Curtiss, F. Weinhold, *Chem. Rev. 88* (1988) 899.
[13] E. C. Ashby, J. T. Laemmle, *Chem. Rev. 75* (1975) 521.

Reduction of Azobenzene by Naphthalene-ytterbium: A Tetranuclear Ytterbium(III) Complex Combining 1,2-Diphenylhydrazido(2−) and Phenylimido Ligands**

By *Alexander A. Trifonov, Mikhail N. Bochkarev,* Herbert Schumann,** and *Jörg Loebel*

Ytterbium halides are able to reduce N_2 in the presence of alkali-metal naphthalides under mild conditions to the −3 oxidation level (N^{3-}).[1-3] Attempts to separate a nitrogen-containing intermediate have been unsuccessful so far. The first N_2 complex of a lanthanide element, $[\{Sm(\eta^5\text{-}C_5Me_5)_2\}_2N_2]$, was formed during the recrystallization of $[Sm(\eta^5\text{-}C_5Me_5)_2]$ in a N_2 atmosphere.[4] Decamethylsamarocene also reacted with azobenzene to give three different samarium(III) complexes, which contain reduced azobenzene moieties as bridging ligands.[5, 6] Dicyclopentadienylytterbium(II) also reduces azobenzene to give $[\{Yb(\eta^5\text{-}C_5H_5)(thf)\}_2](N_2Ph_2)_2$.[6] We have investigated the reduction of azobenzene by mixtures of ytterbium(II) iodide and lithium naphthalide as a possible model of N_2 fixation and reduction. Here we report on the isolation of a stable intermediate and the X-ray crystallographic determination of this tetranuclear ytterbium(III) complex.

Ytterbium(II) iodide reacts with lithium naphthalide in THF to give a black pyrophoric powder, which contains $[Yb(C_{10}H_8)(thf)_3]$ (**1**).[7] Addition of **1** to a THF solution of azobenzene at room temperature results in the formation of a red-brown solution from which, after one week, deep red crystals of **2** separate.[8] These crystals are no longer soluble in organic solvents.

$$4[\underset{\mathbf{1}}{Yb(C_{10}H_8)(thf)_3}] + 5\,PhN{=}NPh \xrightarrow{THF} \underset{\mathbf{2}}{[Yb_4(\mu\text{-}\eta^2{:}\eta^2\text{-}Ph_2N_2)_4(\mu_3\text{-}PhN)_2(thf)_4]} + 4\,C_{10}H_8$$

At room temperature **2** shows a magnetic moment of $\mu_{eff} = 4.3$ BM, characteristic of Yb(III) compounds. It is extremely sensitive towards moisture and air. Hydrolysis results in the evolution of some hydrogen and the formation of $Yb(OH)_3$ and THF as well as $PhNH_2$, PhN=NPh, and PhNHNHPh (ratio around 1:2:2). When heated above 76 °C, **2** looses THF; it decomposes above 154 °C with darkening.

Crystallization from THF yielded single crystals of **2** containing two molecules of THF per formula unit. An X-ray crystal structure determination[8, 9] shows four ytterbium atoms forming a planar rhombus with a center of inversion. The Yb atoms are connected by four $\eta^2{:}\eta^2$-bridging azobenzene units and two μ^3-bridging NPh groups, the latter resulting from the reduction of one azobenzene by four electrons (Figs. 1, 2). One N atom of each bridging $[PhNNPh]^{-2}$ lig-

[*] Prof. Dr. M. N. Bochkarev, Dr. A. A. Trifonov
Institute of Organometallic Chemistry
USSR Academy of Sciences Nizhny Novgorod (USSR)
Prof. Dr. H. Schumann, Dipl.-Chem. J. Loebel
Institut für Anorganische und Analytische Chemie
der Technischen Universität
Strasse des 17. Juni 135, W-1000 Berlin 12 (FRG)

[**] Organometallic Compounds of the Lanthanides. Part 65. This work was supported by the Fonds der Chemischen Industrie and the Deutsche Forschungsgemeinschaft. Part 64: L. Esser, J. Loebel, A. Dietrich, D. van der Helm, Xinhua Ji *Organometallics*, in press.

and lies in the plane of the four Yb atoms (maximum deviation 3 pm); the other is below or above this plane. The N–N bond distance (147 pm) corresponds to a N–N single bond as in hydrazine[10] and is considerably longer than the N=N bond in azobenzene (124.7 pm[10]). Each nitrogen coordinates two ytterbium atoms, one by a short N–Yb single bond (221–229 pm) and the second by a longer coordinative bond (254–259 pm).[11, 12] This bonding situation corresponds very well with that of the PhNNPh ligand in the dinuclear complex $[\{Yb(\eta^5\text{-}C_5H_5)(thf)\}_2(N_2Ph_2)_2]$.[6] The phenyl rings of the PhNNPh units have a *cis* orientation with dihedral angles of 72(2) and 81(2)°. The average N–C(Ph) distance is in the same range as in *trans*-azobenzene.[13]

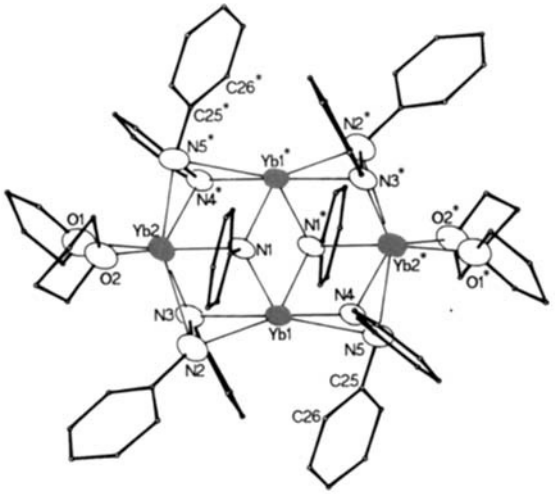

Fig. 1. Molecular structure of **2**. The Yb, N, and O atoms, as well as the important C atoms, are numbered. For clarity, the C atoms are drawn in a simplified way (H atoms omitted). Selected distances [pm] and angles [°]: Yb1···Yb2 336.5(2), Yb1···Yb2* 336.9(2), Yb1-N1* 223(1), Yb1-N3 254(1), Yb1-N5 259(1), Yb1···C26 286(2), Yb2-N2 257(1), Yb2-N4* 235(1), Yb2-O1 236(1), N2-N3 147(2), N2-C7 143(2), N3-C13 143(2), N1-C1 144(2), Yb1···Yb1* 344.1(2), Yb1-N1 221(2), Yb1-N2 227(1), Yb1-N4 229(1), Yb1···C25 280(2), Yb2-N1 229(1), Yb2-N3 220(2), Yb2-N5* 229(1), Yb2-O2 235(1), N4-N5 147(2), N4-C19 146(2), N5-C25 141(2), N1···N1* 280(2); Yb1-Yb2-Yb1* 61.46(3), Yb2-Yb1-Yb2* 118.54(3), Yb1-N1-Yb1* 101.7(6), N1-Yb1-N1* 86.8(4), N2-Yb1-N3 34.9(5), O1-Yb2-O2 78.3(5), C1-N1-Yb2 107(1), C7-N2-N3 118(1), C13-N3-N2 115(1).

Each of the nitrogen atoms N1 and N1*, originating from the reductive cleavage of a fifth azobenzene molecule (N1-N1* = 280 pm), occupies the apex of a trigonal pyramid, the base of which is formed by Yb1, Yb1*, and Yb2 or by Yb1, Yb1*, and Yb2*, respectively. N1 lies above and N1* below the Yb_4 plane. The bonds to the central Yb1 and Yb1* are shorter (221 pm) than to the peripheral Yb2 or Yb2* (229 pm), which are further coordinated by the oxygens of two THF molecules. In addition, there are two Yb_3N_3 rings of approximate chair conformation formed by Yb2, N3, Yb1, N1*, Yb1*, N4* and Yb2*, N3*, Yb1*, N1, Yb1, N4 and connected via Yb1 and Yb1*.

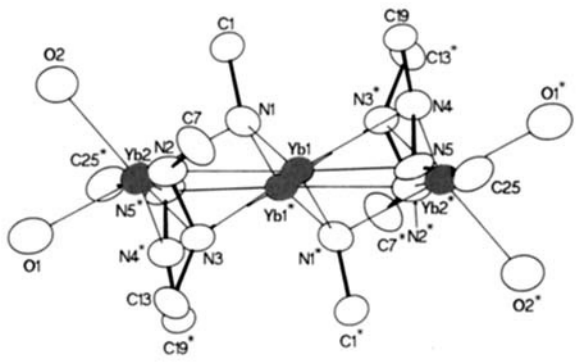

Fig. 2. View of the $Yb_4N_{10}O_4$ skeleton and the tertiary C atoms of **2**.

The coordination number 7 for Yb2 and Yb2* cannot be attained by Yb1 and Yb1* because the bulky arrangement of the phenyl groups does not allow any further coordination by THF molecules. To close this gap, the Yb–C contacts between Yb(1) and C25 (280 pm) or Yb1 and C26 (286 pm) are very short and are in the range of the η^2 interactions between Yb and the phenyl groups in $[Yb_2(\eta^2\text{-}C_6H_5)_5(thf)_4]$[14] or between Sm and the arene ligands in, for example, $[Sm(\eta^6\text{-}C_6H_6)](AlCl_4)_3$ (290 pm),[15] $[Sm(\eta^6\text{-}C_6H_4Me_2)](AlCl_4)_3$ (279 pm),[16] or $[Sm(\eta^6\text{-}C_6Me_6)](AlCl_4)_3$ (283 pm).[17] This interaction explains the unexpectedly short Yb2*–N4 bond (235 pm) and the larger C19–N4–N5–C25 dihedral angle (81°) in comparison to C7–N2–N3–C13 (72°), because there is no short contact between Yb1 and the carbon atoms C7 and C13 of the phenyl ring bonded to N3.

Experimental Procedure

All operations were performed under an argon atmosphere using carefully degassed solutions: **1** (1.23 g, 2.4 mmol) was added to a solution of azobenzene (0.43 g, 2.4 mmol) in 60 mL of THF at room temperature. The reaction mixture was stirred for 45 min, filtered, and stored at room temperature for one week. Deep red crystals of **2** (0.54 g, 45%) were separated by decantation and dried for 1 h in vacuo. Decomposition point: 76 to 154 °C. Correct C, H, N analysis. IR (CsI): $\tilde{\nu}$ [cm^{-1}] = 3060 (m), 1580 (s), 1460 (s), 1250 (s), 1040 (s), 930 (m), 870 (m), 780 (s), 750 (s), 690 (s).

Received: March 12, 1991 [Z 4492 IE]
German version: *Angew. Chem. 103* (1991) 1170

CAS Registry numbers:
1, 123923-16-0; **2**, 135258-02-5; **2**·2 THF, 135283-79-3; PhN=NPh, 103-33-3.

[1] M. N. Bochkarev, A. A. Trifonov, G. A. Razuvaev, M. A. Ilatovskaya, V. B. Shur, *Izv. Akad. Nauk SSSR Ser. Khim. 1986*, 1898, *Bull. Acad. Sci. USSR Div. Chem. Sci. (Engl. Transl.) 1986*, 1726.

[2] M. N. Bochkarev, A. A. Trifonov, G. A. Razuvaev, M. A. Ilatovskaya, V. B. Shur, M. E. Volpin, *Dokl. Akad. Nauk SSSR Ser. Khim. 295* (1987) 1381; *Dokl. Chem. (Engl. Transl.) 295* (1987) 378.

[3] M. N. Bochkarev, A. A. Trifonov, G. A. Razuvaev, M. A. Ilatovskaya, V. B. Shur, M. E. Volpin, *Proc. 2nd Int. Conf. on f-Elements., Lisboa 1987, Abstracts of papers vol. 2* (1987) 13.

[4] W. J. Evans, T. A. Ulibarri, J. W. Ziller, *J. Am. Chem. Soc. 110* (1988) 6877.

[5] W. J. Evans, D. K. Drummond, S. G. Bott, J. L. Atwood, *Organometallics 5* (1986) 2389.

[6] W. J. Evans, D. K. Drummond, L. R. Chamberlain, R. J. Doedens, S. G. Bott, H. Zhang, J. L. Atwood, *J. Am. Chem. Soc. 110* (1988) 4983.

[7] M. N. Bochkarev, A. A. Trifonov, E. A. Fedorova, N. S. Emelyanova, T. A. Basalgina, G. S. Kalinina, G. A. Razuvaev, *J. Organomet. Chem. 372* (1989) 217.

[8] **2**: air-sensitive red crystals, $C_{76}H_{82}N_{10}O_4Yb_4 \cdot (C_8H_{16}O_2)$, M = 2035.94, triclinic, space group $P\bar{1}$, a = 1328.2(5), b = 1362.1(4), c = 1364.9(3) pm, α = 61.08(2), β = 86.45(2), γ = 64.28(2)°, $V = 1912.6(9) \times 10^{-30}$ m^3, Z = 1, $\rho_{calcd.}$ = 1.768 $g\,cm^{-3}$, $F(000)$ 1000, Syntex $P2_1$, $Mo_{K\alpha}$ radiation, 71.069 cm^{-1}, graphite monochromator, θ-2θ scans in the range $0 \le 2\theta \le 48°$ at 138(5) K, 5256 independent reflections, 3540 observed ($F_o > 5\sigma(F_o)$), R = 0.0461, R_w = 0.0403, $w = 1.8516/[\sigma^2(F) + 0.000095 \times F^2]$, free electron density in the last F map: max. 0.97, min. −1.41 e 10^{-6} pm^{-2}). Data corrected for Lorentz and polarization effects, empirical absorption correction applied (min./max. correction factor 0.9882/1.0313). Solution by Patterson and Fourier techniques and refinement by full-matrix least-squares methods. Non-hydrogen atoms were refined with anisotropic temperature factors. Hydrogen atoms were inserted in calculated (d(C-H) = 95 pm) positions with a common isotropic temperature factor. Calculations with SHELX-76 and anomalous dispersion terms applied [9]. Further details of the crystal structure investigation may be ob-

tained from the Fachinformationszentrum Karlsruhe, Gesellschaft für wissenschaftlich-technische Information mbH, W-7514 Eggenstein-Leopoldshafen 2 (FRG), on quoting the depository number CSD-55365, the names of the authors, and the journal citation.
[9] G. M. Sheldrick: *SHELX-76, Program for Crystal Structure Determination*, University of Cambridge (England).
[10] R. Allman: *The Chemistry of the Hydrazo, Azo and Azoxy groups*, Wiley, New York 1975, p. 36.
[11] M. N. Bochkarev, G. S. Kalinina, L. N. Zakharov, S. Ya. Khorshev: *Organicheskie proizvodnye redkozemel'nyk elementov*, Nauka, Moscow 1989, chap. 5.1 and references therein.
[12] W. J. Evans, T. P. Hanusa, J. H. Meadows, W. E. Hunter, J. L. Atwood, *Organometallics 6* (1987) 295.
[13] C. J. Brown, *Acta Crystallogr. 21* (1966) 146.
[14] M. N. Bochkarev, V. V. Khramenkov, Yu. F. Radkov, L. N. Zakharov, Yu. T. Struchkov, *Metalloorg. Khim. 3* (1990) 1438.
[15] B. Fan, Q. Shen, Y. Lin, *J. Organomet. Chem. 377* (1989) 51.
[16] B. Fan, Q. Shen, Y. Lin, *J. Organomet. Chem. 376* (1989) 61.
[17] F. A. Cotton, W. Schwotzer, *Organometallics 6* (1987) 1275.

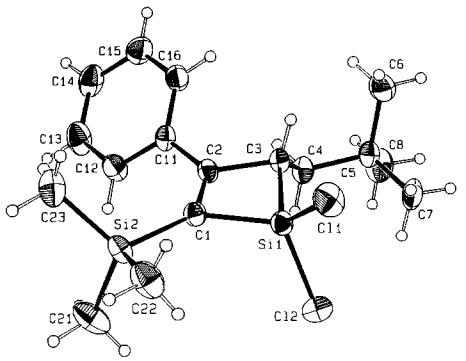

Fig. 1. Structure (ORTEP plot, ellipsoids at the 50% probability level) of **6** in the crystal. The hydrogen atoms are drawn with arbitrary radii. Selected bond lengths [pm] and angles [°]: Si1-Cl1 204.6(1), Si1-Cl2 205.0(1), Si1-C1 182.8(1), Si1-C3 186.4(1), C1-Si2 187.2(1), C1-C2 135.4(1), C2-C3 155.4(1), C2-C11 148.1(2), C3-C4 152.4(1), C1-Si1-C3 80.7(1), Cl1-Si1-Cl2 105.1(1), Si1-C1-Si2 134.7(1), Si1-C1-C2 87.8(1), Si2-C1-C2 137.5(1), C1-C2-C3 110.4(1), C1-C2-C11 129.8(1), C3-C2-C11 119.8(1) Si1-C3-C4 124.2(1), C2-C3-C4 115.0(1), transannular distances: Si1 ··· C2 239.0(1), C1 ··· C3 239.0(1).

Facile Synthesis of Si-Functional Silacyclobutenes**

By *Norbert Auner,* Claudia Seidenschwarz,* and *Eberhardt Herdtweck*

The synthesis, structure, and reactions of monosilacyclobutanes have been the subject of numerous investigations in the last thirty years.[1, 2] In comparison, very little has been reported about silacyclobutenes;[3] the reason for this obviously being their poor accessibility. They can be prepared on a laboratory scale, but only with great effort and in low yield by multistep organosilicon synthesis[4] or by gas-phase pyrolysis of suitable Si-precursors.[5] This is also true in the case of cycloaddition reactions of silenes with acetylenic derivatives.[6] Moreover, Si-halogenated silacyclobutenes, from which substituted derivatives are accessible by simple reaction sequences, are unknown.

In earlier work, *Jones*[7] reported on the cycloaddition reactions of dimethylneopentylsilene. In our studies, however, we used the combination vinyltrichlorosilane/Li*t*Bu for the regioselective synthesis of [2 + 2] cycloadducts of dichloroneopentylsilene **1**, and for the preparation of Diels-Alder adducts with dienes of low activity.[8, 9] The unusually high synthetic potential of this silene has now manifested itself also in its reactivity towards 1,2-disubstituted acetylene derivatives.

By reaction of equimolar amounts of $Cl_3SiCH{=}CH_2$ and Li*t*Bu in the presence of acetylene derivatives R−C≡C−R′ the silacyclobutenes **2**–**7** can be prepared in 50–80% yield (Scheme 1). The spectroscopic data are in good agreement with those reported in the literature.[10]

Surprisingly, the silacyclobutenes are thermally very stable; they do not decompose even on heating for several days at 200 °C. Upon synthesis the derivatives **2**–**5** and **7** are obtained as viscous, colorless liquids, whereas **6** is isolated as a sublimable, crystalline compound. The colorless, almost slightly air-sensitive crystals are readily soluble in nonpolar solvents, and a suitable single crystal could be investigated by X-ray crystallography (Fig. 1).[11]

The central, markedly distorted SiC four-membered ring is almost planar, the bond lengths and angles are largely determined by the influence of the two chlorine substituents at the Si atom and the shortness of the endocyclic C=C double bond. Due to the chlorine substituents the Si1–C1 and Si1–C3 bond lengths—in comparison to the structural parameters of other silacyclobutenes[10]—are clearly shortened to 182.8(1) and 186.4(1) pm, respectively, and consequently the endocyclic angle at Si1 is widened to 80.7(1)°, whereas the C=C bond distorts the angle Si1–C1–C2 to 87.8(1)°. As a result there are two external angles of 134.7(1) and 137.5(1)° at C1. The C1=C2 double bond with a length of 135.4(1) pm is slightly stretched.

The [2 + 2] cycloaddition most likely proceeds in two steps via 1,4-dipoles $[Cl_2Si(\overset{\ominus}{\underset{\cdot\cdot}{C}}HCH_2tBu)C(R){=}\overset{\oplus}{C}(R')]$, and is impressively regioselective (Scheme 1); in no case can isomeric products $Cl_2SiC(R'){=}C(R)CHCH_2tBu$ be detected. This finding suggests a polarization in the silene **1**, with the positive partial charge localized at the Si atom, and the negative partial charge at the C atom. The strong electrophilic character of **1** can be attributed to the influence of the two chlorine substituents on the Si atom.[8, 12] The three reactions leading to formation of the silacyclobutenes **3**, **5** and **6** also yield the *trans*-ethene compounds **8**–**10** (*cis*-orientation of R,R′) in amounts between 10 and 30% (Scheme 1).[13]

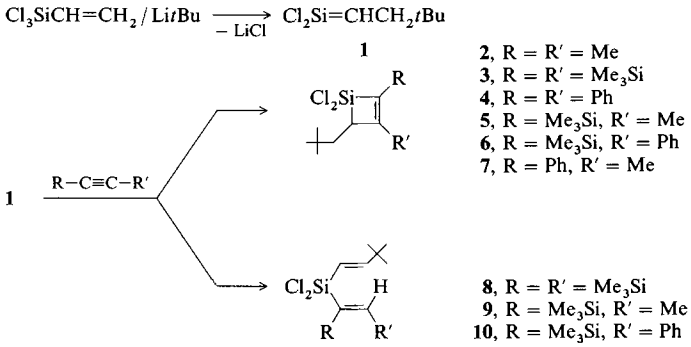

Scheme 1.

Their formation can be explained in terms of an ene reaction, in which **1** as ene reacts with the acetylenes as enophile.[14]

If the electrophilicity of neopentylsilenes of type **1** is reduced by substituent effects at the Si or α-C atom, the [2 + 2]

[*] Prof. Dr. N. Auner, Dipl.-Chem. C. Seidenschwarz, Dr. E. Herdtweck
Anorganisch-chemisches Institut der Technischen Universität München
Lichtenbergstrasse 4, W-8046 Garching (FRG)

[**] Silaheterocycles, Part 12. This work was supported by the Volkswagen-Stiftung, the Deutsche Forschungsgemeinschaft, the Fonds der Chemischen Industrie.—Part 11: [15].

cycloaddition does not take place: $R_2Si{=}CHCH_2tBu$ (R = Me or Ph)[15] and $Cl_2Si{=}C(SiMe_3)CH_2tBu$[16] do not react with the acetylenes mentioned here.

The facile entry to Si-dichlorinated silacyclobutenes opens up further synthetic possibilities through their derivatization; this is exemplified by the preparation of the H- and F-substituted derivatives **11** and **12** in good yields by reaction of **6** with $LiAlH_4$ and of **3** with SbF_3, respectively.

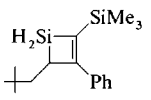

11

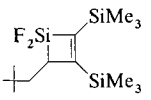

12

Experimental

General procedure for **2**–**7**: A mixture of 15 mmol of $Cl_3SiCH{=}CH_2$ and 45 mmol of acetylene derivative in *n*-pentane at −78 °C (for the synthesis of **5**: 0 °C) was treated with 15 mmol of Li*t*Bu in *n*-pentane (1.4 mmol mL^{-1}) and slowly warmed to room temperature, whereupon LiCl precipitated. For completion of reaction the mixture was stirred for a further 12 h at 20 °C, and then filtered. After removal of pentane by distillation, the residue was subjected to short path distillation at 10^{-2} mbar (b.p. [°C]/yield [%]: **2**: 52/46; **3**: 87/55; **4**: 200/85; **5**: 70/60; **7**: 116/65; **6**: 56 (m.p.)/78) or, for the isolation of pure **6**, recrystallized from pentane or ether.

For the preparation of **11**, **6** (3 mmol) was allowed to react with $LiAlH_4$ in ether at 0 °C according to the procedure described in Ref. [17]; for the synthesis of **12**, a solution of **3** (5 mmol) in toluene was allowed to react with SbF_3 at 0 °C and the mixture was then warmed to 60 °C for 6 h[18]. B.p./*p*/yield: **11**: 100 °C/10^{-2} mbar/60%; **12**: 40 °C/10^{-2} mbar/80%.

The purity of the four-membered ring compounds **2**–**7** and **11**, **12** was checked by elemental analysis; their mass spectroscopic fragmentation (70 eV) was as expected.

NMR data of the silacyclobutenes: ^{1}H NMR (100 MHz, $CDCl_3$, 25 °C, TMS) of **6**: δ = 7.25 (m, 5H; Ph), 3.20 (m, 1H; CH), 1.40 (m, 2H; CH_2), 0.84 (s, 9H; *t*Bu), 0.02 (s, 9H; $SiMe_3$); δ(*t*Bu and CH_2) of **2**–**5**, **7**, **11** and **12** are very similar to the parameters of **6**, the δ values of R and R′ lie in the expected ranges. Merely, δ(CH) varies between 2.30 (in **2**) and 3.20 (in **6** and **7**); ^{13}C- and ^{29}Si-NMR data (^{13}C NMR: 90.6 MHz, $CDCl_3$, DEPT, TMS; ^{29}Si NMR: 79.4 MHz, $CDCl_3$, TMS); assignment: $\overset{1}{>}Si\overset{2}{C}(R){=}\overset{3}{C}(R')\overset{4}{C}H_2tBu$; **6**: δ = 173.0 (C^2), 149.5 (C^3), 46.3 (C^4), 40.8 (CH_2), 30.5 ($C(CH_3)_3$), 29.3 ($C(CH_3)_3$), −0.2 ($SiMe_3$), 137.2 (=*C*(Ph)), 129.2 (*CH*(Ph)), 127.6, 128.3 (each 2 *CH*(Ph)); ^{29}Si NMR: δ = −1.4 (Cl_2Si), −12.4 (Me_3Si). Compound/ δ (C^2)/ δ (C^3)/ δ (C^4)/ δ (Cl_2Si): **2**/ 158.8/ 141.0/ 43.2/ 18.9; **3**/ 186.3/ 169.4/ 51.3/ −1.3; **4**/ 157.1/ 143.6/ 42.1/ −7.0; **5**/ 174.1/ 148.4/ 48.6/ −6.8; **7**/ 157.9/ 141.6/ 42.1/ −2.3; **11**/ 175.5/ 143.0/ 28.1/ H_2Si:−33.9 (t, J(Si,H) = 200 Hz); **12**/ 189.5 (t, ^2J(C,F) = 3 Hz)/ 173.6/ 51.4 (t, ^2J(C,F) = 10 Hz)/ F_2Si:−45.5 (t, ^1J(Si,F) = 417 Hz).

NMR data of Cl_2Si ($C_AH_A = C_BH_BtBu$)(R)C = CHR′ **8**–**10**: ^{1}H NMR; compound/ δ (H_A)/ δ (H_B)/ J(A,B) in Hz: **8**/ 5.41/ 6.25/ 19.44; **9**/ 5.71/ 6.65/ 18.66; **10**/ 5.65/ 6.19/ 18.5; ^{13}C-/ ^{29}Si NMR: Compound/ δ (C_A)/ δ (C_B)/δ (=*C*(R))/ δ (=*C*H(R′))/ δ (Cl_2Si): **8**/ 117.8/ 164.4/ 159.9/ 171.8/ 5.2; **10**/ 117.7/ 166.0/ 164.67/ 141.0/ −1.37.

Received: December 27, 1990;
revised: May 27, 1991 [Z 4357 IE]
German version: *Angew. Chem. 103* (1991) 1172

[1] Reviews: R. Damrauer, *Organomet. Chem. Rev. Sect. A 8* (1972) 67; L. E. Gusel'nikov, N. S. Nametkin, V. M. Vdovin, *Acc. Chem. Res. 8* (1975) 18.
[2] Silacyclobutanes as silene precursors: G. Raabe, J. Michl, *Chem. Rev. 85* (1985) 419; for the reactivity of the Si-C bond in silacyclobutanes: N. Auner, J. Grobe, *Z. Anorg. Allg. Chem. 500* (1983) 132. Gas phase structure of $F_2SiCH_2CH_2CH_2$: B. Rempfer, G. Pfafferott, H. Oberhammer, N. Auner, J. E. Boggs, *Acta Chem. Scand. Ser. A 42* (1988) 352.
[3] The first publications appeared in 1964/1965: H. Gilman, W. H. Atwell, *J. Am. Chem. Soc. 86* (1964) 5589; *ibid. 87* (1965) 2678. To our knowledge 23 original papers have so far been published, in which 14 different silacyclobutenes are described.
[4] See Ref. [3]; C. Eaborn, D. R. M. Dalton, M. Chan, *J. Organomet. Chem. 9* (1967) 25; P. B. Valkovich, W. P. Weber, *Tetrahedron Lett. 26* (1975) 2153.
[5] T. J. Barton, B. L. Groh, *J. Am. Chem. Soc. 107* (1985) 8297; G. T. Burns, T. J. Barton, *ibid. 105* (1983) 2006; S. A. Burns, G. T. Burns, T. J. Barton, *ibid. 104* (1982) 6140; G. T. Burns, T. J. Barton, *J. Organomet. Chem. 216* (1981) C5; E. Block, L. K. Revelle, *J. Am. Chem. Soc. 100* (1978) 1630.
[6] R. T. Conlin, Y.-W. Kwak, H. B. Huffaker, *Organometallics 2* (1983) 343; A. G. Brook, J. W. Harris, J. Lennon, M. E. Sheitch, *J. Am. Chem. Soc. 101* (1979) 83.
[7] P. R. Jones, T. F. O. Lim, *J. Am. Chem. Soc. 99* (1977) 8447; P. R. Jones, T. F. O. Lim, R. A. Pierce, *ibid. 102* (1980) 4970.
[8] N. Auner, *Habilitationsschrift*, Münster 1987.
[9] N. Auner, C. Seidenschwarz, E. Herdtweck, *Angew. Chem. 103* (1991) 425; *Angew. Chem. Int. Ed. Engl. 30* (1991) 444.
[10] M. Ishikawa, S. Matruzawa, K. Hirotsu, S. Kamitori, T. Higuchi, *Organometallics 3* (1984) 1930; M. Ishikawa, H. Sugisawa, H. Akimoto, K. Matsusaki, *ibid. 5* (1986) 2447; M. Weidenbruch, B. Brand-Roth, S. Pohl, W. Saak, *J. Organomet. Chem. 379* (1989) 271; D. B. Puranik, M. P. Johnson, M. J. Fink, *J. Chem. Soc. Chem. Commun. 1989*, 706; M. J. Fink, D. B. Puranik, M. P. Johnson, *J. Am. Chem. Soc. 110* (1988) 1315.
[11] P. Kiprof, E. Herdtweck, R. E. Schmidt, M. Birkhahn, W. Massa: STRUX-III program system for refinement of X-ray data, Technische Universität München/Universität Marburg, 1989/1985. **6** crystallizes as colorless platelets from *n*-pentane. The extinctions ($h01$: $1 = 2n + 1$; $0k0$: $k = 2n + 1$) are consistent with the monoclinic space group $P2_1/c$. The lattice constants are refined on the basis of 25 reflection positions ($\theta > 39.8°$; $\pm h$, $\pm k$, $\pm l$) to a = 963.2(4), b = 1178.9(2), c = 1777.9(6) pm, β = 78.04(2)°; $V = 1975 \times 10^6$ pm^3; $C_{17}H_{26}Cl_2Si_2$; $Z = 4$; ϱ_{calcd} = 1.202 g cm^{-3}. The collection of the intensities was carried out at 193 K on an automatic four-circle diffractometer (CAD4-Enraf-Nonius; λ = 71.073 pm; graphite monochromator) in the measuring range $1.0° \le \theta \le 25.0°$ in the ω-scan at variable width and maximum measuring time t_{max} = 60 s. Of 3856 measured intensities (477 with $I < 0$ were classed as unobserved), after averaging 3178 (NO) independent reflections with $I > 0$ and 291 (NV) parameters were refined by full matrix least squares. $R = \sum(||F_o|-|F_c||)/\sum|F_o| = 0.037$; $R\omega = [\sum\omega(|F_o|-|F_c|)^2/\sum\omega F_o^2]^{1/2} = 0.032$; GOF = $[\sum\omega(|F_o|-|F_c|)^2/(NO-NV)]^{1/2} = 3.423$. The solution of the structure was carried out by direct methods and difference Fourier technique. The positions of the hydrogen atoms were refined free (only the hydrogens on C3 and C4 were given a fixed, collective deviation parameter). Anomalous dispersion was taken into account. After the last refinement cycle (shift error < 0.001) the maximum/minimum residual electron density was + 0.31/−0.27 e_0 Å^{-3}. Further details of the crystal structure investigation are available on request from the Fachinformationszentrum Karlsruhe, Gesellschaft für wissenschaftlich-technische Information mbH, W-7514 Eggenstein-Leopoldshafen 2 (FRG), on quoting the depository number CSD-55625, the names of the authors, and the journal citation.
[12] An alternative reaction path for the formation of the silacyclobutenes involves a carbanionic attack of the α-lithioadduct $Cl_3Si\overset{\ominus}{\underset{\cdot\cdot}{C}}HCH_2tBuLi^{\oplus}$ on the acetylenes followed by cyclization with elimination of LiCl. However, an addition of Me_3SiOMe to the reaction mixture leads to preferential formation of the Si=C trapping product $Cl_2Si(OMe)CH(SiMe_3)CH_2tBu$ (a reaction which proceeds quantitatively in the absence of acetylenes); moreover, $F_3Si\overset{\ominus}{\underset{\cdot\cdot}{C}}HCH_2tBuLi^{\oplus}$, which is markedly more stable in comparison to the chlorine analogue, does not react with dienes and acetylenes: N. Auner, C. Seidenschwarz, A. Wolff, unpublished results.
[13] N. Auner, *J. Organomet. Chem. 336* (1987) 59.
[14] M. Ishikawa, M. Kumada, *Adv. Organomet. Chem. 19* (1981) 51; N. Wiberg, *J. Organomet. Chem. 272* (1984) 141.
[15] N. Auner, W. Ziche, E. Herdtweck, *J. Organomet. Chem.*, in press.
[16] N. Auner, W. Ziche, unpublished results.
[17] N. Auner, J. Grobe, *J. Organomet. Chem. 188* (1980) 25.
[18] N. Auner, J. Grobe, *Z. Anorg. Allg. Chem. 485* (1982) 53.

$BPh_4^{\ominus}$ as a Ligand in Cationic Zirconium Complexes: Novel Bonding Mode and Fluxionality

By *Andrew D. Horton** and *John H. G. Frijns*

It is now fairly well established that a cationic complex, $[Cp_2MR]^{\oplus}$, is the active species of Group 4 metallocene/alkylaluminoxane catalysts and related systems in alkene polymerization.[1] The excess alkylaluminoxane presumably functions partly as a Lewis acidic precursor of a poorly coordinating anion, and so alternative anions are of interest for one-component catalysts.[2, 3] Although Lewis base adducts,

[*] Dr. A. D. Horton, J. H. G. Frijns
Koninklijke/Shell-Laboratorium Amsterdam
P.O. Box 3003, NL-1003 AA Amsterdam (The Netherlands)

$[Cp_2MR(L)][BPh_4]$, have been extensively studied,[2] attempts to synthesize more reactive base-free complexes have led to phenyl metalation giving $[(C_5Me_5)_2Zr(C_6H_4BPh_3)]$.[3] *Bochmann* et al. recently generated the complexes $[Cp_2MMe][BPh_4]$ at low temperature in dichloromethane, and provided evidence for solvent coordination.[4] In contrast, in the new complexes presented here, coordination of the tetraphenylborate anion occurs. Like the alkylaluminoxane systems, the complexes are soluble in aromatic solvents and catalyze the isotactic polymerization of propene.

Attempted isolation of $[Cp'_2ZrMe][BPh_4]$ in aromatic solvents has previously led either to phenyl transfer (non-crowded system, $Cp' = C_5H_5$)[5] or to anion metalation (crowded system, $Cp' = C_5Me_5$).[3] Cyclopentadienyl ligands of intermediate steric bulk were expected to stabilize complexes by allowing anion coordination as an alternative to the sterically less demanding C–H activation,[6] whilst hindering the sterically more demanding phenyl transfer. Complexes with chiral ligands were of relevance to stereospecific polymerization catalysis.[1a, 2b] The new complexes **1**–**4** were synthesized by protonolysis of Cp'_2ZrMe_2 between -30 and 25 °C [Eq. (a)] and were obtained as orange (**1**) or yellow (**2**–**4**), THInd = tetrahydroindenyl) precipitates, indefinitely stable in the solid state at -40 °C.[7] The stability in bromobenzene decreases in the order: **2** (40 h) > **1** (20 h) >> **3** (90 min) > **4** (50 min) ($t_{1/2}$ at 25 °C).

$$Cp'_2ZrMe_2 \xrightarrow[C_6H_5Br]{[PhNMe_2H][BPh_4]} Cp'_2ZrMe(BPh_4) + CH_4 + PhNMe_2 \quad (a)$$

1: $Cp'_2 = rac\text{-}C_2H_4(Ind)_2$
2: $Cp'_2 = rac\text{-}C_2H_4(THInd)_2$
3: $Cp' = (Me_3C)C_5H_4$
4: $Cp' = (Me_3Si)C_5H_4$

Low temperature ^{1}H-NMR studies in aromatic solvents showed that the tetraphenylborate anion is coordinated to the central zirconium. The proton chemical shifts for the coordinated phenyl ring and the three equivalent non-coordinated rings of $[BPh_4]^{\ominus}$ are compared in Table 1 with the "free" anion resonances. Complexes **3** and **4** possess an

Table 1. ^{1}H NMR chemical shifts (300 MHz) of $[BPh_4]^{\ominus}$ in C_7D_8 at -30 °C.

Cp-ligand	δ(*o*-H)		δ(*m*-H)		δ(*p*-H)	
	Ph [a]	BPh_3	Ph [a]	BPh_3	Ph [a]	BPh_3
$C_2H_4(Ind)_2$ [b]	8.24 *o*1	7.86	6.69 *m*1	7.34	5.50	7.36
1	6.53 *o*2		4.77 *m*2			
$C_2H_4(THInd)_2$	8.40 *o*1	8.01	6.81 *m*1	7.43	6.07	7.23
2	7.64 *o*2		6.22 *m*2			
$(Me_3C)C_5H_4$	8.09	7.96	6.80	7.52	6.31	7.35
3						
$(Me_3Si)C_5H_4$	8.09	7.96	6.71	7.49	6.25	7.32
4						
$[HNBu_3][BPh_4]$	7.89		7.21		7.00	

[a] Coordinated phenyl ring. [b] **1** was measured in C_7D_8/C_6D_5Cl.

equatorial plane of symmetry, as shown by the observation of equivalent cyclopentadienyl groups and of three resonances in the ratio 2:2:1 for the coordinated phenyl group. The *ortho*-protons of the coordinated phenyl ring are shifted ca. $\delta = 0.15$ further downfield than those of the three non-coordinated Ph groups, whereas the signals of the *meta*- and *para*-protons are detected ca. $\delta = 0.75$ and 1.05, respectively, further upfield. Complexes **1** and **2**, with a chiral zirconium center, show five signals for the coodinated phenyl ring. The average chemical shifts for the *ortho*-, *meta*- and *para*-hydrogens of the tetrahydroindenyl complex **2** are similar to those for complexes **3** and **4** with C_s symmetry, suggesting similar interactions between the *meta*- and *para*-carbon atoms and the zirconium atom. The extreme upfield location of the signals for H_{o2}, H_{m2} and H_p in **1** are due to the ring-current effect of an indenyl six-membered ring on part of the adjacent phenyl ring (Fig. 1).

The upfield shifts of the *meta*- and *para*-hydrogens and downfield shifts of the *ortho*-hydrogens are consistent either with unusual $\eta^3(m,p)$-coordination of the phenyl ring (Fig. 1),[8] or with the rapid equilibration of two enantiomers (**3**, **4**) or diasteroisomers (**1**, **2**) with $\eta^2(m,p)$-coordinated

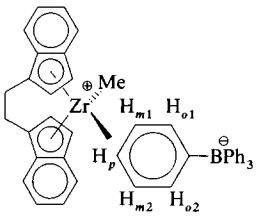

Fig. 1. $[\{rac\text{-}C_2H_4(Ind)_2\}ZrMe(BPh_4)]$ **4**.

phenyl rings. The average structure, in which the B–C_{ipso}–C_p axis of the phenyl ring lies in the equatorial plane with BPh_3 pointing away from the cyclopentadienyl rings, is the same in either case. Interconversion of two η^2-coordinated aromatics can be a low-energy process.[9] Broadening of the cyclopentadienyl and anion ^{1}H-NMR signals of **3** and **4** observed at -70 °C may well be due to restricted rotation of the RC_5H_4 ligand. The fact that resonances due to a static "η^2-"structure for **3** or **4** are not observed, even at -70 °C, and that sharp resonances due to only one (rather than the expected two) diastereoisomer(s) of **2** are seen at -65 °C, does not allow us to entirely rule out the presence of two rapidly intercoverting η^2-forms. Coordination of $[BPh_4]^{\ominus}$ in the η^6-[10] and η^2-models[11] has been observed previously, especially in the case of late transition metal complexes.

Two novel fluxional processes have been observed. The chiral environment at zirconium in the thermally stable complex **2** allows exchange of the hydrogens of the unique phenyl ring above and below the equatorial plane to be probed. Each of the two *ortho*- and two *meta*-H resonances for the unique phenyl group is sharp at -65 °C, but broadens at -30 °C and coalesces at -10 to -5 °C. At 25 °C two relatively sharp resonances (relative intensity 2) are obtained. This lower energy process ($\Delta G^{\neq} \cong 12.1$ kcal mol^{-1}) leaves the *p*-Ph and the BPh_3 resonances unchanged between -65 and 25 °C. Above 25 °C broadening and partial collapse of all Ph and BPh_3 resonances occur, but decomposition is evident above 75 °C, before the high temperature limit is reached. This apparent exchange of all anion phenyl groups leaves the tetrahydroindenyl resonances unchanged.

The NMR results show that in **2** the environments of each of two *ortho*- as well as of the two *meta*-hydrogens exchange more rapidly than phenyl exchange. Since oxidative addition to Zr^{IV} of the phenyl *para*-C–H bond is not possible, a remarkable fluxional process appears to be operative, involving flipping of the coordinated face of the unique phenyl ring, whilst the ring remains coordinated to zirconium, perhaps via a Zr-H-C interaction involving H_p (Fig. 2) or H_m. Such an electrostatically assisted "intermolecular" interaction is known in the structure of $[(EtC_5Me_4)_2ZrMe(C_2B_9H_{12})]$,[3] in which a carborane anion is coordinated solely via a Zr–H–B bond. That ring flipping in **2** occurs

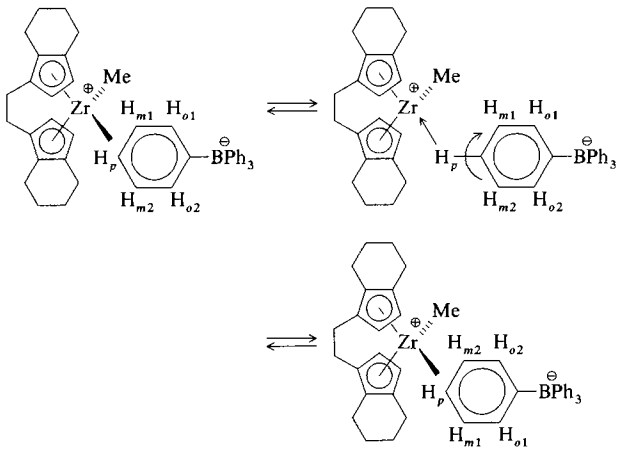

Fig. 2. A possible mechanism of phenyl-group flipping in complex **2**.

faster than ring exchange is surprising, but may be due to the steric crowding at zirconium, which disfavors simultaneous coordination of two phenyl groups.

Use of the good polar solvent 1,1,2,2-tetrachloroethane[12] allows observation of the anion ^{13}C-NMR resonances which are partially obscured or weak in C_6D_5Br. The downfield *ipso*- and *ortho*-resonances and (generally) upfield *meta*- and *para*-resonances of the anion coordinated ring in **1**–**4** are again consistent with η^3- or (fluxional) η^2-coordination of a phenyl ring. However, additional resonances due to the "free" anion are also observed in this solvent. The "free" anion (**1**: *ca.* 35%; **2**: *ca.* 25%; **3**: *ca.* 20%; **4**: *ca.* 10%) gives resonances identical to those of the anion in Lewis base adducts of the type $[Cp'_2ZrMe(L)][BPh_4]$ (formed, e.g., on addition of THF to the complexes). Resonances due to the corresponding cation cannot be unambiguously identified, but the cation is presumably $[Cp'_2ZrMe(C_2D_2Cl_4)]^{\oplus}$, containing η^1- or η^2-coordinated solvent. Previous studies of related metallocene cations, generated *in situ* in CD_2Cl_2, suggested that the anion is not coordinated to the metal, but instead is present as a mixture of "solvated" and "ion paired" species;[4] in contrast, the fluxional anion in $[Zr(CH_2Ph)_3(\eta^6\text{-}PhBPh_3]$ apparently remains coordinated to the Zr atom in CD_2Cl_2.[10c]

Complexes **1** and **2** react with propene at 15°C to give isotactic polypropylene with melting points (**1**: 142°C, **2**: 143°C) comparable to that of polymer formed using methylaluminoxane as cocatalyst.[13] The modest polymerization rate is explained by the difficulty of anion displacement by the weakly coordinating alkene. The electrostatic attraction between anion and cation clearly compensates for the loss of aromatic stabilization on coordination of the anion. High-activity one-component catalysts will require more poorly coordinating anions.

Experimental

C_6H_5Br (4 mL) was added to a mixture of *rac*-$[C_2H_4(Ind)_2ZrMe_2]$ (150 mg; 0.40 mmol) and $[PhMe_2NH][BPh_4]$ (172 mg; 0.39 mmol) at −30°C; the mixture was then warmed to 25°C and stirred for ten minutes. Filtration and addition of hexane gave an orange oil, which was washed twice with hexane, with vigorous stirring, to give **1** as an orange solid (280 mg; 77%). Complexes **2**–**4** were obtained similarly, except that **4** was precipitated at 10°C. A trace impurity of $PhNMe_2$ was removed by re-precipitation. ^{1}H-NMR resonances for **1** and **2** have been assigned using 2D-COSY-NMR techniques. Selected ^{1}H NMR for cations (1:1 C_6D_5Cl:C_7D_8, −30°C): **1**: δ = 6.22, 5.05, 4.83, 3.52 (d, 1H; Ind-C_5), −0.70 (s, 3H; Zr-*Me*); (C_7D_8, −30°C): **2**: δ = 5.72, 4.36, 4.32, 3.26 (d, 1H; THind-C_5), 0.18 (s, 3H; Zr-*Me*); **3**: δ = 5.82, 5.18, 4.95, 4.64 (br, 2H; $(Me_3C)C_5H_4$), 0.88 (s, 18H; $(Me_3C)C_5H_4$), 0.33 (s, 3H; Zr-*Me*); **4**: δ = 5.98, 5.26, 5.17, 5.03 (br, 2H; $(Me_3Si)C_5H_4$), 0.32 (s, 3H; Zr-*Me*), 0.02 (s, 18H; $(Me_3Si)C_5H_4$). Selected ^{13}C-NMR data for the anions ($C_2D_2Cl_4$, −35°C): free $BPh_4^{\ominus}$: δ = 164.5 (*ipso*-C), 136.5 (*o*-C), 126.3 (*m*-C), 122.0 (*p*-C); **2**: δ = 180.8 (*ipso*-Ph), 161.7 (*ipso*-BPh_3), 144.8, 139.7 (*o*-Ph), 136.1 (*o*-BPh_3), 133.1 (*m*-Ph), 127.0 (*m*-BPh_3), 123.1 (*p*-BPh_3), 120.4 (*m*-Ph), 116.0 (*p*-Ph), 46.9 (Zr-*Me*); **4**: δ = 181.0 (*ipso*-Ph), 161.3 (*ipso*-BPh_3), 141.5 (*o*-Ph), 136.0 (*o*-BPh_3), 126.9 (*m*-BPh_3), 123.6 (*m*-Ph), 123.1 (*p*-BPh_3), 120.0 (*p*-Ph), 44.9 (Zr-*Me*). The anion in **1** and **3** gives similar resonances to **2** and **4**, respectively.

Polymerization experiments: A solution of complex **1** (100 mg) in C_6H_5Br/toluene (20 ml, 1/4) was added to toluene (150 ml) and propene (*ca.* 6 atm) in a steel autoclave at 15°C. After 1.9 h, the propene was removed and isooctane (150 ml) and MeOH (100 ml) were added to give a fine precipitate of polypropylene (3.6 g). Similarly, complex **2** (2.6 h) gave 7.2 g of polypropylene. Polymer **1**: M_n = 25,500; M_w = 45,600; M_z = 63,500; M_w/M_n = 1.8. Polymer **2**: M_n = 10,900; M_w = 28,600; M_z = 43,800; M_w/M_n = 2.6.

Received: March 15, 1991 [Z 4506 IE]
German version: *Angew. Chem. 103* (1991) 1181

[1] a) J. A. Ewen, *J. Am. Chem. Soc. 106* (1984) 6355; b) P. G. Gassman, M. R. Callstrom, *ibid. 109* (1987) 7875; c) J. J. Eisch, A. M. Piotrowski, S. K. Brownstein, E. J. Gabe, F. L. Lee, *ibid. 107* (1985) 7219.

[2] a) R. F. Jordan, P. K. Bradley, N. Baenziger, R. E. LaPointe, *Organometallics 8* (1989) 2892; b) R. F. Jordan, R. E. LaPointe, N. Baenziger, G. D. Hitch, *ibid. 9* (1990) 1539; c) M. Bochmann, L. M. Wilson, M. B. Hursthouse, M. Motevalli, *ibid. 7* (1988) 1148; d) R. Taube, L. Krukowka, *J. Organomet. Chem. 347* (1988) C9.

[3] G. G. Hlatky, H. W. Turner, R. R. Eckman, *J. Am. Chem. Soc. 111* (1989) 2728.

[4] M. Bochmann, A. J. Jaggar, N. J. Nicholls, *Angew. Chem. 102* (1990) 830; *Angew. Chem. Int. Ed. Engl. 29* (1990) 780.

[5] Sparingly soluble $[(C_5H_5)_2ZrMe(BPh_4)]$ may be generated in C_6H_5Br, but decomposes ($t_{1/2}$ (25°C) = 5 min) to $[(C_5H_5)_2Zr(Me)Ph]$.

[6] M. E. Thompson, S. M. Baxter, A. R. Bulls, B. J. Burger, M. C. Nolan, B. D. Santarsiero, W. P. Schaefer, J. E. Bercaw, *J. Am. Chem. Soc. 109* (1987) 203.

[7] The isolated complexes contain up to 1.0 equiv. C_6H_{14}; **1** and **2** contain 0.5–1.0 equiv. C_6H_5Br. Solvent removal *in vacuo* leads to decomposition.

[8] a) K. Jonas, G. Koepe, L. Schieferstein, R. Mynott, C. Krüger, Y.-H. Tsay, *Angew. Chem. 95* (1983) 637; *Angew. Chem. Int. Ed. Engl. 22* (1983) 620; b) D. R. Neithamer, L. Párkányi, J. F. Mitchell, P. T. Wolczanski, *J. Am. Chem. Soc. 110* (1988) 4421.

[9] a) J. R. Sweet, W. A. G. Graham, *Organometallics 2* (1983) 135; b) R. Cordone, W. D. Harman, H. Taube, *J. Am. Chem. Soc. 111* (1989) 2896.

[10] a) P. Albano, M. Aresta, M. Manassero, *Inorg. Chem. 19* (1980) 1069; b) G. J. Kruger, A. L. du Preez, R. J. Haines, *J. Chem. Soc. Dalton Trans. 1974*, 1302; c) M. Bochmann, G. Karger, A. J. Jaggar, *J. Chem. Soc. Chem. Commun. 1990*, 1038.

[11] M. Pasquali, C. Floriani, A. Gaetani-Manfredotti, *Inorg. Chem. 19* (1980) 1191.

[12] Complex decomposition to $[Cp'_2Zr(Me)Cl]$ and $[Cp'_2ZrCl_2]$ (ca. 2:1) is much slower in $C_2D_2Cl_4$ than in CD_2Cl_2.

[13] B. Rieger, X. Mu, D. T. Mallin, M. D. Rausch, J. C. W. Chien, *Macromolecules 23* (1990) 3559.

Reactivity of a (Diazomethylene)phosphorane with Alkylating Agents and Lewis Acids; Synthesis of the First α-Diazoalkylborates**

By *Jean-Marc Sotiropoulos, Antoine Baceiredo, Klaus Horchler von Locquenghien, Françoise Dahan,* and *Guy Bertrand**

The Lewis acid catalyzed decomposition of diazo compounds has been the subject of numerous studies.[1] The

[*] Dr. G. Bertrand, J.-M. Sotiropoulos,
Dr. A. Baceiredo, Dr. K. Horchler von Locquenghien[+],
Dr. F. Dahan
Laboratoire de Chimie de Coordination du CNRS
205, route de Narbonne, F-31077 Toulouse Cédex (France)

[+] New address:
BASF AG, W-6700 Ludwigshafen (FRG)

[**] This work was supported by the Centre National de la Recherche Scientifique, the Alexander von Humboldt-Foundation, and the Conseil Régional Midi-Pyrénées (postdoctoral fellowship for *K. H. v. L.*).

interaction between catalyst and diazo derivatives has been postulated to be initiated by electrophilic attack of the Lewis acid MX_n at the diazo carbon, with simultaneous or subsequent loss of N_2. None of the postulated primary adducts **A** or **B** has so far been isolated. Thus, it was of interest to study the reactivity of the stable bis(diisopropylamino)chlorodiazomethylenephosphorane **1**[2] towards Lewis acids and alkylating agents, in the hope of obtaining **A**- and **B**-type complexes **C** and **D**, which should be stable due to the possible π electron delocalization.[3, 4]

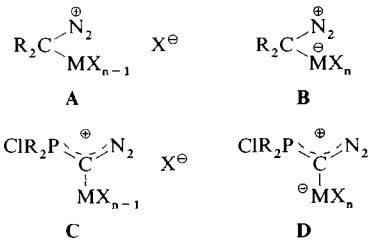

A **B**

C **D**

Among the possible Lewis acids, we first chose mercury dichloride, which is known to be moderately reactive toward diazo decomposition.[5] In toluene at room temperature it reacts smoothly with the (diazomethylene)phosphorane **1** to give the bis{[chlorobis(diisopropylamino)phosphonio]diazomethyl}mercury salt **2** [Eq. (a)]. The ionic nature of **2** was

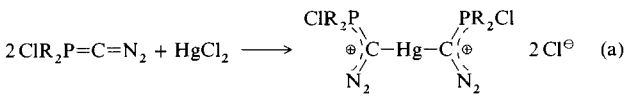

(a)

1 **2**

R = iPr$_2$N

demonstrated by anion exchange with potassium hexafluorophosphate. The PF_6 salt formed could be isolated as a solid (m.p. 130 °C (decomp.)) in 90% yield. The presence of diazo groups was confirmed by an IR absorption at 2083 cm^{-1} and the $[P-C(N_2)]_2Hg$ skeleton was apparent from the ^{31}P-NMR ($\delta = +61.7$, $^2J_{^{199}Hg^{31}P} = 181.3$ Hz) and ^{199}Hg-NMR[6] ($\delta = +1234$, t) spectra. Since Lewis acids are known to react with phosphorus ylides at carbon,[7] it is reasonable to postulate the primary formation of a transient adduct $ClR_2P(N_2)CHgCl_2$, which would rearrange into a salt $[ClR_2P(N_2)CHgCl]Cl$. Repetition of this reaction sequence could explain the formation of **2**.

The alkylation of **1** was then investigated. With methyl trifluoromethanesulfonate and triphenylcarbenium hexafluorophosphate clean reactions occurred, leading to the expected salts **3** (m.p. 135 °C decomp.)) and **4** (m.p. 180 °C (decomp.)) in 85 and 70% isolated yield, respectively [Eq. (b)].

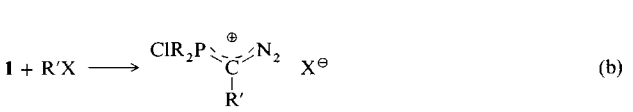

(b)

3: R′ = Me, X = F_3CSO_3
4: R′ = Ph_3C, X = PF_6

R = iPr$_2$N

These compounds were fully characterized by spectroscopic methods (Table 1) and in the case of **4**, by an X-ray crystal study (Fig. 1).[8] The molecular structure of **4** is illustrated in Figure 1, together with the atom numbering scheme

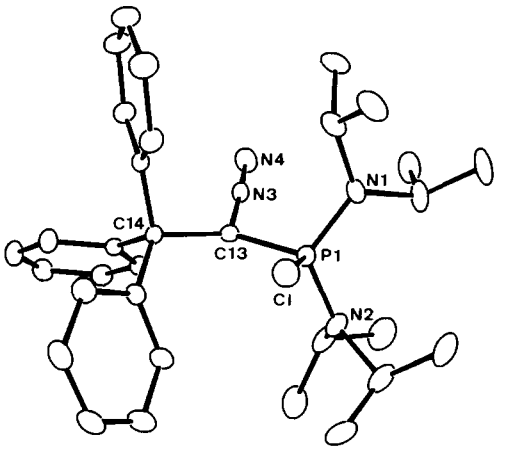

Fig. 1. Molecular structure of **4** (ORTEP, ellipsoids at the 25% probability level. Selected bond lengths [Å] and angles [°]: P1-N1 1.622(4), P1-N2 1.607(3), P1-C1 2.006(2), P1-C13 1.763(4), C13-C14 1.567(5), C13-N3 1.332(4), N3-N4 1.124(4), P1-C13-C14 135.1(2), P1-C13-N3 110.0(3), C14-C13-N3 111.8(3), C13-N3-N4 176.2(4).

and the pertinent metric parameters. Interestingly, the C13–N3 bond length (1.332 Å) is at the upper limit (1.28–1.32 Å) and the N3–N4 bond length (1.124 Å) is at the lower limit (1.12–1.14 Å) for a diazo compound, but they are shorter and longer, respectively, than those observed for diazonium salts (C–N 1.38–1.43; N–N 1.09–1.11 Å).[1b] From the structural data-available,[9] a $P-C_{ylide}$ bond length of 1.63–1.64 Å can be estimated, which is much shorter than the P–C bond length observed for **6** (1.763 Å). These data indicate that in the ground state, although the diazonium form is not negligible, the phosphonium form clearly predominates. This assumption is confirmed by the rather low IR frequency (2090 cm^{-1}).

Table 1. Selected spectroscopic data of **3**–**8**. [a]

3: ^{31}P NMR ($CDCl_3$): $\delta = +60.6$. ^1H NMR ($CDCl_3$): $\delta = 2.17$ (12.9) (d, 3H, $C(N_2)CH_3$). ^{13}C NMR ($CDCl_3$): $\delta = 11.8$ (10.8) (d, $C(N_2)CH_3$), 43.8 (202.0) (d, CN_2), 120.5 (q, $^1J(^{19}F^{13}C) = 320.4$ Hz, CF_3). IR ($CDCl_3$): $\tilde{\nu}$ [cm^{-1}] = 2093 cm^{-1} (CN_2)

4: ^{31}P NMR (CD_3CN): $\delta = +65.0$, -145.1 (sept., $^1J(^{31}P^{19}F) = 707.1$ Hz). ^{13}C NMR (CD_3CN): $\delta = 58.9$ (194.7) (d, CN_2), 64.5 (6.8) (d, CPh_3).

6: ^{31}P NMR (C_6D_6): $\delta = +64.8$. ^{11}B NMR (C_6D_6): $\delta = -29.1$ (q, $^1J(^{11}B^1H) = 92.8$ Hz). IR (C_6D_6): $\tilde{\nu}$ [cm^{-1}] = 2065 (CN_2), 2350 (BH_3) cm^{-1}.

7: ^{31}P NMR ($CDCl_3$): $\delta = +45.5$. ^{11}B NMR ($CDCl_3$): $\delta = -0.4$ (q, $^1J(^{19}F^{11}B) = 20$ Hz). ^{13}C NMR ($CDCl_3$): $\delta = 37.4$ (26.7) (d, CH_2), 53.0 (s, OCH_3), 61.7 (5.4) (d, CH_{ring}), 170.6 (s, CO). ^1H NMR ($CDCl_3$): $\delta = 3.34$ ($^3J_{^1H^1H} = 10.1$ Hz), 3.72 ($^3J(^1H,^1H) = 9.9$ Hz) (d of AB systems $^2J(^1H^1H)$ not resolved, each 1H; CH_2), 3.77 (s, OCH_3), 4.88 (t-like, $^3J(^1H,^1H) = 10.0$ Hz, 1H, CH_{ring}). IR ($CDCl_3$): 1742 cm^{-1} (CO). –

8: ^{31}P NMR ($CDCl_3$): $\delta = +48.0$; ^{11}B NMR ($CDCl_3$): $\delta = -1.2$ (br); ^{13}C NMR ($CDCl_3$): $\delta = 52.5$, 52.6 (s, OCH_3), 53.8 (4.8) (d, CH_{ring}), 54.2 (5.8) (d, CH_{ring}), 117.0 (221.5) (d, PC), 169.9, 170.1 (s, CO); ^1H NMR ($CDCl_3$): $\delta = 3.64$, 3.66 (s, 6H, OCH_3), 4.14, 4.80 (each d, $^3J(^1H,^1H) = 7.5$ Hz, each 1H, CH_{ring}). IR ($CDCl_3$): $\tilde{\nu}$ [cm^{-1}] = 1740 cm^{-1} (CO).

[a] Numbers given in round brackets after the δ values are coupling constants of the respective nucleus from couplings with ^{31}P.

The formation of stable compounds of type **C** prompted us to attempt the synthesis of derivatives of type **D**. Indeed, the reaction of **1** with diethylether-trifluoroborane led to the desired adduct **5** in 83% yield as a water-sensitive reddish orange oil. The presence of the diazo group was confirmed by an IR absorption at 2080 cm^{-1}, the P–C–B skeleton was shown to be present by a 1:1:1:1 quartet at $\delta = +63.4$ ($^1J_{^{31}P^{11}B} = 9$ Hz) in the ^{31}P-NMR spectrum, and the BF_3

moiety gave typical ^{11}B- ($\delta = +0.9$, q, $^1J_{^{19}F^{11}B} = 32$ Hz) and ^{19}F-NMR ($\delta = +38$, q) signals. Similarly, addition of tetrahydrofurane-borane complex to **1** furnished the adduct **6** as a yellow oil in 87% yield. Note that only one example

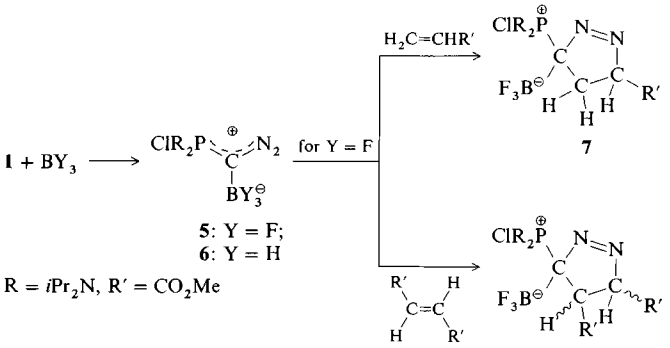

of an isolated α-diazoalkylborane is known,[10, 11] and that compounds **5** and **6** are the first α-diazoalkylborates. Compound **5** undergoes a regiospecific but also stereospecific [2 + 3] cycloaddition with methylacrylate, leading to **7** (m.p. 155°C, 70% yield) in the form of only one of the diastereoisomers (according to NMR data). With dimethyl fumarate, the *trans* geometry is maintained but two diastereoisomers **8** are formed in a 70/30 ratio (Table 1).

Experimental

Diazomethylenephosphorane adducts **2**–**6** were prepared by adding the Lewis acid or alkylating agent to a toluene solution of **1**, at room temperature for $HgCl_2$, Ph_3CPF_6, $BF_3{\cdot}OEt_2$ and $BH_3{\cdot}THF$, and at 0°C for $MeOSO_2CF_3$. After stirring for 1 h at room temperature, the solvent was removed in vacuo and the residue was washed several times with pentane. Adduct **2** was recrystallized from acetonitrile, **3** from 1,2-dichloroethane/ether, and **4** from toluene/acetonitrile, while adducts **5** and **6** were obtained as oils. Cycloadducts **7** and **8** were obtained by adding the stoichiometric amount of the corresponding alkene to a toluene solution of **5** at −80°C. After stirring for 1 h at room temperature, the solvent was removed and **7** was recrystallized from 1,2-dichloroethane/ether, while **8**, owing to its instability, was spectroscopically characterized in solution.

Received: April 2, 1991 [Z 4548 IE]
German version: *Angew. Chem. 103* (1991) 1174

CAS Registry numbers:
1, 109065-32-9; **2**, 135256-12-1; **2** [P(V)], 135227-19-9; **2** (PF_6 statt Cl), 135227-18-8; **3**, 135227-15-5; **3** [P(V)], 135227-20-2; **4**, 135227-16-6; **5**, 135227-21-3; **6**, 135227-22-4; **7**, 135227-23-5; **8** (isomer 1), 135227-24-6; **8** (isomer 2), 135271-28-2; $H_2C{=}CHCO_2Me$, 96-33-3; (*E*)-MeOCOCH=$CHCO_2Me$, 624-49-7; $HgCl_2$, 7487-94-7; Ph_3CPF_6, 437-17-2; $BF_3{\cdot}OEt_2$, 109-63-7; $BH_3{\cdot}THF$, 14044-65-6.

[1] a) G. Maas, *Top. Curr. Chem. 137* (1987) 75; b) J. B. Moffat in S. Patai (Ed.): *The Chemistry of the Diazonium and the Diazo groups*, Wiley, London, 1977; c) M. Regitz, G. Maas: *Diazo Compounds, Properties and Synthesis*, Academic Press, London 1986.

[2] J. M. Sotiropoulos, A. Baceiredo, G. Bertrand, *J. Am. Chem. Soc. 109* (1987) 4711.

[3] A few examples of phosphoniodiazomethanes obtained by diazo group transfer to phosphonium salts have been reported: M. Regitz, A. El-R. M. Tawfik, H. Heydt, *Liebigs Ann. Chem. 1981*, 1865.

[4] Reactions of Lewis acids with other phosphacumulene ylides have been reported: a) H. J. Bestmann, *Angew. Chem. 89* (1977) 361; *Angew. Chem. Int. Ed. Engl. 16* (1977) 349; b) C. N. Matthews, G. H. Birum, *Acc. Chem. Res. 2* (1969) 373.

[5] D. S. Crumrine, T. J. Haberkamp, D. J. Suther, *J. Org. Chem. 40* (1975) 2274.

[6] The ^{199}Hg-NMR spectrum has been measured in CD_3CN at 297 K on a Bruker AM 300 spectrometer. The δ-values are referred to 0.1 M $Hg(ClO_4)_2$ in 0.1 M $HClO_4$ ($\Xi(^{199}Hg) = 17870535$ Hz).

[7] a) H. Schmidbaur, *Acc. Chem. Res. 8* (1975) 62; b) H. Schmidbaur, *Angew. Chem. 95* (1983) 980; *Angew. Chem. Int. Ed. Engl. 22* (1983) 907.

[8] Space group $P2_1/c$, $a = 12.308(2)$, $b = 17.478(3)$, $c = 16.541(3)$ Å, $\beta = 106.74(1)°$, $V = 3407.5$ Å^3, $Z = 4$; 4969 measured reflections, 3271 independent observed ($I > 3\sigma(I)$), 406 refined parameters, $R = 0.041$ ($R_w = 0.040$). Further details of the crystal structure investigations are available on request from the Fachinformationszentrum Karlsruhe, Gesellschaft für wissenschaftlich-technische Information mbH, W-7514 Eggenstein-Leopoldshafen 2 (FRG), on quoting the depository number CSD-55592, the names of the authors, and the journal citation.

[9] Usually the P=C bond lengths in carbodiphosphoranes are about 3 pm shorter than in the corresponding ylides c.f. $Me_3P{=}CH_2$/$Me_3P{=}C{=}PMe_3$: E. A. V. Ebsworth, D. W. H. Rankin, T. E. Fraser, *Chem. Ber. 110* (1977) 3494/E. A. V. Ebsworth, T. E. Fraser, D. W. H. Rankin, O. Gasser, H. Schmidbaur, *ibid. 110* (1977) 3508; $Ph_3P{=}CH_2$/$Ph_3P{=}C{=}PPh_3$: J. C. J. Bart, *J. Chem. Soc. B 1969*, 350/A. T. Vincent, P. J. Wheatley, *J. Chem. Soc. Dalton Trans. 1972*, 617; In $(Me_2N)_2FP{=}C{=}PF(NMe_2)_2$: $d_{(P=C)} = 1.60$ Å, E. Fluck, B. Neumüller, R. Braun, G. Heckmann, A. Simon, H. Z. Borrmann, *Z. Anorg. Allg. Chem. 567* (1988) 23.

[10] M. P. Arthur, A. Baceiredo, G. Bertrand, *J. Am. Chem. Soc.* **113** (1991) 5856.

[11] Two other examples of diazoalkylboranes characterized only by IR in solution have been reported: a) A. Tapper, T. Schmitz, P. Paetzold, *Chem. Ber. 122* (1989) 595; b) U. Schöllkopf, B. Banhidai, H. Frasnelli, R. Meyer, H. Beckhaus, *Justus Liebigs Ann. Chem. 1974*, 1767.

Structure of an Organometallic Intercalate: Single Crystal X-Ray and Powder Neutron Diffraction Study of $[SnS_2\{Co(\eta\text{-}C_5H_5)_2\}_{0.31}]$ and $[SnS_2\{Co(\eta\text{-}C_5D_5)_2\}_{0.31}]$**

By *Dermot O'Hare,* John S. O. Evans, Philip J. Wiseman* and *Keith Prout*

Since the intercalation of an organometallic species into a layered host lattice was first reported by *Dines*[1] in 1975, there has been considerable interest in the intercalation of organometallic guests, e.g. $[Co(\eta\text{-}C_5H_5)_2]$, $[Cr(\eta\text{-}C_5H_5)_2]$, $[Zr(\eta\text{-}C_7H_7)(\eta\text{-}C_5H_5)]$, into layered host lattices, such as MS_2 (M = Nb, Ta, Ti, Mo), MPS_3 (M = Cd, Mn, Fe, Ni) and FeOCl.[2] In particular, the intercalation of electron-rich organometallic guests has been shown to greatly enhance the conductivity of the host lattice through guest-host electron transfer, and in the case of intercalation of $[Cr(\eta\text{-}C_5H_5)_2]$ or $[Co(\eta\text{-}C_5H_5)_2]$ into TaS_2 the superconducting critical temperature (T_c) of the host material was significantly increased.[3] We have also recently reported that the intercalation of $[Co(\eta\text{-}C_5H_5)_2]$ into $SnSe_2$ converts the host lattice, a semiconductor with a relatively large band gap, into a type II superconductor with $T_c = 6.1$ K.[4]

Whilst there has been a considerable amount of research into the physical properties of metallocene intercalates, the inherent disorder of these materials, problems due to extreme preferred-orientation effects, and the difficulty of synthesizing crystals of a suitable quality for conventional diffraction methods have severely limited work on structural determination. Fundamental questions such as the orientation of the guest molecule remain unanswered, as due to the almost spherical van der Waals surface of the unsubstituted metallocenes, little can be deduced from lattice expansion measurements alone (Fig. 1).

[*] Dr. D. O'Hare, J. S. O. Evans, Dr. P. J. Wiseman
Inorganic Chemistry Laboratory,
South Parks Road, GB-Oxford, OX1 3QR (UK)
Dr. C. K. Prout
Chemical Crystallography Laboratory,
9 Parks Road, GB-Oxford, OX1 3PD (UK)

[**] This work was supported by the Science and Engineering Research Council. We thank Dr. *J. Meyers* (Rutherford Laboratory) for assistance in recording the neutron diffraction experiments.

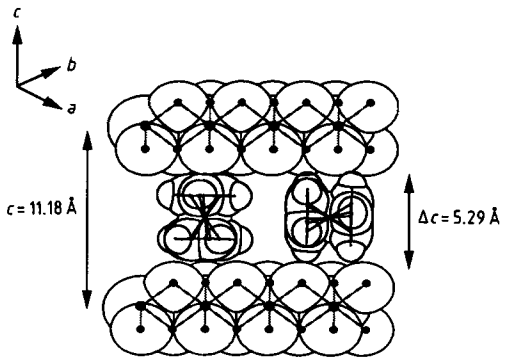

Fig. 1. Intercalated metallocene molecules could adopt two extreme orientations, with their principle axis either perpendicular or parallel to the host lattice planes.

Recently, variable-temperature solid-state ^2H NMR investigations on microcrystalline samples of $[TaS_2\{Co(\eta\text{-}C_5H_5)_2\}_{0.33}]$ have indicated that the guest molecules may be dynamically exchanging between a range of extreme orientations.[5] In this communication we describe the first three-dimensional structure determination of an organometallic intercalate, namely $[SnS_2\{Co(\eta\text{-}C_5H_5)_2\}_{0.31}]$, using single-crystal X-ray film techniques and neutron diffraction studies of both powdered and aligned samples.

Single crystals of phosphorus-doped (1%) 2H-SnS_2 were grown by vapor-phase transport methods using bromine as a transporting agent (5 mg per cm^3).[6] We found that relatively large single crystals of SnS_2 (typically 2 mm × 2 mm × 0.1 mm) could be intercalated with $[Co(\eta\text{-}C_5H_5)_2]$ in 4–5 days by heating the crystals to 60 °C in a concentrated solution of $[Co(\eta\text{-}C_5H_5)_2]$ in dimethoxyethane. The elemental composition was found by microanalysis to be $[SnS_2\{Co(\eta\text{-}C_5H_5)_2\}_{0.31}]$.[1]

Preliminary X-ray photographs of single crystals of this compound indicated that the diffraction patterns obtained were not of a suitable quality to use conventional 4-circle automated diffractometers. For this reason we employed more traditional Weissenberg film methods to record the diffraction pattern. By mounting the crystal along its *a* axis it was possible to record *hkl* reflections for $h = 0$, 1 and 2. A total of 21 photographs of different exposure times were taken to obtain a reasonable intensity range, and the relative intensities of the diffraction peaks were then estimated using the intensity strip method.[7] It proved possible to index and obtain the relative intensities of a total of 177 reflections.

From the photographs obtained it is clear that these materials retain a remarkable degree of order on intercalation. The diffraction "spots" remain sharp in θ, but are up to 30° wide in ω. This suggests that the structural integrity of the host remains essentially intact during intercalation. The fact that the diffraction spots are sharp in θ indicates that the layer sequence, ABABAB, where A and B represent individual SnS_2 layers, is well preserved on intercalation. If the layers were to stack randomly, the diffraction peaks would be diffuse in θ as well as ω. The diffuseness of the spots in the ω direction indicates that the layers show some rotational disorder about the *c* axis. That the lines remain sharp in θ indicates that this diffuseness is more due to increased mosaic spread than to the rotation of individual layers. We therefore conclude that the crystal is made up of relatively well-ordered slabs, which are ca. 200 Å thick and prone to periodic stacking faults along the *c* axis. The total "smeared" pattern is then made up of many sharp patterns, due to the individual mosaics, superposed with different ω translations.

From the systematic absences observed on the films (00*l*, $l = 2n + 1$) it was apparent that as well as the documented increase of the interlamellar distance from 5.89 to 11.18 Å ($\Delta c = 5.29$ Å) on intercalation, there is also a doubling along the *c* axis. The unit cell parameters, measured from Weissenberg and oscillation photographs, are $3.62 \times 3.62 \times 22.36$ Å. The inherent accuracy of the intensity measurements, due to factors such as reflection overlap and absorption, was $00l > 0kl > hkl$; therefore the analysis of the X-ray data was performed in three stages. Initially the estimated intensities of the ten observed 00*l* reflections from the zero-level Weissenberg were used to perform a one-dimensional Fourier synthesis phased on approximate tin and sulfur positions. Least-squares refinement was then used to optimize the sulfur *z* coordinate.

Inclusion of all the intensity information derived from the zero-level photograph enabled two-dimensional Patterson and Fourier maps to be computed. From this tin, sulfur, and cobalt positions could be clearly resolved. We also observed a doubling along the *c* axis caused by a relative shift of adjacent tin disulfide layers along the crystallographic *b* axis.

When we included intensity information from all three Weissenberg photographs, we concluded that consecutive tin disulfide layers are shifted in both the *a* and *b* directions relative to pure SnS_2. This shift necessarily leads to the destruction of the threefold symmetry of the host lattice, and the loss of crystallographic symmetry was confirmed by a series of Laue and Precession photographs.

When the heavy atoms were located satisfactorily, we attempted to determine the relative orientation of the guest molecules between the layers. Initially using the one-dimensional data we compared the observed and calculated electron densities for both the parallel and perpendicular arrangements of the cyclopentadienyl rings relative to the SnS_2 layers (see Fig. 1). The scattering of X-rays from a cyclopentadienyl ring undergoing rapid rotation around the metallocene C_5 axis was described using an appropriate Bessel function. Agreement factors for the two extreme orientations of $R_{I(\text{parallel})} = 0.137$ and $R_{I(\text{perpendicular})} = 0.347$ indicated that the parallel model gives much better agreement with the experimental data. Refinement of a model in which the occupancy of the two extreme orientations is allowed to vary converged to a parallel occupancy of 0.33(5) cobaltocenes per half unit cell and perpendicular of −0.02(5); this agrees

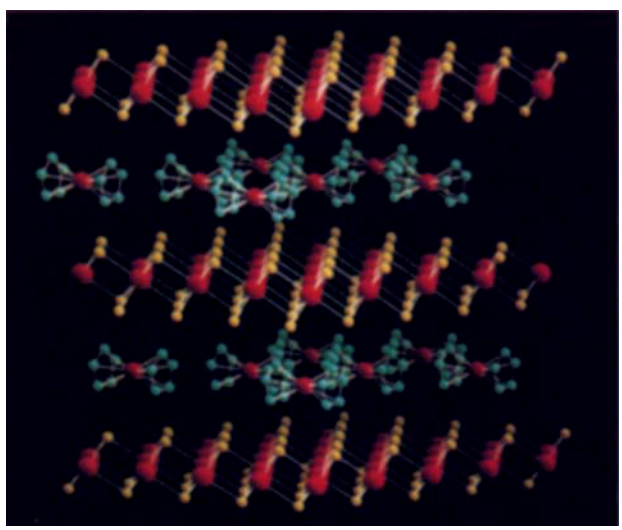

Fig. 2. A view of the three dimensional structure of $[SnS_2\{Co(\eta\text{-}C_5H_5)_2\}_{0.31}]$.

 © VCH Verlagsgesellschaft mbH, W-6940 Weinheim, 1991 0570-0833/91/0909-1157 $ 3.50+.25/0

well with the experimentally observed occupancy of 0.31 molecules per SnS_2.

The parallel orientation of the $[Co(\eta\text{-}C_5H_5)_2]$ was confirmed by analysis of the time-of-flight neutron diffraction pattern of an aligned sample of single crystals of $[SnS_2\{Co(\eta\text{-}C_5D_5)_2\}_{0.31}]$, recorded at the Rutherford Appleton Laboratory. Using the neutron data we calculated an agreement factor for the parallel orientations of $R_{I(\text{parallel})} = 0.106$. The occupancies of an initial model containing both extreme orientations refined to a parallel occupancy of 0.302(5) and a perpendicular of 0.008(5). Attempts to refine a model containing solely the perpendicular orientation failed to produce good agreement with the observed data.

Figure 2 shows the final structure based on refinement of both the X-ray and neutron data. Since both sets of data were collected at room temperature, the carbon atoms of the cyclopentadienyl ring have large thermal parameters to account for the undoubtedly large degree of cyclopentadienyl ring disorder in the *a,b* plane. However, we can conclude from our data that the metallocene molecules all adopt the parallel orientation. We also have preliminary evidence that the guests are ordered in the *a,b* plane of SnS_2 layers which have commensurate interlayer spacing.

Received: March 13, 1991 [Z 4495 IE]
German version: *Angew. Chem. 103* (1991) 1175

[1] M. B. Dines, *Science 188* (1975) 1210.
[2] R. P. Clement, W. B. Davies, K. A. Ford, M. L. H., Green, A. J. Jacobson, *Inorg. Chem. 17* (1978) 2754.
[3] F. R. Gamble, A. H. Thompson, *Solid State Commun. 27* (1978) 379.
[4] C. A. Formstone, E. F. Fitzgerald, D. O'Hare, P. A. Cox, M. Kurmoo, J. W. Hodby, D. Lillicrap, M. Goss-Custard, *J. Chem. Soc. Chem. Commun. 1990*, 501.
[5] S. J. Heyes, N. J. Clayden, C. M. Dobson, M. L. H. Green, P. J. Wiseman, *J. Chem. Soc. Chem. Comm. 1987*, 1560.
[6] F. A. S. Al-Alamy, A. A. Balchin, *J. Cryst. Growth 28* (1977) 221–232.
[7] N. F. M. Henry, H. Lipson, W. A. Wooster: *The Interpretation of X-ray Diffraction Photographs, 2nd ed.*, Macmillan, London 1960.
[8] E. K. Davies, *CHEM-X Users Manual*, Chemical Crystallography Laboratory, Oxford 1975.

Pressure-Assisted Formation of a Cobalt–Carbon σ Bond: A High-Pressure Pulse Radiolysis Study**

By *Rudi van Eldik, Haim Cohen,* and *Dan Meyerstein**

The study of the kinetics of formation of transient complexes with metal–carbon σ bonds through the reaction of aliphatic free radicals with transition metal complexes, and of the homolysis of the metal–carbon σ bond, is of interest due to the role of these processes in a variety of catalytic and biological processes.[1, 2] Of particular significance is the study of the reaction mechanisms of the formation and decomposition of complexes with cobalt–carbon bonds due to the biological role of the homolysis of cobalt–carbon bonds in vitamin B_{12} catalyzed reactions.[1a–c, e, 3] It is therefore not surprising that the kinetics of the reaction of a variety of free radicals with several cobalt complexes [k_1 in Eq. (1)] has been studied.[4–6] The detailed mechanisms of these reactions, that is, whether interchange or dissociative, have not been resolved.[7] The kinetics of the homolysis of cobalt–carbon σ bonds [k_{-1} in (1)] was also studied in a series of investigations,[1e, 2, 3a, 6, 8, 9] partly in order to determine the

$$[L_mCo^{II}] + {}^{\bullet}R \underset{k_{-1}}{\overset{k_1}{\rightleftharpoons}} [L_mCo^{III}\text{-}\langle c^- \rangle R^-] \quad (1)$$

cobalt–carbon bond dissociation energy. It was suggested that this energy equals $\Delta H^{\neq}$ (k_{-1}) as the bond formation step in reaction (1) approaches the diffusion controlled limit, i.e. has a small activation barrier.[1e, 2, 3a, 9] However, it should be noted that this assignment will depend on the intimate nature of the bond breakage process.

The application of high-pressure kinetic techniques to the study of inorganic, organometallic, and bioinorganic reactions has greatly assisted the elucidation of the underlying mechanisms in recent years.[10] Furthermore, pulse radiolysis techniques enable the study of metal–carbon bond formation in a direct way.[4–6] We have therefore combined both techniques and performed pulse radiolysis studies at high pressure (up to 150 MPa)[11] in order to study the interaction of methyl radicals with $[Co^{II}(nta)(H_2O)_2]^-$ (nta = nitrilotriacetate) during which $[Co^{III}(nta)(H_2O)(CH_3)]^-$ is produced. The results reported here enable us to comment on the mechanism of the cobalt–carbon bond-formation and homolysis reactions and clearly demonstrate that pressure assists the formation of this bond.

Irradiation of a N_2O saturated (0.011 M) solution containing $(1-5)\times10^{-3}$ M $CoSO_4$, 6×10^{-3} M nta, 0.1 M DMSO, and 1.2×10^{-4} M O_2 at pH 6.5, results in the following sequence of reactions:[6, 13]

$$e_{aq}^- + N_2O \xrightarrow{H^+} {}^{\bullet}OH + N_2 \quad k_2 = 8.7\times10^9\ M^{-1}s^{-1}\ [14] \quad (2)$$

$${}^{\bullet}OH + (CH_3)_2SO \longrightarrow (CH_3)_2\dot{S}OOH \quad k_3 = 7.0\times10^9\ M^{-1}s^{-1}\ [15] \quad (3)$$

$$(CH_3)_2\dot{S}OOH \longrightarrow {}^{\bullet}CH_3 + CH_3SOOH \quad k_4 = 1.5\times10^7\ s^{-1}\ [15] \quad (4)$$

$$[Co^{II}(nta)(H_2O)_2]^- + {}^{\bullet}CH_3 \rightleftharpoons [Co^{III}(nta)(H_2O)(CH_3)]^- + H_2O \quad (5)$$
$$k_5 = 1.6\times10^8\ M^{-1}s^{-1}\ [6]$$
$$K_5 = k_5/k_{-5} = 2.7\times10^6\ M^{-1}\ [6]$$

$$[Co^{III}(nta)(H_2O)(CH_3)]^- + {}^{\bullet}CH_3 \xrightarrow{H_2O} [Co^{II}(nta)(H_2O)_2]^- + C_2H_6 \quad (6)$$
$$2k_6 = 7.5\times10^7\ M^{-1}s^{-1}\ [6]$$

$${}^{\bullet}CH_3 + O_2 \longrightarrow {}^{\bullet}O_2CH_3 \quad k_7 = 4.7\times10^9\ M^{-1}s^{-1}\ [6] \quad (7)$$

$${}^{\bullet}O_2CH_3 + [Co^{II}(nta)(H_2O)_2]^- \longrightarrow [Co^{III}(nta)(H_2O)(O_2CH_3)]^- + H_2O$$
$$k_8 = 1.0\times10^8\ M^{-1}s^{-1}\ [6] \quad (8)$$

The kinetics of formation of $[Co^{III}(nta)(H_2O)(O_2CH_3)]^-$ under the selected experimental conditions obey the rate law in (9),[6, 13] from which it follows that K_5 and k_{-5} can be

[*] Prof. Dr. R. van Eldik
Institut für Anorganische Chemie
Universität Witten/Herdecke
Stockumer Strasse 10, W-5810 Witten (FRG)
Prof. Dr. D. Meyerstein
R. Bloch Coal Research Center and Chemistry Department
Ben Gurion University of the Negev
Beer-Sheva (Israel)
Prof. Dr. H. Cohen
Nuclear Research Center Negev
and
R. Bloch Coal Research Center and Chemistry Department
Ben Gurion University of the Negev
Beer Sheva (Israel)

[**] This work was supported by the German–Israeli Foundation for Scientific Research and Development, the Israeli Academy of Sciences, the Planning and Granting Committee of the Council for Higher Education, the Israel Atomic Energy Commission, the Deutsche Forschungsgemeinschaft, Fonds der Chemischen Industrie, and Volkswagen-Stiftung. We thank *D. Carmi, Y. Nahon,* and *Y. Nehemia* for technical assistance.

calculated from a plot of k_{obs}^{-1} versus the concentration of Co^{II} at constant O_2 concentration as indicated in (10). Thus

$$-\frac{dc([Co^{III}(nta)(H_2O)(CH_3)]^-)}{dt} = \frac{k_7 k_{-5}\, c(O_2) c([Co^{III}(nta)(H_2O)(CH_3)]^-)}{k_5 c([Co^{II}(nta)(H_2O)_2]^-) + k_7 c(O_2)} \quad (9)$$

$$k_{obs}^{-1} = \frac{K_5 c([Co^{II}(nta)(H_2O)_2]^-)}{k_7 c(O_2)} + k_{-5}^{-1} \quad (10)$$

by repeating such experiments as a function of pressure, it is in principle possible to measure the pressure dependence of K_5 and k_{-5},[16] from which the reaction volume for equilibrium (5) and the activation volume for both the formation and homolysis of the Co^{III}–CH_3^--bond, can be calculated.

The experimental data in Figure 1 depict the relationship suggested by Equation (10). The pressure dependence

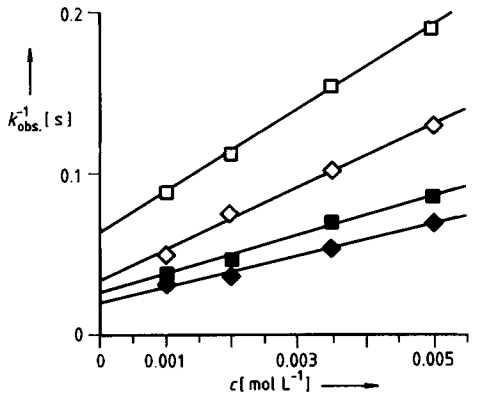

Fig. 1. Plots of k_{obs}^{-1} vs. concentration c of $[Co(nta)(H_2O)_2]^-$ at different pressures: □ p = 150 MPa, ◇ p = 100 MPa, ■ p = 50 MPa, ● p = 0.1 MPa.

of K_5 and k_{-5} is presented in Figure 2, from which it follows that $\Delta\bar{V}(K_5) = -16.4 \pm 1.6\ cm^3\,mol^{-1}$ and $\Delta V^{\neq}(k_{-5}) = +18.6 \pm 2.0\ cm^3\,mol^{-1}$. A combination of these values results in $\Delta V^{\neq}(k_5) = +2 \pm 4\ cm^3\,mol^{-1}$. In order to corroborate the latter value, the pressure dependence of k_5 was measured directly by observing the rate of formation of $[Co^{III}(nta)(H_2O)(CH_3)]^-$ at 264 nm.[17] The observed rate data are $(1.9 \pm 0.1) \times 10^8$ and $(1.3 \pm 0.1) \times 10^8\ M^{-1}s^{-1}$ at 0.1 and 150 MPa, respectively, which result in a $\Delta V^{\neq}(k_5)$ value of $+6.0 \pm 2.5\ cm^3\,mol^{-1}$. The latter value is in good agreement with that calculated in an indirect way (see above).

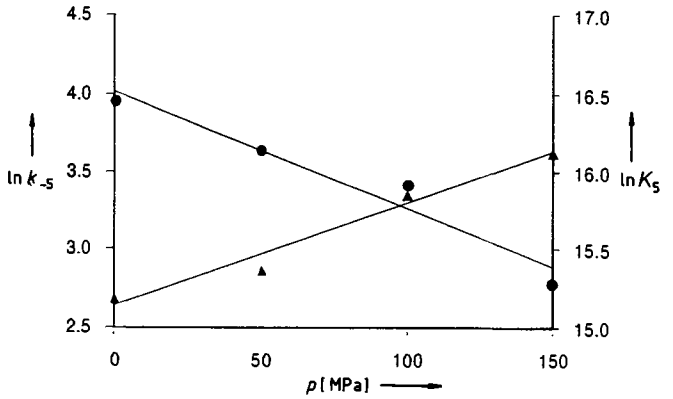

Fig. 2. Pressure dependence of ln k_{-5} (●) and ln K_5 (△).

The effect of pressure on reaction (8) was measured in a similar way,[18] and the results are $k_8 = (1.00 \pm 0.12) \times 10^8$, $(0.96 \pm 0.06) \times 10^8$, $(0.80 \pm 0.10) \times 10^8$, and $(0.68 \pm 0.06) \times 10^8\ M^{-1}s^{-1}$ at 0.5, 50, 100, and 150 MPa, respectively. From these data it follows that $\Delta V^{\neq}(k_8) = +6.0 \pm 1.0\ cm^3\,mol^{-1}$, which is very close to that reported above for k_5.

As reflected by the significantly negative value of $\Delta\bar{V}(K_5)$ (see Equation 5), pressure strongly assists the formation of the cobalt–carbon bond. This value indicates that the product state is considerably more compressed than the reactant state, from which we conclude that the hydrophobic methyl radical has a considerably larger solvation sphere than the water molecule that is released during the bond-formation process. In addition, cobalt–carbon bond formation can be considered an oxidative addition reaction since Co^{II} is oxidized to Co^{III}, which will also result in a significant decrease in volume. The measured activation volumes for k_5, k_{-5} and k_8 are all in line with a dissociative reaction mode. The largest effect ($+18.6 \pm 2.0\ cm^3\,mol^{-1}$) was observed for k_{-5}, which is in good agreement with data reported in the literature for homolysis reactions of the metal–carbon bond.[12a, 19, 20] The observed effect can partly be ascribed to the desolvation of the aliphatic free radicals formed in this process.[9, 20] The observed volumes of activation for k_5 and k_8 are very similar to those generally reported for solvent-exchange and complex-formation reactions of aquated Co^{II} ions[9, 21] and are characterisitc for a dissociative interchange (I_d) mechanism. This conclusion is further underlined by the insensitivity of $\Delta V^{\neq}$ to the nature of the binding radical. From these results we conclude that metal–carbon bond formation is very similar to a ligand-exchange process in terms of volume changes, and follows an I_d mechanism in the case of cobalt(II). Homolysis of the cobalt–carbon bond is presumably accompanied by an additional contribution arising from the breakup of the solvent cage. It is questionable whether this reaction can be considered a limiting dissociative mechanism whose activation enthalpy corresponds to the bond dissociation energy, as suggested previously.[1e, 2, 3a, 9]

We conclude that through a unique combination of pulse radiolysis and high-pressure techniques it was possible to gain insight into the mechanism of metal–carbon bond formation and homolysis. In addition, it is clear that the formation of the cobalt–carbon bond is assisted by pressure since the homolysis reaction exhibits a much larger activation volume than the bond-formation reaction, resulting in a significantly negative overall reaction volume.

Received: January 29, 1991
Revised: June 3, 1991 [Z 4411 IE]
German version: *Angew. Chem. 103* (1991) 1177

CAS Registry numbers:
$[Co^{II}(nta)(H_2O)_2]^-$, 34523-69-8; $[Co^{III}(nta)(H_2O)(CH_3)]^-$, 116053-28-2; $^{\bullet}CH_3$, 2229-07-4.

[1] a) J. K. Kochi in J. K. Kochi (Ed.): *Free Radicals, Vol. 1*, Wiley, New York 1973, Chapter II.; b) J. K. Kochi: *Organometallic Mechanisms and Catalysis*, Academic, New York 1978; c) R. A. Sheldon, J. K. Kochi: *Metal Catalysed Oxidations of Organic Compounds*, Academic, New York 1981; d) J. Halpern, *Acc. Chem. Res. 15* (1982) 238; e) J. Halpern: *Pure Appl. Chem. 51* (1979) 2171; f) M. D. Johnson, *Acc. Chem. Res. 16* (1983) 343; g) R. Scheffold, *Chimia 39* (1985) 203.
[2] J. Halpern, *Pure Appl. Chem. 55* (1983) 1059.
[3] a) R. G. Finke, D. A. Schiraldi, B. Mayer, *Coord. Chem. Rev. 54* (1984) 1; b) N. Bresciani-Pahor, M. Foriolin, L. G. Marzilli, L. Randaccio, M. F. Summers, P. Toscano, *ibid. 63* (1985) 1.
[4] a) G. M. Schrauzer, M. Hashimoto, A. Maihub, *Z. Naturforsch. B35* (1980) 588; b) J. Halpern, H. U. Blaser, *J. Am. Chem. Soc. 102* (1980) 1684; c) V. E. Stel'mashok, A. L. Poznyak, *Russ. J. Inorg. Chem. 26* (1981) 1324; d) G. Ferraudi, L. K. Patterson, *J. Chem. Soc. Dalton Trans. 1980*, 476.

[5] a) W. A. Mulac, D. Meyerstein, *J. Am. Chem. Soc. 104* (1982) 4124; b) Y. Sorek, H. Cohen, W. A. Mulac, K. H. Schmidt, D. Meyerstein, *Inorg. Chem. 22* (1983) 3040; c) Y. Sorek, H. Cohen, D. Meyerstein, *J. Chem. Soc. Faraday Trans. I 85* (1989) 1169.
[6] a) D. Meyerstein, H. A. Schwarz, *J. Chem. Soc. Faraday Trans. I 84* (1988) 2933; b) A. Sauer, H. Cohen, D. Meyerstein, *Inorg. Chem. 28* (1989) 2155.
[7] A. Bakac, J. H. Espenson, *Inorg. Chem. 28* (1989) 4319.
[8] a) F. T. T. Ng, G. L. Rempel, J. Halpern, *J. Am. Chem. Soc. 104* (1982) 621; b) J. Halpern, S. H. Kim, T. W. Leung, *ibid. 106* (1984) 8317; c) M. K. Geno, J. Halpern, *ibid. 109* (1987) 1238; d) H. B. Gjerde, J. H. Espenson, *Organometallics 1* (1982) 435.
[9] a) R. G. Finke, B. L. Smith, B. J. Mayer, A. A. Molinero, *Inorg. Chem. 22* (1983) 3679; b) R. G. Finke, B. P. Hay, *ibid. 23* (1984) 3043; c) B. P. Hay, R. G. Finke, *J. Am. Chem. Soc. 108* (1986) 4820; d) B. P. Hay, R. G. Finke, *ibid. 109* (1987) 8012.
[10] a) R. van Eldik (Ed.): *Inorganic High Pressure Chemistry: Kinetics and Mechanisms*, Elsevier, Amsterdam 1986; b) R. van Eldik, T. Asano, W. J. le Noble, *Chem. Rev. 89* (1989) 549; c) R. vanl Eldik, A. E. Merbach, *Acc. Chem. Res.*, submitted.
[11] Details of the experimental setup are given elsewhere [10, 12]. A further modification of the high-pressure cell was undertaken. The sapphire window through which the radiation entered the cell was replaced with a 10 mm thick steel window into which a hole (9 mm deep, 8 mm diameter) was drilled. In this way sufficient radiation for accurate experiments could penetrate the cell. A Xe–Hg arc lamp was used to follow the reaction at 313 nm. the high light intensity of this lamp helped to increase the signal-to-noise ratio of the kinetic traces. All experiments were performed at 17 °C.
[12] a) R. van Eldik, H. Cohen, A. Meshulam, D. Meyerstein, *Inorg. Chem. 29* (1990) 4156; b) H. Cohen, R. van Eldik, M. Masarwa, D. Meyerstein, *Inorg. Chim. Acta 177* (1990) 31.
[13] A. Sauer, H. Cohen, D. Meyerstein, *Inorg. Chem. 27* (1988) 4578.
[14] G. V. Buxton, C. L. Greenstock, W. P. Helman, A. B. Ross, *J. Phys. Chem. Ref. Data 17* (1988) 513.
[15] D. Veitwisch, E. Janata, K. D. Asmus, *J. Chem. Soc. Perkin Trans. 2 1980*, 146.
[16] According to equation (10) the slope of the plot of k_{obs}^{-1} versus c (Co^{II}) equals $K_5/k_7\, c\,(O_2)$; thus the pressure dependence of the slope arises from the pressure dependence of K_5 and k_7. Fortunately, reaction (7) is diffusion-controlled and k_7 will therefore vary with pressure in the same way as the viscosity of the solvent. Over the investigated pressure range the variation in the viscosity of water is negligible and the pressure dependence of the slope must reflect the pressure dependence of K_5.
[17] This wavelength is near the absorption maximum of the product [6a] and is a line of the Xe–Hg arc lamp used to study the reaction. The light intensity at this wavelength is considerably lower than at 313 nm, and the error limit is therefore larger.
[18] For this purpose N_2O saturated solutions containing 2×10^{-4} M $CoSO_4$, 4×10^{-4} M nta, 0.1 M DMSO and 1.2×10^{-4} M O_2 at pH 6.5 were irradiated. Under these conditions k_8 can be measured directly.
[19] M. J. Sisley, W. Rindermann, R. van Eldik, T. W. Swaddle, *J. Am. Chem. Soc. 106* (1984) 7432.
[20] K. Ishihara, T. W. Swaddle, *Can. J. Chem. 64* (1986) 2168.
[21] R. Mohr, R. van Eldik, *Inorg. Chem. 64* (1986) 2168.

Solvation Effects on Geometry and Chemical Shifts. An Ab Initio/IGLO Reconciliation of Apparent Experimental Inconsistencies on $H_3B\cdot NH_3$ **

By *Michael Bühl, Thomas Steinke, Paul von Ragué Schleyer,** and *Roland Boese*

Redetermination of the X-ray structure of the parent borane-ammonia complex $H_3B\cdot NH_3$ **1**[1] confirms the B–N separation of 1.564 Å,[2] which is surprisingly short for such a dative complex.[3] In contrast, the B–N distance determined in the gas phase by microwave spectroscopy (r_0 = 1.672 Å)[4] is more than 0.1 Å longer. The MW value is reproduced quite accurately by ab initio calculations at various levels[5] (cf. our MP2(Full)/6-31G* data,[6] Fig. 1). While some longer B–N separations in the 1.64–1.67 Å range are found in the crystal structure (and by ab initio calculations) of substituted borane-amine complexes,[7] a recent review recommended 1.58 Å as the reference value.[8] However, the potential energy surface of **1** is quite flat. When the X-ray B–N distance is employed (and the other parameters fully optimized), the energy is only ca. 1.5 kcal/mol higher (Fig. 1).

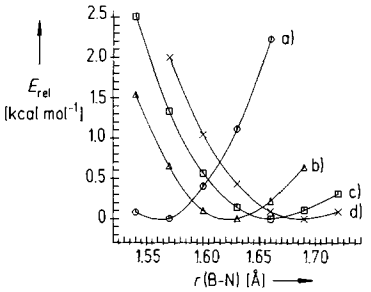

Fig. 1. Relative energy E_{rel} of $H_3B\cdot NH_3$ as a function of the B–N distance r computed with the 6-31G* basis set and various procedures: for the isolated molecule at the SCF (d) and MP2 levels (c), all other parameters optimized; with the SCRF continuum method in the solvents hexane (b) and water (a), single point calculations on the MP2 geometries. Note the pronounced bond-shortening in the polar solvent, water.

There is also a discrepancy between the experimentally determined chemical shift $\delta(^{11}B)$ for **1**, measured in water solution,[9] and the value calculated (IGLO[10]) for the isolated molecule. As shown in Figure 2, the correlation between measured and IGLO $\delta(^{11}B)$ chemical shifts for a large series of borane complexes is generally quite satisfactory (correlation coefficient 0.991, standard deviation δ = 2.0). The ^{11}B IGLO chemical shift for **1**, calculated using the

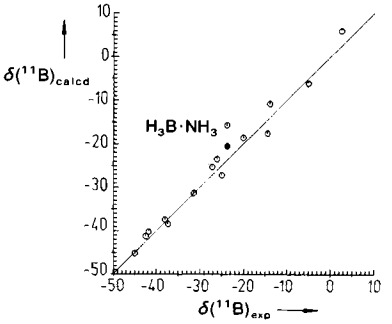

Fig. 2. Plot of the calculated (IGLO) vs. experimentally determined chemical shifts $\delta(^{11}B)$ of borane-adducts H_3B-L (L = CO, PH_3, $CN^{\ominus}$, PMe_3, $PH_2^{\ominus}$, $CH_3^{\ominus}$, $NC^{\ominus}$, $NCS^{\ominus}$, NH_3, $SH^{\ominus}$, SMe_2, $N_3^{\ominus}$, $OH^{\ominus}$, NMe_3, OMe_2 [11]). The theoretical values were computed employing a TZP basis (denoted II') and MP2/6-31G* fully optimized geometries. Without **1**, the standard deviation is δ = 2.0 (correlation coefficient 0.991). The ideal slope = 1 is shown. Blackened point: $H_3B\cdot NH_3$ **1** employing a B–N distance of 1.57 Å according to the SCRF calculations (see Fig. 1).

[*] Prof. Dr. P. v. R. Schleyer, Dipl.-Chem. M. Bühl, Dr. T. Steinke
Institut für Organische Chemie der Universität Erlangen-Nürnberg
Henkestrasse 42, W-8520 Erlangen (FRG)
Prof. Dr. R. Boese
Institut für Anorganische Chemie
der Universität-Gesamthochschule Essen
Universitätsstrasse 57, W-4300 Essen 1 (FRG)

[**] This work was supported by the Deutsche Forschungsgemeinschaft, the Fonds der Chemischen Industrie, the Stiftung Volkswagenwerk, and Convex Computer Corporation. *M. B.* acknowledges a grant from the Studienstiftung des deutschen Volkes.

MP2(Full)/6-31G* B–N distance of 1.66 Å, deviates from the experimental value in water by $\Delta\delta = 8.1$ (Fig. 1, Table 1). However, if the X-ray separation, 1.57 Å, is used instead, the IGLO error is only 3.3. The experimental $\delta(^{11}B)$ value can be matched if a B–N distance of ca. 1.50 Å is assumed.

Table 1. Dependence of the calculated (IGLO) chemical shift $\delta(^{11}B)$ of $H_3B \cdot NH_3$ **1** on the B–N distance; in italics: experimentally determined values.

r (B–N) [Å]	μ [D] [a]	$\delta(^{11}B)$ [b]
1.66 [c]	5.67	– 15.7
1.63	5.73	– 17.5
1.60	5.79	– 19.1
1.57	5.84	– 20.5
1.54	5.90	– 21.8
1.51	5.93	– 23.0
Experiment	*5.22* [d]	*– 23.8* [e]

[a] Dipole moment, calculated at the HF/6-31G*//MP2/6-31G* level; note that the high dipole moment does not change to a great extent with the B–N distance. [b] IGLO basis II': B,N 9s5p1d {51111,2111,1}, H 3s {21} (cf. Ref. [10c]); the geometric parameters (except the B–N distance) were optimized at the MP2/6-31G* level. [c] Fully optimized. [d] Gas phase (Ref. [3]). [e] Ref. [6].

These data suggest that the geometry of **1** (and to a lesser extent of other borane-amine complexes) may depend on the environment. We investigated this possibility for **1** by means of self-consistent reaction field (SCRF) calculations,[12, 13] a modern adaption to the ab initio framework of the Onsager-Kirkwood-Westheimer ellipsoidal cavity model for medium effects.[14] As implemented by *Tomasi* and his group,[12] SCRF provides a means for modeling continuum effects. Simulations can be carried out with parameters for various solvents; those for hexane and for water were employed here.[13] (It should be noted that hydrogen bonding effects for water are not included specifically in this treatment.[15]) The results, summarized in Figure 1, are quite significant. Reoptimization of the B–N distance of **1** in the SCRF field simulated for hexane (6-31G* basis set) results in a reduction of the B–N bond length to 1.62 Å; for water the reduction is even more dramatic (1.57 Å, Fig. 1). As the B–N distance decreases with increasing solvent polarity, we suggest that the dipolar field in the crystal (like the dielectric reaction field of water) may be responsible for the B–N bond shortening. This conclusion is supported by additional findings. In the weaker dipolar crystal fields of more voluminous complexes, the B–N distance is substantially longer, e.g. 1.60 Å in the $H_3B \cdot NH_3 \cdot$ 18-crown-6 complex.[16] Longer B–N separations are also found in complexes of substituted boranes and/or substituted amines in the solid state, e.g. 1.656, 1.648 and 1.616 Å for $Me_3B \cdot NHMe_2$, $Me_3B \cdot NH_3$ and $H_3B \cdot NMe_3$, respectively.[7] For the latter, the B–N bond shortening with respect to the gas phase ($r_0 = 1.637$ Å,[17] MP2/6-31G* value 1.645 Å[18]) is less pronounced than for **1**.

Several important inferences follow. Medium effects on NMR chemical shifts, which occasionally are observed, may be indirect. Solvent molecules are too remote to influence nuclear shielding directly.[15, 18] Instead, solvation may change the geometry (and the electronic structure), and this influences the chemical shifts. Particularly for systems with flat potential energy surfaces, even highly accurate X-ray structures may provide misleading information concerning geometrical parameters, if these are considered to be characterized by the equilibrium values in isolated, unperturbed systems.

Received: March 19, 1991 [Z 4515 IE]
German version: *Angew. Chem. 103* (1991) 1179

CAS Registry numbers:
$H_3B \cdot NH_3$, 13774-81-7; B, 7440-42-8; N_2, 7727-37-9.

[1] Structure determination of **1** at 200 K (further cooling reduced the crystal quality dramatically): Cell dimensions: $a = 5.421(5)$, $b = 4.945(4)$, $c = 5.023(6)$ Å, orthorhombic, space group $Pmn2_1$, $Z = 2$, 705 intensities measured, $2\theta_{max} = 45°$, 198 unique and 191 observed ($F_0 \geq 4\sigma(F)$), 24 parameters, angular constraints on hydrogen positions with common isotropic ADP's and anisotropic ADP's for boron and nitrogen, $R = 0.0926$, $R_w = 0.0939$, maximum residual electron intensity 0.63 eÅ^{-3}. Refinements with higher weights given to reflections with higher 2θ angles resulted in no significant changes. B–N distance: 1.564(6) Å.
[2] Earlier determinations: a) S. G. Shore, R. W. Parry, *J. Am. Chem. Soc. 77* (1955) 6084; b) E. W. Hudges, *ibid. 78* (1956) 502; c) E. L. Lippert, W. N. Lipscomb, *ibid. 80* (1958) 503.
[3] A. Haaland, *Angew. Chem. 101* (1989) 1017; *Angew. Chem. Int. Ed. Engl. 28* (1989) 992.
[4] L. R. Thorne, R. D. Suenron, F. J. Lovas, *J. Chem. Phys. 78* (1983) 167.
[5] For example a) J. D. Dill, P. v. R. Schleyer, J. A. Pople, *J. Am. Chem. Soc. 97* (1975) 3402; b) J. S. Binkley, L. R. Thorne, *J. Chem. Phys. 79* (1983) 2932; c) P. Brint, B. Sangchakr, P. W. Fowler, *J. Chem. Soc. Farad. Trans. II 85* (1989) 29, and references cited therein.
[6] Standard procedures and basis sets were employed, cf. W. J. Hehre, L. Radom, P. v. R. Schleyer, J. A. Pople: *Ab Initio Molecular Orbital Theory*, Wiley, New York 1986.
[7] R. Boese, unpublished results.
[8] P. Paetzold, *Adv. Inorg. Chem. Radiochem. 31* (1987) 123.
[9] D. F. Gaines, R. Schaefer, *J. Am. Chem. Soc. 86* (1964) 1505.
[10] a) W. Kutzelnigg, *Isr. J. Chem. 19* (1980) 193; M. Schindler, W. Kutzelnigg, *J. Chem. Phys. 76* (1982) 1919; for a review see c) W. Kutzelnigg, U. Fleischer, M. Schindler: *NMR, Basic Principles and Progress, Vol. 23*, Springer, Berlin 1990, p. 165; For IGLO applications to boron compounds see d) P. v. R. Schleyer, M. Bühl, U. Fleischer, W. Koch, *Inorg. Chem. 29* (1990) 886; e) M. Bühl, R. v. R. Schleyer, *Angew. Chem. 102* (1990) 962; *Angew. Chem. Int. Ed. Engl. 29* (1990) 886; f) M. Bühl, P. v. R. Schleyer in G. A. Olah, K. Wade, R. E. Williams (Eds.): *Electron Deficient Boron and Carbon Clusters*, Wiley, New York 1991, p. 113; g) M. Bühl, P. v. R. Schleyer, M. L. McKee, *Heteroatom Chem.*, in press.
[11] Ordering of the ligands with respect to experimental chemical shifts. The experimental data were taken from H. Nöth, B. Wrackmeyer: *NMR, Basic Principles and Progress, Vol. 14*, Springer, Berlin 1978; B. Wrackmeyer: *Ann. Rep. NMR Spectrosc. 20* (1988) 61; except L = CO: B. F. Spielvogel, A. T. McPhail, J. A. Knight, C. G. Moreland, C. L. Gatchell, K. W. Morse, *Polyhedron 2* (1983) 1345 and L = $N_3^{\ominus}$ and $NCS^{\ominus}$: M. Thomann, H. Nöth, unpublished results.
[12] See e.g. a) S. Miertus, E. Scrocco, J. Tomasi, *Chem. Phys. 55* (1981) 117; b) J. L. Pascal-Ahuir, J. Tomasi, R. Bonaccorsi, *J. Comput. Chem. 8* (1987) 778; c) J. L. Rivail, B. Terryn, D. Rinaldi, M. F. Ruiz-Lopez, *THEOCHEM 120* (1985) 387; for a recent application see e.g. d) T. Steinke, E. Hänsele, T. Clark, *J. Am. Chem. Soc. 111* (1989) 9107.
[13] *Tomasi*'s SCRF procedure using spherical cavities around the atoms was installed in the Convex version of Gaussian 82 (J. S. Binkley, R. A. Whiteside, K. Raghavachari, R. Seeger, D. J. DeFrees, H. B. Schlegel, M. J. Frisch, J. A. Pople, L. Kahn, Gaussian 82, Carnegie-Mellon University, Pittsburgh, PA, USA 1982). Note that in this version the SCRF calculations are performed at the SCF level. The sphere radii used for the atoms were 20% larger than the van der Waals radii. The solvent effect calculations employed the temperature (298.15 K), as well as the following physical constants: the solvent diameters, densities, thermal expansion coefficients, and the dielectric constants (taken from: J. A. Riddick, W. B. Bunger, T. K. Sahano, *Organic Solvents, Vol. 2*, Wiley, New York 1986).
[14] a) L. Onsager, *J. Am. Chem. Soc. 58* (1936) 1486; b) J. G. Kirkwood, F. H. Westheimer, *J. Chem. Phys. 6* (1938) 506.
[15] We tried to assess the direct influence of solvent molecules by optimizing $H_3B \cdot NH_3 \cdot 3H_2O$ with C_3 symmetry (**2**, which is a minimum at 6-31G*). MP2/6-31G* separations: B–N 1.614, NH···O 2.042, BH···HO 2.101 Å; IGLO $\delta(^{11}B) = -18.9$. The IGLO value for **1** employing the structural parameters of **2** (i.e. **2** without the H_2O molecules) is $\delta = -18.3$. Note the considerable bond-shortening induced by the ligands, and the small direct effect of these on $\delta(^{11}B)$: $\Delta\delta \approx 0.6$.
[16] H. M. Colquhoun, G. Jones, J. M. Maud, J. F. Stoddart, D. J. Williams, *J. Chem. Soc. Dalton Trans. 1984*, 63.
[17] P. Cassoux, R. L. Kuczkowski, P. S. Bryan, R. C. Taylor, *Inorg. Chem. 14* (1975) 126.
[18] E.g. it has been shown that the effect of electric fields on $\delta(^{13}C)$ of saturated hydrocarbons is very small: K. Seidman, G. E. Maciel, *J. Am. Chem. Soc. 99* (1977) 3254.

5-Lithio-2*H*-tetrazolium Carbenoids: NMR Spectroscopic Detection and Reactions with Nitrogen Electrophiles**

By *Robert Weiss** and *Rainer H. Lowack*

2*H*-Tetrazolium ions of type **2** are part of the tetrazolium/formazanide redox system, which is distinguished by an excellent charge stabilization within both the cationic and the anionic oxidation state. As a consequence, the 2*H*-tetrazolio substituent should facilitate redox umpolung.[1] We have examined nucleophilic reagents for the introduction of the 2*H*-tetrazolio group into electrophilic substrates[2] and report trapping reactions of the 5-lithiotetrazolium ion **3** and its spectroscopic detection by ^{13}C NMR spectroscopy.

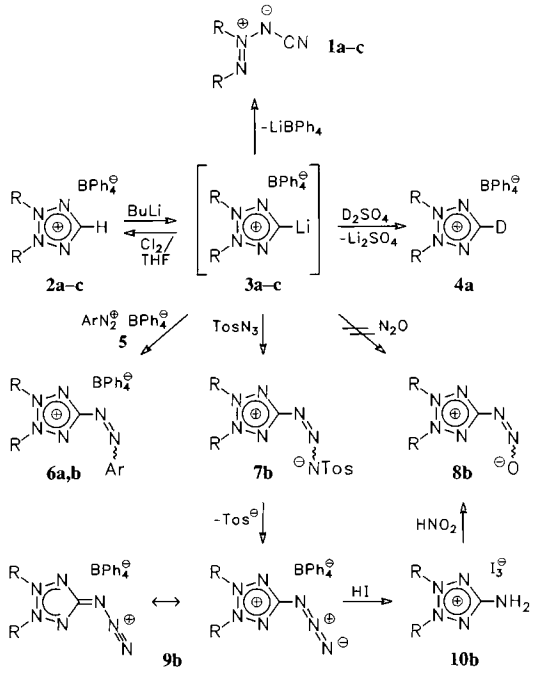

Scheme 1. **a**: R = *p*-tolyl, **b**: R = *p*-anisyl, **c**: R = *p*-dimethylaminophenyl, Tos = *p*-toluenesulfonyl, Ar = *p*-dimethylaminophenyl.

^1H NMR spectra show that tetrazolium salts **2**, dissolved in tetrahydrofuran, are deprotonated quantitatively at − 90 °C by *n*- or *tert*-butyllithium. The 5-lithiotetrazolium salts **3** thus formed can be considered as carbenoids.[3] At − 100 °C they are sufficiently stable for their ^{13}C NMR spectra to be recorded.[4] The ^{13}C NMR spectrum of **2b** had no signals between $\delta = 165$ and 250, whereas, after lithiation, a single unstructured multiplet appeared at $\delta = 202.4$ and vanished when the solution was heated up to room temperature. IGLO/DZ//6-31G* calculations[5] indicate that this multiplet is the ^{13}C NMR signal of the solvated carbenoid's tetrazolium ring.[6] According to the calculations, this shift of 48 ppm to lower field upon lithiation of **2b** can be explained mainly by the decrease of π-electron density at the tetrazolium C atom and by the weakening of the two N–C σ bonds to this atom.[7] Corresponding changes in the chemical shift have been observed upon deprotonation of an imidazolium salt[3] and lithiation of benzene[7] or halogen alkanes.[8]

Above ca. − 60 °C the 5-lithiotetrazolium salts **3** open up by an intramolecular E_{1cB} elimination to yield the (2*Z*)-1-cyano-2,3-diaryltriaz-2-en-2-ium-1-idenes **1**.[1] Nevertheless, **3** could be trapped at − 90 °C with either D_2SO_4, aryldiazonium tetraphenylborate **5**,[9] or tosyl azide in good yields.[10] The new tetrazolium salts **6** and **9b** thus formed had not been accessible before, among other reasons because the reactivity[11] of 1,5-diarylformazans towards **5** is too low. On the other hand, this sole method to derivatize tetrazolium ions of type **2** failed when strongly oxidizing electrophiles like chlorine (or bromine) were used. In this case not the desired product but ion **2** as its chloride (bromide) was isolated in a yield of 67% (79%). We assume that **3** was oxidized by the halogen to the corresponding radical cation which abstracted an H atom from the solvent THF to re-form **2**.[12]

The azide **9b** was identified spectroscopically[13] and by its reduction with iodide to amine **10b** and subsequent diazotization to the known[14] tetrazolium-5-diazotate **8b**. Reduction of **9b** with triphenylphosphane/water led to fission of the C–N bond. In contrast to *Balli's* azidinium salts,[15] **9b** did not react with azide ions. Thus, from the intensely yellow, shock-insensitive tetraphenylborate salt **9b**, the corresponding colorless chloride or azide salt could be prepared with tetrabutylammonium chloride or azide, respectively.

Experimental Procedure

9b: To **2b** (4.64 mmol) dissolved in 50 mL of THF, *n*-butyllithium (5.1 mmol, 1.6 molar in hexane) and then tosyl azide (10 mmol) were added dropwise at − 90 °C. The initially dark brown solution turned dark red within a few minutes. After warming to 20 °C over 10 h the solvent was evaporated. The green brown residue, which contained a small amount of **7b** according to mass spectrometry, was chromatographed with dichloromethane/methanol (1 : 0 to 10 : 1) on silica gel. From acetonitrile/ether or dichloromethane/ether 2.00 mmol (43%) of yellow air-stable crystals were obtained.

6b: As above, from **2b** (1.44 mmol) in 30 mL of THF, *n*-butyllithium (1.50 mmol) and **5** (1.87 mmol, added undissolved in portions). After chromatography and hydrolysis of the anion in hydrochloric acid, the product was precipitated as its tetrafluoroborate from water/methanol (2 : 1) with $LiBF_4$. Recrystallization from dichloromethane/ether yielded 0.81 mmol (56%) of an oxygen-sensitive, dark red crystalline powder.

10b: To **9b** (0.688 mmol) in 2 mL of acetonitrile, an HI solution (3.5 mmol, 50% in H_2O) was added dropwise at − 40 °C. The solution turned dark brown with strong evolution of gas. After slow warming to 20 °C the solvent was evaporated. The residue was dissolved in 3 mL of dichloromethane and filtered. Concentrated aqueous hydrochloric acid (4 mL) was added, followed by titration with H_2O_2 solution (30%) till the color changed from brown to purple. The organic layer was chromatographed with dichloromethane/methanol (1 : 0 to 10 : 1) on silica gel. From methanol, 0.608 mmol (88%) of the colorless chloride crystallized.

Received: March 15, 1991 [Z 4500 IE]
German version: *Angew. Chem. 103* (1991) 1183

[*] Prof. Dr. R. Weiss, Dr. R. H. Lowack
Institut für Organische Chemie der Universität Erlangen-Nürnberg
Henkestrasse 42, W-8520 Erlangen (FRG)

[**] This work was supported by the Fonds der Chemischen Industrie. We thank Dr. *W. Bauer*, Dr. *T. Clark*, and *M. Bühl* for assistance with NMR measurements and ab initio calculations.

[1] R. H. Lowack, R. Weiss, *J. Am. Chem. Soc. 112* (1990) 333.
[2] R. H. Lowack, *Dissertation*, Universität Erlangen-Nürnberg, 1990; R. Weiss, R. H. Lowack, *Bull. Soc. Chim. Belg. 100* (1991) 483.
[3] A. J. Arduengo, III, R. L. Harlow, M. Kline, *J. Am. Chem. Soc. 113* (1991) 361.
[4] The sample was prepared in a 5-mm NMR tube by reaction of **2b** (98 mg dissolved in 0.4 mL of [D_8]THF) with *n*-Bu^6Li^{28} (0.17 mmol, in 0.3 mL of [D_8]THF) at − 98 °C under argon and measured at − 100 °C; cf. W. Bauer, P. von R. Schleyer, *J. Am. Chem. Soc. 111* (1989) 7191.
[5] M. Schindler, *Magn. Res. Chem. 26* (1988) 394; M. Bühl, N. J. R. van Eikema Hommes, P. von R. Schleyer, U. Fleischer, W. Kutzelnigg, *J. Am. Chem. Soc. 113* (1991) 2459.
[6] **2** measured for six different aryl substituents R, $\delta = 154.9 \pm 0.8$, **2** calculated (IGLO/DZ//6-31G*) for R = H, 161.8; 2,3-diaryltetrazolium-5-olate measured, 173.2, 2*H*-tetrazolium-5-olate calculated, 169.6; **3b** measured, 202.4, **3** calculated (R = H), 196.5, **3** · $2H_2O$ calculated (R = H), 204.7. However, the calculations do not take into account configuration interac-

tions and therefore do not allow reliable predictions concerning the solvation and aggregation of carbenoids 3.
[7] Cf. D. Seebach, R. Hässig, J. Gabriel, *Helv. Chem. Acta 63* (1983) 308.
[8] D. Seebach, H. Siegel, K. Müllen, K. Hiltbrunner, *Angew. Chem. 91* (1979) 844; *Angew. Chem. Int. Ed. Engl. 18* (1979) 784.
[9] In contrast to other aryldiazonium salts, **5** decomposes only slowly in THF; other nitrogen electrophiles, cf. H. Quast, E. Schmitt, *Justus Liebigs Ann. Chem. 732* (1970) 43.
[10] No reaction was observed, for example, with dinitrogen oxide or palladium dichloride.
[11] J. N. Ashley, B. M. Davis, A. W. Nineham, R. Slack, *J. Chem. Soc. 1953*, 3881.
[12] The insolubility of **2** in solvents like 1,2-dimethoxyethane plus its instability towards ring opening in dichloromethane necessitated the use of THF.
[13] Selected physical data of the 2,3-*p*-anisyltetrazolium systems **6**, **8**–**10**. **6b** as its BF_4 salt: m.p. 148–149 °C (dec.); UV/VIS (CH_3CN): $\lambda_{max.}$ [nm] (ε) = 512 (5.3×10^4); ^1H NMR (400 MHz, CD_3CN): δ = 3.24 (s, 6H), 3.88 (s, 6H), 6.93 (d, J = 9.2 Hz, 2H), 7.12 (d, J = 9.2 Hz, 4H), 7.61 (d, J = 9.2 Hz, 4H), 8.02 (d, J = 9.2 Hz, 2H); ^{13}C NMR (100.6 MHz, CD_3CN): δ = 41.07, 56.99, 116.51, 126.59, 128.61, 145.12, 157.77, 164.54, 171.58; MS (EI, 70 eV, Ar = $MeOC_6H_4$): *m/z* 431 ($MH^{\oplus}$, 6%), 415 ($M^{\oplus}$ – Me, 5), 401 ($MH^{\oplus}$ – 2Me, 83), 387 (18), 322 (15), 309 (66), 299 (17), 295 (13), 281 (66), 269 (24), 266 (59), 251 (26), 242 (Ar_2N_2, 94), 227 (63), 214 (Ar_2, 39), 161 (39), 148 ($Me_2NC_6H_4N_2$, 99), 135 (ArN_2, 82), 121 (ArN, 75), 108 (ArH, 73), 107 (Ar, 100), 92 (62), 77 (59). **9b**: m.p. = 158–168 °C (dec.); IR (11% in CH_3NO_3, 42 μm): $\tilde{\nu}$[cm^{-1}] = 2164; UV/VIS: $\lambda_{max.}$ [nm] (ε) = 325 (1.0×10^4) ^1H NMR (CD_3CN): δ = 3.82 (s, 6H), 6.83 (t, J = 7.3 Hz, 4H), 6.98 (t, J = 7.4 Hz, 8H), 7.05 (d, J = 9.2 Hz, 4H), 7.27 (m, 8H), 7.50 (*d*, J = 9.2 Hz, 4H) ^{13}C NMR (CD_3CN): δ = 57.05, 116.66, 122.75, 126.53, 126.56, 126.59, 128.44, 136.74, 163.48, 164.51 (q, J = 49 Hz), 164.82. **10b** as its chloride: m.p. >250 °C (dec.); ^1H NMR (CD_3OD): δ = 3.30 (s, 2H), 3.85 (s, 6H), 7.09 (d, J = 9 Hz, 4H), 7.58 (d, J = 9 Hz, 4H) ^{13}C NMR (CD_3OD): δ = 56.61, 116.20, 127.14, 128.78, 164.47, 167.46 MS: *m/z* 299 ($M^{\oplus}$, 8%), 269 ($M^{\oplus}$ –2Me, 7), 229 (Ar_2NH, 13), 214 (Ar_2, 19), 162 (ArN_3CH, 7), 148 (ArN_2CH, 13), 135 (ArN_2, 49), 122 (ArNH, 33), 107 (Ar, 100), 92 (49), 77 (61). **8b**: m.p. = 157–165 °C (dec.) ^1H NMR ($CDCl_3$): δ = 3.90 (s, 6H), 7.18 (d, J = 8.9 Hz, 4H), 7.70 (d, J = 8.9 Hz, 4H) ^{13}C NMR ($CDCl_3$): δ = 56.77, 116.61, 126.82, 128.96, 165.27, 166.71; MS: *m/z* 326 ($M^{\oplus}$, 1.4%), 298 (Ar_2N_4CO, 2.9), 282 (Ar_2N_3CN, 2.2), 270 ($Ar_2N_4CO - N_2$, 2.1), 255 (Ar_2N_2CO – Me, 1.3), 242 (Ar_2N_2, 1.3), 229 (Ar_2NH, 1.1), 214 (Ar_2, 1.5), 161 (ArN_3C, 1.7), 135 (ArN_2, 80), 107 (Ar, 100), 92 (33), 77 (43).
[14] E. Bamberger, R. Padova, E. Ormerod, *Justus Liebigs Ann. Chem. 446* (1926) 260.
[15] H. Balli, F. Kersting, *Justus Liebigs Ann. Chem. 647* (1961) 11.

Galactosyltransferase-Catalyzed Synthesis of 2′-Deoxy-*N*-acetyllactosamine **

By *Joachim Thiem** and *Torsten Wiemann*

Dedicated to Professor Burchard Franck on the occasion of his 65th birthday

2-Deoxy sugars are components of cardiac glycosides[1a] and many antibiotics.[1b] The synthesis of their glycosides and the use of these in medicine and as enzyme inhibitors has attracted great interest.[1c] Since a neighboring group capable of directing the reaction is absent, the stereoselective synthesis of 2-deoxyglycosides poses problems. Several methods have been proposed to solve them.

Whereas 2-deoxy α-glycosides are still obtainable with good results by using the *N*-iodosuccinimide (NIS) method[2a–c] or analogous procedures,[2d–f] 2-deoxy β-glycosides are especially difficult to synthesize owing to the anomeric effect. Here, an auxiliary substituent is usually employed, such as in the dibromomethyl methyl ether method[3a] (DBE method) and other procedures,[3b–e] or, after glycosylation, the 2′-OH function is removed by reduction.[4] To the best of our knowledge, there is only one reported example of an enzymatic synthesis of a 2-deoxy sugar. *Lehmann* et al.[5] observed that D-glucal is accepted by β-glucosidase and were able to isolate a 2′-deoxy-β-disaccharide in 8% yield.

We have used galactosyltransferase (EC 2.4.1.22) for the synthesis of a 2′-deoxy β-D-disaccharide. The galactosyltransferase catalyzes the in vivo transfer of galactose from uridine 5′-diphosphate galactose to terminal *N*-acetylglucosamine residues. The acceptor substrate has been successfully varied in numerous preparative syntheses.[6] However, an example of the synthetic application of a modified donor substrate in not yet known. We have now found that the galactosyltransferase accepts uridine diphosphate (UDP) 2-deoxygalactose, whereby 2-deoxygalactose is transferred to *N*-acetylglucosamine both stereo- and regiospecifically to form a β(1-4) glycosidic bond.

The starting material, 2-deoxy-D-*arabino*-hexose 6-phosphate (**2**), was synthesized by enzymatic phosphorylation of 2-deoxy-*arabino*-hexose (**1**) with in situ regeneration of adenosine triphosphate (ATP) (Scheme 1). Both the hexokinase and the pyruvate kinase had been immobilized on VA-epoxy.[7] The 6-phosphate **2** was isolated by chromatography on DEAE cellulose (80% yield).

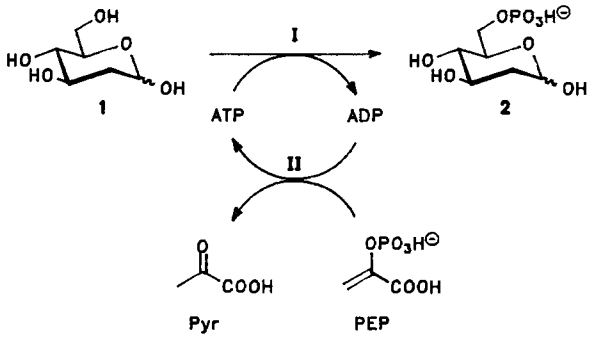

Scheme 1. Synthesis of 2-deoxyglucose-6-phosphate (enzymes: I hexokinase on VA-epoxy, II pyruvate kinase on VA-epoxy).

The reactions were performed in a one-pot synthesis using immobilized enzymes (Scheme 2). The reaction cycle results in constant regeneration of the cofactor uridine triphosphate (UTP), thereby minimizing inhibition effects and costs. Such a cycle—with a different support and different substrates—was first employed by *Whitesides* et al.[8a] and later by other research groups as well.[8b,c] Phosphoglucomutase (**III**) establishes an equilibrium between the 6-phosphate **2** and the 1-phosphate **3**, which is shifted toward **3** by UDP-glucose pyrophosphorylase (**IV**) and inorganic pyrophosphatase (**V**). In this way, *Withers* et al.[9] were able to isolate the extremely hydrolysis-sensitive 2-deoxy 1-phosphate **3**. UDP-galactose-4-epimerase (**VI**) then establishes an equilibrium between the UDP 2-deoxyglucose (**4**) thus synthesized and UDP 2-deoxygalactose (**5**). The kinetic parameters for this reaction have already been determined by *Kochetkov* et al.[10] Compound **5** is accepted as a donor substrate by galactosyltransferase (**VII**), resulting in transfer of 2-deoxygalactose to *N*-acetylglucosamine (**6**). The product, 2′-deoxy-*N*-acetyllactosamine (**7**), was obtained in 40% yield (150-μmol scale). The structure was established by ^1H NMR and ^{13}C NMR spectroscopy as well as by FAB mass spectroscopy (Table 1). The UDP formed as side product is phosphorylated to UTP with phosphoenolpyruvate (PEP) as phosphate donor in a reaction catalyzed by pyruvate kinase (**VIII**). UTP can then

[*] Prof. Dr. J. Thiem, Dipl.-Chem. T. Wiemann
Institut für Organische Chemie der Universität
Martin-Luther-King-Platz 6, W-2000 Hamburg 13 (FRG)

[**] This work was supported by the Fonds der Chemischen Industrie and by the Bundesministerium für Forschung und Technologie. *T. W.* thanks *Sabine Fänger* for her assistance.

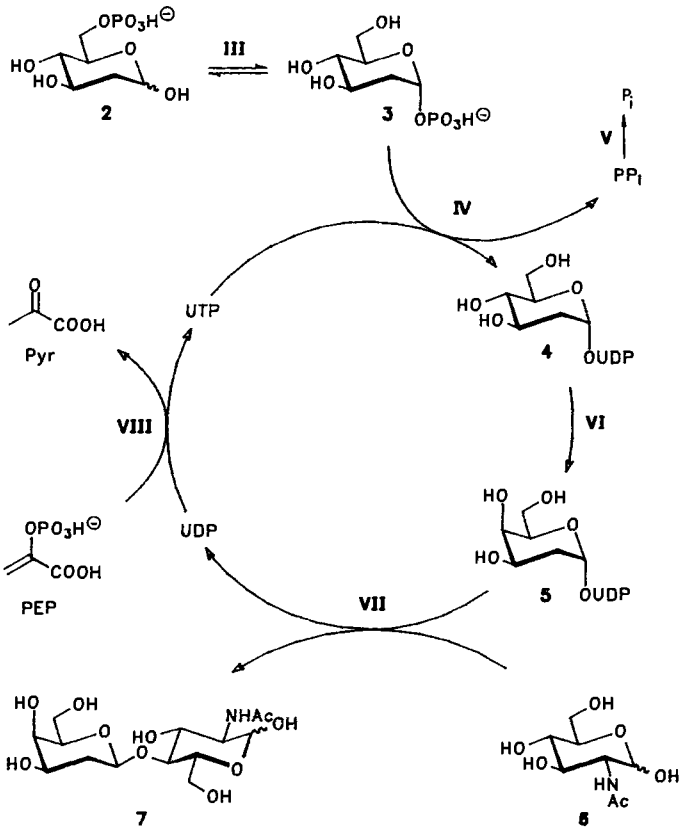

Scheme 2. Enzymatic glycosylation (enzymes: **III**, phosphoglucomutase; **IV**, UDP-glucose-pyrophosphorylase; **V**, inorganic pyrophosphatase; **VI**, UDP-galactose-4-epimerase; **VII**, galactosyltransferase; **VIII**, pyruvate kinase; all enzymes were immobilized on activated CH-sepharose 4B).

Table 1. Spectroscopic data for 7. ^{1}H NMR (400 MHz, [D_6]acetone, [D_5]acetone as internal standard); ^{13}C NMR (63 MHz, H_2O, CH_3CN as internal standard).

^{13}C NMR (free sugar 7): δ = 89.59 (C-1, α form), 93.93 (C-1, β form), 99.42 (C-1′), 52.80 (C-2, α form), 55.29 (C-2, β form), 32.54 (C-2′), 68.30 (C-3, α form), 71.48 (C-3, β form), 66.72 (C-3′), 77.87 (C-4, α form), 77.44 (C-4, β form), 65.73 (C-4′), 69.17 (C-5, α form), 73.79 (C-5, β form), 74.65 (C-5′), 59.18 (C-6), 60.43 (C-6′), 173.31 (NH-*CO*-CH_3), 20.97 (NHCO-CH_3, α form), 21.25 (NHCO-CH_3 β form)

^{1}H NMR (heptaacetate of 7): δ = 5.77 (d, $J_{1a,2}$ = 8.8 Hz, H-1, β form), 6.06 (d, $J_{1e,2}$ = 3.6 Hz, H-1, α form), 7.15 (d, $J_{NH,2}$ = 9.4 Hz, NH, α form), 7.11 (d, $J_{NH,2}$ = 9.4 Hz, NH, β form), 4.33 (ddd, $J_{2,3}$ = 10.4 Hz, H-2, α form), 4.07 (m, H-2, β form), 5.23 (m, 1 H, H-3), 3.95 (t, $J_{3,4} = J_{4,5}$ = 9.6 Hz, 1 H, H-4), 3.83 (ddd, $J_{5,6a}$ = 4.4 Hz, $J_{5,6b}$ = 2.2 Hz, 1 H, H-5), 4.34 (dd, $J_{6a,6b}$ = 12.2 Hz, 1 H, H-6a), 4.23 (dd, 1 H, H-6b), 4.83 (dd, $J_{1',2a'}$ = 9.6 Hz, $J_{1',2'e}$ = 2.2 Hz, 1 H, H-1′), 1.76 (ddd, $J_{2'a,2'e}$ = 12.4 Hz, $J_{2'a,3'}$ = 12.5 Hz, 1 H, H-2′a), 1.95 (m, 1 H, H-2′e), 5.04 (ddd, $J_{2'e,3'}/J_{3',4'}$ = 3.2/5.0 Hz, 1 H, H-3′), 5.23 (m, 1 H, H-4′), 4.00 (ddd, $J_{4',5'}$ = 5.6 Hz, 1 H, H-5′), 4.20 (dd, $J_{5',6'a}$ = 3.6 Hz, $J_{6'a,6'b}$ = 12.2 Hz, 1 H, H-6′a), 4.11 ppm (dd, $J_{5',6'b}$ = 2.0 Hz, 1 H, H-6′b)

FAB-MS (free sugar 7): $M^{\oplus}$ + 1 = 368, $M^{\oplus}$ + Na = 390

reenter the reaction to form UDP 2-deoxyglucose. The amount of conversion in the reaction can be quantified by using the Fiske–Subbarov method for photometric determination of phosphate.[11] All enzymes used in the cycle are immobilized on activated CH-sepharose and can be employed repeatedly.

Experimental Procedure

The reaction was carried out in Tris buffer (100 mM, pH 7.5, 9 mL). The buffer contained $MgCl_2$ (10 mM), $MnCl_2$ (5 mM), KCl (40 mM), NaN_3 (0.02%), and bovine serum albumin (0.5%). After addition of 2-deoxy-D-*arabino*-hexose 6-phosphate (**2**, $NH_4^{\oplus}$ salt, 100 mg, 40 mM), *N*-acetylglucosamine (**6**, 120 mg, 60 mM), PEP (82 mg, 44 mM), glucose 1,6-diphosphate (0.1 mg, catalytic), and UTP (11 mg, 2 mM), adjustment of the pH value, and deoxygenation with helium, the immobilized enzymes were added (phosphoglucomutase (rabbit muscle), 20 U; UDP-glucose-pyrophosphorylase (bovine liver), 10 U; inorganic pyrophosphatase (yeast), 20 U; UDP-galactose-4-epimerase (yeast), 5 U; galactosyltransferase (cow's milk), 2 U; pyruvate kinase (rabbit muscle), 50 U). The mixture was incubated in a shaking apparatus for two weeks at 30 °C. The enzyme, after collection by filtration and washing, could be reused. After removal of phosphate on an ion-exchange column (Dowex 1 × 8, $H^{\oplus}$ form), the product was isolated by gel permeation chromatography (Fractogel TSK HW-40 (S), 2 × 110 cm) (53 mg, 144 μmol, 40% yield).

Received: March 15, 1991 [Z 4497 IE]
German version: *Angew. Chem. 103* (1991) 1184

CAS Registry numbers:
1, 154-17-6; **2**, 3573-50-0; **6**, 7512-17-6; 7, 135190-02-2; 7 heptaacetate, 135190-03-3; EC 2.4.1.22, 9030-11-9.

[1] a) T. Reichstein, E. Weiss, *Adv. Carbohydr. Chem. 17* (1962) 65; b) J. S. Brimacombe, *Angew. Chem. 83* (1971) 261; *Angew. Chem. Int. Ed. Engl. 10* (1971) 236; c) J. Thiem, W. Klaffke, *Top. Curr. Chem. 154* (1990) 285.
[2] a) J. Thiem, H. Karl, J. Schwentner, *Synthesis 1978*, 696; b) J. Thiem, J. Elvers, *Chem. Ber. 112* (1979) 818; c) J. Thiem, P. Ossowski, J. Schwentner, *ibid. 113* (1980) 955; d) R. U. Lemieux, A. R. Morgan, *Can. J. Chem. 43* (1965) 2190; e) K. Tatsuta, K. Fujimoto, M. Kinoshita, S. Umezawa, *Carbohydr. Res. 54* (1977) 85; f) P. J. Garegg, B. Samuelsson, *ibid. 84* (1980) C1.
[3] a) K. Bock, C. Pedersen, J. Thiem, *Carbohydr. Res. 73* (1979) 85; b) R. Preuss, R. R. Schmidt, *Synthesis 1988*, 694; c) M. Perez, J.-M. Beau, *Tetrahedron Lett. 30* (1989) 75; d) K. C. Nicolaou, T. Ladduwahetty, J. L. Randall, A. Chucholowski, *J. Am. Chem. Soc. 108* (1986) 2466; e) H. Jin, R. Tsai, K. Wiesner, *Can. J. Chem. 61* (1983) 2442.
[4] T. Hayashi, T. Iwaoka, N. Takeda, E. Ohki, *Chem. Pharm. Bull. 26* (1978) 1786; b) J. Thiem, H. Karl, *Chem. Ber. 113* (1980) 3039.
[5] a) J. Lehmann, T. Schröter, *Carbohydr. Res. 58* (1977) 65.
[6] a) H. A. Nunez, R. Barker, *Biochemistry 19* (1980) 489; b) S. David, C. Augé, *Pure Appl. Chem. 59* (1987) 1501; c) M. M. Palcic, O. P. Srivastava, O. Hindsgaul, *Carbohydr. Res. 159* (1987) 315; d) C. Augé, C. Gautheron, H. Pora. *ibid. 193* (1989) 288; e) J. Thiem, T. Wiemann, *Angew. Chem. 102* (1990) 78; *Angew. Chem. Int. Ed. Engl. 29* (1990) 80.
[7] a) Product information, Riedel-de Haën, Seelze 1987; b) K. Burg, O. Mauz, S. Noetzel, K. Sauber, *Angew. Makromol. Chem. 157* (1988) 105.
[8] a) S. L. Haynie, C.-H. Wong, G. M. Whitesides, *J. Org. Chem. 47* (1982) 5416; b) C. Augé, S. David, C. Mathieu, C. Gautheron, *Tetrahedron Lett. 25* (1984) 1467; c) J. Thiem, W. Treder, *Angew. Chem. 98* (1986) 1100; *Angew. Chem. Int. Ed. Engl. 25* (1986) 1096.
[9] M. D. Percival, S. G. Withers, *Can. J. Chem. 66* (1988) 1970.
[10] T. N. Druzhinina, Y. Y. Kusov, V. N. Shibaev, N. K. Kochetkov, P. Biely, S. Kucar, S. Bauer, *Biochim. Biophys. Acta 381* (1975) 301.
[11] T. G. Cooper, *Biochemische Arbeitsmethoden*, de Gruyter, Berlin 1981, p. 53.

Direct Location of the Hydrido Ligands in the Dianion $[H_4Os_{10}(CO)_{24}]^{2-}$ by a Neutron Diffraction Study of Its $[(Ph_3P)_2N]^+$ Salt at 20 K **

By *Alan Bashall, Lutz H. Gade, Jack Lewis,* Brian F. G. Johnson, Garry J. McIntyre,** and *Mary McPartlin**

Large hydrido carbonyl clusters of transition metals provide ideal model systems for the study of the chemisorp-

[*] Prof. M. McPartlin, A. Bashall
School of Chemistry, The Polytechnic of North London
Holloway Road, GB-London N7 8DB (UK)
Prof. Lord Lewis, L. H. Gade, Dr. B. F. G. Johnson
University Chemical Laboratory
Lensfield Road, GB-Cambridge CB2 1EW (UK)
Dr. G. J. McIntyre
Institut Laue-Langevin
156X, F-38042 Grenoble Cedex (France)

[**] We acknowledge financial support from the Science and Engineering Research Council (*M.McP.*) and the Foreign and Commonwealth Office (Kurt Hahn Scholarship for *L. H. G.*). We thank Professor *J. W. Lauher* (Stony Brook, USA) for his molecular graphics programme CHEM-RAY.

tion of a "synthesis gas" on the surface of bulk metals or colloidal particles.[1] Several decanuclear hydrido clusters of osmium and ruthenium have been structurally characterized by X-ray diffraction,[2-4] and most exhibit tetracapped octahedral metal cores with what appear to be closed-packed arrays of carbonyl ligands approximately perpendicular to the four six-metal atom surfaces of the core. None of these clusters shows the marked displacement of carbonyl ligands invariably associated with surface-bonded hydride ligands in smaller clusters,[5-8] and it has therefore been thought, until now, that the hydride ligands were probably all located in interstitial sites. A neutron diffraction study of one of these

$[H_4Os_{10}(CO)_{24}]^{2-}$ **1**

decametal clusters, the dianion **1**, has now established that all four hydride ligands are located on the surface of the metal framework.

Single crystal X-ray studies do not allow direct location of H atoms in polynuclear carbonyls of the third-row transition metals, but they often lead to successful deduction of hydrogen sites using indirect methods based on detecting 'gaps' in the carbonyl ligands,[5-8] or on determination of potential energy minima.[9] For example, a μ_3 site on the surface of the octahedral cluster monoanion **2** was deduced from the surface ligand distribution observed in the X-ray analysis,[6] and was later confirmed by neutron diffraction studies.[10] The first interstitial H atom to be reported in a carbonyl cluster

$[HOs_6(CO)_{18}]^-$ **2** $[HRu_6(CO)_{18}]^-$ **3**

was sited in the octahedral cavity of **3**, the ruthenium analogue of **2**.[11] The unexpected location was originally deduced indirectly from the extremely compact arrangement of the carbonyl ligands which left no space for a surface H atom and from the NMR data. This structural assignment initially proved controversial,[12] but was vindicated by later neutron diffraction studies.[13] A similar octahedral hydride environment was revealed in neutron diffraction studies of the hexacobalt cluster $[HCo_6(CO)_{15}]^-$.[14]

Analogous observations in X-ray studies of the decanuclear monoanion **4**[2] were also consistent with an interstitial location for the H atom, because they showed a complete coverage of the metal core by carbonyl ligands very similar to that of the corresponding non-hydrido dianion **5**.[15]

$[HOs_{10}C(CO)_{24}]^-$ **4** $[Os_{10}C(CO)_{24}]^{2-}$ **5**

As the only octahedral site in **4** is occupied by the carbido atom, the possible location of a hydrido ligand in a slightly enlarged tetrahedral cavity of the cluster was proposed, and the ^{187}Os satellite pattern associated with the hydride signal in the ^1H NMR spectrum was consistent with this assignment.[16]

Carbide formation during formation of these high nuclearity clusters is suppressed by thermolyzing the Os_3 precursors in high boiling protic solvents. The X-ray study of **1**,[3] originally obtained in low yield from the reaction of $Os_3(CO)_{12}$ with *i*BuOH,[17] again showed an overall structure almost indistinguishable from that of the carbido dianion **5** but without the central C atom. It was formulated as $[H_4Os_{10}(CO)_{24}]^{2-}$ because the hydrides were essential to give the 134 cluster valence electrons required for the observed tetracapped octahedral geometry,[15, 18] and the presence of hydrido ligands was confirmed by ^1H NMR spectroscopy. The close similarity of the carbonyl distribution in **1** to that of the non-hydrido dianion **5** was consistent with an interstitial location of the four hydrogen ligands. The cluster also showed significant lengthening of a number of metal–metal distances which were attributed to the cavity expansion produced by internal hydrides. Variable-temperature ^1H and ^{13}C NMR studies showed a high degree of ligand fluctionality in solution at ambient temperatures (CD_2Cl_2, 295 K). On cooling to 198 K the single broad hydride reso-

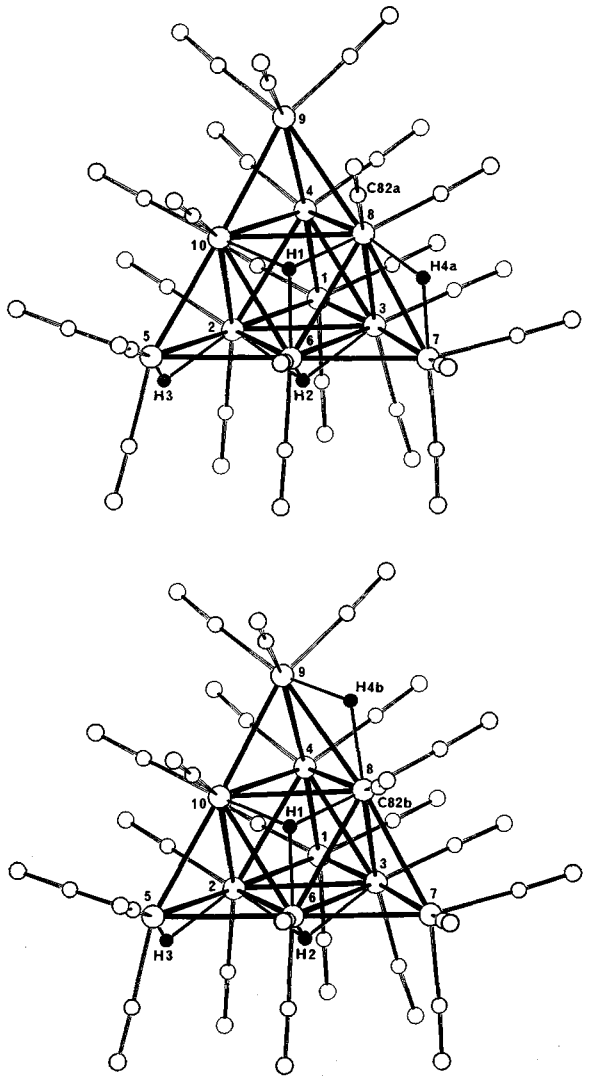

Fig. 1. Perspective views of the structures of the two isomers of the tetrahydrido dianion **1**, showing the surface location of the hydrogen ligands; for clarity only the numbers of the osmium atoms are shown: Top: isomer **1a** which has a virtual C_2 axis through Os6 and Os4; bottom: isomer **1b** which has no symmetry. Principal bond lengths [Å] and angles [°]: (estimated standard deviations in parantheses): Os1-Os2 2.801(8); Os1-Os3 2.772(8); Os1-Os4 2.745(9); Os2-Os3 2.868(7); Os2-Os4 2.816(8); Os2-Os5 2.862(8); Os2-Os6 2.900(8); Os2-Os10 2.805(9); Os3-Os4 2.755(8); Os3-Os6 2.881(8); Os3-Os7 2.733(8); Os3-Os8 2.815(9); Os4-Os8 2.798(8); Os4-Os9 2.739(9); Os4-Os10 2.789(8); Os5-Os6 2.793(7); Os5-Os10 2.778(8); Os6-Os7 2.779(7); Os6-Os8 2.910(8); Os6-Os10 2.858(8); Os7-Os8 2.855(8); Os8-Os9 2.888(8); Os8-Os10 2.894(7); Os9-Os10 2.754(8); Os2-H2 1.87(2); Os2-H3 1.82(3); Os3-H2 1.89(2); Os5-H3 1.81(4); Os6-H1 1.88(3); Os6-H2 1.85(3); Os7-H4a 1.80(5); Os8-H1 1.82(2); Os8-H4a 1.70(4); Os8-H4b 1.77(6); Os9-H4b 1.82(5); Os10-H1 1.89(2); Os6-H1-Os8 104(2); Os10-H1-Os6 99(1); Os10-H1-Os8 103(1); Os3-H2-Os2 100(1); Os6-H2-Os2 103(1); Os6-H2-Os3 101(1); Os5-H3-Os2 104(2); Os8-H4a-Os7 109(2); Os9-H4b-Os8 107(3).

nance at $\delta = -16.48$ split into two signals of equal intensity at -14.70 and -19.08.[19] This signal pattern could not be be explained in terms of a model in which the four hydride ligands occupy interstitial sites (four tetrahedral, one octahedral) within the cluster; therefore their location on the cluster surface, though not apparent from the X-ray study could not be ruled out. Despite persistent attempts to grow crystals of a decanuclear hydrido species suitable for neutron studies using a range of different counterions, none has been obtained until now.

In the present neutron study of the $[(Ph_3P)_2N)]^+$ salt of **1** at 20 K, the hydrido H atoms were directly located in a difference-Fourier synthesis, and were found to be on the cluster surface, two in μ_3 and two in μ_2 sites.[20] The four hydride ligands gave rise to five negative peaks, three of approximately equal height and two of half height. These were attributed to two isomers of the tetrahydrido dianion **1a** and **1b**, differing in the position of the fourth H ligand, and distributed randomly through the crystal. The first isomer **1a** has virtual C_2 symmetry (Fig. 1 top) and the fourth H ligand, H4a, bridges the edge Os7–Os8; in isomer **1b** the corresponding hydride, H4b, bridges Os8–Os9 (Fig. 1 bottom). Significantly, two alternative orientations for a carbonyl ligand on Os8 were resolved and the two components, CO82a and CO82b, were assigned to isomers **1a** and **1b**, respectively.[21] The bridged Os–Os distances show the characteristic lengthening associated with hydrogen ligands (range for H-bridged 2.855 to 2.910(8); for unbridged 2.733 to 2.816 Å). The results from this study demonstrate an essential role for neutron diffraction in full characterization of large hydrido metal clusters.[22] Preliminary results with neutron data collected for **1** at 295 K show a similar hydride distribution to that in the low-temperature study.

The two μ_3 sites occupied by the H ligands in **1** are the first examples of cluster hydrides located in the center of a large planar array of surface metal atoms. Their very congested locations correspond to potential energy minima which are an order of magnitude greater than that associated with the μ_3 H site in the hexanuclear cluster **2** (calculated using the HYDEX programme written by *Orpen*[9]). Computed space filling models[23] (Fig. **2**) show that the H atoms are partially

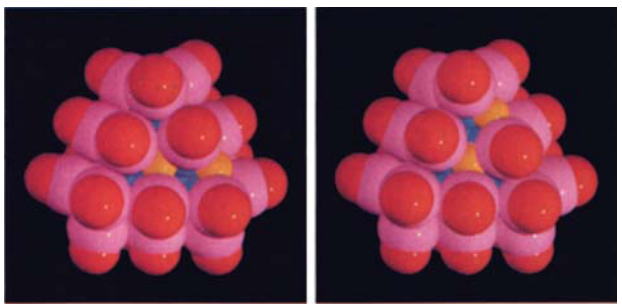

Fig. 2. Computed space-filling models of the two isomers viewed perpendicular to the faces at the front of the views in Fig. 1, that is onto the H1 μ_3 site defined by Os6, Os8, and Os10: (a) isomer **1a** showing the μ_2 H atom H4a; (b) isomer **1b** showing the μ_2 H atom H4b.

submerged under the van der Waals spheres of the three nearest CO ligands in a completely different arrangement from that observed on the surface of smaller clusters.[6, 8, 10] The nearly close-packed distribution of the carbonyl ligands round the μ_3 H atoms in **1** gives rise to some remarkably short C···H contact distances (2.23 to 2.35 Å), compared to a range of 2.48 to 2.70 Å for the three shortest C···H contacts in the neutron study of $[HOs_6(CO)_{18}]^-$ at 20 K.[10] Incipient C···H interaction between the CO ligands and the H atoms on the faces may be deduced from the concerted slight displacement of the oxygen atoms of the carbonyl ligands away from the occupied μ_3 sites which can be seen in Figure 2; this feature is absent in the two unbridged faces of the cluster. These results provide the best molecular model so far for chemisorption at high density of carbon monoxide and hydrogen on (111) or (001) surfaces of metals.

Reveived: April 5, 1991 [Z 4555 IE]
German version: *Angew. Chem. 103* (1991) 1186

CAS Registry number:
$[H_4Os_6(CO)_{24}][(Ph_3P)_2N]_2$, 110371-99-8.

[1] Representative references are: E. L. Muetterties, *Angew. Chem. 90* (1978) 577; *Angew. Chem. Int. Ed. Engl. 17* (1978) 545; E. L. Muetterties, T. N. Rhodin, E. Band, C. F. Brucker, W. R. Pretzer, *Chem. Rev. 79* (1979) 91; G. Ertl, *Gazz. Chim. Italiana 109* (1979) 217.
[2] P. F. Jackson, B. F. G. Johnson, J. Lewis, M.-C. Malatesta, M. McPartlin, W. J. H. Nelson, *J. Chem. Soc. Chem. Commun. 1982*, 49.
[3] D. Braga, B. F. G. Johnson, J. Lewis, M. McPartlin, W. J. H. Nelson, M. D. Vargas, *J. Chem. Soc. Chem. Commun. 1983*, 241.
[4] P. J. Bailey, B. F. G. Johnson, J. Lewis, M. McPartlin, H. R. Powell, *J. Organomet. Chem. 377* (1989) C17.
[5] M. R. Churchill, J. Wormald, *J. Am. Chem. Soc. 93* (1971) 5670.
[6] M. McPratlin, C. R. Eady, B. F. G. Johnson, J. Lewis, *J. Chem. Soc. Chem. Commun. 1976*, 883.
[7] D. Braga, K. Henrick, B. F. G. Johnson, J. Lewis, M. McPartlin, W. J. H. Nelson, M. D. Vargas, *J. Chem. Soc. Chem. Commun. 1982*, 419; *J. Chem. Soc. Dalton Trans. 1984*, 2151.
[8] K. Henrick, M. McPartlin, J. Morris, *Angew. Chem. 97* (1986) 843; *Angew. Chem. Int. Ed. Engl. 25* (1986) 853.
[9] A. G. Orpen, *J. Chem. Soc. Dalton Trans. 1980*, 2509.
[10] A. G. Orpen, T. F. Koetzle, *Acta Crystallogr. C43* (1987) 2084.
[11] C. R. Eady, B. F. G. Johnson, J. Lewis, M.-C. Malatesta, P. Machin, M. McPartlin, *J. Chem. Soc. Chem. Commun. 1976*, 945; C. R. Eady, B. F. G. Johnson, J. Lewis, M.-C. Malatesta, M. McPartlin, W. J. H. Nelson, *J. Chem. Soc. Dalton Trans. 1980*, 383.
[12] P. Chini, G. Longoni, S. Martinengo, A. Ceriotti, *Adv. Chem. Ser. 167* (1978) 1.
[13] P. F. Jackson, B. F. G. Johnson, J. Lewis, P. Raithby, M. McPartlin, W. J. H. Nelson, K. D. Rouse, J. Allibon, S. Mason, *J. Chem. Soc. Chem. Commun. 1980*, 295.
[14] D. W. Hart, R. G. Teller, C. Y. Wei, R. Bau, G. Longoni, S. Campanella, P. Chini, T. F. Koetzle, *Angew. Chem. 91* (1979) 86; *Angew. Chem. Int. Ed. Engl. 18* (1979) 80.
[15] P. F. Jackson, B. F. G. Johnson, J. Lewis, M. McPartlin, W. J. H. Nelson, *J. Chem. Soc. Chem. Commun. 1980*, 224; *J. Chem. Soc. Dalton Trans. 1982*, 2099.
[16] E. C. Constable, B. F. G. Johnson, J. Lewis, G. N. Pain, M. J. Taylor, *J. Chem. Soc. Chem. Commun. 1982*, 754.
[17] More efficient routes to **1**, giving substantially higher yields of the cluster (>20%), have recently been developed and involve the thermolysis of derivatives of $Os_3(CO)_{12}$ in alcohols: A. J. Amoroso, L. H. Gade, B. F. G. Johnson, J. Lewis, unpublished.
[18] K. Wade, *Adv. Inorg. Chem. Radiochem. 18* (1976) 1; R. Mason, K. M. Thomas, D. M. P. Mingos, *J. Am. Chem. Soc. 95* (1973) 3802.
[19] The ^{13}C NMR spectrum of **1** recorded in CD_2Cl_2 at 295 K consists of two (exchange-broadened) carbonyl resonance signals at $\delta = 175.8$ and 192.9 which coalesce at 230 K. Below that temperature the spectra display a complicated pattern of exchange processes which have to date not been fully understood. It proved impossible to obtain a low temperature limit spectrum even at 170 K.
[20] Crystal data for $[(PPh_3)_2N]$-**1** (neutron, 20 K): $C_{96}H_{64}N_2O_{24}P_4Os_{10}$, $M_r = 3655.5$, triclinic, space group $P\bar{1}$ (No. 2), $a = 26.641(1)$, $b = 17.234(1)$, $c = 10.428(1)$ Å, $\alpha = 96.701(2)$, $\beta = 100.672(3)$, $\gamma = 86.148(3)°$, $Z = 2$, $V = 4667.75$ Å^3, ϱ_{calcd} (20 K) = 2.600 g cm^{-3}, $\lambda = 1.3150(2)$ Å (Ge(115) monochromatic thermal neutrons), $T = 20$ K (Displex cryorefrigerator), $\mu = 1.25$ cm^{-1}. Crystal size ca. $0.15 \times 0.20 \times 0.35$ cm; four-circle neutron diffractometer D19, equipped with a position-sensitive detector. A total of 8125 data were recorded, of which 4875 were unique. 4131 absorption corrected data [$I/\sigma(I) > 2.0$] were used in full-matrix refinement of the atomic parameters obtained previously from X-ray data [2] together with those located from this study ($R = 0.0897$; $R_w = 0.0941$). Further details of the crystal structure investigation are available on request from the Director of the Cambridge Crystallographic Data Centre,

University Chemical Laboratory, Lensfield road, GB-Cambridge CB2 1EW (UK), on quoting the full journal citation.

[21] After inclusion of the hydrido H atoms in the model, the highest residual peak was positive (of height approximately 0.2 that of a C atom) and very close to the center of the Os_6 octahedron. The ^{13}C NMR spectra of **1** from the batch used in the neutron study indicated the presence of ca. 20% of the carbido dianion, (**5**) (known to be isomorphous with **1** as its $[(Ph_3P)_2N]^+$ salt). The residual density was therefore interpreted as due to a random 20% occupation of the cluster site by the virtually isostructural carbido dianion. The parameters of the carbido C atom (occupancy 0.2) refined satisfactorily, and the hydrido H atoms and the disordered carbonyl ligand CO82 were therefore assigned overall 0.8 total occupancy.

[22] This study clearly demonstrates that negative evidence for surface location of H ligands in large clusters is unreliable, and the question of the exact location of all the H atoms formerly assigned to interstitial tetrahedral sites must be re-examined. For example the X-ray evidence for the interstitial nature of the H ligand in $[HOs_{10}C(CO)_{24}]^-$ can, with hindsight, be explained by an external μ_2 H and threefold disorder of the cluster anion in the Ph_4As^+ salt and sixfold disorder in the Ph_3PMe^+ salt [2]. Significantly, preliminary X-ray results for the dihydride $[H_2Os_{10}C(CO)_{24}]$ show a similar disorder of two carbonyl ligands to that observed in **1** and have been interpreted as indicating two μ_2 H ligands on the surface (D. Braga, University of Bologna, personal communication).

[23] Calculated using a molecular graphics programme CHEM-RAY: J. W. Lauher, *J. Mol. Graphics 8* (1990) 34. The osmium atoms were assigned covalent radii of 1.5 Å to give a clearer view of the surface ligands. All other atoms have spheres of van der Waals radii [8].

Metal-Centered Coupling of Two Carbyne Ligands To Form an Alkyne Ligand**

By *Alexander Constantin Filippou,* Walter Grünleitner, Christian Völkl,* and *Paul Kiprof*

The coupling of two carbyne ligands to form an acetylene ligand according to $M(CH)_2 \rightarrow M(C_2H_2)$ is symmetry-allowed for d^4 metal centers.[1a] In fact, MO calculations [1b] on the hypothetical 18-electron d^4 complexes $[W(CH)_2Cl_2(CO)_2]$ and $[W(CH)_2Cp(CO)]^+$[2] predict a spontaneous rearrangement to the 16-electron acetylene complexes $[W(\eta^2\text{-}HC{\equiv}CH)Cl_2(CO)_2]$ and $[W(\eta^2\text{-}HC{\equiv}CH)Cp(CO)]^+$, which may be stabilized by complexation with further ligands. However, these calculations also indicate that π-donor substituents on the carbyne carbon stabilize the bis(carbyne) form relative to the alkyne complex. Mononuclear bis(carbyne) complexes are extremely rare, but are often postulated as intermediates in C–C coupling reactions that form alkyne complexes from carbyne precursors.[3]

We have now prepared the first bis(carbyne) complexes of tungsten and selectively converted them into alkyne complexes. The starting materials for the three-stage synthesis are the η^5-C_5Me_5 tungsten complexes **1a** and **1b**[4] (Scheme 1). Treatment of **1a** with *t*BuNC leads to the displacement of the CO ligand to form **2**, which is then reduced to **4** with sodium amalgam in the presence of *t*BuNC. A similar reaction sequence for **1b** leads via **3** to the ethyl isocyanide derivative **5**. The monocarbyne complexes **4** and **5** are finally alkylated with $[Et_3O]BF_4$ to yield selectively the yellow bis(carbyne) derivatives **6** and **7**, respectively.

Nucleophilic reagents induce coupling of the two carbyne ligands in **7** to form an alkyne unit. Thus reaction of **7** with

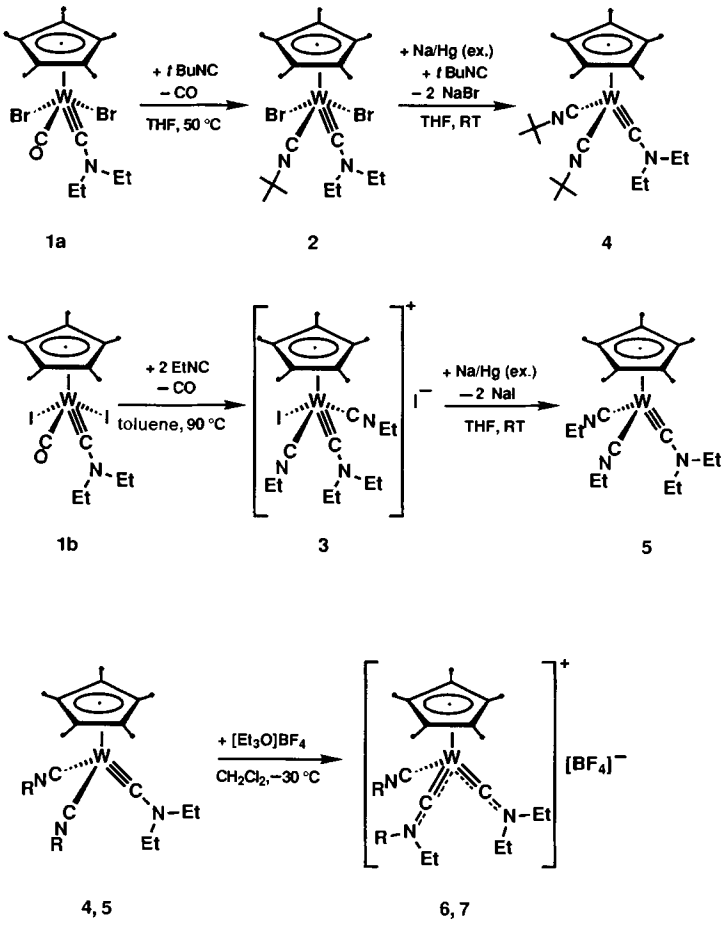

Scheme 1. RT = room temperature, ex. = excess.

ethyl isocyanide yields the W^{II} complex **8** (Scheme 2). A coupling of the two carbyne ligands is also induced by oxidizing agents, as shown by the reaction of **7** with Br_2 which affords the W^{IV}-alkyne complex **9** (Scheme 2).

The bis(carbyne) complexes **6** and **7**[2] are unusually thermally stable: compound **6** decomposes only after several

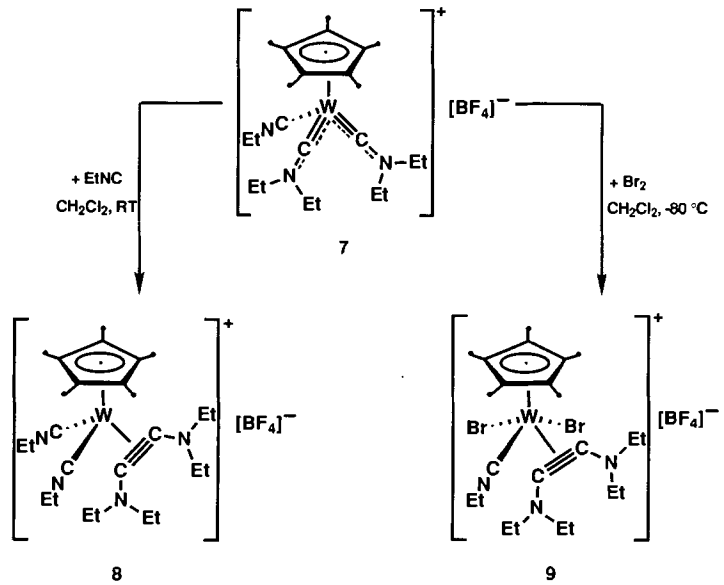

Scheme 2.

[*] Dr. A. C. Filippou, Dr. W. Grünleitner, Dipl.-Chem. C. Völkl, Dipl.-Chem. P. Kiprof
Anorganisch-Chemisches Institut der Technischen Universität München
Lichtenbergstrasse 4, W-8046 Garching (FRG)

[**] This work was supported by the Volkswagen-Stiftung and the Leonhard-Lorenz-Stiftung. We thank Prof. *W. A. Herrmann* and Prof. *E. O. Fischer* for support of our work and Prof. *P. Hofmann* for discussions.

hours in CH_2Cl_2 at room temperature and **7** in the solid state only above 63 °C. In contrast to the IR spectra of the monocarbyne precursors **4** and **5**, two characteristic absorption bands at ca. 1530 and 1600 cm^{-1} for the stretching vibration ν(CN) of the aminocarbyne ligands are found for both **6** and **7** (Table 1).[4] Furthermore, the ^{13}C NMR spectrum of **6** shows two characteristic resonance signals for the carbyne-C atoms at low field, and that of **7** one ($\delta \approx 280$). The $^1J_{WC}$ coupling constants for **6** and **7** (ca. 230 Hz) lie within the expected range for a W–C triple bond.[5a] In the ^{13}C NMR spectra of the coupling products **8** and **9**, however, resonance signals are observed at $\delta \approx 200$, which is typical of a 4-electron alkyne ligand (see also the alkyne-C resonance signals of **12**–**14**).[3c, d, 5b] Evidence of the formation of another W^{II}-bis(carbyne) complex (**11**) in the reaction of the carbyne complex **10** (accessible from $[W(EtNC)_6]$)[3e] with $[Et_3O]BF_4$ is found in the IR spectrum (Scheme 3). Further experimental proof for the formation of **11** is provided by its nucleophile-induced carbyne–carbyne coupling reaction with NEt_4Br to yield the alkyne complex **13** (W^{II}), by the alternative synthesis of **13** from $W(CO)_6$ and $Et_2NC{\equiv}CNEt_2$ (Scheme 4, DME = dimethoxyethane), and by the X-ray structure of the analogous coupling product **14** (Fig. 1).[6]

Table 1. Selected spectroscopic data of **2**–**9** and **11**–**14** [a].

2: IR: $\tilde{\nu}$[cm^{-1}] = 2134s (ν(C≡N*t*Bu)), 1578 m (ν(C=N)); $^{13}C\{^1H\}$ NMR: δ = 164.0 (*t*BuN*C*), 304.4 (W≡*C*, ^1J(W,C) = 219.7 Hz)

3: IR: $\tilde{\nu}$[cm^{-1}] = 2200 w,sh, 2174 s (ν(C≡NEt)), 1596 m (ν(C=N)); $^{13}C\{^1H\}$ NMR: δ = 146.8 (EtN*C*), 298.3 (W≡*C*)

4: IR (pentane): $\tilde{\nu}$[cm^{-1}] = 1926 m, 1811 s (ν(C≡N*t*Bu)), 1506 m (ν(C=N)); ^1H NMR (C_6D_6, 20 °C): δ = 1.19 (t, 6H, ^3J(H,H) = 7.3 Hz; N(CH_2CH_3)$_2$), 1.34 (s, 18H; Me_3C), 2.23 (s, 15H; C_5Me_5), 2.70 (q, 4H, ^3J(H,H) = 7.3 Hz; N(CH_2CH_3)$_2$); $^{13}C\{^1H\}$ NMR (C_6D_6, 20 °C): δ = 221.8 (*t*BuN*C*), 258.0 (W≡*C*); EI MS (70 eV): *m/z* 570 ($[M + H]^+$, basis peak), 540 ($[M - Et]^+$), 513 ($[M - Me_2C{=}CH_2]^+$), 457 ($[M - 2Me_2C{=}CH_2]^+$)

5: IR (pentane): $\tilde{\nu}$[cm^{-1}] = 1915 m, 1823 s (ν(C≡NEt)), 1511 m (ν(C=N)); $^{13}C\{^1H\}$ NMR (C_6D_6, 20 °C): δ = 223.9 (EtN*C*), 257.9 (W≡*C*)

6: IR: $\tilde{\nu}$[cm^{-1}] = 2157 s (ν(C≡N*t*Bu)), 1601 m, 1522 s (ν(C=N)); $^{13}C\{^1H\}$ NMR: δ = 152.6 (*t*BuN*C*), 276.2 (W≡*C*. ^1J(W,C) = 233.0 Hz), 278.1 (W≡*C*, ^1J(W,C) = 230.4 Hz)

7: IR: $\tilde{\nu}$[cm^{-1}] = 2174 s (ν(C≡NEt)), 1610 m, 1539 s (ν(C=N)); ^1H NMR (CD_2Cl_2, −80 °C): δ = 1.18 (t, 12H, ^3J(H,H) = 7.3 Hz; 2 × N(CH_2CH_3)$_2$), 1.35 (t, 3H, ^3J(H,H) = 7.3 Hz; CH_3CH_2NC), 2.06 (s, 15H; C_5Me_5), 3.15 (dq, 4H, $^2J(H_BH_A)$ = 13.4, ^3J(H,H) = 7.3 Hz; 2 × N($CH_AH_BCH_3$)$_2$), 3.31 (dq, 4H, $^2J(H_A,H_B)$ = 13.4, ^3J(H,H) = 7.3 Hz; 2 × N($CH_AH_BCH_3$)$_2$), 3.84 (q, 2H, ^3J(H,H) = 7.3 Hz; CH_3CH_2NC); $^{13}C\{^1H\}$ NMR (CD_2Cl_2, −80 °C): δ = 154.8 (EtN*C*), 276.2 (W≡*C*, ^1J(W,C) = 229.8 Hz); FD MS (CH_2Cl_2): *m/z* 542 (M^+)

8: IR: $\tilde{\nu}$[cm^{-1}] = 2196 w,sh, 2169 s, 2146 s (ν(C≡NEt)), 1629 m, 1579 m (ν(C=N)); $^{13}C\{^1H\}$ NMR: δ = 147.9, 152.0 (EtN*C*), 206.6, 210.0 (C≡C); FD MS (CH_2Cl_2): *m/z* 597 (M^+)

9: IR: $\tilde{\nu}$[cm^{-1}] = 2209 s, 2192 m (ν(C≡NEt)), 1647 vs (ν(C=N)); $^{13}C\{^1H\}$ NMR (CD_2Cl_2, −80 °C): δ = 142.9 (EtN*C*), 200.2, 207.6 (C≡C); FD MS (CH_2Cl_2): *m/z* 700 (M^+)

11: IR: $\tilde{\nu}$[cm^{-1}] = 2195 w, 2144 vs, (ν(C≡NEt)), 1558 w (ν(C=N))

12: IR: $\tilde{\nu}$[cm^{-1}] = 2210 m, 2193 m, sh, 2172 vs, 2141 w, sh, (ν(C≡NEt)), 1984 s (ν(C≡O)), 1661 s (ν(C=N)); $^{13}C\{^1H\}$ NMR: δ = 143.1 (1 × EtN*C*), 145.5 (2 × EtN*C*), 185.6 (C≡C), 206.3 (CO)

13: IR: $\tilde{\nu}$[cm^{-1}] = 2198 w, 2145 vs, 2095 w,br (ν(C≡NEt)), 1657 m (ν(C=N)); $^{13}C\{^1H\}$ NMR: δ = 152.0 (EtN*C*), 186.7 (C≡C); FD-MS (CH_2Cl_2): *m/z* 651 (M^+)

14: IR: $\tilde{\nu}$[cm^{-1}] = 2176 w, 2125 vs, 2055 w,br (ν(C≡N*t*Bu)), 1655 m (ν(C=N)); $^{13}C\{^1H\}$ NMR: δ = 152.6 (*t*BuN*C*), 187.7 (C≡C)

[a] Correct elemental analyses of all compounds have been obtained. IR spectra in CH_2Cl_2 (if not stated otherwise); ^1H (400 MHz) and ^{13}C (100.5 MHz) NMR spectra in CD_2Cl_2 at 20 °C (if not stated otherwise); mass spectra: *m/z* values relative to the ^{184}W and ^{79}Br isotopes.

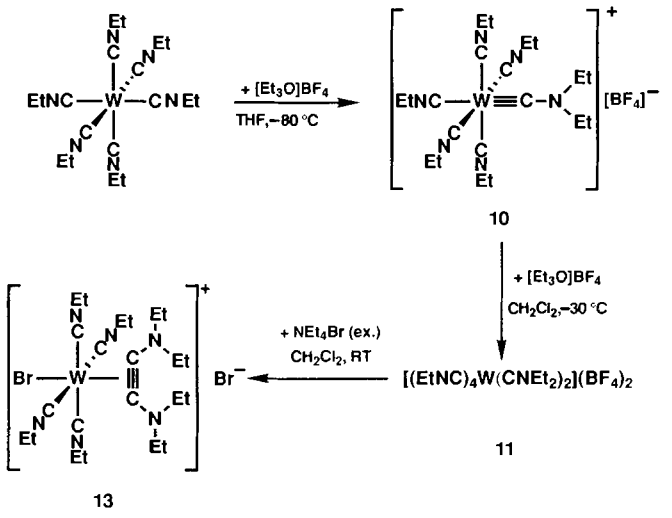

Scheme 3. ex. = excess.

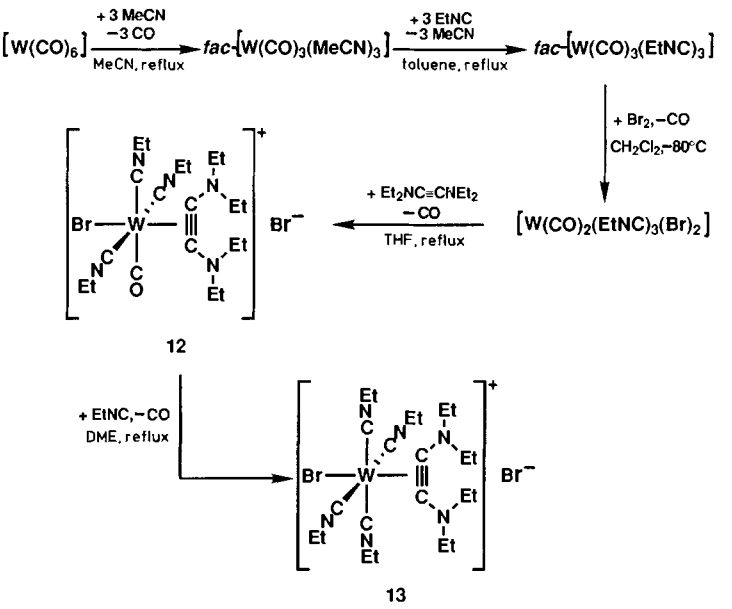

Scheme 4. DME = dimethoxyethane.

$[W(\eta^2\text{-}Et_2NC{\equiv}CNEt_2)Br(t\text{BuNC})_4]PF_6$ **14**

Outstanding features of **14**, the first structurally characterized complex of bis(diethylamino)acetylene, are the bond distances and angles in the alkyne ligand, which suggest strong π-bond delocalization.[5b] The octahedral geometry of the cation is distorted: the four equatorial isocyanide groups tilt toward the bromine ligand (Fig. 1).

These results support our hypothesis[3c–e] that bis(carbyne) complexes are key intermediates in the electrophilically induced carbyne–isocyanide coupling reaction of electron-rich carbyne complexes and in the reductive isocyanide–isocyanide coupling reaction of $[M(RNC)_6X]^+$ complexes (X = halogen) to form the alkyne complexes, $[M\{\eta^2\text{-}R(H)NC{\equiv}CN(H)R\}X(RNC)_4]^+$. This new mechanistic information is particularly important with respect to the stoichiometric reductive coupling of CO ligands in low-valent niobium and tantalum complexes[3g] and the catalytic hydrogenation of carbon monoxide (Fischer–Tropsch synthe-

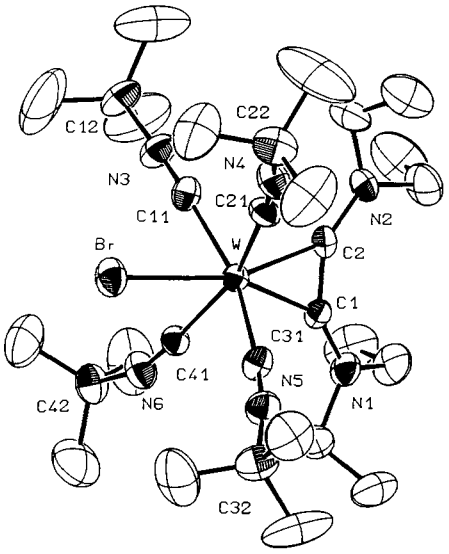

Fig. 1. Structure of the cation of **14** in the crystal (ORTEP). Selected bond lengths [pm] and angles [°]:W-Br 265.9(1), W-C1 204.6(5), W-C2 203.7(5), C1-C2 137.7(7), C1-N1 132.5(7), C2-N2 133.3(7); Br-W-C11 82.9(2), Br-W-C21 80.4(2), Br-W-C31 81.8(1), Br-W-C41 81.3(1), N1-C1-C2 144.3(5), C1-C2-N2 142.7(5).

sis),[7] since the factors promoting such processes are now better understood.

Experimental Procedure

2: A solution of **1a** (0.28 g, 0.47 mmol) in THF (50 mL) was treated with *t*BuNC (0.044 g, 0.06 mL, 0.53 mmol) and heated for 3 h at 50 °C. Evaporation of the solvent yielded the product as a red-violet solid. Yield: 0.30 g (98%); m.p. 148 °C.

4: A solution of **2** (0.35 g, 0.54 mmol) in THF (50 mL) was treated with *t*BuNC (0.052 g, 0.07 mL, 0.62 mmol) and Na/Hg (0.40 mL, 0.85% w/w, 1.99 mmol Na) and stirred at room temperature for 5 h. Thereafter, the red solution was filtered to remove the amalgam and precipitated NaBr, the filtrate evaporated to dryness, and the residue purified by chromatography on neutral alumina (45 × 1.5 cm; eluant pentane/Et_2O, 1/1) at 0 °C. Yield: 0.185 g (60%) of a yellow microcrystalline solid; m.p. 35 °C.

7: A solution of **5** (0.13 g, 0.25 mmol) in CH_2Cl_2 (30 mL) was treated at −78 °C with a solution of $[Et_3O]BF_4$ (0.048 g, 0.25 mmol) in CH_2Cl_2 (5 mL), warmed to −30 °C, and stirred for 2 h. After removal of the solvent at −30 °C, complex **7** was isolated as a yellow solid. Yield: 0.16 g (quantitative); m.p. 63 °C (dec.).

9: A solution of **7** (0.18 g, 0.29 mmol) in CH_2Cl_2 (25 mL) was treated at −78 °C with a solution of Br_2 (0.046 g, 0.015 mL, 0.29 mmol) in CH_2Cl_2 (10 mL), warmed to room temperature, and stirred for 1 h. The lilac solution was then evaporated to dryness, and the residue recrystallized from CH_2Cl_2/pentane. Yield: 0.22 g (97%); m.p. 135 °C.

13: A solution of **12** (0.36 g, 0.51 mmol) in dimethoxyethane (80 mL) was treated with EtNC (0.031 g, 0.042 mL, 0.56 mmol), heated for 5 h under reflux, and thereafter evaporated to dryness. The residue was recrystallized from THF/Et_2O. Yield: 0.34 g (91%) of a lilac solid; m.p. 136 °C.

Received: May 8, 1991 [Z4617 IE]
German version: *Angew. Chem. 103* (1991) 1188

CAS Registry numbers:
1a, 121795-91-3; **1b**, 121795-92-4; **2**, 135004-63-6; **3**, 135004-64-7; **4**, 135004-65-8; **5**, 135004-66-9; **6**, 135004-68-1; **7**, 135004-70-5; **8**, 135004-12-7; **9**, 135004-74-9; **11**, 135004-76-1; **12**, 135004-77-2; **13**, 135004-78-3; **14**, 135004-80-7; *t*BuNC, 7188-38-7; EtNC, 624-79-3; $Et_2NC{\equiv}CNEt_2$, 5323-13-7; $[W(CO)_2(EtNC)_3(Br)_2]$, 129232-08-2.

[1] a) C. N. Wilker, R. Hoffmann, O. Eisenstein, *Nouv. J. Chim. 7* (1983) 535; b) P. Hofmann, H. R. Schmidt, unpublished; H. R. Schmidt, *Dissertation*, Technische Universität München 1988.

[2] The carbyne unit (CH, CR) is here considered a neutral 3e donor ligand (see also [1a]). The resulting d^4 tungsten center cannot form two dπ-pπ back bonds to each carbyne ligand in these compounds for electronic reasons: H. Fischer, P. Hofmann, F. R. Kreißl, R. R. Schrock, U. Schubert, K. Weiss: *Carbyne Complexes*, VCH, Weinheim 1988, p. 59.

[3] a) J. Chatt, A. J. L. Pombeiro, R. L. Richards, *J. Chem. Soc. Dalton Trans. 1980*, 492; b) G. A. McDermott, A. Mayr, *J. Am. Chem. Soc. 109* (1987) 580; c) A. C. Filippou, W. Grünleitner, *Z. Naturforsch. B44* (1989) 1023; *ibid. 46* (1991) 216; d) A. C. Filippou, *Polyhedron 9* (1990) 727; e) A. C. Filippou, W. Grünleitner, *J. Organomet. Chem. 393* (1990) C10; f) A. Mayr, C. M. Bastos, *J. Am. Chem. Soc. 112* (1990) 7797; g) R. N. Vrtis, S. J. Lippard, *Isr. J. Chem. 30* (1990) 331.

[4] A. C. Filippou, W. Grünleitner, *J. Organomet. Chem. 407* (1991) 61.

[5] a) F. H. Köhler, H. J. Kalder, E. O. Fischer, *J. Organomet. Chem. 113* (1976) 11; b) J. L. Templeton, *Adv. Organomet. Chem. 29* (1989) 1.

[6] **14**: Red-violet needles from CH_2Cl_2/pentane; systematic absences: (*h*00) (*h* = 2n + 1), (0*k*0) (*k* = 2n + 1); space group $P2_1/a$ (no. 14); lattice constants from a least-squares refinement of 15 reflections at high diffraction angles; $a = 1791.8(2)$, $b = 1489.3(2)$, $c = 1542.0(2)$ pm, $\beta = 90.71(1)°$; $V = 4115 \times 10^6$ pm^3; molecular formula: $C_{30}H_{56}BrF_6N_6PW$, $M_r = 909.5$, $Z = 4$, $\varrho_{calcd} = 1.47$ g cm^{-3}; $F_{000} = 1824$; Syntex $P2_1$ diffractometer, $Mo_{K\alpha}$ radiation ($\lambda = 71.073$ pm), graphite monochromator; $T = -50 \pm 3$ °C; $1.0° \leq \theta \leq 25°$; ω scan; scan speed 0.8–29.3° min^{-1}; 7787 measured reflections ($+h, +k, \pm l$); empirical absorption correction (10 reflections), $\mu = 37.1$ cm^{-1}; structure solution by Patterson methods and difference Fourier techniques; 7235 independent reflections of which 6438 with $I > 2.0\sigma(I)$ were used for refinement; 467 parameters, full-matrix least-squares refinement, $R = \Sigma(\|F_o| - |F_c\|)/\Sigma|F_o| = 0.042$; $R_w = [\Sigma(w|F_o| - |F_c|)^2/\Sigma wF_o^2]^{1/2} = 0.041$ ($w = 1/\sigma^2[F_o]$; shift/err < 0.01 in the last refinement cycle; Δe_0 Å$^{-3} = +0.94, -0.70$; hydrogen atoms calculated in ideal geometry ($d_{C,H} = 95$ pm) and not refined, anomalous dispersion taken into account. Further details of the crystal structure investigation may be obtained from the Fachinformationszentrum Karlsruhe, Gesellschaft für wissenschaftlich-technische Information mbH, W-7514 Eggenstein-Leopoldshafen 2 (FRG) on quoting the depository number CSD-55623, the names of the authors and the journal citation.

[7] a) E. L. Muetterties, J. Stein, *Chem. Rev. 79* (1979) 479; b) K. M. Nicholas, *Organometallics 1* (1982) 1713.

The Synthesis and Structure of Some New Sodalites: The Lithium Haloberyllophosphates and -Arsenates**

By *Thurman E. Gier, William T. A. Harrison,* and *Galen D. Stucky**

The arrangement of atoms in the sodalite structure, first elucidated in 1930 by *Pauling*[1] for its mineral namesake, $Na_8Cl_2(Al_6Si_6O_{24})$, is a remarkably versatile one. The sodalite cage occurs as a building block in the commercially important zeolites X, Y, A, and related zeolite structures such as "hexagonal Y",[2] and may occur in other aluminosilicates whose structures have not yet been determined. Since the first structure determination, several elements (other than the Al/Si pair) have been found to be capable (along with oxygen) of forming sodalite-like structures: $(B_{12}O_{24})$,[3] $(Si_{12}O_{24})$,[4] $(Al_{12}O_{24})$,[5] $(Al_6P_6O_{24})$,[6] $(Be_6Si_6O_{24})$,[7] $(Be_6Ge_6O_{24})$,[8] $(Al_2Be_2Si_8O_{24})$,[9] $(Ga_6Si_6O_{24})$,[10] and more recently, $(Zn_6(P,As)_6O_{24})$.[11] Substitutions on the extra-framework sites are also possible; at least some of the cage centers tolerate all of the chalcogenides[3, 8, 9] including polysulfides and selenides,[12] the larger halides,[14] and oxyanions such as SO_4^{2-} and WO_4^{2-}.[5] The sodium sites may be fully or partially occupied by Li^+, K^+, Rb^+, or Ag^+[15] and Zn^{2+}, Mn^{2+}, Co^{2+}, and Cd^{2+}.

In the course of exploring new molecular sieves and open framework structures based on $(MXO_4)^-$ framework units, including $BePO_4^-$,[16–18] $BeAsO_4^-$,[13] $ZnPO_4^-$,[11, 13] and $ZnAsO_4^-$[11, 13] which have the same net framework charge

[*] Prof. Dr. G. D. Stucky, T. E. Gier, W. T. A. Harrison
Department of Chemistry, University of California
Santa Barbara, CA 93106-9510 (USA)

[**] The authors gratefully acknowledge the support of the National Science Foundation through a Division of Materials Research (DMR) Grant and The National Science Foundation Quantized Electronic Structures Center.

as the well-known aluminosilicates, analogues of zeolite X, Li–A(BW) and Rho as well as the zincophosphate and zincoarsenate sodalite have been prepared.[13] Here we report the synthesis and structure of the lithium haloberyllophosphates and -arsenates as additions to the sodalite family.

Microcrystalline powders suitable for Rietveld structure determination were prepared hydrothermally in sealed gold capsules at elevated temperatures and pressures; for instance, $Li_8Br_2(Be_6P_6O_{24})$ was prepared from $LiBePO_4$ and LiBr (see *Experimental Procedure*). If LiCl or LiI are substituted for the bromide salt under the same conditions, the corresponding chloro- (a = 8.025(2) Å) or iodo- (a = 8.162(2) Å) congeners are formed. Similarly, if $LiBeAsO_4$ is used, the corresponding chloro- or bromoarsenates result. (a = 8.238(2) Å and 8.286(2) Å respectively). One species, the iodoarsenate, could not be prepared in this fashion, because the iodide ion was extensively oxidized to free iodine by As^V. For reasons not presently known, the hydroxo hydrate analogues, commonly known in the aluminosilicate structure field, have also resisted synthesis.

Only the boralite sodalites (e.g. $Zn_8O_2(B_{12}O_{24})$, a = 7.4659(3) Å) have a smaller unit cell than these new phases, and the corresponding small size of the 6-ring "windows" militates against ion exchange. Apparently no sodium will exchange for the lithium in the lithium bromoberyllophosphate (molten $NaNO_3$, 325 °C, 3 days), but silver exchanges very slowly (molten $AgNO_3$, 265 °C, 5 days) and the cell edge increases to 8.350(3) Å. The extent of silver exchange is unknown, but under these conditions of "stuffing", the structure is marginally stable since traces of AgBr and Ag_3PO_4 appear among the products.

The second harmonic generation (Nd: YAG laser) of these materials was measured and a small but distinct response found (about three times as intense as that of quartz) confirming the acentric space group. Final observed, calculated and difference profile plots for Li/Br-BePO are illustrated in Figure 1.

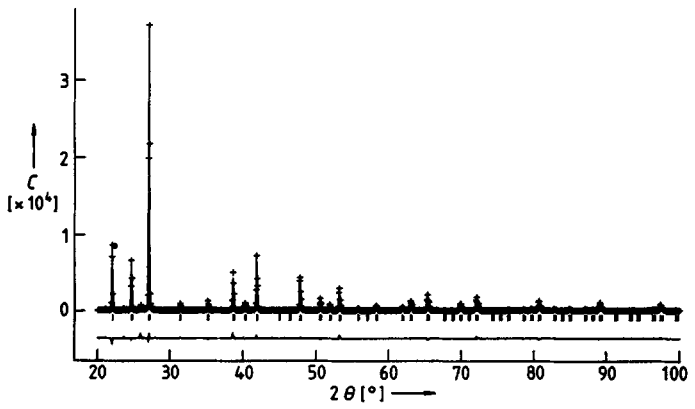

Fig. 1. Structure determination of $Li_8Br_2(Be_6P_6O_{24})$: Final observed (+), calculated (−), and difference profile plots. Allowed reflection positions are indicated by tick marks (|). C = count rate.

The new composition (see *Experimental Procedure*) of the sodalite framework[21] of $[Li_8Br_2(Be_6P_6O_{24})]$ consists of face-sharing truncated octahedra, built up from ordered BeO_4 and PO_4 tetrahedral units. The Be : P ratio is 1 : 1 and the BeO_4 and PO_4 units alternate throughout the structure, as indicated by the bond-distance results (see legend of Fig. 2). Consequently, no refinements of a disordered framework model were attempted. This Be/P/O topology results in spherical cavities (β cages) of approximate diameter 5.5 Å,

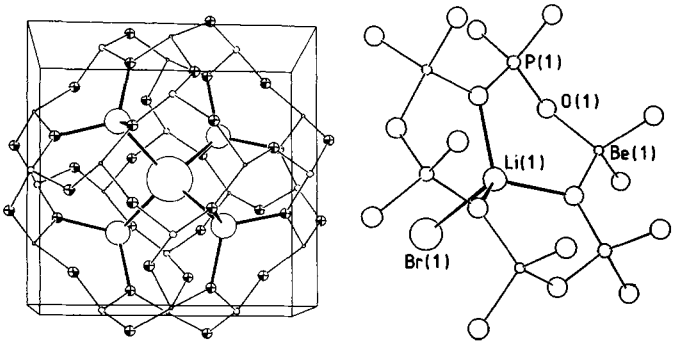

Fig. 2. Left: ORTEP view of the Be/P/O sodalite cage framework, enclosing the tetrahedral Li_4Br unit. For the framework, Be atoms are small circles, P atoms medium circles, and O atoms shaded circles. The large bromide anion is tetrahedrally surrounded by four lithium cations, which in turn make three bonds to the oxygen atoms of the framework. Right: Environment of the Li cation. Selected bond lengths [Å] (standard deviations in parentheses): Be(1)-O(1) 1.620(3), P(1)-O(1) 1.548(3); Li(1)-O(1) 1.923(6); Li(1)-Br(1), 2.685(18).

interconnected via six-rings of approximate diameter 2.2 Å. The $(BePO_4)_6$ framework has an overall negative charge which is compensated by the positive charge of the two $(Li_4Br)^{3+}$ units which reside in the β cages, giving an overall unit cell stoichiometry of $Li_8Br_2(Be_6P_6O_{24})$.

The lithium cations approximately occupy the sodalite 6-ring windows (site symmetry .3.), and are threefold coordinated by framework oxygens. Each also sees the bromine anion at the center of the β cage resulting in distorted tetrahedral geometry (Fig. 2). The bromine anion sees a regular tetrahedron of four lithium cations (23. symmetry). The closest lithium–lithium contact between cages is 4.255(9) Å. The average O–Be–O and O–P–O tetrahedral angles are 110.3(3)° and 110.7(3)° respectively. The Be–O–P framework bond angle is 128.9(2)°, compared with an average of 136(2)° in the zeolite-X analogue, BePO-X,[18] and 134.2(6)° in the zeolite rho analogue, pahasapaite.[16]

By using low temperature synthesis (< 80 °C) the sodalite cage structure was previously found in structures of zeolite X-analogues containing only either Group 2 or Group 12 metal atoms (beryllium and zinc).[18] The synthesis of zinc[11] and beryllium phosphate/arsenate structures analogous to sodalite is further evidence for the existence of an extensive field of molecular-sieve structures based on Group 2 and 12 metals.

Experimental Procedure

A typical preparation may be carried out as follows: for $Li_8Br_2(Be_6P_6O_{24})$, 2.664 g (24 mmol) of $LiBePO_4$ (prepared by standard solid-state techniques) and 2.084 g (24 mmol) of LiBr were sealed in a gold tube (9.5 mm diameter, 102 mm long) with 1.7 ml of H_2O. The tube was then heated in a commercial Tem-Pres (LECO) apparatus to 550 °C (3723 bar–54000 psi) for 36 h and the furnace cooled to ambient over 6 h. After thorough washing and drying of the white microcrystals, 3.305 g (yield = 98.5%) of material exhibiting the powder diffraction pattern of a clean primitive cube (a = 8.081(2) Å) was recovered.

Structure Determination: The crystal structure of $[Li_8Br_2(Be_6P_6O_{24})]$ was established by Rietveld refinement of X-ray powder data (Scintag automated powder diffractometer, θ–θ geometry, flat-plate sample, $Cu_{K\alpha}$ radiation, λ = 1.54178 Å, 20° < 2θ < 100°, step size = 0.02°, T = 25(1) °C). All data analysis was carried out using the program GSAS[19] on a DEC μVAX-II computer. The structure[20] of aluminosilicate hydroxy sodalite $[Na_8(OH)_2(Si_6Al_6O_{24})]$ was used as the starting model for this new $[M_8X_2(A_6B_6O_{24})]$-type sodalite, in space group $P\bar{4}3n$ (No. 218). The usual profile (scale factor, lattice parameter (refined value = 8.0823(4) Å), zero-point error, Voigtian peak-shape-width variation coefficients), atomic positions and isotropic thermal parameters were optimized to convergence, resulting in final agreement factors of R = 0.0867, R_w = 0.1449 and χ^2 = 5.9 for 21 variables and 1998 parameters, largest atomic Δ/σ < 0.01. Difference Fourier syntheses at the end of the refinement revealed no significant regions of extra-atomic electron density, and joint site–population refinements

for Li and Br, constrained to maintain charge neutrality, revealed no significant difference from full occupation. No corrections for preferred orientation or absorption were considered. Final observed, calculated, and difference profile plots for the Li/Br-BePO are illustrated in Figure 1. Further details of the crystal structure investigation my be obtained from the Fachinformationszentrum Karlsruhe, Gesellschaft für wissenschaftlich-technische Information mbH, W-7514 Eggenstein-Leopoldshafen 2 (FRG) on quoting the depository number CSD-55624, the names of the authors and the journal citation.

Received: January 28, 1991
Revised: June 6, 1991 [Z 4407 IE]
German version: *Angew. Chem. 103* (1991) 1191

[1] L. Pauling, *Z. Kristallogr. 74* (1930) 213.
[2] J. M. Newsam, M. M. Tracy, D. E. W. Vaughan, K. G. Strohmaier, W. J. Mortier, *J. Chem. Soc. Chem. Commun. 1989*, 493.
[3] C. Fouassier, A. Levasseur, J. C. Joubert, P. Hagenmüller, *Z. Anorg. Allg. Chem. 375* (1970) 202.
[4] D. M. Bibby, P. M. Dale, *Nature (London) 317* (1985) 157.
[5] N. Setter, M. E. Mendoza-Alvarez, W. Depmeier, H. Schmid, *Ferroelectrics 56* (1984) 49.
[6] S. T. Wilson, B. M. Lok, C. A. Messina, T. R. Cannan, E. M. Flanigen, *J. Am. Chem. Soc. 104* (1982) 1186.
[7] J. J. Glass, R. H. Jahns, R. E. Stevens, *Am. Mineral. 29* (1944) 163.
[8] O. K. Mel'nikov, B. N. Litvin, S. P. Fedosova in A. N. Lobacher (Ed.): *Hydrothermal Synthesis of Crystals*, Consultants Bureau, New York 1971.
[9] M. Dano, *Acta Crystallogr. 20* (1966) 812.
[10] L. B. McCusker, W. M. Meier, K. Suzuki, S. Shin, *Zeolites 6* (1986) 388.
[11] T. M. Nenoff, W. T. A. Harrison, T. E. Gier, G. D. Stucky, *J. Am. Chem. Soc. 113* (1991) 378.
[12] R. J. H. Clark, T. J. Dines, M. Kurmoo, *Inorg. Chem. 22* (1983) 2766.
[13] T. E. Gier, G. D. Stucky, *Nature (London) 349* (1991) 508.
[14] D. Taylor, C. M. B. Henderson, *Phys. Chem. Miner. 2* (1978) 325.
[15] A. Stein, G. Ozin, G. D. Stucky, *J. Am. Chem. Soc. 112* (1990) 904.
[16] R. C. Rouse, D. R. Peakor, S. Merlino, *Am. Mineral. 74* (1989) 1195.
[17] G. Harvey, W. M. Meier in P. A. Jacobs, R. A. van Santen (Eds.) *Zeolites: Facts, Figures, Future: Studies in Surface Science and Catalysis, Vol. 49*, Elsevier, Amsterdam 1989.
[18] W. T. A. Harrison, T. E. Gier, K. L. Moran, J. M. Nicol, H. Eckert, G. D. Stucky, *Chem. Mater., 3* (1991) 27.
[19] A. C. Larson, R. B. Von Dreele, *GSAS User Guide*, Los Alamos National Laboratories, Los Alamos, NM 87545, USA 1985–1990.
[20] S. Luger, J. Felsche, P. Fischer, *Acta Crystallogr. C43* (1987) 1.
[21] D. W. Breck in *Zeolite Molecular Sieves*, Krieger Publishing Company, Malabar, FL, USA 1984.

Reversible Isomerization of the Dinuclear Complex $[(\eta^6\text{-}p\text{-cymene})RuCl(\mu\text{-pz})_2Ir(CO)_2]$ with Formation of a Ruthenium–Iridium Bond**

By *Daniel Carmona, Joaquina Ferrer, Ana Mendoza, Fernando J. Lahoz, Josefa Reyes*, and *Luis A. Oro**

Pyrazoles have been actively investigated as versatile ligands that can yield dinuclear homo- or heterometallic, homo- or heterovalent complexes with interesting photochemical, redox, and catalytic properties.[1] These dinuclear complexes often contain two bridging pyrazolyl ligands forming a six-membered MN_4M' ring in a boat conformation. The unusual flexibility of this ring permits a wide range of intermetallic separations.[2]

[*] Prof. Dr. L. A. Oro, Dr. D. Carmona, J. Ferrer, A. Mendoza, Dr. F. J. Lahoz
Departamento de Química Inorgánica
Instituto de Ciencia de Materiales de Aragón
Universidad de Zaragoza-C.S.I.C
Pl. San Francisco s/n, E-50009 Zaragoza (Spain)
Dr. J. Reyes
Centro Politécnico Superior de Ingenieros
Instituto de Ciencia de Materiales de Aragón
Universidad de Zaragoza-C.S.I.C

[**] This work was supported by the Dirección General de Investigación Científica y Técnica. pz = pyrazolyl.

The reversible cleavage and formation of a metal–metal bond usually implies the addition or removal of small molecules.[3] Nevertheless, Jones *et al.* have recently reported the synthesis of $[(CO)_2Rh(\mu\text{-}t\text{Bu}_2P)_2Rh(CO)_2]$, a unique system in which simple geometrical isomerism occurs with reversible formation and cleavage of a metal–metal bond.[4] Here we describe a double-bridged Ru-Ir pyrazolyl system which easily isomerizes with reversible metal–metal bond formation accompanied by halide migration. The analogous Ru-Rh system was also analyzed for comparison.

Carbonylation of the complexes $[(\eta^6\text{-}p\text{-cymene})RuCl(\mu\text{-pz})_2M(cod)]$ (M = Ir, Rh; cod = 1,5-cyclooctadiene)[5] proceeds rapidly at room temperature when CO is bubbled through dichloromethane or THF solutions. The products are the dicarbonyl complexes **1** and **2**. Complex **1** was ob-

$[(\eta^6\text{-}p\text{-cymene})RuCl(\mu\text{-pz})_2M(CO)_2]$ **1**, M = Ir; **2**, M = Rh

$[(\eta^6\text{-}p\text{-cymene})RuCl(\mu\text{-pz})_2Ir(CO)_2]$ **1a** $[(\eta^6\text{-}p\text{-cymene})\overline{RuCl(\mu\text{-pz})_2}Ir(CO)_2]$ **1b**

tained as a mixture of two isomers, **1a** and **1b**, according to spectroscopic and analytical data.[6] The relative amount of each isomer isolated from solution is variable from one preparation to another and sometimes pure **1a** was obtained. Pure **1b** spontaneously precipitates from methanolic solutions of mixtures of **1a** and **1b**. According to ^1H NMR measurements, an equilibrium between **1a** and **1b** is reached in solution. The K value at room temperature for the process **1a** $\rightleftharpoons$ **1b** is 2.4 ± 0.1 in $CDCl_3$. The isomerization **1b** $\rightarrow$ **1a** was monitored by ^1H NMR spectroscopy. The reaction obeys a second-order rate law in **1b** ($k = 3 \times 10^{-3}$ mol^{-1} dm^3 min^{-1}) and was inhibited by addition of benzyltriphenylphosphonium chloride. These findings support an ionic mechanism for the isomerization.

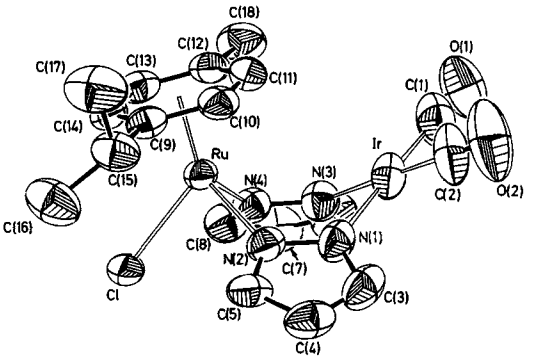

Fig. 1. Molecular structure (ORTEP) of **1a**. Selected bond lengths [Å] and angles [°]: Ru-N(4) 2.079(4), Ru-N(2) 2.088(4), Ru-Cl 2.403(1), Ru-CY 1.678(2), Ir-N(3) 2.062(4), Ir-N(1) 2.062(4), Ir-C(1) 1.872(8), Ir-C(2) 1.838(7), C(1)-O(1) 1.129(10), C(2)-O(2) 1.148(10); N(2)-Ru-N(4) 85.0(1), N(2)-Ru-Cl 86.9(1), N(4)-Ru-Cl 85.1(1), N(1)-Ir-N(3) 89.3(1), N(3)-Ir-C(1) 90.5(3), C(1)-Ir-C(2) 90.2(3), N(1)-Ir-C(2) 90.0(2). CY represents the centroid of the arene ligand.

Both isomers of complex **1** have been completely characterized by X-ray diffraction (Figs. 1, 2).[7] Only one isomer of the related Ru-Rh complex **2** could be detected and was also characterized by X-ray crystallography (Fig. 3).[8] There are no significant structural differences between **1a** and **2**. In both cases the molecular structure of the dinuclear complex consists of a pseudooctahedral ruthenium(II) atom and a square-planar iridium(I) (**1a**) or rhodium(I) (**2**) atom connected by two bridging pyrazolyl ligands. The resulting six-

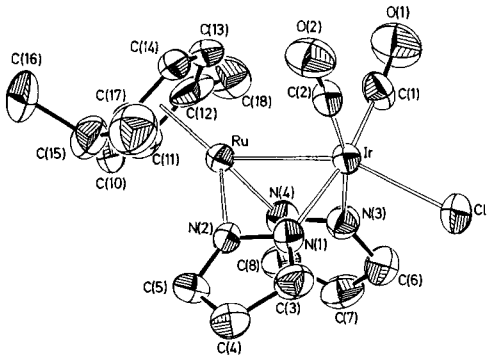

Fig. 2. Molecular structure (ORTEP) of **1b**. Selected bond lengths [Å] and angles [°]: Ru-Ir 2.6962(6), Ru-N(4) 2.075(6), Ru-N(2) 2.083(5), Ru-CY 1.675(3), Ir-N(3) 2.059(5), Ir-N(1) 2.069(5), Ir-Cl 2.517(2), Ir-C(1) 1.844(6), Ir-C(2) 1.831(8), C(1)-O(1) 1.169(8), C(2)-O(2), 1.178(10); Ir-Ru-CY 139.4(1), N(2)-Ru-N(4) 82.9(2), Ir-Ru-N(2) 70.6(2), Ir-Ru-N(4) 70.6(1), N(1)-Ir-N(3) 83.7(2), N(3)-Ir-C(1) 90.3(3), C(1)-Ir-C(2) 92.4(3), N(1)-Ir-C(2) 90.7(3), Ru-Ir-Cl 154.77(3). CY represents the centroid of the arene ligand.

membered RuN_4M ring adopts a boat conformation. The Ru–M distance excludes any significant metal–metal interaction. (Ru-Ir = 3.6636(4), Ru-Rh = 3.6153(5) Å). In particular, the Ru–Cl distance is similar for both complexes (**1a**, Ru-Cl = 2.403(1); **2**, 2.397(1) Å). Isomer **1b** has a dinuclear structure with a metal–metal bond (Ru-Ir = 2.6962(6) Å) bridged by two pyrazolyl ligands. If we consider the metal–metal bond as a coordination position, the pseudooctahedral coordination of the ruthenium metal is completed by an η^6-coordinated *p*-cymene ligand. The distorted octahedral coordination of iridium is completed by two terminal CO ligands and a chlorine atom *trans* to the metal–metal bond

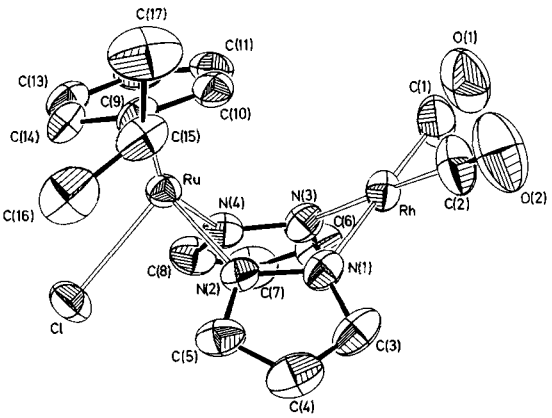

Fig. 3. Molecular structure (ORTEP) of **2**. Selected bond lengths [Å] and angles [°]: Ru-N(4) 2.086(3), Ru-N(2) 2.086(3), Ru-Cl 2.397(1), Ru-CY 1.668(2), Rh-N(3) 2.068(4), Rh-N(1) 2.056(4), Rh-C(1) 1.875(5), Rh-C(2) 1.847(5), C(1)-O(1) 1.108(7), C(2)-O(2) 1.127(7); N(2)-Ru-N(4) 84.5(1), N(2)-Ru-Cl 87.0(1), N(4)-Ru-Cl 87.1(1), N(1)-Rh-N(3) 89.1(1), N(3)-Rh-C(1) 90.5(2), C(1)-Rh-C(2) 91.7(2), N(1)-Rh-C(2) 88.8(2). CY represents the centroid of the arene ligand.

(Ru-Ir-Cl 154.77(3)°). The long Ir–Cl bond 2.517(2) Å) can be explained by the high *trans* influence of the metal–metal bond.[9] From a structural point of view, the isomerization **1a** → **1b** formally implies the migration of the chloride ligand from the ruthenium to the iridium accompanied by a strong compression along the Ru–Ir vector of about 1 Å.

Mixtures of both isomers of **1** react with NaX (X = Br, I) in methanol to give the corresponding bromide and iodide complexes **3** and **4**. From their spectroscopic properties,[10]

$[(\eta^6\text{-}p\text{-cymene})\overline{Ru(\mu\text{-pz})_2}IrX(CO)_2]$ **3**, X = Br; **4**, X = I

we assume that **3** and **4** have similar structures to **1b** with a Ru–Ir metal–metal bond.

The ν(CO) bands of **1b**, **3**, and **4** are shifted to slightly higher wave numbers than the corresponding vibrations of the related compound **1a**. Although a partial oxidation of Ir in the former complexes is thereby implied and a covalent M–M′ bond between d^7 Ru^I and d^7 Ir^{II} centers cannot be ruled out, the most reasonable formulation of these metal–metal complexes involves d^6 Ru^{II} and d^8 Ir^I centers with a polar donor–acceptor bond from the iridium to the ruthenium.

It is noteworthy that only in the Ru-Ir chloride system does the isomerization equilibrium **1a** ⇌ **1b** take place. Neither the homologous bromide or iodide complex nor the Ru-Rh chloride analogue exhibits such reactivity, even under more drastic conditions (reflux in toluene).

Experimental Procedure

1 and **2**: Carbon monoxide (1 atm) was bubbled through a solution of $[(\eta^6\text{-}p\text{-cymene})RuCl(\mu\text{-pz})_2M(cod)]$ (M = Ir, Rh) (2.5 mmol) in 25 mL of THF or CH_2Cl_2 over 3 h. The solution was concentrated under vacuum to about 3 mL and the complex was precipitated by addition of hexane. Yields: **1**, 75%; **2**: 90%.

3: NaBr (131.4 mg, 1.277 mmol) was added to a solution of **1** (278.0 mg, 0.426 mmol) in 25 mL of methanol. After 10 min of stirring an orange solid slowly precipitates. The suspension was stirred for 1 day. The solid was filtered off, washed with methanol and diethyl ether, and air-dried. Yield: 225.0 mg (76%). Complex **4** was prepared analogously. Yield: 73%.

Received: March 7, 1991 [Z 4476 IE]
German version: *Angew. Chem. 103* (1991) 1192

[1] S. Trofimenko, *Prog. Inorg. Chem. 34* (1986) 115.
[2] G. W. Bushnell, D. O. Kimberley Fjeldsted, S. R. Stobart, M. J. Zaworotko, S. A. R. Knox, K. A. Macpherson, *Organometallics 4* (1985) 1107 and references cited therein.
[3] See, for example: a) W. C. Mercer, R. R. Whittle, E. W. Burkhardt, G. L. Geoffroy, *Organometallics 4* (1985) 68; b) M. J. Breen, P. H. Shulman, G. L. Geoffroy, A. L. Rheingold, W. C. Fultz, *ibid. 3* (1984) 782; c) R. Poilblanc, *Inorg. Chim. Acta 62* (1982) 75.
[4] R. A. Jones, T. C. Wright, J. L. Atwood, W. E. Hunter, *Organometallics 2* (1983) 470.
[5] The comlexes $[(\eta^6\text{-}p\text{-cymene})RuCl(\mu\text{-pz})_2M(cod)]$ were prepared as described for the related compound $[(C_5Me_5)RhCl(\mu\text{-pz})_2Rh(cod)]$: L. A. Oro, D. Carmona, J. Reyes, C. Foces-Foces, F. H. Cano, *J. Chem. Soc. Dalton Trans. 1986*, 31.
[6] Relevant spectroscopic data. **1a**: ^{1}H NMR (200 MHz, $CDCl_3$, 25°C, TMS): δ = 7.72 (dd, ^3J(H,H) = 2.2 Hz, ^4J(H,H) = 0.7 Hz, 2H; H3/5 pz), 7.62 (dd, ^3J(H,H) = 2.2 Hz, 2H; H5/3 pz), 6.25 (t, 2H; H4 pz); $^{13}C\{^1H\}$NMR (50.3 MHz): δ = 174.5 (CO). IR (CH_2Cl_2): $\tilde{\nu}$ [cm^{-1}] = 2066, 1994 (C≡O). **1b**. ^{1}H NMR: δ = 7.57 (d, ^3J(H,H) = 2.1 Hz, 2H; H3/5 pz), 7.42 (d, ^3J(H,H) = 2.1 Hz, 2H; H5/3 pz), 5.97 (t, 2H; H4 pz); $^{13}C\{^1H\}$NMR: δ = 169.6 (CO). IR: $\tilde{\nu}$ [cm^{-1}] = 2076, 2021 (C≡O). **2**. ^{1}H NMR: δ = 7.70 (d, ^3J(H,H) = 2.0 Hz, 2H; H3/5 pz), 7.50 (d, ^3J(H,H) = 2.0 Hz, 2H; H5/3 pz), 6.21 (t, 2H; H4 pz). IR: $\tilde{\nu}$ [cm^{-1}] = 2080, 2010 (C≡O). Correct elemental analysis (C, H, N).
[7] X-ray structure analyses. Orange (**1a**) and red (**1b**) single crystals were grown from THF/hexane and MeOH/Et_2O solutions, respectively, of mixtures of **1a** and **1b**. Crystal data for **1a**: $C_{18}H_{20}ClIrN_4O_2Ru$, monoclinic, space group $P2_1/c$, a = 11.861(1), b = 13.759(1), c = 13.220(1) Å, β = 101.39(1)°, V = 2115.0(3) Å^3, Z = 4; crystal size 0.217 × 0.340 × 0.667 mm^3, orange transparent prismatic block; $\mu(Mo_{K\alpha})$ = 71.10 cm^{-1}. Numerical absorption corrections (minimum and maximum transmission factors 0.102 and 0.453). Siemens-Stoe four-circle diffractometer, $Mo_{K\alpha}$ radiation (λ = 0.71069 Å), graphite monochromator; measuring range $3 \le 2\theta \le 50°$, $\omega/2\theta$ scan; 9210 measured reflections, 3679 unique and 3287 observed reflections ($F \ge 5.0\sigma(F)$). Structure solution by Patterson and difference Fourier methods. Anisotropic thermal parameters for all non-hydrogen atoms. Hydrogen from found positions, refined riding on the parent atom with one overall isotropic thermal parameter; 247 parame-

ters, full-matrix least-squares refinement, SHELX76 program [11]. $R = 0.0286$, $R_w = 0.0326$. Weighting scheme: $w = k/[\sigma^2(F) + g F^2]$, with $k = 3.2061$ and $g = 0.000183$. Crystal data for 1b: monoclinic, Cc, $a = 15.084(2)$, $b = 10.414(2)$, $c = 13.844(2)$ Å, $\beta = 109.07(1)°$, $V = 2055.3(6)$ Å^3, $Z = 4$; crystal size $0.418 \times 0.313 \times 0.373$ mm^3, red transparent irregular block; $\mu(Mo_{K\alpha}) = 73.17$ cm^{-1}. Empirical absorption correction (minimum and maximum correction factor 0.781 and 1.192). Data collection, solution, and refinement as described for **1a**; 3837 measured, 3607 unique and 3492 observed reflections; 243 parameters. $R = 0.0192$, $R_w = 0.0208$. Weighting scheme: $k = 0.5160$ and $g = 0.000931$. The enantiomorph was chosen on the basis of a lower weighted R factor. Further details of the crystal structure investigations are available on request from the Director of the Cambridge Crystallographic Data Centre, University Chemical Laboratory, Lensfield Road, GB-Cambridge CB2 1EW (UK), on quoting the full journal citation.

[8] Crystal data for **2**: $C_{18}H_{20}ClN_4O_2RhRu$, monoclinic, space group $P2_1/n$, $a = 12.024(1)$, $b = 13.983(1)$, $c = 12.471(1)$ Å, $\beta = 99.74(1)°$, $V = 2066.5(3)$ Å^3, $Z = 4$; crystal size $0.625 \times 0.521 \times 0.612$ mm^3, orange transparent cubic block; $\mu(Mo_{K\alpha}) = 16.54$ cm^{-1}. Empirical absorption correction (minimum and maximum correction factors 0.917 and 1.112). Data collection, solution and refinement as described in [7]; 7390 measured, 3629 unique and 3536 observed reflections ($F \geq 4.0\sigma(F)$); 245 parameters. $R = 0.0313$, $R_w = 0.0348$. Weighting scheme: $k = 1.0000$ and $g = 0.00001$. See [7] for further details.

[9] E. Rotondo, S. Lo Schiavo, G. Bruno, C. G. Arena, R. Gobetto, F. Faraone. *Inorg. Chem. 28* (1989) 2944 and references cited therein.

[10] Relevant spectroscopic data. **3**. ^{1}H NMR (200 MHz, $CDCl_3$, 25 °C, TMS): $\delta = 7.58$ (d, ^3J(H,H) = 2.1 Hz, 2H; H3/5 pz), 7.44 (d, ^3J(H,H) = 2.1 Hz, 2H; H5/3 pz), 5.95 (t, 2H; H4 pz). ^{13}C{^{1}H}NMR (50.3 MHz): $\delta = 169.9$ (CO). IR (CH_2Cl_2): ν [cm^{-1}] = 2077, 2020 (C≡O). **4**. ^{1}H NMR: $\delta = 7.58$ (d, ^3J(H,H) = 2.1 Hz, 2H; H3/5 pz), 7.45 (d, ^3J(H,H) = 2.1 Hz, 2H; H5/3 pz), 5.93 (t, 2H; H4 pz); ^{13}C{^{1}H}NMR: $\delta = 170.7$ (CO). IR (CH_2Cl_2): ν [cm^{-1}] = 2076, 2022 (C≡O). Correct elemental analysis (C, H, N).

[11] G. M. Sheldrick, SHELX 76, Program for Crystal Structure Determination, University of Cambridge 1976.

[7.7]Circulene, a Molecule Shaped Like a Figure of Eight**

By *Koji Yamamoto,* Yasuhiro Saitho, Daisuke Iwaki,* and *Takayuki Ooka*

We have been interested in the synthetic studies of twisted π-electron systems,[1] and previous papers described the synthesis of the saddle-shaped [7]circulene (**1**), which has a circular arrangement of seven benzene rings.[2] An obvious extension of our interests in these studies directed our efforts to the preparation of the unique 8-shaped and saddle-shaped [7.7]circulene (**2**)[3, 4] with contiguous benzoannelated rings around a central bicyclo[5.5.0]dodecane framework. This molecule consists of ten fused benzene rings and has a total of forty π electrons. However, the canonical structure **2b** suggests that the molecule might behave as a heptalene[5] with a 28 π-electron periphery. The canonical form **2b** is unique for it can in principle, be converted into an aromatic system by the addition or removal of electrons. The consideration of these structural factors led us to synthesize the novel 8-shaped [7.7]circulene (**2**) and its quinonoid derivative (**3**), which has revealed the strained nonplanar and unusual saddle-shaped geometry anticipated from the examination of its molecular model.

[*] Prof. Dr. K. Yamamoto
Department of Chemistry, Faculty of Integrated Arts and Sciences
University of Osaka Prefecture
Sakai, Osaka 591 (Japan)
Y. Saitho, D. Iwaki, T. Ooka
Department of Chemistry, Faculty of Engineering Science
Osaka University
Toyonaka, Osaka 560 (Japan)

[**] This work was supported by a Grant-in-Aid for Scientific Research (No. 01540424) from Japanese Ministry of Education, Science, and Culture.

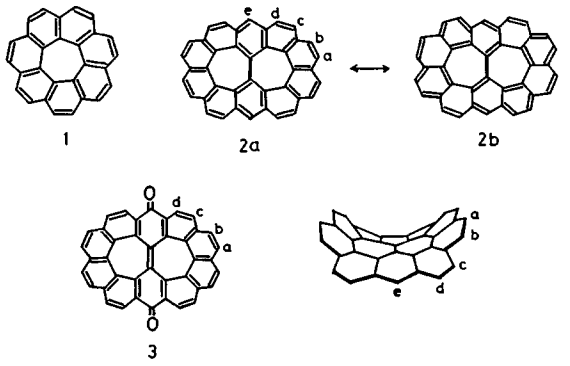

The termolecular coupling of the tetrathiol **5**[6] and two equivalents of 2,7-bis(bromomethyl)naphthalene (**4**)[7] was carried out in dimethylformamide with cesium carbonate[8] to give the tetrathiacyclophane **6**,[9] (m.p. > 300 °C, 40% yield). Reaction of **6** with dimethoxycarbenium tetrafluoroborate in dichloromethane yielded the tetrasulfonium salt **7**. Subsequent Stevens rearrangement mediated by sodium hydride provided a 21% yield of the tetrasulfide **8** as a yellow oil. Oxidation of **8** with *m*-chloroperbenzoic acid gave the tetrasulfoxide **9** whose pyrolysis at 300 °C (0.001 mm) produced the unsaturated cyclophane **10** (yellow prisms, m.p. 176–178 °C, 16% yield from **8**). A cyclohexane solution of **10**

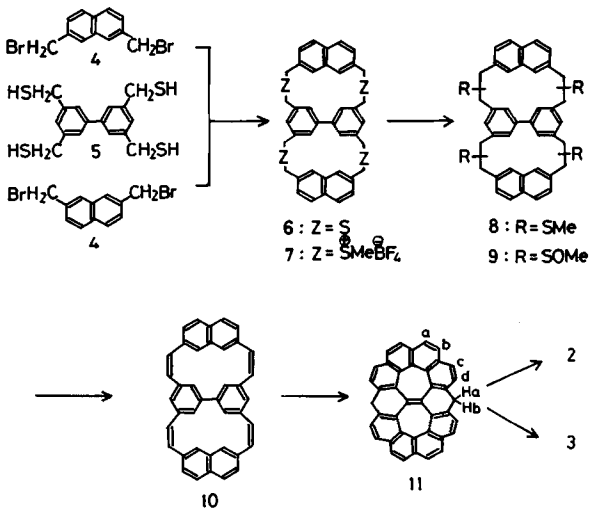

containing a trace amount of iodine was irradiated using a high-pressure mercury lamp[10] for 2 h to afford the dihydro[7.7]-circulene (**11**)[11] (yellow prisms, m.p. 350 °C, 12% yield), which was isolated by chromatography on silicagel. The ^{1}H NMR ($CDCl_3$) revealed that two methylene groups showed an AB quartet at $\delta = 4.50$ (4H) and two sets of AB quartet aromatic resonances (H^a, H^b and H^c, H^d). This evidence, supported by its mass spectrum and its correct elemental analysis, pointed to dihydro[7.7]circulene (**11**) as the product, which seems to be a saddle-shaped nonplanar molecule.[12]

The existence of two methylene groups of **11** was also confirmed by its oxidation with selenium oxide in dioxane which gave the novel quinonoid derivative **3** in 21% yield (as well as 14% of the monoketone, m.p. 210–212 °C)[13] stable orange prisms (from benzene) m.p. > 300 °C).[16]

For the introduction of the final two benzene rings into the circular arrangement, we found that dehydrogenation of **11** with triphenylmethyl perchlorate[14] in acetic acid afforded

a 25% yield of [7.7]circulene (**2**; stable pale orange prisms, m.p. > 300 °C; from benzene).[17] The NMR data are characteristic: The ^{1}H NMR spectrum has a single peak at $\delta = 7.61$ and two sets of AB systems and the ^{13}C NMR spectrum exhibits twelve peaks. These spectral properties of **2** and its thermal stability indicate that this molecule is best represented by the structure **2a** consisting of two hexa[7]circulene units.[15]

We are at present investigating the chemical and physical properties of [7.7]circulene (**2**) and its derivatives.

Received: March 6, 1991
German version: *Angew. Chem. 103* (1991) 1202

[1] M. Nakazaki, K. Yamamoto, K. Naemura, *Top. Curr. Chem. 125* (1984) 1.
[2] K. Yamamoto, T. Harada, Y. Okamoto, H. Chikamatsu, M. Nakazaki, Y. Kai, T. Nakao, M. Tanaka, S. Harada, N. Kasai, *J. Am. Chem. Soc. 110* (1988) 3578.
[3] According to the nomenclature proposed by *H. Wynberg* [4], we call a series of these circulenes by the name of [m.n]circulene where m and n indicate number of ring surrounding each central ring of the system.
[4] H. Wynberg, J. H. Dopper, *Tetrahedron Lett. 1972*, 763.
[5] H. J. Dauben, D. J. Bertelli, *J. Am. Chem. Soc. 83* (1961) 4659.
[6] F. Vögtle, G. Hohner, E. Weber, *J. Chem. Soc. Chem. Commun. 1973*, 366.
[7] W. Baker, F. Glockling, J. F. W. McOmie, *J. Chem. Soc. 1951*, 1118.
[8] J. Buter, R. M. Kellogg, *J. Chem. Soc. Chem. Commun. 1980*, 466.
[9] Satisfactory analytical and spectroscopic data have been obtained for all new compounds.
[10] Halos, ET-500, Eikosha Co., Osaka, Japan.
[11] **11**: MS (EI, 70 eV): *m/z* 500 ($M^{\oplus}$); ^{1}H NMR (270 MHz, 25 °C, $CDCl_3$, TMS) AB system: $\delta_a = 4.29$, $\delta_b = 4.72$ ($J_{ab} = 12.86$ Hz, 4H; CH_2), AB system: $\delta_a = 7.52$, $\delta_b = 7.54$ ($J_{ab} = 8.66$ Hz, 8H; ArH^a, ArH^b), AB system: $\delta_d = 7.53$, $\delta_c = 7.59$ ($J_{cd} = 8.66$ Hz, 8H; ArH^c, ArH^d); ^{13}C NMR ($CDCl_3$) δ = 39.6, 125.0, 125.8, 126.1, 127.8, 128.7, 130.3, 132.3, 134.9, 136.0, 136.9, 139.7; UV/VIS (cyclohexane): λ_{max}[nm] (ε) = 262 (54400), 298 (28600), 313 (33100), 350 (8300), 380sh (5300).
[12] The ^{1}H NMR spectrum of **11** in hexachloro-1,3-butadiene also revealed that two methylene groups showed typical AB quartets whose shapes did not change much on heating up to 160 °C. This indicates a rather rigid saddle-shaped geometry.
[13] IR (KBr): $\tilde{\nu}$[cm^{-1}] = 1671 (C=O); MS: *m/z* 514 ($M^{\oplus}$); ^{1}H NMR ($CDCl_3$) AB system: $\delta_a = 4.28$, $\delta_b = 4.70$ ($J_{ab} = 12.84$ Hz, 2H; CH_2), 7.52–8.15 (m, 16H; ArH).
[14] W. Bonthrone, D. H. Reid, *J. Chem. Soc. 1959*, 2773.
[15] P. J. Jessup, J. A. Reiss, *Aust. J. Chem. 29* (1976) 173.
[16] **3**: IR (KBr): $\tilde{\nu}$[cm^{-1}] = 1670 (C=O); MS: *m/z* 528 ($M^{\oplus}$); ^{1}H NMR ($CDCl_3$): $\delta = 7.69$ (d, $J = 8.37$ Hz, 4H; ArH^a), 7.79 (d, $J = 8.64$ Hz, 4H; ArH^c), 7.90 (d, $J = 8.37$ Hz, 4H; ArH^b), 8.07 (d, $J = 8.64$ Hz, 4H; ArH^d); ^{13}C NMR ($CDCl_3$): δ = 114.0, 126.2, 127.1, 127.9, 129.1, 131.0, 132.6, 135.2, 136.4, 137.2, 139.5, 195.1; UV/VIS (CH_2Cl_2): λ_{max}[nm] (ε) = 273 (111200), 306 (57300), 321 (48700), 462 (7500).
[17] **2**: MS: *m/z* 498 ($M^{\oplus}$). ^{1}H NMR ($CDCl_3$): $\delta = 7.61$ (s), $\delta_a = 7.45$, $\delta_b = 7.48$ ($J_{ab} = 6.22$ Hz, 8H; ArH^a, ArH^b), $\delta_c = 7.47$, $\delta_d = 7.56$ ($J_{cd} = 7.72$ Hz, 8H; ArH^c, ArH^d). ^{13}C NMR: δ = 126.4, 126.8, 127.2, 127.7, 131.2, 131.7, 132.3, 132.8, 136.0, 136.4, 136.9, 137.3; UV/VIS (CH_2Cl_2): λ_{max}[nm] (ε) = 274 (122200), 301 (56400), 316 (8770), 362 (10200), 415 (5700), 440 (3200).

2-Triphenylmethyldicyclohept[*cd,g*]indene: A Novel *cata-peri* Condensed Nonalternant Hydrocarbon**

By *Yoshikazu Sugihara,* Junji Saito*, and *Ichiro Murata**

Due to the unique annelation mode, the *cata-peri*-condensed nonalternant hydrocarbons are endowed with intriguing properties.[1] Our recent studies on cyclohepta[*a*]phenalene **1**[2] and 7-methoxycyclopenta[*a*]phenalene **2b**[3] have been concerned with their high electron donating and accepting properties as a function of their molecular orbital characteristics.[4] Dicyclohept[*cd,g*]indene **3a**, an isomer of **1**, is a new class of compound in the series, since **3** is formally composed of two prototype nonalternant hydrocarbons, azulene and heptafulvene. We report herein the first synthesis of a derivative, **3b**, of this ring system and on its physical properties, which may illustrate the intrinsic character of the parent hydrocarbon **3a**.

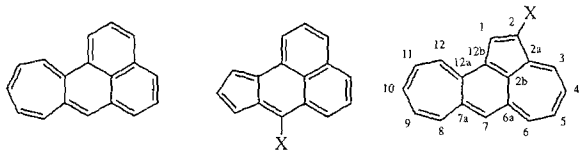

1 **2a**, X = H; **2b**, X = OCH_3 **3a**, X = H; **3b**, X = CPh_3

4-Methylazulene **4**[5] was deprotonated with lithium dicyclohexylamide (LDCHA) in ether (Scheme 1) and the resulting carbanion was quenched with diphenyl disulfide to give 4-phenylthiomethylazulene **5** in 66% yield.[6] The cycloheptatrienyl group could effectively be introduced at the desired position by deprotonation of **5** with lithium diisopropylamide (LDA) in ether followed by treatment with tropylium tetrafluoroborate to afford **6**, which was oxidized with *meta*-chloroperbenzoic acid (MCPBA) to give a mixture of diastereoisomeric sulfoxides **7**. To our surprise, upon thermolysis in a degassed benzene solution at 55 °C, sulfoxides **7** were transformed into a tetracyclic azulene derivative **10**, which consists of the desired carbon skeleton. Although no information could be obtained from ^{1}H-NMR monitoring of the thermolysis (in [D_6]benzene), the formation of **10** was rationalized as shown in Scheme 1. Thus, the heptafulvene

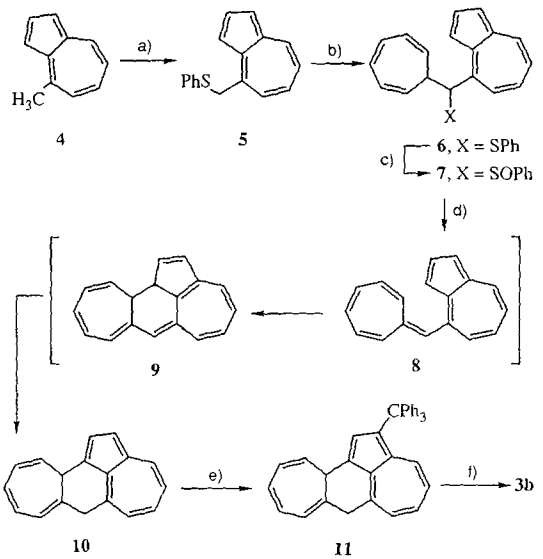

Scheme 1. Synthesis of **3b**. Reaction conditions: a) LDCHA (1.3 equiv.), ether, ice-cooling, 40 min, then PhSSPh (1.3 equiv.), ether, ice-cooling → room temperature, 10 min, 66%. b) LDA (1.2 equiv.), ether, ice-cooling, 10 min, then $C_7H_7^{\oplus}BF_4^{\ominus}$ (1.1 equiv.), −78 °C, 1 h, 54%. c) MCPBA (1.34 equiv.), CH_2Cl_2, −78 °C, 71%. d) heated at 54–65 °C, degassed benzene, 3 h, 82%. e) $Ph_3C^{\oplus}BF_4^{\ominus}$ (0.99 equiv.), CH_2Cl_2, −90 → −78 °C, 1.5 h, 56%. f) $Ph_3C^{\oplus}BF_4^{\ominus}$ (1.0 equiv.), CH_2Cl_2, 0 °C → room temperature, 15 min, then ether, 21%.

[*] Prof. Dr. I. Murata, Dr. Y. Sugihara, J. Saito
Department of Chemistry, Faculty of Science
Osaka University
Toyonaka, Osaka 560 (Japan)

[**] This work was supported by a Grant-in-Aid for Scientific Research on Priority Areas (No. 02230103) from the Ministry of Education, Science and Culture, Japan.

chromophore, initially formed by elimination of sulfenic acid, collapses to the tetracyclic intermediate **9** by a facile electrocyclic 14π reaction.[7] This undergoes a preferential [1,7]-hydride shift with formation of the stable, conjugated azulene **10**. To abstract hydride ion from **10**,[8] this was treated with trityl tetrafluoroborate; however, the product obtained was a triphenylmethyl-substituted derivative **11**,[9] since a reactive site of the azulene skeletal framework in **10** remains free to attack by electrophiles. Finally, **11** was dehydrogenated[10] by sequential treatment with trityl tetrafluoroborate and diethyl ether to afford **3b** as black needles (m.p. = 200 °C (decomp.)).[11]

The UV/VIS spectrum of **3b** in benzene exhibits a long wavelength absorption up to 750 nm, and moderate hypsochromic shifts of 2–6 nm were observed for all the maxima above 300 nm upon using acetonitrile instead of benzene as solvent. The ^{1}H-NMR chemical shifts and the vicinal coupling constants of the skeletal hydrogens (Fig. 1) indicate

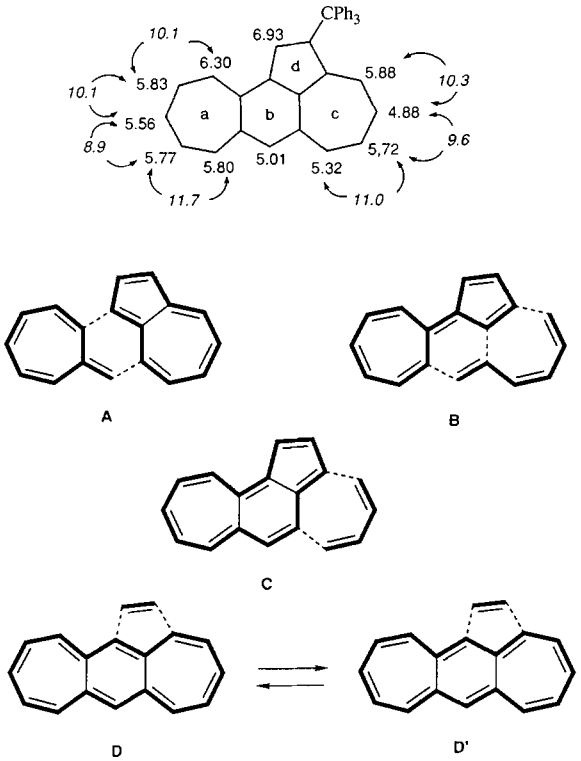

Fig. 1. Above: ^{1}H-NMR data (500 MHz, $CDCl_3$, TMS) of **3b**: chemical shifts (δ values) and vicinal coupling constants [Hz] (in italics). Below: possible bonding structure of **3b**.

some interesting properties: as far as the chemical shifts (δ = 5.56–6.30) and the coupling constants (J_{vic} = 8.9–11.7 Hz) of the ring a are concerned, these NMR parameters are quite similar to those of 8-phenyl-[12] and 8,8-diphenylheptafulvenes.[12] However, the chemical shift of the hydrogens attached to the ring c and ring d, which constitute formally an azulene chromophore, are substantially higher than those of azulene itself. This means that the bonding structure of **3b** cannot be described in terms of a simple composite of azulene and heptafulvene (model **A**). Other possible descriptions are as sesquifulvalene/hexatriene (model **B**) or a cyclohept[*e*]indene/butadiene system (model **C**). However, these models are also unsuitable for a description the real structure of **3b**, since the seven-membered ring hydrogens of sesquifulvalene (δ = 6.2–7.05)[13a] and 4-phenyl-

Table 1. Some physical data of the compounds **10**, **11** and **3b**.

10: a blue oil, exact mass, calcd for $C_{18}H_{14}$ 230.1096, found 230.1089; ^{1}H NMR (400 MHz, $CDCl_3$, TMS): δ = 8.30 (d, J = 9.5 Hz, 1H, H-3), 7.84 (d, J = 3.8 Hz, 1H, H-1), 7.53 (dd, J = 9.9, 9.7 Hz, 1H, H-5), 7.47 (d, J = 3.8 Hz, 1H, H-2), 7.04 (dd, J = 9.7, 9.5 Hz, 1H, H-4), 6.97 (d, J = 9.9 Hz, 1H, H-6), 6.74 (t-like, 2H, H-9 and -10), 6.40 (br. s, 1H, H-8), 6.27–6.31 (m, 1H, H-11), 5.41 (dd, J = 9.0, 5.9 Hz, 1H, H-12), 4.30 (d, J = 21.8 Hz, 1H, H-7), 4.08 (d, J = 21.8 Hz, 1H, H-7'), 3.11 (d, J = 5.9 Hz, 1H, H-12a).

11: blue columnar crystals, m.p. = 210 °C (decomp.); MS: m/z 472 ($M^{\oplus}$, 12%), 395 ($M^{\oplus}$ − Ph, 17), 229 ($M^{\oplus}$ − CPh_3, 4); ^{1}H NMR (400 MHz, $CDCl_3$, TMS): δ = 7.63 (d, J = 9.9 Hz, 1H, H-3), 7.58 (s, 1H, H-1), 7.35 (t, J = 9.9 Hz, 1H, H-5), 7.14–7.26 (m, 15H, trityl), 6.88 (d, J = 9.9 Hz, 1H, H-6), 6.66–6.74 (m, 2H, H-9, 10), 6.58 (t, J = 9.9 Hz, 1H, H-4), 6.37 (d-like, J = 4.2 Hz, 1H, H-8), 6.23 (dd, J = 9.0, 4.8 Hz, 1H, H-11), 5.37 (dd, J = 9.0, 5.9 Hz, 1H, H-12), 4.29 (d, J = 21.8 Hz, 1H, H-7), 4.04 (d, J = 21.8 Hz, 1H, H-7'), 3.01 (d, J = 5.9 Hz, 1H, H-12a).

3b: black crystals, m.p. = 200 °C (decomp.); exact mass, calcd for $C_{37}H_{26}$, 470.2036, found 470.2043; UV/VIS (CH_3CN): λ_{max} [nm] (lg ε) = 268 (4.04), 307 (4.44), 391 (3.89), 412 (3.91), 437 (3.97), 474 (sh, 3.20), 518 (sh, 3.17), 616 (sh, 3.37), 668 (3.63); ^{1}H NMR (500 MHz, $CDCl_3$, TMS): see Fig. 1. ^{13}C-NMR (125.8 MHz, $CDCl_3$, TMS): δ = 130.9, 127.3, 125.8 (phenyl), 142.6 (C-3), 140.6 (C-5), 137.9 (C-8), 136.4 (C-11), 134.7 (C-9), 130.2 (C-10), 129.4 (C-6), 128.2 (C-12), 123.9 (C-1), 122.0 (C-4), 121.1 (C-7).

cyclohept[*e*]indene-2,3-dicarbonitrile (δ = 7.85–9.5)[13b] resonate at substantially lower field than those of the ring a hydrogens of **3b**. A most likely possibility would be a bond shift equilibrium between two Kekulé structures of the hitherto unknown dicyclohepta[*a*,*d*]benzene,[14] which should sustain a paramagnetic ring current associated with its peripheral 16π elelctrons, perturbed by an external double bond (model **D** ⇄ **D'**).[15]

The redox properties of **3b** were examined by cyclic voltammetry,[16] and are characterized by two oxidation waves at 0.43 and 1.10 V as well as a reduction wave at − 1.18 V. As expected from its high Hückel HOMO level (0.1778 β), the first oxidation potential of **3b** is close to that of **1** (E^{ox} = 0.39 V; HOMO = 0.1055 β).[2] Furthermore, the reduction potential of **3b** is clearly more positive than that of **2b** (E^{red} = − 1.27 V) suggesting that the hydrocarbon **3b** is seemingly amphoteric (E^{sum} = 1.61 V).[17]

Since the electronic perturbation caused by the triphenylmethyl substituent in **3b** is presumably small, the physical properties of the unknown parent compound **3a** could be similar to those of **3b**.[18]

Received: April 5, 1991 [Z 4552 IE]
German version: *Angew. Chem. 103* (1991) 1203.

[1] R. Zahradník, J. Michl, *Collect. Czech. Chem. Commun. 30* (1965) 520–536; B. A. Hess, Jr., L. J. Schaad, *J. Org. Chem. 36* (1971) 3418–3423.
[2] Y. Sugihara, H. Yamamoto, K. Mizoue, I. Murata, *Angew. Chem. 99* (1987) 1283–1285; *Angew. Chem. Int. Ed. Engl. 26* (1987) 1247–1249.
[3] Y. Sugihara, H. Fujita, I. Murata, *J. Chem. Soc. Chem. Commun. 1986*, 1130–1131.
[4] Y. Aoki, A. Imamura, I. Murata, *Tetrahedron 46* (1990) 6659–6672.
[5] K. Hafner, H. Weldes, *Justus Liebigs Ann. Chem. 606* (1957) 90–99. We thank Prof. *K. Hafner* for a generous gift of azulene.
[6] For a similar procedure see: M. Müller, S. Braun, K. Hafner, *Angew. Chem. 92* (1980) 633–635; *Angew. Chem. Int. Ed. Engl. 19* (1980) 621–623.
[7] H. Prinzbach, H. Bingmann, D. Hunkler, *Tetrahedron Lett. 1978*, 649–652; H. Prinzbach, H. Bingmann, A. Beck, D. Hunkler, E. Sauter, E. Hädicke, *Chem. Ber. 114* (1981) 1697–1722; H. Prinzbach, L. Knothe, *Pure Appl. Chem. 58* (1986) 25–37.
[8] Generally, hydride abstraction from a tertiary center as in **10** is an unfavorable process under normal conditions and therefore the hydrogen to be eliminated has to be moved thermally or photochemically. In the present case, attempts to migrate a hydrogen atom in **10** resulted in the formation of a tarry material.
[9] K. Hafner, A. Stephan, C. Bernhard, *Justus Liebigs Ann. Chem. 650* (1961) 42–62.
[10] For the conversion **10** → **3a**, we examined dehydrogenation with either *p*-chloranil or 2,3-dichloro-5,6-dicyano-1,4-benzoquinone. An unstable

greenish product was obtained which showed a similar UV/VIS spectrum to that of **3b**; however, its structure could not be characterized due to the low yield.

[11] All the new compounds were fully characterized by spectral data together with satisfactory elemental analyses.

[12] K. Komatsu, M. Fujimori, K. Okamoto, *Tetrahedron 33* (1977) 2791–2797; K. Komatsu, private communication.

[13] a) W. K. Schenk, R. Kyburz, M. Neuenschwander, *Helv. Chim. Acta 58* (1975) 1099–1119. b) H. Prinzbach, H.-W. Schneider, *Angew. Chem. 85* (1973) 1112–1114; *Angew. Chem. Int. Ed. Engl. 12* (1973) 1007–1009.

[14] For theoretical studies see: R. Zahradnik, J. Michl, J. Kopecky, *Collect. Czech. Chem. Commun. 31* (1966) 640–648; *ibid. 29* (1964) 1932–1944; R. Zahradnik, J. Michl, *ibid. 30* (1965) 3550-3559; T. Nakajima, *Pure Appl. Chem. 28* (1971) 219–238; A. Toyota, *Bull. Chem. Soc. Jpn. 48* (1975) 1152–1156; Z. Zhou, R. G. Parr, *J. Am. Chem. Soc. 111* (1989) 7371–7379. For an attempted synthesis see: J. Beeby, P. J. Garratt, *J. Org. Chem. 38* (1973) 3051–3052.

[15] HMO π-bond orders for **3a**: $p_{1,2} = 0.6957$, $p_{2,2a} = 0.5681$, $p_{2a,3} = 0.5236$, $p_{3,4} = 0.7236$, $p_{4,5} = 0.5589$, $p_{5,6} = 0.7362$, $p_{6,6a} = 0.4941$, $p_{6a,7} = 0.6033$, $p_{7,7a} = 0.5974$, $p_{7a,8} = 0.5346$, $p_{8,9} = 0.6960$, $p_{9,10} = 0.6059$, $p_{10,11} = 0.6617$, $p_{11,12} = 0.6344$, $p_{12,12a} = 0.6118$, $p_{12a,12b} = 0.4737$, $p_{1,12b} = 0.5623$, $p_{2a,2b} = 0.4839$, $p_{2b,12b} = 0.5379$, $p_{2b,6a} = 0.5096$, $p_{7a,12a} = 0.4709$.

[16] Measured against SCE in CH_3CN with 0.1 M nBu$_4$NClO$_4$ as supporting electrolyte at room temperature, Pt working electrode, $n = 200\ mVs^{-1}$. The peak separations are 50, 100, and 60 mV for the first and second oxidation and first reduction waves, respectively.

[17] For amphoteric hydrocarbons see: K. Nakasuji, K. Yoshida, I. Murata, *J. Am. Chem. Soc. 104* (1982) 1432–1433; *ibid. 105* (1983) 5136–5137; *Chem. Lett. 1982*, 969–970; S. Sasaki, K.-U. Klabunde, I. Murata, J. Toyoda, K. Nakasuji, *Angew. Chem. 103* (1991) 198–199; *Angew. Chem. Int. Ed. Engl. 30* (1991) 172–173.

[18] Attempts to convert **3b** into **3a** through protonation and detriphenylmethylation were unsuccessful.

Alkane Cascade Polymers Possessing Micellar Topology: Micellanoic Acid Derivatives**

By *George R. Newkome,* Charles N. Moorefield, Gregory R. Baker, Andrew L. Johnson,* and *Rajani K. Behera*

The synthesis of high molecular weight, highly branched, multifunctional molecules possessing a predetermined three-dimensional morphology has been the focus of a growing number of research groups.[1] To develop synthetic strategies for such cascade polymers, diverse factors must be considered; these include the initial core, building blocks (or repeat units), spacers, branching integers, dense packing limits, and porosity. Selection of the appropriate building block(s) is governed by the type of branching desired (e.g., carbon vs. heteroatom) as well as the technology used to attach each successive layer (or tier). Thus far, building-block units have relied predominantly on heteroatom chemistry for either a center of branching or attachment of additional building blocks. We herein report the first example of an alkyl carbon cascade polymer, a derivatized "micellane" possessing the characteristics of a globular micelle.

Our interest[2] in the design and application of cascade polymers initially led us to synthesize high molecular weight molecules containing quaternary carbon branching points and a maximum number of terminal functional groups, and focused on the formation of the amide bond. Work revolved around a multiplicative approach utilizing two building blocks, a trialkyl methanetricarboxylate[3] and 2-amino-2-hydroxymethyl-1,3-propanediol (tris(hydroxymethyl)-aminomethane, "tris"). The inertness of nucleophilic substitution at the neopentyl carbons required the incorporation of spacer moieties; these extraneous steps were circumvented by the preparation of "bis-homotris".[4] Subsequently it was determined that in general, three carbon atoms are necessary to ensure an appropriate distance to minimize the reaction retardation caused by an adjacent quaternary center. Therefore, $C[(CH_2)_3Br]_4$ and $XC[(CH_2)_3Y]_3$ were selected as the ideal alkyl core[5] and building blocks, respectively, for iterative cascade polymer construction.

Since nitrotriol **1**[6] was pivotal to the preparation of bis-homotris,[4] it was chosen as the starting point for construction of the desired reagents (core and building blocks). Application of an unexploited procedure[7] provided the three-carbon homologation[8] from a quaternary center by addition of a tertiary radical to an electron-deficient alkene, such as acrylonitrile or methyl acrylate. Although the yields associated with this reaction are moderate (30–65%), a novel series of tetra(bis-homologated) analogues of pentaerythritol was readily prepared.

The triol **1** (Scheme 1) was treated[9] with benzyl chloride to give (78%) the trisether **2**, which was subsequently cyanoethylated[7] affording (61%) the nitrile **3**. The characteristic ^{13}C NMR chemical shifts for the quaternary carbon ($\delta = 36.5$), cyano moiety ($\delta = 120$), and CH_2CN ($\delta = 11.6$) and loss of the peak at $\delta = 94.0$ for the nitro-substituted carbon support the assignment.

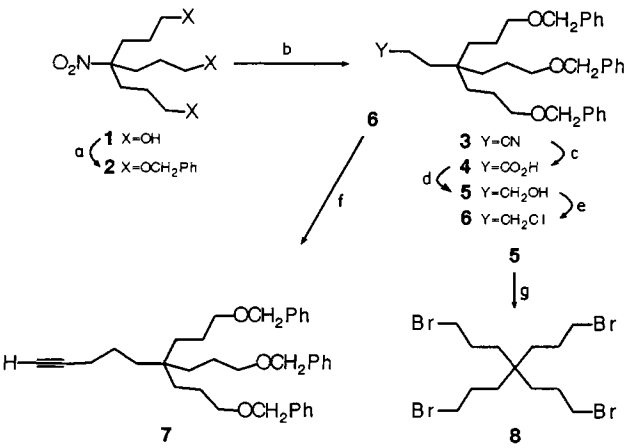

Scheme 1. a) $PhCH_2Cl$, Me_2SO, KOH; b) acrylonitrile, nBu$_3$SnH, azobisisobutyronitrile, $PhCH_3$, 110°C; c) KOH, EtOH/H_2O, H_2O_2, Δ; d) $BH_3 \cdot THF$, THF, Δ; e) $SOCl_2$, CH_2Cl_2, pyridine; f) HC≡CLi · en, Me_2SO, 40°C; g) HBr, H_2SO_4, 100°C.

Hydrolysis[10] of nitrile **3** proceeded cleanly to give (92%) carboxylic acid **4**, as indicated by the appearance (^{13}C NMR) of a peak at $\delta = 179.8$ (CO_2H). Conversion of acid **4** into alcohol **5** proceeded quantitatively with excess 1.0 M $BH_3 \cdot THF$ solution (>95%; ^{13}C NMR: $\delta(CH_2OH) = 63.3$). Transformation into chloride **6** was smoothly achieved in CH_2Cl_2 with excess $SOCl_2$ and a catalytic amount of pyridine[11] (92%; ^{13}C NMR: $\delta(CH_2Cl) = 45.6$). Reaction of lithium acetylide ethylenediamine complex[12] in dimethylsulfoxide with **6** gave the terminal alkyne **7** (87%;

[*] Prof. G. R. Newkome, C. N. Moorefield, G. R. Baker, A. L. Johnson, R. K. Behera
Center for Molecular Design and Recognition
Department of Chemistry
University of South Florida
Tampa, FL 33620 (USA)

[**] Chemistry of Micelles, Part 11. The results were first presented at the Symposium on Self-Assembling Structures (by *G. R. N.*) at the 199th National Meeting of the American Chemical Society, Boston, MA, USA, April 1990 (Abstracts ORGN 317). This work was supported by the Petroleum Research Fund, administered by the American Chemical Society, and the National Science Foundation (DMR-86-00929; 89-06792). For Part 10 see: C. D. Weis, G. R. Newkome, *J. Org. Chem. 55* (1990) 5801.

^{13}C NMR: $\delta(CH_2C{\equiv}CH) = 84.0$ and $\delta(CH_2C{\equiv}CH) = 68.1$).

An improved synthesis of the core tetrabromide **8** from alcohol **5** was achieved by bromination with HBr/H_2SO_4; thus, **8** was obtained in eight steps from nitromethane (24% overall yield) versus 17 steps from citric acid[13] (<2% overall yield) or 12 steps from tetrahydropyran-4-one[5] (<5% overall yield).

Alkylation of the four-directional core **8** with 6 equivalents of terminal alkyne building block **7** (Scheme 2) gave the purified dodecabenzyl ether **9** (67%),[14] as evidenced by the disappearance of the terminal alkyne absorptions and the appearance of a peak $\delta = 80.9$ (C≡C).

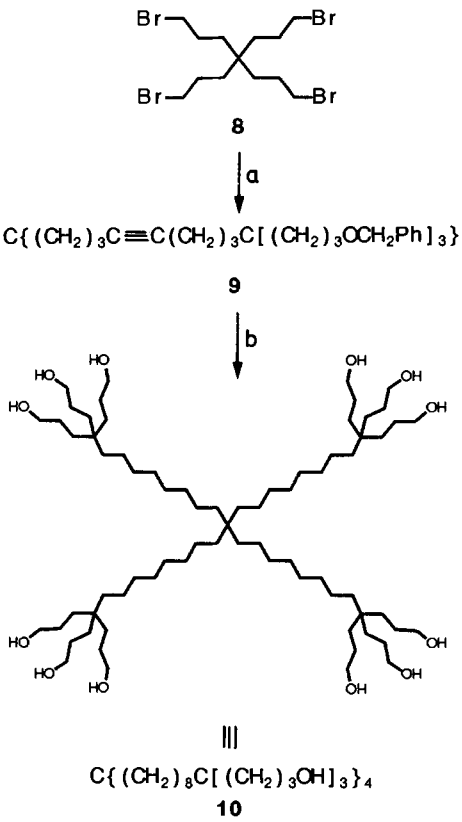

Scheme 2. a) Hexamethylphosphoric triamide (HMPA), lithium diisopropylamide (LDA), 6 equiv alkyne **1**, tetramethylethylenediamine (TMED), 0–40 °C, 1.5 h; b) EtOH, THF, 10% Pd-C/H_2 (4 atm), 60 °C, 4 d.

The dodecabenzyl ether (**9**) was soluble in $CHCl_3$ and CH_2Cl_2 and insoluble in CH_3CN and EtOH. Simultaneous reduction of the triple bonds and deprotection of **9** with Pd–C/H_2 afforded (91%) dodecaalcohol **10**, as indicated in the ^{13}C NMR spectrum by the disappearance of resonances assigned to the alkyne carbons and to their α-carbon atoms ($\delta = 19.8$), as well as the appearance of a peak at $\delta = 64.1$ (CH_2OH). Alcohol **10**, which is slightly soluble in $CHCl_3$ or H_2O but very soluble in EtOH or MeOH, was smoothly converted (53%) into the dodecabromide (^{13}C NMR: $\delta(CH_2Br) = 34.8$) employing $SOBr_2$ at 40 °C for 12 h. A second tier (Scheme 3) was readily obtained by alkylation of the dodecabromide[15] with 18 equivalents of alkyne **7** to give 49% of hexatricontabenzyl ether **11**, which was similarly reduced and deprotected in one step yielding 89% of hexatricontaalcohol **12**, an [$8^2 \cdot 3$]micellanol.[16] Both polyether **11** and polyol **12** exhibited the same solubilities and many of the same ^{13}C and ^1H NMR signals as their lower analogues (**9** and **10**). Aqueous solubility was increased by RuO_4 oxidation[17] of **12** affording 85% of hexatricontacarboxylic acid **13** ([$8^2 \cdot 3$]micellanoic acid), followed by treatment with NH_4OH or $(CH_3)_4NOH$. Disappearance of the ^{13}C NMR signal for the hydroxymethyl moiety at $\delta = 64.0$ and the appearance of the carboxylate signal at $\delta = 187.4$, as well as the high water solubility of its ammonium salt confirm that the transformation has occurred. The micellar properties of **13** have been investigated and will be reported in the following communication.[18]

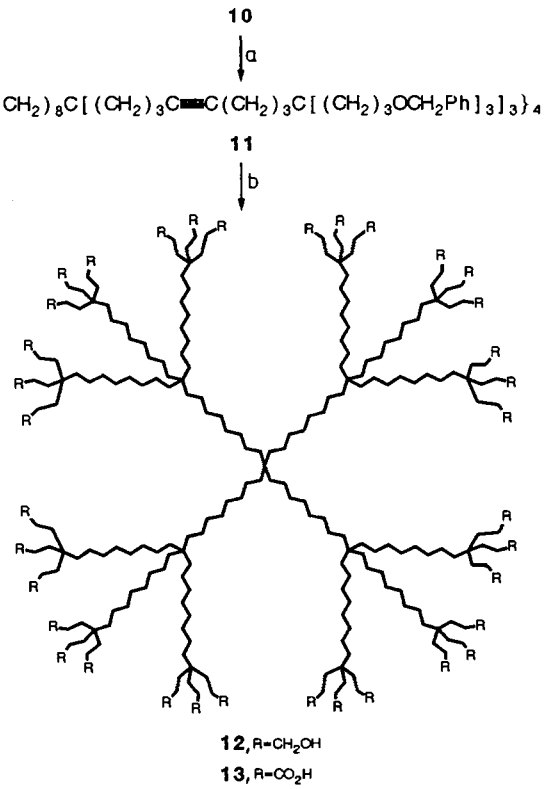

Scheme 3. a) 1. CH_2Cl_2, $SOBr_2$, pyridine; 2. 18 equiv alkyne **1**; b) EtOH/THF, 10% Pd-C/H_2 (4 atm), 60 °C, 4 d.

In view of the diversity of these reagents, we are continuing our efforts towards the synthesis of related macromolecules based on this cascade technology.

Received: March 29, 1991 [Z 4546 IE]
German version: *Angew. Chem. 103* (1991) 1205

[1] D. A. Tomalia, A. M. Naylor, W. A. Goddard III, *Angew. Chem. 103* (1990) 119; *Angew. Chem. Int. Ed. Engl. 29* (1990) 138; Y. H. Kim, O. W. Webster, *J. Am. Chem. Soc. 112* (1990) 4592; C. J. Hawker, J. M. J. Frechet, *ibid. 112* (1990) 7638; see also I. Amato, *Sci. News 138* (1990) 288; Y.-X. Chen, *Youji Huaxue 10* (1990) 289.

[2] G. R. Newkome, Z.-q. Yao, G. R. Baker, V. K. Gupta, *J. Org. Chem. 50* (1985) 2003; G. R. Newkome, Z.-q. Yao, G. R. Baker, V. K. Gupta, P. S. Russo, M. J. Saunders, *J. Am. Chem. Soc. 108* (1986) 849; G. R. Newkome, G. R. Baker, M. J. Saunders, P. S. Russo, V. K. Gupta, Z.-q. Yao, J. E. Miller, K. Bouillion, *J. Chem. Soc. Chem. Commun. 1986*, 752; G. R. Newkome, G. R. Baker, S. Arai, M. J. Saunders, P. S. Russo, K. J. Theriot, C. N. Moorefield, J. E. Miller, T. R. Lieux, M. E. Murray, B. Phillips, L. Pascal, *J. Am. Chem. Soc. 112* (1990) 8458; G. R. Newkome, X. Lin, *Macromolecules 24* (1991) 1443; G. R. Newkome, Y. Hu, F. R. Fronczek, *Tetrahedron Lett. 32* (1991) 1133.

[3] G. R. Newkome, G. R. Baker, *Org. Prep. Proced. Int. 18* (1986) 451; J. Skarzewski, *Tetrahedron 45* (1989) 4593.

[4] G. R. Newkome, C. N. Moorefield, K. J. Theriot, *J. Org. Chem. 53* (1988) 5552.

[5] G. R. Newkome, V. K. Gupta, R. W. Griffin, S. Arai, *J. Org. Chem. 52* (1987) 5480.

[6] Available from Aldrich Chemical Co.

[7] N. Ono, H. Miyake, A. Kamimura, I. Hamamoto, R. Tamura, A. Kaji, *Tetrahedron 41* (1985) 4013.

[8] L. M. Rice, B. S. Sheth, T. B. Zalucky, *J. Pharm. Chem. 60* (1971) 1760.

[9] I. Iwashige, H. Saeki, *Chem. Pharm. Bull. 15* (1967) 1803.

[10] A. I. Vogel: *Textbook of Practical Organic Chemistry*, 4th ed., Longmans, London 1978, p. 478.
[11] J. S. Pizey: *Synthetic Reagents, Vol. 1*, Wiley, New York 1974, pp. 321–357.
[12] W. N. Smith, O. F. Beumel, Jr., *Synthesis 1974*, 441.
[13] C. K. Ingold, L. C. Nickolls, *J. Chem. Soc. Trans. 1922*, 1646.
[14] ^{13}C NMR was extremely useful because of the characteristic chemical shifts of the interior carbons and the expected T_1 increases [19] of the quaternary carbons. All "cascade" compounds were purified by non-aqueous, reverse-phase flash column chromatography. Correct elemental analyses were obtained for all new compounds. ^{13}C NMR assignments are based on calculated values, signal intensities, and DEPT NMR experiments; consecutive numbering beginning at the central quaternary carbon simplifies description due to symmetry. Selected physical data for **9**–**13**: **9**: ^1H NMR (360 MHz, $CDCl_3$): δ = 1.10–1.65 (m, 80H), 2.00–2.21 (m, 16H), 3.35 (br t, 24H), 4.45 (s, 24H), 7.28 (s, 60H); ^{13}C NMR (360 MHz, $CDCl_3$): δ = 19.3 (C4, C7), 22.8 (C3, C8), 23.3 (C12), 32.4 (C11), 35.6 (C2, C9), 36.4 (C10), 36.7 (C1), 71.1 (C13), 72.6 (C14), 80.1 (C5, C6), 127.2, 127.3, 128.1, 138.4 (C_6H_5); IR (neat): $\tilde{\nu}$ = 3080, 3030, 2925, 2860, 1100, 745, 699 cm^{-1}. **10**: ^1H NMR (CD_3OD): δ = 1.08–1.32 (m, 112H), 3.37 (t, 24H, J = 6.5 Hz); ^{13}C NMR (CD_3OD): δ = 23.9, 24.1 (C3, C8), 27.4 (C12), 30.8 (C5, C6), 31.7, 31.8 (C4, C7), 33.6 (C11), 37.5 (C10), 37.8, 37.9 (C2, C9), 38.1 (C1), 63.8 (C13); IR (neat): $\tilde{\nu}$ = 3700–3000, 2850, 2920, 1480, 1575, 1065 cm^{-1}. **11**: ^1H NMR ($CDCl_3$): δ = 1.05–1.70 (m, 300H), 2.00–2.22 (m, 48H), 3.36 (br t, 72H), 4.43 (s, 72H), 7.27 (s, 180H); ^{13}C NMR ($CDCl_3$): δ = 19.3 (C13, C16), 22.8 (C12, C17), 23.2 (C3, C8, C21), 29.0 (C5, C6), 32.0 (C4, C7), 32.3 (C20), 35.5 (C11, C18), 35.8 (C2, C9), 36.3 (C19), 36.4 (C10), 36.5 (C1), 71.0 (C22), 72.6 (C23), 80.1 (C14, C15), 127.2, 127.3, 128.0, 138.3 (C_6H_5); IR (neat): $\tilde{\nu}$ = 3080, 3030, 2925, 2860, 1100, 745, 700 cm^{-1}. **12**: ^1H NMR (CD_3OD): δ = 1.15–1.87 (m, 400H), 3.50 (t, 72H, J = 6.5 Hz); ^{13}C NMR (CD_3OD): δ = 23.8 (C3, C8), 24.7 (C12, C17), 27.4 (C21), 29.5 (C5, C6), 30.7, (C14, C15), 30.8 (C4, C7), 31.6 (C13, C16), 33.6 (C20), 37.5 (C11, C18), 37.6 (C2, C9), 37.7 (C1, C10, C19), 63.9 (C22); IR (neat): $\tilde{\nu}$ = 3700–3000, 2850, 2920, 1480, 1575, 1065 cm^{-1}. **13**: ^1H NMR ($NaOD/D_2O$): δ = 1.11–1.70 (m, 328H), 2.05–2.20 (m, 72H); ^{13}C NMR ($NaOD/D_2O$): δ = 24.9 (C3, C8), 25.3 (C12, C17), 28.5 (C5, C6), 32.1 (C4, C7), 32.9, (C14, C15), 33.0 (C13, C16), 34.8 (C21), 35.2 (C20), 38.0 (C2, C9), 38.3 (C11, C18), 39.2 (C1, C10, C19), 187.4 (C22); IR (neat): $\tilde{\nu}$ = 3400–2700, 2920, 2850, 1715 cm^{-1}.
[15] Alkylation [12] of the corresponding chloro and iodo derivatives was equally effective.
[16] [$8^2 \cdot 3$]-nomenclature: 8 denotes the number of carbons between each branching locus, 2 denotes tiers, and 3 denotes the carbons after the outermost branching center; micellanol denotes a hydrocarbon infrastructure and hydroxylic terminal moieties.
[17] H. Irngartinger, W. Reimann, P. Garner, P. Dowd, *J. Org. Chem. 53* (1988) 3046.
[18] For micellar properties, see: G. R. Newkome, C. N. Moorefield, G. R. Baker, M. J. Saunders, S. H. Grossman, *Angew. Chem. 103* (1991) 1207; *Angew. Chem. Int. Ed. Engl. 30* (1991) 1178.
[19] E. Breitmaier, W. Voelter: *Carbon-13 NMR Spectroscopy*, VCH, New York 1987, pp. 183–186.

structures depend not only on the molecular architecture of the amphiphile, but also on diverse factors such as temperature and concentration.[2] Based on work by *Shinkai* et al.[3] and *Menger* et al.[4] who synthesized water-soluble calixarenes and "hexapus", respectively, which possess micellar characteristics, our investigations[5] as well as others,[6] concerning the design and synthesis of cascade polymers, seemed well suited for the control of molecular topology, stability, and the associated micellar properties. In particular, we have prepared the first, symmetrical, four-directional, saturated hydrocarbon cascade polymer ([$8^2 \cdot 3$]micellanoic acid)[7] containing 36 carboxylic acid moieties equidistant from a central neopentyl core. Due to the obvious micellar topology, the acid groups were converted into their corresponding ammonium (**1**) and tetramethylammonium (**2**) carboxylate derivatives (see Fig. 1) to facilitate the study of their properties.

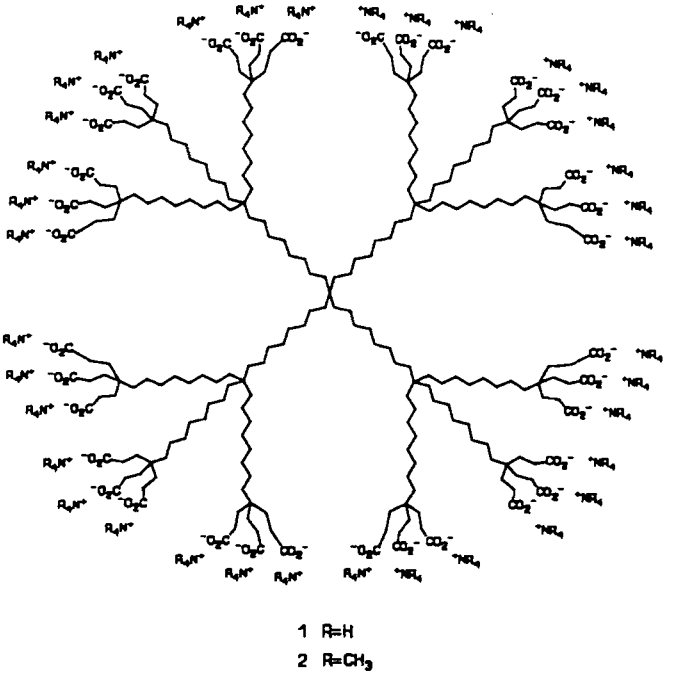

Fig. 1. Two-tier cascade polymer.

Unimolecular Micelles**

By *George R. Newkome,* Charles N. Moorefield, Gregory R. Baker, Mary J. Saunders,* and *Steven H. Grossman*

Aggregation phenomena of amphiphiles and their resultant micellar chemistry are well documented.[1] Micelle

Investigation of possible aggregation was initially facilitated by electron microscopy (EM) of unstained samples of **1** and **2**.[8] Examination of **1** revealed a range of particle sizes; the majority (monomers) were 30 to 50 Å in diameter and the largest (aggregates) were ca. 1000 Å. We attribute the aggregation of **1** to intermolecular H-bonding promoted by solution evaporation on the EM grid, since the size distribution and pattern reflect concentration increases during evaporation. The $Me_4N^{\oplus}$ analogue (**2**), however, exhibited no aggregation (see Fig. 2), but rather the entire field of view consisted of uniform particles (30 Å ± 5 Å). Since the $Me_4N^{\oplus}$ cation is known to reduce H-bonding significantly,[9] aggregation was minimized or totally circumvented during evaporation. Observed diameters agree well with calculated diameters[10] (see Fig. 3), which indicated a minimum of 30 Å and a maximum of 48 Å corresponding to contracted and extended conformations, respectively. This physical observation supports the following spectral evidence that polycarboxylate **2** exists as single molecules.

Phase-resolved anisotropy values for lipophilic probes such as diphenylhexatriene (DPH) in micelles provide a mea-

[*] Prof. G. R. Newkome, C. N. Moorefield, G. R. Baker, M. J. Saunders, S. H. Grossman
Center for Molecular Design and Recognition
Department of Chemistry
University of South Florida
Tampa, FL 33620 (USA)

[**] Chemistry of Micelles, Part 13. The results were first presented at the Symposium on Self-Assembling Structures at the 199th National Meeting of the American Chemical Society, Boston, MA, USA, April 1990 (Abstracts ORGN 317). This work was supported by the Petroleum Research Fund, administered by the American Chemical Society, and the National Science (*G. R. N* Grant Nos. DMR 86-00929 & 89-06792; *M. J. S.* Grant No. DCB 88-02011) as well as the Florida High Technology and Industrial Council. We also thank Professors *J. Rebek, Jr.* (MIT), *P. S. Russo* (LSU), and *R. Potter* (USF) for their invaluable discussions. Part 12: G. R. Newkome, Y. Hu, M. J. Saunders, F. R. Fronczek, *Tetrahedron Lett. 32* (1991) 1133.

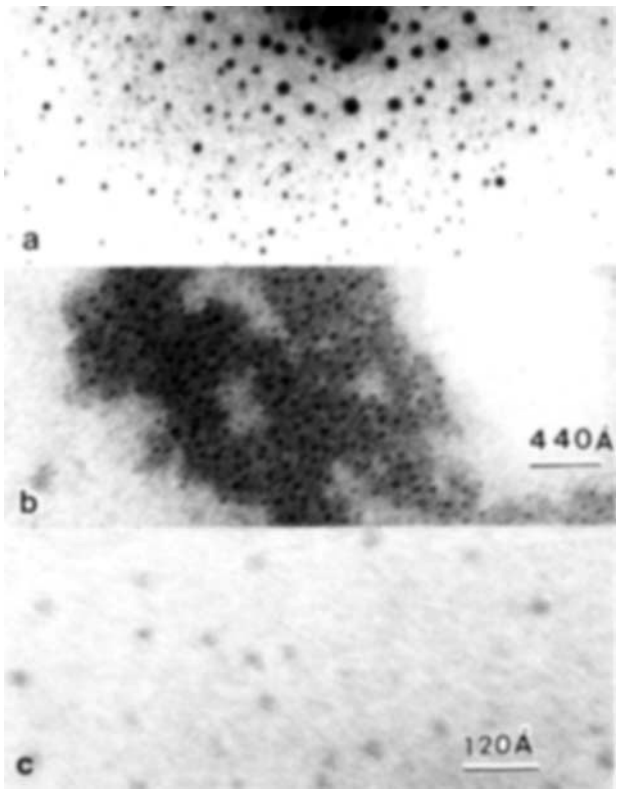

Fig. 2. Electron micrographs of **1** (a) and **2** (b, c). Note aggregation of **1** after solvent evaporation in (a) whereas **2** [(b) and (c)] remains dispersed (darkened background is caused by excess salt). Final magnification for (a) and (b) is 225000× and (c) 820000×.

sure of internal rotational freedom.[11] Models used to describe the data[12] correspond to an isotropic rotator, a two-component anisotropic rotator, and to restricted or hindered rotation. In an independent experiment,[13] the fluorescence lifetime of DPH with **2** was determined to be 1.2 ns (17%) and 6.9 ns (83%) ($\chi^2 = 1.30$). The single-term decay law

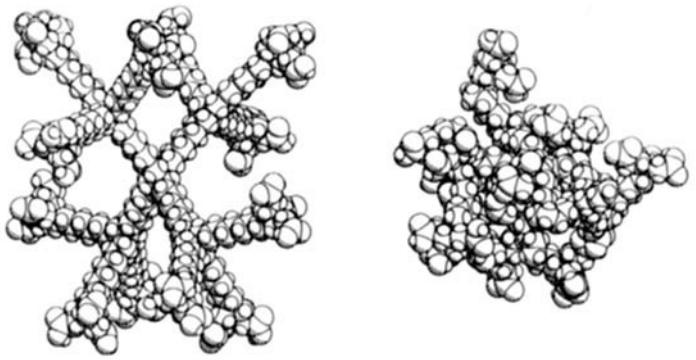

Fig. 3. Idealized representations of the 36-carboxylic acid in extended (left) and contracted (right) conformations, respectively.

was inadequate and the three-term discrete exponential and single-term Lorentzian distribution decay laws were not a significant improvement on the two-term discrete decay law. Anisotropy data were fit to a one-term (θ_1), a two-term (θ_1, θ_2; f_1, f_2), or a single-term decay law with a hindered anisotropy component (θ_1, r_∞). The results are shown in Table 1.

Table 1. Phase-resolved anisotropy values for DPH and micellanoate **2**. θ is the rotational correlation time, f the fractional contribution, and r_∞ the limiting anisotropy for the hindered rotation model. χ^2 is based on the standard deviation for a phase and demodulation ratio of 0.5° and 0.005°, respectively. Data obtained for the a) single discrete anisotropy decay model, b) double discrete anisotropy decay model, and c) hindered rotation model.

	θ_1	f_1	θ_2	f_2	r_∞	χ^2
a	2.90					102.
b	0.23	0.57	4.67	0.43		2.31
c	2.21				0.018	2.51

The values obtained in the two-term lifetime decay law indicate that DPH molecules are predominately associated within the lipophilic interior of the polycarboxylate microenvironment. The fast component could arise from distribution of some DPH near the surface of the micellanoate or more likely, some DPH not embraced by the micellanoate yet and still in the aqueous phase. The differential phase and demodulation ratio data could be equally well fitted to a two-term discrete exponential decay or a single-term decay with hindered rotation. Restricted motion by the probe molecule is insignificant as suggested by the magnitude of the hindered anisotropy. The two-term discrete model shows the presence of two distinct modes of rotational motion. The fast correlation time is similar to that previously observed with DPH in mineral oil (0.76) or dioleoyl-L-α-phosphatidylcholine (DOPC) vesicles (0.8) above the transition temperature,[11] as is the correlation time for the slower rotation (3.9). In fact, both the lifetime and anisotropy decay laws for DPH with micellanoate **2** and DOPC vesicles are remarkably similar[11] demonstrating the host–guest relationship between **2** and DPH.

The commonly employed techniques of optical fluorescence microscopy and photometry revealed the absorption and subsequent fluorescence (at 520 nm) of chlortetracycline (CTC, 5 mM, pH 11),[14] in an aqueous solution of **2**. There was no detectable fluorescence from aqueous solutions of CTC or the spherical polymer **2** alone. When combined, the fluorescence intensity increased linearly with increasing concentrations of **2**.[15] Since CTC fluoresces only in lipophilic environments,[16] this fluorescent probe must be interacting within the infrastructure of the cascade polymer.

Phenol blue (PB),[3, 17] and pinacyanol chloride (PC)[4] have more traditionally been used as spectrophotometric probes to study micellar properties: PB as a solvent property indicator (λ_{max} ranges from 658 nm in water to 552 nm in cyclohexane), and PC as a probe for aggregation. A deep violet aqueous solution of PB (5.5×10^{-6} M) changed to light blue upon addition of micellanoate **1** (3.1×10^{-4} M). The UV spectrum of this solution displayed only a slight frequency shift ($\Delta\lambda_{max} = 5$ nm) for the absorption band, which decreased in intensity, and broadened markedly.

In the presence of anionic micelles, the color of an aqueous solution of PC changes from pink to blue;[18] in the absence of amphiphiles, an aqueous solution of PC (3.9×10^{-6} M) has absorptions at 554 and 600 (λ_{max}) nm. In solutions of PC (3.9×10^{-6} M) and of sodium dodecylsulfate (NaDS) at concentrations above the critical micelle concentration (cmc, $>10^{-2}$ M) these absorptions shift to 564 and 610 nm; NaDS solutions at concentrations below 10^{-2} M show an absorption at 478 nm. Upon addition of micellanoate **1** or **2** (6.8×10^{-4} M and 3.3×10^{-4} M, respectively) to an aqueous solution of PC (3.9×10^{-6} M, pH 10.0), λ_{max} shifts to 610 nm and the absorption becomes more intense and narrowed. In both cases, this absorbance ($\lambda_{max} = 610$ nm) gradually shifts

(toward $\lambda_{max} = 600$ nm) as the concentration of either decreases to 1.6×10^{-6} M; absorptions appear at 478 nm when concentrations fall below 3.9×10^{-7} M. These results are consistent with those of *Shinkai* et al.[3] and *Menger* et al.[4] Furthermore, if a cmc exists, it must be $< 3.9 \times 10^{-7}$ M.

Added evidence of molecular inclusion[4] was provided by the resultant UV spectrum ($\lambda = 214$, 276 nm) of an aqueous solution of micellanoate **2** (2.3×10^{-4} M) with naphthalene ($\lambda = 214$, 276 nm; 3:1 H_2O/EtOH). Also, the intensity of the absorbance for **2** and naphthalene at 276 nm is ca. four times greater (3.35) than that observed for naphthalene in a 2:1 mixture of water and ethanol (0.844).

The interactions of these novel cascade polymers with CTC, PC, DPH, and naphthalene demonstrated the inclusion of these guest molecules within the lipophilic infrastructures of micellanoates **1** and **2**. The interaction of PC with **1** or **2** indicated the formation of 1:1 complexes. In addition, the tetramethylammonium salt **2** was shown not to aggregate in basic solution. The data strongly suggest that these spherical polymers ([$8^2 \cdot 3$]micellanoates) exist as single molecules[19] capable of molecular inclusion and therefore act as unimolecular micelles.

Received: April 2, 1991 [Z4549]
German version: *Angew. Chem. 103* (1991) 1207

[1] For a review see: H. Ringsdorf, B. Schlarb, J. Venzmer, *Angew. Chem. 100* (1988) 117; *Angew. Chem. Int. Ed. Engl. 27* (1988) 113.
[2] a) J. N. Israelachvili, S. Marčelja, R. G. Horn, *Q. Rev. Biophys. 13* (1980) 121; b) J. N. Israelachvili, in V. Degiorgio, M. Corti (Eds.): *Physics of Amphiphiles: Micelles, Vesicles and Microemulsions*, North-Holland, Amsterdam 1985, p. 24; c) D. F. Evans, B. W. Nimham, *J. Phys. Chem. 90* (1986) 226.
[3] S. Shinkai, S. Mori, H. Koreishi, T. Tsubaki, O. Manabe, *J. Am. Chem. Soc. 108* (1986) 2409.
[4] F. M. Menger, M. Takeshita, J. F. Chow, *J. Am. Chem. Soc. 103* (1981) 5938.
[5] a) G. R. Newkome, Z.-q. Yao, G. R. Baker, V. K. Gupta, *J. Org. Chem. 50* (1985) 2003; b) G. R. Newkome, Z.-q. Yao, G. R. Baker, V. K. Gupta, P. S. Russo, M. J. Saunders, *J. Am. Chem. Soc. 108* (1986) 849; c) G. R. Newkome, G. R. Baker, M. J. Saunders, P. S. Russo, V. K. Gupta, Z.-q. Yao, J. E. Miller, K. Bouillion, *J. Chem. Soc. Chem. Commun. 1986*, 752; d) G. R. Newkome, G. R. Baker, S. Arai, M. J. Saunders, P. S. Russo, K. J. Theriot, C. N. Moorefield, J. E. Miller, T. R. Lieux, M. E. Murray, B. Phillips, L. Pascal, *J. Am. Chem. Soc. 112* (1990) 8458; e) G. R. Newkome, X. Lin, *Macromolecules 24* (1991) 1443.
[6] Y. H. Kim, O. W. Webster, *J. Am. Chem. Soc. 112* (1990) 4592. For reviews see: I. Amato, *Science News 138* (1990) 288; Y.-X. Chen, *Youji Huaxue 10* (1990) 289; [*Chem. Abstr. 113* (1990) 190809t]; D. A. Tomalia, A. M. Naylor, W. A. Goddard III, *Angew. Chem. 102* (1990) 119; *Angew. Chem. Int. Ed. Engl. 29* (1990) 138.
[7] For synthetic details see: G. R. Newkome, C. N. Moorefield, G. R. Baker, A. L. Johnson, R. K. Behera, *Angew. Chem. 103* (1991) 1205; *Angew. Chem. Int. Ed. Engl. 30* (1991) 1176.
[8] Experiments were performed on a Hitachi H500 electron microscope at 50 kV to the enhance the contrast of the unstained samples. Sample films were prepared by exposing formar-coated grids to aqueous solutions of **1** and **2** (initial concentrations: 5.9×10^{-7} M; 6.1×10^{-6} M, respectively) adjusted to pH 11.8 with 1 N KOH followed by evaporation. Electron micrographs were taken at 100000× and 240000× and further magnified to 225000× and 818000× photographically.
[9] J. Rebek, Jr., personal communication.
[10] Theoretical diameters were obtained using a Silicon Graphics 4D50GT graphics workstation with Quanta molecular modeling software available from Polygen Corporation.
[11] J. R. Lakowicz, H. Cherek, B. P. Maliwal, E. Gratton, *Biochem. 24* (1985) 376.
[12] For a discussion of these models and pertinent terminology, see J. R. Lakowicz: *Principles of Fluorescence Spectroscopy*, Plenum, New York 1983.
[13] Phase-resolved lifetimes and anisotropies were determined with an SLM Model 48000s spectrofluorometer equipped with two frequency synthesizers capable of attaining 200 MHz. The excitation was a Liconix HeCd laser operated at 325 nm. The emission was collected through a Schott 408 nm cuton filter. The lifetime standard was POPOP (1.32 ns). The samples were stirred continuously during data acquisition and temperature was maintained at 30°C using thermostatted water. The estimated error used in the decay law fittings (SLM Instrument software, Urbana, IL) was 0.005 in the demodulation and 0.4° in the phase shift. Each sample was read three times at each of 22 frequencies (3–70 MHz for lifetime and 10–140 MHz (12 frequencies) for anisotropy determinations). In the minimization used to establish the anisotropy decay law, either the lifetime or the limiting anisotropy (0.38), or for DPH both, were fixed parameters. The sample was prepared by sonicating excess DPH in a 1.76×10^{-4} M aqueous solution of tetramethylammonium carboxylate for 10 min. Excess DPH was removed by filtration through glass wool.
[14] M. J. Saunders, P. K. Helper, *Planta 152* (1981) 272.
[15] **2** was diluted successively with 5 mM CTC (1.2×10^{-5} M to 5.3×10^{-6} M). Fluorescence was viewed on a Nikon fluorescence microscope. Excitation was < 510 nm emission (520 nm) was measured using a Leitz MPV photometer.
[16] A. Caswell, *Int. Rev. Cytol. 56* (1979) 145.
[17] L. G. S. Brooker, R. H. Sprague, *J. Am. Chem. Soc. 63* (1941) 3214.
[18] F. M. Menger, C. E. Portnoy, *J. Am. Chem. Soc. 89* (1967) 4698; F. M. Menger, C. A. Littau, *J. Am. Chem. Soc. 113* (1991) 1451.
[19] Original hypothesis: G. R. Newkome, V. Gupta, G. R. Baker et al., 189th National Meeting of the American Chemical Society, Miami, FL, USA, April 1985 (Abstracts ORGN 166).

Structural Changes on Twofold Oxidation of Tetrakis(dimethylamino)-*p*-benzoquinone: A Sterically Overcrowded Electron-Rich "Chair" Compound Turns into a "Twist" Dicyanine Salt**

By *Hans Bock,* Klaus Ruppert, Christian Näther,* and *Zdenek Havlas*

Dedicated to Kurt Dehnicke on the occasion of his 60th birthday

The textbook example[1a] for a reversible one-electron reduction[1b] of organic π systems, *p*-benzoquinone, can be "umgepolt" by four dimethylamino substituents[1c] (Scheme 1). Tetrakis(dimethylamino)-*p*-benzoquinone, therefore, can be both reduced to its semiquinone radical anion[1c]—and oxidized to its semiquinone radical cation.[1c,d] This extraordinary redox behavior of the sterically overcrowded and electron-rich compound, which can stabilize positive charges by delocalization into the dimethylamino substituents, stimulated us to determine the structures of both the black neutral molecule[2,3] and its black dication salt, which can be prepared by $SbCl_5/CH_2Cl_2$ oxidation (Fig. 1).

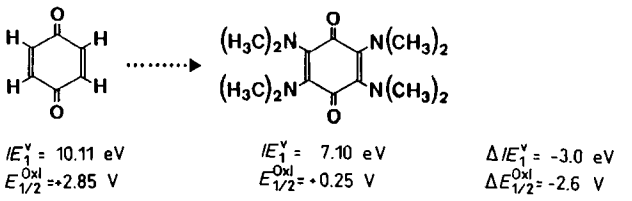

Scheme 1.

[*] Prof. Dr. H. Bock, Dipl.-Chem. K. Ruppert, Dipl.-Chem. C. Näther, Dr. Z. Havlas[+]
Institut für Anorganische Chemie der Universität
Niederurseler Hang, W-6000 Frankfurt am Main 50
[+] Permanent address:
Institut of Organic Chemistry and Biochemistry of the Czechoslovakian Academy of Sciences

[**] Structures of Sterically Overcrowded or Charge-Perturbed Molecules, Part 8. This work was supported by the State of Hesse, the Fonds der Chemischen Industrie, and the Alexander von Humboldt Foundation (*Z. H.*). Part 7: [11a].

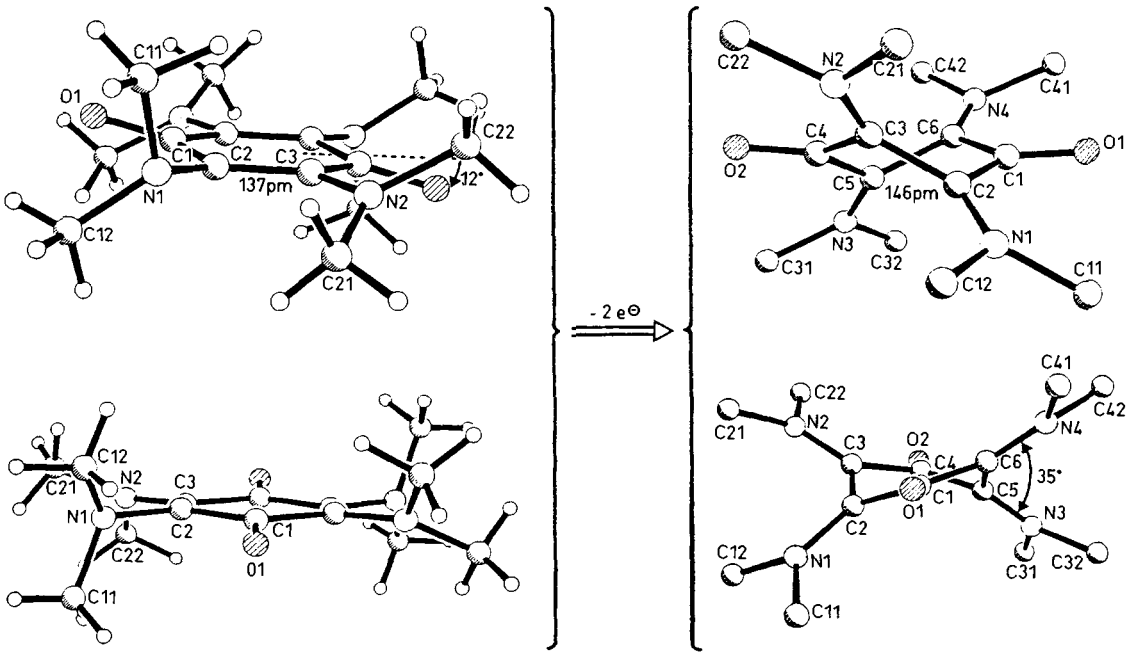

Fig. 1. Left: Crystal structure of tetrakis(dimethylamino)-*p*-benzoquinone [3]. Important distances [pm] (±0.5) and angles [°] (±0.5) (average values): C1-O 123, C1-C2 145, C1'-C3 151, C2-C3 137, C2-N1 142, C3-N2 137, N1-C12 146; O1-C1-C2 120, C1-C2-C3 119; torsion angles, C1C2-N1C11 84, C1'C3-N2C22 45, OC1(C2C3')-C2C3/C2'C3' 12. Right: Crystal structure of tetrakis(dimethylamino)-*p*-benzoquinone bis(hexachloroantimonate) [5]. Important distances [pm] (±1) and angles [°] (±1) (average values): C1-O 123, C1-C2 148, C1-C6 148, C2-C3 146, C2-N1 132, C3-N2 132; O1-C1-C2 123, C2-C1-C6 114; torsion angles, C1C2-N1C11 10, C4C3-N2C22 8, O1C1(C2C6)-O2C4(C3C5) 35.

The steric overcrowding in molecules containing vicinal $(H_3C)_2N$ substituents at a C=C bond,[6] which can be traced to the van der Waals radii of about 200 pm for each of the methyl groups, is also pronounced in the title compound (Fig. 1, left). The space-filling $(H_3C)_2N$ molecular subunits press the C=O groups between them from above and below the central C_4 quinone skeletal plane at interplanar angles of 12° and, in addition, they are either partly or even completely planarized (sums of angles around N1 and N1′ 346° and around N2 and N2′ 359°). This energetically preferred angle distortion is further emphasized by the C=C and C=O bond lengths, $d_{C=C}$ = 137 pm and $d_{C=O}$ = 123 pm, which remain within the usual range.[7] Exciting are the deformations of the quinone skeleton, caused by the different n/π and σ_{CN} interactions of the differently twisted (dihedral angle ω(CC-NC) = 35°, torsion angles φ(CC-NC) = 85°, 136°) and differently planarized dimethylamino substituents (sum of angles C–N–C = 346° and 359°), which are connected by C–N bonds of different lengths (Scheme 1).

The lengths of the C–C bonds on both sides of the C=O groups differ by 5 pm. Analogous "mericyanine"-like[8a] distortions are well-known for 2,5-dialkylamino substituted quinones[8] and can be rationalized by MO perturbation arguments.[8a] The special feature of the structure presented here (see Scheme 2), which can be satisfactorily reproduced quantum-chemically by AM1 energy hypersurface calculations[9] and whose calculated charge distribution q_μ^{AM1} is also displayed in Scheme 2, therefore, consists in the skeletal deformation of tetrakis(dimethylamino)-*p*-benzoquinone structurally "frozen" in its single crystal[1c] and caused by the steric overcrowding of conformationally different $(H_3C)_2N$ substituents.

Oxidation of tetrakis(dimethylamino)-*p*-benzoquinone by $SbCl_5$ in CH_2Cl_2[4] under aprotic conditions yields black crystals of the bis(hexachloroantimonate) salt. Its structure determination (Fig. 1, right) proves that the molecular skeleton remains intact in the dication and that the removal of two electrons produces the two six-electron five-center cyanine chains hoped for, which by their twisting of 35° relative to each other rather elegantly relieve the steric overcrowding in the neutral molecule (Scheme 3).

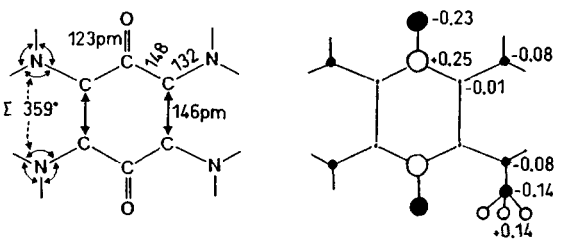

Scheme 3.

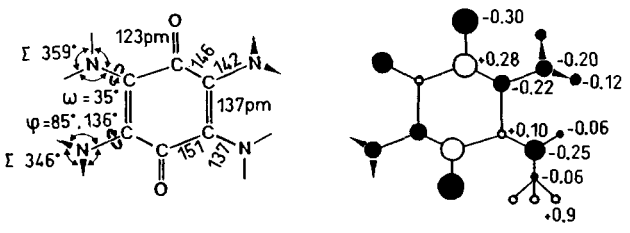

Scheme 2.

The two C=C bonds in tetrakis(dimethylamino)-*p*-benzoquinone, each 137 pm in length, are thus stretched in the dication by 9 pm(!); the CC bonds on either side of the C=O groups become more equal in length, the C–N bonds of 142 and 137 pm are shortened to 132 pm, and all dimethylamino groups become planar (sum of CNC angles 359° to 360°). The ring centers remain planar and the $(H_3C)_2N$ substituents

are only slightly twisted, with dihedral angles between 1 and 10°. The calculated charge distribution q_μ^{AM1} (Scheme 3) for the quantum-chemically reproducible, geometry-optimized structure[10] is in accord with the delocalization of the positive charges along the two N-C-C(O)-C-N$^\oplus$ chains and their considerable transfer to the peripheral methyl groups.

The general and powerful "cyanine" structure perturbation principle[11b] has been pointed out already in the discussion of the 2,4,6,7-tetramethoxythianthrene dication, the structure of which—despite the same number of 14 π electrons as in anthracene—does not exhibit an increased charge delocalization over the three annelated six-membered rings, but rather prefers stretching perpendicular to its long molecular axis with formation of two H_3CO-CCC-S$^\oplus$-CCC-OCH_3 chains.[11a] Of the numerous examples, in which an even number of π electrons are distributed over an odd number of π centers, the following structural changes shown in Scheme 4 are particularly spectacular.[11c-f]

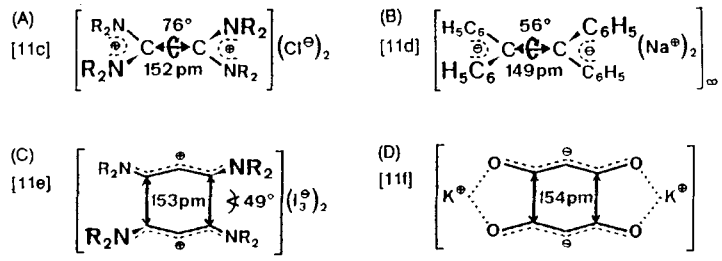

Scheme 4.

The bond skeletons of the starting compounds are always considerably deformed—independent of the formal number of π centers (Scheme 4: three in A and B, five in C and D), the resulting chains and the π electrons delocalized in them (Scheme 4: four in A and B, six in C and D), the type of compounds (Scheme 4: open-chain ethene derivatives such as A and B, those containing six-membered rings such as the dication of tetrakis(dimethylamino)benzene, C, or the dianion of 2,5-dihydroxy-*p*-benzoquinone, D) and independent of their method of preparation (Scheme 4: A, C, oxidation; B, reduction; D, salt formation). Conversely, these deformations permit an energetically favorable "cyanine" charge delocalization.[12] This rationalization can be straightforwardly extended to both structures presented here, the chairlike one of the tetrakis(dimethylamino)-*p*-benzoquinone with differently rotated $(H_3C)_2N$ groups (Scheme 2) and, especially, the one of its dication exhibiting a "twist" conformation and elongated C=C bonds.

In general, a change in the electron distribution and, unalterably, the energy of a compound has to be accompanied by structural changes—as required even in a simplified consideration of the individual states of a molecule,[13a] which always will be superior to the many and misleading so-called bond models. These structural distortions can be surprisingly severe especially on two-electron redox reactions (cf. Fig. 1 as well as Scheme 4; A–D) and, therefore, a search for other striking examples should be quite rewarding.[13b]

Received: March 25, 1991 [Z 4531 IE]
German version: *Angew. Chem. 103* (1991) 1194

[1] a) Cf., e.g., H. Beyer, W. Walter: *Lehrbuch der Organischen Chemie*, 21st ed., Hirzel, Stuttgart 1988, p. 519f.; b) cf., e.g., H. Bock, *Angew. Chem. 101* (1989) 1679; *Angew. Chem. Int. Ed. Engl. 28* (1989) 1646, and references cited therein; c) H. Bock, P. Hänel, W. Kaim, U. Lechner-Knoblauch, *Tetrahedron Lett. 26* (1985) 42. The reversible half-wave reduction potentials of *p*-benzoquinones, O=C(RC=CR)$_2$C=O, are −0.40 V (R = H) and −1.07 V (R = NMe_2); according to its ENDOR spectrum, the Me_2N-substituted radical anion, generated at a sodium mirror, is stabilized in THF solutions as a Na$^\oplus$ contact-ion pair; d) The first dications of tetraamino-*p*-benzoquinone derivatives (1,4,5,8-tetramethylbis(ethylene)- and tetrapiperidino-*p*-benzoquinone, have been prepared and isolated by *R. Gompper, R. Binder*, and *H. U. Wagner, Tetrahedron Lett. 27* (1986) 691.

[2] Tetrakis(dimethylamino)-*p*-benzoquinone was prepared as described by *K. Wallenfels* and *W. Draber* (*Justus Liebigs Ann. Chem. 667* (1963) 55) from tetrafluoro-*p*-benzoquinone and dimethylamine as follows (P. Hänel, *Dissertation*, Universität Frankfurt am Main 1987): A 30% aqueous dimethylamine solution (7 mL) was added dropwise to fluoranil (1 g, 5.56 mmol) (Aldrich) in 40 mL of diethyl ether at 300 K. After stirring for 1 h, the precipitated solid was filtered off, washed with water, and recrystallized from benzene/petroleum ether; yield 0.8 g (63%) 2,5-difluoro-3,6-bis-(dimethylamino)-*p*-benzoquinone. This (3.5 mmol) was heated in a mixture of a 30% aqueous solution of dimethylamine (10 mL), triethylamine (4 mL), and methanol (16 mL) for 4 h to about 350 K. The reaction mixture was poured into 80 mL of water and the precipitated solid filtered off. Sublimation at 10^{-2} mbar yielded 0.45 g (92%) of black crystals (m.p. 378–379 K); ^{1}H NMR ($CDCl_3$, TMS): δ = 2.85 (s, CH_3).

[3] a) Crystal structure analysis: $C_{14}H_{24}N_4O_2$, black crystals by sublimation at 368 K and 10^{-2} mbar; a = 1760.65(9), b = 1075.32(5), c = 832.09(4) pm, $\alpha = \beta = \gamma = 90°$, $V = 1575.36 \times 10^6$ pm^3 (200 K), orthorhombic, space group P_{bca} (No. 61), Z = 4, Siemens AED II four-circle diffractometer, $Mo_{K\alpha}$, graphite monochromator, 3038 measured reflections in the range $3 < 2\theta < 50°$, of which 952 were independent with $I > 1.5\sigma(I)$, $\mu(Mo_{K\alpha}) = 0.8$ cm^{-1}; structure determination by direct methods (SHELXTL-Plus), N = 952, NP = 140, R = 0.039, R_w = 0.035, $w = 1/\sigma^2(F) + 0.000106\,F^2$. All C,N, and O atoms were refined anisotropically, all H atoms were found and refined isotropically. The molecule is situated around a crystallographic inversion center. Further details of the crystal structure investigation are available on request from the Fachinformationszentrum Karlsruhe, Gesellschaft für wissenschaftlich-technische Information mbH, W-7514 Eggenstein-Leopoldshafen 2 (FRG), by quoting the depository number CSD-55493, the names of the authors and, the journal citation.

[4] The oxidizing agent is presumably the chloromethyl carbocation formed by the reaction $SbCl_5 + CH_2Cl_2 \rightarrow SbCl_6^\ominus + CH_2Cl^\oplus$, oxidation potential $E_{1/2}^{ox} \approx +1.6$ V (H. Bock, U. Lechner-Knoblauch, *J. Organomet. Chem. 294* (1985) 295). *Experimental procedure*: Tetrakis(dimethylamino)-*p*-benzoquinone (160 mg) were dissolved in 20 mL of dry CH_2Cl_2 and $SbCl_5$ (1 g) was added dropwise under argon. After 2 d of reaction at room temperature, the solvent was removed from the resulting suspension in vacuo. The violet residue was dissolved in 5 mL of dry CH_3CN; after addition of 10 mL of dry CH_2Cl_2, black needles with a metallic luster began to grow within 12 h.

[5] Crystal structure analysis: $[C_{14}H_{24}N_4O_2]^{\oplus\oplus}[SbCl_6^\ominus]_2 \cdot [CH_3CN] \cdot [CH_2Cl_2]_x$, black needles with a metallic luster from CH_3CN/CH_2Cl_2; a = 1248.4(10), b = 1977.3(5), c = 1566.6(3) pm, β = 97.71(4)°, $V = 3832.29 \times 10^6$ pm^3 (room temperature), monoclinic, space group $P2_1/c$ (No. 14), Z = 4, Siemens AED II four-circle diffractometer, $Mo_{K\alpha}$, graphite monochromator, 8816 measured reflections in the range $3° < 2\theta < 50°$, of which 4135 were independent with $I > 2\sigma(I)$, $\mu(Mo_{K\alpha}) = 22.9$ cm^{-1}. Structure determination by Patterson methods (SHELXTL-Plus), N = 4135, NP = 352, R = 0.059, R_w = 0.06, $w = 1/\sigma(F) + 0.001999\,F^2$; empirical absorption correction; C,N,O,Cl, and Sb atoms refined anisotropically, H atoms at calculated positions (d_{CH} = 96 pm) refined isotropically using a common temperature factor. Dichloromethane molecules statistically disordered [3b].

[6] Cf., e.g., the extreme case of tetrakis(dimethylamino)ethene, which, according to its −30 °C single-crystal structure analysis, exhibits a rather twisted bond as well as largely planarized $(H_3C)_2N$ groups (H. Bock, H. Borrmann, Z. Havlas, K. Ruppert, A. Simon, unpublished results).

[7] Electron diffraction in the gas phase (K. Hagen, K. Hedberg, *J. Chem. Phys. 59* (1973) 158) yields, for example, for the unsubstituted parent molecule *p*-benzoquinone $d_{C=O}$ = 122.5 pm, $d_{C=C}$ = 134.4 pm, d_{C-C} = 148.1 pm, CCC = 118°. Single-crystal structure analysis (I. Bolhius, C. T. Kiers, *Acta Crystallogr. Sect. B34* (1978) 1015) yields $d_{C=O}$ = 133.4 pm, d_{C-C} = 147.0 pm, CCC = 120.9°.

[8] Examples given: a) 2,5-diamino-3,6-dichloro-*p*-benzoquinone (S. Kulpe, D. Leupold, S. Dähne, *Angew. Chem. 78* (1966) 639; *Angew. Chem. Int. Ed. Engl. 5* (1966) 599) with $d_{C(N)/C(O)}$ = 150 pm and $d_{C(Cl)/C(O)}$ = 141 pm; b) 2,5-diaziridino-*p*-benzoquinone (T. Ito, T. Sakurai, *Acta Crystallogr. Sect. B29* (1973) 1594) with $d_{C(N)/C(O)}$ = 152 pm and $d_{C(H)/C(O)}$ = 146 pm.

[9] Geometry-optimized AM1 calculations yield for the energy minimum (ΔH_f°(AM1) = +13.5 kcal mol^{-1}) the following selected structure parameters (distances in pm, angles in °; experimental data in parentheses; cf. Fig. 1, left, as well as Scheme 2): C=O 124 (123), C=C 138 (137), C1-C2 148 (146), C1'-C3 152 (151), C2-N1 143 (142), C3-N2 138 (137), sum of angles CN1C 339 (346), sum of angles CN2C 359 (359), ω_1(C1C2-N1C11) 76 (84), ω_2(C1'C3-N2C22) 29 (45), bending angle OC1(C2C3')-C2-C3/C2'-

C3') 32 (12). Obviously, a satisfactory agreement results; nevertheless, the minimum of the total energy calculated for a "boat" conformation is 6 kcal mol^{-1} below that of the "chair" conformation.

[10] For the dication, a complete geometry optimization also yields a twist conformation with an enthalpy of formation ΔH_f°(AM1) = + 424 kcal mol^{-1}; the resulting structure parameters for the planarized dication skeleton agree largely with the experimental data (cf. Fig. 1 right, as well as Scheme 3): C=O 123 (123), C=C 147 (146), C-C 149 (148), C-N 134 (132), sum of angles CNC 360 (359).

[11] a) H. Bock, A. Rauschenbach, K. Ruppert, Z. Havlas, *Angew. Chem. 103* (1991) 706; *Angew. Chem. Int. Ed. Engl. 30* (1991) 714; b) S. Dähne, D. Leupold, *ibid. 78* (1966) 1029 and *5* (1966) 984; cf. also S. Dähne, F. Moldenhauer, *Prog. Phys. Org. Chem. 15* (1985) 1–130, and references cited therein; c) H. Bock, K. Ruppert, K. Merzweiler, D. Fenske, H. Goesmann, *Angew. Chem. 101* (1989) 1715; *Angew. Chem. Int. Ed. Engl. 28* (1989) 1684; K. Elbl, C. Krieger, H. A. Staab, *ibid. 102* (1990) 183 and *29* (1990) 211; d) H. Bock, K. Ruppert, D. Fenske, *ibid. 101* (1989) 1717 and *28* (1989) 1685; e) K. Elbl, C. Krieger, H. A. Staab, *ibid. 98* (1986) 1024 and *25* (1986) 1023; *102* (1990) 183 and *29* (1990) 211; f) S. Kulpe, *J. Prakt. Chem. 316* (1974) 353.

[12] S. Shaik, P. C. Hiberty, J.-M. Lefour, G. Ohanessian, *J. Am. Chem. Soc. 109* (1987) 363.

[13] a) Cf., e.g., H. Bock, *Angew. Chem. 101* (1989) 1659; *Angew. Chem. Int. Engl. 28* (1989) 1627; *ibid. 89* (1977) 631 and *16* (1977) 613; *Pure Appl. Chem. 62* (1990) 383; b) "Organic chemists will encounter quite some surprises, if the removal of only a few electrons from their compounds can change the structures so tremendously": *J. M. Lehn* on the occasion of a lecture in Frankfurt am Main on May 30, 1990.

What will be formed on reduction of 1,1'-diphenylethene [Eq. (c)], which contains an $(H_5C_6)_2C$ unit only on one side, by lithium and sodium metal under comparable aprotic conditions? Isolated in each case are orange, air-sensitive crystals of the title compounds.

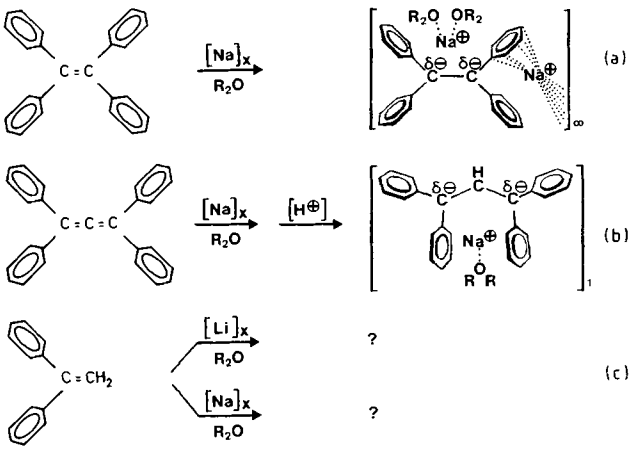

The Two-Electron Reduction of 1,1'-Diphenylethene by Lithium or Sodium to Different 1,1,4,4-Tetraphenylbutane-1,4-diide Salts via C–C Bond Formation— A Monomeric Dilithium Contact Ion Triple and a Polymer String of "Hydrocarbon Oysters Containing Solvated Sodium Pearls"**

By *Hans Bock,* Klaus Ruppert, Zdenek Havlas, Wolfgang Bensch, Wolfgang Hönle,* and *Hans Georg von Schnering*

Dedicated to Professor Hanskarl Müller-Buschbaum on the occasion of his 60th birthday

The "ocean" of known alkali-metal organic compounds with often surprising structures[1] hides numerous details in its "dark depths". Thus, their preparation involves largely unknown redox processes, which include both solvation and contact-ion pair formation. Also unknown is the influence of the respective countercation and its solvation on the crystallization of the reduction product.[3, 4] On allowing unsaturated hydrocarbons containing twofold phenyl-substituted π centers to react with sodium mirrors [Eqs. (a) and (b)], we discovered that Na countercations[5] repeatedly preferred an inter- or intramolecular six-membered-ring sandwich coordination.[3d–f]

The structures (Fig. 1) suggest that both reactions involve two-electron reduction to a 1,1,4,4-tetraphenylbutane-1,4-diide via C–C bond formation,[10, 11] because this dianion is the hydrolysis-sensitive intermediate of a 1,1,4,4-tetraphenylbutane synthesis. The dilithium and disodium salts, although prepared under nearly identical reduction conditions,[6, 7] display rather large structural differences. The monomeric dilithium contact ion triple (Fig. 1 A) contains doubly ether-solvated $Li^{\delta\oplus}$ countercations, which are π-coordinated to the almost trigonal-planar C1 anion centers as well as to adjacent centers of the less twisted ($\omega = 8°$) phenyl ring. Its butane-1,4-diide chain shows an antiperiplanar conformation and contains a central C–C bond of 156 pm length. In contrast, the sodium salt (Fig. 1 B) consists of contact-ion aggregates, the ether-solvated $Na^{\delta\oplus}$ countercations of which (Na1 and Na3) are partly encapsulated as a π sandwich between two phenyl rings, inclined towards each other owing to the synclinal conformation ($\omega = 69°$) of the butane-1,4-diide chain. The central C2–C3 bond of the latter is lengthened to 158 pm presumably because of the decreased $Na^{\oplus} \leftarrow C^{\ominus}$ delocalization of the negative charges. The resulting "hydrocarbon oysters with solvated $Na^{\oplus}$ pearls" are threaded together on crystallization by π-allyl coordination through additional $(R_2O)Na^{\delta\oplus}$ centers (Na2 and Na4) to form an infinite string. Taking into account contact distances up to 300 pm, the coordination numbers are 11 and 12 for the sandwich centers Na1 and Na3 and 8 for the chain-connecting centers Na2 and Na4.[9] The crystal structures of both salts show additional remarkable features. The angles around the nearly planar anion centers C1 and C4 range from 116 to 125°; that is, they differ by up to 9°. The torsion angles of the differently twisted planar phenyl rings are between 9 and 35°. Especially on countercation contact, they are severely distorted; for example the *ipso* angles at the anion substitution centers are decreased to values as low as 112° (cf. Ref. [4c]) and the ring CC bonds vary in length from 136 to 146 pm (Fig. 1 B). For some of the $Li^{\oplus}$ and $Na^{\oplus}$ countercation-solvating diethyl ethers, a bending of one of their external C–C bonds out of the W conformation is observed with torsion angles up to 79° (Fig. 1 B).

[*] Prof. Dr. H. Bock, Dipl.-Chem. K. Ruppert, Dr. Z. Havlas[+], Dr. W. Bensch
Institut für Anorganische Chemie der Universität
Niederurseler Hang, W-6000 Frankfurt am Main 50 (FRG)
Dr. W. Hönle, Prof. Dr. H. G. von Schnering
Max-Planck-Institut für Festkörperforschung
Heisenbergstrasse 1, W-7000 Stuttgart 80 (FRG)

[+] Permanent address:
Institute for Organic Chemistry and Biochemistry
of the Czechoslovakian Academy of Sciences

[**] Structures of Sterically Overcrowed and Charge-Perturbed Molecules, Part 9. This work was supported by the Deutsche Forschungsgemeinschaft, the Fonds der Chemischen Industrie, and the State of Hesse. Part 8: H. Bock, K. Ruppert, D. Fenske, H. Goesmann, *Z. Anorg. Allg. Chem. 595* (1991) 275.

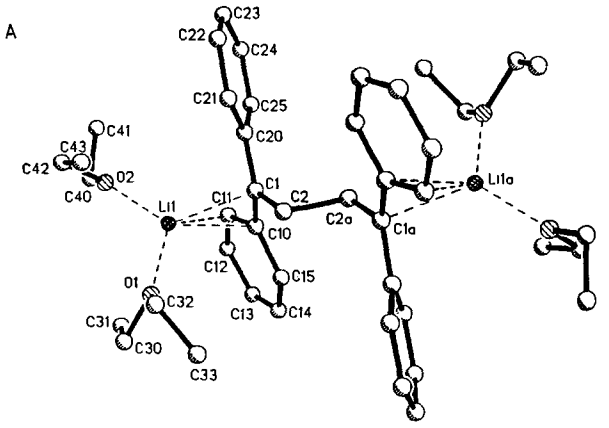

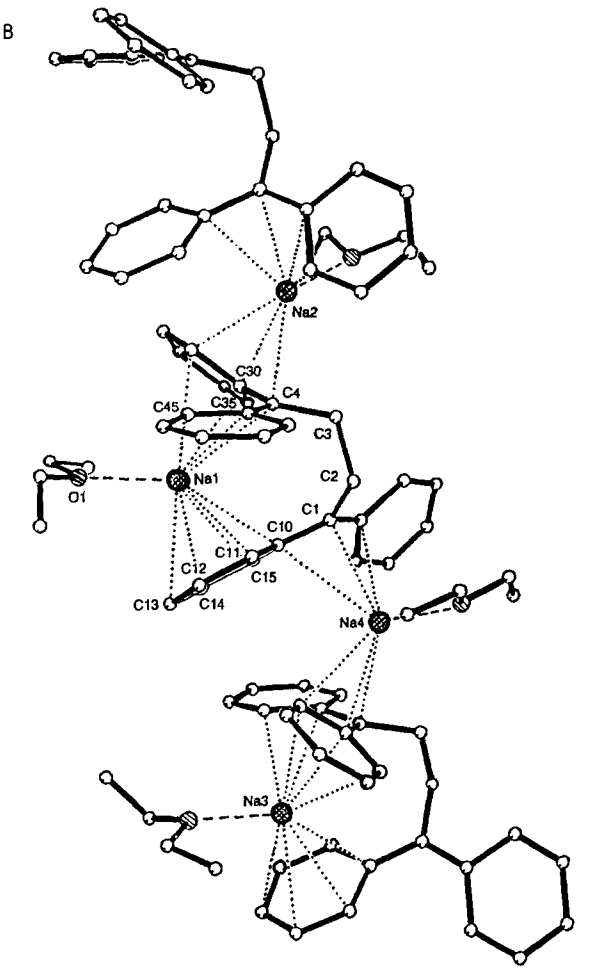

Fig. 1. A) Crystal structure of dilithium 1,1,4,4-tetraphenylbutane-1,4-diide tetrakis(diethylether) [8]. Important distances [pm] (± 0.8) and angles [°] (± 0.5) of the salt, which exhibits a center of inversion: C2-C2a 156, C1-C2 151, C1-C10 144, C1-C20 146, C1-Li1 228, C10-Li1 232, C11-Li1 258, Li1-O1 193, Li1-O2 193; C2a-C2-C1 114, C2-C1-C10 118, C10-C1-C20 123, C1-C10-C11 125, C11-C10-C15 113, C10-C11-C12 124; torsion angles C1C2-C2aC1a 180, C2C1-C10C11 172, C2C1-C20C21 143, C30O1-C32C33 70, C42O2-C40C41 79. B) Crystal structure of disodium 1,1,4,4-tetraphenylbutane-1,4-diide bis-(diethylether) [9]: section of the infinite chain in which the contact ion pairs containing Na1 and Na2 are connected through the likewise solvated centers Na2 and Na4. The tetraphenylbutane-1,4-diide contains a rather long central C2–C3 bond of 158.4 pm, torsion angles ω(C1C2-C3C4) = 69° and ω(CC-phenyl) = 9°–29° a well as partly rather distorted, planar benzene rings (e.g., C10-C11 146 pm versus C12-C13 136 pm or C11-C10-C15 = 112°). The coordination of the Na1 center comprises the sandwich Na1-C10 to Na1-C15 with contact distances of 284, 273, 276, 289, 289 and 279 pm, an allyl unit with Na–C distances of Na1-C35 = 300 pm, Na1-C30 = 267 pm and Na1-C4 = 303 pm, and the single bonds Na1-C45 (305 pm) and Na1-O1 (235 pm).

On viewing the different structures of the tetraphenylbutane-1,4-diide salts, which we have isolated here for the first time as single crystals, it is especially striking that the $Na^{\oplus}$ countercations partly prefer to complex in *intra*molecular sandwiches as observed before in tetraphenylallylsodium diethyl ether.[3e] This obviously renders possible the optimum charge distribution for the formation of contact-ion aggregates. For this reason and starting from the experimentally determined structure (Fig. 1 B), we have approximatively calculated the differences in the enthalpies of formation $\Delta(\Delta H_f^{MNDO})$ and in the charge distributions q_μ^{MNDO} between the 1,1,4,4-tetraphenylbutane-1,4-diide $M^{\ominus\ominus}$, its—for the sake of computing time—"hydrated" sodium contact-ion-pair anion $[M^{\ominus\ominus}Na^{\oplus}(OH_2)_2]^{\ominus}$, and the chain structure unit $\{Na^{\oplus}\cdots[M^{\ominus\ominus}Na^{\oplus}(OH_2)_2]^{\ominus}\cdots Na^{\oplus}\}$ (Scheme 1).

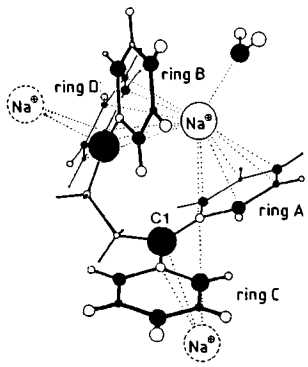

	$M^{\ominus\ominus}$	$[M^{\ominus\ominus}Na^{\oplus}(OH_2)]^{\ominus}$	$\{Na^{\oplus}\cdots[M^{\ominus\ominus}Na^{\oplus}(OH_2)]\cdots Na^{\oplus}\}$
$\Delta(\Delta H_f^{MNDO})$ [kcal mol^{-1}]	0	−269	−471
$\sum q^{MNDO}(M)$	−2	−1.53	−1.15
ring A	−0.30	−0.27	−0.12
ring B	−0.30	−0.21	−0.06
ring C	−0.36	−0.19	−0.13
ring D	−0.36	−0.23	−0.09
q_{C1}	−0.37	−0.34	−0.41

Scheme 1.

The calculated enthalpy of formation for the dianion $M^{\ominus\ominus}$ decreases considerably on additional contact-ion interaction. Simultaneously, the charges $\sum q_\mu^{MNDO}$ of the individual $M^{\ominus\ominus}$ phenyl rings also decrease rather strongly, especially within the simulated chain structure unit $(Na^{\oplus}\cdots[]^{\ominus}\cdots Na^{\oplus})$, whereas q_{C1} of the butane-1,4-diide centers remains approximately constant. The preferred formation of an intramolecular $(R_2O)Na^{\delta\oplus}$ sandwich,[3e] therefore, is supported quantum-chemically for tetraphenylbutane-1,4-diide as well.

Again, there remains the open question concerning the pathway of the two-electron reduction of 1,1′-diphenylethene in ether solutions by the alkali metals lithium and sodium,[6, 7] which presumably starts heterogeneously. Of special interest is the C–C bond formation, for which speculative possibilities range from a surface reaction at the bare metal to a dimerization within a solvent cage. ESR/ENDOR spectroscopic investigations in aprotic ether solutions[2b, 3a–c, 13] confirm that $Li^{\oplus}$ or $Na^{\oplus}$ contact-ion pairs of radical anions $M^{\bullet\ominus}$ of suitable molecules M can be generated by their alkali-metal reduction and identified beyond doubt by their ^7Li or ^{23}Na couplings. The aggregation, possibly required for dimerization of sodium contact-ion pairs via C–C bond for-

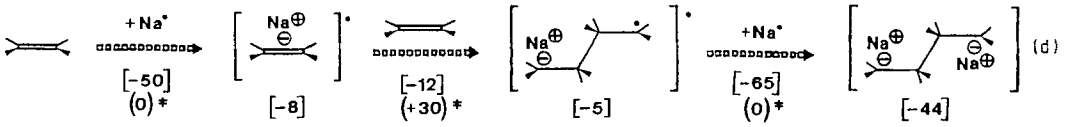

mation, is supported, for example, by the structure determination of the dimer salt [fluorenone$^{\bullet\ominus}$Na$^{\oplus}$(dme)$_2$]$_2$ (dme = dimethoxyethane).[3c] Because of the analogy to anionic styrene copolymerization,[11] we have performed extensive MNDO/CI hypersurface calculations[13] for the network of imaginable reaction steps involved in the C–C bond formation. Equation (d) shows the most probable pathway with the lowest enthalpy differences ($\Delta(\Delta H_f^{MNDO})$) and enthalpies of activation ($\Delta(\Delta H_f^{\neq(MNDO)})$) (all values in kcal mol^{-1}).

Accordingly, the energetically preferred contact-ion-pair radical $\{[H_2C=CH_2]^{\bullet\ominus}Na^{\oplus}\}$ should first form at the sodium metal mirror; addition of excess ethene then leads to the $Na^{\oplus}$ butanyl-4-ide, which is further reduced to the diamagnetic triple ion $[Na^{\oplus}H_2C^{\ominus}\text{-}CH_2\text{-}CH_2\text{-}CH_2^{\ominus}Na^{\oplus}]$. Phenyl substituents lower all enthalpy values.[14]

Thus, despite increasing detailed preparative and quantum-chemical knowledge, a full understanding of contact-ion crystals and their formation is—as emphasized at the beginning—still far away and additional investigations with selected model compounds like the analogous 1,1,4,4-tetraphenylbutadiene, in which the negative charges can be additionally stabilized within the unsaturated C4 chain,[15] are needed.

Received: March 27, 1991 [Z 4543 IE]
German version: *Angew. Chem. 103* (1991) 1197

[1] Recent overviews: a) C. Schade, P. von R. Schleyer, *Adv. Organomet. Chem. 27* (1988) 169; b) W. Setzer, P. von R. Schleyer, *ibid. 24* (1985) 353, and references cited therein.

[2] a) J. M. Lehn, *Angew. Chem. 102* (1990) 1347; *Angew. Chem. Int. Ed. Engl. 29* (1990) 1304; *ibid. 100* (1988) 91 and *27* (1988) 89; b) H. Kurreck, B. Kirste, W. Lubitz: *Electron Nuclear Double Resonance Spectroscopy of Radicals in Solution*, VCH, New York 1988; c) Y. Inone, G. W. Gokel (Eds.): *Cation Binding by Macrocycles*, Marcel Dekker, New York 1990, and references cited therein.

[3] Selected contributions from our group: a) H. Bock, B. Solouki, P. Rosmus, R. Dammel, B. Hierholzer, U. Lechner-Knoblauch, H.-P. Wolf in H. Sakurai (Ed.): *Organosilicon and Bioorganosilicon Chemistry*, Horwood, Chichester 1985, p. 59f.; H. Bock, *Polyhedron 7* (1988) 2429; *Angew. Chem. 101* (1989) 1679; *Angew. Chem. Int. Ed. Engl. 28* (1989) 1646; b) H. Bock, H.-F. Herrmann, *J. Am. Chem. Soc. 111* (1989) 7622; c) H. Bock, H.-F. Herrmann, D. Fenske, H. Goesmann, *Angew. Chem. 100* (1988) 1125; *Angew. Chem. Int. Ed. Engl. 27* (1988) 1067; d) H. Bock, K. Ruppert, D. Fenske, *ibid. 101* (1989) 1717 and *28* (1989) 1685; e) H. Bock, K. Ruppert, Z. Havlas, D. Fenske, *ibid. 102* (1990) 1095 and *29* (1990) 1042, and references cited therein; f) cf. also K. Ruppert, *Dissertation*, Universität Frankfurt 1991.

[4] Among the remarkable exceptions are (1) all alkali methyls (E. Weiss, S. Corbelin, J. K. Cockroff, A. N. Fitch, *Angew. Chem. 102* (1990) 728; *Angew. Chem. Int. Ed. Engl. 29* (1990) 650 and references cited therein; cf. also [1]), (2) the $Li^{\oplus}$, $Na^{\oplus}$, $K^{\oplus}$, and $Rb^{\oplus}$ acetylides [1], (3) $Li^{\oplus}$ and $Na^{\oplus}$ phenyls (T. Maezke, D. Seebach, *Helv. Chim. Acta 72* (1989) 624 and [1] and references cited therein, as well as $Li^{\oplus}$ and $Na^{\oplus}$ cyclopentadienyls [1], and the tetracyanoethene anion salts with $Na^{\oplus}$, $K^{\oplus}$, and $Cs^{\oplus}$ countercations (H. Bock, K. Ruppert, D. Fenske, H. Goesmann, *Z. Anorg. Allg. Chem. 595* (1991) 275, as well as H. Bock, C. Näther, K. Ruppert, unpublished; cf. also D. A. Dixon, J. S. Miller, *J. Am. Chem. Soc. 109* (1987) 3656).

[5] The preferred formation of $Na^{\oplus}$ sandwich-structure subunits may be caused by (1) a favorable average solvation energy of $Na^{\oplus}$ cations, also in diethyl ether (cf., e.g., $\Delta H_{hydr.}$ [kJ mol^{-1}]: $[Li(OH_2)_{25}]^{\oplus}$ −499,5; $[Na(OH_2)_{17}]^{\oplus}$ −390; $[K(OH)_2)_{11}]^{\oplus}$ −306; N. Wiberg: *Hollemann-Wiberg Lehrbuch der Anorganischen Chemie*, 91st–100th ed., de Gruyter, Berlin 1985, p. 954) and (2) possibly also by favorable radii ratios. For the latter, ab initio SCF calculations using 6-31* basis sets are quoted, which suggest an 80% ionic character and yield radii estimates for the countercations of $Li^{\delta\oplus} \approx 75$ pm and $Na^{\delta\oplus} \approx 115$ pm (see [1a], Table on p. 174). The inner circle radius of a hexagon with edge length d amounts to $r_{inside} = d\sqrt{3}/2$; thus, for benzene ($d_{CC} = 139$ pm), about 120 pm should result for the maximum π charge density.

[6] Preparation of the dilithium salt: anhydrous degassed diethyl ether (15 mL) and degassed 1,1'-diphenylethene (310 mg) were placed in a Schlenk trap (preheated under vacuum) under argon and Li powder (100 mg) was added. After 1 d, the reaction solution had turned red and, after 3 d, orange, air- and moisture-sensitive crystals had grown.

[7] Preparation of the sodium salt: A metal mirror was generated in a Schlenk trap, preheated under vacuum, by vacuum distillation of sodium (170 mg). Anhydrous diethyl ether (30 mL) and degassed 1,1'-diphenylethene (500 mg) were then added under argon. After 1 h, the reaction solution had turned red and, after 24 h, the metal mirror had largely vanished. On slow cooling (1 K h^{-1}) from 293 K to 263 K, orange, air- and moisture-sensitive crystals grew.

[8] a) Crystal structure analysis: $[(H_5C_6)_2CCH_2CH_2C(C_6H_5)_2]^{\ominus\ominus}2Li^{\oplus}\cdot 4Et_2O$, $a = 833.4(4)$, $b = 1109.5(6)$, $c = 1194.9(9)$ pm, $\alpha = 79.45(5)$, $\beta = 87.25(5)$, $\gamma = 71.92(4)°$, $V = 1032.54 \times 10^6$ pm^3 (170 K), $Z = 1$, $\varrho_{calcd} = 1.079$ g cm^{-3}, $\mu(Mo_{K\alpha}) = 0.6$ cm^{-1}, triclinic, space group $P\bar{1}$, Siemens AED II four circle diffractometer, 3492 measured reflections within $3° < 2\theta < 48°$, of which 1795 are independent with $I > 1\sigma(I)$. Structure determination by direct methods (SHELXTL-PLUS), $N = 1795$, $NP = 351$, $R = 0.087$, $R_w = 0.061$, $w = 1/\sigma^2(F) + 0.000715\,F^2$. C, O, and Li atoms found anisotropically; H atoms refined isotropically. Insufficient scattering of the single crystal subjected to measurement leads to an unfavorable N/NP ratio. The dianion is centered around a crystallographic inversion center. b) Further details of the crystal structure determination are available on request from the Fachinformationszentrum Karlsruhe, Gesellschaft für wissenschaftlich-technische Information mbH, W-7514 Eggenstein-Leopoldshafen 2 (FRG), by quoting the depository number CSD-55492, the names of the authors, and the journal citation.

[9] Crystal structure analysis: $[(H_5C_6)_2CCH_2CH_2C(C_6H_5)_2]^{\ominus\ominus}2Na^{\oplus}\cdot 2Et_2O$, $a = 1653.1(2)$, $b = 1126.9(4)$, $c = 1762.8(7)$ pm, $\beta = 104.99(5)°$, $V = 3172.03 \times 106$ pm^3 (200 K), $Z = 8$, $\varrho_{calcd} = 1.161$ g cm^{-3}, $\mu(Mo_{K\alpha}) = 0.9$ cm^{-1}, monoclinic, space group $P2_1$, Siemens AED II four-circle diffractometer, 5461 measured reflections within $3° < 2\theta < 48°$, of which 4918 are independent with $I > 1\sigma(I)$. Structure determination by direct methods (SHELXTL-PLUS), $N = 4918$, $Np = 622$, $R = 0.097$, $R_w = 0.093$, $w = 1/\sigma^2(F) + 0.004844\,F^2$. Na and C atoms of the tetraphenylbutane-diide skeleton refined anisotropically; O and C atoms of the ether molecules refined isotropically. Hydrogen atoms are isotropically refined groupwise, each with a fixed temperature factor. The crystal structure (Fig. 1B) shows four different $Na^{\oplus}$ centers, all of which are solvated by one diethyl ether molecule with Na–O contact distances between 229 and 235 pm, and which can be formally characterized by the following four types of bonding: a one-sided phenyl sandwich (Na1 and Na3), coordination to four adjacent C centers (Na2 and Na3), allyl-anion-type interactions (Na1 and Na4), and single $Na^{\oplus}$–C bonds (Na1, Na3, and Na4). Thus, the four different $(R_2O)Na^{\oplus}$ centers are surrounded as follows: Na1 by one C_6 sandwich, one C_3 chain, and one Na–C single bond; Na2 by one C_4 and one C_3 chain; Na3 by one C_6 sandwich, one C_4 chain, and one Na–C single bond; Na4 by two allyl subsystems and one Na–C single bond [8b].

[10] The reductive C–C bond formation of ethenes by reaction with alkali metals has been reported, for example, for $Ph_3SiHC=CH_2$ (J. J. Eisch, R. J. Beuhler, *J. Org. Chem. 28* (1963) 2876) and for $(Me_3Si)_2C=CH_2$ (M. Kira, T. Hino, Y. Kubota, N. Matsuyama, H. Sakurai, *Tetrahedron Lett. 29* (1988) 6939). A literature search produced no known crystal structures; the course of the reaction has been deduced from deuterolysis, reoxidation, and ring closure by R_2SiCl_2 to yield silacyclopentane derivatives.

[11] Cf., e.g., M. Swarć (Ed.): *Carbanions, Living Polymers and Electron Transfer Processes*, Wiley-Interscience, New York 1968, p. 367f. Contrary to the thermally initiated industrial-scale polymerization of styrene, styrene/butadiene copolymerisates are prepared using lithium alkyl compounds; also, sodium naphthalide is applicable (Dr. Brandstetter (BASF, Ludwigshafen), personal communication).

[12] For some organolithium compounds, $Li^{\oplus}$ six-membered-ring sandwiches have also been structurally proven [1b]: for example, on both sides in lithium-7*bH*-indeno[1,2,3-*j*,*k*]fluorenide (D. Bladauski, W. Broser, H. J. Hecht, D. Rewicki, H. Dietrich. *Chem. Ber. 112* (1979) 1380) or one-sided in bis[(tetramethylethenediamine)lithium]naphthalene and -anthracene salts (J. J. Brooks, W. Rhine, G. D. Stucky, *J. Am. Chem. Soc. 94* (1972) 7346; W. E. Rhine, J. Davis, G. D. Stucky, *ibid. 97* (1975) 2079). Die $Li^{\oplus}$–C_6 contact distances are between 228 and 266 pm; in the double sandwich structure, the planes of the six-membered rings are only 386 pm apart. In

the disodium salt presented here, the $Na^{\oplus}$–C_6 distances are between 265 pm and 305 pm and the ones between the nearest-neighbor phenyl rings within the contact-ion-pair subunit are about 470 pm.

[13] a) H. Bock, B. Hierholzer, P. Schmalz, *Angew. Chem. 99* (1987) 811; *Angew. Chem. Int. Ed. Engl. 26* (1987) 791; b) H. Bock, P. Dieckmann, H.-F. Herrmann, *Z. Naturforsch. B46* (1991) 326; c) H. Bock, H.-F. Herrmann, *J. Nouv. Chim.*, in press. Cf. also the *Dissertations* of P. Hänel, B. Hierholzer, H.-F. Herrmann, and R. Baur (Universität Frankfurt 1987, 1988, 1989, and 1990, respectively).

[14] All quantum-chemical calculations have been performed using the MNDO program SCAMP and the parameters given in [3e]. For disodium tetraphenylbutane-1,4-diide, the experimental structure has served as the starting point and all ether ethyl groups have been substituted by H to save computing time. The energy hypersurface calculations for the anionic ethene dimerization have been carried out with all configurations resulting from the six inner and partly occupied molecular orbitals. The C···C distance between the C-connecting centers has been chosen as reaction coordinate and every point of it has been completely geometry-optimized.

[15] H. Bock, C. Näther, K. Ruppert, Z. Havlas, unpublished results.

SiI_2—A Novel Triatomic Molecule with a Relativistic Touch**

By *Hans Bock,* Matthias Kremer, Michael Dolg,** and *Heinz-Werner Preuß*

Dedicated to Don Weyenberg on the occasion of his 60th birthday

Combination of the 13 most important nonmetal elements (H, B, C, Si, N, P, O, S, F, Cl, Br, I, Xe) allows the construction of 1638 triatomic molecules, of which 1183 are linear and 455 are cyclic. With rather few exceptions—including the title compound—they are already known; thus the other dihalogen silanediyls (silylenes), too, are accessible via different routes[1] (Fig. 1).

The still-unpublished He(I) photoelectron (PE) spectrum of $SiBr_2$,[1g] which exhibits a Br–Si–Br angle of 103° and Si–Br bond lengths of 224 pm,[1f] will be discussed by way of introduction without considering relativistic effects, which probably can no longer be neglected for SiI_2. According to a useful rule of thumb,[3] six radical-cation states of low energy are expected for the altogether twelve $3p_{Si}$ and $4p_{Br}$ valence electrons; the additional band at 15.3 eV, therefore, results from a $3s_{Si}$ ionization (Fig. 1, bottom: $2a_1$). As the MNDO diagrams illustrate (Fig. 1, bottom), the following straightforward and plausible assignment results: the $M^{\cdot\oplus}$ ground state $\tilde{X}(^2A_1)$ is generated by electron expulsion from the silicon electron pair (Fig. 1: $4a_1$) followed by four n_{Br} bromine-electron-pair (Fig. 1: $3b_2$, $1a_2$, and $3a_1$) and two σ_{SiBr} ionizations (Fig. 1: $2b_2$ und $2a_1$), the latter with a dominant 3 s_{Si} contribution. On PE spectroscopic comparison of SiF_2, $SiCl_2$, and $SiBr_2$ (Fig. 1), especially striking is the lowering of the halogen-electron-pair ionizations $n_F > n_{Cl} > n_{Br}$, which reflects the tremendous influence of the decreasing effective nuclear charge of the halogen substituents[3] and their increasingly smaller difference from that of the Si center. What additional information will be supplied by the PES band pattern of SiI_2, the preparation of which is best accomplished by the reaction of SiI_4 with elemental silicon?[4]

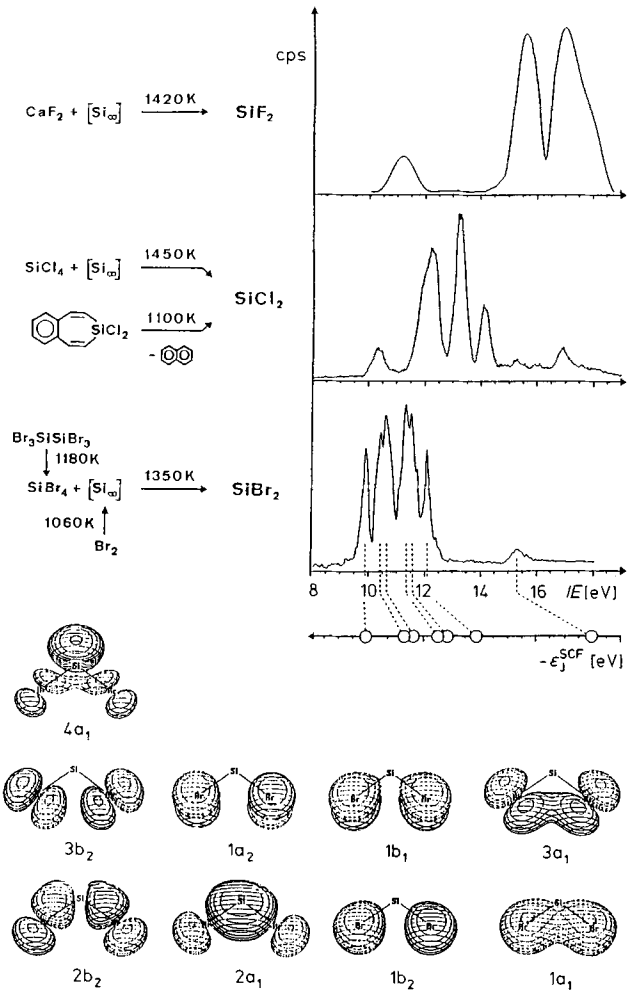

Fig. 1. Preparation and PE spectroscopic characterization of SiF_2 [1c], $SiCl_2$ [1d, e], and $SiBr_2$ [1f, g] (top) as well as Koopmans' assignment of the radical-cation states of $SiBr_2$ based on MNDO eigenvalues and eigenfunctions (bottom) [2].

The comparison of the radical-cation-state pattern of SiI_2 (Fig. 2) with those of the other dihalogen silylenes (Fig. 1) shows that only the $3s_{Si}$ ionization has shifted significantly to lower energies, but a distinct spread to largely isolated bands can be recognized, which now are $\Delta IE^{v}_{n,m} = 0.4$ to 0.7 eV apart (Table 1). For the assignment of the vertical ionization energies IE^{v}_{n} of SiI_2 via Koopmans' correlation, $IE^{v}_{n} = -\varepsilon^{SCF}_{j}$, based on SCF eigenvalues (Table 1), therefore, the relativistic effects caused by the two heavy-atom substituents I necessarily have to be taken into account. The relativistic influence comprises direct effects through the mass/velocity term, the Darwin term, and the spin/orbit term, as well as indirect ones through the relativistic changes in the electron distribution within the core electron system and thus in the field for the valence electrons. In comparison to nonrelativistic Hartree–Fock calculations, the effects for relativistic Dirac–Fock calculations lead to a contraction of the 5s and $5p_{1/2}$ orbitals by 3.9 and 4.0%, whereas the $5p_{3/2}$ orbital expands relative to radii expectation values only slightly by 0.6%. Energetically, the 5s and $5p_{1/2}$ orbitals are stabilized

[*] Prof. Dr. H. Bock, Dipl. Chem. M. Kremer
Institut für Anorganische Chemie der Universität
Niederurseler Hang, W-6000 Frankfurt am Main 50 (FRG)
Dr. M. Dolg, Prof. Dr. H. W. Preuß
Institut für Theoretische Chemie der Universität
Pfaffenwaldring 55, W-7000 Stuttgart 80 (FRG)

[**] Gas-Phase Reactions, Part 81, and Surface Reactions, Part 15. This work was supported by the Land Hessen and the Fonds der Chemischen Industrie. Part 80 and Part 14, respectively: H. Bock, L. S. Cederbaum, W. von Niessen, P. Paetzold, P. Rosmus, B. Solouki, *Angew. Chem. 101* (1989) 77, *Angew. Chem. Int. Ed. Engl. 28* (1989) 88 and H. Bock, M. Bankmann, *Phosphorus, Sulfur Silicon Relat. Elements 53* (1990) 167.

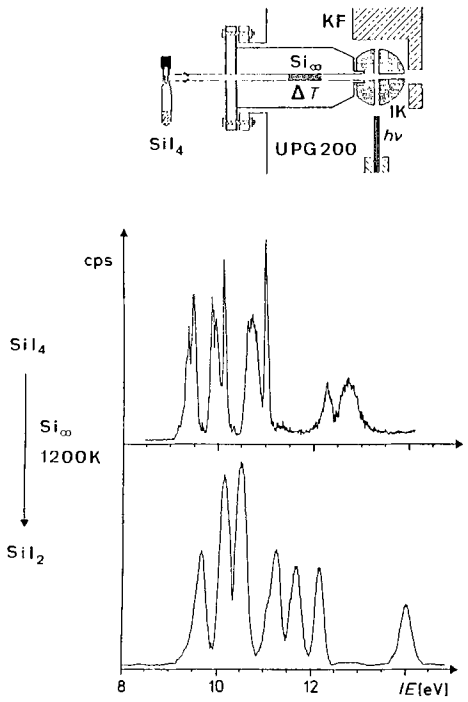

Fig. 2. Short-path apparatus (schematic) for the gas-phase preparation of SiI_2 in the electron-bombardment oven (ΔT) of the Leybold Heraeus UPG 200 PE spectrometer ($h\nu$, He(I) lamp; IK, ionization chamber; KF, cooling trap) as well as He(I) PE spectra of SiI_4 and SiI_2.

by 1.52 and 0.7 eV, whereas the $5p_{3/2}$ orbital is destabilized by 0.39 eV.[7] The experimentally observed hyperfine structure splitting of the ($5s^2$, $5p^5$) states of the iodine atom, $^2P_{3/2}$ and $^2P_{1/2}$, amounts to 0.94 eV.[3b] These relativistic effects can be successfully incorporated into quantum-chemical investigations—as demonstrated by a test calculation for HI (exp./calcd: $IE_1^v(^2P_{3/2})$ = 10.38/10.14 eV; $IE_2^v(^2P_{1/2})$ = 11.05/10.86 eV; $\Delta IE_{1/2}^v$ = 0.67/0.73 eV[3b, 6])—by using a quasi-relativistic two-component pseudopotential SCF method and a double zeta (DZ) polarization function (p) basis set[6] (Table 1).

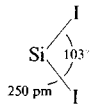

1

Table 1. Experimental and calculated data for SiI_2.

IE_n^v [eV]	C_{2v}^*/C_{2v}	$-\varepsilon_j^{SCF}$ [eV]	$\Delta\varepsilon_j^{SCF}$ (rel.) [eV]
9.70	$9e_{1/2}/4a_1$	9.37	0.02
10.16	$8e_{1/2}/3b_2$	10.00	−0.07
10.54	$7e_{1/2}/1a_2$	10.31	−0.05
11.25	$6e_{1/2}/1b_1$	11.30	0.05
11.70	$5e_{1/2}/3a_1$	11.72	0.06
12.18	$4e_{1/2}/2b_2$	12.37	0.02
14.10	$3e_{1/2}/2a_1$	17.67	0.05

Obviously, the Koopmans' defects amount—with the exception of the $2a_1(3s_{Si})$ ionization—to a maximum deviation of only 0.33 eV. In contrast, the first SiI_2 ionization energy predicted by semiempirical MNDO calculations is too low by 1.1 eV and that predicted by relativistic EHMO calculations using the program ITEREX 85 is even 1.6 eV too low.[1g] Eye-catching is the rather small effect of spin/orbit coupling within the C_{2v} molecular symmetry (**1**, $\Delta\varepsilon_j^{SCF}$ (rel.)) of only at most 0.07 eV, whereas, in the analogous GeI_2, the relativistic effects increase to 0.3 eV and thus can no longer be neglected. The SiI_2 structural parameters from the geometry-optimized DZP-SCF calculation[7] are supported by the satisfactory agreement between the values also calculated for the other dihalogen silylenes and their known experimental values (exp./calcd, e.g., for $SiBr_2$: Si–Br = 224/221 pm, Br–Si–Br = 103/106°[1d, 7]). The population analysis for SiI_2 based on the optimized structure yields for the Si center a charge of + 0.54 and, correspondingly, for each of the I centers − 0.27. Comparison with the values obtained for the Si centers of the other dihalogen silylenes (SiF_2, + 0.91; $SiCl_2$, + 0.78, $SiBr_2$, + 0.66[7]) further supports the assumption that the steady decrease in the valence-electron ionization energies, clearly visible in their PE spectra (Figs. 1 and 2), can be traced back to the effective nuclear charges of halogen substituents, which decrease from F to I.

Could the novel molecule SiI_2 be of some use? Speculations range from the oligomerization of the species, generated here thermally under unimolecular conditions, to give compounds $(SiI_2)_n$ with $n < 6$,[1a, 9] for example, which are stable at room temperature and under normal pressure and which would further enlarge polysilane chemistry, to known silylene additions to unsaturated hydrocarbons[10] as well as subsequent products. More technologically minded proposals[11] concern uses in chemical vapor deposition (CVD), surface etching, or Si_x transport reactions, because the generation temperature for SiI_2 from SiI_4 and Si_x requires only 1200 K (Fig. 2), which is considerably below those necessary for the other dihalogen silylenes, and also because Si–I bonds are supposedly easier to split. Until such proposals are realized for SiI_2, however, its charm consists in being one of the few still unknown triatomic main-group-element molecules.

Received: April 8, 1991 [Z 4559 IE]
German version: *Angew. Chem. 103* (1991) 1200

[1] a) Historical overview: W. H. Atwell, D. R. Weyenberg, *Angew. Chem. 81* (1969) 485; *Angew. Chem. Int. Ed. Engl. 8* (1969) 469, and references cited therein, especially M. Schmeißer, K. Friedrich, *ibid. 76* (1964) 782 and *3* (1964) 699; b) recent review: H. Bock, B. Solouki, "Photoelectron Spectra of Silicon Compounds" in S. Patai, Z. Rappoport (Eds.): *The Chemistry of Organosilicon Compounds*, Wiley, Chichester 1989; c) SiF_2: T. P. Fehlner, D. W. Turner, *Inorg. Chem. 13* (1974) 754; N. P. C. Westwood, *Chem. Phys. Lett. 25* (1974) 588; our spectrum (Fig. 1) was plotted using the program PES [2]; d) Structure of $SiCl_2$: I. Hargittai, G. Schultz, J. Tremmel, N. D. Kagramov, A. K. Maltsev, O. M. Nefedov, *J. Am. Chem. Soc. 105* (1983) 2895; e) PE spectrum of $SiCl_2$: H. Bock, B. Solouki, G. Maier, *Angew. Chem. 97* (1985) 205; *Angew. Chem. Int. Ed. Engl. 24* (1985) 205; f) Structure of $SiBr_2$: [1d]; g) PE spectrum of $SiBr_2$: *Dissertation*, M. Kremer, Universität Frankfurt 1991, which also reports in detail on the generation and characterization of SiI_2.

[2] The PE spectra of $SiBr_2$ and SiI_2 were recorded using the recently developed program PES, which is available on request. It is adaptable to personal computers (ATARI-ST; ≥ 2-Mb hard disc, HPGL plotter, DMA interface) and supports the on-line registration of He(I) PE spectra for the Leybold Heraeus PE spectrometers UPG 200 and Mini-UPG. Well over 50 program functions serve the representation, administration, and interactive manipulation of the measurement data and allow, for example, calibration, baseline correction, and FFT noise suppression as well as weighted subtractions from multicomponent spectra.

[3] a) H. Bock, *Angew. Chem. 89* (1977) 631; *Angew. Chem. Int. Ed. Engl. 16* (1977) 613; b) K. Wittel, H. Bock, "Photoelectron Spectra of Organic Halogen Compounds" in S. Patai, Z. Rappoport (Eds.): *The Chemistry of Functional Groups, Supplement D*, Wiley, Chichester 1983, pp. 1499–1603; cf. also [1b].

[4] a) Pure SiI_4 is an absolute necessity. Therefore, the brownish, waxy raw material obtained from reaction of the elements (G. Brauer: *Handbuch der Präparativen Anorganischen Chemie*, de Gruyter, Berlin 1985) is twice distilled at 500 K after adding 10 wt% of copper powder before each distilla-

tion. The resulting, slightly violet solid can be sublimed under 10^{-3} mbar pressure at 370 K to yield white crystalline needles, which have to been stored in sealed ampoules at low temperature and under exclusion of light. b) Reaction of the silicon tetrahalides SiI_4 and $SiBr_4$ with silicon powder: An 8-mm-long layer of Si powder dispersed in quartz wool was placed into the heatable molybdenum tube (inner diameter 4 mm) of the electron-bombardment oven in the PE spectrometer between two quartz-wool stoppers. After removal of surface water by heating to 370 K under 10^{-5} mbar pressure, the silicon tetrahalides were evaporated from either a trap with a Teflon stopcock ($SiBr_4$, twice distilled at 427 K/1 bar) or from the heatable solid evaporator of the PE spectrometer (SiI_4); the pressure in the inlet system remained below 10^{-4} mbar. After recording of the SiX_4 PE spectra, the reaction zone was heated in 50 K steps until the SiX_4 ionization patterns disappear.

[5] P. Pyykkö, *Chem. Rev. 88* (1988) 563; W. H. E. Schwarz in Z. B. Maksic (Ed.): *Theoretical Models of Chemical Bonding, Part 2, The Concept of the Chemical Bond*, Springer, Berlin 1990. Cf. also P. Pyykkö, J.-P. Desclaux, *Acc. Chem. Res. 12* (1979) 276.

[6] J. P. Desclaux, *At. Data Nucl. Data Tables 12* (1973) 311.

[7] The one- and two-component ab initio pseudopotential calculations are performed using the programs TURBOMOLE (R. Ahlrichs, M. Bär, M. Häser, H. Horn, C. Kölmel, *Chem. Phys. Lett. 162* (1989) 165) or UHREL (P. Hafner, W. H. E. Schwarz, *Chem. Phys. Lett. 65* (1979) 537). The energy-adjusted quasi-relativistic pseudopotentials used comprise in satisfying approximation the most essential relativistic effects resulting from the Dirac equation (mass/velocity term, Darwin term, and spin/orbit term of the Pauli equation). Si and I are treated as systems of four and seven valence electrons and for both atoms energy-optimized (4s4p)GTO-valence basis sets of double zeta quality are employed. The geometry optimizations have been performed within one-component SCF calculations using the program TURBOMOLE and applying a gradient procedure. The effects of spin/orbit interactions were subsequently investigated by two-component SCF calculations using the program UHREL starting from the equilibrium geometries determined.

[8] G. Jonkers, S. M. van der Kerk, R. Mooyman, C. A. de Lange, J. G. Snijders, *Chem. Phys. Lett. 94* (1983) 585, and references cited therein.

[9] Cf., e.g., E. Hengge, *Phosphorus, Sulfur, Relat. Elements 28* (1986) 43; M. Coffin, T. P. Hamilton, P. Pulay, I. Hargittai, *Inorg. Chem. 28* (1989) 4092, although [1 c–1 e] are not quoted.

[10] Cf. G. Raabe, J. Michl in S. Patai, Z. Rappoport (Eds.): *The Chemistry of Organic Silicon Compounds*, Wiley, Chichester 1989; p. 1021 ff., and references cited therein. Cf. also D. H. Pae, M. Xiao, M. Y. Chiang, P. Gaspar, *J. Am. Chem. Soc. 113* (1991) 1281.

[11] Cf. N. Auner, *Nachr. Chem. Tech. Lab. 38* (1990) 1372.

Superconductivity in Layered Structures of Rare-Earth Carbide Halides

By *Arndt Simon,* Hansjürgen Mattausch, Roland Eger,* and *Reinhard K. Kremer*

The structures of superconducting oxocuprates contain without exception CuO_2 layers.[1] For $YBa_2Cu_3O_{6.6}$ (transition temperature $T_c \approx 60$ K), the anisotropy of the decrease of T_c in a magnetic field corresponds to the behavior of two-dimensionally metallic, and at low temperatures superconducting, niobium and tantalum dichalcogenides.[3] Crystals of these phases consist of MX_2 planes, connected by van der Waals bonds. TaS_2 is superconducting at $T_c = 1.8$ K;[4] the highest transition temperature in dichalcogenides (T_c = 7.3 K) is found for $NbSe_2$.[5] Since these systems are two-dimensional and can be modified by intercalation reactions, extensive investigations on superconducting dichalcogenides have been undertaken.[6, 7]

We now report on the superconductivity of similar layered compounds of the composition $Y_2C_2Br_2$, $Y_2C_2I_2$, $La_2C_2Br_2$, and $Lu_2C_{2-x}Cl_2$. Monophasic samples are prepared like $Gd_2C_2Br_2$[8, 9] as moisture-sensitive, microcrystalline, bronze-colored platelets by heating stoichiometric quantities of trihalide, metal, and graphite powder in gas-tight, welded tantalum ampules for several days at ca. 1300 K.[10] The phase analysis[11, 12] was performed with the modified Guinier technique.[13] As Figure 1 shows, the structures of the crystals, which cleave like graphite, are characterized by close-packed double sheets of metal atoms (M). The octahedral interstices are occupied by C_2 units and the metal double layers are sandwiched by layers of halogen atoms (X). Such XMC_2MX slabs are joined together by van der Waals forces.[8, 9] The crystals show good metallic conductivity within the layers. The conductivity is orders of magnitude smaller in the perpendicular direction.[15]

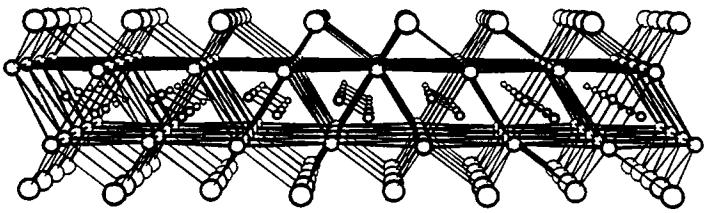

Fig. 1. Central projection of a slab of $M_2C_2X_2$ along [010] of the monoclinic structure (X, M, and C atoms are drawn in decreasing size; the diagram is based on the positional parameters of $Gd_2C_2Br_2$).

Figure 2 shows the onset of superconductivity for $Y_2C_2Br_2$ as indicated by resistance measurements; the diamagnetic shielding[16] displayed in Figure 3 confirms the

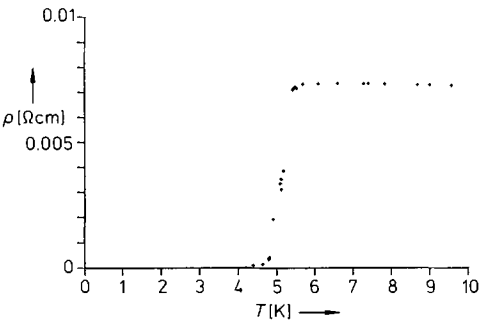

Fig. 2. Dependence of the electrical resistance ϱ of $Y_2C_2Br_2$ on temperature [16].

superconducting state of all four phases. The carbide halides are interesting not only because superconductivity is observed in a two-dimensionally delocalized electronic system. An analysis of their very special electronic structure and bonding could also contribute to the understanding of the chemical prerequisites for the phenomenon of superconductivity.

Extending an earlier idea about high-temperature superconductors,[17, 18] we attribute the attractive interaction between conducting electrons through electron–phonon coupling[19] to a tendency toward localization of the electrons in pairs in special band states. These band states may be bonding (covalent M–M bonds, for example in Nb, Nb_3Sn, $NbSe_2$), nonbonding (lone pairs in Sn, Pb, $(Ba,K)(Bi,Pb)O_3$) or antibonding in character (d states in oxocuprates). The carbide halides described here fall into the last category.

[*] Prof. Dr. A. Simon, R. Eger, Dr. H. Mattausch, Dr. R. K. Kremer
Max-Planck-Institut für Festkörperforschung
Heisenbergstrasse 1, W-7000 Stuttgart 80 (FRG)

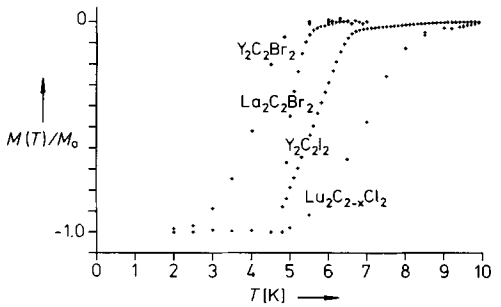

Fig. 3. Magnetization measurements on rare-earth carbide halides. All data points are normalized in such a way that at the lowest temperature the maximal diamagnetic shielding is achieved. For $Y_2C_2Br_2$ it is 40% of the ideal value.

The C–C distance of 127 pm[8] and 130 pm[9] in $Gd_2C_2Br_2$ determined by X-ray crystallography on single crystals—neutron diffraction on a powder sample of $Tb_2C_2Br_2$ gives a C–C distance of 129 pm[20]—corresponds approximately to a double bond and leads to a formal bond description[21] as $(M^{3+})_2C_2^{4-}(X^-)_2$ for the phases $M_2C_2X_2$. Semiconductor behavior is therefore expected unless a strong overlap of M-d and C-p states closes the band gap. Metallic behavior results, in terms of molecular chemistry, from the backbonding of occupied π^* states of the C_2 groups into empty d states on the M atom. This backbonding is already indicated by shortened C–C distances. Such a view of the bonding in $Gd_2C_2Cl_2$ was substantiated by calculations of the band structure using the Extended Hückel method.[23] They led to a density of states at the Fermi edge, and their COOP (*c*rystal *o*rbital *o*verlap *p*opulation)[24] confirmed the C–C antibonding ($C\pi^*$) and the Gd–C bonding character of these states.

Thus, a picture of the pairwise attractive interaction between the conduction electrons in the compounds $M_2C_2X_2$ results. The electrons are delocalized in covalently mixed p-d band states and have a tendency to pairwise occupation of the molecular π^* states of the C_2 units. In this sense, the stretching and wagging vibrations of the C_2 unit should promote an effective electron–phonon coupling through variations of the energy of the π^* level or variation of the p-d overlap. The parallels to other superconducting systems such as, for instance, type $BaBiO_3$ are obvious.[25, 26] Here too, the electrons are delocalized in a band of covalently mixed O–Bi states and have a tendency to occupy in pairs the (in this case nonbonding and metal-centered) lone-pair states.

As anticipated, superconductivity in $M_2C_2X_2$ phases does not occur with magnetic lanthanoid ions; the corresponding, similarly metallic compounds of Gd and Tb undergo magnetic ordering at temperatures around 28 and 78 K respectively, but show no superconductivity. The lowering of the valence electron concentration in $Y_2C_2Br_2$ by replacing 10% of the Y atoms by calcium atoms lowers T_c to 4 K. The particular halogen involved is critical: T_c is ca. 1 K higher for $Y_2C_2I_2$ than for $Y_2C_2Br_2$; however, $Y_2C_2Cl_2$, $La_2C_2I_2$, and $Lu_2C_{2-x}Br_2$ are not superconducting.

For completeness we add that superconductivity also occurs in binary rare-earth metal carbides of the composition M_2C_3 and MC_2.[6] For example, a transition temperature of 17 K is observed for $C_{1.55}Th_{0.3}Y_{0.7}$.[27] Their structures also contain C_2 units as is required for this composition, and the observed C–C distances suggest strong p-d mixing.[28]

Received: May 13, 1991 [Z4626 IE]
German version: *Angew. Chem. 103* (1991) 1210

CAS Registry numbers:
$Y_2C_2Br_2$, 135257-93-1; $Y_2C_2I_2$, 135257-94-2; $La_2C_2Br_2$, 135257-95-3; $Lu_2C_{2-x}Cl_2$, 135339-36-5; YBr_3, 13469-98-2; $LaBr_3$, 13536-79-3; $LuCl_3$, 10099-66-8; Y, 7440-65-5; La, 7439-91-0; Lu, 7439-94-3; graphite, 7782-45-5; YI_3, 13470-38-7.

[1] K. Yvon, M. Francois, *Z. Phys. B: Condens Matter 76* (1989) 413.
[2] W. Bauhofer, W. Biberacher, B. Gegenheimer, W. Joss, R. K. Kremer, H. Mattausch, A. Müller, A. Simon, *Phys. Rev. Lett. 63* (1989) 2520.
[3] R. V. Coleman, G. K. Eiserman, S. J. Hillenius, A. T. Mitchell, J. L. Vincent, *Phys. Rev. B: Condens. Matter 27* (1983) 125.
[4] M. H. van Maaren, G. M. Schaeffer, *Phys. Lett. 29A* (1969) 571.
[5] P. Detrey, S. Gygax, J.-P. Jan, *J. Low Temp. Phys. 11* (1973) 421.
[6] B. W. Roberts, *J. Phys. Chem. Ref. Data 5* (1976) 581.
[7] R. Schöllhorn, *NATO ASI Ser. Ser. B. 172* (1987) 149.
[8] U. Schwanitz-Schüller, A. Simon, *Z. Naturforsch. B40* (1985) 710.
[9] H. Mattausch, R. K. Kremer, R. Eger, A. Simon, *Z. Anorg. Allg. Chem.*, in press.
[10] The Ta ampules charged with ca. 2 g of starting materials were sealed by welding under 1 atm Ar, and heated in quartz ampules for 10 days at 1370 K ($Y_2C_2Br_2$), 12 days at 1320 K ($Y_2C_2I_2$), 10 days at 1220 K ($La_2C_2Br_2$), or 10 days at 1420 K ($LuC_{2-x}Cl_2$). For Lu, no monophasic products have been isolated.
[11] $Y_2C_2Br_2$: *C2/m*; $a = 695.1(1)$, $b = 376.39(5)$, $c = 993.0(2)$ pm, $\beta = 100.03(1)°$. $Y_2C_2I_2$: *C2/m*; $a = 721.7(3)$, $b = 387.9(1)$, $c = 1042.8(2)$ pm, $\beta = 93.47(3)°$. $La_2C_2Br_2$: *C2/m*; $a = 747.6(2)$, $b = 406.07(4)$, $c = 1005.4(3)$ pm, $\beta = 94.11(2)°$. $Lu_2C_{2-x}Cl_2$: $R\bar{3}m$; $a = 360.57(3)$, $c = 2721.7(2)$ pm.
[12] The phase $Lu_2C_{2-x}Cl_2$ has the same Lu/Cl substructure and approximately the same lattice constants as Lu_2CCl_2 ($a = 360.17$, $c = 2716.0$ pm) [14]. The absence of monoclinic symmetry suggests that C^{4-} and C_2^{4-} occur side by side. The presence of C_2 units is indicated by Raman spectra (preliminary measurements: *C. Thomsen*). Lu_2CCl_2 itself is semiconducting according to our studies.
[13] A. Simon, *J. Appl. Crystallogr. 3* (1970) 11.
[14] T. Schleich, G. Meyer, *Z. Anorg. Allg. Chem. 552* (1987) 90.
[15] A. Simon, H. Mattausch, G. J. Miller, W. Bauhofer, R. K. Kremer in K. A. Gschneidner, Jr., L. Eyring (Eds.): *Handbook on the Physics and Chemistry of Rare Earths*, Elsevier, Amsterdam 1991, Chapter 14.
[16] The temperature dependence of the electrical conductivity was measured with the four point method on a pressed pellet (van der Pauw method). The magnetic susceptibilities were determined in an MPMS quantum design SQUID magnetometer at 50 G.
[17] A. Simon, *Angew. Chem. 99* (1987) 602; *Angew. Chem. Int. Ed. Engl. 26* (1987) 579.
[18] A. Simon, *Chem. Unserer Zeit 22* (1988) 1.
[19] In our opinion specific dynamic lattice deformations are essential for the coupling.
[20] J. K. Cockcroft, unpublished results.
[21] A detailed comparison with other carbide halides and a discussion of the bonding relationships is given in [22]. A premonition guided the choice of the structure of $Gd_2C_2Cl_2$ for the cover picture for that article!
[22] A. Simon, *Angew. Chem. 100* (1988) 163; *Angew. Chem. Int. Ed. Engl. 27* (1988) 159.
[23] G. J. Miller, J. K. Burdett, C. Schwarz, A. Simon, *Inorg. Chem. 25* (1986) 4437.
[24] R. Hoffmann, *Angew. Chem. 99* (1987) 871; *Angew. Chem. Int. Ed. Engl. 26* (1987) 846.
[25] A. W. Sleight, J. L. Gilsson, P. E. Bierstedt, *Solid State Commun. 17* (1975) 27.
[26] R. J. Cava, B. Batlogg, J. J. Krajewski, R. Farrow, L. W. Rupp, Jr., A. E. White, K. Short, W. F. Peck, T. Kometani, *Nature 332* (1988) 814.
[27] M. C. Krupka, A. L. Giorgio, N. H. Krikorian, E. G. Szklarz, *J. Less-Common Met. 19* (1969) 113.
[28] The idea mentioned here of pairwise attraction of conducting electrons in systems with C_2 units is naturally not applicable to all carbides. Transition-metal carbides like NbC belong in our opinion to the first category.

Book Reviews are written by invitation from the editor. Suggestions for books to be reviewed and for book reviewers are welcome. Publishers should send brochures or (better) books to the following address: Redaktion Angewandte Chemie, Postfach 101161, D-6940 Weinheim, Federal Republic of Germany. The editor reserves the right of selecting which books will be reviewed. Uninvited books not chosen for review will not be returned.

Profiles, Pathways and Dreams. Autobiographies of Eminent Chemists. Edited by *J. I. Seeman*. American Chemical Society, Washington, D. C. 1990. **D. J. Cram. From Design to Discovery.** xxi, 146 pp., hardcover $ 24.85.—ISBN 0-8412-1768-8; **C. Djerassi. Steroids Made it Possible.** xxiv, 205 pp., hardcover $ 24.85.—ISBN 0-8412-1773-4; **E. L. Eliel. From Cologne to Chapel Hill.** xxxi, 138 pp., hardcover $ 24.95.—ISBN 0-8412-1767-X; **J. D. Roberts. The Right Place at the Right Time.** xix, 299 pp., hardcover $ 24.95.—ISBN 0-8412-1766-1

Jeffrey I. Seeman, an American industrial chemist who tells us that he has always been interested in the human side of scientific developments, suggested to the books department of the American Chemical Society (ACS) in 1986 that they should publish a volume of autobiographical essays by eminent chemists. The ACS took up this idea, but both they and the editor soon found that the project began to develop a life of its own, so that by the time it is finished (at least for the time being!) there will be no less than 22 individual volumes. The series has now been given the general title "Profiles, Pathways and Dreams", and the first four autobiographies (consisting of nearly 800 pages altogether!) have appeared and are reviewed here. My verdict can be summarized in one sentence: please let us have more soon! (Since this was written the number of volumes has in fact grown to ten).

The clever and carefully-considered choice of authors means that the level of interest in the series is unlikely to fade soon. As well as applying the criterion that each author must have made fundamental contributions to organic chemistry over a long period, much importance has also been placed on maintaining the international quality of the project. The authors eventually enlisted (ominously, it is stated in the preface that "Not all who were invited chose to participate, and not all who should have been invited could be asked") represent experiences of teaching and research in thirteen countries altogether.

These first volumes of the series can be read at several quite different levels, and this is likely to be true also of later volumes. In the first place, of course, they are the life stories of the authors, in which the human dimension and the dreams come out to a varying degree depending on temperament and frankness, sometimes strongly (*Djerassi*) and sometimes with more reserve (*Cram*). Here each reader will develop his or her own particular affinities. For me it was *Roberts*' autobiography that pleased most: his sober style and absence of illusions, his modesty ("Memory of the titans of any given era of modern chemistry tends to fade rapidly from generation to generation"), the humor, both overt and veiled, and the occasional adverse comments about colleagues.

Secondly, these "blue volumes" (each with a profile on the cover in gold of the author portrayed therein!) are also excellent textbooks of chemistry, since their authors describe in detail how their research aims have developed over the decades: by studying the classic examples one gains mastery of a science. In this connection it is also interesting to note at how early a stage each author discovered his (scientific) leitmotif in every case, and how steadfastly he continued to pursue it over a very long period and developed it further using the latest techniques. This possibly characterizes one of the main differences compared with present-day research in organic chemistry: the research of the fifties to seventies which is described in these autobiographies (the average age of the authors being around seventy) was more noticeably "inner-directed" (to use a term coined by *David Riesman*, a sociologist of that period), in contrast to the strongly "outer-directed" research of today. The main reason for this could be the considerable changes that have occurred in the system of supporting and rewarding research. The scarcity of financial support and of material resources in general in those earlier years forced researchers to be more self-reliant. Here again *Roberts* provides a good example, constructing his own glass apparatus, and later his own NMR spectrometers which he continued to develop. In those days there was no talk of creativity prizes, reagents of the year, or other such gimmicks originating from the world of scientific marketing.

Thirdly, these volumes are a tribute to the American university system. This is at the same time both very elitist and democratic in character, has a strong internationalist tradition, as is clearly shown by the experiences of the immigrants *Djerassi* and *Eliel* during their first years in American universities, and provides academic freedom (researchers remain almost exclusively researchers, rather than administrators as tends to happen in Germany).

This series of volumes will not add up to a history of modern organic chemistry; that purpose cannot be achieved through autobiographies, and it will certainly not be attempted. On the other hand, when the series is complete we shall have a very rich and colorful patchwork of chemistry, made up additionally of many interesting and sometimes amusing snapshots, together with many brilliant highlights.

Henning Hopf [NB 1159 IE]
Institut für Organische Chemie
der Technischen Universität Braunschweig (FRG)

Heteroatom Chemistry. Edited by *E. Block*. VCH Publishers, New York 1990. xii, 376 pp., hardcover DM 178.00.–ISBN 0-89573-743-4

"Heteroatom chemistry" is usually understood to mean the organoelement chemistry of the elements in main-groups 3 to 7 of the Periodic Table (i.e. the 13th to 17th groups). This book is based on twenty plenary lectures delivered at the International Conference on Heteroatom Chemistry (ICHAC) held in Albany, NY, in 1989. The presentation of this material in book form is almost beyond reproach.

This very extensive subject could not be covered in a mere 376 pages; the editor has therefore limited the contents to an overview of the current situation regarding the applications of heteroatom compounds (excluding those of nitrogen and

 © VCH Verlagsgesellschaft mbH, W-6940 Weinheim, 1991 0570-0833/91/0909-1190 $ 3.50+.25/0

oxygen), mainly in synthetic organic chemistry. In addition a few articles are devoted to unusual types of bonding in compounds of main-group elements. The choice of eminent authors has ensured that the book is successful in meeting these aims.

Y. Apeloig deals with bonding and structure in some unusual silicon compounds. This article is a good summary of the same author's contribution to "The Chemistry of Organic Silicon Compounds" (edited by *S. Patai* and *Z. Rappoport*), which appeared in 1989. *A. J. Arduengo III* and *D. A. Dixon* present experimental and theoretical evidence showing that trivalently bonded compounds of the "pnictogen" elements can undergo not only the familiar textbook vertex inversion process (tetrahedron–trigonal-planar intermediate–tetrahedron), but also an "edge inversion process" (tetrahedron–square-planar intermediate–tetrahedron). This new process is illustrated by the example of *Arduengo*'s T-shaped compounds of main-group elements. In discussing the problem of color in pentaarylbismuth compounds *K. Seppelt* draws attention to the unusual bismuth-carbon bonding in these hypervalent species; relativistic effects must be invoked to account for the phenomena that are observed. This group of contributions dealing mainly with theoretical and physical chemical aspects ends with an article by *J. B. Lambert, G. Wang* and *E. C. Chelius* in which they discuss the β-effect of trimethylsilyl, -germyl and -stannyl groups in the solvolysis of cyclohexyl and cyclopentyl derivatives.

Four articles are devoted to the reactivity and synthetic applications of sulfoxides. Those by *H. B. Kagan* and *A. Ohno* are concerned with chiral sulfoxides, whereas *O. De Lucchi* et al. discuss atropisomeric binaphthylsulfones and -sulfoxides as chiral auxiliaries. *N. Furukawa* describes an investigation into the question of whether sulfuranes are formed as intermediates in the reaction of sulfoxides with organometallic reagents, and considers the possible synthetic applications of these experiments.

A further contribution on the chemistry of hypervalent heteroatoms is provided by *D. H. R. Barton*, who describes ligand coupling reactions applied to pentacoordinated bismuth compounds. *Y.-Z. Huang* et al. give an impressive account of the use of arsene ylides in synthesizing polyenes and sensitive natural products. Some insights into the chemistry of organoselenium compounds are provided by *W. Ando* and *N. Tokitoh*, who describe the photolysis and pyrolysis of selenium- and sulfur-containing heterocycles to form highly reactive intermediates. The section on polyselenium and polysulfur heterocycles is especially interesting, and includes some hitherto unpublished results. *T. G. Back* et al. report on the selenosulfonation of alkenes and alkynes and some applications of this method in steroid chemistry. *A. Krief* et al. have succeeded in synthesizing molecules in which quaternary carbon atoms are linked together, by proceeding via α-lithioselenides.

Two articles deal with the chemistry of low-valency compounds of main-group elements. In the first of these *M. Regitz* discusses the synthesis of phosphaalkynes and the chemistry based on these. Although detailed and up-to-date reviews of this topic already exist,[*] the fascinating possibilities opened up by this chemistry simply had to be included in this book. The second article is an updated survey of the chemistry of siloxy-substituted silenes, an area which is the specialty of *A. G. Brook*. *T. Cohen* describes the use of phenylthioethers to synthesize carbanions which would otherwise be accessible only with great difficulty or not at all. The sections on the preparation of dianions from epoxides and dioxetanes are particularly interesting. These anions are very useful building blocks, for example in synthesizing spiroketals.

Some results obtained in the very promising field of polydentate Lewis acids, which in contrast to that of polydentate Lewis bases is still only in its infancy, are described with the help of examples by *H. G. Kuivala*. Some new sterically strained boron compounds are described by *M. Lappert* et al. Nearly all these results are previously unpublished; however, the coverage is rather too brief for my taste (9 pages), especially as this is the only article dealing with boron chemistry. *H. Sakurai* gives a brief account of some interesting metal-induced cyclooligomerizations of silylated cyclic polyalkynes, and of the synthesis and structure of hexakis(trimethylsilyl)benzene. The book ends with an article by *K. Tang* on copper and silver complexes with sulfur ligands, which is certainly worth reading, although it does not really fit into the subject of the book.

The literature citations in all the articles are, without exception, fairly recent or very recent; references to reviews are also included. The choice of topics and their treatment give no cause for criticism. As the book is essentially a conference proceedings report, it provides insights into the current state of research in selected areas rather than comprehensive reviews. In so doing it succeeds, briefly but succinctly, in conveying an appreciation of the principles underlying the reactivity of each element or molecule discussed. In general it is exactly the personal points of view expressed in the treatment of the topics that give the book its appeal, and the authors' love of their special fields of research is evident between the lines. The fact that the dominant heteroatom elements are sulfur and selenium (at least in nine of the twenty articles), may be a consequence of the editor's area of interest. This excellent book can be recommended to anyone who wants a rapid survey of the currently "hot" topics in main-group chemistry. However, the price is already approaching the "pain threshold" (and is well above it for students), which means that for future volumes, if the basic concept is to be maintained, the possibility of paperback editions should be considered.

Hansjörg Grützmacher [NB 1134 IE]
Anorganisch-chemisches Institut
der Universität Heidelberg (FRG)

[*] M. Regitz, P. Binger, *Angew. Chem. 100* (1988); *Angew. Chem. Int. Ed. Engl. 27* (1988); M. Regitz, *Chem. Rev. 90* (1990).

Chemistry of Alicyclic Compounds. Structure and Chemical Transformations. (Series: Studies in Organic Chemistry, Vol. 38). By *G. Haufe* and *G. Mann*. Elsevier, Amsterdam 1989. 468 pp., hardcover DFl 350.00.—ISBN 0-444-98878-5

This book lives up to the authors' claim: it is suitable as a standard text and guide for the student, and it can be used by a practising chemist to increase the depth of his knowledge of alicyclic compounds. Obviously, the chemistry of alicyclic compounds is so large a subject that it is not possible for the authors to cover it completely. Their treatment is therefore concentrated mainly on small to medium-sized ring systems.

The book, which is practically free of errors that affect the meaning, is divided into six self-contained chapters. The first chapter, and also the two that follow it, are written in textbook style and should therefore be easily understandable even by second-year chemistry undergraduates. Chapter 1 deals with the systematic description of the structures of alicyclic compounds. The topological and topographical as-

pects of alicyclic structures are explained with the help of examples (although the diagrams in Figure 1.11 on page 41 are mirror images of the correct structures). The chapter is completed by detailed tables of compounds arranged according to increasing numbers and sizes of rings, including structural formulas and literature references.

In Chapter 2, after explaining kinetic and thermodynamic stability, results of theoretical calculations on alicyclic compounds by ab initio, semiempirical and force field methods are presented, and their structure-energy relationships are discussed. Unfortunately the treatment in this chapter is very superficial and uncritical. For example, it is wrongly stated on page 84 that in organic chemistry compounds with exceptionally high energies are described as being strained, and molecules with distorted structures are described as being sterically hindered. Also one would expect to find more than is offered here under the title "Relationships Between Strain and Reactivity"; there are no mentions or citations of pioneering studies such as those by *P. von R. Schleyer* (1961), *C. S. Foote* (1964) or *C. J. M. Stirling* (1985).

Chapter 3 is concerned with dynamic processes in alicyclic compounds, such as intramolecular motions, vibrations, internal rotations and ring inversions, conformational transformations (e.g. pseudorotation) and configurational transformations (double-bond isomerizations and inversions), as well as valence isomerizations (π-bond shifts).

The remaining three chapters (4–6) contain detailed discussions of a wide variety of ring-reducing, ring-enlarging and transannular reactions of alicyclic compounds, together with their energetic and stereochemical aspects. Regrettably, one searches in vain in this part of the book for information or literature references concerning modern free radical cyclization chemistry. The structural formulas, which are clearly drawn and also include perspective views where necessary, enable the reader to easily find his or her way around the text, despite the very high information density. This is further helped by the detailed contents list and the 33-page subject index. For those who wish to read up special topics in greater depth there is a bibliography at the end of each chapter, containing between 110 and 430 citations including recently published work.

The printing quality is unsatisfactory. For example, the reproduction of some of the figures is incomplete or of very poor quality (pages 56, 147, 315 and 319), and several pages are marred by blotches. Moreover, owing to the poor quality of the paper the book is not well suited for use in the laboratory.

To summarize, the first three chapters contain stimulating treatments of structural and energetic aspects of alicyclic compounds. This is followed by a compilation of a wide variety of ring-reducing, ring-enlarging and transannular reactions, illustrated by many examples, which should be a useful source, mainly for the synthetic chemist.

Wolfgang Luef and *Reinhart Keese* [NB 1112 IE]
Institut für Organische Chemie
der Universität Bern (Switzerland)

Correspondence

Re: The communication entitled, "The Structure of 'Organic Permanganate'" by M. L. Burgess, D. C. Craig, and M. J. Gallagher, *Angew. Chem. 103* (1991) 723; *Angew. Chem. Int. Ed. Engl. 30* (1991) 704.

The structure reported in this article had previously been established and an alternative preparation devised by H. H. Wasserman, H. W. Ackerman, H. H. Wotiz, and T.-C. Liu (*J. Am. Chem. Soc. 77* (1955) 973). The present results serve only to confirm in all details the earlier work. We are grateful to Professor E. Schmitz, Berlin, for drawing our attention to this crucial reference.

M. J. Gallagher
University of New South Wales
Australia

Registered names, trademarks, etc. used in this journal, even when not marked as such, are not to be considered unprotected by law.

© VCH Verlagsgesellschaft mbH, W-6940 Weinheim, 1991. – Printed in the Federal Republic of Germany by Konrad Triltsch Druck- und Verlagsanstalt Würzburg.

All rights reserved (including those of translation into foreign languages). No part of this issue may be reproduced in any form — by photoprint, microfilm, or any other means — nor transmitted or translated into a machine language without written permission from the publishers. Only single copies of contributions, or parts thereof, may be made for personal use. This journal was carefully produced in all its parts. Nevertheless, authors, editors and publisher do not warrant the information contained therein to be free of errors. Readers are advised to keep in mind that statements, data, illustrations, procedural details or other items may inadvertently be inaccurate.

Valid for users in the USA: The appearance of the code at the bottom of the first page of an article (serial) indicates the copyright owner's consent that copies of the article may be made for personal or internal use, or for the personal or internal use of specific clients. This consent is given on the condition, however, that the copier pay stated per-copy fee through the Coypright Clearance Center, Inc. (CCC), for copying beyond that permitted by Sections 107 or 108 of the U.S. Copyright Law. This consent does not extend to other kinds of copying, such as copying, for general distribution, for advertising or promotional purposes, for creating new collective works, or for resale. For copying from back volumes of this journal see 'Permissions to Photo-Copy: Publisher's Fee List' of the CCC.

Editorial office: Postfach 10 11 61, W-6490 Weinheim, Federal Republic of Germany, Telephone (06201) 60 23 15, Telex 465 516 vchwh d, Telefax (06201) 602 328, E-Mail Z16@DHDURZ2 in Earn Bitnet.

Editor: *Peter Gölitz*

Associate editors: *D. I. Loewus, K. J. Schneider, A. Stimson.* **Editorial assistant:** *E. Schweikart*

Publishers: VCH Verlagsgesellschaft mbH. (Managing Director: *Hans Dirk Köhler.*), Pappelallee 3, W-6940 Weinheim, Federal Republic of Germany.

Advertising office (Advertising Manager *R. J. Roth*): Postfach 10 11 61, W-6940 Weinheim, Federal Republic of Germany, Telephone (0 62 01) 60 61 36, Telex 4 67 155, Telefax (0 62 01) 606 156.

ANGEWANDTE CHEMIE
International Edition in English
Volume 30 · Number 10
October 1991
Pages 1193–1386

Chirality and Crop Protection

By Gerardo M. Ramos Tombo* and Daniel Belluš*

Dedicated to Professor Kurt Schaffner on the occasion of his 60th birthday

The modern agrochemical industry is searching, more intensively than ever, for new substances to combat pests (weeds, deleterious insects, plant pathogens, etc.). In the complex and costly selection and optimization process, state-of-the-art scientific methods are always needed. The aims of the interdisciplinary optimization are mainly the reduction of the rate of application of the new substance, an increase in the selectivity against the target organism, and the optimal ecological profile. If a promising crop protection compound is a racemate or a diastereoisomeric mixture, the chemist has a unique opportunity to contribute to this optimization process through the synthesis of enantiomerically pure isomers for testing purposes. If the single isomer proves to be biologically superior to the racemate, the development of an economical and ecologically sound process for the production of the single isomer presents an even greater challenge. The average price of a crop protection compound is much lower than that for a pharmaceutical product, and this fact imposes a severe limitation upon the flexibility of the chemist who is concerned with the synthesis and production of a stereochemically pure agrochemical. This forces the crop protection chemist to make full use of both his scientific and creative capabilities. Fortunately, parallel to the development of the above optimization aims of a modern and ecologically sound crop protection research, there has been a continuous and worldwide advance in the area of asymmetric synthesis. Due to the interplay of these two parallel efforts there has been a great accumulation of chemical, biological, and agronomical knowledge in recent years, which should have implications beyond merely the synthesis of enantiomerically pure agrochemicals.

1. Introduction

The pioneering work on the resolution of racemic tartaric acid by *Louis Pasteur* in the middle of the 19th century allowed chemists to realize that optical activity is a result of molecular asymmetry. Since then, the significance of stereoisomerism, not only in relation to physicochemical but also to biological properties, has been gradually recognized by scientists.[1] Chirality is not a requirement for biological activity, but in those cases in which the bioactive molecule contains one or more stereogenic centres, the desired biological property is often strongly related to a given absolute configuration.[2, 3]

Besides this so-called principal activity[4] of stereoisomers, there are often differences in their uptake, transportation, metabolic behavior, elimination, and toxicological properties. Accordingly, the advantages of using stereochemically pure compounds have been recognized for many years, first for pharmaceuticals[2] and later for agrochemicals.[3] However, due to practical limitations, only a few substances, mainly of natural origin, have been developed as single stereoisomers.

For a long time, there were no general methodologies for the synthesis of enantiomerically pure compounds, and the separation of racemates on an industrial scale was, in gener-

[*] Dr. G. M. Ramos Tombo, Prof. Dr. D. Belluš
Research and Development Plant Protection
Agro Division, Ciba-Geigy AG
CH-4002 Basel (Switzerland)

 © VCH Verlagsgesellschaft mbH, W-6940 Weinheim, 1991 0570-0833/91/1010-1193 $ 3.50+.25/0

al, difficult, inefficient, and expensive. Over the past 15 years, however, significant advances have been made in both these fields.[5] *Seebach*[6] recently stated that almost no aspect of organic synthesis is generating as many publications as the preparation of enantiomerically pure compounds.

The dramatic improvements in synthesis and analysis have provided the scientific basis for a systematic investigation of the implications of stereoisomerism as one of the many determinant factors of biological properties. Not surprisingly, the industries involved in the synthesis, development, and marketing of biologically active compounds are becoming more and more active in this area. Many examples of the successful development of economically feasible industrial syntheses of enantiomerically pure compounds are now known, and catalytic processes are likely to emerge as a major focus for research in this field in the near future.[8]

In modern agrochemical R & D all four principal methods of introducing chirality (Fig. 1) are now used for obtaining small samples of pure stereoisomers for testing purposes, as well as for commercial-scale syntheses. In many cases the development and use of enantiomerically pure compounds can bring great economic and environmental advantage over the use of a racemate or a diastereoisomeric mixture: for example, lower application rates, and fewer or no side effects or phytotoxicity; the possibility of precise mode of action studies; reduced capital requirements for production, transportation, storage. In addition, this represents an exciting and motivating research field!

It is difficult to obtain precise data on the number of chiral synthetic agrochemicals which are at present used in enantiomerically pure form, but from various sources it can be estimated that approximately 10% for the presently marketed agrochemicals,[3, 9] and 20–30% of the compounds in the development pipelines of leading agrochemical companies[10] contain one or more stereogenic centres. Although the majority of these products will presumably be marketed as a single isomer, examples in this paper will show convincingly that the real situation in crop protection is far from black-and-white ("good enantiomer, bad racemate"). Six principal possibilities are frequently met in agrochemical research and development:

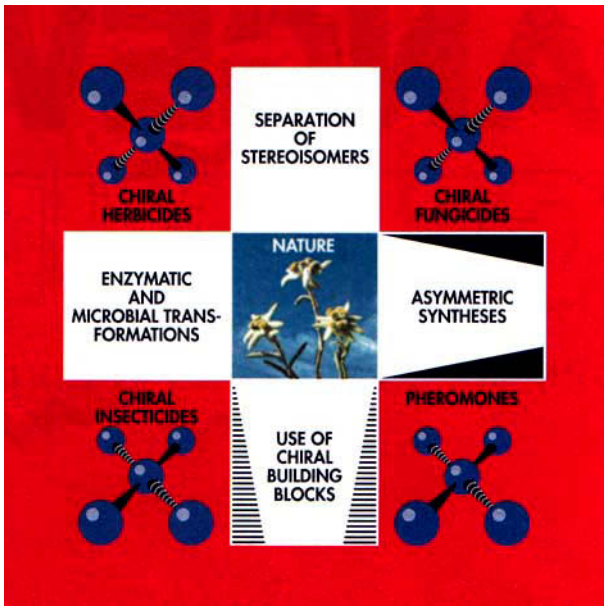

Fig. 1. A chiral Swiss tetrahedron containing Nature in the center as the sole source of chirality for four principal approaches (inside the cross) to enantiomerically pure compounds of importance for crop protection (outside the cross). For 700 years now (1291–1991), the absolute configuration of the Swiss cross is determined regularly by voting, either by a show of hands or by ballot; it is clearly the *R* one (*right*: dextrorotatory) [7]. The centerpiece as well as the overall design is a tribute to the origins of *Kurt Schaffner*.

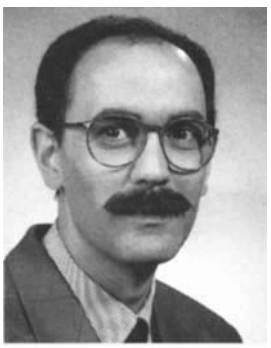

Gerardo M. Ramos Tombo was born in 1952 in Rosario, Uruguay. He studied chemistry in Montevideo (B. Sc., 1976) and at the ETH, Zürich (Diploma, 1979), where he completed his dissertation entitled "Intramolecular additions to isolated C–C double bonds in sterically compressed olefin-alcohols and amines" in 1983 under the guidance of Professors O. Jeger and C. Ganter. This work was honoured with the Silver Medal of the ETH. In 1983 he joined the Central Research Laboratories of Ciba-Geigy Ltd. in Basel and in 1987 he transferred to the Agrochemical Division where he leads the Basic Synthesis Research section. His research interests lie in the conception and development of industrially useful synthetic methods and asymmetric syntheses.

Daniel Belluš was born in 1938 in Trnava, Czechoslovakia and studied chemistry at the Slovak Technical University in Bratislava. He obtained his Dipl. Ing. in 1960 and completed his Ph. D. in 1967 in the area of the photochemistry of polymers. In the same year, he went as a postdoctoral fellow to the ETH Zürich to work with O. Jeger and K. Schaffner. Since 1969 he has been with Ciba-Geigy Ltd. in Basel, 1985–1991 as head of Plant Protection R & D and currently as head of the Corporate Research Units. From 1980 he has lectured at the University of Freiburg (Switzerland). His research interests lie in the reactions of small rings, photochemistry, cycloadditions and rearrangements (reactions without reagents), heterocyclic and metal-catalyzed reactions, and crop protection chemicals (1985–1991). Amongst his honours he prizes the Scientific Award of the City of Basel (1982) and an honorary doctorate (Dr. sc. techn. h.c.) from his Alma Mater (1991) the highest.

1. The stereoisomers have complementary biological acitvity (a common case within the triazole fungicides, e.g. propiconazole **25** and **34**–**37**).
2. All stereoisomers possess nearly identical qualitative and quantitative biological activity (i.e., the fragment containing the chiral center does not interact with the receptor, e.g. **62**).
3. The stereoisomers have qualitatively similar but quantitatively different potencies (a common case, e.g., within pyrethroids containing two or three chiral centers, Section 4.5).
4. Several stereoisomers are equally active (e.g., O.D.P. **125**).
5. The stereoisomers have qualitatively different biological activities (e.g. (*R*)- and (*S*)-**22**).
6. All the biological activity resides in one stereoisomer (e.g., **63**, (*R*)-**78**).

However, in the modern agrochemical industry it is no longer enough to pursue biological activity only. In order to make the very costly decision whether or not to develop a single stereoisomer, it is necessary to adopt a multidisciplinary approach by investigating the translocation, mode of action, nontarget toxicity, crop safety, and environmental behavior of each specific substance. If, for insurmountable economic reasons, a racemate or a mixture of diastereoisomers is chosen for further development, they must exhibit a clean toxicological and environmental record and offer solutions to specific agronomical problems which are clearly superior to the existing ones.[10]

The complexity of the synthetic route to a given stereoisomer and its amenability to scale-up will also play a central role in this decision-making process. Our purpose is to illustrate, for the chemistry of crop protection, the activities in this very dynamic field by means of examples critically selected from recent publications and patents. Apart from a few important examples from the older literature, only structures, syntheses, and activities of chiral herbicides, fungicides, and insecticides which have been published in the last four to five years will be considered. Rich sources of very recent results were the Brighton Crop Protection Conference 1990[11] and the 7th IUPAC International Conference of Pesticide Chemistry, Hamburg, 1990.[12] We have tried to include only compounds with rigorously proven biological activities. The enormous number of chiral natural products with potential usefulness for crop protection are not described,[13] as such a task would exceed the scope of this review.

2. Disease Control

The implications of stereoisomerism for the biological activity of fungicides[14] are difficult to characterize, since the system involved is a complex one. Receptors and metabolic pathways must be considered in both the pathogen and the host plant.

2.1. Acylalanines and Related Acylanilides

The origin of the acylanilide fungicides is closely linked with research in the herbicide field of the chloroacetanilides such as metolachlor **1**, the most active stereoisomer of which has the (αR, 1 *S*) absolute configuration (Scheme 1).[15]

Replacement of the alkoxyalkyl substituent in **1** by an ester group led to the prototype racemic compound (**2**) with the code number CGA 29212, which exhibited curative and systemic activity against *Phytophtora infestans*.[16] Resolution

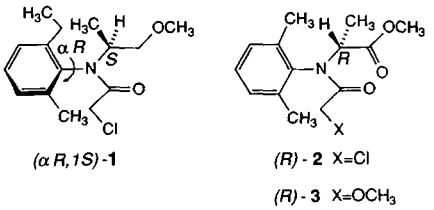

Scheme 1. The most active stereoisomers of the herbicide metolachlor ((α*R*, 1*S*)-**1**) and the structurally related fungicides CGA 29212 ((*R*)-**2**) and metalaxyl ((*R*)-**3**).

and biological testing of the single isomers showed that (*R*)-**2** was an excellent fungicide with low herbicidal activity, whilst its enantiomer (*S*)-**2** exhibited high herbicidal but no fungicidal activity (Fig. 2).[16]

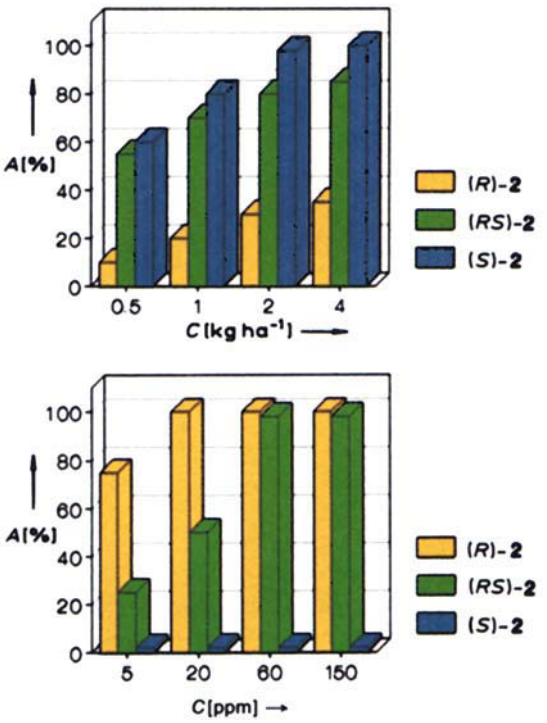

Fig. 2. Biological activity *A* (% relative to untreated control samples) of the stereoisomers of CGA 29212(**2**) [16]. Top: mean herbicidal activity on eight grassy weeds with pre-emergent application. *C* = herbicide concentration. Bottom: fungicidal activity against grape downy mildew. *C* = concentration of the fungicide in the spray solution.

First attempts at a technically feasible large-scale separation of the racemate CGA 29212 (**2**) or an enantioselective synthesis of (*R*)-**2** were unsuccessful. Further work in this direction was discontinued once the biologically more powerful analogue metalaxyl (*rac*-**3**) was discovered, as a result of an intensive optimization program.[17]

In this case the enantiomerically pure stereoisomers of **3** were obtained by the resolution of a racemic precursor through diastereoisomeric salt crystallization.[17] In vitro biological testing against *Phytophthora infestans* and *Phytium ultimum* showed that (*R*)-**3** was approximately 1000 times more active than (*S*)-**3**. However, in vivo trials revealed smaller differences in activity: (*R*)-**3** was 3–10 times more active than (*S*)-**3**, depending on the pathogens tested.[16, 18] Unlike **2**, metalaxyl (*rac*-**3**) shows no phytotoxic effects, and therefore a separation of the single enantiomers was not necessary.

As indicated by a range of biological studies,[14] it seems that a dual mode of action is associated with the acylanilide fungicides. The effects on fungal growth appear to be dependent on the stereochemistry of the agent; however, the effects on the plasma membrane and germination are independent of stereochemical homogeneity.[16] Furthermore, a comparative study of the biochemical and physiological effects of the stereoisomers of **3** indicated that (*R*)- and (*S*)-**3** have the same mode of action but show considerable differences in their effectiveness in reaching, or binding to, the receptor.[19]

Clozylacon (**4**)[20] is a new experimental acylanilide fungicide especially suited for soil application against *Oomycetes*,[21] where protection from these pathogens is required for relatively long periods.

Because of the stereogenic centre at C3 and the atropisomerism due to hindered rotation around the aryl carbon–nitrogen bond (marked with an arrow in Scheme 2), **4** consists of four stereoisomers. These stereoisomers have been separated by several methods.[22]

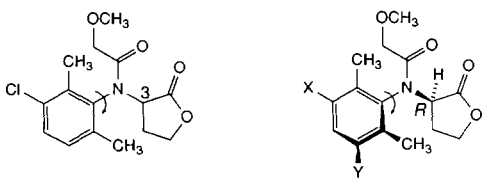

Scheme 2. Stereoisomerism in the experimental fungicide clozylacon (**4**) and its precursor **7**.

The diastereoisomeric pairs of enantiomers **5**, *ent*-**5** and **6**, *ent*-**6** were separated either by crystallization or chromatography on silica gel, and the resulting racemates were subsequently separated on an MPLC column packed with triacetyl cellulose. A more efficient, one-step analytical separation was possible on an HPLC column packed with tris(3-methylbenzoyl) cellulose.[22]

Biological tests showed that the desired fungicidal activity arises mainly from **5**, the isomer with the absolute configuration α *S*, 3 *R*.[22] Work towards an economically feasible process for the stereoselective synthesis of **5** focused on developing enantioselective access to precursor **7**. It was known that **7** is easily chlorinated to afford a diastereoisomeric mixture of **5** and **6**, which can be separated by crystallization. Furthermore, a method had been established to epimerize compound **6** to a mixture of **5** and **6**, thus allowing a recycling of the undesired isomer.[22]

Two conceptionally different synthetic routes to the target molecule **7** were developed:[23]

a) using (*S*)-malic acid (**8**) from the "chiral pool", which provides both the required absolute configuration and the correct number of C atoms for the lactone ring of **7** via the hydroxylactone (*S*)-**10** (Scheme 3).

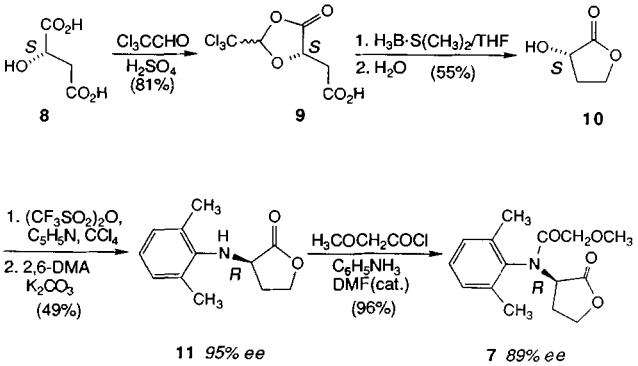

Scheme 3. Synthesis of **7** starting from (*S*)-malic acid (**8**). 2,6-DMA = 2,6-dimethylaniline, DMF = dimethylformamide.

b) in an enantioselective modification of the existing pilot plant synthesis of **4**,[22] introducing the chiral information in a key Rh- or Ru-catalyzed asymmetric hydrogenation of the prochiral enamide intermediate **15** (Scheme 4).[15]

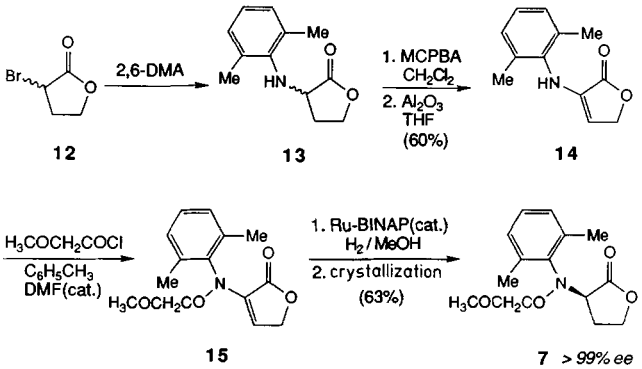

Scheme 4. Syntheses of **7** by catalytic homogeneous hydrogenation of **15**. MCPBA = *meta*-chloroperbenzoic acid.

The key intermediate in route a) is the (*S*)-3-hydroxybutyrolactone **10**, which has the opposite absolute configuration to the target molecule **7**. A nucleophilic subsitution at the activated 3-position, with inversion of the configuration, provides the correct stereochemistry. The final acylation step (→**7**) was accompanied by some racemization. One single recrystallization from a 1:1 mixture of hexane and ethyl methyl ketone (MEK) provided optically pure **7**.

Route b) presents, as a key step, the enantioselective hydrogenation of the enamide **15**. This type of *N*-acyl substituted enamide has never been hydrogenated before. Therefore, several chiral Rh- and Ru-catalysts were tested and an extensive screening of experimental conditions carried out. The best results were obtained with the [Ru(OAc)$_2$(*S*)-BINAP]

catalyst (BINAP = 2,2'-bis(diphenylphosphino)-1,1'-binaphthyl; 95% yield, 66% *ee*). As before, optically pure **7** was obtained by a single recrystallization of the crude hydrogenation product. Since no deactivation, even at a substrate/catalyst ratio of 4000:1, was observed for this system, it was well-suited for industrial production. This fact made [$Ru(OAc)_2$–(*S*)-BINAP] the catalyst of choice for this synthesis.

2.2. Triazole Fungicides

The triazole fungicides are the most important group amongst the ergosterol biosynthesis inhibitors (EBI).[14] The primary mode of action of the 1,2,4-triazole fungicides is the inhibition of the cytochrome P-450 dependent C14-demethylation of lanosterol (**16**, Fig. 3) or 24-methylene-24,25-dihydrolanosterol, which are intermediates in fungal sterol biosynthesis.[24] Besides their fungicidal activity, some of these compounds also show plant growth regulating activity. This can often be explained by the inhibition of the cytochrome P-450 dependent oxidation of the methyl group at C4 of *ent*-kaurene (**17**, Fig. 3), an intermediate in the biosynthesis of gibberellin, and was used for the development of several triazole-containing plant growth regulators.[24]

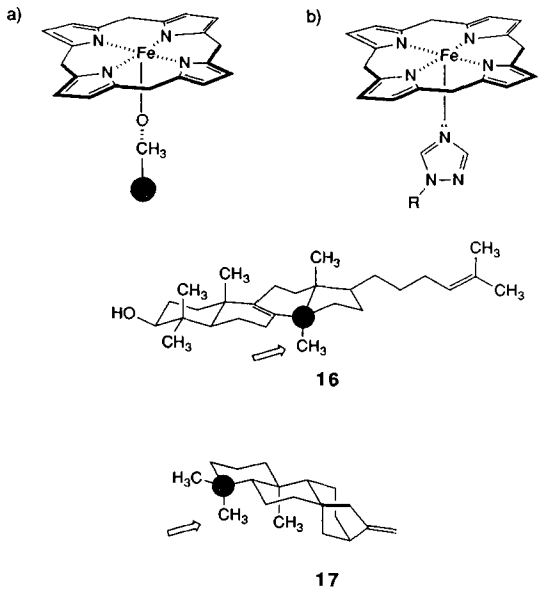

Fig. 3. Hypothetical inhibition model for the system trizaole–cytochrome P-450 [24]: a) normal oxidative process for the C14-demethylation of lanosterol (**16**) (EBI) or C4-oxidation of *ent*-kaurene (**17**) (PGR); b) strong binding of a 1,2,4-triazole moiety, inhibiting oxidation.

Among the 1,2,4-triazole fungicides most extensively investigated with respect to implications of stereoisomerism in their biological activity are triadimefon (**18**) and triadimenol (**19**).

Triadimefon (**18**) is a very weak fungicide for which no significant activity differences have been found between the enantiomers (*S*)- and (*R*)-**18**.[25] The carbonyl group in **18** is reduced to afford **19**, in fungi as well as in plants. This reduction is accompanied by a considerable increase in the fungicidal potency—triadimenol **19** is the active principle.

In contrast to **18**, the fungicidal activity of the resulting triadimenol (**19**) can clearly be attributed to the (1*S*, 2*R*)-**19** isomer. The stereochemical outcome of the reduction, **18** → **19**, and therefore also the resulting biological activity, are highly dependent on the fungal organism involved. The experimental work regarding the relationship between fungitoxicity and the nature and rate of the stereoselective metabolic transformation of **18** into **19** has been recently reviewed.[14, 24]

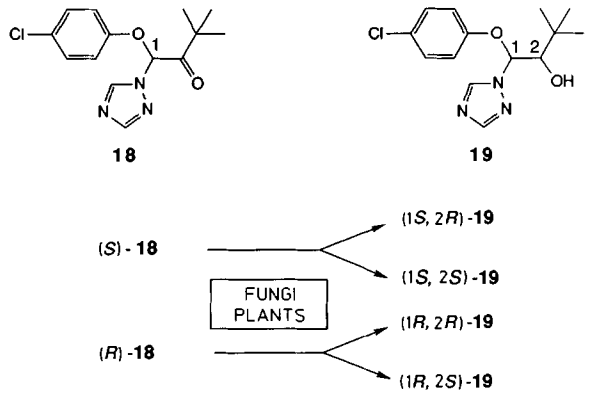

Scheme 5. The isomers of triadimefon (**18**) and triadimenol (**19**).

The 1-vinyltriazoles are a group of compounds which has also been developed as fungicides or plant growth regulation agents. The influence of stereoisomerism on both activities has been thoroughly investigated for the compounds **20** and **21**.[26] The biological activity is concentrated in the *E* isomer (**21**). For the racemate **21** (diniconazole), the fungicidal activity is restricted to the *R* isomer, whilst the *S* isomer is a plant growth regulator, which acts by inhibiting gibberellin biosynthesis.

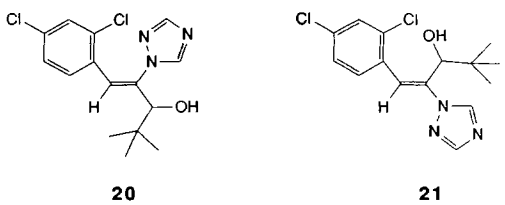

Scheme 6. Isomeric 1-vinyltriazoles: the biological activity is concentrated in the *E* isomer **21** (diniconazole).

Very recently, the synthesis and biological properties of the isomers of a related vinyltriazole, triapentenol (**22**) have been reported (Scheme 7).[27] Small quantities of both enantiomers (*S*)- and (*R*)-**22** were obtained by the chromatographic separation of the diastereoisomeric ester mixture **23**. The synthesis of (*S*)- and (*R*)-**22** was based on enantioselective reduction of the corresponding enone **24** by metal hydrides in the presence of chiral amino alcohols (Scheme 8). In the case of **22**, the fungicidal activity was again restricted to the isomer (*R*)-**22**, whereas (*S*)-**22** was responsible for the plant growth regulating effect.[27]

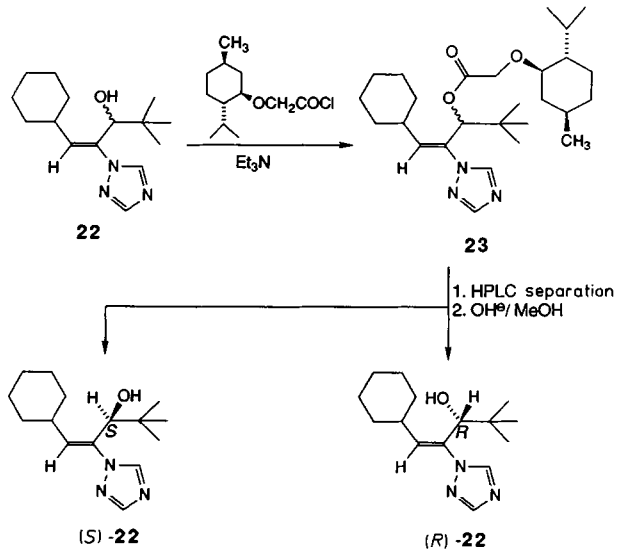

Scheme 7. Small-scale separation of the enantiomers of triapentenol (**22**).

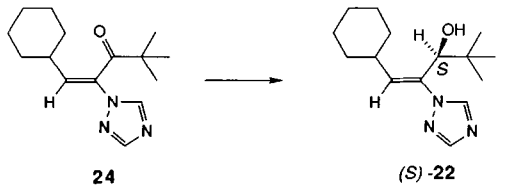

Scheme 8. Enantioselective reduction of **24** to (*S*)-**22** [27]. With $LiAlH_4$/(−)-*N*-methylephedrine the yield is 85% (*ee* > 95%) with $BH_3 \cdot THF$/(*S*)-diphenylprolinol 87% (*ee* = 83%).

Very remarkable differences in the in vitro activity against *Ustilago madis* were recently reported for the stereoisomers of the dioxolano-1,2,4-triazole fungicide propiconazole (**25**).[28] The isomers with the 2*S* absolute configuration were shown to be more efficient inhibitors of ergosterol biosynthesis.

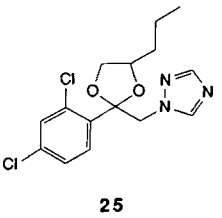

Scheme 9. The broad-spectrum fungicide propiconazole (**25**). See also Scheme 12.

Since the described synthesis of all stereoisomers of **25** included an inefficient preparation of enantiomerically pure (*R*)- and (*S*)-1,2-pentanediol (**27**) starting from the corresponding 2-aminovaleric acid, and a subsequent chromatographic separation of the diastereoisomeric products,[28] a synthesis more amenable to scale-up was needed. A novel stereoselective synthesis of all four stereoisomers **34**–**37** of propiconazole (**25**) was therefore developed.[29] A key step in this process is the catalytic enantioselective preparation of pentanediol ((*R*)-**27** and (*S*)-**27**) from a common achiral precursor. Two different approaches were investigated, both of them returning encouraging results:

a) the hydrogenation of 1-hydroxypentan-2-one (**26**) catalyzed by a Ru–BINAP complex (Scheme 10).
b) the enzymatic reduction of 2-oxopentanoic acid (**28**) using L-lactate dehydrogenase (Scheme 11).

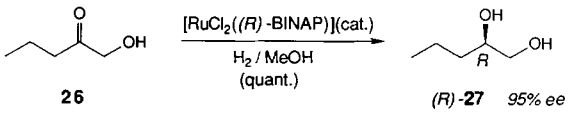

Scheme 10. Enantioselective catalytic homogeneous hydrogenation of 1-hydroxypentan-2-one (**26**).

The enantioselective hydrogenation of **26** using a Ru–BINAP[30] complex as a catalyst proceeds with excellent enantioselectivity and efficiency. The high dilution of the catalyst relative to the substrate makes this process very attractive for the large-scale production of (*R*)- or (*S*)-**27**.[31] The use of [$RuCl_2${(*S*)–BINAP}] affords quantitatively (2*S*)-pentanediol ((*S*)-**27**) with 95% *ee*. (*R*)-**27** can be obtained in similar optical and chemical yields by using the Ru complex with the enantiomeric ligand (*R*)-BINAP.

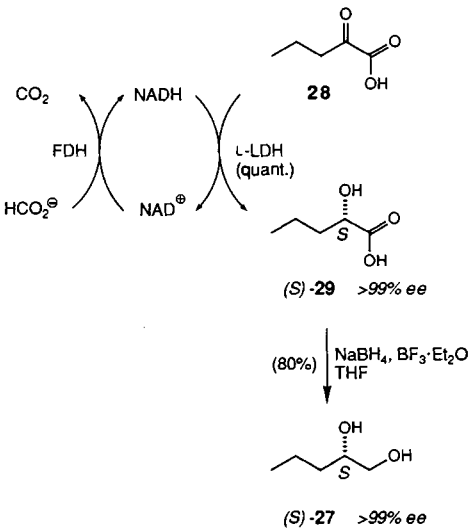

Scheme 11. Enantioselective enzymatic reduction of 2-oxopentanoic acid (**28**). L-LHD = lactate dehydrogenase from bovine heart; FDH = formate dehydrogenase from yeast.

The enantioselective reduction of α-keto acids by means of L-lactate dehydrogenase (L-LDH) is a well-known process.[32] For the synthesis of (*S*)-**29** from **28**, the required NADH cofactor was recycled using formate dehydrogenase (FDH) (Scheme 11). The process was performed either batchwise, or continuously in an enzyme membrane reactor.[33] The enantiomerically pure (*S*)-hydroxy acid **29** was obtained quantitatively and was subsequently reduced, in high yield, to (*S*)-**27** with borane generated in situ. Similarly, by using D-LDH (obtained from yeast) the enantiomeric (*R*)-**27** was produced from the same precursor **27**, again with high optical and chemical yields.

The synthesis of the diastereoisomeric mixtures **32** and **33** was carried out using standard procedures (Scheme 12).[28] The separation of the mixtures of **32** and **33** into the single isomers **34**, **35** and **36**, **37**, respectively, was performed by crystallization of the corresponding nitrates. Field trials of the thus available large quantities of the individual stereoisomers **34**–**37** have shown that the different pathogen species discriminate between each stereoisomer. However, the fungicidal activity as well as the small plant growth regulating effect were not constant across the spectrum of target organisms (Fig. 4). Consequently, the mixture of all four stereoisomers was the prerequisite for the extraordinary commercial success of propiconazole (**25**), which demonstrates strong activity across a broad spectrum of pathogens.

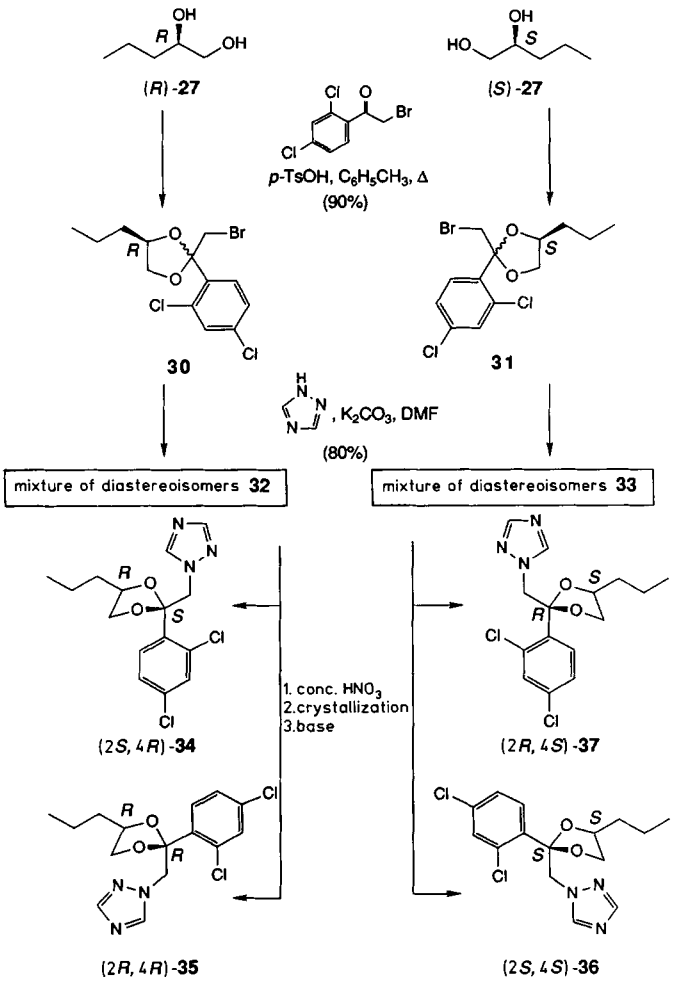

Scheme 12. The stereoisomers (**34**–**37**) of propiconazole (**25**). *p*-TsOH = *p*-toluenesulfonic acid.

Triazole fungicides with novel structures continue to be developed and in some cases the fungicidal activity is clearly connected with a single isomer. For example, the *R* enantiomer of tetraconazole (**41**) has been found to be clearly more fungitoxic than the corresponding *S* enantiomer. Both compounds, (*R*)-**41** and (*S*)-**41**, were prepared with *ee* > 95% by hydrolysis of the racemate **38**, catalyzed by procine pancreas lipase (PPL), or by PPL-catalyzed monoacetylation of the prochiral precursor **42** (Scheme 13).[34]

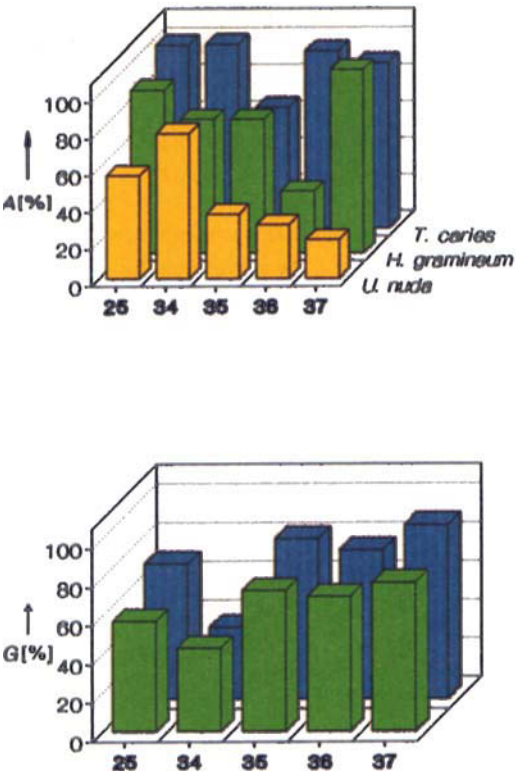

Fig. 4. Biological activity of propiconazole (**25**) and its stereoisomers (**34**–**37**) on seed treatment (rates: 2.5 g a.i. per 100 kg seed). Top: fungicidal activity *A* against *Ustilago nuda, Helminthosporium, and Tilletia caries* as percentage relative to the untreated control sample. Bottom: plant growth regulating effect on barley (green) and wheat (blue) as growth (*G*) relative to the untreated sample [%] at growth stage 11–12.

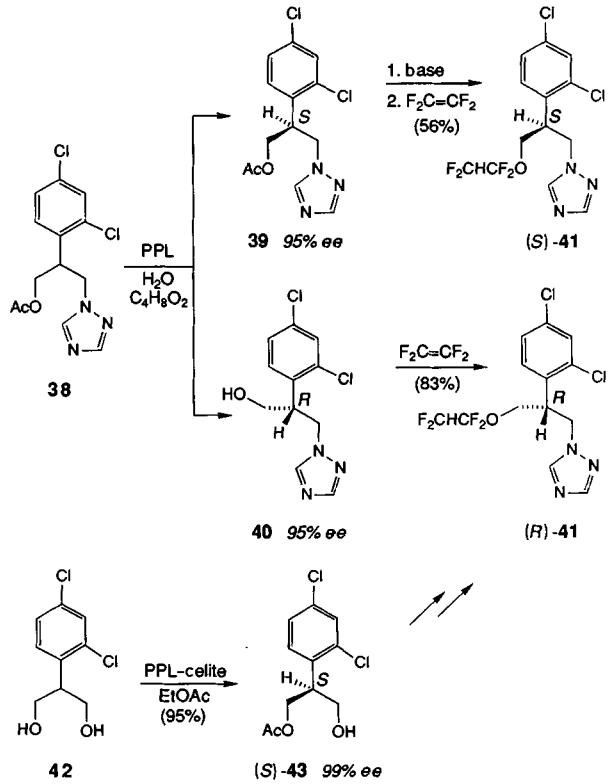

Scheme 13. Chemoenzymatic synthesis of both enantiomers of tetraconazole (**41**).

The new triazole fungicide **47** with the code number SSF-109 contains a cycloheptane ring, which is a unique substructure within the biologically active 1,2,4-triazole fungicides. The *cis* compound **47** exhibited generally stronger in vitro and in vivo fungicidal activity than its *trans* isomer **50**. The latter, on the other hand, showed a much stronger plant growth regulating effect.[35]

This *cis* compound **47** was synthesized by a chelation-controlled addition of the corresponding Grignard compound to the triazolylcycloheptanone **46** (Scheme 14). The *trans* isomer **50** was prepared in poor yield from the bromohydrin **48** via an oxirane intermediate.[36]

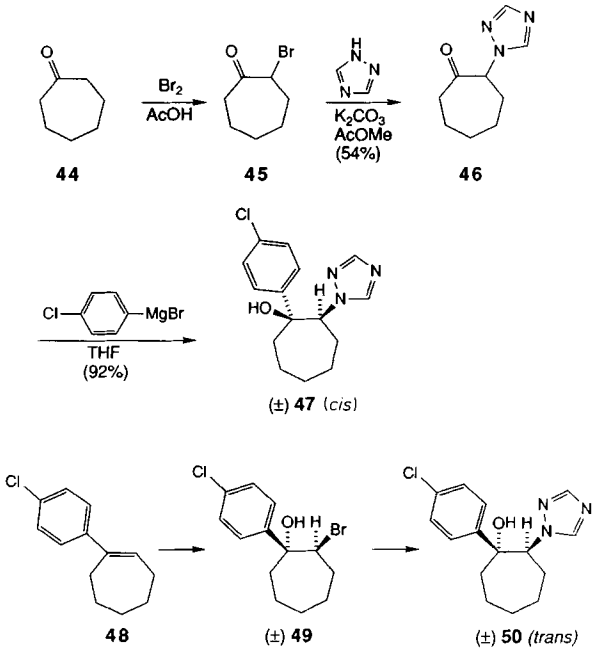

Scheme 14. Synthesis of *cis*- and *trans*-triazolylcycloheptanols **47** and **50**.

This *cis*-racemate **47** was resolved by separation of the corresponding diastereoisomeric L-menthoxyacetates using column chromatography. The absolute configuration of the individual enantiomers has not yet been reported. Nevertheless, biological tests revealed that the enantiomer (−)-**47** was 2–4 times more active than the (+)-enantiomer, curiously both as a fungicide and as a plant growth regulator.[35]

On considering the diversity of structures discussed above, a rather high structural flexibility of the sterol binding site at the cytochrome P-450 oxygenase involved in C14-demethylation is evident. This flexibility in the chemical structure of the inhibitor is generally accompanied by a remarkable stereochemical selectivity. At the moment, conclusions or generalizations on structural or stereochemical requirements for activity must remain tentative, since detailed substrate–receptor studies are lacking.

2.3. Morpholine Derivatives

Whereas triazole fungicides (see Section 2.2) disturb sterol biosynthesis in fungi by inhibition of the C14-demethylation of lanosterol or 24-methylene-24,25-dihydrolanosterol, the morpholine fungicides inhibit sterol biosynthesis at two different sites of the same pathway, namely the Δ^{14}-reductase and the $\Delta^8 \rightarrow \Delta^7$-isomerase enzymes.[37]

Because of their high activity against cereal powdery mildew and rusts, the morpholine fungicides were mainly developed for use in cereals. Due to their different mode of action they also evolved as valuable mixing partners for triazole fungicides. Thus, the morpholine fungicides are able to control strains of cereal powdery mildew which have become less sensitive to triazole fungicides.[38] This mixing of fungicides, each acting by inhibition of different enzymes of the same biochemical pathway, proved to be a very successful antiresistance concept. The most important representative of this class is fenpropimorph (**51**), which was selected from a great number of *p*-alkyl substituted 3-phenyl propylamines for further development as a fungicide for use in cereals.[39]

It was shown earlier that the racemic compound **51**, with a *cis*-2,6-dimethylmorpholine moiety, has a clearly superior fungicidal activity to the corresponding **52**, which contains a *trans*-2,6-dimethylmorpholine substituent.[39] The *cis* and

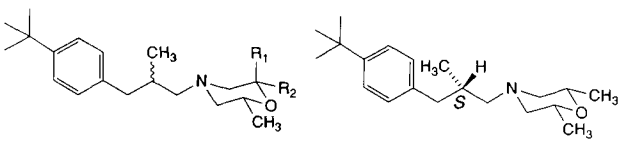

51 $R_1 = H$, $R_2 = CH_3$ *(S)*-**51**

52 $R_1 = CH_3$, $R_2 = H$

Scheme 15. The stereoisomers of fenpropimorph (**51**).

trans isomers **51** and **52** are separable by distillation. Also the transformation of **52** into the thermodynamically more stable **51** could be achieved by using Pd-containing catalysts at high temperatures.[40] Hence, the production of the *cis* stereoisomer **51** of a purity higher than 98% is possible on a large scale.

The *cis* racemate **51** was resolved by crystallization of the diastereoisomeric salts formed with (−)-camphorsulfonic acid.[41] The absolute configuration of the single isomers was determined by X-ray structural analysis.[39]

Extensive biological testing showed that the *S* enantiomer of **51** is equivalent to racemic **51** in its effect against barley mildew and is superior to racemic **51** against mildew and brown rust of wheat. On the other hand the *R* enantiomer of **51** is comparable to *rac*-**51** in its effect against barley mildew, but clearly inferior against mildew and wheat brown rust.[39,42]

Recently the design of new putative inhibitors of the $\Delta^8 \rightarrow \Delta^7$ sterol isomerase in the fungal ergosterol biosynthesis pathway was reported.[43] As neither the fungal nor the yeast $\Delta^8 \rightarrow \Delta^7$ isomerase have been purified to homogeneity or crystallized, this approach was based upon the assumed mechanism of the enzymic transformation and on the structure of the natural substrate.

The proposed detailed mechanism of the $\Delta^8 \rightarrow \Delta^7$ isomerization is depicted in Scheme 16. The process starts with protonation of **53** from the α face, which generates an unstable carbocation at C8 (**54**). This is followed by removal of the α hydrogen at C7, to produce episterol (**55**).

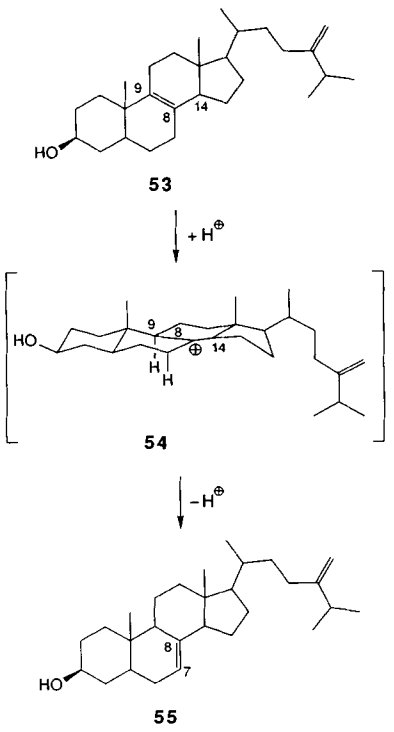

Scheme 16. Conversion of fecosterol (**53**) into episterol (**55**) catalyzed by the enzyme $\Delta^8 \rightarrow \Delta^7$ sterol isomerase.

On this basis, the working hypothesis originally outlined by *Benveniste*[44] included the following points:

a) mimicry of the C8 carbocation by a positively charged nitrogen, despite the resulting different geometries;
b) use of tertiary amines with p*K*a values which allow them to be applied as free bases (advantageous for their permeability through biological membranes) and, on the other hand, to be protonated at the N atom under physiological p*H* to develop the positive charge on the nitrogen atom;
c) simulation of structural elements of the steroid, e.g., rings B and D, including stereochemistry and lipophilicity.

Based on these three principles *Huxley-Tencer* et al.[43a] designed the perceived transition state analogues of the general structure **I** (Scheme 17) and synthesized many compounds. Maximum fungicidal activity was found when the

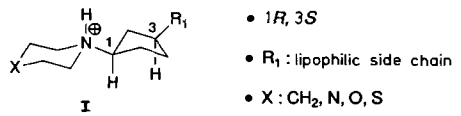

Scheme 17. General structure of an inhibitor of the enzyme $\Delta^8 \rightarrow \Delta^7$ sterol isomerase.

amine moiety was *cis*-2,6-dimethylmorpholine and the substituent at C3 was a *para-tert*-butylphenyl group. The compounds were first synthesized in a nonstereoselective way, with the aim of obtaining, after separation, all possible stereoisomers (Scheme 18).

The absolute configuration of this series was assigned by comparison of the optical rotations of the enantiomeric ketones (*R*)- and (*S*)-**57** with known values.[45] The latter were obtained by preparative chromatographic (HPLC) on triacetyl cellulose. The introduction of the *tert*-butyl group into the *para* position of the phenyl ring of (*R*)- and (*S*)-**57** was achieved regioselectively and without racemization. Reductive amination of the enantiomerically pure ketones (*R*)- and (*S*)-**58** produced the desired compounds **59** and **60** as a diastereoisomeric mixture, which could be separated by chromatography on silica gel. In each case the relative *cis* or *trans* stereochemistry of the cyclopentane rings was assessed from the ^{1}H NMR data (NOE).[43a]

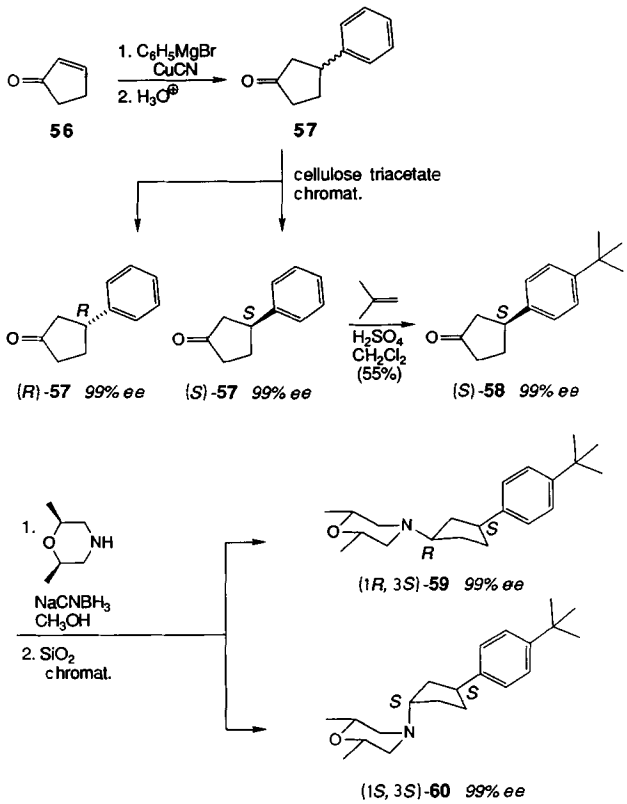

Scheme 18. Stereoselective synthesis of $\Delta^8 \rightarrow \Delta^7$ sterol isomerase inhibitors (1*R*, 3*S*)-**59** and (1*S*, 3*S*)-**60**. The corresponding compounds with the opposite absolute configuration at C3 were obtained analogously from (*R*)-**57**. Chromat. = Chromatography.

In vitro and in vivo tests showed that (1*R*, 3*S*)-**59** was the most potent compound, as expected from the natural absolute configuration of the steroidal ring D. In greenhouse tests against *Erisyphe graminis* on barley, the compound (1*R*, 3*S*)-**59** showed an ED_{50-85} value[46] which was approximately 20 times lower than that of fenpropimorph (**51**). The fungicidal activity in this series (in vitro and in vivo) followed the sequence: (1*R*, 3*S*) > (1*R*, 3*R*) > (1*S*, 3*S*) > (1*S*, 3*R*).[43a]

The *R* absolute configuration at C1 of the designed inhibitor, which corresponds to the stereochemistry at C14 of the natural substrate, seems more important for the inhibitory activity of **59** than the absolute configuration at C3. The latter should simulate the rather flexible side chain in **54**.

3. Weed Control

The structural variability of compounds having herbicidal activity is large. For many of the herbicidal compounds which have sterogenic centers the relationship between stereoisomerism and biological activity is generally not well understood. The stereoselectivity of herbicides interfering with auxin activity, for example 2-aryloxypropionic acid derivatives, has been recently reviewed.[47] A very interesting example within this class of compounds was presented by *Amrein* et al. and *Cornes* et al. in 1989.[48] The combination of the compounds **61** and **62**, with the code numbers CGA 184927 and CGA 185072, respectively, in a ratio of 4:1, is a herbicide(**61**)–safener(**62**) mixture for the selective postemergence control of annual grass weeds in wheat, rye, and triticale. The herbicidal activity of **61** is concentrated in its *R* enantiomer, whereas the enantiomers of the safener showed practically no differences in activity.[48] It was shown that the ability of **62** to protect wheat from injury by the herbicide **61**, and to confer partial protection to barley, is related to the ability of the safener to stimulate herbicide metabolism in these crop species.[49]

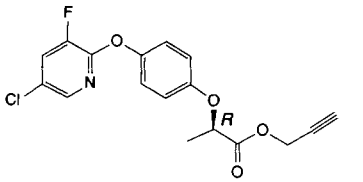

61

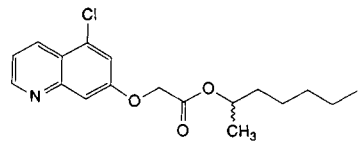

62

Scheme 19. A 4:1 mixture of the herbicide **61** and the safener **62** exhibits excellent postemergence control of annual grass weeds in wheat, rye, and triticale.

Reseach work on the stereoselectivity of the few older chiral compounds belonging to the important group of the photosynthesis inhibitors (mainly ureas and cyanoacrylate derivates) has been the subject of a recent review.[50]

In the following section we shall concentrate on a few new chiral herbicides with high biological potential and whose enantioselective synthesis was accomplished after a great deal of effort.

3.1. (*S*)-Phosphinotricin

(*S*)-Phosphinotricin (**63**) is a naturally occurring phosphorus-containing amino acid. It was first obtained by hydrolysis of the antibiotic tripeptide bialaphos (**64**).[51]

Racemic phosphinotricin is the active component of the broad-spectrum nonselective herbicide with the common name glufosinate ammonium. Its herbicidal action is apparently due to the inhibition of the ammonia-fixing enzyme

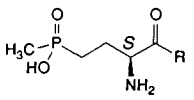

63 R = OH

64 R = Ala-Ala-OH

Scheme 20. (*S*)-Phosphinotricin (**63**), a naturally occurring phosphorus-containing amino acid, was first isolated from the antibiotic tripeptide **64**.

glutamine synthetase.[52] This activity is associated with the isomer (*S*)-**63**.[53]

Besides the synthetic approaches through chiral imine alkylation[54] and enzyme-catalyzed racemate resolution,[55] there are recent reports on the enantioselective syntheses of **63** that use methods with preparative potential. For example, alkylation of the enantiomerically pure Schöllkopf's bislactime ether **65** obtained from (*R*)-valine afforded, after a standard two-step hydrolysis and recovery of (*R*)-methylvalinate, (*S*)-phosphinotricin **63** with 93% *ee* (Scheme 21).[56, 58]

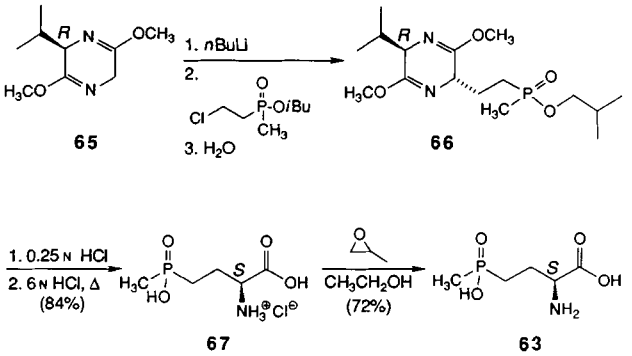

Scheme 21. The bislactime ether route to phosphinotricin (**63**).

Another approach takes advantage of the accessibility of the chiral pool substance (*S*)-glutamic acid (**68**). The conversion of **68** into the protected (*S*)-vinylglycine derivate **69** can be accomplished in three steps according to a known procedure.[59] Regioselective addition of ethyl methyl phosphonite to **69** gives, after deprotection, (*S*)-**63** in high yields with 98% *ee* (Scheme 22).[56]

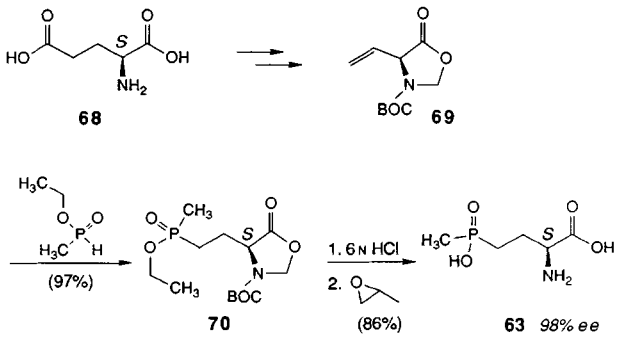

Scheme 22. A chiral-pool approach to phosphinotricin (**63**). BOC = *tert*-butoxycarbonyl.

Finally, an alternative enzymatic process with better prospects for large-scale production of **63** (Scheme 23) was described recently.[57] An aminotransferase capable of transaminating the α-keto acid **71** to **63** was isolated from *Escherichia coli K-12*. Substrate-specific studies suggest that this enzyme is identical with the 4-aminobutyrate–2-ketoglutarate transaminase (EC 2.6.1.19). The transaminase was immobilized by coupling to an epoxide-activated carrier and was used in a column enzyme reactor for the continuous production of **63**. A fourfold molar excess of glutamate over the

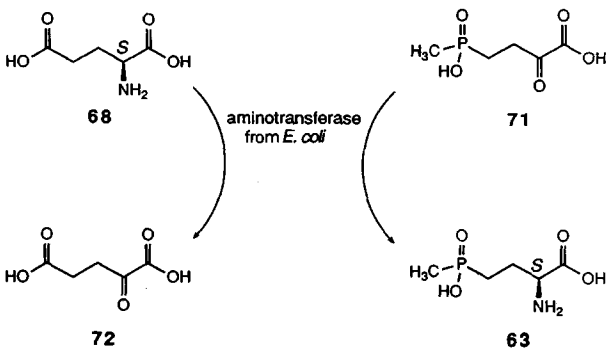

68 **71** **72** **63**

Scheme 23. Enzymatic synthesis of phosphinotricin (**63**).

α-keto acid **71** was used to shift the reaction equilibrium to the desired product **63**. Yields of more than 90% of **51** with production rates of 50 g L^{-1} h^{-1} were then achieved. The unreacted glutamate could be recycled.[57a]

Furthermore, the gene encoding the transaminase was cloned and expressed in *E. coli*. The transaminase expression in transformants of *E. coli* could be increased up to 80-fold compared with that of a wild-type control. The expressed transaminase consituted up to 20% of the total protein of the bacteria. The protein crude extract of the transformants was used, after a heat precipitation step, as described above for the production of **63** in an enzyme reactor.[57b]

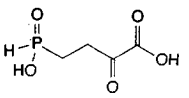

73

Scheme 24. The biosynthetic precursor of phosphinotricin (**63**).

Interestingly, the amino acid forming step in the biosynthesis of bialaphos (**64**) is the transamination of **73** (Scheme 24), which in a later step is methylated at phosphorus.[60]

3.2. 2-Dimethylphosphinoyl-2-hydroxyacetic Acid

A new, interesting phosphorus-containing experimental nonselective herbicide is racemic 2-dimethylphosphinoyl-2-hydroxyacetic acid (**74**), code number HOE 063 704.[61] The herbicidal activity of **74** comes from the inhibition of acetolactate reductoisomerase, an important enzyme in the biosynthesis of branched-chain acids.[62]

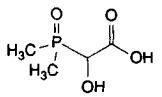

74

Scheme 25. The experimental herbicide HOE 063 704 (**74**).

The racemic ester **75** was enantioselectively hydrolyzed by porcine liver esterase (PLE) to (+)-**74**. The remaining ester **76** racemized spontaneously under the reaction conditions, thus attaining a conversion rate of 95% (→ (+)-**65**).[61] The absolute configurations shown in Scheme 26 are assumed in analogy to (*R*)-acetolactate, but are not yet experimentally determined.

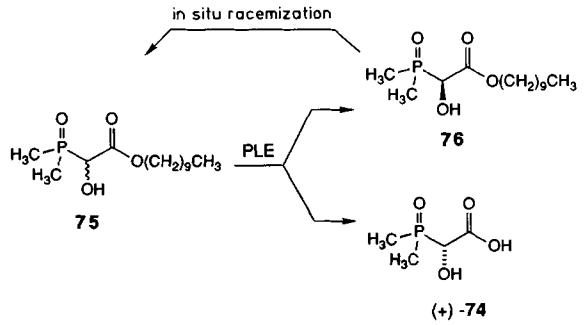

75 **76** (+)-**74**

Scheme 26. Enzymatic resolution of **75**. Absolute configurations and *ee*'s have not yet been reported.

The isolated (+)-**74** is the biologically active isomer, as demonstrated by in vivo studies. Also in vitro experiments with isolated acetolactate reductoisomerase from *Daucus carota* and *Escherichia coli*, indicated that (+)-**74** is twice as active as the racemic compound **74**.[61]

3.3. Imidazole-5-carboxylic Esters

In the course of a standard herbicide screening program, unexpected activity was found in compound **77**, which belongs to a group of imidazole-5-carboxylic esters with hypnotic and antimycotic activity.[63]

As a result of the synthetic work to optimize the herbicidal activity of **77**, a sterol biosynthesis inhibitor, the compound **78** (Scheme 27) was found to be the most active substance in

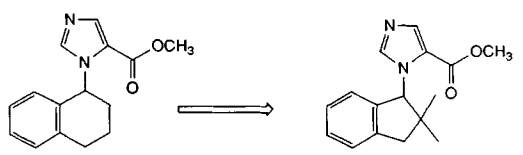

77 **78**

Scheme 27. The herbicide **78**, the result of intensive synthetic work to optimize the herbicidal activity of **77** [62].

this series. In the standard test (against *Digitaria sanguinalis*) **78** was four times more active than **77**.

The stereoisomers of **78** were synthesized in enantiomerically pure form starting from the corresponding amines, (*R*)- or (*S*)-**79**, in a multistep synthesis using either a Thorpe[64] or a Jones[65] cyclization procedure to construct the imidazole moiety. The required enantiomerically pure amines were prepared by resolution of the racemic compound **79** with L-*N*-benzoylglutamic acid.[63] A method of recycling of the undesired isomer in high yields (> 90%) was also developed,[66] based on treatment of the latter with Raney cobalt catalyst at 190 °C without added solvent (Scheme 28). The

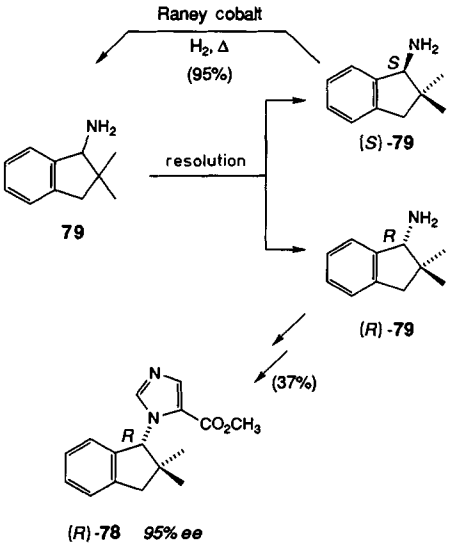

Scheme 28. Stereoselective synthesis of (*R*)-**78** via racemate resolution with (*S*)-*N*-benzoylglutamic acid and recycling of the undesired stereoisomer (*S*)-**79**.

compound (*R*)-**78** proved to be twice as active as the racemate **78**. Its enantiomer (*S*)-**78** was completely inactive in the *D. sanguinalis* test. Similar results were obtained with the stereoisomers of **77**, although in this case the *S*-isomer exhibited a measurable activity (Fig. 5).

A herbicidal pharmacophore structure was proposed based on conformational analysis, force field and MO calculations, and CAMM (*C*omputer-*A*ssisted-*M*olecular *M*odeling) superpositioning studies of **77** with sets of analogues of high activities and low or zero activity.[63]

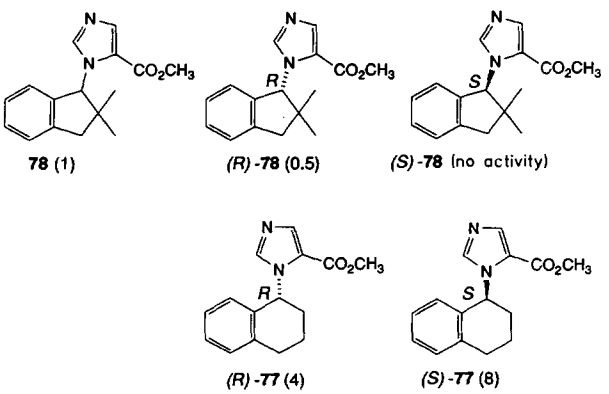

Fig. 5. Activities of some imidazole-5-carboxylic acid derivatives expressed as relative application rates (in parantheses) against *Digitaria sanguinalis*.

Consideration of an optimized orientation of the phenyl ring with respect to the imidazole moiety revealed a lipophilic pocket which seems to be relevant for activity. The methyl ester group points away from the lipohilic groups and the region below the phenyl ring must remain unoccupied (Fig. 6).[63]

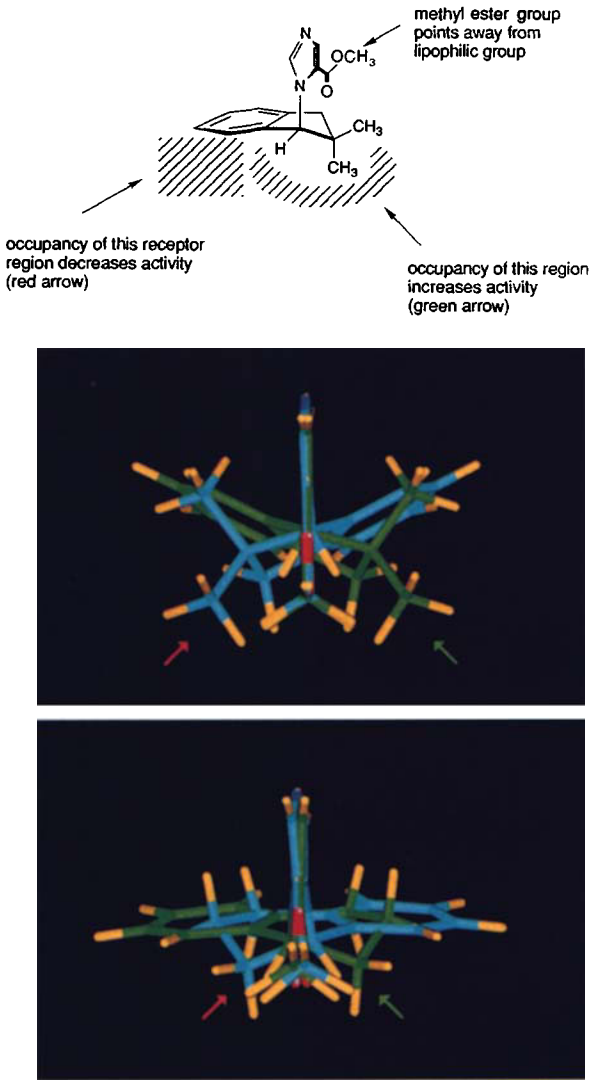

Fig. 6. CAMM studies of **77** and **78**. a) Proposed herbicidal pharmacophore structure, illustrated with the compound (*R*)-**78**. b) Superposition of the imidazole rings of (*R*)-**78** (green) and (*S*)-**78** (blue). c) Superposition of the imidazole rings of (*R*)-**77** (green) and (*S*)-**77** (blue).

The differences in biological activity observed for the stereoisomers of **77** and **78** fit this model. Superposition of the completely inactive (*S*)-**78** with the active (*R*)-**78** shows that the methyl group *trans* to the imidazole ring occupies the region below the phenyl plane in (*S*)-**78**. On the other hand, although (*R*)-**77** is twice as active as (*S*)-**77**, the latter exhibits some activity. In this case, superpositioning studies show that the less active stereoisomer does not occupy the receptor's forbidden region, but that the lipophilic pocket is less occupied. Superposition studies were also used to predict the inactivity of the racemic compounds **80** and **81**. Neither four- nor seven-membered rings were able to provide the

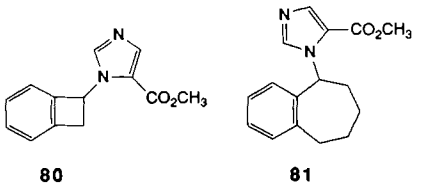

Scheme 29. Imidazole-5-carboxylic acid derivatives which are inactive as herbicides.

correct orientation of the phenyl ring plane relative to the imidazole moiety (Scheme 29).[63]

3.4. Further Structural Types

An interesting example of the optimization of in vitro activity using computer modelling was recently reported by *Mitchell* and *Bartlett*.[67]

The ketomorpholine **82** (Scheme 30) is a newly discovered inhibitor of phytoene desaturase, and shows pre-emergence herbicidal activity. A structural model was constructed by studying the overlap of a number of structurally diverse inhibitors for which structure–activity relationships were available. By comparing **82** with the model, a pseudoaxial orientation of the benzylic substituent at C2 was postulated. The model also predicted that a methyl substituent at C5, *trans* to the benzyl group, should be tolerated. The two *trans* stereoisomers **83** and **84** were prepared selectively, and in an in vitro test the activity was found to reside solely in the (2*R*, 5*S*)-isomer **83** (Scheme 30).[67]

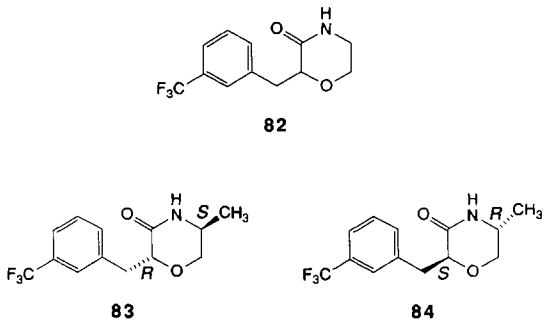

Scheme 30. The herbicidal active ketomorpholine **82** and structural analogues **83** and **84**. Only the stereoisomer **83** shows herbicidal activity.

The *N*-phenyltetrahydrophthalimides are a known class of pre- and postemergence herbicides now experiencing a renaissance. Within this class, the compound **85**, (code number S 23121) is a potent postemergence herbicide for cereals.[68] The selectivity of this compound is apparently related to the 1-methyl-2-propynyloxy substituent.

The stereoisomers of **85** have been prepared enantioselectively from the precursors **87** and **88** (Scheme 31).[69] The single isomers (*S*)- and (*R*)-**85** exhibited no selectivity in the inhibition of protoporphyrin IX synthesis.[68]

The bicyclic compounds **92** is a potent herbicide of a new structural class with an as yet undetermined mode of action.[70] It can be ingeniously synthesized in stereoisomerically pure form from waste paper in four steps, starting with a pyrolysis at 350 °C (Scheme 32).[70]

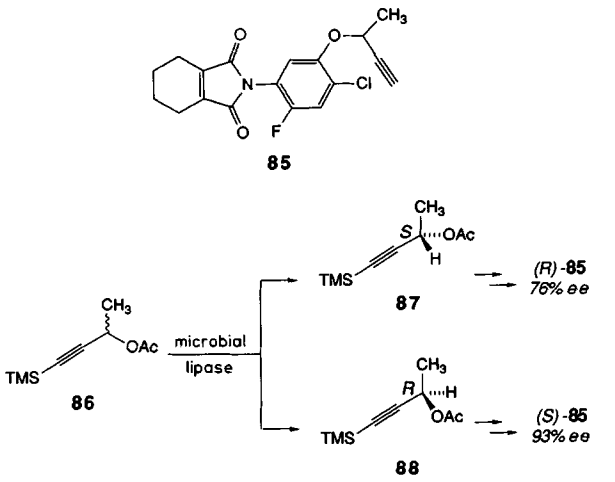

Scheme 31. Chemoenzymatic approach to the stereoisomers of **85**.

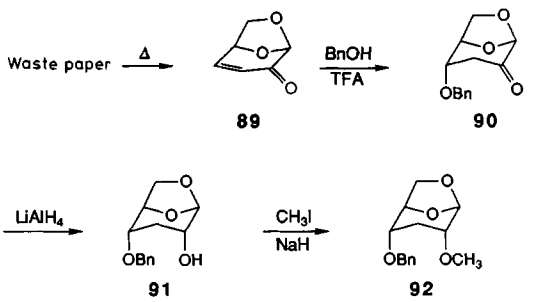

Scheme 32. Stereoselective synthesis of the 6,8-dioxabicyclo[3.2.1]octane derivative **92**. The starting material **89** is obtained from cellulose by pyrolysis. Bn = benzyl; TFA = trifluoroacetic acid.

A number of structural analogues, mainly of the types **d** and **e**, and also some with different configurations as C2 and C4, were prepared stereoselectively.[71] The key step was an aldol reaction between a chiral aldehyde of type **a** and an enolate of type **b** (Scheme 33). In spite of considerable synthetic work, compound **92** remained the most potent in this series.

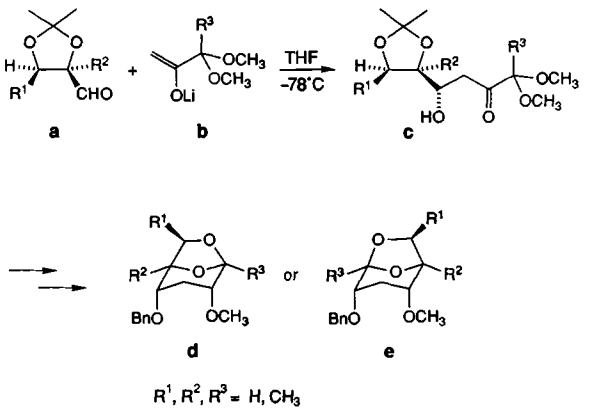

Scheme 33. Aldol approach to polysubstituted 6,8-dioxabicyclo[3.2.1]octane derivatives.

The newly described herbicide hydantocidin (**93**) possesses an unique structural feature, namely a spiro hydantoin ring at C1 of D-ribofuranose.[72]

The compound **93** was isolated from a *Streptomyces hygroscopicus* (SANK 63584) culture. Interesting properties were described for **93**: very low toxicity, systemic mode of action, broad spectrum, and low selectivity. Its weed-control activity is similar to that of glyphosate (**94**).[72, 73]

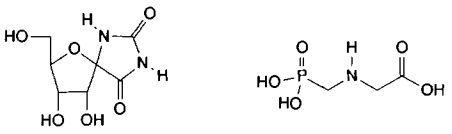

93 **94**

Scheme 34. Two herbicides with similar weed control activity: hydantocidin (**93**) and glyphosate (**94**).

Hydantocidin (**93**) and all its 15 stereoisomers were synthesized starting from derivatives of tartaric acid. The synthesis of the D series, starting from ethyl D-tartrate is described in Scheme 35.[73]

The L series was synthesized analogously, starting from ethyl L-tartrate.[73] Not only the preparative effort of *S. Sugai* et al., but also the stereoselectivity of the biological activity is impressive: only the N^1-β-D isomer **93**, and to a much lesser extent the N^1-α-D isomer **108**, exhibit herbicidal properties.[73]

4. Insect Control

Much work has been done over the past years trying to understand the interrelation of stereochemistry and biological activity of synthetic and natural insect controlling agents. The topic has been recently reviewed for most of the important classes of insecticides.[3]

4.1. Organophosphates

The biochemical and toxicological properties of chiral organophosphate enantiomers differ widely.[74] A very recent study from *Hirashima* et al.[75] illustrates the complex interplay of stereochemical, toxicological, and metabolic factors for the insecticide salithion (**112**) and its oxidation product salioxon (**113**) (Scheme 36).

Enantiomerically pure (*S*)- and (*R*)-**112** was obtained via (*S*)-proline methyl ester derivatives; the diastereomers were separated by crystallization and subsequent acid catalyzed methanolysis.[75a] The corresponding salioxon enantiomers (*R*)- and (*S*)-**113** were obtained from the salithion enantiomers by *meta*-chloroperbenzoic acid (MCPBA) oxidation as shown in Scheme 36.[75b]

(*S*)-**112** was a more potent insecticide by topical application than (*R*)-**112** on *Musca domestica* female adults correlating with the acetylcholine esterase (AChE) inhibition in vivo. However, against *Tribolium castaneum* the *R* enantiomer of **112** had a stronger larvicidal activity than the *S* enantiomer three days after treatment.

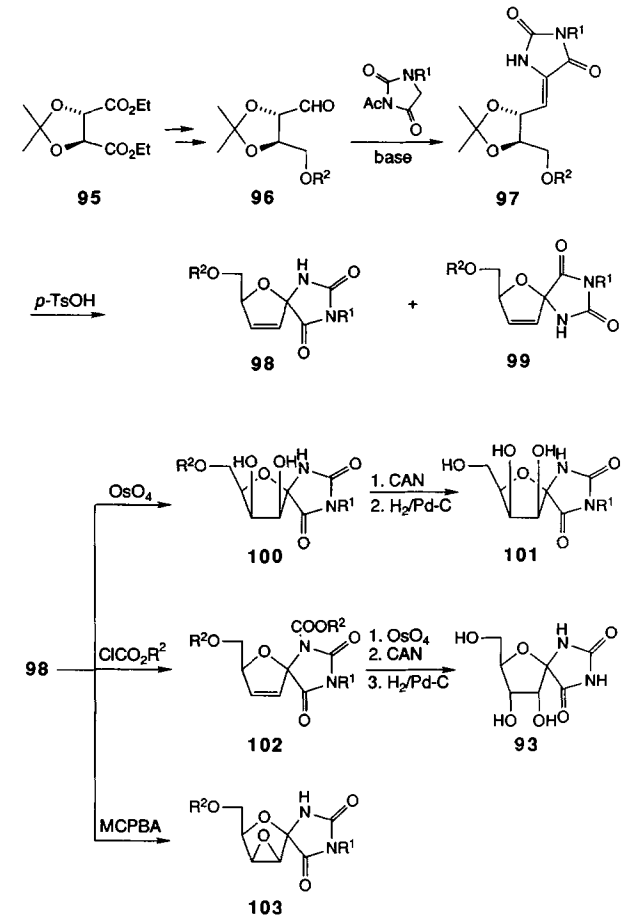

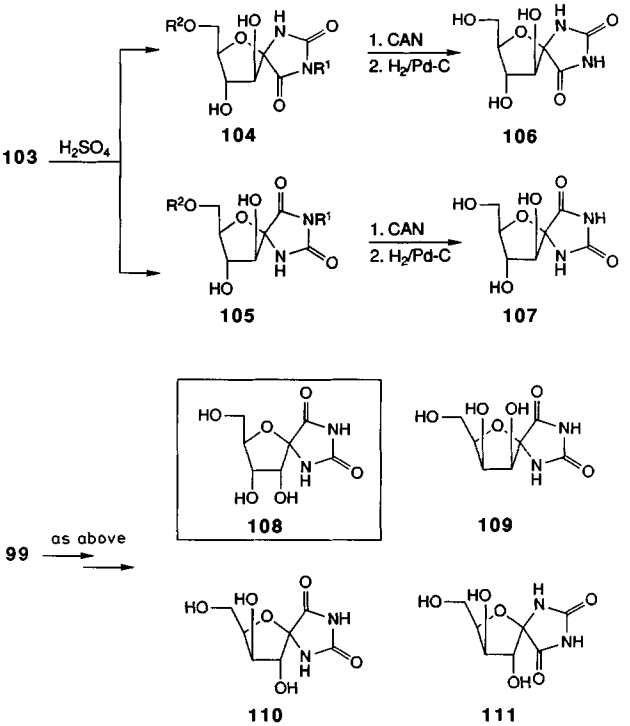

Scheme 35. Stereoselective synthesis of hydantocidin (**93**) and all its 15 stereoisomers. CAN = cerium(IV) ammonium nitrate.

On the other hand, (*R*)-**113** was a stronger house fly AChE inhibitor in vitro than the *S* enantiomer, whereas the latter ((*S*)-**113**) was a more potent *T. castaneum* larval AChE inhibitor than the *R* enantiomer. In all the discussed cases, the oxidized form **113** occurs during metabolism in the insect. The

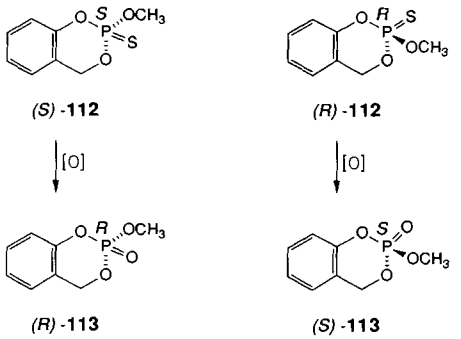

Scheme 36. The stereoisomers of salithion (**112**) and salioxon (**113**).

reversed stereospecificity between *M. domestica* insecticidal and *T. castaneum* larvicidal activity of salithion enantiomers ((*R*)- and (*S*)-**112**) might be a result of a stereospecific difference in the intrinsic potency of salioxon enantiomers ((*S*)- and (*R*)-**113**) as AChE inhibitors of the two species.[75c]

4.2. Benzoylureas

Benzoylureas are insect growth regulators, acting by inhibition of chitin synthesis and so interfering with the formation of the cuticle.[76] An interesting example of a compound of this class possessing stereoisomerism was recently reported by *Drabek* et al. (Scheme 37).[77]

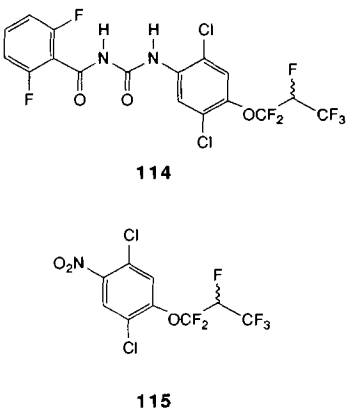

Scheme 37. The benzoylurea insecticide **114**. Its precursor **115** was resolved by chromatography on a tribenzoyl cellulose column.

The compound **114** with the code number CGA 184699 is a benzoylurea with good environmental behavior and interesting activity. Both enantiomers of compound **114** were obtained in pure form from the corresponding intermediates (+)- and (−)-**115**, which were obtained by chromatographic separation of the racemic **115** on a tribenzoyl cellulose column.[77] The absolute configuration could not be determined for this series.

The enantiomers of **114** showed a different insecticidal activity in laboratory trials against *Heliothis virescens L-1*. The (+)-isomer was a factor of 1.7 better than the racemate **114** and 2.2 times better than the (−)-enantiomer. However, the differences in the biological activities of the enantiomers of **114** were practically nonexistent in field trials and did not justify the very expensive and tedious chromatographic separation. As a consequence, compound **114** will be developed as a racemate.

4.3. Pheromones

Pheromones are semiochemicals (*semion* (greek) = a mark or signal) which act between members of the same species. Since the first isolation of a pheromone from the silkworm moth by *Butenand* et al. in 1959,[78] over 100 chiral pheromones have been isolated and identified. Outstanding synthetic work has been performed to obtain enantiomerically pure pheromones, mainly aimed at the determination of the absolute configuration of the natural products. An excellent review of this topic was published recently by *Mori*.[79]

Pheromones are very often blends, the components of which may act synergically and should be present in a definite ratio. This synergism frequently relates double-bond isomers and/or isomerism due to the presence of one or more stereogenic centers in the molecule. The interrelation between stereoisomerism and biological activity can be manifold. In some cases only one isomer is active, in others both, either as synergist, inhibitor, or independently active compounds.[80]

4.3.1. (*S*)-*Ipsenol*

Various species of bark beetles are dangerous pests for coniferous forests throughout the world. Among these are beetles of the genus *Ips* and *Pityokteinus*. (*S*)-ipsenol (**124**) is an aggregation pheromone of several species belonging to these genera.[81] The absolute configuration was established by *Mori* in 1976 by chemical correlation.[82]

The enantioselective synthesis of large amounts (50 g) of (*S*)-ipsenol (**124**) was recently reported by *Oertle* et al.[83] (Schema 38). The material was used for extended field trials to control the population of *Pityokteinus curvidens*. The key hydroxyacid intermediate **121** was obtained in enantiomerically pure form (*ee* > 99%) by an enantioselective aldol reaction using the chiral titanium complex **118**.[85] The subsequent transformation of the carboxy group of **121** followed, with some modifications on the silicon directed diene synthesis described by *Jenkins* et al.[86] In this way 56 g of enantiomerically pure (*ee* > 99%) (*S*)-ipsenol (**124**) has been prepared in one batch, starting from 160 g of β-hydroxyacid **121**.

4.3.2. *The Oviposition-Deterring Pheromone (ODP) in Rhagoletis cerasi*

The cherry fruit fly (*R. cerasi*) lays one single egg into halfripe cherries. It was demonstrated in field tests that double or

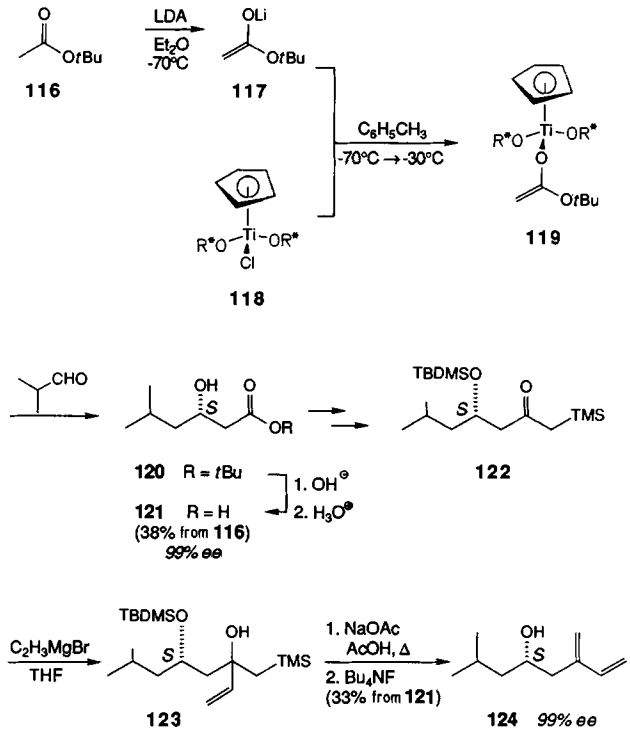

Scheme 38. Enantioselective synthesis of (*S*)-ipsenol (**124**) on a large scale (2 mol). LDA = Lithium diisopropylamide, OR* = 1,2:5,6-di-*O*-isopropylidene-α-D-glucofuranos-3-*O*-yl, TBDMS = *tert*-butyldimethylsilyl.

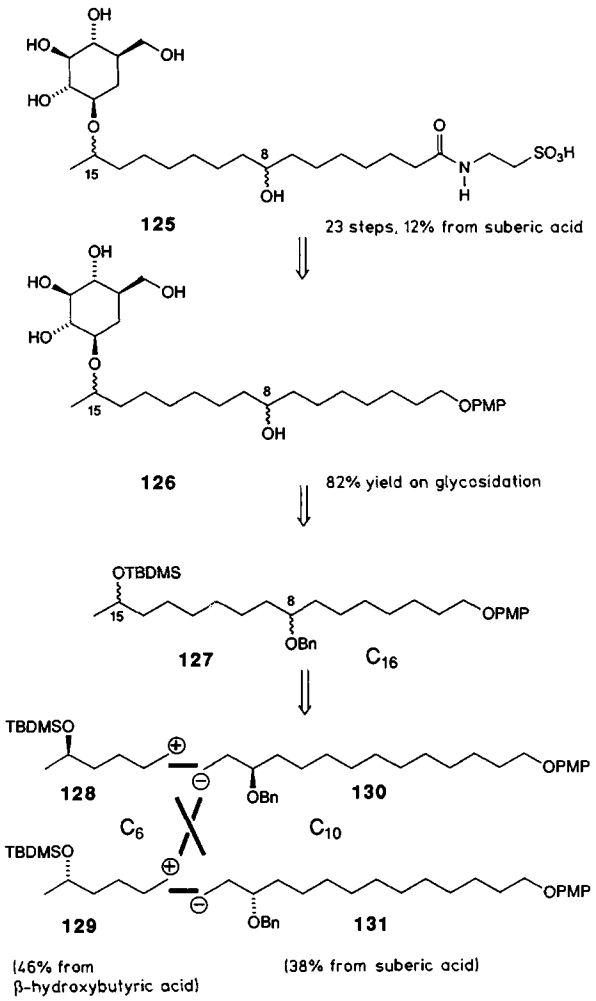

Scheme 39. Retrosynthetic concept of an enantioselective synthesis of all four stereoisomers C8/C15 of **125**. PMP = *p*-methoxyphenyl.

triple oviposition into the same fruit occurred with a much lower frequency than would be expected if deposition had taken place randomly.[87] Consequently, the hypothesis was put forward that the females mark the fruit.[88] Since fruits infested by maggots are not accepted by the consumer, cherries have to be protected against the oviposition of fruit flies.

Isolation and purification of the active component from the faeces made possible a partial structural analysis of the ODP (**125**).[89] ODP contains two stereogenic centres at C8 and C15 besides the sugar moiety. Since the assignment of the absolute configuration was not possible by spectroscopic means, an enantioselective synthesis of all four stereoisomers at C8/C15 was carried out.[90] The general retrosynthetic concept is illustrated in Scheme 39.

As anticipated, the glycosidation to a β-glycoside derivative proved to be an extremely difficult step. Finally, an excellent and highly stereoselective glycosidation was achieved by using tetra-*O*-pivaloylglucopyranosyl fluoride according to *Kunz* et al.[91] The absolute stereochemistry of the natural ODP was assigned by employing both spectroscopic methods and comparative studies of the biological activity. It was demonstrated that the natural ODP is a diastereomeric mixture, namely, (8 *RS*, 15 *R*)-**125**.[92] Since the stereochemistry at C8 need not be controlled, a much shorter synthesis, suitable for large-scale production of "natural" ODP could be developed.[92]

By spraying (8 *RS*, 15 *R*)-**127** (10 mg L^{-1}) on cherry trees, the infestation rate of cherry fruit fly eggs was reduced (i.e., 1.85–2.5% infestation of treated trees against 21.4–23.35% infestation of untreated trees) in summer field trials in Switzerland in 1989.[92]

4.4. Insect Antifeedants

Insect antifeedants are currently attracting much research interest owing to their effect on a range of major crop pests.[93] An antifeedant is a chemical which inhibits feeding but does not kill the insect directly.[94] The insect often remains near the antifeedant source and possibly dies through starvation. The limited information presently known does not allow generalizations on the mode of action of antifeedants.[95]

Considerable attention has been focused recently on the extremely potent natural antifeedant azadirachtin (**132**, Scheme 40).[96]

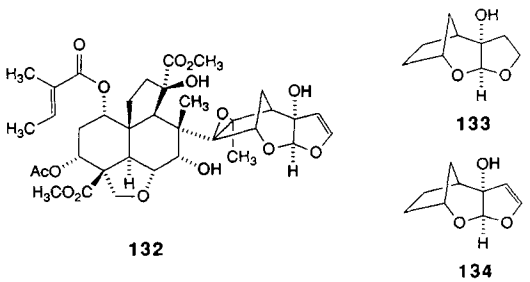

Scheme 40. Azadirachtin **132** and two synthetic substructures with similar antifeedant activity against *S. littoralis*.

The high level of interest in **132**, which has been isolated from the neem tree *Azadirachta indica*, stems from its exceptional biological activity. Compound **132** is the most potent antifeedant against *Lepidopterus* species isolated to date. It is 100 per cent lethal at only 10 ppm concentration through a variety of processes including antifeedancy, growth disruption, and moulting inhibition. Despite such high toxicity towards certain insects, azadirachtin is apparently harmless to higher forms of life and exhibits no phytotoxicity.[94b]

Although it is possible to use extracts of neem seeds for crop protection, **132** itself is quite unstable and its low abundance in the plant makes it difficult to obtain pure **132** for agricultural use. Efforts are being made to synthesize **132**;[97] however, any synthesis of such a structurally complex and chemically unstable molecule containing 16 chiral centers is not going to be amenable to commercial development. In an alternative approach, substructures of **132**, for example **133** and **134**, were synthesized and screened for antifeedant activity.[97a] Both of these compounds were found to be active against *Spodoptera littoralis* and **134** was almost as potent as the natural product **132** at 10 ppm concentration.

4.5. Pyrethroids

The insecticidal properties of the pyrethrum powder extract from the flower heads of *Chrysanthemum cinerariefolium* have been well documented for over 100 years. A few years ago about 23000 tons were produced annually.[98a] The flowers, grown in Kenya, contain on average 1.3% of enantiomerically pure esters of (1 *R*)-*trans*-chrysanthemic acid **135**–**137** and (1 *R*)-*trans*-*E*-pyrethric acid **138**–**140** (Table 1).[99]

Table 1. The mixture of natural enantiomerically pure insecticides present in *Chrysanthemum cinerariefolium* flower heads.

No.	structure	name (% in mixture) stereochemistry [98]
135	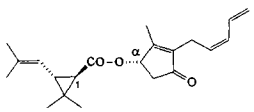	pyrethrin I (35) 1*R trans*; α*S*
136	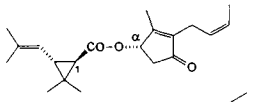	cinerin I (10) 1*R trans*; α*S*
137	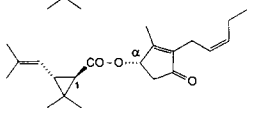	jasmolin I (5) 1*R trans*; α*S*
138	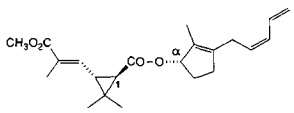	pyrethrin II (32) 1*R trans*, *E*; α*S*
139	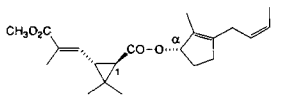	cinerin II (14) 1*R trans*, *E*; α*S*
140	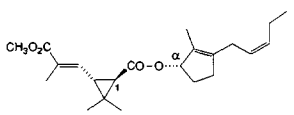	jasmolin II (4) 1*R trans*; *E*; α*S*

The mixture of compounds shown in Table 1 is responsible for their remarkable and rapid action on a wide range of insects. Pyrethrin I (**135**) is especially effective for kill and pyrethrin II (**138**) for the rapid knockdown of flying insects.

Early attempts at synthesizing compounds similar to the natural pyrethrins produced a range of products which, although having an inherent problem of instability to light, did find significant success as insecticides in the household sector. Whereas **141**–**143** (Table 2) are esters of chrysanthemic acid and have the natural (1 *R*)-*trans* configuration (which is conferred on its precursor by the chiral enzymatic microenvironment in the flower heads, Fig. 7), the majority of commercial household chrysanthemates are racemic and take advantage of the elegant and simple access to the racemic chrysanthemic esters (Scheme 41).

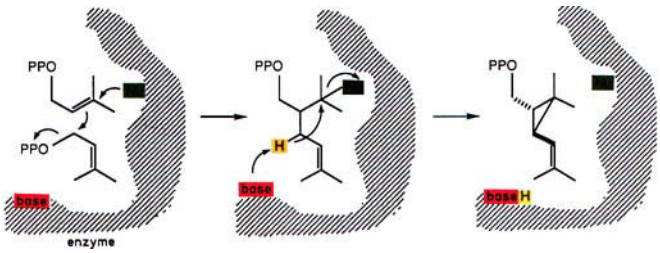

Fig. 7. 1,3-Cycloelimination in nature: suggested enantioselective pathway for (1 *R*)-*trans*-chrysanthemol pyrophosphate formation from isopentenol pyrophosphate in the flower heads of *Chrysanthemum cin.*, according to *Naumann* [98b] and *Crombie* [100].

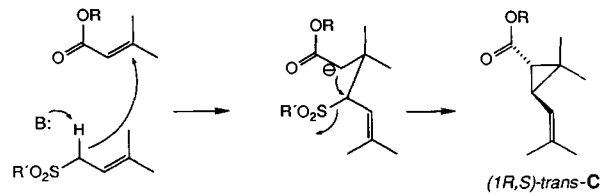

Scheme 41. 1,3-Cycloelimination in the chemical industry: Synthesis of racemic *trans*-chrysanthemic ester **C** according to *Martell* [101], ingeniously utilising the simplest starting materials, and the arylsulfonyl group as both an activating and a leaving group.

However, the pyrethroids started to gain commercial importance as agricultural insecticides only when at the beginning of the 1970's *Elliot*[102] combined phenoxybenzyl alcohols with photostable derivatives of chrysanthemic acid, containing dihalovinyl moieties instead of the dimethylvinyl substituent on C3, thus creating the very potent insecticides permethrin **155** (4 stereoisomers), cypermethrin **156** (8 stereo-

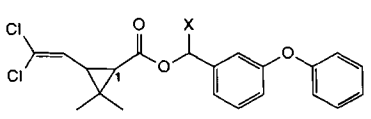

(1R, S)-cis, trans-**155** X = H

(1R, S)-cis, trans-(αR, S)-**156** X = CN

Scheme 42. The potent insecticides permethrin (**155**) and cypermethrin (**156**).

Table 2. Commercially used semisynthetic (**141**–**143**) and synthetic (**144**–**154**) enantiomerically pure pyrethroids [103]

No.	structure	stereochemistry[98]	common name	application
141 [a]	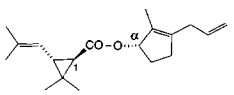	1*R trans*; α*S*	bioallethrin	domestic and industrial hygiene
142	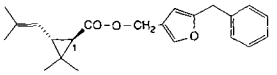	1*R trans*	bioresmethrin	as **141**
143	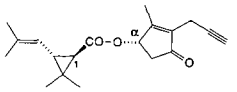	1*R trans*; α*S*	(*S*)-prallethrin[104]	household use
144	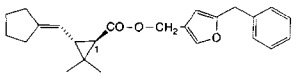	1*R trans*	bioethanomethrin[105]	as **143**
145	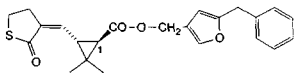	1*R cis*	kadethrin[106]	as **143**
146	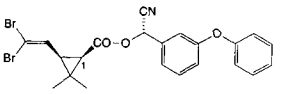	1*R cis*; α*S*	deltamethrin	against lepidoptera, coleoptera in cotton, vegetables, fruits etc.
147	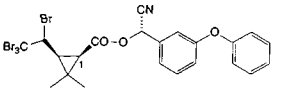	1*R cis*, 1'*RS*; α*S*	tralomethrin	as **146**
148[a]	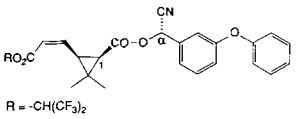	1*R cis*, *Z*; α*S*	acrinathrin[107]	against mites in citrus, fruits, grapes etc.
149	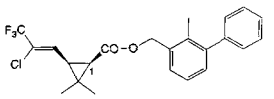	1*R cis*, *Z*	bifenthrin	as **146**
150	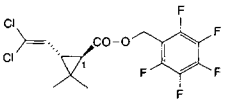	1*R trans*	fenfluthrin	
151	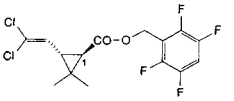	1*R trans*	benfluthrin[108]	mosquitos, flies, moths in the air
152[b]	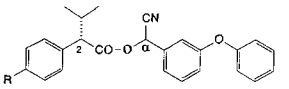	2*S*; α*RS*	esfenvalerate	as **146**
153[c]		2*S*; α*RS*	flucythrinate	against *Aphididae*, *Lepidoptera* in broad range of crops
154	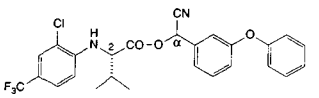	2*S*; α*RS*	(tau)-fluvalinate	against *Aphididae*, *Cicadellidae* in cotton fruits sunflowers, etc.

[a] R = $CH(CF_3)_2$. [b] R = Cl. [c] R = $OCHF_2$.

isomers) and especially the enantiomerically pure ester deltamethrin **146** (Table 2). *Elliot's* discovery triggered an enormous synthetic activity all over the world, aiming in the 1970's mainly at the search for new, improved derivatives and analogues of the archetypal esters **135** and **155**, as well as on the circumvention of existing patents. The emphasis in the 1980's shifted to the cost-effective and enantioselective synthesis of selected leading compounds, as well as to the fine-tuning of their biological and ecotoxicological properties, for example, to decrease their toxicity to fish.

An excellent overview of the wealth of splendid pyrethroid chemistry, performed mostly by industrial chemists, was published in 1990 by *Naumann*.[98] He critically evaluated about 2600 references from the scientific patent literature published until 1987. Therefore we selected only a few recent examples with an emphasis on enantioselective synthesis.

Complete transformation of racemic constituents into a single enantiomer or diastereoisomer without loss of any material, requires refinement of many resolution methods and their adaptation to industrial scale. The underlying principle of all industrially successful separations of stereoisomers is the removal of the target product (or its diastereomeric salt or chiral precursor) in crystalline state from the reaction mixture, on the basis of its relative insolubility. This is accompanied by a continuous epimerization of the undesired stereoisomer in the solution, utilizing the mobility of an activated hydrogen. A striking example of the application of this methodology is the preparation of deltamethrin **146**: the most active, enantiomerically pure (1 *R*)-*cis*-α*S* isomer is now produced at a rate of 200 t per annum from the eight possible isomers, despite of the involvement of two racemates (racemic *trans*-chrysanthemic acid and racemic cyanhydrine).[109]

Eight diastereoisomerically and enantiomerically related isomers of **156** have different biological properties, the (1 *R*)-*cis*-α*S* being the most active.[110] To achieve an economic synthesis of its consituent (1 *R*)-*cis*-**162**, a cost-effective resolution of a cyclobutanone derivative into pure enantiomers had to be accomplished on an industrial scale for the first time (Scheme 43).[111] The easily available racemic cyclobutanone

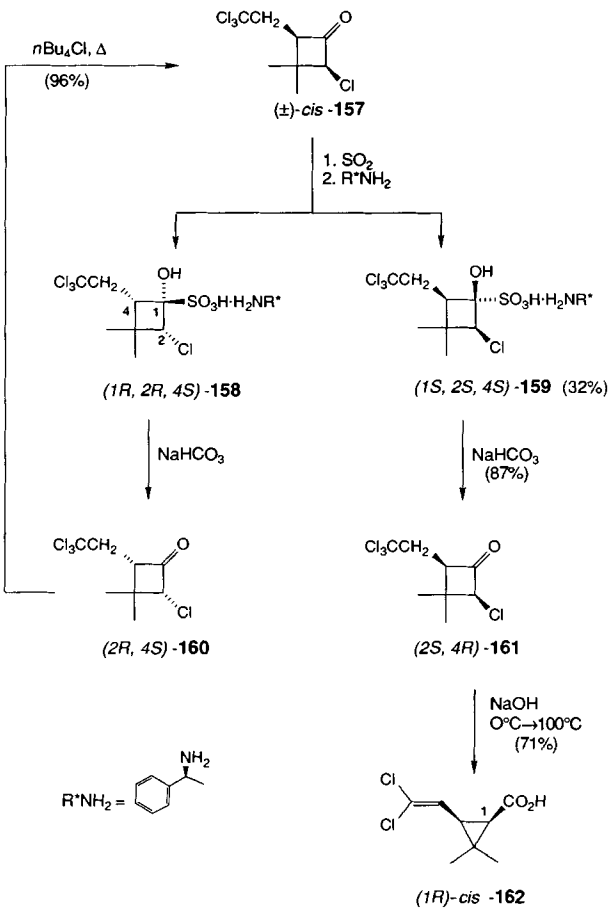

Scheme 43. A "cyclobutanone" route to (1 *R*)-*cis*-permethric acid (**162**).

157 was converted into the bisulfite adducts.[112] Fortunately, by using the cheap auxiliary (1 *S*)-phenylethylamine only two of the four possible diastereomeric salts were formed. Isomers **158** and **159** could be readily separated by fractional crystallization. The mild hydrolysis liberated the properly configurated (2 *S*, 4 *R*)-cyclobutanone **161** for the subsequent enantioselective Favorskii rearrangement to (1 *R*)-*cis*-**162**. The unwanted enantiomer (2 *R*, 4 *S*)-**160** could be readily racemized with Bu_4NCl to (±)-*cis*-**157** and utilized again in the separation steps. Thus, the whole procedure represents a chirally economic synthesis of (1 *R*)-*cis*-**162** (permethric acid).

An approach incorporating an inversion of configuration by an S_N2 substitution of C-α of the undesired alcohol enantiomer was chosen in the industrial synthesis of the new household insecticide (*S*)-prallethrin **143**.[104] Principally, it represents a combination of an enzyme-catalyzed reaction and a chemical reaction, which ensures no loss of valuable starting material (Scheme 44). At a substrate concentration

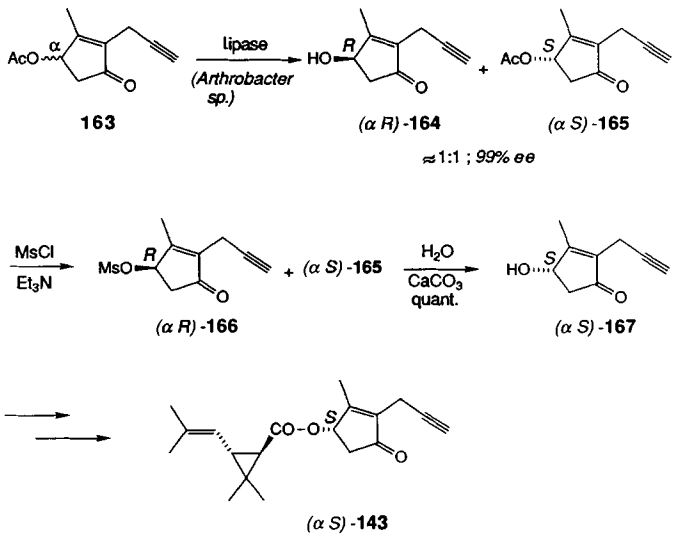

Scheme 44. A complete conversion of a racemic acetate **163** into the enantiomerically pure alcohol **167** by a chemoenzymatic approach.

of 8.8 w/v % (α *R*, *S*)-**163**, an enzyme concentration of 3 mg L^{-1}, pH 7.0, and 40 °C, a lipase from *Arthrobacter* species yielded enantiomerically pure (α *R*)-**164** and the (α *S*)-acetate **165**. This mixture of products was then esterified with methanesulfonyl chloride to afford a mixture of the corresponding (α *R*)-sulfonate **166** along with unaffected (α *S*)-**165** acetate. Both esters were hydrolyzed in the presence of a small amount of $CaCO_3$. The (α *R*)-sulfonate **166** was converted into the desired (α *S*)-cyclopentenolone **167** with inversion of configuration, while (α *S*)-**165** was hydrolyzed with retention of configuration. Consequently, all the racemic acetate was converted with maximum efficiency into (α *S*)-**167**.

A similar chemoenzymatic approach was recently applied to the complete transformation of racemic α-cyano-3-phenoxybenzyl alcohol into the (α *S*) enantiomer.[104]

(1 *R*)-*trans*-caronaldehyde **168** can be prepared by ozonolysis of chrysanthemic acid. Compound **168** and its (1 *R*)-*cis*-isomer **169**, or, more precisely, the lactolic form **170**, are mutually interconvertible.

Both caronaldehyde isomers are extremely valuable chiral building blocks, because many versatile transformations, especially olefinations of the Wittig type, lead ultimately to a variety of interesting pyrethroid acids.[98b] For this reason, new synthesis of caronaldehydes **168** and **169** from natural

compounds like (+)-α-pinene, α-limonene, and (+)-Δ-3-carene are frequently reported. None of them seem to be technically attractive as yet, because several more or less laborious degradation steps are necessary in each case to remove one or more supernumerary atoms of the carbon skeleton.

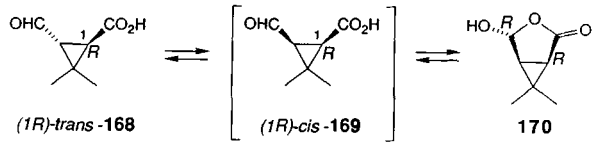

Scheme 45. Interconversion of (1 *R*)-*trans*-caronaldehyde (**168**) and its (1 *R*)-*cis*-lactolic isomer **170**.

Recent syntheses by *Krief* of (1 *R*)-*cis*-**175** lack this disadvantage,[113] as shown in Scheme 46. The optically active unsaturated esters **171** and **173** are derived from easily available (*S*)-2,3-*O*-isopropylidene glyceraldehyde and (*R*,*R*)-2,3-*O*-isopropylidene tartaric acid.

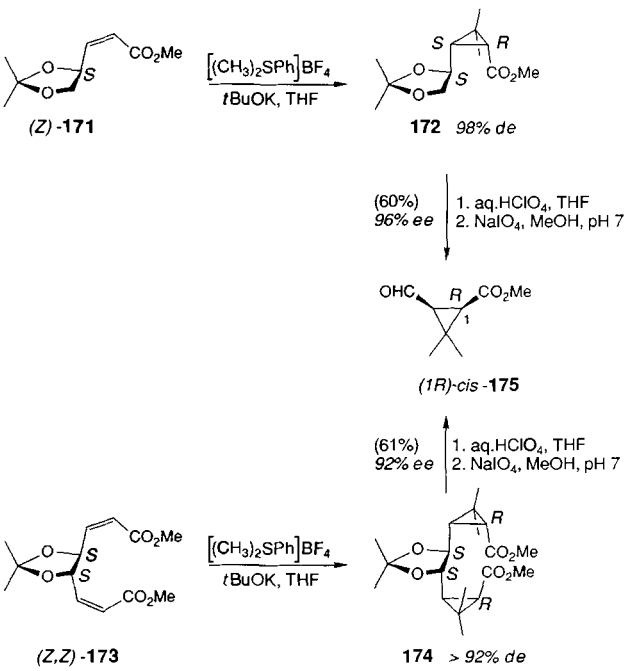

Scheme 46. Synthesis of (1 *R*)-*cis*-caronaldehyde methyl ester **175**.

Very recently, the *tert*-butyl ester of (1 *R*)-*cis*-caronaldehyde **169** was used for the synthesis of the new pyrethroid acrinathrin (**148**) according to Scheme 47.[107]

Finally, the successful preparation of the alcohol constituent of the enantiomerically pure experimental pyrethroid CGA 221 869 (**180**) which has diminished fish toxicity[114] is worth mentioning for at least two reasons.[115] Firstly, 2-phenylethynylzinc bromide was applied for the first time in an asymmetric addition to an aldehyde in the presence of a chiral amino alcohol, the lithium salt of (−)-*N*-methylephedrine (Scheme 48). Secondly, the optical induction (88% *ee*) in this easy addition reaction, **181** → **182**, is considerably higher than the enantioselectivities usually reported for the

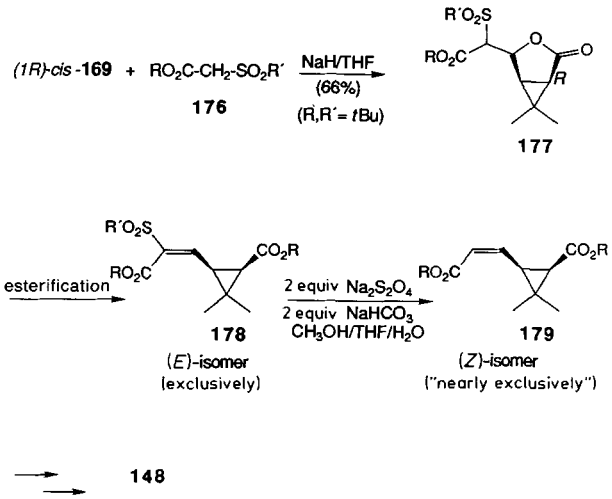

Scheme 47. Enantioselective synthesis of the acid part of acrinathrin (**148**) from the caronaldehyde derivative (1 *R*)-*cis*-**169**.

addition of dialkynyl zinc reagents to aldehydes in the presence of chiral amino alcohols.[116]

Pyrethroid insecticides have achieved a high share (19.4% in 1989) of the total insecticide world market, which amounted to 9.6 billion Swiss Francs in 1989.[117] Alongside the

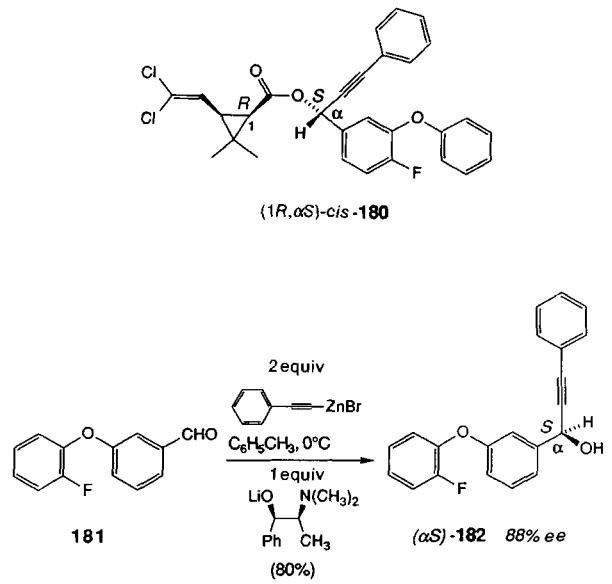

Scheme 48. The use of 2-phenylethylzinc bromide as alkynyl-delivering reagent in asymmetric synthesis of experimental pyrethroid **180**.

natural mixture of esters **135**–**140** and the enantiomerically pure synthetic esters **141**–**154**, there are more than 15 other, constitutionally uniform although stereochemically heterogeneous, pyrethroids on the market. As the wealth of products brought to the market by two decades of synthetic efforts is impressively large, suggestive of exhaustiveness, the impression may arise that there is no longer anything new to discover in this area, either in terms of structure or activity. This is probably largely true. At the same time, however, investigations are being undertaken to overcome some of the deficiencies of the current products and explore new market niches.

For example, the new pyrethroids which have neither an ester group nor a cyclopropane residue (their low fish toxicity makes them appropriate for use in rice fields) have nothing in common structurally with the archetypal pyrethrin **135**, except the outer surface of the molecules which is important for recognition by the binding site.[118]

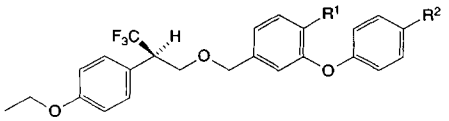

183 $R^1 = R^2 = H$

184 $R^1 = F, R^2 = H$

185 $R^1 = H, R^2 = Br$

Scheme 49. Pyrethroids containing neither ester nor cyclopropane groups.

The only enantiomerically pure derivatives **183**–**185** are missing even the usual geminal methyl group![119] (See Scheme 48; (2 *R*) enantiomers are more active than (2 *S*) ones.)

5. Conclusions and Outlook

As the above results indicate, the syntheses and investigations of enantiomerically pure agrochemicals have developed from isolated curiosities to become serious aims of modern agrochemical research and development. Clearly, the phenomenon of chirality will play an increasingly important role in crop protection by influencing both the thinking and the direction of the research programs of the scientists involved.

From an *agrochemist's* point of view, it is still an important and rewarding task to discover and develop new and inexpensive methods of introducing chirality which are a) applicable not only to model substances, but b) also take account of the chiral-economic requirements of both industry and environment (for instance, by the recycling of unwanted stereoisomers or by using catalytic reactions whenever possible). The examples shown above have been selected to demonstrate what has been achieved to date in this respect.

From an *agrobiologist's* point of view, performing mode-of-action studies with pure stereoisomers improves the understanding of the factors that influence biological activity, and hence enables the best compounds to be discovered more rapidly. The complex interaction of chiral substrates with natural chiral receptors, as well as their uptake, transportation, metabolism, etc., inside the chiral constituents of target organisms (e.g., peptides, polysaccharides, polynucleotides) may frequently lead to surprising insights and stimulate synthetic chemistry by the design of bioactive substances.

From an *agronomist's* point of view, the use of a single stereoisomer may offer an additional possibility for the solution of certain agronomical problems (e.g., reduction in phytotoxicity, fewer effects on beneficial insects and other non-target organisms, etc.). First and foremost, however, one principal question has always to be answered: To which of the six principal categories (see Section 1) does the investigated crop protection product containing one or more centers of chirality belong? Thus, the increasing flow of racemic and diastereoisomeric experimental compounds as well as their enantiomerically pure constituents from chemical laboratories will assist the agronomists in the refinement of their greenhouse and field testing evaluations.

Thanks to these interdisciplinary interactions, further exciting scientific progress, as well as economical and ecological benefits, can be expected in the fledging area of "Chirality in Crop Protection" in the near future.

The authors would like to thank heartily their colleagues Drs. Urs Burckhardt, Hans-Peter Buser, Philippe Chemla, John Dingwall, Hanspeter Fischer, Robert Nyfeler and David Wadsworth, who critically read this article, and Christa Fletcher and Dr. Victor Flück who helped to prepare the manuscript, drawings, and figures.

Received: March 22, 1991 [A 834];
German version: *Angew. Chem. 103* (1991) 1219

[1] The discipline of understanding the interplay of chiral substrates with living matter has a long history. For fascinating reading see: B. Holmstedt in H. Frank, B. Holmstedt, B. Testa (Eds.): *Chirality and biological activity*, H. R. Liss Inc., New York, 1990, pp. 1–14.

[2] I. W. Wainer, D. E. Drayer (Eds.): *Drug Stereochemistry*, Dekker, New York 1988; M. Gross, *Annu. Rep. Med. Chem. 25* (1990) 323.

[3] E. J. Ariens, J. J. S. van Rensen, W. Welling (Eds.): *Stereoselectivity of Pesticides*, Elsevier, Amsterdam 1988.

[4] B. Testa, W. F. Trager, *Chirality 2* (1990) 129.

[5] J. D. Morrison (Ed.): *Asymmetric Synthesis, Vol. 1–5*, Academic, Orlando, Fl, 1983–1985.

[6] D. Seebach, *Angew. Chem. 102* (1990) 1363; *Angew. Chem. Int. Ed. Engl. 29* (1990) 1320.

[7] To the best of our knowledge, *A. Eschenmoser's* suggestion (*Lectures on Organic Synthesis*, Technion, Haifa, 1969) to synthesize the highly strained and delightfully symmetric "helvetane" represents the only attempt to deplanarize the Swiss cross so far. It is cited and depicted in G. Dinsburg (for D. Ginsburg), *Nachr. Chem. Tech. Lab. 30* (1982) 289, as well as *Nouveau J. Chim. 6* (1982) 175. *A. Nickon* and *E. F. Silversmith* write in *Organic Chemistry: The Name Game*, Pergamon, New York 1987, pp. 87–88: "If you read his delightful article, you will go to bed chuckling—and feeling good about chemists."

[8] a) R. Sheldon, *Chem. Ind. (London) 1990 212*; b) H. B. Kagan, *Bull. Soc. Chim. Fr. 1988*, 846; c) W. Oppolzer, *Pure Appl. Chem. 62* (1990) 1241; d) E. J. Corey, *ibid.62* (1990) 1209. For a very recent, extensive, and competent discussion of the subject containing many literature citations see [6].

[9] Ch. R. Worthing (Ed.): *The Pesticide Manual*, The British Crop Protection Council, Farnham 1991.

[10] D. Belluš in *Workshop on Chirality in Crop Protection*, 7th IUPAC Int. Congr. Pestic. Chem. Hamburg 1990.

[11] a) *Proc. Brighton Crop Prot. Conf. Weeds—1989*, The British Crop Protection Council, Brighton 1989; b) *Proc. Brighton Crop Prot. Conf. Pests and Dis. 1990*, The British Crop Protection Council, Brighton 1990.

[12] H. Frehse, E. Kesseler-Schmitz, S. Conway (Eds.): *7th IUPAC Int. Congr. of Pestic. Chem., Book of Abstracts, Vol. I–III*, Hamburg 1990.

[13] Recently, however, papers full of enthusiasm for this theme have appeared: a) H.-P. Fischer, *Nachr. Chem. Tech. Lab. 38* (1990) 732; b) D. J. Chadwick, J. Marsh (Eds.): *Bioactive Compounds from Plants*, Ciba Foundation Symp. 154, Wiley, Chichester 1990.

[14] A. Fuchs in [3], p. 203.

[15] H. Moser, G. Rihs, H. P. Sauter, B. Böhner in J. Miyamoto, P. C. Karney (Eds.): *Proc. 5th Int. Congr. Pestic. Chem., Kyoto, 1982, Vol. 1*, Pergamon, Oxford 1983, p. 315.

[16] A. Hubele, W. Kunz, W. Eckhardt, E. Sturm in J. Miyamoto, P. C. Karney (Eds.): *Proc. 5th Int. Congr. Pestic. Chem., Kyoto, 1982, Vol. 1*, Pergamon, Oxford 1983, p. 233.

[17] H. Moser, C. Vogel, *4th Int. Congr. Pestic. Chem. Zürich 1978*, Abstract Volume, Abstract II-310.

[18] a) R. Nyfeler, P. Huxley in I. M. Smith (Ed.): *Fungicides for Crop Protection, 100 Years of Progress*, Monograph No. 31, BCPC Publication, Croydon 1985, p. 45; b) R. Nyfeler, P. Huxley, *Proc. Brighton Crop Prot. Conf. Pests and Diseases—1986*, BCPC Publications, Thornton Heath 1986, p. 207.

[19] D. J. Fisher, A. L. Hayes, *Crop. Prot. 4* (1985) 501.

[20] a) W. Kunz, W. Eckhardt, A. Hubele, *GB 1577702*, 1977, Ciba-Geigy; b) W. Eckhardt, H. Suess, *US-A 4721797*, 1986, Ciba-Geigy.
[21] P. Margot, W. Eckhardt, H. Dahmen, *Proc. Brighton Crop Prot. Conf., Pests and Diseases—1988*, BCPC Publications, Brighton 1988, p. 527.
[22] a) W. Eckhardt, E. Francotte, W. Kunz, A. Hubele, *EP 275523*, 1988, Ciba-Geigy; b) W. Eckhardt, E. Francotte, P. Margot in [12], Poster No. O1B-11.
[23] H. P. Buser, M. Sutter, F. Spindler, B. Pugin in [12], Poster No. OB-10; H. P. Buser, B. Pugin, F. Spindler, M. Sutter, *Tetrahedron 47* (1991) 5709.
[24] W. Köller, *Pestic. Sci. 18* (1987) 129.
[25] W. Krämer, K. H. Büchel, W. Draber in J. Miyamoto, P. C. Karney (Eds.): *Proc. 5th Int. Congr. Pestic. Chem. Kyoto 1982, Vol. 1*, Pergamon, Oxford, 1983, p. 223.
[26] H. Takano, Y. Oguni, T. Kato *Pestic. Sci. 11* (1986) 373.
[27] a) U. Kraatz, L. Born, *Pflanzenschutz-Nachr. Bayer (Ger. Ed.) 41* (1988) 3; b) U. Kraatz, L. Born in [12], Poster No. O1B-06.
[28] E. Ebert, W. Eckhardt, K. Jäkel, P. Moser, D. Sozzi, C. Vogel, *Z. Naturforsch. C. 44* (1989) 85.
[29] G. M. Ramos Tombo, R. Nyfeler, J. Speich in [12], Poster No. O1B-38.
[30] M. Kitamura, T. Ohkuma, S. Inoue, N. Sayo, H. Kumobayashi, S. Akutagawa, T. Ohta, H. Takaya, R. Noyori, *J. Am. Chem. Soc. 110* (1988) 629.
[31] F. Spindler, Ciba-Geigy AG, Basel, private communication.
[32] M. J. Kim, G. M. Whitesides, *J. Am. Chem. Soc. 110* (1988) 2959.
[33] O. Ghisalba, D. Gygax, R. Lattmann, H. P. Schär, E. Schmidt, G. Sedelmeier, *EP-B 347374*, 1989, Ciba-Geigy.
[34] a) D. Bianchi, P. Cesti, S. Spezia, C. Garavaglia, L. Mirenna, *J. Agric. Food Chem. 39* (1991) 197; b) D. Bianchi, P. Cesti, S. Spezia, C. Garavaglia, L. Mirenna in [12], Poster O1B-07, p. 99.
[35] N. Shirane, A. Murabayashi, M. Masuko, A. Uomori, Y. Yoshimura, S. Seo, K. Uchida, K. Takeda, *Phytochemistry 29* (1990) 2513.
[36] A. Murabayashi, Y. Makisumi, *Heterocycles 31* (1990) 537.
[37] R. I. Baloch, E. I. Mercer, T. E. Wiggins, B. C. Baldwin, *Phytochemistry 23* (1984) 2219.
[38] J. K. Brent in C. J. Delp (Ed.): *Fungicide Resistance in North America*, APS Press, St. Paul, Minnesota 1988, p. 19.
[39] W. Himmele, E.-H. Pommer, *Angew. Chem. 92* (1980) 176; *Angew. Chem. Int. Ed. Engl. 19* (1980) 184.
[40] N. Götz, W. Himmele, L. Hupfer, *DE-B 2830998*, 1978, BASF.
[41] W. Himmele, H. Siegel, E.-H. Pommer, *DE-B 2907614*, 1979, BASF.
[42] G. Lorenz, E.-H. Pommer, W. Himmele, *Tagungsber. Akad. Landwirtschaftswiss. DDR 222* (1984) 233.
[43] a) A. Huxley-Tencer, E. Francotte, M. Bladocha-Moreau, *Pestic. Sci.*, in press; b) W. M. Anthony, C. J. Urch, A. C. Elliot, *EP-B 259977*, 1986, ICI.
[44] P. Benveniste, *Annu. Rev. Plant. Physiol. 37* (1986) 275.
[45] a) D. F. Traber, K. Raman, *J. Am. Chem. Soc. 105* (1983) 5935; b) G. H. Posner, M. Hulce *Tetrahedron Lett. 25* (1984) 379; c) L. A. Paquette, J. P. Gilday, C. S. Ra, *J. Am. Chem. Soc. 109* (1987) 6858.
[46] EC_{50-85} represents the effective concentration inhibiting 50–85% of the pathogen population.
[47] J. D. Naber, J. J. S. van Rensen in [3], p. 263.
[48] a) J. Amrein, A. Nyffeler, J. Rufener in [11a], p. 71; b) D. W. Cornes, T. Scott, E. J. Henderson, P. J. Ryan in [11a], p. 729.
[49] K. Kreuz, J. Gaudin, J. Stingelin, E. Ebert, *Z. Naturforsch. C46* (1991) 164.
[50] J. N. Phillips in [3], p. 183.
[51] E. Bayer, K. H. Gugel, K. Haegele, H. Hagenmeier, S. Jessipow, W. A. Koenig, W. A. Zaehner, *Helv. Chim. Acta 55* (1972) 224.
[52] a) A. Fraser, S. M. Ridley, *Planta 161* (1984) 470; b) M. Leason, D. Cunliffe, D. Parkin, P. J. Lea, B. J. Miflin, *Phytochemisty 21* (1982) 855.
[53] a) T. Takumatsu, M. Konnai, K. Tachibana, T. Tsumoka, S. Inonye, T. Watanabe, *US-A 4265654*, 1981, Meiji Seika Kaisha; b) L. Maier, P. J. Lea, *Phosphorus Sulfur Relat. Elem. 17* (1983) 1.
[54] N. Minowa, M. Hirayama, S. Fukatsu, *Bull. Chem. Soc. Jpn. 60* (1987) 1761.
[55] a) S. Grabley, K. Sauber, *US-A 4389488*, 1983, Hoechst; b) I. A. Natcher, *J. Chem. Soc. Perkin Trans. I 1989* 125.
[56] H. J. Zeiss in [12], Poster O1B-13, p. 105.
[57] a) A. Schulz, P. Taggeselle, D. Tripier, K. Bartsch, *Appl. Environ. Microbiol. 56* (1990) 1; b) K. Bartsch, R. Dickmann, P. Schmitt, E. Uhlmann, A. Schulz, *ibid. 56* (1990) 7.
[58] H.-J. Zeiss, *Tetrahedron Lett. 28*(1987) 1255.
[59] S. Hanessian, S. P. Sakov, *Tetrahedron Lett. 25* (1984) 1425.
[60] H. Seto, S. Imai, T. Tsuruoka, H. Ogawa, A. Sato, T. Sasaki, N. Otake, *Biochem. Biophys. Res. Commun. 111* (1983) 1008.
[61] K. Bauer, H. Bieringer, H. Bürstell, J. Kocur, *EP-B 106114*, 1983, Hoechst.
[62] A. Schulz, P. Spoenemann, H. Koecher, F. Wengenmeyer, *FEBS Lett. 238* (1988) 375.
[63] G. van Lommen, W. Lutz, V. Sipido, P. Huxley, J. van Gestel, H. Fischer in [12], Poster O1D-03, p. 169.
[64] W. Töpfl, *EP-B 314852*, 1987, Ciba-Geigy.
[65] R. Jones, *J. Am. Chem. Soc. 71* (1949) 644.
[66] G. M. Ramos Tombo, unpublished results.
[67] G. Mitchell, D. L. Bartlett in [12], Poster O1D-04, p. 170.
[68] E. Najano, T. Haja, M. Enomoto, K. Kamoshita, S. Hashimoto, R. Sato, R. Yoshida, H. Oshio, in [12], Poster O1C-15, p. 155.
[69] N. Yoshida, M. Kaneoya, M. Uchida, *EP-B. 290878*, 1988, Chisso Corp.
[70] a) R. H. Furneaux, J. M. Mason, P. C. Tyler, R. Blattner, K. R. Lawson, E. J. T. Chrystal, M. Glynn, B. L. Pilkington, *EP-B 302599*, 1988, DSIR, New Zealand; b) R. F. Henzell, R. H. Furneaux, P. C. Tyler, *Pestic. Sci. 30* (1990) 59; c) R. Blattner, R. H. Furneaux, J. M. Mason, P. C. Tyler, *ibid. 31* (1991) 419.
[71] K. R. Lawson, L. M. Prior in [12], Poster O1B-15, p. 107.
[72] M. Mizukai, S. Mio, *JP-B 2085287*, 1989, Sankyo; M. Nakajima, K. Itoi, Y. Takamatsu, T. Kinoshita, T. Okazaki, K. Kawakubo, M. Shindo, T. Honma, M. Tohjigamori, T. Hneishi, *J. Antibiotics* 44 (1991) 293.
[73] S. Sugai, S. Mio, S. Sato, M. Shindo, K. Kawakubo, T. Honma, in [12], Poster O1A-71, p. 83; S. Mio, R. Ichinose, K. Goto, S. Sugai, *Tetrahedron 47* (1991) 2111; S. Mio, M. Shiraishi, S. Sugai, H. Haruyama, S. Sato, *ibid. 47* (1991) 2121; S. Mio, Y. Kumagawa, S. Sugai, *ibid.* 47 (1991) 2133; S. Mio, M. Ueda, M. Hamura, J. Kitagawa, S. Sugai, *ibid. 47* (1991) 2145.
[74] L. P. A. de Jong, H. P. Benshop in [3], p. 109.
[75] a) S. Y. Wu, A. Hirashima, M. Eto, K. Yanagi, E. Nishioka, K. Moriguchi, *Agric. Biol. Chem. 53* (1989) 157; b) A. Hirashima, I. Ishaaya, R. Ueno, Y. Ichiyama, S. Y. Wu, M. Eto, *ibid 53* (1989) 175; c) A. Hirashima, R. Ueno, K. Oyama, H. Koga, M. Eto, *ibid 54* (1990) 1013.
[76] W. Maas, R. van Hes, A. C. Groscurt, D. H. Deul in R. Wegler (Ed.): *Chemie der Pflanzenschutz- und Schädlingsbekämpfungsmittel, Vol. 6*, Springer, Berlin 1980, p. 424.
[77] J. Drabek, E. Francotte, D. Lohmann, F. Bourgeois, *DE-B 4000335*, 1990, Ciba-Geigy.
[78] A. Butenandt, R. Beckmann, D. Stamm, E. Hecker, *Z. Naturforsch. B14* (1959) 283.
[79] K. Mori, *Tetrahedron 45* (1989) 3233.
[80] F. J. Ritter in [2], p. 327.
[81] C. M. Harving, *Z. Angew. Entomol. 85* (1978) 281, and references cited therein.
[82] K. Mori, *Tetrahedron 32* (1976) 1101.
[83] K. Oertle, H. Beyeler, R. O. Duthaler, W. Lottenbach, M. Riediker, E. Steiner, *Helv. Chim. Acta 73* (1990) 353. For other reports on the enantioselective synthesis of (*S*)-ipsenol (**124**) which appeared also in 1990, see [84].
[84] a) T. Imai, S. Nishida, *J. Org. Chem. 55* (1990) 4849; b) H. C. Brown, R. S. Randad, *Tetrahedron Lett. 31* (1990) 455.
[85] R. O. Duthaler, P. Herold, W. Lottenbach, K. Oertle, M. Riediker, *Angew. Chem. 101* (1989) 490; *Angew. Chem. Int. Ed. Engl. 28* (1989) 495.
[86] a) P. A. Brown, P. R. Jenkins, *J. Chem. Soc. Perkin Trans I 1986*, 1303; b) P. A. Brown, R. V. Bonnert, P. R. Jenkins, M. R. Selim, *Tetrahedron Lett. 28* (1987) 693.
[87] a) R. Wiesmann, *Landwirtsch. Jahrb. Schweiz 51* (1937) 1080; b) E. Haefliger, *Mitt. Schweiz. Entomol. Ges. 26* (1953) 258; c) U. Remund, B. I. Katsoyannos, E. F. Boller, W. Berchtold, *ibid 53* (1980) 401.
[88] B. I. Katsoyannos, *Environ. Ent. 4* (1975) 801.
[89] J. Hurter, E. F. Boller, E. Städler, B. Blattmann, H. R. Buser, N. U. Bosshard, L. Damm, M. W. Kozlowski, R. Schöni, R. Raschdorf, R. Dahinden, E. Schlumpf, H. Fritz, W. J. Richter, J. Schreiber, *Experientia 43* (1987) 157.
[90] B. Ernst, B. Wagner, *Helv. Chim. Acta 72* (1989) 165.
[91] a) H. Kunz, A. Harrens, *Liebigs Ann. Chem. 1982*, 41; b) H. Kunz, W. Sager, *Helv. Chim. Acta 68* (1985) 283.
[92] E. F. Boller, B. Ernst, H. Fritz, J. Hurter, F. Raschdorf, W. J. Richter, J. Schreiber, E. Städler, U. Burckhardt, in [12], Poster O2C-12.
[93] T. A. Van Beek, A. De Groot, *Recl. Trav. Chim. Pays Bas 105* (1986) 513.
[94] a) D. M. Norris in W. S. Bowers, W. Ebing, T. R. Fukuto, D. Martin, R. Wegler, I. Yamamoto (Eds.): *Chemistry of Plant Protection, Vol. 1*, Springer, Berlin 1986, p. 97; b) S. V. Ley, P. L. Toogood, *Chem. Brit. 26* (1990) 31.
[95] L. M. Schoonhoven in [3], p. 289.
[96] S. V. Ley, J. C. Anderson, W. M. Blaney, P. S. Jones, Z. Lidert, E. D. Morgan, N. G. Robinson, D. Santafianos, M. S. J. Simmonds, P. L. Toogood, *Tetrahedron 45* (1989) 5175.
[97] a) S. V. Ley, D. Santafianos, W. M. Blaney, M. S. J. Simmonds, *Tetrahedron Lett. 28* (1987) 221; b) Y. Nishimi, T. Iimori, M. Sodeoka, M. S. J. Shinabashi, *J. Org. Chem. 54* (1989) 3354; c) S. V. Ley in [13b], p. 80–98.
[98] Two outstanding new books, treating all aspects of pyrethroid chemistry and neurotoxic activity against insects, appeared in the series *Chemistry of Plant Protection* (W. S. Bowers, W. Ebing, D. Martin, R. Wegler (Eds.), Springer, Berlin 1990: a) *Vol. 4* by K. Naumann: *Synthetic Pyrethroid Insecticides: Structures and Properties;* b) *Vol. 5* by K. Naumann: *Synthetic Pyrethroid Insecticides: Chemistry and Patents.*
[99] For the most part we follow in this paper the unambiguous designation of chiral pyrethroids proposed by N. F. Janes (*Pestic Sci. 18* (1987) 149). The "1 *R*, *cis*" system of designation of stereochemistry of the cyclopropane ring substituents, avoids a confusing *R* vs. *S* change at C3,

required by Cahn–Ingold–Prelog convention, when priority orders of the side-chain substituents are changed.
[100] L. Crombie in G. G. Lund (Ed.): *NEUROTOX '88, Molecular Basis of Drug and Pesticide Action*, Excerpta Medica, Amsterdam 1988, pp. 3–25.
[101] J. Martel, C. Huynh, *Bull. Soc. Chim. Fr. 1967*, 985.
[102] M. Elliott, *Pestic. Sci. 27* (1989) 337 and references cited therein.
[103] There are, however, four exceptions in this table: three non-cyclopropane pyrethroids (**152**–**154**) are marketed apparently as esters containing racemic 3-phenoxybenzaldehyde cyanohydrin [98a], whereas commercial tralomethrin **147** is a 60:40 mixture of two diastereoisomers arising from the brominated side chain at C 3. In contrast to other cases, the two diastereoisomers of **147** are about equally effective because they act first by losing bromine, thus behaving as 'propyrethroids' for **146**.
[104] a) T. Umemura, H. Hirohara, *ACS Symp. Ser. 389* (1989) 371; H. Danda, Y. Fukuwara, T. Umemura, *Synlett 1991*, 441.
[105] **144** is sometimes called 'bioethanoresmethrin'; see e.g., J. P. Leahey (Ed.): *The Pyrethroid Insecticides*, Taylor & Francis, London 1985.
[106] Marketed always in mixtures with **142** or **146**.
[107] B. Babin, J. Demassey, J. P. Demonte, P. Deutheil, J. Tessier, in [12], p. 93.
[108] W. Behrenz, J. Hartwig, B. Homeyer, K. Naumann in [12], p. 18.
[109] J. Tessier, *Chem. & Ind. (London) 1984*, 199 and references cited therein.
[110] P. Ackermann, F. Bourgeois, J. Drabek, *Pestic Sci. 11* (1980) 169.
[111] D. Belluš, B. Ernst, *Angew. Chem. 100* (1988) 820; *Angew. Chem. Int. Ed. Engl. 27* (1988) 797.
[112] H. Greuter, J. Dingwall, P. Martin, D. Belluš, *Helv. Chim. Acta 64* (1981), 2812.
[113] A. Krief, Ph. Lecomte, J. P. Demoute, W. Dumont, *Synthesis 1990*, 275, and references cited therein.
[114] L. Gsell, S. Farooq, *EP 311565* 1989, Ciba-Geigy; *Chem. Abstr. 111* (1989) 148927.
[115] G. M. Ramos Tombo, E. Didier, B. Loubinoux, *Synlett 1990*, 547.
[116] S. Niwa, K. Soai, *J. Chem. Soc. Perkin Trans. 1 1990*, 937.
[117] *County Nat West, Agrochemical Service*, Agrochemical Product Section, Edinburgh, April 1990.
[118] M. H. Bushell in L. Crombie (Ed.): *Recent Advances in the Chemistry of Insect Control II* (Spec. Publ. 79), Royal Society of Chemistry, Cambridge 1990, p. 125, and references cited therein.
[119] K. Tsushima, T. Yano, T. Takagaki, N. Matsuo, M. Hirano, N. Ohno, *Agric. Biol. Chem. 52* (1988) 1323.

Phytochrome, the Visual Pigment of Plants

By Wolfhart Rüdiger* and Fritz Thümmler

Dedicated to Professor Kurt Schaffner on his 60th birthday

Plants require light for photosynthesis. In order to adapt to the light conditions in their particular habitat, they have developed various photoreceptor systems. Of these, phytochrome allows even two-color vision in the red/far-red region. The photoreceptor phytochrome is of interest not only to botanists, but also to natural product chemists, photochemists, biochemists, photobiologists, and recently molecular biologists. Despite numerous studies, there are still considerable gaps in our knowledge of this photoreceptor. This article first describes the basic structural studies of the tetrapyrrole chromophore and its photochemical *cis–trans* isomerization, which is the source of the chromoprotein's photochromism. In the section on the protein moiety, beside other topics, the domain structure of phytochrome and the conformational changes during phototransformation are discussed. Finally, the known phytochrome genes are used to derive phylogenetic relationships, and possible structure-function relationships are discussed.

1. Introduction

After germination, higher plants remain firmly rooted in one place. They have therefore developed strategies to adapt themselves to their particular environmental surroundings. One important environmental factor is light, which is required for photosynthesis. The adaptation of the photosynthetic apparatus to light quality is well known ("light" and "shade" plants or leaves). Many other processes in the life of the plant are also controlled by light, from germination, growth, and greening to flower formation. These may be collected under the term photomorphogenesis.[1] Photomorphogenesis is regulated by photoreceptors. The effective spectral region can be measured as an action spectrum corresponding to the absorption of the particular photoreceptor; by this means at least three photoreceptors may be distinguished in plants. These are active in the UV-B, UV-A/blue, and red/far-red regions. The first two of these photoreceptors have been only poorly characterized to date, but the red/far-red receptor, "phytochrome", has been identified and already studied in detail.

Phytochrome was discovered forty years ago in Beltsville (Maryland).[2] *Borthwick*, *Hendricks*, and their colleagues were interested in the photoperiodic control of flower formation and the light regulation of seed germination. The decisive discovery was that in both cases—with an almost identical action spectrum—red light (λ_{max} = 660 nm) displayed an induction effect which could be abolished by subsequent far-red illumination (λ_{max} = 730 nm).[3,4] A photochromic photoreceptor was postulated, which was thought to exist in a physiologically inactive, red-absorbing form (Pr) and in a physiologically active, far-red absorbing form (Pfr). This was subsequently confirmed by isolation of the photoreceptor. The substance is a chromoprotein which is present in only very low levels in plants; even in seedlings grown in the dark and therefore free of chlorophyll, the photoreceptor cannot be seen with the naked eye. On the other hand, because of its photochromic nature it can readily be detected in such tissue with sensitive spectroscopic methods.

$$\mathrm{Pr} \underset{730\ \mathrm{nm}}{\overset{660\ \mathrm{nm}}{\rightleftharpoons}} \mathrm{Pfr} \rightarrow \text{physiological reaction}$$

The preferred starting material for isolation of phytochrome was dark-grown ("etiolated") oat seedlings, which contain relatively high levels of this photoreceptor in the tips of the coleoptiles (seed leaf sheaths). Because of proteases, which act when the plant cell is broken open, for many years only proteolysis products of the native photoreceptor were isolated ("small phytochrome", 60 kDa; "large phytochrome", 114–118 kDa). Not until 1982 was it possible to determine the size of the intact molecule (monomer size of oat phytochrome, 124 kDa), and to isolate it successfully.[5,6] The photochromic properties are retained on isolation; saturating illumination with far-red light (λ_{max} = 730 nm) transforms 99% of the phytochrome into the Pr form, while saturating illumination with red light yields about 85% Pfr with 15% Pr. Figure 1 shows the absorption spectra of the two

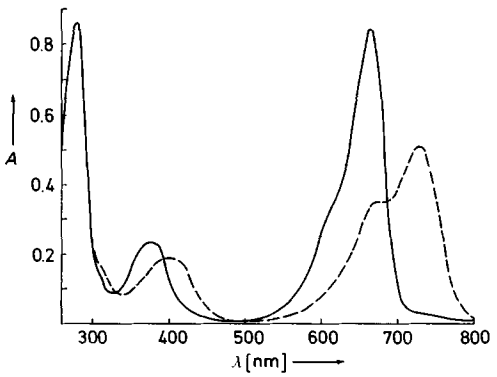

Fig. 1. Absorption spectra of 124 kDa phytochrome from etiolated oat in 10 mM phosphate buffer, pH 7.8 (from ref. [7]). The spectra were determined at 4°C after saturating illumination with far-red (—) and red (– – –) light. The A_{667}/A_{280} ratio of the Pr form (here 0.99) is a measure of the purity of the isolated phytochrome.

[*] Prof. Dr. W. Rüdiger, Dr. F. Thümmler
Botanisches Institut der Universität
Menzingerstrasse 67, W-8000 München 19 (FRG)

forms. Native phytochrome is a dimer consisting of two identical subunits. Each subunit is made up of an *N*-terminal domain containing the chromophore (N in Fig. 2) and a *C*-terminal domain (C in Fig. 2). The quaternary structure of

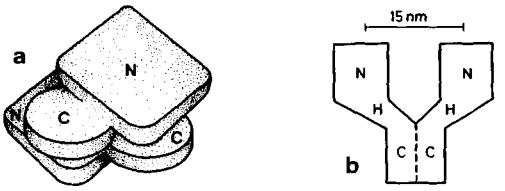

Fig. 2. Model of the dimeric phytochrome molecule, derived from a) small-angle X-ray scattering and electron microscopy (redrawn from ref. [8]) and b) electron microscopy (from ref. [9]).

pea phytochrome has been derived from small-angle X-ray scattering and electron microscopy[8] (cf. Fig. 2). For oat phytochrome, a very similar Y form has also been established by electron microscopy.[9]

2. The Tetrapyrrole Chromophore

2.1. The Structure of Phytochromobilin

The absorption of visible light was an early indication of a nonprotein chromophore in phytochrome, but for a long time there was only speculation about its chemical nature. An open-chain tetrapyrrole structure was not demonstrated until 1969,[10] by oxidative degradation and identification of the products.

Oxidative degradation with chromic acid or dichromate had already been developed as a simple, analytical micromethod for the determination of bile pigment structures, and requires no more than 1 nmol of a tetrapyrrole.[11] This method measures the kinetics of pigment decolorization, which proceeds considerably more rapidly for open-chain tetrapyrroles (bile pigments) than for porphyrins and chlorophyll derivatives. In addition, characteristic degradation products were identified (e.g. by thin-layer chromatography and specific staining), and consisted of β-substituted pyrroledialdehydes, maleimides, and succinimides. The original β-substituents of the tetrapyrrole are retained in the degradation products. Many tetrapyrroles have been studied by this method.[12]

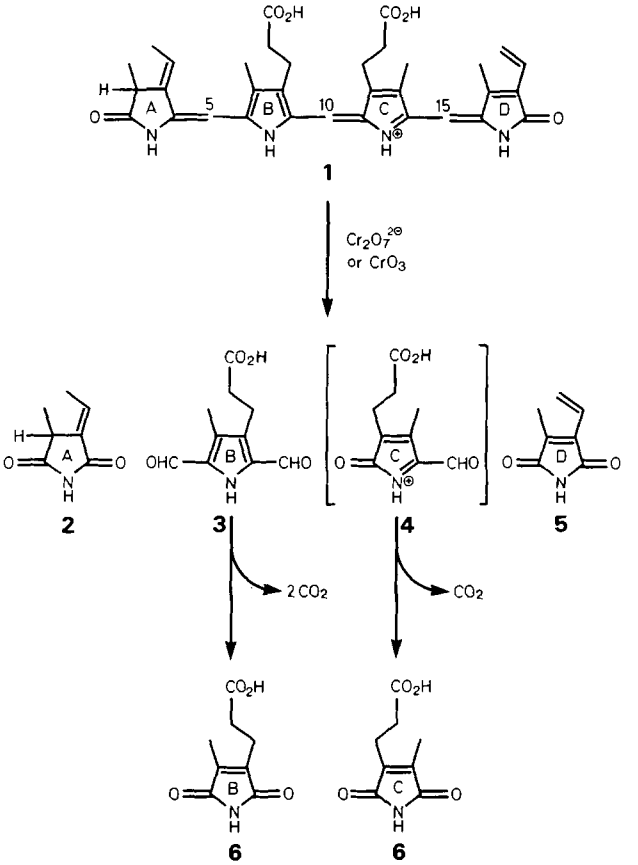

Fig. 3. Chromic acid and dichromate degradation of phytochromobilin (**1**). The degradation is shown here for synthetic **1**. The reactions for the analytical studies are shown in Fig. 4.

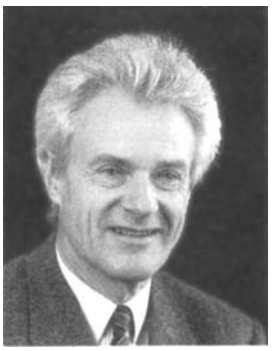

Wolfhart Rüdiger was born in 1933 in Stolp/Pommern, and studied chemistry from 1953 to 1959 at the University of Würzburg. He obtained his doctorate in 1961 under F. G. Fischer on a chlorophyll-related subject and then spent two years at the Max-Planck-Institut for Medicinal Research, Heidelberg, and at the marine biological station in Naples. His work there concerned the biochemistry of vanadium, in particular hemovanadium, in a group of marine animals (tunicates). From 1963 he was a postdoctoral research assistant at the Institute of Biochemistry at Saarbrücken University, where he habilitated in 1969 with a study on open-chain tetrapyrroles in animals and plants. Since 1971 he has been Professor for Phytochemistry and Chairman of the Institute of Botany at Munich University. Besides phytochrome his interests include the regulation of chlorophyll biosynthesis and the structure and function of novel plant germination inhibitors.

Fritz Thümmler was born in 1953 in Rosenheim, and studied biology from 1975 to 1981 at Munich University. After obtaining his doctorate in 1984 on a subject from the phytochrome field under Professor Rüdiger, he went for two years to Professor D. P. S. Verma at the McGill University, Montreal. There he worked on nodulins (plant proteins which are induced on symbiosis with rhizobial bacteria). Since 1987 he has been a postdoctoral assistant at the Institute of Botany, Munich University.

The oxidative degradation of the phytochrome chromophore was first carried out without cleaving the covalent bond to the protein.[10] The only products identified were **3** and **6**, derived from rings B and C (Fig. 3). In order to study the covalent bond to Ring A, thioethers (e.g. **7**) were synthesized as model substances[13] (Fig. 4a). Alkaline cleavage of these thioethers, or of their sulfone products from chromic acid degradation, was optimized.[14] Thus, degradation product **2** from Ring A of the tetrapyrrole was released and identified in a two-step reaction (Fig. 4b). The configurations of

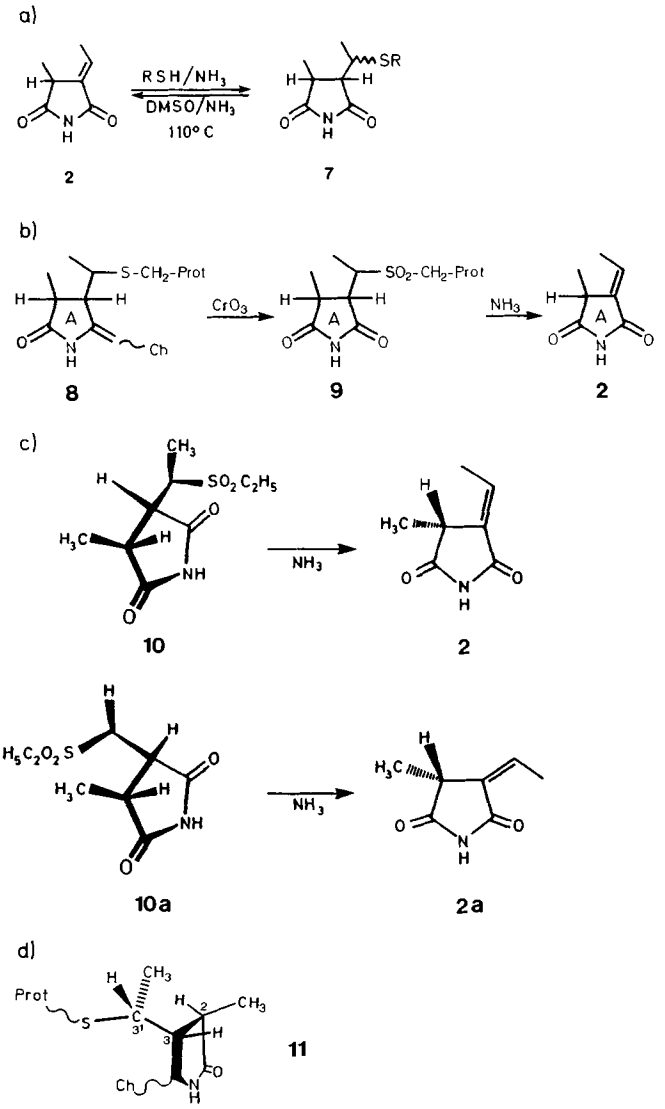

Fig. 4. Model experiments and degradation reactions for structure determination of ring A of phytochromobilin. a) Model synthesis of **7** from **2** and elimination of the thiol [13]. b) Isolation of **2** from phytochrome **8** via the protein-bound **9** [16]. c) Stereoselectivity of the elimination reaction of sulfones **10** or **10a** to olefins **2** or **2a** [14,15]. d) Derived configuration of ring A of the tetrapyrrole chromophore [16]. DMSO = dimethyl sulfoxide, Prot = protein, Ch = chromophore.

the model sulfones **10** and **10a** (determined by X-ray crystallography)[15] and the appearance of *Z,E*-isomeric degradation products **2** and **2a** (Fig. 4c) even yielded some evidence for the absolute configuration of the thioether bond in phytochrome. Stereoselective elimination from phytochrome affords only **2** and not **2a**; from this a 2*R*,3*R*,3*R'* configuration was deduced for Ring A and its substituents in phytochrome (Fig. 4d).[16]

The intact tetrapyrrole chromophore is not cleaved from the protein under the alkaline conditions described in Figure 4b. Clearly, oxidation to the succinimide and, in particular, oxidation of the thioether to the sulfone are required for a facile elimination. In contrast, the thioether was successfully cleaved, while retaining the tetrapyrrole, by using HBr in glacial acetic acid (Scheme 1).[17] However, a complication

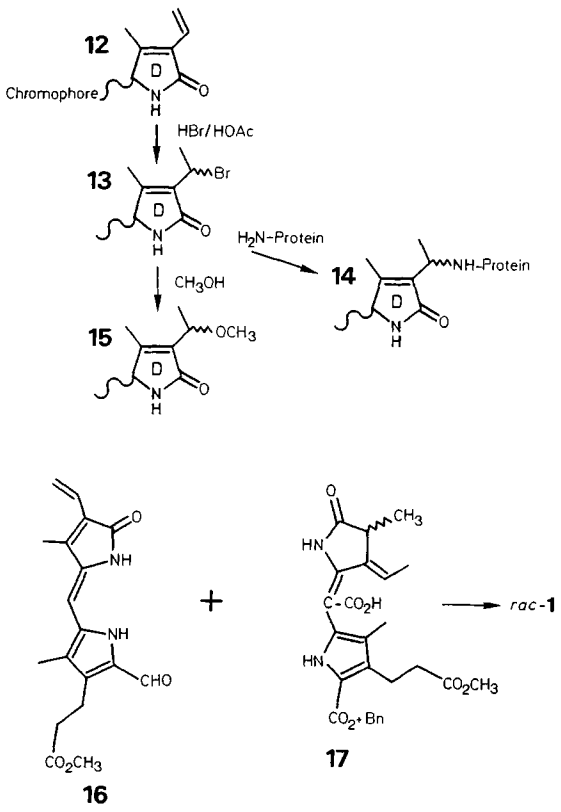

Scheme 1.

arose at Ring D (**12** in Scheme 1); HBr obviously adds very readily to the vinyl group, and the resulting bromo derivative **13** then reacts with nucleophilic groups on the protein to give **14**. This difficulty was avoided by not using the intact chromoprotein for cleavage of the chromophore, but only a chromopeptide obtained by proteolysis, consisting of eight to eleven amino acids in addition to the chromophore. Workup with methanol yielded mainly methanol adducts of the chromophore (**15**). The reaction steps from **12** to **15** were repeated with synthetic **1**.[17,18] This sequence of reactions, together with the total synthesis of **1** from **16** and **17**,[18] can be regarded as a "classical chemical" structure determination of the phytochrome chromophore.

Independently of these studies in Munich, *J. C. Lagarias* in Berkeley has investigated chromopeptides from phycocyanin and phytochrome by ^{1}H NMR spectroscopy. The chromoprotein phycocyanin is a light-harvesting pigment in cyanobacterial photosynthesis.[19] It contains several phycocyanobilin chromophores (one in the α subunit, two in the β subunit), which are closely related to phytochromobilin. Since phycocyanin is easily obtained in large quantities, it

has been used by several groups as a model for studies on phytochrome. *Lagarias* et al. made use of synthetic peptides and in order to assign the amino acid signals synthesized the sequence of one chromopeptide from phytochrome, Leu-Arg-Ala-Pro-His-(Ser,Cys)-His-Leu-Gln-Tyr, which had already been reported in 1971.[20] They also made a heptapeptide corresponding to a chromopeptide from phycocyanin.

By comparison with the known ^{1}H NMR spectrum of free phycocyanobilin, the structure of the bound phycocyanobilin was confirmed to be **18**, thus localizing the thioether bond.[21] A subsequent study of the phytochromopeptide **19**[22] showed that the only structural difference in the chromophore was in the substituents of Ring D: in phytochromobilin, a vinyl group replaces the ethyl group of phycocyanobilin.

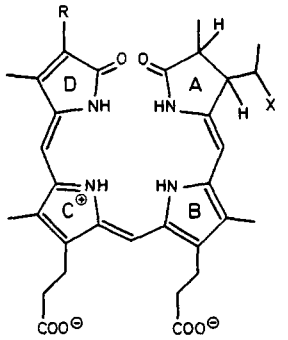

18 R = Ethyl X = Ala-Ala-Cys-Leu-Arg-Asp-Hsl
19 R = Vinyl X = Leu-Arg-Ala-Pro-His-Ser-Cys-His-Leu-Gln-Tyr

Scheme 2. Hsl = homoserine lactone.

2.2. The Chromophore Structure in the Pfr Form

The interaction of the chromophore with the native protein is essential for the photochemistry of phytochrome, since neither free phytochromobilin nor denatured phytochrome in the Pr form show any spectral changes on illumination. Several authors have suggested[22, 23] that photoconversion of phytochrome does not represent a permanent change in the chemical structure of the chromophore, but that only protein interactions or binding to amino acids are altered. This was disproved, however, by our observation that when the reactions were performed in the dark, denaturation with urea[24] or proteolysis with pepsin[25] led to products with different spectral properties from the Pr and Pfr forms (Fig. 5). The products from Pfr are light-sensitive; on illumination they are immediately converted into the products that are obtained from the Pr form. This light-sensitivity could be the reason why other authors[20] have failed to observe the difference between Pr and Pfr peptides. The difference is not limited to spectral properties—Pr and Pfr peptides can be separated by chromatography, even though they have the same amino acid composition. The difference must therefore lie in the chromophore. Since the same tetrapyrrole oxidation products are obtained from the Pr and Pfr

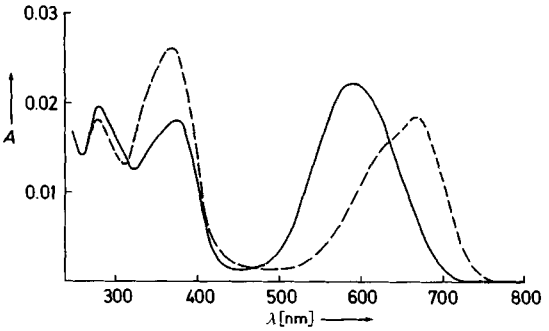

Fig. 5. Absorption spectrum of the Pfr chromopeptide in 1% aqueous formic acid. The spectrum was recorded first after isolation of the peptide by chromatography in the dark (—) and then after illumination with white light for 10 s (– – –). The second spectrum is identical to that of the Pr peptide (from ref. [28]).

peptides,[25] the difference must be located in the methine bridges, which are destroyed on chromic acid oxidation. Various model compounds[26] had to be rejected, since they did not display the light-sensitivity of the Pfr peptide. Eventually, the *Z,E* isomerization of tetrapyrroles proved to be a suitable model reaction; by using a method of *Falk* and co-workers[27] (Fig. 6a), this isomerization can also be carried out on chromopeptides from phycocyanin and phytochrome.[28] The position of the isomerization in the Pfr peptide was then traced to the C15–C16 double bond by ^{1}H NMR spectroscopy[29] (Fig. 6b). Hence, the Pr chromophore is in the 15*Z*,*syn*-form and the Pfr chromophore in the 15*E*,*anti*-form.

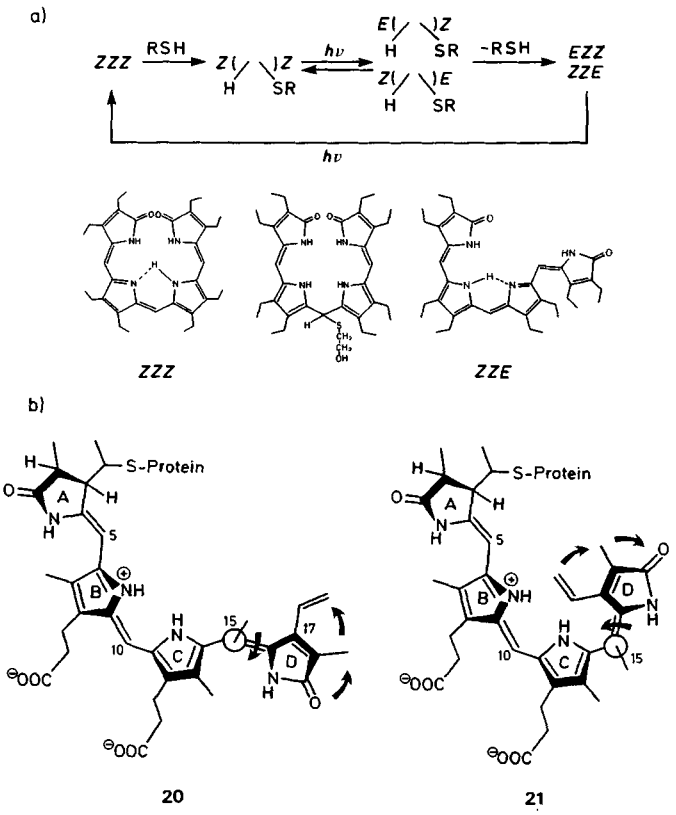

Fig. 6. *Z,E* isomerism in open-chain tetrapyrroles. a) Octaethylbiliverdin as example of the preparation of a bilatriene with *E* configuration according to ref. [27]. b) Structure of phytochromobilin in the Pr form **20** and the Pfr form **21**. Conformation **20** corresponds to the configuration of phycocyanobilin in native phycocyanin, as determined by X-ray analysis [54]. The arrows show the displacement of ring D on conrotation of the C14–C15 and C15–C16 bonds from **20** (*Z,syn*) to **21** (*E,anti*) and vice versa (cf. Section 2.3).

phore can be assigned the 5*Z*,10*Z*,15*Z* configuration **20**, and the Pfr chromophore the 5*Z*,10*Z*,15*E* configuration **21**.

One possible objection to this conclusion is that the 15*E* configuration might arise merely as an artifact of the proteolysis of Pfr. The reasoning behind this objection is, for example, the marked shift in the long-wavelength absorption maximum from 730 nm to 600 nm on proteolysis (cf. Figs. 1 and 5). This spectral shift will be discussed in Section 2.3. The objection ignores the fact that the 15*E* isomer is converted into the 15*Z* isomer in an exergonic reaction (ΔG° is at least $-20\ kJ\,mol^{-1}$).[30] The reverse reaction is not possible with free phytochromobilin. This is related to the steric requirements of the β substituent. Only for the *E* isomer does a significant torsion angle arise, leading to partial decoupling of the π system and a hypsochromic shift in the absorption bands. In bilatrienes methylated at N21 and N24, similar steric hindrance yields a torsion in both the *Z* and the *E* configurations. Correspondingly, the photoisomerization ($Z \rightleftharpoons E$) occurs in both directions here, to give a measurable equilibrium; for example, for a 21,24-dimethyl bilatriene to $Z,Z,Z \rightleftharpoons E,Z,Z \rightleftharpoons E,Z,E$.[31]

Differences between native Pr and Pfr have since been measured by resonance Raman spectroscopy[32] and by SERSS (Surface-Enhanced Resonance Raman Scattering Spectroscopy).[33] In both cases, the differences measured were interpreted in the sense of a 15*Z* configuration for the chromophore in the Pr form and a 15*E* configuration for the Pfr form. This confirmed the data and conclusions from the chromopeptides. Fourier transform difference infrared spectroscopy[34] shows similarities, at least, between *Z*,*E*-isomeric model chromophores and the two phytochrome forms. According to the infrared spectra, the chromophore is protonated in both the Pr and the Pfr forms.

We discussed the *Z*,*E* isomerization of the chromophore as a candidate for the primary photochemical reaction of phytochrome as early as 1985.[35] A *Z*,*E* isomerization of the chromophore retinal is believed to be the primary photoreaction in the visual pigment of humans and mammals. By convergent evolution, the same principle thus seems to be realized in chemically quite divergent chromophores (a tetrapyrrole for phytochrome, an isoprenoid for rhodopsin). The actual photoconversion consists of the isomerization of a C–C double bond, which requires only minimal activation energy from an excited state. The reverse reaction in the dark is blocked because of the higher thermal activation energy for the isomerization (ca. $108\ kJ\,mol^{-1}$ for the tetrapyrrole[30]), and a stable photoproduct is generated. Stepwise dark reactions then take place through interactions with the protein. Both in rhodopsin and in phytochrome, the intermediates of these reactions can be observed in the phototransformation.

2.3. Intermediates

Relaxation products on the pathways Pr → Pfr or Pfr → Pr, which differ from one another in their absorption spectra, are described as intermediates. The absorption spectra of linear tetrapyrroles can be affected by very many factors;[36] for phytochrome, interactions of the apoprotein with phytochromobilin must be taken into consideration. Both for phytochrome and for rhodopsin, discontinuous spectral changes are noticeable; the individual intermediates are hence clearly distinct from one another. On the pathway from Pr to Pfr at least four intermediates can be distinguished,[37] while at least two can be seen on the way from Pfr to Pr.[38] The scheme of intermediates (Fig. 7) was initially derived from absorption measurements at low temperatures, where the individual intermediates are "frozen". The

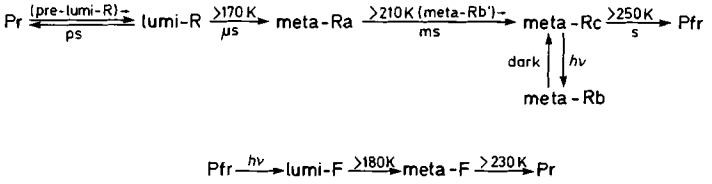

Fig. 7. Schematic diagram of the photointerconversion of the two phytochrome forms via several intermediates (from ref. [38], expanded). The temperatures given are the minimum values for the individual relaxation steps; the times indicate the order of magnitude of the relaxation times at room temperature.

absorption measurements required a clear glass, which was obtained in buffer with 66% glycerine. All the data in Figure 7 and Table 1 refer to this solvent mixture. Thus, below 170 K illumination of Pr affords only lumi-R as intermediate (since $\lambda_{max} \approx 700$ nm it is called I_{700} by some authors), which on warming without further illumination is gradually transformed into Pfr, via the subsequent intermediates. At suitable higher temperatures, the intermediates meta-Ra or meta-Rc are obtained immediately; meta-Rb is formed only in native phytochrome under constant illumination, and relaxes in the dark to meta-Rc. With progressive proteolysis to phytochrome fragments of size 114/118 kDa, 60 kDa, and 39 kDa, the proportion of meta-Rb increases steadily. Many authors combine the products meta-Ra, meta-Rb, and meta-Rc into the intermediate Ibl (= bleached phytochrome), but different absorption spectra are quite distinguishable (Table 1).

Table 1. Spectroscopic data for the phytochrome forms, measured at −140 °C in glycerine buffer solution (from ref. [38]). f_1 and f_2 = relative oscillator strength of the first and second absorption bands.

phytochrome form	first absorption band λ_{max} [nm]	ε [$dm^3mol^{-1}cm^{-1}$]	second absorption band λ_{max} [nm]	ε [$dm^3mol^{-1}cm^{-1}$]	f_2/f_1
Pr	667	140000	380	50000	1.10
Pfr	741	119000	403	41000	1.10
a) path Pr → Pfr					
lumi-R	693	190000	384	47000	0.86
meta-Ra	663	86000	386	52000	1.37
meta-Rb (P_{bl})	665	40000	380	57000	2.29
meta-Rc	725	80000	387	50000	1.45
b) path Pfr → Pr					
lumi-F	673	105000	388	44000	1.02
meta-F	660	133000	381	55000	1.15

The same (or at least very similar) intermediates also occur at room temperature, and can be studied by time-resolved spectroscopy.[39] The intermediates pre-lumi-R[40] and meta-R'b[37] have been described, which had not been found previously by other authors. The times given in Figure 7 only

show the order of magnitude of the duration of intermediate transitions. Both Pr fluorescence[41,42] and absorption changes for the early intermediates[43] can only be explained by at least two parallel but kinetically distinct components. However, complex kinetics can also appear in absorption measurements when intermediates that follow one another overlap strongly in their absorption.[37,44]

Up till now, no direct experimental data is available on the chemistry of the intermediates. The following general observations can be made. The primary photochemical reaction, which is possible even in an ice matrix at temperatures below 170 K, must take place in a protein pocket which protects the chromophore from outside. The chromophore is better protected from attack by chemical agents in the Pr form than in the Pfr form.[45] The protein pocket must be large enough to allow, for example, the *Z,E* isomerization of the chromophore, but not so large that the isomerization can occur quite freely, without any interaction with the protein environment. A complete rotation of Ring D, which also requires temporarily a large space at right angles to the plane of the ring is very hard to imagine—at least not on the picosecond time scale. Conrotation of the C14/C15 single bond with the C15/C16 double bond (Fig. 6) would require the least space. Ring D is thereby displaced with respect to the rest of the molecule only within the plane of the ring, and does not rotate. This model was proposed by us in 1985[35] and is supported by recent resonance-Raman studies,[32] which show that the chromophore possesses a C15-*Z,syn* conformation in the Pr form, and a C15-*E,anti* conformation in the Pfr form.

In the picosecond range this movement only has to reach the activation threshold for the *Z,E* isomerization; the tetrapyrrole will then continue to relax in the direction given by the arrow. If the protein pocket is small enough, the protein must follow this relaxation. The consequence of this would be the conformational changes which eventually lead, via the intermediates, to physiologically active Pfr. As well as these purely steric interactions, however, ionic interactions between the protonated, positively charged chromophore and the charged amino acid residues could well play a part in the conformational changes enforced by the chromophore, as could hydrogen bond interactions.

Comparing the oscillator strengths (Table 1) reveals that the ratio f2/f1 has a particularly high value for the intermediate meta-Rb. This high value corresponds to a protein-free tetrapyrrole in a cyclic–helical conformation, while Pr, Pfr, and the other intermediates appear from the oscillator strengths to be present in a more extended conformation, brought about by interactions with the protein. *H. Falk*[36] has pointed out that because of the many different influences on the electronic spectra of open-chain tetrapyrroles, such data cannot be used alone to draw conclusions on conformation. However, there is other evidence for a particularly small interaction between chromophore and protein in illuminated phytochrome, where meta-Rb is preferentially accumulated; the chromophore and its binding site are more accessible to chemical agents during illumination than in the dark for the Pr or the Pfr form.[45,46]

The data in Table 1 also indicates that the characteristic long-wavelength absorption band of the Pfr form appears only during the last relaxation steps, and thus is not directly associated with the primary photoreaction. By acid denaturation of the meta-Rb intermediate and spectral measurements, we have been able to show that the *Z,E* isomerization takes place before the Pfr band appears.[47] In a 39 kDa fragment, which is still photoreversible and in principle forms the same intermediate as Pr, the long-wavelength absorption is completely absent.[48] Clearly, this fragment is lacking the portion of the peptide chain which needs to interact with the chromophore in order to generate the long-wavelength absorption band. A possible candidate for such an interaction is a point charge, which can effect a bathochromic shift if it is placed in a defined spatial position relative to the π system.[49]

3. Studies of the Protein

3.1. Domain Structure

Electron microscopy and small-angle X-ray scattering studies can only reveal the rough outlines of the shape of the phytochrome molecule (Fig. 2). Biochemical studies, however, have yielded information on the domain structure of phytochrome. Partial proteolysis, electrophoretic separation of the fragments, and studies with monoclonal antibodies or monospecific antisera[50,51] have yielded a picture of a relatively compact chromophore-containing 64 kDa domain which is relatively inert to further proteolytic digestion. This domain lies in the *N*-terminal half of the peptide chain (Fig. 8a), and corresponds to the "small" phytochrome iso-

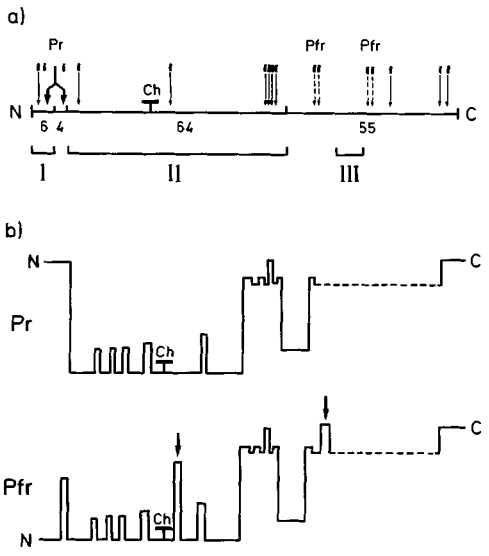

Fig. 8. Domain structure of phytochrome A from etiolated oat. The peptide chain is indicated by a continuous line from the *N*-terminus (N) to the *C*-terminus (C). Ch = tetrapyrrole chromophore. a) The roman numerals refer to three classes of antibodies, whose epitopes have been localized in the regions indicated. The arabic numerals indicate the size of the corresponding domains in kDa (from ref. [50]). The arrows mark sites of proteolytic attack on partial proteolysis: Pfr = preferred attack in the Pfr form, Pr = preferred attack in the Pr form (from ref. [51]). b) Schematic diagram of the conformation of the peptide chain in the Pr and Pfr forms, obtained from kinetic partial proteolysis experiments. Exposed parts of the peptide chain, which contain early proteolytic cleavage sites, are raised. Regions drawn lowered, which are in the interior of the globular protein, contain potential proteolytic cleavage sites which are only attacked later. The dashed region of the peptide chain is cleaved rapidly and often, and therefore yields no defined fragments. Two regions that are only exposed in the Pfr form are marked with arrows (from ref. [54]).

lated at the beginning of phytochrome research. The peptide regions responsible for direct interactions with the chromophore and hence for photochromism are localized here. The area between amino acids 65 and 400, or 200 and 400,[52, 53] is essential for the spectral properties of the Pr chromophore, while the region from 420 to 600[53] is required for the long-wave absorption of the Pfr chromophore. Of all the amino acids essential for interaction with tetrapyrrole in this region, arginine-316 (five residues *N*-terminal to the chromophore-binding site cysteine-321) should be specially mentioned, as it is conserved in all known phytochrome sequences and is also found in the corresponding position in all phycocyanin sequences. Through electrostatic interaction with a propionic acid side chain on the chromophore, this arginine (together with the chromophore-binding cysteine) is responsible for the extended conformation of the tetrapyrrole in phycocyanin.[54] We also assume a similar extended conformation for the phytochrome-chromophore (Fig. 6b). In contrast, the *C*-terminal chromophore-free domain (ca. 55 kDa in size) is readily attacked by proteases, and is therefore rapidly degraded to small, poorly defined peptides. The connection between the chromophore-containing domain and the chromophore-free domain ("hinge region") is attacked particularly rapidly by proteases. Similarly, a proteolytic attack can occur at a series of sites in the extreme *N*-terminal region (ca. 10 kDa) of phytochrome (Fig. 8a).

After elucidation of the primary structure of oat phytochrome (cf. Section 4.1) the *N*-terminal sequences of the peptide fragments were determined and then assigned within the total sequence. The points of protease attack on the amino acids could then be determined precisely.[53, 55] Since the *N*-terminus of the entire peptide chain is blocked, the phytochrome sequence cannot be determined by the Edman method. Mass spectrometry of the *N*-terminal peptides showed acetylserine to be the *N*-terminus of oat phytochrome; the methionine situated immediately before the serine in the DNA sequence is obviously removed before acetylation.[56] By following the kinetics of proteolytic attack at given sites, highly exposed regions of the peptide chain can be distinguished from those situated within the molecule in regions better shielded from proteolytic attack (Fig. 8b). Preferential protease attack is observed in the "hinge region", close to the *C*-terminus and—only in the Pr form—close to the *N*-terminus.

The 6–10 kDa *N*-terminal region of the peptide chain plays a special role. If it is removed by proteolysis[57] or blocked by antibody binding,[58] the absorption maximum of the Pfr form is shifted from 730 to ca. 722 nm, the rate of dark reversion of Pfr to Pr is increased by a factor of at least 10, the chromophore in the Pfr form is more accessible to external chemical agents, and the circular dichroism (CD) spectrum of Pfr in the 200–230 nm region approaches that of the Pr form. This all suggests that there is a direct interaction between this part of the peptide chain and the chromophore in the Pfr form;[59] however, an indirect influence of this region on the protein–chromophore interaction cannot be ruled out.

The *C*-terminal 55 kDa domain does not take part in chromophore–protein interactions. Instead it is responsible for dimerization of phytochrome. On gel chromatography, phytochrome displays an apparent molecular mass of 320–360 kDa;[51] equilibrium centrifugation gives a value of 253 kDa.[60] The data suggest a dimer of nonglobular nature (cf. Fig. 2). After partial proteolysis, only the fragments containing the *C*-terminal domain migrate on gel chromatography at 2–3 times the value of their molecular mass determined by sodium dodecyl sulfate (SDS)-gel chromatography; *N*-terminal, chromophore-containing fragments show the same molecular mass on gel chromatography and SDS-gel chromatography.[60] Experiments on cross-linking the peptide chains with glutaraldehyde or "dimethyl suberimidate" (dimethyl octanediimidate)[60] also suggest contact sites in the *C*-terminal domain for the phytochrome dimer. The schematic diagram of phytochrome dimers (Fig. 2) was partly derived from these experiments.

3.2. Differences between Pr and Pfr

Although conformational effects in the protein as a result of phototransformation have long been postulated, clear changes in shape[8] or protein conformation[61, 62] have not been found. Even the 3% increase in α-helix content,[58 or 59] which was determined from the circular dichroism spectrum in the UV, could not be confirmed by Fourier transform difference-IR spectroscopy.[34] Presumably the tetrapyrrole chromophore also contributes to the CD spectrum in the UV region. The differences between Pr and Pfr in retention time on gel chromatography, which were at first interpreted as a change in shape of the molecule,[51] can also be traced to other causes, presumably a change in the surface charge.[63]

In contrast, local changes in the surface structure of phytochrome on phototransformation have been demonstrated by various methods. Among these are, for example, preferential phosphorylation of the Pr form in the *N*-terminal region,[64] a more negative surface charge on the Pfr form (associated with the exposed site of the aspartate and glutamate residues in the region between amino acids 340–355),[63] better accessibility of the chromophore in the Pfr form,[45] differences in the affinity of various antibodies to Pr and Pfr,[58, 65] differences in the exposure of aromatic amino acids,[66] and differences in partial proteolysis, as discussed above. As can be seen in Figure 8b, the *N*-terminal region (ca. 10 kDa) is easily accessible to proteolysis in the Pr form, but not in the Pfr form. Two regions around amino acids 354 and 753 are especially conspicuous, and are attacked preferentially in the Pfr form.[55] Such regions are of interest as potential components of an "active site" on the surface of the Pfr form; however, neither an active site nor a function associated with one has yet been demonstrated.

3.3. Studies with Antibodies

Phytochrome is probably the plant protein that has been explored most thoroughly with monoclonal antibodies.[67] Of these investigations just a few are presented here.

Phytochrome can be measured quantitatively with the help of antibodies. One application is the measurement of phytochrome distribution within a seedling (Fig. 9).[67, 68] The concentration of the photoreceptor is highest in the

coleoptile tip, the shoot tip, and the root tip. This distribution had also been found by using spectroscopy[69] and immunocyto-chemistry.[70] When the intracellular localization in etiolated seedlings was studied, the Pr form was found to be evenly distributed in the cytoplasm. On conversion into the Pfr form, however, it is rapidly bound to discrete, as yet unidentified sites in the plasma membrane (plasmalemma).[71] In green, lower plants (e.g. the fern *Adiantum*[72] and the alga *Mougeotia*[73]), however, phytochrome appears to be permanently localized, in a dichroic conformation, in or near the plasma membrane.

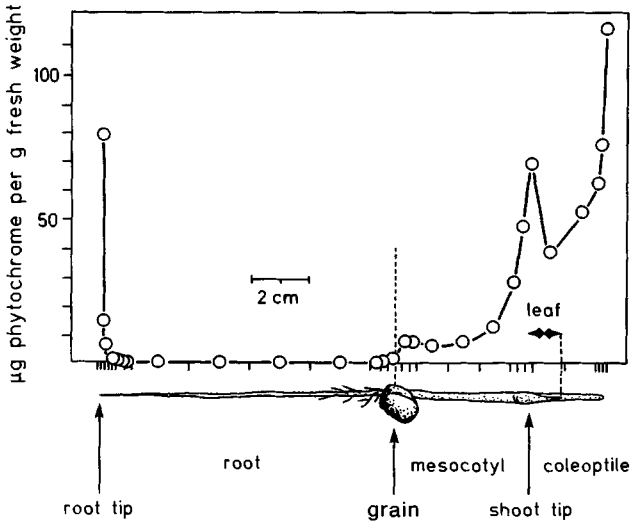

Fig. 9. Distribution of phytochrome in an etiolated, 5-day old maize seedling. The plant was cut into sections, which were then each extracted, and the phytochrome content of the extracts measured using antibodies. The divisions on the abscissa indicate the length of each section analyzed (from ref. [68]).

It has long been known that the photoreversible phytochrome of etiolated plants disappears on illumination, leaving only a small residue (1–5% of the initial amount).[1] Studies with antibodies also showed that not only the chromophore is degraded, but also the phytochrome-protein.[74] The remaining phytochrome proved to be immunologically heterogeneous.[75–78] The dominant photoreceptor in etiolated plants was originally called phytochrome type I; in the meantime, the term used by molecular biologists, type A (*phy*A), has become usual. The dominant phytochrome in light-grown, green plants (originally called type II[79]) is also heterogeneous.[80] It is probably a product of genes *phy*B and *phy*C (cf. Section 4), although differences due to post-translational modifications cannot yet be ruled out.

3.4. Distribution of Phytochrome in the Plant Kingdom

The operational criterion for the presence of phytochrome is a physiological effect inducible by red light which can be reversed by far-red light. From observations in many plants, it is assumed that phytochrome is generally present in higher plants (seed plants). In contrast, for lower plants (ferns, mosses, algae), the evidence indicates only sporadic occurrence. Identification of phytochrome by isolation or partial purification and identification of the protein band has only been possible for a few species; for example, for etiolated seedlings of oat, rye, pea, zucchini, rice,[81, 82] and for several green plants (oat;[75, 78] pea,[76] the moss *Atrichum undulatum*,[83] the green algae *Mesotaenium caldariorum*[84] and *Chaetomorpha linum*[85]).

Table 2. Identification of phytochrome by Western blotting [a].

Type of plant	N [b]	ref.
seed plants		
monocotyledons	17	[86–89]
dicotyledons	21	[86–89]
ferns	3	[89]
mosses	5	[83, 86, 89]
red algae	2	[85, 90]
brown algae	2	[85, 90]
green algae	7	[83, 85, 86, 90]

[a] Plant extracts were separated by SDS gel electrophoresis. The proteins were transferred to a suitable membrane (usually nitrocellulose) and treated with cross-reacting monoclonal antibodies. Specific reaction of a protein band in the size range 120–130 kDa was regarded as a positive result. The monoclonal antibodies were directed against phytochrome from oat [85–87, 89, 90], maize [83, 85, 89, 90], rye [88], or pea [86, 88]. Epitopes of the cross-reacting antibodies lie either in the *N*- or *C*-terminal region of the peptide chain for all examples studied so far. [b] Number of species in which phytochrome has been detected to date.

The distribution of phytochrome has been studied with the aid of monoclonal antibodies directed against phytochrome from etiolated oat,[65, 87] maize,[65] rye, or pea,[86, 88] which show a good cross-reaction with phytochrome from other plants (Table 2). Here, too, the higher plants studied showed a generally broad distribution, while many of the lower plants gave a negative result. This need not necessarily imply the absence of phytochrome. If phytochrome is present, however, the peptide chain must be so different from that in phytochrome of higher plants that it contains no epitope recognizable by the antibodies used. Interestingly, phytochrome is present in several algae where no phytochrome-dependent reaction was previously known. For the green alga *Ulva rigida* we subsequently found phytochrome-dependent protein synthesis, probably associated with the phytochrome-regulated uptake and reduction of nitrate.[91, 92]

4. Phytochrome Genes

4.1. Structure of the Phytochrome Genes, Phylogeny

Information about the primary structure of large protein molecules can be obtained most simply by analyzing the genes coding for the corresponding proteins. The *phy*A protein from oat was the first phytochrome molecule whose primary structure was elucidated in this way by the group of *Quail*.[93, 94]

With the information from this fundamental paper, it was now possible to isolate and characterize other phytochrome genes. By heterologous screening, cDNA clones were identified that code for *phy*A in zucchini,[95] maize,[96] and *Arabidopsis thaliana*.[97] With the help of synthetic oligonucleotide primers, *Kay* et al.[98] were able to isolate cDNA clones coding for rice phytochrome. Independently, *Tomizawa* et al.[99] identified a cDNA clone for pea *phy*A in an expression bank by immunoscreening with a specific antibody.

Once again, it was *Quail* and co-workers who were the first to elucidate the primary structure of the light-stable, "green" phytochrome of higher plants. Using a *phy*A DNA probe from zucchini, they screened a cDNA bank constructed from poly(A)$^{\oplus}$-RNA from green *A. thaliana* leaves, at low stringency, and were thus able to isolate the corresponding cDNA clones (*phy*B and *phy*C).[97] Further genes coding for light-stable phytochrome have since been isolated from rice, pea, and tobacco.[100] A fragment of a fourth phytochrome gene from *A. thaliana* (*phy*D) has also been cloned and sequenced.[101, 102]

Recently, *Thümmler* et al.[103a] have for the first time obtained phytochrome sequences (*phy*Cer) from a lower plant, the moss *Ceratodon purpureus*, using the polymerase chain reaction. The Pfr-dependent phototropism of this plant has been well studied.[103b] The oligonucleotide primers used were directed against conserved DNA sequences in the chromophore-binding region of phytochrome genes of higher plants (see Table 3). Since then, a phytochrome cDNA clone has also been isolated from the fern *Selaginella martensii*, by immunoscreening a λgt11-expression bank with the cross-reacting antibody Z3B1, which is directed against maize phytochrome.[104]

The primary structure of the corresponding genes was determined for *phy*A from oat,[107] rice,[98] maize,[96] and pea,[105] and for *phy*Cer from the moss *Ceratodon*.[106, 108] In Figure 10, the organization of these genes is presented

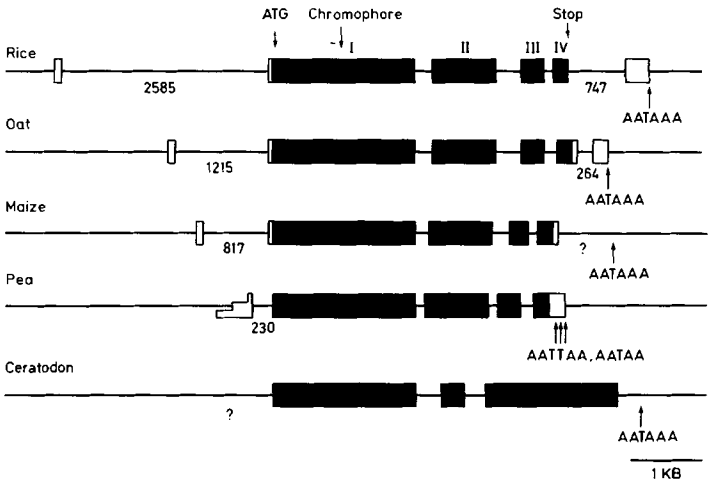

Fig. 10. Comparative schematic diagram of the phytochrome genes of rice, oat, maize, pea, and *C. purpureus*. (—) represents intron and flanking sequences; the numbers indicate the length of the introns in the untranslated exons, in base-pairs (Bp); □ untranslated exon sequences; ■ translated exon sequences I, II, III, IV; references for the corresponding genes: rice [98], oat [107], maize [96], pea [105], and *C. purpureus* [108].

Table 3. Percentage of identical amino acid sequences in different phytochrome proteins. The peptide regions coded for by exons I to IV (see Fig. 10) are listed separately [a].

		maize	pea	Ara A	Ara B	Ara C	Ara D	Selag	Cerat
oat	I	90	69	69	52	55	53	[b]	57
	II	82	60	58	47	43	[b]	55	47
	III	85	49	45	29	33	[b]	33	[c]
	IV	79	56	60	46	39	[b]	43	[c]
maize	I	–	70	70	53	56	56	[b]	58
	II	–	59	57	46	43	[b]	51	47
	III	–	44	40	27	30	[b]	29	[c]
	IV	–	57	57	36	34	[b]	37	[c]
pea	I		–	84	56	58	55	[b]	60
	II		–	77	52	45	[b]	62	50
	III		–	63	31	35	[b]	40	[c]
	IV		–	67	40	41	[b]	47	[c]
Ara A	I			–	56	58	63	[b]	61
	II			–	52	44	[b]	60	47
	III			–	30	37	[b]	41	[c]
	IV			–	44	41	[b]	49	[c]
Ara B	I				–	57	64	[b]	61
	II				–	46	[b]	64	49
	III				–	42	[b]	41	[c]
	IV				–	52	[b]	60	[c]
Ara C	I					–	53	[b]	58
	II					–	[b]	46	38
	III					–	[b]	40	[c]
	IV					–	[b]	51	[c]
Ara D [d]	I						–	[b]	64
Selag [e]	I							–	[b]
	II							–	53
	III							–	[c]
	IV							–	[c]

[a] Comparison of pairwise homology was carried out with the FASTA program [119]. Abbreviations: Selag = *S.martensii*, Cerat = *C.purpureus*, Ara = *Arabidopsis thaliana*. [b] The derived polypeptide sequences do not overlap in the correspondig regions. [c] The FASTA program finds no homology between the given amino acid sequences within the prescibed cut-off range. [d] For *phy*D, only a ca. 500 Bp DNA fragment is known, which is located in exon I. [e] The phytochrome gene from *S. martensii* has only been sequenced in the 3'-terminal region, from ca. 130 base pairs after the start of exon II. References for the phytochrome genes: maize [96], pea [105], Ara A,B,C = *A. thaliana phy*A, *phy*B, and *phy*C [97], Ara D = *A. thaliana phyD* [102], Selag = *S. martensii* [104], Cerat = *C. purpureus* [108].

schematically. For zucchini phytochrome, and for the two light-stable phytochrome types *phy*B and *phy*C from *A. thaliana*, only the cDNA sequence is known, while for *S. martensii* only a partial, 3'-terminal cDNA sequence has yet been published.

As Figure 10 shows, the phytochrome genes illustrated consist of several exons interspersed by shorter introns. The oat *phy*A gene, for example, is 5.94 kilobases (KB) long and consists of six exons and five introns. The *phy*A genes also show unusual, long intron sequences in the 5'- and 3'-flanking, untranslated regions of the gene. In rice, the 5'-terminal intron is 2585 base pairs (Bp) in length, and is therefore one of the longest introns yet found in a plant gene. In contrast to the phytochrome genes of monocotyledonous plants, the pea phytochrome gene lacks the 3'-terminal intron entirely and is made up of only five exons and four short introns. For the maize phytochrome gene, the existence of a 3'-terminal gene was not investigated. In the *phy*A genes of rice and oat, the nucleotide sequence at the boundary between exon 5 and intron 5 (5'TCAAATG/gtat3') is conserved, and the existence of this sequence at a corresponding site in the maize phytochrome gene is strong evidence for the presence of the intron in the maize gene as well. The organization of the *phy*Cer gene differs clearly from the pattern of the *phy*A genes. Unlike the latter, the *phy*Cer gene comprises just two large coding exons, on either side of a short, central exon. It is not known whether the 5'- and 3'-flanking, untranslated regions also contain introns in *phy*Cer. The *phy*A genes in oat, maize, rice, and pea contain sequence motifs which are found in the promoter region of many eukaryotic genes, and which play an important role in regulation of their expression. These include a TATA-motif, a CCAAT-motif, and a GC-element.[109] These genes (including the *S. martensii* and

C. purpureus genes) also reveal AATAAA or related motifs in the 3′-untranslated region, which are responsible for polyadenylation of the corresponding transcripts.

Genes for multidomain proteins are, without exception, built up of several exons. The sites corresponding to the exon–intron boundaries often appear to lie at the surface of the protein, and are hence especially sensitive to protease attack.[110] In phytochrome A, coding exon I corresponds to the chromophore-containing, *N*-terminal domain, probably including the "hinge region", so that several "early cleavage sites" (amino acid residues 600–700) fall into this region of the sequence (cf. Fig. 8). Exons II, III, and IV code for the *C*-terminal, chromophore-free domain. Perhaps the preferential proteolytic cleavage of these domains (cf. Section 3.1) is related to the many exon–intron transitions in this region. It is not known whether the 3′-exons code for different functional subdomains in the *C*-terminus of the phytochrome proteins. Interestingly, *Schneider-Poetsch* et al.[111] have found structural homologies to bacterial sensor proteins in the 250-amino acid, *C*-terminal polypeptide part of *Selaginella* phytochrome; in the oat *phy*A gene this part is encoded in the last two exons.

In Table 3, sequence homologies for phytochrome proteins are presented, divided according to the individual exons. Figure 11 shows the amino acid sequences at the exon–intron boundaries. The high amino acid sequence homology at

4.2. Expression of Phytochrome Genes

The expression of many light-regulated genes is modulated by phytochrome.[112] For most of these genes, expression is stimulated by light, but in the case of protochlorophyllide reductase[113] and the *phy*A genes themselves[114, 115, 98] expression is negatively influenced by Pfr. The point of regulatory action is primarily transcription. In the case of monocotyledonous plants such as oat[114, 115] and rice,[98] this negative control is very dramatic, while in maize and dicotyledonous plants it is much less pronounced. In oat or rice, the *phy*A transcription is suppressed within five minutes of Pfr formation, even in the absence of protein synthesis; hence all the necessary factors for the signal transduction must already be present.[115] In *Arabidopsis* the down-regulation of *phy*A–mRNA is only seen in continuous white light,[97] while in oat or rice a short, inductive period of red light suffices.

Compared to monocotyledonous plants, the Pfr-dependent *phy*A expression is complex in dicotyledonous plants. In *Arabidopsis*, gene probes specific to *phy*A hybridize to two *phy*A transcripts of different length, and in pea to three different species. This is caused by the presence of several transcription start sites within the complex *phy*-promoter (see Fig. 10).[105, 116] Transcription from one of these sites is strongly light-dependent, while the others are expressed in a

	I				II				III				IV			
	<	AS	>	< Bp >	<	AS	>	< Bp >	<	AS	>	< Bp >	<	AS	>	AS
Oat	MSSS	686	LALQ	203	GKEE	273	DSITEK	341	SSCLDL	99	DLELR	137	IKHQG	71	*	1129
Rice	MSSS	692	LALQ	222	GKEE	269	DSVMNK	281	SSCLDL	99	DLELR	102	IKHQG	68	*	1128
Maize	MSSS	689	LALQ	144	GREE	273	DNITDK	189	SSCLDL	99	DFELR	106	IKHRG	71	*	1132
Pea	MSTT	685	LALQ	82	GEEE	272	DGIID	78	GYLDL	98	NLELS	136	ITHGG	69	*	1124
Zucc	MSTS	684	LALQ	?	GQEE	272	DKIID	?	GFIDL	98	HLEFR	?	ITYAG	70	*	1124
Ara A	MSGS	686	NALE	?	GTEE	272	ESIIE	?	GCLDL	98	NLEIR	?	LTHTG	66	*	1122
Ara B	MVSG	721	RALR	90	GDEE	269	ESIED	?	GSFVL	98	RTEFR	?	MACPG	84	*	1172
Ara C	MSSN	672	LALE	?	GSEE	273	EGIEE	?	GYVEL	100	ELEFR	?	IIHPA	66	*	1111
Selag	?	?	?	?	--	>229	ESIED	?	GYLEL	98	HLEFR	?	ITHPG	79	*	406
Cer	MSAT	678	LALQ	303	GEEE	≈100	?	?	?			≈530 AS			*	≈1300

Fig. 11. Comparison of the amino acid sequences from the known exon–intron boundaries in *phy*A from oat, rice, maize, and pea with the amino acid sequences from the presumed exon–intron boundaries in *phy*A from zucchini and *A. thaliana*, *phy*B and *phy*C from *A. thaliana*, and with phytochrome from *C. purpureus* and *S. martensii*. AS = number of amino acids coded for by exons I, II, III, and IV, or the number of amino acids in the entire phytochrome polypeptide; Bp = length of the corresponding intron in basepairs; references for the phytochrome genes: oat [107], rice [98], maize [96], pea [105], zucc = zucchini [95], Ara A,B,C = *A. thaliana phy*A, *phy*B, and *phy*C [97], Selag = *S. martensii* [104], Cer = *C. purpureus* [108]

the transition from exon to intron suggests that the phytochrome genes of higher plants and of the fern show the exon–intron structure illustrated in Figure 10. In the *Arabidopsis phy*B gene, this has been confirmed for the transition from Exon I to Exon II.[108]

In this context, the phytochrome gene from the moss *Ceratodon* is an exception. As in all other *phy* genes, the transition from Exon I to Exon II is conserved. Exon II, however, which in this region shows high homology to the other phytochromes, breaks off after about 100 amino acids; it is followed by an intron of unknown length (probably 300 Bp). This is followed by a long open reading frame of some 530 amino acids.[108] This presumed protein shows no homology at all to the *C*-terminal peptide sequences of the known phytochrome proteins.

more or less light-independent manner.[97, 105, 116] A further peculiarity of dicotyledonous plants is the unidentified open reading frames (URF's), which are oriented "in frame" to the long reading frame of the phytochrome polypeptides. These URF's also exist in *phy*B and *phy*C of *Arabidopsis*, and their function is unknown.[97, 105] In contrast to *phy*A, *phy*B and *phy*C are only expressed very weakly in *Arabidopsis*, in a practically light-independent manner.[97] It is unclear which phytochrome type controls the expression of *phy*A, but in pea the light-stable phytochrome type is certainly also involved in this effect.[117] Conserved sequence motifs have been found in various *phy*A promoters from higher plants.[112] These motifs presumably play a functional role in the expression of the *phy*A genes and are currently the subject of intensive research.[112, 118]

4.3. Possible Structure–Function Relationships

Since biochemical methods have not yet yielded any detailed knowledge of the function of phytochrome or of the signal transduction sequence leading from it, a few considerations based on the structure of known phytochrome genes are in order. All the known phytochrome genes can be traced back to a common "primeval" phytochrome gene, which at least in the 5'-terminal region displayed a similar structure to that shown in Figure 10. In the chromophore domain (Exon I), all the phytochromes (*phy*A, *phy*B, *phy*C, *phy*D, *phy*Cer) show 50–60% homology to one another (the *phy*A types display 70–90% homology; see Table 3). This shows that the light-regulatory domain of the phytochrome molecule is subject to strong evolutionary pressure. The function of this domain, namely reversible photoconversion by interaction with the tetrapyrrole chromophore, should be the same in all phytochromes.

The similarity in the hydropathy profiles (which are a measure of the hydrophobicity of the individual amino acids along the sequence) of *phy*A, *phy*B, *phy*C, and *Selaginella*-phytochrome[97, 111] also suggests general similarity in the *C*-terminal region. Of the exons coding for the *C*-terminal domain of phytochrome, Exons II and IV are somewhat more highly conserved; Exon III is the most variable. In contrast, the phytochrome from *Ceratodon* is strongly divergent from this group of phytochromes. The lack of obvious homology in the *C*-terminal half of the protein and the divergent gene structure in this region are evidence for a different mode of regulatory function for the phytochrome in moss. However, a related phytochrome type has perhaps not yet been discovered either in higher plants or in ferns.

The existence of many phytochrome-dependent reactions, which include examples as varied as the rapid changes in membrane properties and the complex regulation of gene expression, as well as the occurrence of different phytochrome types suggest that there are different signal transduction chains for a single light stimulus.

Signal transduction in animal cells has been thoroughly studied. Many animal hormone functions depend on the binding of the hormone molecule to hormone receptors in the plasma membrane, which causes an activation of G-proteins. The G-proteins activate enzymes such as the phospholipase C, an effector enzyme of the phosphoinosite cascade, or the adenylate cyclase. This activation finally causes the opening of calcium channels and a temporary increase in the cytosolic calcium concentration, which is, however, immediately decreased again by a calcium/calmodulin-dependent calcium-ATPase to the initial concentration. The transient changes in calcium concentration then coupled to a phosphorylation cascade initiated by calcium-regulated kinases bound to the membrane. The signal chain leads to the corresponding answer of the target cells. An increasing number of indications suggest that analogous signal transduction chains also exist in plant cells. The participation of calcium has been proved for many phytochrome-dependent reactions;[125] thus, for example, the calcium/calmodulin system plays a role in the light-dependent expression of the chlorophyll a/b-binding proteins[122] as well as in the Pfr-dependent chloroplast rotation in the alga *Mougeotia*.[73, 120] Similarly red/far red-dependent phosphorylation processes and changes in the cellular concentrations of phosphatidyl inositols have been observed.[126, 123] Experiments with specific inhibitors and activators suggest that regulatory proteins like G-proteins, calmodulin, phospholipase C, protein kinase C, or adenylate cyclase are also involved in the phytochrome-dependent swelling of wheat protoplasts.[121] A phytochrome-dependent phospholipase C has been found in mosses,[123] and a protein kinase C is suspected to be involved in the protein phosphorylation in oat protoplasts that is dependent on red light.[127] Receptor molecules with tyrosine kinase activity play a central role in growth regulation of animal tissue. The participation of similar signal chains in the transmission of phytochrome-dependent stimulation in plant cells has not yet been studied.

Hormone function in the animal kingdom depends without exception on transmission of signals through membranes. As in plants the activated phytochrome is formed in the target cells themselves, such transmission across membrane barriers is not necessary. Thus applying animal signal paths noncritically to plant cells is extremely problematic. The phytochrome-dependent signal transmission should be considered in the light of intracellular signal transmission. *Schneider-Poetsch* et al. established a homology between *phy*A, *phy*B, *phy*C, and *Selaginella*-phytochrome and bacterial sensor proteins, which is interesting.[111] It implies that signal chains for phytochrome reactions exist that are similar to those for the signal transduction for chemical stimulation in bacteria.[128] There is, however, no experimental evidence for the existence of such signal chains in plants. One indication that the regulation of the gene expression by phytochrome is based on different paths is found in the experiments of *Lam* et al.[129] They showed that cycloplasmatic protein synthesis is essential for the Pfr-dependent expression of the genes for the chlorophyll a/b-binding protein and the genes for the small subunit of ribulose-1,5-biphosphate carboxylase, whereas no protein synthesis is required for the Pfr-dependent inhibition of the expression of protochlorophyllide reductase gene and the *phy*A gene. Hints that different phytochromes may have different functions come from experiments with phytochrome mutants.[124] Continuation and extension of these experiments are especially promising directions for further work.

5. Summary and Outlook

The plant photoreceptor phytochrome has proved a rewarding subject for interdisciplinary research in the fields of chemistry, physics, and biology. For natural product chemists, structure and synthesis of the tetrapyrrole chromophore are at the fore. Whether the interactions with the protein can be simulated by coupling the tetrapyrrole to suitable model structures is still an interesting question. Photochromism and the fixing of certain conformations of the flexible tetrapyrrole can be invoked as important criteria for such interactions. For the biochemist, the defined conformational changes in the protein, induced quite reversibly by specific illumination, are of interest. Phytochrome is a suitable model for studying certain aspects of the folding process in proteins. The discovery of various phytochrome genes and the possibility of reconstituting the chromoprotein from the

apoprotein and the chromophore have raised new questions for spectroscopists and biologists. The recently discovered phytochromes have not yet been studied in detail either spectroscopically or with regard to their specific biological effects. The signal transduction sequence induced by phytochrome is still unknown. The old question of whether phytochrome exerts a single primary effect or undergoes a multitude of direct reactions with other components of the plant cell must be reinvestigated with regard to the various phytochromes.

Without the trusting cooperation of colleagues and the committed efforts of the numerous co-workers who are named as coauthors in the original papers, the authors could never have achieved the results cited. We thank all of those who have taken part in the study of phytochrome. The research was supported by the Deutsche Forschungsgemeinschaft and the Fonds der Chemischen Industrie.

Received: April 17, 1991 [A836 IE]
German version: Angew. Chem. 103 (1991) 1242
Translated by Dr. Michael Kertesz, Zürich

[1] W. Shropshire, Jr., H. Mohr (Eds.): *Photomorphogenesis (Encycl. Plant Physiol. New Ser. 16A, B)*, Springer, Berlin 1983.
[2] H. A. Borthwick in K. Mitrakos, W. Shropshire, Jr., (Eds.): *Phytochrome*, Academic Press, London 1972, p. 3–23.
[3] H. A. Borthwick, S. B. Hendricks, M. W. Parker, E. H. Toole, V. K. Toole, *Proc. Natl. Acad. Sci USA 38* (1952) 662–666.
[4] H. A. Borthwick, S. B. Hendricks, M. W. Parker, *Proc. Natl. Acad. Sci USA 38* (1952) 929–934.
[5] L. Kerscher, S. Nowitzki, *FEBS Lett. 146* (1982) 173–176.
[6] R. D. Vierstra, P. H. Quail, *Proc. Natl. Acad. Sci USA 79* (1982) 5272–5276.
[7] R. Grimm, W. Rüdiger, *Z. Naturforsch. C41* (1986) 988–992.
[8] M. Nakasako, M. Wada, S. Tokutomi, K. T. Yamamoto, J. Sakai, M. Kataoka, F. Tokunaga, M. Furuya, *Photochem. Photobiol. 52* (1990) 3–12.
[9] A. M. Jones, H. P. Erickson, *Photochem. Photobiol. 49* (1989) 479–483.
[10] W. Rüdiger, D. L. Correl, *Justus Liebigs Ann. Chem. 723* (1969) 208–212.
[11] W. Rüdiger, *Hoppe-Seyler's Z. physiol. Chem. 350* (1969) 1291–1300.
[12] W. Rüdiger, *Angew. Chem. 82* (1970) 527–534; *Angew. Chem. Int. Ed. Engl. 9* (1970) 473–480; *Naturwissenschaften 57* (1970) 331–337.
[13] S. Schoch, G. Klein, U. Linsenmeier, W. Rüdiger, *Tetrahedron Lett. 1974*, 2465–2468.
[14] S. Schoch, G. Klein, U. Linsenmeier, W. Rüdiger, *Justus Liebigs Ann. Chem. 1976*, 549–558.
[15] H. Lotter, G. Klein, W. Rüdiger, H. Scheer, *Tetrahedron Lett. 1977*, 2317–2320; G. Klein, W. Rüdiger, *Justus Liebigs Ann. Chem. 1978*, 267–279.
[16] G. Klein, S. Grombein, W. Rüdiger, *Hoppe-Seyler's Z. physiol. Chem. 358* (1977) 1077–1079.
[17] W. Rüdiger, T. Brandlmeier, I. Blos, A. Gossauer, J.-P. Weller, *Z. Naturforsch. C35* (1980) 763–769.
[18] J.-P. Weller, A. Gossauer, *Chem. Ber. 113* (1980) 1603–1611.
[19] H. Scheer, *Angew. Chem. 93* (1981) 230–250; *Angew. Chem. Int. Ed. Engl. 20* (1981) 241–260; A. N. Glazer, A. Melis, *Annu. Rev. Plant. Physiol. 38* (1987) 11–45.
[20] K. T. Fry, F. E. Mumford, *Biochem. Biophys. Res. Commun. 45* (1971) 1466–1473.
[21] J. C. Lagarias, A. N. Glazer, H. Rapoport, *J. Am. Chem. Soc. 101* (1979) 5030–5037.
[22] J. C. Lagarias, H. Rapoport, *J. Am. Chem. Soc. 102* (1980) 4821–4828.
[23] P.-S. Song in D. J. Cosens, D. Vince-Price (Eds.): *The Biology of Photoreception*, Soc. Exp. Biol. 1983, pp. 181–206.
[24] S. Grombein, W. Rüdiger, H. Zimmermann, *Hoppe-Seyler's Z. physiol. Chem. 356* (1975) 1709–1714.
[25] F. Thümmler, T. Brandlmeier, W. Rüdiger, *Z. Naturforsch. C36* (1981) 440–449.
[26] W. Rüdiger, H. Scheer in [1], pp. 119–151.
[27] H. Falk, N. Müller, T. Schladerer, *Monatsh. Chem. 111* (1980) 159–175.
[28] F. Thümmler, W. Rüdiger, *Tetrahedron 39* (1983) 1943–1951.
[29] W. Rüdiger, F. Thümmler, E. Cmiel, S. Schneider, *Proc. Natl. Acad. Sci USA 80* (1983) 6244–6248; F. Thümmler, W. Rüdiger, E. Cmiel, S. Schneider, *Z. Naturforsch. C38* (1983) 359–368.
[30] H. Falk, K. Grubmayr, *Monatsh. Chem. 110* (1979) 1237–1242.
[31] H. Falk, K. Thirring, *Z. Naturforsch. B34* (1979) 1448–1453; *ibid. B 34* (1979) 1600–1605; *ibid. B 35* (1980) 376–380.
[32] S. P. A. Fodor, J. C. Lagarias, R. A. Mathies, *Photochem. Photobiol. 48* (1988) 129–136; *Biochemistry 29* (1990) 11141–11146.
[33] D. L. Farrens, R. E. Holt, B. N. Rospendowski, P.-S. Song, T. M. Cotton, *J. Am. Chem. Soc. 111* (1989) 9162–9169.
[34] F. Siebert, R. Grimm, W. Rüdiger, G. Schmidt, H. Scheer, *Eur. J. Biochem. 194* (1990) 921–928.
[35] W. Rüdiger, P. Eilfeld, F. Thümmler in G. Blauer, H. Sund (Eds.): *Optical Properties and Structure of Tetrapyrroles*, de Gruyter, Berlin 1985, pp. 349–366.
[36] H. Falk: *The Chemistry of Linear Oligopyrroles and Bile Pigments*, Springer, New York 1989.
[37] Y. Inoue, W. Rüdiger, R. Grimm, M. Furuya, *Photochem. Photobiol. 52* (1990) 1077–1083.
[38] P. Eilfeld, W. Rüdiger, *Z. Naturforsch. C40* (1985) 109–114.
[39] Reviews: K. Schaffner, S. E. Braslavsky, A. Holzwarth, *Pure Appl. Chem. 62* (1990) 1421–1426; *Adv. Photochem. 15* (1990) 229–277.
[40] M. E. Lippitsch, H. Riegler, F. R. Aussenegg, G. Hermann, E. Müller, *Biochem. Physiol. Pflanz. 183* (1988) 1–6.
[41] H. Brock, B. P. Ruzsicska, T. Arai, W. Schlamann, A. R. Holzwarth, S. E. Braslavsky, K. Schaffner, *Biochemistry 26* (1987) 1412–1417.
[42] G. Hermann, M. E. Lippitsch, H. Brunner, F. R. Aussenegg, E. Müller, *Photochem. Photobiol. 52* (1990) 13–18.
[43] B. P. Ruzsicska, S. E. Braslavsky, K. Schaffner, *Photochem. Photobiol. 41* (1985) 681–688.
[44] P. Eilfeld, P. Eilfeld, J. Vogel, R. Maurer, *Photochem. Photobiol. 45* (1987) 825–830.
[45] F. Thümmler, P. Eilfeld, W. Rüdiger, D. K. Moon, P.-S. Song, *Z. Naturforsch. C40* (1985) 215–218.
[46] P. Eilfeld, W. Rüdiger, *Z. Naturforsch. C39* (1984) 742–745.
[47] F. Thümmler, W. Rüdiger, *Physiol. Plant. 60* (1984) 378–382.
[48] U. Reiff, P. Eilfeld, W. Rüdiger, *Z. Naturforsch. C40* (1985) 693–698.
[49] C. Scharnagl, *Dissertation*, Technische Universität München 1986; S. Schneider, C. Scharnagl, M. Duerring, T. Schirmer, W. Bode in H. Scheer, S. Schneider (Eds.): *Photosynthetic Light-Harvesting systems, Organization and Functions*, de Gruyter Berlin 1988, pp. 483–490.
[50] S. M. Daniels, P. H. Quail, *Plant Physiol. 76* (1984) 622–626.
[51] J. C. Lagarias, F. M. Mercurio, *J. Biol. Chem. 260* (1985) 2415–2423.
[52] A. M. Jones, P. H. Quail, *Planta 178* (1989) 147–156.
[53] R. Grimm, F. Lottspeich, H. A. W. Schneider, *Z. Naturforsch. C41* (1986) 993–1000.
[54] T. Schirmer, W. Bode, R. Huber, *J. Mol. Biol. 195* (1987) 677–695; T. Schirmer, W. Bode, R. Huber in H. Scheer, S. Schneider (Eds.): *Photosynthetic Light-Harvesting systems Organization and Functions*, de Gruyter, Berlin 1988, pp. 195–199.
[55] R. Grimm, C. Eckerskorn, F. Lottspeich, C. Zenger, W. Rüdiger, *Planta 174* (1988) 396–401.
[56] R. Grimm, J. Kellermann, W. Schäfer, W. Rüdiger, *FEBS Lett. 234* (1988) 497–499.
[57] A. M. Jones, R. D. Vierstra, S. M. Daniels, P. Quail, *Planta 164* (1985) 501–506.
[58] M. M. Cordonnier, H. Greppin, L. H. Pratt, *Biochemistry 24* (1985) 3246–3253; Y.-G. Chai, P. S. Song, M.-M. Cordonnier, L. H. Pratt, *ibid. 26* (1987) 4947–4952.
[59] P. S. Song, I. Yamazakin in M. Furuya (Eds.): *Phytochrome and Photoregulation in Plants*, Academic Press, New York 1987, pp. 139–156.
[60] A. M. Jones, P. H. Quail, *Biochemistry 25* (1987) 2987–2995.
[61] L. H. Pratt, *Annu. Rev. Plant Physiol. 33* (1982) 557–582.
[62] W. O. Smith in [1], pp. 96–118.
[63] R. Schendel, W. Rüdiger, *Z. Naturforsch. C44* (1989) 12–18.
[64] a) Y.-S. Wong, H. C. Cheng, D. A. Walsh, J. C. Lagarias, *J. Biol. Chem. 261* (1986) 12089–12097; b) R. W. McMichael, Jr., J. C. Lagarias, *Biochemistry 29* (1990) 3872–3878.
[65] H. A. W. Schneider-Poetsch, B. Braun, W. Rüdiger, *Planta 177* (1989) 511–514.
[66] B. R. Singh, P.-S. Song, P. Eilfeld, W. Rüdiger, *Eur. J. Biochem. 184* (1989) 715–721.
[67] H. A. W. Schneider-Poetsch, *Naturwissenschaften 75* (1988) 132–139; M.-M. Cordonnier, *Photochem. Photobiol. 49* (1989) 821–831.
[68] H. Schwarz, H. A. W. Schneider-Poetsch, *Planta 170* (1987) 152–160.
[69] N. Kondo, Y. Inoue, K. Shibata, *Planta Sci. Lett. 1* (1973) 165–168.
[70] L. H. Pratt, R. A. Coleman, *Proc. Natl. Acad. Sci USA 68* (1971) 2431–2435.
[71] J. M. Mackenzie, Jr., R. A. Coleman, W. R. Briggs, L. H. Pratt, *Proc. Natl. Acad. Sci USA 72* (1975) 799–803.
[72] M. Wada, K. Kadota, M. Furuya, *Plant Cell Physiol. 24* (1983) 1441–1447.
[73] W. Haupt in K. Mitrakos, W. Shropshire, Jr. (Eds.): *Phytochrome*, Academic Press, London 1972, pp. 553–569; *Ber. Dtsch. Bot. Ges. 99* (1986) 251–262.
[74] R. A. Coleman, L. H. Pratt, *Planta 121* (1974) 119–131.
[75] J. G. Tokuhisa, S. M. Daniels, P. H. Quail, *Planta 164* (1985) 321–332.

[76] H. Abe, K. T. Yamamoto, A. Nagatani, M. Furuya, *Plant Cell Physiol 26* (1985) 1387–1399.
[77] Y. Shimazaki, L. H. Pratt, *Planta 164* (1985) 333–344; *ibid. 168* (1986) 512–515.
[78] M.-M. Cordonnier, H. Greppin, L. H. Pratt, *Biochemistry 25* (1986) 7657–7666.
[79] A. Nagatani, P. J. Lumsden, K. Konomi, H. Abe in M. Furuya (Eds.): *Phytochrome and Photoregulation in Plants*, Academic Press, New York 1987, pp. 95–115.
[80] L. H. Pratt, Vortrag auf dem NATO-Workshop "*Phytochrome, Properties and Biological Action*" Chichester (England), July 1990.
[81] R. E. Kendrick, G. H. M. Kronenberg (Eds.): *Photomorphogenesis in Plants*, Nijhoff, Dordrecht 1986.
[82] R. Schendel, Z. Tong, W. Rüdiger, *Z. Naturforsch. C44* (1989) 757–764.
[83] P. Lindemann, S. E. Braslavsky, E. Hartmann, K. Schaffner, *Planta 178* (1989) 436–442.
[84] D. G. Kidd, J. C. Lagarias, *J. Biol. Chem. 265* (1990) 7029–7035.
[85] F. López-Figueroa, P. Lindemann, S. E. Braslavsky, K. Schaffner, H. A. W. Schneider-Poetsch, W. Rüdiger, *J. Plant. Physiol. 136* (1990) 84–87.
[86] M.-M. Cordonnier, H. Greppin, L. H. Pratt, *Plant Physiol. 80*, 982–987; *ibid. 74* (1984) 123–127.
[87] G. C. Whitelam, M. L. Anderson, E. E. Billett, H. Smith, *Photochem. Photobiol. 42* (1985) 793–796.
[88] H. Saji, A. Nagatani, K. T. Yamamoto, M. Furuya, T. Fukumoto, A. Yamashita, *Plant Sci. Lett. 37* (1984) 57–61.
[89] H. A. W. Schneider-Poetsch, H. Schwarz, R. Grimm, W. Rüdiger, *Planta 173* (1988) 61–72.
[90] F. López-Figueroa, P. Lindemann, S. E. Braslavsky, K. Schaffner, H. A. W. Schneider-Poetsch, W. Rüdiger, *Bot. Acta 102* (1989) 178–180.
[91] F. López-Figueroa, W. Rüdiger, *Photochem. Photobiol. 52* (1990) 111–114.
[92] F. López-Figueroa, W. Rüdiger, *J. Phycol. 27* (1991) 389–394.
[93] H. P. Hershey, J. T. Colbert, J. L. Lissemore, R. F. Baker, P. H. Quail, *Proc. Natl. Acad. Sci. USA 81* (1984) 2332–2337.
[94] H. P. Hershey, R. F. Baker, K. B. Idler, J. L. Lissemore, P. H. Quail, *Nucleic Acids Res. 13* (1985) 8543–8559.
[95] R. A. Sharrock, J. L. Lissemore, P. H. Quail, *Gene 47* (1986) 287–295.
[96] A. H. Christensen, P. H. Quail, *Gene 85* (1989) 381–390.
[97] R. A. Sharrock, P. H. Quail, *Genes Dev. 3* (1989) 1745–1757.
[98] S. A. Kay, B. Keith, K. Shinozaki, M.-L. Chye, N.-H. Chua, *Plant Cell 1* (1989) 351–360.
[99] K.-I. Tomizawa, Y. Komeda, N. Sato, A. Nagatani, T. Iino, M. Furuya, *Plant Cell Physiol. 27* (1986) 1101–1108.
[100] a) S. A. Kay, Rockefeller University, New York, M. Furuya, RIKEN Institute, Wako/Japan, personal communication; b) K. Dehesh, J. Tepperman, A. H. Christensen, P. H. Quail, *MGG, Mol. Gen. Genet. 255* (1991) 305–313.
[101] S. Fiedel, *Diplomarbeit*, Universität München 1990.
[102] W. Rüdiger, F. Thümmler in B. Thomas (Eds.): *Phytochrome, Properties and Biological Function*, NATO Workshop Chichester 1990, Academic Press, 57–70.
[103] a) F. Thümmler, A. Beetz, W. Rüdiger, *FEBS Lett. 275* (1990) 125–129; b) E. Hartmann, E. Weber, *Planta 175* (1988) 39–49.
[104] H. A. W. Schneider-Poetsch, B. Braun, *J. Plant Physiol. 137* (1991) 576–580.
[105] N. Sato, *Plant Mol. Biol. 11* (1988) 697–710.
[106] A. Beetz, *Diplomarbeit*, Universität München 1990.
[107] H. P. Hershey, R. F. Barker, K. B. Idler, M. G. Murray, P. H. Quail, *Gene 61* (1987) 339–348.
[108] F. Thümmler, unpublished.
[109] C. Kuhlemeier, P. J. Green, N.-H. Chua, *Annu. Rev. Plant Physiol. 38* (1987) 221–257.
[110] W. Gilbert, *Science (Washington DC) 228* (1985) 823–827.
[111] H. A. W. Schneider-Poetsch, B. Braun, S. Marx, A. Schaumburg, *FEBS Lett. 281* (1991) 245–249.
[112] P. M. Gilmartin, L. Sarokin, J. Memelink, N.-H. Chua, *Plant Cell 2* (1990) 369–378.
[113] E. Mösinger, A. Batschauer, E. Schäfer, K. Apel, *Eur. J. Biochem. 147* (1985) 137–142.
[114] P. H. Quail, J. T. Colbert, N. K. Peters, A. H. Christensen, R. A. Sharrock, J. L. Lissemore, *Philos. Trans. R. Soc. London B314* (1986) 469–480.
[115] J. L. Lissemore, P. H. Quail, *Mol. Cell. Biol. 8* (1988) 4840–4850.
[116] K.-I. Tomizawa, N. Sato, M. Furuya, *Plant Mol. Biol. 12* (1989) 295–299.
[117] M. Furuya, N. Ito, K.-I. Tomizawa, E. Schäfer, *Planta 183* (1991) 218–221.
[118] K. Dehesh, W. B. Bruce, P. H. Quail, *Science (Washington DC) 250* (1990) 1397–1399.
[119] W. R. Pearson, D. J. Lipman, *Proc. Natl. Acad. Sci USA 85* (1988) 2444–2448.
[120] F. Grolig, G. Wagner, *Planta 177* (1989) 169–177.
[121] M. E. Bossen, R. E. Kendrick, W. J. Vredenberg, *Physiol. Plant 80* (1990) 55–62; A. Tretyn, R. E. Kendrick, M. E. Bossen, *ibid. 78* (1990) 230–235.
[122] E. Lam, M. Benedyk, N.-H. Chua, *Mol. Cell. Biol. 9* (1989) 4819–4823.
[123] E. Hartmann, H. Pfaffmann in D. J. Morré, W. F. Boss, F. A. Loewus (Eds.): *Inositol Metabolism in Plants*, Wiley-Liss, New York, 1990, pp. 259–275.
[124] P. Adamse, R. E. Kendrick, M. Koorneef, *Photochem. Photobiol. 48* (1988) 833–841.
[125] S. J. Roux, R. O. Wayne, N. Datta, *Physiol. Plant 66* (1986) 344–348.
[126] B. R. Singh, P. S. Song, *Photochem. Photobiol. 52* (1990) 249–254.
[127] M.-H. Park, Q. Chae, *Biochem. Biophys. Res. Commun. 169* (1990) 1185–1190.
[128] C. W. Ronson, B. T. Nixon, F. M. Ausubel, *Cell 49* (1987) 579–581.
[129] E. Lam, P. J. Green, M. Wong, N.-H. Chua, *EMBO J. 8* (1989) 2777–2783.

The Elucidation of Peroxyl Radical Reactions in Aqueous Solution with the Help of Radiation-Chemical Methods

By Clemens von Sonntag* and Heinz-Peter Schuchmann

Dedicated to Professor Kurt Schaffner on the occasion of his 60th birthday

Whenever free radicals are formed, independent of whether this occurs thermally, is induced by UV or ionizing irradiation, or takes place in redox reactions, they are converted rapidly into the corresponding peroxyl radicals in the presence of oxygen. Peroxyl radical reactions in aqueous environments are observed not only in aquatic systems (e.g., rivers, lakes and oceans) but also in the living cell and to a considerable degree even in the atmosphere (in water droplets). The peroxyl radical chemistry occurring in this medium is often very different from that observed in the gas phase or in organic solvents. In spite of the great importance of these reactions in medicine (for example in anti-cancer irradiation therapy and ischaemia) there have been comparatively few studies of peroxyl reactions in aqueous media. Radiation-chemical techniques such as pulse radiolysis offer the best means for carrying out such studies, so that it is not surprising that the majority of the information available in this area has been obtained with the help of radiation-chemical methods. The radiation chemistry of water can be controlled in such a manner that the main products are $^{\bullet}OH$ radicals (90% yield), which react with substrate molecules to give substrate radicals and in the presence of oxygen to give substrate peroxyl radicals. The experimental conditions can also be varied in such a way that $HO_2^{\bullet}/O_2^{\bullet\ominus}$ radicals can be formed in 100% yield and caused to react with substrates. We therefore have a simple access to these intermediates, which are extremely important in biological systems. A detailed product analysis, supported by kinetic studies carried out with the help of pulse radiolysis, has been used to clarify the chemistry of a series of peroxyl radicals, so that sufficient material is now available to justify a review of the variety of the peroxyl radical reactions studied by means of radiation-chemical methods. A more general survey of the physical properties of the peroxyl radicals and their unimolecular and bimolecular reactions will be followed by a discussion of selected examples of various classes of substance. Because of the great biological importance of radical-induced DNA damage this area will also be treated briefly.

1. Introduction

Peroxyl radicals play an important role in many naturally occurring processes, since almost all free radicals which are formed thermally, photochemically, by ionizing radiation or in the course of oxidation processes react rapidly with oxygen to form the corresponding peroxyl radicals. In addition, many processes which are vital for life as we know it occur in aqueous media, as the living cell consists of ca. 70% water. It is thus particularly surprising that the chemistry of free radical reactions has been studied almost solely under artificial conditions in which oxygen is absent, while that of peroxyl radicals has been studied almost exclusively in organic solvents.[1-3] This became clear to us some years ago when we began to concern ourselves with radical-induced damage to DNA caused by ionizing radiation. The destruction of the cells, which is the required effect in anti-cancer radiation therapy, is intensified by oxygen.[4-8] This means that peroxyl radicals must play a decisive role in those processes occurring in living organisms which are induced by ionizing radiation.

It is becoming ever more clear that some illnesses, even ageing, involve peroxyl radicals.[9] This is true in particular for the effects of ischaemia,[10] where oxygen impoverishment due to blockage of a blood vessel is followed by the development of a high reductive potential as a result of the anaerobic cell metabolism. If the cells are reoxygenated after removal of the blockage, electron transfer leads to the formation of the superoxide radical anion, $O_2^{\bullet\ominus}$, in such a high concentration, physiologically speaking, that the cells are damaged by products formed from it, particularly by the $^{\bullet}OH$ radical; this cell damage involves both the DNA and radical peroxidation of the lipids contained in the cell membranes.[10] $O_2^{\bullet\ominus}$, the smallest of all the peroxyl radicals, also plays a part in inflammatory processes,[10] while it is also an important intermediate in the formation of hypochloric acid, one of the chemical weapons used by the cells of our immune system.[10-12]

Our biological existence is indeed a finely tuned compromise. We need oxygen in order to be able to live, but an increase in its concentration by only a factor of five (pure oxygen rather than air) renders it toxic.[10] Thus animals used for experimental purposes die after a few days in an oxygen atmosphere as a result of peroxyl radical reactions which cannot be compensated for.[13]

Some types of forest damage have also been suggested to be due in part to reactions of $O_2^{\bullet\ominus}$ occurring subsequent to initial damage caused by other agents.[10] The phenolic species found in plant cells, in particular α-tocopherol, act as antioxidants; this is also true for ascorbic acid and glutathione.[10, 14] These antioxidants are also found in animal cells.

[*] Prof. Dr. C. von Sonntag, Dr. H.-P. Schuchmann
Max-Planck-Institut für Strahlenchemie
Stiftstrasse 34–36, W-4330 Mülheim an der Ruhr (FRG)

Peroxyl radicals also play an important part in environmental processes, which often involve an initial photochemical step or a reaction of an ·OH radical. This applies to atmospheric chemistry,[15] where reactions occurring in an aqueous phase (clouds, fog, precipitation) are the subject of increasing interest.[16, 17] The nitrate photolysis induced in surface waters by the UV component of sunlight, which leads to ·OH radicals as well as other species, can play a role in self-cleansing; the sequence of reactions involved naturally proceeds via peroxyl radicals.[18]

·OH radicals are also formed in the course of ozone treatment of drinking water;[19, 20] they attack organic substances in the water, and are also formed under the influence of ultrasound, the application of which leads to the formation of microscopic bubbles (cavitation). Their collapse leads to intense local heating, temperatures of ca. 4000 K being reached, so that water molecules are split into H· atoms and ·OH radicals.[21, 22]

Attack by ·OH radicals also represents the main source in the radiation-chemical formation of organic radicals, and thus of peroxyl radicals, in aqueous solution. The advantages of the radiation-chemical method for the investigation of peroxyl radicals in comparison with other techniques will be discussed in the following section.

2. Radiation-chemical Formation of Peroxyl Radicals

A conventional method of forming peroxyl radicals in aqueous solution makes use of the Fenton reaction,[23, 24] in which $Fe^{2\oplus}$ or $Ti^{3\oplus}$ ions react with H_2O_2 to give ·OH radicals, which in turn react with substrates RH via H-abstraction or add to C=C double bonds to yield substrate radicals (reaction rates for the ·OH radicals are collected in Ref. [25], and unless otherwise stated are taken from this source). The substrate radicals are converted into peroxyl radicals in the presence of O_2 [reactions (1)–(3)]. This simple reaction,

$$Fe^{2\oplus} + H_2O_2 \longrightarrow Fe^{3\oplus} + {}^{\cdot}OH + OH^{\ominus} \quad (1)$$

$$^{\cdot}OH + RH \longrightarrow H_2O + R^{\cdot} \quad (2)$$

$$R^{\cdot} + O_2 \longrightarrow RO_2^{\cdot} \quad (3)$$

which can be carried out in any laboratory, does however have a number of drawbacks. Product analysis is often complicated, as apart from an excess of the substrate $Fe^{2\oplus}$, $Fe^{3\oplus}$, H_2O_2 and frequently additives such as EDTA are present. More serious is the fact that $Fe^{2\oplus}$, $Fe^{3\oplus}$ and H_2O_2 can react with intermediate radicals and reactive products, often in an unclear manner. ·OH radicals can also react with H_2O_2 to give $HO_2^{\cdot}/O_2^{\cdot\ominus}$ radicals [reaction (4), $k_4 = 10^7\ dm^3\ mol^{-1}\ s^{-1}$], so that larger amounts of the latter may also be present and may in turn interfere in the reaction pathways. Examples are known which show clearly that the products can be very

$$^{\cdot}OH + H_2O_2 \longrightarrow H_2O + HO_2^{\cdot} \quad (4)$$

different depending on whether Fenton's reagent or "cleanly" radiation-chemically produced ·OH radicals are used.[26, 27] A further disadvantage of Fenton's reagent is that kinetic studies can only be carried out in exceptional circumstances.

A clean generation of ·OH is in principle possible via a flash-photolytic cleavage of H_2O_2 [reaction (5)]. The disad-

$$H_2O_2 \xrightarrow{h\nu} 2\ ^{\cdot}OH \quad (5)$$

Clemens von Sonntag, born 1936 in Stuttgart, studied Chemistry in Heidelberg, Vienna, and Karlsruhe, where he was awarded his doctorate for research carried out at the Kernforschungszentrum Karlsruhe. After a spell at the University of Leeds, England, doing postdoctoral work with Professor F. S. Dainton, he returned to Karlsruhe where he took up a post as group leader at the Institut für Strahlenchemie des Kernforschungszentrums. In 1970 he habilitated at the Universität Karlsruhe and was appointed professor in 1977. Since 1970 Clemens von Sonntag has been group leader at the Max-Planck-Institut (MPI) for Kohlenforschung, Abteilung Strahlenchemie, today MPI für Strahlenchemie, Mülheim an der Ruhr. In 1984 he was awarded the Weiss Medal of the Association for Radiation Research for his studies on the radiation chemistry of DNA. His main interests center on the radiation chemistry of biologically relevant compounds and photochemistry, especially in vacuum-UV.

Heinz-Peter Schuchmann, born 1937 in Darmstadt, studied Chemistry in Darmstadt and Ottawa, Canada (doctorate 1970 in Ottawa for research in gas kinetics). Since 1971 he has worked at the Max-Planck-Institut für Strahlenchemie, Mülheim an der Ruhr. His fields of interest include the radiation chemistry of aqueous solutions and photochemistry in the far UV.

vantage of this procedure is that the absorption coefficient of H_2O_2 is very low (e.g., only 20 $dm^3\ mol^{-1}\ cm^{-1}$ at 254 nm); thus the concentration of H_2O_2 must be high in order that a sufficient amount of UV light can be absorbed. This however means that reaction (4) can gain in importance. A further problem is caused by substrates which absorb UV light and thus protect the H_2O_2 against decomposition by acting as an inner filter. If, however, (in the absence of H_2O_2) UV-sensitive substrates are to be used as the source of radicals, the substrate-specific photochemistry is accompanied by further problems caused by laser excitation. In aqueous solution the ionization potential is ca. 3 eV lower than in the gas phase,[28, 29] so that the biphotonic photoionization process becomes very important. The spectra of the radical cations, which often react slowly or not at all with oxygen, can then make the kinetic evaluation of the parallel reactions of the peroxyl radicals more difficult.

The above discussion leads us to expect that the radiation-chemical method of production will in many ways be superior to both the Fenton reaction and the photolytic method. In a typical radiation-chemical experiment[7, 30–34] dilute aqueous solutions of a substrate ([substrate] $\approx 10^{-3}$ mol dm^{-3}) is irradiated with ^{60}Co-γ-radiation or with fast electrons from an electron accelerator. The irradiation energy is almost entirely absorbed by the solvent. In contrast to the radiolysis of organic solvents, water provides only a small number of extremely reactive free radical intermediates, which thus generally react rapidly with substrates. This makes it possible to carry out kinetic studies even in the submicrosecond range (pulse radiolysis). A further advantage of water as a solvent is that it is not attacked by organic radicals. Its radiation chemistry is simple: ionization and electronic excitation lead to the formation of solvated electrons $e_{aq}^{\ominus}$, $^{\bullet}OH$ radicals and $^{\bullet}H$ atoms as the primary radicals[35] [reactions (6)–(10)]. In addition, small amounts of H_2 and H_2O_2 are formed in centers of high radical density (the so-called "spurs") [reactions (11)–(13)]. In the

$$H_2O \xrightarrow[\text{radiation}]{\text{ionizing}} H_2O^{\bullet\oplus} + e^{\ominus} \quad (6)$$

$$H_2O \xrightarrow[\text{radiation}]{\text{ionizing}} H_2O^{*} \quad (7)$$

$$H_2O^{\bullet\oplus} \longrightarrow {}^{\bullet}OH + H^{\oplus} \quad (8)$$

$$e^{\ominus} \xrightarrow{H_2O} e_{aq}^{\ominus} \quad (9)$$

$$H_2O^{*} \longrightarrow H^{\bullet} + {}^{\bullet}OH \quad (10)$$

$$H^{\bullet} + H^{\bullet} \longrightarrow H_2 \quad (11)$$

$$e_{aq}^{\ominus} + e_{aq}^{\ominus} \longrightarrow H_2 + 2\,OH^{\ominus} \quad (12)$$

$$^{\bullet}OH + {}^{\bullet}OH \longrightarrow H_2O_2 \quad (13)$$

$$e_{aq}^{\ominus} + O_2 \longrightarrow O_2^{\bullet\ominus} \quad (14)$$

$$H^{\bullet} + O_2 \longrightarrow HO_2^{\bullet} \quad (15)$$

presence of O_2 the solvated electrons and the $^{\bullet}H$ atoms react rapidly with the former to give $O_2^{\bullet\ominus}/HO_2^{\bullet}$ radicals [reactions (14) and (15), $k_{14} = 1.9 \times 10^{10}$ $dm^3\ mol^{-1}\ s^{-1}$, $k_{15} = 2.1 \times 10^{10}$ $dm^3\ mol^{-1}\ s^{-1}$], which are in equilibrium [$pK_a(HO_2^{\bullet}) = 4.8$].[36]

The $^{\bullet}OH$ radicals do not react with O_2 but normally with added organic substrates, as indicated above. The reaction of the $H^{\bullet}$ atoms and in many cases also of the solvated electrons with organic substrates is slower (see Ref. [25]). Thus, in oxygen-saturated solutions the reactions (14) and (15) lead to approximately equal amounts of organic peroxyl radicals and $HO_2^{\bullet}/O_2^{\bullet\ominus}$ radicals. This high proportion of $HO_2^{\bullet}/O_2^{\bullet\ominus}$ radicals is advantageous when the reactions of $RO_2^{\bullet}$ radicals with $HO_2^{\bullet}/O_2^{\bullet\ominus}$ are to be studied, although this is not normally the primary subject of interest. When the solvated electrons are to be converted into $^{\bullet}OH$ radicals their

$$e_{aq}^{\ominus} + N_2O \longrightarrow {}^{\bullet}OH + N_2 + OH^{\ominus} \quad (16)$$

rapid reaction with N_2O can utilized [reaction (16), $k_{16} = 9.8 \times 10^9$ $dm^3\ mol^{-1}\ s^{-1}$]. Because of the much higher solubility of N_2O (2.4×10^{-2} mol dm^{-3} at 1 atm) compared to O_2 (1.3×10^{-3} mol dm^{-3}) the conversion of $e_{aq}^{\ominus}$ into $^{\bullet}OH$ radicals is almost complete when a 4:1 mixture of these gases is used, and reaction (14) can be neglected. Thus, the system now consists of ca. 90% $^{\bullet}OH$ radicals and ca. 10% $HO_2^{\bullet}/O_2^{\bullet\ominus}$ radicals.

It will be shown (Section 5.1) that a series of peroxyl radicals eliminate $HO_2^{\bullet}/O_2^{\bullet\ominus}$. This elimination is fast and quantitative in the case of the reaction of the $CO_2^{\bullet\ominus}$ radical with O_2, so that the system formate/N_2O/O_2 provides a source of 100% $HO_2^{\bullet}/O_2^{\bullet\ominus}$ radicals [reactions (17) and (18)].[37] The

$$HCO_2^{\ominus} + {}^{\bullet}OH \longrightarrow CO_2^{\bullet\ominus} + H_2O \quad (17)$$

$$CO_2^{\bullet\ominus} + O_2 \longrightarrow CO_2 + O_2^{\bullet\ominus} \quad (18)$$

$HO_2^{\bullet}/O_2^{\bullet\ominus}$ radicals thus produced can be caused to react with organic and inorganic substrates in an unambiguous manner when suitable experimental conditions are used. $HO_2^{\bullet}/O_2^{\bullet\ominus}$ radicals are prepared conventionally by enzymatic action of xanthine oxidase on xanthine in the presence of oxygen.[38, 39] In this system other reactive species are formed apart from $HO_2^{\bullet}/O_2^{\bullet\ominus}$. The nature of these is much less well understood than that of the radiation-chemical system; thus use of the xanthine/xanthine oxidase system can under certain conditions simulate a nonexistent high $HO_2^{\bullet}/O_2^{\bullet\ominus}$ reactivity (cf. Ref. [40] with Ref. [41, 42]).

The G-values[**] of the primary radicals are well known ($G(^{\bullet}OH) = 2.9 \times 10^7$ mol J^{-1}; $G(e_{aq}^{\ominus}) = 2.9 \times 10^{-7}$ mol J^{-1}; $G(H^{\bullet}) = 0.6 \times 10^{-7}$ mol J^{-1}; $G(H_2) = 0.45 \times 10^7$ mol J^{-1}; $G(H_2O_2) = 0.8 \times 10^{-7}$ mol J^{-1}). The dose rate [unit of dose: 1 Gray (Gy) = 1 J kg^{-1}] of a radiation source can be determined very simply and rapidly[30] (in the case of a ^{60}Co-γ source this must in principle be done only once, since the decay constant of the nuclide is known). Since the yields of primary radicals, and thus also of primarily formed peroxyl radicals, are known from the dose rate and the irradiation time, it is possible to obtain a material balance subsequent to product analysis. Apart from the formation of the products the oxygen consumption can also be measured. The data thus obtained provide important information: a) when in an

[**] The G value is a measure of the radiation-chemical yield. It was originally defined as the number of molecules formed (consumed) per 100 eV absorbed energy. Since the eV is a non-SI unit, the G value is now given in units of mol J^{-1}. In the older literature the G values are always given in units of molecules/100 eV, but in this review the new SI units will be used.

N_2O/O_2-saturated solution (taking the stoichiometry into account) G(products) is lower than the G value of their primary radical precursors [$G(^{\bullet}OH + H^{\bullet}) \approx 6 \times 10^{-7}$ mol J^{-1}], it is clear that not all the products have been accounted for; b) when the value of G(products) is considerably greater than this value a free-radical chain reaction is involved.

The pulse radiolysis method makes it possible to impart the irradiation energy within less than 1 μs. The reactions (2), (3) and (5)–(15) leading to the peroxyl radicals are often nearly diffusion-controlled ($k \geq 10^9$ dm^3 mol^{-1} s^{-1}), so that at oxygen concentrations of $\geq 10^{-4}$ mol dm^{-3} the organic peroxyl radicals are formed within 2–3 microseconds. Several methods are available for following the kinetics of the subsequent peroxyl radical reactions. In some cases UV/VIS spectroscopy can be used; however, peroxyl radicals generally do not have particularly characteristic absorption spectra but typically exhibit only broad absorptions at $\lambda < 300$ nm.[43] The products formed from them may in some cases show characteristic spectra.

Many peroxyl radicals are uncharged but are converted into charged particles by unimolecular and bimolecular processes; thus for example the elimination of $HO_2^{\bullet}$ leads to $H^{\oplus}$ and $O_2^{\bullet\ominus}$. Since these reactions involve a conductivity change they can be followed by conductometric methods. The range of measurement lies between the submicrosecond and the minute domains, i.e. more than eight powers of ten on the time scale.[44] The conductivity signal at weakly acidic pH is positive when acids are formed (increase in conductivity because of additional $H^{\oplus} + A^{\ominus}$) but negative in alkaline solution (replacement of $OH^{\ominus}$ by $A^{\ominus}$ because of the neutralization of $OH^{\ominus}$ by $H^{\oplus}$; the equivalent conductivity of $OH^{\ominus}$, $\lambda^0(OH^{\ominus}) = 180$ dm^3 val^{-1} Ω^{-1} cm^{-1}, is greater than that of other monoanions, $\lambda^0(A^{\ominus}) = 40$–$60$ dm^3 val^{-1} Ω^{-1} cm^{-1}). The increase in conductivity is reduced parallel to the suppression of the dissociation when the pH of the solution falls below the pK_a of the intermediate.

Studies of polymers in solution can be carried out when the pulse radiolysis apparatus is combined with a light-scattering measurement device[45] (if possible a low-angle laser light-scattering apparatus[46, 47]) in order to carry out a kinetic resolution of the peroxyl radical-induced change (lowering) of the molecular weight. In the case of charged polymers, e.g. polynucleotides, single-stranded DNA or hyaluronic acid the formation of breaks in the strand can also be followed by the change in the conductivity.[48] Because of the high charge density a large proportion of the counterions are condensed on the polyanionic species and play no part in determining the conductivity. When strand cleavage occurs the charge density in the neighborhood of the break is lowered and counterions are set free. When, for example, the counterion is $Na^{\oplus}$, the formation of breaks leads to an increase in conductivity in both acidic and basic solutions (in contrast to the formation of an acid).

The radiation-chemical techniques thus provide us with two complementary tools: a quantitative product analysis and a good set of kinetic data. The use of ^{60}Co-γ radiolysis (and, in a completely different dose rate range, of pulse radiolysis) permits the variation of the dose rate by several orders of magnitude. This is important for studies of chain reactions, and can also provide information on whether particular radicals undergo reactions which are first or second order (in radicals) and which products are formed in the various reaction pathways. The influence of the temperature on the reactions can be studied relatively easily across the temperature range 0–80 °C, while the use of pressure cells allows us to work at higher temperatures;[49, 50] however, this latter possibility has so far been used only rarely.

Having discussed the advantages of the radiation-chemical methods for the study of peroxyl radical reactions, we must now turn to their limitations. Such studies are in general restricted to dilute solutions (typically $\leq 10^{-3}$ mol dm^{-3}), since only under these conditions can we be sure that a conversion of the solvated electrons subsequent to saturation with N_2O into $^{\bullet}OH$ radicals or with O_2 into $O_2^{\bullet\ominus}$ is quantitative. At higher concentrations reactions of the electrons with the substrates are often observed. In addition, at substrate concentrations above 0.1 mol dm^{-3} a *direct* absorption of the ionizing radiation by the substrate is detectable (approximately in proportion to its weight percentage), while in the molar concentration range the formation of products from this source becomes so important that it is no longer possible to obtain a clear interpretation of the data. This, however, means that important processes that can only be reliably measured at substrate concentrations in the molar range (i.e., at concentrations higher by a factor of 1000) because of their low rate constants cannot be studied using radiation-chemical methods or can be studied only in a limited manner. Such processes include the extensive and important area of autoxidation reactions (H transfer reactions and intermolecular addition of peroxyl radicals to double bonds). This subject will thus be referred to only occasionally in the present account. Reactions which occur subsequently to oxidation processes will also not be discussed, as radiation-chemical methods have (until now) not been used to study them. This article is intended to make the reader familiar with the possibilities offered by radiation-chemical methods and with the results obtained so far. A general acount of the chemistry of peroxyl radicals would exceed the scope of the present report.

3. Peroxyl Radicals: Formation and Properties

3.1. Formation of Peroxyl Radicals and the Reversibility of the O_2 Addition

Radicals formed via an attack by $^{\bullet}OH$ radicals often have high absorption coefficients in the UV-visible range, while the peroxyl radicals formed from them absorb only slightly or not at all in this wavelength range.[43] The radical **1** formed from glycine anhydride is a typical example, being formed in virtually quantitative yield in the reaction between an $^{\bullet}OH$ radical and glycine anhydride (see also Section 6.3);

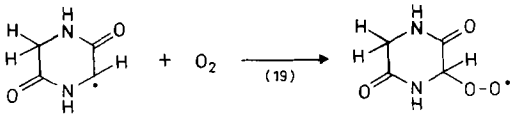

1 **2**

its spectrum shows clear maxima at 270 and 360 nm (Fig. 1). The peroxyl radical **2** formed in reaction (19) shows practically no absorption in this range. If the observed first order rate constant for the decomposition of the radical **1** is plotted as a function of the oxygen concentration the result is a straight line (insert in Fig. 1), the slope of which gives the bimolecular rate constant ($k_{19} = 2 \times 10^9$ dm^3 mol^{-1} s^{-1}).[51]

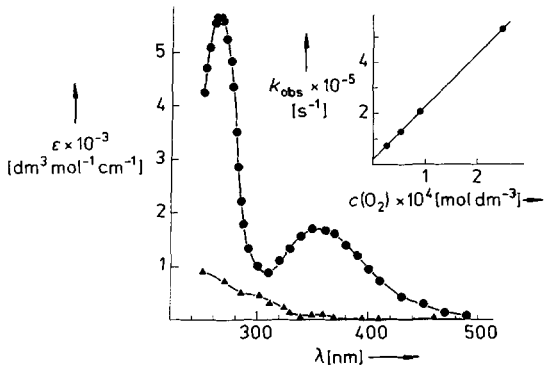

Fig. 1. Pulse radiolysis of glycine anhydride in aqueous solution [51] (10^{-3} mol dm^{-3}, pH 6.5). (●) UV/VIS spectrum of the glycine anhydride radical **1** 6.5 μs after the pulse (N_2O-saturation). (△) spectrum of the glycine anhydride peroxyl radical **2** 15 μs after the pulse (N_2O/O_2-(4:1)-saturation). *Inset:* observed rate constant k_{19} of the disappearance of **1** as a function of the oxygen concentration measured at 360 nm.

Experiments of this type have provided rate constants for reactions of a large variety of radicals with O_2 (a survey can be found in Ref. [43]). These rate constants often lie close to 2×10^9 dm^3 mol^{-1} s^{-1}, i.e., the reaction is virtually diffusion-controlled, and the formation of peroxyl radicals is practically irreversible.[52] There are however also cases in which the formation of the peroxyl radicals is noticeably reversible even at room temperature.[53] Such a reversibility in the gas phase has long been discussed for the hydroxycyclohexadienyl radical **3** which is formed from benzene and ·OH radicals,[15] and has also been demonstrated recently for aqueous solutions.[54]

The spectrum of the radical **3** is shown in Figure 2 (right-hand scale), and shows a clear maximum at 310 nm. This absorption disappears rapidly in the presence of O_2 ($k_{20/22} = 3.1 \times 10^8$ dm^3 mol^{-1} s^{-1}), though it does not disappear completely. A residual absorption dependent on the oxygen concentration is approached at ca. 30 μs; afterwards this disappears only very slowly (Fig. 2). A kinetic evaluation gives a value of $k_{21/23} = 1.2 \times 10^4$ s^{-1} for the back reac-

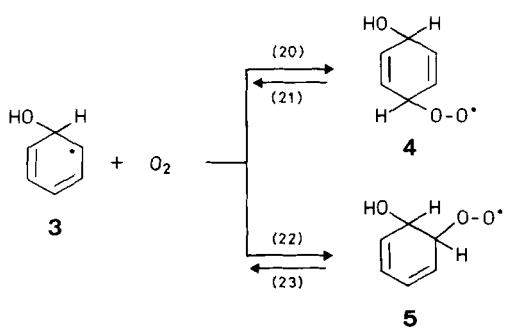

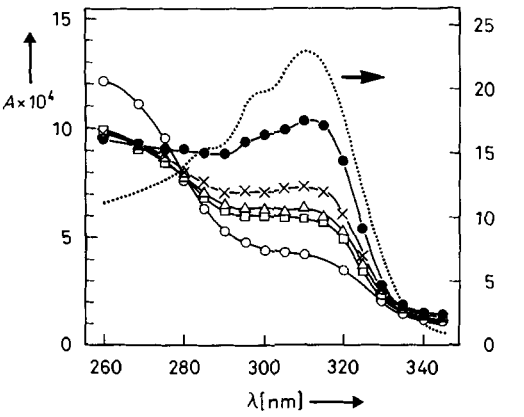

Fig. 2. Pulse radiolysis of benzene in aqueous solution [54] (2×10^{-3} mol dm^{-3}). Right-hand scale: (...) absorption 2 μs after the pulse (N_2-saturation). Left-hand scale: (●) 10 μs, (×) 20 μs, (△) 30 μs, (□) 40 μs and (○) 170 μs after the pulse (N_2O/O_2-4:1-saturation).

tion. There are clear indications that the peroxyl radical with the 1,4-cyclohexadiene structure **4** is dominant and that only a small amount of **5** is present in the equilibrium mixture.[54] This is surprising, since in the case of the open-chain pentadienyl radicals **6** formed from unsaturated fatty acids, which are also in equilibrium with their peroxyl radicals in the presence of O_2 [reactions (24) and (25)],[55, 56] conjugation of the double bonds is observed: thus the peroxyl radical **7** is formed preferentially and nonterminal peroxyl radicals with isolated double bonds appear to be of no importance.[57]

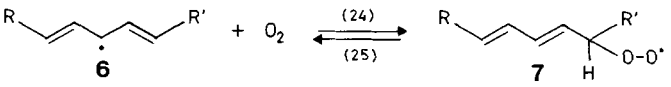

When a hydroxycyclohexadienyl radical contains a strongly electron-attracting group (as for example in the case of the adduct between benzonitrile and an ·OH radical) it is no longer possible to detect the formation of peroxyl radicals, perhaps because of a high rate of the back reaction.[58]

Further examples of oxygen addition which is reversible at room temperature are provided by benzyl[59] and thiyl radicals.[60] In the case of less strongly labilized peroxyl radicals, such as the allylperoxyl radical[61] or the trichloromethylperoxyl radical[62] (in the gas phase) the equilibrium becomes measurable only at higher temperatures.

3.2. Taft Constant σ^*, Dipole Moment and Spin Distribution of the Peroxyl Radical Group

The charge state of an —OH or —NHR group at a position next to the peroxyl radical function is of great importance in aqueous solution, since it has a considerable influence on the rate of the $HO_2^{\cdot}/O_2^{\cdot\ominus}$ elimination (see Section 5.1). The acidity (pK_a value) of these neighboring groups can be calculated for a large number of peroxyl radicals on the basis of increments if the Taft constant σ^* of the peroxyl radical group is known.[63] This constant was measured for the acetic acid system by means of pulse radiolysis; it could

be shown that the pK_a value of the peroxyl radical derived from acetic acid is 2.1 [equilibrium (28/29)],[64] i.e., considerably lower than that of acetic acid itself ([equilibrium (26/27)], $pK_a = 4.8$). The σ^* value for $-CH_2O_2^\bullet$ calculated from

$$CH_3CO_2H \underset{(27)}{\overset{(26)}{\rightleftharpoons}} CH_3CO_2^\ominus + H^\oplus \qquad pK_a = 4.8$$

$$^\bullet O_2CH_2CO_2H \underset{(29)}{\overset{(28)}{\rightleftharpoons}} {}^\bullet O_2CH_2CO_2^\ominus + H^\oplus \qquad pK_a = 2.1$$

these figures is 1.55, which is higher than the σ^* values for $-CH_2F$ (1.10) and $-CH_2CN$ (1.30). The peroxyl radical group is thus a strongly electron-attracting group. A σ^* value of 1.55 for $-CH_2O_2^\bullet$ corresponds to a σ^* value of 3.88 for the $^\bullet O_2$ increment. The pK_a values calculated for the peroxyl radicals derived from malonic acid and glycine anhydride using this increment do indeed agree well with the experimental values.[65]

As expected on the basis of the high σ^* value of the $^\bullet O_2CH_2$ group the alkylperoxyl radicals have a large dipole moment;[66] a value of 2.6 Debye has been estimated.[67]

No data from experiments in aqueous solution are available which would give us information on the spin distribution in peroxyl radicals; it is however known from other measurements that the spin density is not concentrated on the terminal oxygen atom but that a considerable spin density is found at the internal oxygen atom.[67-70] This is also the case for thiylperoxyl radicals $RSOO^\bullet$.[71]

3.3. Redox and Hydrogen Transfer Reactions of Peroxyl Radicals

Peroxyl radicals generally possess oxidizing properties. They thus react rapidly with good electron donors such as *N,N,N',N'*-tetramethylphenylenediamine (TMPD) or ascorbic acid via electron transfer [e.g., reaction (30)].[43, 72-79] Electron-attracting substituents at the peroxyl radical accelerate the electron transfer, so that $CCl_3O_2^\bullet$,[79] and $CH_3C(O)O_2^\bullet$.[77] are reduced by TMPD in a practically diffusion-controlled manner. The redox potential of the $CH_3O_2^\bullet$

$$RO_2^\bullet + TMPD \longrightarrow RO_2^\ominus + TMPD^{\bullet\oplus} \qquad (30)$$

radical has been estimated to be 0.6–0.7 V; $CCl_3O_2^\bullet$ must have a redox potential which is above 1.0 V.[75] The living cell contains two important antioxidants, the C and E vitamins. The rather unreactive radicals formed from these by oxidation have much lower redox potentials (0.28 and 0.48 V respectively[76]) than the peroxyl radicals, so that the latter can be deactivated by the two vitamins. While vitamin C is found in the aqueous phase, vitamin E is localized in the lipid phase. The concentration of vitamin E in the cell is generally much lower than that of vitamin C (in liver cells 2×10^{-5} mol dm^{-3} compared with 2×10^{-3} mol dm^{-3}).

The phenoxyl radical of vitamin E formed by attack of peroxyl radicals is rapidly repaired in vitro by vitamin C ($k = 1.6 \times 10^6$ dm^3 mol^{-1} s^{-1}),[80] and it had thus always been assumed that the latter would also have a protecting effect on vitamin E in vivo. Surprisingly, however, this is not the case.[81].

Halogenated peroxyl radicals react with dimethyl sulfide via electron transfer,[82] but in addition considerable amounts of dimethyl sulfoxide are also formed [reaction (31)].[83] The ROO–H bond energy (ΔH(HOO–H) = 376 ± 5 kJ mol^{-1}[84])

$$R(Hal)COO^\bullet + (CH_3)_2S \longrightarrow R(Hal)CO^\bullet + (CH_3)_2SO \qquad (31)$$

is comparable with the C–H bond energy of compounds which have only weakly bonded hydrogen atoms. For this reason peroxyl radicals can undergo hydrogen abstraction reactions [reaction (32)]. This reaction is one of the steps in

$$RO_2^\bullet + RH \longrightarrow RO_2H + R^\bullet \qquad (32)$$

the well-known chain reactions which play an important part in the autoxidation of, for example, unsaturated fatty acids[55] and ethers.[85, 86]. The increase of the chain length with increasing temperature is due to acceleration of reaction (32). Almost no data have been published for aqueous systems. This is understandable, since reaction (32) is in general slow and concentrations in the molar range are necessary for a proper kinetic analysis; such concentrations are three orders of magnitude greater than those used for typical radiation-chemical studies in aqueous solution. A comparison with data from experiments in organic solvents (hydrogen donors) is thus not possible; however, the data in Ref. [87] allow us to estimate an activation energy of ca. 55 kJ mol^{-1} for the 2-methyltetrahydrofuran system. Similar activation energies were found in organic solvents for a series of readily oxidizable compounds;[88] however, the kinetic parameters depend on the polarity of the medium because of the highly polar structure of the peroxyl radicals[57] and thus cannot simply be transferred uncritically from the organic phase to aqueous solutions.

The $HO_2^\bullet/O_2^{\bullet\ominus}$ radicals occupy a special place within the family of peroxyl radicals, since they have not only oxidizing properties but also, in the case of $O_2^{\bullet\ominus}$ in particular, reducing ones. Their reactions in aqueous solutions will be discussed in the next section. A comparison with the radical chemistry of $O_2^{\bullet\ominus}$ in organic solvents, which is different from that in aqueous media[89-91] cannot be treated here for lack of space.

4. The $HO_2^\bullet/O_2^{\bullet\ominus}$ System, a Special Case

There are hardly any peroxyl radical systems in aqueous solution in which $HO_2^\bullet/O_2^{\bullet\ominus}$ radicals do not play a part, since many peroxyl radicals decompose unimolecularly with formation of $HO_2^\bullet/O_2^{\bullet\ominus}$, or the latter are formed by bimolecular reactions of the peroxyl radicals. Thus, before the reactions of organic peroxyl radicals are covered it is necessary to discuss the properties of $HO_2^\bullet/O_2^{\bullet\ominus}$. A recently published review article surveys this area in detail;[92] here we shall only emphasize some important aspects and refer to some facts not mentioned in that article.

The hydroperoxyl radical $HO_2^\bullet$ has a pK_a value of 4.8 [reactions (33/34)] (the best value,[36] based on a series of radiation-chemical studies.[93-98]). Thus, the superoxide radical $O_2^\bullet$ predominates in neutral solution.

$$HO_2^{\bullet} \underset{(34)}{\overset{(33)}{\rightleftharpoons}} O_2^{\bullet\ominus} + H^{\oplus} \quad pK_a = 4.8$$

$O_2^{\bullet\ominus}$ absorbs much more strongly in the UV ($\lambda_{max} = 243$ nm; $\varepsilon = 2350\ dm^3\ mol^{-1}\ cm^{-1}$) than does $HO_2^{\bullet}$ ($\lambda_{max} = 228$ nm; $\varepsilon = 1400\ dm^3\ mol^{-1}\ cm^{-1}$); this difference can be put to use for the detection of $HO_2^{\bullet}/O_2^{\bullet\ominus}$, for example by following the pH-dependence of the absorption at 260 nm.[36, 92]

The $HO_2^{\bullet}$ radical is an acid, so that its formation can be followed in weakly acid media (pH > 4.8, the pK_a of $HO_2^{\bullet}$) by measuring the increase in conductivity, in alkaline solution, by following the decrease in conductivity. Since these conductivity changes are only observed for short periods of time because of the bimolecular termination of $HO_2^{\bullet}/O_2^{\bullet\ominus}$ they must be followed by the pulse radiolysis technique; an example is shown in Figure 3.

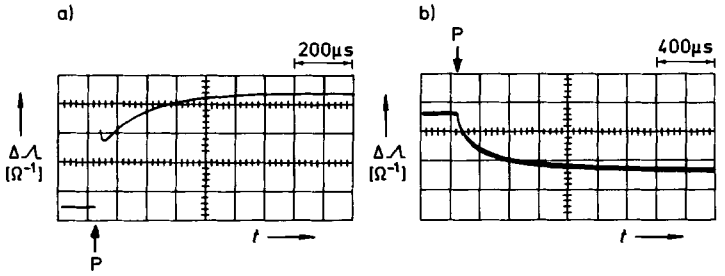

Fig. 3. Pulse radiolysis of diethyl ether in aqueous solution; diagram from Ref. [149] (10^{-3} mol dm^{-3}, N_2O/O_2-(4:1)-saturation). Conductivity change $\Delta\Lambda$ as a function of time. A: pH 6.5, dose 15 Gy, 100 µs/division. B: ph 9.8, dose 10 Gy, 200 µs/division.

This bimolecular termination involves a disproportionation of $HO_2^{\bullet}$ and $O_2^{\bullet\ominus}$ to give hydrogen peroxide and oxygen [reactions (35) and (36); $k_{35} = 8.6 \times 10^5\ dm^3\ mol^{-1}\ s^{-1}$; $k_{36} = 1.0 \times 10^8\ dm^3\ mol^{-1} s^{-1}$]. No reaction (37) between two $O_2^{\bullet\ominus}$ radicals is observed, so that such a reaction must be slower than $0.35\ dm^3\ mol^{-1}\ s^{-1}$.[36] The rate constant of

$$HO_2^{\bullet} + HO_2^{\bullet} \longrightarrow H_2O_2 + O_2 \quad (35)$$
$$HO_2^{\bullet} + O_2^{\bullet\ominus} \longrightarrow HO_2^{\ominus} + O_2 \quad (36)$$
$$2\,O_2^{\bullet\ominus} \longrightarrow O_2^{2\ominus} + O_2 \quad (37)$$

bimolecular disproportionation of the $HO_2^{\bullet}/O_2^{\bullet\ominus}$ radicals is plotted in Figure 4 in logarithmic units against the pH value. Under strongly acid conditions the reaction is controlled by the $HO_2^{\bullet}$ radical. As long as this is virtually the only species present, the observed rate constant (k_{obs}) has the value of

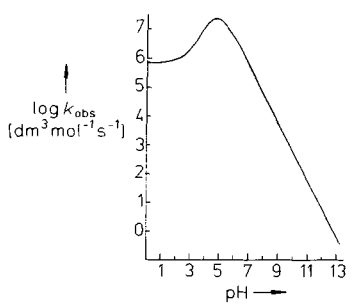

Fig. 4. Observed rate constant (second order) of the decay of $HO_2^{\bullet}/O_2^{\bullet\ominus}$ as a function of pH (after Ref. [36]).

k_{35}. Reaction (36) becomes more important as the pH increases, and k_{obs} also increases. The large linear decrease at high pH reflects the fact that $O_2^{\bullet\ominus}$, which is now dominant, can only react with the $HO_2^{\bullet}$ radicals which are present in ever decreasing quantities in the equilibrium mixture. If a reaction between two $O_2^{\bullet\ominus}$ radicals (37) were of importance then a plateau would be observed at high pH values, as is the case in strongly acid conditions for the disproportionation of two $HO_2^{\bullet}$ radicals.

The question whether singlet oxygen is formed in the disproportionation of $HO_2^{\bullet}/O_2^{\bullet\ominus}$ radicals (e.g., Ref. [99]; a survey given in Ref. [100]) must, according to recent results,[101, 102] be answered in the negative.

In contrast to organic peroxyl radicals, which have only oxidizing properties, the $HO_2^{\bullet}/O_2^{\bullet\ominus}$ radical can both be reduced to hydrogen peroxide and oxidized to oxygen. Tetranitromethane is rapidly reduced by $O_2^{\bullet\ominus}$ to the nitroform anion [reaction (38); $k_{38} = 1.9 \times 10^9\ dm^3\ mol^{-1}\ s^{-1}$], while the reaction of the $HO_2^{\bullet}$ radical is slower by more than five orders of magnitude.[103]

$$O_2^{\bullet\ominus} + C(NO_2)_4 \longrightarrow O_2 + C(NO_2)_3^{\ominus} + NO_2^{\bullet} \quad (38)$$

Since $O_2^{\bullet\ominus}$ is the only peroxyl radical which can reduce tetranitromethane, reaction (38) provides us with a clear proof of the existence of $O_2^{\bullet\ominus}$ in pure peroxyl radical systems (i.e., when no other reducing radicals are present). The nitroform anion is stable and absorbs strongly at 350 nm (ε(350 nm) = $15000\ dm^3\ mol^{-1}\ cm^{-1}$[104]), a wavelength at which peroxyl radicals normally absorb hardly at all. Thus, reaction (38) is suitable for the quantitative determination of $O_2^{\bullet\ominus}$ both in pulse-radiolytic experiments and during continuous γ-irradiation.

The $O_2^{\bullet\ominus}$ radical makes its reducing properties felt in its reactions with other peroxyl radicals, with which it reacts via electron transfer to give hydroperoxides [reaction (39)]. The

$$RO_2^{\bullet} + O_2^{\bullet\ominus} + H^{\oplus} \longrightarrow RO_2H + O_2 \quad (39)$$

rate constant of this reaction depends strongly on the redox potential of the peroxyl radical. The strongly oxidizing acetylperoxyl radical reacts at a rate of $10^9\ dm^3\ mol^{-1}\ s^{-1}$,[77] for the $HO_2^{\bullet}$ radical the rate is $10^8\ dm^3\ mol^{-1}\ s^{-1}$ [reaction (36)], while for the more weakly oxidizing α-hydroxyethylperoxyl radical the rate was estimated to be only $10^7\ dm^3\ mol^{-1}\ s^{-1}$.[105]

Ozone reacts with $O_2^{\bullet\ominus}$ according to reaction (40) via electron transfer to give $^{\bullet}OH$ radicals;[106, 107] this reaction plays a very important role in the purification of drinking water by ozone.[20] The self-exchange reaction (41) of $O_2^{\bullet\ominus}$ is also an

$$O_3 + O_2^{\bullet\ominus} + H_2O \longrightarrow {}^{\bullet}OH + 2\,O_2 + OH^{\ominus} \quad (40)$$

electron transfer reaction. An attempt to estimate its rate using available data and the Marcus theory led to an uncertainty of almost 14 orders of magnitude (10^{-8}–$10^{5.7}\ dm^3\ mol^{-1}\ s^{-1}$).[108] Radiation-chemical techniques have recent-

ly been used to determine this value more exactly, the result being $450 \pm 160\,dm^3\,mol^{-1}\,s^{-1}$.[109]

$$O_2^{\bullet\ominus} + O_2 \longrightarrow O_2 + O_2^{\bullet\ominus} \quad (41)$$

In contrast to $O_2^{\bullet\ominus}$, which undergoes no hydrogen abstraction reactions,[87,91,110] the $HO_2^{\bullet}$ radical behaves like a "normal" peroxyl radical. For example, it reacts with linoleic acid[110] to give radicals of the pentadienyl type ($k \approx 300\,dm^3\,mol^{-1}\,s^{-1}$) with a rate constant very similar to that found for 1,4-cyclohexadiene in acetonitrile ($k = 160\,dm^3\,mol^{-1}\,s^{-1}$).[111]

It is thus particularly surprising that $O_2^{\bullet\ominus}$ reacts relatively rapidly with phenolic antioxidants such as pyrogallol **8a** or the propyl ester of gallic acid **8b** ($k = 3.4 \times 10^5$ and $2.6 \times 10^5\,dm^3\,mol^{-1}\,s^{-1}$ respectively) to give the phenoxyl radicals **10** and **11**.[112] For energetic reasons[113–115] the latter cannot be formed via a hydrogen transfer reaction. It must be assumed that $O_2^{\bullet\ominus}$ adds to the benzene ring and that the adduct radical **9** splits off $HO_2^{\ominus}$ or H_2O_2 subsequent to protonation at the peroxyl function [reactions (42) and (43)]. Moreover, the $HO_2^{\bullet}$ radical reacts much more slowly with such phenolic antioxidants.[112] This observation supports the suggested mechanism, since the $HO_2^{\bullet}$ radical should be the more reactive in a hydrogen transfer reaction. Furthermore $O_2^{\bullet\ominus}$ is also able to oxidize the phenoxyl radical **11** (probably via **12**) to the quinone **13** [reactions (46) and (47)].

Phenols which contain two rather than three OH groups react noticeably slower with $O_2^{\bullet\ominus}$. Thus, for example, the rate constant k for catechol was found to be $< 8 \times 10^4\,dm^3\,mol^{-1}\,s^{-1}$.[112] The oxidation of 3,4-dihydroxymandelic acid **14** by $O_2^{\bullet\ominus}$ leads via decarboxylation to 3,4-dihydroxybenzaldehyde **22**.[116] In this case again, the initial step is presumably an addition of $O_2^{\bullet\ominus}$ [reaction (48)]. The adduct radical **16** must have a high pK_a value, and **15** will thus undergo rapid protonation of the peroxylate function [reaction (49)]. At high oxygen concentration (i.e., in O_2-saturated solution) **16** will be converted into the peroxyl radical **17**; this type of peroxyl radical rapidly splits off $HO_2^{\bullet}$. Loss of H_2O_2 then gives the quinone **18** [reactions (50) and (51)]. $O_2^{\bullet\ominus}$ is reformed, and a chain reaction occurs. In competition with reaction (50) **16** can split off H_2O_2 (via **19**) to give the phenoxyl radical **20** [reactions (52) and (53)]. This does not react with O_2, but disproportionates with a second radical to give 3,4-dihydroxymandelic acid **14** and its quinone **18** [reaction (54)]. The latter can now undergo decarboxylation and forms the final product 3,4-dihydroxybenzaldehyde **22** via the enol **21**. The reation steps from **20** to **22** were established by means of pulse radiolysis.[117] The reaction scheme makes clear that at the stage of intermediate **16** a branching occurs, which allows a chain reaction via reaction (50). Reaction (52) does not lead to a chain reaction; it can be accelerated by the

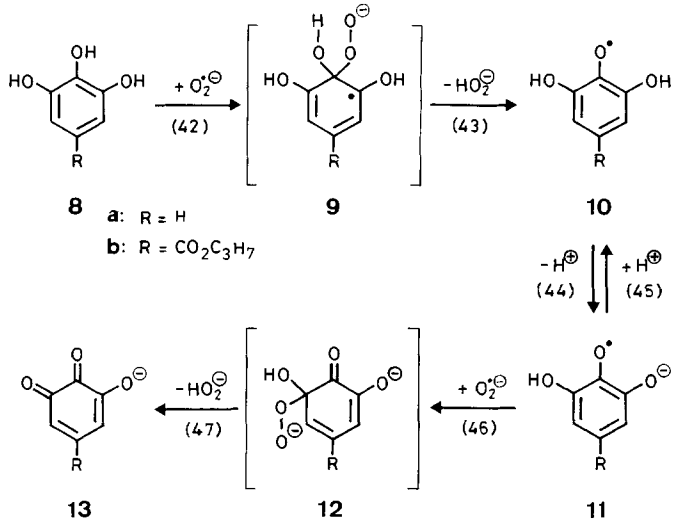

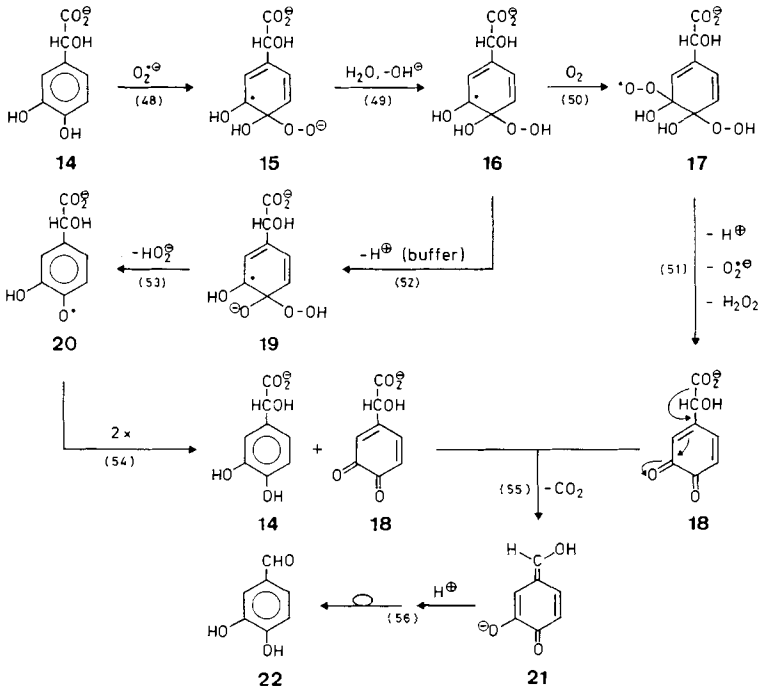

addition of a borate buffer to such an extent that the chain reaction is suppressed.

Adrenalin belongs to the same class of compounds, so that it is not surprising that $O_2^{\bullet\ominus}$ also causes its oxidation.[116, 118]

A remarkable process is the cleavage of the ketomalonate anion **23** by $O_2^{\bullet\ominus}$ to give CO_2 and monoperoxalic acid **25**.[119] The dependence of $G(CO_2)$ on the reciprocal square root of the dose rate shown in Figure 5 (left) and the dependence on the concentration of ketomalonic acid (right) [$G(CO_2) > 200 \times 10^{-7}$ mol J^{-1} can be achieved!] are good indications for the occurrence of a chain reaction.

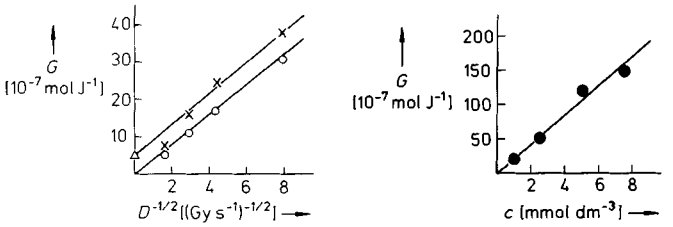

Fig. 5. γ-Radiolysis of ketomalonate [119] (10^{-3} mol dm^{-3}) in the presence of sodium formate (10^{-2} mol dm^{-3}) in aqueous solution (pH 10, N_2O/O_2-4:1-saturation). G Values of CO_2 (×) and monoperoxalic acid (o) as a function of (dose rate)$^{-1/2}$. The zero value for CO_2 (Δ) is the value from the radiolysis of formate in the absence of ketomalonate. *Inset:* G value of monoperoxalic acid as a function of ketomalonate concentration.

This reaction was unexpected; it may perhaps involve the adduct **24**, which is subject to the β-cleavage typical of oxyl radicals [reaction (58)]. The $CO_2^{\bullet\ominus}$ thus formed propagates the chain by means of its rapid reaction with oxygen to give $O_2^{\bullet\ominus}$ [reaction (18)]. It is not known with certainty how the adduct **24** is formed. The rate constant for the propagation is ca. 150 dm^3 mol^{-1} s^{-1}.

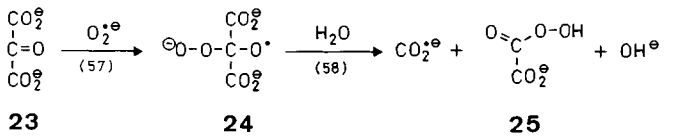

The reaction of $O_2^{\bullet\ominus}$ with thiolate ions, studied for the example of 1,4-dithiothreitol, is also a chain reaction;[42] its final products are water and the disulfide **31**. Since $O_2^{\bullet\ominus}$ can neither abstract a hydrogen atom from the thiol (present in equilibrium) nor accept an electron from the thiolate anion, another mechanism must be involved. Thiolate ions readily form complexes with radicals (e.g. **32** with its three-electron bond typical of complex sulfur radicals[120]). The formation of **26** is thus probably the initial step [reaction (59)]. Rapid protonation of **26** at the peroxylate function would be followed by decomposition of the adduct radical **27** to give the sulfinyl radical **28** and hydroxide ion [reaction (62)]. Chain propagation occurs via reactions (64)–(66); sulfenate ions **29** and thiyl radicals **30** are also intermediates in the reaction.

It was mentioned in the Introduction that the $O_2^{\bullet\ominus}$ radical is a dangerous poison for the living cell. The concentration in the cell of $O_2^{\bullet\ominus}$, which is continually formed in a number of reactions, is therefore kept low by special enzymes, the superoxide dismutases (SOD).[121, 122] The SODs are metal-

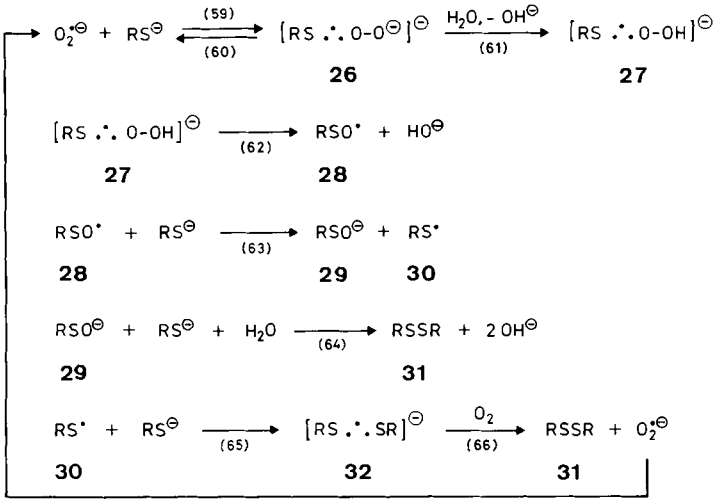

loenzymes which can contain Cu/Zn, Fe or Mn.[122, 123] Common to all these enzymes is that the oxidation state of the metal can change, as in the two reactions (67) and (68).

$$SOD\text{–}Cu^{2\oplus} + O_2^{\bullet\ominus} \longrightarrow SOD\text{–}Cu^{\oplus} + O_2 \quad (67)$$

$$SOD\text{–}Cu^{\oplus} + O_2^{\bullet\ominus} + 2H^{\oplus} \longrightarrow SOD\text{–}Cu^{2\oplus} + H_2O_2 \quad (68)$$

This is not the place to discuss the interesting chemistry of the SODs, but it should be pointed out that pulse radiolytic methods have played an important part in understanding the kinetics of the $O_2^{\bullet\ominus}$/SOD reactions (e.g., Refs. [124–135]).

As is so often the case for electron transfer processes, the transition metal/$O_2^{\bullet\ominus}$ reaction generally involves adducts. As a result of the reactions of such transition metal ion/$O_2^{\bullet\ominus}$ complexes reactive intermediates (or •OH radicals) can be formed, which are able for example to induce damage to DNA.[136] They could be a cause of the toxicity of $O_2^{\bullet\ominus}$. Such intermediates have been well characterized in many cases.[92]

5. Reactions of Peroxyl Radicals: a Survey

Studies of the reactions of peroxyl radicals in aqueous solution have made clear that a series of reaction pathways are possible which do not occur, or if so only very slowly, in the gas phase and in nonpolar solutions. This also applies to some secondary reactions, for example those of oxyl radicals. The two following sections will provide a brief survey of the various types of reaction, while Section 6 will be concerned with particular aspects of the peroxyl radical chemistry of certain classes of compound.

5.1. Monomolecular Reactions

A number of peroxyl radicals are able to eliminate $O_2^{\bullet\ominus}$. In order for the rate of this reaction to be measurable the positive charge must be stabilized by a heteroatom [reaction (69)]. The influence of the substituents is much more pronounced in charge stabilization than in the stabilization of radical centers.[137] An alkoxy group situated next to the

peroxyl radical function (**33**, X = O) does not suffice to make the reaction much faster than 1 s^{-1},[138] while two alkoxy groups (**33**, X = O, R′ = OR) accelerate the reaction to almost 10^5 s^{-1};[139] with a dimethylamino group as the stabilizer of the positive charge (**34**, X = NR) the reaction is so fast that an intermediate peroxyl radical (**33**, X = NR) can no longer be detected.[140] The rapid formation of $HO_2^{\bullet}/O_2^{\bullet\ominus}$ from the peroxyl radicals of aldehyde hydrates (**35**, R = H) and hemiacetals **35**[77, 141, 142] may also involve an elimination of $O_2^{\bullet\ominus}$, although in these cases the proton is split off in a concerted manner together with $O_2^{\bullet\ominus}$ [reaction (70)]. The $HO_2^{\bullet\ominus}$-elimination reactions starting from α-hydroxyalkylperoxyl radicals **37** [reaction (71)] are mechanistically different, and a five-membered transition state has been assumed to be involved.[143] This type of reaction possibly also includes the formation of $HO_2^{\bullet}$ from cyclohexadienylperoxyl radicals **42** [reaction (76)].[27, 144] In this case the driving force would

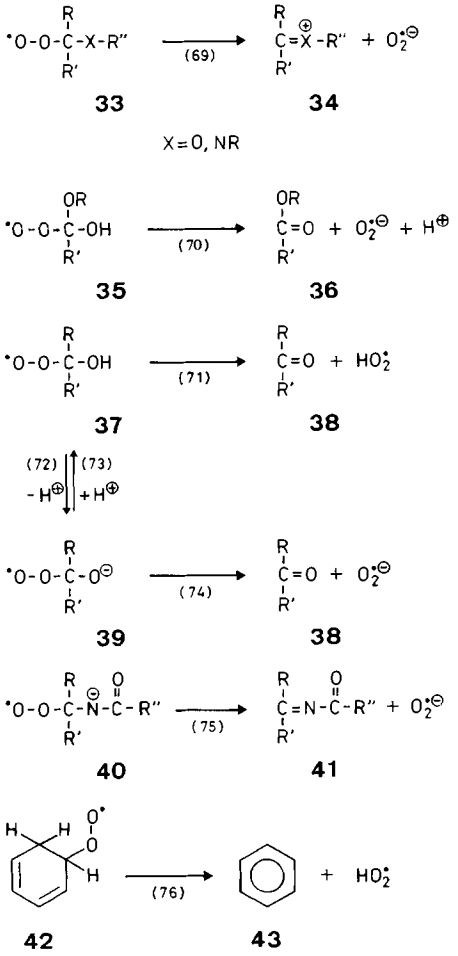

33 **34** **35** **36** **37** **38** **39** **38** **40** **41** **42** **43**

be the increase in conjugation energy as the aromatic product **43** is formed. A deprotonation of the α-hydroxyalkylperoxyl radicals **37** leads to their anions **39**, which very rapidly eliminate $O_2^{\bullet\ominus}$ [reaction (74); $k_{74} > 10^6 s^{-1}$].[105, 145, 146] This is also true for the peroxyl radical anions derived from the peptides **40**, which are however noticeably more stable ($k_{75} < 3.7 \times 10^6$ s^{-1})[147] than the peroxyl radical anions of the alcohols **39**.

If weakly bonded hydrogen atoms are in a suitable position (**44**, six-membered ring as the transition state) intramolecular hydrogen transfer reactions can become more important at low dose rates (i.e., long lifetime of the peroxyl radical with respect to termination reactions [reaction (77)].[138, 148, 149] Peroxyl radicals of type **46** can also add intramolecularly to double bonds[150] [reaction (78)]; in the benzene system this reaction leads to endoperoxide radicals

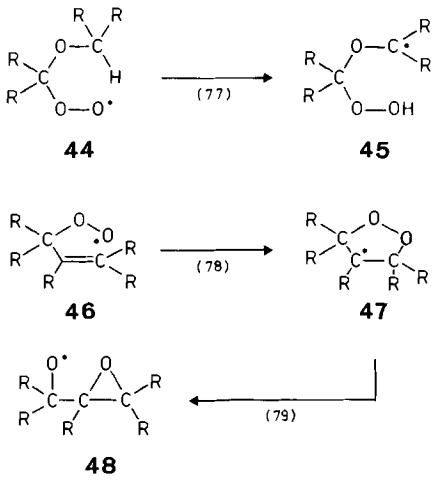

44 **45** **46** **47** **48**

(Section 6.7). The peroxyadduct radicals can decompose with formation of the epoxides **48** [reaction (79)].[150, 151]

5.2. Bimolecular Reactions

Peroxyl radicals undergo a head-to-head termination reaction[152] to form intermediate tetroxides **49**, which are in equilibrium with the peroxyl radicals at low temperatures in organic solvents [reactions (80) and (81)].[153–158]

An equilibrium is possible because the decomposition of the tetroxide **49** to form products [reactions (82)–(85)] has a higher activation energy than decomposition to give two peroxyl radicals [reaction (81)].[*] At higher temperatures the decomposition of the tetroxide to form products becomes more important. Tetroxides **49** have so far not been observed during pulse radiolysis experiments in aqueous solution [$c(RO_2^{\bullet}) < 5 \times 10^{-5}$ mol dm^{-3}], and under these conditions the formation of products always shows second-order kinetics.[149] The formation of tetroxides in higher concentrations would have made itself felt by the presence of a noticeable first-order component.

Bimolecular rate constants for product formation of $> 10^9$ dm^3 mol^{-1} s^{-1} were determined in water for a series of primary ($RCH_2O_2^{\bullet}$) and secondary ($R_2CHO_2^{\bullet}$) peroxyl radicals.[149, 159] This indicates that in these cases the rate of decomposition of **49** to give products must be comparable with that of the back reaction to give two peroxyl radicals. This is however not the case for all primary and secondary peroxyl radicals and in particular not for tertiary peroxy radicals ($R_3CO_2^{\bullet}$). Thus the rate constant for the bimolecular

[*] *Note added in proof* (September 5, 1991): It has recently been proposed [S. L. Khursan, V. S. Martem'yanov, E. T. Denisov, *Kinetics Catalysis (Engl. Transl.) 31* (1990) 899–907] that the product-forming reactions of the tetroxide have their origin in the asymmetric homolysis ROOOOR → RO• + •OOOR

termination of the tertiary peroxyl radical derived from diisopropyl ether has been estimated as $2k \leqq 2\times10^7\ dm^3\,mol^{-1}\,s^{-1}$.[138] The tert-butylperoxyl radical reacts even more slowly ($2k = 2\times10^4\ dm^3\,mol^{-1}\,s^{-1}$).[160] A smaller number of reaction pathways is available to tertiary peroxyl radicals than to primary or secondary radicals [reactions (82) and (83) are not possible]; this may be *one* reason for their slow bimolecular decay. It has recently been demonstrated for certain organic solvents that the rate of bimolecular recombination of tertiary[161] and secondary[162] peroxyl radicals increases when the Taft σ^* constants of their substituents increase. A similar systematic dependence was however not found for primary peroxyl radicals.[162]

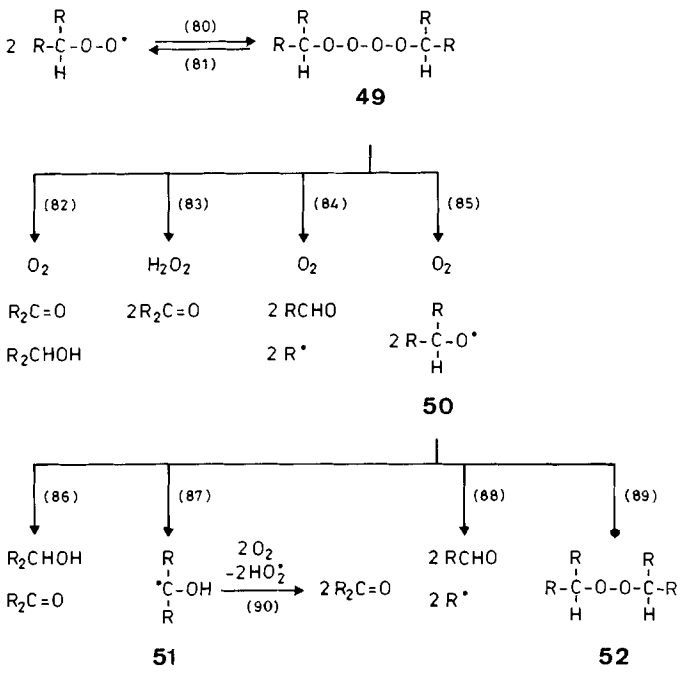

The fact that primary and secondary peroxyl radicals generally terminate several orders of magnitude faster than tertiary radicals has been explained in terms of the ability of the former to disproportionate to the hydroperoxide and the Criegee intermediate RR'COO (R' = H, R),[163], one of these species then being responsible for a chain reaction.[164]. In the case of the methylperoxyl radical it was possible to show that in aqueous solution such a reaction cannot play an important role under these conditions.[165]

The best known reaction is the Russell reaction, in which two primary or secondary peroxyl radicals undergo an electrocyclic reaction (i.e., without the formation of free radicals as intermediates) to give molecular oxygen, a product with a C=O function and one with an OH function [reaction (82)].[166] A six-membered transition state **53** has been postulated. Two decomposition pathways are possible, which both obey the spin conservation postulate: either decomposition into a singlet carbonyl compound, an alcohol and singlet oxygen ($^1O_2$), or into a triplet carbonyl compound,[167] alcohol and triplet (ground state) oxygen. In organic solvents $^1O_2$ could be detected in peroxyl reactions,[168, 169] but not in aqueous solution. The short lifetime of $^1O_2$ in aqueous solutions makes such experiments more difficult.

A further electrocyclic process leads to the formation of H_2O_2 and two carbonyl compounds [reaction (83)]. The transition state could involve two five-membered rings as in **54**, while in water the inclusion of two water molecules to form two six-membered rings as in **55** is also possible. This interesting reaction was first described for the reaction of two cyclopentylperoxyl radicals in cyclopentane at low temperatures,[170] while it is of general importance in aqueous solution. In the case of the bimolecular decay of the hydroxymethylperoxyl radicals this reaction is in fact the major one.[143]

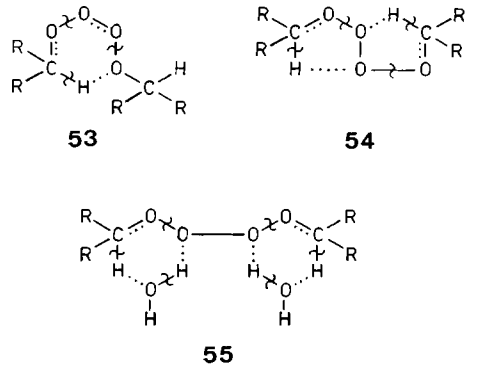

The decomposition of peroxyl radicals to give molecular oxygen and two oxyl radicals **50** [reaction (85)] is a further well-known reaction pathway.[1] A disproportionation of the oxyl radicals in the solvent cage (reaction (86); see Ref. [171]) leads to the same products as the Russell mechanism, so that these two processes cannot be clearly separated. A recombination of two oxyl radicals to give peroxides **52** [reaction (89)] is not of great importance in aqueous solution,[160, 172] since reaction (85) probably leads preferentially to $^3O_2$ and a triplet oxyl radical pair and to only a small degree to $^1O_2$ and a singlet radical pair. Thus the probability of recombination in the solvent cage is reduced and the probability that the oxyl radicals **50** can leave it is high.

A further reaction thus gains in importance, i.e. the water-catalyzed rearrangement of an oxyl radical **50** to the tautomeric α-hydroxyalkyl radical **51** [reaction (87)].[173–176] Hydrogen shifts of this type have not been observed in the gas phase or in organic solvents;[177] this is in agreement with theoretical predictions[178] which indicate it to have an activation energy that is too high. In water the reaction is, however, very fast ($t_{1/2}$ < several μs). Mechanistic details have not so far been elucidated. Reaction (87) is of particular interest, since $HO_2^•/O_2^{•\ominus}$ is formed in the subsequent reaction (90). Since the latter can be very fast, the rate of formation of $HO_2^•/O_2^{•\ominus}$ is in this case determined by the bimolecular termination reaction (80).

In the case of primary and secondary oxyl radicals **50** the 1,2-H shift is generally so fast that it can take precedence over the long-known β-fragmentation of the oxyl radicals **50** [reaction (88)]. In the case of tertiary oxyl radicals the latter is however the typical decomposition pathway. The solvent water also has a considerable influence here. Thus, in the gas phase the decay constant of the *tert*-butoxy radical $k = 10^3\ s^{-1}$;[179] it increases in solution with increasing polarity of the solvent[180] and in water reaches a value of $k >$

$10^6\ s^{-1}$.[181] For this reason H-abstraction reactions [reaction (91)], which are typical of oxyl radicals in organic solvents, do not take place in dilute aqueous solution. Frag-

$$RO^{\bullet} + RH \longrightarrow ROH + R^{\bullet} \quad (91)$$

mentation products such as those shown in the sequence of reaction (85) followed by reaction (88) could perhaps also be formed via a "zipper" mechanism [reaction (84)]; evidence for this will be discussed in Section 6.2.

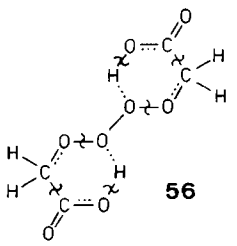

56

A further electrocyclic fragmentation reaction was observed in the acetate system.[182] It leads to formaldehyde and CO_2, perhaps via the transition state **56** (or ionized analogues).

6. The Peroxyl Radical Chemistry of Individual Classes of Compound

In any real system it is never the case that merely one of the possible processes discussed above is observed; various processes always occur in parallel. It would exceed the limits of the present article to give a detailed account of the decomposition pathways followed in each of the cases studied together with their percentage contributions. Such figures, as far as they have been measured, can be found in the original literature. In the following sections we shall attempt to emphasize particular aspects as well as to make the reader acquainted with the scope of the material available.

The manner in which we have ordered the following sections may appear arbitrary; we have however attempted to group together compounds with functions that are structurally related and which thus often induce a similar peroxyl radical chemistry. The sections bear the names of the substrate molecules involved. We have devoted a section to DNA and its model systems because of their importance for radiation biology and cancer radiation therapy.

6.1. Alkanes

The only unsubstituted alkylperoxyl radicals which have so far been studied are the methylperoxyl[165] and the cyclopentyl- and cyclohexylperoxyl radicals.[183] The alkanes from which these are derived have only one type of hydrogen atom, so that ·OH-radical-induced hydrogen abstraction leads to only one single alkyl radical species.

The low solubility of the alkanes in water plays a not unimportant part in these studies, since product analysis

Table 1. Products of methane radiolysis in aqueous solution [165] ($c(CH_4)$ = 0.08 mol dm^{-3}, $c(N_2O)$ = 0.1 mol dm^{-3}, $c(O_2) = 1.3 \times 10^{-3}$ mol dm^{-3}) and their G values in units of 10^{-7} mol J^{-1}.

Product	G (pH ≤ 6)	G (pH 8)[a]	Product	G (pH ≤ 6)	G (pH 8) [a]
CH_2O	2.9	3.3	HCOOH	0.3	0.0 5
CH_3OH	1.6	–	CH_3OOCH_3	0.1	–
CH_3OOH	0.8	0.7	H_2O_2	2.2	2.4

[a] Buffered.

requires that the radiation-chemically produced ·OH radicals do not react with the products but only with the alkanes even at higher doses. This is a particular problem in the case of methane, which is only slightly soluble at atmospheric pressure. Since it must also be mixed with N_2O/O_2, its concentration in water is reduced accordingly. In addition methane reacts relatively slowly with ·OH radicals ($k = 1.1 \times 10^8$ $dm^3\ mol^{-1}\ s^{-1}$) while the products derived from it react an order of magnitude faster. For this reason the γ-radiolysis was carried out in an autoclave at a methane pressure of 50 bar.[165] The products are listed in Table 1.

This method is less suitable for pulse radiolysis studies, for which it is possible to make use of the reaction of the ·OH radical with dimethyl sulfoxide;[184] this produces methyl radicals (and methylsulfinic acid) in 92% yield[172] [reaction (92), $k_{92} = 6.6 \times 10^9\ dm^3\ mol^{-1}\ s^{-1}$]. This methyl radical

$$^{\bullet}OH + (CH_3)_2SO \longrightarrow [(CH_3)_2S(O^{\bullet})OH] \longrightarrow {}^{\bullet}CH_3 + CH_3SO_2H \quad (92)$$

source was used to measure the rate constants $k(^{\bullet}CH_3 + O_2 \rightarrow CH_3O_2^{\bullet}) = 1.7 \times 10^9\ dm^3\ mol^{-1}\ s^{-1}$ and $2k(2\ CH_3O_2^{\bullet} \rightarrow \text{products}) = 1.8 \times 10^8\ dm^3\ mol^{-1}\ s^{-1}$.[185] Since the methylperoxyl radical is only a weak oxidizing agent[75] the reaction with $O_2^{\bullet\ominus}$ is slow and the rate constant cannot be measured by means of pulse radiolysis; however, the value for the bimolecular termination of the methylperoxyl radicals and the data from the product analysis (Table 1) lead to an estimated value for $k(CH_3O_2^{\bullet} + O_2^{\bullet\ominus} + H^{\oplus} \rightarrow CH_3O_2H)$ of $2.5 \times 10^7\ dm^3\ mol^{-1}\ s^{-1}$.[185]

The formation of the products listed in Table 1 can readily be explained on the basis of the general reaction scheme given above [reactions (80)–(90)], the methoxyl/hydroxymethyl rearrangement[176] playing an important role. The hydroxymethylperoxyl radicals undergo spontaneous elimination of $HO_2^{\bullet}$ (see Section 6.2) only slowly, so that they are also subject to bimolecular termination reactions which lead to the production of formic acid. If the solution is buffered at pH 8, the elimination of $HO_2^{\bullet}/O_2^{\bullet\ominus}$ is accelerated by reactions (72) and (74). Thus G(formaldehyde) increases while G(formic acid) decreases correspondingly (Table 1).

The peroxides **52** formed according to reaction (89) are generally not detected, since they are often formed in low yields, their detection is difficult, and in the main no material is available for comparison in order to confirm their identity. In the case of methane radiolysis the yield of dimethyl peroxide is less than 4% of the methylperoxyl radicals originally formed, which demonstrates that this reaction pathway is indeed unimportant. The peroxide yield is comparably low for the termination of *tert*-butylperoxyl radicals.[160]

The cyclopentylperoxyl radical in cyclopentane decomposes to give only cyclopentanone and cyclopentanol.[170] In

aqueous solution, however, various reactions occur in parallel; the most important single process (40%) is ring cleavage.[183] Cyclohexylperoxyl radicals also decompose in aqueous solution with ring cleavage, though since the cyclohexane system is less strained the contribution of this pathway is only 15%.[183] This ring cleavage is particularly interesting; were intermediate oxyl radicals **57** to be formed, these would rapidly rearrange to give α-hydroxycyclopentyl radicals **58** [reaction (93)], so that β-fragmentation [reaction (94)] would not be able to compete.[175] The formation of fragmentation products in such a high yield has been explained on the basis of the "zipper mechanism" [reaction (84)].[183] The sole formation of α-hydroxycyclopentyl radicals **58** as established by ESR spectroscopy could be an artefact[186], since the reversibility of reaction (94) [reaction (95)][187] with a subsequent fast and irreversible 1,2-H shift [reaction (93)] should make the detection of the intermediate ring-opened radical **59** impossible. This indicates that further evidence for the suggested zipper mechanism is required.

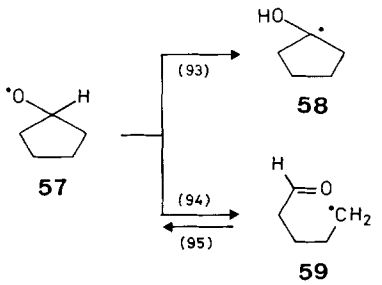

6.2. Alcohols, Ethers, Acetals, Aldehyde Hydrates and Carbohydrates

Attack of •OH radicals on the alcohols methanol, ethanol and 2-propanol lead to the preferential formation of α-hydroxyalkyl radicals.[188] It has already been mentioned that the peroxyl radicals derived from the latter eliminate $HO_2^{\bullet}$[105, 145, 146, 189] [reaction (71)] or split off $O_2^{\bullet\ominus}$ subsequent to deprotonation of the OH function [reaction (74)].

The elimination of $O_2^{\bullet\ominus}$ from the radical anion must occur very rapidly ($k > 5 \times 10^5\ s^{-1}$; the temporal resolution is limited by the rate of the O_2-addition), since a pre-equilibrium has not so far been observed (but compare the analogous peptide-peroxyl radicals, Section 6.3). The spontaneous $HO_2^{\bullet}$ elimination depends to a large extent on the neighboring substituents; thus it cannot be measured for the peroxyl radical $HOCH_2O_2^{\bullet}$ derived from methanol ($k < 3\ s^{-1}$), while that derived from ethanol, $CH_3CH(OH)O_2^{\bullet}$, eliminates $HO_2^{\bullet}$ at a rate of $50\ s^{-1}$ and that from 2-propanol at a rate of $650\ s^{-1}$.[146] $HO_2^{\bullet}/O_2^{\bullet\ominus}$ is formed within 10 μs from the peroxyl radicals $(HO)_2CHO_2^{\bullet}$ derived from formaldehyde hydrate and $CH_3C(OH)_2O_2^{\bullet}$ derived from acetaldehyde hydrate.[77, 141]

Since the $HO_2^{\bullet}$ elimination from hydroxymethylperoxyl radicals is so slow in neutral solution, the latter react with one another at the high dose rate of a pulse radiolysis experiment to give two molecules of formic acid and one of hydrogen peroxide [reaction (83)].[143] This type of reaction is also observed in the ethanol system, though other processes (such as the Russell mechanism) occur here as well.[105]

β-Hydroxyalkylperoxyl radicals are formed to the extent of about 15% in the ethanol and 2-propanol systems.[188] Their chemisty can be studied separately, as •OH radicals react quantitatively with ethylene to give β-hydroxyethyl radicals,[190] and in the presence of oxygen to give the corresponding peroxyl radicals **60** [reactions (96) and (97)].[191] Radicals of this type are also formed from *tert*-butanol [reactions (98) and (99), 95% yield,[188, 192] $k_{99} = 1.8 \times 10^9\ dm^3\ mol^{-1}\ s^{-1}$.[193] The chemistry of the peroxyl radicals **60** and

$$\bullet OH + H_2C{=}CH_2 \longrightarrow HOCH_2CH_2^{\bullet} \xrightarrow{O_2} \underset{\mathbf{60}}{HOCH_2CH_2O_2^{\bullet}} \quad (96/97)$$

$$\bullet OH + (CH_3)_3COH \xrightarrow{-H_2O} {}^{\bullet}CH_2C(CH_3)_2OH \xrightarrow{O_2} \underset{\mathbf{61}}{{}^{\bullet}O_2CH_2C(CH_3)_2OH} \quad (98/99)$$

61 has been cleared up in detail by means of product analysis, and their reaction kinetics determined by means of pulse radiolysis.[159, 191] A series of reactions occur via an undetected tetroxide [see the general scheme, reactions (80)–(90)]. The fragmentation reaction observed in both systems [e.g. reaction (100)] is noteworthy: it leads to α-hydroxyalkylperoxyl radicals (•CH_2OH or •$C(CH_3)_2OH$), which eliminate $HO_2^{\bullet}/O_2^{\bullet\ominus}$ subsequent to oxygen addition. Thus, the β-hydroxyalkylperoxyl radicals also produce superoxide radicals in considerable amounts, though in contrast to the α-hydroxyalkylperoxyl radicals this occurs according to second order rather than first order kinetics. The formation of $HO_2^{\bullet}$ subsequent to bimolecular termination is also important in the case of ethers [reactions (101)–(103)].[149] It can be estimated from the data available that in the case of the oxyl radical **62** the 1,2-H shift [reaction (102)] occurs at about double the rate at which the methyl group is cleaved [reaction (104)]. In the case of the polymeric ether polyethylene oxide the bimolecular decay of the peroxyl radicals leads to rupture of the polymer chain.[194] Since no oxyl/α-hydroxyalkyl rearrangement was observed here[149] the C–C fragmentation [analoguous to reaction (104)] must be much faster. This is understandable, as the fragmentation of poly(ethylene oxide) leads to an alkoxymethyl radical which is more stable than the methyl radical. At lower dose rates the bimolecular disappearance of these peroxyl radicals must compete with an intramolecular hydrogen transfer, which can take place via a

$$\underset{\mathbf{60}}{2\ HOCH_2CH_2O_2^{\bullet}} \longrightarrow 2\ {}^{\bullet}CH_2OH + O_2 + 2\ CH_2O \quad (100)$$

$$2\ CH_3CH(O_2^{\bullet})OEt \longrightarrow \underset{\mathbf{62}}{2\ CH_3CH(O^{\bullet})OEt} + O_2 \quad (101)$$

$$\underset{\mathbf{62}}{CH_3CH(O^{\bullet})OEt} \longrightarrow CH_3C^{\bullet}(OH)OEt \xrightarrow{O_2} CH_3CO_2Et + HO_2^{\bullet} \quad (102/103)$$

$$\underset{\mathbf{62}}{CH_3CH(O^{\bullet})OEt} \longrightarrow {}^{\bullet}CH_3 + HCO_2Et \quad (104)$$

sterically more favored six-membered transition state [reaction (77)].[138, 149] The rate constant of this reaction is of the order of magnitude of $1\ s^{-1}$;[138] since it is a genuine unimolecular reaction it is independent of the ether concentration in the dilute solutions studied.[149, 195] Only at higher ether concentrations do the known intermolecular hydrogen transfer reactions (ether autoxidation) become important.

The tertiary peroxyl radical derived from diisopropyl ether also seems to be able to eliminate $HO_2^{\bullet\ominus}$ at a rate similar to that of the slow intramolecular hydrogen transfer (and thus not amenable to kinetic study). This reaction is presumably so slow because of the low stabilization energy of the ether carbocation: the introduction of a second ether function as in the tertiary peroxyl radical **63** derived from acetaldehyde dimethyl acetal causes this reaction to become very fast [reaction (105), $k_{105} = 6.5 \times 10^4\ s^{-1}$].[139] The relatively high stabilization energy of this acetal carbocation **64** is demonstrated by its easily measurable reaction with water [reaction (106)], the rate k_{106} of which was determined by pulse radiolysis to be $1.3 \times 10^5\ s^{-1}$.[196]

$$\underset{\mathbf{63}}{CH_3C(OCH_3)_2O_2^{\bullet}} \longrightarrow O_2^{\bullet\ominus} + \underset{\mathbf{64}}{CH_3C(OCH_3)_2^{\oplus}} \qquad (105)$$

$$\underset{\mathbf{64}}{CH_3C(OCH_3)_2^{\oplus}} + H_2O \longrightarrow CH_3C(OCH_3)_2OH + H^{\oplus} \qquad (106)$$

•OH radicals are unselective in their reactions with carbohydrates, and abstract hydrogen atoms bonded to carbon in an almost statistical manner; reactions with OH groups are observed hardly at all.[197] Thus the reaction with D-glucose leads to six different radicals in similar yields. Five of the latter lead to α-hydroxyalkylperoxyl radicals and thus to elimination of $HO_2^{\bullet}$. The elimination rates are different, but the various processes can be only partially resolved kinetically.[142] The elimination of $HO_2^{\bullet}$ from the C(1)-peroxyl radical is an extremely rapid process ($k > 10^5\ s^{-1}$), in agreement with the reactions of aldehyde hydrates reported above. Not all types of glucose peroxyl radical eliminate $HO_2^{\bullet}$ within 10 ms.[198] It appears that the C(5)-peroxyl radical can eliminate $HO_2^{\bullet}$ either only slowly (after or concertedly with a ring-opening) or not at all. It is thus capable of bimolecular termination, a reaction which leads to the fragment products glycolic acid and L-*threo*-tetrodialdose as well as *xylo*-pentodialdose and formaldehyde (Table 2).

The C(5)-peroxyl radical can also be reduced by $HO_2^{\bullet}$ to the corresponding hydroperoxide. This is possible because in neutral solution the stationary concentration of $O_2^{\bullet\ominus}$ can be relatively high. After ring opening the C(5)-hydroperoxide should split off H_2O_2, a reaction typical of α-hydroxyhydroperoxides.[105, 141, 199, 200] The fact that no organic hydroperoxides can be detected after irradiation[87] thus does not necessarily contradict the suggested reaction pathway.

It was mentioned in the introduction that •OH radicals are formed in the ultrasound irradiation of aqueous solutions and that they are also formed in the decomposition of ozone in this medium. Thus ultrasound[201, 202] and ozone treatment[198] of aqueous glucose solutions should yield the same products as γ-irradiation, and this is indeed the case.

The reactions of peroxyl radicals which lead to the cleavage of the glycosidic linkage in di- and poly-saccharides are much less well understood. In the case of polysaccharides this reaction leads to a lowering of the molecular weight; thus ca. 22% of the peroxyl radicals induced in alginic acid lead to chain rupture.[203] The polysaccharide hyaluronic acid is of great biological importance, being present in many types of tissue. It is also converted into low molecular weight fragments by free-radical attack,[47, 204–206] so that the viscosity of its aqueous solutions undergoes a considerable decrease; this effect could lead to an impairment of its biological function. The kinetics of strand rupture were followed by pulse radiolysis[47] and are basically second order. They are however not yet understood in detail, particularly since no product analysis has been carried out. Equally in the case of cellobiose, mechanistic details are not yet fully clear even though a product analysis exists.[207]

Carbohydrates contain a set of relatively weak C–H bonds, as do aldehydes and ethers, and should thus also undergo autoxidation in aqueous solution. This is however not the case,[87] because most sugar peroxyl radicals readily split off $HO_2^{\bullet}/O_2^{\bullet\ominus}$. The $O_2^{\bullet\ominus}$ does not undergo hydrogen abstraction reactions, so that no chain reaction takes place, and autoxidation is prevented.

6.3. Amines, Amino Acids, and Peptides

The free-radical chemistry of such simple amines as trimethylamine is surprisingly complex. In aqueous solution three

Table 2. γ-Radiolysis of D-glucose (5×10^{-3} mol dm^{-3} in aqueous solution) [197] in the presence of oxygen. Dose rate 0.18 Gy s^{-1}. Products and G values (in units of 10^{-7} mol J^{-1}).

Product	G (N_2O/O_2)[a]	G (O_2)[b]	Product	G (N_2O/O_2)[a]	G (O_2)[b]
D-Gluconic acid	0.93	0.38	D-Erythrose	0.01	0.01
D-*arabino*-Hexosulose	0.93	0.50	D-Erythronic acid	0.01	
D-*ribo*-Hexos-3-ulose	0.59	0.36	D-Glyceraldehyde	0.06	[c]
D-*xylo*-Hexos-4-ulose	0.52	0.32	D-Glyceric acid	0.07	[c]
D-*xylo*-Hexos-5-ulose	0.62	0.24	Glyoxal	0.11	[c]
D-*gluco*-Hexodialdose	1.61	0.82	Glyoxylic- and glycolic acid	0.4	[c]
D-Glucuronic acid	0.05	[c]	Formaldehyde	0.12	0.07
D-Arabinose	0.07	0.015	Formic acid	0.6	0.2
D-Arabinonic acid	0.03		Hydrogen peroxide	3.1	3.1
xylo-Pentodialdose	0.07	0.02	Hydrogen	0.38	[c]
D-Xylose	0.01		Carbon dioxide	[c]	[d]
L-*threo*- Tetrodialdose	0.21	0.12	D-*arabino*-Hexulonic acid	[d]	[c]

[a] Mixture 4:1 (saturated: c (N_2O) = 1.8×10^{-2} mol dm^{-3}, c (O_2) = 2.6×10^{-4} mol dm^{-3}). [b] c (O_2) = 2×10^{-3} mol dm^{-3} (saturation and irradiation at 0°C). [c] Not determined. [d] Secondary product.

radicals are in equilibrium, the neutral radical $^{\bullet}CH_2N(CH_3)_2$ **65** and the two protonated forms $(CH_3)_3N^{\bullet\oplus}$ **66** and $^{\bullet}CH_2N(CH_3)_2H^{\oplus}$ **67**.[208] In neutral and acid conditions **66** predominates, as its pK_a lies above that of **67** [pK_a(**66**) = 8, pK_a(**67**) = 3.6]. The neutral form **65** dominant in alkaline conditions reacts rapidly with O_2 to give the immonium ion **68** and $O_2^{\bullet\ominus}$ [$k_{107} = 3.5 \times 10^9$ dm^3 mol^{-1} s^{-1}), apparently without the formation of an intermediate peroxyl radical.[140] The formation of $O_2^{\bullet\ominus}$ is accompanied by a change in

$$^{\bullet}CH_2N(CH_3)_2 + O_2 \longrightarrow CH_2{=}N(CH_3)_2^{\oplus} + O_2^{\bullet\ominus} \quad (107)$$
65 **68**

the conductivity of the solution. The subsequent reactions can also easily be followed by pulse radiolysis using conductometry [reactions (108/109)], $k_{108} = 2.8 \times 10^8$ dm^3 mol^{-1} s^{-1}; $k_{109} = 4$ s^{-1}). Reaction (109) is of more general interest because this type of reaction plays a part in the condensation of aldehydes with amines, which is an equilibrium reaction.

$$CH_2{=}N(CH_3)_2^{\oplus} \xrightarrow{OH^{\ominus}} HOCH_2N(CH_3)_2 \longrightarrow CH_2O + HN(CH_3)_2 \quad (108/109)$$

Peroxyl radicals derived from amino acids also eliminate $HO_2^{\bullet}/O_2^{\bullet\ominus}$. In the case of the peroxyl radical of the glycine zwitterion the elimination rate is 1.5×10^5 s^{-1} at pH 7.9.[209]

The only peptides which have so far been studied in detail are glycine anhydride, alanine anhydride and sarcosine anhydride.[65, 147, 210, 211] In these compounds hydroxyl radicals abstract a hydrogen atom bonded to a ring carbon atom; sarcosine anhydride also undergoes abstraction of a hydrogen from the exocyclic methyl group (20%). The pK_a-values of the corresponding peroxyl radicals are 10.7 and 11.2 in the case of glycine anhydride **69a** and alanine anhydride **69b** [equilibrium (110/111)]; these agree very well with the values calculated using the σ^* value of the peroxyl increment. An elimination of $HO_2^{\bullet}$, which has been demonstrated for the corresponding α-hydroxylalkylperoxyl radicals [reaction (71)] is not observed here ($k < 0.1$ s^{-1}). However, the perox-

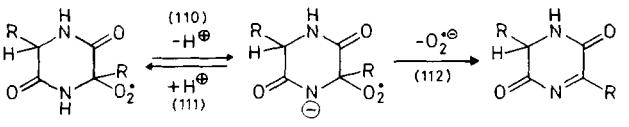

69 **70** **71**

a: R = H, **b**: R = CH$_3$

yl radical anions **70** eliminate $O_2^{\bullet\ominus}$; $k_{112} = 1.6 \times 10^5$ s^{-1} for the anion derived from glycine anhydride **70a** and 3.7×10^6 s^{-1} for that from alanine anhydride **70b**. The electron-donating effect of the methyl group thus makes itself felt both in the pK_a value and in the rate of elimination of $O_2^{\bullet\ominus}$. This elimination leads to the formation of unstable 3,4-dehydro-2,5-diketopiperazines **71**; these undergo $H^{\oplus}$- and $OH^{\ominus}$-catalyzed addition of water, a process which has also been studied by means of pulse radiolysis.[212]

The peroxyl radicals derived from sarcosine anhydride cannot eliminate $HO_2^{\bullet}/O_2^{\bullet\ominus}$, so that their disappearance is described by a second-order rate law; the products were determined both qualitatively and quantitatively.[65]

In the case of proteins the $^{\bullet}OH$ radical-induced peroxyl radical formation is followed by chain rupture. It is interesting to note that predetermined fracture points apparently exist; these are responsible for a nonstatistical distribution of the possible fragments.[213] The reasons for this behavior are as yet unknown.

6.4. Aldehydes and Ketones

Aldehydes such as formaldehyde and acetaldehyde are hydrated to a considerable extent in aqueous solution. In the case of formaldehyde the equilibrium lies almost completely on the side of the hydrate, and its peroxyl radical chemistry is thus described in Section 6.2. The hydrate **73** of acetaldehyde **72** is also very important; at 20 °C, 56% of the total aldehyde exists in the form of the hydrate [equilibrium (113/114)]. Reaction (113) is relatively slow ($k = 9 \times 10^{-3}$ s^{-1}). If the acetyl radical **74** is formed via hydrogen abstraction the rate of hydration is increased by many orders of magnitude ($k_{115} = 2 \times 10^4$ s^{-1}), but the dehydration reaction (116) may also be accelerated.[77, 214]

$$CH_3CHO + H_2O \underset{(114)}{\overset{(113)}{\rightleftharpoons}} CH_3CH(OH)_2$$
72 **73**

$$CH_3C(O)^{\bullet} + H_2O \underset{(116)}{\overset{(115)}{\rightleftharpoons}} CH_3C(OH)_2^{\bullet}$$
74 **75**

The reaction with oxygen leads to the formation of a mixture of acetylperoxyl radicals **76** and acetylhydrate peroxyl radicals. The latter rapidly eliminate $HO_2^{\bullet}$ (Section 6.2), so that after a few microseconds $O_2^{\bullet\ominus}$ radicals are present as well as **76**. Since **76** is one of the strongest oxidizing agents in the peroxyl radical family, it reacts rapidly with $O_2^{\bullet\ominus}$ to give the peracetate ion **77** ($k_{117} = 10^9$ dm^3 mol^{-1} s^{-1}). Peracetic acid **78** reacts with the acetaldehyde to give two molecules of acetic acid ($k_{118} = 1.2 \times 10^{-2}$ dm^3 mol^{-1} s^{-1}[215]). The value of 1.5×10^{-2} dm^3 mol^{-1} s^{-1} obtained from the radiation-chemical experiment is in good agreement with the literature.[77]

$$CH_3C(O)O_2^{\bullet} + O_2^{\bullet\ominus} \longrightarrow CH_3C(O)O_2^{\ominus} + O_2 \quad (117)$$
76 **77**

$$CH_3C(O)OOH + CH_3CHO \longrightarrow 2\,CH_3CO_2H \quad (118)$$
78

The isomer of the acetyl radical **74** is the formylmethyl radical **80**, which is formed by elimination of water from the 1,2-dihydroxyethyl radical **79** [reaction (120)].[216–219] The

$$^{\bullet}OH + HOCH_2CH_2OH \xrightarrow{(119)} H_2O + {}^{\bullet}CH(OH)CH_2OH$$
79

$$\mathbf{79} \xrightarrow[(120)]{-H_2O} {}^{\bullet}CH_2CHO \xrightarrow[(121)]{O_2} {}^{\bullet}O_2CH_2CHO$$
80 **81**

water elimination is acid- and base-catalyzed.[220-222] Under alkaline conditions (pH $\geq$ 12) the 1,2-dihydroxyethyl radical anion (the anion of **79**) rapidly eliminates $OH^{\ominus}$ ($3.1 \times 10^6\ s^{-1}$),[221] so that at low O_2 concentrations only formylmethylperoxyl radicals **81** are formed. These decompose bimolecularly, the main products being formaldehyde and formic acid.[116]

A detailed study of the acetonylperoxyl radical (from acetone and $^{\bullet}OH$) has been carried out.[223] Apart from other reactions, fragmentation following a bimolecular reaction occurs to give formaldehyde and the acetyl radical mentioned above. The latter is the precursor of the carbon dioxide also observed.[77].

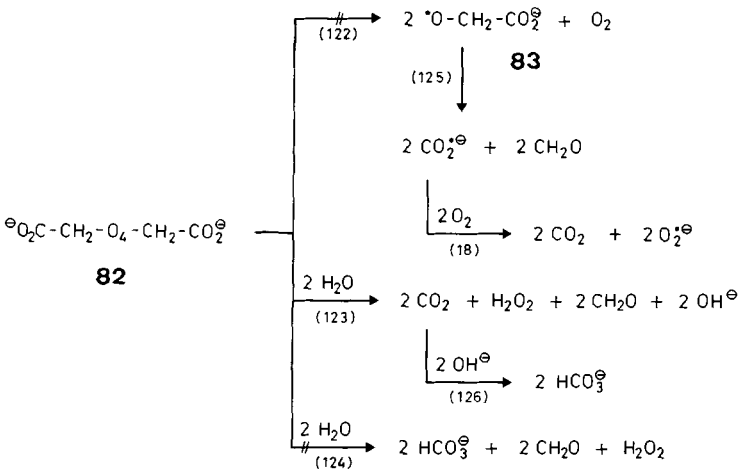

6.5. Carboxylic Acids

The radical $CO_2^{\bullet\ominus}$ derived from formic acid ($pK_a(^{\bullet}CO_2H) = 1.4$[224]) reacts rapidly to give CO_2 and $O_2^{\bullet\ominus}$;[37] an intermediate peroxyl radical has so far not been detected [reaction (18)]. The latter could perhaps be observed through pulse radiolysis if high oxygen pressure (in a pressure cell) were used to accelerate the reaction between $CO_2^{\bullet\ominus}$ and O_2, so that a high concentration of the intermediate could be built up; under such conditions the decay would perhaps be observable in the nanosecond range.

The main products derived from the peroxyl radicals of the acetate ion are glyoxylic acid, glycolic acid, formaldehyde and CO_2[64, 182, 209, 225-228] (Table 3). It is noticeable that much more glyoxylic acid is formed than glycolic acid, i.e. the Russell mechanism [reaction (82)] is unimportant in comparison with reaction (83); this is also confirmed by the high yield of H_2O_2. The reaction pathway to give formaldehyde and CO_2 is however surprising. "Classically" one could formulate the decomposition of the assumed tetroxide intermediate **82** to give O_2 and two oxyl radicals **83** [reaction (122)], and **83** should rapidly decompose into $CO_2^{\bullet\ominus}$ and formaldehyde [reaction (125)]. The $CO_2^{\bullet\ominus}$ reacts immediately according to reaction (18) to give CO_2 and $O_2^{\bullet\ominus}$. However, it was shown by pulse radiolysis that this reaction pathway is not the main one,[182] since although some $O_2^{\bullet\ominus}$ is formed in the course of the bimolecular decay of the acetate peroxyl radicals, its yield is much too small to explain the production of formaldehyde and CO_2 as being due to this process. It is probable that the reaction is a concerted one [reaction (123)]. One of the possible transition states has been indicated above (formula **56**), while deprotonated analogues and multistep processes could also be involved. The process certainly involves the formation of CO_2, which is only slowly[229] converted into bicarbonate according to reaction (126). Reaction (124) can thus be excluded. This possibility had to be checked, since this reaction pathway would involve the presence of a transition state (**84**) similar to that of (**56**) postulated for pathway (123).

Table 3. γ-Radiolysis products of sodium acetate [182] (0.01 mol dm^{-3}, pH 7.8) in N_2O/O_2-(4:1)-saturated solution and their G values (in units of 10^{-7} mol J^{-1}).

Product	G	Product	G
Glyoxylic acid	2.8	Organic (hydro)peroxides	0.7
Glycolic acid	0.7	Hydrogen peroxide	2.6
Formaldehyde	1.4	Oxygen uptake	5.5
Carbon dioxide	1.4		

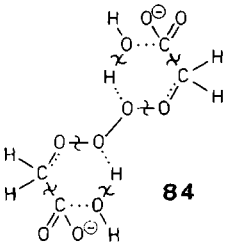

The acetate peroxyl radical reacts with $O_2^{\bullet\ominus}$ via electron transfer, while the reaction with the $HO_2^{\bullet}$ radical leads via a tetroxide to C—C fragmentation.[64]

As expected the peroxyl radical derived from malonic acid ($pK_a(HCO_2CH(O_2^{\bullet})CO_2^{\ominus}) \leq 3$) has a pK_a much lower than that of the parent compound ($pK_a(HCO_2CH_2CO_2^{\ominus}) = 5.7$);[62] this behavior parallels that of acetic acid (see Section 3.2). The pK_a-value agrees well with that of 2.9 calculated from the σ^* value of the peroxyl group.

6.6. Lipids

The radical-induced lipid peroxidation (oxidation of polyunsaturated fatty acids) has mainly been studied in organic solvents,[56] but aqueous solutions have also provided interesting results. In very dilute solutions the salts of fatty acids are predominantly homogeneously dissolved; however, above the critical micelle concentration[230] (which, for example, in the case of linoleic acid lies at 2.3×10^{-3} mol dm^{-3}) the fatty acids begin to form aggregates; at higher concentration rod-shaped micelles are formed, this second transition occurring at ca. 1.2×10^{-2} mol dm^{-3} for linoleic acid.[231]

Only relatively few radicals of the pentadienyl type **6** (10%[232]) are formed primarily as a result of initiation by $^{\bullet}OH$ radicals (see Section 3.1); most of the $^{\bullet}OH$ radicals react

by addition to a double bond. These radicals generate (intramolecularly if the geometry is favorable) pentadienyl-type radicals. Within the micelles the rate of this conversion is slower because of the lower mobility of the radicals in such a matrix; however, the conversion is almost quantitative because of the intermolecular hydrogen transfer reaction which now takes place.[232–234] This should also be true for the corresponding peroxyl radicals.

The lipid peroxidation is a radical chain reaction, the rate-limiting step being a hydrogen transfer reaction which has a considerable energy of activation [reaction (26)]. Oxygen addition to the pentadienyl radicals **6** is however fast ($k_{24} = 3 \times 10^8$ dm^3 mol^{-1} s^{-1}), as is the bimolecular termination of the lipid peroxyl radicals **7** ($2k \approx 10^7$ dm^3 mol^{-1} s^{-1}).[233] As expected, it is found that the chain length increases both with increasing temperature and with a decrease in the steady-state concentration of the radicals, i.e. if the radicals are formed by irradiation it is proportional to (dose rate)$^{-1/2}$.[231, 235]

As long as the fatty acids are not aggregated the chain length is short and the peroxidation ineffective. The chain length increases drastically when the critical micelle concentration is exceeded.[231, 236] A second increase is observed at the transition to rod-shaped micelles.[231] On the basis of the postulate that bimolecular termination occurs mainly via two monomeric peroxyl radicals or via the reaction of a monomer with a micellar peroxyl radical, while a termination via two micellar peroxyl radicals is improbable, it was possible from pulse radiolysis data to estimate that the monomeric peroxyl radicals are incorporated into the micelles with a rate constant $k = 8 \times 10^8$ dm^3 mol^{-1} s^{-1} but that they also leave the micelles at a rate of 1.6×10^5 s^{-1}.[232]

Little is known about the products of radiation-induced lipid peroxidation in aqueous solution. Material balances have not yet been established. The oxygen consumption is much higher than that expected for the formation of organic hydroperoxides and "malondialdehyde".[238] It is not known which reaction is responsible for the formation of $HO_2^{\bullet}/O_2^{\bullet\ominus}$ in the decomposition of fatty aid peroxyl radicals [$G \approx (2.2–4.7) \times 10^{-7}$ mol J^{-1}].[239]

6.7. Benzene and its Derivatives

Benzene and its derivatives rapidly add $^{\bullet}$OH radicals and hydrogen atoms to give cyclohexadienyl-type radicals such as **3**. As described in Section 3.1, addition of oxygen to these radicals can be reversible [reactions (20)–(23)]. In the case of the unsubstituted cyclohexadienyl radical (formed from the reaction of $^{\bullet}$OH radicals with 1,4-cyclohexadiene[240]) a subsequent $HO_2^{\bullet}$ elimination analogous to reaction (127) or the direct hydrogen transfer from this radical to O_2 with direct formation of $HO_2^{\bullet}$ [reaction (128)] is so fast ($k > 8 \times 10^5$ s^{-1}[58]) that a back reaction can no longer be detected. These reactions have been discussed for the autoxidation of cyclohexadiene.[241, 242] In the polar solvent water a decomposition to give an $O_2^{\bullet\ominus}$ radical and a cyclohexadienyl cation could provide a possible alternative to an electrocyclic $HO_2^{\bullet}$ elimination; however, this pathway has been excluded.[58] The $HO_2^{\bullet}$ elimination must involve a transition state in which the hydrogen to be eliminated and the terminal oxygen of the peroxyl radical function can approach very closely. Of the two possible peroxyl radicals **4** and **5**, only **5** with its 1,3-cyclohexadiene structure permits this (distance ca. 1.8 A); for **4**, which has a 1,4-cyclohexadiene structure, the distance is ca. 3.9 A. The yield of $HO_2^{\bullet}$ elimination product (benzene from the cyclohexadienylperoxyl radicals, phenol **85** from

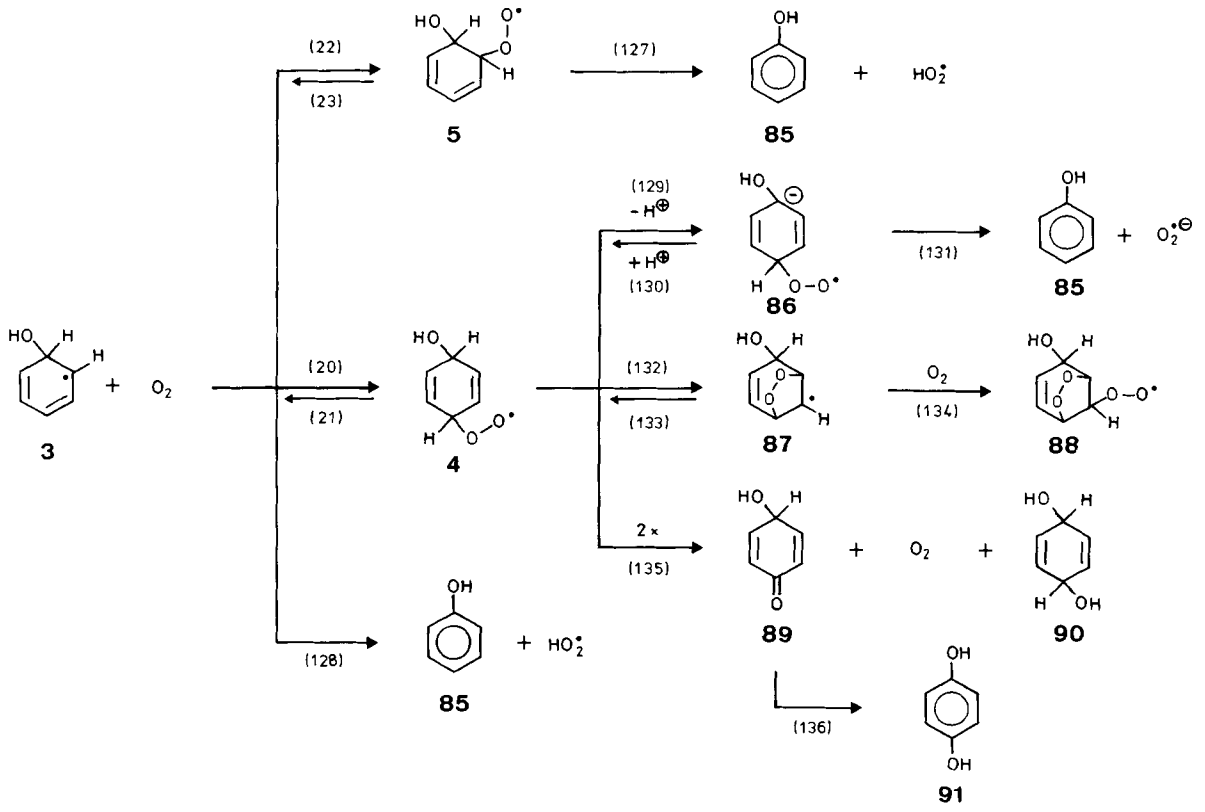

the hydroxycyclohexadienylperoxyl radicals **5**) reaches only about 60% of the expected value[27] (see also earlier radiation-chemical studies of this system[243-251]). The $HO_2^•$ elimination is thus not the only unimolecular reaction. In Table 4, the presence of fragment products (altogether about thirty) with one to six carbon atoms is indicated. They are thought to derive from intermediate endoperoxides **87** and **88** [reactions (132)–(134)].

Table 4. γ-Radiolysis of benzene in aqueous solution [27] (pH 6.5), c (benzene) = 2×10^{-3} mol dm^{-3}, c (N_2O) = 1.8×10^{-2} mol dm^{-3}, c (O_2) = 2.6×10^{-4} mol dm^{-3}, dose rate 0.14 Gy s^{-1}. Products and their G values (in units of 10^{-7} mol J^{-1}).

Product	G (C_6H_6)	G (C_6D_6)
Phenol	3.1	2.3
Hydroquinone	0.1	0.07
3,6-Dihydroxy-1,4-cyclohexadiene	0.1	0.07
Catechol	0.05	≤0.03
Mucondialdehyde	<0.01	<0.01
Fragmentation products with 3 to 6 carbon atoms	2.2	3.0
Glyoxal	0.2	[a]
Acetaldehyde	0.3	[a]
Formaldehyde	0.7	0.9
Formic acid	0.9	1.4
Oxygen uptake	5.6	9.0
Hydrogen peroxide	1.7	1.4
$HO_2^•$	4.0[b]	[a]

[a] Not determined. [b] Determined by the TNM method (see Section 4).

In the system hydroxycyclohexadienyl radical/O_2 the observed $HO_2^•$ elimination is much slower than in the unsubstituted case ($k \approx 800$ s^{-1}).[27, 144] Because of the occurrence of reactions (20)–(23) the observed decay constant is smaller than the rate constant which corresponds to reaction (127). When reaction (128) is neglected, a value of ca. 4×10^4 s^{-1} can be estimated for k_{127}, showing that after this correction the rate of elimination of $HO_2^•$ from **5** approaches the value found for the unsubstituted peroxyl radical.

Pathway (127) via equilibrium (22)/(23) could not be distinguished from a slow reaction (128) which might proceed alongside processes (20)/(21) and (22)/(23), and the question as to which of these constitutes the route to phenol must remain open. The fact that perdeuterated benzene gives a smaller phenol yield than the undeuterated compound, and that at the same time the oxygen consumption is higher, may be attributed to the isotope effect that is expected for reactions (127) and (128). In the case of the deuterated benzene this will lead to a longer lifetime of peroxyl radical **5** with respect to reaction (127), and thus will favor the reaction sequence (20 → 132 → 134), causing the oxygen consumption to be higher.

At high pH the yield of phenol approaches the G value of the primarily attacking $^•OH$ radical. It thus follows that the 4-hydroxy-2,5-cyclohexadienylperoxyl radical **86** deprotonated at C4 can also eliminate $O_2^{•\ominus}$ [reactions (129) and (131)].

Further reactions may be involved at the high dose rate of pulse radiolysis. The peroxyl radical **4**, which is by far the dominant one, is now also subject to bimolecular termination [reaction (135)]. Important products are then 3,6-dihydroxy-1,4-cyclohexadiene **90** and hydroquinone **91**, which is formed via the short-lived (see below) 4-hydroxy-2,5-cyclohexadienone **89** [reaction (136)].

It is noteworthy that muconaldehyde is a prominent product when the $^•OH$ radicals are formed via a Fenton reagent,[252] while in the radiolytic system no muconaldehyde is formed (< 0.5%).[27] The use of $^{36}O_2$ does not lead to incorporation of ^{18}O into the phenol in the radiolytic system, though this is the case of the Fenton system.[253] This is a further indication of the problems which can occur in the interpretation of results obtained with Fenton systems.

The amino acid phenylalanine behaves similarly to benzene, its radiation chemistry being dominated by the phenyl group.[254] The system phenol/$^•OH$/O_2 has also been studied by pulse radiolysis.[255] It was reported that the peroxyl radicals **92** formed in this system eliminate $HO_2^•$. An undefined non-radical intermediate is postulated; this rearranges to give hydroquinone and could be 4-hydroxy-2,5-cyclohexadienone **89** [reaction (137)]. Cyclohexadienones are indeed short-lived in water and rearrange rapidly to give the corresponding phenols [reaction (136)].[256, 257]

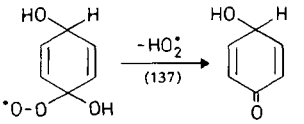

92 **89**

It was mentioned above that the hydroxycyclohexadienyl radicals derived from some benzene derivatives, e.g. benzonitrile, show only a slight reaction or even no reaction at all with oxygen. This has been confirmed by oxygen consumption measurements at low dose rates (^{60}Co-γ-radiolysis).[58]

6.8. Sulfur Compounds

The simplest sulfur radicals, the thiyl radicals, react very rapidly with oxygen; the RS–$O_2^•$ bond is however very weak, so that an equilibrium is set up at room temperature [reactions (138) and (139)];[60] this equilibrium does not lie completely on the side of the thiylperoxyl radicals **93** even under the conditions of air saturation [$c(O_2) = 2.5 \times 10^{-4}$ mol dm^{-3}].[258] The latter exhibit a definite absorption at ca. 540 nm[259] which permits their observation; they have very recently also been observed by ESR spectroscopy.[71] The

$$RS^• + O_2 \underset{(139)}{\overset{(138)}{\rightleftharpoons}} RSOO^• \quad \mathbf{93}$$

isomeric sulfonyl radical RS(O)O$^•$ **94** is however much more stable than **93**, the calculated energy difference being about 210 kJ mol^{-1}.[260] It can thus be assumed that **93** should rearrange to **94**. This can easily be achieved under photolytic conditions;[261, 262] the thermal rearrangement is however slowed to such an extent by the activation energy (calc. 105 kJ[260]) that the rate of this strongly exothermic reaction (140) can no longer be measured with certainty at room temperature by pulse radiolysis ($k_{140} < 10^4$ s^{-1}[258]). The

measurement of this unimolecular reaction is made more difficult by bimolecular termination processes (**93** + **93**; **93** + RS$^{\bullet}$; RS$^{\bullet}$ + RS$^{\bullet}$) and by a reaction with the thiol which can lead to sulfinyl radicals **28** [reaction (141)]. ESR measurements at low temperatures have provided good evidence for the occurrence of **28** in irradiated thiol/O_2 systems.[71, 262–265] This reaction also cannot be very fast; a first estimate for a value of $k_{141} \approx 5 \times 10^5$ dm^3 mol^{-1} s^{-1} was obtained for the 2-mercaptoethanol system.[266] As is to

$$\underset{\mathbf{93}}{\text{RSOO}^{\bullet}} \longrightarrow \underset{\mathbf{94}}{\text{RS(O)O}^{\bullet}} \qquad (140)$$

$$\underset{\mathbf{93}}{\text{RSOO}^{\bullet}} + \text{RSH} \longrightarrow \text{RSOH} + \underset{\mathbf{28}}{\text{RSO}^{\bullet}} \qquad (141)$$

be expected for such a complex mechanism, the yields of the products in the 2-mercaptoethanol system depend strongly on the concentrations of the thiol and of oxygen (Table 5 and Fig. 6).

Table 5. γ-Radiolysis of 2-mercaptoethanol in aqueous solution at different concentrations [258] (c (N_2O) = 1.8×10^{-2} mol dm^{-3}, c (O_2) = 2.6×10^{-4} mol dm^{-3}, pH 5.7). Dose rate 0.3 Gy s^{-1}. G values in units of 10^{-7} mol J^{-1}.

Products	G at 2.8×10^{-4} M	G at 1.12×10^{-2} M	Products	G at 2.8×10^{-4} M	G at 1.12×10^{-2} M
RSO_3H	3.7	1.2	HCHO	0.7	0.97
RSSR	1.2	4.9	CH_3CHO	0.2	0.27
RSO_2H	0.09	0.08	$HOCH_2CHO$	0.12	0.48
H_2SO_4	0.79	0.65	OHCCHO	0.10	0.04
HCOOH	0.10	0.15			

Two main products are noteworthy, the disulfide and the sulfonic acid. However, almost no sulfinic acid is formed. This indicates that a further oxygenation beyond the $RSO_2^{\bullet}$ stage must take place. ESR measurements at low temperatures provide evidence for a reaction of the RS(O)O$^{\bullet}$ radicals with oxygen to give $RSO_4^{\bullet}$ radicals.[262] This intermediate could be the precursor for the sulfonic acid and the sulfuric acid, but details are still obscure.

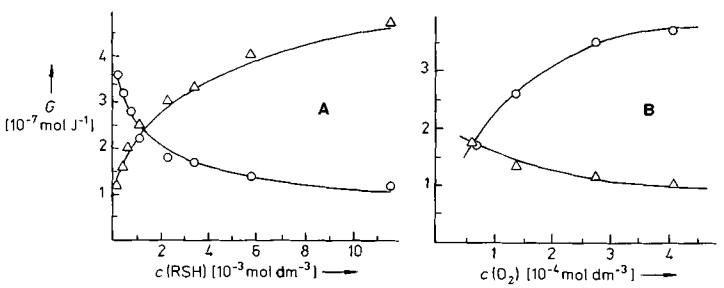

Fig. 6. γ-Radiolysis of 2-mercaptoethanol in aqueous solution [258] (pH 5.6, N_2O/O_2, dose rate 0.3 Gy s^{-1}). Concentration dependence of the G values of disulfide (△) and sulfonic acid (○). A: as a function of the thiol concentration; c (O_2) = 2.6×10^{-4} mol dm^{-3}. B: as a function of the oxygen concentration; c (RSH) = 2.8×10^{-4} mol dm^{-3}.

In alkaline solution, when sufficient thiolate anions are present in equilibrium, the disulfide radical anion and its reaction with oxygen [reactions (65)[267] and (66)[268, 269] become important. The $O_2^{\bullet\ominus}$ radical can then enter into a chain reaction with the thiolate ion (see Section 4).

Radical cations ($R_2S^{\bullet\oplus}$, $(R_2S)_2^{\bullet\oplus}$, $RSSR^{\bullet\oplus}$) play an important role in the radical chemistry of sulfur; just as for other radical cations,[270–272] these are unreactive or only slightly reactive towards oxygen.[273]

6.9. Halogen Compounds

The peroxyl radical chemistry of the halogens has attracted particular interest for two reasons. The well-known liver toxicity of this class of compounds, which also includes some anaesthetics such as halothane, is suggested to be due in part to reactions of intermediate peroxyl radicals.[74] Secondly they are intermediates in the ozone-induced decomposition (in aqueous media by the $^{\bullet}$OH radical route) of the haloethenes, which are nowadays omnipresent in ground-water.[274, 275] The addition of $^{\bullet}$OH radicals to halogenated ethenes gives $^{\bullet}$OH adduct radicals **95** which rearrange rapid-

$$^{\bullet}\text{OH} + \text{Cl}_2\text{C}{=}\text{CCl}_2 \xrightarrow{(142)} \underset{\mathbf{95}}{\text{HOCCl}_2\text{CCl}_2^{\bullet}} \underset{(144)}{\overset{(143)}{\rightleftharpoons}} \underset{\mathbf{96}}{^{\bullet}\text{C(OH)ClCCl}_3}$$

$$\underset{\mathbf{96}}{^{\bullet}\text{C(OH)ClCCl}_3} \xrightarrow[(145)]{\text{O}_2,\ -\text{HO}_2^{\bullet}} \underset{\mathbf{97}}{\text{CCl}_3\text{COCl}} \xrightarrow[(146)]{\text{H}_2\text{O}} \underset{\mathbf{98}}{\text{CCl}_3\text{CO}_2\text{H}} + \text{HCl}$$

$$\text{HOC(Cl)}_2\text{CCl}_2^{\bullet} \xrightarrow{(147)} \text{HCl} + \text{OCClCCl}_2^{\bullet}$$

ly [reaction (143)]. This rearrangement has been postulated because of the formation (via **96** and **97** as intermediates) of trichloroacetic acid **98** [reactions (145) and (146)].[275] **95** can split off HCl rather than undergoing rearrangement and addition of O_2 [reaction (147)]. According to pulse radiolysis measurements the latter reaction is very fast ($k_{147} > 7 \times 10^5$ s^{-1}).[276]

Halogenated peroxyl radicals are also formed from the reaction of $^{\bullet}$OH radicals with partially halogenated ethanes.[277] Another route to these intermediates is provided by solvated electrons,[74, 78, 277, 278] which react with halogen compounds via dissociative electron capture [e.g. reaction (148)]. The

$$\text{HCCl}_3 + \text{e}_{\text{aq}}^{\ominus} \xrightarrow{(148)} {^{\bullet}\text{CHCl}_2} + \text{Cl}^{\ominus}$$

oxyl radicals **99** formed in the bimolecular termination reactions can undergo decomposition via two routes, i.e., 1,2-H shift and β-fragmentation [reactions (149) and (152)]. In bro-

$$\cdot OCHCl_2 \xrightarrow[(149)]{} HOC\cdot Cl_2 \xrightarrow{-HCl} ClC\cdot=O \xrightarrow[(151)]{} Cl\cdot + CO$$
99

$$\cdot OCHCl_2 \xrightarrow{(152)} HCOCl + Cl\cdot$$
99

mine-containing oxyl radicals the β-fragmentation is the only decomposition route observed because the C–Br bond is considerably weaker than the C–Cl bond.[278, 279] C–C bond cleavage has also been observed in the peroxyl radical chemistry of halogenated ethanes, though this reaction is not yet understood in detail.[280]

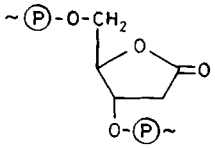

100

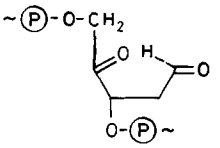

101

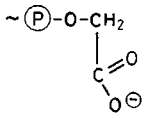

102

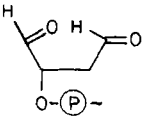

103

6.10. Nucleic Acids and Their Building Blocks

Radical-induced changes in the DNA of the living cell can trigger mutations and carcinogenesis and even lead to reproductive cell death. The latter is the goal of cancer therapy, since the actual danger is the uncontrolled growth of cancer cells and not their presence as such. For this reason the field of radical-induced DNA modifications has been the subject of much research.[7]

In the cell most DNA damage can be repaired enzymatically. However, an unrepaired break in the DNA double helix prevents the transmission of the complete information to the daughter cells, which generally in turn prevents cell multiplication. Unrepaired base changes can in principle lead to a point mutation. In the cell the radiation energy can either be absorbed by the DNA (*direct* effect), or by the water surrounding it (*indirect* effect) whereby the 'OH radicals, solvated electrons and 'H atoms formed in reactions (6)–(10) react with the DNA. The direct effect has so far been little studied, while a good deal more is known about the indirect effect.[7]

The solvated electrons (and also the H' atoms) react only with the nucleobases. The 'OH radicals react preferentially with these as well, though about 10–20% of them also react at the sugar component (in poly(U) 7%[282]). The sugar radicals are then the precursors for the strand breaks and for unchanged free nucleobases. A small proportion of the sugar radicals which cause a single strand rupture can subsequently react with the complementary strand and thus lead to a double-strand break.[283] In the absence of O_2 the strand breakage in DNA is mainly due to a β-elimination of the phosphate groups from the C4' radical[284, 285] (see also Refs. [286–288]). This process is however so slow that the corresponding peroxyl radical is formed in the presence of O_2.

A radical-induced chain rupture is of necessity accompanied by a chemical change in the sugar component. A set of such sugar products has been identified in irradiated DNA (**100**–**103**).[289–292] It is by no means easy to generate one single sugar radical selectively.[293] It is not possible here to discuss mechanistic suggestions regarding the formation of these products in DNA (for the reactions of the peroxyl radicals of the alkyl phosphates see Refs. [294, 295]).

The base-derived radicals can be studied in much more detail in model systems, e.g. DNA subunits; however, the results thus obtained cannot be transferred with complete confidence to DNA itself. We know for example from the poly(U) system that base radicals react with the sugar component both in the presence and in the absence of oxygen, these reactions leading to strand rupture and the liberation of unchanged bases.[282, 296–304] Hydrogen transfer reactions of this type are less efficient in DNA. However, the often extremely detailed model studies are also very relevant to the chemistry of DNA peroxyl radicals.

The reaction of a solvated electron with a nucleobase leads to the formation of the electron adduct. In the case of derivatives of cytosine, adenine and guanine these electron adducts are rapidly protonated by water.[305–308] The subsequent reactions with oxygen are not yet well understood.[305, 309] In the uracil/thymine system **104** the electron adduct **105** reacts more slowly with water [pK_a (**106**) $\approx$ 7[310, 311]], initial protonation occurring at the heteroatom [reaction (154)]. A protonation at C6 [reaction (156)] is slower, but at the same time the deprotonation is much more difficult (pK_a (**107**) $\gg$ 7).[312–314] As a result **107** eventually dominates. The electron adduct **105** itself and its *O*-protonated form **106** react rapidly with oxygen, resulting in the formation of $O_2^{\cdot\ominus}/HO_2^{\cdot}$ and restitution of the base **104** [reactions (157) and (158)], no intermediate peroxyl radical being observed. The C-protonation [reaction (156)] can be accelerated by phosphate catalysis.[313] The resultant radicals **107** react with O_2 [reaction (159)] without regeneration of the pyrimidine chromophore.[315]

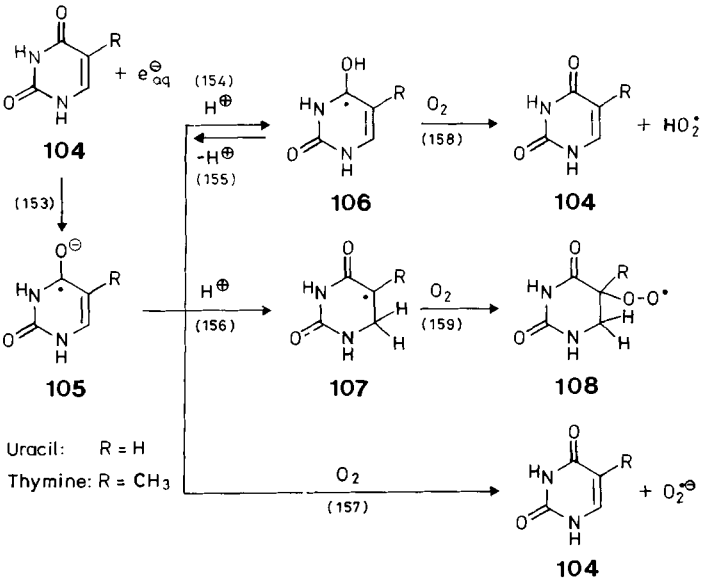

The C6-yl radicals isomeric to **107** are formed via addition of an ·H atom;[316] they are also formed when ·OH radicals are allowed to react with dihydrouracil.[317] The addition of ·OH radicals to the pyrimidines also leads preferentially to this type of radical.[318, 319] The reaction of the latter with O_2 leads to peroxyl radicals **109**, the structure of which is similar to that of the peptide peroxyl radicals (Section 6.3) and which behave in a similar manner. As in the case of the latter these peroxyl radicals eliminate $O_2^{\cdot\ominus}$ from their anion **110** with the formation of very short-lived isopyrimidines **111** [reactions (160)–(162)], the reactions of which with water have been established by means of product analysis and pulse radiolysis.[320, 321] Since the $O_2^{\cdot\ominus}$ elimination occurs only from the anion **110**, while elimination of $HO_2^{\cdot}$ from the neutral form **109** is very slow, the peroxyl radicals **109** decompose under acid conditions according to a second-order rate law, which leads to a different product distribution. Thus, one of the products formed from **109** is the keto form of barbituric acid **112** [reaction (163)]. As the latter is a C–H acid it dissociates only relatively slowly in spite of its low pK_a of 4.0 [reaction (164)];[322, 323] this reaction can be followed very readily by pulse radiolysis.[229]

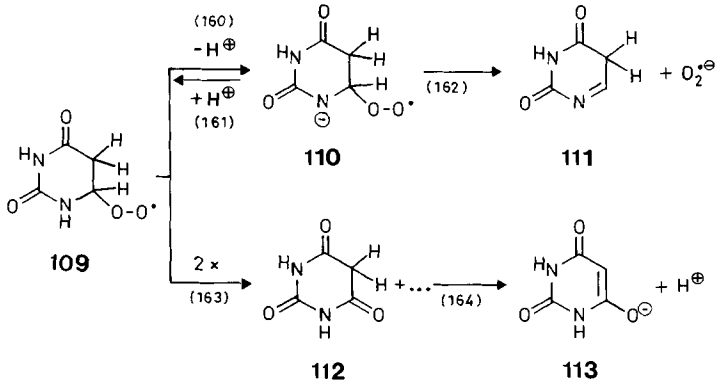

The ·OH radical-induced radical chemistry of the purines leads to conjugated radicals with a high spin density at the heteroatom.[324] Such radicals are often (but not always) unreactive towards oxygen. It is thus not surprising that a fraction of the purine radicals does not react with oxygen, as could be shown both by pulse radiolysis[195, 325] and by measurement of the O_2 uptake during the irradiation.[195]

In the cells, aside from the enzymatic repair of the damaged DNA, a faster "chemical" repair of the DNA radicals via thiols/thiolate ions plays an important role (the glutathione concentration in the cell can be as high as 10^{-2} mol dm^{-3}), by suppressing the dangerous formation of DNA peroxyl radicals.[6, 8, 326] The latter can however also react with thiols, as was recently shown by means of kinetic ESR spectroscopy for the DNA (polynucleotide)/thiol system.[301, 304, 327] Since the peroxyl radicals derived from polymers, e.g. the DNA peroxyl radicals, have a very long lifetime (with respect to a bimolecular termination) their reaction with glutathione in the cell must be of great importance because of its high concentration. Thus the final products of the peroxyl radicals would in the main be determined by this reaction. In Sections 4 and 6.8 we referred to the very complex sulfur/peroxyl radical chemistry. The question of the $RO_2^{\cdot}$/thiol(thiolate) reaction requires further study because of its great biological significance which is becoming apparent.

7. Future Prospects

The present survey is intended to provide an impression of the possibilities afforded by radiation-chemical techniques in the field of peroxyl radical chemistry. The fact that these studies have been carried out mostly using *dilute aqueous solutions* is due to the method used. The radiolysis of water is a simple process chemically which provides only three radicals, ·OH, ·H and the solvated electron; the reactions of these can be carried out in such a way that either $RO_2^{\cdot}$ radicals are formed in 90% yield or $O_2^{\cdot\ominus}$ radicals formed quantitatively. The possibility of using very dilute solutions has the advantage that even many hydrocarbons dissolve at the concentrations required; if not, derivatives are often available which are sufficiently water-soluble. One example is Trolox C, a functionalized water-soluble analogue of vitamin E.

There is certainly no better method for studying $O_2^{\cdot\ominus}$, which is so important in biological systems. The variety of reactions which have recently been uncovered indicates that we are entering a very interesting area of chemistry, interesting in particular because $O_2^{\cdot\ominus}$ forms very reactive complexes with a series of transition metal ions. A better understanding of the chemistry of antioxidants is also important, not only for elucidating the processes occurring in the living cell but also for technical processes, e.g. food technology.

In spite of the considerable progress so far made in studies of radical-induced DNA damage, which could be referred to only briefly here, this area will be the subject of further research. Because of their long lifetimes these polymer radicals can be subject to a number of unimolecular reactions which are not observed clearly in low molecular weight model systems[138, 300, 303] as their peroxyl radicals undergo much faster bimolecular termination. Synthetic polymers will be of use in investigating this point. An exact understanding of their peroxyl radical chemistry is certainly of technical interest.[45, 328]

In environmental technology radical-forming agents such as ozone are increasingly being used in the rehabilitation of former industrial sites to remove unwanted pollutants from both the soil and the ground-water. Here as well, radiation-chemical techniques provide the best method for mechanistic studies.

Received: April 26, 1991 [A 835IE]
German version: *Angew. Chem. 103* (1991) 1255
Translated by Prof. Dr. *T. N. Mitchell*, Dortmund

[1] K. U. Ingold, *Acc. Chem. Res. 2* (1969 1–9.
[2] J. A. Howard in G. H. Williams (Ed.): *Advances in Free Radical Chemistry, Vol. 4*, Logos, London 1972, pp. 49–173.
[3] J. A. Howard, J. C. Scaiano in H. Fischer (Ed.): *Landoldt-Börnstein, Neue Serie, Gruppe II, Vol. 13d*, Springer, Berlin 1984, pp. 5–431.
[4] G. Schwarz, *Muench. Med. Wochenschr. 56* (1909) 1217–1218.
[5] H. Dertinger, H. Jung: *Molekulare Strahlenbiologie*, Springer, Berlin 1969.
[6] T. Alper: *Cellular Radiobiology*, University Press, Cambridge 1979.
[7] C. von Sonntag: *The Chemical Basis of Radiation Biology*, Taylor and Francis, London 1987.
[8] D. Schulte-Frohlinde, E. Bothe, *Int. J. Radiat. Biol. 58* (1990) 603–611.
[9] B. N. Ames, *Science 221* (1983) 1256–1264.
[10] E. F. Elstner: *Der Sauerstoff. Biochemie, Biologie, Medizin*, B. I. Wissenschaftsverlag, Mannheim 1990, pp. 1–529.

[11] T. G. Gabig, B. M. Babior in L. W. Oberley (Ed.): *Superoxide Dismutase, Vol. 2*, CRC Press, Boca Raton, FL, USA 1982, pp. 1–13.
[12] M. N. Hamers, D. Roos in H. Sies (Ed.): *Oxidative Stress*, Academic, London 1985, pp. 351–381.
[13] J. H. Forman, A. B. Fisher in R. A. Greenwald (Ed.): *CRC Handbook of Methods for Oxygen Radical Research*, CRC Press, Boca Raton, FL, USA 1985, pp. 359–364.
[14] B. Halliwell in L. W. Oberley (Ed.): *Superoxide Dismutase, Vol. 1*, CRC Press, Boca Raton, FL, USA 1982, pp. 89–123.
[15] R. Atkinson, A. C. Lloyd, *J. Phys. Chem. Ref. Data 13* (1984) 315–444.
[16] J. Lelieveld, P. J. Crutzen, *Nature 343* (1990) 227–233.
[17] G. V. Buxton, *Int. J. Radiat. Biol. 59* (1991) 1–13.
[18] R. G. Zepp, J. Hoigne', H. Bader, *Environ. Sci. Technol. 21* (1987) 443–450.
[19] J. Hoigne', H. Bader, *Water Res. 10* (1976) 377–386.
[20] J. Hoigne', in S. Stucki (Ed.): *Progress Technologies for Water Treatment*, Plenum, New York 1988, pp. 121–143.
[21] P. Riesz, D. Berdahl, C. L. Christman, *Environ. Health Perspect. 64* (1985) 233–252.
[22] A. Henglein, *Ultrasonics 25* (1987) 6–16.
[23] H. J. H. Fenton, H. Jackson, *J. Chem. Soc. Trans. 75* (1899) 1–11.
[24] G. Cohen in R. A. Greenwald (Ed.): *CRC Handbook of Methods for Oxygen Radical Research*, CRC Press, Boca Raton, FL, USA 1985, pp. 55–64.
[25] G. V. Buxton, C. L. Greenstock, W. P. Helman, A. B. Ross, *J. Phys. Chem. Ref. Data 17* (1988) 513–886.
[26] J. F. Mouret, M. Berger, C. Anselmino, M. Polverelli, J. Cadet, *J. Chim. Phys. Phys. Chim. Biol.* (1991), in press.
[27] X.-M. Pan, M. N. Schuchmann, C. von Sonntag, unpublished results.
[28] A. Bernas, M. Gauthier, D. Grand, G. Parlant, *Chem. Phys. Lett. 17* (1972) 439–443.
[29] A. Bernas, J. Blais, M. Gauthier, D. Grand, *Chem. Phys. Lett. 30* (1975) 383–386.
[30] A. Henglein, W. Schnabel, J. Wendenburg: *Einführung in die Strahlenchemie*, Verlag Chemie, Weinheim 1969.
[31] I. G. Draganic, Z. D. Draganic: *The Radiation Chemistry of Water*, Academic, New York 1971.
[32] A. J. Swallow: *Radiation Chemistry. An Introduction*, Longman, London 1973.
[33] Farhataziz, M. A. Rodgers (Eds.): *Radiation Chemistry. Principles and Applications*, VCH, Weinheim 1987.
[34] J. W. T. Spinks, R. J. Woods: *An Introduction to Radiation Chemistry* 3rd Edit., Wiley, New York 1990.
[35] G. V. Buxton in Farhataziz, M. A. Rodgers (Eds.): *Radiation Chemistry: Principles and Applications*, VCH, Weinheim 1987, pp. 321–349.
[36] B. H. J. Bielski, D. E. Cabelli, R. L. Arudi, A. B. Ross, *J. Phys. Chem. Ref. Data 14* (1985) 1041–1100.
[37] G. E. Adams, R. L. Willson, *Trans. Faraday Soc. 65* (1969) 2981–2987.
[38] A. O. Allen, B. H. J. Bielski in L. W. Oberley (Ed.): *Superoxide Dismutase, Vol. 1*, CRC Press, Boca Raton, FL, USA 1982, pp. 125–141.
[39] I. Fridovich in R. A. Greenwald (Ed.): *CRC Handbook of Methods for Oxygen Radical Research*, CRC Press, Boca Raton, FL, USA 1985, pp. 51–53.
[40] K. Asada, S. Kanematsu, *Agric. Biol. Chem. 40* (1976) 1891–1892.
[41] B. H. J. Bielski, G. G. Shiue: *Oxygen Free Radicals and Tissue Damage (Ciba Found. Symp. 65)* Excerpta Medica, Amsterdam 1979, pp. 43–56.
[42] N. Zhang, H.-P. Schuchmann, C. von Sonntag, *J. Phys. Chem. 95* (1991) 4718–4722.
[43] P. Neta, R. E. Huie, A. B. Ross, *J. Phys. Chem. Ref. Data 19* (1990) 413–513.
[44] K.-D. Asmus, E. Janata in J. H. Baxendale, F. Busi (Eds.): *The study of fast processes and transient species by electron pulse radiolysis*, Reidel, Dordrecht 1982, pp. 91–113.
[45] W. Schnabel, *Radiat. Phys. Chem. 28* (1986) 303–313.
[46] M. Liphard, E. Bothe, D. Schulte-Frohlinde, *Int. J. Radiat. Biol. 58* (1990) 589–602.
[47] D. J. Deeble, E. Bothe, H.-P. Schuchmann, B. J. Parsons, G. O. Philips, C. von Sonntag, *Z. Naturforsch. C45* (1990) 1031–1043.
[48] E. Bothe, D. Schulte-Frohlinde, *Z. Naturforsch. C37* (1982) 1191–1204.
[49] H. Christensen, K. Sebested, *Radiat. Phys. Chem. 16* (1980) 183–186.
[50] G. V. Buxton, N. D. Wood, S. Dyster, *J. Chem. Soc. Faraday Trans. 1 84* (1988) 1113–1121.
[51] C. von Sonntag in M. G. Simic, K. A. Taylor, J. F. Ward, C. von Sonntag (Eds.): *Oxygen Radicals in Biology and Medicine*, Plenum, New York 1988, pp. 47–54.
[52] A. Marchaj, D. G. Kelley, A. Bakac, J. H. Espenson, *J. Phys. Chem. 95* (1991) 4440–4441.
[53] E. I. Finkel'shtein, G. N. Gerasimov, *Russ. J. Phys. Chem. (Engl. Transl.) 58* (1984) 570–572.
[54] X.-M. Pan, C. von Sonntag, *Z. Naturforsch. B45* (1990) 1337–1340.
[55] N. A. Porter, L. S. Lehman, B. A. Weber, K. J. Smith, *J. Am. Chem. Soc. 103* (1981) 6447–6455.
[56] E. N. Frankel in M. G. Simic, K. A. Taylor, J. F. Ward, C. von Sonntag (Eds.): *Oxygen Radicals in Biology and Medicine*, Plenum, New York 1988, pp. 265–282.
[57] L. R. C. Barclay in F. Minisci (Ed.): *Free Radicals in Synthesis and Biology*, Kluwer, Dordrecht 1989, pp. 391–406.
[58] X.-M. Pan, C. von Sonntag, unpublished results.
[59] P. S. Nangia, S. W. Benson, *Int. J. Chem. Kinet. 12* (1980) 29–42.
[60] M. Tamba, G. Simone, M. Quintiliani, *Int. J. Radiat. Biol. 50* (1986) 595–600.
[61] C. A. Morgan, M. J. Pilling, J. M. Tulloch, R. P. Ruiz, K. D. Bayes, *J. Chem. Soc. Faraday Trans. 2 78* (1982) 1323–1330.
[62] J. J. Russell, J. A. Seetula, D. Gutman, F. Danis, F. Caralp, P. D. Lightfoot, R. Lesclaux, C. F. Melius, S. M. Senkan, *J. Phys. Chem. 94* (1990) 3277–3283.
[63] D. D. Perrin, B. Dempsey, E. P. Serjeant: *pK_a Prediction for Organic Acids and Bases*, Chapman and Hall, New York 1981.
[64] M. N. Schuchmann, H.-P. Schuchmann, C. von Sonntag, *J. Phys. Chem. 93* (1989) 5320–5323.
[65] O. J. Mieden, *Dissertation*, Universität Bochum 1989 (Schriftenreihe Max-Planck-Institut für Strahlenchemie No. 51).
[66] R. W. Fessenden, P. M. Carton, H. Shimamori, J. C. Scaiano, *J. Phys. Chem. 86* (1982) 3803–3811.
[67] L. R. C. Barclay, K. U. Ingold, *J. Am. Chem. Soc. 103* (1981) 6478–6485.
[68] K. Adamic, K. U. Ingold, J. R. Morton, *J. Am. Chem. Soc. 92* (1970) 922–923.
[69] E. Melamud, B. L. Silver, *J. Phys. Chem. 77* (1973) 1896–1900.
[70] E. Melamud, S. Schlick, B. L. Silver, *J. Magn. Reson. 14* (1974) 104–111.
[71] S. G. Swarts, D. Becker, S. DeBolt, M. D. Sevilla, *J. Phys. Chem. 93* (1989) 155–161.
[72] R. E. Huie, D. Brault, P. Neta, *Chem. biol. Interact. 62* (1987) 227–235.
[73] J. E. Packer, R. L. Willson, D. Bahnemann, K.-D. Asmus, *J. Chem. Soc. Perkin Trans. 2 1980*, 296–299.
[74] J. Mönig, K.-D. Asmus in W. Bors, M. Saran, D. Tait (Ed.): *Oxygen Radicals in Chemistry and Biology*, de Gruyter, Berlin 1984, pp. 57–63.
[75] R. E. Huie, P. Neta, *Int. J. Chem. Kinet. 18* (1986) 1185–1191.
[76] S. V. Jovanovic, M. G. Simic in M. G. Simic, K. A. Taylor, J. F. Ward, C. von Sonntag (Eds.): *Oxygen Radicals in Biology and Medicine*, Plenum, New York 1987, 115–122.
[77] M. N. Schuchmann, C. von Sonntag, *J. Am. Chem. Soc. 110* (1988) 5698–5701.
[78] M. Lal, C. Schöneich, J. Mönig, K.-D. Asmus, *Int. J. Radiat. Biol. 54* (1988) 773–785.
[79] P. Neta, R. E. Huie, S. Mosseri, L. V. Shastri, J. P. Mittal, P. Maruthamuthu, S. Steenken, *J. Phys. Chem. 93* (1989) 4099–4101.
[80] J. E. Packer, T. F. Slater, R. L. Willson, *Nature 278* (1979) 737–738.
[81] G. W. Buton, U. Wronska, L. Stone, D. O. Foster, K. U. Ingold, *Lipids 25* (1990) 199–210.
[82] J. Mönig, M. Göbl, K.-D. Asmus, *J. Chem. Soc. Perkin Trans. 2 1985*, 647–651.
[83] C. Schöneich, A. Aced. K.-D. Asmus, *J. Am. Chem. Soc. 113* (1991) 375–376.
[84] P. S. Nangia, S. W. Benson, *J. Phys. Chem. 83* (1979) 1138–1142.
[85] J. A. Howard, K. U. Ingold, *Can. J. Chem. 47* (1969) 3809–3815.
[86] J. A. Howard, K. U. Ingold, *Can. J. Chem. 48* (1970) 873–880.
[87] M. N. Schuchmann, C. von Sonntag, *Z. Naturforsch. B33* (1978) 329–331.
[88] F. R. Mayo, *Acc. Chem. Res. 1* (1968) 193–201.
[89] J. S. Valentine in W. S. Caughey (Ed.): *Biochemical and Clinical Aspects of Oxygen*, Academic, San Francisco 1979, pp. 659–677.
[90] D. T. Sawyer, J. S. Valentine, *Acc. Chem. Res. 14* (1981) 393–400.
[91] A. A. Frimer in S. Patai (Ed.): *The Chemistry of Functional Groups, Peroxides*, Wiley, Chichester 1983, pp. 429–461.
[92] B. H. J. Bielski, D. E. Cabelli, *Int. J. Radiat. Biol. 59* (1991) 291–319.
[93] B. H. J. Bielski, H. A. Schwarz, *J. Phys. Chem. 72* (1968) 3836–3841.
[94] J. Rabani, S. O. Nielsen, *J. Phys. Chem. 73* (1969) 3736–3744.
[95] D. Behar, G. Czapski, J. Rabani, L. M. Dorfman, H. A. Schwarz, *J. Phys. Chem. 74* (1970) 3209–3213.
[96] G. C. Barker, P. Fowles, *Trans. Faraday Soc. 66* (1970) 1661–1669.
[97] B. H. J. Bielski, A. O. Allen, *J. Phys. Chem. 81* (1977) 1048–1050.
[98] N. Getoff, M. Prucha, *Z. Naturforsch. A38* (1983) 589–590.
[99] A. U. Khan, *J. Am. Chem. Soc. 103* (1981) 6516–6517.
[100] A. A. Frimer in L. W. Oberley (Ed.): *Superoxide Dismutase*, CRC Press, Boca Raton, FL, USA 1982, pp. 83–125.
[101] C. S. Foote, F. C. Shook, R. A. Abakerli, *J. Am. Chem. Soc. 102* (1980) 2503–2504.
[102] J. R. Kanofsky, H. Sugimoto, D. T. Sawyer, *J. Am. Chem. Soc. 110* (1988) 3698–3699.
[103] J. Rabani, W. A. Mulac, M. S. Matheson, *J. Phys. Chem. 69* (1965) 53–70.
[104] A. Henglein, J. Langhoff, G. Schmidt, *J. Phys. Chem. 63* (1959) 980.
[105] E. Bothe, M. N. Schuchmann, D. Schulte-Frohlinde, C. von Sonntag, *Z. Naturforsch. B38* (1983) 212–219.
[106] K. Sehested, J. Holcman, E. J. Hart, *J. Phys. Chem. 87* (1983) 1951–1954.
[107] R. E. Bühler, J. Staehelin, J. Hoigne' *J. Phys. Chem. 88* (1984) 2560–2564.

[108] M. S. McDowell, J. H. Espenson, A. Bakac, *Inorg. Chem. 23* (1984) 2232–2236.
[109] J. Lind, X. Shen, G. Merenyi, B. I. Jonsson, *J. Am. Chem. Soc. 111* (1989) 7654–7655.
[110] J. M. Gebicki, B. H. J. Bielski, *J. Am. Chem. Soc. 103* (1981) 7020–7022.
[111] D. T. Sawyer, M. S. McDowell, K. S. Yamaguchi, *Chem. Res. Toxicol. 1* (1988) 97–100.
[112] D. J. Deeble, B. J. Parsons, G. O. Phillips, H.-P. Schuchmann, C. von Sonntag, *Int. J. Radiat. Biol. 54* (1988) 179–193.
[113] G. Merenyi, J. Lind, *J. Phys. Chem. 94* (1990) 5412.
[114] C. P. Nash, D. H. Volman, *J. Phys. Chem. 94* (1990) 5412–5413.
[115] D. M. Golden, V. M. Bierbaum, C. J. Howard, *J. Phys. Chem. 94* (1990) 5413–5415.
[116] D. J. Deeble, C. von Sonntag, unpublished results.
[117] M. Bouheroum, J. M. Bruce, E. J. Land, *Biochim. Biophys. Acta 998* (1989) 57–62.
[118] H. P. Misra, I. Fridovich, *J. Biol. Chem. 247* (1972) 3170–3175.
[119] M. N. Schuchmann, H.-P. Schuchmann, M. Hess, C. von Sonntag, *J. Am. Chem. Soc. 113* (1991), in press.
[120] K.-D. Asmus, *Acc. Chem. Res. 12* (1979) 436–442.
[121] I. Fridovich, *Annu. Rev. Biochem. 44* (1975) 147–159.
[122] L. W. Oberley (Ed.): *Superoxide Dismutase*, CRS Press, Boca Raton, FL, USA 1982.
[123] J. A. Fee in M. A. J. Rodgers, E. L. Powers (Eds.): *Oxygen and Oxy-Radicals in Chemistry and Biology*, Academic, New York 1981, pp. 205–231.
[124] D. Klug, J. Rabani, I. Fridovich, *J. Biol. Chem. 247* (1972) 4839–4842.
[125] D. Klug-Roth, I. Fridovich, J. Rabani, *J. Am. Chem. Soc. 95* (1973) 2786–2790.
[126] M. Pick, J. Rabani, F. Yost, I. Fridovich, *J. Am. Chem. Soc. 96* (1974) 7329–7333.
[127] E. M. Fielden, P. B. Roberts, R. C. Bray, D. J. Lowe, G. N. Mautner, G. Rotilio, L. Calabrese, *Biochem. J. 139* (1974) 49–60.
[128] F. Lavelle, M. E. McAdam, E. M. Fielden, P. B. Roberts, K. Puget, A. M. Michelson, *Biochem. J. 161* (1977) 3–11.
[129] M. E. McAdam, F. Lavelle, R. A. Fox, E. M. Fielden, *Biochem. J. 165* (1977) 81–87.
[130] M. E. McAdam, E. M. Fielden, F. Lavelle, L. Calabrese, D. Cocco, G. Rotilio, *Biochem. J. 167* (1977) 271–274.
[131] M. E. McAdam, R. A. Fox, F. Lavelle, E. M. Fielden, *Biochem. J. 165* (1977) 71–79.
[132] J. A. Fee, G. J. McClune, P. O'Neill, E. M. Fielden, *Biochem. Biophys. Res. Commun. 100* (1981) 377–384.
[133] P. O'Neill, E. M. Fielden, D. Cocco, G. Rotilio, L. Calabrese, *Biochem. J. 205* (1982) 181–187.
[134] P. O'Neill, E. M. Fielden, D. Cocco, L. Calabrese, G. Rotilio in G. Cohen, R. A. Greenwald (Eds.): *Oxy Radicals and Their Scavenger Systems*, Elsevier, Amsterdam 1983, pp. 316–319.
[135] S. Goldstein, C. Michel, W. Bors, M. Saran, G. Czapski, *Free Radical Biol. Med. 4* (1988) 295–303.
[136] G. Czapski, S. Goldstein, *Free Radical Res. Commun. 1* (1986) 157–161.
[137] G. Koltzenburg, cited in C. von Sonntag, *The Chemical Basis of Radiation Biology*, Taylor and Francis, London 1987, p. 172.
[138] M. N. Schuchmann, C. von Sonntag, *Z. Naturforsch. B42* (1987) 495–502.
[139] M. N. Schuchmann, H.-P. Schuchmann, C. von Sonntag, *J. Am. Chem. Soc. 112* (1990) 403–407.
[140] S. Das, M. N. Schuchmann, H.-P. Schuchmann, C. von Sonntag, *Chem. Ber. 120* (1987) 319–323.
[141] E. Bothe, D. Schulte-Frohlinde, *Z. Naturforsch. B35* (1980) 1035–1039.
[142] E. Bothe, D. Schulte-Frohlinde, C. von Sonntag, *J. Chem. Soc. Perkin Trans. 2 1978*, 416–420.
[143] E. Bothe, D. Schulte-Frohlinde, *Z. Naturforsch. B33* (1978) 786–788.
[144] S. Das, O. J. Mieden, X.-M. Pan, M. Repas, M. N. Schuchmann, H.-P. Schuchmann, C. von Sonntag, H. Zegota in M. G. Simic, K. A. Taylor, J. F. Ward, C. von Sonntag (Eds.): *Oxygen Radicals in Biology and Medicine*, Plenum, New York 1988, pp. 55–58.
[145] Y. Ilan, J. Rabani, A. Henglein, *J. Phys. Chem. 80* (1976) 1558–1565.
[146] E. Bothe, M. N. Schuchmann, D. Schulte-Frohlinde, C. von Sonntag, *Photochem. Photobiol. 28* (1978) 639–644.
[147] O. J. Mieden, M. N. Schuchmann, C. von Sonntag, *Free Radical Res. Commun. 6* (1989) 127–128.
[148] A. Fish in D. Swern (Ed.): *Organic Peroxides*, Wiley Interscience, New York 1970, pp. 181–198.
[149] M. N. Schuchmann, C. von Sonntag, *J. Phys. Chem. 86* (1982) 1995–2000.
[150] D. C. Nonhebel, J. C. Walton: *Free Radical Chemistry, Structure and Mechanism*, University Press, Cambridge 1974, p. 405.
[151] A. J. Bloodworth, J. L. Courtneidge, A. G. Davies, *J. Chem. Soc. Perkin Trans. 2 1984*, 523–527.
[152] J. E. Bennett, J. A. Howard, *J. Am. Chem. Soc. 95* (1973) 4008–4010.
[153] P. D. Bartlett, G. Guaraldi, *J. Am. Chem. Soc. 89* (1967) 4799–4801.
[154] K. Adamic, J. A. Howard, K. U. Ingold, *Can. J. Chem. 47* (1969) 3803–3808.
[155] J. E. Bennett, D. M. Brown, B. Mile, *Trans. Faraday Soc. 66* (1970) 397–405.
[156] J. A. Howard, J. E. Bennett, *Can. J. Chem. 50* (1972) 2374–2377.
[157] J. A. Howard, *ACS Symp. Ser. 69* (1978) 413–432.
[158] E. Furimsky, J. A. Howard, J. Selwyn, *Can. J. Chem. 58* (1980) 677–680.
[159] M. N. Schuchmann, C. von Sonntag, *J. Phys. Chem. 83* (1979) 780–784.
[160] J. E. Bennett, *J. Chem. Soc. Faraday Trans. 86* (1990) 3247–3252.
[161] S. L. Khursan, V. S. Martemyanov, *React. Kinet. Catal. Lett. 40* (1989) 253–258.
[162] S. L. Khursan, V. S. Martemyanov, *React. Kinet. Catal. Lett. 40* (1989) 269–275.
[163] P. S. Bailey: *Ozonation in Organic Chemistry. Olefinic Compounds*, Academic, London 1978, p. 57.
[164] P. S. Nangia, S. W. Benson, *Int. J. Chem. Kinet. 12* (1980) 43–53.
[165] H.-P. Schuchmann, C. von Sonntag, *Z. Naturforsch. B39* (1984) 217–221.
[166] G. A. Russell, *J. Am. Chem. Soc. 79* (1957) 3871–3877.
[167] S.-H. Lee, G. D. Mendenhall, *J. Am. Chem. Soc. 110* (1988) 4318–4323.
[168] M. Nakano, K. Takayama, Y. Shimizu, Y. Tsuji, H. Inaba, T. Migita, *J. Am. Chem. Soc. 98* (1976) 1974–1975.
[169] Q. Niu, G. D. Mendenhall, *J. Am. Chem. Soc. 112* (1990) 1656–1657.
[170] J. E. Bennett, R. Summers, *Can. J. Chem. 52* (1974) 1377–1379.
[171] G. D. Mendenhall, E. M. Y. Quinga, *Int. J. Chem. Kinet. 17* (1985) 1187–1190.
[172] D. Veltwisch, E. Janata, K.-D. Asmus, *J. Chem. Soc. Perkin Trans. 2 1980*, 146–153.
[173] V. M. Berdnikov, N. M. Bazhin, V. K. Fedorov, O. V. Polyakov, *Kinet. Catal. (Engl. Transl.) 13* (1972) 986–987.
[174] B. C. Gilbert, R. G. G. Holmes, H. A. H. Laue, R. O. C. Norman, *J. Chem. Soc. Perkin Trans. 2 1976*, 1047–1052.
[175] B. C. Gilbert, R. G. Holmes, R. O. C. Norman, *J. Chem. Res. Synop. 1977*, 1.
[176] H.-P. Schuchmann, C. von Sonntag, *J. Photochem. 16* (1981) 289–295.
[177] L. Batt, *Int. Rev. Phys. Chem. 6*(1987) 53–90.
[178] S. Saebo, L. Radom, H. F. Schaefer, III, *J. Chem. Phys. 78* (1983) 845–853.
[179] K. Y. Choo, S. W. Benson, *Int. J. Chem. Kinet. 13* (1981) 833–844.
[180] C. Walling, P. J. Wagner, *J. Am. Chem. Soc. 86* (1964) 3368–3375.
[181] B. C. Gilbert, P. D. R. Marshall, R. O. C. Norman, N. Pineda, P. S. Williams, *J. Chem. Soc. Perkin Trans. 2 1981*, 1392–1400.
[182] M. N. Schuchmann, H. Zegota, C. von Sonntag, *Z. Naturforsch. B. 40* (1985) 215–221.
[183] H. Zegota, M. N. Schuchmann, C. von Sonntag, *J. Phys. Chem. 88* (1984) 5589–5593.
[184] G. Meissner, A. Henglein, G. Beck, *Z. Naturforsch. B22* (1967) 13–19.
[185] M. N. Schuchmann, C. von Sonntag, unpublished results.
[186] We thank *K. U. Ingold* for this information.
[187] A. L. J. Beckwith, B. P. Hay, *J. Am. Chem. Soc. 111* (1989) 230–234.
[188] K.-D. Asmus, H. Möckel, A. Henglein, *J. Phys. Chem. 77* (1973) 1218–1221.
[189] E. Bothe, G. Behrens, D. Schulte-Frohlinde, *Z. Naturforsch. B32* (1977) 886–889.
[190] T. Söylemez, C. von Sonntag, *J. Chem. Soc. Perkin Trans. 2 1980*, 391–394.
[191] A. Piesiak, M. N. Schuchmann, H. Zegota, C. von Sonntag, *Z. Naturforsch. B39* (1984) 1262–1267.
[192] H.-P. Schuchmann, C. von Sonntag, *Radiat. Phys. Chem. 32* (1988) 149–156.
[193] G. Mark, M. N. Schuchmann, H.-P. Schuchmann, C. von Sonntag, *J. Photochem. Photobiol. A55* (1990) 157–168.
[194] U. Gröllmann, W. Schnabel, *Makromol. Chem. 181* (1980) 1215–1226.
[195] M. Isildar, M. N. Schuchmann, D. Schulte-Frohlinde, C. von Sonntag, *Int. J. Radiat. Biol. 41* (1982) 525–533.
[196] R. A. McClelland, S. Steenken, *J. Am. Chem. Soc. 110* (1988) 5860–5866.
[197] M. N. Schuchmann, C. von Sonntag, *J. Chem. Soc. Perkin Trans. 2 1977* (1958–1963.
[198] M. N. Schuchmann, C. von Sonntag, *Aqua (London) 38* (1989) 311–317.
[199] B. L. Dunicz, D. D. Perrin, D. W. G. Style, *Trans. Faraday Soc. A 197* (1951) 1210–1215.
[200] C. N. Satterfield, L. C. Case, *Int. Eng. Chem. 46* (1954) 998–1001.
[201] H. Heusinger, *Z. Lebensm. Unters. Forsch. 185* (1987) 106–110.
[202] H. Heusinger, *Z. Lebensm. Unters. Forsch. 185* (1987) 447–456.
[203] M. S. Akhlaq, H.-P. Schuchmann, C. von Sonntag, *Environ. Sci. Technol. 24* (1990) 379–383.
[204] H. B. Lamberts, P. Alexander, *Biochim. Biophys. Acta 88* (1964) 642–644.
[205] P. Myint, D. J. Deeble, P. C. Beaumont, S. M. Blake, G. O. Philips, *Biochim. Biophys. Acta 925* (1987) 194–202.
[206] M. Lal, *J. Radioanalyt. Nucl. Chem. 92* (1985) 105–112.
[207] M. N. Schuchmann, C. von Sonntag, *Int. J. Radiat. Biol. 34* (1978) 397–400.
[208] S. Das, C. von Sonntag, *Z. Naturforsch. B41* (1986) 505–513.
[209] S. Abramovitch, J. Rabani, *J. Phys. Chem. 80* (1976) 1562–1565.

[210] E. Hayon, M. Simic, *J. Am. Chem. Soc. 93* (1971) 6781–6786.
[211] O. J. Mieden, C. von Sonntag in P. Beaumont, D. J. Deeble, B. Parsons, C. Rice-Evans (Ed.): *Free Radicals, Metal Ions and Biopolymers*, Richelieu, London 1989, pp. 85–89.
[212] O. J. Mieden, C. von Sonntag, *J. Chem. Soc. Perkin Trans. 2 1989*, 2071–2078.
[213] H. Schuessler, K. Schilling, *Int. J. Radiat. Biol. 45* (1984) 267–281.
[214] D. J. Nelson, *J. Phys. Chem. 83* (1979) 2186–2195.
[215] J. T. Allan, *J. Phys. Chem. 68* (1964) 2714–2716.
[216] N. M. Bazhin, E. V. Kuznetsov, N. N. Bubnov, V. V. Voevodskii, *Kinet. Catal. (Engl. Transl.) USSR 7* (1966) 643–645.
[217] R. Livingston, H. Zeldes, *J. Am. Chem. Soc. 88* (1966) 4333–4336.
[218] F. Seidler, C. von Sonntag, *Z. Naturforsch. B24* (1969) 780–781.
[219] C. von Sonntag, E. Thoms, *Z. Naturforsch. B25* (1970) 1405–1407.
[220] K. M. Bansal, M. Grätzel, A. Henglein, E. Janata, *J. Phys. Chem. 77* (1973) 16–19.
[221] S. Steenken, *J. Phys. Chem. 83* (1979) 595–599.
[222] S. Steenken, M. J. Davies, B. C. Gilbert, *J. Chem. Soc. Perkin Trans. 2 1986* 1003–1010.
[223] H. Zegota, M. N. Schuchmann, D. Schulz, C. von Sonntag, *Z. Naturforsch. B41* (1986) 1015–1022.
[224] G. V. Buxton, R. M. Sellers, *J. Chem. Soc. Faraday Trans 1 69* (1973) 555–559.
[225] W. M. Garrison, H. R. Haymond, W. Bennett, S. Cole, *J. Chem. Phys. 25* (1956) 1282.
[226] W. M. Garrison, H. R. Haymond, W. Bennett, S. Cole, *Radiat. Res. 10* (1959) 273–282.
[227] L. Josimovic, I. Draganic, *Int. J. Radiat. Phys. Chem. 5* (1973) 505–512.
[228] L. R. Josimovic, I. G. Draganic, V. M. Markovic, *Glas. Khem. Drus. Beograd 41* (1976) 75–79.
[229] M. N. Schuchmann, C. von Sonntag, *Z. Naturforsch. B37* (1982) 1184–1186.
[230] B. Lindman, H. Wennerström, *Top. Curr. Chem. 87* (1980) 1–83.
[231] M. AlSheikhly, M. G. Simic, *J. Phys. Chem. 93* (1989) 3103–3106.
[232] L. K. Patterson, K. Hasegawa, *Ber. Bunsenges. Phys. Chem. 82* (1978) 951–956.
[233] K. Hasegawa, L. K. Patterson, *Photochem. Photobiol. 28* (1978) 817–823.
[234] L. K. Patterson in M. A. J. Rodgers, E. L. Powers (Eds.): *Oxygen and Oxy-Radicals in Chemistry and Biology*, Academic, New York 1981, pp. 89–96.
[235] M. Al-Sheikhly, M. G. Simic in C. Rice-Evans, B. Halliwell (Eds.): *Free Radicals: Methodology and Concepts*, Richelieu, London 1988, pp. 481–497.
[236] J. M. Gebicki, A. O. Allen, *J. Phys. Chem. 73* (1969) 2443–2445.
[237] J. A. Raleigh, W. Kremers, B. Gaboury, *Int. J. Radiat. Biol. 31* (1977) 203–213.
[238] J. A. Raleigh in T. L. Walden, Jr., H. N. Hughes (Eds.): *Prostaglandin and Lipid Metabolism in Radiation Injury*, Plenum, New York 1987, pp. 3–27.
[239] M. I. AlSheikhly, M. G. Simic in G. Rotilio (Ed.): *Superoxide and Superoxide Dismutase in Chemistry, Biology and Medicine*, Elsevier, New York 1986, pp. 32–34.
[240] X.-M. Pan, E. Bastian, C. von Sonntag, *Z. Naturforsch. B43* (1988) 1201–1205.
[241] J. A. Howard, K. U. Ingold, *Can. J. Chem. 45* (1967) 785–792.
[242] D. G. Hendry, D. Schuetzle, *J. Am. Chem. Soc. 97*(1975) 7123–7127.
[243] M. Daniels, G. Scholes, J. Weiss, *J. Chem. Soc. 1956*, 832–834.
[244] E. V. Barelko, L. I. Kartasheva, P. D. Novikov, M. A. Proskurnin: *Proc. All-Union Conf. Radiat. Chem. 1st 1957* (1959) 81–85.
[245] I. Loeff, G. Stein, *J. Chem. Soc. 1963*, 2623–2633.
[246] L. I. Kartasheva, A. K. Pikaev, *Russ. J. Phys. Chem. (Engl. Transl.) 41* (1967) 1534–1536.
[247] T. K. K. Srinivasan, I. Balakrishnan, M. P. Reddy, *J. Phys. Chem. 73* (1969) 2071–2073.
[248] I. Balakrishnan, M. P. Reddy, *J. Phys. Chem. 74* (1970) 850–855.
[249] L. I. Kartasheva, A. K. Pikaev, *High Energy Chem. (Engl. Transl.) 6* (1972) 76–77.
[250] I. Balakrishnan, M. P. Reddy, *J. Phys. Chem. 76* (1972) 1273–1279.
[251] G. Ramanan, *J. Indian Chem. Soc. 53* (1976) 957–964.
[252] L. Latriano, A. Zaccaria, B. D. Goldstein, G. Witz, *J. Free Radicals Biol. Med. 1* (1985) 363–371.
[253] G. Cohen, S. E. Ofodile in G. Cohen, R. A. Greenwald (Eds.): *Oxy-Radicals and Their Scavenger Systems*, Elsevier, New York 1983, pp. 74–83.
[254] D. Wang, C. von Sonntag in J. J. Raffi, J.-J. Beliardo (Eds.): *Potential New Methods of Detection of Irradiated Food*, Commission of the European Communities, Luxembourg 1991, pp. 207–212.
[255] O. I. Micic, M. T. Nenadovic, *J. Phys. Chem. 80*(1976) 940–944.
[256] R. Bausch, H.-P. Schuchmann, C. von Sonntag, R. Benn, H. Dreeskamp, *J. Chem. Soc. Chem. Commun. 1976*, 418–419.
[257] R. Benn, H. Dreeskamp, H.-P. Schuchmann, C. von Sonntag, *Z. Naturforsch. B34* (1979) 1002–1009.
[258] C. von Sonntag, X. Zhang, H.-P. Schuchmann, *J. Chim. Phys. Phys. Chem. Biol.* (1991), in press.
[259] G. G. Jayson, D. A. Stirling, A. J. Swallow, *Int. J. Radiat. Biol. 19* (1971) 143–156.
[260] C. Chatgilialoglu, M. Guerra in C. Chatgilialoglu, K.-D. Asmus (Eds.): *Sulfur-Centered Reactive Intermediates in Chemistry and Biology*, Plenum, New York 1990, pp. 31–36.
[261] M. D. Sevilla, M. Yan, D. Becker, *Biochem. Biophys. Res. Commun. 155* (1988) 405–410.
[262] M. D. Sevilla, D. Becker, M. Yan, *Int. J. Radiat. Biol. 57* (1990) 65–81.
[263] M. D. Sevilla, D. Becker, S. Swarts, J. Herrington, *Biochem. Biophys. Res. Commun. 144* (1987) 1037–1042.
[264] D. Becker, S. Swarts, M. Champagne, M. D. Sevilla, *Int. J. Radiat. Biol. 53* (1988) 767–786.
[265] M. D. Sevilla, M. Yan, D. Becker, S. Gillich, *Free Radical Res. Commun. 6* (1989) 99–102.
[266] C. von Sonntag, N. Zhang, H.-P. Schuchmann, *Int. J. Radiat. Biol. 59* (1991) 585.
[267] G. E. Adams, G. S. McNaughton, B. D. Michael in G. R. A. Johnson, G. Scholes (Eds.): *The Chemistry of Ionization and Excitation*, Taylor and Francis, London 1967, pp. 281–293.
[268] P. C. Chan, B. H. J. Bielski, *J. Am. Chem. Soc. 95* (1973) 5504–5508.
[269] J. L. Redpath, *Radiat. Res. 54* (1973) 364–374.
[270] K. Sehested, J. Holcman, *J. Phys. Chem. 82* (1978) 651–653.
[271] J. Holcman, K. Sehested, *J. Phys. Chem. 80* (1976) 1642–1644.
[272] D. J. Deeble, M. N. Schuchmann, S. Steenken, C. von Sonntag, *J. Phys. Chem. 94* (1990) 8186–8192.
[273] K. Schäfer, M. Bonifacic, D. Bahnemann, K.-D. Asmus, *J. Phys. Chem. 82* (1978) 2777–2780.
[274] G. R. Peyton, F. Y. Huang, J. L. Burleson, W. H. Glaze, *Environ. Sci. Technol. 16* (1982) 448–453.
[275] W. H. Glaze, *Environ. Health Perspect. 69* (1986) 151–157.
[276] R. Köster, K.-D. Asmus, *Z. Naturforsch. B26* (1971) 1108–1116.
[277] M. Lal, J. Mönig, K.-D. Asmus, *J. Chem. Soc. Perkin Trans. 2 1987*, 1639–1644.
[278] K.-D. Asmus, D. Bahnemann, K. Krischer, M. Lal, J. Mönig, *Life Chem. Rep. 3* (1985) 1–15.
[279] M. Lal, H. S. Mahal, *Radiat. Phys. Chem. 32* (1988) 599–603.
[280] K.-D. Asmus, M. Lal, J. Mönig, C. Schöneich in M. G. Simic, K. A. Taylor, J. F. Ward, C. von Sonntag (Eds.): *Oxygen Radicals in Biology and Medicine*, Plenum, New York 1989, pp. 67–73.
[281] G. Scholes, R. L. Willson, M. Ebert, *J. Chem. Soc. D 1969*, 17–18.
[282] D. J. Deeble, D. Schulz, C. von Sonntag, *Int. J. Radiat. Biol. 49* (1986) 915–926.
[283] M. A. Siddiqi, E. Bothe, *Radiat. Res. 112* (1987) 449–463.
[284] M. Dizdaroglu, C. von Sonntag, D. Schulte-Frohlinde, *J. Am. Chem. Soc. 97* (1975) 2277–2278.
[285] F. Beesk, M. Dizdaroglu, D. Schulte-Frohlinde, C. von Sonntag, *Int. J. Radiat. Biol. 36* (1979) 565–576.
[286] G. Behrens, G. Koltzenburg, A. Ritter, D. Schulte-Frohlinde, *Int. J. Radiat. Biol. 33* (1978) 163–171.
[287] G. Behrens, G. Koltzenburg, D. Schulte-Frohlinde, *Z. Naturforsch. C37* (1982) 1205–1227.
[288] G. Koltzenburg, G. Behrens, D. Schulte-Frohlinde, *J. Am. Chem. Soc. 104* (1982) 7311–7312.
[289] M. Dizdaroglu, D. Schulte-Frohlinde, C. von Sonntag, *Z. Naturforsch. C30* (1975) 826–828.
[290] M. Dizdaroglu, D. Schulte-Frohlinde, C. von Sonntag, *Int. J. Radiat. Biol. 32* (1977) 481–483.
[291] M. Dizdaroglu, D. Schulte-Frohlinde, C. von Sonntag, *Z. Naturforsch. C32* (1977) 1021–1022.
[292] W. D. Henner, L. O. Rodriguez, S. M. Hecht, W. A. Haseltine, *J. Biol. Chem. 258* (1983) 711–713.
[293] A. Hissung, M. Isildar, C. von Sonntag, H. Witzel, *Int. J. Radiat. Biol. 39* (1981) 185–193.
[294] M. N. Schuchmann, C. von Sonntag, *J. Chem. Soc. Perkin Trans. 2 1984*, 699–704.
[295] M. N. Schuchmann, H. Zegota, C. von Sonntag in W. Bors, M. Saran, D. Tait (Eds.): *Oxygen Radicals in Chemistry and Biology*, de Gruyter, Berlin 1984, pp. 629–635.
[296] D. G. E. Lemaire, E. Bothe, D. Schulte-Frohlinde, *Int. J. Radiat. Biol. 45* (1984) 351–358.
[297] D. G. E. Lemaire, E. Bothe, D. Schulte-Frohlinde, *Int. J. Radiat Biol. 51*(1987) 319–330.
[298] D. J. Deeble, C. von Sonntag, *Int. J. Radiat. Biol. 46* (1984) 247–260.
[299] C. P. Murthy, D. J. Deeble, C. von Sonntag, *Z. Naturforsch. C43* (1988) 572–576.
[300] M. Adinarayana, E. Bothe, D. Schulte-Frohlinde, *Int. J. Radiat. Biol. 54* (1988) 723–737.
[301] E. Bothe, G. Behrens, E. Böhm, B. Sethuram, D. Schulte-Frohlinde, *Int. J. Radiat. Biol. 49* (1986) 57–66.
[302] D. Schulte-Frohlinde, E. Bothe, *Z. Naturforsch. C.39* (1984) 315–319.

[303] D. J. Deeble, C. von Sonntag, *Int. J. Radiat. Biol. 49* (1986) 927–936.
[304] K. Hildenbrand, G. Behrens, D. Schulte-Frohlinde, *Bioelectrochem. Bioenerg. 18* (1987) 147–153.
[305] A. Hissung, C. von Sonntag, *Int. J. Radiat. Biol. 35* (1979) 449–458.
[306] A. Hissung, C. von Sonntag, D. Veltwisch, K.-D. Asmus, *Int. J. Radiat. Biol. 39* (1981) 63–71.
[307] K. J. Visscher, M. P. de Haas, H. Loman, B. Vojnovic, J. M. Warman, *Int. J. Radiat. Biol.* 52 (1987) 745–753.
[308] C. von Sonntag, X.-M. Pan, unpublished results.
[309] C. von Sonntag in W. A. Glass, M. Varma (Eds.): *Proceedings of the Conference at Wood Hole (1990)*, in press.
[310] E. Hayon, *J. Chem. Phys. 51* (1969) 4881–4892.
[311] L. M. Theard, F. C. Peterson, L. S. Myers, Jr., *J. Phys. Chem. 75* (1971) 3815–3821.
[312] S. Das, D. J. Deeble, M. N. Schuchmann, C. von Sonntag, *Int. J. Radiat. Biol. 46* (1984) 7–9.
[313] D. J. Deeble, S. Das, C. von Sonntag, *J. Phys. Chem. 89* (1985) 5784–5788.
[314] H. M. Novais, S. Steenken, *J. Am. Chem. Soc. 108* (1986) 1–6.
[315] D. J. Deeble, C. von Sonntag, *Int. J. Radiat. Biol. 51* (1987) 791–796.
[316] S. Das, D. J. Deeble, C. von Sonntag, *Z. Naturforsch. C40* (1985) 292–294.
[317] M. N. Schuchmann, S. Steenken, J. Wroblewski, C. von Sonntag, *Int. J. Radiat. Biol. 46* (1984) 225–232.
[318] S. Fujita, S. Steenken, *J. Am. Chem. Soc. 103* (1981) 2540–2545.
[319] D. K. Hazra, S. Steenken, *J. Am. Chem. Soc. 105* (1983) 4380–4386.
[320] M. Al-Sheikhly, A. Hissung, H.-P. Schuchmann, M. N. Schuchmann, C. von Sonntag, A. Garner, G. Scholes, *J. Chem. Soc. Perkin Trans. 2 1984*, 601–608.
[321] M. N. Schuchmann, M. Al-Sheikhly, C. von Sonntag, A. Garner, G. Scholes, *J. Chem. Soc. Perkin Trans. 2 1984*, 1777–1780.
[322] M. Eigen, G. Ilgenfritz, W. Kruse, *Chem. Ber. 98* (1965) 1623–1638.
[323] H. Koffer, *J. Chem. Soc. Perkin Trans. 2 1975*, 819–821.
[324] S. Steenken, *Chem. Rev. 89* (1989) 503–520.
[325] R. L. Willson, *Int. J. Radiat. Biol. 17* (1970) 349–358.
[326] C. von Sonntag, H.-P. Schuchmann in C. Chatgilialoglu, K.-D. Asmus (Eds.): *Sulfur-centered Reactive Intermediates in Chemistry and Biology*, Plenum, New York 1990, pp. 409–414.
[327] D. Schulte-Frohlinde, G. Behrens, A. Oenal, *Int. J. Radiat. Biol. 50* (1986) 103–110.
[328] W. Schnabel: *Polymer Degradation. Principles and Practival Applications*, Hanser, München 1981.

VCH Index Library

The electronic index comes with the search module of the literature-management program, VCH Biblio. You can use this index on all PCs running with MS-DOS.

ANGEWANDTE CHEMIE
International Edition in English

Soon available

At the press of a button

The annual index of "Angewandte" is soon available on 5 1/4" and 3 1/2" diskettes.

Yearly updates will keep this invaluable electronic library complete. You can search the cumulative contents in mere seconds.

Price: ca. DM 34.00 plus shipping and handling.

Special news! In honor of the 30th anniversary of "Angewandte Chemie I.E." the cumulative index will also be available on diskette.

VCH
Software
P.O. Box 101161
D-6940 Weinheim

VCH

Single-Crystal X-Ray Diffraction Studies of Oligonucleotides and Oligonucleotide–Drug Complexes

By Olga Kennard* and William N. Hunter

Nucleic acids constitute the library of genetic information for all living organisms. They also play a regulatory role in many biological events concerned with the utilization of genetic information. The double-helical model of DNA, proposed by *Watson* and *Crick* in 1953, suggested the structural basis for its biological role, but this insight into nucleic acid structures seems to have generated as many questions as it has provided answers. Experimental studies, in particular fiber diffraction work, yielded a wealth of information on the conformational flexibility of nucleic acids and on the importance of interactions with water and cations. Major advances in synthetic organic chemistry, with implications for molecular biology, propelled nucleic acid research forward in the late 1970s. The availability of milligram quantities of synthetic oligonucleotides of defined sequence and high purity paved the way for detailed and accurate structural analysis using single-crystal X-ray diffraction methods and, in more recent times, NMR spectroscopy. This article is a detailed survey of the structural results generated by crystallographic techniques as applied to DNA, RNA, and nucleic acid–drug complexes over the period 1979–1990. The appendix lists important definitions used in the characterization of oligonucleotide structures.

1. Introduction

The aim of a review is not only to present a factual survey of a field but to try and define the fundamental problems which are being tackled, to indicate how far these have yielded to solutions, and to discuss the possibilities opened up for future research. While factual aspects can be presented with relatively little bias, the definition of the field and the relative importance attached to the various results is necessarily colored by the reviewer's interests and prejudices, to say nothing of the very human tendency of attaching too much significance to the results from the reviewer's own laboratory. Striving for impartiality, on the other hand, produces a bland review far removed from the rough and tumble of the actual research.

In this review we present a factual account of some of the results which seem to us of crucial importance to the role of DNA and RNA structure in biological systems and discuss how far these have helped us to understand the fundamental mechanisms which are being investigated. Areas highlighted include a variety of sequence-specific model structures, RNA helices, hydration patterns, and the continuum of right-handed DNA conformation. We present detailed models for DNA with base-pair mismatches and other errors and review the interactions of a variety of drugs and antibiotics with oligonucleotides.

This is admittedly a very personal and ephemeral view of what we find of greatest interest in looking back over the work of the past decade and the way we see the success and failure of prodigious work in a score of laboratories in answering some fundamental questions about oligonucleotide structure and function. Other, possibly equally personal, views can be found in some of the reviews cited and we hope that readers will be encouraged to consult them and thus gain a more rounded view of the field. We also present a brief nontechnical account of the experimental and computational techniques used in the single-crystal X-ray determinations of oligonucleotides, as well as their scope and limitations. There is a comprehensive list of references to individual structure determinations, to complementary studies where appropriate, and to reviews and textbooks. To help the general reader to evaluate our review and the detail given in the references, we have compiled an appendix with numeric tables summarizing the main crystallographic results. For the same reason the important definitions of geometric features used to describe oligonucleotide structure are given and are translated into visual terms through a variety of diagrams. We include references to some recent conference abstracts to alert readers to important work in progress which is likely to be published in the near future.

2. The Single-Crystal X-Ray Structure Determination of Oligonucleotides

The principal references to structure determinations of oligonucleotide fragments containing four or more bases, published in the last decade or so, are given in Tables 1–3. Tables 1–3 are fairly comprehensive, although in isolated cases several structure determinations were reported for the same molecule, but carried out at different temperatures, with different counterions, or with oligonucleotides containing some brominated, methylated, or otherwise modified bases. Because the essential findings of such multiple determinations are very similar, not all references are cited.

Oligonucleotide structures fall into three main categories: the right-handed A and B forms and the left-handed Z form. Figures 1–3 show examples of each family based on a single-crystal structure determination. Throughout this article we will use global conformation to designate the helix type (e.g.,

[*] Dr. O. Kennard
University Chemical Laboratory
Lensfield Road, GB-Cambridge, CB2 1EW (UK)

Dr. W. N. Hunter
Department of Chemistry, Manchester University (UK)

Table 1. Right-handed double helices.

Sequence [a]	Global form	Ref.
d(pATAT)		[1,2]
d(IoCCGG)	A	[3,149]
d(CCGG)	A	[4]
d(GGTATACC)	A	[5,6]
d(GGBrUABrUACC)	A	[7]
d(GGCCGGCC)	A	[8]
d(GGGGCCCC)	A	[9]
d(GGGATCCC)	A	[10]
d(CTCTAGAG)	A	[11]
d(GGGCGCCC)	A	[12,13]
d(GCCCGGGC)	A	[14]
d(CCCCGGGG)	A	[15]
d(GGmCCGGCC)	A	[16]
d(GTGTACAC)	A	[17,18]
d(GTGCGCAC)	A	[155]
d(GGATGGGAG)	A	[19]
d(ACCGGCCGGT)	A	[20]
d(CpsCGTACGTACGG)	A	[21]
d(CCGTACGTACGG)	A	[157]
r(GCG)d(TATACGC)	A	[22]
r(UUAUAUAUAUAA)	A	[23,88]
d(GpsCGpsCGpsC)	B	[24]
d(CGCGAATTCGCG)	B	[25,26,142]
d(CGCAAATTTGCG)	B	[27]
d(CGCAAAAAAGCG)	B	[28]
d(CGCATATATGCG)	B	[29]
d(CCAGGCCTGG)	B	[30]
d(CGCAAAAATGCG)	B	[31]
d(CGCGAm6ATTCGCG)	B	[32]
d(ACCGGCGCCACA)	B	[33]
d(CGATCGATCG)	B	[34]
d(CCAACGTTGG)	B	[35]
d(CGCGTTAACGCG)	B	[154]
d(CCCCCGCGGGGG)	B	[159]

[a] IoC = 5-iodocytosine, BrU = 5-bromouridine, mC = 5-methylcytosine, ps = Rp-phosphorothioate, m6A = 6-methyladenine.

Table 2. Z-form left-handed double helices.

Sequence [a]	Comment	Ref.
d(CGCG)	high-salt	[36–38]
d(CGCG)	low-salt, disordered	[39]
d(CGCGCG)	spermine, Mg and Na	[40]
d(CGCGCG)	Mg and Na	[41]
d(CACGTG)	two forms	[42]
d(BrCGBrCGBrCG)		[43]
d(BrCGATBrCG)		[44]
d(mCGATmCG)		[44]
d(BrCGTABrCG)		[45]
d(mCGTAmCG)		[45]
d(mCGmCGmCG)		[46]
d(CG)r(CG)d(CG)		[47]
d(CG)(araC)d(GCG)		[47]
d(CGCGCGCG)	disordered	[48]
d(CGCATGCG)	disordered	[48]
d(CGTACCTACG)	disordered	[49]

[a] BrC = 5-bromocytosine, mC = 5-methylcytosine, araC = arabinose cytosine.

A-DNA, B-DNA, or Z-DNA). These polymorphic forms are quite distinct.

The A form (Fig. 1) has 11 base pairs per turn of helix with 32.7° twist between adjacent base pairs. The rise per base pair is 2.9 Å. The bases are oriented *anti* about the glycosidic bond and the furanose ring adopts C3′-*endo* conformation. The global helix axis lies in the major groove with the bases displaced some distance away. The overall effect is that of a ribbonlike structure wrapped around a pole. The structure has a wide and shallow minor groove and a narrow, deep major groove.

Olga Kennard was born in Budapest, Hungary, in 1924. She was educated at the University of Cambridge (B.A., 1944; M.A., 1948; Sc.D. 1973) She was the recipient of the Royal Society of Chemistry Prize in 1980, was elected a Fellow of the Royal Society in 1987, and was awarded the Order of the British Empire in 1988. She has been a member of the scientific staff of the Medical Research Council since 1948 and worked until 1961 in London at the Institute of Ophthalmology and the National Institute for Medical Research. In 1961 she was seconded to the University of Cambridge to set up a laboratory of Crystallographic Chemistry to study the structure of molecules of biological interest, which, over the years, increased in complexity from simple steroids to large antibiotics. Since the early 1970s her laboratory has focused on the analysis of DNA fragments and DNA–drug complexes. She also pioneered the compilation and utilization of scientific data through the establishment, in 1965, of the Cambridge Crystallographic Data Centre. Currently she is Scientific Director of the Centre and Visiting Professor of University of London and is working on the structure of oligonucleotides, particularly RNA fragments.

William N. Hunter was born in Greenock, Scotland, in 1958. He studied Chemistry at Paisley College (B.Sc., 1979). Further research in synthetic inorganic chemistry and crystallography at the University of Glasgow with Prof. D. W. A. Sharp and Dr. K. W. Muir led to the award of a Ph.D. in 1982. For the next two years he was Henry Bertie and Florence Mabel Gritton fellow at the University of Sydney, working in protein crystallography in Prof. H. C. Freeman's laboratory. From 1985 to 1989 he was a research associate with Olga Kennard in Cambridge studying nucleic acid structure. He is now a lecturer in the Structural Chemistry section in Manchester with research interests centered on macromolecular crystallography.

Table 3. Double helices with non-Watson–Crick base pairs or extra-helical bases.

Sequence [a]	Comment	Form	Ref.
d(TGCGCG)	G · T	Z	[50]
d(BrUGCGCG)	BrU · G	Z	[51]
d(CGCGFUG)	FU · G	Z	[53]
d(CGTDCG)	T · 2-aminoadenine	Z	[52]
d(CDCGTG)	T · 2-aminoadenine	Z	[52]
d(CGCGXG)	G · X	Z	[54]
d(CGCGTG)	G · T	Z	[55]
d(GGGGTCCC)	G · T	A	[56]
d(GGGGCTCC)	G · T	A	[57, 58]
d(GGGTGCCC)	G · T	A	[12]
d(GGIGCTCC)	I · T	A	[59]
d(CCAAGATTGG)	G(*anti*) · A(*anti*)	B	[60, 61]
d(CGCGAATTTGCG)	G · T	B	[62]
d(CGCGAATTAGCG)	G(*anti*) · A(*syn*)	B	[63, 64]
d(CGCAAATTCGGG)	C · A	B	[65, 66]
d(CGCIAATTAGCG)	I · A	B	[67]
d(CGCAAATTGGCG)	A(*anti*) · G(*syn*)	B	[68]
d(CGCAGAATTCGCG)	extra A	B	[69]
d(CGCGAAATTTACGCG)	extra A	B	[70]
d(CGCGCGTTTTCGCGCG)	hairpin	Z	[71]

[a] FU = 5-fluorouridine, D = 2-aminoadenine, X = N4-methoxycytosine.

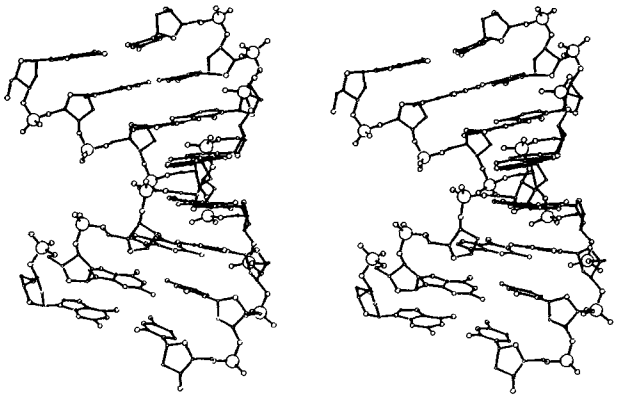

Fig. 1. Stereoview illustrating the A-form DNA as represented by the octamer d(GGGGCCCC) [9]. In this view the shallow but wide minor groove is seen at the bottom and the narrow, deep major groove above.

The B form (Fig. 2) has 10 base pairs per turn, a helix twist of 36.0° and a rise per base pair of 3.4 Å. The glycosidic orientation is *anti* and the sugar conformation tends to C2′-*endo*. The global helix axis is through the base pairs. The minor groove tends to be narrow and deep, the major groove much more open in comparison to the A form.

The Z form (Fig. 3) is a left-handed helix with a zigzag sugar-phosphate backbone, hence the name. The Z form is mostly adopted by alternating cytosine/guanine sequences and can be considered as a repeat of d(CpG) steps. There are 12 base pairs per turn and a rise of 3.7 Å. The helix twist, glycosidic orientation, and sugar conformation depend on whether the pyrimidine or purine is being considered or whether it is the first or second base pair of the dinucleotide step.

Within each family there are a number of structural subsets, denoted by A′, B′, etc. These conformations depend on small structural differences. Comparative values are presented in Table 11 in the appendix.

The number of distinct structures that have been successfully crystallized and analyzed during the past decade is still relatively limited. There are several types of B-DNA structures,

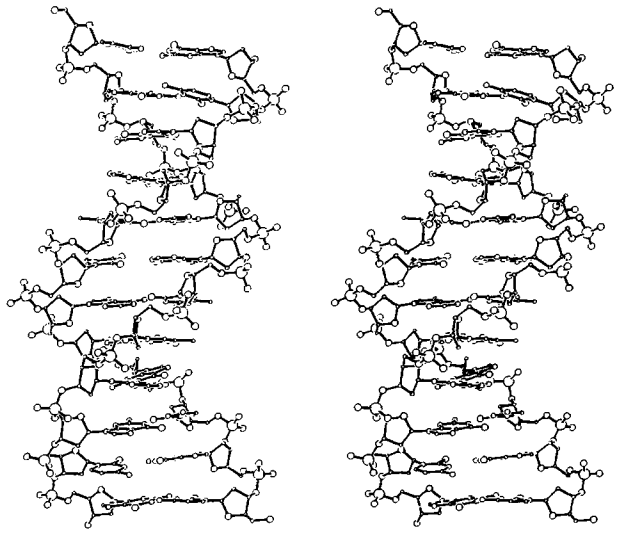

Fig. 2. Stereoview of B-form DNA as depicted by the Drew–Dickerson dodecamer d(CGCGAATTCGCG). Numerous references to this structure are given in the text.

represented by two dodecamers, d(CGCGAATTCGCG)[26] and d(ACCGGCGCCACA),[33] a hexamer d(GpsCpGpsCpGpsC),[24] decamers, d(CCAGGCCTGG)[30] and d(CGATCGATCG)[34] (Table 1), and two sequences with extra adenines[70, 71] (Table 3). These structure types make use of different interactions between adjacent double helices to create the regular crystal lattice. In contrast, all the A-

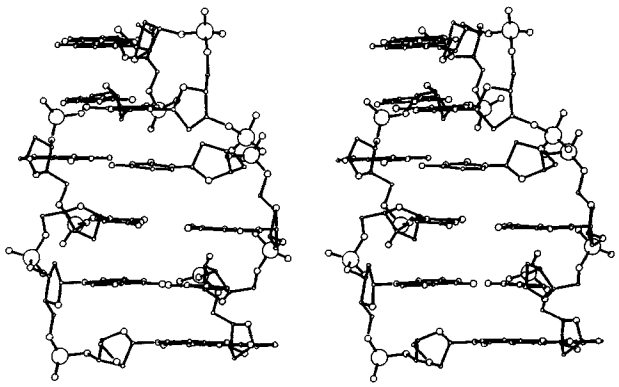

Fig. 3. The left-handed polymorph, Z-DNA, formed by the hexamer d(CGCGCG) [40, 41, 150]. Note the zigzag appearance of the phosphate-sugar backbone, from which the name is derived.

DNA helices that have been crystallized utilize a very similar packing motif involving hydrogen bonding and van der Waals contacts in the flat minor grooves. Such interactions can be accommodated in unit cells with a variety of symmetry operators, including sixfold, fourfold, and twofold screw axes. The same packing motif is utilized by a hybrid DNA–RNA decamer which forms an orthorhombic crystal.[22] Left-handed Z-DNA helices crystallize in essentially the same way, with end-to-end contacts between the helices in an orthorhombic space group (hexanucleotides) and two other closely related space groups (tetranucleotides). Selected references to deoxyoligonucleotides containing mismatched

(non-Watson–Crick) base pairs and extra bases, all utilizing the various crystal packing arrangements discussed above, are listed in Table 3. Table 4 (Section 8) gives selected references to deoxyoligonucleotide–drug complexes.

The limited number of crystal types has raised some fundamental questions about the relationship between the length of the sequence, the base composition, and the influence of crystal lattice forces in determining the type of global conformation adopted and whether or not the global conformation is identical in the crystal structures and in solution. We shall discuss these questions and some relevant experimental findings later in this review.

3. Techniques of X-Ray Analysis

3.1. Synthesis, Purification, Crystallization, and Data Collection

Techniques of synthesizing deoxyoligonucleotides in the milligram quantities required for X-ray analysis have greatly advanced since the original solution methods,[72, 73] which yielded large quantities, but which were very labor-intensive. Modern automatic solid-phase equipment based on the phosphoramidite technique[74] allows for the rapid synthesis of deoxyoligonucleotides up to 20–24 base pairs in length and of reasonable homogeneity. Stringent purification appears to be an essential prerequisite for successful crystallization. Generally, the deprotected oligonucleotide is subjected to high-pressure liquid chromatography on a strong anion-exchange resin and eluted with a phosphate buffer gradient at neutral pH. This process separates uncharged molecules from DNA and removes the shorter DNA fragments, which are by-products of the synthesis, from the main fragment by charge-based separation. A second HPLC run on C18-reverse-phase material and elution with an acetonitrile gradient separates the partially protected DNA segments of the same lengths as the target molecule from the main deprotected product, utilizing the differences in hydrophobicity. This second HPLC step also removes the phosphate salts. The pure oligonucleotide is then lypohilized to give typically 5–15 milligrams of the ammonium salt of the target DNA.

Anion-exchange separation on a preparative scale, however, is not ideal for purification of oligonucleotides longer than 10–12 nucleotides. Instead, the "trityl on" procedure is used. The acid-labile and highly lipophilic dimethoxytrityl protecting group at the 5′ terminus is left intact on the crude sample and is used to differentiate between the target sequence and the shorter sequences, where the protecting group has already been removed. A high degree of purification is achieved during the first HPLC run on a C18-reverse-phase column with acetonitrile elution. After detritylation with aqueous acetic acid and lyophilization, the sample is further purified by HPLC on an anion-exchange resin. The entire process takes about three to four days, most of which is spent on purification. Problems often arise with purification of self-complementary sequences by anion-exchange chromatography due to the formation of secondary structures such as DNA duplexes or hairpin loops, which elute at different rates. In such cases, heat and/or the use of phosphate buffer solutions, containing 20 % acetonitrile, helps to generate and maintain single strands only.

This rather detailed description of purification procedures is included to give chemists (and crystallographers) a better perspective of the problems involved in the preparation of the quantities of ultrapure compounds needed for crystallization. Even so, we would also like to note that the chances of obtaining diffraction-quality crystals on any sequence is generally less than 10 %, and crystallization remains the rate-determining step in many structure analyses.

The most common method of crystallization is to diffuse a precipitating agent into a solution containing the DNA, an associated cation, a buffer, and in many cases, spermine. Alternatively, water is diffused out of the solution by a desiccant such as hexane-1-6-diol or 2-methyl-2,4-pentanediol. In either method approximately 5- to 10-μL droplets of the oligonucleotide solution are suspended as hanging drops over a reservoir or up to 50-μL droplets are placed as "sitting drops" in hollowed-out glass plates. A wide range of conditions are commonly set up with variations in oligonucleotide concentration, the nature and concentration of the counterions, and pH, at either room temperature or at 4 °C. Remarkably, the only RNA fragment so far analyzed was crystallized at 37 °C![23] Once the approximate conditions are determined, they are refined until diffraction-quality crystals are obtained. With care, reproducible conditions are found, and more crystals can generally be grown.

The success rate of crystallization, as discussed above, is very low. Disordered crystals are often formed or none at all. Even crystals with good optical order, as indicated by sharp extinction when viewed with a polarized light source, may only give poor-quality X-ray diffraction patterns. This is most likely a consequence of rotational disorder of the cylindrical DNA helixes in the adjacent unit cells which form the crystal. The problem is further exacerbated by the extensive hydration of the crystals, which commonly contain about 50 % solvent. The limited diffracting power of many of the oligonucleotides, discussed in the next section, is the consequence of both solvent and DNA disorder.

Certain crystals are unstable at room temperature and diffraction measurements are frequently carried out at 4 °C on samples sealed in glass capillary tubes to prevent loss of solvent. Recently, several structures were measured at 115 K without a capillary, using a fast-freezing technique.[75, 76] Although this technique does not improve the diffracting resolution, it stabilizes the crystals and allows data collection from a single crystal.

The quality of the diffraction data and the attainable resolution are determined by the size and, most importantly, by the perfection of the crystals used for measurements. The Z hexamers form the most perfect crystals, often diffracting to 1 Å or better. Shorter or longer Z-forming sequences tend to be disordered. In general, the right-handed deoxyoligonucleotide crystals diffract in the range of 1.7- to 2.5-Å resolution except for the B-DNA decamer,[60] which diffracts to 1.3-Å resolution. The use of synchrotron radiation can lead to improvements in effective resolution[7] and is likely to be used more frequently in the future to aid structure solution by anomalous dispersion methods.[77, 152] A typical data collection on a diffractometer would result in some 2500 reflections to a resolution of about 2.0 Å, which would be used in

the structure analysis. The recent availability of area detectors designed for the simultaneous measurement of very large numbers of reflections is revolutionizing this aspect of the subject.[78, 79]

3.2. Structure Solution and Refinement

A variety of experimental and computational techniques can be applied to solve oligonucleotide structures, such as molecular replacement, multiple isomorphous replacement, and anomalous dispersion (see *Blundell* and *Johnson*[80]). The object is to find the correct model for the fundamental structural motif: the asymmetric unit. In many cases this motif consists of two independent oligonucleotide strands which coil about each other to form a duplex. Less frequently, the motif is a single strand and the double helix is formed by a twofold symmetry operation. Occasionally, the asymmetric unit contains four or more strands which may complicate the structure solution.[152]

Most of the successful structure determinations to date have employed the molecular replacement method with a model based on fiber diffraction coordinates or on coordinates from a related crystal structure.[4, 81] A notable exception is the use of maximum entropy methods for a 15-mer containing an extra base.[70]

Once the phase problem is solved, the refinement process begins. This procedure is directed towards reducing discrepancies between structure amplitudes calculated from the model and the experimentally determined values derived from intensity measurements. When a crystal does not diffract to atomic resolution, the number of measurements is small compared to the number of variables. In such cases constrained/restrained methods of refinement are employed and certain variables such as bond lengths and angles are held constant in an attempt to make the best use of the experimental observations.

Solvent molcules are an essential part of the oligonucleotide crystal structures. Refinement will, if the resolution warrants, include the location of solvent molecules from various electron density maps, often with the aid of computer graphics. Usually around three to eight solvent molecules are found for each nucleotide in the molecule. Counterions have only been positively identified in the Z-DNA hexamers, the B-DNA decamers, and some of the DNA–drug complexes. It is common practice to assign solvent positions as water oxygen atoms. The refinement process is terminated when there is optimal fit of the model structure with the electron density maps, when no further solvent molecules can be located, and when there is no further improvement in the crystallographic residual R. This residual is defined as $R = \sum(|F_o| - |F_c|)/\sum|F_o|$, where F_o is the observed and F_c the calculated structure amplitude. Most oligonucleotide structures are refined to an R factor of between 0.12 for well-resolved structures and 0.25 for poorly resolved structures.

The effective resolution limits the degree of structural detail that can be accurately determined. Coordinates for individual atoms can only be determined reliably for structures which diffract close to 1 Å. For most oligonucleotide structures, resolution limits the analysis to the accurate determination of structural features such as sugar conformation, orientation of bases, and the principal torsion angles. Information about the position of solvent molecules, particularly in the first hydration shell, is sufficiently reliable to allow for some generalizations of the role of hydration and its relation to global conformations.

A variant of the techniques described above has been used to analyze structures with base-pair mismatches. In these structures the contributions of the atoms of the mismatched bases were initially omitted from the calculations. At an intermediate stage in the refinement the positions of the atoms in the mismatched base pairs were located from electron density maps and their contributions were included in the calculations. In this way the analysis is not biased by a preconceived model of the base-pair mismatch. Similar techniques were used for several other structures, including some oligonucleotide–drug complexes and have led to the discovery of novel features such as Hoogsteen base-pairing in DNA fragments complexed with bifunctional intercalators.[82, 83]

4. Sequence-Specific Model Structures

4.1. Alternating B-DNA

The relation between sequence and variations in local helical parameters was analyzed in detail by *Calladine* and *Drew*[84–86] and by *Shakked* and *Rabinovich*[87] and some tentative "rules" were proposed. The rules, which relate variations in helix twist and roll angles to steric clash between base pairs, proved to be too simple and were contradicted by later X-ray structures.

An interesting generalization that has emerged, however, is the existence of regular alternation in the local helical parameters of d(AT) tracts. Such alternations, first observed in the tetramer d(pTATA),[1, 2, 89] led to the proposal of an alternating B-DNA helix for poly d(AT). In such a model the helix twist angle is smaller at the ApT step than at the TpA step. Similar alternation was reported in the central AT region of d(CGCATATATGCG).[29] Alternating backbone conformation was also observed in the phosphorothioate analogue of d(GCGCGC)[24] and, when examined closely, in the CGCG segments of the dodecamer d(CGCGAATTCGCG). DNAse footprinting experiments give good correlation with the notion that this nuclease is able to cut preferentially at ApT and GpC steps (low twist) rather than at TpA and CpG steps (high twist), suggesting that modulations of the backbone conformation may act as recognition signals, directing interactions with proteins.

4.2. Homopolymer d(A)–d(T) Tracts

The special characteristics of d(A)–d(T) tracts were first demonstrated crystallographically by *Nelson* et al.[28] who analyzed the duplex formed by d(CGCAAAAAAGCG) and d(CGCTTTTTTGCG). Although the crystals are isomorphous with the Dickerson–Drew dodecamer, the double helix has some interesting structural variations. The A·T base pairs of the central region have unusually large propeller twists (approximately 25°), which permit the formation of a three-centered hydrogen-bonding network in the

major groove between the N6 atoms of adenines and the O4 atoms of two thymines, one the Watson–Crick partner and the other the base in the 3′ direction of the opposing strand. Similar three-centered bonds were subsequently observed in d(CGCAAATTTGCG), both when crystallized by itself and when complexed with distamycin.[27] The presence of such interstrand hydrogen bonds, in addition to a marked purine–purine base overlap, confers a certain rigidity to the homopolymer tract and could well provide an explanation as to why long runs of adenines are not located in the more sharply curved tracks of chromosomes, but are found at the end of the nucleosomal DNA with decreased supercoiling.[90] The rigidity and mode of bending of DNA is a highly controversial subject and a number of different theories have been proposed to account for the many experimental observations. For a recent discussion see *Calladine* et al.[91]

4.3. Ribonucleotide Double Helices

Structural studies on transfer-RNA have been detailed elsewhere (see *Saenger*[92]), and our review is restricted to duplex RNA. There are only two examples of well-characterized crystals containing RNA double helices. They are the hybrid decamer r(GCG)d(TATACGC) studied by *Wang* et al.[22] and the 14-mer r(UUAUAUAUAUAUAA).[23, 88] Stereoviews of these structures are given in Figures 4 and 5, respectively. In both cases the major groove is narrow and deep, the minor groove broad and shallow. RNA adopts conformations similar to those observed for A-form DNA. The hydroxyl substituent on the furanose ring is implicated in restricting the sugar conformation to C3′-*endo*.

The decamer structure (Fig. 4) consists of two hybrid DNA–RNA segments on either side of duplex DNA. All three sections display a conformation similar to the fiber-based model for the 11-fold RNA duplex. Water molecules bridge the ribose O2′-hydroxyl group and the cytosine O2 group on the minor-groove side of the base pair and may contribute to the particular ribo conformation. The 14-mer RNA duplex (Fig. 5) allows for the most detailed analysis of an RNA helix. This structure can be treated as three segments separated by kinks in the sugar-phosphate backbone. The kinks influence the major-groove dimensions and result in a structure quite distinct from the fiber models. The O2′-hydroxyl group, while playing a structural role, is directed towards the minor groove and thus provides a functional group able to interact with proteins. The access to this functional group is facilitated by the relatively open minor groove in the A-form structures.

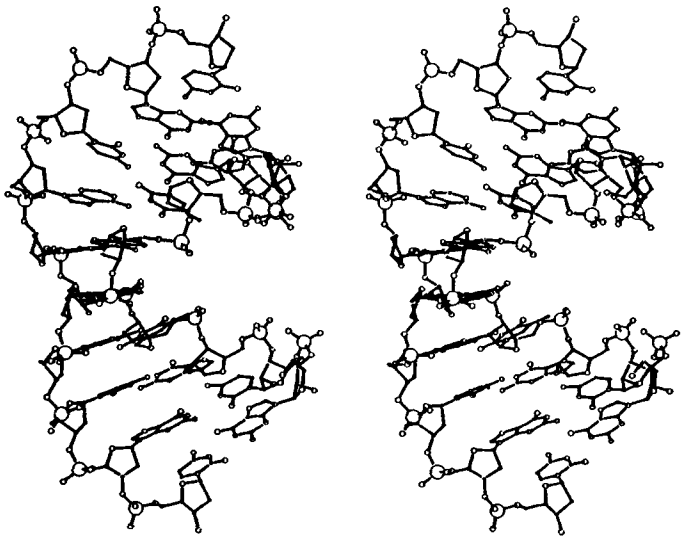

Fig. 4. A stereoview of the RNA–DNA hybrid decamer r(CGC)-d(TATAGCG), analyzed by *Wang* et al. [22].

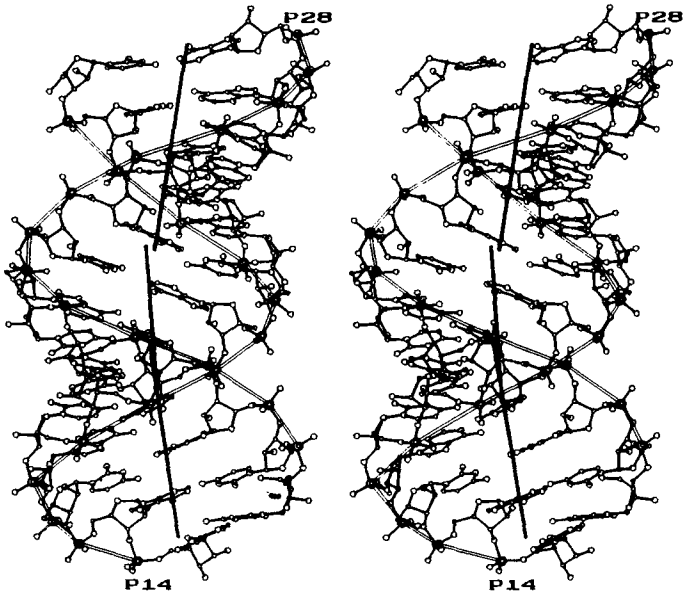

Fig. 5. A stereoview of the RNA structure r(UUAUAUAUAUAUAA), studied by *Dock-Bregeon* et al. [23]. Phosphorus atoms 14 and 28 are labeled. This structure can be considered as consisting of three segments and the three optimal helix axes corresponding to each section are drawn. Note the A form and how the bases tend to wrap around these helical axes. We thank Prof. *D. Moras* for providing this diagram.

5. Hydration

DNA crystals, as already mentioned, contain around 50 % solvent. The extensive hydration contributes to the difficulties of obtaining well-ordered crystals and precise X-ray diffraction data. It does, however, allow for the experimental study of nucleic acid hydration and extrapolation from the crystal-structure results to in vivo structures, in much the same way as is common for protein structures.

In DNA, distinct hydration patterns are observed around the sugar-phosphate backbone as well as in the major and minor grooves. An examination by *Saenger* et al.[93] of the water structure reported in numerous DNA fragments led to the proposal that in mixed-sequence DNA the hydration of the backbone is related to the global conformation. The typical backbone hydration patterns of A-, B-, and Z-DNA helices are illustrated in Figures 6–8. As can be seen, in both A- and Z-DNA a continuous chain of water molecules links the phosphate oxygens along the backbone. The water molecules are shared between adjacent phosphate groups, result-

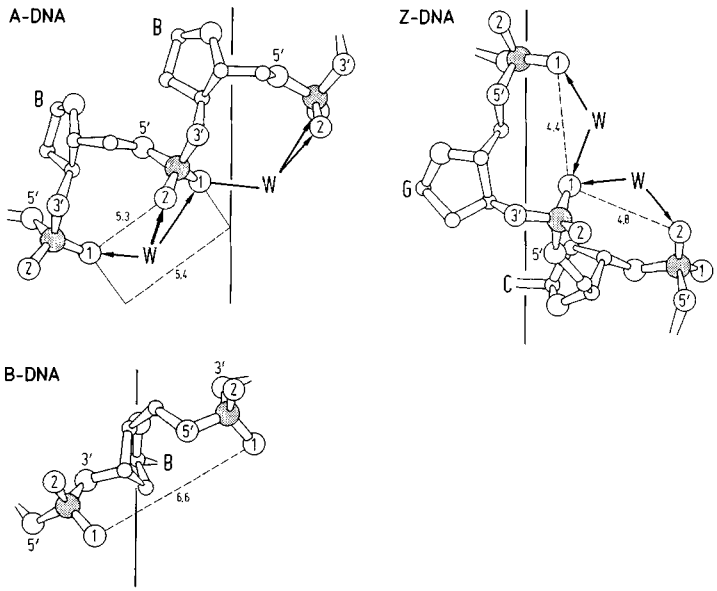

Fig. 6. A comparison of deoxyribose 3',5'-diphosphate fragments in A-form, B-form, and Z-form DNA. Phosphorus atoms are shaded, phosphate oxygens are numbered. The vertical line is a representation of the helix axis calculated for each polymorph, the dashed lines and distances [Å] represent the shortest separations between free phosphate oxygen atoms. The base position for the right-handed forms is indicated by "B" and by "G" and "C" for Z-DNA. "W" represents water molecules able to bridge free phosphate oxygens in A- and Z-form DNA [93].

ing in an effectively greater economy of hydration. In the B form there are more water molecules around each phosphate group and virtually no water bridges between adjacent phosphate oxygens. These observations can be rationalized very

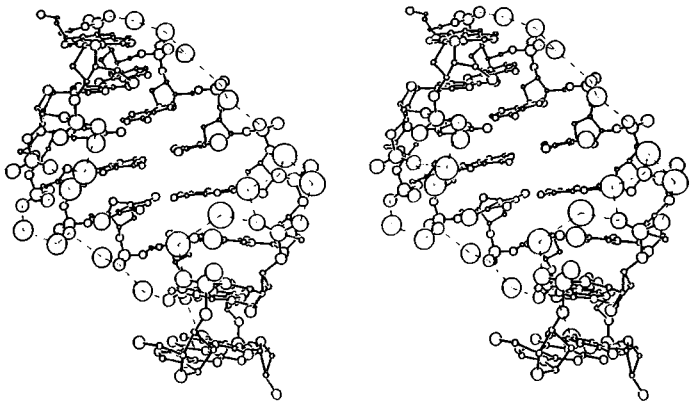

Fig. 7. The hydration of phosphate groups in the A-form fragment d(GGBrUABrUACC). This stereoview shows a view into the major groove. Waters are represented by the largest spheres with possible hydrogen bonds as dashed lines. Note that there is an almost continuous linking of phosphate groups by water molecules [93].

simply by considering the O1P/O2P···O1P/O2P distances in the three global conformations. In A- and Z-DNA the distances are about 5.4 Å and 4.6 Å, respectively, short enough to be bridged by a single water molecule. The pattern of backbone hydration in A-DNA can be affected by local changes, which appear to be related to specific sequences. In two octamers with global A conformations the backbone hydration pattern was found to be discontinuous at the central pyrimidine–purine step.[11, 14] At this step the structures deviate most markedly from standard "textbook" A-DNA. In B-DNA the corresponding phosphate oxygen distances are 6.5 Å or more, too great for a single water bridge to form. The extended sugar-phosphate backbone of the B form is either responsible for or a direct consequence of the more variable hydration under high water activity.

The hydration of the grooves appears more sequence-dependent than the hydration of the backbone. *Dickerson* and colleagues were the first to observe a regular pattern of hydration in the central AATT segment of the dodecamer d(CGCGAATTCGCG). A string of well-ordered water molecules is hydrogen-bonded to nitrogen and oxygen atoms

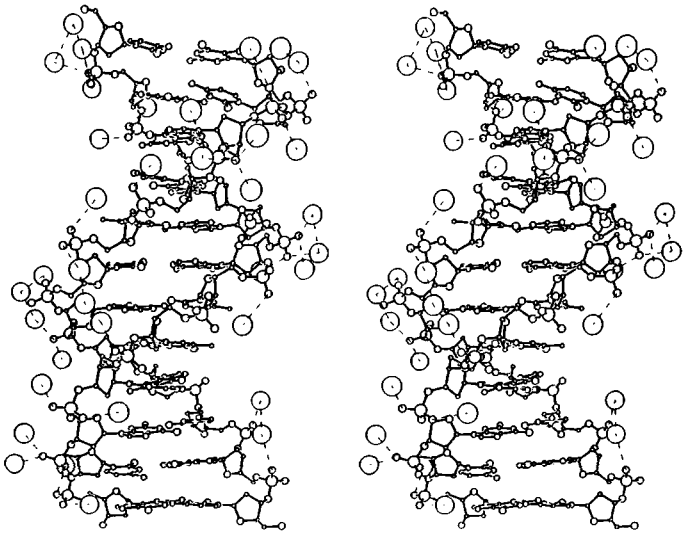

Fig. 8. Hydration of phosphate groups in the B-form dodecamer d(CGCGAATTCGCG). As in Fig. 7, the waters are the largest spheres and attendant hydrogen bonds are shown as dashed lines. The phosphate groups tend to have clusters of water molecules around them rather than bridging waters [93].

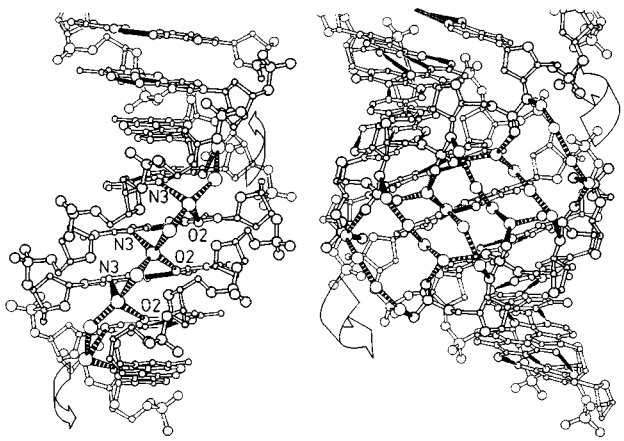

Fig. 9. Schematic illustration of the minor-groove hydration, the "spine of hydration" observed in the narrow AATT section of the B-form dodecamer (left), and the major-groove hydration observed in A-form d(loCCGG) (right). Broken lines show possible water–water hydrogen bonds, filled lines show hydrogen bonds between atoms on the DNA bases and the water molecules. Note that in the B-form the purine N3 and pyrimidine O2 atoms form the hydrophilic attachments [92].

lining the minor groove, which is very narrow in this region.[94, 95] As the groove widens at the CGCG ends, the regular arrangement of water molecules is disrupted (Fig. 9, left). This so-called spine of hydration probably plays a significant role in stabilizing the B-DNA conformation, particularly of this AT-rich region.

In A-DNA structures some sequence-specific hydration patterns were observed in the major groove . In d(IoCCGG) there are strings of water molecules across the groove linking the phosphates of each strand (Fig. 9, right).[3] The hydration pattern in the major groove of the octamer d(GGBrUABrUACC) and in d(GGTATACC)[7] consists of a series of fused pentagons involving hydrogen bonds between water oxygen atoms and the functional groups of the bases (Fig. 10). This pattern is related to the base sequence

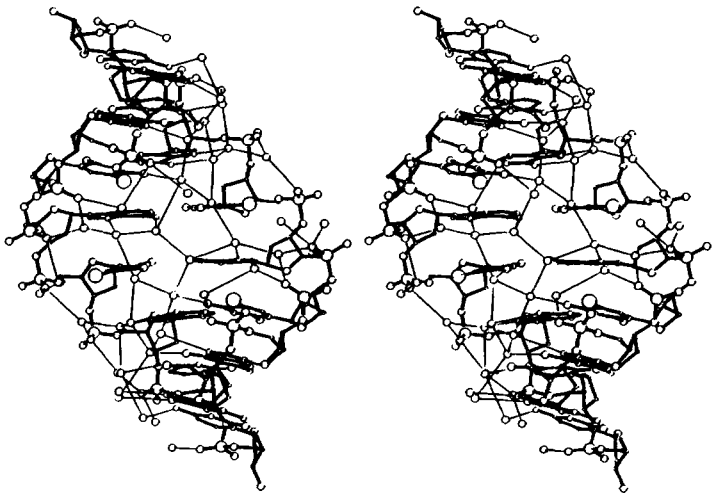

Fig. 10. The major-groove hydration of d(GGBrUABrUACC). Hydrogen bonds are shown as thin lines. Note the series of fused pentagons which fill the major groove of this A-DNA fragment.

and is disrupted in octamers with different sequences. The diagrams depicting the fused pentagons and the role of water in stabilizing non-Watson–Crick base pairs are given in Figures 13 and 14. More detailed accounts of hydration are given by *Saenger*[92, 96] and *Westhof*.[97, 98]

6. The Continuum of Right-Handed DNA Conformation

The archetypal concept that the various global conformations of right-handed DNA represent discontinuous states, which are only stable in very different environments, has undergone a marked change. Single-crystal studies have shown that the global characteristics of individual sequences are more variable than indicated by fiber diffraction studies. Refer, for example, to Table 10 in the appendix, which shows that in A-type helices the minor-groove width can vary from 10.2 to 8.7 Å and that of the major groove from 10.1 to 3.2 Å. Extrapolations from the single-crystal studies of short fragments such as d(GGGGCCCC) to models of poly(dG)·poly(dC) led to the suggestion that the homopolymer utilizes the preferred stacking of the purines and adopts a double-helical form which resembles the A form[9] even in environmental conditions where the classical B form may be expected. Preferred stacking of purines was also observed in the crystal structure formed by the nonamer d(GGATGGGAG) and its complementary strand d(CTCCCATCC).[19] This oligonucleotide structure, which represents the essential DNA binding site of the transcription factor TF III A of *Xenopus*, adopts an A-type conformation. It is worth noting that TF III A is a protein able to bind both DNA and RNA.

The question arises as to whether these structures are an artifact of the crystalline state induced by lattice forces which distort the DNA structure from the solution equilibrium conformation. For a number of years the global conformations observed in the solid state and solution could not be reconciled. For example, when sequences known to adopt an A-type conformation in the crystal were examined by NMR or CD spectroscopy, the spectra could only be interpreted as arising from the B form.[99] An important study was published by *Fairall* et al.[100] comparing the CD spectra of a number of short DNA fragments of known solid-state conformation. In these experiments carefully selected reference spectra were used and the variations in conformation in relation to the solution conditions were monitored. The results show clearly that in solution there is a continuum of helix conformations which is sequence-dependent. The CD experiments find that the complete TF III A binding site of 54 base pairs, as well as the 9-mer fragment examined crystallographically,[19] adopt a conformation which is intermediate between the canonical A- and B-DNA conformations. In addition, the study successfully correlates the CD spectra, which range from the B form, represented by the Dickerson–Drew dodecamer, to the A form characterized by calf thymus DNA in 80 % ethanol, with the experimentally determined helix parameters such as groove width, base-pair tilt, rise, and displacement.

6.1. The Coexistence of A and B Conformations

A new twist was given to the question of the influence of the environment on the stabilization of the various global forms of DNA by the observation[101] that the crystal structure of d(GGBrUABrUACC) contains double helices of both the A and B forms. The crystal lattice of this sequence is built up from A-DNA double helices which form a helical arrangement about the crystallographic sixfold screw axes and enclose a large channel approximately 26 Å in diameter (Fig. 11). The presence of DNA double helices in these channels was indicated by diffuse reflections observed on some high-intensity synchrotron photographs (Fig. 12) which are reminiscent of fiber patterns. The diffuse reflections were interpreted as originating from disordered B-form DNA helices and were successfully modeled by computer simulation experiments. The coexistence of these two DNA polymorphs of the same sequence in the same crystal structure confirms, if such confirmation is required, that the two conformations are near equivalent in energy. It further shows that different global conformations can be adequately stabilized by intramolecular interactions, such as stacking forces between bases and hydrogen bonding of base pairs as well as first- and possibly second-order hydration effects already discussed.

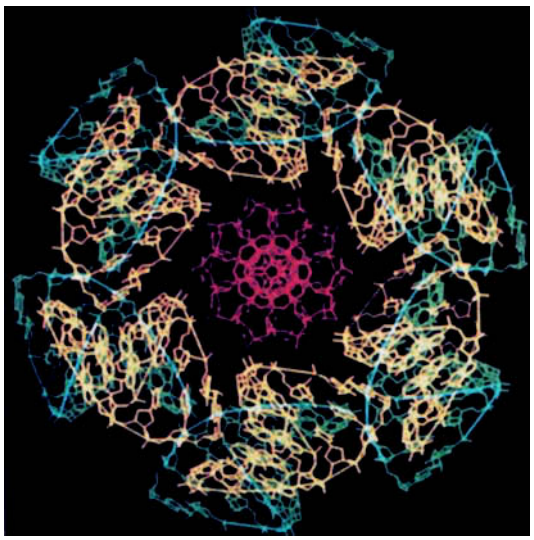

Fig. 11. A view down the 6_1 screw axis in the crystal structure of d(GGBrUABrUACC) showing the channel filled with B-form DNA (in red) and six surrounding A-form helices (in yellow and green). There are no unacceptable intermolecular contacts between the A- and B-form helices.

On the basis of this observation it is possible to conceive that in the biological situation adjacent stretches of DNA might adopt different global conformations or structures of intermediate conformation in response to the mutual adaptation between a protein and the DNA base sequence at the appropriate recognition site. Conformational shifts could occur without the drastic change of environment needed in fiber transformations. One such situation might arise at the

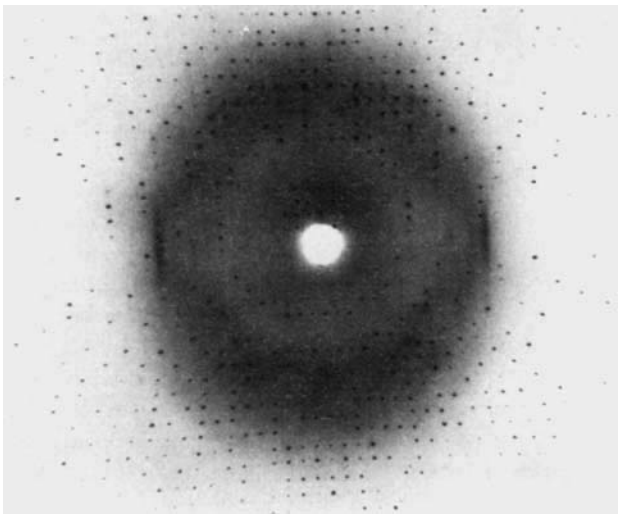

Fig. 12. A 2° oscillation photograph from a single crystal of d(GGBrUABrUACC) [101]. Discrete Bragg reflections give rise to well-defined spots. The streaks are representative of B-DNA fiber patterns. The darkening due to diffuse scattering from the glass capillary and bulk solvent is evident.

TFIIIA binding site discussed previously, which shows a strong tendency to adopt an A-type structure both in solution and in the crystal structure. A further example is the similarity between the structure of d(CTCTAGAG), the central part of which forms an important section of the *trp* repressor site[111] and the *trp* repressor/operator complex analyzed by *Sigler* and co-workers.[102]

7. Errors in the DNA Duplex

The genetic code as encapsulated in the sequence and structure of DNA is constantly under attack from chemical and physical forces present in our environment. Carcinogenic materials, ultraviolet light, and ionizing radiation, to quote but a few examples, can directly damage nucleic acid structures or induce biosynthetic errors during replication or genetic recombination. Such errors include strand breaks, missing or additional bases, chemically modified bases, or the formation of base pairs which are not complementary in the Watson–Crick sense. Biosynthetic errors may also occur as a random event even in the absence of external factors.

While modifications to DNA may provide a useful evolutionary adaptation, the mutagenic process, if unchecked, may run out of control, reduce the fidelity of replication and produce unacceptably high rates of point mutations with deleterious consequences for a given organism. Nature has evolved a complicated and as yet poorly understood recognition and repair system to process errors in DNA.[103] In recent years X-ray diffraction analyses of synthetic deoxyoligonucleotides containing a variety of errors have contributed important structural information to aid our understanding of the nature of these errors and the implication for error recognition and processing. We detail the various "error" studies in this section.

7.1. Base-Pair Mismatches

The incorporation of non-Watson–Crick base pairs in the double helix is the most common error occurring on replication. The classical theory of such mispair formation, initially proposed by *Watson* and *Crick*[140] and subsequently extended by *Topal* and *Fresco*,[104, 105] postulated the involvement of rare tautomer forms of the bases. The resultant mispairs are sterically equivalent to Watson–Crick base pairs and thought unlikely to destabilize the double helix to any significant extent. The rare tautomer hypothesis is the subject of a recent review by *Strazewski* and *Tamm*.[106]

The X-ray analysis of DNA fragments with potential mispairs cannot give any information about the transient occurrence of rare tautomer forms at the time of replication. It can, however, define the structure of a DNA double helix which incorporates mismatched base pairs and provide details concerning the nature of the hydrogen-bonding scheme between noncomplementary bases, the manner in which such base pairs are accommodated in the duplex, the influence of neighboring sequences on the structure and stability of the mispairs, and the effect of global conformation on the mispair as well as, most importantly, provide clues about the way mismatches might be recognized by proteins which constitute the enzyme repair systems.

Table 8 in the appendix presents details of the various mispair-containing structures that have been characterized. Consideration of Tables 1–3 indicates that in each case a

corresponding Watson–Crick structure is available for comparative purposes.

The purine–pyrimidine G·T, and A·C mismatches form "wobble" base pairs with hydrogen bonding between the functional groups on the bases. For the G·T mispair there is no need to invoke the presence of minor tautomer forms to explain this pairing. Two of the three functional groups of guanine that are involved in hydrogen-bonded G·C pairs are utilized. The third functional group, N2, is free and projects into the minor groove. The thymine is displaced towards the major grove, bringing the O2 group within hydrogen-bonding distance of N1 of guanine. The free functional groups are hydrogen-bonded to solvent molecules. The pattern of solvation around the G·T mispair is remarkably similar in the various G·T-containing structures which have been analyzed. These include exampes of A-, B-, and Z-form helices. These solvent molecules are likely to play an important role in stabilizing certain base-pair mismatches. The global conformation adopted by the double helix appears to have little influence on mispair formation. The G·T pair can be accommodated with minimal distortion in any of the helices studied.

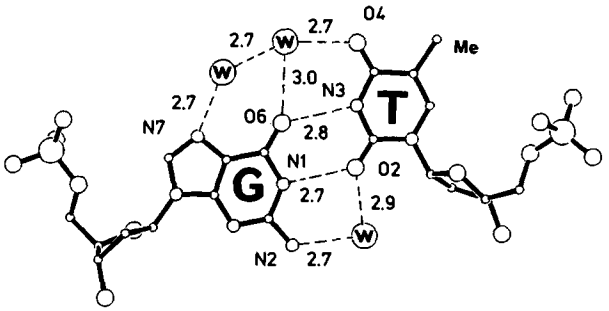

Fig. 13. One of the G·T mispairs observed in d(CGCGAATTTGCG). Distances are given in Å, hydrogen bonds are shown as dashed lines. Note the water molecules which bridge the mispaired bases in both the major and minor grooves [62].

The A·C wobble mismatch shows a close contact between two hydrogen-bond accepting groups, namely, the O2 of cytosine and the N1 of adenine. There are a variety of hydrogen-bonding schemes which can be constructed utilizing minor tautomeric forms of the bases. Because of the high-energy requirements for tautomerization, it was thought that the most likely formation of the A·C mispair involves the protonation of the adenine at the N1.[65, 66] This suggestion was later substantiated by NMR studies.[107] A bridging water, such as observed in the G·T pair, was found in the major groove of the A·C mispair. Figures 13 and 14 show these mispairs as determined in the crystal structures; Figure 15 gives the structural formulae.

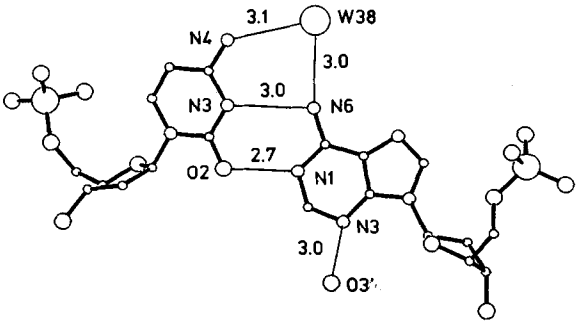

Fig. 14. One of the C·A mispairs observed in d(CGCCAATTAGCG). For comparison see Figure 13. In this case there is only bridging water molecule between the functional groups of the base in the major groove [65, 66].

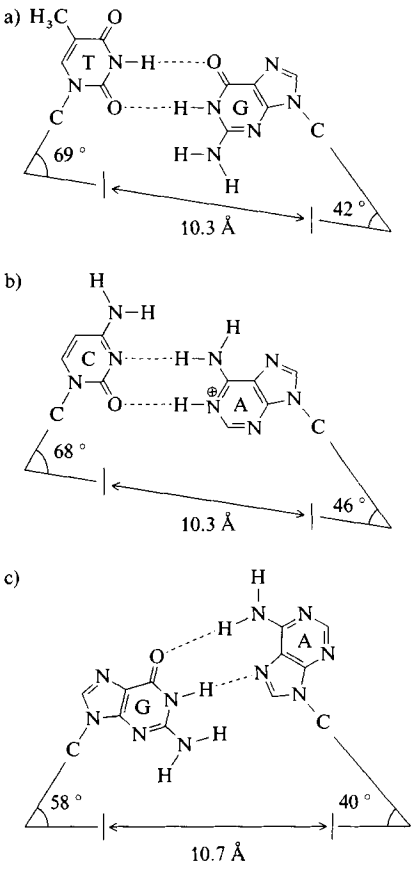

Fig. 15. Structural formulae and geometric details of three mispairs analyzed in the same crystallographic environment, namely, positions four and nine of the dodecamer sequence d(CGC_AATT_GCG). a) T·G; b) C·A; c) the G·A (*syn*). Distances [Å] represent the C1′–C1′ separation, the angles represent the N(base)–C1′–C1′ angle and highlight the asymmetry of the mispairs. Compiled from references [62–67].

The purine–purine G·A pair is more variable than the G·T and A·C mismatches. This is interesting in view of what we know about mutational hot spots and the variability of G·A mismatch repair. It was *Fresht* et al.[108] who showed that G·A was the most likely mismatch to escape detection by polymerase III. This mispair has been observed in three different hydrogen-bonding arangements (Scheme 1).

G(*anti*)·A(*syn*) in d(CGCGAATTAGCG)[63, 64]
G(*syn*)·A(*anti*) in d(CGCAAATTGGCG)[68]
G(*anti*)·A(*anti*) in d(CCAAGATTGG)[60, 61]

Scheme 1. Hydrogen-bonding arrangements in G·A mispairs.

The structural formulae for these purine–purine pairs are illustrated in Figure 16. The G(*anti*)·A(*syn*) base pair is illustrated in Figure 17. All three types of base pairs can be accommodated in the B-DNA double helix with the G(*anti*)·A(*anti*) pair causing the largest distortions to the sugar-phosphate backbone. The variation in the mutual

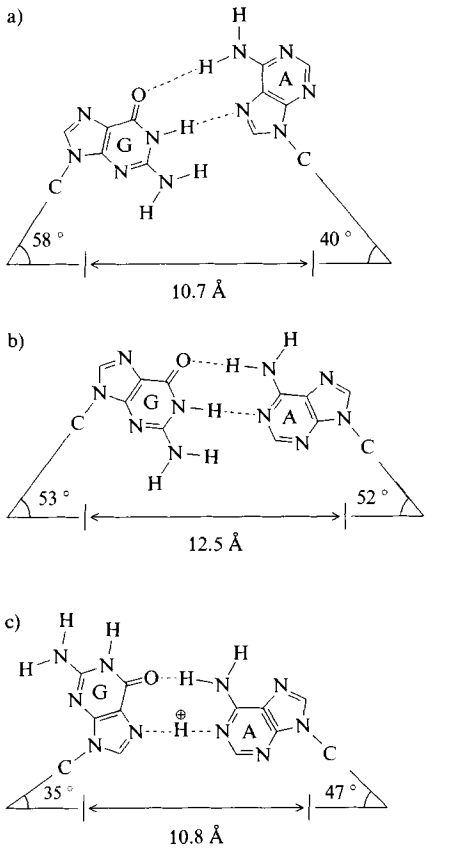

Fig. 16. Structural formulae and geometric details of three types of G·A pairing with the attendant C1′–C1′ distances and N(base)–C1′–C1′ angles. a) G(*anti*)·A(*syn*); b) G(*anti*)·A(*anti*); c) protonated G(*syn*)·A(*anti*). The largest distortions of the sugar-phosphate backbone are observed for the G(*anti*)·A(*anti*) pairing where the C1′–C1′ separation increases by almost 2 Å. Compiled from references [60, 61, 63, 68].

orientation of the bases appears to be related to both the sequence environment of the mispair and to pH. In solution the G(*anti*)·A(*anti*) pair is observed at neutral pH[109] whereas the G(*syn*)·A(*anti*) base pair with a protonated adenine is the dominant form at pH values of 4.0 to 5.5.[110]

The neighbor dependence can to some extent be rationalized by the hypothesis that this purine–purine mispair formation is strongly influenced by dipole–dipole interactions with the adjacent bases.[68] The importance of sequence environment is clearest for the G(*anti*)·A(*anti*) pair, which is stabilized by an inter-base-pair hydrogen bond from the amino N2 of the guanine to the O2 of thymine in the base pair above on the opposing strand (Fig. 18). Without a thymine in this position the mismatch stability would be lowered and another orientation could be adopted.

There is evidence[111] of differential recognition of the G·A mispair in vivo in different sequence environments. This may well be a consequence of the very different functional groups which are free to interact with polymerase or a repair enzyme in the different structural arrangements of the G·A pair. Given this variability it is perhaps not so surprising that G·A is the least well corrected mismatch.

These structural studies of mismatches have been extended to include the base inosine. This base occurs at the 5′-hydroxyl end of some tRNA anticodons, where it can pair with adenine, cytosine, or uracil. Despite the absence of the N2 amino group, this base behaves very like guanine and forms wobble pairs with thymine[60] and an I(*anti*)·A(*syn*) base pair with adenine.[67]

Extensive efforts to crystallize fragments that contain the other mismatches, A·A, G·G, C·C, C·T, or T·T, have so far met with little success. The T·T pairing has been observed

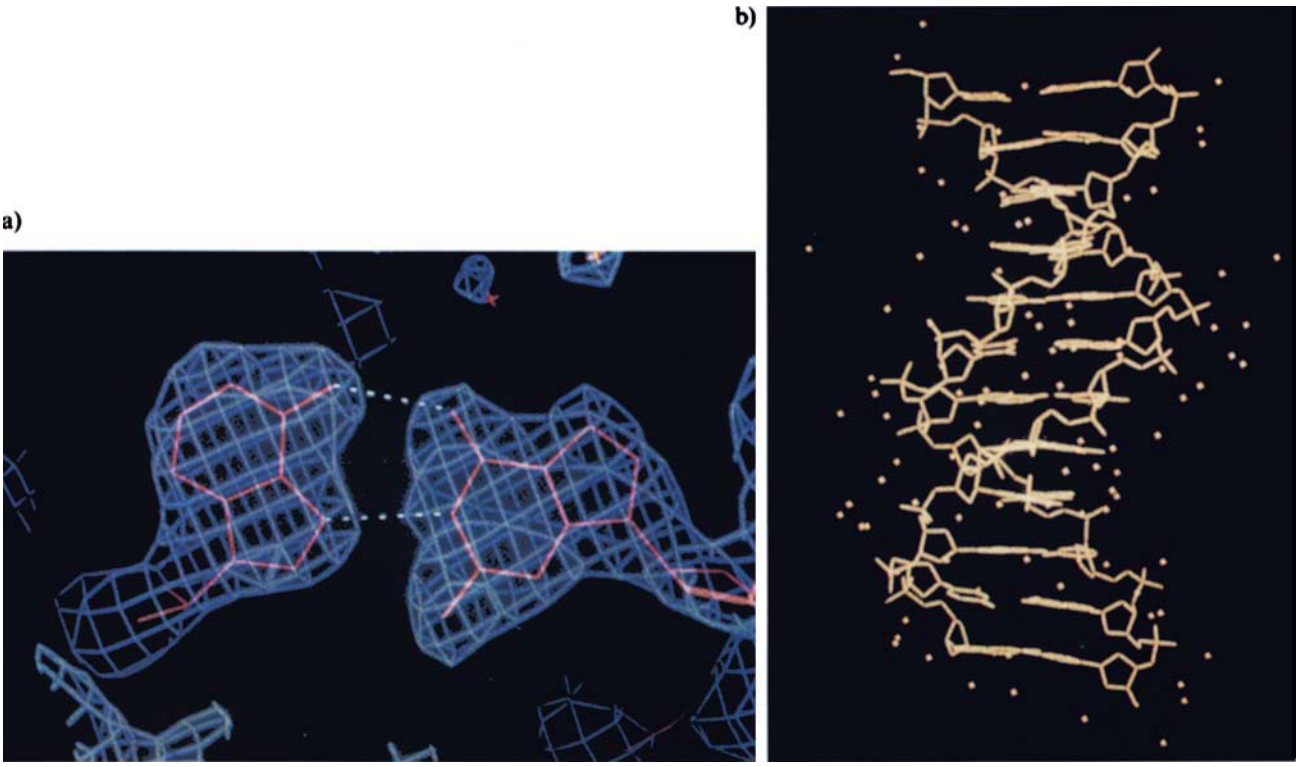

Fig. 17. The G(*anti*)·A(*syn*) base pair in the B-DNA dodecamer [63, 64]. a) The G(*anti*)·A(*syn*) mismatch viewed perpendicular to the plane of the bases G(04) and A(21), together with the electron density in the plane of the base pairs (calculated from a $2F_o-F_c$ map). b) A view of the double helix and associated solvent positions. Note that there is no distortion of the sugar-phosphate backbone in the region of the mismatch.

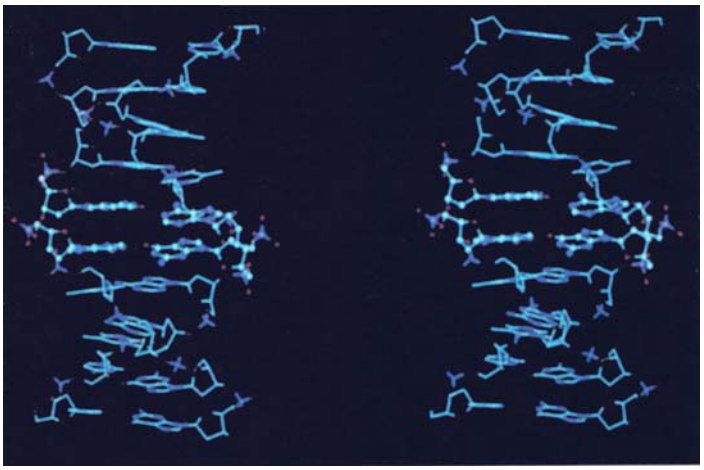

Fig. 18. The B-form decamer d(CCAAGATTGG) with the G(*anti*)·A(*anti*) base pairs [60, 61]. The mispairs in the center of the helix are highlighted. Note the cross-strand interactions of thymines in adjacent base pairs.

not in a duplex base pair but in intermolecular interactions in the sequence d(CGCGCGTTTTCGCGCG).[71] A symmetry-related molecule is positioned so that two thymines are brought into a pairing arrangement in a manner which could represent the non-Watson–Crick pair. In this structure the T·T pairing is such that the enol tautomeric form may be present for one of these bases. There is more information on mispairs from NMR experiments and readers are referred to reviews by *Patel* et al.[112] and to *van der Ven* and *Hilbers*.[160]

7.2. Extra-helical Bases and Mutation Hotspots

Three structures of oligonucleotide fragments that contain extra-helical bases have been published. Two of these were the sequences d(CGCGAAATTTACGCG)[70] and d(CGCAGAATTCGCG).[69] In both structures B-form double helices with 14 and 12 base pairs, respectively, were formed with adenines looped out from the helices. Crystal packing forces have been identified as playing a role in determining the positions of these extra-helical adenines. Nevertheless, despite the prominent role attributed to crystal packing forces, these studies illustrate how unpaired bases can be associated with a stable duplex and may give clues to the relevant properties of certain sequences that undergo frameshift mutations.

The sequence d(CGCGCGTTTTCGCGCG) referred to above was studied by *Chattopadhyaya* et al.[71] It adopts a monomeric hairpin conformation with a six-base-pair Z-DNA stem. The extra thymines form a loop which caps the left-handed helical section. A study by *Timsit* et al.[33] on the nonpalindromic sequence d(ACCGGCGCCACA) showed a structure where the crystal lattice contacts involve groove–backbone interactions which are responsible for a partial opening of G·C base pairs. This structure may be a valid model for the DNA–DNA interactions associated with such processes as genetic recombination. The partial opening of the G·C base pairs promotes a high propeller twist and sequence-dependent three-center hydrogen bonds. We would expect this section of the duplex to be less stable and this may explain the propensity of the sequence to be a hotspot for frameshift mutagenesis. Perhaps more than anything else it may highlight the importance of proteins such as recombinases in maintaining the fidelity of the genetic code.

7.3. Recognition of Mistakes in DNA

It appears from the crystallographic analysis that the DNA duplex has sufficient flexibility to incorporate mispairs or extra-helical bases in a stable duplex where the conformation of the sugar–phosphate backbone remains essentially indistinguishable from that of the native helix with no mispairs. Any distortions are highly localized. The structural studies suggest that the recognition of mispairs is likely to occur at the level of the bases. One aspect of such recognition is the distribution of donor and acceptor groups in the major and minor grooves of the helix. The discrimination of the G·C and A·T base pairs by such a mechanism was suggested by *Seeman* et al.[113] and has been supported by a number of recent crystallographic studies on DNA–protein complexes. This mechanism is likely to play a role in mismatch recognition since the functional group disposition is characteristic of the different mismatches (Fig. 19).

A second recognition feature may be the asymmetry of the glycosyl angles between the bases and the sugar on each side

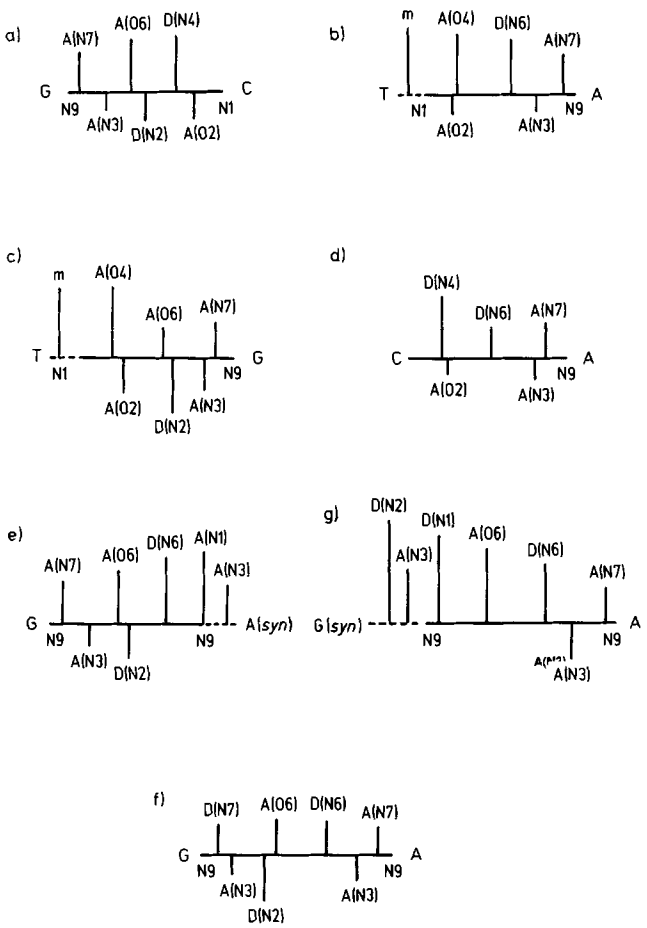

Fig. 19. Stick representations, as given in Figure 28, of the Watson–Crick base pairs G·C (a) and A·T (b) and mispairs G·T (c), C·A (d), G(*anti*)·A(*syn*) (e), G(*anti*)·A(*anti*) (f), and G(*syn*)·A(*anti*) (g). Note the varied positions of the donor and acceptor groups. Compiled from references [60–67].

of a base pair. The glycosyl angles in Watson–Crick base pairs are symmetrical but they become increasingly asymmetrical as we examine the A·G, A·C, and G·T mispairs (see Fig. 15 and 16). This asymmetry is paralleled by the repair efficiencies for these mismatches. Whether such a structural-biological correlation is significant or not will become clearer when more mispairs in different sequence environments are characterized and when there is more information about the mismatch repair enzymes and their complexes with oligonucleotide fragments containing mispairs.

8. DNA–Drug Complexes

DNA is a logical target for chemotherapy. The binding of peptides, as well as small organic and inorganic molecules, to DNA can interfere with the numerous processes, including transcription and replication, in which DNA participates. Such interference can retard or prevent cell growth. There is an extensive literature on the chemical and biochemical studies of molecules able to bind to DNA and numerous antibiotics of this type have been characterized.[114] Some of these molecules have clinical applications but most have toxic side effects.

With an increasing knowledge of the detailed structure of DNA at the molecular level, derived from X-ray and NMR studies, the challenge now is to obtain similar information about drug–DNA complexes. The hope is that such studies will lead to an improved understanding of the rules governing sequence-specific binding and an insight into the correlation between DNA structure, sequence, and activity. Such information is important for rational drug design[115] and may well lead to more useful antibiotics and antitumor agents. One must, however, beware of too simplistic a belief in structural studies. The delivery of a drug to the target site, and only the target site, is a complex problem which calls for solution studies, biological experiments, and a different type of insight into drug design requirements.

Table 4. DNA complexed with drugs.

Complex [a]	Ref.
d(CGCGAATTCGCG)/cisplatin	[131]
d(CGCGAATTBrCGCG)/netropsin	[134]
d(CGCGATATCGCG)/netropsin	[146]
d(CCCAAATTTGCG)/distamycin	[27]
d(CGCGAATTCGCG)/berenil	[144]
d(CGCGAATTCGCG)/DAPI	[145]
d(CGCGAATTCGCG)/Hoechst 33258	[126, 127]
d(CGCGATATCGCG)/Hoechst 33258	[129]
d(CGTACG)/daunomycin	[147]
d(CGATCG)/adriamycin	[164]
d(CGATCG)/daunomycin	[118, 164]
d(CGTpsACG)/11-deoxydaunomycin	[161]
d(CGATCG)/4′-epiadriamycin	[162]
d(CGTACG)/triostin A	[123]
d(CGTACG)/echinomycin	[82]
d(GCGTACGC)/triostin A	[83]
d(BrCGBrCG)/proflavin	[148]
d(CGTpsACG)/nogalamycin	[121, 122]
d(mCGTpsAmCG)/nogalamycin	[163]
d(TBrUGGCCAA)/chromomycin	[152, 158]
d(ATGCATATGCAT)/actinomycin	[153]
d(CGCAAATTTTGCG)/netropsin	[156]

[a] ps = Rp-phosphorothioate, mC = 5-methylcytosine, BrC = 5-bromocytosine, BrU = 5-bromouracil.

The X-ray structure analysis of DNA–drug complexes made a slow start. Up to 1984 the structure of only one complex was published, as a preliminary report,[116] but increasingly (as shown in Table 4) the crystal structures of more complexes have been solved. Progress was particularly rapid in 1988/89 when the number of papers more than doubled. Many of these have only appeared in conference reports but the main results from the studies are included here.

8.1. Drug Categories

Three categories of drugs have been studied crystallographically, intercalators, minor-groove binders, and an inorganic compound which coordinates to DNA. All these drugs can

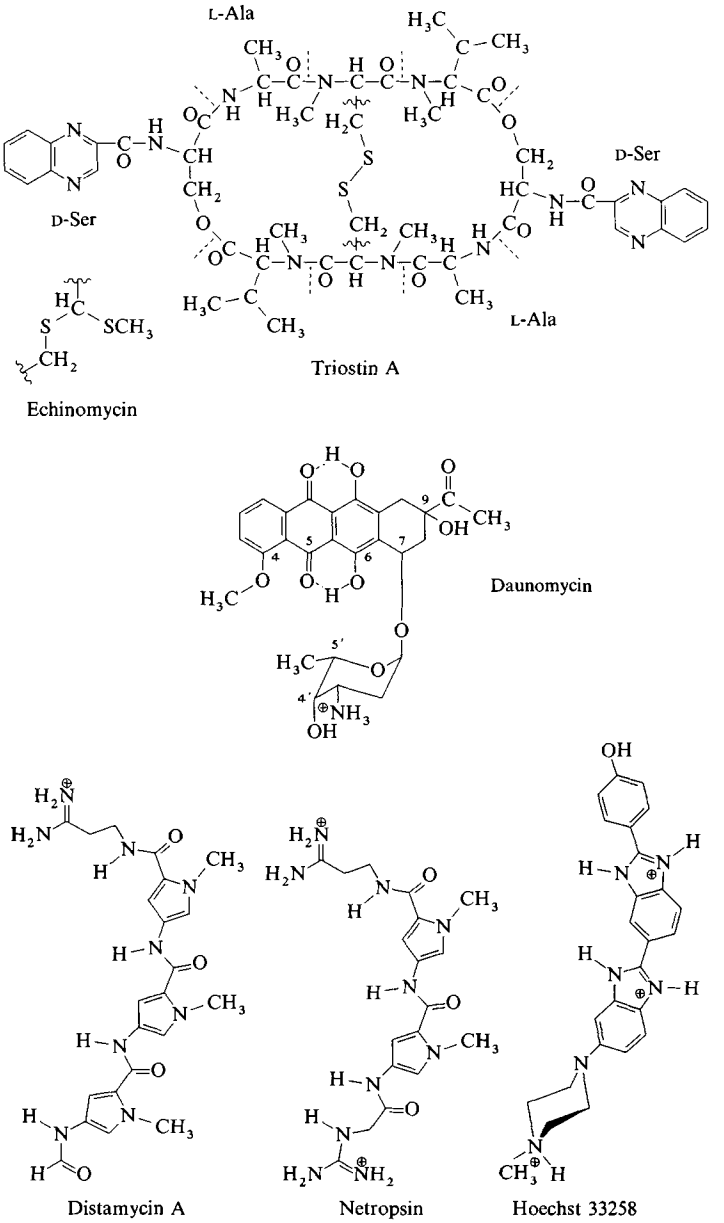

Fig. 20. Structural formulae for selected DNA-binding antibiotics which have been studied complexed to oligonucleotides. (a) shows the intercalators, (b) the minor-groove binders. The groove binders are arranged with the left side as the one which interacts with the minor-groove side of the bases while the right side is directed away from the duplex. Reference [151] contains further information concerning nucleic acid–antibiotic interactions.

bind to double-stranded DNA. The structural formulae of selected antibiotics is given in Figure 20.

Prior to describing the results of the X-ray analyses, it may be useful to recall the structural features of the DNA duplex which may be important in sequence-specific recognition by other molecules, be they large or small. They include the negatively charged phosphate backbone, the hydrogen-bond-accepting and -donating functional groups in the major and minor grooves, and aromatic, hydrophobic components able to promote van der Waals and hydrophobic interactions. There are additional structural aspects to be considered: the physical shapes and dimensions of the minor and major grooves, which are to some extent sequence-dependent, the hydration patterns, and the extreme structural flexibility of the double helix.

8.2. Intercalators

The phenomena of intercalation was first described by *Lerman*.[117] It involves the aromatic portion of a drug molecule positioning itself between base pairs. Intercalation increases the separation of adjacent base pairs and the resultant helix distortion is compensated for by adjustments in the sugar-phosphate backbone and an unwinding of the duplex. Aromatic stacking interactions between the bases and the intercalating molecule are the major stabilizing feature of the complexes formed.

Simple mono-intercalators like acridine have only been examined crystallographically in dinucleoside phosphates, which are too short for reliable extrapolation to intercalation of the double helix. More complex monofunctional intercalators, such as daunomycin, adriamycin, and their derivatives, which have a planar chromophore and a sugar residue, have been successfully cocrystallized with hexanucleotides, principally d(CGTACG), d(CGATCG), and variants of d(CGTACG) with methylated cytosines and/or a phosphorothioate linkage. Table 4 lists selected references to some of the structure determinations, Table 13 (appendix) to crystallographic details. In all these structures two drug molecules are intercalated, one at each CpG step. The chromophores are inserted in a "head-on" fashion with the long axis of the aglyclone moiety oriented at right angles to the long axis of adjacent base pairs and with the cyclohexene ring A protruding into the major groove. The amino sugar lies in the minor groove. Within this general pattern the individual contacts between drug and DNA depend both on the sequence of the bases adjacent to the intercalation site and on the chemical modifications of the intercalating drug.

The studies already reported give us an opportunity of evaluating these various factors, since we have, as indicated in Table 4, examples of complexes between different drugs and the same sequence, such as the sequence d(CGATCG) complexed to daunomycin, 4'-deoxyadriamycin, and adriamycin and the same drug analyzed in different sequence environments—for example, daunomycin complexed to d(CGTACG) and d(CGATCG). We even have two independent analyses of the same complex, daunomycin–d(CGATCG).[118, 119] It is reassuring that these two determinations led to the same structure within the relatively small experimental errors expected at the resolution of the studies.

We also have data on the X-ray structures of many of the uncomplexed drugs themselves, but as yet no structural information on the hexamers used in these studies. Figure 21 shows a daunomycin hexamer structure and Figure 22 the hydrogen-bonding system between the DNA and daunomycin, observed in the d(CGATCG) and the d(CGTACG) complexes.[118] This latter diagram emphasizes the flexibility

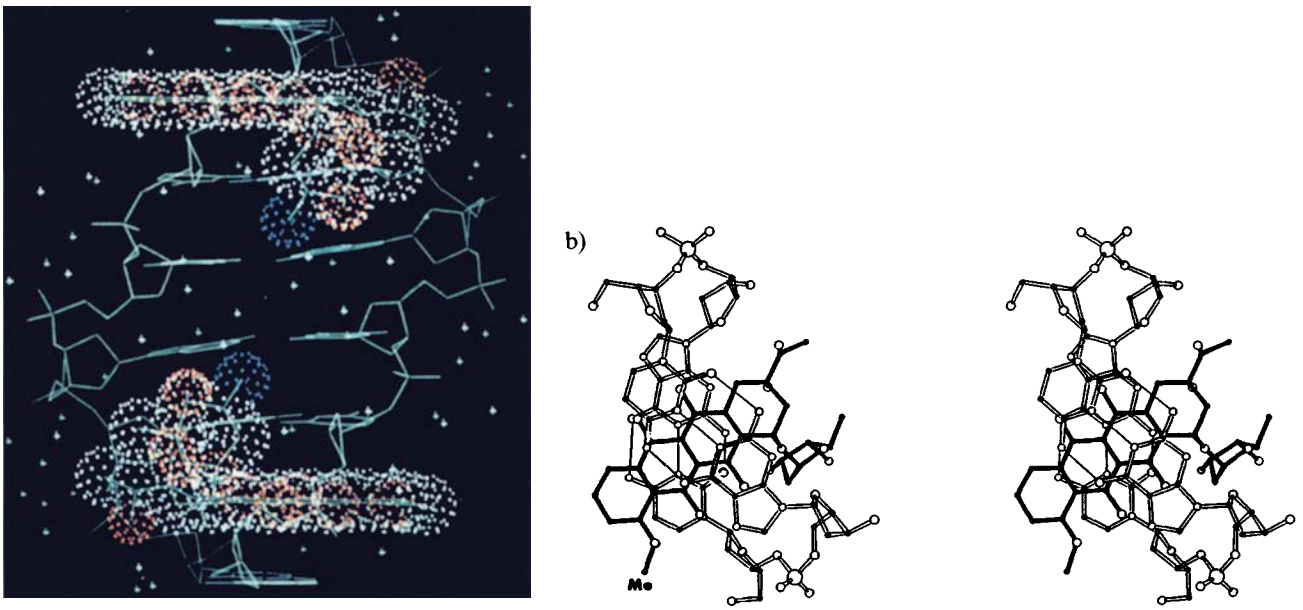

Fig. 21. The d(CGATCG)–daunomycin complex studied by *Moore* et al. [118]. (a) is a view from the minor-groove side of the complex. The drug is depicted with a dot surface representing 50 % van der Waals area. Note how the daunosamine moiety covers a large section of the minor groove. (b) is a view perpendicular to the chromophore of the drug and includes the CpG intercalation site. The drug is shown with dark bonds. This diagram illustrates the "head on" intercalation.

of the hydrogen-bonding arrangements in these complexes. Hydrogen-bond interactions can be directly between the functional groups of the drug and the DNA as, for example, between the hydroxyl group of ring A (essential for drug action) and the functional groups N2 and N3 of guanine at the intercalation site.

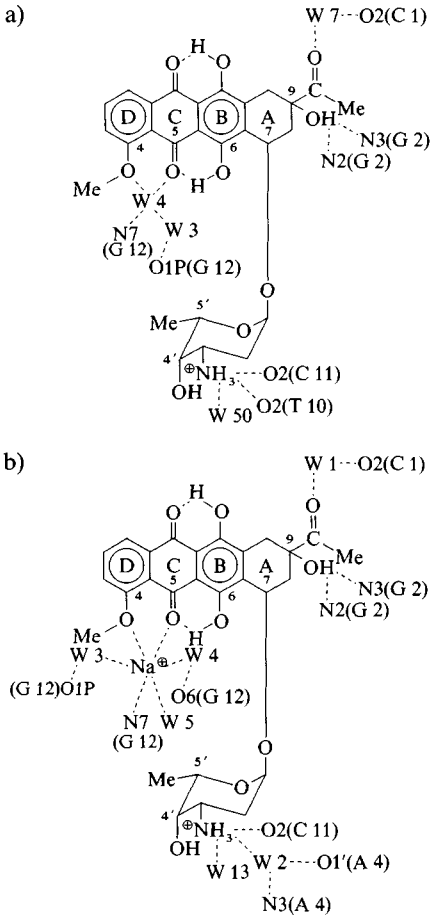

Fig. 22. Schematics of the hydrogen-bonding systems observed in a) the d(CGATCG)–daunomycin complex and (b) the d(CGTACG)–daunomycin complex [118]. The nucleobases belonging to the coordinated atoms are given in parentheses.

There is also hydrogen-bond interaction between the $NH_3^{\oplus}$ group and O2 of cytidine. The inversion of the base sequence adjacent to the intercalation site is accommodated by having a water-mediated rather than a direct hydrogen-bond interaction of the appropriate base with the $NH_3^{\oplus}$ group. Daunomycin also interacts with DNA in the major groove through water or through sodium-mediated interactions involving O4 and O5 of the chromophore substituents.

The two structure determinations show clearly why d(CpG) is the observed intercalation site for this drug and suggest that only the d(TpG) step could provide a similar hydrogen-bonding environment on intercalation.[118] Such a step has been identified as a possible binding site by *Chaires* et al.[120] and is being characterized crystallographically (*Kennard*, private communication). In addition to the hydrogen-bonding and stacking interactions at the intercalation site, the complex is further stabilized by a number of van der Waals contacts of less than 3.4 Å. These contacts are more numerous in the d(CGATCG) complex than in the d(CGTACG) complex and may possibly compensate for the somewhat weaker hydrogen-bond interactions mediated through water instead of the direct $NH_3^{\oplus}$ contact observed in the AT complex. Predictions about the importance of electrostatic interactions between the negatively charged phosphates and positively charged sugar substituent have not been substantiated by the results of the crystal structure analyses.

Two other aspects of these high-resolution studies are worthy of mention; changes in the drug structure and the distortion of the DNA double helix. Daunomycin and related molecules consist of a rigid aromatic system and a flexible sugar substituent. Comparison of the crystal structures of free and complexed drug molecules show that alterations in the structure are almost exclusively localized on the sugar moiety. The comparisons between daunomycin complexed to the two DNA hexamers show that structural differences are minimal but again localized on the flexible sugar. The distortion of the DNA can only be estimated indirectly since the structures of the uncomplexed hexamers are not yet known. There are marked asymmetric distortions of the double helix and it is possible to estimate the total unwinding angle, which is approximately 8° per daunomycin molecule. It is not yet possible to detail the effect of different drugs bound to the same oligomer since only preliminary reports of the other structures are available.

Recently, a complex between d(CGTpsACG) and the mono-intercalator nogalamycin has been reported.[121, 122] This drug has two sugars attached to the aglycone chromophore with the nogalose substituent in the minor groove and an aminoglucose in the major groove. In common with the daunomycin family there are extensive hydrophobic interactions to stabilize the complex. A close inspection of the aglycone rings of the nogalamycin and the daunomycin reveals that in the former the drug is positioned more towards the minor groove side of the duplex. This can perhaps be rationalized by the need to accommodate a section of the nogalamycin in the major groove. The shift thus enhances hydrophobic interactions on that side of the molecule and the flexible sugar on the minor-groove side is able to adjust once again to maximize interactions with the DNA.

The principal features of the DNA–drug structures discussed above are substantiated and extended in studies of complexes with the bifunctional intercalators triostin A and echinomycin (Fig. 20).[83, 123, 124] These molecules, illustrated in Figure 20, have two planar quinoxaline groups separated by a fairly rigid cyclic depsipeptide system. The two chromophores are optimally aligned (with the aid of a D-serine) to intercalate and bracket two adjacent base pairs from the minor-groove side of the B-DNA helix. Two views of an octamer bis-intercalator complex are given in Figure 23. In this complex the unwinding of the double helix is much more drastic than in the complexes with monofunctional intercalators. The DNA now resembles a ladder more closely than a double helix. As with the monofunctional intercalators, there are specific hydrogen bonds between the functional groups of the drug, the alanine amide groups, and the nucleotide bases (guanines) at the intercalation site, which account for the specificity of the drug. The most surprising feature of these structures, and one which was not predicted by the numerous theoretical studies of bifunctional interca-

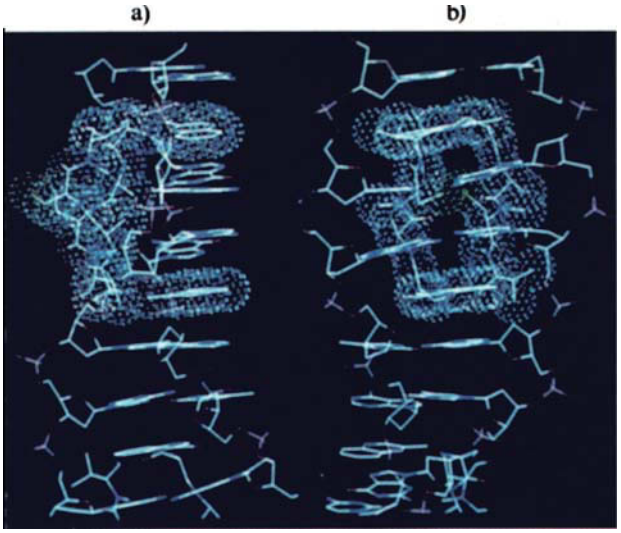

Fig. 23. Views of the d(GCGTACGC)–triostin complex characterizd by *Quigley* et al. [83]. The high degree of distortion of the DNA produces a ladder-like duplex. a) Side view of the drug highlighting the bis-intercalation. b) View from the major-groove side of the DNA. In both cases the drug is depicted with a dot surface representing a 50 % van der Waals area.

lation, is the disruption of the Watson–Crick hydrogen bonding of the base pairs adjacent to the intercalated quinoxaline rings. The central A·T base pair and the G·C pairs at each end now adopt Hoogsteen geometry.[125] This pairing arises when the purines adopt a *syn* orientation about the glycosidic bond as opposed to the normal *anti* orientation. The altered base-pairing allows the DNA to approach the drug more closely and results in extensive van der Waals interactions. Such interactions appear to be the dominant forces in the stabilization of these DNA–drug complexes.

8.3. Minor-Groove Binders

A number of studies have been reported on the structure of minor-groove binders, notably distamycin, netropsin, Hoechst 33258 (see Fig. 20), DAP1 (4′,6-diamidine-2-phenylindole),

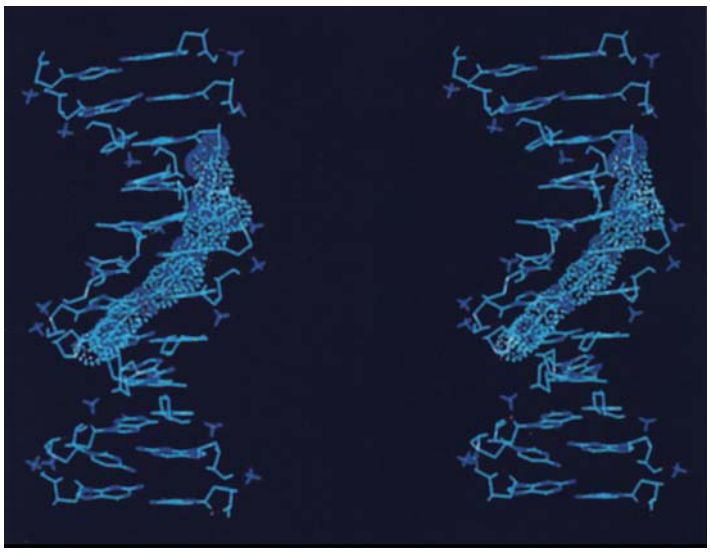

Fig. 24. A view of the d(CGCAAATTTGCG)–distamycin complex [27]. The overall B form of the DNA is retained and the drug highlighted with a dot surface representing a 50 % van der Waals area fits into the minor groove.

and, most recently, berenil, all of them complexed to either to the Dickerson–Drew dodecamer d(CGCGAATTCGCG) or one of its variants. The formulae of three of the groove binders are given in Figure 20. The diagrams presented in Figures 24 and 25 shows how this class of drugs interact with DNA. References and crystallographic constants are listed in Table 13 in the appendix. Unlike the complexes discussed in the previous section, the structure determinations were carried out at a lower resolution of between 2.2 and 2.4 Å, and thus some of the details and conclusions need to be treated with caution. In the case of one oligomer, d(CGCGAATTCGCG) complexed to Hoechst 33258, two independent determinations gave different results. In one determination[126] the drug was found to bind to the central four AATT base pairs, while in the other determination[127] the drug bound asymmetrically to the ATTC region. Only the symmetric AATT binding mode was observed in NMR studies.[128]

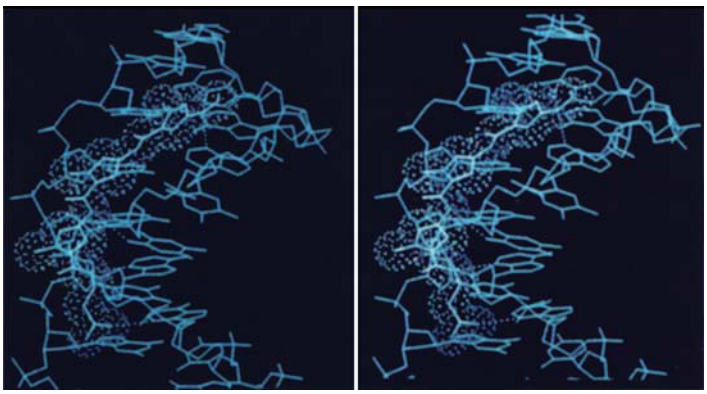

Fig. 25. A closeup view of the distamycin–d(CGCAAATTTGCG) interactions. Dashed bonds show the hydrogen bonds between the drug and the DNA.

Interestingly, the same drug, when complexed with the modified DNA dodecamer d(CGCGATATCGCG), binds in the opposite orientation and covers the GATAT region.[129] This study also contradicts previous findings that groove binders have little influence on the DNA structure itself and merely displace the so-called spine of hydration in the minor groove. In the d(CGCGATATCGCG) complex the helical twist between the ApT and the TpA steps is reversed from that described in the section on alternating DNA. An additional change involves the rotation of a thymine to facilitate hydrogen bonding to the drug.

Changes induced in the conformation of some of the groove-binding drugs themselves are surprisingly large. They include changes in the dihedral angles between the four rigid units of the Hoechst compound. It may well be that, while in some complexes the drug is a passive replacement for the ordered water structure in the narrow minor groove, in other sequences the narrow minor groove is not a feature of the native solvated sequences but is induced through an active interaction with the appropriate drug.

8.4. Cisplatin

The fortuitous discovery that *cis*-diamminedichloroplatinum(II) interacts with DNA[130] has produced one of the

most successful drugs for the treatment of cancer, albeit with serious side effects. The platinum coordinates to purines, especially adjacent guanines. Heavy-atom soaking experiments with d(CGCGAATTCGCG) produced evidence that the platinum atom was coordinating to the N7 atom of guanines.[131] Work on the drug interacting with pGpG has indicated the large degree of local distortion that this drug is likely to induce in duplex DNA.[132, 133]

8.5. General Principles of DNA–Drug Interactions

The drugs in the DNA–antibiotic complexes so far examined have all interacted mainly in the minor groove of B-DNA but have also, to some extent, perturbed the major groove. No direct electrostatic contacts have so far been observed between charged portions of a drug and the negatively charged sugar-phosphate backbone. Interactions between the drug and DNA generally involve direct hydrogen bonds linking the functional groups of the two components and hydrogen-bond contacts between such groups mediated by water molecules or by counterions. van der Waals forces contribute significantly to the stabilization of the complexes and may lead to serious perturbations of the DNA helix from the normal Watson–Crick geometry. At their most extreme, such perturbations can lead to the formation of Hoogsteen base pairs instead of the normal Watson–Crick pairs. Interaction with the DNA also induces some changes in the conformation of the drugs themselves.

Intercalation at specific base steps can be rationalized in terms of the hydrogen-bond interactions. The preference of minor-groove binders for A·T-rich regions seems to be related to the need to maximize van der Waals contacts. In some sequences the minor grooves in this region are intrinsically narrow. This produces a narrow canyon with hydrophobic walls and a polar floor which is well-suited to interaction with the types of organic molecules being discussed. In other sequences the drug itself induces the narrowing of the minor groove in the A·T-rich region to allow for close van der Waals contacts. It would be very much more difficult to induce a narrowing of a groove in a region containing guanines since the N2 group of guanine would hinder the entry of the drug into the minor groove.[134, 135] These general principles, deduced from structural studies, provide useful guidelines to synthetic chemists developing more effective and sequence-specific DNA-binding drugs.

9. Future Directions

Crystallographers, unlike other crystal gazers, claim no insight into the future. However, the upsurge of successful structure determinations in the past few years and the spread of work among a larger number of laboratories suggests that the next decade will bring a multitude of new results. We anticipate that a wealth of data will accumulate on the conformation of the various base steps in different sequence and crystal environments. It is possible that some rules characterizing the conformation of various steps will emerge, but we should not be too disappointed if, because of the extreme flexibility of the DNA double helix, there are no simple deductions. The range of oligonucleotide structures which can successfully be analyzed by X-ray diffraction methods will be extended by the development of synthetic techniques which will facilitate the preparation of much larger quantities of pure oligomers, the improved technology of X-ray data collection (synchrotron sources, area detectors, etc.), and the use of anomalous dispersion methods for structure solution.

There will undoubtedly be increased activity on the structure analysis of DNA–drug complexes with the major types of antibiotics and antitumor agents. Work on other classes of drugs such as those which form covalent or cross-strand linkages is already underway in a number of laboratories. Such studies will certainly lead to a much better understanding of the interaction between DNA and various drugs and possibly inspire the development of new anticancer agents.

Attempts may also be made at synthesizing novel molecules which would interact in the major rather than the minor groove. Ideas for such new compounds may arise from studies such as the analysis of drugs like nogalomycin, which affect the major groove and through a better characterization of DNA–protein interactions, which primarily occur in the major groove. We foresee an explosion in the number of protein–DNA complexes analyzed.

One of the largest growth areas is likely to be in the field of RNA structures. After years of mostly unsuccessful endeavors the synthesis of RNA fragments has now become a practical proposition and further developments in RNA chemistry hold out the bright hope of a similar review listing scores of RNA structures in 10 years time.

Close collaboration between workers from many disciplines using different approaches and techniques will be an essential prerequisite for all these studies if we are to gain an improved understanding of the structural basis of DNA and RNA function in the myriad biological events in which these unique polymers participate.

10. Appendix

Tables 5–13 give numeric information derived from X-ray diffraction analyses of selected oligonucleotide fragments, published between 1980 and 1990.

Tables 5–7 give selected data for DNA fragments crystallizing as A, B, or Z helices. For each crystal structure the following information is quoted: temperature of X-ray measurement, space group, cell dimensions, the resolution of the analysis, R factor, the number of solvent molecules located in the analysis, $N_{solv.}$ and the volume per base pair. The volume per base pair is calculated by dividing the asymmetric unit volume by the number of base pairs. In all these crystals two strands of the oligomer form the double helix and in many cases the double helix has no imposed crystallographic symmetry.

Table 8 lists similar data for DNA fragments containing mispairs. Comparison of Table 8 with Tables 5–7 shows that within each conformation type (A, B, or Z) the structures containing mismatches crystallize isomorphously with the native structures containing Watson–Crick complementary base pairs only. Table 9 gives data for three structures with extra bases.

Table 5. Crystallographic details of selected A-form structures. IoC=5-iodocytosine

Sequence	[°C] [c]	Space group	Unit Cell dimensions [Å]			Resolution [Å]	R	N_{solv}	V [Å^3]
d(IoCCGG)	−2	$P4_32_12$	41.1	41.1	26.7	2.2	0.16	86	1409
d(GGTATACC)	RT	$P6_1$	45.0	45.0	41.5	2.2	0.20	66	1519
d(GGBrUABrUACC) [a]	RT	$P6_1$	45.1	45.1	41.7	1.8	0.14	84	1530
d(GGGGCCCC)	RT	$P6_1$	45.3	45.3	42.3	2.5	0.14	104	1566
d(GGGATCCC)	RT	$P6_1$	46.8	46.8	44.5	2.5	0.17	9	1615
d(GCCCGGGC) [b]	RT	$P4_32_12$	43.2	43.2	24.6	1.8	0.17	68	1435
d(GGGTACCC) [b]	RT	$P4_32_12$	43.3	43.3	24.7	1.7	0.16	88	1447
d(GTGTACAC) [b]	4	$P4_32_12$	42.4	42.4	24.8	2.0	0.12	86	1393
d(GGGCGCCC)	RT	$P4_32_12$	43.3	43.3	24.7	1.8	0.16	88	1444
d(GGGCGCCC)	−158	$P4_32_12$	42.7	42.7	24.6	1.7	0.21	62	1403
d(GGGCGCCC)	RT	$P6_1$	47.0	47.0	44.3	2.9	0.12	45	1763
d(GGGCGCCC)	−158	$P6_1$	43.6	43.6	41.5	1.9	0.16	100	1424
d(CTCTAGAG) [b]	RT	$P4_32_12$	42.5	42.5	24.3	2.2	0.15	70	1315
d(GGCCGGCC) [b]	RT	$P4_32_12$	42.0	42.0	25.1	2.2	0.18	80	1383
d(CCCCGGGG) [b]	RT	$P4_32_12$	43.4	43.4	24.8	2.2	0.15	82	1459
d(GGATGGGAG)	RT	$P4_3$	45.3	45.3	24.7	3.0	0.33	–	1410
d(ACCGGCCGGT)	10	$P6_122$	39.2	39.2	78.0	2.0	0.18	36	1772
d(CpsCGTACGTACGG)	RT	$P6_122$	46.2	46.2	71.5	2.5	0.14	71	1836
r(GCG)d(TATACGC)	0	$P2_12_12_1$	24.2	43.5	49.4	2.0	0.16	179	1300
r(UUAUAUAUAUAUAA)	RT	$P2_12_12_1$	34.1	44.6	49.1	2.2	0.13	86	1334

[a] Synchrotron radiation used in the analysis. [b] The asymmetric unit consists of a single strand or four base pairs. A twofold axis is coincident to the octamer duplex twofold axis of symmetry. [c] RT signifies room temperature (specified in the original publication).

Table 6. Crystallographic details of selected B-form structures [a].

Sequence	[°C]	Space group	Unit cell dimensions [Å]			Resolution [Å]	R	$N_{solv.}$	V [Å^3]
d(CGCGAATTCGCG)	RT	$P2_12_12_1$	24.9	40.4	66.2	1.9	0.18	80	1385
d(CGCGAATTCGCG)	−257	$P2_12_12_1$	23.4	29.3	65.3	2.7	0.15	83	1253
d(CGCGAATTBrCGCG)	7	$P2_12_12_1$	24.2	40.1	63.9	2.3	0.17	114	1293
d(CGCAAATTTGCG)	RT	$P2_12_12_1$	25.2	41.7	65.8	2.5	0.16	32	1440
d(CGCAAAAAAGCG)	4	$P2_12_12_1$	25.4	40.7	65.8	2.5	0.20	27	1417
d(CGCATATATGCG)	6	$P2_12_12_1$	23.5	38.9	66.6	2.2	0.19	43	1268
d(CGCAAAAATGCG)	12	$P2_12_12_1$	24.5	40.3	65.9	2.6	0.20	23	1355
d(CGCGAm6ATTCGCG)	RT	$P2_12_12_1$	25.6	40.7	67.3	2.0	0.17	87	1461
d(GpsCGpsCGpsC)	RT	$P2_12_12_1$	34.9	39.2	20.6	2.2	0.14	72	1175
d(CCAGGCCTGG)	RT	$C2$, $\beta = 117°$	32.2	25.5	34.8	1.6	0.17	–	1275
d(ACCGGCGCCACA)	4	$R3$	65.9	65.9	47.1	2.8	0.15	20	1640
d(CGATCGATCG)	RT	$P2_12_12_1$	38.9	39.6	33.2	1.8	0.22	42	1278

[a] BrC = 5-bromocytosine, m6A = 6-methyladenine, pS = Rp-phosphorothioate. [b] RT signifies room temperature.

Table 7. Crystallographic details of selected Z-form structures [a]

Sequence (cations present)	Space group	Unit cell dimensions [Å]			Resolution [Å]	R	$N_{solv.}$	V [Å^3]
d(CGCGCG) (Na, Mg, spermine)	$P2_12_12_1$	17.9	31.5	44.6	0.9	0.14	68	1048
d(CGCGCG) (Na, Mg)	$P2_12_12_1$	18.0	31.0	44.8	1.0	0.18	88	1043
d(mCGmCGmCG) (Mg, spermine)	$P2_12_12_1$	17.8	30.6	45.4	1.3	0.16	98	1027
d(mCGTAmCG) (Mg, Na)	$P2_12_12_1$	17.9	30.4	44.9	1.2	0.16	98	1021
d(CG)r(CG)d(CG)	$P2_12_12_1$	18.3	30.9	43.1	1.5	0.20	82	1015
d(CG)(araC)d(GCG)	$P2_12_12_1$	18.6	30.7	42.9	1.5	0.17	91	1020
d(CGCG) (Mg and/or Na)	$C222_1$	19.5	31.3	64.7	1.5	0.21	84	1232
d(CGCGCGCG) (Mg and/or Na)	$P6_5$	31.3	31.3	43.6	1.6	0.19	85	1025
d(CGCATGCG) (Mg and/or Na)	$P6_5$	30.9	30.9	43.1	2.5	0.16	–	991

[a] mC = 5-methylcytosine, araC = arabinose cytosine.

Table 10 contains the global helical parameters for A- and B-type helices observed in typical single-crystal studies and, for comparison, values derived from fiber diffraction. Table 10 is restricted to helices with Watson–Crick base pairs only. The parameters include the helix twist, rise per base pair, x, base-pair tilt, propeller twist groove width, and the displacement of the base pairs from the helix axis, D. These parameters can best be understood by reference to Figures 26–32 and the definitions given in Section 10.1. Note that there are quite substantial variations for each of these parameters in the different DNA fragments analyzed. These variations can be attributed to differences in base sequence, particularly when oligonucleotides crystallizing with the same structural motif are compared. The groove width is one of the parameters particularly affected. In A-type crystals the width of the minor groove ranges from 10.2 to 8.7 Å compared to the fiber value of 11.0 Å and the width of the major groove from 10.1 to 3.2 Å compared to the fiber value of 2.4 Å. Recently, two accounts[13, 18] have appeared on variations in the global and local parameters of the same sequence when crystal-

Table 8. Crystallographic details of some structures containing non-Watson–Crick base pairs [a].

Sequence	Mispair	DNA form	Space group	Unit cell dimensions [Å]			Resolution [Å]	R	$N_{solv.}$	V [Å^3]
d(GGGGCTCC)	G · T	A	$P6_1$	45.2	45.2	42.9	2.2	0.14	52	1584
d(GGGGTCCC)	G · T	A	$P6_1$	44.7	44.7	42.4	2.1	0.14	104	1529
d(GGGTGCCC)	G · T	A	$P6_1$	45.6	45.6	41.0	2.5	0.15	63	1507
d(GGIGCTCC)	I · T	A	$P6_1$	45.1	45.1	45.5	1.7	0.14	81	1600
d(CCAAGATTGG)	G · A	B	$C2$, $\beta = 119°$	32.5	26.2	34.3	1.3	0.17	48	1278
d(CGCGAATTAGCG)	G · A	B	$P2_12_12_1$	25.7	41.9	65.2	2.5	0.17	83	1464
d(CGCAAATTGGCG)	G · A	B	$P2_12_12_1$	25.2	41.2	65.0	2.3	0.16	94	1406
d(CGCIAATTAGCG)	I · A	B	$P2_12_12_1$	25.8	41.9	65.1	2.5	0.19	64	1466
d(CGCAAATTCGCG)	C · A	B	$P2_12_12_1$	25.4	41.4	65.2	2.5	0.19	82	1428
d(CGCGAATTTGCG)	G · T	B	$P2_12_12_1$	25.5	41.2	65.6	2.5	0.18	71	1436
d(TGCGCG)	G · T	Z	$P2_12_12_1$	17.9	30.7	45.1	1.5	0.18	–	1033
d(BrUGCGCG)	BrU · G	Z	$P2_12_12_1$	17.9	30.9	49.9	2.2	0.16	64	1152
d(CGCGTG)	G · T	Z	$P2_12_12_1$	17.5	31.6	45.6	1.0	0.20	91	1048
d(CGCGFUG)	G · FU	Z	$P2_12_12_1$	17.8	31.3	45.4	1.5	0.20	64	1047
d(CGCGXG)	G · X	Z	$P2_12_12_1$	18.2	30.4	43.9	1.7	0.16	79	1012

[a] BrU = 5-bromouridine, FU = 5-fluorouridine, X = *N*4-methoxycytosine.

Table 9. Crystallographic data on DNA structures containing extra bases.

Sequence	T [°C] [a]	Space group	Unit cell dimensions [Å]			Resolution [Å]	R
d(CGCAGAATTCGCG)	−150	$C2$, $\beta = 99°$	78.5	42.8	25.2	2.8	0.15
d(CGCGAAATTTACGCG)	4	$I222$	37.0	53.7	101.6	3.0	0.24
d(CGCGCGTTTTCGCGCG)	RT	$C2$, $\beta = 95°$	57.2	21.6	36.4	2.1	0.23

[a] RT = room temperature.

Table 10. Average helical parameters for selected right-handed structures [a]

	Helix twist [°]	x [Å]	Base-pair tilt [°]	Propeller twist [°]	Minor [Å]	Major [Å]	D [Å]
A form							
d(GGTATACC)	32	2.9	13	10	10.2	6.3	4.0
d(GGGGCCCC)	32	2.9	13	10	10.1	6.8	4.1
d(GGGCGCCC)	32	3.3	7	12	9.5	10.1	3.7
d(GGCCGGCC)	33	3.1	12	13	9.8	7.5	3.5
d(IoCCGG)	34	2.8	14	16	9.5	4.8	3.5
d(CTCTAGAG)	32	3.1	10	11	8.7	8.0	3.6
r(GCG)d(TATACGC)	33	2.5	19	12	10.2	3.2	4.5
r(UUAUAUAUAUAUAA)	33	2.8	17	19	10.2	3.7	3.6
Fiber A-DNA [b]	33	2.6	22	6	11.0	2.4	4.4
B form							
d(CGCGAATTCGCG)	36	3.3	2	13	5.3	11.7	−0.2
d(CGCGAATTBrCGCG)	36	3.4	−2	18	4.6	12.2	−0.2
d(GpSCGpSCGpSC) [c]	37/34	3.5/3.3	0	9	6.4	10.2	−0.6
Fiber B-DNA [b]	36	3.4	2	13	6.0	11.4	−0.6

[a] IoC = 5-iodocytosine, BrC = 5-bromocytosine. [b] Based on fiber diffraction data [143]. [c] There are two conformational states in this structure.

Table 11. Comparison of A-, B- and Z-DNA.

	A-DNA [a]	B-DNA [a]	B′-DNA [b]	Z-DNA[c]
Helix sense	right-handed	right-handed	right-handed	left-handed
Base pairs per turn	11	10	10	12 (6 dimers)
Helix twist [°]	32.7	36.0	34.1, 36.8	−10, −50
Rise per base pair [Å]	2.9	3.4	3.5, 3.3	3.7
Helix pitch [Å]	32	34	34	45
Base-pair tilt [°]	13	0	0	−7
P distance from helix axis [Å]	9.5	9.3	9.1	6.9, 8.0
Glycosidic orientation	*anti*	*anti*	*anti*	*anti, syn*
Sugar conformation	C3′-*endo*	wide range	C2′-*endo*	C2′-*endo*, C3′-*endo* [d]

[a] Numerical values for each form were obtained by averaging the global parameters of the corresponding double-helix fragments. [b] B′-DNA values are for a double helix backbone conformation alternating between conformational states I and II [24]. [c] The two values given correspond to CpG and GpC steps for the helix twist and P distance values, to cytidine and guanosine for the others. [d] Two values correspond to the two conformational states.

lized in two different space groups, that is, in two different crystal environments. These studies throw some light on the relative influence of base sequence and lattice forces on conformation.

Table 11 lists the most important parameters of A-, B-, and Z-DNA. Table 12 contains the torsion angles of selected oligonucleotides and Table 13 important structural parameters of DNA–drug complexes.

10.1. Definitions Used in the Characterization of Oligonucleotide Structures

Here we present the most important definitions used in the detailed geometric characterization of oligonucleotide struc-

Table 12. Average torsion angles [°] for selected right-handed structures (see Fig. 27).

Sequence	α(P-O5′)	β(O5′-C5′)	γ(C5′-C4′)	δ(C4′-C3′)	ε(C3′-O3′)	ζ(O3′-P)	χ(glycosyl)
A form							
d(GGTATACC)	−62	173	52	88	−152	−78	−160
d(GGGGCCCC)	−76	178	63	84	−156	−70	−158
d(IoCCGG)	−73	180	64	89	−157	−66	−157
d(GGCCGGCC) [a]	−67	170	58	80	−142	−76	−162
d(CCCCGGGG) [a]	−87	182	72	79	−153	−66	−162
d(CTCTAGAG) [a]	−76	170	52	79	−175	−54	−156
d(GCCCGGGC) [a]	−71	177	55	85	−165	−64	−159
d(GGGCGCCC) [a]	−71	178	62	80	−158	−70	−163
d(GGGATCCC)	−101	181	81	81	−164	−63	−164
r(GCG)d(TATACGC)	−69	175	58	82	−151	−75	−162
r(UUAUAUAUAUAUAA)	−61	169	53	80	−148	−79	−159
A-DNA [b]	−50	172	42	79	−146	−78	−159
A-RNA [b]	−68	178	54	82	−153	−71	−158
B form							
d(CGCGAATTCGCG)	−63	171	54	122	−169	−108	−117
d(CGCGAATTBrCGCG)	−62	170	55	120	−169	−109	−120
d(GpsCGpsCGpsC) [c]	−53	154	46	138	−164/−114	−102/−192	−109
B-DNA [b]	−33	138	33	142	−141	−157	−139

[a] Excluding α and γ of the fifth nucleotide. [b] Based on fiber diffraction data [143]. [c] Two values correspond to conformational states I and II.

Table 13. Crystallographic details of selected DNA-antibiotic structures. BrC = 5-bromocytosine.

Complex	T [°C] [c]	Space group	Unit cell dimensions [Å]			Resolution [Å]	$N_{solv.}$	R
d(CGTACG)/triostin A [a]	−16	$F222$	31.4	62.4	61.3	1.7	137	0.19
d(CGTACG)/echinomycin [a]	−16	$F222$	30.7	62.6	61.7	1.8	88	0.20
d(GCGTACGC)/triostin A [a]	12	$P6_322$	40.9	40.9	80.7	2.2	91	0.20
d(CGTACG)/daunomycin [a]	−15	$P4_12_12$	27.9	27.9	52.7	1.2	83	0.18
d(CGATCG)/daunomycin [b]	4	$P4_12_12$	28.0	28.0	52.9	1.5	40	0.25
d(CGCGAATTCGCG)/Hoechst 33258 [b]	RT	$P2_12_12_1$	25.0	40.3	65.9	2.2	175	0.14
d(CGCGAATTCGCG)/Hoechst 33258 [b]	RT	$P2_12_12_1$	25.2	40.6	66.1	2.2	126	0.16
d(CGCGAATTBrCGCG)/netropsin	RT	$P2_12_12_1$	24.3	39.6	63.6	2.2	75	0.25
d(CGCGATATCGCG)/netropsin	RT	$P2_12_12_1$	25.5	41.3	66.9	2.4	60	0.20
d(CGCAAATTTGCG)/distamycin	RT	$P2_12_12_1$	25.2	41.1	64.7	2.2	70	0.20
d(CGCGAATTCGCG)/cisplatin	RT	$P2_12_12_1$	24.2	39.9	66.1	2.6	128	0.17

[a] Two drugs per duplex. [b] There are two determinations of this structure. [c] RT = room temperature.

tures. They include the IUPAC-IUB recommendations,[136] the definitions introduced by *Dickerson* and co-workers,[137, 38] and implemented in the widely used HELIB/NEWHELIX suite of computer programs. The major groups engaged in developing algorithms for the analysis of oligonucleotide structures have recently agreed on a revised nomenclature.[139] We use the new terms in this text.

10.2. The Single Oligonucleotide Strand

Figure 26 illustrates a fragment of DNA with the sequence adenosine (A), guanosine (G), cytosine (C), and thymine (T). The bases are linked by 3′,5′-phosphodiester bonds. The fragment can be written as d(5′ApGpCpT3′) or, more usually, d(AGCT). Note that the fragment is self-complementary in the Watson–Crick sense. Figure 27 shows the atomic-numbering scheme and the definition of the torsion angles. Figure 28 illustrates aspects of nucleoside geometry with the purines in two alternative orientations, *syn* and *anti*, and also the intermolecular phosphorus distances associated with the two sugar conformations.

10.3. The Base Pairs

The Watson–Crick base pairs[140] are illustrated in Figure 29. Figures 30 and 31 illustrate the definitions associated

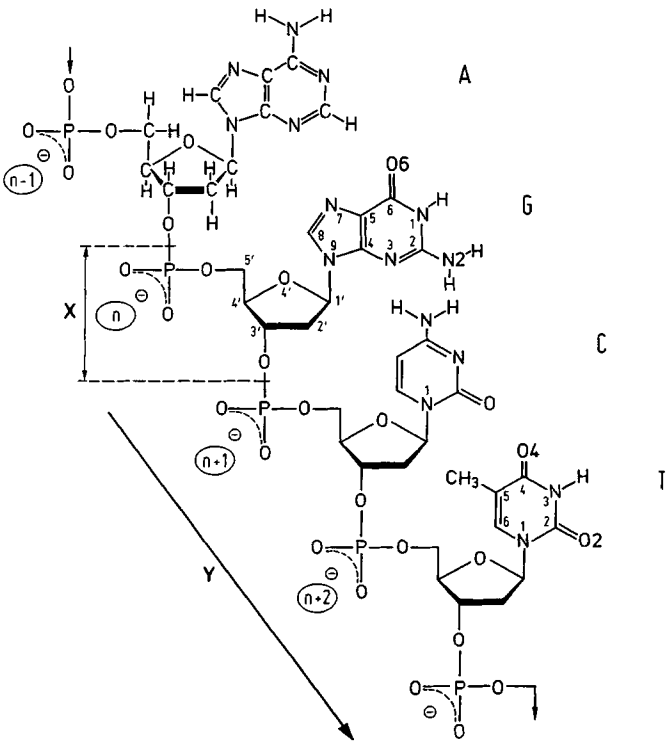

Fig. 26. The formula for a fragment of DNA with sequence adenosine (A), guanosine (G), cytosine (C), and thymidine (T) linked by 3′,5′-phosphodiester bonds [92, 136]. X indicates a nucleotide residue, Y the direction of the chain.

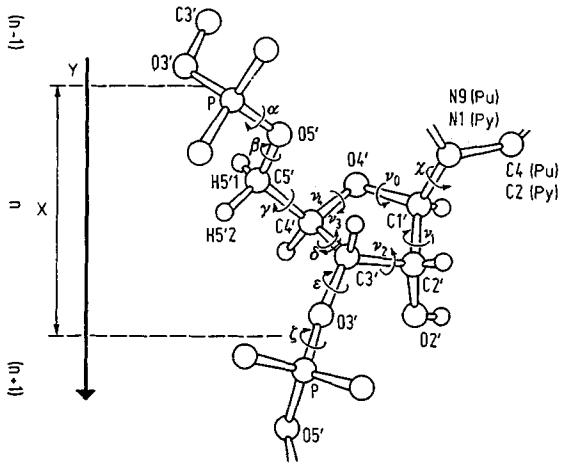

Fig. 27. An illustration of the sugar-phosphate backbone with the atomic-numbering scheme and definition of the torsion angles [92, 136] (for X and Y see Fig. 26). Pu = purine, Py = pyrimidine.

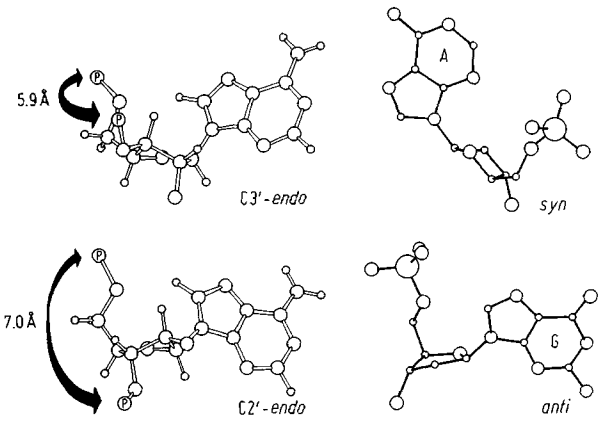

Fig. 28. Nucleoside geometry. Left: Drawings to show the two major furanose conformations encountered in structural studies and the effect each has on the phosphorus–phosphorus distances. Right: The *syn* and *anti* conformations of purines with respect to the furanose rings [92, 136].

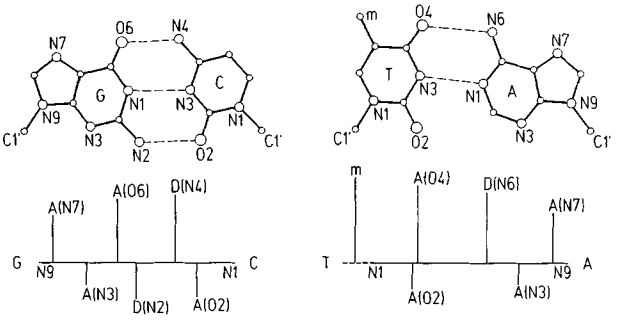

Fig. 29. The Watson–Crick base pairs G·C and A·T. Stick representations are used to convey some idea about the displacement of the functional groups of the bases. D indicates a hydrogen-bond donor and A a possible acceptor group. Base pairs are represented by a line parallel to the N9–N1 vector. The major groove is above this vector, the minor groove below.

with individual base pairs, Figure 32 with successive base pairs. These parameters are as follows:

Displacement represents the perpendicular displacement of the C6(pyrimidine–C8(purine) vector from the helix axis.

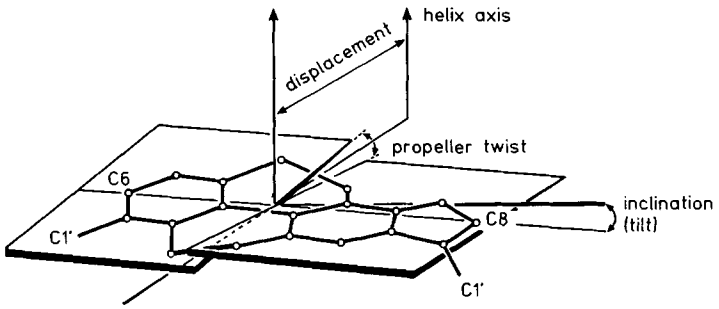

Fig. 30. Schematic drawing to show displacement, propeller twist, and inclination (formerly tilt) for a G·C base pair. The C6(pyrimidine–C8(purine) vector is drawn. This is often used as a point of reference.

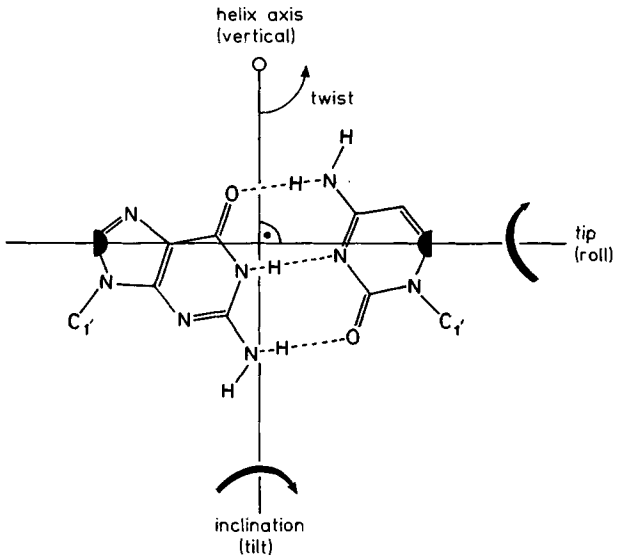

Fig. 31. An illustration of twist, inclination (formerly tilt), and tip (formerly roll) for a G·C base pair. The dark semicircles represent the positions of the C6 and C8 atoms of the pyrimidine and purine, respectively.

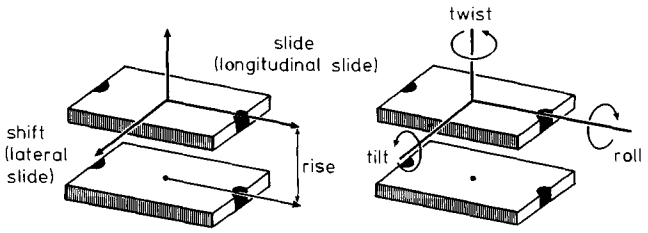

Fig. 32. Definitions for successive base pairs. This drawing shows slide, shift (formerly named lateral slide), twist, tilt, and roll. The base pairs are represented by blocks with the minor-groove side shaded and the C6(pyrimidine)/C8(purine) atoms depicted as dark semicircles on the short edges.

Propeller twist is the dihedral angle formed between individual base planes when viewed along the C6–C8 vector of the base pair.

Inclination (formerly base-pair tilt) defines the orientation of a base pair relative to the helix axis. It represents a rotation of the base-pair plane about the pseudodyad axis.

Tip (formerly base-pair roll) is used to define the orientation of a base pair relative to the helix axis and is denoted by a rotation of the base-pair plane about a line approximated

by the C6–C8 vector. This vector is perpendicular to both the helix axis and pseudodyad.

Helix twist also defines orientation of the base pair with respect to the helix axis. It is calculated by projecting successive C1′–C1′ vectors down a plane normal to the helix axis and measuring the angle between the two vectors. Alternatively, a local helix axis can be determined and by projecting the C6–C8 vectors in a similar fashion the local helix twist can be calculated.

Properties of successive base pairs

Roll and tilt define the angles between successive base pairs in the directions of the short and long axes, respectively.

Rise is the distance between successive base pairs along the helix axis.

Shift (formerly lateral slide) is the relative displacement of the C6–C8 vector midpoints of successive base pairs perpendicular to the long axis of the base pair.

Slide is the relative displacement of the C6–C8 vector midpoints of successive base pairs parallel to the long axis of the base pair.

Analytical expressions are given in Refs. [137, 138 141]. For calculations of the global helix axis the reader is directed to Ref. [6].

10.4. Properties of Grooves

Characterization of the shape of the major and minor grooves of the double helix is important since in many cases it will influence access to the functional groups of the bases by some sequence-specific agent such as a drug or protein. Shape will also influence the pattern of hydration. It is generally presented in terms of groove width and depth. The groove width can be estimated as the shortest phosphorus–phosphorus distance across a groove less 5.8 Å to compensate for the van der Waals radii of two phosphate groups Minor-groove depth is determined by the distance between phosphorus and the N2 of guanine, N3 of adenine, or O2 of either cytosine and thymine, less the sum of the van der Waals radii. The major-groove depth is quoted as the direct distance between the phosphorus and O6 atoms of guanine, N6 of adenine, O4 of thymine, and N4 of cytosine less the sum of their respective van der Waals radii. The van der Waals radii of oxygen and nitrogen atoms are generally taken as 1.4 and 1.5 Å, respectively.

We thank our colleagues, past and present, who worked in the crystallographic chemistry group, University Chemical Laboratory, Cambridge, and contributed to many of the studies cited in this review and to our friends in various laboratories who made their papers available to us prior to publication. We thank Springer-Verlag for permission to use diagrams from the Landolt-Bornstein Tables. The studies in Cambridge have been funded by the Medical Research Council. W.N.H. gratefully acknowledges the support of the Department of Chemistry at the University of Manchester, the Science and Engineering Research Council, and the Wellcome Trust.

Received: September 6, 1990;
German version: *Angew. Chem. 103* (1991) 1280

[1] M. A. Viswamitra, O. Kennard, P. G. Jones, G. M. Sheldrick, S. A. Salisbury, L. Favello, Z. Shakked, *Nature 273* (1978) 687–688.
[2] M. A. Viswamitra, Z. Shakked, P. G. Jones, G. M. Sheldrick, S. A. Salisbury, O. Kennard, *Biopolymers 21* (1982) 513–532.
[3] B. N. Conner, T. Takano, S. Tanaka, K. Itakura, R. E. Dickerson, *Nature 295* (1982) 294–299.
[4] R. Chattopadhaya, P. Chakrabarti, *Acta Crystallogr. Sect. B44* (1988) 651–657.
[5] Z. Shakked, D. Rabinovich, W. B. T. Cruse, E. Egert, O. Kennard, G. Sala, S. A. Salisbury, M. A. Viswamitra, *Proc. R. Soc. London B213* (1981) 479–487.
[6] Z. Shakked, D. Rabinovich, O. Kennard, W. B. T. Cruse, S. A. Salisbury, M. A. Viswamitra, *J. Mol. Biol. 166* (1983) 183–201.
[7] O. Kennard, W. B. T. Cruse, J. Nachman, T. Prange, Z. Shakked, D. Rabinovich, *J. Biomol. Struct. Dyn. 3* (1986) 623–648.
[8] A. H.-J. Wang, S. Fujii, J. H. van Boom, A. Rich, *Proc. Natl. Acad. Sci. USA 79* (1982) 3968–3972.
[9] M. McCall, T. Brown, O. Kennard, *J. Mol. Biol. 183* (1985) 385–396.
[10] H. Lauble, R. Frank, H. Blocker, U. Heinemann, *Nucleic Acids Res 16* (1988) 7799–7816.
[11] W. N. Hunter, B. Langlois d'Estaintot, O. Kennard, *Biochemistry 28* (1989) 2444–2451.
[12] D. Rabinovich, T. E. Haran, M. Eisenstein, Z. Shakked, *J. Mol. Biol. 200* (1988) 151–161.
[13] Z. Shakked, G. G. Guzikevich, M. Eisenstein, F. Frolow, D. Rabinovich, *Nature 342* (1989) 456–460.
[14] U. Heinemann, H. Lauble, R. Frank, H. Blocker, *Nucleic Acids Res. 15* (1987) 9531–9550.
[15] T. E. Haran, Z. Shakked, A. H.-J. Wang, A. Rich, *J. Biomol. Struct. Dyn. 5* (1987) 199–217.
[16] C. A. Frederick, D. Saal, G. A. van der Marel, J. H. van Boom, A. H.-J. Wang, A. Rich, *Biopolymers 26* (1987) 145–160.
[17] S. Jain, G. Zon, M. Sundaralingam, *J. Mol. Biol 197* (1987) 141–145.
[18] S. Jain, M. Sundaralingam, *J. Biol. Chem. 264* (1989) 12780–12784.
[19] M. McCall, T. Brown, W. N. Hunter, O. Kennard, *Nature 322* (1986) 661–664.
[20] C. A. Frederick, G. J. Quigley, M.-K. Teng, M. Coll, G. A. van der Marel, J. H. van Boom, A. Rich, A. H.-J. Wang, *Eur. J. Biochem. 181* (1989) 295–307.
[21] C. A. Bingman, S. Jain, D. Jebaratnuam, M. Sundaralingam, *Conf. abstr. sixth conversation Biomol. Stereodyn. 28* (1989) 28–29.
[22] A. H.-J. Wang, S. Fujii, J. H. van Boom, G. A. van der Marel, S. A. A. van Boeckel, A. Rich, *Nature 299* (1982) 601–604.
[23] A. C. Dock-Bregeon, B. Chevrier, A. Podjarny, D. Moras, J. S. de Bear, G. R. Gough, P. T. Gilham, J. E. Johnson, *Nature 335* (1988) 375–378.
[24] W. B. T. Cruse, S. A. Salisbury, T. Brown, F. Eckstein, R. Costick, O. Kennard, *J. Mol. Biol. 192* (1986) 891–905.
[25] R. Wing, H. Drew, T. Takano, C. Broka, S. Tanaka, K. Itakura, R. E. Dickerson, *Nature 287* (1980) 755–758.
[26] H. R. Drew, R. M. Wing, T. Takano, C. Broka, S. Tanaka, K. Itakura, R. E. Dickerson, *Proc. Natl. Acad. Sci. USA 78* (1981) 2179–2183.
[27] M. Coll, C. A. Frederick, A. H.-J. Wang, A. Rich, *Proc. Natl. Acad. Sci. USA 84* (1987) 8385–8389.
[28] H. C. M. Nelson, J. T. Finch, B. E. Luisi, A. Klug, *Nature 330* (1987) 221–226.
[29] C. Yoon, G. G. Prive, D. S. Godsell, R. E. Dickerson, *Proc. Natl. Acad. Sci. USA 85* (1988) 6332–6336.
[30] U. Heinemann, C. Alings, *J. Mol. Biol. 210* (1989) 369–373.
[31] A. Di Gabriele, M. Sanderson, T. A. Steitz, *Proc. Natl. Acad. Sci. USA 86* (1989) 1816–1820.
[32] C. A. Frederick, G. J. Quigley, G. A. van der Marel, J. H. van Boom, A. H.-J. Wang, A. Rich, *J Biol. Chem. 263* (1988) 17872–17879.
[33] Y. Timsit, E. Westhof, R. P. P. Fuchs, D. Moras, *Nature 341* (1989) 459–462.
[34] K. Grzeskowiak, K. Yanagi, G. G. Prive, K. M. Grzeskowiak, M. L. Kopka, R. G. Harvey, R. E. Dickerson, *Conf. abstr. sixth conversation Biomol. Stereodyn. 20* (1989) 120–124.
[35] G. G. Prive, R. E. Dickerson, *Conf. abstr. sixth conversation Biomol. Stereodyn. 259* (1989).
[36] H. R. Drew, R. E. Dickerson, K. Itakura, *J. Mol. Biol. 125* (1978) 535–543.
[37] H. R. Drew, T. Takano, S. Tanaka, K. Itakura, R. E. Dickerson, *Nature 286* (1980) 567–573.
[38] H. R. Drew, R. E. Dickerson, *J. Mol. Biol. 152* (1981) 723–736.

[39] J. L. Crawford, E. J. Kolpak, A. H.-J. Wang, G. J. Quigley, J. H. van Boom, G. A. van der Marel, A. Rich, *Proc. Natl. Acad. Sci. USA 77* (1980) 4016–4020.
[40] A. H.-J. Wang, G. J. Quigley, R. J. Kolpak, J. L. Crawford, J. H. van Boom, G. A. van der Marel, A. Rich, *Nature 282* (1979) 680–686.
[41] R. V. Gessner, C. A. Frederick, G. J. Quigley, A. Rich, A. H.-J. Wang, *J. Biol. Chem. 264* (1989) 7921.
[42] M. Coll, I. Pita, J. Lioveras, J. A. Subirana, P. Bardella, T. Huynh-Dinh, J. Iglolen, *Nucleic Acids Res. 16* (1988) 8695–8705.
[43] B. Chevrier, A. C. Dock, B. Hartmann, M. Leng, D. Moras, M. T. Thoung, E. Westhof, *J. Mol. Biol. 188* (1986) 707–711.
[44] A. H.-J. Wang, R. V. Gessner, G. A. van der Marel, J. H. van Boom, A. Rich, *Proc. Natl. Acad. Sci. USA 82* (1985) 3611–3615.
[45] A. H.-J. Wang, T. Hakoshima, G. A. van der Marel, J. H. van Boom, A. Rich, *Cell. 37* (1984) 321–331.
[46] S. Fujii, A. H.-J. Wang, G. A. van der Marel, J. H. van Boom, A. Rich, *Nucleic Acids Res. 10* (1982) 7879–7892.
[47] M.-K. Teng, Y.-C. Liaw, G. A. van der Marel, J. H. van der Boom, A. H.-J. Wang, *Biochemistry 28* (1989) 4923–4928.
[48] S. Fujii, A. H.-J. Wang, G. A. van der Marel, J. H. van Boom, A. Rich, *Biopolymers 24* (1985) 243–250.
[49] R. G. Brennan, E. Westhof, M. Sundaralingam, *J. Biomol. Struct. Dyn. 3* (1986) 649–666.
[50] O. Kennard, *J. Biomol. Struct. Dyn. 3* (1985) 205–225.
[51] T. Brown, G. Kneale, W. N. Hunter, O. Kennard, *Nucleic Acids Res. 14* (1986) 1801–1809.
[52] M. Coll, A. H.-J. Wang, G. A. van der Marel, J. H. van Boom, A. Rich, *J. Biomol. Struct. Dyn. 4* (1986) 157–172.
[53] M. Coll, D. Saal, C. A. Frederick, J. Aymami, A. Rich, A. H.-J. Wang, *Nucleic Acids Res. 17* (1989) 911–923.
[54] L. Van Meervelt, M. H. Moore, L. P. Kong Thoo, D. M. Brown, O. Kennard, *J. Mol. Biol. 216* (1990) 773–778.
[55] P. S. Ho, C. A. Frederick, G. Quigley, G. A. van der Marel, J. H. van Boom, A. H.-J. Wang, A. Rich, *EMBO J. 4* (1985) 3617–3623.
[56] G. Kneale, T. Brown, O. Kennard, D. Rabinovich, *J. Mol. Biol. 186* (1985) 805–814.
[57] T. Brown, O. Kennard, G. Kneale, D. Rabinovich, *Nature 315* (1985) 604–606.
[58] W. N. Hunter, G. Kneale, T. Brown, D. Rabinovich, O. Kennard, *J. Mol. Biol. 190* (1986) 605–618.
[59] W. B. T. Cruse, J. Aymami, O. Kennard, T. Brown, A. G. C. Jack, G. A. Leonard, *Nucleic Acids Res. 17* (1989) 55–72.
[60] G. G. Prive, U. Heinemann, S. Chandrasegaran, L. S. Kan, M. L. Kopka, R. E. Dickerson, *Science 238* (1987) 498–504.
[61] G. G. Prive, U. Heinemann, S. Chandrasegaran, L. S. Kan, M. L. Kopka, R. E. Dickerson in W. K. Olson, R. H. Sarma, M. H. Sarma, M. Sundaralingam (Eds.): *Structure and Expression, Vol. 2*, Adenine Press, Guilderland, NY, USA (1988) S. 27.
[62] W. N. Hunter, T. Brown, G. Kneale, N. N. Anand, D. Rabinovich, O. Kennard, *J. Biol. Chem. 262* (1987) 9962–9970.
[63] T. Brown, W. N. Hunter, G. Kneale, O. Kennard, *Proc. Natl. Acad. Sci. USA 83* (1986) 2402–2406.
[64] W. N. Hunter, T. Brown, O. Kennard, *J. Biomol. Struct. Dyn. 4* (1986) 173–191.
[65] W. N. Hunter, T. Brown, N. N. Anand, O. Kennard, *Nature 320* (1986) 552–555.
[66] W. N. Hunter, T. Brown, O. Kennard, *Nucleic Acids Res. 15* (1987) 6589–6606.
[67] P. W. R. Corfield, W. N. Hunter, T. Brown, P. Robinson, O. Kennard, *Nucleic Acids Res. 15* (1987) 7935–7949.
[68] T. Brown, G. A. Leonard, E. D. Booth, J. Chambers, *J. Mol. Biol. 207* (1989) 455–457.
[69] L. Joshua-Tor, D. Rabinovich, H. Hoppe, F. Frolow, E. Appella, J. L. Sussman, *Nature 334* (1988) 82–84.
[70] M. Miller, R. W. Harrison, A. Wlodawer, E. Appella, J. L. Sussman, *Nature 334* (1988) 85–86.
[71] R. Chattopadhyaya, S. Ikuta, K. Grzeskowiak, R. E. Dickerson, *Nature 344* (1988) 175–179.
[72] M. J. Gait, H. W. D. Matthes, M. Singh, B. S. Sproat, R. C. Titmus, *Nucleic Acids Res. 10* (1982) 6243–6248.
[73] R. Arentzen, C. A. A. van Boeckel, G. A. van der Marel, J. H. van Boom, *Synthesis 1979* 137–139.
[74] L. J. McBride, M. H. Caruthers, *Tetrahedron Lett. 24* (1983) 245–248.
[75] H. Hope, *Acta Crystallogr. Sect. B44* (1988) 22–26.
[76] M. Eisenstein, H. Hope, T. E. Haran, F. Frolow, Z. Shakked, D. Rabinovich, *Acta Crystallogr. Sect. B44* (1988) 625–628.
[77] W. Hendrickson, J. L. Smith, S. Sheriff, *Methods Enzymol. 115* (1985) 41–55.
[78] U. W. Arndt, *Methods Enzymol. 114* (1985) 472–485.
[79] R. Hamlin, *Methods Enzymol. 114* (1985) 416–452.
[80] T. Blundell, L. N. Johnson: *Protein Crystallography* Academic Press, New York 1986.
[81] D. Rabinovich, Z. Shakked, *Acta Crystallogr. Sect. A40* (1984) 195–200.
[82] G. Ughetto, A. H.-J. Wang, G. J. Quigley, G. A. van der Marel, J. H. van Boom, A. Rich, *Nucleic Acids Res. 13* (1985) 2305–2323.
[83] G. J. Quigley, G. Ughetto, G. A. van der Marel, J. H. van Boom, A. H.-J. Wang, A. Rich, *Science 232* (1986) 1255–1258.
[84] C. R. Calladine, *J. Mol. Biol. 161* (1982) 343–352.
[85] C. R. Calladine, H. R. Drew, *J. Mol. Biol. 178* (1984) 773–782.
[86] C. R. Calladine, H. R. Drew, *J. Mol. Biol. 192* (1986) 907–918.
[87] Z. Shakked, D. Rabinovich, *Prog. Biophys. Mol. Biol. 47* (1986) 159–195.
[88] A. C. Dock-Bregeon, B. Chevrier, A. Podjarny, J. Johnson, J. S. de Bear, G. R. Gough, P. T. Gilham, D. Moras, *J. Mol. Biol. 209* (1989) 459–463.
[89] A. Klug, A. Jack, M. A. Viswamitra, O. Kennard, Z. Shakked, T. A. Steitz, *J. Mol. Biol. 131* (1979) 669–680.
[90] S. C. Satchwell, H. R. Drew, A. A. Travers, *J. Mol. Biol. 191* (1986) 659–675.
[91] C. R. Calladine, H. R. Drew, M. J. McCall, *J. Mol. Biol. 201* (1988) 127–137.
[92] W. Saenger: *Principles of Nucleic Acid Structure*, Springer, New York 1984.
[93] W. Saenger, W. N. Hunter, O. Kennard, *Nature 324* (1986) 385–388.
[94] H. R. Drew, R. E. Dickerson, *J. Mol. Biol. 151* (1981) 535–556.
[95] M. L. Kopka, A. V. Fratini, H. R. Drew, R. E. Dickerson, *J. Mol. Biol. 163* (1983) 129–146.
[96] W. Saenger, *Annu. Rev. Biophys. Chem. 16* (1987) 93–114.
[97] E. Westhof, *Annu. Rev. Biophys. Chem. 17* (1987) 125–144.
[98] E. Westhof, *J. Biol. Macromol. 9* (1987) 185–192.
[99] J. M. Gottesfeld, J. Blanco, L. L. Tennant, *Nature 329* (1987) 460–462.
[100] L. Fairall, S. Martin, D. Rhodes, *EMBO J. 8* (1989) 1809–1817.
[101] J. Doucet, J.-P. Benoit, W. B. T. Cruse, T. Prange, O. Kennard, *Nature 337* (1989) 190–192.
[102] Z. Otwinowski, R. W. Schevitz, R.-G. Zhang, C. L. Lawson, A. Joachimiak, R. O. Marmorstein, B. F. Luisi, P. B. Sigler, *Nature 355* (1988) 321–329.
[103] M. Modrich, *Annu. Rev. Biochem. 56* (1987) 435.
[104] M. D. Topal, J. R. Fresco, *Nature 263* (1976) 285.
[105] M. D. Topal, J. R. Fresco, *Nature 263* (1976) 290–293.
[106] P. Strazewski, C. Tamm, *Angew. Chem. 102* (1990) 37–59; *Angew. Chem. Int. Ed. Engl. 29* (1990) 36–57.
[107] L. C. Sowers, G. V. Frazakerly, H. Kim, L. Dalton, M. F. Goodman, *Biochemistry 25* (1986) 3983–3988.
[108] A. R. Fersht, T. K. Knill-Jones, W. C. Tsui, *J. Mol. Biol. 156* (1982) 37–51.
[109] L.-S. Kan, S. Chandrasegaran, S. M. Pulford, P. S. Miller, *Proc. Natl. Acad. Sci. USA 80* (1983) 4263–4265.
[110] X. Gao, D. Patel, *J. Am. Chem. Soc. 110* (1988) 5178–5182.
[111] G. V. Fazakerly, E. Quignard, A. Woisard, W. Guschlbauer, G. A. van der Marel, J. H. van Boom, M. Radman, *EMBO J. 5* (1986) 3697–3703.
[112] D. J. Patel, L. Shapiro, D. Hare in F. Eckstein D. M. J. Lilley (eds.): *Nucleic Acids and Molecular Biology*, Springer, Berlin (1987) S. 70–84.
[113] N. C. Seeman, J. M. Rosenberg, A. Rich, *Proc. Natl. Acad. Sci. USA 73* (1976) 804–808.
[114] J. F. Fisher, P. A. Aristoff, *Prog. Drug. Res. 32* (1988) 412–415.
[115] W. Hol, *Angew. Chem. 98* (1986) 765–777; *Angew. Chem. Int. Ed. Engl. 25* (1986) 767–778.
[116] G. J. Quigley, A. H.-J. Wang, G. Ughetto, G. A. van der Marel, J. H. van Boom, A. Rich, *Proc. Natl. Acad. Sci. USA 77* (1980) 7204–7208.
[117] L. S. Lerman, *J. Mol. Biol. 3* (1961) 18–30.
[118] M. H. Moore, W. N. Hunter, B. Langlois d'Estaintot, O. Kennard, *J. Mol. Biol. 206* (1989) 693–705.
[119] R. V. Gessner, D. L. Williams, A. Rich, C. A. Frederick, *Conf. abstr. sixth conversation Biomol. Stereodyn.* (1989) 104–105.
[120] J. B. Chaires, K. R. Fox, J. E. Herrera, M. Britt, M. J. Waring, *Biochemistry 26* (1987) 8227–8232.
[121] Y.-C. Liaw, Y.-G. Gao, H. Robinson, G. A. van der Marel, J. H. van Boom, A. H.-J. Wang, *Biochemistry 28* (1989) 9913–9918.
[122] L. D. Williams, M. Egli, Q. Gao, P. Bash, G. A. van der Marel, J. H. van Boom, A. Rich, C. A. Frederick, *Proc. Natl. Acad. Sci. USA 87* (1990) 2225–2230.
[123] A. H.-J. Wang, G. Ughetto, G. J. Quigley, T. Hakoshima, G. A. van der Marel, J. H. van Boom, A. Rich, *Science 225* (1984) 1115–1121.
[124] A. H.-J. Wang, G. Ughetto, G. J. Quigley, A. Rich, *J. Biomol. Struct. Dyn. 4* (1986) 319–342.
[125] K. Hoogsteen, *Acta Crystallogr. 16* (1963) 907–916.
[126] M.-K. Teng, N. Usman, C. A. Frederick, A. H.-J. Wang, *Nucleic Acids Res. 16* (1988) 2671–2690.
[127] P. E. Pjura, K. Grzeskowiak, R. E. Dickerson, *J. Mol. Biol 197* (1987) 257–271.
[128] J. A. Parkinson, J. Barber, K. T. Douglas, J. Rosamund, D. Sharples, *J. Chem. Soc. Chem. Commun. 1989*, 1023–1025.
[129] M. A. A. F. Carondo, M. Coll, J. Aymami, A. H.-J. Wang, G. A. van der Marel, J. H. van Boom, A. Rich, *Biochemistry 28* (1989) 7849–7852.
[130] B. Rosenberg, J. van Camp, J. E. Trosko, V. H. Mansour, *Nature 222* (1969) 385–386.

[131] R. M. Wing, P. Pjura, H. R. Drew, R. E. Dickerson, *EMBO J. 3* (1984) 1201–1206.
[132] S. E. Sherman, D. Gibson, A. H.-J. Wang, S. J. Lippard, *Science 230* (1985) 412–417.
[133] S. E. Sherman, D. Gibson, A. H.-J. Wang, S. J. Lippard, *J. Am. Chem. Soc. 110* (1988) 7368–7381.
[134] M. L. Kopka, C. Yoon, D. Goodsell, P. Pjura, R. E. Dickerson, *Proc. Natl. Acad. Sci. USA 82* (1985) 1376–1380.
[135] M. L. Kopka, C. Yoon, D. Goodsell, P. Pjura, R. E. Dickerson, *J. Mol. Biol. 183* (1985) 553–563.
[136] IUPAC-IUB Joint Commission on Biochemical Nomenclature, *Eur. J. Biochem. 131* (1983) 9–11 (Abbreviations and Symbols for the Description of Conformations of Polynucleotide Chains).
[137] A. V. Fratini, M. L. Kopka, H. R. Drew, R. E. Dickerson, *J. Biol. Chem. 257* (1982) 14686–14707.
[138] R. E. Dickerson, *J. Mol. Biol. 166* (1983) 419–441.
[139] R. E. Dickerson, *EMBO J. 8* (1989) 1–4.
[140] J. D. Watson, F. H. C. Crick, *Nature 171* (1953) 737–738.
[141] R. E. Dickerson, H. R. Drew, *J. Mol. Biol. 149* (1981) 761–786.
[142] H. R. Drew, S. Samson, R. E. Dickerson, *Proc. Natl. Acad. Sci. USA 79* (1982) 4040–4044.
[143] S. Arnott, D. W. J. Hukins, *Biochem. Res. Commun. 47* (1972) 1504–1509.
[144] D. G. Brown, M. R. Sanderson, J. V. Skelly, T. C. Jenkins, T. Brown, E. Garman, D. I. Stuart, S. Neidle, *EMBO J. 9* (1990) 1329–1333.
[145] T. A. Larsen, D. S. Goodsell, D. Cascio, K. Grzeskowiak, R. E. Dickerson, *J. Biomol. Stereodyn. 7*(1989) 477–483.
[146] M. Coll, J. Aymami, G. A. van der Marel, J. H. van Boom, A. Rich, A. H.-J. Wang, *Biochemistry 28* (1989) 310–320.
[147] A. H.-J. Wang, G. Ughetto, G. J. Quigley, A. Rich, *Biochemistry 26* (1987) 1152–1163.
[148] E. Westhof, M. V. Hosur, M. Sundaralingam, *Biochemistry 27* (1988) 5742–5747.
[149] B. N. Conner, C. Yoon, J. L. Dickerson, R. E. Dickerson, *J. Mol. Biol. 174* (1984) 663–695.
[150] A. Rich, A. Nordheim, A. H.-J. Wang, *Annu. Rev. Biochem. 53* (1984) 791–846.
[151] S. Neidle, L. Pearl, J. V. Skelly, *Biochem. J. 243* (1987) 1–9.
[152] C. M. Ogata, W. Hendrickson, X. Gao, D. J. Patel, *Abstr. Am. Crystallogr. Assoc. Meet. 17* (1989) 53–57.
[153] S. C. Jain, H. M. Sobell, *Abstr. Am. Crystallogr. Assoc. Meet. 18* (1990) 86–92.
[154] K. Baldendran, C. Bingman, M. Sunderalingam, *Abstr. Am. Crystallogr. Assoc. Meet. 18* (1990) 86–90.
[155] X. Li, C. Bingman, M. Sunderaralingam, *Abstr. Am. Crystallogr. Assoc. Meet. 18* (1990) 87–95.
[156] L. Tabernero, J. Aymami, J. A. Subirana, *Abstr. XVth Int. Congr. Int. Union Crystallogr. C-147* (1990) 04.02.08.
[157] M. Sundaralingam, K. Baldendran, C. Bingman, G. Zon, *Abstr. XVth Int. Congr. Int. Union Crystallogr. C-147* (1990) 04.02.05.
[158] C. M. Ogata, W. A. Hendrickson, *Abstr. XVth Int. Congr. Int. Union Crystallogr. C-146* (1990) 04.02.03.
[159] N. Verdaguer, J. Aymami, I. Fita, J. A. Subirana, *Abstr. XVth Int. Congr. Int. Union Crystallogr. C-148* (1990) 04.02.07.
[160] F. J. M. van der Ven, C. W. Hilbers, *Eur. J. Biochem. 178* (1988) 1–7.
[161] L. D. Williams, M. Egli, G. Ughetto, G. A. van der Marel, J. H. van Boom, G. J. Quigley, A. H.-J. Wang, A. Rich, C. A. Frederick, *J. Mol. Biol. 215* (1990) 313–319.
[162] L. D. Williams, C. A. Frederick, G. Ughetto, A. Rich, *Nucleic Acids Res. 18* (1990) 5533–5540.
[163] Y.-G. Gao, Y.-C. Liaw, H. Robinson, A. H.-J. Wang, *Biochemistry 29* (1990) 10307–10311.
[164] C. A. Frederick, L. D. Williams, G. Ughetto, G. A. van der Marel, J. H. van Boom, G. J. Quigley, A. H.-J. Wang, *Biochemistry 29* (1990) 2538–2542.

Medicinal Chemistry in the Golden Age of Biology: Lessons from Steroid and Peptide Research**

By Ralph Hirschmann*

In memory of Max Tishler (1906–1989), mentor and longtime friend

Collaboration between biologists and chemists has generated medicines of enormous benefit to society. The dynamics of this synergistic interaction combines two strengths: the rigor of chemistry and the ability of biologists to construct unifying concepts from diverse fields of investigation. The resulting contributions to the practice of medicine have reduced morbidity and mortality while increasing the quality of life. Building on the work of chemists such as *Robinson, Prelog, Woodward,* and *Pauling*, medicinal chemists have advanced rational drug discovery, especially of enzyme inhibitors, to a degree unthinkable even twenty years ago. Some of the major contributions of medicinal chemistry to human and animal health stem directly from the creative application of structural and electronic reasoning, from advances in instrumentation, and from spectacular progress in biology. However, medicinal chemists have only begun to scratch the surface of the opportunities made possible by the impact of the "double-helix revolution" of the 1950s.

The most fundamental and lasting objective of synthesis
is not production of new compounds,
but production of properties.

George S. Hammond
Norris Award Lecture, 1968

1. Introduction

That effective collaboration between biologists and chemists fuels the drug discovery process is the underlying assumption of this article. To optimize this collaboration, it is desirable that chemists identify problems in biology that can be effectively and seminally solved through chemistry—which, as the molecular science, is in a position to play a central role in our understanding of biological events at the molecular level. Suffice it to say that the names of over forty biological journals include the word "Molecular". I will use the term *medicinal chemistry* to encompass whatever is of interest to those leading chemists in academia, at research institutes, and in industry who contribute to the biomedical sciences and/or drug discovery. I believe that chemists, though properly awed by developments in molecular biology stemming from the discovery of the double helix, have not, in their own minds, enjoyed the pride and self-esteem fully justified by their remarkable contributions to medicine and by their critical role in bringing about the "double-helix revolution" in biology.

This article is intended as a review of selected lessons in biomedicine-related chemistry that have been learned during the past 40 years. The items selected are developments that were of particular interest to the author. Thus, the examples are chosen subjectively and are based for the most part on research with the anti-inflammatory steroids (glucocorticoids) and with a small number of both large and small peptides.

[*] Prof. R. Hirschmann
Department of Chemistry, University of Pennsylvania
Philadelphia, PA 19104-6323 (USA)

[**] This paper is based, in part, on the 1986 ACS Medicinal Chemistry Award Lecture and the 1988 Nichols Award Lecture of the New York Section of the American Chemical Society.

Three landmarks of the late 1940s and early 1950s make the past four decades a suitable time frame for review. First, *Sir Robert Robinson*'s electronic interpretation of organic chemistry, already the basis for the mechanistic thinking of the organic chemist, was introduced to medicinal chemistry. Secondly, the 1950s saw the application to medicinal chemistry of what was to become another of its major pillars, *structural chemistry*, resulting from the pivotal work of *Pauling, Prelog,* and *Woodward*. Had I chosen to view the past 40 years through a different glass (e.g., β-lactam antibiotics rather than the glucocorticoids), the same principles and strategies—electronic and structural—would still have been cited, but I would also be discussing the discoveries of *Fleming, Florey, Chain*, and *Abraham* and the synthetic contributions of *Woodward, Sheehan, Christensen, Morin*, and many others. Thirdly, the past forty years coincided with unprecedented developments in physical methods of characterization. As exemplified by steroid research, medicinal chemistry benefited enormously from the expanding applications of ultraviolet spectroscopy (*Dannenberg, Dorfman, Gillam, Woodward*), molecular rotation relationships (*Barton, Braude, Djerassi, Wallis, Young*), and mass spectroscopy (*Djerassi*), from the developing application of rotatory dispersions (*Djerassi*) and infrared spectroscopy (*Cookson, R. N. Jones, Dobriner, E. R. Katzenellenbogen*), and, finally, from the nuclear magnetic resonance technique (*Shoolery*).

2. The Cortisone Era

The discovery by *Hench* et al.[1] of the dramatic effect of cortisone (**1**) on patients incapacitated by rheumatoid arthritis opened the door to the cortisone era of the 1950s. Besides its great importance in physiology and medicine,

cortisone had an enormous impact on chemistry, both medicinal and otherwise. The isolation and characterization of this glucocorticoid steroid hormone—with which we associate the names of *Wintersteiner*, *Reichstein*, and *Kendall*—were remarkable achievements. Later on, it was recognized

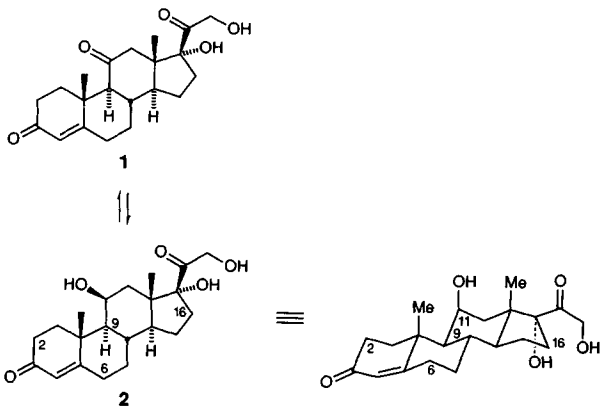

1 ⇌ **2**

that cortisone (**1**) and cortisol (**2**) are interconvertible in vivo and that the latter is the biologically active compound.[2a]

2.1. Synthetic Challenges

Cortisone was first synthesized by *Sarett*.[2b] To make the 37-step conversion of cholic acid (**3**) to cortisone practical on a commercial scale, *Tishler* at Merck introduced process re-

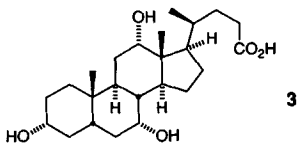

3

search as a sophisticated form of organic chemistry. He proved that esoteric reactions discovered in university laboratories can be reproduced effectively on a pilot-plant or even factory scale to manufacture molecules that possess medical and thus social value. Thereby he expanded enormously the horizons of the pharmaceutical industry.

The partial synthesis of **1** incorporated advances from the laboratories of many distinguished synthetic organic chemists of the international steroid community, including *Bergmann, Djerassi, Fieser, Gallagher, Julian, van de Kamp, Kendall, Marker, Mattox, Meystre, Miescher, Reichstein, Riegel, Robinson, Rosenkranz, Ruzicka, Sarett, Schwenk, Turner, Wallis, Wettstein, Woodward*, and their collaborators. As reported by *Fieser* and *Fieser*[3] in their well-known 1959 treatise *Steroids*, the research conferences sponsored by the National Research Council helped assure collaboration between many of the principal participants. The synthesis of **1** was preceded by that of *Kendall*'s Compound A (**4**). *Tishler*

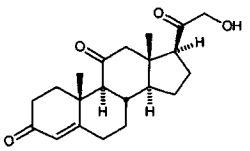

4

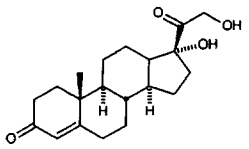

5

and three associates undertook the production of **4** in February 1944. By the summer of 1945, about 100 g had been prepared. In collaboration with *Kendall* and *Turner*, the laboratory production of cortisone was begun in March 1946 by three chemists and a technician, with early steps supported by the pilot plant. A total of 576 kg of the bile acid starting material **3** was processed. The hormone became available about two years later (April 1948), and the classic clinical study by *Hench*[1] at the Mayo Clinic began that same month. The original plan had been to assess the potential of cortisone by making 25 g available for testing. Fortunately, the highly successful process research, which raised the yield by more than two orders of magnitude, provided more than the targeted 25 g. This proved to be very important, because—as reported by *Tishler*—about 100 g was required to demonstrate the hormone's usefulness. Ultimately, 938 g of cortisone was produced! The production of the first 1000 kg of cortisone from bile acid was completed in about 30 months in the pilot plant. The extraordinary chemical and engineering accomplishments aside, it seems remarkable in retrospect—the interest of the Air Force in the adrenal steroids notwithstanding—that Merck undertook this task even prior to the first clinical success in arthritic patients and despite the fact that neither *Kendall*'s Compound A (**4**) nor *Reichstein*'s Substance S (**5**), which between them contain all of the oxygenated functions of **1**, possessed noteworthy biological activity. Indeed, the absence of such activity in the

Ralph Hirschmann is Research Professor of Chemistry at the University of Pennsylvania in Philadelphia. He has a concurrent appointment as University Professor of Biomedical Research at the Medical University of South Carolina in Charleston. Born in Germany in 1922, he came to the United States in 1937 and received an A. B. degree from Oberlin College in 1943. After three years of service in the U. S. Army during World War II, he began graduate studies at the University of Wisconsin in Madison, receiving a Ph.D. degree with William S. Johnson in 1950. He joined Merck & Co. that year and retired as a Senior Vice President in 1987.

former compound had been a source of profound disappointment to those involved in the program.

The complexity of the synthesis of cortisone sparked an intensive search by many of the leading chemists in industry and in universities to discover alternative starting materials, and thus simpler routes and, later on, safer analogues. This interest generated novel chemistry in many laboratories principally in Switzerland, the United Kingdom, the United States, and Mexico. During the early and mid 1950s, at Gordon Research Conferences on the Chemistry of Steroids (now the Conference on Natural Products), investigations by many other organic chemists were also discussed—among them *Bernstein, Bowers, Chemerda, Fried, Henbest, Hershberg, Heusser, Herzog, H. Hirschmann, Hogg, Johnson, Laubach, Oliveto, Ringold, Schneider, Sondheimer, Stork, Taub*, and *Wendler*. It was an unusually exciting time, when one was always apprehensive about the competition's latest advances.

The complexity of the conversion of the bile acids to cortisone produced still another fringe benefit, in that the search for alternative starting materials and shorter routes enabled microbiologists—principally at Upjohn, Squibb, and Pfizer—to demonstrate that microbial transformations

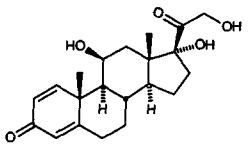

6

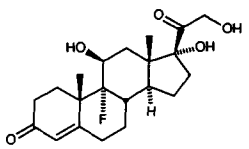

7

can be invaluable adjuncts to the repertoire of the chemist. Two of the important early synthetic analogues, prednisolone (**6**) and 9α-fluorocortisol (**7**), stemmed from serendipitous observations resulting from microbial transformations.

2.2. Electronic and Structural Issues

During the 1950s, *Sir Derek Barton*,[4] building on *Hassel*'s[5] analysis of the stereochemistry of cyclohexane with its interconverting boat and chair forms, contributed uniquely to our understanding of the chemical behavior of the steroids as it is affected by the geometry of the molecule with its axial, equatorial, and pseudoequatorial substituents. Steroids, with their rigid backbones, became a proving ground for conformational analysis. Earlier, *Reichstein* had observed that there are two kinds of α and two kinds of β substituents. Almost overnight, *Barton*'s insights systematized a multitude of seemingly unrelated observations, such as the fact that a 3β-hydroxyl substituent in the allopregnane series (A/B rings *trans*) behaves chemically like a 3α-hydroxyl in the pregnane series (A/B rings *cis*). Both are equatorial substituents (Fig. 1). Building on *Barton*'s concepts, *Hirschmann* and co-workers[6] were able to explain their unexpected observation that solvolysis of the equatorial 12β-mesylate of rockogenin led to the unprecedented rearrangement to a C- nor D-homo ring system, rather than to methyl migration or to dehydration without rearrangement (Fig. 2). It was one

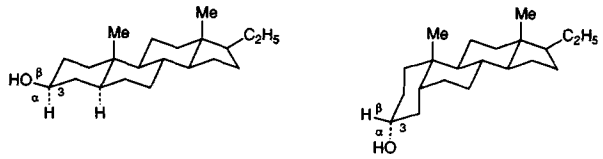

Fig. 1. The 3β-hydroxyl of the allopregnanes (left) and the 3α-hydroxyl of the pregnanes (right) are equatorial.

of the first, if not *the* first, rearrangement explicitly[6a] recognized to be under stereoelectronic control; it also allowed us to propose a pathway for the biosynthesis of the alkaloid jervine (**8**).

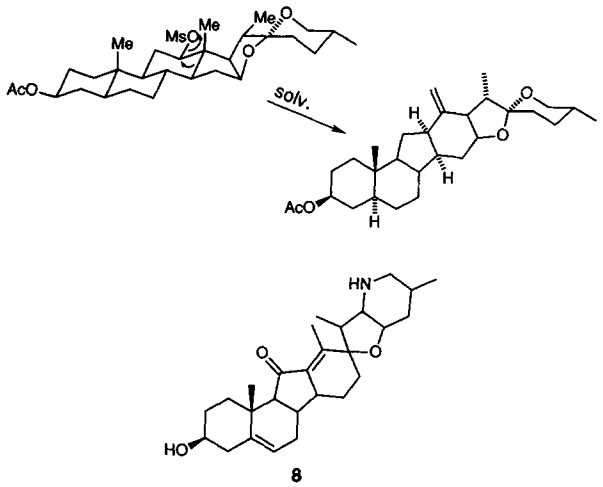

Fig. 2. The solvolytic rearrangement of the 12β-mesylate of rockogenin is under stereoelectronic control[6a] and suggested a biosynthetic route to jervine (**8**).

Barton's and *Robinson*'s insights, combined with the understanding of steric hindrance effects, studied especially by *M. Newman* and *H. C. Brown*, enabled chemists to rationalize steroidal structure–activity relationships (SARs). It became understandable why equatorial 2α-, 6α-, and 16α-methyl substituents enhanced the biological activity of cortisol, whereas the axial 2β and 6β substituents decreased such activity (for numbering, see **2**). Activity enhancement by the 2α and 6α substituents was thought to be due to decreased metabolism of the α,β-unsaturated 3-ketone, whereas the axial 2β- and 6β-methyls interfered with the binding of the 11β-hydroxyl to the glucocorticoid receptor. That both the 16α- and the 16β-methyl groups enhanced potency came as no surprise to anyone cognizant of the fact that, because the D ring is five-membered, both methyls occupy quasi-equatorial positions, thus protecting the C-17 side chain from metabolism without interfering with the binding of the 11β-hydroxyl to the receptor. *Fried* at Squibb explained the SARs of 9α-halogen substitution on the basis of electronic effects;[7] steric effects of large 9α substituents may also play a role. That 9α-fluorocortisol (**7**) is ten times more potent than cortisol (**2**) was attributed[7] to the increased acidity of the important 11β-hydroxyl. As electronegativity decreased and the size of the halogen increased, potency decreased: 9α-chloro, 4.7; 9α-bromo, 0.28; 9α-iodo, 0.1 (cortisol = 1). It is interesting that crystallographic

analysis of **7** by *Weeks* et al.[8] revealed that the 9α-fluorine substituent also has a structural effect on the A ring.

The creative application of electronic and steric concepts enabled the chemist in the pharmaceutical industry to reduce the number of compounds which had to be synthesized and tested in going from a lead to a candidate for clinical trial. *Sarett* referred to this as the "minimum systematic approach" to drug discovery.

2.3. Biological Issues

It soon became clear that cortisone caused multiple side effects, such as loss of calcium, a negative nitrogen balance, renal salt and water retention, and occasionally adverse mental effects. Initially this came as a surprise, since in the 1940s several vitamin-deficiency diseases had been cured—without side effects—by giving pharmacologic doses of the deficient vitamins. At first biologists and chemists hoped that enhancing potency would improve the therapeutic index (T. I.) of cortisol. They hoped that enhanced potency, by allowing one to lower dosage, would thereby reduce side effects. Unfortunately, this proved to be illusory, as shown by the fact that such early synthetic analogues as 2α-methyl and 9α-fluorocortisol (**7**), though more potent anti-inflammatory compounds than cortisol, did not possess an improved T. I. On the contrary, the unwanted salt retention had increased even more than the desired anti-inflammatory activity.

On the other hand, *Hershberg, Herzog,* and their associates at Schering discovered prednisolone (**6**) in 1955,[9] the first clinically important glucocorticoid that combined enhanced anti-inflammatory activity with a T. I. superior to that of cortisone/cortisol, in that prednisolone caused less salt retention.

Taken together, these results taught the medicinal chemists and the biologists two important lessons: first, that treating a patient with a pharmacologic dose of a hormone is likely to cause side effects when the disease is not due to a deficiency of that hormone; second, that the synthesis of analogues of a natural product such as cortisol, or of any other drug or potential drug, has a chance of improving the therapeutic index only if the receptor that mediates the desired effect is not the same as the receptor that causes a side effect.[10] The observation that the 2α-methyl and the 9α-fluoro substituents as well as the 1,2 double bond of **6** affected anti-inflammatory potency differently from salt retention potency suggested that this particular side effect of cortisol might be due to a receptor that is not the same as the receptor that results in anti-inflammatory activity. The biologists were able to make this important discovery because of the chemists' ability to produce molecules with novel properties. At about the same time (1955), *Reichstein*'s isolation and characterization of aldosterone (**9**),[11] the steroid hormone that regulates salt metabolism, lent further support to this idea.

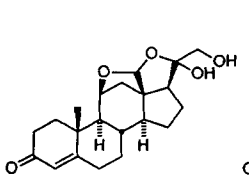

9

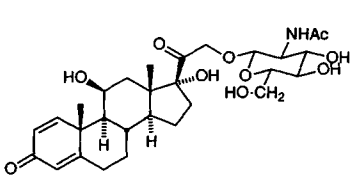

10

The term *receptor*[12a] had been defined in pharmacologic terms by *Langley*.[12b] At the molecular level, however, it was a black box. When there was some molecular understanding, a proper name such as trypsin was used rather than a term such as "the receptor for lysine-containing peptides".

A great many potent analogues were synthesized by industrial laboratories, and several of them became clinically important products. That no progress could be made in separating the remaining side effects of cortisone made it likely that these side effects were mediated via the same receptor that mediated the desired anti-inflammatory activity, though this interpretation was not, to my knowledge, explicitly stated at the time. In the 1950s, therefore, *Hirschmann, Sarett* et al. applied *drug latentiation* as a novel and "rational" approach toward a safer glucocorticoid.[13] We sought to design and synthesize a biologically inactive steroid (a prodrug), which would be *selectively*, or at least *preferentially*, converted into the active steroid at the site of inflammation. The 21-*N*-acetylglucosamide of prednisolone, **10**, was synthesized with the presumption that it would be biologically inactive and also with the anticipation that it would be *preferentially* converted into the active compound **6** in inflamed joints by *N*-acetylglucosaminidase. The basis for these expectations was the knowledge that the 21-ethers of the glucocorticoids are inactive and that the levels of *N*-acetylglucosaminidase are higher in inflamed joint fluids than in normal joints or in plasma. Our hope was at least partially borne out, because in animals the glycoside **10** has a better T. I. than prednisolone (**6**). Lack of oral bioavailability, however, led to the decision that the compound did not justify a clinical trial in humans. Still, the concept of drug latentiation—that is, *selective* conversion at a target of a prodrug to a drug—has been repeatedly explored since then.

The successful synthesis of the medically important water-soluble 21-phosphate ester of cortisol for use in intravenous administration and ophthalmic formulations was reported by *Chemerda, Poos, Hirschmann* et al.[14] The synthesis proved to be nontrivial, because the presence of the 17α-hydroxyl group in potential precursors resulted in a propensity to give the unwanted 17α,21-epoxides.[15]

By 1963 it had been established that an oxygen at C-3 is not required for steroidal anabolic-androgenic or progestational activity. Indeed *Clinton* et al. at the Sterling-Winthrop Research Institute had reported in 1959 that androst-4-eno- and androstano[3,2-*c*]pyrazoles are potent anabolic compounds.

On the other hand, a wide body of data seemed to support the belief that a C-3 oxo group is required for the anti-inflammatory activity. Nevertheless, *Hirschmann, Steinberg, Tishler* et al.[16] undertook the synthesis of pregnadiene derivatives containing a fused pyrazole ring, such as **11** and **12**, and found them to be highly active. Indeed, the phenylpyrazoles, typified by **12**, proved to be the most powerful activity-enhancing pharmacophores discovered to date for steroidal anti-inflammatory compounds. Because one of these phenylpyrazoles was marketed by Roussel-Uclaf in France, the discovery of this class of compounds may either be regarded as "irrational-though-successful drug discovery" or as a reminder that at times it is desirable to question

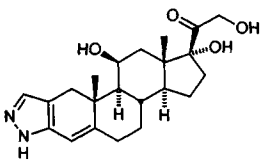

11

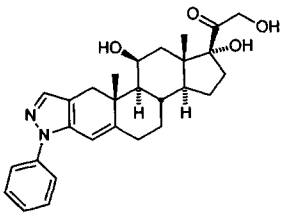

12

accepted but unproven dogma. Initially we[17] interpreted the high activity of the pyrazoles in terms of electron distribution around the 3-position, but later it appeared more likely to us that the observed potency was an early example of the existence of alternative or accessory binding sites. The latter has been a recurring theme in medicinal chemistry during the past twenty years, although, to my knowledge, it has been principally applied in the discussion of antagonists. The concept suggests that a function believed to be required for biological activity, such as the 3-oxo group of a glucocorticoid, may in fact not be needed if some other substituent, such as an aromatic ring, introduced elsewhere in the molecule, is complementary to the receptor. In general, then, novel structures have provided new insights into steroid interactions with receptors.

During the mid-fifties, the work of the Syntex and the Searle groups under the leadership of *Djerassi* and *Rosenkranz*[18] and *Colton* and *Riegel*,[19] respectively, with the progestins 17α-ethynyl-19-nortestosterone (**13**) and its isomer with a 5(10) double bond, was to become of great importance because these compounds can serve as orally effective anovulatory agents. Pharmaceutical preparations

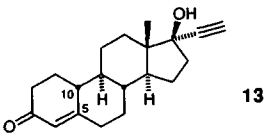

13

used in the United States combine a progestin with an estrogen. This work serves as a persuasive reminder, if any is needed, that medicinal chemists are in a position to synthesize molecules with properties that profoundly affect not only medicine, but also societal behavior.

2.4. Recent Developments

By the early 1960s, the chemistry of the anti-inflammatory steroids appeared to have largely realized its potential. Clinically, the nonsteroidal anti-inflammatory drugs replaced the steroids as the treatment of choice for most inflammatory diseases. However, other aspects of steroid chemistry and medicinal chemistry continued to flourish. For example, *W. S. Johnson*'s brilliant biomimetic cyclizations are already regarded as classics.[20] Another noteworthy example, which generated great interest in the 1970s, is research related to vitamin D. Studies in several laboratories, including those of *Haussler*,[21] *Kodicek* and *Lawson*,[22] *DeLuca*,[23] and *Norman*,[24] culminated in the recognition that vitamin D_3 (**14**), after absorption from the gut, is hydroxylated in position 25 by a liver enzyme to give **15** and then in position 1α by a kidney enzyme to afford **16**. It is this latter dihydroxylated metabolite of vitamin D_3 that initiates calcium absorption. Subsequent to these biochemical accomplishments, which resulted in the characterization of **16**, organic chemists contributed elegantly to the solution of the resulting synthetic challenges as exemplified by the work of the laboratories of *Hesse*,[25] *DeClerq*,[26] *Dauben*,[27] *Mazur*,[28] *Uskovic*,[29] and others. These workers, as well as *Seki*[30] and others, have also helped to clarify the role of 1α,14(*R*),25-trihydroxyvitamin D_3 (**17**).

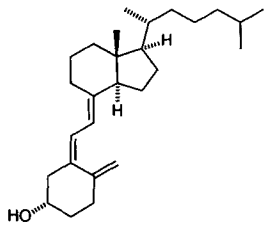

14

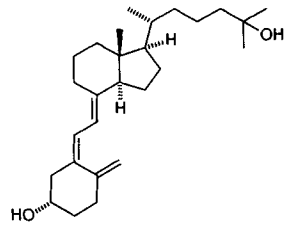

15

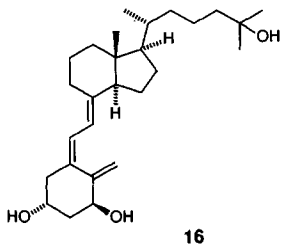

16

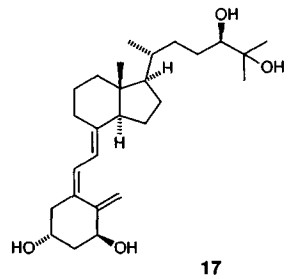

17

Steroid hormone antagonists and steroid-related enzyme inhibitors remain of the greatest interest today. Further, the understanding of cholesterol biosynthesis from acetate has recently led to one of the most important drugs approved during the 1980s, lovastatin (**18a**), which inhibits cholesterol biosynthesis. Its introduction in 1987[31] was hailed as a significant advance in the treatment of hypercholesterolemia (see Section 5, where **18b** is also discussed).

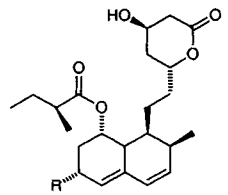

18a, R = Me
18b, R = H

Mifepristone (**19**)[32] is a progesterone antagonist developed by Roussel-Uclaf. Administration of this steroid, followed by a small amount of prostaglandin, has been found to be a safe and effective method for the early termination of pregnancy. It has been approved for distribution in France as a tightly controlled prescription drug.

Among the promising drugs currently in advanced clinical trials is Proscar (**20**), an inhibitor of the enzyme human pro-

static 5α-reductase. Proscar was designed and synthesized by *Rasmusson* et al.[33] to block the conversion of testosterone (**21**) to dihydrotestosterone (**22**). Unlike **21**, compound **22** stimulates prostate hyperplasia, but serves no known desirable purpose in the adult male. This eminently "rational" approach to the discovery of a drug for reducing the size of an enlarged prostate was first suggested in the 1950s by the late *Glen Arth* at Merck.

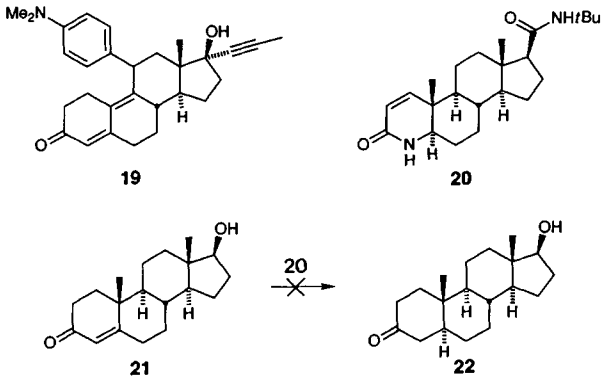

Other steroids of current interest include inhibitors of human placental aromatase, antiestrogens devoid of agonism, and compounds (21-amino steroids) with the potential to protect against central nervous system trauma, or amino steroids with the potential to be of benefit in adult-onset diabetics.

Finally, molecular biology has opened an important and fruitful new direction in steroid-related research, designed to gain an understanding of the molecular basis for the ability of intracellular steroid receptor proteins and their hormonal ligands to alter the transcriptional efficiency of networks of specific genes.[34] It will be interesting to see to what extent such investigations will add to our understanding of the SARs of steroid hormones and their antagonists, especially if crystalline receptors become available. At present it is interesting, but not surprising, that the cDNAs of diverse steroid receptors reveal three highly conserved regions.[35a] The structural unity in nuclear hormone receptors has been reviewed recently.[35b]

3. Peptides Large (Proteins) and Small (Hormones)

Steroids and peptides share an importance in both physiology and medicine. The peptide field had its inception about ninety years ago, when *Franz Hofmeister* and *Emil Fischer* (who was to receive a Nobel Prize that year for his work with sugars and purines) reported independently at a meeting in Karlsbad in 1902 that proteins are made up of amino acids linked via "peptide bonds" (*Fischer*'s term). *Fruton* has provided an interesting account of these scientists and of this event.[36] Yet despite *Fischer*'s reputation, this field of study did not quickly "catch on". Indeed, many hard-core organic and medicinal chemists continued to hold peptide research in low esteem well beyond the 1950s. In recent years, peptide research has enjoyed an explosive growth, but why did it have a relatively slow beginning? I believe several factors contributed to this.

One is that organic chemists considered peptide chemistry boring, largely because of the repetitious pattern of the amide backbone. In addition, most organic chemists tend to be uncomfortable with water-soluble organic molecules, because normally the aqueous layer is the one they discard. The pharmaceutical industry was also not sanguine about peptides, because peptides lack adequate oral bioavailability and often possess unacceptably short biological half-lives. Another deterrent was the suspicion that peptide hormones are a *Gemisch* of chemically related substances. *Sanger*'s elucidation of the sequence of bovine insulin[37] was a major milestone, in part because it drove home the fact that bovine insulin is as well-defined a chemical entity as are benzoic acid and cholesterol.

In spite of the reluctance of organic chemists to regard peptide chemists as bona fide members of their discipline, the early history of peptide research testifies to the extraordinary creativity and skill of such pioneers as *Fischer*, *Bergmann*, *Zervas*, and *Curtius*. Indeed, the history of peptide research abounds with the elegant contributions to organic chemistry by many peptide chemists whose names could not be cited herein because of the limited nature of this review.[*]

3.1. Structure Determination and Synthesis of Peptide Hormones

The isolation, characterization, and synthesis of the peptide hormones oxytocin (**23**)[38] and vasopressin (**24**)[39] was reported in 1953 by *du Vigneaud*, who was awarded a Nobel Prize for this achievement. The characterization of these two

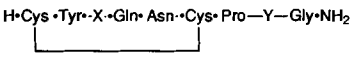

23, X = Ile, Y = Leu
24, X = Phe, Y = Arg

hormones was an impressive accomplishment if we consider that both are cyclic peptides and that the structures had to be determined without benefit of Edman[40] degradation. The syntheses of these hormones in pure form was an equally noteworthy achievement, since it was not until later on that *Wieland*'s mixed anhydride method, the use of active esters pioneered by *Wieland*, *Schwyzer*, *Bodanszky*, *G. Anderson*, and others, as well as *Sheehan*'s carbodiimide method, really came into their own.

The oxytocin/vasopressin research by *du Vigneaud* and his collaborators provided an enormous impetus to peptide research (see Section 3.3 for medicinal chemical studies on oxytocin and vasopressin). By 1963 advances in synthesis enabled *Schwyzer* and *Sieber*[41] to announce the total synthesis of a chemically homogeneous peptide with the sequence proposed[42] for porcine ACTH (**25**), a hormone containing 39 amino acids. This synthesis was carried out by the stepwise method from the C-terminus to the N-terminus,

[*] An excellent survey of this area is given in a recent book: T. Wieland, H. Bodanszky: *The World of Peptides. A Brief History of Peptide Chemistry*, Springer, Heidelberg 1991. See also [36] and [151].

with purification at each step and without recourse to fragment condensation. Each amino acid was protected by the benzyloxycarbonyl protecting group, which could be removed by catalytic hydrogenation since ACTH has only one sulfur-containing amino acid, a methionine, near the N-terminus. The synthesis of the pure peptide of 39 amino acids remains a major milestone to this day.

H-Ser-Tyr-Ser-Met-Glu-His-Phe-Arg-Trp-Gly-Lys-Pro-Val-Gly-Lys-Lys-Arg-Arg-Pro-Val—
—Lys-Val-Tyr-Pro-Asp^{25}-Gly-Ala-Glu-Asp^{30}-Gln-Leu-Ala-Glu-Ala-Phe-Pro-Leu-Glu-Phe-OH

25

It was discovered later[43] that the synthetic peptide with the C-terminal amino acid sequence of **25** does not undergo deamidation under weakly alkaline conditions where natural porcine ACTH is completely deamidated. Further, this rapid deamidation was not satisfactorily explained by structure **25**. These observations led to a revision[43] of the structure originally assigned[42] to porcine ACTH, with Asn replacing Asp in position 25 and Glu replacing Gln in position 30. The revised structure explains the loss of ammonia under mild conditions, because the Asn–Gly bond is known[44] to undergo succinimide formation (Fig. 3).

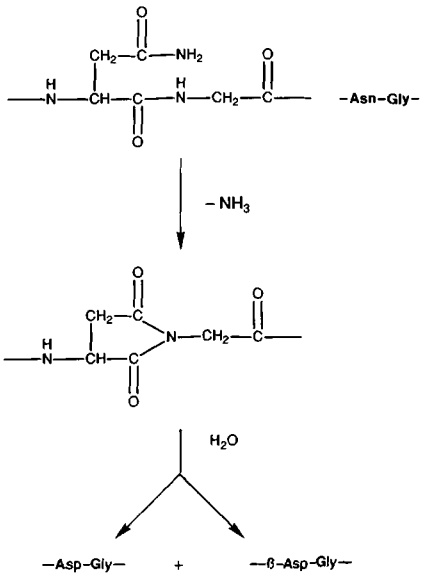

Fig. 3. The instability of the Asn–Gly bond, a pitfall in peptide chemistry. The dipeptide is present, for example, in ACTH, ribonuclease A, and secretin.

ACTH has found clinical use in treating inflammatory disease and as a diagnostic agent. It was found that the tetracosapeptidoamide lacking the amino acid sequence 25–39 possesses approximately 75% of the steroidogenic potency of the native hormone, demonstrating that drastic deletion of amino acids is sometimes permissible with little or no loss of biological activity.

Schwyzer's synthetic achievement notwithstanding, important and formidable problems still awaited solutions in the mid-1960s. Insulin (**26**) remained a challenge. The elucidation of the structure of bovine insulin by *Sanger*[37] had been completed in 1955. It had required the determination of

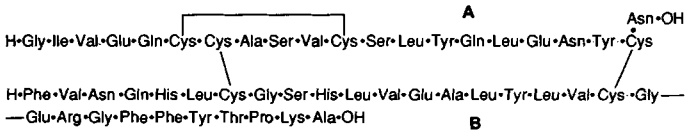

26

the linear sequences of its two chains, utilizing partial acid hydrolysates and partial enzyme digests to generate overlapping fragments. It was also necessary to distinguish Asn from Asp, and Gln from Glu, and to locate the one intrachain and the two interchain disulfide bonds.

Announcements of the total chemical synthesis of insulin were made in Germany by *Zahn* et al.[45] in 1963, in the United States by *Katsoyannis* et al.[46] in 1964, and in China by *Wang, Du* et al.[47] in 1965. The yields were low, however. This was attributed to the fact that the final step involved the uncontrolled formation of the three disulfide bridges, leading to the formation of undesired isomers and polymers. Interestingly, however, *Katsoyannis* et al.,[48] using an excess of A chain, were eventually able to obtain a yield of 60–80% for the simultaneous formation of the three cystine bridges. High yields were obtained later on also by investigators at Eli Lilly[49] and Genentech[50] for the combination of the A and B chains prepared by biotechnology. In 1974, *Sieber, Kamber* et al.[51] at Ciba attained another milestone in chemical design with a total synthesis of crystalline human insulin, in which the correctly paired disulfide bonds were formed in a controlled manner. This accomplishment was made possible through techniques developed by *Zervas* and *Photaki*[52] in Greece, by *Hirschmann, Veber* et al.[53] at Merck, and especially by *Hiskey* and his associates at Chapel Hill.[54]

The low yield (less than 4%) of insulin initially obtained in the "uncontrolled" oxidation of its reduced A and B chains proved to be a blessing in disguise. Because the low yield was contrary to *Anfinsen*'s principle of self-assembly (see Section 3.2), which states that a peptide sequence encodes proper folding, *Steiner* and his co-workers[55] considered the possibility that the biosynthesis of insulin might proceed via a *single-chain* hexahydro precursor, a prohormone. Indeed, *Steiner* was able to isolate a single-chain proinsulin in 1967 and to show that a fragment consisting of 29–35 amino acids (depending on the species) connects the A and B chains. He also demonstrated that fully reduced proinsulin can be oxidized to proinsulin in high yield and that proinsulin is convertible into insulin in vitro. The successful search for a prohormone exemplifies again the impact of chemical experimentation (in this instance, low yields in the combination of the two chains) on biological understanding (the discovery of prohormones). *Steiner*'s discovery of proinsulin started peptide research on the road to prohormones generally, and later to the preprohormones, which molecular biologists like to call the "gene products". Scientists at Eli Lilly and Genentech have synthesized insulin via proinsulin prepared by biotechnology. Studies by *Brandenburg* et al.[229] and by *Markussen*[230] with "miniproinsulins" led to the suggestion that the role of the connecting peptide of proinsulin in biosynthesis is simply to render the formation of the first interchain disulfide bridge a monomolecular process.

A profound contribution of molecular biology was the isolation, cloning, and expression of the insulin receptor and the recognition that it possesses kinase activity.

Insulin holds a very special place in the annals of peptide research. It was the first complex peptide of profound importance in medicine (life-saving in the case of the juvenile diabetic) to be sequenced.[56] Insulin played a central role in numerous other scientific discoveries as well. It established that peptide hormones are pure chemical entities and showed that a peptide lacking a prosthetic group can still generate biological activity.[57] Insulin was also the first peptide hormone to be crystallized (*Abel*, 1926);[58] in 1969, *D. C. Hodgkin* et al.[59a] reported its X-ray structure (see Ref. [215]). *Blundell*, *Hodgkin* et al.[59b] used X-ray crystallography to show that replacement of the B10-histidine can have a pronounced effect on the tertiary structure of the hormone, thus providing an explanation for the low potency of guinea-pig insulin in rodents or rodent tissues. Human insulin of porcine insulin origin became the first naturally occurring protein to be manufactured by semisynthesis.[231] Insulin became the first clinically significant product to be prepared by recombinant DNA technology.[50]

3.2. Chemical Syntheses of Enzymes

The first total syntheses of an enzyme (ribonuclease) were simultaneously but independently announced by *Merrifield* and *Gutte*[60] and by our group at *Merck*.[61] *Merrifield* and *Gutte* used the new solid-phase technique,[62] while we employed the fragment condensation method,[63–67] extensively utilizing the *N*-carboxyanhydrides[68] as building blocks. Selecting ribonuclease as the synthetic target, rather than seeking to improve the synthesis of insulin, had been a very deliberate choice for both groups. Insulin was the smaller molecule and thus presumably the less difficult to synthesize, and for that reason it appeared to be the more obvious one to pursue. However, the lure of an enzyme synthesis vis-à-vis a hormone synthesis proved decisive.

The de novo chemical syntheses of enzymes[160, 161] with good specific activity from their amino acid building blocks was highly satisfying in two respects (though it failed to fulfill its promise in a third). First, despite the brilliant demonstration by *Anfinsen* and *Haber* that a protein's *primary* sequence also contains the information for its *tertiary* structure,[69] many scientists in the mid-1960s still believed that the total chemical synthesis of an enzyme would prove impossible in the absence of some form of a template. A linear peptide containing eight cysteine residues can, on oxidation, form theoretically as many as 105 isomers, each possessing four cystine bridges. The two successful total chemical syntheses of the right isomer thus provided powerful affirmation of the Anfinsen/Haber principle of self-assembly.

Second, it was highly satisfying to know that the combined efforts of the international community of peptide chemists had made it possible by 1968 to synthesize an enzyme, a longtime goal of synthetic organic chemistry. Twelve years later *Yajima* et al.[70] were able to report the total synthesis of crystalline ribonuclease A by solution chemistry; they introduced trifluoromethanesulfonic acid as a deprotecting agent.

The unfulfilled promise relates to the fact that the total chemical syntheses of enzymes remained an arduous undertaking. Except for *Yajima*'s synthesis of crystalline ribonuclease A[70a] in 1981, no successful enzyme synthesis was announced between 1969 and 1988, notable efforts in the United States and abroad notwithstanding. It had been our hope, and also *Merrifield*'s, that the synthesis of ribonuclease would be followed by the syntheses of analogues of enzymes not found in nature, and that this would contribute to the understanding of protein structure and function. Unfortunately, the synthesis of an analogue of a protein can be an even more challenging task than that of the natural product itself, because there is no reference sample with which one can compare the physical, chemical, and biological properties of the synthetic product. Thus, criteria of purity are even harder to establish.[71] In addition, purification procedures developed for the natural substance, including, importantly, affinity chromatographic techniques, may not be applicable to the analogue. It remained for biotechnology to make site-directed mutagenesis into the powerful tool for protein analogue synthesis that we know it to be today. Reports by, for example, *Benkovic*,[72] *Fersht*,[73] *Knowles*,[74] and *Wells*[75] and their associates elegantly exemplify that enzyme analogue synthesis does indeed extend our understanding of enzyme mechanisms and of protein folding. In retrospect, *Anfinsen*'s pioneering work proved to be as important to biotechnology as it had been to the chemical enzyme syntheses of the 1960s.[75, 232]

In 1988, *Nutt*, *Veber* et al.[76a] described the total chemical synthesis of a 99-residue peptide with the sequence proposed by *Ratner* et al. at the NIH for the AIDS-related HIV protease. At the same time, *Schneider* and *Kent*[76b] reported the synthesis of an analogue of this enzyme in which L-α-aminobutyric acid replaced the two cysteine residues.

When *Merrifield* and *Gutte*, as well as we at Merck, selected protecting groups for our proposed enzyme syntheses, really general orthogonal protection had not been worked out. In particular, the then-current literature notwithstanding, the all-important acid-labile *tert*-butyloxycarbonyl (Boc)[77–79] protecting group could not be removed from an α-amino group without partial loss of the carbobenzoxy group (Cbz) from the ε-position of lysine. Even a partial loss of Cbz protection from any of the multiple lysine side chains of ribonuclease can lead to unwanted branching in the next coupling step. General orthogonality was subsequently achieved through the combined contributions of chemists such as *Carpino*, who introduced the acid-stable, piperidine-labile 9-fluorenylmethoxycarbonyl (Fmoc) group,[80] *Sieber* and *Iselin*, who used the biphenylisopropyloxycarbonyl (Bpoc) group,[81] and *Hiskey*, who employed selective cystine-bridge formation,[82] as well as through the work of *Barany*.[83]

3.3. More Recent Chemical and Biological Developments

The most notable advance in peptide synthesis since the introduction of the benzyloxycarbonyl protecting group by *Bergmann* and *Zervas*, and of the azide coupling reaction by *Curtius*, was *Merrifield*'s invention of solid-phase peptide

synthesis.[62] Subsequent improvements in this new technique, in *Merrifield*'s laboratory and by countless investigators worldwide, and improvements in the fragment-condensation method[61,67] in combination with the introduction of the HF reaction by *Sakakibara* and co-workers[84] and the application of HPLC to peptide synthesis, principally by *Rivier*, have brought peptide synthesis to a point where, in the late 1980s, the peptide chemists possessed the techniques to synthesize complex peptides/proteins of about 100 amino acids quite rapidly. For example, *Sakakibara* et al. used the fragment condensation method to synthesize both human parathyroid hormone, hPTH(1–84),[84b] and angiogenin, which contains 123 amino acids.[84c] The HIV protease mentioned above became available[76] in sufficient quantity by total chemical synthesis for urgently needed inhibitor screening at a time when the viral enzyme had not yet been provided by biotechnology. Similarly, *Garsky* et al.[85] accomplished the chemical synthesis of echistatin, a potent inhibitor of platelet aggregation, composed of 49 amino acids, including four cystine bridges. These authors were, in addition, able to draw meaningful conclusions about SARs for novel analogues of this peptide. These advances, made possible by the research over a period of time of physical organic chemists such as *Kemp*,[86], *Benoiton*,[87] and *Tam*,[88] led to many of our current procedures that permit racemization-free, high-yield coupling reactions and the high-yield removal of protecting groups with minimal side reactions. Advances in the chemical syntheses of peptides and proteins remain of great importance, in part because biotechnology has so far been confined to use of the 20 coded amino acids, although recent work, especially by *Schultz*, suggests that this limitation will eventually be overcome.

In the 1960s, electronic theory and structural chemical concepts were having a marked effect on peptide chemistry. The impact of conformational analysis was to be as great on peptide research as it had been on steroid research. Gaining insight into peptide conformation was complicated by the greater flexibility of peptides and their greater structural diversity. Thus, whereas steroid conformational analysis is restricted to the relatively[89] rigid cyclopentanoperhydrophenanthrene skeleton, peptide conformations include helices, extended structures, turns, and other chain foldings less readily classified. The basis for peptide conformational analysis was provided by the seminal work of *Ramachandran*,[90] *Scheraga*,[91] and *Blout*,[92] who set forth many exciting ideas about solutions to problems in peptide conformation and protein folding. Using a range of physical methods, *Goodman*[93] initiated studies of conformational transitions in polypeptide systems. *Schwyzer* pointed out that cyclic peptides might have conformation-defining secondary structure,[94] opening a fertile field for conformational study of cyclic oligopeptides, exploited by *Blout*,[95a] *Kopple*,[95b] *Prelog*,[95c] *Ovchinnikov*,[95d] and others. The increasing capability of nuclear magnetic resonance spectroscopy to investigate peptide conformation was important to this effort. It has been reviewed by *Kessler*.[96] *Marshall*[97] pointed out the value of conformation-restricting amino acid residues in identifying biologically important peptide conformations. One of the first applications of cyclic peptide conformational analysis to problems in medicinal chemistry was made by *Urry, Ohnishi,* and *Walter*[98] in the oxytocin series. More recent elegant examples of conformational study of biologically active cyclic peptides come from the laboratories of *Hruby*,[99] *Kessler*,[100] and *Fesik* and *Rich*.[101] The classic review by *Rose, Gierasch,* and *Smith*[102] examines conformation from the perspective of "Turns in Peptides and Proteins". This review has recently been updated.[103]

As pointed out earlier (see ACTH and insulin, Section 3.1), the peptide hormones, like their steroidal counterparts, proved important in biology and in medicine. Oxytocin has been used widely for the induction of labor. *du Vigneaud* himself followed his synthesis of the neurohypophyseal hormones with medicinal chemical investigations into the importance of their side chains for biological activity. *Rudinger* and *Jost* in Czechoslovakia, in seminal studies,[104] showed that a monocarba (i.e., methylene) analogue of oxytocin is biologically active, proving that neither a sulfur–sulfur bond per se nor a *reducible* cyclic structure is required for activity. These empirical investigations laid the foundation for the subsequent, elegant medicinal chemical research by the Prague group,[105] by *Walter*,[106] by *Manning*,[107] and by *Hruby*.[108] Of clinical interest is the vasopressin analogue [1-deamino, D-Arg[8]]vasopressin (DDAVP, **27**), synthesized by *Huguenin* and *Boissonas*[109] and also by *Zaoral* et al.[110] as a potent, *selective*, long-lasting antidiuretic, of value in the treatment of diabetes insipidus. It is selective for the V_2 (kidney) receptor. It is interesting in terms of the molecular mechanisms of hormone action that *Manning*'s Val[4] analogue[111] (**28**), a potent V_2 agonist, is also a weak V_1 (vasopressor receptor) antagonist. *Berde, Huguenin*, and *Boissonas* at Sandoz in Basel prepared vasopressin analogues that are preponderantly either vasopressors or antidiuretics. The chemists' ability to generate new molecules again promoted the biologists' understanding of receptor subclasses. It is important to stress that by generating molecules possessing greater selectivity and potency, chemists have also provided the clinicians with better medicines and the biologists with more useful *labeled* ligands.

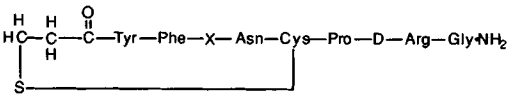

27, X = Gln
28, X = Val

In 1971, *Urry* and *Walter*[112] proposed a three-dimensional solution structure for oxytocin, thus applying structural thinking to this peptide hormone. They made several insightful observations, including the statement that there is no evidence that the amide backbone of peptide hormones participates directly in receptor occupation and activation. They recognized the importance of specific conformational assignments of structured sequences and the consequence of such assignments to side-chain conformations. Building on *Ramachandran*'s theoretical calculations of the early 1960s[90] and the later work by *Geddes* et al.,[113] *Walter* and *Urry* brought to medicinal chemistry an understanding of the effects of different types of turns on the conformation (equatorial, pseudoequatorial, axial, etc.) of substituents at

the α carbons in the $i + 1$ and $i + 2$ positions of such turns (Fig. 4).

Hruby, Manning, Walter, and others have called attention to the important fact that there can be considerable divergence in the SARs of hormone agonists and their antagonists. This is consistent with *Jencks'* insightful analysis of the "economics of binding energies",[114a] which states that agonists bind tightly to the receptor in its activated conformation, whereas antagonists bind tightly to the receptor in the ground state. In his commentary on "Binding Energy and the Activation of Hormone Receptors", *Franklin*[114b] built on and expanded these concepts.

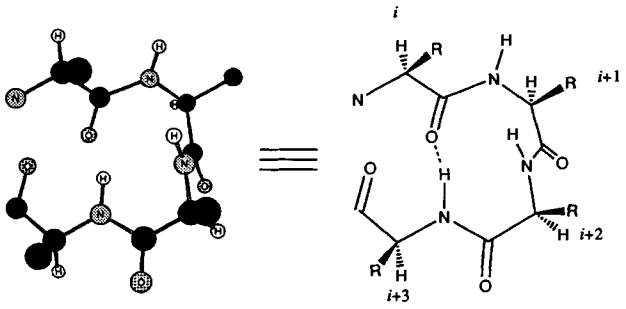

Fig. 4. Orientation of side chains in a type I β-turn.

At about the same time when *Urry* and *Walter* questioned the importance of hydrogen bonding between the amide backbone of the peptide hormones and their receptors, *Rudinger*[105] called attention to the crystallographic evidence for just such an interaction between proteolytic enzymes and their substrates/inhibitors. This distinction first became clear to me during a conversation with *D. Rich.*

The research in the 1960s and 1970s by *Guillemin*,[115, 116] *Rivier*,[117] *Schally*,[118, 119] and their collaborators typifies the ever-growing impact of peptide research on physiology and medicine. Their investigations culminated in the isolation, characterization, and synthesis of three hypothalamic hormones: gonadoliberin (GnRH, **29**), somatostatin (SRIF, **30**), and thyroliberin (TRH, **31**). These achievements were recognized by the award of a Nobel Prize to *Guillemin* and *Schally*. Equally significant were the subsequent isolation, characterization, and synthesis by *Rivier, Spiess, Thorner,* and *Vale*[120] and by *Guillemin* et al.[121] of growth-hormone-releasing factor (GHRF, **32**) and of the long-sought corticotropin-releasing hormone (CRF, **33**) by *Vale, Spiess, Rivier,* and *Rivier*.[122] Studies in humans have demonstrated that GnRH is useful in both the diagnosis and treatment of infertility, since it stimulates the release of luteinizing hormone (LH) and of follicle-stimulating hormone (FSH). As is so frequently the case, the discovery of a pure antagonist, in this case a GnRH antagonist, proved at least as significant as the discovery of novel agonists. GnRH antagonists are being tested clinically as antifertility agents.[123] Biologists also made the interesting discovery that, whereas superagonist analogues of GnRH initially act (as expected) as potent agonists, superagonism then results in downregulation of the receptors, and thus the long-term effect is to *prevent* the release of LH and of FSH, an effect of interest in the treatment of prostate cancer. Superagonists like ICI's Zoladex have been approved in certain markets.

pGlu–His–Trp–Ser–Tyr–Gly–Leu–Arg–Pro–Gly•NH_2

29, GnRH

H•Ala–Gly–Cys–Lys–Asn–Phe–Phe–Trp–Lys–Thr–Phe–Thr–Ser–Cys•OH

30, SRIF

pGlu–His–Pro•NH_2

31, TRH

H•Tyr–Ala–Asp–Ala–Ile–Phe–Thr–Asn–Ser–Tyr–Arg–Lys–Val–Leu–Gly–Gln–Leu–
–Ser–Ala–Arg–Lys–Leu–Leu–Gln–Asp–Ile–Met–Ser–Arg–Gln–Gln–Gly–Glu–Ser–
Asn–Gln–Glu–Arg–Gly–Ala–Arg–Ala–Arg–Leu•NH_2

32, GHRF

H•Ser–Gln–Glu–Pro–Pro–Ile–Ser–Leu–Asp–Leu–Thr–Phe–His–Leu–Leu–Arg–
–Glu–Val–Leu–Glu–Met–Thr–Lys–Ala–Asp–Gln–Leu–Ala–Gln–Gln–Ala–His–Asn–
–Ser–Arg–Lys–Leu–Leu–Asp–Ile–Ala•NH_2

33, CRF

A major development of the 1970s was the report in 1975 by *Hughes, Kosterlitz,* and their collaborators[124] of the isolation of two related pentapeptides, the now well-known enkephalins, Met-enkephalin (**34**) and Leu-enkephalin (**35**).

H•Tyr–Gly–Gly–Phe–Met•OH

34

H•Tyr–Gly–Gly–Phe–Leu•OH

35

Their discovery attracted much attention because the enkephalins are the long-sought endogenous ligands for the "morphine receptor". The presence of a tyrosine in the enkephalins prompted peptide chemists to do the "logical" thing, that is, to superimpose the phenolic hydroxyls of morphine and of the enkephalins. Unhappily, as is so often the case, the receptors lack the chemists' "insights"; that is, the overlap of the two acidic hydroxyls does not appear to explain why morphine and the enkephalins bind to the same receptor. The question still remains unanswered.

The hope of finding a nonaddicting analgesic led to an intensive effort to find enkephalin analogues that are more selective, bioavailable, and biostable. Indeed, Sandoz's FK 33-824[125] and Lilly's methkephamid[126] possess improved in vivo stability, but these early compounds were nonselective and caused side effects. Enkephalin-related research, notably by *Schiller*,[127] *Hruby*,[128] and their collaborators, employed the principles of conformational restriction in an effort to achieve receptor selectivity. Taken together, studies with classical opiates, and with synthetic enkephalin analogues, have demonstrated the existence of several subclasses of opiate receptors, but the physiological function of these receptors is not yet understood.

In Section 1, I referred to the subjective scope of this article. Suffice it to mention here that in his excellent 1980 review[129] of peptide and protein hormones, *Meienhofer* provides valuable information about such additional compounds as the endorphins, melanostatin, melanoliberin, Substance P, neurotensin, lipotropin, melanotropin, prolactin, growth hormone, parathyrin, calcitonin, thymic factors, glucagon, gastric inhibitory polypeptides, vasointestinal polypeptides, motilin, the placental hormones, relaxin, angiotensin, the kinins, and the growth factors. A more recent review was provided by *Schmidt*.[123] I cite these here to provide a better sense of the ever-expanding scope of peptide research.

As pointed out by *Reichlin*,[237] SRIF (**30**) is a major regulatory peptide with an extraordinary range of actions. A possible clinical application is acromegaly. Another was suggested by an early observation at the Karolinska Institute by *Luft* et al. that growth hormone (GH) may play a permissive role in the development of retinopathy in diabetes. Later, *Unger* pointed out that inappropriately high levels of glucagon may contribute to the complications of diabetes.[130] Because **30** suppresses both glucagon and GH release, I sought to discover an analogue of SRIF with a half-life suitable for the evaluation of such an agent in the treatment of juvenile diabetes. This was not possible with the short-lived **30**.

Veber and his collaborators approached this problem by seeking to gain insight into the conformation of **30** at its receptor. Building on the observation by *Rivier* et al.[131] that an analogue of somatostatin in which Trp^8 is replaced by D-Trp is significantly more potent than the hormone, and on *Ramachandran*'s[132] theoretical studies, suggesting that D-amino acids in the $i+1$ position stabilize β-turns, *Veber* et al.[133] proposed a model wherein Trp occupies an $i+1$ position (**36**, Fig. 5). This model resembled in several respects the solution conformation of SRIF that had been proposed earlier by *Holladay* and Puett,[134] but differed from it in other details, in that the Merck model suggested that the side chains of Asn^5 and Thr^{12}, as well as those of Phe^6 and Phe^{11}, are within bonding distance. In a systematic approach, these proposed relationships were then tested via the design, synthesis, and biological testing of relevant bicyclic compounds in which cystine bridges replaced Asn^5/Thr^{12} or Phe^6/Phe^{11}. An even greater conformational constraint was incorporated into a third bicyclic compound, **37**.

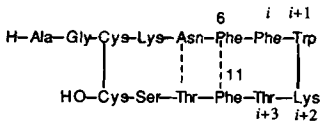

36

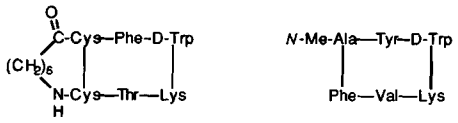

37

38

Fig. 5. The conformation proposed [133] for **30** at its receptor includes a β-turn, shown in **36**. This turn is supported by the fact that Asn^5/Thr^{12} or Phe^6/Phe^{11} may be replaced by cystine bridges, indicated by the dotted lines. The most compact bicyclic analogue is **37**. The correctness of the model is convincingly supported by the high activity of the cyclic hexapeptide **38**.

That high activity was retained in all three bicyclic structures strongly supported the proposed model. This led ultimately to the design and synthesis by *Freidinger*, *Veber*, *Nutt*, *Hirschmann* et al.[135] of the cyclic hexapeptide **38**, which contains only 2 of the 14 amino acids found in **30** but which is nevertheless 50 to 100 times more potent than the hormone. That the replacement of Phe^6 and Phe^{11} by a cystine bridge in **30** resulted in an analogue more potent than SRIF is of interest because *Rivier* and *Vale* had shown that replacement of either Phe^6 or Phe^{11} led to the loss of 97–99% of activity. Taken together, these paradoxical findings suggested that the two phenyalanines may stabilize the β-turn via a "herringbone" stacking of two phenyl rings. Presumably, the β-turn that is stabilized in SRIF by Phe^6 and Phe^{11} is stabilized by the cystine bridge of **37**. Clinical trials with **38** were terminated because, after short-term administration to humans, steatorrhea (fat malabsorption) was observed. In addition, when the drug was given to patients at bedtime, the insulin requirements the following morning were not lowered as much as had been hoped. This account reminds us that in drug discovery it is often easier to achieve scientific success, including encouraging results in model animal experiments, than to prevail in the clinic. On the other hand, *Bauer* et al.[136a,b] at Sandoz designed and synthesized octreotide (**39**)[136c], a cyclic octapeptide. The Swiss investigators found that the initial steatorrhea disappeared on continued administration of **39**. Octreotide was approved by the FDA for treatment of acromegalics and for use in patients with metastatic carcinoid and vasoactive intestinal-peptide-secreting tumors.

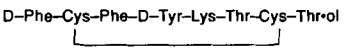

39

3.4. Peptidomimetics

A remarkable achievement in medicinal chemistry was the work by *Evans*, *Anderson*, *Bock*, *Freidinger*, *Veber*, and their collaborators[137] which led to the design and synthesis of

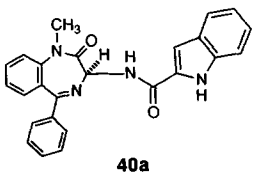

40a

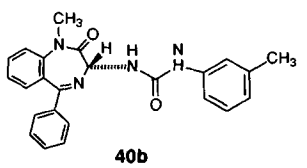

40b

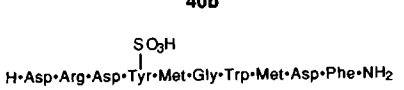

41

40a, a selective, potent, orally effective, peptidomimetic antagonist of the peptide hormone cholecystokinin (CCK, shown as the highly active decapeptide **41**).

Building on an astute analysis[137b] of the structure of the cholecystokinin antagonist and fungal screening lead asperlicin (**42**),[137c] these workers were successful in improving on its properties. They reasoned that a structure combining the elements of diazepam with D-tryptophan might bind to the CCK receptor. Given the similarities between the structures of CCK and gastrin (**43**), it is pleasing that they were subsequently able to design and synthesize selective gastrin antagonists as well,[138] typified by **40b**. It appears to be an important and generally valid concept that if two distinct hormones or neurotransmitters have structural similarities, their receptors are also likely to resemble each other (see also Section 2.3).

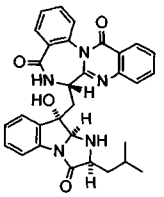

42

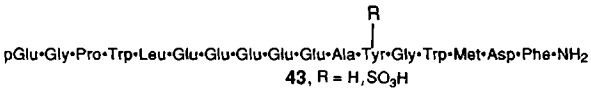

43, R = H, SO_3H

The discovery of asperlicin (**42**) falls into the realm of one of the most active areas of current peptide research, peptidomimetics. Peptidomimetic research owes its impetus to the desire to discover nonpeptides that bind to peptide receptors, but which have better bioavailability, biostability, and possibly greater selectivity than endogenous or synthetic peptide ligands.

Discovery of peptidomimetics falls into one of two broad categories. They may be discovered either via broad screening of chemical sample collections, microbial broths, fungal metabolites, etc., or via design. Peptidomimetics discovered by screening include the above-mentioned fungal product, asperlicin (**42**), and compounds from chemical sample collections such as the 1-benzylimidazoles, typified by S-8308 (**44**),

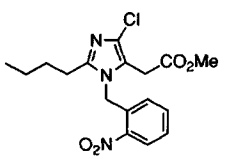

44

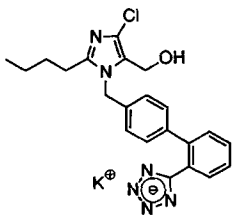

45

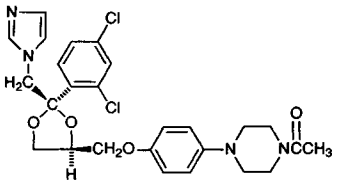

46

reported by *Furukawa* et al.[139] in Japan to be an angiotensin-II antagonist. At du Pont, *Chiu, Duncia, Timmermans et al.*,[140] in a series of important medicinal chemical studies, explored this peptidomimetic screening lead and were able to achieve increased potency (IC_{50} in the nM range) without loss of specificity. (The IC_{50} value denotes the concentration of an antagonist at which the maximal effect of the agonist is reduced by 50%.) DuP 753 (**45**), now in clinical trial, is orally active and devoid of any agonistic activity. It will be interesting to learn the clinical effects of renin inhibitors and of angiotensin II antagonists (see Fig. 6, Section 4.2) and to compare them with those of the established angiotensin-converting enzyme (ACE) inhibitors.

Another example of a screening lead is the antifungal drug ketoconazole (**46**), which was reported by *Biswanath* et al.[141] to be a GnRH antagonist. Compounds **44** and **45** are devoid of any amide bond, and **46** contains but one. All are orally bioavailable. The number of such nonpeptide antagonists of peptide hormones/neurotransmitters is steadily increasing.

In designing peptidomimetics, many laboratories have investigated the replacement of one amide bond at a time by such amide look-alikes as the ketomethylene isosteres, amines, ethylene bonds, α-difluoro ketones, cyclopropane isosteres, and many others. Stabilization of bioactive conformations via cyclization[97, 142] can also fall into the category of amide bond modification. The isostere approach has indeed succeeded in generating compounds with significantly greater biostability. Notable contributions have been made by *Barany, Bradbury, Coy, Goodman, Hoover, Martin, Morgan, Nagel, Rich, Rodriguez, Rosen, Sato, Spatola, Szelke, Thorsett, Wyvratt,* and others. *Spatola* has reviewed this field.[143] The isosteric replacement approach has generally not allowed one to predict which particular peptide bond might be replaceable by what mimetic as one goes from one peptide to the next. Few active compounds with more than two amide replacements have been reported.

A complementary approach involves the design of new scaffolding. Thus, *Nagai* and *Sato* described the synthesis of a bicyclic dipeptide derivative, **47**, mimicking the *i* and *i* + 1 positions of a β-turn, without including side chains at these positions. Compounds **47**–**52** do, however, contain handles for incorporation of the β-turn mimics into antiparallel β-pleated sheets. *Feigel*[144a] used the rigid tricycle **48** as well as the biphenyl derivative **49** to simulate a β-turn, again with-

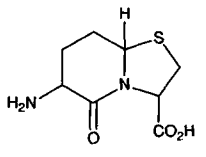

47

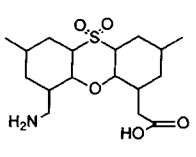

48

out incorporation of side chains. Similarly, *Kemp* et al.[145] described the synthesis of mimetic **50**, *Olson* et al.[146] of **51**, and *Kahn* et al.[147] of **52**. Both **51** and **52** incorporate a phenyl side chain.

Nicolaou, Hirschmann et al.[148] reported the *design* of a peptidomimetic, **53**, in which a β-D-glucose scaffolding re-

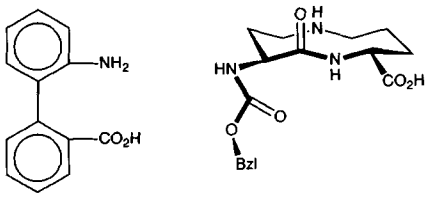

49

50

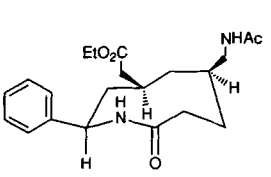

51

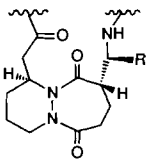

52

placed a β-turn and which incorporates the three critical side chains (i, $i+1$, and $i+2$) of the β-turn of a highly active cyclic hexapeptide analogue (**38**) of SRIF. Compound **53** was found by *Reisine* and *Raynor*[148] to bind to an endocrine (pituitary) SRIF receptor with an IC_{50} of 1 μM. However, **53** does not provide handles for the incorporation of the β-turn mimetic into a pleated sheet. Conceptually, the design of **53** resembles that of **54**, reported at about the same time by *Olson* et al.[149a] at Hoffmann-La Roche (Nutley), who at-

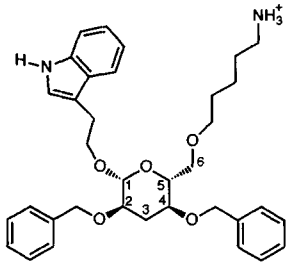

53

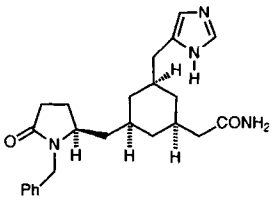

54

tached the side chains of the tripeptide thyrotropin-releasing hormone (TRH) to a cyclohexane scaffolding. The Roche compound is devoid of endocrine activity, but it exhibits oral activity in animal models of cognitive dysfunction. Consistent with these results, **54** bound to the low-affinity TRH receptors in the CNS but not to the high-affinity *endocrine* receptors of the pituitary brain stem.[149b]

Throughout the past 40 years, both biologists and organic chemists contributed to the biomedical sciences not by only advancing their respective fields of research but also by interacting with each other. For example, the structure determination and the total syntheses of the steroid and peptide hormones could not have been achieved without the prior isolation of these molecules, which was often guided by *biological* assays. Thus, biologists have prepared the ground for some of the great achievements in natural product synthesis by chemists such as *Corey*, *Danishefsky*, *du Vigneaud*, *Eschenmoser*, *W. S. Johnson*, *Kishi*, *Masamune*, *Stork*, and *Woodward*. These chemists, in turn, through their profound impact on synthetic methods and structural thinking, have helped to set the stage for many of the medicinal chemical achievements mentioned in this article. The award of the Nobel Prize to *Corey* in 1990[150] provides satisfying recognition of the importance of chemical methodology and synthesis to, inter alia, the biomedical sciences.

The spectacular, technological-intensive achievements of the recent past should not cause us to forget the extraordinary accomplishments of earlier workers, who solved problems of great complexity without access to modern techniques. Many examples may be found in *Fruton's* essays describing the interplay of chemistry and biology between 1800 and 1950.[151] Consider, for example, the elucidation of the molecular basis of sickle-cell anemia. As early as 1910, *James B. Herrick*[152] had surmised some connection between this disease and a peculiar, elongated form of red blood cells. In 1949, *Linus Pauling*[153] described a difference in electrophoretic mobilities between normal and sickle-cell hemoglobin and suggested a difference in ionizable groups as the cause. By 1957, *V. M. Ingram*[154] had found the molecular explanation by comparing trypsin digests of normal and abnormal hemoglobin: out of nearly 300 amino acids, one glutamic acid residue is replaced by a valine, a discovery well ahead of its time.

4. Drug Discovery in the Golden Age of Biology

It is desirable to define the word "drug" as used herein. Activity in relevant in vitro and in vivo assays does not mean that a compound is a drug. A drug is a substance approved by a regulatory agency in a medically sophisticated country. Many a promising compound has failed in safety studies, or in the clinic, because of poor bioavailability, rapid metabolism, species differences, and so forth. Discovering an active compound is relatively easy, discovering an important new drug remains unbelievably difficult.

The exciting recent developments in receptor research to be discussed below were made possible by two major discoveries that, in 1953, ushered in the modern era of biology. Of foremost significance, it was the year in which *James D. Watson* and *Francis Crick* proposed the double-helical structure of DNA and suggested that the sequence of nucleotide units in DNA carries encoded genetic information. It was also the year in which *Frederick Sanger* announced the structure of insulin. Taken together, these two discoveries suggested[155] that there is a connection between nucleotide and peptide sequences. These discoveries led within a decade to our understanding of the genetic code words that determine the amino acid sequence of proteins. Thus, the discovery of the double-helical structure of DNA became a revolutionary event in biology, with a profound impact on the vitality of all biomedical research.

It is difficult to overstate the impact of the double helix on the biomedical sciences. The dynamics between molecular biology and chemistry may be summarized rather simply: the discovery of the double helix was principally an accomplishment of the physical sciences. The roles played by X-ray crystallography, by chemical analyses (which provided information about the ratios of the building blocks of DNA), and by the chemical concept of complementarity are well known. Biochemists had to play a further role before biotechnology could come into its own. They discovered many

of the enzymes now taken for granted in the practice of genetic engineering, such as restriction endonucleases, ligases, polymerases, transcriptases, and reverse transcriptases. Similarly, chemists provided the techniques for the microsequencing of peptides and proteins and for the syntheses of nucleic acids. These operations are all taken for granted today. Having said all this, I hasten to add that molecular biologists are well on the road to repaying the biologically oriented chemists for their services, in that medicinal chemists are only beginning to build on the opportunities generated by molecular biology. The ability of biotechnology to facilitate the discovery and synthesis of proteins such as receptors and receptor subclasses can be cited as an illustration.

4.1. Complementarity and Rational Drug Design

The term *complementarity*, meaning molecular recognition, has already been used twice in this article. As *Arnett, Harvey,* and *Rose*[156] pointed out recently, "... molecular recognition has become one of the most evocative buzz terms in the chemistry of the late 1980s, with enzymes as the model of perfection for catalytic efficiency and specificity." They go on to list enzyme mimetic systems such as *Cram*'s crown ethers, *Lehn*'s cryptands, *Breslow*'s cyclodextrins, and *Rebek*'s convergent cleft molecules as designed artificial receptor sites. Simply put, molecular recognition is what biochemistry and bioorganic chemistry are all about. Therefore, it seems to me more noteworthy when molecular recognition is not involved, than when it is. There is even reason to expect that in the not-too-distant future the concept of complementarity will allow one to predict from the analysis of sequence data made possible by the polymerase chain reaction that a certain gene may be regulated by a given protein.

Another popular, and possibly overworked, buzzword is *rational drug design. Patchett* has drawn a useful distinction between rational drug discovery and rational drug design. Screening, often thought of as the antithesis of the rational approach, continues to play a very productive role in drug *discovery*, as is repeatedly illustrated throughout this review. On the other hand, the identification of the target enzymes, receptors, transport proteins, etc., for such screening has become much more mechanism-based, more sophisticated, and thus more "rational". In addition, the introduction of receptor displacement assays has dramatically increased the scope of screening. Mixtures of microbial and fungal products can be screened today as readily for central nervous system (CNS) or anti-inflammatory activity as they could be used forty years ago for the sole purpose of discovering new antibiotics. Another recent development with great potential stems from the ability of chemists and of molecular biologists readily to generate large libraries of polypeptides and of polynucleotides. These libraries can be quickly evaluated by sophisticated screening techniques. It remains the task of medicinal chemists to transform screening leads into candidates for clinical trial. Today they benefit enormously from computer-based molecular modeling in these endeavors.

Examples of rational drug discovery are typified by *D. Wood*'s observation in 1940 that the inhibition of bacterial growth by sulfonamide is competitively overcome by *p*-aminobenzoic acid. This observation established the latter as a growth factor and led to the synthesis of many structurally related antimetabolites. The synthesis in 1947 of aminopterin (4-aminopteroylglutamic acid) by *Seeger, Smith,* and *Hultquist* as an antimetabolite of folic acid, the structure of which had just been elucidated, serves as another example of rational drug discovery. Aminopterin was later found effective in inhibiting the growth of certain tumors. The synthesis of methyldopa, one of the most widely prescribed antihypertensives during the past 40 years, exemplifies both a reasoned choice of a synthetic target by *Pfister* and *Stein* and of rational drug testing by *Udenfriend* and *Sjoerdsma* at the NIH. The discovery of the thiazide diuretics by *Beyer, Novello,* and *Sprague*, a milestone in the treatment of hypertension, is another notable illustration. Many of the analogues of steroid and peptide hormones cited above serve as additional examples.

Rational drug *design*, on the other hand, implies that an enzyme or other receptor target has been identified in sufficient structural or mechanistic detail that a chemist can use such information to perfect a screening lead or to design de novo molecules that uniquely bind to and inhibit (or activate) the target protein. Such design from first principles, based solely on structural information about the macromolecule, is today a goal for the future, not as yet a reality. Therefore, research directors in the pharmaceutical industry with responsibility for keeping "pipelines" filled with product candidates, still do not commit a significant share of their resources to de novo design.

4.2. Enzyme Inhibitors

Enzyme inhibitors represent the area of medicinal chemistry where drug discovery has approached rational design most successfully. Research in laboratories such as those of *Abeles, Benkovic, Bloch, Bruice, Cleland, Fersht, Jencks, Knowles, Rose, Santi, Walsh,* and *Westheimer* has greatly increased our understanding of enzyme mechanisms. Central is the concept that an enzyme is able to enhance reaction rates by lowering the energy of the transition state of the reaction that it catalyzes. Enzyme-inhibitor design has been more successful than hormone-antagonist design because the former can take advantage of the transition-state analogue (TSA) concept. *Pauling* described the application of the TSA concept to enzyme-inhibitor design more than 50 years ago:[157]

> This picture of the nature of enzymes may well make us optimistic about the future of chemotherapeutics, for it predicts that for every enzyme... it would be possible to find an inhibiting molecule that is more closely complementary in structure to the enzyme than is the substrate itself, and which would accordingly be an effective inhibitor. The picture even presents us with ideas as to the nature of substances that would be effective inhibitors—they should resemble the activated complex.

Wolfenden, recognizing the importance of *Pauling*'s teachings, successfully explored its promise. *Byers* and *Wolfenden* pointed out[158] that "unusual potency is expected of inhibitors bearing a structural resemblance to chemically acti-

vated intermediates in catalysis or incorporating the binding characteristics of several reactants in a single inhibitor molecule." He designed and synthesized (*R*)-2-benzyl-3-carboxypropionic acid, which proved to be a potent inhibitor of carboxypeptidase A. He concluded that the inhibitor resembles the collected substrates for the reverse reaction, that is, the collected products. Taken together, the concepts of collected substrates, collected products, and transition-state analogues have proven to be exceptionally useful in the discovery of potent enzyme inhibitors. Examples of potent TSA inhibitors of enzymes include the fermentation product pepstatin (see below) and phosphorus-containing inhibitors described by several laboratories, including those of *Bartlett, Patchett* and *Thorsett, Portoghese, Petrillo,* and *Walsh.*

The design of the angiotensin-converting enzyme (ACE) inhibitors captopril (**55**) and enalapril (**56**) represents the most notable contribution to date of the Pauling–Wolfenden concepts to the practice of medicine. These ACE inhibitors

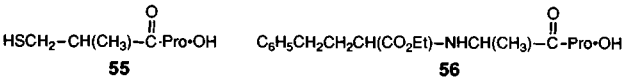

have revolutionized the treatment of hypertension and congestive heart failure. The achievements that they represent climaxed a series of worldwide investigations over a period of about 30 years, which included the isolation in the United States of the biologically inactive decapeptide angiotensin I (Fig. 6) and of the potent pressor substance angiotensin II, an octapeptide. It was shown[159] that a mammalian enzyme can convert angiotensin I to angiotensin II (Fig. 6).

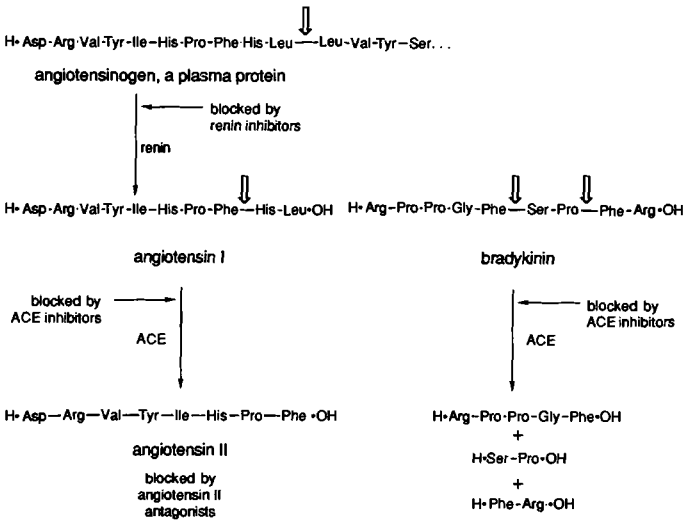

Fig. 6. ACE inhibitors, including the "bradykinin potentiating peptides", block formation of the pressor substance angiotensin II. ACE inhibitors also block the metabolism of bradykinin, a hypotensive peptide. The double arrow denotes site of enzymatic cleavage. Renin inhibitors block the formation of angiotensin I and thus, indirectly, of angiotensin II.

Later, scientists in Brazil discovered a series of peptides in snake venom, which potentiated the ability of a plasma nonapeptide, bradykinin, to lower blood pressure by inhibiting kininase I.[238] The seemingly unrelated studies in the United States and Brazil were linked when biochemists at Tulane University and the Albert Einstein College of Medicine purified and characterized ACE, and when studies at American, Brazilian, and British universities demonstrated that ACE is identical with kininase II and that it both inactivates (cleaves) the hypotensive bradykinin, and cleaves angiotensin I to give the hypertensive angiotensin II (Fig. 6).

Early studies by *Skeggs* had suggested that ACE is a metalloprotease. *Ferreira* and *Rocha Silva*, as well as *Erdös* and *Whales*, had therefore employed sulfhydryl compounds to potentiate bradykinin. In an important advance, *Lipscomb* and co-workers were able to identify precisely the groups of the above-mentioned carboxypeptidase A which interact directly with zinc(II). Astutely recognizing the relevance of *Wolfenden*'s carboxypeptidase A inhibitor to the design of an inhibitor of the carboxydipeptidase ACE, and being aware of the snake venom inhibitors with their C-terminal prolines, *Ondetti, Cushman* et al.[160] at Squibb designed and synthesized captopril (**55**) and demonstrated its ability to lower blood pressure in animals. It was the beginning of a new era for the treatment of hypertension. Side effects seen in a small number of patients after administration of captopril, such as development of a rash and loss of taste, were reminiscent of side effects seen with penicillamine and made it appear reasonable to attribute these side effects to the mercapto groups common to **55** and penicillamine. A worldwide effort ensued to find a mercaptomimetic that would retain the ability of the mercapto group to bind zinc effectively without loss of oral bioavailability. No such mimetic has been found. However, *Patchett* et al.[161] ingeniously finessed the problem. They accepted partial loss of potency (three orders of magnitude) by replacing sulfhydryl with carboxyl, but gained potency (three orders of magnitude) by introducing phenethyl, which presumably recognizes the S_1 binding site. Monoesterification led to the prodrug **56**, which exhibits good bioavailability.

All in all, the ACE story is a beautiful illustration of successful interaction on an international scale between chemists, biochemists, X-ray crystallographers, and biologists in both academic and industrial environments. It is one of innumerable examples of the critical need for high quality, long-term basic research by individual academic investigators and for industry's ability, practicing research of equal excellence, to convert such basic research into products of societal value.

The contrasting clinical status of renin inhibitors is instructive. Renin is a mammalian aspartate protease that cleaves the protein angiotensinogen to generate angiotensin I (Fig. 6). As expected, renin inhibitors are effective in lowering blood pressure. In both academia and industry, the quality of the search for renin inhibitors has been superb. Of fundamental importance in this research was the recognition, which occurred almost concurrently in the laboratories of *Marciniszyn*,[162] *Marshall*,[163] and *Rich*,[164] that the statine residue, (3*S*,4*S*)-4-amino-3-hydroxy-6-methylheptanoic acid (Sta), in inhibitors of mammalian aspartic proteases such as pepstatin, functions as a transition-state bioisostere. *Boger* et al.[165] recognized that the statine residue replaces a dipeptide unit. Medicinal chemists in many laboratories have succeeded in designing and synthesizing a host of potent inhibitors of *human* renin based on

this understanding, yet to date there is no approved renin inhibitor, because the dual problems of oral bioavailability and adequate biological half-life have not been solved. This reminds us that bioavailability can remain a formidable obstacle to drug discovery even today.

The design of mechanism-based enzyme inhibitors,[166] pioneered by *Bloch*, *Abeles*, *Rando*, and *Walsh*, represents an intellectually highly satisfying achievement. Generally, but not necessarily, they lead to covalent bond formation. Two such inhibitors have recently become drugs, that is, approved for use in therapy. One is vigabatim (**57**), a selective, enzyme-activated, irreversible inhibitor of γ-aminobutyric acid (GABA) transaminase, for treatment of epilepsy. The other is ornidyl (**58**), which is used for the treatment of sleep-

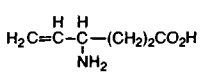

57

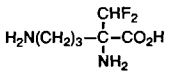

58

ing sickness. It acts by blocking enzymes essential for the proliferation of trypanosome peptides transmitted by tsetse flies. In addition, a number of drugs have been determined retrospectively to belong in the category of mechanism-based enzyme inhibitors.[166]

5. What Has Chemistry Done for Us Lately?

I shall restrict myself to first-generation compounds discovered during the past 20 years that are widely considered to represent milestones in therapy.

(1) I have already mentioned the discovery of captopril (**55**) (Section 4.2) and that its antihypertensive effect is mediated via a novel biochemical mechanism. Captopril provides effective treatment for a significantly broader patient population than prior antihypertensive therapy, suggesting that it treats a basic pathophysiology. In addition, its relative freedom from side effects, as well as its potential to reduce the incidence of strokes and the recurrence of heart attacks, makes its discovery an outstanding advance in medicine.

(2) Of equal importance was the isolation and the chemical and biochemical characterization of the fungal metabolite lovastatin (**18a**) by *Alberts*, *Patchett*, *Monaghan*, *Albers-Schonberg* et al.[31a] It is an inhibitor of HMG-CoA reductase and therefore blocks the conversion of 3-hydroxy-3-methylglutaryl coenzyme A (HMG-CoA) to mevalonate, the first committed intermediate in cholesterol biosynthesis. Importantly, it dramatically lowers the plasma levels of the cholesterol associated with the low-density lipoprotein (LDL), the principal contributor to atherosclerosis, the underlying condition responsible for coronary heart disease. A 1% decrease in the LDL cholesterol levels decreases the risk of coronary heart disease by 2%. Lovastatin was the first such enzyme inhibitor to be approved by a sophisticated regulatory agency. It is interesting that *Brown*, *Goldstein* et al. were able to show that the mechanism of **18b** is indirect, in that it stimulates, at the transcription level, the synthesis of the LDL cholesterol receptors.[31b] Mevastatin (**18b**, compactin) had actually been described before **18a** by *Endo* et al.[167] at Sankyo, who had built on the same biochemical rationale. Mevastatin, however, had encountered problems in safety assessment, another reminder that the road from a potent compound that is active both in vitro and in vivo to an approved drug is a hazardous one.

(3) The discovery of cimetidine (**59**) for the safe treatment of duodenal and gastric ulcers culminated research carried out at SKF (UK), to discover compounds which would block the histamine receptor subtype (H_2) involved in gastric acid secretion. Its discovery by *Black*[168] and by *Ganellin*,[239] pharmacologist and chemist, respectively, followed the prototypes burimamide and metiamide, discovered earlier by the same team. Cimetidine greatly reduces ulcer-related morbidity, pain, and the need for expensive hospitalization. Cimetidine and second-generation compounds are thus of great benefit to both the patient and society. In 1988, *Black* was awarded a Nobel Prize for his role in the discovery of cimetidine and for his earlier discovery of the β-adrenergic blocking agent propranolol.

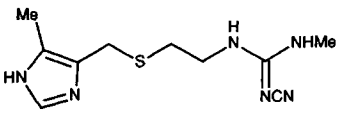

59

(4) Synthetic β-adrenergic blocking agents have long been established as cardiovascular drugs. The more recent discovery that one of them, timolol (**60**, blocadren),[169] synthesized by *B. K. Wasson* et al. at Merck (Canada), is a safe and effective agent for the topical treatment of glaucoma, represented another breakthrough in therapy. The compound has fulfilled its promise to revolutionize the management of open angle glaucoma because it can slow the progression of the disease.

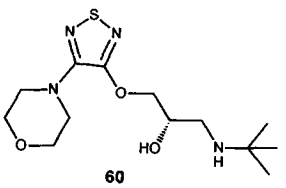

60

(5) The discovery of acyclovir (**61**), an effective antiherpes drug, by *H. J. Schaeffer*, *G. Elion* et al.[170a] at the Wellcome Research Laboratories (USA) provided a potent inhibitor of the replication of the herpes simplex virus. Acyclovir is a prodrug that is monophosphorylated at the primary alcohol, but only by the viral thymidine kinase, not by human kinases. The triphosphate derived from this monophosphate

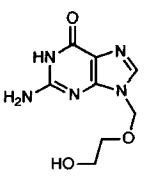

61

by host-cell enzymes inhibits the viral DNA polymerase more effectively than it inhibits the host polymerase. This twofold specificity apparently ensured a favorable T. I. The discovery of acyclovir built on the earlier antimetabolite research of *Elion* and *Hitchings*, which was recognized with the award of a Nobel Prize in 1988.[170b,c]

(6) The fungal metabolite cyclosporin (**62**)[171,172] has had a remarkable impact on the survival rates after organ and bone marrow transplants, because it greatly reduces the likelihood of near-term rejection induced by T cells. Isolated and chemically characterized by *Rüegger* et al. at Sandoz (Basel), this cyclic peptide has been adopted as the immunosuppressive agent of choice at a growing number of treatment centers worldwide.

Later, another more potent immunosuppressant, *Fujisawa*'s FK-506 (**63**), a 23-membered macrolide lactone, also discovered via the screening of fungal metabolites, was isolated and characterized by *Tanaka* et al.[173] Although it has not yet been approved for therapy by a regulatory agency, it is appropriate to discuss it here. Both **62** and **63** inhibit T-cell activation mediated by the T-cell receptor and, at the cellular level, inhibit remarkably similar steps in signal transduction.

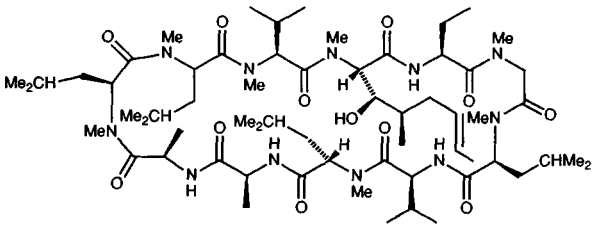

62

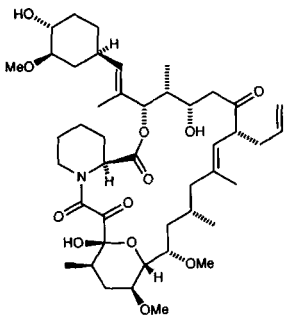

63

They hold promise for the treatment of a variety of diseases with an immunological etiology. Thus, an intensive effort is underway to find safer analogues and to identify biochemical mechanisms. Both immunosuppressants have been synthesized.[174,175] Cyclophilin has been shown[176] to be a receptor for cyclosporin. Cyclophilin was recognized to be identical to peptidyl-prolyl *cis-trans* isomerase by *Takahashi* et al.[177a] and by *G. Fischer* et al.[177b] *Fischer* et al. had also been the first[177c] to isolate that enzyme, which is now under investigation also by the groups of *Stein*,[178] *Schreiber*,[179] *Rich*,[181] and *Walsh*.[180] Through synthesis of cyclosporin analogues, *Rich*[181a] and also *Sigal* et al.[181b] have sought to determine the relevance of this receptor to the immunosuppressant activity of cyclosporin. Interestingly, an FK-506 binding protein called FKBP, under investigation by the groups of *Siekierka*,[182] *Schreiber*,[183a-c] and *Tropschug*,[184] is also a proline isomerase. Cyclosporin inhibits the isomerase activity of cyclophilin, and FK-506 that of FKBP. However, these inhibitory activities do not appear to be the full explanation of the immunosuppressant effects[181a,183a,c] of these compounds. Very recently, *Moore* et al.[240] and *Michnick* et al.[183d] have investigated the solution structure of FKBP and *Van Duyne* et al.[241] have succeeded in elucidating by X-ray crystallography the FKBP/FK-506 complex. The latter revealed a striking difference in conformation between FK-506 determined earlier[173] and bound FK-506. Very recently, *Schreiber* et al. have shown that cyclophilin and FKBP complexed with their respective ligands inhibit calcineurin. Taken together, these studies strikingly exemplify the ability of chemists to address problems of the greatest importance in biology and medicine.

(7) Mankind is also benefiting enormously from the discovery at Merck[185] of the avermectins in a broth produced by a culture of streptomyces originating from a Kitasato Institute actinomycete. They represent a family of compounds exhibiting a broad spectrum of potent antiparasitic properties. Chemically, they are related to the milbemycins discovered earlier in a search for pesticidal fermentation products at Sankyo. The Merck research involved fermentation and isolation, structure determination, parasitology, and synthetic organic chemistry. Under the leadership of *Chabala, M. H. Fischer,* and *Mrozik*, the medicinal chemistry program culminated in the further remarkable discovery that both the potency and the T. I. could be improved by the selective reduction of the single disubstituted, isolated *cis* double bond of the avermectins A/B to give the semisynthetic 22,23-dihydroavermectin B (**64**) containing some dihydroavermectin A. A mixture thereof, with a prescribed

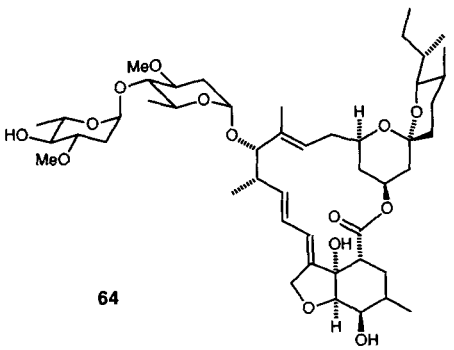

64

composition, is known as ivermectin.[185] The screening at Merck of a novel broth generated at the Kitasato Institute has thus led to molecules which are safe and effective not only against endoparasites such as roundworms, but also against ectoparasites such as ticks, lice, mites, and insects.

Best of all, in addition to their value in veterinary medicine, these compounds hold the exciting promise of eradicating river blindness, one of the most dreaded diseases in certain countries of the Third World. This latter fact alone should make every medicinal chemist feel proud of his profession, as should the fact that Merck & Co., Inc. is making the drug available to the Third World without charge.

Chemists, collaborating with biologists and physicians, have played a critical role in bringing about these breakthrough discoveries, either by isolation chemistry, by design and synthesis, or by contributing to the design of sophisticated screening assays and by analogue synthesis. These achievements of the last 20 years follow such earlier milestones as the discovery of the antibiotics, antiasthmatics, antidepressants, anti-Parkinson drugs, antipsychotics, antitumor drugs, anxiolytics, diuretics, steroids, peptides, and the nonsteroidal anti-inflammatory agents. Taken together, these discoveries represent a sustained record of service to the practice of medicine and to scientific progress.

6. Summary and Outlook

It is tempting to speculate about the future, although it is the unexpected discoveries that often have the greatest impact. Nevertheless, certain recent developments may foreshadow advances. I shall cite two examples to illustrate the potential of molecular biology to provide new opportunities for medicinal chemists to intervene in pathophysiology. Until recently we had no understanding at all about cancer at the molecular level. Discoveries[186] in the laboratories of *Weinberg* at MIT, *Scolnick* at the NIH, and later *Sigal, Gibbs*, and *Scolnick* at Merck have opened the door to new approaches to cancer therapy. These workers determined the amino acid sequences of ras proteins in human tumors and showed how such sequences differ from the sequences in the normal protein. They found, for example, that a mutation causing Gly^{12} to be replaced by Val^{12} in the p-21 protein generates a mutant with the capacity to transform normal colon cells into malignant ones. Since both Gly and Pro are α-helix breakers, conformational analysis predicted[187] that only Pro would fail to convert the normal ras gene into an active oncogene. Experimental results were in good agreement with this prediction, but X-ray crystallography revealed later that helix-breaking is not involved. It was found by biochemists that the p-21 proteins are monomeric G-proteins, enzymes which are known to bind guanine nucleotides and to hydrolyze GTP to GDP, especially in the presence of GAP.[186] In the oncogenic mutants, the ratio of bound GTP to bound GDP is greater than in the normal protein, either because of a slower rate of enzymatic hydrolysis of GTP by the transformed G-protein or because of an increased exchange of GDP by GTP.[188, 189] Either way, these defective molecular switches cause the transformed cells to be "turned on" to an inappropriate degree. It has not yet been possible to apply this new understanding, but several approaches can now be contemplated. In this context it is particularly interesting that the processing of ras proteins has recently been found to involve the addition of a farnesyl residue.[190] This post-translational event is proving to be of great importance generally for membrane association. In the case of the monomeric ras G-proteins discussed above, such farnesylation appears to be required before their transforming properties can come into play. *Reiss* et al.[191] have recently defined the sequence requirements for peptide recognition by rat brain $p21^{ras}$ protein transferase. Inhibition of the farnesylation reaction thus offers a further potential target for intervention. It remains to be determined whether this particular post-translational event can be inhibited selectively.

At the DNA/RNA level, the application of the so-called antisense technology[192, 193] and the related "triple helix" approach[194a] have great potential,[194b] but also pose a profound challenge to chemists. This approach to drug design seeks to prevent the expression of unwanted proteins, rather than to inhibit their actions. This is also true of the strategies to deliver oxidative cleaving agents selectively to the unwanted DNA sequence, typified by the work of *Dervan*.[195] *Hurley*[196] has recently reviewed other opportunities provided by DNA-associated drug targets, which are by no means restricted to cancer.

An equally spectacular example of new understanding at the molecular level made possible by biotechnology is the work of *Lefkowitz* and his co-workers and that of *Dixon, Sigal, Strader*, and their co-workers, who have rescued the adrenergic receptors from the status of a black box. The work with the β-adrenergic receptors (βARs) at Duke University and at Merck built on the earlier investigations into visual pigments and into the far-more-accessible bacteriorhodopsin, which mediates light-driven proton transport across the purple membrane from *Halobacterium halobium*. These studies have taken place over a 100-year period, but significant advances into the structures of these proteins occurred only since the 1970s when *Henderson* and *Unwin*[197] used electron microscopy to show that the protein in the purple membrane contains seven closely packed, α-helical segments that extend roughly perpendicular to the plane of the membrane and that the lipid bilayer fills the spaces around the protein segments. The structure of this membrane protein in atomic detail was recently reported by *Henderson* et al.[198] Studies by *Ovchinnikov*,[199] *Hargrave*,[200] *Khorana*,[201] *Crouch*,[202] *Nakanishi*,[203] and their co-workers, as well as investigations in other laboratories,[243] established that the pathway of visual excitation in vertebrate retina involves the protein opsin, which is linked through a Schiff base derived from a lysine side chain and the aldehyde of 11-*cis*-retinal (rhodopsin). The presence of the seven-helix motif in rhodopsin was inferred by *Hargrave* et al.[243] through hydrophobic matching and other physical measurements. A photon induces a conformational change in rhodopsin via isomerization of 11-*cis*- to 11-*trans*-retinal. This isomerization in the photoreceptor results in binding of the hetero-trimeric G-protein (G_t, t = transducing; see Fig. 7 and below), initiating a series of events that ultimately affect the intracellular levels of the second messenger, cyclic AMP (cAMP).

The cloning of the gene and cDNA for a mammalian β_2 AR enabled *Dixon, Sigal, Strader* et al.[204] to discern that the amino acid sequence predicted for the receptor had significant homology with bovine rhodopsin, and to suggest that, like rhodopsin, the β_2 AR possesses multiple membrane-spanning regions. Application of the concept of hydrophobic matching led to a proposed structure for the β_2 AR which thus also contains seven transmembrane α-helical segments composing a single peptide chain. In this proposed structure, the seven hydrophobic domains are again connected by short hydrophilic segments, forming extramembranous loops. These structural similarities suggested also functional similarities between rhodopsin and the β_2 AR; that is,

both are linked to their G-proteins (G_t and G_s, respectively), with a photon serving as the agonist for rhodopsin and adrenaline for the β_2 AR.

An impressive subsequent accomplishment, made possible by site-directed mutagenesis, was the identification by *Dixon, Sigal, Strader* et al.[205] of aspartate-113 in transmembrane helix 3 as the amine binding site for β-adrenergic agonists and antagonists.[205] Later on, it was shown[206] that hydrogen bonding between the *m*-hydroxyl of the catecholamine adrenaline with Ser^{204} of the receptor and the *p*-hydroxyl of adrenaline with Ser^{207}, both in helix 5, is required for the expression of agonism.

Lefkowitz et al.[207] have deduced the complete primary amino acid sequences of mammalian β_1 ARs and of α ARs. It should be remembered, however, that medicinal chemists had discovered selective ligands for ARs long before the amino acid sequences of the relevant receptors had become known. The cardioselective (β_1) adrenergic blocking agents atenolol and metoprolol, which have greater affinity for the cardiac (β_1) receptors than for the bronchial (β_2) receptors, are well-known examples. At present, the new knowledge about the sequences and probable structures of both the cardiac (β_1) and bronchial (β_2) β receptors, however satisfying, does not yet allow us to explain the selectivity of these adrenergic blocking drugs, let alone to design, for example, a new cardioselective β blocker or a selective β_2-receptor agonist. This represents a significant challenge for the future. On the other hand, the work by *Strader* et al.[206] allows one to speculate why β-adrenergic blocking agents such as propranolol, pronethalol, and atenolol are β-blockers devoid of the so-called "intrinsic sympathomimetic activity (ISA)", that is, of β-adrenergic agonism, whereas β-blockers such as pindolol, dichloroisoprenaline, and practolol do possess ISA. The latter contain heteroatoms that may be able to mimic one of the phenolic hydroxyls of adrenaline and may thus hydrogen-bond with a serine hydroxyl in helix 5. Admittedly, one would have to invoke alternative explanations, such as allosteric effects, to explain why compounds such as alprenolol exhibit ISA.

The β ARs are among the best-characterized members of a family of receptors which mediate their actions through signal transduction pathways involving guanine nucleotide regulatory proteins (G-proteins; Fig. 7). In a series of elegant studies, which built on *Rodbell*'s suggestions of the transducer concept,[208] *A. G. Gilman*[209] and *Stryer* and *Bourne*[210] showed that receptors do not directly activate the effector enzymes or ion channels, but that G-proteins act as transducers of information across cell membranes, by coupling receptors with effectors inside the cell. These effectors thus respond to the original stimulation of the receptors (R) by hormones, neurotransmitters, and other agonists (H) via the intervention of the hetero-trimeric G-proteins. For example, after adrenaline binds to a β-adrenergic receptor, the conformational change thereby induced causes the H·R complex to become associated with the appropriate G·GDP complex. In the case of the β receptor, G is the so-called stimulatory G-protein (G_s). This interaction with the receptor causes GTP to replace GDP on the H·G·G_s complex, generating H·R·G_s·GTP. Formation of the latter complex triggers two further events. First, the G_s loses its affinity for H·R, regenerating free hormone and unoccupied receptor, and, second,

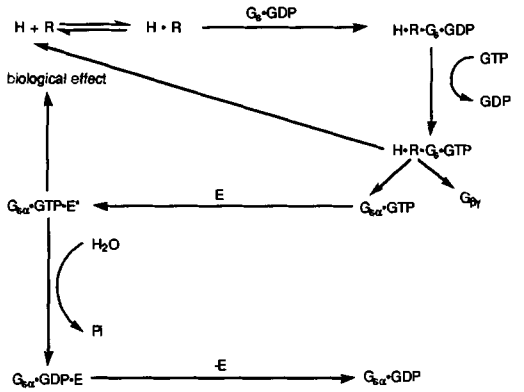

Fig. 7. The signal transduction pathway whereby stimulated membrane receptors are coupled to intracellular receptors via hetero-trimeric G-proteins, composed of α,β, and, γ subunits. For the β-adrenergic receptor, the relevant G-protein is the stimulatory G-protein G_s, and the enzyme (E) is adenylate cyclase. For the visual receptor rhodopsin, the G protein is transducin (G_t), and E is phosphodiesterase. E* denotes an activated enzyme, R a receptor, and H a hormone, neurotransmitter, or other agonist.

the β,γ subunits of the G_s·GTP complex dissociate from $G_{s\alpha}$·GTP.

It is this remaining complex between GTP and the α subunit of G_s that now binds and activates the relevant enzyme (E), which for the β ARs is adenylate cyclase, the enzyme that generates the "second messenger" cAMP. At this point another control mechanism intervenes. The $G_{s\alpha}$ protein is also an enzyme, irreversibly hydrolyzing GTP to GDP. The resulting $G_{s\alpha}$·GDP lacks affinity for the enzyme E, which is thus deactivated. As pointed out by *Jencks*,[114a] the system works because an effective agonist is complementary to the active conformation of the receptor, thus pulling the system forward. By analogy the system can be "cooled off" because the enzyme E is not complementary to the $G_{s\alpha}$ when the latter is bound to GDP. It has recently been shown[211] that farnesylation of γ subunits of G-proteins is required for GTP binding. Such farnesylation, and the opportunity for its selective inhibition was already mentioned above as a goal for the medicinal chemist in the case of the monomeric ras p21 protein.

In the case of the visual pigments, the G-protein is G_t (transducin), and the enzyme that it activates is a phosphodiesterase rather than adenylate cyclase. As pointed out by *Applebury* and *Hargrave*, nature has thus capitalized on a general biochemical mechanism for control of second messengers in the cytoplasm of cells. The diversity of the known ligands for cloned G-protein-linked receptors has been found to be remarkable.

These advances in our molecular understanding of the G-protein-linked receptors—typified above by the β_2-adrenergic receptor, like the advances in our understanding of the ras oncogenes—were made possible by biotechnology. In neither case has the medicinal chemist as yet used this information to design a new drug, but the opportunities are there. Specificity may well prove to be the critical requirement for success.

Rational drug design (in contrast to rational drug discovery) will have come fully into its own when the structural information about enzymes or other receptors permits the discovery of a new drug that would not have been possible without such structural information about the macro-

molecule. Analysis of X-ray crystal structures, in combination with other physical measurements, molecular modeling, and chemical intuition, will play a major role in this process in the years ahead. Biotechnology greatly increases the likelihood that the relevant crystalline protein will be available to the crystallographer at the right time, helping to connect the biochemistry and structural biology of a system. The initial success stories may well come from X-ray information about enzymes with a bound inhibitor. Promising advances include inhibitors of the enzyme dihydrofolate reductase.[212] The ability to make correct predictions continues to be the critical measure of success. Indeed, the design by *Baldwin, Navia, Anderson* et al.[213] of MK-927, a novel, topically active, carbonic anhydrase inhibitor for the treatment of glaucoma, represents an important step in that direction.

One well-recognized problem in such endeavors was cited by *Beddell, Goodford* et al.[214] in their search for substituted benzaldehydes designed to increase the oxygen affinity for human hemoglobin: "the structure of the receptor site is not rigid and it is often difficult to take account of the flexibility of both the designed ligands and the receptor site itself in predicting the properties of the ligand-receptor complex." The problem is compounded by the fact that the conformation of a ligand on its receptor may not correspond to a minimum-energy conformation of the ligand in solution. This was the situation reported by *Baldwin, Navia, Anderson* et al.[213] for their most potent inhibitor of carbonic anhydrase and for its optical antipode. Thus, the conformation of the receptor–ligand complex will minimize the energy of the complex, but not necessarily that of its components. This analysis suggests that it will, at times, prove undesirable to impose a conformational constraint on the solution minimum-energy conformation or on the conformation revealed by X-ray analysis of the small molecule. For example,[215] a recent X-ray study of an isomorphic, but completely inactive insulin analogue, miniproinsulin,[230] has led to the conclusion that insulin crystals can represent inactive conformers. Thus, 2 D NMR is emerging as a valuable, complementary technique to X-ray crystallography. Yet imposing a constraint on a minimum-energy conformation of a small molecule has often proved fruitful. In a recent review, *Schiller*[216] addresses some of these and related problems. *Knowles*[217] concluded from his studies with the enzyme triosephosphate isomerase that there are important "elements of precision" beyond the well-known[157, 218] fit of the transition state into the active site of an enzyme. For the interactions of hormones/neurotransmitters, such elements of precision are suggested by the finding of *Strader* et al.[219] that the replacement of Asp^{113} of the β_2-adrenergic receptor by Glu results in a mutant receptor which now recognizes several known β-adrenergic antagonists (β-blockers) as partial agonists.

An early example of chemical site-directed mutagenesis[220] was described by *Polger* and *Bender* in 1966, who converted the enzyme subtilisin into thiosubtilisin, containing a thiol group rather than a hydroxyl group as the essential nucleophile of the active site. This protein still hydrolyzes nitrophenyl acetate but fails to react with any of the classical substrates of subtilisin.[220, 221] These results can serve as a reminder that a de novo design might be creative to the point of being inspired, and yet miss the mark.

These difficulties notwithstanding, there is no doubt that the information provided by X-ray crystallography about receptor–ligand complexes is already proving invaluable to drug discovery. The same can be said about site-directed mutagenesis. One has every reason to expect that the combination of these techniques will prove to be synergistic. The studies of the interaction of human GH with its receptor by *Cunningham, Wells*, and their associates[222] at Genentech are of great current interest in this regard, since the atomic structure of the complex between GH and its binding protein (receptor) has just been solved.[223] It will be a major event when the information provided by X-ray crystallography and 2 D NMR, combined with site-directed mutagenesis, will permit, for example, the de novo design of an allosteric GH mimetic, or a novel inhibitor of FKBP, or an erythropoietin (EPO) mimetic. Such achievements would indeed represent rational drug design.

One can have the greatest expectations for the discoveries in biomedical science that will be made during the last decade of this century and during the 21st century. The challenges are formidable, and too many to enumerate, but they include autoimmune diseases, mental health, cancer, geriatric medicine, diabetes, and viral infections. And no challenge is greater than that posed by the clear and present danger of AIDS, where a formidable, multipronged attack is underway. For the time being the reverse transcriptase inhibitor 3′-azido-3′-deoxythymidine (AZT)[170d, 224] represents a welcome first step.

The staple of basic research discoveries that are waiting to be applied to the solution of these problems is impressive. In addition to the examples of advances in our understanding of cell signaling already mentioned, the elegant research of the phosphatidylinositol system, notably by the laboratories of *Berridge*[225] and *Irvine*[226] in Cambridge (UK) with IP_3 (based on observations made by *Mitchell*[227]) and by *Nishizuka*'s[228] laboratory in Japan with protein kinase C, provide opportunities for the medicinal chemist.

Small molecules are certain to continue to play a very important role among the drugs of the future. The new class of therapeutic small molecules might include, for example, compounds of value in the treatment of asthma, such as inhibitors of enzymes involved in leukotriene synthesis and antagonists of the leukotrienes. Success with any such compounds would bring to fruition years of long-term basic research in academia and industry. Promising results are also being reported with compounds for the treatment of migraine and osteoporosis. Selective inhibitors of reverse transcription, of phospholipase A_2, and of enzymes regulating lymphokine biosynthesis are other promising active research areas. This is also true of compounds with the potential to regulate thrombosis and clot lysis.

On the other hand, biotechnology is also certain to continue to add macromolecules to the armamentarium of the physician. As we approach the 21st century, there is the expectation of a growing list of proteins for use in therapy and the hope that gene therapy will also become a reality. At the present it seems likely to this reviewer that biotechnology will contribute to therapy at least as much by facilitating the discovery of small molecules as through the therapeutic use of macromolecules themselves.

Promises for the future are most likely to be fulfilled if neither biologists, nor chemists, nor molecular biologists view the other disciplines as a mere handmaiden of their own. As this article makes evident, we need each other.

The author is deeply grateful to the many colleagues who have read either sections of this manuscript or the entire paper. Their suggestions have truly been invaluable. It is also a pleasure to thank Paul Friese and Key Payton for their technical expertise in the typing of the manuscript and for the patience and good humor with which they accepted one revision after another. I am particularly indebted to Dr. Andreas Lender for his insightful and careful checking of the German and English versions of the galley proofs of this manuscript.

Received: February 12, 1991 [A 838 IE]
German version: *Angew. Chem. 103* (1991) 1305

[1] P. P. Hench, E. C. Kendall, C. H. Slocumb, H. F. Polley, *Proc. Staff Meet. Mayo Clin. 24* (1949) 181.
[2] a) J. E. Bush, A. A. Sandberg, *J. Biol. Chem. 205* (1953) 783; J. E. Bush, *Experientia 12* (1956) 325; b) L. H. Sarett, *J. Biol. Chem. 162* (1946) 601.
[3] L. F. Fieser, M. Fieser: *Steroids*, Reinhold Publishing Company, New York 1959, p. 634f; *Steroide*. Verlag Chemie, Weinheim 1961.
[4] a) D. H. R. Barton, *J. Chem. Soc. 1953*, 1027; b) *Angew. Chem. 82* (1970) 827.
[5] O. Hassel, *Q. Rev. Chem. Soc. 7* (1953) 221.
[6] a) R. Hirschmann, C. S. Snoddy, Jr., N. L. Wendler, *J. Am. Chem. Soc. 74* (1952) 2693; b) R. Hirschmann, C. S. Snoddy, Jr., C. F. Hiskey, N. L. Wendler, *ibid. 76* (1954) 4013; c) C. F. Hiskey, R. Hirschmann, N. L. Wendler, *ibid. 75* (1953) 5135.
[7] a) J. Fried, *Cancer 10* (1957) 752; b) J. Fried, A. Borman, *Vitam. Horm. 16* (1958) 303.
[8] C. M. Weeks, W. L. Duax, M. D. Wolff, *J. Am. Chem. Soc. 95* (1973) 2865.
[9] a) H. L. Herzog, A. Nobile, S. Tolksdorf, W. Charney, E. B. Hershberg, P. L. Perlman, *Science (Washington, D. C.) 121* (1955) 176; b) A. Nobile, W. Charney, P. L. Perlman, H. L. Herzog, C. C. Payne, M. E. Tully, M. A. Jevnik, E. B. Hershberg, *J. Am. Chem. Soc. 77* (1955) 4184.
[10] An exception to this generalization would be an analogue which reaches the receptor only at the desired target tissues, but not at those mediating side effects.
[11] a) S. A. Simpson, J. F. Tait, A. Wettstein, R. Nehr, J. von Euw, O. Schindler, T. Reichstein, *Experientia 10* (1954) 132; b) *Helv. Chim. Acta 37* (1954) 1200.
[12] a) The term receptor is used herein to include acceptors and enzymes; b) J. N. Langley, *J. Physiol. (London) 1* (1878) 339; *33* (1905) 374.
[13] R. Hirschmann, R. G. Strachan, P. Buchschacher, L. H. Sarett, S. L. Steelman, R. Silber, *J. Am. Chem. Soc. 86* (1964) 3903.
[14] G. I. Poos, R. Hirschmann, G. A. Bailey, F. A. Cutter, Jr., L. H. Sarett, J. M. Chemerda, *Chem. Ind. (London) 1958*, 1260.
[15] R. Hirschmann, G. A. Bailey, G. I. Poos, R. Walker, J. M. Chemerda, *J. Am. Chem. Soc. 78* (1956) 4814; B. G. Christensen, N. G. Steinberg, R. Hirschmann, *Chem. Ind. (London) 1958*, 1259.
[16] a) R. Hirschmann, N. G. Steinberg, P. Buchschacher, J. H. Fried, G. J. Kent, M. Tishler, S. L. Steelman, *J. Am. Chem. Soc. 85* (1963) 120; b) R. Hirschmann, P. Buchschacher, N. G. Steinberg, J. H. Fried, R. Ellis, G. J. Kent, M. Tishler, *ibid. 86* (1964) 1520.
[17] S. L. Steelman, R. Hirschmann in A. Eisenstein (Ed.): *The Adrenal Cortex*, Little, Brown & Co., Boston 1967.
[18] C. Djerassi, L. Miramontes, G. Rosenkranz, F. Sondheimer, *J. Am. Chem. Soc. 76* (1954) 4092.
[19] F. B. Colton, L. N. Nysted, B. Riegel, A. L. Raymond, *J. Am. Chem. Soc. 79* (1957) 1123.
[20] a) W. S. Johnson, *Bioorg. Chem. 5* (1976) 51; b) W. S. Johnson, S. J. Telfer, S. Cheng, U. Schubert, *J. Am. Chem. Soc. 109* (1987) 2517; c) W. S. Johnson, S. D. Lindell, J. Steele, *ibid. 109* (1987) 5852.
[21] a) M. R. Haussler, J. F. Myrtle, A. W. Norman, *J. Biol. Chem. 243* (1968) 4055; b) M. R. Haussler, J. E. Verwekh, R. H. Hesse, E. Rizzardo, M. M. Pachet, *Proc. Natl. Acad. Sci. USA 70* (1973) 2248.
[22] a) D. E. M. Lawson, P. W. Wilson, E. Kodicek, *Nature (London) 222* (1969) 171; b) *Biochem. J. 115* (1969) 269; c) E. Kodicek, D. E. M. Lawson, P. W. Wilson, *Nature (London) 228* (1970) 763; d) D. E. M. Lawson, D. R. Fraser, E. Kodicek, H. R. Morris, D. H. Williams, *ibid. 230* (1971) 228.
[23] a) G. Ponchon, H. F. DeLuca, *J. Clin. Invest. 48* (1969) 2373; b) M. F. Holick, H. K. K. Schnoes, H. F. DeLuca, T. Suda, R. J. Cousins, *Biochemistry 10* (1971) 2799.
[24] a) J. F. Myrtle, A. W. Norman, *Science (Washington, D. C.) 171* (1971) 79; b) A. W. Norman, J. F. Myrtle, R. J. Midgett, H. G. Nowicki, V. Williams, G. Popjak, *ibid. 173* (1971) 51.
[25] a) D. R. Andrews, D. H. R. Barton, K. P. Cheng, J. Finet, R. H. Hesse, G. Johnson, M. M. Pechet, *J. Org. Chem. 51* (1986) 1635; b) D. H. R. Barton, R. H. Hesse, M. M. Pechet, E. Rizzardo, *J. Chem. Soc. Dalton Trans. 1974*, 203.
[26] L. J. Vanmaele, P. J. DeClerq, M. Vanderwalle, S. J. Halkes, W. R. M. Overbeek, *Tetrahedron 40* (1984) 1179.
[27] W. G. Dauben, R. B. Phillips, P. Jeffries, *Proc. Natl. Acad. Sci. USA 79* (1982) 5115.
[28] M. Sheves, N. Friedman, Y. Mazur, *J. Org. Chem. 42* (1977) 3597.
[29] E. G. Baggiolini, J. A. Jacobelli, B. M. Hennessy, A. D. Batcho, J. F. Soreno, M. R. Uskovic, *J. Org. Chem. 51* (1986) 3098.
[30] M. Seki, N. Koizumi, M. Morisaki, N. Ikekawa, *Tetrahedron Lett. 1975*, 15.
[31] a) A. W. Alberts, J. Chen, G. Kuron, V. Hunt, J. Huff, C. Hoffman, J. Rothrock, M. Lopez, H. Joshua, E. Harris, A. Patchett, R. Monaghan, S. Currie, E. Stapley, G. Albers-Schonberg, O. Hensens, J. Hirschfeld, K. Hoogsteen, J. Liesch, J. Springer, *Proc. Natl. Acad. Sci. USA 77* (1980) 3957; b) P. A. Dawson, J. E. Metherall, N. D. Ridgway, M. S. Brown, J. L. Goldstein, *J. Biol. Chem. 266* (1991) 9128, and references cited therein.
[32] A. Bélanger, D. Philibert, G. Teutsch, *Steroids 37* (1981) 361.
[33] G. H. Rasmusson, G. F. Reynolds, N. G. Steinberg, E. Walton, G. F. Patel, T. Liang, M. A. Cascieri, A. H. Cheung, J. R. Brooks, C. Berman, *J. Med. Chem. 29* (1986) 2298.
[34] K. R. Yamamoto, *Annu. Rev. Genet. 19* (1985) 209.
[35] a) T. Ojasoo, J. Delettré, J. P. Mornon, C. Turpin-Van Dyke, J. P. Raynaud, *J. Steroid Biochem. 11* (1979) 93; b) W. Wahli, E. Martinez, *FASEB J. 5* (1991) 2243.
[36] See J. S. Fruton, *Proc. Am. Philos. Soc. 129* (1985) 313.
[37] a) F. Sanger, E. O. P. Thompson, R. Kitai, *Biochem. J. 59* (1955) 509; b) A. P. Ryle, F. Sanger, L. F. Smith, R. Kitai, *ibid. 60* (1955) 541, and references cited therein.
[38] V. du Vigneaud, C. Ressler, J. M. Swan, C. W. Roberts, P. G. Katsoyannis, S. Gordon, *J. Am. Chem. Soc. 75* (1953) 4879.
[39] a) V. du Vigneaud, H. C. Lawler, E. A. Popenone, *J. Am. Chem. Soc. 75* (1953) 4880; b) V. du Vigneaud, D. T. Gish, P. G. Katsoyannis, *ibid. 76* (1954) 4751.
[40] P. Edman in S. B. Needleman (Ed.): *Protein Sequence Determination*, Springer, Berlin 1970, p. 211.
[41] R. Schwyzer, P. Sieber, *Helv. Chim. Acta 49* (1966) 134.
[42] R. G. Shepherd, S. D. Wilson, K. S. Howard, P. H. Bell, D. S. Davies, S. B. Davis, E. A. Eigner, N. E. Shakespeare, *J. Am. Chem. Soc. 78* (1956) 5067.
[43] B. Riniker, P. Sieber, W. Rittel, *Nature New Biol. 235* (1972) 114.
[44] a) E. E. Haley, B. J. Corcoran, *Biochemistry 6* (1967) 2668; b) K. Weber, W. Konigsberg, *J. Biol. Chem. 242* (1967) 3563; c) M. A. Ondetti, A. Deer, J. T. Sheehan, J. Plûscek, O. Kocy, *Biochemistry 7* (1968) 4069; d) S. R. Jenkins, R. F. Nutt, R. S. Dewey, D. F. Veber, F. W. Holly, W. J. Paleveda, Jr., T. Lanza, Jr., R. G. Strachan, E. F. Schoenewaldt, H. Barkmeyer, M. J. Dickinson, J. Sondey, R. Hirschmann, E. Walton, *J. Am. Chem. Soc. 91* (1969) 505.
[45] J. Meienhofer, E. Schnabel, H. Bremer, O. Brinkhoff, R. Zabel, W. Sroka, H. Klostermeyer, D. Brandenburg, T. Okuda, H. Zahn, *Z. Naturforsch. B 18* (1963) 1120.
[46] P. G. Katsoyannis, K. Fukuda, A. Tometsko, K. Suzuki, M. Tilak, *J. Am. Chem. Soc. 86* (1964) 930.
[47] a) Y. C. Du, R. Q. Jiang, C. L. Tsou, *Sci. Sinica (Peking) 14* (1965) 229; b) Y. Kung, Y. Du, W. Huang, C. Chen, L. Ke, S. Hu, R. Jiang, S. Chu, C. Niu, J. Hsu, W. Chang, L. Chen, H. Li, Y. Wang, T. Loh, A. Chi, C. Li, P. Shi, Y. Yieh, K. Tang, C. Hsing, *Sci. Sinica (Peking) 15* (1966) 544.
[48] P. G. Katsoyannis, A. C. Trakatellis, S. Johnson, C. Zalut, G. Schwartz, *Biochemistry 6* (1967) 2642.
[49] A. D. Riggs, K. Itakura, H. W. Boyer in A. P. Bollon (Ed.): *Recombinant DNA Products: Insulin, Interferon and Growth Hormone*, CRC Press, Boca Raton, FL 1984, p. 43.
[50] R. E. Chance, J. A. Hoffmann, E. P. Kroeff, M. G. Johnson, E. W. Schirmer, W. W. Bromer, M. J. Ross, R. Wetzel, *Pept. Synth., Struct., Func., Proc. Am. Pept. Symp.* 7th, 1981, 721.
[51] P. Sieber, B. Kamber, A. Hartmann, B. Jöhl, B. Riniker, W. Rittel, a) *Helv. Chim. Acta 57* (1974) 2617; b) *60* (1977) 27.
[52] a) L. Zervas, I. Photaki, *J. Am. Chem. Soc. 84* (1962) 3887; b) I. Photaki in P. K. Katsoyannis (Ed.): *The Chemistry of Polypeptides*, Plenum, New York 1973, p. 59.
[53] D. F. Veber, J. D. Milkowski, R. G. Denkewalter, R. Hirschmann, a) *Tetrahedron Lett. 1968*, 3057; b) *J. Am. Chem. Soc. 94* (1972) 5456.
[54] a) R. G. Hiskey, V. R. Rao, W. G. Rhodes in J. F. W. McOmie (Ed.): *Protective Groups in Organic Chemistry*, Plenum, New York 1973, p. 235; b) R. G. Hiskey, A. Wittinghofer, A. N. Goud, R. R. Vunnam, *Pept. Chem., Struct. Biol. Proc. Am. Pept. Symp. 4th 1975*, 487.
[55] D. F. Steiner, P. E. Oyer, *Proc. Natl. Acad. Sci. USA 57* (1967) 473; D. F. Steiner, D. Cunningham, L. Spigelman, B. Aten, *Science (Washington,*

D.C.) 157 (1967) 697; C. Nolan, E. Margoliash, J. D. Peterson, D. F. Steiner, *J. Biol. Chem. 246* (1971) 2780; D. F. Steiner in J. A. Parsons (Eds.): *Peptide Hormones*, University Park Press, Baltimore 1976, p. 49.
[56] a) A. P. Ryle, F. Sanger, L. F. Smith, R. Kitai, *Biochem. J. 60* (1955) 541; b) H. Brown, F. Sanger, E. O. P. Thompson, *ibid. 60* (1955) 556.
[57] a) O. Wintersteiner, V. du Vigneaud, H. Jensen, *J. Pharmacol. Exp. Ther. 32* (1928) 367, 287, 297; b) K. Freudenberg, W. Dirscherl, H. Eyer, *Hoppe-Seyler's Z. Physiol. Chem. 202* (1931) 128.
[58] J. J. Abel, *Proc. Natl. Acad. Sci. USA 12* (1926) 136.
[59] a) M. J. Adam, T. L. Blundell, E. J. Dodson, G. G. Dodson, M. Vijayan, E. N. Baker, M. M. Harding, D. C. Hodgkin, B. Rimmer, S. Skeat, *Nature (London) 224* (1969) 491; b) T. L. Blundell, G. G. Dodson, D. C. Hodgkin, D. A. Mercola, *Adv. Protein Chem. 26* (1972) 279.
[60] a) B. Gutte, R. B. Merrifield, *J. Am. Chem. Soc. 91* (1969) 501; b) *J. Biol. Chem. 246* (1971) 1922.
[61] a) R. G. Denkewalter, D. F. Veber, F. W. Holly, R. Hirschmann, *J. Am. Chem. Soc. 91* (1969) 502; b) R. G. Strachen, W. J. Paleveda, Jr., R. F. Nutt, R. A. Vitali, D. F. Veber, M. J. Dickinson, V. Garsky, J. E. Deak, E. Walton, S. R. Jenkins, F. W. Holly, R. Hirschmann, *ibid. 91* (1969) 503; c) S. R. Jenkins, R. F. Nutt, R. S. Dewey, D. F. Veber, F. W. Holly, W. J. Paleveda, Jr., T. Lanza, Jr., R. G. Strachan, E. F. Schoenewaldt, H. Barkemeyer, M. J. Dickinson, J. Sondey, R. Hirschmann, E. Walton, *ibid. 91* (1969) 505; d) D. F. Veber, S. L. Varga, J. D. Milkowski, H. Joshua, J. B. Conn. R. Hirschmann, R. G. Denkewalter, *J. Am. Chem. Soc. 91* (1969) 506; e) R. Hirschmann, R. F. Nutt, D. F. Veber, R. A. Vitali, S. L. Varga, T. A. Jacob, F. W. Holly, R. G. Denkewalter, *ibid. 91* (1969) 507; f) R. Hirschmann, *Intra-Sci. Chem. Rep. 5* (1971) 203; g) R. Hirschmann, R. G. Denkewalter, *Naturwissenschaften 57* (1970) 145; h) R. Hirschmann: *Peptides 1969*, North-Holland, Amsterdam 1971, p. 138.
[62] a) R. B. Merrifield, *J. Am. Chem. Soc. 85* (1963) 2149; b) *Adv. Enzymol. 32* (1969) 221.
[63] V. du Vigneaud, C. Ressler, J. M. Swan, C. W. Roberts, P. G. Katsoyannis, S. Gordon, *J. Am. Chem. Soc. 75* (1953) 4879.
[64] W. Rittel, B. Iselin, H. Kappeler, B. Riniker, R. Schwyzer, *Helv. Chim. Acta 40* (1957) 614.
[65] H. Schwarz, F. M. Bumpas, I. H. Page, *J. Am. Chem. Soc. 79* (1957) 5697.
[66] S. Guttman, R. A. Boissonas, a) *Helv. Chim. Acta 41* (1958) 42; b) *42* (1959) 1257.
[67] H. Romovacek, S. R. Dowd, K. Kawasaki, N. Nishi, K. Hoffmann, *J. Am. Chem. Soc. 101* (1979) 6081.
[68] T. J. Blacklock, R. Hirschmann, D. F. Veber in S. Udenfriend, J. Meienhofer (Eds.): *The Peptides: Analysis, Synthesis, Biology, Vol. 9, Part C*, Academic Press, Harcourt Brace Jovanovich, San Diego, CA 1987, p. 39.
[69] E. Haber, C. B. Anfinsen, *J. Biol. Chem. 236* (1961) 422.
[70] a) H. Yajima, N. Fujii, *J. Am. Chem. Soc. 103* (1981) 5867; b) *J. Chem. Soc. Chem. Commun., 1980* 115.
[71] The discussion about the structure of porcine ACTH illustrates that proof of structure can be a nontrivial task with any large peptide.
[72] S. J. Benkovic, C. A. Fienke, A. M. Naylor, *Science (Washington, D. C.) 239* (1988) 1105.
[73] See, e.g., T. N. C. Wells, A. R. Fersht, *Biochemistry 25* (1986) 1881; R. J. Leatherbarrow, A. R. Fersht, G. Winter, *Proc. Natl. Acad. Sci. USA 82* (1985) 7840; M. D. Jones, D. M. Lowe, T. Borgford, A. R. Fersht, *Biochemistry 25* (1986) 1887.
[74] J. D. Hermes, S. C. Blacklow, J. R. Knowles, *Proc. Natl. Acad. Sci. USA 87* (1990) 696; see also W. J. Alberty, J. R. Knowles, *Biochemistry 15* (1976) 5631.
[75] D. A. Estell, T. P. Graycar, J. A. Wells, *J. Biol. Chem. 260* (1985) 6518; J. A. Wells, D. B. Powers, R. R. Bott, T. P. Graycar, D. A. Estell, *Proc. Natl. Acad. Sci. USA 84* (1987) 1219.
[76] a) R. F. Nutt, S. F. Brady, P. L. Drake, T. M. Ciccarone, C. Dylion Colton, E. M. Nutt, J. A. Rodkey, C. D. Bennett, L. H. Waxman, I. S. Sigal, P. S. Anderson, D. F. Veber, *Proc. Natl. Acad. Sci. USA 85* (1988) 7129; b) J. Schneider, S. B. H. Kent, *Cell 54* (1988) 363.
[77] a) L. A. Carpino, *J. Am. Chem. Soc. 79* (1957) 98; b) *79* (1957) 4427.
[78] F. C. McKay, N. F. Albertson, *J. Am. Chem. Soc. 79* (1957) 4686.
[79] G. W. Anderson, A. C. McGregor, *J. Am. Chem. Soc. 79* (1957) 6180.
[80] a) L. A. Carpino, G. Y. Han, *J. Am. Chem. Soc. 92* (1970) 5748; b) E. Atherton, R. C. Sheppard in [68], p. 1.
[81] P. Sieber, B. Iselin, *Helv. Chim. Acta 51* (1968) 614, 622.
[82] R. G. Hiskey, A. M. Thomas, R. S. Smith, W. C. Jones, Jr., *J. Am. Chem. Soc. 91* (1969) 7525.
[83] D. G. Mullen, G. Barany, *J. Org. Chem. 53* (1988) 5240, and references cited therein.
[84] a) S. Sakakibara, Y. Shimonishi, *Bull. Chem. Soc. (Jpn.) 38* (1965) 1412; b) T. Kimura, M. Takai, Y. Masui, T. Morikawa, S. Sakakibara, *Biopolymers 20* (1981) 1823; c) T. Kimura, N. Chino, S.-I. Kumagaye, H. Kuroda, J. Emura, S. Sakakibara, *Biochem. Soc. Trans. 18* (1990) 1297.
[85] V. M. Garsky, P. K. Lumma, R. M. Freidinger, S. M. Pitzenberger, W. C. Randall, D. F. Veber, R. J. Gould, P. A. Friedman, *Proc. Natl. Acad. Sci. USA 86* (1989) 4022.
[86] D. S. Kemp in E. Gross, J. Meienhofer (Eds.): *The Peptides, Vol. 1*, Academic Press, New York 1979, p. 315.
[87] N. L. Benoiton in E. Gross, J. Meienhofer (Eds.): *The Peptides, Vol. 5*, Academic Press, New York 1983, p. 217.
[88] a) J. P. Tam, R. B. Merrifield in [68], p. 185; b) J. P. Tam in D. H. Schlesinger (Ed.): *Macromolecular Sequencing and Synthesis, Selected Methods and Applications*, Alan R. Liss, New York 1988, p. 153.
[89] It is worth noting, however, that *Barton* had introduced the concept of "conformational transmission", showing that steroidal D-ring substituents affect the rate of aldol couplings at C-2 of steroidal 3-ketones (see also [8]).
[90] G. N. Ramachandran, V. Sasisekharan, *Adv. Protein Chem. 23* (1968) 283.
[91] H. A. Scheraga, *Chem. Rev. 71* (1971) 195.
[92] S. M. Bloom, G. D. Fasmna, C. DeLoze, E. R. Blout, *J. Am. Chem. Soc. 84* (1961) 458.
[93] M. Goodman, R. P. Saltman, *Biopolymers 20* (1981) 1929.
[94] R. Schwyzer, P. Sieber, B. Gorup, *Chimia 12* (1958) 90.
[95] a) C. M. Deber, V. Madison, E. R. Blout, *Acc. Chem. Res. 9* (1976) 106; b) K. D. Kopple, M. Ohnishi, A. Go, *J. Am. Chem. Soc. 91* (1969) 4264; c) H. Gerlach, J. A. Owtschinnikow, V. Prelog, *Helv. Chim. Acta 47* (1964) 2294; d) Y. A. Ovchinnikov, V. T. Ivanov in H. Neurath, R. L. Hill (Eds.): *The Cyclic Peptides: Structure, Conformation and Function, Vol. V*, Academic Press, New York 1982, p. 307; Y. A. Ovchinnikov, V. T. Ivanov, *Tetrahedron 31* (1975) 2209.
[96] H. Kessler, *Angew. Chem. 94* (1982) 509; *Angew. Chem. Int. Ed. Engl. 21* (1982) 512.
[97] G. R. Marshall, H. E. Bosshard, *Circulation Res. 30/31 Suppl. II* (1972) 143.
[98] D. W. Urry, M. Ohnishi, R. Walter, *Proc. Natl. Acad. Sci. USA 66* (1970) 111; D. W. Urry, R. Walter, *ibid. 68* (1971) 956.
[99] V. J. Hruby, „Conformationally Directed Drug Design", *ACS Symp. Ser. 251* (1984) 9–27.
[100] H. Kessler, W. Bermel, A. Müller in S. Udenfried, J. Meienhofer (Eds.): *The Peptides, Vol. 7*, Academic Press, New York 1985, p. 437.
[101] S. W. Fesik, R. T. Gampe, Jr.; T. F. Holzman, D. A. Egan, R. Edalji, J. R. Luly, R. Simmer, R. Helfrich, V. Kishore, D. H. Rich, *Science (Washington, D.C.) 250* (1990) 1406.
[102] G. D. Rose, L. M. Gierasch, J. A. Smith, *Adv. Protein Chem. 1* (1985) 1.
[103] J. Rizo, M. Dhingra, L. M. Gierasch in P. Balram, S. Ramaseshan (Eds.), in press.
[104] J. Rudinger, K. Jost, *Experientia 20* (1964) 570.
[105] J. Rudinger in E. J. Ariens (Ed.): *Drug Design, Vol. 2*, Academic Press, New York 1971, p. 319.
[106] R. Walter, *Fed. Proc. 36* (1977) 1872.
[107] M. Manning, J. Lowbridge, J. Haldar, W. H. Sawyer, *Fed. Proc. 36* (1977) 1848; W. H. Sawyer, M. Manning, *Annu. Rev. Pharmacol. 13* (1973) 5; *Atlas of Science*, 1988, p. 252.
[108] V. J. Hruby in M. Margoulies, F. C. Greenwood (Ed.): *Structure-Activity Relationships of Proteins and Polypeptide Hormones*, Excerpta Medica, Amsterdam 1972, p. 458.
[109] R. Huguenin, R. A. Boissonas, *Helv. Chim. Acta 49* (1966) 695.
[110] I. Vavra, A. Machova, V. Holecek, J. H. Cort, M. Zaoral, F. Sorm, *Lancet 1* (1968) 948.
[111] M. Manning, L. Balaspiri, M. Acosta, *J. Med. Chem. 16* (1973) 975.
[112] D. W. Urry, R. Walter, *Proc. Natl. Acad. Sci. USA 68* (1971) 956.
[113] A. J. Geddes, D. K. Parker, E. D. T. Atkins, E. Beighton, *J. Mol. Biol. 32* (1968) 343.
[114] a) W. P. Jencks in G. van Binst (Ed.): „Design and Synthesis of Organic Molecules Based on Molecular Recognition", *Proc. Solvay Conf. Chem. 18th*, Springer, Berlin 1986, p. 59; b) T. J. Franklin, *Biochem. Pharmacol. 29* (1980) 853.
[115] R. Burgus, T. F. Dunn, D. Desiderio, D. Ward, W. Vale, R. Guillemin, *Nature (London) 26* (1970) 321.
[116] P. Brazeau, W. Vale, R. Burgus, N. Ling, M. Butcher, J. Rivier, R. Guillemin, *Science (Washington, D. C.) 179* (1973) 77.
[117] J. Rivier, *J. Am. Chem. Soc. 96* (1974) 2986.
[118] J. Boler, F. Enzmann, K. Folkers, C. Y. Bowers, A. V. Schally, *Biochem. Biophys. Res. Commun. 37* (1969) 705.
[119] A. W. Schally, A. Arimura, Y. Baba, R. M. G. Nair, H. Matsuo, T. W. Redding, L. Debeljuk, W. F. White, *Biochem. Biophys. Res. Commun. 43* (1971) 393.
[120] J. Rivier, J. Spiess, M. Thorner, W. Vale, *Nature (London) 300* (1982) 276.
[121] R. Guillemin, P. Brazeau, P. Böhlen, F. Esch, N. Ling. W. B. Wehrenberg, *Science (Washington, D. C.) 218* (1982) 585.
[122] W. Vale, J. Spies, C. Rivier, J. Rivier, *Science (Washington, D. C.) 213* (1981) 1394.
[123] See, for example, G. Schmidt, *Top. Curr. Chem. 136* (1986) 109.
[124] J. Hughes, T. W. Smith, H. W. Kosterlitz, A. Fothergill, B. A. Morgan, H. R. Morris *Nature (London) 258* (1975) 577.
[125] J. Pless, W. Bauer, F. Cardinaux, A. Closse, D. Hauser, R. Huguenin, D. Roemer, H.-H. Buescher, R. C. Hill, *Helv. Chim. Acta 62* (1979) 398.
[126] R. C. A. Frederickson, E. L. Smithwick, R. Shuman, K. G. Bemis, *Science (Washington, D. C.) 211* (1981) 603.
[127] P. W. Schiller, J. Mimaio, *Nature (London) 297* (1982) 74; P. W. Schiller,

T. M.-D. Nguyen, L. Maziak, C. Lemieux, *Biochem. Biophys. Res. Commun. 127* (1985) 558, and references cited therein.
[128] H. J. Mosberg, R. Hurst, V. J. Hruby, K. Gee, H. I. Yamamura, J. J. Galligan, T. F. Burks, *Proc. Natl. Acad. Sci. USA 80* (1983) 5871.
[129] J. Meienhofer in M. E. Wolff (Ed.): *Burger: Medicinal Chemistry, Part II*, 4th ed., Wiley, New York 1979.
[130] R. H. Unger, *Diabetes 25* (1976) 36.
[131] J. Rivier, M. Brown, W. Vale, *Biochem. Biophys. Res. Commun. 65* (1975) 746.
[132] R. Chamdrasekaren, A. V. Lakshminarayanau, U. V. Pandya, G. N. Ramachandran, *Biochim. Biophys. Acta 303* (1973) 14.
[133] a) D. F. Veber, F. W. Holly, W. J. Palveda, R. F. Nutt, S. J. Bergstrand, M. Torchiana, M. S. Glitzer, R. Saperstein, R. Hirschmann, *Proc. Natl. Acad. Sci. USA 75* (1978) 2636; b) D. F. Veber, R. G. Strachan, S. J. Bergstrand, F. W. Holly, C. F. Homnick, R. Hirschmann, *J. Am. Chem. Soc. 98* (1976) 2367.
[134] L. A. Holladay, D. Puett, *Proc. Natl. Acad. Sci. USA 73* (1976) 1199.
[135] D. F. Veber, R. Saperstein, R. F. Nutt, R. M. Freidinger, S. F. Brady, P. Curley, D. S. Perlow, W. J. Palveda, C. D. Colton, A. G. Zacchei, D. J. Tocco, D. R. Hoff, R. L. Vandlen, J. E. Gerich, L. Hall, L. Mandarino, E. H. Cordes, P. S. Anderson, R. Hirschmann, *Life Sci. 34* (1984) 1371.
[136] a) W. Bauer, U. Briner, W. Doepner, R. Haller, R. Hugenin, P. Marbach, T. J. Petcher, J. Pless, *Life Sci. 31* (1982) 1133; b) S. W. J. Lamberts, P. Uitterlinden, L. Verschoor, K. J. van Dongen, E. del Pozo, *N. Engl. J. Med. 313* (1985) 1576; c) The C-terminal Thr-ol denotes a derivative of threonine in which the carboxyl has been reduced to a primary alcohol.
[137] a) B. E. Evans, M. G. Bock, K. E. Rittle, R. M. DiPardo, W. L. Whitter, D. F. Veber, P. S. Anderson, R. M. Freidinger, *Proc. Natl. Acad. Sci. USA 83* (1986) 4918; b) B. E. Evans, K. E. Rittle, M. G. Bock, R. M. DiPardo, R. M. Freidinger, D. F. Veber, P. S. Anderson, R. S. L. Chang, V. J. Lotti, D. J. Cerino, J. P. Springer, J. Hirshfield, *J. Med. Chem. 31* (1988) 2235; c) J. M. Liesch, O. D. Hensens, J. P. Springer, R. S. L. Chang, V. J. Lotti, *J. Antibiot. 38* (1985) 1638.
[138] M. G. Bock, R. M. DiPardo, B. E. Evans, K. E. Rittle, W. L. Whitter, D. F. Veber, P. S. Anderson, R. M. Freidinger, *J. Med. Chem. 32* (1989) 13.
[139] Y. Furukawa, S. Kishimoto, K. Nishikawa, US-Pat. 4355040 (1982).
[140] J. V. Duncia, A. T. Chiu, D. J. Carini, G. B. Gregory, A. L. Johnson, W. A. Price, G. J. Wells, P. C. Wong, J. C. Calabrese, P. B. M. W. M. Timmermans, *J. Med. Chem. 33* (1990) 1312.
[141] D. Biswanath, J. J. Plattner, E. N. Bush, H. Jae, G. Diaz, E. S. Johnson, T. J. Perun, *J. Med. Chem. 32* (1989) 2036.
[142] The earliest examples of the employment of the concept of conformational constraint in peptide medicinal chemistry are probably the synthesis of carba analogues of oxytocin [104], and, more explicitly, the synthesis of a biscarba analogue of SRIF [133b]. The synthesis of bicyclic analogues of SRIF [133a] again employed conformational constraints to help elucidate bioactive conformations. The seminal work by *Freidinger* and *Veber* [see R. M. Freidinger, D. F. Veber, *Science (Washington, D. C.) 210* (1980) 656] and later by *Hruby*'s group [see T. K. Sawyer, W. L. Cody, J. J. Knittel, V. J. Hruby, M. E. Hadley, M. D. Hirsch, T. L. O'Donohue, *Pept. Struct. Funct. Proc. Am. Pept. Symp. 8th 1984*, 323] and by P. W. Schiller and J. DiMaio [*ibid.*, p. 269] are excellent examples of a different approach to conformational constraint. An early example of the use of conformational constraint in enzyme inhibitor design is the work of *Thorsett* und *Patchett* et al. [E. D. Thorsett, E. E. Harris, S. Aster, E. R. Peterson, D. Taub, A. A. Patchett, E. H. Ulm, T. C. Vassil, *Biochem. Biophys. Res. Commun. 111* (1983) 166].
[143] A. F. Spatola in B. Weinstein (Ed.): *Chemistry and Biochemistry of Amino Acids, Peptides and Proteins*, Marcel Dekker, New York 1983, 267; see also D. B. Sherman, A. F. Spatola, *J. Am. Chem. Soc. 112* (1990) 433, and references cited therein.
[144] a) U. Nagai, K. Sato, *Pept. Struct. Funct. Proc. Am. Pept. Symp. 9th 1985*, 465; b) M. Feigel, *J. Am. Chem. Soc. 108* (1986) 181; c) *Angew. Chem. 101* (1989) 466; *Angew. Chem. Int. Ed. Engl. 28* (1989) 486.
[145] D. S. Kemp, W. E. Stites, *Tetrahedron Lett. 29* (1988) 5057.
[146] G. L. Olson, M. E. Voss, D. E. Hill, M. Kahn, V. S. Madison, C. M. Cook, *J. Am. Chem. Soc. 112* (1990) 323.
[147] M. Kahn, S. Wilke, B. Chen, K. Fujita, *J. Am. Chem. Soc. 110* (1988) 1638; M. Kahn, S. Wilke, B. Chen, K. Fujita, Y. Lee, M. E. Johnson, *J. Mol. Recogn. 1* (1988) 75; M. Kahn, S. Bertenshaw, *Tetrahedron Lett. 30* (1989) 2317.
[148] K. C. Nicolaou, J. M. Salvino, K. Raynor, S. Pietranico, T. Reisine, R. M. Freidinger, R. Hirschmann, *Pept. Chem. Struct. Biol. Proc. Am. Pept. Symp. 11th 1989* (1990) 881.
[149] a) G. L. Olson, H.-C. Cheung, M. E. Voss, D. E. Hill, M. Kahn, V. S. Madison, C. M. Cook, J. Sepinwall, G. Vincent, *Proc. Biotechnol (USA)*, Conference Management Corporation, Norwalk, CT 1989, S. 348; b) G. L. Olson private communication.
[150] E. J. Corey, *Angew. Chem. 103* (1991) 479; *Angew. Chem. Int. Ed. Engl. 30* (1991) 455.
[151] J. S. Fruton: *Molecules of Life*, Wiley-Interscience, New York 1972.
[152] J. B. Herrick, *Arch. Intern. Med. 6* (1910) 517.
[153] L. Pauling, H. A. Itano, S. J. Linger, J. C. Wells, *Science (Washington, D. C.) 110* (1949) 543.
[154] V. M. Ingram, *Nature (London) 180* (1957) 326.
[155] A. L. Lehninger: *Principles of Biochemistry*, Worth Publishers, New York 1982, p. 129.
[156] E. M. Arnett, N. G. Harvey, P. L. Rose, *Acc. Chem. Res. 22* (1989) 131.
[157] L. Pauling, *Am. Sci. 36* (1948) 51; *Chem. Eng. News 24* (1946) 1375.
[158] L. D. Byers, R. Wolfenden, *Biochemistry 12* (1973) 2070.
[159] Y. S. Bakhle, *Nature (London) 220* (1968) 919.
[160] M. A. Ondetti, B. Rubin, D. W. Cushman, *Science (Washington, D. C.) 196* (1977) 441.
[161] A. A. Patchett, E. Harris, E. W. Tristram, M. J. Wyvratt, M. T. Wu, D. Taub, E. R. Peterson, T. J. Ikeler, J. ten Broeke, L. G. Payne, D. L. Ondeyka, E. D. Thorsett, W. J. Greenlee, N. S. Lohr, R. D. Hoffsommer, H. Joshua, W. V. Ruyle, J. W. Rothrock, S. D. Aster, A. L. Maycock, F. W. Robinson, R. Hirschmann, C. S. Sweet, E. H. Ulm, D. M. Gross, T. C. Vassil, C. A. Stone, *Nature (London) 288* (1980) 280.
[162] J. Marciniszyn, J. A. Hartsuck, J. Tang, *J. Biol. Chem. 251* (1976) 7088.
[163] G. R. Marshall, *Fed. Proc. 75* (1976) 2494.
[164] a) D. H. Rich, E. T. Sun, J. Singh, *Biochem. Biophys. Res. Commun. 74* (1977) 762; b) D. H. Rich ("Inhibitors of Aspartic Proteinases") in Barrett, Salversen (Eds.): *Proteinase Inhibitors*, Elsevier, Amsterdam, 1986, p. 179; c) D. H. Rich ("Peptidase Inhibitors") in P. G. Sammes, J. B. Taylor (Eds.): *Comprehensive Medicinal Chemistry, Vol. 2*, Pergamon, New York 1990, p. 391.
[165] J. Boger, N. S. Lohr, E. H. Ulm, M. Poe, E. H. Blaine, G. M. Fanelli, T.-Y. Lin, L. S. Payne, T. W. Schorn, B. I. LaMont, T. C. Vassil, I. I. Stabilito, D. F. Veber, D. H. Rich, A. S. Boparai, *Nature (London) 303* (1983) 81.
[166] R. B. Silverman, S. J. Hoffman, *Med. Res. Rev. 4* (1984) 415.
[167] A. Endo, M. Kuroda, Y. Tsujita, *J. Antibiot. 29* (1976) 1346.
[168] Sir J. W. Black, *Angew. Chem. 101* (1989) 910; *Angew. Chem. Int. Ed. Engl. 28* (1989) 886.
[169] B. K. Wasson, W. K. Gibson, R. S. Stuart, H. W. R. Williams, C. H. Yates, *J. Med. Chem. 15* (1972) 651.
[170] a) H. J. Schaeffer, L. Beauchamp, P. de Miranda, G. Elion, D. J. Bauer, P. Collins, *Nature (London) 272* (1978) 583; b) G. B. Elion, *Angew. Chem. 101* (1989) 893; *Angew. Chem. Int. Ed. Engl. 28* (1989) 870; c) G. H. Hitchings, Jr., *ibid. 101* (1989) 903 bzw. *28* (1989) 879. d) It is appropriate to mention in this context another prodrug, 3'-azido-3'-deoxythymidine (AZT), first synthesized by *T. S. Lin* and *W. H. Prusoff* at Yale [*J. Med. Chem. 21* (1978) 109], the first reverse transcriptase inhibitor and the first anti-AIDS drug to be approved by the FDA. Its effectiveness against the AIDS virus was first described in a paper from the NCI, Duke University Medical Center and the Wellcome Research Laboratories [H. Mitsuya, K. J. Weinhold, P. A. Furman, M. H. St. Clair, S. Nusinoff Lehrmann, R. C. Gallo, D. Bolognesi, D. W. Barry, S. Broder, *Proc. Natl. Acad. Sci. USA 82* (1985) 7096].
[171] A. Ruegger, M. Kuhn, H. Lichti, H. R. Loosli, R. Huguenin, C. Quiquerez, A. von Wortburg, *Helv. Chim. Acta 59* (1976) 1075; T. J. Pechter, H.-P. Weber, A. Rüegger, *ibid. 59* (1976) 1480.
[172] R. M. Wenger, *Angew. Chem. 97* (1985) 88; *Angew. Chem. Int. Ed. Engl. 24* (1985) 77.
[173] A. Tanaka, A. Kuroda, H. Marusawa, H. Hatanaka, T. Kino, T. Goto, M. Hashimoto, *J. Am. Chem. Soc. 109* (1987) 5031.
[174] R. M. Wenger, *Helv. Chim. Acta 66* (1983) 2308, 2672.
[175] T. K. Jones, S. G. Mills, R. A. Reamer, D. Askin, R. Desmond, R. P. Volante, J. Shinkai, *J. Am. Chem. Soc. 111* (1989) 1157.
[176] R. E. Handschumacher, M. W. Harding, J. Rice, R. Drugge, D. Speicher, *Science (Washington, D. C.) 226* (1984) 544.
[177] a) N. Takahashi, T. Hayano, M. Suzuki, *Nature (London) 337* (1989) 473; b) G. Fischer, B. Wittmann-Liebold, K. Lang, T. Kiefhaber, F. X. Schmid, *ibid. 337* (1989) 476; c) G. Fischer, H. Bang, C. Mech., *Biomed. Biochim. Acta 43* (1984) 1101.
[178] a) R. K. Harrison, R. L. Stein, *Biochemistry 29* (1990) 684; b) R. K. Harrison, C. G. Caldwell, A. Rosegay, D. Melillo, R. L. Stein, *J. Am. Chem. Soc. 112* (1990) 7063.
[179] M. K. Rosen, R. F. Standaert, A. Galat, M. Nakatsuka, S. L. Schreiber, *Science (Washington, D. C.) 248* (1990) 863.
[180] J. Liu, M. W. Albers, C. Chen, S. L. Schreiber, C. T. Walsh, *Proc. Natl. Acad. Sci. USA 87* (1990) 2304.
[181] a) J. D. Aebi, D. T. Deyo, C. Q. Sun, D. Guillaume, B. Dunlap, D. H. Rich, *J. Med. Chem. 33* (1990) 999; F. J. Kofron, P. Kumič, V. Kishore, E. Colón-Bomilla, D. H. Rich, *Biochem. 30* (1991) 6127. b) N. H. Sigal, F. Dumont, P. Durette, J. J. Siekieska, J. Peterson, D. H. Rich, B. E. Dunlap, M. J. Staruch, M. R. Melino, S. L. Koprak, D. Williams, B. Witzel, J. M. Pisano, *J. Exp. Med. 173* (1991) 619.
[182] J. J. Siekierka, S. H. Y. Hung, M. Poe, C. S. Lin, N. Sigal, *Nature (London) 341* (1989) 755.
[183] a) M. W. Harding, A. Galat, D. E. Uehling, S. L. Schreiber, *Nature (London) 341* (1989) 758; b) M. K. Rosen, R. F. Standaert, A. Galat, M. Nakatsuka, S. L. Schreiber, *Science (Washington, D. C.) 248* (1990) 863; c) S. L. Schreiber, *ibid. 251* (1991) 283, and references cited therein;

d) S. W. Michnick, M. K. Rosen, T. J. Wandless, M. Karplus, S. L. Schreiber, *Science (Washington, D. C.) 252* (1991) 836.
[184] M. Tropschug, E. Wachter, S. Mayer, E. R. Schoenbrunner, F. X. Schmid, *Nature (London) 346* (1990) 674.
[185] a) J. C. Chabala, H. Mrozik, R. L. Tolman, P. Eskola, A. Lusi, L. H. Peterson, W. C. Campbell, J. R. Egerton, D. A. Ostlind, *J. Med. Chem. 23* (1980) 1134; b) M. H. Fischer, H. Mrozik in S. Ōmura (Ed.): *Macrolide Antibiotics*, Academic Press, New York 1984, p. 553.
[186] M. Barbacid, *Annu. Rev. Biochem. 56* (1987) 779.
[187] P. H. Seeburg, W. W. Colby, D. J. Capon, D. V. Goeddel, A. D. Levinson, *Nature (London) 312* (1984) 71.
[188] J. B. Gibbs, I. S. Sigal, M. Poe, E. M. Scolnick, *Proc. Natl. Acad. Sci. USA 81* (1984) 5704.
[189] J. P. McGrath, D. J. Capon, D. V. Goeddel, A. D. Levinson, *Nature (London) 310* (1984) 644.
[190] J. F. Hancock, A. I. Magee, J. E. Childs, C. J. Marshall, *Cell* 57 (1989) 1167; P. J. Casey, P. A. Solski, C. J. Der, J. E. Buss, *Proc. Natl. Acad. Sci. USA 86* (1989) 8323.
[191] Y. Reiss, S. J. Stradly, L. M. Gierasch, M. S. Brown, L. J. Goldstein *ibid. 88* (1991) 732.
[192] C. A. Stein, J. S. Cohen, *Cancer Res. 48* (1988) 2659.
[193] A. R. Van der Krol, J. N. M. Mol, A. R. Stuitje, *BioTechniques 6* (1988) 958.
[194] a) D. A. Horne, P. D. Dervan, *J. Am. Chem. Soc. 112* (1990) 2435; b) M. L. Riordan, J. C. Martin, *Nature (London) 350* (1991) 442.
[195] a) P. B. Dervan, *Science (Washington, D. C.) 232* (1986) 464; b) P. B. Dervan, R. Scott, *J. Am. Chem. Soc. 109* (1987) 7564; c) M. G. Oakley, P. B. Dervan, *Science (Washington, D. C.) 248* (1990) 847.
[196] L. H. Hurley, *J. Med. Chem. 32* (1989) 2027.
[197] R. Henderson, P. N. T. Unwin, *Nature (London) 257* (1975) 28.
[198] R. Henderson, J. M. Baldwin, T. A. Ceska, F. Zemlin, E. Beckman, K. H. Downing, *J. Mol. Biol. 213* (1990) 899.
[199] Y. A. Ovchinnikov, N. G. Abdulaev, M. Y. Feigina, I. D. Artamonov, A. S. Zolotarev, M. B. Kostina, A. S. Bogachuk, A. I. Miroshinkov, A. B. Kudelin, *Bioorg. Khim. 8* (1982) 1011.
[200] a) P. A. Hargrave, *J. Prog. Retinal Res. 1* (1982) 1; b) P. A. Hargrave, J. H. McDowell, D. R. Curtis, J. K. Wang, E. Juszczak, S.-L. Fong, J. K. M. Rao, P. Argos, *Biophys. Struct. Mech. 9* (1983) 235, and references cited therein.
[201] a) C. Altenbach, T. Marti, H. G. Khorana, W. L. Hubbell, *Science (Washington, D. C.) 248* (1990) 1088; b) T. Marinetti, S. Subramaniam, T. Mogi, T. Marti, H. G. Khorana, *Proc. Natl. Acad. Sci. USA 86* (1989) 529, 8309; c) T. A. Nakayama, H. G. Khorana, *J. Biol. Chem. 265* (1990) 15762, and references cited therein.
[202] G. E. Renk, Y. S. Or, R. K. Crouch, *J. Am. Chem. Soc. 109* (1987) 6163, and references cited therein.
[203] V. Balogh-Nair, K. Nakanishi in C. Tamm (Ed.): *New Comprehensive Biochemistry, Vol. 3*, Elsevier Biomedical, Amsterdam 1982, pp. 283–334.
[204] R. A. F. Dixon, B. K. Kobilka, D. J. Strader, J. L. Benovic, H. G. Dohlman, T. Frielle, M. A. Bolanowski, C. D. Bennett, E. Rands, R. E. Diehl, R. A. Mumford, E. E. Slater, I. S. Sigal, M. G. Caron, R. J. Lefkowitz, C. D. Strader, *Nature (London) 321* (1986) 75.
[205] a) C. D. Strader, I. S. Sigal, R. B. Register, M. R. Candelore, E. Rands, R. A. F. Dixon, *Proc. Natl. Acad. Sci. USA 84* (1987) 4384; b) C. D. Strader, I. S. Sigal, M. R. Candelore, E. Rands, W. S. Hill, R. A. F. Dixon, *J. Biol. Chem. 263* (1988) 10267.
[206] C. D. Strader, M. R. Candelore, W. S. Hill, I. S. Sigal, R. A. F. Dixon, *J. Biol. Chem. 264* (1989) 13572.
[207] R. J. Lefkowitz, A. G. Caron, *J. Biol. Chem. 263* (1988) 4993, and references cited therein.
[208] M. Rodbell, L. Brinbraumer, S. L. Pohl, H. M. J. Krans, *J. Biol. Chem. 246* (1971) 1877.
[209] a) A. G. Gilman, *Cell 36* (1984) 577; b) Annu. Rev. Biochem. 56 (1987) 615; c) M. Freissmuth, P. J. Cassey, A. G. Gilman, *FASEB J. 3* (1989) 2125.
[210] a) L. Stryer, H. R. Bourne, *Annu. Rev. Cell. Biol. 2* (1986) 391; b) H. R. Bourne, D. A. Sanders, F. McCormick, *Nature (London) 349* (1991) 117.
[211] Y. Fukada, T. Takao, H. Ohguro, T. Yoshizawa, T. Akino, Y. Shimonishi, *Nature (London) 346* (1990) 658, and references cited therein.
[212] B. Roth, *Fed. Proc. 45* (1986) 2765.
[213] J. J. Baldwin, G. S. Ponticello, P. S. Anderson, M. E. Christy, M. A. Murcko, W. C. Randall, H. Schwam, M. F. Sugrue, J. P. Springer, P. Gautheron, J. Grove, P. Mallorga, M.-P. Viader, B. M. McKeever, M. A. Navia, *J. Med. Chem. 32* (1989) 2510, 2548.
[214] C. R. Beddell, P. J. Goodford, G. Kneen, R. D. White, S. Wilkinson, R. Wooton, *Br. J. Pharmacol. 82* (1984) 397.
[215] K. Derewenda, Z. Derewenda, E. J. Dodson, G. G. Dodson, X. Bing, J. Markussen, *J. Mol. Biol. 259* (1991) 1406.
[216] P. W. Schiller in C. G. Wermuth (Ed.): *Medicinal Chemistry for the 21st Century*, IUPAC, Blackwell Scientific Publications, Oxford, in press.
[217] J. R. Knowles, *Nature (London) 350* (1991) 121.
[218] R. J. Leatherbarrow, A. R. Fersht, G. Winter, *Proc. Natl. Acad. Sci. USA 82* (1985) 7840.
[219] C. D. Strader, M. R. Candelore, W. S. Hill, R. A. F. Dixon, *J. Biol. Chem. 264* (1989) 16470.
[220] L. Polgar, M. L. Bender, *J. Am. Chem. Soc. 88* (1966) 3153; *Biochemistry 6* (1967) 610.
[221] K. E. Neet, A. Nanci, D. E. Koshland, *J. Biol. Chem. 243* (1968) 6392.
[222] B. C. Cunningham, J. A. Wells, *Proc. Natl. Acad. Sci. USA 88* (1991) 3407, and references cited therein; B. C. Cunningham, W. G. Mulkerrin, J. A. Wells, *Science (Washington, D. C.)* (1991), in press; M. Ultsch, A. M. de Vos, M. G. Mulkerin, B. C. Cunningham, J. A. Wells, unpublished.
[223] A. M. de Vos, M. Ultsch, A. A. Kossiakoff, unpublished.
[224] J. P. Horowitz, J. Chua, M. Noel, *J. Org. Chem. 29* (1964) 2076; R. P. Glinski, M. S. Kahn, R. L. Kalamas, *ibid. 38* (1973) 4299; Editorial, *Lancet 2* (1989) 483.
[225] a) See, e.g., M. J. Berridge, *Phil. Trans. R. Soc. Lond. B317* (1987) 525; b) M. J. Berridge in N. A. Thorn, M. Treiman, O. H. Petersen (Eds.): *Molecular Mechanisms in Secretion, Alfred Benzon Symposium 25*, Munksgaard, Kopenhagen 1988, pp. 117–119; c) M. J. Berridge, P. H. Cobbold, K. S. R. Cutherbertson, *Phil. Trans. R. Soc. Lond. B320* (1988) 325; d) M. J. Berridge, *J. Physiol (London) 403* (1988) 589; e) M. J. Berridge, R. F. Irvine, *Nature (London) 341* (1989) 197.
[226] a) L. Changya, D. V. Gallacher, R. F. Irvine, B. V. L. Potter, O. H. Peterson, *J. Membrane Biol. 109* (1989) 85; b) L. Changya, D. V. Gallagher, R. F. Irvine, O. H. Peterson, *FEBS Lett. 251* (1989) 43; c) R. F. Irvine, R. M. Moor, *Biochem. J. 240* (1986) 917, and references cited therein.
[227] R. H. Mitchell, *Biochim. Biophys. Acta 415* (1975) 81.
[228] a) Y. Nishizuka, *Science (Washington, D. C.) 203* (1986) 305; b) *Nature (London) 334* (1988) 661; c) *Annu. Rev. Biochem. 58* (1989) 31.
[229] A. Wollmer, D. Brandenburg, H. P. Vogt, W. Schermutzki, *Hoppe-Seyler's Z. Physiol. Chem. 355* (1974) 1471.
[230] J. Markussen, *Int. J. Pept. Protein Res. 25* (1985) 431.
[231] J. Markussen: *Human Insulin by Tryptic Transpeptidation of Porcine Insulin and Biosynthetic Precursors*, MTP Press, Norwell, MA, 1987.
[232] Following *Haber* and *Anfinsen*'s successful refolding of ribonuclease in vitro in 1961 [69], attention has more recently shifted to protein folding in vivo [233–235]. Building on seminal studies by *Kauzmann* and by *Richards*, *Behe*, *Lattman* and *Rose* [236] concluded that in globular proteins the native fold determines packing, but packing does not determine the native fold.
[233] G. Fischer, F. X. Schmid, *Biochemistry 29* (1990) 2205.
[234] R. J. Ellis, *Semin. Cell Biol. 1* (1990) 1.
[235] S. J. Landry, L. M. Gierasch, *Trends Biochem. Sci. 16* (1991) 159.
[236] M. J. Behe, E. E. Lattman, G. D. Rose, *Proc. Natl. Acad. Sci. USA 88* (1991) 4195.
[237] S. Reichlin, *N. Engl. J. Med. 309* (1983) 1495, 1556.
[238] S. H. Ferreira, *Brit. J. Pharmacol. 24* (1965) 163.
[239] R. W. Brimblecombe, W. A. M. Duncan, G. J. Durant, J. C. Emmett, C. R. Ganellin, M. E. Parsons, *J. Intern. Med. Res. 3* (1975) 86.
[240] J. M. Moore, D. A. Peattie, M. J. Fitzgibbon, J. A. Thomson, *Nature (London) 351* (1991) 248.
[241] G. D. van Duyne, R. F. Standaert, P. A. Karplus, S. L. Schreiber, J. Clardy, *Science (Washington, D. C.) 252* (1991) 839.
[242] J. Lin, J. D. Farmer, Jr., W. S. Lane, J. Friedman, J. Weissman, S. L. Schreiber, *Cell 66* (1991) 807.
[243] P. A. Hargrave, *J. Prog. Retinal, Res. 1* (1982); M. L. Applebury, P. A. Hargrave, *Vision Res. 26* (1987) 1881.

The Extraordinary Enzymes Involved in Erythromycin Biosynthesis

By *James Staunton* *

The polyketides form a family of compounds which have very diverse structures and no obvious structural relationship, at least on superficial examination. Representatives of some of the main classes are presented in Scheme 1. Many of these compounds are of great commercial interest. For example, erythromycin, tetronasin, and oxytetracycline are all antibiotics which are used in medical practice and in animal husbandry. Another polyketide metabolite, FK 506 (not shown), is currently causing great excitement for its ability to act as an immunosuppressant following organ transplant surgery.[**]

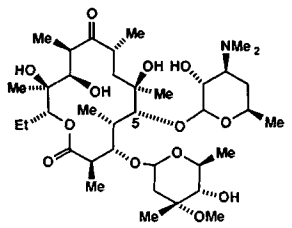

Erythromycin A

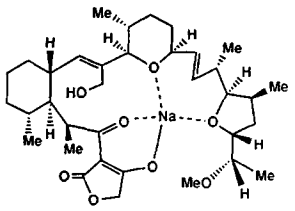

Tetronasin

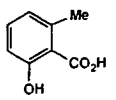

6-MSA

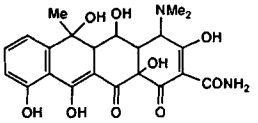

Oxytetracycline

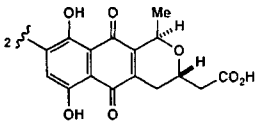

Actinorhodin

Scheme 1. Types of polyketide metabolites. 6-MSA = 6-methylsalicylic acid.

Despite their structural diversity the polyketides are thought to be related in biosynthesis, at least in the early steps of the pathways in which the essential core of the structure is assembled. This assembly process is thought to involve a variation of the standard biosynthetic cycle by which fatty acids are produced. In this cycle the growing fatty acyl chain is extended by the repeated addition of two methylene groups.[1] A representative reaction sequence is shown in Scheme 2. Initially, acetate is condensed with malonate to give acetoacetate with simultaneous loss of CO_2. Steps 2, 3, and 4 follow an unexceptional strategy to convert the ketone carbonyl to a methylene. The resulting extended acyl group then reenters at the starting point, and the cycle is repeated until the appropriate length of chain is reached. A special characteristic of these systems is that the growing chain is bonded via a thioester link to a protein thiol group at all stages, until the final product is released. The system of enzymes which carries out these steps is known as the fatty acid synthase (FAS) system.

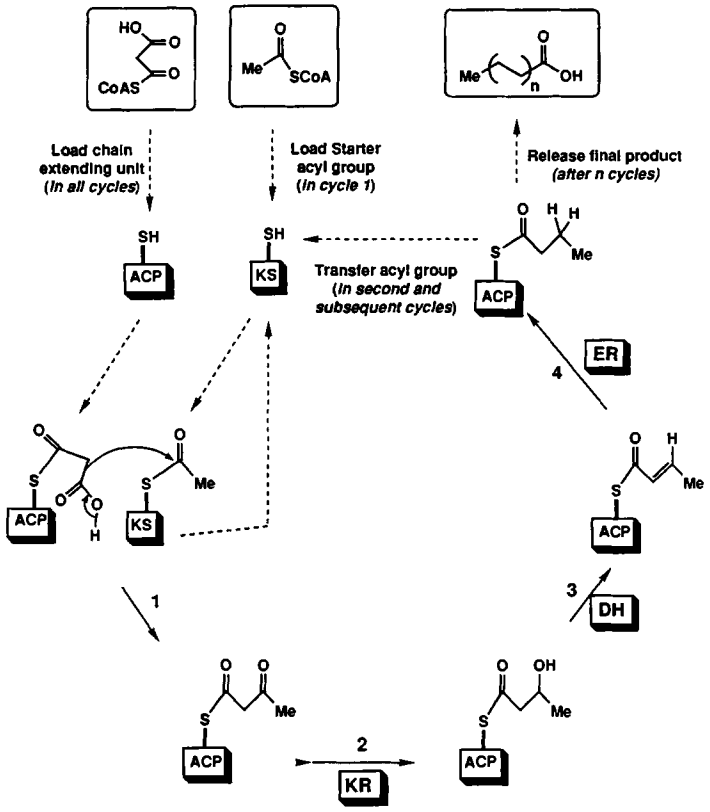

Scheme 2. Reactions and enzymes of fatty acid biosynthesis. KS = ketoacyl-synthetase; KR = ketoreductase; DH = dehydratase; ER = enoylreductase; ACP = acyl-carrier protein; CoA = Coenzyme A.

On casual inspection it may seem improbable that any of the polyketides of Scheme 1 is related to the simple fatty acids, but ample evidence has been accumulated to support this proposition. Studies with mutants have provided important though indirect evidence. When a mutant of a polyketide-producing organism lacks the ability to produce one of the biosynthetic enzymes, the preceding intermediate may accumulate in sufficient quantities for it to be isolated and identified. Such experiments with the erythromycin producer, *Saccharopolyspora erythraea* (formerly *Streptomyces erythraea*), led to the identification of several late intermediates of the biosynthetic pathway.[2] These compounds lacked some of the features of the erythromycin A structure, but nothing simpler than the macrocyclic lactone 6-deoxyerythronolide B was discovered. These experiments therefore indicate that the biosynthesis of erythromycin takes place in two phases, as is shown in Scheme 3, linked by the pivotal first enzyme-free intermediate, 6-deoxyerythronolide B. Al-

[*] Dr. J. Staunton
University Chemical Laboratory
Lensfield Road, GB-Cambridge CBZ 1EW (UK)

[**] See the Highlight in Number 8/1991: H. Kessler, D. F. Mierke, D. Donald, M. Furber, *Angew. Chem. 103* (1991) 968; *Angew. Chem. Int. Ed. Engl. 30* (1991) 954.

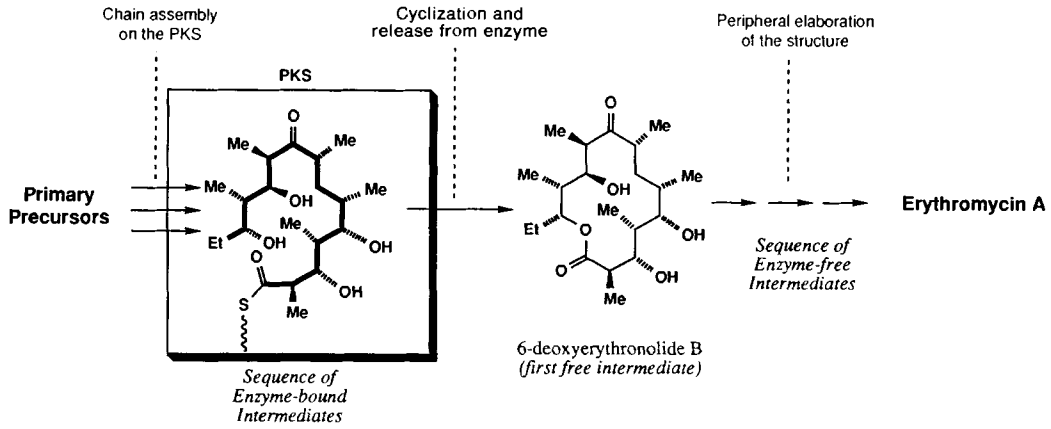

Scheme 3. Overview of the erythromycin A biosynthetic pathway. PKS = polyketide synthetase system.

though they throw no light on the mode of assembly of the key macrolide core of the molecule, these results support the idea that the early intermediates remain enzyme-bond, and so cannot accumulate in sufficient quantities for detection. By analogy with FAS systems, the enzymes involved in the chain assembly stage of a polyketide biosynthetic pathway are collectively known as the polyketide synthase (PKS) system.

The structure of the proposed final intermediate bound to the PKS in Scheme 3 is highlighted with heavy lines to emphasize that it contains a chain of carbons terminating in a carboxyl residue, and so has some structural resemblance to a simple fatty acid. Greater structural complexity is conferred on the antibiotic precursor by a series of branching methyl groups and by oxygen substituents. Both of these structural features can easily be introduced by a variation of the fatty acid biosynthetic cycle. The use of propionate rather than acetate as the chain starter acyl, and methyl malonate instead of malonate for the chain extension steps in Scheme 2 results in the formation of a carbon skeleton with methyl branching. Hydroxyl or ketone substituents could be left at the appropriate sites by omitting some or all of the steps normally used to convert each new ketone group to a methylene. In the case of 6-deoxyerythronolide B, the sequence of reactions catalyzed by the PKS would then take the form outlined in Scheme 4. The heavy arrows indicate where acyl groups need to be transferred in the various cycles, in order to leave the appropriate array of oxygen functions in the final enzyme-bound intermediate. Subsequent lactonization, perhaps catalyzed by a component of PKS, would then lead to the release of 6-deoxyerythronolide B. There are many classical biosynthetic incorporation studies using simple primary precursors variously labeled with isotopes of carbon, hydrogen, and oxygen in support of this scheme, and more recent incorporation studies with 'partly formed' chains, corresponding to enzyme-bound intermediates, have provided added insights.[3]

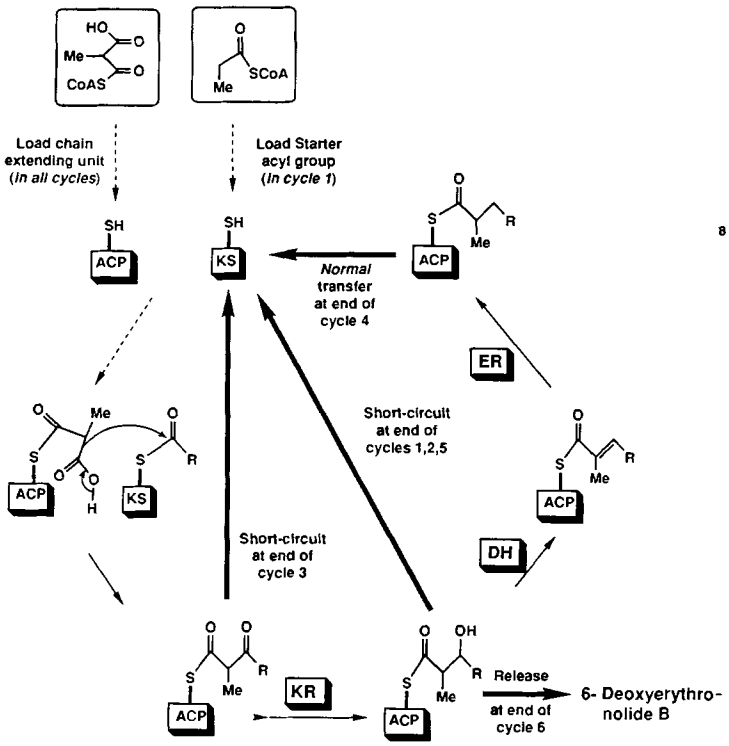

Scheme 4. Proposed mode of operation of the erythromycin PKS.

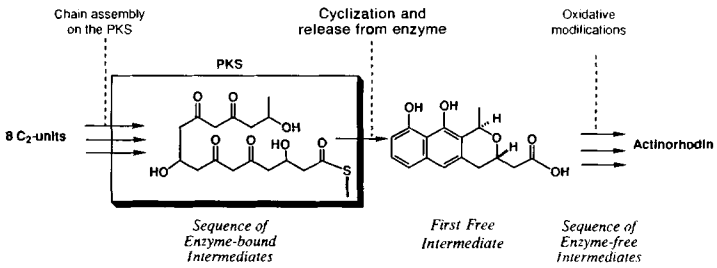

Scheme 5. Proposed biosynthesis pathway for actinorhodin.

Encouraged by progress made in studies of the genetics of the actinorhodin pathway by the Hopwood group in Norwich, many groups engaged in studies of polyketide biosynthesis have recently turned to a genetic approach in an effort to gain a clearer understanding of the molecular basis of chain assembly.[4] Actinorhodin has a structure consistent with a derivation from C_2-units via the enzyme-bound polyketide intermediate shown in Scheme 5. Since most of the ketone residues of this chain have been left unmodified by PKS, subsequent cyclization and dehydration reactions could take place to form the second intermediate shown. The

proposed pathway leads to actinorhodin by further oxidative steps involving other enzymes.

Many genes coding for proteins involved in this biosynthesis pathway have now been identified. Of particular interest here are a set of four which code for proteins having a strong sequence homology with protein components of various fatty acid synthases, and a fifth which is thought to be the cyclase responsible for the process of aromatization. These proteins are very probably the components of PKS. Interestingly, the individual genes are discrete and therefore the corresponding enzyme activities are not covalently linked to each other as they are formed. The actinorhodin PKS therefore probably resembles the FAS systems of most bacteria in consisting of a dissociable set of cooperating enzymes. Several other PKS gene clusters associated with the generation of polyacetate aromatic compounds in various *Streptomyces* species show a similar organization.[4] In contrast, the PKS for biosynthesis of 6-methylsalicylic acid (6-MSA), which has been isolated, is composed of a similar set of enzymes activities, linked covalently to form a large multifunctional protein.[5] The active form of the PKS is formed by the aggregation of four such multifunctional proteins. This more elaborate molecular architecture, which has precedents in the FAS systems of yeasts, mammals, and certain bacteria, probably leads to a more efficient and possibly more robust catalytic apparatus. In all of these polyacetate PKS systems, only one gene codes for each catalytic activity in the FAS cycle, which means that individual active sites in the PKS complex participate in successive cycles of chain extension.

The breakthrough in locating the actinorhodin PKS genes has stimulated a search for PKS genes in other organisms. In one approach genetic probes based on the actinorhodin genes were used with considerable success to locate the PKS genes for various aromatic polyacetate metabolites.[4] A second approach, also based on the pioneering work of the Norwich group, proved successful with the erythromycin genes, although the size of the task proved much greater than anyone imagined at the outset.[6, 7] Firstly, the gene coding for erythromycin resistance in the producing organism was located. By working initially on the assumption that the biosynthetic genes would be clustered in the vicinity of the resistance gene, as had been observed for the actinorhodin genes, the neighboring DNA was sequenced in a search for genes coding for FAS type proteins. This search was encouraged by the finding stemming from the Abbott laboratories in Chicago that mutations that prevented synthesis of 6-deoxyerythronolide B could all be localized to near the resistance gene.

The resulting picture which has emerged for the gene structure of the enzyme system for erythromycin biosynthesis is outlined in Scheme 6. On both sides of the resistance gene there are regions containing about 10000 pairs (10 kbp) of DNA which contain genes thought to code for proteins involved in the late stages of the pathway, in which 6-deoxyerythronolide B is converted into the erythromycin A. In confirmation, deletion of individual genes in these regions produced mutant organisms from which late intermediates have been isolated.

Sequencing further away from the resistance gene has subsequently revealed a region of DNA which contains sections corresponding to the elusive PKS gene cluster (Scheme 6). It became clear that the erythromycin PKS is much more elaborate than that associated with the biosynthesis of actinorhodin and other polyacetate aromatic compounds. The first indication of this extra complexity came with the discovery that there are several different genes coding for specific components of the PKS (e.g., there is more than one acyl-carrier protein (ACP) gene). This suggested that different cycles of chain extension might employ different versions of specific component enzymes.

What is perhaps even more surprising is the complexity of the organization of the enzyme activities. This was first revealed when a group from Cambridge published the complete sequence of one of the open reading frames (i.e., a potential gene) coding for part of the erythromycin PKS.[6] This exceptionally large open reading frame, containing more than 10 kbp of DNA, codes for a single giant protein of molecular weight 332472 Da, particular segments of which show sequence homology with individual FAS proteins. In all there are eight catalytic activities, corresponding to two different sets of the enzymes required for chain extension, together with a thioesterase.

More recently the complete sequence of the erythromycin PKS genes has been published by *Katz* and co-workers from the Abbott Laboratories.[7] It consists of three large open reading frames each coding for a large multifunctional protein having sufficient catalytic sites to carry out two chain extension cycles. It would appear, therefore, that there is an individual enzyme for each and every step carried out by the erythromycin PKS. The activities seem to be organized in six "modules", all of which contain the active sites for a condensation step, and all but one contain some or all of the active sites associated with conversion of the ketone group into a methylene in the fatty acid biosynthetic cycle. These modules are further linked in pairs, for which I suggest the term cassette. Three such cassettes collaborate in some undefined way to produce the first enzyme-free-intermediate, 6-de-

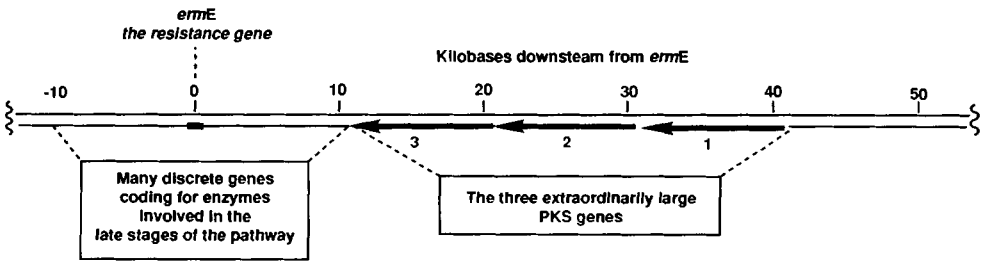

Scheme 6. Outline map of the cluster of genes coding for enzymes involved in erythromycin biosynthesis.

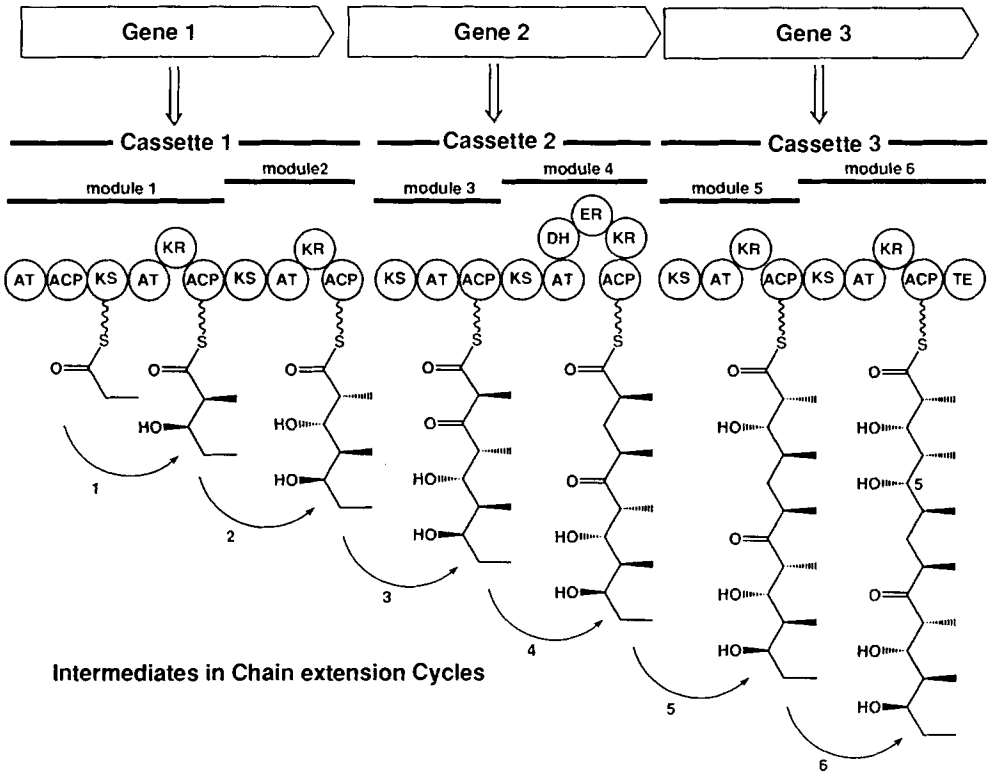

Scheme 7. The erythromycin polyketide synthetase system (PKS): primary organization of the genes and their corresponding protein cassettes. Examples of intermediates in the chain extension cycles are given. However, see caveat in text.

oxyerythronolide B, from one unit of propionate and six of methylmalonate.

Scheme 7 shows in more detail how the PKS genes are arranged on the genome, and how the catalytic sites are ordered in the primary structure of the protein chain in each corresponding cassette. A ligand is shown attached to each module to indicate how the modules may operate in assembling the polyketide chain. It should be stressed, however, that there are many possible ways for the cassettes to fold, possibly bringing complementary activities sited in different modules close together. In the functioning of the cassettes, therefore, the various activities which cooperate in a particular chain extension cycle may be drawn from different modules. Consequently, individual active sites with a particular function (e.g., the ACP's) need not necessarily come into play in the order in which they appear in the primary sequence of the protein, as is assumed in Scheme 7. At this time only one catalytic site, the ketone reductase (KR) site in module 5, has been firmly linked to a specific role in the elaboration of the erythromycin chain.[7] This was achieved by selective disruption of the DNA coding for this activity. The resulting mutant organism generated, instead of erythromycin, an analogue carrying a keto group at C5 of the macrolide ring. It is safe to conclude, therefore, that this reductase operates in the fifth cycle of chain extension, but not that its nearest neighbors in the primary sequence of the protein are its functioning partners.

In its size and sheer complexity this extraordinary PKS system breaks new ground, although in passing it should be mentioned that giant multifunctional proteins have also been implicated in the nonribosomal biosynthesis of some peptide secondary metabolites, and further examples may emerge as efforts to identify enzymes involved in other pathways of secondary metabolism gather pace.[8] The information obtained from sequencing the genes gives a fascinating insight into the primary organization of the PKS proteins, and some indication of how they function. An enormous multidisciplinary effort is required, however, to uncover fully the molecular basis of their action, and this will have to include direct studies of the proteins themselves. Encouraging progress on the isolation of PKS proteins from the erythromycin PKS has been reported from Cambridge.[9] A section of the open reading frame for cassette 3, corresponding to the thioesterase (TE) and ACP activities at the C-terminus, has been expressed at high levels in *Escherichia coli*. The resulting protein had the expected molecular mass (38019 Da), according to the electrospray mass spectrum, and it showed an ability to bind a standard inhibitor (phenylmethylsulphonyl fluoride) in a manner consistent with its expected thioesterase activity. More recently, the complete open reading frame coding for cassette 3 has been expressed in *E. coli* as a single protein with a molecular weight in the required range (ca 300 kDa by electrophoresis), confirming that these large genes are capable of expression as large single proteins.[10] Now that PKS proteins are becoming available, there is the exciting prospect that the activity of the constituent active sites may be demonstrated in vitro. The Cambridge group has already succeeded with a FAS ACP derived from the erythromycin producer, and in doing so has developed methodology appropriate to studying the PKS system.[11]

What other developments should we look for in the near future? It will be interesting to see if the organization of the erythromycin PKS as a series of modules arranged in cas-

settes holds good for other macrolide PKS's, and also possibly for ionophore-producing PKS's. This ordering of proteins in cassettes, which need not be exclusively bimodular, may hold the key to the precise control exercised by the synthase as a whole in carrying out its synthetic operations. It would, for example, help rationalize both the early observations of *Celmer* et al. on the common patterns of structure and stereochemistry which run through families of macrolides,[12, 13] and more recent related analyses of ionophore structures.[14] Perhaps regions with common structure in diverse metabolites are produced in different organisms by closely related cassettes derived from a common ancestral protein. Looking ahead, it may be possible to engineer organisms to produce novel chimeric metabolites by switching genes coding for specific cassettes from one producer to another.

If substantial amounts of active PKS proteins can be isolated by overexpression, it will be possible to investigate the molecular mechanisms by which the cassettes carry out their specific tasks. The protein–protein interactions which must play a major part in the collaboration between cassettes will make a fascinating study. Equally interesting are the molecular interactions which occur between protein components and substrates, which presumably help define the substrate specificity of the enzymic reactions. Progress in such studies could be of particular significance to synthetic chemists who have made great efforts in recent years to develop new methodology for macrolide synthesis.[15] Isolated PKS cassettes used in vitro may well prove to be convenient and efficient alternative synthetic tools for carrying out limited transformations on natural substrates and substrate analogues. In the longer term, it may be feasible to employ different combinations of cassettes in vitro, to generate complex chimeric products with greater control than would be possible in vivo. Chemists as well as biologists have reason to watch developments in this field.

German version: *Angew. Chem. 103* (1991) 1331

[1] S. Numa (Ed.): *Fatty Acid Metabolism and its Regulation* (in *Comprehensive Biochemistry, Vol. 7*) Elsevier, Amsterdam 1984.
[2] E. T. Seno, C. R. Hutchinson in S. W. Queener, I. E. Day (Eds.): *The Bacteria, Vol. 9*, Academic Press, New York p. 231.
[3] D. E. Cane, C. Yang, *J. Am. Chem. Soc. 109* (1987) 1255.
[4] D. A. Hopwood, D. H. Sherman, *Annu. Rev. Genet. 24* (1990) 37.
[5] J. Beck, S. Ripka, A. Siegner, E. Schiltz, E. Schweizer, *Eur. J. Biochem. 192* (1990) 487.
[6] J. Cortes, S. F. Haydock, G. A. Roberts, D. J. Bevitt, P. F. Leadlay, *Nature 348* (1990) 176.
[7] S. Donadio, M. J. Staver, J. B. McAlpine, J. B. Swanson, L. Katz, *Science 252* (1991) 675.
[8] H. Kleinkauf, H. von Doehren, *FEBS Lett. 268* (1990) 405.
[9] P. Caffrey, B. Green, L. C. Packman, B. J. Rawlings, J. Staunton, P. F. Leadlay, *Eur. J. Biochem. 195* (1991) 823.
[10] G. A. Roberts, personal communication.
[11] A. M. Bridges, P. F. Leadlay, W. P. Revill, J. Staunton, *J. Chem. Soc. Chem. Commun. 1991*, 778.
[12] W. D. Celmer, *J. Am. Chem. Soc. 87* (1965) 1801.
[13] D. E. Cane, W. D. Celmer, J. W. Westley, *J. Am. Chem. Soc. 105* (1983) 3594.
[14] D. O'Hagan, *Nat. Prod. Rep. 1989*, 205.
[15] Editorial comment: see also the Highlight by *J. Mulzer* in the November issue.

$LiClO_4$ in Ether—an Unusual Solvent

By *Herbert Waldmann**

Many reactions can be influenced in a variety of ways by the solvent employed. This is especially the case when polarized transition states or ionic intermediates are involved in the reaction and when the solvent is nucleophilic or electrophilic. A case to the contrary is the Diels-Alder reaction, which remains largely unaffected by the surrounding organic medium. In the mid-eighties, however, *Breslow* et al.[1] and *Grieco* et al.[2] demonstrated that Diels-Alder reactions proceed with increased reaction rate and with improved *endo-exo* selectivity when they are carried out, not in organic solvents but in aqueous solutions. The effect is further enhanced by salts such as LiCl (salting-in effect), whereas the addition of guanidinium chloride has the opposite effect (salting-out effect). The use of water as solvent for such cycloadditions had already been described earlier by *Alder* et al.[3a] and later by *Koch* et al.[3b] The accelerating effect of this reaction medium is also manifested in many other reactions,[4] e.g. asymmetric hetero-Diels-Alder reactions[4b] and asymmetric nonhetero-Diels-Alder reactions,[4c, d] nucleophilic additions to iminium ions[4e] and carbonyl compounds,[4f] Claisen rearrangements,[4g] the benzoin condensation,[1b] and aldol reactions.[4h] It is attributed to the fact that a suitable aggregation is generated by hydrophobic interactions between the reaction partners (hydrophobic effect), and so exercises an "internal pressure" on the reactants encapsulated in "solvent cavities" whose effects are, in turn, comparable with a high external pressure, at least in the case of the Diels-Alder reaction.

Last year, *Grieco* et al.[5] described a solvent system, namely a 5 M solution of $LiClO_4$ in diethyl ether, which has a comparable, if not greater accelerating effect on Diels-Alder reactions. Already in 1986 *Sauer* et al.[6] investigated the steric course of Diels-Alder reactions in such solvent systems in order to determine the polarity of ethereal $LiClO_4$ solutions, and had already recommended them as polar solvents for organic chemical reactions. *Grieco* et al. then demonstrated the astounding properties of these solutions (see Scheme 1), which according to *Pocker* et al.[7] must be regarded as mixtures of the mono- and diether adduct of $LiClO_4$. The reaction of cyclopentadiene **1** with ethyl acrylate **2**

[*] Prof. Dr. H. Waldmann
Institut für Organische Chemie und Biochemie der Universität
Gerhard-Domagk-Strasse 1
W-5300 Bonn (FRG)

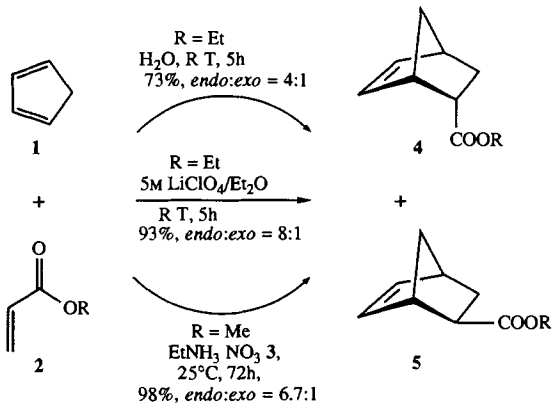

Scheme 1.

(R = Et) to give the bicycloheptenes **4** and **5** proceeds more rapidly and with higher *endo*-selectivity in 5 M $LiClO_4$/diethyl ether (*endo*:*exo* = 8:1) than in water (Scheme 1). Particularly advantageous is the compatibility of the $LiClO_4$/ether system with substances sensitive to hydrolysis. Thus, the azadiene **6** reacts with methyl acrylate at room temperature in the presence of the Li-salt to give the desired cycloadduct **7** in 80% yield in 5 h, whereas the same reaction in benzene affords **7** in 75% yield only after 72 h at 60 °C (Scheme 2). Particularly impressive is the reaction of furan **8**, which, owing to its aromaticity does not react with the thiophene derivative **9** under normal conditions (Scheme 2). In $LiClO_4$/ether,

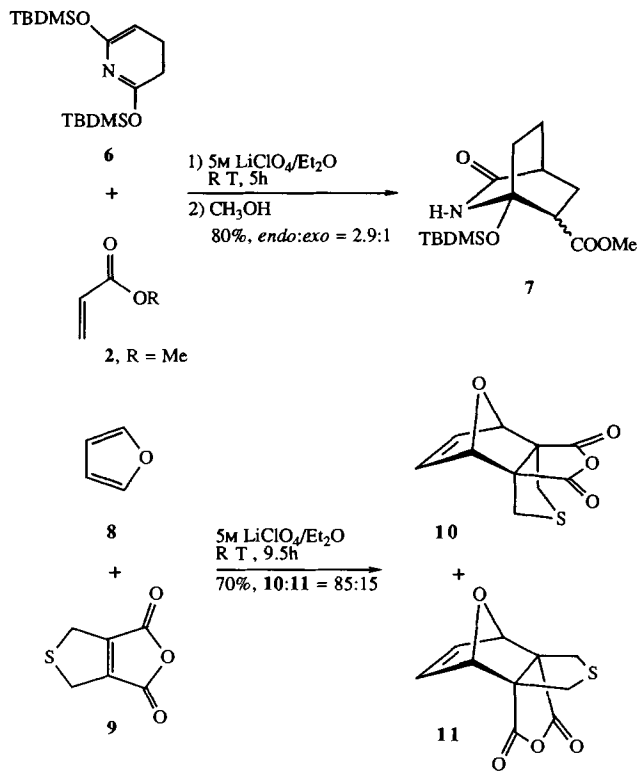

Scheme 2. RT = room temperature.

however, the cycloadducts **10** and **11** are formed in 70% yield in the ratio 85:15 after 9.5 h at room temperature and under atmospheric pressure. These values must be compared with those reported by *Dauben* et al.,[8] who required 6 h and 15 kbar in order to achieve the same product ratio in their synthesis of cantharidin by the same reaction in CH_2Cl_2. To explain their results *Grieco* et al. assume that $LiClO_4$/ether solutions, in analogy to water, generate an internal pressure and press the reactants together. However, the stabilization of a polarized transition state by the salt is not ruled out.

The latter possibility is not improbable, since, on the one hand, the rate- and selectivity-enhancing effect of Lewis acids on Diels-Alder reactions is well known, so that such an effect could be attributed to the presence of Li^+ ions in higher concentration. On the other hand, it has already been possible, with ethereal solutions of $LiClO_4$, to accelerate a number of reactions which proceed via polarized intermediates. Thus, *Winstein* et al.[9] found that the ionization of *p*-methoxyneophyl tosylate and a *p*-nitrobenzoate in a 0.1 M solution of $LiClO_4$ in ether is respectively 10^5 and 10^6 times faster than in ether itself. *Pocker* et al.[7] have investigated the properties of concentrated solutions of $LiClO_4$ in ether, developed concepts about their structure, showed that the ionization of *tert*-butyl chloride in 5.5 M $LiClO_4$/diethyl ether occurs about 10^6 times more rapidly than in ether, and found that the rearrangement of 1-phenylallyl chloride to 3-phenylallyl chloride takes place 85600 times more rapidly in a 3.39 M solution than without added salt ("electrostatic catalysis").

Already in the early eighties *B. Föhlisch* et al.[10] exploited the advantageous effects of the medium presented here in their detailed investigations of the [4 + 3] cycloadditions of α-halogeno- or α-sulfonyloxy-substituted ketones **12** to 1,3-dienes, in particular to furan (Scheme 3). The 8-oxabicy-

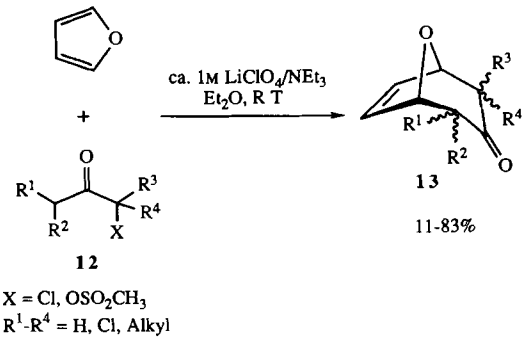

Scheme 3.

clo[3.2.1]oct-6-en-3-ones **13** formed thereby are of interest, inter alia, as starting materials for the synthesis of tropones and other natural products. For the cycloadditions with the α-halogeno- or the α-mesyloxyketones **12**, room temperature suffices, and inter- and intramolecular reactions can be carried out in satisfactory to good yields. A possible use of this method for the synthesis of natural terpenes, e.g. of the guajanolide, azulene, and hydroazulene type, seems very promising.

The favored acceleration of ionic conversions and reactions with polarized transition states by the system $LiClO_4$/diethyl ether also follows from the surprising observation made by *Grieco* et al.[11] that allyl vinyl ethers, contrary to expectation, do not undergo [3,3]-sigmatropic rearrange-

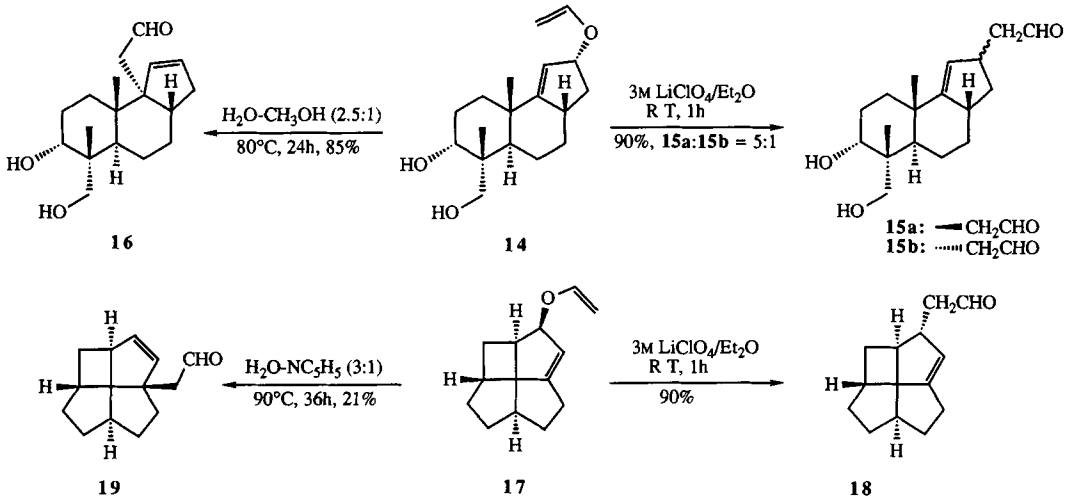

Scheme 4.

ments in 3 M $LiClO_4$/diethyl ether solutions, but give aldehydes in [1,3]-sigmatropic rearrangements (Scheme 4). Thus, e.g., **14** reacts under these conditions to give **15** in 90% yield within 1 h at room temperature (in 5 M salt solution the reaction is already complete after 10 min), and also the fenestrane **17** is transformed into the aldehyde **18** in high yield. These observations, particularly the steric course of the rearrangements, are in sharp contrast to the findings that **14** undergoes the expected Claisen rearrangement to **16** in water-methanol (2.5:1) at 80 °C and that also the fenestrane **17** rearranges to **19** in water-pyridine (3:1) at 90 °C.

In all cases the [1,3]-sigmatropic rearrangements take place at room temperature and make the products available in high yields under the mildest conditions. The authors demonstrate on the basis of crossover experiments that ionic intermediates must indeed be involved, and they verify the importance of Li^+ ions being present: the use of a 1.8 M tetrabutylammonium perchlorate solution as solvent has no advantageous effect on the rearrangement.

The solvent system $LiClO_4$/diethyl ether has already proven to be an excellent medium for diverse reactions. It is to be expected that further uses will be found. The fantasy of the experimentalist must not be confined to the concentrated solutions of $LiClO_4$ in ether, which also can be regarded as a salt with little ether additive.[7] Thus, *Jaeger* et al.[12] have recently reported that the low-melting (m.p. $\approx$ 12 °C) ethylammonium nitrate **3** (Scheme 1) likewise offers advantages as solvent; Diels-Alder reactions are considerably accelerated and proceed more selectively in this salt than in organic solvents. The effect is, however, less pronounced than on changing over to water or $LiClO_4$/ether.

German version: *Angew. Chem. 103* (1991) 1336

[1] a) R. Breslow, U. Maitra, *Tetrahedron Lett. 25*(1984) 1239–1240, and references cited therein; b) review: R. Breslow, *Acc. Chem. Res. 24* (1991) 150–164.

[2] P. A. Grieco, P. Galatsis, R. F. Spohn, *Tetrahedron 42* (1986) 2847–2853, and references cited therein.

[3] a) O. Diels, K. Alder, *Justus Liebigs Ann. Chem. 490* (1931) 243–257; b) H. Koch, J. Kotlan, H. Markert, *Monatsh. Chem. 96* (1965) 1646–1657.

[4] a) Review: H. U. Reissig, *Nachr. Chem. Tech. Lab. 34* (1986) 1169–1171; b) H. Waldmann, *Liebigs Ann. Chem. 1989*, 231–238, and references cited therein; c) H. Waldmann, M. Dräger, *ibid. 1990*, 681–685; d) A. Lubineau, Y. Queneau, *Tetrahedron 45* (1989) 6697–6712; e) S. D. Larsen, P. A. Grieco, W. F. Fobare, *J. Am. Chem. Soc. 108* (1986) 3512–3513; f) H. Waldmann, *Synlett 1990*, 627–628, and references cited therein; g) P. A. Grieco, E. B. Brandes, S. McCann, J. D. Clark, *J. Org. Chem. 54* (1989) 5849–5851; h) A. Lubineau, *ibid. 51* (1986) 2142–2144.

[5] P. A. Grieco, J. J. Nunes, M. D. Gaul, *J. Am. Chem. Soc. 112* (1990) 4595–4596.

[6] R. Braun, J. Sauer, *Chem. Ber. 119* (1986) 1269–1274.

[7] Y. Pocker, D. L. Ellsworth, *J. Am. Chem. Soc. 99* (1977) 2276–2284, 2284–2293, and references cited therein.

[8] W. G. Dauben, C. R. Kessal, K. H. Takemura, *J. Am. Chem. Soc. 102* (1980) 6893–6894.

[9] S. Winstein, S. Smith, D. Darnisch, *J. Am. Chem. Soc. 81* (1959) 5511–5512.

[10] a) R. Herter, B. Föhlisch, *Synthesis 1982*, 976–979; b) B. Föhlisch, D. Krimmer, E. Gerlach, D. Käshammer, *Chem. Ber. 121* (1988) 1585–1593, and references cited therein.

[11] P. A. Grieco, J. D. Clark, C. T. Jagoe, *J. Am. Chem. Soc. 113* (1991) 5488–5489.

[12] D. A. Jaeger, C. E. Tucker, *Tetrahedron Lett. 30* (1989) 1785–1788.

Communications may be submitted in English *or* in German. Further details regarding the submission of communications can be found in the "Notice to Authors" reproduced in the January issue of the journal. Copies thereof may be obtained from the editorial office upon request.

Globe-trotting Hydrogens on the Surface of the Fullerene Compound $C_{60}H_6(N(CH_2CH_2)_2O)_6$**

By *Andreas Hirsch, Qiaoying Li,* and *Fred Wudl**

Dedicated to Professor Michael Hanack on the occasion of his 60th birthday

We discovered recently that a variety of dienes, dipoles, and a number of nucleophiles react with buckminsterfullerene (C_{60}) to yield adducts.[1] Among the nucleophiles, primary and secondary amines such as *n*-propylamine, *n*-dodecylamine, *tert*-butylamine, ethylenediamine, and morpholine (H morph) readily react with C_{60} to give the amino addition compounds $C_{60}H_n(NRR')_n$ (predominantly $n = 6$ as determined by elemental analysis and titration experiments with 0.1 N HCl).[1] This might be due to the fact that C_{60} consists of six independent pyracyclene units to which the amines can be added most easily. In the case of the reaction with *n*-propylamine, however, also minor amounts of higher addition products (up to twelve amino groups) have been found by FAB mass spectrometry.[1] Whereas the other amino adducts of C_{60} are soluble in the neat amine, $C_{60}H_6(morph)_6$ precipitates from the solution and therefore evades further additions. All those carbon atoms in these "hairy balls" to which either a hydrogen or a nitrogen atom has been added change their state of hybridization from pseudo-sp^2 to pseudo-sp^3. The mechanism of the amino addition is stepwise (Scheme 1). A single electron transfer (SET) precedes the covalent bond formation and proton transfer, as determined by UV/VIS and ESR spectroscopy.[1]

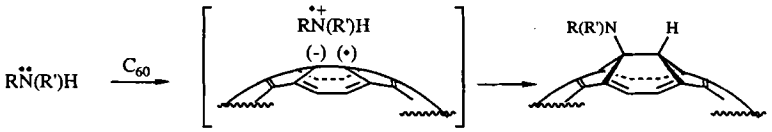

Scheme 1. Proposed mechanism of amine addition to C_{60}.

In this paper we report the remarkable dynamic behavior of the morpholine adduct $C_{60}H_6(morph)_6$, which has been studied by ^1H NMR spectroscopy and deuterium exchange experiments. This compound was prepared by stirring C_{60} in neat morpholine for 2 days, whereupon it precipitated as an orange-brown solid from the red-brown solution. The $C_{60}H_6(morph)_6$ composition of this solid has been confirmed by elemental analysis and thermogravimetric analysis.[2] The IR spectrum[3] of $C_{60}H_6(morph)_6$ shows complete substitution of the NH by CH hydrogens (C_{60}–H, no NH vibrations) and is typical for *N*-substituted morpholine compounds.[4] Two broad peaks in the room-temperature ^1H NMR spectrum (relative to TMS) at $\delta = 3.84$ and 3.27, which are not resolved as triplets, are due to the methylene groups of the morpholine substituent. The attachment of the morpholine unit to C_{60} causes a downfield shift from $\delta = 2.87$ (free morpholine) to 3.27 for the CH_2 protons α to nitrogen, whereas the CH_2 protons α to oxygen are affected to a smaller extent ($\Delta\delta = 0.2$). This behavior demonstrates clearly the electron-withdrawing influence of the C_{60} core. The signal for the "bucky ball" protons is very broad and symmetrical at $\delta = 1.84$, indicating already a rapid exchange of these hydrogens. The ^1H NMR spectrum (in $CDCl_3$, δ relative to TMS), as a function of temperature, shows very interesting features (Fig. 1). Upon cooling, the signals of the

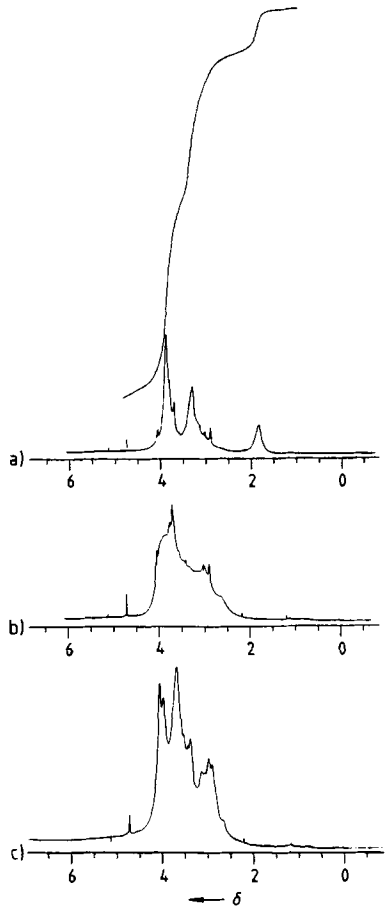

Fig. 1. Temperatur-dependent ^1H NMR spectra (500 MHz) of $C_{60}H_6(morph)_6$ in $CDCl_3$. a) 25 °C, b) −25 °C, c) −60 °C.

CH_2 groups of the morpholine substituents become broader, and at the same time the signals of the "bucky ball" protons shift downfield from $\delta = 1.84$ at room temperature to about 2.6 at −20 °C. At −25 °C only one broad and little struc-

[*] Prof. Dr. F. Wudl, Dr. A. Hirsch, Dr. Q. Li
Institute for Polymers and Organic Solids
Department of Physics and Chemistry, University of California
Santa Barbara, California 93106 (USA)

[**] This work was supported by the Deutsche Forschungsgemeinschaft (postdoctoral fellowship for *A. H.*) as well as NSF Grants DMR-88-20933 and CHE89-08323 to *F. W.*

tured resonance region reaching from $\delta = 2.5$ to 4.2 appears in the spectrum. Further stepwise cooling down to $-60\,^{\circ}C$ results in a sharpening and formation of new signals. The main peaks appear at $\delta = 4.04$, 3.97, 3.96, 3.38, and 3.15. This relatively complex spectrum shows that $C_{60}H_6(morph)_6$ at $-60\,^{\circ}C$ consists of a mixture of constitutional and, perhaps, conformational isomers; different arrangements of the morpholine groups and "bucky ball" protons cause slightly different chemical shifts. At $-90\,^{\circ}C$ in CD_2Cl_2 even individual triplets between $\delta = 2.7$ and 3.4 can be resolved (CH_2 α to N). Heating up to $50\,^{\circ}C$ leads just to a small extent of further line sharpening compared to the spectrum at room temperature, but the chemical shift of the fullerene protons remains constant.

Whereas the observed dynamic phenomenon of the morpholine units can be conformational in character (ring inversion), the reversible shift of the "bucky ball" protons shows their very high mobility on the surface of the fullerene. The dynamic effect is independent of concentration (in the range 1×10^{-2}–8×10^{-4} M), indicating that it is an intramolecular process. It is possible, as suggested by a referee, that the process is assisted by the basic N atoms, particularly since the pK_a of the C_{60} surface C–H bonds is rather low (see below the discussion on H–D exchange). Therefore the spherical structure and the remaining conjugated π system of the C_{60} core is expected to allow multiple, almost degenerate [1,5]-sigmatropic hydrogen shifts (Scheme 2) which make these hydrogens on fullerene "globe trotters".[5]

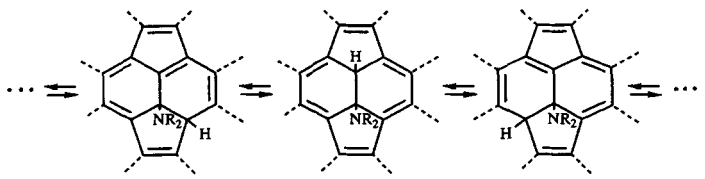

Scheme 2. [1,5] sigmatropic hydrogen shift in $C_{60}H_6(N(CH_2CH_2)_2O)_6$.

In typical cases of [1,5]-sigmatropic hydrogen shifts the activation enthalpies $\Delta H^{\neq}$ are in the neighborhood of 30 kcal mol^{-1} but ca. 10 kcal mol^{-1} for cyclopentadiene, whereas the entropies $\Delta S^{\neq}$ are[6] -5 to -10 cal mol^{-1} K^{-1}. Although the activation entropies $\Delta S^{\neq}$ for [1,5]-sigmatropic shifts on the surface of C_{60} are expected to be very low (preorganized arrangement), the activation enthalpies $\Delta H^{\neq}$ must be extraordinarily low and lie below 10 kcal mol^{-1} since a rapid exchange is occurring above $-25\,^{\circ}C$. This result is puzzling, because considerable geometric changes must accompany the hydrogen motion; the carbon atom bearing the migrating hydrogen must move back down to the sphere's surface while a new carbon atom must rise to meet the incoming atom.

The reaction of C_{60} with *N*-deuterated morpholine leads to $C_{60}D_6(morph)_6$. The ^1H NMR spectrum of this compound shows just the CH_2 signals at $\delta = 3.9$ and 3.3. The deuterium on the C_{60}, however, can be easily exchanged by addition of methanol to the chloroform solution resulting in the formation of $C_{60}H_6(morph)_6$. Conversely, $C_{60}D_6(morph)_6$ has also been prepared by treatment of $C_{60}H_6(morph)_6$ with CH_3OD.[7] This behavior is in accordance with the line shape of the C_{60}-bound protons in the ^1H NMR spectrum and also supports the low $\Delta H^{\neq}$ values for [1,5]-sigmatropic hydrogen shifts. With the deuterated product in hand, we found that within experimental error there is no measurable deuterium isotope effect in this dynamic process.

That the CH bond in $C_{60}H_6(morph)_6$ is still covalent in character is shown by cyclic voltammetry in CH_2Cl_2. Two reversible reduction peaks at high scan rates (1 V s^{-1}) can be observed at 880 and 1319 mV vs. commercial Ag/AgCl (Fig. 2). Dissociated protons would have been reduced to H_2

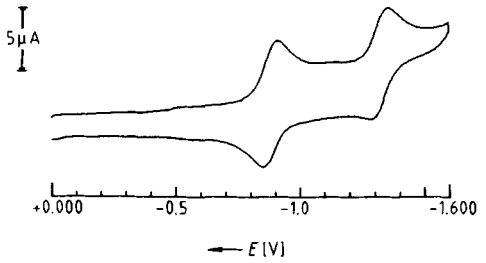

Fig. 2. Cyclic voltammogram of $C_{60}H_6(N(CH_2CH_2)_2O)_6$ at a platinum electrode in CH_2Cl_2; supporting electrolyte, 0.1 M Bu_4NBF_4; scan rate, 1 V s^{-1}; reference electrode, Ag/AgCl.

and at least one peak would have been irreversible. Although the reduction potentials are much higher than those for natural C_{60},[8] the cyclic voltammogram of $C_{60}H_6(morph)_6$ demonstrates that there is still a large amount of π conjugation of a substantially *electronegative* set of carbon atoms. The sharpness of the cyclic voltammogram waves shows also that a fairly uniform compound is present at room temperature; the substituents are very likely regularly distributed (one can postulate that the six morpholine substituents, due to steric requirements, are as far from each other as possible) or averaged through the globe-trotting hydrogens.

In summary, we report the discovery of a novel, facile dynamic process, very likely characteristic of C_{60} addition products where the elements of R_2N and **H** are added across the pyracyclene units. The scope and generality [R_nX–**H**, X = N, O, S, C(?), etc] of this phenomenon remain to be determined.

Received: July 26, 1991 [Z 4827 IE]
German version: *Angew. Chem. 103* (1991) 1339

[1] A. Hirsch, K. Khemani, T. Suzuki, P.-M. Allemand, A. Koch, G. Srdanov, F. Wudl in: *Large Carbon Clusters* (*ACS Symp. Ser.* (1991)).

[2] Analysis calcd for $C_{60}H_6(OC_4H_8D)_6 \cdot 1/2\,CHCl_3$: C 78.67, H 3.77, N 6.47; found: C 78.84, H 3.84, N 6.44. thermogravimetric analysis (10 K per min): Weight loss calcd for $C_{60}H_6(OC_4H_8N)_6 \cdot 1/2\,CHCl_3$: 44.69%; found (between 25 and 540 °C) 44.42%. $T_{max} = 250\,^{\circ}C$.

[3] IR (KBr) $\tilde{\nu}$ = 3040(w), 2950(s), 2880(w), 2840(s), 2810(sh), 2740(w), 2670(w), 1450(s), 1390(m), 1360(vw), 1290(m), 1270(s), 1210(w), 1120(s), 1070(w), 1010(s), 910(w), 870(m), 730(m), 550(m), 520(m) cm^{-1}.

[4] Compare, for example: *N*-methylmorpholine in C. J. Pouchert: *The Aldrich Library of FT-IR Spectra, Vol. 1*, 1st ed., 1985, p. 382.

[5] We could have chosen the term "ring-whizzing" but it is restricted to *two* dimensions; the phenomenon described here occurs in three dimensions on a spherical molecule.

[6] a) A. P. ter Borg, H. Kloosterziel, *Recl. Trav. Chim. Pays-Bas 82* (1963) 741; b) D. S. Glass, R. S. Boikess, S. Winstein, *Tetrahedron Lett. 1966*, 999; c) R. W. Roth, *Justus J. Liebigs Ann. Chem. 671* (1964) 25.

[7] This set of experiments allowed us to assign unambiguously the C_{60}-H and C_{60}-D stretching frequency as 3040 and 2240 cm^{-1}, respectively.

[8] P.-M. Allemand, A. Koch, F. Wudl, Y. Rubin, F. Diederich, M. M. Alvarez, S. J. Anz, R. L. Whetten, *J. Am. Chem. Soc. 113* (1991) 1050.

$[Mo(CO)_2(^{tbu}S'_2)_2]$ and $[MoCO(PPh_3)(^{tbu}S'_2)_2]$: CO Coordination at [Mo–S] Centers Where Mo Is in a High Oxidation State**

By *Dieter Sellmann,* Franz Grasser, Falk Knoch,* and *Matthias Moll*

Carbonyl complexes of metals in high oxidation states are usually unstable[1] and therefore rare.[2] Can such species occur in nitrogenases? The sulfur-coordinated Mo atoms of the active centers of Fe/Mo nitrogenases are probably in the high oxidation state + IV.[3] Nevertheless, they are postulated as coordination sites for the nitrogen molecule and the nitrogenase inhibitor CO.[4] In order to obtain model compounds for Fe/Mo nitrogenases, attempts have often been made to bind N_2 or CO to high-valent [Mo–S] centers.[5]

We have now obtained such a CO complex [see Eq. (a)]. In an unusual redox elimination the Mo^{II} complex $[Mo(CO)_3(^{tbu}S'_4)_2]$ (**1**, $^{tbu}S'^{2\ominus}_4$ = 1,2-bis(3,5-di-*tert*-butyl-2-mercaptophenylthio)ethane(2 −))[6] loses CO and C_2H_4 under high vacuum conditions to form $[Mo(CO)_2(^{tbu}S'_2)_2]$ (**2**). Complex **2** has a Mo^{IV} center; the only other ligands besides CO which are bound to the metal are biologically relevant dithiolato donors.

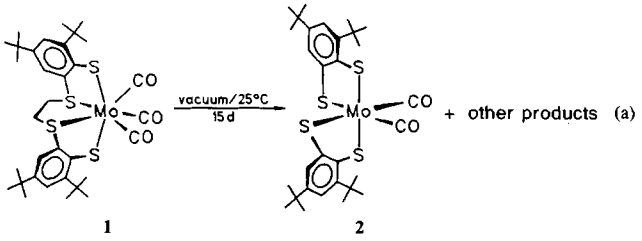

1 **2**

The bright blue-violet **2** is stable at room temperature and its IR spectrum in *n*-pentane shows two intense high-frequency CO bands at $\tilde{\nu}$ = 2041 and 2006 cm^{-1}. The number of bands, their absolute position, and their significant shift to higher frequency relative to the bands of **1** (for which $\tilde{\nu}$ = 2028, 1951 cm^{-1} in *n*-pentane) indicate that in **2** *cis* CO ligands are bound to an electron-deficient, high-valent [Mo–S] center.

^1H and $^{13}C\{^1H\}$ NMR spectra show that the $^{tbu}S'_2$ ligands are symmetry-equivalent, as are the CO ligands. The four *tert*-butyl groups give rise to only two sharp singlets in the ^1H NMR spectrum; the CO ligands show one signal and the C atoms of the $^{tbu}S'_2$ ligands ten in the $^{13}C\{^1H\}$ NMR spectrum. The IR and NMR data therefore confirm that **2** has a C_2 axis as indicated in Equation (a).

From the PPh_3 derivative $[Mo(CO)(PPh_3)(^{tbu}S'_2)_2]$ (**3**) we obtained single crystals, which enabled a molybdenum–sulfur–carbon monoxide complex in a high oxidation state to be characterized not only by spectroscopic methods, but for the first time also by X-ray crystallography.[7] Compound **3** forms in a similar way to **2** from $[Mo(CO)_2(PPh_3)(^{tbu}S'_2)]$ (**4**) ($\tilde{\nu}$(CO) = 1939(sh), 1930, 1882(sh), 1864 cm^{-1} in KBr)[6] and also shows a high-frequency CO band (1978 cm^{-1} in KBr). The released C_2H_4 was detected directly by NMR spectroscopy.

$$[Mo(CO)_2(PPh_3)(^{tbu}S'_4)] \xrightarrow[75\ min]{THF/65°C} [Mo(CO)(PPh_3)(^{tbu}S'_2)_2] + C_2H_4 + CO \quad (b)$$

4 **3**

As shown in Figure 1a, the C_1-symmetrical structure of compound **3** exhibits almost ideal pseudo-trigonal-prismatic coordination at the molybdenum center (Fig. 1b).[7] The average deviations of the atoms from tetragonal planes lie between 2.0 and 6.7 pm, the trigonal planes P1-S2-S3 and C1-S1-S4 are practically parallel (dihedral angle 2.1°), and the torsion angle between them is close to the limiting value of 0° for an ideal trigonal prism. The *tert*-butyl groups are as far apart as possible, giving rise to C_2 symmetry for the $[Mo(^{tbu}S'_2)_2]$ framework of **3**.

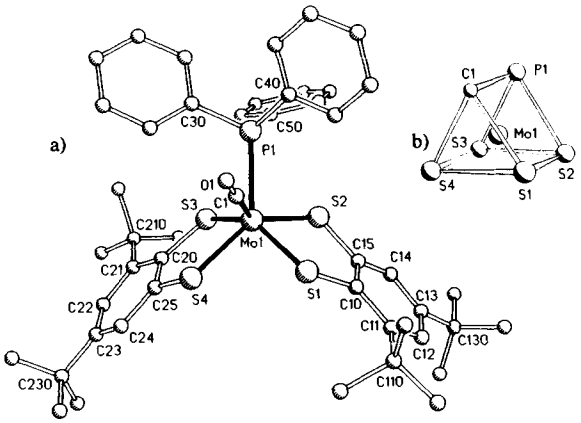

Fig. 1. a) Structure of **3** in the crystal (H atoms omitted); b) pseudo-trigonal-prismatic coordination at the molybdenum center. Important bond lengths [pm] and angles [°]: Mo1-C1 204.2(6), Mo1-S1 234.9(2), Mo1-S2 235.8(2), Mo1-S3 236.4(2), Mo1-S4 235.0(2), Mo1-P1 251.7(2), S1-C10 173.8(5), S2-C15 173.6(6), S3-C20 174.5(5), S4-C25 172.9(6), C1-O1 113.4(7); C1-Mo1-S1 79.0(2), S1-Mo1-S2 81.4(1), S2-Mo1-S3 86.8(1), S3-Mo1-S4 80.8(1), S1-Mo1-S4 84.2(1), C1-Mo1-P1 82.3(2), Mo1-C1-O1 178.8(5).

Not only the high-frequency CO absorptions of **2** and **3**, but also the interatomic distances of **3** indicate a high oxidation state for the Mo center and exclude an oxidation of the benzenedithiolato ligands to dithioketones according to Equation (c). Such ligand-centered redox steps are often discussed in connection with compounds containing dithioethylene ligands of the type $S_2C_2R_2$ and are deduced from bond shortening.[8] The relevant C–S distances in **3** and related $^tS'_4$ ($^tS'^{2\ominus}_4$ = 1,2-bis(2-mercaptophenylthio)ethane(2 −)) and $^{tbu}S'_4$ complexes with metals in low oxidation states, such as $[Mo(CO)_2(PMe_3)(^tS'_4)]$ (**5**), $[Mo(NO)(NH_2O)(^tS'_4)]$ (**6**), $[Mo(NO)_2(^tS'_4)]$ (**7**),[9] and $[Fe(CO)_2(^{tbu}S'_4)]$ (**8**),[10] all lie within the range 172.9(6) to 176.2(6), and no shortening of the C–S bond in **3** is evident. The same holds for the C–C distances in the C_6 rings. These findings are supported by calculations which indicate that 1,2-benzenedithiolate(2 −) also functions as dianion on coordination to high-valent metal centers,[11] by our results for Fe^{IV}–benzenedithiolato complexes,[12] and last but not least by the expectation that

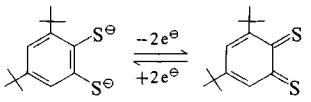

(c)

[*] Prof. Dr. D. Sellmann, Dipl.-Chem. F. Grasser, Dr. F. Knoch, Dr. M. Moll
Institut für Anorganische Chemie II der Universität
Egerlandstrasse 1, W-8520 Erlangen (FRG)

[**] $^{tbu}S'^{2-}_2$ = 3,5-di-*tert*-butyl-1,2-benzenedithiolate(2 −). Transition-metal Complexes with Sulfur-Containing Ligands, Part 74. This work was supported by the Deutsche Forschungsgemeinschaft and the Fonds der Chemischen Industrie. Part 73: D. Sellmann, P. Lechner, F. Knoch, M. Moll, *Z. Naturforsch.*, in press.

the resonance stabilization energy of the aromatic system would hinder a reaction such as described in Equation (c).[8] The Mo^{IV} centers of **2** and **3** thus have formal 14e configurations.

What stabilizes these electronically highly unsaturated metal centers? One answer is found in the comparison of the Mo–S distances in **3** and the previously mentioned complexes. The average Mo–S distances in **3** (235.5 pm) are significantly shorter than the average Mo–S(thiolato) distances in, for example, **5** (250.6 pm), **6** (247.8 pm), and **7** (245.1 pm).[9] They indicate that S → Mo π-donor bonds between occupied p orbitals of the thiolato ligands and empty Mo d orbitals decrease the electron deficit at the Mo center in **3**.

The ^1H and $^{13}C\{^1H\}$ NMR spectra of **3** each show exactly half the number of signals anticipated from the C_1 symmetry of the solid. Thus, in solution **3** has firstly a different structure than in the solid, and secondly a C_2 axis (as, for instance, in the *trans* structure of **3**.)

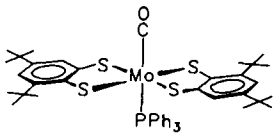

trans-**3**

$[Mo(CO)_2(^{tbu}S'_2)_2]$ shows that CO can indeed coordinate to Mo^{IV} centers that are surrounded exclusively by (biologically relevant) dithiolato donors. Do the Mo^{IV} centers in Fe/Mo nitrogenases have accordingly to be the coordination sites for the nitrogenase inhibitor CO as well as for the N_2 molecule? Even after the discovery of nitrogenases containing only iron as metal centers,[13] this possibility cannot be entirely ruled out. It is, however, also possible that N_2 is bound to the Fe center and CO to the Mo center. This arrangement could primarily impede the electron flow within the Fe–Mo clusters and as a result prevent the reduction of the N_2 molecule that becomes cut off from a further supply of electrons, although it is already bound. So the role of molybdenum in Fe/Mo nitrogenases can remain a topic of speculation!

Experimental Procedure

All operations were carried out under a nitrogen atmosphere in anhydrous, N_2-saturated solvents. **2**: Solid **1** (100 mg, 0.14 mmol) was decomposed at room temperature under high vacuum over 15 days. The resulting deep violet solid was purified by chromatography on SiO_2 (ICN Silica 100–200 60A) at 15 °C (eluant *n*-pentane/CH_2Cl_2, 19:1). Compound **2** is eluted as a blue-violet zone. Yield: 60%; IR(KBr): $\tilde{\nu}$(CO) [cm^{-1}] = 2035, 1997; ^1H NMR (270 MHz, $CDCl_3$, TMS): δ = 8.30 (d, 2H; C_6H_2), 7.64 (d, 2H; C_6H_2), 1.77 (s, 18H; C_4H_9), 1.42 (s, 18H; C_4H_9); $^{13}C\{^1H\}$ NMR (67.94 MHz, $CDCl_3$, TMS): δ = 222.04 (CO), 160.84, 153.26, 149.67 (2 peaks overlap), 125.63, 122.47 (C_{Aryl}), 38.39, 35.61, 32.02, 31.24 (C_{Alkyl}); FD-MS: *m/z* 658 ($M^{\oplus}$).

3: Compound **4** (950 mg, 1.0 mmol) was heated in THF (75 mL) for 75 min at boiling point, during which time the color changed from orange to red-violet. Evaporation of all volatile components afforded a violet-red solid, which was dried for 12 h and then redissolved in CH_2Cl_2 (10 mL). Filtration over SiO_2, evaporation of the filtrate to dryness and subsequent recrystallization from CH_2Cl_2/MeOH (1:1.5, 25 mL, 25– – 30 °C) yielded a deep red microcrystalline solid. Yield:44%; IR(KBr):$\tilde{\nu}$(CO) [cm^{-1}] = 1978; ^1H NMR (270 MHz, $CDCl_3$, TMS): δ = 8.16 (d, 2H; C_6H_2), 8.0–6.9 (br. s, 12H; C_6H_5), 7.45 (d, 2H; C_6H_2), 6.9–6.3 (br. s, 3H; C_6H_5), 1.61 (s, 18H; C_4H_9), 1.36 (s, 18H; C_4H_9); $^{31}P\{^1H\}$-NMR (109.38 MHz, $CDCl_3$, H_3PO_4): δ = 55.56 (*s*; PPh_3); $^{13}C\{^1H\}$-NMR (67.94 MHz, $CDCl_3$, TMS): δ = 231.73 (d, $^2J(^{31}P,^{13}C)$ = 11.5 Hz; CO), 159.39, 152.05, 147.63, 135.30 (d, $^2J(^{31}P,^{13}C)$ = 8.6 Hz), 130.95, 129.06, 128.91, 125.10, 120.83 (C_{Aryl}), 38.08, 35.43, 32.17, 31.21 (C_{Alkyl}); FD-MS: *m/z* 892 ($M^{\oplus}$).

Received: May 6, 1991 [Z4604 IE]
German version: *Angew. Chem. 103* (1991) 1346

CAS Registry numbers:
1, 135823-49-3; **2**, 135823-50-6; **3**, 135823-51-7; **4**, 135823-52-8; $^{tbu}S'^{2\ominus}_4$, 126979-36-0.

[1] See: F. A. Cotton, G. Wilkinson: *Inorganic Chemistry*, 4. ed., Wiley-Interscience, New York 1980, p. 1049ff.
[2] a) J. A. Crayston, M. J. Almond, A. J. Downs, M. Poliakoff, J. J. Turner, *Inorg. Chem. 23* (1984) 3051; b) R. J. Haines, R. S. Nyholm, M. H. B. Stiddard, *J. Chem. Soc. A 1966*, 1606; c) M. L. H. Green, W. E. Lindsell, *ibid. 1967*, 686; d) B. S. Erler, J. C. Dewan, S. J. Lippard, *Inorg. Chem. 20* (1981) 2719; e) N. J. Lazarowych, R. H. Morris, *Can. J. Chem. 68* (1990) 558; f) M. M. Millar, T. O'Sullivan, N. de Vries, *J. Am. Chem. Soc. 107* (1985) 3714.
[3] B. K. Burgess, *Chem. Rev. 90* (1990) 1377.
[4] R. L. Richards in A. Müller, W. E. Newton (Eds.): *Nitrogen Fixation*, Plenum, New York 1983; p. 275ff.
[5] a) E. Roland, E. C. Walborsky, J. C. Dewan, R. R. Schrock, *J. Am. Chem. Soc. 107* (1985) 5795; b) E. C. Walborsky, D. E. Wigley, E. Roland, J. C. Dewan, R. R. Schrock, *Inorg. Chem. 26* (1987) 1615; c) M. Kamata, T. Yoshida, S. Otsuka, *J. Am. Chem. Soc. 103* (1981) 3011.
[6] D. Sellmann, F. Grasser, M. Moll, *J. Organomet. Chem.*, in press.
[7] X-ray crystal structure of **3**: Single crystals obtained from a saturated solution of **3** in CH_2Cl_2/MeOH (1:1) on cooling from 35° to room temperature. $P2_12_12_1$, a = 1446.7(9), b = 1645.8(7), c = 1922.2(10) pm, V = 4577(4) × 10^6 pm^3, Z = 4, T = 200 K, $\lambda(Mo_{K\alpha})$, ω scan, 3.0 < $\dot{\omega}$ < 15° min^{-1}, 3° < 2θ < 54°. Of 8881 independent reflections, 7421 with $F > 4\sigma(F)$. SHELXTL-PLUS, direct methods, R = 0.062, R_w = 0.047. Further details of the crystal structure investigation may be obtained from the Fachinformationszentrum Karlsruhe, Gesellschaft für wissenschaftlich-technische Information mbH, W-7514 Eggenstein-Leopoldshafen 2 (FRG) on quoting the depository number CSD-320252, the names of the authors, and the journal citation.
[8] U. T. Mueller-Westernhoff, B. Vance in G. Wilkinson, R. D. Gillard (Eds.): *Comprehensive Coordination Chemistry, Vol. 2*, Pergamon, Oxford 1987, p. 595ff.
[9] a) D. Sellmann, J. Keller, M. Moll, C. F. Campana, M. Haase, *Inorg. Chim. Acta 141* (1988) 243; b) D. Sellmann, B. Seubert, M. Moll, F. Knoch, *Angew. Chem. 100* (1988) 1221; *Angew. Chem. Int. Ed. Engl. 27* (1988) 1164; c) D. Sellmann, J. Keller, M. Moll, H. P. Beck, W. Milius, *Z. Naturforsch. B41* (1986) 1551.
[10] D. Sellmann, G. Freyberger, R. Eberlein, E. Böhlen, G. Huttner, L. Zsolnai, *J. Organomet. Chem. 323* (1987) 21.
[11] S. Alvarez, R. Vicente, R. Hoffmann, *J. Am. Chem. Soc. 107* (1985) 6253.
[12] D. Sellmann, M. Geck, F. Knoch, G. Ritter, J. Dengler, *J. Am. Chem. Soc. 113* (1991) 3819.
[13] J. R. Chrisnell, R. Premakumar, P. E. Bishop, *J. Bacteriol. 170* (1988) 27.

Formation of Colloidal Transition Metals in Organic Phases and Their Application in Catalysis**

By *Helmut Bönnemann,* Werner Brijoux, Rainer Brinkmann, Eckard Dinjus, Thomas Joußen,* and *Barbara Korall*

Dedicated to Professor Kurt Schaffner on the occasion of his 60th birthday

Colloidal transition metals with a narrow particle size range are interesting for catalysis, because they enable cata-

[*] Prof. Dr. H. Bönnemann, Dr.-Ing. W. Brijoux, Dipl.-Ing. R. Brinkmann, Dr. T. Joußen, Dipl.-Chem. B. Korall
Max-Planck-Institut für Kohlenforschung
Postfach 101353, W-4330 Mülheim an der Ruhr (FRG)
Dr. E. Dinjus
Chemische Fakultät, Universität Jena.

[**] We thank Dr. *G. Block* and *E. Schauf* (Krupp Industrie Technik GmbH, Essen) for TEM photographs taken on a Hitachi H 600/2 electron microscope at 100 kV, and Dr. *B. Tesche* (Fritz-Haber-Institut, Berlin) for TEM photographs on a Siemans Elmiskop 102 at 100 kV and DEEKO 100 at 100 kV. We are grateful to Drs. *R. Brand, B.M. Despeyroux, A. Freund,* and *U. Ohlrogge* (Degussa AG, Hanau) for catalyst test procedures and noble metal chemicals.

lytic processes in homogeneous and heterogeneous phase to be studied on largely uniform metal particles.[1] The formation and stabilization of noble metal colloids in water is widely known[2] and was recently improved substantially by the use of special complex ligands.[3] Here we report on a general method for the preparation of metal colloids of elements of Groups 6–11 in the organic phase. The metal salts were suspended in THF and treated with tetraalkylammonium hydrotriorganoborates [Eq. (a)], which is readily accessible from ammonium halides and alkali-metal hydroorganoborates.[4] Brown-red metal colloid solutions are generated with hydrogen evolution, from which only a small proportion of the reduced metal precipitates. The ammonium salt that forms in the process functions as a protective atmosphere for the metal particles obviating the need for external stabilizers. The filtered colloid solutions are stable for months.

$$MX_n + nNR_4BEt_3H \xrightarrow{THF} M_{colloid} + nNR_4X + nBEt_3 + n/2\,H_2 \quad (a)$$

M: metal of groups 6–11; X: Cl, Br; n: 2, 3; R: alkyl, C_4–C_{20}.

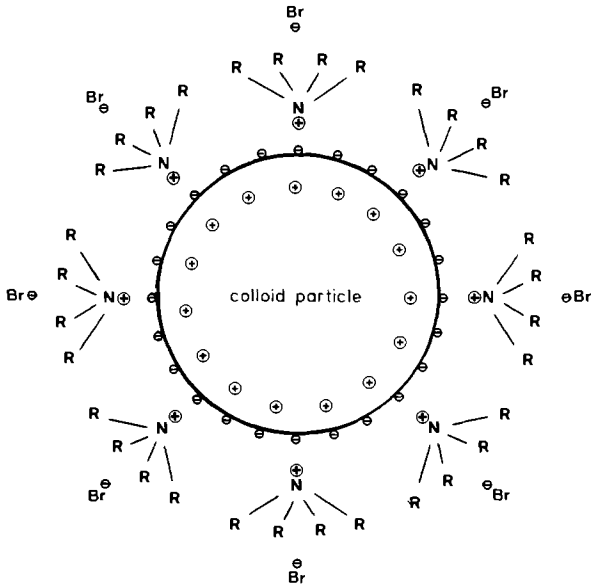

Fig. 1. Stabilization of the metal nucleus with NR_4Br.

In some cases we were able to isolate the metal colloids in powder form. The solution was evaporated to dryness under high vacuum, the waxy residue was taken up in ether or ethanol, and the colloid precipitated by addition of a third solvent (for particulars see Table 1 and Experimental Procedure). The gray-black metal colloid powder is very soluble in THF and other organic solvents (up to 1 g at metal L^{-1}). Elemental analysis of the isolated metal colloid and results from mass spectrometry indicate that NR_4X is present. The results hitherto suggest that tetraalkylammonium ions surround the presumably negatively charged metal nucleus (Fig. 1). The screening of the metal nucleus by large lipophilic alkyl groups explains the remarkable solubility of the metal colloids in organic solvents and their extraordinary stability.

The isolated metal colloids were examined by electron microscopy and preliminary results for Ru, Co, Rh, Pd, and Pt colloids and the coreduction product Pt/Rh are available. An estimation of the size of particle from transmission electron spectroscopy (TEM) pictures of the isolated colloids (at a magnification of 2.5×10^5:1, 3.6×10^5:1, and 1.2×10^6:1) revealed a narrow particle range (Table 1). With rhodium and ruthenium the size distribution maximum indicates that relatively small metal aggregates are formed, while for platinum and palladium they are larger. TEM photographs of the Pt/Rh coreduction product show a colloid with a narrow particle size distribution and a maximum size of approximately 2 nm. Whether this colloid is a Pt/Rh alloy must still

Table 1. Preparation of metal colloids in solution or as an isolated powder.

no.	starting material	reducing agent	conditions t [h]	conditions T [°C]	product colloid solution's color	workup solvent	solvent added for precipitation	metal content in isolated colloid [%]	particle size [nm][a]
1	$CrCl_3$	NBu_4BEt_3H	1	23	deep red to black				
2	$MnCl_2$	NBu_4BEt_3H	1	23	deep red to black				
3	$RuCl_3$	$N(octyl)_4BEt_3H$	2	53	dark red-brown to black Ru almost completely dissolved	ethanol	pentane	68.72	1–2
4	$OsCl_3$	NBu_4BEt_3H	1	23	deep red to black				
5	$CoBr_2$	$N(octyl)_4BEt_3H$	3	23	dark brown to black Co completely dissolved	ethanol	ether	60.50	1.2–2 4.5–5.5 [b]
6	$RhCl_3$	$N(octyl)_4BEt_3H$	3	40	deep red to black Rh completely dissolved	ether	ethanol	73.40	1.3–2 3–4 [b]
7	$IrCl_3$	$N(octyl)_4BEt_3H$	1	50	dark red to black Ir almost completely dissolved	ethanol	ether	65.55	
8	$NiBr_2$	$N(octyl)_4BEt_3H$	6	23	dark red to black Ni completely dissolved	ethanol	ether	66.13	1–5
9	$PdCl_2$	$N(octyl)_4BEt_3H$	1	23	dark brown to black Pd completely dissolved	ether	ethanol	83.62	1–6
10	$PtCl_2$	$N(hexyl)_4BEt_3H$	2	23	dark brown to black Pt up to 80% dissolved				
11	$PtCl_2$	$N(octyl)_4BEt_3H$	2	23	dark brown to black Pt up to 80% dissolved	ether	ethanol	64.46	1–5
12	$PtCl_2$	$N(decyl)_4BEt_3H$	2	23	dark brown to black Pt up to 80% dissolved				
13	$PtCl_2/RhCl_3$	$N(octyl)_4BEt_3H$	1	50	deep red to black Rh completely and Pt almost completely dissolved	ether	ethanol	Pt: 24.45 Rh: 24.09	1–4

[a] 10% error; [b] additional maximum.

be determined by X-ray diffraction and electron spectroscopy (ESCA) studies.

The metal colloids can be adsorbed on the surface of supports. The metal aggregates do not coalesce during the process: electron microscope investigations show that the particle size remains the same and a very uniform distribution of the metal particles on the support is achieved. The supported metal colloids are effective catalysts for the hydrogenation of unsaturated compounds such as CO and C–C, C–O, C–N multiple bond systems, as well as for the hydrogenation of aromatic compounds. Furthermore, the free Pd and Ni colloids are suitable for the selective hydrogenation of naturally occurring products and product mixtures such as soya bean oil. The activity a of the rhodium colloid on an activated carbon support for the hydrogenation of *n*-butyronitrile, determined under controlled conditions[5] and quoted as volume H_2 taken up per g catalyst and per minute, was compared in a series of experiments with the activity of a conventionally prepared rhodium catalyst. Both systems contained 5% Rh on activated carbon from the same batch. The average activity of the Rh colloid catalyst (a = 140 N mL) exceeded the technical standard (a = 80 N mL) by a factor of 1.75. If the activated carbon support is doped with 0.2% titanium by initial treatment with bis(η-toluene)titanium[6] in THF and then covered with 5% Rh colloid, the measured hydrogenation activity (a = 195 N mL) of the Rh colloid catalyst on the support increases to a factor of 2.4 higher than that of the technical standard catalyst. A palladium colloid catalyst doped with 1% Ti (5% on activated carbon) surpasses the corresponding technical standard for the hydrogenation of cinnamic acid by a factor of 1.7 (a = 600 N mL). The corresponding Pt colloid catalyst (1% Ti, 5% Pt on activated carbon; a = 810 N mL) is a factor 2.1 better than the technical standard for the hydrogenation of crotonic acid. Attempts to isolate and characterize further colloid catalysts, to apply them in catalysis, and to determine the doping effects of low-valent early transition metals are in progress.

Experimental Procedure

Tetraoctylammonium triethylhydroborate: To a solution of $N(C_8H_{17})_4Br$ (160.04 g, 292.67 mmol) in THF (350 mL) under an inert atmosphere, was added a solution of $K[BEt_3H]$ in THF (250 mL, 1.17 M) within 30 min at room temperature and with constant stirring. KBr precipitated. After 1 h the reaction mixture was cooled for 16 h at 0°C. The bulky white precipitate was filtered off on a glass frit and washed with ca. 150 mL THF. The tetraoctylammonium hydridotriethylborate was obtained as colorless solution (0.371 M), which was stored below 0°C.

Rhodium colloid: To a suspension of $RhCl_3$ (2.79 g, 13.33 mmol) in THF (500 mL) was added a solution of $N(C_8H_{17})_4BEt_3H$ in THF (0.4 M, 100 mL) within 1 h at 40°C under an inert atmosphere and with stirring. The $RhCl_3$ dissolved completely within 2 h at 40°C. After 15 h at room temperature, the dark red-black solution was completely clear. The volatile components were removed by evaporation, and the black-brown, waxy residue was dried for 3 h at 40°C and 10^{-3} mbar. The product (22.3 g) was soluble in THF, ether, toluene, and acetone, but insoluble in ethanol, and contained 6.1% Rh. The residue was dissolved (in air) in 500 mL technical quality ether. Addition of 50 mL pure ethanol causes a gray-brown precipitate to form. It was left to stand for 1 h, before removing the clear supernatant solution by pressure of inert gas on the liquid surface. The precipitate was washed twice with a mixture of 90 mL ether/10 mL ethanol. Drying in vacuum (10^{-3} mbar, 20 min, 25°C) yields a gray rhodium colloidal powder (1.24 g), very soluble in THF, soluble in acetone, less soluble in toluene, and insoluble in ether. Elemental analysis: Rh: 73.40%, N: 0.30%, C: 16.57%, H: 3.13%; mass spectrum: characteristic ions at 36 (HCl, cleavage at high temperature); 353 ($N(C_8H_{17})_3$, major peak).

Charging of activated carbon with rhodium colloid: activated carbon (3.0 g) was pretreated under argon with bis(η^6-toluene)titanium (30.6 mg) in pentane (50 mL), dried, and suspended in dry THF (ca. 50 mL). Rhodium colloid (234 mg) in THF (50 mL) is added over 30 min with vigorous stirring. The completely metal-free, colorless solution is filtered through a D4 glass frit and the rhodium covered activated carbon is dried under high vacuum (10^{-3} mbar) for 16 h at room temperature. Approximately 10% of the solvent remains adsorbed. The activated carbon so charged contains 5% Rh and 0.2% titanium (relative to the solvent-free product). The catalyst is ready for use after treatment with inert gas that contains 0.2 vol% O_2 for 2 h.

Received: May 24, 1991 [Z4649 IE]
German version: *Angew. Chem. 103* (1991) 1344

[1] G. Schmid in R. Ugo (ed.): *Aspects of Homogeneous Catalysis, Vol. 7*, Kluwer, Dordrecht 1990, pp. 1–77.
[2] G. Lagaly, *Ullmanns Encycl. Ind. Chem., 5. Aufl., Vol. A 7* (1986) 341–367.
[3] G. Schmid, A. Lehnert, *Angew. Chem. 101* (1989) 733; *Angew. Chem. Int. Ed. Engl. 28* (1989) 780.
[4] R. Köster, *Methoden Org. Chem.* (Houben-Weyl) 4th Ed. *Band XIII/3b* (1983) 789.
[5] Hydrogen pressure 1 bar, temperature 40°C ± 0.5°, concentration of substrate 1.04 mol L^{-1}, catalyst used 0.3–1 g, stirring rate 2000 revolutions per minute, solvent 100 mL ethanol DAB 7.
[6] a) F. G. N. Cloke, M. F. Lappert, G. A. Lawless, A. C. Swain, *J. Chem. Soc. Chem. Commun. 1987*, 1667–1668; b) M. T. Anthony, M. L. H. Green, D. Young, *J. Chem. Soc. Dalton Trans. 1975*, 1419; c) P. N. Hawker, E. P. Kündig, P. L. Timms, *J. Chem. Soc. Chem. Commun. 1978*, 730.

Herbicide Resistance in Transgenic Plants through Degradation of the Phytotoxin to Urea**

By *Ursula H. Maier-Greiner, Christian B. A. Klaus, Lydia M. Estermaier, Guido R. Hartmann**

Herbicide resistance in transgenic plants has been achieved by three approaches:[1] 1) overproduction of the target protein, 2) expression of a mutant target protein that is resistant to the herbicidal action and 3) expression of an enzyme which inactivates the herbicide by modification. In each case residues of the phytotoxin or derivatives of it remain in the plant, causing possible drawbacks in its use as a nutrient. We describe here a new method of engineering resistance by converting the herbicide into an innocuous physiological compound. The relevant herbicide is cyanamide which is degraded to urea in transgenic tobacco.

In the soil fungus *Myrothecium verrucaria* an inducible enzyme was discovered which hydrates the herbicide cyanamide (brand name alzodef®) quantitatively to urea.[2, 3] This cyanamide hydratase (EC 4.2.1.69) is encoded by the 732 base-pair *cah* gene which is located on a 900 base-pair *Eco*RI fragment isolated from a cDNA gene bank of *Myrothecium verrucaria*.[3]

For expression in plants, a gene cassette was constructed by placing this *Eco*RI fragment between the 35S promoter of cauliflower mosaic virus and the polyA signal of the nopaline synthetase gene. The vector pRT101[4] may be used for this purpose. Two constructs were obtained, one with the gene in correct orientation with respect to the promoter (designated cah^+), the other with the gene in opposite orientation (cah^-). Transfer into plants was achieved by using standard binary vector systems, for example, pBin19[5] containing the cah^+ or cah^- gene cassette and *Agrobacterium tumefaciens* strain LBA4404[6] (Clontech Laboratories, Palo Alto, CA, USA). Triparental mating, transformation, and

[*] Prof. Dr. G. R. Hartmann, Dr. U. H. Maier-Greiner, Dipl.-Chem. C. B. A. Klaus, Dipl.-Chem. L. M. Estermaier
Institut für Biochemie der Ludwig-Maximilians-Universität
Karlstrasse 23
W-8000 München 2 (FRG)

[**] We thank *Reinhard Töpfer*, Max-Planck-Institut für Züchtungsforschung, Cologne, for the plasmid vector pRT101. This work was supported by SKW Trostberg AG and the Fonds der Chemischen Industrie.

regeneration were carried out as described.[7, 8] Developing shoots were selected on 100 $\mu g\,mL^{-1}$ kanamycin.

Fifteen kanamycin resistant plants were tested for cyanamide hydratase activity.[3] Enzyme activity was found in all plants, the level of expression ranging from 0.03 to 0.79 units per mg protein in the cell extract. The highest value corresponds to about a fifth of the specific activity measured in induced *Myrothecium verrucaria* extracts. Although the specific activity was highest in the roots, the total enzyme activity per gram fresh weight was distinctly higher in the leaves than in the other plant organs (Table 1). No activity was found in plants transgenic for *cah*$^-$.

Table 1. Activity of cyanamide hydratase in extracts of various organs of tobacco plants transgenic for *cah*$^+$. The organs were frozen in liquid nitrogen, pulverized, and then extracted with 5 mM phosphate buffer pH 8 (1 $mL\,g^{-1}$ fresh weight) (specific enzymatic activity in the extract of the total plant: 0.276 $U\,mg^{-1}$). No activity above background could be measured in *cah*$^-$ transgenic plants.

plant organ	activity [units per g fresh weight]	specific activity [units mg^{-1} protein]
cah$^+$ roots	0.073	0.660
cah$^+$ stem	0.437	0.469
cah$^+$ leaves	0.643	0.202

Rooting of wild type or *cah*$^-$ transgenic tobacco shoots is completely depressed with 1.2 mM cyanamide in the medium. In contrast, root formation of *cah*$^+$ transgenic axillary shoots was observed even when the growth medium was supplemented with 12 mM cyanamide. Thus in respect to root formation, the tolerance to cyanamide is increased at least by a factor 10. Rooted *cah*$^+$ transgenic plants grow well on at least 2.4 mM cyanamide, a concentration that kills nontransformed or *cah*$^-$ transgenic plants within six weeks. Plants nontransformed or transgenic only for the vector pBin19 are completely bleached within 15 days after being sprayed once with 0.5% cyanamide solution. In contrast *cah*$^+$ transgenic plants tolerate distinctly higher concentrations, which correlate with the level of *cah*$^+$ gene expression. For example, a plant with a specific enzymatic activity of 0.58 units per mg protein in the cell extract showed no necrosis after being sprayed once with 5% cyanamide solution, which is the herbizide concentration recommended for use in agriculture (Fig. 1). Additional evidence for the expressed cyanamide hydratase activity being responsible for the increased tolerance is the formation of urea in the plant. Extracts from leaves of *cah*$^+$ transgenic plants grown for several weeks in the presence of 2.4 mM cyanamide contain 10–32 μmol urea per g leaves (fresh weight), which is absent in controls grown without cyanamide.

Fig. 1. Cyanamide tolerance in transgenic tobacco. *Nicotiana tabacum* SR1 plants transgenic for *cah*$^+$ or pBin19 with 6–8 leaves were sprayed once with 5% cyanamide solution. The plants were maintained under sterile conditions in a growth chamber (16 h photo-period, 25/18°C). The photographs were taken after 15 days. Left: plant transgenic for pBin19; right: plant transgenic for *cah*$^+$.

These results clearly demonstrate that expression of cyanamide hydratase confers tolerance to cyanamide in transgenic tobacco by its degradation to urea. In the presence of the urea-degrading enzyme urease found in many plants,[9–12] the subsequent product of hydrolysis NH_4^+ may be used by the plant as a nitrogen source.

Received: July 5, 1991 [Z4778 IE]
German version: *Angew. Chem. 103* (1991) 1353

CAS Registry numbers:
cyanamide hydratase, 50812-20-9; cyanamide, 156-62-7; urea, 57-13-6.

[1] J. Botterman, J. Leemans, *Trends Genet. 4* (1988) 219–222.
[2] H. Stransky, A. Amberger, *Z. Pflanzenphysiol. 70* (1973) 74–87.
[3] U. H. Maier-Greiner, B. M. M. Obermaier-Skrobranek, L M. Estermaier, W. Kammerloher, C. Freund, C. Wülfing, U. I. Burkert, D. H. Matern, M. Breuer, M. Eulitz, Ö. I. Küfrevioglu, G. R. Hartmann, *Proc. Natl. Acad. Sci. USA 88* (1991) 4260–4264.
[4] R. Töpfer, V. Matzeit, B. Gronenborn, J. Schell, H.-H. Steinbiss, *Nucleic Acids Res. 15* (1987) 5890.
[5] M. Bevan, *Nucleic Acids Res. 12* (1984) 8711–8721.
[6] A. Hoekema, P. R. Hirsch, P. J. J. Hooykaas, R. A. Schilperoort, *Nature (London) 303* (1983) 179–180.
[7] R. B. Horsch, J. E. Fry, N. L. Hoffmann, D. Eichholtz, S. G. Rogers, R. T. Fraley, *Science (Washington D.C.) 227* (1985) 1229–1231.
[8] J. Draper, R. Scott, (Eds.): *Plant Genetic Transformation and Gene Expression: A Laboratory Manual*, Blackwell, Oxford 1988.
[9] M. Damodaran, P. M. Sivaramakrishnan, *Biochem. J. 31* (1932) 1041–1052.
[10] T. A. Skokut, P. Filner, *Plant Physiol. 65* (1980) 995–1003.
[11] H. M. Davis, L. M. Shih, *Phytochemistry 23* (1984) 2741–2745.
[12] Y. Chen, T. M. Ching, *Plant Physiol. 86* (1988) 941–945.

On the Enigma of Chlorophyll Degradation: The Constitution of a Secoporphinoid Catabolite**

By *Bernhard Kräutler,* Bernhard Jaun, Karlheinz Bortlik, Maja Schellenberg,* and *Philippe Matile*

Dedicated to Professor Vladimir Prelog on the occasion of his 85th birthday

The degradation of the green plant pigment chlorophyll, which lies behind the impressive natural phenomenon of fall colors of trees and shrubs, is still not understood.[1, 2] This gap in our knowledge[3] exists because the degradation of chlorophyll "apparently takes place without leaving any traces",[1a] although annually on earth probably over 10^9 t of chlorophyll is catabolized.[3] Only lately did the prospect of gaining insights into the chlorophyll metabolism arise out of the discovery of almost colorless plant metabolites, the most important of which were characterized as tetrapyrrole

[*] Priv.-Doz. Dr. B. Kräutler, Dr. B. Jaun
Laboratorium für Organische Chemie
der Eidgenössischen Technischen Hochschule
Universitätstrasse 16, CH-8092 Zürich (Switzerland)
Prof. Dr. P. Matile, Dr. K. Bortlik, M. Schellenberg
Institut für Pflanzenphysiologie der Universität Zürich.

[**] This work was supported by the Schweizerischen Nationalfonds und der ETH-Zurich. We thank Prof. *A. Eschenmoser* for stimulating discussions and Dr. *W. Amrein* and *R. Häfliger* for acquiring the mass spectra.

derivatives by isotope labeling.[1, 4–6] Among these metabolites the "fluorescent compounds" ("FC's") were suggested as precursors of the "rusty pigments" ("RP's"),[4] based on their appearance first in the chloroplasts and then in the vacuoles of yellowing barley primary leaves. The RP's owe their name (and their discovery) to the observation that on isolation in air and in the presence of acid they are transformed into easily visible, rust-colored secondary products.[1, 4, 5] We report here on the research resulting from cooperation between a botanical and a chemical laboratory, which led to the elucidation of the constitution of "RP-14",[5] the major representative of the rusty pigments from senescent barley primary leaves. The proposed constitution of RP-14 as the 1-formyl-19-oxobilane (**3**)[7] substantiates its relationship with chlorophyll a (**1**) and provides the first structural guideline which may help to unravel the mystery of how chlorophyll is catabolized.

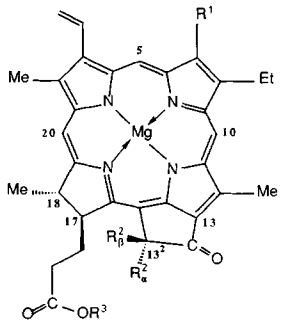

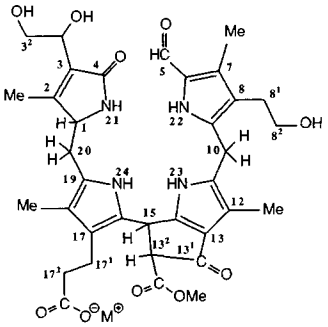

1 (Chlorophyll a): R^1 = Me, R^2_α = C(O)OMe, R^2_β = H, R^3 = phytyl
2 (Chlorophyll b): R^1 = CH(O), R^2_α = C(O)OMe, R^2_β = H, R^3 = phytyl,
4 (Chlorophyllide a, Na salt): R^1 = Me, R^2_α = C(O)OMe, R^2_β = H, R^3 = Na
5 (13-Hydroxychlorophyll a): R^1 = Me, R^2_α = C(O)OMe, R^2_β = OH, R^3 = phytyl
6 (Pyrochlorophyllide a, Na salt): R^1 = Me, R^2_α = H, R^2_β = H, R^3 = Na

3-K: "RP-14" (K salt): $M^\oplus = K^\oplus$

To obtain a sample of the plant metabolite RP-14 (**3**), the primary leaves of the barley mutant *Hordeum vulgare* cv. Gerbel were aged in the dark as described before[4a, 5] (Fig. 1), and the cryosap isolated from it was separated by HPLC. The eluate that contained the potassium salt **3**-K as major component (94%, HPLC analysis) was lyophilized, and the salts removed from the residue on C-18 cartridges. The metabolite **3**-K was isolated as a powdery lyophilization residue (see *Experimental Procedure*).

The constitution of RP-14 (1-formyl-19-oxobilane, **3**) was deduced from MS, ^{1}H and ^{13}C NMR, UV/VIS, CD, and IR spectra: the molecular formula of **3**-K was given as $C_{35}H_{41}N_4O_{10}K$ in the FAB mass spectrum[8a] in positive-ion mode: molecular ion at *m/z* 717.266 ($C_{35}H_{42}N_4O_{10}K$ 717.254); base peak at *m/z* 679.287 ($C_{35}H_{43}N_4O_{10}$ 679.298); in negative-ion mode the base peak was at *m/z* 677.4. The absorption maximum of the longest wavelenth band in the UV/VIS spectrum of **3**-K (cf. ref. [5]) at 315 nm is consistent with an α-formylpyrrole unit, but not with an extended, conjugated chromophore. In the ^{1}H NMR (400 MHz) spectrum of **3**-K in D_2O ([D_6]DMSO), the signals of 33 (40) of the 41 protons can be seen (Figs. 2 and 3a): a singlet for the formyl proton and five singlets for methyl protons, including, according to the chemical shift, an ester methyl group; signals due to unsubstituted ethyl and vinyl groups are not observed. The signal at higher field of an AX system in the

Fig. 1. Primary leaves of barley (*Hordeum vulgare* cv. Gerbel and the structural formulas for chlorophyll a (**1**) and for the catabolite "RP-14" (**3**); left: freshly cut; right: as left, after 7 days aging in darkness [4a, 5]).

spectrum in [D_6]DMSO ($\delta_A = 4.63$, $\delta_X = 3.91$, $J_{A,X} = 3.3$ Hz, assigned to H-C15 and H-C13^2) is missing in the D_2O system as a result of H/D exchange. Of the 35 carbon atoms, signals for 33 are resolved in the ^{13}C NMR spectrum (100 MHz) of **3**-K in D_2O: the signal of C13^2, deuterated in D_2O, cannot be found; the spectrum in [D_6]DMSO shows 32 signals including that for C13^2 at $\delta = 64.99$.

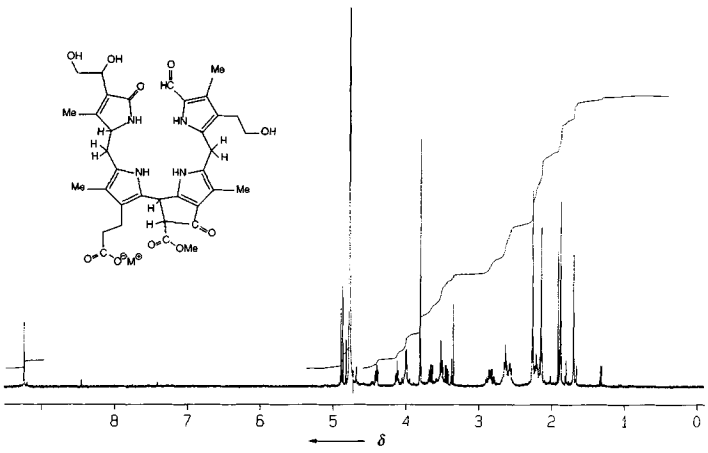

Fig. 2. ^{1}H NMR spectrum (400 MHz) of **3**-K in D_2O at 25 °C. (δ_{HDO} 4.72, *c* = ca. 3.5 mM): The signal of H-C13^2 is missing because of H–D exchange; the signal of H-C15 at $\delta = 4.83$ is therefore a singlet.

In addition to the five methyl groups, the H atoms bound to O and N atoms, and the formyl-H atom, six isolated spin systems of **3**-K are recognized on applying homonuclear ^{1}H chemical shift correlation (DFQ-COSY, TOSCY[8b–e]). The corresponding ^{13}C NMR signals were identified by ^{1}H,^{13}C–$^1J_{H,C}$ chemical shift correlation.[8f, g] Through information about the spatial neighborhoods from ^{1}H nuclear Overhauser measurements (NOESY,[8b, h, i] Fig. 3a) and support-

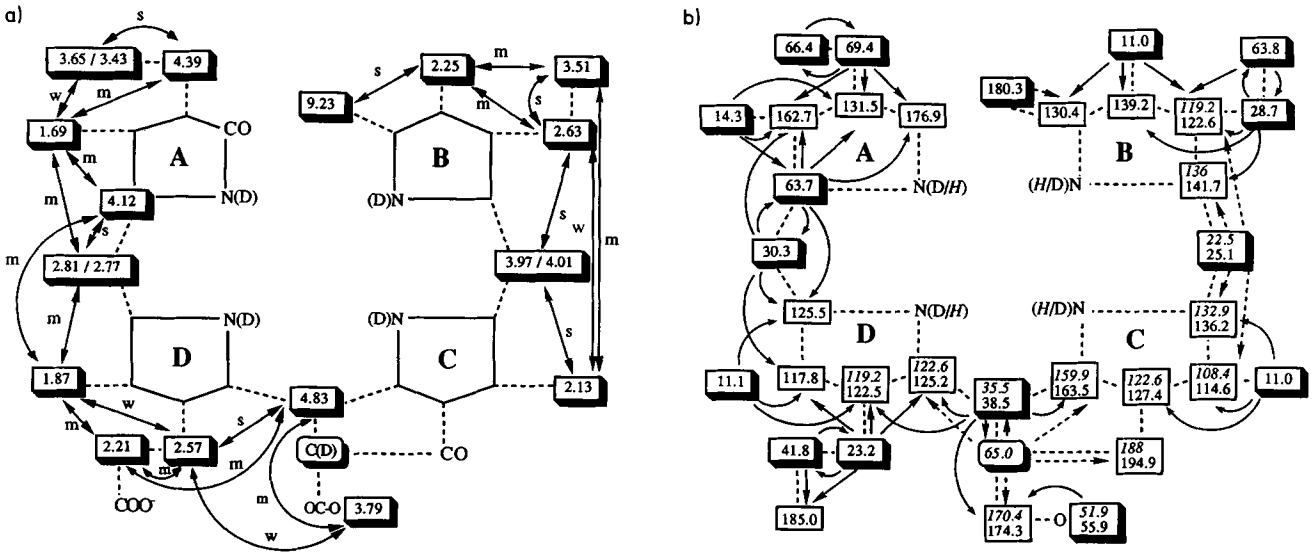

Fig. 3. a) Assignments and chemical shifts of the proton signals of **3**-K (D_2O, 25 °C, N_2) and NOE correlations observed in the NOESY spectrum [8b] (D_2O/MeOH 1:1, −7.5 °C, N_2; w = weak, m = medium, s = strong); b) assignments and chemical shifts of the ^{13}C NMR signals of **3**-K (D_2O, 25 °C, N_2; additional values in italics are for those signals in the spectrum of **3**-K in [D_6]DMSO that show additional correlations to those in D_2O in the HMBC spectrum [8i, j]). $^{2/3}J$(C,H) correlations are represented as arrows that start at protons and point to the correlated ^{13}C atoms (solid for D_2O, dashed for [D_6]DMSO). In the [D_6]DMSO spectrum the H-N21 and H-N24 show additional $^{2/3}J$(C,H) correlations to all four C atoms of the corresponding pyrrole rings A and D.

ed by H–C long-range connectivities from HMBC spectra (HMBC = Heteronucluear Multiple-Bond Connectivity,[8j] Fig. 3b), the connectivities of the C-centers and the *C*- and *N*-bonded H atoms of the B–C part (C5 to C13) and the A–D region (C14 to C4, including $C13^1$ and $C13^2$) of **3**-K were deduced, to which the four pyrrole N atoms could be fitted in a satisfactory way. The three O atoms which were not already assigned to carbonyl, ester, or carboxylato groups could be identified as hydroxy substituents at positions 3^1, 3^2, and 8^2 from FAB-MS, ^{13}C, and ^1H NMR data. The coupling of the A–D and B–C halves through an annelated cyclopentanone ring was concluded from the following: a) The molecular formular of **3**-K implies 17 double-bond equivalents, of which three are involved in the coupling in question. b) The ^{13}C chemical shifts of the three C atoms involved (δ = 127.4, 163.5, and 194.9) indicate that two are olefin (arene) atoms for which two σ bonds are observed and another is a ketone C atom for which the second C–C bond is missing. The exclusion of highly strained systems leads to the coupling through the cyclopentanone annelated to the pyrrole ring C, and the three C atoms are identified as C13, C14, and $C13^1$. (A related structural problem has been described.[10])

The analysis of all the spectroscopic data suggests that the constitution of **3**-K is that of a potassium-4,5-seco-4,5-dioxo-3^1,3^2,8^2-trihydroxy-13^2-methoxycarbonyl-1,4,5,10,15,20-(22H,24H)-octahydrophytoporphyrinate. The configuration of the four stereogenic centers, which apparently are largely uniform in optically active **3**-K, has still not been ascertained. However, from ^1H NMR data the methoxycarbonyl group at the 13^2-position of the cyclopentanone ring is *trans* to the AD half. Thus **3**-K presumably is the thermodynamically more stable diastereomer with respect to this part of the molecule (but it possibly forms in vitro on H exchange in a protic milieu).

A feature of **3** is the methoxycarbonyl-substituted cyclopentanone ring, which is a structural characteristic of the chlorophyll derivatives such as **1** and **2**. This and the occurrence of four methyl groups bonded to the chromophore in **3** shows a close structural correspondence between **3** and **1** (and less so with **2**), but not with the chlorins **5**[11a] and **6**[11b] suspected to be chlorophyll catabolites: compound **3** is formally accessible from chlorophyllide a (**4**), which has been postulated as the first degradation product of chlorophyll a (**1**),[1a, 12, 13] by demetalation and addition of one oxygen molecule and three water molecules; its chiroptic properties suggest an enzyme-controlled formation (cf. the current speculations on chlorophyll degradation[3, 14]).

Recently the light-emitting substance of krill (a part of the sea plankton) and luciferin from dinoflagellates have been characterized as the first examples of naturally occurring "bile pigments" structurally derived from chlorophyll.[10] In these substances the chlorin macrocycle is interrupted at the *meso* position C20, a site of the chlorin ring which is readily attacked by electrophilic reagents.[15] In contrast, the macrocycle in **3** is opened at the *meso* position C5, which recalls the oxygenolytic degradation of the iron porphyrin heme [7b, 16] to bile pigments.

The constitution of the 4,5-seco-4,5-dioxophytoporphyrinate **3**-K provides for the first time a structural guideline which may contribute to the understanding of the apparently complex process of chlorophyll degradation.

Experimental Procedure

For the cultivation of *Hordeum vulgare* cv. Gerbel and the conditions of the senescence induced in the dark, see [4a, 5]: 115 g of leaves were aged in continuous darkness for 7 d; the cryosap from 5 g batches of leaf material (ca. 4 mL) was treated with acetone (ca. 16 mL) and centrifuged to separate the protein material (5 min per 2300 g). The supernatant was treated with chloroform (20 mL), briefly shaken, and the aqueous phase separated into two portions (HPLC column, Stagroma, Wallisellen, Switzerland): Nucleosil RP-8, 10 μm, 20 × 250 mm; eluant: 27 vol% methanol/73 vol% 50 mM potassium phosphate pH 7; flow rate 14.6 mL min^{-1}; detection at 320 nm. The fraction with a retention of ca. 17.3 min was collected at 0 °C under an inert atmosphere (N_2). The crude fractions of **3**-K were lyophilized in three portions at room temperature, the residue extracted three times with ca. 3 ml portions 20 vol% aqueous methanol and the extracts purified in five portions by HPLC as described. The HPLC eluates were stored for 3–8 days under nitrogen at −20 °C and then lyophilized in two portions at $T < 0$ °C; the pale yellow residue of each batch was placed on a Waters C_{18} Sep-pak cartridge with ca. 2 mL destilled water and washed with ca. 25 mL destilled water. A pale yellow fraction was eluted with ca. 20 mL 20 vol% aqueous methanol and the eluate lyophilized under high vacuum at $T < 0$ °C. The light yellow residue of powdery **3**-K was dried under high vacuum at room temperature for ca. 4 h. Yield 13 mg (> 94%; analytical HPLC, cf. [5]).

Spectroscopic data: (NMR: Bruker AMX-400, ^{1}H NMR in D_2O: cf. Fig. 2 and 3a, ^{13}C NMR in D_2O: cf. Fig. 3b). ^{1}H NMR (400 MHz, ca. 4 mM solution under N_2, [D_6]DMSO): δ = 1.84, 1.85 (2s, H_3C (2^1 and 18^1)), 2.00, 2.17 (2s, H_3C (12^1, 7^1)), overlapping with 2.0–2.2 (m, H_2C (17^2)), 2.31 (dd, J(H,H) = 8.7/14.5 Hz, $H_aC(20)$), 2.4–2.6 (m, $H_2C(8^2)$ and $H_aC(17^1)$), 2.6–2.7 (m, $H_bC(17^1)$), 2.72 (dd, J(H,H) = 4.9/14.5 Hz, $H_bC(20)$), 3.2–3.3 (m, $H_2C(8^2)$), 3.3–3.5 (m, $H_2C(3^2)$), 3.62 (s, ester CH_3), 3.70/3.79 (AB spin system, J(H,H) = 15.8, $H_2C(10)$), 3.91 (d, J(H,H) = ca. 3.5 Hz, $HC(13^2)$) overlapping with 3.94 (dd, J(H,H) = 4.9/8.7 Hz, HC(1)), 4.33 (t, J(H,H) ca. 5.6 Hz, $HC(3^1)$), 4.63 (d, J(H,H) = 3.3 Hz, HC(15)), overlapping with 4.6–4.7 (br, 1H), 4.7–5.0 (br, 1H), 7.79 (s, HN(21)), 9.49 (s, HC(5)), 9.85 (s, HN(24)), 11–13 (br, ca. 1H), 13.0–13.2 (br, 1H)); ^{13}C NMR (100 MHz, ca. 15 mM solution under N_2, [D_6]DMSO): δ = 9.04(7^1,12^1), 9.30(18^1), 12.20(2^1), 21.68(17^1), 22.47(10), 27.35(8^1), 29.66(20), 35.52(15), 39.6(17^2), 51.92 (ester CH_3), 60.15(1), 61.01(8^2), 64.63(3^2), 64.99(13^2), 67.64(3^1), 108.42(12), 113.25(18), 119.20(8,17), 122.54, 122.62(13,16), 122.99(19), 127.9 (br, 6), 130.86(3), 132.95(11), 136 (br, 9), 154.94(2), 159.86(14), 170.43(13^3), 172.52(4), 177.30(17^3), 178 (br, 5), 188.15(13^1). UV/VIS and CD (0.02 M sodium phosphate, pH 7, $c = 8.10^{-5}$ M): λ_{max}[nm] (rel. ε) = 243 (0.83), 272 (sh, 0.59), 315 (1.0, log ε = 4.2); λ_{max}[nm]($\Delta\varepsilon$) = 223 (15), 247 (– 4), 282 (– 14), 317 (4). FAB-MS (3-nitrobenzyl alcohol matrix, ZAB-2 SEQ, cesium bombardment, 35 keV): a) positive-ion mode: m/z 755.1 (10%); 719.2 (20), 718.2 (60), 717.2 (90, $C_{35}H_{42}N_4O_{10}K$, $[M + 1]^{\oplus}$); 681.2 (12), 680.2 (55), 679.2 (100, $C_{35}H_{43}N_4O_{10}$, $[M + 2 - K]^{\oplus}$), 678.2 (30), 677.2 (12), 560.1 (12, $C_{28}H_{31}N_3O_7K$, $[M + 1 - \text{Ring A}]^{\oplus}$), 523.2 (28), 522.2 (65, $C_{28}H_{32}N_3O_7$, $[M + 2 - K - \text{Ring A}]^{\oplus}$); exact mass determination (OPUS-V 1.5D software, internal matching with matrix references at m/z 651.134, 613.178, 498.091, 460.136; resolution: ca. 1500): m/z C 717.266 (95%, $C_{35}H_{42}N_4O_{10}K$, 717.254); 679.287 (100, $C_{35}H_{43}N_4O_{10}$, 679.298); 522.213 (65, $C_{28}H_{32}N_3O_7$, 522.224); b) negative-ion mode: m/z 679.4 (15%), 678.4 (46), 677.4 (100, $C_{35}H_{41}N_4O_{10}$, $[M - K]^{\ominus}$), 676.4 (30); IR (0.3%, Perkin Elmer-983, KBr): $\tilde{\nu}$[cm^{-1}] = 2950(m), 2920(m), 2860(m), 1725(m), 1670(s), 1630(s), 1560(m), 1490(m), 1445(m), 1390(m), 1345(m), 1310(m), 1275(m).

Received: May 29, 1991 [Z4664 IE]
German version: *Angew. Chem. 103* (1991) 1354

CAS Registry numbers:
1, 479-61-8; **3**, 135972-64-4; **3**·K, 136144-63-3.

[1] a) P. Matile, *Chimia 41* (1987) 376; b) P. Matile, T. Düggelin, M. Schellenberg, D. Rentsch, K. Bortlik, C. Peisker, H. Thomas, *Plant Physiol. Biochem. 29* (1989) 595.
[2] W. Rüdiger, S. Schoch, *Naturwissenschaften 76* (1989) 453.
[3] G. A. Hendry, J. D. Houghton, S. B. Brown, *New Phytol. 107* (1987) 255.
[4] a) P. Matile, S. Ginsburg, M. Schellenberg, H. Thomas, *J. Plant Physiol. 129* (1987) 219; b) T. Düggelin, M. Schellenberg, K. Bortlik, P. Matile, *J. Plant Physiol. 133* (1988) 492; c) P. Matile, S. Ginsburg, M. Schellenberg, H. Thomas, *Proc. Natl. Acad. Sci. USA 85* (1988) 9529.
[5] K. Bortlik, C. Peisker, P. Matile, *J. Plant Physiol. 136* (1990) 161.
[6] C. Peisker, H. Thomas, F. Keller, P. Matile, *J. Plant Physiol. 136* (1990) 544.
[7] For tetrapyrrole nomenclature see a) G. P. Moss, *Pure Appl. Chem. 59* (1987) 779–832; b) H. Falk: *The Chemistry of Linear Oligopyrroles and Bile Pigments*, Springer, Wien 1989.
[8] a) C. Fenselau, R. J. Cotter, *Chem. Rev. 87* (1987) 501; b) H. Kessler, M. Gehrke, C. Griesinger, *Angew. Chem. 100* (1988) 507; *Angew. Chem. Int. Ed. Engl. 27* (1988) 490; c) M. Rance, O. W. Sørensen, G. Bodenhausen, G. Wagner, R. R. Ernst, K. Wüthrich, *Biochem. Biophys. Res. Commun. 117* (1983) 479; d) L. Braunschweiler, R. R. Ernst, *J. Magn. Reson. 53* (1983) 521; e) A. Bax, D. G. Davis, *ibid. 65* (1985) 355; f) L. Müller, *J. Am. Chem. Soc. 101* (1979) 4481; g) A. Bax, S. Subramanian, *J. Magn. Reson. 67* (1986) 565; h) J. Jeener, B. H. Meier, P. Bachmann, R. R. Ernst, *J. Chem. Phys. 71* (1979) 4546; i) S. Macura, R. R. Ernst, *Mol. Phys. 41* (1980) 95; j) A. Bax, M. F. J. Summers, *J. Am. Chem. Soc. 108* (1986) 2093.
[9] a) A. Gossauer: *Chemie der Pyrrole*, Springer, Berlin 1974; b) C. Pasquier, A. Gossauer, W. Keller, C. Kratky, *Helv. Chim. Acta 70* (1987) 2098.
[10] a) H. Nakamura, B. Musicki, Y. Kishi, *J. Am. Chem. Soc. 110* (1988) 2683; b) H. Nakamura, Y. Kishi, O. Shimomura, D. Morse, J. W. Hastings, *ibid. 111* (1989) 7607.
[11] a) M. J. Maunders, S. B. Brown, H. W. Woolhouse, *Phytochemistry 22* (1983) 2443; b) R. Ziegler, A. Blaheta, N. Guha, B. Schönegge, *J. Plant Physiol. 132* (1988) 327.
[12] H. Thomas, K. Bortlik, D. Rentsch, M. Schellenberg, P. Matile, *New Phytol. 111* (1989) 3.
[13] D. Amir-Shapira, E. E. Goldschmidt, A. Altman, *Proc. Natl. Acad. Sci. USA 84* (1987) 1901.
[14] S. B. Brown, K. M. Smith, G. M. F. Bisset, R. F. Troxler, *J. Biol. Chem. 255* (1980) 8063.
[15] a) R. B. Woodward, V. Skaric, *J. Am. Chem. Soc. 83* (1961) 4676; b) J.-H. Fuhrhop, J. Subramanian, *Philos. Trans. R. Soc. London B 273* (1976) 335.
[16] R. Schmid, A. F. McDonagh in D. Dolphin (Eds.): *The Porphyrins, Vol. VI*, Academic Press, New York 1979, p. 258.

Anti-Selective and Diastereofacially Selective Aldol Reactions with (*R*)-2-Siloxy-1,2,2-triphenylethyl propionate**

By *Manfred Braun** and *Hubert Sacha*

Dedicated to Professor Leonhard Birkofer on the occasion of his 80th birthday

The directed synthesis of the enantiomeric *syn*-β-hydroxycarbonyl compounds **1** and *ent*-**1** is achieved today with highly efficient variants of the aldol reaction, mostly starting from chiral propionamides. In contrast, *anti*-selective aldol reactions, based on the addition of chiral propionic acid esters to aldehydes RCHO, are known to be problematic partly because of poor simple diastereoselectivity (*anti*-**1** versus *syn*-**1**) and partly unsatisfactory diastereofacial selectivity (**2** versus *ent*-**2**).[1] Lately more effective enolates and silyl

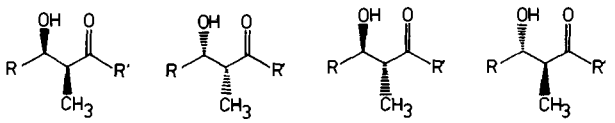

1 *ent*-**1** **2** *ent*-**2**

ketene acetals have been developed as starting materials, but their synthesis has been hampered by the difficult access to the required chiral auxiliaries.[2] We now report the first *anti*-selective and diastereofacially selective aldol additions of the propionate **4b**; its chiral building block, triphenylglycol, is easily accessible in both enantiomeric forms (**3** and *ent*-**3**) and it has repeatedly proved its worth as the acetate.[3]

The esterification of the (*R*)-diol **3** with propionyl chloride took place as anticipated, exclusively at the secondary hydroxy group, and afforded the propionate **4a**, which was transformed into the propionate **4b** by *O*-silylation[4] in 90% total yield (Scheme 1, Table 1). The lithium enolate **5a**, formed in situ from 2-siloxy-1,2,2-triphenylethyl propionate (**4b**) deprotonated by lithium cyclohexylisopropylamide, undergoes transmetalation with [Cp_2ZrCl_2] to form **5b**. Subsequent addition of an aldehyde yields predominantly the *anti* diastereomers **6**/**7** (Table 1). Their contribution to the product distribution was determined by NMR spectroscopy (Table 2). At the same time this aldol addition shows a high diastereofacial selectivity: the diastereomeric ratio of **6**:**7** lies between 97:3 and > 98:2.

Table 1. Adducts **6**/**7**, formed by addition of the enolate **5b** to an aldehyde RCHO.

R		**6**–**9** Yield [a]	**6**/**7**:**8**/**9** (*anti*:*syn*)	**6**/**7**
Ph	**a**	90	89:11	97.5:2.5
$(CH_3)_2CH$	**b**	82	>98:2	97:3
$(CH_3)_3C$	**c**	75	>98:2	>98:2

[a] Crude yield in [%].

[*] Prof. Dr. M. Braun, Dipl.-Chem. H. Sacha
Institut für Organische und Makromolekulare Chemie der Universität
Universitätsstrasse 1, W-4000 Düsseldorf 1 (FRG)

[**] This work was supported by the Deutsche Forschungsgemeinschaft, the Fonds der Chemischen Industrie, and BASF AG (gift of chemicals).

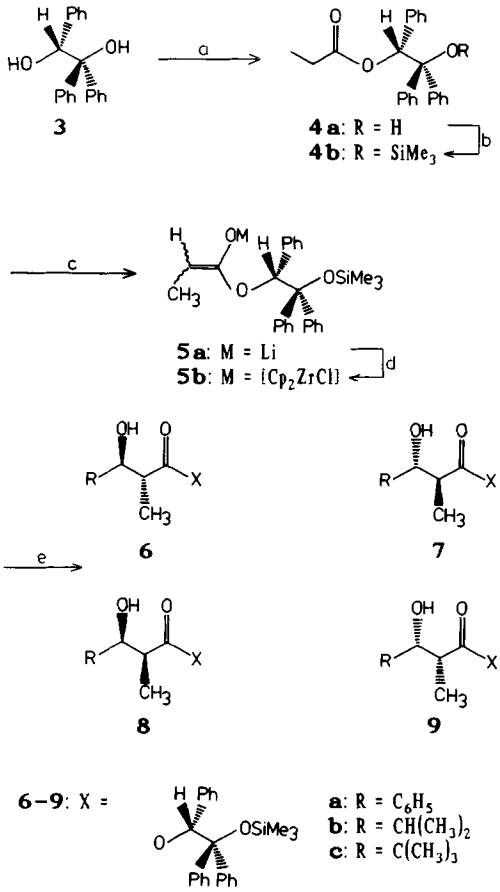

Scheme 1. Synthesis and aldol addition of the propionate **4b**. a) CH_3CH_2COCl, CH_2Cl_2, pyridine. b) 2 equiv lithium diisopropylamide, 3 equiv chlorotrimethylsilane; 1 M HCl. c) Lithium cyclohexylisopropylamide, THF. d) $[Cp_2ZrCl_2]$. e) RCHO, THF.

Table 2. Physical and spectroscopic data of compounds **4** and **6**.

4a: m.p. = 208–209 °C; $[\alpha]_D^{25}$ (c = 1.5, $CHCl_3$) = 199.8; ^{1}H NMR (60 MHz, $CDCl_3$, TMS int.): δ = 0.97 (t, J = 7.4 Hz, 3H), 2.18 (q, J = 7.4 Hz, 2H), 2.78 (s, 1H), 6.62 (s, 1H), 6.87–7.60 (m, 15H). – **4b**: m.p. = 77–79 °C; $[\alpha]_D^{25}$ (c = 1.15, $CHCl_3$) = 39.3; ^{1}H NMR (300 MHz, $CDCl_3$, TMS int.): δ = – 0.13 (s, 9H), 1.04 (t, J = 7.6 Hz, 3H), 2.27 (q, J = 7.3 Hz, 2H), 6.60 (s, 1H), 6.8–7.3 (m, 15H). – **6a**: ^{1}H NMR (300 MHz, $CDCl_3$, TMS int.): δ = – 0.13 (s, 9H), 0.88 (d, J = 7.3 Hz, 3H), 2.79 (m, 1H), 2.94 (d, J = 4.8 Hz, 1H), 4.66 (dd, J = 8.2, 4.8 Hz, 1H), 6.59 (s, 1H), 6.79–7.33 (m, 20H). – **6b**: ^{1}H NMR (300 MHz, $CDCl_3$, TMS int.): δ = – 0.15 (s, 9H), 0.77 (d, J = 6.6 Hz, 3H), 0.90 (d, J = 6.8 Hz, 3H), 1.08 (d, J = 7.3 Hz, 3H), 1.62 (m, 1H), 2.51 (d, J = 8.4 Hz, 1H), 2.63 (dq, J = 7.3, 5.5 Hz, 1H), 3.19 (m, 1H), 3.19 (m, 1H), 6.60 (s, 1H), 6.77–7.33 (m, 15H). – **6c**: ^{1}H NMR (300 MHz, $CDCl_3$, TMS int.): δ = – 0.13 (s, 9H), 0.84 (s, 9H), 1.17 (d, J = 7.3 Hz, 3H), 2.67 (dq, J = 7.3, 1.9 Hz, 1H), 3.11 (dd, J = 9.8, 1.9 Hz, 1H), 3.75 (d, J = 9.9 Hz, 1H), 6.55 (s, 1H), 6.78–7.31 (m, 15H).

The alkaline hydrolysis of the adduct mixture **6a**/**7a**/**8a**/**9a** obtained with benzaldehyde yields carboxylic acid **10a**, and subsequent treatment with diazomethane affords after purification by column chromatography (to separate off the *syn* isomer) the methyl ester **10b** (85% yield) in 96% *ee*. Comparison of the optical rotation[5] reveals the (2*R*,3*S*) configuration for **10b** and its optical purity was confirmed by ^{1}H NMR measurements with the shift reagent $[Eu(hfc)_3]$.[6] The reduction by $LiAlH_4$ of the crude products **6b**/**7b**/**8b**/**9b** and **6c**/**7c**/**8c**/**9c** which are formed by addition of the zirconium enolate **5b** to isobutyraldehyde or pivalaldehyde, respectively, affords the diols **11a** and **11b** (chemical yields: 63% and 68% respectively) in diastereomeric purity of 98% *de* after column chromatography on silica gel (to separate off both **3** and the *syn* isomer in each case); the enantiomeric excess is 94% and > 97%, respectively. The (2*S*,3*R*) configuration for 2,4-dimethylpentane-1,3-diol (**11a**) and (2*S*,3*S*) for 2,4,4-trimethylpentane-1,3-diol (**11b**)[7] are assigned by comparison of optical rotations.[8] Confirmation of the *ee* values is achieved by esterification of both the hydroxy groups with Mosher's reagent[9] and subsequent ^{19}F NMR spectroscopy.

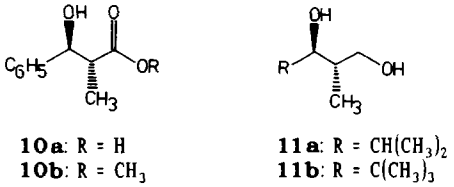

Although the zirconium enolate **5b** of the (*R*)-propionate **4b** always shows a large preference to attack the *Si* side of the aldehyde, the opposite topicity results from addition of the silyl ketene acetal **5** (M = $SiMe_3$) under Mukaiyama conditions.[10] However, the diastereofacial selectivity is smaller than with zirconium enolate (**5b**). The lithium enolate also affords predominantly *anti* adducts, but shows almost no diastereofacial selectivity. The highly stereoselective *anti* addition of **5b**[11] is all the more astounding, because the zirconium enolates used so far, sometimes independent of their configuration (*E* or *Z*), have reacted with *syn* selectivity.[12] The chiral auxiliary triphenylglycol (**3**) is recovered without racemization after both the hydrolysis to carboxylic acid **10a** and the reduction to the diols **11**, and is reusable. Access from (*S*)-**3**[13] to the enantiomeric products is possible as well.

Experimental Procedure

6c: A solution of lithium isopropylcyclohexylamide generated from isopropylcyclohexylamine (0.36 mL, 2.1 mmol) and butyllithium (2.1 mmol, 1.6 M in hexane) in THF (10 mL) was treated under an inert atmosphere of nitrogen with **4b** (0.84 g, 2.0 mmol) in THF (10 mL) and stirred for 90 min at – 105 °C to – 78 °C. The mixture was cooled to – 105 °C, and $[Cp_2ZrCl_2]$ (1.84 g, 6.3 mmol) in THF (26 mL), precooled to – 78 °C, was added dropwise. The resulting mixture was stirred for 2 h at – 60 °C, again cooled to – 105 °C, whereupon a solution of 2,2-dimethylpropanal (0.33 mL, 3.0 mmol) in THF (10 mL) was added dropwise. After stirring for 1 h at – 100 °C and 3 h at – 78 °C, the solution was treated successively with hydrochloric acid (15 mL, 1 M), saturated NH_4Cl solution (10 mL), and water (40 mL), stirred for 1 h at 25 °C, and worked up with ethyl acetate. Removal of the solvent gave crude **6c** (0.76 g, 75%), which according to the 300 MHz ^{1}H NMR spectrum was still contaminated with ca. 1% of **7c** and ca. 1% of the *syn* isomers **8c**/**9c**.

11b: The crude product **6c** was treated for 20 h at 25 °C with $LiAlH_4$ (1.15 g, 30.0 mmol) in diethyl ether. After aqueous workup and separation from **3** by column chromatography (silica gel, ethyl acetate/*n*-hexane 3:2; R_f of **3** = 0.38), **11b** (0.18 g, 80%) is eluted. $[\alpha]_D^{25}$ = – 5.1 (c = 1.78, $CHCl_3$).

Received: May 13, 1991 [Z4624 IE]
German version: *Angew. Chem. 103* (1991) 1369

CAS Registry numbers:
3, 95061-46-4; **4a**, 135789-36-5; **4b**, 135789-37-6; **5**, 135822-23-0; **6a**, 135789-38-7; **6b**, 135789-39-8; **6c**, 135789-40-1; **10a**, 36041-79-9; **10b**, 36041-80-2; **11a**, 97906-32-6; **11b**, 105497-75-4; PhCHO, 100-52-7; **b**, *i*PrCHO, 78-84-2; *t*BuCHO, 630-19-3; propionyl chloride, 79-03-8.

[1] Reviews: a) D. A. Evans, J. V. Nelson, T. R. Taber, *Top. Stereochem. 13* (1982) 1; b) C. H. Heathcock in D. J. Morrison (Eds.): *Asymmetric Synthesis, Vol. 3, Part B*, Academic, New York 1984, Chap. 2; c) S. Masamune, W. Choy, J. S. Petersen, L. R. Sita, *Angew. Chem. 97* (1985) 1;

Angew. Chem. Int. Ed. Engl. 24 (1985) 1; d) M. Braun in V. Snieckus (Eds.): *Advances in Carbanion Chemistry*, JAI Press, Greenwich, CT, USA, in press.
[2] G. Helmchen, U. Leikauf, I. Taufer-Knöpfel, *Angew. Chem. 97* (1985) 874; *Angew. Chem. Int. Ed. Engl. 24* (1985) 874; S. G. Davies, I. M. Dordor-Hedgecock, P. Warner, *Tetrahedron Lett. 26* (1985) 2125; W. Oppolzer, J. Marco-Contelles, *Helv. Chim. Acta 69* (1986) 1699; C. Palazzi, L. Colombo, C. Gennari, *Tetrahedron Lett. 27* (1986) 1735; S. Masamune, T. Sato, B. M. Kim, T. Wollmann, *J. Am. Chem. Soc. 108* (1986) 8279; M. T. Reetz, E. Rivadeneira, C. Niemeyer, *Tetrahedron Lett. 31* (1990) 3863; E. J. Corey, S. S. Kim, *J. Am. Chem. Soc. 112* (1990) 4976; R. O. Duthaler, P. Herold, S. Wyler-Helfer, M. Riediker, *Helv. Chim. Acta 73* (1990) 659. Recently the use of chiral amides in *anti*-selective aldol additions was also described: A. G. Myers, K. L. Widdowson, *J. Am. Chem. Soc. 112* (1990) 9672; C. H. Heathcock, H. Danda, M. M. Hansen, *J. Org. Chem. 55* (1990) 173.
[3] M. Braun, *Angew. Chem. 99* (1987) 24; *Angew. Chem. Int. Ed. Engl. 26* (1987) 24 and [1 d] and references cited therein; K. Prasad, K.-M. Chen, O. Repic, G. E. Hardtmann, *Tetrahedron Asymmetry 1* (1990) 703; T. Allmendinger, E. Felder, E. Hungerbühler, *Tetrahedron Lett. 31* (1990) 7301.
[4] The silyl ketene acetal **5** (M = $SiMe_3$) is formed first and is transformed into the propionate **4b** during workup (1 N HCl). Absence of the acid treatment allows the silyl ketene acetal to be isolated.
[5] C. Gennari, L. Colombo, G. Bertolini, G. Schimperna, *J. Org. Chem. 52* (1987) 2754.
[6] [Eu(hfc)$_3$]: Tris[3-(2,2,3,3,4,4-heptafluoro-1-hydroxybutylidene)-*d*-camphorato]europium (Aldrich).
[7] Formal inversion of configuration at C3, since the *tert*-butyl group in **11b**, in contrast to the isopropyl residue in **11a**, has a higher priority than the carbon atom C2.
[8] I. Taufer-Knöpfel, *Dissertation*, Universität Würzburg 1986; W. R. Roush, K. Ando, D. B. Powers, A. D. Palkowitz, R. L. Halterman, *J. Am. Chem. Soc. 112* (1990) 6339.
[9] J. A. Dale, D. L. Dull, H. S. Mosher, *J. Org. Chem. 34* (1969) 2543.
[10] Cf. T. Mukaiyama, *Org. React. (N.Y.) 28* (1982) 203.
[11] Also in the reaction of **5b** with acetaldehyde the proportion of the *anti*-configurated major diastereomer in the crude product is ca. 95%.
[12] Cf. [1 a] and references cited therein; T. Katsuki, M. Yamaguchi, *Tetrahedron Lett. 26* (1985) 5807; G. Iwasaki, M. Shibasaki, *ibid. 28* (1987) 3257. Only in the case of α-disubstituted zirconium enolates of ketones has *anti* selectivity been observed: S. Yamago, D. Machii, E. Nakamura, *J. Org. Chem. 56* (1991) 2098.
[13] R. Devant, U. Mahler, M. Braun, *Chem. Ber. 121* (1988) 397.

Addition of Chiral Nucleophiles to Pyridine Compounds: Total Synthesis of (−)-Isovallesiachotamine and (+)-Vallesiachotamine**

By *Robert Amann* and *Dietrich Spitzner**

In the syntheses of indole alkaloids of the yohimbane, heteroyohimbane, or corynanthe type, the procedure of *Wenkert* (addition of a nucleophile—preferably malonate—to an *N*-tryptophylpyridinium derivative, protonation of the intermediate 1,4-dihydropyridine, and Pictet–Spengler ring closure) has proved its worth.[1] This reaction sequence generates two chiral centers in the prochiral pyridine residue. Stereoelectronic effects control the relative configuration of these centers.

We can now demonstrate that enantiomerically pure frameworks of indole alkaloids can be constructed with this reaction cascade when chiral nucleophiles are added to the pyridinium compound **1** and the Pictet–Spengler ring closure is performed according to *Wenkert*'s one-pot procedure in benzene with dry hydrogen bromide.[2] The (−)-(2*R*,6*R*)-2-*tert*-butyl-6-methyl-1,3-dioxan-4-one (**2**), formed from poly-(*R*)-3-hydroxybutyric acid according to *Seebach* et al.,[3] is particularly suitable as chiral nucleophile. The reaction procedure to form hexahydroindolo[2,3-*a*]quinolizine (**3**) is very simple, and also in this case no protecting group is required on the indole nitrogen. However, **2**-Li must be added in excess so that the indole is also deprotonated. As the addition proceeds, the reaction mixture, which is at first heterogeneous at −78 °C, becomes homogeneous.[4]

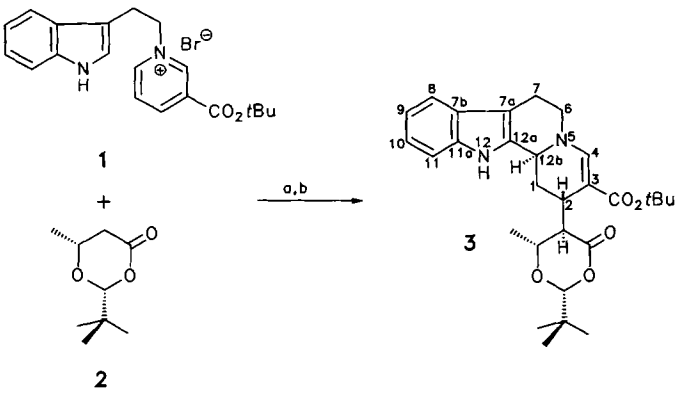

Scheme 1. Synthesis of **3**. Reagents and conditions: a) 2.2 equiv lithium diisopropylamide (LDA) and **2**, THF, −78 °C to 0 °C, 3.0 h; b) HBr(g), benzene, pH 6.5, 0 °C, 0.5 h, 27%.

Nonreacted pyridinium salt **1** can be recovered to a large extent. Analysis by chromatography (DC, silica gel 60, petroleum ether:ethyl acetate 4:1) and by ^{1}H NMR spectroscopy (250 MHz) of the chromatographed components of the crude product show that only one diastereomer (> 95%) is formed. It is remarkable that the chiral nucleophile is directed exclusively to C4 of **1**. This addition can be formulated by ionic as well as by radical steps (Single Electron Transfer, SET). To establish the stereochemical course (*lk* or *ul* addi-

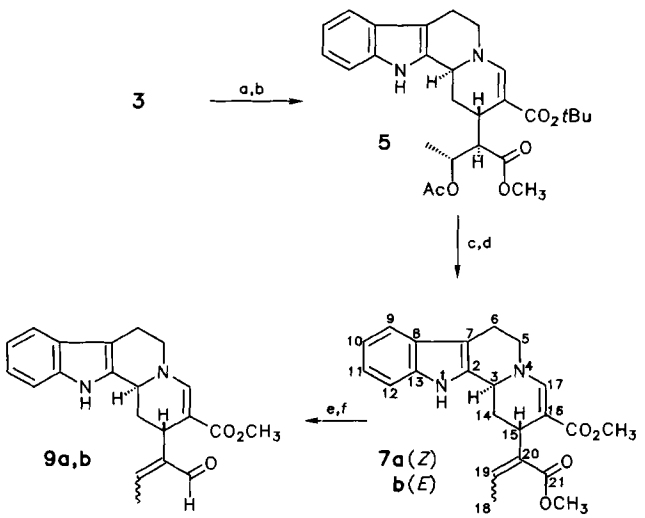

Scheme 2. Synthesis of **9a, b**. Reagents and conditions: a) 4 equiv $NaOCH_3$, CH_3OH, 20 °C, 0.5 h, 98%, **4**; b) 1.5 equiv Ac_2O, pyridine, 120 °C, 30 h, argon, 88%, **5**; c) 6 equiv 1,8-diazabicyclo[5.4.0]undec-7-ene (DBU), toluene, 115 °C, 1.5 h, argon, 88%, **6a, b**; d) 1 N HCl, CH_3OH, 20 °C, 2.5 h, 100%, **7a, b**; e) 4 equiv $LiAlH_4$, THF, 0 °C, 2.0 h, 78%, **8a, b**; f) 4 equiv MnO_2, CH_2Cl_2, 20 °C, 6.0 h, 60%, **9a, b**.

[*] Prof. Dr. D. Spitzner, Dipl.-Chem. R. Amann
Institut für Chemie der Universität Hohenheim
Garbenstrasse 30, W-7000 Stuttgart 70 (FRG)

[**] This work was supported by the Deutsche Forschungsgemeinschaft, the Fonds der Chemischen Industrie and the firms Marlborough Biopolymers Ltd, Billingham (UK), and Chemetall GmbH, Frankfurt am Main (through gifts of chemicals).

tion) of the reaction, the biosynthetically "early" alkaloids (−)-isovallesiachotamine (**9a**) and (+)-vallesiachotamine (**9b**), which can be isolated from *Vallesia*, *Rhazia*, and *Strychnos* species or obtained by mild hydrolysis from the alkaloid strictosidine,[5] were synthesized in few steps, starting from hexahydroquinolizine **3**. These natural products are formed along known biosynthetic pathways from tryptamine and secologanin.[6]

Compound **3** reacts with sodium methoxide in methanol by loss of pivalaldehyde to form the hydroxyester **4**, which is subsequently acylated. Acetate **5** forms the croton esters **6a, b** (3:1 *Z*/*E* mixture) by β elimination in toluene. Transesterification (MeOH/HCl) to **7a, b**[7] and selective reduction yield the alcohols **8a, b**, which are oxidized with MnO_2 to form the natural products **9a, b**. The proportion of the major isomer is increased by fractional crystallization.[8] These chemically very labile compounds isomerize on attempts to separate them by chromatography on silica gel.

The multifunctional hexahydroindolo[2,3-*a*]quinolizine **3** can be transformed in such a way that other enantiomerically pure indole alkaloids can also be prepared from it. Particularly attractive, however, are the homologous hexahydroindolo[2,3-*a*]quinolizines, which are derived from 2-methylnicotinic acid esters, since for these compounds the C_2 side chain typical of many indole alkaloids can be introduced very directly by a Winterfeldt lactam rearrangement.[9]

Received: May 23, 1991 [Z4643 IE]
German version: *Angew. Chem. 103* (1991) 1373

CAS Registry numbers:
1, 10052-60-5; **2**, 100017-18-3; **3**, 135887-51-3; **4**, 135887-52-4; **5**, 135887-53-5; **6a**, 135866-36-3; **6b**, 135866-37-4; **7a**, 136085-12-6; **7b**, 136029-92-0; **8a**, 34384-66-2; **8b**, 5523-49-9; **9a**, 34384-71-9; **9b**, 5523-37-5.

[1] J. E. Saxton, *Nat. Prod. Rep. 6* (1989) 433, and references cited therein.
[2] a) E. Wenkert, C.-J. Chang, H. P. S. Chawla, D. W. Cochran, E. W. Hagaman, J. C. King, K. Orito, *J. Am. Chem. Soc. 98* (1976) 3645; b) E. Wenkert, *Pure Appl. Chem. 53* (1981) 1271; c) D. Spitzner, E. Wenkert, *Angew. Chem. 96* (1984) 972; *Angew. Chem. Int. Ed. Engl. 23* (1984) 984; d) D. Spitzner, T. Zaubitzer, Y.-J. Shi, E. Wenkert, *J. Org. Chem. 53* (1988) 2274.
[3] D. Seebach, M. F. Züger, *Helv. Chim. Acta 65* (1982) 495; *Tetrahedron Lett. 25* (1984) 2747; D. Seebach, R. Imwinkelried, G. Stucky, *Angew. Chem. 98* (1986) 182; *Angew. Chem. Int. Ed. Engl. 25* (1986) 178; D. Seebach, J. Zimmermann, *Helv. Chim. Acta 69* (1986) 1147; D. Seebach, R. Imwinkelried, G. Stucky, *ibid. 70* (1987) 448; J. Zimmermann, D. Seebach, T.-K. Ha, *ibid. 71* (1988) 1143.
[4] **3**: Yield 27%; colorless crystals, m.p. = 266°C. $[\alpha]_D^{27} = +34$ ($c = 0.11$; 1,2-dichloroethane/isopropanol 8:2); ^{1}H NMR (250 MHz, $CDCl_3$, 25°C, TMS): $\delta = 0.9$ (s, 9H, acetal-*t*Bu), 1.4 (d, $J = 6.1$ Hz, 3H, CH_3), 1.5 (s, 9H, ester-*t*Bu), 1.8–1.9 (m, 1H, C1-H), 2.1–2.2 (m, 1H, C1-H), 2.4–2.5 (dd, $J = 9.5$, 1.2 Hz, 1H, C5′-H), 2.7–2.9 (m, 2H, C7-H), 2.9–3.0 (m, $J = 5.2$, 1H, C2-H), 3.6-3.7 (m, 2H, C6-H), 4.6–4.7 (dq, $J = 9.5$, 6.1 Hz, 1H, C6′-H), 5.0–5.1 (d, br, $J = 13$ Hz, 1H, C12b-H), 5.1 (s, 1H, C2′-H), 7.1–7.5 (m, 5H, C8-,9-,10-,11-H + C4-H), 7.9 (s, 1H, NH). – ^{13}C NMR (62.77 MHz, $CDCl_3$/[D$_6$]DMSO 5:1, 25°C): $\delta = 20.1$ (q, CH_3), 21.1 (t, C7), 22.9 (3q, acetal-C(CH_3)$_3$), 27.6 (3q, ester-C(CH_3)$_3$, 30.7 (d, C2), 33.4 (t, C1), 34.0 (s, acetal-C(CH_3)$_3$), 48.2 (d, C12b), 50.2 (t, C6), 55.0 (d, C5′), 74.6 (d, C6′), 77.3 (s, ester-C(CH_3)$_3$), 94.4 (s, C3), 106.1 (s, C7a), 106.5 (d, C2′), 110.3 (d, C11), 117.0 (d, C8), 118.1 (d, C9), 120.4 (d, C10), 125.9 (s, C7b), 132.8 (s, C12a), 135.8 (s, C11a), 146.4 (d, C4), 167.0 (s, ester carbonyl), 169.4 (s, lactone carbonyl). – MS (70 eV): *m/z* 494 ($M^{\oplus}$, 7%), 351 (18), 322 (14), 321 (13), 267 (31), 266 (49), 265 (100), 221 (19), 57 (17).
[5] a) C. Djerassi, H. J. Monteiro, A. Walser, L. J. Durham, *J. Am. Chem. Soc. 88* (1966) 1792; b) D. A. Evans, J. A. Joule, G. F. Smith, *Phytochemistry 7* (1968) 1429; c) Atta-ur-Rahman, S. Malik, *J. Nat. Prod. 47* (1984) 388; d) P. G. Waterman, S. Zhong, *Planta Med. 45* (1982) 28; e) K. T. D. DeSilva, G. N. Smith, K. E. H. Warren, *J. Chem. Soc. Chem. Commun. 1971*, 905. As far as we know, an enantioselective synthesis for **9a** or **9b** has not yet been published. We thank Prof. G. Höfle, Gesellschaft für Biotechnologische Forschung mbH (GBF), Braunschweig, for natural (+)-vallesiachotamine. Unfortunately is was not possible to obtain authentic (−)-isovallesiachotamine.
[6] J. D. Phillipson, M. H. Zenk: *Indole and Biogenetically Related Alkaloids*, Academic, London 1980; L.-F. Tietze, *Angew. Chem. 95* (1983) 840; *Angew. Chem. Int. Ed. Engl. 22* (1983) 828.
[7] Biogenetic numbering in Scheme 2 from J. Le Men, W. I. Taylor, *Experientia 21* (1965) 508.
[8] The 5.2:1-mixture of **9a, b** has an optical rotation of $[\alpha]_D^{25} = -105$ ($c = 0.34$, $CHCl_3$) ([5e]: **9a**: $[\alpha]_D = -180$; **9b**: $[\alpha]_D = +220$ in $CHCl_3$); [5d]: **9a**: $[\alpha]_D^{25} = -54$ ($c = 0.06$, $CHCl_3$), probably after partial isomerization to **9b**.
[9] J. Müller, E. Winterfeldt, *Chem. Ber. 111* (1978) 1540; C. Bohlmann, R. Bohlmann, E. G. Rivera, C. Vogel, M. D. Manandhar, E. Winterfeldt, *Liebigs Ann. Chem. 1985*, 1752; I. Ninomiya, T. Naito, O. Miyata, T. Shinada, E. Winterfeldt, R. Freund, T. Ishida, *Heterocycles 30* (1990) 1031, and references cited therein.

2,2-Dimethyl-α,α,α′,α′-tetrakis(β-naphthyl)-1,3-dioxolan-4,5-dimethanol (DINOL) for the Titanate-Mediated Enantioselective Addition of Diethylzinc to Aldehydes**

By *Beat Schmidt* and *Dieter Seebach**

We reported recently[1a] that addition of diethylzinc to aldehydes in the presence of 1 equivalent $Ti(OCHMe_2)_4$ and 0.1 equivalents spirotitanate **1** is highly enantioselective.[2] The compatibility of this Lewis acid mediated process with the donor solvent diethylether[3] allowed us to use dialkylzinc compounds which had been generated in situ from conventionally prepared primary Grignard reagents.[1b] With aliphatic aldehydes the selectivity was rather below 90% *ee* while it reached 99% with aromatic ones. We have now found that the monocyclic naphthyl-substituted titanate **2** is a far more effective catalyst.[4,5]

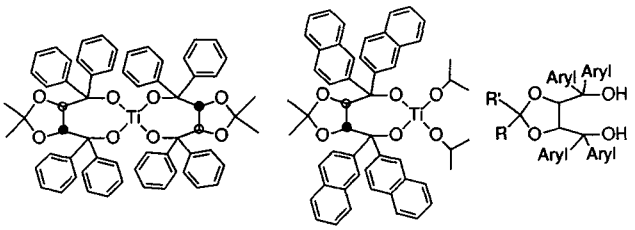

1 **2** (M_r = 830.87) **3**

In the course of mechanistic studies of the reaction carried out with $Ti(OCHMe_2)_4$/**1**, we noticed that simply adding diols **3** to the achiral titanate led to appreciable enantioselectivities and that a seven-membered ring titanate was formed upon mixing these components (NMR spectroscopy). Tetraaryldioxolanedimethanol (TADDOL) derivatives of titanium such as **2** can be isolated as colorless solids.[4]

The procedure using **2** and the product analysis followed those described for the spirotitanate[1] (see Eq. (a) and Table 1). The *Si* selectivity of Et_2Zn addition to benzaldehyde is > 99:1 with 0.2 equivalents of **2**; the product **4** is still formed with a 96:4 preference, when 5 mol% of **2** and

[*] Prof. Dr. D. Seebach, Dipl.-Chem. B. Schmidt
Laboratorium für Organische Chemie der Eidgenössischen Technischen Hochschule
ETH-Zentrum, Universitätstrasse 16, CH-8092 Zürich (Switzerland)
[**] Part of the projected Ph. D. thesis of *B. Schmidt*. We thank *Y. Wang* for carrying out some experiments and *D. Felix* for assistance with *ee* determinations by gas chromatography. Financial support and gifts of chemicals by the Sandoz AG (CH-Basel), Dynamit-Nobel, Hüls Troisdorf (Bergkamen, FRG) are gratefully acknowledged.

an excess of Et_2Zn is used.[8] With terephthalic aldehyde one of the four possibilities, the (*S,S*) stereoisomer **5**, is obtained exclusively (>99% *ds*, 98% *ee*), while the reaction with isophthalic aldehyde is a little less selective, furnishing the (*S,S*) diol **6** with 93% *ds* and > 99% *ee* (see Fig. 1). Especially with saturated (→ **7**–**9**), olefinic (→ **10**–**12**), and acetylenic (→ **13**) aliphatic aldehydes the improvement obtained with **2** over the reagent with the tetraphenyl-substituted ligand is essentially an order of magnitude. The highest selectivity was observed with phenylpropinal: the (*R*) enantiomer was not detectable by gas chromatography (see Fig. 1), a promising result if one considers the multitude of interesting conversions that propargyl alcohols are capable of undergoing.

To test the influence of a stereogenic center in the α-carbonyl position of the aldehyde we added diethylzinc to (*R*)-2-methyl-4-hexenal (**14**). [Equation (b)]:[10] with the catalyst **2** a 97 : 3 *Si* addition ensued, with *ent*-**2** a > 96 : 4 *Re* addition. The assignment of configuration to the epimers **15** and **16**[11]

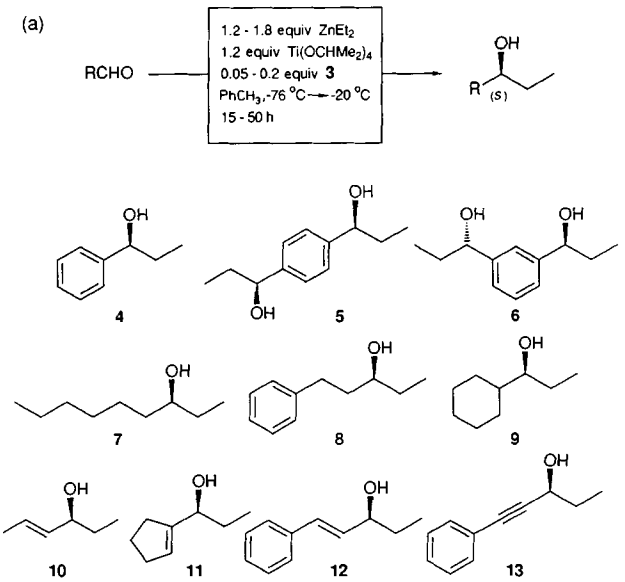

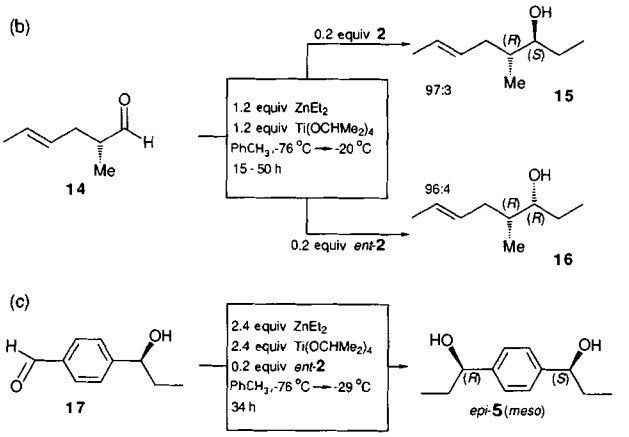

that formed is based on the sign of optical rotations and in analogy to the other reactions carried out.[12] The high selectivity of addition allowed us to construct the two centers of opposite sense of chirality in the *meso* diol *epi*-**5**[9] by first using the (*R/R*) ligand (→ **17**; *S/R* = 98.2 : 1.8) and then the (*S/S*) ligand (*ent*-**2**) on terephthalic aldehyde (see Fig. 1).

Table 1. Reactions of benzaldehyde, phthalic aldehydes, heptanal, 3-phenylpropanal, cyclohexanecarbaldehyde, crotonaldehyde, cyclopentene-1-carbaldehyde, cinnamaldehyde, and 3-phenylpropanal (5–10 mmolar runs). All secondary alcohols, except **5**, **6**, and **11**, have been previously described, and their configurations assigned; the sense of chirality follows from comparison of the sense of optical rotation with literature data [6]. Thus, we assign all alcohols the (*S*), and the diols **5** and **6** the (*S,S*) configuration. The ratios of enantiomers were determined by GC (cf. the specifications in [1b], for which the trifluoroacetates of **6**, **7** and **8** had to be prepared [7]).

product	equivalents		Temp.	reaction time	yield	*S/R*
	Et_2Zn	**2**	[°C]	[h]	[%]	
4	1.2	0.2	−25	30	76	99.3:0.7
4	1.2	0.1	−20	19	88	93:7
4	1.8	0.05	−24	22	95	96:4
5	2.4[a]	0.4	−76→−23	42	79	99.5:0.5[b,c]
6	2.4[a]	0.4	−76→−25	50	95	99.5:0.5[c]
7	1.2	0.2	−28	50	70	98.5:1.5
8	1.2	0.2	−22	15	87	>99:1[b,d]
9	1.2	0.2	−27	30	77	99.5:0.5
10	1.2	0.2	−76→−27	20	56	>99:1
11	1.2	0.2	−29	20	79	99.5:0.5[c]
12	1.2	0.2	−27	24	87	95.5:4.5
13	1.2	0.2	−27	22	83	>99.5:0.5[e]

[a] 2.4 equiv of $Ti(OCHMe_2)_4$ were used. [b] Only one diastereoisomer detectable. [c] See Fig. 1. [d] Racemate in GC not quite baseline separated. [e] The amount of the enantiomer lies below GC detection limits.

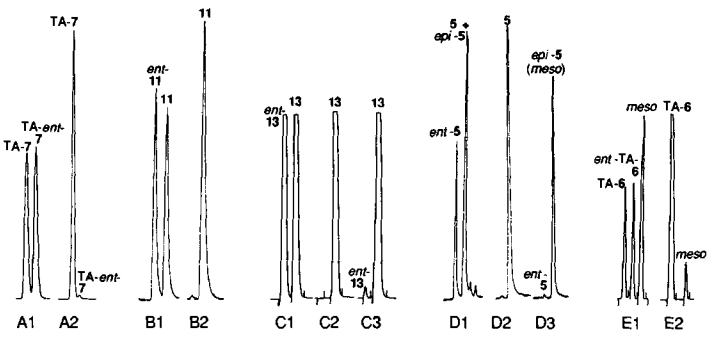

Fig. 1. Gas chromatograms for determination of the enantiomer ratios [1b]. A (**7**, trifluoroacetate); A1: racemic mixture; A2: product from reaction Eq. (a). B (**11**); B1: racemic mixture; B2: product from reaction. C (**13**); C1: racemic mixture; C2: product from reaction; C3: product "diluted" with ca. 3% *rac*. **13** (integration 1.5 : 98.5). D (**5**) [9]; D1: *meso*/*rac* mixture from terephthalic aldehyde and EtMgBr (integration ratio 22.9/58.0; on an achiral GC column a 29.1 : 38.0 *meso*/*dl* ratio was determined in this sample); D2: product from reaction; D3: *meso* product from **17**, Equation (c). E (**6**, bistrifluoroacetates) [9]; E1: *meso*/*rac* mixture from isophthalic aldehyde and EtMgBr (integration ratio 22.2/21.1/45.0); E2: product from reaction.

As can be seen from the diagram in Figure 2, the Lewis acid cocktail **2**/$(Me_2CHO)_4Ti$ provides the first case of a linear correlation between the enantiopurity of the catalyst and of the product in a Et_2Zn addition to an aldehyde, suggesting that a single DINOL ligand is involved in the rate-determining step.[13]

We are confident that organozinc compounds other than Et_2Zn will give similar results[1b] with the DINOL titanate **2**.

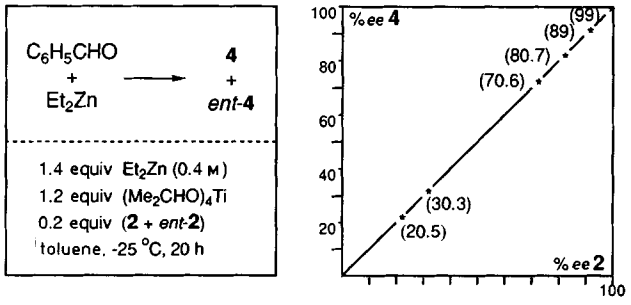

Fig. 2. Reactions of benzaldehyde with the DINOL derivative **2** of different enantiopurity. The molarity of Et_2Zn refers to the reaction mixture. Aliquots of (*R,R*)- and (*S,S*)-**3**, aryl = 2-$C_{10}H_7$, R = R′ = CH_3 were mixed for the preparation of **2** (see procedure). The numbers in brackets in the diagram were calculated from GC integrations measured with the samples of **4** obtained.

Experiments with aldehydes and zinc derivatives containing additional functional groups are under way.

Typical Procedure

8: Diol **3** (aryl = 2-$C_{10}H_7$, R = R′ = Me)[4], 0.933 g (1.4 mmol) is placed under argon in a dry 100 mL flask with side arm (serum cap). $Ti(OCHMe_2)_4$ (0.48 g, 1.7 mmol) and $PhCH_3$ (10 mL) are added by syringe, and after stirring at room temperature for 5 h the $PhCH_3$ and isopropanol are removed (40 °C/100–3×10^{-2} Torr). The solid residue is combined at room temperature with $PhCH_3$ (20 mL) and $Ti(OCHMe_2)_4$ (2.5 mL, 2.4 g, 8.4 mmol), and the solution cooled to − 25 °C (cryostat). Et_2Zn (4.2 mL, 8.4 mmol, 2 M in $PhCH_3$), and then 3-phenylpropanal (0.92 mL, 0.94 g, 7.0 mmol) are added dropwise. After 15 h at − 22 °C (TLC sampling) the reaction mixture is quenched with saturated aqueous NH_4Cl (10 mL), and Et_2O (40 mL) is added. Stirring for 30 min is followed by filtration through Celite, washing with saturated aqueous NaCl, drying over Na_2SO_4, and removal of the solvent. The residue is chromatographed through a short SiO_2 column (C_6H_{14}/Et_2O 3:1), and the resulting mixture of **3** and **8** heated in a Kugelrohr oven (100 °C air temp./0.3 mbar) to expel the alcohol **8**, the absence of which in the residue [14] is ascertained by NMR spectroscopy: 1.0 g colorless crystals, m.p. 40 °C.

Received: April 15, 1991 [Z 4578 IE]
German version: *Angew. Chem. 103* (1991) 1383

[1] a) B. Schmidt, D. Seebach, *Angew. Chem. 103* (1991) 100; *Angew. Chem. Int. Ed. Engl. 30* (1991) 99; b) D. Seebach, L. Behrendt, D. Felix, *Angew. Chem. 103* (1991) 991; *Angew. Chem. Int. Ed. Engl. 30* (1991) 1008.

[2] For an up-to-date review on enantioselective catalytic Et_2Zn additions to aldehydes, see R. Noyori, M. Kitamura, *Angew. Chem. 103* (1991) 34–55; *Angew. Chem. Int. Ed. Engl. 30* (1991) 49–69. See also the discussion in: D. A. Evans, *Science 240* (1988) 420–426.

[3] For the use of THF in such reactions, see also: J. Hübscher, R. Barner, *Helv. Chim. Acta 73* (1990) 1068.

[4] Preparation of tetraaryldioxolanedimethanols (TADDOLs) on a several-hundred-gram scale: A. K. Beck, B. Bastani, D. A. Plattner, D. Seebach, H. Braunschweiger, P. Gysi, L. LaVecchia, *Chimia 45* (1991) 238. See also: D. Seebach, A. K. Beck, R. Imwinkelried, S. Roggo, A. Wonnacott, *Helv. Chim. Acta 70* (1987) 954.

[5] For another example of a bis(β-naphthyl)methanol-containing chiral auxiliary see E. J. Corey, J. O. Link, *Tetrahedron Lett. 30* (1989) 6275.

[6] *Beilstein Handbook of Organic Chemistry, Bände 1, 6*, 1.–4. Ergänzungswerk, Springer, Heidelberg; R. C. Weast, M. J. Astle, W. H. Beyer: *CRC Handbook of Chemistry and Physics*, CRC Press, Boca Raton, Florida 1985. For **13** see K. Ishihara, A. Mori, I. Arai, H. Yamamoto, *Tetrahedron Lett. 27* (1986) 983.

[7] W. A. König, S. Lutz, G. Wenz, E. von der Bey, *HRC & CC J. High Resol. Chromatogr. & Chromatogr. Commun. 11* (1988) 506.

[8] Cf. also P. A. Chaloner, E. Langadianou, *Tetrahedron Lett. 31* (1990) 5185.

[9] So far only mixtures of (*rac*-**5** and *epi*-**5**) and (*rac*-**6** and *epi*-**6**) have been described [6]. We determined the following properties ($[\alpha]_D^{RT}$ in $CHCl_3$): **5** M.p. 51 °C, $[\alpha]_D^{RT} = -59.5$; *epi*-**5**: *meso*-configuration, m.p. 114 °C, $[\alpha]_D^{RT} = +0.3$; **6**: M.p. 59 °C, $[\alpha]_D^{RT} = -59.7$).

[10] R. M. Wenger, *Helv. Chim. Acta 66* (1983) 2308.

[11] The *Re* face of **14** is more reactive according to Cram's rule (with EtMgBr, **16** is formed preferentially by 8:5) D. J. Cram, F. A. Abd Elhafez, *J. Am. Chem. Soc. 74* (1952) 5828. See also: J. Mulzer, H.-J. Altenbach, M. Braun, K. Krohn, H.-U. Reissig: *Organic Synthesis Highlights*, VCH, Weinheim 1991, p. 3–8, and references cited therein.

[12] **14** was freshly prepared by Swern oxidation from the corresponding alcohol; the enantiopurity of **14** was ≥ 85% (GC). Since all four stereoisomeric products could be seperated on a chiral capillary GC column [1 b, 7], the ratio **15**:**16** could be accurately determined, and extrapolated for enantiopure aldehyde. The isolated sample of **15** is levorotatory, that of **16** dextrorotatory.

[13] Nonlinear correlations between % *ee* and optical properties or enantioselectivities: A. Horeau, *Tetrahedron Lett. 1969*, 3121; C. Puchot, O. Samuel, E. Dunach, S. Zhao, C. Agami, H. B. Kagan, *J. Am. Chem. Soc. 108* (1986) 2353. For "chirality enhancement" in additions of Et_2Zn see the review [2] and references cited therein.

[14] **3** (aryl = 2-naphthyl, R = R′ = CH_3) holds on to **4** and **9** especially stubbornly. Cf. F. Toda, *Top. Curr. Chem. 149* (1988) 211, and earlier papers by *Toda*'s group cited therein.

The Radical Cations of Silaketene and Several Isomers of $[C,H_2,Si,O]^{\cdot\oplus}$: An Ab Initio MO Investigation**

By *Jan Hrušák, Ragampeta Srinivas, Diethard K. Böhme,* and *Helmut Schwarz**

Recently, during systematic studies of the gas-phase chemistry of unsaturated silicon molecules,[1] we produced a radical cation with the elemental composition $[C,H_2,Si,O]^{\cdot\oplus}$ by the electron-impact ionization of $Si(OCH_3)_4$.[2] Although it was possible in analogous cases to establish ion connectivities by using tandem mass spectrometry,[1] the $[C,H_2,Si,O]^{\cdot\oplus}$ ion derived from $Si(OCH_3)_4$ could not be characterized in this way with certainty. The analysis of the collisional-activation spectra pointed toward the presence of several structures such as **1** and **4**, and ab initio calculations revealed an

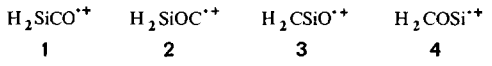

energy surface rich in isomers. Here we present structures **1** to **4** which exhibit unusual structural features and show differences in geometry, symmetry, electronic structure, and order of stability from the "analogous" radical cations $CH_2{=}C{=}O^{\cdot\oplus}$ and $CH_2{=}O{=}C^{\cdot\oplus}$. These differences are also seen for the corresponding neutral molecules, and are much more pronounced than is implied by the similarities in Lewis structures.[3, 4]

[*] Prof. Dr. H. Schwarz
Institut für Organische Chemie der Technischen Universität
Strasse des 17. Juni 135, W-1000 Berlin 12 (FRG)
Dr. J. Hrušák
Institute of Macromolecular Chemistry
Czechoslovak Academy of Sciences
Heyrovsky Square 2, CS-16202 Prague (Czechoslovakia)
Dr. R. Srinivas
Council of Scientific and Industrial Research
Indian Institute of Chemical Technology
Hyderabad (AP) 500007 (India)
Prof. D. K. Böhme
Department of Chemistry and
Centre for Research in Earth and Space Science
York University
North York, Ontario M3J IP3 (Canada)

[**] This work was supported by the Deutsche Forschungsgemeinschaft and the Fonds der Chemischen Industrie. *R. Srinivas* is grateful to DAAD for a stipend und *D. K. Böhme* to the Humboldt Foundation for a Humboldt Senior Award.

All MO calculations were carried out with the GAUSSIAN 88 program package[5] within the unrestricted Hartree–Fock (UHF) formalism.[6] Stationary points were characterized by analyzing the force constant matrix. Complete geometry optimizations were accomplished with a 6-31G** basis set[7] and second-order Møller-Plesset perturbation theory (MP2).[8] Zero-point vibrational energies (ZPVE) were derived from harmonic frequencies calculated at the MP2/6-31G** level. The ZPVE were scaled by a factor of 0.89. The data for the energies obtained in this way (MP2/6-31G**//MP2/6-31** + ZPVE) for **1** to **4** are summarized in Table 1, and the geometric and electronic structures, as well as the relative stabilities of the $[C,H_2,Si,O]^{\bullet\oplus}$ radical ions, are adequately described[9] at this level of theory. This also follows from a comparison of calculated bond dissociation energies with experimentally available data.[2] Inconsistent results are obtained with smaller basis sets or when correlation effects are not included. On the other hand, an increase in the basis sets beyond 6-31G** does not seem necessary.

Table 1. Absolute [in Hartree] and relative energies [kcal mol^{-1}] for isomers of $[C, H_2, Si, O]^{\bullet\oplus}$ [a].

isomer	symmetry/ state	MP2/6-31G**// MP2/6-31G**	MP2/6-31G**// MP2/6-31G**+ZPE [b]
1	$C_s/^2A'$	− 402.876262 (5.7)	− 402.855192 (1.1)
1' [c]	$C_{2v}/^2B_1$	− 402.865087 (12.7)	− 402.840662 (10.1)
2	$C_s/^2A'$	− 402.839944 (28.5)	− 402.817705 (24.5)
3	$C_{2v}/^2A_1$	− 402.838988 (29.1)	− 402.819463 (23.4)
4	$C_{2v}/^2A_1$	− 402.885364 (0.0)	− 402.856762 (0.0)

[a] For structural details see text and Scheme 1. [b] ZPVE: Zero-point vibrational energy. [c] The planar structure **1'** corrsponds to a transition state (one imaginary frequency) for the degenerate transformation **1** ⇄ **1'*** ⇄ **1**.

From many points of view, the radical cation of 1-silaketene ($H_2SiCO^{\bullet\oplus}$, **1**) is related to the neutral silaketene recently calculated by *Hamilton* and *Schaefer*.[10] The ketene-like *planar* C_{2v} structure **1'** (Scheme 1) is in both cases not a minimum but corresponds to a transition state of the degenerate isomerization **1** ⇄ **1'** ⇄ **1**. While for the neutral species an activation energy of 18.5 kcal mol^{-1} was calculated,[10] for the radical cations the energy difference between **1'** and **1** amounts to 9.0 kcal mol^{-1} (see Table 1). The imaginary frequency of the out-of-plane deformation is 598 cm^{-1} for the radical cation **1'** (Table 2) and 592 cm^{-1} for the neutral molecule.[10] Both the radical cation and the neutral form of **1** have a nonplanar C_s structure at the minimum. From a comparison of the vibrational frequencies (Table 2), the formal charges derived from the Mulliken population analysis and the geometrical details (Scheme 1) it follows that **1** corresponds to a complex of $SiH_2^{\bullet\oplus}$ and a largely "unperturbed" CO molecule. As is the case for the neutral species,[11] the Si–C bond can be understood in terms of an interaction between the empty p orbital of the silicon that is perpendicular to the SiH_2 plane and the pair of electrons on the carbon. A relatively long Si–C bond (1.979 Å) results. As expected, the unpaired electron occupies the sp^2-hybridized orbital of $SiH_2^{\bullet\oplus}$. In **1** Si is both the radical site (spin density ϱ = 1.01 e) and the center of charge (q = 0.78 e). The changes in structure which result as a consequence of the "complexation" of the $SiH_2^{\bullet\oplus}$ and CO parts are quite small compared with the structures of the separate building blocks: the C–O bond distance of 1.138 Å in **1** is not significantly shorter than that of the free CO (1.150 Å), and the Si–H bond is shortened by 0.008 Å and the HSiH angle is opened by 0.56 degrees. The vibrational frequencies summarized in Table 2 are also consistent with these changes in geometry. The energy for the dissociation of **1** into $SiH_2^{\bullet\oplus}$ and CO is 41.1 kcal mol^{-1}.

Table 2. Comparison of the vibrational frequencies of the planar and nonplanar silaketene radical cations (**1**) calculated at the MP2/6-31G**//MP2/6-31G** level with the CCSD results [10] for the neutral system [a].

system	vibration	cation ω_i[cm^{-1}]	neutral ω_i[cm^{-1}]
H_2Si-CO	torsion	271	270
	SiCO bending	293	280
	SiC stretching	410	410
	SiH_2 twisting	681	791
1	SiH_2 wagging	710	744
	SiH_2 scissoring	906	1021
	CO stretching	2261	2252
	SiH_2 asymm. stretching	2388	2200
	SiH_2 symm. stretching	2446	2200
H_2Si-CO	out-of-plane	−598	− 592
	in-plane linear bending	299	356
	out-of-plane linear bending	371	511
	Si-C stretching	551	732
1a	SiH_2 rocking	633	710
	SiH_2 scissoring	849	906
	CO stretching	2422	2202
	SiH_2 symm. stretching	2439	2448
	SiH_2 asymm. stretching	2516	2488
CO	CO stretching	2124	2245
SiH_2 [b]	SiH_2 bending	951	1072
	SiH_2 asymm. stretching	2334	2144
	SiH_2 symm. stretching	2414	2146

[a] For structural details see text and Scheme 1. [b] Calculated for the isolated cation and neutral species, respectively.

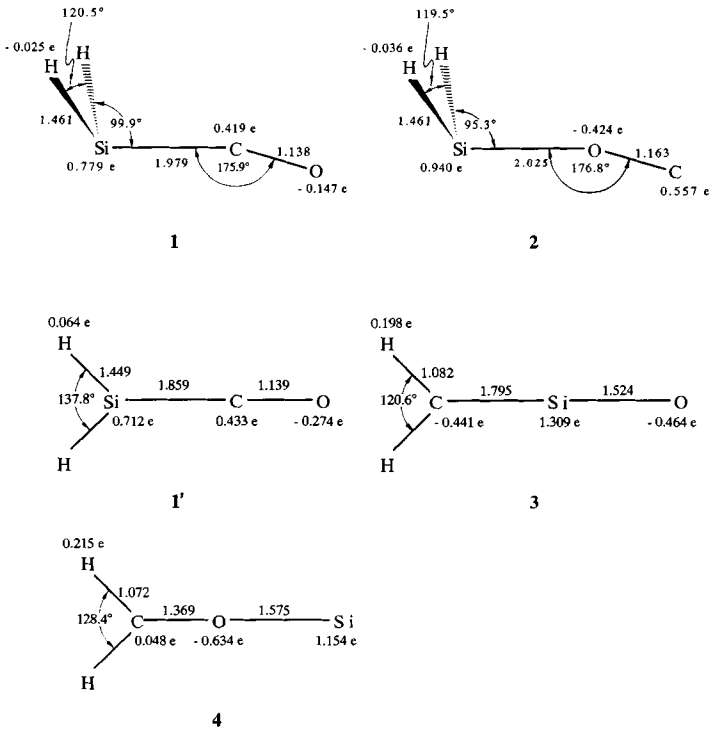

Scheme 1. The structural parameters and charge distribution calculated for the $[C, H_2, Si, O]^{\bullet\oplus}$ isomers **1**–**4**.

The coordination of $SiH_2^{\bullet\oplus}$ with the oxygen end of CO also results in a minimum in the energy surface for a nonplanar structure **2**. Although the isomer **2** is 23.4 kcal mol^{-1} less stable than **1**, the bond relationships and the geometries are

quite similar. The radical site and the charge are again mainly localized on the silicon ($\varrho = 0.98$ e; $q = 0.94$ e). The $SiH_2^{\bullet\oplus}$ segment is strongly bent (95.3°), and the Si–H and C–O bond lengths of 1.461 and 1.163 Å, respectively, are very similar to those found for **1**. Furthermore, the analysis of the vibrational frequencies supports a description of **2** as a complex of $SiH_2^{\bullet\oplus}$ and OC. The normal vibration of CO for **2** (2047 cm^{-1}) points towards an "unperturbed" CO bond, which is also consistent with the observed increase in the C–O bond length in **2** by 0.025 Å compared to **1**. The long Si–O separation of 2.025 Å and the low-lying frequency of 298 cm^{-1} for the SiO vibration correspond to a small perturbation. The symmetric and asymmetric SiH vibrations of 2383 and 2454 cm^{-1}, respectively, for **2** are very close to the vibrations of the free $SiH_2^{\bullet\oplus}$ (2334 and 2414 cm^{-1}, respectively). We obtain a value for the energy of dissociation of **2** into $SiH_2^{\bullet\oplus}$ and CO of 17.7 kcal mol^{-1}. As expected, the interaction of the empty p orbital of the $SiH_2^{\bullet\oplus}$ fragment with a free electron pair on the oxygen is energetically less attractive than the interaction with the electron pair on the carbon atom of CO.

The radical cation of 2-silaketene ($H_2CSiO^{\bullet\oplus}$, **3**) is a minimum on the energy surface. The energy of **3** is comparable to that of **2**. Several structural details deserve to be emphasized: 1) In contrast to **1** and **2**, the minimum in **3** can be described by a *planar* form with C_{2v} symmetry. 2) The Si–O bond in **3** of 1.524 Å is somewhat shorter than in the isolated $^2\Sigma^+$ $SiO^{\bullet\oplus}$ (1.542 Å). This corresponds to an increase in the SiO vibrational frequency (1321 cm^{-1}) of 271 cm^{-1} compared to $SiO^{\bullet\oplus}$. 3) The Si–C distance in **3**, 1.795 Å, lies between those of a Si–C bond in methylsilane (1.867 Å) and a Si–C double bond in silavinylidene (1.709 Å).[12] All of these data indicate that **3** formally corresponds to a silaketene derivative in which an electron has been removed from the Si–C double bond. The centers of spin and charge are formally separated in the resulting radical ion (a "distonic" ion[13]). The carbon atom carries the unpaired electron ($\varrho = 1.08$ e) and the silicon the charge (q = 1.30 e).

That the global minimum on the $[C,H_2,Si,O]^{\bullet\oplus}$ energy surface corresponds to a planar C_{2v} structure $H_2COSi^{\bullet\oplus}$ (**4**) is surprising, because in the ketene analogue the $H_2COC^{\bullet\oplus}$ structure is about 63 kcal mol^{-1} more energetic than $H_2CCO^{\bullet\oplus}$.[4c] It follows from the analysis of the geometry data and the charge distribution that **4** is not really a complex of $CH_2O/Si^{\bullet\oplus}$ but a combination of $CH_2/OSi^{\bullet\oplus}$. For example, the C–O separation in **4** of 1.369 Å clearly is larger than in a typical C–O double bond (H_2CO: 1.208 Å), while the Si–O bond in **4** is only 0.033 Å longer than in isolated $^2\Sigma^+$ $SiO^{\bullet\oplus}$. The C–H bond length and the HCH angle are also much closer to the parameters calculated for $^3CH_2$ (1.073 Å and 131°, respectively). Like **3**, structure **4** represents a distonic ion. The carbon carries the spin (1.292 e) and the silicon the charge ($q = 1.154$ e). Attempts to localize a bent form for **4** were unsuccessful; the C_s structure found at the UHF level does not correspond to a stationary point at the MP2/6-31G** level.

Received: May 27, 1991 [Z 4652]
German version: *Angew. Chem. 103* (1991) 1396

CAS Registry numbers:
1, 136034-35-0; **3**, 136034-36-1; **4**, 136034-37-2; SiH_2, 13825-90-6; $SiH_2^{\bullet+}$, 28149-31-7; CO, 630-08-0; $CO^{\bullet+}$, 12144-04-6.

[1] a) R. Srinivas, D. Sülzle, H. Schwarz, *Chem. Phys. Lett. 175* (1990) 575; b) *J. Am. Chem. Soc. 113* (1991) 52; c) R. Srinivas, D. Sülzle, T. Weiske, *Int. J. Mass Spectrom. Ion Processes*, 107 (1991) 369; d) R. Srinivas, D. Sülzle, W. Koch, C. H. DePuy, H. Schwarz, *J. Am. Chem. Soc.* 113 (1991) 5970.
[2] R. Srinivas, D. K. Böhme, J. Hrušák, D. Schröder, H. Schwarz, *J. Am. Chem. Soc.*, submitted.
[3] For excellent reviews see a) H. F. Schaefer III, *Acc. Chem. Res. 15* (1982) 283; b) G. Raabe, J. Michl, *Chem. Rev. 85* (1985) 419; c) H. Bock, *Angew. Chem. 101* (1989) 1659; *Angew. Chem. Int. Ed. Engl. 28* (1989) 1627; d) S. Patai, Z. Rappoport (Eds.): *The Chemistry of Functional Groups: The Chemistry of Silicon Compounds*, Wiley Interscience, New York 1989.
[4] a) K. Tanaka, M. Yoshimine, *J. Am. Chem. Soc. 102* (1980) 7655; b) W. J. Bouma, R. H. Nobes, L. Radom, C. E. Woodward, *J. Org. Chem. 47* (1982) 1869; c) W. J. Bouma, P. M. W. Gill, L. Radom, *Org. Mass Spectrom. 19* (1984) 610; d) G. Vacek, B. T. Colegrove, H. F. Schaefer III, *Chem. Phys. Lett. 177* (1991) 468.
[5] M. J. Frisch, M. Head-Gordon, H. B. Schlegel, K. Raghavachari, J. S. Binkley, C. Gonzales, D. J. DeFrees, D. J. Fox, R. A. Whiteside, R. Seeger, C. F. Melius, J. Baker, R. L. Martin, L. R. Kahn, J. J. P. Stewart, E. M. Fluder, S. Topiol, J. A. Pople: Gaussian Incl., Pittsburgh, PA, USA 1988.
[6] J. A. Pople, K. Raghavachari, M. J. Frisch, J. S. Binkley, P. von R. Schleyer, *J. Am. Chem. Soc. 105* (1983) 6389.
[7] R. Krishnan, J. S. Binkley, R. Seeger, J. A. Pople, *J. Chem. Phys. 72* (1980) 650.
[8] C. Møller, M. S. Plesset, *Phys. Rev. 46* (1934) 618.
[9] a) J. A. Pople, *Ber. Bunsenges. Phys. Chem. 86* (1982) 806; b) H. Guo, M. Karplus, *J. Chem. Phys. 91* (1989) 1719; c) Y. Apeloig in [3d], Chap. 2; d) H. Bock, B. Solouki in [3d], Chap. 9.
[10] T. P. Hamilton, H. F. Schaefer III, *J. Chem. Phys. 90* (1989) 1031.
[11] C. A. Arrington, J. T. Petty, S. E. Payne, W. C. K. Haskins, *J. Am. Chem. Soc. 110* (1988) 6240.
[12] G. Frenking, R. B. Remington, H. F. Schaefer III, *J. Am. Chem. Soc. 108* (1986) 2169.
[13] For a definition and an overview see a) B. F. Yates, W. J. Bouma, L. Radom, *J. Am. Chem. Soc. 106* (1984) 5805; b) S. Hammerum, *Mass Spectrom. Rev. 7* (1988) 123.

$K_2Cu_5Te_5$, a Novel Mixed-Valence Layered Compound with Metallic Properties**

By *Younbong Park, Donald C. Degroot, Jon Schindler, Carl R. Kannewurf,* and *Mercouri G. Kanatzidis**

Since the discovery of high temperature superconductivity, mixed-valence Cu compounds have received considerable attention with the aim of discovering related materials with even higher transition temperatures. Although mixed-valence solid state Cu–chalcogenide compounds have been known for some time, they remain relatively rare. For example, the only mixed-valence compounds known so far are $Na_3Cu_4S_4$,[1] ACu_4Q_3 (A = K, Rb, Cs, Tl; Q = S, Se),[2] $A_3Cu_8S_6$ (A = K, Rb),[3] $A_3Cu_8Se_6$ (A = Rb, Cs),[4] $Cs_2Cu_5Se_4$,[5] $TlCu_2Q_2$ (Q = S, Se),[6] $TlCu_6S_4$,[7] $Tl_5Cu_{14}Se_{10}$.[8] Even though the a priori design of a superconducting material that has a high T_c is not yet possible, it is still worthwhile to pursue the synthesis of mixed-valence Cu compounds, since their electronic features generally play an important role for high electrical conductivity. Furthermore, compared with ternary sulfides and selenides, tellurides are even rarer. To the best of our knowledge, there are

[*] Prof. M. G. Kanatzidis, Y. Park
Department of Chemistry and
Center for Fundamental Materials Research
Michigan State University
East Lansing, MI 48824 (USA)
Prof. C. R. Kannewurf, D. C. Degroot, J. Schindler
Department of Electrical Engineering and Computer Science
Northwestern University

[**] Financial support from the Center for Fundamental Materials Research (CFMR) Michigan State University and the National Science Foundation (Presidential Young Investigator Award CHE-8958451) is gratefully acknowledged. The X-ray instrumentation was purchased in part with funds from the National Science Foundation (grant no. CHE-8908088). This work made use of the scanning electron microscope facilities of the Center for Electron Optics at Michigan State University.

only four known phases ($NaCu_3Te_2$,[9] KCu_3Te_2,[10] KCuTe,[11] and NaCuTe[11]) in the ternary A/Cu/Te (A = alkali metal) system, none of which have mixed Cu oxidation states. With these ideas in mind, we decided to use the now proven polychalcogenide flux method (150–450 °C)[12, 13] to explore similar new compounds. In our hands, this synthetic method has been quite successful in preparing novel structural types of (poly)sulfides and (poly)selenides of various transition metals.[12] Thus, we extended it to the telluride systems and report here the synthesis of a novel layered material, $K_2Cu_5Te_5$, the first mixed-valence Cu/Te compound, which possesses high metallic conductivity.

The reaction of K_2Te (0.309 g, 1.5 mmol), Cu (0.032 g, 0.5 mmol), and Te (0.508 g, 4.0 mmol) in an evacuated pyrex tube at 350 °C for three days followed by cooling (2 °C/h) afforded black parallelepiped crystals of $K_2Cu_5Te_5$ in 77% yield.[14] A quantitative microprobe analysis performed on a large number of crystals with a scanning electron microscope/EDS system gave the composition as $KCu_{2.4}Te_{2.6}$.[15] The product was isolated by removing the excess K_2Te_x with dimethylformamide (DMF) under inert atmosphere and is insoluble in all common organic solvents and stable in water and air. The nature of $K_2Cu_5Te_5$ was established by a single-crystal X-ray diffraction study.[16]

The structure of $K_2Cu_5Te_5$ is anisotropic. Anionic $[Cu_5Te_5]_n^{2n-}$ corrugated layers alternate with charge compensating K^+ ions (Fig. 1). The $[Cu_5Te_5]_n^{2n-}$ layers are

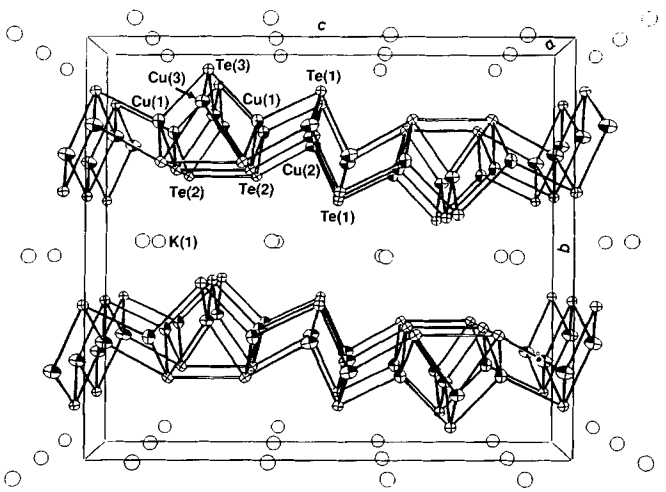

Fig. 1. ORTEP representation and labeling scheme of unit cell of $K_2Cu_5Te_5$. Selected bond distances (Å) and angles (°): Cu(1)-Te(1) 2.644(2), Cu(1)-Te(2) 2.701(1), Cu(1)-Te(3) 2.713(1), Cu(2)-Te(1) 2.637(1), Cu(2)-Te(1) 2.582(1), Cu(2)-Te(2) 2.760(2), Cu(3)-Te(2) 2.625(1), Cu(3)-Te(3) 2.540(2), Te(2)-Te(2) 2.960(1); Te(1)-Cu(1)-Te(2) 113.90(4), Te(1)-Cu(1)-Te(3) 108.38(4), Te(2)-Cu(1)-Te(2) 99.74(6), Te(2)-Cu(1)-Te(3) 110.37(4), Te(1)-Cu(2)-Te(1) 118.04(4), Te(1)-Cu(2)-Te(1) 106.24(6), Te(1)-Cu(2)-Te(2) 85.86(4), Te(1)-Cu(2)-Te(2) 113.96(4), Te(2)-Cu(3)-Te(2) 68.63(5), Te(2)-Cu(3)-Te(3) 118.74(2), Te(3)-Cu(3)-Te(3) 108.79(7), Cu(1)-Te(1)-Cu(2) 89.10(5), Cu(1)-Te(1)-Cu(2) 67.63(4), Cu(2)-Te(1)-Cu(2) 61.96(4), Cu(2)-Te(1)-Cu(2) 106.24(6), Te(2)-Te(2)-Cu(1) 98.57(3), Te(2)-Te(2)-Cu(2) 151.19(3), Te(2)-Te(2)-Cu(3) 55.68(2), Cu(1)-Te(2)-Cu(1) 99.74(6), Cu(1)-Te(2)-Cu(2) 64.35(4), Cu(1)-Te(2)-Cu(3) 64.29(3), Cu(1)-Te(2)-Cu(3) 95.51(4), Cu(1)-Te(3)-Cu(1), 87.89(6), Cu(1)-Te(3)-Cu(3) 65.22(3), Cu(3)-Te(3)-Cu(3) 108.79(7).

formed by edge-sharing rhombic $[Cu_2Te_2]$ units to form a distorted anti-PbO type structure. The structure of $[Cu_5Te_5]_n^{2n-}$ can also be viewed as a derivative of the CuTe lattice,[17] into which K^+ ions have been inserted and the electrons absorbed into the lattice. Based on the formula $K_2Cu_5Te_5$ and on the assumption that the oxidation state on each Te atom is −2, the formal oxidation state on copper would be +1 (two atoms) and +2 (three atoms). However, the coexistence of Cu^{2+} and Te^{2-} is most likely thermodynamically unstable with respect to electron transfer from the reducing Te^{2-} to the oxidizing Cu^{2+}. If all copper atoms are assigned the +1 oxidation state, the average oxidation state of Te is −1.4. This electron deficiency (holes) at Te can be either delocalized in the valence band, or localized through a structural distortion as ditelluride, or both. This situation is reminiscent of that found in CuS, a known metallic mixed-valence compound formulated as $(Cu^+)_2Cu^{2+}(S_2)^{2-}S^{2-}$ or as $(Cu^+)_3(S_2)^{2-}S^{-}$.[18] In $K_2Cu_5Te_5$ there are three crystallographically independent copper atoms, each of which possess a distorted tetrahedral geometry. The average Cu–Te distances for Cu1, Cu2, and Cu3 are 2.69(3) Å, 2.64(7) Å, and 2.58(4) Å respectively, which compare favorably with those found in KCu_3Te_2,[10] NaCuTe,[11] and CuTe.[17] However, the Cu2–Te1 and Cu3–Te3 distances (along the crystallographic *a* axis) are short at 2.582(1) Å and 2.540(2) Å respectively, suggesting that the holes might be constrained but delocalized on rows made from these atoms parallel to the *a* axis. Based on the +1 oxidation state for Cu, three electron vacancies exist per five Te. As a result, a structural distortion from the ideal anti-PbO structure occurs in which two vicinal Te2 atoms move closer together along the *c* axis to form a bond. Structural distortions in the electronegative element network as a response to changes in electronic structure of the electropositive metal are at the core of the Zintl concept[19] and are found in other ternary chalcogenide and pnictide systems.[20] The short Te2–Te2 bonds of 2.960(1) Å are formed by localizing two holes. In the absence of an additional distortion we can expect the remaining electron vacancy to be delocalized in the valence

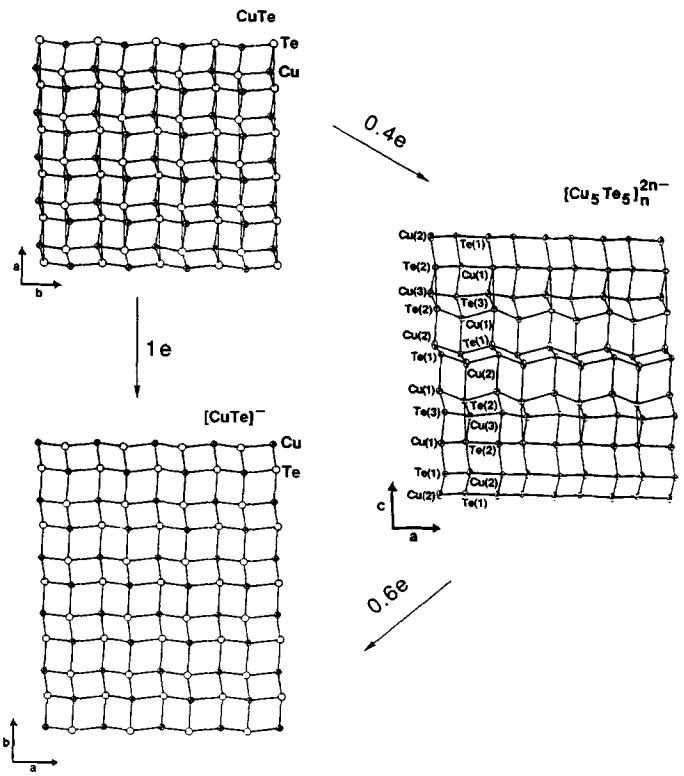

Fig. 2. Structural relationship of the $[Cu_5Te_5]_n^{2n-}$ layers (viewed down the (010) direction) to those of CuTe (above) and $[CuTe]_n^{n-}$ (below), as a function of oxidation state.

band, which consists mainly of p orbitals of the remaining three Te atoms, giving rise to a partially empty band. The Te2–Te2 bond is longer than normal Te–Te single bonds found in known polytellurides[21] by ca. 0.20 Å due to the multibonded nature of the Te2–Te2 unit. Each Te atom binds four Cu atoms which pull a significant fraction of the electron density from the Te–Te bond. The next shortest distance is between Te2 and Te1 and is in the nonbonding range of 3.667(1) Å. Te–Te bonds exist in the related layered structure of CuTe, which formally is better described as $(Cu^{+})_n(Te_n^{n-})$ rather than $(Cu^{2+})(Te^{2-})$. The structure of the $[Cu_5Te_5]_n^{2n-}$ layers can be rationalized as being derived from that of CuTe by reduction with 0.4 electrons. This reduction breaks some of the Te–Te bonds in CuTe. Further reduction by one electron breaks all the Te–Te bonds and gives rise to the ideal anti-PbO structure type found in NaCuTe.[11] Thus, $[Cu_5Te_5]_n^{2n-}$ is a true intermediate oxidation state compound between CuTe and $[CuTe]_n^{n-}$ (Fig. 2). The square-pyramidal geometry around Te1 and Te3 in $K_2Cu_5Te_5$ and their comparable average Cu–Te distances (2.61(3) Å for Te1, 2.63(9) Å for Te3) suggest indistinguishable oxidation states on Te1 and Te3 even though they are crystallographically distinct atoms. $K_2Cu_5Te_5$ can therefore be reasonably formulated as $(K^{+})_2(Cu^{+})_5(Te_2^{2-})_2(Te^{-1.67})_3$. Of course these are only formal oxidation states. The actual description is more complex due to the small electronegativity difference between the Cu and Te atoms. The geometry around K1 is square prismatic and the average K–Te distance is 3.63(5) Å.

Electrical conductivity and thermopower measurements on several single crystals of $K_2Cu_5Te_5$ show that it is a p-type metallic conductor within the temperature range 5–300 K (Fig. 3). The conductivity increases from 1.5×10^4 Scm^{-1} at room temperature to 3.2×10^5 Scm^{-1} at 5 K. The p-type conductivity is expected in view of the band filling argument advanced above.

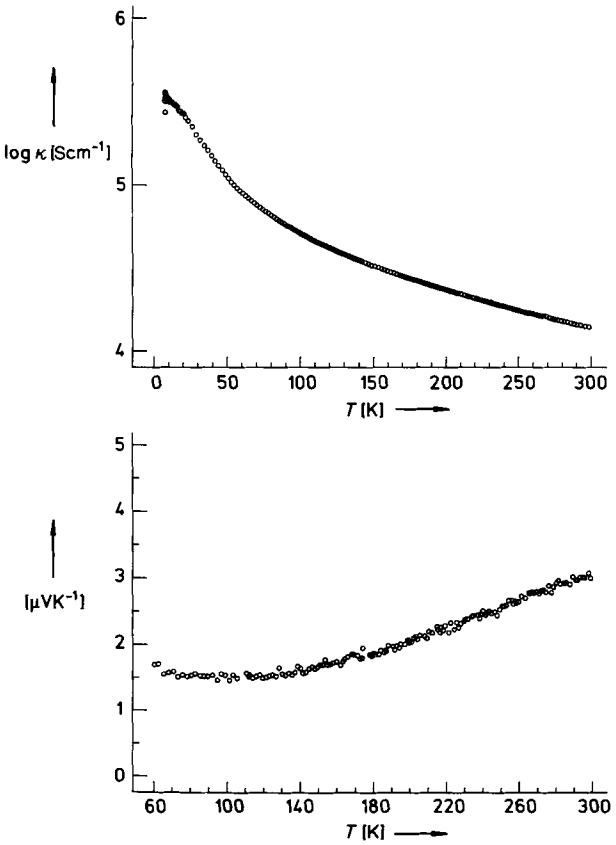

Fig. 3. Top: Four probe electrical conductivity (Scm^{-1}) data as a function of temperature for a single crystal of $K_2Cu_5Te_5$. Bottom: Thermoelectric power data as a function of temperature for a single crystal of $K_2Cu_5Te_5$. The measurements were made parallel to the *ac* plane.

Magnetic susceptibility data for $K_2Cu_5Te_5$ in the temperature range 2–300 K are shown in Figure 4. When plotted as

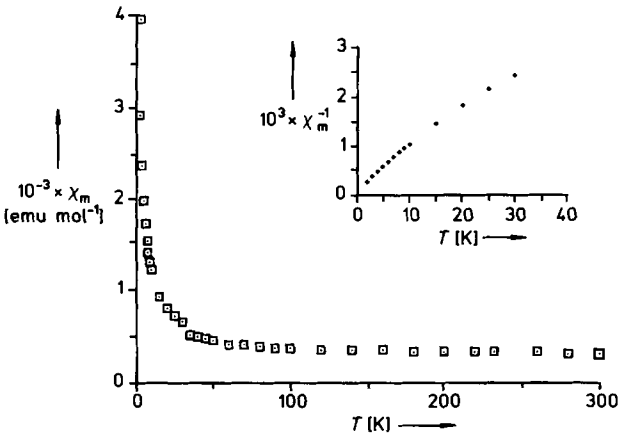

Fig. 4. Variable-temperature magnetic susceptibility data χ_m for polycrystalline $K_2Cu_5Te_5$. Insert: χ_m^{-1} [molemu^{-1}] vs. T.

χ^{-1} vs temperature (see insert), the data above 30 K show temperature-independent paramagnetism, while below 30 K the data follow a Curie–Weiss Law. This behavior is characteristic of metals (Pauli paramagnetism) containing a low concentration of paramagnetic impurities. The calculated Pauli paramagnetism is 25.6×10^{-5} emu mol^{-1}.[22]

Received: March 4, 1991 [Z 4466 IE]
German version: *Angew. Chem. 103* (1991) 1404

CAS Registry numbers:
DMF, 68-12-2; K_2Te, 12142-40-4; Cu, 7440-50-8; $K_2Cu_5Te_5$, 136059-93-3; $KCu_{2.4}Te_{2.6}$, 136059-94-4.

[1] a) C. Burschka, *Z. Naturforsch. B34* (1979) 396–397; b) Z. Peplinski, D. B. Brown, T. Watt, W. E. Hatfield, P. Day, *Inorg. Chem. 21* (1982) 1752–1755; c) M. H. Whangbo, E. Canadell, *ibid. 29* (1990) 1395–1397.
[2] a) W. Rüdorff, H. G. Schwarz, M. Walter, *Z. Anorg. Allg. Chem. 269* (1952) 141–152; b) D. B. Brown, J. A. Zubieta, P. A. Vella, J. T. Wrobleski, T. Watt, W. E. Hatfield, P. Day, *Inorg. Chem. 19* (1980) 1945–1950; c) K. Klepp, H. Boller, H. Völlenkle, *Monatsh. Chem. 111* (1980) 727–733; d) C. Burschka, *Z. Anorg. Allg. Chem. 463* (1980) 65–71.
[3] a) C. Burschka, *Z. Naturforsch. B34* (1979) 675–677; b) L. W. Haar, F. J. Di Salvo, H. E. Bair, R. M. Fleming, J. V. Waszczak, W. E. Hatfield, *Phys. Rev. B35* (1987) 1932–1938; c) R. M. Fleming, L. W. Haar, F. J. Di Salvo, *ibid. 35* (1987) 5388–5391.
[4] H. Schils, W. Bronger, *Z. Anorg. Allg. Chem. 456* (1979) 187–193.
[5] W. Bronger, H. Schils, *J. Less Common Met. 83* (1982) 279–285.
[6] a) R. Berger, C. F. Van Bruggen, *J. Less Common Met. 99* (1984) 113–123; b) R. Berger, *ibid. 147* (1989) 141–148.
[7] R. Berger, L. Eriksson, *J. Less Common Met. 161* (1990) 165–173.
[8] R. Berger, *Eur. J. Solid State Inorg. Chem. 25* (1988) 279–288.
[9] G. Savelsberg, H. Schäfer, *Mater. Res. Bull. 16* (1981) 1291–1297.
[10] K. O. Klepp, *J. Less Common Met. 128* (1987) 79–89.
[11] a) G. Savelsberg, H. Schäfer, *Z. Naturforsch. B33* (1978) 370–373; b) Y. Park, M. G. Kanatzidis, unpublished.
[12] a) M. G. Kanatzidis, *Chem. Mater. 2* (1990) 353–363; b) M. G. Kanatzidis, Y. Park, *J. Am. Chem. Soc. 111* (1989) 3767–3769; c) M. G. Kanatzidis, Y. Park, *Chem. Mater. 2* (1990) 99–101; d) Y. Park, M. G. Kanatzidis, *Angew. Chem. 102* (1990) 945–947; *Angew. Chem. Int. Ed. Engl. 29* (1990) 914–915.
[13] a) S. A. Sunshine, D. Kang, J. A. Ibers, *J. Am. Chem. Soc. 109*(1987) 6202–6204; b) D. Kang, J. A. Ibers, *Inorg. Chem. 27* (1988) 549–551.
[14] The yield was calculated with respect to Cu metal used.
[15] The ratio was calibrated using known K/Cu/Te compounds. The error limit is 3%. Y. Park, M. G. Kanatzidis, unpublished.

[16] Crystal data for $K_2Cu_3Te_5$: orthorhombic *Cmcm*, $Z = 4$, $a = 4.130(3)$, $b = 16.004(2)$, $c = 18.533(3)$ Å, $V = 1225.0(4)$ Å^3, $2\theta_{max}(Mo_{K\alpha}) = 50°$. Number of reflections measured: 2255; number of unique reflections (averaged): 652; number of data with $F_0^2 > 3\sigma(F_0^2)$:569, number of variables: 40; number of atoms: 7. $\mu = 209$ cm^{-1}. $R = 0.025$ and $R_w = 0.034$. An empirical absorption correction based on ψ scans followed by DIFABS [23] was applied to the unique data set. In order to ensure product homogeneity, the X-ray powder diffraction diagram of $K_2Cu_3Te_5$ was compared and found to be identical with that calculated from the single-crystal data. Further details of the crystal structure investigations may be obtained from the Fachinformationszentrum Karlsruhe, Gesellschaft für wissenschaftlich-technische Information mbH, W-7514 Eggenstein-Leopoldshafen 2 (FRG), on quoting the depository number CSD-55341, the names of the authors, and the journal citation.

[17] a) K. Anderko, K. Schubert, *Z. Metallkd. 45* (1954) 371–378; b) I. Patzak, *ibid. 47* (1956) 418–420; c) F. Hulliger in F. Levy (Ed.): *Structural Chemistry of Layer-Type Phases, Vol. 5*, Reidel, Dordrecht 1976, pp. 133–135.

[18] a) F. Jellinek in D. W. A. Sharp (Ed.): *MTP International Review of Science, Inorganic Chemistry Series One, Vol. 5*, Butterworths, London 1972, pp. 339–396; b) J. C. W. Folmer, F. Jellinek, *J. Less Common Met. 76* (1980) 153–162.

[19] H. Schäfer, *Annu. Rev. Mater. Sci. 15* (1985) 1–41; b) H. G. von Schnering, *Angew. Chem. 93* (1981) 44–63; *Angew. Chem. Int. Ed. Engl. 20* (1981) 33–51; c) H. G. von Schnering, W. Hönle, *Chem. Rev. 88* (1988) 243–273; c) W. Bronger, P. Müller, *J. Less Common Met. 100* (1984) 241–247; d) W. Bronger, *Angew. Chem. 93* (1981) 12–23; *Angew. Chem. Int. Ed. Engl. 20* (1981) 52–62.

[20] a) R. Hoffmann, C. Zheng, *J. Phys. Chem. 89* (1985) 4175–4181; b) J. K. Burdett, *Chem. Rev. 88* (1988) 3–30; c) W. Tremel, R. Hoffmann, J. Silvestre, *J. Am. Chem. Soc. 108* (1986) 5174–5187.

[21] a) L. C. Roof, W. T. Pennington, J. W. Kolis, *J. Am. Chem. Soc. 112* (1990) 8172–8174; b) R. D. Adams, T. A. Wolfe, B. W. Eichhorn, R. C. Haushalter, *Polyhedron 21* (1989) 701–703; c) R. C. Haushalter, *Angew. Chem. 97* (1985) 414–415; *Angew. Chem. Int. Ed. Engl. 24* (1985) 433–435.

[22] Corrections for diamagnetic contribution from atomic constituents were made using values tabulated by Mulay: L. N. Mulay in E. A. Boudreaux, L. N. Mulay (Eds.): *Theory and Applications of Molecular Paramagnetism*, Wiley, New York 1976, pp. 494–495.

[23] N. Walker, D. Stuart, *Acta Crystallogr. Sect. A 39* (1983) 158–166.

Amino-substituted β-Benzyl-*C*-glycosides; Novel β-Glycosidase Inhibitors

By *Richard R. Schmidt** and *Hansjörg Dietrich*

Glycosides and saccharides fulfill many biological functions; they serve as protective and skeletal substances, and as nutritional and reserve foodstuffs, they are components of nucleic acids, and they occur on the surfaces of cell membranes in the form of complex glycoconjugates.[1, 2] Biosynthesis and degradation of the saccharide chain are accomplished by complicated enzyme systems. Interference of the glycosidase-catalyzed degradation by specific enzyme inhibitors therefore allows conclusions to be drawn about the function of the carbohydrates and a planned modification of this function. High and low molecular weight glycosidase inhibitors have been found.[3] The low molecular weight inhibitors such as cyclites, mono- and oligosaccharides, and alkaloids provide a wide field of interest for chemistry, biology, and medicine, because α-glycosidase inhibitors might be effective against virus diseases. For instance, activity against HIV viruses has been found for the very potent glycosidase inhibitors, 1-deoxynojirimycin and castanospermine.[4, 5] Another excellent glycosidase inhibitor is acarbose, which is used in the treatment of diabetes.[3, 6]

The inhibitory action of these substances, which are similar to substrates or intermediates, respectively, is attributed particularly to the interaction of the amine nitrogen atom of the inhibitor with the acid groups AH of the active site of the enzyme, which initiates the hydrolysis of the glycoside bond of the substrate or (as carboxylate anion) stabilizes the glycosyl cation (Scheme 1).[7] Because phenylglycosides are often

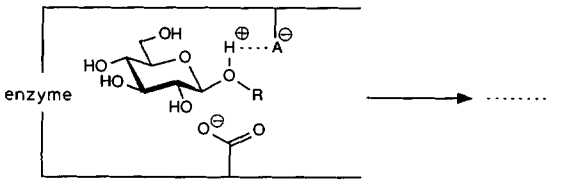

Scheme 1.

accepted as substrates by glycosidases, we planned to prepare novel amino-substituted β-benzyl-*C*-glycosides of the structure **1a, b** (Scheme 2) as potential β-glucosidase inhibitors. Their inhibitory action should be compared with

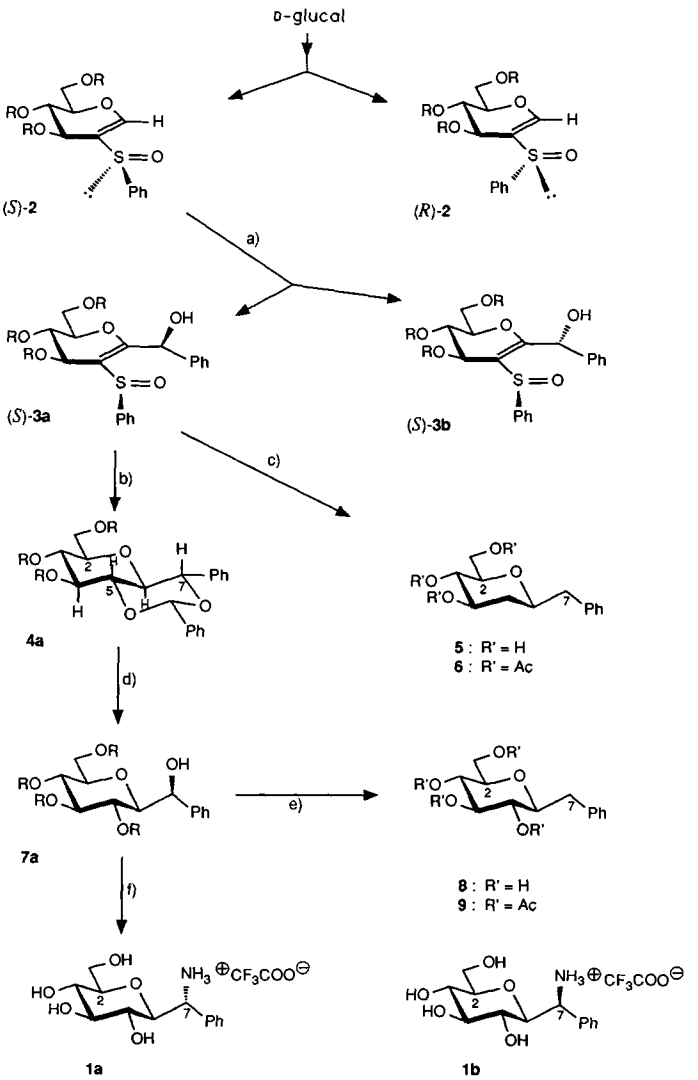

Scheme 2. R = Benzyl. a) LDA, THF/hexamethylphosphoric triamide (HMPT), −100 °C; PhCHO (86%); (*S*)-**3a**:(*S*)-**3b** ≈ 4:1. b) 1. Raney nickel W II (50%); 2. $H_3B \cdot SMe_2$; H_2O_2, NaOH (80%); 3. $PhCH(OMe)_2$, $(p\text{-}O_2NC_6H_4O)_2P(O)OH$ (96%). c) 1. Raney nickel W II (57%); 2. Pd/C, H_2 (quantitative). d) $LiAlH_4$, $AlCl_3$ (80%). e) 1. $(ClCH_2CO)_2O$, pyridine (quantitative); 2. Pd/C, H_2 (80%). f) 1. MesCl, pyridine (80%); 2. $Bu_4N^{\oplus}N_3^{\ominus}$, toluene (81%); 3. $LiAlH_4$ (86%); 4. Boc_2O (82%); 5. Pd/C, H_2; CF_3COOH (quantitative).

[*] Prof. Dr. R. R. Schmidt, Dipl.-Chem. H. Dietrich
Fakultät für Chemie der Universität
Postfach 55 60
W-7760 Konstanz 1 (FRG)

that of the *C*-glucoside derivatives not substituted at the benzyl group.

The direct C1 lithiation of the 2-phenylsulfinyl substituted glycals (**2**, readily obtained from D-glucal,[8, 9] Scheme 2) was used to synthesize the *C*-glucosides. Thus the C1-lithiated species was formed from the *S* isomer, (*S*)-**2**, with lithium diisopropylamide (LDA) in THF/HMPT at $-100\,^{\circ}C$ and subsequent reaction with benzaldehyde afforded an easily separable mixture of diastereomers, (*S*)-**3a** and (*S*)-**3b** (ca. 4:1, 86%) (Table 1). Treatment of the major product (*S*)-**3a** with Raney nickel W II and thereafter with hydrogen in the presence of Pd/C as catalyst yielded directly, through loss of the *O*-benzyl protecting groups and the benzylic hydroxy group, the dideoxy derivative **5**, whose structure was ascertained by *O*-acetylation to form **6**. If borane addition and alkaline oxidation with hydrogen peroxide followed the Raney nickel treatment, which causes the cleavage of the phenylsulfinyl group, a 5,7-dihydroxy derivative was obtained stereoselectively. Its structure was determined by ^1H NMR spectroscopy after transformation into the benzylidene derivative **4a** ($J_{4,5} = J_{5,6} = J_{6,7} = 9$ Hz. The reductive opening of the benzylidene group with $LiAlH_4/AlCl_3$ proceeded chemoselectively and afforded the 1,3,4,5-tetra-*O*-benzyl derivative **7a**. Here the hydrogenolytic *O*-debenzylation yielded the deoxy compound **8** directly and the derivative **9** on *O*-acetylation. The target molecule **1a** was obtained in good yield from **7a** by 7-*O*-mesylation, introduction of azide with tetrabutylammonium azide, release of the amino group by reduction with $LiAlH_4$, introduction of a *tert*-butoxycarbonyl(Boc) protecting group, hydrogenolytic *O*-debenzylation, and acid-catalyzed cleavage of the Boc protecting group. Compound **1a** was isolated as trifluoroacetate. The diastereoisomer **1b** was synthesized analogously from (*R*)-**2** via (*R*)-**3b** (the transformation with benzaldehyde afforded (*R*)-**3a** and (*R*)-**3b** in a 1:4 ratio and 94% yield) and the intermediates **4b** and **7b** (diastereomeric to **4a** and **7a**).

Table 1. Selected physical data of the compounds **4a**, **6**, **9**, and **1a**, **b** [a].

4a: $[\alpha]_D + 22.5$ ($c = 1.0$, $CHCl_3$); $\delta_H = 3.28$ (dd, $J_{5,6} = J_{6,7} = 9.0$ Hz; H-6), 3.77 (dd, $J_{2,3} = J_{3,4} = 9.5$ Hz; H-3), 3.86 (dd, $J_{4,5} = 9.0$ Hz; H-4), 3.92 (dd, $J_{4,5} = J_{5,6} = 9.0$ Hz; H-5), 4.79 (d, $J_{1,2} = 9.0$ Hz; H-7).
6: $[\alpha]_D + 10.1$ ($c = 1.0$, $CHCl_3$); $\delta_H = 2.72$ (dd, $J_{6,7'} = 6$, $J_{7,7'} = 13.8$ Hz; H-7'), 2.98 (dd, $J_{6,7} = 6$, $J_{7,7'} = 13.8$ Hz; H-7), 3.56 (ddd, $J_{1,2} = 5.2$, $J_{1',2} = 2.3$, $J_{2,3} = 9.6$ Hz; H-2), 3.68 (dddd, $J_{5a,6} = 11.4$, $J_{5e,6} = 1.9$, $J_{6,7} = 6$, $J_{6,7'} = 6$ Hz; H-6); 4.07 (dd, $J_{1,1'} = 12.1$, $J_{1',2} = 2.3$ Hz; H-1'), 4.26 (dd, $J_{1,1'} = 12.1$, $J_{1,2} = 5.2$ Hz; H-1), 4.90–4.98 (m; H-3,4).
9: $[\alpha]_D - 4.6$ ($c = 1.0$, $CHCl_3$); $\delta_H = 3.59$ (ddd, $J_{1,2} = 5.2$, $J_{1,2} = 2.4$, J_2,3 = 9.9 Hz; H-2), 3.66 (ddd, $J_{5,6} = 9.8$, $J_{6,7} = 6.5$, $J_{6,7'} = 5.6$ Hz; H-6), 4.95 (dd, $J_{4,5} = J_{5,6} = 9.4$ Hz; H-5), 5.04 (dd, $J_{2,3} = J_{3,4} = 9.4$ Hz; H-3), 5.18 (dd, $J_{3,4} = J_{4,5} = 9.4$ Hz; H-4).
1a: $[\alpha]_D - 9.4$ ($c = 1.0$, H_2O); $\delta_H = 3.27$–3.31 (m, 4H; H-2,3,4,5), 3.56–3.68 (m, 2 H; H-1',6), 3.74 (d, $J_{1,1'} = 12.0$ Hz; H-1), 4.49 (d, $J_{6,7} = 4.5$ Hz; H-7), 7.27–7.33 (m, 5H; C_6H_5).
1b: $[\alpha]_D + 20.8$ ($c = 1.0$, H_2O); $\delta_H = 2.63$ (dd, $J_{4,5} = J_{5,6} = 9.5$ Hz; H-5), 2.88 (dd, $J_{2,3} = J_{3,4} = 9.5$ Hz; H-3), 3.24–3.32 (m, 2H; H-2, 4), 3.48 (dd, $J_{1,1'} = 12.1$, $J_{1,2} = 7.5$ Hz; H-1), 3.64 (dd, $J_{5,6} = 9.5$, $J_{6,7} = 3.2$ Hz; H-6), 3.76 (dd, $J_{1,1'} = 12.1$, $J_{1',2} = 1.9$ Hz; H-1'), 4.56 (d, $J_{6,7} = 3.1$ Hz; H-7), 7.24–7.34 (m, 5H; C_6H_5).

[a] Optical rotations recorded at 20 °C, ^1H NMR spectra at 250 MHz in $CDCl_3$ (**4a**, **6**, **9**) or D_2O (**1a**, **b**).

For the inhibition studies, the cleavage of *O*-nitrophenyl-β-D-glucoside with β-glucosidase (cellobiase) from sweet almonds[10] was employed.[11] The resulting types of inhibition and the inhibition constants (K_i) are listed in Table 2. It is remarkable that the amino compound **1a** yields a K_i value similar to that of 1-deoxynojirimycin. The diastereomer **1b**, however, has an enzyme affinity two orders of magnitude smaller. This observation gives an indication of the relative position of the acid groups (AH) of the active site of the enzyme which participate in the glycoside cleavage. The K_i values of the deoxy compounds **5** and **8** lie in the same region as that of **1b**.

Table 2. Type of inhibition and inhibition constants (K_i) [a].

compound	pH	T [°C]	inhibition type	K_i [M]
1-deoxynojirimycin	6.8	27	competitive	1.8×10^{-5} [b]
1a	6.8	30	competitive	7.0×10^{-5} [c]
δ-gluconolactone	6.2	27	competitive	2.0×10^{-4} [b]
5	6.8	30	competitive	2.6×10^{-3}
8	6.8	30	mixed	6.1×10^{-3}
1b	6.8	30	competitive	7.6×10^{-3}
D-glucal	6.2	27	competitive	2.0×10^{-2} [b]
cellobiose	6.2	27	(substrate)	6.3×10^{-1} [b]

[a] For method see [11]. [b] See [5]. [c] Measurement range up to an inhibitor concentration of I = 1.0 mM.

Received: June 4, 1991 [Z4673 IE]
German version: *Angew. Chem. 103* (1991) 1348

CAS Registry numbers:
1a base, 136034-25-8; **1a** salt, 136034-26-9; **1b** base, 136087-43-9; **1b** salt, 136171-90-9; **2** *S* isomer, 118916-46-4; **2** *R* isomer, 118798-67-7; **3a** *S* isomer, 136034-18-9; **3a** *R* isomer, 136087-42-8; **3b** *S* isomer, 136087-41-7; **3b** *R* isomer, 136087-44-0; **4a**, 136034-19-0; **5**, 136034-20-3; **6**, 136034-21-4; **7a**, 136034-22-5; **8**, 136034-23-6; **9**, 136034-24-7; benzaldehyde, 100-52-7; β-glucosidase, 9001-22-3.

[1] R. R. Schmidt, *Angew. Chem. 98* (1986) 213; *Angew. Chem. Int. Ed. Engl. 25* (1986) 212; *Pure Appl. Chem. 61* (1989) 1257; H. Paulsen, *Angew. Chem. 102* (1990) 851; *Angew. Chem. Int. Ed. Engl. 29* (1990) 823, and references cited therein.
[2] S. Hakomori, *J. Biol. Chem. 265* (1990) 18713, and references cited therein.
[3] E. Truscheit, W. Frommer, B. Junge, L. Müller, D. D. Schmidt, W. Wingender, *Angew. Chem. 93* (1981) 738; *Angew. Chem. Int. Ed. Engl. 20* (1981) 741.
[4] T. Feizi, M. Larkin, *Glycobiology 1* (1990) 17.
[5] M. P. Dale, *Biochemistry 24* (1985) 3530; R. Saul, R. J. Mulyneux, A. D. Elbein, *Arch. Biochem. Biophys. 230* (1984) 668.
[6] H. Mehnert, *Arzneimitteltherapie 8* (1990) 378.
[7] L. M. Sinnott in M. I. Page, A. Williams (Eds.): *Enzyme Mechanisms*, The Royal Society of Chemistry, London 1987, p. 259; P. Lalegerie, G. Legler, J. M. You, *Biochimie 64* (1982) 977.
[8] R. Preuß, R. R. Schmidt, *Liebigs Ann. Chem. 1989*, 429; S. Maier, R. Preuß, R. R. Schmidt, *ibid. 1990*, 483; R. R. Schmidt, R. Preuß, *Tetrahedron Lett. 30* (1989) 3409.
[9] The configuration for (*R*)-**2** was established by X-ray structure analysis: H. Dietrich, *Diplomarbeit*, Universität Konstanz, 1990.
[10] Obtained from Boehringer Mannheim GmbH.
[11] J. Lehmann, L. Ziser, *Carbohydr. Res. 188* (1989) 45; we thank Prof. Lehmann for support during the introduction of this method.

HETLOC, an Efficient Method for Determining Heteronuclear Long-Range Couplings with Heteronuclei in Natural Abundance**

By *Michael Kurz*, *Peter Schmieder*, and *Horst Kessler**

Heteronuclear long-range couplings such as $^3J(C,H)$ and $^3J(N,H)$ are among the most important NMR parameters

[*] Prof. Dr. H. Kessler, Dipl.-Chem. M. Kurz, Dipl.-Chem. P. Schmieder Organisch-Chemisches Institut der Technischen Universität München Lichtenbergstrasse 4, W-8046 Garching (FRG)

[**] This work was supported by the Deutsche Forschungsgemeinschaft and the Fonds der Chemischen Industrie. *Peter Schmieder* thanks the Fonds der Chemischen Industrie for a fellowship.

for determining conformation and configuration.[1] However, their intensive use has been hindered by the difficulty in measuring them. Either the sensitivity of the existing methods of determination[2] is too low or the methods are limited to well-resolved proton spectra. Here we propose a procedure that can be used to determine the couplings to proton-bearing heteroatoms without the disadvantages mentioned above and without the necessity of a cumbersome enrichment of the heteronucleus (^{13}C, ^{15}N).

An efficient method for determining these long-range couplings should meet the following requirements: highest sensitivity, applicability to overlapped proton and carbon signals, and measurement of the coupling constants within the detection time (dimension with the better resolution). All of these conditions are fulfilled by the method of *Montelione* et al.,[3] in which an E. COSY pattern[4] is obtained in the conventional TOCSY or NOESY spectra of *isotopically enriched* proteins. In the incremented dimension ($F1$ in 2D spectra, $F2$ in 3D spectra), the cross peaks show the direct, large coupling to the heteronucleus ($^1J(C,H)$, $^1J(N,H)$) and, in the detected dimension ($F2$ in 2D spectra, $F3$ in 3D spectra), they show the desired heteronuclear long-range coupling to the same heteronucleus through the shift of the multiplet. In this way, coupling constants smaller than the line widths may be measured.

In order to determine couplings to nuclei in *natural abundance*, it is necessary to suppress the signals of protons that are not bonded to a magnetically active heteronucleus. We suggest the use of a ω_1 hetero half-filter,[5] which selects for such nuclei in $F1$ via the phase cycle. The pulse sequences are shown in Figure 1. BIRD presaturation[6] of the protons bonded to ^{12}C allows a rapid pulse sequence[7] (ca. two scans per second). The resulting 2D spectra are TOCSY spectra in which the cross peaks show the desired "E. COSY" pattern. The pulse sequence b in Figure 1 is the three-dimensional variant[8] in which the chemical shift is allowed to evolve

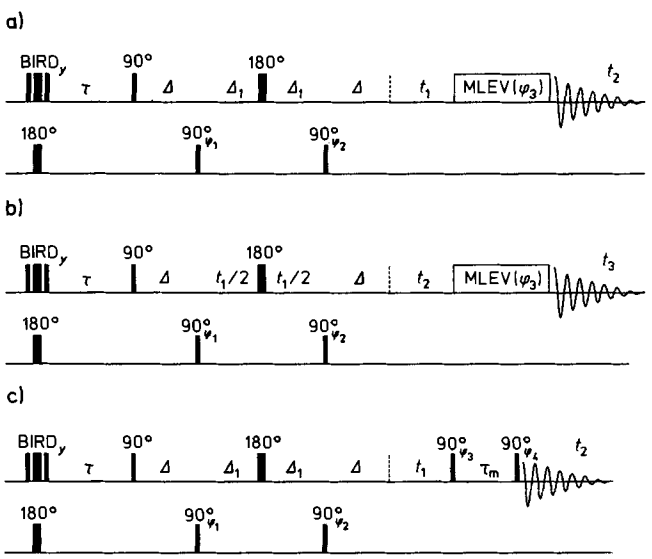

Fig. 1. Pulse sequences of the NMR experiments discussed in the text. a) ω_1 hetero half-filtered TOCSY without heteronuclear decoupling (HETLOC, determination of *het*eronuclear *l*ong-range *c*ouplings). b) 3D HMQC-TOCSY without heteronuclear decoupling. c) ω_1-filtered NOESY without heteronuclear decoupling. In all sequences, the BIRD pulse serves to suppress the signals of C^{12}-bonded protons and makes it possible to perform the experiment rapidly with two repetitions per second. The delay times are $\Delta = 3.57$ ms, $\Delta_1 = 3$ μs; τ has to be optimized for each compound. The phase cycle is $\Phi_1 = x, -x, x, -x$, $\Phi_2 = x,x, -x, -x$, receiver = +,−,−,+. In (c), the phase cycle corresponds to the phases Φ_3 and Φ_4 in the usual NOESY experiment. In the case of TOCSY transfer, MLEV-17 was used as mixing sequence.

further. This technique is especially applicable for overlapping signals. However, the method proposed here is restricted to systems in which the heteronucleus is bonded to a proton belonging to the same spin system as the $^nJ(H,X)$-coupled proton. If this is not the case, then the NOE cross peaks obtained with the pulse sequence shown in Figure 1 can be used: for example, between the amide proton of an amino acid and H^α of the preceding amino acid. For small molecules, however, the sensitivity is limited by the efficiency of the NOE mixing process.

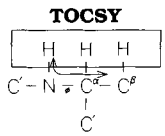

Fig. 2. Schematic representation of the determination of $^3J(H^N,C^\beta)$ in a peptide. H^N is linked to H^β through the TOCSY transfer. If ^{13}C-bonded H^β is selected for in the experiment, the H^N show long-range coupling to C^β.

The method to obtain $^nJ_{AX}$ is illustrated here to determine the Φ angle in peptides, the dihedral angle between the two carbonyl C atoms along the peptide chain. Figure 2 shows that the $^3J(H^N,C^\beta)$ coupling, just like the homonuclear $^3J(H^N,H^\alpha)$ coupling, is correlated with the angle Φ through a Karplus relation. The relevant Karplus–Bystrov relations

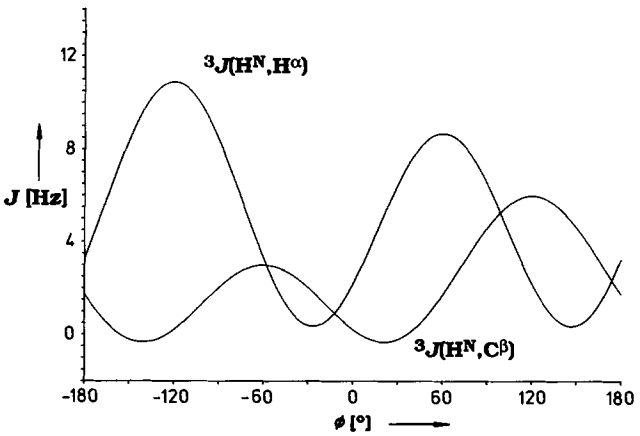

Fig. 3. Graphical representation of the Karplus–Bystrov relations (a) and (b). The curves shown pertain to the middle of an allowed range.

are given in Equations (a) and (b).[9] A graphical representation is shown in Figure 3.

$$^3J(H^N,H^\alpha) = 9.4\cos^2(\phi - 60) - 1.1\cos(\phi - 60) + 0.4 \quad \text{(a)}$$

$$^3J(H^N,C^\beta) = 4.7\cos^2(\phi + 60) - 1.5\cos(\phi + 60) - 0.2 \quad \text{(b)}$$

This approach will be exemplified with the cyclic pentapeptide *cyclo*(-Ala^1-Ala^2-Ala^3-Pro^4-Pro^5-), which exists in two conformations (53 and 47 %). Figure 4a shows the H^N, H^β region of the ω_1 hetero half-filtered TOCSY (HETLOC) spectrum. The cross peak of Ala^2-H^N in Figure 4a clearly reveals the E. COSY pattern.[4] Coupling constants can be determined either directly from the cross peak or, analogously to the DISCO procedure,[10] from slices through the spectrum (Fig. 4c).

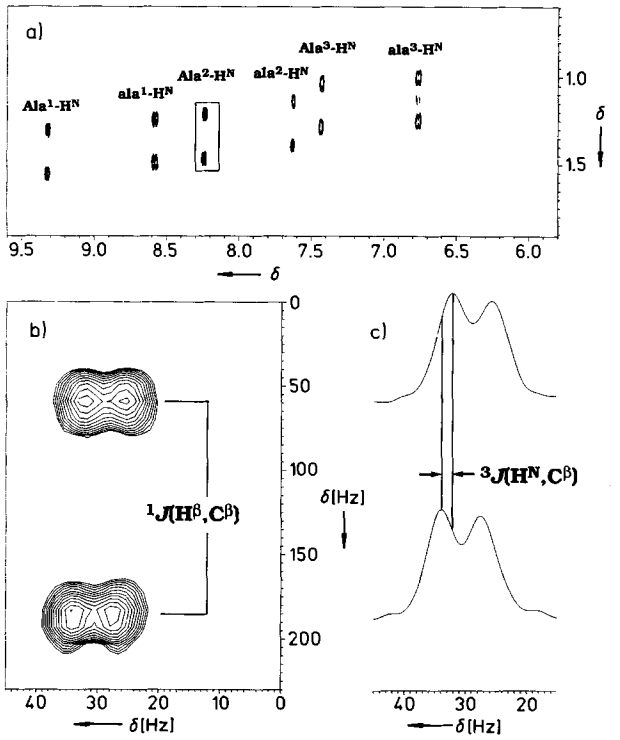

Fig. 4. Application of the pulse sequence shown in Figure 1a to the cyclic pentapeptide *cyclo*(-Ala[1]-Ala[2]-Ala[3]-Pro[4]-Pro[5]-). The sample contains 10 mg of peptide in 0.5 mL of [D_6]DMSO (ca. 25 mM per conformation); the measurements were carried out at 300 K with a Bruker AMX-500 spectrometer. 512 t_1 increments with 128 repetitions each were carried out ($\tau = 198$ ms, $\Phi_3 = x$); the total measuring time was 9.5 hours. 4096 points were recorded in the acquisition dimension; the spectrum was apodized in both dimensions with a 90°-shifted quadratic sine function and, after the calculation, had a size of 8192 × 1024 real points. a) Region of the H^N, H^β cross peaks of the ^{13}C ω_1-filtered TOCSY spectrum. b) Cross peaks of Ala[2]; the E. COSY pattern is clearly evident. c) Two slices through the cross peak of (b); the slices were inverse Fourier transformed, zero-filled, and Fourier transformed once again. The shift of the signals with respect to one another gives the long-range coupling.

Table 1 compares the angles obtained from both couplings. Combination of the two relations allows the number of possible angles to be reduced to one or two. The final determination can be made by using two additional long-range couplings, $^3J(H^N, C'_{(i)})$ and $^3J(H^\alpha, C'_{(i-1)})$, which need to be determined only qualitatively from a selective HMBC experiment.[11] The possible angles thus determined are given in boldface in Table 1; they are in good agreement with those obtained from MD simulations.

The experiment presented here provides a simple method for determining heteronuclear coupling constants. For the determination of structures in solution by NMR spectroscopy, these coupling constants are a valuable adjunct to the distances obtained from NOESY spectra.

Table 1. Coupling constants [Hz] and corresponding angles [°] for the three alanines in *cyclo*(-Ala[1]-Ala[2]-Ala[3]-Pro[4]-Pro[5]-) for the major and minor conformers (Ala and ala, respectively).

	$^3J(H^N,H^\alpha)$	→ angle	$^3J(H^N,C^\beta)$	→ angle	MD angle [a]
Ala[1]	8.0	−153, −87, 44, **76**	2.0	−90, −30, **63**, 177 [b]	63
Ala[2]	6.7	−160, −**80**, 32, 88	3.0	−**60**, 73, 167 [c]	−99
Ala[3]	6.6	−161, −**79**, 31, 89	2.5	−**81**, −39, 68, 172 [c]	−67
ala[1]	9.6	−**141**, −**99** [d]	0.2	−160, −**120**, 0, 40	−95
ala[2]	5.6	−167, −**73**, 24, 96	2.6	−**79**, −41, 69, 171 [c],	−51
ala[3]	10.0	−**137**, −**103** [d]	0.4	−163, −**117**, −3, 43	−100

[a] From restrained MD simulation with GROMOS [12] over 100 ps in vacuum. Eighteen and seventeen distances were used for the major and minor conformer, respectively. [b] Because of a very intense cross peak between the carbonyl C atom of the preceding amino acid and Ala[1] H^α, the alternative (−87°/90°) can be ruled out. [c] Owing to the weak or absent cross peak between the carbonyl C atom of the preceding amino acid and H^α of the amino acid being considered, the alternative with positive Φ angle (88°/73°, 89°/68°, or 96°/69°) can be ruled out. [d] Both angles determined from the $^3J(H^N, H^\alpha)$ coupling constants are consistent with the angles in boldface determined from the $^3J(H^N, C^\beta)$ relation. A more precise distinction is not possible, not even by using the other two long-range couplings, $^3J(H^N, C'_{(i)})$ and $^3J(H^\alpha, C'_{(i-1)})$.

Received: June 7, 1991 [Z 4682IE]
German version: *Angew. Chem. 103* (1991) 1341

CAS Registry number:
cyclo(-Ala-Ala-Ala-Pro-Pro-), 135866-42-1.

[1] J. L. Marshall: *Carbon-Carbon and Carbon-Proton NMR couplings*, Verlag Chemie International, Deerfield Beach, FL, USA 1983; A. Demarco, M. Llinas, K. Wüthrich, *Biopolymers 17* (1978) 2727–2742.
[2] A. Bax, R. Freeman, *J. Am. Chem. Soc. 104* (1982) 1099–1100; M. Ochs, S. Berger, *Magn. Reson. Chem. 28* (1990) 994–997; R. C. Crouch, G. E. Martin, *J. Magn. Reson. 92* (1991) 189–194; H. Kessler, M. Gehrke, C. Griesinger, *Angew. Chem. 100* (1988) 507–554; *Angew. Chem. Int. Ed. Engl. 27* (1988) 490–536, and references cited therein.
[3] G. T. Montelione, M. E. Winkler, P. Rauenbuehler, G. Wagner, *J. Magn. Reson. 82* (1989) 198–204.
[4] C. Griesinger, O. W. Sørensen, R. R. Ernst, *J. Magn. Reson. 75* (1987) 474–492.
[5] G. Otting, H. Senn, G. Wagner, K. Wüthrich, *J. Magn. Reson. 70* (1986) 500–505.
[6] J. R. Garbow, D. P. Weitkamp, A. Pines, *Chem. Phys. Lett. 93* (1982) 504–509.
[7] A. Bax, S. Subramanian, *J. Magn. Reson. 67* (1986) 565–569.
[8] G. Wider, D. Neri, G. Otting, K. Wüthrich, *J. Magn. Reson. 85* (1989) 426–431; A. S. Edison, W. M. Westler, J. L. Markley, *ibid. 92* (1991) 434–438; P. Schmieder, M. Kurz, H. Kessler, *J. Biomol. NMR*, unpublished.
[9] V. F. Bystrov, *Prog. Nucl. Magn. Reson. Spectrosc. 10* (1976) 41–81.
[10] H. Kessler, A. Müller, H. Oschkinat, *Magn. Reson. Chem. 23* (1985) 844–852.
[11] W. Bermel, K. Wagner, C. Griesinger, *J. Magn. Reson. 83* (1989) 223–232; H. Kessler, P. Schmieder, M. Köck, M. Kurz, *ibid. 88* (1990) 615–618.
[12] W. F. van Gunsteren, H. J. C. Berendsen, *Angew. Chem. 102* (1990) 1020–1055; *Angew. Chem. Int. Ed. Engl. 29* (1990) 992–1017.

A New Macrobicyclic Tris-bipyridine Ligand and Its Cu^I_2 and Ag^I_3 Complexes**

By *Javier de Mendoza,* Esther Mesa, Juan-Carlos Rodríguez-Ubis, Purificación Vázquez, Fritz Vögtle,* Paul-Michael Windscheif, Kari Rissanen, Jean-Marie Lehn,* Daniel Lilienbaum*, and *Raymond Ziessel*

The remarkable complexation properties of tris(2-aminoethyl)amine (Tren) **1**[1] towards transition-metal cations

[*] Prof. Dr. J. de Mendoza, E. Mesa, Dr. J.-C. Rodríguez-Ubis, Dr. P. Vázquez
Departamento de Química, Universidad Autónoma de Madrid
Cantoblanco, E-28049 Madrid (Spain)
Prof. Dr. F. Vögtle, Dipl.-Chem. P.-M. Windscheif
Institut für Organische Chemie und Biochemie der Universität
Gerhard-Domagk-Strasse 1, W-5300 Bonn 1 (FRG)
Priz.-Doz. Dr. K. Rissanen
Department of Chemistry, University of Jyväskylä
Kyllikinatu 1–3, SF-40100 Jyväskylä (Finland)
Prof. Dr. J.-M. Lehn, D. Lilienbaum, Dr. R. Ziessel
Institut Le Bel, Université Louis Pasteur
4, rue Blaise Pascal, F-67000 Strasbourg (France)

[**] This work was supported by Comisión Interministerial de Ciencia y Tecnologia (CICYT PB87-0109), by the Bundesministerium für Forschung und Technologie (BMFT-0329120A), by the CNRS (URA422) and by the Academy of Finland (No. 1031002). Since our three groups in Madrid, Bonn, and Strasbourg, supplemented by a Finnish group, had been working independently on this same topic, we decided to publish our results jointly, in a European spirit!

raised an interest in cryptands containing such binding subunits, and several were prepared during the past decade.[2] More recently, an efficient synthetic alternative, based on the high-yield, one-step Schiff base condensation of **1** with suitable dicarbonyl compounds, has been developed.[3] The importance of 2,2′-bipyridine metal complexes in photochemistry, photophysics, and in the splitting of water[4] led us to investigate the synthesis and properties of the cryptand **3**, which incorporates three such subunits and is derived form Tren (**1**) and 5,5′-diformyl-2,2′-bipyridine (**2**).

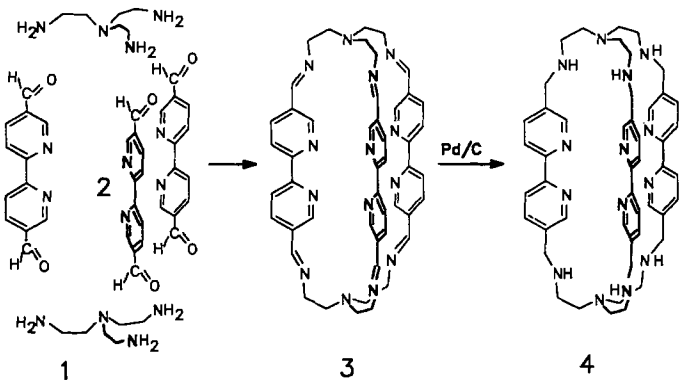

1 3 4

The dialdehyde **2** was obtained in 50% yield from 5,5′-bis(bromomethyl)-2,2′-bipyridine[5] by a Sommelet reaction or in 93% yield by Swern oxidation[6] of the corresponding dialcohol. Condensation of **2** with **1** under mild conditions gave the macrobicycle **3** in 78% yield. This one-pot cyclization, in which six new bonds are created in a single step to give a cage containing up to 14 nitrogen-donor centers, does not need high-dilution conditions. The cryptand **3** precipitates from the reaction mixture as soon as it is formed. Reduction of **3** with Pd/H_2 afforded the macrobicyclic polyamine **4** (>50% yield).

The dinuclear bis-Cu^I and trinuclear tris-Ag^I complexes **5** (78% yield) and **6** (67% yield) were prepared readily from **3** and two- or threefold molar amounts of $[Cu\text{-}(CH_3CN)_4BF_4$[7] or $AgBF_4$, respectively. The ^1H NMR spectra of these complexes were markedly different from those of the free ligand **3**, all signals being shifted downfield. The strongest effect ($\Delta\delta = 1.23$) was observed for the bipyridine C6 proton in complex **6** (anisotropic effect).

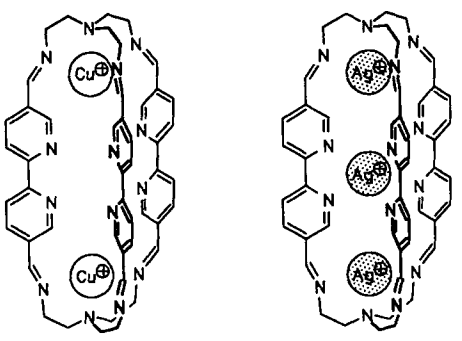

5 6

Crystal structure analyses of the free ligand **3** and its tris-Ag^I complex **6** showed *endo-endo*[8] conformations for the capping Tren units (Fig. 1).

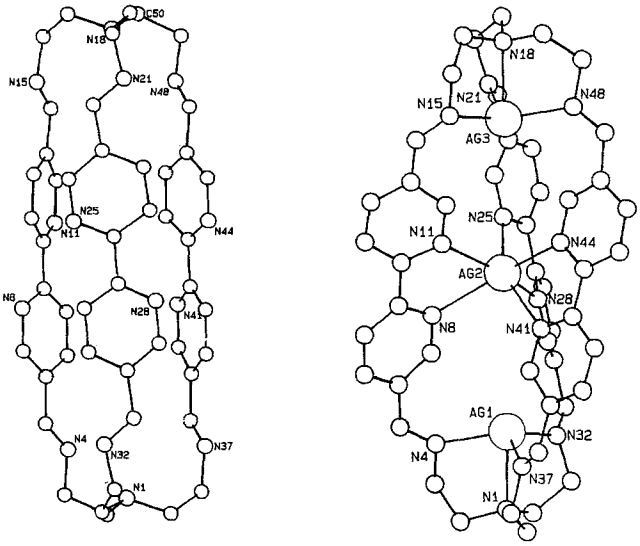

Fig. 1. Crystal structures of ligand **3** (left) and the Ag^I_3 cryptate **6** (right). Bond distances [pm] and bond angles [°] for the trinuclear Ag^I centers of **6**: Ag1-N1 244.6(7), Ag1-N4 231.6(8), Ag1-N32 229.0(9), Ag1-N37 228.0(8), Ag2-N8 250.4(7), Ag2-N11 248.1(6), Ag2-N25 244.4(6), Ag2-N28 250.6(7), Ag2-N41 248.9(6), Ag2-N44 247.7(7), Ag3-N15 229.3(8), Ag3-N18 243.1(7), Ag3-N21 229.9(7), Ag3-N48 229.3(9); Ag3-Ag2-Ag1 176.43(4); N4-Ag1-N1 76.5(3), N32-Ag1-N1 76.2(3), N32-Ag1-N4 113.3(3), N37-Ag1-N1 77.9(3), N37-Ag1-N4 112.2(3), N37-Ag1-N32 119.5(3), N11-Ag2-N8 66.3(2), N25-Ag2-N8 107.6(2), N25-Ag2-N11 99.3(2), N28-Ag2-N8 97.5(2), N28-Ag2-N11 155.7(2), N28-Ag2-N25 67.4(2), N41-Ag2-N8 96.3(2), N41-Ag2-N11 106.0(2), N41-Ag2-N25 150.6(2), N41-Ag2-N28 93.2(2), N44-Ag2-N8 149.1(2), N44-Ag2-N11 93.7(2), N44-Ag2-N25 98.5(2), N44-Ag2-N28 107.9(2), N44-Ag2-N41 65.5(2), N18-Ag3-N15 77.4(3), N21-Ag3-N15 116.1(3), N21-Ag3-N18 76.9(3), N48-Ag3-N15 115.2(3), N48-Ag3-N18 76.4(3), N48-Ag3-N21 113.7(3).

The distances between the bridgehead nitrogen atoms of **3** and **6** are about the same (1470 and 1466 pm, respectively). Similar donor distances in the cryptand and the cryptate (1550 pm) have also been reported for the tris(diphenylmethane) macrobicycle and its dinuclear Cu^I complex.[3a] The C_3 symmetry of the free ligand **3** changes to nearly D_3 symmetry in complex **6** (Fig. 2.). Whereas in **3** the bipyridine

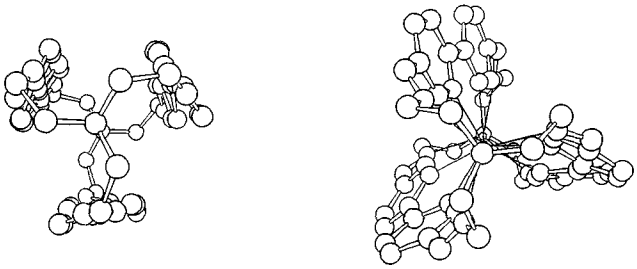

Fig. 2. Crystal structures of **3** (left) and **6** (right) projected along the bridgehead N–N axis.

subunits show the most favored *anti* conformation, which minimizes lone-pair repulsion, all nitrogen atoms are turned inside in **6** for complexing the central Ag^I ion in an almost octahedral way.[9] The torsion angles of the bipyridine units in **3** and **6** are changed from −163.3°, −160.9°, and −166.9° to −21.9°, −27.7°, and 1.0°, respectively. The imino nitrogen atoms are complexed by the Ag^I ions, so that their average N–N distance decreases from 443–452 pm in the free ligand **3** to 382–394 pm in complex **6**. The N–Ag^I distances to the bridgehead centers are 244 and 243 pm, and

the Ag^I–Ag^I distances are 493 and 490 pm. Finally, the N–Ag^I distances to the bipyridine N atoms are 244–251 pm. The coordination sphere around the central Ag^I ion can be regarded as a distorted octahedron, that around each of the two other Ag^I ions as a heavily distorted trigonal pyramid.

A mononuclear[10] and two dinuclear[3a] Ag^I complexes of related macrobicyclic ligands have been reported earlier. The cryptate **6** constitutes the first trinuclear Ag^I complex. The three metal ions are arranged in a row, held at well-defined distances, and bound in two different environments, the central one being a tris-bipyridine Ag^I site. Cryptand **3** offers the possibility of preparing homo- or heterometallic trinuclear metal cryptates that should display different binding, electrochemical, and photophysical properties for the terminal and the central metal ions, making available a range of novel features. For instance, a Cu^I-Ag^I-Cu^I heterodinuclear complex has already been prepared. Further development of the present work will also include the encapsulation of organic substrates inside the cavities of macrobicycles **3** and **4** either as free bases or as protonated and alkylated derivatives.

Experimental Procedures

3: To a stirred solution of Tren (**1**: 0.047 g, 0.32 mmol) in 5 mL of anhydrous acetonitrile was added dropwise at room temperature under argon a suspension of the dialdehyde **2** (colorless crystals, m.p. 228 °C; 0.1 g, 0.47 mmol) in acetonitrile (5 mL). The orange solid was filtered and recrystallized from methanol. Colorless crystals; m.p. 280 °C (CH_3OH); yield 78%; UV-VIS ($CHCl_3$/CH_3OH, 99:1): λ_{max} [nm] (ε) = 308 (85300) 263 (40100); ^{1}H NMR (200 MHz, CD_2Cl_2, 25 °C): δ = 2.80 (m, 12H; $CH_2N<$), 3.79 (m, 12H; $CH_2N=$), 7.73 (dd, ^3J = 8.25 Hz, ^4J = 2.40 Hz, 6H; H4), 7.89 (d, ^3J = 8.25 Hz, 6H; H3), 8.24 (s, 6H; CH = N), 8.40 (d, ^4J = 2.40 Hz, 6H; H6); ^{13}C NMR (50.3 MHz, CD_2Cl_2/CD_3OD, 99:1, 25 °C); δ = 53.5 ($CH_2N<$), 58.3 ($CH_2N=$), 121.3 (C3), 131.5 (C5), 134.3 (C4), 150.3 (C2), 156.5 (C6), 159.8 (CH = N); MS (FAB$^+$, *m*-nitrobenzylalcohol): *m/z* 821.4 ($M^{\oplus}$ + H).

4 · HBr: yield 52%; ^{1}H NMR (200 MHz, $CDCl_3$, CD_3OD, 25 °C): δ = 2.7 (m, 12H; $CH_2N<$), 3.3 (m, 12H; CH_2NH–), 4.15 (s, 12H; Ar-CH_2-NH), 8.00 (d, ^3J = 8.25 Hz, 6H; H3), 8.40 (dd, ^3J = 8.25 Hz, ^4J = 2.40, 6H; H4), 8.60 (d, ^4J = 2.40, 6H; H5); MS (FAB$^+$, *m*-nitrobenzylalcohol): *m/z* 833.6 ($M^{\oplus}$ + H):

5: yield 78%; UV-VIS ($CHCl_3$/CH_3OH, 99:1): λ_{max} [nm] (ε) = 373 sh (15100), 303 sh (47300), 282 sh (49000), 263 (50200); ^{1}H NMR (200 MHz, CD_2Cl_2, 25 °C): δ = 3.19 (m, 12H; $CH_2N<$), 3.90 (m, 12H; $CH_2N=$), 8.05 (dd, ^3J = 8.20 Hz, ^4J = 2.00 Hz, 6H; H4), 8.21 (d, ^3J = 8.20 Hz, 6H; H3), 8.70 (s, 6H; CH = N), 8.94 (d, ^4J = 2.00 Hz, 6H; H6).

6: yield 67%; UV-VIS ($CHCl_3$/CH_3OH, 99:1): λ_{max} [nm] (ε) = 306 (73700), 274 sh (47800); ^{1}H NMR (200 MHz, CD_3CN, 25 °C): δ = 3.10 (m, 12H; $CH_2N<$), 3.84 (m, 12H; $CH_2N=$), 8.24 (dd, ^3J = 8.20 Hz, ^4J = 2.30 Hz, 6H; H4), 8.42 (d, ^4J = 8.20 Hz, 6H; H3), 8.77 (br. s, 6H; CH = N), 9.63 (d, ^4J = 2.30 Hz, 6H; H6); ^{13}C NMR (50.3 MHz, CD_3CN, 25 °C): δ = 51.6 ($CH_2N<$), 58.8 ($CH_2N=$), 123.9 (C3), 132.8 (C4), 140.9 (C5), 145.3 (C2), 154.0 (C6), 162.0 (CH = N).

Received: May 21, 1991 [Z 4636 IE]
German version: *Angew. Chem. 103* (1991) 1365

CAS Registry numbers:
1, 4097-89-6; **2**, 135822-72-9; **3**, 135852-89-0; **3**·4H_2O, 135822-73-0; **4**·xHBr, 135877-62-2; **5**, 135822-75-2; **6**, 135852-91-4.

[1] J. E. Prue, G. Schwarzenbach, *Helv. Chim. Acta 33* (1950) 963.
[2] a) J.-M. Lehn, S. H. Pine, E. Watanabe, A. K. Willard, *J. Am. Chem. Soc. 99* (1977) 676; b) B. Dietrich, M. W. Hosseini, J.-M. Lehn, R. B. Sessions, *Helv. Chim. Acta 68* (1985) 289; c) R. J. Motekaitis, A. E. Martell, I. Murase, J.-M. Lehn, M. W. Hosseini, *Inorg. Chem. 27* (1988) 3630.
[3] a) J. Jazwinski, J.-M. Lehn, D. Lilienbaum, R. Ziessel, J. Guilhem, C. Pascard, *J. Chem. Soc. Chem. Commun. 1987*, 1691; b) J.-M. Lehn, R. Meric, J.-P. Vigneron, I. Bkouche-Waksman, C. Pascard, *ibid. 1991*, 62; c) D. MacDowell, J. Nelson, *Tetrahedron Lett. 29* (1988) 385; d) D. MacDowell, J. Nelson, V. McKee, *Polyhedron 8* (1989) 1143; e) O. Kocian, R. J. Mortimer, P. D. Beer, *Tetrahedron Lett. 31* (1990) 5069.
[4] See for instance: a) K. Kalyanasundaram, *Coord. Chem. Rev. 46* (1982) 159; b) A. Juris, V. Balzani, F. Barigelleti, S. Campagna, P. Belser, A. von Zelewsky, *ibid. 84* (1988) 85; c) F. Barigelleti, L. de Cola, V. Balzani, P. Belser, A. von Zelewsky, F. Vögtle, F. Ebmeyer, S. Grammenudi, *J. Am. Chem. Soc. 111* (1989) 4662.
[5] F. Ebmeyer, F. Vögtle, *Chem. Ber. 122* (1989) 1725.
[6] A. J. Mancuso, D. Swern, *Synthesis 1981*, 165.
[7] B. J. Hathaway, D. G. Holah, J. D. Postlethwaite, *J. Chem. Soc. 1961*, 3215.
[8] Crystal structure data for **3**: $C_{48}H_{48}N_{14}4\ H_2O$, colorless crystals, monoclinic, space group $P2_1/c$ (No. 14); M_r = 893.06; a = 1721.6(3), b = 1631.0(2), c = 1719.6(3) pm, β = 97.98(4)°; V = 4782(1) × 10^6 pm^3, Z = 4; ϱ_{calcd} = 1.241 g cm^{-3}; $Cu_{K\alpha}$ (λ = 1.5418 Å); μ = 0.63 mm^{-1}; $F(000)$ = 1896; T = 296 ± 1 K; crystal dimensions, 0.20 × 0.20 × 0.30 mm; CAD4 diffractometer (Enraf Nonius); corrections: Lorentz polarization, linear ca. 45% decrease (corrected with factors 1.00 to 1.53 on I), empirical absorption correction (DIFABS) with minimum and maximum correction coefficients 0.884 and. 1.254; 2θ = 4–100°; *hkl* range h = −1 → 17, k = −1 → 16, l = −17 → 17; 6085 measured, 4918 unique reflections, 3642 with $I > 2.0\ \sigma(I)$. The structure was solved using SHELXS. Refinement: full-matrix least-squares, R = 0.053, R_w = 0.061 ($w = w'[1.0-(\Delta F/6 \cdot \sigma F)^2]^2$, with w' = Chebychev polynomial for F_c with three coefficients (10.8, 4.3 und 7.95)), R_{int} = 0.020. Crystal structure data for **6**: $[C_{48}H_{48}N_{14}Ag_3](BF_4)_3$, pale yellow crystals, triclinic, space group $P\bar{1}$ (No. 2); M_r = 1405.02; a = 1358.0(1), b = 1433.3(3), c = 1576.7(2) pm, α = 106.95(1), β = 99.98(1), γ = 82.99(1)°; V = 2894(1) × 10^6 pm^3, Z = 2; ϱ_{calcd} = 1.612 g cm^{-3}; $Cu_{K\alpha}$ (λ = 1.5418 Å); μ = 8.97 mm^{-1}; $F(000)$ = 1396; T = 296 ± 1 K; crystal dimensions, 0.15 × 0.15 × 0.20 mm; CAD4 diffractometer (Enraf Nonius); corrections: Lorentz polarization, empirical absorption correction (DIFABS) with minimum and maximum correction coefficients 0.759 and 1.532; 2θ = 4–130°; *hkl* range h = −1 → 15, k = −16 → 16, l = −18 → 18; 10488 measured, 9596 unique reflections, 5415 with $I > 3.0\ \sigma(I)$. The structure was solved using SHELXS. Refinement: block-matrix least-squares (three blocks), R = 0.058, R_w = 0.070 ($w = w'[1.0-(\Delta F/6 \cdot \sigma F)^2]^2$, with w' = Chebychev polynominal for F_c with three coefficients (16.3, −0.097 and 12.9)), R_{int} = 0.045. Non-hydrogen atoms refined anisotropically, H atoms calculated at their idealized positions (C–H distance 1.00 Å) and included in the final structure factor calculations but not refined (CRYSTALS and PLUTO programs). Further details of the crystal structure investigations are available on request from the Director of the Cambridge Crystallographic Data Centre, University Chemical Laboratory, Lensfield Road, GB-Cambridge CB2 1 EW (UK), on quoting the full journal citation.
[9] The energy difference (steric energy) between the two conformations of the free ligand **3** and the conformation of the tris-Ag^I complex **6** calculated by MM2 can be estimated to be approximately 57 kJ mol^{-1} [on an HP9000 model 825SSRX; as option of the molecular modeling program MOLEK9000 (version February 1991), P. Bischof, ISKA (Bensheim)].
[10] J. C. Rodríguez-Ubis, B. Alpha, D. Plancherel, J.-M. Lehn, *Helv. Chim. Acta 67* (1984) 2264; b) B. Alpha, *Thèse de Doctorat des Sciences*, Univeristé Louis Pasteur, Strasbourg, 1987.

Endoreceptors with Convergent Phenanthroline Units: A Molecular Cavity for Six Guest Molecules**

By *Fritz Vögtle,** *Ingo Lüer, Vincenzo Balzani,* and *Nicola Armaroli*

The cagelike bridging of three 2,2′-bipyridine units has so far afforded ligands whose conformational flexibility allows the nitrogen donor centers to be twisted.[1] The use of 1,10-phenanthroline instead of 2,2′-bipyridine promised to increase the preorganization of the binding sites directed toward the interior of large molecular cavities, as *Lehn* et al.[2a] have described for smaller ligands. In this way, it should be

[*] Prof. Dr. F. Vögtle, Dipl.-Chem. I. Lüer
Institut für Organische Chemie und Biochemie der Universität
Gerhard-Domagk-Strasse 1, W-5300 Bonn 1 (FRG)
Prof. Dr. V. Balzani, Dr. N. Armaroli
Dipartimento di Chimica dell'Università
via Selmi 2, I-40126 Bologna (Italy)

[**] This work was supported by the Bundesministerium für Forschung und Technologie (BMFT-0329120A). We thank Dr. *G. Eckhardt* and Dr. *S. Schuth*, Universität Bonn, for recording the FAB mass spectra and Prof. Dr. *E. Steckhan* and Dipl.-Chem. *M. Frede*, Universität Bonn, for recording and interpreting the cyclic voltammograms.

possible to confine several organic guest molecules in the interior of a *single* host molecule, thereby bringing them into close proximity—a prerequisite for controlled reactions in the cavities of tailored catalysts.

In the new endoreceptors[2b] **2** and **3**, the convergent arrangement of the donor centers realizes the desired extent of *endo* preorganization of the binding sites, while the conformational flexibility made possible by the ether bridges should result in little hindrance to the inclusion of guest molecules. The synthesis of **2** and **3** was accomplished in a one-step reaction of 2,9-bis(4-hydroxyphenyl)-1,10-phenanthroline (**1**), introduced by *Sauvage* et al.,[3] with **4**[4a] and **5**,[4b] respectively, in 11% und 2.3% yield. The ^{1}H NMR spectra, the FAB mass spectra, and the elemental analyses are consistent with the host structures proposed; the formation of the corresponding macrobicyclic hosts containing the spacers **6**–**10**[4c–e] was confirmed by FAB MS.

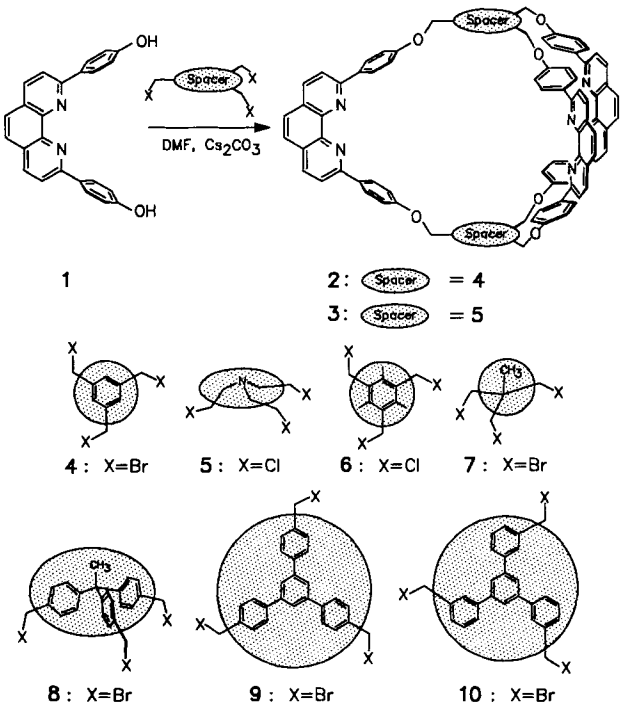

Like the bipyridine cavities described earlier,[1b] **2** and **3** were expected to form inclusion compounds with trihydroxybenzenes. However, attempts to complex 1,3,5-trihydroxybenzene were unsuccessful, as were efforts involving 1,3,5-tris(4-hydroxyphenyl)benzene, which fits better into the cavity. These results underline the demands of host/guest complementarity.

Surprisingly, however, inclusion of 2,9-disubstituted 1,10-phenanthrolines such as **11**–**14**, as their Cu^I complexes, takes place in the interior of the macrobicyclic host **2**. Treatment of a solution of **2** in dimethylformamide (DMF) with $[Cu(CH_3CN)_4]BF_4$ in CH_3CN, followed by addition of a solution of **11** or **12** in CH_2Cl_2, results in quantitative formation of complex **15** or **16**, respectively, both of which are stable in solution and to air. Elemental analysis gave the correct empirical formulas for $[\mathbf{15}(BF_4)_3] \cdot 3\,H_2O$ and $[\mathbf{16}(BF_4)_3] \cdot 3\,H_2O$ and FAB MS and ^{1}H NMR spectroscopy established the presence of *endo* complexes. FAB mass spectra confirmed the composition of **15** and **16**: peaks at *m/z* 2765 and *m/z* 2307 correspond to $[\mathbf{15}(BF_4)_2]^{\oplus}$ and $[\mathbf{16}(BF_4)_2]^{\oplus}$, respectively; further peaks correspond to the fragmentation products formed by stepwise loss of phenanthroline and $Cu^{\oplus}$. The ^{1}H NMR spectrum of **15** (5×10^{-3} M in CD_2Cl_2) indicates a symmetric arrangement of the guests in the cavity: the signals of the OCH_2 protons are shifted to higher field compared with those of the free ligand **2** by $\Delta\delta = 0.38$ to give a single, somewhat broad signal at $\delta = 5.00$. The signals of the mutually interacting phenylene groups of the bis(4-methylphenyl)phenanthroline (**11**) guest and the bis(oxyphenyl)phenanthroline unit of the ligand are both shifted to higher field.[3b] The signals of the methyl groups of the phenanthroline guest are shifted by $\Delta\delta = 0.06$ to higher field ($\delta = 1.90$) compared with those of the complex **11a**; the signal intensities are those expected for a complex with three $Cu^{\oplus}$ centers and three phenanthroline guests.

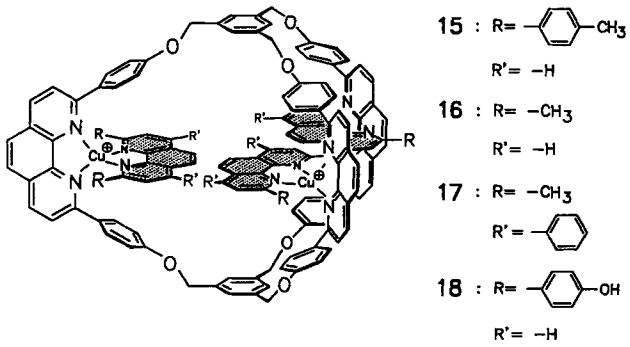

In complex **16**, the signals of the OCH_2 protons ($\delta = 4.78$) are shifted more strongly to higher field than those in **15** ($\Delta\delta = 0.6$). The inclusion of neocuproine (**12**) also causes high-field shifts of the signals for the phenylene protons of the bis(oxyphenyl)phenanthroline. The signals of the methyl groups of neocuproine are at higher field compared with those of complex **12a**[3b] by $\Delta\delta = 0.2$ and their intensity ratios are those expected. Accordingly, **2** is a true endoreceptor. The convergent arrangement of the donor centers forces the guest molecules to "dock" within the cavity. Steric factors prevent the guests from swinging freely.

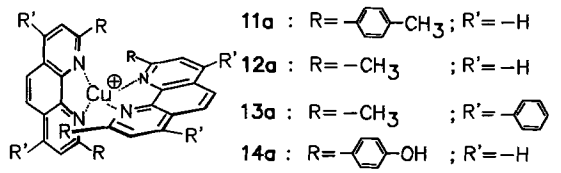

The space available in the cavity of **2** is not unlimited, however. Whereas three 2,9-disubstituted phenanthroline molecules fit into the cavity, only two molecules of bathocuproine (**13**, R' = phenyl), which is larger, were found by FAB MS to undergo inclusion under analogous conditions.

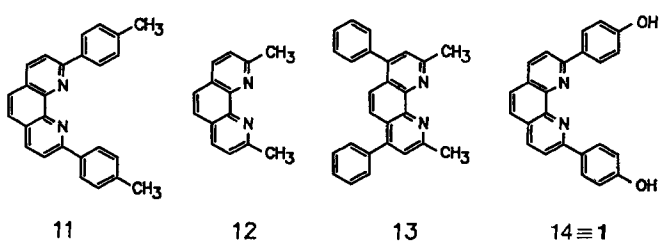

Although host **2** is sparingly soluble in CH_2Cl_2, complexes **15** and **16**, obtained by inclusion of **11** and **12**, respectively, are readily soluble. Attempts to synthesize **18**, on the other hand, led to a substance that was sparingly soluble in CH_2Cl_2 and could not be purified any further. ^1H NMR spectra indicate the presence of a mixture of **18** and **14a**.

Table 1. Absorption and luminescence data for **11a**, **12a**, **15**, and **16** [a].

Complex	λ_{max}^{abs} [nm] [b]	λ_{max}^{em} [nm] [c]	$\varphi^{em} \times 10^3$ [d]	τ_{em} [ns] [e]
11a	440	720	1.70	237
12a [f]	457	750	0.40	73
15	437	730	0.70	170
16	443	760	0.08	50

[a] Room temperature, degassed CH_2Cl_2 solution. [b] Absorption maximum at the longest wavelength. [c] From corrected emission spectra; estimated error $\pm$ 5 nm. [d] Quantum yield; estimated error ca. 25 %. [e] Lifetime; estimated error $\leq$ 10 %. [f] See also [5b].

The absorption and luminescence data for **11a** and **12a** as well as for **15** and **16** are summarized in Table 1; the emission maxima are corrected. Figure 1 shows the absorption and (uncorrected) luminescence spectra of **15** and **16**. The photophysical properties of **12a** and similar complexes, including the Cu^I catenate, are well-investigated.[5] The intense absorp-

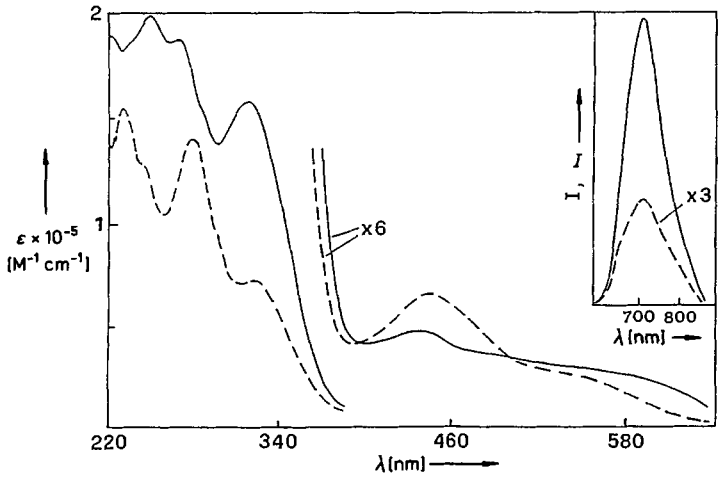

Fig. 1. Absorption and (superimposed) uncorrected luminescence spectra of **15** (——) and **16** (– – –) in CH_2Cl_2.

tion bands in the UV region are due to π–π^* ligand-centered transitions, while the bands appearing in the visible region are assigned to metal-to-ligand charge-transfer (MLCT) transitions. The three metal-containing chromophoric units of the trinuclear complexes **15** and **16** are equivalent. The luminescence bands of **15** and **16** should be assigned to an MLCT-excited state involving the ligands **11** and **12**, respectively. This assumption is based on the observed redshift of the luminescence bands of **15** and **16** with respect to those of **11a** and **12a**, respectively, which is expected on replacing a ligand in **11a** and **12a** by the more basic[5e] bis(anisyl)-phenanthroline unit of the macrobicyclic host. The tolyl substituents in **15** and **11a** protect the excited state against the formation of short-lived exciplexes and this is reflected in an increase in the luminescence intensity and lifetime compared to those of **16** and **12a**.[5d]

The stabilizing effect of tolyl substituents in the guest is also evident in the cyclic voltammetry measurements on **15** and **16**. Although adsorption effects at the glassy-carbon working electrode make the investigation of the complexes difficult, a chemically largely reversible reduction was detected for **15** and can be assigned to the formal transition $Cu^I \rightarrow Cu^0$. In contrast, **16** is reduced irreversibly.

The new type of complex offers the possibility of using the methods developed by *Sauvage* et al.[3d–e] to synthesize a previously unknown type of catenane in which **2** would be symmetrically interlaced with three crown ethers. The confinement and orientation of three guests in close proximity in a *single* cavity, achieved here for the first time, opens up new possibilities for the development of catalysts for selective reactions between several oriented guests within a molecular cavity.

Experimental Procedure

2: A solution of **1** (3.3 g, 9 mmol) in 250 mL of dry DMF and a solution of **4** (2.14 g, 6 mmol) in 250 mL of DMF were added simultaneously to a solution of $CsCO_3$ (8 g) in 1.2 L of DMF under argon at 70 °C over 15 h. The reaction mixture was then stirred for an additional 15 h at 70 °C. After removal of the solvent, the residue was extracted into $CHCl_3$ and purified by chromatography on silica gel (eluent: CH_2Cl_2/MeOH, 10 : 1) (R_f value: 0.63); m.p. 282–285 °C. ^1H NMR (200 MHz, $CDCl_3$/TFA): δ = 5.38 (s, 12 H), 7.35 (d, 12 H, ^3J = 9 Hz), 7.63 (s, 6 H), 8.08 (d, 12 H, ^3J = 9 Hz), 8.37 (s, 6 H), 8.5 (d, 6 H, ^3J = 8 Hz), 9.07 (d, 6 H, ^3J = 8 Hz). FAB-MS (matrix: *m*-nitrobenzyl alcohol): *m/z* 1321 ($M^{\oplus}$ + H). The extreme low solubility of **2** in pure $CDCl_3$ only allowed an ^1H NMR spectrum of unsatisfactory quality to be recorded; it is clearly evident, however, that the shift of the OCH_2 protons is unchanged with respect to the measurement in $CDCl_3$/TFA (δ = 5.39). the aromatic protons absorb at δ = 7.17–8.33.

3: Synthesized analogously to **2**. The product was obtained by column chromatography on silica gel (eluent: CH_2Cl_2/MeOH, 40 : 1) (R_f value: 0.27); m.p. 263 °C. ^1H NMR (90 MHz, CD_2Cl_2): δ = 3.2 (t, 12 H, ^3J = 5 Hz), 4.26 (t, 12 H, ^3J = 5 Hz), 7.06 (d, 12 H, ^3J = 9 Hz), 7.55 (s, 6 H), 7.82 (d, 6 H, ^3J = 8 Hz), 8.04 (d, 6 H, ^3J = 8 Hz), 8.26 (d, 12 H, ^3J = 9 Hz). FAB-MS (matrix: dithioerythritol/dithiothreitol + 2 N HCl): *m/z* 1283 (100 %), ($M^{\oplus}$ + H), 1256 (17 %).

15–17: $[Cu(CH_3CN)_4BF_4$ (95 mg, 0.3 mmol) [6] in 15 mL of degassed CH_3CN was added to **2** (132 mg, 0.1 mmol) in 20 mL of degassed DMF with stirring under argon. The solution turned red-brown. It was stirred for a further 10 min, after which the phenanthroline guest (0.3 mmol), dissolved in 15 mL of degassed CH_2Cl_2, was added continuously over 1 h. After 3 h, the reaction mixture was evaporated to dryness and the residue dissolved in CH_2Cl_2. The product was isolated by preparative layer chromatography (PLC) (eluent: CH_2Cl_2/methanol, 10 : 1) and recrystallized from CH_2Cl_2/benzene. [**15**$(BF_4)_3$] · 3 H_2O: Fp = 302–303 °C; [**16**$(BF_4)_3$] · 3 H_2O: Fp = 285–287 °C. **11a**, **13a**, **14a**: Synthesized analogously to **12a** [3b].

The absorption spectra were recorded with a Perkin-Elmer λ6 spectrophotometer; the luminescence spectra were obtained with a Perkin-Elmer 650-40 spectrofluorimeter. The emission lifetimes were measured with an Edinburgh single photon counting apparatus. The quantum yields were determined with $[Os(bpy)_3]^{2\oplus}$ as standard ($\Phi = 5 \times 10^{-3}$ in CH_3CN at room temperature) [7].

Received: June 4, 1991 [Z 4674IE]
German version: *Angew. Chem. 103* (1991) 1367

CAS Registry numbers:
1, 88498-43-5; **2**, 136034-17-8; **3**, 136059-97-7; **4**, 18226-42-1; **5**, 555-77-1; **11**, 116287-98-0; **11a**, 136059-96-6; **12**, 484-11-7; **13**, 4733-39-5; **13a**, 111290-82-5; **14a**, 128039-68-9; **15**, 136088-30-7; **16**, 136088-32-9; **17**, 136088-34-1.

[1] S. Grammenudi, F. Vögtle, *Angew. Chem. 98* (1986) 1119; *Angew. Chem. Int. Ed. Engl. 25* (1986) 1122; b) F. Ebmeyer, F. Vögtle, *ibid. 101* (1989) 95 bzw. *28* (1989) 79; c) J. M. Lehn, D. Lilienbaum, J. de Mendoza, E. Mesa, J.-C. Rodriguez-Ubis, P. Vasquez, P.-M. Windscheif, R. Ziessel, K. Rissanen, F. Vögtle, *ibid. 103* (1991) 1365 and *30* (1991) 1333; d) F. Ebmeyer, F. Vögtle in: *Bioorganic Chemistry Frontiers, Vol. 1*, Springer, Berlin 1990, p. 145.

[2] a) J.-C. Rodriguez-Ubis, B. Alpha, D. Planchel, J. M. Lehn, *Helv. Chim. Acta 67* (1984) 2264; b) J. M. Lehn, *Angew. Chem. 100* (1988) 91; *Angew. Chem. Int. Ed. Engl. 27* (1988) 89.

[3] a) C. O. Dietrich-Buchecker, J. P. Sauvage, *Tetrahedron Lett. 24* (1983) 5091; b) C. O. Dietrich-Buchecker, P. A. Marnot, J. P. Sauvage, J. P. Kintzinger, P. Maltese, *Nouv. J. Chim. 8* (1984) 573; c) C. O. Dietrich-Buchecker, P. A. Marnot, J. P. Sauvage, J. R. Kirchhoff, D. R. McMillin, *J. Chem. Soc. Chem. Commun. 1983*, 513; d) J. C. Chambron, C. O. Dietrich-

Buchecker, C. Hemmert, A. K. Khemiss, D. Mitchell, J. P. Sauvage, J. Weiss, *Pure Appl. Chem. 62* (1990) 8002; e) J. P. Sauvage, *Acc. Chem. Res. 23* (1990) 319.

[4] a) F. Vögtle, M. Zuber, R. G. Lichtenthaler, *Chem. Ber. 106* (1973) 717; b) K. Ward, *J. Am. Chem. Soc. 57* (1935) 914; c) H. Stetter, W. Böckmann, *Chem. Ber. 84* (1951) 834; d) B. Dung, F. Vögtle, *J. Inclusion Phenom. 6* (1988) 429; e) N. Sendhoff, W. Kißener, F. Vögtle, S. Franken, H. Puff, *Chem. Ber. 121* (1988) 2179.

[5] a) A. K. Ichinaga, J. R. Kirchhoff, D. R. McMillin, C. O. Dietrich-Buchecker, P. A. Marnot, J. P. Sauvage, *Inorg. Chem. 26* (1987) 4290; b) A. K. I. Gushurst, D. R. McMillin, C. O. Dietrich-Buchecker, J. P. Sauvage, *ibid. 28* (1989) 4070; c) R. M. Everly, R. Ziessel, R. Suffert, D. R. McMillin, *ibid. 30* (1991) 559; d) R. M. Everly, D. R. McMillin, *Photochem. Photobiol. 50* (1989) 711; e) N. Armaroli, V. Balzani, L. De Cola, J. P. Sauvage, C. O. Dietrich-Buchecker, J. M. Kern, unpublished; f) N. Armaroli, V. Balzani, F. Barigeletti, L. De Cola, J. P. Sauvage, C. Hemmert, *J. Am. Chem. Soc. 113* (1991) 4033; g) Overview: V. Balzani, F. Scandola: *Supramolecular Photochemistry*, Ellis Horwood, Chichester 1991.

[6] H. Meerwein, V. Hederich, K. Wunderlich, *Arch. Pharm. Ber. Dtsch. Pharm. Ges. 291* (1958) 541.

[7] E. M. Kober, J. V. Caspar, R. S. Lumpkin, T. J. Meyer, *J. Phys. Chem. 90* (1986) 3722.

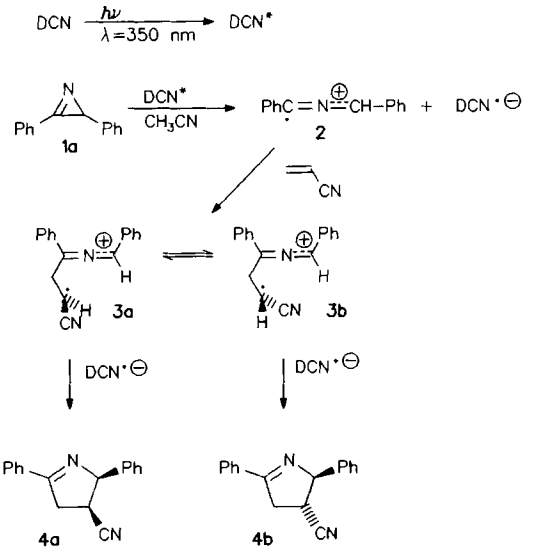

Scheme 1. Products **4a** and **b** are formed in a 50:50 ratio.

[3 + 2] Cycloadditions with Azirine Radical Cations: A New Synthesis of *N*-Substituted Imidazoles**

By *Felix Müller* and *Jochen Mattay**

Dedicated to Professor Kurt Schaffner on the occasion of his 60th birthday

Recently, much attention has been focused on the investigation of reactions involving photoinduced electron transfer (PET), especially the PET-catalyzed ring opening of highly strained carbo- and heterocycles.[1] Here we report on the reactions of azirines, a group of compounds frequently used in 1,3-dipolar cycloaddition reactions,[2] under photosensitized (electron-transfer) irradiation conditions.

Photochemical irradiation usually results in energy transfer to a substrate either by direct excitation or through a triplet sensitizer. PET, however, generally proceeds by the irradiation of an electron acceptor. For this purpose cyanoarenes such as 1,4-napthalenedicarbonitrile (DCN) are very useful.

Since the n–π^* transition of azirines such as **1a** occurs at a wavelength of 280 nm,[2] irradiation with light of 350-nm wavelength does not lead to the direct excitation of the substrate. However, DCN is excited and abstracts an electron from the azirine.[3] As observed for direct excitation,[2] the C–C bond of azirine is thereby broken. We regard the formation of the 2-azaallenyl radical cation **2** as an intermediate. This species reacts with acrylonitrile under ring closure and back electron transfer to give the five-membered ring **4**. The addition thus proceeds via a two-step mechanism. The photoinduced 1,3-dipolar cycloaddition of azirines described by *Padwa* et al.[4] leads to a very high diastereoselectivity. Compound **4b** is formed in a yield of 90%, whereas that of **4a** is just 10%. In contrast, we found a product ratio of 50:50 when DCN catalysis was used.

Scavenging with 2,2,2-trifluoroethanol resulted in **5** and **6** as products.[5] Compound **5** is the trapped product of the 2-azaallenyl radical cation **2**. The formation of **6** is easily explained by the trapping of **3a/3b**, which were formed through reaction of **2** with acrylonitrile. Thus, dihydropyrroles **4** are not formed via a concerted [3 + 2] cycloaddition, as is the case for direct irradiation.[4]

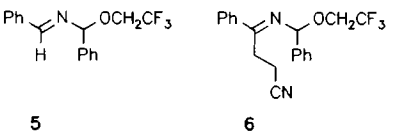

The reaction does not proceed upon 350-nm irradiation in the absence of DCN or in the presence of a triplet sensitizer (benzophenone). When we compared the reactivity of **2** with nitrile ylides generated by direct irradiation, we noted that the reaction is favored for olefins substituted with electron-withdrawing groups; for instance, the reaction with vinyl ethers does not lead to five-membered rings. If there is no suitable reaction partner, azirines will dimerize, via [3 + 2] cycloaddition[4,6] to give **9**. Both nitrile ylides and 2-azaallenyl radical cations react with aldehydes and ketones to form 3-dihydrooxazoles.[6]

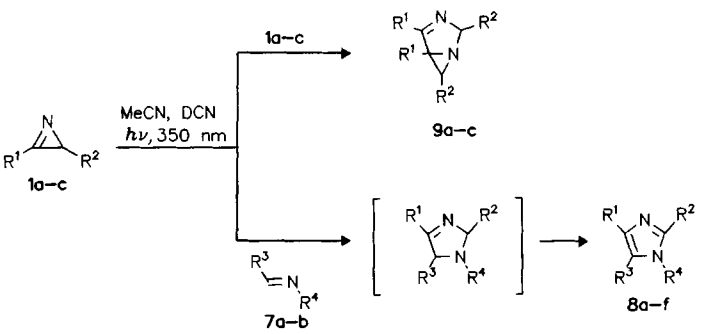

Scheme 2. **1a**, $R^1 = R^2$ = phenyl; **1b**, R^1 = phenyl, R^2 = H; **1c**, R^1 = *n*-butyl, R^2 = H; **7a**, R^3 = phenyl, R^4 = *n*-propyl, **7b**, $R^3 = R^4$ = *n*-propyl.

[*] Prof. Dr. J. Mattay, Dipl.-Chem. F. Müller
Organisch-Chemisches Institut der Universität Münster
Orleansring 23, W-4400 Münster (FRG)

[**] Radical Ions and Photochemical Charge-Transfer Phenomena (Series A), Part 31, and Cycloadditions (Series B), Part 35. This work was supported by the Deutsche Forschungsgemeinschaft, the Fonds der Chemischen Industrie, and the state of Nordrhein-Westfalen. We also thank Bayer AG for generous gifts of materials. *F. M.* would like to thank the Studienstiftung des deutschen Volkes for a predoctoral grant. Series A, Part 30: J. Mattay, M. Vondenhof, *Top. Curr. Chem. 159* (1991) 219. Series B, Part 34: M. Conrads, J. Mattay, *Chem. Ber. 124* (1991) 1425.

The radical cation **2** is also able to attack the C–N double bond in imines in an intermolecular fashion, a reaction not possible for photochemical 1,3-dipolar cycloaddition.[6] The reaction of azirines with imines leads to the formation of the *N*-substituted imidazoles.

The course of the reaction is as follows: Addition of the radical cation **2** to the imine is followed by ring closure to form a dihydroimidazole. Under these reaction conditions the dihydroimidazole is not stable and undergoes subsequent aromatization, so that, even in the crude product, no dihydroimidazole is detected. *Huisgen*[7] did not find a dihydroimidazole under comparable conditions either. The reaction of azirines with imines offers a ready approach for the synthesis of *N*-substituted imidazoles with a wide variety of substituents.

Since the C–N double bonds of the imine and the azirine compete for reaction, the yields of imidazoles vary rather widely (Table 1). The remaining products are the azirine dimers. Nevertheless, compared to classical procedures,[8] the yields of this direct synthesis are quite high. Furthermore, the ready availability of starting materials offers plenty of new synthetic opportunities.

Table 1. Yields of the new imidazoles **8**.

Compd	R^1	R^2	R^3	R^4	Yield
8a	phenyl	phenyl	phenyl	*n*-propyl	87% [8] [a]
8b	phenyl	H	phenyl	*n*-propyl	12% [b]
8c	*n*-butyl	H	phenyl	*n*-propyl	3% [c]
8d	phenyl	phenyl	*n*-propyl	*n*-propyl	25% [d]
8e	phenyl	H	*n*-propyl	*n*-propyl	35% [e]
8f	*n*-butyl	H	*n*-propyl	*n*-propyl	40% [f]

[a] **9a**, 12%; [b] **9b**, 85%; [c] **9c**, 95%; [d] **9a**, 74%; [e] **9b**, 60%; [f] **9c**, 57%.

Experimental Procedure

The azirines were prepared according to [9], the imines according to [10]. The synthesis of DCN is described in [11]. A solution of the azirine (0.3 mmol) and the imine (1.0 mmol, in 10 mL of acetonitrile was poured into a Pyrex tube. 1,4-Naphthalenedicarbonitrile (0.1 mmol, 18 mg) was added, the reaction solution deoxygenated by argon bubbling, and the tube sealed. Irradiation was carried out by means of a Rayonet photochemical reactor and 350-nm radiation lamps. Irradiation was maintained for 6–10 hours. The solvent was then evaporated and the residue separated by flash chromatography on alumina (Merck Neutral Act. I) using diethyl ether as eluent. The new compounds gave satisfactory ^{1}H NMR, ^{13}C NMR, and mass spectroscopic data, which are similar to the data of comparable compounds [12].

Received: March 15, 1991 [Z 4501 IE]
German version: *Angew. Chem. 103* (1991) 1352

[1] J. Mattay, *Synthesis 1989*, 233; H. Tomioka, D. Kobayashi, A. Hashimoto, S. Murata, *Tetrahedron Lett. 30* (1989) 4685; P. Clawson, P. M. Lunn, D. A. Whiting, *J. Chem. Soc. Perkin Trans. 1 1990* 153, *ibid. 1990*, 159; E. Palomino, A. P. Schaap, M. J. Heeg, *Tetrahedron Lett. 31* (1990) 6861; K. Gollnick, M. Weber, *ibid. 31* (1990) 4585; N. Ichimose, K. Mizuno, T. Tamai, Y. Otsuji, *J. Org. Chem. 55* (1990) 4079; M. Kamata, H. Furukawa, T. Miyashi, *Tetrahedron Lett. 31* (1990) 681.

[2] R. Huisgen in A. Padwa (Ed.): *1,3 Dipolar Chemistry, Vol. I*, Wiley, New York 1984, p. 1; A. Padwa in W. Horspool (Ed.): *Synthetic Organic Photochemistry*, Plenum, New York 1984, p. 313; H. Heimgartner, *Angew. Chem. 103* (1991) 271; *Angew. Chem. Int. Ed. Engl. 30* (1991) 238.

[3] We assume that the first step is the oxidation of the azirine to the azirine radical cation, since the energy for the electron-transfer process estimated from the Weller equation (D. Rehm, A. Weller, *Isr. J. Chem. 8* (1970) 259) is negative and, therefore, the process is thermodynamically allowed.

[4] A. Padwa, J. Smolanoff, *J. Am. Chem. Soc. 93* (1971) 548; A. Padwa, M. Dharan, J. Smolanoff, S. I. Wetmore Jr. *ibid. 95* (1973) 1945, *ibid. 95* (1973) 1954; A. Padwa, J. Smolanoff, A. Tremper, *ibid. 97* (1975) 4682.

[5] Scavenging by addition of 1 mL of 2,2,2-trifluoroethanol to the reaction mixture (see *Experimental Procedure*). The yield of **5** and **6** was 8% and 7%, respectively. Direct irradiation just led to the formation of **5**. When nucleophilic alcohols were added, no compound similar to **6** could be detected.

[6] H. Giezendanner, M. Märky, B. Jackson, H.-J. Hansen, H. Schmid, *Helv. Chim. Acta 55* (1972) 745; H. Giezendanner, H. Heimgartner, B. Jackson, T. Winkler, H. Schmid, *ibid. 56* (1973) 2611; U. Gerber, H. Heimgartner, H. Schmid, H.-J. Hansen *Heterocycles 6*(1977) 143.

[7] R. Huisgen, H. Gotthardt, B. O. Bayer, *Chem. Ber. 103* (1970) 2370; K. Bünge, R. Huisgen, R. Raab, H. J. Sturm, *ibid. 105* (1972) 1307.

[8] V. Stoeck, W. Schunack, *Arch. Pharm. (Weinheim, Ger.) 307* (1974) 922, *ibid. 309* (1976) 421.

[9] G. Smolinsky, *J. Org. Chem. 27* (1962) 3557; F. W. Fowler, A. Hassner, L. A. Levy, *J. Am. Chem. Soc. 89* (1967) 2077.

[10] L. F. Tietze, T. Eicher: *Reaktionen und Synthesen*, Thieme, Stuttgart 1981, p. 69.

[11] A. Albini, D. R. Arnold, *Can. J. Chem. 56* (1978) 2985.

[12] H. J. Sattler, V. Stoeck, W. Schunack, *Arch. Pharm. (Weinheim, Ger.) 308* (1975) 795; *ibid. 311* (1978) 736.

Laser Flash Photolysis Generation, Spectra, and Lifetimes of Phenylcarbenium Ions in Trifluoroethanol and Hexafluoroisopropyl Alcohol. On the UV Spectrum of the Benzyl Cation**

By *Robert A. McClelland,* Christopher Chan, Frances Cozens, Agnieszka Modro*, and *Steen Steenken* *

Dorfman and co-workers have reported reactivities of $Ph_3C^{\oplus}$, $Ph_2CH^{\oplus}$, and $PhCH_2^{\oplus}$ with various nucleophiles in chlorinated hydrocarbon solvents.[1–3] The experiments were performed using the pulse radiolysis technique, with the cations obtained upon fragmentation of the initially formed radical cations. In the case of $Ph_3C^{\oplus}$ and $Ph_2CH^{\oplus}$, there were excellent matches of spectra of the transients observed in the pulse radiolysis experiments with ones obtained for solutions of authentic cations in concentrated acid and there

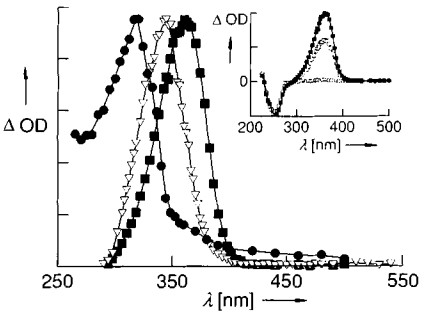

Fig. 1. Absorption spectra of the *p*-methoxycumyl cation (in TFE, ■), the *p*-methoxyphenethyl cation (in TFE, △), and the *p*-methoxybenzyl cation (in HFIP, ●). The precursors *p*-methoxy-α-methylstyrene, *p*-methoxystryrene, and *p*-methoxybenzyltrimethylammonium tetrafluoroborate were photolyzed at 248 nm with 20-ns pulses. Spectra were recorded 50–100 ns after the pulse. The insert shows the formation and decay of the cation and the (permanent) depletion of parent in the experiment with *p*-methoxy-α-methylstyrene, at 100 ns, 45 μs, and 500 μs after the pulse.

[*] Prof. Dr. R. A. McClelland, C. Chan, F. Cozens, Dr. A. Modro
Department of Chemistry, University of Toronto
Toronto, Ontario M5S 1A1 (Canada)
Prof. Dr. S. Steenken
Max-Planck-Institut für Strahlenchemie
Stiftstrasse 34–36, W-4330 Mülheim (FRG)

[**] This work was supported by the Donors of the Petroleum Research Fund, administered by the American Chemical Society, and by NSERC (Canada).

can be no question that the particular cations were being studied. With $PhCH_2^{\oplus}$, however, no spectrum from a "classical" source is available. The transient that was observed had an absorption maximum at 363 nm. Arguments that this represented $PhCH_2^{\oplus}$ were based upon the analogy with the other two systems, the observation of the same transient with different precursors, and the characteristic quenching by nucleophiles.[1] Using nanosecond laser flash photolysis ($\lambda = 248$ nm) we now have observed a number of substituted benzyl cations in trifluoroethanol (TFE) and hexafluoroisopropyl alcohol (HFIP). Our results lead to the conclusion that the 363-nm transient is unlikely to have been the benzyl cation.

The λ_{max} and rate constant data for the benzyl cations are summarized in Table 1, and spectra are shown in Figures 1 and 2 for the parent and *p*-methoxy series. In the case of the cumyl (**2**, R^1 = Me) and arylethyl (**2**, R^1 = H) cations, the styrenes **1** (R^1 = Me, H) were the precursors, with cation generation involving protonation of the electronically excited styrene by the solvent SOH [Eq. (a)]. This process, which

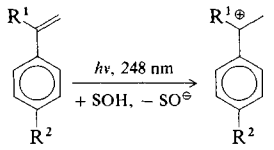

(a)

1 **2**

R^1 = H, Me; R^2 = H, Me, MeO; S = CF_3CH_2, $(CF_3)_2CH$

has previously been described for *p*-methoxystyrene in TFE,[4, 5] has now proved to be a general one for styrenes in these fluorinated alcohols, HFIP being particularly efficient. This weakly nucleophilic solvent[6] also permits the observation of the more reactive cations.

The benzyl cations were generated by photoheterolysis of appropriate precursors, *p*-methoxybenzyl from *p*-methoxybenzyltrimethylammonium fluoroborate[7, 8] and *p*-methoxybenzyl chloride and *p*-methylbenzyl from *p*-methylbenzyl chloride and bromide [Eq. (b)]. In these cases radicals arising from a competing photohomolysis[4, 7, 8] were also observed [Eq. (c)].

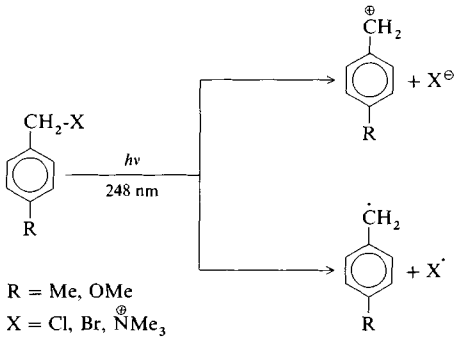

(b)

(c)

R = Me, OMe
X = Cl, Br, $\overset{\oplus}{N}Me_3$

Identification of transients as benzylic cations took several forms. (1) They were quenched in a manner characteristic of carbenium ions, with large rate accelerations upon addition of methanol and bromide (see insert to Figure 2 and Table 1 for the rate constants). Oxygen, on the other hand, had no effect. (2) The cations were formed in monophotonic processes, which shows that they are not derived from cation radicals, which could only be generated via biphotonic processes.[9] (3) The appropriate products were observed, for example, *p*-methoxybenzyl trifluoroethyl ether upon photolysis of $4\text{-}MeOC_6H_4CH_2N(CH_3)_3 \cdot BF_4$ in TFE, and the Markovnikov adducts of both styrene and α-methylstyrene with the solvent HFIP. (4) For the *p*-methylbenzyl cation, which decays in HFIP with $k_s = 2 \times 10^6\ s^{-1}$, a rate constant of $1.0 \times 10^{10}\ M^{-1}\,s^{-1}$ was measured for reaction with bromide (added as the $nBu_4N^{\oplus}$ salt, Table 1), giving $k_{Br^{\ominus}}/k_s = 5 \times 10^3\ M^{-1}$. The solvolysis of *p*-methylbenzyl bromide in HFIP containing nBu_4NBr showed pronounced common ion inhibition, from which the $k_{Br^{\ominus}}/k_s$ ratio was calculated to be $5 \times 10^3\ M^{-1}$, identical with the number obtained from observation of the cation. (5) For the parent cumyl cation, the spectrum of the transient in HFIP is virtually identical to that reported by *Olah* et al. for the same cation in SO_2–SbF_5–FSO_3H ($\lambda_{max} = 390$ nm, $\varepsilon = 1400$; $\lambda_{max} = 326$, $\varepsilon = 11\,000$).[10] With the latter extinction coefficient, the quantum yield for formation of the cumyl cation upon irradiation of α-methylstyrene in HFIP was calculated, using a previously described technique,[11] as 0.08.

Table 1. λ_{max} [nm] and rate constants (20 °C) for reaction of derivatives of benzyl cations with solvent (k_s) and with $Br^{\ominus}$ ($k_{Br^{\ominus}}$) and MeOH (k_{MeOH}) in TFE and HFIP. The cations were generated by 248-nm laser flash photolysis according to Equations (a) and (b).

Cation	Cumyl	Phenethyl	Benzyl
4-Methoxy			
λ_{max}	360	340	320, ~360 [a]
k_s (TFE) [b]	1.6×10^4	3.9×10^5	4.3×10^6 (9×10^6) [c]
k_s (HFIP) [b]	$<10^2$	$<10^2$	3.2×10^2
$k_{Br^{\ominus}}$ [d]	1.1×10^8 (TFE) [e]	4.5×10^9 (TFE)	4.8×10^9 (HFIP)
k_{MeOH} [d]	9.1×10^5 (TFE)	5.6×10^6 (TFE)	5.8×10^5 (HFIP)
4-Methyl			
λ_{max}	340, ~380 [a]	325, ~390 [f]	310 [g]
k_s (TFE) [b]	1×10^7	$>5 \times 10^7$	$>5 \times 10^7$
k_s (HFIP) [b]	6×10^2	5×10^4 [h]	2×10^6
$k_{Br^{\ominus}}$ (HFIP) [d]	1.3×10^9	7.2×10^9	1.0×10^{10}
k_{MeOH} (HFIP) [d]	3.4×10^5 [j]	1.1×10^7	6.5×10^7
4-H			
λ_{max}	325, ~410 [f]	315, ~430 [f]	
k_s (HFIP) [b]	9×10^3	6×10^5 [h]	
$k_{Br^{\ominus}}$ (HFIP) [d]	6.7×10^9	8.2×10^9	
k_{MeOH} (HFIP) [d]	4.1×10^6	4.3×10^7	

[a] Shoulder. [b] Units s^{-1}. [c] The rate constant $9 \times 10^6\ s^{-1}$ was obtained in 1:1 TFE/acetonitrile with both $4\text{-}MeOC_6H_4CH_2N(CH_3)_3 \cdot BF_4$ and $4\text{-}MeOC_6H_4CH_2Cl$ as precursors. In 100% TFE and 100% HFIP, the choride undergoes rapid thermal solvolysis. [d] Units $M^{-1}s^{-1}$. [e] The reaction is reversible (F. Cozens, to be published). [f] λ_{max} approximate, peak is about 10% of major one (see Fig. 2). [g] Weak absorbance also at higher λ, but this is obscured by other weak transient(s). [h] Extrapolated to zero styrene concentration. These cations also react with excess styrene remaining after photolysis. [j] The k_{obsd} vs. [MeOH] plot is curved upwards. The number indicated is from a linear fit in the [MeOH] range 0.1 to 0.35 M.

These experiments establish that simple benzyl cations such as cumyl and phenethyl do exist as free ions in HFIP. However, the benzyl cation itself was not observed in this solvent when precursors such as benzyl halides were used. We estimate its lifetime to be in the range 2–20 ns, just beyond the limit of detection of our apparatus. The spectra of the other eight cations have a major peak with λ_{max} in the range 310–360 nm, with the trend λ_{max} (4-MeO) > λ_{max} (4-Me) > λ_{max} (H) for a given type of cation (as is also observed for $Ar_3C^{\oplus}$ and $Ar_2CH^{\oplus}$),[11, 12] while for a given *para* substituent, λ_{max}(cumyl) > λ_{max}(phenethyl) > λ_{max}(benzyl). There is also absorbance at higher wavelengths that is associated with the cation, as concluded from the identity of the decay and quenching characteristics with those of the major peak, and as observed in strong acids with the cumyl cation.[10] This absorbance appears as a shoulder or weak peak with

most of the cations, the exceptions being *p*-methoxycumyl and *p*-methoxyphenethyl. The dependence of λ_{max} on structure is less precisely defined because of the weakness of this absorbance, but it appears to be exactly opposite to that seen in the stronger peaks at lower wavelength. Examination of the trends in both bands leads to the prediction that the parent benzyl cation has a strong band with λ_{max} 300–310 nm and a weak peak (about 10% of the strong band) at 430–460 nm. In contrast, the transient observed in the pulse radiolysis experiments by *Dorfman* et al.[1] was a single broad peak with λ_{max} at 363 nm and weak absorbance at 320 and 420 nm (see Figure 2 of Ref. [1]). We conclude that this was not the benzyl cation. One possibility is that the transient observed was due to a cyclohexadienyl cation arising from coupling of an initially generated cation or cation radical with unreacted precursor. Cyclohexadienyl cations of this type would absorb in this region.[3] Consistent with a bimolecular mechanism for its formation, the amplitude of the 363-nm transient was larger at higher concentrations of precursor.[1]

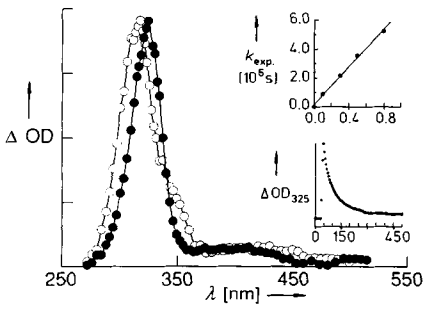

Fig. 2. Absorption spectra of the cumyl cation (•) and the phenethyl cation (○) in HFIP, obtained on photolysis of α-methylstyrene and styrene, respectively, recorded at ≈ 100 ns after the pulse. The inserts show the decay of the cumyl cation at 325 nm (time scale in [μs]), and first-order rates for decay of cation measured in the presence of Bu_4NBr [mM]; the slope of the line yields the rate constant 6.7×10^9 $M^{-1} s^{-1}$ for the reaction cumyl$^{\oplus}$ + $Br^{\ominus}$.

From an analysis of reactivities with alkenes, *Mayr* et al. have recently arrived at a similar conclusion; that is, the rate constants for the 363-nm transient are not consistent with it being the benzyl cation.[14] In addition there is a recent example showing that the technique of pulse radiolysis to produce cations is not a general one, particularly for less stable cations. The radical cation of 9-chlorofluorene[15] does not fragment to the 9-fluorenyl cation.[6]

Received: March 8, 1991 [Z 4484 IE]
German version: *Angew. Chem. 103* (1991) 1389

CAS Registry numbers:
p-methoxy-α-methylstyrene, 1712-69-2; *p*-methoxystyrene, 637-69-4; (*p*-methoxybenzyl)trimethylammonium tetrafluoroborate, 136033-67-5; α-methylstyrene, 98-83-9; styrene, 100-42-5; *p*-methylbenzyl chloride, 104-82-5; *p*-methylbenzyl bromide, 104-81-4; 4-methoxycumyl cation, 22666-71-3; 4-methoxyphenethyl cation, 18207-33-5; 4-methoxybenzyl cation, 29180-19-6; 4-methylcumyl cation, 20605-66-7; 4-methylphenethyl cation, 31042-87-2; 4-methylbenzyl cation, 57669-14-4; cumyl cation, 16804-70-9; phenethyl cation, 25414-93-1; bromide, 24959-67-9; methanol, 67-56-1.

[1] R. L. Jones, L. M. Dorfman, *J. Am. Chem. Soc. 96* (1974) 5715.
[2] L. M. Dorfman, R. J. Sujdak, R. Bockrath, *Acc. Chem. Res. 9* (1976) 352.
[3] Y. Wang, L. M. Dorfman, *Macromolecules 13* (1980) 63.
[4] R. A. McClelland, V. M. Kanagasabapathy, S. Steenken, *J. Am. Chem. Soc. 110* (1988) 6913.
[5] R. A. McClelland, F. Cozens, S. Steenken, *Tetrahedron Lett. 31* (1990) 2821.
[6] R. A. McClelland, N. Mathivanan, S. Steenken, *J. Am. Chem. Soc. 112* (1990) 4857.
[7] M. A. Ratcliff, J. K. Kochi, *J. Am. Chem. Soc. 93* (1971) 3112.
[8] B. Foster, B. Gaillard, N. Mathur, A. L. Pincock, J. A. Pincock, C. Sehmbey, *Can. J. Chem. 65* (1987) 1599.
[9] S. Steenken, R. A. McClelland, *J. Am. Chem. Soc. 111* (1989) 4967.
[10] G. A. Olah, C. U. Pittman, R. Waack, M. Doran, *J. Am. Chem. Soc. 88* (1966) 1488.
[11] J. Bartl, S. Steenken, H. Mayr, R. A. McClelland, *J. Am. Chem. Soc. 112* (1990) 6918.
[12] R. A. McClelland, V. M. Kanagasabapathy, N. Banait, S. Steenken, *J. Am. Chem. Soc. 111* (1989) 3966.
[13] a) G. P. Smith, A. S. Dworkin, R. M. Pagni, S. P. Zingg, *J. Am. Chem. Soc. 111* (1989) 525; b) S. Steenken, R. A. McClelland, *ibid. 112* (1990) 9648.
[14] H. Mayr, R. Schneider, B. Irrgang, C. Schade, *J. Am. Chem. Soc. 112* (1990) 4460.
[15] E. Gaillard, M. A. Fox, P. Wan, *J. Am. Chem. Soc. 111* (1989) 2180.

ACRL Toxin I: Convergent Total Synthesis of Its 3-Methyl Enol Ether from D-Glucose**

By *Frieder W. Lichtenthaler,** *Jürgen Dinges*, and *Yoshimasa Fukuda*

A pathogenic type of the fungus *Alternaria citri*, found host-specifically on rough lemon and Rangpur lime citrus species, produces a number of toxins, which cause a rapidly spreading, harvest-threatening necrosis (brown spot disease) on the leaves and fruits of infected plants.[1] The main component of this mixture of toxins and, at the same time, the substance with the highest biological activity is ACRL Toxin I (**1a**), which, after laborious isolation, was characterized as a light orange oil.[2, 3a] Since it is present as a mixture of keto and enol tautomers (^{1}H NMR) and, moreover, readily undergoes decarboxylation, **1a** is converted for convenience into the stable methyl enol ether **1b**. Intensive CD and NMR spectroscopic investigation of **1b**, together with X-ray structure analysis of the decarboxylation product, established its constitution and absolute configuration.[3]

Our strategy for the total synthesis of **1b** involves the preparation of enantiopure,[4] connective segments from D-glucose. The key feature of the retrosynthetic analysis was the expectation that the dihydro-α-pyrone ring could be introduced via a suitable acetoacetic ester derivative. Thus, the molecule was dissected into the segments **A**, **B**, and **C** (Scheme 1). The advantage of this segmentation is the possibility of carrying out a convergent reaction sequence, since both the twofold methyl-branched C_6 chain of synthon **A** and the adipaldehyde building block **B** are derivable—each in the correct absolute configuration—from the 1,2-acetonide of 3-deoxy-3-*C*-methyl-α-D-allofuranose (**2**), which, in turn, is accessible from D-glucose by a known route.

In order to synthesize the key starting material **2** on a scale of 50–100 grams, the diacetone glucose **3** was first oxidized with pyridinium dichromate/acetic anhydride.[5] The resulting ulose **5**, formed in practically quantitative yield, was converted into **4** by reaction with methyl(triphenyl)phosphonium bromide. Hydrogenation of **4** over Pd/C followed by

[*] Prof. Dr. F. W. Lichtenthaler, Dipl.-Ing. J. Dinges, Dr. Y. Fukuda[+]
Institut für Organische Chemie der Technischen Hochschule
Petersenstrasse 22, W-6100 Darmstadt (FRG)
[+] Research fellow on leave of absence from Meiji Seika Kaisha, Kawasaki, Japan (1988–1989).

[**] Enantiopure [4] Building Blocks from Sugars, Part 13. This work was supported by the Deutsche Forschungsgemeinschaft and the Fonds der Chemischen Industrie. Part 12: F. W. Lichtenthaler, *Zuckerindustrie (Berlin) 115* (1990) 762.

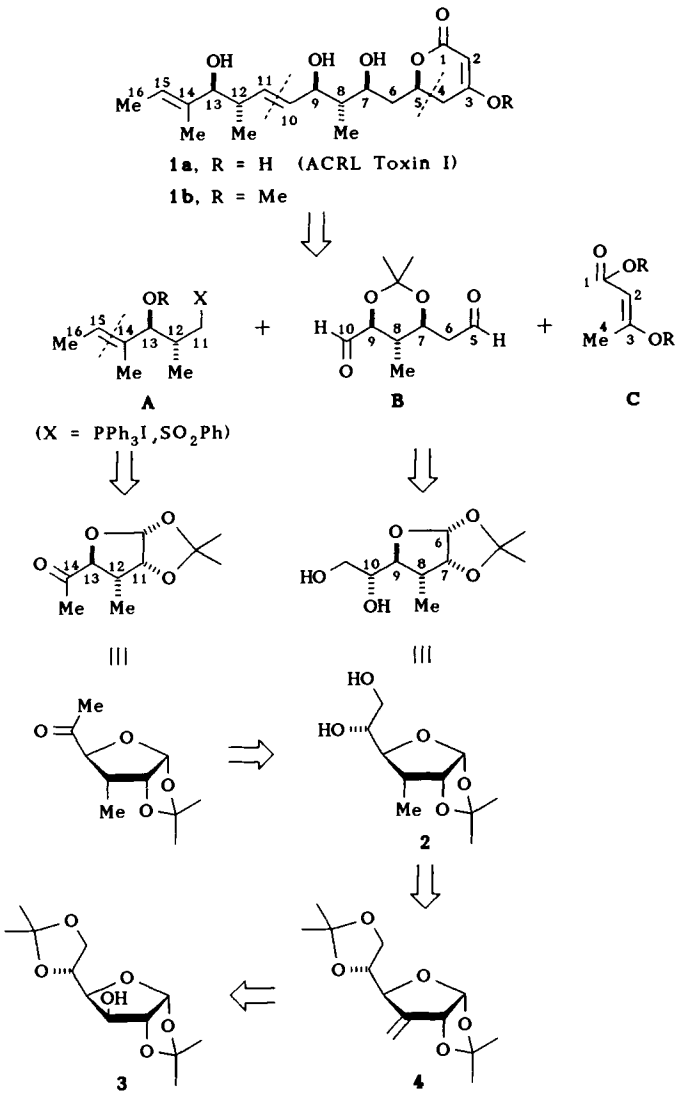

Scheme 1. Retrosynthetic analysis of the ACRL toxin I (**1a**) to D-glucose.

acid cleavage of the 5,6-isopropylidene group gave **2** (Scheme 2). This four-step process, optimized with respect to reaction conditions and procedure, affords an overall yield of 58% (previously 22%[6]).

The synthesis of the C_5–C_{10} building block **B** in an OH-protected form suitable for coupling at either end starts with the periodate oxidation of **2** followed by hydride reduction to give 3-deoxy-3-*C*-methyl-D-ribose (**6**), which was converted by benzoylation into the well-crystallizing **7**[7]—in contrast to **2** and **6**, characterizable only as syrups. The unmasking of the aldehyde group in **7** and its protection as the dithio acetal was smoothly accomplished with ethanethiol/conc. HCl at 0°C. The 1,3-diol thereby formed was immediately protected: acid-catalyzed acetonation smoothly led to the *O,O*-isopropylidene-blocked *S,S*-acetal **8** (syrup, $[\alpha]_D^{20}$ 13, $CHCl_3$, 92%). Alkylating hydrolysis of the *S,S*-acetal **8** by the methyl iodide/cadmium carbonate variant,[8] in this case, proved to be preparatively satisfactory (93%) for unmasking the aldehyde group to yield the suitably *O*-protected 3-*C*-methyl-3-deoxy-*aldehydo*-D-ribose **9**.[7] The C_1 extension required for conversion of **9** to the desired C_5–C_{10} segment **11** was accomplished by reaction with methylthiomethyl(triphenyl)phosphonium chloride/sodium amide to give the thio enol ether **10**, which was obtained as a 1:1 *E*/*Z* mixture and could be desulfurized in the presence of mercury salts. The synthesis of compound **11**[7] thus makes accessible the C_5–C_{10} fragment of ACRL Toxin I in a suitably functionalized, enantiopure form. Steps **2** → **6** and **7** → **8** can be carried out in a one-pot reaction, the overall yield for the eight-step synthesis of **11** being 33%.

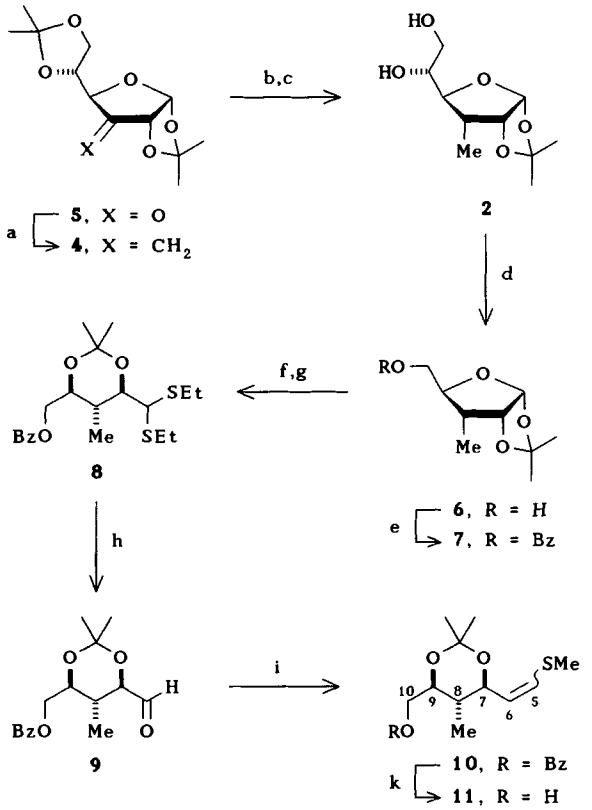

Scheme 2. a) $MePPh_3Br$, *n*BuLi, THF, 22°C, 2 h, 84%; b) H_2, 10% Pd/C, Et_3N, MeOH, 22°C, 5 h, 85%; c) 0.1 N H_2SO_4, MeOH, 22°C, 5 h, 84%; d) $NaIO_4$, C_2H_5OH/H_2O (2:1), 5°C, 30 min, then $NaBH_4$, 5°C, 30 min, 81%; e) BzCl, pyridine, 22°C, 2 h, 88%; f) conc. HCl, C_2H_5SH, 0°C, 6 h, 79%; g) *p*-TsOH, acetone/$Me_2C(OMe)_2$ (4:1), 22°C, 2 h, 92%; h) MeI, $CdCO_3$, acetone/H_2O (4:1), 22°C, 24 h, 93%; i) $MeSCH_2PPh_3$, $NaNH_2$, THF, 22°C, 2 h, 71%; k) 0.1 N NaOH, MeOH, 22°C, 3 h, 83%.

The C_{11}–C_{16} building block **B** (Scheme 1) can also be obtained from **2** in a suitably functionalized form (Scheme 3). Tosylation[9] of the primary hydroxyl group in **2** was accomplished in a highly regioselective fashion (93%). Subsequent hydride reduction (**12** → **13**) and oxidation with pyridium chlorochromate (PCC) on aluminum oxide[10] afforded **14** in a yield of 76% over the three steps. Olefination of the carbonyl group in **14** with ethyl(triphenyl)phosphonium bromide/butyllithium led to **15** as a 4.1:1 mixture of the *Z*/*E* isomers,[11] a ratio that can be shifted towards the *E* compound (→ 1:6.6) by light-induced diphenyl sulfide-aided isomerization. Thus, **15** was obtained as the pure *E* isomer (m.p. 35°C; $[\alpha]_D^{20}$ 26, $CHCl_3$) in 67% yield (based on **14**). Acid hydrolysis of the isopropylidene protecting group in **15**, subsequent periodate oxidation, hydride reduction of the aldehyde, and saponification of the resulting 3-formyl ester of **16** were performed in one continuous operation and afforded 2,4-dimethylhex-4-ene-1,3-diol (**6**)[7] in an overall yield of 77%. Compound **6** has the *S,S* configuration required for the C_{11}–C_{16} segment. Differentiation between the hydroxyl groups in **16** was accomplished by virtually re-

giospecific tosylation of the primary OH group (→ **17**) and protection of the secondary OH group as the *tert*-butyl dimethylsilyl ether **18**. Substitution of the tosyloxy group by iodine proceeded smoothly upon heating **18** with sodium iodide in butanone to give the distillable iodide **19** (b.p. 125 °C/0.04 Torr; 94%), which, on reaction with triphenylphosphane, afforded the C_{11}–C_{16} building block **20**,[7] suitable for subsequent Wittig reaction.

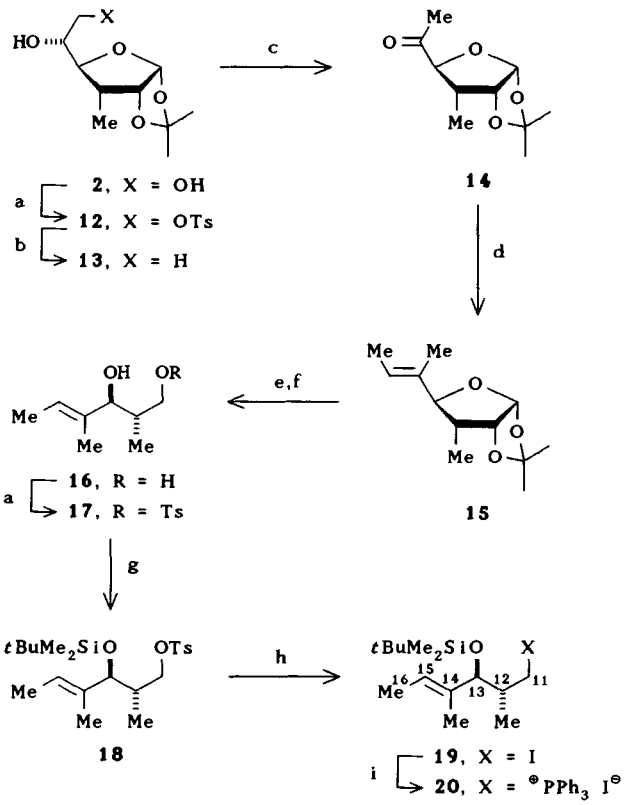

Scheme 3. a) *p*-TsCl, pyridine, 22 °C, 20 h, 93%; b) $LiAlH_4$, Et_2O, 35 °C, 3 h, 88%; c) PCC/Al_2O_3, NaOAc, CH_2Cl_2, 22 °C, 24 h, 93%; d) $C_2H_5PPh_3Br$, *n*BuLi, THF, 22 °C, 2 h, then $(PhS)_2$, *hv*, benzene, 22 °C, 30 min, 67%; e) 1.4 N H_2SO_4, dioxane, 22 °C, 2 d, 76%; f) $NaIO_4$, dioxane/H_2O (1:1), 5 °C, 2 h, then $NaBH_4$, dioxane, 0 °C, 2 h, and saponification of the formyl ester by $KHCO_3$, MeOH, 22 °C, 2 d, 77%; g) *t*$BuMe_2SiCl$, DMF, imidazole, 22 °C, 15 h, 92%; h) NaI, butanone, reflux, 8 h, 94%; i) PPh_3, 80 °C, 25 h, 65%.

The expectation that the phosphonium salt **20** would couple with the aldehyde **22** prepared from **11** by oxidation proved to be delusive. The ylide generated by treatment of **20** with butyllithium reacted with **22** as well as with a number of simple model aldehydes to give disappointingly complex mixtures. Even extensive variation of the reaction conditions did not improve the preparative outlook.[12] Since the Julia coupling[13] has proved itself superior to the Wittig reaction in a variety of cases,[14] the C_{11}–C_{16} fragment was generated as its phenylsulfone **21** by reaction of the tosylate **18** with thiophenol followed by oxidation. The coupling of the lithium derivative of **21** with model aldehydes, as well as with the C_5–C_{10} aldehyde **22**, proceeded smoothly; the diastereomeric β-acetoxysulfones initially formed after acetylation were transformed by subsequent sodium amalgam reduction into a 4:1 *E*/*Z* mixture (^{1}H NMR) of the two C_{10}–C_{11} olefins, from which the *trans E* isomer **23** (syrup, $[\alpha]_D^{20}$ 19, $CHCl_3$) could be separated in 70% yield (based on sulfone **21**) (Scheme 4).

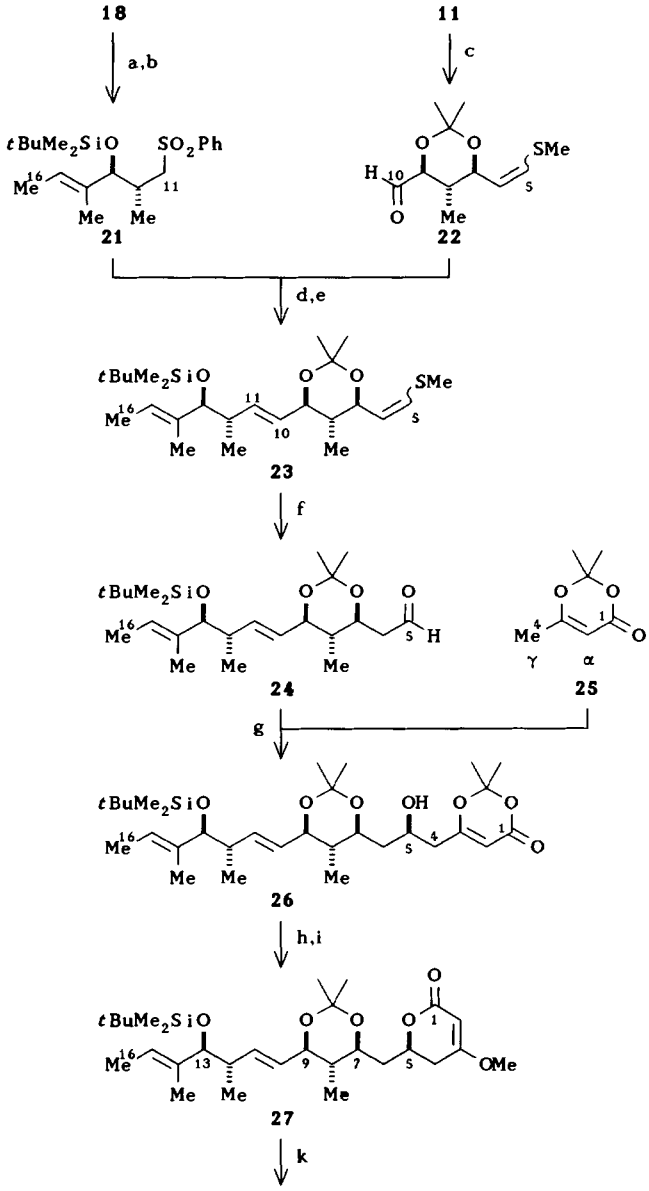

Scheme 4. a) PhSH, KO*t*Bu, DMF, 45 °C, 1 h, 75%; b) $(PhSe)_2$, H_2O_2, 15% CH_2Cl_2/Et_2O, 22 °C, 4 h, 89%; c) DMSO, $(COCl)_2$, CH_2Cl_2, −78 °C, 15 min, then Et*N*i-Pr_2, 90%; d) *n*BuLi, THF, −78 °C, 1 h, then Ac_2O, 22 °C, 90 min; e) 6% Na/Hg, MeOH/EtOAc (2:1), −30 °C, 17 h, 87% (for d + e); f) $HgCl_2$, HgO, acetone/H_2O, (2:1), 50 °C, 16 h, 65%; g) LDA, THF, −78 °C, 2 h, 35%, h) 0.1 N NaOH, MeOH, 22 °C, 2 h, then 2 N HCl to pH 5; i) $(MeO)_2SO_2$, K_2CO_3, acetone, 22 °C, 1 h, 24% (for h + i); k) 0.1 N H_2SO_4, EtOAc, 22 °C, 6 d, 71%.

For annelation of the C_1–C_4 unit as an acetoacetic ester derivative (building block **C** in Scheme 1), several standard methods were tested with respect to the diastereoselectivity of the addition to the carbonyl group of **24** as well as the α,γ regioselectivity in the acetoacetic ester. The obvious use of the acetoacetic ester dianion[15] under otherwise successful conditions[16] led, in the case of **24**, to complex mixtures; the same holds for attempts to add the bistrimethylsilyl enol ether[17] of acetoacetate to **24** in a $TiCl_4$-induced reaction. Likewise, extensive variations of reaction conditions successfully employed in other systems[18] led nowhere. At long last, in order to form the dihydro-α-pyrone ring, the inexpensive[19] trimethyl-1,3-dioxinone (**25**) was evaluated. Al-

though **25** has not been used previously for aldol additions, in two cases (pentyl iodide[20a] and chloroacetyl chloride[20b]) it gave terminal alkylation products. Reaction of **24** with the lithium enolate generated by deprotonation of **25** with lithium diisopropylamide (LDA) in THF at $-78\,^{\circ}C$ led to a mixture of the C_5-epimeric (ca. 2:1 in favor of **26**) γ and α adducts (3.5:1 according to ^1H NMR); the desired product **26** (syrup; $[\alpha]_D^{20} = -18$, $CHCl_3$) is surprisingly simple to obtain by chromatography in a yield of 45% (based on **24**). Although the aldol addition step **24** → **26** is still not preparatively satisfactory, current investigations with the menthone-protected, enantiopure acetoacetic ester analogues of **25**[21] indicate that better results are attainable with respect to the diastereoselectivity of carbonyl addition as well as the α, γ regioselectivity at the acetoacetic ester.

Alkaline saponification of the ester group in **26**, which, on acidification, spontaneously lactonizes, and standard methylation afforded a 64% yield of the 3-methyl enol ether **27** (Scheme 4), crystallizing as long needles. Compound **27** differs from **1b** only in two protecting functions. The X-ray structure analysis[22] (Fig. 1) established unequivocally the

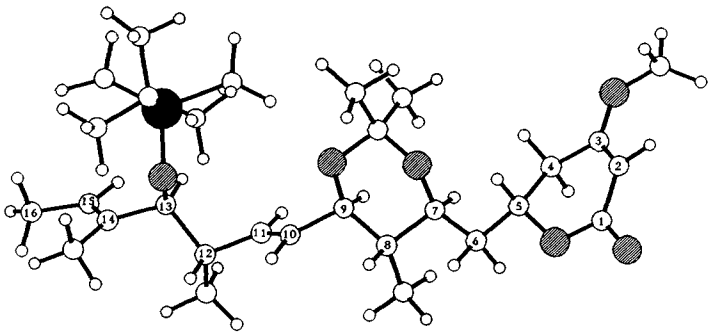

Fig. 1. Structure of the protected ACRL toxin **27** [22]. The O-1 atom and the C-5 atom lie 0.2 Å and 0.8 Å from the four-atom ring plane (C-1 to C-4) and thus the conformation of the dihydropyranone ring is between a boat ($B_{0,5}$) and an envelope (E_5).

structural and configurational integrity of the compound. Subsequent deprotection of **27**, cleavage of the silyl moiety, and hydrolysis of the acetal group was accomplished in one step by treatment with 0.1 N sulfuric acid at room temperature. The 3-methyl enol ether of ACRL toxin I (**1b**) was thereby obtained in 71% yield in crystalline form with an $[\alpha]_D^{20}$ value of -42 ($c = 1$, MeOH). The identity of synthetic **1b** with that obtained from the ACRL Toxin **1a**, characterized so far only as a syrup of $[\alpha]_D^{20} = -26$ ($c = 1$, MeOH),[3b] was established by ^1H and ^{13}C NMR spectroscopic and CD data;[3, 7] the higher optical rotation measured for the synthetic sample is undoubtedly due to its higher purity, which also induced the substance to crystallize.

Conclusion: A convergent synthesis has been developed for ACRL Toxin I as its stable enol ether **1b**; the C_5–C_{10} and C_{11}–C_{16} segments are prepared in an enantiopure form, suitable for coupling, from D-glucose, in both cases via the acetonide of 3-*C*-methyl-D-allose. The outcome of the synthesis is quite satisfactory: 16% overall yield for the thirteen steps from diacetone glucose to the C_5–C_{10} building block (as C_5 aldehyde) and 10% for the preparation of the C_{11}–C_{16} segment (as C_{11} sulfone) from the same starting material. The C_1–C_4 unit was introduced through an acetoacetic ester derivative; the connective steps were effected through Julia and aldol coupling, requiring another seven steps (15%) to the target molecule **1b**. This synthesis represents the first preparatively variable route to structures of type **1** and now enables the synthesis of analogues for the study of the largely unexplained toxin activity. Also noteworthy is an observation made during the synthesis: alkyl(triphenyl)phosphonium salts with a 3-alkoxy-4-ene group in the aliphatic portion of the molecule deprotonate abnormally and thus are unsuitable for a Wittig reaction, whereas the analogous phenylsulfones in the Julia coupling are not subject to this limitation.

Received: June 24, 1991;
revised: July 16, 1991 [Z 4745/6/7]
German version: *Angew. Chem. 103* (1991) 1385

CAS Registry numbers:
1b, 107655-60-7; **2**, 26291-75-8; **3**, 582-52-5; **4**, 21665-16-7; **5**, 2847-00-9; **6**, 30080-46-7; **7**, 59896-06-9; **8**, 136061-37-5; **9**, 136061-38-6; **10**(*E*), 136061-39-7; **10**(*Z*), 136172-04-8; **11**(*E*), 136061-40-0; **11**(*Z*), 136172-05-9; **12**, 56982-94-6; **13**, 114183-16-7; **14**, 114144-66-0; **15**(*E*), 136061-41-1; **15**(*Z*), 136172-06-0; **16**, 136061-42-2; **17**, 136061-43-3; **18**, 136061-44-4; **19**, 136061-45-5; **20**, 136061-46-6; **21**, 136088-41-0; **22**(*E*), 136061-47-7; **22**(*Z*), 136061-52-4; **23**(*E*), 136061-48-8; **23**(10-OAc, 11-SO_2Ph), 136061-53-5; **23**(*Z*), 136172-07-1; **24**, 136061-49-9; **25**, 5394-63-8; **26**, 136061-50-2; **27**, 136061-51-3; methyltriphenylphosphonium bromide, 1779-49-3; methylthiomethyltriphenylphosphonium chloride, 1779-54-0; ethyltriphenylphosphonium bromide, 1530-32-1; D-glucose, 50-99-7.

[1] J. O. Whiteside, *Plant Dis. Rep. 60* (1976) 326; K. Kohmoto, R. P. Scheffer, J. O. Whiteside, *Physiol. Biochem. 69* (1979) 667; K. Kohmoto, T. Kohguchi, Y. Kondoh, H. Otani, S. Nishimura, S. Nakatsuka, T. Goto, *Proc. Jpn. Acad. Ser. B61* (1985) 269; K. Akimitsu, K. Kohmoto, H. Otani, S. Nishimura, *Plant Physiol. 89* (1989) 925.

[2] ACRL: Abbreviation for *A*lternia *C*itri *R*ough *L*emon.

[3] a) J. M. Gardner, Y. Kono, J. H. Tatum, Y. Suzuki, S. Takeuchi, *Agric. Biol. Chem. 49* (1985) 1235; b) *Phytochemistry 24* (1985) 2861; c) Y. Kono, J. M. Gardner, K. Kobayashi, Y. Suzuki, S. Takeuchi, T. Sakurai, *ibid. 25* (1986) 69.

[4] After enantioselective, enantiospecific, enantio-enriched, and enantio-economic, the term enantiopure, in place of the longish enantiomerically pure, is a logically consistent term that we will use henceforth, although it will require some getting used to (cf. E. L. Eliel, S. H. Wilen, *Chem. Eng. News 68* (1990) No. 37, p. 2).

[5] F. Andersson, B. Samuelsson, *Carbohydr. Res. 129* (1984) C1.

[6] A. Rosenthal, M. Sprinzl, *Can. J. Chem. 47* (1969) 3941.

[7] All new compounds were characterized by elemental analyses and by ^1H (300 MHz, $CDCl_3$) and ^{13}C NMR spectra as well as mass spectra. For example, **7**: colorless crystals m.p. 49 °C; $[\alpha]_D^{20}$ 25 ($c = 2$, $CHCl_3$). ^1H NMR: $\delta = 1.16$ (d, 3H; 3-Me), 1.35, 1.54 (each 3H; CMe_2), 2.00 (ddq, 1H; 3-H), 4.08 (ddd, 1H; 4-H), 4.36 (dd, 1H; 5-H), 4.56 (dd, 1H; 5'-H), 4.59 (dd, 1H; 2-H), 5.85 (d, 1H; 1-H), 7.41–8.08 (m, 5H; C_6H_5); $J_{1,2} = 3.7$, $J_{2,3} = 4.5$, $J_{3,3\text{-Me}} = 6.8$, $J_{3,4} = 10.3$, $J_{4,5} = 5.4$, $J_{4,5'} = 2.7$, $J_{5,5'} = 12.2$ Hz. **9**: syrup, $[\alpha]_D^{20}$ 85 ($c = 1$, $CHCl_3$). ^1H NMR: $\delta = 1.02$ (d, 3H; 3-Me), 1.50 (s, 6H, CMe_2), 1.86 (ddq, 1H; 3-H), 3.91 (dd, 1H; 2-H), 3.92 (ddd, 1H; 4-H), 4.40 (dd, 1H; 5-H), 4.49 (dd, 1H; 5'-H), 7.43–8.07 (m, 5H; C_6H_5), 9.56 (d, 1H; 1-H); $J_{1,2} = 2.0$, $J_{2,3} = 11.0$, $J_{3,3\text{-Me}} = 6.6$, $J_{3,4} = 10.4$, $J_{4,5} = 4.9$, $J_{4,5'} = 2.6$, $J_{5,5'} = 12.0$ Hz. **14**: colorless oil, b.p. 107 °C/0.03 Torr; $[\alpha]_D^{20} = -56.3$ ($c = 1$, $CHCl_3$). ^1H NMR: $\delta = 1.16$ (d, 3H; 3-Me), 1.35, 1.51 (each 3H; CMe_2), 2.00 (ddq, 1H; 3-H), 2.22 (s, 3H; 6-H_3), 4.08 (d, 1H; 4-H), 4.58 (dd, 1H; 2-H), 5.91 (d, 1H; 1-H); $J_{1,2} = 3.5$, $J_{2,3} = 4.5$, $J_{3,3\text{-Me}} = 6.8$, $J_{3,4} = 10.6$ Hz. **16**: colorless crystals, m.p. 56 °C; $[\alpha]_D^{20}$ 19.3 ($c = 1$, $CHCl_3$). ^1H NMR: $\delta = 0.62$ (d, 3H; 2-Me), 1.55 (d, 3H; 4-Me), 1.55 (d, 3H; 6-H_3), 1.85 (dddq, 1H; 2-H), 2.62 (s, 1H; 3-OH), 3.22 (s, 1H; 1-OH), 3.57 (dd, 1H; 1-H), 3.64 (dd, 1H; 1'-H), 3.79 (d, 1H; 3-H), 5.40 (qq, 1H; 5-H); $J_{1,1'} = 10.8$, $J_{1,2} = 7.9$, $J_{1',2} = 3.6$, $J_{2,2\text{-Me}} = 7.0$, $J_{2,3} = 9.1$, $J_{4\text{-Me},5} = 0.8$, $J_{5,6} = 6.7$ Hz. **21**: syrup; $[\alpha]_D^{20} = -21$ ($c = 1$, $CHCl_3$). ^1H NMR: $\delta = 0.08$, -0.05 (each 3H; $SiMe_2$), 0.79 (s, 9H; *t*Bu), 0.99 (d, 3H; 2-Me), 1.52 (d, 3H; 4-Me), 1.56 (d, 3H; 6-H_3), 2.19 (ddq, 1H; 2-H), 2.80 (dd, 1H; 1-H), 3.66 (dd, 1H; 1'-H), 4.07 (d, 1H; 3-H), 5.33 (qq, 1H; 5-H), 7.56–8.04 (m, 5H; C_6H_5); $J_{1,1'} = 13.9$, $J_{1,2} = 10.5$, $J_{1',2} = 1.7$, $J_{2,2\text{-me}} = 6.8$, $J_{2,3} = 9.4$, $J_{5,6} = 6.9$, $J_{5,8} = 1.3$ Hz. **27**: colorless needles, m.p. 125 °C; $[\alpha]_D^{20} = -65$ ($c = 1$, $CHCl_3$). ^1H NMR: $\delta = -0.12$, -0.06 (2s, 6H; $SiMe_2$), 0.72 (d, 3H; 8-Me), 0.77 (d, 3H; 12-Me), 0.81 (s, 9H; *t*Bu), 1.31, 1.39 (2s, 6H; CMe_2), 1.48 (s, 3H; 14-Me), 1.49 (m, 1H, 8-H), 1.52 (d, 3H; 16-H_3), 1.94 (m, 2H; 6/6'-H), 2.28 (ddq, 1H; 12-H), 2.33 (dd, 1H; 4-H), 2.52 (ddd, 1H; 4'-H), 3.56 (d, 1H; 13-H), 3.63 (dd, 1H; 7-H), 3.69 (s, 3H; OMe), 3.80 (dd, 1H; 9-H), 4.59 (dddd, 1H; 5-H), 5.08 (d, 1H; 2-H), 5.24 (dd, 1H; 10-H), 5.27 (q, 1H; 15-H), 5.78 (dd, 1H; 11-H); $J_{2,4'} = 1.1$, $J_{4,4'} = 17.1$, $J_{4,5} = 3.9$, $J_{4',5} = 12.0$, $J_{5,6} = 6.7$, $J_{5,6'} = 4.8$, $J_{6,6'} = 9.5$, $J_{6,7} = 10.9$, $J_{6',7} = 4.8$, $J_{7,8} = 7.7$, $J_{8,8\text{-Me}} = 6.6$, $J_{8,9} = 9.9$, $J_{9,10} = 7.4$, $J_{10,11} = 15.5$, $J_{11,12} = 6.3$, $J_{12,12\text{-Me}} = 6.8$, $J_{12,13} = 8.1$, $J_{15,16} = 6.5$ Hz. **1b**: colorless crystals, m.p. 129–132 °C; $[\alpha]_D^{20} = -42$ ($c = 1$, MeOH); CD ($c = 1.0$, MeOH): $\lambda_{max} = 245$ nm, $\Delta\varepsilon = -8.86$. ^1H NMR: $\delta = 0.78$ (d, 3H; 8-Me), 0.82 (d, 3H; 12-Me), 1.59 (s, 3H; 14-Me), 1.62 (d, 3H; 16-H_3), 1.67 (ddq, 1H; 8-H), 1.90 (ddd, 1H; 6-H), 2.00 (ddd, 1H;

6'-H), 2.31 (ddq, 1H; 12-H), 2.51 (dd, 1H; 4-H), 2.54 (dd, 1H; 4'-H), 3.63 (d, 1H; 13-H), 3.74 (s, 3H; OMe), 3.80 (ddd, 1H; 7-H), 3.98 (dd, 1H; 9-H), 4.70 (dddd, 1H; 5-H) 5.13 (s, 1H; 2-H), 5.44 (q, 1H; 15-H), 5.47 (dd, 1H; 10-H), 5.55 (dd, 1H; 11-H); $J_{4,4'} = 16.8$, $J_{4,5} = 4.6$, $J_{4',5} = 10.3$, $J_{5,6} = 6.2$, $J_{5,6'} = 2.7$, $J_{6,6'} = 13.8$, $J_{6,7} = 8.4$, $J_{6',7} = 7.0$, $J_{7,8} = 7.3$, $J_{8,8\text{-Me}} = 7.0$, $J_{8,9} = 7.9$, $J_{9,10} = 7.3$, $J_{10,11} = 15.1$, $J_{11,12} = 7.7$, $J_{12,12\text{-Me}} = 6.9$, $J_{12,13} = 9.1$, $J_{15,16} = 6.7$ Hz.

[8] M. Fetizon, M. Jurion, *J. Chem. Soc., Chem. Commun. 1972*, 382; H. Redlich, B. Schneider, *Liebigs Ann. Chem. 1983*, 412.

[9] M. Kinoshita, S. Mariyama, *Bull. Chem. Soc. Jpn. 48* (1975) 2081.

[10] Y. S. Cheng, W. L. Liu, S. Chen, *Synthesis 1980*, 223.

[11] The isomeric ratio was determined by ^{1}H NMR spectroscopy by integration of the 4-H signals ($\delta_{4\text{-H,Z}} = 4.70$, $\delta_{4\text{-H,E}} = 4.04$) and their assignment was confirmed by NOE experiments.

[12] a) An approach to explaining these difficulties is provided by the finding that, on treatment with butyllithium in hexamethylphosphoramide (HMPA) or THF/HMPA at −78 °C in the absence of a carbonyl component, **20** affords the diphenylphosphane oxide (i) (m.p. = 92 °C, $[\alpha]_D^{20}$ − 5 ($CHCl_3$); 53%). This abnormal course of a phosphonium salt deprotonation, which has not been previously documented, is possibly due to the fact that deprotonation does not occur in a position α to phosphorus, but rather at the allylic C atom bearing the alkoxy group. This, together with participation of the 4,5 double bond, seemingly results in formation of the cyclic intermediate (ii); the subsequent elimination of benzene, without precedent at pentavalent phosphorus [12b], then leads, after aqueous workup, to the hydroxyphosphorane (iii), which undergoes cleavage of the P–C bond to give (i), thereby forming the best resonance-stabilized moiety [12c]. The abnormal course of the deprotonation seems to be limited to alkenyl(triphenyl)phosphonium salts with a 3-alkoxy-4-ene group in the aliphatic moiety. Compounds without 3-alkoxy groups undergo normal deprotonation and smoothly afford the desired olefination products [12d]; b) D. Seyferth, J. K. Heeren, W. B. Hughes Jr., *J. Am. Chem. Soc. 84* (1962) 1764; c) H. J. Bestmann, *Angew. Chem. 77* (1965) 609; *Angew. Chem. Int. Ed. Engl. 4* (1965) 583; d) see, e.g., H. J. Bestmann, K. H. Koschatzky, O. Vostrowsky, *Liebigs Ann. Chem. 1982*, 1478; J. Balsevich, *Can. J. Chem. 61* (1983) 1053; K. Sato, O. Miyamoto, S. Inoue, F. Furusawa, Y. Matsuhashi, *Chem. Lett. 1983*, 725.

[13] M. Julia, J. M. Paris, *Tetrahedron Lett. 1973*, 4833; P. J. Kocienski, B. Lythgoe, S. Ruston, *J. Chem. Soc. Perkin Trans 1, 1978*, 829; P. J. Kocienski, B. Lythgoe, I. Waterhouse, *ibid. 1980*, 1045.

[14] D. A. Evans, R. L. Dow, T. L. Shih, J. M. Takacs, R. Zahler, *J. Am. Chem. Soc. 112* (1990) 5290.

[15] J. F. Wolfe, T. M. Harris, C. R. Hauser, *J. Org. Chem. 29* (1964) 3249; S. N. Huckin, L. Weiler, *Tetrahedron Lett. 1971*, 4835; *Can. J. Chem. 52* (1974) 2157.

[16] H. Meyer, D. Seebach, *Justus Liebigs Ann. Chem. 1975*, 2261; T. Reffstrup, P. M. Boll, *Acta Chem. Scand. B30* (1976) 613; H. Achenbach, J. Witzke, *Z. Naturforschg. B35* (1980) 1459; Y. Tanabe, M. Miyakado, N. Ohno, H. Yoshioka, *Chem. Lett. 1982*, 1543; W. C. Groutas, T. L. Huang, M. A. Stanga, M. J. Brubaker, M. K. Moi, *J. Heterocycl. Chem. 22* (1985) 433.

[17] P. Brownbridge, T. H. Chan, M. A. Brook, G. J. Kang, *Can. J. Chem. 61* (1983) 688.

[18] H. Hagiwara, K. Kimura, H. Uda, *J. Chem. Soc. Chem. Commun. 1986*, 860; W. S. Johnson, A. B. Kelson, J. D. Elliot, *Tetrahedron Lett. 29* (1988) 3757.

[19] Fluka Chemie AG, Buchs, Schweiz.

[20] a) A. B. Smith, P. A. Levenberg, P. J. Jerris, R. M. Scarborough, Jr., P. M. Wovkulich, *J. Am. Chem. Soc. 103* (1981) 1501; b) S. Sakaki, Y. Sugita, M. Sato, C. Kaneko, *J. Chem. Soc. Chem. Commun. 1991*, 434.

[21] M. Demuth, A. Palomer, H.-D. Dhuna, A. K. Dey, C. Krüger, Y.-H. Tsay, *Angew. Chem. 98* (1986) 1093; *Angew. Chem. Int. Ed. Engl. 25* (1986) 1117.

[22] The X-ray structure analysis was performed by Prof. *H. J. Lindner*, Technische Hochschule Darmstadt.

mer-[Cr(CO)$_3$(η^4-norbornadiene)(η^2-ethene)]: A Key Compound in Understanding the Mechanism of the Photocatalytic Diene Hydrogenation with Chromium Carbonyl Complexes**

By *Dietmar Chmielewski, Friedrich-Wilhelm Grevels,* Jürgen Jacke,* and *Kurt Schaffner*

Dedicated to Professor Horst Prinzbach on the occasion of his 60th birthday

The photocatalytic hydrogenation of norbornadiene (NBD) with [Cr(CO)$_6$] or [Cr(CO)$_4$ (η^4-nbd)] as precursor of the catalytically active species[1–4] affords norbornene (NBN) and nortricyclene (NTC) in a ratio of about 1 : 3 (Scheme 1). Conjugated dienes undergo selective *cis* 1,4-hydrogenation.[5–8] Much work has addressed questions about the photochemical activation as well as the subsequent course of the reaction. The most recent IR spectroscopic results,[9,10] obtained both by conventional spectroscopy at low temperature in noble-gas matrices and in liquid noble gases and by time-resolved spectroscopy at room temperature, indicate that [Cr(CO)$_4$(η^4-nbd)] is transformed into *fac*- and *mer*-[Cr(CO)$_3$(η^4-nbd)] by photolytic detachment of CO. Both complex fragments[11] add hydrogen,[10] which is subsequently transferred to the norbornadiene ligand. This provides a plausible explanation for the formation of the two hydrogenation products (*mer* isomer, 1,2-hydrogenation → NBN; *fac* isomer, *homo* 1,4-hydrogenation → NTC; Scheme 2).

Scheme 1. Norbornene (NBN) and nortricyclene (NTC) are formed in a ratio of approximately 1 : 3. Norbornadiene = NBD.

Scheme 2.

We describe here the photochemical synthesis and the use of the thermally labile complex *mer*-[Cr(CO)$_3$(η^4-nbd)(η^2-ethene)] (**1**), whose ethene ligand is readily exchanged. Thus, **1** offers a potential source of the reactive [Cr(CO)$_3$ (η^4-nbd)] fragment, which, in turn, obviates the photochemical induc-

[*] Prof. Dr. F.-W. Grevels, Dipl.-Chem. D. Chmielewski, Dr. J. Jacke, Prof. Dr. K. Schaffner
Max-Planck-Institut für Strahlenchemie
Stiftstrasse 34–36, W-4330 Mülheim an der Ruhr (FRG)

[**] This work was supported by the Commission of the European Community (contract SCI-0007-C, EDB).

tion step. The catalytic hydrogenation of norbornadiene can then be carried out in the dark, thus affording deeper insight into the reaction mechanism.

Complex **1** is obtained in crystalline, analytically pure form by irradiation of $[Cr(CO)_4(\eta^4\text{-nbd})]$ in ethene-saturated solution at $-50\,^{\circ}C$, followed by workup below $-30\,^{\circ}C$ (Scheme 3). The structural assignment is supported by a comparison of the spectroscopic data with those of the analogous tungsten complex,[12] which was investigated by X-ray analysis. Solid **1** is stable for a limited period of time even at room temperature. Its lability is revealed in solution, where it decomposes above $-10\,^{\circ}C$ to give insoluble products and $[Cr(CO)_4(\eta^4\text{-nbd})]$. If other ligands are present (L = trimethylphosphite, *E*-cyclooctene, CO, ^{13}CO), they smoothly displace the coordinated ethene to form $[Cr(CO)_3(\eta^4\text{-nbd})(L)]$.

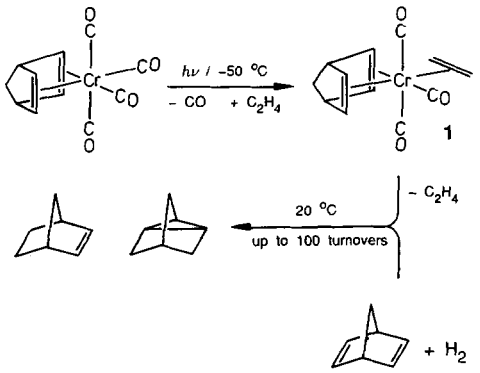

Scheme 3. Product distribution after catalysis: NBN : NTC = 1 : 3.2.

In H_2-saturated solution, **1** catalyzes the hydrogenation of norbornadiene present in excess. Without irradiation, roughly 100 turnovers take place for a substrate-to-catalyst ratio of 200 : 1, until catalysis ceases after about 2 h. The product distribution (NBN : NTC = 1 : 3.2) is nearly identical to that obtained in the photoinduced catalysis with $[Cr(CO)_4(\eta^4\text{-nbd})]$. Detachment of ethene from **1** seems to be the rate-determining step, since the gradual loss of catalytic activity parallels the decrease in concentration of **1** observable by IR spectroscopy. Complex **1** decomposes with formation of $[Cr(CO)_4(\eta^4\text{-nbd})]$ together with traces of $[Cr(CO)_6]$, both of which are catalytically inactive in the dark. When the reaction is performed with D_2 instead of H_2, *endo*-[D_2]NBN and [D_2]NTC are formed in a ratio of 1 : 2.2. Both this H/D isotope effect and the selective *endo* deuteration are consistent with the results of the photoinduced catalysis with $[Cr(CO)_4(\eta^4\text{-nbd})]$, which was carried out earlier by others[11] and was repeated by us.

Our results indicate that photolytic CO detachment from $[Cr(CO)_4(\eta^4\text{-nbd})]$ and loss of ethene from **1** generate the same catalyst system. Earlier suggestions that *cis*-vacant $[Cr(CO)_4$ (*endo*-η^2-nbd)] is the active species[2-4] in the formation of norbornene (NBN) are not supported by our results. Moreover, we have obtained no evidence that the *mer*-$[Cr(CO)_3]$ structure of **1** is retained in the active catalyst and thus could favor even transiently the 1,2-hydrogenation ($\rightarrow$ NBN). Instead, a rapid *mer*/*fac* rearrangement of the $[Cr(CO)_3(\eta^4\text{-nbd})]$ fragment presumably occurs, so that the catalysis affords the two products, NBN and NTC, in a constant ratio from the very beginning. It is unlikely, therefore, that the product ratio will be controllable by selective photochemical generation of *mer*- or *fac*-$[Cr(CO)_3(\eta^4\text{-nbd})]$.

Analogous conclusions apply to the hydrogenation of conjugated dienes,[5-8] as shown by catalytic experiments with **1** in which, instead of norbornadiene, isoprene was used as the substrate (Scheme 4). After displacement or hydrogenative release of the NBD ligand ($\rightarrow$ NBN : NTC = 1 : 3 to 1 : 3.5), the $[Cr(CO)_3]$ unit is available for hydrogenation of isopropene. Without irradiation, up to 15 turnovers took place. As observed in the photoinduced catalysis,[6] isoprene almost selectively undergoes 1,4-hydrogenation ($\rightarrow$ 2-methyl-2-butene), despite the *mer* structure of the $[Cr(CO)_3]$ skeleton in complex **1**. From this we conclude that the stereoselective photolytic formation of the *fac*-$[Cr(CO)_3(\eta^4$-1,3-diene)] fragment[13] is not a necessary condition for the photocatalytic selective 1,4-hydrogenation of conjugated dienes.

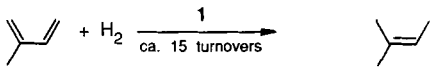

Scheme 4. The NBD contained in **1** is partly hydrogenated (NBD: NTC ≈ 1:3), partly displaced without hydrogenation.

With respect to the pressure dependence of the NBD hydrogenation,[4] the use of **1** also provides new insight. First of all, it should be noted that, by analogy with the photoinduced catalysis,[4] a high pressure of H_2 also favors the formation of norbornene when the reaction is carried out in the dark with **1** as catalyst (NBN : NTC = 1 : 1.4 under 50 bar H_2; a small amount of norbornane is also formed). When D_2 is used, the ratio of products formed under high pressure is likewise shifted in favor of 1,2-addition ([D_2]NBN : [D_2]NTC = 1 : 1.1 under 60 bar D_2; Scheme 5).

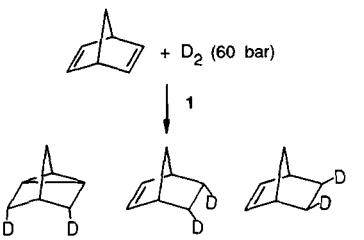

Scheme 5. [D_2]NTC *endo*-[D_2]NBN *exo*-[D_2]NBN

Surprisingly, however, the ^1H NMR spectrum of [D_2]NBN, isolated by preparative gas chromatography, reveals that exclusive *endo* 1,2-deuteration has not taken place here. Instead, a mixture of 52 % *endo* and 48 % *exo* 1,2-deuterated norbornene is present. This finding clearly shows that the increased formation of NBN under high pressure is not due to a favoring of the *mer*-$[Cr(CO)_3$ (η^4-nbd)] species over the *fac* species, but rather to an additional reaction path involving *exo* η^2-coordinated norbornadiene. Owing to the absence of the stabilizing chelate effect, an intermediate of this kind should have an considerably shorter lifetime compared with the above-mentioned species with η^4-NBD, in consequence of which this hydrogenation path becomes kinetically important only at higher H_2 or D_2 pressures.

The *mer*-$[M(CO)_3(\eta^4\text{-nbd})(\eta^2\text{-olefin})]$ complexes are generally more stable than the corresponding *fac* isomers because of the *trans*-orthogonal orientation of the olefin with respect to one of the C=C bonds of norbornadiene.[12] Identification of the *fac* isomer in the case of chromium complexes was achieved only with *E*-cyclooctene (ECO),

which has elsewhere[14] manifested a special coordination ability. Irradiation ($\lambda = 289$ nm) of [Cr(CO)$_4$(η^4-nbd)] and ECO in 2-methylpentane at $-40\,^\circ$C affords *mer*- and *fac*-[Cr(CO)$_3$(η^4-nbd)(η^2-eco)], which are easily distinguished on the basis of their CO stretching bands (*mer* complex, $\tilde{\nu}$[cm^{-1}] = 1997(m), 1925 (sst); *fac* complex $\tilde{\nu}$[cm^{-1}] = 1968, 1904, 1876). The *mer* complex, which is more stable, is the only observed product at room temperature. In order to determine the quantum yield ($\Phi = 0.18$ at 300 nm, 0.11 at 365 nm), its formation was followed quantitatively by IR spectroscopy. If this reaction is assumed to serve as a model for the generation of the catalytically active [Cr(CO)$_3$] complex (Φ_{ind}), then the relation $\Phi_{cat} = \Phi_{ind} \times$ (turnovers) gives a rough estimate of 10 to 20 for the quantum yield of the photocatalytic hydrogenation of norbornadiene (Φ_{cat}). The experimentally determined values (1.9,[2] ca. 0.3[4]) are considerably lower, probably because the active [Cr(CO)$_3$] complex generated in situ is rapidly transformed into inactive [Cr(CO)$_4$(η^4-nbd)] by the CO still present in the system.

The stability of [M(CO)$_3$(η^4-nbd)(η^2-olefin)] complexes increases markedly in the series Cr $\ll$ Mo $<$ W. As a result, the catalytically active species is trapped by excess substrate (NBD) as [M(CO)$_3$ (η^4-nbd)(η^2-nbd)] in the cases of tungsten and molybdenum.[10] The analogous chromium complex, by contrast, has not yet been detected. Thus, the drastic decrease in the catalytic activity in the series Cr $\gg$ Mo $>$ W[3] is readily explained.

In analogy to the hydrogenation, norbornadiene can also be hydrosilylated with silanes (R_3SiH), both photocatalytically with [Cr(CO)$_4$ (η^4-nbd)] and in the dark with **1**. As we will report in detail elsewhere, both variants afford *endo* 1,2-, *exo* 1,2-, and *homo* 1,4-adducts with comparable product distributions.

Experimental Procedure

Preparation of **1**: [Cr(CO)$_4$(η^4-nbd)] (1.00 g, 3.9 mmol) was irradiated in 200 mL of ethene-saturated pentane at $-50\,^\circ$C in an immersion lamp apparatus (Solidex glass, $\lambda \geq 280$ nm; Philips HPK 125-W Hg lamp) for about 3 h, until the starting material ($\tilde{\nu}_{CO}$ [cm^{-1}] = 2043, 1961, 1946, 1917) had largely reacted. The temperature was maintained at $\leq -30\,^\circ$C during workup. After addition of about 2 g of silica gel (to absorb readily decomposable by-products), the solution was stirred for several minutes and then evaporated to dryness under vacuum. The residue was extracted into 3 × 10 mL of ethene-saturated pentane, transferred to a column (silica gel 60, Merck; 2 × 15 cm), and eluted with additional solvent. The first of the two yellow fractions was concentrated under vacuum to about 50 mL and cooled to $-78\,^\circ$C, whereupon pure *mer*-[Cr(CO)$_3$(η^4-nbd)(η^2-ethene)] (0.46 g, 46%) crystallized out. M.p. = 46 °C; correct elemental analysis (C, H, Cr); IR (*n*-hexane): $\tilde{\nu}$[cm^{-1}] = 2005(m), 1933 (sst) (CO). ^{1}H NMR (400 MHz, C_7D_8, 243 K): $\delta = 0.85$ (m, 2 H), 1.85 (s, br, 4 H, ethene), 3.00 (s, br, 2 H), 3.16 (s, br, 2 H), 3.89 (s, br, 2 H). ^{13}C NMR (100.6 MHz, C_7D_8, 243 K): $\delta = 47.41$ (CH), 52.78 (ethene), 55.66 (CH), 59.95 (CH_2), 79.47 (CH), 229.45 (CO), 232.62 (2 CO). The second yellow fraction of the chromatographic run contained residual, unreacted starting material.

Catalytic hydrogenations with **1**: A solution of **1** (4–6 mM) and NBN (0.2–0.8 M) or isoprene in *n*-hexane (with addition of *n*-octane as internal standard) was prepared at $-35\,^\circ$C and hydrogen was admitted to the solution, which was warmed to room temperature and then stirred in the dark. Samples were treated with aqueous cerium(IV) ammonium nitrate solution to destroy the complex and then analyzed by gas chromatography. In pressure experiments, the precooled solution was sucked rapidly into a previously evacuated autoclave and H_2 or D_2 was admitted.

Received: May 6, 1991 [Z 4611 IE]
German version: *Angew. Chem. 103* (1991) 1361

CAS Registry numbers:
1, 124815-42-5; NBN, 498-66-8; NBD, 121-46-0; NTC, 279-19-6; [Cr(CO)$_4$($\eta^{3/4}$-nbd)], 12146-36-0; isoprene, 78-79-5; 2-methyl-2-butene, 513-35-9.

[1] G. Platbrood, L. Wilputte-Steinert, *Bull. Soc. Chim. Belg. 82* (1973) 733–735.
[2] G. Platbrood, L. Wilputte-Steinert, *J. Organomet. Chem. 70* (1974) 393–405.
[3] D. J. Darensbourg, H. H. Nelson, III, M. A. Murphy, *J. Am. Chem. Soc. 99* (1977) 896–903.
[4] a) M. J. Mirbach, D. Steinmetz, A. Saus, *J. Organomet. Chem. 168* (1979) C13–C15; b) M. J. Mirbach, T. N. Phu, A. Saus, *ibid. 236* (1982) 309–320.
[5] a) J. Nasielski, P. Kirsch, L. Wilputte-Steinert, *J. Organomet. Chem. 27* (1971) C13–C14; b) G. Platbrood, L. Wilputte-Steinert, *Tetrahedron Lett. 1974*, 2507–2508.
[6] M. Wrighton, M. A. Schroeder, *J. Am. Chem. Soc. 95* (1973) 5764–5765.
[7] a) G. Platbrood, L. Wilputte-Steinert, *J. Organomet. Chem. 70* (1974) 407–412; b) G. Platbrood, L. Wilputte-Steinert, *J. Mol. Catal. 1* (1975/76) 265–273.
[8] I. Fischler, M. Budzwait, E. A. Koerner von Gustorf, *J. Organomet. Chem. 105* (1976) 325–330.
[9] F.-W. Grevels, J. Jacke, W. E. Klotzbücher, K. Schaffner, R. H. Hooker, A. J. Rest, *J. Organomet. Chem. 382* (1990) 201–224.
[10] a) S. A. Jackson, P. M. Hodges, M. Poliakoff, J. J. Turner, F.-W. Grevels, *J. Am. Chem. Soc. 112* (1990) 1221–1233; b) P. M. Hodges, S. A. Jackson, J. Jacke, M. Poliakoff, J. J. Turner, F.-W. Grevels, *ibid. 112* (1990) 1234–1244.
[11] The occupation of the free coordination site by a solvent molecule is omitted for clarity.
[12] F.-W. Grevels, J. Jacke, P. Betz, C. Krüger, Y.-H. Tsay, *Organometallics 8* (1989) 293–298.
[13] W. Gerhartz, F.-W. Grevels, W. E. Klotzbücher, E. A. Koerner von Gustorf, R. N. Perutz, *Z. Naturforsch. B40* (1985) 518–523.
[14] a) F.-W. Grevels, V. Skibbe, *J. Chem. Soc. Chem. Commun. 1984*, 681–683; b) H. Angermund, F.-W. Grevels, R. Moser, R. Benn, C. Krüger, M. J. Romão, *Organometallics 7* (1988) 1994–2004; c) F.-W. Grevels, J. Jacke, W. E. Klotzbücher, S. Özkar, V. Skibbe, *Pure Appl. Chem. 60* (1988) 1017–1024.

The Mechanism of Interaction of Triplet 3-Methylcyclohex-2-en-1-one with Maleo- and fumarodinitrile: Evidence for Direct Formation of Triplet 1,4-Biradicals in [2 + 2] Photocycloadditions without the Intermediacy of Exciplexes**

By *David I. Schuster,* George E. Heibel, and Jan Woning*

Dedicated to Professor Kurt Schaffner on the occasion of his 60th birthday

The mechanism of [2 + 2] photocycloaddition reactions between cyclic enones and alkenes continues to be of interest.[1] There seems to be general agreement that triplet 1,4-biradicals are intermediates in these reactions.[1–5] However, the question of whether exciplexes of enone triplet excited states (T_1) and alkenes are precursors to the 1,4-biradicals remains unresolved.[6,7]

In acetonitrile, the high-energy triplets of acetophenone ($E_T = 73.8$ kcal mol^{-1}),[8] benzophenone ($E_T = 68.6$ kcal mol^{-1}),[8] and bicyclo[4.3.0]non-1(6)-en-2-one (BNEN, $E_T = 74$ kcal mol^{-1})[9] interact with maleo- (MN) or fumarodinitrile (FN, $E_T = 48$ kcal mol^{-1})[10] exclusively by energy transfer. Thus, in acetonitrile the T_1 state of BNEN is quenched by both FN and MN at the diffusion-controlled rate ($k_q = (4.5 \pm 0.7) \times 10^9$ M^{-1} s^{-1}).[11] Irradiation of these ketones in the presence of FN leads exclusively to *cis–trans* isomerization of the alkene. The MN:FN photostationary state ratios are 49:51, 48:52, and 44:56, respectively. No [2 + 2] cycloadducts could be detected in these systems. On

[*] Prof. D. I. Schuster, Dr. G. E. Heibel, Dr. J. Woning
New York University, Faculty of Arts and Science
Department of Chemistry
New York, NY 10003 (USA)

[**] This work was supported by the National Science Foundation (Grant CHE-890099). We thank Prof. *D. Wink* and Dr. *J. Dewan* for X-ray studies and Dr. *M. Barra* and Dr. *J. C. Scaiano* (National Research Council, Canada) for their cooperation in obtaining flash photolysis data.

the other hand, irradiation of conformationally flexible cyclohexenones ($E_T = 63-69$ kcal mol^{-1})[12] or cyclopentenone[12] in the presence of FN or MN gives rise to both *cis–trans* isomerization of the alkene and the formation of [2 + 2] cycloadducts.

We previously reported[6] that the rate constants for quenching of enone triplets by alkenes are higher for electron-poor than for electron-rich alkenes. This is inconsistent with the hypothesis of *Corey*[4] and *de Mayo*[5,13] that donor–acceptor complexes, with the alkene acting as the donor and the enone as the acceptor, are involved in the reaction. Such exciplexes have been invoked even in reactions involving electron-deficient alkenes.[1,4,5] However, the possibility that triplet energy transfer might be responsible for the high quenching rates observed with electron-poor alkenes could not be previously ruled out. Here we report new evidence that triplet 3-methylcyclohex-2-en-1-one (3-MCH) reacts with MN and FN to yield triplet 1,4-biradicals directly and that exciplexes of the type proposed by *Corey*[4] and *de Mayo*[5,13] are not involved in this system.

Irradiation of 3-MCH in the presence of either MN or FN gives four [2 + 2] cycloadducts, **1**–**4** (Scheme 1).[14] The

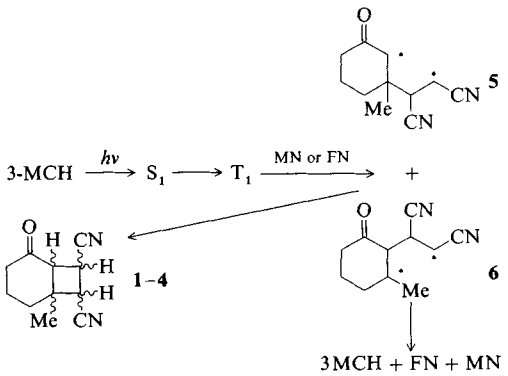

Scheme 1.

yields of these adducts increase linearly with the irradiation time (Fig. 1), while their ratio (**1**:**2**:**3**:**4** = 29:15:21:35) is

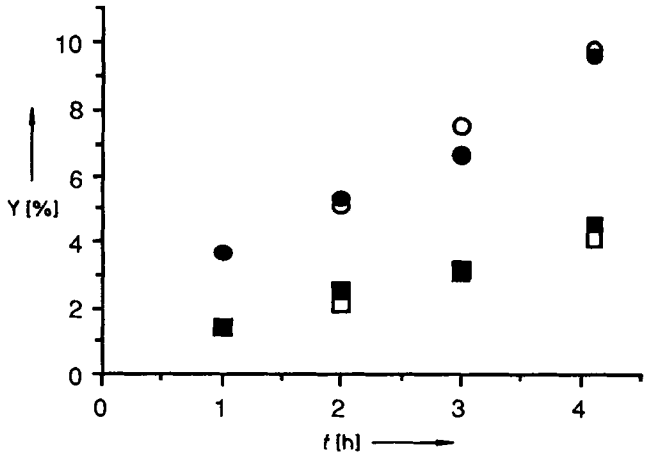

Fig. 1. Yield (Y) vs. time curves (GC) for **2** (squares) and **4** (circles) obtained from irradiations (300 nm, merry-go-round, max. 28% conversion) of 3-MCH (0.087 M) in the presence of stoichiometric quantities of FN (closed plot symbols) and MN (open plot symbols). Similar curves for **1** and **3** have been omitted for clarity.

independent of the conversion of the alkene (FN or MN) used. This indicates that the stereochemistry on the alkene moiety is completely lost in the course of the reaction. The loss of stereochemistry is also evident from the crystal structure (Fig. 2)[15] of the major [2 + 2] cycloadduct **4** originating from irradiation of 3-MCH and FN, which unambiguously establishes a *cis* configuration for the two CN groups.

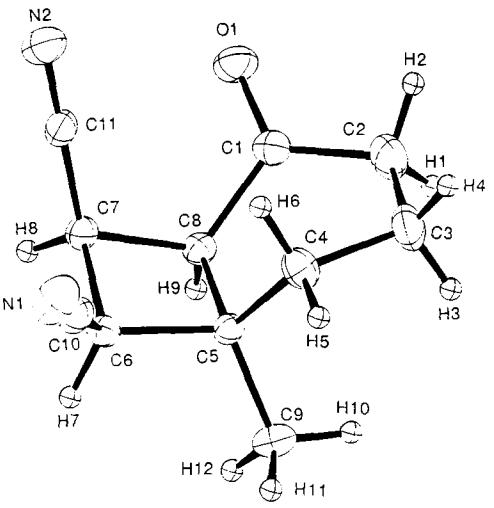

Fig. 2. The molecular structure of [2 + 2] cycloadduct **4** [15].

The quantum yields for adduct formation (Φ_{prod}) and alkene isomerization (Φ_{iso}) from 3-MCH in the presence of MN or FN are presented in Table 1.

Table 1. Rate constants (k_q) or quenching of 3-MCH by alkene and quantum yields [a] of **1**–**4** (Φ_{prod}), alkene isomerization (Φ_{iso}), and triplet capture (Φ_{tc}) from irradiation of 3-MCH and MN or FN in acetonitrile.

Alkene	k_q [M^{-1}s^{-1}]	Φ_{prod}	Φ_{iso}	Φ_{tc}	$\Phi_{tc} - \Phi_{prod}$
FN	$(5 \pm 1) \times 10^8$	0.28 ± 0.05	0.19 ± 0.04	0.95	0.67
MN	$(7 \pm 1) \times 10^8$	0.36 ± 0.06	0.42 ± 0.08	0.96	0.60

[a] Concentrations: 0.015 M (3-MCH), 0.5 M (alkene). Irradiation wavelength: 313 nm. Apparatus: PTI QUANTACOUNT, calibrated using the photochemical transformation of valerophenone (*n*-butyl phenyl ketone) into acetophenone in benzene ($\Phi = 0.33$).

The rate constants (k_q) for quenching of the 3-MCH triplet ($\tau_T = 75$ ns) by MN and FN in acetonitrile, determined by transient absorption spectroscopy,[16] are 7×10^8 and 5×10^8 M^{-1}s^{-1}, respectively. The quantum yields Φ_{tc} for

$$\Phi_{tc} = k_q[\text{alkene}] \times (\tau_T^{-1} + k_q[\text{alkene}])^{-1} \quad \text{(a)}$$

capture of 3-MCH triplets by MN and FN under the conditions stated in Table 1 are 0.96 and 0.95. The quantity Φ_{tc} is the sum of the quantum yields Φ_{bir} for formation of the 1,4-biradical intermediate and Φ_{et} for triplet energy transfer from the 3-MCH triplet. In addition to energy transfer from triplet 3-MCH, alkene isomerization can arise from reversion of the intermediate 1,4-biradicals **5** and **6** to ground-state 3-MCH and MN or FN. Depending on the extent of

this reversion, $\Phi_{prod} \leq \Phi_{bir}$. Therefore, the minimum value of Φ_{et} is zero and the maximum value is $\Phi_{tc} - \Phi_{prod}$.

The maximum quantum yields for biradical reversion to 3-MCH, FN, and MN equal $\Phi_{tc} - \Phi_{prod}$ and are collected in Table 1. These quantities would be reduced to the extent that concomitant alkene isomerization by triplet energy transfer occurs. From these data one can also calculate the minimum fraction F of intermediates (triplet adduct 1,4-biradicals or perpendicular 1,2-dicyanoethene triplets) which revert to FN. From the values of Φ_{iso} and $\Phi_{tc} - \Phi_{prod}$ given in Table 1 these fractions F are calculated to be 0.70 ($\Phi_{iso}/[\Phi_{tc} - \Phi_{prod}]$) and 0.72 ($[\Phi_{tc} - \Phi_{iso} - \Phi_{prod}]/[\Phi_{tc} - \Phi_{prod}]$) for the addition of MN and FN, respectively, to the 3-MCH triplet. The excellent agreement between these two values, and their deviation from the *cis–trans* decay ratio of ca. 1:1 for triplet-sensitized FN and MN isomerizations, provide strong evidence for the direct formation of a common set of rotationally equilibrated triplet 1,4-biradicals (**5** and **6**) in the photoreactions of 3-MCH with MN and FN. The fact that the stereochemistry on the alkene moiety is entirely lost in the course of formation of the cycloadducts **1**–**4** indicates that rotational equilibration in the intermediate triplet 1,4-biradicals is complete. This supports the conclusion that alkene isomerization predominantly, if not exclusively, arises from reversion of the biradicals **5** and **6**.

If one were to assume, for the sake of argument, that the isomerization of MN and FN induced by 3-MCH triplets occurs entirely by energy transfer, despite the large discrepancy observed in the *cis–trans* decay ratios, minimum rate constants $k_{add} = k_q \Phi_{prod}$ of 2.5×10^8 and 1.4×10^8 s^{-1} are derived for the addition of MN and FN, respectively, to triplet 3-MCH. These lower limits to k_{add} are two orders of magnitude larger than the rate constants[6] for interception of the T_1 states of 3-MCH and other enones by typical electron-rich alkenes. This finding is clearly inconsistent with the Corey–de Mayo exciplex hypothesis, according to which higher rate constants for the interception of enone triplets should be expected for the more electron-rich alkenes. In the present system the possible involvement of a reverse exciplex, with the electron-deficient enone triplet acting as the donor toward MN or FN, is improbable, but not rigorously ruled out by the experimental data. However, the high rate constants observed for addition of MN and FN to the 3-MCH triplet are completely consistent with formation of stabilized (by the neighboring CN group) triplet 1,4-biradicals **5** or **6** directly from the enone triplet. The fact that triplet energy transfer from 3-MCH to FN or MN does not occur despite the favorable energetics of this process remains puzzling. This could be an example of inefficiency in triplet energy transfer[17] due to twisting of the π system of the triplet donor 3-MCH,[9,18] since planar enone triplets such as BNEN are quenched by MN and FN at a diffusion-controlled rate by an energy-transfer mechanism.[11]

As stated previously,[2,6] direct physical evidence for the involvement of exciplexes in the mechanism of [2 + 2] photocycloaddition reactions of enones has not been forthcoming from studies using transient absorption spectroscopy[18] and time-resolved photoacoustic calorimetry.[9] In the present case and earlier studies,[6] photophysical data do not support the intermediacy of donor–acceptor enone–alkene exciplexes of the type repeatedly invoked in the literature concerning enone photocycloaddition to alkenes.[1,4,5] Although we do not dispute the heuristic value of the Corey–de Mayo exciplex hypothesis in rationalizing product ratios in such reactions, we note that all efforts to directly observe enone–alkene triplet exciplexes have failed thus far. Hence, the exciplex hypothesis should, in our opinion, be regarded with skepticism, at least until compelling experimental evidence supporting its validity is presented.

Experimental Procedure

1–**4**: A deaerated solution of 3-MCH (1.103 g, 10.0 mmol) and FN (782 mg, 10.0 mmol) in acetonitrile (50 mL) was irradiated (300 nm, Pyrex) to > 98% conversion. The solvent was evaporated and traces of 3-MCH, FN, and MN were thoroughly removed under vacuum. Purification of the remaining residue by column chromatography (silica gel, EtOAc–cyclohexane 1:3) afforded isomer **1** (250 mg, GC purity 99.3%) and two fractions containing **2** and **3** (1:2 ratio) and **3** and **4** (1:2 ratio), respectively. Slow evaporation of the solvent from the latter fraction afforded crystals (300 mg), which, upon repeated fractional crystallization from EtOAc–cyclohexane 4:1, gave single crystals of **4** containing < 6% of **3**.

Received: February 18, 1991;
revised: May 3, 1991 [Z 4449 IE];
Publication delayed at authors' request
German version: *Angew. Chem. 103* (1991) 1381

CAS Registry numbers:
4, 135911-49-8; 3-MCH, 1193-18-6; MN, 928-53-0; FN, 764-42-1; 6-methyl-2-oxobicyclo[4.2.0]octane-7,8-dinitrile, 135823-13-1.

[1] Reviews: a) S. W. Baldwin, *Org. Photochem. 5* (1981) 123; b) A. C. Weedon in W. M. Horspool (Ed.): *Synthetic Organic Chemistry*, Plenum, New York 1984, p. 61; c) H. A. J. Carless in J. D. Coyle (Ed.): *Photochemistry in Organic Synthesis*, Royal Soc. Chem., London 1986, p. 95; d) P. A. Wender, *ibid.*, p. 163.
[2] D. I. Schuster in S. Patai, Z. Rappoport (Eds.): *The Chemistry of Enones*, Wiley, Chichester 1989, p. 623.
[3] P. G. Bauslaugh, *Synthesis 1970*, 287.
[4] E. J. Corey, J. D. Bass, R. LeMahieu, R. B. Mitra, *J. Am. Chem. Soc. 86* (1964) 5570.
[5] P. de Mayo, *Acc. Chem. Res. 4* (1971) 41.
[6] D. I. Schuster, G. E. Heibel, P. B. Brown, N. J. Turro, C. V. Kumar, *J. Am. Chem. Soc. 110* (1988) 8261.
[7] G. Cruciani, H.-J. Rathen, P. Margaretha, *Helv. Chim. Acta 73* (1990) 856.
[8] J. C. Scaiano (Ed.): *CRC Handbook of Organic Photochemistry, Vol. I*, CRC Press, Boca Raton, Fl, USA 1989, pp. 376–378.
[9] D. I. Schuster, G. E. Heibel, R. A. Caldwell, W. Tang, *Photochem. Photobiol. 52* (1990) 645.
[10] J. A. Lavilla, J. L. Goodman, *Chem. Phys. Lett. 141* (1987) 149.
[11] J. Woning, D. I. Schuster, M. Barra, unpublished.
[12] G. E. Heibel, *Ph. D. Thesis*, New York University 1990.
[13] R. O. Loutfy, P. de Mayo, *J. Am. Chem. Soc. 99* (1977) 3559.
[14] **4** (See Fig. 2 for the numbering of the atoms): m.p. 133–137 °C. ^{1}H NMR (300 MHz, $CDCl_3$): $\delta = 3.81$ (t, J(H-7,H-8) = J(H-8,H-9) = 9.9 ± 0.4 Hz, 1 H; H-7), 3.32 (d, 1 H, H-7), 2.99 (d, 1 H; H-9), 2.72–2.19 (m, 4 H; H-1, H-2, H-5, H-6), 1.95–1.81 (m, 2 H; H-3, -4), 1.39 (s, 3 H, CH_3). ^{13}C NMR (75 MHz, $CDCl_3$): $\delta = 205.73$ (C-1), 115.15, 114.85 (*C*N), 50.12 (C-8), 43.88 (C-5), 39.41 (C-2), 34.94 (C-6), 31.33 (C-4), 27.71 (*C*H$_3$), 26.45 (C-7), 19.46 (C-3). MS (70 eV): m/z 188 ($M^{\oplus}$, 4%), 173 ($M^{\oplus} - CH_3$, 2), 118 ($M^{\oplus} - (CH_2)_3CO$, 4), 110 ($M^{\oplus}$ – NCCH = CHCN, 21), 82 ($M^{\oplus}$ – CO – NCCH=CHCN, 100). Correct C, H, N analysis. The ^{1}H, ^{13}C, and 2 D (COSY, NOESY) NMR data of **1**–**3** indicate that in two of these isomers the six-membered ring possesses a *trans* geometry, but they do not allow an unambiguous assignment of the stereochemistry of the CN groups.
[15] **4**: space group $P2_12_12_1$, $a = 9.710(7)$, $b = 15.452(5)$, $c = 6.488(4)$ Å, $V = 973(1)$ Å^3, $Z = 4$, 846 observed reflections ($I > 2\sigma(I)$, Rigaku AFC-6S diffractometer, $Mo_{K\alpha}$ radiation, ω scan). The refinement (C, N, O anisotropic, H isotropic) gave $R = 0.036$, $R_w = 0.040$. Further details of the crystal structure investigation are available on request from the Director of the Cambridge Crystallographic Data Centre, University Chemical Laboratory, Lensfield Road, GB-Cambridge CB2 1EW (UK), on quoting the full journal citation.
[16] These measurements were made at the National Research Council of Canada. For the experimental details, see: J. C. Scaiano, *J. Am. Chem. Soc. 102* (1980) 3559.
[17] J. C. Scaiano, W. J. Leigh, M. A. Meador, P. J. Wagner, *J. Am. Chem. Soc. 107* (1985) 5806.
[18] D. I. Schuster, D. A. Dunn, G. E. Heibel, P. B. Brown, J. M. Rao, J. Woning, R. Bonneau, *J. Am. Chem. Soc. 113* (1991) 6245.

6-Deoxy-6-*N*-histamino-β-cyclodextrin Copper(II) Complex, a New Enantioselective Receptor for Aromatic Amino Acids**

By *Giuseppe Impellizzeri, Giuseppe Maccarrone, Enrico Rizzarelli,* Graziella Vecchio, Roberto Corradini,* and *Rosangela Marchelli**

Cyclodextrins have been widely used as chiral discriminating agents in gas[1] and liquid[2] chromatography, either covalently bound to the stationary phase or as chiral additives to the eluent. Recently, β-cyclodextrins with both positive and negative charges on the C6 carbons of two adjacent glucose rings have shown enantioselective recognition of L- and D-tryptophan based on a three-point interaction (two polar sites and the hydrophobic cavity).[3]

However, other types of interactions, such as those occurring in ligand exchange chromatography (LEC),[4] can be exploited by chemically modifying the cyclodextrin structure. Accordingly, we have synthesized[5] 6-deoxy-6-*N*-histamino-β-cyclodextrin (β-CDhm), which was opportunely designed in order to coordinate transition-metal ions. β-CDhm was shown to form a 1:1 complex with a copper(II) ion,[5] giving rise to an ideal receptor site for the enantiomeric recognition of aromatic amino acids.

Here we report the direct HPLC enantiomeric resolution of D,L-tryptophan by using the copper(II) complex of β-CDhm as additive to the mobile aqueous phase in combination with a conventional achiral reversed-phase (RP-18) column. To obtain quantitative information about the interactions responsible for the chiral recognition, we have investigated the formation and the stability of the ternary complexes between copper(II), β-CDhm, and L- and D-trptophan, respectively, in aqueous solution by means of potentiometric and spectroscopic measurements (CD).

Indeed, baseline separation of D- and L-Trp was obtained by eluting with H_2O:MeOH (80:20) at pH 7.5 in the presence of Cu^{II} (β-CDhm), with an enantioselectivity factor $\alpha = 1.41$ (elution order $k'_D < k'_L$). In contrast, D,L-alanine was eluted much faster and was not separated. This can be regarded as the first example of mixed inclusion-ligand exchange chromatography for the separation of optical isomers. When β-CDhm was used in the mobile phase without the addition of copper(II) at pH 7.5, the reversed elution order was observed, suggesting that both inclusion and complexation at the metal ion were effective in the former case.

Furthermore, this seems to be one of the few examples in which the discrimination process occurs in the aqueous mobile phase, with the more strongly bound enantiomer eluting first. It is thus possible to approach the problem of enantioselectivity on the basis of molecular thermodynamics in aqueous solution.

Potentiometric titrations were carried out in aqueous solution with β-CDhm (L), Cu^{II}, and two amino acids (A), D- and L-Trp or D- and L-Ala, as a function of pH; three mixed species were detected: $[CuLAH_2]^{3\oplus}$, $[CuLAH]^{2\oplus}$, and $[CuLA]^{\oplus}$, whose stability constants are listed in Table 1. No

Table 1. Logarithm of the overall stability constants (lg β) [a] for the ternary complexes containing Cu^{II}, β-CDhm (L), and D- and L-amino acids (A) at 25 °C and $I = 0.1$ M (KNO_3).

$A^{\ominus}$	$[CuLAH_2]^{3\oplus}$	$[CuLAH]^{2\oplus}$	[CuLA]
L-Trp$^{\ominus}$	25.03(1)	20.78(1)	16.12(1)
D-Trp$^{\ominus}$	25.02(3)	20.82(2)	16.47(2)
L-Ala$^{\ominus}$	25.12(4)	20.68(3)	15.53(4)
D-Ala$^{\ominus}$	25.12(5)	20.67(5)	15.51(2)

[a] The generalized reaction for formation of the complexes is given by the following equation:

$$m\mathrm{Cu} + l\mathrm{L} + a\mathrm{A}^{\ominus} + h\mathrm{H}^{\oplus} \overset{\beta_{mlah}}{\rightleftharpoons} [\mathrm{Cu}_m\mathrm{L}_l\mathrm{A}_a\mathrm{H}_h]^{(m+h-a)\oplus}.$$

The stability constants for the simple complex with protons or copper(II) have been reported elsewere [5, 6] lg $K_{HL^{\oplus}} = 8.01$, lg $K_{H_2L^{2\oplus}} = 5.81$, lg $K_{AlaH} = 9.69$, lg $K_{AlaH_2^{\oplus}} = 2.44$, lg $K_{TrpH} = 9.37$, lg $K_{TrpH_2^{\oplus}} = 2.41$, lg $K_{CuL^{2\oplus}} = 7.26$, lg $K_{Cu(Ala)^{\oplus}} = 8.17$, lg $K_{Cu(Ala)_2} = 6.77$, lg $K_{Cu(Trp)^{\oplus}} = 8.29$, lg $K_{Cu(Trp)_2} = 7.13$.

enantioselectivity was observed for the $[CuLAH_2]^{3\oplus}$ and $[CuLAH]^{2\oplus}$ species for both amino acids, whereas a significant difference in the stability of the two mixed species was shown to occur only with tryptophan in the case of the $[CuLA]^{\oplus}$ species. In the last complex, both tryptophan and β-CDhm act as bidentate ligands, with the two amino groups most likely arranged in the *cis* position, as generally observed in the ternary complexes formed by histamine and other amino acids.[6] The relative stability is governed by the position of the aromatic side chain of tryptophan relative to the cyclodextrin cavity, so that inclusion may be allowed only for D-Trp and not for L-Trp (Fig. 1). In fact, the small bulk of the alanine side chain is irrelevant to the size of the cavity, so that there is neither discrimination in HPLC nor enantioselectivity in the ternary complex formation.

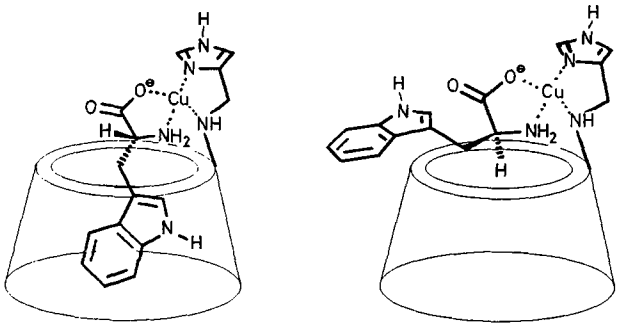

Fig. 1. Schematic model for the ternary complexes $[CuLA)^{\ominus}$ containing D- (left) and L-tryptophan (right).

Indeed, the D-Trp side chain experiences a more highly asymmetric environment than the L-Trp moiety, as evidenced by circular dichroism spectroscopy, both in the UV and in the visible regions (Fig. 2): at pH 7.5, both chromophores (Cu^{II} and the tryptophan aromatic side chain) showed an abnormal CD intensity enhancement for the ternary complex containing D-Trp, whereas much weaker effects were observed in the case of the L-Trp diastereomeric complex. The more favorable interaction of the D-Trp aromatic side chain with the cavity also drags the copper ion inside, thus enhancing the CD intensity of the d–d transitions compared to the corresponding ones in the binary $[Cu(\beta\text{-CDhm})]^{2\oplus}$ complex.

On the basis of these results, other experiments for estimating the different contributions to the process, as well as

[*] Prof. Dr. E. Rizzarelli, G. Impellizzeri, G. Maccarrone, G. Vecchio
Dipartimento di Scienze Chimiche dell'Università
and
Istituto per lo Studio delle Sostanze Naturali di Interesse Alimentare e Chimico Farmaceutico del CNR
Viale A. Doria 6, I-95125 Catania (Italy)
Prof. Dr. R. Marchelli, R. Corradini
Istituto di Chimica Organica dell'Università
Viale delle Scienze, I-43100 Parma (Italy)

[**] This work was partially supported by the Consiglio Nazionale delle Ricerche (Progetto Finalizzato Chimica Fine e Secondaria II).

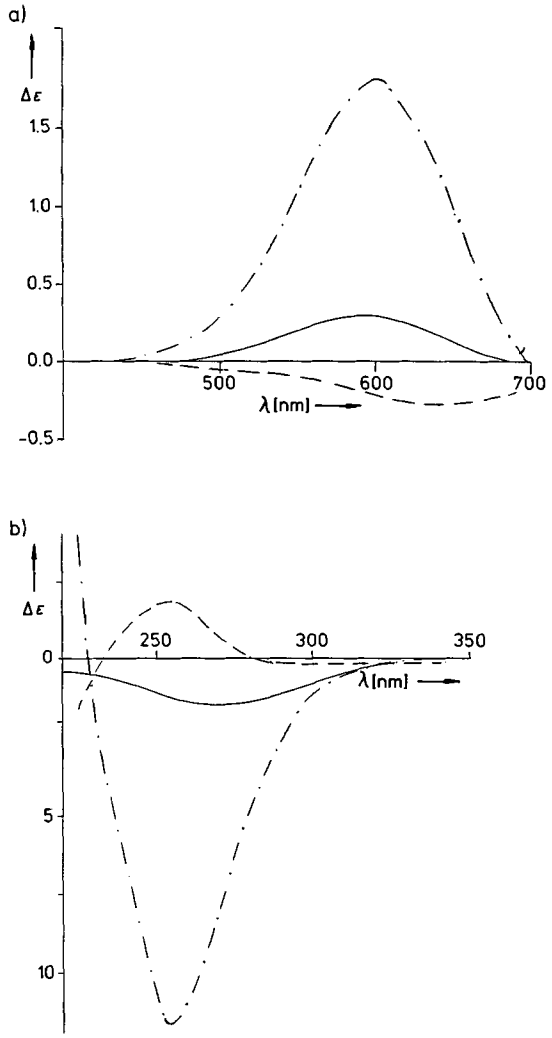

Fig. 2. Circular dichroism spectra in aqueous solution at pH = 7.5 in the visible (a) and UV region (b). — $[Cu(\beta\text{-CDhm})]^{2\oplus}$, - - - $[Cu(\beta\text{-CDhm})(L\text{-Trp}^{\ominus})]^{\oplus}$, -·-·- $[Cu(\beta\text{-CDhm})(D\text{-Trp}^{\ominus})]^{\oplus}$.

for determining whether the method can be extended to other amino acids, are warranted.

Experimental Procedure

β-CDhm was prepared from dried 6-*O*-(p-tosyl)-β-cyclodextrin [7] (1 g, 0.77 mmol), converted into the iodo derivative by reaction with NaI (10-fold excess) in anhydrous DMF (40 mL) at 90 °C for 5 h under stirring, then allowed to reacted with histamine (10-fold excess) in DMF at 60° for 24 h under nitrogen. After purification on CM-Sephadex C-25, β-CDhm was obtained with a total yield of 40%. β-CDhm was characterized by ^1H and ^{13}C NMR and by elemental analysis [5].

Chromatographic separations were performed on a Waters model 6000A HPLC pump, using a Radialpak C_{18} cartridge (10 × 0.8 cm) and a model 440 UV detector, set at 280 nm. The mobile phase was prepared as described previously [4c]. β-CDhm can be subsequently recovered from the eluent, after precipitation of copper(II) as CuS, by filtration and HPLC purification using a Technosphere 5 Amino (30 × 0.4 cm) column and a mixture of CH_3CN and water (1/1) as eluent.

Potentiometric titrations were carried out in aqueous solution by means of two fully automated computer-controlled meters (Metrohm E654) using a combined glass electrode (Metrohm 125). All potentiometric data were handled by the program SUPERQUAD [8].

CD Measurements were performed on a JASCO J-500A spectropolarimeter equipped with a DP-500N data processor.

Received: February 4, 1991
revised: May 29, 1991 [Z 4419 IE]
German version: *Angew. Chem. 103* (1991) 1363

[1] V. Schurig, H. P. Nowotny, *Angew. Chem. 102* (1990) 969; *Angew. Chem. Int. Ed. Engl. 29* (1990) 939.
[2] T. J. Ward, D. W. Armstrong, *J. Liq. Chromatogr. 9* (1986) 407.
[3] I. Tabushi, Y. Kuroda, T. Mizutani, *J. Am. Chem. Soc. 108* (1986) 4514.
[4] a) P. E. Hare, E. Gil-Av, *Science 204* (1979) 1226; b) V. A. Davankov, A. A. Kurganov, A. S. Bochkov, *Adv. Chromatogr. 22* (1983) 71; c) E. Armani, L. Barazzoni, A. Dossena, R. Marchelli, *J. Chromatogr. 441* (1988) 287.
[5] R. P. Bonomo, V. Cucinotta, F. D'Alessandro, G. Impellizzeri, G. Vecchio, E. Rizzarelli, *Inorg. Chem., 30* (1991) 2708.
[6] G. Borghesani, F. Pulidori, M. Remelli, R. Purello, E. Rizzarelli, *J. Chem. Soc. Dalton Trans. 1990*, 2095.
[7] I. Tabushi, N. Shimizu, T. Sugimoto, M. Shiozuka, K. Yamamura, *J. Am. Chem. Soc. 99* (1977) 7100.
[8] P. Gans, A. Sabatini, A. Vacca, *J. Chem. Soc. Dalton Trans. 1985*, 1195.

Competing Occurrence of Isomeric (Dialkyltartrato)zirconocene Dimers with Dimetallatricyclic and Ten-Membered Dimetallamonocyclic Frameworks**

By *Gerhard Erker,** *Stefan Dehnicke, Mathias Rump, Carl Krüger, Stefan Werner,* and *Matthias Nolte*

Dinuclear (dialkyltartrato)titanium alkoxides are starting substances for the generation of important enantioselective catalysts.[1] It is still an open question, however, whether the catalytically active species is derived only from the dimetallatricyclic structure type **1** found in the solid state[2, 3] or whether the isomeric ten-membered dimetallamonocyclic structure **2**[4] is also present in equilibrium. We have investigated the structure and dynamic behavior of (dialkyltartrato)zirconocenes as catalytically inactive model systems for **1**/**2** and have made a surprising observation.

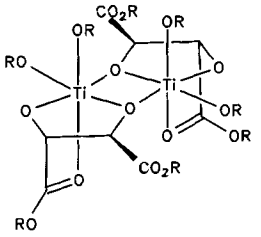

1

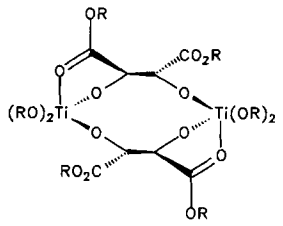

2

Reaction of (2*R*, 3*R*)-(+)-diisopropyl tartrate (**4a**) with dimethylzirconocene (**3**) results in loss of methane and dimerization to give the dimetallatricyclic complex **5a**. The dimetallatricyclic structure is confirmed in the solid state by the crystal structure analysis (Fig. 1) and in solution by the symmetry properties of the complex revealed by the low-temperature NMR spectra. For example, the ^1H NMR spec-

[*] Prof. Dr. G. Erker, Dipl.-Chem. M. Rump
Organisch-Chemisches Institut der Universität
Corrensstrasse 40, W-4400 Münster (FRG)
Dr. S. Dehnicke
Institut für Organische Chemie der Universität Würzburg
Prof. Dr. C. Krüger, Dipl.-Chem. S. Werner, Dipl.-Chem. M. Nolte
Max-Planck-Institut für Kohlenforschung, W-4330 Mülheim a. d. Ruhr (FRG)

[**] This work was supported by the Fonds der Chemischen Industrie, the Alfried Krupp von Bohlen und Halbach-Stiftung, and the Bundesminister für Forschung und Technologie.

trum (4.7 T) of **5a** at 233 K in CD_2Cl_2 shows two sets of signals for the methine protons of the isopropoxy groups at $\delta = 5.2$ and 4.9 in a ratio of 1:1; the framework methine protons (the protons of the CH(E)CH(E) unit, E = $-CO_2CHMe_2$) appear as an AX system at $\delta = 4.67$ and 4.17 ($^3J = 8.3$ Hz). When the monitoring temperature is raised, pairwise coalescence of the signals of the ester groups, as well as those of the framework methine protons, is observed. Above the coalescence temperature of 255 K, the framework methine protons appear as a singlet. An activation barrier of $\Delta G^{\neq} = 12 \pm 1$ kcal mol^{-1} at 255 K was estimated for the underlying exchange process from the temperature-dependent ^{1}H NMR spectra (C*H*(E) coalescence).

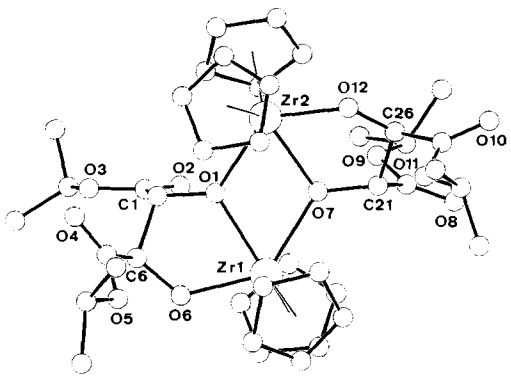

Fig. 1. Molecular structure of the dimetallatricyclic complex **5a**. Selected bond distances [Å] and angles [°]: Zr1-O1 2.239(5), Zr1-O6 2.066(6), Zr1-O7 2.268(5), Zr2-O1 2.244(6), Zr2-O7 2.258(5), Zr2-O12 2.032(6); C1-O1-Zr2 127.8(5), Zr1-O1-Zr2 113.7(2), Zr1-O1-C1 118.2(5), C21-O7-Zr1 127.2(5), Zr1-O7-Zr2 112.1(2), Zr2-O7-C21 116.8(5). Folding of the central Zr_2O_2 four-membered ring, 157°; angle of the Cp centroids with Zr1 and Zr2, 122.5 and 121.2°, respectively.

A quite analogous dynamic behavior in solution has long been known for the "Sharpless system" **1** ($\Delta G^{\neq} \approx 15$ kcal mol^{-1}).[2a, b] As in the case of our zirconocenes, it is also an open question there whether an inter- or an intramolecular equilibration is involved. Therefore, we allowed dimethylzirconocene to react with (2*S*, 3*S*)-(−)-diisopropyl tartrate to give *ent*-**5a**. ^{1}H NMR spectroscopy can be easily used to follow and to analyze kinetically the intermolecular exchange reaction of the monomeric five-membered metallacyclic complex *trans*-$Cp_2\overline{ZrOCH(E)CH(E)O}$, starting from the racemate prepared from the components **5a** and *ent*-**5a**, by monitoring the appearance of, for example, the singlet of the framework methine protons of the complex *meso*-**5a** at 268 K in CD_2Cl_2 (equilibrium *rac*-**5a**/*meso*-**5a** ≈ 1:1, $\Delta G^{\neq} = 21 \pm 1$ kcal mol^{-1} at 268 K).[5]

The products of the reaction of dimethyl tartrate (**4b**) with dimethylzirconocene behave analogously. At 233 K, the ^{1}H NMR spectrum of the optically active (dimethyltartrato)zirconocene dimer **5b** displays an AX spin system ($\delta = 4.81$, 4.11, $^3J = 9.5$ Hz) for the framework methine protons, which coalesces above 255 K to a singlet ($\Delta G^{\neq}_{intra} = 12 \pm 1$ kcal mol^{-1} at 262 K). The intermolecular exchange reaction **5b** + *ent*-**5b** ⇌ *meso*-**5b** proceeds about seven orders of magnitude slower ($\Delta G^{\neq}_{inter} = 20 \pm 2$ kcal mol^{-1} at 268 K).

The chiral (*rac*-**5a**, *rac*-**5b**) and achiral (*meso*-**5a**, *meso*-**5b**) diastereomeric (tartrato)zirconocene dimers show very different dynamic behavior. In the case of the racemic compounds (see above), the singlet of the framework methine protons ($\delta = 4.45$, *rac*-**5a**; $\delta = 4.56$, *rac*-**5b**) is split into an AX spin system on cooling, whereas, in the case of *meso*-**5a** and *meso*-**5b**, a corresponding intramolecular exchange process cannot be frozen out on the NMR time scale. Down to the lowest temperature attainable, the signals of the framework methine protons of the *meso* diastereomers remain unchanged ($\delta = 4.39$ (202 K), *meso*-**5a**; $\delta = 4.49$ (213 K), *meso*-**5b**). This simple stereochemical variation results, at least for the dimeric (dialkyltartrato)zirconocenes, in a dramatic change in the activation barrier for the intramolecular equilibration process; possibly, the diastereomers *rac*-**5** and *meso*-**5** have completely different structures. The NMR spectra of these *meso* compounds are fully consistent with a ten-membered dimetallacylic structure.

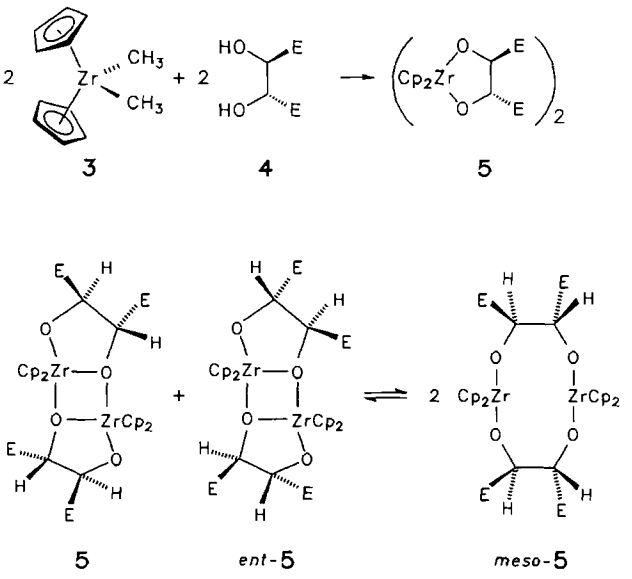

4,5: E = $-CO_2CHMe_2$ (a) ; $-CO_2CH_3$ (b)

For the chiral compound **5b**, obtained by reaction of dimethylzirconocene with (2*R*, 3*R*)-(+)-dimethyl tartrate, we demonstrated that external effects alone could cause a change in the preferred dimeric structure. The NMR spectra (see above) of **5b** indicate a C_2-symmetric dimetallatricyclic structure in solution (CD_2Cl_2). In the solid state, on the other hand, the ten-membered dimetallamonocyclic structure is favored, as shown by the crystal structure analysis of **5b** (Fig. 2, crystals from CH_2Cl_2).

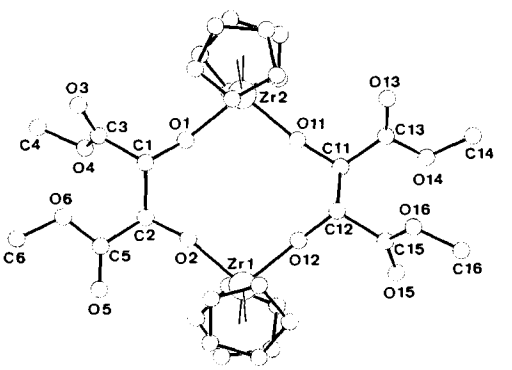

Fig. 2. Molecular structure of the ten-membered dimetallacyclic complex **5b**. Selected bond angles [°]: O2-Zr1-O12 99.4(2), O1-Zr2-O11 100.8(2)°. Angle of the Cp centroids with Zr1 and Zr2 126.7 and 127.4°, respectively.

In the crystal, **5b** displays a crown-shaped ten-membered ring framework. The ester groups are arranged pairwise in a nearly C_2-symmetric fashion. For both pairs, the Zr–O (carbonyl) distances are too large for an interaction (Zr1-O5, 3.88; Zr2-O3 4.48, Zr1-O15 4.18, Zr2-O13 4.00 Å). Noteworthy are the short bonds of the zirconium atoms to the ring oxygen atoms (Zr1-O2 1.952(3), Zr1-O12 1.952(8), Zr2-O11 1.941(3), Zr2-O1 1.974(6) Å) and the substantially increased Zr–O–C angles in the metallacycle (Zr1-O2-C2 152.9(2), Zr1-O12-C12 158.8(3), Zr2-O1-C1 148.2(2), Zr2-O11-C11 169.9(4)°). Accordingly, the formation of energetically favorable metal–oxygen π interactions can compensate for the energy difference between a ten-membered dimetallacyclic and the commonly observed dimetallatricyclic structure.[6]

If it is equally facile to effect the change between a ten-membered dimetallacyclic and a dimetallatricyclic structure through external influences in the case of the dinuclear (dialkyltartrato)titanium catalysts,[2, 3] then the question of the detailed structure of the active species in these important enantioselective catalyst systems is again open. Since, in such a case, it is problematic to draw conclusions about the structural parameters from direct observation, we are trying to obtain this information on modified catalyst systems in which stereochemical probes are incorporated.

Experimental Procedure

5a: Reaction of **3** (1.52 g, 6.04 mmol) with **4a** (1.39 g, 5.92 mmol) ($[\alpha]_D^{25}$ = + 17.0) in 80 mL of CH_2Cl_2 gave, after removal of the solvent and recrystallization twice from toluene, 2.50 g (93 %) of **5a**; m.p. 146–153 °C (dec.). $[\alpha]_D^{25}$ = + 28.0 (c = 0.82, CH_2Cl_2). Correct C, H analysis. ^{1}H NMR (200 MHz, CD_2Cl_2, 300 K): δ = 6.25 (s, 20 H; Cp), 5.09 (sept, 4H; $CHMe_2$), 4.45 (s, 4H; CH(metallacycle), 1.36 (d, 12 H; CH_3), 1.34 (d, 12 H; CH_3).

Crystal structure analysis of **5a**: $C_{40}H_{52}O_{12}Zr_2$, crystal size, 0.25 × 0.36 × 0.29 mm; M = 907.3, a = 9.692(1), b = 9.784(1), c = 21.105(2) Å, β = 93.88(1)°, V = 1996.9 Å^3, ϱ_{calcd} = 1.51 g cm^{-3}, μ = 5.71 cm^{-1}, Z = 2, space group $P2_1$, λ = 0.71069 Å, Enraf-Nonius CAD4 diffractometer, 4933 measured reflections ($\pm h, +k, +l$), $[(\sin\theta)/\lambda]_{max}$ = 0.65 Å^{-1}, 4803 independent and 4439 observed reflections ($I > 2\sigma(I)$), 487 refined parameters, R = 0.053, R_w = 0.062, residual electron density 1.82 e Å^{-3}.

ent-**5a**: Reaction of **3** (1.72 g, 6.84 mmol) and *ent*-**4a** (1.60 g, 6.84 mmol) ($[\alpha]_D^{25}$ = − 16.5) gave 2.72 g (88 %) of *ent*-**5a**; m.p. 149–151 °C (dec.); $[\alpha]_D^{25}$ = − 28.2 (c = 0.93, CH_2Cl_2). Correct C, H analysis.

5b: Reaction of **3** (2.14 g, 8.51 mmol) and **4b** (1.52 g, 8.51 mmol) ($[\alpha]_D^{25}$ = + 21) gave 3.08 g (91%) of **5b**; m.p. 149 °C (dec.); $[\alpha]_D^{25}$ = +6.5 (c = 1.11, CH_2Cl_2). Correct C, H analysis. ^{1}H NMR (200 MHz, 300 K, CD_2Cl_2): δ = 6.24 (s, 20 H; Cp), 4.56 (s, 4 H; CH) 3.71 (s, 12 H; CH_3) ^{13}C NMR (50 MHz, 300 K, CD_2Cl_2): δ = 173.9 (C=O), 112.9 (Cp), 84.8 (CH), 52.0 (OCH_3). Crystal structure analysis of **5b**: $C_{32}H_{36}O_{12}Zr_2$; crystal size, 0.39 × 0.49 × 0.49 mm, M = 795.1, a = 8.222(1), b = 18.842(2), c = 11.240(1) Å, β = 107.85(1)°, V = 1657.4 Å^3, ϱ_{calcd} = 1.59 g cm^{-3}, μ = 6.76 cm^{-1}, Z = 2, space group $P2_1$, λ = 0.71069 Å, Enraf-Nonius CAD4 diffractometer, 4092 measured reflections ($\pm h, +k, +l$), $[(\sin\theta)/\lambda]_{max}$ = 0.65 Å^{-1}, 3892 independent and 3805 observed reflections ($I > 2\sigma(I)$), 416 refined parameters, R = 0.022, R_w = 0.029, residual electron density 0.22 e Å^{-3}. Further details of the crystal structure investigations are available on request from the Fachinformationszentrum Karlsruhe, Gesellschaft für wissenschaftlich-technische Information mbH, W-7514 Eggenstein-Leopoldshafen 2, (FRG) on quoting the depository number CSD-55411, the names of the authors, and the journal citation.

ent-**5b**: Reaction of **3** (1.34 g, 5.34 mmol) and *ent*-**4b** (0.95 g, 5.34 mmol) ($[\alpha]_D^{25}$ = − 21) gave 2.12 g (quant.) of *ent*-**5b**; correct C, H analysis; m.p. 149 °C (dec.); $[\alpha]_D^{25}$ = − 6.1 (c = 0.95, CH_2Cl_2).

Received: May 21, 1991 [Z 4637 IE]
German version: *Angew. Chem. 103* (1991) 1371

[1] a) T. Katsuki, K. B. Sharpless, *J. Am. Chem. Soc. 102* (1980) 5974; b) M. Hayashi, T. Matsuda, N. Oguni, *J. Chem. Soc. Chem. Commun. 1990*, 1364.

[2] Proposals for the dinuclear catalytically active species: a) M. G. Finn, K. B. Sharpless, in J. D. Morrison (Ed.): *Asymmetric Synthesis, Vol. 5*, Academic Press, New York 1985, p. 247; b) S. S. Woodard, M. G. Finn, K. B. Sharpless, *J. Am. Chem. Soc. 113* (1991) 106; M. G. Finn, K. B. Sharpless, *ibid. 113* (1991) 113; c) I. D. Williams, S. F. Pedersen, K. B. Sharpless, S. J. Lippard, *ibid. 106* (1984) 6430; S. F. Pedersen, J. C. Dewan, R. R. Eckman, K. B. Sharpless, *ibid. 109* (1987) 1279; d) K. A. Jorgensen, R. Wheeler, R. Hoffmann, *ibid. 109* (1987) 3240; e) C. Puchot, O. Samuel, E. Dunach, S. Zhao, C. Agami, H. B. Kagan, *ibid. 108* (1986) 2353.

[3] An opposing proposal has been given: E. J. Corey, *J. Org. Chem. 55* (1990) 1693. See also: S. Takano, Y. Iwabuchi, K. Ogasawara, *J. Am. Chem. Soc. 113* (1991) 2786.

[4] K. B. Sharpless, S. S. Woodard, M. G. Finn, *Pure Appl. Chem. 55* (1983) 1823. See also: R. B. Ortega, R. E. Tapscott, C. F. Campana, *Inorg. Chem. 21* (1982) 672; P. G. Potvin, P. C. C. Kwong, M. A. Brook, *J. Chem. Soc. Chem. Commun. 1988*, 773; P. G. Potvin, P. C. C. Kwong, R. Gau, S. Bianchet, *Can. J. Chem. 67* (1989) 1523.

[5] A similar exchange experiment with labeled ("two-dimensionally chiral") metallacyclic (catecholato)zirconocenes: G. Erker, R. Noe, *J. Chem. Soc. Dalton Trans. 1991*, 685.

[6] D. W. Stephan, *Organometallics 9* (1990) 2718; T. T. Nadisdi, D. W. Stephan, *Can. J. Chem. 69* (1991) 167; see for comparison: J. C. Huffman, K. G. Moloy, K. G. Caulton, *Inorg. Chem. 27* (1988) 2190; B. Bachand, J. D. Wuest, *Organometallics 10* (1991) 2015.

Bis(hydroperoxy)naphthaldiimide as a "Photo-Fenton Reagent": Sequence-Specific Photocleavage of DNA

By *Seiichi Matsugo, Shosuke Kawanishi, Koji Yamamoto, Hiroshi Sugiyama, Teruo Matsuura,* and *Isao Saito**

Dedicated to Professor Kurt Schaffner on the occasion of his 60th birthday

In view of the high level of interest in the role of the hydroxyl radical (HO•) in biological systems,[1] several approaches toward the development of efficient methods for HO• generation without using transition-metal ions and hydrogen peroxide have been investigated.[2, 3] Our objectives are to design an efficient organic precursor that generates pure HO• by low-energy irradiation, such as long-wavelength UV (>350 nm) or visible light irradiation. Such molecules, referred to as "photo-Fenton reagents", are particularly attractive as a controllable and mechanistically less complicated HO• source for applications in a number of biologically important reactions such as cross-linking of biopolymers[4] and cleavage of DNA[5] and proteins.[6] The design criteria include the ease of synthesis, stability at ambient temperature, solubility in aqueous solvents, and ability to produce free HO• by irradiation with long-wavelength light. Our initial studies have indicated that hydroperoxyphthalimides can photogenerate HO• upon irradiation at λ > 280 nm.[3] In the present work, a naphthaldiimide derivative bearing a symmetrical bis-hydroperoxy group was designed in order to improve the efficiency of HO• generation per molecule and to enhance the absorption at longer-wavelengths. It acts as an effective photogenerator of HO• and can induce sequence-specific cleavage of duplex DNA at the 5′ site of 5′-GG-3′ sequences.

Bis(hydroperoxide) **1** was prepared from the corresponding dimethyl ketal **2** by treatment with excess ethereal hydro-

[*] Prof. Dr. I. Saito, Dr. H. Sugiyama, Prof. T. Matsuura
Department of Synthetic Chemistry, Faculty of Engineering
Kyoto University
Kyoto 606 (Japan)
Dr. S. Matsugo
Kobe University of Mercantile Marine
Kobe 658 (Japan)
Dr. S. Kawanishi, K. Yamamoto
Department of Public Health, Faculty of Medicine
Kyoto University
Kyoto 606 (Japan)

gen peroxide in the presence of triflic acid (1 equivalent) in dichloromethane at 0°C followed by recrystallization (67%). The thermally stable hydroperoxide **1**[7] was soluble in aqueous organic solvents (up to 0.25 mM in acetonitrile–water 8:92) and exhibited a strong absorption at 377 nm (lg $\varepsilon = 4.45$).

Photolysis of **1** in acetonitrile at 366 nm under nitrogen proceeded rapidly to give the ester **3** quantitatively with a quantum yield of $\Phi = 0.18$.[8] In the presence of adamantane (5 equivalents) as HO• acceptor, 1-adamantanol, 2-adamantanol, and adamantanone were obtained in 30, 15, and 6% yields, respectively, based on **1**, and their formation was inhibited by addition of an HO• scavenger such as dimethyl sulfoxide. Generation of HO• during this photodecomposition was confirmed by an ESR spin trapping method using 4,5-dihydro-5,5-dimethyl-3*H*-pyrrole-*N*-oxide (DMPO).[3] Upon brief exposure of a solution of **1** (100 μM) and DMPO (1.5 mM) in sodium cacodylate buffer (pH 7.0) to 366-nm light, intense ESR signals (1:2:2:1 four-line pattern, $a_N = a_H = 14.8$ G, $g = 2.0058$) characteristic of a hydroxyl radical–DMPO adduct[9] were detected. Exclusive formation of **3** accompanied by HO• generation is consistent with a mechanism involving γ-hydrogen abstraction by the naphthalimide carbonyl followed by β cleavage of the labile O–O bond of the biradical **4**,[10] and cannot be explained by direct homolysis of the O–O bond initiated by intramolecular energy transfer from the photoexcited naphthaldiimide chromophore.[3]

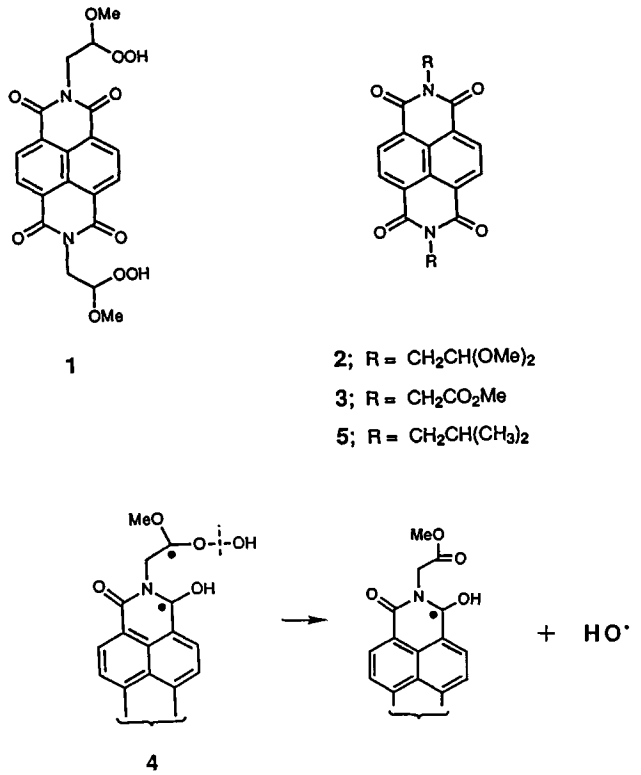

We have examined the strand scission of DNA in the presence of **1** by using supercoiled circular φX174RFI DNA (form I). Single-strand breaks and a small amount of double-strand breaks at higher conversion were observed, as evidenced by the production of form II and form III DNA, respectively (Table 1). Addition of sodium benzoate as HO• scavenger to the reaction system considerably inhibited the DNA cleavage.[11] The base and sequence specificity of

Table 1. Cleavage of supercoiled circular ØX 174 RFI DNA (form I) into nicked circular (form II) and linear DNA (form III) by photoirradiation of **1** [a].

Conc. of **1** [μM]	% form I[b]	% form II[b]	% form III[b]
100	–	88.0	12.0
10	23.8	72.4	3.8
1	69.5	28.4	2.1
0 [c]	83.1	16.9	–

[a] The reaction mixtures containing 25 μM DNA (form I) and varying concentrations of **1** in 50 mM sodium cacodylate buffer (pH 7.0) were irradiated at a distance of 10 cm from the light source at 0°C for 20 min and analyzed by agarose gel electrophoresis. [b] The values were determined by densitometry reading after ethidium staining. [c] The DNA used contained a small amount of form II DNA.

DNA cleavage was analyzed by using ^{32}P-end-labeled DNA fragments obtained from human c-Ha-*ras*-1 protooncogene[12] (Fig. 1). Hydroperoxide **1** induced DNA strand cleavage preferentially at the 5′ site of 5′-GG-3′ sequences after piperidine treatment. No cleavage was observed at other sites, including single G residues. This is in marked contrast to the photocleavage of DNA mediated by singlet oxygen, where the cleavage occures equally at each G residue after piperidine treatment.[13] In control experiments, photoirradiation of the related naphthaldiimide derivatives **2** and **5** did not induce DNA cleavage, even after piperidine treatment. These results indicate the crucial role of the hydroperoxy group of **1** in the specific photocleavage and clearly eliminate the possibility of oxidative DNA cleavage with singlet oxygen generated from the photoexcited naphthaldiimide.

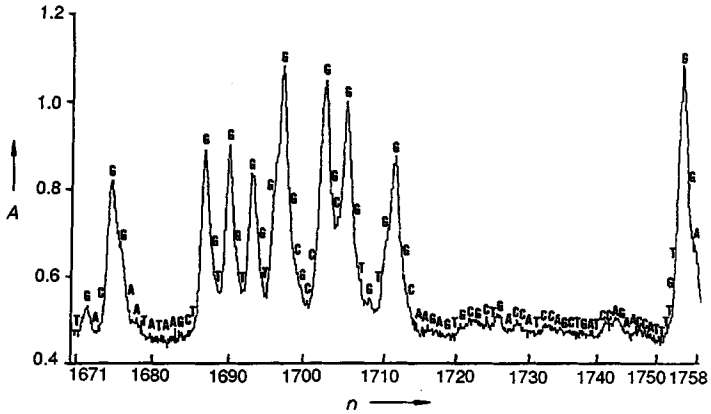

Fig. 1. Site specificity of the DNA cleavage in the photoirradiation of **1**. A solution containing the ^{32}P-5′-end-labeled 261-bp fragment (*Ava*I *1645-*Xba*I 1905) of human c-Ha-*ras*-1 protooncogene[12] and 10 μM of **1** in 50 mM sodium cacodylate buffer (pH 7.0) was photoirradiated for 20 min under the conditions shown in Table 1. After piperidine treatment (1 M, 90°C, 20 min) the DNA fragments were separated by electrophoresis on an 8% polyacrylamide/8 M urea gel. The relative amounts of oligonucleotides produced by the photoreaction and following piperidine treatment were measured by a laser densitometer. The horizontal axis shows the nucleotide number of the DNA fragment (from left to right, 5′ → 3′). *A* = absorption.

The DNA cleavage was enhanced approximately 10-fold upon treatment with piperidine at 90°C, suggesting that HO• reacts preferentially with the DNA base, particularly with the guanine base rather than the sugar backbone.[5c, d, e, 14] The cleavage of double-stranded DNA by HO• with piperidine treatment usually occurs at every nucleotide position with some preference for G and T.[5c, 15b] We therefore propose that the observed specific cleavage is a consequence of the selective binding of **1** to 5′-GG-3′ sequences.[16]

This method of HO• generation is very efficient and could be quite attractive for the use in applications requiring HO• in a number of other biological systems.

Received: March 5, 1991 [Z 4472 IE]
German version: *Angew. Chem. 103* (1991) 1343

CAS Registry numbers:
1, 133503-07-8; **2**, 136144-94-0; **3**, 136144-95-1; **5**, 136144-96-2; HO•, 3352-57-6.

[1] a) B. H. Bielski, J. M. Gebicki, *Free Radicals Biol. 1* (1977) 1; b) W. A. Pryor (Ed.): *Free Radicals in Biology, Vol. 1–4*, Academic Press, Orlando, FL, USA 1976–1978; c) B. Halliwell, M. C. Guntteridge, *Biochem. J. 219* (1984) 1; d) H. Sies: *Oxidative Stress*, Academic Press, New York 1985; e) D. Shulte-Frohlinde, K. Hildenbrand in F. Minisci (Eds.): *Free Radicals in Synthesis and Biology*, Kluwer, Dordrecht 1989, p. 335.

[2] For photolysis or radiolysis of water, see [1].

[3] I. Saito, M. Takayama, T. Matsuura, S. Matsugo, S. Kawanishi, *J. Am. Chem. Soc. 112* (1990) 883.

[4] a) S. A. Lesko, J. L. Drocourt, Y. Shu Uin, *Biochemistry 21* (1982) 5010; b) K. J. A. Davis, *J. Biol. Chem. 26* (1987) 9895; c) T. M. Rana, C. F. Meares, *Bioconjugate Chem. 1* (1990) 357.

[5] a) R. P. Herzberg, P. B. Dervan, *Biochemistry 23* (1984) 3934; b) J. D. Tullius, B. A. Dombroski, *Science 230* (1985) 679; c) S. Inoue, S. Kawanishi, *Cancer Res. 47* (1987) 6522; d) C. von Sonntag: *The Chemical Bases of Radiation Biology*, Taylor and Francis, London 1987, S. 221; e) R. Prigodich, C. T. Martin, *Biochemistry 29* (1990) 8017; f) D. P. Mack, J. P. Sluka, J. A. Shin, J. H. Griffin, M. I. Simon, P. B. Dervan, *ibid. 2* (1990) 6561.

[6] a) T. M. Rana, C. F. Meares, *J. Am. Chem. Soc. 112* (1990) 2457; b) A. Schepartz, B. Cuenoud, *ibid. 112* (1990) 3247; c) D. Hoyer, H. Cho, P. G. Schultz, *ibid. 112* (1990) 3249.

[7] M.p. 142–145 °C (dec.); UV: (CH_3CN) λ_{max} [nm] = 340 nm (lg ε = 4.20), 357 (4.38), 377 (4.45); ^{1}H NMR ($CDCl_3$): δ = 3.59 (s, 6H), 4.40 (dd, J = 2.8, 14 Hz, 2H), 4.67 (dd, J = 8.2, 14 Hz, 2H), 4.91 (dd, J = 2.8, 8.2 Hz, 2H), 8.85 (s, 4H), 9.56 (s, 2H, OOH); MS: m/z 446 ($M^{\oplus}$), 410.

[8] The quantum yield was determined by using phenylglyoxylic acid (ϕ = 0.72 at 365 nm) as an actinometer.

[9] E. Finkelstein, G. M. Rosen, E. J. Rauckman, *Arch. Biochem. Biophys. 20* (1980) 1.

[10] Intramolecular electron transfer from the methoxy group of the side chain would provide a similar biradical, **4**; see a) P. H. Mazzochi, *Org. Photochem. 5* (1981) 421; b) W. M. Horspool in J. D. Coyle (Ed.): *Photochemistry in Organic Synthesis*, Royal Society of Chemistry, London 1986, S. 61.

[11] Addition of sodium benzoate (1 mM) in the presence of 10 μM of **1** resulted in a complete inhibition of the formation of form III DNA with a diminished yield of form II DNA.

[12] K. Yamamoto, S. Kawanishi, *J. Biol. Chem. 264* (1989) 15435.

[13] a) T. Friedman, D. M. Brown, *Nucleic Acids Res. 5* (1978) 615; b) S. Kawanishi, S. Inoue, S. Sano, *J. Biol. Chem. 261* (1986) 6090; c) W. Blau, D. T. Croke, J. M. Kelly, D. J. McCornnell, C. OhUigin, W. J. M. Van der Putten, *J. Chem. Soc. Chem. Commun. 1987*, 751.

[14] The reactivity of hydroxyl radicals toward the ribose moiety, leading to direct DNA cleavage, is known to be considerably less than that toward the purine and pyrimidine bases [15].

[15] a) S. Steenken, *Chem. Rev. 89* (1989) 503; b) M. Dizdaroglu, O. I. Aruoma, B. Halliwell, *Biochemistry 29* (1990) 8447, and references therein.

[16] The binding constant of **1** to calf thymus DNA as measured by the equilibrium dialysis method was 1.50×10^4.

The Interaction of Tri-*tert*-butylgallium with White Phosphorus: Isolation of an Unusual Gallium Phosphorus Cluster**

By *Michael B. Power* and *Andrew R. Barron**

Despite the vast quantity of literature concerning compounds containing both group 13 and 15 elements, and their proposed relevance to electronic materials,[1] there has been surprisingly little variation in the chemistry of these compounds since they were first reported nearly 30 years ago.[2] Thus, the vast majority of the compounds fall into one of two classes of compound, i.e., $[MR_x(ER'_2)_{3-x}]_n$ (x = 0, 1, 2 and n = 1, 2, 3)[3] and $(RMER)_n$ (n = 2 → ∞)[4] where M is a group 13 metal, Al, Ga, or In and E is one of the group 15 elements N, P, As, or Sb. Two notable exceptions are the unusual gallium-arsenic and gallium-phosphorus clusters reported by the groups of *Wells* et al.[5] and *Power* et al.,[6] $[(GaR_2)(GaR)_4(AsHPh)(AsPh)_6]$ and $[Ga(GaR)_3(PR')_4(PHR')]$ (R = CH_2SiMe_3, R' = 1-adamantyl, Ar = 2,4,6-$iPr_3C_6H_2$).

In an effort to develop new classes of mixed 13/15 compounds we have investigated the reaction of group 13 alkyls with elemental phosphorus. The results for $GatBu_3$ are presented herein.

The reaction of white phosphorus, P_4, with two molar equivalents of $GatBu_3$,[7] in pentane at room temperature, affords a colorless solid with a composition corresponding to $Ga_2P_4tBu_6$ **1**. The medium-resolution mass spectrum (70 eV, CI, NH_3) of **1** exhibits a fragmentation pattern m/z consistent with loss of tBu (m/z = 566) and $GatBu_3$ (m/z = 365).

The ^{1}H and ^{13}C-{^{1}H}-NMR spectra of **1**[8] indicate the presence of three different *tert*-butyl environments with an integrated ratio of 3:2:1, the latter showing coupling to a single phosphorus atom. The ^{31}P-{^{1}H}-NMR spectrum of **1**[8] consists of three signals which exhibit P–P one-bond coupling to give two triplets and a doublet of doublets. The one-bond connectivity of the phosphorus atoms is confirmed by the homonuclear 2D-^{31}P-NMR-COSY[9] spectrum. The shift of the downfield triplet (δ = −50.73) is close to that observed for "tBuP" fragments in the polycyclodiphosphanes tBu_6P_8 (δ = −45),[10] while the two upfield signals (δ = −226.81 and −327.43) are indicative of a tetrahedrane type phosphorus environment, and may be compared with those for the transition metal complexes **2** (δ = −258.2, −335.9, and −376.9),[11] **3** (δ = 166.1 and −206.5),[12] and **4** (δ = −247.0).[13]

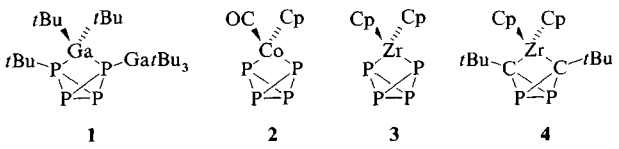

1 **2** **3** **4**

The similarity of the ^{31}P-NMR spectrum for **1** to that of **2** suggests that they are structurally related, however, since the structure of **1** could not be established unequivocally from NMR spectroscopy, an X-ray crystal structure analysis was performed,[14] the result of which is presented in Figure 1. The X-ray structure is entirely consistent with analytical and spectroscopic data. All the P–P distances [2.197(2)–2.214(2) Å] are consistent with that of a P–P single bond. The Ga(1)–P(1) and Ga(1)–P(4) distances, 2.515(2) and 2.476(2) Å respectively, are towards the long end of the range previously observed for Ga–P bonds, 2.370(3)–2.475(4) Å,[6, 15] consistent with the strain imposed by the small P(1)–Ga(1)–P(4) angle, 68.8(1)°. The dative P(4)–Ga(2) bond [2.619(2) Å] is significantly longer than those associated with the P–Ga–P bridge, and is presumably a result of the steric crowding at Ga(2) due to the three *tert*-butyl ligands.

Since little is known about ring opening reactions of white phosphorus with Lewis acids we can, at present, only speculate as to how **1** is formed. Presumably the initial reaction

[*] Prof. Dr. A. R. Barron, Dr. M. B. Power
Department of Chemistry
Harvard University
Cambridge, MA 02138 (USA)

[**] This work was supported by the US-Petroleum Research Fund.

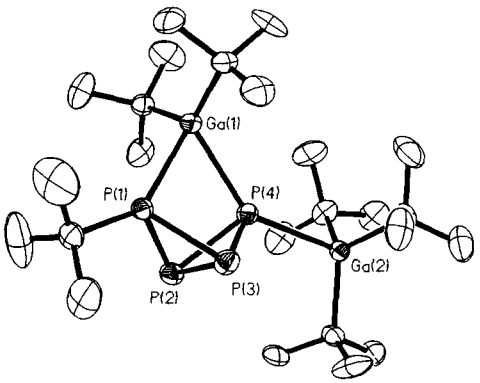

Fig. 1. Structure of **1** in the crystal (ORTEP). Important bond lengths and angles, see text.

involves the addition of a Ga–C bond across one of the P–P bonds in P_4 since a related addition of alkyllithium reagent across P_4 has previously been described.[16] Finally, we note that thermolysis (75–80 °C in C_6D_6) of **1** results in the liberation of $GatBu_3$ and the decomposition of the remaining GaP_4tBu_3 moiety.

Experimental Procedure

1: $GatBu_3$ (3.89 g, 16.13 mmol) in pentane (40 mL) was stirred for 3 to 4 h with P_4 (1.0 g, 8.07 mmol) at room temperature under nitrogen. After all the P_4 had been visibly consumed by the reaction a pale yellow solution resulted. Some solvent was then removed under vacuum (ca. 10 mL), and the resulting solution set aside in the freezer overnight (−25 °C). A large mass of white crystalline material was deposited, which was filtered and dried under vacuum. More crystalline material was obtained from the filtrate. Yield: 4.10 g, 84%. m.p. 120–121 °C.

Received: May 22, 1991 [Z 4641 IE]
German version: *Angew. Chem. 103* (1991) 1403

CAS Registry numbers:
1, 135989-55-8; P_4, 12185-10-3; $GatBu_3$, 55681-99-7.

[1] For a review, see: A. H. Cowley, R. A. Jones, *Angew. Chem. 101* (1989) 1235; *Angew. Chem. Int. Ed. Engl. 28* (1989) 1208, and references therein.
[2] a) G. E. Coates, J. Graham, *J. Chem. Soc. 1963*, 223; b) O. T. Beachley, Jr., G. E. Coates, *J. Chem. Soc. 1965*, 3241.
[3] a) R. L. Wells, A. P. Purdy, A. T. McPhail, C. G. Pitt, *J. Organomet. Chem. 308* (1986) 281; b) A. M. Arif, B. L. Benac, A. H. Cowley, R. L. Geerts, R. A. Jones, K. B. Kidd, J. M. Power, S. T. Schwab, *J. Chem. Soc. Chem. Commun 1986*, 1543; c) O. T. Beachley, Jr., J. P. Kopasz, H. Zhang, W. E. Hunter, J. L. Atwood, *J. Organomet. Chem. 325* (1987) 69; d) C. G. Pitt, K. T. Higa, A. T. McPhail, R. L. Wells, *Inorg. Chem. 25* (1986) 2483; e) K. M. Waggoner, P. P. Power, *J. Am. Chem. Soc. 113* (1991) 3385.
[4] a) K. M. Waggoner, H. Hope, P. P. Power, *Angew. Chem. 100* (1988) 1765; *Angew. Chem. Int. Ed. Engl. 27* (1988) 1699; b) R. A. Bartlett, P. P. Power, *J. Am. Chem. Soc. 112* (1990) 3660.
[5] R. L. Wells, A. P. Purdy, A. T. McPhail, C. G. Pitt, *J. Chem. Soc. Chem. Commun. 1986*, 487.
[6] K. M. Waggoner, S. Parkin, D. C. Pestana, H. Hope, P. P. Power, *J. Am. Chem. Soc. 113* (1991) 3597.
[7] R. A. Kovar, H. Derr, D. Brandau, J. O. Callaway, *Inorg. Chem. 14* (1975) 2809.
[8] ^1H NMR (500 MHz, C_6D_6, TMS ext.): $\delta = 1.36$ (s, 27 H; $GaC(CH_3)_3$), 1.26 (s, 18 H; $GaC(CH_3)_3$), 0.511 (d, $J(P,H) = 13.87$ Hz, 9 H; $PC(CH_3)_3$); ^{13}C NMR (125.72 MHz, C_6D_6, TMS ext.): $\delta = 40.60$ (d, $J(P,C) = 49.55$ Hz, $PC(CH_3)_3$), 33.63 ($GaC(CH_3)_3$), 31.53 ($GaC(CH_3)_3$), 31.08 ($GaC(CH_3)_3$), 27.93 (d, $J(P,C) = 9.05$ Hz, $PC(CH_3)_3$), 27.76 ($GaC(CH_3)_3$); $^{31}P\{^1H\}$-NMR (202.40 MHz, C_6D_6, H_3PO_4 ext.): $\delta = -50.73$ (t, $J(P,P) = 212.45$ Hz, 1 P; P*t*Bu), −226.81 (t, $J(P,P) = 205.71$ Hz, 1 P; $PGatBu_3$), −327.43 (overlapping dd, $J(P,P) = 207.52$ Hz, 209.74 Hz, 2P; P_2PtBu). IR (KBr, Nujol): $\tilde{\nu}$ [cm^{-1}] = 2357(w), 2165(w), 1973(w), 1686(w), 1164(s), 1072(w), 1005(s), 935(m), 897(sh), 850(w), 805(s), 725(m), 685(w), 597(m), 568(w), 526(m), 398(m).
[9] a) W. P. Ave, E. Bartholidi, R. R. Ernst, *J. Chem. Phys. 64* (1976) 2229; b) K. Nagayama, A. Kumar, K. Wüthrich, R. R. Ernst, *J. Magn. Reson. 40* (1980) 321.
[10] M. Baudler, J. Hellmann, P. Bachmann, K.-F. Tebbe, R. Fröhlich, M. Fehér, *Angew. Chem. 93* (1981) 415; *Angew. Chem. Int. Ed. Engl. 20* (1981) 406.
[11] O. J. Scherer, M. Swarowsky, G. Wolmershäuser, *Organometallics 8* (1989) 841.
[12] O. J. Scherer, M. Swarowsky, H. Swarowsky, G. Wolmershäuser, *Angew. Chem. 100* (1988) 738; *Angew. Chem. Int. Ed. Engl. 27* (1988) 694.
[13] P. Binger, B. Biedenback, C. Krüger, M. Regitz, *Angew. Chem. 99* (1987) 798; *Angew. Chem. Int. Ed. Engl. 26* (1987) 764.
[14] X-ray structure analysis of **1**: space group $P\bar{1}$, $a = 9.436(4)$, $b = 12.331(4)$, $c = 15.866(4)$, $\alpha = 70.76(2)$, $\beta = 81.21(3)$, $\gamma = 69.95(3)°$, $V = 1635(1)$ Å^3, $\varrho_{calcd} = 1.230$ g cm^{-3}, $\mu(Mo_{K_\alpha}) = 18.44$ cm^{-1}, 4242 unique reflections, 3342 observed ($I > 4\sigma(I)$), $R = 0.0412$, $R_w = 0.0536$. Further details of the crystal structure investigation may be obtained from the Fachinformationszentrum Karlsruhe, Gesellschaft für wissenschaftlich-technische Information mbH, W-7514 Eggenstein-Leopoldshafen 2 (FRG), on quoting the depository number CSD-15575, the names of the authors, and the journal citation.
[15] A. H. Cowley, P. R. Harris, R. A. Jones, C. M. Nunn, *Organometallics 10* (1991) 652.
[16] R. Riedel, H.-D. Hausen, E. Fluck, *Angew. Chem. 97* (1985) 1050; *Angew. Chem. Int. Ed. Engl. 24* (1985) 1056.

A Simple Way to Predict the Products of Topochemical Photoreactions on the Basis of Force Field Calculations

By *Klaus Angermund,* Ingo Klopp, Carl Krüger,* and *Matthias Nolte*

Dedicated to Professor Kurt Schaffner on the occasion of his 60th birthday

Photoreactions in organic solids are for the most part highly selective and, in many cases, enable access to unusual compounds.[1] For the interpretation of such solid-state reactions the relationship between the packing of the molecules in the crystal and the resulting photoproducts is very important. These relationships were first studied systematically by *Schmidt* et al.[2] on substituted *trans*-cinammic acids. The investigations led to the establishment of the topochemical postulate, according to which "reactions in organic crystals take place with minimal atomic and molecular movement".

Recently, however, reactions have also been observed which take place with considerable reorganization of the molecules in the crystal lattice.[1, 3] They can be described in terms of an extension of the topochemical postulate proposed by *Cohen*.[4] According to this *reaction cavity principle*, "lattice-controlled reactions proceed with minimal distortion of the surface of the reaction cavity". The reaction cavity is the space which is formed by the molecules surrounding the transition state of the reaction complex in the lattice.

If several reaction products are conceivable a prediction of the products on the basis of force field calculations or theoretical methods should be possible via a determination of the cavity deformation. The result of such calculations, however, crucially depends on the formulation of the transition state and on the size of the crystal lattice section ("thickness of cavity wall") used in describing the reaction cavity, and thus significantly limits the practical application of this principle.

We have therefore modified the Cohen model to the effect that the deformation of the cavity by the transition state of

[*] Dr. K. Angermund, Prof. Dr. C. Krüger, Dipl.-Chem. M. Nolte
Max-Planck-Institut für Kohlenforschung
Kaiser-Wilhelm-Platz 1, W-4330 Mülheim an der Ruhr (FRG)
Dr. I. Klopp
Max-Planck-Institut für Strahlenchemie
Stiftstrasse 34–36, W-4330 Mülheim an der Ruhr (FRG)

the reaction complex is approximated as deformation of the product in the reaction cavity assumed to be rigid. This leads to some essential advantages in the practical application of the concept: The smallest crystal lattice section to be set as reaction cavity is unequivocally given by the nearest neighbors of the starting compounds in the crystal. Inclusion of further parts of the crystal lattice has no significant influence on the result. The computational effort required is comparatively small because only the deformation of the potential products instead of that of the whole reaction cavity, as in the classical Cohen model, has to be determined. The energy difference $\Delta E = E_K - E_G$ between the potential energy of the most stable conformation of the product in the cavity (E_K) and that of the isolated molecule (E_G) serves as a relative measurement. It is obtainable by known methods of molecular modeling.[5] For topochemically-controlled reactions before the recrystallization, ΔE is a measure of the solid-state solubility (stabilization) of the products in the reacting crystal. A comparison of the ΔE values should afford information about the expected reaction products, which exceeds the prediction by topochemical considerations.

In the class of compounds including the 3-cyclohexylidene-5-phenyl-2(3*H*)furanones, lattice-controlled photoreactions are known which cannot be explained by the topochemical rules[6] and are therefore especially suitable for checking the predictions made by using our approach. For this purpose the homologous esters **1a** and **1b** were chosen and prepared from *p*-hydroxy-substituted β-benzoylpropionic acids by a method analogous to the Erlenmeyer azalactone synthesis (Scheme 1).[6, 7]

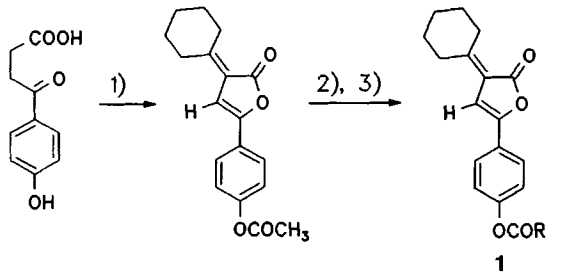

1

Scheme 1. Synthesis of the esters **1** [6, 7]. 1) Cyclohexanone, Ac_2O, lead(II) acetate, 4 h at 150 °C; 2) $Al(OiPr)_3$, CH_2Cl_2, MeOH, 2 h reflux; 3) acid chloride RCOCl, triethylamine, CH_2Cl_2.

The crystalline esters were then irradiated with UV light (λ = 360 nm) and the product distribution was determined NMR spectroscopically.[6] Whereas the propionate **1a** forms only the symmetrical [2 + 2]-photoproduct **2a**, the homologous butyrate **1b** forms the corresponding product **2b** in similar yields together with the unsymmetrical [2 + 2]-dimer **3b** (Scheme 2).

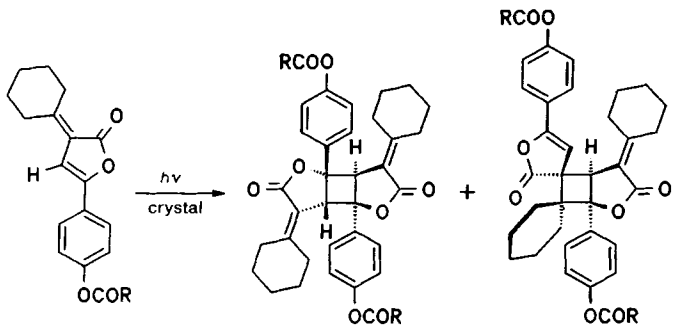

1a : R = C_2H_5 **2a** (21.2%) **3a** (−/−)

1b : R = C_3H_7 **2b** (20.4%) **3b** (16.6%)

Scheme 2. Photoreactions of the crystalline esters **1a** and **1b**.

To find an explanation for the different reaction behavior, the X-ray crystal structures of **1a** and **1b** were determined.[8] The packing of the two compounds in the crystal reveals two different arrangements of monomers around the inversion centers from which the reactions could take place (Fig. 1).

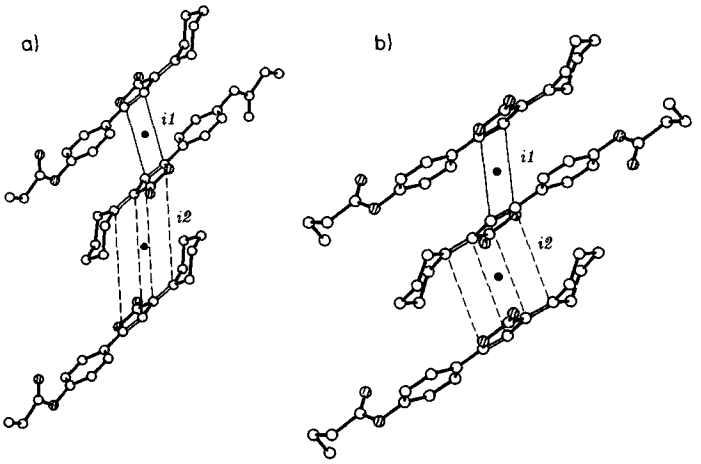

Fig. 1. Sections from the crystal structures of the butenolides **1a** (a) and **1b** (b). investigated. C: white spheres; O: shaded spheres; inversion centers: black spheres. The potential reaction routes leading to the symmetrical *endo* dimers are indicated by unbroken lines, those to the unsymmetrical dimers **3** by broken lines, via the corresponding inversion centers *i1* and *i2*, respectively. Coordinates of the inversion centers: a) $i1 = (0, \frac{1}{2}, \frac{1}{2})$, $i2 = (0, 0, \frac{1}{2})$; b) $i1 = (\frac{1}{2}, \frac{1}{2}, 1)$, $i2 = (\frac{1}{2}, \frac{1}{2}, \frac{1}{2})$. Distances of the midpoints of the double bonds from a) *i1* 3.88(1) Å, *i2* 6.25(1) Å; b) *i1* 3.88(1) Å, *i2* 4.92(1) Å. Distances between the planes of the π-systems a) *i1* 3.52(1) Å, *i2* 4.82(1) Å; b) *i1* 3.43(1) Å, *i2* 4.50(1) Å.

According to the topochemical rules, the reaction leading to the symmetrical *endo*-dimers **2a** and **2b** is allowed at inversion center 1 (*i1*) but forbidden at inversion center 2 (*i2*).[2] A formation of the unsymmetrical dimers **3a** and **3b** is similarly topochemically forbidden, since bonds over distances of more than 4.9 Å would have to be coupled for a reaction at both inversion centers (Fig. 1). The deviating reaction behavior of **1b** should, however, be understandable in terms of the reaction cavity concept and, in principle, should be predictable according to our method.

The most stable of all potential dimers were determined using the program SYBYL,[9] and the relevant energy values E_K and E_G were calculated (Table 1).

As can be seen from Table 1, the symmetrical dimers **2a** and **2b** are stabilized by the crystal assembly in a reaction at

Table 1. Potential energies [kcal mol^{-1}] of the possible dimers of **1** and **4** in the reaction cavity (E_K) and as isolated molecules (E_G).

Reaction at	Product	E_K	E_G	ΔE	Product	E_K	E_G	ΔE
i1	**2a**	−15	50	−65	**2b**	−26	49	−75
	3a	57	51	6	**3b**	56	51	5
i2	**2a**	211	50	161	**2b**	70	49	21
	3a	53	51	2	**3b**	17	51	−34
	5	9	68	−59	**6**	166	58	108
	7	65	32	33				

i1 (ΔE negative). A conceivable reaction at the inversion center *i2*, on the other hand, leads to a destabilization (ΔE positive) of the products in the cavity. The energy differences between the two routes indicate that the dimerization to the symmetrical product should proceed at *i1*, which is consistent with the results of the topochemical consideration. In the case of the dimer **3a**, both formations at *i1* as well as at *i2* are associated with a slight destabilization. Since an energetically much more favorable reaction route exists with the formation of **2a** at *i1*, **3a** should not be formed, or only in very small amounts.

For the formation of the dimer **3b** at the inversion center *i2*, however, we found a stabilization by the crystal lattice. Hence, the reaction leading to the unsymmetrical dimer **3b** should also be possible in the case of the butyrate **1b**, but, due to the greater stabilization by the cavity, **2b** should be formed preferentially. Thus, a qualitatively correct prediction of the photoproducts is possible with the modified Cohen model also in the case of the topochemically forbidden reactions leading to **3a** and **3b**.

The limited application of this purely energetic approach is manifested in the photodimerization of crystalline 2,5-dibenzylidenecyclopentanone **4** (Scheme 3).[10, 11] Whereas

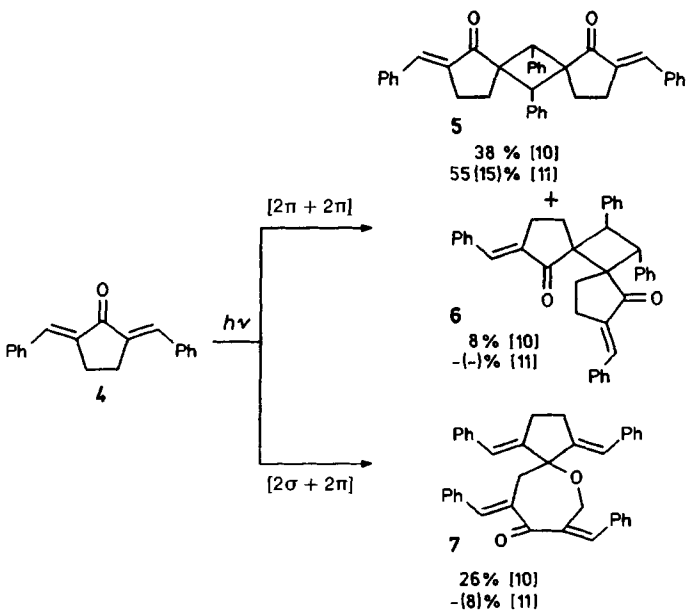

Scheme 3. Photoreactions of crystalline **4**. The yields quoted in brackets refer to 25% conversion.

the results of the simulation correlate with the experimental findings of the $[2\pi + 2\pi]$ cycloaddition leading to **5** and **6**,[10, 11] **7** formed by radical $[2\sigma + 2\pi]$ addition[10] is significantly stabilized by the crystal assembly (see Table 1). Its high ΔE value, together with the experimental finding that **7** could only be isolated at incomplete (25%) conversion,[11] points to a kinetically controlled reaction for which the modified Cohen model is of limited application. Reversal of the product distribution upon carrying out the reaction in solution[10, 11]—a kinetic inhibition of the formation of **7** presupposed[10]—follows from a comparison of the E_G-values of **5** and **6**, in agreement with the experiment (Table 1).

That only two energy values are necessary per potential product molecule in the method presented here enables a simpler calculation, with generally accessible force-field programs, compared to the classical Cohen model. This possibility of predicting products, is together with the simulation of molecular packings, an important step on the way to a rational design of organic solid-state reactions and thus also to their application in synthetic chemistry.

Received: April 27, 1991 [Z 4591 IE]
German version: *Angew. Chem. 103* (1991) 1379

[1] General overviews of organic solid-state reactions: G. R. Desiraju (Ed.): *Organic Solid State Chemistry*, Elsevier, New York 1987; M. D. Cohen, *Tetrahedron 43* (1987) 1211; V. Ramamurthy, K. Venkatesan, *Chem. Rev. 87* (1987) 433; V. E. Shklover, T. V. Timofeeva, Yu. T. Struchkov, *Russ. Chem. Rev. 55* (1986) 721; V. Ramamurthy, *Tetrahedron 42* (1986) 5753.

[2] A summary of the works by *G. M. J. Schmidt* are to be found in D. Ginsburg (Ed.): *Solid State Photochemistry*, Verlag Chemie, Weinheim 1976.

[3] S. Mohr, W. R. Balzer, D. Lawrenz in H. Sixl, J. Friedrich, C. Bräuchle (Eds.): *Photoreaktive Festkörper*, M. Wahl, Karlsruhe 1984, p. 455; S. Mohr, *Tetrahedron Lett. 1979*, 2461, 3139; *ibid. 21* (1980) 593; *Fresenius Z. Anal. Chem. 304* (1980) 280; C. Krüger, S. Mohr, I. Ortmann, K. Schaffner, unpublished; G. Kaupp, H. Frey, G. Behmann, *Chem. Ber. 121* (1988) 2135, and references cited therein.

[4] M. D. Cohen, *Angew. Chem. 87* (1975) 439; *Angew. Chem. Int. Ed. Engl. 14* (1975) 386.

[5] H. Frühbeis, R. Klein, H. Wallmeier, *Angew. Chem. 99* (1987) 413; *Angew. Chem. Int. Ed. Engl. 26* (1987) 403, and references cited therein.

[6] I. Klopp. *Dissertation*, Universität Wuppertal 1991.

[7] W. I. Awad, S. M. A. Omran, A. I. Hashem, *J. Chem. U. A. R. 10* (1967) 287; *Chem. Abstr. 69* (1968) 86677k.

[8] a) Crystallographic data of **1a**: $P2_1/n$, $a = 6.542(1)$, $b = 11.479(1)$, $c = 22.263(2)$ Å, $\beta = 97.66(1)°$, $V = 1656.9$ Å^3, $Z = 4$, $\varrho_{calcd} = 1.25$ g cm^{-3}, $\lambda = 1.54178$ Å, $\mu = 6.72$ cm^{-1}, $R = 0.058$, $R_w = 0.063$; 3593 measured reflections, 3334 independent reflections, 2228 observed ($I > 2\sigma(I)$), 209 refined parameters, residual electron density 0.48 eÅ^{-3}. b) Crystallographic data of **1b**: $P2_1/c$, $a = 6.512(1)$, $b = 29.347(3)$, $c = 9.534(1)$ Å, $\beta = 109.29(1)°$, $V = 1719.7$ Å^3, $Z = 4$, $\varrho_{calcd} = 1.26$ g cm^{-3}, $\lambda = 1.54178$ Å, $\mu = 6.67$ cm^{-1}, $R = 0.086$, $R_w = 0.097$; 3598 measured reflections, 3324 independent reflections, 2507 observed ($I > 2\sigma(I)$), 217 refined parameters, residual electron density 0.58 eÅ^{-3}.—Further details of the crystal structure investigations are available on request from the Fachinformationszentrum Karlsruhe, Gesellschaft für wissenschaftlich-technische Information mbH, W-7514 Eggenstein-Leopoldshafen 2 (FRG), on quoting the depository number CSD-55331, the names of the authors, and the journal citation.

[9] SYBYL 5.3, Tripos Associates, Inc., St. Louis, USA; Force Field: Tripos (Version 5.2)[||]; minimization algorithm: conjugate gradient; convergence criterion: gradient of standard deviation < 0.01 kcal mol^{-1} Å^{-1}; nonbonded cutoff 8 Å.

[10] G. Kaupp, I. Zimmermann, *Angew. Chem. 93* (1981) 1107; *Angew. Chem. Int. Ed. Engl. 20* (1981) 1018.

[11] C. R. Theocharis, W. Jones, J. M. Thomas, M. Motevalli, M. B. Hursthouse, *J. Chem. Soc. Perkin Trans. II 1984*, 71.

Flash Photolytic Generation and Study of Ynamines. First Observation of Primary and Secondary Ynamines in Solution**

By *Yvonne Chiang, Andrew S. Grant, A. Jerry Kresge,* Przemyslaw Pruszynski, Norman P. Schepp*, and *Jakob Wirz*

Although tertiary ynamines **1** are well-known stable substances,[1] primary and secondary ynamines **2** and **3**, because

[*] Prof. Dr. A. J. Kresge, Y. Chiang, Dr. A. S. Grant, Dr. P. Pruszynski
Department of Chemistry, University of Toronto
Toronto, Ontario M5S 1A1 (Canada)
Dr. N. P. Schepp, Prof. Dr. J. Wirz
Institute für Physikalische Chemie der Universität
CH-4056 Basel (Switzerland)

[**] This work was supported by the Natural Sciences and Engineering Research Council of Canada, the Donors of the Petroleum Research Fund, administered by the American Chemical Society, the National Institutes of Health, and the Swiss National Science Foundation (Project No. 2000-5.515)

of their facile isomerization to ketenimines, have heretofore been observed only in the gas phase or in low-temperature matrices.[2, 3] We wish to report that we have now developed a method for generating all three classes of ynamines in aqueous solution and have begun to study their chemistry in that medium.

$RC{\equiv}CNR_2$ (1) $RC{\equiv}CNH_2$ (2) $RC{\equiv}CNHR$ (3)

We have found that flash photolysis[4] of phenylaminocyclopropenones **4** in aqueous solution gives carboxylic acid amides as the ultimate reaction products [Eq. (a)], via short-lived transient intermediates with strong absorbance in the region $\lambda = 270-290$ nm, which, from their behavior as well as by analogy with our previous flash photolytic generation

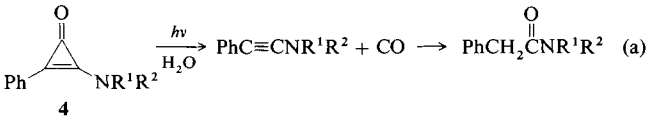

$$\xrightarrow[H_2O]{h\nu} PhC{\equiv}CNR^1R^2 + CO \longrightarrow PhCH_2\overset{O}{\overset{\|}{C}}NR^1R^2 \quad (a)$$

4

a: $R^1 = R^2 = H$; **b**: $R^1 = R^2 = C_6H_5$; **c**: $R^1 = H$, $R^2 = C_6F_5$; **d**: $R^1 = H$, $R^2 = C_6H_{11}$; **e**: $R^1 = H$, $R^2 = CH(CH_3)_2$; **f**: $R^1/R^2 = (CH_2)_5$; **g**: $R^1/R^2 = [(CH_2)_2]_2O$; **h**: $R^1/R^2 = C(N(CH_3)_2)_2$.

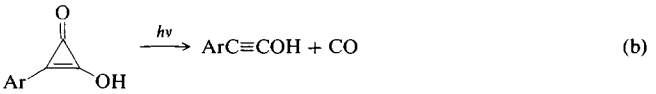

$$\xrightarrow{h\nu} ArC{\equiv}COH + CO \quad (b)$$

of ynols from arylhydroxycyclopropenones,[5] [Eq. (b)], we conclude are ynamines.[6] Ynamines produced in this way with at least one hydrogen substituent on amine nitrogen are transformed into still other transient species which we have identified as ketenimines from their rates of reaction: the hydration of ketenimines to amides [Eq. (c)], has been studied before[8, 9] and the rate constants reported, e.g. $k = 100$ and 2200 $M^{-1}s^{-1}$ for the hydrogen-ion catalyzed reactions

$$PhCH{=}C{=}NR \xrightarrow{H_2O} PhCH_2\overset{O}{\overset{\|}{C}}NHR \quad (c)$$

of phenylketene-*N*-phenylimine and phenylketene-*N*-isopropylimine respectively, are in good agreement with our values, $k = 98$ and 2190 $M^{-1}s^{-1}$. Ynamines without amino hydrogen, i.e. tertiary ynamines, cannot isomerize to ketenimines, but their direct hydration has also been studied before,[11] and again the rates we measure are consistent with those reported, e.g. $k = 1.03\ s^{-1}$ for the "uncatalyzed" reaction of phenylpiperidinoacetylene in 8.6% dioxane-water vs. our $k = 1.84\ s^{-1}$ for wholly aqueous solution.

These reactions of primary, secondary, and teriary ynamines are acid catalyzed, and the conversion of primary and secondary ynamines into ketenimines is base catalyzed, as well. The acid-catalyzed reactions show general catalysis and give sizeable kinetic isotope effects, e.g. $k_{H_2PO_4^\ominus}/k_{D_2PO_4^\ominus} = 5.9$ for phenylpiperidinoacetylene. This is classic evidence for rate-determining proton transfer to carbon and suggests that the reaction is initiated by electrophilic addition of a proton to acetylenic carbon, as shown in [Eq. (d)]. Such a mechanism is further supported by the correlation illustrated in Figure 1, which shows that the rate of reaction increases with increasing basicity, and therefore cation stabilizing ability, of the amino portion of the substrate. This step in the case of tertiary ynamines is then followed by hydration of the cation and amide formation, as shown in [Eq. (e)], and in the case of primary and secondary ynamines, by loss of a proton from nitrogen, [Eq. (f)]. The fact that primary, secondary,

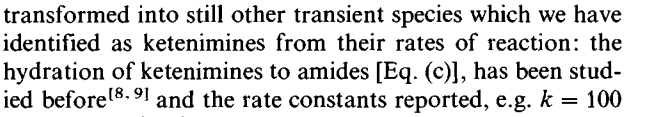

$$PhCH{=}CNR_2^\oplus \xrightarrow[-H^\oplus]{H_2O} PhCH{=}\overset{OH}{\overset{|}{C}}NR_2 \longrightarrow PhCH_2\overset{O}{\overset{\|}{C}}NR_2 \quad (e)$$

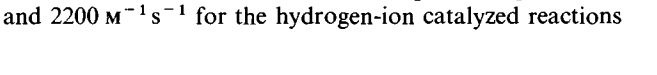

$$PhCH{=}CNHR^\oplus \longrightarrow PhCH{=}C{=}NR + H^\oplus \quad (f)$$

and tertiary ynamines obey the same correlation (Fig. 1) implies that this proton loss from nitrogen is not concerted with proton addition to carbon, for such proton loss cannot occur in the case of tertiary ynamines. The slope of the correlation is 0.34, which suggests an early transition state consistent with the rapid nature of these reactions.

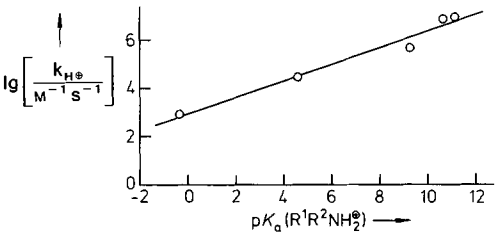

Fig. 1. Relationship between rate constants for the reaction of ynamines with hydronium ion in aqueous solution at 25 °C and acid dissociation constants of the conjugate acids of amines corresponding to the amino portion of the ynamines; from left to right: $R^1 = H$, $R^2 = C_6F_5$; $R^1 = H$, $R^2 = C_6H_5$; $R^1 = R^2 = H$; $R^1 = H$, $R^2 = C_6H_{11}$, and $R^1R^2 = (CH_2)_5$.

In sufficiently acidic solutions, ynamines can be expected to experience reversible protonation on nitrogen in addition to rate-detemining proton transfer to carbon [Eq. (g)]. The *N*-protonated species will be much less susceptible to elec-

$$PhC{\equiv}CNHR_2^\oplus \overset{K_a}{\rightleftharpoons} PhC{\equiv}CNR_2 + H^\oplus \xrightarrow{[a]} PhCH{=}CNR_2^\oplus \quad (g)$$

[a] rate determining

trophilic attack on carbon, and carbon protonation will consequently be inhibited. We detected no such inhibition up to the most acidic solutions we examined, e.g. $[H^\oplus] = 0.5$ M for phenylcyclohexylaminoacetylene. This sets an upper limit of $pK_a < 0.3$, i.e. $-\lg 0.5$, for the conjugate acid of this ynamine, and that makes the ynamine more than ten orders of magnitude less basic than cyclohexylamine ($pK_a(BH^\oplus) = 10.6$). This strong base-weakening effect of the acetylenic group parallels the remarkable acid-strengthening effect which we found in the case of ynols,[5, 12] and which is also evident in the ionization of ynamines as acids (*vide infra*).

The base-catalyzed isomerization of primary and secondary ynamines to ketenimines shows only specific hydroxide-ion catalysis. This suggests a mechanism, shown in [Eq. (h)],

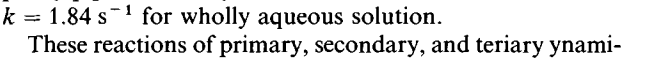

$$PhC{\equiv}CNHR + HO^\ominus \overset{K}{\rightleftharpoons} PhC{\equiv}CNR^\ominus + H_2O \xrightarrow{k[a]} PhCH{=}C{=}NR + HO^\ominus \quad (h)$$

[a] rate-determining

$$PhC{\equiv}CNR_2 + HA \longrightarrow PhCH{=}CNR_2^\oplus + A^\ominus \quad (d)$$

consisting of proton transfer from the substrate to base in a rapid and reversible reaction, whose position of equilibrium is governed by the hydroxide ion concentration, followed by an "uncatalyzed" rate-determining protonation at carbon by water. The hydroxide-ion catalytic coefficient for such a process is equal to the equilibrium constant for the first step times the rate constant for the second: $k_{HO}^{\ominus} = Kk$. This equilibrium constant is also equal to the acidity constant of the ynamine ionizing as an acid divided by the autoprotolysis constant of water, $K = K_a/K_w$. Use of $k = 10^{11}\ s^{-1}$ as an upper limit for this rate constant[13] combined with the experimentally determined value of $k_{HO^{\ominus}} = 6.5 \times 10^6\ M^{-1}s^{-1}$ for phenylaminoacetylene then gives $pK_a \leq 18.0$ as an upper limit for the acid dissociation of this ynamine [Eq. (i)]. This

$$PhC{\equiv}CNH_2 \overset{K_a}{\rightleftharpoons} PhC{\equiv}CNH^{\ominus} + H^{\oplus} \qquad \text{(i)}$$

makes phenylaminoacetylene at least 17 pK units more acidic than ammonia ($pK_a = 35$[15]) and provides another example of the dramatic acidifying effect of the acetylenic group.

Received: May 8, 1991 [Z 4618 IE]
German version: *Angew. Chem. 103* (1991) 1407

[1] H. G. Viehe in H. G. Viehe (Ed.): *Chemistry of Acetylenes*, Marcel Dekker, New York 1969, Chapter 12; J. M. Z. Gladych, D. Hartley in D. Barton, W. D. Ollis (Eds.): *Comprehensive Organic Chemistry*, Pergamon, New York 1979, pp. 75–79.

[2] H.-W. Winter, C. Wentrup, *Angew. Chem. Int. Ed. Engl. 19* (1980) 720; J. M. Buschek, J. L. Holmes, *Org. Mass Spectrom. 21* (1986) 729; B. van Baar, W. Koch, C. Lebrilla, J. K. Terlouw, T. Weiske, H. Schwarz; *Angew. Chem. Int. Ed. Engl. 25* (1986) 827; J. K. Terlouw, P. C. Bergers, B. L. M. van Baar, T. Weiske, H. Schwarz, *Chimia 40* (1986) 357; C. Wentrup, H. Briehl, P. Lorenčak, U. J. Vogelbacher, H.-W. Winter, A. Maquestiau, R. Flammang, *J. Am. Chem. Soc. 110* (1988) 1337.

[3] Ethynamine has also been characterized by high level *ab-initio* calculations: S. Saebo, L. Farnell, N. Riggs, L. Radom, *J. Am. Chem. Soc. 106* (1984) 5047; B. J. Smith, L. Radom, unpublished results; R. D. Brown, E. H. N. Rice, M. Rodler, *Chem. Phys. 99* (1985) 347; P. von R. Schleyer (Universität Erlangen-Nürnberg (FRG)), private communication.

[4] Two different flash systems were used: 1) a conventional apparatus with excitation flash produced by capacitor discharge through a pair of xenon flash lamps, 50 μs pulse width, 0.5 to 2.0 kJ per pulse. 2) a KrF eximer laser system, $\lambda_{exc} = 248$ nm, 25 ns pulse width, 200 mJ per pulse; monitoring wavelengths varied from $\lambda = 265$ to 315 nm.

[5] Y. Chiang, A. J. Kresge, R. Hochstrasser, J. Wirz, *J. Am. Chem. Soc. 111* (1989) 2355.

[6] Cyclopropenone substrates were prepared by reaction of phenylchlorocyclopropenone[7] with amines and were characterized by their NMR, IR, and mass spectra.

[7] J. S. Chickos, E. Patton, R. West, *J. Org. Chem. 39* (1974) 1647.

[8] A. F. Hegarty, D. G. McCarthy, *J. Am. Chem. Soc. 101* (1979) 1345; *J. Chem. Soc. Perkin Trans. 2 1980*, 579.

[9] Although ketenimines substituted at nitrogen are hydrated to amides directly[8], we have found that phenylketenimine, whose nitrogen substituent is hydrogen, is first converted into the corresponding nitrile; i.e., the cationic intermediate formed by protonation of the ketenimine at carbon loses a proton from nitrogen more rapidly than it reacts with water:

$$PhCH{=}C{=}NH \xrightarrow[-A^-]{HA} PhCH_2C{\equiv}NH^{\oplus} \xrightarrow{-H^{\oplus}} PhCH_2CN$$

This is consistent with the generally accepted mechanism for acid catalyzed hydrolysis of nitriles in which rapid and reversible protonation on nitrogen is followed by rate-determining reaction of the *N*-protonated intermediate with water[10].

[10] M. Liler: *Reaction Mechanisms in Sulfuric Acid and other Strong Acid Solutions*, Academic Press, New York 1971, pp. 205–208.

[11] W. F. Verhelst, W. Drenth, *J. Am. Chem. Soc. 96* (1974) 6692.

[12] B. J. Smith, L. Radom, A. J. Kresge, *J. Am. Chem. Soc. 111* (1989) 8297.

[13] This upper limit is for a diffusion-controlled reaction governed by the rotational correlation time of water[14].

[14] D. Eisenberg, W. Kauzmann: *The Structure and Properties of Water*, Oxford University Press, New York, 1969, pp. 206–214.

[15] R. P. Bell: *The Proton in Chemistry*, Second Edition, Cornell University Press, Ithaca, NY 1973, p. 86.

Solvent Dependence of Photoinduced Intramolecular Electron Transfer: Criteria for the Design of Systems with Rapid, Solvent-Independent Charge Separation**

By *Jan Kroon, Jan W. Verhoeven,* Michael N. Paddon-Row,** and *Anna M. Oliver*

Dedicated to Professor Kurt Schaffner on the occasion of his 60th birthday

Photoinduced electron transfer constitutes one of the most versatile and potentially efficient methods for converting light energy into useful (electro)chemical energy, as unequivocally demonstrated by its successful implementation in the photosynthetic apparatus. The ongoing extensive investigations[1] of such processes have made clear that, e.g., in synthetic D(onor)-bridge-A(cceptor) systems very large charge separation distances can be realized but at the same time it has become evident that the success is critically dependent upon a number of factors relating to the structure of the system itself as well as that of its environment. We and others have addressed, via both experimental and theoretical methods, the structural requirements to be met by the "bridge" in order to sustain sufficient electronic coupling over long distances.[2–9] During these studies we have also occasionally noted the remarkable difference in solvent sensitivity that the rate of charge separation may show in structurally quite closely related D-bridge-A systems and we have pointed out the decisive role that the interdependence of solvent stabilization and solvent reorganization may play.[5, 10] In the present paper this important point is quantified by comparison of the solvent effect on the rate of photoinduced charge separation in the fully rigid and structurally related systems **1a** and **1b** (Scheme 1), for which kinetic data could be collected in a wide variety of solvents. Furthermore, as will be shown, consideration of the interplay between solvent stabilization and solvent reorganization leads to the formulation

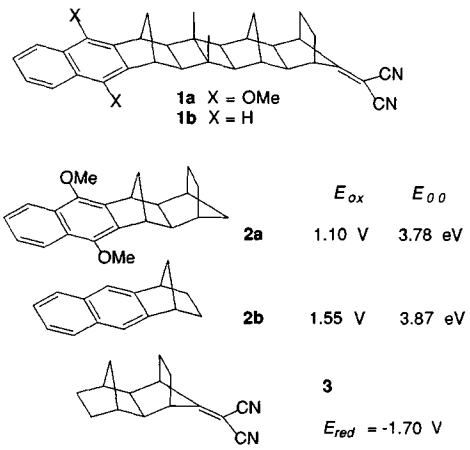

Scheme 1. Structure and relevant physicochemical properties of the systems investigated.

[*] Prof. Dr. J. W. Verhoeven, Drs. J. Kroon
Laboratory of Organic Chemistry, University of Amsterdam
Nieuwe Achtergracht 129, NL-1018 WS Amsterdam (The Netherlands)
Prof. Dr. M. N. Paddon-Row, Dr. A. M. Oliver
Department of Chemistry, University of New South Wales
P. O. Box 1, Kensington, N.S.W. 2033 (Australia)

[**] The present investigations were supported in part by the Netherlands Foundation for Chemical Research (SON) with financial aid from the Netherlands Organization for the Advancement of Research (NWO). We also thank the Australian Research Council for support.

of design criteria for systems capable of undergoing virtually medium-independent charge separation at the maximum rate feasible for a particular D/A distance.

As shown by *Rehm* and *Weller*[11, 12] the standard Gibbs free energy change ("driving force") for photoinduced electron transfer between neutral D and A species in a medium with static dielectric constant ε_s can be estimated via Equation (1),

$$\Delta G = e[E_{ox}(D) - E_{red}(A)] - E_{00} - \frac{e^2}{\varepsilon_s R_c} - \frac{e^2}{r}\left(\frac{1}{37} - \frac{1}{\varepsilon_s}\right) \quad (1)$$

which we can rewrite in the form of Eq. (2):

$$\Delta G = P - \frac{e^2}{\varepsilon_s R_c} - \frac{e^2}{r}\left(\frac{1}{37} - \frac{1}{\varepsilon_s}\right) \quad (2)$$

The parameter P ("polar driving force") represents the limiting value of ΔG for charge separation across an infinite distance in polar media and is readily accessible from the independently determined redox potentials and excitation energies (E_{00}) of the separate D and A units.

Oxidation potentials (measured in acetonitrile relative to SCE) and excitation energies for relevant model D systems **2a** and **2b** as well as the reduction potential of the model A system **3** are given in Scheme 1. Applying $R_c = 11.4$ Å for the center-to-center distance[13] and $r = 4.5$ Å for the average ionic radius,[5] the plots of ΔG versus ε_s in Figure 1 were constructed. From these plots it is evident that photoinduced charge separation in **1a** should be thermodynamically feasible in virtually all solvents, including saturated hydrocarbons ($\varepsilon_s \approx 2$), while for **1b** additional solvent stabilization ($\varepsilon_s \geq 3$) is required.

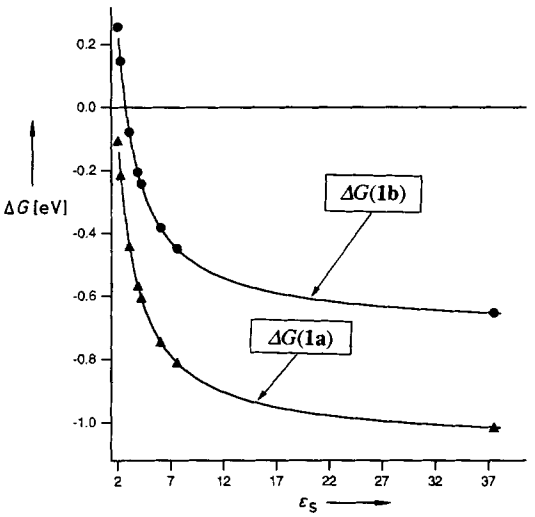

Fig. 1. Standard Gibbs free energy change (ΔG) for photoinduced charge separation in **1a** and **1b** as a function of the solvent dielectric constant (ε_s). Markers (▲ for **1a**, ● for **1b**) correspond to the solvents employed (see Table 1).

Our experimental results (see Table 1) are in line with this prediction. Thus, for **1a**, as reported earlier,[5] photoinduced charge separation occurs with a high rate (k_{et}) in all solvents investigated, but for **1b** we now find that it can only be detected if $\varepsilon_s > 3.1$, with the exception of benzene ($\varepsilon_s = 2.28$). The latter is obviously due to specific solvation effects that cannot be accounted for by Equation (1), but the overall

Table 1. Rate data (k_{et}) for photoinduced charge separation in **1a** and **1b** as calculated from fluorescence lifetimes in various solvents.

Solvent	ε_s	n^2	**1a** $10^{-7} \times k_{et}$ [s^{-1}] [a]	**1b** $10^{-7} \times k_{et}$ [s^{-1}] [b]
cyclohexane	2.02	2.03	2100	<0.1
benzene	2.28	2.25	5200	1.4
di-*n*-butyl ether	3.10	1.96	4700	<0.1
diisopropyl ether	3.88	1.87	–	0.5
diethyl ether	4.20	1.83	4700	1.4
ethyl acetate	6.02	1.88	4500	3.9
tetrahydrofuran	7.58	1.98	6700	6.5
acetonitrile	37.5	1.81	3000	11

[a] Data from Ref. [5]. [b] Analogous to the procedure used for **1a** (Ref. [5]), rates for **1b** were calculated from comparison of the naphthalene fluorescence lifetimes of **1b** and **2b** as k_{et} (**1b**) = $(\tau(\mathbf{1b}))^{-1} - (\tau(\mathbf{2b}))^{-1}$. Compound **2b** shows little solvent dependence of its fluorescence lifetime (59 ± 3 ns) over the range of solvents investigated while the lifetime of **1b** decreases from 60 ns in cyclohexane to 8 ns in acetonitrile.

data once more underline[14] the remarkable usefulness of this equation for estimating ΔG.

Closer inspection of the data in the Table reveals a dramatic difference in solvent dependence of k_{et} for **1a** and **1b** in the region where ΔG is negative for both molecules. While k_{et} in **1a** shows very minor ε_s dependence over the whole range of solvents, in **1b** it increases by more than an order of magnitude in response to a tenfold increase of ε_s (i.e. from diisopropyl ether to acetonitrile). Even more strikingly, under conditions of virtually identical ΔG, such as constituted by comparison of **1a** in di-*n*-butyl ether ($\Delta G = -0.44$ eV) and **1b** in tetrahydrofuran ($\Delta G = -0.45$ eV), the rate in **1a** is almost three orders of magnitude higher than in **1b**.

This observation leads to the important generalization that while a lower intrinsic driving force (ΔG), such as that in **1b** as compared to **1a**, can be compensated by use of a solvent with high ε_s, this evidently does not proportionally decrease the barrier ($\Delta G^{\neq}$) to electron transfer.

We have presented earlier[10] a rationalization of a similar difference in solvent sensitivity between two other rigid D-bridge-A systems via qualitative energy surface intersection diagrams. We now pursue this aspect more quantitatively in terms of the Marcus[15] expression for $\Delta G^{\neq}$ [Eq. (3)], which quantifies the relation between $\Delta G^{\neq}$, ΔG, and the overall reorganization energy, λ. The latter can be written as the sum of an internal part and a solvent dependent part ($\lambda = \lambda_{in} + \lambda_s$). Using approximations similar to those used in deriving Equation (1) above, the solvent reorganization energy, λ_s,[16] can be expressed by Equation (4), where n is the solvent refractive index.

$$\Delta G^{\neq} = \frac{(\Delta G + \lambda)^2}{4\lambda} \quad (3)$$

$$\lambda_s = e^2\left(\frac{1}{r} - \frac{1}{R_c}\right)\left(\frac{1}{n^2} - \frac{1}{\varepsilon_s}\right) \quad (4)$$

In Figure 2, the $\Delta G^{\neq}$ values for **1a** and **1b**, which were calculated from Equations (1)–(4), are plotted for the solvents experimentally employed (see Table 1) and also as a continuous function of ε_s at a fixed value of $n^2 = 2$, which is a reasonable approximation for most (organic) solvents. In calculating the $\Delta G^{\neq}$ values, the previously determined[5] λ_{in} value of 0.6 eV for **1a**, was used.

In agreement with experiment $\Delta G^{\neq}$ for **1a** is predicted to be low for all values of ε_s. In contrast, $\Delta G^{\neq}$ for **1b** initially

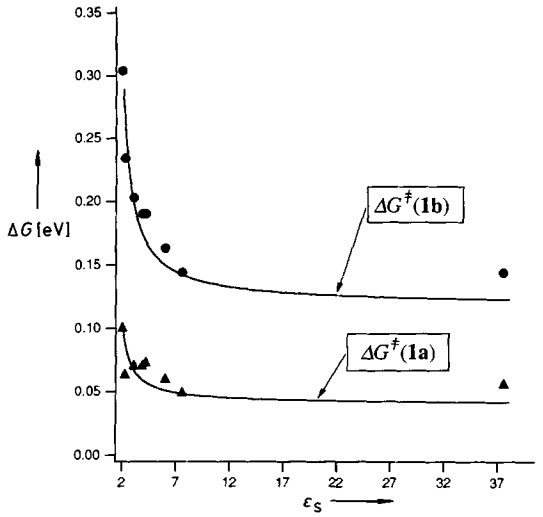

Fig. 2. Activation barrier for photoinduced charge separation in **1a** (▲) and **1b** (●) in various solvents as calculated from Equations (1)–(4). Continuous lines were calculated for $n^2 = 2$.

falls sharply with increasing ε_s, but it soon reaches a constant value of ca. 0.14 eV, owing to the compensating effects of changes in λ_s and ΔG. Thus, in (very) polar solvents the difference between **1a** and **1b** approaches 0.1 eV, implying a ratio $k_{et}(\mathbf{1a})/k_{et}(\mathbf{1b}) = 50$, thereby accounting for the major part of the experimental ratio, which amounts to about 300 (see Table 1). The latter would imply a barrier difference of 0.15 eV, but it should be borne in mind, that part of the discrepancy may in fact be due to a difference between **1a** and **1b** in electronic coupling as a result of different orbital-coefficients and/or -symmetry at the donor site.[17] The latter point is currently under further study.

From the experimental and theoretical results presented above it can be concluded that the same design criteria with regard to $E_{ox}(D)$, $E_{red}(A)$ and E_{00} that allow a system to undergo optimally fast photoinduced charge separation also make this rate virtually solvent independent. Thus, a check for solvent (in)dependence also provides a convenient experimental method to test whether optimization with respect to the rate of charge separation has been achieved. This intriguing interdependence between the degree of sensitivity of the electron transfer rate to solvent polarity and the extent by which the rate deviates from its optimal value is visualized in Figure 3, which plots the energy barrier for electron transfer in systems with the geometrical properties of **1a** and **1b** (i.e. $R_c = 11.4$ and $r = 4.5$ Å) as a function of both ε_s and the polar driving force P. The $\Delta G^{\neq}$ plots in Figure 2 represent sections through the three dimensional plot of Figure 3 at two specific values of P (i.e. $P = -0.98$ eV for **1a** and $P = -0.62$ eV for **1b**).

The observation that a unique valley, running parallel to the ε_s axis, occurs with $\Delta G^{\neq} = 0$ in Figure 3 demonstrates that a single P value ($= P_{opt}$) can be found at which both optimally fast electron transfer and virtual solvent independence of the rate of this process can be achieved. From the equations given above, together with the condition that $\Delta G^{\neq} = 0$, expression (5) can be derived:

$$P_{opt} = -\lambda_{in} - \frac{e^2}{n^2}\left(\frac{1}{r} - \frac{1}{R_c}\right) + \frac{e^2}{37r} \approx -\lambda_{in} - \frac{e^2}{n^2}\left(\frac{1}{r} - \frac{1}{R_c}\right) \quad (5)$$

This demonstrates that P_{opt} is independent of the solvent dielectric constant, but depends on the charge separation distance. On the other hand, since λ_{in} and the average ionic radius r are mainly determined by the structure of the D and A units employed while n varies only marginally with solvent, this also implies that for any given D/A combination the condition defined by Equation (5) can only be fulfilled at a single charge separation distance R_c, irrespective of the solvent employed. In fact at the distance $R_c = 11.4$ Å dictated by the structure of compounds **1a** and **1b** a $P_{opt} = -1.57$ eV (see Fig. 3) would be required (assuming the same λ_{in} and r) to make electron transfer barrierless in all solvents. Clearly, **1a** ($P = -0.98$ eV) comes closer to meeting this requirement than does **1b** ($P = -0.62$ eV), which is in agreement with our experimental results. Interestingly, Equation (5) also allows definition of the P_{opt} for very large charge separation ($R_c \gg r$), leading to $P_{opt}(R_c \rightarrow \infty) = -\lambda_{in} - e^2/n^2 r$ which amounts to 2.2 eV for the present type of D/A combinations.

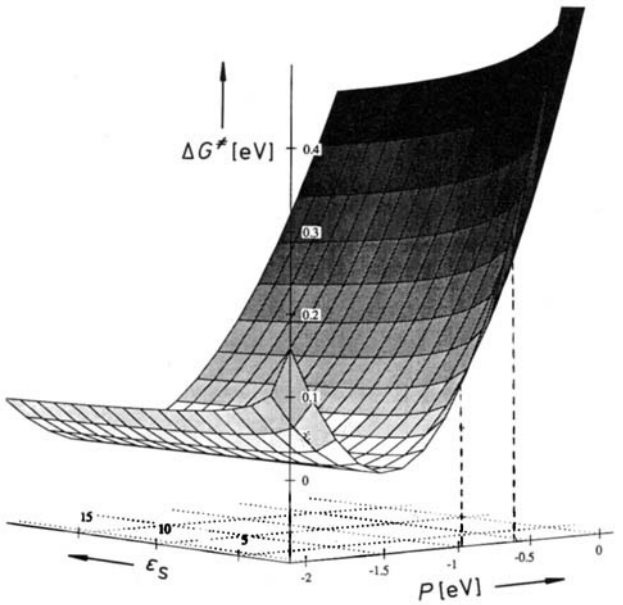

Fig. 3. Activation barrier, $\Delta G^{\neq}$ (in eV), of photoinduced charge separation for systems with $\lambda_{in} = 0.6$ eV, $R_c = 11.4$ Å and $r = 4.5$ Å as a function of the solvent dielectric constant ε_s and the "polar driving force" P [eV], at a fixed value of the refractive index ($n^2 = 2$). Vertical dashed lines indicate P values for **1a** (-0.98 eV) and **1b** (-0.62 eV).

In conclusion we propose that application of Equation 5 provides useful design criteria for systems intended to display optimally fast charge separation across a given distance that is also virtually independent of both medium effects and temperature, since under the barrierless conditions existing at P_{opt} the reorganization energy exerts only a weak ($\lambda^{-0.5}$) influence on the rate, via the pre-exponential component, and so does the temperature. Since in such systems the transition state for charge separation can be reached without solvent reorientation, it may be predicted that for systems designed to work at P_{opt}, the viscosity and dielectric relaxation rate of the medium are of minor importance.[18–20]

Received: April 12, 1991 [Z 4567 IE]
German version: *Angew. Chem. 103* (1991) 1398

[1] M. A. Fox, M. Chanon, (Eds.): *Photoinduced Electron Transfer*, Elsevier, Amsterdam 1988.
[2] P. Pasman, F. Rob, J. W. Verhoeven, *J. Am. Chem. Soc. 104* (1982) 5127–5133.

[3] M. N. Paddon-Row, K. D. Jordan in J. Liebman, A. Greenberg (Eds.): *Molecular Structure and Energetics, Vol. 6*, VCH Publishers, New York 1989, Chap. 3.
[4] D. N. Beratan, J. J. Hopfield, *J. Am. Chem. Soc. 106* (1984) 1584–1594.
[5] H. Oevering, M. N. Paddon-Row, M. Heppener, A. M. Oliver, E. Cotsaris, J. W. Verhoeven, N. S. Hush, *J. Am. Chem. Soc. 109* (1987) 3258–3269.
[6] A. M. Oliver, D. C. Craig, M. N. Paddon-Row, J. Kroon, J. W. Verhoeven, *Chem. Phys. Lett. 150* (1988) 366–373.
[7] J. M. Lawson, D. C. Craig, M. N. Paddon-Row, J. Kroon, J. W. Verhoeven, *Chem. Phys. Lett. 164* (1989) 120–125.
[8] M. N. Paddon-Row, S. S. Wong, *Chem. Phys. Lett. 167* (1990) 432–438.
[9] A. Broo, S. Larsson, *Chem. Phys. 148* (1990) 103–115.
[10] P. Pasman, G. F. Mes, N. W. Koper, J. W. Verhoeven, *J. Am. Chem. Soc. 107* (1985) 5839–5843.
[11] D. Rehm, A. Weller, *Ber. Bunsenges. Phys. Chem. 73* (1969) 834–845.
[12] A. Weller, *Z. Phys. Chem. 133* (1982) 93–98.
[13] D. C. Craig, M. N. Paddon-Row, *Aust. J. Chem. 40* (1987) 1951–1964.
[14] G. L. Gaines, M. P. O'Neil, W. A. Svec, M. P. Niemczyk, M. R. Wasielewski, *J. Am. Chem. Soc. 113* (1991) 719–721.
[15] R. A. Marcus, *J. Chem. Phys. 43* (1965) 679–701.
[16] N. S. Hush, *Trans. Faraday Soc. 57* (1961) 557–580.
[17] H. Oevering, J. W. Verhoeven, M. N. Paddon-Row, J. M. Warman, *Tetrahedron 45* (1989) 4751–4766.
[18] E. M. Kosower, *J. Am. Chem. Soc. 107* (1985) 1114–1118.
[19] H. Heitele, M. E. Michel-Beyerle, P. Finckh, *Chem. Phys. Lett. 138* (1987) 237–243.
[20] M. J. Weaver, G. E. McManis III, *Acc. Chem. Res. 23* (1990) 294–300.

A General Entry to Rigid Systems with Alternatingly Orthogonal Arene Units via Diels-Alder Reactions**

By *Burkhard König, Jürgen Heinze, Klaus Meerholz,* and *Armin de Meijere**

Dedicated to Professor Horst Prinzbach on the occasion of his 60th birthday

Unconventional materials with novel features are of interest worldwide,[1] and new and unusual properties can be expected for polycyclic aromatic systems with alternatingly orthogonal subunits. One basic system of this sort is realized in 1:2,9:10-dibenzo[2.2]paracyclophane-1,9-diene.[1] In fact di- and tetraphenyl derivatives of dibenzo[2.2]paracyclophanediene do exhibit uncommon features in that the odd electrons in their radical anions and dianions reside in the annelated biphenyl units and are isolated from each other by the intersecting [2.2]paracyclophane moiety.[2] Consequently, the triplet diradical dianions of these systems appear to be energetically favored over the singlet states. Our recently reported octaphenyldibenzo[2.2]paracyclophane-1,9-diene can be reversibly reduced to its hexaanion.[3] Extended systems containing several dibenzo[2.2]paracyclophanediene units linked through electroactive arene groups can be envisaged to accept an even larger number of charges which would be partitioned in groups by the intersecting orthogonal units. We therefore wanted to develop a versatile methodology that makes such molecules accessible from relatively simple starting materials.

The mixture of 1,1,9,9- and 1,1,10,10-tetrabromo[2.2]-paracyclophane **1** can readily be obtained in virtually quantitative yield from commercially available [2.2]paracyclophane.[4] Fourfold dehydrobromination of **1** with potassium *tert*-butoxide in tetrahydrofuran leads to the stepwise generation of two triple bonds in the bridges of the molecule which rapidly add to dienes present.[3] Furan readily cycloadds to the reactive intermediates to give a mixture of *anti*- and *syn*-isomeric bisendooxides *anti*/*syn*-**2** in 23% yield (Scheme 1). Flash vacuum pyrolysis (FVP) at 240 °C (2 mbar) via double *retro Diels-Alder*-reaction with evolution of ethyne afforded 1:2,9:10-bis-(3,4-furano)[2.2]paracyclophane **4** in 60% yield. When the pyrolysis was carried out at lower pressure (0.01 mbar), corresponding to a shorter contact time in the hot tube, a mixture of **2** (20%), **4** (34%) and 1:2-(1,4-epoxybenzo)-9:10-(3,4-furano)[2.2]paracyclophan-1-ene **3** (27%) was obtained. The starting material **2** and two products **3**/**4** can be separated by column chromatography on silica gel (dichloromethane/hexane 1:1).[5] This two-step procedure starting from **1** easily affords mono- and difurano-annelated [2.2]paracyclophanes **3** and **4** on a gram scale. The new compounds are stable, crystalline solids, and can be stored without noticeable alteration for months.

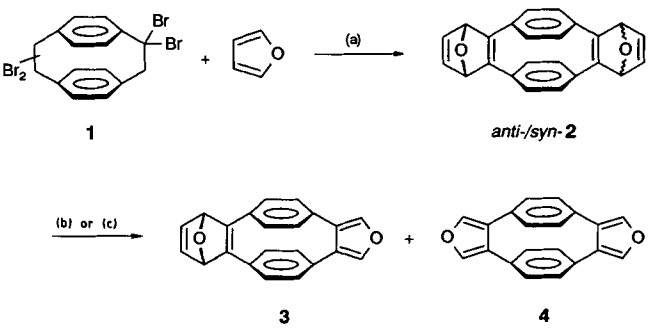

Scheme 1. a) KO*t*Bu, THF, room temperature, 23%. b) FVP, 240 °C, 0.01 mbar; 20% *anti*/*syn*-**2**, 27% **3**, 34% **4**. c) FVP, 240 °C, 2 mbar; 60% **4**.

Both **3** and **4** were allowed to react with a variety of dehydroarenes and bisdehydroarenes generated in situ from the corresponding vicinal dibromoarenes with *n*-butyllithium in close analogy to procedures described in the literature (Scheme 2, Table 1).[6–8] Treatment of a mixture of **3** (1 equiv.) and 1,2,4,5-tetrabromo-3,6-di-*n*-hexylbenzene **5**[9] (0.5 equiv.) with 1.1 equivalents of *n*-butyllithium at low temperatures gave, after warming to room temperature, a complex mixture of isomeric cycloadducts. This mixture was deoxygenated with low-valent titanium ($TiCl_4/LiAlH_4$)[11] without further purification to give bis-2:3,6:7-[1:2-benzo[2.2]paracyclophane-1,9-dieno]-9,10-di-*n*-hexylanthracene **6** (overall yield 25%). In solution, **6** adds oxygen, when exposed to light and air at room temperature; the corresponding 9,10-endoperoxide is formed in quantitative yield. As a solid, "bisphane" **6** can be stored indefinitely without any change.

Upon reaction of 1,2,3,4-tetrabromo-5,6-dimethylbenzene **7** (0.5 equiv.) with *n*-butyllithium (1.1 equiv.) in the presence of **3** (1 equiv.) and subsequent deoxygenation with $TiCl_4/LiAlH_4$, 2:3,6:7-bis[1:2-benzo[2.2]paracyclophane-1,9-dieno]-1,2-dimethylphenanthrene **8** was obtained (15%). As in all these cases, it was not necessary to separate the

[*] Prof. Dr. A. de Meijere[+], Dipl.-Chem. B. König
Institut für Organische Chemie der Universität Hamburg
Martin-Luther-King-Platz 6, W-2000 Hamburg 13 (FRG)
Prof. Dr. J. Heinze, Dipl.-Chem. K. Meerholz
Institut für Physikalische Chemie der Universität Freiburg
Albertstrasse 21, W-7800 Freiburg (FRG)
[+] New address:
Institut für Organische Chemie der Universität Göttingen
Tammannstrasse 2, W-3400 Göttingen (FRG)

[**] This work was supported by the Fonds der Chemischen Industrie as well as by BASF AG, Bayer AG and Hoechst AG by generous gifts of chemicals. *B. K.* thanks the Studienstiftung des Deutschen Volkes for a graduate student fellowship.

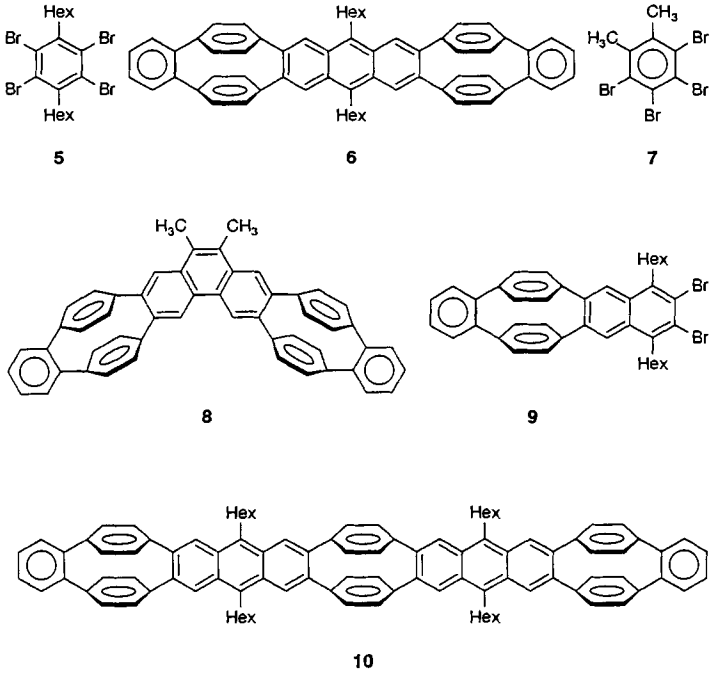

Scheme 2. (For conditions see Table 1).

Table 1. New arene-annelated [2.2]paracyclophane-1,9-diene derivatives[5] from furan-annelated compounds **3**, **4** and dehydroarenes as well as bisdehydroarenes (see Scheme 2).

Reactants		Reaction Conditions	Product [a, b] (m.p. [°C])	Yield [%]
Diene	Aryne precursor			
3	1,2,4,5-tetrabromo-3,6-di-*n*-hexylbenzene **5**	1) 0.5 equiv. **5**, 1.1 equiv. *n*BuLi, toluene, −90 °C → 25 °C, 6 h 2) $TiCl_4$, $LiAlH_4$, NEt_3, THF, 25 °C, 1 h	**6** (> 290)	25
3	1,2,3,4-tetrabromo-5,6-dimethylbenzene **7**	1) 0.5 equiv. **7**, 1.1 equiv. *n*BuLi, toluene, −90 °C → 25 °C, 6 h 2) $TiCl_4$, Zn, NEt_3, THF, 25 °C, 1 h	**8** (> 290)	15
3	1,2,4,5-tetrabromo-3,6-di-*n*-hexylbenzene **5**	1) 1.0 equiv. **5**, 1.1 equiv., *n*BuLi, −90 °C → 25 °C, 6 h 2) $TiCl_4$, $LiAlH_4$, NEt_3, THF, 25 °C, 1 h	**9** (> 290)	40
4	**9**	1) 2.5 equiv. **9**, 2.7 equiv. *n*BuLi, toluene, −90 °C → 25 °C, 6 h 2) $TiCl_4$, $LiAlH_4$, NEt_3, THF, 25 °C, 1 h	**10** (> 290)	18

[a] *Anti*- and *syn*-isomers were not separated in the first step. Where applicable, the ratio of isomers was about 1 : 1. [b] Isolation of the pure Diels Alder adducts is not necessary for the deoxygenation step.

stereoisomeric endooxides before the reductive deoxygenation.

In order to obtain the one-sided cycloadduct **9**, a 1 : 1 mixture of **3** and **5** was treated with 1.1 equivalents of *n*-butyllithium at low temperature and the mixture warmed to room temperature. Reductive deoxygenation of the crude mixture of *anti*- and *syn*-isomers without affecting the bromine substituents was achieved with $TiCl_4$ and zinc in refluxing tetrahydrofuran according to a procedure described by *Hart* et al.[6] 1:2-Benzo-9:10-(1,4-di-*n*-hexyl-2,3-dibromo-6,7-naphtho)[2.2]paracyclophane-1,9-diene **9** was isolated as a crystalline compound with an overall yield of 40%. According to its substitution pattern, **9** can be used to generate an aryne again. Thus, reaction of **9** with 1.1 equivalents of *n*-butyllithium in the presence of **4** at low temperature afforded a mixture of two isomeric cycloadducts (*anti*/*syn*), from which the extended "trisphane" hydrocarbon **10** was obtained in 18% yield by reductive deoxygenation with $TiCl_4/LiAlH_4$. In solution, **10** exhibits the same reactivity toward oxygen and light as the anthracene derivative **6**.

All the new hydrocarbons are white crystalline solids with melting points higher than 290 °C. In solution, the "bisphane" **6** and the "trisphane" **10** show intense fluorescence. Compared with the spectra of anthracene,[10] bathochromic shifts of 25 to 34 nm are observed for all bands in the UV spectra, and shifts of 37 to 42 nm as well as remarkable increases in quantum yields to $\Phi = 0.8$ (excitation wave length 388 nm) in the fluorescence spectra.[5]

The cyclic voltammogram of the "bisphane" **6** shows four reversible one-electron reduction waves at $E^0 = -1.93$, -2.43, -3.03 and -3.10 V, when measured in dimethylamine with 0.1 M tetrabutylammonium bromide[11] versus Ag/AgCl.[12] Since anthracene can only be reduced to a dianion in the accessible region, this means that **6** accepts two electrons in the central anthracene moiety and one each in its two phane units. In spite of its four *n*-hexyl groups, the 38 Å long "trisphane" **10** caused severe solubility problems. Nevertheless, two reversible one-electron and one reversible two-electron reduction waves were detected in the cyclic voltammogram of **10** at $E^0 = -1.93$, -2.06 and -2.41 V. A slight rise in the current at the limit of the supporting electrolyte reduction indicates a further charge-transfer step below -3.19 V. Obviously, the two anthracene units are again reduced to their dianionic redox states. The fifth redox step then leads to the charging of the phane units, which occurs at extremely negative potentials due to the strong Coulombic repulsion of the already existing excess charges.

Experimental[5]

3: M.p. = 234 °C (decomp.); ^{1}H NMR (250 MHz, $CDCl_3$): $\delta = 6.70$ (s, 8H), 7.51 (s, 4H); ^{13}C NMR (63 MHz, $CDCl_3$): $\delta = 130.79$ and 132.85 (C_{quart}), 133.07 and 134.55 (+); MS (70 eV): *m/z* 284 ($M^{\oplus}$, 100%).—**4**: M.p. = 220 °C; ^{1}H NMR (250 MHz, $CDCl_3$): $\delta = 6.70$ (s, 8H), 7.51 (s, 4H, 1′(3′,1″,3″)); ^{13}C NMR (63 MHz, $CDCl_3$): $\delta = 130.79$ and 132.85 (C_{quart}), 133.07 and 134.55 (+); MS (70 eV): *m/z* 284 ($M^{\oplus}$, 100%).—**6**: ^{1}H NMR (400 MHz, $CDCl_3$): $\delta = 0.88$ (t, 6H), 1.2–2.0 (m, 16H), 3.74 (t, 4H), 6.82 (AB system: $\delta_A = 6.78$, $\delta_B = 6.87$, $^3J_{AB} = 8$ Hz, 16H), 7.50 and 7.73 (AA′BB′ system, 8H), 8.60 (s, 4H); ^{13}C NMR (63 MHz, $CDCl_3$): $\delta = 13.86$ (+), 22.47, 28.22, 29.63, 31.36 and 31.56 (−), 120.69, 125.60 and 126.70 (+), 131.47 and 131.79 (+), 129.50, 134.95, 140.02, 140.12, 142.12 and 145.04 (C_{quart}); MS (70 eV): *m/z* 798.4221 ($M^{\oplus}$, calcd. 798.4226, 100%); UV/VIS (CH_2Cl_2): λ_{max} [nm] (ε) = 280 (118000), 350 (4000), 368 (6000), 388 (9150), 412 (8050); fluorescence (CH_2Cl_2; excitation at 388 nm): λ_{max} [nm] (rel. intensity) = 417 (0.9), 442 (0.8), 468 (0.3); $\Phi_F = 0.8$.—**8**: ^{1}H NMR (250 MHz, $CDCl_3$): $\delta = 2.29$ (s, 6H), 6.78 (AB system, $\delta_A = 6.74$, $\delta_B = 6.82$, $^3J_{AB} = 8.0$ Hz, 16H, phane arene-H), 7.50 and 7.70 (m, AA′BB′ system, 8H), 8.50 (s, 2H), 9.12 (s, 2H); ^{13}C NMR (63 MHz, $CDCl_3$): $\delta = 16.25$ (+), 119.64, 121.49, 125.78 and 127.10 (+), 128.16, 130.15 and 131.10 (C_{quart}), 131.57, 131.83, 131.89 (+), 140.49, 140.57, 142.57, 143.47 and 144.94 (C_{quart}); MS (70 eV): *m/z* 658 ($M^{\oplus}$, 100%).—**9**: ^{1}H NMR (250 MHz, $CDCl_3$): $\delta = 0.92$ (t, 6H), 1.30–1.85 (m, 16H), 3.45 (t, 4H), 6.77 (AB system: $\delta_A = 6.74$, $\delta_B = 6.80$, $^3J_{AB} = 8.6$ Hz, 8H), 7.51 and 7.72 (AA′BB′ system, 4H), 8.30 (s, 2H); ^{13}C NMR (63 MHz, $CDCl_3$): $\delta = 14.07$ (+), 22.64, 29.49, 29.67, 31.59 and 35.01 (−), 121.53 and 125.76 (+), 126.12 (C_{quart}), 127.16 (+), 130.63 (C_{quart}), 131.66 and 131.73 (+), 139.19, 139.87, 140.79, 143.40 and 144.75 (C_{quart}); MS (70 eV): *m/z* 681/679 ($M^{\oplus}$, 58/100%).—**10**: ^{1}H NMR (250 MHz, $CDCl_3$): $\delta = 0.90$ (m, 12H), 1.30–2.05 (m, 32H), 3.72 (m, 12H), 6.78 and 6.90 (m, 24H), 7.50 and 7.72 (AA′BB′ system, 8H), 8.52 and 8.57 (s, 8H); MS (FD): *m/z* 1292 ($M^{\oplus}$, 100%); UV/VIS (CH_2Cl_2): λ_{max} [nm] (ε) = 280 (118600), 351 (3480), 368 (5160), 388 (6960), 410 (6200); fluorescence (CH_2Cl_2; excitation at 388 nm): λ_{max} [nm] (rel. intensity) = 418 (0.7), 442 (0.7), 468 (0.3); $\Phi_F = 0.8$.

Received: April 4, 1991 [Z 4550 IE]
German version: *Angew. Chem. 103* (1991) 1350

[1] H. N. C. Wong, C. W. Chan, *J. Am. Chem. Soc. 110* (1988) 463.
[2] F. Gerson, A. de Meijere, O. Reiser, B. König, T. Wellauer, *J. Am. Chem. Soc. 112* (1990) 6827.
[3] A. de Meijere, B. König, J. Heinze, K. Meerholz, *Angew. Chem. 102* (1990) 1443; *Angew. Chem. Int. Ed. Engl. 29* (1990) 1418.
[4] M. Stöbbe, O. Reiser, R. Näder, A. de Meijere, *Chem. Ber. 120* (1987) 1667.
[5] All new compounds were fully characterized by $^1H/^{13}C$ NMR spectroscopy, (high resolution) mass spectrometry, and elemental analysis. Assignment of ^{13}C NMR signals by the DEPT technique, positive (CH_3, CH) and negative signals (CH_2) are designated + /− respectively, quaternary carbons (C_{quart}) show no signal in the DEPT spectra.
[6] H. Hart, C. Lai, G. C. Nwokogu, S. Shamouilian, *Tetrahedron 43* (1987) 5203.
[7] H. Hart, B. Hashewi, J. Luo, M. Meader, *Tetrahedron 42* (1986) 1641.
[8] For example, by treating a mixture of **4** and 2.5 equivalents of 1,2-dibromobenzene or 2,3-dibromonaphthalene with *n*-butyllithium at − 90 °C and warming the mixture up to room temperature, the *anti*- and *syn*-isomeric Diels Alder adducts were obtained in 82 and 71 % yield, respectively. Subsequent reductive deoxygenation with $TiCl_4/LiAlH_4$ afforded the yet unknown[1] fully aromatic 1:2,9:10-bisnaphtho[2.2]paracyclophane-1,9-diene and 1:2,9:10-bisanthraceno[2.2]paracyclophane-1,9-diene, respectively.
[9] K. Blatter, A. D. Schlüter, *Chem. Ber. 122* (1989) 1351.
[10] Cf. B. M. Krasovitskii, B. M. Bolatin: *Organic Luminescent Materials*, VCH, Weinheim 1988, p. 277.
[11] K. Meerholz, J. Heinze, *J. Am. Chem. Soc. 111* (1989) 2325.
[12] Three of these reduced species have also been detected by ESR/ENDOR spectroscopy, but the interpretation requires deuterium labeled compounds with a reduced set of protons. F. Gerson, T. Wellauer, B. König, A. de Meijere, unpublished results.

Metal-Ion Dependent Regioselectivity in Cyclometalation Reactions**

By *Edwin C. Constable,* Roland P. G. Henney, Paul R. Raithby,* and *Lynn R. Sousa*

Cyclometalated compounds contain chelated ligands in which one of the donor sites is an anionic carbon center.[1] Recently, there has been particular interest in species in which the carbon center is formally an aryl anion,[2] and we have been investigating the features which favor the formation of such compounds.[3,4] The ligand 6-(2-thienyl)-2,2′-bipyridine (HL) has proved to be of particular interest, and forms complexes in which it behaves as an N-, N,N-, N,N,S- or N,N,C-donor ligand.[3,4] In this communication we wish to describe the behavior of HL with d^8 metal centers, and correct an earlier misassignment of the structure of a gold(III) complex.[4]

The reaction of HL with $K_2[MCl_4]$ (M = Pd or Pt) in aqueous acetonitrile at room temperature results in the direct and near-quantitative formation of the cyclometalated complexes [MLCl] **1** as yellow-brown microcrystalline solids. Each compound exhibits peaks assigned to $[ML]^+$ and $[MLCl]^+$ in their FAB mass spectra (3-nitrobenzyl alcohol matrix). The ^1H-NMR spectra of CD_2Cl_2 solutions of the complexes are sharp and well-resolved, and may be fully assigned using a double quantum filtered phase-sensitive COSY experiment. In each case only two resonances, a pair of doublets, are assigned to H4″ and H5″ of the metalated thienyl ring. In the platinum complex H4″ and H5″ also exhibit satellites due to coupling with ^{195}Pt of 20 Hz and 8 Hz respectively. The $^3J_{H\text{-}H}$ coupling constant of 4.8 Hz establishes the site of metalation as C3′, because in thiophenes $^3J_{2,3}$ ($\equiv {}^3J_{4,5}$) lies in the range 4.90–5.80 Hz, whereas $^3J_{3,4}$ is in the range 2.45–4.35 Hz.[5]

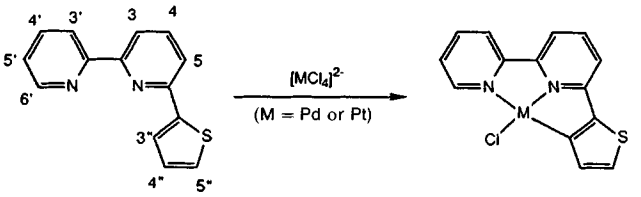

HL **1**

In contrast to the above, the reaction of $Na[AuCl_4]$ with HL in aqueous acetonitrile results in the precipitation of a non-metalated complex $[Au(HL)Cl_3]$ **2** as an orange microcrystalline solid in 95 % yield. The ^1H-NMR spectrum of this complex clearly exhibits three resonances assigned to the non-metalated thienyl ring. We believe the compound to be similar in structure to $[Au(bipy)Cl_3]$.[6]

The reaction of HL with $Na[AuCl_4]$ at 90 °C in aqueous acetonitrile results in the formation of a red-brown crystalline product **3**; the same compound is obtained by heating **2** under similar conditions. Microanalysis indicates a formulation $[AuLCl_2]$ to be appropriate, and the ^1H-NMR spectrum confirms the presence of a metalated thienyl ring showing only two doublet resonances (CD_2Cl_2, $\delta = 7.06$, 7.44, $^3J_{HH}$ 3.9 Hz). A detailed analysis of the ^1H-NMR spectrum of **3** suggested that only the terminal pyridine ring was coordinated, whilst the central pyridine was not. Furthermore, the coupling constants within the metalated ring (3.9 Hz) are indicative of a compound containing H3″ and H4″ rather than one which is metalated at the expected 3″-position. These observations are at odds with our previous belief that the complex was analogous to those formed with palladium(II) and platinum(II), and in order to clarify the position we have determined the crystal and molecular structure of **3**.[7] It proved to be extremely difficult to grow crystals of **3**, but eventually one poor quality crystal was obtained.

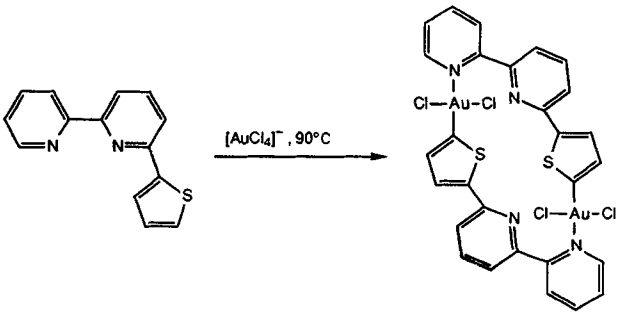

3

[*] Dr. E. C. Constable, Dr. R. P. G. Henney, Dr. P. R. Raithby
University Chemical Laboratory
Lensfield Road, Cambridge, CB2 1EW (UK)
Professor L. R. Sousa,
Department of Chemistry
Ball State University
Muncie, IN 47306 (USA)

[**] This work was supported by the U.K. Science and Engineering Research Council (Studentship for *R.P.G.H.*). We also thank the Royal Society of Great Britain for assistance in the purchase of spectrometers and Johnson Matthey p.l.c. for support and the loan of precious metal salts.

The crystal and molecular structure of **3** is shown in Figure 1. The compound is dimeric and contains two crystallographically non-equivalent $[AuLCl_2]$ units. Each thiophene is metalated at the 5″-position; the C–Au distances 1.95(3) and 2.00(4) Å are unremarkable and typical of gold(III) organometallic compounds. The two gold centers are approximately square-planar (the greatest deviation of any atom from each of the square planes is 0.1 Å), with the coordination sphere being completed by two *trans* chlorines and the nitrogen of the terminal pyridine ring of the second ligand. The gold–chlorine and gold–nitrogen distances are typical for gold(III) complexes. Each ligand acts as a bridging C,N-donor to two gold centers; the ligands are metalated but not *cyclo*metalated. The central pyridine ring of each ligand is noncoordinated. The dimeric structure is achieved by twisting the molecule about the internuclear C–C bonds between the pyridyl (33.4°, 41.5°) and the pyridyl and thienyl rings (14.8°, 4.4°).

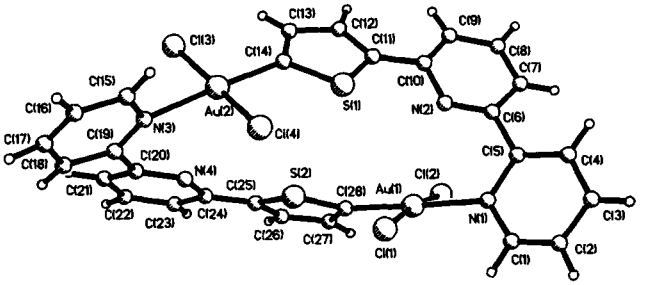

Fig. 1. The crystal and molecular structure of **3** showing the numbering scheme adopted. Important bond lengths [pm] and angles [°]: Au(1)-Cl(1) 227.9(14), Au(1)-Cl(2) 2279(12), Au(1)-N(1) 206.3(26), Au(1)-C(28) 195.3(29), Au(2)-Cl(3) 225.4(12), Au(2)-Cl(4) 227.9(12), Au(2)-C(14) 200.0(39), Au(2)-N(3) 211.1(34), Cl(1)-Au(1)-Cl(2) 172.5(5), Cl(1)-Au(1)-N(1) 90.2(10), Cl(2)-Au(1)-N(1) 88.3(9), Cl(1)-Au(1)-C(28) 88.8(13), Cl(2)-Au(1)-C(28) 93.0(12), N(1)-Au(1)-C(28) 177.7(17), Cl(3)-Au(2)-Cl(4) 173.7(4), Cl(4)-Au(2)-C(14) 92.3(12), Cl(4)-Au(2)-N(3) 89.6(10), Cl(3)-Au(2)-C(14) 91.2(12), Cl(3)-Au(2)-N(3) 87.2(10), C(14)-Au(2)-N(3) 176.2(16)

We have no evidence for the formation of 5″-metalated complexes with palladium(II) or platinum(II) compounds, or of 3″-metalated compounds with gold(III). Significantly, reactions of 2-(2′-thienyl)pyridine (HL′) appear to parallel this behavior; reaction with palladium(II) acetate or with $Li_2[PdCl_4]$ results in clean metalation at C3″ ($^3J_{4,5}$ 4.9 Hz), whereas reaction with $Na[AuCl_4]$ results in the formation of the non-metalated compound $[Au(HL')Cl_3]$ **4**.[8, 9] Upon heating **4** to 90 °C in aqueous acetonitrile a mixture of products derived from a range of reactions (chlorination, oxidative dimerization *etc.*) at C5″ are obtained in low yield. This is compatible with the formation of the non-strained chelated cyclometalated ring in the case of the metal(II) centers, and reflects the inability of the Au^{II} center to form either a complex cyclometalated at C3″ or a dimer in this case.

It has previously been noted that 2-(2′-thienyl)-pyridine forms a kinetic 3-lithio and a thermodynamic 5-lithio derivative.[10] In the case of the HL ligand, we believe that all of the metalated products are obtained under thermodynamic control; there is no evidence for the formation of other metalated species. We suggest that the differences in reactivity with isoelectronic d^8 ions result from the interplay between the differing sizes of the metal ions and the fixed 'bite' of the cyclometalated N,C donor mode. We are currently investigating the photochemical and photophysical properties of these unusual gold(III) complexes.

Experimental Procedure

The gold complexes **2** and **3** and the ligand HL were prepared as reported previously [4]. X-ray quality crystals of **3** were obtained by the diffusion of diethyl ether vapor into a solution of **3** in *N,N*-dimethylformamide.

1 (M = Pd): A solution of HL (0.016 g, 0.066 mmol) in acetonitrile (1.5 mL) was added to an aqueous solution of $K_2[PdCl_4]$ (0.022 g, 0.066 mmol in 1 mL water). The resulting solution was heated to 60 °C for 2 h., whereupon a yellow solid precipitated. This was collected by filtration to give **1** (M = Pd) [Yield 0.026 g, 99 %]. Correct C, H, N, Cl analysis. ^{1}H NMR (CD_3SOCD_3) δ = 8.62 (m, $^3J(5,6)$ = 5.1 Hz; H 6′, 7.80 (dd, $^3J(5,6)$ = 5.1, $^3J(5,4)$ = 7.6 Hz; H 5′), 8.28 (dd, $^3J(4,5)$ = 7.6, $^3J(3,4)$ = 7.9 Hz; H 4″), 8.49 (d, $^3J(3,4)$ = 7.9 Hz; H 3′) 8.05 (m, $^3J(x,4)$ = 7.9 Hz; H 4 and H 3 or H 5), 7.60 (d, $^3J(x,4)$ = 7.9 Hz; H 3 or H 5) 7.07 (d, $^3J(4,5)$ = 4.8 Hz; H 4″) 7.67 (d, $^3J(4,5)$ = 4.8 Hz; H 5″); FAB-MS (3-nitrobenzyl alcohol matrix) m/z = 378, 380 (PdLCl), 343 (PdL).

1 (M = Pt): A solution of HL (0.050 g, 0.21 mmol) in acetontrile (3 mL) was added to an aqueous solution of $K_2[PtCl_4]$ (0.085 g, 0.205 mmol in 4 mL water). The resulting solution was heated to reflux for 20 h., whereupon a brown solid precipitated. This was collected by filtration to give **1** (M = Pt) [Yield 0.086 g, 97 %]. Correct C, H, N, Cl analysis. ^{1}H NMR (CD_3SOCD_3) δ = 8.85 (m, $^3J(5,6)$ = 5.2 Hz; H 6′), 7.91 (dd, $^3J(5,6)$ = 5.2, $^3J(5,4)$ = 7.8 Hz; H 5′), 8.35 (t, $^3J(4,5)$ = 7.8, $^3J(3,4)$ = 7.8 Hz; H 4′), 8.47 (d, $^3J(3,4)$ = 7.8 Hz; H 3′), 7.98 (m, $^3J(x,4)$ = 7.9 Hz; H 4 and H 3 or H 5), 7.56 (d, $^3J(x,4)$ = 7.9 Hz; H 3 or H 5), 6.97 (d, $^3J(4,5)$ = 4.7 Hz; H 4″), 7.83 (d, $^3J(4,5)$ = 4.7 Hz; H 5″); FAB-MS (3-nitrobenzyl alcohol matrix) m/z = 468, 470 (PtLCl + H), 432 (PtL).

Received: May 16, 1991 [Z 4633 IE]
German version: *Angew. Chem. 103* (1991) 1401

CAS Registry numbers:
1 (M = Pd), 136044-30-9; **1** (M = Pt), 136044-31-0; **2**, 136044-32-1; **3**, 136044-33-2; HL, 123760-40-7; HL′, 3319-99-1; $K_2[PtCl_4]$, 10025-98-6; $K_2[PdCl_4]$, 10025-99-7; $Na[AuCl_4]$, 15189-51-2; $Li_2[PdCl_4]$, 15525-45-8; Palladium(II)-acetate, 3375-31-3.

[1] I. Omae: *Organometallic Intramolecular-coordination Compounds, Journal of Organometallic Chemistry Library, 18*, Elsevier, Amsterdam 1986; J. Dehand, M. Pfeffer, *Coord. Chem. Rev. 18* (1976) 327; A. K. Prokof'ev, B. I. Brezasze, O. Yu. Okhlobystin, *Usp. Khim. Akad. Nauk SSSR, 39* (1970) 412; G. W. Parshall, *Acc. Chem. Res. 3* (1970) 139; M. Nonoyama, *Kagaku no Ryoiki 28* (1974) 674; M. I. Bruce, *Angew. Chem. 89* (1977) 75; *Angew. Chem. Int. Ed. Engl. 16* (1977) 73.
[2] E. C. Constable, *Polyhedron 3* (1984) 1037.
[3] E. C. Constable, *J. Chem. Soc. Dalton Trans 1985*, 1719; E. C. Constable, J. M. Holmes, *J. Organomet. Chem. 301* (1986) 203; E. C. Constable, T. A. Leese, *J. Organomet. Chem. 335* (1987) 293; *J. Organomet. Chem. 363* (1989) 419; E. C. Constable, T. A. Leese, D. A. Tocher, *J. Chem. Soc. Chem. Commun. 1989*, 570; *Polyhedron 9* (1990) 1613; E. C. Constable, R. P. G. Henney, D. A. Tocher, *J. Chem. Soc. Chem. Commun. 1989*, 913; *J. Chem. Soc. Dalton Trans*, in press; E. C. Constable, R. P. G. Henney, T. A. Leese, D. A. Tocher, *J. Chem. Soc. Dalton Trans. 1990*, 443; E. C. Constable, C. E. Housecroft, *Polyhedron 9* (1990) 1939; E. C. Constable, R. P. G. Henney, T. A. Leese, D. A. Tocher, *J. Chem. Soc. Chem. Commun. 1990*, 513; E. C. Constable, A. M. W. Cargill Thompson, T. A. Leese, D. G. F. Rees, D. A. Tocher, *Inorg. Chim. Acta 182* (1991) 93.
[4] E. C. Constable, R. P. G. Henney, T. A. Leese, *J. Organomet. Chem. 361* (1989) 277.
[5] S. Gronowitz, *Adv. Heterocycl. Chem. 1* (1963) 1.
[6] W. Micklitz, B. Lippert, G. Muller, P. Mikulcik, J. Riede, *Inorg. Chim. Acta 165* (1989) 57.
[7] Crystal data for **3**: $C_{28}H_{18}N_4S_2Cl_4Au_2$, triclinic, $P\bar{1}$, a = 9.271(5), b = 14.214(10), c = 16.194(10) Å, α = 108.11(5), β = 96.55(5), γ = 111.46(5)°, V = 1824(2) Å^3, M = 1010.3, Z = 2, ϱ_{calcd} = 1.840 g cm^{-1}, $F(000)$ = 944, $Mo_{K\alpha}$ radiation, λ = 0.71069 Å, $\mu(Mo_{K\alpha})$ = 8.449 mm^{-1}. The structure was solved by direct methods and refined by blocked full-matrix least squares; Au, S, Cl, N atoms anisotropic; H atoms riding on appropriate carbon atom with fixed isotropic U. A disordered solvent molecule was present for which no good model could be found. 5170 reflections measured ($5 < 2\theta < 45°$), corrected for absorption, 4668 unique observed reflections with $F > 5\sigma(F)$, R = 0.068, wR = 0.087. Further details of the crystal structure investigation are available on request from the Director of the Cambridge Crystallographic Data Centre, University Chemical Laboratory, Lensfield Road, GB-Cambride CB2 1EW (UK) on quoting the full journal citation.
[8] M. Nonoyama, S. Kajita, *Transition Met. Chem. (Weinheim, Ger.) 6* (1981) 163; T. J. Giordiano, P. G. Rasmussen, *Inorg. Chem. 14* (1975) 1628.
[9] E. C. Constable, L. R. Sousa, unpublished results.
[10] T. Kauffmann, A. Mitschker, *Tetrahedron Lett. 1973*, 4039.

Novel Reactions of Disubstituted 1,2-Dioxetanes with Olefins as π-Nucleophiles: Cycloadditions via 1,6-Dipoles**

By *Waldemar Adam,** *Simone Andler,* and *Markus Heil*

In view of their ability to serve as an efficient source of excited carbonyl products, 1,2-dioxetanes have been the subject of intensive investigation for almost twenty years.[1] However, aside from unimolecular fragmentations in excited carbonyl compounds, only little was hitherto known about the chemical transformations of these strained peroxides. One of the first reactions of 1,2-dioxetanes with heteroatomic nucleophiles to be reported was their deoxygenation by phosphanes.[2] Biphylic insertion into the peroxide bond first yields a pentacovalent intermediate, which, after thermal elimination of phosphane oxide affords the epoxide. Also the reaction of dioxetanes with sulfides[3] generates epoxides, whereas lithium aluminum hydride,[4] thiols[5] and biologically relevant reductants,[6] such as ascorbic acid or NADH, reduce 1,2-dioxetanes to 1,2-diols. Moreover, although reactions of cyclic acyl peroxides[7] with π-nucleophiles, e.g. olefins, are quite common, such transformations do not appear to be known in the case of dioxetanes. In this communication we report the cycloaddition of 3,3-disubstituted 1,2-dioxetanes **1** with electron-rich olefins **2** to afford unusual products, whose structure depend on the type of olefin and solvent employed (Scheme 1, Table 1).

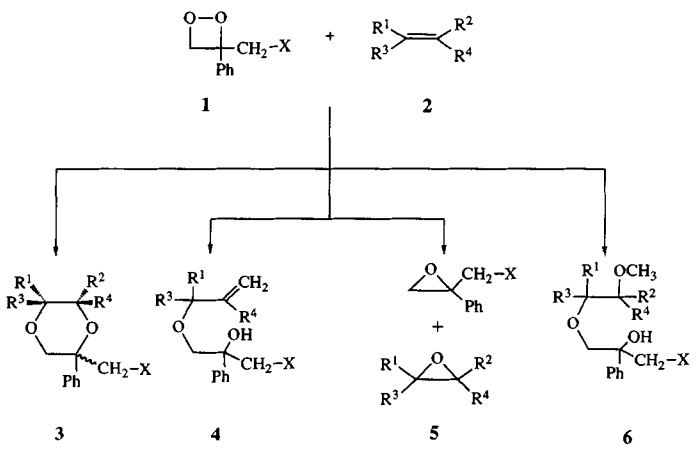

Scheme 1. **1a**: X = H; **1b**: X = Cl; **1c**: X = Br; **2a**: $R^1 = R^2 = R^3 = R^4 = OEt$; **2b**: $R^1 + R^2 = -OCH_2CH_2O-$, $R^3 = R^4 = H$; **2c**: $R^1 = R^2 = CH_3$, $R^3 + R^4 = o\text{-}OC_6H_4O$; **2d**: $R^1 = R^2 = CH_3$, $R^3 + R^4 = (CH_2)_3$; **2e**: $R^1 = R^2 = R^3 = R^4 = CH_3$; **3a**: $R^1 = R^2 = R^3 = R^4 = OEt$, X = Br; **3b**: $R^1 + R^2 = -OCH_2CH_2O-$, $R^3 = R^4 = H$, X = Br; **4a**: $R^1 = CH_3$, $R^3 + R^4 = o\text{-}OC_6H_4O$, X = Br; **4b**: $R^1 = CH_3$, $R^3 + R^4 = (CH_2)_3$, X = Br; **4c**: $R^1 = R^3 = R^4 = CH_3$, X = Br; **4d**: $R^1 = R^3 = R^4 = CH_3$, X = H; **4e**: $R^1 = R^3 = R^4 = CH_3$; X = Cl; **5a**: $R^1 = R^2 = CH_3$, $R^3 + R^4 = (CH_2)_3$; **5b**: $R^1 = R^2 = R^3 = R^4 = CH_3$; **6**: $R^1 = R^2 = R^3 = R^4 = CH_3$; X = Br.

The dioxetane **1a** was synthesized as described in the literature.[8] The previously unknown halogen-substituted derivatives **1b** and **1c**[9] were prepared from the corresponding β-bromohydroperoxides according to the usual Kopecky method.[4]

[*] Prof. Dr. W. Adam, S. Andler, Dipl.-Chem. M. Heil
Institut für Organische Chemie der Universität
Am Hubland, W-8700 Würzburg (FRG)

[**] This work was supported by the Deutsche Forschungsgemeinschaft (SFB 172 "Molekulare Mechanismen kanzerogener Primärveränderungen") and the Wilhelm-Sander-Stiftung. We are grateful to Prof. Dr. *R. Saalfrank*, Erlangen, for a sample of tetraethoxyethene.

The reaction of dioxetane **1c** with tetraethoxyethene **2a** and 1,4-dioxene **2b**, electron-rich olefins without allylic hydrogen, afforded the dioxane derivatives **3** in good yields; cleavage of the dioxetane into carbonyl fragments occurred only to a small extent (Table 1), and deoxygenation to epoxides was not observed. The moisture-sensitive orthoester product **3a** (m.p. 47–48 °C) showed characteristic singlets at $\delta = 108.8$ and 109.4 in the ^{13}C-NMR spectrum ($CDCl_3$, 63 MHz) for the orthoester carbon atoms. The cycloadduct **3b** formed from dioxetane **1c** and 1,4-dioxene **2b**, was established as its *cis* isomer (coupling between the acetal protons: $J = 1.6$ Hz) and was isolated as the diastereomeric mixture (52:48).

Table 1. Reaction of dioxetane **1c** [a] with olefins **2**.

Olefin	Reaction Conditions: solvent	T [°C]	t [h]	Product Distribution [%] [b]: Adduct [c]	Epoxide [d]	Ketone [e]
2a	CH_2Cl_2	−30	0.5	**3a**: 83 (74)	0	17
2b	CH_2Cl_2	−20	1	**3b**: 78 (59) (*dr* = 52:48)	0	22
2c	CH_2Cl_2	−20	2	**4a**: 78 (38) (*dr* = 59:41)	0	22
2d	CH_2Cl_2	−20	8	**4b**: 80 (65) (*dr* = 77:23)	4	16
2e	CH_2Cl_2	−10	2	**4c**: 73 (58)	6	21
2e	CH_3OH	−20	1	**4c**: 10 **6**: 84 (73)	0	6

[a] For the reaction of **1a**, **b** with 2,3-dimethyl-2-butene cf. Ref. [13]. [b] Determined by ^{1}H-NMR spectroscopy (250 MHz) and yields refer to 100% dioxetane consumption; mass balance > 90%. [c] The adducts were isolated by column chromatography and the yields are given in parenthesis; *dr* = diastereomeric ratio. [d] 2-Bromomethyl-2-phenyloxirane and [e] ω-Bromoacetophenone were not isolated but identified by means of their characteristic ^{1}H-NMR signals.

In contrast, reaction of the 2,3-dimethylbenzo-1,4-dioxene **2c** with dioxetane **1c** furnished the ene product **4a** as the main product (two diastereomers, 59:41), together with appreciable amounts of ω-bromoacetophenone as cleavage product from dioxetane **1c** (Table 1). Epoxides or cycloadducts **3** were not observed. In a similar way, 1,2-dimethylcyclopentene **2d** and 2,3-dimethyl-2-butene **2e** gave with dioxetane **1c** the corresponding ene products, namely the β-methylene-β′-hydroxy ethers **4b**, **c**; two diasteromers (77:23) were found for the ene product derived from olefin **2d**. No cycloadducts **3** were detected, but cleavage into carbonyl products and deoxygenation of the dioxetane **1c** leading to 2-bromomethyl-2-phenyloxirane, together with the corresponding oxygen transfer products 1,2-dimethyl-1,2-epoxycyclopentane **5a**[11a] and 2,3-dimethyl-2,3-epoxybutane[11b] **5b**, were observed. Likewise, reaction of the dioxetanes **1a**, **b** with 2,3-dimethyl-2-butene **2e** resulted mainly in the formation of the ene products **4d**, **e** and small amounts of the corresponding epoxides,[12] besides considerable quantities of ketones from dioxetane cleavage. When the reaction of olefin **2e** and dioxetane **1c** was carried out in methanol, hydroxy ether **6** was obtained as the main product, the ene product **4c** was formed in only ca. 10% yield.

The two-step character of the reaction between dioxetanes **1** and olefins is evident from the observation of the cycloadducts **3**, the ene products **4**, and the methanol adduct **6**. The 1,6-dipole **7**, which is formed by attack of the π-nucleophile on the peroxide bond of the dioxetane, and is stabilized by the epoxide valence-isomeric structure **7′**, presumably operates as bona fide intermediate. All products can be convincingly explained via this dipolar intermediate. When the car-

bocation center does not bear methyl groups (olefins **2b**, **c**), the 1,6-dipole **7** cyclizes to the cycloadducts **3** (Scheme 1). Methyl groups at the carbocation center (olefins **2c**, **e**) lead exclusively to the ene product **4** by hydrogen atom abstraction. In presence of methanol, the 1,6-dipole is trapped as the hydroxy ether **6**.

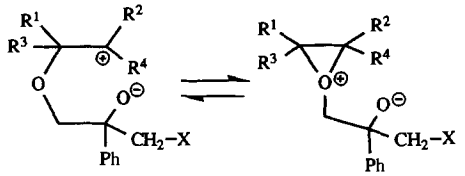

7 **7′**

In the case of the halogen-substituted dioxetanes **1b** and **1c**, instead of proton abstraction to afford the corresponding ene product, the 1,6-dipole might have also extruded halogen to give a terminal epoxide, but we did not detect it. From the point of view of energy, halogen elimination seems unfavorable compared with deprotonation, because in the former case an ion pair is formed, whereas in the latter case the charges of dipole **7** are annihilated in one step and the stable ene product **4** is formed.

It remains to explain the formation of the side products. Epoxide **5** and the expoxide derived from the dioxetane are formed by nucleophilic attack of the alkoxide center on the methylenic carbon of the dioxetane moiety of the epoxide-like 1,6-dipole **7′**. The carbonyl fragmentation products ω-bromoacetophenone and formaldehyde suggest a catalytic decomposition of the dioxetane **1**, which might arise by fragmentation of the 1,6-dipole **7** with regeneration of the olefin.

To summarize, we have found that 3,3-disubstituted 1,2-dioxetanes are quite different from the tetrasubstituted derivatives in their reactivity towards π-electron donors. For example, the reaction of tetramethyldioxetane with electron-rich olefins leads exclusively to fragmentation into carbonyl compounds instead of cycloaddition (Scheme 1). This difference in behavior is rationalized in terms of the transition states **A** or **B**. We postulate these in the attack of the 3,3-di-

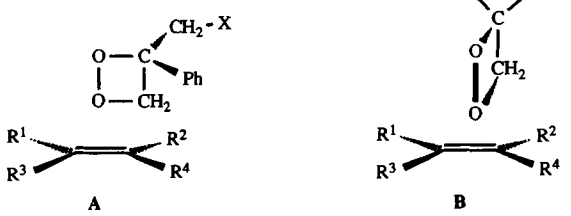

A **B**

substituted dioxetane on the olefin, but for steric reasons they are unlikely in the case of tetrasubstituted dioxetanes. Of the two possibilites, again on steric grounds, transition state **A** should be preferred. A comprehensive theoretical study of these novel reactions is necessary.

Received: April 30, 1991 [Z 4602 IE]
German version: *Angew. Chem. 103* (1991) 1395

CAS Registry numbers:
1c, 136132-07-5; **2a**, 40923-93-1; **2b**, 543-75-9; **2c**, 79792-92-0; **2d**, 765-47-9; **2e**, 563-79-1; **3a**, 136132-01-9; **3b** (isomer 1), 136132-02-0; **3b** (isomer 2), 136132-08-6; **4a** (isomer 1), 136132-03-1; **4a** (isomer 2), 136132-09-7; **4b** (isomer 1), 136132-04-2; **4b** (isomer 2), 136132-10-0; **4c**, 136132-05-3; **6**, 136132-06-4; ω-bromoacetophenone, 70-11-1.

[1] a) G. Cilento, W. Adam, *Photochem. Photobiol. 48* (1988) 361; b) W. Adam, T. Mosandl, C. R. Saha-Möller in W. Ando (Ed.): *Organic Peroxides*, Wiley, Chichester, England, in press.
[2] P. D. Bartlett, M. E. Landis, M. J. Shapiro, *J. Org. Chem. 42* (1977) 1661.
[3] a) H. H. Wasserman, I. Saito, *J. Am. Chem. Soc. 97* (1975) 905; b) W. Adam, L. Hadjiarapoglou, T. Mosandl, C. R. Saha-Möller, D. Wild, *Angew. Chem. 103* (1991) 187; *Angew. Chem. Int. Ed. Engl. 31* (1991) 200; F. Vargas, *Dissertation*, Universität Würzburg 1989.
[4] K. R. Kopecky, J. E. Filby, C. Mumford, P. A. Lockwood, J.-Y. Ding, *Can. J. Chem. 53* (1975) 1103.
[5] W. Adam, B. Epe, D. Schiffmann, F. Vargas, D. Wild, *Angew. Chem. 100* (1988) 443; *Angew. Chem. Int. Ed. Engl. 27* (1988) 249.
[6] W. Adam, B. Epe, D. Schiffmann, F. Vargas, D. Wild, *Free Radical Res. Commun. 5* (1989) 253.
[7] a) F. D. Greene, W. W. Rees, *J. Am. Chem. Soc. 80* (1958) 3432; b) W. Adam, A. Griesbeck, D. Kappes, *J. Org. Chem. 51* (1986) 4479.
[8] M. A. Umbreit, E. H. White, *J. Org. Chem. 41* (1976) 479.
[9] The dioxetane **1b** (m.p. 31–33 °C) was prepared from 3-chloro-2-phenyl-1-propene in 27% yield, [10a] while **1c** (m.p. 58–59 °C) was prepared from 3-bromo-2-phenyl-1-propene [10b], also in 27% yield.
[10] a) H. E. Zimmerman, R. A. Bunce, *J. Org. Chem. 47* (1982) 3377; b) J. Mulzer, G. Brüntrup, U. Kühl, G. Hartz, *Chem. Ber. 115* (1982) 3453.
[11] a) L. E. Friedrich, R. A. Fiato, *J. Am. Chem. Soc. 96* (1974) 5783; b) E. L. Eliel, M. N. Rerick, *ibid. 82* (1960) 1362.
[12] a) 2-Methyl-2-phenyloxirane: F. Francesco, F. Pizzo, R. Germani, G. Savelli, *Org. Prep. Proced. Int. 21* (1989) 757; b) 2-Chlormethyl-2-phenyloxirane: J. Barluenga, J. L. Fernandez-Simon, J. M. Concellon, M. Yus, *J. Chem. Soc. Perkin Trans. 1 1989*, 77.
[13] Reaction of the dioxetane **1a** with 2,3-dimethyl-2-butene in CH_2Cl_2 at −20 °C gave the ene product **4d** (44%), 2-methyl-2-phenyloxirane (20%), and acetophenone (36%), while dioxetane **1b** led under these conditions to ene product **4e** (72%), 2-chloromethyl-2-phenyloxirane (1%), and ω-chloroacetophenone (28%).

The Mechanism of Acylcarbene Insertion into O–H Bonds—Direct Observation of the Enol of a Carboxylic Acid Ester in Aqueous Solution**

By *Yvonne Chiang, A. Jerry Kresge,* Przemyslaw Pruszynski, Norman P. Schepp,** and *Jakob Wirz*

One of the most common reactions of carbenes is their insertion into X–H bonds,[1] especially into the O–H bonds of alcohols and water.[2] A number of different mechanisms have been proposed for the O–H insertion reaction,[2, 3] all of which involve direct and exclusive attack of the alcohol or water at the carbene carbon atom. We wish to report that we have observed the formation of an enol intermediate in the reaction of phenylcarbomethoxycarbene **1**[4] with water, and have been able to demonstrate that "insertion" in this case involves the carbonyl group as well [Eq. (a)]; the process

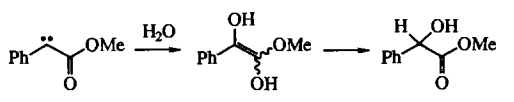

1 **2** **3** (a)

may therefore be more accurately described as conjugate addition of water across the entire acylcarbene function. The enol intermediate observed is the enol tautomer **2** of methyl mandelate **3**, and our detection of this species constitutes the

[*] Dr. N. P. Schepp, Prof. Dr. J. Wirz
Institut für Physikalische Chemie der Universität
CH-4056 Basel (Switzerland)
Prof. Dr. A. J. Kresge, Y. Chiang, Dr. P. Pruszynski
Department of Chemistry, University of Toronto
Toronto, Ontario M5S 1A1 (Canada)

[**] This work was supported by the Natural Sciences and Engineering Research Council of Canada, of the Donors of the Petroleum Research Fund, administered by the American Chemical Society, and the Swiss National Science Foundation.

first direct observation of a carboxylic acid ester enol in aqueous solution.

We generated the carbene **1** by photolysis of methyl phenyldiazoacetate **4**,[5] [Eq. (b)]. The product **3** expected

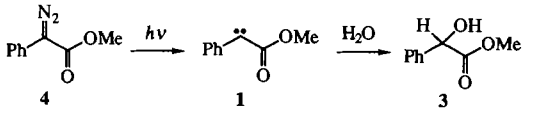

(b)

from the insertion of **1** into the O–H bond of water was the only material produced by photolysis in aqueous solution over the pH range from 1 to 13. When the photolysis was conducted in ^{18}O-enriched water, the isotopic label appeared exclusively in the α-hydroxy group of **3**, thus confirming the occurrence of an O–H "insertion" reaction.

Laser flash photolysis of **4** in aqueous solution produces two transient species (Fig. 1). The longer-lived transient

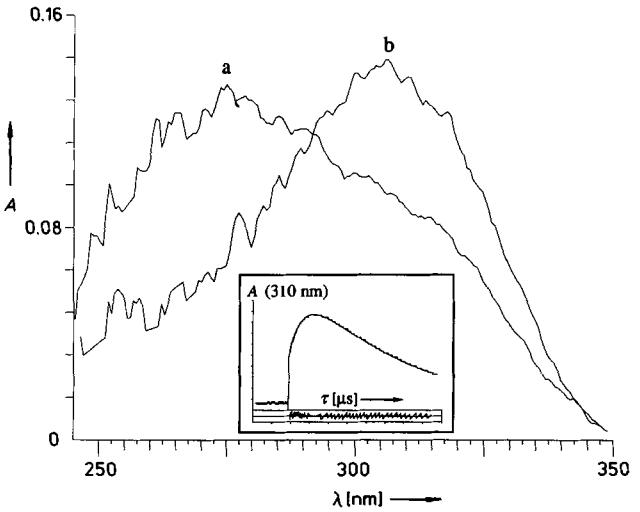

Fig. 1. Absorption spectra of the transients generated upon flash photolysis of **4** in ca. 0.0001 M NaOH at 25 °C (I = 0.10 M) using an excitation pulse from a KrF-excimer-laser (λ_{exc} = 248 nm, 20 ns pulse width, 100 mJ per pulse). Curve a represents the absorption immediately after the laser pulse; curve b represents the absorption 1 μs after the pulse. The inset shows the time-dependent absorbance changes at λ = 310 nm; the bottom trace shows residuals from a least squares fit of the data to a double exponential expression which gives the rate constants $k_{formation} = 2.3 \times 10^6\ s^{-1}$ and $k_{decay} = 4.3 \times 10^5 s^{-1}$.

shows an absorption band with $\lambda_{max} \approx 280$ nm in acidic solution which shifts to $\lambda_{max} \approx 310$ nm in basic solution (Fig. 1., curve b), as expected for conversion of an enol into its enolate ion.[6] Decay of this transient is catalyzed by both acids and bases, showing general catalysis in both cases, and it gives the rate dependence on the concentration of the solvent-related species, $H^{\oplus}$ and $OH^{\ominus}$, depicted by curve a in Figure 2. Such behavior is typical for the ketonization of enols,[7] and in particular the rate profile is closely similar, both in shape and in magnitude of rate constants, to that for the ketonization of the enol of mandelic acid.[8] The saturation of the base catalysis observed between $[H^{\oplus}] = 10^{-6}$ and 10^{-7} M is the result of the ionization of enol **2** as an oxygen acid [Eq. (c)] to give the enolate ion $\mathbf{2}^{\ominus}$, and the kinetic data obtained in this region plus a spectrophotometric titration curve[9] lead to the acidity constant, $pK_a^E = 6.45 \pm 0.14$; this value is similar to that obtained for the first ionization of the

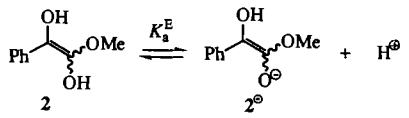

(c)

enol of mandelic acid ($pK_a^E = 6.62 \pm 0.07$).[8] The flat portion of the rate profile at $[H^{\oplus}] < 10^{-7}$ M represents ketonization through reaction of the anion $\mathbf{2}^{\ominus}$ with water [Eq. (d)]. A comparison of the rates of reaction in this region measured in H_2O with those measured in D_2O gives the isotope effect $k_H/k_D = 7.5$, which is consistent with expectation for this kind of reaction and similar again to values obtained for other enols: $k_H/k_D = 6.9$ (mandelic acid enol)[9] and $k_H/k_D = 7.5$ (isobutyrophenone enol).[10]

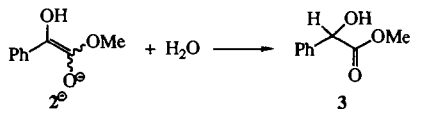

(d)

These observations indicate that the longer-lived transient species observed upon flash photolysis of **4** in aqueous solution is the enol **2** of methyl mandelate **3**. This assignment then suggests that the shorter-lived transient is the carbene **1**. The absorption spectrum of this transient in aqueous solution, $\lambda_{max} \approx 275$ nm (Fig. 1, curve a), is similar to that previously reported for **1** in Freon 113.[4] However, unlike in the previous study, we did not observe any influence of oxygen concentration on the rate of decay of **1**, nor did we detect the presence of the carbonyl oxide produced by reaction of **1** with oxygen.[4] This change upon going from Freon 113 to aqueous solutions may be attributed to the low solubility of oxygen in water, or to a shift of the carbene singlet-triplet equilibrium more to the side of the singlet carbene in water.[11]

Hydration of the carbene **1** to the enol **2** is catalyzed by both acids and bases, and both catalyses are once again general in type. The rate profile for reaction through solvent-related species is shown by curve b in Figure 2. The catalytic

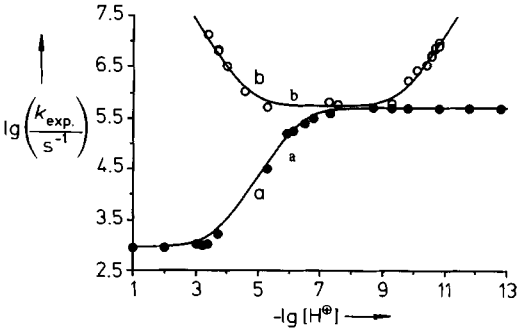

Fig. 2. Rate profile for a) the ketonization of **2** and b) the hydration of **1** in aqueous solution at 25 °C, I = 0.10 M. Data for the pH range 4–11 were obtained from measurements in HOAc, $H_2PO_4^{\ominus}$, $NH_4^{\oplus}$, $HCO_3^{\ominus}$ and $Et_3NH^{\oplus}$ buffers extrapolated to zero buffer concentration.

coefficients for general base catalysts give a shallow Brønsted relation with the exponent $\beta = 0.2$, and the isotope effect for catalysis by hydronium ions in H_2O and $D_3O^{\oplus}$ in D_2O is $k_H/k_D = 1.3$. These results are similar to those obtained for the hydration of simple carbonyl compounds,[12] and thus

imply a not unexpected mechanistic similarity between these two hydration reactions. A more detailed investigation of this carbene hydration is presently underway.

Received: April 5, 1991 [Z 4554 IE]
German version: *Angew. Chem. 103* (1991) 1391

CAS Registry numbers:
1, 16904-42-0; **2**, 135943-37-2; $2^{\ominus}$, 135943-38-3; **4**, 22979-35-7; D, 7782-39-0; H_2O, 7732-18-5.

[1] T. L. Gilchrist, C. W. Rees: *Carbenes and Nitrenes*, Nelson, London 1969, pp. 72–75.
[2] W. Kirmse: *Carbene Chemistry*, 2nd ed., Academic, New York 1971, pp. 423–430.
[3] W. Kirmse, K. Loosen, H.-D. Sluma, *J. Am. Chem. Soc. 103* (1981) 5935; M. Regitz (Ed.): *Methoden Org. Chem. (Houben-Weyl)* 4th Edit., *Vol. E19b, Carbene (oide), Carbine*, 1989; H. Tomioka, K. Hirai, K. Tabayashi, S. Murata, Y. Izawa, S. Inakaki, T. Okajima, *J. Am. Chem. Soc. 112* (1990) 7692.
[4] Y. Fujiwara, Y. Tanimoto, M. Itoh, K. Hirai, H. Tomioka, *J. Am. Chem. Soc. 109* (1987) 1942.
[5] E. Ciganek, *J. Org. Chem. 35* (1970) 862.
[6] P. Haspra, A. Suter, J. Wirz, *Angew. Chem. 91* (1979) 652; *Angew. Chem. Int. Ed. Engl. 18* (1979) 617.
[7] J. R. Keeffe, A. J. Kresge in Z. Rappoport (Ed.): *The Chemistry of Enols*, Wiley, New York 1990, Chapter 7.
[8] Y. Chiang, A. J. Kresge, P. Pruszynski, N. P. Schepp, J. Wirz, *Angew. Chem. 102* (1990) 810; *Angew. Chem. Int. Ed. Engl. 29* (1990) 792.
[9] N. P. Schepp, unpublished results.
[10] Y. Chiang, A. J. Kresge, P. A. Walsh, *Z. Naturforsch. A 44* (1989) 406.
[11] E. V. Sitzmann, J. Langan, K. B. Eisenthal, *J. Am. Chem. Soc. 106* (1984) 1868.
[12] R. P. Bell, *Adv. Phys. Org. Chem. 4* (1966) 1; L. H. Funderburk, W. P. Aldwin, W. P. Jencks, *J. Am. Chem. Soc. 100* (1978) 5444; P. Sorenson, W. P. Jencks, *ibid. 109* (1989) 4675.

In unsaturated alcohols so constructed that a single chiral center is present and features conducive to the independent induction of π-facial selectivity are lacking, the resulting transition state structures will differ energetically only by virtue of oxido-group orientation. Furthermore, if the alcohol is geometrically and optically pure, oxido-group orientation in the transition state can be directly inferred from the absolute configuration of the newly created stereogenic center in the product. These criteria are met by **2** and **6** (Scheme 1).

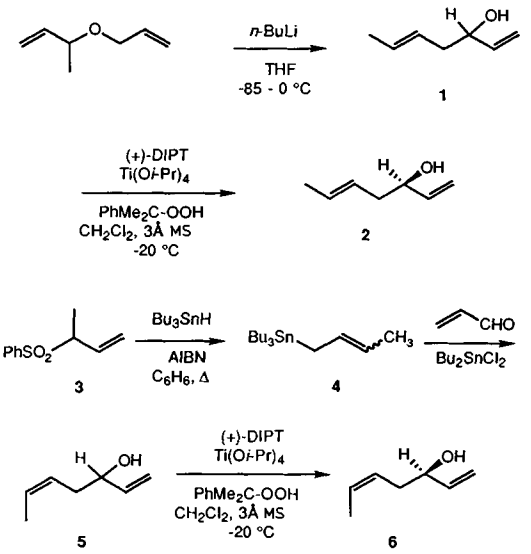

Scheme 1. DIPT = diisopropyl tartrate, MS = molecular sieve, AIBN = azobisisobutyronitrile.

Importance of Oxyanion Orientation to the Stereochemical Control of Anionic Oxy-Cope Rearrangements**

By *Leo A. Paquette** and *George D. Maynard*

Dedicated to Professor Horst Prinzbach on the occasion of his 60th birthday

The anionically-accelerated oxy-Cope rearrangement[1] is widely recognized to proceed via a highly dissociative transition state having a substantially weakened C3–C4 bond.[2] Where possible, chair conformations are preferred,[3] although structural constraints that demand passage through a boat geometry do not arrest [3,3] sigmatropy.[4] Despite extensive synthetic application of this useful reaction,[5] little is known about the factors that determine the orientation of the oxido-groups in the associated transition states[6] and the importance of this orientation to chirality transfer.[6, 7] Several well-documented cases have been reported in which chair-like transition states having both pseudoequatorial[6a, 8] and pseudoaxial oxyanion substituents[9] are involved. However, analysis of the relative importance of the oxido-group orientation to stereochemical control requires that other steric demands on the particular system be absent or at least well defined.

Base-promoted condensation of racemic 3-buten-2-ol with allyl bromide followed by [2,3]-Wittig rearrangement provided (*E*)-1,5-heptadien-3-ol (**1**) admixed with 2–5% of the (*Z*)-isomer.[10] Subsequent kinetic resolution according to *Sharpless* et al.[11] gave optically pure **2** ($[\alpha]_D^{25} = +3.4°$ ($c = 3.4$, $CHCl_3$)), as determined by analysis of the Mosher ester.[12] The most efficient route to **5** involved allylic stannylation of 3-(phenylsulfonyl)-1-butene **3** under free radical conditions,[13] followed by coupling of **4** with acrolein in the presence of 2.5 equiv. of di-*n*-butyltin dichloride. Optically pure **6** free from detectable isomeric contamination ($[\alpha]_D^{25} = +2.0°$ ($c = 3.4$, $CHCl_3$)), was obtained by analogous kinetic resolution.

The action of KH and [18]crown-6 on **2** and **6** at 50 °C in THF or DME promoted efficient oxy-Cope rearrangement provided that quenching was carried out with methanol at −78 °C. Although the pure (*R*)- and (*S*)-enantiomers of 4-methyl-5-hexenal have been described earlier,[14] their optical rotations have never been reported. Accordingly, pure (*S*)-**8** ($[\alpha]_D^{25} = +14.4°$ ($c = 3.6$, $CHCl_3$)) was prepared from (*S*)-(+)-citronellene **7** as shown (Scheme 2, above). This information permitted ready calculation of the distribution of pathways followed by the potassium alkoxides of **2** and **6**. Independent verification of these data was realized by hydride reduction of the aldehydes so obtained,[15] hydrogenation of the unsaturated alcohols, and Mosher ester analyses of the products **9** (Scheme 2, below). The agreement between the two forms of measurement is very good (Table 1).

Several relevant control experiments were also undertaken. In order to eliminate from consideration the possibility that the intermediate potassium enolates experience partial racemization by reversible allylic proton abstraction (per-

[*] Prof. Dr. L. A. Paquette, Dr. G. D. Maynard
Evans Chemical Laboratories, The Ohio State University
Columbus, OH 43210 (USA)

[**] Grateful acknowledgement is made to the National Science Foundation for support of this research. *G. D. M.* has served as an Ohio State University Fellow (1986–1987), National Need Fellow (1988–1989) and American Chemical Society Organic Division Fellow (1989–1990).

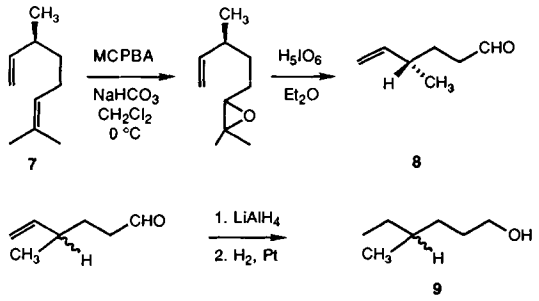

Scheme 2. MCPBA = *meta*-chlorobenzoic acid.

haps accelerated by the neighboring oxido group), (*S*)-**8** was heated with KH (8 equiv.) and [18]crown-6 (3 equiv.) in dry THF under argon at 50 °C for 8 h, isolated as before, and converted into **9**. Since the optical purity of this sample was unchanged relative to a reference sample formed directly from untreated **8**, the enantiomer ratios are *not* lowered by adventitious epimerization of this type.

The operational assumption of chairlike transition states to the exclusion of boat conformations for [3,3]-sigmatropic rearrangements in *acyclic* systems has become routine[6c, 16] because of the widely disparate energy differences involved.[17] Although no ambiguities are expected for **2** and **6**, their associated chair transition states **10**–**13** do lead to pairs of (*E*)- and (*Z*)-enolates, respectively, that differ mutually in absolute configuration and should be enantiomerically pure if no subsequent isomerization of the stereogenic center or enolate double bond takes place. Knowledge of the absolute configuration and (*E*/*Z*)-enolate geometry, if these are unperturbed, would serve to dismiss unequivocally boat conformations from consideration. When **2** was rearranged and treated with *tert*-butyldimethylsilyl chloride (−78 °C to 0 °C), a 64:36 mixture of *cis* (J = 5.9 Hz) and *trans* (J = 11.9 Hz) silylenol ethers was obtained (71%). Hydrogenation of each pure isomer ($H_2/PtO_2/CH_2Cl_2/CH_3OH$) gave samples of **9** identically enriched (60%) in the (*R*)-enantiomer (Mosher ester analysis). These results establish that enolate geometry is not preserved following oxy-Cope rearrangement and unilateral use of this method probing the mechanism is therefore not recommended. Nevertheless, the intimate consequences of transition state geometry depicted in Table 1 are consistent with all available facts.

Table 1. Data for the anionic oxy-Cope rearrangement of **2** and **6**.

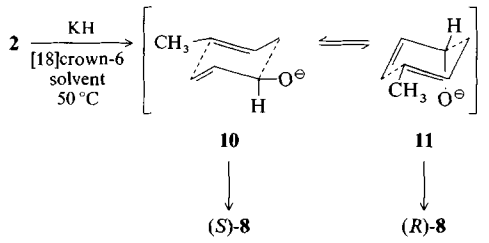

10 → (*S*)-**8**; **11** → (*R*)-**8**

Solvent	Yield [%][a]	$[\alpha]_D^{25}$ [b]	Amount of **10** [%] based on $[\alpha]_D$	Mosher ester of **9**
THF	69	+4.0°	64	61
DME	92	+3.7°	63	61

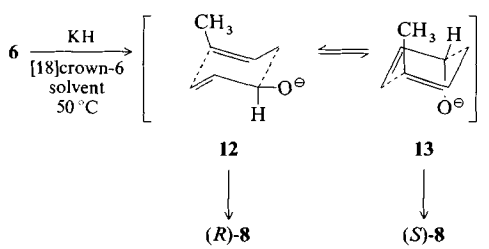

12 → (*R*)-**8**; **13** → (*S*)-**8**

Solvent	Yield [%][a]	$[\alpha]_D^{25}$ [b]	Amount of **12** [%] based on $[\alpha]_D$	Mosher ester of **9**
THF	78	−2.7	59	57
DME	98	−2.5	59	55
C_6H_6	83	−2.4	58	55

[a] GC analysis values as averaged over two experiments. [b] Samples purified by preparative GC before measurement.

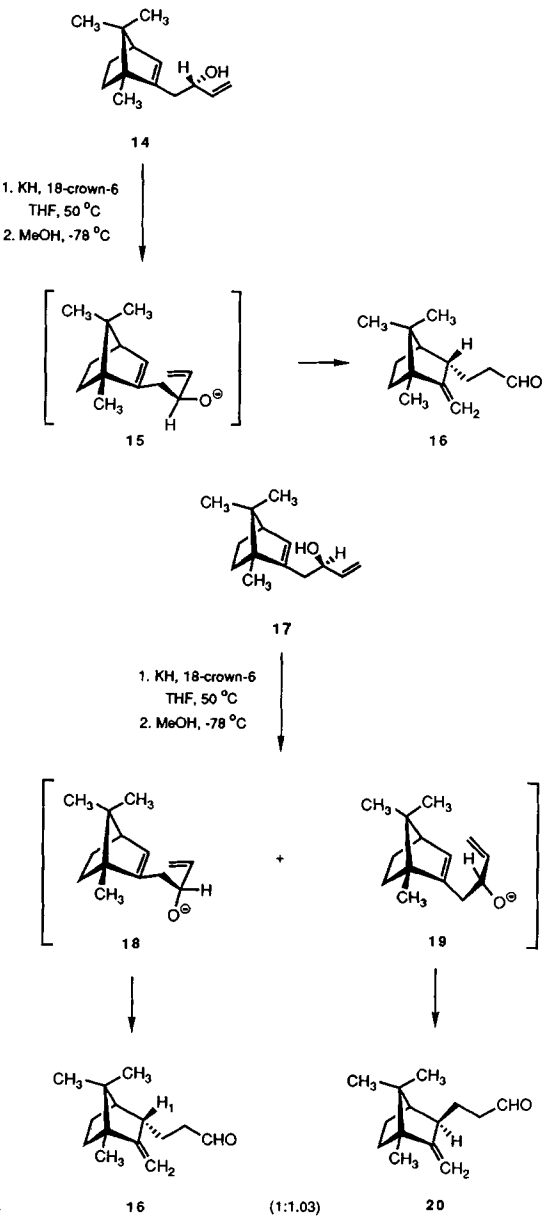

Scheme 3.

The $[\alpha]_D$ values of the products are seen to remain relatively constant irrespective of solvent. Significantly, both stereoisomeric alcohols show a preference for electronic reorganization via that chairlike species where the oxido-group is equatorially disposed. However, the extent of this bias is not especially dramatic. One possible explanation for the low selectivity is that a positive stereoelectronic contribution

from the axial C–O$^{\ominus}$ bond to the LUMO of the system offsets to some degree the steric advantages enjoyed by its equatorial C–O counterpart.

Whatever the actual underlying cause(s) in these *acyclic* examples, related studies have shown that the steric demand of the oxido-group can gain considerably greater importance when *cyclic* systems are involved. Thus, alcohol **14**[18] isomerizes by way of **15** to **16**, avoiding in the process that transition state option involving *exo* C–C bond formation with axial oxido-group orientation. In contrast, stereoisomer **17**[18] must project the alkoxide group axially as in **18** to arrive at **16**. This less favorable state of affairs allows for the competitive formation of **20** via **19**. Therefore, a change in relative carbinol configuration can have significant impact on product distribution.

Received: March 22, 1991;
revised: July 24, 1991 [Z 4524 IE]
German version: *Angew. Chem. 103* (1991) 1392

CAS Registry numbers:
1, 136034-27-0; **2**, 136087-45-1; **3**, 136034-28-1; (*Z*)-**4**, 35998-94-8; **5**, 136034-29-2; **6**, 136087-46-2; **7**, 10281-55-7; (*R*)-**8**, 63215-85-0; (*S*)-**8**, 93904-58-6; (*S*)-**8** (*E*-*tert*-butyldimethylsilylenol ether), 136034-30-5; (*S*)-**8** (*Z*-*tert*-butyldimethylsilylenol ether), 136034-31-6; (*R*)-**9**, 53353-04-1; **14**, 136034-33-8; **16**, 136034-34-9; **17**, 136034-32-7; **20**, 136087-47-3; (*rac*)-3-buten-2-ol, 6118-14-5; allyl bromide, 106-95-6; acrolein, 107-02-8.

[1] D. A. Evans, A. M. Golob, *J. Am. Chem. Soc. 97* (1975) 4765.
[2] a) J. J. Gajewski, K. R. Gee, *J. Am. Chem. Soc. 113* (1991) 967; b) D. A. Evans, D. J. Baillargeon, *Tetrahedron Lett. 19* (1978) 3315, 3319; c) M. L. Steigerwald, W. A. Goddard, III, D. A. Evans, *J. Am. Chem. Soc. 101* (1979) 1994.
[3] a) W. von E. Doering, W. R. Roth, *Tetrahedron 18* (1962) 67; b) R. K. Hill, N. W. Gilman, *Chem. Commun. 1967*, 619; c) K. J. Shea, R. B. Phillips, *J. Am. Chem. Soc. 100* (1978) 654; d) J. J. Gajewski, L. K. Hoffman, C. N. Shih, *ibid. 96* (1974) 3705.
[4] a) L. A. Paquette, R. E. Maleczka, Jr., *J. Org. Chem. 56* (1991) 912; b) L. A. Paquette, J. A. Oplinger, *Tetrahedron 45* (1989) 107.
[5] a) R. K. Hill in J. D. Morrison (Ed.): *Asymmetric Synthesis. Vol. 3*, Academic Press, New York 1984, p. 503; b) L. A. Paquette, *Angew. Chem. 102* (1990) 642; *Angew. Chem. Int. Ed. Engl. 29* (1990) 609.
[6] a) E. Lee, I.-J. Shin, T.-S. Kim, *J. Am. Chem. Soc. 112* (1990) 260; b) M.-h. Lin, W. H. Watson, R. P. Kashyap, W. J. leNoble, *J. Org. Chem. 55* (1990) 3597; c) K. Tomooka, S.-Y. Wei, T. Nakai, *Chem. Lett. 1991*, 432.
[7] a) F. M. Hauser, V. M. Baghdanov, *Tetrahedron 40* (1984) 4719; b) L. K. Truesdale, D. Swanson, R. C. Sun, *Tetrahedron Lett. 26* (1985) 5009.
[8] D. A. Evans, J. V. Nelson, *J. Am. Chem. Soc. 102* (1980) 774.
[9] a) M. Koreeda, Y. Tanaka, A. Schwartz, *J. Org. Chem. 45* (1980) 1172; b) D. L. J. Clive, G. C. Russell, S. C. Suri, *ibid. 47* (1982) 1632.
[10] a) T. Nakai, K. Mikami, S. Taya, Y. Fujita, *J. Am. Chem. Soc. 103* (1981) 6492; b) T. Nakai, K. Mikami, N. Kishi, *Tetrahedron 42* (1986) 2911.
[11] a) K. B. Sharpless, Y. Gao, R. M. Hanson, J. M. Klunder, S. Y. Ko, S. Masamune, *J. Am. Chem. Soc. 109* (1987) 5765; b) K. B. Sharpless, R. M. Hanson, *J. Org. Chem. 51* (1986) 1922; c) K. B. Sharpless, P. R. Carlier, W. S. Mungall, G. Schröder, *J. Am. Chem. Soc. 110* (1988) 2978.
[12] H. S. Mosher, J. A. Dale, D. L. Dull, *J. Org. Chem. 34* (1969) 2543.
[13] a) Y. Ueno, S. Aoki, M. Okawara, *J. Am. Chem. Soc. 101* (1979) 3413; b) G. Tagliavini, A. Boaretto, D. Marton, *Inorg. Chim. Acta 77* (1983) L 196; c) G. Tagliavini, A. Boaretto, D. Marton, P. Ganis, *J. Organomet. Chem. 321* (1987) 199.
[14] a) R. E. Ireland, S. Thaisrivongs, P. H. Dussault, *J. Am. Chem. Soc. 110* (1988) 5768; b) R. E. Ireland, L. C. Anderson, R. Badoud, B. J. Fitzsimmons, G. J. McGarvey, S. Thyisrivongs, C. S. Wilcox, *ibid. 105* (1983) 1988.
[15] K. Mori, S. Kuwahara, H. Z. Levinson, A. R. Levinson, *Tetrahedron 38* (1982) 2291.
[16] For recent examples, consult: a) E. J. Corey, D.-H. Lee, *J. Am. Chem. Soc. 113* (1991) 4026; b) R. E. Ireland, P. Wipf, J.-N. Xiang, *J. Org. Chem. 56* (1991) 3572; c) S.-Y. Wei, K. Tomooka, T. Nakai, *J. Am. Chem. Soc.*, in press.
[17] W. von E. Doering, W. R. Roth, *Angew. Chem. 75* (1963) 27; *Angew. Chem. Int. Ed. Engl. 2* (1963) 115.
[18] The alcohols **14** and **17** were prepared by subjecting (1*R*)-(+)-camphor trishydrazone to the Shapiro reaction and condensing the resultant vinyl anion with butadiene monoxide. After chromatographic enrichment of the (α*R*,1 *R*,4 *S*) and (α*R*, 1 *S*, 4 *R*) diastereomers, pure samples of the individual alcohols were obtained by appropriate Sharpless epoxidation to remove the unwanted minor constituent.

π-Coordination of Diorganotin Dications**

By *Bernd Wrackmeyer,* Gerald Kehr,* and *Roland Boese*

Alkynyl groups have fascinating properties, both as bridging ligands of transition metals[1] as well as of main group elements.[2] During the organoboration of alkynylmetal compounds,[3] intermediates are presumed to occur in which an alkyne moiety bridges metal and boron atom. Thus, we recently found in the case of **A** the first example of the π-coordination of a C≡C bond of an alkynyl borate moiety to a triorganolead cation.[4] Tin compounds analogous to **A**

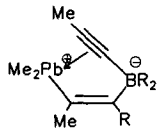

A (R = *i*Pr)

could, however, only be postulated on the basis of NMR spectroscopic data.[5] We report here on a new type of compound **3**, in which a diorganotin dication is stabilized by π-coordination to two C≡C bonds. These compounds are of special interest for gaining insight into the mechanisms of organoboration.

The reaction of tetraalkynylstannanes **1** with triethylborane **2** affords the *spiro*-compounds **5b–e** in high yields[6, 7] (Scheme 1). Monitoring of the reaction of **1** and **2** by ^{119}Sn-

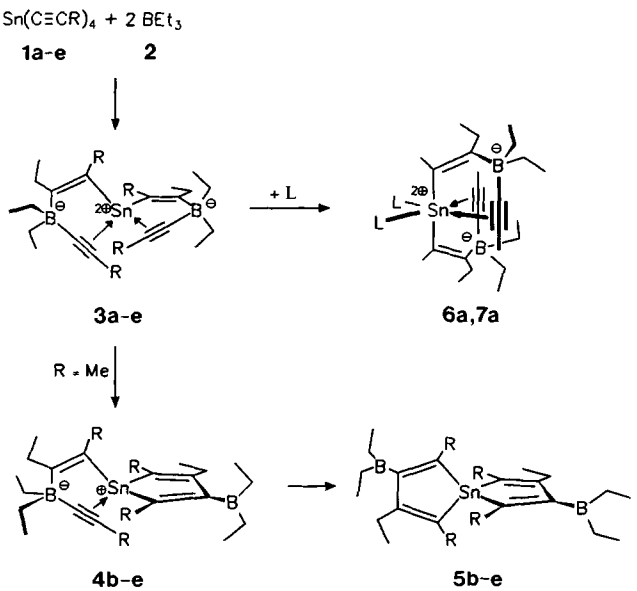

Scheme 1. **a**: R = Me, **b**: R = Et, **c**: R = Pr, **d**: R = *i*Pr, **e**: R = Bu. **6**, **7**: L = py, bipy.

NMR spectroscopy in the temperature range −78 to 25 °C provided the first indications of the formation of intermediates **3** and **4** (cf. Table 1). The compound **3a** can be isolated as a crystalline, colorless solid,[8] which decomposes above

[*] Prof. Dr. B. Wrackmeyer, Dipl.-Chem. G. Kehr
Laboratorium für Anorganische Chemie der Universität
Postfach 101251, W-8580 Bayreuth (FRG)
Dr. R. Boese
Institut für Anorganische Chemie der Universität-Gesamthochschule
Universitätsstr. 5–7, W-4300 Essen 1 (FRG)

[**] This work was supported by the Deutsche Forschungsgemeinschaft, the Fonds der Chemischen Industrie, and the Volkswagen Stiftung.

Table 1. ^{13}C-, ^{11}B-, ^{119}Sn-NMR data [a] of **3a**, **4b**, **6a** and **7a**.

	3a	**6a** [b]	**7a** [c]	**4b** [d]
Sn-*C*=	130.8	138.0	138.2	142.2
	[552.6]	[795.6]	[1060.0]	[576.6]
B-*C*=	190.0(br)	165.9(br)	176.9(br)	184.5(br)
B-*C*≡C	109.1(br)	91.7	104.9(br)	106.9(br)
	[70.0]	[382.6]		
B-C≡*C*	124.9	104.2	125.5	119.7
	[66.7]	[64.3]		[56.7]
R^1-C=	25.7	22.8	20.1	26.5, 17.9
	[154.0]	[86.7]	[164.0]	[141.7] [59.0]
R^1-C≡	6.8	5.3 [7.6]	7.9 [<10]	15.5, 14.4
Et-C=	19.5	26.6	25.1	26.7
	[174.0]	[137.3]	[204.0]	[146.0]
	14.0 [14.1]	13.8 [16.4]	13.8	14.4 [19.5]
B*Et*$_2$	16.8(br)	13.2(br)	18.2(br)/ 18.8(br)	18.3(br)
	13.0	9.9{br}	13.5/13.9	12.7
$\delta(^{11}B)$	− 5.6	− 8.0	− 4.8	+89.5, − 4.2
$\delta(^{119}Sn)$	+165.6	− 277.4	− 190.9	+130.2

[a] ca. 20% in CD_2Cl_2, Bruker AC 300, 243 K; δ values versus Me_4Si (^{13}C), Et_2O–BF_3 (^{11}B), Me_4Sn (^{119}Sn), external; [ ]: $^nJ(^{119}Sn,^{13}C)$ in Hz; (br): broad ^{13}C resonances due to partly relaxed scalar couplings $^1J(^{13}C,^{11}B)$; {}: broad ^{13}C resonanecs due to dynamic effects. [b] Pyridine, $\delta(^{13}C)$ = 146.1 (C^2), 124.7 (C^3), 139.3 (C^4). [c] ca. 10% in C_7D_8; 2,2'-bipy, $\delta(^{13}C)$ = 148.5 (C^2), 121.6 (C^3), 139.8 (C^4), 126.0 (C^5), 149.7 (C^6). [d] ^{13}C NMR (293 K) of the stannacyclopentadiene rings in **4b**: $\delta(^{13}C)$ [$^nJ(^{119}Sn,^{13}C)$] = 140.6 [321.5] C(2), 164.4 (br) C(3)-B, 152.6 [130.8] C(4), 140.1 [379.3] C(5), 23.0 (br), 9.6 (BEt_2), 27.0 [55.6], 14.6 [7.4] (= C(4)*Et*), 24.7 [70.8], 17.5 [16.9], 28.3 [80.7], 17.7 [16.9] (C(2/5)*Et*).

− 20 °C. The compounds **3b–e**[9] are also present in the mixture at 0 °C together with **1**, **2** and **4**, but are finally converted into **5** without signs of decomposition.

Owing to the ready decomposition of **3a**, both in solution as well as in the solid state, the preparation of crystals was carried out in a vessel[10] specially designed for the purpose of performing an X-ray structure analysis at 115 K (Fig. 1).[11]

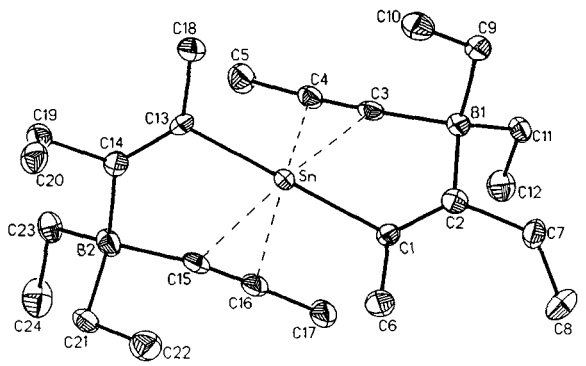

Fig. 1. Structure of **3a** in the crystal, ellipsoids drawn at the 50% probability level. Important bond lengths [Å] and angles [°]: Sn-C1 2.117(3), Sn-C3 2.355(3), Sn-C4 2.511(3), Sn-C13 2.122(3), Sn-C15 2.351(3), Sn-C16 2.535(3), B1-C2 1.634(5), B1-C3 1.643(5), B2-C14 1.630(5), B2-C15 1.647(5), C1-C2 1.337(4), C3-C4 1.227(5), C4-C5 1.459(5), C13-C14 1.347(4), C13-C18 1.509(4), C15-C16 1.222(5), C16-C17 1.479(5); C1-Sn-C3 84.0(1), C1-Sn-C4 111.5(1), C3-Sn-C4 29.0(1), C1-Sn-C13 140.9(1), C3-Sn-C13 118.8(1), C4-Sn-C13 99.1(1), C1-Sn-C15 115.7(1), C3-Sn-C15 114.9(1), C4-Sn-C15 93.8(1), C13-Sn-C15 84.8(1), C1-Sn-C16 95.0(1), C3-Sn-C16 94.6(1), C4-Sn-C16 83.3(1), C13-Sn-C16 112.8(1), C15-Sn-C16 28.7(1), C2-B1-C3 108.6(3), C14-B2-C15 109.5(3), Sn-C1-C2 113.5(2), B1-C2-C1 125.5(3), Sn-C3-B1 104.4(2), B1-C3-C4 172.7(3), C3-C4-C5 175.8(3), Sn-C13-C14 112.3(2), B2-C14-C13 126.6(3), Sn-C15-B2 104.9(2), B2-C15-C16 171.0(3), C15-C16-C17 177.2(3).

In addition, the ^{13}C- and ^{119}Sn-CP/MAS-NMR spectra of crystalline **3a** were recorded at − 30 °C.[12] The agreement of the NMR data in solution with $\delta(^{13}C)$ and $\delta(^{119}Sn)$ values obtained from the solid-state NMR measurements confirmed that the π-coordination at the $R_2Sn^{2\oplus}$ dication remains intact in solution. The double set of ^{13}C resonance signals in the case of solid **3a** is consistent with the result of the X-ray structure analysis,[11] according to which there are slight differences in the bond lengths and angles in the two halves of the molecule.

For a free diorganotin dication, the bond angle at the tin should be 180°. But the angle measured for C(1)–Sn–C(13) is 140.9°, which is unprecedented for organotin compounds. The coordination of the tin to the C≡C bond is unsymmetrical with the distance to the boron-bound alkyne carbons being on average 0.17 Å shorter. Even these distances are significantly longer than all known tin–carbon single bond lengths. With $d_{C\equiv C}$ distances of 1.227 and 1.222 Å and almost linear geometry at the alkyne carbon atoms, the C≡C bond is little influenced by the coordination to the tin atom. Remarkably, the distances B1–C3 and B2–C15 for the ≡C–B bonds are even greater than the B–C(sp^2) and B–C(sp^3) bond lengths. This weakening of the B-C(sp) bond is in accord with the observed exchange of the propynyl moiety of **3a** in solution (see below). The unexpectedly large B–C–C angles, with an average value of 116.5(5)°, are consistent with quantum mechanical calculations and the experimental results of other structural analyses with B-C-C fragments.[13]

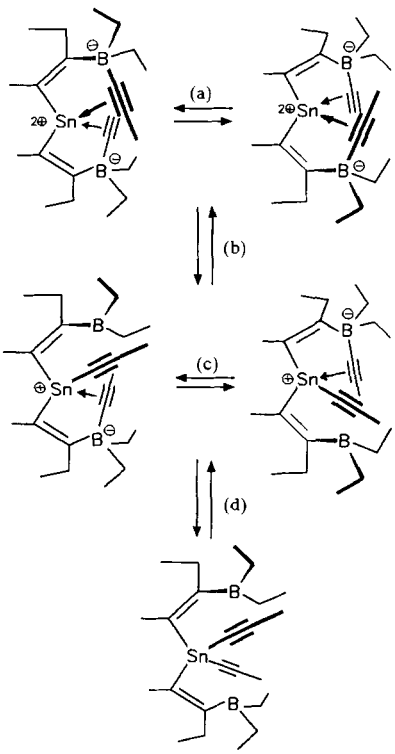

Scheme 2. Dynamic processes in **3** (**3a** as example). a) Ring inversion, b)–d) exchange of the propynyl groups.

^1H-NMR spectra of **3a** between − 20 °C and − 90 °C indicate dynamic behavior of the compound in solution. Two processes are discernable, namely exchange of the propynyl group between the tin and the boron atoms, and, at lower temperature, ring inversion (Scheme 2).

Slow exchange of the propynyl groups leads to diastereotropism of the B–CH_2 protons (below − 35 °C), and hindered inversion finally results in nonequivalence of the Et_2B methyl groups and the diastereotopism of the C=C–CH_2 protons (below −60 °C and −90 °C, respectively).

The electrophilic character of tin in the new compounds **3** is manifested in reactions with nucleophiles.[14] With pyridine and with 2,2'-bipyridyl, **3a** forms the adducts **6a** and **7a**,[15] in which the tin atom is coordinatively saturated (cf. Table 1, ^{119}Sn resonance signals at high field). As in the case of **3a**, dynamic processes can also be demonstrated for **6a** and **7a** by ^{1}H- and ^{13}C-NMR spectroscopy. The structure for the intermediates **4** is based on consistent sets of NMR data (cf. Table 1 for **4b**) and is confirmed by the isolation of the final product **5**. The results suggest that the formation of compounds **4** and **5** from **3** and **4** respectively proceeds via an Sn-Substituted vinyl cation **8**.

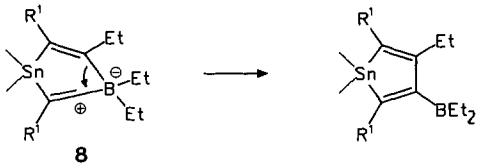

Received: April 22, 1991;
revised: July 16, 1991 [Z 4586 IE]
German version: *Angew. Chem. 103* (1991) 1374

CAS Registry numbers:
1a, 1692-20-2; **1b**, 135989-68-3; **2**, 97-94-9; **3a**, 136015-67-3; **3b**, 135989-64-9; **3c**, 135989-65-0; **3d**, 135989-66-1; **3e**, 135989-67-2; **4b**, 135989-63-8; **5b**, 135952-83-9; **5c**, 135952-84-0; **5d**, 135952-85-1; **5e**, 135952-86-2; **6a**, 135989-61-6; **7a**, 135989-62-7.

[1] a) A. J. Carty, *Pure Appl. Chem. 54* (1982) 113; b) E. Sappa, A. Tiripicchio, P. Braunstein, *Coord. Chem. Rev. 65* (1985) 219; c) G. Consiglio, F. Morandini, *Chem. Rev. 87* (1987) 761; d) A. A. Cherkas, L. H. Randall, S. A. Maclaughlin, G. N. Mott, N. J. Taylor, A. J. Carty, *Organometallics 7* (1988) 969.

[2] a) N. A. Bell, I. W. Nowell, H. M. M. Shearer, *J. Chem. Soc. Chem. Commun. 1982*, 147; b) P. N. V. P. Kumar, E. D. Jemmis, *J. Am. Chem. Soc. 110* (1988) 125; c) P. Jutzi, *Adv. Organomet. Chem. 26* (1986) 217.

[3] a) B. Wrackmeyer, *Rev. Silicon Germanium Tin Lead Compd. 6* (1982) 75; b) B. Wrackmeyer in S. Hermanek (Ed.): *Boron Chemistry*, World Scientific, Singapore 1987, p. 387–415.

[4] B. Wrackmeyer, K. Horchler, R. Boese, *Angew. Chem. 101* (1989) 1563; *Angew. Chem. Int. Ed. Engl. 28* (1989) 1500.

[5] L. Killian, B. Wrackmeyer, *J. Organomet. Chem. 148* (1978) 137.

[6] a) Only in the case of tetra-1-propynylstannane **1a** and triethylborane **2** and upon using the pure intermediate **3a** could no well-defined products be obtained. Various solutions of **3a** [concentration between 0.5 M down to 0.001 M (in order to suppress intermolecular reactions) in CH_2Cl_2, THF, hexane or toluene at $-78\,^{\circ}C$ afford elemental tin and red, highly viscous oils on warming to room temperature. The large number of broad ^{13}C- and ^{1}H-resonances point to complex mixtures with polymeric constituents. Separation into pure components could not be achieved by distillation. An analogous behavior was observed upon heating the compounds **6a** and **7a**.—b) In contrast, spiro compounds analogous to **5** are formed smoothly from tetra-1-propynylsilane or -germane and excess triethylborane: R. Köster, G. Seidel, MPI für Kohlenforschung, Mülheim a.d. Ruhr (FRG), private communication.

[7] **5b**: A solution of **1b** (3.10 g, 9.37 mmol) in toluene (20 mL) was cooled to $-78\,^{\circ}C$, treated with **2** (3.00 mL, 21.3 mmol), and the stirred mixture was slowly warmed to room temperature. After heating to 60 °C for 24 h the solvent and unchanged **2** were removed in vacuo. Kugelrohr distillation of the residue afforded 3.85 g (78%) of **5b** (b.p. 175–180 °C/10^{-3} torr). **5c** (180–190 °C/10^{-3} torr), **5d** (b.p. 200 °C/10^{-3} torr), and **5e** (b.p. 185–190 °C/10^{-3} torr) were obtained analogously. ^{1}H- and ^{13}C-NMR data are consistent with the proposed structures. ^{119}Sn/^{11}B-NMR (111.9 MHz, CD_2Cl_2, 298 K): (^{119}Sn)/(^{11}B) = − 19.7/83.0 (**5b**), − 13.7/84.3 (**5c**), − 48.3/86.3 (**5d**), − 15.7/85.2 (**5e**).

[8] **3a**: A solution of **1a** (3.2 g, 11.6 mmol) in toluene (40 mL) was cooled to $-78\,^{\circ}C$, treated with 4 mL (28 mmol) of **2** and the stirred mixture warmed to 0 °C. After ca. 30 min the solvent and excess **2** were removed in vacuo. The remaining yellow solid was crystallized from pentane at $-78\,^{\circ}C$; 3.8 g (69%); decomp. above − 20 °C. **3a**: ^{1}H NMR (300 MHz, C_7D_8, 243 K): $\delta(^{1}H)[^{n}J(^{119}Sn^{1}H)] \approx 0.80$ m, 1.10 t (20H; BEt_2) 2.22 q, 0.96 t (10H; =CEt), 1.42[7.3] s(6H; ≡CMe), 1.81[107.6] s(6H; =CMe).

[9] **3b**, **3c**, **3d**, **3e**: relevant ^{1}H- and ^{13}C NMR data correspond to the values for **3a**. ^{119}Sn/^{11}B NMR (CD_2Cl_2, 298 K): $\delta(^{119}Sn)/\delta(^{11}B)$ = + 207.5/−4.9 (**3b**); + 203.1/−4.5 (**3c**); + 223.2/−4.3 (**3d**); + 202.1/−4.4 (**3e**).

[10] R. Boese, D. Bläser, *J. Appl. Crystallogr. 22* (1989) 394.

[11] X-ray structure analysis of **3a** at 115 K: $P2_1/c$, $a = 11.924(2)$, $b = 14.512(3)$, $c = 14.299(2)$ Å, $\alpha = \gamma = 90°$, $\beta = 97.29(1)°$, $V = 2454.4(7)$ Å^3, $Z = 4$, $\varrho_{calcd} = 1.274$ g cm^3, $\mu = 1.05$ mm^{-1}, $Mo_{K\alpha}$ radiation (graphite monochromator), $\lambda = 0.71069$ Å; 3414 independent reflections. 2979 observed ($F_0 \geq 4\sigma(F)$); $2\theta(max) = 45°$; absorption correction: empirical, Ψ scans in the 2θ range, (°): 3 2 35 max/min. Transmission: 0.926/0.815, R_{merg} before/after the correction: 0.0303/0.0203; $R = 0.029$, $R_w = 0.026$. Further details of the crystal structure analysis are available on request from the Fachinformationszentrum Karlsruhe, Gesellschaft für wissenschaftlich-technische Information mbH, W-7514 Eggenstein-Leopoldshafen 2 (FRG), on quoting the depository number CSD-320291, the names of the authors, and the journal citation.

[12] ^{13}C- and ^{119}Sn-CP/MAS-NMR (Bruker MSL 300). We thank Drs. *A. Sebald* and *L. H. Merwin* for recording the spectra.

[13] R. Boese, M. Bühl, P. von R. Schleyer, unpublished results.

[14] A report of the reaction of **3a** with ammonia, amines, and alcohols will be reported elsewhere.

[15] **6a**: A solution of **3a** (0.5 g, 1.1 mmol) in toluene (ca. 20 mL) was treated with pyridine (0.3 mL, 3.7 mmol) at $-78\,^{\circ}C$. After removal of solvent and excess pyridine in vacuo at 0 °C their remained 0.6 g (95%) of a colorless solid (> 20 °C, decomp.). **7a** was obtained analogously as a yellow solid (> 40 °C, decomp.), whereby **3a** already reacts at $-78\,^{\circ}C$.

Stable Phosphazenium Ions in Synthesis—an Easily Accessible, Extremely Reactive "Naked" Fluoride Salt**

By *Reinhard Schwesinger,* Reinhard Link, Gerhard Thiele, Heinz Rotter, Dieter Honert, Hans-Heinrich Limbach,* and *Ferdinand Männle*

Dedicated to Professor Horst Prinzbach on the occasion of his 60th birthday

Lipophilic organic cations are of exceptional importance in preparative organic chemistry; however, their breadth of application has hitherto been limited owing to their modest stability towards bases and nucleophiles.[1] This is especially true in the case of organic fluoride salts,[2] efficient auxiliary bases and indispensable reagents in organosilicon chemistry. The only unsolvated organic ("naked") fluoride salt that has proven reliable[3] is tetramethylammonium fluoride,[6] certainly the most reactive source of fluoride known so far.[7] However, it is only sparingly soluble, and the cation is particularly unstable towards strong nucleophiles. We now report on the stable, easily accessible phosphazenium fluoride **1**-F, a source for THF solutions of naked fluoride ions.

In connection with our studies on the preparation of novel, extremely basic polyaminophosphazenes we found that peralkylated cations such as **1** and particularly **2** are many orders of magnitude more stable than conventional organic cations towards nucleophiles.[8, 9] In the meantime we have been able to simplify the synthesis of **1**[8, 10] considerably: reaction of PCl_5 with NH_4Cl and subsequently with

[*] Priv.-Doz. Dr. R. Schwesinger, Dipl.-Chem. R. Link
Institut für Organische Chemie und Biochemie der Universität
Albertstr. 21, W-7800 Freiburg (FRG)
Prof. Dr. G. Thiele, Dr. H. Rotter, Dr. D. Honert
Institut für Anorganische Chemie der Universität Freiburg (FRG)
Prof. Dr. H.-H. Limbach, Dipl.-Chem. F. Männle
Institut für Physikalische Chemie der Universität Freiburg (FRG)

[**] This work was supported by the Deutsche Forschungsgemeinschaft and the Fonds der Chemischen Industrie.

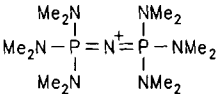

1

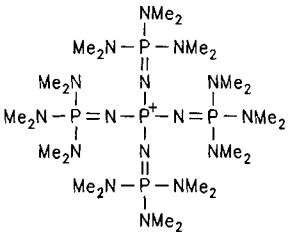

2

dimethylamine and $NaBF_4$ to give **1**-BF_4 via **3**[11] can be carried out in a one-pot process; hexamethylphosphoric triamide (HMPA) and salts of **4** are formed as by-products via complex routes from the aminolysis product of PCl_6^- and CH_3NO_2 (Scheme 1).

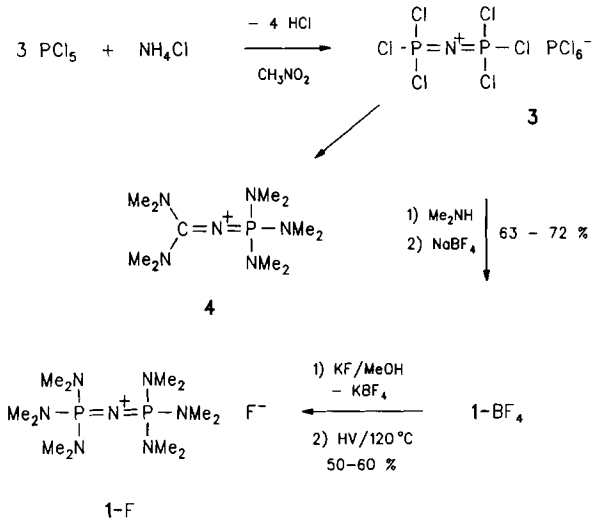

Scheme 1. HV = high vacuum.

On attempting to obtain **1**-F by double reaction of **1**-BF_4 with KF in methanol/water and drying in a vacuum, partial hydrolysis of the cation and formation of **1**-FHF was observed. However, on using anhydrous methanol a product was obtained from which the solvent could be largely removed at 120 °C. After washing with THF, colorless, extremely hydroscopic **1**-F was obtained in 50–60% yield and could be recrystallized from THF.

According to the X-ray structure analysis,[12] the very first of an organic unsolvated fluoride salt, **1**-F crystallizes with FeS_2-(in the broadest sense NaCl-)type structure, hitherto unprecedented for organic compounds, with discrete phosphazenium and fluoride ions. The cation–anion distance (6.3 Å) is the largest observed in any known solvent-free fluoride salt (KF 2.67 Å, CsF 3.01 Å, NMe_4F presumably 4.2 Å[6]), which immediately allows conclusions to be drawn about the solubilities and reactivities of the ion pairs or ion aggregates. Six P–N bonds point almost exactly (P1–N2–F = 178°) to a fluoride ion, which is surrounded approximately icosahedrally by one proton each of the twelve methyl groups. The F–H distances (2.37 and 2.57 Å), however, are in the region of the sum of the van-der-Waals radii and are too large for hydrogen bridges, i.e. the fluoride ion here (in agreement with IR data) can be regarded as "naked". The cation has crystallographic C_{3i} (S_6) symmetry, its conformation is almost the same as that of the isoelectronic oxa compound[14] and, with respect to the linearity of the bridge, also that of the carba compound.[15] The PNP bridges in the cation of **5**[8] are indeed bent (141 and 143°[16]), but in the case of **1** there is no evidence of disordered bent conformers, for example the P–N1 distance is very similar to the P–N distances in the bridges of **5** (1.55–1.58 Å), and the standard deviation is small. The dimethylamino groups are turned through about 39° from the N1–P–N2 plane, their six N atoms staggered with respect to the P–N1–P bridge and slightly pyramidal (sum of angles 358.2°).

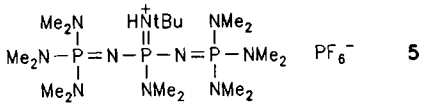

5

Crystalline **1**-F is stable indefinitely at room temperature in the absence of moisture, and is stable to a limited extent on heating; above 144 °C, however, it melts with decomposition and formation of **1**-FHF.

At 20 °C, **1**-F dissolves in THF to give an approximately 2 mM solution, which rapidly becomes inactive in the absence of the corresponding solid phase, even in fired glass vessels; at boiling temperature it is markedly more soluble and, for a few hours, is stable except for the reaction with the glass surface. The solutions of **1**-F are more basic than the corresponding solutions of previously known phosphazene bases.[8] Triphenylmethane-containing, deep-red solutions of **1**-F (with solid phase) are decolorized within a minute already at −55 °C upon treatment with an excess of tetrabutylammonium hexafluorophosphate; this suggests that "naked tetrabutylammonium fluoride" was no more than a myth.[2b]

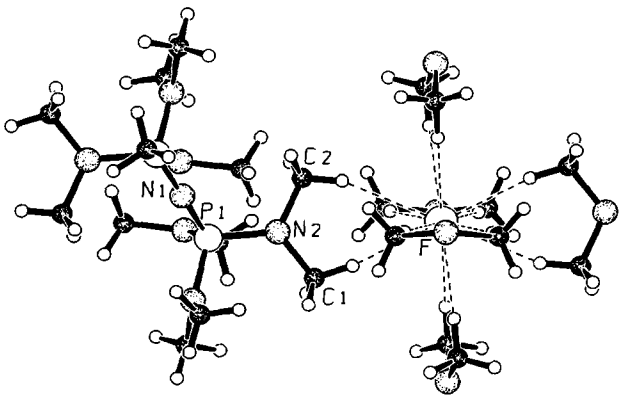

Fig. 1. Structure of **1**-F in the crystal [17]. Bond lengths [Å] and angles [°]: P–N1 1.536(2), P–N2 1.644(5), N2–C1 1.471(9), N2–C2 1.483(8); N1–P–N2 110.8(2), P–N2–C1 122.3(4), P–N2–C2 118.9(4).

Compared with solvated fluorides,[2a] potassium *tert*-butoxide[18] or phosphazene bases,[8] the fluoride ion in **1**-F shows unique E2 reactivity (with formation of **1**-FHF) with comparatively unusually low nucleophilicity, and is excellently suitable for the generation of 1-alkenes from 1-halides; e.g., three equivalents of **1**-F react with 1-iodoundecane already at −70 °C to give a 9:1 mixture of 1-undecene and 1-fluoroundecane. The benzenesulfonate of lanost-8(9)-en-3β-ol reacts in THF within 30 minutes at room temperature

to give lanosta-2,8(9)-diene exclusively, a reaction which with potassium *tert*-butoxide in dimethyl sulfoxide/THF (1:1) furnishes the diene in only 75% yield after four days at 80 °C.[19]

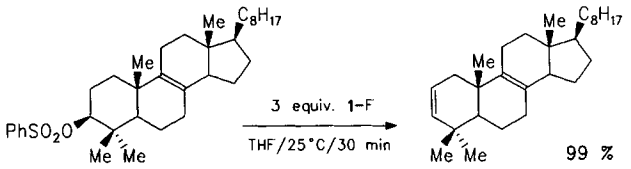

1-F enables, for the first time, the alkylation of an allyl anion species generated from allyltrimethylsilane. The addition of one equivalent of a 1:1 mixture of allyltrimethylsilane and 1-iodoundecane to 2.2 equivalents of **1**-F at −78 °C leads (not optimized) to **1**-tetradecene in 70% yield; only the aforementioned reaction of **1**-F with alkyl halide competes to any significant extent.

No extensive conversion can be achieved with one equivalent of **1**-F; the difluorotrimethylsilicate monoanion[21] formed after alkyl transfer (presumably from the allyldifluorotrimethylsilicate dianion[20]) is here apparently neither sufficiently reactive as source of fluoride nor as source of methyl anions; in the absence of electrophiles, however, even the methyl groups of the silane are transferred to other compounds, as recognizable by the formation of a precipitate of

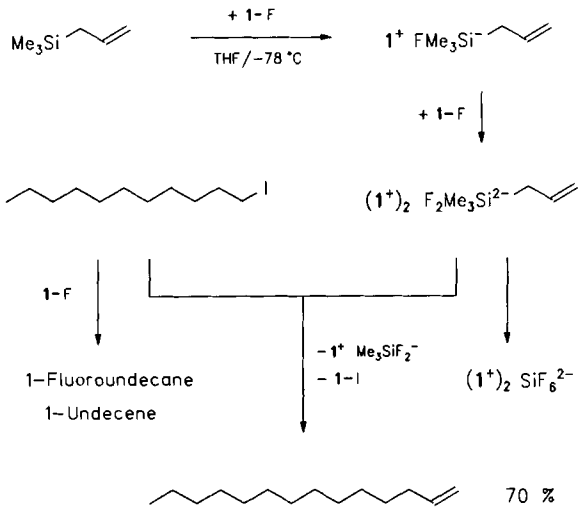

$(\mathbf{1})_2$-SiF_6; the supernatant orange solution decolorizes on thawing and **1** can be recovered from the mixture almost quantitatively as tetrafluoroborate by aqueous work-up. Further studies will be concerned with elucidating the mechanisms of the reactions involved ("naked" allyl anion or hypervalent Si species), exploring the scope of application of this alkylation (and analogous reactions of other silanes) particularly in cyclization reactions, and investigating, in general, the possible use of "naked" phosphazenium salts for the anion-activation of main group organometallic compounds.

Experimental

1-BF_4: A suspension of PCl_5 (208.5 g, 1.00 mol) and NH_4Cl (17.83 g, 0.333 mol) in anhydrous CH_3NO_2 (330 mL) under N_2 was slowly heated to 100 °C. After evolution of HCl had ceased (ca. 1 h), the mixture was cooled to − 10 °C (dry-ice bath, **3** crystallized as pale yellow, robust needles). Dimethylamine (330 g, 7.33 mol, free of primary amines) was then passed (after drying over Na_2O) into the mixture at − 10 °C (delivery tube above solution). After storage at 20 °C for 2 d the mixture, which had turned yellow-orange, was treated with a solution of $NaBF_4$ (73 g, 0.67 mol) in water (330 mL) and stirred vigorously. The mixture was then adjusted to pH 8 by addition of H_3PO_4. The heavier, organic phase was separated off, the aqueous phase extracted once with a little CH_3NO_2, and the combined organic phases washed once with water (170 mL). The organic phase was then evaporated down in vacuo and dried in a high vacuum. The orange-brown, partly crystalline residue (Caution! contains ca. 0.2 mol HMPA) was treated with a 5% $NaBF_4$ solution (330 mL), and the mixture stirred vigorously, cooled to − 5 °C for 30 min, and finally filtered. The colorless crystals were then washed with ice-cooled 5% $NaBF_4$ solution (170 mL) and with a little ice-water. For the further reaction to give **1**-F, the crude crystals of **1**-BF_4 were recrystallized from THF (800 mL) and dried in a high vacuum. Yield 90–102 g (63–72%); m.p. 260 °C (decomp). Correct elemental analysis (C,H,N). ^{1}H NMR (250 MHz, $CDCl_3$, 30 °C, TMS): $\delta = 2.69$ (m).

1-F: A solution of **1**-BF_4 (25.63 g, 60.00 mmol) in MeOH (60 mL, < 50 ppm water) was treated with a solution of KF (3.486 g, 60.00 mmol, dried for 12 h at 240 °C in a high vacuum) in MeOH (40 mL) under N_2. After removal of KBF_4 by suction, the majority of MeOH was removed by evaporation in vacuo at room temperature. The residue was dried in a high vacuum for 1 h at 100 °C (initially with stirring until the contents of the flask became solid, no Teflon used, vacuum apparatus with 10-mm flow cross-section) and 1–2 h at 120 °C bath temperature (until constant weight, if necessary with ^{1}H-NMR monitoring of MeOH), and finally digested and washed with THF (distilled over Na/K/anthracene). After drying in a high vacuum at room temperature, 11–13 g (50–60%) of almost colorless crystals were obtained; according to titration (with HPF_6 salt of 1,8-bis(dimethylamino)naphthalene against *N*-ethyl-4-nitroaniline in THF) at least 88–93% in strongly basic fluoride; ca. 20% **1**-BF_4 could still be recovered from the mother liquor. The crude product was sufficiently pure for most reactions, but could be recrystallized from THF, whereupon the titer increased. M.p. 144 °C (decomp.). IR [perfluorokerosine]: $\tilde{\nu}$ [cm^{-1}] = 2978, 2910, 2886, 2850, 2798, 2478, 2386, 2340, 2214, 1866, 1806, 1736, 1464. ^{19}F-NMR (282 MHz, HMPA, 77 °C, polyethylene ampule in NMR-tube, CCl_3F external): $\delta = -81$ (s, $\nu_{1/2} = 97$ Hz) [22].

1-Tetradecene from allyltrimethylsilane and 1-iodoundecane: A suspension of crude **1**-F (832 mg, at least 2.05 mmol of strongly basic fluoride, see above) in anhydrous THF (3.5 mL) was degassed by removal of 0.5 mL of solvent in a high vacuum. The degassed solution was cooled to − 80 °C, treated dropwise with a mixture of 1-iodoundecane (296 mg, 242 µL, 1.05 mmol) and allyltrimethylsilane (120 mg, 168 µL, 1.05 mmol), and the mixture warmed to room temperature. After addition of water (10 mL), the mixture was extracted with 4 × 5 mL of pentane, the combined pentane extracts washed four times with water, dried over Na_2SO_4, and then the solvent was removed in vacuo. Yield: 208 mg of crude product, according to GC and ^{1}H-NMR analysis consisting of 144 mg of 1-tetradecene (70% yield), 1-iodoundecane (2%), trimethylsilanes (ca. 2%), 1-undecene (22%), and 1-fluoroundecane (2–3%).

Received: May 27, 1991 [Z 4656 IE]
German version: *Angew. Chem. 103* (1991) 1376

[1] W. K. Musker, *J. Org. Chem. 32* (1967) 3189; H. J.-M. Dou, R. Gallo, P. Hassanaly, J. Metzger, *ibid. 42* (1977) 4275; D. Landini, A. Maia, A. Rampoldi, *ibid. 51* (1986) 3187.
[2] a) C. Rieux, B. Langlois, R. Gallo, *C. R. Acad. Sci. Ser. 2 310* (1990) 25; b) D. Landini, A. Maia, A. Rampoldi, *J. Org. Chem. 54* (1989) 328.
[3] Salts of naked fluoride ions have already been reported which apparently were obtained from acetonitrile solutions [4] or extracted into $CDCl_3$ [5]. The very high basicity already found for the tetramethylammonium fluoride, however, indicates that naked fluoride ions could not be capable of existing in such acidic solvents [6].
[4] J. E. Richman, R. B. Flay, *J. Am. Chem. Soc. 103* (1981) 5265.
[5] S. J. Brown, J. H. Clark, *J. Chem. Soc. Chem. Commun. 1983*, 1256.
[6] K. O. Christe, W. W. Wilson, R. D. Wilson, R. Bau, J.-an Feng, *J. Am. Chem. Soc. 112* (1990) 7619, and references cited therein.
[7] R. F. Cunico, Y.-K. Han, *J. Organomet. Chem. 162* (1978) 1, and references cited therein.
[8] R. Schwesinger, H. Schlemper, *Angew. Chem. 99* (1987) 1212; *Angew. Chem. Int. Ed. Engl. 26* (1987) 1167; R. Schwesinger, *Chimia 39* (1985) 269; R. Schwesinger, *Nachr. Chem. Tech. Lab. 38* (1990) 1212.
[9] E. V. Dehmlow, V. Knufinke, *J. Chem. Res. (S) 1989*, 224.
[10] A. P. Marchenko, S. I. Shaposhnikov, G. N. Koidan, A. V. Kharchenko, A. M. Pintchuk, *Zh. Obshch. Khim. 58* (1988) 2230.
[11] M. Becke-Goehring, W. Lehr, *Chem. Ber. 94* (1961) 1591.
[12] X-ray structure analysis: $C_{12}H_{36}N_7P_2 \cdot F$, space group *Pa*3 (No. 205), $a = 12.603(1)$ Å from 25 reflections with $19.5 < 2\theta < 39°$, $V = 2001.33$ Å^3, $Z = 4$, crystal dimensions 0.16 × 0.1 × 0.08 mm^3, $\mu(Mo_{K\alpha}) = 2.3$ cm^{-1}, 296 K, no absorption correction, ω-2θ scan, Nonius CAD4 diffractometer, 7346 measured reflections, 589 independent reflections,

471 with $F_0 > 6\sigma(F_0)$. Direct methods [13], $R = 0.0534$ ($R_w = 0.0461$), anisotropic temperature factors for all atoms except hydrogen. Weighting scheme $\omega^{-1} = \sigma^2(F_0) + 0.000024\,F_o^2$, 35 free parameters. Maximum electron density in subsequent difference Fourier synthesis $\pm$ 0.3 eÅ^3. Further details of the crystal structure investigation are available on request from the Fachinformationszentrum Karlsruhe, Gesellschaft für wissenschaftlich-technische Information mbH, W-7514 Eggenstein-Leopoldshafen 2 (FRG), on quoting the depository number CSD-55496, the names of the authors, and the journal citation.

[13] SHELXTL PC for Siemens Crystallographic Research Systems, Siemens Analytical X-Ray Systems Madison, WI, USA 1990.

[14] A. Aaberg, T. Gramstad, S. Husebye, *Acta Chem. Scand. A 34* (1980) 717.

[15] R. Appel, U. Baumeister, F. Knoch, *Chem. Ber. 116* (1983) 2275.

[16] D. Putzas, H. Rotter, H. Schlemper, R. Schwesinger, unpublished; cf. H. R. Allcock, N. M. Tollefson, R. A. Arcus, R. R. Whittle, *J. Am. Chem. Soc. 107* (1985) 5166.

[17] Diagram: SCHAKAL, a Fortran Program for the Graphical Representation of Molecular and Crystallographic Models; E. Keller, *J. Appl. Cryst. 22* (1989) 19.

[18] E. V. Dehmlow, M. Lissel, *Synthesis 1979*, 372.

[19] R. Schwesinger, J. Willaredt, unpublished.

[20] C. Chuit, R. J. P. Corriu, C. Reyé, *J. Organomet. Chem. 358* (1988) 57.

[21] W. J. Middleton, US-A 3940402 (1976) Dupont; T. Hiyama, M. Obayashi, M. Sawahata, *Tetrahedron Lett. 24* (1983) 4113.

[22] Because of the relatively high proportion of entrained water associated with the sparing solubility of **1**-F, considerable amounts of FHF^- were recognizable, in particular, in the THF spectra ($\delta = -91$) (in HMPA: $\delta = -145$ (d, $^1J(F,H) = 120$ Hz) (so far, best F^-:FHF^- ratio in THF = 1:1, in HMPA 2.3:1).

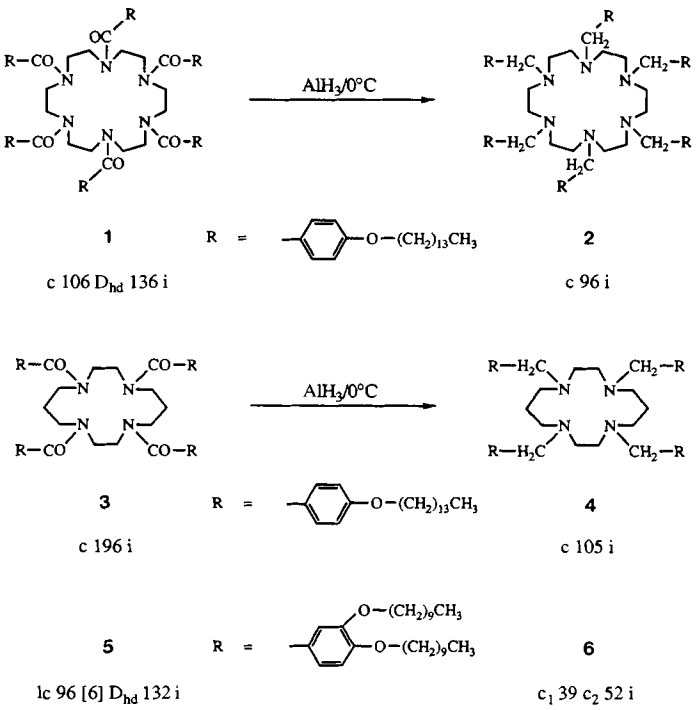

Scheme 1. Temperatures in °C.

Complexation of Transition Metal Ions with Substituted Aza Macrocycles: Induction of Columnar Mesophases by Molecular Recognition

By *Andrea Liebmann, Carlo Mertesdorf, Thomas Plesnivy, Helmut Ringsdorf,** and *Joachim H. Wendorff*

Coronands, as for example [18]crown-6, readily complex metal ions. Whereas crown ethers can incorporate both alkali-metal ions and alkaline-earth-metal ions with high complexation constants, the nitrogen analogues show special affinity for transition metal ions.[1] Furthermore, the aza macrocycles can be converted by substitution at the nitrogen atom into discoid compounds, which in the case of acylated compounds can form discotic liquid crystal phases;[2] however, their complexing ability is only modest. The results presented in this contribution show that both of these aspects of coronand chemistry can be combined, namely the formation of host/guest complexes and their self-assembly to liquid crystalline phases.

At temperatures between 106 and 136 °C, hexa(*p*-tetradecyloxybenzoyl)hexacyclene **1** forms a columnar discotic mesophase (D_{hd}),[3] which, owing to the central cavity in the columns, has been described by *Malthête* et al. as tubular.[2] With the help of gas-volumetrically calibrated solutions of AlH_3 in THF it was possible to carry out the reduction of **1** to the *non*liquid crystalline amine **2** in high yields (83%) (Scheme 1).[4]

The cyclam derivatives **4** and **6**[5] were prepared analogously from the acylated tetraaza macrocycles **3**[3] and **5**[6] respectively (Scheme 1), of which only the derivative **5** bearing eight wing groups forms a mesophase.

With exception of compound **6**, complexation of transition metal salts by the highly flexible cyclic amines induces a liquid crystalline phase which is absent for the free amines. We attribute this phenomenon in part to a stiffening of the macrocycle. This interpretation is consistent with the fact that the stiffer, structurally analogous amides can form mesophases. The phase behavior of the metal complexes is given in Table 1.

Table 1. Phase behavior of the transition metal complexes [a].

Complex	Ratio host/guest	Phase T [°C]
2 · $Co(NO_3)_2$	2:1 [7]	c 30 N_c 60 [b] i
2 · $Ni(NO_3)_2$	1:1	c 29 lc 95 i
4 · $Cu(NO_3)_2$	1:1	c 18 lc [c]
6 · $Cu(NO_3)_2$	1:1	g 67 i

[a] Abbreviations: c = crystalline; N_c = nematic-columnar; i = isotropic; lc = liquid crystalline; g = glassy. [b] First cooling curve of the DSC thermogram. [c] Decomposition above 160 °C.

In the following communication we shall deal more closely with the 1:2 $Co(NO_3)_2$/amine **2** system, which has been characterized as liquid crystalline by polarization microscopy, differential calorimetry, and X-ray diffraction analysis. Upon heating under the polarization microscope the birefringence of the enantiotropic liquid crystal phase is visible up to a temperature of about 53 °C. Initially, no specific texture is recognizable, but tempering at ca. 40 °C leads after 3 h to the formation of characteristic schlieren. The texture depicted in Figure 1 shows the singularities of $s = -1/2$ and $s = -1$ typical for a nematic phase. The enthalpy for the transition between the liquid crystalline and isotropic phase, which is obtainable from the cooling curve of the DSC thermogram is of an order of magnitude that is consistent with a transition into a slightly ordered nematic phase. A macroscopic planar orientation of the mesophase can easily be achieved by mechanical shearing. Under crossed polarizers it

[*] Prof. Dr. H. Ringsdorf, Dipl.-Chem. C. Mertesdorf, T. Plesnivy
Institut für Organische Chemie der Universität
J.-J.-Becher-Weg 18–20, W-6500 Mainz (FRG)
Dipl.-Phys. A. Liebmann, Prof. Dr. J. H. Wendorff
Deutsches Kunststoff-Institut
Schlossgartenstrasse 6 R, W-6100 Darmstadt (FRG)

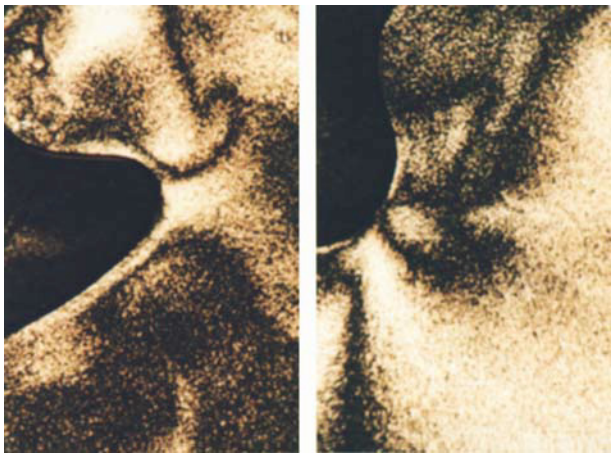

Fig. 1. Nematic schlieren texture of the **2** · $Co(NO_3)_2$ complex with singularities of s = −1/2 (left) and s = −1 (right).

is characterized by extinction perpendicular to and parallel to the direction of stress.

The X-ray scattering diagram of the complex shows a diffuse reflection at small angles and a halo in the wide angle region. The distance of 4.5 Å corresponding to the halo in the wide angle region compares with the typical scattering behavior of paraffin chains in liquid crystals and liquids. The reflection at 39.0 Å can be assigned to the average distance between the disk-shaped mesogens. Formally, the scattering behavior of the liquid crystal would thus suggest a discotic nematic ordering (N_D) of the complexed aza macrocycles, whereas the planar orientation of the highly viscous mesophase observable under the polarizing microscope, which is readily achievable by mechanical shearing, would suggest a columnar ordering. The diffuse reflection at 39.0 Å would then correspond to the average distance between the columns. There is no scattering reflection which can be attributed to the distance between the macrocycles in the columns. On the one hand, this could be indicative of a general disordering of the mesogenic units in the columns, which would correspond to a new nematic-columnar phase (N_{Cd}). Equally interesting

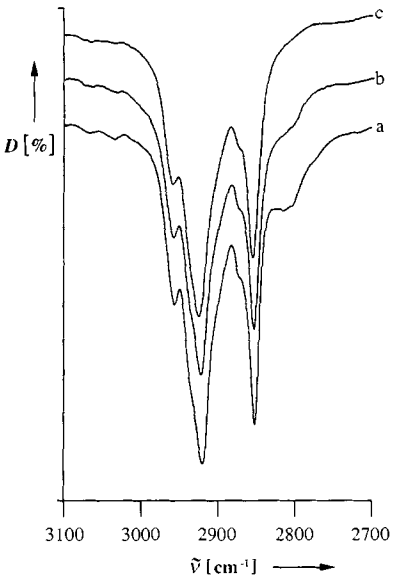

Fig. 2. FT-IR spectra of pure ligand **2** (a) and the complexes **2** · $Co(NO_3)_2$ (3:1) (b), and **2** · $Co(NO_3)_2$ (2:1) (c).

is the possibility of a jumping of the metal cations between the ligand molecules, which has already been proposed for the oxygen coronands in solution.[8]

In this connection the absence of the C–H stretching vibration of the methylene groups neighboring the donor centers (compare the IR spectra of amine **2** and amine **2**/$Co(NO_3)_2$ system) indicates that the ligand is completely complexed (cf. Fig. 2). This could be a result of the previously mentioned dynamic process.[9] In comparison, in the case of a 3:1 mixture the shoulder observable for the free ligand reappears. In principle, this observation could be explained by the formation of a sandwich complex. However, due to the absence of a scattering reflection which would result from the distance between the cobalt ions in such a structure, this possibility seems unlikely; hence the single macrocycle must be regarded as the repeat unit of the liquid crystal.[10]

Further spectroscopic investigations are needed to completely determine the molecular structure of this system. The process of phase induction and a possible supermolecular structure of the complex in the mesophase is shown schematically in Figure 3.

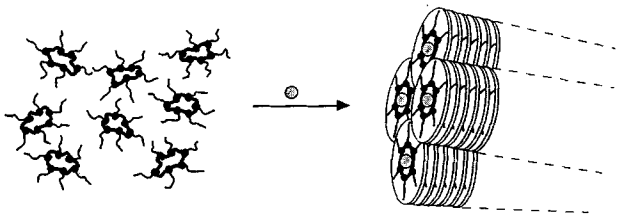

Fig. 3. Schematic representation of the induction of a columnar discotic mesophase by complexation of transition metal ions with substituted aza macrocycles.

A comparison of the substituted hexacyclenes **1** and **2** clearly reveals the influence of molecular dynamics on phase properties and provides an insight into the causes of the phase induction described here. As a result of the partial double bond character of the exocyclic C–N bond in the amide **1**, rotation about this bond axis is considerably restricted, and the macrocycle thus has an essentially rigid conformation. In comparison, in the case of the amine **2** a rapid change of conformation is possible due to the unhindered rotation of the wing groups and to the nitrogen inversion vibration.[11] Converting the amine into the complex decisively influences these dynamics; by coordination to the cobalt ion, the hexacyclene framework experiences substantial conformational rigidification and in this way forms the constitutional unit of the liquid crystal. Herein, this system differs fundamentally from the phthalocyanines, which, even as free ligands, are rigid and form liquid crystalline phases.

However, the occurrence of a broad mesophase in the case of the Cu^{II} complex of the amine **4**,[12] whose parent amide **3** is not liquid crystalline due to an insufficient space filling of the peripheral alkyl chains also demonstrates that the described induction of a mesomorphic phase is not only an effect of the conformational rigidification. Possibly, in this case the interaction between the central units is sufficiently large to compensate for the disadvantage of a smaller packing density of the alkyl chains. Preliminary susceptibility measurements on this system would seem to indicate a possible electronic coupling between the metal ions. The multifarious possibilities of variation with regard to ring size and substitution pattern of the aza macrocycles on the one hand,

and of the central ions and counterions on the other, open up a broad spectrum of novel metallomesogens.[13]

Received: April 24, 1991
revised: July 19, 1991 [Z 4589 IE]
German version: *Angew. Chem. 103* (1991) 1358

CAS Registry numbers:
1, 125498-89-7; **2**, 135866-19-2; **2**·$[CO(NO_3)_2]_2$, 136316-39-7; **2**·$Ni(NO_3)_2$, 135866-25-0; **3**, 125482-02-2; **4**, 135866-20-5; **4**·$Cu(NO_3)_2$, 135866-27-2; **5**, 125362-00-7; **6**, 135866-21-6; **6**·$Cu(NO_3)_2$, 135866-23-8.

[1] R. D. Hancock, A. E. Martell, *Chem. Rev. 89* (1989) 1875.
[2] J. M. Lehn, J. Malthête, A. M. Levelut, *J. Chem. Soc. Chem. Commun. 1985*, 1794.
[3] C. Mertesdorf, H. Ringsdorf, *Liq. Cryst. 5* (1989) 1757.
[4] N. M. Yoon, H. C. Brown, *J. Am. Chem. Soc. 90* (1968) 2927. *Procedure* for **2**: A solution of **1** (216 mg, 0.10 mmol) in THF (2 mL) was slowly added dropwise under nitrogen to a 0.35 M solution of aluminum hydride in THF (2.20 mL) cooled to 0 °C; the mixture was then stirred for 2 h at 0 °C. The reaction was terminated by addition of 0.5 mL THF/water (1:1). By addition of a small amount of dilute caustic soda, the reaction product could be filtered much more easily from the aluminum hydroxide precipitate. The hydroxide precipitate was thoroughly washed with cloroform, the filtrate dried with sodium sulfate, and the solvent finally removed by evaporation. The almost pure product obtained in this way was then recrystallized twice from ethyl acetate. Yield 172 mg (83%) of a white crystalline powder; m.p. 96 °C; elemental analysis in agreement with the calculated values. ^{1}H NMR (200 MHz, $CDCl_3$): $\delta = 0.86$ (t, 18H; CH_3), 1.20–1.50 (m, 132H; $(CH_2)_{11}$), 1.76 (m, 12H; O-CH_2-CH_2), 2.56 (s, 24H; CH_2-N-CH_2), 3.37 (s, 12H; N-CH_2), 3.91 (t, 12H; CH_2-O), 6.75 (d, 12H; aromat. 3,5), 7.04 (d, 12H; aromat. 2,6); IR (KBr): $\tilde{\nu}$ [cm^{-1}] = 1250 (ν, C-O), 1514, 1613 (ν, C = C).
[5] *Procedure* for **4**: The reaction was conducted in the same way as in the synthesis of **2**. The purification of the crude product, after washing the hydroxide precipitate with THF, ether, and chloroform, combination of the organic phases, drying with sodium sulfate and removal of the solvent in a rotary evaporater was carried out by flash chromatography (chloroform/methanol, 80:1) and recrystallization from ethyl acetate. Yield: 61.5%; m.p. 105 °C (DSC; 20 °C per min); R_f (chloroform/methanol, 10:1) = 0.52; elemental analysis compared favorably with the calculated values. ^{1}H NMR (200 MHz, $CDCl_3$): $\delta = 0.86$ (t, 12H; CH_3), 1.10–1.50 (m, 88H; $(CH_2)_{11}$), 1.78 (m, 12H, O-CH_2-CH_2 + N-CH_2-CH_2), 2.47, 2.56 (m, 16H; N-CH_2-CH_2-CH_2-N + N-CH_2-CH_2-N), 3.36 (s, 8H; N-CH_2), 3.86 (t, 8H; CH_2-O), 6.77 (d, 8H; aromat.), 7.13 (d, 8H; aromat.); IR (KBr): $\tilde{\nu}$ [cm^{-1}] = 1257 (ν, C-O), 1513, 1612 (ν, C = C).
Procedure for **6**: Reaction and work-up were carried out as in the synthesis of **4**. The purification of the crude product was accomplished by flash chromatography (chloroform/methanol, 80:1) and subsequent recrystallization from acetone. Yield 72.8%; m.p. 52 °C (DSC; 20 °C per min); R_f (chloroform/methanol, 10:1) = 0.52; elemental analysis consistent with calculated values.
^{1}H NMR (200 MHz, $CDCl_3$): $\delta = 0.86$ (t, 24H; CH_3), 1.10–1.55 (m, 112H; $(CH_2)_7$), 1.74 (m, 20H; O-CH_2-CH_2 + N-CH_2-CH_2), 2.41, 2.51 (m, 16H; N-CH_2-CH_2-CH_2-N + N-CH_2-CH_2-N), 3.26 (s, 8H;N-CH_2), 3.78 (t, 8H; CH_2-O), 3.91 (t, 8H; CH_2-O), 6.69 (s, 8H; aromat. 2,5), 6.93 (s, 4H; aromat. 6); IR (KBr): $\tilde{\nu}$ [cm^{-1}] = 1261 (ν, C-O), 1516, 1590 (ν, C = C).
[6] G. Lattermann, *Liq. Cryst. 6* (1989) 619. According to *G. Lattermann* further phase transitions occur in the case of the cyclam derivative **5**, the nature of which is still unclear: S. Schmidt, G. Lattermann, 19th Freiburger Working Conference on Liquid Crystals, April 4–6, 1990.
[7] The complexation of the transition metal ions with the amines was accomplished by dissolution of the appropriate equivalents of ligand and metal salt in dry THF and two days' stirring at room temperature in the case of amine **2** and one hours' stirring in the case of cyclam derivatives. After removal of the solvent in a rotary evaporator and drying under oil-pump vacuum the **2**-complexes precipitated as brownish ($Co(NO_3)_2$) or pale-green ($Ni(NO_3)_2$) substances. In the case of the tetraaza macrocycles an immediate change in color of the initially blue $Cu(NO_3)_2$ solution to green could be observed upon addition of the ligand; this is associated with the occurrence of a charge transfer band in the UV/VIS spectrum. The solid complexes are likewise intense green. In the case of the $Co(NO_3)_2$-complex an oxidation of the central ion by atmospheric oxygen occurs during the complexation, which is of decisive importance for the phase induction. Upon complete exclusion of atmospheric oxygen, and thus of any oxidation, no color change could be observed; nor could any signs of a complexation be recognized in the IR spectrum. The solid precipitating after removal of the solvent in a rotary evaporator showed merely a melting point depression as compared to the pure ligand, and no formation of a mesophase.
[8] F. L. Dickert, W. Gmeiner, W. Gumbrecht, H. Meissner, *Angew. Chem. 99* (1987) 238; *Angew. Chem. Int. Ed. Engl. 26* (1987) 228.
[9] In addition, the IR spectrum of the complex shows an intense band at 1384 cm^{-1}, which can be assigned to the twofold degenerate stretching vibration of ionically coordinated nitrate. Cf. also N. F. Curtis, Y. M. Curtis, *Inorg. Chem. 4* (1965) 804.
[10] Cf. for example the investigations on the bis(octaalkoxyphthalocyaninato)lutetium coordination compounds that form discotic mesophases in which sandwich complexes are the repeat units of the liquid crystal: C. Piechocki, J. Simon, J. J. Andre, D. Guillon, P. Petit, A. Skoulios, P. Weber, *Chem. Phys. Lett. 122* (1985) 124.
[11] This difference in the molecular dynamics of amide and amine is immediately apparent on comparing the ^{1}H-NMR spectra recorded in solution. In the case of the acylated hexacyclene **1** the aromatic protons as well as the methylene protons of the macrocycle show extremely broad signals at room temperature, whereas in the case of the amine sharp bands occur as a result of the rapid change of conformation, which in the case of the amide can first be observed at elevated temperature. A description of the coalescence phenomena occurring in benzoyl-substituted hexacyclenes is given in: D. Tatarsky, K. Banerjee, W. T. Ford, *Chem. Mater. 2* (1990) 138.
[12] Preliminary X-ray scattering measurements indicate a D_{hd} phase.
[13] For a review of metal-containing liquid crystals see: A. M. Giroud-Godquin, P. M. Maitlis, *Angew. Chem. 103* (1991) 370; *Angew. Chem. Int. Ed. Engl. 30* (1991) 375.

Azarhoda-*closo*-dodecaborane **

By *Hans-Peter Hansen, Jens Müller, Ulrich Englert,* and *Peter Paetzold**

Of the heteroboranes with nitrogen as heteroatom in the cluster framework, the compounds *arachno*-$N_2B_8H_{12}$,[1] *nido*-$NB_{10}H_{13}$ **1**,[2] and *closo*-$NB_{11}H_{12}$,[3] derive structurally from an icosahedron as the corresponding *closo*-polyhedron. The N atom in these azaboranes is four-, five- and six-coordinate, respectively; consequently classical two-center, two-electron bonds do not suffice for a description of the bonding of the N atom in the *nido*- and the *closo*-compound. We now report on the first representative of an azametallaborane from the series of icosahedra. Following *Hawthorne*'s classical route to the *closo*-dicarbametallaboranes from *nido*-$C_2B_9H_{11}^{2-}$ and suitable transition-metal compounds,[4] we first deprotonated **1** according to Equation (a) (tmeda = 1,2-bis(dimethylamino)ethane) to give the anion $NB_{10}H_{12}^-$, whose structure with C_s symmetry follows unequivocally from the 2D-^{11}B-^{11}B-NMR spectrum. The NH group detectable ^{1}H-NMR and IR spectroscopically is especially informative, since it indicates that a bridge proton and not an *N*-bound proton is cleaved from **1**. The remaining non-terminal H atom shows a correlation with B9 and B10 in the 2D-^{11}B-^{1}H experiment, that is either bridges B9 and B10, or undergoes, as *endo*-H-atom, a rapid exchange equilibrium between the degenerate isomers with a BH_2 group in the 9 or 10 position. A broad ^{1}H-NMR signal at $\delta = -3.59$ suggests a bridge position on the mirror plane of $NB_{10}H_{12}^-$. The position of the corresponding H atom in the isoelectronic anion $C_2B_9H_{12}^-$ could recently be established unequivocally as *endo*, i.e. this anion contains a BH_2 group on its symmetry plane.[5] A renewed deprotonation of **2** to give the dianion $NB_{10}H_{11}^{2-}$ isoelectronic with the dianion $C_2B_9H_{11}^{2-}$ can indeed be accomplished unproblematically with $LiBHEt_3$, but is unnecessary for the synthesis of the target molecule **3**, since **3** is formed directly from **2** when the latter is allowed to react

[*] Prof. Dr. P. Paetzold, J. Müller, H.-P. Hansen, Dr. U. Englert
Institut für Anorganische Chemie der Technischen Hochschule
Templergraben 55, W-5100 Aachen (FRG)

[**] This work was supported by the Deutsche Forschungsgemeinschaft.

with $[(Ph_3P)_3RhCl]$ according to Equation (b). The nonterminal H atom of **2** is bound, in **3**, terminally to Rh as hydrido ligand. The anion $NB_{10}H_{12}^-$ thus behaves like the anion $C_2B_9H_{12}^-$, which reacts directly with $[(Ph_3P)_3RhCl]$ analogous to reaction (b) to give *closo*-$[\{(Ph_3P)_2RhH\}C_2B_9H_{11}]$ **4**.[6]

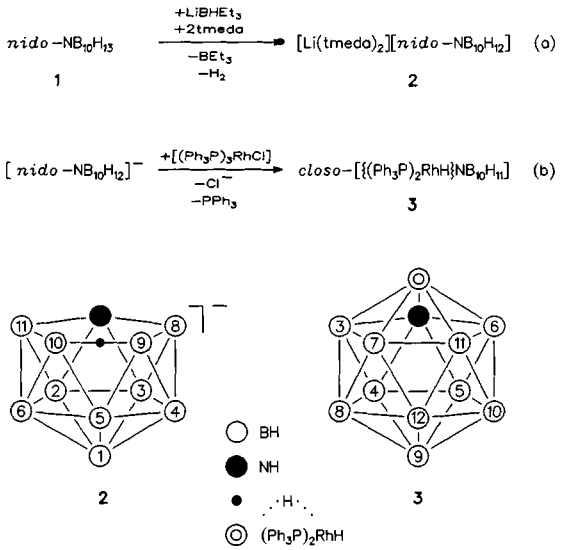

An X-ray structure analysis was carried out on crystals which still contained 1 mol of CH_2Cl_2 and 0.5 mol of pentane per mol of **3**.[7] The central structural unit of **3** consists of a distorted $RhNB_{10}$ icosahedron (Fig. 1). The Rh atom, because of its size, lies well outside the ideal icosahedral position, and consequently the angles subtended by the five triangles apexing at the Rh atom are significantly smaller than 60° (41.8–47.3°). For electronic reasons the smaller N atom is obviously more distant from the Rh atom (2.40 Å) than the four larger B atoms neighboring the Rh atom (2.23–2.26 Å). The planarity of the pentagon, which is capped by the Rh atom with formation of a pentagonal pyramid, is thereby lost (angle between the planes through B3–N–B6 and B3–B7–B11–B6 13.2°). In contrast to the Rh atom, the N atom, because of its smallness, lies more central than would correspond to the ideal position, so that the angles subtended by the five triangles apexing at the N atom are greater than 60° (62.8–64.3°). The pentagonal pyramid capped by the atom B9 opposite the Rh atom more closely approaches the ideal icosahedral geometry and has an almost planar base (angle between the planes B8–B12–B10 and B8–B4–B5–B10: 3.7°). With exception of the triangles B3–B4–B8 and B5–B6–B10 the ten remaining triangles formed by B atoms deviate only slightly from the regular geometry. The structure of **3** is related with that of **4** and, in the icosahedral region, also with that of $[\{(C_5Me_5)Rh\}C_2B_9H_{11}]$.[8]

3 is a cluster compound of the *closo* type with a six-coordinate N atom. With the elucidation of the structure of **3**, also the *nido* structure of **1** which we previously deduced from 2D-NMR spectra is indirectly confirmed.[2] The orange solid **3**, which can be handled at least briefly whilst exposed to air, is stable up to 100 °C.

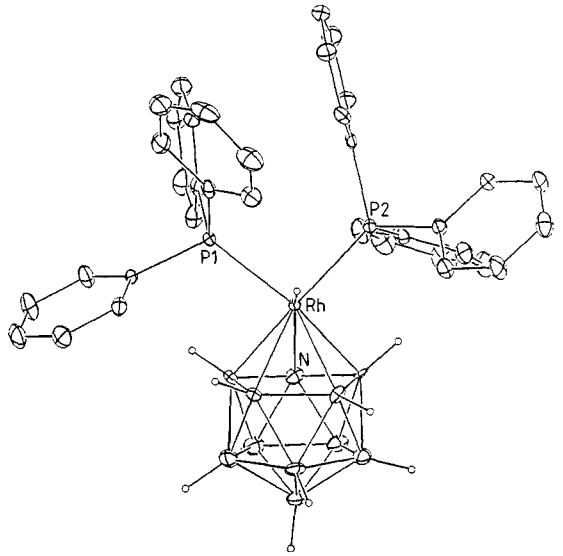

Fig. 1. Structure of 3 in the crystal. Selected bond lengths [Å] and angles [°], standard deviations in brackets, numbering of framework atoms as in Equation (b): Rh–N 2.400(4), Rh–B3 2.249(4), Rh–B6 2.227(5), Rh–B7 2.241(4), Rh–B11 2.262(4), Rh–P1 2.3386(9), Rh–P2 2.3652(9), Rh–H 1.61(6), N–B3 1.663(6), N–B4 1.695(5), N–B5 1.691(5), N–B6 1.728(5), B3–B4 1.851(7), B3–B7 1.800(7), B3–B8 1.776(6), B4–B5 1.782(6), B4–B8 1.726(9), B4–B9 1.738(6), B5–B6 1.886(7), B5–B9 1.736(7), B5–B10 1.758(8), B6–B10 1.792(6), B6–B11 1.772(8), B7–B8 1.828(8), B7–B11 1.790(6), B7–B12 1.786(6), B8–B9 1.789(7), B8–B12 1.786(6), B9–B10 1.764(6), B9–B12 1.774(8), B10–B11 1.783(8), B10–B12 1.777(7), B11–B12 1.782(6); Rh–N–B3 64.3(2), N–Rh–B3 41.8(1), Rh–N–B6 62.8(2), N–Rh–B6 43.7(1), B3–N–B4 66.9(3), N–B3–B4 57.4(3), B4–N–B5 63.5(2), N–B4–B5 58.1(2), B5–N–B6 67.0(3), N–B5–B6 57.5(2), B3–Rh–B7 47.3(2), Rh–B3–B7 66.1(2), B6–Rh–B11 46.5(2), Rh–B6–B11 67.8(2), B7–Rh–B11 46.8(1), Rh–B7–B11 67.2(2), B7–B3–B8 61.5(3), B3–B7–B8 58.6(3), B11–B6–B10 60.0(3), B6–B11–B10 60.5(3), B4–B8–B9 59.3(3), B8–B4–B9 62.2(3), B5–B10–B9 59.1(3), B10–B5–B9 60.6(3), B4–B3–B8 56.8(3), B3–B4–B8 59.4(3), B5–B6–B10 57.0(3), B6–B5–B10 58.8(3), B5–B4–B9 59.1(3), B4–B5–B9 59.2(3), B9–B8–B12 59.5(3), B8–B9–B12 60.2(3), B9–B10–B12 60.1(3), B10–B9–B12 60.3(3), B8–B7–B12 59.2(3), B7–B8–B12 59.2(3), B11–B10–B12 60.1(3), B10–B11–B12 59.8(3), B11–B7–B12 59.8(2), B7–B11–B12 60.0(2), P1–Rh–P2 96.38(3), P1–Rh–H 78(2), P2–Rh–H 92(2).

Experimental

2: A solution of **1** [2] (66 mg) in THF (3 mL) was treated at −78 °C with 0.49 mL of 1 M $Li[BHEt_3]$ in THF. After 5 minutes' stirring at room temperature, all volatile components were removed in vacuo; the residue was taken up in 3 mL of THF and the resulting solution treated with 0.38 g of tmeda. After evaporation to dryness the residue was washed three times with pentane, and, after drying, contained 0.180 g (99%) of **2**.—NMR spectra in $[D_8]$THF at 25 °C; ^{1}H NMR (299.95 MHz, TMS): δ = −3.59 (br, μ-H), 0.16 (H1), 0.53 (H9/10), 0.75 (H5), 1.34 (H4/6), 1.70 (H2/3), 1.85 (H8/11) (measurement and assignment of the BH signals as cross peaks in the 2D-^{11}B-^{1}H-NMR spectrum), 2.15 and 2.31 (2s in the ratio 3:1, tmeda), 4.08 (br, NH); ^{11}B NMR (96.23 MHz, $Et_2O \cdot BF_3$): δ = −42.8 (d, J = 147 Hz, B1 (B5, B2/3, B4/6)), −25.0 (d, J = 147 Hz, B9/10 (B5, B4/6, B8/11)), −22.8 (d, J = 147 Hz, B5 (B1, B9/10, B4/6)), −17.6 (d, J = 171 Hz, B2/3 (B1, B6/4)), −15.4 (d, J = 146 Hz, B4/6 (B1, B9/10, B5, B3/2, B8/11)), −10.9 (d, J = 147 Hz, B8/11 (B9/10, B4/6)) (in brackets, the B atoms correlated in the 2D-^{11}B-^{11}B-NMR spectrum pulse, sequence COSY 45; as expected [2], no cross peak is observable between B2/3 and B11/8 due to the common neighborhood of the N atom). IR(CH_2Cl_2): $\tilde{\nu}$ [cm^{-1}] = 3365 (NH), 2522 (BH).

3: Starting with a solution of **1** (0.24 g) in THF (4 mL), the same procedure was followed as in the preparation of **2** except that, instead of treatment with tmeda, the product taken up in THF (5 mL) was added dropwise at −78 °C to a suspension of $[(Ph_3P)_3RhCl]$ (1.62 g) in toluene (10 mL). The mixture was stirred for 3 h at room temperature, filtered, and the orange solid washed with toluene (2 × 5 mL). After column chromatographic purification in CH_2Cl_2 on silica gel the solution was evaporated down to 20 mL and layered with 20 mL of pentane. At −40 °C there crystallized 0.83 g (54%) of $3 \cdot CH_2Cl_2 \cdot 0.5C_5H_{12}$.—NMR spectra of **3** in CD_2Cl_2 at 25 °C; ^{1}H NMR (299.9 MHz, TMS): δ = −14.70 (d/t, ^1J(Rh,H) = 29 Hz, ^2J(P,H) = 20 Hz, 1H; RhH), 1.19–3.02 (10H; BH), 3.05 (s, 1H; NH), 7.06–7.26 (30H; Ph); ^{11}B NMR (96.23 Hz, $Et_2O \cdot BF_3$): δ = −19.21 and −15.01 (d, J = 146 Hz, and s resp., br, 4B), −2.59 and 1.86 (m and d resp., J = 146 Hz, 6B). IR (CH_2Cl_2): $\tilde{\nu}$ [cm^{-1}] = 3318 (NH).

Received: June 3, 1991 [Z 4670 IE]
German version: *Angew. Chem. 103* (1991) 1357

CAS Registry numbers:
1, 131179-98-1; **2**, 135952-56-6; **3**, 135989-30-9; $LiBHEt_3$, 22560-16-3; $[(Ph_3P)_3RhCl]$, 14694-95-2.

[1] B. Štibr, J. D. Kennedy, T. Jelinek, *J. Chem. Soc. Chem. Commun. 1990*, 1309.

[2] J. Müller, P. Paetzold, R. Boese, *J. Heteroat. Chem. 1* (1990) 461.

[3] J. Müller, J. Runsink, P. Paetzold, *Angew. Chem. 103* (1991) 201; *Angew. Chem. Int. Ed. Engl. 30* (1991) 175.

[4] M. F. Hawthorne, D. C. Young, P. A. Wegener, *J. Am. Chem. Soc. 87* (1965) 1818.

[5] J. Buchanan, E. J. M. Hamilton, D. Reed, A. J. Welch, *J. Chem. Soc. Dalton Trans. 1990*, 677.

[6] T. E. Paxson, M. F. Hawthorne, *J. Am. Chem. Soc. 96* (1974) 4674; G. E. Hardy, K. P. Callahan, C. E. Strouse, M. F. Hawthorne, *Acta Crystallogr. Sect. B 32* (1976) 264.

[7] Crystallographic data: $a = 9.807(4)$, $b = 18.512(6)$, $c = 24.152(9)$ Å, $\beta = 96.57(3)°$. $V = 4365(5)$ Å^3, $Z = 4$, $\varrho_{calcd} = 1.346$ g cm^{-3}, $P2_1/n$ (No. 14); ENRAF-Nonius CAD 4; measuring temperature 228 K; $\mu(Cu_{K\alpha}) = 53.2$ cm^{-1}, $F(000) = 1812$; 6179 reflections with $5 < \theta < 59°$, 4706 symmetry independent with $I > 2\sigma(I)$ in the solution of structure and refinement for 507 parameters; empirical absorption correction with DIFABS [9]; pentane disordered about $\bar{1}$; $R = 0.061$, $R_w = 0.076$, $w^{-1} = 1/\sigma^2(F_0)$; H atom on Rh refined with fixed isotropic temperature factor, the remaining atoms in the structure factor calculation. Further details of the crystal structure investigation are available on request from the Fachinformationszentrum Karlsruhe, Gesellschaft für wissenschaftlich-technische Information mbH, W-7514 Eggenstein-Leopoldshafen 2 (FRG), on quoting the depository number CSD-55495, the names of the authors, and the journal citation.

[8] X. L. R. Fontaine, N. N. Greenwood, J. D. Kennedy, K. Nestor, M. Thornton-Pett, *J. Chem. Soc. Dalton Trans. 1990*, 681.

[9] N. Walker, D. Stuart, *Acta Crystallogr. Sect. A 39* (1983) 159.

Surface Fractality of Dendrimers**

By *Dina Farin* and *David Avnir**

We provide evidence that a conjecture made in this journal on the fractal nature of the surface of polymeric dendrimer molecules[1] is correct. The chemistry and physical properties of dendritic polymers (starburst dendrimers) have been the topic of intensive recent research activity in several laboratories[2] and were reviewed recently in this journal by *Tomalia* et al.[1]. These macromolecules are constructed from various initiator cores upon which radially branched layers, termed generations, are covalently attached, thus yielding a three-dimensional highly ordered polymeric compound. The final exterior layer may be further modified chemically to provide a variety of terminal functionalities. The interest in starburst dendrimers is due to an ever-rising demand for materials with special properties, a demand which can be approached through the controlled hierarchical molecular architecture, layer after layer, of these novel polymers.

Since most of the specific applications of starburst dendrimers involve interaction with their outer exposed surface, their full characterization is of prime importance, as indeed stressed by *Tomalia* et al.[1] In particular, these authors drew attention to the importance of the *morphological* characteristics of the surface of dendrimers. The hierarchical self-similarity suggested to them that this morphology may be fractal in its nature. We now provide direct evidence that *Tomalia* et al. were right in their intuition and that the highly clefted surfaces of starburst dendrimers are indeed fractal. This finding is in accordance with the evidence accumulated over the past decade that the complex morphologies of surfaces of both man-made and natural materials are, by and large, describable by fractal geometry.[3,4] Of particular relevance is the evidence that the surfaces of many enzymes and proteins are fractal;[5] we recall that one of the potential applications of starburst dendrimers is to mimic these biomolecules.[1]

We have applied two different fractal analyses. The first method[6] is based on Equation (a), where A is the surface

$$A \sim \sigma^{(2-D)/2} \qquad (a)$$

area accessible to probe spheres of cross-sectional area σ. The degree of surface irregularity is quantified through D, the surface fractal dimension. For a smooth surface ($D = 2$), A becomes independent of the size of the yardstick used to measure it, but for $D > 2$ surface accessibility to external spheres does depend on their size.

The second method[6] is based on Equation (b), in which

$$A \sim d^D \qquad (b)$$

the surface area of an object, as determined with a fixed yardstick (sphere), is measured as a function of the object size, d. For objects with surfaces which are mainly external, the D values from both equations coincide. Many materials[5g] obey Equations (a) and (b), not only in terms of surface area but also in terms of the effective area which participates in a reaction.[3,5g]

Of the starburst dendrimers described in Ref. [1], starburst polyamidoamine (PAMAM) is accompanied by data which allow a comparative fractal analysis based on Equations (a) and (b). Figure 27 in Ref. [1] describes the relation between the (square root of the) solvent-accessible surface-area of PAMAM and the size of probe spheres (Fig. 1). For the larger

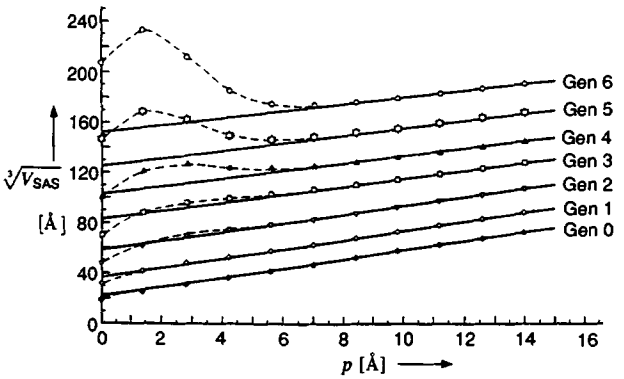

Fig. 1. Relationship between the solvent-accessible surface area and the probe-sphere diameter p (Figure 27 in [1]).

spheres (those with cross-sectional areas much larger than the size of a surface atom), there is a smooth weak increase in surface area with probe size, which actually reflects the increase in the area of enveloping contours with probe size. The fine details of the surface are probed by the smaller probes, and here it is clearly seen, for instance for the highest (sixth) generation, that the area *decreases* with increase in probe size, as is indeed expected for a rough surface. Using the data for the highest generation over the area-yardstick range of 7–158 Å^2 (radii of 1.5–7.0 Å), one finds that Equation (a) is obeyed nicely (Fig. 2a) with $D = 2.41 \pm 0.04$ (correlation coefficient 0.988). The authenticity of this result is corroborated by applying now the second method [Eq. (b)].

[*] Prof. D. Avnir, Dr. D. Farin
Department of Organic Chemistry
The Hebrew University of Jerusalem
Jerusalem 91904 (Israel)

[**] This work was supported by grants from the US-Israel Binational Foundation, the Wolfson Foundation, and the Valatzi-Pikowski Foundation. *D. F.* thanks the Minerva Foundation for a study-grant in Germany.

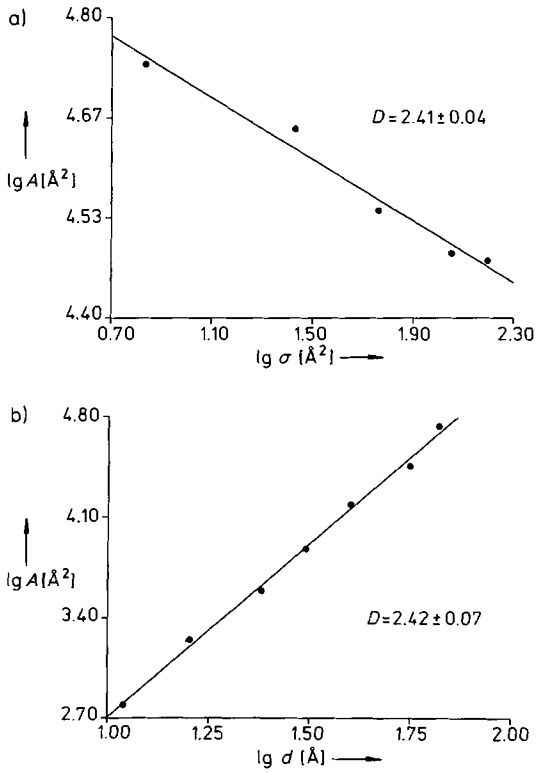

Fig. 2. Solvent-accessible surface area A of PAMAM dendrimers (a) as a function of probe cross-sectional area σ [Eq. (a)] and (b) as a function of dendrimer diameter d [Eq. (b)].

Figure 1 provides also the change in area with the generation number, and Table 6 in Ref. [1] links the generation number with the size, d (d_{exp} in the table). As explained elsewhere,[5] it is more accurate to use the smallest available yardstick, which, in our case, is a sphere with a cross-sectional area of 7 Å^2 (radius of 1.5 Å). We find that this data obeys Equation (b) (Fig. 2b) with $D = 2.42 \pm 0.07$ (correlation coefficient 0.998), practically the same value obained by the first method. Interestingly, *Lewis* and *Rees* obtained $D = 2.4$ as a general value for the surfaces of various enzymes.[5b]

Similar data is available for polyether dendrimers (Fig. 28 in Ref. [1]), but the range is too limited (four generations compared with six for PAMAM). Nevertheless, it is interesting to notice that the different apparent D value obtained from this limited data, namely, $D = 1.96 \pm 0.02$ (correlation coefficient 0.999), is in agreement with the difference in the structural properties between the two types of dendrimers as described in Ref. [1] (p. 155): "The polyether system quickly becomes congested and has little in the way of internal cavities," while the "PAMAM dendrimers have a great deal of internal surface area and solvent-filled volume"; that is, the latter have a porous structure leading to a rough surface, whereas the former is densely compact with much smoother surface cavities.

The demonstrated ability to quantify the surface roughness of starburst dendrimers in terms of their surface fractal dimension opens the possibility of applying several theoretical approaches that have been developed for the physical-chemistry properties of such surfaces. Examples include adsorption[7a, b] and diffusion[7c] on fractal surfaces, their derivatization,[7d] and their catalytic[7e] and noncatalytic[7f] reactivity.

Received: May 7, 1991 [Z 4616 IE]
German version: *Angew. Chem. 103* (1991) 1409

[1] D. A. Tomalia, A. M. Naylor, W. A. Goddard III, *Angew. Chem. 102* (1990) 119; *Angew. Chem. Int. Ed. Engl. 29* (1990) 138.
[2] D. A. Tomalia, M. Hall, D. M. Hedstrand, *J. Am. Chem. Soc. 109* (1987) 1601; D. A. Tomalia, V. Berry, M. Hall, D. M. Hedstrand, *Macromolecules 20* (1987) 1167; A. M. Naylor, W. A. Goddard III, *J. Am. Chem. Soc. 111* (1989) 2339; C. J. Hawker, J. M. J. Frechet, *ibid. 112* (1990) 7638; G. Caminati, N. J. Turro, D. A. Tomalia, *ibid. 112* (1990) 8515.
[3] D. Avnir (Ed.): *The Fractal Approach to Heterogeneous Chemistry: Surfaces, Colloids, Polymers*, Wiley, Chichester 1989 (reprinted 1990).
[4] H. Takayasu: *Fractals in the Physical World*, Manchester University Press, Manchester 1989.
[5] a) P. Pfeifer, U. Velz, H. Wipperman, *Chem. Phys. Lett. 113* (1985) 535; b) M. Lewis, D. C. Rees, *Science 230* (1985) 1163; c) C. Abad-Zapatero, C. T. Lin, *Biopolymers 29* (1990) 1745; d) D. Fushman, *J. Biomol. Struct. Dyn. 7* (1990) 1333; e) J. Aqvist, O. Tapia, *J. Mol. Graphics 5* (1987) 30; f) D. Farin, S. Peleg, D. Yavin, D. Avnir, *Langmuir 1* (1985) 399; g) D. Farin, D. Avnir, *New J. Chem. 14* (1990) 197.
[6] P. Pfeifer, D. Avnir, *J. Chem. Phys. 79* (1983) 3558; *ibid. 80* (1984) 4573.
[7] a) M. W. Cole, N. S. Holter, P. Pfeifer, *Phys. Rev. B 33* (1986) 8806; b) M. Jaroniec, X. Lu, R. Madey, D. Avnir, *J. Chem. Phys. 92* (1990) 7589; c) S. Havlin, D. Ben-Avraham, *Adv. Phys. 36* (1987) 695; d) D. Farin, D. Avnir, *J. Chromatogr. 406* (1987) 317; e) *J. Am. Chem. Soc. 110* (1988) 2039; f) *J. Phys. Chem. 91* (1987) 2039.

Book Reviews are written by invitation from the editor. Suggestions for books to be reviewed and for book reviewers are welcome. Publishers should send brochures or (better) books to the following address: Redaktion Angewandte Chemie, Postfach 101161, D-6940 Weinheim, Federal Republic of Germany. The editor reserves the right of selecting which books will be reviewed. Uninvited books not chosen for review will not be returned.

Acronyms and Abbreviations in Molecular Spectroscopy. An Encyclopedic Dictionary. By *D. A. W. Wendisch*. Springer, Berlin 1990. 314 pp., hardcover DM 98.00.—ISBN 3-540-51348-5

This book entitled "Acronyms and Abbreviations in Molecular Spectroscopy: An Encyclopedic Dictionary" by *D. A. W. Wendisch* is a comprehensive collection of the jargon used by spectroscopists, which is rich in abbreviations. Of the approximately 500 entries, an overwhelming majority are concerned with abbreviations used in NMR spectroscopy; other spectroscopy methods such as ESR, NQR, IR, Raman, optical spectroscopy, and polarized light methods receive only minor coverage. To that extent, therefore, the description "Molecular Spectroscopy" in the title promises more than is contained in the book.

Each entry includes an explanation varying in length from a few lines to several pages. At the end of each section there are relevant literature references, mostly to recent publications. The choice of keywords is very comprehensive for the field of NMR, but is rather limited for the other areas of spectroscopy. Of the NMR keywords that occurred to this reviewer, not a single one had been omitted. On the other hand, though, many terms that are not normally abbreviated have been forced to fit into the procrustean bed of abbreviations and acronyms, and have thereby been altered out of recognition in some cases. Thus, POF stands for "product operator formalism", WST for "water suppression technique", and CDRE for "convolution difference resolution enhancement". I have not previously encountered the abbreviation POF in any publication, but have certainly seen "product operator formalism" for which there is no entry in this encyclopedia. This shortcoming detracts a little from the book's value as a reference source.

The explanations vary greatly in their extent and depth. For example, under CYCLOPS I would expect to find not only that it provides a way of avoiding instrumental errors in data acquisition, but also an additional line of text giving the phase cycle. WALTZ is described as a pulse sequence for heteronuclear decoupling, but again the pulse sequence is not given. Some rather unimportant sequences such as UPT are given the rare distinction of a detailed description with a diagram of the pulse sequence, whereas important sequences such as HMQC or DEPT are described by text alone; only four lines are devoted to DEPT, the most important of all editing sequences! This very uneven treatment of different entries does not appear to follow any kind of system, and it is regrettable that there is no correlation with the relative importance of the entries.

Apart from these imbalances in the descriptions, which could give non-specialists a wrong impression of the relative importance of the various techniques, the explanations are in general accurate and provide a good starting point, not least through the literature references given. However, it would be unreasonable to expect a complete coverage of all the important publications relevant to a given entry.

A further positive feature is the references that are given to software packages for the analysis or simulation of NMR spectra, such as LAOCOON, DAISY, SPHINX, or SMART; on the other hand, commercial programs such as Felix or the nmri products are not mentioned.

An index of keywords at the end of the book allows one to quickly assign each term to the relevant area of spectroscopy. Here the extreme bias of the encyclopedia towards NMR becomes obvious, even if it has not been noticed earlier. The book is printed on glossy paper with a hard cover. The printing error on the cover is not typical of the rest of the book. The figures are of good quality.

Despite the weaknesses mentioned above, the book can be recommended as a work of reference for NMR spectroscopists. It provides an alternative to the recently published book "A Handbook of Nuclear Magnetic Resonance" by *R. Freeman*; although the explanations in the latter are more detailed and well-balanced, the number of terms included is much smaller.

Christian Griesinger [NB 1122 IE]
Institut für Organische Chemie
der Universität Frankfurt am Main (FRG)

Challenges in Synthetic Organic Chemistry. By *T. Mukaiyama*. Oxford University Press, Oxford 1990. 225 pp., hardcover £ 27.50.—ISBN 0-19-855644-6

To mark his 60th birthday *Teruaki Mukaiyama* wrote a comprehensive review of his research efforts during the last forty years. He describes all his research achievements chronologically. Thanks to *J. E. Baldwin*, who has written a fitting foreword, we can now read this fine book in English.

The importance of *Mukaiyama*'s contributions becomes immediately clear just by browsing through the book. The development of the oxidation–reduction condensation was a real breakthrough in the development of organic synthetic methods. Many macrolide syntheses still rely on the use of the combination of triphenylphosphine and dipyridyl disulfide for the ring closure. The *Mitsunobu* reaction, developed by a former collaborator of *Mukaiyama*, is one of the most reliable transformations to obtain a carbon–heteroatom bond with inversion. Finally 2-halopyridinium salts as reagents for esterification and macrolactonization have been widely used in organic synthesis. The titanium(IV) chloride catalyzed crossed aldol reaction between silyl enol ethers and acetals is one of the most important C–C bond-forming reactions in organic chemistry. Since the first pioneering reports of *Mukaiyama*'s group an enormous number of applications of titanium(IV) chloride have been reported. The use of Lewis acids for the aldol reaction made it possible to achieve high and synthetically useful stereoselectivities. At least as important are the contributions of *Mukaiyama*'s group to the development of the tin and boron enolates. Finally, the

use of proline-derived chiral auxiliaries for the stereoselective reduction of ketones and for the stereoselective addition of organometallic reagents to carbonyl compounds is yet another achievement of *Mukaiyama*'s group.

That the author succeeds in accurately and impartially describing all these results and many more which have been accomplished in his laboratories is an astonishing achievement. Personal views intrude only rarely, and the results are reported in essentially chronological order. Only in the prologue and in the epilogue does *Mukaiyama* allow himself some personal remarks. In the first, poetic sentence of his prologue he proclaims the importance of purely exploratory experimentation. He advocates the importance of the unpredictable as a tool to achieve major breakthroughs in chemical research. One of the most fascinating parts of his book is the well-documented change of *Mukaiyama*'s interest from mechanistic questions to the development of synthetic methods. A series of unexpected results led him to develop the oxidation–reduction condensation. In spite of the clear distinction made between the different research projects described in the individual chapters, a Western reader is surprised to find how all the innumerable experimental results seem to be connected by an invisible network of associations. The fact that most of *Mukaiyama*'s inventions of new reactions can be traced to the concept of "dehydration" may be astonishing for Western chemists, but perhaps reflects some of the Japanese traditions.

Keeping this in mind, the book is not only a source book for the synthetic chemist about the results of one of the most successful research groups in Japan, but also affords some insights into the Japanese way of doing research.

Reinhard Neier [NB 1163 IE]
Institut für Organische Chemie
der Universität Fribourg (Switzerland)

Atomic and Molecular Clusters. Edited by *E. R. Bernstein*. Elsevier, Amsterdam 1990. 806 pp., hardcover DFl 495.00.—ISBN 0-444-88193-X

Although research on clusters is still a relatively young field, its close connections with atomic and molecular physics, solid state physics, and not least with chemistry, have resulted in it already becoming an extensive field of study in its own right. This book does not attempt to present a superficial review of all the different areas of cluster physics. Instead some of the most important aspects of cluster physics have been selected and described in detail in eight independent chapters. Each chapter is carefully constructed and thoughtfully worked out, presenting valuable information in a clearly comprehensible style.

The first chapter, by *R. E. Smalley*, gives a comprehensive 62-page review of studies on clusters of carbon atoms. Special attention is devoted to the cluster C_{60}, which according to the author will possibly "come to be recognized as one of the most abundant and most important molecules in the universe". If this raises some doubts in the reader's mind, he or she will presumably feel a need to read this fascinating chapter.

The next chapter is a comprehensive and well-written account of clusters of main group elements. In preparing this the authors, *M. L. Mandich, W. D. Reents, Jr.* and *V. E. Bondybey*, have performed an important service for the clusters research community. This substantial 290-page review is packed with useful information, and contains nearly 500 literature references. It is the only such report in the clusters literature, and is enough in itself to make the book a worthwhile purchase.

Chapter 3 is devoted to a specialist topic, the structures of weakly bound complexes. In this 34-page article *S. E. Novick, K. R. Leopold*, and *W. Klemperer* have tabulated the most important properties of 144 complexes.

In Chapter 4 *R. O. Watts* reports on recent advances in the IR spectroscopy of van der Waals clusters. Reducing the temperature of such clusters by adiabatic expansion and laser cooling makes it possible to obtain IR spectra of previously unattainable resolution.

The following chapter is also concerned with van der Waals clusters, though in this case with a special class, namely clusters made up of inert gas atoms and halogen atoms. *K. C. Janda* and *C. R. Bieler* describe how such clusters exhibit a wealth of interesting effects, including the so-called "rotational rainbows" and quantum interference effects associated with vibrational predissociation.

In Chapter 6 *A. W. Castlemann, Jr.* and *R. G. Keese* describe a number of important techniques for observing clusters in a cluster beam, together with the interpretation of the results from such measurements. Special attention is given to the technique of resonance enhanced multiphoton ionization of clusters followed by detection in a time-of-flight mass spectrometer.

Chapter 7 represents another substantial contribution by this book. In this 200-page article the editor, *E. R. Bernstein*, describes the properties of a special class of molecular clusters consisting of two or more different molecular species, usually organic, one of which is spectroscopically active. By applying absorption and emission spectroscopy to molecular clusters of this type, together with computer simulations, one can investigate the ground and excited states.

The eighth and final chapter is a well-written review by *R. L. Whetten* and *M. Y. Hahn* of the spectroscopy of large molecular clusters. It includes discussions of the liquid drop model, the elementary excitations, and the liquid-solid transition in molecular clusters.

This book succeeds in the aim of filling the gap between international conference reports and general reviews. The wealth of information that it contains should make it a welcome addition to the library of every cluster physicist.

Thomas Lange and *T. Patrick Martin* [NB 1114 IE]
Max-Planck-Institut für Festkörperforschung,
Stuttgart (FRG)

Quasicrystals, Networks, and Molecules of Fivefold Symmetry. By *I. Hargittai*. VCH Verlagsgesellschaft, Weinheim/ VCH Publishers, New York 1990. xiii, 314 pp., hardcover, DM 148.00.—ISBN 3-527-27927-X/0-89573-723-X

The discovery by *Shechtman* et al. in 1984 of a material that exhibited the diffraction properties of an ordinary crystal (Bragg peaks) and yet seemed to display perfect fivefold rotational symmetry has brought on a surge of activity in solid state chemistry and physics. The output of the scientific community in this area has been very large indeed, and the need for monographs, both as introductions to the field and as overviews, is obvious. The present book is therefore timely (although not unique, as a fair number of monographs on the subject have already appeared).

The book covers an area ranging from pure mathematics to organic chemistry, thus providing a good overview to newcomers and experts alike. Like any monograph consisting of a number of papers by different authors, it suffers

from a certain amount of disjointedness, but this is well counterbalanced by the thus widened scope of the book.

In the first chapter *Mackay* reviews the history of fivefold symmetry in crystallography and discusses its philosophical implications. The chapter is a good introduction to the general problem of the meaning of the terms order and disorder in flat and curved spaces of different dimensionalities. *Senechal* discusses the impact of the one-dimensional quasicrystal, pointing out that even this, the simplest of cases, is very incompletely elucidated, and that our understanding of noncrystallographic symmetry is indeed rather poor. In the excellent second chapter current knowledge of the one-dimensional case is summarized in a clear and thorough way. Chapter 3 is an account of the connections between stochastic web mappings and quasicrystalline symmetry. The authors *Sagdeev* and *Zaslavsky* exploit the connections between the chaotic behavior of self-similar fractals and the self-similarity of quasicrystalline systems.

Chapters 4 to 6 deal more closely with experimental chemistry. High resolution electron microscopic (HREM) images of quasicrystals have been published by many authors, and to build models of the atomic arrangement in these materials based on the information from HREM images has been the method of choice for many. In Chapter 4 *Lin* and *Bursill* show how computer-simulated images of clusters of different sizes can be compared to experimental images. The other major method to get structural information from quasicrystals is by X-ray diffraction studies. This is used on a single crystal by *Dénoyer* et al. in Chapter 5 to characterize a slowly cooled icosahedral alloy and on a powder by *Dunlap* et al. in Chapter 6 to distinguish between the cubic crystal model and the quasicrystal model for aluminum based samples.

There exist a number of different ways of generating quasilattices. One of these is to use a set of substitution rules on a finite lattice that generates the infinite lattice. This procedure is well known for the Fibonacci sequence, and it has recently been generalized to higher dimensions. In Chapter 7 *Allouche* and *Salon* prove that such a 2-D substitution can generate the Robinson tiling. Chapters 8 to 10 deal with the connection between quasilattices and higher space. *Whittaker* and *Whittaker* give a general overview of symmetry in higher space; *Baake* et al. discuss 2-D quasilattices as projections from regular 4-D root lattices; and *McMullen* deals with nondiscrete regular apeirotopes. The grid method is discussed by *Nissen* in Chapter 11 and *Stampfli* in Chapter 12.

The rest of the articles in the monograph deal with fivefold symmetry in a rather different concept. Potential energy hypersurfaces have been studied extensively by *Mezey*, and in Chapter 13 he discusses the impact of fivefold symmetry on these structures.

The last six chapters are devoted to the C_{60} carbon cluster found by *Kroto* et al. in laser vaporized graphite and christened buckminsterfullerene, a somewhat more manageable name than that which IUPAC nomenclature would require. This molecule, which takes the form of a truncated icosahedron, has prompted an avalanche of theoretical papers and further experimental work. In this volume *Klein* and *Schmalz* give an introductory overview.

As early as 1910, astronomers analyzing light received from stars found diffuse absorption bands whose origin was later proved to be interstellar. The source of these bands has long been a matter of controversy, and *Léger* et al. argue here in favor of buckminsterfullerene as a possible source.

The buckminsterfullerene molecule poses some rather interesting theoretical problems. In the present volume *Brendsdal* et al. analyze its Hückel energy levels, *Elser* et al. study the Kekulé structures (there are exactly 12500 of them), and *Brendsdal* et al. discuss the vibrational spectrum of the molecule. The last chapter is devoted to the subject of polyindans, organic systems of fused five-membered rings. The author, *Kuck*, discusses several different features of the centropolyindans: classification, synthesis, and structural aspects.

In all the present monograph covers a very wide scope indeed, and it prompts the reader to go far beyond the narrower interests of one's own field. The book should be a valuable addition to the library of anyone with an interest in the implications of fivefoldedness.

Sven Lidin [NB 1150 IE]
Inorganic Chemistry 2
Chemical Centre
Lund (Sweden)

Basic One- and Two-Dimensional NMR Spectroscopy. By *H. Friebolin*. VCH Verlagsgesellschaft, Weinheim/VCH Publishers, New York 1991. xxi, 344 pp., hardcover DM 58.00—ISBN 3-527-28108-8/0-89573-972-0

This book is intended to provide a simple introduction to the world of one- and two-dimensional NMR spectroscopy, taking the reader from a limited knowledge base to a general understanding of the NMR methods and applications available today. There are fourteen chapters ranging from a general introduction, through spectral parameters, relaxation, simple pulsed methods, and the nuclear Overhauser effect (NOE) to finally medical applications.

The general introduction discusses the basic theory and principles behind the NMR phenomenon and briefly introduces the spectral parameters of shift and scalar coupling. This, as always, is important groundwork to cover initially. Some of the figures in this section are less than adequate. In particular the resolution in the spectra in some cases is so poor that it is difficult to decide whether the discrepancies in peak heights are due to this or to potential strong coupling effects. As with other introductory texts, a more detailed description of the rotating frame transformation and its consequences would be beneficial. Certainly, it seems that those people learning this subject for the first time have a good deal of difficulty in grasping the impact of this point.

Chapters 2 and 3 dealing with chemical shift and spin–spin coupling respectively follow on well from Chapter 1. Throughout Chapter 2 there are an unusually large number of excellent examples, and substituent effects and stereochemical aspects are covered in precise detail. Chapter 3 continues along the same lines with many useful tables of coupling constants. A particularly useful inclusion is the in-depth description of dihedral angle effects and Karplus curves, vital in much structure determination work. The section on the "theory" of coupling would, however, have been much better suited at the beginning of this chapter than at the end. A useful chapter on spectral analysis (two, three, and four spin systems) is followed by Chapter 5 outlining double resonance procedures. Homonuclear spin decoupling is covered, but it should be noted that this technology has been all but eclipsed by the ease and speed of running COSY-type spectra. Most importantly, proton decoupling in carbon experiments is addressed. Chapter 6 deals with the assignments of proton and carbon shifts and the prediction of shifts by empirical methods.

Chapter 7, covering relaxation processes, appears to be directed almost exclusively towards the study of carbon-13

nuclei. It is never completely clear, especially to a novice audience, that methods such as inversion-recovery and Carr-Purcell-Meiboom-Gill experiments are general methods for observing general phenomena. One-dimensional experiments using pulse sequences are covered in Chapter 8. Spin-echoes are covered well, and the treatment of the INEPT and refocussed INEPT experiments is particularly good. Unfortunately, several vector pictures in this chapter are extremely confusing and detract from the lucid description in the text. It is important to remember that trying to oversimplify problems often results in overloading the reader with too much information at one time. Two-dimensional NMR experiments are covered in Chapter 9. Particularly good here is the slow development of the heteronuclear correlation experiment, taking the method from its intuitive beginnings through to a usable pulse sequence. Descriptions of spectral widths as related to the incrementable delay period and phase sensitive spectra would make a useful addition here. Only basic two-dimensional experiments are covered, and many of the recent and powerful two-dimensional methods are not presented.

Chapter 10, developing the idea of the NOE, is well explained and very understandable and leads nicely into Chapter 11 on dynamic NMR. This section, including lineshape analysis and coalescence, is packed with informative examples. Rotations about bonds, ring inversion, tautomerism, and exchange effects are all described with clarity. Bringing the book to a close are chapters on shift reagents, macromolecular applications (synthetic polymers) and, surprisingly, medical applications including in vivo studies and magnetic resonance tomography.

In summary, this text provides a reasonably successful introduction to basic NMR ideas. Its greatest asset is that it is written at a level that is accessible to students across a wide range of disciplines and consequently would make a useful basis for an introductory teaching course. The reservations that exist include the lack of clarity and accuracy in some of the figures and the fact that the enormous power of two-dimensional NMR is not conveyed to an appropriate extent.

John Cavanagh [NB 1175 IE]
Department of Chemistry
University of Cambridge
Cambridge (United Kingdom)

Computational Chemistry Using the PC. By *D. W. Rogers*. VCH Verlagsgesellschaft, Weinheim 1990. viii, 224 pp., hardcover DM 98.00. – ISBN 3-527-27937-7

The term "computational chemistry" does not have a very precise definition. In the title of this book it essentially means molecular mechanics and molecular orbital calculations and the numerical methods on which these are based. In contrast to the numerous monographs dealing with the theory of molecular and quantum mechanics, this book aims to give an introduction to programming such methods and applying them. This seems a very sensible approach, and the book succeeds in its aims. Most "computer chemists" have become involved in this field in an unplanned way through modifying already existing programs to perform new tasks, and have had to acquire the necessary expertise in numerical mathematics from a variety of sources. This book now offers a systematic introduction, ranging from the basic numerical methods to working with ready-made HMO and SCF programs. Each chapter includes many exercise problems, for which solutions are provided in most cases. The book also includes "computer projects", a form of learning aid which is an innovation, at least in the context of a textbook. Each one consists of a set of guidelines for solving a physical chemical problem using a computer program. The programs, most of which are written in BASIC, are supplied with the book on a $5^1/_4$-inch diskette suitable for running on any IBM-compatible PC operating under DOS.

The book is divided into two parts. The first six chapters present the basic principles of programming numerical methods. Iterative methods and numerical integration methods are explained with the help of examples from physical chemistry (e.g. the van der Waals equation, Wien's law, and the Maxwell–Boltzmann distribution). These are followed by matrix operations and curve-fitting. The last seven chapters of the book are concerned with molecular orbital calculations, molecular mechanics, and molecular graphics. In the treatment of MO theory, if not even earlier, the author encounters a basic difficulty that is inherent in the task he has undertaken, namely whether to introduce the reader to quantum theory (and thereby make the book considerably more bulky), or to assume this knowledge. He decides in favor of a middle road. The theoretical introductions are short and very condensed. Consequently, if the book is to be used as a self-study text one must already be familiar with the main fundamentals, or must use it in conjunction with a textbook of theoretical or physical chemistry. Subject to these preconditions, the chapters on molecular mechanics and MO methods (Hückel, EHT, PPP, MNDO, ab initio, etc.) provide a deeper insight into how these programs function.

The book fills an important gap that has existed between those (very few) books dealing with the application of the most popular molecular mechanics and MO programs to chemical problems (e.g. *T. Clark*'s "Handbook of Computational Chemistry") and the actual textbooks of theoretical chemistry. It is shown here that as a result of the present state of development of PCs, the excellent programs already available can now be usefully run on cheap hardware that nearly all students can afford. The high price of the book is in marked contrast to this, but on the other hand the perfect typography that is typical of the publishers, VCH, is a delight to the eye. The book is outstandingly suitable as a self-study text for lecturers and students of graduate level and beyond. It is especially recommended for users of black box program systems such as GAUSS or MOPAC who would like (and indeed ought) to gain a somewhat better understanding of what they are calculating.

Rainer Herges [NB 1132 IE]
Institut für Organische Chemie
der Universität Erlangen-Nürnberg (FRG)

Metals and Ligand Reactivity. By *E. C. Constable*. Ellis Horwood, New York 1990. xii, 246 pp., hardcover $54.50. – ISBN 0-13-577222-2

The rapid development from about 1960 onwards of the new organometallic chemistry with its sometimes exotic structures and bonding situations, temporarily pushed the study of classical coordination compounds into the background. During the 1950s the latter were at the center of attention in molecular inorganic chemistry as a result of the successful combination of spectroscopy, reactivity studies, and ligand field theory. Now their importance is gradually

becoming generally appreciated once again, especially through the rise of bioinorganic chemistry as a new field of research. However, even leaving aside the remarkable catalytic capabilities of the metal centers in enzymes, many organic chemical transformations that are made possible or are catalyzed by non-organometallic coordination compounds are indispensable in laboratory synthesis and technological processes. Whether one already has an interest in the subject or has previously regarded classical coordination chemistry as boring, weighed down with theory, and irrelevant, it will be found that Constable's account is a thoroughly readable one that offers an agreeable way of catching up on developments. The main emphasis in this monograph is on using (transition) metal centers to influence the reactivities of organic compounds that have coordination sites formed by heteroatom donors.

The particular features that make this an easy book to read are its emphasis on synthetically useful reactions and the absence of lists of physico-chemical data and literature citations in the main text. References for further reading are collected at the end of the book under topic headings—where the author gives more detailed information.

Constable begins with a very brief introduction to the orbital models needed. Regrettably, however, the qualitative description of chemical reactivity does not include catalytic aspects. Coordinative bonding, both with and without π interaction, is described from the standpoint of electrostatic interactions and geometry in a clearly understandable way. The descriptions of examples begin with the chapters on attack by nucleophiles, including H_2O and $OH^{\ominus}$, on metal-coordinated carbonyl compounds and their derivatives (nitriles, imines), on sulfur compounds, and on phosphoric acid esters. These are followed by a chapter discussing electrophilic attack on metal-stabilized anions such as enolates or thiolates and on neutral bases (e.g. metal-induced amine–imine transformations).

Another chapter describes template reactions that lead to ring closure, with a general discussion of the special characteristics of macrocyclic systems with regard to stability, resistance to attack, metal selectivity, and geometric strains caused by imperfectly matching metal ions. Supramolecular structures, including knotted molecules, continue to be a source of fascination. The special characteristics of aromatic substrates are discussed, with particular emphasis on the substitution reactions of metal-coordinated *N*-heterocycles of the pyridine type. The description of redox processes is limited to transition metal catalyzed reactions with O_2, which are of practical importance, but whose mechanisms are not always as they seem at first sight. It is pleasing to note that here, at last, a clear distinction has been made between the processes of electron transfer, dehydrogenation, and oxygen transfer. The final chapter, entitled "Envoi", contains a very brief, and consequently rather simplified account of the search for an overall rationalization of the catalytic capabilities of coordinated metal ions in enzymes.

The contents of the book are clearly arranged and well presented, matching the author's excellent lecturing style. The many formulas are well prepared, except for a few ring systems and the inconsistent use of arrows for coordinative bonds. The popular structure diagrams as reproduced from X-ray diffraction studies are few in number so that the reader obtains a rather limited appreciation of the complex geometries. On the other hand, the summaries given at the end of each chapter and the pithy critical evaluations scattered throughout the text are especially useful. Thus, for the reader who, for a relatively small cost in time and money, wishes to acquire as much practical, useful knowledge of coordination chemistry as possible, this book is recommended unreservedly.

Wolfgang Kaim [NB 1131 IE]
Institut für Anorganische Chemie
der Universität Stuttgart (FRG)

Sonochemistry: The Uses of Ultrasound in Chemistry. Edited by *T. J. Mason*. The Royal Society of Chemistry, London 1990. 151 pp., paperback \$ 89.25.—ISBN 0-85186-293-4

Chemical applications of ultrasonic waves, often referred to as sonochemistry, enjoyed a renaissance in the eighties. These books are introductory in nature, intended for the chemist with a potential interest in the field. The first is more general, while the second will be of more interest to synthetic chemists.

There are nine contributors covering an important range of topics in eleven chapters: *T. J. Mason* provides an overview of the field in the first chapter (8 pages, 10 references) dealing with historical aspects, non-chemical uses of ultrasound (diagnostics), power ultrasound, and specific examples of ultrasound enhanced chemical reactions. The incorrect attribution of *Regen*'s work on dichlorocarbene to *Repic* is unfortunate. Chapter 2 ("Sonochemistry, the General Principles", *J. P. Lorimer*, 18 pages, 5 references) offers a lucid discussion of wave propagation, particle displacement due to a longitudinal wave, factors affecting cavitation, and the fate of a bubble in a sound field. It is one of the best chapters in the book, marred only by the conspicuous absence of a discussion of the "hot spot" theory and *Suslick*'s vapor shell.

The third chapter ("Ultrasound in Diagnosis, Inspection, and Monitoring", *C. S. Gartside* and *M. M. Robins*, 20 pages, 6 references) is simply out of place and dilutes the effort of such a small book. Chapter 4, ("Power Ultrasound", *J. P. Perkins*, 13 pages, 5 references) deals with some important fundamental concepts such as monitoring acoustic input and output, construction of the transducer, cavitation phenomena, health and safety aspects, and large scale applications, but would be more effective if blended efficiently with topics in Chapters 2 (see above), 5 ("A Survey of Commercially Available Sources of Ultrasound Suitable for Sonochemistry", *T. J. Mason*, 9 pages, no references), 10 ("The Uses of Ultrasound in Chemical Technology", *T. J. Mason*, 6 pages, 13 references), and 11 ("Scale-up Considerations", *T. J. Goodwin*, 14 pages, 4 references). There is a good deal that is useful in these chapters but the fragmentation of information and unnecessary repetition detract from them.

Chapters 6 ("Ultrasound in Organic Synthesis", *R. S. Davidson*, 17 pages, 38 references), 7 ("Free Radical Reactions under Sonochemical Conditions", *J.-L. Luche*, 15 pages, no references) and 8 ("Ultrasound in Heterogeneous Catalysis", *J. Lindley*, 8 pages, 89 references) discuss much of the important literature of interest to synthetic chemists. It is distracting that a number of the references in Chapters 6 and 8 are simply incorrect and others have an author's name misspelled.

There is overlap among the chapters that a small book can ill afford. As examples, precious space is wasted on two discussions with schemes by *Davidson* and *Luche*, of *Luche*'s free radical ring closure of benzamide and of his elegant preparation of dialkylzinc compounds. Likewise, *Davidson*'s treatment of continuous ultrasonic hydrogenation of soy-

bean oil and platinum catalyzed hydrosilation belong only in *Lindley*'s chapter where they are also discussed. Chapter 9 ("Ultrasound in Polymer Chemistry", *J. P. Lorimer*, 20 pages, 10 references) covers theory of high frequency waves (>1 MHz) as well as applications in providing information on relaxation phenomena. Uses of low frequency waves (polymerization/depolymerization) are also given.

Ultrasound in Synthesis. By *S. V. Ley* and *C. M. Low*. Springer, Berlin 1989. 133 pp., hardcover, $ 79.50.— ISBN 0-387-51023.

Following a very brief introductory chapter (1 page), Chapter 2 ("The Physical Basis of Sonochemistry", 27 pages) provides a qualitative discussion of the origin of and the factors influencing sonochemical reactivity. The current thinking on the cavitation process and the roles of frequency, intensity, temperature, and cell and probe design are presented, along with a discussion of methods of measuring ultrasonic intensity. This chapter will be useful to the novice in the field.

The remainder of the book summarizes applications of ultrasonic waves to synthesis, and covers organic, inorganic and organometallic examples. The chapter titles and page count illustrate the organization of the book. The treatment is broad with only the highlights in each area covered: Chapter 3 ("Aqueous Sonochemistry", 4 pages); Chapter 4 ("Preparation of Activated Magnesium", 6 pages); Chapter 5 ("Preparation of Organoaluminum Compounds", 1 page); Chapter 6 ("Application of Ultrasound to the Preparation of Organolithiums", 11 pages); Chapter 7 ("Reactions with Other Alkali Metals", 11 pages); Chapter 8 ("Organozinc Reagents", 16 pages); Chapter 9 ("Intercalation Reactions", 1 page); Chapter 10 ("The Effects of Ultrasound on Enzyme-Catalyzed Reactions", $1\frac{1}{4}$ pages); Chapter 11 ("Ultrasonic Acceleration of Organic Reactions", 19 pages); Chapter 12 ("Ultrasonic Acceleration of Redox Reactions", 6 pages); Chapter 13 ("The Effects of Ultrasound on Transition Metal Catalysts", 2 pages); Chapter 14 ("Transition Metal Carbonyls and Ultrasound", 15 pages).

Chapters 11 and 12 emphasize homogeneous phase-transfer and nonmetal reactions, although there is some overlap with metal-based reactions. Perhaps a different organization of material would have avoided this and the need for the one- and two-page chapters (5, 9, 10 and 13). Considering the hefty price tag, a more judicious use of space is required for good value. For example, the diagrams and schemes are too large for a book this size, as are the spaces allotted for chapter headings, leading to far too much white space. The aim of this book is to familiarize a wider audience with the background of chemical applications of ultrasound. This is accomplished at the "acquaintance" level.

Philip Boudjouk [NB 1139 IE]
Department of Chemistry, North Dakota State University
Fargo, ND (USA)

Corrigendum

In the communication "On a Metathesis Reaction of Tetrathiafulvalene (TTF)" by *Henning Hopf* et al. (*Angew. Chem. Int. Ed. Engl. 30* (1991) 1127), the first sentence in the discussion of the crystal structure of compound **4a** should read as follows: Its structure in the crystal is characterized by an almost orthogonal arrangement of the phenyl ring and of the heterocycle containing S1 and S2 with respect to the largely planar rest of the molecule (dihedral angle between the best planes, 96 and 79°, respectively). In reference [9] the lattice constant *b* is 1443.3(3) pm.

Registered names, trademarks, etc. used in this journal, even when not marked as such, are not to be considered unprotected by law.

© VCH Verlagsgesellschaft mbH, W-6940 Weinheim, 1991. – Printed in the Federal Republic of Germany by Konrad Triltsch Druck- und Verlagsanstalt Würzburg.

All rights reserved (including those of translation into foreign languages). No part of this issue may be reproduced in any form — by photoprint, microfilm, or any other means — nor transmitted or translated into a machine language without written permission from the publishers. Only single copies of contributions, or parts thereof, may be made for personal use. This journal was carefully produced in all its parts. Nevertheless, authors, editors and publisher do not warrant the information contained therein to be free of errors. Readers are advised to keep in mind that statements, data, illustrations, procedural details or other items may inadvertently be inaccurate.

Valid for users in the USA: The appearance of the code at the bottom of the first page of an article (serial) indicates the copyright owner's consent that copies of the article may be made for personal or internal use, or for the personal or internal use of specific clients. This consent is given on the condition, however, that the copier pay stated per-copy fee through the Copyright Clearance Center, Inc. (CCC), for copying beyond that permitted by Sections 107 or 108 of the U.S. Copyright Law. This consent does not extend to other kinds of copying, such as copying, for general distribution, for advertising or promotional purposes, for creating new collective works, or for resale. For copying from back volumes of this journal see 'Permissions to Photo-Copy: Publisher's Fee List' of the CCC.

Editorial office: Postfach 10 11 61, W-6490 Weinheim, Federal Republic of Germany, Telephone (06201) 60 23 15, Telex 465 516 vchwh d, Telefax (06201) 602 328, E-Mail Z16@DHDURZ2 in Earn Bitnet.

Editor: *Peter Gölitz*

Associate editors: *D. I. Loewus, K. J. Schneider, A. Stimson.* **Editorial assistant:** *E. Schweikart*

Publishers: VCH Verlagsgesellschaft mbH. (Managing Director: *Hans Dirk Köhler.*), Pappelallee 3, W-6940 Weinheim, Federal Republic of Germany.

Advertising office (Advertising Manager *R. J. Roth*): Postfach 10 11 61, W-6940 Weinheim, Federal Republic of Germany, Telephone (0 62 01) 60 61 36, Telex 4 67 155, Telefax (0 62 01) 606 156.

ANGEWANDTE CHEMIE
International Edition in English
Volume 30 · Number 11
November 1991
Pages 1387–1530

Chemistry and Biology of the Enediyne Anticancer Antibiotics

By K. C. Nicolaou* and W.-M. Dai

Novel, biologically active substances from nature often provide excitement, stimulation, challenges, and opportunities for the scientific and medical communities. Experience and wisdom dictate investigation of their chemistry and pursuit of their chemical synthesis for more often than not, the rewards for both chemistry and medicine are great. The enediyne anticancer antibiotics are a rapidly emerging class of such compounds derived from bacterial sources. Combining unprecedented and highly unusual molecular architecture, phenomenal biological activities and fascinating modes of action, these DNA cleaving compounds burst onto the scene in the latter half of the 1980s when their structures became known, and they rapidly moved to center stage. Today the enediyne family includes the neocarzinostatin chromophore, the calicheamicins, the esperamicins, and the dynemicins, and soon the number of family members is certain to increase. These molecules elicited extensive research activities in chemical, biological, and biomedical circles and inspired the design of a number of novel molecular assemblies to probe and mimic their chemical and biological actions. A new body of synthetic technology and several novel synthetic strategies have already been devised to address the challenges posed by these molecules, and several new DNA cleaving agents have been designed and synthesized. This article summarizes the chemistry and biology of the enediynes and discusses mechanistic, synthetic, molecular design, and DNA cleavage aspects associated with the field.

1. Introduction

In 1985 *Edo* et al.[1] disclosed the structure of neocarzinostatin chromophore **1** (Scheme 1) possessing a novel bicyclo[7.3.0]dodecadiynene system. This seminal contribution received little attention until 1987 when the structures of two other novel families of natural products, the calicheamicins (**2**: calicheamicin γ_1^I, Scheme 1) and the esperamicins (**3**: esperamicin A_1, Scheme 1) possessing an enediyne moiety, were reported by scientists from the Lederle Laboratories[2] and Bristol-Myers,[3] respectively. In 1989 a fourth novel structure, dynemicin A (**4**, Scheme 1) was reported by Bristol-Myers, Japan.[4] Thus began the story of this rapidly emerging class of anticancer antibiotics known today as the enediynes. The apparent failure of neocarzinostatin chromophore to immediately spark the interest of the synthetic community despite its structural novelty may be partially explained by the absence of an X-ray crystallographic analysis that left unresolved a number of stereochemical issues, not to mention suspicions about its, at the time, seemingly unlikely structure. Today, however, all these novel compounds and their relatives are in the forefront of chemical, biological and medical research.

The excitement surrounding these molecules lies in their novel molecular architecture, their important biological activity, and their fascinating mode of action. All four types of compounds mentioned above exert their biological action by virtue of their ability to cleave DNA. Furthermore, their DNA

[*] Prof. Dr. K. C. Nicolaou, Dr. W.-M. Dai
Department of Chemistry, The Scripps Research Institute
10666 N. Torrey Pines Road, La Jolla, CA 92037 (USA)
and
Department of Chemistry, University of California at San Diego
La Jolla, CA 92093 (USA)

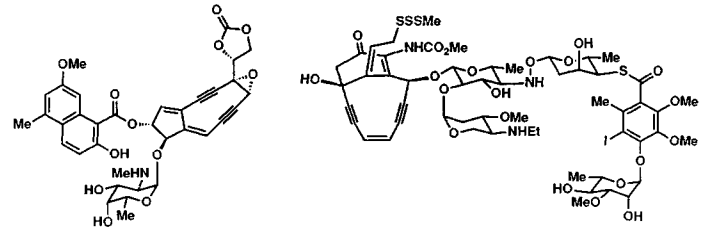

1

2

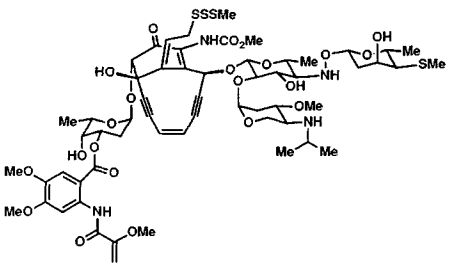

3

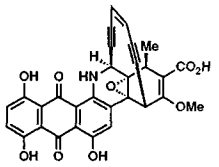

4

Scheme 1. Structures of the enediyne antibiotics, neocarzinostatin chromophore **1**, calicheamicin γ_1^I **2**, esperamicin A_1 **3**, and dynemicin A **4**.

cleaving properties are derived from their common ability to generate sp^2 carbon-centered radicals upon suitable activation. It has been widely recognized that these molecules are equipped with at least three important functional domains: a) a "warhead" destined to "explode" upon suitable activation, thus providing the fragments that damage DNA; b) a "delivery system" which apparently delivers the warhead to its target, DNA; and c) a triggering device, which upon suitable activation, initiates the cascade of reactions that leads to the generation of the damaging radicals.

Before discussing the chemistry of these remarkable antibiotics, it is perhaps appropriate to review some interesting observations made in the 1960s and 1970s by a number of investigators pursuing research in the area of physical organic chemistry and theoretically interesting molecules. Thus, in 1972 *Bergman*[5] reported his elegantly designed studies with model enediynes, showing clearly their cycloaromatization via 1,4-benzenoid diradicals (e.g. structure **5**, Scheme 2).

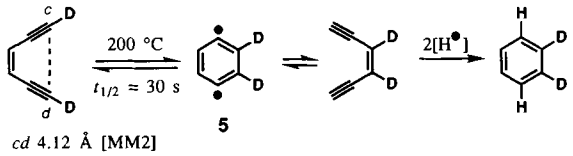

5

Scheme 2. The Bergman cyclization (1972). The distance between the centers *c* and *d* in the educt calculated by MM2 is 4.12 Å.

This is precisely the reaction that nature is apparently using as the crucial process to generate the fragments that inflict the lethal blows on DNA. Prior to *Bergman*'s studies, *Masamune* et al.[6] described the conversion of the two cyclic enediynes **6** (Scheme 3) into benzenoid systems, but without

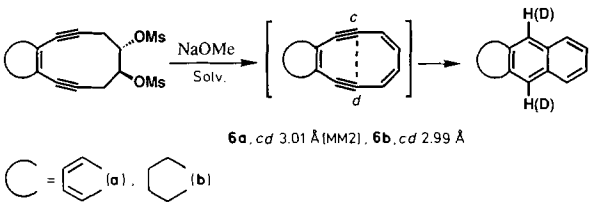

Scheme 3. Observations by *Masamune* et al. (1971). Ms = mesyl.

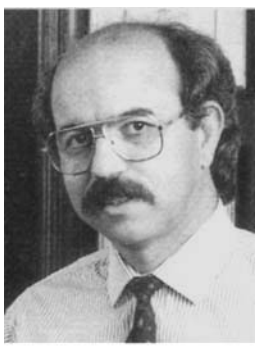

K. C. Nicolaou was born in Cyprus in 1946 and received his Ph.D. degree from the University of London under Professors F. Sondheimer and P. Garratt. After postdoctoral work at Columbia University with Professor T. Katz and at Harvard University with Professor E. J. Corey, in 1976 he joined the faculty at the University of Pennsylvania, where he was promoted to Rhodes-Thompson Professor of Chemistry. He moved to La Jolla in 1989 to fill an unprecedented joint appointment as a Professor of Chemistry at the University of California San Diego and as the Darlene Shiley Professor of Chemistry and Chairman of the Department of Chemistry at the Scripps Research Institute. The recipient of numerous awards, including the Alfred P. Sloan Award, a Guggenheim Fellowship, and a Humboldt Senior American Scientist Award, Nicolaou has been involved with the development of new ways of synthesizing complex organic molecules of natural or nonnatural origin. He is the author or co-author of over 250 publications, 16 patents, and one book. His hobbies include walking on the beach and playing tennis.

W.-M. Dai was born in 1957 in Ninghai, China. He received his B. S. in 1982 from Hangzhou University (China) and then moved to the Shanghai Institute of Organic Chemistry, Academia Sinica for his graduate studies with Professor W.-S. Zhou, receiving his M. S. in 1984. In 1985 he joined Professor Y. Nagao's group at Kyoto University (Japan) where he worked in the area of asymmetric synthesis utilizing chiral Tin(II) enolates and applying this chemistry to the total synthesis of alkaloids. After gaining his Ph.D. degree from Kyoto University in 1990 he joined Professor Nicolaou's group in La Jolla, California where he is currently a Research Associate. His research interests include the development of novel asymmetric reactions and the synthesis of natural products and biomedically interesting molecules. He is currently engaged in the design, synthesis, and study of novel enediynes. W.-M. Dai speaks fluent Chinese, Japanese, and English, and his hobbies include chinese cooking and reading the literature.

mentioning the involvement of a diradical intermediate. Subsequent to these studies and prior to the discovery of the naturally occurring enediynes, *Wong* and *Sondheimer*[7] had also observed the cycloaromatization of in situ generated strained cyclic enediynes such as **7** (Scheme 4) and postulated benzenoid 1,4-diradicals as intermediates. This process is now widely known as the Bergman cyclization reaction. Even earlier (1966) *Mayer* and *Sondheimer*[8] described a rearrangement (Scheme 5) which most likely involved a similar type of cyclization reaction of **8** and a diradical intermediate.

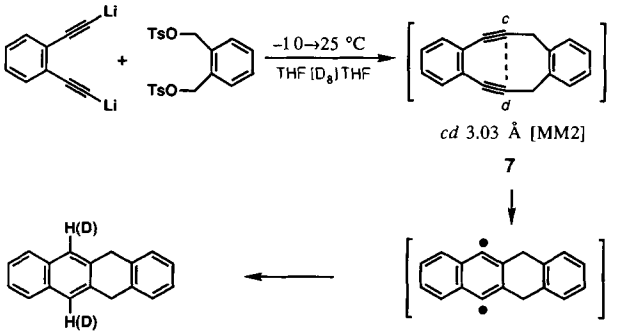

Scheme 4. Observations by *Wong* and *Sondheimer* (1980). Ts = tosyl.

Although it was known for some time that reactive benzenoid diradicals are formed from enediynes, no one took up the challenge to engineer this chemistry for the design of molecules with potential biological and medical significance. It took nature once again to show us the way to what now, of course, looks so obvious! This recognition should serve as

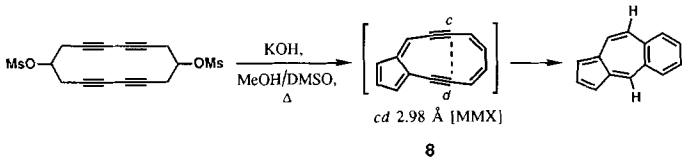

Scheme 5. Observations by *Mayer* and *Sondheimer* (1966). Ms = mesyl, DMSO = dimethyl sulfoxide. The $c\cdots d$ distance here was calculated by MMX.

a constant reminder to those who do not have, or have lost their appreciation for natural products chemistry: This discipline continues, and will continue for a long time, to uncover invaluable leads and knowledge from nature that become the guiding lights in our search for new scientific ventures and wonder drugs of tomorrow. At the same time we should also salute the discipline of physical organic chemistry and those who champion its course, for they often open pathways for others to follow, or should follow, in related disciplines such as synthetic and bioorganic chemistry. Let us now return to the fascinating chemistry and biology of the enediynes.

2. Isolation, Biological Properties, Structures, and Mechanisms of Action of the Enediyne Anticancer Antibiotics

The announcement of the structures of the calicheamicins[2] and esperamicins[3] in 1987 aroused a great deal of interest in chemical and biological circles. The newly discovered compounds combined unprecedented and intriguing molecular structures with striking biological activities. At the same time, mechanistically intriguing proposals relating to their mode of action were put forward by the authors.[2, 3] Synthetic chemists throughout the world became immediately interested in these structures. Furthermore, the neocarzinostatin chromophore[1] that had earlier failed to fully capture the chemist's imagination was now viewed with renewed interest because of its structural and biological similarities with the newly discovered enediynes.

2.1. Neocarzinostatin

Neocarzinostatin (NCS) is a naturally occurring antibiotic complex consisting of a 1:1 mixture of a protein component (NCS apoprotein) and a chromophoric molecule (NCS chromophore) isolated from *Streptomyces carzinostaticus* Var. F-41. First reported in 1965 by *Ishida* et al.,[9] this antibiotic complex was later resolved into its components, NCS apoprotein and NCS chromophore.[10, 11] It was soon recognized that essentially all the biological activity of NCS resides in its chromophoric moiety and that the protein component plays an important role in transporting and stabilizing the drug.[12, 13] NCS apoprotein binds tightly and specifically to NCS chromophore ($K_D = 1 \times 10^{-10}$ M)[14] and delivers the active chromophore to its target, DNA, by controlled release.[15] The biological activities of NCS include potent antitumor and antibacterial actions and they are exerted via DNA cleavage. The DNA damaging activity of the labile, free NCS chromophore, results primarily in single strand cuts and proceeds via an oxygen-dependent reaction.[16] Thiols[17] and ultraviolet radiation[18] greatly enhance the DNA cleaving properties of NCS chromophore.

The novel structural skeleton of NCS chromophore was first proposed by *Edo* et al. in 1985.[1] The first proposal for

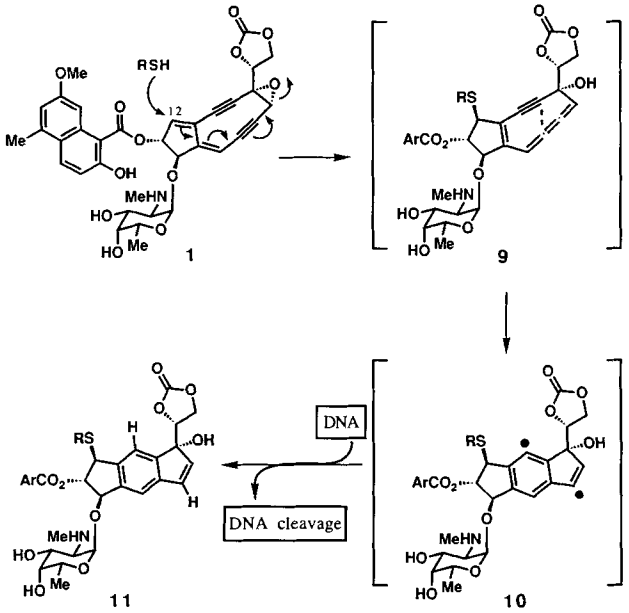

Scheme 6. Mechanism of DNA cleavage by **1**. RSH = thionucleophile, Ar = naphthyl substituent.

the mechanism of action of NCS chromophore was put forward by *Myers* in 1987.[19] According to this elegant hypothesis (Scheme 6) the cascade of reactions leading to DNA damage is initiated by stereospecific nucleophilic attack at C12, probably assisted by the basic nitrogen of the carbohydrate moiety of the agent. This triggering event is accompanied by rearrangement of the ring skeleton with epoxide opening and formation of cumulene **9** as shown in Scheme 6. The highly strained and labile intermediate **9** then suffers rapid cycloaromatization to form diradical **10** which proceeds to attack DNA by hydrogen atom abstraction resulting in **11**. This scenario has been demonstrated in the laboratory using $HSCH_2COOMe$[19–22] and $NaBH_4$[22] as nucleophiles, and the cumulene intermediate **9** has been observed at low temperature by ^1H NMR spectroscopy.[21] Furthermore, the methyl thioglycolate adducts of NCS chromophore have been isolated and fully characterized, leading to complete structural elucidation of the molecule including the absolute configuration.[20]

It is now accepted that NCS chromophore intercalates into DNA via its naphthoate group and positions the rest of the molecule in the minor groove[23–25] ready for activation (Fig. 1). Triggering is thought to occur upon nitrogen-assisted nucleophilic attack[26] by thiol at C12 of the chromophore as discussed above. The NCS chromophore preferentially attacks at adenine and thymine sites.[27]

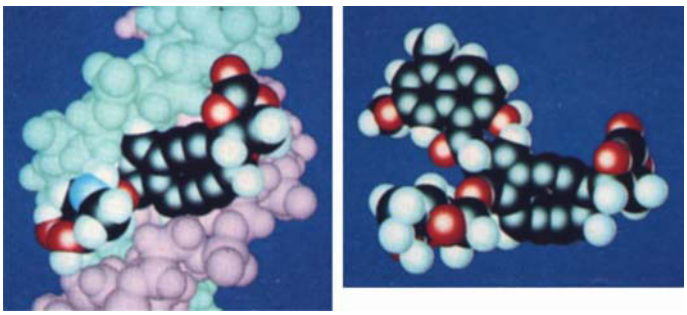

Fig. 1. Computer-generated space-filling models of free **1** (right) and DNA-bound **1** (left).—These and the following pictures in this article were obtained as follows: Molecular models were elicited using Sybyl Version 5.4 (Tripos Associates, Inc.) on a Personal Iris 40/25 Super Turbo (Silicon Graphics) computer terminal. The files were then submitted to a Stardent ST 1040 (Stardent) terminal and visualized using Stardent AVS (Version 3.0). The models were then photographed from the screen.

It has been demonstrated that at least 80% of the DNA cleavage by NCS chromophore leads to the 5′-aldehyde of the A and T residues selectively.[27] The chemistry leading to these breaks involves hydrogen atom abstraction from C5′ by the diradical species **10** and oxygen atom transfer from molecular oxygen to the resulting DNA radical and eventually, the aldehyde residues are formed according to the pathway shown in Scheme 7. Less than 20% of the strand breaks result from pathways initiated by hydrogen atom abstraction from C4′ (Scheme 8)[28–32] and C1′ (Scheme 9).[29]

Biosynthetic studies[33] with neocarzinostatin chromophore showed that the C_{14} dienediyne ring skeleton incorporates six intact acetate units and two terminal acetate units which suffer C–C bond cleavage, and suggested that the C_{14} chain is derived from degradation of oleate via the oleate-crepenylate pathway for polyacetylenes. Similar proposals have been made for the C_{15} ring skeleton of the calicheamicin/esperamicin families.[33]

Interesting synthetic studies and designed molecules inspired by NCS chromophore will be discussed in Section 3.1.

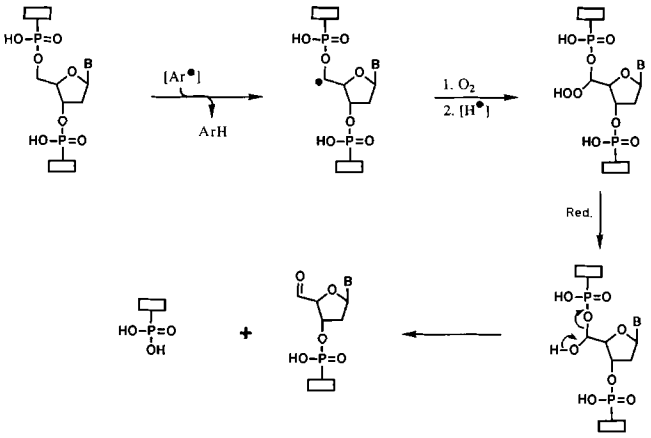

Scheme 7. DNA strand cleavage initiated by C5′ hydrogen atom abstraction. B = nucleobase, Ar• = **10**, Red. = reduction.

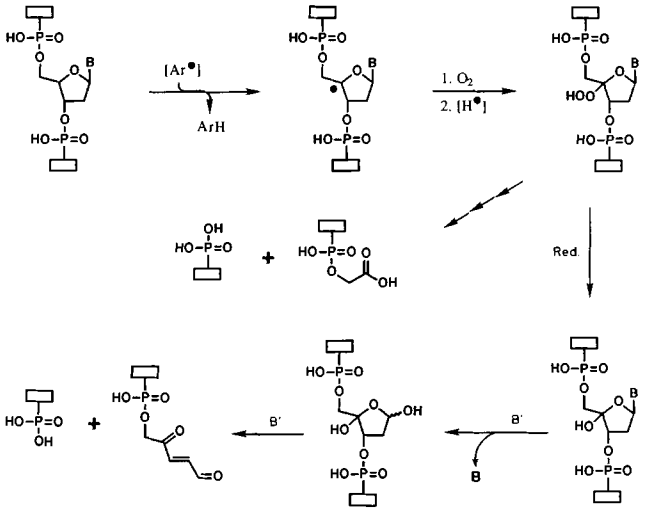

Scheme 8. DNA strand cleavage initiated by C4′ hydrogen atom abstraction. B′ = external base, e.g. OH^-.

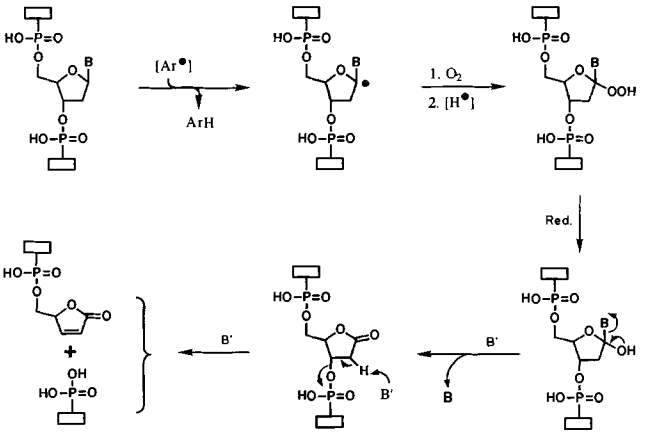

Scheme 9. DNA strand cleavage initiated by C1′ hydrogen atom abstraction.

2.2. Calicheamicins

The calicheamicins (Table 1) are a family of enediyne antibiotics isolated from *Micromonospora echinospora* ssp. calichensis. Their structures were first reported in 1987 by *Lee* et al.[2] and revised (one stereochemical center) in 1989.[34] Calicheamicin γ_1^I **2** is the most prominent member of this class of compounds.[34] The iodine-containing

Table 1. The calicheamicin family.

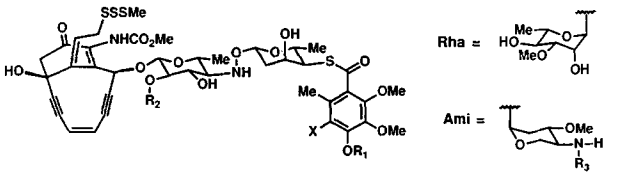

Calicheamicin	X	R_1	R_2	R_3
Calicheamicin β_1^{Br}	Br	Rha	Ami	$CHMe_2$
Calicheamicin γ_1^{Br}	Br	Rha	Ami	Et
Calicheamicin α_2^I	I	H	Ami	Et
Calicheamicin α_3^I	I	Rha	H	–
Calicheamicin β_1^I	I	Rha	Ami	$CHMe_2$
Calicheamicin γ_1^I **2**	I	Rha	Ami	Et
Calicheamicin δ_1^I	I	Rha	Ami	Me

calicheamicins were discovered when sodium iodide was added to the fermentation medium, resulting not only in the new compounds containing iodine rather than bromine, but also in much improved fermentation yields.[34] The calicheamicins are active[2, 34] in the biochemical prophage induction assay at concentrations below 1 pg mL^{-1}, extremely active against Gram-positive bacteria, and highly active against Gram-negative bacteria. Most importantly, they exhibit extraordinary potency[2, 34] against murine tumors such as P338 and L1210 leukemias and solid neoplasms such as colon 26 and B-16 melanoma with optimum doses of 0.15–5 μg/kg. These compounds are thought to exert their biological activities by damaging DNA. Indeed, the calicheamicins are highly potent DNA cleaving agents giving rise primarily to sequence specific double strand cuts.[35, 36]

The molecule of calicheamicin γ_1^I **2** is a masterpiece of "natural" ingenuity. Its structure can be roughly divided into three components: a) the enediyne system with its potential power to wreak havoc on any biological target, but cleverly locked in place until activated; b) the oligosaccharide fragment which is thought to serve as a delivery system to bring the lethal warhead to its intended target, DNA; and c) the trisulfide moiety, which acts as a triggering device allowing the initiation of the crucial chemical events which lead to the generation of highly aggressive species that cause fatal damage to the genetic material. But the beauty of this molecule must extend beyond this simplistic picture, for we still marvel at its biological actions without fully understanding its precise mode of action. How does binding to DNA, for example, initiate activation, and how does the producing organism protect itself from such a dangerous molecule?

Nevertheless, from the information gathered so far, the following scenario[2, 3] accounts for its damaging action on DNA. Calicheamicin γ_1^I **2** binds to the minor groove of

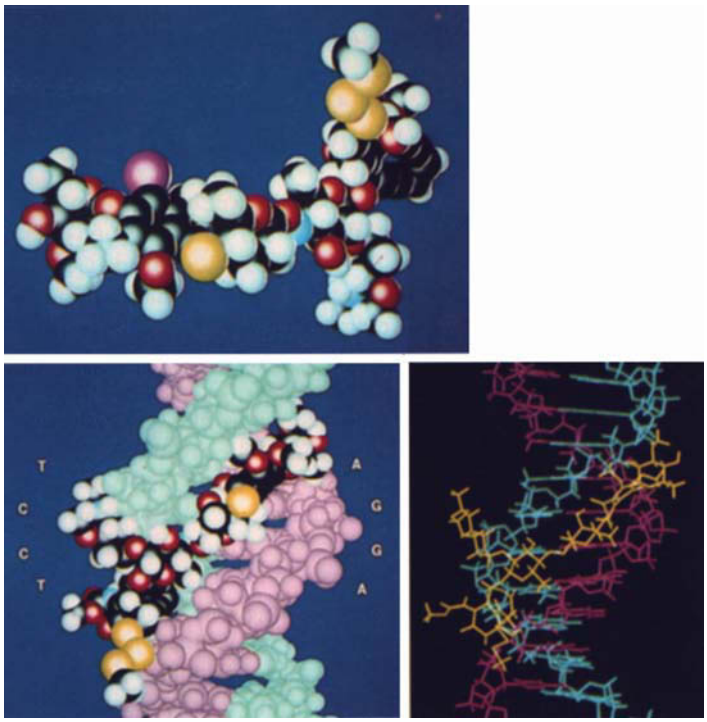

Fig. 2. Computer-generated models of free **2** (top) and DNA-bound **2** (bottom).

double helical DNA specifically at TCCT sites and by orienting its oligosaccharide tail towards the 3′-ends of DNA fragments (Fig. 2).[37] The oligosaccharide fragment is thought to be the molecule's main recognition and binding moiety.[38, 39] A nucleophile (e.g. glutathione), probably activated by an internal basic nitrogen, then attacks the central sulfur atom[2, 40] of the trisulfide group, causing the formation of a thiolate (bioreduction) which finds itself in a perfect position, due to the proper geometry of the allylic double bond, to attack intramolecularly the α,β-unsaturated ketone embedded in the adjacent six-membered ring to give compound **12** (Scheme 10). This reaction, converting the sp^2 carbon atom at the point of attack to an sp^3 carbon paves the

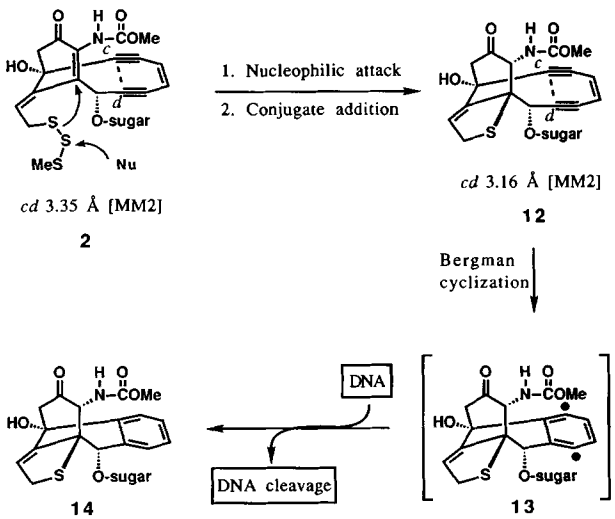

Scheme 10. Mechanism of DNA cleavage by **2**.

way for a Bergman cyclization reaction, leading to the benzenoid diradical **13**. It is interesting to note that the distance between the *c* and *d* carbon atoms (Scheme 10) is significantly shortened in going from calicheamicin γ_1^I **2** [3.35 Å, MM2] to the highly strained intermediate **12** [3.16 Å, MM2].[41] The reactive diradical **13** is capable, and well positioned, to abstract two hydrogen atoms, one from the C5′ position of deoxycytidine (C) and the other from a ribose position of the opposing strand.[37, 42] The DNA radicals so generated then proceed to react with molecular oxygen leading to double strand cleavages according to the mechanism depicted in Scheme 7.[37] Carefully designed experiments led to observation of the proposed intermediate **12** (estimated half-life at 37 °C ca. 4.5 s).[43] Furthermore, it was shown that the majority of the cleavage within the T *C*CT recognition sequence is initiated by hydrogen abstraction from the C5′ position of deoxycytidine (*C*) and transfer to the C4′ position (site nearest to the oligosaccharide segment) of the cycloaromatized calicheamicin γ_1^I molecule.[37] Other experiments confirmed the requirements of thiols for the high potency of calicheamicin γ_1^I **2** in DNA cleavage and the crucial role of the ethyl amino group on the terminal carbohydrate unit.[34]

Although the natural calicheamicins exhibit unacceptable delayed organ toxicity in animals,[44] antibody conjugates of modified derivatives show exceptional promise as drug candidates. Thus, calicheamicin γ_1^I derivatives attached to tumor-selective monoclonal antibodies are currently under development for clinical use, having shown high potency against tumors with low toxicity.[44]

Much synthetic work has been inspired by calicheamicin γ_1^I **2**. A number of novel strategies and model systems will be discussed in Section 3.2.

2.3. Esperamicins

The esperamicins are a subclass of naturally occurring enediynes with extremely high activities as broad spectrum antibiotics and antitumor agents. These compounds were isolated[45] from cultures of *Actinomadura verrucosospora* and their molecular structures were elucidated in 1987 (Table 2).[3, 46] The similarities between the esperamicins and the calicheamicins are quite striking, extending over structure, biological activity, and mode of action. Thus, like the calicheamicins, the esperamicins contain in their structure a bicyclo[7.3.1]tridecadiynene ring system, an allylic trisulfide, (or tetrasulfide), a 1,5-diyn-3-ene moiety as part of the ring system, and an α,β-unsaturated ketone in which the double bond is at the bridgehead of the bicyclic core. The absolute configuration of esperamicin A_1 **3** and its relatives has been determined.[47–49] The esperamicins, together with the calicheamicins, are amongst the most potent anticancer agents known, exhibiting powerful activity[47] against a number of murine tumor models such as P388, B16, M5076 at injected doses in the 100 ng/kg range.[3] Like calicheamicins, the esperamicins are thought to exert their biological action by damaging DNA. The mechanism of the DNA cleavage by esperamicin A_1 **3** is identical to that of the cleavage by calicheamicin γ_1^I **2** (see Scheme 10), as proposed simultaneously by the Lederle[2] and Bristol-Myers[3] groups. Esperamicin A_1 **3**, however, exhibits less sequence selectivity[50, 51] than calicheamicin γ_1^I **2** and shows[50, 51] preference for T > C > A > G. As in the case of calicheamicin γ_1^I **2**, the activity of esperamicin A_1 **3** towards DNA is significantly enhanced by thiols such as dithiothreitol[50, 51] and results in both single and double strand cuts. The carbohydrate fragments are thought to assist in the binding of the drug to the minor groove of DNA[50, 51] (Fig. 3), as in the case of calicheamicin γ_1^I **2**. Light-induced DNA cleavage by esperamicin A_1 **3** has also been demonstrated.[18]

Table 2. The esperamicin family.

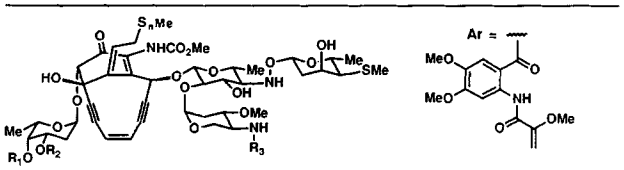

Esperamicin	n	R_1	R_2	R_3
Esperamicin A_1 **3**	3	H	Ar	$CHMe_2$
Esperamicin A_{1b}	3	H	Ar	Et
Esperamicin A_{1c}	3	H	Ar	Me
Esperamicin P	4	H	Ar	$CHMe_2$
Esperamicin A_2	3	Ar	H	$CHMe_2$
Esperamicin A_{2b}	3	Ar	H	Et
Esperamicin A_{2c}	3	Ar	H	Me

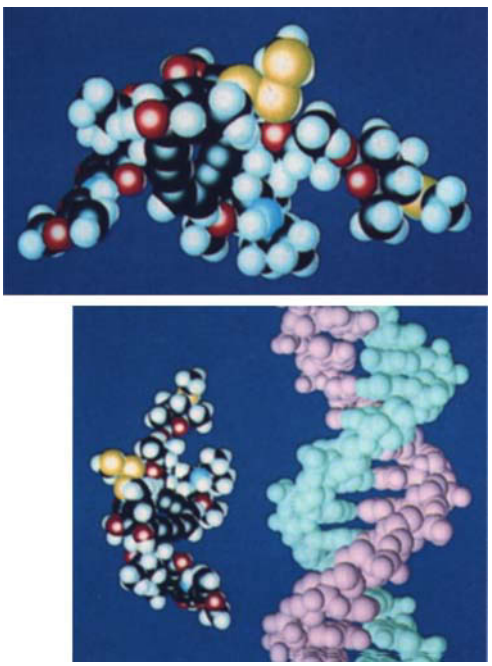

Fig. 3. Computer-generated models of free **3** (top) and of **3** on approaching DNA (bottom).

Despite a number of side effects, esperamicin A_1 has successfully passed phase I[47, 51] and is currently in phase II clinical trials.[52]

2.4. Dynemicins

The first member of this subclass of enediynes, dynemicin A **4**, was reported in 1989.[4] This novel, violet-colored anticancer antibiotic was discovered in the fermentation broth of

Table 3. The dynemicin family.

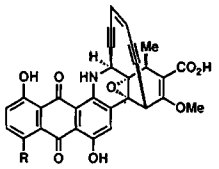

Compound No.	Name	R
4	Dynemicin A	OH
15	Deoxydynemicin A	H

Micromonospora chersina.[4] Its molecular structure, with exception of the absolute configuration, was fully determined by spectroscopic and X-ray crystallographic analysis.[53] Dynemicin A **4** exhibits very potent activity against a variety of cancer cell lines and prolongs significantly the life span of mice inoculated with P388 leukemia and B16 melanoma cells.[53] Furthermore, dynemicin A **4** and its derivatives exhibit promising in vivo antibacterial activity with low toxicity.[4] More recently, a second member of this family, deoxydynemicin A **15** (Table 3), a bioactive compound with similar biological profile to dynemicin A **4**, was isolated from *Micromonospora globosa* MG331-hF6.[54] Like the calicheamicins and esperamicins, the dynemicins include in their molecular structures a ten-membered ring with a 1,5-diyn-3-ene bridge. They are, however, distinctly unique in combining the enediyne unit with the anthraquinone chromophore of the anthracycline[55] anticancer antibiotics.

It has been shown that dynemicin A **4** cleaves double-stranded DNA, causing both single and double strand cuts.[56, 57] The potency of the drug as a DNA cleaving agent is significantly enhanced by thiols[56] and by visible light irradiation.[57] Dynemicin A **4** preferably attacks the 3′ side of purine bases such as 5′-AG, 5′-GC, 5′-GT and 5′-AT with

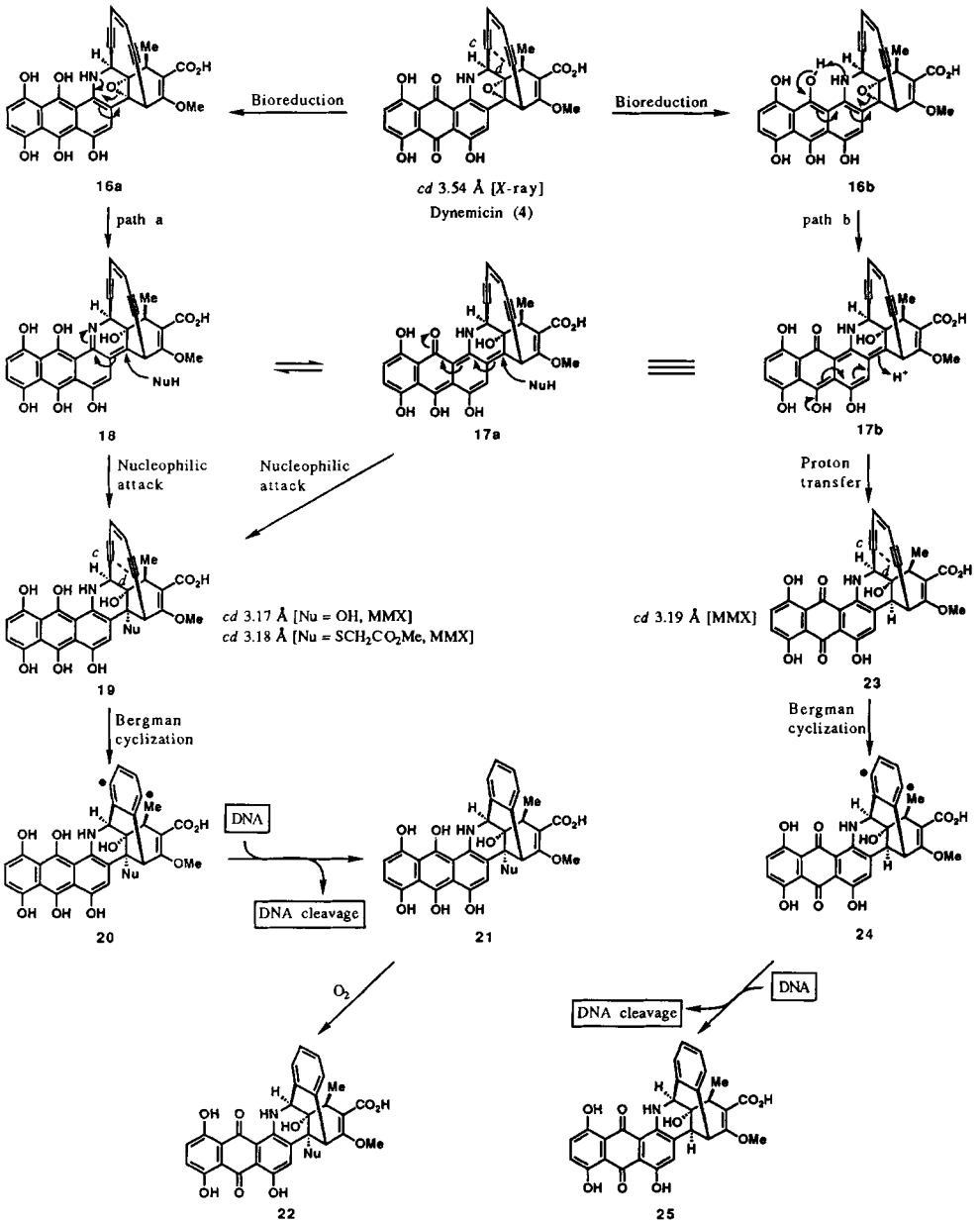

Scheme 11. Proposed mechanism of DNA cleavage by **4**.

clear selection for G and to a lesser extent A.[56, 58] Intercalators and minor groove binders interfere with DNA cleavage by dynemicin A **4**, suggesting both intercalation and minor groove binding for this agent.[56] A mechanism of action of dynemicin A **4** involving several pathways has been suggested (Scheme 11).[56–61] This mechanism combines features of the modes of action of the enediyne and the anthracycline antibiotics.

The hypothesis for the mode of action of dynemicin A **4** postulates minor groove binding and intercalation (Fig. 4), bioreduction, epoxide opening, trapping of generated intermediates, cycloaromatization with benzenoid diradical formation, and hydrogen atom abstraction from DNA. This

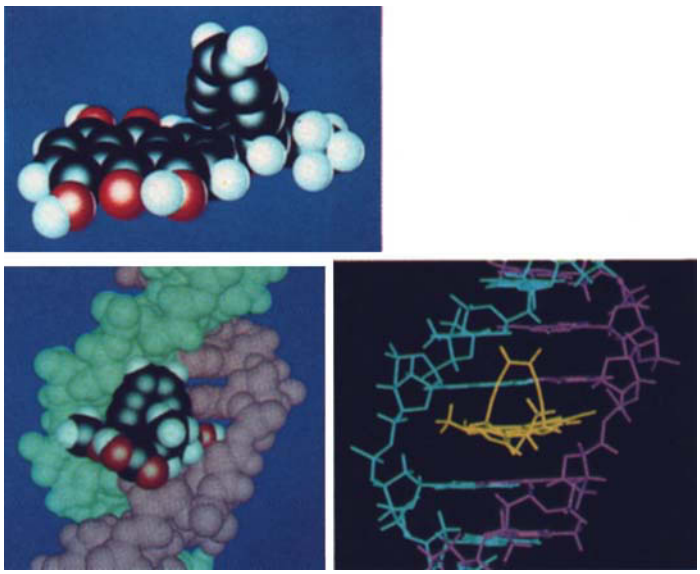

Fig. 4. Computer-generated models of free **4** (top) and DNA-bound **4** (bottom).

remarkable chemical cascade (Scheme 11) is triggered by a reduction process (**4** → **16**) which unleashes two lone pairs of electrons, one on nitrogen and one on oxygen (structures **16a** and **16b**) providing two alternative pathways for epoxide opening (path a and path b). Path a leads to the conjugated quinone methide intermediate **17** which may suffer nucleophilic attack (structure **17a**) or proton transfer (structure **17b**) to form intermediates **19** and **23**, respectively. Molecular mechanics calculations on **19** and **23** revealed considerable shortening of the $c \cdots d$ distance (3.17–3.19 Å) compared to the X-ray crystallographically determined valued 3.54 Å for **4**,[4] suggesting and explaining their rapid collapse to benzenoid diradicals, **20** and **24**, respectively, via Bergman cyclization. Alternatively, path b may lead to the *ortho*-iminoquinone methide **18** (tautomeric with **17**), which could suffer nucleophilic attack (or proton shift) via intermediate **19** (or **23** after tautomerization). The benzenoid diradicals generated are thought to be responsible for initiating DNA rupture by hydrogen abstraction, although direct alkylation of DNA by intermediates **17** and/or **18** may also contribute to DNA damage.[56, 60, 61] Compound **21** may suffer spontaneous oxidation to **22**. Both compounds **22** (Nu = OH, SCH_2CO_2Me) and **25** were isolated as final products of this cascade.[53, 56, 57, 61]

Synthetic studies in the area of the dynemicins as well as other enediyne antibiotics are discussed in Section 3.3.

3. Synthesis of Enediyne Antibiotics

3.1. Neocarzinostatin Chromophore Model Systems

The basic reaction[19] involved in the generation of radicals from neocarzinostatin chromophore was demonstrated with the parent system (*Z*)-1,2,4-heptatrien-6-yne **26**, (Scheme 12) by *Myers* et al.[62] in 1989. This cycloaromatiza-

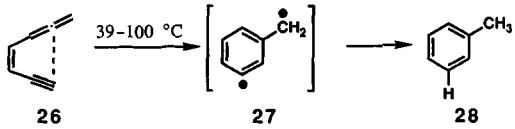

Scheme 12. The Myers cyclization (1989).

tion, now recognized as the Myers reaction, proceeds via α,3-didehydrotoluene **27** and leads to toluene **28** upon hydrogen atom abstraction (Scheme 12). In his elegant studies,[62] *Myers* determined the following activation parameters for this process: $\Delta H^{\neq} = 21.8 \pm 0.5$ kcal mol^{-1}, $\Delta S^{\neq} = -11.6 \pm 1.5$ cal K^{-1} mol^{-1} ($E_a = 22.5$ kcal mol^{-1}, lg $A = 10.7$).

Saito et al.[63, 64] demonstrated the chemistry shown in Scheme 13 as well as DNA cleaving properties for compound **30** and its phenylsulfoxide.[64]

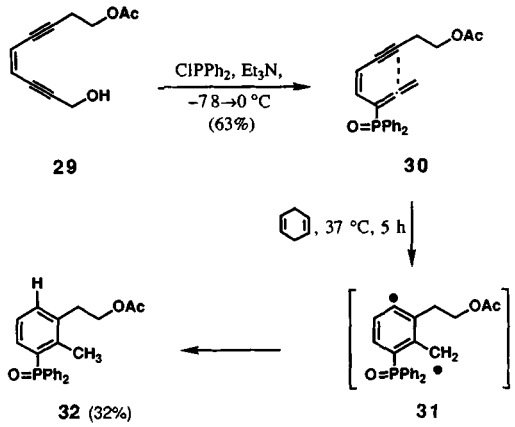

Scheme 13. Neocarzinostatin chromophore related studies by *Saito* et al. (1989).

A very imaginative and skilfull choice of model compound by *Myers* and *Dragovich*[65] resulted in the chemistry depicted in Scheme 14. Compound **33** was triggered under basic conditions to form the (*Z*)-1,2,4-heptatrien-6-yne derivative **34**, which was observed to decay below room temperature, forming, in the presence of cyclohexadiene, aromatized derivative **36** via diradical **35**.

The *Myers* group has also reported[66] an enantioselective synthesis of the epoxy diyne core of the neocarzinostatin chromophore (**46**, Scheme 15). Key features in this synthesis include Pd^0/Cu-catalyzed construction of the enediyne moiety (**37** → **38**), Sharpless asymmetric epoxidation (**39** → **40**), dia-

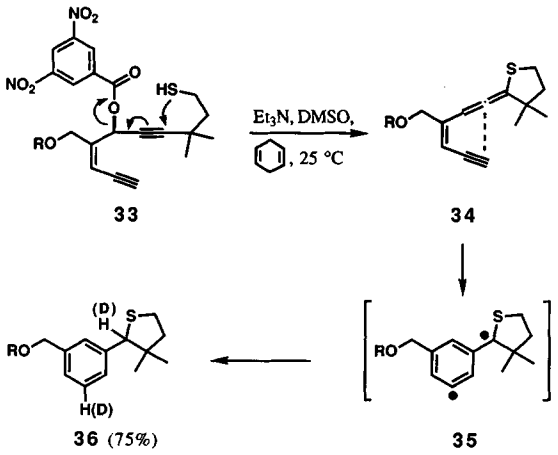

Scheme 14. Model studies related to neocarzinostatin chromophore by *Myers* et al. (1989). R = Si*t*BuPh$_2$.

stereomeric resolution by crystallization (**42**, obtained from **41**) and intramolecular acetylide addition to an aldehyde (**45** → **46**) to close the nine-membered ring.

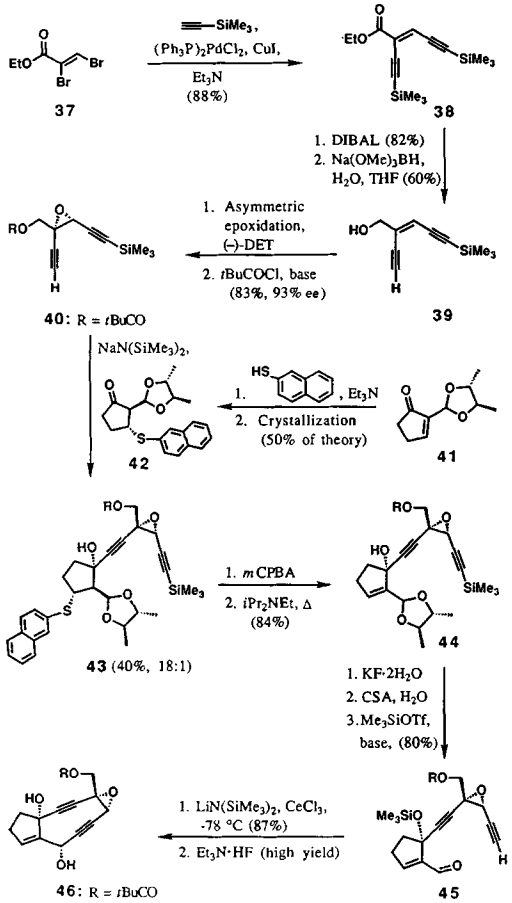

Scheme 15. Synthesis of the epoxy diyne core **46** of neocarzinostatin chromophore by *Myers* et al. (1991). DIBAL = diisobutylaluminum hydride, DET = diethyl tartrate, *m*CPBA = *meta*-chloroperbenzoic acid, CSA = camphorsulfonic acid, Tf = trifluoromethanesulfonate; R = *t*BuCO.

Our work[67] in this area focused on the design of DNA-cleaving molecules which react both by way of a radical mechanism as well as by way of an alkylation mechanism (Scheme 16). This mechanistically supported reaction cascade starts from **47** and incorporates a [3,2]sigmatropic rearrangement (**48** → **49**) and a Myers cyclization reaction[62] leading to a diradical (**49** → **50**), or to a nucleophilic attack of a DNA base at the allene system (**49** → **51**). The by-products of the DNA cleavage are then **52** and **53**, respectively.

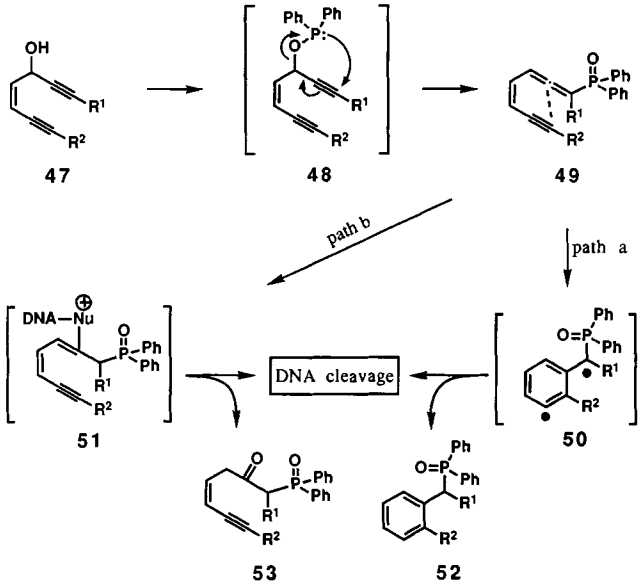

Scheme 16. Design of DNA-cleaving molecules with dual mode of action: a) radical mechanism; b) alkylation mechanism (*Nicolaou* et al., 1990).

Scheme 17 shows a number of synthesized compounds and their cyclizations to aromatic systems with half-lives ranging from 8 h to 117 h at 37 °C. Experiments with supercoiled

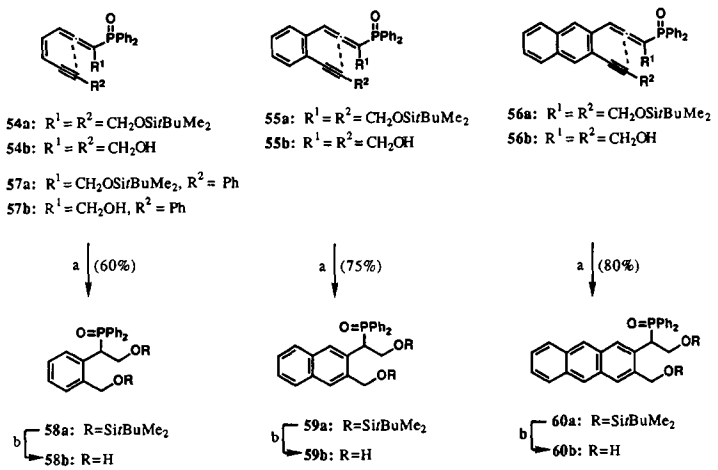

Scheme 17. Cycloaromatization of conjugated phosphane oxide allene-eneynes synthesized by *Nicolaou* et al. (1990). a) 0.01 M in 1,4-cyclohexadiene, 37 °C; **54a**, $t_{1/2}$ = 8 h; **55a**, $t_{1/2}$ = 23 h; **56a**, $t_{1/2}$ = 117 h, b) 48 % aq. HF, CH_3CN, 20 °C, 100 %.

ΦX174DNA (form I) demonstrated thermally-induced DNA cleavage by these compounds (Fig. 5)[67] and mechanistic studies[67] confirmed their dual mode of action. Figure 6 shows computer-generated space-filling models of compound **54b** and of **54b** approaching double helical DNA.

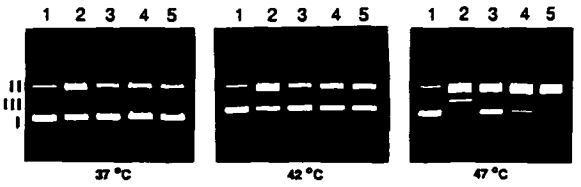

Fig. 5. DNA cleavage by the compounds **54**–**57**. ΦX174 form I DNA (50 μM/base pair) was incubated for 48 h at the specified temperatures with various compounds (1 mM in 20% ethanol in phosphate buffer, pH 8.5, 50 mM) and analyzed by gel electrophoresis (1 % agarose, ethidium bromide stain). Lane 1, DNA alone; lanes 2–5, DNA with compounds **54b**, **55b**, **56b**, and **57b**, respectively. Forms I, II, and III used in this article correspond to supercoiled, relaxed, and linear DNA, respectively.

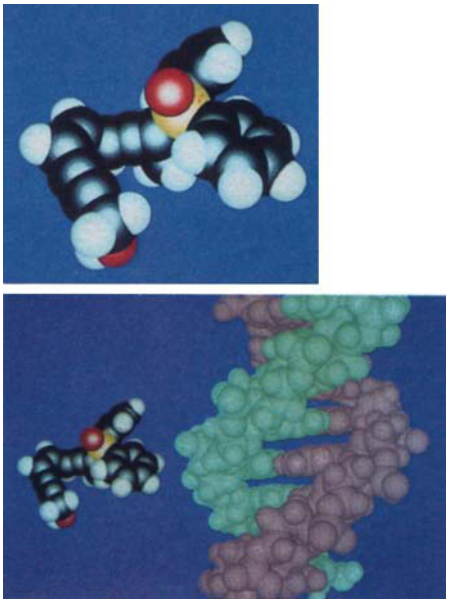

Fig. 6. Computer-generated models of free **54b** (top) and of **54b** on approaching DNA (bottom).

Golfomycin A **61** is a novel, designed molecule reported from our laboratories with DNA-cleaving properties and antitumor activity.[68] Two mechanistic rationales, shown in Scheme 18, led to the design of this intriguing molecule. The

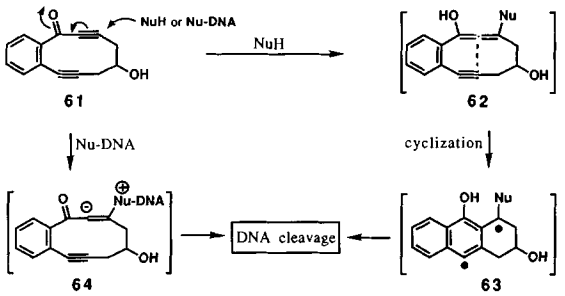

Scheme 18. Mechanism-based design of golfomycin A **61** (*Nicolaou* et al., 1990).

neocarzinostatin chromophore-inspired rationale (**61** → **62** → **63**) postulated a Myers type[62] cyclization, whereas the nucleophilic attack (**61** → **64**) had plenty of examples.[69] The construction of golfomycin A **61** (Scheme 19) involved base-induced intramolecular C–C bond formation within **65**, followed by mild oxidation (**65** → **66**) and deprotection (**66** → **61**).[68]

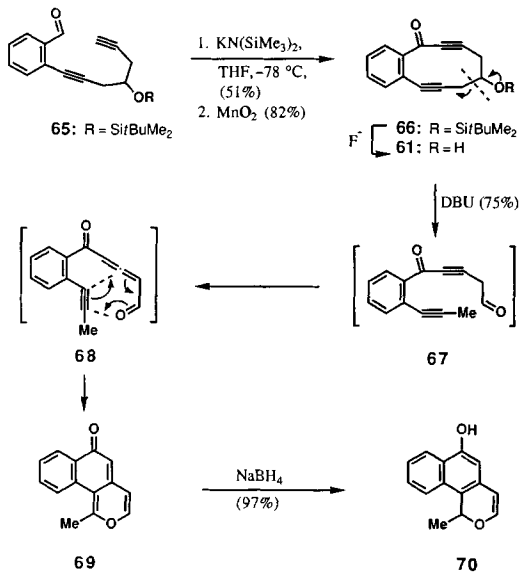

Scheme 19. Synthesis and reactions of **61** (*Nicolaou* et al., 1990). DBU = diazabicyclo[5.4.0]undecene.

Golfomycin A **61** and its protected precursor **66** exhibit unusual chemistry[68] upon treatment with base and methyl thioglycolate, respectively. Thus, upon treatment with DBU, **61** entered into the cascade shown in Scheme 19 (**61** → **67** → **68** → **69**) with **69** isolated as the final product and **67** detected by ^{1}H NMR spectroscopy. The structure of **69** was confirmed by its reaction with sodium borohydride to give **70**, whose *p*-bromobenzoate was characterized X-ray crystallographically. On the other hand, derivative **66** reacts with DBU and methyl thioglycolate to give the unusual thiophene derivatives **72** and **73**, presumably via intermediate **71** (Scheme 20).

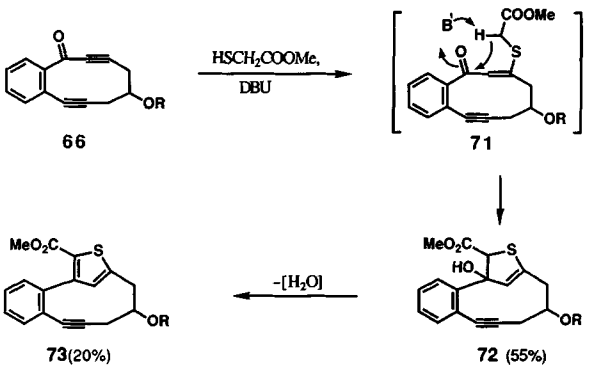

Scheme 20. Reaction of the golfomycin A precursor **66** with methyl thioglycolate (*Nicolaou* et al., 1990). R = Si*t*BuMe$_2$.

Figure 7 shows space-filling models of golfomycin A **61**, whereas Figure 8 depicts the molecule's DNA-cleaving activity against supercoiled DNA at various pH's.[68] Preliminary results with golfomycin A indicated growth inhibition of MB49 murine bladder carcinoma cells with an IC_{50} of

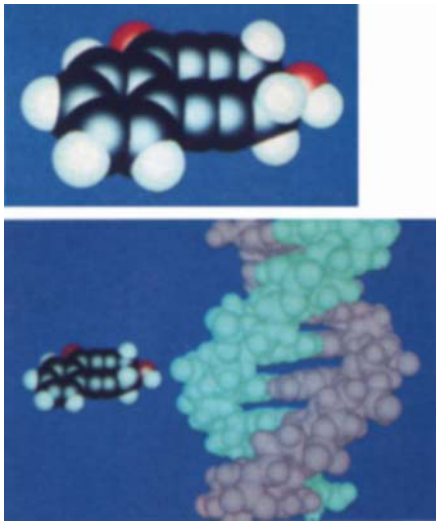

Fig. 7. Computer-generated models of free **61** (top) and of **61** on approaching DNA (bottom).

3.4 μmol L^{-1} during 4 days of exposure.[68] These properties fulfilled the expectations of the molecular design and elevated the compound to a significant lead for further developments.

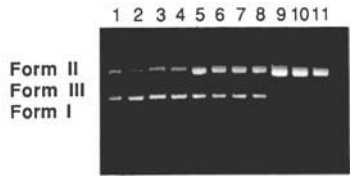

Fig. 8. DNA cleavage by golfomycin A **61** at various pH values. ΦX174 form I DNA (50 μM/base pair) was incubated for 20 h at 37 °C with **61** (1000 μM) in various pH buffers and analyzed by electrophoresis (1 % agarose gel, ethidium bromide stain). Lane 1, DNA alone at pH 8.5; lanes 2–11 correspond to pH 5.0, 6.0, 7.0, 7.4, 8.0, 8.5, 9.0, 9.5, 10.0, and 10.7, respectively. Control experiments at the above pH's in the absence of agent demonstrated no DNA cleavage.

Elegant studies by the *Hirama* group[70] culminated in the synthesis of neocarzinostatin chromophore-related model systems **76** and **77** (Scheme 21). Key to the success of this scheme was an intramolecular, Pd^0-catalyzed coupling of a vinyl bromide with an acetylenic stannane. The reaction of ketone **77** with methyl thioglycolate in AcOH/EtOH under aerobic conditions proved to be quite fascinating, leading to compounds **80**–**82**, presumably via intermediates **78** and **79** (Scheme 21). The acetate **76** (Scheme 22) reacted similarly under the same conditions to afford compounds **85a** and **85b** via the postulated intermediates **83** and **84** (Scheme 22). Under anaerobic conditions, compounds **88a–d** were isolated in the indicated yields (Scheme 22). Compounds **88a–c** are presumably formed via pathway **76b** → **86** → **87** as shown in Scheme 22. The regioisomeric ketone **89** (Scheme 23) was also synthesized by *Hirama* et al.[71] and its reaction with methyl thioglycolate explored under aerobic and anaerobic conditions, leading to compounds **91a–c** (aerobic, path a via **90**) and **94a–c** (anaerobic, path b via **92** and **93**) as shown in Scheme 23.

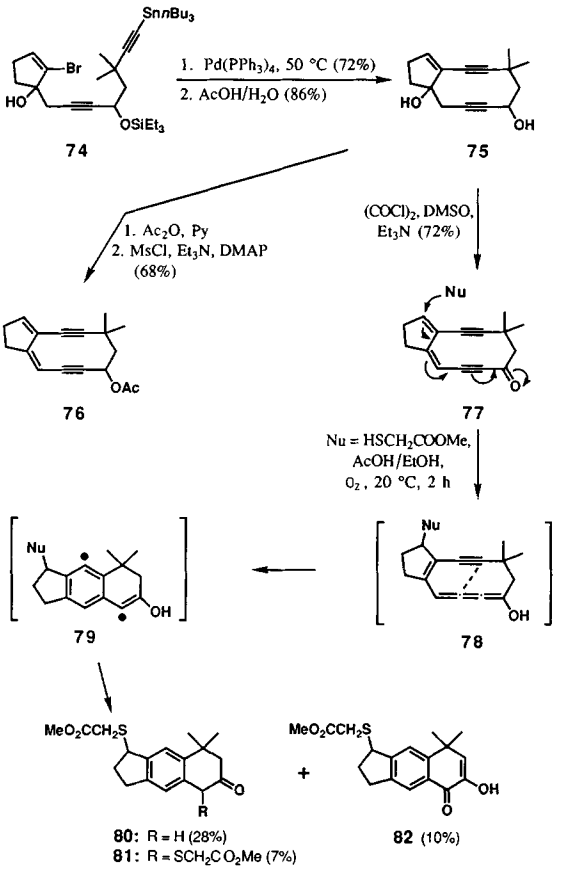

Scheme 21. Neocarzinostatin chromophore related model studies by *Hirama* et al. (1989). Synthesis and cycloaromatization of the ketone **77**. Py = pyridine, DMAP = dimethylaminopyridine.

The interesting enyne[3]cumulene **96** was synthesized by *Hirama* et al.[72] as shown in Scheme 24 (**95** → **96**). This compound exhibited the expected reactivity towards a Myers-type cyclization,[62] leading to **98** via **97** as well as forming compound **100**. The latter compound is thought to be formed via the indicated pathway (Scheme 24) initiated by a formal [2 + 2] intramolecular cycloaddition (**96b** → **99** → **100**). The half-life of **96** at 80 °C was found to be 1.1 h.[72, 73]

The team led by *Toshima* and *Tatsuta* recently reported[74] an interesting ten-membered sulfur-containing ring system (**102**, Scheme 25) with Myers-type reactivity reminiscent of the chemistry of neocarzinostatin chromophore. Thus, deprotection and dehydration of **101**[75] led to the stable crystalline compound **102** in high yield, which upon reaction with basic methanol furnished compound **104** via the postulated intermediate **103a** and the presumed polar mechanism shown in Scheme 25. On the other hand, DBU-induced isomerization of **102** in the presence of CCl_4 and oxygen furnished compounds **106**–**109**, presumably via **103b** and the diradical **105**.

The parent hydrocarbon representing the carbocyclic framework of neocarzinostatin chromophore (**115**, Scheme 26) was synthesized by *Wender* et al. in 1988.[76] In these studies,[76] the Wender group demonstrated the viability of a number of reactions (**111** → **112** → **113** → **114** → **115**) for the synthesis of such systems. Compound **115** was found to be rather labile ($t_{1/2}$ = 48 h at room temperature), suffering polymerization upon removal of solvent.[76] In a more recent

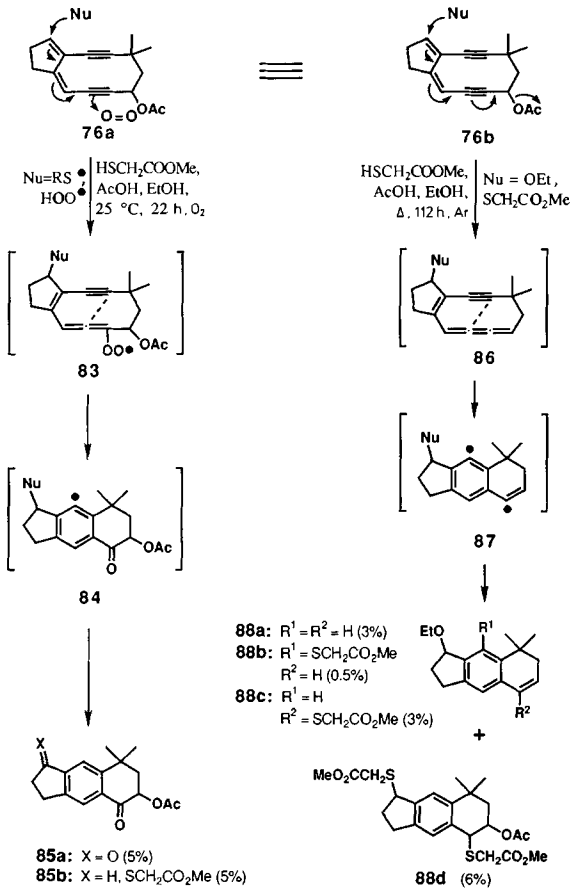

Scheme 22. Neocarzinostatin chromophore related model studies by *Hirama* et al. (1989). Cycloaromatization of compound **76** under aerobic and anaerobic conditions.

study[77] the same group demonstrated the utilization of a chromium-induced intramolecular condensation[78] (**116** → **117**, Scheme 27) and a ring contraction strategy based on the Wittig rearrangement[79] (**119** → **117**, Scheme 27). Selective acetylation of **117** followed by dehydration resulted in the formation of the model compound **120**.

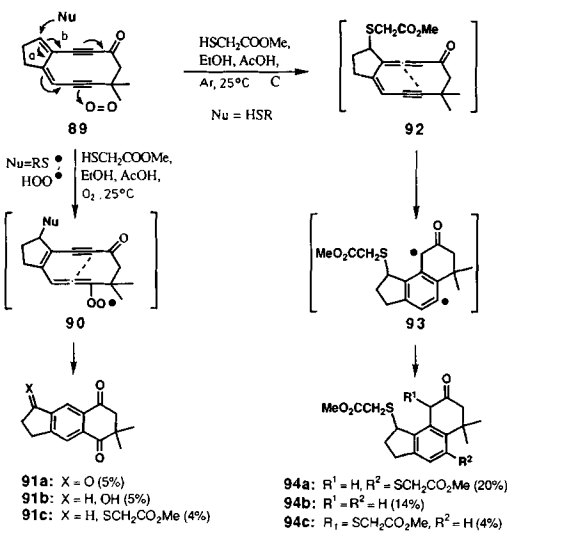

Scheme 23. Neocarzinostatin chromophore related model studies by *Hirama* et al. (1990). Cycloaromatization of ketone **89**.

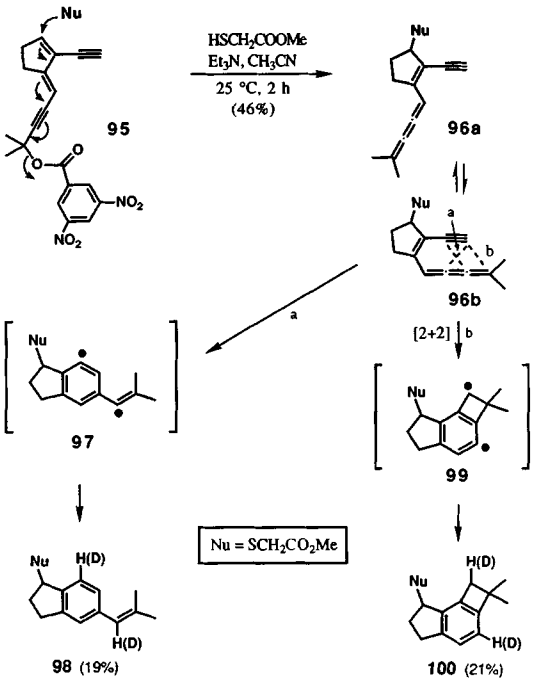

Scheme 24. Synthesis and cycloaromatization of enyne[3]cumulene **96** (*Hirama* et al., 1991).

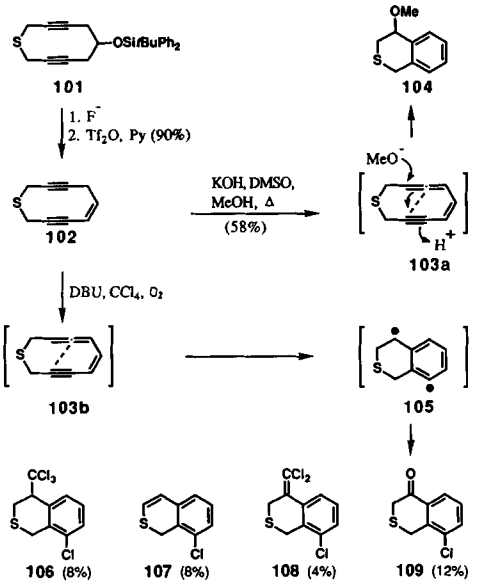

Scheme 25. Neocarzinostatin chromophore related model studies by *Toshima, Tatsuta* et al. (1991).

The *Takahashi* group[80] has also cleverly utilized the Wittig rearrangement reaction to contract the macrocyclic rings **121** to the smaller rings **122** (Scheme 28), which served as precursors to the neocarzinostatin related model systems **123** and **124**. The enediyne **123** underwent smooth Bergman-type[5] cyclization to afford compounds **126** via diradical **125**, whereas compound **124** was triggered by methyl thioglycolate to undergo a Myers-type[62] ring closure affording **129** via **127** and **128**.

The synthesis of the twelve-membered macrocyclic ether **131** from **130** was also reported by *Krebs* et al.[81] (Scheme

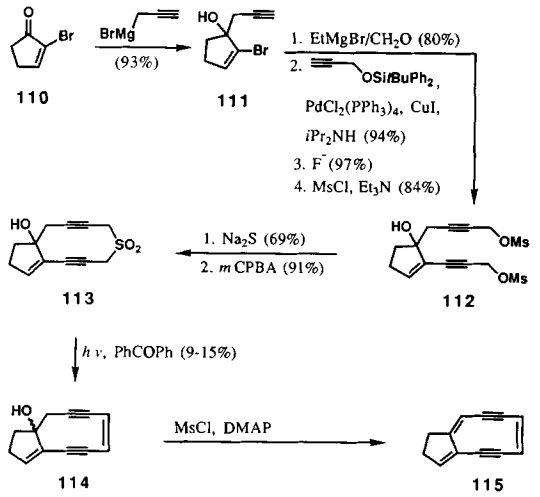

Scheme 26. Synthesis of the parent carbocycle **115** of the neocarzinostatin chromophore by *Wender* et al. (1988).

29). The same group also reported[82] the synthesis of the interesting neocarzinostatin chromophore related systems **133** and **135** from **132** employing intramolecular aldol-type ring closures by the routes outlined in Scheme 29.

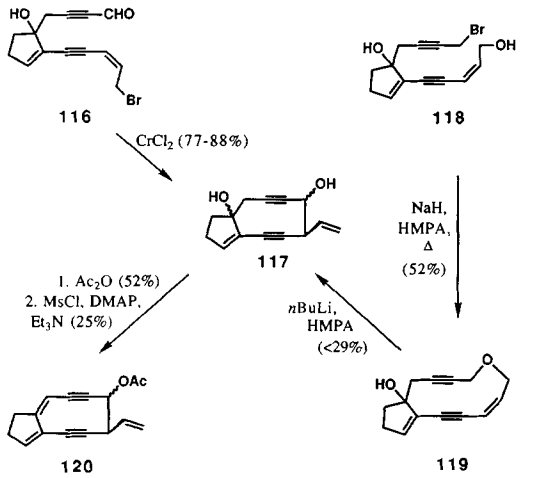

Scheme 27. Neocarzinostatin chromophore related model studies by *Wender* et al. (1990). HMPA = Hexamethylphosphoric acid triamide.

An intramolecular allylsilane-aldehyde cyclization was successfully employed by *Suffert*[83] to synthesize compound **137** (1:1 mixture of diastereoisomers from compound **136** (Scheme 30). The acyclic neocarzinostatin chromophore-related derivatives **138** and **139** (Scheme 31) were synthesized by *Terashima* et al.[84] Interestingly, the (*Z*)-isomer **138** exhibited stronger cytotoxicity against P388 leukemia cells than the (*E*)-isomer **139**.[84]

Scheme 32 summarizes recent studies by *Magnus* et al.[85] with neocarzinostatin models in which an intramolecular aldol-type addition was used to convert the organocobalt compound **140** into the nine-membered ring enediyne precursor **141**. In situ generation of **142** resulted in Bergman cyclization and trapping as tricyclic system **143**.[85]

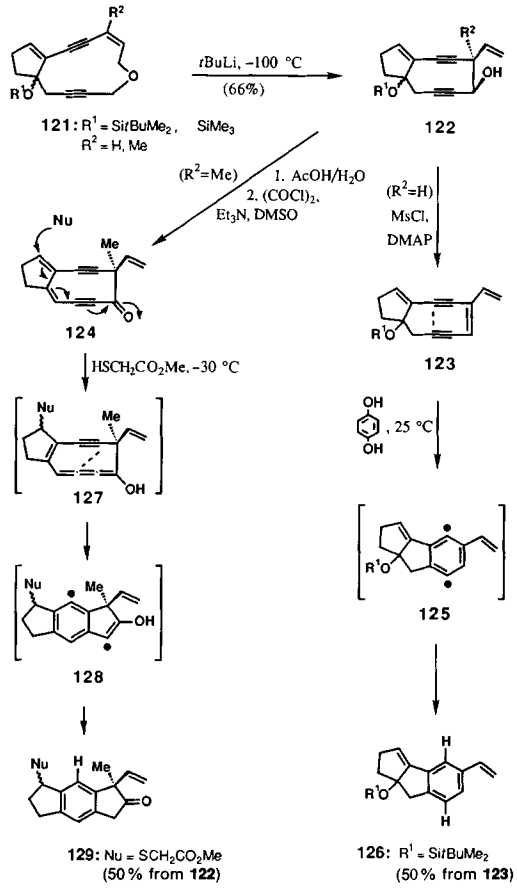

Scheme 28. *Takahashi*'s neocarzinostatin chromophore related model studies (1991).

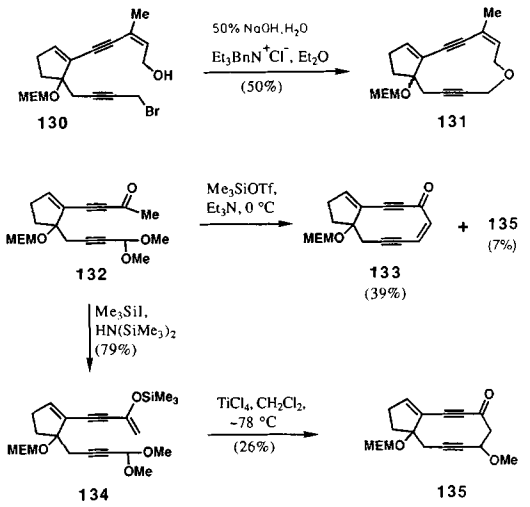

Scheme 29. Neocarzinostatin chromophore related model studies by *Krebs* et al. (1990). MEM = methoxyethoxymethyl, Bn = benzyl.

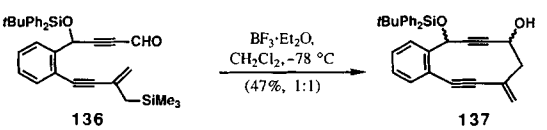

Scheme 30. Synthesis of the neocarzinostatin chromophore related system **137** (*Suffert*, 1990).

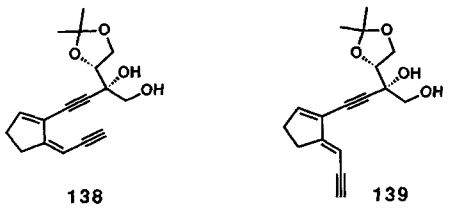

Scheme 31. Structures of acyclic neocarzinostatin chromophore related derivatives **138** and **139** (*Terashima* et al., 1990).

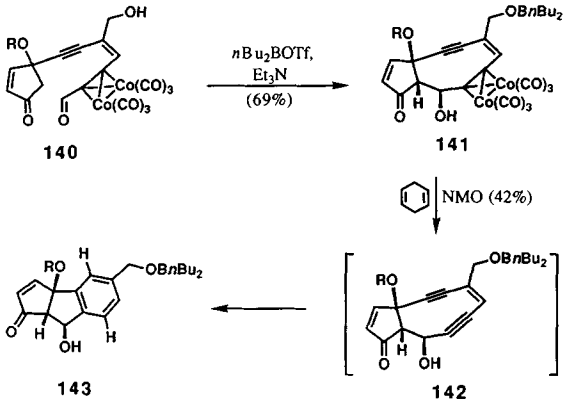

Scheme 32. Intramolecular aldol-based construction of a model system related to neocarzinostatin by *Magnus* et al. (1991). NMO = *N*-methylmorpholine *N*-oxide; R = $SiBuMe_2$.

Two syntheses of the naphthalene moiety of neocarzinostatin chromophore have been reported.[86]

3.2. Calicheamicin/Esperamicin Model Systems

3.2.1. Enediyne Systems

Intrigued by the novel molecular architecture and fascinating mode of action of the calicheamicin/esperamicin enediyne antiobiotics, we initiated in 1987 a program directed toward their total synthesis, an understanding of their chemistry, and the design of novel mimics of their biological actions. Our initial studies focused on monocyclic conjugated enediynes[41] of the type present in these naturally occurring substances. Thus, a series of compounds with formula **145** were synthesized by the Ramberg–Backlund reaction (Scheme 33) and studied. Table 4 lists a number of such compounds together with some other related systems and summarizes selected parameters and properties.

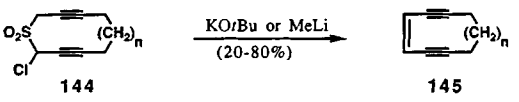

Scheme 33. Synthesis of monocyclic enediynes **145** via Ramberg–Backlund reaction (*Nicolaou* et al., 1988).

On the basis of these data it was surmised that, as a general rule at least in monocyclic systems, the distance between the remote acetylenic carbons ($c \cdots d$ distance, see Table 4 and some Schemes) provides a useful guide for determining the ease of cyclization, since it correlates with the strain energy (see Section 4). It must be emphasized, however, that this hypothesis is based on first approximations and is meant for simple systems, and that exceptions, particularly in bicyclic systems with complex frameworks and centers, do exist.[87] The rule works well for a large number of examples and it has been useful in molecular design and in making predictions regarding the stability of certain members of a given series of compounds. As expected from inspection of Table 4, enediyne **145** (n = 2) cyclized smoothly at 37 °C in the presence of cyclohexadiene via the diradical **149** to give the tetralin **150** (Scheme 34) (and two isomeric adducts with cyclo-

Table 4. Calculated $c \cdots d$ distances and stabilities of conjugated enediynes.

Entry	Compound	Ring size	$c \cdots d$ Distance [Å]	Stability	Ref.
1	**145** (n = 1)	9	2.84	unknown compound	[41]
2	**145** (n = 2)	10	3.25	$t_{1/2}$ = 18 h at 37 °C	[41]
3	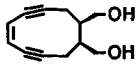 **146**	10	3.20	$t_{1/2}$ = 11.8 h at 37 °C	[90]
4	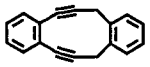 **7**	10	3.03	cyclized at 25 °C	[7]
5	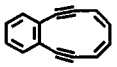 **6a**	10	3.01	cyclized < 25 °C	[6]
6	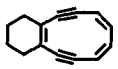 **6b**	10	2.99	cyclized < 25 °C	[6]
7	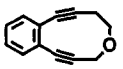 **147**	10	3.40 [a]	$t_{1/2}$ = 52 h at 37 °C	[88a]
8	**145** (n = 3)	11	3.61	stable at 25 °C	[41]
9	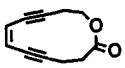 **148**	12	3.77	stable at 25 °C	[88b]
10		–	4.12	stable at 25 °C; $t_{1/2}$ = 30 s at 200 °C	[5a]
11		–	3.94	stable at 25 °C; $k_{obs} = 6.4 \times 10^{-4}\,s^{-1}$ at 156 °C	[5c]

[a] For *trans* conformer, see Ref. [88a].

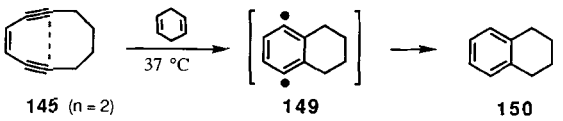

Scheme 34. Bergman-type cyclization of enediyne **145** (n = 2) (*Nicolaou* et al., 1988). $t_{1/2}$ = 18 h, E_a = 23.8 kcal mol^{-1}.

hexadiene). The oxaenediyne system **147** (Table 4, entry 7) also cyclizes at 37 °C, as reported recently by *Just* et al.[88a]

The eleven-membered ring (**145**, $n = 3$), again as anticipated from a $c \cdots d$ distance of 3.61 Å (Table 4, entry 8), was found to be quite stable at ambient temperature and, furthermore, it crystallized nicely from pentane. An X-ray crystallographic analysis of **145** (n = 3) revealed an interesting conformation (Fig. 9) and a $c \cdots d$ distance of 3.66 Å, agreeing

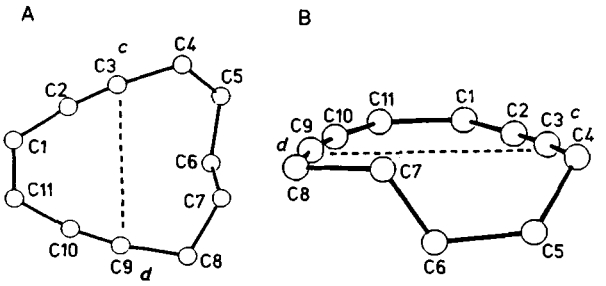

Fig. 9. ORTEP drawing of **145** (n = 3): A) top view, B) side view. $c \cdots d$ distance = 3.661(5) Å.

remarkably well with the calculated value and thus boosting our confidence in such calculations. Interestingly the nine-membered ring **145** (n = 1) could not be synthesized; instead, the diacetylene **153** was isolated. The latter compound presumably arose from the unusual pathway shown in Scheme 35.[89]

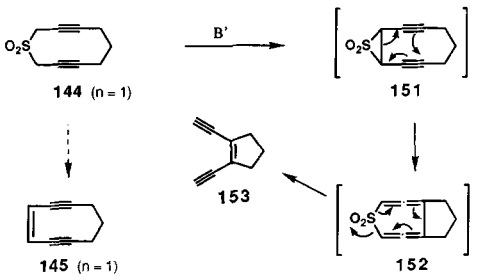

Scheme 35. Attempted synthesis of **145** (n = 1). Formation of compound **153** (*Nicolaou* et al., 1988).

On the basis of the studies described above, the conjugated cyclodecenediyne **146** was designed as a potential DNA-cleaving agent.[90] Its synthesis proceeded along the lines presented in Scheme 36. The compound **146** was sufficiently stable for handling but decayed at 37 °C in the presence of cyclohexadiene into the benzenoid product **160** via diradical **159** (Scheme 37) with a half-life of 11.8 h (E_a = 23.6 kcal mol^{-1}). Most significantly, enediyne **146** demonstrated marked temperature- and time-dependent DNA cleaving properties, re-

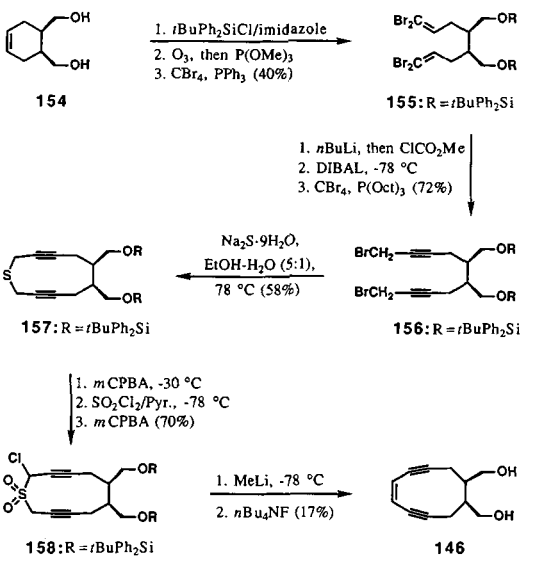

Scheme 36. Synthesis of the enediyne **146** (*Nicolaou* et al., 1988). Oct = octyl; R = Si*t*BuPh$_2$.

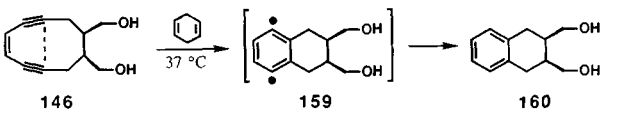

Scheme 37. Bergman-type cyclization of the enediyne **146** (*Nicolaou* et al., 1988).

sulting in both single and double strand DNA cuts (Fig. 10).[90] Figure 11 shows computer-generated space-filling models of enediyne **146** and its target, DNA.

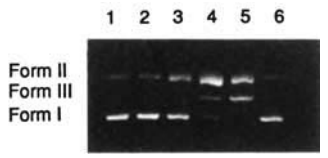

Fig. 10. DNA cleavage by **146** and **160**. ΦX174 form I DNA (50 μM/base pair) was incubated with **146** or **160** in Tris-acetate buffer (pH 8.5, 50 mM) at 37 °C for 12 h and analyzed by agarose gel electrophoresis. Lane 1, DNA alone; lanes 2–5, DNA + 1.0, 10, 100, and 500 μM **146**, respectively; lane 6, DNA + 2 mM **160**.

These results provided the first confirmation for the proposed mode of action of calicheamicins and esperamicins and supported our previous hypothesis[41] that simple cyclic conjugated enediynes should spontaneously cleave DNA in the absence of any cofactors such as metals or thiols, and should therefore serve as "warheads" for designed systems against preselected targets such as specific DNA segments and tumor cells. The incorporation of structures of the type **146** into larger molecular assemblies equipped with delivery systems may, therefore, be worthwhile and may result in powerful biotechnological tools and useful therapeutic agents.

Encouraged by the results with the model ten-membered ring enediynes and inspired by chemistry previously discovered by *Garratt*[91] and *Braverman*,[92] we proceeded to de-

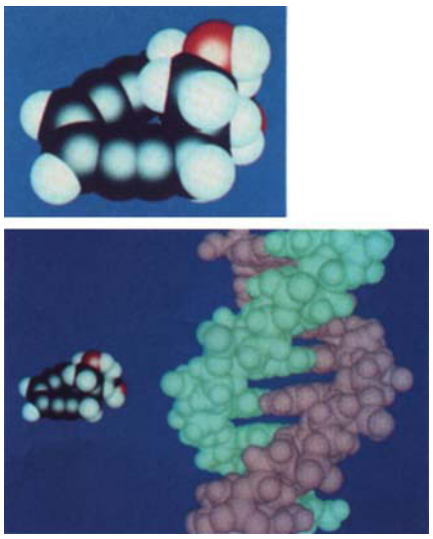

Fig. 11. Computer-generated models of free **146** (top) and of **146** on approaching DNA (bottom).

sign a new class of DNA-cleaving molecules containing propargylic or allenic sulfone moieties.[75] Scheme 38 shows the mechanistic rationale, which led to the design of this class of compounds. Specifically, it was hypothesized that the

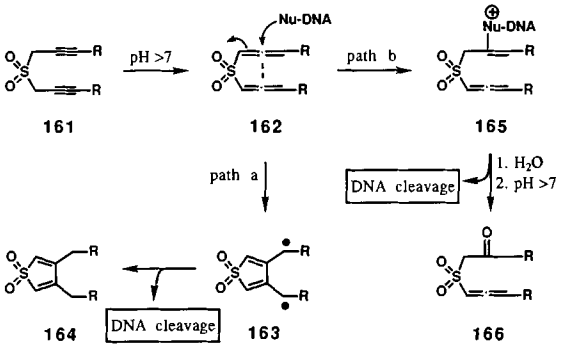

Scheme 38. Mechanistic rationale for the design of DNA-cleaving molecules of the propargylic and allenic sulfone type (*Nicolaou* et al., 1989).

Garratt–Braverman cascade would proceed in aqueous solution at pH > 7, converting a bis(propargylic) sulfone **161** first into a bis(allenic) sulfone **162** and subsequently into a diradical species **163** (path a) which might cause DNA damage (→ **164**). Alternatively, it was reasoned that nucleophilic attack (path b) by DNA on the conjugated allenic

Table 5. Structures of propargylic and allenic sulfones **167a–d**.

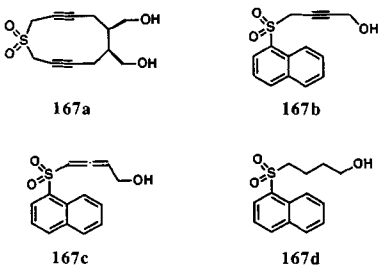

acceptor **162** may lead to structures such as **165** which were then expected to undergo Maxam–Gilbert[69] type reactions (→ **166**) causing DNA rupture as shown in Scheme 38.

Table 5 presents the structures of some of the most interesting molecules of this series, whereas Figure 12 outlines DNA-cleaving action with these molecules.[93] Exploring

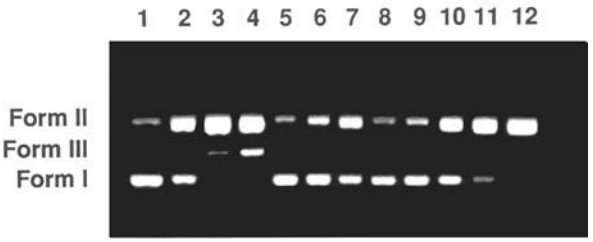

Fig. 12. DNA cleavage by **167**. ΦX174 form I DNA (50 μM/base pair) was incubated for 24 h at 37 °C with **167a–c** in buffer solution (50 mM Tris/HCl, pH 8.5) and analyzed by electrophoresis (1% agarose gel, ethidium bromide stain). Lane 1: DNA control; lane 2: DNA + 100 μM **167a**; lane 3: DNA + 5 μM **167b**; lane 4: DNA + 5 μM **167c**; lane 5: DNA + 10 mM **167d**; lane 6: DNA + 100 μM ethidium bromide; lane 7: DNA + 100 μM **167a** + 100 μM ethidium bromide; lane 8: DNA + 5 μM **167b** + 5 μM ethidium bromide; lane 9: DNA + 5 μM **167c** + 5 μM ethidium bromide; lane 10: DNA + 100 μM **167a** + 10 mM **167d**; lane 11: DNA + 5 μM **167b** + 10 mM **167d**; lane 12: DNA + 5 μM **167c** + 10 mM **167d**.

structure–activity relationships, base and sequence selectivity, and other mechanistic aspects, led to the conclusion that the most likely mechanism for the mode of action of these com-

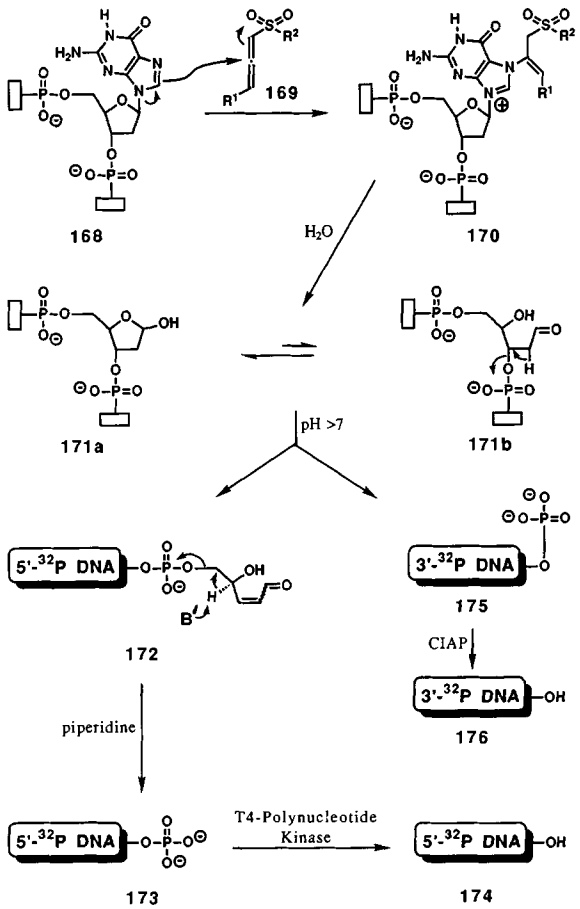

Scheme 39. Mechanism of DNA cleavage by propargyl and allenic sulfones (e.g. **169**) (*Nicolaou* et al., 1989). CIAP = calf intestine alkaline phosphatase.

pounds is the alkylation pathway (**168**–**176**) depicted in some detail in Scheme 39.[93] Furthermore, it was established that compound **167a** (Table 5) shows preferential attack at guanine sites and, significantly, high selectivity for 5′-GCA, 5′-GCG, and 5′-GCC sequences.[93] These results render these types of compounds quite attractive as "warheads" for further manipulation and development.

The *Danishefsky* group has been very active in the calicheamicin/esperamicin area.[94–98] Their synthesis of calicheamicinone **186** shown in Scheme 40[94] represents the first arrival at this target and a major achievement in the field.

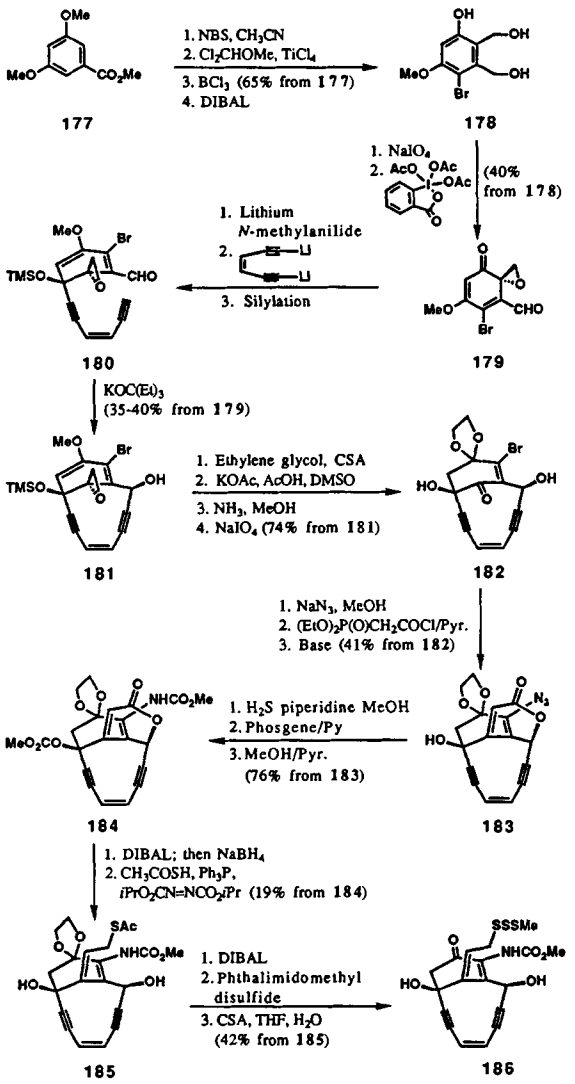

Scheme 40. *Danishefsky*'s synthesis of calicheamicinone **186** (1990). NBS = *N*-bromosuccinimide.

Key steps in this sequence, which begins with **177**, are: a) the formation of the quinone epoxide **179** from **178**; b) the regioselective addition of dilithioenediyne to ketoaldehyde **179**; c) the intramolecular acetylide addition to the aldehyde group of **180** to give **181**; and d) the intramolecular Emmons condensation (**182** → **183**) to keep the allylic functionality in the correct configuration for **186**.

Simulation of the calicheamicin/esperamicin cascade has been amply demonstrated by *Danishefsky* et al. with a variety of compounds (Scheme 41).[95, 97] Furthermore, comparisons of calicheamicin γ_1^I **2** and calicheamicinone **186** in DNA cleavage experiments pointed to the importance of the carbohydrate fragment of the natural product in the molecular recognition of its target sequence.[39]

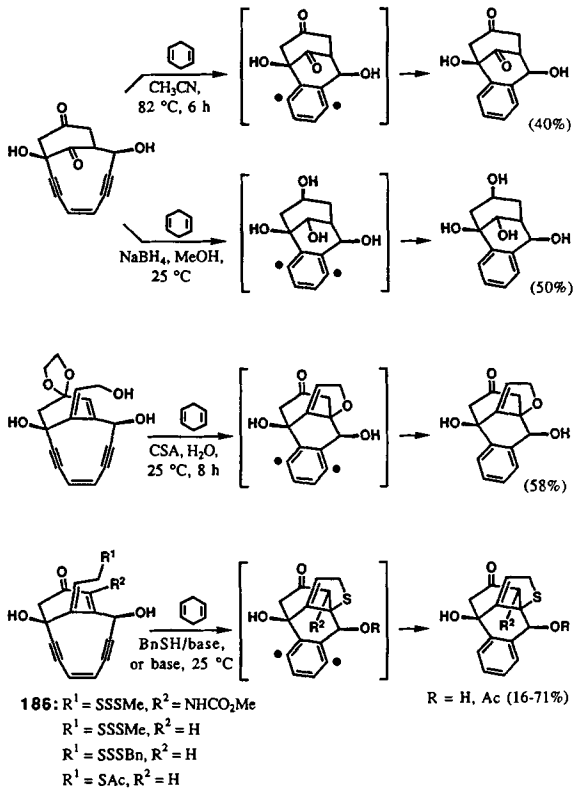

Scheme 41. Bergman cyclization of calicheamicinone **186** and related analogues (*Danishefsky* et al., 1989–1990). Bn = benzyl.

Kende and *Smith*[99] also utilized the intramolecular acetylide/aldehyde condensation (**190** → **191**, Scheme 42) to construct an enediyne model system (**191**) related to the calicheamicin/esperamicin core from **187**.

Magnus's approach to the enediyne model of the calicheamicin/esperamicin core cleverly exploited some intriguing

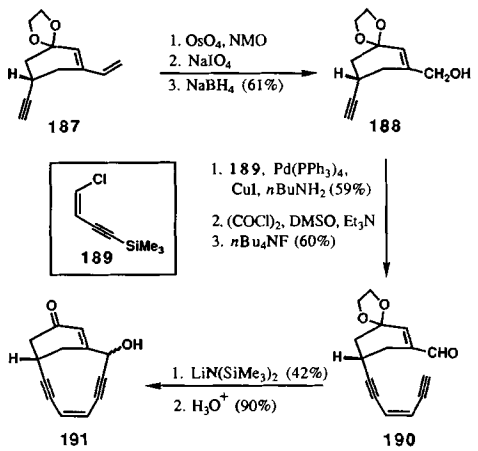

Scheme 42. The Kende synthesis of the calicheamicin/esperamicin related model system **191** as 3:1 mixture of epimers (*Kende* et al., 1988).

organocobalt chemistry to construct the ten-membered ring.[100-104] Schemes 43 and 44 show the synthesis of the model compounds **202** (from **192**)[100,101] and **205** (from **203**)[102] utilizing a $TiCl_4$/DABCO-induced ring closure of methoxy precursor **195** to give **196** and an intramolecular aldol reaction of the keto aldehyde **203** to give **204**, respectively. The *Magnus* group was the first[103a] to demonstrate

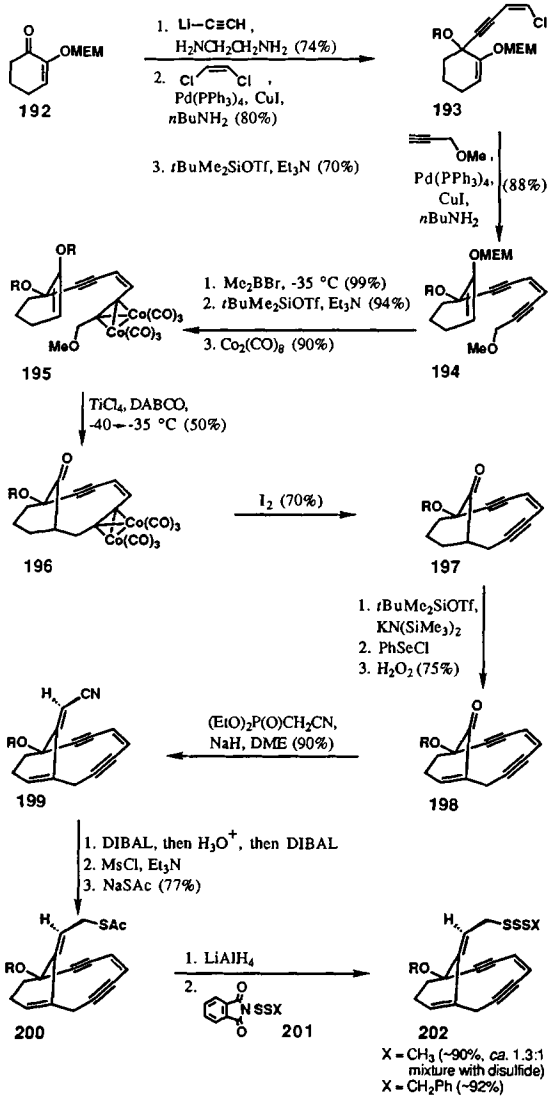

Scheme 43. Synthesis of calicheamicin/esperamicin related models by *Magnus* et al. (1988–1989). DABCO = diazabicyclooctane, DME = dimethoxyethane; R = Si*t*BuMe$_2$.

the construction of the trisulfide moiety in such systems using reagents of type **201** (Scheme 43). The same group also synthesized a number of other model systems such as **207**,[101] **211**,[87] and **213**[87] (Scheme 45) and demonstrated the cycloaromatization of a series of these compounds as shown in Schemes 44 (**204** → **206**)[102] and 45 (**207** → **208**;[101] **197** → **209**;[100] **198** → **210**;[104] **211** → **212**;[87] and **213** → **214**[87]).

The same approach towards for the synthesis of **197** has been reported by *Tomioka* et al.[105]

Schreiber's entry to the calicheamicin/esperamicin enediyne studies was based on an intramolecular Diels–Alder reac-

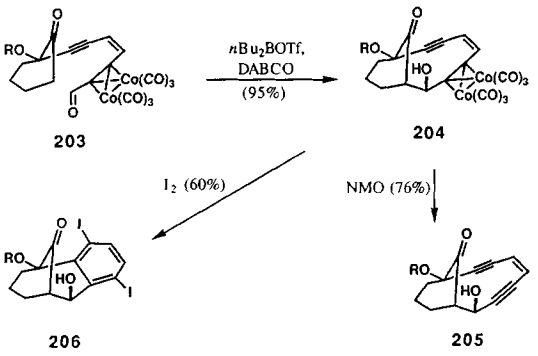

Scheme 44. Intramolecular aldol-based construction of a model system related to calicheamicin/esperamicin by *Magnus* et al. (1990). R = Si*t*BuMe$_2$.

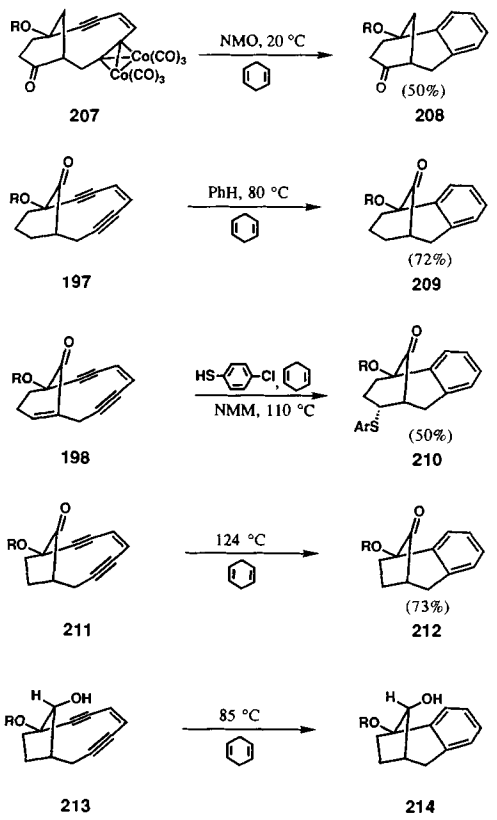

Scheme 45. Calicheamicin/esperamicin related systems synthesized and studied by *Magnus* et al. (1988–1990). NMM = *N*-methylmorpholine; R = Si*t*BuMe$_2$.

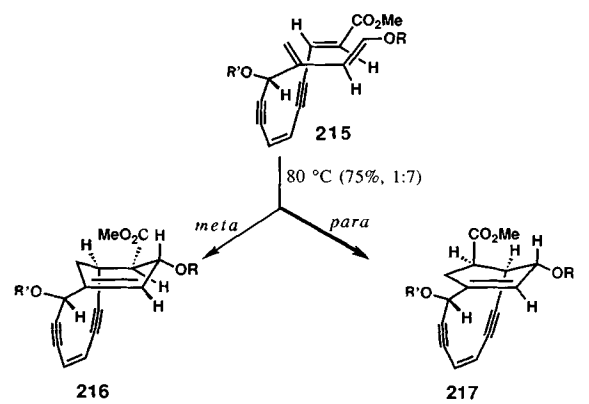

Scheme 46. The synthesis of the calicheamicin/esperamicin enediyne core skeleton by intramolecular Diels–Alder reaction according to *Schreiber* et al. (1988–1989). R = Si*t*BuMe$_2$. **216** present only as by-product.

tion. This approach initally met with a disappointing regiochemical outcome, as indicated in Scheme 46.[106, 107] Thus, heating the polyunsaturated substrate **215** to 80 °C resulted in the unfavorable ratio of 1:7 for the *meta*- and *para*-products (**215** → **216** + **217**). This outcome, however, was swiftly corrected in subsequent work[108] by a clever maneuver involving a Tsuchihashi pinacol rearrangement[109] with con-

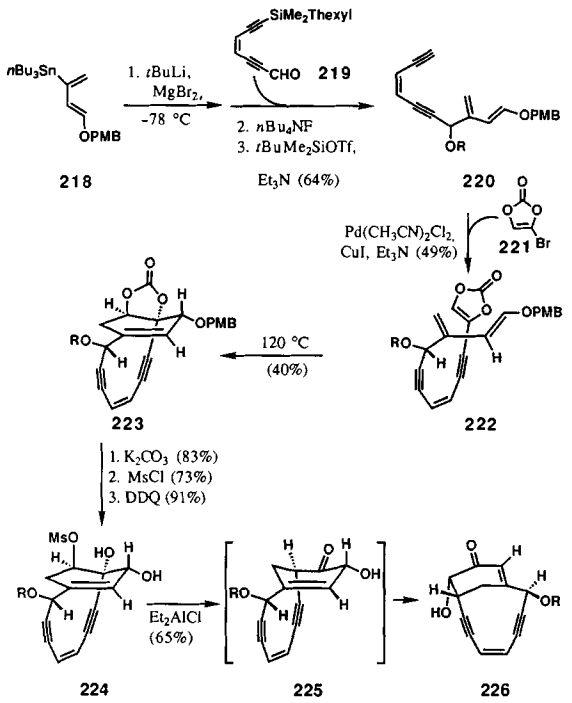

Scheme 47. The intramolecular Diels–Alder approach to the calicheamicin/esperamicin enediyne model **226** by *Schreiber* et al. (1989). Thexyl = Me_2CH-CMe_2, PMB = *para*-methoxybenzyl, DDQ = dichlorodicyanobenzoquinone; R = Si*t*BuMe$_2$.

comitant diastereoselective acyloin shift to secure the desired ring skeleton (**224** → **225** → **226**, Scheme 47).

3.2.2. *Carbohydrate Fragments*

The implication of the calicheamicin γ_1^I oligosaccharide segment as a minor groove binder and recognition element for sequence specificity in DNA cleavage coupled with the challenge of the calicheamicin γ_1^I total synthesis prompted us to undertake its construction.[110–114] Focusing on the oligosaccharide fragment of calicheamicin γ_1^I, we identified the following novel and challenging structural features shown in model **227** (Scheme 48)[110, 111]: a) the unusual alkoxylamine bond (β) linking carbohydrate units A and B through bonds α and γ; b) the *β*-configuration of the glycoside bond γ, which, taken in combination with the 2-deoxy nature of saccharide B, presents a unique challenge to synthetic construction; c) the sulfur bridge, linking carbohydrate unit B with the fully substituted aromatic ring via bonds δ and ε; and d) the α-configuration of the N- and S-bearing stereogenic centers of carbohydrate units A and B, respectively.

Targeting model system **227** (Scheme 48) provided rather novel solutions to all the above synthetic challenges. The synthetic design for this construction was based on the retrosynthetic disconnections indicated in structure **227** (Scheme 48) which led to diimidazolylthioketone (Im_2C=S) as the sulfur source, *N*-hydroxyphthalimide (HO–NPhth) as the ori-

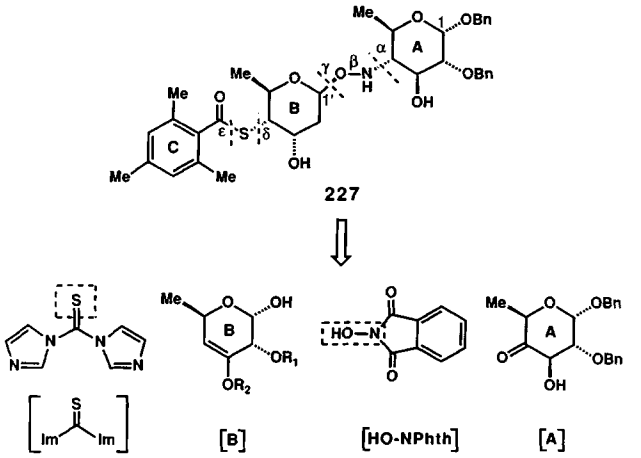

Scheme 48. Retrosynthetic analysis of the ABC model fragment **227** of the calicheamicin γ_1^I oligosaccharide moiety (*Nicolaou* et al., 1990).

gin of the alkoxyamino group, and precursors to rings A, B, and C as potential starting materials. Scheme 49 outlines the strategy utilized in this synthesis as designed from the above analysis and which, in addition to solving the above mentioned problems, avoids a potentially difficult deoxygenation step to generate the desired methylene group of the B ring. Thus, intermediate **228** was designed with an ester group at position 2 to assure the desired stereochemical outcome of the glycosidation reaction (**228** → **229**, *β*-configuration) as well as to serve as a device to stereoselectively deliver the sulfur atom at position 4 via a sigmatropic rearrangement (**229** → **230** → **231**). Compound **231** was then expected to serve as a

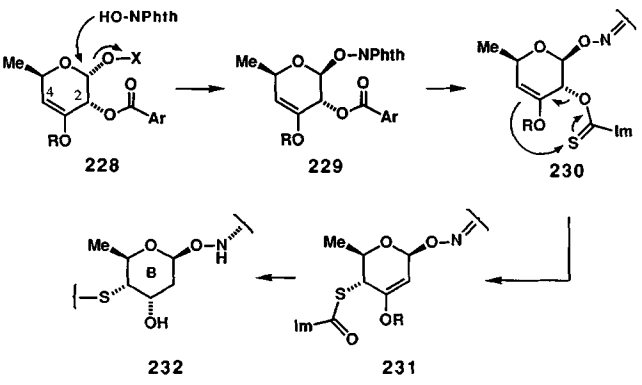

Scheme 49. Synthetic strategy for the construction of the central ring region **232** of the calicheamicin γ_1^I oligosaccharide moiety (*Nicolaou* et al., 1990).

precursor to **232**. The execution of the synthesis proceeded as planned (Scheme 50). In addition to the above mentioned highlights, the synthesis featured stereoselective reductions of both the C=O and the C=N bonds (**242** → **227**) to afford the desired product in high overall yield.[110, 111]

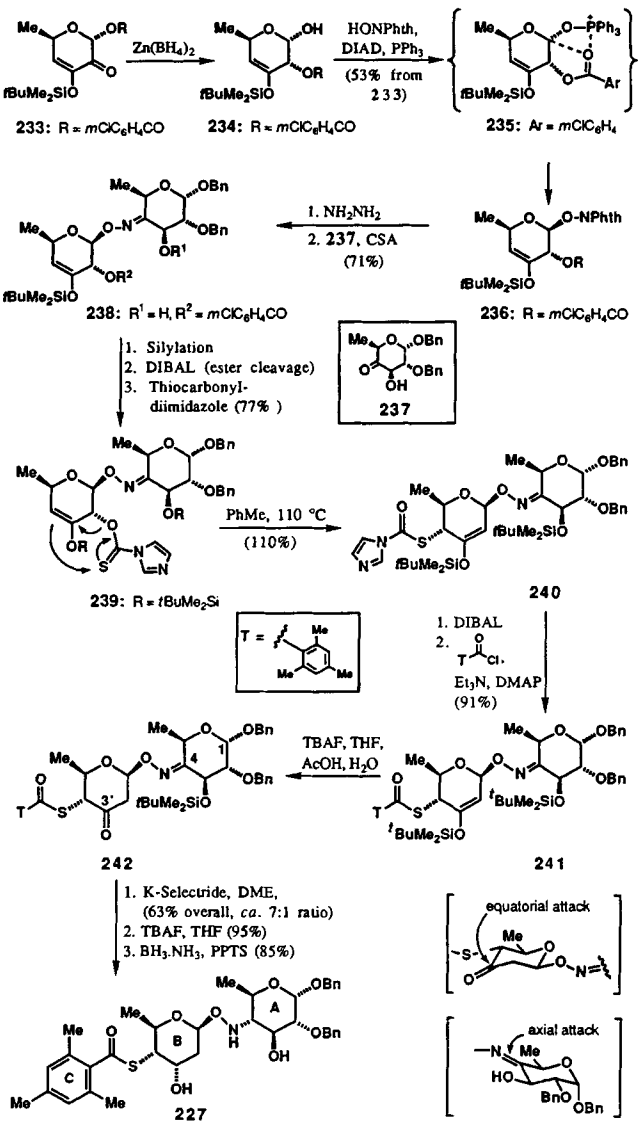

Scheme 50. Synthesis of the calicheamicin γ_1^I oligosaccharide model system **227** (*Nicolaou* et al., 1990). DIAD = diisopropylazodicarboxylate, TBAF = tetrabutylammonium fluoride, PPTS = pyridinium *p*-toluenesulfonate.

Application of this synthetic technology featuring the novel [3,3]sigmatropic rearrangement to the construction of the natural calicheamicin γ_1^I oligosaccharide methyl glycoside **243** followed swiftly. Designated on structure **243** (Scheme 51) are the strategic bond disconnections that allowed the tracing of the requisite intermediates to the readily available

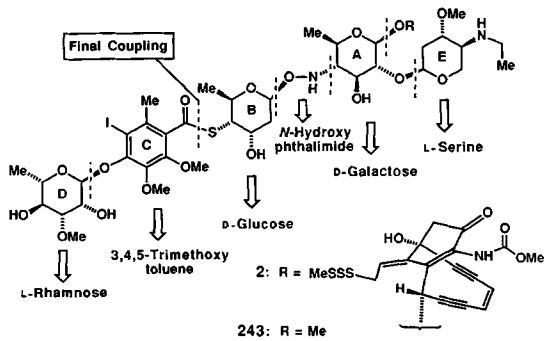

Scheme 51. Strategic bond disconnections and retrosynthetic analysis of the calicheamicin γ_1^I oligosaccharide derivative **243** (*Nicolaou* et al., 1990).

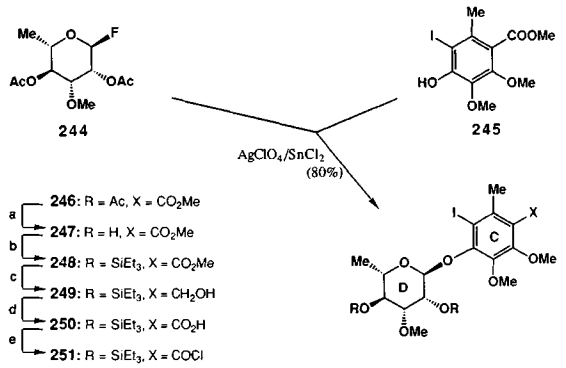

Scheme 52. Synthesis of the DC ring system **251** of the calicheamicin γ_1^I oligosaccharide moiety (*Nicolaou* et al., 1990). a: K_2CO_3, MeOH (100 %); b: Et_3SiOTf, 2,6-lutidine (92 %); c: DIBAL (90 %); d: $RuCl_3 \cdot H_2O$, $NaIO_4$, $CCl_4/CH_3CN/H_2O$ (2/2/3) (75 %); e: $(COCl)_2$ (95 %).

starting materials: L-rhamnose (ring D); 3,4,5-trimethoxytoluene (ring C); D-glucose (ring B); *N*-hydroxypthalimide (O–NH group); D-galactose (ring A); and L-serine (ring E). The thioester linkage (CO–S) was reserved as the key bond for the final coupling reaction. Schemes 52–54 summarize

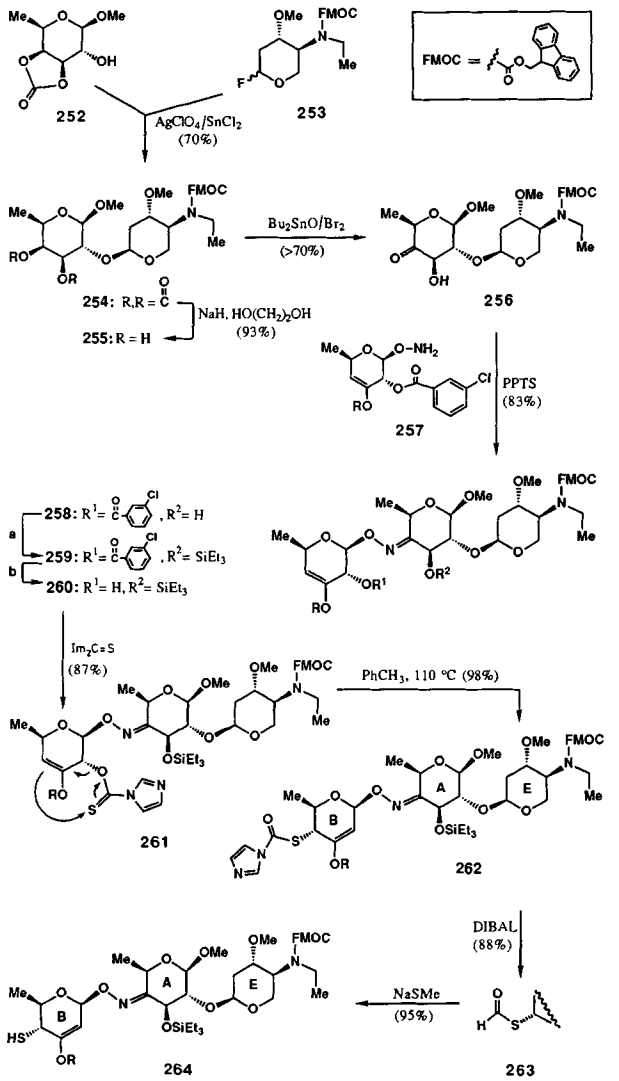

Scheme 53. Synthesis of EAB ring systems **263** and **264** of the calicheamicin γ_1^I oligosaccharide moiety (*Nicolaou* et al., 1990). a: Et_3SiOTf, 2,6-lutidine (100 %); b: DIBAL (91 %). R = *Si*BuMe$_2$.

the total synthesis of **243** with the intermediates **244**, **245**, **252**, **253** and **257** as key building blocks. Despite the encouraging results with model system **227**, the final reduction of the C=N bond in **266** proceeded with rather low stereoselectivity to afford a mixture of products (1:2 in favor of the wrong isomer). Efforts to improve this outcome are continuing.

Molecular recognition studies involving **243** *and DNA* segments are now possible and so are projected total syntheses of calicheamicin γ_1^I **2** and other hybrid structures.

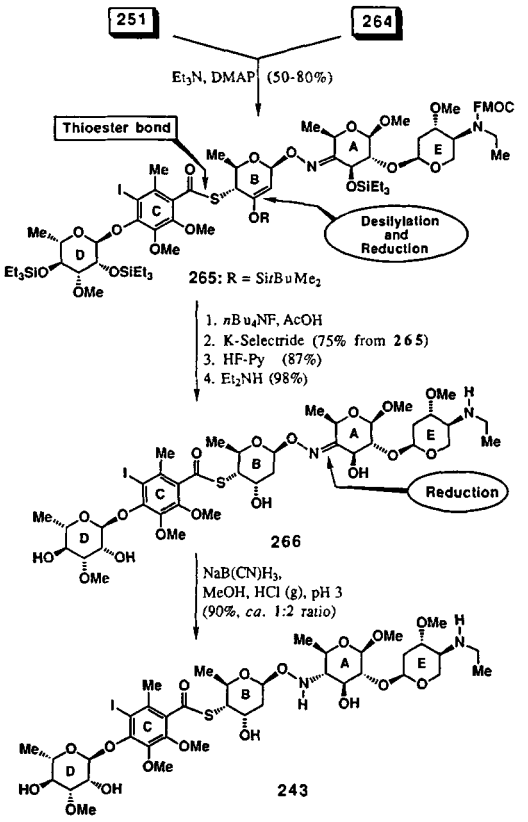

Scheme 54. Total synthesis of the calicheamicin γ_1^I oligosaccharide compound **243** (*Nicolaou* et al., 1990).

A synthesis of the trisaccharide segment **273** of esperamicin A_1 **3**, was recently completed by *Danishefsky* et al.[115, 116] as summarized in Scheme 55. Highlights of this construction include: a) the utilization of glycals in glycosidation reactions, and b) the use of a urethane anion to construct the crucial C–N bond (**270** + **271** → **272a, b**), as demonstrated by the *Kahne* group.[117] An interesting observation in the *Danishefsky* work[115] was the rearrangement of the central pyranose ring to a five-membered nitrogen-containing ring system (**272b** → **274**) upon liberation of both the anomeric and the NH–O position of the central sugar unit.[48]

The *Kahne* group was the first to publish a synthesis of the 4-ethylamino sugar (ring E) of calicheamicin γ_1^I **2** and to assign its absolute configuration.[118] The same group has recently reported a new method for the construction of N–O linkages for oligosaccharides based on urethane anion chemistry and applied it to the construction of the calicheamicin/esperamicin core trisaccharide **281** as shown in Scheme 56.[117]

Subunits of the calicheamicin γ_1^I oligosaccharide were also synthesized by *Laak* and *Scharf*.[119]

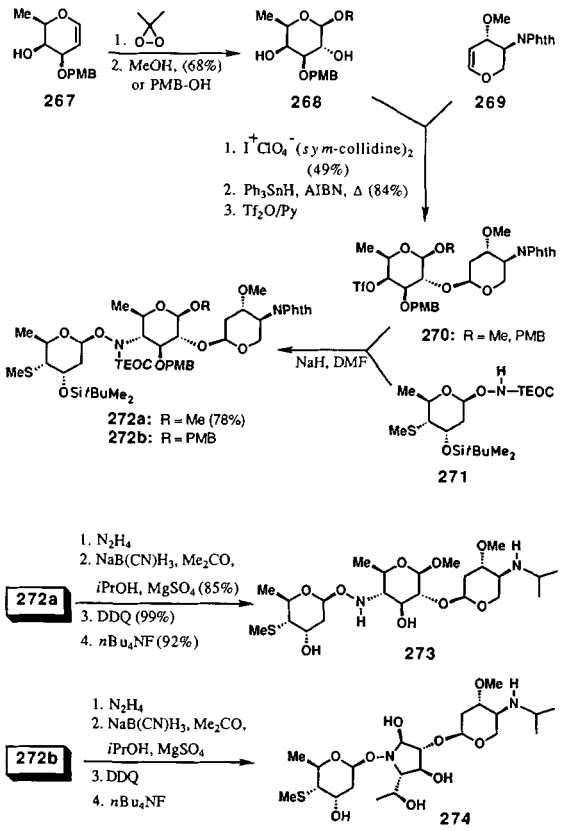

Scheme 55. The Danishefsky synthesis of the core trisaccharide fragment **273** of esperamicin (1991). AIBN = azodiisobutyronitrile. TEOC = $Me_3Si(CH_2)_2OC(O)$–

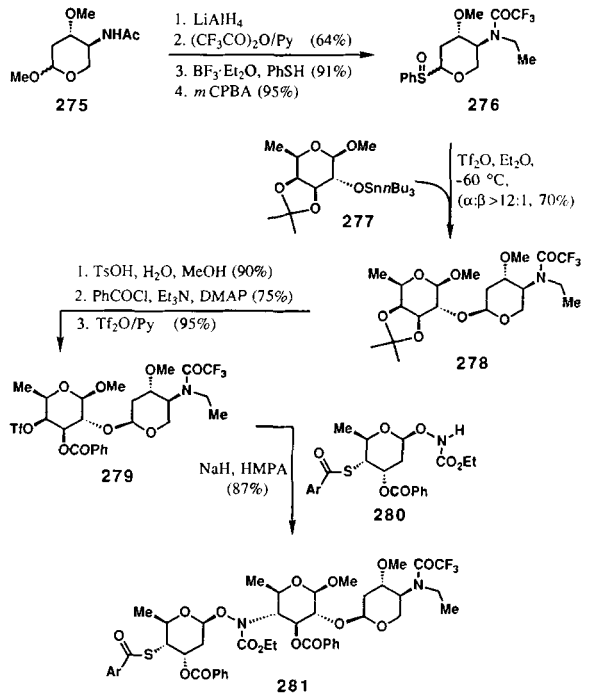

Scheme 56. The Kahne synthesis of the calicheamicin/esperamicin core trisaccharide fragment **281** (1991).

3.3. Dynemicin A Model Systems

The elegance and challenging nature of the dynemicin A structure combined with its potent antitumor and antibiotic

activity prompted immediate response from the synthetic chemistry community. We decided to pursue the design, synthesis, and study of models for dynemicin A in order to gain further insight into the mechanism of action of this fascinating molecule and to pave the way for an eventual total synthesis as well as to lay the foundations for the development of biotechnological tools and therapeutic agents.

The model system **282** was initially designed[120, 121] for its simplicity and flexibility to generate a library of related structures. It was traced retrosynthetically as outlined in Scheme 57, to tetrahydrophenanthridine **283.** The synthetic strategy

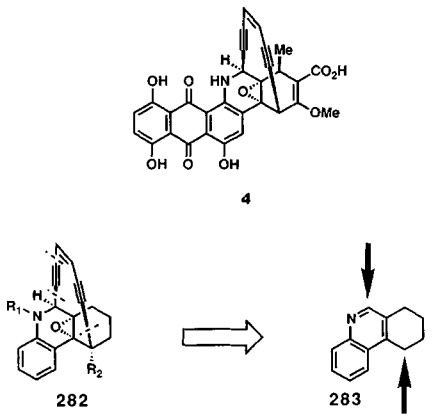

Scheme 57. Strategic bond disconnections and retrosynthetic analysis of the dynemicin model compounds **282** (*Nicolaou* et al., 1990). The positions to be activated in **283** are indicated by arrows.

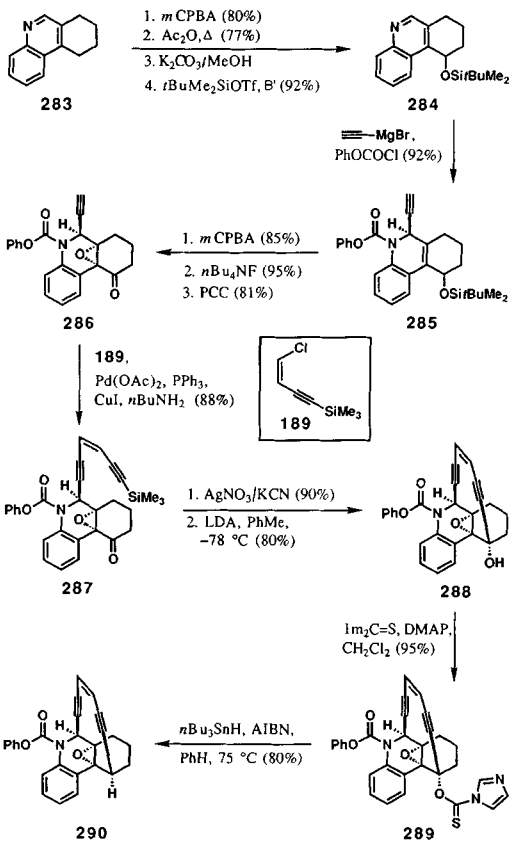

Scheme 58. Synthesis of dynemicin A model systems **288**–**290** (*Nicolaou* et al., 1990). PCC = pyridinium chlorochromate, LDA = lithium diisopropylamide.

for its construction is summarized in Scheme 58.[120, 121] Highlights of this synthesis include: a) the functionalization of the tetrahydrophenanthridine ring (**283** → **284** and **284** → **285**); b) the palladium-catalyzed construction of the enediyne moiety (**286** → **287**); c) the intramolecular acetylide–ketone condensation to close the ten-membered ring; and d) the radical-induced deoxygenation step (**289** → **290**). The structures of both **288** and **290** were confirmed by X-ray crystallographic analysis revealing interesting geometrical parameters. Figure 13 shows the ORTEP drawing of **290** and lists some of these

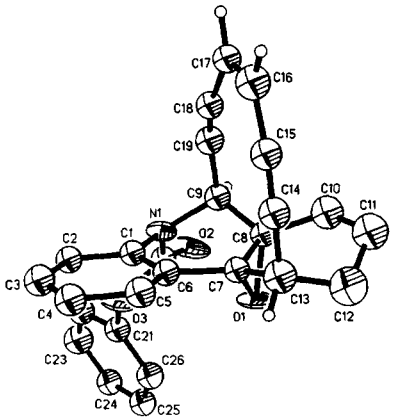

Fig. 13. Structure of **290** in the crystal. $c \cdots d$ distance ($r_{C_{14}-C_{19}}$) = 3.59 Å. Angles at the sp carbon atoms: C14 163.7, C15 170.1, C18 170.2, C19 162.0°.

parameters. Figure 14 shows computer-generated space-filling models of compounds **290** and its target, DNA.

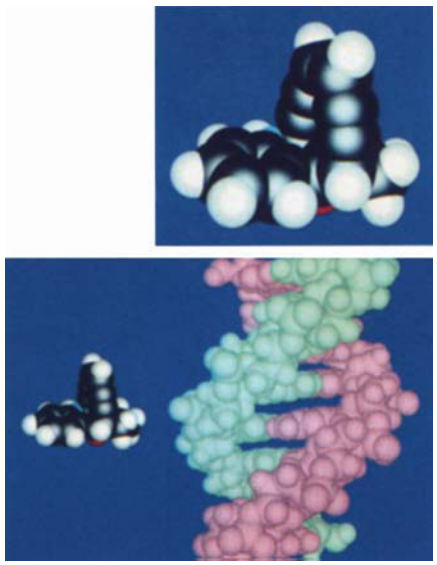

Fig. 14. Computer-generated models of free **290** (top) and of **290** on approaching DNA (bottom).

The chemistry of these dynemicin A model systems proved to be quite fascinating.[120, 121] Thus, upon triggering with acid, the hydroxy compound **288** entered the reaction cascade shown in Scheme 59, involving: a) epoxide opening leading to **292a** [calculated $c \cdots d$ distance = 3.19 Å]; b) Berg-

man cycloaromatization to give **293**; and c) spontaneous pinacol rearrangement under the reaction conditions furnishing ketone **294**. It is interesting to speculate about the timing of the bond migration leading to ring construction, in relation to the cascade coordinate, and whether the sequence includes structure **295**. Blocking the final rearrangement step (R = H or OAc) results in the isolation of structures **293b–e** (Scheme 59).[120, 121]

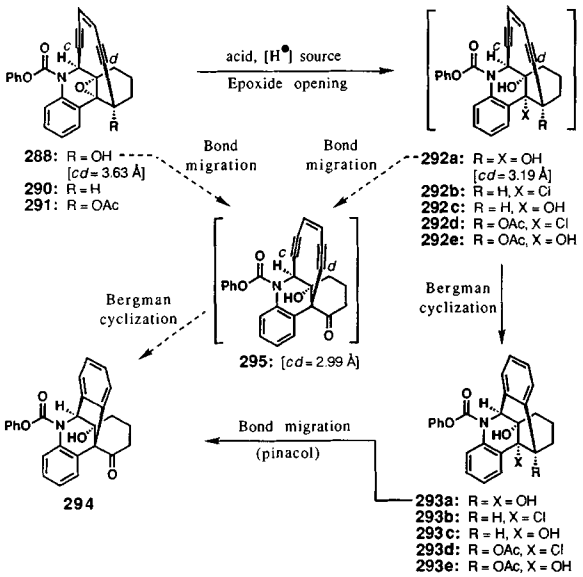

Scheme 59. Chemistry of dynemicin A model systems. Triggering the Bergman cyclization/pinacol rearrangement cascade (*Nicolaou* et al., 1990–1991).

An organometallic-based mode of triggering the dynemicin A cascade was devised as shown in Scheme 60.[121] This pathway was designed so as to prevent the enediyne unit from spontaneously collapsing to a benzenoid diradical upon epoxide opening and allow isolation of the postulated resulting *cis*-diol in the form of its cobalt complex. Accordingly, the cobalt complex **296** was prepared from **288**.[121] Surprisingly, acid treatment of **296** led to the highly strained compound **297** in which epoxide opening had apparently

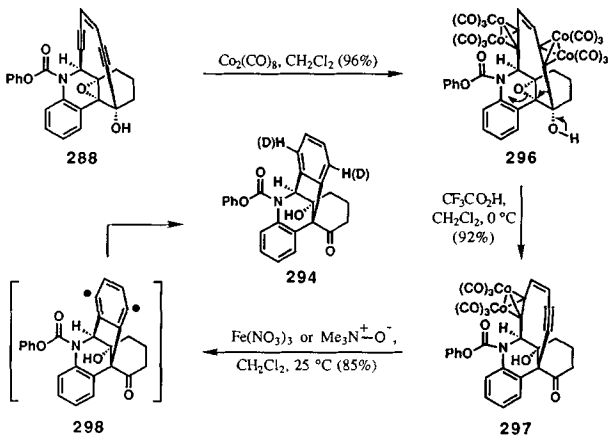

Scheme 60. Synthesis and chemistry of cobalt complexes of dynemicin A model systems. Triggering of Bergman cyclization by decomplexation (*Nicolaou* et al., 1991).

been accompanied by bond migration–ring contraction and regiospecific loss of one of the cobalt groups.[121] Structure **297** was supported by X-ray crystallographic analysis of its acetate derivative which revealed some interesting topological data (Fig. 15). As expected, oxidative decomplexation of

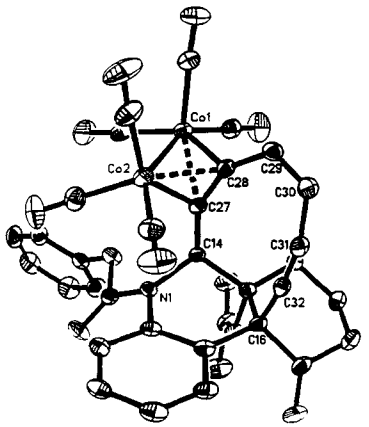

Fig. 15. Structure of the acetyl derivative of **297** in the crystal. Hydrogen atoms are omitted for clarity. $c \cdots d$ distance ($r_{C_{27}-C_{32}}$) = 3.08 Å. Angles at the sp carbon atoms: C27 151.7, C28 151.1, C31 158.3, C32 166.8°.

297 precipitated spontaneous Bergman cyclization leading to product **294** via the presumed nine-membered enediyne **295** (Scheme 59) and diradical **298** (Scheme 60).[121]

Recent work from our laboratories[60] resulted in a number of second generation enediyne systems of the dynemicin type, equipped with acid-, base-, and photo-sensitive trigger-

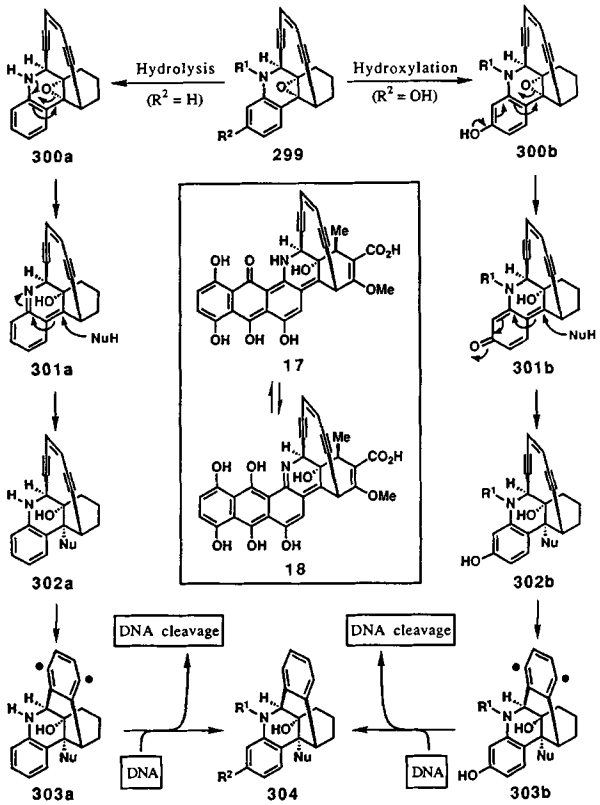

Scheme 61. Simulation of the dynemicin cascade by model compounds (*Nicolaou* et al., 1991).

ing devices. The designed structures (**299**) were considered as candidates for laboratory simulation of the two cascade scenarios shown in Scheme 61 under mild conditions. These two sequences involving iminoquinone methide species **301 a** (related to the dynemicin-derived species **18**, Schemes 11 and 61) or quinone methide species **301 b** (related to the dynemicin-derived species **17**, Schemes 11 and 61) may, in fact be initiated in vivo by enzymatic action and are, therefore, of value in the design of potential prodrugs.

The enediyne system **306** was designed so as to allow easy access to the parent compound **300 a**. Its preparation and conversion to **300 a** are shown in Scheme 62.[60] The parent

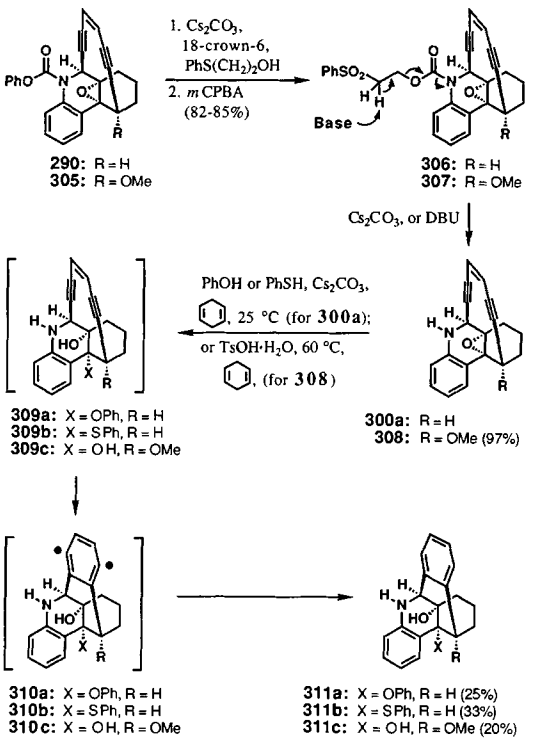

Scheme 62. Chemistry of dynemicin A model systems. Triggering the dynemicin cascade with base or acid (*Nicolaou* et al., 1991).

enediyne **300 a** proved too labile for isolation but its reactivity and ability to cleave DNA (see Figs. 17 and 18) support the notion of the involvement of path a (Scheme 11) and the

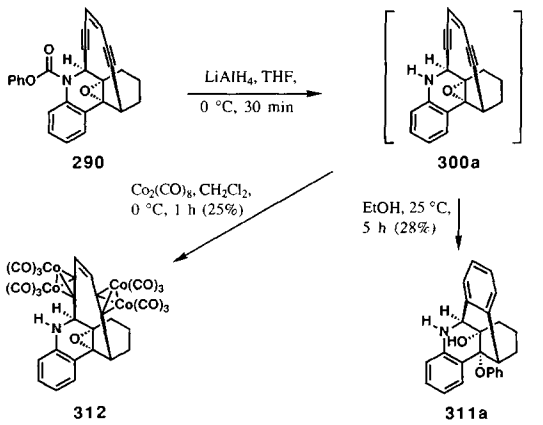

Scheme 63. Chemistry of dynemicin A model systems. Triggering the dynemicin cascade by reduction (*Nicolaou* et al., 1991).

participation of an *ortho*-iminoquinone methide species in the dynemicin A cascade at least as a partially contributing pathway. The structure of **300 a**, which was also generated in solution by LAH reduction of **290** (Scheme 63), was deduced from a number of trapping experiments as summarized in Schemes 62[60] and 63.[121] In contrast to **300 a**, the methoxy compound **308** (Scheme 62) proved to be a stable, crystalline solid. Its structure was confirmed by X-ray crystallographic analysis (Fig. 16) and under acidic conditions **308** followed the expected dynemicin-type cascade (Scheme 62).

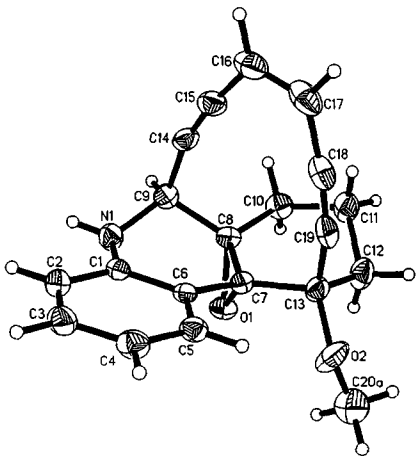

Fig. 16. Structure of **308** in the crystal. $c \cdots d$ distance ($r_{C_{14}-C_{19}}$) = 3.63 Å. Angles at sp carbon atoms: C14 163.2, C15 173.0, C18 169.3, C19 160.5°.

The enediyne model system **313** (Scheme 64) was designed and synthesized[60] for its potential to generate species **314** upon photolysis. Indeed, irradiation of **313** resulted in its clean conversion to **314** as detected by TLC and ^1H NMR spec-

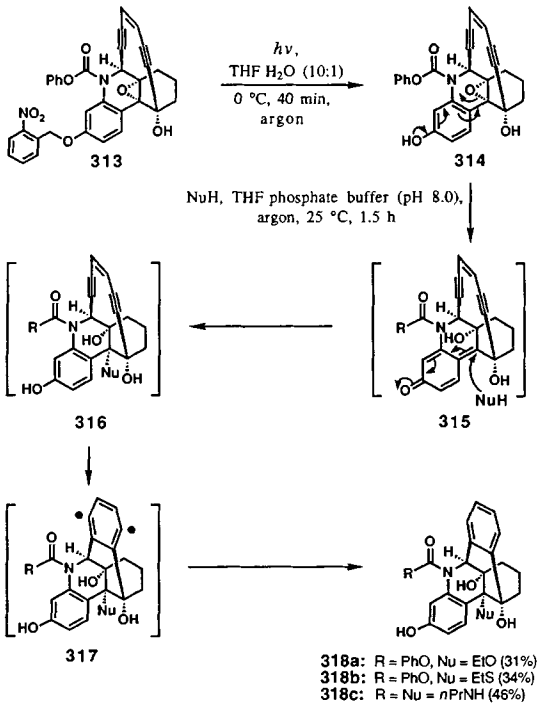

Scheme 64. Chemistry of dynemicin A model systems. Triggering the dynemicin cascade by photo-deprotection (*Nicolaou* et al., 1991).

troscopy. Attempted isolation of **314** led to decomposition, whereas treatment of crude **314** with nucleophiles (e.g. EtOH, EtSH, nPrNH$_2$) furnished the aromatized products **318a–c** as shown in Scheme 64. Interesting observations in these experiments include the isolation of the novel quinone–epoxide structure **319** (Scheme 65) from the reaction with ethanol in air (along with **318a**) as a sensitive but stable molecule under neutral conditions. The isolation of **319** provides support for the intermediacy of quinone methide **315** (Scheme 64), which when trapped with oxygen could provide **319**. Equally remarkable was the isolation of **321** and **322** as stable molecules upon treatment of **320** with O_2 (Scheme 65).

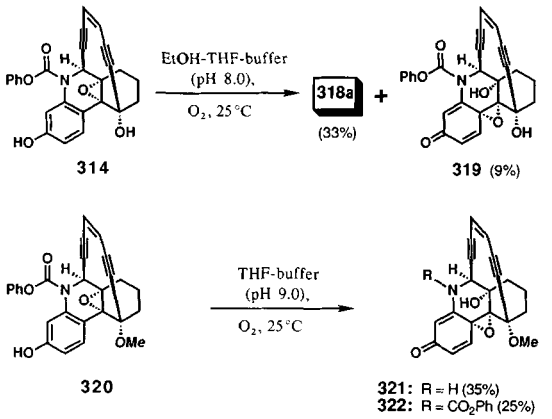

Scheme 65. Chemistry of dynemicin A model systems. Trapping quinone methide intermediates by molecular oxygen (*Nicolaou* et al., 1991).

The pivaloate protected enediyne systems **323** and **324** (Scheme 66) were also synthesized[60] for their potential to liberate phenolic species under basic conditions, thus presenting yet another triggering mechanism to initiate the dynemicin A cascade. Not surprisingly, exposure of **323** and **324**

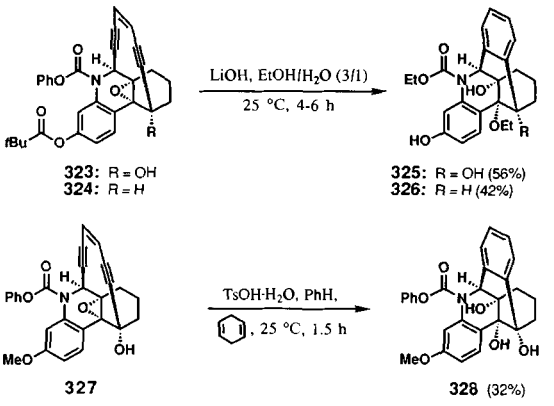

Scheme 66. Chemistry of dynemicin A model systems. Triggering the dynemicin cascade with base or acid (*Nicolaou* et al., 1991).

to lithium hydroxide in aqueous ethanol resulted in the formation of compounds **325** and **326**, respectively, via benzenoid diradicals and concomitant carbamate exchange (PhO → EtO, Scheme 64). The methoxy compound **327** was found to be reasonably stable under neutral and basic conditions but cyclized rapidly under acidic conditions to give aromatized product **328** (Scheme 66) as expected.

Molecules **300a**, **314**, and **319** caused significant DNA cleavage when incubated with supercoiled ΦX174 DNA (Fig. 17 and 18).[60, 121] Noteworthy in these experiments is the

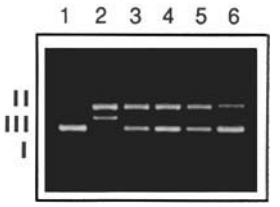

Fig. 17. DNA cleavage by **300a**. ΦX174 form I DNA (50 μM/base pair) was incubated for 12 h at 37 °C with **300a** (in 20% THF in phosphate buffer, pH 7.4, 50 μM) and analyzed by electrophoresis (1% agarose gel, ethidium bromide stain). Lane 1: DNA control; lanes 2–6: DNA + 5000, 2000, 1000, 500, and 100 μM of **300a**, respectively.

observation of both single and double strand cuts, as is the case with dynemicin A.[50, 51] As expected from their chemical profiles, the methoxy compounds **308**, **320**, **321**, and **322** exhibited diminished activity against DNA.[60] The potency of these DNA-cleaving molecules is expected to increase by attaching them to suitable DNA-binding moieties.

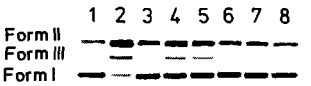

Fig. 18. DNA cleavage by dynemicin A model compounds. ΦX174 form I DNA (50 μM/base pair) was incubated for 24 h at 37 °C with **300a**, **308**, **314**, **319**, **320**, **321**, or **322** in buffer (50 mM Tris/HCl, pH 8.0) and analyzed by electrophoresis (1% agarose gel, ethidium bromide stain). Lane 1: DNA control; lane 2: DNA + 5 mM **300a**; lane 3: DNA + 5 mM **308**; lane 4: DNA + 5 mM **314**; lane 5: DNA + 5 mM **319**; lane 6: DNA + 5 mM **320**; lane 7: DNA + 5 mM **321**; lane 8: DNA + 5 mM **322**.

These studies provided support for the viability of both paths a and b of Schemes 11 and 61 as triggering mechanisms for the dynemicin A cascade by demonstrating that a lone pair of electrons on a heteroatom (nitrogen or oxygen) strategically positioned on the aromatic ring in relation to the epoxide moiety serves well to initiate the Bergman cyclization reaction. Such reactive species may be generated within cells from natural or designed molecules of the enediyne type, or as discussed above, be released from suitable precursors in the laboratory under mild conditions. Furthermore, the observation and relative stability of certain intermediates in these studies is intriguing in that it allows for the possibility of bioreduction prior to intercalation as well as a nucleophilic attack by a DNA base on a quinone methide and/or an *ortho*-iminoquinone methide species such as **17** and/or **18** (tautomeric structures, see Scheme 11). Thus, the proposition[51] that dynemicin A **4** may be interacting with DNA by a dual mechanism (nucleophilic and radical) appears attractive, not only because of the observed preference[50, 51] for cleavage at adenine and guanine but also in light of the chemistry of **314** (Scheme 64).[60]

A number of hybrid molecules between the dynemicin A model system **334** (Scheme 67) and potential DNA binding moieties were recently synthesized in our laboratories.[122] Scheme 67 summarizes the construction[122] of the two diastereomeric, enatiomerically pure hybrids **338a** and **338b** containing a dynemicin A enediyne model system and the AE disaccharide segment of calicheamicin γ_1^I **2**. The highlights of this technology include a stereoselective glycosidation using Schmidt's trichloroacetimidate method[123] (**333** + **334** → **335a, b**, Scheme 67) and a highly efficient and stereoselec-

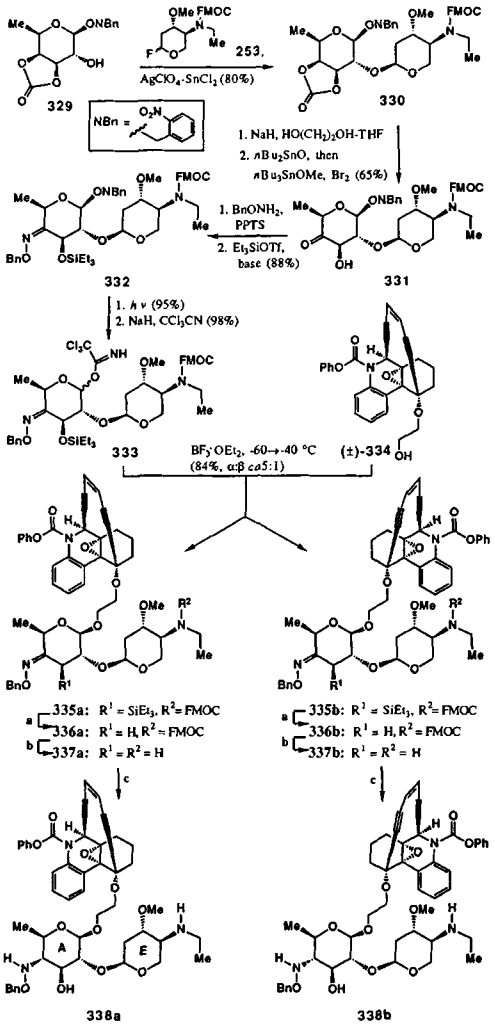

Scheme 67. Synthesis of calicheamicin–dynemicin model hybrid structures (*Nicolaou* et al., 1991). a: HF · Py (98 %); b: Et_2NH (98 %); c: $Ti(OiPr)_4$, Ph_2SiH_2 (90 %).

tive reduction of the C=N bond with $Ti(OiPr)_4/Ph_2SiH_2$ (**337a, b** → **338a, b**, Scheme 67).[122] In addition to providing these novel compounds, this chemistry demonstrated potential synthetic technology for the coupling of the carbohydrate and aglycone fragments of the calicheamicins and esperamicins.

Aiming for higher binding constants, we designed and synthesized hybrid structures **339** and **340** (Scheme 68).[124] These molecules, containing anthraquinone and distamycin units as respective intercalating and minor groove binding moieties, as well as the oligosaccharide-containing hybrids

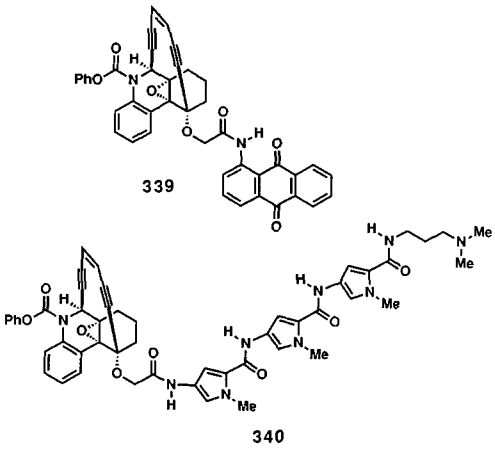

Scheme 68. Hybrid structures of dynemicin A model compound and DNA binding molecules (*Nicolaou* et al., 1990).

discussed above and other recently synthesized molecules are currently under investigation in our laboratories with regard to their biological activity and molecular recognition profiles. Figure 19 shows computer-generated space-filling models of these compounds and their target, DNA.

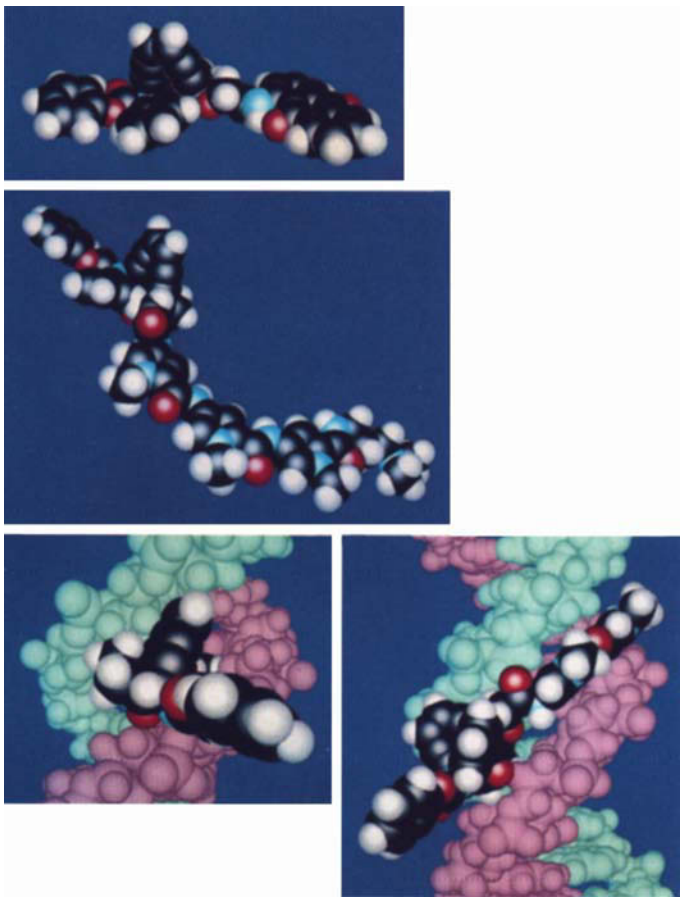

Fig. 19. Computer-generated models of the compounds **339** (top) and **340** (center) and DNA-bound **339** (bottom right) and **340** (bottom left).

Wender's group has recently published[125] the dynemicin A model studies summarized in Scheme 69.

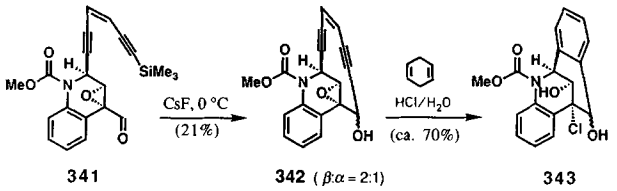

Scheme 69. The Wender synthesis of dynemicin A model compounds (1991).

Schreiber et al.[126] have been able to apply their enediyne intramolecular Diels–Alder approach to the synthesis of the dynemicin A model system **352** (Scheme 70). In addition to the ring skeleton assembly, interesting points in this elegant synthesis include: a) a regioselective allylic oxidation (**349** → **350**); b) a stereospecific hydride delivery with concomitant S_N2' displacement of a hydroxyl group (**350** → **351**); and c) a chemoselective epoxidation (**351** → **352**). *Schreiber*'s group has also recently reported[127] a synthesis of an anthraquinone subunit of dynemicin A.

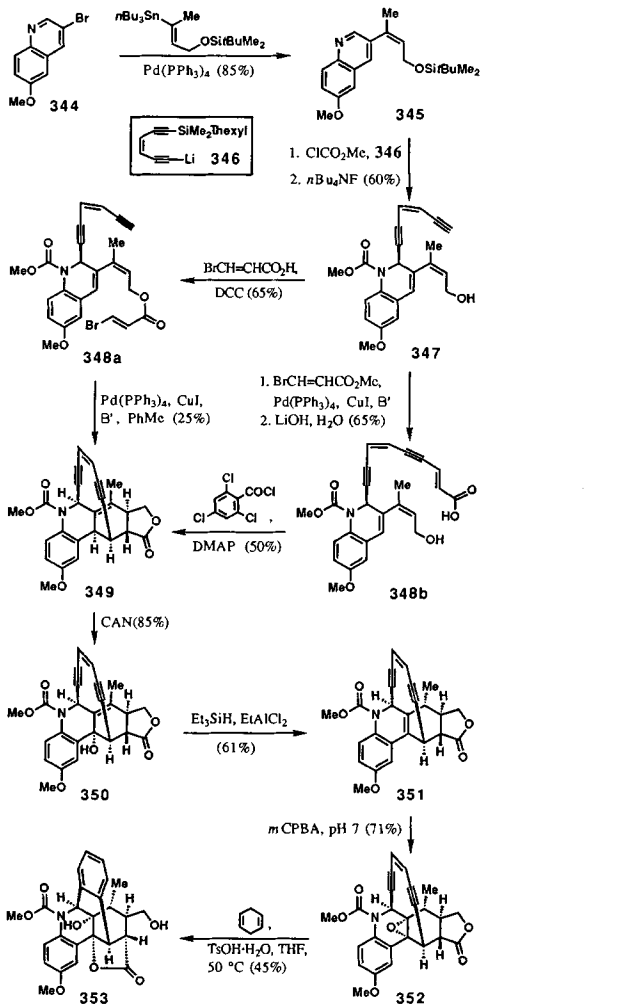

Scheme 70. The Schreiber synthesis of dynemicin A model compounds (1990). DCC = dicyclohexylcarbodiimide, CAN = cerium ammonium nitrate.

Magnus et al. synthesized[128] and studied the core tetrahydroquinoline diynene structure **358** utilizing a cobalt acetylene complex as a precursor as summarized in Scheme 71.

Model studies by *Isobe* et al.[129] with open enediynes related to dynemicin A have recently been published.

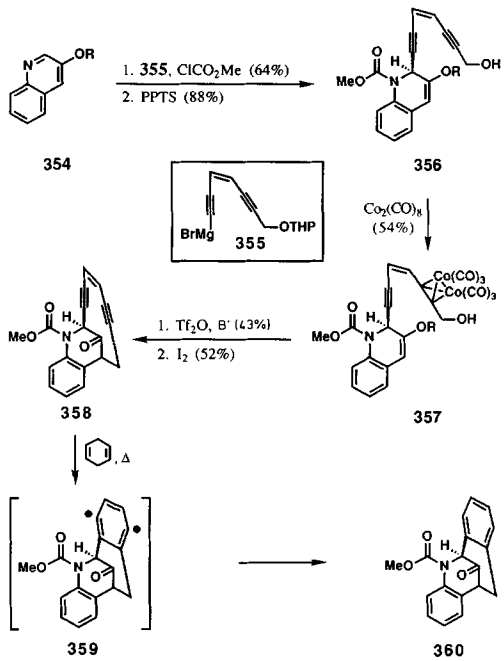

Scheme 71. The Magnus synthesis of dynemicin A model compound **358** (1991). THP = tetrahydropyranyl; R = $SiBuMe_2$.

4. Theoretical Studies

The fascinating enediyne structures did not fail to attract the attention of theorists. Extending the initial, first approximation attempts to correlate the distance between the remote acetylenic carbons and reactivity in simple acyclic and monocyclic enediynes, *Snyder*[130] carried out broader calculations linking reactivity in monocyclic and polycyclic enediynes with molecular strain in the ground and transition states. *Snyder* also described a quantum mechanical model for the cycloaromatization of a number of calicheamicin/esperamicin models[131] and evaluated two distinct pathways of dynemicin A activation involving acid-catalyzed epoxide opening and quinone methide formation.[132] *Semmelhack* et al. also reported[59] on the mechanism of action of dynemicin A with supportive calculations on $c \cdots d$ distances.

Koga and *Morokuma*[133] compared the energetics of the Bergman (enediyne) and Myers (enyne–allene) cyclizations and found that the enyne–allene reaction is more exothermic and is associated with a lower activation energy than the enediyne process, consistent with experimental data.

It is certain that these systems will stimulate many more theoretical studies in the years to come.

5. Concluding Remarks

With their unprecented molecular stuctures, fascinating mode of action, and phenomenal biological activities, the enediyne anticancer antibiotics have excited the creative im-

pulses and imagination of many researchers and thus established a vibrant field of investigations. Research in this rapidly evolving field spans areas from computational chemistry, molecular design, chemical synthesis, molecular recognition, DNA chemistry, and medicine.

Rarely before has a newly discovered class of natural products created such stimulation and excitement in chemistry, biology, and medicine as the enediynes. Equally rare is the beauty and fascination associated with the molecular architecture and mode of action of these naturally occurring substances. The opportunities they offer for challenging and creative scientific endeavors may be overshadowed only by their potential therapeutic and biotechnological applications. It is, therefore, not surprising that so much exciting science could be written in this first comprehensive review of the subject, even though the field is only about four years old. Judging from the present momentum driven by their promise as targets of opportunity, these structures are sure to occupy the minds of an increasing number of investigators in academia and industry. It is certain that shortly a number of these formidable synthetic targets will be conquered and that some of them or their analogs may even be in the hands of clinicians before too long. No doubt many more pages will be needed to cover the entire field a few years from now.

A comparison of the enediynes with the β-lactams, the macrolides, and the polyether antibiotics may well be appropriate. In terms of their chemistry, the enediynes compare well with the very best nature has shown us so far. With regard to medical applications, an affirmative prediction may seem at present too daring. But one should remember that fertile ground combined with persistent cultivation often bring forth a good harvest.

Finally, this topic serves as a reminder to us of the beauty of the natural products and their value in opening up new fields of investigation. Who can deny in this instance, nature's "pioneering" role in this area of research even though, in principle, man could have done it all! The molecules of nature are still serving as initiating sparks and guiding lights, which when followed with wisdom and modern ideas may result in highly satisfying and rewarding scientific endeavors. Natural products synthesis and related chemistry, when pursued wisely with the proper perspective and with the right blend of originality and imagination, will remain a valid and exciting practice for a long time to come.

Addendum (October 1, 1991)

After submission of the original manuscript several articles have appeared in the literature. These works are briefly mentioned below under the appropriate sections where they should be inserted.

Section 2.1.:

A review article on the mechanism of action of the neocarzinostatin chromophore has recently appeared.[134] The protein/chromophore complex of neocarzinostatin was examined by 2D-NMR spectroscopy.[135]

Section 2.2.:

A review article on all aspects of calicheamicins has recently appeared.[136] Hydrophobic interaction of calicheamicin γ_1^I with DNA has been suggested and studied using inorganic salts and temperature variations to probe the rate of DNA cleavage and binding.[137] DNA cleavage by esperamicins, calicheamicin γ_1^I, and DNase I has been compared showing that single strand action predominates in the case of esperamicin A_1 and DNase, whereas esperamicin C and calicheamicin γ_1^I operate mainly through double-strand cleavage.[138] The action of calicheamicin γ_1^I on the ataxia-telangiectasia derived cell lines has been studied.[139]

Section 2.3.:

Based on energy minimizations and molecular dynamics techniques, a model for dynemicin A has been proposed and and its absolute stereochemistry was deduced from this model [2*S*, 3*S*, 4*S*, 7*R*, 8*R*].[140]

Section 3.1.:

Seco dienediyne compounds related to the neocarzinostatin chromophore have been prepared via Pd(0)–Cu(I) mediated coupling reactions of bis(enoltriflate) intermediates with alkynes.[141, 142]

Section 3.2.:

A Cr(II)–Ni(II) mediated ring closure reaction was utilized to construct simple 10- and 11-membered ring enediynes.[143] A sulfur-containing 10-membered ring enediyne has been synthesized and studied.[144] An oxidative formation of an enediyne unit from a 1,5-diyne precursor demonstrating a new triggering device for the in situ generation of the enediyne moiety has been published.[145]

Section 3.3.:

Two new dynemicin A model systems have been reported.[146]

We wish to thank our many talented and motivated collaborators without the contributions of whom this article could not have been written: A. L. Smith, C.-K. Hwang, P. Maligres, G. Skokotas, S. V. Wendeborn, R. D. Groneberg, N. A. Stylianides, W. Stahl, E. P. Schreiner, S. Furuya, T. Miyazaki, G. Zuccarello, Y. Ogawa, K. Toshima, Y. Torisawa, J. Shin, E. De Leon, D. Rideout, H. Suemune, E. J. Schweiger, D. C. Nicolaou. We thank Janise Petrey for her speedy typing and patience, and Professors Reza Ghadiri, C.-H. Wong and Richard Lerner for useful discussions. Thanks are also due to Professors S. J. Danishefsky (Yale), P. Magnus (Texas) and D. Kahne (Princeton) for kindly providing us with some of their results prior to publication. In acknowledging financial support for the work described in this article we extend our gratitude and many thanks to the following: The National Institutes of Health (USA), the National Science Foundation (USA), Merck Sharp & Dohme (USA), Smith Kline Beecham (USA), Hoffmann-LaRoche (USA), Glaxo (USA), Lederle Laboratories (USA), Takeda Co. (Japan), Ono Pharmaceutical Co. (Japan), Sanraku Co. (Japan), Johnson & Johnson (USA), the Humboldt Foundation (FRG), the SERC-NATO (UK), and the Fonds der Chemischen Industrie (FRG).

Received: May 14, 1991 [A 841 IE]
German version: *Angew. Chem. 103* (1991) 1453

[1] K. Edo, M. Mizugaki, Y. Koide, H. Seto, K. Furihata, N. Otake, N. Ishida, *Tetrahedron Lett. 26* (1985) 331.
[2] M. D. Lee, T. S. Dunne, M. M. Siegel, C. C. Chang, G. O. Morton, D. B. Borders, *J. Am. Chem. Soc. 109* (1987) 3464; M. D. Lee, T. S. Dunne,

C. C. Chang, G. A. Ellestad, M. M. Siegel, G. O. Morton, W. J. McGahren, D. B. Borders, *ibid. 109* (1987) 3466.
[3] J. Golik, J. Clardy, G. Dubay, G. Groenewold, H. Kawaguchi, M. Konishi, B. Krishnan, H. Ohkuma, K. Saitoh, T. W. Doyle, *J. Am. Chem. Soc. 109* (1987) 3461; J. Golik, G. Dubay, G. Groenewold, H. Kawaguchi, M. Konishi, B. Krishnan, H. Ohkuma, K. Saitoh, T. W. Doyle *ibid. 109* (1987) 3462.
[4] M. Konishi, H. Ohkuma, K. Matsumoto, T. Tsuno, H. Kamei, T. Miyaki, T. Oki, H. Kawaguchi, G. D. VanDuyne, J. Clardy, *J. Antibiot. 42* (1989) 1449.
[5] a) R. R. Jones, R. G. Bergmann, *J. Am. Chem. Soc. 94* (1972) 660; b) R. G. Bergman, *Acc. Chem. Res. 6* (1973) 25; c) T. P. Lockhart, P. B. Comita, R. G. Bergman, *J. Am. Chem. Soc. 103* (1981) 4082; d) T. P. Lockhart, R. G. Bergman, *ibid. 103* (1981) 4091.
[6] N. Darby, C. U. Kim, J. A. Salaün, K. W. Shelton, S. Takada, S. Masamune, *Chem. Commun. 1971*, 1516.
[7] H. N. C. Wong, F. Sondheimer, *Tetrahedron Lett. 21* (1980) 217.
[8] J. Mayer, F. Sondheimer, *J. Am. Chem. Soc. 88* (1966) 602.
[9] N. Ishida, K. Miyazaki, K. Kumagai, M. Rikimaru, *J. Antibiot. 18* (1965) 68.
[10] M. A. Napier, B. Holmquist, D. J. Strydom, I. H. Goldberg, *Biochem. Biophys. Res. Commun. 89* (1979) 635.
[11] a) W. Koide, F. Ishii, K. Hasuda, Y. Koyama, K. Edo, S. Katamine, F. Kitame, N. Ishida, *J. Antibiot. 33* (1980) 342; b) H. Suzuki, K. Miura, K. Kumada, T. Takeuchi, N. Tanake, *Biochem. Biophys. Res. Commun. 94* (1980) 225.
[12] M. A. Napier, L. S. Kappen, I. H. Goldberg, *Biochemistry 19* (1980) 1767.
[13] L. S. Kappen, M. A. Napier, I. H. Goldberg, *Proc. Natl. Acad. Sci. USA 77* (1980) 1970.
[14] L. F. Povirk, I. H. Goldberg, *Biochemistry 19* (1980) 4773.
[15] G. Jung, W. Köhnlein, *Biochem. Biophys. Res. Commun. 98* (1981) 176.
[16] L. F. Povirk, I. H. Goldberg, *Biochemistry 23* (1984) 6304.
[17] L. S. Kappen, I. H. Goldberg, *Nucleic Acids Res. 5* (1978) 2959.
[18] Y. Uesawa, J. Kuwahara, Y. Sugiura, *Biochem. Biophys. Res. Commun. 164* (1989) 903.
[19] A. G. Myers, *Tetrahedron Lett. 28* (1987) 4493.
[20] A. G. Myers, P. J. Proteau, T. M. Handel, *J. Am. Chem. Soc. 110* (1988) 7212.
[21] A. G. Myers, P. J. Proteau, *J. Am. Chem. Soc. 110* (1989) 1146.
[22] O. D. Hensens, I. H. Goldberg, *J. Antibiot. 42* (1989) 761.
[23] L. F. Povirk, N. Dattagupta, B. C. Warf, I. H. Goldberg, *Biochemistry 20* (1981) 4007.
[24] S. H. Lee, I. H. Goldberg, *Biochemistry 28* (1989) 1019.
[25] I. H. Goldberg, *Free Radicals Biol. Med. 3* (1987) 41.
[26] A. G. Myers, (Pasadena, CA, USA), private communication.
[27] L. S. Kappen, I. H. Goldberg, *Biochemistry 22* (1983) 4872.
[28] D. H. Chin, L. S. Kappen, I. H. Goldberg, *Proc. Natl. Acad. Sci. USA 84* (1987) 7070.
[29] L. S. Kappen, I. H. Goldberg, S. H. Wu, J. Stubbe, L. Worth, Jr., J.W. Kozarich, *J. Am. Chem. Soc. 112* (1990) 2797.
[30] L. S. Kappen, I. H. Goldberg, B. L. Frank, L. Worth, Jr., D. F. Christner, J. W. Kozarich, J. Stubbe, *Biochemistry 30* (1991) 2034, and references cited therein.
[31] I. Saito, H. Kawabata, T. Fujiwara, H. Sugiyama, T. Matsuura, *J. Am. Chem. Soc. 111* (1989) 8302.
[32] B. L. Frank, L. Worth, Jr., D. F. Christner, J. W. Kozarich, J. Stubbe, L. S. Kappen, I. H. Goldberg, *J. Am Chem. Soc. 113* (1991) 2271.
[33] O. D. Hensens, J.-L. Giner, I. H. Goldberg, *J. Am. Chem. Soc. 111* (1989) 3295.
[34] M. D. Lee, J. K. Manning, D. R. Williams, N. Kuck, R. T. Testa, D. B. Borders, *J. Antibiot. 42* (1989) 1070; W. M. Maiese, M. P. Lechevalier, H. A. Lechevalier, J. Korshalla, N. A. Kuck, A. Fantini, M. J. Wildey, J. Thomas, M. Greenstein, *ibid. 42* (1989) 558.
[35] N. Zein, A. M. Sinha, W. J. McGahren, G. A. Ellestad, *Science 240* (1988) 1198.
[36] N. Zein, M. Poncin, R. Nilakantan, G. A. Ellestad, *Science 244* (1989) 697.
[37] J. J. De Voss, C. A. Townsend, W.-D. Ding, G. O. Morton, G. A. Ellestad, N. Zein, A. B. Tabor, S. L. Schreiber, *J. Am. Chem. Soc. 112* (1990) 9669.
[38] S. Walker, K. G. Valentine, D. Kahne, *J. Am. Chem. Soc. 112* (1990) 6428.
[39] J. Drak, N. Iwasawa, S. Danishefsky, D. M. Crothers, *Proc. Natl. Acad. Sci. USA 88* (1991) 7464.
[40] G. A. Ellestad, P. R. Hamann, N. Zein, G. O. Morton, M. M. Siegel, M. Pastel, D. B. Borders, W. J. McGahren, *Tetrahedron Lett. 30* (1989) 3033.
[41] K. C. Nicolaou, G. Zuccarello, Y. Ogawa, E. J. Schweiger, T. Kumazawa, *J. Am. Chem. Soc. 110* (1988) 4866.
[42] N. Zein, W. J. McGahren, G. O. Morton, J. Ashcroft, G. A. Ellestad, *J. Am. Chem. Soc. 111* (1989) 6888.
[43] J. J. De Voss, J. J. Hangeland, C. A. Townsend, *J. Am. Chem. Soc. 112* (1990) 4554.
[44] Drs. G. Ellestad und J. Upeslacis, Lederle Laboratories, NY, USA, private communication.
[45] M. Konishi, H. Ohkuma, K. Saitoh, H. Kawaguchi, J. Golik, G. Dubay, G. Groenewold, B. Krishnan, T. W. Doyle, *J. Antibiot. 38* (1985) 1605.
[46] J. Golik, H. Wong, D. M. Vyas, T. W. Doyle, *Tetrahedron Lett. 30* (1989) 2497.
[47] T. W. Doyle, J. Golik, H. Wong, K. S. Lam, D. Langley, S. Forenza, D. Vyas, S. Kelley in L. Baker, F. Valeriote, T. Corbett, (Eds.): *Proc. 22nd Ann. Cancer Symp. Anticancer Drug Discovery and Development-1*, Kluwer Acad. Publishers, Boston, MA, USA, in press.
[48] J. Golik, H.Wong, B. Krishnan, D. M. Vyas, T. W. Doyle, *Tetrahedron Lett. 32* (1991) 1851.
[49] J. Golik, T. W. Doyle, G. VanDuyne, J. Clardy, *Tetrahedron Lett. 31* (1990) 6149.
[50] B. H. Long, J. Golik, S. Forenza, B. Ward, R. Rehfuss, J. C. Dabrowiak, J. J. Catino, S. T. Musial, K. W. Brookshire, T. W. Doyle, *Proc. Natl. Acad. Sci USA 86* (1989) 2.
[51] Y. Sugiura, Y. Uesawa, Y. Takahashi, J. Kuwahara, J. Golik, T. W. Doyle, *Proc. Natl. Acad. Sci, USA 86* (1989) 7672.
[52] T. W. Doyle (Wallingford, CT, USA), private communication.
[53] M. Konishi, H. Ohkuma, T. Tsuno, T. Oki, G. D. VanDuyne, J. Clardy, *J. Am. Chem. Soc. 112* (1990) 3715.
[54] K. Shiomi, H. Iinuma, H. Naganawa, M. Hamada, S. Hattori, H. Nakamura, T. Takeuchi, Y. Iitaka, *J. Antibiot. 43* (1990) 1000.
[55] a) H. S. El Khadem (Ed.): *Anthracycline Antibiotics*, Academic Press New York 1982; b) T. R. Kelly (Ed.): *Recent Aspects in Anthracyclinone Chemistry (Tetrahedron Symposia-in-Print, Tetrahedron 40* (1980) 4537).
[56] Y. Sugiura, T. Shiraki, M. Konishi, T. Oki, *Proc. Natl. Acad. Sci. USA 87* (1990) 3831.
[57] T. Shiraki, Y. Sugiura, *Biochemistry 29* (1990) 9795.
[58] T. Shiraki, Y. Sugiura, *Nucleic Acids Res. Symp. Ser. 21* (1989) 53.
[59] M. F. Semmelhack, J. Gallagher, D. Cohen, *Tetrahedron Lett. 31* (1990) 1521.
[60] K. C. Nicolaou, W.-M. Dai, S. V. Wendeborn, A. L. Smith, Y. Torisawa, P. Maligres, C.-K. Hwang, *Angew. Chem. 103* (1991) 1034; *Angew. Chem. Int. Ed. Engl. 30* (1991) 1032.
[61] Y. Sugiura, T. Arakawa, M. Uesugi, T. Shiraki, H. Ohkuma, M. Konishi, *Biochemistry 30* (1991) 2989.
[62] A. G. Myers, E. Y. Kuo, N. S. Finney, *J. Am. Chem. Soc. 111* (1989) 8057.
[63] R. Nagata, H. Yamanaka, E. Okazaki, I. Saito, *Tetrahedron Lett. 30* (1989) 4995.
[64] R. Nagata, H. Yamanaka, E. Murahashi, I. Saito, *Tetrahedron Lett. 31* (1990) 2907.
[65] A. G. Myers, P. S. Dragovich, *J. Am. Chem. Soc. 111* (1989) 9130.
[66] A. G. Myers, P. M. Harrington, E. Y. Kuo, *J. Am. Chem. Soc. 113* (1991) 694; A. G. Myers, M. M. Alauddin, M. A. M. Fuhry, *Tetrahedron Lett. 30* (1989) 6997.
[67] K. C. Nicolaou, P. Maligres, J. Shin, E. de Leon, D. Rideout, *J. Am. Chem. Soc. 112* (1990) 7825.
[68] K. C. Nicolaou, G. Skokotas, S. Furuya, H. Suemune, D. C. Nicolaou, *Angew. Chem. 102* (1990) 1066; *Angew. Chem. Int. Ed. Engl. 29* (1990) 1064.
[69] A. M. Maxam, W. Gilbert, *Methods Enzymol. 65* (1980) 499; A. M. Maxam, W. Gilbert, *Proc. Natl. Acad. Sci. USA 74* (1977) 560.
[70] M. Hirama, K. Fujiwara, K. Shigematsu, Y. Fukazawa, *J. Am. Chem. Soc. 111* (1989) 4120.
[71] K. Fujiwara, A. Kurisaki, M. Hirama, *Tetrahedron Lett. 31* (1990) 4329.
[72] K. Fujiwara, H. Sakai, M. Hirama, *J. Org. Chem. 56* (1991) 1688.
[73] Review: K. F. Fujiwara, M. Hirama, *Gendai Kagaku 1990*, 14.
[74] K. Toshima, K. Ohta, T. Ohtake, K. Tatsuta, *Tetrahedron Lett. 32* (1991) 391.
[75] K. C. Nicolaou, G. Skokotas, P. Maligres, G. Zuccarello, E. J. Schweiger, K. Toshima, S. Wendeborn, *Angew. Chem. 101* (1989) 1255; *Angew. Chem. Int. Ed. Engl. 28* (1989) 1272.
[76] P. A. Wender, M. Harmata, D. Jeffrey, C. Mukai, J. Suffert, *Tetrahedron Lett. 29* (1988) 909.
[77] P. A. Wender, J. A. McKinney, C. Mukai, *J. Am. Chem. Soc. 112* (1990) 5369.
[78] Y. Okude, S. Hirano, T. Hiyama, H. Nozaki, *J. Am. Chem. Soc. 99* (1977) 3179; see also P. A. Wender, J. W. Grissom, U. Hoffmann, R. Mah, *Tetrahedron Lett. 31* (1990) 6605.
[79] Review: T. Nakai, K. Mikami, *Chem. Rev. 86* (1986) 885.
[80] T. Doi, T. Takahashi, *J. Org. Chem. 56* (1991) 3465.
[81] A. Krebs, T. Wehlage, C.-P. Kramer, *Tetrahedron Lett. 31* (1990) 3533.
[82] T. Wehlage, A. Krebs, T. Link, *Tetrahedron Lett. 31* (1990) 6625.
[83] J. Suffert, *Tetrahedron Lett. 31* (1990) 7437.
[84] K. Nakatani, K. Arai, N. Hirayama, F. Matsuda, S. Terashima, *Tetrahedron Lett. 31* (1990) 2323.
[85] P. Magnus, T. Pitterna, *J. Chem. Soc. Chem. Commun. 1991*, 541.
[86] M. Shibuya, K. Toyooka, S. Kubota, *Tetrahedron Lett. 25* (1984) 1171; K. Shishido, A. Yamashita, K. Hiroya, K. Fukumoto, T. Kametani, *Tetrahedron Lett. 30* (1989) 111; *Tetrahedron 45* (1989) 5791.
[87] P. Magnus, S. Fortt, T. Pitterna, J. P. Snyder, *J. Am. Chem. Soc. 112* (1990) 4986.
[88] a) R. Singh, G. Just, *Tetrahedron Lett. 31* (1990) 185; b) D. Guillerm, G. Linstrumelle, *ibid. 26* (1985) 3811.

[89] G. Zuccarello, Ph.D. Thesis, University of Pennsylvania 1990; K. C. Nicolaou, Y. Ogawa, G. Zuccarello, unpublished.
[90] K. C. Nicolaou, Y. Ogawa, G. Zuccarello, H. Kataoka, *J. Am. Chem. Soc. 110* (1988) 7247.
[91] P. J. Garratt, S. B. Neoh, *J. Org. Chem. 44* (1979) 2667; Y. S. P. Cheng, P. J. Garratt, S. B. Neoh, V. M. Rumjanek, *Isr. J. Chem. 26* (1985) 101.
[92] S. Braverman, D. Segev, *J. Am. Chem. Soc. 96* (1974) 1245; S. Braverman, Y. Duar, D. Segev, *Tetrahedron Lett. 1976,* 3181.
[93] K. C. Nicolaou, S. Wendeborn, P. Maligres, K. Isshiki, N. Zein, G. Ellestad, *Angew. Chem. 103* (1990) 462; *Angew. Chem. Int. Ed. Engl. 30* (1991) 418.
[94] M. P. Cabal, R. S. Coleman, S. J. Danishefsky, *J. Am. Chem. Soc. 112* (1990) 3253; J. N. Haseltine, M. P. Cabal, N. B. Mantlo, N. Iwasawa, D. S. Yamashita, R. S. Coleman, S. J. Danishefsky, G. K. Schulte, *J. Am. Chem. Soc., 113* (1991) 3850.
[95] J. N. Haseltine, S. J. Danishefsky, *J. Org. Chem. 55* (1990) 2576.
[96] S. J. Danishefsky, N. B. Mantlo, D. S. Yamashita, *J. Am. Chem. Soc. 110* (1988) 6890.
[97] J. N. Haseltine, S. J. Danishefsky, G. Schulte, *J. Am. Chem. Soc. 111* (1989) 7638; N. B. Mantlo, S. J. Danishefsky, *J. Org. Chem. 54* (1989) 2781.
[98] S. J. Danishefsky, D. S. Yamashita, N. B. Mantlo, *Tetrahedron Lett. 29* (1988) 4681.
[99] A. S. Kende, C. A. Smith, *Tetrahedron Lett. 29* (1988) 4217.
[100] P. Magnus, R. T. Lewis, J. C. Huffman, *J. Am. Chem. Soc. 110* (1988) 6921.
[101] P. Magnus, P. A. Carter, *J. Am. Chem. Soc. 110* (1988) 1626.
[102] P. Magnus, H. Annoura, J. Harling, *J. Org. Chem. 55* (1990) 1709.
[103] a) P. Magnus, R. T. Lewis, F. Bennett, *J. Chem. Soc, Chem. Commun. 1989*, 916; b) P. Magnus, F. Bennett, *Tetrahedron Lett. 30* (1989) 3637.
[104] P. Magnus, R. T. Lewis, *Tetrahedron Lett. 30* (1989) 1905.
[105] K. Tomioka, H. Fujita, K. Koga, *Tetrahedron Lett. 30* (1989) 851; see also J. F. Kadow, M. G. Saulnier, M. M. Tun, D. R. Langley, D. M. Vyas, *ibid. 30* (1989) 3499.
[106] S. L. Schreiber, L. L. Kiessling, *J. Am. Chem. Soc. 110* (1988) 631.
[107] S. L. Schreiber, L. L. Kiessling, *Tetrahedron Lett. 30* (1989) 433.
[108] F. J. Schoenen, J. A. Porco, Jr., S. L. Schreiber, *Tetrahedron Lett. 30* (1989) 3765.
[109] K. Suzuki, E. Katayama, G. Tsuchihashi, *Tetrahedron Lett. 24* (1983) 4997; K. Suzuki, T. Ohkuma, M. Miyazawa, G. Tsuchihashi, *ibid. 27* (1988) 373.
[110] K. C. Nicolaou, R. D. Groneberg, *J. Am. Chem. Soc. 112* (1990) 4086.
[111] K. C. Nicolaou, T. J. Caulfield, R. D. Groneberg, *Pure Appl. Chem. 63* (1991) 555.
[112] K. C. Nicolaou, R. D. Groneberg, T. Miyazaki, N. A. Stylianides, T. J. Shultze, W. Stahl. *J. Am. Chem. Soc. 112* (1990) 8193.
[113] K. C. Nicolaou, R. D. Groneberg, N. A. Stylianides, T. Miyazaki, *J. Chem. Soc. Chem. Commun. 1990,* 1275.
[114] K. C. Nicolaou, T. Ebata, N.A. Stylianides, R. D. Groneberg, P. J. Carrol, *Angew. Chem. 100* (1988) 1138; *Angew. Chem. Int. Ed. Engl. 27* (1988) 1097.
[115] M. D. Wittman, R. L. Halcomb, S. J. Danishefsky, *J. Org. Chem. 55* (1990) 1979.
[116] R. L. Halcomb, M. D. Wittman, S. H. Olson, S. J. Danishefsky, J. Golik, H. Wong, D.Vyas, *J. Am. Chem. Soc. 113* (1991) 5080.
[117] D. Yang, S.-H. Kim, D. Kahne, *J. Am. Chem. Soc. 113* (1991) 4715.
[118] D. Kahne, D. Yang, *Tetrahedron Lett. 31* (1990) 21.
[119] K. V. Laak, H.-D. Scharf, *Tetrahedron Lett. 30* (1989) 4505.
[120] K. C. Nicolaou, C.-K. Hwang, A. L. Smith, S. V. Wendeborn, *J. Am. Chem. Soc. 112* (1990) 7416.
[121] K. C. Nicolaou, A. L. Smith, S. V. Wendeborn, C.-K. Hwang, *J. Am. Chem. Soc. 113* (1991) 3106.
[122] K. C. Nicolaou, E. P. Schreiner, W. Stahl, *Angew. Chem. 103* (1991) 566; *Angew. Chem. Int. Ed. Engl. 30* (1991) 585.
[123] R. R. Schmidt, *Angew. Chem. 98* (1986) 213; *Angew. Chem. Int. Ed. Engl. 25* (1986) 212.
[124] K. C. Nicolaou, C.-K. Hwang, S. V. Wendeborn, unpublished results.
[125] P. A. Wender, C. K. Zercher, *J. Am. Chem. Soc. 113* (1991) 2311.
[126] J. A. Porco, Jr., F. J. Schoenen, T. J. Stout, J. Clardy, S. L. Schreiber, *J. Am. Chem. Soc. 112* (1990) 7410.
[127] H. Chikashita, J. A. Porco, Jr., T. J. Stout, J. Clardy, S. L. Schreiber, *J. Org. Chem. 56* (1991) 1962.
[128] P. Magnus, S. M.Fortt, *J. Chem. Soc. Chem. Commun. 1991,* 544.
[129] T. Nishikawa, M. Isobe, T. Goto, *Synlett 1991*, 99.
[130] J. P. Snyder, *J. Am. Chem. Soc. 112* (1990) 5367.
[131] J. P. Snyder, *J. Am. Chem. Soc. 111* (1989) 7630.
[132] J. P. Snyder, G. E. Tipsword, *J. Am. Chem. Soc. 112* (1990) 4040.
[133] N. Koga, K. Morokuma, *J. Am. Chem. Soc. 113* (1991) 1907.
[134] I. H. Goldberg, *Acc. Chem. Res. 24* (1991) 191.
[135] T. Tanaka, M. Hirama, M. Ueno, S. Imajo, M. Ishiguro, M. Mizugaki, K. Edo, H. Komatsu, *Tetrahedron Lett. 32* (1991) 3175.
[136] M. D. Lee, G. A. Ellestad, D. B. Borders, *Acc. Chem. Res. 24* (1991) 235.
[137] W.-D. Ding, G. A. Ellestad, *J. Am. Chem. Soc. 113* (1991) 6617.
[138] H. Kishikawa, Y.-P. Jiang, J. Goodisman, J. C. Dabrowiak, *J. Am. Chem. Soc. 113* (1991) 5434.
[139] N. Sullivan, L. Lyne, *Mutat. Res. 1990*, 245.
[140] D. R. Langley, T. W. Doyle, D. L. Beveridge, *J. Am. Chem. Soc. 113* (1991) 4395.
[141] a) R. Brückner, S. W. Scheuplein, J. Suffert, *Tetrahedron Lett. 32* (1991) 1449; b) J. Suffert, R. Brückner, *ibid. 32* (1991) 1453.
[142] K. Nakatani, K. Arai, K. Yamada, S. Terashima, *Tetrahedron Lett. 32* (1991) 3405.
[143] C. Crevisy, J.-M. Beau, *Tetrahedron Lett. 32* (1991) 3171.
[144] Y. Sakai, E. Nishiwaki, K. Shishido, M. Shibuya, *Tetrahedron Lett. 32* (1991) 4363.
[145] M. E. Maier, T. Brandstetter, *Tetrahedron Lett. 32* (1991) 3679.
[146] a) T. Nishikawa, A. Ino, M. Isobe, T. Goto, *Chem. Lett. 1991*, 1271; b) T. Nishikawa, M. Isobe, T. Goto, *Synlett 1991*, 393.

Mechanisms of Molecular Recognition: Investigations of Organic Host–Guest Complexes

By Hans-Jörg Schneider*

Dedicated to Professor Michael Hanack on the occasion of his 60th birthday

Noncovalent interactions constitute the basis for information transfer between molecules in living systems as well as in synthetic supramolecular structures. Despite ever more accurate descriptions of biological systems and a dramatically increasing diversity of synthetic host–guest complexes, a systematic and general understanding of the underlying intermolecular forces is still in its infancy. Organic chemistry makes possible the targeted construction of infinitely variable host compounds with multiple centers interacting in complementary ways. This in turn opens the door to systematic experimental analyses based on binding increments, which can be shown to have a high degree of additivity. Even in the case of relatively simple ion pairs, several mechanisms are at work simultaneously, and either entropy or enthalpy contributions may prove to be decisive. Nevertheless, it is possible to identify individual interactions and then use them to practical advantage in ways analogous to the free-energy relationships of physical organic chemistry. Contributions due to solvophobic effects, to interactions with permanent and induced dipoles, and to hydrogen bonds lend themselves to a high degree of empirical quantification on the basis of classical physical-chemical principles. Water as a solvent plays a special role due to its low polarizability, apart from hydrophobic effects. Quantification of pairwise interactions and ultimate control over them through manipulation of the microenvironment should prove useful not only in the design of new synthetic host–guest complexes but also, for example, in the rational development of biologically active substances, molecular switches (e.g., for sensor technology), and catalysts that function analogously to enzymes. The results should also assist in the planning and analysis of biochemical experiments including techniques of genetic engineering.

1. Introduction, Goals, and Methods

The growing significance of supramolecular chemistry is already documented in a number of monographs,[1–20] with the early emphasis more on the complexation of inorganic ions.[17–19] For further orientation with respect to the vigorous development of this highly interdisciplinary subject the reader is referred to more recent review articles and the original literature.[21–76] Noncovalent interactions between host and guest molecules lie at the heart not only of synthetic supramolecular complexes but also much of biomimetic and biological chemistry too.[6, 7, 51, 77–93] Elucidation of these interactions is also the basis of promising new approaches in pharmacy, medicine, chemical analysis,[15, 55–58, 82, 86–93] and chromatography,[94] as well as catalysis[22b, 23a, 24, 28c, 29a, c, 35d, 75b, 95] and materials science.[55–58, 96] The principal advantage of synthetic host–guest chemistry is that it permits targeted construction of supramolecular complexes with infinitely variable noncovalent interactions arranged in conformationally defined ways. To analyze and to plan, for example, the genetically engineered exchange of amino acids in a protein is obviously a more difficult problem given the complexity and flexibility of typical biopolymers. With respect to interaction analyses in biological systems we cite only a few illustrative references.[81–84]

Despite the large (and exponentially increasing) number of known synthetic host–guest systems, systematic description of the underlying mechanisms has so far developed only to roughly the point reached by the mechanistic chemistry of covalent bonds decades ago. The goal of this overview is to classify as completely as possible the most important interactions found in organic host–guest complexes, and more particularly to quantify these interactions. Parameters that can be established in this way are applicable not only in a host of biological and industrial contexts (cf. Table 1), but also to the process of designing and synthesizing new supramolecular complexes with structures and energy contents that are predictable. Our methodology is aimed primarily at characterizing as far as possible pairwise interactions by targeted variation of the experimental systems. A model for this approach exists in the semiempirical methods of physical-organic chemistry, where analogous free-energy relationships play a major heuristic and practical role.

Table 1. A few potential applications arising from the studies of interaction mechanisms in organic host–guest complexes.

1) Synthetic planning for supramolecular complexes
2) Quantification for systems of biological or medicinal interest: enzymes, pharmacological receptors, immunoglobulins, antigen–antibody systems, nucleic acids
3) Genetic engineering/modification of proteins
4) Drug design
5) New analytical and diagnostic procedures
6) Selective phases for affinity chromatography
7) Development of molecular sensors, switches, etc.
8) Enzyme-analogous catalysis in water as solvent

[*] Prof. Dr. H.-J. Schneider
Fachrichtung Organische Chemie der Universität
W-6600 Saarbrücken 11 (FRG)

The physicochemical basis of intermolecular interactions is treated in a number of classical monographs;[97-100] nevertheless, exact description is possible, even today, only in the case of relatively small systems.[101, 102] Recent dramatic advances in computer technology and the application of semiempirical molecular-mechanics (MM) methods now offer the prospect of quantitative simulations of larger molecular systems as well, including biopolymers.[103-115] Especially in the case of relatively small metal complexes of crown ethers and cryptands,[112] satisfactory agreement already exists between calculated and experimental *structures*. Quite recently this has also come to be true for larger systems, in some cases ones containing organic substrates.[112-114] The introduction of molecular dynamics (MD) and Monte Carlo (MC) methods has led here to significant advances.[103-111] The application of statistical perturbation theory (SPT or FEP)[92b, 111a] makes it possible to calculate *changes in free energy* (ΔG) between similar states. Statistical mechanics is used here to provide a description of the substrate and receptor or the solvent separately, which then constitutes a reference state, and associations are treated as a perturbed state. This approach requires extensive calculation even for relatively small complexes, and comparisons should be restricted to similar molecules. On the basis of appropriate thermodynamic cycles, and with the inclusion of discretely describable solvent molecules and the free energy of desolvation of host and guest molecules (**H** and **G**), the method becomes applicable to systems in *solution*.

In this overview we limit ourselves to noting only a few of the—often overlooked—problems that arise during the simulation of complex molecules. The extremely high degree of freedom associated with multiparticle systems, even ones of limited size, imposes limitations with respect to the localization of optimal geometries in terms of energy minima, even if one is willing to devote massive amounts of computational effort to the problem.[116] For example, 262 discrete minima with ΔH differences $< 13\ kJ\,mol^{-1}$ were found for cycloheptadecane ($C_{17}H_{34}$),[116c] and a nine-membered lactam gave as many as 39 minima,[116d] 12 of them falling within only $< 13\ kJ\,mol^{-1}$ of each other. Equally serious—and often underestimated, even in comparisons between two simple conformations—are shortcomings in the potentials assigned to individual interactions, which constitute the basis for all such calculations. Thus, descriptions of electrostatic or van der Waals interactions are to some extent quite arbitrary (cf. Sections 5–7), and induction of di- or polypoles, without which the binding of aromatic substrates would often be impossible (cf. Section 7), is not taken into account by the force fields in use, particularly those available commercially. Such inductions are difficult to include in the calculations, in part due to the anisotropy of polarizability.[115] Different force fields sometimes lead to widely diverging energies even for the same structure;[114] for example, ΔH values computed for the *cis* and *trans* amide conformations in the above-mentioned lactam differ by more than $10\ kJ\,mol^{-1}$, depending on the method used.[116d] It is to be hoped that systematic measurements with organic host–guest complexes will contribute to some improvement and extension in the force-field potentials for noncovalent binding.

Results presented in this review relate primarily to host–guest complexes in solution, although the many analyses of corresponding crystal structures reported in conjunction with supramolecular solid-state chemistry[1a, b, 11, 25-27] naturally represent essential starting points with respect to the geometric boundary conditions for complex formation. The many *functions* of synthetic and biological supramolecular systems often require a dissolved or "mobile" state. Information regarding energy changes during complex formation or, for example, in allosteric phenomena (for molecular switches, etc.) is accessible in any event only from the solution state. Furthermore, a liquid medium is often required to establish a solvophobic driving force for association between host and guest molecules, and it opens the way to a large degree of control over the complexation process.

To obtain reliable results on host–guest complexes in solutions it is necessary to employ suitable methods of measurement. At this point we limit our comments to a few brief observations. Spectroscopic titrations[117] are preferable for establishing equilibrium constants and the corresponding values of ΔG. Compared to UV/VIS and fluorescence spectroscopy (which are also utilized),[117b] NMR methods offer the advantage of supplying several independent signals for the determination of a single constant K.[41b, 118] This often leads to the discovery that a particular solution actually contains more than simply one type of 1:1 complex, a conclusion that may be subject to verification by optical methods with data collected at several wavelengths.[117-119] Typical complexation constants tend to be smaller than those for biochemical systems, which limits the applicability of standard biochemical methods. In working with titration curves it is usually necessary that one first optimize the experimental conditions and then apply nonlinear curve-fitting techniques in order to obtain complexation constants and intrinsic spec-

Hans-Jörg Schneider was born in Stuttgart, Germany in 1935. He studied chemistry in Tübingen, Munich, and Berlin and received his Ph.D. under Michael Hanack at the Tübingen Institut Walter Hückels in 1967. After conducting postdoctoral research at the University of California, San Diego (1967–1969) he worked on his habilitation and other research until 1971 in the laboratory of Walter Hückel. In 1971 he completed his habilitation in Saarbrücken and since 1973 he has been Professor of Organic Chemistry at the Universität des Saarlandes. His areas of interest include: conformational analyses, quantitative structure–reactivity relationships for aliphatic compounds, including steroids, NMR spectroscopic methods with an emphasis on ^{13}C and ^{1}H NMR shielding parameters, selective functionalization of paraffins, and in the last few years supramolecular receptor and enzyme models.

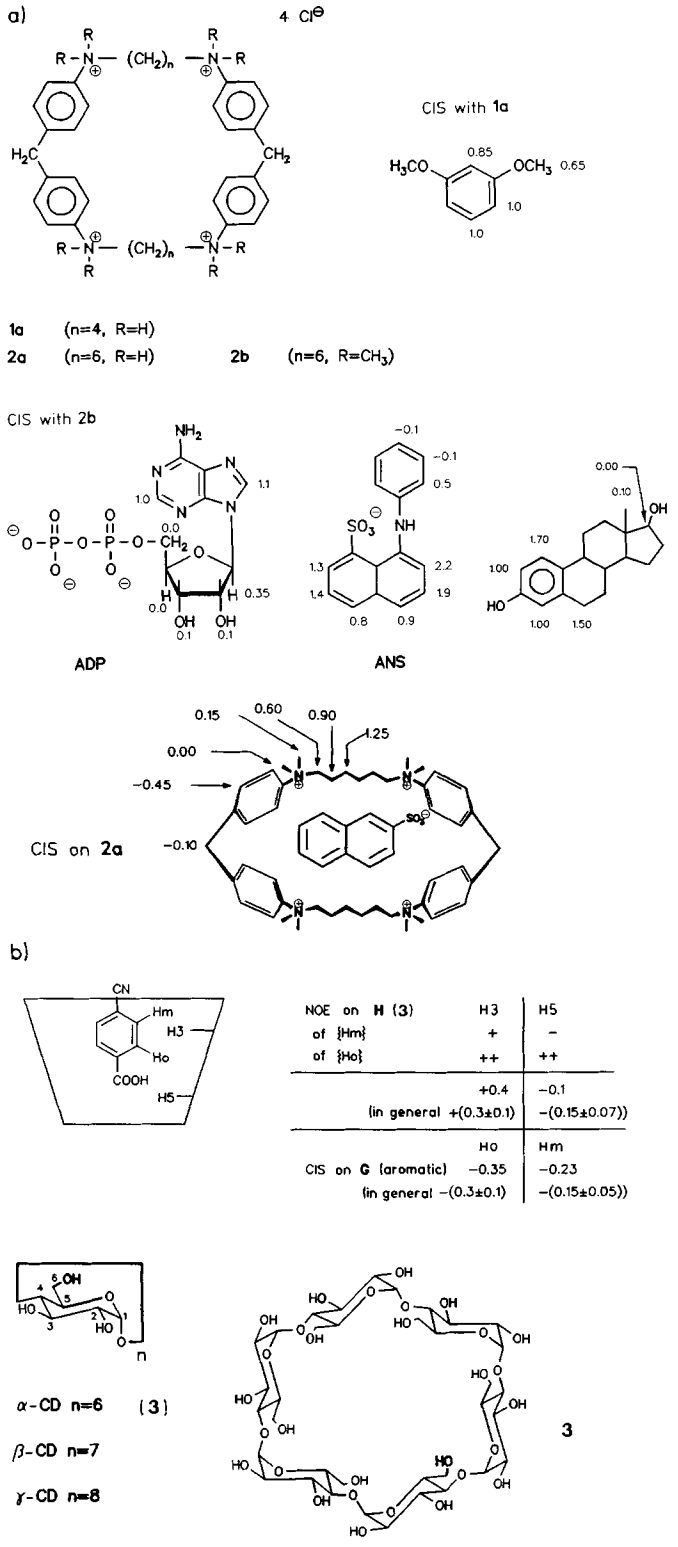

Scheme 1. Typical ^{1}H NMR CIS values in D_2O on complexation. (CIS > 0: upfield shift, CIS < 0: downfield shift). a) Complexation in azoniacyclophanes **1a**, **2a**, **2b**; b) complexation of 1,4-disubstituted aromatics in α-cyclodextrin **3**. NOE effects are indicated as + + (very strong), + (weaker), and − (absent). Hm = *meta*-H atoms and Ho = *ortho*-H atoms of the benzene ring, **H** = host, **G** = guest. ADP = adenosine diphosphate, ANS = 1-anilido-8-naphthylsulfonate, CD = cyclodextrin.

troscopic values x characteristic of the fully complexed system, a state that in most cases is not accessible experimentally.[41b, 117, 118] Scheme 1 includes a selection of typical NMR complexation-induced shifts (CIS values: + refers to upfield shifts, − to downfield shifts). Quantitative interpretation of such shifts requires explicit calculations, in particular of anisotropy and field effects.[43a, 120] These can only be parameterized on the basis of appropriate model investigations with geometrically fixed substrates such as steroids.[121] Spectral shifts can be analyzed with respect to both guest and host molecules, although the latter approach has often been neglected. CIS values obtained with curve-fitting methods (cf. Scheme 1) provide considerable information regarding whether (or to what extent) molecules **G** are actually complexed within an **H** cavity. Unfortunately, intermolecular NOE effects (NOE = *N*uclear *O*verhauser *E*nhancement) for organic host–guest systems at least in water usually fall between the positive NOE values (signal increases) for *intra*molecular interactions in smaller molecules and the numerically much larger negative NOEs of biopolymers.[122] Small NOE effects, caused by unfavorable relaxation times and by high magnetic fields, can be enhanced by application of such spin-lock techniques as ROESY,[122a] (ROESY = *R*otating frame nuclear *O*verhauser *E*ffect *S*pectroscop*y*) thereby permitting (with cyclodextrin complexes, for example) at least semiquantitative conclusions (Scheme 1). Taken together with CIS chemical shifts, these have led in the case of cyclodextrins to considerable modification of the lock-and-key principle.[43c, 119]

2. The Additivity of Noncovalent Binding Increments

Polytopic host compounds **H** and guest molecules **G** with multiple complementary centers A,B,C,... and K,L,M,..., respectively, for pairwise noncovalent binding A · · · K, B · · · L, etc., (Scheme 2) offer the important opportunity for

Scheme 2.

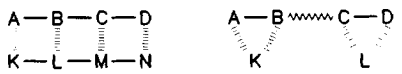

increasing to the nth power the effect of even weak individual interactions through incorporation of n such centers. The basis for this phenomenon is the additivity of the corresponding individual free energies [Eq. (1a)] and formation constants [Eq. (1b)] well known in inorganic coordination

$$\Delta G_{HG} = \Delta G_{AK} + \Delta G_{BL} + \Delta G_{CM} \cdots \quad (1a)$$

$$K_{HG} = K_{AK}\, K_{BL}\, K_{CM} \cdots \quad (1b)$$

chemistry as the "chelate effect". Incidentally, here no recourse to entropy arguments is necessary.[47] Organic substrates, too, are subject to the principle that multiple binding to natural or synthetic receptors leads to greater efficiency and selectivity in complexation. The familiar "lock-and-key" model of *Emil Fischer*, dealt with extensively elsewhere,[43c, 123] implies a close steric approach of the individual centers for optimal ΔG values. Conformational changes during the course of complexation can assist in the process ("induced fit"[124]) and can also result in allosteric systems, which are particularly interesting from a functional standpoint.

The use of host–guest systems containing at least two binding centers offers significant advantages in the experi-

mental determination of intrinsic interactions, which in turn facilitate the reverse process: predicting on the basis of Equations (1a) and (1b) previously unknown complexation strengths and selectivities. In addition to supplying an experimentally desirable increase in what might be an inconveniently small complexation constant in the presence of only one interaction, the incorporation of an additional center makes it possible to analyze the effects of that particular center more fully through systematic variation of substituents, assuming all other interactions and the solvent are left unchanged. In particular, this makes it easier to maintain a constant entropy effect. The reduction in translational freedom of **H** and **G** that accompanies formation of a complex **H** · **G** leads to a reduction in the entropy, with typical $T\Delta S$ values of 150 kJ mol^{-1}.[125] The entropy disadvantages accompanying the association of host and guest molecules with only one different interaction site can be kept quite similar, although rotatory degrees of freedom also influence complex formation.[125] With this strategy we in fact frequently observe a linear correlation between measured free energy of complexation ΔG_{HG} and the number n of analogous binding centers (see Sections 5–8). When this is the case, the slope of a best-fit line provides the intrinsic binding increment ΔG_i per interaction.

The principle of additive binding increments can be applied even in a case with only two centers, which makes it valuable for noncovalent interactions of a wide variety of types. It is important here to ensure that the primary interaction—the one held constant—is larger than the secondary interaction that is to be quantified on the basis of variation ($\Delta G_{AK} > \Delta G_{BL}$), in part to minimize possible entropy differences. The free energies of complexation ΔG_{HG} established for the azoniacyclophane **2b** with a series of substituted naphthalene derivatives (Scheme 3), for example, reveals a

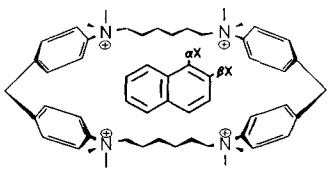

	ΔG_{HG}
X = H, OH, NH_2	19
βX = $CO_2^{\ominus}$, $SO_3^{\ominus}$, $OPO_3H^{\ominus}$	22
αX = $CO_2^{\ominus}$	20
αX = $CH_2CO_2^{\ominus}$, $OPO_3H^{\ominus}$	22

Scheme 3. Complexation of azoniacyclophane **2b** with naphthalene derivatives. ΔG_{HG} values in kJ mol^{-1}.

large contribution from the hydrocarbon residue that is held constant ($\Delta G_{AK} \approx 19$ kJ mol^{-1}), and for a variety of anionic substituents X at the β position a relatively constant electrostatic increment (cf. Section 5) of $\Delta\Delta G_{BL} \approx 3$ kJ mol^{-1}. These increments are significantly smaller for substituents in the α position ($\Delta\Delta G'_{BL} = 1-2$ kJ mol^{-1}); introduction of spacer elements (–O– or $-CH_2-$), however, leads to an increment similar to that observed for βX, since optimal contact is once again possible between $X^{\ominus}$ and the positively charged N atom of the receptor. This example illustrates a further prerequisite to the application of additive binding increments: the host–guest system must be so conceived that mutual disturbances of the individual interactions are minimized. Molecular-mechanics simulations can be helpful in controlling this factor, and permit, if necessary, numerical corrections for conformational strain energy changes.

The analysis of pairwise interactions led earlier already to the identification of specific types of interactions,[72] also in biologically significant complexes,[89–91] but it is subject particularly to influences related to differences between cavities (cf. Sections 4 and 8). Only the systematic application of constant binding increments under the conditions described above leads to comprehensive comparisons between experiment and prediction covering a large number of complexes of varying type. The value of this approach has already been demonstrated (cf. Sections 5–8) in the analysis of Coulombic interactions,[126] hydrogen bonding,[127] higher-order field (van der Waals) effects, and charge-transfer (CT) interactions,[128] the latter being mostly insignificant. The linear correlations that usually result are different from earlier Hammett correlations, as found, for example, by *Connors* et al.[129] for inclusion of phenyl derivatives in cyclodextrins. Here not only the substituents themselves but also the arenes whose π systems they modify participate in binding within the same cyclodextrin cavity. For this reason it becomes necessary also to introduce terms for molar refraction and dipole moments in order to obtain linear energy relationships.[129]

3. Receptor Structures: Open, Half-Open, and Closed

The examples[128, 130–133] in Scheme 4 show that multiplicative pairwise interactions can also lead to strong complexation at open, extended receptor surfaces. Contrary to

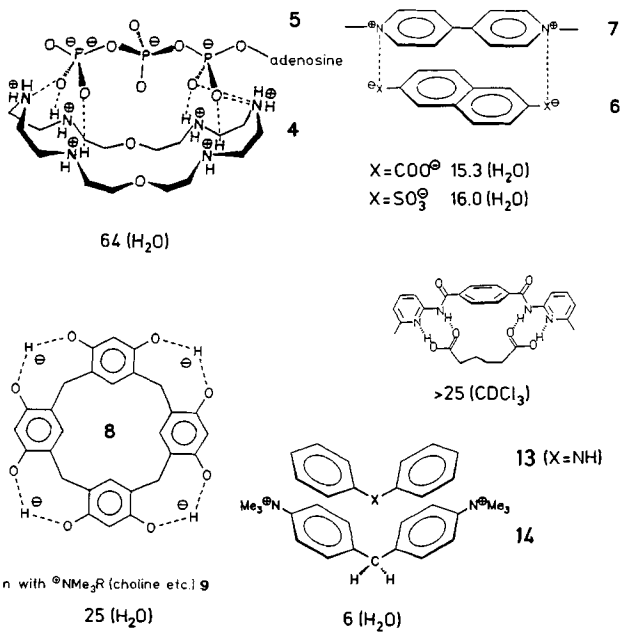

Scheme 4. Complexation on open, extended receptor surfaces. Numbers indicate ΔG_{HG} [kJ mol^{-1}] for the solvent given in parentheses.

simplifying expectations,[42a] the provision of a more completely enclosed cavity does *not* necessarily lead to increased complex stability even in those cases where the interactions are primarily solvophobic. This is illustrated by a comparison of the monocyclic host compound **2a** with its bicyclic

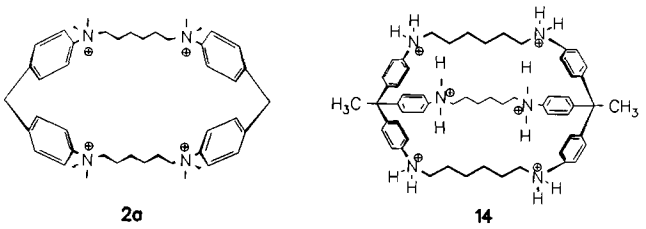

2a + ANS $K = 2.0\times10^5\ M^{-1}$ **14** $K = 0.4\times10^5\ M^{-1}$

Scheme 5. Complexation of ANS (Scheme 1) in a mono- and a bicyclic receptor in D_2O at 300 K.

analogue **14**[134] (Scheme 5). What then are the prerequisites for increased effectiveness with concave or closed cavities? In addition to solvophobic effects (see below) it is important also to take into account the fact that spherical particles are subject, in a hemispherical cavity, to four times as much dispersive binding force (cf. Section 7) as on a planar surface, and that this factor increases to six with a cylindrical cavity and approximately eight with a fully encompassing spherical cavity.[135] Especially in the case of vectorially directed interactions (indicated by the arrows in Scheme 6) like those involved in hydrogen bonding, binding efficiencies are found to be particularly high when the binding is so arranged as to avoid linear attachment with parallel vectors, unlike, for example, the systems in Schemes 2 and 4. This principle underlies many of the so-called cleft-receptors[35h, 41c, 66b, 74, 136, 137] (Scheme 7), in which a convergent arrangement of binding centers at the same time hinders self-association of the host compound. Cavities that are more completely enclosed, as in the case of cyclodextrin **3** or many cyclophanes[28, 29, 33, 72, 118, 138] (Schemes 1 and 8), generally lead to significantly higher ΔG_{HG} values even in the absence of solvophobic forces, and with increasing encapsulation of the guest molecule the result may actually be immeasurably low levels of complex dissociation.[138]

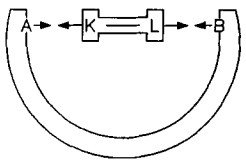

Scheme 6. Vectoral interactions between substrate and the sites in the cavity of a hemispherical receptor.

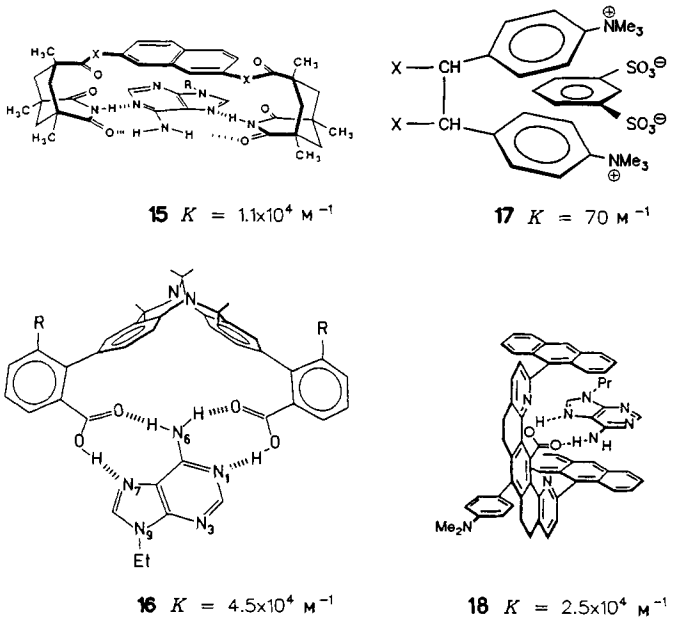

15 $K = 1.1\times10^4\ M^{-1}$ **17** $K = 70\ M^{-1}$ **16** $K = 4.5\times10^4\ M^{-1}$ **18** $K = 2.5\times10^4\ M^{-1}$

Scheme 7. Complexation constants with cleft receptors [with **15** in CD_3CN/$CDCl_3$ (30/70), **16** and **18** in $CDCl_3$, and **17** in D_2O].

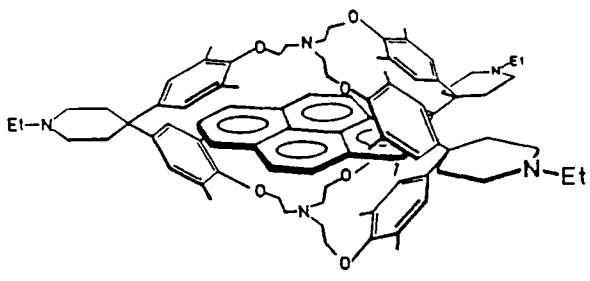

19

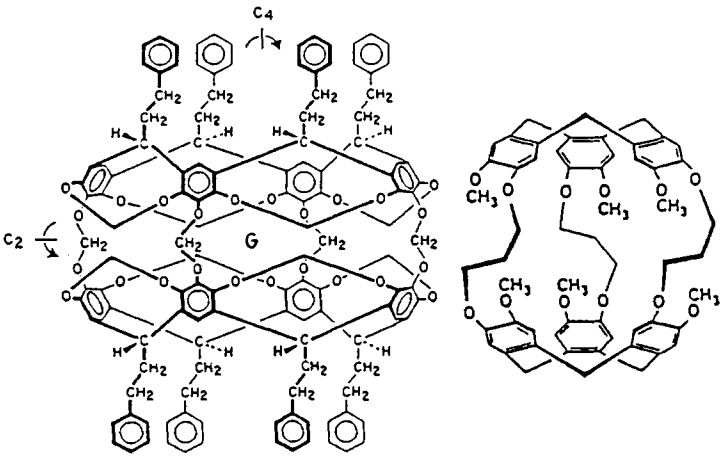

20 **21**

Scheme 8.

The sections that follow introduce those host–guest complexes in which specific types of interaction mechanisms dominate. The treatment is intended to be illustrative rather than exhaustive.

4. Solvophobic Forces: Contributions from Both Enthalpy and Entropy

The most important host–guest interaction in aqueous solution consists of attraction between lipophilic regions in the host and guest molecules. The "classical"[79] hydrophobic effect[139, 140] is caused by a release of water molecules and a corresponding gain in entropy ΔS°. Prior to association of the lipophilic particles water solvates the particle surfaces in the form of highly organized solvation shells.[141] There can be no better example of the continuing state of uncertainty with respect to the physical principles that govern molecular recognition than the conflicting explanations offered for the behavior of lipophilic particles in water: in addition to (or

even in place of) the entropy factor already cited, claims are made for a purely enthalpic basis for the solvophobic effect (see below). In particular, some authors regard dispersive interactions (cf. Section 7) as entirely[142] or partially[143] sufficient to explain thermodynamic data obtained with noble gases or alkanes in water. On the other hand, even the most recent edition of a well-known monograph[139] on the hydrophobic effect barely mentions dispersive interactions. Without going further into the extensive and in some respects controversial literature on this subject,[79, 139, 140, 142] we note that in the case of complex formation with proteins[145] as well as, for example, cyclodextrins[146] in water, significantly positive ΔS° values have in fact frequently been observed—even overall losses in ΔH° (cf. Section 7). A further characteristic of such associations is a decrease in heat capacity ΔC_p,[143, 144] since the release of water of solvation leads to a reduction in the number of heat-absorbing bonds. One important consequence for supramolecular equilibria is that the corresponding $\Delta H^\circ/\Delta S^\circ$ values show significant dependence on the temperature, and like the changes in ΔCp such values can only be established by very precise measurements of equilibrium constants over a wide range of temperatures[147] or, better, by direct calorimetric studies.[146, 148]

The determination of individual thermodynamic parameters for organic host–guest complexes suffers from more than simply experimental difficulties (which are often underestimated!); interpretations are complicated further by the previously noted temperature dependency—including variable temperature coefficients for different interactions. Linear free-energy relationships (LFER) such as the Hammett correlation are subject to similar problems with respect to $\Delta H/\Delta S$ distinctions. For example, the observed pK values for substituted acids and bases owe their magnitudes at least as much to differences in entropy as in enthalpy. Despite this fact, it is the additivity of ΔG increments that is the basis of the practical success of LFER analyses. An analogous approach appears to be justified in the case of noncovalent binding, particularly since here there is also a tendency toward compensation between ΔH and ΔS;[146, 148b] a given molecular interaction frequently gives rise to enthalpy and entropy effects of the same sign, as for example with the solvophobic effect.

One model based on a gain in enthalpy ΔH° describes the solvophobic effect in terms of cohesive forces—usually hydrogen bonds—between solvent molecules, for which an experimental measure can be deduced from the surface tension.[149] The approach of two particles at a surface A, solvated before association by, for example, water, leads according to *Sinanoglu*[149] to a release of solvent molecules and creation of a single cavity in the water where before there were two. This in turn implies an increase in cohesive energy described by Equation (2)[149] where γ is the surface tension, M the number of solvent molecules per kg, and ϱ the solvent density.

$$\Delta H = 0.43\,\gamma A T^{-1} - 1.36\,M\varrho \qquad (2)$$

Investigations have already been carried out on the association of relatively nonpolar substrates as a function of solvent.[149, 150] Agreement in principle with this theory has been reported by *Diederich* et al.[151] for a large number of solvents ranging from water to benzene for the complex **19**, among others (Scheme 8). Thus, a roughly continuous increase is observed in the free energy of complexation ΔG_{HG} with the cohesive pressure of the solvent or the related Hildebrand–Scott parameter,[152] as well as with decreasing polarizability of the solvent. As is often observed with solvent effects, the best (linear) correlation of the ΔG_{HG} values for **19** was obtained with empirical parameters, in this particular case,[151] in fact, with the polarity factors E_T.[152a] It will continue to be necessary to use such empirical parameters as long as it remains impossible to carry out satisfactory calculations of, for example, even solvation enthalpies for simple halobenzenes, irrespective of whether one uses reaction field theory or the classical Kirkwood–Westheimer approach.[153]

What effect does *substrate structure* have on the magnitude of solvophobic effects? *Connors, Cohen* et al. found for associations between planar aromatic molecules an approximately linear relationship between ΔG_{HG} and the contact surface A linking **H** with **G**.[150a, b, 154] Even more definitive evidence of the dominance of cohesive forces in water comes from the slope of the observed linear correlation, which is reported to have a value of 64 dyn cm^{-1}, close to the macroscopic surface tension of water (72 dyn cm^{-1}).[154] The assumption that association is due almost entirely to desolvation of the individual particles (**H** and **G**) is supported by the absence of larger specific effects or dependence, for example, on whether the aromatic substrates are ionic or neutral: although there was considerable scatter, the value of ΔG_{cplx} for ca. 50 different association pairs appeared to be determined exclusively by the surface area A.[154] In the absence of substrate-specific solvation, therefore, the hydrophobic effect can be computed solely from the energy required to create a free surface of 1 Å^2 in water (γ = 72 mN m^{-1}); this amounts to 7.2×10^{-12} J or, after multiplication by Avogadro's number N, to 0.43 kJ Å^{-2}mol^{-1}.

Is there a specific effect dominated by hydrophobicity with respect to cavities? With the help of the host molecules **2b** and **12** shown in Scheme 9 it becomes possible for the first time to examine structurally equivalent receptors both in the presence and in the absence of cavities.[133] The results indi-

	2b		**12**
	ΔG_{HG}	$\Delta\Delta G$	ΔG_{HG}
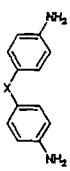 X = CH_2	14.5	*7.6*	6.9
X = NH	14.5	*8.5*	6.0
CH_2I_2	7.5	*5.8*	1.7
	10.0	*7.3*	2.7

Scheme 9. Differences in the energy of complexation ΔG [kJ mol^{-1}] (in D_2O) between host compounds with cavities (**2b**) or without cavities (**12**). $\Delta\Delta G$ is on average 7.3 kJ mol^{-1}.

cate a surprisingly constant increase in ΔG_{HG} of $7 \pm 1\ kJ\,mol^{-1}$ for a wide variety of guest molecules **G** as a consequence of the cavity that is present only in **2b**. For the complexation of diiodomethane this value is significantly larger than the maximum increase $\Delta G_{HG} \leq 4\ kJ\,mol^{-1}$ that can be ascribed to total surface contact with the surface A through total inclusion of **G**. Simulations of the macrocyclic system **2b** in a water box with the aid of the CHARMm force field[108] suggest, as the possible cause of this special cavity effect, five water molecules located in or near the cavity (Fig. 1) that participate in an average of only two hydrogen bonds as opposed to the four typical for "free" water.[155] That a loss of water hydrogen bonds within a cavity might be a source of the hydrophobic effect gains support from crystal structure analyses of cyclodextrins[156] as well as peptides.[157] Dependence of the extent of the hydrophobic effect on the form of the cavity can lead to considerable divergence in comparisons of pairwise interactions[89-91] within biopolymers (cf. Section 8).

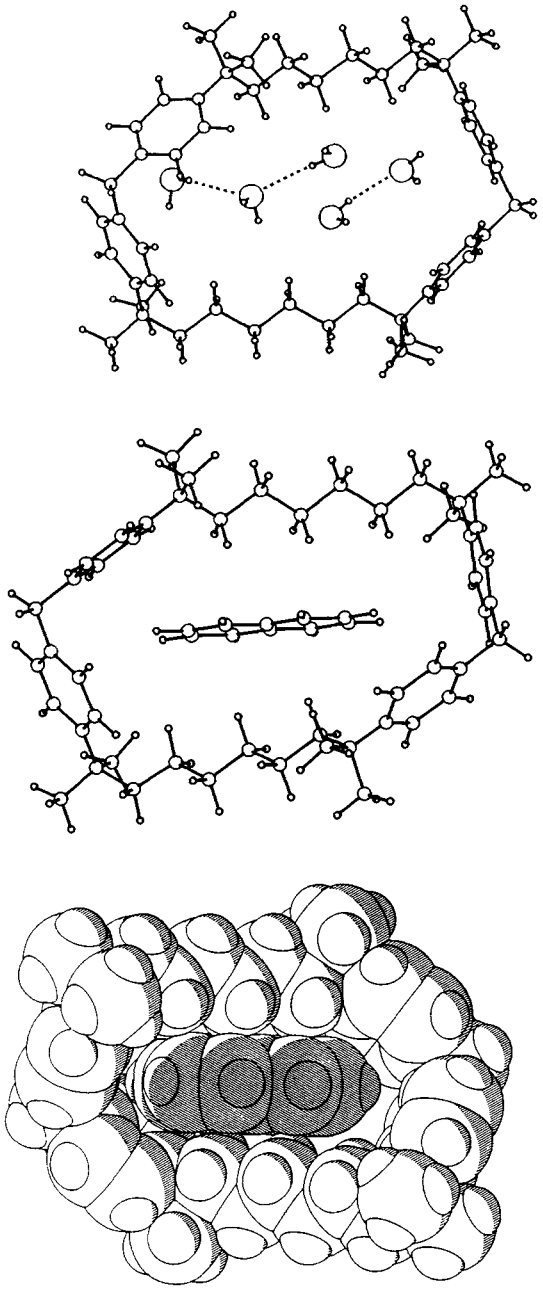

Fig. 1. Molecular graphics representation (CHARMm/QUANTA) of the azoniacyclophane **2b**; top: with 5 water molecules in or partially within the cavity; the (on average) two, rather than the normal four, hydrogen bonds are indicated by dotted lines [133]; for comparison (center and bottom): **2b** with naphthalene in its cavity.

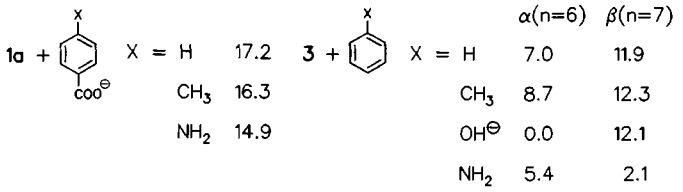

Scheme 10. Energies of complexation [$kJ\,mol^{-1}$] in H_2O or D_2O for the reaction of azoniocyclophane **1a** [158b] and of α-cyclodextrin **3** [159, 160] with arenes.

The limitations of a nonspecific model of cohesive solvent forces appear as soon as there are significant differences in the natures of the particles. Despite similar surface areas A and volumes, the various cyclophane[158] and cyclodextrin complexes[159, 160] in Scheme 10 display ΔG_{HG} values that differ markedly, sometimes opposing the anticipated trend. There is likewise no satisfactory correlation between stabilities of cyclodextrin complexes and either the water solubilities of the corresponding substrates or their distribution coefficients between water and lipophilic solvents,[129] as illustrated by a comparison of benzene derivatives (Scheme 10). These apparently substrate-specific interactions between **H** and **G** or between solvent and either **H** or **G** can be attributed largely to higher order electrical effects (cf. Section 7).

Despite cavities of geometrically similar size, complexes with **22**[161] (Scheme 11) are considerably weaker than those with **2a**. This means that desolvation of a cavity containing primarily hydrophilic N atoms requires especially large amounts of energy. Furthermore, bonding with cyclophanes can be affected by portions of the guest molecules **G** that extend beyond the cavities and are therefore unable to contribute to contact between **H** and **G**. This *extracavity* effect[162] is apparent, for example, in the regular increase in complexation constants K for **1a** in water from $K_{rel} =$

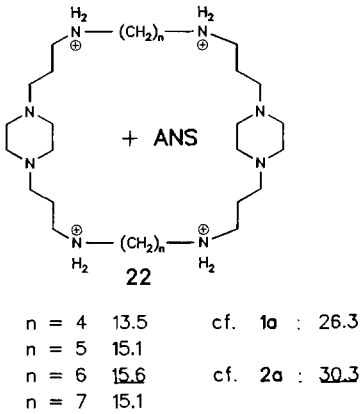

Scheme 11. Energy of complexation [$kJ\,mol^{-1}$] in H_2O for the reaction of the macrocycle **22** with ANS (see Scheme 1).

$1.0\ M^{-1}$ for benzene to $K_{rel} = 8.0\ M^{-1}$ for biphenyl.[162] Similar considerations apply to the association of steroids with **2b**, which bind more effectively than the corresponding tetralin derivatives.[163] Substituents like the phenyl group in the fluorescence dye ANS or the C- and D-rings in estradiol[163] definitely fall outside the cavity of **2b**, as shown not only by a study of models but also from observed NMR shifts (Scheme 1). The fact that such molecular fragments displaying no contact with the host can nonetheless cause complexation to increase by a factor of as much as ca. 30[162] is an indication of the important role played by entropy in the hydrophobic effect; it also illustrates the problems associated with the usual computer-generated geometric-fit predictions for host and guest molecules.

Better relative values for the extent of the hydrophobic contribution to ΔG_{HG} with various host–guest complexes can be anticipated from studying changes in ΔG_{HG} or K as a function of solvent composition, rather than relying solely on individual measurements in water.[150] The corresponding relationship (3)[118] is intended to characterize the sensitivity of contributions from hydrophobic interactions (in terms of the slope a), where S_p is an empirical parameter

$$\lg K_{HG} = a S_p + \lg K^\circ \qquad (3)$$

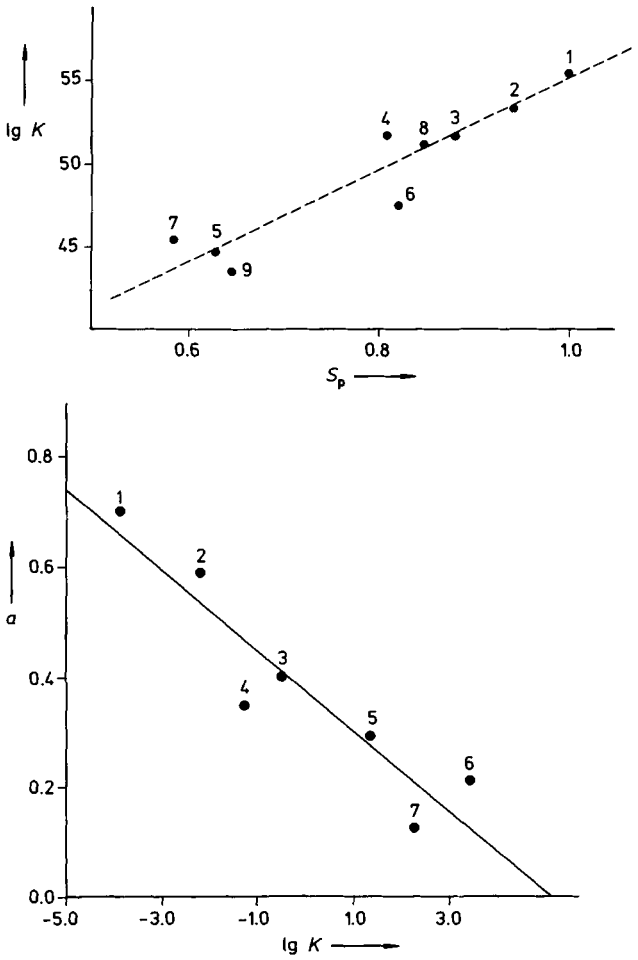

Fig. 2. Solvophobic effects on the association constants K; the numbers refer to complexes described in the literature, corresponding to Equation (3) [118]. Top: correlation for lg K vs. the solvophobicity parameter S_p for **2b** · ANS; bottom: correlation for the slope a (a measure of sensitivity) vs. lg K° (corresponding to complexation in hydrocarbon solvent, $S_p \equiv 0.0$).

describing the solvophobicity of the medium. Free energies of transfer ΔG_t for hydrocarbons for instance, from the gas phase into a particular medium[143a] and the related ΔG_t values from water to the same medium have been found on the basis of various investigations to constitute a suitable measure of S_p.[164, 127b] Using parameters ranging from $S_p \equiv 0.00$ for hexane as solvent to $S_p \equiv 1.00$ for water, we have obtained correlations with about ten complexes of **2b**, **3**, and **8** that are significantly more linear than with E_T parameters.[118] The slopes a provide a similarly satisfactory correlation with the intercepts lg K°, which correspond to extrapolations to the thus accessible complexation in a hexane medium (Fig. 2). As expected, complexes with **3** (cyclodextrin complexes), which have, for example, $a = 7.0$ and lg $K^\circ = -3.9$, represent one extreme, those with **8** (e.g., $a = 1.25$, lg $K^\circ = +2.3$) the other. The latter complex can in fact be described essentially as an ion pair (cf. Section 5).

While the solvophobic effects discussed above do increase the stability of supramolecular associations, they necessarily lead to a simultaneous reduction in the *selectivity* of interactions between host and guest molecules. Water as a medium brings about these entropic and/or cohesive hydrophobic effects largely through the desolvation of individual particles. At the same time, however, it also promotes complexation through induction of di- or polypoles as a result of its extremely low polarizability-forces that once again show relatively little directional character (cf. Sections 6 and 7). By contrast, highly directional and thus selective Coulombic effects, including hydrogen bonding (Sections 5 and 8), are *reduced* by water and other polar media, and *increased* by nonpolar media.

5. Electrostatic (Coulombic) Interactions with Permanent Charges

Electrostatic (ES) forces play a central role in molecular association not only with respect to inorganic systems but also in biological phenomena, for example in the case of nucleic acids and proteins. Such systems have been the subject of extensive investigation particularly by *Warshel*[109] and by *Williams* et al.[165] Electrostatic interactions have also been shown to provide a suitable basis for developing organic host–guest complexes that illustrate particularly efficient and straightforward approaches to molecular recognition. According to the Debye–Hückel theory in the classical point-charge model, the potential between two ions is a function of the separation r, the charge numbers z, the unit charge e_0, and the dielectric constant ε, which is assumed to be uniform [Eq. (4)]. The variable χ includes changes in the

$$\psi = z_i e_0 \frac{1}{\varepsilon r} e^{-\chi r} \qquad (4)$$

activity coefficient—and thus also the salt effect (see below)—by way of the ionic strength $I = \frac{1}{2}\sum c_i z_i^2$ [Eq. (5)].

$$\chi = \left[\frac{8\pi N e_0^2 \cdot I}{1000 \cdot \varepsilon k T} \sum c_i z_i^2\right]^{1/2} \qquad (5)$$

According to *Bjerrum* the association constant between spherical ions $A^{\oplus}$ and $B^{\oplus}$ can be described as a function of the charge product $z_A \cdot z_B$ and a mean effective distance a between $A^{\oplus}$ and $B^{\ominus}$, which in addition to z_A, z_B, and ε determines the magnitude of the factor $Q(b)$ [Eq. (6)]. For a

$$K = \frac{4\pi N}{1000}\left[\frac{|z_A z_B|}{\varepsilon k T}\right]^3 \cdot Q(b) \qquad (6)$$

mean separation a of 5–7 Å Equation (6) predicts a relatively linear dependence of $\lg K$ on $z_A z_B$, which is in agreement with experimental equilibrium constants for numerous inorganic complexes—for example, with $[A^{2\oplus}B^{2\oplus}]$ for which $z_A z_B = 4$, $K \approx 10^2\ M^{-1}$.[165] Associations involving different metal ions, such as $Ca^{2\oplus}$ and $Mg^{2\oplus}$, especially with complicated organic anions, show considerable deviations, however, and these can be explained only partially on the basis of known ionic radii.[165] Problems related to the selection of a mean ionic distance[165, 167e] are also encountered in the description of contact ion pairs according to *Fuoss*, *Eigen*, *Denison*, *Ramsey*, et al.[167] for which the simplified relationship of Equation (7) is applicable.[167a]

$$pK = -2.6 - 3\lg a - \frac{560|z_A z_B|}{a\varepsilon} \qquad (7)$$

Empirically determined stability constants K include the sum of the constants for contact (K_{CIP}) and solvent-separated (K_{SSIP}) ion pairs, which in some cases can be distinguished spectroscopically.[167a] Other limitations associated with the above-described models [Equations (4)–(7)] include neglect of specific interactions between ions and solvent molecules. Thermodynamic measurements reveal that ion-pair formation, especially in water, usually results in an increase in entropy and sometimes even in an unfavorable value of ΔH°.[167a] Similar to the situation with solvophobic effects (see above), association here is favored primarily by the release of highly ordered solvent molecules from solvation shells surrounding the separated ions. Other forces responsible for ion-pair formation include (in addition to the classical Coulombic interaction) those resulting from induced dipoles, especially with highly polarizable electron clouds.[167] Thorough analysis of ion association is further hampered by serious measurement and evaluation problems, for example with conductometric procedures. The result can be differences of 50–100% in experimental K values,[168a, 169] especially at high concentrations and in the presence of foreign salts.[168b]

In view of the difficulty of characterizing inorganic ion pairs, it is surprising to find that equilibrium constants for currently known organic ionic host–guest complexes turn out to be predictable on the basis of simple rules.[126a] With water as the solvent a plot of ΔG_{HG} versus the number n of possible ionic interactions or salt bridges results in a linear correlation [Fig. 3 and Eq. (8)]. The slope here corresponds

$$\Delta G_{HG(ES)}[kJ\,mol^{-1}] = (5 \pm 1)\,n \qquad (8)$$

roughly to the constant calculated according to Equation (6) or (7) for $a = 5$ to 7 Å,[165] for example in the region of $z_A = z_B = 2$, but is surprisingly independent of the sizes and

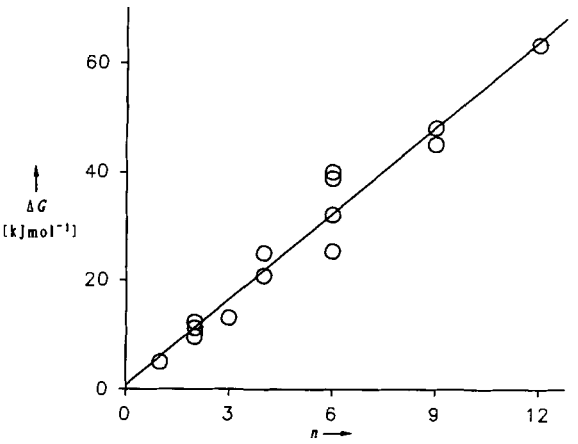

Fig. 3. Electrostatic interactions in ion pairs ($H^{x\oplus}G^{y\ominus}$); ΔG_{HG} vs. number of salt bridges n [Eq. (5)]; based on measurements in H_2O or D_2O at 300 K [126, 128].

polarizabilities of the ions involved: the examples presented in Schemes 4 and 12 as well as Figure 3 include (among others) $R_2NH^{2\oplus}$, $R_4N^{\oplus}$, pyridinium-$N^{\oplus}$, $R_4P^{\oplus}$, $-COO^{\ominus}$, $-SO^{3\ominus}$, $-OPO(OH)O^{\ominus}$, $-OPOO_2^{2\ominus}$, and phenolate-$O^{\ominus}$. Organic ion pairs with flexible alkane chains, examined by *Tam* and *Williams*,[169] also fall into the linear correlation (Fig. 2), since contrary to the expectations of the authors[169] entropy effects do not result in deviations greater than the limits of experimental error. The fact that a regular difference of $\Delta G_{HG} = 3$ rather than 5 kJ mol^{-1} was observed in complexes of the azoniacyclophane **2b** with electrically neutral and anionic naphthalene derivatives (Scheme 3) can be explained by assuming that in these complexes the dominant hydrophobic contribution to binding is diminished by the hydrophilic anionic substituent X. The prerequisites to correlations on the basis of Equation (1) are that a) for the electrostatic part comparisons are made to electrically neutral partner molecules that are as nearly isosteric as possible (e.g., Me_3COH with $Me_4N_{\oplus}$ in **8**, Schemes 4 and 12), and b) that n will be limited to salt bridges, which are based on direct $A^{\oplus}/B^{\ominus}$ contacts.

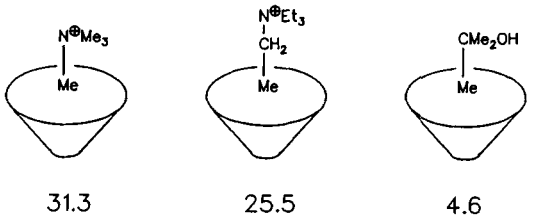

Scheme 12. Energies of complexation ΔG_{HG} [kJ mol^{-1}] with host **8** in D_2O (cf. with choline: 30 kJ mol^{-1}).

For straightforward systems such as the ion pair **8** · $^{\oplus}NMe_3R$ ($R = H_3C(CH_2)_n$) (Scheme 12, left for $n = 0$) the expected decrease in ΔG_{HG} with distance r^{-1} for a simple Coulombic relationship [Eq. (9)] can be verified experimentally (Fig. 4). In this case the distance r between the charge centers $O^{\ominus}$ and $N^{\oplus}$ was established from model geometries.

$$\Delta G_{HG(ES)} = \frac{q_A q_B}{\varepsilon r} \qquad (9)$$

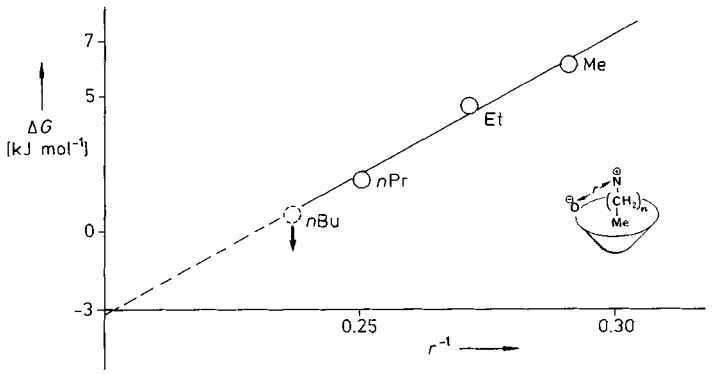

Fig. 4. Electrostatic interaction as a function of separation r in the ion-pair complex $\mathbf{8} \cdot {}^{\oplus}NR_4$ (R = $(CH_2)_nMe$) [131a] from data acquired in D_2O at 300 K.

The slope of the line derived from experiments in water led to $\varepsilon = 30$, providing evidence that the concept is realistic.

Charge distribution within the ions, which in the case of alkylammonium ions, for example, implies considerable delocalization onto the C and H atoms, has little influence on the total Coulomb energy. This has been demonstrated by simulations with various point charges using MO calculations, as well as[128] by the observed relative lack of dependence of the empirical correlations in Equation (8) on the nature of the ionic groups.[126a]

The principle of multiple salt bridges between charges situated in a complementary way permits the construction of receptors like **4** or **8** (Scheme 4) that bind such species as $ATP^{4\ominus}$ ($K = 10^{11}\ M^{-1}$) or the singly charged choline ($K = 5 \times 10^{4}\ M^{-1}$). This approach can be exploited for both catalysis (as in the case of **4**)[23a, 130] and inhibition (with **8**)[170] in appropriate reactions of these substrates.

Allosteric systems containing the elements of a simple proton pump can be conceived provided 1) the creation of a charge (and therefore a salt bridge) through uptake or release of a proton can be controlled and is accompanied by conformational changes in the receptor caused by the corresponding salt bridges or hydrogen bonds, and 2) these conformational changes lead to association or dissociation of another guest molecule. The macrocyclic resorcinol derivative **23** (Scheme 13) features optimal conformational coupling between precisely such processes.[131a] Since only the half-open conformation **23b** is suitable for binding choline, for example, (more generally: any species $^{\oplus}NMeR^3$), addition of a substance like this to a solution of the corresponding octaphenolate (**23a**), the latter dominating for reasons of strain, leads to the creation of two hydrogen bonds in **23b** and to the uptake of two protons from the solution. In a reversal of the process, an increase in pH causes release of the positively charged guest molecule from complex **23b** into the solution. The phenomenon is completely reversible and can be characterized unambiguously by NMR spectroscopy as a result of the differing symmetries of the conformers.

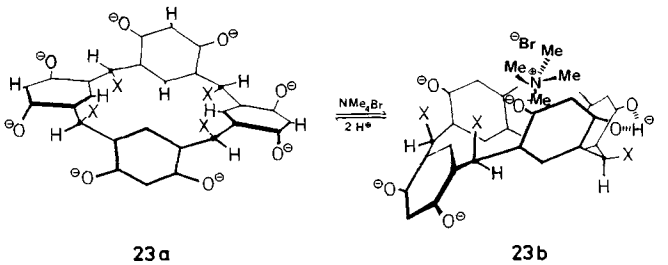

23a 23b

Scheme 13.

What influence does the microenvironment exert upon the stability of organic ion pairs?[167] A decrease in solvent polarity causes a considerable increase in association constants due to the reduction in dielectric shielding: with tetraethylammonium bromide, for example, from $K \approx 10\ M^{-1}$ in methanol to $K \approx 1000\ M^{-1}$ in 2-butanone.[167f] The simple $1/\varepsilon$ (ε = dielectric constant) relationship predicted by Equations (4) through (7) is seldom observed, however, in part due to solvent-dependent changes in the effective ionic separation a as well as specific donor and acceptor characteristics of the solvent molecules.[167] On the other hand, salt effects do induce ΔG_{HG} changes that are predictable from Debye–Hückel Equations (4) and (5), even for complicated anisotropic complexes like those with **2b** or **8**.[118] The observed lg K values show a linear dependence on ionic strength consistent with Equation (5) and have slopes remarkably close to those calculated from the charge numbers z for isotropically spherical ions or cavities (Fig. 5). This is true even with

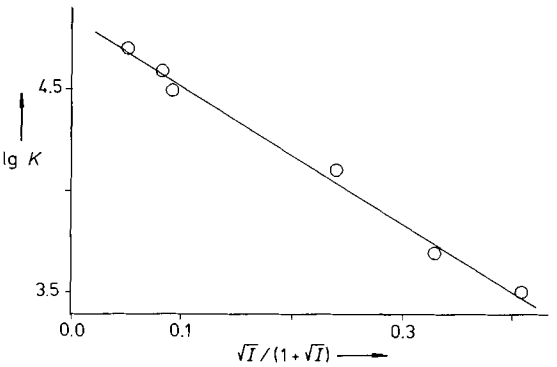

Fig. 5. Debye–Hückel plot of salt effects on the complex $\mathbf{8} \cdot {}^{\oplus}Et_4N$; slope: theoretical −4.07; observed −3.3. I = ionic strength [118].

foreign salt concentrations up to 0.5 M provided the correspondingly modified Debye–Hückel equation is used. Specific salt effects outside these correlations arise if foreign salt ions associate selectively with the host compound. Thus, with 0.1 M glycine solution, which is often used as a buffer, reduction in the association constant by a factor of 70 is observed with **2b** · ANS (Scheme 1).[118] Consideration of the salt effect, especially when there are significant electrostatic contributions to the binding (under some circumstances even with complex titrations) is therefore required for the interpretation of supramolecular complexation constants. On the other hand, salt effects can make it possible to quantify ionic contributions to binding. In the presence of nonionic binding forces the effect of even high concentrations of foreign salts is quite limited.[166, 167a, c, f] For example, 1 M NaCl leads to only a 15% increase in the association constant for a cyclodextrin complex (**3** · *p*-nitrophenolate).[118]

Although the analysis of complex ion pairs in terms of additive salt-bridge increments appears straightforward, quantitative description of systems with *partial* charges and di- or polypoles has proven difficult, even with the aid of MC, MD, and, more recently, FEP methods[103-111] (cf. Section 1). The situation is complicated partly because of the underlying charge distribution. Treatment of the solvent as a dielectric continuum according to *Kirkwood* or *Tanford* is increasingly being displaced by an explicit consideration of discrete solvent molecules,[105, 106, 109, 111] and several suggestions have been made for reducing the degree of computational effort entailed.[171] The inherent difficulty of a theoretical approach for a secure assignment of significant noncovalent forces becomes apparent, for example, with cyclodextrin complexes,[48-50, 52, 53] which have been regarded as being dominated either by electrostatic[50, 172] or dispersive factors[173] (cf. Section 7). We limit ourselves here to a consideration of electrostatic interactions with aromatic rings in host–guest complexes.

The charge distribution in benzene is characterized by partial positive charges on the hydrogen atoms and partial negative charges on the carbon atoms, the latter residing primarily in the π system[174] (Scheme 14). This distribution has

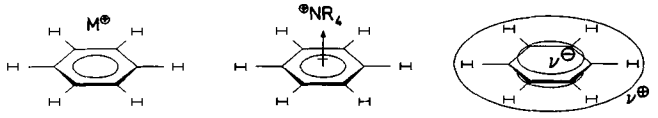

Scheme 14.

been quantified by means of various ab initio calculations[174, 175] and can be confirmed on the basis of the experimental quadrupole moment, whose direction lies in the C_6 symmetry axis z of the ring. The resulting Coulomb interactions are attractive for positively charged particles perpendicular to the plane of the ring and for negatively charged particles in the plane of the ring. Such interactions have been quantified[175, 176] with model calculations, and have also been measured, for example, for the association of potassium ion with benzene in the gas phase.[176a] Here again, entropy changes are responsible for much or all of the free energy of complexation.[176a] Model calculations[176a] for the energetically most favorable axial orientation of $K^{\oplus}$ over a benzene ring, once again using experimentally based parameters for charge and polarizability, reveal that interactions via induced dipoles (Section 6) play as large a role as Coulombic forces, and the role of dispersive forces (Section 7) is greater still.

All known organic host–guest compounds with charges vis-a-vis π systems demonstrate, due to the polarizable solvents, much weaker complexation than in the previously described gas-phase associations.[176] They are nevertheless stabilized by both electrostatic and induced dipole interactions (see below). Positive *partial* charges are probably also capable of associating with the negatively charged π faces of arenes. The best-known example is the however still controversial "edge-to-face" dimer of benzene itself.[177] Because of their low charge content such complexes are significantly less stable even in the gas phase. For this reason no definitive examples yet exist of "edge-to-face" stabilization within host–guest complexes in solution. On the other hand, systematic analysis of crystal structures does reveal a statistically significant accumulation of preferred conformations of this type.[91] *Hunter, Sanders*, et al.[67] have predicted in the case of porphyrin complexes not only solid-state but also solution structures on the basis of simplified calculations of Coulombic energies. They emphasize that the inevitably repulsive π–π interactions between arenes in a centrosymmetric stack—a consequence, of course, of the known charge distribution (Scheme 14)[91, 174-176]—can be transformed into attractive interactions by geometric displacement of the ring planes, or through appropriate charge redistribution brought about by heteroatoms within the ring systems.

In supramolecular structures such as **2b** · naphthalene, **24**, and **25** (Scheme 15), ammonium ions are so situated with respect to the π systems that they experience electrostatic attraction and can at the same time induce dipoles in the arenes. Whereas in **24** (R = H)[68] it is possible to envision a

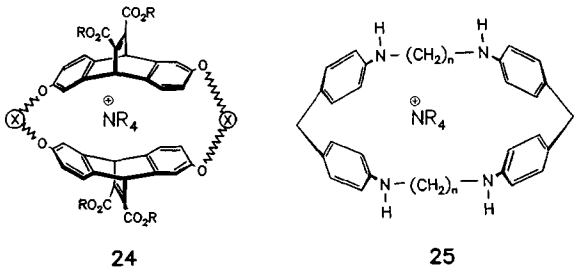

Scheme 15.

contribution from the potentially far-reaching Coulombic interaction[178] between the guest molecule and the external carboxylate group of the host, this cannot be the case with complexes such as **2b** · naphthalene or **25**. *Dougherty* et

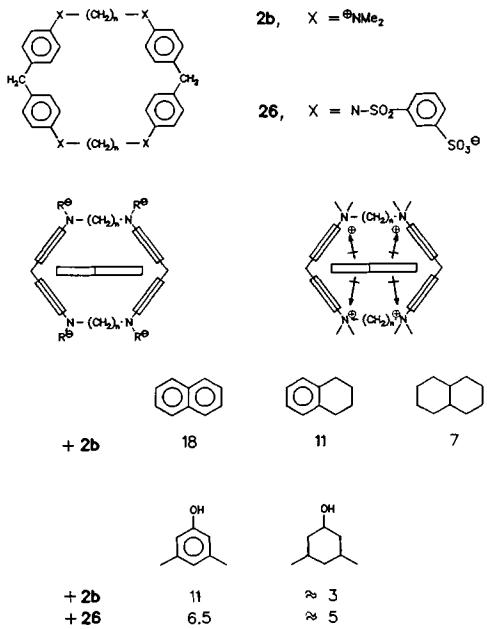

Scheme 16. Energy of complexation ΔG_{HG} [kJ mol^{-1}] for the reaction of the macrocyclic hosts **2b** and **26** with arenes and completely or partially hydrogenated arenes.

al.[68] have established for complexes of the type **24** a dominant influence of special $N^{\oplus}\cdots\pi$ interactions through the observed increase in ΔG_{HG} with addition of supplementary arenes as spacers ⊗ in the host compounds, as well as by complexation of positively charged substrates with the neutral receptor **24** (R = CH_3) in chloroform rather than water as solvent.[179]

In contrast to the otherwise similar **2b**, cyclophane **26** (Scheme 16) possesses no $N^{\oplus}$ unit in its cavity. The cavity is thus considerably more lipophilic, despite which **26** is *less effective* at binding naphthalene in water than **2b** with its hydrophilic cavity![180a] Only with aliphatic guest molecules does lipophilicity lead to the anticipated reverse order.[180b] These results can only be explained through special $N^{\oplus}$–π interactions, the various ΔG_{HG} values for which (Scheme 16) permit estimation of an increment ($\Delta G_{N^{\oplus}/\pi}$) of about 2 kJ mol^{-1} as the cause of the interaction (in water). The relative contributions of the individual electrostatic and dipole-induced mechanisms to this interaction, however, need to be discussed further (Section 6).

6. Van der Waals Interactions: Induced Dipoles (IN Interactions)

The notion that complex stabilization through the interaction of charged particles is due largely to induction of dipoles in easily polarizable electron clouds is supported by more than empirically based calculations on gas-phase associations.[176] The azoniacyclophane **2b** in aqueous solution binds diiodomethane, but not dichloromethane (Scheme 17) even though the latter has a C–Hal dipole moment that is equally well suited to Coulombic attraction. Moreover, *negative* charges can also lead to attractions through dipole induction in π systems, as illustrated by **19b**[181] in Scheme 17. Observed NMR shifts indicate a geometry for the complex with **19a** similar to that of **19b**. In view of what are presumably repulsive electrostatic interactions in **19b** between X = $SO_3^{\ominus}$ and the π cloud the stability demonstrated by this complex is rather high, which together with the other observations supports the conclusion that the increments $\Delta G_{N^{\oplus}/\pi} \approx 2$ kJ mol^{-1} derived in Section 5 should be ascribed largely to induction of a dipole.

A similar increment for the interaction between charges and π systems emerges from the equilibria for association of di- and trications with corresponding di- and trianions containing varying numbers of benzene rings (for examples see Scheme 18).[128] The structures were selected in such a way that contact would always be possible between the cationic and anionic centers. Geometries were tested in some cases by molecular simulation with the CHARMm force field,[108] and the results agree qualitatively with observed NMR shieldings. Neglecting two complexes in which the conformational fits were inadequate, results obtained for nine ion pairs with various experimental techniques (NMR[128] and UV/VIS[128] spectroscopy, conductivity[168b]) showed not only the expected dependence of complex stability on the number *n* of salt bridges [Eq. (5)] but also a dependence on the number *m* of aromatic rings present in the ion pair. If one subtracts from the experimental ΔG_{HG} values the electrostatic increment $\Delta G_{ES} = 4.8$ kJ mol^{-1} per salt bridge *n* obtained by studying ion pairs lacking supplementary interactions (for example zinc sulfate, cf. Section 5), one then ob-

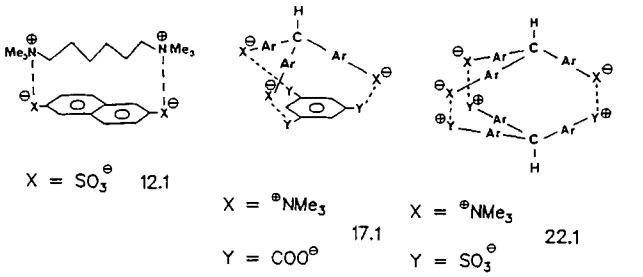

Scheme 18. ΔG_{HG} values [kJ mol^{-1}] of associations of di- and trianions in H_2O or D_2O at 300 K. Ar = aryl.

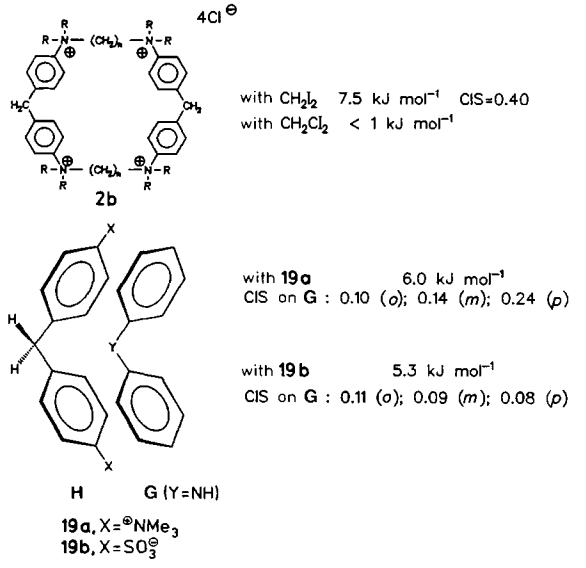

Scheme 17. Energies of complexation and CIS values for complexation of CH_2I_2 and CH_2Cl_2 with **2b** and for **G** with **19a** or **19b**. (*o*), (*m*), (p): *ortho*, *meta*, and *para* protons of the phenyl rings of **G**.

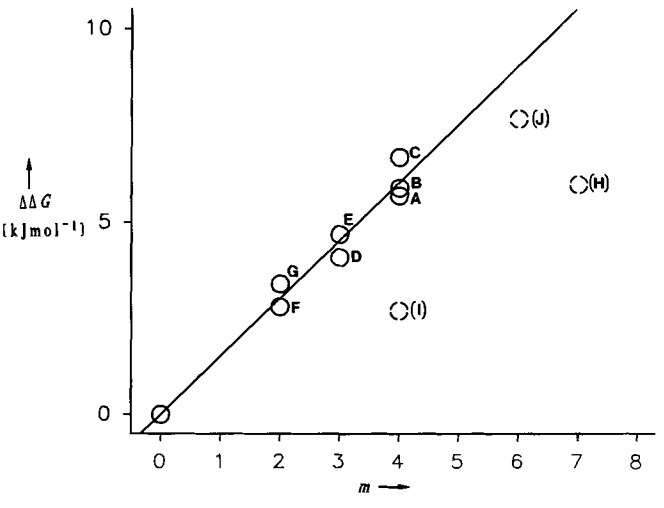

Fig. 6. Additional van der Waals interactions $\Delta\Delta G$ in aromatic ion-pair complexes (examples in Scheme 18) as a function of the number *m* of phenyl rings (based on measurements in H_2O/D_2O at 300 K, [128]); deviations in the case of *I*, *H*, *J* (not taken into account in the correlation): cf. text.

tains a linear correlation between the induced-dipole increment, $\Delta G_{IN} = (\Delta G_{HG(exp)} - 4.8n)$, and the number m (Figure 6).[128] The slope of the linear correlation that results from applying the principle of additive increments [Eq. (1)] corresponds to ca. 1.5 kJ mol^{-1} per arene, and it agrees once again reasonably well with the increments reported above even though these were obtained quite independently. The linear correlation implies that the small conformational shifts required for optimal attraction (i.e., shifts of the arenes relative to one another as well as to the available charges) are always achieved thanks to the flexibility of the complexes. This in turn explains why repulsive interactions such as those between centrosymmetrically arranged stacks of aromatic systems do not develop in supramolecular complexes, which are instead stablilized by a multitude of attractive interactions of the electrostatic and induced-dipole type.

Induced dipoles can also be identified as probable causes of the binding differences between different nucleosides and nucleotides in azoniacyclophanes such as **2b**, since complex stability increases with the polarizability of the nucleobase (Scheme 19).[181] Observed NMR shifts prove that, in con-

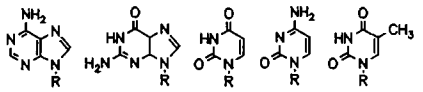

	A	G	U	C	T
for R=					
ribose	10	≈6.5	≈6	≈7	–
ribose–$OPO_2^{2\ominus}$	19.3	15.9	17.3	18.3	17.6

Scheme 19. Energies of complexation ΔG_{HG} [kJ mol^{-1}] for nucleotides and nucleosides with **2b**.

trast to the adenosine phosphate receptor **4** of *Lehn, Hosseini*, et al.,[23a] the nucleobases are bound by **2b** *within* the van der Waals cavity, whereas the hydrophilic sugar residues remain on the periphery of the cavity. It is remarkable in this context that the permethylated azoniacyclophane **2b** proves to be one of the strongest complexation agents of the polyamine type with respect to DNA, as shown by fluorescence titration with ethidium bromide as indicator.[181]

7. Van der Waals Interactions: Dispersive (DI) and Charge-Transfer (CT) Contributions; "Stacking"

Numerous studies of organic host–guest complexes make reference to electron donor–acceptor (EDA) interactions, although these actually represent nothing more than the sum of highly variable electrostatic (Coulombic and induced, Sections 5 and 6) and higher-order (e.g., dispersive and CT, see below) effects.[97, 182] Ab initio SCF calculations for simple EDA complexes suggest primarily electrostatic contributions in the case of "hard" Lewis acid–base complexes such as $H_3N \cdot BH_3$, but for "soft" combinations like $C_6H_6 \cdot Cl_2$ roughly comparable electrostatic, dispersive, and CT contributions. It should be noted that we are referring here to gas-phase calculations, and that partitioning of the energy is to some extent arbitrary.[182]

Charge-transfer (CT) complexes are stabilized by the transfer of electrons from high-lying occupied MOs into low-lying unoccupied MOs.[183] Increases in complexation constants have occasionally been observed as a result of alternating electron-withdrawing and electron-donating groups,[196] but these are presumably also due to electrostatic and induced-dipole contributions: even for the strongest CT complexes between 1,3,5-trinitrobenzene and, for example, hexamethylbenzene in CCl_4 solution ΔG_{HG} is only 4.6 kJ mol^{-1}, and with toluene in fact -2 kJ mol^{-1}[183]—that is to say, a negligible effect, especially in polar solvents. Complexation constants for various arene-containing ionic associations (Scheme 18) are subject to correlation *without* reference to CT contributions simply on the basis of electrostatic and induced-dipole increments (cf. Fig. 6), although the complexes, for example, with the unusually electron-poor species methylviologen (Scheme 4) do show typical CT bands in their electronic spectra.[128]

The π–π or "stacking" complexes are subject to stabilization from the three sources, namely electrostatic, induced dipole, and dispersive contributions, in addition to solvophobic effects. Various complexes with a face-to-face arrangement between host and guest—stable even in lipophilic media—have recently been described [Scheme 7 compound **17** and Scheme 8 compound **20**]. They suggest that there may be an increase in ΔG_{HG} with increasing surface of the π system, a significant observation with respect to DNA intercalations as well. The hydrogen bonds in *Rebek*'s complexes[35h] (Scheme 20) function in the sense of Equation (1) as a fixed interaction; each benzene unit then supplies a reasonably constant binding increment of $\Delta G_{\pi/\pi} = 1.8$ kJ mol^{-1}.

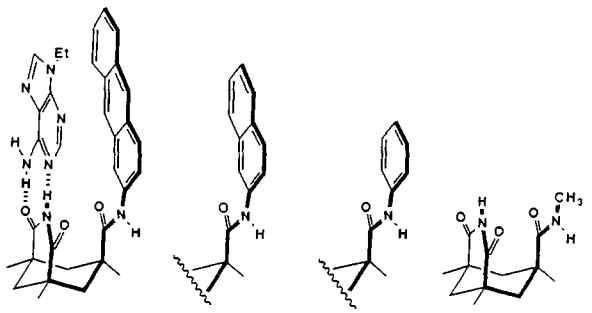

K	440	220	100	50
$\Delta\Delta G_{HG}$		1.72	1.96	1.72

Scheme 20. Complexation constants K [M^{-1}] and $\Delta\Delta G_{HG}$ values [kJ mol^{-1}] in $CDCl_3$ for associations of the derivatives of *Rebek*'s tricarbonic acids and 9-ethyladenine [35h].

Dispersive or London–Eisenschitz interactions result from attraction between fluctuating transient dipoles that also develop in nonpolar bonds. The dependence of such interactions upon the actual separation r relative to the van der Waals distance r_0 is usually given by the Lennard-Jones potential [Eq. (10a)] or the Buckingham equation [Eq. (10b)].

$$V = C\left[\left(\frac{r_0}{r}\right)^{12} - 2\left(\frac{r_0}{r}\right)^{6}\right] \quad (10a)$$

$$V = Ce^{-112.5\,r_0/r} - C'\left(\frac{r_0}{r}\right)^{6} \quad (10b)$$

The first terms in these equations represent repulsion due to approach closer than the distance r_0; the applicable constants (C and C') can be derived from polarizability parameters among other sources. The extent of the calculated gas-phase interaction between two relatively nonpolarizable C–H bonds amounts to only ca. 0.2 kcal mol^{-1} even at the optimal distance, but the cumulation in the case of organic molecules as a result of the large number of bonds present leads, for example, to 25 kJ mol^{-1} in the case of two *n*-hexane chains. Determinations of transfer energies for linear alkanes from the gas phase into water give average values $\Delta H = 1.5$ and $T\Delta S = 0.5$ kJ mol^{-1} for the hydrophobic contribution per CH_2 group, whereas CH_3 groups make equivalent contributions (1.4 kJ mol^{-1}) to both the enthalpy and the entropy terms. Despite their sometimes high ΔG values, dispersive forces contribute only slightly to *selectivity* in molecular recognition. Potentials (10a) and (10b) require only a single—though narrowly defined—contact distance between **H** and **G**, and are much less orientation-dependent than the other intermolecular forces discussed previously.

Intermolecular London–Eisenschitz interactions are not reduced as much in water as they are in organic solvents, which are much more polarizable. Complex formation with the cryptophanes of *Collet* et al.[33] is therefore observed only when the lipophilic solvent molecule is chosen so large that it cannot enter the cavity. The cleft compound **17** described by *Zimmerman* et al.[74] represents one of the rare examples to date of purely hydrophobic π–π complex formation in chloroform despite the fact that the cavity in this case permits the entry of solvent molecules.[74, 111c] Nevertheless, association is limited to species like tetranitrofluorenone, which is both polar and polarizable; with the less polar and polarizable adenine complexation requires the presence of a supplementary hydrogen bond:[74a] introduction of a carboxyl group into receptor **17** causes adenine binding in chloroform with the remarkably high complexation energy of 24 kJ mol^{-1}.[74a] A simple carboxylic acid function adds only $\Delta G_{HG} = 7$ kJ mol^{-1}, so the net gain in stacking energy for adenine is 17 kJ mol^{-1}, a value in good agreement with calculations based on perturbation theory.[111c]

Dispersive forces between **H** and **G** generally play a significant role only in aqueous medium due to the low polarizability of water. At the same time, these become difficult to distinguish from solvophobic effects (cf. Section 4). The literature on cyclodextrin complexes is almost impossible to summarize, but an attempt will nonetheless be made to demonstrate on the basis of a few examples the ways in which binding mechanisms can be distinguished in aqueous solution. Calorimetric measurements[185] suggest negligibly small entropy contributions for the complexes of α- and β-cyclodextrin (**3** and **4** respectively) with adamantane-1-carboxylate.[185a] In contrast to these results, association with γ-cyclodextrin (**5**) is favorable only because of entropy factors, (ΔH is in fact unfavorable; Scheme 21), since here the large size of the cavity relative to the α and β compounds makes it unsuitable for effective dispersive forces. Similar conclusions can be drawn from equilibrium studies with *p*-nitrophenol and its anion[159, 186] (Scheme 21); anion formation, with the resulting accumulation of a highly polarizable charge, is considerably more advantageous with the narrower α-cyclodextrin cavity, since here dispersive forces

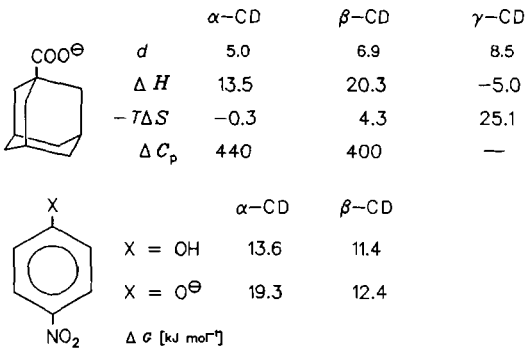

Scheme 21. Energy of complexation [kJ mol^{-1}] and change in heat capacity ΔC_p [J mol^{-1}K^{-1}] in H_2O or D_2O for the complexation of cyclodextrins **2**, **3**, and **4** (α-, β-, and γ-CD respectively) with adamantane-1-carboxylate and nitrobenzene derivatives, from calorimetric measurements [185a].

which require a close contact predominate. These experiments show that at least two different mechanisms govern the formation of cyclodextrin complexes, but they do not allow secure predictions as to which cavity will be most effective for the complexation of a particular substrate. Competition experiments with guest molecules containing simultaneously larger and smaller residues (e.g. naphthyl and phenyl; cf. Scheme 22) show by NMR shifts and NOEs that, in general, binding within larger cavities is preferred over binding in those cavities that offer the best fit. This is consis-

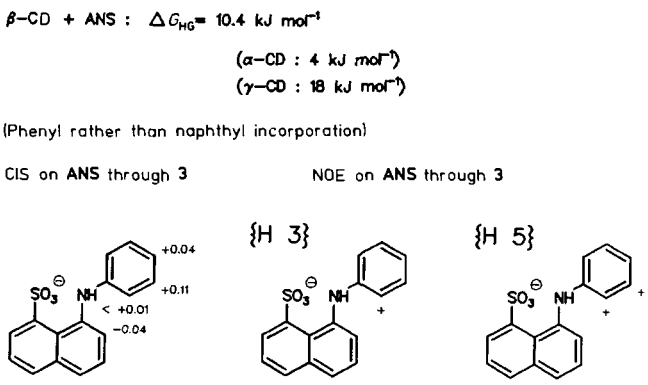

Scheme 22. **3** = α-CD.

tent with the observation that many monosubstituted benzene derivatives associate more strongly with β- than with α-cyclodextrin[159] (Scheme 10).

8. Hydrogen Bonds

Similarly to EDA complexes, hydrogen-bonded associations[187] involve the participation of at least three interaction mechanisms: electrostatic (Coulombic), dispersive, and charge-transfer. The predominant role of Coulombic forces has become increasingly apparent through quantum-chemical calculations utilizing larger basis sets, and it is supported by experimental evidence of a stability dependence for appropriate complexation systems on the acidity of the donor X–H and the basicity of the acceptor Y.[189] For this reason, structures and energies of such complexes (Schemes 23 and

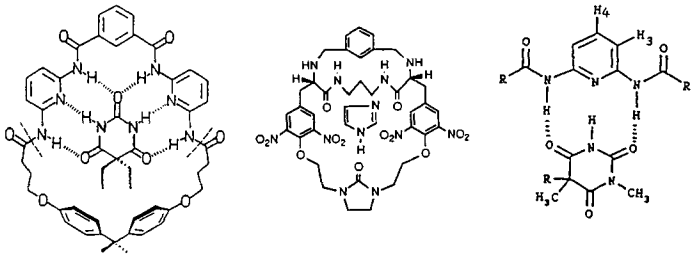

27 28 29

Scheme 23. Host–guest complexes with hydrogen bonds (see also **15** in Scheme 7).

24) are most often calculated on the basis of Coulomb potentials. Interactions of this type are relatively insensitive to changes in charge separation distance (cf. Section 5), but the central role of positively charged hydrogen leads to the highest directional specificity of all the interactions, as demonstrated by calculations based either on point charges (Scheme 24, model **a**) or on the presence of two dipoles (Scheme 24, model **b**). A significant factor in this directional specificity is anisotropy in the charge distribution at typical acceptor atoms Y (e.g., for lone pairs), a factor that is neglected in most force fields.

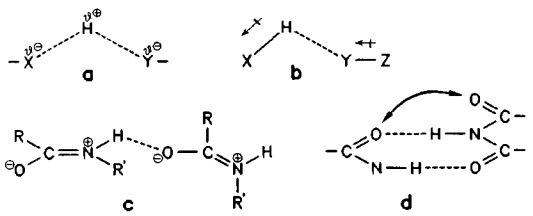

Scheme 24.

Due to their charge distributions, carboxylic acid amides are predestined for hydrogen bonding (Scheme 24). Such bonds dominate therefore not only in proteins[91] but also in the most successful known cases of selective binding in organic host–guest complexes. The groups of *Rebek*,[35] *Hamilton*,[39] and *Still*[76] (Schemes 4, 23) have been especially active in designing systems containing multiple complementary hydrogen donor–acceptor sites, which are also well suited for chiral recognition. The strength of a simple amide hydrogen bond[190] was until now derived, for example, from measurements with *N*-methylacetamide in carbon tetrachloride, with results that varied between 4[190b] and 7 kJ mol^{-1}[190c] depending upon the method. The principle of additive binding increments [Eq. (1)] makes it possible to establish a more reliable ΔG value,[127] one that is free of the problems associated with the stoichiometry and geometry of simple dimers.[190b,c] A plot of a large number of literature values for ΔG_{HG} determined in chloroform versus the number n of possible hydrogen bonds in each case leads to a straight line (Fig. 7), the slope of which provides the increment $\Delta G_{HB} = 5 \pm 1$ kJ mol^{-1}.[127a] The solvent chloroform itself associates with amides ($K \approx 1$ M^{-1}[190a]); therefore, experiments were also conducted in CCl_4 and carried out with reference to self-association using the simpler model **29** (Scheme 23), leading to an increment $\Delta G_{HB} \approx 10$ kJ mol^{-1}.[127] Addition of methanol leads in the case of **29** to a linear decrease in complexation, and with only 10% (v + v) CH_3OH in CCl_4 the complexation constants are reduced by a factor of about 100.[127b] In the presence of the even more efficient hydrogen-bonding component water only an extremely strong acid–base pair such as $FH\cdots F^{\ominus}$ ($K = 4$ M^{-1})[187,189] forms complexes of this type; there is a total absence of complexation under aqueous conditions in the case of amides.[79,111a,187] Were it not for supplemental contributions toward association from the entropy,[79,84] peptide fragments would be capable of forming hydrogen bonds only in the hydrophobic interiors of proteins. Possible interferences due to polar or polarizable amino acids, as well as cavity-dependent solvophobic effects, can lead here to variable incremental values per hydrogen bond. For this reason pairwise interactions determined experimentally with peptides and proteins vary between ca. 2[91,191] and ca. 20 kJ mol^{-1}[90c] per amide bridge!

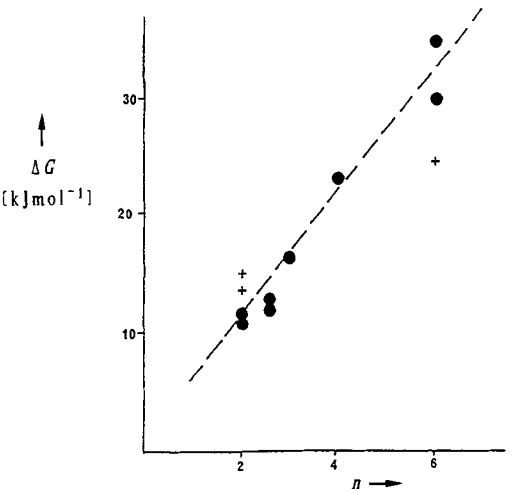

Fig. 7. Complexation energies ΔG for compounds containing the structure R–CONHR′– (mostly amides) in $CDCl_3$ as a function of the number n of hydrogen bonds [127]. The compounds indicated on the graph as + show additional stabilization through stacking or destabilization through entropy losses.

Linear correlation of ΔG_{HG} with n (Fig. 7) ignores such positive secondary interactions as the stacking effects that result from the presence of additional π systems,[35] as well as negative factors accompanying unusually large losses in entropy.[39] *Rebek* et al.[192] recently observed systematically higher association values for amide–amide and lactam–lactam bridges relative to imide–imide or imide–lactam bridges. Destabilization of the latter by about 1.5 kJ mol^{-1} (in $CDCl_3$) can be interpreted in terms of electrostatic repulsion by the additional carbonyl groups present in the imides (cf. **d** in Scheme 24) and can be reproduced quantitatively by MC–FEP calculations.[193]

In the case of interactions in nucleic acids, the distinction between Watson–Crick and Hoogsteen base pairs is of particular significance.[194] *Rebek* et al.[35h] have succeeded in demonstrating with the adenine receptors not only the Watson–Crick pairing illustrated in Scheme 20, but also (by varying the arenes involved in stacking in the host com-

pound) Hoogsteen complexation, as well as the simultaneous presence of both types of interaction with the cleft compound **15** (Scheme 7). Model systems of this sort should make it possible to achieve a clearer understanding of the distortion of the DNA double helix caused by intercalated substances, and eventually permit its exploitation for medicinal purposes.[195]

9. Conclusions and Prospects

The systematic investigation of organic host–guest compounds in solution permits positive identification of important noncovalent interactions. Departing from the crystalline state does have its price, however: one must be content with imprecise descriptions of aggregates equilibrating in solution. Similarly, the advantages connected with studying complicated associations in solution instead of simple complexes in the gas phase come at the expense of precise statements on the relevant mechanisms and their energy contributions (cf. Table 2). Even inorganic ion pairs, and even more so organic substrate–receptor complexes, owe their existence to a multitude of noncovalent forces; in solution it is the entropy term that often proves decisive. Nevertheless, synthetic complexes allow extensive and planned variation of functionalities and shape in controlled conformations, and are in principle better suited for the isolation and manipulation of individual mechanisms than biological systems. As in classical physical-organic chemistry, systematic variation of host and guest structures and their microenvironments in solution permits the identification of generalizable parameters that can subsequently be applied to problems of even greater complexity. The increments listed in Table 2 can be of assistance in the design of new supramolecular complexes, allowing one to make quantitative predictions on behavior, on the basis, for example, of salt bridges and hydrogen bonds between subunits and reflecting, at least in principle, infinite variability with respect to stability and function.

One important group of complexes has so far been ignored in this overview even though it represents a subject of increasing importance. The combination of metals with organic ligands has led not only to fascinating template-synthesis strategies[37, 70]—with promising technical, analytical, and pharmaceutical implications—but also to the construction, for example, of a fully synthetic double helix.[23f] Conformational coupling of metallic binding centers[196] with other

Table 2. Typical intermolecular interactions [a] in organic host–guest complexes.

Type		Geometric factor	Example	Medium	Typical ΔG_{HG} [kJ mol^{-1}]	Ref.
ES	ion–ion	$\frac{q_A q_B}{r}$	$RCOO^{\ominus} + {}^{\oplus}NR'_4$	H_2O	5 ± 1	[126a]
			$Br^{\ominus} + {}^{\oplus}NR_4$	EtCOMe	17	[167f]
			$Br^{\ominus} + {}^{\oplus}NR_4$	MeOH	6	[167f]
	ion–dipol	$\frac{q\mu}{r^2}$	$(-CH_2)_2O + {}^{\oplus}NR_4$	$CHCl_3$	≈ 3	[72c]
	ion–quadrupol	$\frac{qQ}{r^3}$	${}^{\oplus}NR_4$ + Aren	H_2O	≈ 1	[128, 180b, 181]
IN	ion–dipole$_{IN}$	$\frac{q^2\alpha}{2r^4}$	${}^{\oplus}NR_4$ + Aren	H_2O	1–2	"
			${}^{\oplus}NR_4 + CH_2I_2$	"	"	"
DI	dipole$_{IN}$–dipole$_{IN}$	$A\left[\frac{r_0}{r}\right]^6$	C–H/C–H	(gas)	0.2 (calcd.)	[97–99]
			arene + arene	$CDCl_3$	1.75	[35h]
CT			$Ph(NO_2)_3$ + PhMe	CCl_4	−2	[183]
HB-hydrogen bond			amide + amide	$CHCl_3$	5 ± 1	[127]
			amide + amide	CCl_4	≈ 10	[127]
			$(-CH_2)_2O + {}^{\oplus}NHR_3$	$CHCl_3$	≈ 9	[72c]
hydrophobic effect			$-CH_2-$ + alkane	H_2O	2.3	[143]
			$-CH_3$ + alkane	H_2O	1.4	[143]
			arene + arene	H_2O	0.4 (per Å^2)	[154]

[a] Abbreviations: ES = electrostatic or permanent charges, IN = induced dipoles, DI = dispersive; q = charge; r = distance.

centers opens the way to the formation of allosteric systems possessing more effective cooperativity than that found in proteins. For example, we have recently synthesized various receptors containing coordination centers for transition-metal ions in the form of ethylene diamine or amino acid units in conjunction with a second lipophilic or polar binding center (Scheme 25, **30**–**32**).[197] System **30** displays the greatest degree of positive cooperativity between a polar and a lipophilic center yet recorded (Scheme 26),[197a] whereas **31** is characterized by somewhat less pronounced negative cooperativity, releasing a second ionically bound substrate upon binding, for example, a cadmium ion.[197c]

Finally, we touch upon the question of which of the interactions discussed will play a key role in the development of enzyme-analogous catalysts. In principle all of the mechanisms are capable of assisting in stabilization not only of the essential binary or ternary complexes but also of transition states for the reactions subject to catalysis, with multiple interactions again potentiating the efficiency consistent with Equation (1). It must be noted, however, that higher-order

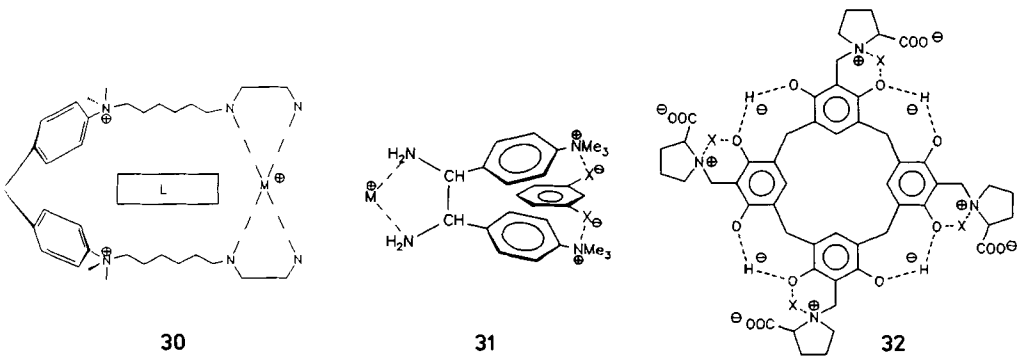

30 **31** **32**

Scheme 25. Receptors containing coordination centers for transition-metal ions in conjunction with lipophilic or polar binding sites.

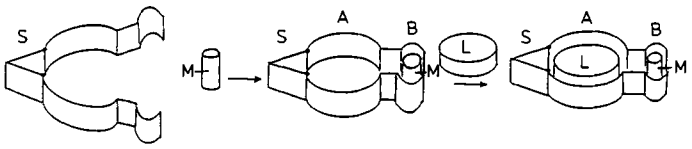

Scheme 26. Schematic representation of the cooperativity displayed by binding sites. S = hinge, M = metal ion, B = polar binding site, L = lipophilic guest molecule.

interactions (Section 7) demand a particularly precise geometrical fit between catalyst and substrate due to the rapid decline of such forces with increasing intermolecular separation r (cf. Table 2). A close fit is especially difficult to achieve in the stabilization of short-lived transition states. Nature alone has succeeded in meeting this challenge through millions of years of evolution, taking advantage of cooperative interactions of all the various mechanisms. In particular, electrostatic interactions with their extremely long-range character are especially promising in the development of synthetic enzyme-analogous systems, which should also be suitable for more than just one specific substrate.

Our work in Saarbrücken was supported by the Deutsche Forschungsgemeinschaft, the Fonds der Chemischen Industrie, and in part by the Volkswagen-Stiftung. I am particularly grateful for the efforts of all the co-workers cited in our publications. They have not only learned to apply, both intellectually and in practice, a wide diversity of methods, but in the course of overcoming a multitude of synthetic problems they have also provided the prerequisites without which the actual experiments and their subsequent interpretation would have been impossible.

Received: April 22, 1991 [A840 IE]
German version: *Angew. Chem. 103* (1991) 1419
Translated by: Dr. W. Russey Huntingdon PA (USA)

[1] J. L. Atwood, J. E. D. Davies, D. D. MacNicol (Eds.): *Inclusion Compounds*; a) Vol. 1: *Structural Aspects of Inclusion Compounds Formed by Inorganic and Organometallic Hosts*; b) Vol. 2: *Structural Aspects of Inclusion Compounds Formed by Organic Host Lattices*; c) Vol. 3: *Physical Properties and Applications*, Academic Press, London 1984; d) Vol. 4: *Key Organic Host systems*; e) Vol. 5: *Inorganic and Physical Aspects of Inclusion*, Oxford Universitzy Press, Oxford 1991.

[2] F. Vögtle: *Supramolekulare Chemie*, Teubner, Stuttgart 1989; *Supramolecular Chemistry*, Wiley, Chichester 1991.

[3] F. Vögtle (Ed.): *Host Guest Complex Chemistry*; a) Part I: *Top. Curr. Chem. 98* (1981); b) Part II: *ibid 101* (1982); Part III: *ibid. 121* (1984).

[4] F. Vögtle (Ed.): *Cyclophanes*; a) Part I: *Top. Curr. Chem. 113* (1983); b) Part II: *ibid. 115* (1983).

[5] F. Vögtle, E. Weber (Eds.): *Host Guest Complex Chemistry – Macrocycles, Synthesis, Structures, Applications*, Springer, Berlin 1985.

[6] Z.-I. Yoshida, N. Ise (Eds.): *Biomimetic Chemistry*, Kodansha, Tokio Elsevier, Amsterdam 1983 (Proc. 2nd Int. Kyoto Conf.).

[7] *Biomimetic and Bioorganic Chemistry*; a) F. L. Boschke (Ed.): Part I: *Top. Curr. Chem. 128* (1985) b) F. Vögtle, E. Weber (Eds.): Part II: *ibid. 132* (1986); c) F. Vögtle, E. Weber (Eds.): Part III: *ibid. 136 (1986)*.

[8] Y. Murakami (Ed.): *New Frontiers in Supramolecular Chemistry (Supramolecular Assemblies)*, Mita Press, Tokyo 1990.

[9] J. F. Stoddart (Ed.): *Monographs in Supramolecular Chemistry*; a) C. D. Gutsche: *Calixarenes*; b) F. Diederich: *Cyclophanes*, Royal Soc. Chem., Cambridge 1989, 1991.

[10] S. M. Roberts (Ed.): *Molecular Recognition: Chemical and Biochemical Problems*, Royal Soc. Chem., Cambridge 1989.

[11] J. L. Atwood (Ed.): *Inclusion Phenomena and Molecular Recognition*, Plenum, New York 1990.

[12] H.-J. Schneider, H. Dürr (Eds.): *Frontiers in Supramolecular Organic Chemistry and Photochemistry*, VCH, Weinheim 1991.

[13] J. Vicens, V. Böhmer (Eds.): *Calixarenes*, Kluwer, Dordrecht 1990.

[14] *Host-Guest Molecular Interactions: From Chemistry to Biology* (Ciba Foundation Symposium 158), Wiley, Chichester 1991.

[15] M. L. Bender, M. Komiyama: *Cyclodextrin Chemistry*, Springer, Berlin 1977.

[16] a) J. Szejtli: *Cyclodextrins and their Inclusion Complexes*, Akademiai Kiado, Budapest 1982; b) J. Szejtli: *Cyclodextrin Technology*, Kluwer, Dordrecht 1988; c) D. Duchene (Ed.): *Cyclodextrins and Their Industrial Uses*, Ed. Santé, Paris 1987.

[17] L. F. Lindoy: *The Chemistry of Macrocyclic Ligand Complexes*, Cambridge University Press, Cambridge 1989.

[18] R. M. Izatt, J. J. Christensen (Eds.): *Progress in Macrocyclic Chemistry*, a) Vol. 1; b) Vol. 2; c) Vol. 3 Wiley, New York 1979, 1982, 1986.

[19] Y. Inoue, G. W. Gokel (Eds.): *Cation Binding by Macrocycles* (Complexation of Cationic Species by Crown ethers); Marcel Dekker, New York, 1990.

[20] E. Weber (Ed.): *Molecular Inclusion and Molecular Recognition Clathrates*; a) Part I: *Top. Curr. Chem. 140* (1987); b) Part II: *ibid. 149* (1988).

[21] a) D. D. MacNicol in [1b], p. 1, p. 123; b) J. E. D. Davies, P. Finocchiario, F. H. Herbstein in [1b], p. 407; c) F. Toda, *Top. Curr. Chem. 149* (1988) 211.

[22] a) D. J. Cram, *Angew. Chem. 98* (1986) 1041; *Angew. Chem. Int. Ed. Engl. 25* (1986) 1039; b) *Science 240* (1988) 760; c) D. J. Cram, K. N. Trueblood in [5], p. 125; d) D. J. Cram, *J. Inclusion Phenom. 6* (1988) 397; e) D. J. Cram, K. N. Trueblood in [3a], p. 43.

[23] a) J.-M. Lehn, *Angew. Chem. 100* (1988) 91; *Angew. Chem. Int. Ed. Engl. 27* (1988) 89; b) in [6], p. 1, p. 163; c) *Science 227* (1985) 849; d) *J. Inclusion Phenom. 6* (1988) 351; e) in [12], p. 1; f) *Angew. Chem. 102* (1990) 1347; *Angew. Chem. Int. Ed. Engl. 29* (1990) 1304.

[24] a) R. Breslow in [1c], p. 473; b) *Science 218* (1982) 552; c) in [6], p. 1; d) *Adv. Enzymol. Relat. Areas Mol. Biol. 58* (1986) 1; e) in [14] S. 115.

[25] I. Tabushi, K. Yamamura in [4a], p. 145; b) I. Tabushi, Y. Kuroda, *Adv. Catal. 32* (1983) 417; c) I. Tabushi, *Tetrahedron 40* (1984) 269; d) *Pure Appl. Chem. 58* (1986) 1529; e) in [1c], p. 445.

[26] a) F. Vögtle, W. M. Müller, W. H. Watson, *Top. Curr. Chem. 125* (1984) 131; b) E. Weber, F. Vögtle in [3a], p. 1; c) F. Vögtle, H. Sieger, W. M. Müller in [3a], p. 107; d) L. Rossa, F. Vögtle, in [4a], p. 1; e) J. Franke, F. Vögtle in [7a], p. 137; f) F. Vögtle, H.-G. Löhr, J. Franke, D. Worsch, *Angew. Chem. 97* (1985) 721; *Angew. Chem. Int. Ed. Engl. 26* (1985).

[27] a) Y. Murakami in [4b], p. 107; b) in [11], p. 107; c) in [8], p. 173; d) *Pure Appl. Chem. 66* (1988) 549; e) in [12], p. 145.

[28] a) K. Odashima, K. Koga in: P. M. Keehn, S. M. Rosenfeld (Eds.): *Cyclophanes, Vol. 2*, Academic Press, New York 1983, p. 629; b) K. Koga in: *Proc. 31st IUPAC Congr. Sofia 1987*, Section 6, p. 100; c) K. Koga, S. Sasaki, *Pure Appl. Chem. 60* (1988) 539; d) S. Sasaki, K. Koga, *J. Inclusion Phenom. Mol. Recognit. Chem. 7* (1989) 267.

[29] a) F. Diederich, *Angew. Chem. 100* (1988) 372; *Angew. Chem. Int. Ed. Engl. 27* (1988) 362; b) in [11], p. 93; c) in [12], p. 167; d) *J. Chem. Educ. 67* (1990) 813; e) D. B. Smithrud, E. M. Sanford, I. Chao, S. B. Ferguson, J. D. Evanseck, K. N. Houk, F. Diederich, *Pure Appl. Chem. 62* (1990) 2227.

[30] a) J. F. Stoddart in [10], p. 243; b) *Pure Appl. Chem. 60* (1988) 467; c) H. M. Colquhoun, J. F. Stoddart, D. J. Williams *Angew. Chem. 98* (1986) 483; *Angew. Chem. Int. Ed. Engl. 25* (1986) 487; d) F. H. Kohnke, J. P. Mathias, J. F. Stoddart, *Angew. Chem. Adv. Mater. 101* (1989) 1129; *Angew. Chem. Int. Ed. Engl. Adv. Mater. 28* (1989) 1103; *Adv. Mater. 1989*, 275; e) in [11], p. 41, f) in [12], p. 251; f) in [14], p. 5.

[31] a) I. O. Sutherland, *Chem. Soc. Rev. 15* (1986) 63; b) *Methods Stereochem. Anal. 6* (1986) 1; c) *Heterocycles 21* (1984) 235; d) *J. Inclusion Phenom. Mol. Recognit. Chem. 7* (1989) 213.

[32] a) D. N. Reinhoudt, *J. Coord. Chem. 18* (1988) 21; b) D. N. Reinhoudt, H. J. Den Hertog, *Bull. Soc. Chim. Belg. 97* (1988) 645; c) in [12], p. 83; d) D. N. Reinhoudt, P. J. Dijkstra, *Pure Appl. Chem. 60* (1988) 477; in [14], p. 51.

[33] a) A. Collet in [1b], p. 97; b) *Tetrahedron 43* (1987) 5725.

[34] a) C. D. Gutsche, *Top. Curr. Chem. 123* (1984) 1; b) *Acc. Chem. Res. 16* (1983) 161; c) in [18c], p. 93; d) C. D. Gutsche, M. Iqbal, K. S. Nam, K. See, I. Alam, *Pure Appl. Chem. 60* (1988) 483; e) C. D. Gutsche in [13], p. 3; f) C. D. Gutsche in [1d], p. 27; g) C. D. Gutsche, J. S. Rogers, D. Stewart, K. A. See, *Pure Appl. Chem. 62* (1990) 485.

[35] a) J. Rebek, Jr., *Science 235* (1987) 1478; b) *Acc. Chem. Res. 17* (1984), 258; c) *J. Inclusion Phenom. Mol. Recognit. Chem. 7* (1989) 7; d) *Pure Appl. Chem. 61* (1989) 1517; e) in [24b], p. 189; f) *J. Heterocycl. Chem. 27* (1990) 111; g) *Heterocycles 30* (1990) 707; h) *Angew. Chem. 102* (1990) 261; *Angew. Chem. Int. Ed. Engl. 29* (1990) 245; i) in [11], p. 1; j) *Top. Curr. Chem. 149* (1988) 189; k) *Acc. Chem. Res. 23* (1990) 399; l) in [14], p. 109.

[36] a) S. Shinkai, *Pure Appl. Chem. 59* (1987) 425; b) *J. Inclusion Phenom. Mol. Recognit. Chem. 7* (1989) 193; c) in [11], p. 125; d) in [13], p. 173; e) in [8], p. 301.

[37] a) R. M. Kellog, *Angew. Chem. 96* (1984) 769; *Angew. Chem. Int. Ed. Engl. 23* (1984) 782; b) in [3b], p. 111.

[38] a) F. M. Menger in [7c], p. 1; b) in [12], p. 193; c) *Angew. Chem. 103* (1991) 1104; *Angew. Chem. Int. Ed. Engl. 30* (1991) 1086.

[39] a) A. D. Hamilton, N. Pant, A. Muehldorf, *Pure Appl. Chem. 60* (1988)

533; b) A. D. Hamilton in [11], p. 57; c) A. D. Hamilton *J. Chem. Educ. 67* (1990) 821.
[40] a) R. Ungaro in [11], p. 135; b) R. Ungaro, A. Pocchini in [12] p. 57; c) in [13], p. 127; d) G. D. Andreeti, F. Ugozzoli, R. Ungaro, A. Pochini in [1d], p. 64; e) G. D. Andreeti in [13], p. 57.
[41] a) C. Wilcox in [11], p. 27; b) in [12], p. 123; c) J. C. Adrian, C. S. Wilcox, *J. Am. Chem. Soc. 113* (1991) 678, and references cited therein.
[42] a) F. P. Schmidtchen in [7b], p. 101; b) *Nachr. Chem. Tech. Lab. 36* (1988) 8; c) *Pure Appl. Chem. 61* (1989) 1535.
[43] a) H. J. Schneider, T. Blatter, R. Kramer, S. Kumar, U. Schneider, I. Theis in [11], p. 65; b) H.-J. Schneider, R. Busch, R. Kramer, U. Schneider, I. Theis, *Adv. Chem. Ser. 215* (1987) 457; c) H.-J. Schneider, T. Blatter, U. Cuber, R. Juneja, T. Schiestel, U. Schneider, I. Theis, P. Zimmermann in [12], p. 29.
[44] a) J. L. Atwood in [1a], p. 375; b) J. L. Atwood, S. G. Bott in [13] p. 199; c) in [19], p. 581.
[45] a) V. Böhmer, J. Vicens in [13] p. 39; b) H. Goldmann, W. Vogt, E. Paulus, V. Böhmer, *J. Am. Chem. Soc. 110* (1988) 6811, and references cited therein.
[46] a) G. W. Gokel, K. A. Arnold, M. Delgaab, L. Echevierra, V. J. Gatto, D. A. Gustowski, J. Hernandez, A. Kaifer, S. R. Miller, L. Echegoyen, *Pure Appl. Chem. 60* (1988) 461; b) G. W. Gokel in [1d], p. 283; c) G. W. Gokel, J. E. Trafton in [19], p. 253.
[47] R. D. Hancock, A. E. Martell, *Chem. Rev. 89* (1989) 1875.
[48] a) W. Saenger, *Angew. Chem. 92* (1980) 343; *Angew. Chem. Int. Ed. Engl. 21* (1980) 344; b) in [1b], p. 231.
[49] R.-J. Bergeron in [1a], p. 391; R. J. Clarke, J. H. Coates, S. F. Lincoln, *Adv. Carbohydr. Chem. Biochem 46* (1988) 205.
[50] Y. Yamamoto, Y. Inoue *J. Carbohydr. Chem. 8* (1989) 29.
[51] M. I. Page (Ed.): *The Chemistry of Enzyme Action,* Elsevier, Amsterdam 1984.
[52] M. Komiyama, M. L. Bender in [51], p. 505.
[53] Y. Matsui, T. Nishioka, T. Fujita in [7a], p. 61.
[54] U. Tonellato, *Bull. Soc. Chim. Fr. 1988*, 277.
[55] a) H. Ringsdorf, B. Schlarb, J. Venzmer, *Angew. Chem. 100* (1988) 117; *Angew. Chem. Int. Ed. Engl. 27* (1988) 113; b) I. Cabrera, M. Engel, L. Häußling, C. Mertesdorf, H. Ringsdorf in [12], p. 311; c) M. Ahlers, W. Müller, A. Reichert, H. Ringsdorf, J. Venzmer, *Angew. Chem. 102* (1990) 1310; *Angew. Chem. Int. Ed. Engl. 29* (1990) 1269.
[56] a) J.-H. Fuhrhop, D. Fritsch, *Acc. Chem. Res. 19* (1986) 130; b) J.-H. Fuhrhop, J. Mathiew, *Angew. Chem. 96* (1984) 124; *Angew. Chem. Int. Ed. Engl. 23* (1984) 100; c) J.-H. Fuhrhop, U. Krull in [12], p. 223.
[57] a) T. Kunitake in [8], p. 17; b) K. Kurihara, K. Ohto, Y. Tanaka, Y. Aoyama, T. Kunitake, *J. Am. Chem. Soc. 113* (1991) 444, and references cited therein.
[58] a) Y. Hui, W. Zou in [12], p. 203; b) Y. Hui, W. Zou *Makromol. Chem. 190* (1989) 1531, and references cited therein.
[59] a) A. W. Czarnik in [12], p. 109; b) M. E. Huston, C. Engleman, A. W. Czarnik, *J. Am. Chem. Soc. 112* (1990) 7054, and references cited therein.
[60] a) J. L. Sessler, D. Magda in [11], p. 17; b) H. Furuta, D. Magda, J. L. Sessler, *J. Am. Chem. Soc. 113* (1991) 978; and references cited therein.
[61] a) C. J. Burrows in [11], p. 199; b) H. Yoon, T. R. Wagler, K. J. O'Connor, C. J. Burrows, *J. Am. Chem. Soc. 112* (1990) 4568, and references cited therein.
[62] a) K. Kano in [11], p. 243; b) K. Kano, K. Mori, B. Uno, M. Goto, T. Kubota, *J. Am. Chem. Soc. 112* (1990) 8645, and references cited therein.
[63] a) Ueno, F. Morinaki, A. Azuma, T. Osa in [11], p. 269; b) A. Ueno, I. Suzuki, T. Osa *J. Am. Chem. Soc. 111* (1989) 6391.
[64] a) K. Saigo in [8], p. 75; b) K. Saigo, N. Kihara, Y. Hashimoto, R.-J. Lin, H. Fujimura, Y. Suzuki, M. Hasegawa, *J. Am. Chem. Soc. 112* (1990) 1144, and references cited therein.
[65] a) Y. Aoyama in [8], p. 307; b) Y. Aoyama, M. Asakawa, A. Yamagishi, H. Toi, H. Ogoshi, *J. Am. Chem. Soc. 112* (1990) 3145, and references cited therein.
[66] a) T. W. Bell, S. K. Sahni in [1d], p. 325; b) T. W. Bell, J. Lin, *Angew. Chem. 102* (1990) 931; *Angew. Chem. Int. Ed. Engl. 29* (1990) 923.
[67] a) C. A. Hunter, J. K. M. Sanders, *J. Am. Chem. Soc. 112* (1990) 5525; b) H. L. Anderson, C. A. Hunter, M. N. Meah, J. K. M. Sanders, *ibid. 112* (1990) 5780, and references cited therein.
[68] a) D. A. Stauffer, R. E. Barrans, D. A. Dougherty, *J. Org. Chem. 55* (1990) 2762; b) D. A. Dougherty, D. A. Stauffer *Science 250* (1990) 1558.
[69] A. Echavarren, A. Galán, J.-M. Lehn, J. de Mendoza in [11], p. 119, and references cited therein.
[70] J.-P. Sauvage, *Acc. Chem. Res. 23* (1990) 319, and references cited therein.
[71] J. W. H. Smeets, L. Van Dalen, V. E. M. Kaats-Richter, R. J. M. Nolte *J. Org. Chem. 55* (1990) 454, and references cited therein.
[72] a) W. L. Mock, N.-Y. Shih, *J. Am. Chem. Soc. 110* (1988), 4706; b) W. L. Mock, T. A. Irra, J. P. Wepsiec, M. Adhya, *J. Org. Chem. 54* (1989) 5302, and references cited therein.; c) J. M. Timko, S. S. Moore, D. M. Walba, P. C. Hiberty, D. J. Cram, *J. Am. Chem. Soc. 99* (1977) 4207; d) T. M. Fyles in [19], p. 203.
[73] K. M. Neder, H. W. Whitlock, Jr., *J. Am. Chem. Soc. 112* (1990), 9412, and references cited therein.
[74] a) S. C. Zimmermann, W. Wu, Z. Zeng, *J. Am. Chem. Soc. 113* (1991) 196; b) S. C. Zimmerman, C. M. Van Zyl, G. S. Hamilton, *ibid. 111* (1989) 1373, and references cited therein.
[75] a) T. A. Kaden in [3c], p. 157; b) *Pure Appl. Chem. 60* (1988) 1117; c) *ibid. 61* (1989) 879.
[76] K. T. Chapman, W. C. Still, *J. Am. Chem. Soc. 111* (1989) 3075, and references cited therein.
[77] G. van Binst (Ed.): *Design and Synthesis of Organic Molecules Based on Molecular Recognition*, Springer, Berlin 1986.
[78] H. Dugas: *Bioorganic Chemistry,* 2nd ed. Springer, New York 1989.
[79] W. P. Jencks: *Catalysis in Chemistry and Enzymology,* McGraw Hill, New York 1969.
[80] a) B. Pullman (Ed.): *Molecular Associations in Biology,* Academic Press, New York 1968; b) B. Pullman (Ed.): *Intermolecular Interactions: From Diatomics to Biopolymers,* Wiley, New York 1978; c) B. Pullman (Ed.): *Intermolecular Forces,* Reidel, Dordrecht 1981.
[81] R. M. Burnett, H.-J. Vogel: *Biological Organizations/Macromolecular Interactions at High Resolutions,* Academic Press, New York 1987.
[82] P. M. Dean: *Molecular Foundation of Drug Receptor Interaction*, Cambridge University Press, Cambridge 1987.
[83] S. Benner (Ed.): *Redesigning the Molecules of Life,* Springer, Berlin 1988.
[84] A. Fersht: *Enzyme Structure and Mechanism,* Freeman, San Francisco 1985.
[85] J. F. Liebman, A. Greenberg (Ed.): *Mechanistic Principles of Enzyme Activity,* VCH, New York 1988.
[86] J. J. Langone (Ed.): *Antibodies, Antigens and Molecular Mimicry* Chapter 4: *Engineered Antibodies* (*Methods. Enzymol. 178* (1989)).
[87] a) G. Schmidt, *Top. Curr. Chem. 136* (1986) 109; b) M. Mutter, S. Vuilleumier, *Angew. Chem. 101* (1989) 551; *Angew. Chem. Int. Ed. Engl. 28* (1989) 535.
[88] Catalytic antibodies: a) P. G. Schultz, *Acc. Chem. Res. 22* (1989) 287; b) K. M. Shokat, M. K. Ko, T. S. Scanlan, L. Kochersperger, S. Yonkovich, S. Thaisrivongs, P. G. Schultz, *Angew. Chem. 102* (1990) 1339; *Angew. Chem. Int. Ed. Engl. 29* (1990) 1296; c) A. Plückthun *Kontakte (Darmstadt) 1990*, 40; d) A. Plückthun *Chem. Unserer Zeit 24* (1990) 182; e) B. S. Green *Adv. Biotechnol. Processes 11* (1989) 359; f) R. A. Lerner, S. J. Benkovic *BioEssays 9* (1988) 107.
[89] Interactions in proteins modified by genetic engineering: a) A. R. Fersht, *Proc. R. A. Welch Found. Conf. Chem. Res. 31* (1987) 158; b) A. R. Fersht, *Biochemistry 26* (1987) 8031; c) R. J. Leatherbarrow, A. R. Fersht, *Protein Eng. 1* (1986) 7; d) J. A. Gerlt, *Chem. Rev. 87* (1987) 1079; e) A. Warshel, F. Sussman, J.-K. Hwang, *J. Mol. Biol. 201* (1988) 139.
[90] Peptide–antibiotica interactions: a) D. H. Williams, J. P. Waltho, *Pure Appl. Chem. 61* (1989) 585; b) *Biochem. Pharmacol. 37* (1988) 133, and references cited therein.
[91] S. K. Burley, G. A. Petsko: *Weakly Polar Interactions in Proteins* (*Adv. Protein Chem. 39* (1988) 125).
[92] a) A. S. V. Burgen, G. C. K. Roberts, M. S. Tute (Eds.): *Molecular Graphics and Drug Design,* Elsevier, Amsterdam 1986; b) M. Pettitt, M. Karplus: *Interaction Energies: Their Role in Drug Design* in [92a], p. 75.
[93] Saccharide–protein interactions: a) R. U. Lemieux, *Chem. Soc. Rev. 18* (1989) 347; b) R. U. Lemieux, L. T. J. Delbaere, H. Beierbeck, U. Spohr in [14], p. 213.
[94] Molecular recognition in chromatography: a) K. B. Lipkowitz, D. A. Demeter, R. Zegarra, R. Larter, T. Darden, *J. Am. Chem. Soc. 110* (1988) 3446; b) B. Sellergren, M. Lepistö, K. Mosbach, *J. Am. Chem. Soc. 110* (1988) 5853; c) V. Schurig, H.-P. Nowotny, *Angew. Chem. 102* (1990) 969; *Angew. Chem. Int. Ed. Engl. 29* (1990) 939; and references cited therein. Interaction mechanisms may change significantly upon immobilization of the host compound: d) H.-J. Schneider, W. Müller, D. Güttes *Angew. Chem. 96* (1984) 909; *Angew. Chem. Int. Ed. Engl. 23* (1984) 910.
[95] S. a) V. T. D'Souza, M. L. Bender, *Acc. Chem. Res. 20* (1987) 146; b) M. P. Mertes, K. Bowman, K. B. Mertes, *ibid. 23* (1990) 413, and references cited therein.
[96] a) T. E. Edmonds (Ed.): *Chemical Sensors,* Chapman & Hall, New York 1988; b) R. Szostak: *Molecular Sieves,* Van Nostrand Reinhold, New York 1988; c) P. Bergreld, A. Sibbald: *Analytical and Biomedical Applications of Ion- Selective Field-Effect Transistors,* Elsevier, Amsterdam 1988; d) D. N Reinhoudt, E. J. R. Sudhoelter, *Adv. Mater. 2* (1990) 23; e) W. J. Albery in [14], p. 55; f) K. Cammann, U. Lemke, A. Rohen, J. Sander, H. Wilken, B. Winter, *Angew. Chem. 103* (1991) 519; *Angew. Chem. Int. Ed. Engl. 30* (1991) 516.
[97] P. Hobza, R. Zahradnik: *Intermolecular Complexes,* Elsevier, Amsterdam 1988.
[98] J. N. Israelachvili: *Intermolecular and Surface Forces,* Academic Press, London 1985.
[99] A. Weber (Ed.): *Structure and Dynamics of Weakly Bound Molecular Complexes,* Reidel, Dordrecht 1987.
[100] M. Rigby, E. B. Smith, W. A. Wakeham, G. C. Maitland: *The Forces Between Molecules,* Clarendon, Oxford 1986.
[101] Cf. Editorial *Chem. Rev. 88* (1988) 813; review of the status of both theory and methods applicable to "non-bonded" interactions: pp. 815–988.
[102] M. Badertscher, M. Welti, P. Portmann, E. Pretsch, *Top. Curr. Chem. 136* (1986).
[103] K. B. Lipkowitz, D. B. Boyd (Eds.): *Reviews in Computational Chemis-*

try, a) P. G. Mezey, Chap. 7, p. 265; b) T. P. Lybrand, Chap. 8, p. 295; c) D. B. Boyd, Chap. 9, p. 321, VCH, New York 1990.
[104] a) W. F. van Gunsteren, P. K. Weiner: *Computer Simulations of Biomolecular systems* Escom Science Publ., Leiden 1989; b) J. G. Winter, M. R. Sanders in [14], p. 249.
[105] J. A. McCammon, S. C. Harvey: *Dynamics of Proteins and Nucleic Acids*, Cambridge University Press, Cambridge 1987.
[106] P. Kollman, W. F. van Gunsteren, *Methods. Enzymol 154* (1987) 430.
[107] K.-C. Chou, G. Nemethy, H. A. Scheraga, *Acc. Chem. Res. 23* (1990) 134, and references cited therein.
[108] a) C. L. Brooks, M. Karplus *Methods Enzymol. 127* (1986) 369; b) A. T. Brünger, M. Karplus *Acc. Chem. Res. 24* (1991) 54, and references cited therein.
[109] A. Warshel, S. T. Russel, *Q. Rev. Biophys. 17* (1984) 283.
[110] A. T. Hagler in V. J. Hruby, J. Meienhofer (Eds.): *The Peptides*, Academic Press, New York 1985.
[111] a) W. J. Jorgensen, *Acc. Chem. Res. 22* (1989) 184; b) W. L. Jorgensen, D. L. Severance, *J. Am. Chem. Soc. 112* (1990) 4768; c) J. F. Blake, W. L. Jorgensen, *ibid. 112* (1990) 7269; and references cited therein.; d) W. L. Jorgensen, D. L. Severance *ibid. 113* (1991) 209.
[112] Recent references on metal-complex simulations: a) P. A. Kollman, P. D. J. Grootenhuis, M. A. Lopez, *Pure Appl. Chem. 61* (1989) 593; b) L. X. Dang, P. A. Kollman, *J. Am. Chem. Soc. 112* (1990) 5716; c) M. H. Mazor, J. A. McCammon, T. P. Lybrand, *ibid. 112* (1990) 4411; d) G. Wipff *Stud. Phys. Theor. Chem. 71* (1990) 143; e) G. Wipff, *J. Coord. Chem.*, in press; f) H. Bruning, D. Feil, *J. Comput. Chem. 12* (1991) 1.
[113] Recent articles on simulations of cyclodextrin complexes: a) M. Ohashi, K. Kasatani, H. Shinohara, H. Sato, *J. Am. Chem. Soc. 112* (1990) 5824; b) C. Jaime, J. Redoudo, F. Sanchez-Ferrando, A. Virgili, *J. Org. Chem. 55* (1990) 4772; c) C. A. Venanzi, P. M. Canzius, Z. Zhang, J. B. Bunce, *J. Comput. Chem. 10* (1989) 1038.
[114] P. D. J. Grootenhuis, P. A. Kollman, L. C. Groenen, D. N. Reinhoudt, G. J. van Hummel, F. Ugozzoli, G. D. Andreeti, *J. Am. Chem. Soc. 112* (1990) 4165.
[115] a) C. H. Faerman, S. L. Price, *J. Am. Chem. Soc. 112* (1990) 4915 (also with respect to polarization functions); b) see also K. B. Lipkowitz, R. Zegarra, *J. Comput. Chem. 10* (1989) 595.
[116] Recent references dealing with minimization problems: a) A. E. Howard, P. Kollman, *J. Med. Chem. 31* (1988) 1669; b) G. T. Montelione, H. A. Scheraga, *Acc. Chem. Res. 22* (1989) 70 (protein folding); c) M. Saunders, K. N. Houk, Y.-D. Wu, W. C. Still, M. Lipton, G. Chang, W. C. Guida, *J. Am. Chem. Soc. 112* (1990) 1419; d) H.-J. Böhm, G. Klebe, T. Lorenz, T. Mietzner, L. Sigel, *J. Comput. Chem. 11* (1990) 1021; see also e) K. Gundertofte, J. Palm, I. Petterson, A. Stamvik, *ibid. 12* (1991) 200, and references cited therein.
[117] a) K. A. Connors: *Binding Constants*, Wiley, New York 1987; b) J. Polster, H. Lachmann: *Spectrometric Titrations*, VCH, Weinheim 1989.
[118] H.-J. Schneider, R. Kramer, S. Simova, U. Schneider, *J. Am. Chem. Soc. 110* (1988) 6442, and references cited therein.
[119] H.-J. Schneider, T. Blatter, S. Simova, *J. Am. Chem. Soc. 113* (1991) 1996.
[120] H.-J. Schneider, J. Pöhlmann, *Bioorg. Chem. 15* (1987) 183.
[121] H.-J. Schneider, U. Buchheit, N. Becker, G. Schmidt, U. Siehl, *J. Am. Chem. Soc. 107* (1985) 7278, and references cited therein.
[122] a) D. Neuhaus, M. Williamson: *The Nuclear Overhauser Effect* VCH, New York 1989; b) K. Wuethrich, *Acc. Chem. Res. 22* (1989) 36.
[123] a) R. Breslow, *Adv. Chem. Ser. 191* (1980) 1; b) A. C. Coxon, W. D. Curtis, D. A. Laidler, J. F. Stoddart, *Carbohydrates, Nucleosides, Nucleotides 6* (1979) 167.
[124] D. E. Koshland, *Proc. Natl. Acad. USA 44* (1958) 98.
[125] a) M. I. Page in [51], p. 1 ff; b) W. P. Jencks, *Proc. Natl. Acad. Sci. USA 78* (1981) 4046, and references cited therein.
[126] a) H.-J. Schneider, I. Theis, *Angew. Chem. 101* (1989) 757; *Angew. Chem. Int. Ed. Engl. 28* (1989) 753; b) cf. H.-J. Schneider, K. Philippi, J. Pöhlmann, *ibid. 96* (1984) 907 and *23* (1984) 908.
[127] a) H.-J. Schneider, R. K. Juneja, S. Simova, *Chem. Ber. 112* (1989); b) unpublished.
[128] H.-J. Schneider, T. Schiestel, P. Zimmermann, unpublished.
[129] a) K. A. Connors, D. D. Pendergast, *J. Am. Chem. Soc. 106* (1984) 7607; b) K. A. Connors, A. Paulson, D. Toledo-Velasquez, *J. Org. Chem. 53* (1988) 2033.
[130] M. W. Hosseini, J.-M. Lehn, M. P. Mertes, *Helv. Chim. Acta 66* (1983) 2454.
[131] a) H. J. Schneider, D. Güttes, U. Schneider, *J. Am. Chem. Soc. 110* (1988) 6449; b) *Angew. Chem. 98* (1986) 635; *Angew. Chem. Int. Ed. Engl. 25* (1986) 647.
[132] F. Garcia-Tellado, S. Goswami, S.-K. Chang, S. J. Geib, A. D. Hamilton, *J. Am. Chem. Soc. 112* (1990) 7393.
[133] H.-J. Schneider, T. Blatter, P. Zimmermann, *Angew. Chem. 102* (1990) 1194; *Angew. Chem. Int. Ed. Engl. 29* (1990) 1161.
[134] J. Franke, T. Merz, H.-W. Losensky, W. M. Müller, U. Werner, F. Vögtle, *J. Inclusion Phenom. 3* (1985) 471.
[135] J. H. de Boer, J. F. H. Custers, *Z. Phys. Chem. Abt. B 25* (1934) 225.
[136] C. W. Chen, H. W. Whitlock, Jr., *J. Am. Chem. Soc. 100* (1978) 4921.
[137] For additional cleft compounds see, for example: a) H. M. Colquhoun, J. F. Stoddart, D. J. Williams, *Angew. Chem. 98* (1986) 483; *Angew. Chem. Int. Ed. Engl. 25* (1986) 487; b) A. Echavarren, A. Galán, J.-M. Lehn, J. de Mendoza, *J. Am. Chem. Soc. 111* (1989) 4994.
[138] J. C. Sherman, D. J. Cram, *J. Am. Chem. Soc. 111* (1989) 4527.
[139] C. Tanford: *The Hydrophobic Effect*, 2nd ed., Wiley New York 1980 (for critical remarks see L. R. Pratt, *J. Am. Chem. Soc. 103* (1981) 7700).
[140] a) A. Ben-Naim: *Hydrophobic Interactions*, Plenum, New York 1980; b) A. Ben-Naim: *Solvation Thermodynamics*, Plenum, New York 1987.
[141] H. S. Franck, M. W. Evans, *J. Chem. Phys. 13* (1945) 507.
[142] R. D. Cramer III, *J. Am. Chem. Soc. 99* (1977) 5408, and references cited therein.
[143] M. H. Abraham, *J. Am. Chem. Soc. 104* (1982) 2085, and references cited therein.
[144] a) M. J. Blandamer *Adv. Phys. Org. Chem. 14* (1977) 204; b) V. Zaslavsky, E. A. Masimov *Top. Curr. Chem. 146* (1988) 171; c) W. Blokzijl, J. B. F. N. Engberts, M. J. Blandamer, *J. Am. Chem. Soc. 112* (1990) 1197; d) N. Muller, *Acc. Chem. Res. 23* (1990) 28; e) P. Backx, S. Goldman, *Chem. Phys. Lett. 113* (1985) 578, and references cited therein.; f) P. L. Privalov, S. J. Gill, *Adv. Protein Chem. 39* (1988) 191; g) R. Wolfenden, *Science 222* (1983) 1087.
[145] J. Sturdevant, *Proc. Natl. Acad. Sci. USA 74* (1977) 2236, and references cited therein.
[146] a) J. C. Harrison, M. R. Eftink, *Biopolymers 21* (1982) 1153; b) M. R. Eftink, M. L. Andy, K. Bystrom, H. D. Perlmutter, D. S. Kristol, *J. Am. Chem. Soc. 111* (1989) 6765; c) A. F. D. de Namor, R. Trabulssi, D. F. V. Lewis, *ibid. 112* (1990) 8442; d) R. M. Izatt, D. J. Eatough, J. J. Christensen, *Struct. Bonding (Berlin) 16* (1973) 161.
[147] D. A. Stauffer, R. E. Barrans, D. A. Dougherty, *J. Org. Chem. 55* (1990) 2762.
[148] a) J. F. Liebman (Ed.): *Molecular Structure and Energetics, Vol. 1–4*, VCH, New York 1987; b) Y. Inoue, Y. Liu, T. Hakushi in [19], p. 1.
[149] O. Sinanoglu in [80], p. 427.
[150] a) K. A. Connors, S. Sun, *J. Am. Chem. Soc. 93* (1971) 7239; b) K. A. Connors, M. H. Infeld, B. J. Kline, *ibid. 91* (1969) 3597, 5697; and references cited therein. c) M. J. Lowe, J. Schellman, *J. Mol. Biol. 65* (1972) 91.
[151] D. B. Smithrud, F. Diederich, *J. Am. Chem. Soc. 112* (1990) 339, and references cited therein.
[152] a) C. Reichardt: *Solvents and Solvent Effects in Organic Chemistry*, 2nd ed., VCH, Weinheim 1988; b) J. H. Hildebrand, R. C. Scott: *Regular Solutions*, Prentice-Hall, Englewood Cliffs, NJ, USA 1962; c) A. I. M. Barton: *Handbook of Solubility Parameters and Other Cohesion Parameters*, CRC Press, Boca Raton, FL, USA 1983, p. 139 ff.
[153] See, for example, Z. Friedl, J. Biros, O. Exner, *J. Chem. Soc. Perkin Trans. 2 1990*, 459, and references cited therein.
[154] J. L. Cohen, K. A. Connors, *J. Pharm. Sci. 59* (1970) 1271.
[155] F. Franks (Ed.): *Water: A Comprehensive Treatise*, Plenum, New York 1979.
[156] T. Steiner, S. A. Mason, W. Saenger, *J. Am. Chem. Soc. 112* (1990) 6184, and references cited therein.
[157] See, for example, z. B. I. L. Karle, P. Balaram, *Biochemistry 29* (1990) 6747; I. Karle, J. L. Flippen-Anderson, K. Uma, M. Sukumar, P. Balaram, *J. Am. Chem. Soc. 112* (1990) 9350, and references cited therein.
[158] a) H.-J. Schneider, T. Blatter, S. Simova, I. Theis, *J. Chem. Soc. Chem. Commun. 1989*, 580; b) I. Theis, *Dissertation*, Universität Saarbrücken 1989.
[159] a) S. F. Lin. K. Connors *J. Pharm. Sci 72* (1983) 1333; b) A. Buvari, L. Barcza, *J. Chem. Soc. Perkin Trans. 2* (1988) 543; c) A. Wong, S.-F. Liu, K. Connors, *J. Pharm. Sci. 72* (1983) 388.
[160] I. Sanemasa, Y. Akamine, *Bull. Chem. Soc. Jpn. 60* (1987) 2059, and the references cited therein to ΔG determination for benzene–cyclodextrin complexes, some of which led to differing values.
[161] H.-J. Schneider, A. Tretter, unpublished.
[162] H.-J. Schneider, R. Kramer, I. Theis, M.-q. Zhou *J. Chem. Soc. Chem. Commun. 1990*, 276.
[163] S. Kumar, H.-J. Schneider, *J. Chem. Soc. Perkin Trans. 2 1989*, 245.
[164] a) M. H. Abraham, P. L. Grellier, R. A. McGill, *J. Chem. Soc. Perkin Trans. 2 1988*; b) N. K. Sangwan, H.-J. Schneider, *ibid. 1989*, 113, and references cited therein.
[165] See, for example S.-C. Tam, R. J. P. Williams, *Struct. Bonding (Berlin) 63* (1985) 103.
[166] a) J. O'M. Bockris, A. K. N. Reddy: *Modern Electrochemistry*, Plenum New York 1970; b) G. Kortüm: *Lehrbuch der Elektrochemie* 2nd Edit., Verlag Chemie, Weinheim 1957.
[167] a) J. E. Gordon: *The Organic Chemistry of Electrolyte Solutions*, Wiley, New York 1975; b) A. Marcus: *Ion Solvation*, Wiley, Chichester 1986; c) K. Burger: *Solvation, Ionic and Complex Formation Reactions in Non-Aqueous Solvents*, Elsevier, Amsterdam 1983; d) M. Szwarc (Ed.): *Ions and Ion Pairs in Organic Reactions*, Wiley, New York 1972; e) Y. Marcus, *Chem. Rev. 88* (1988) 1475; f) U. Meyer, *Coord. Chem. Rev. 21* (1976) 159.
[168] a) See, for example A. D. Pethybridge, S. S. Taba, *J. Chem. Soc. Faraday Trans. 1 78* (1982) 1331; b) G. Schwitzgebel, P. Zimmermann, unpublished.

[169] S. C. Tam, R. J. P. Williams, *J. Chem. Soc. Faraday Trans. 1 80* (1984) 2255.
[170] H.-J. Schneider, U. Schneider, *J. Org. Chem. 52* (1987) 1613.
[171] S. a) M. Schaefer, C. Froemmel, *J. Mol. Biol. 216* (1990) 1045; b) U. Dinur. A. T. Hagler, *J. Am. Chem. Soc. 111* (1989) 5149, and references cited therein.
[172] M. Kitagawa, H. Hoshi, M. Sakurai, Y. Inoue, R. Chujo, *Bull. Chem. Soc. Jpn. 61* (1988) 4225, and references cited therein.
[173] a) I. Tabushi, T. Mizutani, *Tetrahedron 43* (1987) 1447; b) R. I. Gelb, L. M. Schwartz, B. Cardelino, H. S. Fuhrman, R. F. Johnson, D. A. Laufer, *J. Am. Chem. Soc. 103* (1981) 1750.
[174] a) A. D. Buckingham in [80b], p. 20; b) P. Claverie in [80b], p. 167, and references cited therein.
[175] a) S. L. Price, A. J. Stone *J. Chem. Phys. 86* (1987) 2859; I. Petterson, T. Liljefors, *J. Comput. Chem. 8* (1987) 1139.
[176] a) J. Sunner, K. Nishizawa, P. Kebarle *J. Phys. Chem. 85* (1981) 1814. Similar studies also exist for benzene as an $X-H^+$ acceptor: b) M. Meot-Ner, C. A. Deakyne, *J. Am. Chem. Soc. 107* (1985) 469; C. A. Deakyne, M. Meot-Ner, *ibid. 107* (1985) 474; c) B. V. Cheney, M. W. Schulz, J. Cheney, W. G. Richards, *ibid. 110* (1988) 4195; d) J. L. Brédas, G. B. Street, *ibid. 110* (1988) 7001, and references cited therein.
[177] a) The 4–6 kJ mol^{-1} preference for the edge-to-face conformation for the benzene dimer in the gas-phase assumed earlier (cf. [91] and sources cited therein) actually amounts to only ca. 0.7 kJ mol^{-1} according to recent ab initio calculations. The relevant experimental information is also quite contradictory: see [175] and sources cited therein; b) MC simulations for benzene complexes in water—albeit without consideration of induced dipoles—also lead to virtual equivalence in the energies for approximately edge-to-face and face-to-face conformations: W. L. Jorgensen, D. L. Severance, *J. Am. Chem. Soc. 112* (1990) 4768.
[178] H.-J. Schneider, N. Becker, *J. Phys. Org. Chem. 2* (1989) 679, and references cited therein.
[179] D. A. Stauffer, D. A. Dougherty, *Tetrahedron Lett. 29* (1988) 6039.
[180] a) H.-J. Schneider, T. Blatter, *Angew. Chem. 100* (1988) 1211; *Angew. Chem. Int. Ed. Engl. 27* (1988) 1163; b) H.-J. Schneider, T. Blatter, S. Simova, I. Theis, *J. Chem. Soc. Chem. Commun. 1989*, 580.
[181] H.-J. Schneider, T. Blatter, I. Theis, unpublished.
[182] a) A. E. Reed, L. A. Curtiss, F. Weinhold, *Chem. Rev. 88* (1988) 899; b) P. W. Fowler, A. D. Buckingham, J. M. Hutson, *ibid. 88* (1988) 963; c) K. Morokuma *Acc. Chem. Res. 10* (1977) 294.
[183] a) R. Foster: *Organic Charge-Transfer Complexes* Academic Press, London 1969; b) G. Briegleb *Elektronen-Donator-Acceptor-Komplexe*, Springer, Berlin 1961; c) R. L. Strong in [80c], p. 217–232; d) R. Paetzold, *Z. Chem. 15* (1975) 377; e) C. J. Bender, *Chem. Soc. Rev. 15* (1986) 475; f) M. H. Schwartz, *J. Inclusion Phenom. Mol. Recognit. Chem. 9* (1990) 1.
[184] S. B. Ferguson, F. Diederich, *Angew. Chem. 98* (1986) 1127; *Angew. Chem. Int. Ed. Engl. 25* (1986) 1127.
[185] [185] a) W. C. Cromwell, K. Byström, M. R. Eftink, *J. Phys. Chem. 89* (1985) 326 and references cited therein. Recent calorimetric measurements apparently lead to satisfactory agreement—cf. b) L.-E. Briggner, X.-R. Ni, F. Tempesti, I. Wadsö, *Thermochim. Acta 109* (1986) 139—whereas earlier studies gave inconsistent values: c) E. A. Lewis, L. D. Hansen, *J. Chem. Soc. Perkin Trans. 2 1973*, 2081. The problems associated with $\Delta H/\Delta S$ measurements as a result of temperature dependence of the equilibrium constants, discussed in Section 4, are apparent in the great differences between reported values and recent [185a] calorimetric data: d) R. Gelb, L. M. Schwartz, B. Cardelino, H. S. Fuhrman, R. F. Johnson, D. A. Laufer, *J. Am. Chem. Soc. 103* (1981) 1750. Calorimetric studies of linear alcohols with α-cyclodextrin (G. Barone, G. Castronuovo, P. Del Vecchia, V. Elia, M. Muscetta, *J. Chem. Soc. Farad. Trans. 1 1986*, 2089) reveal inclusion that is dominated generally by ΔH; however, in this case and for most other cyclodextrin complexes[160] there is a lack of any (NMR) investigation into the question of intracavity inclusion vs. external association.
[186] M. R. Eftink, J. C. Harrison, *Bioorg. Chem. 11* (1982) 420.
[187] a) M. D. Joesten, L. J. Schaad: *Hydrogen Bonding*, Dekker, New York 1974; b) A. C. Legon, D. J. Millen, *Acc. Chem. Res. 20* (1987) 39; c) C. E. Dykstra, *ibid. 21* (1988) 355; d) M. C. Etter, *ibid. 23* (1990) 120; e) P. Dauber, A. T. Hagler, *ibid. 13* (1980) 105, f) L. A. Curtiss, M. Blander *Chem. Rev. 88* (1988) 827, and references cited therein.
[188] a) A. D. Buckingham, P. W. Fowler, *Can. J. Chem. 63* (1985) 2018; b) S. M. Cybulski, S. Scheiner, *J. Am. Chem. Soc. 111* (1989) 23; c) H. Basch, W. J. Stevens, *ibid. 113* (1990) 95.
[189] a) J. Hine *J. Am. Chem. Soc. 94* (1972) 5766; J. Hine, S. Hahn, J. Hwang, *J. Org. Chem. 53* (1988) 884; b) N. Stahl, W. P. Jencks, *J. Am. Chem. Soc. 108* (1986) 4196; c) M. H. Abraham, P. L. Grellier, D. V. Prior, R. W. Taft, J. J. Morris, P. J. Taylor, C. Laurence, M. Bertheldt, R. M. Doherty, M. J. Kamlet, J.-L. M. Abboud, K. Sraidi, G. Guihéneuf, *ibid. 110* (1988) 8534, and references cited therein.
[190] a) See, for example, G. E. Schulz, R. H. Schirmer, *Principles of Protein Structure*, Springer, New York 1979; b) I. M. Klotz, J. S. Franzen, *J. Am. Chem. Soc. 84* (1962) 3461; c) J. N. Spencer, R. C. Garrett, F. J. Mayer, J. E. Merkle, C. P. Powell, M. T. Tran, S. K. Berger, *Can. J. Chem. 58* (1980) 1372.
[191] A. R. Fersht, J.-P. Shi, J. Knill-Jones, D. M. Lowe, A. J. Wilkinson, D. M. Blow, P. Brick, P. Carter, M. M. Y. Waye, G. Winter *Nature 314* (1985) 235.
[192] K. S. Jeong, T. Tjivikua, A. Muehldorf, G. Deslongchamps. M. Famulok, J. Rebek, Jr., *J. Am. Chem. Soc. 113* (1991) 201.
[193] W. L. Jorgensen, D. L. Severance, *J. Am. Chem. Soc. 113* (1991) 209.
[194] a) W. Saenger: *Principles of Nucleic Acid Structure*, Springer New York 1984.
[195] a) N. R. Kallenbach (Eds.): *Chemistry and Physics of DNA-Ligand Interaction*, Adenine Press, Guilderland, NY, USA 1989; b) W. A. Denny, *Anti-Cancer Drug Des. 4* (1989) 241; c) L. P. G. Wakelin, *Med. Res. Rev. 6* (1980) 275; d) M. J. Waring in [14], p. 142.
[196] Earlier work on allosteric binding centers involving only metal ions: a) J. F. Stoddart in [51], p. 544; b) Ref. [35b]; c) P. D. Beer, A. S. Rothin, *J. Chem. Soc. Chem. Commun. 1988*, 52.
[197] a) H.-J. Schneider, D. Ruf, *Angew. Chem. 20* (1990) 1192; *Angew. Chem. Int. Ed. Engl. 29* (1990) 1159; b) H.-J. Schneider, U. Schneider, unpublished; c) H.-J. Schneider, U. Werner, unpublished.

Protease-Catalyzed Kinetically Controlled Peptide Synthesis

By Volker Schellenberger and Hans-Dieter Jakubke*

In spite of the enormous progress in the synthesis of peptides and proteins using commercial peptide synthesizers and the immense technological possibilities of recombinant DNA technology, a C-N ligase is an indispensable tool for the racemization-free fragment condensation of peptides. Since activation of the C-terminal α-carboxyl group of a peptide segment could cause partial racemization, chemical condensations of peptide fragments are prone to racemization. For the synthesis of the huge number of peptides and proteins, however, nature has only developed the ribosomal peptidyltransferase, which exhibits its full catalytic function independent of the side-chain functions of the amino acids being coupled. However, its function requires coordination with numerous other ribosomal factors. Besides the limited possibilities of using multienzyme complexes of bacterial peptide synthesis systems, the only alternatives to peptidyltransferase are proteases, which, based on their in vivo function as hydrolases, cannot act as ideal ligases. However, by exploiting the intrinsic reversibility of hydrolytic reactions and by adjusting appropriate physicochemical reaction parameters, the protease acitivity can be used in the direction of ligation. Undoubtedly, the course of kinetically controlled, serine and cysteine protease-catalyzed reactions can be more efficiently influenced than the equilibrium-controlled protease-catalyzed synthesis. This article describes the influence of the enzyme specificity on the efficiency of kinetically controlled synthesis and points the way toward a broad exploitation of serine and cysteine proteases for the catalysis of C–N bond formation.

1. Introduction

In principle, the use of enzymes for peptide bond formation offers great advantages over chemical procedures. Thus, because of the regiospecificity of enzymes, the reversible protection of side-chain functions of the amino acid building blocks is not necessary. The mild reaction conditions of the enzyme-catalyzed reactions guarantee racemization-free syntheses. Owing to the stereospecificity of enzymes, chirally homogeneous products are obtained even when racemic N-protected amino acid derivatives are used as starting material.

A prerequisite, however, is a C-N ligase which can be simply handled like a coupling reagent to form a peptide bond. Since such an ideal ligase is not available, even the proponents of this strategy do not regard the enzymatic approach as a real alternative to chemical procedures in peptide synthesis. There are, however, a number of convincing arguments which vigorously support the necessity for further basic research to find other—although certainly not so favorable—enzymes.

In spite of the high efficiency of the now virtually automatic solid-phase peptide synthesis and the development of coupling reagents that do not cause racemization in model syntheses, the high optical purity required of pharmaceutical products cannot be guaranteed by this approach. In particular, the danger of racemization is strongly dependent on the amino acid sequence adjacent to the residues undergoing peptide bond formation. Therefore, the standard racemization tests do not possess general validity. Chemical fragment condensations are specially at risk.[1] In the stepwise solid-phase synthesis using urethane-type protecting groups, moreover, the danger of partial racemization cannot be excluded and is often revealed by employing increasingly sensitive analytical methods.

The use of enzymes is above all necessary for (1) the coupling of fragments obtained from natural proteins in semisynthesis, (2) the condensation of peptide fragments synthesized by stepwise chemical procedures, and (3) the modification of products prepared by recombinant DNA technology.

The ribosomal peptidyltransferase is not suitable for practical use and also the multienzyme complexes involved in bacterial peptide synthesis do not seem to possess a general applicability at present. Consequently, only the proteases come into consideration. Their fundamental suitability for peptide synthesis is based on the principle of reversibility and was predicted by *van't Hoff* more than 90 years ago[2] and proved experimentally by *Bergmann* and *Fraenkel-Conrat* in 1937.[3]

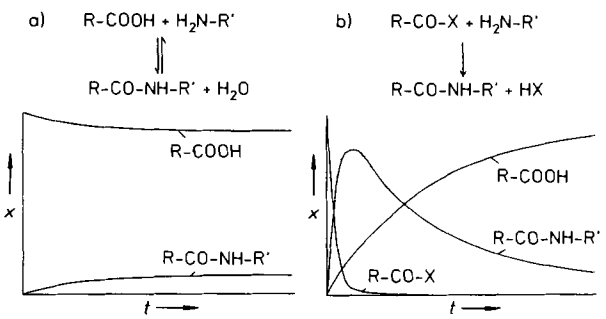

Fig. 1. Comparison of an equilibrium (a) and a kinetically controlled (b) peptide synthesis. In the kinetically controlled reaction, besides the product R-CO-NH-R', the acid R-COOH is formed.

[*] Prof. Dr. H.-D. Jakubke, Dr. V. Schellenberger
Fachbereich Biowissenschaften der Universität
Talstrasse 33, O-7010 Leipzig (FRG)

[**] In this article the amino acid residues of the peptide substrate, *p,p'*, and the binding sites on the enzyme, *S, S'*, are abbreviated in italics to avoid confusion with S = substrate and P = product or leaving group (Scheme 1).

Two strategies for protease-catalyzed peptide synthesis are distinguished in the literature (cf. recent reviews[4-8]). While the equilibrium-controlled synthesis represents the direct reversal of the proteolysis, the kinetically controlled synthesis makes use of weakly activated carboxy components. Both methods are compared in Figure 1.

2. Is Protease-Catalyzed Kinetically Controlled Fragment Condensation Preferential to Other Methods?

The equilibrium-controlled peptide synthesis, as direct reversal of the protease-catalyzed hydrolysis of a peptide bond, has the advantage that all the proteases, independent of their catalytic mechanism, can be used. However, the high enzyme requirements and the low reaction velocity are disadvantages. Furthermore, high concentrations of organic solvents are usually required in order to suppress the ionization of the fragments being condensed. In spite of these limitations, this strategy proved to be worthwhile in the trypsin-catalyzed semisynthesis of human insulin as well as the aspartame synthesis using thermolysin (cf. reviews[4-8]). On the other hand, if one plans to carry out equilibrium-controlled reactions involving reactants with unprotected side-chain functions in aqueous media, then the specificity-determining C-terminal amino acid residue of the carboxy component should not occur once more in the fragments.

It has been known for a long time that, besides the hydrolysis of peptides and proteins, serine and cysteine proteases can also catalyze acyl transfer to various acceptors.[9, 10] This is a direct consequence of the reaction mechanism of these enzymes. The acyl-enzyme intermediate formed during catalysis can be deacylated competitively by water and also by other nucleophiles. The use of peptide esters for the acyl transfer to other peptide derivatives has special significance. This is described in the literature as kinetically controlled peptide synthesis. By using acylamino acid esters as the carboxy components, it is possible to achieve a temporary product accumulation lying far above the thermodynamically determined equilibrium concentration (see Fig. 1).

Kinetically controlled enzymatic fragment couplings with unprotected side-chain functions can be carried out in aqueous systems with a modest addition of organic solvents. This is due to the decisively improved solubility of the fragments in aqueous medium. Unfavorable conformational effects of the peptides, which occur during the chemical condensation of fully protected fragments, can thereby be avoided. The application of proteases to protein synthesis, however, necessitates a knowledge of the kinetics of the acyl-transfer reactions and the introduction of a few kinetic parameters to describe the reaction course. Methods for determining the individual parameters will be compared and their significance explained in the following discussion.

3. Survey of Protease-Catalyzed Acyl-Transfer Reactions

The first protease-catalyzed acyl-transfer experiments were mainly performed in order to investigate the mechanism of the catalysis.[11, 13] Since the middle of the 1970s the preparative use of such reactions has been the focus of interest.[14-20] The influence of reactant structure and reaction conditions on the yield of the peptide product has been investigated. However, the variable conditions (type and concentration of the employed solvents, pH, ionic strength, reactant concentration, and temperature) make it difficult to compare the results. In many investigations only the concentration of the peptide product at a fixed time is given, but not the initial relationship between the formation of aminolysis

Hans-Dieter Jakubke, born in 1933 in Mosau (Mark Brandenburg), studied chemistry at the Universität Halle-Wittenberg from 1952 to 1958. He received his Ph.D. in 1961 under W. Langenbeck for work on enzyme models and cyclic peptides. After doing research in Prague for one year with J. Rudinger, he completed his habilitation in 1968 on racemization-free peptide synthesis. In 1970 he was appointed lecturer at the Institut für Biochemie at the Universität Halle-Wittenberg and was appointed Ordinarius für Biochemie at the Universität Leipzig in 1977. Since 1990 Jakubke has been a member of the Council of the European Peptide Society. He is the coauthor of several books. The focus of his research is peptide chemistry, enzymatic peptide synthesis, and studies on the specificity of proteases.

Volker Schellenberger, born in 1960 in Leipzig, studied biochemistry from 1979 to 1983 at the Universität Leipzig and received his Ph.D. in 1986 under H.-D. Jakubke for work on protease-catalyzed peptide synthesis. After doing research with Yu. V. Mitin (Puschchino, USSR) and A. Aaviksaar (Tallinn, USSR) and working as an FEBS postdoctoral fellow with V. Kasche (Hamburg), he completed his habilitation in 1991 at the Universität Leipzig. After doing research with H.-J. Fritz (Göttingen), he began his current work with W. J. Rutter at the Hormone Research Institute (San Francisco, USA).

and hydrolysis products. Consequently, it is virtually impossible to draw conclusions about the enzyme specificity for the different amino components.

The nomenclature for protease specificity, which was introduced by *Schechter* and *Berger*,[21] is explained in Figure 2. A characterization of the *S'*-subsite specificity of the

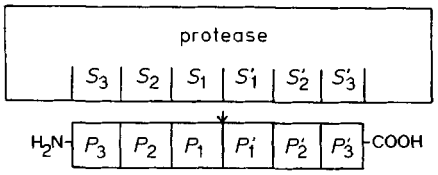

Fig. 2. Schematic representation of the nomenclature of protease specificity according to *Schechter* and *Berger* [21]. The amino acid residues are denoted by *P* and *P'*, respectively. They interact with the corresponding *S* and *S'* subsites of the enzyme active site, respectively. The arrow indicates the site of proteolytic cleavage. Starting at this site, *P* or *S* are numbered.

proteases requires a large series of acyl-transfer reactions, which must be investigated under standardized reaction conditions. The fundamental studies on the serine- and cysteine-protease-catalyzed acyl transfer are summarized in Table 1.

An extensive discussion of the results of these studies is beyond the scope of this article. Some generalizations, however, seem to be possible, although the individual experiments differ regarding the reaction conditions and analytical procedures.

The ratio between aminolysis and hydrolysis of the acyl-enzyme is generally more favorable for cysteine proteases than for serine proteases. This is in accordance with the finding that the ratio of the esterase to amidase activity of cysteine proteases is clearly less than that of serine proteases.[35]

In the class of serine proteases, the enzymes of the trypsin family show a higher acyltransferase efficiency than the enzymes of the subtilisin type, which generally constitute very good esterases.[36]

Hydrolysis of the initially formed acyl-enzyme–nucleophile complex (EAN, see Schema 1) has seldom been observed.[31, 37–39] This is of special significance in the trypsin-catalyzed reactions.[28] At present, most of the available

Table 1. Representative examples of protease-catalyzed acyl-transfer reactions characterizing the efficiency of different nucleophiles.

Protease	Nucleophile	Method [a]	Ref.
papain	oligoglycin amides	A	[22]
	n-alcohols	A	[23]
	amino acid amides	A	[24]
	amino acid amides, alcohols, amines	A	[25]
leukocyte elastase	amino acid amides	A	[26]
pancreatic elastase	amino acid amides, peptides	B	[27]
bovine trypsin	amino acid amides	D	[28]
α-chymotrypsin	amines, alcohols	A	[11]
	amino acid amides, peptides	D	[29]
	amino acid amides, peptides	B	[30]
	amino acid amides	C	[31]
δ-chymotrypsin	amino acid amides, amines	A	[32]
V8 protease	amino acid amides, peptides	C	[33]
endoproteinase Glu/Asp-C (*Actinomycetes*)	amino acid amides	C	[34]

[a] Methods for analysis of the acyl-transfer efficiency: A, acceleration of the deacylation by the nucleophile; B, measuring apparatus discussed in Section 5.2.2; C, product analysis using HPLC; D, photometric measurement of the product ratio (see Section 5.2.1).

information concerns the acyl-transfer efficiency of chymotrypsin. These data will be discussed in Section 7.

4. Competitive Reactions during Acyl Transfer

Proteases are not perfect acyltransferases. Owing to their limited specificity, other reactions can take place parallel to acyl transfer (Fig. 3).

The acyl-enzyme formed in the course of the reaction can undergo hydrolysis. The resulting hydrolysis product possesses a very low acylation potential and consequently is not available for formation of the desired product. For this reason, the ratio between aminolysis and hydrolysis of the acyl-donor ester is of utmost importance in protease-catalyzed acyl-transfer reactions. It is essentially determined by the *S'*-subsite specificity of the enzyme. The peptide bond formed by acyl transfer corresponds to a cleavage site for the enzyme. In the literature, enzymatic attack on this bond is denoted as secondary hydrolysis.

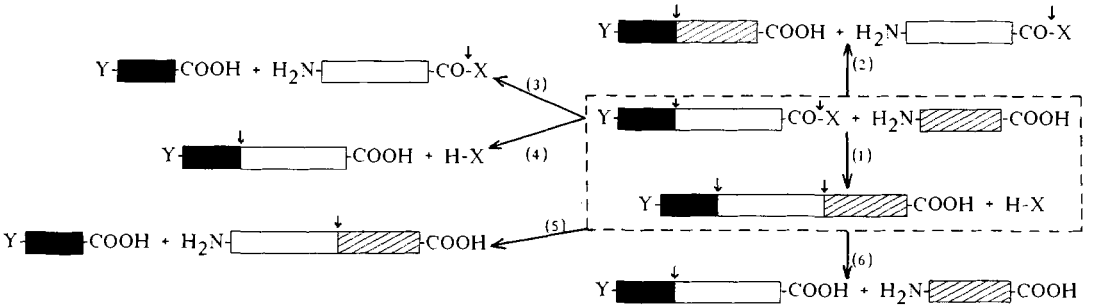

Fig. 3. Reaction paths of the protease-catalyzed acyl transfer. The peptide synthesis (1), starting from the acyl donor and amino component, is framed. Cleavage sites of the individual compounds are indicated by arrows. Parallel to the synthesis reaction (1), hydrolysis of the ester bond (CO-X) of the acyl donor also occurs (4). Besides the ester bond, the acyl donor is presumed to possess a further cleavage site in the acyl part. If the peptide bond of the acyl donor is attacked by the protease, then, besides hydrolysis (3), an acyl transfer (2) to the amino component can take place. The newly formed bond of the synthesized product may undergo a secondary hydrolysis (6); moreover, hydrolysis of another peptide bond is possible (5). Many of the depicted products can undergo further protease-catalyzed reactions because they contain cleavage sites for the enzyme; alternatively, owing to the presence of a free α-amino group, they can behave as a nucleophilic acceptor.

With increasing length of the peptide to be synthesized, the possibility grows that the sequence will contain further peptide bonds that meet the specificity of the protease employed. In the reaction shown in Figure 3, it was assumed that the acyl donor contains only one further cleavage site for the enzyme. It is obvious that there are a large number of reaction pathways, only a few of which are presented in Figure 3.

For the suppression of this kind of undesired side reaction, therefore, enzymatic attack at the ester bond of the acyl donor should be preferred over attack at all other bonds in the reactants and products. The crucial parameters of the enzyme specificity responsible for such side reactions will be discussed in Section 8.

5. Amino Component and Water Compete for the Acyl-Enzyme

5.1. Definition and Significance of the Partition Constant

As already mentioned, the ratio of the formation of aminolysis and hydrolysis products is of decisive importance in preparative peptide synthesis. Moreover, it allows conclusions to be drawn about the *S'*-subsite specificity of the protease. A parameter that describes the acyl-transfer efficiency of the protease must therefore be introduced.

The kinetics of protease-catalyzed acyl-transfer reactions can be described by Scheme 1. The nucleophilic amino component first binds to the acyl-enzyme. The resulting acyl-enzyme–nucleophile complex can undergo aminolysis as well as hydrolysis.[23] The ratio of the formation of aminolysis and hydrolysis products, which is also denoted as selectivity,[40] is determined by the acyl-transfer efficiency of the protease for the corresponding reactants.

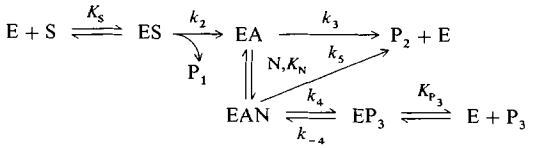

Scheme 1. Protease-catalyzed acyl-transfer reaction. E = enzyme, S = acyl-donor ester (carboxy component), N = nucleophile (amino component), P_1 = leaving group of the acyl-donor ester, P_2 = hydrolysis product, P_3 = peptide product, EA = acyl-enzyme, EAN = acyl-enzyme–nucleophile complex.

In analogy to the definition of the Michaelis constant, we decided to introduce the partition constant p defined in Equation (1).[41] The partition constant corresponds to the

$$\frac{v_H}{v_A} = \frac{d[P_2]}{d[P_3]} = \frac{p}{[N]} \quad (1)$$

nucleophile concentration at which aminolysis and hydrolysis of the acyl-enzyme proceed with the same velocity. Such a definition of the partition constant has the advantage that it is not based on a particular kinetic scheme. Moreover, p allows a rapid estimation of the yield of the acyl-transfer reaction. Only if $[N] > p$ is valid can the peptide be produced in a high yield.

The partition constant is an empirically introduced measure. Its definite significance ensues from the kinetic pattern of the reaction. If an equilibrium is assumed between the acyl-enzyme and the acyl-enzyme–nucleophile complex, Equations (2) and (3) can be derived from Scheme 1 for the velocities of hydrolysis and aminolysis of the acyl-enzyme.

$$v_H = [EA]k_3 + [EA][N]\frac{k_5}{K_N} \quad (2)$$

$$v_A = [EA][N]\frac{k_4}{K_N} \quad (3)$$

By combining Equations (1)–(3), one obtains Equation (4).

$$p = \frac{[N]k_5}{k_4} + \frac{K_N k_3}{k_4} \quad (4)$$

Accordingly, Scheme 1 yields a linear correlation between the partition constant and the nucleophile concentration. The quotient k_5/k_4 corresponds to the ratio of hydrolysis to aminolysis of the EAN complex. The term $K_N k_3/k_4$ is a measure for the nucleophilic efficiency.

The concept of the partition constant has been accepted by several research groups.[42, 43] *Gololobov* et al.[44] have proposed the parameter β, which is the reciprocal of the partition constant. Other authors prefer to characterize the nucleophilic efficiency by means of quotients of different rate constants.[22, 26, 29, 31, 32] A disadvantage of the latter method is the lack of comparable results, since they depend on the particular kinetic pattern of each reaction.

5.2. Methods for Determining the Partition Constant

5.2.1. Product Ratio for an Excess of Nucleophile

According to Equation (1), the partition constant is determined by the ratio of the velocities of aminolysis and hydrolysis of the acyl-enzyme. If the reaction is carried out in the presence of a large excess of nucleophile, ($[N]_0 \gg [S]_0$), then the decrease of the nucleophile concentration during the reaction course can be ignored. Under these conditions the ratio is $v_H/v_A = [P_2]/[P_3]$. This relation allows a simple calculation of the partition constant according to Equation (5).

$$p = \frac{[P_2][N]}{[P_3]} \quad (5)$$

The determination of the product ratio is preferentially carried out by HPLC analysis.

By employing appropriate acyl-donor esters it is possible to establish the ratio of hydrolysis to aminolysis from the change of the absorption during the reaction course,[29, 37] provided that the absorption changes differ for the two reactions ($\varepsilon_{P_2} \neq \varepsilon_{P_3} - \varepsilon_N$).

5.2.2. Apparatus for the Determination of p

The determination of the partition constant p by means of HPLC analysis is a discontinuous method. Moreover, it is

necessary to adjust the separation conditions for each product mixture. In order to characterize the applicability of the proteases for peptide synthesis, however, it is necessary to perform extensive investigations on the acyl transfer. In this process a large number of acyl-donor esters and nucleophiles in various combinations have to be examined.

An apparatus was developed by us, especially for the broad screening of the S'-subsite specificity of proteases.[45] The velocity of hydrolysis is determined by titration. The aminolysis of the acyl-enzyme is indirectly determined by the decrease of the nucleophile concentration in the reaction mixture. For this purpose, the amino groups are allowed to react with *o*-phthalaldehyde and photometrically evaluated.[46]

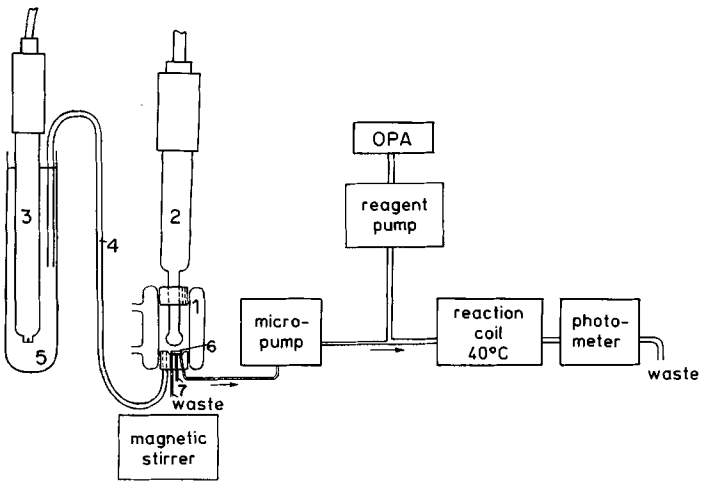

Fig. 4. Apparatus for the continuous monitoring of protease-catalyzed acyl-transfer reactions. The reactions are carried out in a thermostated vessel (1) equipped with a magnetic stirrer and a cannula for the titrant (7). The pH measurement is carried out using a miniature glass electrode (2). In order to keep the reactor volume small, the reference electrode (3) was connected via a salt bridge (4) to the vessel. The reference electrode and the polyethylene tube are inserted into a reagent glass filled with saturated potassium chloride solution (5). The reaction sample is continuously pumped from the reaction vessel and is mixed with *o*-phthalaldehyde solution by means of a second pump. The absorption of the mixture running through a reaction loop is continously recorded at 340 nm.

The apparatus schematically shown in Figure 4 was used to carry out numerous series of acyl-transfer reactions and to investigate the S'-subsite specificity of α-chymotrypsin and porcine pancreatic elastase.[27, 30]

5.2.3. *Acceleration of the Deacylation by the Nucleophile*

In the serine- and cysteine-protease–catalyzed hydrolysis of specific ester substrates, the deacylation of the acyl-enzyme generally constitutes the rate-limiting step (i.e., $k_2 \gg k_3$ and $k_{cat} = k_3$). Under these conditions, the catalytic constant $(k_{cat})_{app}$ increases in the presence of an added nucleophile according to Equation (6).

$$(k_{cat})_{app} = k_3\frac{K_N}{K_N + [N]} + (k_4 + k_5)\left(1 - \frac{K_N}{K_N + [N]}\right) \quad (6)$$

If $k_5 = k_3$ or $k_4 \gg k_3$ is valid, then it is possible to simplify Equation (6) to Equation (7).

$$(k_{cat})_{app} = k_3 + k_4\frac{K_N}{K_N + [N]} \quad (7)$$

If an acyl-donor ester with a chromogenic leaving group is used, then, from the k_{cat} increment due to the nucleophile addition, the efficiency of the employed nucleophile can be calculated. Applications of this method are described in a series of publications.[22, 24, 26, 32, 38] For nonspecific ester substrates it is possible to isolate the acyl-enzyme and to follow the deacylation directly.[25]

5.2.4. *Determination of p from the Integrated Rate Equation*

As mentioned in Section 3.2.1, an excess of the nucleophilic amino component over the acyl donor is used in the analysis of acyl-transfer reactions by HPLC. In the preparative use of acyl-transfer reactions, however, a large excess of the nucleophile is not useful because a complete turnover of both reactants is desired. For this reason, we developed a method which allows the partition constant to be determined from HPLC data, even when the nucleophile concentration significantly decreases during the reaction.[47]

For the initial nucleophile concentration Equation (8) is valid. By substituting Equations (8) and (4) into Equation (1) and subsequent integration, Equation (9) is obtained.

$$[N] = [N]_0 - [P_3] \quad (8)$$

$$\frac{[P_2]}{[P_3]} = \frac{k_5}{k_4} + K_N\frac{k_3}{k_4}\frac{\ln([N]_0/([N]_0 - [P_3]))}{[P_3]} \quad (9)$$

According to Equation (9), a plot of $[P_2]/[P_3]$ versus $\ln([N]_0/[N]_0 - [P_3]))/[P_3]$ gives a straight line with the slope $K_N k_3/k_4$ and an intercept with the y axis at k_5/k_4. Figure 5 shows a plot according to Equation (9) for the acyl-transfer reaction catalyzed by V8 proteinase.[47]

This method permits a determination of the partition constant under the conditions employed in a preparative peptide synthesis. Therefore, it should be especially useful for the optimization of the reaction conditions.

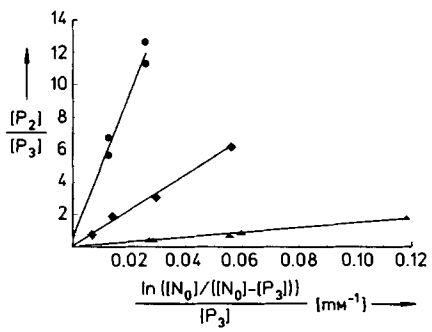

Fig. 5. Plot according to Equation (9) for the V8-protease-catalyzed acyl transfer using Z-Glu-OMe as the acyl donor. Nucleophiles: ▲, H-L-Leu-NH_2; ●, H-D-Leu-NH_2; ■, H-L-Val-NH_2.

It is a further advantage of this method that the reactions can be carried out in the presence of an excess of the acyl donor. This allows the analysis of reactions in which the peptide product is subjected to further protease-catalyzed reactions. For example, this type of reaction is known for the thiolprotease papain.[35,48] An excess of the acyl donor protects the peptide product from secondary hydrolysis by the enzyme and allows an exact determination of the partition constant.

6. The *S'*-Subsite Specificity for the Acyl Transfer and Peptide Hydrolysis Are Equal

Acylation of the enzyme by a peptide substrate represents the reversal of the aminolysis of the acyl-enzyme by the corresponding nucleophile. For the illustration of this case, the hydrolysis of two peptide substrates, YA and YB, will be compared [Eqs. (a) and (b)]. The course of the free energy for

$$E + YA \rightleftharpoons EY + A \rightleftharpoons E + Y + A \quad (a)$$

$$E + YB \rightleftharpoons EY + B \rightleftharpoons E + Y + B \quad (b)$$

both reactions is depicted in Figure 6. During the hydrolysis of both substrates the same acyl-enzyme EY is formed as an intermediate. Consequently, the free energy of the acyl-enzyme hydrolysis, ΔG_{deac}, is identical for both substrates.

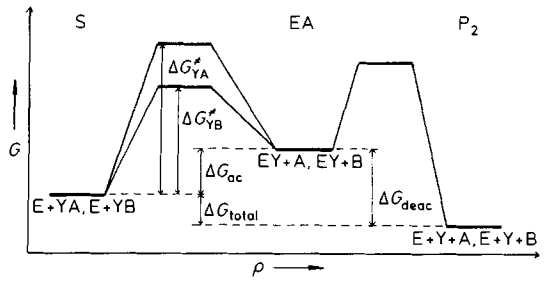

Fig. 6. Comparison of the reaction coordinates ρ for the enzymatic hydrolysis of the two peptide substrates YA and YB with the same acyl moiety. EA = acyl-enzyme, P_2 = hydrolysis product.

Fersht and *Requena*[49] carried out numerous investigations concerning the influence of the structure of peptides on the equilibrium constants of their hydrolysis. The results showed that the free energy of peptide hydrolysis is only minimally influenced by the structure of the amino acid side-chains, as long as the pK values of the amino acids released by hydrolysis do not differ significantly. This leads to the assumption that the free energy of hydrolysis of both substrates, ΔG_{total}, scarcely differs.

The free energy of the enzyme acylation by the substrate is obtained from Equation (10). ΔG_{ac} must be identical for

$$\Delta G_{ac} = \Delta G_{total} - \Delta G_{deac} \quad (10)$$

both substrates, because the substrates do not differ in ΔG_{total} and ΔG_{deac}. Furthermore, aminolysis of the acyl enzyme and peptide hydrolysis pass through the same transition state. Assuming the substrate YB possesses the higher specificity constant k_{cat}/K_M (i.e., $\Delta G^{\ddagger}_{YB} < \Delta G^{\ddagger}_{YA}$), then the nucleophilic efficiency of the leaving group B must lie above the efficiency of A by the same magnitude.

If only peptides whose free energies of hydrolysis do not differ significantly are compared, then there exists a strict relationship between the *S'*-subsite specificity of peptide hydrolysis and aminolysis of the acyl-enzyme. Therefore, it becomes possible to investigate the *S'*-subsite specificity of serine and cysteine proteases via acyl-transfer reactions. This is a significant point since analysis of the specificity of proteases in peptide hydrolysis encounters several problems. This type of measurement requires the preparation of numerous series of peptide substrates. Especially in large peptides, several peptide bonds in the sequence may be simultaneously cleaved. Moreover, peptide hydrolysis is not generally accompanied by an absorption change which can be spectrophotometrically measured. Since in the acyl-transfer reactions comparatively reactive esters are used as acyl donors, one can even determine the specificity for peptide sequences which are not hydrolyzed by the corresponding protease at detectable rates.[32]

7. Chymotrypsin-Catalyzed Acyl Transfer

α-Chymotrypsin is one of the most intensively investigated enzymes.[10] Its three-dimensional structure has been determined by X-ray crystallography.[50–52] α-Chymotrypsin is an endopeptidase with a distinct primary specificity for peptide substrates bearing aromatic amino acids in the P_1 position.[53]

The specificity of α-chymotrypsin for the leaving groups of the substrates has been intensively investigated. In these reactions substituted phenyl esters, anilides, or aliphatic alkyl esters of various structures have been employed.[54–58] However, there is a lack of information on the *S'*-subsite specificity of α-chymotrypsin in the hydrolysis of peptides. Investigations have so far been restricted to substrates with aromatic amino acids in the P_1 position and small hydrophobic amino acids in the P'_1 position.[17,18,59–62]

7.1. Specificity of the *S'* Subsites

A large number of chymotrypsin-catalyzed acyl-transfer reactions are described in the literature.[29,30–32,37] In accordance with the endopeptidase character of chymotrypsin, no acyl transfer to free amino acids has been ascertained.[29] Also, when H-β Ala-Gly-OH and D-amino acid derivatives are used as nucleophiles, aminolysis of the acyl-enzyme was barely observed[30,31] Obviously, efficient acyl transfer requires nucleophiles containing α-amino acids of the L configuration.

In order to characterize the specificity of the enzyme S'_1 subsite, a large number of amino acid amides were investigated as nucleophilic amino components. The results of these measurements are summarized in Table 2. The values demonstrate a preference of the S'_1 subsite for amino acids with hydrophobic side chains. An exception is H-Arg-NH_2, which clearly shows a higher efficiency than all the other amino acid amides. This is believed to be due to electrostatic

Table 2. Partition constants [mM] for the chymotrypsin-catalyzed acyl transfer to amino acid amides [a].

Nucleophile	Ac-Tyr-OEt [31]	Ac-Phe-ONp [32], [b]	Mal-Phe-OMe [30]	Mal-Leu-OBzl [30]
H-Met-NH_2	–	–	3.3	4.9
H-Tyr-NH_2	–	8.5	–	–
H-Trp-NH_2	–	22	–	–
H-Leu-NH_2	19 [c]	–	4.2	10
H-Val-NH_2	21 [c]	–	6.7	15
H-Ala-NH_2	23 [c]	23	9.3	18
H-Ser-NH_2	49	–	–	–
H-Gly-NH_2	104	87	44	90
H-Arg-NH_2	–	–	0.11	0.24
H-D-Ala-NH_2	5500	–	–	–

[a] The acyl-donor esters and the references are given in the table head. All acyl-transfer experiments were carried out under comparable conditions (25 °C; pH 9.0–10.0; solvent content < 5 %; ionic strength = 0.19–0.95). Mal = maleyl (3-carboxyacryloyl). [b] δ-Chymostrypsin was used. All the other reactions were carried out with α-chymotrypsin. [c] The partition constant is dependent on the nucleophile concentration (i.e., $k_3/k_4 > 0$).

interactions with the enzyme, which will be separately discussed in the following section.

The S'_1-subsite specificity of chymotrypsin can be explained in terms of the structure of complexes of the enzyme with protein inhibitors. These inhibitors constitute specific substrates for the proteases, whose hydrolysis proceeds reversibly owing to the structure of the inhibitor molecule.[63] The structures of such inhibitors and of enzyme–inhibitor complexes can serve as models for the interactions of proteases with peptide substrates.

From the model of the complex between bovine pancreatic trypsin inhibitor and chymotrypsin, it was deduced that the P'_1 side chain of the substrate is directed away from the enzyme.[64] Accordingly, larger amino acid side chains can also be bound. The same model also explains the low efficiency of H-D-Ala-NH_2.

Investigations on the acyl transfer to dipeptide amides revealed that additional interactions in the S'_2 binding site slightly influence the specificity of the S'_1 subsite.[30] A series of dipeptide nucleophiles with different residues in the P'_2 position showed that amino acids with hydrophobic side chains are preferred at this site.[29, 65]

7.2. Ionic Interaction in the S' Subsites

Nucleophiles containing charged groups clearly show a different behavior in the α-chymotrypsin-catalyzed acyl-transfer reactions when compared with uncharged compounds (see Table 3). Thus, for H-Arg-NH_2, the p values lie more than one order of magnitude lower than the values of the other amino acid amides. Also, the high partition constants of nucleophiles containing free carboxyl groups are conspicuous. We believe that the influence of the charged groups on the nucleophilic efficiency is due to a negative electrostatic potential at the S' subsites of the enzyme.[37]

A statistical analysis of proteolysis data confirmed that α-chymotrypsin possesses a specificity for peptide bonds bearing arginine or lysine in the P'_1 position.[66] Furthermore, the analysis showed that α-chymotrypsin cleaves Leu–Asp bonds of proteins considerably less frequently than one expects from the frequency of occurrence of this bond.

The X-ray crystallographic analysis of a chymotrypsin complex with a protease inhibitor from ovomucoid showed that a salt bridge is formed between the P'_3 arginine residue of the inhibitor and Asp-64 of the enzyme.[67]

A comparison of the oligoglycines in Table 3 shows the influence of the distance between the nucleophilic amino group and the charged carboxyl group. With increasing length of the nucleophile, the electrostatic interactions with the negatively charged residues of the α-chymotrypsin S' subsites are reduced. Favorable interactions of the nucleophiles with the S'_3 and S'_4 subsites cannot explain the influence of the nucleophile length on the p value, since for H-Gly-NH_2 a higher efficiency has been established than for H-Gly-Gly-Gly-Gly-OH (compare Tables 2 and 3).

Table 3. Influence of charged groups in the nucleophile on the aminolysis of Mal-Phe-α-chymotrpysin.

Nucleophile	p [mM]	Ref.
H-Arg-NH_2	0.11	[30]
H-Leu-NH_2	4.2	[30]
H-Arg-OMe	22 [a]	[37]
H-Leu-OMe	> 600	[37]
H-Ala-Ala-OH	58	[30]
H-Ala-Ala-NH_2	4.9	[30]
H-Gly-Gly-OH	214	[30]
H-Gly-Gly-Gly-OH	138	[30]
H-Gly-Gly-Gly-Gly-OH	103	[30]

[a] The partition constant is dependent on the nucleophile concentration.

For a series of model reactions, it could be shown that the nucleophilic efficiency of dipeptides with free carboxyl groups can be improved by more than one order of magnitude by adding inorganic salts to the reaction medium.[65] This is supposed to be due to the shielding of the unfavorable electrostatic interactions between the negatively charged carboxyl group of the nucleophile and the negative potential of the acyl-enzyme S' subsites. The interaction of the arginine residues in the nucleophile with the enzyme can similarly be influenced by the addition of various salts.[68]

All the above-mentioned examples prove that proteolysis, the binding of the inhibitors, and acyl transfer are governed by the same factors. Consequently, an understanding of the molecular interaction between the acyl-enzyme and the nucleophile allows an optimization of the acyl-transfer efficiency.

7.3. Influence of the Acyl-Donor Structure on the Partition Constant

For the planning of protease-catalyzed peptide syntheses, it is of importance to determine whether the nucleophilic specificity of a protease is influenced by the structure of the acyl donor. For this reason, we compared the α-chymotrypsin-catalyzed acyl transfer from two different acyl-donor esters to a series of nucleophiles.[30]

As Figure 7 shows, the partition constants for a particular nucleophile do not differ by more than one order of magnitude, whereas for different nucleophiles and the same acyl donor, differences of more than three orders of magnitude

are observed. The structure of the residues occupying the S subsites obviously has little influence on the binding of the nucleophile in the S' subsites. An investigation of the acyl transfer from fourteen acyl-donor esters to four different nucleophiles confirmed this conclusion.[30]

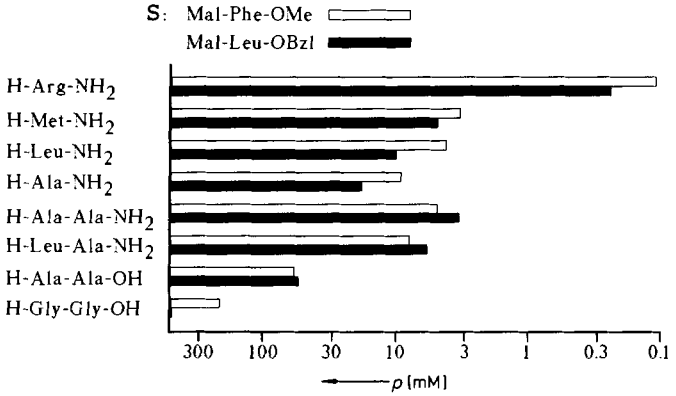

Fig. 7. Comparison of the partition constants for the α-chymotrypsin-catalyzed acyl transfer with two different acyl-donor esters [30].

Accordingly, for the characterization of the S' subsite specificity of α-chymotrypsin, it is sufficient that a series of nucleophiles be allowed to react with a single acyl donor. The resulting data can be applied with an accuracy sufficient for preparative purposes to other acyl donor esters.

8. Competition for the Free Enzyme

Besides the hydrolysis of the acyl-enzyme, which was already discussed in detail, an attack of the enzyme on the peptide product has practical relevance (cf. Fig. 3). This process can result in secondary hydrolysis of the peptide bond formed. With increasing number of peptide bonds the probability grows that other peptide bonds in the product will meet the specificity of the enzyme. If in the course of the reaction a product containing a protease-labile bond is accumulated, then the desired product can undergo further enzymatic reaction. A kinetic analysis of this type of reaction is a prerequisite for the optimization of the peptide yield.

In considering the reactions that can occur subsequent to proteolysis, it is sufficient to assume that the peptide product possesses, besides the newly formed peptide bond, only one additional protease-labile peptide bond. The corresponding reaction mechanism is presented in Scheme 2. Despite the large number of velocity and equilibrium constants in Scheme 2, it is possible to discuss the kinetic relationships in a simple manner, provided that a small number of parameters for the enzyme specificity are introduced. All the kinetic parameters used and their significance are summarized in Table 4.

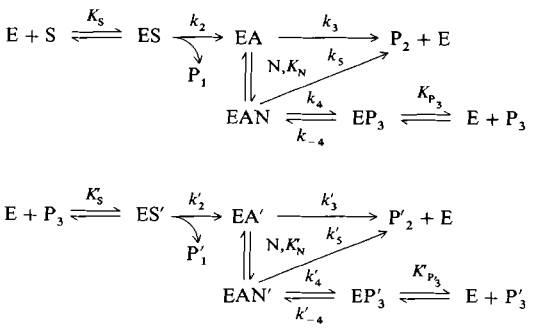

Scheme 2. Protease-catalyzed acyl-transfer and competitive reactions of the peptide product P_3. In the reaction of P_3 to EA', the bond cleaved is different from the one formed in the upper part of the scheme.

Table 4. Kinetic parameters for the description of protease-catalyzed acyltransfer reactions. Each parameter characterizes the competition between two reaction paths in Scheme 2. The quotients k_2/K_S, k'_2/K'_S, k_4/K_{P_3}, and k'_{-4}/K'_{P_3} correspond to the rate constants for the second-order reactions given in the last two columns of the table. They are therefore equal to the specificity constants k_{cat}/K_M of these reactions.

Parameter	Equation [a]	Competitive reactions	
p	$p = [N]\frac{k_5}{k_4} + K_N\frac{k_3}{k_4}$	EA ⟶ P_2	EA + N ⟶ P_3
p'	$p' = [N]\frac{k'_5}{k'_4} + K'_N\frac{k'_3}{k'_4}$	EA' ⟶ P'_2	EA' + N ⟶ P'_3
α	$\alpha = \frac{k_{-4}/K_{P_3}}{k_2/K_S}$	E + P_3 ⟶ EA	E + S ⟶ EA
α'	$\alpha' = \frac{k'_{-4}/K'_{P_3}}{k_2/K_S}$	E + P'_3 ⟶ EA	E + S ⟶ EA'
α_1	$\alpha_1 = \frac{k'_2/K'_S}{k_2/K_S}$	E + P_3 → EA'	E + S ⟶ EA

[a] The equation gives the parameter according to Scheme 2.

8.1. Parameter α of Secondary Hydrolysis

The attack of the enzyme on the newly formed peptide bond is the reversal of the aminolysis of the acyl-enzyme. Consequently, this side reaction may occur during every enzymatic peptide synthesis. For the understanding of the kinetics, it is important that the acyl donor employed and the resulting peptide compete for the free enzyme. Accordingly, the concentration ratio and the specificity constants, k_{cat}/K_M, determine which substance will be preferably attacked.

In kinetically controlled reactions, the tendency for the occurrence of a secondary hydrolysis is characterized by the parameter α[44] (see Table 4). A small value of α signifies a low risk of secondary hydrolysis.

If serine proteases are used for the synthesis, a secondary hydrolysis of the product should not generally be expected as long as a small concentration of the acyl-donor ester is still available in the reaction mixture. For these enzymes esters constitute much better substrates than peptides with the same acyl part. In the case of cysteine proteases, the preference for ester substrates is lower[35] and proteolytic side reactions are observed.[48]

8.2. Parameter α_1 of Specificity

If one compares the variety of peptide sequences to be synthesized with the limited number of proteases available for preparative purposes, it becomes clear that enzymes with an absolute specificity for the bond formation will not be available. Consequently, segment coupling must be feasible, although the peptide product possesses several cleavage sites for the enzyme.

For the reaction depicted in Scheme 2, it was assumed that the peptide product P_3, besides the newly formed bond, contains one further protease-labile bond. To explain the competition between this bond and the acyl donor for the free enzyme, we introduced the parameter α_1,[48] as shown in Table 4.

8.3. Calculation of the Reaction Course

By applying the steady-state principle and on the basis of the parameters in Table 4, Equations (11)–(16) can be

$$\frac{d[P_2]}{dt} = [E]\frac{k_2}{K_s}\frac{[S] + \alpha[P_3]}{1 + [N]/p} \tag{11}$$

$$\frac{d[P_3]}{dt} = [E]\frac{k_2}{K_s}\frac{[S][N]/p - (\alpha + \alpha_1 + \alpha_1[N]/p)[P_3]}{1 + [N]/p} \tag{12}$$

$$\frac{d[P'_2]}{dt} = [E]\frac{k_2}{K_s}\alpha_1\frac{[P_3] + \alpha'[P'_3]}{1 + [N]/p'} \tag{13}$$

$$\frac{d[P'_3]}{dt} = [E]\frac{k_2}{K_s}\alpha_1\frac{[P_3][N]/p' - \alpha'[P'_3]}{1 + [N]/p'} \tag{14}$$

$$[N] = [N]_0 - [P_3] - [P'_2] - 2[P'_3] \tag{15}$$

$$[S] = [S]_0 - [P_2] - [P_3] - [P'_2] - [P'_3] \tag{16}$$

derived. The numerical solution of this system of equations allows the yield of the peptide product to be calculated from a given set of initial conditions (concentration of the nucleophile and the acyl donor).

The term $[E]k_2/K_S$ appears in all four differential equations and, therefore, has no influence on the concentration ratios of the individual products. The enzyme concentration only influences the velocity of the reaction, but not its course and the yield of P_3.

In order to explain the significance of the individual parameters, it is helpful to consider the conditions at the product maximum, which is attained if $d[P_3]/dt = 0$ is valid. If one denotes the concentrations of the acyl donor and nucleophile at the time of the maximum product concentration with [S]* and [N]*, respectively, then Equation (12) gives Equation (17). In order to achieve high product yields,

$$[P_3]_{max} = \frac{[N]^*[S]^*}{p(\alpha + \alpha_1 + \alpha_1[N]^*/p)} \tag{17}$$

the following conditions must be fulfilled: $[N] > p$, $\alpha < 1$ and $\alpha_1 < 1$.

The procedure described above corresponds to the approach of *Gololobov* et al.[44], which has been extended to the analysis of subsequent reactions. Another approach to estimate the product concentration has been proposed by *Bratovanova* et al.[69]

8.4. Determination of the α Parameters

The formally simplest way to determine the individual α parameters follows from the equations given in Table 4. Accordingly, the hydrolysis kinetics of the acyl-donor ester and the peptide products P_3 and P'_3 must be investigated. In the hydrolysis of the peptide product, several cleavage sites can be attacked. These individual cleavage sites can be dealt with as competitive substrates; that is, the occurrence of cleavage is proportional to the specificity constants of the enzyme for the individual bonds.

It is easier to carry out an analysis of the product mixture at the time of the yield maximum. The α parameters can be calculated from the concentration ratios by using Equation (17). For the separate determination of α and α_1, several reactions with various nucleophile concentrations must be investigated.

8.5. Possibilities to Suppress Competitive Reactions

If undesired subsequent reactions are observed in a kinetically controlled protease-catalyzed synthesis, then it is of minor importance which bond is cleaved by the enzyme. These reactions merely show that the specificity of the enzyme for the acyl donor does not lie sufficiently above its specificity for the peptide product. Since structural changes in the amino acid building blocks of the reactants are ruled out, the leaving group of the acyl donor remains as the only variable to suppress these competitive reactions. *Leaving group variations at the carboxy components*, therefore, are of great importance in order to counteract undesired side reactions. For syntheses using carboxypeptidase Y[70] and papain,[71] the proper choice of the leaving groups of the carboxy component allowed the subsequent reactions to be suppressed.

We studied the chymotrypsin-catalyzed synthesis of the chromogenic chymotrypsin substrate Mal-Leu$\overset{\downarrow}{-}$Phe$\underset{\uparrow}{-}$pNA (the arrow from above shows the newly formed peptide bond) as a peptide model with a highly sensitive cleavage site. In this case the subsequent chymotryptic cleavage of the anilide bond (arrow from below) can be easily detected spectrophotometrically.[72] Table 5 shows the relationship between the specificity of the acyl donor ester and the yield of the synthesis. When Mal-Leu-OMe is employed as acyl donor, the velocity of the product cleavage reaches the velocity of its formation after a short time. By using more specific acyl-donor esters a clear product accumulation is attained. Only after almost complete consumption of Mal-Leu-ONb was there an indication that a reaction involving the product took place. This result proves that by choosing a specific leaving group for the acyl donor, protease-labile products can be obtained in good yield.

Table 5. Influence of the specificity of the acyl donor on the α-chymotrypsin-catalyzed synthesis of Mal-Leu-Phe-pNA [72].

Acyl donor	k_{cat}/K_M [$M^{-1}s^{-1}$]	Yield [%]
Mal-Leu-OMe	4.7×10	3
Mal-Leu-OBzl	3.2×10^3	65
Mal-Leu-ONb	1.5×10^4	80.5

The use of "inverse substrates" in trypsin-catalyzed peptide synthesis allows a still more effective suppression of the

subsequent reactions to be achieved. In inverse substrates[73] the positive charge required for the trypsin catalysis is not located in the P_1 position but on the leaving group. These acyl-donor esters allow a nearly irreversible trypsin-catalyzed peptide synthesis.[74] Of the acylamino acid esters with positively charged leaving groups synthesized so far, the *p*-guanidinophenyl esters proved to be especially suitable. The extremely low specificity of trypsin for the acyl part of such inverse substrates enables even the formation of peptide bonds with proline, which, in general, is not simple to achieve by protease catalysis. The concept of inverse substrates therefore allows the trypsin-catalyzed synthesis of peptides, independent of the side-chain groups in the P_1 position. Furthermore, the newly formed peptide bond is practically resistant toward secondary hydrolysis, with the exception of trypsin-labile Arg(Lys)–Xaa bonds. Whether this strategy can be developed into a standard method depends on further optimization of the synthesis of inverse substrates.

The reaction conditions influence the course of kinetically controlled synthesis in various ways. High pH values favor an increase of the nonprotonated form of the amino component and, consequently, enhance the efficiency of the aminolytic deacylation of the acyl-enzyme. Furthermore, high pH values may effect an increased proteolytic stability of the newly formed peptide bonds. In a papain-catalyzed synthesis, a temperature decrease from 40 °C to 5 °C led to a noticeable lowering of undesired subsequent reactions.[48]

The protease-catalyzed synthesis of peptides in frozen aqueous medium opens completely new possibilities.[75] At temperatures down to − 25 °C, a dramatically improved ratio between aminolysis and hydrolysis of the acyl-enzyme was observed, presumably resulting from a high local concentration of the nucleophile. This procedure even allowed the chymotrypsin-catalyzed coupling of free amino acids, which yield no detectable amount of product at 25 °C.

The possibility of protease-catalyzed peptide synthesis in organic solvents has been intensively investigated.[76] Chymotrypsin-catalyzed acyl-transfer reactions in nonpolar solvents in the presence of salt hydrates have been described.[77, 78] Besides a minimization of the undesired proteolytic side reactions and an improvement of the reactant solubility, the protease-catalyzed synthesis in monophasic organic solvent offers favorable conditions for adjusting the reaction media between the enzymatic and chemical synthetic steps. This is in accordance with the attempts to achieve an enzymo-chemical synthesis. Enzymatic syntheses in monophasic organic solvents are frequently described as reactions with "solvent-modified enzymes". Besides such apparent modifications, the proteases can be chemically modified to become soluble in organic solvents; examples include chymotrypsin[79, 80] and papain[81] modified with polyethylene glycol (PEG). Under these conditions, generally the proteolytic reactions can be completely eliminated. Reactions in monophasic organic systems also possess disadvantages, such as drastic lowering of the velocity of the catalyzed reaction, extensive loss of the regiospecificity and thus the necessity to protect the side-chain functions, and change of the substrate specificity, as well as the necessity for waste disposal of the organic solvents.

On the basis of elevated solvent tolerance and also owing to the lowered amidase and protease acitivity, chemically and genetically engineered proteases have been successfully used for synthetic purposes. The use of cyanomethyl esters and methylchymotrypsin[82] proved to be an advantageous synthesis variant, which, on the basis of the reduced esterolytic activity, also allows the coupling of amino components with C-terminal alkyl ester groups. Thiolsubtilisin[83] is active against specific ester substrates, but shows no amidase and peptidase activities. It proved to be useful for the synthesis of Leu-enkephalin and a partial-segment synthesis of ribonuclease T_1. Good results were also obtained in the synthesis of various L,D-dipeptides using [Met(O)^{192}]chymotrypsin as catalyst.[84] Using multiple site-directed mutagenesis, *Wong* et al.[85] converted subtilisin into so-called subtilisin 8350, which allows kinetically controlled syntheses to be performed in the presence of high concentrations of dimethylformamide. This development has certainly opened the way for a new phase of protease-catalyzed peptide synthesis.

Nonproteases are supposed to possess favorable prerequisites for the enzymatic peptide synthesis because undesired proteolytic cleavages in the reactants and products can be ruled out. Besides other hydrolases, several synthetases can be used as alternatives to proteases. Lipases that contain the catalytic triade typical of serine proteases[86, 87] seem to be especially suitable. Peptide derivatives have been synthesized using various lipases as well as pig liver esterase.[88–90] In accordance with the investigations of *Wong* and co-workers,[88, 89] acyl-donor esters with long-chain leaving groups such as glycerol or *n*-octanol are more suitable than simple alkyl esters. Lipases also accept D-amino acid derivatives as substrates. Thus, the dipeptide N^{α}-phenacetyl-L-cysteinyl-D-valine was synthesized by lipase catalysis.[89] It could be converted into penicillin G by a cyclase.[91]

The use of synthetases for peptide synthesis has the advantage that the formation of the peptide bond is practically irreversible. Besides the aminoacyl-tRNA-synthetase–aminoadenylate complex[92, 93] and the arginyl-tRNA:protein arginyltransferase,[94] further synthetase complexes have been tested for the C–N coupling, especially for the synthesis of microbiologically active peptides.[95] Enzymatic syntheses of cyclosporin and its analogues, gramicidin S, special β-lactam antibiotics, etc., support the increasing importance of such multienzyme complexes.

9. Planning and Optimization of Protease-Catalyzed Syntheses

In the synthesis of a peptide, enzymes can only make a meaningful contribution to a synthesis strategy if the full advantages of the enzymatic reactions can be utilized. To compare the stepwise protease-catalyzed assembly of a peptide chain with solid-phase peptide synthesis is a priori completely unrealistic. On the other hand, di- and tripeptides can be prepared enzymatically on a large scale, even in a continuous fashion.[96, 97] For the assembly of biologically active peptides of medium size, it has to be examined in each case whether the formation of peptide bonds, which are especially prone to racemization, is more amenable to enzymatic

procedures. From an ecological point of view, enzymatic steps should be included wherever possible in large-scale syntheses. Proteolysis studies, carried out in advance, can provide information about the specificity of the enzymes employed in the different coupling steps.

Of special interest are also protease-catalyzed acyl-transfer modification of peptide chains prepared by recombinant-DNA technology. For example, the knowledge of the S' specificity of α-chymotrypsin allows specific cleavage sites to be inserted into a peptide chain. As exemplified by a model peptide with a chymotrypsin-labile sequence, it can be shown experimentally that chymotrypsin-catalyzed modification of the C-terminus is possible via transpeptidation.[98]

Apart from the enzyme specificity, the solubility of the components being coupled also dramatically influences the application of enzymes. The spectrum of solvents ranges from water, the ideal medium, to monophasic organic solvents. The character of the peptide components as well as the protecting groups always determines the compromise adopted with regard to the choice of solvent.

The kinetic parameters for the course of an enzymatic synthesis are often not available. These parameters can at best be estimated from data for similar substrates or nucleophiles. Such estimates are usually sufficient for establishing an optimum synthesis strategy. The measures required for an optimization of the peptide yield are obtained by analyzing the reaction course of the acyl transfer. The concentration ratios of the reactants and products furnish the information necessary to decide which parameter limits the product yield. Here, the following rules have to be considered:

(1) In the initial phase of the reaction the product concentration is low. Accordingly, the subsequent reactions of the product can be ignored, and the partition constant can be calculated from the ratio of the peptide product P_3 to the hydrolysis product P_2. If $p > [N]_0$ is met, then a large part of the acyl donor is hydrolyzed. Thus, the nucleophile concentration has to be increased or the reaction conditions (temperature, addition of the solvents or inorganic salts) have to be optimized.

(2) Information about the occurrence of subsequent reactions is obtained from the analysis of the reaction mixture at the maximum recovery point for P_3. If at this point a high concentration of the acyl-donor ester is still present, then the specificity constant k_{cat}/K_M for the acyl donor is small. In this case, an improvement of the yield can be achieved by increasing the concentration of the acyl donor, or more favorably, by choosing a more specific leaving group of the acyl-donor ester.

(3) In enzymatic synthesis it is generally reasonable to use the acyl donor in excess. In the presence of the acyl donor the peptide product is largely protected against enzymatic attack. Furthermore, a certain loss of the acyl donor through hydrolysis is unavoidable.

The employment of this strategy allowed us to achieve a rapid optimization of the (D-Phe)^6-GnRH synthesis by means of a chymotrypsin-catalyzed (3 + 7) segment condensation.[99] By using a small amount of substance for the optimization of the process, we succeeded in finding reaction conditions that led to a yield of more than 97%. If a reaction is to be carried out on a large scale, then it seems reasonable to determine the fundamental kinetic parameters in advance. In order to facilitate an estimation of the expected yield on the basis of these parameters, we have calculated the diagram presented in Figure 8. If the parameters α_1 and p as well as the concentration of the amino component are given, then from the graph it can be determined what concentration of the acyl donor is required in order to obtain a peptide yield of 90%, based on the starting amino component.

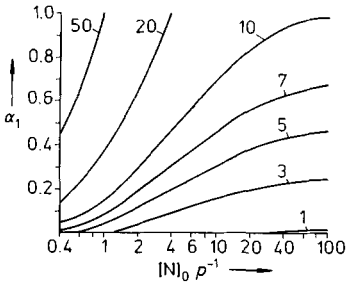

Fig. 8. Correlation between the kinetic parameters of the reaction and the reactant concentrations necessary for preparative peptide synthesis. If α_1, $[N]_0$, and p are given, the ratio $[S]_0/[N]_0$ for which a 90% yield of the peptide product is obtained, can be read from the diagram. The values are calculated from the system of equations in Section 8.3 by using numerical integration. For that, an iterative procedure described by to *Runge-Kutta* is employed [100]. Further kinetic parameters are obtained from Table 4 and are treated in the following way: A value of 0.001 is assumed for α. This value is consistent with the fact that in the majority of the kinetically controlled peptide syntheses the secondary hydrolysis of the formed bond takes place slowly (if this condition is not met, α_1 can be replaced in good approximation by $\alpha_{app} = (\alpha + \alpha_1 + \alpha_1 [N]_0/p)$). Furthermore, it is assumed that $p = p'$. As shown in Section 7.3., the partition constant is not significantly dependent on the structure of the transferred acyl component. The α' value is set to 1, since this parameter corresponds to the quotients of the specificity constants of a second peptide substrate with the same acyl part. The values of the parameters α', p' have a very small influence on the results of calculations. Changing these parameters by about one order of magnitude does not significantly alter the calculated peptide yield. This is understandable because both parameters describe the subsequent reactions of the peptide product. If a 90% yield is desired, the occurrence of these subsequent reactions must be minimized.

10. Outlook

Protease-catalyzed kinetically controlled peptide synthesis has a series of advantages which renders its use in peptide and protein chemistry attractive. Especially, the stereo- and regiospecificity of the proteases, which guarantee racemization-free fragment condensation and require only minimal side-chain protection, are of great significance for preparative purposes.

At present, model investigations on the synthesis of small peptides aim to characterize the enzyme specificity and the parameters which determine the reaction course. Further measurements, especially for the specificity of the S' subsites of the proteases, are required. For the future, it seems quite conceivable to adapt the specificity of the proteases, by means of site-directed mutagenesis, to the practical requirements of the synthesis. Another possibility is the use of catalytic antibodies whose specificity can be adapted to the synthesis objectives.

A further broad field of application for protease-catalyzed reactions ensues from the rapid development of recombinant-DNA techniques. These methods allow the preparation of long peptide sequences; however, they are limited to the 20 proteinogenic amino acids. A selective chemical modification of the genetically prepared peptides and proteins is barely possible due to the numerous unprotected side-chain functions. A combination of gene expression followed by protease conversion could represent an important method to prepare long-chain peptides in the future.

Received: October 31, 1990 [A 839 IE]
German version: *Angew. Chem. 103* (1991) 1440

[1] See, for example, J. Meienhofer, *Biopolymers 20* (1981) 1761–1784.
[2] J. H. van't Hoff, *Z. Anorg. Chem. 18* (1898) 1–13.
[3] M. Bergmann, H. Fraenkel-Conrat, *J. Biol. Chem. 119* (1937) 707–720.
[4] H.-D. Jakubke, P. Kuhl, A. Könnecke, *Angew. Chem. 24* (1985) 85–93; *Angew. Chem. Int. Ed. Engl. 24* (1985) 85–93.
[5] W. Kullmann: *Enzymatic Peptide Synthesis*, CRC, Boca Raton, USA 1987.
[6] H.-D. Jakubke in S. Udenfriend, J. Meienhofer (Eds.): *The Peptides: Analysis, Synthesis, Biology, Vol. 9*, Academic New York 1987, pp. 103–165.
[7] K. Morihara, *Trends Biotechnol. 5* (1987) 164–170.
[8] V. Kasche, in R. J. Beynon, J. S. Bond (Eds.): *Proteolytic Enzymes: a practical approach*, IRL, Oxford 1989, pp. 125–143.
[9] C. Walsh: *Enzymatic Reaction Mechanisms*, Freeman, San Francisco 1979.
[10] A. R. Fersht: *Enzyme structure and mechanism*, Freeman, New York 1985.
[11] P. W. Inward, W. P. Jencks, *J. Biol. Chem. 240* (1965) 1986–1996.
[12] M. L. Bender, G. E. Clement, C. R. Gunter, F. J. Kezdy, *J. Am. Chem. Soc. 86* (1964) 3697–3703.
[13] B. Zerner, M. L. Bender, *J. Am. Chem. Soc. 86* (1964) 3669–3674.
[14] a) F. Widmer, J. T. Johansen, *Carlsberg Res. Commun. 44* (1979) 37–46; b) K. Bredam, F. Widmer, J. T. Johansen, *ibid. 45* (1980) 361–367; c) F. Widmer, K. Breddam, J. T. Johansen, *ibid. 45* (1980) 453–463; d) *ibid. 46* (1981) 91–106.
[15] T. Oka, K. Morihara, *J. Biochem. 82* (1977) 1055–1062.
[16] G. Fortier, S. L. MacKenzie, *Biotechnol. Lett. 8* (1986) 777–782.
[17] K. Morihara, T. Oka, *Biochem. J. 183* (1977) 531–538.
[18] S. A. Bizzozero, B. A. Rovagnati, H. Dutler, *Helv. Chim. Acta 65* (1982) 1707–1719.
[19] Yu. V. Mitin, N. P. Zapevalova, E. Yu. Gorbunova, *Int. J. Pept. Protein Res. 23* (1984) 528–534.
[20] E. N. Lysogorskaya, I. Yu. Philipova, S. E. Boytsova, E. S. Oksenoit, L. A. Lyublinskaya, V. M. Stepanov, *Bioorg. Khim. 9* (1983) 470–477.
[21] I. Schechter, A. Berger, *Biochem. Biophys. Res. Commun. 27* (1967) 157–162.
[22] L. J. Brubacher, M. L. Bender, *Biochem. Biophys. Res. Commun. 27* (1967) 176–182.
[23] A. L. Fink, M. L. Bender, *Biochemistry 8* (1969) 5109–5118.
[24] M. R. Alecio, M. L. Dann, G. Lowe, *Biochem. J. 141* (1974) 495–501.
[25] L. J. Brubacher, M. L. Bender, *J. Am. Chem. Soc. 88* (1966) 5871–5899.
[26] R. L. Stein, A. M. Strimpler, *Biochemistry 26* (1987) 2238–2242.
[27] V. Schellenberger, U. Schellenberger, Yu. V. Mitin, H.-D. Jakubke, *Eur. J. Biochem. 179* (1989) 161–163.
[28] U.-K. Hanisch, A. Könnecke, V. Schellenberger, H.-D. Jakubke, *Biocatalysis 1* (1987) 129–136.
[29] D. D. Petkov, I. Stoineva, *Biochem. Biophys. Res. Commun. 118* (1984) 317–323.
[30] V. Schellenberger, U. Schellenberger, Yu. V. Mitin, H.-D. Jakubke, *Eur. J. Biochem. 187* (1990) 163–167.
[31] L. Riechmann, V. Kasche, *Biochem. Biophys. Res. Commun. 120* (1984) 686–691.
[32] A. R. Fersht, D. M. Blow, J. Fastrez, *Biochemistry 12* (1973) 2035–2041.
[33] M. Schuster, A. Aaviksaar, V. Schellenberger, H.-D. Jakubke, *Biochim. Biophys. Acta 1036* (1990) 245–247.
[34] M. Schuster, A. Aaviksaar, V. M. Stepanov, G. N. Rudenskaya, H.-D. Jakubke, *Biomed. Biochim. Acta 50* (1991) 139–143.
[35] B. Asboth, L. Polgar, *Acta Biochim. Biophys. Acad. Sci. Hung. 12* (1977) 329–333.
[36] M. Ottesen, I. Svendsen, G. E. Perlmann, L. Lorand (Hrsg.): *Methods in Enzymology, Band 19*, Academic, New York 1970, S. 199–215.
[37] V. Schellenberger, H.-D. Jakubke, *Biochim. Biophys. Acta 869* (1986) 54–60.
[38] A. L. Fink, M. L. Bender, *Biochemistry 8* (1969) 5109–5118.
[39] M. Yu. Gololobov, V. K. Svedas, *Biokhimiya (Moscow) 53* (1988) 1174–1180.
[40] A. Schwarz, D. Steinke, M.-R. Kula, C. Wandrey, *Biotechnol. Appl. Biochem. 12* (1990) 188–195.
[41] A. Könnecke, V. Schellenberger, H.-J. Hofmann, H.-D. Jakubke, *Pharmazie 39* (1984) 785–786.
[42] J. B. West, W. J. Hennen, J. L. Labonde, J. A. Bibbs, Z. Zhong, E. F. Meyer, Jr., C.-H. Wong, *J. Am. Chem. Soc. 112* (1990) 5313–5320.
[43] P. Clapes, G. Valencia, J. L. Torres, F. Reig, J.-M. Garcia-Anton, J. Mata-Alvarez, *Biochim. Biophys. Acta 953* (1988) 157–163.
[44] M. Yu. Gololobov, I. L. Borisov, V. M. Belikov, V. K. Svedas, *Biotechnol. Bioeng. 32* (1988) 866–872.
[45] V. Schellenberger, U. Schellenberger, Yu. V. Mitin, H.-D. Jakubke, *Anal. Biochem. 165* (1987) 327–330.
[46] V. K. Svedas, I. J. Galaev, I. L. Borisov, I. V. Berezin, *Anal. Biochem. 101* (1980) 188–195.
[47] V. Schellenberger, M. Schuster, H.-D. Jakubke, *Biocatalysis 4* (1990) 105–111.
[48] M. Yu. Gololobov, U. Schellenberger, V. Schellenberger, H.-D. Jakubke, V. K. Svedas, *Biokhimiya (Moscow) 55* (1990) 338–345.
[49] A. R. Fersht, Y. Requena, *J. Am. Chem. Soc. 93* (1971) 3499–3504.
[50] B. W. Matthews, P. B. Sigler, R. Henderson, D. M. Blow, *Nature 214* (1967) 652–656.
[51] P. B. Sigler, D. M. Blow, B. W. Matthews, R. Henderson, *J. Mol. Biol. 35* (1968) 143–164.
[52] J. J. Birktoft, D. M. Blow, *J. Mol. Biol. 68* (1972) 187–240.
[53] J. Kraut, *Annu. Rev. Biochem. 46* (1977) 331–358.
[54] G. H. Nelson, J. L. Miles, W. J. Canady, *Arch. Biochem. Biophys. 96* (1962) 545–549.
[55] R. M. Epand, I. B. Wilson, *J. Biol. Chem. 238* (1963) 1718–1723.
[56] R. E. Williams, M. L. Bender, *Can. J. Biochem. 49* (1971) 210–217.
[57] D. D. Petkov, E. Christova, I. Stoineva, *Biochim. Biophys. Acta 527* (1978) 131–141.
[58] C. Grieco, C. Hansch, C. Silipo, R. N. Smith, A. Vittoria, K. Yamada, *Arch. Biochem. Biophys. 194* (1979) 542–551.
[59] W. K. Baumann, S. A. Bizzozero, H. Dutler, *FEBS Lett. 8* (1970) 257–260.
[60] C.-A. Bauer, R. C. Thompson, E. R. Blout, *Biochemistry 15* (1976) 1291–1295.
[61] E. D. Djachenko, L. J. Volkova, L. V. Kozlov, V. K. Antonov, *Bioorg. Khim. 2* (1976) 1665–1671.
[62] C. R. Hill, G. C. Tomalin, *Arch. Biochem. Biophys. 221* (1983) 324–328.
[63] M. Laskowski Jr., I. Kato, *Annu. Rev. Biochem. 49* (1980) 593–626.
[64] D. M. Blow, C. S. Wright, D. Kukla, A. Rühlmann, W. Steigemann, R. Huber, *J. Mol. Biol. 69* (1972) 137–144.
[65] V. Schellenberger, A. Aaviksaar, H.-D. Jakubke, *Biocatalysis 4* (1991) 291–296.
[66] B. Keil, *Protein Sequences Data Anal. 1* (1987) 13–20.
[67] M. Fujinaga, A. R. Sielecki, R. J. Read, W. Ardelt, M. Laskowski, Jr., M. N. G. James, *J. Mol. Biol. 195* (1987) 397–418.
[68] a) V. Schellenberger, M. Kosk, H.-D. Jakubke, A. Aaviksaar, *Biochim. Biophys. Acta 1078* (1991) 1–7; b) V. Schellenberger, H.-D. Jakubke, V. Kasche, *ibid. 1078* (1991) 8–11.
[69] E. K. Bratovanova, I. B. Stoineva, D. D. Petkov, *Tetrahedron 44* (1988) 3633–3637.
[70] K. Breddam, F. Widmer, J. T. Johansen, *Carlsberg Res. Commun. 48* (1983) 231–237.
[71] V. Schellenberger, U. Schellenberger, Yu. V. Mitin, H.-D. Jakubke, *Monatsh. Chem. 120* (1989) 437–443.
[72] V. Schellenberger, U. Schellenberger, A. Kucharski, H.-D. Jakubke in G. Jung, E. Bayer (Eds): *Peptides 1988*, de Gruyter, Berlin 1989, pp. 247–249.
[73] a) K. Tanizawa, Y. Kasaba, Y. Kanaoka, *J. Am. Chem. Soc. 99* (1977) 4484–4488; b) K. Tanizawa, Y. Kanaoka, W. Lawson, *Acc. Chem. Res. 20* (1967) 337–343.
[74] a) V. Schellenberger, H.-D. Jakubke, N. P. Zapevalova, Yu. V. Mitin, *Biotechnol. Bioeng. 38* (1991) 104–108; b) V. Schellenberger, U. Schellenberger, H.-D. Jakubke, N. P. Zapevalova, Yu. V. Mitin, in E. Giralt, D. Andreu (Eds.): *Peptides 1990*, Escom, Leiden 1991, 287–288.
[75] M. Schuster, A. Aaviksaar, H.-D. Jakubke, *Tetrahedron 46* (1990) 8093–8102.
[76] See, for example, A. M. Klibanov, *Chemtech. 16* (1986) 354–359.
[77] P. Kuhl, S. Posselt, H.-D. Jakubke, *Pharmazie 36* (1981) 463–465.
[78] P. Kuhl, P. J. Halling, H.-D. Jakubke, *Tetrahedron Lett. 31* (1990) 5213–5216.
[79] A. Matsushima, M. Okada, Y. Inada, *FEBS Lett. 178* (1984) 275–277.
[80] H. F. Gaertner, A. J. Puigserver, *Proteins 3* (1988) 130–137.
[81] H. Lee, K. Takahashi, Y. Kodera, T. Ohwada, T. Tsuzuki, A. Matsushima, Y. Inada, *Biotechnol. Lett. 10* (1988) 403–407.
[82] J. B. West, J. Scholten, N. J. Stolowich, J. L. Hogg, A. I. Scott, C.-H. Wong, *J. Am. Chem. Soc. 110* (1988) 3709–3710.
[83] T. Nakatsaka, T. Sasaki, E. T. Kaiser, *J. Am. Chem. Soc. 109* (1987) 3808–3810.
[84] J. B. West, C.-H. Wong, *J. Chem. Soc. Chem. Commun. 1986*, 417–418;

J. B. West, W. J. Hennen, J. L. Lalonde, J. A. Bibbs, Z. Zhong, E. F. Meyer, Jr., C.-H. Wong, *J. Am. Chem. Soc. 112* (1990) 5313–5320.
[85] C.-H. Wong, S.-T. Chen, W. J. Hennen, J. A. Bibbs, Y.-F. Wang, J.-C. Liu, M. W. Pantoliano, M. Whitlow, P. N. Bryan, *J. Am. Chem. Soc. 112* (1990) 945–953.
[86] F. K. Winkler, A. D'Acry, W. Hunzicker, *Nature 343* (1990) 771.
[87] L. Brady, A. M. Brzozowski, Z. S. Derewenda, E. Dodsen, G. Dodsen, S. Tolley, J. P. Turkenberg, L. Christiansen, B. Huge-Jensen, L. Norskov, L. Thim, U. Menge, *Nature 343* (1990) 767–770.
[88] J. B. West, C.-H. Wong, *Tetrahedron Lett. 28* (1987) 1629–1632.
[89] J. R. Matos, J. B. West, C.-H. Wong, *Biotechnol. Lett. 9* (1987) 233–236.
[90] A. L. Margolin, A. M. Klibanov, *J. Am. Chem. Soc. 109* (1987) 3802–3804.
[91] J. M. Lugeno, M. T. S. Alemany, F. Salto, F. Ramos, M. J. Lopez-Nieto, J. F. Martin, *Biotechnology 4* (1986) 44.
[92] H. Nakajima, S. Kitabake, R. Tsurutani, I. Tomiaka, K. Yamamato, K. Imahori, *Biochim. Biophys. Acta 790* (1984) 197–199.
[93] M. Dombou, H. Nakashima, S. Kitabake, K. Tomita, K. Imahori, *Agric. Biol. Chem. 50* (1986) 2967–2971.
[94] M. Kato, T. Takanashi, *Agric. Biol. Chem. 48* (1984) 2577–2578.
[95] H. Kleinkauf, H. von Döhren (Eds.): *Biochemistry of Peptide Antibiotics*, de Gruyter, Berlin, New York 1990.
[96] A. Flörsheimer, M.-R. Kula, H.-J. Schütz, C. Wandrey, *Biotechnol. Bioeng. 33* (1989) 1400–1405.
[97] G. Hermann, A. Schwarz, C. Wandrey, G. Knaub, K. H. Drauz, *Biotechnol. Appl. Biochem. 13* (1991) 346–353.
[98] V. Schellenberger, W. Tegge, K.-D. Klöppel, R. Frank, unpublished.
[99] V. Schellenberger, U. Schellenberger, H.-D. Jakubke, A. Hänsicke, M. Bienert, E. Krause, *Tetrahedron Lett. 31* (1990) 7305–7306.
[100] I. N. Bronstein, K. A. Semendjajew: *Taschenbuch der Mathematik*, Teubner, Leipzig 1983, S. 769–771.

Helices, Supramolecular Chemistry, and Metal-directed Self-Assembly

By *Edwin C. Constable**

Chemists have been concerned with shape ever since the realization that molecules possess three-dimensional structure. An aspect of shape which has attracted recent attention is conveniently categorized under the title molecular topology and is concerned with the interlinking and intertwisting of molecular threads.[1] The spatial orientation of the molecular threads is critical and has been the subject of some very elegant organic chemistry. More recently, it has been recognized that the required pre-organisation of molecular threads may be achieved by utilization of the specific stereochemical requirements of transition metal ions. All that is required is the incorporation of suitable donor atoms into the molecular threads, and this approach has been exploited in the synthesis of many "exotic" molecular systems. The beauty of using transition metal ions as the templates for the spatial control of molecular threads lies in the fact that all of the stereochemical information is contained at the metal center. The result is that the chemist is then a *passive* observer of the assembly of the organized molecular system—a phenomenon termed spontaneous self-assembly.

The helical geometry is particularly appealing, and this structural motif appears in many important biological molecules. The metal-directed assembly of double helices has been established by a number of groups, and in a paper in this issue, *Williams* et al. report the extension of this methodology to the synthesis of a binuclear triple-helical complex.[2] The principle used for the assembly of the triple helix is very simple. A bis-bidentate ligand is allowed to react with a metal ion which favors six-coordinate octahedral geometry; each of two such metal ions coordinates to one bidentate grouping at each end of three such ligands (Fig. 1).

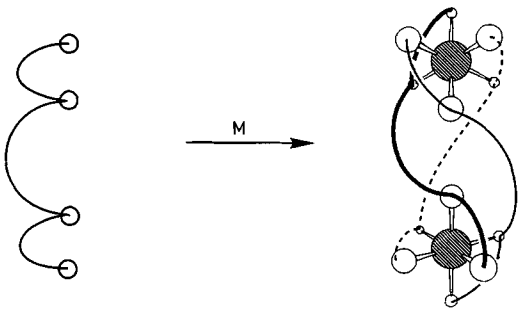

Fig. 1. The formation of a triple-helical complex by interaction of a bis-bidentate ligand with a six-coordinate metal center.

The key to assembling helicate structures lies in the design of a ligand with the correct linker groups between the metal-binding termini. *Williams, Piguet,* and *Bernardinelli*[2] have now shown that the relatively rigid bis-bidentate ligand **1**, consisting of two 2-(2′-pyridyl)benzimidazolyl units linked together, each of which can act as a bidentate N_2 donor, spontaneously forms a triple-helical complex cation $[Co_2(\mathbf{1})_3]^{4+}$ upon treatment with cobalt(II) salts. The X-ray crystal structure of the organge-red complex $[Co_2(\mathbf{1})_3][ClO_4]_4 \cdot 2.5$ MeCN reveals that the complex is indeed a triple helix. The two cobalt(II) centers are in slightly distorted octahedral environments, and the ligand-imposed geometry places the metals over 8 Å apart within the triple-helical array.

1

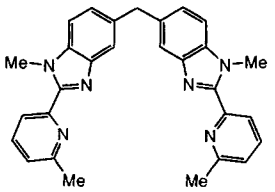

This paper is important for a number of reasons beyond the remarkable beauty of the resultant structure. *Williams* et al.[2] has demonstrated that new molecular topologies may be *designed* and *synthesized* by a logical combination of ligands and metals with specific donor and acceptor properties. The spontaneous manner in which the highly ordered structure assembles illustrates the efficacy and the remarkable potential of this approach. This is the first example of a triple-helical coordination compound, although *Shanzer* et al. have described a diiron triple helix resulting from the metal-controlled intermolecular twisting of a tripodal ligand[3] and *Lehn* et al. have mentioned in passing a diiron complex with a bis-bidentate ligand which may well possess this geometry.[4]

The synthesis of this triple-helical structure is a logical extension of investigations by a number of groups into the metal-controlled intertwisting of molecular threads to give double helical arrays. Although a considerable variety of ligands have been used for the preparation of double-helical coordination compounds, they all exhibit structural features

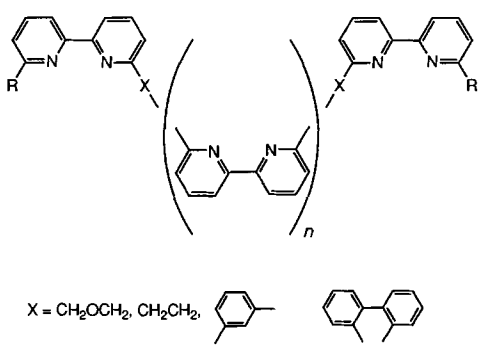

2

[*] Dr. E. C. Constable
University Chemical Laboratory
Lensfield Road, Cambridge, CB21EW (UK)

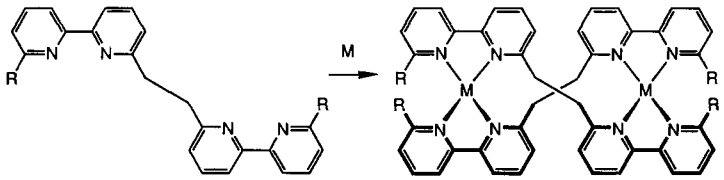

Fig. 2. The formation of a double-helical complex by interaction of a bis-bidentate ligand with a four-coordinate metal center M.

in common with **1**. The basic pattern consists of two or more polydentate ligands linked by spacer groups. Ligands which have been shown to give rise to double-helical structures include tetrapyrroles,[5] cyclohexane-1,2-diimines,[6] bishydrazones,[7] quater-,[8] quinque-,[9] and sexipyridines[10]. But the essential structural features are most simply seen in the linked oligobipyridines (**2**)[4, 11] and oligophenanthrolines[12]. In the same way that a triple helix is built up by coordination of bis-bidentate ligands to a six-coordinate metal center, a double helix is assembled by interaction with a four-coordinate (usually tetrahedral) one (Fig. 2).[12]

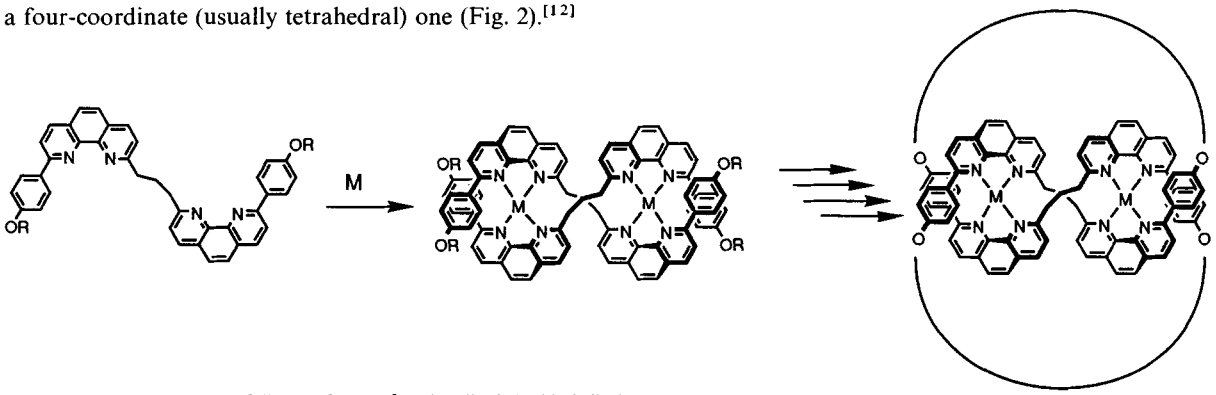

Fig. 3. The assembly of a trefoil knot from a functionalized double helical precursor. R = H, ∩ = $CH_2(CH_2OCH_2)_5CH_2$, M = Cu.

3

Why is there such interest in this esoteric activity? There are a number of answers to this question. Perhaps the simplest answer lies in the aesthetic beauty of the molecules which are obtained— helices and interlinked networks have long been associated with artistic works, and the molecular analogues are equally satisfying to the observer. A more serious reason to investigate these systems arises from some of the consequences of intertwisting molecular threads. *Sauvage* and *Dietrich-Buchecker* have demonstrated that the key intermediate for the synthesis of the trefoil knot **3** is a suitably functionalized double helix, and have used the metal-directed assembly of a double-helical complex as the key step in their elegant preparation of a molecular knot.[12] The important step is the formation of a double-helical dicopper(I) complex of a functionalized bis-1,10-phenanthroline ligand, followed by cyclization in a conventional macrocyclization step (Fig. 3).

The functionalization of helicate complexes offers another reason for their investigation. These are the first examples of a new class of chiral molecules, which may possess novel optical or electronic properties. *Lehn* et al. are investigating extrahelical interactions in which substituents on the external surface of a double-helical structure may interact with other molecules, of which helicate–nucleic acid interactions are an obvious area of interest.[13]

The future for metal-directed topological chemistry is very bright. The wide variety of coordination numbers and stereochemistries which are available offer a new "playground" for molecular chemists to prepare new structures in designed and high-yielding syntheses. A fusion of inorganic and organic chemistry is leading to an exciting and beautiful new interdisciplinary area.

[1] C. O. Dietrich-Buchecker, J.-P. Sauvage, *Chem. Rev. 87* (1987) 795; *Bioorg. Chem. Front. 2* (1991) 195; J.-P. Sauvage, *Acc. Chem. Res. 23* (1990) 319; V. I. Sokolov, *Russ. Chem. Rev. 42* (1973) 452.

[2] A. F. Williams, C. Piguet, G. Bernardinelli, *Angew. Chem. 103* (1991) 1530; *Angew. Chem. Int. Ed. Engl. 30* (1991) 1490.

[3] J. Libman, Y. Tor, A. Shanzer, *J. Am. Chem. Soc. 109* (1987) 5880.

[4] M. T. Youinou, R. Ziessel, J.-M. Lehn, *Inorg. Chem. 30* (1991) 2144.

[5] W. S. Sheldrick, J. Engel, *Acta Crystallogr. Sect. B 37* (1981) 250; G. Struckmeier, U. Thewalt, J.-H. Fuhrhop, *J. Am. Chem. Soc. 98* (1976) 278; D. Dolphin, R. L. N. Harris, J. L. Huppatz, A. W. Johnson, I. T. Kay, J. Leng, *J. Chem. Soc. C 1966*, 98.

[6] G. C. van Stein, G. van Koten, F. Blank, L. C. Taylor, K. Vrieze, A. L. Spek, A. J. M. Duisenberg, A. M. M. Schreurs, B. Kojić-Prodić, C. Brevard, *Inorg. Chim. Acta 98* (1985) 107; G. C. van Stein, G. van Koten, K. Vrieze, A. L. Spek, E. A. Klop, C. Brevard, *Inorg. Chem. 24* (1985) 1367, and references therein.

[7] D. Wester, G. J. Palenik, *Inorg. Chem. 15* (1976) 755; *J. Chem. Soc. Chem. Commun. 1975*, 74; E. C. Constable, J. M. Holmes, P. R. Raithby, *Polyhedron 10* (1991) 127.

[8] J.-P. Gisselbrecht, M. Gross, J.-M. Lehn, J.-P. Sauvage, R. Ziessel, C. Piccinni-Leopardi, J. M. Arrieta, G. Germain, M. van Meerssche, *Nouv. J. Chim. 8* (1984) 661; J.-M. Lehn, J.-P. Sauvage, J. Simon, R. Ziessel, C. Piccinni-Leopardi, G. Germain, J.-P. Declercq, M. van Meerssche, *ibid. 7* (1983) 413.

[9] E. C. Constable, S. M. Elder, P. R. Raithby, M. D. Ward, *Polyhedron 10* (1991) 1395, and references therein.

[10] E. C. Constable, M. D. Ward, D. A. Tocher, *J. Chem. Soc. Dalton Trans. 1991*, 1675, and references therein.

[11] T. M. Garrett, U. Koert, J.-M. Lehn, A. Rigault, D. Meyer, J. Fischer, *J. Chem. Soc. Chem. Commun. 1990*, 557; J.-M. Lehn, A. Rigault, J. Siegel, J. Harrowfield, B. Chevrier, D. Moras, *Proc. Natl. Acad. Sci. USA 84* (1987) 2565; J.-M. Lehn, A. Rigault, *Angew. Chem. 100* (1988) 1121; *Angew. Chem. Int. Ed. Engl. 27* (1988) 1095; C. Piguet, G. Bernardinelli, A. F. Williams, *Inorg. Chem. 28* (1989) 2920.

[12] C. O. Dietrich-Buchecker, J. Guilhem, C. Pascard, J.-P. Sauvage, *Angew. Chem. 102* (1990) 1202; *Angew. Chem. Int. Ed. Engl. 29* (1990) 1154; C. O. Dietrich-Buchecker, J.-P. Sauvage, *ibid. 101* (1989) 192 and *28* (1989) 189.

[13] E. C. Constable, *Nature (London) 346* (1990) 319; U. Koert, M. M. Harding, J.-M. Lehn, *ibid. 346* (1990) 339.

Erythromycin Synthesis—A Never-ending Story?

By *Johann Mulzer**

The synthesis of the macrolide antibiotics, erythromycin A (**1**) and B (**2**), which are highly effective against gram-positive pathogens, is probably the most extensive single project in the history of synthetic organic chemistry.[1] This phenomenon is not rational as **1** and **2** are accessible in large quantities from fermentation by the microorganism *Streptomyces erythreus*. It is the complexity of the molecule's structure, the plethora of stereocenters and functional groups, and the magic of the medium ring that has fascinated about 15 large research groups worldwide for more than a decade. All total syntheses followed the same pattern. They first aimed at the aglycons (erythronolides A and B, **3** and **4** respectively). The final glycosidation, and with it the synthesis of **1**, has been achieved only by the Woodward group.[2] The protected aglycons are formed by lactonization of the seco acids; for example, **3** is prepared from **5**–**7**, and **4** from **8**–**11**. The seco acids are constructed by coupling smaller chiral fragments that are obtained from the chiral pool, by optical resolution, or by enantioselective synthesis.

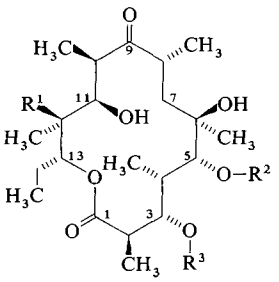

1, R^1 = OH, R^2 =

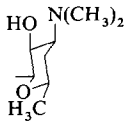

R^3 =

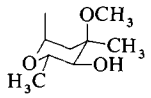

2, R^1 = H, R^2 =

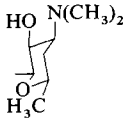

R^3 =

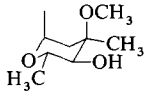

3, R^1 = OH, R^2 = R^3 = H

4, R^1 = R^2 = R^3 = H

Over the years the priorities have shifted several times. Initially the attention focused on the seco acid fragments and therefore on the stereocontrolled construction of the often recurring β-hydroxycarbonyl and 1,3-diol units of **3**/**4**. The development of methods for enantio- and diastereomeric control (acyclic stereoselection[9]) proved to be unbelievably fruitful. Whereas the first syntheses of seco acids[2,6] required cyclic intermediates and optical resolution, and often resorted to "relay compounds" recovered from the degradation of the natural product, today in ca. 15 steps derivatives such as **10** and **11** can be constructed stereoisomerically pure in gram amounts.[7,8]

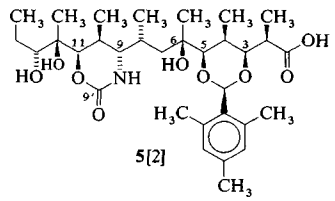

5[2]

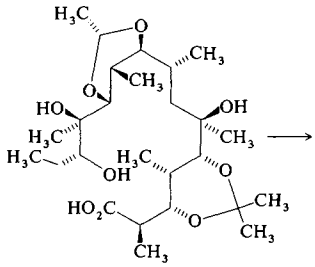

6[3]

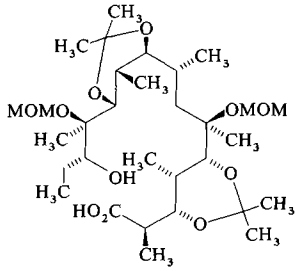

7[4]

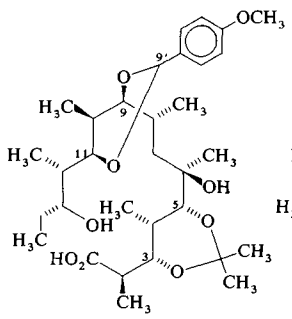

8[5]

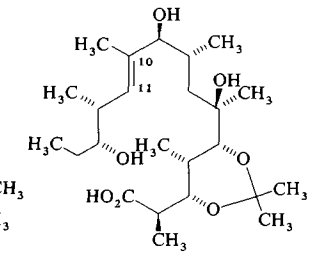

9[6]

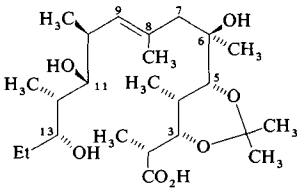

10[7]

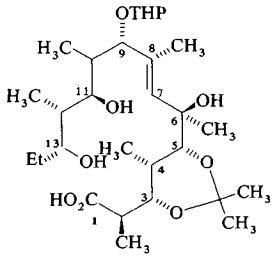

11[8]

In the last two years the growing number of easily accessible seco acids shifted the attention more and more toward the lactonization step. In general this was carried out via an activated ester intermediate (**12**, Table 1). However, the formation of a 14-membered ring proved to be not straightforward; dimerization and polymerization are significant side reactions. The thiopyridyl activation (via the intermediates

[*] Prof. A. J. Mulzer
Institut für Organische Chemie
Fachbereich Chemie der Freien Universität
Takusstrasse 3, W-1000 Berlin 33 (FRG)

12a, b)[10] was the standard procedure for the macrolactonization for ten years, but has now been replaced by the Yamaguchi lactonization via the mixed anhydride **12c**. Next to activation the hydroxyl protecting groups play a central role. They not only suppress the formation of rings of unwanted size, but may also be used to induce conformations favorable for cyclization. Thus the 3,5-acetal or ketal unit in **5**–**11** locks the C2–C6 fragment of the molecule into a rigid, linear structure, due to the diequatorial arrangement around the 1,3-dioxane chair. In this case the 6-OH function may remain unprotected, because it can only be lactonized after flipping the acetonide to the diaxial conformation. The 9- and 11-hydroxyl groups are often protected by a cyclic acetal (as in **5**–**8**), which induces considerable transannular strain by the 9′-substituent. In fact, 9′-disubstituted derivatives such as **7** are substantially more difficult to cyclize than the corresponding 9′-monosubstituted seco acids **5**, **6**, and **8** (Table 1).[3,4] Moreover, the configuration at C9 is important: (9*S*) seco acids behave much more favorably than (9*R*)

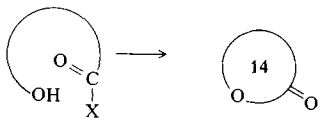

12

Table 1. Macrolactonization to form the 14-membered ring in the erythromycin synthesis.

12	Activating group X	Product yield in [%]
a[10]		**5** (70)[2]
b[10]	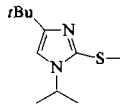	**8** (65)[5], **9** (50)[6]
c[11]	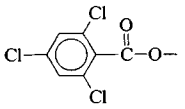	**7** (27)[4], **10** (89)[7], **11**(>95)[8]

isomers.[2] Many of these hitches may be avoided by the introduction of a CC double bond in the critical region between C7 and C11 (see **9**–**11**). At least one OH function and its protecting group is then missing; in addition the two sp^2 centers on the periphery of the ring decrease the transannular ring strain. Trisubstituted olefins display the phenomenon of allylic 1,3 strain.[12] In seco acid **10** this leads to a sickle-like curve in the carbon chain at C7–C10. Thus simple rotations of the rigid C1–C6 fragments around the C5/6 and C6/7 axes lead to an optimal conformation for cyclization (**13**). The 11-OH group is out of reach of the carboxyl function and can remain free.[7]

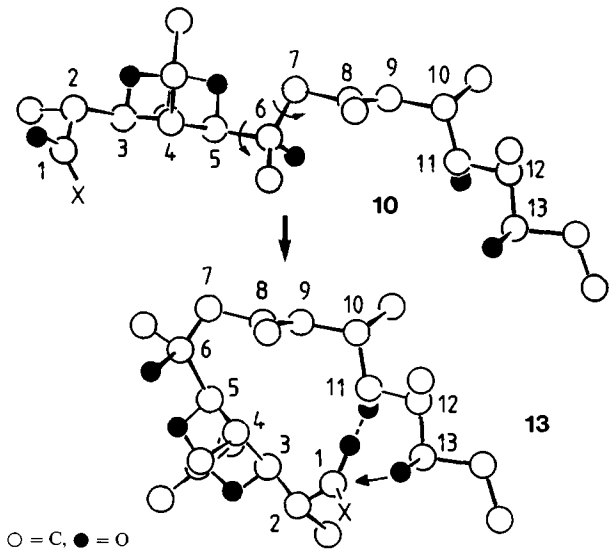

The high macrolactonization yields for **10**/**11** (Table 1) leave as the last aspect of the erythromycin synthesis to be solved the **3** → **1** and **4** → **2** glycosations, which are indispensible for the physiological activity. As was shown early by the Woodward group[2] both the monosaccharide blocks desosamine (**15**) and cladinose (**16**), in suitably protected and activated form, can be coupled to an almost "naked" aglycon (**14**). Only the 5- and the 3-OH groups can be glycosidated and the 5-OH group has a clear kinetic advantage over the 3-OH.

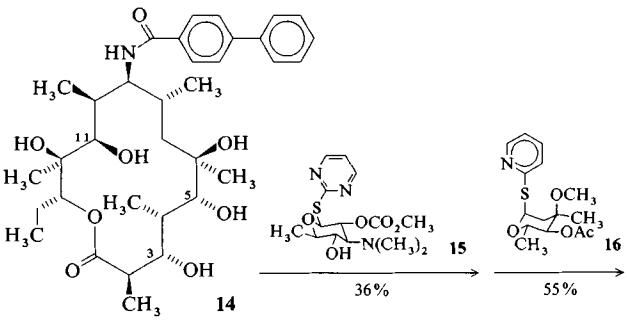

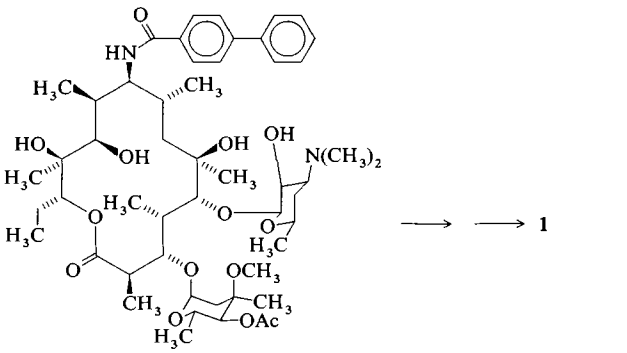

Recently in a remarkable experiment *S. F. Martin* and *M. Yamashita*[13] have broken with the accepted sequence of lactonization followed by glycosidation. In ten steps the diglycosidated seco acid **17** was prepared from **2** by *partial*

synthesis and subjected to the Yamaguchi conditions. However, the procedure afforded only small amounts of the desired macrolide **18**. The major products were seven-membered lactones **19** epimeric at C2. This is not surprising because the seven-membered ring is favored and can form readily, since the 6-OH function is not protected and also not blocked by a 3,5-ketal. As predicted, the Yamaguchi lactonization of the 6-OMe derivative of **17** (14 steps from **2**) affords exclusively the 6-OMe derivative of **18**, but in only 53% yield.

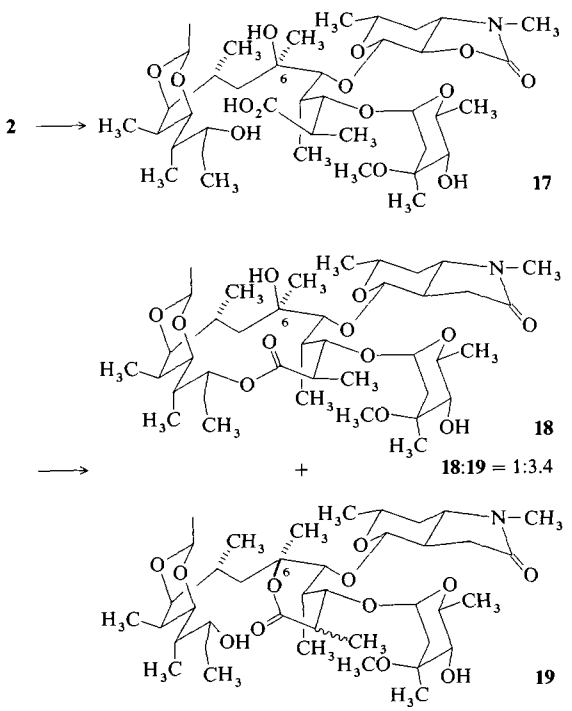

Have *Martin* and *Yamashita* solved the problem of erythromycin B synthesis? Hardly, because 1) the protecting groups of 6-OMe-**18** must still be removed and a mild 6-*O*-demethylation will probably be difficult, and 2) **17** is only partially synthesized; the necessary 3,5-differentiation for the total synthesis will be considerably more troublesome in the acyclic form than in the aglycon, where it occurs unaided.[2]

Therefore at the moment it seems more promising to stay with the traditional sequence and to optimize the glycosidation of **3**/**4** derivatives, perhaps by enzyme catalysis. After all, the biosynthesis follows this pathway: first **4**, and from it **2**.[14]

German version: *Angew. Chem. 103* (1991) 1482

[1] Review: I. Paterson, M. M. Mansuri, *Tetrahedron 41* (1985) 3569.
[2] R. B. Woodward et al. *J. Am. Chem. Soc. 103* (1981) 3210, 3213, 3215.
[3] G. Stork, S. D. Rychnovsky, *J. Am. Chem. Soc. 109* (1987) 1564, 1565.
[4] H. Tone, T. Nishi, Y. Oikawa, M. Hikota, O. Yonemitsu, *Tetrahedron Lett. 28* (1987) 4569; M. Hikota, H. Tone, K. Horita, O. Yonemitsu, *Tetrahedron 46* (1990) 4613.
[5] N. K. Kochetkov, A. Sviridov, M. S. Ermolenko, D. V. Yashunsky, V. S. Borodkin, *Tetrahedron 45* (1989) 5109.
[6] E. J. Corey et al., *J. Am. Chem. Soc. 100* (1978) 4618.
[7] J. Mulzer, H. M. Kirstein, J. Buschmann, C. Lehmann, P. Luger, *J. Am. Chem. Soc. 113* (1991) 910.
[8] J. Mulzer, P. A. Mareski, J. Buschmann, P. Luger, *Synthesis 1992*, in press.
[9] P. A. Bartlett, *Tetrahedron 36* (1980) 1.
[10] E. J. Corey, K. C. Nicolaou, *J. Am. Chem. Soc. 96* (1974) 5614; E. J. Corey, D. J. Brunelle, *Tetrahedron Lett. 1976*, 3409.
[11] J. Inanaga, K. Hirata, H. Saeki, T. Katsuki, M. Yamaguchi, *Bull. Chem. Soc. Jpn. 52* (1979) 1989.
[12] R. W. Hoffmann, *Chem. Rev. 89* (1989) 1841.
[13] S. F. Martin, M. Yamashita, *J. Am. Chem. Soc. 113* (1991) 5478.
[14] J. Staunton, *Angew. Chem. 103* (1991) 1331; *Angew. Chem. Int. Ed. Engl. 30* (1991) 1302.

Communications may be submitted in English *or* in German. Further details regarding the submission of communications can be found in the "Notice to Authors" reproduced in the January issue of the journal. Copies thereof may be obtained from the editorial office upon request.

[3-Bromo-2-lithio-1-phenylsulfonylbenzofuran · Diisopropyl Ether]$_2$ and 3-Fluoro-2-lithio-1-phenylsulfonylbenzene · Pentamethyldiethylenetriamine: Crystal Structures of Compounds with Lithium and Halogen on Neighboring Carbon Atoms**

By *Ferdinand Bosold, Peter Zulauf, Michael Marsch, Klaus Harms, John Lohrenz,* and *Gernot Boche**

The elimination of a metal halide, MX (M = Li, Na, K, MgX, etc.; X = F, Cl, Br, I) from neighboring sp^3- or sp^2-hybridized carbon atoms (β-elimination) is a standard reaction for the preparation of (cyclo)olefins and (cyclo)acetylenes. A similar approach is used for the generation of arynes (dehydroaromatic compounds)[1] and heteroarynes.[2] As expected, the stability of the organometallic compound containing the α-halogen atom correlates with the instability of the corresponding unsaturated compound. This is observed, for example, on going from six-membered to five-membered ring compounds containing a "triple" bond.[1-3] It is of historical interest that 2,3-dehydrobenzofuran (**2**), which *Stoermer* and *Kahlert* formulated in 1902 as the reaction product of 3-bromo-2-sodio/potassiobenzofuran (**1b**), was the first (hetero)aryne to be postulated.[4] *Wittig* and *Kolb*[5], on the other hand, observed that 3-bromo-2-lithiobenzofuran (**1a**)—like other five-membered ring compounds of this structural type[6-9]—is stable at 20 °C. Trapping of **2** upon reaction of **1a, b** at higher temperature[4, 5] has been essentially ruled out in the meantime.[2]

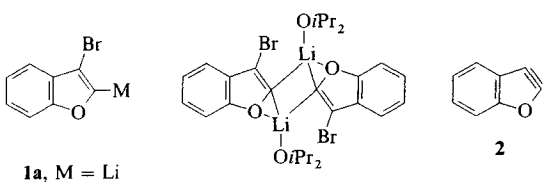

The number of successful attempts to prepare dehydrobenzene and substituted dehydrobenzenes from the corresponding α-halogen-substituted organometallic benzene derivatives, in contrast, is legion. For instance, 1-fluoro-2-lithiobenzene decomposes at -60 °C to give LiF and dehydrobenzene.[1] A remarkable substituent effect is observed for 3-fluoro-2-lithio-1-phenylsulfonylbenzene (**3**), which only eliminates LiF on warming to $+60$ °C, affording phenylsulfonyl-substituted dehydrobenzene (**4**).[1, 10]

Here we report on the crystal structures of **1a**, which crystallizes from diisopropyl ether as [**1a** · O*i*Pr$_2$]$_2$, and **3** · PMDETA (Figs. 1 and 2, respectively).

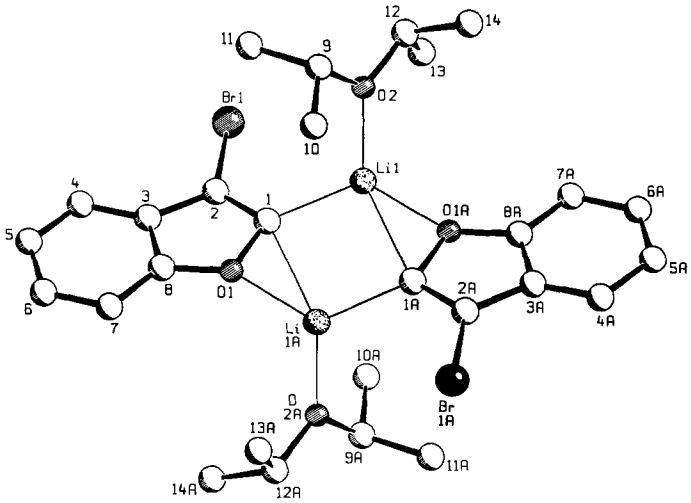

Fig. 1. Molecular structure of [**1a** · O*i*Pr$_2$]$_2$ [11, 13]. Selected bond lengths [pm] and angles [°]: Li1A-O1 195.4(6), O1-C1 147.0(4), C1-C2 134.9(4), C2-Br1 189.3(3), C1-Li1 212.2(7), C1-Li1A 250.2(6), Li1-O2 194.7(6), O1-C8 137.5(4), C2-C3 144.4(5), C3-C8 139.4(4), Li1-Br1 386.7(6), Li1A-Br1 533.3(6); C8-O1-C1 109.6, O1-C1-C2 102.9(3), C1-C2-C3 113.9(3), C1-C2-Br1 124.2(3), Li1-C1-C2 130.3(3), C1-O1-Li1A 92.8(2), O1-C1-Li1A 51.3(2); Li1-C1-C2-Br1 28.9(5), Li1A-C1-C2-Br1 $-151.5(4)$, O1-C1-C2-Br1 $-179.5(2)$, C2-C1-O1-Li1A 162.4(3).

As Figure 1 shows, [**1a** · O*i*Pr$_2$]$_2$ is present as a *trans* dimer whose anionic C atoms are bridged through lithium. C1-Li1 (212.2(7) pm) is markedly shorter than Li1-C1A (250.2(6) pm). The preferred tetracoordination of the Li atoms is achieved through one bond to the oxygen atom of the diisopropyl ether (Li1-O2 194.7(6) pm) as well as to the oxygen atom of the bromobenzofuranyl anion (Li1-O1A 195.4(6) pm). This *intra*molecular O–C bridging through Li is also found in [2-lithiobenzofuran · TMEDA]$_2$ for *one* of the two anions with pentacoordination of the bridging Li.[18, 19] The two bromobenzofuranyl anions of [**1a** · O*i*Pr$_2$]$_2$ lie in the same plane; the Li1–Li1A axis is bent out of this plane by an angle of 62.7°. The C1–O1 bond (147.0(4) pm) is relatively long—the O1–C8 bond is 137.5(4) pm long[20]—in accord with the situation for [2-lithiobenzofuran · TMEDA]$_2$ (145.3 pm)[18] and our observations for two other α-oxygen-substituted organolithium compounds.[21] A lengthening of this bond, as well as the bridging of O1 and the anionic C1 atom through Li, is in agreement with model calculations on $LiCH_2OH$.[22]

The stability of [**1a** · O*i*Pr$_2$]$_2$ toward β-elimination of LiBr (as well as the stability of other lithiated five-membered ring

[*] Prof. Dr. G. Boche, F. Bosold, Dipl.-Chem. P. Zulauf, M. Marsch, Dr. K. Harms, Dipl.-Chem. J. Lohrenz
Fachbereich Chemie der Universität
Hans-Meerwein-Strasse, W-3550 Marburg (FRG)

[**] This work was supported by the Deutsche Forschungsgemeinschaft (SFB 260) and the Fonds der Chemischen Industrie.

compounds containing α-halogen atoms[1, 2, 6–9]) indicates that, as observed here, the structure is not favorable for elimination. Thus, the C2–Br1 bond length (189.3(3) pm) corresponds roughly to the C–Br distance found in nonlithiated 4-bromo-2-formylburan (189.9 and 190.3 pm).[23, 24] Furthermore, no close approach of Li and Br is evident, as revealed by the Br1–C2–C1 (124.2(3)°) and C2–C1–Li1 (130.1(3)°) angles and the Li1–Br1 (386.7(6) pm) and Li1A–Br1 (533.3(6) pm) distances. Li1 (Li1A) lies outside the Br1–C2–C1 plane, as shown by the Li1(Li1A)–C1–C2–Br1 torsion angle of 28.9(5)° (– 151.5(4)°).

The crystal structure of **3** · PMDETA (Fig. 2) shows that the greater ease of MX elimination is also reflected structurally. In **3** · PMDETA, which is present as a monomer, the

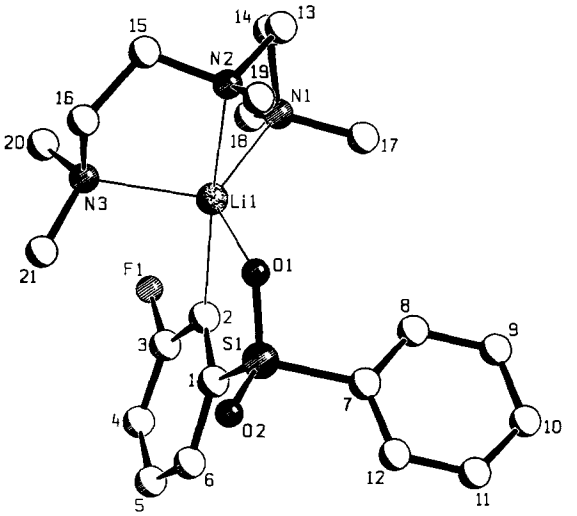

Fig. 2. Molecular structure of **3** · PMDETA [25, 26]. Selected bond lengths [pm] and angles [°]: Li1-N1 227.8(7), N2-Li1 228.6(8), N3-Li1 219.4(8), C1-C2 139.5(5), C2-C3 138.2(6), C3-C4 136.7(6), C4-C5 137.0(6), C5-C6 138.9(6), C1-C6 138.5(6), C1-S1 177.0(4), C7-S1 176.5(4), S1-O1 145.0(3), S1-O2 144.2(3), Li1-O1 217.0(8), C2-Li1 225.8(8), C3-F1 138.9(5), Li1-F1 367.2(7); F1-C3-C2 117.9(4), C3-C2-Li1 133.8(4), S1-C1-C2 116.3(3); F1-C3-C4-C5 – 179.3(4), Li1-C2-C3-F1 25.7(6), C2-C1-S1-O1 149.7(3).

Li1 atom exhibits, besides the three contacts to the N atoms of the amine ligand, an additional contact to the anionic C2 atom (Li1-C2 225.8(8) pm) and to the O1 atom of the sulfonyl group (O1-Li1 217.0(8) pm). Li1 lies outside the plane of C1 to C6 and F1: Li1-C2-C3-F1 25.7(6)°. We have previously observed a five-membered ring structure such as that formed by C2-C1-S1-O1-Li1.[28a] This complexation of lithium by the neighboring phenylsulfonyl group explains why the LiF elimination in **3** occurs only at + 60 °C.[1, 28b] Despite the very large Li1–F1 distance (367.2(7) pm), the C3–F1 distance (138.9(5) pm) is still lengthened compared to the average value of 160 C_{aryl}–F distances (135.4 pm; Cambridge Structural Database). Interestingly, another α-fluoro-substituted organometallic compound also exhibits a lengthened C–F distance: in bis(2-fluorophenyl)triphenylbismuth, this distance is 138.2 pm.[29] Accordingly, it is reasonable to assume that the observed LiF elimination from **3** in solution to give the aryne **4** is structurally reflected, in the sense of the correlation principle,[30] in the crystal structure of **3** · PMDETA, in total contrast to the situation found for [**1a** · O*i*Pr$_2$]$_2$ and **1a**.

Received: July 3, 1991;
Supplemented: August 10, 1991 [Z 4771 IE]
German version: *Angew. Chem. 103* (1991) 1497

CAS Registry numbers:
1, M = Br, 64150-61-4; [**1a** · O*i*Pr$_2$]$_2$, 136569-63-6; **3** (H instead of Li), 40154-94-7; **3** · PMDETA, 136569-64-7.

[1] R. W. Hoffmann: *Dehydrobenzene and Cycloalkynes*, Verlag Chemie, Weinheim/Academic Press, New York 1967.
[2] M. G. Reinecke, *Tetrahedron 38* (1982) 427.
[3] a) Calculations for (hetero)arynes: L. Radom, R. H. Nobes, D. J. Underwood, W.-K. Li, *Pure Appl. Chem. 58* (1986) 75; b) MNDO calculations for five- and six-membered ring compounds led to the following dehydrogenation energies [kcal mol^{-1}]: benzene, 118.0, cyclopentadiene, 148.7, cyclopentadienyl anion, 150.3, furan 166.4.
[4] R. Stoermer, B. Kahlert, *Chem. Ber. 35* (1902) 1633 "Die Nichtauffindbarkeit der Acetylenverbindung (**2**), auf deren Isolierung wir viel Mühe verwendet haben, hat ihren Grund offenbar in der großen Instabilität infolge sehr starker Spannungen innerhalb des Moleküls. Vielleicht ist der stets beobachtbare, sonderbare, etwas zum Husten reizende Geruch des Reaktionsgemisches beim Öffnen des Autoklaven auf die Anwesenheit geringer Reste davon zurückzuführen." [The inability to find the acetylene compound (**2**), to whose isolation we have devoted much effort, apparently is due to its great instability as a result of very strong strains within the molecule. Perhaps the consistently observed, unusual, cough-inducing smell of the reaction mixture on opening the autoclave is due to the presence of small amounts of it.]
[5] G. Wittig, G. Kolb, unpublished results; see [1], p. 291; see also G. Wittig, M. Rings, *Justus Liebigs Ann. Chem. 719* (1968) 127; E. A. Karakhanov, S. K. Shapirova, M. I. Rozhkova, E. A. Vikrorova, *Chem. Heterocycl. Comp. (Engl. Transl.) 14* (1978) 15.
[6] For 1-bromo-2-cyclopent-1-enyllithium as well as other cyclopent(adi)enes of this kind, see [1] and also G. Wittig, H. Heyn, *Chem. Ber. 97* (1964) 1609; G. Wittig, J. Weinlich, E. R. Wilson, *ibid. 98* (1965) 458; K. Rasheed, *Tetrahedron 22* (1966) 2957.
[7] 2-Chloro-3-bicyclo[2.1.1]hept-2-enyllithium: P. G. Gassman, J. Gennick, *J. Am. Chem. Soc. 102* (1980) 6864.
[8] 2-Chloro(bromo)-3-bicyclo[2.2.1]heptadienyllithium: J. W. Kenndorf, *Dissertation*, Universität München, 1990. I thank Professor Dr. *G. Szeimies*, for providing us with this work; see also J. Kenndorf, K. Polborn, G. Szeimies, *J. Am. Chem. Soc. 112* (1990) 6117.
[9] 1-Chloro-5-tetracyclo[3.2.0.0^{2,7}.0^{4,6}]heptyllithium only undergoes elimination of LiCl at room temperature to give 1,5-dehydroquadricyclane [8].
[10] a) W. E. Truce, M. F. Amos, *J. Am. Chem. Soc. 73* (1951) 3013; b) K. Grohmann, *Dissertation*, Universität Heidelberg 1965.
[11] Preparation of [**1a** · O*i*Pr$_2$]$_2$: 2,3-Dibromobenzofuran (250 mg, 0.91 mmol) was dissolved in 3 mL of diisopropyl ether and treated at – 78 °C with 0.6 mL (0.96 mmol) of a 1.6 M solution of *n*BuLi in hexane. After 20 min, the solvent was removed from the precipitated Li compound and the solid was washed twice with 1 mL of hexane and then dissolved in 9 mL of diisopropyl ether at 50 °C. After 24 h at 4 °C, single crystals suitable for X-ray structure analysis had formed. ^{1}H NMR ([D$_8$]THF, 293 K): δ = 7.19 (d, J = 9 Hz, 1 H), 7.18 (d, J = 9 Hz, 1 H), 6.95 (t, J = 7 Hz, 1 H), 6.86 (t, J = 7 Hz, 1 H) (H5-H8), 3.69 (sept, J = 7 Hz, 2H; C*H*(CH$_3$)$_2$); 1.07 (d, J = 7 Hz, 12H; CH(C*H*$_3$)$_2$). ^{13}C-NMR ([D$_8$]THF, 173 K): δ = 218.4 (q, J(^{13}C,^{7}Li) = 40 Hz; C2), 160.5 (C9), 130.4 (C4), 111.6 (C3), 120.4, 119.6, 116.2, 109.9 (C5-C8), 67.4 (*C*H(CH$_3$)$_2$), 22.9 (CH(*C*H$_3$)$_2$). The quartet of the ^{13}C–^{7}Li coupling shows that only *one* C–Li bond is still present when [**1a** · O*i*Pr$_2$]$_2$ is dissolved in [D$_8$]THF and investigated by NMR spectroscopy at 173 K. We still do not know which C1–Li bond is broken or whether a dimer or monomer is present [12]. Note added in proof (September 24, 1991): A cryoscopic determination of the aggregation state of [**1a** · O*i*Pr$_2$]$_2$ in THF at – 108 °C revealed a monomeric **1a** (F. Haller, Universität Marburg 1991).
[12] For comparison: ^{13}C NMR spectrum of 3-bromobenzofuran ([D$_8$]THF, 173 K), δ = 155.1 (C9), 144.7 (C2), 127.6 (C4), 126.5, 124.5, 120.2, 112.6 (C5-C8), 98.5 (C3).
[13] Crystal structure data for [**1a** · O*i*Pr$_2$]$_2$: $C_{14}H_{18}BrLiO_2$, M = 305.14; forms triclinic crystals, space group $P\bar{1}$, a = 8.200(4), b = 8.916(5), c = 11.315(4) Å, α = 72.87(3), β = 69.01(3), γ = 74.97(4)°, Z = 2, ϱ_{ber} = 1.394 g cm^{-3}, μ = 2.788 mm^{-1}. 2761 reflections were measured on an Enraf-Nonius diffractometer (Mo$_{K\alpha}$ radiation, graphite monochromator, T = 179 K) of which 2563 were unique (R_{int} = 0.0194) und 2271 with $F_o > 4\sigma(F_o)$ were regarded as observed. Empirical absorption correction. Solution by direct methods (SHELXTL Plus), refinement (SHELXTL Plus) to R = 0.0314, wR = 0.0322, $w = 1/\sigma^2(F_o)$. Non-hydrogen atoms refined anisotropically, position of the hydrogen atoms determined and refined with groupwise common temperature factors. 221 parameters. All calculations were performed on a MicroVAX II [14–17].
[14] SHELXTL PLUS Software, Siemens.
[15] A. L. Spek: *Platon 88, Program for Geometrical Analysis of Crystal Structures*, Utrecht 1988.
[16] E. Keller: *SCHAKAL-88B. A Fortran Program for the Graphic Representation of Molecular and Crystallographic Models*, Freiburg 1988.
[17] Further details of the crystal structure investigation are available on re-

quest from the Fachinformationszentrum Karlsruhe, Gesellschaft für wissenschaftlich-technische Information mbH, W-7514 Eggenstein-Leopoldshafen 2 (FRG), on quoting the depository number CSD-320276, the names of the authors, and the journal citation.

[18] S. Harder, J. Boersma, L. Brandsma, J. A. Kanters, W. Bauer, R. Pi, P. von R. Schleyer, H. Schöllhorn, U. Thewalt, *Organometallics 8* (1989) 1688.

[19] On the basis of model calculations on *intra*molecular solvation in *monomeric* 2-furanyllithium, *Harder* concluded that the O–C bridging through Li is considerably overestimated and is overcome by solvent molecules (three OH_2 on Li); I thank Dr. *S. Harder*, University of Utrecht, for sending us his dissertation (1990). This result, however, is not directly comparable with the crystal structures of the *dimeric* $[\mathbf{1a} \cdot O i Pr_2]_2$ and [2-lithiobenzofuran · TMEDA]$_2$ [18], since in the calculated monomer Li lies *in* the plane of the furan ring, while in the crystalline dimers the Li atoms lie *above* and *below* the planes of the benzofuran rings (private communication, *A. Harder*, September 7, 1991).

[20] The average value of the bond lengths corresponding to O1-C1 (O1-C8) is 138.5 (137.1) pm for 27 benzofurans (Cambridge Structural Database).

[21] M. Marsch, K. Harms, O. Zschage, D. Hoppe, G. Boche, *Angew. Chem. 103* (1991) 338; *Angew. Chem. Int. Ed. Engl. 30* (1991) 321.

[22] T. Clark, P. von R. Schleyer, K. N. Houk, N. G. Rondan, *J. Chem. Soc. Chem. Commun. 1981*, 579; P. von R. Schleyer, T. Clark, A. J. Kos, G. W. Spitznagel, C. Rohde, D. Arad, K. N. Houk, N. G. Rondan, *J. Am. Chem. Soc. 106* (1984) 6467.

[23] C. Riche, *Acta Crystallogr. Sect. B 29* (1973) 756.

[24] Average value of C–Br for 1121 bromarenes: 189.7 pm (Cambridge Structural Database).

[25] Preparation of **3** · PMDETA: 3-(fluorophenyl)phenylsulfone (150 mg, 0.63 mmol) was dissolved in 0.5 mL tetrahydrofuran, deprotonated at −75 °C with 0.4 mL (0.64 mmol) of a 1.6 M solution of *n*BuLi in hexane, and then treated immediately with 0.2 mL of PMDETA. After 30 min, the reaction solution was warmed to 20 °C and 1 mL of hexane was added. After 6 h at 0 °C, crystals suitable for X-ray structural analysis were obtained. ^{1}H NMR ([D$_8$]THF, 258 K) δ = 7.92 (d, J = 7 Hz, 2H), 7.50 (m, 3H), 7.34 (dd, $J(^1H, ^1H)$ = 7 Hz, $J(^1H, ^{19}F)$ = 2.6 Hz), 6.98 (dt, $J(^1H, ^1H)$ = 7 Hz, $J(^1H, ^{19}F)$ = 7 Hz), 6.72 (d, J = 7 Hz, 1H), 2.53 (s, 4H; CH_2-PMDETA), 2.52 (s, 4H; CH_2-PMDETA), 2.44 (s, 3H, CH_3-PMDETA), 2.23 (s. 12H, CH_3-PMDETA). ^{13}C-NMR ([D$_8$]THF, 253 K) δ = 176.2 (d, ^2J(C,F) = 133.3 Hz; C2), 172.2 (d, ^1J(C,F) = 217.5 Hz; C3), 153.9 (d, ^3J(C,F) = 39.0 Hz; C1), 145.0 (C7), 132.6 (C10), 129.4 (C9-C11), 128.0 (C8-C12), 126.2 (d, ^3J(C,F) = 5.0 Hz; C5), 122.4 (d, ^4J(C,F) = 3.8 Hz; C6), 114.2 (d, ^2J(C,F) = 42.7 Hz; C4), 57.7, 55.1, 46.1, 44.4 (PMDETA). For comparison: ^{13}C NMR spectrum of 3-(fluorophenyl)phenylsulfone ([D$_8$]THF, 253 K): δ = 163.2 (d, ^1J(C,F) = 250.3 Hz; C3), 145.2 (d, ^3J(C,F) = 6.3 Hz; C1), 142.3 (C7), 134.4 (C10), 132.5 (d, ^3J(C,F) = 7.8 Hz; C5), 130.3 (C9-C11), 128.6 (C8-C12), 124.6 (d, ^4J(C,F) = 3.4 Hz; C6), 121.2 (d, ^2J(C,F) = 21.4 Hz; C4), 115.5 (d, ^2J(C,F) = 23.9 Hz, C2). Particularly noteworthy is the difference in the ^2J(C2,F) coupling in the "anion" **3** · PMDETA (133.3 Hz) and in the neutral compound 3-(fluorophenyl)phenylsulfone (23.9 Hz). *Harder*, in his dissertation [19], described this phenomenon for the first time in 1990 for several other fluorinated pairs of compounds and explained it in terms of a through-space interaction of fluorine with the "lone pair" of the C–Li bond. Related couplings have been explained in a similar way by *F. B. Mallory, C. W. Mallory* und *W. M. Ricker* (*J. Org. Chem. 50* (1985) 457). The ^3J(C1,F) coupling in the "anion" is also markedly larger (39.0 Hz) than in the neutral compound (6.3 Hz); not quite as large is the difference in the ^2J(C4,F) couplings: "anion", 42.7 Hz; neutral compound: 21.4 Hz. The C2–Li coupling could not be resolved in the temperature range 198–253 K, a result also found by *Harder* for 2-fluorophenyllithium at lower temperatures [19].

[26] Crystallographic data for **3** · PMDETA: $C_{21}H_{31}FLiN_3O_2S$, M = 415.5, monoclinic, space group $P2_1/n$, a = 889.4(3), b = 1997.2(2), c = 1304.6(4) pm, β = 101.34(1)°, Z = 4, $\varrho_{ber.}$ = 1.215 gcm^{-3}, μ($Cu_{K\alpha}$ radiation) = 14.62 cm^{-1}. Measurement carried out an Enraf-Nonius CAD4 diffractometer ($Cu_{K\alpha}$ radiation, λ = 1.54184 Å, graphite monochromator, T = 190 K); 3137 measured reflections, of which 2807 were unique (R_{int} = 0.0667) and 2579 with $F > 4\sigma(F)$ were regarded as observed. Solution by direct methods and refinement with the Siemen's SHELXTL-PLUS(VMS) program package, R = 0.0636, wR = 0.0693 ($w = 1/\sigma^2(F)$), all non-hydrogen atoms refined anisotropically, H atoms refined in a "riding" model with groupwise common isotropic temperature factors [15, 16]. The measurement data were corrected empirically with the program DIFABS [27]. Further details of the crystal structure investigation are available on request from the Fachinformationszentrum Karlsruhe, Gesellschaft für wissenschaftlich-technische Information mbH, W-7514 Eggenstein-Leopoldshafen 2 (FRG), on quoting the depository number CSD-320305, the names of the authors, and the journal citation..

[27] N. Walker, D. Stuart, *Acta Crystallogr. Sect. A 39* (1983) 158.

[28] a) W. Hollstein, K. Harms, M. Marsch, G. Boche, *Angew. Chem. 99* (1987) 1279; *Angew. Chem. Int. Ed. Engl. 26* (1987) 1287. This article contains comprehensive references on the directing effects of RSO_2 groups and on the complex-induced proximity effect; b) The energy difference between conformation **5**, which is the global minimum, and **6** (ΔE = 38.7 kcal mol^{-1}; 3-21G*) provides an indication of the "stabilization" of Li by the neighboring phenylsulfonyl group in $[\mathbf{1a} \cdot O i Pr_2]_2$.

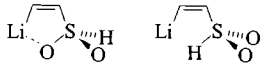

5 **6**

[29] A. Schmuck, P. Pyykkö, K. Seppelt, *Angew. Chem. 102* (1990) 211; *Angew. Chem. Int. Ed. Engl. 29* (1990) 213.

[30] H. B. Bürgi, J. D. Dunitz, *Acc. Chem. Res. 16* (1983) 153, and references cited therein.

Extension of Free Energy Correlations to Gas-Phase Ionic Reactions. Competitive Alkylation of Substituted Benzonitriles by $(CH_3)_2Cl^+$ Ions**

By *Marina Attinà, Fulvio Cacace,** and *Andreina Ricci*

The study of structure–reactivity relationships is greatly complicated in solution by the effects of the reaction medium, which are quantitatively reflected in the Hammett equation and in other free energy correlations by the strong dependence of the reaction constant on the nature of the solvent.[1] The substantially reduced impact of such complicating factors in gaseous media is a strong incentive to extend the study to the gas phase, especially in the case of charged species whose reactivity is deeply affected and diversified by the effects of solvation, ion pairing, viscosity, etc.

So far, experimental approaches to the problem have met with considerable problems, since in the low-pressure range accessible to mass spectrometry operation of a unique "electrostatic activation" mechanism prevents ion–molecule reactions from obeying thermal kinetics, a necessary prerequisite for the construction of free energy correlations. In fact, without efficient collisional thermalization, the energy released by the electrostatic interaction of the reactants remains stored in the ion–molecule complex formed and is available to overcome the activation barrier of the reaction.[2, 3] This explains why most exothermic ion–molecule reactions have been found to proceed at the collision rate, often with *negative* temperature coefficients, when investigated by mass-spectrometric techniques.

Here we report the construction of a free energy correlation in a typical gas-phase ionic reaction by a different approach, based on the combination of mass-spectrometric and high-pressure radiolytic techniques successfully exploited in the study of thermal ion–molecule kinetics.[4]

Since it was deemed important to follow in the gas phase exactly the same procedure adopted in solution for the derivation of the original Hammett[5] equation, a suitable ionic process was sought, involving a side-chain reaction center bound to a *meta*- or *para*-substituted aromatic ring.

The reaction chosen [Eq. (a)], the counterpart of the Ritter reaction long known in solution[6] and previously investigat-

[*] Prof. Dr. F. Cacace, Dr. M. Attinà, Dr. A. Ricci
Dipartimento di Studi di Chimica e Tecnologia delle Sostanze Biologicamente Attive
Università di Roma "La Sapienza"
P.le A. Moro, 5, I-00185 Rome (Italy)

[**] This work was supported by the Italian Ministero dell'Università e della Ricerca Scientifica e Tecnologica (MURST) and the National Research Council (CNR).

ed in the gas phase,[7] involves *N*-alkylation of substituted benzonitriles by $(CH_3)_2Cl^+$ ions, obtained upon ionization of gaseous CH_3Cl according to a well-established[8] reaction sequence.

$$XC_6H_4CN + (CH_3)_2Cl^+ \longrightarrow \underset{\mathbf{1}}{XC_6H_4C{\equiv}\overset{+}{N}CH_3} + CH_3Cl \qquad (a)$$

Even in the absence of specific thermochemical data for all the substrates involved, it can be asserted with confidence that reaction (a) is generally exothermic (e.g., a ΔH° value of -163 kJ mol^{-1} can be estimated for X=H[9]). The nitrilium ions **1** can subsequently be captured by a gaseous nucleophile (e.g., water), eventually yielding the corresponding *N*-methylbenzamides [Eq. (b)].

$$\mathbf{1} \xrightarrow{+H_2O} XC_6H_4\overset{+}{C}(OH_2)NCH_3 \xrightarrow[-H^+]{} XC_6H_4\overset{+}{C}(OH)NHCH_3 \xrightarrow[-BH^+]{+B} XC_6H_4CONHCH_3 \qquad (b)$$

Chemical ionization (CI) mass spectrometry of appropriate gaseous mixtures demonstrates the occurrence of processes (a) and (b), in particular the CH_3Cl/CI spectra of benzonitriles diplay ions **1** as major charged adducts.

Whereas the CI experiments allow the mechanistically informative detection of the charged reactants and intermediates, they are not equally useful from the kinetic standpoint; that is, no meaningful selectivity data could be obtained from the competitive alkylation of nitriles under the conditions ($p(CH_3Cl) = 67$ Pa, $T = 330$ K) prevailing in the CI ion source.

The radiolytic experiments, representative examples of which are illustrated in Table 1, involved γ irradiation of CH_3Cl gas (100 kPa, 320 K) containing traces of the nitriles and of water, followed by analysis of the neutral end products by GC and GC/MS. The results show that indeed *N*-methylbenzamides are obtained in high yields, accounting for up to 30% of the radiolytically formed $(CH_3)_2Cl^+$ ions, depending on the composition of the irradiated systems, where the nitriles compete with other nucleophiles (e.g., the water vapor added to trap the nitrilium ions) for the $(CH_3)_2Cl^+$ ions. The ionic character of the alkylation is ensured by a large excess of an effective radical scavenger (O_2) and independently demonstrated by the depression of the yields upon addition of a gaseous base which intercepts the $(CH_3)_2Cl^+$ ions (see Table 1).

The results of the competition experiments conform to a Hammett-type equation, $\lg k/k_0 = \rho\sigma^+$, characterized by a reaction constant $\rho = -1.9$, a correlation of 0.98, and a zero intercept (Fig. 1). The quality of the correlation is quite reasonable if one considers that the σ^+ constants used are the ones derived from conventional solution kinetics[1] and their values may be somewhat different in a gaseous reaction medium. Furthermore, the largest deviation from linearity, observed for the OCF_3 substituent, may reflect, at least in part, the uncertainty of its σ^+ constant measured in solution.

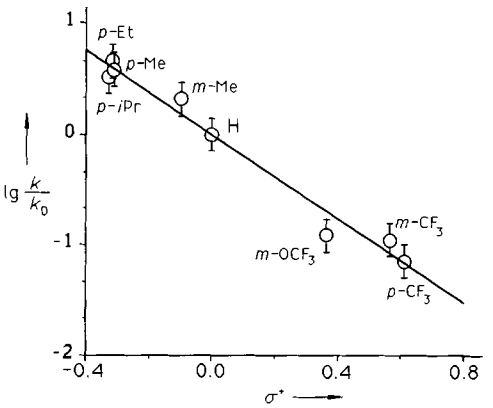

Fig. 1. Hammett-type plot of the relative reactivity of substituted benzonitriles, XC_6H_4CN, toward gaseous $(CH_3)_2Cl^+$ ions in CH_3Cl gas at 100 kPa, 320 K.

The selectivity of $(CH_3)_2Cl^+$ characterizes the gaseous reagent as a typical, if rather indiscriminate, electrophile, as shown by the small and negative value of its ρ constant.

As to the general problem addressed in this study, it seems fair to conclude that the results are definitely encouraging. In fact, a typical ion–molecule reaction, whose selectivity is inappreciable under mass-spectrometric conditions, when studied in a pressure domain where thermal kinetics are obeyed, lends itself to the construction of a free energy correlation analogous to those established in solution.

Extension of the approach outlined here to other reactants, and to different reference reactions, can be a useful step toward unified structure–reactivity relationships, unaffected by the complicating effects of the medium that influence ionic processes in solution, and hence amenable to direct correlation with theoretical results.

Table 1. Methylation of benzonitriles, XC_6H_4CN, by $(CH_3)_2Cl^+$ ions in CH_3Cl at 320 K, 100 kPa.

X	Partial pressures of the components [Pa] [a]				Yields [nmol J^{-1}] [b]		k/k_0
	XC_6H_4CN	C_6H_5CN	H_2O	NEt_3	$C_6H_5CONHCH_3$	$XC_6H_4CONHCH_3$	
p-CH_3	42.1	52.7	307		17.6	53.8	3.8
p-CH_3	37.1	37.3	395		25.6	79.8	3.2
p-CH_3	42.7	40.3	355	35.2	4.0_4	16.6	3.8
p-CH_3	37.1	50.8	375	124	0.1_5	0.4_7	3.8
p-CH_3	47.2	43.1	419	240	[c]	[c]	–
m-CH_3	36.3	46.0	367		36.2	63.2	2.2
p-C_2H_5	42.8	46.9	411		12.4	51.8	4.6
p-iC_3H_7	34.9	54.5	323		29.0	62.2	3.4
p-CF_3	50.1	53.6	433		30.0	2.0	0.07
m-CF_3	46.7	55.5	377		40.4	3.7	0.11
m-OCF_3	35.3	35.5	372		38.3	4.7	0.12

[a] All systems contained O_2 (1.33 kPa) as a radical scavenger. SF_6 (0.667 kPa) was used in certain irradiations as a thermal-electron scavenger. [b] Standard deviation ± 10%. [c] Not detectable.

Experimental Procedure

Pyrex ampules containing premixed gaseous systems of the desired composition, preheated for 22 h at 320 K to ensure complete evaporation of relatively involatile nitriles, were irradiated (9.6×10^3 Gy, 1.9×10^4 Gy h^{-1}) in a Gammacell (Nuclear Canada Ltd.), equipped with a thermostatic device, at 320 K, suitable blanks being run to rule out the occurrence of "dark" reactions. The products were analyzed by GC and GC/MS, using a HP 5970 B mass-selective detector and a TRIO 1/QMD 1000 (VG Micromass). The CI measurements were carried out in CH_3Cl at 67 Pa, 330 K, using a HP 5982 A quadrupole instrument or a VG Micromass ZAB-2F magnetic spectrometer.

Received: May 31, 1991 [Z 4665 IE]
German version: *Angew. Chem. 103* (1991) 1527

CAS Registry numbers:
p-$CH_3C_6H_4CN$, 104-85-8; *m*-$CH_3C_6H_4CN$, 620-22-4; *p*-$C_2H_5C_6H_4CN$, 25309-65-3; *p*-*i*-$C_3H_7C_6H_4CN$, 13816-33-6; *p*-$CF_3C_6H_4CN$, 455-18-5; *m*-$CF_3C_6H_4CN$, 368-77-4; *m*-$OCF_3C_6H_4CN$, 52771-22-9; C_6H_5CN, 100-47-0; $(CH_3)_2Cl^{\oplus}$, 24400-15-5.

[1] R. Taylor: *Electrophilic Aromatic Substitution*, Wiley, Chichester 1990, and references therein.
[2] W. N. Olmstead, J. L. Braumann, *J. Am. Chem. Soc. 99* (1977) 4219.
[3] T. F. Magnera, P. Kebarle in A. Ferreira (Ed.): *Ionic Processes in the Gas Phase*, Reidel, Dordrech 1983, and references therein.
[4] F. Cacace, *Acc. Chem. Res. 21* (1988) 215, and references therein.
[5] L. P. Hammett, *J. Am. Chem. Soc. 59* (1937) 96.
[6] J. J. Ritter, P. P. Minieri, *J. Am. Chem. Soc. 70* (1948) 4045.
[7] F. Cacace, G. Ciranni, P. Giacomello, *J. Am. Chem. Soc. 104* (1982) 2258.
[8] J. L. Beauchamp, D. Holz, S. D. Woodgate, S. L. Patt, *J. Am. Chem. Soc. 94* (1972) 2798.
[9] Estimated from the methyl-cation affinity of CH_3CN and the proton affinity of CH_3CN and C_6H_5CN, according to C. A. Deakine, M. Meot-Ner (Mautner), *J. Phys. Chem. 94* (1990) 232.

Observation of a Direct Sn–Li Bond; The Crystal and Molecular Structure of Monomeric [$Ph_3SnLi \cdot PMDETA$] and the Detection of $^{119,117}Sn$–^7Li NMR Coupling in Solution**

By *David Reed, Dietmar Stalke*, and *Dominic S. Wright**

Stannyl-metal reagents (R_3SnM, R = alkyl or aryl; M = Li, Na, K, MgX, X = halogen) have been used widely by organic chemists for some years.[1] Such reagents have been prepared prior to use by low-temperature in situ reactions of organotin halides (R_3SnX), hexaorganoditins (R_3SnSnR_3), or organotin hydrides (R_3SnH) with the metals (M) or organometallics (RM).[2] They are particularly useful in the formation of tin–carbon bonds by stannylation of electrophilic substrates (e.g., ketones, epoxides, and vinyl halides) and many of these reactions occur with control of regio- and stereoisomerism.[2] However, despite such synthetic utility, even the simple and widely employed trialkyl and triaryl derivatives have not been systematically studied in solution and the solid state. Reflecting such lack of data on these species, there has been some controversy as to whether the lithium ion is bound to the tin or whether a solvent-separated ion pair is present.[2, 3] We describe here the synthesis of [$Ph_3SnLi \cdot$ PMDETA] (**1**; PMDETA = $(Me_2NCH_2CH_2)_2NMe$) from the metalation reaction of Ph_3SnH with *n*BuLi in the presence of PMDETA and its characterization in solution and in the solid state. In the crystal, **1** is monomeric (n = 1) and contains a Sn–Li bond between the pseudotetrahedral Ph_3Sn^- anion and the (PMDETA)Li^+ cation. This is the first simple triaryl- or trialkylstannyllithium reagent to be structurally characterized and the first clear identification of a Sn–Li bond, or indeed, we believe, of any bond between tin and an alkali metal or alkaline-earth metal. Cryoscopy measurements show that **1** is similarly monomeric in solution. The maintenance of Sn–Li bonding is proved by the first observation, in low-temperature ^7Li NMR studies, of direct $^{119,117}Sn$–^7Li coupling.

Addition of *n*BuLi to a chilled solution of Ph_3SnH and PMDETA in toluene (1:1:1 equivalents) leads to the formation of a white precipitate. This dissolves on heating and, from the clear yellow solution produced, colorless crystals of **1** were grown in good yield (see *Experimental Procedure*).

Crystals of **1**, mounted directly from the mother liquor, were investigated by X-ray diffraction.[4] The structure (Fig. 1) is that of a monomer, [$Ph_3SnLi \cdot$ PMDETA]. The two crystallographically independent molecules within the asymmetric unit differ essentially only in the stereochemistry of the coordinated tridentate amine ligand. The main feature

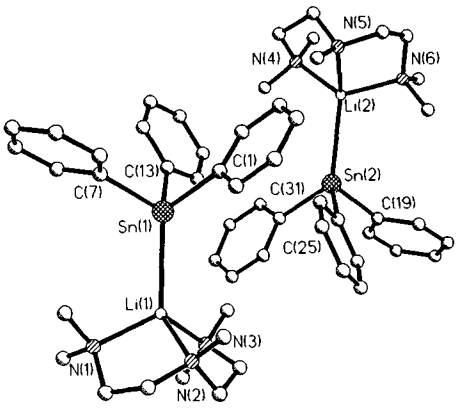

Fig. 1. The molecular structure of both monomer molecules of **1** in the asymmetric unit. Hydrogen atoms have been omitted for clarity. Selected distances [Å] and angles [°]: Li(1)-Sn(1) 2.861(7), Li(2)-Sn(2) 2.882(7), Sn(1)-C(1) 2.221(4), Sn(1)-C(7) 2.210(4), Sn(1)-C(13) 2.212(3), Sn(2)-C(19) 2.205(4), Sn(2)-C(25) 2.210(4), Sn(2)-C(31) 2.180(4); C-Sn-C 96.1(2) (average); Li-Sn-C 120.7(2) (average).

is the clear occurrence of a Sn–Li bond (Sn-Li, average 2.817(7) Å). This bond is only slightly longer than expected for pure covalent bonding (sum of covalent radii of Sn and Li, ca. 2.74 Å). Although a considerable number of alkali and alkaline-earth stannate complexes have been structurally characterized, *none* of these contain metal–Sn contacts; rather, these are ion-separated species or else bridging heteroatoms (e.g., O, P, Cl) hold the metal and Sn centers together. The closest analogue to **1** is the only other lithium triorganostannate thus far characterized in the solid, [Li(dioxane)$_4$]$^+$ [Sn(furyl)$_3$ · Li(furyl)$_3$Sn]$^-$ [furyl = $-\overline{C(CH)_3O}$], the anion of which consists of two pyramidal Sn(furyl)$_3^-$ ions linked via their furyl O atoms to a central six-coordinate Li center; there is no obvious Sn–Li contact.[3] Also, within the structure of the trialkoxystannate, [Li(μ-2,6-

[*] Dr. D. S. Wright, Dr. D. Stalke
University Chemical Laboratory
Lensfield Road, GB-Cambridge CB2 1EW (UK)
Dr. D. Reed
Department of Chemistry,
University of Edinburgh, GB-Edinburgh EH9 3JJ (UK)

[**] This work was supported by Gonville and Caius College Cambridge (Research Fellowship for *D. S. W.*) and by the DAAD (NATO Scholarship for *D. S.*).

$Ph_2C_6H_3O)_3Sn]$, μ_2-bridging of the three O atoms is probably responsible for the close approach of Li to Sn (Sn-Li, 2.784(4) Å).[5] However, the absence of further intermolecular association involving the donor-deficient and highly distorted pyramidal Li centers may, in the light of our current work, imply some degree of Sn–Li intramolecular bonding, rather than the hinted-at agostic aryl $\cdots$ Li interactions.[5] In marked contrast to the few hitherto known Sn–Li complexes, there are certainly no bridging phenyl $\cdots$ Li interactions in **1**. Indeed, the phenyl groups bend *away* from the Sn–Li contact (average Li-Sn-C 120.7(2)°), so that the average C–Sn–C angle (96.1(2)°) is well below that expected for pure tetrahedral geometry about the Sn center (cf. ca. 109° in $Ph_3SnSnPh_3$[6]). A similar pyramidal geometry has been observed for the "naked" Ph_3Sn^- ion in the solid-state structure of $[(18\text{-crown-6})K^+ \cdots SnPh_3^-]$ (closest K $\cdots$ Sn contact > 6 Å; average C-Sn-C 96.9(2)°).[7] This suggests that, within this ion (whether separated or, as in **1**, contacted), a high degree of p character is employed in Sn–C bonding. As a result, the lone pair on the Sn center has mainly s character. The trend towards planarity of the central atoms observed in the Ph_3C^- system[8] is not found here.

Finally, cryoscopic relative molecular mass measurements show that **1** is also monomeric in benzene (number of formula units 0.96 ± 0.05, $c = 0.013$ mol L^{-1}). Thus, the Sn–Li contact observed in the crystal structure is maintained. Evidencing this, low-temperature 139.96-MHz ^{7}Li NMR spectra of **1** in [D_8]toluene (-90 °C, $c \approx 0.020$ mol L^{-1}, PhLi external standard in [D_8]toluene) clearly show the presence of unresolved ^{119,117}Sn ($I = 1/2$)–^{7}Li coupling, as an apparent 1:1 doublet ($J \approx 412$ Hz[9]) (Fig. 2).[10] The integral ratio

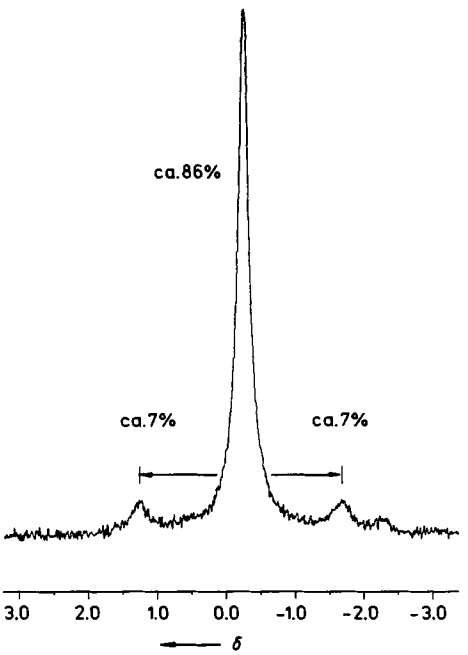

Fig. 2. The low-temperature 139.96-MHz ^{7}Li NMR spectrum of **1**. The average coupling constant $J(^{119,117}Sn\text{-}^7Li)$ is 412 Hz. For further details see text.

of these satellites to the central ^{118}Sn($I = 0$)–^{7}Li signal tallies with the natural abundance ratios of ^{119,117}Sn to ^{118}Sn (ca. 14:86). To our knowledge, this is the first observation of such direct coupling, although very weak long-range ^{119,117}Sn–^{7}Li coupling ($J = 6.2$ Hz) has been observed in the low-temperature ^{7}Li NMR spectrum of 6-substituted 3-trimethylstannylbicyclo[3.2.1]octa-2,6-dienyllithium in THF.[11]

We are now extending this initial work by similarly investigating a variety of alkali-metal (Li, Na, K, Rb, Cs) and alkaline-earth-metal (Mg, Ca, Sr, Ba) triphenylstannate complexes. The hope is to further elucidate the nature of these bonds between p-block metals and early-main-group metals and to assess the structural trends within these compounds.

Experimental Procedure

1: *n*BuLi (2.6 mmol, in hexanes) was added to a chilled solution (ca. -10 °C) of Ph_3SnH (0.91 g, 2.6 mmol) in toluene (12 mL) and PMDETA (0.55 mL, 2.6 mmol) under nitrogen. An exothermic reaction ensued as the reaction mixture warmed to 20 °C, giving a yellow solution and a white precipitate, which dissolved on heating to 70 °C. Slow cooling of the resulting yellow solution (12 h) gave air-sensitive, colorless crystals, identified as [$Ph_3SnLi \cdot$ PMDETA] (**1**). First batch yield 52%, m.p. 145 °C, dec. 230–235 °C to black oil ^{1}H NMR (C_6D_6): $\delta = 8.12$ (m, 5H; phenyl H), 7.30 (m, 10H; phenyl H), 1.86 (s, 3H; CH_3-N), 1.76 (s, 12H; $(CH_3)_2$N-), 1.50 (m, 8H; $(CH_2)_2$). Correct C, H analysis.

Received: June 17, 1991 [Z 4722 IE]
German version: *Angew. Chem. 103* (1991) 1539

CAS Registry numbers:
1, 130445-35-7; PMDETA, 3030-47-5; Ph_3SnH, 892-20-6.

[1] M. Fieser: *Reagents for Organic Synthesis, Vol. 15*, Wiley, New York 1990, and earlier volumes.
[2] a) M. Pereyre, J.-P. Quintard, A. Rahm: *Tin in Organic Synthesis*, Butterworths, London 1987; b) I. Omae: *Organotin Chemistry*, Elsevier, Amsterdam 1989; c) Y. Yamamoto (Ed.): Organotin Compounds in Organic Synthesis, *Tetrahedron 45* (1989) 909–1230; d) P. G. Harrison: *Chemistry of Tin*, Chapman and Hall, New York 1989.
[3] M. Veith, C. Ruloff, V. Huch, F. Töllner, *Angew. Chem. 100* (1988) 1418; *Angew. Chem. Int. Ed. Engl. 27* (1988) 1381.
[4] X-ray structure data: $C_{27}H_{38}LiN_3Sn$, $M = 530.2$, monoclinic, space group $P2_1$, $a = 12.327(2)$, $b = 17.571(4)$, $c = 12.676(3)$ Å, $\beta = 101.71(3)°$, $V = 2688.4(13)$ Å^3, $Z = 4$, $\varrho_{calcd} = 1.310$ Mg m^{-3}, $F(000) = 1096$, $\lambda = 0.71073$ Å), $T = 153$ K, $\mu(Mo_{K\alpha}) = 0.968$ mm^{-1}. Data were collected on a Siemens-Stoe AED using an oil-coated shock-cooled crystal of dimensions $0.8 \times 0.8 \times 0.2$ mm^3 by the $2\theta/\omega$ method $8° \leq 2\theta \leq 50°$). From 5888 collected reflections, 5550 are unique and 5548 have been employed in the structure refinement (data-to-parameter ratio 9.6:1.) The structure was solved by direct methods (G. M. Sheldrick, *Acta Crystallogr., Sect. A 46* (1990) 467) and refined by the full-matrix least-squares procedure to R and R_w values of 0.023 and 0.031, respectively. All hydrogen atoms were located on a difference map and were refined using a riding model with equivalent group U values. Refinement of the alternative enantiomorph resulted in a far higher R value and higher estimated standard deviations, so that it is assumed that the presented enantiomorph is the correct one. Further details of the crystal structure investigation are available on request from the Director of the Cambridge Crystallographic Data Centre, University Chemical Laboratory, Lensfield Road, GB-Cambridge CB2 1EW, on quoting the full journal citation.
[5] G. D. Smith, P. E. Fanwick, I. P. Rothwell, *Inorg. Chem. 28* (1989) 618.
[6] V. H. Preut, H.-J. Haupt, F. Huber, *Z. Anorg. Allg. Chem. 396* (1973) 81.
[7] T. Brichall, J. A. Vetrone, *J. Chem. Soc. Chem. Commun. 1988*, 877.
[8] a) J. J. Brooks, G. D. Stucky, *J. Am. Chem. Soc. 94* (1972) 273; b) H. Köster, E. Weiss, *J. Organomet. Chem. 168* (1979) 273; c) R. A. Bartlett, H. V. R. Dias, P. P. Power, *ibid. 341* (1988) 1; d) M. M. Olmstead, P. P. Power, *J. Am. Chem. Soc. 107* (1985) 2174; e) D. Hoffmann, P. von R. Schleyer, D. Stalke, $[K \cdot PMDETA \cdot THF]^+ Ph_3C^-$, unpublished results.
[9] a) $^1J(Si,Li) = 51$ Hz for a related Si system, $PhMe_2SiLi$, in ether solvents at low temperatures: U. Edlund, T. Lejon, *J. Am. Chem. Soc. 107* (1985) 6408; b) U. Edlund, T. Lejon, P. Pyykkö, T. K. Venkatachalam, E. Buncel, *ibid. 109* (1987) 5982.
[10] At 25 °C the same solution gave only a singlet at $\delta = -0.38$ and no ^{119,117}Sn–^{7}Li coupling was resolvable. The temperature dependence of this system is currently being studied.
[11] N. Hertkorn, F. H. Koehler, *Z. Naturforsch. B 45* (1990) 848.

Investigation of the Light-Induced Charge Transfer between Covalently Linked Porphyrin and Quinone Units by Time-Resolved EPR Spectroscopy**

By *Friedhelm Lendzian,* Jenny Schlüpmann, Jörg von Gersdorff, Klaus Möbius,** and *Harry Kurreck**

The efficiency of the light-induced charge separation in the primary step of photosynthesis is governed by the molecular and electronic structure of the chlorophyll donor and the pheophytin and quinone acceptors and by their mutual separations and orientations. Covalently linked porphyrin quinones (P-Q's) have proven particularly suitable as model compounds for the investigation of these complex electron-transfer (ET) processes.[1] In liquid solvents at room temperature, these compounds generally show rapid ET from the optically excited singlet state of the porphyrin component to the quinone in a time range of several 10 to several 100 ps.[1] Current interest has focused increasingly on the influence of the static and dynamic properties of the surrounding medium on the ET rates. The reorientation of the polar solvent molecules (dielectric relaxation) as a result of Coulomb interaction on transition from ^{S}*P-Q to ^{S}($P^{\bullet+}$-$Q^{\bullet-}$) affects, according to Marcus theory,[2] the free energy ΔG^0 of the reaction and particularly the reorganization energy λ_0.[3] With increasing viscosity (decreasing temperature) the dielectric relaxation time τ_l of the solvent increases and can strongly decrease the rate of the ET reaction. The adiabaticity parameter[4] κ [Eq. (a)] is the decisive factor, where V is the

$$\kappa = 4\pi V^2 \tau_l/(\lambda_0 \hbar) \qquad \text{(a)}$$

electronic interaction between the initial state ^{S}*P-Q and the charge-separated state ^{S}($P^{\bullet+}$-$Q^{\bullet-}$) (Fig. 1) and τ_l is the longitudinal dielectric relaxation time[4] of the solvent. For $\kappa \ll 1$, a nonadiabatic ET results; this is usually assumed for P-Q's in low-viscosity solvent at around 300 K. For $\kappa \gg 1$, the reaction proceeds adiabatically. The ET rate is proportional to τ_l^{-1}[4] and therefore strongly temperature-dependent. Thus, the ET reaction from the excited singlet state of a P-Q could be sufficiently slowed down in a polar solvent at low temperature to observe the competing reaction via intersystem crossing (ISC) to the excited triplet state of the porphyrin component, followed by ET to the charge-separated triplet state of the radical pair ^{T}($P^{\bullet+}$-$Q^{\bullet-}$) (Fig. 1). Both triplet states could be detected for the first time in a P-Q by time-resolved EPR spectroscopy in the time range of several 100 ns to several 10 μs.[5]

A recent report discusses picosecond fluorescence spectroscopy of PQ's, covalently bridged by, among others, cyclohexylene units, in low-viscosity, liquid solution.[6] Under these conditions, the fluorescence lifetimes, are in the picosecond time range. Here we report on time-resolved EPR measurements on two P-Q's[7] in highly viscous solution with a continuous wave (cw) EPR spectrometer equipped for direct detection (without field modulation) of transient signals.[6, 8] The comparison of *trans*- and *cis*-cyclohexylene-linked P-Q's, **1** and **2**, respectively (Fig. 2), seemed especially attractive, since the arrangement of donor and acceptor differs despite the same number of bonds in the cyclohexylene bridges.[9]

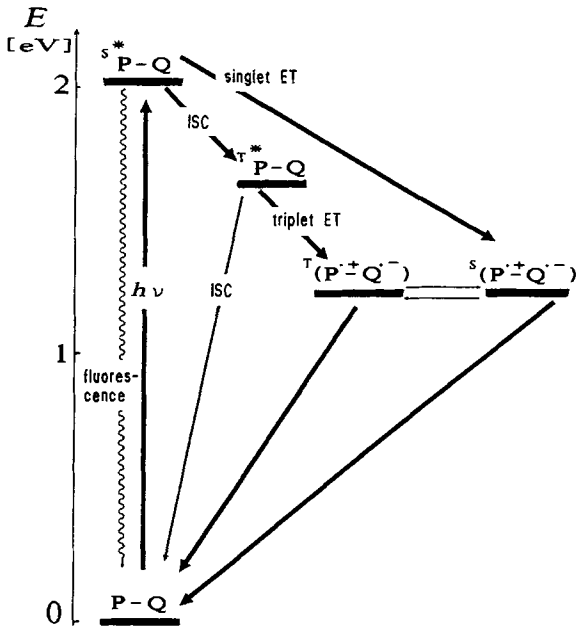

Fig. 1. Energy levels and ET reaction scheme for the P-Q's **1** and **2**. In low-viscosity solution at room temperature, the reaction pathway is "singlet ET"; in highly viscous solution at lower temperature, the favored pathway is "ISC" with subsequent "triplet ET" (see also text).

The ethanolic solutions of the P-Q's were irradiated at about 150 K in situ, that is, in the EPR resonator, with a pulsed dye laser at 584 nm. In the time range of 0.2 μs to several 10 μs after the laser pulse, both compounds show spin-polarized transient EPR spectra, which clearly reveal a broad signal of about 70-mT width (Fig. 2a) and a narrow group of signals of about 6-mT width (Fig. 2a and c). Whereas the intensity of the broad signal decreases in less than 1 μs, the inner group of signals increases, its polarization pattern changing with time.

These results can be interpreted in terms of the energy level and reaction scheme in Figure 1. Laser irradiation results in the initial generation of the (EPR-inactive) excited singlet state of the porphyrin quinone, ^{S}*P-Q, from which the charge-separated singlet-state radical pair ^{S}($P^{\bullet+}$-$Q^{\bullet-}$) is formed in low-viscosity solution at 300 K within several 10 ps.[6] In highly viscous solution at 150 K, a slower, adiabatic, solvent-controlled reaction is expected. An estimate based on Equation (a) with the values $\lambda_0 = 1$ eV,[6] $V = 2.4 \times 10^{-3}$ eV,[6] and $\tau_l \approx 5 \times 10^{-9}$ s (calculated from $\tau_l = (\varepsilon_\infty/\varepsilon_S)\tau_D$[4] with the values for ethanol at 150 K[10]) gives an adiabaticity parameter of $\kappa_{150K} \approx 5.5 \times 10^2$. At 150 K the ET reaction from the excited singlet state of the porphyrin moiety can no longer compete effectively with the temperature-independent singlet-triplet ISC, induced by spin-orbit coupling, to the triplet porphyrin ^{T}P-Q ($\tau_{ISC} = 1.9$ ns[11]). The triplet porphyrin undergoes subsequent ET reaction to give the charge-separated radical pair ^{T}($P^{\bullet+}$-$Q^{\bullet-}$) in its triplet state. If the values for V and λ_0 are assumed to be similar to those for the reaction from the excited singlet state, this reaction is likewise adiabatic. Both triplet species are in principle detectable by EPR spectroscopy. Indeed, the broad EPR signal (Fig. 2a) corresponds to the known EPR powder spectrum of the triplet state of zinc tetraphenylporphyrin (ZnTPP), where the z and y components happen to coincide at the outer edges of the

[*] Dr. F. Lendzian, Prof. Dr. K. Möbius, Dipl.-Phys. J. Schlüpmann
Institut für Molekülphysik, Freie Universität Berlin
Arnimallee 14, W-1000 Berlin 33 (FRG)
Prof. Dr. H. Kurreck, Dipl.-Chem. J. von Gersdorff
Institut für Organische Chemie, Freie Universität Berlin
Takustrasse 3, W-1000 Berlin 33 (FRG)

[**] This work was supported by the Deutsche Forschungsgemeinschaft (SFB 337 and normal grants) and the Fonds der Chemischen Industrie (*H. K.*). We thank Priv.-Doz. *B. Kirste*, Freie Universität Berlin, for the conformational calculations using the Alchemy II program, and Professor Dr. *F. Willig*, Fritz-Haber-Institut, Berlin, as well as Dr. *M. Plato* and Dr. *B. von Maltzan*, Freie Universität Berlin, for fruitful discussions.

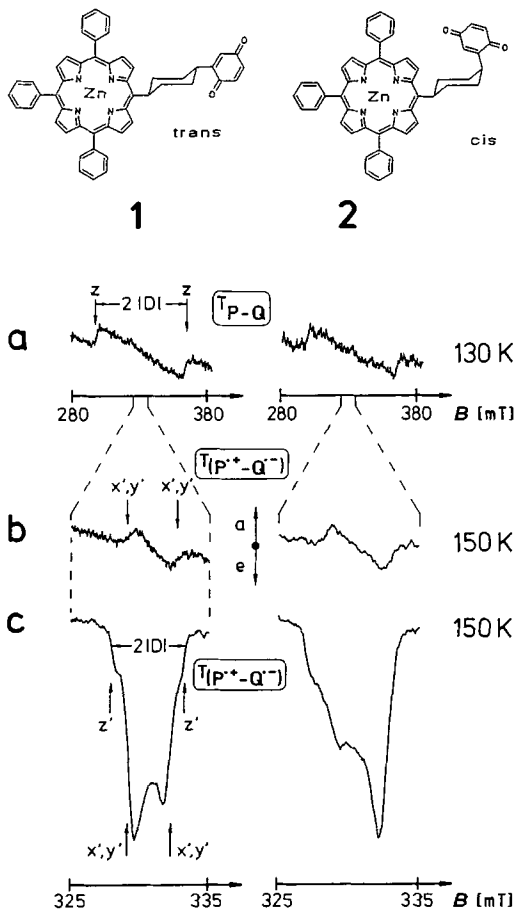

Fig. 2. Spin-polarized transient EPR spectra of the P-Q's **1** and **2** after pulsed laser excitation of the porphyrin moiety (10 ns, 584 nm, 8 mJ, repetition rate 20 Hz). a) Spectra of ^{T}P-Q; delay times: **1**, 0.2 μs; **2**, 0.4 μs; integration time, 0.5 μs. b) Early spectrum of $^{T}(P^{\bullet+}\text{-}Q^{\bullet-})$; delay time, 0.5 μs; integration time, 0.5 μs. c) Late spectrum of $^{T}(P^{\bullet+}\text{-}Q^{\bullet-})$: delay time, 5 μs; otherwise as in b). For interpretation see text. a = absorption, e = emission.

spectrum, while the x components (xyz is a coordinate system intrinsic to the molecule, the z axis lying perpendicular to the molecular plane; Fig. 3) coincide at the center of the spectrum but cannot be observed because they cancel each other owing to opposite polarization.[12] From the positions of the signals the electron dipole–dipole interaction can be determined in terms of the zero-field splitting parameters D and E, where E describes the nonequivalence of the x and y axes.[13] The D values obtained for *trans* and *cis* ^{T}P-Q, are equal within experimental error and agree with the data reported for ^{T}ZnTPP[12] (**1**, 32.6(4) mT; **2**, 32.8(4) mT with $|D| \approx 3|E|$).

The group of signals at the center (Fig. 2b, c) can be assigned to the charge-separated state $^{T}(P^{\bullet+}\text{-}Q^{\bullet-})$ formed by subsequent ET. The measured D values for the *trans* (2.65(5) mT) and *cis* compounds (3.75(5) mT) are significantly smaller than those for ^{T}P-Q and are of similar magnitude to those of another P-Q with comparable porphyrin–quinone separation.[5] The expected magnetic dipole–dipole interaction of $^{T}(P^{\bullet+}\text{-}Q^{\bullet-})$ was estimated using the point dipole model,[14] whereby the two electrons were assumed to be localized at the respective centers of gravity of the porphyrin and quinone moieties and the vector joining them forms the z′ axis of the radical pair (Fig. 3). Using the measured D values of $^{T}(P^{\bullet+}\text{-}Q^{\bullet-})$, electron separations of 10.2 Å are calculated for the radical pair of **1** and 9.1 Å for that of **2**, both values being in good agreement with the midpoint separations (10.7 Å and 8.8 Å, respectively) between porphyrin and quinone obtained with the molecular modeling program Alchemy II.

In addition to the detection of the ET reaction from the porphyrin triplet state by identification of the transient triplet species ^{T}P-Q and $^{T}(P^{\bullet+}\text{-}Q^{\bullet-})$ via the dipolar interactions, the observed spin polarization patterns are of particular interest. The pattern obtained for ^{T}P-Q (aaa eee, starting on the low-field side) agree well with spectra reported for the triplet state of ZnTPP,[12] which can be understood by assuming a spin-selective ISC resulting in exclusive population of the T_z level[12] (see Fig. 3). In the high-field limit, then, the T_0 level for BIIx and BIIy is not populated, whereas this level is predominantly populated for BIIz.

The polarization pattern (aa ee) appearing for the radical pair $^{T}(P^{\bullet+}\text{-}Q^{\bullet-})$ after a short delay time (ca. 0.5 μs, Fig. 2b) can be interpreted with the following assumptions: (1) During ET, the spin polarization in the porphyrin moiety ^{T}P-Q is transferred to the biradical formed. (2) The z′ principal axis is tilted by 90° with respect to the z axis (Fig. 3), whereby T_0 is empty for BIIz′ and overpopulated for BIIx′, y′. (3) $D < 0$, as expected for two separated, localized electrons (biradical)[13] (see Fig. 3).

The polarization effects described so far are similar to those observed previously for another P-Q with a conjugated bridge.[5] The essential structural difference of the systems investigated here is the aliphatic cyclohexylene bridge. In comparison to the P-Q with a conjugated bridge, therefore, the singlet–triplet splitting parameter (exchange energy) $|J|$ of the radical pair $^{T}(P^{\bullet+}\text{-}Q^{\bullet-})$ is appreciably smaller and is of the same order of magnitude as the Zeeman energy. This leads to a mixing of the radical-pair triplet states T_0, T_-, and T_+ with the radical-pair singlet state S (Fig. 3), whereby the respective admixture of singlet character depends on the energy separation between the radical-pair singlet state and the respective triplet sublevel.[15] Owing to their differing singlet character, the radical-pair states T_0 and T_- recombine with different rates to the singlet ground state P-Q (the recombination from the pure radical-pair triplet state is spin-forbidden). Thus, the initial spin polarization pattern in the EPR spectrum of the radical pair $^{T}(P^{\bullet+}\text{-}Q^{\bullet-})$ is governed by the

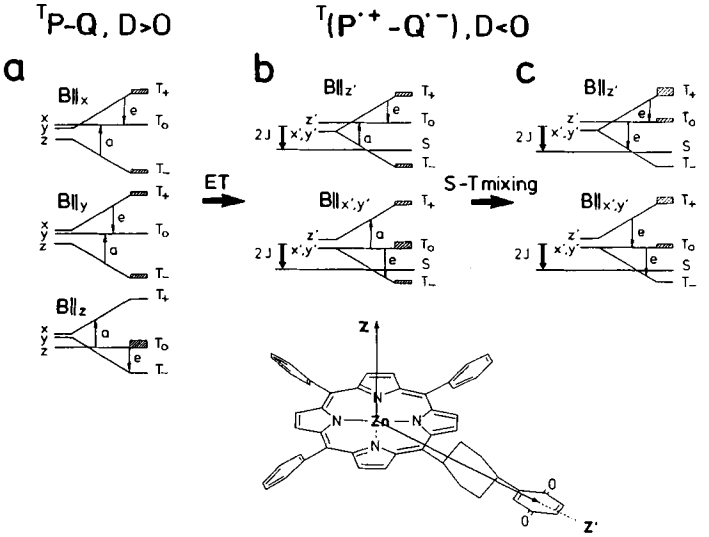

Fig. 3. Zeeman energy levels and excess spin populations for the three canonical orientations (B field in each case parallel to one of the three principal axes x, y, z of the zero-field splitting tensor) of the triplet states ^{T}P-Q ($D > 0$, $E \neq 0$) and $^{T}(P^{\bullet+}\text{-}Q^{\bullet-})$ ($D < 0$, $E = 0$). a) Starting high-field population of ^{T}P-Q due to spin-selective ISC [12]. b) Starting populations of the radical pair $^{T}(P^{\bullet+}\text{-}Q^{\bullet-})$. c) Later populations formed by different recombination rates to the ground state P-Q (see text).

polarization transfer from ^{T}P-Q, whereas after longer times spectra in pure emission develop owing to the differing recombination rates from the triplet sublevels (cf. Figs. 2 and 3). A more exact analysis of the amplitude ratios of the high-field and low-field x',y' signals of **1** and **2** reveals a stronger mixing of the singlet and T_- state in **2**, which, in turn, indicates a larger $|J|$ in comparison to **1**. This is likewise expected because of the smaller porphyrin–quinone distance in **2** compared to **1**.

The kinetics of primary ET reactions in covalently linked P-Q's have been investigated up to now almost exclusively by time-revolved optical spectroscopy.[1] Only in multistep complex donor–acceptor cascades have states with far-separated charges been found to be sufficiently long-lived for detection by time-resolved EPR spectroscopy.[16] The strong decrease of ET in polar solvents of high viscosity (ethanol, 150 K), however, also enables the observation of primary ET reactions in covalently linked, simple P-Q's from the excited triplet state of the porphyrin to the triplet state of the charge-separated radical pair $^{T}(P^{\bullet+}\text{-}Q^{\bullet-})$ by time-resolved EPR spectroscopy in the time range of 0.1 μs to several 10 μs.[5] Augmenting optical spectroscopy, EPR allows an unequivocal identification of both triplet species on the basis of the measured electron dipole–dipole interaction. The observed spin polarization in the transient radical pairs of these model compounds contains information about these interactions, which also determine the ET and spin dynamics of the transient radical pairs in photosynthetic organisms.[16]

Received: July 1, 1991 [Z 4763 IE]
German version: *Angew. Chem. 103* (1991) 1536

CAS Registry numbers:
1, 127572-82-1; **2**, 136844-72-9; $\mathbf{1}^{\bullet+} \cdot \mathbf{1}^{\bullet-}$, 136762-48-6; $\mathbf{2}^{\bullet+} \cdot \mathbf{2}^{\bullet-}$, 136844-75-2.

[1] See, e.g., S. Boxer, *Biochim. Biophys. Acta 726* (1983) 265; M. R. Wasielewski, *Photochem. Photobiol. 47* (1988) 923; J. L. Sessler, M. R. Johnson, T. Y. Lin, *Tetrahedron 45* (1989) 4767; J. S. Connolly, J. R. Bolton in M. A. Fox, M. Chanon (Eds.): *Photoinduced Electron Transfer Part D*, Elsevier, Amsterdam 1988, p. 303.
[2] R. A. Marcus, N. Sutin, *Biochim. Biophys. Acta 811* (1985) 265.
[3] J. A. Schmidt, J. Y. Liu, J. R. Bolton, M. D. Archer, V. P. Y. Gadzekpo, *J. Chem. Soc. Faraday Trans. 1* 85 (1989) 1027; M. R. Wasielewski, D. G. Johnson, W. A. Svec, K. M. Kersey, D. W. Minsek, *J. Am. Chem. Soc. 110* (1988) 7219.
[4] R. A. Marcus, H. Sumi, *J. Electroanal. Chem. 204* (1986) 59; I. Rips, J. Jortner, *J. Chem. Phys. 87* (1987) 2090; I. Rips, J. Jortner, *Chem. Phys. Lett. 133* (1987) 411; P. Finckh, H. Heitele, M. E. Michel-Beyerle, *Chem. Phys. 138* (1989) 1.
[5] F. Lendzian, B. von Maltzan, *Chem. Phys. Lett. 180* (1991) 191.
[6] J. von Gersdorff, M. Huber, H. Schubert, D. Niethammer, B. Kirste, M. Plato, K. Möbius, H. Kurreck, R. Eichberger, R. Kietzmann, F. Willig, *Angew. Chem. 102* (1990) 690, *Angew. Chem. Int. Ed. Engl. 29* (1990) 670.
[7] The synthesis of P-Q (**1**) was described in [6]. Compound **2** was obtained in a similar way, whereby it was particularly important to avoid in all reaction steps the isomerization of the *cis*-cyclohexane-1,4-dicarboxylic acid to the *trans* products.
[8] F. Lendzian, P. Jaegermann, K. Möbius, *Chem. Phys. Lett. 120* (1985) 195.
[9] The structural formulas give the energetically most favorable conformations according to the molecular modeling program Alchemy II (Tripos).
[10] F. X. Hassion, R. H. Cole, *J. Chem. Phys. 23* (1955) 1756.
[11] A. Harriman, G. Porter, N. Searle, *J. Chem. Soc. Faraday Trans. 2 75* (1979) 1515.
[12] H. Levanon, *Rev. Chem. Intermediates 8* (1987) 287; J. H. van der Waals, W. G. van Dorp, T. J. Schaafsma in D. Dolphin (Ed.): *The Porphyrins Vol. IV*, Academic Press, New York 1979, p. 257.
[13] E. Wasserman, L. C. Snyder, W. A. Yager, *J. Chem. Phys. 41* (1964) 1763.
[14] N. Hirota, S. I. Weissman, *J. Am. Chem. Soc. 86* (1964) 2538; B. Kirste, *Dissertation*, Freie Universität Berlin 1977; H. van Willigen, B. Kirste, H. Kurreck, M. Plato, *Tetrahedron 38* (1982) 758.
[15] P. J. Hore, D. A. Hunter, C. D. McKie, A. J. Hoff, *Chem. Phys. Lett. 137* (1987) 495; D. Stehlik, C. H. Bock, J. Petersen, *J. Phys. Chem. 93* (1989) 1612.
[16] K. Hasharoni, H. Levanon, J. Tang, M. K. Bowman, J. R. Norris, D. Gust, T. A. Moore, A. L. Moore, *J. Am. Chem. Soc. 112* (1990) 6477.

Unique Reactivity of Heterodinuclear Pentacarbonyl(fulvalene)molybdenumruthenium with Alkynes: Fluxionality, Rearrangements, Structures, and First Reversible Conversion of a "Side-on"- to a Semi-Bridging Alkenylidene Ligand **

By *Roland Boese*,* *Mark A. Huffman*, and *K. Peter C. Vollhardt**

We report on the unique reactivity of the heterodinuclear fulvalene (Fv) cluster **1** with alkynes,[1] the dynamic behavior of the resulting alkyne complexes, the direct observation of alkyne–alkenylidene rearrangements mediated by a heterodinuclear core,[2] and the unprecedented reversible conversion of an alkenylidene ligand from the "side-on"- to the semi-bridging mode.[3]

Irradiation of $[(Fv)MoRu(CO)_5]$ (**1**)[4] in the presence of diphenylethyne (THF, 300 nm, 5.5 h) gave **2** (48%) and traces of **3**.[5,6] The former is readily carbonylated (CO,

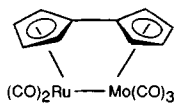

1

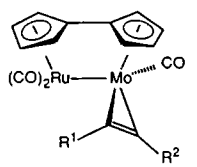

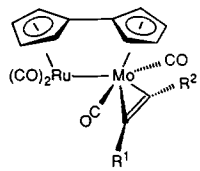

2: $R^1 = R^2 = C_6H_5$
4: $R^1 = R^2 = 4\text{-}CH_3\text{-}C_6H_4$
5a: $R^1 = Si(CH_3)_3$, $R^2 = C_6H_5$
5b: $R^1 = C_6H_5$, $R^2 = Si(CH_3)_3$
10a: $R^1 = H$, $R^2 = C_6H_5$
10b: $R^1 = C_6H_5$, $R^2 = H$

3: $R^1 = R^2 = C_6H_5$
6: $R^1 = Si(CH_3)_3$, $R^2 = C_6H_5$

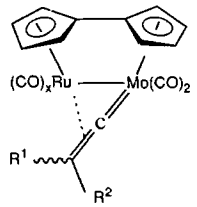

7a,b: $R^1 = C_6H_5$, $R^2 = H$, $x = 1$
8a,b: $R^1 = Si(CH_3)_3$, $R^2 = H$, $x = 1$
9: $R^1 = R^2 = H$, $x = 1$
11: $R^1 = C_6H_5$, $R^2 = H$, $x = 2$

1 atm, 23 °C, 100%) to its likely precursor **3**, a process that is reversible (75 °C). The analogues **4**–**6** were prepared in the same way (20–56%). The unusual end-on, parallel (to the Fv ligand) assignment of the two-electron-donating alkynes

[*] Prof. Dr. K. P. C. Vollhardt, Dr. M. A. Huffman
Department of Chemistry, University of California at Berkeley
and
the Chemical Sciences Division
Lawrence Berkeley Laboratory
Berkeley, CA 94720 (USA)
Prof. Dr. R. Boese
Institut für Anorganische Chemie der Universität-Gesamthochschule
Universitätsstrasse 5–7, Postfach 103764, W-4300 Essen 1 (FRG)

[**] This work was supported by the Director, Office of Energy Research, Office of Basic Energy Sciences, Materials Sciences Division of the U.S. Department of Energy (DE-AC03-76SF00098).

in **3** and **6** rests on the ^1H and ^{13}C NMR spectra, which reveal the symmetrical patterns expected for **3** and the appropriate lack thereof for **6**. In contrast, the NMR spectra indicate that the four-electron donor alkynes in **2**, **4**, and the two (inseparable) isomers of **5** (assignments by NOE experiments at $-30\,^{\circ}C$, **5a**:**5b** = 7:1) adopt a terminal, perpendicular configuration, a conclusion corroborated by an X-ray structural analysis of **2** (Fig. 1).[5] Noteworthy (with respect to the observed isomer ratio for **5**) is the relatively unencumbered environment of the phenyl group *syn* to the Fv moiety, a location preferred by the more bulky silyl substituent in **5**.

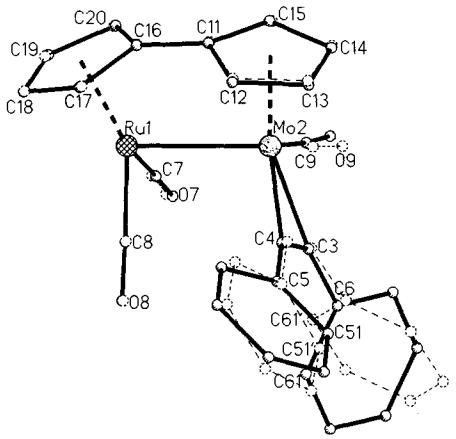

Fig. 1. Molecular structure of **2**, hydrogen atoms omitted. The two independent molecules are drawn superpositioned (fitted on the metal atoms and the fulvalene moiety), with the coordinates of the atoms of one molecule inverted (dashed lines). Atomic labeling is given for only two atoms of the phenyl rings. Selected bond lengths [Å] and angles [°] (interplanar angles defined as best planes of the given atomic positions in parentheses, separated by virgules): Ru1'–Mo2' 2.840(1), Ru1'–Mo2' 2.860(1), Mo2–C3 2.055(5), Mo2'–C3' 2.060(5), Mo2–C4 2.026(4), Mo2'–C4' 2.023(5), C3–C4 1.304(7), C3'–C4' 1.322(5), C3–C6 1.466(7), C3'–C6' 1.464(5), C11–C16 1.451(7), C11'–C16' 1.453(6); Mo2–Ru1–C7 92.0(2), Mo2'–Ru1'–C7' 93.8(2), Mo2–Ru1–C8 86.0(2), Mo2'–Ru1'–C8' 84.7(2), Ru1–Mo2–C9 90.2(1), Ru1'–Mo2'–C9' 93.8(1), Ru1–Mo2–C3 106.6(1), Ru1'–Mo2'–C3' 107.7(1), Ru1–Mo2–C4 105.4(1), Ru1'–Mo2'–C4' 107.7(1), C3–Mo2–C4 37.3(2), C3'–Mo2'–C4' 37.8(2), C3–C4–C5 141.3(4), C3'–C4'–C5' 138.7(5), C4–C3–C6 138.0(4), C4'–C3'–C6' 142.1(5), (C11–C15)/(C16–C20) 29.1, (C11'–C15')/(C16'–C20') 27.2, (C3,C4,C5,C6)/(C5,C51–C55) 147.5, (C3',C4',C5',C6')/(C5',C51'–C55') 14.9, (C3,C4,C5,C6)/(C6,C61–C65) 43.6, (C3',C4',C5',C6')/(C6',C61–C65) 56.5, C12–C11–C16–C17 0.7, C12'–C11'–C16'–C17' −2.4, C3–C4–C5–C51 −24.2, C3'–C4'–C5'–C51' 12.7, C4–C3–C6–C61 −36.8, C4'–C3'–C6'–C61' 123.0.

Interestingly, **2** and **4** exhibit fluxionality via two different processes, one that equilibrates the two sides of the Fv ligand (i.e., C(14,15,20,19) with C(13,12,17,18)) at the same rate as CO(9) with *one* of the Ru carbonyls (presumably CO(8); $\Delta G^{\ddagger}_{25\,^{\circ}C} = 15.5 \pm 0.1$ kcal mol^{-1}), a second ($\Delta G^{\ddagger}_{25\,^{\circ}C} = 17.6 \pm 1.0$ kcal mol^{-1}) that in addition reveals coalescence of the signals of the respective arylcarbyne halves of the alkynes. The most plausible mechanism for the first involves stereospecific access to a hitherto undetected doubly bridging carbonyl (e.g., CO(8) and CO(9)) intermediate containing a perpendicular terminal alkyne group, the second process being alkyne rotation. The latter should interconvert **5a** and **b**, an expectation verified through spin-saturation transfer experiments at 50 °C.

In contrast to the photosubstitution chemistry of **1** with internal alkynes which leaves the Ru center as a seemingly innocent spectator, their terminal analogues (e.g., PhC_2H and $(CH_3)_3SiC_2H$) provide the first heterodinuclear, side-on-bridging four-electron-donating alkenylidenes **7** and **8** (40–50%).[5] Unlike previous systems which were stereochemically biased,[2] they exist as (inseparable) mixtures of the two possible diastereomers (ratio: 3.5:1 for **7**, 4:1 for **8**; relative configuration undetermined). Both compounds are also available thermally from **2** by treatment with the corresponding alkynes (42–53%). The two respective isomers of **7** and **8** are in equilibrium, as indicated by line-broadening of their NMR spectra at 75 °C (**7**) or 23 °C (**8**) and ready crystallization in (presumably) one form, a finding that allowed the X-ray structural analysis of crystalline **7** (Fig. 2).[5]

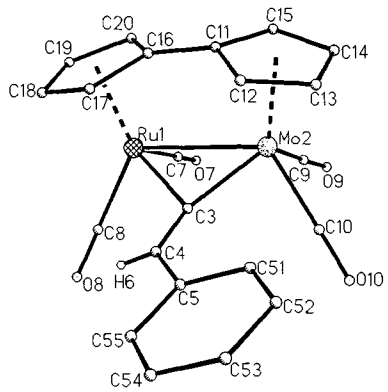

Fig. 2. Molecular structure of **7**, hydrogen atoms except H6 omitted. Selected bond lengths [Å] and angles [°] (interplanar angles given as in Fig. 1): Ru1–Mo2 2.847(1), Mo2–C3 1.918(4), Ru1–C3 2.091(4), C3–C4 1.388(5), C4–C5 1.478(5), C11–C16 1.452(6); Mo2–Ru1–C7 103.3(1), Ru1–Mo2–C9 88.9(1), Ru1–Mo2–C3 47.3(1), Mo2–Ru1–C3 42.4(1), Ru1–C3–Mo2 90.4(1), C3–C4–C5 123.6(4), (C11–C15)/(C16–C20) 26.7, (C3,C4,C5)/(C5,C51–C55) 1.5, (Ru1–Mo2–C3)/(C3–C4–C5) 69, C12–C11–C16–C17 −7.2, C3–C4–C5–C51 1.1.

To gain further insight into this isomerization process, it was desirable to scrutinize the dynamic behavior of the parent structure **9**, available by ready protodesilylation of **8a, b** (Bu_4NF, THF, 23 °C, 65%). On heating **9**, the ^1H NMR signals for the two vinylidene hydrogens ($\delta = 2.37, 2.84$, $J = 14$ Hz) suffer extensive line-broadening, while the Fv absorptions remain unchanged. The molecule's thermal sensitivity required spin-saturation transfer techniques to establish the occurrence of vinylidene H–H site exchange (20–60 °C; $\Delta H^{\ddagger} = 14.8 \pm 0.8$ kcal mol^{-1}; $\Delta S^{\ddagger} = -15.3 \pm 2.4$ cal K^{-1} mol^{-1}, $\Delta G^{\ddagger}_{25\,^{\circ}C} = 19.4 \pm 0.1$ kcal mol^{-1}). This observation is significant in light of the mechanism proposed for the similar fluxional behavior of $[Cp_2M_2(CO)_4(\mu\text{-}\eta^1\text{:}\eta^2\text{-}C{=}CMe_2)]$ (M = Mo, W),[7] the cornerstone of which is the intermediacy of a symmetrical μ_2-η^1-structure, insufficient to explain the dynamics of **9** because of the asymmetry imparted by the heterodinuclear backbone. Rather, vinylidene rotation has to be postulated, perhaps featuring a non-bridging isomer[8] or a dipolar semibridging form (see below).

That the precursors to **7** and **8** are most likely terminal alkyne complexes was indicated by protodesilylation of **5a, b** as above (7:1) at −78 °C to give first **10a** and **b** (not isolated) in varying ratios. ^1H NMR analysis at −57 °C revealed the composition **10a**:**10b** = 2:1, changing to the equilibrium ratio (1:5) at −40 °C. The diastereomer assignments are tentative, resting on the presumed steric preference of the phenyl group to be *syn* to the Fv unit. Remarkably, even at −40 °C, these compounds are unstable with respect to alkyne–alkenylidene isomerization (**7a, b** 3.5:1), a facility that is unprecedented.[2, 3a]

In analogy to side-on- and semi-bridging CO,[3] the corresponding alkenylidenes should be readily displaced by added ligands. Indeed, exposure of **7** to CO (5 atm, CH_3COCH_3,

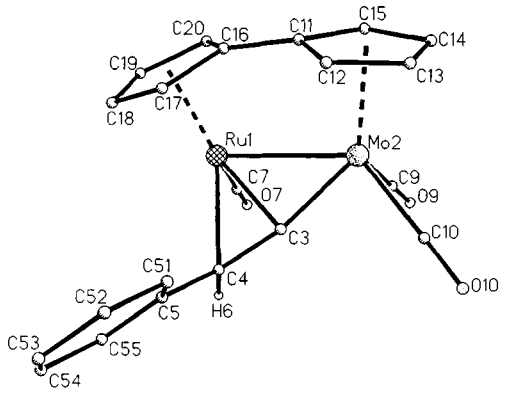

Fig. 3. Molecular structure of **11**, hydrogen atoms except H6 omitted. Selected bond lengths [Å] and angles [°] (interplanar angles given as in Fig. 1): Ru1–Mo2 2.906(1), Mo2–C3 2.053(2), Ru1–C3 2.191(3), C3–C4 1.340(4), C4–C5 1.478(4), C11–C16 1.452(5); Mo2–Ru1–C7 81.2(1), Mo2–Ru1–C8 116.3(1), Ru1–Mo2–C9 96.3(1), Ru1–Mo2–C3 48.8(1), Mo2–Ru1–C3 44.8(1), Ru1–C3–Mo2 86.3(1), Ru1–C3–C4 121.3(2), Mo2–C3–C4 148.3(3), C3–C4–C5 129.2(3), (C11–C15)/(C16–C20) 25.4, (C3,C4,C5)/(C5,C51–C55) 2.3, (Ru1–Mo2–C3)/(C3–C4–C5) 160, C12–C11–C16–C17 4.2, C3–C4–C5–C51 2.6.

75 °C, 20 h) effected monocarbonylation (60%) to isomerically pure **11**,[5] a process that is reversible under vacuum. The IR spectrum exhibited only terminal CO absorptions, suggesting the formation of a nonbridging structure containing a terminal, Mo-bound alkenylidene or alkyne ligand. However, the ^{13}C NMR data were inconsistent with either view. This ambiguity was resolved by an X-ray structural analysis revealing the presence of a semi-bridging Ph(H)CC moiety (Fig. 3).[5]

The most outstanding feature of the structure is its general resemblance to that of **7**, particularly with respect to the asymmetric disposition of the alkenylidene, C(3) being attached to Mo by a relatively short and to Ru by a correspondingly long bond. Moreover, C(4) is strongly tilted towards the Ru atom, while the carbonyls maintain their terminal coordination mode.[9] These similarities notwithstanding, there is a large change in the "twist" angle of the terminal methylene group relative to the metallacyclopropane core when going from **7** (69°) to **11** (160°). It is curious that, while both experience an unusually large distortion (typically only about 10°)[3, 9] from the "ideally" expected perpendicular and coplanar configurations, respectively, the net "rotation" is exactly that predicted: 90°. The equilibrium **7** ⇄ **11** is the first of its kind to be observed. Interestingly, **11** is also readily generated from **6** by protodesilylation.

In stark contrast to the chemistry of **1**, under the same conditions its homodinuclear analogues give rise to distinctly different products,[1, 6, 10] some exhibiting behavior[11] that is not unlike that of the related Cp_2M_2 (M = Ru, Mo) systems.[12]

Received: May 22, 1991 [Z 4642 IE]
German version: *Angew. Chem. 103* (1991) 1542

[1] For a summary of recent work, see: P. A. McGovern, K. P. C. Vollhardt, *Synlett 1990*, 493.

[2] a) J. Silvestre, R. Hoffmann, *Helv. Chim. Acta 68* (1985) 1461; b) A. B. Antonova, A. A. Joganson, *Russ. Chem. Rev. (Engl. Transl.) 58* (1989) 693; c) M. I. Bruce, *Chem. Rev. 91* (1991) 197.

[3] This mode of binding is known for other, related ligands, especially CO; a) H. Werner, *Angew. Chem. 102* (1990) 1109; *Angew. Chem. Int. Ed. Engl. 29* (1990) 1077; b) A. L. Sargent, M. B. Hall, *J. Am. Chem. Soc. 111* (1989) 1563; c) R. A. Doyle, L. M. Daniels, R. J. Angelici, *ibid. 111* (1989) 4995; d) Y. Chi, F.-J. Wu, B.-J. Liu, C.-C. Wang, S.-L. Wang, *J. Chem. Soc. Chem. Commun. 1989*, 873.

[4] K. P. C. Vollhardt, T. W. Weidman, *Organometallics 3* (1984) 82.

[5] All new isolated compounds were fully characterized. For example **2**: green prisms, m.p. = 225 °C (dec.); ^1H NMR (300 MHz, CD_3COCD_3): δ = 7.61–7.34 (m, 10 H), 6.17 (br s, 1 H), 5.75 (br s, 1 H), 5.65 (br s, 1 H), 5.44 (br s, 1 H), 5.16 (br s, 1 H), 5.06 (br s, 1 H), 4.08 (br s, 1 H), 3.98 (br s, 1 H), $^{13}C\{^1H\}$ NMR (75 MHz, [D$_8$]THF): δ = 241.9, 208.1, 205.0, 203.7, 199.4, 140.8, 138.7, 129.3, 129.2, 129.1, 128.4, 127.7 (2 C), 103.5, 96.0, 95.8, 90.3, 89.1, 85.2, 84.7, 81.2, 77.7, 76.8; IR (THF): $\tilde{\nu}_{CO}$ = 1985, 1935 cm^{-1}; MS (70 eV): *m/z* 587 ($M^{\oplus}$, 3.0), 559 ($M^{\oplus}$ − CO, 19.4) 502 ($M^{\oplus}$ − 3 CO, 100). Space group $P2_1/c$, a = 18.966(5), b = 16.003(4), c = 16.265(3) Å, α = 90, β = 114.93(2), γ = 90°, V = 4477(2) Å^3, Z = 8, μ = 1.234 mm^{-1}, ϱ_{calcd} = 1.74 g cm^{-3}; $Mo_{K\alpha}$ radiation; scan range 3° ≤ 2θ ≤ 50°; 7203 unique reflections, 5982 treated as observed [$F_o \geq 4\sigma(F)$], R = 0.030, R_w = 0.036. – **7**: red needles, m.p. = 155.5–156.5 °C; ^1H NMR (3.5:1 ratio of interconverting diastereomers in solution; 300 MHz, [D$_8$]THF major isomer): δ = 7.11–6.72 (m, 5 H), 6.26 (m, 1 H), 5.60 (m, 1 H), 5.57 (m, 1 H), 5.54 (s, 1 H), 5.17 (m, 1 H), 4.84 (m, 1 H), 4.75 (m, 1 H), 4.45 (m, 1 H), 2.37 (m, 1 H); (minor isomer): δ = 7.11–6.72 (m, 5 H), 6.05 (m, 1 H), 5.80 (m, 1 H), 5.57 (m, 1 H), 5.52 (m, 1 H), 5.29 (m, 1 H), 4.86 (m, 1 H), 4.70 (s, 1 H), 4.23 (m, 1 H), 3.08 (m, 1 H); $^{13}C\{^1H\}$ NMR (75 MHz, [D$_8$]THF major isomer): δ = 319.3, 229.1, 228.5, 206.5, 144.2, 128.8, 126.2, 125.3, 97.5, 96.4, 94.7, 88.4, 88.0, 87.2, 86.6, 86.1, 86.0, 72.6, 61.5; IR (KBr): $\tilde{\nu}_{CO}$ = 1989, 1931, 1894 cm^{-1}; MS (70 eV): *m/z* 511 ($M^{\oplus}$, 8.3), 483 ($M^{\oplus}$ − CO, 23.0), 455 ($M^{\oplus}$ − 2 CO, 4.2), 427 ($M^{\oplus}$ −3 CO, 100). Space group $P1$, a = 7.201(2), b = 11.523(2), c = 14.940 Å, α = 79.99(2), β = 76.60(2), γ = 76.54(2)°, V = 1163.3(4) Å^3, Z = 2, μ = 1.19 mm^{-1}, ϱ_{calcd} = 1.46 g cm^{-3}; $Mo_{K\alpha}$ radiation; scan range 3° ≤ 2θ ≤ 45°; 2953 unique reflections, 2652 treated as observed [$F_o \geq 4\sigma(F)$], R = 0.031, R_w = 0.035; disorder as shown in Fig. 1. – **11**: dark red crystals, m.p. = 115 °C (dec.); ^1H NMR (300 MHz, [D$_8$]THF, − 40 °C): δ = 7.36 (m, 2 H), 7.17 (m, 2 H), 7.14 (s, 1 H), 6.98 (m, 1 H), 6.42 (m, 1 H), 6.04 (m, 1 H), 5.87 (m, 1 H), 5.75 (m, 1 H), 5.55 (m, 1 H), 5.44 (m, 1 H), 4.72 (m, 2 H); $^{13}C\{^1H\}$ NMR (75 MHz, [D$_8$]THF, − 50 °C): δ = 247.4, 243.4, 241.5, 205.7, 203.2, 152.1, 141.0, 128.5, 126.5, 125.6, 97.5, 96.8, 96.0, 95.7, 93.1, 90.0, 88.6, 87.3, 85.2, 84.1; IR (KBr): $\tilde{\nu}_{CO}$ = 2039(s), 1984(s), 1954(m), 1903(s), 1827(s) cm^{-1}; FAB-MS (NBA): *m/z* 540 ($M^{\oplus}$), 512 ($M^{\oplus}$ − CO), 485 ($M^{\oplus}$ − 2 CO). Space group $P2_1/n$, a = 15.931(2), b = 8.176(1), c = 16.463(2) Å, α = 90, β = 117.79(1), γ = 90°, V = 1896.8(4) Å^3, Z = 4, μ = 1.45 mm^{-1}, $\varrho_{calcd.}$ = 1.889 g cm^{-3}; $Mo_{K\alpha}$ radiation; scan range 3° ≤ 2θ ≤ 55°; 5518 unique reflections; 4992 treated as observed [$F_o \geq 3.5\sigma(F)$], R = 0.031, R_w = 0.038. Further details of the crystal structure investigations may be obtained from the Fachinformationszentrum Karlsruhe, Gesellschaft für wissenschaftlich-technische Information mbH, W-7514 Eggenstein-Leopoldshafen 2 (FRG) on quoting the depository numbers CSD-320235 (**2**), 320236 (**7**) and 320237 (**11**), the names of the authors, and the journal citation.

[6] Compound **2** reacts with oxygen to give [(Fv)Ru(CO)$_2$Mo(PhC$_2$Ph)(O)], previously observed under reaction conditions that evidently allowed air contamination: J. S. Drage, M. Tilset, K. P. C. Vollhardt, T. W. Weidman, *Organometallics 3* (1984) 812.

[7] S. F. T. Froom, M. Green, R. J. Mercer, K. R. Nagle, A. G. Orpen, S. Schwiegk, *J. Chem. Soc. Chem. Commun. 1986*, 1666.

[8] See D. R. Senn, A. Wong, A. T. Patton, M. Marsi, C. E. Strouse, J. A. Gladysz, *J. Am. Chem. Soc. 110* (1988) 6096, and the references therein.

[9] For a seminal study, see: H. Werner, F. J. Garcia Alonso, H. Otto, K. Peters, H. G. von Schnering, *Chem. Ber. 121* (1988) 1565.

[10] J. S. Drage, K. P. C. Vollhardt, *Organometallics 5* (1986) 280.

[11] M. A. Huffman, K. P. C. Vollhardt, unpublished results.

[12] See a) D. L. Davies, A. F. Dyke, A. Endesfelder, S. A. R. Knox, P. J. Naish, A. G. Orpen, D. Plaas, G. E. Taylor, *J. Organomet. Chem. 198* (1980) C43; b) R. E. Colborn, D. L. Davies, A. F. Dyke, A. Endesfelder, S. A. R. Knox, A. G. Orpen, D. Plaas, *J. Chem. Soc. Dalton Trans. 1983*, 2661; c) R. J. Mercer, M. Green, A. G. Orpen, *J. Chem. Soc. Chem. Commun. 1986*, 567.

1,2-Asymmetric Induction in the Ketene Claisen Rearrangement of Allyl Sulfides

By *Udo Nubbemeyer, Reinhold Öhrlein, Jozef Gonda, Beat Ernst,** and *Daniel Belluš**

The preparative potential of even such old reactions as the [3,3]-sigmatropic Claisen rearrangement[1] still seems far from exhausted. The stereochemical course of this intra-

[*] Prof. Dr. D. Belluš, Dr. B. Ernst, Dr. J. Gonda, Dr. U. Nubbemeyer, Dr. R. Öhrlein
CIBA-GEIGY AG
Schwarzwaldallee 211, CH-4002 Basel (Switzerland)

molecular reaction has been thoroughly investigated,[2] so that it can be incorporated into sophisticated synthetic sequences.[3] We recently showed that the ketene Claisen rearrangement of allyl sulfides (allyl thioethers),[4] a novel "intramolecular" variant of the [3,3]-sigmatropic rearrangement, proceeds chemoselectively (allyl thioether versus allyl ether) with excellent chirality transfer from a C–S to a C–C bond.[5] Here we report on the 1,2-asymmetric induction in this new type of reaction. We chose the optically active allyl thioethers **4**, **8**, and **12** (Scheme 1) as starting compounds for our investigations.

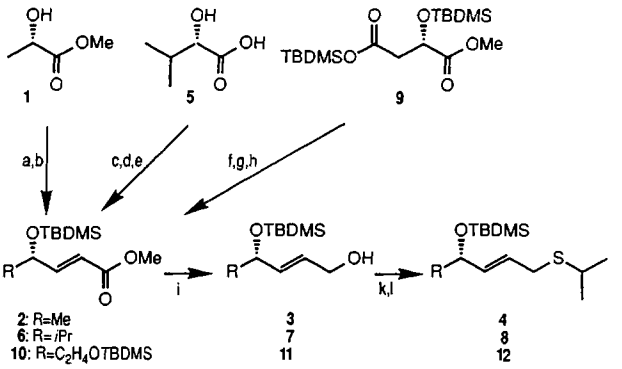

Scheme 1. Synthesis of allyl thioethers **4**, **8**, and **12**. **4**: a) TBDMSCl, imidazole, dimethylformamide (DMF), 20 °C (98%) [9]; b) DIBAH, hexane, −78 °C, 1 h [6], then $Ph_3P{=}CHCO_2Me$, THF, CH_2Cl_2, −78 °C to 20 °C, 1 h, 51% *E*, 7% *Z* [6b, c] (see *Experimental Procedure*); i) DIBAH, THF, 0 °C, 30 min (92%) [10]; k) AcSH, Ph_3P, diethyl azodicarboxylate (DEAD), THF, 0 °C (95%) [11] (see *Experimental Procedure*); l) NaOEt, EtOH, 20 °C, 1 h then *i*PrBr, 20 °C, 12 h (92%). **8**: c) TBDMSCl, imidazole, DMF, 20 °C (quant.) [12]; d) DIBAH, THF, −78 °C, 1 h (93%); e) $(COCl)_2$, dimethyl sulfoxide (DMSO), CH_2Cl_2, NEt_3, then $Ph_3P{=}CHCO_2Me$, −78 °C to 20 °C (81% *E*, 1% *Z*); i) (83%); k) (81%); l) (82%).

The methyl ester of L-(−)-lactic acid (**1**, *ee* ≥ 99%), after silylation with *tert*-butyldimethylsilyl chloride (TBDMSCl), was reduced with diisobutylaluminum hydride (DIBAH) to the known lactaldehyde[6a] and lengthened via in situ Wittig olefination[6b] to the α,β-unsaturated ester **2**.[6c] A second DIBAH reduction then led to the allyl alcohol **3**, whose corresponding Mosher ester[7] was used to determine its optical purity (*de* ≥ 94%).

Subsequently, **3** was converted into the thioacetate by reaction with thioacetic acid under Mitsunobu conditions. Saponification and in situ alkylation with isopropyl bromide afforded thioether **4**.[8]

An analogous reaction sequence, starting from L-(+)-hydroxyisovaleric acid (**5**, *ee* ≥ 98%), was used to synthesize the allyl alcohol **7**, whose Mosher ester showed *de* ≥ 90% according to the ^{1}H NMR spectrum. The thioether **8**[8] was then prepared as described above.

L-(−)-Malic acid (*ee* ≥ 99%) was first converted by a known procedure[13] into the 1-methyl ester **9** (Scheme 1). Mild hydrolysis resulted in selective cleavage of the silyl ester.[14] Reduction of the acid function with borane–dimethyl sulfide, silylation of the resulting alcohol, DIBAH reduction of the methyl ester function, and subsequent Wittig olefination then led to isolation of the disilyl ether **10**, from which the allyl alcohol **11** was obtained. The corresponding Mosher ester showed *de* ≥ 90% according to the ^{1}H NMR spectrum. The allyl alcohol **11** was finally transformed into the allyl thioether **12**.[8] The chiral allyl thioethers **4** (*ee* ≥ 94%), **8** (*ee* ≥ 90%), and **12** (*ee* ≥ 90%) were thus available for the ketene Claisen rearrangement. Dichloroketene, generated in situ by reductive elimination of chlorine from trichloroacetyl chloride upon treatment with activated zinc,[4] was allowed to react with the allyl thioethers **4**, **8**, and **12**. In all three cases, as expected,[5] the rearrangement proceeded with high chemoselectivity.

Compound **4** afforded thioester **14** (*de* ≥ 94%),[8] **8** gave **15** (*de* ≥ 90%),[8] and **12** yielded **16** (*de* ≥ 90%)[8] (Scheme 2). The retention of configuration in the ketene Claisen rearrangement was examined by ^{1}H NMR spectroscopy of γ-butyrolactone **17**, obtained by reduction of **14**. For racemic **17**, the methyl groups give rise to two signals in the presence of *R*-(−)-1-(9-anthryl)-2,2,2-trifluoroethanol. This splitting is not observed for **17**, so that the optical purity is ≥ 95%.

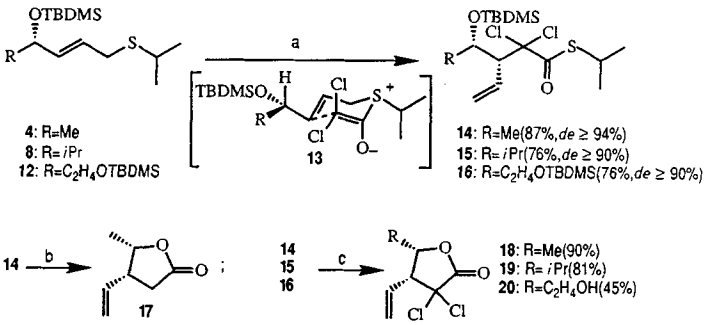

Scheme 2. Reaction of **4**, **8**, and **12** with dichloroketene via **13** and subsequent lactonization of the reaction products **14**–**16**. a) CCl_3COCl, Et_2O, Zn/Cu, 40 °C, 3–5 h; b) AcOH, Zn, 110 °C, 1 h; c) 48% HF, CH_3CN, 20 °C, 2 h.

In contrast, the intramolecular [3,3]-sigmatropic rearrangement of analogous silylketene acetals, prepared from L-lactaldehyde[16] or D-glyceraldehyde,[17] proceeds with diastereomeric excesses of only 50 and 13%, respectively, in favor of the *syn* product. In view of these results and the model for the steric and electronic course of [3,3]-sigmatropic reactions proposed by *Felkin* et al., *Houk* et al.[18] and *Kahn* and *Hehre*,[19] the rearrangement products **14**–**16** should have a *syn* structure, since the reaction should occur via transition state **13** with minimal 1,3-diaxial interactions. Examination of the postulated *syn* selectivity in the formation of ester **14** was carried out by ^{1}H NMR spectroscopic investigation of the corresponding cyclization product **17**.[20] Irradiation of the methyl protons in lactone **17** resulted in a positive NOE effect in the vinyl CH signal, which supports a *syn* selectivity in the formation of thioesters **14**–**16**.[21] Under nonreducing conditions, these esters afforded chlorolactones **18**–**20**, which likewise were *cis* isomers.

The less reactive chloromethylketene also reacted with thioether **4**. The resulting thioester **21**,[8] which possesses a further stereocenter in the α position to the carbonyl group, was obtained as an inseparable mixture of diastereomers (*de* ≈ 50%). After desilylation, the chromatographically separable lactones **22a** and **22b** were obtained in a ratio of 3:1 (Scheme 3).

The stereochemistry of these lactones could again be assigned by NOE measurements. Reduction of ester **21** in zinc/acetic acid yielded the chlorine-free lactones **23a** and **23b** in a ratio of 1:3.[22] This ratio was also obtained when either the diasteromeric mixture **22a**, **b** or either one of the pure isomers, **22a** or **22b**, was dehalogenated with zinc in acetic acid. The radical dechlorination of **22a** or **22b** with tributylzinc hydride at various temperatures led to the same ratio of lactones **23**.

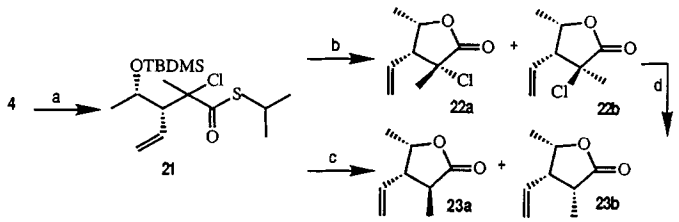

Scheme 3. Reaction of **4** with chloromethylketene and subsequent lactonization. a) CH_3CCl_2COCl, Et_2O, Zn/Cu, 40 °C, 7 h (82%); b) 48% HF, CH_3CN, 20 °C, 2 h (**22a**: 65%, **22b**: 22%); c) AcOH, Zn, 110 °C, 1 h (**23a**: 19%, **23b**: 53%); d) nBu$_3$SnH, toluene, *hv*, −78 °C, 1.5 h (89%); for further conditions see text.

This novel, "intermolecular" ketene Claisen rearrangement is characterized not only by its excellent chemoselectivity but also by its excellent 1,2-*syn* selectivity (ca. 20:1). By choice of suitably substituted precursors, such as **8** or **12**, this reaction offers a route to optically active γ-butyrolactones, a class of substances of use in numerous natural product syntheses.[23]

Experimental Procedure

One-pot procedure for the synthesis of α,β-unsaturated esters **2** and **6** [6b]: The α-siloxy ester (60 mmol), dissolved in 60 mL of dry hexane at −78 °C, was treated dropwise over 30 min with 65 mL of a 1 M solution of DIBAH in hexane under argon. After 1 h, methoxycarbonylmethylene(triphenyl)phosphorane (60 mmol) in 40 mL of THF and 50 mL of CH_2Cl_2 was added. The reaction mixture was then allowed to warm over 1 h to room temperature, poured into ice water, and extracted with diethyl ether. The organic phase was washed with a saturated aqueous NaCl solution and the *E*/*Z* mixture separated by chromatography on silica gel.

Mitsunobu variant for the synthesis of the allyl thioacetate: Freshly distilled DEAD (20 mmol) was injected into a solution of triphenylphosphane (20 mmol) in 20 mL of dry THF at 0 °C under argon. After 40 min, allyl alcohol (10 mmol) and freshly distilled thioacetic acid (20 mmol), each dissolved in 5 mL of THF, were successively added dropwise. Monitoring by thin layer chromatography revealed that the reaction was over after about 1 h. Pentane was added and the mixture was filtered through silica gel with pentane/ether (1:1) as eluent. After removal of the solvent, the thioester was chromatographed or purified by distillation.

Ketene Claisen rearrangement of allyl thioether: Allyl thioether (1.5 mmol) and about 15 mmol of Zn/Cu alloy [4] were placed in 15 mL of vigorously stirred ether under argon and the mixture was heated to reflux. A solution of 3 mmol of freshly distilled trichloroacetyl chloride in 5 mL of ether was added dropwise to the solution over 4 h by means of a syringe pump (7 h infusion for the generation of chloromethylketene from 2,2-dichloropropionyl chloride). After cooling, the reaction solution was decanted from the residue. Purification of the thioester was accomplished by chromatography on silica gel.

Received: March 7, 1991;
Revised version: August 19, 1991 [Z 4480 IE]
German version: *Angew. Chem. 103* (1991) 1533

[1] L. Claisen, *Chem. Ber. 45* (1912) 3157.
[2] a) R. Hill, *Asymmetric Synth. 3B* (1984) 503, and references cited therein; b) F. E. Ziegler, *Chem. Rev. 88* (1988) 1423.
[3] R. E. Ireland, P. G. M. Wuts, B. Ernst, *J. Am. Chem. Soc. 103* (1981) 3205; R. E. Ireland, R. C. Anderson, R. Badoud, B. J. Fitzsimmons, G. J. McGarvey, S. Thaisrivongs, C. S. Wilcox, *ibid. 105* (1983) 1988.
[4] R. Malherbe, D. Belluš, *Helv. Chim. Acta 61* (1978) 3096; R. Malherbe, G. Rist, D. Belluš, *J. Org. Chem. 48* (1983) 860; G. Rosini, G. G. Spineti, E. Foresti, G. Pradella, *ibid. 46* (1981) 2228; E. Vedejs, R. A. Buchanan, *ibid. 49* (1984) 1840.
[5] R. Öhrlein, R. Jeschke, B. Ernst, D. Belluš, *Tetrahedron Lett. 30* (1989) 3517.
[6] a) S. K. Massad, L. D. Hawkins, D. C. Baker, *J. Org. Chem. 48* (1983) 5180; b) A. Krief, W. Dumont, P. Pasau, *Tetrahedron Lett. 29* (1988) 1079; c) R. Annunziata, M. Cinquini, F. Cozzi, G. Dondio, L. Raimondi, *Tetrahedron 43* (1987) 2369.
[7] J. A. Dale, D. L. Dull, H. S. Mosher, *J. Org. Chem. 34* (1969) 2543.
[8] **4**: $[\alpha]_D^{20}$ −4.0 (c = 1, $CHCl_3$); **8**: $[\alpha]_D^{20}$ −3.7 (c = 0.75, $CHCl_3$); **12**: $[\alpha]_D^{22}$ −7.6 (c = 1, $CHCl_3$); **14**: $[\alpha]_D^{20}$ −27.4 (c = 0.9, $CHCl_3$); **15**: $[\alpha]_D^{23}$ −23.5 (c = 1.6, $CHCl_3$); **16**: $[\alpha]_D^{23}$ −7.6 (c = 1.2, $CHCl_3$); **21**: $[\alpha]_D^{23}$ −39.4 (c = 0.5, $CHCl_3$).
[9] E. J. Corey, A. Venkateswarlu, *J. Am. Chem. Soc. 94* (1972) 6190.
[10] E. Winterfeldt, *Synthesis 1975*, 617.
[11] R. P. Volante, *Tetrahedron Lett. 22* (1981) 3119.
[12] T. Rosen, M. Watanabe, C. H. Heathcock, *J. Org. Chem. 49* (1984) 3657.
[13] a) M. J. Miller, J. S. Bajwa, P. G. Mattingly, K. Peterson, *J. Org. Chem. 47* (1982) 4928; b) M. J. Smith, *Tetrahedron Lett. 30* (1989) 313.
[14] D. R. Morton, J. L. Thompson, *J. Org. Chem. 43* (1978) 2102.
[15] S.-J. Shiuey, J. J. Partridge, M. R. Uskokovic, *J. Org. Chem. 53* (1988) 1040.
[16] S. Hatakeyama, K. Saijo, S. Takano, *Tetrahedron Lett. 26* (1985) 865.
[17] J. K. Cha, S. C. Lewis, *Tetrahedron Lett. 25* (1984) 5263.
[18] M. Chérest, H. Felkin, N. Prudent, *Tetrahedron Lett. 1968*, 2199; K. N. Houk, S. R. Moses, Y.-D. Wu, N. G. Rondan, V. Jäger, R. Schohe, F. R. Fronczek, *J. Am. Chem. Soc. 106* (1984) 3880.
[19] S. D. Kahn, W. J. Hehre, *J. Org. Chem. 53* (1988) 301.
[20] The NMR data for **17** are identical with published values [16].
[21] The *Z* isomer of the sulfide **4** afforded exclusively cyclobutanone under the rearrangement conditions.
[22] Methylation of **17**, as described by *Fleming* et al. (I. Fleming, I. Paterson, *Synthesis 1979*, 736) led to isomer **23a** and thereby allowed the absolute configuration of the lactones **23** to be confirmed.
[23] C. W. Jefford, A. W. Sledeski, J. Boukouvalas, *Helv. Chim. Acta 72* (1989) 1362; K. Koseki, T. Ebata, H. Kawakami, H. Matsushita, Y. Naoi, K. Itoh, *Heterocycles 31* (1990) 423.

Directed Synthesis of Peptides from α-Amino Acid Esters at Metal Centers**

By *Wolfgang Beck** and *Roland Krämer*

Dedicated to Professor Viktor Gutmann on the occasion of his 70th birthday

The first directed synthesis of peptides from nonactivated α-amino acid esters at a metal center was accomplished with cobalt(III) amine complexes.[1] The cobalt atom acts as an amino protecting group and, at the same time, activates the carboxyl group.[1] However, the preparation of oligopeptides by this route is relatively laborious, since the peptide has to be liberated from the metal and isolated before it is allowed to react with the next α-amino acid ester complex of cobalt.[2]

Several metal salts, particularly those of copper(II), catalyze the formation of peptides (up to tetrapeptides) from α-amino acid esters.[3] Different α-amino acid esters, however, cannot be linked in a defined sequence; instead, a mixture of the corresponding peptides is obtained.[3,4] An interesting model for the prebiotic formation of peptides is the recently described Cu^{II}-catalyzed synthesis of peptides from α-amino acids in aqueous NaCl solution.[5]

We have now found a way to extend metal-coordinated peptide esters from the amino terminus in a controlled manner. In the course of our work on chiral organometallic compounds containing α-amino acids,[6] we obtained the diglycine ester complexes **1** and **2**, in which the amide N atom is deprotonated.

These chelate complexes react with α-amino acid esters such as Gly-OEt, L-Ala-OMe, L-Leu-OMe, L-Asp-$(OMe)_2$, and L-Ser-OMe in the presence of triethylamine at 20 °C to give the corresponding tripeptide ester complexes **3** and **4**,

[*] Prof. Dr. W. Beck, Dipl.-Chem. R. Krämer
Institut für Anorganische Chemie der Universität
Meiserstrasse 1, W-8000 München 2 (FRG)

[**] Metal Complexes Containing Biologically Important Ligands, Part 62. This work was supported by the Deutsche Forschungsgemeinschaft and the Fonds der Chemischen Industrie. We thank Professor Dr. *E. Wünsch*, Max-Planck-Institut für Biochemie, Martinsried, for amino acid analyses and for valuable and encouraging discussions. Part 61: [16].

respectively, in yields of 70–90% (crystalline products).[7] Complex **3b** was also prepared in a one-pot reaction from $[\{Cp^*RhCl_2\}_2]$ ($Cp^* = \eta^5$-C_5Me_5), Gly-Gly-OMe · HCl, and Ala-OMe with Na_2CO_3 as base (80% yield). Treatment of complexes **3b, c** (see *Experimental Procedure*) with 0.2 N methanolic HCl solution liberated the tripeptide esters L-Ala-Gly-Gly-OMe · HCl and L-Leu-Gly-Gly-OEt · HCl, respectively, which were then isolated; $[\{Cp^*RhCl_2\}_2]$ was thereby re-formed. The tripeptides in **3b, c** are formed without almost any racemization. For comparison, **3a**, which cannot be isolated in pure form, was synthesized directly from Gly-Gly-Gly-OEt and $[\{Cp^*RhCl_2\}_2]$ and characterized by X-ray structure analysis.[8] The tetrapeptide ester complex **5** is formed via a triglycine methyl ester complex as intermediate when Gly-OEt and Ser-OMe are added successively to **1a**.

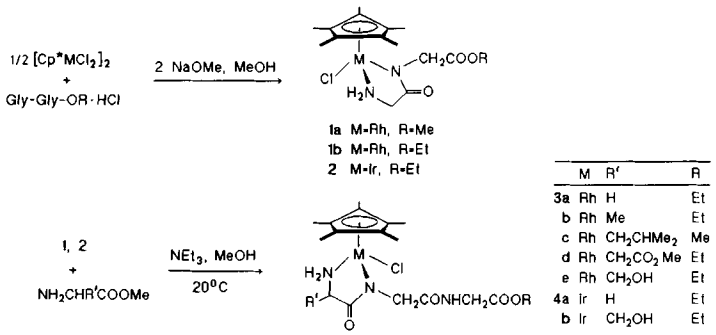

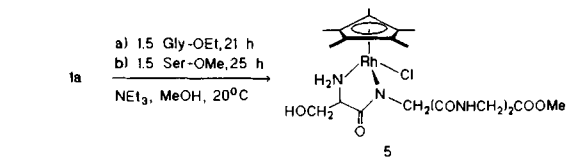

Further peptide ester complexes are formed as side products (ca. 15%) in these reactions. Independently, **5** was obtained from [Cp*(Cl)Rh(Gly-Gly-Gly-OMe − H^+)] and Ser-OMe in the presence of NEt_3 and its structure was determined by X-ray analysis.[9] The principle illustrated in Scheme 1 should allow still longer peptide chains to be constructed at the complex in a one-pot procedure.

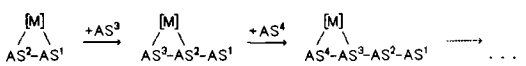

Scheme 1. AS = α-amino acid building block, AS^1 = *C*-terminal amino acid, [M] = metal complex fragment.

A template reaction is plausible for the mechanism of peptide formation. The synthesis of the tripeptide at the metal center affords complexes with three accessible (here, facially arranged) coordination sites. The crucial step is a nucleophilic attack of the coordinated amino anion in **B** on the carbonyl group of the N-coordinated amino acid ester. *Yamada* et al. have suggested such a step for peptide formation at Cu^{II}.[3c] The base serves only as catalyst. The intermediacy of **C** (M = Rh, R = Et, R′ = CH_2CO_2Me) could be established by reaction of **1b** with asparagine dimethyl ester and sodium methoxide instead of NEt_3. The complex [Cp*Rh{L-Asp(β-OMe)-Gly-Gly-OEt − $2H^+$}] (**6**) was characterized by crystal structure analysis;[10] it contains an unusual structural element, a bridgehead peptide N atom surrounded in a pyramidal fashion (sum of angles at N atom: 346.1°).[11]

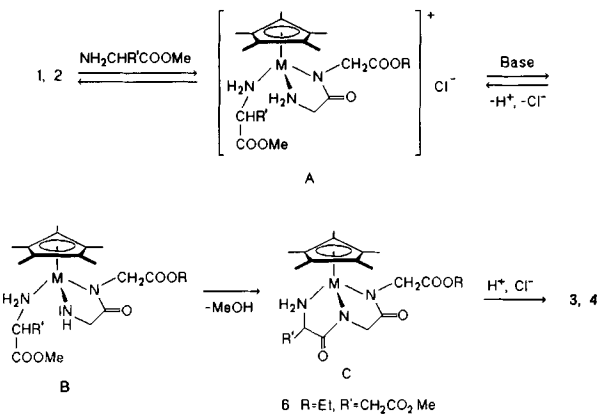

Of particular interest is the question whether optically active dipeptide ester complexes preferentially incorporate only one enantiomer of an α-amino acid ester present as a racemate. The reactions of [Cp*(Cl)Rh(L-Ala-Gly-OMe − H^+)] with D,L-Leu-OMe and D,L-Ser-OMe indicate that the tripeptide esters L-Leu-L-Ala-Gly-OMe and L-Ser-L-Ala-Gly-OMe are formed somewhat faster at the complex than the corresponding diastereoisomers D-Leu-L-Ala-Gly-OMe and D-Ser-L-Ala-Gly-OMe, respectively.

Experimental Procedure

NEt_3 (1.00 mmol, 139 μL) was added to a solution of **1a** (0.20 mmol, 84 mg; prepared from $[\{Cp^*RhCl_2\}_2]$[12], Gly-Gly-OMe · HCl, and two equivalents of NaOMe in methanol) and L-Leu-OMe (0.21 mmol, 32 μL) in 5 mL of absolute methanol. The reaction mixture was stirred for 15 h at 20°C and then concentrated to about 0.5 mL. Addition of 20 mL of ether and 30 mL of hexane resulted in precipitation of the orange complex. The isolated and dried complex **3c** (yield 92%) was dissolved in 5 mL of 0.2 N methanolic HCl and the solution was then concentrated to about 1.5 mL and kept at −78°C for 2 h. The precipitate of $[\{Cp^*RhCl_2\}_2]$ was filtered off and the filtrate was concentrated to about 0.5 mL and treated with 50 mL of ether. The resulting solution was cooled with liquid nitrogen until it began to solidify and then allowed to warm to room temperature with stirring. The precipitated tripeptide ester hydrochloride was centrifuged, washed with 30 mL of $CHCl_3$/hexane (1/1), and reprecipitated from methanol/ether (yield 61% based on **1a**). ^1H NMR of L-Leu-Gly-Gly-OMe · HCl [13] (400 MHz, CD_3OD, 22°C, TMS): δ = 3.92 (m, 1H, partly overlapped; Leu-Hα), 1.7 (m, 3H; CH-CH_2, $CH(CH_3)_2$), 1.01 (m, 6H; $CH(CH_3)_2$), 3.92, 4.05 (d, $^2J(H,H)$ = 16.3 Hz, 1H; $NHCOCH_2$, diastereotopic), 3.98 (s, 2H; $CH_2CO_2CH_3$), 3.72 (s, 3H; CO_2CH_3).

Amino acid analysis [14]: $Leu_{0.87}Gly_2$. TLC (*n*BuOH/glacial acetic acid/water 4/1/1; silica gel): R_f = 0.47. Gas-chromatographic racemate test [15]: 1.5% D-Leu-OMe. Racemate test for L-Ala-Gly-Gly-OEt · HCl isolated from **3b**: 1.0% D-Ala.

The reaction of [Cp*Rh(Cl)(L-Ala-Gly-OMe · HCl)] with D,L-Leu-OMe or D,L-Ser-OH was carried out analogously to the preparation **3c**. The reaction times were chosen so that only a small amount of the added amino acid ester reacted. After 3.5 and 2 h, respectively, the complexes were isolated and treated with 0.2 N methanolic HCl solution. In the liberated peptide esters (nonreacted serine methyl ester could not be separated quantitatively from the complex), amino acid ratios of $Leu_{0.15}Ala_{0.96}Gly_{1.00}$ and $Ser_{0.60}Ala_{0.98}Gly_{1.00}$, respectively, and L-proportions of L-Leu (52.3%)/L-Ala (99.1%) and L-Ser (61.3%)/L-Ala (99.1%), respectively, were determined.

Received: April 25, 1991 [Z 4594 IE]
German version: *Angew. Chem. 103* (1991) 1492

[1] D. A. Buckingham, L. G. Marzilli, A. M. Sargeson, *J. Am. Chem. Soc. 89* (1967) 2772; J. P. Collman, E. Kimura, *ibid. 89* (1967) 6096; P. A. Sutton, D. A. Buckingham, *Acc. Chem. Res. 20* (1987) 357.
[2] D. R. Knighton, D. R. K. Harding, M. J. Friar, W. S. Hancock, G. D. Reynolds, C. R. Clark, R. F. Tasker, D. A. Buckingham, *J. Am. Chem. Soc. 103* (1981) 7025.

[3] a) S. Yamada, M. Wagatsuma, Y. Takeuchi, S. Terashima, *Chem. Pharm. Bull. 19* (1971) 2380; S. Yamada, S. Terashima, M. Wagatsuma, *Tetrahedron Lett. 1970*, 1501; b) S. Terashima, M. Wagatsuma, S. Yamada, *Tetrahedron 29* (1973) 1487; c) M. Wagatsuma, S. Terashima, S. Yamada, *ibid. 29* (1973) 1497.
[4] H. Schmidt, *Diplomarbeit*, Universität München 1984; M. Maurus, *Diplomarbeit*, Universität München 1991.
[5] M. G. Schwendinger, B. M. Rode, *Anal. Sci. 5* (1989) 411; B. M. Rode, *Spektrum Wiss. 1991*, No. 3, p. 26; B. M. Rode, M. G. Schwendinger, *Origins Life Evol. Biosphere 20* (1990) 401.
[6] R. Krämer, K. Polborn, H. Wanjek, I. Zahn, W. Beck, *Chem. Ber. 123* (1990) 767; W. Beck, W. Petri, *J. Organomet. Chem. 127* (1977) C 40. Cf. also D. Carmona, A. Mendoza, F. J. Lahoz, L. A. Oro, M. P. Lamata, E. San Jose, *ibid. 396* (1990) C 17.
[7] a) In **3**–**5** (CD_3OD solution, 20 °C), the epimerization at the metal atom is fast on the NMR time scale. For the complexes [Cp*(Cl)M(L-amino acid anion)], M = Rh, Ir, on the other hand, the expected diastereoisomers (S_cR_m, S_cS_m) were detected by NMR spectroscopy [6]; b) We found that the corresponding complexes with coordinated glycinamide and glycinate as bidentate ligands also react with α-amino acid esters according to this principle.
[8] B. Wagner, R. Krämer, W. Beck, unpublished. The synthesis and structure of a comparable complex, [(η^6-C_6H_6)(Cl)Ru(Gly-Gly-Gly-OH − H^+)] has been described: W. S. Sheldrick, S. Heeb, *J. Organomet. Chem. 377* (1989) 357.
[9] K. H. Sünkel, R. Krämer, W. Beck, unpublished.
[10] C. Robl, R. Krämer, W. Beck, unpublished.
[11] As in free peptides, the coordinated, deprotonated peptide N atoms here usually show planar environments: H. C. Freeman, *Adv. Protein Chem. 22* (1967) 257; H. Sigel, R. B. Martin, *Chem. Rev. 82* 385; S. H. Laurie in G. Wilkinson, R. D. Gillard, J. A. McCleverty (Eds.): *Comprehensive Coordination Chemistry, Vol. 2*, Pergamon, Oxford 1987, p. 759.
[12] J. W. Kang, K. Moseley, P. M. Maitlis, *J. Am. Chem. Soc. 91* (1969) 5970; B. L. Booth, R. N. Haszeldine, M. Hill, *J. Chem. Soc. A 1969*, 1299.
[13] The ^1H NMR data are similar to those of Leu-Gly-GlyH · HCl. Cf. M. Anteunis, R. Callens, *J. Magn. Reson. 15* (1974) 317.
[14] Hydrolysis with half-concentrated hydrochloric acid; amino acid analyzer Biotronic LC 6001.
[15] The racemate test was performed with the N-(pentafluoropropionyl)-amino acid propyl esters on Chirasil-Val® (Carlo Erba HR GC 4160): H. Frank, G. J. Nicholson, E. Bayer, *J. Chromatogr. 167* (1978) 187.
[16] I. Zahn, K. Polborn, W. Beck, *J. Organomet. Chem. 412* (1991) 397.

Synthesis of Ethenyl(phenyl)iodonium Triflate, $[H_2C{=}CHIPh][OSO_2CF_3]$, and Its Application as a Parent Vinyl Cation Equivalent**

By *Peter Stang** and *Jörg Ullmann*

Dedicated to Professor Michael Hanack on the occasion of his 60th birthday

Vinylations are well recognized and widely employed in organic chemistry. However, most known vinylating agents are nucleophilic, such as vinylmetals of the first and second main-group elements as well as vinylsilanes and -stannanes.[1] Vinylations have also been carried out with acetylene[2] and by metal-catalyzed processes.[3] However, there are only few examples for the electrophilic introduction of the parent vinyl moiety (e.g., vinyl ethers, acetates, and halides[1]).

Ethenyl(phenyl)iodonium triflate (**3**) is a novel electrophilic vinylating agent with promising applications in vinylation reactions that are not covered by the known reagents mentioned above. For example, **3** may be employed to synthesize the hitherto unknown parent vinyl triflate (**4**),[4] a possible precursor for the generation of the parent vinyl cation[5] as well as for metal-catalyzed vinylic couplings.[6] Compound **3** should also undergo oxidative addition to organometallic substrates, serving formally as a vinyl cation equivalent. Such a synthesis complements the more traditional methods for the introduction of the σ-bonded parent vinyl substituent into organometallic complexes, mainly the use of vinylmagnesium bromide in displacement reactions[7] and the equilibration of π-ethene complexes.[7a, 8]

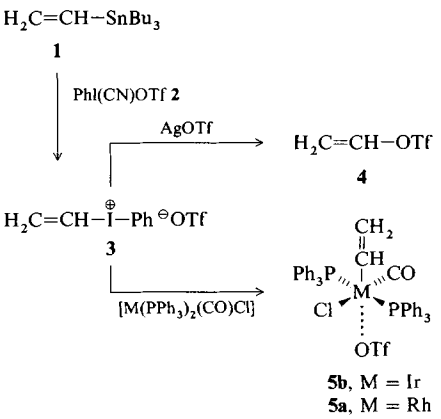

Salt **3** was obtained from tri-*n*-butyl(vinyl)tin (**1**) and cyano(phenyl)iodonium triflate (**2**) in 75% isolated yield.[9, 10] The previously unknown parent vinyl triflate (**4**) was formed from **3** by cleavage of the C–I bond in the presence of catalytic amounts of silver triflate. Isolation of **4** was possible from benzonitrile by distilling **4** directly from the reaction mixture (15 to 20% yield). Compound **4** is fully characterized. Noteworthy is the ^{13}C NMR spectrum, where the signals of the vinyl carbons of **4** have changed positions with respect to **3** (**3**, $\delta_{CH_2} = 133.4$, $\delta_{CH} = 109.5$; **4**, $\delta_{CH_2} = 106.4$, $\delta_{CH} = 143.5$).

Iodonium salt **3** is also a strong electrophilic substrate in organometallic reactions. Treatment of Vaska's complex or its rhodium analogue with **3** yields the new octahedral hexacoordinate rhodium and iridium species **5a**, **b** in 84 and 75% yield, respectively. The IR spectrum reveals a strong CO vibration at $\tilde{\nu} = 2063\ cm^{-1}$ for **5a** and at $\tilde{\nu} = 2088\ cm^{-1}$ for **5b**. In the far-infrared region of **5a**, an Ir–Cl stretch at $\tilde{\nu} = 307\ cm^{-1}$ indicates a *trans* arrangement between the Cl and CO ligands.[12] Likewise, the *trans* relationship of the phosphane ligands and the octahedral symmetry is confirmed in the ^{31}P NMR spectrum by the typical high-field position of the Rh doublet ($\delta = 15.1$) for **5b** and the singlet ($\delta = -8.3$) for **5a**.

The introduction of the parent vinyl substituent into organometallic substrates via **3** constitutes a significant change in methodology. Rather than vinylmagnesium bromide reacting as a nuclephile due to the carbanionic character of the vinyl substituent, **3** shows an umpolung of the vinyl reactivity, making it employable as an electrophile in oxidative additions. Traditionally, oxidative additions are well established as a method for the introduction of alkyl substituents,[13] but could not be used for vinylations owing to the unreactivity of simple vinyl substrates.[14]

Other applications of **3** are under investigation (e.g., cycloadditions). Preliminary results show that **3** reacts with cyclopentadiene. Isolation of the expected product, however, is not possible owing to the thermal instability of alkyliodonium salts.

[*] Prof. Dr. P. J. Stang, Dr. Jörg Ullmann
Department of Chemistry, University of Utah
Salt Lake City, UT 84112 (USA)

[**] This work was supported by the National Cancer Institute of the National Institutes of Health (2ROCA16903). *J. U.* thanks the Alexander von Humboldt Foundation for the award of a Feodor Lynen Fellowship.

Experimental Procedure

3: Salt **2** [10] (0.60 g, 1.58 mmol), suspended in CH_2Cl_2 (30 mL) under N_2, was cooled to $-40\,^{\circ}C$. Compound **1** [15] (0.46 mL, 1.58 mmol), dissolved in CH_2Cl_2 (10 mL), was added dropwise. After the addition was complete, the cooling bath was removed and the heterogeneous mixture was allowed to warm to room temperature, turning into a clear, slightly yellow solution. By adding hexane under vigorous stirring, a yellowish oil separated out and was washed with hexane twice to remove tri-*n*-butyltin cyanide. Crystallization occurred by adding the oil, dissolved in a small amount of CH_2Cl_2, to vigorously stirring hexane. After decantation of the solvent, the precipitate was dried in vacuo, yielding 0.45 g (1.18 mmol; 75%) of white microcrystalline **3**. M.p. 32 °C. ^{1}H NMR (300 MHz, CD_2Cl_2): $\delta = 6.22$ (dd, $J_{H\text{-}1,H\text{-}2} = 5.2$, $J_{H\text{-}1,H\text{-}3} = 15.0$ Hz, 1H; H-1), 6.95 (dd, $J_{H\text{-}2,H\text{-}1} = 5.2$, $J_{H\text{-}2,H\text{-}3} = 6.8$ Hz, 1H; H-2, *trans* to I), 7.20 (dd, $J_{H\text{-}3,H\text{-}2} = 6.8$, $J_{H\text{-}3,H\text{-}1} = 15$ Hz, 1H; H-3, *cis* to I), 7.57 (t, $J = 7.8$ Hz, 2H; H_{meta}), 7.75 (*t*, $J = 7.3$ Hz, 1H; H_{para}), 7.99 (d, $J = 8.4$ Hz, 2H; H_{ortho}). ^{13}C NMR (75 MHz, CD_2Cl_2): $\delta = 109.5$ (s; =CH), 110.1 (s; C_{arom}), 120.5 (q, $J_{C,F} = 320$ Hz; CF_3), 132.5, 133.2, 136.6 (3s; CH_{arom}), 133.4 (s; $=CH_2$). IR [16]: $\tilde{\nu}$ [cm^{-1}] = 3087, 3072, 3004, 2946, 1588, 1568, 1474, 1446, 1379, 1253, 1223, 1165, 1156, 1025, 992, 733. MS(FAB): *m/z* 231 ($M^{\oplus}$). High-resolution MS: calcd for $C_9H_8F_3IO_3S^{\oplus}$, 230.96707; found, 230.96655.

4 [17]: To **3** (0.84 g, 2.21 mmol), dissolved in benzonitrile, was added 10 mol % of silver triflate (0.06 g). After the mixture was stirred for 3 d, colorless **4** (0.06 g, 0.34 mmol) was distilled off in 15% yield. B.p. 80 °C. ^{1}H NMR (300 MHz, CD_3CN): $\delta = 5.14$ (dd, $J_{H\text{-}2,H\text{-}3} = 3.7$, $J_{H\text{-}2,H\text{-}1} = 5.5$ Hz; H-2, *trans* to OTf), 5.36 (dd, $J_{H\text{-}3,H\text{-}2} = 3.7$, $J_{H\text{-}3,H\text{-}1} = 13.0$ Hz, 1H; H-3, *cis* to OTf), 6.84 (dd, $J_{H\text{-}1,H\text{-}2} = 5.5$, $J_{H\text{-}1,H\text{-}3} = 13.1$ Hz, 1H; H-1). ^{13}C NMR (75 MHz, CD_3CN): $\delta = 106.4$ (s; $=CH_2$), 119.4 (q, $J_{C,F} = 319$ Hz; CF_3), 143.5 (s; =CH). IR: $\tilde{\nu}$ [cm^{-1}] = 3111, 2994, 1646, 1428, 1309, 1250, 1215, 1145, 1086, 963, 798; MS(EI): *m/z* 176 ($M^{\oplus}$). High-resolution MS: calcd for $C_3H_3F_3O_3S^{\oplus}$, 175.97550; found, 175.97532.

5: $[M(PPh_3)_2(CO)Cl]$ [18] (13 mg, M = Rh; 15 mg, M = Ir; 0.019 mmol) was stirred with **3** (8.7 mg, 0.023 mmol) in C_6H_6 (20 mL) at room temperature for 30 min (for **5a**) or 5 h (for **5b**) under N_2 and with protection from light. Precipitation with hexane afforded **5** containing small impurities of decomposed **3**. After recrystallization from CH_2Cl_2/hexane (or ether/hexane), **5a** is obtained as off-white crystals in 84% yield and **5b** as yellow crystals in 75% yield. **5b**: M.p. 178–210 °C (dec). ^{1}H NMR (300 MHz, CD_2Cl_2): $\delta = 4.43$ (dm, $J_{H\text{-}3,H\text{-}1} = 16.4$ Hz, 1H; H-3, *cis* to Ir), 5.41 (dm, $J_{H\text{-}2,H\text{-}1} = 8.2$ Hz, 1H; H-2, *trans* to Ir), 6.67 (dd, $J_{H\text{-}1,H\text{-}2} = 8.3$, $J_{H\text{-}1,H\text{-}3} = 16.5$ Hz, 1H; H-1). ^{31}P NMR (121 MHz, CD_2Cl_2): $\delta = -8.3$. IR [16]: $\tilde{\nu}$ [cm^{-1}] = 3061, 2063, 1579, 1484, 1436, 1315, 1265, 1230, 1202, 1093, 1004, 744, 693. MS(FAB): *m/z* 807 [$M^{\oplus} - OTf$]. High-resolution MS: calcd for $C_{39}H_{33}ClIrOP_2^{\oplus}$, 807.13280; found 807.13285. **5b**: M.p. 55–120 °C (dec). ^{1}H NMR (300 MHz, CD_2Cl_2): $\delta = 4.40$ (dm, $J_{H\text{-}3,H\text{-}1} = 16.4$ Hz, 1H; H-3, *cis* to Rh), 4.97 (m, 1H; H-2, *trans* to Rh), 6.67 (m, 1H; H-1), 7.39–7.82 (m, 30H; H_{arom}). ^{31}P NMR (121 MHz, CD_2Cl_2): $\delta = 15.1$ (d, $^1J_{P,Rh} = 88.5$ Hz). IR [16]: $\tilde{\nu}$ [cm^{-1}] = 3069, 2088, 1574, 1482, 1436, 1324, 1259, 1233, 1204, 1171, 1029, 1016, 746, 692, 685. MS(FAB): *m/z* 627 $[Rh(PPh_3)_2^{\oplus}]$. High-resolution MS: calcd for $C_{36}H_{30}P_2Rh^{\oplus}$, 627.08778; found, 627.08708.

Received: April 29, 1991 [Z 4597 IE]
Publication delayed at authors' request
German version: *Angew. Chem. 103* (1991) 1549

[1] For a review see: T. Ohnuma, *Yuki Gosei Kagaku Kyokaishi 41* (1983) 768; *Chem. Abstr. 99* (1983) 157378w. Recent papers include: N. P. Lebedeva, I. V. Kalaus, *Khim Geterotsikl. Soedin. 1989*, 856; *Chem. Abstr. 112* (1990) 178801f; V. D. Sheludyakov, V. I. Zhun, M. I. Shumilin, V. N. Bochkarev, T. F. Slyusarenko, *Zh. Obshch. Khim. 58* (1988) 1583; *Chem. Abstr. 110* (1989) 212906q; K. Tamao, K. Maeda, T. Yamaguchi, Y. Ito, *J. Am. Chem. Soc. 111* (1989) 4984.

[2] a) B. A. Trofimov, S. E. Korostova, S. G. Shevchenko, E. A. Polubentsev, A. I. Mikhaleva, *Zh. Org. Khim. 26* (1990) 1110; *J. Org. Chem. USSR Engl. Transl. 26* (1990) 956; b) B. V. Trzhtsinskaya, N. D. Abramova, E. V. Rudakova, A. V. Afonin, V. V. Keiko, *Izv. Akad. Nauk SSSR, Ser. Khim. 1988*, 1882; *Chem. Abstr. 110* (1989) 231516d.

[3] See, for example: a) F. L. Wang, W. Ueda, Y. Morikawa, T. Ikawa, *Chem. Lett. 1989*, 281; b) K. Karabelas, A. Hallberg, *J. Org. Chem. 53* (1988) 4909; c) A. Arcadi, E. Bernocchi, A. Burini, S. Cacchi, F. Marinelli, B. Pietroni, *Tetrahedron Lett. 30* (1989) 3465, and references cited therein.

[4] P. J. Stang, M. Hanack, L. R. Subramanian, *Synthesis 1982*, 85.

[5] a) P. J. Stang, Z. Rappoport, M. Hanack, L. R. Subramanian: *Vinyl Cations*, Academic Press, New York 1979; b) P. Vogel: *Carbocation Chemistry*, Elsevier, Amsterdam 1985.

[6] J. M. Brown, N. A. Cooley, *Chem. Rev. 88* (1988) 1031, and references therein.

[7] For some recent papers, see: a) P. O. Stoutland, R. G. Bergman, *J. Am. Chem. Soc. 110* (1988) 5732; b) J. Martinez, J. B. Gill, H. Adams, N. A. Bailey, J. M. Saez, G. J. Sunley, P. M. Maitlis, *J. Organomet. Chem. 394* (1990) 583.

[8] Some recent examples: a) P. O. Stoutland, R. G. Bergman, *J. Am. Chem. Soc. 107* (1985) 4581; b) T. W. Bell, D. M. Haddleton, A. McCanley, M. G. Partridge, R. N. Perutz, H. Willner, *ibid. 112* (1990) 9212.

[9] The formation of bis(ethenyl)phenyliodonium hexachlorostannate from trichloro(vinyl)tin and iodosobenzene dichloride in 5% yield was reported previously. A. N. Nesmeyanov, T. P. Tolstaya, A. V. Petrakov, *Dokl. Akad. Nauk SSSR 197* (1971) 1337; *Dokl. Chem. Engl. Transl. 197* (1971) 343. Several other counterions were introduced by anion exchange.

[10] Compound **2**, a mild iodonium transfer reagent, was developed recently: V. V. Zhdankin, C. M. Crittell, P. J. Stang, N. S. Zefirov, *Tetrahedron Lett. 31* (1990) 4828. It offers an elegant way to prepare several new classes of alkynyl(phenyl)iodonium triflates [11].

[11] a) P. J. Stang, V. V. Zhdankin, *J. Am. Chem. Soc. 112* (1990) 6437; *ibid. 113* (1991) 4571; b) P. J. Stang, J. Ullmann, *Synthesis 1991*, in press.

[12] a) J. P. Collman, C. T. Sears, *Inorg. Chem. 7* (1968) 27; b) J. M. Jenkins, B. L. Show, *J. Chem. Soc. 1965*, 6789.

[13] F. R. Hartley, S. Patai (Eds.): *The Chemistry of the Metal Carbon Bond*, Wiley, London 1985.

[14] a) Z. Rappoport, *Recl. Trav. Chim. Pays-Bas 104* (1985) 309; b) Z. Rappoport, *Acc. Chem. Res. 14* (1981) 7; c) P. J. Stang, A. K. Datta, *J. Am. Chem. Soc. 111* (1989) 1358.

[15] D. Seyferth, F. G. A. Stone, *J. Am. Chem. Soc. 79* (1957) 515.

[16] Powder, dispersed between NaCl plates.

[17] The parent vinyl nonaflate was obtained by reacting nonafluorobutanesulfonic acid with acetylene. E. Eckes, L. R. Subramanian, M. Hanack, *Tetrahedron Lett. 1973*, 1967. No yield was reported.

[18] a) D. Evans, J. A. Osborn, G. Wilkinson, *Inorg. Synth. 11* (1968) 99; b) K. Vrieze, J. P. Collman, C. T. Sears, M. Kubota, *ibid. 11* (1968) 101.

Fischer Carbene Complexes Facilitate the Intramolecular Pauson–Khand Reaction**

By *Francisco Camps, Josep M. Moretó,* Susagna Ricart,* and *Josep M. Viñas*

The $[Co_2(CO)_8]$-mediated carbonylative cycloaddition of acetylenes and olefins (Pauson–Khand reaction) is one of the most straightforward methods for preparation of cyclopentenone derivatives.[1] This procedure has been successfully applied to the synthesis of a variety of bioactive natural products.[2] Recently, the first efficient enantioselective synthesis of a hirsutene precursor has also been reported.[3]

However, there are still some unsolved drawbacks that limit the scope of application of the Pauson–Khand reaction. For example, low yields are often obtained owing to the high temperatures required to further activate the alkyne–$Co_2(CO)_6$ intermediate complex, which, in addition, may preclude the presence of certain thermally labile moieties in the starting reagents. To overcome these problems, different modifications have been put forth such as the use of silica gel,[4] nitrogen oxides,[5] sonication,[6] or UV irradiation.[7] Yields can be substantially improved in intramolecular reactions.[2–5, 7, 8] As an example of its potential practical importance, an efficient catalytic synthesis of jasmone by application of this reaction has been recently published.[9]

In connection with our current studies of the applications of Fischer carbene complexes to organic synthesis, we have proved, in agreement with results described by other authors,[10] that a triple bond conjugated to a transition-metal carbene moiety becomes highly polarized, resulting in easy

[*] Dr. J. M. Moretó, Prof. Dr. F. Camps, Dr. S. Ricart, Dr. J. M. Viñas
Departament de Química Orgànica Biològica
Consell Superior d'Investigacions Cientifiques
Centre d'Investigació i Deseuvolupament
J. Girona, 18–26, E-08034 Barcelona (Spain)

[**] This work was supported by Direccion General de Investigación Científica y Técnica (DGICYT) (Project No. PB87-0201-C-03-03). *J. M. V.* thanks the Spanish Ministry of Education and Science for a postdoctoral fellowship.

cycloadditions and Michael additions with a variety of substrates.[11] We anticipated that this approach might be used to facilitate the intramolecular Pauson–Khand reaction by activation of the corresponding acetylenic moiety in a similar strategy to that reported for analogous olefin complexes in Diels–Alder cycloadditions.[12]

When alkynyl allylamino carbene complexes **1a–d** were treated with one equivalent of $[Co_2(CO)_8]$ in dry THF *for a few hours at room temperature*, the expected cyclopentenone derivatives **2a–d** were obtained in 70–75% yields. Moderate yields of tricyclic derivative **2e** were obtained by performing the reaction with cyclohexenylamine complex **1e** (Table 1).

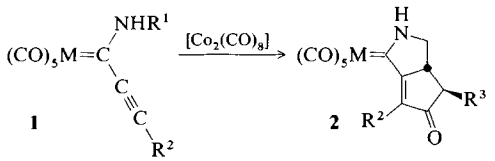

1 **2**

	M	R^1	R^2	R^3
a	W		Ph	H
b	Cr		Ph	H
c	W		Et	H
d	W	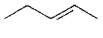	Ph	Me
e	W		Ph	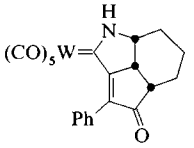

2e

Table 1. Pauson-Khand reaction at alkynyl allylamino carbene complexes **1** to give cyclopentenone derivatives **2**.

Enyne complex	Reaction time [h]	Product	Yield [%]
1a	3	**2a**	75
1b	3	**2b**	72
1c	2.5	**2c**	70
1d	2	**2d**	72
1e	12	**2e**	35
1f	8	**3**	84

Surprisingly, unlike the report of previous authors on high yields of Pauson–Khand cycloadducts from trimethylsilylacetylenic derivatives,[13, 2b, c, g] carbene complex **1f** afforded only $[Co_2(CO)_6]$–alkyne complex **3** in good yields. We attribute this failure mainly to the steric encumbrance of the trimethylsilyl group, which should push the olefin moiety towards coordination with the transition metal of the carbene.

The activating role of the carbene-metal functionality was made clear by an independent experiment in which one equivalent of the enyne amide was stirred with one equivalent of $[Co_2(CO)_8]$ in dry THF for three days at room tem-

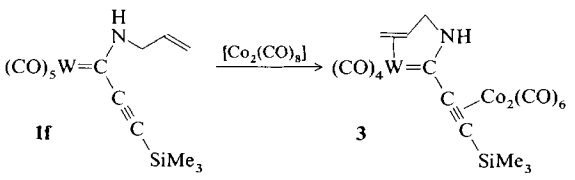

1f **3**

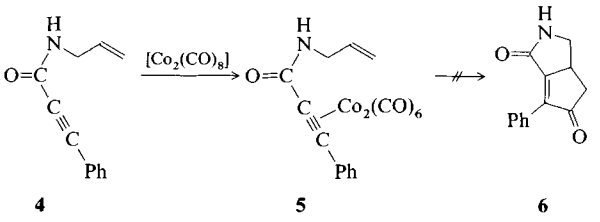

4 **5** **6**

perature and the $[Co_2(CO)_6]$–amide complex **5** was obtained instead of the expected cycloadduct **6**.

A few remarkable points deserve further comment. Good yields of cycloaddition products are obtained despite the fact that disubstituted acetylenes bearing electron-withdrawing substituents (the metal-carbene group may be considered to fall into this category) usually give mainly linear diene adducts and low yields of cycloadducts.[1, 13] Furthermore, the reaction occurs at room temperature with high stereoselectivity (in cases **2d** and **2e** the formation of only one stereoisomer was detected[14]). This stereoselectivity control might be expected from the defined coordination geometries around both metal centers.

In conclusion, we have proved that intramolecular Pauson–Khand reactions can be efficiently performed on a metal-carbene-activated enyne derivative in a stereoselective manner under very mild conditions. The resulting cycloadducts still bearing the Fischer carbene functionality may be used to carry out further reactions (such as benzannulation[15] or cyclopropanation[16]).

Experimental Procedure

$[Co_2(CO)_8]$ (1 mmol) was added to the allylamino carbene complex (1 mmol) in 25 mL of dry THF and the reaction mixture was left at room temperature for 2–12 h (Table 1). The reaction course was monitored by thin layer chromatography (hexane/ethyl acetate 2/1). After the starting product had completely disappeared, the solvent was removed and the residue passed through a flash chromatography column using the mentioned eluent. The cyclopentenone complexes crystallize upon concentration. All compounds (**2a–e, 3**) gave satisfactory spectroscopic data and elemental analysis. Those for **2d** and **2e** are given as representative: **2d**: IR ($CHCl_3$): $\tilde{\nu}$ [cm^{-1}] = 2058(m), 1989(w), 1943(vs), 1925(sh), 1755(m), 1725(m); ^1H NMR (300 MHz, $CDCl_3$): δ = 9.05 (br. s, 1H), 7.45 (m, 5H), 4.12 (ddd, J = 2.1, 8.4, 11.4 Hz, 1H), 3.53 (dd, J = 8.1, 11.4 Hz, 1H), 3.25 (ddd, J = 4.2, 8.4, 8.1 Hz, 1H), 2.54 (dq, J = 7.3, 4.2 Hz, 1H), 1.39 (d, J = 7.3 Hz, 3H); ^{13}C NMR (75.4 MHz, $CDCl_3$): δ = 232.9, 209.7, 202.7, 198.2, 178.1, 143.0, 131.9, 131.2, 131.1, 129.3, 128.5, 59.6, 51.4, 47.6, 13.7. **2e**: IR ($CHCl_3$): $\tilde{\nu}$ [cm^{-1}] = 2060(m), 1970(w), 1920(vs), 1705(m); ^1H NMR (80 MHz, $(CD_3)_2CO$): δ = 9.02 (br.s, 1H), 7.45 (m, 5H), 4.25 (dd, J = 8, 16 Hz, 1H), 3.5 (t, J = 8 Hz, 1H), 3.0 (dd, J = 8, 16 Hz, 1H), 1.1–2.8 (m, 6H); ^{13}C NMR (75.4 MHz, $CDCl_3$): δ = 363.3, 210.9, 201.9, 197.5, 174.9, 145.0, 130.3, 130.2, 129.5, 128.4, 63.8, 45.7, 43.1, 31.2, 25.8, 20.0.

Received: June 3, 1991 [Z 4683 IE]
German version: *Angew. Chem. 103* (1991) 1540

CAS Registry numbers:
1a, 136658-86-1; **1b**, 136658-87-2; **1c**, 136675-75-7; **1d**, 136658-88-3; **1e**, 136658-89-4; **1f**, 136658-98-7; **2a**, 136658-91-8; **2b**, 136658-92-9; **2c**, 136658-93-0; **2d**, 136658-94-1; **2e**, 136675-76-8; **3**, 136658-95-2; $[Co_2(CO)_8]$, 10210-68-1.

[1] a) P. L. Pauson, *Tetrahedron 41* (1985) 5855; b) N. E. Schore, *Chem. Rev. 88* (1988) 1081.

[2] a) N. E. Schore, E. G. Rowley, *J. Am. Chem. Soc. 110* (1988) 5224; b) P. Magnus, L. M. Principe, M. J. Slater, *J. Org. Chem. 52* (1987) 1483; c) P. Magnus, C. Exon, P. Albaugh-Robertson, *Tetrahedron 41* (1985) 5861; d) D. C. Billington, P. L. Pauson, *Organometallics 1* (1982) 1560; e) D. C. Billington, *Tetrahedron Lett. 24* (1983) 2905; f) J. Mulzer, K. D. Graske, B. Kirste, *Liebigs Ann. Chem. 1988*, 891; g) P. Magnus, D. P. Becker, *J. Am. Chem. Soc. 109* (1987) 7945; h) H. Jaffer, P. L. Pauson, *J. Chem. Res. (S) 1983*, 244.

[3] J. Castro, H. Sörensen, A. Riera, C. Morin, A. Moyano, M. A. Pericás, A. E. Greene, *J. Am. Chem. Soc. 112* (1990) 9388.

[4] S. O. Symonian, W. A. Smit, A. S. Gybin, A. S. Shashkov, G. S. Mikaelian, V. A. Tarasov, I. I. Ibragimov, R. Caple, D. E. Froen, *Tetrahedron Lett. 27* (1986) 1245.

[5] S. Shambayati, W. E. Crowe, S. L. Schreiber, *Tetrahedron Lett. 31* (1990) 5289.
[6] D. C. Billington, I. M. Helps, P. L. Pauson, W. Thomson, D. Willison, *J. Organomet. Chem. 354* (1988) 233.
[7] S. C. Brown, P. L. Pauson, *J. Chem. Soc. Perkin Trans. 1 1990*, 1205.
[8] N. E. Schore, M. C. Croudace, *J. Org. Chem. 46* (1981) 5436.
[9] V. Rautenstrauch, P. Mégard, J. Conesa, W. Küster, *Angew. Chem. 102* (1990) 1441; *Angew. Chem. Int. Ed. Engl. 29* (1990) 1413.
[10] W. D. Wulff, K. S. Chan, *J. Am. Chem. Soc. 108* (1986) 5229.
[11] a) F. Camps, J. M. Moretó, S. Ricart, J. M. Viñas, E. Molins, C. Miravitlles, *J. Chem. Soc. Chem. Commun. 1989*, 1560; b) F. Camps, A. Llebaría, J. M. Moretó, S. Ricart, J. M. Viñas, *Tetrahedron Lett. 31* (1990) 2479; c) K. L. Faron, W. D. Wulff, *J. Am. Chem. Soc. 110* (1988) 8727; d) E. O. Fischer, H. J. Kalder, *J. Organomet. Chem. 131* (1977) 57; e) F. Camps, A. Llebaría, J. M. Moretó, S. Ricart, J. M. Viñas, J. Ros, R. Yáñez, *ibid. 401* (1991) C17; f) H. Fischer, T. Meisner, J. Hofmann, *Chem. Ber. 123* (1990) 1799.
[12] K. H. Dötz, R. Noack, K. Harms, G. Müller, *Tetrahedron 46* (1990) 1235.
[13] M. E. Krafft, C. A. Juliano, I. L. Scott, C. Wright, M. D. McEachin, *J. Am. Chem. Soc. 113* (1991) 1693.
[14] The structural assignment has been made on basis of NMR data as well as structural and mechanistic considerations. Particular significance has been given to the different coupling constants for **2d** and **2e** for the bridgehead proton with the vicinal α-ketonic proton. These values (J = 4.2 Hz for **2d** and J = 8 Hz for **2e**), although slightly higher than those reported by *Schore* et al. for related organic structures (N. E. Schore, M. J. Kundsen, *J. Org. Chem. 52* (1987) 569), are complementary and in the same order of assignment (the larger for the *cis*-vicinal coupling constant and the smaller for the corresponding *trans*). Furthermore, the stereoisomers thus obtained are those which are to be expected starting from a *trans* olefin (*E*-crotylamine) and a *cis* one (2-cyclohexenylamine) in a stereospecific process.
[15] K. H. Dötz, *Angew. Chem. 96* (1984) 573; *Angew. Chem. Int. Ed. Engl. 23* (1984) 587.
[16] A. Wienandt, H. U. Reissig, *Organometallics 9* (1990) 3133, and references therein.

Crown Ethers with a Lewis Acidic Center: A New Class of Heterotopic Host Molecules**

By *Manfred T. Reetz,* Christof M. Niemeyer,* and *Klaus Harms*

Many cation-selective crown ethers and cryptands are known,[1] but only a few host compounds bind anions selectively. Naturally, the latter are electronically inverse macrocycles that usually contain suitably positioned protonated or quaternary nitrogen functions.[2] Here we report a new class of anion-selective receptors, **2**, which in addition to a conventional crown ether moiety for complexation of cations, contain a σ-bonded Lewis acidic metal center—in this case, boron— for complexation of anions. Our concept is based on the expectation that, for example, potassium salts, KX (X = F, Cl, Br, I, SCN, CN, OCH_3) should be able to bind to the host **2** in either a monotopic (**3**) or a heterotopic (**4**) fashion. The selectivity would then be governed by quite diverse factors, such as the strength of the B–X bond in the ate complex **4**, the lattice energy of the salt KX, Coulomb and van der Waals interactions, and solvent effects.

Since potassium salts were to be investigated first, we chose the 21-membered crown ether **2**, which contains six oxygen atoms. The aryl bromide **1a** was used for its synthesis.[4] The corresponding aryllithium compound was borylated with $B(OCH_3)_3$ and the crude product was hydrolyzed to

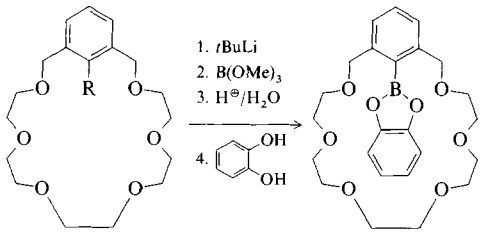

1a, R = Br
1b, R = H

2

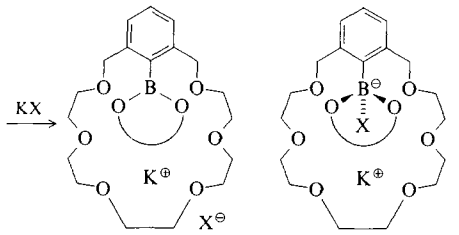

3 **4**

a, X = F; **b**, X = Cl; **c**, X = Br; **d**, X = I
e, X = SCN; **f**, X = CN; **g**, X = OCH_3;

give the arylboronic acid.[5] Treatment of the acid with catechol finally led to the target compound **2** (>95% overall yield), which is stable and easy to handle under an inert atmosphere.

In the first complexation experiment, host **2** was added to a suspension of dry KF (excess) in dichloromethane at room temperature. A stoichiometric amount of the otherwise insoluble salt dissolved within 4 h with quantitative formation of adduct **4a**. This is noteworthy since potassium-specific crown ethers such as [18]crown-6[6] or 1,3-xylyl[21]crown-6 (**1b**)[7] complex at most *catalytic* amounts of KF.[8] In the case of **4a**, the strength of the B–F bond[9] is decisive. The usual interaction between $K^{\oplus}$ and the oxygen atom of the crown ether acts synergistically, since a control experiment with KF and the catechol ester of phenylboronic acid afforded *no* adduct.[10, 11]

The host–guest compound **4a** was investigated in solution particularly by ^{11}B and ^{13}C NMR spectroscopy. The ^{11}B NMR spectrum (CD_2Cl_2) at room temperature with BF_3–ether as external standard shows a single signal at $\delta = 10.0$, which means a shift of $\Delta\delta = 20$ to higher field compared with the signal of the uncomplexed host **2** ($\delta = 30$). This is characteristic of compounds with tetracoordinated boron.[12] The participation of $K^{\oplus}$ as guest is shown by a comparison of the ^{13}C NMR spectra of the free host **2** and the adduct **4a** (Fig. 1). The low-field shift of the signals of the benzylic C atoms (C7 and C18) and the high-field shift of the other ether C atoms are definite indications of cation binding.[13] The fact that the spectra of mixtures of compounds **2** and **4a** exhibit sharp signals shows that, under these conditions, rapid exchange processes do not occur on the NMR time scale. The ^{19}F NMR ($\delta = -124.4$; $CFCl_3$ as external standard) and the ^1H NMR spectrum are also consistent with structure **4a**.

Figure 2 shows the result of an X-ray structure analysis of **4a**.[14] The inclusion of $K^{\oplus}$ and $F^{\ominus}$ is clearly evident (Fig. 2, top), as are intermolecular interactions between the units of the host–guest compound (Fig. 2, bottom). The "unsymmetrical" structure (Fig. 2, top) could be due to a crystal packing effect, since the ^{13}C NMR spectrum of **4a** in solution does *not* show a double set of signals in the range of 40 °C to −80 °C.

[*] Prof. Dr. M. T. Reetz [+], Dipl.-Chem. C. M. Niemeyer, Dr. K. Harms
Fachbereich Chemie der Universität
Hans-Meerwein-Strasse, W-3550 Marburg (FRG)
[+] New address: Max-Planck-Institut für Kohlenforschung
Kaiser-Wilhelm-Platz, W-4330 Mülheim a.d. Ruhr (FRG)

[**] This work was supported by the Deutsche Forschungsgemeinschaft (Leibniz-Program) and the Fonds der Chemischen Industrie.

The salts KCl and KBr do not undergo monotopic or heterotopic interactions with **2**, even after a reaction period of two weeks. This behavior corresponds to that of crown ether **1b**.[15] We ascribe this to the fact that $K^{\oplus}$ complexation is not sufficiently favored energetically and to the weaker B–Cl and B–Br bonds.[9] By contrast, monotopic binding is observed for KI and KSCN (formation of **3d** and **3e**, respectively). After two days, the respective ^{13}C NMR spectra show the signal shifts characteristic of $K^{\oplus}$ inclusion,[13] whereas the position of the ^{11}B NMR signal has hardly changed (**3d**, $\delta = 29.9$; **3e**, $\delta = 29.4$). The formation of the host–guest compound **3** is energetically favored in these cases by the usual $K^{\oplus}$ complexation.[16] This interpretation is consistent with the observation that the reaction of crown ether **1b** with KI or KSCN leads to inclusion of $K^{\oplus}$. In the reactions of host **2** with KCN (reaction time 2 d) and $KOCH_3$ (1 h), **4f**[17] and **4g**, respectively, are formed nearly quantitatively. The ^{11}B NMR spectra (**4f**, $\delta = 10.7$; **4g**, $\delta = 10.6$), as well as ^{13}C NMR signal shifts characteristic of $K^{\oplus}$ binding, confirm a heterotopic behavior.

The selectivity described here for the series of potassium salts KX has not been previously observed for any other receptor.[1–3] Selectivity in competition experiments is also possible. For example, if **2** is allowed to react with a mixture of KF, KCl, KBr, and KI the KF adduct **4a** is formed exclusively within two days. Host **2** is also capable of distinguishing between potassium salts leading to heterotopic host–guest compounds **4**. Thus, upon reacting the host **2** with a KF/KCN mixture for a sufficient length of time,[18] only **4a** is formed. The suitability of host compounds of type **2** with respect to synergistic effects in molecular recognition of organic compounds is the subject of further investigations.[19]

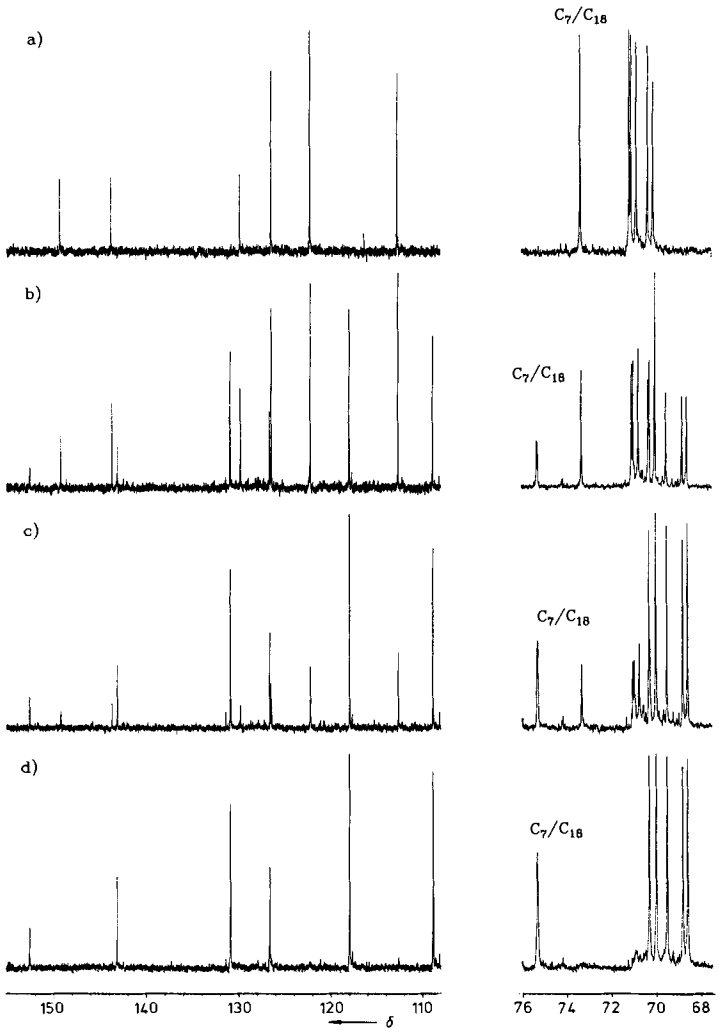

Fig. 1. ^{13}C NMR spectroscopic investigation of the reaction of host **2** with KF to give adduct **4a**: a) Host **2**; b) after about 35% uptake of KF; c) after about 65% uptake of KF; d) host–guest compound **4a**.

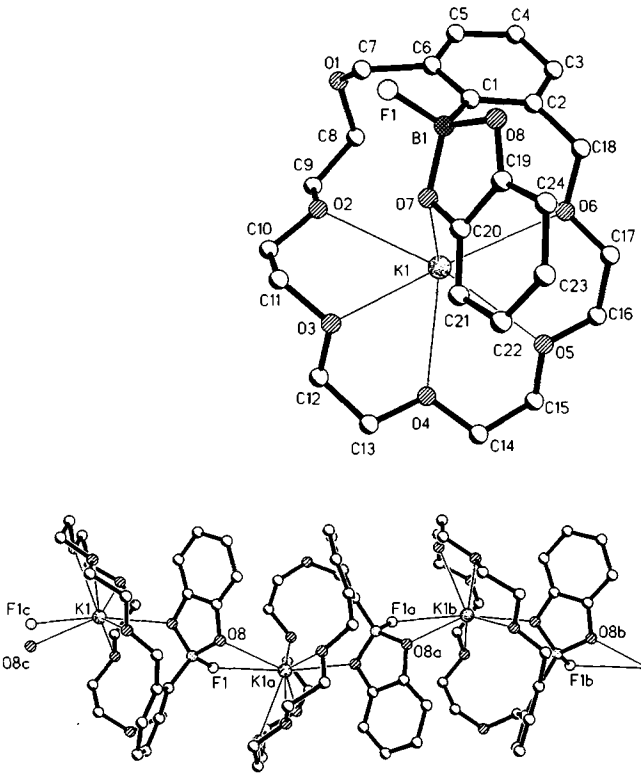

Fig. 2. Top: Asymmetric unit of **4a** in the crystal (H atoms omitted). Bottom: Section of the packing of **4a** in the crystal (H atoms omitted).

Received: June 10, 1991 [Z 4689 IE]
German version: *Angew. Chem. 103* (1991) 1515

CAS Registry numbers:
2, 136426-4; **3d**, 136577-16-7; **3e**, 136577-18-9; **4a**, 136577-15-6; **4f**, 136577-19-0; **4g**, 136577-20-3.

[1] a) D. J. Cram, *Angew. Chem. 100* (1988) 1041; *Angew. Chem. Int. Ed. Engl. 27* (1988) 1009; b) C. J. Pedersen, *ibid. 100* (1988) 1053 and *28* (1988) 1021; c) J.-M. Lehn, *ibid. 100* (1988) 91 and *27* (1988) 89; *ibid. 102* (1990) 1347 and *29* (1990) 1304; d) E. Weber, F. Vögtle, *Top. Curr. Chem. 98* (1981) 1; e) Y. Takeda, *ibid. 121* (1984) 1.

[2] a) Ammonium or guanidinium hosts: J.-M. Lehn, E. Sonveaux, A. K. Willard, *J. Am. Chem. Soc. 100* (1978) 4914; F. P. Schmidtchen, G. Müller, *J. Chem. Soc. Chem. Commun. 1984*, 1115; Y. Murakami, J. Kikuchi, T. Ohno, O. Hayashida, M. Kojima, *J. Am. Chem. Soc. 112* (1990) 7672; J.-M. Lehn, R. Meric, J.-P. Vigneron, I. Bkouche-Waksman, C. Pascard, *J. Chem. Soc. Chem. Commun. 1991*, 62; A. Galan, E. Pueyo, A. Salmeron, J. de Mendoza, *Tetrahedron Lett. 32* (1991) 1827; b) macrocylic Lewis acids: J. D. Wuest, B. Zacharie, *J. Am. Chem. Soc. 109* (1987) 4714; M. T. Blanda, J. H. Horner, M. Newcomb, *J. Org. Chem. 54* (1989) 4626, M. E. Jung, H. Xia, *Tetrahedron Lett. 29* (1988) 297; A. R. Van Doorn, M. Bos, S. Harkema, J. van Eerden, W. Verboom, D. N. Reinhoudt, *J. Org. Chem. 56* (1991) 2371.

[3] *Schmidtchen* has synthesized heterotopic compounds that contain a crown ether moiety and an ammonium macrocycle: F. P. Schmidtchen, *Tetrahedron Lett. 25* (1984) 4361; F. P. Schmidtchen, *J. Org. Chem. 51* (1986) 5161.

[4] M. Newcomb, S. S. Moore, D. J. Cram, *J. Am. Chem. Soc. 99* (1977) 6405.

[5] *Reinhoudt* et al. have carried out a similar borylation and have oxidized the resulting, nonisolated boronic acid to the corresponding phenol: M. Skowronska-Ptasinska, V. M. L. J. Aarts, R. J. M. Egberink, J. van Eerden, S. Harkema, D. N. Reinhoudt, *J. Org. Chem. 53* (1988) 5484.

[6] According to *Liotta* et al., [18]crown-6 binds potassium fluoride (as a suspension in benzene or acetonitrile) only to the extent of 2–5%, which

is nonetheless sufficient to accelerate S_N2 reactions: C. L. Liotta, H. P. Harris, *J. Am. Chem. Soc. 96* (1974) 2250.
[7] D. N. Reinhoudt, R. T. Gray, *Tetrahedron Lett. 1975*, 2105.
[8] When the suspension of KF in CH_2Cl_2 is allowed to react with 1,3-xylyl[21]crown-6 **1b** for several days under ultrasonication, the ^1H and ^{13}C NMR spectra of the solution show no evidence of binding of $K^{\oplus}$ ions.
[9] Since dative bonds are formed in the ate complexes, the usual values of the bonding energies, which refer to diatomic molecules, cannot be used (cf. A. Haaland, *Angew. Chem. 101* (1989) 1017; *Angew. Chem. Int. Ed. Engl. 28* (1989) 1010). The usual trend toward weaker bonding in the order B-F > B-Cl > B-Br > B-I probably still holds, however.
[10] a) Tris(dimethylamino)sulfonium fluoride reacts with 1,8-naphthalenediylbis(dimethylborane) to form an adduct: H. E. Katz, *J. Org. Chem. 50* (1985) 5027; b) [18]crown-6 binds the counterion of pentacoordinated silicon compounds: J. L. Brefort, R. J. P. Corriu, B. J. L. Henner, W. W. C. W. Chi Man, *Organometallics 9* (1990) 2080.
[11] The mixture containing the catechol ester of phenylboronic acid and 1,3-xylyl[21]crown-6 (**1b**) also effects the dissolution of KF. The synergistic effect, however, is smaller. For example, if adduct **4a** is allowed to react with a 1:1 mixture containing **1b** and the catechol ester of phenylboronic acid, an equilibrium is established in favor of **4a** ($\approx$ 70:30).
[12] H. Nöth, B. Wrackmeyer, *NMR: Basic Princ. Prog. 14* (1978).
[13] M. C. Fedarko, *J. Magn. Reson. 12* (1973) 30; D. Live, S. I. Chan, *J. Am. Chem. Soc. 98* (1976) 3769.
[14] Crystallographic data for **4a**: ($C_{24}H_{31}BFKO_8$, M_r = 516.4): monoclinic, space group $P2_1/n$, a = 1022.8(2), b = 2075.7(4), c = 1238(2) pm, β = 106.05(3)°, Z = 4, $\varrho_{calcd.}$ = 1.357 gcm^{-3}, $\mu(Cu_{K\alpha})$ = 23.05 cm^{-1}. Measurement carried out on an Enraf-Nonius CAD4 diffractometer ($Cu_{K\alpha}$ radiation, λ = 1.54184 Å, graphite monochromator, room temperature); 2379 measured reflections, 2164 of which were independent ($R_{int.}$ = 0.0355), 1893 with $F > 3\sigma(F)$ were regarded as observed. Solution by direct methods and refinement with Siemen's-SHELXTL-PLUS(VMS) program package, R = 0.0479, R_w = 0.0355 ($\omega = 1/\sigma^2(F)$), all non-hydrogen atoms anisotropically, H atoms "riding" with groupwise common isotropic temperature factors. Empirical correction of the measurement data with the program DIFABS (N. Walker, D. Stuart, *Acta Crystallogr. Sect. A 39* (1983) 158). Further details of the crystal structure investigation are available on request from the Fachinformationszentrum Karlsruhe, Gesellschaft für wissenschaftlich-technische Information mbH, W-7514 Eggenstein-Leopoldshafen 2 (FRG), on quoting the depository number CSD-320264, the names of the authors, and the journal citation.
[15] No complexation could be observed by NMR spectroscopy. This also holds for samples heated under ultrasonification.
[16] Why the soft anions do not bind to the hard boron in **3d–e** is explained, among other things, by the weak B-I- and B-S bonds as well as by possible steric solvent effects.
[17] In the case of KCN, complex **4f** was formed in about 95% yield; in addition, 5% of a further, unidentified ate complex was obtained.
[18] According to the NMR spectra, different adducts are formed during the first hours of reaction. ^1H, ^{13}C and ^{11}B NMR spectra recorded after 10 d show only the presence of **4a**.
[19] M. T. Reetz, C. M. Niemeyer, K. Harms, *Angew. Chem. 103* (1991) 1517; *Angew. Chem. Int. Ed. Engl. 30* (1991) 1474.

Heterotopic Host Molecules for Binding Two Different Guests **

By *Manfred T. Reetz,* Christof M. Niemeyer,* and *Klaus Harms*

An important aspect of host/guest chemistry is the simulation of biological systems.[1] It is all the more surprising, therefore, that practically no host molecules capable of recognizing and binding *two different* organic guest molecules have been synthesized.[1–3] Here we describe a new concept of molecular recognition in which alcohols and amines are recognized simultaneously and selectively. This work was motivated by the hope that compounds with one acceptor site (e.g., a metal center[3]) and several donor sites (e.g., ether functions) might be potential hosts for alcohols *and* amines, because, after proton transfer, the alkoxide anion and the ammonium cation could bond through reversible dative and hydrogen bonds, respectively (Scheme 1). Such binding would therefore involve heterotopic host molecules whose Lewis acid/base property affects the equilibrium of the Brønsted acid/base pair (alcohol and amine; see Scheme 1).

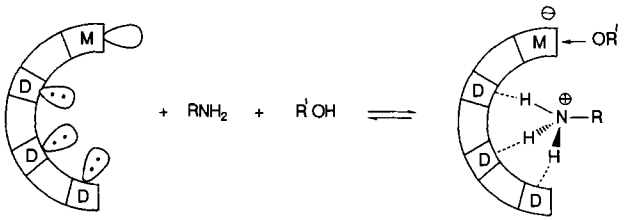

Scheme 1. Simultaneous molecular recognition of amines and alcohols (M = metal center with empty orbital; D = donor site with occupied orbital).

In an initial experiment the boron-containing crown ether **1**[4] was allowed to react with a 1:1 mixture of methanol and benzylamine in dichloromethane. A spontaneous reaction ensued, leading to the formation of **2**. The assumption that methoxide bonds to boron and the ammonium ion to the crown ether moiety was supported by ^{11}B, ^1H, and ^{13}C NMR spectroscopy.[5]

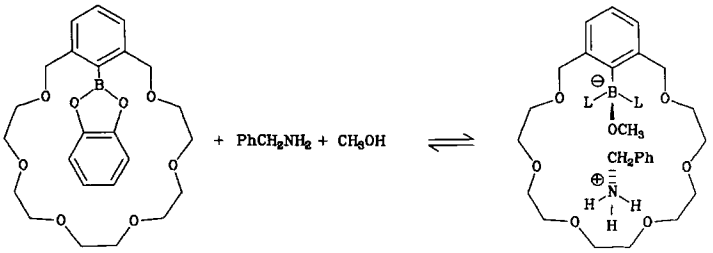

1 **2**

The X-ray structure analysis[6] provided final confirmation and also brought to light some structural details. The ammonium ion is completely embedded in the crown ether moiety, as a space-filling picture reveals (Fig. 1b[7]). This structural element is unique, since ammonium ions are usually situated "outside" the crown ether and form hydrogen bonds to the ether oxygen atoms.[1, 8] In this case, however, the ammonium ion is drawn deeply into the host owing to the formation of a hydrogen bond to the methoxide. The N atom is located exactly in the average plane of the crown ether atoms, the maximum deviation of the ring atoms being ± 0.8 Å.[6] This type of communication between the two guests leads to a rotaxane-type structure.

To determine whether host **1** can distinguish between different alcohols and amines, we first carried out competition experiments involving benzylamine and, in each case, two alcohols.[9] The results summarized in Table 1 establish that steric factors are mainly responsible for the molecular recognition.[10] Thus, host **1** can distinguish between methanol and ethanol (73% in favor of the methanol adduct). Control

[*] Prof. Dr. M. T. Reetz [+], Dipl.-Chem. C. M. Niemeyer, Dr. K. Harms
Fachbereich Chemie der Universität
Hans-Meerwein-Strasse, W-3550 Marburg (FRG)
[+] New address: Max-Planck-Institut für Kohlenforschung
Kaiser-Wilhelm-Platz, W-4330 Mülheim a. d. Ruhr (FRG)

[**] This work was supported by the Deutsche Forschungsgemeinschaft (Leibniz Program) and the Fonds der Chemischen Industrie.

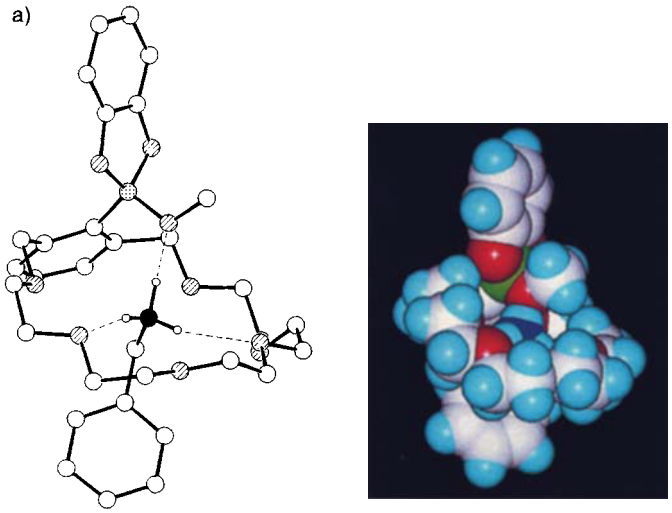

Fig. 1. a) Asymmetric unit of **2** in the crystal. Boron, dotted; carbon, white; oxygen, striped; nitrogen, black (H atoms only shown for ammonium ions). b) Space-filling representation of **2** [7]. Boron, green: carbon, white; oxygen, red; nitrogen, dark blue; hydrogen, light blue.

experiments show that the data were obtained under thermodynamic conditions. Although the exchange processes are reversible, they are slow on the NMR time scale, and two host/guest compounds can be detected simultaneously by NMR spectroscopy.

Table 1. Molecular recognition of alcohols by host **1** in the presence of benzylamine at room temperature [9].

R^1OH	R^2OH	Ratio of complex formation $R^1OH:R^2OH$
CH_3OH	CH_3CH_2OH	73:27
CH_3OH	$Ph(CH_3)CHCH_2OH$	86:14
CH_3OH	$(CH_3)_2CHOH$	93: 7
CH_3OH	$(CH_3)_3COH$	>97: <3
CH_3OH	PhOH	71:29
$PhCH_2OH$	CH_3CH_2OH	56:44
$PhCH_2OH$	$(CH_3)_2CHOH$	88:12

On the basis of the X-ray structure analysis of adduct **2** (Fig. 1), we expected a high degree of molecular recognition of amines. Indeed, competition experiments with the amine pair benzylamine/α-methylbenzylamine and one alcohol (methanol, ethanol, or isopropyl alcohol) show that, in each case, only *one* host/guest[1]/guest[2] combination is realized, namely, **1**/benzylamine/alcohol.

When similar competition experiments were performed with a smaller analogous host containing five oxygen atoms in the 18-membered ring,[11] the amine selectivity turned out to be significantly lower. In the case of methanol as the alcohol component, for example, benzylamine is favored over α-methylbenzylamine to the extent of only 80%. This has to do with the fact that the ammonium ions cannot penetrate as deeply into the smaller crown ether ring,[12] as shown by the result of the X-ray structure analysis of the ethanol/benzylamine adduct **4** (Fig. 2a).[13] Thus difference in steric interactions in the case of different amines is not as great as in the case of the host **1**. In contrast, alcohol selectivity is much higher. In the case of benzylamine as the amine component and methanol/ethanol as alcohols, methanol is complexed exclusively! The smaller ring induces more steric shielding of the boron (see Fig. 2b). Further investigations, involving

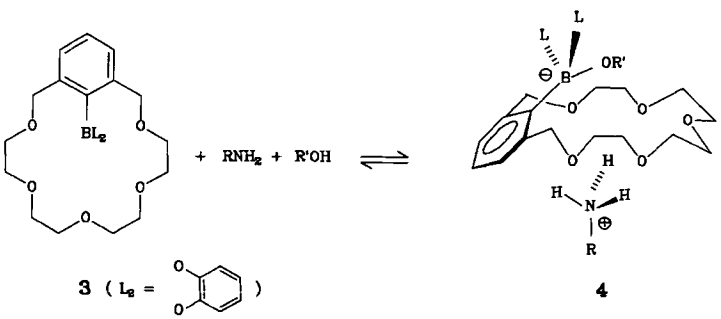

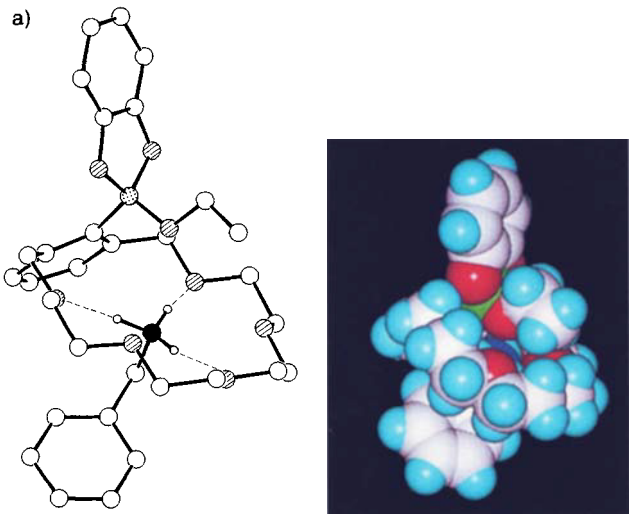

Fig. 2. a) Asymmetric unit of **4** (R = $PhCH_2$, R' = Et) in the crystal. b) Space-filling representation of **4** [7]. Same notation as in Fig. 1.

variation of the guests,[14] the ligands on boron, the topology of the cavity, and the metal, are in progress.

Received: July 26, 1991 [Z 4825 IE]
German version: *Angew. Chem. 103* (1991) 1517

CAS Registry numbers:
1, 136426-45-4; **2**, 136426-48-7; **2**·toluene, 136426-53-4; **3**, 136426-46-5; **4**, 136426-50-1.

[1] See, for example: F. Vögtle: *Supramolekulare Chemie*, Teubner, Stuttgart 1989; *Supramolecular Chemistry*, Wiley, Chichester, England 1991; D. J. Cram, *Angew. Chem. 100* (1988) 1041; *Angew. Chem. Int. Ed. Engl. 27* (1988) 1009; J.-M. Lehn, *ibid. 100* (1988) 91 and *27* (1988) 90; *ibid. 102* (1990) 1347 and *29* (1990) 1304; F. Vögtle, E. Weber (Eds.): *Host Guest Complex Chemistry—Macrocycles*, Springer, Berlin 1985; J. Rebek, Jr., *Top. Curr. Chem. 149* (1988) 189; *Angew. Chem. 102* (1990) 261; *Angew. Chem. Int. Ed. Engl. 29* (1990) 245; E. Weber, *J. Mol. Graphics 7* (1989) 12; R. M. Kellog, *Angew. Chem. 96* (1984) 769; *Angew. Chem. Int. Ed. Engl. 23* (1984) 782.

[2] Systems obtained by molecular biological techniques are not considered here. Several host compounds that bind organic molecules and metal cations simultaneously are known: F. Diederich, M. R. Hester, M. A. Uyeki, *Angew. Chem. 100* (1988) 1775; *Angew. Chem. Int. Ed. Engl. 27* (1988) 1705, and references cited therein; crystalline clathrate compounds with several guests, such as alcohols: E. Weber, M. Hecker, I. Csöregh, M. Czugler, *Mol. Cryst. Liq. Cryst. 187* (1990) 165; see also J. L. Atwood, J. E. D. Davies, D. D. MacNicol (Eds.): *Inclusion Compounds*, Vol. 1–3, Academic Press, London 1984.

[3] Host molecules with metal centers have been reported in recent years. Examples include the following: a) compounds with two zinc-containing porphyrin rings, which complex dipyridines and diamines: S. Kugimiya, *J.*

Chem. Soc. Chem. Commun. 1990, 432; H. L. Anderson, C. A. Hunter, M. N. Meak, J. K. M. Sanders, *J. Am. Chem. Soc. 112* (1990) 5780; b) metallomacrocycles, such as uranium-containing chelates, which form complexes with pyridines: A. R. van Doorn, M. Bos, S. Harkema, J. van Eerden, W. Verboom, D. N. Reinhoudt, *J. Org. Chem. 56* (1991) 2371; c) numerous multidentate Lewis acids that bind two molecules of the same kind, see, e.g.: B. Bachand, J. D. Wuest, *Organometallics 10* (1991) 2015, and references cited therein; d) Note added by the editorial staff: See also the communication by *F. Hawthorne* et al. in this issue, in which a host compound analogous to a [12]crown-4 with four Hg atoms is reported: X. Yang, C. B. Knobler, M. F. Hawthorne, *Angew. Chem. 103* (1991) 1519; *Angew. Chem. Int. Ed. Engl. 30* (1991) 1507.

[4] In the preceding communication we describe the synthesis of the host compound **1** as well as its ability to bind potassium salts, KX (X = F, Cl, Br, I, SCN, CN, OCH_3) selectively: M. T. Reetz, C. M. Niemeyer, K. Harms, *Angew. Chem. 103* (1991) 1515; *Angew. Chem. Int. Ed. Engl. 30* (1991) 1472.

[5] The ^{11}B NMR spectrum (CD_2Cl_2, BF_3-ether as external standard) of **2** shows one signal at $\delta = 9.0$, a reliable indication of the presence of a compound with tetracoordinated boron [4]. The ^1H and ^{13}C NMR spectra exhibit chemical shifts characteristic of cation inclusion [4].

[6] Crystallographic data for **2** · toluene ($C_{39}H_{52}BNO_9$, $M_r = 689.6$): triclinic, space group $P\bar{1}$, $a = 1093.8(1)$, $b = 1392.3(1)$, $c = 1447.7(2)$ pm, $\alpha = 101.16(1)$, $\beta = 109.52(1)$, $\gamma = 104.29(1)°$, $Z = 2$, $\varrho_{calcd} = 1.193\ g\,cm^{-3}$, $\mu(Cu_{K\alpha}) = 6.42\ cm^{-1}$. Measurement carried out on an Enraf-Nonius CAD4 diffractometer ($Cu_{K\alpha}$ radiation, $\lambda = 1.54184$ Å, graphite monochromator, $T = 190$ K); 4666 measured reflections, 4404 of which are independent ($R_{int.} = 0.0185$), 4081 with $F > 4\sigma(F)$ were regarded as observed. Solution by direct methods and refinement with the Siemens SHELXTL-PLUS(VMS) program package, $R = 0.0641$, $R_w = 0.0797$ ($\omega = 1/\sigma^2(F)$); all non-hydrogen atoms refined anisotropically; N- and O-bonded H atoms localized; the others "riding" with groupwise common isotropic temperature factors. Further details of the crystal structure investigation are available on request from the Fachinformationszentrum Karlsruhe, Gesellschaft für wissenschaftlich-technische Information mbH, W-7514 Eggenstein-Leopoldshafen 2 (FRG), on quoting the depository number CSD-320298, the names of the authors, and the journal citation.

[7] In order to generate the space-filling representation, the X-ray data were processed on a Silicon graphics computer using the Sybyl program.

[8] See, e.g.: D. J. Cram, K. N. Trueblood, *Top. Curr. Chem. 98* (1981) 43; I. Goldberg in S. Patai, Z. Rappoport (Eds.): *Crown Ethers and Analogs*, Wiley, Chichester, England 1989, p. 359.

[9] In a typical experiment, 0.1 mmol of host **1** and 0.1 mmol of an amine were placed in 1 mL of dry CD_2Cl_2 at room temperature and treated with 0.2 mmol of each alcohol. The analysis was carried out by ^{13}C NMR spectroscopy at room temperature. When 1, 3, or 5 mmol of the methanol/ethanol pair was used, no change in the selectivity was observed. The selectivities thereby obtained (Table 1) provide no information concerning the absolute magnitudes of the binding constants, which are the subject of a more detailed investigation.

[10] The equilibrium constants for the reaction of boranes and amines to form borane/amine adducts were measured by *Brown* et al. and interpreted on the basis of front strain: H. C. Brown, R. B. Johannesen, *J. Am. Chem. Soc. 75* (1953) 16; H. C. Brown, *Rec. Chem. Prog. 14* (1953) 83; Related studies have recently been reported by *Yamamoto* et al. on this kind of molecular recognition in the complexation of ethers and carbonyl compounds by bulky aluminum compounds: K. Maruoka, S. Nahahara, H. Yamamoto, *J. Am. Chem. Soc. 112* (1990) 6115; K. Maruokoa, S. Nagahara, H. Yamamoto, *Tetrahedron Lett. 31* (1990) 5475.

[11] The host was prepared in the same way as **2** [4].

[12] An indication of the weaker complexation is the fact that rapid exchange processes are detectable by NMR spectroscopy for the ammonium components at room temperature. In this case the competition experiments were therefore carried out at $-40\,°C$.

[13] Crystallographic data for **4** ($C_{31}H_{42}BNO_8$, $M_r = 567.5$): monoclinic, space group $P2/n$, $a = 1535.9(3)$, $b = 994.4(2)$, $c = 2067.8(4)$ pm, $\beta = 105.55(3)°$, $Z = 4$, $\varrho_{calcd} = 1.239\ g\,cm^{-3}$, $\mu(Cu_{K\alpha}) = 6.82\ cm^{-1}$. Measurement carried out on an Enraf-Nonius CAD4 diffractometer ($Cu_{K\alpha}$ radiation, $\lambda = 1.54184$ Å, graphite monochromator, $T = 190$ K); 4290 measured reflections, 3830 of which were independent ($R_{int.} = 0.0660$); 2605 with $F > 4\sigma(F)$ were regarded as observed. Solution by direct methods and refinement in Siemens SHELXTL-PLUS(VMS) program system, $R = 0.0686$, $R_w = 0.0613$ ($\omega = 1/\sigma^2(F)$), all non-hydrogen atoms refined anisotropically; *N*-bonded H atoms localized; the others were refined using the riding model with groupwise common isotropic temperature factors. Further details of the crystal structure determination are available on request from the Fachinformationszentrum Karlsruhe, Gesellschaft für wissenschaftlich-technische Information mbH, W-7514 Eggenstein-Leopoldshafen 2, on quoting the depository number CSD-320335, the names of the authors, and the journal citation.

[14] For example, host **1** can bind water and benzylamine in the same way as **2**. Furthermore, preliminary experiments show that hosts form 1:1 inclusion complexes with amines and even ammonia.

Naphtho[2,3-*d*][1,2,3]oxadiazole**

By *Achim Blocher* and *Klaus-Peter Zeller**

Dedicated to Professor Michael Hanack on the occasion of his 60th birthday

The early history of "diazoanhydrides", obtained on diazotization of α-amino β-keto esters and of *o*-aminophenols, is marked by controversy over the constitution of these compounds.[1] Much evidence initially favored the presence of 1,2,3-oxadiazoles of type **1** and **2**, respectively. In the end, however, the application of spectroscopic methods settled this structural discussion in favor of the isomeric α-diazo carbonyl compounds **3** and the *o*-quinonone diazides **4**, respectively.[2]

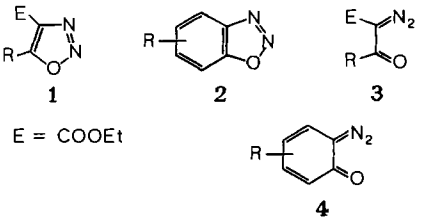

Only recently were *Schulz* and *Schweig*[3, 4] able to detect the formation of an equilibrium[5] between the parent compound, the *o*-quinone diazide **5**, and its valence isomer, the benzo[1,2,3]oxadiazole **6**, in the gas phase and in nonpolar solvents and thus provide the first experimental evidence for the existence of this five-membered heterocycle.

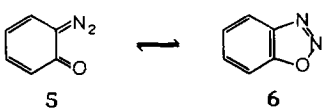

The *o*-quinone diazide **8**, expected on deprotonation of the diazonium tetrafluoroborate **7**, contains the *o*-quinone bismethide substructure A together with the *o*-quinonoid structural element B. On going to naphtho[2,3-*d*][1,2,3]oxadiazole (**9**), both of these energetically unfavorable structures should give way to the more stable naphthalene system. Thus, the cyclization to **9** should be particularly favored.

We have carried out the deprotonation of **7**[6] on basic alumina and sublimed the product (which is slightly colored owing to impurities) at about 10 °C under vacuum. The white to pale lemon yellow solid thereby obtained is stable for several days in the dark at $-20\,°C$. Its spectroscopic data

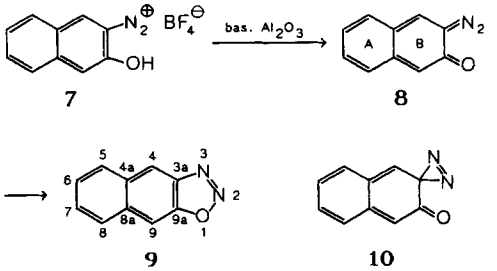

[*] Prof. Dr. K.-P. Zeller, Dipl.-Chem. A. Blocher
Institut für Organische Chemie der Universität
Auf der Morgenstelle, W-7400 Tübingen (FRG)

[**] This work was supported by the Fonds der Chemischen Industrie.

rule out both the *o*-quinone diazide structure **8** and the equally conceivable α-carbonyl diazirine structure **10**,[7] but are consistent with **9**. To the best of our knowledge, **9** is the first 1,2,3-oxadiazole to be isolated in pure form.

In the IR spectrum (KBr), the intense diazo and carbonyl bands typical of *o*-quinone diazides are absent. If the KBr disk is exposed to daylight for a few minutes and the IR spectrum recorded again, intense bands appear at 2090 (ν(C=N=N)) and 1627 cm^{-1} (ν(C=O)), indicative of the photochemical ring opening **9** → **8**. If the disk is kept in the dark for 30 min at 20 °C, the initial spectrum is obtained once again.

The ^1H and ^{13}C NMR spectra indicate that compound **9** is a 2,3-disubstituted naphthalene derivative; this structure is supported in particular by the lowest-field ^{13}C NMR signal ($\delta = 148.7$), which is at markedly higher field than that of a carbonyl C atom of *o*-quinone diazides, which usually show a chemical shift of $\delta = 180$.[8]

In the 70 eV mass spectrum (*m/z*, rel. int.), the molecular-ion peak, M^+ (170, 10%), is accompanied by intense peaks corresponding to the fragment ions $[M - N_2]$ (142, 100%) and $[M - N_2 - CO]^{\oplus}$ (114, 14%).

Table 1. Spectroscopic data for **9**.

IR (KBr): $\tilde{\nu}$ [cm^{-1}] = 1626 (m), 1611 (m), 1594 (m), 1503 (m), 1464 (s), 1457 (s), 1443 (m), 1376 (m),...

After direct irradiation of the KBr disk with sunlight (filtered through a glass window) for 7 min [a]: $\tilde{\nu}$ [cm^{-1}] = 2090 (s), 1718 (s), 1700 (s), 1696 (s), 1684 (s), 1675 (m), 1627 (s), 1617 (m), 1601 (m), 1576 (m), 1565 (m), 1560 (m), 1499 (s), 1457 (s),...

^1H NMR (200 MHz, $CDCl_3$, −20 °C): $\delta = 8.58$ (s, 1H; H-9), 8.04–8.01 (d, 1H, $J = 8.3$ Hz; H-5 or H-8), 7.97–7.94 (d, 1H, $J = 8.5$ Hz; H-5 or H-8), 7.91 (s, 1H; H-4), 7.63–7.57 (t, 1H, $J = 7.6$ Hz; H-6 or H-7), 7.51–7.45 (t, 1H, $J = 7.6$ Hz; H-6 or H-7)

^{13}C NMR (200 MHz, $CDCl_3$, −20 °C): $\delta = 148.7$ (C-9a), 137.6 (C-3a), 135.7, 130.0 (C-4a, 8a), 129.4, 128.8, 128.0, 125.1 (C-5,6,7,8), 121.2 (C-4), 103.8 (C-9)

UV/VIS (*n*-heptane): λ_{max} (log ε) = 358 (3.37), 311 (4.00), 298 (3.84), 286 (3.56), 239 (4.54), 213 (4.54) nm

UV/VIS (95% methanol/5% *n*-heptane) [b]: λ_{max} (log ε) = 547 (3.07), 335 (3.70), 312 (3.76), 298 (3.73), 246 (4.43), 213 (4.33), 198 (4.03), 192 (3.98) nm

[a] Photochemical valence isomerization to **8**. [b] Formation of an equilibrium mixture between the valence isomers **8** and **9**.

The UV/VIS spectrum of **9** in *n*-heptane is similar in structure to that recorded for benzo[1,2,3]oxadiazole **6** in solution.[4] As expected, the positions of the bands are shifted to longer wavelengths. The spectrum of **9** in polar methanol is significantly different. We interpret this change as evidence of partial ring opening to give **8**, in analogy to the system **5** ⇌ **6**.[4] The absorption in the visible ($\lambda_{max} = 547$ nm, $\varepsilon_{max} = 1200$), in contrast to the short-wavelength absorptions, remains unchanged on going back to nonpolar *n*-heptane and is therefore presumably due to a secondary product of the ring-opened *o*-quinone diazide **8**.

Photolysis[9] of a 4.7×10^{-3} molar solution of **9** in methanol affords, as main product, 2-(methoxycarbonyl)indene (**13**) (59% yield).[10] As indicated by the UV/VIS spectrum, **9** forms an equilibrium with its valence isomer **8** in methanol.

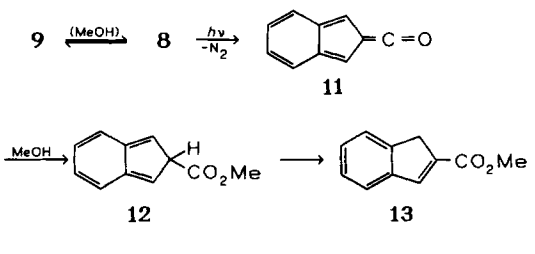

In addition, as already noted, **8** can be formed photochemically from **9**. We assume that the observed loss of N_2 and the ring closure preceed as expected for a Wolff rearrangement[11] of an *o*-quinone diazide, via the ketene **11** and the ester **12**[12] as intermediates.

Experimental Procedure

9: A solution of **7** (100 mg, 0.388 mmol) in about 80 mL of methanol was concentrated to about 3 mL at ca. 20 °C and then transferred to a cooled column (ca. 10 °C) filled with 100 g of basic Al_2O_3 (Woelm B, activity 1) and immediately eluted (eluent: petroleum ether/ethyl acetate 1:1). Concentration of the eluate afforded 74 mg of crude product, which was dissolved in a small amount of dichloromethane and transferred to a sublimation apparatus. The sublimation was carried out in the dark (bath temperature ca. 10 °C, cold finger temperature −70 °C, 0.01 Torr). Yield: 14.3 mg (22%). The product could be stored in the dark at −20 °C for two days without any noticeable spectroscopic changes. At 20 °C, **9** gradually turns brown. Above 77 °C, it decomposes explosively.

Received: December 11, 1990 [Z 4319 IE]
Publication delayed at the authors' request
German version: *Angew. Chem. 103* (1991) 1489

CAS Registry numbers:
7, 136445-42-6; **9**, 70304-47-1; **13**, 17332-04-6.

[1] For a short historical discussion of this intriguing controversy about the constitution, see L. C. Behr in R. H. Wiley (Ed.): *The Chemistry of Heterocyclic Compounds, Vol. 17*, Interscience Publishers, New York 1962, p. 235.
[2] M. Regitz, *Diazoalkane*, Thieme, Stuttgart 1977.
[3] R. Schulz, A. Schweig, *Angew. Chem. 91* (1979) 737; *Angew. Chem. Int. Ed. Engl. 18* (1979) 692.
[4] R. Schulz, A. Schweig, *Angew. Chem. 96* (1984) 494; *Angew. Chem. Int. Ed. Engl. 23* (1984) 509.
[5] The valence isomerization **5** → **6** can be regarded as a pericyclic 1,5-electrocyclization: R. Huisgen, *Angew. Chem. 92* (1980) 979; *Angew. Chem. Int. Ed. Engl. 19* (1980) 947.
[6] Synthesized by diazotization of 3-amino-2-hydroxynaphthalene in analogy to M. P. Doyle, W. J. Bryker, *J. Org. Chem. 44* (1979) 1572. Recrystallization from acetone/*n*-pentane (2:1); yield 82% **7**, m.p. 143–4 °C (dec.). IR (KBr): $\tilde{\nu} = 2244$ cm^{-1} (C=C=N).
[7] Several α-carbonyl diazirines are obtainable by photochemical valence isomerization of α-diazo carboxamides: R. A. Franich, G. Lowe, J. Parker, *J. Chem. Soc. Perkin Trans. I 1972*, 2034; E. Voigt, H. Meier, *Angew. Chem. 87* (1975) 109; *Angew. Chem. Int. Ed. Engl. 14* (1975) 103.
[8] Cf., for example, R. Radeglia, J. Egler, A. Hauser, S. Simova, J. Schraml, *Z. Chem. 24* (1984) 259.
[9] Hanovia 450-W medium-pressure lamp, Pyrex filter.
[10] Identified by comparison with authentic **13** (m.p. 80 °C): J. Vebrel, R. Carrié, *Bull. Soc. Chim. Fr. 1982* 116; ^{13}C NMR: B. Eliasson, U. Edlund, *J. Chem. Soc. Perkin Trans. II 1981* 403.
[11] H. Meier, K.-P. Zeller, *Angew. Chem. 87* (1975) 52; *Angew. Chem. Int. Ed. Engl. 14* (1975) 32.
[12] Both the ketene **11** and the ester **12** display an interesting *o*-quinone bismethide structure. Matrix isolation and trapping experiments are planned.

[{Fe(μ-'S_4')}$_2$(μ-S_2)]: A Model Complex for [Fe–S] Enzymes with a New Type of [2 Fe–2 S] Center**

By *Dieter Sellmann,* Günter Mahr,* and *Falk Knoch*

Enzymes containing iron–sulfur centers are ubiquitous in nature and are found, for example, in ferredoxins, hydro-

[*] Prof. Dr. D. Sellmann, Dipl.-Chem. G. Mahr, Dr. F. Knoch
Institut für Anorganische Chemie II der Universität
Egerlandstraße 1, W-8520 Erlangen (FRG)

[**] 'S_4'$^{2-}$ = 2,2'-(ethylenedithio)dibenzenethiolate. Transition Metal Complexes with Sulfur-Containing Ligands, Part 77. This work was supported by the Deutsche Forschungsgemeinschaft, the Bundesministerium für Forschung und Technologie, and the Fonds der Chemischen Industrie. Part 76: D. Sellmann, S. Fünfgelder, F. Knoch, M. Moll, *Z. Naturforsch. 46b* (1991), in press.

genases, and nitrogenases.[1] The structure of such centers has been determined unambiguously only in the case of a few ferredoxins. In these, iron is always surrounded tetrahedrally by thiolate and sulfide *S*-donors and forms [Fe–S] clusters of the type [2Fe–2S], [3Fe–4S], or [4Fe–4S] (**I**–**III**).[1] The SR ligands are cysteinates in the proteins, and thiolates such as $C_6H_5S^-$ in the synthetic analogues.

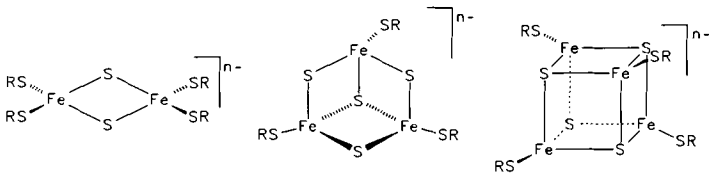

I **II** **III**

In most [Fe–S] enzymes, however, the structure of the active site is as yet undetermined. They possibly contain building blocks completely different from **I**–**III**. This assumption is supported by Mössbauer and EXAFS studies (EXAFS = *E*xtended *X*-ray *A*bsorption *F*ine *S*tructure). They indicate that, for instance, hydrogenases[2] and nitrogenases[3] contain [Fe–S] units that are fundamentally different from types **I**–**III**. Moreover, **I**–**III** interconvert very easily, and consequently no definite conclusions on the structure of the [Fe–S] sites in the native proteins can be drawn from extrusion experiments. Finally, the influence that the peptide chains and their cysteine residues exert on the formation and structure of [Fe–S] centers is still unknown.

It is therefore of basic interest that Fe^{2+} ions, elemental sulfur, and a multidentate thioether–thiolato ligand spontaneously form the novel [Fe–S] cluster $[\{Fe(\mu\text{-}'S_4')\}_2(\mu\text{-}S_2)]$ (**1**) under normal conditions in high yield according to Equation (a).

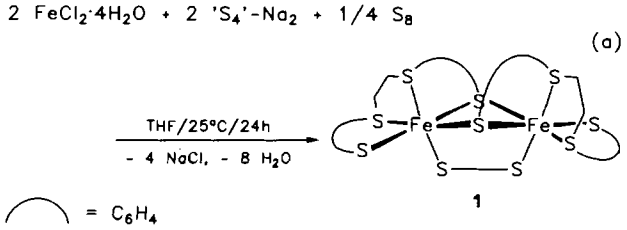

Complex **1** differs distinctly from types **I**–**III** and the organometallic clusters $[Cp_2Fe_2(\mu\text{-}S_2)(\mu\text{-}SR)_2]$ and $[Cp_2Fe_2(\eta^1\text{-}\mu\text{-}S_2)(\eta^2\text{-}\mu\text{-}S_2)]$[4] and has in many aspects prototype character.

The black-green **1** is diamagnetic and is soluble in dimethyl sulfoxide (DMSO), dimethylformamide (DMF), and CH_2Cl_2. The X-ray structure analysis[5] (Fig. 1) shows that both iron centers in **1** are pseudooctahedrally surrounded by six sulfur donors and are linked by two thiolato bridges of the 'S_4' ligands and one S_2 bridge. The Fe–thiolate and Fe–thioether distances of 225.2(4)–233.1(4) pm lie in the region typical for such complexes. The S_2 bridge has a S–S distance of 200.5(3) pm, which corresponds to a stretched interatomic distance in a neutral S_2 molecule (188.7 pm), and the Fe–Fe distance of 331.5 pm excludes a direct Fe–Fe bond. The [Fe1–S1–Fe2–S5] dihedral angle (148.3°) indicates that the four-membered ring is distinctly folded.

Complex **1** is chiral and contains two homochiral [Fe('S_4')] fragments linked through the thiolato-S atoms whose *ortho*

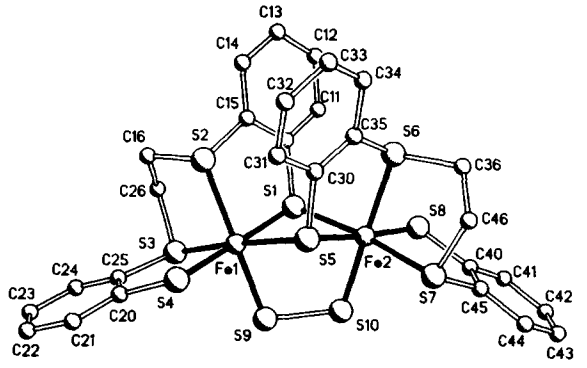

Fig. 1. Crystal structure of **1** (H atoms omitted). Important distances [pm] and angles [°]: Fe1-Fe2 331.5, Fe1-S1 228.3(3), Fe1-S2 229.5(4), Fe1-S3 225.5(4), Fe1-S4 228.2(3), Fe1-S5 233.1(4), Fe1-S9 215.9(5), Fe2-S1 232.1(4), Fe2-S5 228.6(3), Fe2-S6 227.3(5), Fe2-S7 225.2(4), Fe2-S8 231.3(4), Fe2-S10 213.1(5), S9-S10 200.3(5); Fe1-S1-Fe2 92.1(1), Fe1-S5-Fe2 91.8(1), S1-Fe1-S5 83.2(1), S1-Fe2-S5 83.3(1), S2-Fe1-S9 176.2(1), S6-Fe2-S10 178.8(2).

thioether-S atoms on the same benzene ring are *trans* to the μ-S_2 coligand. This α-bridging[6] is apparently electronically favored. The formation of **1** is thus also an interesting case of chiral recognition, since only homochiral fragments combine with one another from a racemic mixture of [Fe('S_4')] precursor complexes that form initially in the reaction represented in Equation (a).

The bonding in the $[\mu\text{-}S_2Fe_2]$ unit may be described as a delocalized 4-center 6-electron π system, formed from occupied Fe d orbitals and the π and π* orbitals of the μ-S_2 ligand. This model plausibly explains the S–S distance in the μ-S_2-bridge that is elongated with respect to uncomplexed S_2 molecules, and the short Fe–S distances in the FeS_2Fe unit (215.9 and 213.1 pm). Also the intense absorptions in the electronic spectrum of **1** (Fig. 2, left) may be attributed to the Fe···S···S···Fe bonding system. They extend into the near IR region and can be assigned to π–π* transitions.

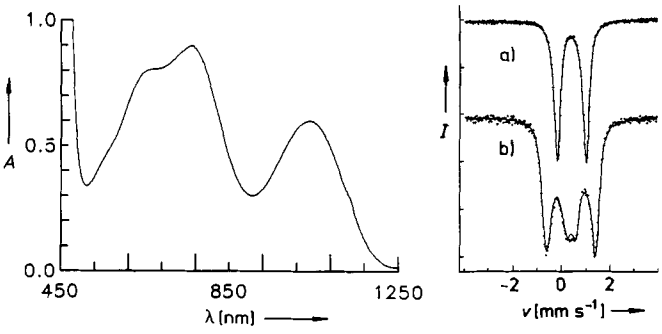

Fig. 2. Left: UV/VIS/near IR spectrum of **1** in CH_2Cl_2; λ_{max}[nm] (ε)[$M^{-1}cm^{-1}$]: 640(1950), 760(2100), 1050(1650); right: Mössbauer spectra of **1** at a) 4.2 K (δ = 0.367 and ΔE_Q = 1.161 mm s^{-1} with respect to metallic iron at 295 K and b) 4.2 K in a magnetic field (4 T) parallel to γ radiation. *I* = relative intensity.

The Mössbauer spectra (Fig. 2, right)[7] indicate that **1** contains low-spin Fe^{II} centers. This follows not only from the spectral parameters, but additionally from the agreement of experimental and calculated curves[8] on perturbation in an external magnetic field. The two Fe^{II} centers distinguish **1** from complexes of type **I**, that are accessible in Fe^{III}/Fe^{III} and Fe^{III}/Fe^{II} but not Fe^{II}/Fe^{II} oxidation states.[1]

Also the electrochemical properties of **1** are worth comment. In contrast to the [2Fe–2S] clusters of type **I**, complex **1** can take up or release several electrons and shows five redox waves in the cyclic voltammogram (Fig. 3).

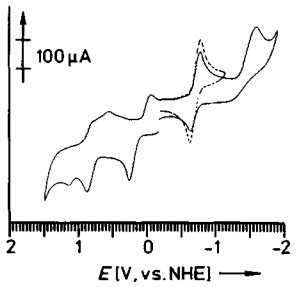

Fig. 3. Cyclic voltammogram of **1**; 10^{-3} mol L^{-1} in CH_2Cl_2, 0.1 mol L^{-1} $[N(C_4H_9)_4]ClO_4$, $v = 100$ mV s^{-1}, NHE = normal hydrogen electrode.

Complex **1** gives a positive methylene-blue reaction.[9] This interesting finding shows that μ-S_2 ligands apparently also undergo this reaction, which is a typical test for S^{2-} ligands. It is thus not surprising that the exact number of S^{2-} ligands in many [metal sulfide] proteins is unknown. The difficulties encountered when determining the S^{2-} content of such proteins were comprehensively reviewed recently.[10] Furthermore, similarly to the H clusters of Fe/Fe hydrogenases,[2] **1** reacts irreversibly with CO under normal conditions. $[\{Fe(CO)(\mu\text{-}'S_4')\}_2]$[6] forms from **1**, showing that the coordinatively saturated Fe centers of **1** are still reactive enough to coordinate CO with concomitant loss of the S_2 bridge.

These results are significant for a more detailed characterization of structurally unknown [Fe–S] sites of proteins, including in particular the M^N, P, and S clusters of nitrogenases and the H clusters of hydrogenases. For example, for the M^N clusters, which probably contain the Fe–Mo cofactor, Mössbauer parameters $\delta = 0.41$ and $\Delta E_Q = 0.8$ mm s^{-1} have been reported,[3] which correlate with octahedral low-spin Fe^{II} centers in sulfur-dominated coordination spheres as found in **1** or $[\{Fe(CO)(\mu\text{-}'S_4')\}_2]$ and $[Fe_2(CO)(NO)(\mu\text{-}'S_4')_2]$.[6] The H clusters of hydrogenases in the reduced form of the protein are diamagnetic in external magnetic fields up to 6.0 T, and EXAFS studies on them yield Fe–Fe distances of 3.3 Å.[2] Both properties agree with those of **1**, but are incompatible with the occurrence of conventional [Fe–S] clusters of type **I**–**III**.

Experimental Procedure

All operations were carried out in an inert atmosphere (N_2) with Schlenk techniques. To a stirred white suspension of 'S_4'-H_2 (2060 mg, 6.7 mmol) and NaOMe (728 mg, 13.4 mmol) in THF (100 mL) was added $FeCl_2 \cdot 4H_2O$ (1320 mg, 6.7 mmol). On subsequent addition of elemental sulfur (215 mg, 6.7 mmol), the red-brown reaction mixture gradually became black-green, and **1** was formed. Complex **1** was filtered off after 24 h, washed with CS_2 and thereafter MeOH, and dried. Yield: 80%; correct elemental analyses; MS(FD): m/z 792 (M^+). ^1H NMR (270 MHz): $\delta = 7.8$–6.8 (m, C_6H_4; in $[D_7]$DMF); 2.9 (m), 2.6 (m, C_2H_4; in CD_2Cl_2); $^{13}C\{^1H\}$ NMR spectra could not be recorded because of the low solubility of **1**.

Received: May 13, 1991 [Z4625 IE]
German version: *Angew. Chem. 103* (1991) 1493

CAS Registry numbers:
1, 136489-55-9; hydrogenase, 9027-05-8.

[1] a) J. B. Berg, R. H. Holm in T. G. Spiro (Ed.): *Metal Ions in Biology, Vol. 4* (Iron Sulfur Proteins), Wiley, New York 1982; b) C. R. Kissinger, E. T. Adman, L. C. Sieker, L. H. Jensen, *J. Am. Chem. Soc. 110* (1988) 8721.
[2] M. W. W. Adams, *Biochim. Biophys. Acta 1020* (1990) 115.
[3] W. H. Orme-Johnson, *Annu. Rev. Biophys. Biophys. Chem. 14* (1985) 419.
[4] a) G. T. Kubas, T. G. Spiro, A. Terzis, *J. Am. Chem. Soc. 95* (1973) 273; b) R. Weberg, R. C. Haltiwanger, M. Rakowski DuBois, *Organometallics 4* (1985) 1315; c) H. Brunner, N. Janietz, W. Meier, G. Sergeson, J. Wachter, T. Zahn, M. L. Ziegler, *Angew. Chem. 97* (1985) 1056; *Angew. Chem. Int. Ed. Engl. 24* (1985) 1060.
[5] X-ray crystallographic data of **1**: $P\bar{1}$, $a = 1093.8(4)$, $b = 1113.2(4)$, $c = 1384.1(10)$ pm, $\alpha = 111.36(5)$, $\beta = 97.60(5)$, $\gamma = 100.71(3)°$; $V = 1504(2) \times 10^6$ pm^3; $Z = 2$. $T = 200$ K, $Mo_{K\alpha}$-radiation; ω scan; $3.0 < \dot{\omega} < 15°$ min^{-1}, $3° < 2\theta < 54°$. 6025 independent reflections of which 3287 have $F > 6\sigma(F)$. SHELXTL-PLUS, direct methods, $R = 0.084$, $R_w = 0.066$. Further details of the crystal structure investigation may be obtained from the Fachinformationszentrum Karlsruhe, Gesellschaft für wissenschaftlich-technische Information mbH, W-7514 Eggenstein-Leopoldshafen 2 (FRG) on quoting the depository number CSD-320253, the names of the authors, and the journal citation.
[6] D. Sellmann, R. Weiss, F. Knoch, G. Ritter, J. Dengler, *Inorg. Chem. 29* (1990) 4107.
[7] We thank Prof. Dr. *G. Ritter* and Dipl.-Phys. *J. Dengler*, Institut für Physik at the Universität Erlangen-Nürnberg, for recording the Mössbauer spectra.
[8] P. Collins, J. Travis in I. Gruverman (Ed.): *Mössbauer Effect Methodology, Vol.3*, Plenum Press, New York 1967, p. 123.
[9] a) J. K. Fogo, M. Popowsky, *Anal. Chem. 21* (1949) 732; b) W. Lovenberg, B. B. Buchanan, J. C. Rabinowitz, *J. Biol. Chem. 238* (1963) 3899; c) K. Suhara, S. Takemori, M. Katagiri, K. Wada, H. Kobayashi, H. Matsubara, *Anal. Biochem. 68* (1975) 632.
[10] B. K. Burgess, *Chem. Rev. 90* (1990) 1377.

The First Persistent β-Silyl-Substituted Vinyl Cation**

By *Hans-Ullrich Siehl*, Frank-Peter Kaufmann, Yitzhak Apeloig, Viviana Braude, David Danovich, Armin Berndt*, and *Nikolaos Stamatis*

Dedicated to Professor Michael Hanack on the occasion of his 60th birthday

The ability of silyl substituents to promote the formation of positive charge at the β-position (the "β-silyl effect") has attracted considerable experimental as well as theoretical interest in the last decade.[1] Gas-phase experiments,[2] solvolysis studies,[3] and high-level ab initio calculations[4] show that the β-silyl stabilization, attributed to strong σ–π interactions (hyperconjugation), is substantial—in the range of 18–22 kcal mol^{-1} (relative to hydrogen) for secondary carbenium ions.

However, attempts to observe β-silyl-substituted carbocations in solution have failed.[5] These failures have been attributed to the higher bond energy of Si–O and Si–halogen bonds compared to the Si–C bond, to the ease of forming five-coordinated silicon intermediates, and to the polar nature of the Si–C bond ($Si^{\delta+}$–$C^{\delta-}$) which makes the silicon prone to attack even by weakly nucleophilic anions of superacids, with subsequent cleavage of the Si–C bond.

In this communication we report the first successful observation of a stable β-silyl-substituted carbocation by ^{13}C NMR. Furthermore, the very efficient hyperconjugative stabilization by the β-silyl groups enables the first characterization by NMR of a vinyl cation which is not stabilized by π-conjugating groups, such as vinyl or aryl substituents.[6]

Protonation of tetrakis-(trimethylsilyl) allene **1**[7] with HSO_3F/SbF_5 under carefully controlled experimental condi-

[*] Priv.-Doz. Dr. H.-U. Siehl, Dipl.-Chem. F.-P. Kaufmann
Institut für Organische Chemie der Universität
Auf der Morgenstelle 18, W-7400 Tübingen (FRG)
Prof. Dr. Y. Apeloig, V. Braude, D. Danovich
Department of Chemistry, Technion – Israel Institute of Technology
Haifa 32000 (Israel)
Prof. Dr. A. Berndt, N. Stamatis
Fachbereich Chemie der Universität Marburg

[**] This work was supported by the Deutsche Forschungsgemeinschaft and the Fonds der Chemischen Industrie (Tübingen, Marburg), the Israel Academy of Sciences and Humanities, the Henri Gutwirth Fund, and the Fund for the Promotion of Research (Technion). *D.D.* thanks the Center for the Absorption of Science, Ministry of Immigrant Absorption, State of Israel, for a scholarship.

tions[8] gives the 1,1,3,3-tetrakis(trimetylsilyl)methylpropen-2-yl cation **2**.[9] The isomeric allyl cation **3** is not formed, as is evident from the ^1H and ^{13}C NMR data[9] (e.g. the chemical shifts, in particular of the β' proton signal at $\delta = 2.81$ ($-100\,^\circ C$), as well as the multiplicities and relative intensities of the carbon signals[9]). This contrasts with the protonation of 1,3-dimethyl, 1,1,3,3-tetramethyl, and 1,3,3-trimethyl 1-phenyl allene with HSO_3F/SbF_5, which yield the corresponding allyl cations.[10] The different reaction courses followed by the silyl- and alkyl-substituted allenes are fully consistent with the hyperconjugation model, which predicts that a β-silyl group is more stabilizing than a β-alkyl group,[2-4] and with previous conclusions[11] that α-silyl substitution as in **3** is destabilizing relative to α-methyl substitution. The larger spatial requirements of the trimethylsilyl groups may also contribute to the kinetic stability of **2**.

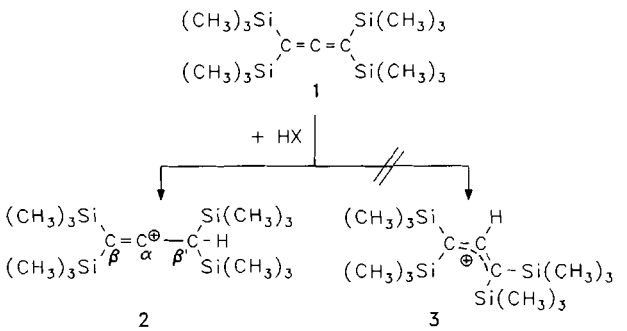

At $-100\,^\circ C$ the ^{13}C NMR spectrum of **2** shows five signals (Fig. 1). Assignments[9] are based on the ^1H-coupled ^{13}C NMR spectra and on comparison of chemical shifts with

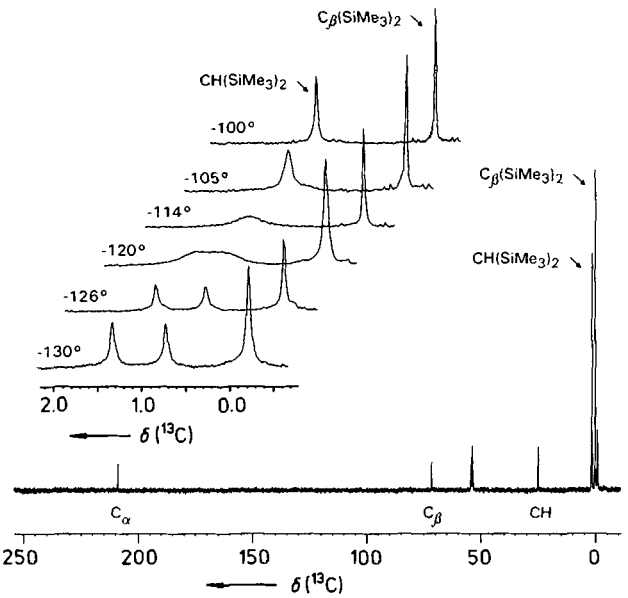

Fig. 1. 100.6 MHz ^{13}C NMR spectrum of **2** ($-100\,^\circ C$, $SO_2ClF/SO_2F_2/CD_2Cl_2$). The insert shows the temperature dependence (-130 to $-100\,^\circ C$) of the $(CH_3)_3Si$ signals.

those of other β-silyl-substituted vinyl cations,[6d] as well as with IGLO chemical shift calculations[12] of model systems such as **4** and **5**. Comparison with NMR data of other vinyl cations, which were obtained in several types of acidic media and with different counterions,[6d] indicates that specific interactions (like ion pairing and fluoride ion complexation to the silicon atom) are not important for **2** under the conditions employed. The good agreement between the experimental and the calculated shifts for **2** (see below) also support this conclusion.

$H_2C=C^\oplus-CH_2(SiH_3)$ **4** $H_2C=C^\oplus-CH(SiH_3)_2$ **5**

The signal at $\delta = 208.7$ assigned to C_α of **2** is strongly shielded (by ca. 250, 198, 186, and 214 ppm) relative to the IGLO calculated shifts for C_α in the parent (nonbridged vinyl cation,[12a] in $H_2C=C^\oplus CH_3$, in $H_2C=C^\oplus CH_2CH_3$, and in $(H_3C)_2C=C^\oplus CH_3$, respectively. Comparable shieldings of C_α have been observed in vinyl cations stabilized by $2p-\pi$ conjugation or by hyperconjugation with cyclopropyl substituents.[6a] Calculations[12b] for model cations confirm the strong shielding effect of β-silyl substituents (Scheme 1).

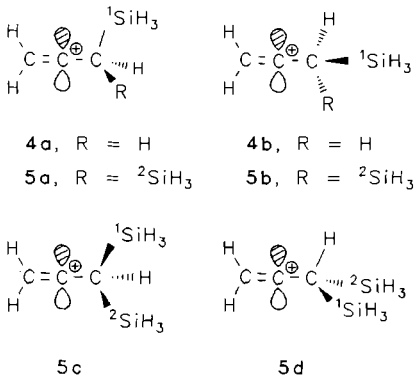

Scheme 1. Conformers of **4** and **5** for which the ab initio and IGLO calculations were performed.

Thus, the calculated chemical shift for C_α in **5c** ($\delta = 331$) is 75 ppm upfield relative to C_α in $H_2C=C^\oplus CH_3$. The vinylic β-silyl groups cause even larger shielding of C_α (123 ppm in $(H_3Si)CH=C^\oplus CH_3$ and 158 ppm in $(H_3Si)_2C=C^\oplus CH_3$ relative to $H_2C=C^\oplus CH_3$). The calculated overall shielding of the four β- and β'-H_3Si groups in **5c** is 233 ppm (158 + 75), 18 ppm higher than the observed shielding of C_α in **2** compared with the IGLO value for C_α in $(H_3C)_2C=C^\oplus CH_3$. These strong shielding effects can be attributed mainly to hyperconjugative charge dispersal and not to the inductive effect of silicon. Thus, IGLO calculations show that C_α is shielded by 75 ppm in **4a** compared to **4b** and by 53 ppm in **5c** relative to **5d**, while in $H_2C=C^\oplus CH_2CH_3$ the difference between conformations analogous to **4a** and **4b** is only 10 ppm. Similar shielding effects attributed to hyperconjugation have been observed for analogous β-silyl methyleneboranes.[13a]

The chemical shift for C_β in **2** ($\delta = 71.39$) is not much different from that in other vinyl cations[6] or from the IGLO values for C_β in $H_2C=C^\oplus H$ ($\delta = 69$),[12a] $H_2C=C^\oplus CH_3$ (73), **5c** (74), or $H_3SiCH=C^\oplus CH_3$ (66). The chemical shift of the methine carbon C_β ($\delta = 25$) is also in line with the IGLO calculations; for example, $\delta = 30$ in $H_2C=C^\oplus CH_3$, 36 in **5c**, and 19 in $H_3SiCH=C^\oplus CH_3$.

At $-100\,^\circ C$ two signals at $\delta = 0.14$ and 1.59 are observed for the four trimethylsilyl groups. However, upon cooling (see insert in Fig. 1) the peak at $\delta = 1.59$ broadens, and below the coalescence temperature of ca. $-114\,^\circ C$ it splits into two peaks, which at $-130\,^\circ C$ are 0.67 ppm apart and have similar line widths to the other peaks at that temperature.

This allows the unequivocal assignment of the signal at $\delta = 0.14$ ($-100\,^{\circ}C$) to the β-$SiMe_3$ groups and the averaged peak at $\delta = 1.59$ ($-100\,^{\circ}C$) to the $CH(SiMe_3)_2$ groups. The free energy barrier for the dynamic process is $\Delta G^{\neq} = 7.5$ kcal mol^{-1} (31 kJ mol^{-1}) at $-114\,^{\circ}C$.

Ab initio calculations[14] on model cations **4**–**6** assist in the interpretation of the equilibration process that leads to the averaged signal.

$(H_3Si)_2C = C^{\oplus} - CH(SiH_3)_2$

6

As expected on the basis of the hyperconjugation concept[4], cation **4** prefers conformation **4a** in which hyperconjugation between the empty 2p orbital on $C^{\oplus}$ and the Si–C bond is maximized. The calculated rotation barrier around the $C^{\oplus}$–CH_2SiH_3 bond is 14.5 kcal mol^{-1} at MP 3/6–31 G*//6–31 G* (12.4 kcal mol^{-1} at 6–31 G*//6–31 G*); conformation **4b** is the highest point along the rotation path.

In the disilyl-substituted cation **5**, the most stable calculated conformation is **5c**, where each of the Si–C bonds forms a dihedral angle θ of ca. 30° with the empty 2p orbital on $C^{\oplus}$, each thus contributing 75 % of the full hyperconjugative stabilization of this group. (This estimation is based on the dependence of the hyperconjugative stabilization on $[1 + \cos 2(90 - \theta)]$,[15] where θ is the dihedral angle $HC_{\beta}C_{\beta'}Si$.) Conformation **5a**, in which the maximal interaction with the empty 2p orbital is possible for one silyl group ($^1SiH_3$) and 25 % for the other ($^2SiH_3$), is 3.1 kcal mol^{-1} (MP 3/6–31 G*//6–31 G*) higher in energy. However, a detailed analysis of the computational results leads us to predict that at higher levels of calculations **5a** is actually the most stable conformation of **5**.[16a] Thus, as a result of hyperconjugation the geometry in **5a** is strongly distorted toward a ^1Si-bridged species $\sphericalangle\, ^1Si{-}C_{\beta'}{-}C_{\alpha} = 102.4°$ and $d(C_{\beta'}{-}^1Si) = 203$ pm, compared to $\sphericalangle\, ^2Si{-}C_{\beta'}{-}C_{\alpha} = 117.1°$ and $d(C_{\beta'}{-}^2Si) = 196$ pm). It is therefore likely that energetically, **5a** will benefit more than **5c** from geometry optimizations at the MP2/6–31 G* level (which are beyond our computing capabilities) making it more stable than **5c**.[16b] MP2/6–31 G* geometry optimizations of **4a** indeed show stronger distortions toward silyl bridging than at 6–31 G*, and $\sphericalangle\, Si{-}C_{\beta'}{-}C_{\alpha}$ is reduced from 102° (6–31 G*) to 92°. In analogy to **5** we expect the most stable conformation of **2** to be **2a**, in which the $^1Si(CH_3)_3$ group is in the $H_2C{=}C^{\oplus}$ plane and strongly bent toward the cationic center.

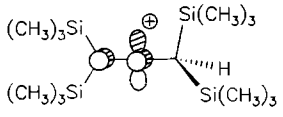

2a

This conclusion is consistent with the experimental observation at $-130\,^{\circ}C$ of two ^{13}C NMR signals for the β'-silyl groups. Recent calculations on tricoordinated carbocations show analogous structural distortions accompanying hyperconjugation[17a] and the same preference for σ–π interaction with one of two seemingly equal β-C–H or β-C–C σ bonds.[17b] Similar distortions due to C–Si hyperconjugation have been observed experimentally in a substituted 1-bis(trimethylsilyl)methyl methyleneborane.[13b]

The calculated barrier to rotation around the $C^{\oplus}$–$CH(SiMe_3)_2$ bond in **5** is 13.6 kcal mol^{-1} (MP 3/6–31 G*//6–31 G*), **5d** being the highest energy conformer along the rotation path. Further stabilization of **5** by two β-silyl groups lowers the electronic demand on the β'-silyl groups and in **6** the calculated rotation barrier is only 5.9 kcal mol^{-1} (3–21 G*//3–21 G*). Computational experience with the smaller cations suggests that at MP 3/6–31 G*, the barrier to rotation in **6** would be higher by 1–2 kcal mol^{-1}. The calculated rotation barrier for **6** is close to the value of 7.5 kcal mol^{-1} determined experimentally for the equilibration of the two β'-$SiMe_3$ groups in **2**. However, this equilibration process can bypass the conformation analogous to **5d**.

In conclusion, we have prepared and observed by NMR spectroscopy the first persistent β-silyl-substituted carbocation and have shown by molecular orbital calculations that rotation around the $C^{\oplus}$–$CH(SiMe_3)_2$ bond is controlled by strong hyperconjugation with the β-silyl groups, and that IGLO calculations nicely account for the observed chemical shifts.

Received: June 3, 1991 [Z 4669]
German version: *Angew. Chem. 103* (1991) 1546

CAS Registry numbers:
1, 3721-17-3; **2**, 136445-13-1; **4**, 95045-34-4; **5**, 136445-14-2; **6**, 136445-15-3.

[1] For a recent review see: J. B. Lambert, *Tetrahedron 46* (1990) 2677.
[2] a) D. Hajdasz, R. Squires, *J. Chem. Soc. Chem. Commun. 1988*, 1212; b) X. Li, A. Stone, *J. Am. Chem. Soc. 111*, (1989) 5586; c) Y. Apeloig, M. Karni, A. Stanger, H. Schwarz, T. Drewello, G. Czekay, *J. Chem. Soc. Chem. Commun. 1987*, 989.
[3] a) J. B. Lambert, R. B. Finzel, *J. Am. Chem. Soc. 104* (1982) 2020; b) J. B. Lambert, G.-T. Wang, R. B. Finzel, D. H. Teramura, *ibid. 109* (1987) 7838; c) J. B. Lambert, G.-T. Wang, *J. Phys. Org. Chem. 1* (1988) 169; d) J. B. Lambert, E. C. Chelius, *J. Am. Chem. Soc. 112* (1990) 8120; e) H. Mayr, R. Pock, *Tetrahedron 42* (1986) 4211; f) R. Biton, Y. Apeloig in *10th IUPAC-Conference on Physical Organic Chemistry*, Haifa, Israel 1990, PO-A-74, p. 186; g) Y. Himeshima, H. Kobayashi, T. Sonoda, *J. Am. Chem. Soc. 107* (1985) 5286.
[4] a) M. R. Ibrahim, W. L. Jorgensen, *J. Am. Chem. Soc. 111* (1989) 819; b) S. G. Wierschke, J. Chandrasekhar, W. L. Jorgensen, *ibid. 107* (1985) 1496; c) Y. Apeloig, D. Arad, *ibid. 107* (1985) 5285.
[5] G. A. Olah, A. L. Berrier, L. D. Field, G. K. S. Prakash, *J. Am. Chem. Soc. 104* (1982) 1349.
[6] a) H.-U. Siehl, E.-W. Koch, *J. Org. Chem. 49* (1984) 575; b) H.-U. Siehl, *J. Chem. Soc. Chem. Commun. 1984*, 635; c) E.-W. Koch, H.-U. Siehl, M. Hanack, *Tetrahedron Lett. 26* (1985) 1493; d) K. Bertsch, *Diplomarbeit*, Universität Tübingen, 1987; F.-P. Kaufmann, *Diplomarbeit*, Universität Tübingen, 1990.
[7] **1**: ^{13}C NMR (100.6 MHz, $CDCl_3$, 27 °C, TMS): $\delta = 203.88$ (central allene-C), 64.27 (terminal allene-C), 0.63 ($^1J(CH) = 118.7$ Hz, methyl groups). ^1H NMR (400 MHz, $CDCl_3$, internal standard $CHCl_3$, $\delta = 7.24$): $\delta = 0.08$ (methyl groups).
[8] 0.35 mL (ca. 6.3 mmol) HSO_3F and 0.1 ml (ca. 0.31 mmol) **1** are cocondensed within 45 min at 2×10^{-5} mbar onto a homogeneous matrix of 0.08 mL (ca. 1.3 mmol) SbF_5, 2.4 mL SO_2ClF, 0.7 mL SO_2F_2, and 0.3 mL CD_2Cl_2 at $-196\,^{\circ}C$. Warming to $-125\,^{\circ}C$ yields a colorless solution of **2**. For experimental details, see: D. Lenoir, H.-U. Siehl in M. Hanack (Ed.), *Methoden Org. Chem. (Houben–Weyl)* 4th Ed. 1952ff, Thieme, Vol. E 19c, (1990), p. 26–32.
[9] **2**: ^{13}C NMR (100.6 MHz, $SO_2ClF/SO_2F_2/CD_2Cl_2$, internal standard CD_2Cl_2, $\delta = 53.80$), :δ ($-100\,^{\circ}C$) = 208.73 ($^2J(CH) = 9.5$ Hz, $C^{\oplus}$), 71.39 ($^3J(CH) < 3.5$ Hz, C_{β}), 25.00 ($^1J(CH) = 121$ Hz, $^3J(CH) < 2.7$ Hz, $C_{\beta'}$), 1.59 ($^1J(CH) = 122$ Hz, C_{β}–$Si(CH_3)$ methyl groups), 0.14 ($^1J(CH) = 121$ Hz, $C_{\beta'}$–$Si(CH_3)$ methyl groups; δ ($-136\,^{\circ}C$) = 208.74 ($C^{\oplus}$), 70.58 (C_{β}), 25.27 ($C_{\beta'}$), 1.35 and 0.70 ($C_{\beta'}$–$Si(CH_3)$ methyl groups), -0.30 (C_{β}–$Si(CH_3)$ methyl groups). ^1H NMR (400 MHz, in $SO_2ClF/SO_2F_2/CD_2Cl_2$, internal standard $CHDCl_2$, $\delta = 5.32$ ppm): δ ($-100\,^{\circ}C$) = 2.81 (β'-H), 0.59 ($C_{\beta'}$–$Si(CH_3)$ methyl groups), 0.47 (C_{β}–$Si(CH_3)$ methyl groups); δ ($-113\,^{\circ}C$) = 2.89 (β'-H). 0.57 (br., $C_{\beta'}$–$Si(CH_3)$ methyl groups), 0.44 (C_{β}–$Si(CH_3)$ methyl groups).
[10] C. U. Pittman, Jr., *J. Chem. Soc. Chem. Commun. 1969*, 122.
[11] Y. Apeloig, A. Stanger, *J. Am. Chem. Soc. 107* (1985) 2806.
[12] a) M. Schindler, *J. Am. Chem. Soc. 109*, (1987) 1020. b) Calculations used fully optimized 6–31 G* geometries. For basis sets used in the IGLO calculations see basis set II in: W. Kutzelnigg, U. Fleischer, M. Schindler, *NMR Basic Princ. and Prog. 23* (1991) 165–262.

[13] a) M. Pilz, M. Stadler, R. Hunold, J. Allwohn, W. Massa, A. Berndt, *Angew. Chem. 101* (1989) 761; *Angew. Chem. Int. Ed. Engl. 28* (1989) 784; b) P. Willershausen, *Diplomarbeit*, Universität Marburg 1990.
[14] The Gaussian 86 series of programs was used: M. J. Frisch, J. S. Binkley, H. B. Schlegel, K. Raghavachari, C. F. Melius, R. L. Martin, J. J. P. Stewart, F. W. Bobrowicz, C. M. Rohlfing, L. R. Kahn, D. J. Defrees, R. Seeger, R. A. Whiteside, D. H. Fox, E. M. Fluder, J. A. Pople, Carnegie-Mellon University, Pittsburgh, PA (USA).
[15] L. Radom, W. J. Hehre, J. A. Pople, *J. Am. Chem. Soc. 94* (1972) 2371; for applications of this function to hyperconjugation, see for example: Z. Rappoport, B. Abramovitch, M. Karni, Y. Apeloig, *Israel J. Chem. 29* (1989) 267.
[16] a) At 6–31G*, the only minimum on the potential energy surface of **5** is **5c** (verified by frequency calculations to be a minimum). The structure reported for **5a** is fully optimized except that ^{1}Si was kept in the $H_2C{=}C^{\oplus}$ plane; b) the 6–31G* optimized structure of **5c** also shows prefered $\sigma-\pi$ interaction by one of the two seemingly equivalent silyl groups (although to a smaller extent than in **5a**): $\sphericalangle$ ^{1}Si–$C_{\beta'}$–C_{α} = 107.5°, d($C_{\beta'}$–^{1}Si) = 201 pm and $\sphericalangle$ ^{2}Si–$C_{\beta'}$–C_{α} = 112.5°, d($C_{\beta'}$–^{2}Si) = 199 pm.
[17] a) P. von R. Schleyer, J. W. de M. Carneiro, W. Koch, D. A. Forsyth, *J. Am. Chem. Soc. 113* (1991) 3990. b) for β-C–H hyperconjugation in cyclopentyl cation, see: P. von R. Schleyer, J. W. de M. Caneiro, W. Koch, K. Raghavachari, *ibid. 111* (1989) 5475; for β-C–C hyperconjugation in the 2,3-dimethyl-2-butyl cation, see: M. Saunders, G. W. Cine, *J. Am. Chem. Soc. 112* (1990) 3955.

Inclusion of Metal Ions within a Tin–Oxygen Cage Stabilized by Organic Residues: Crystal Structure of $[(i\text{PrSn})_{12}O_4(OH)_{24}][Ag_7I_{11}]\cdot NaCl\cdot H_2O\cdot 10\,DMSO$**

By *Hans Reuter**

Dedicated to Professor Heinrich Puff on the occasion of his 70th birthday

As in the case of polyoxovanadates, where it was only recently observed that solvent molecules[1a] and also halide ions[1b] can reside within the vanadium–oxygen cavity, large cagelike units are found in the crystal structures of partially or completely hydrolyzed monoorganotin trichlorides,[2] carboxylates,[3] phosphinates,[3a,4] and phosphates,[3d] which can thus be considered as hosts for ions and small molecules. Although potential inclusion behavior has been long discussed in relation to the tin–oxygen cage,[3a] a preparative access to such supramolecular structures was hitherto unknown.

Only with difficulty could we imagine how a solvated or even a "naked" metal ion could penetrate the apolar organic shell to enter the relatively rigid tin–oxygen framework. We therefore tried to use the metal ion as template around which the tin–oxygen cage could be built.

Already the preliminary experiment in which an organotin compound was treated with sodium and silver ions as potential templates in the molar ratio 1:1:1.5 (see *Experimental Procedure*) proved the value of this strategy. Among the phases that crystallized from the solution over several weeks were compact, dark red crystals, which were shown by a single-crystal X-ray crystallographic analysis[5] to have the composition **1** and in which the sodium ion is included within the oligomeric organotin unit. The reaction can be represented formally by Equation (a).

$$12\,i\text{PrSn(OH)Cl}_2\cdot 3/4\,H_2O + 10\,AgI + NaI \xrightarrow{DMSO} [(i\text{PrSn})_{12}O_4(OH)_{24}][Ag_7I_{11}]\cdot NaCl\cdot H_2O\cdot 10\,DMSO + 5\,H_2O + 3\,AgCl + 8\,HCl \quad (a)$$

1

$[(i\text{PrSn})_{12}O_4(OH)_{24}]^{4+}$ **2** $[Ag_7I_{11}]^{4-}$ **3**

The solid-state structure of **1** (= **2**–**3**·NaCl·H_2O·10 DMSO) contains as novel structural elements cation **2** and anion **3**. The structure of **2** and the position of the encapsulated sodium ion is shown as ball-and-stick model in Figure 1, left. The ion has approximate C_s symmetry. It differs from the known hydrolysis products[2] of monoorganotin trichloride, in which five-coordinate, trigonal-pyramidal or square-planar tin atoms coexist with six-coordinate tin atoms, in that all 12 tin atoms have octahedral coordination. Further primary building units[6] are four oxygen atoms each bridging three tin atoms (the oxygen atoms form the apex of trigonal pyramids) and 24 hydroxyl groups each bridging two tin atoms.

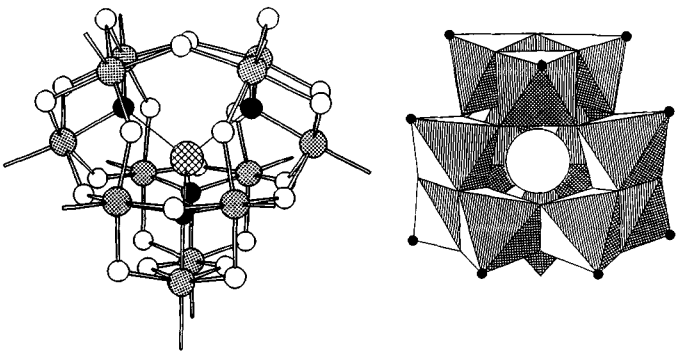

Fig. 1. Crystal structure of the $[(i\text{PrSn})_{12}O_4(OH)_{24}]^{4+}$ ion and the sodium ion encapsulated within it. Left: ball-and-stick model. Open circles = OH groups, filled circles = O atoms, dotted circles = Sn, hatched circle = Na^+ ion; for clarity the atoms of the isopropyl groups have been omitted, but their position relative to the Sn–O framework is indicated by a bonding stick. Observed distances [pm] and angles [°] (averaged values/no. of individual values in parentheses): Na-O 233.9–243.8 (240.2/4), O-Na-O = 104.0–113.6 (109.4/12); Sn-O = 204.3–218.5 (210.8/12), Sn-O-Sn = 101.7–108.9; Sn-OH = 199.1–221.9 (211.5/48), Sn-OH-Sn = 101.4–110.6 (105.3/14), 137.1–146.9 (141.6/10). Right: polyhedral type model. Black spheres = position of an organic residue, open spheres = Na^+ ion; view of the ten-membered Sn–O ring.

The cavity inside the tin–oxygen cage is edged by the four μ_3–O atoms tetrahedrally arranged around the sodium ion. The average O–Na distance is 240.2 pm, and the O-Na-O angle 109.5°. Such a low coordination number for sodium ion is unusual, but not impossible.[7] In this case it is probably forced on the ion by the topological requirements within the Sn–O cage.

Metal–oxygen cagelike clusters with twelve octahedrally coordinated metal atoms and a tetrahedrally coordinated metal or nonmetal ion at the center also occur in hetero- and isopolycations and -anions, to which the different Keggin structural types belong. The structural correspondence of **2** with these compounds becomes clear on considering the polyhedral type model in Figure 1, right. In both, the dodecameric ion comprises four trimeric building blocks. Every octahedral unit of the trimer shares two edges with both the other two.[8] In contrast to the heteropolyanion $[PW_{12}O_{40}]^{3-}$ ($\triangleq[(W^{oct}O)_{12}(\mu_3\text{-}O)_4(\mu_2\text{-}O)_{24}(P^{tetr})]^{3-}$) of the α-Keggin structural type,[9] in which one trimeric building block shares two corners with all three other trimers, and the isopolycation $[Al_{13}O_4(OH)_{24}(H_2O)_{12}]^{7+}$ ($\triangleq[(H_2O\text{-}Al^{oct})_{12}(\mu_3\text{-}O)_4(\mu_2$-

[*] Dr. H. Reuter
Institut für Anorganische Chemie der Universität
Gerhard-Domagk-Strasse 1, W-5300 Bonn 1 (FRG)

[**] The Hydrolysis of Monoorganotin Trihalides Part 4. This work was supported by the Deutsche Forschungsgemeinschaft and the Fonds der Chemischen Industrie. Part 3: H. Puff, H. Reuter, *J. Organomet. Chem. 373* (1989) 173. DMSO = dimethyl sulfoxide.

$OH)_{24}(Al^{tetr})]^{7+}$) analogous to the ε-Keggin structural type, in which each trimeric building block shares an edge with all other three,[10] one trimeric building block in this case shares corners with the three others, which in turn share edges. It is thus isostructural with the heteropolyanion $[PW_{10}V_2O_{40}]^{5-}$ ($\triangleq[(V^{oct}O)_2(W^{oct}O)_{10}(\mu_3\text{-}O)_4(\mu_2\text{-}O)_{24}(P^{tetr})]^{5-}$) of the γ-Keggin type.[11]

Ion **2** is bound to ten DMSO molecules by hydrogen bonds. All μ_2-OH groups, with few exceptions (see below), are involved, but in one case a single water molecule lies between the hydroxyl group and the solvent molecule. As can be seen in Figure 2, the apolar organic shell formed by the isopropyl groups is completed by these solvent molecules. The thus

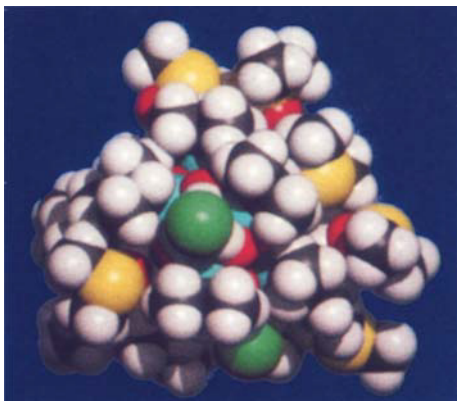

Fig. 2. Space-filling model of $[(i\text{PrSn})_{12}O_4(OH)_{24}]^{4+}$ ion and its immediate surroundings: tin = turquoise, oxygen = red, carbon = black, hydrogen = white, sulfur = yellow, chlorine = green; for a clearer picture of the function of the solvent molecule, the structural model has been extended to include the hydrogen atoms. Intermolecular distances [pm]: DMSO···HO- 246.1–298.6, DMSO···H_2O = 276.6, H_2O···HO- 248.0, Cl···HO- 324.2–345.1.

solvated cation is not isolated in the crystal, but is linked as a strongly puckered one-dimensional string via chloride ions. Also in this case the bonds are hydrogen bonds, which are, however, distinctly longer because of the larger ionic radius of the chloride ion and its weaker acceptor properties.

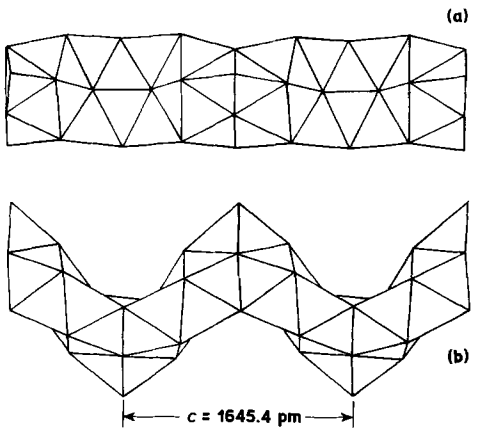

Fig. 3. Polyhedral type model of the $[Ag_7I_{11}]^{4-}$ ion from the top (a) and from the side (b); for clarity only the face-sharing tetrahedrons formed by the iodide ions are shown; the positions of all silver ions are within this one-dimensional double string; interatomic distances [pm] (average/number of individual values in parentheses): I···I 409.5–521.2 (470.6/41), Ag···I 234.8–330.0 (288.9/72); between the individual anion strings and between these and the solvated cation strings are no interactions that are stronger than normal van der Waals interactions.

The second remarkable structural feature of **1** in the crystal is the complex anion $Ag_7I_{11}^{4-}$ (**3**), which may be described as a one-dimensional, twisted double chain $^1_\infty[Ag_7I_{11}^{4-}]$ of face-sharing iodine tetrahedrons. This anion string lies in the *yz* plane (depicted in Fig. 3), strictly parallel to the cation string, although no forces stronger than van der Waals interactions are formed between the strings.

Although the positions of the iodine atoms could be determined very precisely, this was only partly possible for the Ag^+ ions.[12] In the structural model proposed here, 18 Ag^+ sites (occupancy factors from 1.00 to 0.15) were taken into account, some of which are situated at the center of the iodide tetrahedrons and some are displaced towards a shared tetrahedral face. Thus of the total of 19 crystallographically independent tetrahedrons per asymmetric unit, almost all are partly or completely occupied.

These structural characteristics of **3** fulfill the essential conditions for a solid-state electrolyte, and we anticipate that the compound will show a significant one-dimensional silver-ion conductivity.[13]

Experimental Procedure

First NaI (5.64 g, 37.6 mmol) was dissolved in 35 mL DMSO in a 100 mL Erlenmeyer flask. Much heat evolved, and after the solution cooled AgI (12.2 g, 52.0 mmol) was dissolved. Thereafter $i\text{PrSn(OH)}_2\text{Cl}\cdot 3/4\,H_2O$ [2a] (9.22 g, 37.7 mmol) was added. The suspension was stirred and heated to ca. 80 °C, during which time the organotin compound slowly dissolved. After two hours the small amount of undissolved substance was filtered from the hot solution and the clear, dark red solution left to stand open to air. Beside other not yet studied crystalline phases, **1** separated during the course of several weeks as large dark red crystals that slowly decomposed in air [14].

Received: June 3, 1991 [Z4587 IE]
German version: *Angew. Chem. 103* (1991) 1487

CAS Registry numbers:
1, 137007-08-0; **2**·3·NaCl, 137003-10-2; $i\text{PrSn(OH)}_2\text{Cl}$, 125739-94-8.

[1] a) V. W. Day, W. G. Klemperer, O. M. Yaghi, *J. Am. Chem. Soc. 111* (1989) 5959; b) A. Müller, M. Penk, M. Rohlfing, E. Krickmeyer, J. Döring, *Angew. Chem. 102* (1990) 928; *Angew. Chem. Int. Ed. Engl. 29* (1990) 926.

[2] a) H. Puff, H. Reuter, *J. Organomet. Chem. 368* (1989) 173; b) H. Puff, H. Reuter, *ibid. 373* (1989) 173.

[3] a) V. Chandrasekhar, R. O. Day, R. R. Holmes, *Inorg. Chem. 24* (1985) 1970; b) V. Chandrasekhar, C. G. Schmid, S. D. Burton, J. M. Holmes, R. O. Day, R. R. Holmes, *ibid. 26* (1987) 1050; c) R. R. Holmes, C. G. Schmid, V. Chandrasekhar, R. O. Day, J. M. Holmes, *J. Am. Chem. Soc. 109* (1987) 1408; d) R. O. Day, V. Chandrasekhar, K. C. K. Swamy, J. M. Holmes, S. D. Burton, R. R. Holmes, *Inorg. Chem. 27* (1988) 2887.

[4] a) R. O. Day, J. M. Holmes, V. Chandrasekhar, R. R. Holmes, *J. Am. Chem. Soc. 109* (1987) 940; b) K. C. K. Swamy, R. O. Day, R. R. Holmes, *ibid. 109* (1987) 5546; c) R. R. Holmes, K. C. K. Swamy, C. G. Schmid, R. O. Day, *ibid. 110* (1988) 7060; d) K. C. K. Swamy, C. G. Schmid, R. O. Day, R. R. Holmes, *ibid. 110* (1988) 7067.

[5] Compact, dark red crystal; dimensions: $0.28\times0.35\times0.31$ mm^3; $C_{56}H_{170}Ag_7ClI_{11}NaO_{39}S_{10}Sn_{12}$; M_r = 5422.47; monoclinic, space group $P2_1/c$; a = 2602.4(4), b = 3621.7(4), c = 1645.4(1) pm, β = 107.55(1)°, V = 14.786 nm^3, Z = 4, $\varrho_{calcd.}$ = 2.436 g cm^{-3}; $\mu(Mo_{K\alpha})$ = 52.30 cm^{-1}, Enraf Nonius CAD4 diffractometer, $Mo_{K\alpha}$ radiation 0.71069 Å, graphite monochromator, ω-2θ scans to $2\theta_{max}$ = 54.0° at T = 200(2) K; 19530 measured reflections, of which 18765 were symmetry-independent (R_m = 0.0617) and 11550 with $F_o \geq 4\sigma(F_o)$ considered observed, conventional corrections for intensity decay, Lorentz and polarization factor, solution of the structure with direct methods of the program SHELXS-86 [15a] and subsequent difference Fourier maps with the program SHELX-76 [15b]; refinement by least-squares method (block diagonal) of the program SHELX-400 [15c]; 947 refined parameters, ratio of data to parameters: 12.20; $R = \sum||F_o| - |F_c||/\sum|F_o| = 0.103$, $R_w = \sum\sqrt{w}||F_o| - |F_c||/\sum\sqrt{w}|F_o| = 0.088$ with $w = 1/\sigma^2(F_o)$; residual electron density $\leq 1.536\times10^{-6}$ e pm^{-3} within the $[Ag_7I_{11}]^{4-}$ ion; disorder in the region of the solvent molecules and silver ions; the drawings were designed with the program KPLOT [15d] and constructed with the program ORTEP [15e] (Fig. 1a, 3) and SCHAKAL-88 [15f] (Fig. 2). Further details of the crystal structure investigation may be obtained from the Fachinformationszentrum Karlsruhe, Gesellschaft für wissenschaftlich-technische Information mbH, W-7514 Eggenstein-Leopoldshafen 2 (FRG) on quoting the depository number CSD-55576, the name of the author, and the journal citation.

[6] Besides the almost planar four-membered Sn–O rings with acute angles at tin and wide angles at the oxygen atoms, which are characteristic for organotin oxygen compounds, and also the six-membered Sn–O rings in half-chair conformation [2b] the new hitherto unknown structural motifs of more or less strongly puckered, eight- and ten-membered Sn–O rings are found at secondary building units embedded in the molecular structure.
[7] See R. D. Shannon, *Acta Crystallogr. Sect. A 32* (1976) 751.
[8] On the possibilities of corner- and edge-sharing for four trimeric units and their realization in solids, cf. H. G. Wells: *Structural Inorganic Chemistry*, 5th ed., Clarendon, Oxford 1984, p. 520ff.; for the structural description of the Keggin isomers through successive rotation of the trimeric units see M. T. Pope, A. Müller, *Angew. Chem. 103* (1991) 56; *Angew. Chem. Int. Ed. Engl. 30* (1991) 34.
[9] G. M. Braun, M.-R. Noe-Spirlet, W. R. Busing, H. A. Levy, *Acta Crystallogr. Sect. B 33* (1977) 1038.
[10] a) G. Johansson, *Acta Chem. Scand. 14* (1960) 771; b) G. Johansson, *Ark. Kemi 20* (1963) 305; c) G. Johansson, *ibid. 20* (1963) 321.
[11] P. J. Domaille, R. L. Harlow, *J. Am. Chem. Soc. 108* (1986) 2108.
[12] Cf. S. Geller, *Acc. Chem. Res. 11* (1978) 87.
[13] Cf. X. Sishen, S. Geller, *J. Solid State Chem. 68* (1987) 73.
[14] Because of the very inhomogenous composition of the crystallized material, which is accompanied by a strong interpenetrating growth of individual phases, the X-ray crystallographic determination of the Sn, I, and Ag content of the single crystal used was confirmed by energy dispersive X-ray microanalysis (EDX). The ratio thus determined (1:1.02:0.55) agrees well, within the limits of precision of this method, with those calculated from electron densities. The formulation of anion **3** as $[Ag_7I_{11}]^{4-}$ implies that all oxygen atoms bridging two tin atoms in **2** are protonated and that the oxygen atom of the solvate must come from water. This agrees with the observed pattern of hydrogen bonds.
[15] a) G. M. Sheldrick, *SHELXS-86: Program for Crystal Structure Determination*, Göttingen 1986; b) G. M. Sheldrick, *SHELX-76: Program for Crystal Structure Determination*, Cambridge 1976; c) G. M. Sheldrick, *SHELX-400: Program for Crystal Structure Determination*; modified by R. Rabinovich, K. Reich, Rehovot 1976; d) R. Hundt, *KPLOT: Ein Programm zum Zeichnen und zur Untersuchung von Kristallstrukturen*, Bonn 1979; e) C. K. Johnson, *ORTEP: A FORTRAN Thermal Ellipsoid Plot Program for Crystal Structure Illustrations*, Oak Ridge 1965; modified by R. Hundt, Bonn 1969; f) E. Keller, *SCHAKAL-88, A FORTRAN Program for the Graphic Representation of Molecular and Crystallographic Models*, Freiburg 1988.

Ring Inversion in Sterically Hindered Arenes

By *Günther Maier,* Frank Fleischer, Hans-Otto Kalinowski,* and *Roland Boese*

Dedicated to Professor Horst Prinzbach on the occasion of his 60th birthday

The congestion of *tert*-butyl groups in a molecule favors the formation of spherical structures.[1] The most convincing example of this behavior is the "corset effect", which gives tetra-*tert*-butyltetrahedrane its surprisingly high stability.[2] We now report on another phenomenon which is likewise based on the repulsive interactions of neighboring *tert*-butyl groups and which came to our attention on examination of the ^{1}H NMR spectrum of 3,4,5-tri-*tert*-butyl-6-isopropylpyridazine (**1**).

Analogous to the tetra-*tert*-butyl derivative **2**[3], the pyridazine **1** is accessible in almost quantitative yield by heating (tri-*tert*-butyl-2-cyclopropen-1-yl)isopropyldiazomethane to 80 °C. The diazo compound itself is obtained in 12% yield by the reaction of lithiated isopropyldiazomethane with tri-*tert*-butylcyclopropenylium tetrafluoroborate.[4]

[*] Prof. Dr. G. Maier, Dipl.-Chem. F. Fleischer, Dr. H.-O. Kalinowski
Institut für Organische Chemie der Universität
Heinrich-Buff-Ring 58, W-6300 Giessen (FRG)
Priv.-Doz. Dr. R. Boese
Institut für Anorganische Chemie
der Universität-Gesamthochschule Essen (FRG)

At room temperature the ^{1}H NMR signals of both methyl groups of the isopropyl substituent of **1**[5] appear as two separated doublets (J = 6.5 Hz) at δ = 1.26 and 1.55 and the corresponding ^{13}C NMR signals[5] at δ = 22.6 and 25.2. However, a single, sharp signal is observed for the methyl groups of each of the three *tert*-butyl substituents. On heating a sample of **1** in pentadeuterionitrobenzene or [D_{18}]cyclosilane (1,1,3,3,5,5-hexakis(trideuteriomethyl)-1,3,5-trisilacyclohexane), the previously separate doublets of the methyl groups of the isopropyl substituent broaden. At 181 °C (nitrobenzene) and 190 °C (cyclosilane) the coalescence point is reached. From the coalescence temperature and the difference in chemical shift of the separated signals at room temperature, an activation energy barrier of $\Delta G^{\neq}$ = 91.5 kJ mol^{-1} may be estimated for the observed dynamic process.

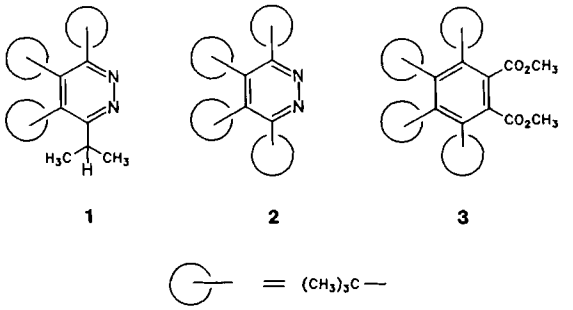

1 **2** **3**

It is tempting to attribute the occurrence of two signals for the methyl groups at room temperature to a hindered rotation of the isopropyl substituent. Such behavior is well known for rotation about C–C bonds.[6] So it is not too surprising, for example, that on cooling three signals appear in the ^{1}H NMR spectrum for the methyl groups of the *tert*-butyl substituents on the sp^3 atom of the adducts **4**, **5**, and **6** of tri-*tert*-butyl(trimethylsilyl)cyclobutadiene[7] and acetylenedicarboxylic acid ester, maleic anhydride, and citraconic anhydride. That steric hindrance, such as that confirmed by the low-temperature spectra of **4**–**6**, may also be observed for rotation about the considerably longer C–Si bond (in **5**, 188 pm) is, however, new. The coalescence temperatures for C–Si rotation are − 80 (**4**), − 93 (**5**), and − 23 °C (**6**). The corresponding free energies of activation derived for **4**–**6** are 35.3 (**4**), 32.5 (**5**), and 50.2 (**6**) kJ mol^{-1}.[8]

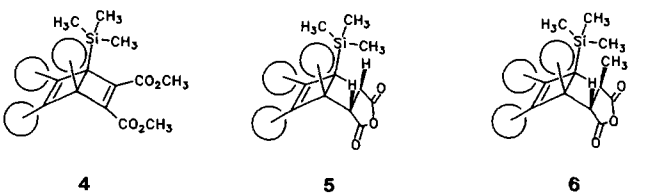

4 **5** **6**

A logical conclusion on the basis of this information would be that the aromatic ring in **1** is planar and the substituents favor a configuration in which the symmetry of the whole molecule is no longer C_s. In such a case, however, the signal for the *tert*-butyl group adjacent to the isopropyl group should also broaden. We therefore propose another explanation: As a result of the congestion of the four bulky groups, the six-membered ring is in a twisted configuration (the C4–C5 axis crosses the N1–N2 axis). The resultant lowering of the symmetry of the ring causes the two methyl groups of the isopropyl substituent to be diastereotropic and they give rise

to separate signals in the ^{1}H NMR spectrum. This should also be true at higher temperatures. If coalescence is nevertheless observed, it must result from inversion of the ring together with its substituents on heating. Above 180 °C this process occurs rapidly on the NMR timescale. Thus the time-averaged arene spectrum has the appearance of that of a planar and achiral ring.

The following findings support this hypothesis: Although the ^{1}H NMR spectrum of **1** does not change on addition of racemic Pirkle's reagent [1-(9-anthryl)-2,2,2-trifluoroethanol, **7**], all signals split again on addition of optically active (*S*)-(+)-**7**; pyridazine **1** is therefore chiral. This was also observed for tetra-*tert*-butylpyridazine **2**[3] (in the presence of (*S*)-(+)-**7** both ^{1}H NMR signals of the *tert*-butyl groups are doubled) and for dimethyl tetra-*tert*-butylphthalate **3**[9] (one of the two signals of the *tert*-butyl groups splits and line broadening for the ester methyl groups is noticeable).

The X-ray structure analysis—to our knowledge the first of an alkyl-substituted pyridazine—reveals the type and extent of the distortion of **1** (Fig. 1). The conformation has an

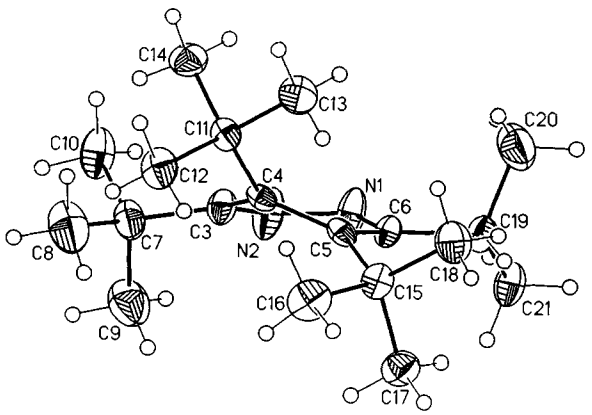

Fig. 1. Structure of **1** in the crystal (side view). Important distances [Å]: N1-N2 1.334(6), N1-C6 1.333(5), N2-C3 1.332(5), C3-C4 1.449(6), C4-C5 1.402(6), C5-C6 1.426(5), C3-C7 1.533(7), C4-C11 1.572(6), C5-C15 1.562(6), C6-C19 1.519(6) [11].

angle of 24.6° between the planes containing the N1, N2, C3, and C4 atoms and the C4, C5, C6, and N1 atoms.[10] Similar to the case for tetra-*tert*-butylcyclopentadienone,[1, 2] the ring C atoms are in an almost planar environment; the sum of the angles at C3, C4, C5, and C6 are 359.6, 358.2, 359.4, and 358.9°, respectively. It must have been easier to deform the ring system than to distort the planar environment of the ring C atoms. The intramolecular H···H contacts between the *tert*-butyl groups and the isopropyl groups lie between 1.75 and 2.16 Å. An additional distortion is observed particularly at the C7 and C19 atoms: angles C7-C3-N2 and C7-C3-C4 are 109.6 and 129.7°, respectively; angles C19-C6-N1 and C19-C6-C5 are 110.0 and 127.4°, respectively.

Received: June 26, 1991 [Z4748 IE]
German version: *Angew. Chem. 103* (1991) 1495

CAS Registry numbers:
1, 136445-37-9; **2**, 136445-38-0; **3**, 136445-39-1; **4**, 136445-40-4.

[1] Overview: G. Maier, H. Rang, D. Born, in G. A. Olah (Ed.): *Cage Hydrocarbons*, Wiley, New York 1990, p. 219–259.
[2] Review: G. Maier, *Angew. Chem. 100* (1988) 317–341; *Angew. Chem. Int. Ed. Engl. 27* (1988) 309–332.
[3] G. Maier, F. Fleischer, *Tetrahedron Lett. 32* (1991) 57.
[4] Analogous to the reaction of the salt with lithiated *tert*-butyldiazomethane: G. Maier, K. A. Reuter, L. Franz, H. P. Reisenauer, *Tetrahedron Lett. 26* (1985) 1845.
[5] Complete NMR data of **1**: ^{1}H NMR (400 MHz, $CDCl_3$, 25 °C, TMS): δ = 3.56 (sept, J = 6.5 Hz, 1 H; $CH(CH_3)_2$), 1.55 (d, J = 6.5 Hz, 3 H; $CH(CH_3)_2$), 1.48 (s, 9 H, *t*Bu), 1.45 (s, 9 H; *t*Bu), 1.37 (s, 9 H; *t*Bu); 1.26 (d, J = 6.5 Hz, 3 H; $CH(CH_3)_2$); ^{13}C NMR (100 MHz, $CDCl_3$, 25 °C, δ = 163.5 (C3), 161.5 (C6), 149.9/149.8 (C4/C5), 41.4/40.2/39.2 34.9/33.8/32.7 ($C(CH_3)_3$), 32.1 ($CH(CH_3)_2$), 25.2/22.6 ($CH(CH_3)_2$).
[6] M. Oki, *Angew. Chem. 88* (1976) 67; *Angew. Chem. Int. Ed. Engl. 15* (1976) 87; *Methods in Stereochemical Analysis 4*, Verlag Chemie, Weinheim 1985.
[7] G. Maier, D. Born, *Angew. Chem. 101* (1989) 1085; *Angew. Chem. Int. Ed. Engl. 28* (1989) 1050;
[8] D. Born, *Dissertation*, Universität Gießen 1989.
[9] G. Maier, K.-A. Schneider, *Angew. Chem. 92* (1980) 1056; *Angew. Chem. Int. Ed. Engl. 19* (1980) 1022.
[10] Boatlike distortions of arenes are already present in the case of a *vic*-tri-*tert*-butyl substitution pattern: G. Maas, J. Fink, H. Wingert, M. Regitz, *Chem. Ber. 120* (1987) 819. The same is valid for 1,3,5-tris(dialkylamino)-2,4,6-trinitrobenzenes: J. M. Chance, B. Kahr, A. B. Buda, J. S. Siegel, *J. Am. Chem. Soc. 111* (1989) 5940.
[11] Structure determination of **1**: crystal dimensions 0.38 × 0.27 × 0.18 mm^3, measured at 110 K on a R3m/V Nicolet four-circle diffractometer with $Mo_{K\alpha}$-radiation (graphite monochromator). Monoclinic, a = 12.127(2), b = 9.547(3), c = 16.085(4) Å, β = 92.97(2)°, V = 1860.3(7) Å^3, space group $P2_1/c$ (No. 14), Z = 4, $\varrho_{calcd.}$ = 1.037 g cm^{-3}, μ = 0.05 mm^{-1}, $2\theta_{max}$ = 50°, 3193 independent reflections, of which 2091 observed ($F_o \geq 4\sigma(F)$), 196 parameters for the refinement with hydrogen atoms in fixed positions with the same isotropic shift factors for identical groups. The anisotropic shift factors, particularly those of N1 and C4, indicate disorder effects, which could not be eradicated. R = 0.088, R_w = 0.090, $w^{-1} = (\sigma^2(F_o) + 0.00068F_o^2)$, maximum residual electron density 0.77 e Å^{-3}. Further details of the crystal structure investigation may be obtained from the Fachinformationszentrum Karlsruhe, Gesellschaft für wissenschaftlich-technische Information mbH, W-7514 Eggenstein-Leopoldshafen 2 (FRG) on quoting the depository number CSD-320273, the names of the authors, and the journal citation.

[FCNF]$^+$[AsF$_6$]$^-$, a Salt of the Linear 22-Valence Electron Cation [FCNF]$^+$ **

By *Inis C. Tornieporth-Oetting, Petra Gowik,* and *Thomas M. Klapötke**

New and very simple inorganic cations are still being found.[1, 2] Recently, *Pyykkö* and *Runeberg*[3] reported an ab initio study of the hitherto unknown 22-valence electron cation [FCNF]$^+$ and predicted a linear arrangement of its constituent atoms. This stimulated our interest in synthesizing an [FCNF]$^+$-salt. As starting material for the synthesis of such a salt we chose [HCNH]$^+$[AsF$_6$]$^-$ **1**, which was prepared according to Equation (a).[4]

The [HCNH]$^+$ cation appeared to be suitable as educt,[5] since, firstly, **1** reacts with KrF_2 in the ratio 1:1 with HF-elimination to give [HCNKrF]$^+$ [AsF$_6$]$^-$,[4] and, secondly, it could be estimated on the basis of a simple Born–Haber cycle that a reaction corresponding to Equation (b) should be thermodynamically allowed [ΔH°_{298} (b) = − 815 kJ mol^{-1}].[6]

[*] Priv.-Doz. Dr. T. M. Klapötke, Dipl.-Chem. I. C. Tornieporth-Oetting, Dr. P. Gowik
Institut für Anorganische und Analytische Chemie
der Technischen Universität
Strasse des 17. Juni 135, W-1000 Berlin 12 (FRG)

[**] This work was supported by the Deutsche Forschungsgemeinschaft (KL-636/2-1), the Fonds der Chemischen Industrie, the Solvay Fluor und Derivate GmbH, and the Bundesminister für Bildung und Wissenschaft im Rahmen des Graduiertenkollegs "Synthese und Strukturaufklärung niedermolekularer Verbindungen". We thank Prof. Dr. *Pyykkö* for stimulating information [3] and Prof. Dr. *H. Bürger* for supplying a preprint [18]. We also thank Prof. Dr. *H. Willner* und Dipl.-Chem. *J. Schaebs* for providing facilities for and carrying out an ^{19}F NMR measurement, and Prof. Dr. *O. Glemser* for a gift of ClF_3.

$$HCN + HF + AsF_5 \xrightarrow{HF} \underset{\mathbf{1}}{[HCNH]^+[AsF_6]^-} \quad (a)$$

$$[HCNH]^+(g) + 2F_2(g) \longrightarrow [FCNF]^+(g) + 2HF(g) \quad (b)$$

Reaction of **1** with an excess of elemental fluorine in anhydrous hydrogen fluoride afforded $[FCNF]^+[AsF_6]^-$ **2**, which could be identified by vibration (IR, Raman[10]) and ^{19}F NMR spectroscopy.[11]

$$\mathbf{1} + 2F_2 \text{ (excess)} \xrightarrow{HF,\ 0\,^\circ C} \underset{\mathbf{2}}{[FCNF]^+[AsF_6]^-} + 2HF \quad (c)$$

Salt **2** is stable at $-196\,^\circ C$, and can be handled with ease at $-78\,^\circ C$; however, the neat substance already decomposes rapidly and irreversibly below room temperature with loss of AsF_5 (IR) to give a yellow oil.[12] The ^{19}F NMR spectrum of an HF solution of **2** shows, after warming to $+10\,^\circ C$, two further multiplets in an intensity ratio of about 3:1 at $\delta = -74$ and -90, which can be assigned to the salt $[CF_3NFH_2]^+[AsF_6]^-$ **3** (cf. the synthesis of **3** in HF from CF_2NF and AsF_5,[13] ^{19}F NMR: $\delta = -74.5$ (d), -92.2 (q)[13]). The formation of **3** as decomposition product in solution is consistent both with the cleavage of AsF_5 from neat **2** as well as with the fact that CF_2NF does not react with AsF_5 to give **2**, but in the absence of HF forms only a loose adduct[13] and can be formulated as in Equations (d) and (e).

$$\mathbf{2} \longrightarrow F_2C{=}NF + AsF_5 \quad (d)$$

$$F_2C{=}NF + AsF_5 \xrightarrow{HF} \underset{\mathbf{3}}{[CF_3\text{-}NFH_2]^+[AsF_6]^-} \quad (e)$$

The vibration spectrum of the $[FCNF]^+$ cation was calculated at the HF/6-31G* level;[3] the calculated, scaled,[14–16] and experimental data are compared in Table 1. From the reasonably good agreement of the calculated and experimental data, as well as from a comparison of the vibration spectrum with that of the very recently prepared isoelectronic difluoroacetylene[17, 18] and that of the $[N_2F]^+$ cation,[19] it can be concluded that the 22-valence electron cation $[FCNF]^+$ in **2** is linear as predicted, and the electronegative F atoms occupy the terminal positions of the heteronuclear species as expected.

Moreover, the appearance of two signals of almost equal intensity in the ^{19}F NMR spectrum of **2**,[11] which can be assigned to the cation, confirms the linear $C_{\infty v}$ structure of the $[FCNF]^+$ cation and, in agreement with the IR and Raman data, rules out a likewise conceivable C_{2v} structure $[F_2CN]^+$. The signals at $\delta = -99$ and -105 are, as expected, shifted substantially downfield compared to that of FCN ($\delta = 157$[20]), and are in good agreement with the value reported for the $[N_2F]^+$ cation. However, owing to the expectedly very similar resonance frequencies of the N–F and C–F fluorine atoms in **2** (cf. $FN{=}CF_2$: $\delta(NF) = -67$; $\delta(CF_2) = -60$[20]) and the unresolved couplings, an extensive assignment cannot be given.

Table 1. Calculated and observed vibration frequencies (relative intensities in brackets) of the $[FCNF]^+$ cation in **2** and, for comparison, of FCCF [18].

Raman [a]	IR [a]	Calcd. [b]	Scaled [c]	FCCF [d]	Assignment
2587 (10)		3017	2565	2450	ν_1 (σ)
	1378 m-s	1544	1312	1349	ν_3 (σ)
729 (8)		911	774	794	ν_2 (σ)
456 (3)		537	457	258	ν_4 (π)
243 (1)		270	230	282	ν_5 (π)

[a] Ref. [10]. [b] HF/6-31 G*, Ref. [1]. [c] Scaling: 0.85, Ref. [14–16]. [d] Ref. [18].

Experimental

2: F_2 (5.69 mmol, 0.22 g) was condensed at $-196\,^\circ C$ onto a frozen solution of **1** (0.41 g, 1.90 mmol) in anhydrous HF (5 mL; dried over BiF_5) in a 15 mL Kel-F reaction vessel (deactivated with ClF_3). The stirred reaction mixture was warmed within 12 h to $0\,^\circ C$. After cooling to $-50\,^\circ C$, all volatile components (excess fluorine, HF) were removed in vacuum and **2** was isolated as a white solid and stored at $-196\,^\circ C$.

Warning: F_2, AsF_5, ClF_3, and N–F compounds are potentially explosive substances and are sensitive to phase transformations and fluctuations in temperature[21]. In another attempt at the synthesis of **2**, we irradiated (UV, 1 h, 254 nm, 900 W) a mixture of F_2, $(CN)_2$, and AsF_5 at $-196\,^\circ C$; the mixture exploded on warming to $-85\,^\circ C$!

Received: June 17, 1991 [Z 4717 IE]
German version: *Angew. Chem. 103* (1991) 1490

CAS Registry numbers:
1, 42039-53-2; **2**, 136750-67-9; **3**, 92745-54-5.

[1] I. Tornieporth-Oetting, T. Klapötke, *J. Chem. Soc. Chem. Commun. 1990*, 132.
[2] I. Tornieporth-Oetting, T. Klapötke, *Angew. Chem. 101* (1989) 1742; *Angew. Chem. Int. Ed. Engl. 28* (1989) 1671.
[3] P. Pyykkö, N. Runeberg, *J. Mol. Struct. THEOCHEM*, in press.
[4] G. J. Schrobilgen, *J. Chem. Soc. Chem. Commun. 1988*, 863.
[5] As main products of the attempted direct fluorination of HCN with F_2 or ClF_3, only $(CN)_2$ and ClCN, respectively, could be isolated.
[6] ΔH^0_{298} ($HCN^+ + H \rightarrow HCNH^+$) set equal to $\Delta H^0_{298}(NH_3^+ + H \rightarrow NH_4^+) = -391$ kJ mol^{-1} [7]; $\Delta H^0_{298}(FCN^+ + F \rightarrow FCNF^+)$ set equal to $\Delta H^0_{298}(NF_3^+ + F \rightarrow NF_4^+) = -418$ kJ mol^{-1}, these values are equivalent to the corresponding FPDE (F^+ detachment energies) [23]; ionization energies: (HCN) = 1312 kJ mol^{-1} [4], FCN = 1284 kJ mol^{-1} [9]; bond energies: B C-H (HCN) = 524 kJ mol^{-1} [22a], F-F = 158 kJ mol^{-1} [8], C-F (FCN) = 464 kJ mol^{-1} [22b], H-F = 568 kJ mol^{-1} [8].
[7] R. Bougon, T. Bui Huy, J. Burgess, K. O. Christe, R. D. Peacock, *J. Fluorine Chem. 19* (1982) 263.
[8] D. A. Johnson: *Some Thermodynamic Aspects of Inorganic Chemistry*, Cambridge University Press, Cambridge 1982, appendix.
[9] V. H. Dibeler, S. K. Liston, *J. Chem. Phys. 47* (1964) 4548.
[10] **2**: Raman ($-20\,^\circ C$, 647.09 nm, 40 mW, rel. int. in brackets): $\tilde{\nu}$ [cm^{-1}] = 243 (1) ν_5-FCNF$^+$, 370 (4) ν_5-AsF_6^-, 456 (3) ν_4-FCNF$^+$, 518 (2), 574 (2) ν_2-AsF_6^-, 684 (7) ν_1-AsF_6^-, 729 (8) ν_2-FCNF$^+$, 2587 (10) ν_1-FCNF$^+$; IR (Nujol): $\tilde{\nu}$ [cm^{-1}] = 390 s (ν_4-AsF_6^-), 700 s (ν_3-AsF_6^-), 1378 m-s (ν_3-FCNF$^+$), 1460 s br.
[11] **2**: ^{19}F NMR (HF, $-10\,^\circ C$, 188.31 MHz, rel. to $CFCl_3$) $\delta = 0.04$ ($CFCl_3$), -62 to -68 (s, br; AsF_6^-), -98.8 (s, FCNF$^+$), -105.0 (s, FCNF$^+$), -196.6 (HF).
[12] AsF_5-detection by gas-IR. Since **2** does not contain protons and is not contaminated with **1** (absence of the v-CN band of **1** at 2116 cm^{-1} [4] in the Raman spectrum of **2**), neither **2** nor its decomposition products attack glass.
[13] D. D. DesMarteau, W. Y. Lam, B. A. O'Brien, A. Shi-Ching Chang, *J. Fluorine Chem. 25* (1984) 387.
[14] J. C. Brahms, W. P. Dailey, *J. Am. Chem. Soc. 111* (1989) 8940.
[15] W. J. Hehre, L. Radom, P. von R. Schleyer, J. A. Pople: *Ab Initio Molecular Orbital Theory*, Wiley, New York 1986.
[16] D. A. Dixon, A. J. Arduengo III, *Inorg. Chem. 29* (1990) 970.
[17] H. Bürger, S. Sommer, *J. Chem. Soc. Chem. Commun. 1991*, 456.
[18] H. Bürger, W. Schneider, S. Sommer, W. Thiel, H. Willner, *J. Chem. Phys.*, in press.
[19] K. O. Christe, R. D. Wilson, W. W. Wilson, R. Bau, S. Sukumar, D. D. Dixon, *J. Am. Chem. Soc. 113* (1991) 3795.
[20] C. H. Dungan, J. R. Van Wazer: *Compilation of Reported F^{19} NMR Chemical Shifts*, Wiley, New York 1970.
[21] W. C. Firth, Jr., *J. Org. Chem. 33* (1968) 3489.
[22] a) D. Koschel in *Gmelin: Handbuch der Anorganischen Chemie, Kohlenstoff Teil D 1*, 8th Edit., Springer, Berlin 1971, p. 175; b) D. Koschel in *Gmelin: Handbuch der Anorganischen Chemie, Kohlenstoff Teil D 3*, Springer, Berlin 1976, p. 179.
[23] K. O. Christe, D. A. Dixon, *J. Fluorine Chem. 54* (1991) 2.

A Metal-Ion- and Cofactor-independent Enzymatic Redox Reaction: Halogenation by Bacterial Nonheme Haloperoxidases**

By *Theodor Haag, Franz Lingens,* and *Karl-Heinz van Pée**

In memorium Richard Kuhn

Haloperoxidases are oxidoreductases, which, with the help of peroxides (e.g. H_2O_2) and halide ions (chloride or bromide) catalyze the halogenation of organic substrates [Eq. (a)]. The halogenation proceeds in two steps. In the first enzyme-catalyzed step the halide ions are oxidized by H_2O_2 or other peroxides. In the second step the Hal^+ species formed thereby attacks electrophilically at the organic substrate in a reaction that is not necessarily enzyme-catalyzed.

$$R\text{-}H + H_2O_2 + Hal^- + H^+ \rightarrow R\text{-}Hal + 2H_2O \qquad (a)$$
$$Hal = Br, Cl$$

In all previously investigated haloperoxidases the electron transfer from the halide ion to the peroxide proceeds via a prosthetic heme group[1] or the cofactor vanadium.[2] The bacterial nonheme haloperoxidases, on the other hand, contain neither a cofactor nor a prosthetic group.[3, 4] They thus differ both from the usual haloperoxidases as well as from all other oxidoreductases, since redox enzymes normally require a cofactor or a prosthetic group for electron transfer. As examples of bacterial nonheme haloperoxidases, two enzymes from antibiotic-producing bacterial strains were investigated: the chloroperoxidase from the pyrrolenitrin producer *Pseudomonas pyrrocinia*[3] and the bromoperoxidase from the 7-chlorotetracyclin-producing strain *Streptomyces aureofaciens*.[4] Since they contain neither a cofactor nor a prosthetic group, the electron transfer must take place from the halide ion to the H_2O_2 on an amino acid. The behavior of the bacterial nonheme haloperoxidases towards cyanide ions played an essential role in the identification of this amino acid.

The incubation of the bacterial nonheme haloperoxidases with cyanide in the presence of H_2O_2 and bromide, i.e. under reaction conditions,[5] led to inactivation of the enzymes by splitting of the proteins into two peptides. By electrophoretic separation of the two peptides it could be shown that they have the same molecular weight as two fragments formed by cleavage of the native enzymes with cyanogen bromide. Since both the enzyme reaction with cyanide as well as the cleavage with cyanogen bromide lead to the same products, the enzymes must be capable of producing cyanogen bromide.

Cyanogen bromide cleaves peptide chains after methionine. Since an excess of methionylglycine could not prevent the self-cleavage of the enzymes, it may be assumed that the reactive methionine is located in or near the active center of the enzyme. In this case the cyanogen bromide formed reacts immediately with the methionine of the enzyme before it can leave the active center. The assumption that this methionine lies in the active center was confirmed by the behavior of chloroperoxidase during the cyanogen bromide cleavage. Cleavage of the denatured chloroperoxidase with cyanogen bromide[7] leads to a large number of peptides, corresponding to the five methionine residues contained in the amino acid sequence. In contrast, cleavage of the native chloroperoxidase with cyanogen bromide leads to the two previously mentioned peptides, which are also formed in the reaction with cyanide and correspond to the cleavage of the enzyme after a single methionine residue (Fig. 1). Bromoperoxidase contains only one methionine residue.

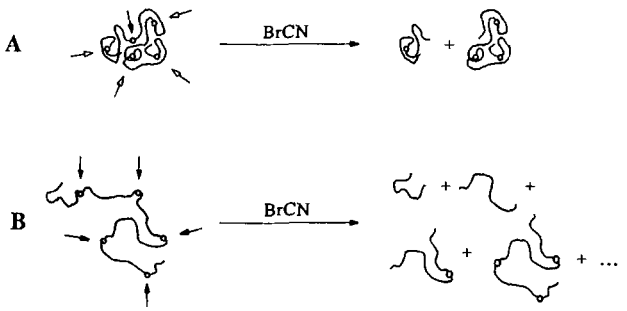

Fig. 1. Cleavage of native (A) and denaturated (B) chloroperoxidase with cyanogen bromide. o = methionine residue of the chloroperoxidase.

Methionine can be readily oxidized by H_2O_2 to methionine sulfoxide. Many enzymes lose their catalytic activity thereby.[8] Therefore, in an enzyme whose substrate is H_2O_2, methionine residues should be protected from the H_2O_2 molecule—and thus also from the similarly large cyanogen bromide molecule. Indeed, four of the five methionine residues of chloroperoxidase in the native enzyme are inaccessible for cyanogen bromide. The only accessible methionine is that after which the enzyme is cleaved by reaction with cyanide. This readily accessible methionine is oxidized to methionine sulfoxide by H_2O_2 under the reaction conditions.

Sulfoxides are reduced to sulfides in HBr solution in a chemical reaction,[9] and Br^- is oxidized by the sulfoxide to Br_2. An analogous reaction, via methionine sulfoxide, can be postulated for the enzymatic oxidation of Br^- to Br^+ by bacterial nonheme haloperoxidases (Scheme 1).

This model also explains the reaction of the haloperoxidases with cyanide: If the bromine atom in **4** is replaced by a cyano group, this leads to an intermediate which also occurs in the cleavage of proteins with cyanogen bromide. The substrate specificity of the chloroperoxidase for the chlorination—the chloroperoxidase can chlorinate substrates from the biosynthesis of pyrrolenitrin, whereas organic substrates such as 2-chloro-4,4-dimethyl-1,3-cyclohexanedione are only brominated[3]—can also be explained by this reaction scheme. The chemical oxidation of Cl^- to give Cl_2 (or HOCl) by sulfoxide is not possible under conditions in which the oxidation of Br^- to Br_2 is observed.[9] The reaction with Cl^- leads only to the intermediate **4**. Only substrates which find access to the active center—i.e. substrates from the pyrrolenitrin biosynthesis for which the enzyme has an affinity—and can react there with the intermediate **4**, are chlorinated. In other compounds the enzyme can only catalyze an unspecific bromination with free Br_2 via **4a**. This explains why the chloroperoxidase only catalyzes the bromination and not the chlorination of 2-chloro-4,4-dimethyl-1,3-cyclohexanedione.

If the enzymes are treated with H_2O_2, methionine is oxidized, and methionine sulfoxide **2** is detectable.[10] This reaction can be carried out quite easily with many enzymes. For the reduction of the resulting methionine sulfoxide back to methionine, reducing agents such as mercaptoethanol must usually be employed. In contrast, the reduction in the case of bacterial nonheme haloperoxidases according to the proposed mechanism with halide ions must take place, i.e. in the

[*] Priv.-Doz. Dr. K.-H. van Pée, Dipl.-Chem. T. Haag, Prof. Dr. F. Lingens
Institut für Mikrobiologie der Universität Hohenheim
Garbenstrasse 30, W-7000 Stuttgart 70 (FRG)

[**] This work was supported by the Bundesministerium für Forschung und Technologie (Grant No. 0319416A) and the Deutsche Forschungsgemeinschaft (Heisenberg Fellowship for *K.-H. van Pée*).

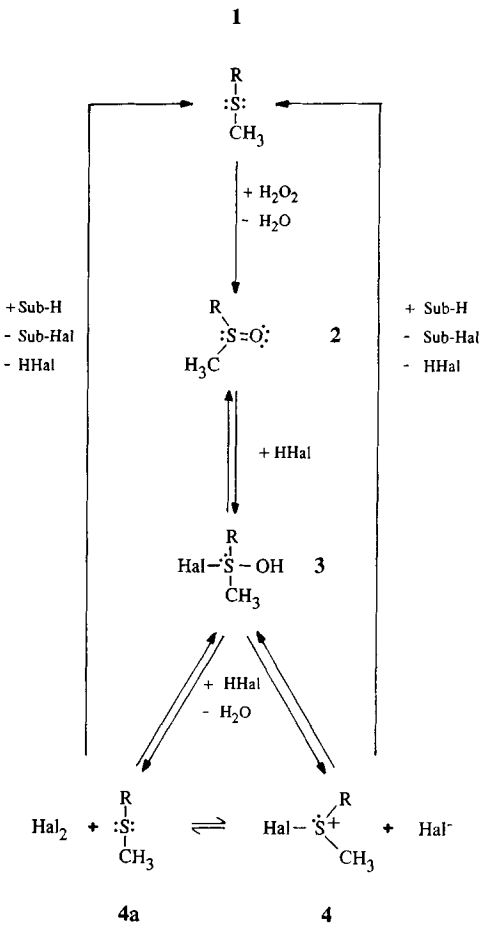

Scheme 1. Reaction cycle of bacterial nonheme haloperoxidases. R = $CH_2CH_2CH(NHR')(COR'')$ with R',R'' = peptide chain of the enzyme; Hal = Br or Cl; Sub-H = organic substrate; Sub-Hal = halogenated product. **4a** is formed only in the case of Hal = Br.

presence of bromide and the organic halogen acceptor (2-chloro-4,4-dimethyl-1,3-cyclohexanedione) in excess compared to H_2O_2, and the reaction cycle must stop at the stage of the methionine **1** after consumption of all of the H_2O_2. This could be confirmed by cleavage with cyanogen bromide and subsequent electrophoresis.[10]

The overall enzyme reaction is certainly much more complex than is depicted in this scheme. There must, for example, still be amino acids in the active center which induce the necessary polarization of the S–O bond during the reaction. These amino acids can be determined by elucidation of the structure of the active center by X-ray structural analysis. For this purpose the bromoperoxidase has already been crystallized, and the first structure investigations have been carried out on these crystals.[11]

Received: July 9, 1991 [Z 4785 IE]
German version: *Angew. Chem. 103* (1991) 1550

CAS Registry numbers: haloperoxidase, 93229-67-5; methionine, 63-68-3.

[1] S. L. Neidleman, J. Geigert: *Biohalogenation: Principles, Basic Roles and Applications*, Ellis Horwood, Chichester, England 1986.
[2] D. Rheder, *Angew. Chem. 103* (1991) 152–172; *Angew. Chem. Int. Ed. Engl. 30* (1991) 148–167.
[3] W. Wiesner, K.-H. van Pée, F. Lingens, *J. Biol. Chem. 263* (1988) 13725–13732.
[4] K.-H. van Pée, G. Sury, F. Lingens, *Biol. Chem. Hoppe Seyler 368* (1987) 1225–1232.
[5] Incubation of the enzymes with cyanide: the enzyme (5 mg mL^{-1}) in 0.1 M ammonium acetate buffer, pH 5.5, was incubated for 6–8 h with 20 mM of NaBr, 8.8 mM H_2O_2 and 100 μM KCN.
[6] Electrophoresis according to: H. Schägger, G. von Jagow, *Anal. Biochem. 166* (1987) 368–378.
[7] BrCN cleavage: the lyophilized enzyme (100 μg) was incubated for about 15 h with 100 μL BrCN (10 mg mL^{-1}) in 0.1 M HCL solution or in 50 mM ammonium acetate buffer (for the BrCN cleavage of the native enzyme).
[8] N. Brot, H. Weissbach in S. Patai, Z. Rappoport, C. Stirling (Eds.): *The Chemistry of Sulphones and Sulphoxides*, Wiley, Chichester, England 1988, p. 851–869.
[9] I. Ookuni, A. Fry, *J. Org. Chem. 36* (1971) 4097–4101.
[10] Methionine can be distinguished from methionine sulfoxide by BrCN cleavage [7] and subsequent electrophoresis [6]. The BrCN cleavage is possible only in the case of methionine [8].
[11] H. Sobek, T. Haag, O. Pfeifer, F. Lingens, D. Schomburg, K.-H. van Pée, *J. Mol. Biol. 221* (1991), 35–37.

Direct Observation of the Central Atom in $[C\{Au[P(C_6H_5)_2(p\text{-}C_6H_4NMe_2)]\}_6](BF_4)_2$ by ^{13}C NMR Spectroscopy**

By *Hubert Schmidbaur,** *Benno Brachthäuser*, and *Oliver Steigelmann*

Previous studies that led to the discovery of hexakis(phosphaneaurio)methanium(2+) cations of the type $[(LAu)_6C]^{2+}$ with a hypercoordinated central carbon atom teach us that direct detection of the interstitial atom is of utmost importance. When such a hexanuclear complex was formed by chance in earlier experiments with gold clusters, the presence of this carbon atom was overlooked and the product was formulated as $[(LAu)_6]^{2+}$.[2] However, since this stoichiometry should, according to theoretical predictions, lead to an edge-shared bi-tetrahedral and not to the octahedral geometry found in the experiment,[3] initial doubts were cast on the validity of the data, especially since the synthesis was not reproducible.[4] Further calculations revealed that C-centered octahedral clusters should be characterized by a particularly stable electron configuration.[5]

Following the successful, directed synthesis of $[(LAu_6)C]^{2+}$ dications with tertiary phosphanes as ligands L, the presence of the central atom could at first only be detected with certainty by high-resolution field desorption (FD) and fast atom bombardment (FAB) mass spectroscopy.[1] Although the X-ray diffraction patterns of all complexes investigated in the meantime[1,6–8] show the expected electron density in the center of the cluster, the information obtained from such diagrams is only of limited value in view of the six large surrounding atoms with their even larger ligand systems. The same is true for the IR/Raman and UV/VIS spectra and the diamagnetism, as well as the ^{197}Au-Mössbauer spectra.[1]

Thus, direct observation of the central C atom by NMR spectroscopy remained a challenge, not least because, in view of the unusual bonding situation of this atom, for which there is no precedent, no predictions were possible regarding the chemical shift and spin-spin coupling values. This prompted

[*] Prof. Dr. H. Schmidbaur, Dipl.-Chem. B. Brachthäuser, Dipl.-Chem. O. Steigelmann
Anorganisch-chemisches Institut der Technischen Universität München
Lichtenbergstrasse 4, W-8046 Garching (FRG)

[**] This work was supported by the Deutsche Forschungsgemeinschaft (Leibniz Program), the Fonds der Chemischen Industrie, and—through gifts of chemicals—by Degussa AG and Heraeus GmbH. We thank Prof. *M. Taylor*, University of Auckland, New Zealand, for helpful discussions, Prof. *J. Shamir*, Hebrew University, Jerusalem and Prof. *W. Preetz*, Universität Kiel, for the first Raman spectroscopic measurements, as well as Dr. *S. Mronga* and Mr. *J. Balbach*, TU München, for high-field NMR measurements.

us to synthesize the title compound starting from ^{13}C-enriched $^{13}CCl_4$. Commercially available $^{13}CCl_4$[8] was diluted with CCl_4 with natural isotopic abundance, for cost reasons, to a ^{13}C-content of 20%, and converted as previously described[9] into $^{13}C[B(OCH_3)_2]_4$. NMR and MS monitoring of this product confirmed the expected ^{13}C-content at the central atom. As the second component required for the synthesis of the title compound the 1:1 complex of $(p\text{-}C_6H_4NMe_2)P(C_6H_5)_2$[10] and AuCl was prepared, the constitution of which was confirmed analytically and structurally (yield 97%, m.p. 218–220 °C (decomp.)[11] (Scheme 1). The *p*-dimethylamino-substituents are meant to improve the solubility and derivatizability in order to facilitate the detection. The reaction of the R_3PAuCl complex with $^{13}CCl_4/CCl_4$ in the presence of CsF in hexamethylphosphoric triamide (HMPT) furnished the title compound in 40% yield in the form of colorless crystals (m.p. 145–152 °C (decomp.)). The FAB mass spectrum (nitrobenzyl alcohol matrix) confirmed the (half) mass of the dication (m/z = 1521.1), the ^{197}Au-Mössbauer spectrum, the equivalence of the six gold atoms in the solid state (IS = 2.5 mms^{-1} and QS = 7.54 mms^{-1} at 4 K). The counterions are identified by a quintet signal in the ^{11}B NMR spectrum ($^1J_{BF}$ = 7.6 Hz).

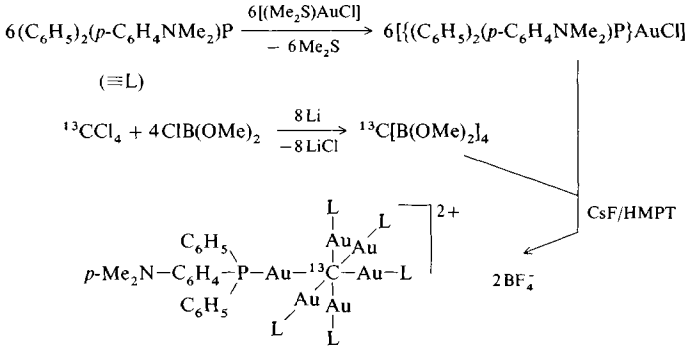

Scheme 1.

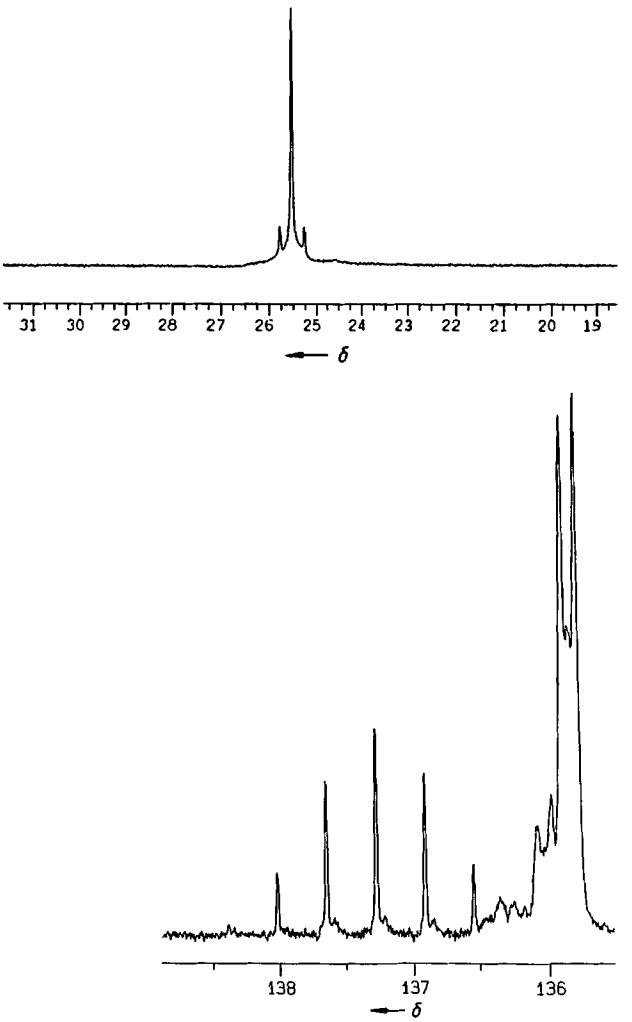

Fig. 1. Above: $^{31}P\{^1H\}$ NMR spectrum (161.84 MHz) of the title compound in CD_2Cl_2 at 300 K. Below: Section from the arene region of the $^{13}C\{^1H\}$-NMR spectrum (150.91 MHz) of the title compound in CD_2Cl_2 at 300 K.

In the ^{31}P NMR spectrum (161.84 MHz) of a solution of the product in CD_2Cl_2 at 300 K the satellite pair expected from the ^{31}P–^{13}C interaction appears symmetrically disposed to the singlet at δ = 25.50 in the intensity ratio 10:80:10 with the coupling constant ^2J = 56.1 Hz (Fig. 1, above). Only with a knowledge of this value could we unambiguously assign a septet signal *in the arene region* of the $^{13}C\{^1H\}$-NMR spectrum (600 MHz spectrometer, 150.91 MHz) at δ = 137.27 to the interstitial C-atom. Parts of this septet are already partly masked by the signals of the phenyl and *p*-dimethylaminophenyl groups in spectra recorded with a 400 MHz spectrometer, and are therefore difficult to locate. In the ^1H-coupled ^{13}C NMR spectrum the resonance of the central C atom experiences no further splitting, whereas the expected multiplicities are recorded for all the remaining signals. The same applies in the case of the ^1H NMR spectrum.[12]

The ^{13}C-resonance of the cluster C atom thus appears in a completely unexpected region, since one would have expected either a very strong or an extremely weak shielding upon coordination of metals, particularly with high coordination numbers. For example, the resonance of the central P atom in the related cluster dication $[(Ph_3PAu)_5P]^{2+}$ is observed at very high field,[13] whereas those of interstitial C atoms in typical carbonyl transition metal carbides appear at $\delta \approx 450$.[14] An explanation for these discrepancies is only to be expected from theoretical calculations, which, in the case of heavy metals—and especially in the case of gold—must take into account strong relativistic effects. The scalar value of the coupling constant $^2J_{PAuC}$ (without determination of sign), on the other hand, is less surprising, since values between 122.6 and 51.5 Hz have been found for organogold compounds such as $[(R_3P)AuCN]$, $[(R_3P)AuR]$, $[(R_3P)Au\{CH(SiR_3)_2\}]$, and $[(R_3P)Au\{C(SiR_3)_3\}]$.[15] The placement in the lower range is in keeping with the electron deficient character of the cluster and a formal hybridization of the interstitial atom with little s-character.[5]

Knowing the δ and J values for the title compound, the resonance of the cluster atom could also be found in the case of the non-^{13}C-enriched parent compound $[\{(Ph_3P)Au\}_6C](BF_4)_2$ (δ = 55.3, J = 54 Hz).

NMR spectroscopic evidence for the central N-atom in $[\{(Ph_3P)Au\}_4N]^+$ ions was obtained in the case of high-purity samples and suitable anions (BF_4^-) by observation of a 1:1:1 triplet splitting of the ^{31}P signal ($^2J_{^{31}P^{14}N}$ = 26 Hz).[16] Responsible for the success of the experiment here, as in the case of the title compound, is a zero-field gradient between the quadrupole nuclei of the gold atoms, determined by high point symmetry of the complex. Polarizing anions and impurities, which can induce exchange processes, lead to eradication of the coupling pattern. Enrichment with ^{15}N

should also enable direct observation of the central atom in the case of $[\{(Ph_3P)Au\}_4N]^+$.

Received: July 3, 1991 [Z 4774 IE]
German version: *Angew. Chem. 103* (1991) 1552

CAS Registry numbers:
$[(LAu)_6\ ^{13}C](BF_4)_2$, 137008-25-4; L, 739-58-2; LAuCl, 137008-26-5; (Me_2S)-AuCl, 29892-37-3; $^{13}CCl_4$, 32488-50-9; $ClB(OMe)_2$, 868-81-5; $^{13}C[B(OMe)_2]_4$, 137051-00-4.

[1] H. Schmidbaur, *Gold Bull. 23* (1990) 11.
[2] P. L. Bellon, M. Manassero, L. Naldini, M. Sansoni, *J. Chem. Soc. Chem. Commun. 1972*, 1035; P. L. Bellon, M. Manassero, M. Sansoni, *J. Chem. Soc. Dalton Trans. 1973*, 2443.
[3] C. E. Briant, K. P. Hall, D. M. P. Mingos, *J. Organomet. Chem. 254* (1983) C18; *J. Chem. Soc. Dalton Trans. 1986*, 687.
[4] J. J. Steggerda, J. J. Bour, J. W. A. van der Velden, *Recl. Trav. Chim. Pays-Bas 101* (1982) 164.
[5] D. M. P. Mingos, *J. Chem. Soc. Dalton Trans. 1976*, 1163; *Nature (London) 345* (1990); J. P. Hall, D. M. P. Mingos, *Prog. Inorg. Chem. 32* (1984) 237; N. Rösch, A. Görling, D. E. Ellis, H. Schmidbaur, *Angew. Chem. 101* (1989) 1410; *Angew. Chem. Int. Ed. Engl. 28* (1989) 1357; *Inorg. Chem.*, in press; P. Pyykkö, Y. Zhao, *Chem. Phys. Lett.* (1991) 103.
[6] F. Scherbaum, A. Grohmann, B. Huber, C. Krüger, H. Schmidbaur, *Angew. Chem. 100* (1988) 1602; *Angew. Chem. Int. Ed. Engl. 27* (1988) 1544.
[7] O. Steigelmann, P. Bissinger, H. Schmidbaur, *Angew. Chem. 102* (1990) 1475; *Angew. Chem. Int. Ed. Engl. 29* (1990) 1399.
[8] MSD Isotopes, Merck Frosst Canada Inc., Montreal.
[9] R. B. Castle, D. S. Matteson, *J. Organomet. Chem. 20* (1969) 19. – MS (EI, 70 eV): *m/z* 272 (M^+); ^{13}C NMR (CD_2Cl_2): $\delta = 53.79$ (q, OCH_3), 9.61 (br. s, CB_4).
[10] H. A. Brune, M. Falck, R. Hemmer, G. Schmidtberg, H. G. Alt, *Chem. Ber. 117* (1984) 2791; S. Trippett, D. M. Walker, *J. Chem. Soc. 1961*, 2130; W. Dreissig, K. Plieth, *Acta Crystallogr. 135* (1972) 294. – M.p. 149–150°C; $\delta(^{31}P) = -6.75$ (in $CDCl_3$).
[11] For methods see: D. B. Dyson, R. V. Parish, C. A. McAuliffe, R. Fields, *Hyperfine Interact. 40* (1988) 327. – $\delta(^{31}P) = 31.72$ (in CD_2Cl_2). The crystal structure analysis will be published elsewhere in connection with other investigations.
[12] ^{13}C NMR (CD_2Cl_2): $\delta = 40.05$ (s, CH_3), 112.25 (C3), 113.10 (C1, $J = 65.6$ Hz), 129.30 (C3'), 131.33 (C4'), 132.11 (C1', $J = 55.8$ Hz), 133.88 (C2'), 135.83 (C2), 152.55 (C4); ^1H NMR (CD_2Cl_2): $\delta = 2.78$ (CH_3), 6.67 (H3), 6.92 (H2), 7.22–7.37 (m, residual H (arom.)).
[13] H. Schmidbaur, G. Weidenhiller, O. Steigelmann, *Angew. Chem. 103* (1991) 442; *Angew. Chem. Int. Ed. Engl. 30* (1991) 450.
[14] B. F. G. Johnson, J. Lewis, W. J. H. Nelson, J. N. Nichols, M. D. Vargas, *J. Organomet. Chem. 249* (1983) 255.
[15] H. Schmidbaur, A. A. M. Aly, *Angew. Chem. 92* (1980) 66; *Angew. Chem. Int. Ed. Engl. 19* (1980) 70; F. Glockling, V. B. Mahale, *J. Chem. Res. (S) 5* (1978) 170; A. L. Hormann-Arendt, C. F. Shaw, *Inorg. Chem. 29* (1990) 4683.
[16] H. Schmidbaur, A. Grohmann, A. Kolb, unpublished results 1990.

A Self-Assembling Triple-Helical Co_2^{II} Complex: Synthesis and Structure**

By *Alan F. Williams,* Claude Piguet,* and *Gérald Bernardinelli*

A theme of considerable interest in supramolecular chemistry is the selective and spontaneous assembly of supermolecules by the complexation of polydentate ligands around two or more metal ions.[1] Double-helical structures may be generated by two "oligobidentate" ligands complexing cations with a preference for tetrahedral coordination—the metal–metal axis is the helical axis about which the ligands are twisted. *Lehn* et al.[2] have synthesized a series of oligobipyridyl ligands which form double-helicates containing as many as five Cu^I ions, while *Sauvage* et al.[3] have used the double-helical complex formed by Cu^I with a ligand containing two phenanthroline units linked by a $(CH_2)_4$-bridge as a precursor for the synthesis of a molecular knot. Tetrahedral coordination of the metal is not an essential requirement for the formation of a helical structure, and we recently reported[4] a double-helical complex of Cu^I in which the ligand 2,6-bis(1-methylbenzimidazol-2-yl)pyridine (mbzimpy) acts essentially as a bis(monodentate) ligand, giving a linear coordination of the two copper ions.

A basic requirement for self-assembly around metal ions is that the coordinating possibilities of the ligands should match the stereochemical preference of the metal ion. We may therefore predict for ions with a preference for octahedral coordination the possible formation of double-helical complexes from bis(terdentate) ligands and of triple helices from bis(bidentate) ligands. The first possibility has recently been shown to occur in the complex $[Cd_2(sexipyridyl)_2]^{4\oplus}$ reported by *Constable*.[5] In this communication we report the crystal structure of a triple-helical complex which is formed on mixing stoichiometric amounts of the bis(bidentate) ligand bis[1-methyl-2-(6'-methyl-2'-pyridyl)benzimidazol-5-yl]methane (L) and cobalt(II) ions.

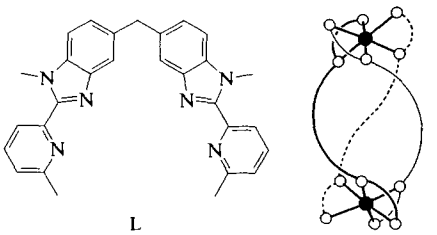

L

Scheme 1. Left: Structure of the ligand L. Right: Schematic representation of the helical complex formed from L and Co^{II} ions. Co atoms are shown as black spheres, N atoms as white spheres.

The ligand L has four coordination sites, but the rigidity of the aromatic rings prevents it from acting as a tetradentate ligand, and repulsion between the hydrogens in position 4 of the benzimidazoles destabilizes a planar structure. It is therefore ideally suited to act as a bis(bidentate) ligand. Reaction with cobalt(II) perchlorate leads to the isolation of orange salts with the composition $[Co_2L_3(ClO_4)_4]$; the rose-orange color of the crystals suggested a probable octahedral coordination of the cobalt, and the stoichiometry is in agreement with a triple-helical structure.

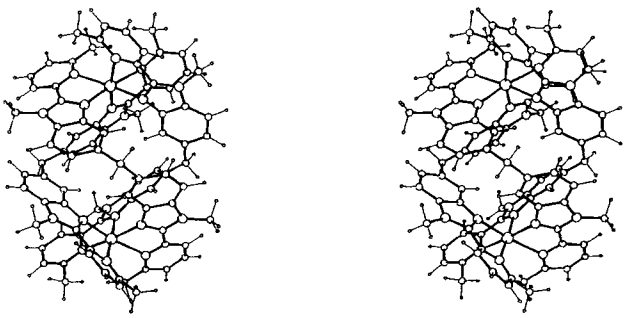

Fig. 1. Stereoview of the triple-helical cation $[Co_2L_3]^{4\oplus}$ along one of the approximate C_2 axes.

[*] Dr. A. F. Williams, Dr. C. Piguet
Département de Chimie Minérale, Analytique et Appliquée
Université de Genève
30 quai Ernest Ansermet, CH 1211 Genève 4 (Switzerland)
Dr. G. Bernardinelli
Laboratoire de Cristallographie aux Rayons-X
Université de Genève

[**] This work was supported by the Swiss National Science Foundation (Grant No. 20.30139.90). We thank Dr. *O. Schaad* and Miss *Anna Quattropani* for their collaboration.

The X-ray crystal structure determination of $[Co_2L_3(ClO_4)_4 \cdot 2.5CH_3CN]$ confirms the existence of a triple-helical cation with approximate D_3 symmetry. Figure 1 shows an ORTEP[6] stereoview of the cation along one of the C_2 axes which passes through one of the methylene carbon atoms and the midpoint between the two cobalt atoms. Figure 2 gives computer-generated representations of the structure in which the different strands are shown in different colors. Figure 3 shows a projection down the Co–Co axis. The perchlorate anions and the acetonitrile molecules have been omitted; one of the perchlorates showed five positions for the oxygens, but the other three were relatively well ordered. Five solvent molecules were found, but the sites were not totally occupied, and they were refined with a population parameter of 0.5.

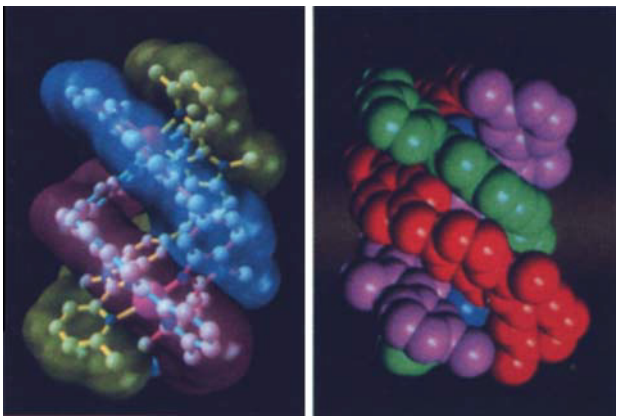

Fig. 2. Left: View [14] of the triple-helical cation $[Co_2L_3]^{4\oplus}$ with the ligands represented by a ball-and-stick model surrounded by a translucent Connolly surface [15]. Right: View [16] of the triple-helical cation $[Co_2L_3]^{4\oplus}$ with the non-hydrogen atoms represented as spheres with radii 80% of the van der Waals radius showing how the ligands wrap round the C_3 axis.

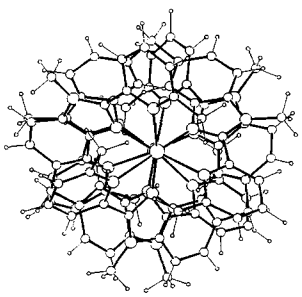

Fig. 3. View along the Co–Co axis showing the approximate C_3 symmetry.

The coordination sites of the two cobalt atoms are very similar, and in Table 1 we give the structural parameters obtained by averaging bond distances and angles related by pseudo D_3 symmetry. The cobalt coordination sphere may best be described as an octahedron flattened along a C_3 axis. The Co–N(benzimidazole) distance (2.07(2) Å) is shorter than the literature value of 2.103 Å[7] for high spin octahedral cobalt(II), but the Co–N(pyridine) distance 2.29(6) Å is longer than the standard value of 2.185 Å. We attribute this distortion to repulsion between the methyl groups on position 6 of the pyridine, since the distances between the carbon atoms of these methyls are quite short (average value 4.05(2) Å). This is supported by the observation that the average pyridine-Co-pyridine angle of 103° is significantly greater than the average benzimidazole-Co-benzimidazole angle (97°). The average ligand "bite angle" is 76.2°, and the cobalt–cobalt distance is 8.427(4) Å.

Table 1. Structural data for the cobalt coordination sphere, py = pyridine, bzim = benzimidazole.

	average [e.s.d.] [a]	minimum	maximum
$Co-N_{py}$	2.29(6)	2.24	2.40
$Co-N_{bzim}$	2.07(2)	2.04	2.10
ligand "bite angle"	76(2)	74.0	78.4
py–Co–py	103(4)	96.9	106.9
bzim–Co–bzim	97(2)	95.2	99.5
bzim–Co–py	172(2)	171.0	174.4
bzim–Co–bzim	84(3)	79.7	89.2

[a] Bond lengths [Å] and angles [°] are averaged assuming D_3 symmetry, and the quoted e.s.d. are obtained from the six values used to obtain the average. The experimental e.s.d are smaller.

The aromatic rings of the ligands are planar within experimental error, and the interplanar angles are given in Table 2. The average angle between the pyridine and the benzimidazole planes of a chelate ring is 22.7°, and between the two benzimidazole planes of one strand is 80°, but the spread of values is several degrees. Although the coordination sites of the cobalt ions are approximately related by D_3 symmetry, the complex as a whole deviates significantly from this high symmetry (Fig. 3). This deviation is essentially due to the spread in torsion angles which are not expected to be strongly constrained, and suggest that the molecule is fairly flexible. In support of this we note the absence of the strong stacking interactions observed[4] in $[Cu_2(mbzimpy)_2]^{2\oplus}$; in $[Co_2L_3]^{4\oplus}$ there is evidence of some slight stacking between benzimidazoles in different strands, but the planes are not parallel, and the distances between the benzimidazoles, calculated using those atoms which show the greatest overlap, lie in the range 4.2 to 4.6 Å compared with the 3.4 Å observed previously.[4] It therefore seems probable that the self

Table 2. Interplane angles [°] between aromatic rings.

Ring [a]	pA1	bA1	bA2	pA2	pB1	bB1	bB2	pB2	pC1	bC1	bC2
bA1	24.0										
bA2	86.6	79.1									
pA2	82.7	87.7	30.5								
pB1	75.1	52.6	52.9	81.3							
bB1	85.6	67.2	32.1	62.3	22.6						
bB2	58.0	70.2	50.5	27.9	87.9	76.3					
pB2	33.2	49.3	66.3	51.7	84.1	81.9	25.0				
pC1	80.7	82.5	22.6	8.6	72.7	53.9	30.8	52.2			
bC1	69.0	76.3	37.0	14.0	81.0	65.7	14.7	37.7	16.1		
bC2	56.3	32.4	68.3	91.3	22.5	43.0	87.3	74.6	83.2	85.9	
pC2	70.1	47.4	54.8	82.0	5.1	26.1	86.1	80.5	73.5	80.45	17.7

[a] The rings are denoted as pyridine p or benzimidazole b, belonging to ligand strand A, B, or C, and bound to Co1 or Co2. Thus pB2 is the pyridine of strand B that is bound to Co2. The error in the angles is typically 1°.

assembly is directed by the coordination requirements of the cation rather than by interligand interactions.

This is, to our knowledge, the first triple-helical coordination compound which has been characterized by X-ray crystallography. *Libman, Tor*, and *Shanzer*[8] reported a triple-helical dinuclear iron complex which was characterized by ^{1}H NMR and CD spectra, but in this case the tripodal nature of the ligand undoubtedly plays an important role in structuring the complex. Another Fe_2 complex composed of two Fe^{II} centers with octahedral coordination and three bidentate ligands was reported recently,[9] but in this case a triple-helical structure was not observed, presumably as a result of the greater flexibility of the ligands.

Experimental

The ligand L was obtained by a Phillips condensation of 3,3'-diamino-4,4'-bis(*N*-methylamino)diphenylmethane (prepared according to a modified literature procedure [10]) with 2-methylpyridine-6-carboxylic acid [11]. Crystals of $[Co_2L_3(ClO_4)_4 \cdot 2.5\,CH_3CN]$ were grown from acetonitrile solution at 40 °C. A red-orange crystal ($0.22 \times 0.32 \times 0.32$ mm^3) was sealed in a capillary tube with some of the supernatant liquid. $M_r = 1994$, triclinic $P\bar{1}$, $a = 14.403(2)$, $b = 16.558(3)$, $c = 21.328(3)$ Å, $\alpha = 78.15(1)°$, $\beta = 81.19(1)°$, $\gamma = 89.02(1)°$ based on 24 reflections ($16° < 2\theta < 31°$), $V = 4919(1)$ Å^3, $Z = 2$. Intensity data were collected at room temperature on an Enraf-Nonius CAD4 diffractometer with $Mo_{K\alpha}$ radiation ($\lambda = 0.71069$ Å), $4° < 2\theta < 38°$, 7877 unique reflections measured. Structure solved by direct methods [12], other calculations made using the XTAL system [13]. Full matrix refinement was performed successively on ligand 1 and cobalt, ligand 2, ligand 3 and perchlorate and solvent molecules (maximum of variables = 335). All atoms other than perchlorate oxygens and carbons of solvent molecules were refined with anisotropic thermal displacement parameters. Final R factor 11.0% ($R_w = 9.7\%$, $w = 1/\sigma^2(F_0)$), for 4980 observed reflections ($|F_0| > 4\sigma(F_0)$). Further details of the crystal structure investigation are available on request from the Director of the Cambridge Crystallographic Data Centre, University Chemical Laboratory, Lensfield Road, GB-Cambridge, CB2 1EW (UK), on quoting the full journal citation.

Received: July 1, 1991 [Z 4764 IE]
German version: *Angew. Chem. 103* (1991) 1530

CAS Registry numbers:
L, 136629-58-8; $[Co_2(L_3)](ClO_4)_4 \cdot 2.5(CH_3CN)$, 136642-58-5; $[Co_2L_3](ClO_4)_4$, 136642-57-4; 3,3'-diamino-4,4'-bis(*N*-methylamino)diphenylmethane, 23816-42-4; 2-methylpyridine-6-carboxylic acid, 934-60-1.

[1] E. C. Constable, *Nature 346* (1990) 314–315.
[2] J.-M. Lehn, A. Rigault, J. Siegel, J. Harrowfield, B. Chevrier, D. Moras, *Proc. Natl. Acad. Sci. USA 84* (1987) 2565–2569; J.-M. Lehn, A. Rigault, *Angew. Chem. 100* (1988) 1121–1122; *Angew. Chem. Int. Ed. Engl. 27* (1988) 1095–1097.
[3] J.-P. Sauvage, *Acc. Chem. Res. 23* (1990) 319–327; C. O. Dietrich-Brücheker, J. Guilhem, C. Pascard, J.-P. Sauvage, *Angew. Chem. 102* (1990) 1202–1204; *Angew. Chem. Int. Ed. Engl. 29* (1990) 1154–1156.
[4] C. Piguet, G. Bernardinelli, A. F. Williams, *Inorg. Chem. 28* (1989) 2920–2925.
[5] E. C. Constable, M. D. Ward, *J. Am. Chem. Soc. 112* (1990) 1256–1258.
[6] C. K. Johnson, ORTEPII Report ORNL-5138, Oak Ridge National Laboratory, TN, USA, 1976.
[7] A. G. Orpen, L. Brammer, F. H. Allen, O. Kennard, D. G. Watson, R. Taylor, *J. Chem. Soc. Dalton Trans. 1989*, S1–S83.
[8] J. Libman, Y. Tor, A. Shanzer, *J. Am. Chem. Soc. 109* (1987) 5880–5881.
[9] B. R. Serr, K. A. Andersen, C. M. Elliott, O. P. Anderson, *Inorg. Chem. 27* (1988) 4499–4504.
[10] V. V. Korshak, A. A. Izyneev, D. M. Mognonov, V. P. Mazurevskii, Zh. P. Mazurevskaya, I. S. Novak, G. F. Slezko, A. I. Prokosova, A. D. Markov, *Tr. Buryat. Inst. Estestv. Nauk. Buryat. Fil., Sib. Otd. Akad. Nauk SSSR 1971*, 143–145.
[11] G. Black, E. Depp, B. B. Corson, *J. Org. Chem. 14* (1949) 14–21.
[12] P. Main, S. J. Fiske, S. E. Hull, L. Lessinger, G. Germain, J.-P. Declercq, M. M. Woolfson, MULTAN 87, Universities of York, England, and Louvain, Belgium, 1987.
[13] S. R. Hall, J. M. Stewart (Eds.): *XTAL 3.0 User's Manual*, Universities of Western Australia and Maryland, 1990.
[14] E. de Castro, S. Edelstein, VISP 2.0, University of Geneva, 1991.
[15] M. L. Connolly, *J. Am. Chem. Soc. 107* (1985) 1118–1124.
[16] J. Brickmann, *MOLCAD molecular modelling package*, Technische Hochschule, Darmstadt (FRG) 1990.

Synthesis, Absolute Configuration and Specific Rotation of (+)- and (−)-Modhephene**

By *Lutz Fitjer,* Honorato Monzó Oltra,* and *Mathias Noltemeyer**

Dedicated to Professor Michael Hanack on the occasion of his 60th birthday

Since its discovery in *Isocoma wrightii*,[1] a plant toxic to sheep and cattle in the south west USA, (−)-modhephene (**5**) has been a popular goal of synthetic studies. Because of a growth-inhibiting function of derivatives,[2] related compounds have also been investigated. Twelve diastereoselective[3] and one enantioselective syntheses[4a–c] document an intense interest.

The only enantioselective synthesis[4a–c] assigns (−)-modhephene a (1*R*,5*S*,8*R*) configuration on the basis of the circular dichroism of a cyclopropyl ketone precursor. The

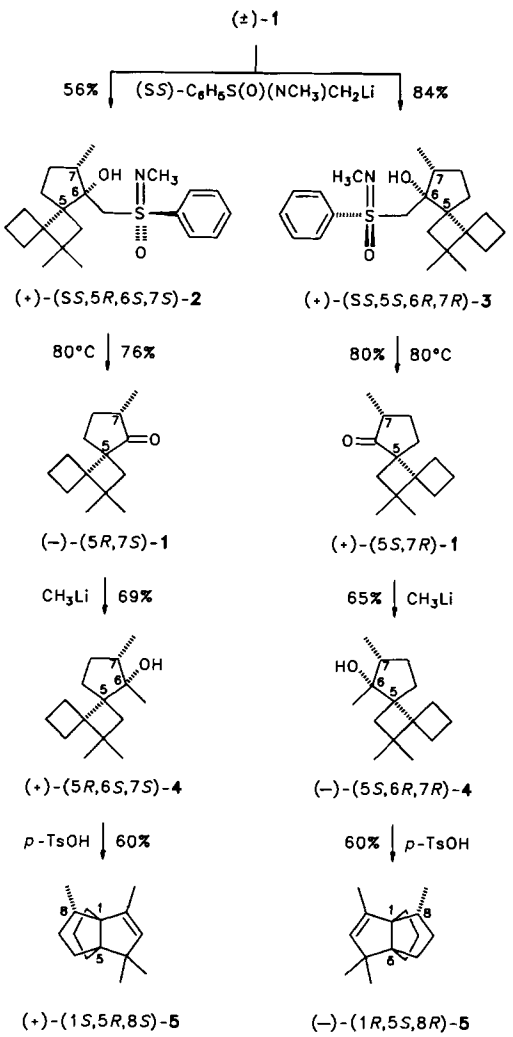

Scheme 1.

[*] Prof. Dr. L. Fitjer, Dipl.-Chem. H. Monzó Oltra
Institut für Organische Chemie der Universität
Tammannstrasse 2, W-3400 Göttingen (FRG)
Dr. M. Noltemeyer
Institut für Anorganische Chemie der Universität
Tammannstrasse 4, W-3400 Göttingen (FRG)

[**] Polyspiranes, Part 21. Rearrangement Cascades; Part 15. This work was supported by the Deutsche Forschungsgemeinschaft and the Fonds der Chemischen Industrie. Part 20: L. Fitjer, K. Justus, P. Puder, M. Dittmer, C. Hassler, M. Noltemeyer, *Angew. Chem. 103* (1991) 431; *Angew. Chem. 30* (1991) 436; Part 16: L. Fitjer, A. Kanschik, M. Majewski, *NATO Adv. Study Inst. Ser. C 273*(1989) 431.

specific rotation ($[\alpha]_D$ − 5.2)[4c] corresponds to that of the natural product ($[\alpha]_D$ − 4.2),[1b, 4c] although the synthetic product (78% *ee*) was contaminated with 17% epimodhephene, whose specific rotation is unknown. A negligible specific rotation for epimodhephene could explain this observation. Contradictions cast doubt on the absolute configuration when a considerably different rotation ($[\alpha]_D$ − 20.5) was determined for modhephene isolated from *Otanthus maritimus*.[5] As there were no reliable criteria for purity, we synthesized both enantiomers and determined the absolute configuration and specific rotation anew.

Our synthesis (Scheme 1) is based on the stereospecificity of the rearrangement of (±)-**4** to (±)-modhephene (**5**)[6] and required separation of racemic (±)-**1**. According to the general method of *Johnson* et al.[7] we treated (±)-**1**[6] with lithiated (+)-(*S*)-*N*,*S*-dimethyl-*S*-phenylsulfoximine (97% *ee*, $[\alpha]_D$ + 178, *c* = 3, acetone; literature value[7] + 184, *c* = 3, acetone) and obtained a liquid and a solid β-hydroxysulfoximine. X-ray crystallography[8] showed the solid ($[\alpha]_D$ + 61, *c* = 1.34, $CHCl_3$) to be (S*S*,5*R*,6*S*,7*S*)-**2**[10] (Fig. 1); the liquid ($[\alpha]_D$ + 34, *c* = 1.39, $CHCl_3$) was therefore (S*S*,5*S*,6*R*,7*R*)-**3**.[10] Cleavage to form the corresponding

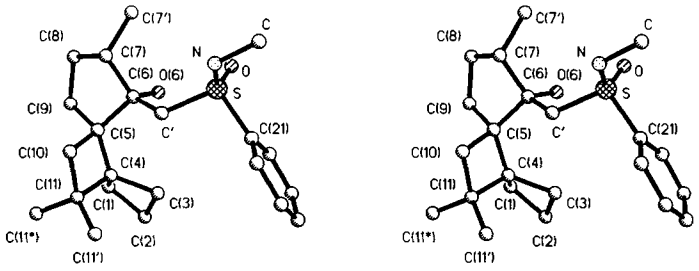

Fig. 1. Stereoscopic view of the crystal structure of (S*S*,5*R*,6*S*,7*S*)-**2** (hydrogen atoms omitted). Selected bond lengths [pm] and angles [°]: cyclobutane rings: C4–C11 158.3, other C–C 152.2–155.6, C-C-C 88.1–91.0; cyclopentane ring: C–C 151.1–154.3, C-C-C 101.5–106.6.

ketones (−)-(5*R*,7*S*)-**1**[10] ($[\alpha]_D$ − 39, *c* = 1.3, $CHCl_3$) and (+)-(5*S*,7*R*)-**1**[10] ($[\alpha]_D$ + 36, *c* = 0.9, $CHCl_3$) was achieved by thermal fragmentation (12 h/80 °C), and the stereospecific addition of methyllithium afforded finally the desired alcohols (+)-(5*R*,6*S*,7*S*)-**4**[10] ($[\alpha]_D$ + 58, *c* = 1.05, $CHCl_3$) and (−)-(5*S*,6*R*,7*R*)-**4**[10] ($[\alpha]_D$ − 57, *c* = 1.09, $CHCl_3$).

For the rearrangement, (+)-(5*R*,6*S*,7*S*)-**4** and (−)-(5*S*,6*R*,7*R*)-**4** were heated with equivalent quantities of a 0.075 M solution of dry *p*-toluenesulfonic acid in benzene for 25 min at 70 °C. Column chromatography on silica gel doped with 20% silver nitrate (eluant pentane/dichloromethane 95:5) afforded (+)-modhephene, (+)-(1*S*,5*R*,8*S*)-**5**,[10] ($[\alpha]_D$ + 16.5, *c* = 0.5, $CHCl_3$) from the rearrangement of (+)-(5*R*,6*S*,7*S*)-**4**, and (−)-modhephene, (−)-(1R,5*S*,8*R*)-**5**,[10] ($[\alpha]_D$ − 15.8, *c* = 1.08, $CHCl_3$) from the rearrangement of (−)-(5*S*,6*R*,7*R*)-**4**.

Since our optical rotation values contradicted every other earlier report, we have reisolated (−)-modhephene from *Othanthus maritimus*[5, 11], determined its specific rotation again ($[\alpha]_D$ − 16.5, *c* = 1.58, $CHCl_3$), and reexamined the chemical and optical purity of all natural and synthetic samples by capillary gas chromatography on permethylated β-cyclodextrin (Fig. 2).[12] With the exception of synthetic (−)-**5** (95% *ee*, $[\alpha]_D^{corr}$ − 16.6), all the samples were chemically and optically pure and therefore the rotation data are conclusive.

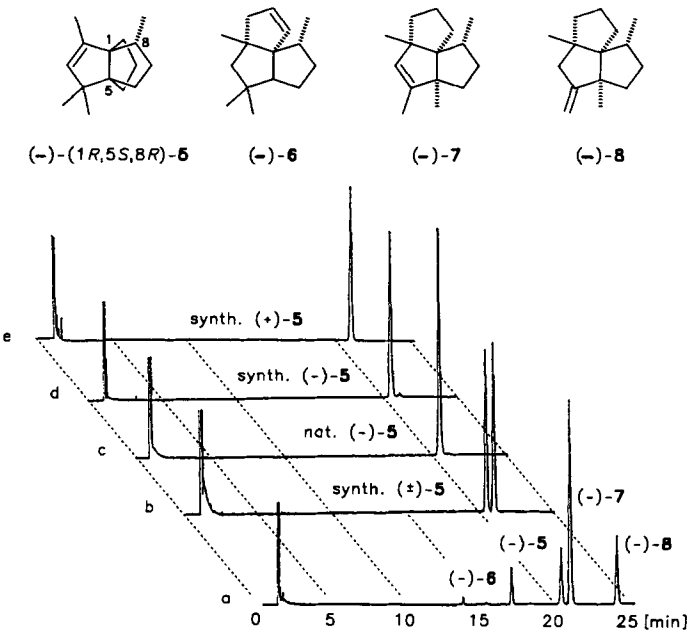

Fig. 2. Capillary chromatograms [25 m × 0.25 mm inner diameter, deactivated fused-silica capillary columns coated with heptakis(2,3,6-tri-*O*-methyl)-β-cyclodextrin in OV-1701 (0.07 M), at 110 °C, carrier gas 0.6 bar H_2]. a) Extract from *Otanthus maritimus* [11] containing (−)-silphinene [(−)-**6**], (−)-modhephene [(−)-**5**], (−)-isocomene [(−)-**7**], and (−)-β-isocomene [(−)-**8**]; b) synthetic (±)-**5** [6]; c) naturally occurring (−)-**5**; d) synthetic (−)-**5**; e) synthetic (+)-**5**.

As our studies show, none of the earlier samples of (−)-modhephene was really pure. Although the assignment of the absolute configuration as 1*R*,5*S*,8*R*[4c] was correct, it was by no means definite. Care should also be taken in establishing the hitherto unknown absolute configurations of (−)-silphinene [(−)-**6**, $[\alpha]_D$ − 21.3,[13] − 46.7[5]], (−)-isocomene [(−)-**7**, $[\alpha]_D$ − 67.8,[1b] − 85,[13] − 85.2[5]] and (−)-β-isocomene [(−)-**8**, $[\alpha]_D$ − 63.2[5]]. Here too, contradictory values exist, although besides (−)-modhephene [(−)-**5**] at least (−)-isocomene [(−)-**7**] is produced enantiomerically pure by *Othanthus maritimus* (Fig. 2).[14] Since (±)-modhephene can be rearranged to (±)-isocomene,[6] we can now determine the absolute configuration of (−)-isocomene also, using (+)- and (−)-modhephene.

Received: March 18, 1991 [Z4508 IE]
German version: *Angew. Chem. 103* (1991) 1534

CAS Registry numbers:
(±)-**1**, 122518-25-6; (+)-**1**, 136655-30-6; (−)-**1**, 136655-31-7; **2**, 136545-66-9; **3**, 136656-55-8; (−)-**4**, 136655-22-8; (+)-**4**, 136655-33-9; (−)-**5**, 68269-87-4; (+)-**5**, 136655-34-0; **6**, 74284-57-4; **7**, 65372-78-3; **8**, 74311-15-2; (+)-(*S*)-*N*,*S*-dimethyl-*S*-phenylsulfoximene, 50635-99-9.

[1] a) L. H. Zalkow, R. N. Harris III, D. Van Derveer, *J. Chem. Soc. Chem. Commun. 1978*, 420; b) L. H. Zalkow, R. N. Harris III, N. I. Burke, *J. Nat. Prod. 42* (1979) 96.
[2] K. Kakiuchi, M. Ue, T. Nagashima, M. Kinugawa, K. Kobiro, Y. Tobe, Y. Odaira, *Chem. Pharm. Bull. 36* (1988) 542, and references cited therein.
[3] a) C. P. Jasperse, D. P. Curran, *J. Am. Chem. Soc. 112* (1990) 5601, and references cited therein; b) C.-K. Sha, T.-S. Jean, D. C. Wang, *Tetrahedron Lett. 31* (1990) 3745.
[4] a) E. A. Mash, S. K. Math, C. J. Flann, *Tetrahedron Lett. 29* (1988) 2147; b) *ibid. 30* (1989) 2; c) *Tetrahedron 45* (1989) 4945.
[5] J. de Pascual Teresa, A. San Feliciciano, A. F. Barrero, M. Medarde, F. Tome, *Phytochemistry 20* (1981) 166.
[6] L. Fitjer, A. Kanschik, M. Majewski, *Tetrahedron Lett. 29* (1988) 5525.
[7] C. R. Johnson, J. R. Zeller, *Tetrahedron 40* (1984) 1225, and references cited therein.

[8] X-ray crystallographic data for (*S,5R,6S,7S*)-**2** ($C_{22}H_{33}NO_2S$): space group $P2_12_12_1$, $a = 933.2(2)$, $b = 1060.2(2)$, $c = 2136.2(5)$ pm, $V = 2.1135(8)$ nm^3, $Z = 4$, $\varrho_{calcd.} = 1.180$ g cm^{-3}, $\mu(Mo_{K\alpha}) = 0.071$ mm^{-1}. Of 1593 independent reflections, 1534 with $|F| > 3\sigma(F)$ were considered for the solution of the structure and refinement. The anisotropic refinement converged at $R = 0.0400$. Refinement according to *Rogers* [9] yielded $\eta = 0.9(3)$ and thus also the correct configuration. Further details of the crystal structure investigation may be obtained from the Fachinformationszentrum Karlsruhe, Gesellschaft für wissenschaftlich-technische Information mbH, W-7514 Eggenstein-Leopoldshafen 2 (FRG) on quoting the depository number CSD-54727, the names of the authors, and the journal citation.

[9] D. Rogers, *Acta Crystallogr. Sect. A 37* (1981) 734.

[10] The new compounds (*S,S,5R,6S,7S*)-**2** and (*S,S,5S,6R,7R*)-**3** gave correct C,H analyses. The IR, ^{1}H NMR, and mass spectrometry data are in accord with the proposed structures. ^{13}C NMR data: (*SS,5R,6S,7S*)-**2** (50.3 MHz, $CDCl_3$): $\delta = 14.84$, 17.80, 26.35, 27.13, 27.65, 27.95, 29.09, 29.54, 33.00, 33.27, 42.05, 42.22, 51.72, 52.71, 62.71, 82.33, 128.82 (coincidence of two signals), 129.48 (coincidence of two signals), 132.86, 140.25; (*S,S,5S,6R,7R*)-**3** (20 MHz, $CDCl_3$): $\delta = 15.53$, 17.89, 26.41, 27.13, 27.58, 27.87, 28.55, 29.51, 32.93, 33.11, 40.44, 41.72, 51.94, 53.07, 60.87, 83.52, 128.53 (coincidence of two signals), 129.51 (coincidence of two signals), 132.94, 139.65. The ^{1}H NMR spectra of the enantiomers of **1**, **4**, and **5** were identical to those of the racemates [6].

[11] We thank Mr. *A. Vizcaino*, Oficina Tecnica Devesa-Albufera, Ctr. Nazaret-Oliva, E-46012 Valencia, Spain for large quantities of fresh roots.

[12] a) V. Schurig, H.-P. Nowotny, *J. Chromatogr. 441* (1988) 155; b) V. Schurig, H.-P. Nowotny, *Angew. Chem. 102* (1990) 969; *Angew. Chem. Int. Ed. Engl. 27* (1990) 939. We thank Prof. Dr. *V. Schurig*, Universität Tübingen for optimizing the separation of (±)-**5** [12b] and for the use of the chromatography column.

[13] F. Bohlmann, J. Jakupovic, *Phytochemistry 19* (1980) 259.

[14] We have ascertained that the enantiomers of (±)-**7** [6] are separable under the conditions given in Figure 2. This test has not yet been undertaken for (±)-**6** and (±)-**8**.

formed thereby is trapped by addition of triethylamine, yields between 84 and 89% can be achieved.[10]

The corresponding iron(III) complexes **2d–f** (yields: 60–90%) can be obtained analogously from the 1-(1-alkyl/aryl-1*H*-tetrazol-5-yl)-2-alkanones **1d–f**.[12] On the basis of the elemental analyses and mass spectrometric data **2a–f** are mononuclear iron(III) complexes of the general composition FeL_3 (HL = **1a–f**). In the reaction of **1a** with aluminum trichloride, the corresponding aluminum complex **3a** is formed.[10]

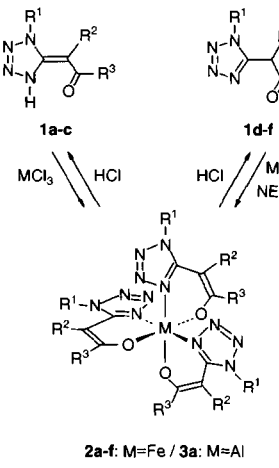

1,2,3	a	b	c
R^1	Me_3CCH_2	$C_6H_5CH_2$	4-EtC_6H_4
R^2	CN	CN	CN
R^3	OMe	OMe	OMe

1,2,3	d	e	f
R^1	Et	$Me(CH_2)_2$	Me_3C
R^2	H	H	H
R^3	C_6H_5	C_6H_5	C_6H_5

Synthetic Siderophores of the Tetrazolylenol Type: Iron(III) Complexes and Three-Dimensional Iron(II) Coordination Polymers**

By *Rolf W. Saalfrank,* Claus-Jürgen Lurz, Klaus Schobert, Oliver Struck, Eckhard Bill,* and *Alfred X. Trautwein**

Dedicated to Professor Hiroshi Taniguchi on the occasion of his 60th birthday

Naturally occurring and synthetically accessible siderophores (iron carriers) contain predominantly bidentate pyrocatechinato- or hydroxamato-ligands and are of special interest because of their high affinity towards trivalent metal ions, especially towards iron(III) ions.[1–8] The methyl (*E*)-2-(1-alkyl/aryl-4,5-dihydro-1*H*-tetrazol-5-ylidene)-2-cyanoacetates **1a–c**, first prepared by us with a completely different intention,[9] appeared to be also suitable as siderophores. Upon reaction of **1a–c** in ether with aqueous iron(III) chloride solutions, a deep blue coloration of the ether phase suddenly occurs, and, after addition of *n*-hexane, **2a–c** separate in the form of deep blue microcrystals. If the hydrochloric acid

The Mössbauer spectra of powdered samples of the complexes **2a,b** at 298 K show relatively poorly resolved quadrupole doublets with quadrupole splittings $\Delta E_Q \approx 0.5$ mms^{-1} and isomeric shifts $\delta \approx 0.45$ mms^{-1} (not shown). The values of the isomeric shifts point to high-spin iron(III) ($S = 5/2$) in a quasi-octahedral environment.[13] The temperature dependence of the Mössbauer spectra is similar to that of the spectra of other siderophore complexes, e.g. ferrichrome A.[14]

X-band-EPR spectra of the complexes **2a,b** confirm the high-spin state ($S = 5/2$) of the iron(III) center. Powdered samples already afford strong resonance signals at lower field, from about $g = 10$, but these were not analyzed further because of their extreme broadening by intermolecular spin-spin interactions. **2a,b** dissolved in dichloromethane, however, show the same spectrum at 10 K with a strong isotropic line at $g = 4.3$ and a weaker anisotropic line at $g = 9.6$ typical for magnetically isolated Fe^{III} centers ($S = 5/2$) with maximum rhombicity, $E/D = 1/3$ (E and D are zero-field interaction parameters in the spin-Hamilton formulation for the description of the electronic fine structure of the iron(III) center).[15] The rhombicity shows that apparently in each case only the statistically most probable (Δ)/(Λ)-*mer*-isomers **2** of the two theoretically possible (Δ)/(Λ)-configurational isomers, FeL_3, are formed. This finding is supported by the ^{13}C-NMR spectrum of the aluminum complex **3a**, which shows the set of signals expected for the three nonequivalent ligands.[10] Whereas **1a–c** function as bidentate ligands towards iron(III) ions and form the *mer*-complexes **2a–c**, the same compounds **1a–c** should function as tridentate ligands towards iron(II) ions and afford, by *spontaneous self-organization*,[16] three-dimensional coordination polymers.[17]

In order to check this assumption we have carried out reactions of **1a–c** in diethyl ether with aqueous iron(II) sulfate solutions. Pale green precipitates are obtained which are almost insoluble in noncoordinating solvents and still show no changes even at 570 K. According to microanalyses, the

[*] Prof. Dr. R. W. Saalfrank, Dipl.-Chem. C.-J. Lurz, Dipl.-Chem. K. Schobert, O. Struck
Institut für Organische Chemie der Universität Erlangen-Nürnberg
Henkestrasse 42, W-8520 Erlangen (FRG)
Prof. Dr. A. X. Trautwein [+], Dr. E. Bill
Institut für Physik der Medizinischen Universität
Ratzeburger Allee 160, W-2400 Lübeck 1 (FRG)

[+] EPR and Mössbauer spectra.

[**] Siderphores, Part 1. This work was supported by the Deutsche Forschungsgemeinschaft and the Fonds der Chemischen Industrie, and would hardly have materialized without the stimulating discussions with J.-M. Lehn, Strasbourg, during a research visit by *R. W. S.* We thank Dr. *M. Moll*, Institut für Anorganische Chemie der Universität Erlangen-Nürnberg, for recording the NMR spectra, and Dr. *A. van Dorsselaer*, Institut de Chimie de l'Universite Strasbourg, for measuring the FAB-MS spectra.

products obtained are compounds of the general composition $[FeL_2]_n$, the FAB-MS data (FAB = Fast Atom Bombardment) of **4a** indicating the presence of a polymer.[10]

The formation of coordination polymers of type **4** is understandable if **1a–c** or their enolates are considered as tridentate chelate ligands and if one assumes intermediary formation of the coordinatively unsaturated iron(II) building block **5**. The monomers are bidentate coordinating through the two CN groups, which leads to linking of monomers and to coordinative saturation at the iron(II) center of **5** with formation of the corresponding three-dimensional coordination polymers **4**.[18] In agreement with a polymeric structure of **4** is the finding that compounds **4** are readily soluble in coordinating solvents such as pyridine, acetonitrile etc. and are depolymerized.

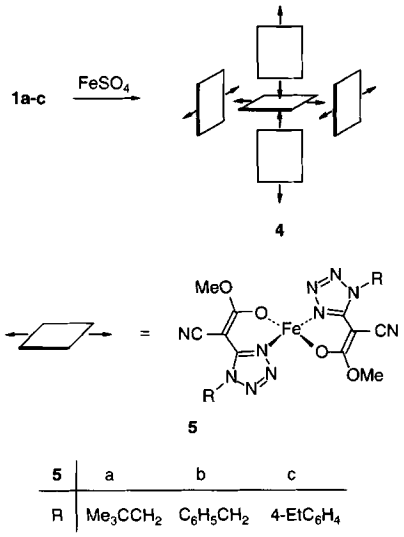

5	a	b	c
R	Me_3CCH_2	$C_6H_5CH_2$	4-EtC_6H_4

In contrast to **1a–c**, the prerequisites for an "internal" coupling are lacking in **1d–f** because of the absence of additional CN groups, so that in these cases the formation of coordination polymers with iron(II) ions does not occur.[20]

The DMSO solutions of compounds **4a,b** in contrast to their powdered samples, belong to the few systems with integer spin $S = 2$, which give EPR spectra (Fig. 1). The broad

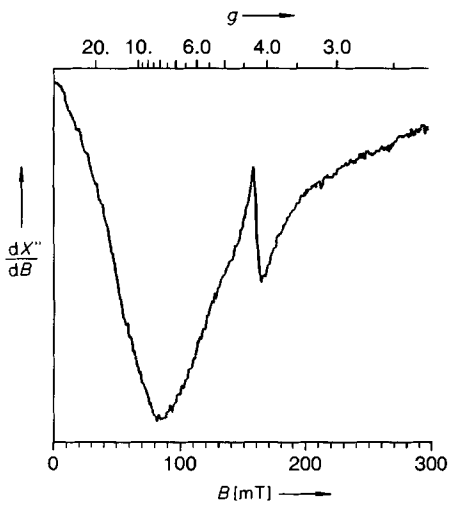

Fig. 1. EPR spectrum of a DMSO solution of compound **4a**. Temperature: 10 K, frequency: 9.434 GHz, power: 20 mW. (The weak resonance signal at $g = 4.3$ arises from slight contamination of the solution with iron(III).)

resonance signals can be explained as quasi "$\Delta m = 4$" transitions between the states "$S_z = +2$" and "$S_z = -2$" of the $S = 2$ quintet.[15] They are only measureable under the condition that the zero-field splitting of the quintet is very small (< 0.3 cm). Possibly the CN bond of the "axial" ligands in the solid, in contrast to the weak coordination in solution, effects too strong a zero-field interaction to allow EPR transitions.

The Mössbauer spectra of powdered samples of the complexes **4a, b** show almost temperature-independent quadrupole doublets with splittings $\Delta E_Q = 3.16\ mms^{-1}$ (**4a**), $3.0\ mms^{-1}$ (**4b**) in the temperature range 4.2 to 300 K and the isomeric shift $\delta = 1.22\ mms^{-1}$ (**4a, b**) typical for high-spin iron(II) at 4.2 K (Fig. 2, left). The high δ value confirms the sixfold coordination of the iron by nitrogen and oxygen ligands in the coordination polymer. A quasi-tetrahedral ligand arrangement would give $\delta < 1\ mms^{-1}$.[13] Below 4.2 K the two complexes **4a** and **4b** behave differently. At 1.6 K without external magnetic field, **4a** shows *spontaneous magnetic ordering*, recognizable by the magnetic hyperfine interaction in the Mössbauer spectrum (Fig. 2, right), which furnishes further proof of the polymeric structure of **4a**. An

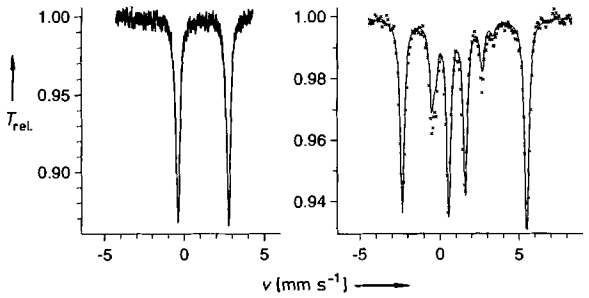

Fig. 2. Left: Mössbauer spectrum of a powdered sample of compound **4a**, recorded at 77 K. The solid line is a best fit with Lorenz lines. Right: Mössbauer spectrum of a powdered sample of compound **4a**, recorded at 1.6 K. The solid line is a simulation with the parameters: $\delta = 1.22\ mms^{-1}$; $\Delta E_Q = 3.10\ mms^{-1}$; $B^{int} = 17.7$ T; $\Gamma = 0.30\ mms^{-1}$; polar angle of B^{int} based on the molecular principal axis system of the electric field gradient: $\theta = 30°$, $\varphi = 90°$ (right). T_{rel} = relative transmission, v = relative velocity.

external field of 0.18 T has no measureable influence on the 1.6 K spectrum of **4a**, thus indicating that the magnetic ordering is of an antiferromagnetic nature. In contrast to the spectrum of **4a**, the spectrum of **4b** at 1.6 K shows no signs of a magnetic hyperfine interaction. The antiferromagnetic interaction in **4b** should thus be weak and only observable below 1.6 K in the Mössbauer spectrum.

Received: June 11, 1991 [Z 4693 IE]
German version: *Angew. Chem. 103* (1991) 1499

CAS Registry numbers:
2a, 136537-84-3; **2b**, 136537-85-4; **2c**, 136568-97-3; **2d**, 136537-86-5; **2e**, 136537-87-6; **2f**, 136537-88-7; **3a**, 136537-89-8; **4a**, 136537-91-2; **4b**, 136537-93-4; **5c**, 136568-98-4.

[1] F. Vögtle: *Supramolekulare Chemie*, Teubner, Stuttgart 1989, p. 103ff.; B. F. Matzanke, G. Müller-Matzanke, K. N. Raymond in T. M. Loehr (Ed.): *Physical Bioinorganic Chemistry Series, Vol. 5, Iron Carriers and Iron Proteins*, VCH, Weinheim 1989, p. 1.
[2] F. Ebmeyer, F. Vögtle in H. G. Dugas (Ed.): *Bioorganic Chemistry Frontiers, Vol. 1*, Springer, Berlin 1990, p. 143ff.; W. Kiggen, F. Vögtle, S. Franken, H. Puff, *Tetrahedron 42* (1986) 1859.
[3] R. D. Hancock, A. E. Martell, *Chem. Rev. 89* (1989) 1875.
[4] Y. Sun, A. E. Martell, *Tetrahedron 46* (1990) 2725; M. J. Miller, J. A. McKee, A. A. Minnick, E. K. Dolence, *Biol. Met. 4* (1991) 62.

[5] T. M. Garrett, T. J. McMurry, M. Wais Hosseini, Z. E. Reyes, F. E. Hahn, K. N. Raymond, *J. Am. Chem. Soc. 113* (1991) 2965.
[6] J. L. Pierre, P. Baret, G. Gellon, *Angew. Chem. 103* (1991) 75; *Angew. Chem. Int. Ed. Engl. 30* (1991) 85; A.-M. Giroud-Godquin, P. M. Maitlis, *ibid. 103* (1991) 370 and *30* (1991) 375.
[7] M. T. Ahmet, C. S. Frampton, J. Silver, *J. Chem. Soc. Dalton Trans. 1988*, 1159.
[8] K. Schreiber, *Mitteilungsbl. Chem. Ges. DDR 37* (1990) 1577; *Nachr. Chem. Tech. Lab. 37* (1990) 1577.
[9] R. W. Saalfrank, C.-J. Lurz, J. Hassa, D. Danion, L. Toupet, *Chem. Ber. 124* (1991) 595.
[10] All the compounds gave satisfactory analytical and spectroscopic data. For example, **2b**: deep blue crystals, m.p. 155°C.—IR(KBr): $\tilde{\nu}$ [cm^{-1}] = 2215 (CN). ^{1}H NMR (270 MHz, CD_2Cl_2): δ = 3.82 (s, 9H; $3OCH_3$), 5.81 (s, 6H, $3CH_2$), 7.44 (s, 15H; Phenyl-H) (simple set of signals, broad); ^{13}C NMR (67.7 MHz, CD_2Cl_2): δ = 29.38 (=C), 29.89 (OCH_3), 52.39 (CH_2), 128.29, 128.56, 129.29, 131.41, 133.18 (Phenyl-C or CN), 133.55 (C=N), 137.72 (=C–O) (simple set of signals, broad). EI-MS (70 eV): *m/z* 824 (M^+). UV/VIS (CH_3CN): λ_{max}[nm] (ε) = 604 (1230), 264 (38904), 208 (50119). **3a**: colorless crystals, m.p. = 154°C (decomp.). – IR (KBr): $\tilde{\nu}$ [cm^{-1}] = 2210 (CN). ^{1}H NMR (400 MHz, $CDCl_3$): δ = 1.00 (s, 9H; $3CH_3$), 1.02 (s, 18H; $6CH_3$, [11]), 3.72, 3.80, 3.93 (s, 3H; OCH_3), 4.33, 4.55 (each 3d, 3H; CH-N diastereotopic); ^{13}C NMR (100.5 MHz, $CDCl_3$): δ = 27.05 (CH_3), 27.09 ($2CH_3$, [11]), 33.56 (3C, [11]), 51.18, 51.61, 51.65 (=C), 53.81, 54.17, 54.29 (OCH_3), 57.61, 57.63, 57.68 (CH_2N), 116.34 (CN), 116.42 (2CN, [11]), 151.17, 151.29, 151.45 (C=N), 173.27, 173.36, 173.84 (=C–O). EI-MS (70 eV): *m/z* 735 (M^+). **4a**: bright green powder m.p. > 300°C (decomp.). – IR (KBr): $\tilde{\nu}$ [cm^{-1}] = 2190 (CN). – EI-MS (70 eV): *m/z* 528 (M^+); FAB-MS: *m/z* 529 [$(FeL_2)_1$ + H]$^+$, 1056 [$(FeL_2)_2$ + H]$^+$, 1584 [$(FeL_2)_3$ + H]$^+$.
[11] Coincidental overlap.
[12] R. T. Chakrasali, H. Ila, H. Junjappa, *Synthesis 1988*, 453.
[13] W. M. Reiff in I. J. Gruverman, C. W. Seidel (Eds.): *Mössbauer Effect Methodology, Vol. 8*, Plenum, New York, London 1973, p. 89ff.
[14] H. H. Wickman, M. P. Klein, D. A. Shirley, *Phys. Rev. 152* (1966) 52.
[15] W. R. Hagen, *Biochim. Biophys. Acta 708* (1982) 82.
[16] J.-M. Lehn, A. Rigault, *Angew. Chem. 100* (1988) 1121; *Angew. Chem. Int. Ed. Engl. 27* (1988) 1095; R. W. Saalfrank, A. Stark, M. Bremer, H.-U. Hummel, *ibid. 102* (1990) 292 and *29* (1990) 311; J.-M. Lehn in H.-J. Schneider, H. Dürr (Eds.): *Frontiers in Supramolecular Chemistry and Photochemistry*, VCH, Weinheim 1991, p. 17ff.
[17] M. Hvastijová, J. Kohout, H. Köhler, G. Ondrejovic, *Z. Anorg. Allg. Chem. 566* (1988) 111.
[18] Note added in proof: This is supported by a recent X-ray structure analysis of an analogous [CuL_2] complex, which shows that the coordination sphere of the Cu^{2+} center is a slightly distorted tetragonal bipyramid with CN groups of neighboring systems in apical positions [19].
[19] R. W. Saalfrank, O. Stuck, C.-J. Lurz, K. Peters, H. G. von Schnering unpublished.
[20] We will report elsewhere about the results achieved by us with 5-cyanosemicorrins [20] and Fe^{3+}/Fe^{2+} ions.
[21] H. Fritschi, U. Leutenegger, K. Siegmann, A. Pfaltz, W. Keller, C. Kratky, *Helv. Chim. Acta 71* (1988) 1541.

Metal-Assisted Organization rather than Preorganization for the Design of Macrocyclic Hosts

By *Yoshiaki Kobuke,* Yasutaka Sumida, Minoru Hayashi,* and *Hisanobu Ogoshi*

The strategy of preorganization of macrocyclic hosts ensures the efficient as well as selective binding of guest molecules.[1] Here, the unfavorable entropy term for assembling ligands around the guest is already overcome during the chemical synthesis so that large changes in free enthalpy, $-\Delta G^0$, and large differences $-\Delta\Delta G^0$ can occur upon host–guest complexation. This is clearly demonstrated in a vast number of publications, in which it is shown that stability and selectivity generally increase along the series podands, coronands, and cryptands.[2] Nevertheless, there are also arguments against strategies with such nicely arranged hosts: 1) the synthesis of such well-organized hosts may not be easy; 2) once synthesized, the hosts can be modified structurally only with difficulty; 3) a host with strong binding generally decomplexes too slowly, and the efficiency of regeneration is low.

We would like to introduce here a new concept for the design of macrocyclic hosts and cooperative metal binding (Scheme 1). A host with two metal binding sites is synthesized in which the binding of M^1 to the first site influences the second site both electronically and conformationally, converting it from an otherwise weak binding site into a potent site for the cooperative binding of M^2. Since the final structure formation is completed with the aid of M^1, the synthesis of the parent host itself becomes much easier and various structural modifications become possible by appropriate selection of M^1. Moreover, the decomplexation of M^1 destroys the final ligand organization and regenerates the starting host. Therefore, all of the negative aspects cited above can be avoided. In this report, the synthesis of hosts according to the above concept and their preliminary binding characteristics will be demonstrated.[3]

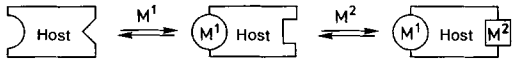

Scheme 1. Cooperative metal binding with influence of the M^2 binding site by binding of M^1.

The catecholate group was chosen as the unit for the M^1 binding site, since it shows the highest degree of chelating ability towards a large variety of metal ions as a result of its *ortho*-dianionic form;[4] a neutral polyether group was used as unit for the coordination of alkali metal ions M^2. Accordingly, both a podand (**1**) and a coronand (**3**) were synthesized as parent hosts (Scheme 2). We employed a benzyl group for protecting the catechol unit.

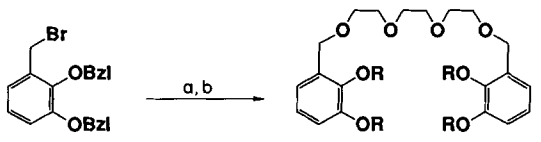

1 (R=H), 2 (R=Bzl)

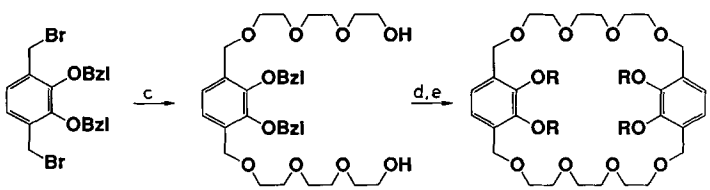

5 **3 (R=H), 4 (R=Bzl)**

Scheme 2. Synthesis of **1** and **3** via **2** and **4**. a) Triethylene glycol, NaH, dioxane; 60%. b) Pd/C, THF; 95%. c) Triethylene glycol (excess), NaH, dioxane; 60%. d) **5**, NaH, dioxane; 30%. e) Pd/C, EtOH; 95%. Bzl = benzyl.

[*] Prof. Dr. Y. Kobuke
Department of Materials Science, Faculty of Engineering
Shizuoka University
Johoku, Hamamatsu 432 (Japan)
Y. Sumida, M. Hayashi, Prof. Dr. H. Ogoshi
Department of Synthetic Chemistry, Faculty of Engineering
Kyoto University
Yoshida, Kyoto 606 (Japan)

The precursor molecule for podand **2** was easily obtained by treatment of 2,3-bis(benzyloxy)benzyl bromide with triethylene glycol. In the synthesis of the coronand precursor **4**, 2,3-bis(benzyloxy)-1,4-bis(bromomethyl)benzene (**5**) was first treated with an excess of triethylene glycol and the resulting intermediate was cyclized under high dilution conditions in dioxane with **5** to give **4**. The benzyl–O bonds of the aryl benzyl ether units were cleaved by controlled hydrogenation over palladium/carbon (5%) without attack at the benzyl–O bonds of the alkyl benzyl ether units in the main chain; this led to quantitative formation of **1** and **3**.

A buffer solution (pH 8.0, phosphate) of **1** was titrated with boric acid to give a smooth change in absorption of the catecholate–boron complex at 290 nm. The titration curve was consistent with formation of a 1:1 complex and the equilibrium constant was estimated to be $3700 \pm 90\ M^{-1}$.

An ethanolic solution of **1** was treated with four equivalents of aqueous KOH and then with one equivalent of boric acid. A colorless precipitate was formed, whose FAB mass spectrum gave a peak at *m/z* 440, corresponding to the ternary complex of the tetranion of **1**, boron, and potassium $(\mathbf{1} - 4H)^{4-} \cdot B^{3+} \cdot K^{+}$ (**6**). In the NMR spectrum of **6** in $CDCl_3$ the benzyl protons give rise to an AB quartet at $\delta = 4.03$ and 4.96 ($J = 9.6$ Hz), while those in the parent podand **1** afford a sharp singlet at $\delta = 4.52$. When the complexation was undertaken in the presence of NaOH, the benzyl protons in the resulting complex **7** gave an AB pattern at slightly different δ values (4.10 and 4.97; $J = 10.0$ Hz). The differences in the chemical shifts and in the coupling constants between **6** and **7** suggest that benzyl protons are close enough to the cationic metal center to be influenced by even the subtle change from K^+ to Na^+. Upon treatment of the Na complex **7** with excess KPF_6, **6** was regenerated (NMR spectroscopic detection). These results clearly indicate that boron is complexed with two catecholate ligands in the same molecule leading to formation of a boron-assisted coronand, in which two anionic oxygen atoms from the catecholate units and four neutral oxygen atoms from the polyether chain are nicely arranged to afford an additional metal binding site. K^+ or Na^+ may be entrapped in this monoanionic crown-like cavity to give the respective neutral species $(\mathbf{1} - 4H)^{4-} \cdot B^{3+} \cdot K^{+}$ or $(\mathbf{1} - 4H)^{4-} \cdot B^{3+} \cdot Na^{+}$. It should be noted that the parent podand possesses the basic structural units for alkali-metal binding but it is inert unless the complexation with boron organizes them into a macrocyclic structure which still bears an anionic charge.

It is well established that boron is generally surrounded tetrahedrally by ligands, and that the metal-assisted coronand is presumably a C_2 symmetric and should be a mixture of *A* and *Δ* isomers. When 0.1 molar equivalents of europium (III) tris[3-(hydroxyl)trifluoromethylmethylene)-(+)-camphorate] was added to **6** in $CDCl_3$ the AB quartet was separated into two sets of AB quartets, one at $\delta = 4.04$ and 5.07

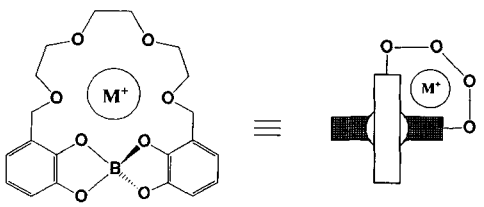

6 (M=K)
7 (M=Na)

Scheme 3. Probable structures of **6** and **7**; right: drawn schematically for one enantiomer.

Table 1. ^1H NMR, mass spectrometric, and elemental analysis data of **1**–**4** and **6**–**8**.

1: ^1H NMR (90 MHz, $CDCl_3$): $\delta = 3.73$ (s, 12H, OCH_2CH_2O), 4.70 (s, 4H, OCH_2Ar), 6.02 (s, 2H, OH), 6.45–6.95 (m, 6H, C_6H_3), 7.81 (s, 2H, OH); MS (FAB): *m/z* 394 (M^+); correct C,H,O analysis.

2: ^1H NMR (90 MHz, $CDCl_3$): $\delta = 3.44$–3.78 (br. s, 12H, OCH_2CH_2O), 4.56 (s, 4H, OCH_2Ar), 5.05 (s, 4H, $PhCH_2OAr$), 5.13 (s, 4H, $PhCH_2OAr$), 7.01 (m, 6H, C_6H_3), 7.26–7.50 (br. s, 20H, C_6H_5); MS (FAB): *m/z* 754 (M^+); correct C,H,O analysis.

3: ^1H NMR (90 MHz, $CDCl_3$): $\delta = 3.72$ (s, 24H, OCH_2CH_2O), 4.61 (s, 8H, OCH_2Ar), 6.64 (s, 4H, C_6H_2), 7.13 (br. s, 4H, OH); MS (FAB): *m/z* 569 ($M^+ + H$), 591 ($M^+ + Na$), 607 ($M^+ + K$).

4: ^1H NMR (90 MHz, $CDCl_3$): $\delta = 3.63$ (s, 24H, OCH_2CH_2O), 4.52 (s, 8H, OCH_2Ar), 5.03 (s, 8H, $PhCH_2OAr$), 7.16 (s, 4H, C_6H_2), 7.34 (s, 20H, C_6H_5); MS (FAB): *m/z* 928 (M^+); correct C,H,O analysis.

6: ^1H NMR (90 MHz, $CDCl_3$): $\delta = 3.37$–3.77 (m, 12H, OCH_2CH_2O), 4.03 and 4.96 (q, 4H, $J = 9.6$ Hz, OCH_2Ar), 6.47–6.88 (m, 6H, C_6H_3); UV ($CHCl_3$): λ_{max} [nm] = 290, MS (FAB): *m/z* 440 (M^+); correct C,H analysis.

7: ^1H NMR (90 MHz, $CDCl_3$): $\delta = 3.51$–3.78 (m, 12H, OCH_2CH_2O), 4.10 and 4.97 (q, 4H, $J = 10.0$ Hz, OCH_2Ar), 6.44–6.87 (m, 6H, C_6H_3); MS (FAB): *m/z* 424 (M^+)

8: MS (FAB): *m/z* 615 ($M^+ + H$), 637 ($M^+ + Na$), 653 ($M^+ + K$)

with $J = 9.6$ Hz and the other at $\delta = 4.09$ and 5.24 with $J = 10.2$ Hz. Further addition of the shift reagent gave a larger downfield shift and a larger broadening of the latter set of signals selectively at the lower field. This observation is in complete agreement with the expectation. Therefore the structures of the complexes may safely be formulated as shown in Scheme 3.

When **3**, which already has a coronand structure, was treated with boric acid in the presence of KOH, a similar neutral triple complex, $(\mathbf{3} - 4H)^{4-} \cdot B^{3+} \cdot K^{+}$ (**8**) was obtained. The FAB mass spectrum showed a peak corresponding to $(\mathbf{8} + H)^+$ together with peaks for $(\mathbf{8} + Na)^+$ and $(\mathbf{8} + K)^+$. The latter two ions must therefore be formed from a quaternary complex $[(\mathbf{3} - 4H \cdot B \cdot K \cdot M]^+$, with M = Na or K. Presumably an additional monovalent metal cation had been entrapped in the vacant coronand cavity of **8** (Scheme 4).

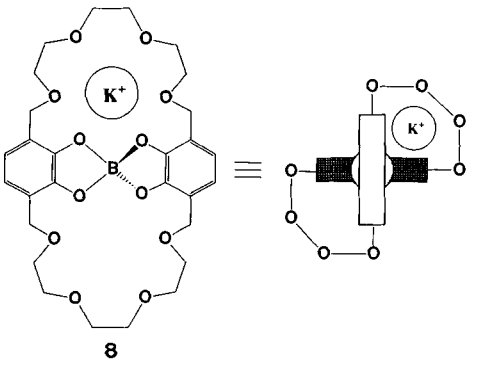

8

Scheme 4. Probable structure **8**; right: drawn schematically for one enantiomer.

In summary, the achiral parent podand or coronand was converted upon complexation with boron into the respective chiral coronand or a chiral bicyclic coronand with a C_2-symmetry. Alkali-metal ions are bound in this newly organized monoanionic cavity. This is a successful example of positive cooperativity for the binding of different metal ions in a single host. It shows a clear distinction from previous reports in which attempts at metal binding showed no cooperativity or if so, in negative or only marginally positive

terms.[5] The use of anionic ligation seems essential for achieving positive cooperativities so that the occurrence of a positive charge in the structure through the first metal cation is carefully avoided.

Received: June 26, 1991 [Z 4749 IE]
German version: *Angew. Chem. 103* (1991) 1513

CAS Registry numbers:
1, 137003-58-8; **2**, 137003-59-9; **3**, 137003-60-2; **4**, 137003-61-3; **5**, 137003-62-4; **6**, 137003-64-6; **6** (M = K^+), 137003-65-7; **7** (M = Na^+), 137003-66-8; **8** (M = K^+), 137003-67-9; **8** (M = Na^+), 137003-68-0; $HO(CH_2CH_2O)_3H$, 112-27-6; 2,3-bis(benzyloxy)-1-(bromomethyl)benzene, 81464-85-9; 2,3-bis(benzyloxy)-1,4-bis[{2-[2-(2-hydroxyethoxy)ethoxy]ethoxy}methyl]benzene, 137003-63-5.

[1] a) D. J. Cram, *Angew. Chem. 98* (1986) 1041; *Angew. Chem. Int. Ed. Engl. 25* (1986) 1039; b) D. N. Reinhoudt, P. J. Dijkstra, *Pure Appl. Chem. 60* (1988) 477.

[2] a) C. J. Pedersen, *J. Am. Chem. Soc. 89* (1967) 2495; b) J. M. Lehn, *Angew. Chem. 100* (1988) 91; *Angew. Chem. Int. Ed. Engl. 27* (1988) 90; c) F. Vögtle (Ed.): *Host Guest Complex Chemistry Vol. I–III*, Springer, Berlin 1981–1984; d) R. M. Izatt, J. J. Christensen (Ed.): *Synthesis of Macrocycles*, Wiley, New York 1987.

[3] *Schepartz* et al. developed an idea of self-assembling ionophores and reported the complexation of two different cations in the assembly: a) A. Schepartz, J. P. McDevitt, *J. Am. Chem. Soc. 111* (1989) 5976. Cocomplexation of a neutral guest and an electrophilic cation immobilized in the macrocycle was reported by *Reinhoudt* et al.: b) C. J. van Staveren, D. E. Fenton, D. N. Reinhoudt, J. van Eerden, S. Harkema, *ibid. 109* (1987) 3456; c) C. J. van Staveren, J. van Eerden, F. C. J. M. van Veggel, S. Harkema, D. N. Reinhoudt, *ibid. 110* (1988) 4994.

[4] a) K. N. Raymond, T. J. MacMurry, T. M. Garrett, *Pure Appl. Chem. 60* (1988) 545, and references cited therein; b) P. Stutte, W. Kiggen, F. Vögtle, *Tetrahedron 43* (1987) 2065; c) J. L. Pierre, P. Baret, G. Gellon, *Angew. Chem. 103* (1991) 75; *Angew. Chem. Int. Ed. Engl. 30* (1991) 85.

[5] a) J. Rebek, Jr., J. D. Trend, R. V. Wattley, S. J. Chakravosti, *J. Am. Chem. Soc. 101* (1979) 4333; b) J. Rebek, Jr., R. V. Wattley, *ibid. 102* (1980) 4853; c) J. Rebek, Jr., R. V. Wattley, T. Costello, R. Gadwood, L. Marshall, *ibid. 102* (1980) 7398; d) *Angew. Chem. 93* (1981) 584; *Angew. Chem. Int. Ed. Engl. 20* (1981) 605; e) J. Rebek, Jr., L. Marshall, *J. Am. Chem. Soc. 105* (1983) 6668; f) J. Rebek, Jr., *ibid. 107* (1985) 7481; g) T. Nabeshima, T. Inaba, N. Furukawa, *Tetrahedron Lett. 28* (1987) 6211; h) F. Gaviña, S. V. Luis, A. M. Costero, M. I. Burguete, J. Rebek, Jr., *J. Am. Chem. Soc. 110* (1988) 7140.

Antiperovskite Structure with Ternary Tetrathiafulvalenium Salts: Construction, Distortion, and Antiferromagnetic Ordering**

By *Patrick Batail,* Carine Livage, Stuart S. P. Parkin, Claude Coulon, James D. Martin*, and *Enric Canadell*

Our present ability to rationally design and prepare molecular solids within a predicted structure type is still in its infancy.[1] Here we report that a series of ternary tetrathiafulvalenium salts of large, divalent all-inorganic hexanuclear molybdenum halides, formulated as $(TTF^{\bullet+})_3[(Y^-)(Mo_6X_{14}^{2-})]$ (X = Y = Cl; X = Br, Y = Cl, Br, I), has been electrochemically assembled and shown to actually adopt a perovskite-type[2] structure. The latter features a unique three-dimensional arrangement of tetrathiafulvalene (TTF) cation radicals, located at the oxygen sites of the $BaTiO_3$ prototypical structure. Thus, a rhombohedrally distorted antiperovskite network is identified, in which, in all four compounds, the unpaired π-electron spins ($S = 1/2$) for each of the tetrathiafulvalenium HOMOs, centered at the vertices of vertex-sharing $\{Y^-(TTF^{\bullet+})_6\}$ octahedra, undergo sharp, long-range antiferromagnetic ordering at roughly 6–8 K. In fact, the initial discovery that antiferromagnetic ordering occurs in $(TTF)_3[(Cl)(Mo_6Cl_{14})]$ **1** prompted the preparation of $(TTF)_3[(Y)(Mo_6Br_{14})]$, Y = Cl (**2**), Br (**3**), and I (**4**) with the two-fold anticipation that they would form the same antiperovskite structure and indeed order antiferromagnetically.

These observations suggest that significant molecular information can be expressed and manipulated by substitution into a predicted target structure in order to design highly ordered, specialized three-dimensional molecular solids. These structures act as efficient receptors for halides with unique magnetic properties, very much along the same approach that has proven so successful in solid state inorganic chemistry. In this respect, such a unique family of compounds bridges the gap between organic and inorganic materials: it is indeed a novel simple structure type recognized[3] in complex molecular solids in the CsCl,[4a] NaCl,[4b,c] and $CdCl_2$ structures.[4d] It is also suggested that the three-dimensional nature of the perovskite structure has played a role in preventing the occurrence of the spin-Peierls transition commonly observed[5] in other cation radical salts, albeit of lower dimensionality, thereby providing a particularly simple example of geometric control of the electronic structure in the solid state. An exchange mechanism by direct, through-space coupling of the organic spins inside the octahedron—unprecedented in the molecular solid state—could be revealed by consideration of structural and antiferromagnetic resonance data and MO calculations.

The electrochemical assembling of the units $[Mo_6Cl_{14}]^{2-}$, $TTF^{\bullet+}$, and Cl^- was purposely attempted in order to demonstrate that the formation of the perovskite framework is a consequence of the divalent character of the large cluster anion (site A). This assumption was based on recent evidence that (a) such associations with the monovalent, isoelectronic, and isostructural hexarheniate cluster anions $[Re_6Q_5Cl_9]^-$ (Q = S, Se)[6] result in the formation of 2:1 binary phases with discrete mixed-valence $[(TTF)_2^{+}]$ dimers;[7] and (b) that the monovalent rhenium cluster-based, paramagnetic perovskite previously obtained by serendipity,[6] was actually a disordered material with only a fraction of the monovalent anions on the A site. Indeed, we have shown that in the latter phase, now formulated as $\{(TTF^{\bullet+})_5(TTF)\}\{(Cl^-)_2\}\{(Re_6Se_6Cl_8^{2-})(Re_6Se_5Cl_9^-)\}$ one spin fails per TTF octahedron and no antiferromagnetic ordering occurs.[7]

Black, rhombohedrally-shaped single crystals of **1**–**4** were grown on a platinum wire anode upon constant low current density (1.3 $\mu A\,cm^{-2}$) oxidation of TTF (0.067 mmol) in anhydrous acetonitrile in the presence of equimolecular amounts (0.045 mmol) of the tetrabutylammonium (TBA) salts of the hexanuclear halomolybdate[8] and of the appropriate halide. The proportions and amounts of the two anionic components in the 30 mL electrochemical cells proved to be critical for the formation of the proper 3:1:1 stoichiometry. While

[*] Dr. P. Batail, Dr. C. Livage
Laboratoire de Physique des Solides Associé au CNRS
Université de Paris-Sud
F-91405 Orsay (France)
Dr. S. S. P. Parkin
IBM Research Division, Almaden Research Center
San Jose, CA 95120 (USA)
Dr. C. Coulon
Centre de Recherche Paul Pascal, CNRS
Avenue Dr. Schweitzer, F-33600 Pessac (France)
Dr. J. D. Martin, Dr. E. Canadell
Laboratoire de Chimie Théorique Associé au CNRS
Université de Paris-Sud

[**] This work was supported by the Ministère de la Recherche et de la Technologie (The "Ingénierie Moléculaire" Program and Research Fellowship to *C. L.*), the Centre National de la Recherche Scientifique (France), and the National Science Foundation Office of International Programs (postdoctoral fellowship for *J.D.M.*). We thank *P. Auban* for her contribution to the ESR experiments.

we have found no evidence so far of other ternary phases with different stoichiometry, single crystals of a binary 11:2 phase (for example, $(TTF)_{5.5}(Mo_6X_{14})$, X = Cl, Br) have been identified, whose formation competes with that of the 3:1:1 antiperovskite; more about this will be described separately. This binary phase was obtained earlier, independently by us and by *Fuchs*,[9] when the electrocrystallization was conducted without TBA^+Y^- in the cells.

The compounds, which crystallize in the space group $R\bar{3}$ (Table 1) are isostructural. Their structure,[10] shown in Figure 1a, emphasizes the analogy with the classical representation of the cubic perovskite-cage (Fig. 1b). Attention is thus drawn to the three-dimensional framework of vertex-sharing $\{(TTF^{\bullet+})_6Y^-\}$ octahedra, with the divalent inorganic cluster anion encapsulated in the organic cage. Both the center of the cage and that of the cluster anion are located at the origin of rhombohedral unit cells (Table 1); the discrete halide ion is found at the center of the unit cell and the $TTF^{\bullet+}$ ions at the middle of the faces.

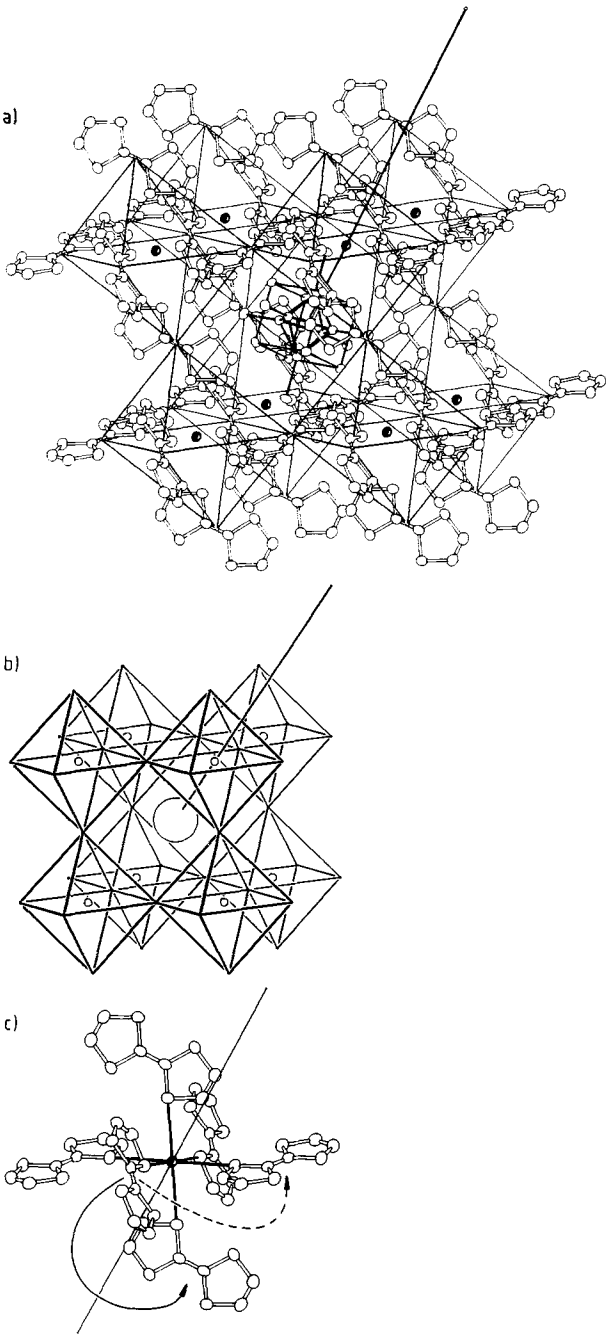

Fig. 1. a) Structural organization of the antiperovskites **1**–**4**. b) The cubic perovskite structure. c) Binding geometry within the $\{(TTF)_6^+Y^-\}$ octahedra (see text). In all figures the unique $\bar{3}$-axis direction of the $R\bar{3}$ unit cell is indicated.

Table 1. Crystallographic and magnetic data for compounds **1**–**4**.

Quantity	Unit	**1** X=Y=Cl	**2** X=Br, Y=Cl	**3** X=Y=Br	**4** X=Br, Y=I
a	Å	10.685(1)	10.899(1)	10.928(1)	11.033(1)
α	°	101.54(1)	100.80(1)	100.95(1)	101.35(1)
V	Å^3	1134(4)	1215(4)	1223(7)	1251(6)
S–Y	Å	3.229(1)	3.313(2)	3.345(3)	3.404(3)
N [a]		808	1187	906	1137
R [b]	%	1.5	2.1	3.2	2.4
R_w [b]	%	1.7	2.3	3.4	3.4
C [c]		0.349	0.357	0.407	0.349
μ_{eff}	μ_B	0.94	0.96	1.09	0.94
θ	K	− 14.6	− 16.7	− 11.5	− 12.1
T_{max}	K	11	13	11	8
T_N	K	8.2	8.2	7.5	6.3

[a] N = number of the observed intensities, corrected for absorption such that $I \geq 3\sigma(I)$. [b] R and R_w are the residuals for the structure factors and their weighted sum, respectively. [c] The observed Curie constants C are given in cgs units per mol TTF (in SI units this is 3.75 JT^{-2}K); the calculated value is 0.3723 emu. mol^{-1} for $S = 1/2$ and $g = 2$.

The analysis of the crystal structures reveals a set of six symmetry-equivalent, short S–Y contacts (Table 1). These might be primarily responsible for the binding geometry inside the octahedral motif, since the orientation of the $TTF^{\bullet+}$ ions on their lattice site is such as to satisfy quasilinear C–$S^{\delta+}\cdots Y\cdots{}^{\delta+}$S–C electrostatic interactions across the central halide ion (Fig. 1c). Therefore, the small rhombohedral distortions in the unit cell would specifically reflect the offset between the former direction of optimum, long range Coulomb forces[11] and that of the unit-cell translational symmetry vector linking the centroids of the TTF ions. This is a novel type of geometrical distortion for the perovskite structure, since the quadratic, rhombohedral, and orthorhombic distortions commonly observed in inorganic compounds result rather from the mismatch between the metal–oxygen and the metal–halide bond lengths.[12]

We then observe that this novel distortion of the perovskite structure demonstrated in this series of isostructural salts allows for a striking crystallographic expression of the anisotropic shape and binding capabilities of their common organic component when assembled with essentially spherical inorganic counterparts. A macroscopic manifestation of this molecular shape-selective binding symmetry is to be found in the actual rhombohedral habit of the single crystals.

The $TTF^{\bullet+}$ centers are 6.754 ($\bar{3}$-axis related) and 8.272 Å (for **1**) to 6.984 and 8.521 Å (**4**) apart along the edges of the $\{Y^-(TTF^{\bullet+})_6\}$ octahedra. This is another remarkable feature of this three-dimensional network of organic cation radicals, given the propensity of such planar aromatic cations to overlap and favor electron delocalization along one-dimensional stacks of closely spaced molecules (3.47 Å). As expected then, the compounds **1**–**4** are insulating.

As follows from the temperature dependence of their static magnetic susceptibilities, the compounds are paramagnetic down to low temperatures (as shown for example for **3** in Fig. 2). Above 50 K, the data obey the Curie–Weiss law, and the observed and calculated Curie constants and effective magnetic moments (Table 1) are in excellent agreement with the assumption of one spin per TTF molecule. The data also reveal (Fig. 2) that the susceptibility of each compound goes through a maximum at the temperatures T_{Max} given in Table 1. The magnetic susceptibilities were measured at var-

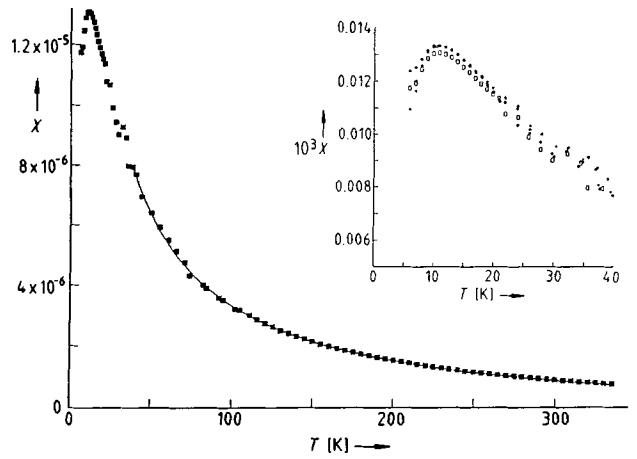

Fig. 2. Temperature dependence of the specific magnetic susceptibilities (in cgs units) measured directly on some single crystals of **3** using a SQUID susceptometer. The solid lines represent the fit of the data to $\chi = \chi_0 + C(T + \theta)^{-1}$. The observed Curie constants and Weiss temperatures for **1**–**4** are given in Table 1. The inset shows that T_{max} is independent of the field strength. o = 1 kOe, ● = 2 kOe, □ = 5 kOe, ■ = 50 kOe. χ in emu g^{-1}.

ious field strengths from 50 kOe (3.98×10^6 A m^{-1}) down to 1 kOe, and T_{Max} values were found to be independant of the field. A typical example is given for **3**, between 5 and 40 K, in the insert of Figure 2. These indications of anisotropic antiferromagnetic (AF) fluctuations suggest the possibility of AF ordering at lower temperature.

This assumption was suppported by single-crystal electron spin resonance (ESR) experiments showing in each case that the narrow single line observed in the paramagnetic regime, with Lorentzian shape and isotropic characteristics typical of $TTF^{\bullet+}$ spins,[13] abruptly vanishes in a few tenths of a degree at Néel temperatures (T_N) lower than T_{max} (Table 1). Finally, the observation of antiferromagnetic resonances (AFMR) below T_N definitely confirms the existence of magnetic ordering.

So far we have only incomplete information on the mechanism of the magnetic interaction. A classical description[14] of the perovskite structure requires, however, that **1**–**4** are built up by the stacking of pseudo-close-packed $(TTF^{\bullet+})_3$-$(Mo_6X_{14}^{2-})$ layers which form octahedral holes occupied by the discrete halide ions Y^-. Owing to the rhombohedral distortion there is only one such stacking direction in the structure, that is the layers of organic spins are stacked along the unique threefold inversion axis. The most likely interactions are either the two through-space interactions symbolized by the arrows in Figure 1c, or the indirect *trans*-coupling across the halide at the center of the octahedron. Extended Hückel-type calculations[15] demonstrate that the latter coupling is extremely weak. Remarkably, the strongest interaction is between the TTF ions related by symmetry by the $\bar{3}$-axis (solid arrow in Fig. 1c). These interactions (5×10^{-2} eV in **2**) are about three times stronger than those between the TTF ions *not* related by symmetry (dashed arrow in Fig. 1c) and indeed thirteen times stronger than the indirect *trans*-coupling. This would suggest that most of the magnetic interaction might occur by direct exchange between spins of successive layers.

The quantitative analysis of the AFMR rotation patterns provides information on the magnetic anisotropy.[16] The AFMR spectrum is complex and composed of several narrow lines, the origin of which will be discussed in a separate paper. However, the evolution of the mean position of the spectrum as a function of the field orientation for **1**–**4** is reminiscent of the room temperature crystal structure symmetry. That is, we find that the single $\bar{3}$-axis, actually the short diagonal of the crystals, is the magnetic hard axis. In addition there exists an easy plane, that is the spin-flop field vanishes ($H_{SF} = 0$). These results agree with the absence of any sizeable field dependence of the magnetic susceptibility below T_N. Thus, with this approximation, we are left with only one adjustable parameter to describe the anisotropy of the system, that is, $H^+ = \hbar\Omega_+/\mu_B$.[16a] Preliminary estimations yield an H^+ field strength on the order of 5 kG, a value similar to those found previously for other TTF-based charge transfer salts.[16b] This convincingly supports the hypothesis that the magnetic anisotropy has the same origin, i.e. is due to magnetic dipolar interactions.[17]

Altogether, the structural analysis and molecular orbital calculations are consistent with the ESR and AFMR experiments and favor a direct exchange mechanism for the antiferromagnetic ordering. Thus, the strength and anisotropy of the magnetic interaction are expected to be very sensitive to even small modifications of the $\{(TTF^{\bullet+})_6Y^-\}$ octahedral geometry. The electrochemical assembling of three components associated with the control of the site location of the molecular ions, allows for many substitutions in these series of compounds. One possible aim is the synthesis of a related molecular equivalent of the K_2NiF_4-type of structure, particularly with the prospect of the occurrence of two-dimensional magnetic ordering reminiscent of the antiferromagnetic phase of La_2CuO_4;[18] this would require the stabilization of single perovskite layers, which might be achieved by decoupling the $(TTF)_6$ octahedra either by alloying with unsymmetrical TTF ions or by using bulkier divalent cluster anions. Such possibilities are being explored.

Received: June 13, 1991 [Z 4700 IE]
German version: *Angew. Chem. 103* (1991) 1508

[1] J. S. Miller, *Adv. Mater. 2* (1990) 98.
[2] J. B. Goodenough, J. M. Longo in *Landolt-Börnstein-Tabellen Vol. 111/4a*, Springer, Berlin 1978, p. 126.
[3] An approach not unlike *Paul Moore*'s perception of structural complexity: P. B. Moore, *Am. Miner. 74* (1989) 918–926. See also P. B. Moore, *ibid. 71* (1986) 540; J. K. Burdett, *Chem. Rev. 88* (1988) 3.
[4] a) L. Ouahab, P. Batail, C. Perrin, C. Garrigou-Lagrange, *Mater. Res. Bull. 21* (1986) 1223; b) A. Pénicaud, P. Batail, P. Davidson, A.-M. Levelut, C. Coulon, C. Perrin, *Chem. Mater. 2* (1990) 117; c) A. Renault, D. Talham, J. Canciell, P. Batail, A. Collet, J. Lajzerowicz, *Angew. Chem. 101* (1989) 1251; *Angew. Chem. Int. Ed. Engl. 28* (1989) 1249; d) P. Batail, K. Boubekeur, A. Davidson, M. Fourmigué, C. Lenoir, C. Livage, A. Pénicaud in G. Saito, S. Kagoshima (Eds.): *The Physics and Chemistry of Organic Superconductors*, Springer, Berlin 1990, p. 353.
[5] J. B. Torrance in D. Jérome, L. G. Caron (Eds.): *Low dimensional Conductors and Superconductors*, NATO ASI Ser. B155, (1987) 113.
[6] P. Batail, L. Ouahab, A. Pénicaud, C. Lenoir, A. Perrin, *C. R. Acad. Sci. Ser. 2 304* (1987) 1111.
[7] K. Boubekeur, *Dissertation*, Université de Rennes (1989).
[8] P. Nanelli, B. P. Block, *Inorg. Synth. 12* (1970) 170.
[9] H. Fuchs, *Dissertation*, Universität München (1987).
[10] Enraf-Nonius CAD-4F, (ω-2θ) scans, $Mo_{K\alpha}$, solution of structures by direct methods and Fourier synthesis. Further details of the crystal structure investigations are available on request from the Fachinformationszentrum Karlsruhe, Gesellschaft für wissenschaftlich-technische Information mbH, W-7514 Eggenstein-Leopoldshafen 2 (FRG), on quoting the depository number CSD-55593, the names of the authors, and the journal citation.
[11] W. F. van Gunsteren, H. J. C. Berendsen, *Angew. Chem. 102* (1990) 1020; *Angew. Chem. Int. Ed. Engl. 29* (1990) 992.
[12] R. A. Wheeler, M. H. Whangbo, T. Hughbanks, R. Hoffmann, J. K. Burdett, T. A. Albright, *J. Am. Chem. Soc. 108* (1986) 2222.
[13] Y. Tomkiewicz, A. R. Taranko, J. B. Torrance, *Phys. Rev. B15* (1977) 101.
[14] A. F. Wells: *Structural Inorganic Chemistry*, Oxford University Press, Oxford, 1986, pp. 179–181.
[15] R. Hoffmann, *J. Chem. Phys. 39* (1963) 1397. Our calculations use double-ζ type orbitals: E. Clementi, C. Roetti, *At. Nucl. Data Tables 14* (1974) 177.
[16] a) T. Nagamiya, *Prog. Theor. Phys. 11* (1954) 309; b) C. Coulon, R. Laversanne, J. Amiell, *Physica B + C (Amsterdam) 143* (1986) 425.
[17] M. Rogers, J.-M. Delrieu, E. Wope Mbougue, *Phys. Rev. B34* (1986) 4952.
[18] D. Vaknin, S. K. Sinha, D. E. Moncton, D. J. Johnston, J. M. Newsam, C. R. Safinya, H. E. King, Jr., *Phys. Rev. Lett. 58* (1987) 2802.

Solvated Electrons in the Synthesis of Ionic Clusters in Zeolites**

By *Paul A. Anderson,* Donald Barr*, and *Peter P. Edwards**

It has long been known that the interaction of alkali metal vapor with certain zeolites results in the formation of paramagnetic centers such as Na_4^{3+}, Na_6^{5+}, and K_4^{3+} within the pores of the zeolite, whose presence can be detected through electron spin resonance (ESR) spectroscopy.[1, 2, 3] As a result of recent studies the existence of two more such centers, Na_5^{4+} and K_3^{2+}, has come to light,[4, 5] suggesting that a whole series of similar species may exist. These unusual ion clusters are of interest both on account of the comparative rarity of alkali metal clusters[6] and because of their potential as basic catalysts.[7] But a major problem associated with their characterization has been that the direct reaction between zeolites and the various metal vapors tends to provide an excess of metal atoms which results in the formation of aggregates or metal particles.[2, 3] The same problem attends the alternative preparation for sodium-containing zeolites devised by *Martens* et al.,[7, 8] which involves the pyrolysis of sodium azide. Although *Yoon* and *Kochi*[9] demonstrated that a simple reduction of the sodium cations in Na-X and Na-Y zeolites by organolithium reagents resulted in the selective formation of Na_4^{3+}, we have found their method to be ineffective in other cases.

Here we present the novel use of solvated electrons, formed in situ by dissolving lithium metal in primary amines, as a welcome solution to this problem. The solvated electron solutions are powerful enough reagents that they have the potential to reduce the cations of virtually any zeolite. Although the reduction of a substantial proportion of the zeolite cations can be achieved in this manner, the concentration of the solutions is easily controlled to enable the preparation of ionic clusters in the absence of excess metal atoms. In fact, the scope of this new method is much wider than that: the solvated electron solutions also facilitate the reduction of certain zeolites (those containing lithium for instance) that tend to decompose when exposed to alkali metal. This has enabled us to compare the ESR parameters of Na_4^{3+} in a range of zeolites and to report the discovery of another new cluster, Na_3^{2+}.

The reduction of three of the zeolites used in this work resulted in compounds whose ESR spectrum exhibited the hyperfine pattern of thirteen lines characteristic of the Na_4^{3+} cluster.[1, 9] The *g*-values and hyperfine splittings are given in Table 1. The selective reduction of the Na-X zeolite to produce the Na_4^{3+} cluster is of particular interest, since that zeolite plays host to different paramagnetic centers when treated with alkali metal vapor.[4] Similar selectivity was observed by *Yoon* and *Kochi*[9] in their reduction of Na-X with organolithium reagents. The origin of these differences must lie either in the fact that the reaction with metal vapor necessarily takes place at temperatures above ambient, or in the presence of solvent molecules within the zeolite structure. The Na_4^{3+} cluster can also be formed through the exposure of dehydrated Na-Y to γ-rays.[10] Having found that the irradiation of dehydrated Na-X did not produce Na_4^{3+}, we conclude that, under vacuum, the zeolite is not disposed to the creation of that cluster, and that the effect of the solvent is critical. Remarkably, Na_4^{3+} was also the product of the reduction of $Li_{44}Na_{12}$-Y. Evidently in this case the valence electron of the cluster prefers to associate with the sodium ions rather than with those of lithium which heavily outnumber them. Since the residual charge on a lithium ion in dehydrated zeolite Y is calculated to be less than one sixth of that on a sodium ion in a similar site,[11] this is perhaps not surprising.

The apparent inertness of lithium in this respect led us to attempt the preparation of new sodium clusters containing fewer than four cations by restricting the concentration of sodium ions in the zeolite to a minimum. Success was achieved in the reduction of $Li_{50}Na_6$-Y and $Li_{82}Na_5$-X, to give the colored solids whose ESR spectra are reproduced in Figure 1.[12] The reduction of $Li_{50}Na_6$-Y produced a purple-gray solid whose spectrum (Fig. 1 a) consisted of a hyperfine pattern of ten lines with $a = 4.50 \pm 0.10$ mT and $g = 2.002 \pm 0.001$. Ten lines are expected from an electron interacting with three equivalent nuclei with nuclear spin $I = 3/2$, but although both the ^{23}Na nucleus and the more abundant isotope of lithium (^7Li) have spin $I = 3/2$, the unambiguous assignment of the hyperfine pattern of reduced $Li_{44}Na_{12}$-Y

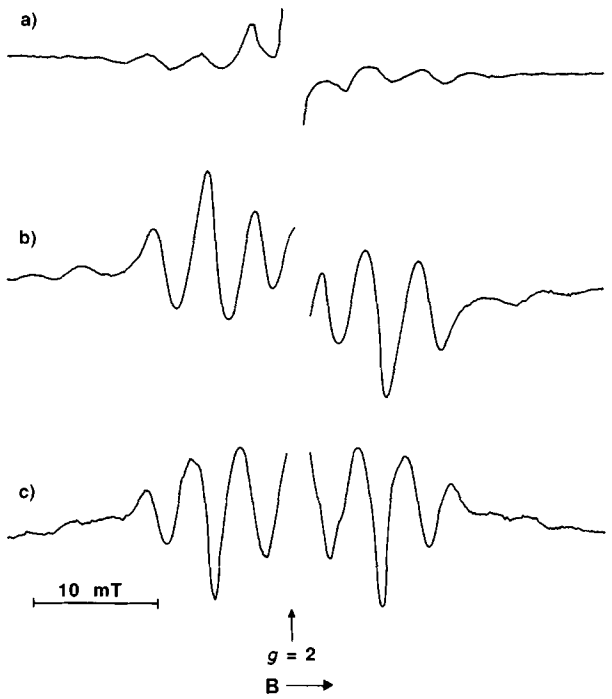

Fig. 1. a) The ESR spectrum of $Li_{50}Na_6$-Y reduced by a solution of lithium metal in propylamine, b) the first derivative, and c) the second derivative spectrum of $Li_{82}Na_5$-X after similar treatment.

Table 1. The *g*-values and hyperfine splittings (*a*) of Na_4^{3+} clusters, prepared by reduction of certain zeolites with solvated electron solutions.

Zeolite[a]	Si/Al	Color	*g*-value	*a* [mT] (298 K)
Na_{56}-Y	2.4	violet-pink	2.003 ± 0.001	3.33 ± 0.10
Na_{87}-X	1.2	purple	2.001 ± 0.001	2.92 ± 0.10
$Li_{44}Na_{12}$-Y	2.4	pinkish gray	2.0025 ± 0.0025	3.75 ± 0.10

[a] The figures represent the number of ions per unit cell.

[*] Prof. Dr. P. P. Edwards [+], Dr. P. A. Anderson, Dr. D. Barr [++]
University Chemical Laboratory
Lensfield Road, GB-Cambridge CB21EW (UK)

[**] Present address: School of Chemistry, University of Birmingham
Edgbaston, GB-Birmingham B152TT (UK)

[+] Present address: The Associated Octal Company Ltd, Ellesmere Port (UK)

[**] We thank the Department of Education for Northern Ireland, B. P. (VRU) and the SERC for financial support and Dr. *R. Snaith* for much advice. The ESR simulation program was written by Dr. *R. J. Singer*.

to Na_4^{3+}, and the lack of other lines due to ^6Li, means that the pattern of ten lines recorded from $Li_{50}Na_6$-Y may be regarded with confidence as the first observation of an Na_3^{2+} cluster.

The deep pink solid obtained from the reduction of $Li_{82}Na_5$-X exhibited a more complex ESR spectrum (Fig. 1 b and c). Although the pattern was symmetric about its midpoint ($g = 2.0028 \pm 0.0005$), the spacing of the lines was not constant, a clue that more than one component was involved. Figure 2 shows simulations of the first and second derivative spectrum expected from a sample containing an equal number of Na_4^{3+} and Na_3^{2+} centers. The simulations reproduce many features of the experimental spectrum (this is particularly clear in the second derivative), suggesting that the zeolite plays host to two such clusters in roughly equal numbers. A similar situation occurs in zeolite Na-X after reaction with alkali metal vapor, where the ESR spectrum provides proof of the presence of both Na_5^{4+} and Na_6^{5+} clusters.[4]

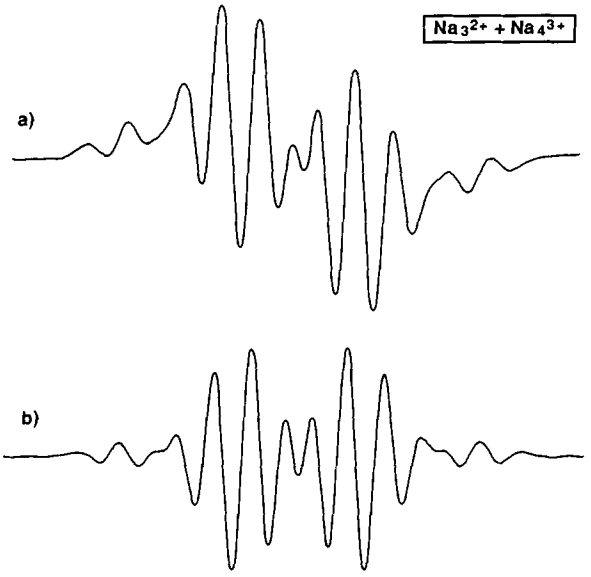

Fig. 2. Simulated ESR spectrum for an equal mixture of Na_3^{2+} and Na_4^{3+} centers: a) first, b) second derivative.

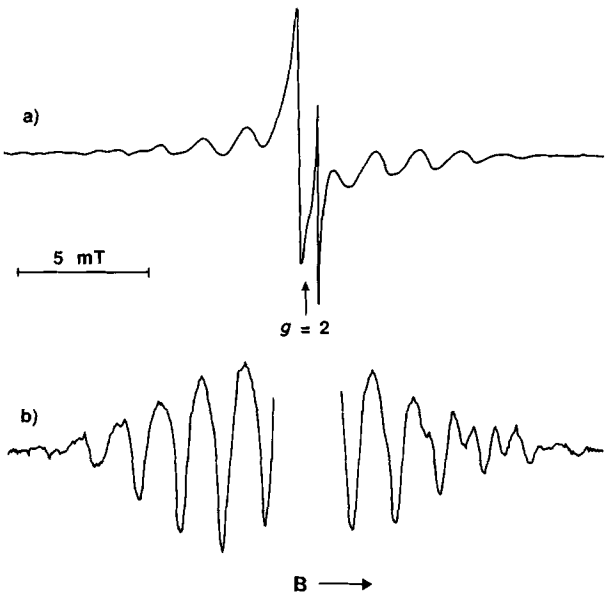

Fig. 3. The ESR spectrum of K_{56}-Y reduced by a solution of lithium metal in butylamine: a) first derivative, b) second derivative.

The reduction of zeolites K_{56}-Y and K_{87}-X produced brilliant blue solids, whose ESR spectra were qualitatively similar to those observed after the reaction of the same zeolites with potassium vapor,[2, 3, 5] and betray the presence of K_4^{3+} and K_3^{2+} respectively. In the absence of excess potassium atoms, the spectrum of K_{56}-Y reduced by the solvated electron solution (Fig. 3) is much better resolved than that obtained after exposure of the same zeolite to potassium vapor. The second derivative in particular clearly shows the secondary lines on the high field side of the spectrum, first noted by *Harrison* et al.[3] These lines may indicate the presence of other paramagnetic centers or may simply result from anisotropy in the spectrum of K_4^{3+} itself. Further studies are in progress to investigate this point.

Experimental Procedure

Zeolites Na_{56}-Y (silicon to aluminum ratio $r = 2.4$) and Na_{87}-X ($r = 1.2$) were supplied by Laporte, from which samples containing potassium and lithium cations were prepared by standard ion exchange.[13] The crystallinity of the resultant solids was checked by powder X-ray diffraction and their composition determined by atomic absorption.

In preparation for reaction, a suitable amount of zeolite (typically ca. 1 g) was placed in a pyrex Schlenk tube, which had been soaked in strong detergent, rinsed thoroughly with tap water and distilled water, and fired overnight at 500 °C. The vessel was then connected to a vacuum line, heated gradually to 450 °C, and evacuated overnight to ca. 10^{-5} mbar. The zeolite was subsequently placed in suspension in propylamine or butylamine, under an argon atmosphere, to await the addition of high-purity lithium shot, which had been cleaned in hexane, toluene, hexane again, and finally by stirring for several hours under argon in the same amine. This cleaning procedure was found to be particularly effective in thoroughly removing the oxide/nitride coating from the surface of the lithium granules. If at any stage the stirrer was switched off, the characteristic blue color of solvated electrons could be seen diffusing from the surface of the lithium into the bulk of the amine. After the suspension was stirred for up to 72 hours, it was filtered to yield a colored solid, which was washed with hexane and taken into an argon glovebox to be loaded into an airtight ESR tube. First and second derivative ESR spectra of the products were recorded at room temperature on a Varian ER-109 spectrometer operating at X-band frequencies (ca. 9.3 GHz).

Received: July 21, 1991 [Z 4741 IE]
German version: *Angew. Chem. 103* (1991) 1511

CAS Registry numbers:
Na_4^{3+}, 12596-68-8; Na_3^{2+}, 103637-08-7; Na, 7440-23-5; K_4^{3+}, 90836-71-8; K_3^{2+}, 103637-07-6; K, 7440-09-7.

[1] J. A. Rabo, C. L. Angell, P. H. Kasai, V. Schomaker, *Discuss. Faraday Soc. 41* (1966) 328.
[2] P. P. Edwards, M. R. Harrison, J. Klinowski, S. Ramdas, J. M. Thomas, D. C. Johnson, C. J. Page, *J. Chem. Soc. Chem. Commun. 1984*, 982.
[3] M. R. Harrison, P. P. Edwards, J. Klinowski, J. M. Thomas, D. C. Johnson, C. J. Page, *J. Solid State Chem. 54* (1984) 330.
[4] P. A. Anderson, P. P. Edwards, *J. Chem. Soc. Chem. Commun. 1991*, 915.
[5] P. A. Anderson, R. J. Singer, P. P. Edwards, *J. Chem. Soc. Chem. Commun. 1991*, 914; P. A. Anderson, Ph.D. thesis, Cambridge University (1990).
[6] U. Westphal, G. Geismar, *Z. Anorg. Allg. Chem. 508* (1984) 165.
[7] L. R. M. Martens, P. J. Grobet, P. A. Jacobs, *Nature 315* (1985) 568; L. R. M. Martens, P. J. Grobet, W. J. M. Vermeiren, P. A. Jacobs, *Stud. Surf. Sci. Catal. 28* (1986) 935.
[8] P. J. Grobet, L. R. M. Martens, W. J. M. Vermeiren, D. R. C. Huybrechts, P. A. Jacobs, *Z. Phys. D 12* (1989) 37.
[9] K. B. Yoon, J. K. Kochi, *J. Chem. Soc. Chem. Commun. 1988*, 510.
[10] P. H. Kasai, *J. Chem. Phys. 43* (1965) 3322.
[11] S. Beran, *J. Phys. Chem. Solids 43* (1982) 221; E. E. Dimukhambetov, V. I. Lygin, E. G. Chadiarov, *Zh. Fiz. Khim. 62* (1988) 226.
[12] The central portions of these spectra, dominated by one or more sharp, intense lines originating from the reductant solution, have been omitted for clarity.
[13] See H. S. Sherry, *J. Phys. Chem. 70* (1966) 1158; The lithium exchanges were carried out at temperatures of 60–70 °C.

Chemoenzymatic Syntheses of Sialyloligosaccharides with Immobilized Sialidase**

By *Joachim Thiem** and *Bernd Sauerbrei*

Sialylated oligosaccharides participate in many biological processes as components of glycoproteins and -lipids.[1a, b] They have essential functions as terminal structures in cell receptors[1c, d] for the specific binding of viruses, blood-group- and tumor-recognizing antibodies, bacterial toxins, and a variety of lectins.[1a, e, f] To understand these recognition phenomena on a molecular basis, studies with comparable substances are needed. Although their syntheses by classical chemical routes is possible, the procedures often still involve many steps and are complicated.[2] The promising chemoenzymatic access through the use of sialyltransferases has already become a preparative technique.[3] The isolation of these enzymes is, however, laborious since especially the (2–3)-sialyltransferases occur in animal tissues only in very low concentrations and are extremely unstable. Furthermore, the pronounced acceptor specificity of the transferases limits their synthetic potential.[2d, 3b]

At first our attention focused mainly on the synthesis of partial structures common in nature in which *N*-acetylneuraminic acid (**1**, Neu5Ac) is terminal and α(2–3)- and α(2–6)-glycosidically bonded to β-galactose. Moreover, we were interested in the preparation of unusual and nonphysiological sialyloligosaccharides.

In order to make sialidase (EC 3.2.1.18) useful for the synthesis of sialyloligosaccharides, it was first necessary to investigate whether it showed transferase activity besides its significant physiological hydrolysis activity. Also, in analogy to successful reactions with other glycosidases,[4] experiments with reverse hydrolysis and transglycosylation were performed (Fig. 1).

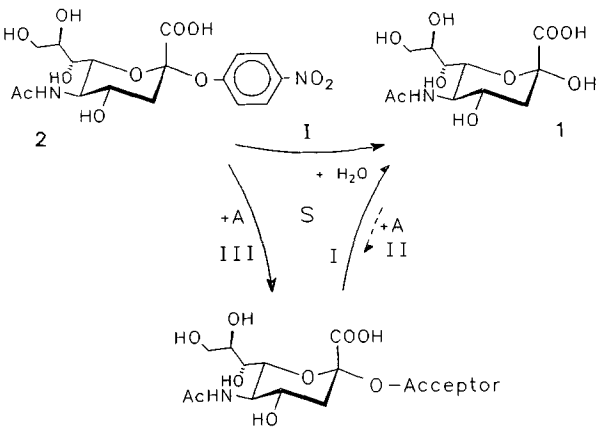

Fig. 1. Sialidase catalysis of transsialylation and potential side reactions. I = hydrolysis, II = reverse hydrolysis, III = transglycosylation; A = acceptor, S = sialidase.

Sialidase from *Vibrio cholerae*[5] (1 U mL^{-1}) was immobilized on a polymeric carrier (VA-epoxy, Riedel-de Haën). In this way the enzyme could be reused several times, and the enzyme incubation could be interrupted at a particular point by separating it completely from the protein. Binding to the carrier was achieved by reaction of the amino functions of the protein with the epoxide groups of the carrier material.[6] After the immobilized enzyme had been freeze-dried, the activity yield was 68% (1.36 U per g carrier). Shaking for six days at 26 °C in the incubation buffer caused an additional activity loss of 24%. The activities of the immobilized enzyme and the free enzyme were determined by hydrolytic cleavage of *p*-nitrophenyl 5-acetamido-3,5-dideoxy-α-D-*glycero*-D-*galacto*-2-nonulopyranosylonic acid (**2**, αNeu5Ac-O(pNPh)). The amount of *p*-nitrophenolate formed was determined photometrically at 400 nm (Fig. 1).[7]

The acceptor molecules for the sialylations are likewise accessible chemoenzymatically. Thus the galactosylation of *N*-acetylglucosamine by galactosyltransferase and UDP-galactose is a proven method for the preparation of *N*-acetyllactosamine (**11**).[8] The donor **2**, on the other hand, can be easily obtained by nonenzymatic techniques from **1** in six steps. In this sequence the transformation of glycosyl chloride by *p*-nitrophenolate is the key reaction.[7]

Transformations according to the principle of reverse hydroloysis are conducted at relatively high temperatures, high acceptor concentrations, and with the free sugar as donor.[4a] This treatment of **1** (lyophilized from aqueous solution after the pH value was adjusted to 6.4 with dilute NaOH) in a 7.8 M solution of methyl β-D-galactopyranoside (**3**, molar ratio 1:13) with sialidase at 44 °C afforded the methyl(5-acetamido-3,5-dideoxy-α-D-*glycero*-D-*galacto*-2-nonulopyranosylonic acid)-β-D-galactopyranoside **4a, b** (αNeu5Ac-βGal-OCH$_3$) in only 1% yield. The ratio of (2–3)- to (2–6)-bonded isomer was 1:10 according to the ^{1}H NMR spectrum.

In contrast to reverse hydrolysis, transglycosylations are usually conducted at low temperatures and in general give higher yields.[4a] However, they require donors in which the sugar to be transferred is in an activated form, for example as glycoside. At first this principle was applied with **2** as donor, **3** as acceptor, and the free enzyme, at 26 °C. The degradation of **2** was followed photometrically at 400 and 303 nm (absorptions of **2**). To minimize the hydrolysis of the products, the incubations were stopped as soon as 65–75% of the starting material had reacted. Variation of the acceptor concentrations had substantial influence on both the yield and the ratio of the isomeric products (Table 1). In all cases, however, the (2–6)-isomer predominated, which probably is attributable to a partial hydrolytic cleavage of the products because sialidase from *Vibrio cholerae* hydrolyses the (2–3)-isomer faster than the (2–6)-isomer.[9] A further increase in yield can be achieved by using immobilized sialidase. The reason for this is not known.

Table 1. Transsialylation with free sialidase. Donor: αNeu5Ac-O(pNPh) **2**; acceptor: βGal-OCH$_3$ **3**.

Molar ratio donor : acceptor	Acceptor concentration [mol L^{-1}]	Total yield [%]	Molar ratio **4a** : **4b**
1 : 4	0.67	1.8	1 : 1.6
1 : 7	2.37	9.5	1 : 5.8
1 : 15	3.37	5.4	1 : 9.0

The incubation conditions and results for the acceptors investigated are listed in Table 2. The coupling pattern of the synthesized di- and trisaccharides have been established by ^{1}H NMR spectroscopy (Table 3). The biologically important (2–3)- and (2–6)-glycosidic bonds of αNeu5Ac to β-galac-

[*] Prof. Dr. J. Thiem, Dipl.-Chem. B. Sauerbrei
Institut für Organische Chemie der Universität
Martin-Luther-King-Platz 6
W-2000 Hamburg 13 (FRG)

[**] This work was supported by the Fonds der Chemischen Industrie and the Bundesministerium für Forschung und Technologie.

Table 2. Transsialylation with immobilized sialidase.

Acceptor	Reaction conditions [a]	t [h]	Product	Ratio of 3- to 6-isomer[b]	Total yield [%]
3	a)	41	**4a, b**	1:2.9	20
3	b)	120	**4a, b**	1:2.0	20
5	a)	45	**6a, b**	1:6.0	24
7	a)	45	**8a, b**	1:3.2	16
9	a)	45	**10a, b**	1:2.0	16
11	a)	68.5	**12a, b**	1:2.8	14

[a] See experimental procedure. [b] Determined by ^{1}H NMR spectroscopy and HPLC.

Table 3. Selected characteristic ^{1}H NMR data of the prepared sialyloligosaccharides (400 MHz, D_2O).

4a: δ = 4.31 (d, 1H, H-1, $J_{1,2}$ = 8.0 Hz), 3.57 (s, 3H, OCH_3), 2.73 (dd, 1H, H-3′ eq., $J_{3'eq,3'ax}$ = 12.2 Hz, $J_{3'eq,4'}$ = 4.7 Hz), 2.04 (s, 3H, NAc), 1.69 (dd, 1H, H-3′ax, $J_{3'ax,4'}$ = 12.2 Hz); **4b**: δ = 4.39 (d, 1H, H-1, $J_{1,2}$ = 8.0 Hz), 4.08 (dd, 1H, H-3, $J_{2,3}$ = 9.7 Hz, $J_{3,4}$ = 3.2 Hz), 3.57 (s, 3H, OCH_3), 2.75 (dd, 1H, H-3′ eq, $J_{3'eq,3'ax}$ = 12.0 Hz, $J_{3'eq,4'}$ = 4.6 Hz), 2.04 (s, 3H, NAc), 1.78 (dd, 1H, H-3′ax, $J_{3'ax,4'}$ = 12.0 Hz); **6a**: δ = 4.81 (d, 1H, H-1, $J_{1,2}$ = 3.3 Hz), 3.41 (s, 3H, OCH_3), 2.73 (dd, 1H, H-3′ eq, $J_{3'eq,3'ax}$ = 12.3 Hz), $J_{3'eq,4'}$ = 4.6 Hz), 2.04 (s, 3H, NAc); 1.68 (dd, 1H, H-3′ax, $J_{3'ax,4'}$ = 12.3 Hz); **6b**: δ = 4.88 (d, 1H, H-1, $J_{1,2}$ = 3.3 Hz), 4.30 (dd, 1H, H-3, $J_{2,3}$ = 10.0 Hz, $J_{3,4}$ = 2.6 Hz), 3.41 (s, 3H, OCH_3), 2.73 (dd, 1H, H-3′eq, $J_{3'eq,3'ax}$ = 12.3 Hz, $J_{3'eq,4'}$ = 4.6 Hz), 2.04 (s, 3H, NAc), 1.81 (dd, 1H, H-3′ax, $J_{3'ax,4'}$ = 12.3 Hz); **8a**: δ = 4.38 (d, 1H, H-1, $J_{1,2}$ = 8.0 Hz), 3.57 (s, 3H, OCH_3), 2.75 (dd, 1H, H-3′eq, $J_{3'eq,3'ax}$ = 12.4 Hz, $J_{3'eq,4'}$ = 4.8 Hz), 2.03 (s, 3H, NAc), 1.72 (dd, 1H, H-3′ax, $J_{3'ax,4'}$ = 12.1 Hz); **8b**: δ = 4.51 (d, 1H, H-1, $J_{1,2}$ = 8.0 Hz), 4.12 (dd, 1H, H-3, $J_{2,3}$ = 10.0 Hz, $J_{3,4}$ = 10.0 Hz), 3.57 (s, 3H, OCH_3), 2.71 (dd, 1H, H-3′eq, $J_{3'eq,3'ax}$ = 12.4 Hz, $J_{3'eq,4'}$ = 4.8 Hz), 2.04 (s, 3H, NAc), 1.77 (dd, 1H, H-3′ax, $J_{3'ax,4'}$ = 12.4 Hz); **10a**: δ = 4.43 (d, 1H, H-1, $J_{1,2}$ = 8.0 Hz), 4.41 (d, 1H, H-1′, $J_{1',2'}$ = 8.0 Hz), 3.58 (s, 3H, OCH_3), 2.71 (dd, 1H, H-3″eq, $J_{3''eq,3''ax}$ = 12.5 Hz, $J_{3''eq,4''}$ = 4.6 Hz), 2.02 (s, 3H, NAc), 1.75 (dd, 1H, H-3″ax, $J_{3''ax,4''}$ = 12.5 Hz); **10b**: δ = 4.52 (d, 1H, H-1′, $J_{1',2'}$ = 7.9 Hz), 4.39 (d, 1H, H-1, $J_{1,2}$ = 8.1 Hz), 4.11 (dd, 1H, H-3′, $J_{2',3'}$ = 10.0 Hz), 3.58 (s, 3H, OCH_3), 2.75 (dd, 1H, H-3″eq, $J_{3''eq,3''ax}$ = 12.5 Hz, $J_{3''eq,4''}$ = 4.9 Hz), 2.02 (s, 3H, NAc), 1.79 (dd, 1H, H-3″ax, $J_{3''ax,4''}$ = 12.5 Hz; **12a**: δ = 5.18 (d, 1H, H-1α, $J_{1,2}$ = 2.2 Hz), 4.44 (d, 1H, H-1′, $J_{1',2'}$ = 8.0 Hz), 2.67 (dd, 1H, H-3″eq, $J_{3''eq,3''ax}$ = 12.4 Hz, $J_{3''eq,4''}$ = 4.5 Hz), 2.07 (s, 3H, NAc (βGlcNAc)), 2.03 (s, 3H, NAc (αNeu5Ac)), 1.71 (dd, 1H, H-3″ax, $J_{3''ax,4''}$ = 12.4 Hz); **12b**: δ = 4.54 (d, 1H, H-1′, $J_{1',2'}$ = 8.0 Hz), 4.11 (dd, 1H, H-3′, $J_{2',3'}$ = 9.1 Hz, $J_{3',4'}$ = 2.8 Hz), 2.77 (dd, 1H, H-3″eq, $J_{3''eq,3''ax}$ = 12.2 Hz, $J_{3''eq,4''}$ = 4.4 Hz), 2.04 (s, 3H, NAc (αNeu5Ac)), 2.05 (s, 3H, NAc (βGlcNAc)), 1.80 (dd, 1H, H-3″ax, $J_{3''ax,4''}$ = 12.2 Hz).

tose are achieved in the products **4a**, **4b**, **10a**, **10b**, **12a**, and **12b** (Table 4). A general rule holds: the larger the acceptor, the smaller the yield.

The acceptor **3** was not only treated under the standard conditions, but also in a 30% by volume dimethylsulfoxide (DMSO)/water mixture. To achieve the same yield the length of the incubation period and the enzyme concentration had to be drastically increased. Nevertheless, organic cosolvents could be of interest for effective sialylation of less polar acceptors.

The saccharide structure of **10b** is a frequently occurring fragment in gangliosides,[1b] while no biological relevance has yet been proved for the (2–6)-bonded analogue **10a** and for **6a**, **6b**, and **8b**. Compounds **12a** and **12b** are universal building blocks, mainly for *N*-glycosidic glycoproteins, but also for gangliosides.[11] The sialylation of β-glucose at the 6-position, realized in **8a**, has as yet been found only sporadically in nature in gangliosides[10a] and in glycolipids from sea urchins of the species *Strongylocentrotus intermedius*.[10b]

In comparison with the other acceptors, the transformation with methyl α-D-galactopyranoside **5** gives not only the highest total yield but also an unusual isomer ratio shifted in favor of the (2–6)-bond. This can be interpreted resulting from as a specific interaction with the enzyme that stems from the larger spatial requirements and higher hydrophobicity of the bottom side of the molecule **5**.

The yields of these syntheses of sialyloligosaccharides are smaller than those of the sialyl transferase catalyzed reactions and the regioselectivity is less pronounced. The latter feature, however, enables an uncomplicated access to the (2–3)-coupled sialyloligosaccharides, whose synthesis is un-

Table 4. Transsialylation with immobilized sialidase.

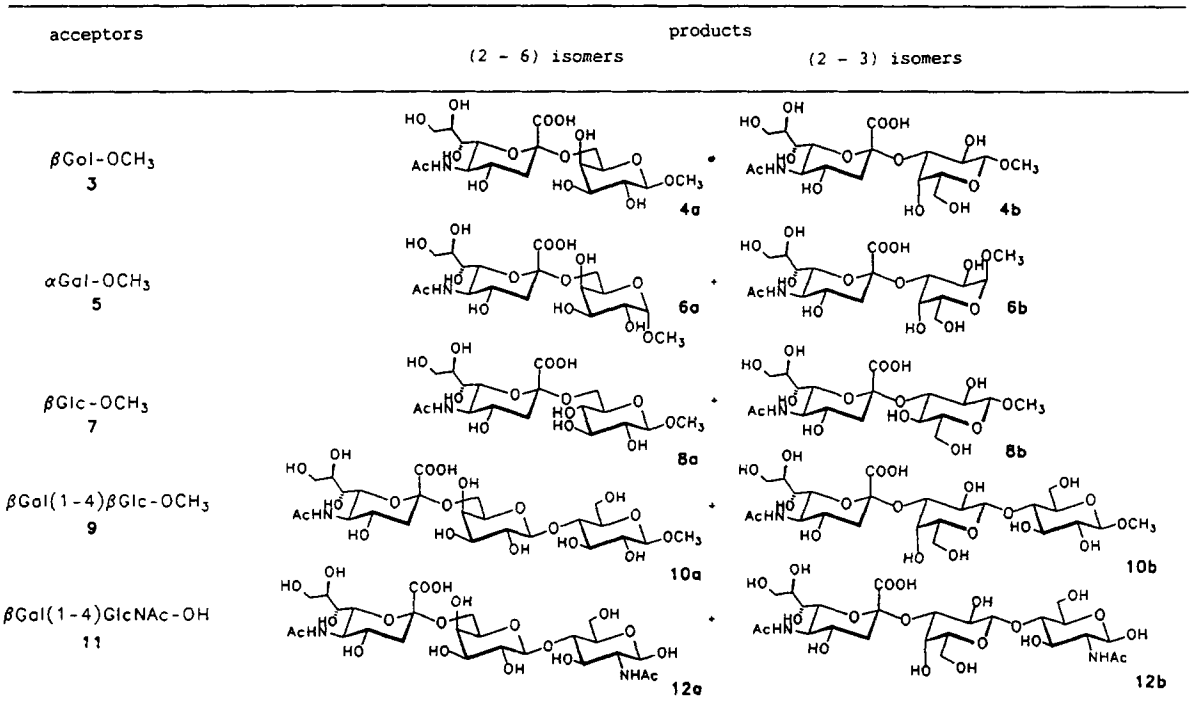

satisfactory not only with classical chemical methods, but also with the (2–3)-sialyl transferase as long as this enzyme cannot be produced in sufficient quantities by genetic engineering techniques. Also the low aglycon specificity of the sialidases proves to be an advantage, because it makes possible the sialylation of nonphysiological acceptors. Moreover, the isolation of sialidases is comparatively trouble-free, they are easy to handle, and require relatively simple substrates.

Experimental Procedure

Immobilization of the sialidases: To 1 mL enzyme solution (1 U^2mL^{-1}) and 4 mL potassium phosphate buffer (1 M, pH 7.5) was added VA-epoxy (500 mg) and the suspension was shaken for 3 d. Thereafter the immobilized enzyme was washed several times with 0.1 M potassium phosphate buffer (pH 7.5) and finally shaken with 2 mL mercaptoethanol solution (5%, pH 8.0) for 3 days at 20 °C. After renewed washing the activity yield of the lyophilized preparation was 68% (1.36 $U g^{-1}$).

Sialylation with immobilized sialidase: a) A paste was made with donor **2** (25 μmol), acceptor (175 μmol), immobilized enzyme (40 mg, 60 mU) and degassed incubation buffer (130 μL, 0.1 M NaOAc, 0.5 mM $CaCl_2$, 0.03% NaN_3, pH 5.5) and incubated at 26 °C (see Table 2). The reaction was interrupted by dilution with doubly distilled water and immediate removal of the immobilized enzyme by centrifugation. Workup by anion exchange chromatography (Dowex 1 × 2, PO_4^{3-} form) [3b] was followed by desalination by gel chromatograpy (Sephadex G15). The product fraction was monitored conductometrically. b) DMSO (30 vol.% in water) was added to the incubation buffer and procedure a) was followed.

Analytical HPLC to determine the relative amounts of the positional isomers [12] (see Table 2): Column Lichrosorb-NH_2 (5 × 240 mm), eluant 15 mM KH_2PO_4/acetonitrile 28:72, flowrate 1.2 mL min^{-1}. Detection at 200 nm.

Received: June 18, 1991 [Z4729 IE]
German version: *Angew. Chem. 103* (1991) 1521

CAS Registry numbers:
2, 26112-88-9; **3**, 1824-94-8; **4a**, 100605-28-5; **4b**, 136378-93-3; **5**, 3396-99-4; **6a**, 136378-91-1; **6b**, 136378-94-4; **7**, 709-50-2; **8**, 136378-92-2; **8b**, 136378-95-5; **9**, 7216-69-5; **10a**, 100605-29-6; **10b**, 100605-31-0; **11**, 32181-59-2; **12a**, 64364-50-7; **12b**, 64317-00-6; sialidase (EC 3.2.1.19), 9001-67-6.

[1] a) R. Schauer, *Adv. Carbohydr. Chem. Biochem. 40* (1982) 131; b) *Sialic Acids Chemistry, Metabolism and Function* (Cell Biology Monographs Vol. 10) Springer, Vienna 1982; c) *Biochem. Soc. Trans. 11* (1983) 270; d) J. C. Paulson, G. N. Rogers, S. M. Carroll, H. H. Higa, T. Pritchett, G. Milks, S. Sabesan, *Pure Appl. Chem. 56* (1984) 797; e) S. Hakomori, *Annu. Rev. Immunol. 2* (1984) 103; f) M. H. Ravindranath, H. H. Higa, E. L. Cooper, J. C. Paulson, *J. Biol. Chem. 260* (1985) 8850.

[2] a) H. Paulsen, H. Tietz, *Carbohydr. Res. 125* (1984) 47; b) T. Ogawa, M. Sugimoto, *ibid. 135* (1985) C5; c) H. Paulsen, U. von Deessen, *ibid. 146* (1986) 147; d) K. Okamoto, T. Goto, *Tetrahedron 46* (1990) 5835.

[3] a) J. Thiem, W. Treder, *Angew. Chem. 98* (1986) 1100; *Angew. Chem. Int. Ed. Engl. 25* (1986) 1096; b) S. Sabesan, J. C. Paulson, *J. Am. Chem. Soc. 108* (1986) 2068; c) E. S. Simon, M. D. Bednarski, G. M. Whitesides, *ibid. 110* (1988) 7159; d) E. J. Toone, E. S. Simon, M. D. Bednarski, G. M. Whitesides, *Tetrahedron 45* (1989) 5365.

[4] a) K. G. J. Nilsson, *Trends Biochem. Sci. 6* (1988) 256; b) S. C. T. Svensson, J. Thiem, *Carbohydr. Res. 200* (1990) 391.

[5] We are grateful to the Behringwerke AG, Marburg for a gift of sialidase from *Vibrio cholerae* (EC 3.2.1.18).

[6] K. Burg, O. Mauz, S. Noetzel, K. Sauber, *Angew. Makromol. Chem. 157* (1988) 105.

[7] V. Eschenfelder, R. Brossmer, *Carbohydr. Res. 162* (1987) 294.

[8] a) S. L. Haynie, C.-H. Wong, G. M. Whitesides, *J. Org. Chem. 47* (1982) 5416; b) J. Thiem, T. Wiemann, *Angew. Chem. 102* (1990) 78; *Angew. Chem. Int. Ed. Engl. 29* (1990) 80.

[9] A. P. Corfield, J.-C. Michalski, R. Schauer in G. Tetamanti, P. Durand, S. DiDonato (Eds.): *Sialidases and Sialidoses, Perspectives in Inherited Metabolic Diseases. Vol. 4*, Edition Ermes, Milan 1981.

[10] a) H. Wiegandt in L. Svennerholm, P. Mandel, H. Dreyfus, P. F. Urban (Eds.): *Structure and Function of Gangliosides*, Plenum Press, New York 1980; b) N. K. Kochetkov, I. G. Zhukova, G. P. Smirnova, I. S. Glukhoded, *Biochim. Biophys. Acta 326* (1973) 74.

[11] a) J. Montreuil, *Adv. Carbohydr. Chem. Biochem. 37* (1980) 158; b) A. Kobata, *Cell. Struct. Funct. 4* (1979) 169; c) B. L. Slomiany, V. L. N. Murty, A. Slomiany, *J. Biol. Chem. 255* (1980) 9719.

[12] M. L. E. Bergh, P. Koppen, D. H. van den Eijnden, *Carbohydr. Res. 94* (1981) 225.

Synthesis and Characterization of a New Binary Deca-Osmium Carbonyl Cluster Anion—An Intermediate in the Formation of Other High-Nuclearity Osmium Carbonyl Clusters; Crystal and Molecular Structure of $(Ph_4P)_2[Os_{10}(CO)_{26}]$**

By *Angelo J. Amoroso, Brian F. G. Johnson, Jack Lewis,* Paul R. Raithby*, and *Wing-Tak Wong*

We are currently interested in the synthesis of high nuclearity Ru and Os carbonyl clusters and the study of the necessary build-up processes.[1] Early work from this group has shown that the vacuum pyrolysis of Os_3 derivatives[2] (such as $[Os_3(CO)_{11}(py)]$ and $[Os_3(CO)_{10}(NCMe)_2]$) at high temperatures (> 220 °C) gives moderate to good yields of a thermodynamically very stable ion $[Os_{10}C(CO)_{24}]^{2-}$ **1**. The chemistry of this carbido cluster has been extensively studied.[3] However, little is known about the mechanism of its formation or the source of the interstitial carbide. Recently, we reported the isolation and characterization of two large osmium carbonyl clusters, $[Os_{17}(CO)_{36}]^{2-}$ **2**[4] and $[Os_{20}(CO)_{40}]^{2-}$ **3**[5] from the same solid-state pyrolysis reaction of $[Os_3(CO)_{10}(NCMe)_2]$ in vacuo. It was thus interesting for us to isolate and study some of the intermediate species that we believe are involved in cluster build-up processes.

Vacuum pyrolysis of $[Os_3(CO)_{10}(NCMe)_2]$ was investigated in the temperature range of 150–210 °C. A typical product distribution at 190 °C is: 20% $[Os_3(CO)_{12}]$, 5% $[Os_5(CO)_{16}]$, 15% $[Os_6(CO)_{18}]$, 5% $[Os_7(CO)_{21}]$, traces of $[Os_8(CO)_{23}]$, and 16% $[Os_9H(CO)_{24}]^-$ (as $(PPh_3)_2N^+$ salt). A previously unknown brown cluster anion, formulated as $[Os_{10}(CO)_{26}]^{2-}$ **4** on the basis of spectroscopic data,[8] can be isolated, as either the $(PPh_3)_2N^+$ or Ph_4P^+ salt, in reasonable yield (10% at 150 °C, 13% at 170 °C, 18% at 190 °C). Above 190 °C, substantial amounts of **1** are formed which impose problems on the purification of **4** since both have very similar chromatographic properties.

The structure of the new anion **4** has been established by an X-ray analysis of its $[Ph_4P]^+$ salt (Fig. 1).[9] The novel metal framework geometry may be described as a tricapped octahedron with an extra $Os(CO)_3$ unit on one of the caps of the octahedron. Although unusual for third row cluster carbonyls, the structure contains two bridging carbonyl ligands [C(43)–O(43) and C(93)–O(93)]. There are also two incipient bridging carbonyls, C(51)–O(51) and C(71)–O(71) [Os(10)···C(51), 2.76(3) Å, Os(10)···C(71), 2.75(3) Å], which presumably help to reduce the electronic imbalance between the formally electron-rich osmium atoms, Os(5) and Os(7) (19 e^- each) and the electron-poor osmium atom, Os(10) (17 e^-). The individual formal electron counts for the metal atoms reflect the uneven electron distribution within the cluster framework; Os(6), Os(8), and Os(10) are formally electron-poor, each with a count of 17 e^- and with three terminal COs bonded to each metal; Os(1) has a count of 18 e^- with two terminal COs bonded to it; Os(2), Os(4), and Os(9) each have a count of 18 e^- and each metal is associated with two terminal and one bridging CO; Os(7) has a count of 19 e^- and is coordinated to two terminal and one

[*] Prof. Lord Lewis, Dr. P. R. Raithby, W.-T. Wong, A. J. Amoroso
University Chemical Laboratory
Lensfield Road, Cambridge, CB2 1EW (UK)
Prof. B. F. G. Johnson
Department of Chemistry, University of Edinburgh
West Mains Road, Edinburgh, EH9 3JJ (UK)

[**] We acknowledge the financial support of the Royal Commission for the Exhibition of 1851, the U.K. Committee of Vice Chancellors and Principals (*W.-T. W.*) and SERC (*A. J. A.*).

bridging CO; Os(5) is also electron-rich with a count of 19 e^- and has two coordinated terminal COs; Os(3) has a count of 19 e^- and has three terminal CO ligands. In terms of overall electron counting, the species is a 134 e^- system, which may be rationalized in terms of the Condensed Polyhedral approach,[6] and is isoelectronic with $[Os_{10}C(CO)_{24}]^{2-}$ **1**.

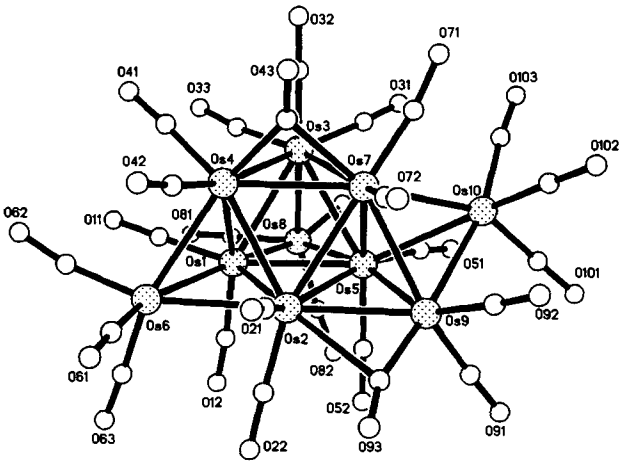

Fig. 1. The molecular structure of **4** in the crystal showing the atom numbering scheme. Selected bond distances [Å] and angles [°]: Os1-Os2, 2.738(2); Os1-Os3, 2.789(2); Os1-Os4, 2.787(2); Os1-Os5, 2.770(2); Os1-Os6, 2.722(2); Os1-Os8, 2.678(2); Os2-Os4, 2.804(2); Os2-Os5, 2.849(2); Os2-Os6, 2.840(2); Os2-Os7, 2.860(2); Os2-Os9, 2.768(2); Os3-Os4, 2.908(2); Os3-Os5, 2.825(2); Os3-Os7, 2.941(2); Os3-Os8, 2.925(2); Os4-Os6, 2.810(2); Os4-Os7, 2.807(2); Os5-Os7, 2.772(2); Os5-Os8, 2.806(2); Os5-Os9, 2.778(2); Os5-Os10, 2.868(2); Os7-Os9, 2.809(2); Os7-Os10, 2.816(2); Os9-Os10, 2.739(2); Os4-C43, 2.04(3); Os7-C43, 2.21(3); Os9-C93, 1.91(3); Os2-C93, 2.55(3); Os4-C43-O43, 143(3); Os7-C43-O43, 134(3); Os4-C43-Os7, 82(1); Os2-C93-O93, 124(2); Os9-C93-O93, 161(3); Os2-C93-Os9, 75(1).

Both the structures for **1** and **4** may be derived from PSEP theory (PSEP = Polyhedral Skeleton Electron Pair) with $S = 7$ and $n = 10$, since the asymmetric structure of **4** is isomeric to the symmetric tetracapped octahedron **1**.[2] However, the more open metal framework of **4** generates additional coordination sites on the periphery of the cluster which can accommodate the two extra carbonyl groups in comparison with **1**. The metal frameworks in both **1** and **4** may be thought of as derived from the tricapped octahedral arrangement recently reported[7] for $[Os_9H(CO)_{24}]^-$ **5** by the addition of the tenth metal atom to a different triangular face.

The subsequent vacuum pyrolysis of **4** as Bu_4P^+ or Ph_4P^+ salts, at 230 °C, leads to **1** (> 85 %), **3** (< 5 %), and other uncharacterized products in trace quantities. The yield of **3** increases as the temperature of the pyrolysis increases. At 300 °C, yields of **1** and **3** are 60 % and 25 % respectively. Both CO and CO_2 evolved in this reaction, have been trapped and identified by their characterized IR absorption spectra (P and R bands centered at 2352 cm^{-1} for CO_2; 2143 cm^{-1} for CO). On the basis of these observations, it is reasonable to believe that **4** is the common precursor for **1** [Eq. (a)] and **3** [Eq. (b)] in the vacuum pyrolysis of $[Os_3(CO)_{10}(NCMe)_2]$ at high temperatures (see Scheme 1).

$$\mathbf{4} \longrightarrow \mathbf{1} + CO_2 \quad \text{(a)}$$

$$2\,\mathbf{4} \longrightarrow \mathbf{3} + 12\,CO \quad \text{(b)}$$

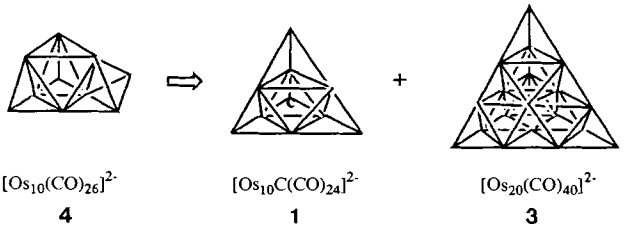

$[Os_{10}(CO)_{26}]^{2-}$ **4** $[Os_{10}C(CO)_{24}]^{2-}$ **1** $[Os_{20}(CO)_{40}]^{2-}$ **3**

Scheme 1. Conversion of **4** into **1** and **3**.

Experimental Procedure

To a flame-dried Carius tube (180 cm^3), solid $[Os_3(CO)_{10}(NCMe)_2]$[10] (1.0 g) was introduced as a suspension in hexane (5 mL). The solvent was removed under reduced pressure to give a thin layer of the Os_3-compound deposited on the inner wall of the tube. It was evacuated to 10^{-3} torr for 2 hours and sealed at this pressure. This compound was pyrolyzed at the required temperature (150–190 °C) for 12 hours to give a dark brown powder, which was first extracted with CH_2Cl_2 (50 mL) to remove $[Os_5(CO)_{16}]$, $[Os_6(CO)_{18}]$, $[Os_7(CO)_{21}]$, and $[Os_8(CO)_{23}]$. The brown CH_2Cl_2 insoluble residue, mainly consisting of $[Os_3(CO)_{12}]$, $[H_2Os_9(CO)_{24}]$, and $[H_2Os_{10}(CO)_{26}]$, was extracted with acetone (10 mL) to give a dark brown solution and a yellow powder of $[Os_3(CO)_{12}]$. Separation of the acetone extract by thin-layer chromatography (silica gel) using acetone/hexane (1/1) as eluent, gave an orange-brown band of $[Os_9H(CO)_{24}]^-$ **5** ($R_f \sim 0.6$) and a dark brown band of $[Os_{10}(CO)_{26}]^{2-}$ **4** ($R_f \approx 0.2$). The $(PPh_3)_2N^+$ salt of **5** (167 mg, 16 %) and Ph_4P^+ salt of **4** (191 mg, 18 %) were obtained through cation metathesis with $[(PPh_3)_2N]Cl$ and $(Ph_4P)Br$ respectively and crystallized by slow evaporation of a solution of the salt in CH_2Cl_2/ethanol (1/1).

Received: June 17, 1991 [Z 4727 IE]
German version: *Angew. Chem. 103* (1991) 1529

CAS Registry numbers:
4, 136919-95-4; **4**·0.74 $CHCl_3$, 136952-94-8; $[Os_3(CO)_{10}(NCMe)_2]$, 61817-93-4; $[Os_3(CO)_{12}]$, 15696-40-9; $[Os_5(CO)_{16}]$, 60109-68-4; $[Os_6(CO)_{18}]$, 37216-50-5; $[Os_7(CO)_{21}]$, 59158-84-8; $[(PPh_3)_2N][Os_9H(CO)_{24}]$, 136575-73-0; $[Ph_4P]_2[Os_{10}(CO)_{26}]$, 136984-74-2.

[1] P. J. Bailey, B. F. G. Johnson, J. Lewis, M. McPartlin, H. R. Powell, *J. Organomet. Chem. 377* (1989) C17; P. J. Bailey, M. J. Duer, B. F. G. Johnson, J. Lewis, G. Conole, M. McPartlin, H. R. Powell, C. E. Anson, *ibid. 383* (1990) 441; B. F. G. Johnson, J. Lewis, W. J. H. Nelson, M. D. Vargas, D. Braga, K. Henrick, M. McPartlin, *J. Chem. Soc. Dalton Trans. 1984*, 2151; B. F. G. Johnson, J. Lewis, M. McPartlin, W. J. H. Nelson, P. R. Raithby A. Sironi, M. D. Vargas, *J. Chem. Soc. Chem. Commun. 1983*, 1476.

[2] P. F. Jackson, B. F. G. Johnson, J. Lewis, W. J. H. Nelson, M. McPartlin, *J. Chem. Soc. Dalton Trans. 1982*, 2099.

[3] B. F. G. Johnson, J. Lewis, W. J. H. Nelson, J. Puga, D. Braga, K. Henrick, M. McPartlin, *J. Organomet. Chem. 266* (1984) 173; R. J. Gouldsmit, P. F. Jackson, B. F. G. Johnson, J. Lewis, W. J. H. Nelson, J. Puga, M. D. Vargas, D. Braga, K. Henrick, M. McPartlin, A. Sironi, *J. Chem. Soc. Dalton Trans. 1985*, 1795; B. F. G. Johnson, J. Lewis, W. J. H. Nelson, M. D. Vargas, D. Barga, K. Henrick, M. McPartlin, *ibid. 1986*, 975.

[4] E. Charalambous, L. H. Gade, B. F. G. Johnson, J. Lewis, M. McPartlin, H. R. Powell, *J. Chem. Soc. Chem. Commun. 1990*, 688.

[5] A. J. Amoroso, L. H. Gade, B. F. G. Johnson, J. Lewis, P. R. Raithby, W. T. Wong, *Angew. Chem. 103* (1991) 102; *Angew. Chem. Int. Ed. Engl. 30* (1991) 107.

[6] D. M. P. Mingos, *J. Chem. Soc. Chem. Commun. 1983*, 706.

[7] A. J. Amoroso, B. F. G. Johnson, J. Lewis, P. R. Raithby, W. T. Wong, *J. Chem. Soc. Chem. Commun. 1991*, 814.

[8] Spectroscopic data for **4**: IR (CH_2Cl_2): $\tilde{\nu}$(CO) [cm^{-1}] = 2077 w, 2047 vs, 2018 s, 1988 s, 1884 w, 1846 w, 1751 w; FAB MS: *m/z* (M^+ obs.) 2630 (calc.) 2630; ^1H NMR (CD_2Cl_2): no hydride signal in the range $\delta = -40$ to 0.

[9] Crystal data for (Ph_4P)-4·074 $CHCl_3$: $C_{74}H_{40}O_{26}P_2Os_{10}$·0.74 $CHCl_3$; $M = 3309.1$ (excluding $CHCl_3$), triclinic, space group $P\bar{1}$ (No. 2), $a = 12.446(4)$, $b = 13.246(5)$, $c = 26.901(6)$ Å, $\alpha = 88.90(1)°$, $\beta = 79.13(1)°$, $\gamma = 68.07(1)°$, $U = 4034(2)$ Å^3, $Z = 2$, $\rho_{calcd} = 2.797$ g cm^{-3}, $F(000) = 3049.96$, ($Mo_{K\alpha}$) radiation, $\lambda = 0.71069$ Å, $\mu(Mo_{K\alpha}) = 158.93$ cm^{-1}, 6119 observed reflections [$F > 3\sigma(F)$]. Structure solved by direct methods and Fourier difference techniques, refined by full matrix least-squares analysis (Os and P anisotropic) to $R = 0.058$, $R_w = 0.058$. Further details of the crystal structure investigation can be obtained from the Director of the Cambridge Crystallographic Data Centre, University Chemical Laboratory, Lensfield Road, Cambridge CB2 1EW (UK). Any request should be accompanied by the full literature citation for this communication.

[10] B. F. G. Johnson, J. Lewis, D. A. Pippard, *J. Chem. Soc., Dalton Trans. 1981*, 407.

"[12]Mercuracarborand-4", the First Representative of a New Class of Rigid Macrocyclic Electrophiles: The Chloride Ion Complex of a Charge-Reversed Analogue of [12]Crown-4 **

By *Xiaoguang Yang, Carolyn B. Knobler,* and *M. Frederick Hawthorne**

Dedicated to Professor Donald J. Cram

Until very recently the field of molecular recognition has been dominated by studies of electrophilic guests surrounded by preorganized nucleophilic host molecules.[1] Molecular recognition of anionic guests by similarly preorganized Lewis acid hosts has only lately been achieved[2-5] and offers new prospects for selective molecular recognition, anion transport, and the catalytic activation of electron-rich organic and inorganic substrates.[3c, 6] In all known cases, electrophilic hosts that employed tin,[2] mercury,[3] silicon,[4] and boron[5] atoms as binding sites for anion guests function as bidentate or bisbidentate Lewis acids, although a few potential tridentate silicon- and tin-containing hosts have been reported.[2d, 2e, 4]

Wuest and co-workers recently described a series of halide complexes of 1,2-phenylenedimercury dihalides that, unlike simple monodentate organomercuric halides, bind additional halide ions.[3a] They have also reported a macrocyclic mercury-containing Lewis acid which functions as an electrophile[3d, e] and binds nucleophilic organic solvents. We here report the first example (**1**) of a portentous new class of macrocyclic, multidentate, and electrophilic host species as well as the structural characterization of the chloride ion complex **1** · Cl^-. The species **1** is a charge-reversed analogue of the well-known [12]crown-4 macrocycle, which we have therefore named [12]mercuracarborand-4.

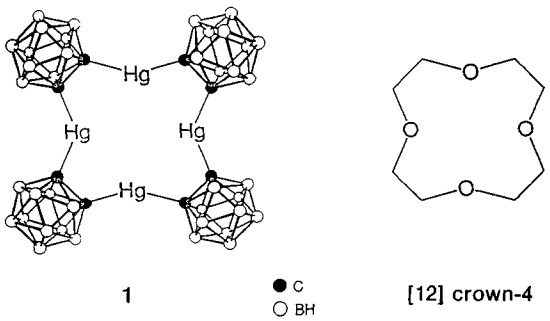

The icosahedral carborane 1,2-$C_2B_{10}H_{12}$ (**2**) contains relatively positive C atoms and can be easily lithiated by *n*BuLi at the carbon positions to give **3**.[7] The reaction of mercury(II) chloride with **3** results in the formation of the cyclic tetramer Li[$(HgC_2B_{10}H_{10})_4Cl$](**1** · ClLi) in 75% yield, in accord with Equation (a).

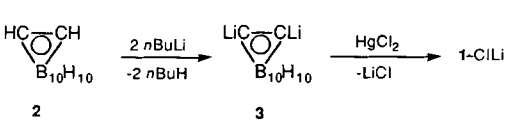

[*] Prof. Dr. M. F. Hawthorne, Dr. X. Yang, Dr. C. B. Knobler
Department of Chemistry and Biochemistry
University of California
Los Angeles, CA 90024 (USA)

[**] This work was supported by the National Science Foundation.

The species **1** · ClLi is quite soluble in most organic solvents except aliphatic hydrocarbons. Like other organomercurials, **1** · ClLi decomposes upon prolonged heating at 300°C or during UV irradiation to form mercury, **2**, and carborane-containing polymers. The ^1H, ^{13}C, ^{11}B, and ^{199}Hg NMR data revealed that **1** · ClLi has a highly symmetrical structure with single types of both carbon and mercury atoms. The negative-ion FAB mass spectrum exhibited an anion with $m/z = 1414$, which corresponds to **1** · Cl^-. The metathesis reaction of **1** · ClLi with $[As(C_6H_5)_4]Cl$ gave **1** · $Cl[As(C_6H_5)_4]$ in ca. 80% yield. The ^1H NMR spectrum of **1** · $Cl[As(C_6H_5)_4]$ displayed resonances due to $[As(C_6H_5)_4]^+$ and B-H in the ratio 1:2, which is consistent with the assigned formulation. The ^{13}C and ^{11}B NMR spectra of **1** · $Cl[As(C_6H_5)_4]$ are identical to those of **1** · ClLi except for the presence of $As(C_6H_5)_4^+$ ^{13}C resonances.

A single crystal of **1** · ClLi grown from *o*-dichlorobenzene/hexane was selected for the X-ray diffraction study.[8] The anion **1** · Cl^- (Fig. 1) consists of four bivalent 1,2-$C_2B_{10}H_{10}$

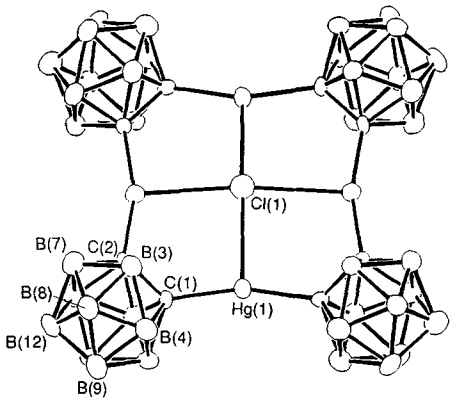

Figure 1. ORTEP representation of **1** · Cl^- with hydrogen atoms removed for clarity. Atoms labeled are in the x, y, z positions, all other atoms are generated by the fourfold and mirror symmetry of the tetramer.

cages linked by four Hg atoms in a cyclic tetramer with a chloride ion located in the center of the array and 2.944(2) Å from each Hg. The anion possesses crystallographically imposed C_{4h} symmetry with the four Hg atoms, the eight cluster carbon atoms, and eight boron atoms in the mirror plane. The chloride ion is displaced 0.383 Å above and below this plane, on the fourfold axis, with half occupancy of each of these two positions. Each Hg atom links carbon atoms of two carborane icosahedra (Hg–C distances: 2.105(13) and 2.080(13) Å). The Hg-C-C angles are 126.0(6) and 125.4(6)°, and the C-Hg-C angle is 162.0(3)°, which is the largest deviation from 180° yet observed in diorganomercurials.[9] The distance between the adjacent mercury atoms is 4.129(1) Å. In comparison, the trimer of *ortho*-phenylenemercury, $(C_6H_4Hg)_3$, has a planar structure with an average C–Hg distance of 2.10 Å, a C-Hg-C angle of 177.7°, and a Hg-C-C angle of 120.5° for the orthorhombic crystal.[10] The deviation from linear coordination of the mercury atoms in **1** · Cl^- is induced by strain in the tetramer ring. The average Hg-C-C angle of 125.7° in **1** is smaller than the 135° required for a strain-free tetramer. Consequently the mercury centers are displaced toward the cavity of the ring, resulting in a conformation of the ring that maximizes the bonding between the chloride ion and the four mercury centers. The deviation from linear mercury coordination requires the mixing of some additional p character into the sp hybrid mercury orbitals involved in bonding to carborane C atoms.

The nearly square planar coordination geometry of the chloride ion in $1 \cdot Cl^-$ is unprecedented. The Hg–Cl distance of 2.944(2) Å is significantly shorter than the van der Waals distance. The structure of the 1:2 adduct of chloride ion with 1,2-diphenylenedimercury dichloride has two short Cl–Hg distances (2.925 Å) and two long Cl–Hg distances (3.167 Å).[3b] In organomercury compounds Hg(II) is normally sp hybridized and forms two linear covalent bonds while retaining two empty and mutually perpendicular p orbitals.[9] The location of Cl^- in the [12]mercuracarborand-4 host maximizes the cooperative interaction of four empty mercury orbitals with two filled p orbitals of the chloride ion, which are essentially within the plane of the macrocycle. The trapped chloride ion is therefore bound to the host by a pair of three-orbital two-electron bonds. Four empty nonparticipating p orbitals perpendicular to the host ring arise from the set of four mercury atoms.

The synthesis of $1 \cdot ClLi$ is significant because it efficiently produces a macrocyclic multidentate Lewis acidic host in a single step. We believe that Cl^- functions as a template which directs the assembly of the host macrocycle, since either a cyclic trimer or a linear polymer is expected to have more favorable geometries for coordination of Hg(II) with the carbon atoms of the carborane cage, as seen in the case of $(C_6H_4Hg)_3$.[10–12] The template effect of metal ions in promoting certain cyclization reactions has been recognized for a very long time.[1c, 13] Two recent examples of the template effect of organic molecules are the syntheses of cyclic porphyrin oligomers[14] and a macrocyclic ligand from a so-called (template)^2 synthesis.[15] As far as we know, the synthesis of $1 \cdot ClLi$ is the first example of a guest anion acting as template for the formation of its organic host structure.[16]

The chloride ion adduct of **1** is the only structurally defined anionic halide complex of a diorganomercury compound.[3b] We suggest that the electron-withdrawing ability of the carborane cages greatly increases the electrophilicity of the four Hg(II) centers and thus enhances the interaction of Cl^- with the four empty in-plane mercury orbitals.[17] The adduct $1 \cdot Cl^-$ is sufficiently stable to be detected in the negative ion FAB mass spectrum with a relative intensity of 100%, and the cation exchange reaction proceeds smoothly without the destruction of the anionic adduct. Unlike crown ethers and cryptands, **1** is a planar preorganized host with a cavity in the uncomplexed state and promises to be an excellent electrophilic host for the complexation of anions or nucleophilic organic substrates. Such a preorganized host should result in higher thermodynamic and kinetic stabilities of its complexes.[18] Moreover, the four mercury binding sites are arranged in such a way that a cooperative interaction with a variety of guests is anticipated. Thus, one of the empty orbitals at each mercury in **1** can be directed into the cavity, as in the case of $1 \cdot Cl^-$, or both empty orbitals can be directed 45° above and below the plane of the host, thus allowing **1** to bind two nucleophiles simultaneously. Preliminary work indicates that chloride ion may be removed from $1 \cdot Cl^-$ by Ag^+ without decomposition of the host, and ^{199}Hg NMR experiments prove that I^- is tightly bound by **1**. We are now studying the ability of **1** and related mercuracarborands to interact with a variety of inorganic anions and organic substrates and are evaluating their capabilities as homogeneous catalysts.

Experimental Procedure

$1 \cdot ClLi$: *n*BuLi (43.7 mmol, 17.5 mL, 2.5 M in hexane) was added to an ethereal solution (50 mL) of *o*-carborane **2** (20.8 mmol, 3.00 g) at 0 °C, and the slurry was stirred at room temperature under argon. After two hours, the mixture was treated with solid $HgCl_2$ (20.8 mmol, 5.65 g) and stirred overnight. The mixture was then treated with 100 mL H_2O, and the organic phase was washed three times with H_2O (100 mL) and dried over $MgSO_4$. The solvent was removed and the residue was recrystallized from ether to give colorless, air-stable crystals of $1 \cdot ClLi$ in 75% yield. M.P. > 300 °C. ^1H NMR (200 MHz, $(CD_3)_2CO$, 25 °C): $\delta = 0.6-3.6$. ^{13}C NMR (50 MHz, $(CD_3)_2CO$, 25 °C, decoupled): $\delta = 94$. ^{11}B NMR (160 MHz, $(CH_3)_2CO$, 25 °C, relative to external $BF_3 \cdot Et_2O$, decoupled): $\delta = 0.3, -6.0, -8.3, -10.2$. ^{199}Hg NMR (89.6 MHz, 0.25 M in $(CD_3)_2CO$, 25 °C; 1.0 M PhHgCl in $[D_6]$DMSO as an external reference at $\delta = -1187$, [19] upfield to neat Me_2Hg, decoupled): $\delta = -1077$; IR (KBr): $\tilde{\nu}$ [cm^{-1}] = 2560 (B-H). Negative ion FAB-MS: *m/z* 1407 ($1 \cdot Cl^-$, 100%), 1204 ($1 \cdot Cl^- - Hg$, 2.5%), 1064 ($1 \cdot Cl^- - HgC_2B_{10}H_{10}$, 18%). A correct elemental analysis was obtained for $1 \cdot ClLi$.

Received: July 15, 1991 [Z 4796]
German version: *Angew. Chem. 103* (1991) 1519

CAS Registry numbers:
1, -ClLi, 136846-47-4; **2**, 16872-09-6; **3**, 22220-85-5.

[1] a) D. J. Cram, *Science 219* (1983) 1177; b) F. Vögtle, E. Weber: *Host-Guest Complex Chemistry/Macrocycles*, Springer, Berlin 1985; c) L. F. Lindoy: *The Chemistry of Macrocyclic Ligands*, Cambridge University Press, Cambridge 1989.

[2] a) M. Newcomb, J. H. Horner, M. T. Blanda, P. J. Squattrito, *J. Am. Chem. Soc. 111* (1989) 6294; b) M. Newcomb, M. T. Blanda, *Tetrahedron. Lett. 29* (1988) 4261; c) M. Newcomb, A. M. Madonik, M. T. Blanda, J. K. Judice, *Organometallics 6* (1987) 145; d) K. Jurkschat, H. G. Kuivila, S. Liu, J. A. Zubieta, *ibid. 8* (1989) 2755; e) K. Jurkschat, A. Rühlemann, A. Tzschach, *J. Organomet. Chem. 381* (1990) C 53.

[3] a) J. D. Wuest, B. Zacharie, *Organometallics 4* (1985) 410; b) A. L. Beauchamp, M. J. Olivier, J. D. Wuest, B. Zacharie, *J. Am. Chem. Soc. 108* (1986) 73; c) J. D. Wuest, B. Zacharie, *ibid. 107* (1985) 6121; d) *ibid. 109* (1987) 4714; e) F. Nadeau, M. Simard, J. D. Wuest, *Organometallics 9* (1990) 1311.

[4] M. E. Jung, H. Xia, *Tetrahedron Lett. 29* (1988) 297.

[5] a) H. E. Katz, *Organometallics 6* (1987) 1134; b) *J. Am. Chem. Soc. 108* (1986) 7640; c) *ibid. 107* (1985) 1420; d) *J. Org. Chem. 54* (1989) 2179; e) editors's comment: *Reetz* et al. report on the latest results with boron-containing host molecules in two communications of this issue: M. T. Reetz, C. M. Niemeyer, K. Harms, *Angew. Chem. 103* (1991) 1515, 1517; *Angew. Chem. Int. Ed. Engl. 30* (1991) 1472, 1474.

[6] a) J. Rebek, Jr., *Science 235* (1987) 1478; b) J. Hine, S.-M. Linden, V. M. Kanagasabapathy, *J. Am. Chem. Soc. 107* (1985) 1082.

[7] R. N. Grimes: *Carboranes*, Academic, New York 1970, p. 66.

[8] Crystallographic data for **1**-ClLi: $C_8H_{40}B_{40}Hg_4ClLi$, tetragonal, space group $P4/mcc$, $a = 14.3233(8)$, $c = 11.2641(7)$ Å, $V = 2311$ Å^3, $Z = 2$ (1/8 of the tetramer per asymmetric unit), $\varrho_{calcd} = 2.03$ g cm^{-3}. $\mu(Mo_{K\alpha}) = 2.03$ cm^{-1}, $T = 25$ °C. Data were collected on a Huber diffractometer, using $Mo_{K\alpha}$ radiation, to a maximum $2\theta = 60°$, giving 1608 unique reflections, and the structure was solved by heavy atom methods. The final discrepancy index was $R = 0.041$, $R_w = 0.060$ für 1207 independent reflections with $I > 3\sigma(I)$. Further details of the crystal structure investigation may be obtained from the Fachinformationszentrum Karlsruhe, Gesellschaft für wissenschaftlich-technische Information mbH, W-7514 Eggenstein-Leopoldshafen 2 (FRG), on quoting the depository number CSD-55584, the names of the authors, and the journal citation.

[9] J. L. Wardell in G. Wilkinson, F. G. A. Stone, E. W. Abel (Eds.): *Comprehensive Organometallic Chemistry, Vol. 2*, Pergamon, Oxford, pp. 863–978.

[10] D. S. Brown, A. G. Massey, D. A. Wickens, *Acta. Crystallogr. B34* (1978) 1695.

[11] C. M. Woodard, G. Hughes, A. G. Massey, *J. Organomet. Chem. 112* (1976) 9.

[12] D. S. Brown, A. G. Massey, D. A. Wickens, *Inorg. Chim. Acta 44* (1980) L 193.

[13] M. DeSousa Healy, A. J. Rest, *Adv. Inorg. Chem. Radiochem. 21* (1978) 1.

[14] H. L. Anderson, J. K. M. Sanders, *Angew. Chem. 102* (1990) 1478; *Angew. Chem. Int. Ed. Engl. 29* (1990) 1400.

[15] C. A. Salata, M.-T. Youinou, C. J. Burrows, *J. Am. Chem. Soc. 111* (1989) 9278.

[16] The formation of complexes of inorganic hosts with encapsulated anions was discussed in A. Müller, M. Penk, R. Rohlfing, E. Krickemeyer, J. Döring, *Angew. Chem. 102* (1990) 927; *Angew. Chem. Int. Ed. Engl. 29* (1990) 926; P. C. H. Mitchell, *Nature 348* (1990) 15; A. Müller, *ibid. 352* (1991) 115; V. W. Day, W. G. Klemperer, O. M. Yaghi, *ibid. 352* (1991) 115; P. C. H. Mitchell, *ibid. 352* (1991) 116.

[17] The cyclic trimer of 1,2-phenylene mercury, $(1,2\text{-}C_6H_4Hg)_3$, does not bind halide anions. See [11] and references therein.

[18] D. J. Cram, *Angew. Chem. 98* (1986) 1041; *Angew. Chem. Int. Ed. Engl. 25* (1986) 1039.

[19] M. A. Sen, N. K. Wilson, P. D. Ellis, J. D. Odom, *J. Magn. Reson. 19* (1975) 323.

Microporous Silica Films

By *Wilhelm F. Maier,* Michael Wiedorn,* and *Herbert O. Schramm*

Thin ceramic films are useful for optical or protective coatings. Microporous ceramic membranes with pore diameters from 5–10 Å are of interest for separations in the food industry, gas separation, nonlinear optics, and for microelectronic sensors. The present activity in the field of microporous ceramic films focuses on zeolites, due to its well-defined pore structure. However, because of the limited crystallite size of zeolites, the preparation of homogeneous, pinhole-free films is still very difficult. We now report the pore size distribution of new, microporous, homogeneous silica films, which can be prepared in any thickness by electron beam evaporation. Such films may be used for the preparation of microporous ceramic membranes.

Our interest in the study of the microporosity of thin silica films originates in heterogeneous catalysis. In studies on the mechanism of hydrogenation and H/D-exchange reactions on hydrocarbons we have used thin silica films (50–200 nm) that covered the surface of the catalyst[1] to shield the catalytically active metal film (Pt film on a Si wafer) from direct interaction with the organic reagent. The silica layer is impervious to the organic reagent, while hydrogen apparently diffuses through the oxide layer and is activated at the Pt–SiO_2 interface. The activated hydrogen diffuses as spill-over hydrogen back to the surface (a steady-state concentration gradient is set up), where it reacts with the organic reagent. However, the mechanism of diffusion remained unclear, since no cracks or holes in the silica film were evident. Because of the small amounts of film material it was not possible to check for micropores, which remained as a possible explanation for our data. Various published discussions document the broad interest in our results.[2]

We have now determined the pore size distribution of the silica films, prepared by electron-beam evaporation, through nitrogen adsorption. Instead of Pt/Si wafers as basis for the silica coatings, commercial aluminum foil was used as substrate for silica deposition, because the silica film could be separated from the substrate mechanically, by immersion in pure water, or by dissolving the aluminum foil in 2 N HCl. It has been shown that the films are amorphous, and that a silica film on platinum can differ from that on alumina only in the first few atomic layers. Their structure should thus be independent of the substrate, especially at thicknesses larger than 50 nm. From the nitrogen adsorption isotherm the specific surface and pore volume was determined according to BET[3] and to *Dubinin*[4]. The pore radius distribution (3–300 Å) was determined from the adsorption data by applying the Kelvin equation[5] as well as by the micropore method.[6]

The N_2-adsorption isotherm of the silica (Fig. 1) documents the microporosity of the material. Figure 2 shows the associated pore radius distribution determined by the Kelvin equation. Although the equation is not valid for pore radii smaller 15 Å,[7] the analysis reveals a very narrow pore size distribution with a maximum clearly below 15 Å and no pores of larger diameter. To analyze the micropores with radii smaller than 10 Å, we relied on the MP method, using the t-plot method of *de Boer*.[8] As a criterium for the quality

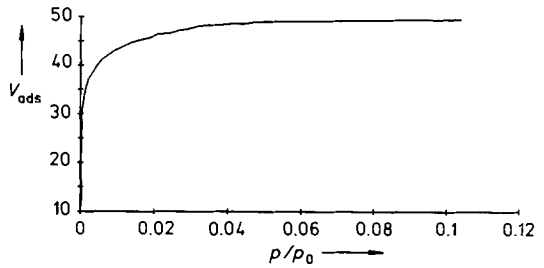

Fig. 1. Section of the nitrogen adsorption isotherm of silica, prepared by electron-beam evaporation. At $p/p_0 > 0.1$ (not shown) there was no further N_2 desorption. Adsorption volume V_{ads} in $cm^2 g^{-1}$

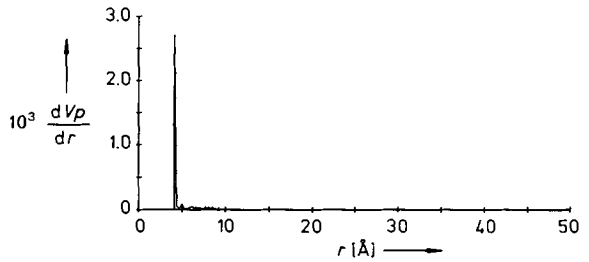

Fig. 2. Pore radii distribution of the silica film from Fig. 1, calculated by applying the Kelvin equation. $d Vp/d r$ in mL Å^{-1}.

of the data produced by the MP method, the surface and pore volume were compared with the data obtained by the BET and Dubinin treatment. Isotherms for the t-plot calculated from the Halsey equation[9] did not result in reasonable surfaces and pore volumes. Good results were obtained by the use of finely ground quartz wool as nonporous reference material. The t-plot[6] shows a decrease in slope at a layer thickness of about 3 Å, which indicates a pore maximum at 3.1 Å (see Fig. 3). This procedure was tested on various molecular sieves. We thus estimate the error of our analysis to better than $\pm$ 1 Å, which points to pore diameters of 6 ± 2 Å[13] for the microporous silica.

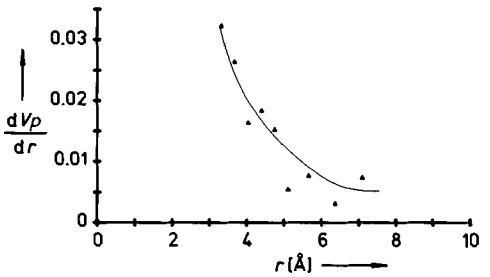

Fig. 3. Pore radius distribution of the silica film of Fig. 1, calculated by applying the MP method.

To test whether the determined pore volume is due to inner pore structure or to surface structure, the adsorption isotherm was obtained from 10 films of different thickness (between 250 and 4000 nm). The total surface of the material varied between 155 and 259 $m^2 g^{-1}$ and the pore volume between 0.055 and 0.09 cm^3/g^{-1}, independent of the film thickness. The maximum of the pore radius distribution was the same in all cases. The measured pore volume is thus not due to surface characteristics of the films, but only to inner pore and channel structures.

[*] Prof. Dr. W. F. Maier, Dipl.-Chem. M. Wiedorn, Dipl.-Chem. H. O. Schramm
Institut für Technische Chemie der Universität-Gesamthochschule Schützenbahn 70, W-4300 Essen 1 (FRG)

[**] This study was supported by the Bundesministerium für Forschung und Technologie.

Table 1. BET analysis of nitrogen adsorption isotherms.

	SiO_2 film	zeolite 3 Å	4 Å	5 Å	NaY
pore volume [$cm^3 g^{-1}$]	0.07	0.003	0.013	0.23	0.34
surface e [$m^2 g^{-1}$]	192	9.3	37.2	661.7	960

Because the size of the pores of our materials was clearly at the limits of the methods used, we were interested in a seperate method to estimate the actual pore size, in particular for pores too small to be determined by nitrogen adsorption. The adsorption isotherms of three molecular sieves and a NaY zeolite were determined (Table 1). While the NaY-zeolite and the 5 Å molecular sieve adsorbed nitrogen readily, the 4 Å and 3 Å molecular sieve showed little N_2 adsorption, confirming that these pores are to small for nitrogen as adsorbate (rotational diameter 4.3 Å).[11]

To test whether the silica films contain similarly small pores we had to use an adsorbate smaller than nitrogen. One of the few suitable molecules is water (rotational diameter 2.6 Å). Because of technical problems with recording the adsorption isotherm of water on our equipment, we have used thermogravimetry (TGA). Two silica films and three molecular sieves were saturated with water, dried for one hour at 120 °C (for the 4000 nm film, 80 °C), and analyzed in a SETARAM TGA92. The temperature-dependent water loss was registered (Table 2). The temperature of maximal

Table 2. Thermogravimetric study of water adsorption by zeolites and silica films

	zeolite 3 Å	4 Å	5 Å	thickness of SiO_2 film 30000 Å	40000 Å
Mass used [mg]	85.0	86.7	85.6	41.7	54.9
ΔM [mg] [a]	11.7	11.9	11.9	2.0	3.9
ΔM [w%] [a]	13.8	13.7	13.9	4.7 (6.6) [b]	7.1
T_{max} [°C] [c]	211.9	206.0	201.9	118.1	121.2

[a] ΔM = change in mass. [b] The value in parentheses includes the weight loss during the predrying stage (see text). [c] T_{max} = temperature of maximal water loss.

water loss increases with decreasing pore size of the molecular sieves. The relatively low temperatures of maximal water loss for the silica films shows that they adsorb water less strongly. In contrast to the pore volume from nitrogen adsorption, but as expected from the identical porosities of the molecular sieves, the pore volume obtained from water loss for the three molecular sieves is virtually identical. In the case of the 5 Å molecular sieve the pore volume obtained from TGA is about 40% below the BET volume (0.23 mL g^{-1}), which corresponds to the known water adsorption capacity of the molecular sieve. The difference can be traced to the predrying procedure of the molecular sieves, because the volume obtained from TGA for the more mildly predried 4000 nm film was identical with its BET pore volume. Therefore, all micropores in the silica films are larger than the critical diameter of nitrogen.

From these studies we conclude that silica films prepared by electron-beam evaporation have a porosity of 14 %, and a very narrow micropore distribution comparable to that of a 5 Å molecular sieve. Silica films are therefore potential materials for the preparation of microporous membranes and surface coatings. The simple preparation procedure and the homogeneity of the films make these materials very promising alternatives to zeolite films.

The extreme microporosity of the silica films supports the interpretation of our previous catalytic studies on silica coated Pt/Si-catalysts.[1] The narrow pore diameter of about 6 Å is readily penetrable by hydrogen, while diffusion of the organic reactant through the silica layer is highly hindered. Also formation of a concentration gradient of spill-over hydrogen as explanation for the observed catalytic phenomenon[1] seems plausible.

Experimental procedure

The films were prepared in a Balzers (BAE 250) evaporation unit, equipped with a 3 kW electron gun (Edwards, E 036-15). The rate of evaporation was 2–20 nm min^{-1} at a pressure smaller than 10^{-5} torr. The silica film was deposited onto aluminum foil, from which it was subsequently removed. After washing and drying of the film, the nitrogen adsorption isotherm was recorded on a modified Sorptomatic 1900 from Carlo Erba (smaller sample volumes, a dosage unit for smaller dosage pressures (p = 0–100 torr), and a pressure gange for the range 0–100 torr). The modifications allowed a reduction of the sample size needed and the recording of more data in the micropore range. For data treatment[12] a makro, programmed for the spreadsheet Excel®, was developed. Repeated measurements showed only small deviations in surface area and pore volume.

Received: June 7, 1991 [Z 4685 IE]
German version: *Angew. Chem. 103* (1991) 1523

CAS Registry number: SiO_2, 7631-86-9.

[1] A. B. McEwen, R. H. Fleming, S. Baumann, W. F. Maier, *Nature 329* (1987) 531; J. M. Cogen, K. Ezaz-Nikpay, R. H. Fleming, S. Baumann, W. F. Maier, *Angew. Chem. 99* (1987) 1222; *Angew. Chem. Int. Ed. Engl. 26* (1987) 1182; W. F. Maier, *ibid. 101* (1989) 135 and 28 (1989) 135.
[2] K. Seshan, *Appl. Catal. 50* (1989) N 14; S. J. Teichner, *ibid. 51* (1989) N 18; *CHEMTECH 1988*, 518.
[3] S. Brunauer, P. H. Emmett, E. Teller, *J. Am. Chem. Soc. 60* (1938) 309; S. Brunauer, L. S. Deming, W. E. Deming, E. Teller, *ibid. 62* (1940) 1723.
[4] M. M. Dubinin, *J. Colloid Interface Sci. 23* (1967) 487.
[5] D. Dollimore, G. R. Heal, *J. Appl. Chem. 14* (1964) 109.
[6] R. S. Mikhail, S. Brunauer, E. E. Bodor, *J. Colloid Interface Sci. 26* (1968) 45.
[7] J. Seifert, G. Emig, *Chem. Ing. Tech. 59* (1987) 475.
[8] B. C. Lippens, J. H. de Boer, *J. Catal. 4* (1965) 319.
[9] G. D. Halsey, *J. Chem. Phys. 16* (1948) 931.
[10] G. Horváth, K. Kawazoe, *J. Chem. Eng. Jpn. 16* (1983) 470.
[11] J. Schröder, *GIT Fachz. Lab. 30* (1986) 978; *ibid. 30* (1986) 1095.
[12] S. Lowell, J. E. Shields: *Powder Surface Area and Porosity*, 3rd ed., Chapman and Hall, London 1991.
[13] Note added in proof (30. 10. 91): We thank Micrometrics for the determination of the micropore distribution of our SiO_2 film with their new ASAP 2000 M, carried out after submission of this manuscript. Data treatment by the method of *Horváth* and *Kawazoe* [10] gave a maximum for the pore diameter distribution at 5.5 Å, confirming our data.

Crystal Structure of Chlorine Dioxide **

By *Anette Rehr* and *Martin Jansen**

By virtue of their small number, stable radicals or radical ions play a subordinate role in the chemistry of the nonmetals. In this setting, the characteristically increasing number of examples found in the case of the triatomic 19-electron systems is striking. These can be homoatomic such as S_3^-,[1] O_3^-,[2] or P_3^{4-}[3] or heteroatomic such as ClO_2, NF_2[4] and SO_2^-,[5] with the more electronegative atom in the terminal position. A gradual change in tendency to dimerize is ob-

[*] Prof. Dr. M. Jansen, Dipl.-Chem. A. Rehr
Institut für Anorganische Chemie der Universität
Gerhard-Domagk-Straße 1, 5300 Bonn 1 (FRG)

[**] This work was supported by the Deutsche Forschungsgemeinschaft (Leibniz Program) and the Fonds der Chemischen Industrie.

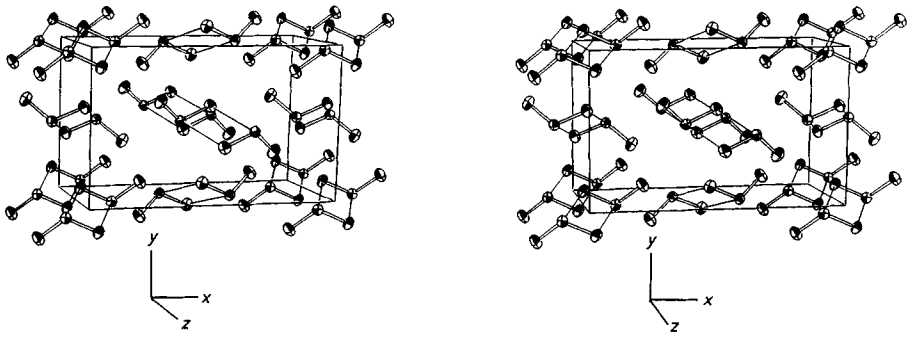

Fig. 1. Stereoview of the crystal structure of ClO_2; intermolecular bond interactions are indicated by lines.

served between the extreme cases: O_3^-, P_3^{4-} are exclusively monomeric, SO_2^- ($S_2O_4^{2-}$) is known only as the dimer, whereas $2\,S_3^- \rightleftarrows S_6^{2-}$ and $2\,NF_2 \rightleftarrows N_2F_4$ are solvent- and temperature-dependent equilibria, respectively. These gradual changes are difficult to interpret. An influential factor is undoubtedly the difference in electronegativity, and thus the site of greatest residence probability for the unpaired electron (antibonding π-orbital $2\,b_1$). Since gas-phase equilibria naturally cannot be investigated in the case of the charged compounds, and electrostatic effects would dominate in the condensed phase, the behavior of NF_2 and ClO_2 is of particular importance. In the case of NF_2 a temperature-dependent equilibrium could be detected, whereas ClO_2 should show no tendency whatsoever to dimerize and should be isotypic with SO_2 in the crystalline state.[6] To check this hypothesis we have determined the crystal structure of ClO_2 and carried out measurements of the magnetic susceptibility of solid ClO_2.

ClO_2, prepared by reaction of sodium chlorite with chlorine, was carefully purified and recondensed into a capillary tube or into the sample tube of the magnetometer. Crystal growth was carried out in situ on a four-circle diffractometer. The X-ray structure analysis[7] confirmed that a molecular crystal was indeed formed, but revealed no signs of isotypy with SO_2. In SO_2, all molecules are oriented equidirectionally with respect to their dipole moments and their relative arrangement can easily be reduced to a cubic face-centered packing. In contrast, the ClO_2 molecules arrange themselves pairwise with oppositely directed dipole moments (cf. Fig. 1). From the spectrum of bond lengths from one ClO_2 molecule to its nearest neighbors there always is a pair of significantly shorter Cl–O bond lengths. The chlorine and one terminal oxygen atom each of the two neighboring molecules approach each other with formation of a head-to-tail dimer. The resulting shortest intermolecular Cl–O bond length (274 pm) is 46 pm shorter than the van der Waals distance; thus, the relative shortening corresponds approximately to that in solid NO (240 compared to 290 pm[8]). The mass centers of the dimers of ClO_2 lie on all corners and face centers of the orthorhombic unit cell and are inversion symmetric, that is the planes through the two molecules are parallel to each other. The bond from chlorine to the "terminal" oxygen atom within the dimer forms an angle of 101.5° with the Cl_2O_2 plane. The structural factors thus clearly indicate an association of two ClO_2 molecules in the crystal; however, a two-electron two-center bond is not formed thereby. Namely, if one bears in mind the S–S bond lengths in $S_2O_4^{2-}$ (239 pm)[9] then a chlorine–chlorine bond length of at most 240 pm would be expected in such a case.

With the aim of independently demonstrating this intermolecular interaction we have carried out magnetic measurements on solid ClO_2.[10] As the plot of χ against T (Fig. 2) shows, ClO_2 is initially paramagnetic below the melting point and becomes diamagnetic below $-108\,°C$. Thus, it is proven beyond doubt that ClO_2 is present in the form of dimers with compensated spin moments at low temperatures. That the observed interaction cannot be of an electrostatic nature (dipole–dipole interactions) follows from the relative arrangement of the molecules with respect to one another. Moreover, SO_2, with the higher dipole moment, would then have to tend to undergo association to a greater extent, which obviously is not the case. Interestingly, two monomers are always so related to each other that the antibonding π-orbitals ($2\,b_1$) can overlap. An intermolecular interaction should increase the electron density in these antibonding orbitals and should thus concomitantly expand the respective Cl–O bond. This is in fact observed: the Cl–O bond, through which the dimerization takes place, is longer (147.5 pm) than the non-bridging bond (146.4 pm). The effect, however, lies almost in the range of experimental error. The bond length determined for gaseous ClO_2 by microwave spectroscopy corresponds exactly to the mean value of the bond lengths found in the crystal; the angle (116.0°) is slightly reduced compared to 117.4° (gaseous).

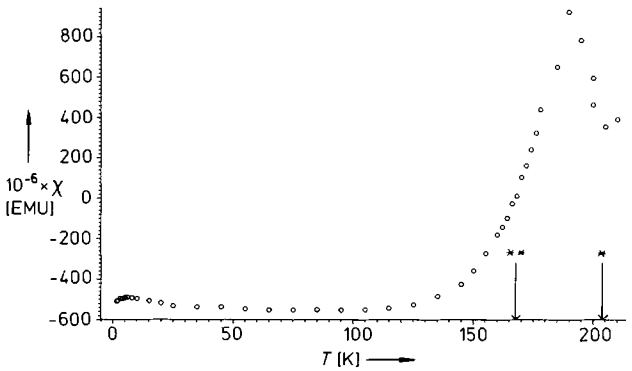

Fig. 2. Relative magnetic susceptibility of ClO_2 in dependence of the temperature (* melting point; ** temperature at which X-ray data was collected.

Experimental

The synthesis was carried out analogously to that described by G. Brauer: *Handbuch der Präparation Anorganischen Chemie*, 3rd ed., Enke, Stuttgart 1974, p. 312.

Warning: Chlorine dioxide is extremely explosive! At temperatures below $-40\,°C$ and pressures below 50 mbar it is relatively safe to handle. When subjected to any source of energy it decomposes explosively; on handling ClO_2, therefore, exposure to light was avoided if possible, otherwise all operations were carried out under a red light. The apparatus was painstakingly cleaned and KEL-F paste was used.

ClO_2 was distilled over ($-50 \rightarrow -120\,^{\circ}C$) from the cooling trap into a capillary tube previously cleaned with aqua regia and sealed onto the trap. The capillary and cooling trap were then cooled to $-196\,^{\circ}C$ and the capillary detached under vacuum (1.3×10^{-3} mbar). Storage and transfer to the diffractometer were carried out under continous cooling to $-196\,^{\circ}C$.

An analogous procedure was used on condensing ClO_2 into the sample tube of the magnetometer except that this was immediately cooled to $-196\,^{\circ}C$ and filled to a height of 3–4 mm. The substance used for crystal growing was purified by zone-refining. At a cooling temperature 0.3 K below the melting point of ClO_2 the intensity of the IR lamp was regulated so that the substance just melted. Several rapid cycles were run through, but always in only one direction. The crystal growth was finally carried out in a zone shortened by about 1/10 mm and the melting zone was moved slowly (1 mm h^{-1}) run. The crystal quality was checked by X-ray diffraction (film methods).

Received: July 8, 1991 [Z 4783 IE]
German version: *Angew. Chem. 103* (1991) 1506

[1] F. Seel, H. J. Güttler, G. Simon, A. Wieckowski, *Pure Appl. Chem. 49* (1977) 45; T. Fuginaga, T. Kuwamoto, S. Okazaki, M. Hojo, *Bull. Chem. Soc. Jpn. 53* (1980) 2851.
[2] W. Schnick, M. Jansen, *Angew. Chem. 97* (1985) 48; *Angew. Chem. Int. Ed. Engl. 24* (1985) 54; W. Schnick, M. Jansen, *Rev. Chim. Miner, 24* (1987) 446.
[3] H. G. von Schnering, M. Hartweg, V. Hartweg, W. Hönle, *Angew. Chem. 101* (1989) 98; *Angew. Chem. Int. Ed. Engl. 28* (1989) 56.
[4] J. P. Freemann, *Inorg. Chim. Acta Rev. 1* (1967) 65.
[5] H. C. Clark, A. Horsfield, M. C. R. Symons, *J. Chem. Soc. 1961* 7.
[6] J.-L. Pascal, A. C. Pavia, J. Potier, *J. Mol. Struct. 13* (1972) 38.
[7] Crystal structure: *Pbca*; $a = 1081.8(5)$, $b = 667.3(3)$, $c = 555.2(1)$ pm, $Z = 8$; four-circle diffractometer Enraf-Nonius, $Mo_{K\alpha}$; data collection at $-110\,^{\circ}C$, 723 independent reflections, 549 with $F > 2\sigma(F)$; $R = 0.052$, $R_w = 0.046$. Further details of the crystal structure investigation are available on request from the Fachinformationszentrum Karlsruhe, Gesellschaft für wissenschaftlich-technische Information mbH, 7514 Eggenstein-Leopoldshafen 2 (FRG), on quoting the depository number CSD-300 221, the names of the authors, and the journal citation.
[8] W. J. Dulmaye, E. A. Meyers, W. N. Lipscomb, *Acta Crystallogr. 6* (1953) 760.
[9] J. D. Dunitz, *J. Am. Chem. Soc. 78* (1956) 878.
[10] A. Rehr, *Dissertation*, Hannover 1991.

sulfur) at room temperature we were able to obtain black crystals of the dimorphous salt **1**.

$(NH_4)_2[Re_2S_2(S_3)_2(S_4)_2] \cdot 4\,H_2O$ **1**

1 was characterized by elemental analysis, thermogravimetry (H_2O content), UV/VIS/NIR and IR spectroscopy, X_α-MO calculations, and powder diffractometry.[5]

In addition, single-crystal structure analyses were carried out on the two crystal modifications **1a** and **1b**.[5] The anion in **1a** has a crystallographic symmetry center, that in **1b** a twofold rotation axis. The idealized symmetry in both cases is C_{2h} (Fig. 1). The anions in each case consist of two Re

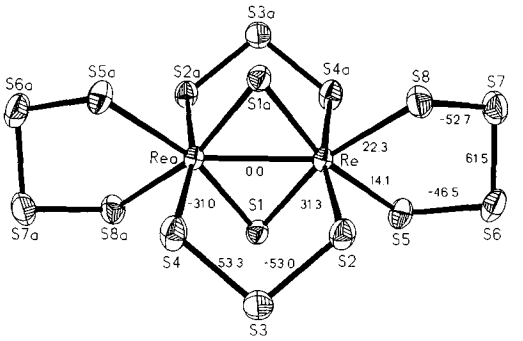

Fig. 1. Structure of the anion of **1a** in the crystal with data of the torsion angles [°] in the ReS_4 ring and the Re_2S_3 ring. Bond lengths [pm] and selected bond angles [°]: Re-Rea 263.6(1), Re-S1 230.7(2), Re-S2 243.2(2), Re-S5 248.3(2) Re-S8 248.3(2), Re-S1a 230.0(2), Re-S4a 243.7(2), S2-S3 206.6(3), S3-S4 208.3(2), S5-S6 206.7(3), S6-S7 205.2(3), S7-S8 207.0(3); S-Re-S 76.3(1)-110.2(1), 163.9(1)-167.2(1), Re-S1-Re 69.8(1), Re-S-S 106.3(1)-109.3(1), S-S-S 99.8(1)-100.2(1). The bond lengths and angles of **1b** do not differ significantly from those of **1a**.

$(NH_4)_2[Re_2S_{16}]$, a Soluble Metal Sulfide with Interesting Electronic Properties and Unusual Reactivity**

By *Achim Müller,* Erich Krickemeyer, Volker Wittneben, Hartmut Bögge,* and *Michael Lemke*

Dedicated to Professor Hans Georg von Schnering on the occasion of his 60th birthday

"Molecular" metal sufides[1] are topical for many reasons: they are the active centers in a number of, in part, ubiquitous proteins that are of importance in fundamental biological processes,[2] and are also used as starting materials for important catalysts;[3] however, only in the last 20 years have they become preparatively accessible.[4] In this communication an unusual sulfide is presented in which the metal–metal bond has largely double-bond character and whose electronic structure can be correlated with its unusual reaction behavior and that of other metal sulfides. A molecular metal sulfide with a metal–metal double bond has heretofore not been described in the literature.

By reaction of ammonium perrhenate with an aqueous ammonium poly-sulfide solution (with a high proportion of atoms linked via two μ_2-S^{2-}-centers and two S_3^{2-} ligands. Each Re atom bears, in addition, a chelating S_4^{2-} ligand, and thus has a distorted octahedral geometry (the angle S1–Re–S1a (110.2(1)°) deviates the most from 90°); two ReS_6 octahedra are linked via one edge (for structure type see Ref. [6]). The Re_2S_3 rings are present in an "envelope" conformation; the ReS_4 rings form approximate "half-chair" conformations in **1a** and exact "half-chair conformations symmetric about the twofold axis in **1b** (torsion angles 17.9; −49.1, 60.6; −49.1, 17.9°). Especially interesting from the structural point of view is the eight-membered Re_2S_6 ring with a strong transannular Re–Re interaction (cf. below).

In the system $[ReO_4]^-/S_x^{2-}$ the formation of **1** competes with that of $[Re^{VII}S_4]^-$, $[Re^{V}S(S_4)_2]^-$, $[Re_4^{IV}S_4(S_3)_6]^{4-}$, and $[Re_4^{IV}S_4(S_3)_4(S_4)_2]^{4-}$.[7a] When the S_x^{2-} solution contains a high proportion of sulfur, **1** is formed preferentially instead of the Re^{IV} clusters, since further reduction is hindered thereby. Accordingly, it contains the highest S/M proportion (M = V, Mo, W, Re) of all multinuclear sulfides of the early transition metals (except some mononuclear species like $[Re^{V}S(S_4)_2]^-$).

1 is a novel type of molecular sulfide not only with regard to structure, but also with regard to electronic properties.[8] Compared to Mo–S and W–S systems, Re–S systems are characterized by the lower energy of the rhenium 5d function[9a] and the possibility thereby of stronger covalent Re–S interactions. Due to the very similar energies of the

[*] Prof. Dr. A. Müller, E. Krickemeyer, Dipl.-Chem. V. Wittneben, Dr. H. Bögge, Dipl.-Chem. M. Lemke
Fakultät für Chemie der Universität
Postfach 8640, W-4800 Bielefeld 1 (FRG)

[**] We thank Degussa AG for gifts of rhenium compounds.

Re-5d and S-3p functions,[9a] ligand and metal functions mix better in Re–S-compounds than in analogous Mo and W compounds.[10] This contributes for example to the high Re–S bond order in $[ReS_4]^-$.[10,11] All "Re-containing" molecular orbitals in **1** are so strongly stabilized that also orbitals with partial δ, δ^*, and π^* character are populated.[9b] The Re–Re π bond is thereby partially compensated, i.e. the metal–metal bond weakened (cf. values for W–W and Re–Re single bond lengths[6,8]).

The presence of orbitals that have not only Re–Re π-bonding character but also a pronounced delocalization of the electrons (with a high proportion of ligand contributions), also explains the characteristic redox behavior of **1**. In all the solvents investigated, a remarkable electron transfer (with exclusion of O_2 !) takes place spontaneously (e.g., in dimethyl sulfoxide with 75 % yield), which has model character for catalytic processes [Eq. (a)]. The S_x^{2-} ligands probably oxi-

$$[Re^{V}_2S_2(S_3)_2(S_4)_2]^{2-} \xrightarrow{DMSO} [Re^{VII}S_4]^- \qquad (a)$$

dize Re^V to Re^{VII} in a complicated reaction pathway (the prerequisite for electron transfer from Re to S is evident, e.g., by virtue of the fact that, in the case of $[Re^VS(S_4)_2]^-$, a relatively high bonding energy is measured for the Re-4$f_{7/2}$ electrons in the ESCA experiment (*E*lectron *S*pectroscopy for *C*hemical *A*nalysis)[7a].

Similar reactions are *not* observed, e.g., in the clusters $[Re_4S_4(S_3)_6]^{4-}$ and $[Re_4S_4(S_3)_4(S_4)_2]^{4-}$,[7a] since in these cases the valence electrons are located in "stable" metal–metal σ bonds and are not available for intramolecular redox reactions (for intramolecular redox reactions in the case of Mo–S compounds, cf. Ref. [12]). This generally confirms our hypothesis that easily displaced electrons in exchange coupled clusters, and also as here in strongly delocalized MOs (i.e. not fixed in strong metal–metal bonds), are of importance for electron transfer in biology and catalysis.[13] Accordingly, Re sulfides have other, and in part better, catalytic properties in redox reactions than the Mo and W analogues.[14]

A further remarkable reaction in this connection takes place when **1** is treated in the presence of air at 90 °C with an aqueous KCN solution [Eq. (b)]. The formation of the

$$[Re_2S_2(S_3)_2(S_4)_2]^{2-} \xrightarrow{CN^-, O_2} [Re_2(SO_2)_2(CN)_8]^{6-} \qquad (b)$$

$K_6[Re_2(SO_2)_2(CN)_8]\cdot 2H_2O$ **2**

anion of **2** (for structure see Fig. 2) proceeds with ligand exchange and S^0-abstraction (NCS^- formation), whereby Re^V is reduced to Re^{III}; cf. Ref. [15].

The highly negative partial charge at the μ_2-S^{2-} bridges facilitates attack by O_2 and the formation of SO_2^{2-} bridges in this reaction (cf. discussion in Ref. [15]), but also hinders a further nucleophilic attack of CN^- with formation of NCS^-, i.e. cleavage of the Re–S–Re bonds. Cyanolysis of amorphous metal sulfide catalysts also permits differentiation of the various metal-bound S_x^{2-} groups.

These results provide an indication of how one can interpret the different influence of nd-metal centers (n = 4 and 5) regarding the reactivity and catalytic activity of metal-sulfur systems. Both the absolute energy of the d function as well as its relative position to the S-3p level are of importance.

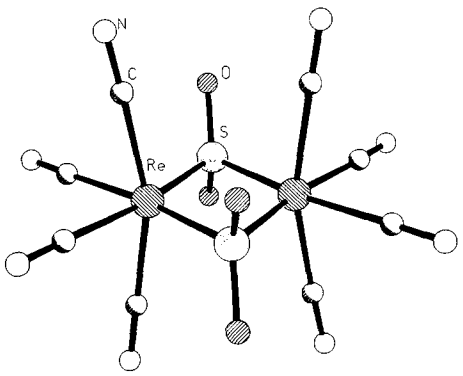

Fig. 2. Structure of the anion of **2** in the crystal. Important bond lengths [pm] and angles [°]: Re-Re 265.3(1), Re-S 232.5(2), 232.6(2), Re-C 209.5(8)-211.8(6), S-O 149.5(6), 149.9(5), S-Re-S, S-Re-C, C-Re-C 78.4(2)-96.2(2), 162.0(2)-171.1(2), Re-S-Re 69.6(1), Re-S-O 118.8(2)-119.3(2), O-S-O 107.5(3), Re-C-N 173.7(6)-179.0(5).

Experimental

1: H_2S gas was passed into a suspension of sulfur powder (150 g) in 500 mL of a 12.5 % aqueous ammonia solution for 4 h (20 $L\,h^{-1}$; the first hour with stirring); the sulfur dissolved almost completely. The polysulfide solution was then treated with a solution of ammonium perrhenate (0.5 g, 1.86 mmol) in H_2O (25 mL) and the mixture kept in a closed 1 L round bottom flask at 20–25 °C. The dark brown precipitate which initially formed after a rapid change in color of the reaction solution from red through dark red to reddish brown went into solution again. The black crystals of **1** which had precipitated after one to one and a half weeks (**1a**: distorted rectangular platelets (ca. 75 %); **1b**: tetragonal bipyramids (ca. 25 %) were filtered off, washed with 2-propanol, carbon disulfide, and 2-propanol, and then dried and stored under argon. Yield: 0.2 g (21.6 % based on $NH_4[ReO_4]$ employed).

Correct elemental analysis. IR (CsI): $\tilde{\nu}[cm^{-1}]$ = ca. 3500(m) ($\nu(H_2O)$); ca. 3130(m) ($\nu_{as}(NH_4^+)$); 1590(m) (br), 1560(m) ($\delta(H_2O)$); 1410(sh)/1390(s) ($\delta_{as}(NH_4^+)$); 455(m), ca. 430(m) (br), 392(s) (ν_{as}(S-S), ν_{as}(Re-S)). UV/VIS/NIR (KBr/transmission): λ[nm] = ca. 1200, 780, 620, 540, 440, and 375 (sh). **1** decomposes according to equation (a) at 30–40 °C in H_2O, dimethyl sulfoxide, *N*,*N*-dimethylformamide, pyridine, and methanol.

2: A solution of potassium cyanide (0.50 g, 7.68 mmol) in H_2O (20 mL) was treated with **1** (0.13 g, 0.13 mmol) in a 100-mL Erlenmeyer flask (wide-necked, covered with a watch glass) and allowed to stand on a hotplate at 90 °C until brown crystals of **2** precipitated from the solution. After filtration of the hot solution, the crystals were washed with aqueous 2-propanol (80 %), then absolute 2-propanol, and dried on filter paper. Yield: 0.10 g (78 % based on initial amount of **1**).

IR (CsI): $\tilde{\nu}[cm^{-1}]$ = 1063(m) (ν_{as}(S-O)); 963(s) (ν_s(S-O)). X-ray structure analysis of **2**: $P\bar{1}$; a = 804.0(2), b = 887.2(3), c = 901.3(3) pm, α = 83.79(2), β = 64.52(2), γ = 81.61(2)°, $V = 573.4 \times 10^6$ pm^3, R = 0.036 (for deposition of structural data see [5]).

Received: March 19, 1991 [Z 4513 IE]
German version: *Angew. Chem. 103* (1991) 1501

CAS Registry numbers:
1, 136504-57-9; **2**, 136536-86-2; NH_4ReO_4, 13598-65-7; $(NH_4)_2S_x$, 9080-17-5; $[ReS_4]^-$, 16829-47-3; S^{2-}, 18496-25-8.

[1] a) S. C. Lee, R. H. Holm, *Angew. Chem. 102* (1990) 868; *Angew. Chem. Int. Ed. Engl. 29* (1990) 840; b) A. Müller, E. Diemann in G. Wilkinson, R. D. Gillard, J. A. McCleverty (Eds.): *Comprehensive Coordination Chemistry, Vol. II*, Pergamon, Oxford 1987, pp. 515, 559; c) M. Draganjac, T. B. Rauchfuss, *Angew. Chem. 97* (1985) 745; *Angew. Chem. Int. Ed. Engl. 24* (1985) 743; d) M. Rakowski Dubois, *Chem. Rev. 89* (1989) 1.

[2] W. E. Newton in A. Müller, B. Krebs (Eds.): *Sulfur – Its Significance for Chemistry, for the Geo-, Bio- and Cosmosphere and Technology*, Elsevier, Amsterdam 1984, p. 409; R. H. Holm, *Chem. Soc. Rev. 10* (1981) 455.

[3] For example for the hydrodesulfurization (HDS), hydrodenitrification and hydrodemetalation of fossil fuels see: W. Eltzner, M. Breysse, M. Lacroix, C. Leclerq, M. Vrinat, A. Müller, E. Diemann, *Polyhedron 7* (1988) 2405 and patent literature. An excellent HDS catalyst can be prepared from $(NH_4)_2[Mo_3S_{13}]$: A. Müller, E. Diemann, A. Branding, F.-W. Baumann, M. Breysse, M. Vrinat, *Appl. Catal. 62* (1990) L 13.

[4] First example of a discrete pure metal sulfide cluster: $[Mo_3S_{13}]^{2-}$, A. Müller, S. Pohl, M. Dartmann, J. P. Cohen, J. M. Bennett, R. M. Kirchner, *Z. Naturforsch. B34* (1979) 434; of a polythiometallate: $[W_3S_9]^{2-}$: E. Königer-Ahlborn, A. Müller, *Angew. Chem. 87* (1975) 598; *Angew. Chem. Int. Ed. Engl. 14* (1975) 573; A. Müller, H. Bögge, E. Krickemeyer, G. Henkel, B. Krebs, *Z. Naturforsch. B37* (1982) 1014; of a heteremetal thioanion: $[Ni(WS_4)_2]^{2-}$: A. Müller, E. Diemann, *J. Chem. Soc. Chem. Commun.* (1971) 65.

[5] **1a:** $P\bar{1}$; $a = 713.4(1)$, $b = 925.6(2)$, $c = 984.1(2)$ pm, $\alpha = 87.31(2)$, $\beta = 84.83(2)$, $\gamma = 70.57(1)°$, $V = 610.1 \times 10^6$ pm^3, $Z = 1$, $\rho_{calcd} = 2.70$ g cm^{-3}, $R = 0.035$ for 2485 independent reflections ($F_0 > 4\sigma(F_0)$). **1b:** $C2/c$; $a = 1379.1(3)$, $b = 1378.1(4)$, $c = 1452.1(4)$ pm, $\beta = 114.07(2)°$, $V = 2519.7 \times 10^6$ pm^3, $Z = 4$, $\rho_{calcd} = 2.62$ g cm^{-3}, $R = 0.058$ for 2380 independent reflections ($F_0 > 4\sigma(F_0)$). Further details of the crystal structure investigation of **1a**, **1b**, and **2** are available on request from the Fachinformationszentrum Karlsruhe, Gesellschaft für wissenschaftlich-technische Information mbH, W-7514 Eggenstein-Leopoldshafen 2 (FRG), on quoting the depository number CSD-55361, the names of the authors and the journal citation. The measured ($Cu_{K\alpha}$) powder diffraction diagram of **1** (ca. 75% **1a** and ca. 25% **1b**) is in good agreement as regards reflection sequence and intensities with that calculated for **1a** and **1b** from data of the X-ray structure analysis (most intense reflections corresponding to interplanar distances d of 980, 930, 873, 670, 663, 645, 637, 631, 593, and 575 pm).

[6] F. A. Cotton, *Polyhedron 6* (1987) 667; S. Shaik, R. Hoffmann, C. R. Fisel, R. H. Summerville, *J. Am. Chem. Soc. 102* (1980) 4555.

[7] a) A. Müller, E. Krickemeyer, H. Bögge, *Z. Anorg. Allg. Chem. 554* (1987) 61; A. Müller, E. Krickemeyer, H. Bögge, *Angew. Chem. 98* (1986) 258; *Angew. Chem. Int. Ed. Engl. 25* (1986) 272; A. Müller et al., unpublished; b) S. Ciurli, M. J. Carney, R. H. Holm, G. C. Papaefthymiou, *Inorg. Chem. 28* (1989) 2696; A. Müller, E. Krickemeyer, H. Bögge, M. Penk, D. Rehder, *Chimia 40* (1986) 50 and unpublished results.

[8] The relatively short distance between the two Re^V centers (electron configuration d^2) (263.6(1) pm in **1a** and 263.2(1) pm in **1b**) points, according to the argument put forward by *Hoffmann* et al. and *Cotton* [6], to the presence of a formal M=M double bond. Example: $[W_2^{IV}S_2(dtc)_4]$ with a W–W distance of 253.0(2) pm; cf. A. Bino, F. A. Cotton, Z. Dori, J. C. Sekutowski, *Inorg. Chem. 17* (1978) 2946; cf. also L. Wei, T. R. Halbert, H. H. Murray III, E. I. Stiefel, *J. Am. Chem. Soc. 112* (1990) 6431 as well as F. A. Cotton, R. A. Wolton: *Multiple Bonds between Metal Atoms*, Wiley, New York 1982, p. 290.

[9] a) Cf., e.g., Hartree-Fock-Slater orbital energies: S–3p: 10.3; Mo–4d: 7.2; W–5d: 9.3; Re–5d: 10.6 eV (J. J. Yeh, I. Lindau, *At. Data Nucl. Data Tables 32* (1985) 1); b) X_α calculations were carried out in spin-unpolarized form using the XASW program by M. Cook and D. A. Case (D. A. Case, *Annu. Rev. Phys. Chem. 33* (1982) 151; *Quantum Chemistry Program Exchange*, Bloomington, IN 47405 (USA), Program 465). In contrast to the markedly localized Re–Re σ-bonding orbital ($E(\sigma) = -7.7$ eV with 61% Re contribution) the expected Re–Re π-bonding orbital splits significantly due to strong Re–S interactions ($E(\pi_1) = -8.1$ eV with 35% Re contribution and $E(\pi_2) = -5.0$ eV with 34% Re contribution, whereby the energetically destabilized orbital (π_2) lies at almost the same energy with the Re–Re δ^* antibonding orbital ($E(\delta^*) = -5.1$ eV with 51% Re contribution) in the region of the frontier orbitals (HOMO-LUMO). This can explain the small μ_{eff} value at room temperature ($\approx 0.4\ \mu_B$) (Further details will be published later).

[10] A. Müller, V. Wittneben, U. Kuetgens, J. Hormes, unpublished.

[11] X_α calculations, XPS data, and energies from XANES spectra in the region of the S–K edge show that, e.g., the HOMO t_1 and the LUMO $2e$ in the simplest system, namely $[ReS_4]^-$ are, e.g., stabilized by about 1 eV compared to $[MoS_4]^{2-}$, whereby the LUMO in the case of $[ReS_4]^-$ contains more S contributions [10] (corresponding to stronger Re–S interaction; cf. also thermodynamic stability corresponding to Equation (a)). This results, e.g., in the Re cluster compounds of the type $[(FeCl_2)_2(MS_4)]^{n-}$ (M = V, Mo, W, Re) taking up one electron "more" under the same conditions [Eq. (c)], and in $[ReS_4]^-$, in contrast to $[MoS_4]^{2-}$ and $[WS_4]^{2-}$, being reduced reversibly [7b]. See also A. Müller, R. Jostes, K. Schmitz, E. Krickemeyer, H. Bögge, E. Bill, A. Trautwein, *Inorg. Chim. Acta 149* (1988) 9.

$$[MS_4]^{n-} \xrightarrow{FeCl_2} [(FeCl_2)_2(MS_4)]^{n-} \qquad (c)$$

M = V, Mo, W: 12 d-electrons;
M = Re: 13 d-electrons,

[12] E. I. Stiefel, T. R. Halbert, C. L. Coyle, L. Wei, W.-H. Pan, T. C. Ho, R. R. Chianelli, M. Daage, *Polyhedron 8* (1989) 1625; A. Müller *ibid. 5* (1986) 323.

[13] Cf. e.g., A. Müller, E. Krickemeyer, M. Penk, V. Wittneben, J. Döring, *Angew. Chem. 102* (1990) 85; *Angew. Chem. Int. Ed. Engl. 29* (1990) 88.

[14] This is true for several processes, e.g., (catalytic) HDS, where the increase in HDS activity on going from Mo/WS_2 to ReS_2 correlates with the results of this work (high degree of mixing of the Re-5d and S-3p functions, whereby, however, the metal–metal interaction in ReS_2 is greater); cf. T. A. Pecoraro, R. R. Chianelli, *J. Catal. 67* (1981) 430; S. Harris, R. R. Chianelli, *ibid. 86* (1984) 400; R. R. Chianelli, *Catal. Rev. Sci. Eng. 26* (1984) 361; S. Kasztelan, *Catal. Lett. 2* (1989) 165; W. H. Davenport, V. Kollonitsch, C. H. Kline, *Ind. Eng. Chem. 60* (1968) 10; R. Colton: *The Chemistry of Rhenium and Technetium*, Wiley, London 1965.

[15] A. Müller, W. Eltzner, R. Jostes, H. Bögge, E. Diemann, J. Schimanski, H. Lueken, *Angew. Chem. 96* (1984) 355; *Angew. Chem. Int. Ed. Engl. 23* (1984) 389, and references cited therein.

Switch Peptides: pH-Induced α-Helix to β-Sheet Transitions of Bis-amphiphilic Oligopeptides**

By *Manfred Mutter,* R. Gassmann, U. Buttkus,* and *K.-H. Altmann*

The de novo design of peptides and proteins exhibiting well-defined structural and functional properties has developed into an area of major theoretical as well as practical interest.[1] Of particular importance for the construction of novel proteins is the understanding of the conformational properties of amphiphilic peptides, where secondary structure formation in aqueous solution is usually associated with the formation of multimeric aggregates.[1a–c, 2] Apart from the intrinsic tendency of the constituent amino acid residues to form α-helix or β-sheet structures, ordered conformations of this type of peptides are stabilized by hydrophobic interactions within the intermolecular aggregates; thus, the process of self-association of amphiphilic peptides in aqueous solution may be regarded as a model for the folding of globular proteins that mimics the effect of long-range interactions in protein folding.[3] While the intrinsic propensity of various types of model peptides (including amphiphilic sequences) for α-helix[4] or β-sheet[5] formation has been studied in great detail, very little is known about α-helix to β-sheet transitions in such systems. Although temperature- and solvent-induced $\alpha \rightarrow \beta$ transitions have been previously observed for homo*poly*peptides[6] and solvent-induced (reversible) $\alpha \rightleftharpoons \beta$ transitions have been recently reported for amphiphilic *oligo*peptides,[2d] amphiphilic sequences exhibiting reversible $\alpha \rightleftharpoons \beta$ transitions under purely aqueous conditions have not been described so far.

We now report on the design and conformational properties of *oligo*peptides that are amphiphilic with respect to α-helix and β-sheet formation. Due to the major contribution of intramolecular hydrophobic interactions to the stabilization of amphiphilic α-helices as well as β-structures, these peptides ("switch peptides") should posses the potential for reversible conformational transitions of the type $\alpha \rightleftharpoons \beta$ in aqueous solution; that is they should switch between two different (ordered) conformational states depending on the experimental conditions such as pH, temperature, salt concentration, etc. (Fig. 1).

The general principles for the design of switch are outlined in Figure 2. Starting from the repetitive pattern of an amphiphilic β-sheet (alternating arrangement of hydrophilic and hydrophobic residues as in **I**), hydrophobic (hydrophilic) residues located on what is supposed to become the

[*] Prof. Dr. M. Mutter, Dr. R. Gassmann, Dipl.-Biochem. U. Buttkus, Dr. K.-H. Altmann
Séction de chimie, Université de Lausanne
Rue de la Barre 2, CH-1005 Lausanne (Switzerland)

[**] This work was supported by the Swiss National Science Foundation and the Agassiz Foundation. We thank Dr. *F. Raschdorf* Ciba-Geigy AG, Basel, for mass spectrometry analyses.

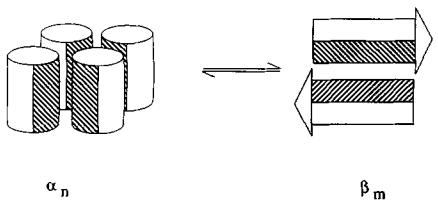

Fig. 1. Schematic representation of the conformational transition between an aggregated α-helical state and a bilayer sheet (β-structure); n, m denote the (unknown) respective degree of aggregation. The conformational transition may be induced by a change in the experimental conditions (concentration, temperature, pH, or solvent).

hydrophilic (hydrophobic) face of the helical cylinder are replaced by indifferent that is, neither polar nor hydrophobic) amino acids (Fig. 2, **II** → **III**). These manipulations result in a primary sequence that is amphiphilic in nature with respect to an α-helical (Fig. 2, **III**) as well as a β-sheet conformation (Fig. 2, **IV**) and the switch peptides obtained in this

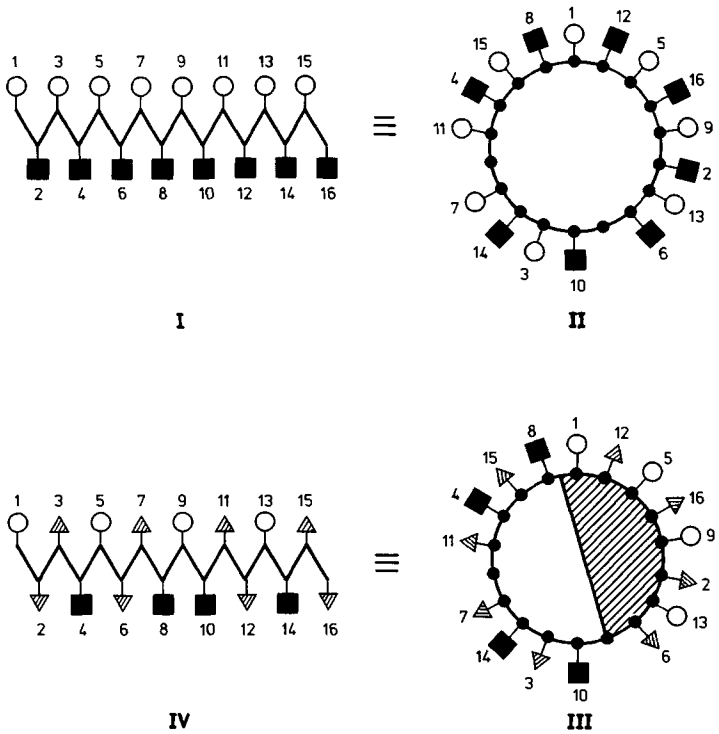

Fig. 2. Design of switch peptides. Left: Schematic representation of a β-sheet conformation for the starting sequence (**I**) and the final switch peptide sequence (**IV**). Right: Helical wheel representation [7] of the starting sequence (**II**) and a final switch peptide sequence (**III**). Note that sequence **II** is still identical with **I** and **IV** with **III**. Cycles, squares, and triangles denote hydrophilic, hydrophobic, and neutral residues, respectively.

way exhibit the following general sequence (shown for a chain length of 16 residues, which is the length of the peptides studied in this paper):

P–N–N–H–P–N–N–H–P–H–N–N–P–H–N–N **A**

P=hydrophilic (polar), H=hydrophobic, N=indifferent (neutral) amino acid residues

As the first representative examples of this new class of peptides, we have designed four sequences comprising 16 amino acid residues each, using Leu, Lys or/and Glu, and Ala as hydrophobic (H), hydrophilic (P), and neutral (N) residues, respectively (Scheme 1). While peptides **1** and **2** contain only one type of ionizable group, **2** and **4** each contain an equal number of Lys and Glu residues in an (i, i+4) sequence relationship.[4b] The chain length of the peptides was chosen to be well above the critical length for α-helix and β-sheet formation[4, 5] in order to ascertain a sufficient general potential for the formation of either secondary structure.

1 Ac-EAALEAALELAAELAA-NH_2
2 Ac-KAALKAALKLAAKLAA-NH_2
3 Ac-KAALEAALKLAAELAA-NH_2
4 Ac-EAALKAALELAAKLAA-NH_2

Scheme 1. Amino acid sequences of switch peptides **1**–**4**. A = alanine, L = leucine, E = glutamic acid, K = lysine, Ac = acetyl.

As a general feature, all peptides investigated undergo pH-induced, reversible conformational transitions from helical to β-sheet conformations and vice versa (Fig. 1). As demonstrated by the CD spectra (Fig. 3, left), peptide **1** clearly exists in a β-structure conformation at pH 4, while it adopts a partially helical conformation at pH ≥ 7. Based on $[\theta]_{222}$ a helix constant of 23% may be calculated at pH 7 and 25 °C by using α-helix poly-L-Lys as a reference.[8] It is interesting that the spectra obtained at pH 5 and pH 6 (transition region) display very unusual curve shapes that are not observed for simple helix-coil or β-structure-coil transitions.[4, 5] For peptide **2** the conformational transition (partial) helix ⇌ β takes place at pH ~ 4.5: peptide **2** exists in a partially helical conformation at pH 2 and pH 3 (helix content at pH 3 ca. 19%), while only β-structure formation is observed for pH ≥ 6. In contrast to peptides **1** and **2**, peptide **3** exhibits *three* pH-induced conformational transitions at pH ≈ 5, pH ≈ 8, and pH ≈ 10. As can be seen in Figure 3, right the CD spectra of peptide **3** at pH 3 and pH 9 are characteristic for peptides in a predominantly α-helical conformation with an estimated helix content of 60% and 53%, respectively. On the other hand, the spectra observed at pH 7 and pH 11 are indicative of predominant and complete β-structure formation, respectively—the assigment of the former spectrum is based on the location of the negative Cotton effect at 218 nm as well as the lack of any pronounced minimum between 200 and 210 nm.[8] Likewise, three conformational transitions are observed for peptide **4**, which, for example, adopts a helical conformation at pH 3 (48% helicity)

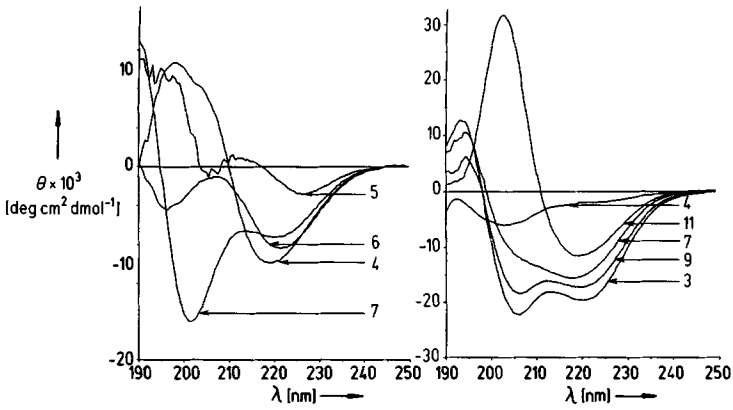

Fig. 3. CD-spectra, left of peptide **1** (c = 0.5 mg mL^{-1}) and right of peptide **3** (c = 0.5 mg mL^{-1}) in aqueous solution at different pH values.

and pH 7 (66 % helicity); β-structure formation occurs at pH 5 and 6 and at pH 10. The high tendency of peptides **1**–**4** to switch between helical and β-sheet conformations is further documented by the sensitivity of the specific conformational features to minor changes in the experimental conditions other than pH. For example, a $\beta \rightarrow \alpha$ transition is observed for peptide **4** at pH 10 upon dilution from 0.5 mg mL^{-1} (Fig. 3, right) to ca. 0.25 mg mL^{-1}. Similarly, addition of increasing amounts of 2,2,2-trifluoroethanol (TFE) to an aqueous solution of peptide **3** at pH 11 results in a $\beta \rightarrow \alpha$ transition between TEF concentrations of 20 and 30 %. In pure TFE only α-helical conformations are observed in all four cases.

In summary, these data demonstrate that peptides displaying sequence regularities that allow for the formation of amphiphilic structures in either a α-helical or a β-sheet conformation do indeed undergo medium-induced conformational transitions of the type $\alpha \rightleftharpoons \beta$ under purely aqueous conditions. What exactly determines the preference for one or the other type of secondary structure under different sets of experimental conditions remains elusive at this stage. However, it is reasonable to conclude that the occurrence of a particular conformation under certain experimental conditions (but not others) is mainly dominated by factors related to the intermolecular association process (i.e. intermolecular hydrophobic interactions) rather than by the intrinsic tendency of the peptides to adopt a specific type of secondary structure (short range interactions). This view is supported by the fact that β-sheet formation is favoured over helix formation under a variety of experimental conditions, despite the much higher probability predicted for a helical conformation ($\langle P_\alpha \rangle = 1.39$, $\langle P_\beta \rangle = 0.92$ for peptides **3** and **4**.[9] Furthermore, a number of recent studies demonstrated that sequential oligopeptides that have similar sequences as peptides **1**–**4** but are nonamphiphilic in nature do not form β-structures in aqueous solution.[4b–d, 4h] In all those cases α-helical structures were observed as the only type of ordered conformation. Conformational transitions of peptides are accompanied by distinct changes in their physicochemical and functional properties like solvation, association state, membrane activity, and catalytic and biological activity.[2, 10] In a very recent report on the CD4-binding properties of 15-residue peptides related to the CD4-binding domain of gp 120 from HIV I it was also suggested that a conformational switch of the type $\beta \rightarrow \alpha$ is essential for binding to the receptor.[11] The detailed elucidation of the structural determinants (e.g., nature of the amino acid residues, chain length) that govern the unique conformational properties of peptides **1**–**4** should make possible the design of peptides exhibiting tailor-made, medium-induced conformational transitions. These switch peptides may then serve as conformational modules (relay systems) in a number of applications. Furthermore, they should be a versatile tool for the investigation of the structural and dynamic factors involved in secondary and tertiary structure formation. Clearly, switch peptides should represent a much more adequate model system than (exclusively) helix-forming nonamphiphilic peptides for promoting a better understanding of the conformational preferences of the different amino acids in proteins. Not only does intermolecular aggregation of switch peptides approximate the occurrence of long-range interactions during protein folding, but in constrast to α-helical model systems[4f–g] they are also unbiased with respect to any particular type of secondary structure. This should, in principle, allow the elucidation of secondary structure potentials not only in relation to a random coil state but also in relation to an alternative type of ordered conformation.

Experimental

Peptide synthesis: All peptides were synthesized by the solid-phase method [12] (Fmoc/*t*Bu strategy [13]) on an Advanced ChemTech ACT II peptide synthesizer (semi-automatic operation) using Rink's amide resin [14]. Double couplings were performed in DMF/CH_2Cl_2 (3:2) for 90 min (first coupling) and in DMF for 60 min (second coupling) by using a 3.5-fold and 2-fold excess, respectively, of the preformed 1-hydroxybenzotriazole (HOBt) ester (preactivation with diisopropylcarbodiimide (DIC)/HOBt in DMF for 15 min). Three equivalents of Hünig's base (DIEA) were added to the reaction mixture directly after active ester addition. The Fmoc group was removed by treatment with 20 % piperidine/DMF for 2 and 15 min. After the last Fmoc removal the *N*-terminus was acetylated and the peptide was cleaved from the resin by treatment with CF_3COOH/CH_2Cl_2/ethanedithiol/thioanisole (75:22:1:2) for 45 min at room temperature. The resin was removed by filtration, washed, and the combined filtrates concentrated in vacuo. The peptides were precipitated with ether and isolated by centrifugation. Crude yields of 230–340 mg were obtained starting from 0.8 g of Fmoc protected resin (0.38 mmol Fmoc g^{-1}). The crude peptides were purified by preparative RP-HPLC (Waters Delta Prep 3000 Preparative Chromatography System) on a Vydac RP C18 column (2.5 × 20 cm). (Gradient elution with 0.05 % CF_3COOH/CH_3CN (B) into 0.05 % CF_3COOH/H_2O (A). **1**: 40 % B to 55 % B in 30 min; **2**: 30 % B to 55 % B in 20 min; **3**: 20 % B to 45 % B in 15 min; **4**: 35 % B to 50 % B in 15 min). According to analytical RP-HPLC the peptides were > 95 % pure and gave correct amino acid analyses.

CD spectroscopy: CD spectra were recorded on a Jobin Yvon Mark VI Dichrograph at 23 °C. Samples were prepared by dilution of stock solutions whose concentrations had been determined by amino acid analysis. Sample concentrations were 0.5 mg mL^{-1}.

Received: June 14, 1991 [Z 4710 IE]
German version: *Angew. Chem. 103* (1991) 1504

CAS Registry numbers:
1, 136795-88-5; **2**, 136795-89-6; **3**, 136795-90-9; **4**, 136822-55-4.

[1] a) M. Mutter, *Angew. Chem. 97* (1985) 639; *Angew. Chem Int. Ed. Engl. 24* (1985) 639; b) W. F. DeGrado, Z. R. Wasserman, J. D. Lear, *Science 243* (1989) 622; c) M. Mutter, S. Vuilleumier, *Angew. Chem. 101* (1989) 551; *Angew. Chem. Int. Ed. Engl. 28* (1989) 535; d) J. S. Richardson, D. C. Richardson, *Trends Biochem. Sci. 14* (1989) 904.

[2] a) E. T. Kaiser, F. J. Kézdy, *Science 223* (1984) 249; b) D. Eisenberg, W. Wilcox, S. M. Eshita, P. M. Pryciak, S. P. Ho, W. F. DeGrado, *Proteins 1* (1986) 16; c) S. P. Ho, W. F. DeGrado, *J. Am. Chem. Soc. 109* (1987) 6751; d) M. Mutter, R. Hersperger, *Angew. Chem. 102* (1990) 195; *Angew. Chem. Int. Ed. Engl. 29* (1990) 185.

[3] For recent reviews on protein folding, see for example: a) G. T. Montelione, H. A. Scheraga, *Acc. Chem. Res. 22* (1989) 70; b) R. L. Baldwin, *Trends Biochem. Sci. 14* (1989) 291; c) T. E. Creighton, *Biochem. J. 270* (1990) 1; d) R. Jaenicke, *Biochemistry 30* (1991) 3147.

[4] See, for example: a) M. Mutter, K.-H. Altmann, A. Flörsheimer, J. Herbert, *Helv. Chim. Acta 69* (1986) 786; b) S. Marqusee, R. L. Baldwin, *Proc. Natl. Acad. Sci. USA 84* (1987) 8898; c) S. Padmanabhan, S. Marqusee, T. Ridgeway, T. M. Laue, R. L. Baldwin, *Nature 344* (1990) 268; d) G. Merutka, W. Lipton, W. Shalongo, S. H. Park, E. Stellwagen, *Biochemistry 29* (1990) 7511; e) K. T. O'Neil, W. F. DeGrado, *Science 250* (1990) 646; f) P. C. Lyu, M. F. Liff, L. A. Marky, N. R. Kallenbach, *ibid. 250* (1990) 669; g) J. Wojcik, K.-H. Altmann, H. A. Scheraga, *Biopolymers 30* (1990) 12; h) G. Merkuta, E. Stellwagen, *Biochemistry 30* (1991) 1591.

[5] See for example: a) M. Mutter, F. Maser, K.-H. Altmann, G. M. Bonora, C. Toniolo, *Biopolymers 24* (1985) 1057; b) D. G. Ostermann, E. T. Kaiser, *J. Cell. Biochem. 29* (1985) 57; c) W. F. DeGrado, J. D. Lear, *J. Am. Chem. Soc. 107* (1985) 7684; d) K.-H. Altmann, A. Flörsheimer, M. Mutter, *Int. J. Pept. Protein Res. 27* (1986) 314; e) G. M. Bonora, C. Toniolo, J. H. Jones, K. N. Rajasekharan, *ibid. 27* (1986) 1.

[6] See for example: a) G. D. Fasman (Ed.): *Poly-α-Amino Acids*, Dekker, New York 1967; b) N. Greenfield, B. Davidson, G. D. Fasman, *Biochemistry 6* (1967) 1630; c) S.-Y. C. Wooley, G. Holzwarth, *ibid. 9* (1970) 3604; d) G. Ebert, Y. Kuroyanagi, *Int. J. Biol. Macromol. 5* (1983) 109; e) G. Ebert, *Top. Curr. Chem. 128* (1985) 1.

[7] M. Schiffer, A. B. Edmundson, *Biophys. J. 7* (1967) 121.

[8] N. Greenfield, G. D. Fasman, *Biochemistry 8* (1969) 4108.

[9] P. Y. Chou, G. D. Fasman, *Adv. Enzymol. 47* (1978) 45.

[10] a) S. Abd El Rahman, H. Anzinger, M. Mutter, *Biopolymers 19* (1980) 173; b) J. W. Taylor, G. Ösapay, *Acc. Chem. Res. 23* (1990) 338; c) A. Seelig, M. Mutter, L. Kürz, unpublished; d) V. Steiner, M. Mutter, *J. Chromatogr.*, in press.

[11] J. Reed, V. Kinzel, *Biochemistry 30* (1991) 4521.

[12] G. Barany, R. B. Merrifield in E. Gross, J. Meienhofer, (Eds.): *Peptides – Analysis, Synthesis, Biology, Vol. 2*, Academic, New York 1980, p. 3.

[13] G. B. Fields, R. L. Noble, *Int. J. Pept. Protein Res. 35* (1990) 161.

[14] H. Rink, *Tetrahedron Lett. 28* (1987) 3787.

Photolytic Cleavage of DNA by $[Pt_2(P_2O_5H_2)_4]^{4-}$ **

By *William A. Kalsbeck, Neena Grover,* and *H. Holden Thorp**

The oxidative cleavage of DNA by metal complexes has attracted the interest of chemists interested in drug applications and the design of synthetic restriction enzymes.[1] Oxidative DNA cleavage reactions mediated by $[Fe(edta)]^{2-}$ have also been used to image unusual structures, such as helical twists and bent DNA, by high-resolution gel electrophoresis.[2] In the $[Fe(edta)]^{2-}$ system, the anionic metal complex does not bind to the DNA and generates $(OH)^{\bullet}$ in the bulk solution. Cleavage via abstraction of ribose H atoms by $(OH)^{\bullet}$ is therefore more efficient in regions of the DNA that are more exposed to the bulk solvent; quantitation of the cleavage efficiency by electrophoresis therefore allows for structural imaging. We hope to develop a highly discriminating imaging reagent by finding an anionic metal complex that can cleave DNA without binding and without generating a high-energy intermediate, such as $(OH)^{\bullet}$, $(O_2)^{\bullet-}$, or $^1O_2$. The excited state of $[Pt_2(pop)_4]^{4-}$ (**1**, pop = $P_2O_5H_2^{2-}$) fulfills these initial criteria.

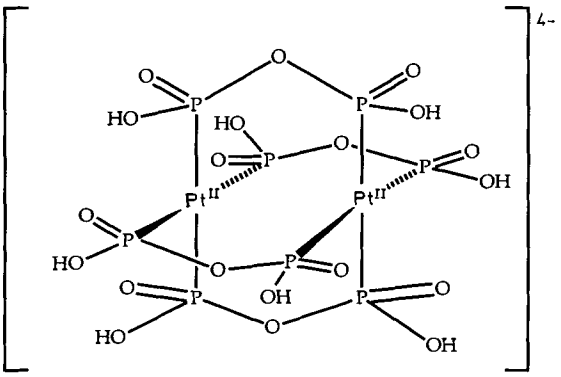

1

The d^8-d^8 dimer **1** is an effective photoreagent for H atom abstraction reactions such as the oxidation of alcohols and hydrocarbons (Eq. (a)–(c)).[3, 4] The reactive ($d\sigma^* \rightarrow p\sigma$) excited state is populated by irradiation at 367 nm ($^1A_{1g} \rightarrow {}^1A_{2u}$, $\varepsilon = 35000\ M^{-1}cm^{-1}$) or 435 nm ($^1A_{1g} \rightarrow {}^3A_{2u}$, $\varepsilon = 110\ M^{-1}cm^{-1}$);[5] the long-lived ($\tau = 9.5\ \mu s$) triplet state is responsible for the oxidative activity. The dihydride species retains the Pt–diphosphonate framework, coordinating the two H^- ligands in open axial positions.[4] Irradiation at 458 nm of **1** in the presence of φX174 DNA leads to complete conversion of supercoiled DNA (form I) into nicked DNA (form II) in 20 min (Fig. 1, lane D) under anaerobic conditions at an ionic strength of 50 mM.[6] As seen in the controls, no significant cleavage occurs upon irradiation in the absence of **1** (lane F) or incubation with **1** in the dark (lane G).

$$[Pt_2^{II}(pop)_4]^{4-} \xrightarrow{h\nu} \{[Pt_2^{II}(pop)_4]^{4-}\}^{\bullet} \quad \text{(a)}$$

1 → **1***

$$\mathbf{1}^* + \text{OH} \xrightarrow{\text{H atom transfer}} [Pt^{II}Pt^{III}(pop)_4H]^{4-} + \text{OH}^{\bullet} \quad \text{(b)}$$

2

$$2\,\mathbf{2} \longrightarrow \mathbf{1} + [Pt_2^{III}(pop)_4H_2]^{4-} \quad \text{(c)}$$

3

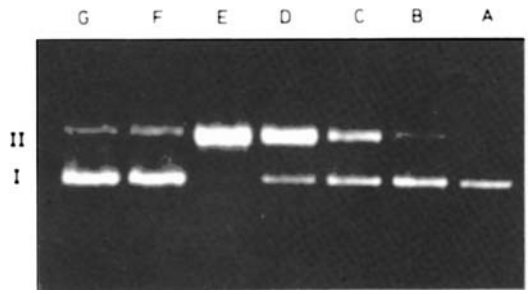

Fig. 1. 1% Agarose gel showing the results of electrophoresis of solutions of 60 μM φX174 DNA (50 mM phosphate, pH 7) containing (A) no platinum and 40 μM $K_4[Pt_2(pop)_4]$ after photolysis at 458 nm for (B) 2 min, (C) 5 min, (D) 10 min, (E) 20 min; (F) 60 μM φX174 DNA that has been photolyzed for 20 min; (G) 60 μM φX174 DNA that has been incubated with 40 μM $K_4[Pt_2(pop)_4]$ for 2 h in the dark. Concentrations of DNA are expressed as nucleotide phosphate.

It is clear that photocleavage is occurring via direct reaction of the excited state of **1** with the DNA. The excited-state, one-electron oxidation potential (ca. 0.7 V vs. saturated calomel electrode) is far too low for generation of $(OH)^{\bullet}$.[3, 7] The reaction is performed in the absence of O_2, so we can rule out the intermediacy of $^1O_2$ and $(O_2)^{\bullet-}$.[8] Furthermore, in the oxidation of organic substrates direct H atom abstraction by the excited state of the complex is the demonstrated reaction pathway [Eq. (b)].[4]

If **1** does not bind to DNA but cleaves by direct collision of the excited state with the double helix, the reaction efficiency should increase with solution ionic strength. At higher ionic strength, electrostatic repulsions between the tetraanionic **1** and the DNA polyanion will be lower,[9] facilitating approach of the excited metal complex to the DNA sugars. Figure 2 shows that increasing the solution ionic strength from 50 mM (lane A) to 150 mM (lane D) significantly in-

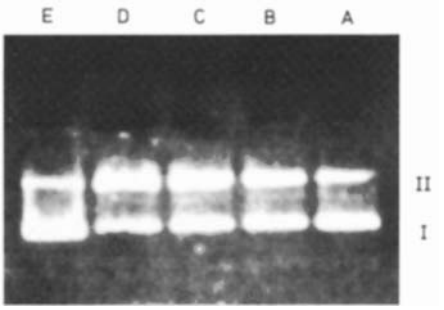

Fig. 2. 1% Agarose gel showing the results of electrophoresis of 60 μM φX174 DNA photolyzed in the presence of 20 μM $K_4[Pt_2(pop)_4]$ for 5 min in pH 7 phosphate buffer at ionic strengths of (A) 50 mM, (B) 75 mM, (C) 100 mM, (D) 150 mM; (E) φX174 DNA control.

[*] Prof. H. H. Thorp, W. A. Kalsbeck, N. Grover
Department of Chemistry
North Carolina State University
Raleigh, NC 27695-8204 (USA)

[**] This work was supported by the National Science Foundation (Presidential Young Investigator Award, CHE-9157411), the Camille and Henry Dreyfus Foundation (New Faculty Award) and the North Carolina Biotechnology Center (Academic Research Initiation Grant).

creases the cleavage efficiency.[10] If the complex were bound to DNA, we would expect to see the efficiency *decrease*; if $(OH)^{\bullet}$ or $^1O_2$ were generated, we would expect at most a very small effect of ionic strength on the cleavage efficiency.

The final product of the reaction is the d^7-d^7 dimer $[Pt_2(pop)_4(H_2O)_2]^{2-}$ (**4**). We have detected the conversion of **1** into **4** by optical spectroscopy of calf thymus DNA solutions irradiated at 458 nm under N_2. This conversion is characterized by an isosbestic point at 306 nm (λ_{max} (**4**) = 245 nm).[5, 11] The $[Pt_2^{III}H_2]^{4-}$ species is known to eliminate H_2 in aqueous solution,[4] and we therefore propose the mechanism shown in Equations (d)–(f).

$$\mathbf{1}^{*} + \text{DNA (form I)} \xrightarrow{\text{H atom transfer}} \mathbf{2} + \text{DNA (form II)} \quad \text{(d)}$$

$$2\,\mathbf{2} \longrightarrow \mathbf{1} + \mathbf{3} \quad \text{(e)}$$

$$\mathbf{3} + 2H_3O^{+} \longrightarrow \underset{\mathbf{4}}{[Pt_2^{III}(pop)_4(H_2O)_2]^{2-}} + 2H_2 \quad \text{(f)}$$

It is now clear that **1** may be a versatile new imaging reagent; approach of the tetraanion excited state to the double helix is certainly more demanding sterically and electrostatically than approach of $(OH)^{\bullet}$, yet not so demanding as to prevent efficient cleavage. Other characteristics of this reaction are also noteworthy because they fulfil a number of general goals in DNA photocleavage.[12] First, we have succeeded in achieving efficient photocleavage with visible light (458 nm), where no background cleavage of the DNA occurs. Second, **1** photocleaves DNA under conditions where there is unambiguously no intervention of species such as $^1O_2$, $(O_2)^{\bullet -}$, or $(OH)^{\bullet}$. Third, the product of the reaction (**4**) still retains the Pt–diphosphonate framework and can be readily converted into **1** with mild reductants. Thus, we might ultimately observe photocatalytic cleavage in the presence of sacrificial reductants, similar to the thermal catalysis of the $[Fe(edta)]^{2-}$[13] and $[Cu(phen)_2]^{2+}$ (phen = 1,10-phenanthroline)[14] systems.

Received: June 24, 1991 [Z 4744 IE]
German version: *Angew. Chem. 103* (1991) 1525

[1] S. M. Hecht, *Acc. Chem. Res. 19* (1986) 83; J. Stubbe, J. W. Kozarich, *Chem. Rev. 87* (1987) 1107; J. K. Barton, *Science (Washington D.C.) 233* (1986) 727; P. B. Dervan, *ibid. 232* (1986) 464; K. Nagai, B. J. Carter, J. Xu, S. M. Hecht, *J. Am. Chem. Soc. 113* (1991) 5099.
[2] T. D. Tullius, B. A. Dombroski, *Science (Washington D. C.) 235* (1985) 679; A. M. Burkhoff, T. D. Tullius, *Nature (London) 331* (1988) 455; A. M. Burkhoff, T. D. Tullius, *Cell (Cambridge, Mass.) 48* (1987) 935.
[3] D. M. Roundhill, H. B. Gray, C.-M. Che, *Acc. Chem. Res. 22* (1989) 55.
[4] E. L. Harvey, A. E. Stiegman, A. Vlcek, H. B. Gray, *J. Am. Chem. Soc. 109* (1987) 5233.
[5] C.-M. Che, L. G. Butler, P. J. Grunthaner, H. B. Gray, *Inorg. Chem. 24* (1985) 4662.
[6] $K_4[Pt_2(pop)_4]$ was prepared as described in [5]. Solutions were irradiated at 458 nm with an Ar ion laser at an incident power of 250 mW. Solutions were degassed with N_2 prior to photolysis and N_2 bubbling was continued throughout the reaction. φX174 DNA was purchased from Pharmacia and used as received. Solutions were electrophoresed for 1 h at 44 V, and the gels were stained with ethidium bromide and photographed under UV light.
[7] We also observe cleavage in the presence of sodium formate, an efficient scavenger of $(OH)^{\bullet}$: J. D. Rush, Z. Maskos, *Inorg. Chem. 29* (1990) 897.
[8] We have performed the photolysis both with and without degassing the solution and find that degassing has no effect on the cleavage efficiency. Thus, it appears that even in aerated solutions, an O_2-dependent pathway is not involved.
[9] C. R. Cantor, P. R. Schimmel: *Biophysical Chemistry. Part III: The Behavior of Biological Macromolecules*, Freeman, New York 1980.
[10] Densitometry shows that the yield of cleavage in Figure 2 is 10% in lane A and 65% in lane D.
[11] Optical spectra were recorded using an HP 8452 diode array spectrophotometer. Calf thymus DNA was purchased from Sigma and used as described in M. T. Carter, M. Rodriguez, A. J. Bard, *J. Am. Chem. Soc. 111* (1989) 8901.
[12] A. M. Pyle, T. Morii, J. K. Barton, *J. Am. Chem. Soc. 112* (1990) 9432; A. M. Pyle, E. C. Long, J. K. Barton, *ibid. 111* (1989) 4520; M. B. Fleisher, K. C. Waterman, N. J. Turro, J. K. Barton, *Inorg. Chem. 25* (1986) 3551.
[13] R. P. Hertzberg, P. B. Dervan, *J. Am. Chem. Soc. 104* (1982) 313.
[14] T. P. Thederahn, M. D. Kuwabara, T. A. Larsen, D. S. Sigman, *J. Am. Chem. Soc. 111* (1989) 4941.

7,7′-Bi(dispiro[2.0.2.1]heptylidene)—the Perspirocyclopropanated Bicyclopropylidene**

By *Stephan Zöllner, Herwig Buchholz, Roland Boese, Rolf Gleiter,* and *Armin de Meijere**

Dedicated to Professor Michael Hanack on the occasion of his 60th birthday

Unsubstituted bicyclopropylidene **1**[1] is in itself already an unusual tetrasubstituted alkene;[2] due to its high-lying HOMO[3] and its strained double bond,[4] it is particularly reactive towards electrophiles.[5] Four or eight methyl substituents, as in **2** and **3**, respectively, lower the π-ionization energy[6] and thus increase the nucleophilicity, though spiroannelated cyclopropane rings are more reactive, as evidenced[8] by the He(I)-photoelectron spectrum of 7-cyclopropylidenedispiro[2.0.2.1]heptane (**4**).[7] The ultimate reactivity in this series may very well be observed in the case of the hitherto unknown perspirocyclopropanated bicyclopropylidene **5**. Even if this should not be reflected in the position of the π-HOMO, the nucleophilicity of **5** could still surpass that of the perspirocyclopropanated bicyclobutylidene **6** described by us in an earlier work.[9]

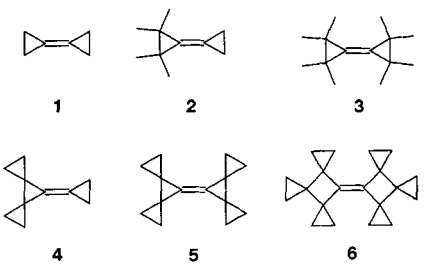

Of several possible routes to **5** that were tried out, one finally led to the target compound (Scheme 1). The starting material was the readily accessible compound **4**,[7] which smoothly furnished—via the dibromocarbene adduct **7**[10]

[*] Prof. Dr. A. de Meijere[+], Dr. S. Zöllner, Dipl.-Chem. H. Buchholz
Institut für Organische Chemie der Universität
Martin-Luther-King-Platz 6, W-2000 Hamburg 13 (FRG)
Dr. R. Boese
Institut für Anorganische Chemie der Universität-GH Essen (FRG)
Prof. Dr. R. Gleiter
Institut für Organische Chemie der Universität Heidelberg (FRG)
[+] New address:
Institut für Organische Chemie der Universität
Tammannstrasse 2, W-3400 Göttingen (FRG)

[**] This work was supported by the Deutsche Forschungsgemeinschaft and the Fonds der Chemischen Industrie. We thank Hoechst AG, Hüls AG and BASF for generous gifts of chemicals. *H. B.* thanks the Hermann-Schlosser-Stiftung for a fellowship.

(66% yield after chromatography)—the cyclopropylidene(dispiro[2.0.2.1]heptylidene)methane **8**[10] (84%). Analogous to the first synthesis of [3]rotane[11] from bicyclopropylidene **1** and diazocyclopropane,[12] the treatment of **8** with diazocyclopropane generated in situ furnished, besides the fourfold spirocyclopropanated [3]rotane **10**[10, 13, 14] (8% yield, based on reacted **8**) and 11-cyclopropylidenetetraspiro[2.0.0.2.0.2.0.1]undecane (**9**)[10] (7%), the title compound 7,7'-bi(dispiro[2.0.2.1]heptylidene) (**5**)[10] as the main product (31% yield, based on reacted **8**). Decisive for a satisfactory conversion of the allene **8** (up to 65%) was that a relatively dilute solution of **8** in *n*-pentane was treated at 0°C with 1.7 equiv of *N*-cyclopropyl-*N*-nitrosourea[15] and 25 equiv of solid sodium methoxide.

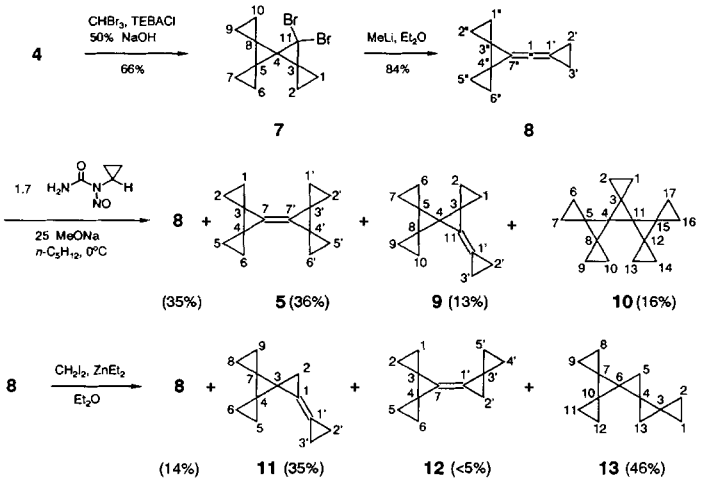

Scheme 1. TEBACl = benzyltriethylammonium chloride.

The selectivity of the attack of diazocyclopropane at the sterically less shielded double bond of **8**, which is favorable for the formation of **5**, is not observed in the Simmons–Smith cyclopropanation with diiodomethane/diethylzinc[16] (Scheme 1, bottom). The smaller reagent preferentially attacks at the central double bond, which is obviously more reactive due to strain; this affords predominantly **11** (35%) and the product of double cyclopropanation **13**[17] (46%), besides small amounts of **12** (<5%).

The products **5**, **9**, and **10** and the main products **11** and **13** of the carbene additions to **8** could be separated by chromatography on silica gel. Upon recrystallization from methanol, **5** and **10** precipitated as crystals that were suitable for X-ray structure analyses (Fig. 1).[18] The most striking structural features of **5** and **10** are the differences in lengths between the proximal and distal bonds in the external cyclopropane rings, while all CC bonds in the internal cyclopropane rings are shortened.[19] Both of these features are a consequence of the increased strain, along with the accompanying changes in hybridization.[20] The double bond in **5** (130.5(4) pm) is almost the same length as that in bicyclopropylidene **1** (130.4(8) pm[4]). Accordingly, the hybridization of the central C atoms is scarcely altered by the fourfold spiroannelation,[20] and the electronic properties of the double bond are largely determined by the four α-cyclopropane groups. The result is an ionization energy of 8.20 eV, which is significantly lower than that of the octamethyl derivative **3** (IE_{iv} = 8.35 eV).[6]

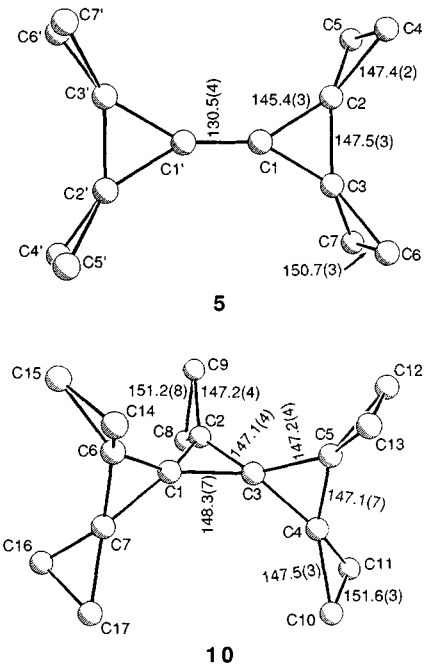

Fig. 1. Structures of **5** and **10** in the crystal. The bond lengths [pm] are determined in each case via the *mmm* symmetry, and in the case of **10** also via two independent molecules in the asymmetric unit. The numbering does not agree with that recommended by IUPAC and used in Table 1.

In contrast to bicyclopropylidene **1**, which reacts with bromine[21] and many other electrophiles[5e] with rearrangement, the perspirocyclopropanated **5** reacts with hydrogen bromide and bromine in *n*-pentane at −15°C to give, without rearrangement, the respective products **15a** (≥95%) and **15b** (≥95%, isolated 71%). This can be taken as an

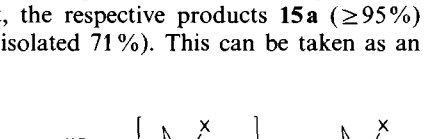

Table 1. Physical and spectroscopic data of important new compounds [10]. Signal assignments marked with an asterisk are uncertain; a dash signifies a negative signal in the DEPT ^{13}C-NMR spectrum.

5: white solid, m.p. 115°C (subl.); Raman (powder): $\tilde{\nu}$ = 1868 cm^{-1} (C=C), 1487, 1448, 1421, 1301, 1004, 956, 914, 887, 791, 620, 410; ^{1}H NMR (250 MHz, $CDCl_3$): δ = 0.99, 1.01 (AA'BB', 16H); ^{13}C NMR (62.9 MHz, $CDCl_3$, additional DEPT): δ = 8.8 (−, C-1(1',2,2',5,5',6,6')), 16.1 (C_{quat}, C-3(3',4,4')), 115.0 (C_{quat}, C-7(7')).—**7**: white solid, m.p. 84°C; IR (KBr): $\tilde{\nu}$ = 3070 cm^{-1}, 2994, 1499, 1436, 1419, 1216, 1138, 1115, 1044, 1002, 948, 913, 893, 766, 707; ^{1}H NMR (250 MHz, $CDCl_3$): δ = 0.68 (m, 2H), 0.76 (m, 2H), 0.88 (m, 2H), 1.12, 1.18 (AA'BB', 4H), 1.43 (m, 2H); ^{13}C NMR (62.9 MHz, $CDCl_3$, additional DEPT): δ = 2.6 (−, C-6(9))*, 3.8 (−, C-7(10)), 9.3 (−, C-1(2)), 21.9 (C_{quat}, C-5(8)), 31.5 (C_{quat}, C-3), 32.9 (C_{quat}, C-4), 41.4 (C_{quat}, C-11). **8**: IR (KBr): $\tilde{\nu}$ = 3073 cm^{-1}, 2993, 2044 (C=C=C), 1415, 1146, 1044, 1000, 951, 885, 811, 758; ^{1}H NMR (250 MHz, C_6D_6): δ = 0.77, 1.06 (AA'BB', 8H), 1.33 (s, 4H); ^{13}C NMR (62.9 MHz, C_6D_6, additional DEPT): δ = 7.6 (−, C-2'(3')), 8.2 (−, C-1''(2'',5'',6'')), 21.3 (C_{quat}, C-3''(4'')), 83.6 (C_{quat}, C-1'), 93.5 (C_{quat}, C-1''), 172.0 (C_{quat}, C-1). **9**: ^{1}H NMR (250 MHz, C_6D_6): δ = 0.60, 0.75 (AA'BB', 4H), 0.94 (m, 4H), 1.02–1.21 (m, 8H); ^{13}C NMR (62.9 MHz, C_6D_6, additional DEPT): δ = 2.4 (−, C-2')*, 2.6 (−, C-3')*, 3.0 (−, C-1(2)), 5.1 (−, C-7(10))*, 6.3 (−, C-6(10))*, 15.9 (C_{quat}, C-3), 21.0 (C_{quat}, C-5(8)), 23.5 (C_{quat}, C-7), 104.5 (C_{quat}, C-1'), 119.1 (C_{quat}, C-11). **10**: m.p. 56–57°C; ^{1}H NMR (250 MHz, $CDCl_3$): δ = 0.47–0.56 (m, 4H), 0.69–0.82 (m, 12H), 0.70 (s, 4H, 9-H_2, 10-H_2); ^{13}C NMR (62.9 MHz, $CDCl_3$, additional DEPT): δ = 1.3 (−, C-1(2)), 3.3 (−, C-6(9,14,16))*, 6.1 (−, C-7(10,13,17))*, 16.7 (C_{quat}, C-3), 17.8 (C_{quat}, C-5-(8,12,15)), 25.9 (C_{quat}, C-4(11)).

indication that a cyclopropyl cation such as **14a**, **b**, or a correspondingly bridged cation survives without *ring opening*. In the ^{13}C NMR spectrum (125 MHz) of the dibromide **15b** at temperatures above + 50 °C two signals are observed for methylene carbon atoms; at lower temperatures (≤ -25 °C) four sharp signals are observed. Accordingly, two conformers of **15b** are present in equilibrium whose interconversion is characterized by a rotation barrier ($\Delta G^{\neq} \approx 14.1$ kcal mol^{-1}, estimated from the coalescence temperature) unusually high for bicyclopropyl derivatives.[22]

Received: July 3, 1991 [Z 4769 IE]
German version: *Angew. Chem. 103* (1991) 1544

[1] a) P. LePerchec, J.-M. Conia, *Tetrahedron Lett. 1970*, 1587; b) L. Fitjer, J.-M. Conia, *Angew. Chem. 85* (1973) 347; *Angew. Chem. Int. Ed. Engl. 12* (1973) 332; c) A. H. Schmitt, U. Schirmer, J.-M. Conia, *Chem. Ber. 109* (1976) 2588; d) W. Weber, A. de Meijere, *Synth. Commun. 16* (1986) 837.
[2] a) R. C. Lord, C. J. Wurrey, *Spectrochim. Acta, Part A 30* (1974) 915; b) F. Gerson, A. de Meijere, X.-Z. Qin, *J. Am. Chem. Soc. 111* (1989) 1135.
[3] R. Gleiter, R. Haider, J.-M. Conia, J.-P. Barnier, A. de Meijere, W. Weber, *J. Chem. Soc. Chem. Commun. 1979*, 130.
[4] M. Traetteberg, A. Simon, E.-M. Peters, A. de Meijere, *J. Mol. Struct. 118* (1984) 333.
[5] a) W. Weber, U. Behrens, A. de Meijere, *Chem. Ber. 114* (1981) 1196; b) D. Kaufmann, A. de Meijere, *ibid. 117* (1984) 3134; c) A. Hofland, H. Steinberg, T. J. de Boer, *Recl. Trav. Chim. Pays-Bas 104* (1985) 350; d) A. de Meijere, H. Wenck, F. Seyed-Mahdavi, H. G. Viehe, V. Gallez, I. Erden, *Tetrahedron 42* (1986) 1291; e) A. de Meijere, I. Erden, W. Weber, D. Kaufmann, *J. Org. Chem. 53* (1988) 152.
[6] F. Seyed-Mahdavi, R. Machinek, R. Gleiter, A. Flatow, M. Spiekermann, A. de Meijere, unpublished results; F. Seyed-Mahdavi, *Diplomarbeit*, Universität Hamburg 1982.
[7] L. Fitjer, *Chem. Ber. 115* (1982) 1035, 1047.
[8] With a value of $IE_{i\pi} = 8.50$ eV, the π-ionization energy of **4** is about 0.1 eV lower than that of **2** ($IE_{v,i} = 8.60$ eV [6]).
[9] H. Wenck, A. de Meijere, F. Gerson, R. Gleiter, *Angew. Chem. 98* (1986) 343; *Angew. Chem. Int. Ed. Engl. 25* (1986) 335.
[10] All the new compounds were completely characterized by spectroscopic methods (^1H NMR, IR, Raman, MS), elemental analyses, and/or crystal structure analyses.
[11] L. Fitjer, J.-M. Conia, *Angew. Chem. 85* (1973) 349; *Angew. Chem. Int. Ed. Engl. 12* (1973) 334.
[12] W. Kirmse, H. Schütte, *Chem. Ber. 109* (1968) 1674.
[13] Systematic name: heptaspiro[2.0.0.2.0.2.0.0.0.2.0.2.0.0]heptadecane. For such hydrocarbons consisting exclusively of spiro-coupled cyclopropane rings the trivial name [n]triangulanes has been proposed: N. S. Zefirov, S. I. Kozhushkov, T. S. Kusnetsova, O. V. Kokoreva, K. A. Lukin, B. I. Ugrak, S. S. Tratch, *J. Am. Chem. Soc. 112* (1990) 7702. **10** is accordingly an [8]triangulane with C_{2v} symmetry [14].
[14] The preparation of the perspirocyclopropanated spiropentane, a [6]triangulane with D_{2d} symmetry, from **4** and diazocyclopropane generated in situ is reported in connection with a general strategy for the synthesis of branched [n]triangulanes. Cf. N. S. Zefirov, S. I. Kozhushkov, B. I. Ugrak, K. A. Lukin, O. V. Kokoreva, D. S. Yufit, Y. T. Struchkov, S. Zöllner, R. Boese, A. de Meijere, *J. Org. Chem. 58* (1992) in press.
[15] *N*-Cyclopropyl-*N*-nitrosourea was obtained by nitrosation of cyclopropylurea analogously to the procedure for *N*-nitroso-*N*-(*trans*-2-methylcyclopropyl)urea: W. Kirmse, H. Urbach, *Chem. Ber. 105* (1972) 8.
[16] Cf. J. Furukawa, N. Kuwabata, J. Nishimura, *Tetrahedron 24* (1968) 53.
[17] The [6]triangulane **13** was prepared independently by another route and thus completely characterized. Cf. [14].
[18] Determination of the crystal structures of **5** and **10**: diffractometer Nicolet R 3m/V, $\lambda(Mo_{K\alpha})$, graphite monochromator, ω-scan, $3° < 2\theta < 45°$, direct methods (SHELXTL-PLUS). **5**: crystal dimensions: $0.24 \times 0.14 \times 0.03$ mm^3, space group $P2_1/c$, $Z = 2$, $T = 210$ K, cell dimensions $a = 696.3(2)$, $b = 1013.4(3)$, $c = 819.1(2)$ pm, $\beta = 102.27(2)°$, 612 independent intensities, 481 observed ($F_0 \geq 4\sigma(F)$), 68 parameters for the structure refinement with hydrogen atoms as rigid groups, $R = 0.037$, $R_w = 0.038$. **10**: crystal dimensions: $0.20 \times 0.12 \times 0.09$ mm^3, space group $P2_1/c$, $Z = 8$, $T = 190$ K, cell dimensions $a = 1135.5(4)$, $b = 888.0(4)$, $c = 2751.5(10)$ pm, $\beta = 100.36(3)°$, 3577 independent intensities, 1803 observed ($F_0 \geq 4\sigma(F)$), 308 parameters for the structure refinement with hydrogen as rigid groups, $R = 0.058$, $R_w = 0.052$. Lower measuring temperatures led, in the case of **5** and **10**, to a deterioration in the quality of the crystals due to reversible phase transformations. Further details of the crystal structure investigations are available on request from the Fachinformationszentrum Karlsruhe, Gesellschaft für wissenschaftlich-technische Information mbH, W-7514 Eggenstein-Leopoldshafen 2 (FRG), on quoting the depository numbers CSD-320287 (for **5**) and CSD-320286 (for **10**), the names of the authors, and the journal citation.
[19] Similar differences in the bond lengths were observed for spiropentane (cf. R. Boese, D. Blaeser, K. Gomann, U. H. Brinker, *J. Am. Chem. Soc. 111* (1989) 1501), [3]rotane (cf. R. Boese, T. Miebach, A. de Meijere, *J. Am. Chem. Soc. 113* (1991) 1743), and for the perspirocyclopropanated spiropentane (cf. [14]).
[20] Cf. M. Eckert-Maksic, S. Zöllner, L. Maksimovic, W. Göthling, R. Machinek, R. Boese, A. de Meijere, *Chem. Ber. 124* (1991) 1591, and references cited therein.
[21] L. Fitjer, unpublished results; private communication to A. de Meijere, May 1991.
[22] R. Stölevik, P. Bakken, *J. Mol. Struct. 197* (1989) 137.

BOOK REVIEWS

Book Reviews are written by invitation from the editor. Suggestions for books to be reviewed and for book reviewers are welcome. Publishers should send brochures or (better) books to the following address: Redaktion Angewandte Chemie, Postfach 101161, D-6940 Weinheim, Federal Republic of Germany. The editor reserves the right of selecting which books will be reviewed. Uninvited books not chosen for review will not be returned.

Organic Synthesis via Organometallics. Edited by *K. H. Dötz* and *R. W. Hoffmann*. Vieweg, Braunschweig 1991. viii, 323 pp., hardcover DM 92.00.—ISBN 3-528-08947-4

This volume contains 17 papers presented at the third symposium on research topics sponsored by the Volkswagen-Stiftung, which was held in Marburg in July 1990. It is a wide-ranging and readable survey of recent applications of organometallic reagents and reactions in organic synthesis. The organizers have once again put together an attractive program of lectures, containing a balanced mixture of "classical" topics and new developments in the field of organometallic chemistry.

R. H. Grubbs reports on the use of titanacyclic compounds and alkylidene complexes in "Living Ring-Opening Metathesis Polymerization" (ROMP) and the application of this method to the preparation of block copolymers and highly conjugated polymers, of which the extreme example is polyacetylene. *W. Keim* et al. give a wide-ranging review of the enantioselective telomerization of 1,3-dienes using palladium and nickel catalysts, including discussions of analytical and mechanistic aspects. A short article by *H. H. Brintzinger* on chiral *ansa*-metallocenes, in which the stereoselectivity of α-olefin polymerizations is explained by mechanistic arguments, is then followed by *H. Fischer*'s contribution on benzylidene complexes as C_1 sources, which is a somewhat longer report describing their stereoselective conversion to give cyclopropane derivatives and heterocycles. In a very interesting and highly imaginative article *D. Astruc* summarizes the work of his group on "Organo-Iron Complexes in Aromatic Synthesis". This describes how simple cationic complexes of hexamethylbenzene with iron are used, in a single-pot reaction, to prepare "tentacle" molecules, and how the benzyl sites are then activated by electron transfer reactions to yield a wide variety of new complexes, many of which are multinuclear. Especially worth mentioning here is a compilation of literature references on the activation of arenes by transition metals. The article by *D. Walther* et al. describes the activation of CO_2 using nickel(0) complexes and alkenes or alkynes to give nickela-cyclic carboxylates, which can also be prepared by reacting a bipyridyl-stabilized diethylnickel species with cyclic anhydrides. Especially interesting here are the cyclizations with alkynes leading to the formation of the preparatively very useful 2-pyrones with selectivities of more than 90%; the trimerization reaction of the alkyne is almost completely suppressed. A description of the use of steroid systems in cross-coupling reactions with nickelacarboxylates and a section on the carboxylation of C–H bonds and of imines as "reversible CO_2 carriers" serve to emphasize the close relationship between organometallic and bioorganic CO_2 chemistry. The next article by *J. K. Kochi* on "Charge-Transfer Activation of Organometallic Reactions" is quite long, and is of fundamental importance to an understanding of many of the reactions of organometallic chemistry. However, the relevance to organic synthesis here is rather tenuous.

The review by *H.-J. Knölker* on the use of dienyliron complexes in synthesizing natural products is very well worth reading and full of information. It is pleasing to find that a large number of the author's published papers, which have appeared within a remarkably short period, are here summarized. The emphasis is again on iron in the article by *P. Eilbracht* et al.; these authors have converted cyclohexadiene derivatives, via their complexes with $Fe(CO)_3$ with insertion of CO, into a wide variety of carbocycles, some of which are quite complicated, and have investigated the mechanisms of the reaction steps. *G. R. Stephenson* et al. are concerned with the control of regiospecificity in alkylation reactions using cyclohexadienyliron complexes, and the very careful and thorough study reported here shows that there are close relationships to alkaloid syntheses. *C. P. Casey* et al. summarize their recent investigations on new reactions of organorhenium compounds, which are very interesting from a mechanistic standpoint; they also discuss the importance of heterobimetallic systems. *J. Okuda* et al. describe the ligand (3-butenyl)tetramethylcyclopentadienyl; as a ligand with an olefinic side-chain this is capable of reversibly blocking one of the coordination sites of the metal atom in the corresponding cyclopentadienyl complexes. The chemical behavior with cobalt is particularly interesting here, since the [2 + 2 + 2]-cycloadduct was formed from two alkyne molecules and the double bond of the ligand, which, however, is irreversibly attached to the ligand. The contribution by *C. Bolm* is concerned with the use of optically active bipyridines in enantioselective synthesis; the author has alkylated aldehydes and α,β-unsaturated ketones with varying degrees of enantioselectivity in the presence of these chiral ligands using palladium or nickel catalysts. In the article by *V. Schurig* the main preparative interest is centered on enantioselective methods for preparing simple oxiranes. The author also discusses aspects of prochiral and chiral recognition using complexation gas chromatography. In the article by *D. Hoppe* we are reminded that "organometallics" are not confined to transition metal compounds: *N,N*-dialkylcarbamoyloxy groups not only facilitate lithiation at the adjacent sites but also, as a result of intramolecular complexation, increase the configurational stability of the ion pairs that are formed, which has very important consequences for enantioselective syntheses. An industrial research team led by *A. Hafner* describes a fruitful combination of transition metal chemistry with carbohydrate chemistry: by forming chiral complexes of carbohydrates with titanium, zirconium and hafnium, the authors were able to prepare a number of enantiomerically pure reactive alkylating agents. In a large number of reactions this good idea yielded enantiomeric excesses and diastereoselectivities that were in most cases very high. Last but not least in this collection of articles, *R. Noyori* et al. present a very lucid contribution on "Multiplication and Amplification of Chirality". Catalytic concentrations of enantiomerically pure 3-*exo*-(dimethylamino)isoborneol (DAIB) cause alkylzinc compounds to react with aldehydes giving secondary alcohols with *ee* values up to 99%. Even when the DAIB present in catalytic amounts has an *ee* value of only 14%, a product with an *ee* value of 98% is obtained.

The 17 articles have been reproduced directly, which means that the publishers have had almost no typesetting or correction work to do. The authors too have done their work thoroughly, and there are very few errors; in the case of the German authors one occasionally comes across idioms carried over from the German language. It would have been desirable in the reaction schemes to give details of yields and reaction conditions wherever possible. The book can be recommended to everyone interested in organometallic chemistry and organometallic methods of synthesis; it is suitable, rather in the manner of an advanced seminar, as an introduction to the areas of work described. A cheaper paperback edition would have been desirable.

Holger Butenschön [NB 1177 IE]
Max-Planck-Institut für Kohlenforschung
Mülheim a. d. Ruhr (FRG)

Materials Science and Technology (A Comprehensive Treatment). Volume 5: Phase Transformations in Materials. Edited by *P. Haasen*. VCH Verlagsgesellschaft, Weinheim/VCH Publishers, New York 1991. xiii, 648 pp., hardcover DM 430.00.—ISBN 3-527-26818-9/0-89573-693-4

This series is planned to consist of 18 volumes altogether; by the end of this year a further six volumes will have been published in addition to Volume 5 which is reviewed here. One can expect this to be an exciting series when complete—and the same also goes for the price. The editors (*R. W. Cahn*, *P. Haasen* and *E. J. Kramer*), on behalf of the authors (of whom there are more than 200), introduce the series as follows: "The new series is intended to mark the coming-of-age

of that new discipline, define its nature and range and provide a comprehensive overview of its principal constituent themes". The series appears at an opportune time and fills a real gap. Can there be anyone who has not already come into contact in some way with the field of "materials science and technology"? This in itself illustrates the interdisciplinary nature of this now virtually "exploding" area of science and technology. In the past we used to refer simply to "materials science", but often the technological and economic implications were underestimated.

It is certainly appropriate here to briefly indicate where Volume 5, which is the first to appear, fits into the overall series. In this way one can explain most clearly the aim of the series and its level (and thus also the position occupied by each individual volume). The topics to be treated in the 18 volumes are as follows: 1. Structure of Solids, 2. Characterization of Materials, 3. Electronic and Magnetic Properties of Metals and Ceramics, 4. Electronic Structure and Properties of Semiconductors, 5. Phase Transformations in Materials, 6. Plastic Deformation and Fracture of Materials, 7. Constitution and Properties of Steels, 8. Structure and Properties of Nonferrous Alloys, 9. Glasses and Amorphous Materials, 10. Nuclear Materials, 11. Structure and Properties of Ceramics, 12. Structure and Properties of Polymers, 13. Structure and Properties of Composites, 14. Medical and Dental Materials, 15. Processing of Metals and Alloys, 16. Processing of Semiconductors, 17. Processing of Ceramics, 18. Processing of Polymers. Thus a picture of materials science embracing both basic research and technology is built up.

Phase equilibria, phase transformations, transport and diffusion processes, reactions at interfaces, decomposition reactions, structure-forming processes, precipitations, superlattices and crystallization processes are, of course, all of fundamental importance to materials science. The volume reviewed here is devoted to this topic area, which is covered in ten chapters of roughly equal length, namely: 1. Thermodynamics and Phase Diagrams of Materials: aspects covered are chemical equilibria and Gibbs free energy, thermodynamics of solutions, binary and ternary phase diagrams (including reciprocal salt pairs), thermodynamics and the analysis of phase diagrams.– 2. Diffusion in Crystalline Solids: this chapter discusses macroscopic and microscopic diffusion, diffusion in solid materials, and experimental methods for determining diffusion coefficients. – 3. Statistical Theories of Phase Diagrams: topics here include phenomenological approaches, computer methods (models) and metastability. – 4. Homogeneous Second Phase Precipitation: this chapter covers experimental methods for studying the kinetics of decomposition reactions, the morphology of precipitates, the kinetics of decomposition reactions, increasing the particle size of primary precipitates, and numerical calculations on nucleation, growth and increasing particle sizes. – 5. Transformations Involving Interfacial Diffusion: the structures of particle and phase boundaries, diffusion (the roles of capillary forces, chemical forces and mechanical forces), chemically induced migration of grain boundaries, and discontinuous precipitations are discussed. – 6. Diffusionless Transformations: here the reader learns about mechanisms, microstructures, morphological changes, dilative and martensitic transformations, shear transformations, techniques of investigation, and finally properties and applications. – 7. Spinodal Decomposition: this chapter discusses separation kinetics, the equation of nonlinear diffusion, spinodal decomposition processes, influence of cooling rates (quenching), systems in the neighborhood of a triple point, spontaneous growth of ordered domains, and some experimental results (selected examples from the fields of metallic alloys, glasses, ceramics, liquid mixtures and polymer mixtures). – 8. High Pressure Phase Transformations: this chapter is concerned with experimental techniques, elements of Group IV, III–V compounds, barium chalcogenides, cesium halides, xenon, semimetal/semiconductor/metal transitions, and molecular solids (iodine, oxygen, hydrogen). – 9. Atomic Ordering: here the topics are atomic configurations, domains and configuration polyhedra, ground states, calculations of phase equilibria (by the cluster variation or Monte-Carlo methods) and applications to real systems. – 10. Solidification: the final chapter discusses first-order phase transformations, experimental methods, dendritic growth, orientated (directional) crystallization, and eutectic growth.

All the chapters, including even the strongly computing-orientated Chapters 3 and 9, are elucidated by describing selected chemical systems as examples wherever possible, thereby ensuring that the discussion is always related to real situations. The topics are dealt with in a rigorous and concise manner throughout; the reader is assumed to already have some basic knowledge of the subject. Adequate and appropriate references to original papers, review articles and books for more advanced or supplementary reading are provided. The choice of topics and their treatment are without doubt appropriate for such an interdisciplinary field of study.

Research groups with interests in materials science will need to have direct access (through their institutes and libraries) not only to Volume 5 but (presumably!) to the entire work. This certainly also applies to groups working in the area of "basic scientific research", whose problems and aims are much closer to materials science than is generally recognized.

This volume can be recommended, and the further volumes in the series that are to follow will be eagerly anticipated!

Rüdiger Kniep [NB 1155 IE]
Eduard-Zintl-Institut
der Technischen Hochschule Darmstadt (FRG)

High Vacuum Techniques for Chemical Synthesis and Measurements. By *P. H. Plesch*. Cambridge University Press, Cambridge 1989. xiii, 167 pp., hardcover £ 35.00.—ISBN 0-521-25756-5

P. H. Plesch discusses the advantages and possible applications of high-vacuum techniques in the research laboratory in a very personal style. "This book may have a slightly old-fashioned look" writes the author in the introduction, and he's not wrong in saying that. Yet the book was written by an experienced practitioner for practical use, and contains countless tips and tricks which are difficult to find elsewhere in comparable literature.

This book is divided into 5 sections, and is very readable throughout. Chapter 1 (Fundamentals) covers first of all the fundamentals of working under an inert gas, as well as the advantages and disadvantages of different working techniques. There then follows a short section on the theoretical principles. Section 1.3 (Essential skills and equipment) introduces the rudiments of glass-blowing, where one is advised not to forget Murphy's Law. In this context I felt the advice on safety in Section 1.4 (General comments on safety) was especially important. Various sources of hazard are mentioned here, which cannot be overemphasized (for example,

the condensation of oxygen in cold traps). I would like to add that substances hazardous to health, such as Na/Pb alloys (p. 8) or chromic acid (p. 75) should no longer be used in a modern research laboratory, and should be replaced by more suitable drying and cleaning agents. Chapter 2 (The main vacuum line) can be considered the heart of the book. It contains detailed descriptions of the building and running of a high-vacuum line. After a short overview, the individual components of this equipment (pumps, cold-traps, taps, valves, manometers) are described and compared. The reader thereby obtains important advice on which device best suits each situation. Here too, *Plesch* succeeds in giving the reader the experience he has gained from many years of working with high-vacuum techniques. Even apparently minor particulars, like the correct greasing of ground glass connections, are not to be underestimated in practice. Practical advice of this kind makes the book useful reading material for every diploma or PhD research student who needs to use some form of vacuum technique. After the construction of the vacuum line the sometimes laborious task of detecting leaks is discussed. In Chapter 3 (Applications and procedure) countless specialized apparatus and additional possible applications for high-vacuum techniques are described. *Plesch* gives particular attention to the filling and melting of glass phials. Much of this equipment (burettes, dilatometers, viscometers, calorimeters, etc.) is useful, but some, in my view, is a little too exotic (e.g., on page 93, the device for simultaneous filling of several dilatometers). On the other hand the section on NMR measurements (p. 96) is a little too short. Sealing NMR tubes under vacuum should be a routine operation for any advanced graduate student. However, I consider the making of NMR tubes (p. 97) a waste of time. Chapter 4 (Purification, including drying) contains countless useful tips for practical work. Every synthetic chemist will daily encounter problems with cleaning and drying reagents and solvents. A book about potential applications of vacuum techniques would therefore be incomplete without advice on drying glass apparatus (p. 119) as well as degassing and drying the solvent to be used. Thus, Section 4.6 (What is so special about drying?) particularly is worth reading attentively. Chapter 5 concludes the book with a few syntheses and measurements, chosen to show the advantages of the high-vacuum technique.

In the introduction *P. H. Plesch* defines the aim of the book: "...to enable a chemist to assess the possible utility of high-vacuum techniques for his purposes, to design and build a high-vacuum system, and to do good chemistry with it". The author has succeeded in doing this.

Frank T. Edelmann [NB 1178 IE]
Institut für Anorganische Chemie
der Universität Göttingen (FRG)

Basic Principles and Techniques of Molecular Quantum Mechanics. By *R. E. Christoffersen*. Springer, Berlin 1990. xiv, 686 pp., hardcover DM 178.00.—ISBN 3-540-96759-1

This book is a comprehensive student text and work of reference on the theoretical fundamentals of quantum chemistry and their practical applications. It differs from other books on this theme in several respects, including the amount of space devoted to describing the mathematical basis of quantum-mechanical methods.

A brief introductory section reminds the reader of some of the concepts of classical mechanics, and describes the experimental observations that led to the formulation of quantum mechanics. This is followed by 140 pages on vector space and function space, matrix algebra, operator algebra, etc. After this come several chapters in which the postulates of quantum mechanics are introduced and the usual model problems are treated (particle in a box, harmonic oscillator, the hydrogen atom, etc.). The Hamiltonian operator for molecular systems is discussed in considerable detail, including the effects of external magnetic fields as well as relativistic effects. The final chapter of the book contains an equally detailed treatment of the approximate methods that are commonly used in quantum chemistry, such as the closed- and open-shell Hartree-Fock SCF approximations, perturbation theory and configuration interaction.

The overall impression is of a sound and competently written book. Explanations are given of many points that are not often covered in comparable textbooks; for example, there are discussions of the Rayleigh-Schrödinger and Brillouin-Wigner perturbation theories, of methods of calculating lower limits for the energy, and of such details as the origin of the s,p,d... nomenclature for atomic orbitals. Nevertheless, there is some doubt as to whether the book entirely succeeds in the ambitious aim of presenting the complex mathematical background in a form which is both detailed and comprehensible to the student. Too often one finds that proofs and theorems are glossed over, and the reader is referred, in one of the many footnotes, to the original literature. Also the mathematics is presented without directly relating it to applications, and one suspects that many students will consequently feel that this part of the book is an unappealing and barren slog.

It is also regrettable that the discussion of quantum-mechanical computational methods is not always completely up-to-date. New developments such as the use of direct SCF methods for calculations on large molecules or of natural atomic orbital basis sets are not described. In the discussion of the multiconfigurational SCF approach one searches in vain for a mention of the CASSCF method that is now most commonly used; also the direct CI methods that have now become so important are treated rather too briefly. A further example of the sometimes rather outdated treatment is the comment by *Christoffersen* that the diagonalization of a 1000×1000 matrix takes several seconds of computation, whereas fast modern computers can in fact perform such tasks in fractions of a second. This tendency towards outdatedness is also reflected in the choice of literature references, which mostly come from the 1970s and early 1980s.

It is also unfortunate that many printing errors have found their way into the text, including some that are rather confusing. For example, "yield" has become "field", a factor of 1/2 has been omitted from one formula, and one suddenly finds that instead of an external force one is dealing with an "external face". With monotonous regularity a trial wave-function becomes a "trail" wave-function, and even the names of authors in the literature citations do not escape distortion. A particularly annoying error is a reference to a figure at the end of Chapter 7, where one looks in vain for it; it is not until four chapters later that one suddenly comes across an identical paragraph, this time with the figure. Blunders such as these could certainly have been avoided with a little care.

However, if one leaves aside these deficiencies in the preparation, the tendency towards outdatedness in some parts, and the fact that the planning of the mathematical part is perhaps not entirely successful, *Christoffersen*'s book is an interesting addition to the range of textbooks on theoretical

chemistry, and is to be welcomed especially for its many-faceted treatment of the subject.

Wolfram Koch [NB 1116 IE]
IBM Deutschland GmbH
Heidelberg Scientific Center
Institute for Supercomputing and Applied Mathematics
Heidelberg (FRG)

Houben-Weyl. Methoden der Organischen Chemie. 4th Edition, supplementary volumes. **Volume E 16a, Parts 1 and 2: Nitrogen Compounds I.** Edited by *D. Klamann*. Thieme, Stuttgart 1990. Part 1: xxxvi, pp. 1–855; Part 2: xiv, pp. 856–1516; hardcover DM 2100.00 (subscription price: DM 1890.00).—ISBN 3-13-218-604-X

The publishing house Thieme continues to press on with the work of updating the Houben-Weyl volumes written in the period from the 1950s to the 1980s, by publishing a supplementary work which takes into account the latest state of development on methods and the most recent literature. In these two part volumes on organonitrogen compounds they have again succeeded in an impressive way.

This work again meets the aim (which has never been explicitly stated) of not only giving an appropriate experimental procedure for each special case, but also providing the reader who has not yet become a specialist in a particular field with an introductory, but nevertheless thoroughly sound, overview of the possibilities. The reader may look up a specific method and gain some additional information as a result, or browse around the special problem of interest, or again may read a few dozen pages almost in the manner of a textbook. Each of these types of readers will get good value from the work, helped by the information-packed and mainly well chosen subject matter, although not necessarily by the arrangement of the contents, which follows an ever more rigid pattern. The strict adherence to the ten hierarchical levels of classification sometimes results in an undue emphasis on unimportant features, and often separates closely related topics. For example, the closely similar procedures of the *N*-alkylation of hydroxylamine and that of *N*-alkylhydroxylamines appear in different sections, as also do the entirely analogous methods used to synthesize mono- and dihalogenated amines.

The limitation to work published during the last twenty to thirty years, which is usually applied very consistently, sometimes results in an emphasis on procedures that have been overrated. Without actually copying "Beilstein" it would have been useful to keep in mind the system used there, in which the variety of routes to a class of compounds is shown under the heading "Bildungsweisen", whereas under "Darstellung" the more generally useful and perhaps less elegant method is chosen. The recommended procedures should always be rather more generally applicable than the reactions described in between these. A welcome feature is the caution that has been applied with regard to mechanisms, avoiding unnecessary embellishments on this theme; in view of the need for "Houben-Weyl" to remain up-to-date for decades, speculations of that nature would be likely to become obsolete more rapidly than the established facts.

The first of the two part volumes contains two very long chapters on organic hydroxylamine compounds (395 pp.) and organic hydrazine compounds (435 pp.), together with much shorter chapters on nitroxyl radicals, nitroxides and amino-oxides. The considerable length of the chapter on the hydroxylamines is no doubt due to the many different types of redox reactions of N–O compounds and the biological activity shown by many individual compounds. In the case of the hydrazines the reason for the length is that the alkylhydrazines have made a welcome appearance in the last few decades; previously these could only be prepared with great difficulty by laborious alkylation of hydrazine or by reduction of nitrosamines, whereas they are now accessible by a variety of interesting reactions, mainly by forming N–N bonds. The lengths of these two chapters are therefore justified. However, the lengths of some of the subsections are not commensurate with the importance of the topics. Addition reactions of nitrones and olefins occupy 20 pages with an enormous table, and the (admittedly interesting) criss-cross cycloaddition of alkenes to hexafluoroacetone is given a six-page table. Such comprehensive treatments of examples that are analogous should be left to specialized monographs. The same also applies to the 16 pages with analogous examples of *Meerwein*'s reaction of diazonium salts with alkenes in Part 2 of the work. On the other hand the work does not give an up-to-date procedure for preparing solutions of chloramine; the conventional procedure giving a yield of 30–40% (reproduced here on p. 250) can be improved to give reproducibly more than 90% simply by adding ammonium chloride (*Z. Anorg. Allg. Chem. 396* (1973) 178).

In the chapter on hydrazines it would have been useful in a number of cases to indicate how precursors that are not altogether commonplace can be prepared, for example, when describing the reduction of alkoxy(alkyl)diazene-*N*-oxides (p. 463). The usefulness of the method for preparing 1,2-diethylhydrazine by reduction of the azo compound (p. 523) could be better appreciated if one knew whether it was possible to make the azo compound by some route other than the reverse of the reaction described, i.e. by oxidation of diethylhydrazine. The interesting synthesis of arylhydrazines by acid hydrolysis of arylsydnones cannot give acetic acid as the secondary cleavage product, as is shown in the formula on page 793. Also, the preparation of methylhydrazine from methylamine (p. 426) should not be described as an oxidation.

In Part 2 the long chapter on *N*-halogenated amines possibly puts too much emphasis on the preparation of pure compounds; it is more important to have straightforward methods for preparing well-defined solutions for use in further reactions. This chapter is followed by the subject of *C*-nitroso compounds, which obviously has a great many subdivisions and requires no less than 129 headings in 47 pages of text. In the description of the nitrosation of arenes it would have been desirable to show a clear division between those nitrosation reactions that are useful for synthetic purposes (e.g. those of phenols) and the nitrosations of simple arenes such as benzene that have also been investigated. The chapter by *J. Goerdeler* on ammonium compounds is excellent; this describes the quaternization of amines of increasing inertness on reaction with alkylating agents of increasing reactivity. A separate chapter is devoted to the hydrazinium compounds, which have only attained importance in recent years. This is followed by the classical diazonium compounds; as these have had a career of more than a hundred years their preparation occupies less space (35 pp.) than their reactions (49 pp.). Next come chapters on a few special classes of compounds such as nitrosamines, triazenes and tetrazenes; the work ends with a chapter on azides.

Finally a few errors and incorrect usages need to be mentioned. On page 462 the statement that the pressure falls from 73 694 torr to 60 765 torr is hardly in accord with the precision of typical pressure measurements in the preparative laboratory. Quoted values such as 101.87 kPa (p. 878) probably

arise from giving the results of calculations with too high a precision. One should not refer to "activated alkenes" without indicating whether they are activated in the direction of electron deficiency (unsaturated esters, nitriles or ketones) or electron excess (vinyl ethers, enamines). In this light many reactions are quickly seen to be plausible. Sodium sulfate is a water-binding agent, not a dehydrating agent (p. 876). On page 947 the precursor of quinuclidine has a carbon atom missing. What is meant by the statement on page 879 that sodium chlorite ($NaClO_2$) is oxidized to chlorine? On page 258 the formula of *O*-sulfohydroxylamine is shown without the crucially important oxygen atom between N and S. In two preparative methods on pages 444 and 468 one of the reagents has been omitted in each case.

The fact that in over 1500 pages only about twenty printing errors could be found is an indication of the high quality of the typesetting. However, one of these is an incorrect spelling of the name *Birkofer*; this is again repeatedly shown with an extra "h", despite this error having been pointed out by *Richard Kuhn* in a review[*] of the 4th Edition.

A tribute must be paid to the hard work by the authors. Since a chemist's range of interests is not nowadays defined in terms of compound classes, a specialist dealing with a particular class of compounds is now a rarity. Despite all the aids that are now available, collecting together the required information is still an arduous task; the essential job of evaluating facts costs time and effort.

Ernst Schmitz [NB 1171 IE]
Zentralinstitut für Organische Chemie
Bereich Organische Synthese
Berlin-Adlershof (FRG)

Crystalline Symmetries. An Informal Mathematical Introduction. By *M. Senechal*. Adam Hilger, Bristol 1990. xi, 137 pp., hardcover £ 79.50.—ISBN 0-7503-0041-8

Chemists are generally comfortable with the geometry of structure, the algebra of stoichiometry, and the calculus of kinetics. Most of them have learned to live with the eigenvalue problems of quantum mechanics. As to the less familiar mathematics of group theory graph theory or topology, many chemists have only a vague concept of the mathematical fundamentals and employ terminology in a manner that is at best intuitive and idiosyncratic. Discussing the application of mathematics to chemistry with a real mathematician can be an uncomfortable, confusing, and humbling experience.

In this small, aptly-titled book Professor *Senechal*, a professional mathematician, provides a friendly introduction to the mathematical fundamentals of crystallography that will entertain and reward casual readers as well as chemists and materials scientists who work with crystallography.

Almost two-thirds of the text involves familiar concepts of symmetry, lattices and space groups, but the treatment is novel: it is written by a mathematician for experimental scientists. Familiar and less familiar concepts, such as orbits, cosets, the Voronoï cell, isometries, and symmorphic space groups, are clearly defined and illustrated. Simple theorems are proven while others are invoked or outlined with reference to an extensive bibliography for more detailed treatment. After reading this book one can feel more comfortable with the assertion that there are 4901 four-dimensional space groups, or with the impossibility of having space groups with fivefold rotation axes. Most of the discussion is clear and satisfying, with only the occasional difficulty, such as on page 56 where an unnatural definition of density in a two-dimensional lattice leads to difficulty in relating the reciprocal lattice to crystal form.

There are appetizing but less complete chapters that introduce the modern topics of color symmetry and *N*-dimensional crystallography, including mention of Penrose tiling and local fivefold symmetry, and a fifteen-page chapter which discusses crystal classification and how to interpret space group information in the *International Tables for X-Ray Crystallography*. The bibliography includes twenty books and journal articles published since 1980.

Throughout the book, particularly in the first chapter, special attention is given to the historical development of crystallography as an experimental, mathematical, and artistic science. This emphasis is effective both for holding the reader's interest and for illuminating the logic of the subject. A four-page appendix provides concise information about the contributions to crystallography by 34 natural philosophers and mathematicians from *Plato* to *Roger Penrose*.

Professor *Senechal* notes that although the French mathematician *Jordan* had combined the proper motions (rotations, translations, and screw rotations) with Bravais' lattices by 1868, it took another 23 years before *Fedorov* and *Schoenflies* completed the 232 space groups by adding the reflections, glides and rotary reflections that interconvert enantiomers. This seems curious because by 1850 *Pasteur* had already demonstrated the need for such improper symmetry elements by revealing the relation between molecular and morphological chirality. *Senechal* wonders, "Was [this delay] due to differences in scientific fields, or differences in language? Are there similar gaps today of which *we* are unaware?". By providing a simple introduction to the mathematics of crystallography this small book should help to bridge one of the gaps between scientific fields that persists today.

J. Michael McBride [NB 1196 IE]
Department of Chemistry, Yale University
New Haven, CT (USA)

Microbial Polyesters. By *Y. Doi*. VCH Verlagsgesellschaft, Weinheim/VCH Publishers, New York 1990. ix, 156 pp., DM 74.00.—ISBN 3-527-27860-5/0-89573-746-9

In the future biopolymers are likely to play an ever increasing role. Such compounds are interesting for several reasons: for one thing they are biodegradable and therefore do not contribute to environmental problems; for another they are produced from renewable resources. Commercial utilization of such materials has already begun: shampoo containers manufactured from polyesters which have been made by biotechnological methods have appeared on the market. A comprehensive review of polyesters that are produced by microbial synthesis is therefore welcome, even if the present author has chosen to give pride of place to his own contributions.

The monograph, which has a convenient A5 format ($8\frac{3}{4} \times 5\frac{1}{2}$ inches), presents in eight chapters a discussion and comparison of the properties of poly-(*R*)-3-hydroxybutyrate (PHB) and of two copolymers, poly(3-hydroxybutyrate-co-3-hydroxyvalerate) (P(3-HB/3-HV)) and poly(3-hydroxybutyrate-co-4-hydroxybutyrate) (P(3-HB/4-HB)), the latter discovered and investigated by the present author.

[*] *Angew. Chem. 72* (1960) 502.

The early chapters deal mainly with biological aspects, while the later chapters emphasize physical properties and applications. A brief introduction (Chapter 1) is followed by a discussion of the preparation of polyesters by fermentation and of current methods of their analysis (Chapter 2) and of the natural occurrence of a wide range of microbial polyhydroxyalkanoates (Chapter 3). The dependence of yield and composition of the copolymers on carbon source, bacterial strain, and culture conditions, as well as the function of PHB as a storage material are also discussed. Regrettably, the occurrence of PHB in cell membranes is not mentioned. Chapter 4 presents an overview of the routes of biosynthesis and of the enzymology of the polyesters. It is interesting to note that several research groups have located the gene responsible for PHB biosynthesis in *Alcaligenes eutrophus*, and have expressed it in *Escherichia coli*, a bacterium which normally does not produce PHB as a storage material. Chapter 5 is devoted entirely to a discussion of the copolymer, P(3-HB/4-HB), whose promising properties have not yet been fully explored. The next two chapters deal with the structure and properties of PHB and P(HB/HV)-copolymers. Investigations of the solids by X-ray diffraction and NMR are described in detail. Also dealt with are mechanical and thermal properties. These are important from the point of view of industrial applications. The current state of knowledge of the structure of the polymers in solution—the existence of secondary structure is still in dispute—is summarized briefly. Chapter 8 deals with the extracellular depolymerases that catalyze the biodegradation of the polyesters. This is followed by a brief discussion of possible uses of the polymers. Here one looks in vain for any indication that depolymerization of PHB generates chiral molecules which are potentially useful as starting materials in stereospecific syntheses. Nor is there any mention of attempts to generate PHB by polymerization.

Throughout the book, experimental data are presented clearly in tables and graphs, but occasionally one wishes there were a better juxtaposition of text and tables. Each chapter concludes with an extensive and up-to-date bibliography (to 1990).

This monograph is a valuable supplement to the numerous reviews of the topic that have appeared. In particular, the book can be recommended to readers who are interested in biological aspects of the field on the one hand, and in macromolecular aspects on the other. In view of the ecological significance of the new materials, the book can be recommended also to environmental scientists.

Hans Michael Bürger, Hans-Martin Müller [NB 1142 IE]
Laboratorium für Organische Chemie
der Eidgenössischen Technischen Hochschule
Zürich (Switzerland)

Essentials of Molecular Photochemistry. By *A. Gilbert* and *J. Baggott*. Blackwell Scientific Publications, Oxford 1991. xii, 538 pp., paperback £ 17.85.—ISBN 0-632-02429-1

More than 13 years have elapsed since the publication of *Turro*'s "Modern Molecular Photochemistry".[1] Although a significant number of monographs on particular areas of organic photochemistry have appeared during that time, there has been no new attempt at a comprehensive treatment of the fundamentals of molecular photochemistry. For that reason alone it is very pleasing that the authors of this book have now undertaken that risky task, and it can be said at the outset that they have succeeded in fulfilling it.

The risk element lies in the need to bring together such widely different aspects as, on the one hand, the basic principles of quantum mechanics, spectroscopy and kinetic methods and, on the other hand, organic photoreactions, their potential applications in synthesis and the reaction mechanisms involved. In contrast to "ground-state chemistry", a knowledge of the underlying quantum mechanical and photophysical principles is essential in order to plan and carry out experimental work on photoreactions, and it is therefore entirely appropriate that these aspects occupy nearly half the book. It begins with lucidly written chapters on the electronic structures of molecules, radiation and molecular orbital theory, which are then followed by two excellent sections on molecular photophysics and the theory of photochemical reactions. However, it is noticeable that in the series of tables listing photophysical properties, much of the data is quite old: the main sources used are *Birks*' classic work "Photophysics of Aromatic Molecules" (Wiley, 1970) and the book by *Turro* that has already been mentioned (1978). It would have been useful to also provide an index of tables, so that one could quickly find the required data. In many cases one is only referred to more recent collections of tables, such as the "Handbook of Photochemistry",[2] although the latter too suffers from some intrinsic defects.

With regard to those photophysical parameters that have long been familiar, such as triplet and singlet state energies, lifetimes of excited states, and IC and ISC rates, one does not expect to find any very significant changes. However, the ability to determine dynamic quantities, through the recent rapid developments in time-resolved laser spectroscopy, has radically extended our understanding of photochemical reactions. The authors have responded to this situation by including separate sections on laser effects and spectroscopic techniques, and also by covering these aspects in each of the photochemically orientated chapters in the second part of the book. This, of course, carries the risk that some of the statements included there may already have been superseded by the time they are printed; for example, this has occurred in the case of the comments on the "Marcus inverted region" in the (unduly short) chapter on photoinduced electron transfer reactions. In the discussion of pericyclic reactions I would have expected to find a detailed treatment of the Salem correlation diagram; admittedly this is introduced later in connection with the α-scission of carbonyl compounds, but this does not do justice to the importance of the concept.

The theoretically orientated first part is followed by five chapters that are arranged according to the different types of chromophores: alkenes and alkynes, carbonyl groups, arenes, nitrogen compounds and "others" (alkyl halides, peroxides and sulfur compounds).

This concept has already proved useful in the past, and it is here applied to a remarkably large number of recent examples (up to 1989 in some cases). Most of the types of reactions mentioned here have been covered in at least one review article during the last few years, and therefore every aspect has not been discussed in detail here—in fact such a thorough treatment would not have been desirable. Each type of chromophore is introduced by describing its photophysical properties; thus the energies, lifetimes and excitation and deexcitation behavior of the excited states are discussed and correlated with the reactivities or selectivities of these "electronic isomers". These characteristics are then illustrated by numerous examples, including detailed descriptions of the analytical methods used (flash photolysis, laser spectroscopy, measurement of quantum yields, Stern–Volmer kinetics, labeling experiments, scavenging experiments, etc.). In my opinion the enormous growth in the importance of photoin-

duced electron transfer processes during the last few years has not yet been as fully appreciated as it should be. However, this subject is currently in a state of flux, and a detailed discussion of these aspects would have been outside the scope of a textbook such as this.

In the area of "ground-state chemistry" many different approaches to the problem of synthesizing diastereomerically or enantiomerically pure compounds (EPC syntheses) have been developed. Photochemistry too is making considerable contributions in this field. This aspect is not adequately covered in the book; for example, there are no detailed descriptions of the important studies that have been carried out on the synthesis of enantiomerically pure compounds using Paternò–Büchi reactions (e.g. the work of *Schreiber* and of *Scharf*), on oxa-di-π-methane rearrangements (*Schaffner, Demuth*), or on *meta* photocycloadditions (*Wender*). One could argue that these topics belong instead to a textbook on organic synthesis, but I believe that this is where the future of organic photochemistry must lie. This subject area should therefore have been given more space.

The final chapter departs from the system adopted up to this point whereby the subject matter is arranged according to chromophores, as it describes aspects of photochemically induced oxygen transfer. Here PET-induced oxygenation reactions are discussed on an equal footing with "pure" singlet oxygen reactions. Regrettably, however, there is no mention of the very interesting chemoluminescence or CIEEL phenomena observed for 1,2-dioxetanes.

The incidence of errors is gratifyingly low for a first edition (although trivial mistakes have crept into some of the formula diagrams), and both the text and the figures are of excellent quality. The book can be thoroughly recommended as a textbook to accompany a course of lectures on photochemistry, and the remarkably low price should serve as an example to other publishers.

Axel G. Griesbeck [NB 1172 IE]
Institut für Organische Chemie
der Universität Würzburg (FRG)

[1] N. J. Turro: *Modern Molecular Photochemistry*, Benjamin/Cummings, Menlo Park, CA, 1978.
[2] J. C. Scaiano (ed.): *Handbook of Photochemistry*, CRC Press, Boca Raton, FL, 1989.

Selective Hydrocarbon Activation. Principles and Progress. Edited by *J. A. Davies, P. L. Watson, J. F. Liebman* and *A. Greenberg*. VCH Verlagsgesellschaft, Weinheim/VCH Publishers, New York 1990. xiv, 568 pp., hardcover DM 275.00.—ISBN 3-527-26959-2

The search for routes whereby hydrocarbons—especially paraffins—can be converted into higher value products by reactions that are as "mild" as possible, stoichiometric, preferably catalytic, and above all selective is, for obvious reasons, one of the most important and ever-present tasks of chemical research. It is only in the last decade that crucial progress has been achieved in the intermolecular activation of C–H bonds in saturated hydrocarbons and related compounds; this has led to an enormous growth in the literature on this topic, especially on homogeneous C–H activation at transition metal centers. Compared with only a few publications per year up to the end of the seventies, there are now well over a thousand papers every year that are concerned with one or other aspect of the subject "C–H activation". Many review articles have appeared in recent years, and the time was undoubtedly ripe for comprehensive treatments in book form.

In the work reviewed here 20 authors have covered, in 15 chapters, every important aspect of the homogeneous activation of hydrocarbons. The form chosen here, that of a multiauthor volume with contributions from relevant specialists, is appropriate to the topicality and interdisciplinary character of this field of research, and offers the most effective way of taking into account to some extent the rapid pace of new developments, without abandoning the claim of providing a sound treatment. The four editors (three of whom are also among the authors) have succeeded in putting together a selection of topics which ensures that this book will be worthwhile reading for everyone who seeks a comprehensive coverage of the subject corresponding (nearly) to the current state of knowledge.

In the first chapter, "The Homogeneous Activation of H–H and X–H Bonds by Metals" (17 pp., 49 references), *R. H. Crabtree* gives a brief summary of the various mechanisms of C–H activation reactions, followed by a more detailed treatment of the related topics of the activation of H_2, silanes and X–H bonds (OH, NH etc.). A section on two-electron/three-center interactions (agostic interactions, H_2 complexes, etc.) and electrophilic X–H activation is followed by a description of the mercury-sensitized photochemistry of C–H and X–H bonds, which the author has himself investigated in detail. *Crabtree*'s contribution is informative and provides a good introduction to the subject, although it is not nearly as good as other reviews on the topic of C–H activation by the same author. In Chapter 2, "Alkane Oxidation: The Oxidation of Alkanes by Group VIII Metal Ions" (21 pp., 66 references), *J. V. Zeile Krevor* is concerned with problems in the partial catalytic oxidation of hydrocarbons and with species bonded to SiO_2 surfaces. The article discusses stoichiometric homogeneous C–H activation reactions using transition metal complexes (the standard examples based on Rh, Ir, Pt and Os), and also briefly touches on the related chemistry of metal ions in the gas phase (see below). The chapter concludes with short digressions into models for biological oxidation systems and the use of inorganic complexes absorbed in zeolites. In *I. P. Rothwell*'s contribution, "The Homogeneous Activation of Carbon-Hydrogen Bonds by Electrophilic Early Transition Metal Systems" (31 pp., 100 references), the main topics are the "early" transition metals in high oxidation states, including intramolecular C–H activations by hydrogen abstraction at the α, β... up to ε positions, and cyclometalations of heteroligands, where the author's own research is concerned especially with aryloxy ligands. Partly anticipating the next contribution, the chapter then deals with C–H activation chemistry based on organometallic compounds of the lanthanoids and actinoids, and concludes with a discussion of mechanistic aspects. Following up the previous topic is *P. L. Watson*'s very interesting review of "C–H Bond Activation with Complexes of Lanthanide Elements" (30 pp., 86 references). The basic principles of electrophilic C–H activation are thoroughly discussed, including thermochemical aspects. This is followed by a detailed treatment of agostic interactions with electron-deficient lanthanoid and actinoid metal centers, and an excellent survey of the relevant activation reactions on C–H bonds of alkanes, alkenes, alkynes, arenes and coordinated ligands, ending with a look at β-elimination processes. In this chapter one clearly recognizes the expertise of this author and coeditor of the book, who has to her credit the discovery of the first well-defined homogeneous reaction of methane with an organometallic compound, and whose experience in basic industrial research has certainly been used to good effect in this review article.

In Chapter 5, "Development of Catalytic Processes for the Synthesis of Organic Compounds that Involve C–H Bond Activation" (32 pp., 75 references), *W. D. Jones* first defines the important (but often overlooked) thermodynamic limitations to the long-term objective described in the title, then addresses the crucial question of the functionalization of C–H bonds in arenes and alkenes, in this case involving mainly the "late" transition metals. After considering the stoichiometric cases, the author goes on to deal with the less common examples of systems having at least short-term catalytic activity, some of which he has investigated himself. A wide variety of complexes and reaction types that have been studied are described in this well-informed review. The next chapter is devoted to thermochemistry, an area already touched on frequently in earlier contributions: *J. F. Liebman* and *C. D. Hoff* deal with "The Thermochemistry of Hydrocarbon Activation Reactions: A View from the Organic and Metal Perspectives" (52 pp., 118 references). This is a detailed and soundly-based, but also very entertainingly written, account of the thermodynamic aspects of insertion reactions in C–H and C–C bonds of hydrocarbons, supported by 15 tables and much additional data. About 20 pages are directly concerned with organometallic thermochemistry, and especially with the role of M–C and M–H bond strengths in complexes of the "late" transition metals in relation to catalysis. This part also includes a critical evaluation of the available data, as well as an up-to-date literature survey and references to relevant results from theoretical chemistry. The sections on ligand effects on L_nM-X bond energies, on the importance of the L_nM-X bond strength in catalytic reactions, and the compilation of important representative data on M–C and M–H bond energies facilitate the important task of estimating thermodynamic relationships in the search for metal-catalyzed reactions of hydrocarbons leading to useful products. The only purely theoretical chapter of the book, "Theoretical Aspects of Alkane C–H Activation by Organometallics" (28 pp., 98 references), has been written by *J.-Y. Saillard*, who puts the main emphasis on the description of qualitative relationships between bonding and reactivity; nearly all of these are based on EH model calculations, interaction and correlation diagrams, fragment MO analyses, frontier orbital considerations and the isolobal concept, and they originate almost exclusively from the published work of *Roald Hoffmann*'s school of theoretical chemistry. However, this section of the book also reviews other, more quantitatively orientated, theoretical work on C–H activation that has appeared up to now; a careful study of this part will also give the reader an appreciation of the limitations of qualitative descriptions and the need for reliable numerical methods for quantum chemical calculations.

L. D. Field's review "Alkane Activation with Superacids" (20 pp., 66 references) then turns to a quite different area of alkane activation, dealing with the chemistry of alkanes exposed to the effects of superacids. This chapter discusses the types of superacid reagents and their strengths, mechanistic aspects of C–H and C–C activation, and especially the conversion of alkanes to higher value products. Naturally the name of *G. Olah* appears prominently in the background of the discussion. The resemblances and differences between these reactions and the alkane activations that occur at metal centers are clearly brought out. The following chapter, "On the Mechanism of Action of Vitamin B_{12}" by *P. Dowd* (35 pp., 62 references), takes us into the area of biological systems, whose ability to activate C–H and C–C bonds first made life possible. The author gives an up-to-date status report and a review of all the important aspects and hypotheses concerning the mechanism of B_{12}-mediated substrate conversions; here C–H abstractions at aliphatic carbon atoms emerge again and again as the most important and least understood of the elementary steps. The variety of biological systems in which processes involving the dissociation of C–H bonds play a crucial role is greatly extended in the following very comprehensive chapter by *S. E. Groh* and *M. J. Nelson* on "Mechanisms of Activation of Carbon-Hydrogen Bonds by Metalloenzymes" (61 pp., 339 references). As well as vitamin B_{12} this covers all the other important enzyme systems that have the ability to catalyze C–H bond activations by means of metal centers. Here the authors not only list such systems according to the types of metal ions involved, but also provide detailed descriptions and critical comments regarding mechanistic experiments, methods of investigation and hypotheses, and point out the differences compared with typical organometallic activation mechanisms. Next the review by *J. A. Davies* and *R. J. Staples* of "Electrochemical Approaches to Transition Metal Mediated C–H Bond Activation" (27 pp., 88 references) returns us to the area of "inorganic or organometallic" C–H activations. These authors describe electrochemically generated low-valency intermediates of the type d^{10}-ML_2 (M=Ni, Pd, Pt), and also the corresponding species for the elements Rh, Ir, Fe and Ru. Although the electrochemical results described here are in themselves very interesting, the number of genuine electrochemically induced intermolecular C–H activation processes is actually very small, and consequently the prospects for electrochemical generation of reactive species, which are also accessible by thermal or photochemical methods, cannot yet be reliably assessed. This chapter ends with a section on the electrochemistry of M–H and M–C bonds.

The next three contributions are concerned with results obtained using specialized physical techniques to study the key elementary processes involved in the activation of C–H and C–C bonds at metal centers. *Z. H. Kafafi* in "Metal Atom/Cluster Reactions via FTIR Matrix Isolation Studies: C–H vs. C–C Bond Activation" (19 pp., 51 references) reports results from studies of the metal atom chemistry of a number of representative hydrocarbons in matrices at 10 K, then compares these with well known organometallic systems and with results from theoretical studies. In Chapter 13, "Ground State Metal Atoms and Clusters in Low-Temperature C–H and C–C Activation: Periodic Trends and Unusual Structural Effects" (30 pp., 85 references), *K. J. Klabunde, G. H. Jeong* and *A. W. Olsen* give a detailed account of the principles involved in studies of low temperature reactions between metal atoms or metal atom clusters (surface models) and alkanes in a matrix. The great value of this article is that it covers all the different transition metal atoms and derives relationships and trends. The importance of the rapidly growing number of studies of C–H and C–C activation in the gas phase using "bare" metal ions is acknowledged by the inclusion of one of the best contributions in the book: Chapter 14, "C–H Bond Activation by Gas Phase Atomic Metal Ions", by *P. B. Armentrout* (62 pp., 119 references). This article is of an exemplary standard with regard to both the breadth and depth of the treatment. The only criticism is that the choice of literature citations seems rather limited; many important publications by other authors, especially in Europe, are not mentioned. The last of these reviews, Chapter 15, "Alkane Acidities and Organosilanes in the Gas Phase: A Silicon Reaction Makes Good", by *R. Damrauer* (20 pp., 30 references), is not directly concerned with metals nor with the activation of hydrocarbons, but the gas phase chemistry of anions and molecules of organosilanes that is described here leads to important new insights

regarding gas phase acidities of alkanes, which are relevant in connection with the scission of their C–H bonds.

A minor weakness of this book is that in many of the chapters there are frequent repeated references to the standard examples of C–H activations that have become well-known. This is, admittedly, almost unavoidable in a collection of individual articles, but it does become a little tedious for the reader. There is a large preponderance of authors from the USA (18 out of 20, although regrettably a few of the greatest names in this field are not included; the remaining two are from Australia and France). This is perhaps not surprising in view of the make-up of the group of editors, but nevertheless it does, unfortunately, reflect to some extent the relative output of contributions from different countries in this area of research. The greatest value of the book lies in the wide and interdisciplinary coverage of the subject, which is what the editors have set out to achieve and have succeeded in producing, without at the same time sacrificing detailed information. The fact that the title of the book describes a hope for future developments rather than the existing situation does not diminish the value of this collection of articles; on the contrary it emphasizes the need for intensive and interdisciplinary research using all the available methods and tools, and provides some pointers in that direction. For a field that is undergoing such rapid developement it is unfortunate that a book of this nature appearing in 1990 cannot include references to the very latest work (i.e. papers published in the latter part of 1989 or in 1990), but one presumably has to accept this as a necessary evil. Obviously in the very near future one could only justify buying the book on the grounds of the "Principles" mentioned in the subtitle rather than "Principles and Progress", but nevertheless one can be confident about the coverage of the former.

This specialized work can definitely be recommended unreservedly for everyone whose work is concerned with the activation and functionalization of hydrocarbons, or who wishes to learn about this field; it is at present the best treatment available on the market. It is certainly essential for appropriate libraries.

Peter Hofmann [NB 1166 IE]
Anorganisch-chemisches Institut
der Technischen Universität München,
Garching (FRG)

Physics and Chemistry of the Upper Atmosphere. By *M. H. Rees*. Cambridge University Press, Cambridge (UK) 1989. ix, 289 pp., paperback £ 15.00.—ISBN 0-521-36848-0

To fully understand the upper atmosphere requires a knowledge of many disciplines: the physics and chemistry of radiation, spectroscopy, fluid dynamics and the chemistry of gases. A typical student of physics or chemistry will have a knowledge of some, but probably not all, of these fields. In the introduction to this book the author sets himself the task of bridging the gap between the material covered in standard physics textbooks and the literature on upper atmosphere research. The resulting book succeeds in this aim. In it the student will find a good survey of the science of the upper atmosphere with useful references to the research literature.

In the introductory chapter *M. H. Rees* defines the upper atmosphere as the zone in which the energy sources consist of solar UV radiation, energetic particles, electric fields and electric currents, where the most important neutral species are O, N_2 and O_2, and the dynamic behavior of the neutral gas atmosphere is largely determined by plasma dynamics. The rest of the chapters consist of explanations and discussions of this theme.

Chapter 2 deals with photochemistry, in particular with the interaction of solar UV photons with N_2 and O_2 molecules, leading to the production of atomic nitrogen and oxygen together with $N_2^{\oplus}$, $O_2^{\oplus}$, $N^{\oplus}$ and $O^{\oplus}$ ions in the upper atmosphere. The basic theory of radiation transfer and photochemistry is described. High-energy electrons that are produced in the upper atmosphere interact strongly with the ions present, and this interaction is the subject of Chapter 3. In Chapter 4 the effects of collisions between particles in the ionosphere are analyzed: the distinction between elastic, inelastic and reactive collisions is explained and the theory of these processes is developed. Chapter 5 describes the composition of the upper atmosphere. The different temperatures of the molecules and ions in the ionosphere are discussed in Chapter 6. Chapter 7 is concerned with the spectroscopy of the emitted radiation, with the night sky light or airglow (which is also important in daytime), and with the polar aurora. Lastly, Chapter 8 describes the dynamics of the thermosphere and ionosphere.

The main emphasis of the book is on interpreting the results of observations on the composition of the upper atmosphere, often also with the help of relatively new data obtained from artificial satellites. Although the theoretical basis is adequately explained, enabling the reader to understand the important processes and to interpret data, some prior knowledge of theoretical physics would also be an advantage. Also it is difficult for a reader with no previous knowledge of the atmosphere to understand some parts of the book: for example, the D and F zones are referred to before they have been defined.

The text contains some inaccuracies. For example, in the treatment of dynamics in Chapter 8 the meaning of the hydrostatic equation is wrongly stated. It is not correct to say that the vertical velocity vanishes in this case; instead one should say that the vertical acceleration is small compared with the vertical gradients of the pressure field and of the gravitational force.

The example problems provided at the end of each chapter are very well chosen, since they are relevant to the main points covered in the chapters. Also at the end of each chapter there are literature references to results of recent research. These are an important help for readers wishing to study the subject at a more advanced level. The book includes a great deal of useful data, e.g. on the structure of the atmosphere and on the effects of solar radiation. To summarize, this is a well written and informative book. It is suitable as a textbook on the complex subject of upper-atmosphere science and can be recommended as such.

Steven Pawson [NB 1111 IE]
Institut für Meteorologie
der Universität Berlin (FRG)

Biocatalysis. (Van Nostrand Reinhold Catalysis Series). Edited by *D. A. Abramovicz*. Van Nostrand Reinhold, New York 1990. xxv, 369 pp., hardcover $ 89.95.—ISBN 0-442-23848-7

This volume, published as part of a series on catalytic methods of synthesis, is based on selected papers presented at an international conference on "Biocatalytic Synthesis of Organic Compounds", held in August 1988 at Saratoga Springs, NY (USA). It contains 17 articles related to different problem areas of biotechnology; without claiming com-

pleteness, the authors discuss some highly topical aspects of biocatalysis, a field that is characterized by very rapid development and increasingly importance. As the articles are written in the form of progress reports the emphasis is, as expected, not so much on completed solutions to general problems as on new lines of research and specific developments.

The range of topics encompasses a wide variety of methods for preparing organic fine chemicals, with a nearly equal balance between processes based on fermentation and those characterized by on applied enzymology. The articles deal with such widely varied problem areas as the application of genetic engineering to the optimization of microbial metabolic systems or the creation of new ones, single-stage and multi-stage enzymic conversions, and the use of free or immobilized enzymes in aqueous or organic media, as well as investigations of a more process-orientated nature on multiphase systems and reactor design, or on the use of thermophilic or other extremophilic organisms. Some examples of the detailed studies described are the use of enzymes in the hydroxylation of arenes, the synthesis of vitamin C, the synthesis of acrylamide by nitrile hydrogenation, the lipase-catalyzed formation of polyesters, the synthesis of amino acids by transamination, enantioselective dehalogenations, and the use of unusual oxidoreductases or of stereoselective aldolases. The main emphasis in most cases is on preparative applications, often supported by relevant enzymological data or by mechanistic evaluations. The first article is a (critical) account of the historical development of enzymology and of the growth in the understanding of biocatalytic processes—a rather unexpected theme in this context, but one that will probably be of particular interest to newcomers to the field.

The articles are, without exception, excellently written, clearly presented and carefully printed; the many tables, schemes, diagrams and even photographic illustrations contribute to the clarity of presentation and to the pleasure of reading the book. Since the topics are mostly very different from each other there is little overlapping, but on the other hand there are few internal cross-references. The bibliographies appended to each article usually list, as well as references to the authors' own research, the most important relevant papers by others, thus directing the reader to suitable background reading on topics that are unfamiliar. A useful feature in this respect, and one that other editors and authors are strongly recommended to copy, is that the citations give the complete title of the original publication in most cases. In contrast to this, however, the subject index is too brief.

Up-to-date information is a perishable commodity, and specialist reviews of rapidly developing subject areas are particularly affected by this problem. Inevitably some of the articles in this volume already no longer represent the latest state of knowledge in every detail, but nevertheless the choice and variety of the topics and the quality of presentation ensure that on average the book will have a "user-friendly expiry date".

To summarize, the book offers the reader, at several different levels, a stimulating cross-section of recent developments in a wide variety of topical areas of biocatalysis research, chosen so as to provide pointers to future trends. It can be recommended (also because of its price) as an addition to existing monographs on related subjects, particularly for libraries and scientists with interests in this area.

Wolf-Dieter Fessner [NB 1167 IE]
Institut für Organische Chemie und Biochemie
der Universität Freiburg (FRG)

Registered names, trademarks, etc. used in this journal, even when not marked as such, are not to be considered unprotected by law.

© VCH Verlagsgesellschaft mbH, W-6940 Weinheim, 1991. – Printed in the Federal Republic of Germany by Konrad Triltsch Druck- und Verlagsanstalt Würzburg.

All rights reserved (including those of translation into foreign languages). No part of this issue may be reproduced in any form — by photoprint, microfilm, or any other means — nor transmitted or translated into a machine language without written permission from the publishers. Only single copies of contributions, or parts thereof, may be made for personal use. This journal was carefully produced in all its parts. Nevertheless, authors, editors and publisher do not warrant the information contained therein to be free of errors. Readers are advised to keep in mind that statements, data, illustrations, procedural details or other items may inadvertently be inaccurate.

Valid for users in the USA: The appearance of the code at the bottom of the first page of an article (serial) indicates the copyright owner's consent that copies of the article may be made for personal or internal use, or for the personal or internal use of specific clients. This consent is given on the condition, however, that the copier pay stated per-copy fee through the Copyright Clearance Center, Inc. (CCC), for copying beyond that permitted by Sections 107 or 108 of the U.S. Copyright Law. This consent does not extend to other kinds of copying, such as copying, for general distribution, for advertising or promotional purposes, for creating new collective works, or for resale. For copying from back volumes of this journal see 'Permissions to Photo-Copy: Publisher's Fee List' of the CCC.

Editorial office: Postfach 10 11 61, W-6490 Weinheim, Federal Republic of Germany, Telephone (06201) 60 23 15, Telex 465 516 vchwh d, Telefax (06201) 602 328, E-Mail Z16@DHDURZ2 in Earn Bitnet.

Editor: *Peter Gölitz*

Associate editors: *D. I. Loewus, K. J. Schneider, A. Stimson.* **Editorial assistant:** *E. Schweikart*

Publishers: VCH Verlagsgesellschaft mbH. (Managing Director: *Hans Dirk Köhler.*), Pappelallee 3, W-6940 Weinheim, Federal Republic of Germany.

Advertising office (Advertising Manager *R. J. Roth*): Postfach 10 11 61, W-6940 Weinheim, Federal Republic of Germany, Telephone (0 62 01) 60 61 36, Telex 467 155, Telefax (0 62 01) 606 156.

ANGEWANDTE CHEMIE
International Edition in English
Volume 30 · Number 12
December 1991
Pages 1531–1750

New Approaches to the Use of Amino Acids as Chiral Building Blocks in Organic Synthesis

New Synthetic Methods (85)

By Manfred T. Reetz*

Dedicated to Professor Karl Heinz Büchel on the occasion of his 60th birthday

α-Amino acids protected at nitrogen in quite different ways can be transformed without racemization into the corresponding α-amino aldehydes. Provided one chooses the right protecting groups (e.g., two benzyl residues on nitrogen) it is possible for the first time to carry out Grignard-like, aldol, and Me_3SiCN additions, and hetero-Diels–Alder reactions with a high degree of nonchelation control. If the reactions of classical carbanions turn out to be nonselective, transmetalation, for example into organotitanium reagents, constitutes an important tool in controlling stereoselectivity. Diastereoselectivity can be reversed by specific variation of the protecting group and reagent. "Protecting-group tuning", "metal tuning", and "ligand tuning" are very useful in reactions of α-amino aldimines as well. The α-amino aldehydes can also be converted by Wittig reactions into electron-poor γ-amino olefins, which in turn undergo stereoselective cuprate, Michael, and cycloadditions.

1. Introduction and Goals

Chiral, nonracemic natural products, including amino acids, have long been utilized as building blocks for organic synthesis.[1] An impressive example is the synthesis of cytochalasine B (**1**) by *Stork* et al.,[2] in which three different natural products are incorporated into the target: L-phenylalanine (**4**), L-malic acid (**3**), and (+)-citronellol (**2**).

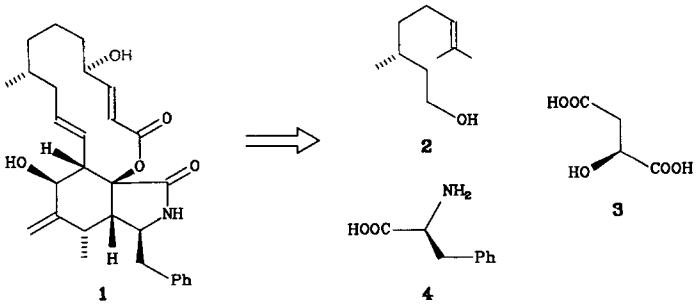

Nearly all the common L-amino acids have been employed in synthesis, and in quite diverse ways.[1] Such a strategy has gained in importance because efficient enzymatic processes, asymmetric syntheses, and new separation procedures have significantly expanded the number of available nonracemic amino acids.[3] The synthetic chemist today has available not only the many natural and synthetic L-amino acids, but also their enantiomeric D forms. An example of a particularly efficient enzymatic "separation procedure" involves the hydrolysis of amino acid amides with the aminopeptidase *Pseudomonas putida*.[4] This enzyme is capable of converting a racemic mixture of amino acid amides (**5**) into the corresponding L-amino acids (**6**) and D-amino acid amides (**7**), which are easily separable. The procedure displays nearly 100% stereoselectivity and is applicable to an unusually wide range of substrates.

[*] Prof. Dr. M. T. Reetz
Fachbereich Chemie der Universität
Hans-Meerwein-Strasse, W-3550 Marburg (FRG)
New Address:
Max-Planck-Institut für Kohlenforschung
Kaiser-Wilhelm-Platz 1, W-4330 Mülheim a. d. Ruhr (FRG)

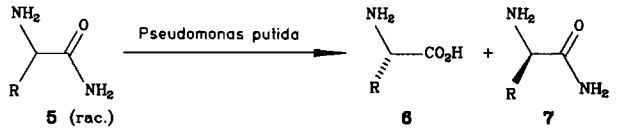

5 (rac.) 6 7

Apart from using amino acids in the synthesis of biologically active compounds and natural products, another goal has also become apparent in recent years: the development of stereoselective synthetic methods for transforming amino acids into other classes of compounds. Efforts to date have been directed particularly toward the preparation of β-amino alcohols **9**/**10** from protected α-amino aldehydes **8**, which in turn are accessible from the corresponding amino acids.[5] A number of highly interesting results have been recorded,[5] but so far no generally applicable method has appeared. For example, Grignard reagents and lithium enolates usually add to α-amino aldehydes **8** bearing *tert*-butoxycarbonyl (Boc) or benzyloxycarbonyl (Cbz) protecting groups with the formation of 1:1 or 2:1 mixtures of the diastereomers **9**/**10**.[5] Notable exceptions include additions

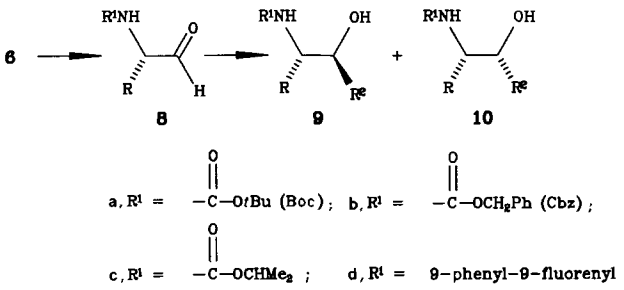

8 9 10

to certain α-amino aldehydes **8**, prepared, for example, from serine (cf. Section 3), as well as reactions of specific α-amino aldehydes with special reagents for the synthesis of particular natural products.[5]

A further complication is the fact that many protected α-amino aldehydes show a tendency to undergo racemization, and need to be handled in cold solvent and subjected to reaction as quickly as possible after their preparation.[5] The very bulky 9-phenyl-9-fluorenyl protecting group confers configurational stability on the aldehydes **8d** at room temperature, but Grignard and aldol additions result in the formation of 2:1 mixtures of diastereomers **9d**/**10d**.[6]

The lack of stereoselective methods is unfortunate, because β-amino alcohols constitute a pharmaceutically and biologically interesting class of substances. The compounds themselves frequently display appreciable biological activity, as in the case of the antibiotic chloramphenicol (**11**);[7] in other cases these structures are found as components of more complex active substances or natural products—for example, in the coronary agent alifedrin (**12**),[8] the aminopeptidase-B inhibitor bestatin (**13**),[9] the blood-pressure-reducing renin inhibitor pepstatin (**14**) and its synthetic analogues,[10] amino sugars [e.g., tolyposamine (**15**)],[11] and sphingolipids[11] and alkaloids.[12]

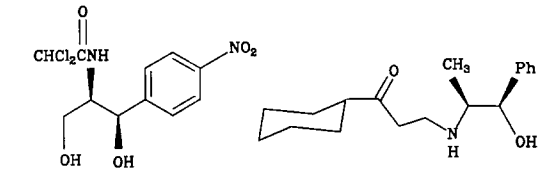

11 12

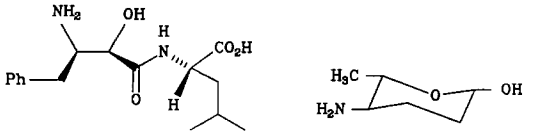

13 15

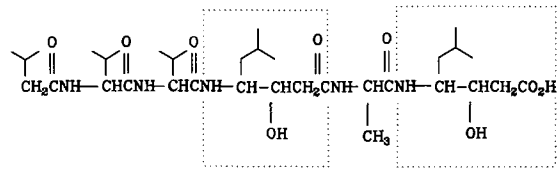

14

The first part of this progress report describes methods by which α-amino aldehydes (and α-amino ketones) can be converted selectively into either of the two diastereomeric forms of β-amino alcohols. Attention will be given not only to Grignard and aldol additions, but also to cyanohydrin- and epoxide-forming reactions of Me_3SiCN and sulfur ylides, respectively, as well as to hetero-Diels–Alder reactions. The emphasis here is on our own recent work; the complete literature on the subject up to 1988 has been summarized elsewhere.[5]

Another class of potentially accessible substances, again starting from α-amino aldehydes or amino acids, includes the

Manfred Reetz was born in Hirschberg, Silesia, studied chemistry at Washington University, St. Louis, and the University of Michigan, and obtained his doctorate under U. Schöllkopf at the Universität Göttingen in 1969. After a post-doctorate in Marburg with R. W. Hoffmann he habilitated there in 1974 in the field of dyotropic rearrangements. From 1978 to 1980 he was professor in Bonn and moved to the Universität Marburg in 1980. Since the summer of 1991 he has been Director at the Max-Planck-Institut für Kohlenforschung in Mülheim an der Ruhr. His research priorities lie in the development of new methods in synthetic organic chemistry, in particular the search for new organometallic reagents for chemo- and stereoselective C–C bond formation. Other fields of interest are peptide chemistry, molecular recognition, and polymer chemistry.

vicinal diamines. In contrast to the many known reactions of α-amino aldehydes, analogous C–C bond-forming reactions of α-amino aldimines as outlined in Scheme 1 have not been attempted until quite recently. Initial results are summarized in Section 5.

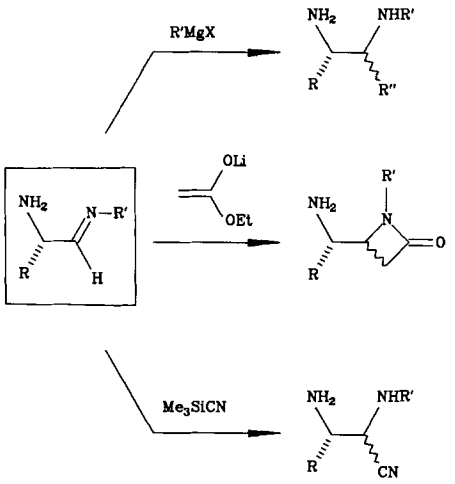

Scheme 1. Reactions of α-amino aldimines (protecting groups omitted).

Finally, in Section 6 attention is paid to stereoselective reactions of electron-poor γ-amino olefins, which can be prepared from the corresponding α-amino aldehydes via Wittig reactions (Scheme 2).

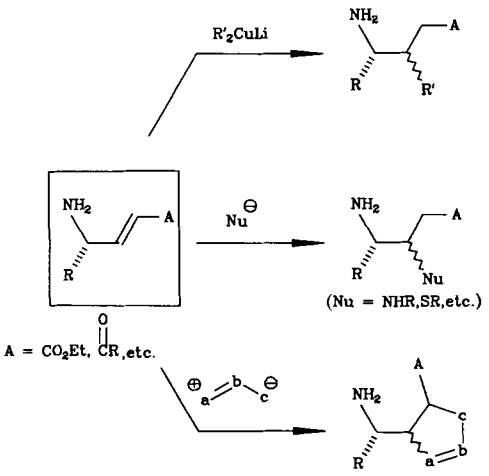

Scheme 2. Reactions of electron-poor γ-amino olefins (protecting groups omitted).

2. Methods

What methods are in fact available to the synthetic organic chemist who wishes to carry out the C–C bond formations outlined above stereoselectively and without racemization? Since most of the reactions discussed here involve organometallic agents, the choice of the metal ("metal tuning") and the ligand ("ligand tuning") must be made at the outset. Thus, unselective classical "carbanions" can be subjected to transmetalation—for example with the titanation reagents $ClTiX_3$ (Scheme 3).[13] This generates a new class of organometallic reagents $RTiX_3$ with electronic and steric properties that depend upon the nature of the ligands X at the metal. Thus, the chlorides $RTiCl_3$ are especially Lewis acidic, a characteristic that proves decisive, for example, in chelation-controlled reactions of chiral α- and β-alkoxy aldehydes.[14] Intermediate chelates form during the process, and these are attacked from the sterically less hindered side.[14] On the other hand, alkoxy and amino ligands increase the electron density at the metal as well as the overall size of the reagent, resulting in compounds of the type $RTi(OiPr)_3$ and $RTi(NEt_2)_3$, which are generally incapable of chelation. In some cases the observed stereochemical consequences then represent what has been interpreted within the framework of the Felkin–Anh model[15] as "nonchelation control".[14] This phenomenon is less general than chelation control, however, because the number of degrees of freedom of the free aldehydes is larger than that of the complexed forms.

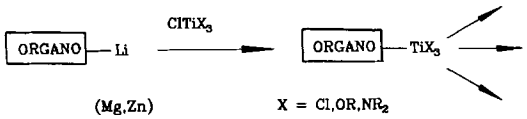

Scheme 3. Control of carbanion selectivity by titanation.

The extensive work in the area of organotitanium reagents as delineated above has stimulated a number of research groups to test other metals in a similar manner,[16] although systematic studies of ligand effects are still lacking. A particularly valuable metal in this context is cerium. Transmetalation of Grignard and organolithium compounds with $CeCl_3$ leads to reagents of the type $RCeCl_2$, which have proven to be especially useful in chemoselective additions to enolizable ketones.[16]

A further possibility for control—one that has generally been neglected—involves careful choice of the protecting groups to be used with polyfunctional molecules that are to be subjected to organometallic reactions.[17] It will be demonstrated below that protecting-group tuning in this sense can become a third and extraordinarily powerful method in the optimization of a stereoselective reaction, often in the proper combination with particular metals and ligands.

3. Preparation and Reactions of α-Amino Aldehydes

3.1. Nonchelation-Controlled Additions

Early attempts to design stereoselective addition reactions like those described above starting with traditionally protected α-amino aldehydes **8** and utilizing organotitanium reagents resulted in only sporadic success.[18] In the hope of evoking a positive protecting-group effect, doubly protected substrates were then synthesized, in particular the *N*,*N*-dibenzylamino aldehydes **18**.[19]

The readily accessible and isolable aldehydes **18** are configuratively stable at room temperature, and thus easy to handle.[19] The surprise actually came in the course of the subsequent reactions with Grignard and organolithium

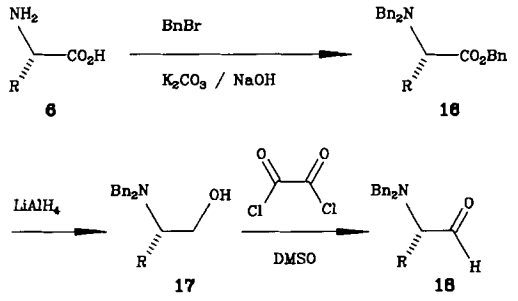

a, R = CH_3 ; **b**, R = $PhCH_2$; **c**, R = $(CH_3)_2CHCH_2$; **d**, R = $(CH_3)_2CH$; **e**, R = $tBu(CH_3)_2SiOCH_2$; **f**, R = $PhCH_2OCH_2$; **g**, R = $Bn_2N(CH_2)_3$; **h**, R = $Bn_2N(CH_2)_4$

Scheme 4. Bn = benzyl, DMSO = dimethylsulfoxide.

reagents. In nearly every case a diastereoselectivity of > 90% was observed in favor of the nonchelation-controlled adduct **20** (Table 1).[19] This result is rather remarkable, because it *cannot* involve chelation-induced reduction of degrees of freedom. Only in the case of the very reactive allylmagnesium chloride was a 1:3 mixture of diastereomers produced (cf. entry 12, Table 1). This particular problem can be solved by prior titanation of the Grignard reagent with $ClTi(NEt_2)_3$ (entries 13, 16). Nonchelation control is also applicable to reactions of cuprates and organocerium compounds (entries 6, 7), albeit with somewhat lower diastereoselectivity. Cyanohydrin-forming reactions can be effected quite generally with $Me_3SiCN/ZnBr_2$ (cf. entry 8, Table 1).[20] Here again the *N*,*N*-dibenzylamino aldehydes

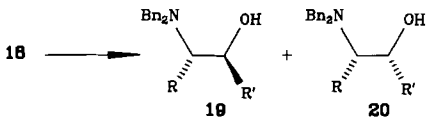

Table 1. Typical examples of nonchelation-controlled additions to the aldehydes **18** [18–20, 22]. (C_3H_5 represents allyl.)

no.	aldehyde	reagent	yield [%]	**19**:**20**
1	**18a**	CH_3MgI	87	5:95
2	**18a**	$CH_3Ti(OiPr)_3$	78	3:97
3	**18a**	PhMgBr	85	3:97
4	**18a**	EtMgBr	85	5:95
5	**18a**	*t*BuLi	88	<3:>97
6	**18a**	$(CH_3)_2CuLi$	80	25:75
7	**18a**	CH_3CeCl_2	70	10:90
8	**18a**	$Me_3SiCN/ZnBr_2$	74	5:95
9	**18b**	CH_3MgI	85	8:92
10	**18b**	PhMgBr	84	3:97
11	**18b**	PhC≡CLi	72	<4:>96
12	**18b**	C_3H_5MgCl	82	28:72
13	**18b**	$C_3H_5Ti(NEt_2)_3$	81	7:93
14	**18c**	CH_3MgI	85	10:90
15	**18c**	PhMgBr	84	3:97
16	**18c**	$C_3H_5Ti(NEt_2)_3$	81	3:97
17	**18d**	CH_3MgI	87	5:95
18	**18d**	PhMgBr	69	9:91
19	**18d**	2-thienyl	85	<5:>95
20	**18d**	$Me_3SiCN/ZnBr_2$	81	5:95
21	**18e**	$n\text{-}C_{13}H_{27}MgBr$	77	6:94
22	**18f**	PhMgBr	78	7:93
23	**18f**	$n\text{-}C_{15}H_{31}MgBr$	79	<5:>95
24	**18g**	CH_3MgI	62	6:94
25	**18g**	EtMgBr	70	8:92
26	**18h**	CH_3MgI	76	4:96

18 prove to be fortuitous representatives, since cyanohydrin-forming reactions with Boc-protected aldehydes **8a** display no selectivity.[9b, 21] The resulting products are key intermediates in the synthesis of such complex molecules as bestatin (**13**), epibestatin, amastatin, and epiamastatin.[9b, 21] Although the reactions proceed under conditions that are either quite basic or Lewis acidic, the C–C bond formations listed in Table 1 occur without any signs of racemization.

Although no organic chemist is likely to replace the inexpensive, naturally occurring norephedrin with a synthetic starting material in the preparation of such compounds as alifedrin (**12**), meaningful synthetic possibilities arise when substituted aryl or heteroaryl analogues are to be prepared (cf. entry 19, Table 1).[22] A further example of an intricate interplay between metal, ligand, and protecting group is illustrated by the synthesis of the amino alcohol **22**, which can be incorporated in modified form into peptide chains as an isosteric component. Whereas the organotitanium reagent **21** (X = O*i*Pr) provides a 60:40 mixture of diastereomers with the Boc-protected aldehyde **8a**,[23] the same reaction with the doubly protected analogue **18** (R = $PhCH_2$) is significantly more stereoselective (86:14 mixture).[24] A further increase in diastereoselectivity to 90% can be effected by the use of amino ligands (X = NEt_2) at titanium.[24]

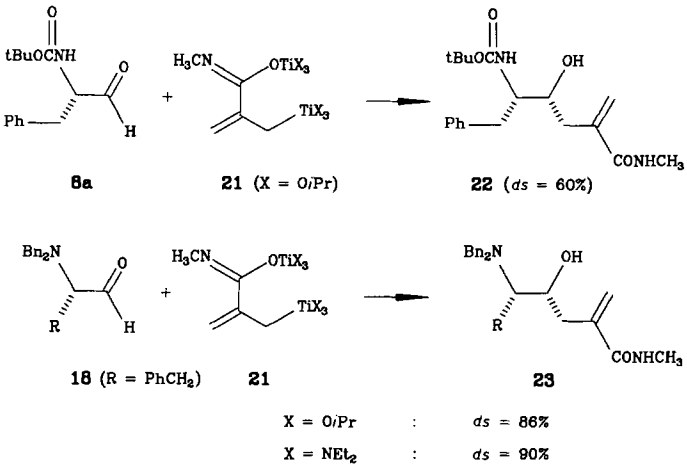

Although many reagents are known for homo-aldol additions,[25] so far only the homoenolate **24** has been subjected to reaction with aldehydes **18**.[26] Nonchelation control of 90–93% (yield 45–65%) has been achieved with several common members of the series (R = CH_3, *i*Bu, $PhCH_2$).

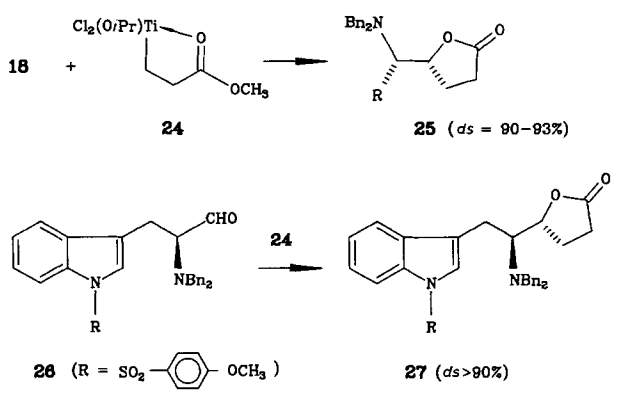

The aldehyde **26** derived from tryptophane reacts similarly.[26]

Ordinary lithium enolates (**28**) add surprisingly stereoselectively to the *N,N*-dibenzyl aminoaldehydes **18** (**29**:**30** = < 10:> 90), again without racemization.[19]

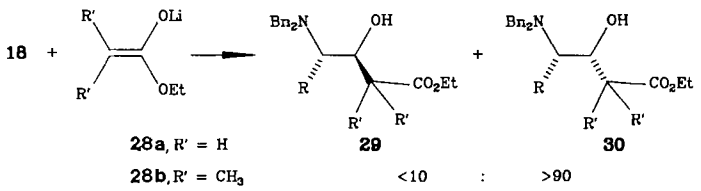

One example of the application of this nonchelation-controlled aldol addition pertains to the synthesis starting from isoleucine (**31**) of the unusual amino acid ester **33** with the (3*R*,4*S*,5*S*) configuration.[27] Compound **33** represents a building block useful in the synthesis of dolastatin 10 (**34**), recently isolated by *Pettit* et al. from the sea hare *Dolabella auricularia*.[28] This peptide is said to have the most powerful antineoplastic activity ever recorded for any natural or synthetic substance, and for this reason effective synthetic approaches to **33** and its analogues are important in cancer research. Aldol addition to aldehyde **32** gives essentially the

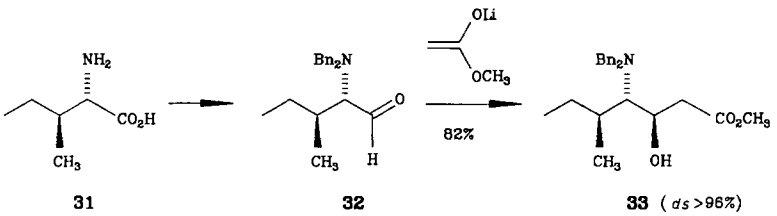

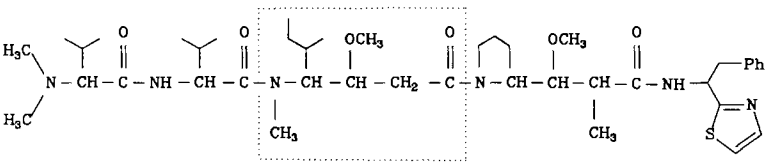

single product **33**, which has the desired absolute and relative configuration.[27] The conventional synthesis starting with Cbz-protected isoleucinal entails unselective lithium enolate addition, with formation of a 3:2 mixture of diastereomers (33% yield).[28] Stereoselective synthesis of similar components found in the peptides didemnin A and B[29] is comparably straightforward.[18]

An attempt was made to add *O*-phenyl-*O*-silylketene ketal (**35**) to the aldehydes **18** and **32**; however, the products isolated were not the aldol adducts **36**, but rather the β-amino γ-lactones **38** in diastereomerically and enantiomerically pure form.[30] This unexpected finding is a consequence of three successive $MgCl_2$-catalyzed reactions: nonchelation-controlled aldol addition to give **36** followed by lactone formation (**37**) and dyotropic rearrangement[31] (→ **38**). β-Amino γ-lactones are of interest in the synthesis of unusual amino acids[32] and amino sugars (cf. ristosamine).[33]

$EtAlCl_2$-induced additions of *O*-alkyl-*O*-silylketene ketals to the aldehydes **18** occur as expected with nonchelation control (94–99%), although under the experimental conditions the aldol adducts **30** undergo no further reactions.[34] Such *O*-silylketene ketals also react with the aldehydes **18** under nonchelation control provided *catalytic* amounts of europium salts like $Eu(fod)_3$ are employed.[18]

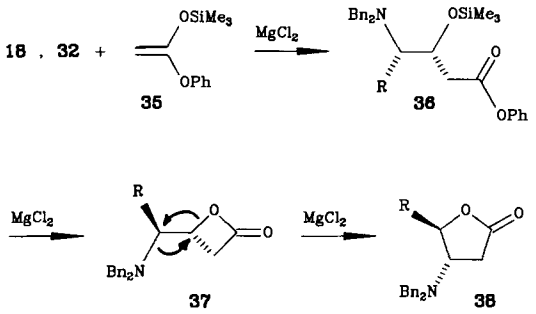

Three different research groups recognized simultaneously the value of *N,N*-dibenzylamino aldehydes **18** in the (formal) hetero-Diels–Alder reactions of electron-rich siloxydienes.[18,35,36] Both the Danishefsky diene **39**[18,36] and the Brassard diene **41**[35] react exclusively under nonchelation control. These reactions may actually involve an aldol addition followed by cyclization to the pyranes **40** and **42**. The

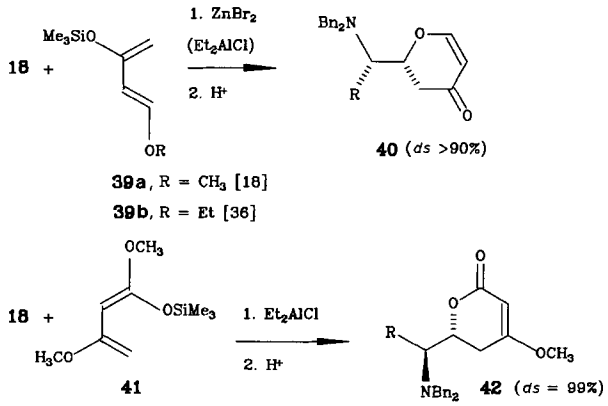

first examples of hetero-Diels–Alder reactions of the aldehydes **18** under high pressure (5 kbar) were recently described.[37]

If the reagents are prochiral, then along with the previously discussed diastereofacial selectivity the so-called simple diastereoselectivity also becomes relevant, and four diastereomeric products are possible. Starting with the titanium reagent **43**, readily accessible from crotylmagnesium chloride and $Ti(OiPr)_4$,[38] diastereomer **44** is essentially the only one formed.[27,39] This implies the usual nonchelation control as well as a predictably high simple diastereoselectivity (*anti*-selectivity). Titanation is absolutely essential, since the Grignard reagent alone reacts in a totally unselective way.

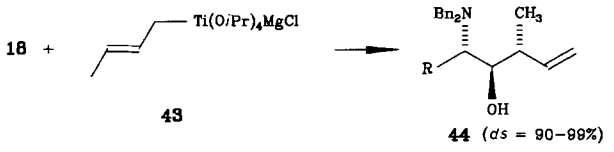

43 **44** (*ds* = 90–99%)

The *anti*-selective Heathcock enolate **45**[18,27] also reacts with complete stereoselectivity. Reversal in simple diastereoselectivity can be achieved with the *syn*-selective Masamune reagent **47**, although a second diastereomer that has not been characterized arises in the case of the bulky aldehydes **18** (R = $CHMe_2$, CH_2CHMe_2).[18]

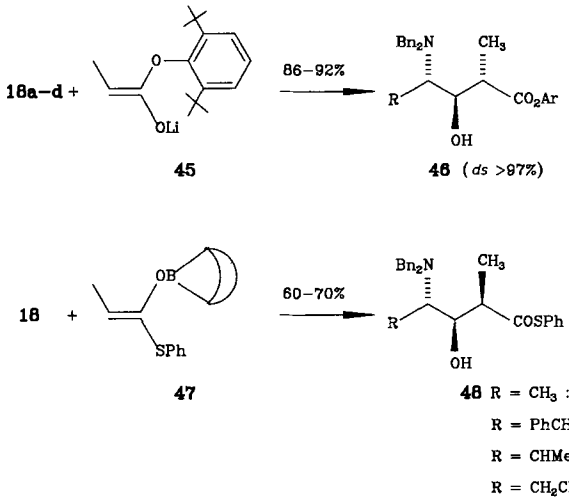

45 **46** (*ds* >97%)

47

48 R = CH_3 : *ds* >97%
R = $PhCH_2$: *ds* >97%
R = $CHMe_2$: *ds* = 76%
R = CH_2CHMe_2 : *ds* = 76%

Furthermore, the zinc enolate **49** derived from isocyanoacetic ester adds in a stereoselective way with formation of the adducts **50**/**51**. These lead after ring opening to the unusual class of α,γ-diamino acids **52**.[40] The crude reaction product consists here of a 10:90 mixture of **50** and **51**. A single recrystallization leads to the diastereomerically and enantiomerically pure ester **51** (81% isolated yield), which can be converted quantitatively into the diamino acid ester **52** by the method of *Schöllkopf* and *Hoppe*.[41]

An elegant one-pot procedure for stereoselective nucleophilic acylation of the aldehydes **18** resulting in the enones **56** takes advantage of the titanium reagent **53**.[42] This again involves a nonchelation-controlled nucleophilic addition,

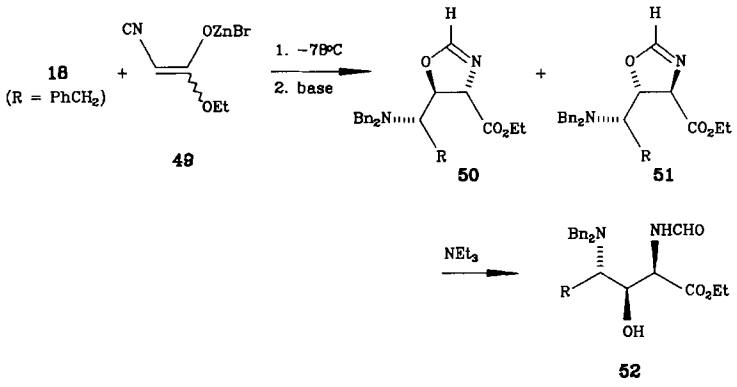

49 **50** **51** **52**

followed in this case by stereospecific elimination and rearrangement **54** → **55** → **56**. The lithium precursor to **53** reacts unselectively.[43]

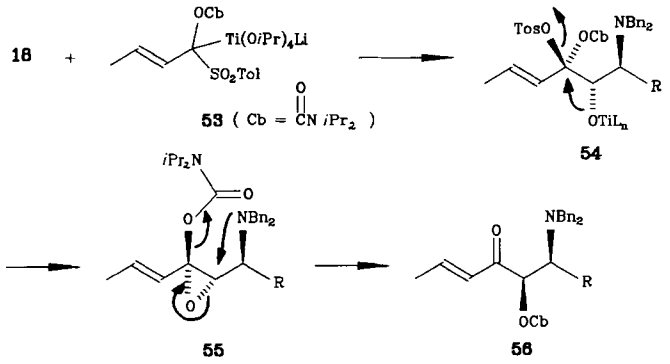

Since aminoalkyl oxiranes are valuable building blocks in the synthesis of dipeptide isosteres and other pharmacologically important amino alcohols, there have been many attempts to perform stereoselective reactions of protected α-amino aldehydes with sulfur ylides.[44] Nevertheless, every case so far reported has led to a 1:1 mixture of the two possible diastereomers and a maximum total yield of 50%.[44] In the hope of achieving stereochemical results comparable to those of the previously investigated organometallic addition reactions, the *N*,*N*-dibenzylamino aldehydes **18** were allowed to react with the ylides **57**, **58**, and **59**. Indeed, the desired adducts **61** were formed as the predominant diastereomers, although the extent of stereoselectivity turned out to be less than 90%.[45] A possible reason why a sterically less demanding reagent like CH_3MgCl produces significantly *higher* diastereoselectivity than ylides of

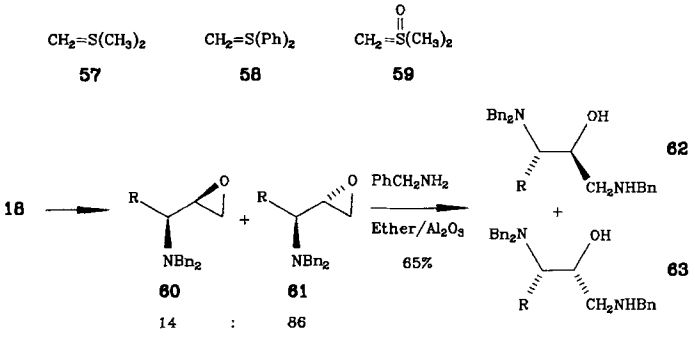

57 **58** **59**

60 : **61**
14 : 86

62

63

the type $CH_2{=}SR_2$ will be discussed in Section 3.2. Only with the bulky arsenic ylide $CH_2{=}As(Ph)_3$ were "normal" diastereoselectivities again observed (90–99%).[45] Whereas oxiranes **60**/**61** cannot be separated easily, the corresponding open-chain compounds resulting from nucleophilic substitution (e.g. **62**/**63**) are readily separable by chromatography.[45]

With respect to cleavage of the benzyl protecting groups by hydrogenolysis, the catalyst originally selected was Pd black (65–90% yield).[19] Problems were occasionally encountered, however, especially with catalysts that were no longer sufficiently fresh.[18] Generally, deprotection is much more efficient with the Pearlman catalyst [$Pd(OH)_2$] according to the method of *Yoshida*[46] (75–95% yields).[18] Since the products **64** are quite polar, careful extraction is essential.

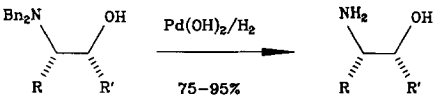

20 **64**

The preceding discussion indicates that the presence of the *N*,*N*-dibenzylamino group is a prerequisite for high diastereoselectivity. There are special situations in which this is not the case, however.[5] For example, serinal has been investigated with quite a wide variety of protecting groups. The Garner aldehyde **65**—accessible in four steps from serine—is of particular preparative significance.[47] A diastereoselectivity of about 88% in favor of the nonchelation-controlled adduct **67** has been achieved with lithium enolates.[48] Diastereoselectivity can be reversed under Lewis acidic conditions (cf. Section 3). Addition of Grignard and alkyllithium reagents occurs under nonchelation control, although there is some scatter in the selectivities (84–95% *ds*).[49] Results achieved in the addition of alkynyllithium compounds are quite acceptable—diastereoselectivities of 95% are the rule. This finding has been exploited in the synthesis of sphingoid bases.[50,51] Since the protecting groups are also easily cleaved, aldehyde **65** can be described as a real winner. It must be noted, however, that the compound cannot be isolated in a state of complete enantiomeric purity (*ee* = 93–95%).[47]

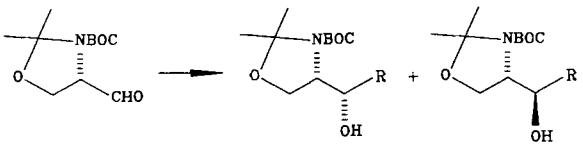

65 **66** **67**

The serinal derivatives **18e** and **18f**[18,52] offer both advantages and disadvantages relative to the Garner aldehyde **65**. On one hand, any olefin residues present in the reaction product are subject to undesirable reduction during cleavage of the protecting groups by hydrogenolysis. On the other, no racemization is observed during either the synthesis or the highly selective reactions of aldehydes **18e**/**18f** (entries 21–23, Table 1).[18,52] Also aldol additions proceed with nonchelation control.[52]

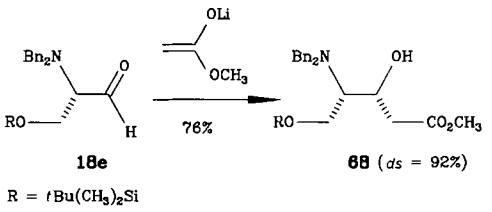

18e **68** (*ds* = 92%)

R = *t*Bu(CH$_3$)$_2$Si

Grignard-type addition to the allothreoninal **69** that has two stereogenic centers proceeds according to the usual pattern, although the observed nonchelation control here is somewhat less pronounced.[52] Apart from studies of the serinal derivatives **18e**/**18f**,[52] allothreoninal (**69**),[52] tryptophanal (**26**),[26] ornithinal (**18g**) (entries 24–25, Table 1),[18] and lysinal (**18h**) (entry 26, Table 1),[18,53] relatively few attempts have been made to transform amino acids containing additional functional groups into the corresponding *N*,*N*-dibenzylamino aldehydes.

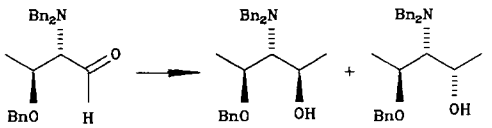

69 **70** **71**

CH_3MgI(−78°C/18h)	86	:	14(88%)
$CH_3Ti(O{i}Pr)_3$(22°C/16h)	93	:	7(73%)

Efforts to synthesize the corresponding aldehyde from methionine (**72**) have proven unsuccessful, since the sulfur function is alkylated under the benzylation conditions. This results in the expected formation of the lactone **73**, an interesting molecule in other contexts.[30]

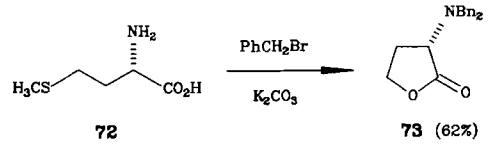

72 **73** (62%)

The desire to extend the spectrum of nonchelation-controlled nucleophilic additions to α-amino aldehydes started a quest for other potential protecting groups. In the course of a search for systems in which the protecting group can be cleaved by hydrolysis, the benzostabase protecting group (BSB) was developed. This group can be introduced smoothly into the amino acid esters **74** under Pd catalysis.[54] A one-pot reaction of the ester **76** protected in this way entails reduction followed by a highly nonchelation-controlled reaction of the intermediate aldehyde with Grignard or organolithium reagents, and subsequent deprotection of the product in the course of acidic workup. The analytically pure products **77** can be isolated in 40–60% yield, which is quite respectable given the three steps involved.

Nonetheless, the development of additional protecting groups remains a worthwhile endeavor.[55]

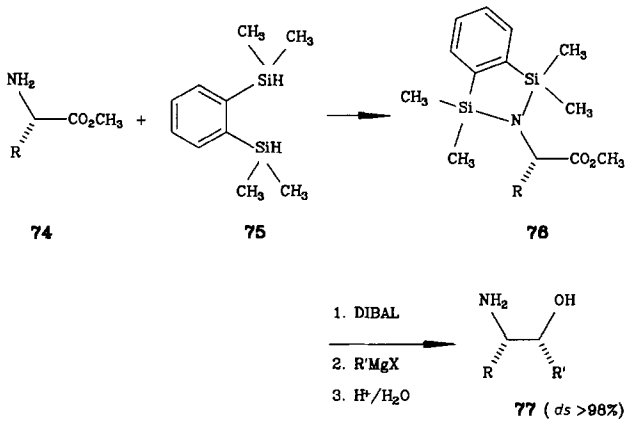

74 75 76

While attempting to uncover the origin of the unanticipated nonchelation control, both smaller and larger protecting groups were investigated. A dramatic influence of steric parameters was especially apparent in the reactions of *N*,*N*-dimethylamino aldehydes **78**:[18] absolutely no useful diastereoselectivity whatsoever was observed!

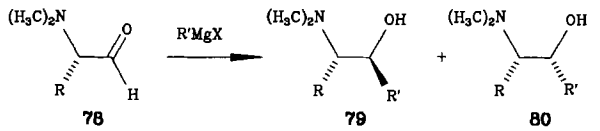

78 79 80

a) R = CH_3 ; R' = Ph	50	:	50
b) R = $PhCH_2$; R' = CH_3	35	:	65
c) R = $PhCH_2$; R' = Ph	48	:	52

The conclusion that the number and size of the protecting groups is decisive has been substantiated by studying the synthesis and reactions of the *ortho*-methylbenzyl-protected aldehydes **81**. The 99% stereoselectivity achieved for Grignard additions in this case exceeds that of analogous additions to the *N*,*N*-dibenzylamino aldehydes **18**.[18] This selectivity-enhancing effect is also applicable to additions of sulfur ylides, although nonchelation control cannot be driven above 92%.[45]

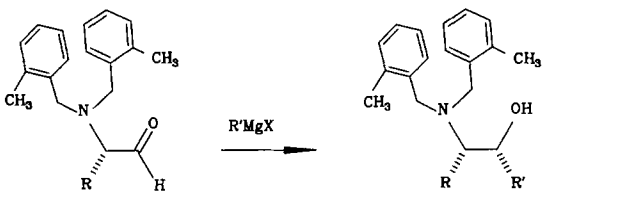

81 82 (ds = 99%)

3.2. Models for Explaining the Observed Nonchelation Control

Theoretical studies concerning the origin of the nonchelation control described in the previous section are not yet complete, but two possible explanations have emerged.[27]

From a formal standpoint the observed stereochemical results are in agreement with the Felkin–Anh model.[15] One particular conformation (in this case **83**) leads to maximum lowering in energy of the LUMO (π^* bond), hence a maximum degree of reactivity.[27] Nevertheless, MO calculations show that the requisite π^*–σ^*_{C-N} conjugation in the parent amino compound **84** (R = NH_2) is nearly insignificant,[56] in contrast to the π^*–σ^*_{C-Cl} conjugation in the chloro compound **84** (R = Cl) (Fig. 1). The σ^*_{C-N} orbital simply lies too

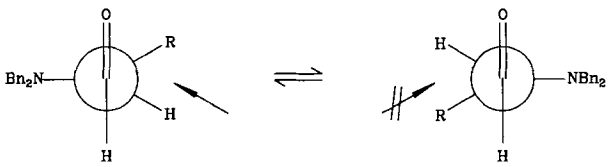

83a 83b

high. However, since metal ions may complex at nitrogen (without necessarily entering into chelation), the possibility of a dramatic change in the electronic nature of the C–N σ bond emerges. Indeed, MO calculations for α-amino aldehydes complexed at nitrogen with BH_3 (where the Lewis acid BH_3 serves as a model for a metal ion) show a drastic lowering in the energy of the π^* orbital (cf. Fig. 1).[56] The Anh model extended in this sense would also explain differences in diastereoselectivity with Grignard and essentially salt-free sulfur ylide reactions. Not so easily interpreted, however, is the enormous protecting-group effect on changing from *N*,*N*-dibenzyl- to *N*,*N*-dimethylamino aldehydes (**18** and **78**, respectively).

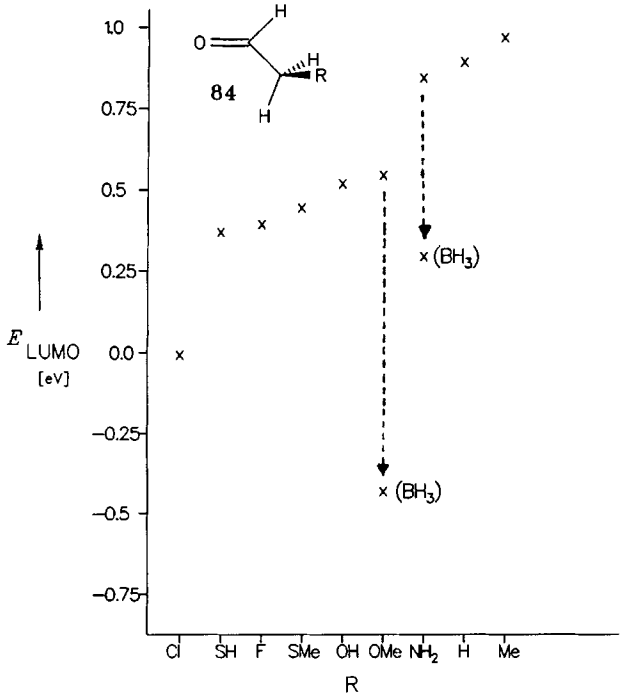

Fig. 1. Location of the LUMOs in aldehyde **84** as a function of substituents R. Dashed arrows indicate lowering of the LUMOs through complexation with BH_3 at the NH_2 or CH_3O groups.

A second model takes into account the ground-state structures of the various α-amino aldehydes.[27,57] Preliminary force-field calculations on the parent structure **18a** show

that conformation **85** represents the most stable form, and that small conformational changes involving the benzyl groups result in certain energy differences. The prediction that the carbonyl function and the α and β C-atoms lie essentially in a single plane is the most significant result. This also

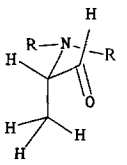

85 R = $PhCH_2$

represents the preferred conformation for propanal and other simple achiral aldehydes, an observation that has been explained by *Wiberg* on the basis of dipole–dipole interactions.[58] A recently completed X-ray structural analysis on the amino aldehyde **18b** confirms the validity of the force-field calculations (Fig. 2).[59] It is apparent that the back side

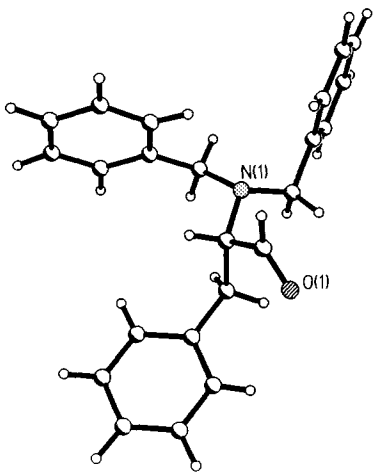

Fig. 2. Crystal structure of the aldehyde **18b**.

of the carbonyl function is sterically shielded. Assuming that the conformation of the ground state corresponds to that of the reacting molecule, front-side attack—and thus nonchelation control—can be rationalized. When the space behind the carbonyl function is less completely occupied, as in the case of the *N,N*-dimethylamino aldehydes **78** or the monoprotected analogues **8**, this model explains the lower diastereoselectivity. Furthermore, larger protecting groups should have the opposite effect, a conclusion consistent with experimental observations (cf. **76** and **81**). The metal complexation at nitrogen considered previously would have the further effect of increasing the passive volumes of the amino groups.[56]

3.3. Chelation-Controlled Additions

Chelation of chiral α- and *β-alkoxy* aldehydes with $TiCl_4$, $SnCl_4$, or $MgBr_2$, followed by diastereoselective addition of appropriate carbon nucleophiles such as R_2Zn, allyl and enol silanes, or Me_3SiCN has become a general principle in stereoselective synthesis.[14] However, attempts to carry out an analogous procedure with the *N,N*-dibenzylamino aldehydes **18** did not always result in diastereoselectivities above 90% (Table 2).[19] In contrast, $TiCl_4$-mediated ene reactions on the same aldehydes lead to high degrees of chelation control.[34] $MgBr_2$-mediated addition of Me_3SiCN to the aldehydes **18** proceeds with modest chelation control (*ds* ≈ 80%).[20]

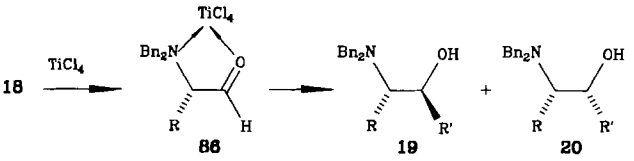

Table 2. Typical examples of chelation-controlled additions to the aldehydes **18** [18–20]. C_3H_5 = allyl

no.	aldehyde	reagent	yield [%]	**19**:**20**
1	**18a**	$TiCl_4/(CH_3)_2Zn$	82	94: 6
2	**18a**	$SnCl_4/C_3H_5SiMe_3$	85	84:16
3	**18b**	$SnCl_4/C_3H_5SiMe_3$	79	87:13
4	**18b**	$TiCl_4/(CH_3)_2Zn$	63	78:22
5	**18b**	$TiCl_4/Me_3SiCN$	58	78:22
6	**18c**	$SnCl_4/C_3H_5SiMe_3$	78	90:10
7	**18c**	$TiCl_4/Me_3SiCN$	63	88:12
8	**18d**	$TiCl_4/(CH_3)_2Zn$	65	65:35
9	**18d**	$SnCl_4/C_3H_5SiMe_3$	79	95:5
10	**18d**	$TiCl_4/Me_3SiCN$	63	84:16

The explanation for these nonuniform findings may be based on steric inhibition of chelation. Whereas chiral α-alkoxy aldehydes form only a single reactive species (chelate) with $TiCl_4$,[14,60] NMR studies reveal that there are actually several species involved with the *N,N*-dibenzylamino aldehyde/$TiCl_4$ complexes **86**.[18] As a result of weaker N–Ti bonding and steric interaction between the chlorine ligands, benzyl groups, and other residues on the five-membered ring, complex **86** opens rather readily. According to the Curtin–Hammett principle, the most reactive species then undergoes reaction, and this need not always lead to the chelation-controlled adduct. Consequently, investigations were undertaken on less sterically demanding protecting groups (cf. **87**[19] and **90**[18]). This approach did in fact result in efficient chelation control in the Grignard-like addition of cuprates. In other words, a change from benzyl protecting groups to the smaller analogues present in **87** and **90** results in complete reversal of diastereoselectivity! This example of

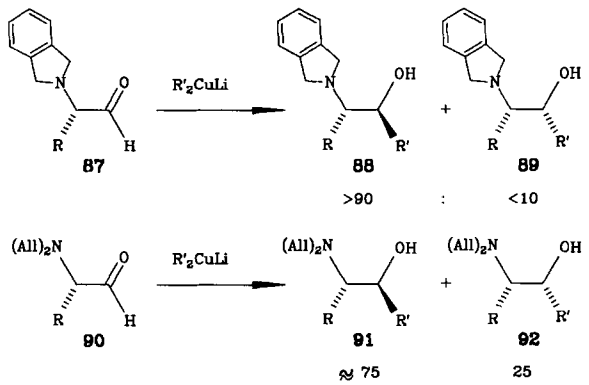

protecting-group tuning is only effective, however, in combination with metal tuning, since alkyllithium reagents react with the aldehydes **87** and **90** (All = allyl) in an unselective way.[18] A relevant observation here is the fact that the *N,N*-dimethyl analogues **78** react with cuprates under 99% chelation control.[18]

In the case of the aldehydes **87** such results are mainly of mechanistic interest, since the protecting groups are not easily cleaved. The situation is different with the monoprotected aldehydes **8a** and **8c**, which after treatment with $SnCl_4$ or $TiCl_4$ undergo particularly facile chelation-controlled allyl[61] and enol silane additions,[62] as well as ene reactions,[34] and the products can be readily deprotected. However, Grignard-like additions with cuprates proceed with nonuniform stereochemical results.[18] Chelation-controlled hetero-Diels–Alder reactions are possible using the Garner aldehyde **65**.[48]

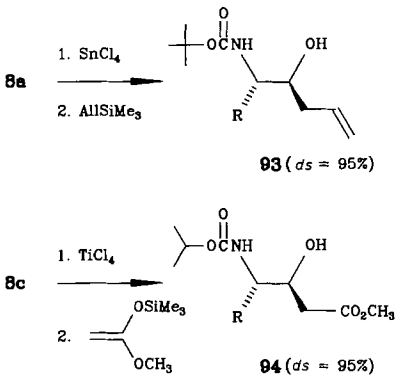

Very effective chirally modified boron enolates add to the aldehydes **18** to give aldol products **29** or **30** depending on the absolute configuration of the reagent.[63] Nevertheless, relying solely on reagent control[64] implies greater effort and cost.

4. Preparation and Reactions of α-Amino Ketones

Stereoselective reductions of α-amino ketones have been studied extensively in the earlier literature.[65] However, the reported cases refer almost exclusively to racemic starting materials or to systems bearing residues on nitrogen that are difficult to cleave (alkyl, aryl). A first systematic study has shown that the activated amino acids **95** can be converted without racemization into the ketones **96**.[66] On using $NaBH_4$ in methanol the reduction occurs under nonchelation control (**19**:**20** > 90:10). The products are the same ones that arise in chelation-controlled C–C bond-forming reactions of the aldehydes **18**. Since the latter processes do not always occur stereoselectively, a route via the ketones **96** is an attractive alternative. Compounds prepared in this way include statin (derivative **98b**), which occurs in pepstatin (**14**).[67]

Boc-protected α-amino ketones **99** undergo chelation-controlled reduction with $Et_3SiH/TiCl_4$.[68] Ketones **101** derived from *N*-phenylsulfonylserine can be transformed selectively into the adducts **102** or **103** depending upon the nature of the reducing agent.[69] It remains unclear whether

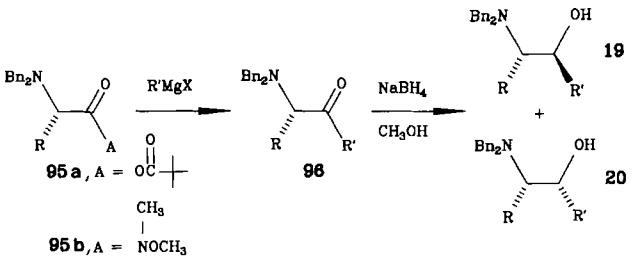

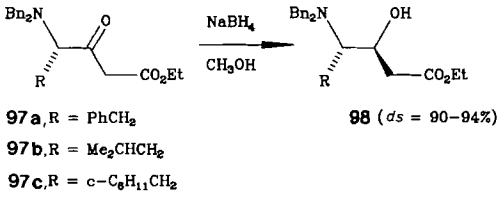

this method can be generalized to substrates derived from other amino acids.

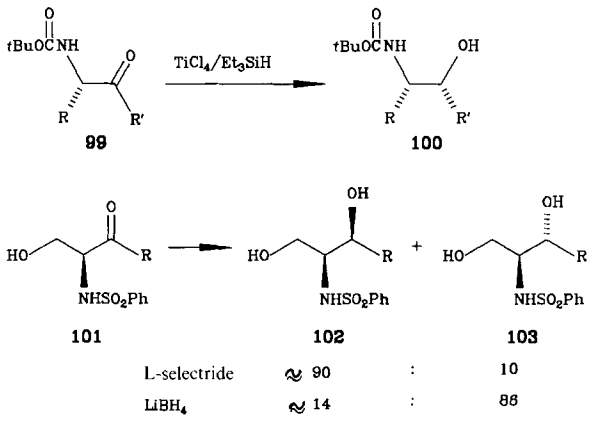

Grignard additions to the *N,N*-dibenzylamino ketones **96** occur with a high degree of nonchelation control (*ds* > 95%).[18]

5. Preparation and Reactions of α-Amino Aldimines and α-Amino Ketimines

The first transformation of chiral α-amino aldehydes into the corresponding aldimines has recently been described using the *N,N*-dibenzyl derivatives **18** → **104**.[70] Since Grignard-like additions to simple aliphatic aldimines are notoriously difficult due to competition from α-deprotonation, it was not expected that corresponding C–C bond formation in the case of the aldimines **104** would be easy. Indeed, essentially no conversion was observed using R_2CuLi/BF_3[71] or Grignard and alkyllithium reagents in THF. In contrast, organocerium compounds $RCeCl_2$[16] are capable of adding to **104**, and they do so under chelation control (cf. **106**).[70] In some instances even alkyllithium reagents add, provided *ether* is used as the solvent. In the case of CH_3Li and $CH_3Li/CeCl_3$, diastereoselectivity is >95%, although the yield does not exceed 40%. This shortcoming can be eliminated with the very reactive reagent $3CH_3Li/CeCl_3$ (>75% yield with >95% diastereoselectivity). It has not yet been established

whether $(CH_3)_3Ce$ or ate complexes are involved.[70] In any event, the intermediacy of chelates of the type **105** is probable. Since the reagents RLi and $RLi/CeCl_3$ add to the analogous aldehydes **18** under nonchelation control, aldimines apparently constitute better chelating agents. This is a consequence, among other things, of the (*E*) configuration of the C–N double bond, which permits only *syn* complexation necessary for chelation. Analogous hydrazones derived from *N*,*N*-dimethylhydrazine also react with alkyllithium reagents under chelation control.[18]

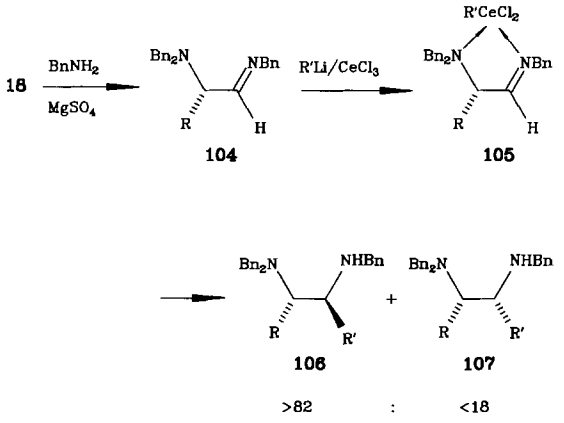

In order to reverse the sense of diastereoselectivity the donor strength of the nitrogen atoms in the α-amino aldimines must be weakened to such an extent that effective chelation is precluded. This can in fact be achieved by replacing the benzyl protecting group on the aldimine nitrogen by the electron-withdrawing tosyl function. Thus, aldimines **108** prepared according to the Weinreb method[72] react with Grignard reagents under nonchelation control to give the adducts **110** (61–95% yield; *ds* = 90–99%).[70] These substrates therefore behave stereochemically like the aldehydes **18**. Adducts **106** and **110** can usually be deprotected without difficulty. In those cases in which difficulties are encountered, other protecting groups must be used. To this end phosphorus-based groups are being developed.[18] It is significant to note that both the preparation and the reactions of the aldimines **104** and **108** occur without racemization.[70] Vicinal diamines are encountered as ligands in metal-induced stereoselective reactions, in various chemotherapeutic contexts (cisplatin analogues and technetium-99 contrasting agents), as well as in a wide variety of natural products.[70]

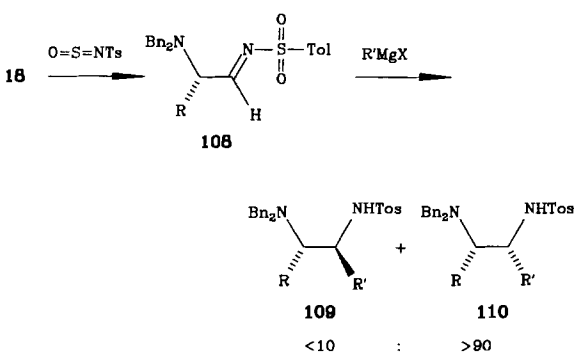

Other very different types of C–C bond-forming reactions of α-amino aldimines are currently under intensive investigation.[18] Preliminary experiments with the aldimines **111** prepared according to the Cainelli method[73] show that stereoselective aldol additions are possible, resulting in formation of the unusual β-lactams **112**. As proven by an X-ray structural analysis of adduct **112** (R = CH_3), the process involves nonchelation control.[18] Since the bulky aldimines **111** are relatively unreactive (failing, for example, to react with the Li enolate of ethyl acetate at low temperature), the more reactive *N*-tosylaldimines **108** were employed. These do in fact react highly selectively with virtually all Li ester enolates to give the diamines **113**.[18] Nonchelation control is likely, but remains to be proven.

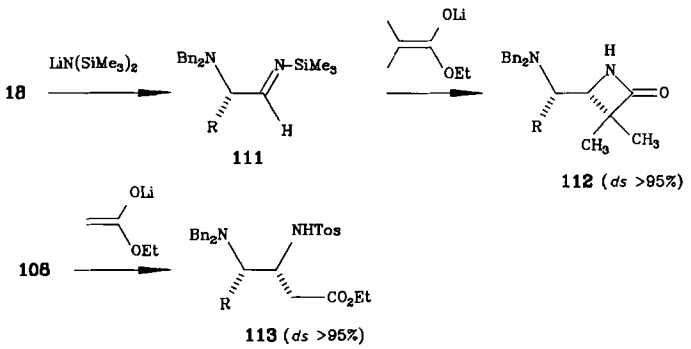

Stereoselective addition of Me_3SiCN to α-amino aldimines (e.g. **104**) would be another important step toward preparative exploitation of this class of compounds. Hydrolysis of the nitrile function, for example, would lead to the biologically important class of α,β-diamino carboxylic acids. As a first example we cite the $TiCl_4$-mediated addition of Me_3SiCN, resulting in formation of the adduct **115**. Definitive proof of the stereochemistry remains to be presented.[18,74] However, since BF_3/OEt_2 also leads to the same product, nonchelation control is likely. This cannot involve a thermodynamically based equilibrium favoring **115**, be

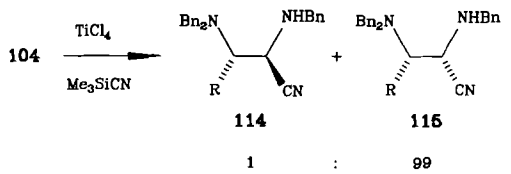

cause higher reaction temperatures result in a 1:1 mixture of **114**/**115**. Whether reversal of diastereoselectivity can be achieved with other protecting groups or alternative reagents remains to be seen. Reaction of the aldimine **108** (R = $PhCH_2$) with $Me_3SiCN/SnCl_4$ leads as expected to the corresponding nonchelation-controlled adduct **115**, the relative configuration of which has been verified by X-ray analysis.[74]

In principle, α-amino ketones **96** should be amenable to reductive amination to give the corresponding vicinal diamines. In practice this actually succeeds only with the methyl ketones **96** (R′ = CH_3); all other substrates are too

bulky or too unreactive.[75] With $NaCN \cdot BH_3$ in the presence of benzylamines, for example, reaction occurs without difficulty, resulting in virtually exclusive formation of the products **106**. It is probable that the process involves reduc-

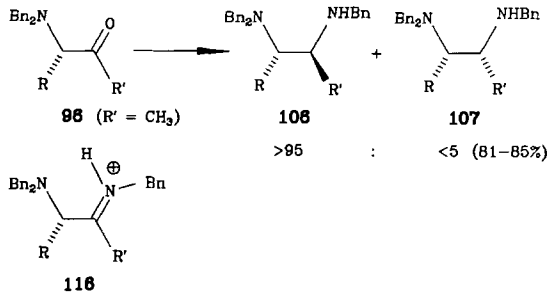

tion of the intermediate ammonium ions **116** under nonchelation control.

6. Preparation and Reactions of Electron-Poor γ-Amino Olefins

6.1. Cuprate and Other Michael Additions

In order to take advantage of the synthetic potential of *N*,*N*-dibenzylamino aldehydes **18** in yet another context, the electron-poor olefins **117** were prepared without racemization by using the Horner–Wittig reaction.[76] This provides an enantiomerically pure class of compounds suitable for cuprate and other 1,4-Michael additions as well as epoxidation and Diels–Alder or 1,3-dipolar cycloadditions. Although not all of our expectations have been fulfilled, results to date are quite promising. For example, cuprates add highly diastereoselectively in the presence of Me_3SiCl to form the enantiomerically pure *syn*-configurated adducts **118**.[76]

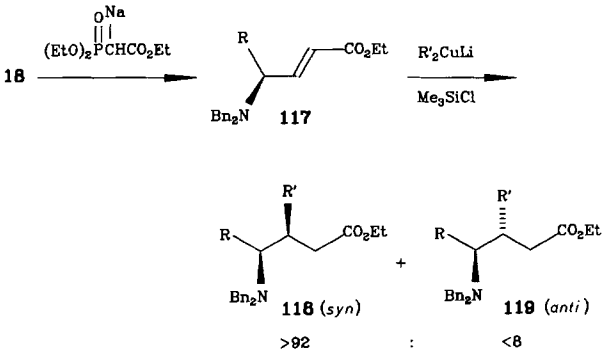

Since γ-aminobutyric acid (GABA) is a compound of considerable biological importance, the products **118** could well be of interest, especially in unprotected form (e.g. **120**).[76]

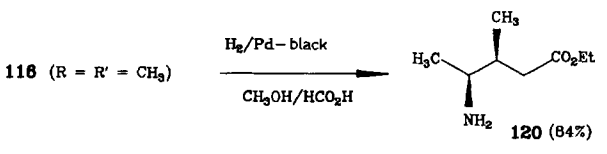

Knoevenagel products **121** were prepared in order to reverse the sense of diastereoselectivity. These proved to be considerably more reactive, with no requirement for Me_3SiCl in cuprate addition, and lead preferentially to the *anti* adducts **123** (*ds* = 79–99%).[76]

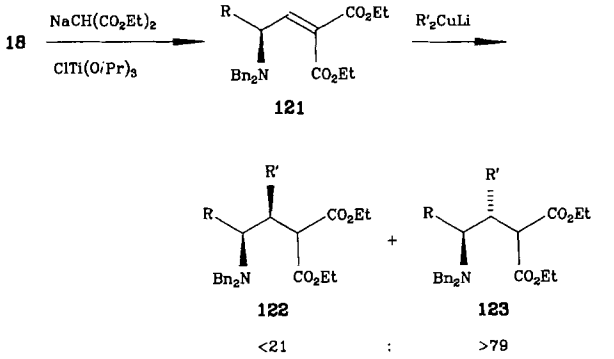

What is the origin of the observed diastereoselectivity in the reactions described above? In the case of the diesters **121** 1,3-allylic strain[77] certainly plays the decisive role.[76] This factor causes conformation **124** to be favored relative to **125**; steric interaction between the residue R and the *cis* ester group would otherwise result in an energetically unfavorable situation, a conclusion supported by force-field calculations.[78] NMR studies reveal that the reaction commences with the formation of Cu–olefin π complexes.[78] Mechanistic interpretation of additions to the ester **117** is more difficult, since force-field calculations show that no particular conformation is favored.[78] For this reason only speculation is possible, for example by assuming a Bürgi–Dunitz trajectory.[79]

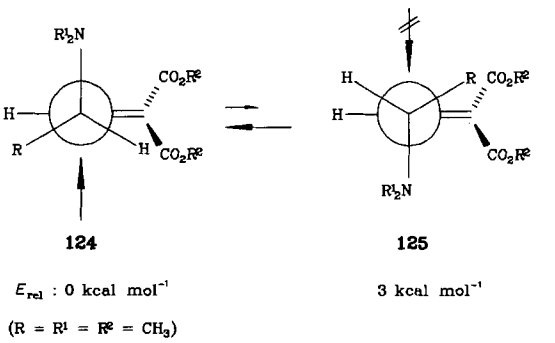

Analogously to the esters **117**, the more reactive ketones **126** also react with cuprates.[78]

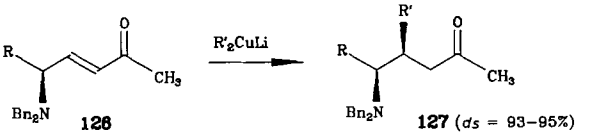

Quite recently the α,β-unsaturated esters have also been subjected to reaction with nitrogen nucleophiles. Whereas amines such as benzylamine react primarily with the ester function to give the undesired amides, the silylated hydroxy-

lamine **128** undergoes smooth and highly stereoselective Michael addition with diesters **121** (though not with **117**).[78] The sense of the diastereoselectivity is the same as in the case of cuprate additions; that is, 1,3-allylic strain is once again the controlling factor (cf. **124**).

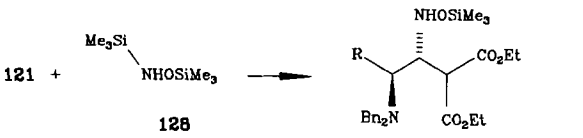

128 **129** (*ds* = 91–95%)

Since epoxides are useful vehicles for subsequent synthetic transformations, special attention has been directed toward epoxidation of the esters **117**.[80] By using special conditions (*tert*-butylhydroperoxide/potassium *tert*-butoxide in ammonia/THF) smooth epoxidation can be effected. From a mechanistic point of view this probably involves 1,4-addition/elimination, in which the same diastereotopic face of the electron-poor π system is attacked as in the case of the cuprates. The conditions employed result in saponification to the corresponding carboxylic acids, which are then esterified to simplify isolation (overall yield of **130** ca. 50%). Epoxidation is also possible with the ketones **126**, providing a significantly higher isolated yield of the epoxides **131** (>80%; *ds* > 95%).[80]

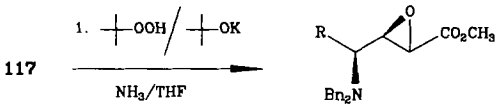

130 (*ds* >95%)

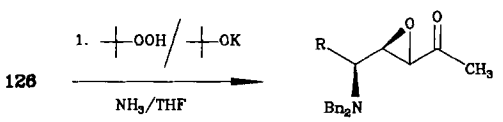

131 (*ds* >95%)

Electrophilic epoxidizing agents such as *m*-chloroperbenzoic acid (MCPBA) oxidize not the double bond, but rather the nucleophilic nitrogen.[81] This entails formation of intermediate amine oxides **132**, which then undergo stereoselective [2,3]sigmatropic rearrangements[82] to the esters **134** with complete 1,3-transfer of chirality.[81] Transition state

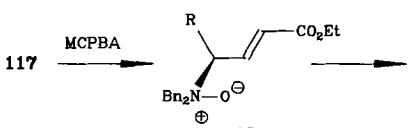

132

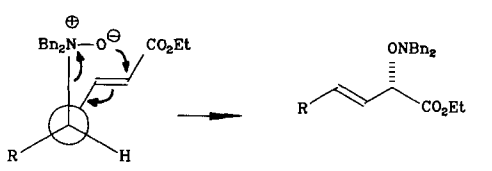

133 **134** (*ee* >95%)

133 is consistent with the stereochemical result[81] and has also been postulated in related cases.[83]

6.2. Cycloadditions

Esters **117** and ketones **126** smoothly undergo $EtAlCl_2$ mediated Diels–Alder reactions with cyclopentadiene (though not with butadiene). Of the four possible diastereomeric products there is a pronounced preference for the adducts **135** and **136**, respectively.[78] In the case of the ketones **126** it was possible to make a definitive assignment of configuration on the basis of X-ray structural analysis. This demonstrates that the Diels–Alder reaction involves attack on the same diastereotopic face of the electron-poor π system as observed during cuprate addition.

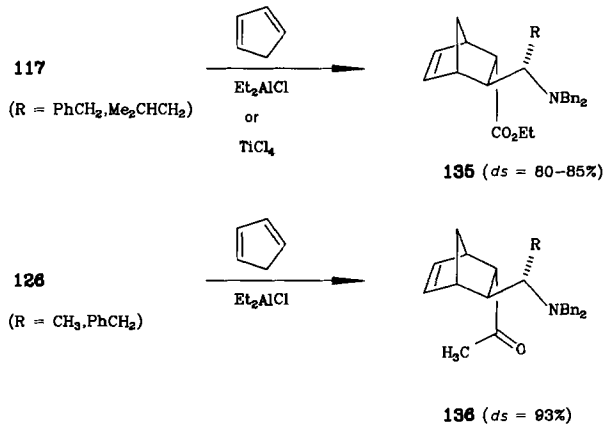

135 (*ds* = 80–85%)

136 (*ds* = 93%)

Nevertheless, it would be premature to conclude that Diels–Alder reactions and Michael additions always follow the same stereoselective course. For example, the diesters **121** react unselectively with cyclopentadiene, providing, in the case of **121** (R = $PhCH_2$), a 58 : 24 : 11 : 7 mixture of four diastereomers. Here both diastereofacial selectivity and *endo* selectivity are relatively low.[78] This is surprising, since 1,3-allylic strain should be an especially important factor as delineated previously in cuprate addition to the diesters **121**. It is not yet clear whether protecting-group tuning might be a last resort in controlling stereoselectivity.[84] The theoretical interpretation is also difficult, because 1,3-dipolar cycloadditions with diazomethane prove to be extraordinarily stereoselective (*ds* = 92–99% in favor of **137**).[78]

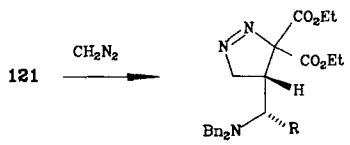

137 R = CH_3; *ds* = 92%
R = $PhCH_2$; *ds* = 99%
R = Me_2CHCH_2; *ds* = 99%

Cycloadditions to the "functionalized" esters **138** have also led to interesting results.[85] A Diels–Alder reaction of **138a** with cyclopentadiene gave a single adduct **139a** with an

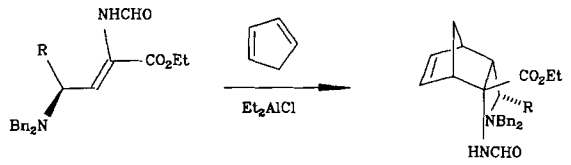

138 **139**

a, R = CH_3 *ds* > 96%

b, R = $PhCH_2$ *ds* = 82%

c, R = Me_2CHCH_2 –

d, R = $tBu(CH_3)_2SiOCH_2$ *ds* = 78%

initially unknown relative configuration. After X-ray structural analysis of the starting material **138a** suggested that it constituted a classic example of a system subject to 1,3-allylic strain (Fig. 3), preferential attack from the upper, sterically less shielded π-face seemed plausible. However, X-ray structural analysis of the product revealed the configuration to be as shown in structure **139a**. This means that the attack of cyclopentadiene occurs not from above (C3-*Si*, C4-*Re*), but from below (C3-*Re*, C4-*Si*)!

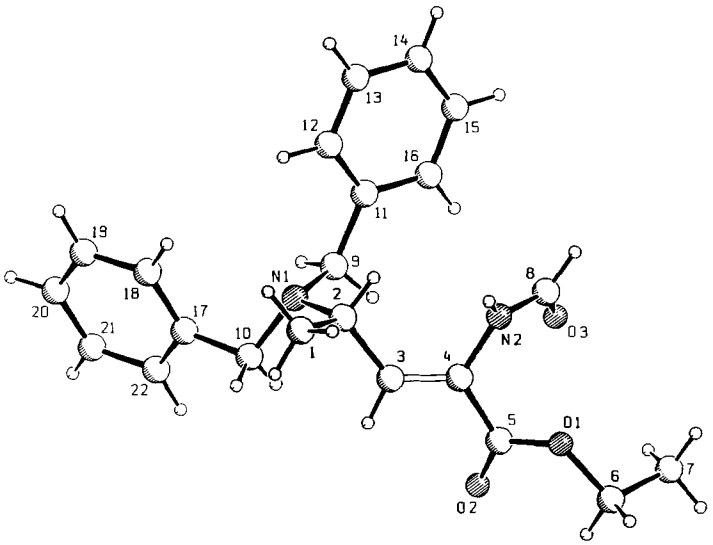

Fig. 3. Crystal structure of the ester **138a**.

Why does the traditional application of the principle of 1,3-allylic strain[77] lead to the wrong conclusion? Perhaps the steric relationships in the transition states of Diels–Alder reactions are different from those in Michael additions. It may be that in the transition state the π system of the diene approaches the dienophile **138** like a flat "board" in a way

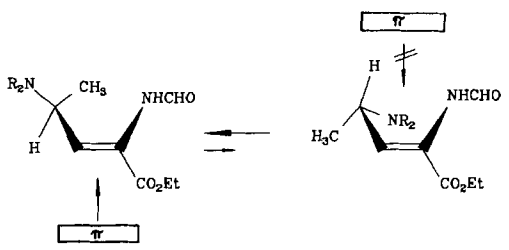

140 (R = $PhCH_2$) **141**

that avoids direct steric interaction with both the amino and benzyl groups. This can be achieved by appropriate rotation of the relevant C–C bond, because then the sterically least demanding H atom would point toward the attacking diene. Of the two possibilities (cf. **140** and **141**), the latter is less energetically favored, since here the larger *N*,*N*-dibenzylamino residue is pressed inward, leading to unfavorable 1,3-allylic strain.

If this analysis is correct,[85,86] then dienophiles **138** with *larger* alkyl residues at the stereogenic center should lead to *lower* diastereoselectivity. This is precisely what is observed (cf. **138b,d**); strict *endo* selectivity of the *N*-formylamino group is maintained. The same trend is apparent in a series of 1,3-dipolar cycloadditions with diazomethane leading to formation of the adducts **142**.[85] Here again the relative

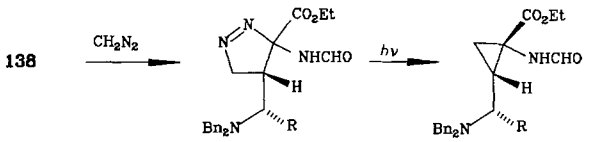

142a, *ds* = 95% **143**

142b, *ds* = 86%

142c, *ds* = 74%

142d, *ds* = 90%

configuration has been verified by X-ray structural analysis. On the synthetic side, compounds **142** can be converted photolytically into cyclopropane derivatives **143** without loss of stereochemical information.[18,85]

7. Conclusions and Prospects

The chemistry described in this progress report constitutes a significant extension of the use of amino acids as chiral, nonracemic building blocks in organic synthesis. The stereochemical results—in some cases unexpected—present a challenge to theoreticians. From a methodological point of view the function of protecting groups is not only to prevent undesirable side reactions; their steric and electronic characteristics can be exploited as important parameters in controlling the stereoselectivity of organometallic and cycloaddition reactions. When protecting groups are called upon to act in this sense they must be carefully tailored to match the nature of particular metals and ligands present. Nevertheless, a number of important problems persist. For example, chelation-controlled additions of Me_3SiCN to α-amino aldimines have yet to be realized. It remains to be seen whether here and in other problematic chemical situations the combination of metal, ligand, and protecting-group tuning will open of new synthetic avenues.

Recently further applications of *N*,*N*-dibenzylamino aldehydes **18** have been described, for example, stereoselective additions of α-phenylselenoalkyllithium reagents,[87] 1-lithiomethoxyallene,[88] and "second generation" Grignard reagents (e.g., RMgOAc).[18,89] Aldol additions to *N*,*N*-dibenzylamino aldehydes that were *not* prepared from amino acids occur diastereoselectively.[90] Finally, α,β-unsaturated esters **117** were converted into the corresponding aldehydes

144; these react with cuprates in the presence of Me_3SiCl/HMPA regioselectively in a 1,2-manner with notable diastereoselectivity in favor of **145** (ds = 79–92%).[91] This surprising result can be explained on the basis of initial diastereoselective π complexation at the C–C double bond followed by a stereoselective "walk" to the π terminus.[91]

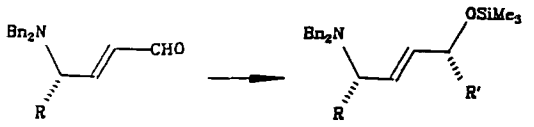

144 **145**

As part of a new project, vinylogous amino acids of the type **117** were incorporated in peptides (cf. **146**). Michael additions, for example with R_2CuLi, occur stereoselectively,

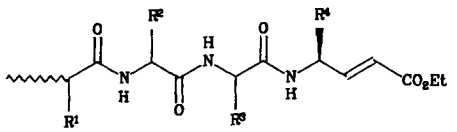

146

depending upon the nature of the R group being transferred and on the configuration of the stereogenic centers along the peptide chain.[89, 92]

I am particularly grateful to my committed co-workers, whose names appear in the works cited from our research group. I wish also to thank the Deutsche Forschungsgemeinschaft (SFB 260 and the Gottfried-Wilhelm-Leibniz Program) and the Fonds der Chemischen Industrie for generous financial support.

Received: April 23, 1991 [A843 IE]
German version: *Angew. Chem. 103* (1991) 1559
Translated by Dr. *W. E. Russey*, Huntingdon, PA (USA)

CAS Registry numbers:
2, 136426-45-4; **3d**, 136577-16-7; **3e**, 136577-18-9; **4a**, 136577-15-6; **4f**, 136577-19-0; **4g**, 136577-20-3.

[1] G. M. Coppola, H. F. Schuster: *Asymmetric Synthesis*, Wiley, New York 1987; J. Martens, *Top. Curr. Chem. 125* (1984) 165; K. Drauz, A. Kleemann, J. Martens, *Angew. Chem. 94* (1982) 590; *Angew. Chem. Int. Ed. Engl. 21* (1982) 584.
[2] G. Stork, Y. Nakahara, Y. Nakahara, W. J. Greenlee, *J. Am. Chem. Soc. 100* (1978) 7775.
[3] R. M. Williams: *Synthesis of Optically Active α-Amino Acids*, Pergamon Press, Oxford 1989.
[4] J. Kamphuis, M. Kloosterman, H. E. Schoemaker, W. H. J. Boesten, E. M. Meijer, *Proc. 4th Eur. Congr. Biotech. 4* (1987) 331.
[5] J. Jurczak, A. Golebiowski, *Chem. Rev. 89* (1989) 149.
[6] W. D. Lubell, H. Rapoport, *J. Am. Chem. Soc. 109* (1987) 236.
[7] *Merck Index*, 8th Ed., Merck, Rahway, NJ, USA 1968, p. 233.
[8] J. Engel, H. Bekel, D. Heiliger, E. Schaumlöffel, *Arch. Pharm. (Weinheim) 318* (1985) 465.
[9] a) R. Nishizawa, T. Saino, *J. Med. Chem. 20* (1977) 510; b) D. H. Rich, B. J. Moon, A. S. Boparai, *J. Org. Chem. 45* (1980) 2288.
[10] D. H. Rich, *J. Med. Chem. 28* (1985) 264.
[11] J. F. Kennedy, C. A. White: *Bioactive Carbohydrates*, Ellis Horwood, Chichester 1983.
[12] G. W. Fleet, P. W. Smith, *Tetrahedron Lett. 26* (1985) 1469.
[13] M. T. Reetz: *Organotitanium Reagents in Organic Synthesis*, Springer, Berlin 1986; B. Weidmann, D. Seebach, *Angew. Chem. 95* (1983) 12; *Angew. Chem. Int. Ed. Engl. 22* (1983) 31.
[14] Review: M. T. Reetz, *Angew. Chem. 96* (1984) 542; *Angew. Chem. Int. Ed. Engl. 23* (1984) 556.
[15] N. T. Anh, *Top. Curr. Chem. 88* (1980) 145.
[16] T. Imamoto, N. Takiyama, K. Nakamura, T. Hatajima, Y. Kamiya, *J. Am. Chem. Soc. 111* (1989) 4392; T. Kauffmann in G. Erker, H. Werner (Eds.): *Organometallics in Organic Synthesis 2*, Springer, Berlin 1989.
[17] The nature of the protecting group plays a decisive role in stereoselective reductions as well as Grignard and aldol additions of *O*-protected α-hydroxyketones; see, for example: L. E. Overman, R. J. McCready, *Tetrahedron Lett. 23* (1982) 2355; T. Nakata, T. Tanaka, T. Oishi, *ibid. 24* (1983) 2653; M. T. Reetz, M. Hüllmann, *J. Chem. Soc. Chem. Commun. 1986*, 1600.
[18] M. T. Reetz, M. W. Drewes, N. Harmat, M. Hübel, K. Lennick, W. Reif, A. Schmitz, A. Wehrsig, T. Wünsch, unpublished.
[19] M. T. Reetz, M. W. Drewes, A. Schmitz, *Angew. Chem. 99* (1987) 1186; *Angew. Chem. Int. Ed. Engl. 26* (1987) 1141.
[20] M. T. Reetz, M. W. Drewes, K. Harms, W. Reif, *Tetrahedron Lett. 29* (1988) 3295.
[21] R. Nishizawa, T. Saino, *J. Med. Chem. 20* (1977) 510; see also [96].
[22] M. T. Reetz, W. Reif, X. Holdgrün, *Heterocycles 28* (1989) 707.
[23] D. J. Kempf, *J. Org. Chem. 51* (1986) 3921.
[24] M. W. Drewes, *Dissertation*, Universität Marburg 1988.
[25] D. Hoppe, *Angew. Chem. 96* (1984) 930; *Angew. Chem. Int. Ed. Engl. 23* (1984) 932.
[26] S. Kano, T. Yokomatsu, S. Shibuya, *Tetrahedron Lett. 32* (1991) 233.
[27] M. T. Reetz, *Pure App. Chem. 60* (1988) 1607.
[28] G. R. Pettit, Y. Kamano, C. L. Herald, A. A. Tuinman, F. E. Boettner, H. Kizu, J. M. Schmidt, L. Baczynskyj, *J. Am. Chem. Soc. 109* (1987) 6883; G. R. Pettit, S. B. Singh, F. Hogan, P. Lloyd-Williams, D. L. Herald, D. D. Burkett, P. J. Clewlow, *ibid. 111* (1989) 5463.
[29] K. L. Rinehart, V. Kishore, S. Nagarajan, R. J. Lake, J. B. Gloer, F. A. Bozich, K. M. Li, R. E. Maleczka, W. L. Todsen, M. H. G. Munro, D. W. Sullins, R. Sakai, *J. Am. Chem. Soc. 109* (1987) 6846.
[30] M. T. Reetz, A. Schmitz, X. Holdgrün, *Tetrahedron Lett. 30* (1989) 5421.
[31] M. T. Reetz, *Adv. Organomet. Chem. 16* (1977) 33; J. Mulzer, G. Brüntrup, *Angew. Chem. 91* (1979) 840; *Angew. Chem. Int. Ed. Engl. 18* (1979) 793; T. H. Black, W. J. DuBay, *Tetrahedron Lett. 29* (1988) 1747.
[32] T. Wakamiya, T. Shiba, T. Kaneko, *Bull. Chem. Soc. Jp. 45* (1972) 3668.
[33] See, for example: S. Hannessian, J. Kloss, *Tetrahedron Lett. 26* (1985) 1261.
[34] K. Mikami, M. Kaneko, T. P. Loh, M. Terada, T. Nakai, *Tetrahedron Lett. 31* (1990) 3909.
[35] M. M. Midland, M. M. Alfonso, *J. Am. Chem. Soc. 111* (1989) 4368.
[36] J. Jurczak, A. Golebiowsky, J. Raczko, *J. Org. Chem. 54* (1989) 2495.
[37] J. Jurczak, *Tetrahedron 47* (1990) 1037, 1045.
[38] M. T. Reetz, R. Steinbach, J. Westermann, R. Peter, B. Wenderoth, *Chem. Ber. 118* (1985) 1441.
[39] M. T. Reetz, M. W. Drewes, A. Schmitz, X. Holdgrün, T. Wünsch, J. Binder, *Phil. Trans. R. Soc. London A 326* (1988) 573.
[40] M. T. Reetz, T. Wünsch, K. Harms, *Tetrahedron Asymm. 1* (1990) 371.
[41] D. Hoppe, U. Schöllkopf, *Liebigs Ann. Chem. 763* (1972) 1.
[42] P. Tebben, M. Reggelin, D. Hoppe, *Tetrahedron Lett. 30* (1989) 2919.
[43] D. Hoppe, personal communication.
[44] B. E. Evans, K. E. Little, C. F. Homnick, J. P. Springer, J. Hirschfield, D. F. Veber, *J. Org. Chem. 50* (1985) 4615.
[45] M. T. Reetz, J. Binder, *Tetrahedron Lett. 30* (1989) 5425.
[46] K. Yoshida, S. Nakajima, T. Wakamatsu, Y. Ban, M. Shibasaki, *Heterocycles 27* (1988) 1167.
[47] P. Garner, J. M. Park, *J. Org. Chem. 52* (1987) 2361.
[48] P. Garner, S. Ramakanth, *J. Org. Chem. 51* (1986) 2609.
[49] P. Garner, J. M. Park, *J. Org. Chem. 53* (1988) 2979.
[50] P. Garner, J. M. Park, E. Malecki, *J. Org. Chem. 53* (1988) 4395.
[51] P. Herold, *Helv. Chim. Acta 71* (1988) 354; G. Casiraghi, L. Colombo, G. Rassu, P. Spanu, *J. Chem. Soc. Chem. Commun. 1991*, 603.
[52] X. Holdgrün, *Dissertation*, Universität Marburg 1989.
[53] M. Hübel, *Diplomarbeit*, Universität Marburg 1990.
[54] R. P. Bonar-Law, A. P. Davis, B. J. Dorgan, M. T. Reetz, A. Wehrsig, *Tetrahedron Lett. 31* (1990) 6725.
[55] We have recently discovered that α-amino acid esters undergo reductive alkylation with 2,4-dimethoxybenzaldehyde with the formation of *N,N*-di(2,4-dimethoxy)benzylamino acid esters. The latter can be transformed into the corresponding α-amino aldehydes [18].
[56] G. Frenking, M. T. Reetz, unpublished.
[57] C. Bolm, A. Wehrsig, M. T. Reetz, unpublished.
[58] K. B. Wiberg, *J. Am. Chem. Soc. 108* (1986) 5817.
[59] K. Harms, E. H. Lauterbach, M. T. Reetz, unpublished.
[60] M. T. Reetz, M. Hüllmann, T. Seitz, *Angew. Chem. 99* (1987) 478; *Angew. Chem. Int. Ed. Engl. 26* (1987) 477.
[61] J. V. N. Vara Prasad, D. H. Rich, *Tetrahedron Lett. 31* (1990) 1803.
[62] Y. Takemoto, T. Matsumoto, Y. Ito, S. Terashima, *Tetrahedron Lett. 31* (1990) 217.
[63] M. T. Reetz, E. Rivadeneira, C. Niemeyer, *Tetrahedron Lett. 31* (1990) 3863.

[64] S. Masamune, W. Choy, J. S. Petersen, L. R. Sita, *Angew. Chem. 97* (1985) 1; *Angew. Chem. Int. Ed. Engl. 24* (1985) 1.
[65] M. Tramontini, *Synthesis 1982*, 605.
[66] M. T. Reetz, M. W. Drewes, K. Lennick, A. Schmitz, X. Holdgrün, *Tetrahedron Asymm. 1* (1990) 375.
[67] M. T. Reetz, M. W. Drewes, B. R. Matthews, K. Lennick, *J. Chem. Soc. Chem. Commun. 1989*, 1474.
[68] S. Kano, T. Yokomatsu, H. Iwasawa, S. Shibuya, *Tetrahedron Lett. 28* (1987) 6331.
[69] R. C. Roemmele, H. Rapoport, *J. Org. Chem. 54* (1989) 1866.
[70] M. T. Reetz, R. Jaeger, R. Drewlies, M. Hübel, *Angew. Chem. 103* (1991) 76; *Angew. Chem. Int. Ed. Engl. 30* (1991) 103.
[71] M. Wada, K. Sakurai, K. Akiba, *Tetrahedron Lett. 25* (1984) 1079.
[72] J. Siko, S. M. Weinreb, *J. Org. Chem. 55* (1990) 393.
[73] G. Cainelli, M. Panunzio, P. Andreoli, G. Martelli, G. Spunta, D. Giacomini, B. Bandini, *Pure Appl. Chem. 62* (1990) 605.
[74] R. Jaeger, *Dissertation*, Universität Marburg 1991.
[75] A. Schmitz, *Dissertation*, Universität Marburg 1991.
[76] M. T. Reetz, D. Röhrig, *Angew. Chem. 101* (1989) 1732; *Angew. Chem. Int. Ed. Engl. 28* (1989) 1706; the α,β-unsaturated ester derived from aldehyde **65** also undergoes cuprate additions: I. Jako, P. Viber, A. Mann, M. Tadei, C. G. Wermuth, *Tetrahedron Lett. 31* (1990) 1011; cf. H. Yoda, T. Shirai, T. Katagiri, K. Takabe, K. Kimata, K. Hosoya, *Chem. Lett. 1990*, 2037.
[77] R. W. Hoffmann, *Chem. Rev. 89* (1989) 1841.
[78] D. Röhrig, *Dissertation*, Universität Marburg 1991.
[79] C. Scolastico, A. Bernardi, *Chemtracts 3* (1990) 413; A. Bernardi, A. M. Capelli, C. Gennari, C. Scolastico, *Tetrahedron Asymm. 1* (1990) 21.
[80] M. T. Reetz, E. H. Lauterbach, *Tetrahedron Lett. 32* (1991) 4477.
[81] M. T. Reetz, E. H. Lauterbach, *Tetrahedron Lett. 32* (1991) 4481.
[82] Review: R. W. Hoffmann, *Angew. Chem. 91* (1979) 625; *Angew. Chem. Int. Ed. Engl. 18* (1979) 563.
[83] Y. Yamamoto, J. Oda, Y. Inouye, *J. Org. Chem. 41* (1976) 303.
[84] *Tamm* et al. were able to show that a Cbz-protected ester related to compound **121** ($R = Me_2CHCH_2$) undergoes a stereoselective Diels–Alder reaction with 4-methyl-2,4-hexadienol (although with opposite diastereofacial selectivity!): T. Schmidlin, P. E. Burckhardt, N. Waespe-Sarcevic, C. Tamm, *Helv. Chim. Acta 66* (1983) 450.
[85] M. T. Reetz, F. Kayser, K. Harms, unpublished.
[86] Related effects have been observed by *Barrett*, who coined the term "stealth effect": A. G. M. Barrett, personal communication.
[87] R. W. Hoffmann, M. Julius, K. Oltman, *Tetrahedron Lett. 31* (1990) 7419.
[88] S. Hormuth, H.-U. Reissig, *Synlett 1991*, 179.
[89] M. T. Reetz, *Pure Appl. Chem.*, in press.
[90] H. Ina, C. Kibayashi, *Tetrahedron Lett. 32* (1991) 4147.
[91] M. T. Reetz, F. Wang, K. Harms, *J. Chem. Soc. Chem. Commun. 1991*, 1309.
[92] J. Kanand, M. T. Reetz, unpublished.

VCH Index Library

The electronic version can be read by all MS-DOS compatible computers. It is accessed by the Search module of the Literature Management Program VCH-Biblio.

ANGEWANDTE CHEMIE
A Journal of the Gesellschaft Deutscher Chemiker
International Edition in English

30 Year Index of Reviews
– in print or on diskette –

The reviews in Angewandte Chemie are amongst the most often cited chemical publications of each year. Many have become classics of the chemical literature. For thirty years they have been available in English as well as German. The 30 year review index now celebrates this anniversary by facilitating access to these important documents of the rapid development of our discipline. The index—both a chemical dictionary and a history book—offers you:

1. A list of all authors, indicating the main author and the title of the review.
2. A subject index giving the main author.
3. Both indexes provide complete information on date of issue and first and last page numbers of the German and English editions.

The electronic version of the index is available on 5¼" and 3½" diskettes.

If you order immediately, you save about 30% since the prepublication price is U.S. $44.00/£26.00 (plus postage) only until the end of January. Please order by telephone or in writing to **VCH, Software und Datenbanken, Postfach 10 11 61, D-W-6940 Weinheim, Tel. 0 62 01/6 02-2 71, Telefax 0 62 01/6 02-3 28.**

Volume Effect or Paddle-Wheel Mechanism—Fast Alkali-Metal Ionic Conduction in Solids with Rotationally Disordered Complex Anions

By Martin Jansen*

Dedicated to Professor Karl Heinz Büchel on the occasion of his 60th birthday

Transport phenomena in the solid state are of equal importance in basic research and practice. In the past two decades particular interest has been directed towards so-called "fast" or "super" ionic conductors because of their attractive potential applications. We have synthesized highly conductive alkali-metal ionic conductors based on ionic crystals in which, on the one hand, high concentrations of the charge carriers can be realized by doping (point defects in the cation substructure) and, on the other, the activation energy of the interchange of sites is decreased by translationally fixed but rotationally mobile complex anions. Mixed crystals with Na_3PO_4 or Na_3AlF_6 structures have proven especially suitable in this connection. With the object of establishing a broader experimental foundation for clarifying the controversially discussed question of whether the higher free transport volume or the rotational motion of the anions is responsible for the high cation mobility in these rotary phases we have systematically varied the type of anions and concentration of defects and monitored the resulting changes in conductivity. Although the macroscopical characteristics investigated are not suitable for explaining mechanisms in detail at the atomic level, the results afford clear support for the assumption of a "paddle wheel mechanism"; but also effects of the enlarged transport volume are not to be disputed. Both these effects enhancing the cationic conductivity are concomitantly operative in amounts varying from system to system; they cannot be totally separated from each other. Seen in this light, the alternative, "volume effect" or "paddle wheel mechanism," is not as sharply defined as was previously discussed.

1. Introduction

The solid state is still the least well understood form of aggregation. Both prognoses as well as the later interpretation of experimental findings leave much to be desired, even with regard to the composition of solids, their structures, their bond behavior, and particularly with respect to certain material properties. Tailormade syntheses aimed at elucidating one or more of the aforementioned differentia specifica are only possible—if at all—in exceptional cases; extrapolations from the known to the unknown are risky. Difficulties are met in going from the fictitious ideal crystal—as a rule fundamental to a discussion of structural features and the calculation of, e.g., band structures or phonon spectra—to the real crystal. The microstructure, determined, inter alia, by the type and number of non-equilibrium defects, mosaic structure, morphology of internal boundary surfaces, can vary widely from one individual sample to another. Thus, in solids of the same chemical composition a broad variation is found with regards to their reactivity and most of their physical properties. This affects in particular the transport properties, which are of utmost importance for the formation and decomposition of solids, and thus play a role in all studies, basic as well as application-oriented areas of solid-state research. The present review is concerned with one aspect of the transport properties of solids, namely the fast transport of ions in ionic crystals. Ionic crystals whose ionic conductivities σ lie between ca. 10^{-10} and $10^{-4}\,S\,cm^{-1}$ are usually referred to as solid electrolytes, those with $\sigma = 10^{-4}$ to $10^{0}\,S\,cm^{-1}$ as fast ionic conductors.[1]

Materials whose electric conductivity is due to charge transport by ions (solid electrolytes), have undoubtedly been known since the end of the last century. Systematic research in this area began with such works as those of *Tubandt* and *Lorenz*,[2] who reported the results of the first quantitative investigations on silver iodide and, inter alia, the unusual finding that the conductivity of AgI is higher below the melting point than above. The theoretical models for ion transport via defects in the crystalline solid state, which, in principle, still apply today, were developed by *Frenkel*[3] and by *Schottky* and *Wagner*[4] in the twenties. Since then our understanding of the mechanisms involved in charge transport has developed so far as to include such mechanisms at the atomic level.[5]

There has been a dramatic revitalization of research in the area of solid-state electrolytes through a pioneering work by *Yao* and *Kummer*:[6] β-aluminum oxide, long known in the solid state and initially considered to be a further modification of aluminum oxide but later identified by X-ray structure analysis as sodium oxoaluminate $NaAl_{11}O_{17}$,[7] is an exceptionally good and still unsurpassed sodium ion conductor. The actual stimulating aspect of these author's work was not the new "record" reached for sodium ion conductivity but rather the concepts developed there from for the technological utilization[8] of such materials. The possible use of such electrolytes in galvanic chains for thermodynamic and kinetic studies in solid-state chemistry and as sensors for direct measurement of the partial pressures of different gases, and especially the prospect of developing efficient energy storage and conversion systems (solid-state batteries and fuel

[*] Prof. Dr. M. Jansen
Institut für Anorganische Chemie der Universität
Gerhard-Domagk-Strasse 1, W-5300 Bonn (FRG)

cells) based on solid-state electrolytes, has motivated the interest of numerous groups world-wide in this area of research.

For practical purposes, most important at present are sodium, lithium, oxygen, and hydrogen ion conductors. The temperature dependence of the conductivity of the respective solid electrolytes, with, in each case, the highest conductivities achieved so far, is reproduced in Figure 1 as an Arrhenius plot ($\log \sigma T$ versus $1/T$). the curves for AgI and conc. H_2SO_4 are included for comparison.

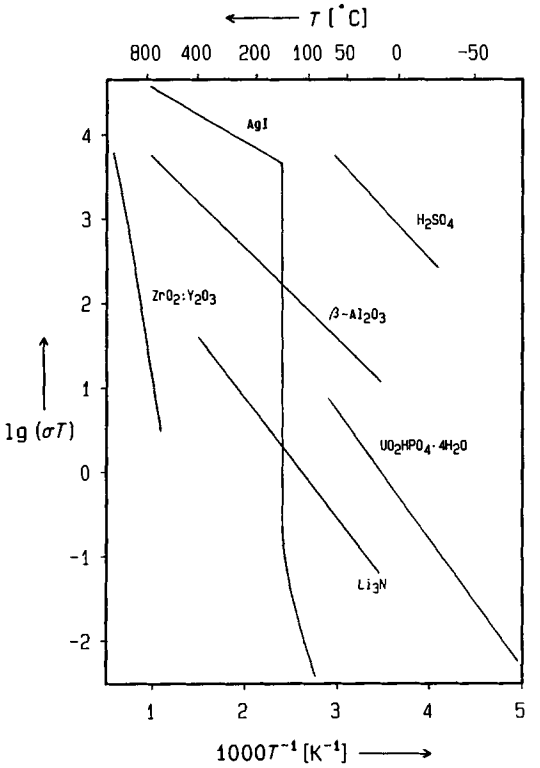

Fig. 1. Temperature dependence of the ionic conductivity in AgI [2,9] conc. H_2SO_4 [10], β-Al_2O_3 [11], ZrO_2: Y_2O_3 [12], Li_3N [13], and $UO_2HPO_4 \cdot 4\,H_2O$ [14]; Arrhenius diagram.

Even though mass-produced devices based on solid-state electrolytes (λ-probes[5] and Na/S batteries[16]) are meanwhile on the market, the ion conductors developed so far do not fulfill all practical requirements, especially with regards to their thermodynamic and mechanical stability and conductivity at low temperatures (300–400 K). Further research into the rudimentary steps of ion transport and the search for new ionic conductors is therefore essential.

2. Concepts in the Search for New Ionic Conductors

The thermodynamic prerequisite for an effective charge transport in solids by ions, namely the presence of a gradient, either in the chemical or electrical potential, is trivial. The kinetic requirement is a high translational mobility of the ions. Three mechanisms[17] of ion migration usually come under discussion:

1. Conventional transport by uncorrelated jump processes of point defect sites. The difference from the diffusive behavior of normal ionic crystals is thereby only of a quantitative nature; the jump rates and defect concentrations are in comparison a few orders of magnitude higher. Examples are β-Al_2O_3 and CeO_2:Y_2O_3.
2. Highly correlated jump processes, in which fast ion transport is brought about by collective movement of several ions. As examples Li_3N and $RbBiF_4$ may be mentioned.
3. A more fluent movement of the cations in a high-grade disordered cation substructure with flat potential surface. This description applies above all in the case of compounds such as silver(I) sulfide.

For by far the greatest number of ionic conductors, the mechanism via uncorrelated, thermally activated jump processes listed under 1 would be the correct mechanism. In this case, the parameters on which the ionic conductivity depends are essentially known.

From the general expression for the conductivity

$$\sigma = nq\mu \tag{a}$$

incorporation of the Nernst–Einstein equation

$$\mu k T = q D \tag{b}$$

and of the expression for the diffusion coefficients

$$D = \gamma(1 - c)\, d^2 \nu_0 \exp(-E_a/kT) \tag{c}$$

gives the relationship

$$\sigma T = N q^2 \gamma c(1 - c)\, d^2 k^{-1} \nu_0 \exp(-E_a/kT) \tag{d}$$

μ = mobility of the charge carrier, N = number of structural sites for the migrating ion, c = degree of occupation of the N positions, $n = Nc$ = charge carrier concentration, q =

Martin Jansen, born on Pellworm in 1944, studied chemistry at the Justus-Liebig-Universität Giessen where he gained his doctorate in 1973 under the supervision of R. Hoppe. After his habilitation in 1978 he was offered and accepted a professorial chair for inorganic chemistry at the Universität Hannover; in 1987 he moved to the Rheinische Friedrich-Wilhelms-Universität in Bonn. His research interests lie in the fields of preparative solid-state chemistry, crystal chemistry, and the structure properties relationships of solid materials.

charge, d = jump distance, ν_0 = characteristic vibration frequency, k = Boltzmann constant, E_a = activation energy, γ = geometry factor (contains activation entropy).

Of the factors included in Equation (d), N, d, q, and ν_0 are the least variable when one attempts to optimize the conductivity, since they are largely fixed, either for the chosen type of structure or for the type of ion. The best possibilities for an optimization are provided by the defect concentration c and activation energy E_a. Table 1 lists a collection of the prerequisites for high ionic mobility in the solid state. If an

Table 1. Prerequisites for high ionic mobility in the solid state.

1) Prerequisites in the structural geometry
   a) vacant sites in the substructure of the migrating particle type and/or corresponding interstitial sites
   b) diffusion paths with flattest possible potential curve
      α) flat potential trough of the regular and/or interstitial site
      β) narrowest site ("bottle neck") in the diffusion path as wide as possible
   c) branched diffusion paths
2) Prerequisites in the chemical nature of the participating species
   a) high polarizability of the migrating ions
   b) high polarizability of the immobile matrix

appropriate number of energetically favorable interstitial sites or defects of the migrating ion type are not available in the pure substance an adequate concentration of defects (50 % of all positions of the migrating ion would be optimal) can generally be realized quite easily by doping. In contrast, the possibilities of decreasing the activation energy for the hopping processes are very limited. A low coordination number for the migrating ions on the regular lattice position has a favorable effect, since in such cases the difference between the space available inside the polyhedron to that on the surface is relatively small. The energy required for elastic deformation of the electron shells upon passage of the cations through one of polyhedra faces ("bottle necks") is then smaller. Of advantage, furthermore, is a high polarizability of the migrating cations and/or of the anionic matrix. These facts explain the generally very high diffusion coefficients of the monovalent coin metals in the solid state[18] and the high lithium conductivity in Li_3N (polarizability of N^{3-}).[13] If alkali-metal ionic conductivity without any electronic contributions is the more important objective regarding the potential application of such electrolytes, there remains only modification of the anionic matrix. However, here also there is little latitude. Only non-metals of the higher periods in lower oxidation states come under consideration as anions with a polarizability greater than N^{3-}; however, their electronic contribution to the total conductivity is frequently undesirable.

Fundamental to our working hypothesis in the search for fast ion conductors is the assumption that in structures with translationally fixed complex anions having increased rotational mobility these facilitate the passage of the alkali metal ions through one of the faces of their coordination polyhedra somewhat in the sense of a "paddle wheel" and thereby drastically decrease the activation energy for ionic conduction. Such a mechanism[19] was first discussed in the case of the high-temperature form of Li_2SO_4,[20] which crystallizes with disordered anions in the cubic anti-fluorite structure. Since rotational diffusion of the sulfate anion with high frequency for this modification and concomitant marked increase of the lithium ion conductivity (by a factor of 10^2) during the phase transformation was established, one assumes a causal relation in the above-mentioned sense, namely a favoring of Li^+ hopping by the quasi freely rotating anions. With the aim of exploiting this effect in the search for new alkali-metal ion conductors, we have chosen ionic crystals of alkali-metal ions and complex oxo or fluoro anions as basic compounds which are susceptible to orientational disorder of the complex anion. In addition, either a sufficient concentration of intrinsic cation defects (not too energy-rich interstitial sites) must be present or corresponding extrinsic defects in the cation substructure must be producible by doping (mixed crystal formation).

The demand for branched, two-dimensionally or better still three-dimensionally cross-linked diffusion routes is generally fulfilled in such materials, since their structural makeup is usually dominated by arrangement of the complex groups in the sense of hexagonal closest, cubic closest, or cubic body-centered packing.

3. Choice of Suitable Basic Structures

The tendency of a complex anion to develop rotational disorder in the crystal is generally deducible from the crystal structure: if the symmetry of the environment is higher than the point symmetry of the (to a first approximation) rigid anion, there are several energetically equivalent orientations for the latter, which, on a time average, are occupied with equal frequency. Transitions between these orientations are brought about by thermally activated rotational jumps (rotational diffusion), which, phenomenologically, are closely related to the elementary steps of translational motion. The jump rates can vary widely, so that all intermediary steps from practically static disorder to quasi free rotation are possible. This spectrum of jump frequencies can also be observed as a function of the temperature on one and the same material, whereby the transition to free rotation is frequently accompanied by a reconstructive phase transformation. Since practically all alkali-metal salts with complex anions convert into such rotary phases at elevated temperature, we have directed special attention in preselection of the salt to a lowest possible transformation temperature and to available or producible concentration of charge carriers (defects). In the systems studied in detail by us, in the case of Na_3PO_4 and Na_3AlF_6 it involved a directed selection[21] on the basis of the above-mentioned criteria; in the case of the antiperovskite-type $(NO_2)ONa_3$, an accidental discovery with regard to high ionic conductivity. At first it was not known in which way the required charge carrier concentration could be achieved in the latter case.

3.1. The Na_3PO_4 Family or the Cryolite Problem

Difficulties in the refinement of the crystal structure[23] of K_3PO_4 as a result of the disorder of the phosphate anion turned our attention to the group of alkali-metal orthophosphates, and with a view to possible practical applications, especially to the air-stable anhydrous Na_3PO_4. To our surprise, on searching through the literature, we established that

in the case of this well-known inorganic salt, the number and stabilities of the polymorphic modifications were highly controversial and, moreover, no structural information was documented.[24] After optimization of the synthesis, which turned out to be unexpectedly lengthy (see below), we have been able to attribute the controversial data for Na_3PO_4 to the different degrees of purity of the samples investigated:[21a] pure Na_3PO_4 exists only in two modifications, a low-temperature and a high-temperature form (L-Na_3PO_4 and H-Na_3PO_4). The phase transformation occurs reversibly at 598 K. Single crystals of H-Na_3PO_4, grown just below the melting point at 1573 K, could be quenched metastably to room temperature and investigated by the usual single-crystal technique. As confirmed by a comparison with the X-ray powder diagram of H-Na_3PO_4 above the transformation temperature, the observed structure (cf. Fig. 2) practically represents the dynamically disordered high-temperature form in the "frozen in" state. If the PO_4^{3-} group is regarded as a pseudoatom, a

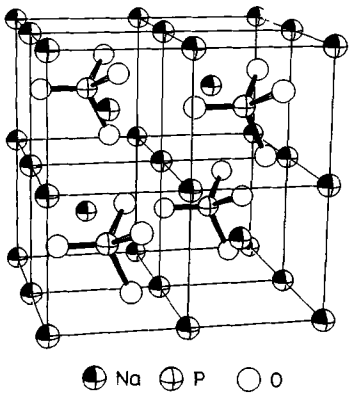

Fig. 2. Perspective plot of the crystal structure of H-Na_3PO_4; phosphate groups in one of the possible orientations.

very simple description of the basic structure is obtained: The particles X^{3-} form a cubic close packed arrangement, whose tetrahedral and octahedral voids are completely occupied by sodium ions. From this structural principle there immediately follow constraints that hinder the formation of an ordered structure and, in retrospect, make the difficulties of synthesizing pure Na_3PO_4 understandable. Easily recognizable in Figure 2 is the incompatibility of the positional symmetry (O_h) and point symmetry (T_d) of the anion, which necessarily leads to disorder. Above the transformation temperature it is dynamic in nature.

The six preferred orientations of the tetrahedron, each with one of its threefold rotational axes parallel to the cubic axes, lead to a displacement of the sodium ions from their ideal positions too; this is so strong that it can no longer be simulated by harmonic temperature parameters.[21a]

The second of the above-mentioned difficulties results from the simultaneous occupation of all tetrahedral and octahedral sites by sodium. Such an arrangement is energetically extremely unfavorable in ionic crystals, because of the short distances between neighboring tetrahedral and octahedral sites. This is recognizable best with sodium ions at the "octahedral sites"; these are first surrounded by eight further sodium ions and only in a secondary coordination sphere by six phosphate groups. Only in the case of less polar compounds, e.g. with predominantly metallic bonding, is this structure realized undistorted and with complete occupation of all positions; the prototype is Li_3Bi.[25] In the case of the ionic crystal Na_3PO_4 this leads to the incorporation of any "impurity" if it is suitable for reducing the number of cations per anion. This holds true for anions with a lower ionic charge than 3− and for cations with a higher charge than 1+. It follows that ionic crystals with this structure are obtainable in pure form only with difficulty if at all. Further examples are Na_3AlF_6[26] ("cryolite problem") and BiF_3,[27] which only occurs in this structure type contaminated with oxygen as $BiF_{3-2x}O_x$; pure BiF_3 has another structure.[28] Na_3PO_4 (and with limitations also Na_3AlF_6) thus fulfills important prerequisites for fast ion conductivity both with respect to its dopability as well as to the potential rotational mobility of the complex anion according to our above-mentioned concept (Section 2).

A further favorable feature is the close relationship of the modification with ordered anions, which is thermodynamically stable at low temperatures (cf. Fig. 3), with the high-

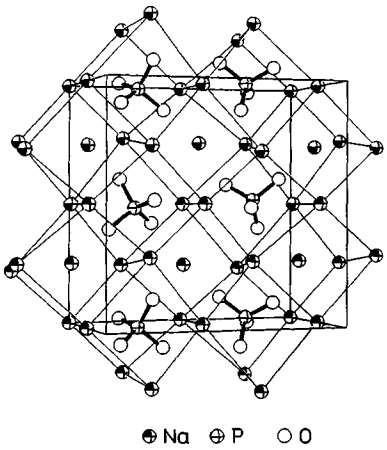

Fig. 3. Section of the crystal structure of L-Na_3PO_4.

temperature form, from which the good dopability also of this modification and a displacive transition in the rotary phase immediately follow.

3.2. The Orthonitrites of the Alkali-Metals and Related Compounds

Na_3NO_3 was originally considered to be the ortho salt of sodium nitrite with NO_3^{3-} ions.[29] In fact these compounds, in contrast to the alkali-metal orthonitrates, are not ortho salts but oxide nitrites[30] with perovskite structure in accordance with the formulation $(NO_2)ONa_3$. Unexpectedly, the crystal structure at room temperature is cubic with one formula unit in the unit cell. This necessarily leads to orientational disorder of the complex NO_2^- anion (point group C_{2v}) located in a cubooctahedron of sodium (positional symmetry O_h). This was confirmed by a single-crystal structure analysis (cf. Fig. 4). The disorder of the anion is apparently of a dynamic nature, confirmed in particular by the behavior upon lowering the temperature.[31, 32] A sequence of phase trans-

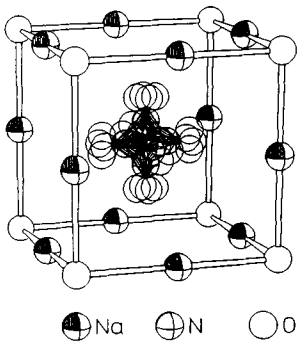

Fig. 4. Crystal structure of H-Na_3NO_3 (≡$(NO_2)ONa_3$); dynamic disorder of the nitrite anion outlined by superposition of 24 orientations.

formations is observed, H-Na_3NO_3 $\xrightarrow{235\,K}$ M-Na_3NO_3 $\xrightarrow{180\,K}$ L-Na_3NO_3 $\xrightarrow{72\,K}$ LL-Na_3NO_3, in the course of which the disorder decreases to complete order in LL-Na_3NO_3 (cf. Fig. 5). In L-Na_3NO_3, still two equivalent

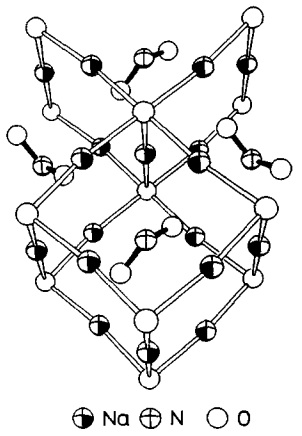

Fig. 5. Crystal structure of LL-Na_3NO_3.

orientations of the nitrite groups occur; the structure can be generated from that of LL-Na_3NO_3 by mirror imaging the latter through an imaginary plane at $z = 1/2$ parallel to (001). Even this disorder is still dynamic in nature: with the help of alternating current techniques, Debye relaxation with jump

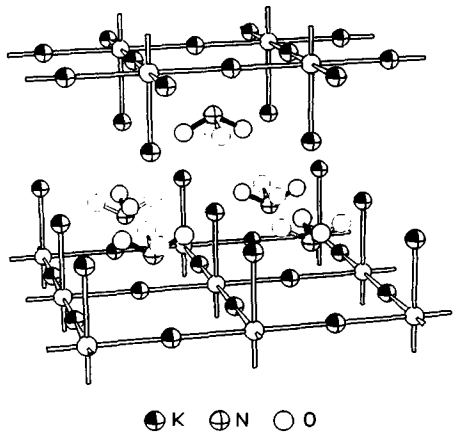

Fig. 6. Crystal structure of $K_4N_2O_5$ ($Na_4N_2O_5$ forms a superstructure of the anti-K_2NiF_4 type), disorder of the nitrite anion illustrated by superposition of the two possible orientations.

rates of $10^{-6}\,s^{-1}$ was established at 100 K.[22] Extrapolation to room temperature, which naturally can afford only a rough approximate value, gives jump rates in the gigahertz range. Since we considered Na_3NO_3 a daltonide compound, the high ionic conductivity established in a routine measurement surprised us (see Section 5).

This discovery incited us to vary $(NO_2)ONa_3$ by changing the individual components and by structural modification—as has been achieved for example in numerous other cases for the perovskite family. The variants obtained, like $(NO_2)_2ONa_4$ (Fig. 6), are to be assigned the anti-K_2NiF_4 structure, or like $(CN)ONa_3$ contain another disordered anion in place of NO_2^-.[32, 33] The close relationship of these compounds is underscored by the mutual solubility[34] of $BrONa_3$[35] and $(NO_2)ONa_3$.

4. Sodium Ionic Conductors with Sodium Orthophosphate or Cryolite Structure

The ionic compounds of the cryolite family, commonly considered to have well-defined formulas (see Section 3.1) already exhibit cation defects to a more or less marked extent, due to the above discussed structural features and the resulting difficulty to realize their ideal composition. In spite of that it appeared meaningful in view of the optimization of the sodium ion conductivity to approximate as close as possible the maximum charge carrier concentration (50 % vacant sites in the cationic substructure) by doping.

Basically, this sodium can be substituted by divalent metal ions[36, 37] such as e.g., Cd^{2+} or Ca^{2+}, or the threefold negatively charged complex anions can be replaced by groups of lower ionic charge. Besides these two possibilities of substitution, there are further possibilities which can generate anionic defects or lead to interstitial cations,[37] which are either undesirable or in view of the nevertheless already overcharged cation substructure in Na_3PO_4, will play no greater role.

Each substituted particle changes the potential on the corresponding lattice site and thus effects, inter alia, a more or less strong deformation of its surroundings and thus lowers the mobility of the charge carrier. Since this effect could be most noticeable in the case of the cation conductivity upon aliovalent exchange in the cation sublattice, we have, in our studies, substituted exclusively the anions. The replacement of a phosphate anion by a sulfate anion with retention of the structure has essentially the following effects with regard to the cation conductivity:

1. Increasing the concentration of defects in the cation substructure.
2. Changing the so-called free transport volume for the cations
3. Increasing the rotational motion of the complex anion ("paddle-wheel effect").

Further, less significant effects, such as the already indicated different trapping of the charge carrier in the proximity of different anions, are not taken into consideration in the following.

The above-mentioned effects are not strictly separable, as would be desirable for their selective exploitation in the opti-

mization of ionic conductors. In order to gain at least some information about how strongly which parameters influence the ionic conduction, we have chosen mixed-crystal systems and compared them with one another, eliminating at most one of the three influential parameters (Table 2).

Table 2. Mixed crystals investigated and effectivity of the factors favoring ionic conduction, minus = no effect, plus = positive effect.

System	Defect site concentration	Transport volume	Paddle-wheel effect
Na_3PO_4/Na_3AlF_6	–	+	+
Na_3PO_4/Na_2SO_4	+	–	+
Na_3PO_4/Na_2CO_3	+	+	+
Na_3AlF_6/Na_2SiF_6	+	–	+
Na_3AlF_6/Na_2SO_4	+	+	+

In connection with our own studies the synthesis of the mixed crystals was in each case accomplished by solid-state reaction of the pseudobinary components. It proved absolutely essential to elucidate the corresponding sections of the phase diagrams. The samples were characterized by X-ray diffraction techniques, and their homogeneity was checked by energy dispersive microanalysis. The characteristic electrical quantities were determined on sintered samples by alternating current techniques, by measurement of the Hebb-Wagner polarization and, on selected samples, by measurement of the sodium ion transference.[38]

The good dopability of both Na_3PO_4 and Na_3AlF_6 predicted on the basis of structural conditions is impressively confirmed by the experimental findings: thus, for example, Na_3AlF_6 dissolves in the cubic high-temperature phase Na_2SO_4 with retention of the structure up to $x_S = 0.8$ (x_S = mole fraction of dissolved component) and at room temperature up to $x_S = 0.125$.

In the case of Na_3PO_4/Na_2SO_4 the formation of mixed crystals extends to $x_S = 0.6$. The range can even be extended to $x_S = 0.75$ by quenching. Figure 7 shows as a typical example the phase diagram of the pseudobinary system Na_3AlF_6/Na_2SO_4.

According to direct current measurements[38] the electronic part of the conductivity always lies about five to six orders of magnitude below the total conductivity. Hereby, and by transference measurements on selected random samples the mixed crystals are characterized as practically pure sodium ion conductors. A confirmation of our working hypothesis is seen in the considerably high values for the conductivities, especially in the case of the mainly cubic high-temperature forms with dynamically disordered anions. In the system Na_3AlF_6/Na_2SO_4 two regions can be differentiated: on the one hand that with miscibility in the low-temperature and high-temperature forms and on the other, that with demixing at low temperatures. In the first case, Arrhenius behavior is observed in the whole temperature range examined with a sudden increase in the conductivity and at the same time decrease in the activation energy at the monoclinic → cubic transformation (cf. Fig. 8).

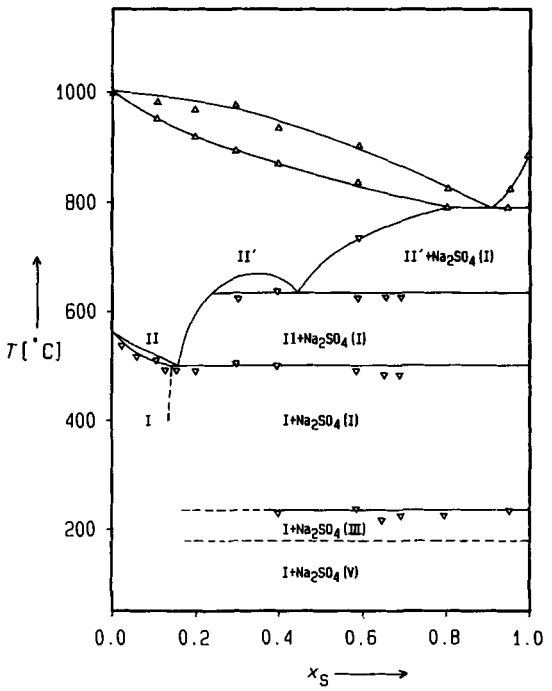

Fig. 7. Phase diagram of the pseudobinary system Na_3AlF_6/Na_2SO_4. x_S = mole fraction of Na_2SO_4, △ = DTA heating mode, ▽ = DTA cooling mode (DTA = differential thermal analysis). I–V represent the different polymorphic modifications of Na_2SO_4.

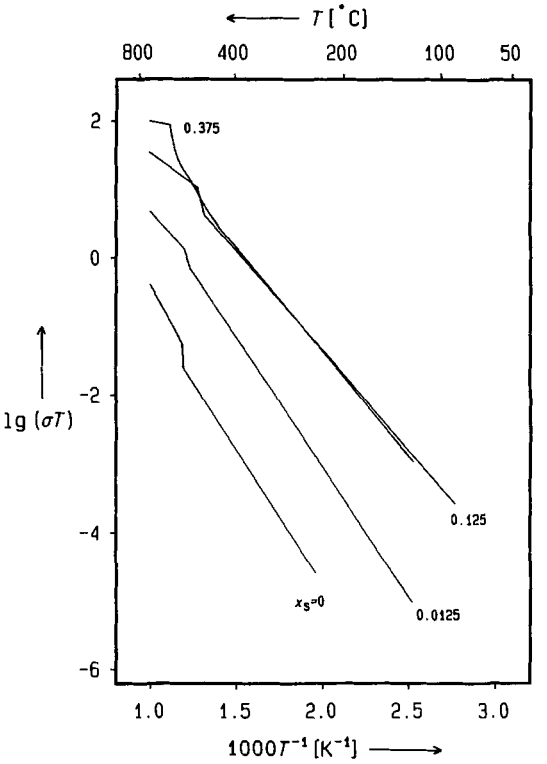

Fig. 8. Temperature dependence of the sodium ion conductivity in the system Na_3PO_4/Na_2SO_4. x_S = mole fraction of Na_2SO_4.

In studies on Na_3PO_4[21a] there were initially discrepancies with respect to the ion conductivity of the mixed crystal systems;[40] in the meantime, however, these have largely been resolved[41, 42] and numerous new systems have been included.[42] In one respect the electrical behavior of the solid solutions based on Na_3PO_4 is fundamentally different from the cryolite solutions. Obviously as a result of the fact

that even very slight doping is enough to stabilize the cubic form at room temperature, the sudden increase in conductivity and the corresponding decrease in the activation energy of the pure Na_3PO_4 during the phase transformation is no longer observed in the mixed crystals.[42] At low temperatures (298 K) the conductivity increases by up to four orders of magnitude with doping. The activation energy corresponds to that of pure Na_3PO_4 at this temperature and decreases constantly on elevating the temperature until the activation energy of pure Na_3PO_4 in the high-temperature form is approximately reached. These facts are illustrated by way of example for the system Na_3PO_4/Na_2SO_4 in Figure 9. Qualitatively, all systems in which Na_3PO_4 participates show an analogous behavior.[43]

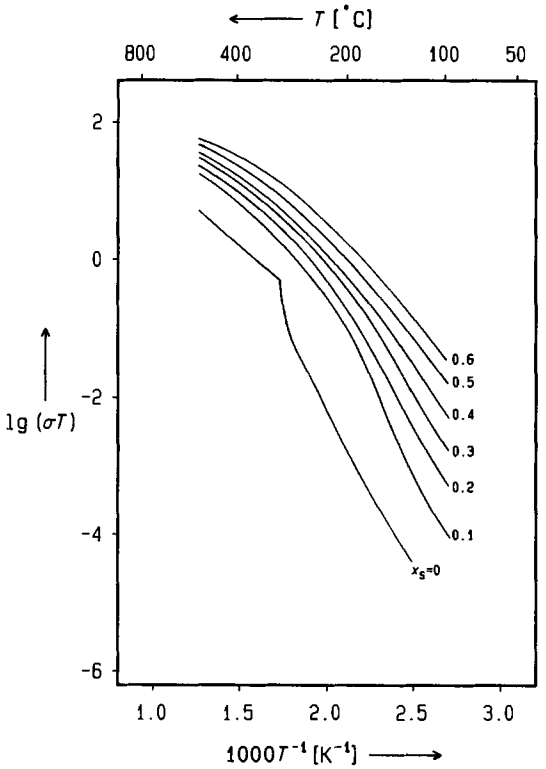

Fig. 9. Temperature dependence of the sodium ion conductivity in the system Na_3PO_4/Na_2SO_4. x_S = mole fraction of Na_2SO_4.

An intermediary position is assumed by Na_3AlF_6/Na_2SiF_6 solid solutions, in which the sudden transition into the cubic modification in the case of pure cryolite smears out more and more and disappears at $x_{Si} = 0.73$ completely[44] (Fig. 10).

The influence of volume and "paddle-wheel effect" without alteration of the charge carrier concentration can be monitored by substitution of the AlF_6^{3-} in Na_3AlF_6 by PO_4^{3-}.[45] As follows from the pseudobinary section (Fig. 11), complete miscibility and cubic structure occurs above ca. 913 K. In the phosphate-rich part, the temperature-dependence of the conductivity shows the nonlinear relationship $\log(\sigma T)$–$1/T$ typical for doped Na_3PO_4, while in the cryolite-rich part, Arrhenius behavior and conductivity jumps are observed in the region of the phase transformations (Fig. 12).

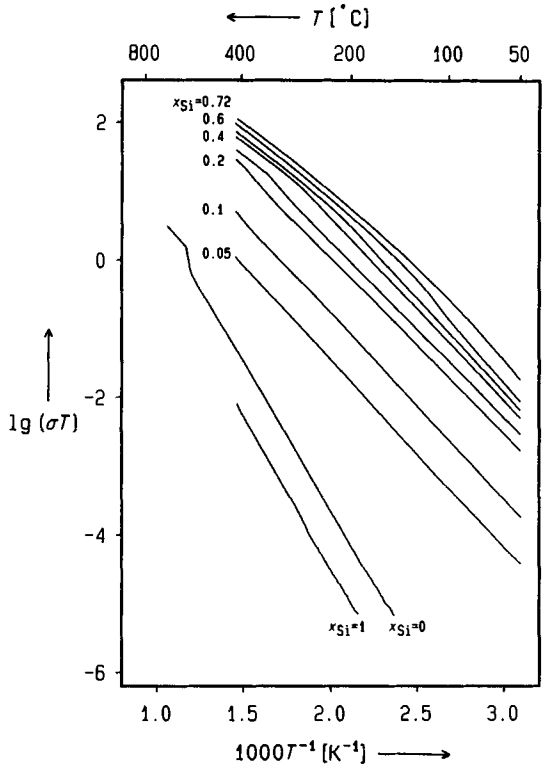

Fig. 10. Temperature dependence of the sodium ion conductivity in the system Na_3AlF_6/Na_2SiF_6. x_{Si} = mole fraction of Na_2SiF_6.

The increase in conductivity by an order of magnitude at unchanged charge carrier concentration, is higher than expected.

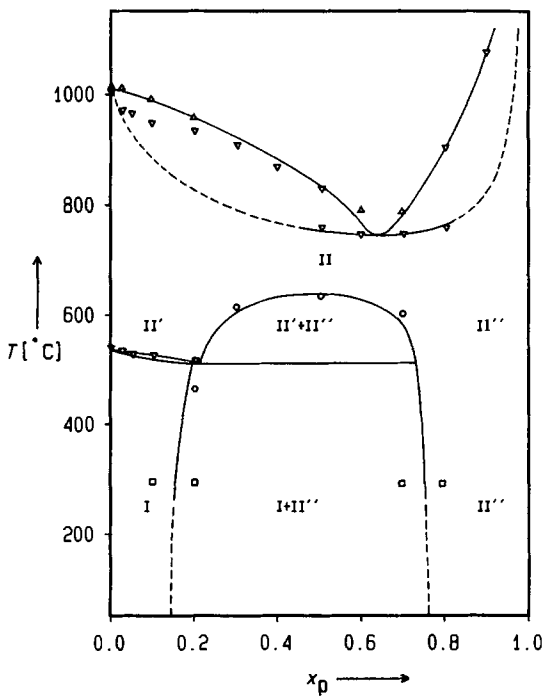

Fig. 11. Phase diagram of the pseudobinary system Na_3AlF_6/Na_3PO_4. x_P = mole fraction of Na_3PO_4, △ = DTA heating mode, ▽ = DTA, cooling mode, ○ = impedance measurements, □ = X-ray diffraction analyses.

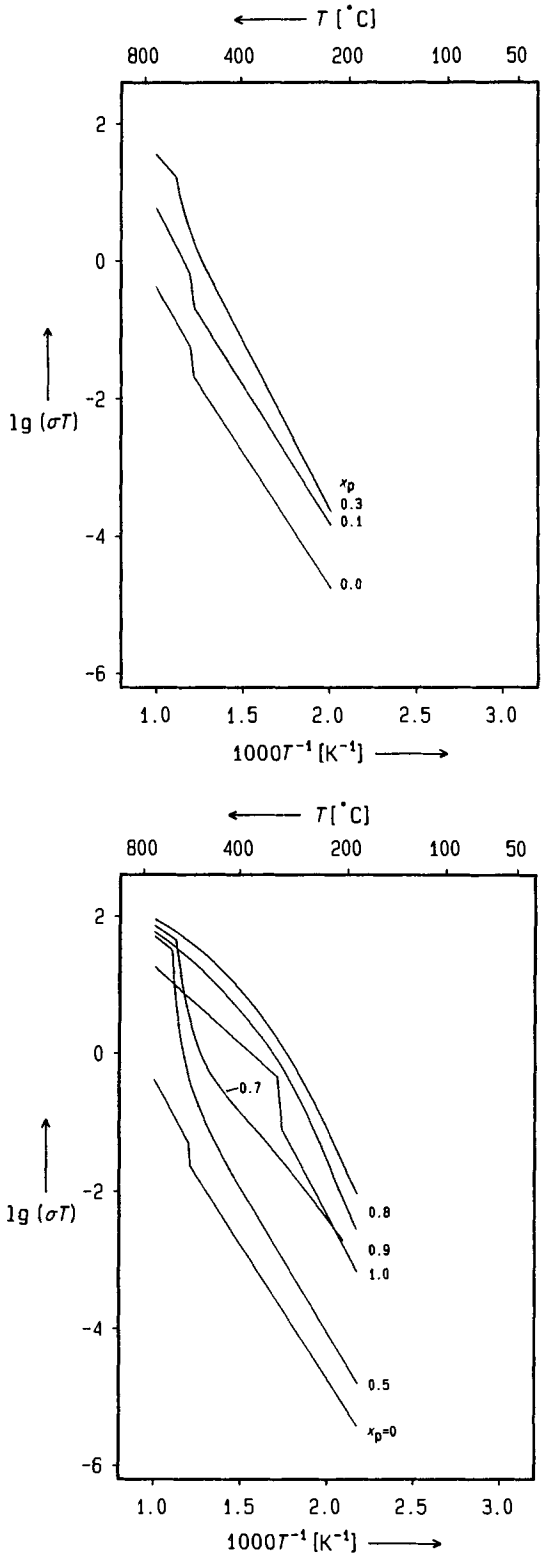

Fig. 12. Temperature dependence of the sodium ion conductivity in the system Na_3AlF_6/Na_3PO_4. Solid solutions of phosphate in cryolite (top) and of cryolite in phosphate (bottom). x_P = mole fraction of Na_3PO_4.

5. Sodium Ion Conduction in anti-Perovskite Variants $XONa_3$ (X = NO_2, Br, CN) and X_2ONa_4 (X = NO_2)

In the above-mentioned attempts to confirm the dynamic nature of the disorder in $(NO_2)ONa_3$ by measurement of the Debye relaxation by alternating current techniques,[22] the temperature range above room temperature to 500 K was also included (at still higher temperatures reactions with all common electrode materials or decomposition are observed). Surprisingly, drastic increases in conductivity by a total of three orders of magnitude occurred in two steps at 500 and 520 K. These at first completely unexplainable observations quite clearly indicate (confirmed by sodium transfer measurements) jumps in the sodium ion conductivity. They are accompanied by strong endothermic effects without mentionable hysteresis and do not coincide with the eutectics of the pseudobinary system $NaNO_2/Na_2O$. Since reconstructive phase transformations (type 1 according to the Ehrenfest classification) are not involved there are only two possible explanations left: Increasing rotational mobility of the NO_2^- anion or melting of the sodium ion substructure. NO_2^- is dynamically disordered with jump rates in the gigahertz range already at room temperature. However, for steric reasons the bent anion can only move around its longitudinal axis. Conceivable now would be that rotations about the other axes are possible at elevated temperatures. This could only happen, however, if the sodium ions leave their regular positions. This would then provide an explanation for their translational mobility and for the high sodium ion conductivity. Independent of the effects of the dynamic behavior of the complex anion, the general structural makeup with a "cubic body-centered" arrangement of the anions, as in α-AgI or Ag_3SBr, which are the best solid-state electrolytes of all, could favor a melting of the cation substructure. Indeed, there are a series of features in common with the behavior of AgI.

An experimental differentiation of the two proposed models can be accomplished by substitution of NO_2^- by anions such as CN^- or Br^- which have fewer degrees of rotational freedom. Indeed the results of the conductivity measurements and of the differential thermal analyses of the two compounds Na_3OCN and Na_3OBr isotypic with Na_3NO_3 (cf. Fig. 13) are very informative:[33] Even without the possibility of rotation diffusion, in the case of Na_3OBr, sudden jumps in conductivity and an endothermic effect are observed, albeit to a lesser extent than in the case of Na_3NO_3 and in one step. Na_3OCN shows qualitatively the same behavior, but with the largest conductivity jump found so far in these systems. These findings can now be explained by assumption of a combination of both effects in Na_3NO_3 and Na_3OCN, in the case of Na_3OBr exclusively as a result of the structurally ("cubic body-centered" arrangement of the anions) promoted premelting of the cation substructure. That Na_3OCN exhibits only one thermal effect is accounted for by the complete activation of the possible rotations of the smaller rod-shaped anions already at room temperature.

A similar argument holds in the case of oxide nitrites of the anti-K_2NiF_4 type[32] (cf. Fig. 6) such as $(NO_2)_2ONa_4$ or $(NO_2)_2OK_4$, in which the ONa_4 structural moieties are topologically related to that of ONa_3 in Na_3NO_3. As follows from Figure 13, the effect here is even more drastic; the activation energy in the high-temperature modification approaches that of liquid electrolytes. This could be connected with the more weakly bound sodium ions at the octahedral apices in the $^2_\infty(ONa_4)$ layers.

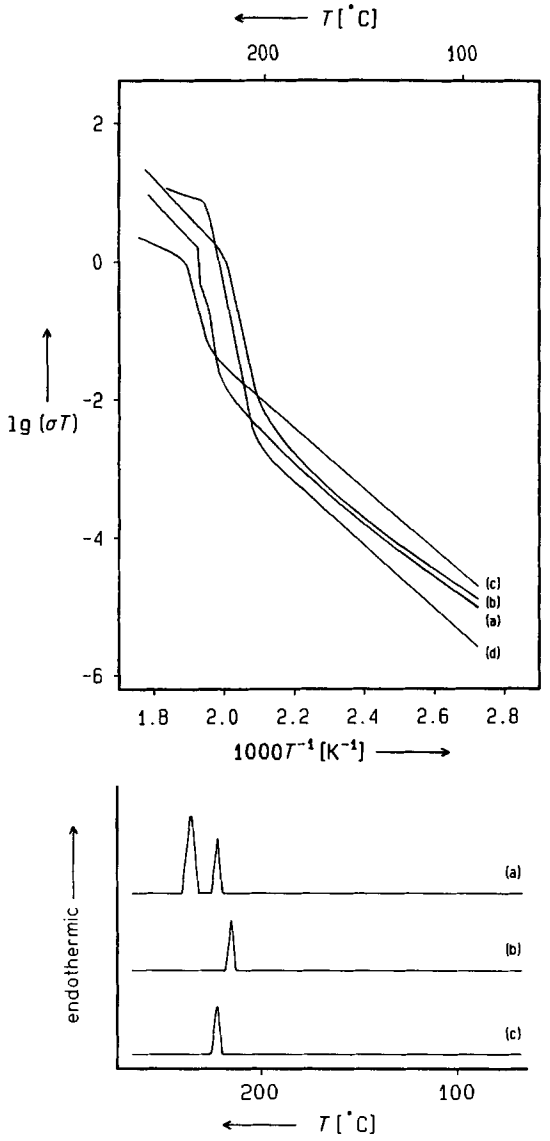

Fig. 13. Sodium ion conductivity in $(NO_2)ON_3$ (a), $(CN)ONa_3$ (b), $BrONa_3$ (c), and $(NO_2)_2ONa_4$ (d) (top) and schematic reproduction of the DTA curves of (a)–(c) (bottom).

6. Trends, Interpretations

The aim of our studies is to collect empirical material through the development of novel alkali-metal ionic conductors by the choice of suitable basic structures and material systems, in order to assess the importance of the parameters influencing ion conduction and their destructive and constructive interplay. The most homogeneous and thus best data for comparison are known for the highly symmetric rotationally dissolved phases of the respective systems. Here, without exception, the maximum achievable defect concentration is highest (in agreement with the findings in the case of Li_2SO_4[46]) and the macroscopic transport behavior can be described in the form of Arrhenius diagrams. In the case of the low-temperature modifications the solubility is lower, and regions of demixing are very soon reached. The conductivities in the two-phase regions are highly dependent on the temperature programs run for the AC measurements. This is accounted for, on the one hand, by the solid-state reactions (demixing) taking place on establishment of equilibrium, and, on the other, by an irregular distribution of the readily and poorly conducting volumes of the electrolyte (percolation phenomena). From the data available, the quantities

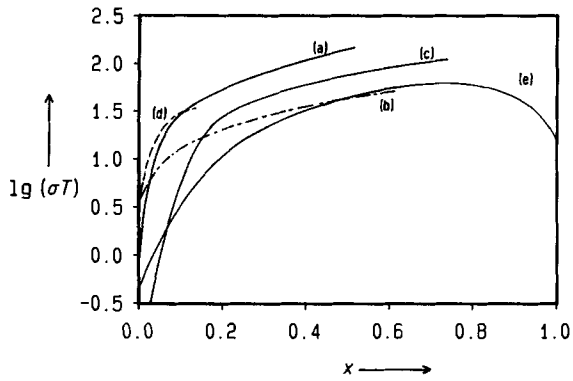

Fig. 14. Sodium ion conductivities in Na_3AlF_6/Na_2SO_4 (a), Na_3PO_4/Na_2SO_4 (b), Na_3AlF_6/Na_2SiF_6 (c), Na_3PO_4/Na_2CO_3 (d) and Na_3AlF_6/Na_3PO_4 (e) as a function of the composition (950 K for cases (a) and (e), 773 K for (b) and (d) 683 K for (c)). x = mole fraction of last named component in each system.

characterizing alkali-metal ionic conductivity, namely the activation energy and the conductivities, for the high-temperature and low-temperature phases have been chosen as the most informative (Fig. 14 and 15). The trends derived from changes in these characteristics with changing composition can be related to the various influencing parameters:

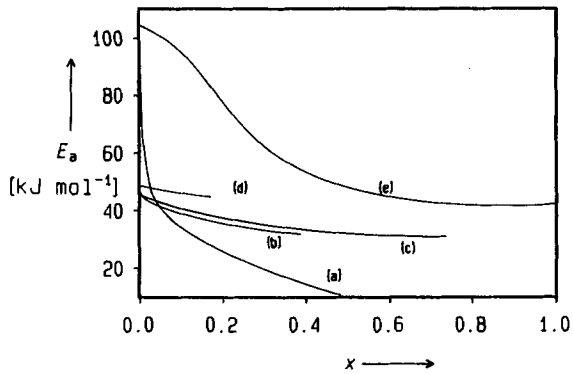

Fig. 15. Activation energies of the sodium conductivity in Na_3AlF_6/Na_2SO_4 (a), Na_3PO_4/Na_2SO_4 (d), Na_3AlF_6/Na_2SiF_6 (c), Na_3PO_4/Na_2CO_3 (d) and Na_3AlF_6/Na_2PO_4 (e) as a function of the composition in the region of the high-temperature modifications. x = mole fraction of last named component in each system.

Extrinsic Disorder in the Cationic Substructure

Increasing the defect concentration in the cationic substructure not unexpectedly (cf. Equation (d)) favors the conductivity quite significantly. As for the aliovalent substitution of cations,[36, 37] this is found also in the previously described (Section 4) solid solutions with anions of different ionic charge. The effect is clearly recognizable in the system Na_3AlF_6/Na_2SiF_6. Here, the volume of the unit cell remains practically constant during the course of doping and at the same time the conductivity at 473 K increases by five orders of magnitude between $x_{Si} = 0$ and $x_{Si} = 0.73$. If all parame-

ters except the term $c(1-c)$ in Equation (d) were fixed, then the maximum conductivity should lie at $c = 0.5$. This is in fact observed (cf. Fig. 14 and 15); however, at small values of doping it increases faster than with the factor $c(1-c)$. Here, it becomes evident that the influenced factors do not act independently of each other.

Volume Effects

The assumption that the increase of lattice constants upon doping leads to an expansion of the "transport volume" for the cations and thus effects a decrease in the activation energy of the ion transport seems plausible. The environment of a vacancy in the cationic lattice experiences a broadening and thus contributes to the expansion of the transport volume. Naturally the volume of the vacancy itself may not be taken into account, since the following consideration concerns primarily the *activation* of the macroscopic ion migration. The former local contributions are hardly measureable exactly. On the other hand, the changes in the lattice constants afford useful information: the increase in volume upon doping could fully augment the transport volume. If, in addition, one takes into account the difference between the volume increment[47] of the regular anion and that of the substituted anion, this could give a quantity which almost correctly measures the change in the free transport volume. In the system Na_3AlF_6/Na_3PO_4 the charge carrier concentration remains constant over the whole range of composition. As a comparison of the trends of σ, E_a, and V (the latter only for the sodium phosphate-rich part) with changing mole fraction x_p shows (cf. Fig. 16), there does in fact seem

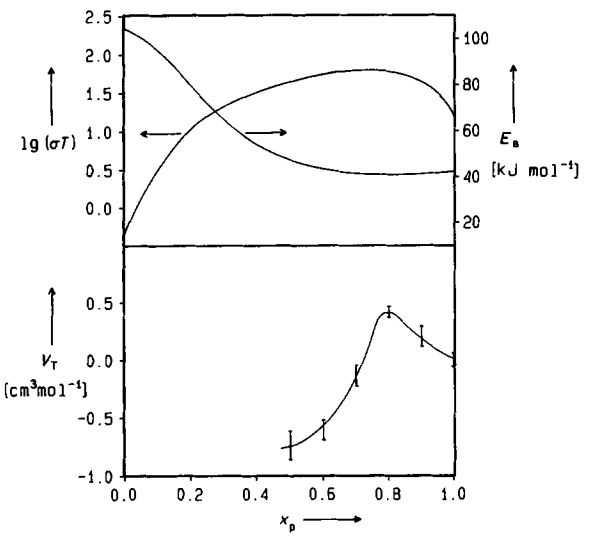

Fig. 16. Course of the sodium ion conductivity, activation energy, and "free transport volume" in a solution of Na_3PO_4 in Na_3AlF_6 and a solution of Na_3AlF_6 in Na_3PO_4. x_P = mole fraction of Na_3PO_4.

to be a connection between ionic conductivity and free transport volume; a volume increment of PO_4^{3-} (39 cm^3 mol^{-1}) is significantly smaller than that of AlF_6^{3-} (46 cm^3 mol^{-1}). On the other hand, it is obvious that the smaller PO_4^{3-} ion at an AlF_6^{3-} lattice site will also exhibit an increased rotational mobility on steric and symmetry grounds.

"Paddle-Wheel Effect"

The effect of the rotational diffusion of complex anions on the activation energy of translational transport is just as difficult to separate from the other influential factors as is the volume effect. Indications of this effect are given by the jumps in conductivity and the generally decreasing activation energies upon transition into the high-temperature phase with dynamically disordered anions. Convincing evidence for the effectiveness of the paddle-wheel effect appears to be derivable from the systems with doped Na_3PO_4 and the NO_2^--containing perovskite variants.

As already mentioned, slight doping of Na_3PO_4 stabilizes the high-temperature form at room temperature. The temperature dependence of the conductivity in the Arrhenius plot is completely different for doped and undoped Na_3PO_4 (cf. Fig. 9). Upon transition into the rotational phase with significant change in structure, pure Na_3PO_4 shows a corresponding increase in conductivity and an activation energy which differs for L- and H-Na_3PO_4 but is constant in their respective regions of existence. In contrast the activation energies in all solid solutions based on Na_3PO_4 change continuously with the temperature. Here, an influence of the volume effect can now be virtually ruled out, since such drastic changes in the activation energy with temperature as a result of the thermal expansion would then have to occur in all ion-conducting materials, and this is not the case.

A logical explanation, on the other hand, is provided by the concept that in H-Na_3PO_4, stabilized at room temperature by doping, the rotation of the anion is "frozen in", and this is gradually excited via thermal activation with increasing temperature up to quasi free rotation. Since, in our opinion, also rotational jumps of complex anions decrease the activation energy of translational cation transport, this model consistently explains the temperature dependence of the activation energy of mixed crystals based on Na_3PO_4.

The influence of the changing distribution of defects with temperature on the octahedral and tetrahedral holes (by means of neutron diffraction a ratio of 75:25 was measured at room temperature, and 100:0 at 673 K),[48] is not forseeable at the present time.

Especially instructive in this connection seems to be the situation in the anti-perovskites of type $XONa_3$ with $X = NO_2^-$, CN^-, Br^-. Due to the packing of the anions (cubic body-centered) we have a structural principle common to all three compounds, which we see as a prerequisite for the surprisingly high ionic conductivity. In addition, a further increase in the conductivity by a few orders of magnitude manifests itself as a result of the rotational degrees of freedom of the anionic groups in $(CN)ONa_3$ and $(NO_2)ONa_3$. We consider the fact that $(NO_2)ONa_3$ shows two jumps (NO_2^- has one more degree of rotational freedom available than CN^-) with endothermic effects as lending support to the opinion that the rotational diffusions of the anions promote the translational mobility of the cations.

Packing of the Anions

The type of packing of the anions to give ideally an immobile matrix has been somewhat neglected in previous work. This aspect has, however, been vividly brought to mind in direct connection with discussions of the electrical behavior

of the anti-perovskites. It is certainly not without good reason that just α-AgI and Ag_3SBr with cubic body-centered arrangement of the anions are the solid-state electrolytes with the highest conductivity found so far. The unforseen high sodium ion conductivity in $BrONa_3$ or $(NO_2)ONa_3$ is certainly accounted for in part in terms of this anionic structure with its characteristically distorted and mutually interpenetrating "tetrahedral" and "octahedral" holes. This can be taken as an indication that also the packing and thus the type and connectivity of the holes for the cations may in no way be ignored when designing fast ion conductors based on large complex anions.

7. Volume Effect or Paddle-Wheel Mechanism?

Parallel to our attempts to develop new solids with high alkali-metal ion conductivity exploiting the rotational mobility of complex anions, a very controversial discussion has developed as to whether the rotational motion of the anions actually and effectively favors the cationic conductivity. *Lunden* et al.[46, 49] are of the opinion that a paddle-wheel mechanism provides the actual explanation for the high conductivity of ionic crystals with dynamically disordered anions, particularly of Li_2SO_4, whereas *Secco* et al.[50] disagree with involvement of such an effect and make the increase in volume during the transition into the rotational phase responsible for the increase in conductivity. The argument in each case is based predominantly on macroscopic material properties. *Lunden* et al. have indeed demonstrated beyond doubt the nature of the high-temperature form of Li_2SO_4 as rotational phase, however direct proof of an immediate interaction between translational mobility of the cations and rotational diffusion of the anions is still lacking. Attempts to come to a decision here were impaired by insufficient employment of local probes responding to the dynamics in solids and by certain limitations coupled with the heterogeneity of the systems investigated. A further deficiency lies in the diffuse definition of the mechanism: Corresponding to the images employed "paddle wheel", "cog wheel", or "revolving door" are different concepts, from the one extreme of an active role of the anions transporting the cations mechanically, to a passive function responding with an evasive motion toward the passage of the cation.

The following classification of the differences would seem meaningful:

1. Cooperative rotational movements of the anions transport the cation actively (paddle-wheel or cog-wheel mechanism).
2. Uncoupled rotational jumps permit passage of the cations according to the random principle and thus lead to a high mobility of the cations.
3. The mobile anions react with an evasive motion towards the passage of the cation (revolving door mechanism).
4. The rotational diffusion generates periodically fluctuating potentials at the cation positions and thus favors cation mobility.

All synchronous mechanisms are less likely. The assumption of coupled motions of neighboring anions ("cog-wheel" mechanism) would signify considerable interaction between these anions, which in turn would not be reconcilable with the suggested quasi free rotation. Comparable jump rates for anions and cations over a greater temperature range are also not conceivable, since this would require matching activation energies.

For differentiation between the remaining models quantitative data for the local dynamics are essential. But already the data available permit a first classification. In agreement with *Lunden* et al. we have, according to our results, no doubt that the rotational diffusion of the anions increases the cationic conductivity and decreases the associated activation energy. In any case the observations on the anti-perovskites $XONa_3$ and the mixed crystals based on Na_3PO_4 are not to be understood otherwise. On the other hand, a favoring of the ion transport by a higher transport volume is equally incontestable. The two effects can not be strictly separated. The phase transformation in a rotational phase is also always accompanied by an increase in volume; conversely an increase in volume at the lattice of the anion promotes its rotational mobility. In this respect the question "volume effect" or "paddle-wheel mechanism" is not so closely defined, as is presently being discussed. Moreover there is no reason to grant Li_2SO_4 a special position. The differences from other ionic crystals with dynamically disordered complex anions such as Na_3PO_4 or Na_2SO_4 are only of a qualitative nature; at correspondingly elevated temperatures PO_4^{3-} in Na_3PO_4 will, e.g., exhibit similarly high jump rates as SO_4^{2-} in Li_2SO_4.

It can be clearly shown that a "paddle-wheel mechanism" is effective during cation transport (albeit to a differing extent from compound to compound); the respective contribution and the mechanism on a microscopic level cannot be determined via the macroscopic properties predominantly determined here.

8. Conclusion

On the basis of the results collected so far we consider our concept to promote the translational motion of cations in ionic crystals by introducing complex anions with rotational mobility as having been validated. Right from the start, material with negligible electronic contributions, showed cation conductivities comparable with those of the so-called "fast-ion conductors". However, the values of the hitherto best sodium ion conductor, β-aluminum oxide, could not be outrun or even reached. The results are concomitantly documentary evidence that the factors influencing ionic conduction appear to be principally understood. Remarkable progress has also been made in our understanding of the microscopic mechanisms and in deducing quantitative relationships.[51] Even if it is difficult to surpass the previous "record marks" through the synthesis of tailormade solids then this in our opinion has nothing to do with the respective optimum compounds being found already, but rather with the difficulties in realizing the required structural and chemical circumstances with the necessary precision. In this context we might only mention the ionic radius of the migrating particle, which must be accurately matched to the free cross

section of the diffusion path; even slight deviations below or above the ideal value lead to drastic breaks in the conductivity.

As shown, for example, by the development of NASICON,[52] our understanding certainly suffices in order to develop suitable material systems with predicted high ionic conductivity in a practically deductive way. On the other hand, the accidental discovery of the high sodium ion conductivity in Na_3NO_3 and in the compounds structurally derived therefrom already in the undoped state demonstrates that a more inductive approach also still has justification.

The systems newly introduced by us broaden the material basis for discussions in connection with the paddle-wheel mechanism. They support the concept according to which the rotational diffusion of the anions favor cation conduction. We expect to acquire further supporting evidence for this interpretation by measuring the local motions in the systems described, e.g. with the help of nuclear magnetic resonance spectroscopy. Although valuable additional atom-specific information might be accessible thereby, the attempt to strictly separate rotational and translational motions from each other or even to establish cause–effect relationships will fail—as much as this would be desirable for an understanding of the processes and their description. It is an essential characteristic of chemical systems and especially of solids that they always respond collectively to external impacts, for example in the course of a physical measurement.

Our own works mentioned in this review were supported by the Fonds der Chemischen Industrie and the Deutsche Forschungsgemeinschaft (SFB 173 and Gottfried Wilhelm Leibniz Program). I wish to thank all co-workers who participated in the individual studies cited in this work. Thanks are also due to Dipl.-Chem. U. Henseler, Dr. R. Hundt, Dipl-Chem. D. Trinschek, and Frau K. Schirop for help in preparing the manuscript.

Received: April 18, 1991 [A 842 IE]
German version: *Angew. Chem. 103* (1991) 1574

[1] H. L. Tuller, P. K. Moon, *Mater. Sci. Eng. B1* (1988) 171.
[2] C. Tubandt, E. Lorenz, *Z. Phys. Chem. 87* (1914) 513.
[3] J. Frenkel, *Z. Phys. 35* (1926) 652.
[4] C. Wagner, W. Schottky, *Z. Phys. Chem. B11* (1930) 163; W. Schottky, *ibid. B29* (1935) 335; C. Wagner, *ibid. B22* (1933) 181.
[5] H. Schmalzried: *Solid State Reactions*, Verlag Chemie, Weinheim 1981, pp. 59–90; M. A. Ratner, A. Nitzan, *Solid State Ionics 28–30* (1988) 3.
[6] Y.-F. Y. Yao, J. T. Kummer, *J. Inorg. Nucl. Chem. 29* (1967) 2453.
[7] R. Ridgway, A. Klein, W. O'Leary, *Trans. Elektrochem. Soc. 70* (1936) 71; C. A. Beevers, M. A. S. Ross, *Z. Kristallgr. 77* (1937) 59; C. Peters, M. Bettman, J. Moore, M. Glick, *Acta Crystallogr. Sect. B27* (1971) 1826.
[8] Cf also: H. Rickert, *Angew. Chem. 90* (1978) 38; *Angew. Chem. Int. Ed. Engl. 17* (1978) 37; T. Takahashi in A. L. Laskar, S. Chandra (Eds.): *Superionic Solids—Solid Electrolytes: Recent Trends*, Academic Press, Boston 1989, pp. 1–41.
[9] K. H. Lieser, *Z. Phys. Chem. NF 9* (1956) 302.
[10] C. Drotschmann, *Batterien 19* (1965) 761.
[11] M. S. Wittingham, R. A. Huggins, *J. Chem. Phys. 54* (1971) 414.
[12] R. E. W. Casselton, *Phys. Status Solidi A2* (1970) 571.
[13] A. Rabenau, *Solid State Ionics 6* (1982) 277.
[14] M. G. Shilton, A. T. Howe, *Mater. Res. Bull. 12* (1977) 701.
[15] D. F. Shriver, G. C. Farrington, *Chem. Eng. News 63* (1985) 42.
[16] B. B. Scholtens, W. van Gool in W. van Gool, P. Hagenmuller (Eds.): *Solid Electrolytes*, Academic Press, New York 1978, pp. 466–473; G. Dahlke, *Prax. Naturwiss. Teil 3 3/38* (1989) 14.
[17] C. Richard, A. Catlow, *J. Chem. Soc. Faraday Trans. 86* (1990) 1167.
[18] D. O. Raleigh, *J. Appl. Phys. 41* (1970) 1876; J. C. Phillips, *J. Electrochem. Soc. 123* (1976) 934; S. Geller, *Acc. Chem. Res. 11* (1978) 87.
[19] A. Kvist, A. Bengtzelius in W. van Gool (Ed.): *Fast Ion Transport in Solids—Solid State Batteries and Devices*, North-Holland, Amsterdam 1973, pp. 193–199.
[20] A. Lundén, *Solid State Commun. 65* (1988) 1237.
[21] a) D. M. Wiench, M. Jansen, *Z. Anorg. Allg. Chem. 461* (1980) 101; *ibid. 468* (1982) 57; b) H. Hruschka, M. Jansen, *Mater. Res. Bull. 22* (1987) 887.
[22] J. Kremmler, *Dissertation*, Universität Hannover 1987; J. Kremmler, M. Jansen, *Z. Kristallogr. 186* (1989) 149.
[23] G. Meyer, R. Hoppe, *Rev. Chim. Miner. 12* (1975) 455.
[24] H. Menzel, E. von Sahr, *Z. Elektrochem. 43* (1937) 104; W. C. Schroeder, A. A. Berk, A. Gabriel, *J. Am. Chem. Soc. 59* (1937) 1783; E. Zintl, W. Morawietz, *Z. Anorg. Allg. Chem. 245* (1940) 12; E. T. Turkdogan, W. R. Maddocks, *J. Iron Steel Inst. London 172* (1952) 1; M. Palazzi, F. Remy, *Bull. Soc. Chim. Fr. 1971*, 2795; M. Kizilyalli, A. J. E. Welch, *J. Inorg. Nucl. Chem. 38* (1976) 1237.
[25] A. F. Wells: *Structural Inorganic Chemistry*, 4th Edit., Clarendon Press, Oxford 1984, p. 176.
[26] E. G. Steward, H. P. Rooksby, *Acta Crystallogr. 6* (1953) 49.
[27] F. Hund, R. Fricke, *Z. Anorg. Allg. Chem. 258* (1949) 198.
[28] O. Greis, M. Matinez-Ripoll, *Z. Anorg. Allg. Chem. 436* (1977) 105.
[29] F. Zintl, W. Morawietz, *Z. Anorg. Allg. Chem. 236* (1938) 372.
[30] M. Jansen, *Z. Anorg. Allg. Chem. 435* (1977) *13*; M. Jansen, *Angew. Chem. 88* (1976) 410; *Angew. Chem. Int. Ed. Engl. 15* (1976) 376.
[31] M. Jansen, *Z. Naturforsch. A37* (1982) 1457.
[32] W. Müller, *Dissertation*, Universität Bonn 1991.
[33] W. Müller, M. Jansen, *Z. Anorg. Allg. Chem.* 591 (1990) 41.
[34] M. Jansen, W. Müller, *Z. Naturforsch. B44* (1989) 996.
[35] H. T. Sabrowsky, K. Pazkowski, D. Reddig, P. Vogt, *Z. Naturforsch. B43* (1988) 238.
[36] E. A. Secco, *Solid State Ionics 28–30 (1988) 168.*
[37] A. R. West, *Ber. Bunsenges. Phys. Chem. 93* (1989) 1235.
[38] The measurement of the total conductivity was carried out with an impedance analyzer HP 4192 A coupled to a central computer HP vectra. The specific conductivity was calculated from the real part at the first minimum found in the Argand plot with increasing frequency. The direct current measurements according to Hebb-Wagner [39] were carried out with a current-voltage generator Advantest TR 6142, double multimeter Keithley 195 A, and Hameg HM 8112-2 as well as a control computer HP 9000. The transport measurements were carried out with the same apparatus. Tungsten bronzes were used as reversible electrodes and Na-β-alumina discs were used as specific sodium permeable membranes between electrode and sample.
[39] M. Hebb, *J. Chem. Phys. 20* (1952) 185; C. Wagner, *Z. Elektrochem. 60* (1956) 4.
[40] A. Hooper, P. McGeehin, K. T. Harrison, B. C. Tofield, *J. Solid State Chem. 24* (1978) 265; B. Majidi, J.-F. Brice, H. Kessler, *Mater. Res. Bull. 19* (1984) 1599.
[41] J. T. S. Irvine, A. R. West, *J. Solid State Chem. 69* (1987) 126; *ibid. 74* (1988) 385; *Mater Res. Bull. 22* (1987) 1047.
[42] H. Hruschka, E. Lissel, M. Jansen *Solid State Ionics 28–30* (1988) 159.
[43] E. Lissel, *Dissertation*, Universität Hannover 1990; E. Lissel, M. Jansen, *Z. Naturforsch. B46* (1991) 393.
[44] D. Trinschek, *Diplomarbeit*, Universität Bonn 1989.
[45] H. Hruschka, M. Jansen, *Mater Res. Bull. 24* (1989) 1279.
[46] A. Lundén, K. Schröder, H. Ljungmark, *Solid State Ionics 28–30* (1988) 262.
[47] W. Biltz: *Raumchemie der festen Stoffe*, Leopold Verlag, Leipzig 1934.
[48] M. Jansen, J. Geb, unpublished.
[49] A. Lundén, *Solid State Ionics 28–30* (1988) 163; A. Lundén, in B. V. R. Chowdari, S. Radhakrishna (Eds.): *Materials for Solid State Batteries*, World Scientific Publ., Singapore 1986, p. 149; A. Lundén, J. O. Thomas in T. Takahashi (Ed.): *High Conductivity Solid Ionic Conductors—Recent Trends and Applications*, World Scientific Publ., Singapore 1989, p. 45; A. Lundén, M. A. K. L. Dissanayake, *J. Solid State Chem. 90* (1991) 179.
[50] E. A. Secco, *Phys. Status Solidi A88* (1985) K 75; M. D. Leblanc, U. M. Gundusharma, E. A. Secco, *Solid State Ionics 20* (1986) 61; U. M. Gudusharma, C. MacLean, E. A. Secco, *Solid State Commun. 66* (1988) 921; A. S. Campbell, K. G. MacDonald, E. A. Secco, *J. Solid State Chem. 81* (1989) 65.
[51] K. Funke, *Z. Phys. Chem. NF154* (1987) 251; A. Bunde, D. K. Chaturvedi, W. Dieterich, *Z. Phys. B47* (1982) 209; K. Funke, R. Hoppe, *Int. Soc. Solid-State Ionics Lett. 1* (1990) 9.
[52] H. Y.-P. Hong, *Mater. Res. Bull. 11* (1976) 173; J. B. Goodenough, H. Y.-P. Hong, J. A. Kafalas, *ibid. 11* (1976) 203.

1,4-Dihydropyridines: Effects of Chirality and Conformation on the Calcium Antagonist and Calcium Agonist Activities

By Siegfried Goldmann* and Jürgen Stoltefuss

Dedicated to Professor Karl Heinz Büchel on the occasion of his 60th birthday

4-Aryl-1,4-dihydropyridine-3,5-dicarboxylic diesters of the nifedipine type have become almost indispensable for the treatment of cardiovascular diseases since they first appeared on the market in 1975. There are some twenty derivatives currently under clinical development worldwide and work in this area is continuing undiminished. The 1,4-dihydropyridines are the most effective of the calcium antagonists or calcium channel blockers. They are valued not only for their pharmacological effect, but also as a tool for the investigation of the calcium channel, particularly since the discovery that this class also includes compounds that have exactly the opposite action profile and are known as calcium agonists. There are even instances in which this reversal of activity is found between enantiomers. In view of the importance of chirality to pharmacological activity, the present article will describe methods for the separation of enantiomers, point out the structural differences between calcium antagonists and calcium agonists, and attempt to explain the difference in their behavior.

1. Introduction

1,4-Dihydropyridines of type **1** were first synthesized by *A. Hantzsch* in 1882 from acetoacetic esters, an aldehyde, and ammonia.[1] It was not until 60 years later, however,

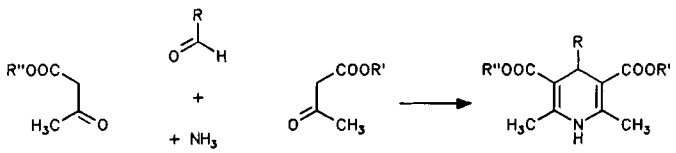

1

that compounds of this class were shown to exhibit pharmacological activity. The 4-quinoline-substituted 1,4-dihydropyridines **2**, which have analgesic, morphine agonist, and spasmolytic properties, were described in a Wellcome patent in 1943.[2] However, this patent had no influence on the present importance of 1,4-dihydropyridines.

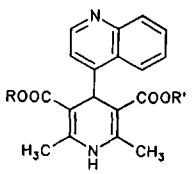

2

Twenty years later, in an investigation on cardioactive compounds of the khellin type, **3**,[3,4] *Bossert* and *Vater* at Bayer AG attempted to produce more effective and more soluble compounds by modification of the basic skeleton.

Starting with **3** and proceeding via the 4-quinolones **4** and the fused dihydropyridine derivatives **5**, they obtained the

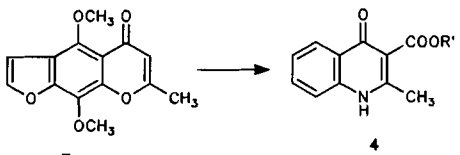

3 **4**

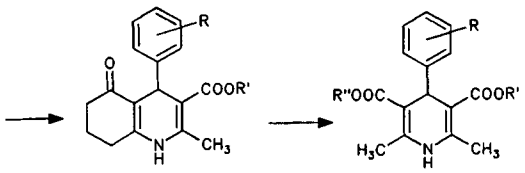

5 **6**

1,4-dihydropyridines **6** of the Hantzsch type,[5] which were characterized by outstanding coronary vasodilator activity.[6] The 2-nitrophenyl derivative **7** was selected as a promising compound for development. As nifedipine (Adalat®), it was successfully introduced in Germany at the beginning of 1975 for the treatment of coronary diseases.[7] *Loev* et al. at Smith, Kline and French independently studied similar derivatives having antihypertensive properties.[8-10]

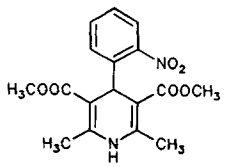

7

Very soon after the discovery of the cardiovascular properties of 1,4-dihydropyridines, it was found that these substances act by inhibiting the entry of Ca^{2+} into the cells of cardiac and vascular muscle through the voltage-dependent calcium channels.[11,12] To this day, the 1,4-dihydropyridines are still the most potent group of calcium channel blockers or "calcium antagonists".

[*] Dr. S. Goldmann, J. Stoltefuss
Bayer AG, Pharma-Forschungszentrum
W-5600 Wuppertal 1 (FRG)

With these early studies as a foundation, many dihydropyridine derivatives have now been synthesized worldwide[5, 13–21] and have led to numerous second-generation commercial products,[16, 22] such as nimodipine (**8**),[23, 24] nisoldipine,[25] nitrendipine,[26] amlodipine (**9**),[27] felodipine,[28] isradipine,[29] manidipine,[30] nicardipine (**10**),[31] and nilvadipine.[32] Some of these compounds are characterized by longer bioavailability or greater tissue selectivity.

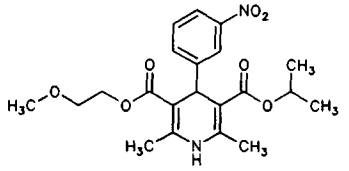

8

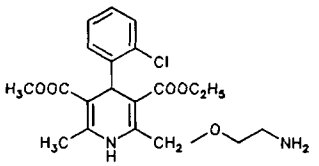

9

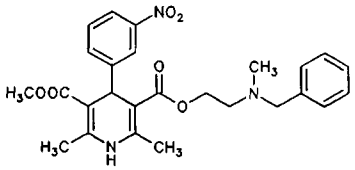

10

Symmetrically substituted dihydropyridines such as nifedipine **7** are achiral compounds. Different substituents in compounds of the second generation lead to chiral derivatives whose enantiomers differ in their pharmacological effects. In the case of the calcium antagonists, the differences are quantitative. However, the introduction of certain substituents in positions 3 or 5 can lead to calcium agonists. The enantiomers exhibit opposite activity, one of them acting as an agonist, the other as an antagonist.[33]

Because of the great importance of chirality in 1,4-dihydropyridines, the present article will be particularly concerned with the synthesis of the enantiomers and the differences in their activities. The question of which of the conformations of 1,4-dihydropyridines could be "pharmacologically active" will also be discussed, and an attempt will be made to explain the differences in pharmacological behavior.

2. Synthesis of Enantiomerically Pure 1,4-Dihydropyridines

The methods used most frequently for the separation of the enantiomers are (1) resolution of the racemic monocarboxylic acids **11** via diastereomeric salts and (2) separation of the diastereomeric esters **12** followed by selective removal

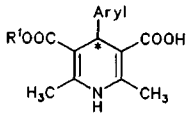

11

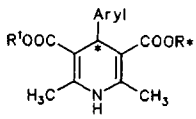

12

of the esterifying group to produce the monocarboxylic acid **11** or direct transesterification to form the desired dihydropyridine. Enantioselective synthesis with a chiral auxiliary group on the nitrogen has also proved to be particularly successful.

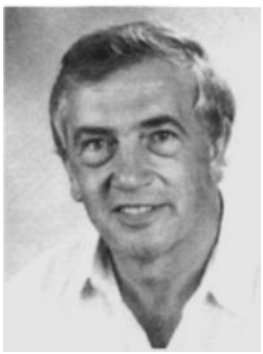

Siegfried Goldmann was born in Mölln in 1947. He studied chemistry at Marburg and was awarded a doctorate with distinction in 1979 for his work on „The stereochemistry of the [2,3]-sigmatropic rearrangement of allyl sulfoxides and the preparation of optically active allyl alcohols" under Prof. R. W. Hoffmann in Marburg. He has been employed in pharmaceutical research for Bayer AG since 1979 and works mainly in the field of 1,4-dihydropyridines for cardiovascular and metabolic indications.

Jürgen Stoltefuss was born in Wuppertal in 1941. After training as a chemical laboratory assistant for Bayer AG, he studied chemistry at Essen Technical College from 1966 until 1969. Since 1969 he has been employed by Bayer AG as a graduate engineer at the Wuppertal Research Center. His work centers mainly on synthetic investigations in the field of deoxynojirimycins and dihydropyridines.

2.1. Resolution of Racemic Dihydropyridinecarboxylic Acids

Most resolutions of racemic dihydropyridines proceed via diastereomeric salts of dihydropyridinecarboxylic acids **11** with chiral bases. A number of special methods have been developed for the preparation of dihydropyridinecarboxylic acids,[34-39] either via readily cleavable esters[35-48] or via *N*-blocked dihydropyridine dialkyl esters.[42,49] The most important of these preparation methods begin with esters of dihydropyridinecarboxylic acids having an electron-attracting group in the β position, so that they readily undergo β eliminations.[35-44] Even sensitive monocarboxylic acids can be obtained in yields of more than 70% by this means.

Cinchonidine, quinidine, cinchonine, and brucine are used as chiral bases, though other enantiomerically pure amines can also be used.[50] The first resolution of racemic dihydropyridinecarboxylic acids was carried out with the *N*-blocked 3-nitrophenyldihydropyridinecarboxylic acid **13** (Scheme 1).[51]

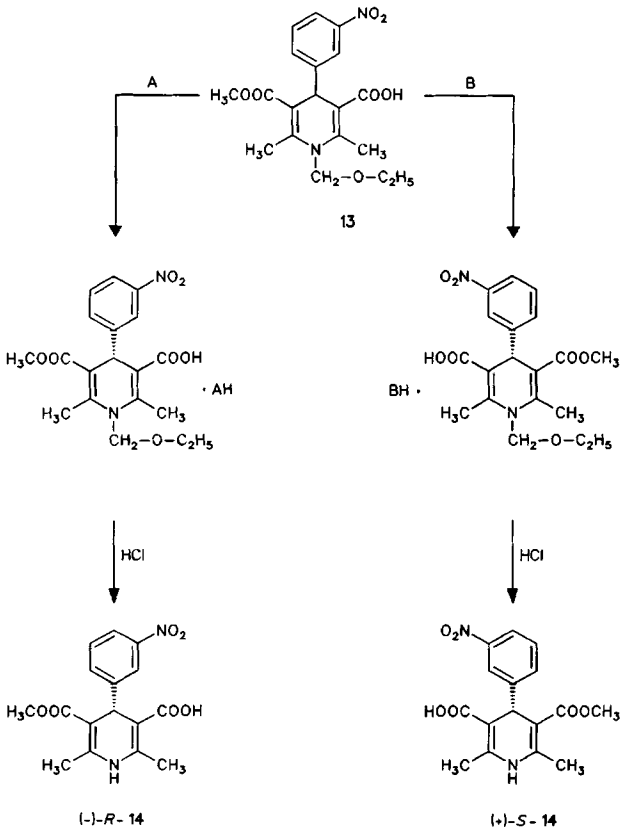

Scheme 1. Path A: Addition of cinchonidine (AH), recrystallization. Path B: Addition of cinchonine (BH), recrystallization.

Compound **13** is allowed to react with cinchonidine to form the diastereomeric salts. The *R* enantiomer **14** is obtained by repeated recrystallization and hydrolysis with hydrochloric acid (path A).[51,52] If cinchonine is used as the chiral base, on the other hand, the (+)-*S* enantiomer forms a sparingly soluble salt (path B).[52] With a suitable choice of the chiral base, therefore, either the *R* or the *S* enantiomer can be obtained by simple purification steps in an overall yield of about 10% and with high enantiomeric purity (*ee* > 99%). In DMF/water mixtures (DMF = *N*,*N*-dimethylformamide), separation of **14** is possible even without prior protection of the NH function.[50]

The resolution of racemates via diastereomeric salts has been successfully used for dihydropyridinecarboxylic acids with various structures, both of the calcium antagonist type[49,53-61] and of the calcium agonist type.[50,62] The enantiomers of the dihydropyridinecarboxylic acids are important starting compounds for the preparation of enantiomerically pure commercial and development products and of other pharmacologically interesting dihydropyridinecarboxylic esters.[49-77]

2.2. Resolution of Racemic Mixtures of Basic Dihydropyridine Derivatives

Chiral acids such as camphorsulphonic acid and substituted tartaric acids have been used to separate the enantiomers of basic dihydropyridine derivatives in yields of up to 30%.[51,55,59,67,68,73,78-79] A resolution by temporary introduction of a basic isothiourea is illustrated in Scheme 2.[45] The enantiomers obtained after separation of **16** with chiral acids may be converted into 2-substituted derivatives or into 2,6-dimethyldihydropyridines. By the use of a suitable ester group (allyl or *tert*-butyl ester), it is possible to obtain *both* enantiomerically pure compounds from *one* diastereomerically pure salt by changing the sequence of the cleavage and esterification steps.[45]

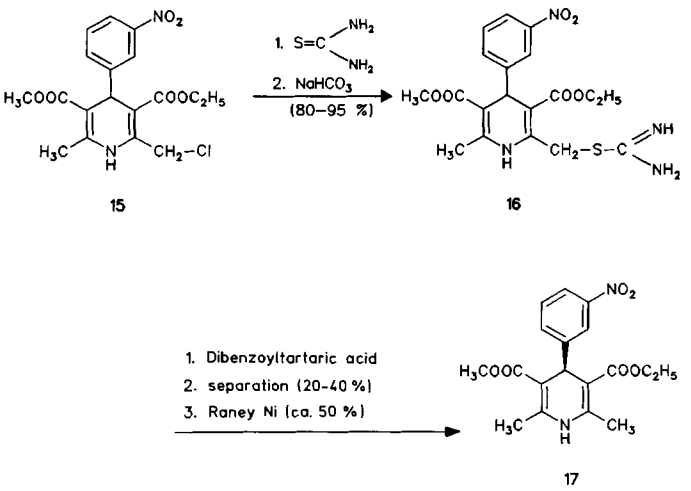

Scheme 2.

This method of enantiomer separation is suitable for many 2-substituted dihydropyridine derivatives (some of them new). However, it offers no advantages over the resolution of racemic dihydropyridinecarboxylic acids for the preparation of the enantiomers of 2,6-dimethyldihydropyridines, simply because of the greater number of steps involved in the synthesis.

In general, the resolution of racemic mixtures of basic dihydropyridines is of minor importance in comparison with that of dihydropyridinecarboxylic acids, mainly because the dihydropyridinecarboxylic acids are easy to prepare and can

be used as starting compounds both for neutral alkyl esters and for acidic and basic esters.

2.3. Separation via Diastereomeric Esters

The separation of enantiomeric dihydropyridines via diastereomeric esters is superior to other separation methods with regard to chemical yield and enantiomeric purity. If diastereomers **12** are produced by esterification with an optically active alcohol R*OH, regioselective removal of the alcohol must be possible after the separation has been performed. Three different variants are known:

1. The chiral ester group is activated, so that it can react selectively.
2. The structure of the chiral esterifying group is such that it can be removed by β elimination.
3. The chiral esterifying group can be removed by hydrogenolysis.

In certain cases the optically active group remains in the pharmacologically active molecule, so that the diastereomers can be separated without further derivatization.[65, 80–89]

2.3.1. *Activation of the Ester Group*

The first synthesis of enantiomerically pure dihydropyridines with activated chiral ester groups was performed by *E. Wehinger* et al. (Scheme 3).[90] With mandelic acid (**18**) as the starting material, the alcohol **19** is obtained in two steps; this alcohol is then used via the corresponding acetoacetic ester, to prepare the dihydropyridine **20**. Recrystallization yields a diastereomerically pure product. By regioselective transesterification with sodium methoxide, the desired enantiomer **21** can be obtained from the ester **20** in enantiomeric purities of *ee* > 99%. The ester group here is presumably activated by chelation with metal ions, so that the transesterification proceeds regioselectively. This method has been successfully used to prepare the enantiomers both of calcium antagonists[54, 91–95] and of calcium agonists.[96]

The use of lactic acid as the ester component has certain advantages. Lactic acid is considerably cheaper than mandelic acid, and it can also be used without derivatization. Esters of lactic acid were first used for the diastereomer separation of 3-(1,3,4-oxadiazol-2-yl)dihydropyridines such as **22**.[97] The isolated diastereomers were transesterified with sodium alkoxide in yields of about 30%.

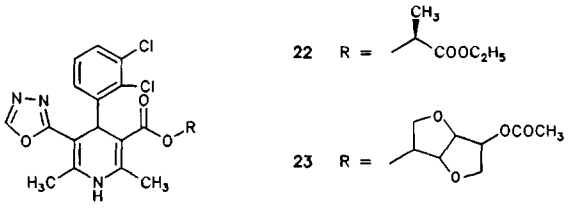

Esters of lactic acid have also been used successfully for the diastereomer separation of dihydropyridine lactones,[98] 3-nitrodihydropyridines,[99–100] and 3-cyanodihydropyridinecarboxylic esters.[101] Here again it is possible that the esters were activated by complex formation with metal ions. The same could be true of the 2-acetate of isosorbide as the alcohol component, as in **23**.[97]

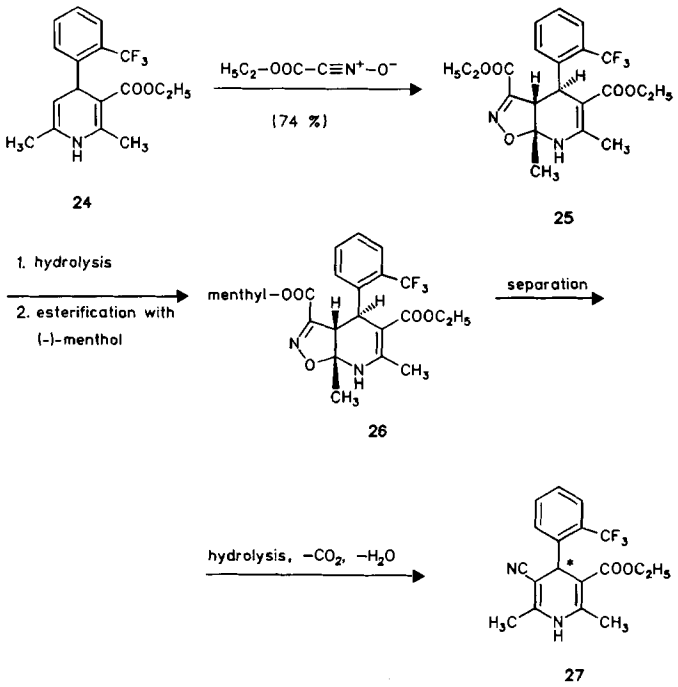

Scheme 4.

A method for the preparation of optically active 3-cyanodihydropyridines has been described with the compound **27** as an example (Scheme 4).[102] With the monoester **24** as the starting material, the isoxazolo[5.4-*b*]tetrahydropyridine **25** is obtained as the sole product of 1,3-dipolar cycloaddition with a nitrile oxide. Hydrolysis of the ester followed by reesterification with (−)-menthol leads to the formation of diastereomers, which are separated by flash chromatography. The enantiomers of the 3-cyanodihydropyridines are then obtained by hydrolysis of the methyl ester followed by decarboxylation.

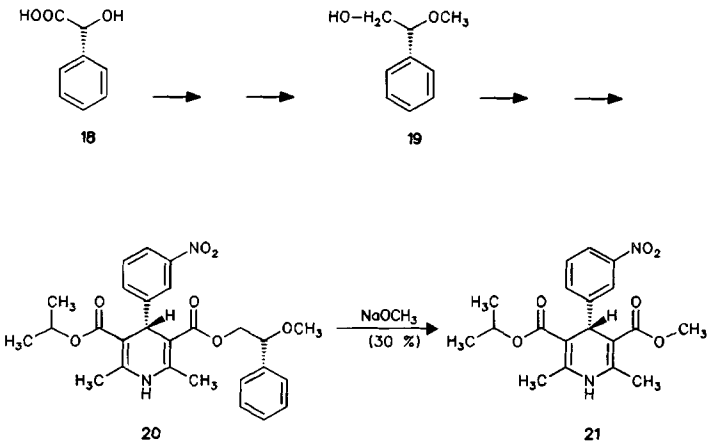

Scheme 3.

2.3.2. Removal of the Esterifying Group by β Elimination

A fundamentally different method for the selective removal of the chiral auxiliary alcohol is β elimination of a chiral esterifying group with a special structure (e.g., **28** → **29**). X in this formula must be an electron-attracting group or must be capable of being converted into such a group. A disadvantage of this method is the often demanding synthesis of the special alcohols, particularly since the chiral auxiliary alcohol is lost and cannot be recycled.

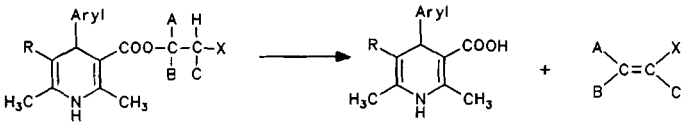

28 **29**

To prepare the enantiomers of felodipine (**34**) (Scheme 5), the dihydropyridine derivative **32** is synthesized from the optically active diol **30** in an overall yield of 50–55%.[103] The chromatographic separation of the diastereomers is advantageously performed after acidic removal of the trityl group. By hydrolysis and esterification, the enantiomers **34** are obtained with an enantiomeric excess of $ee \geq 99\%$.

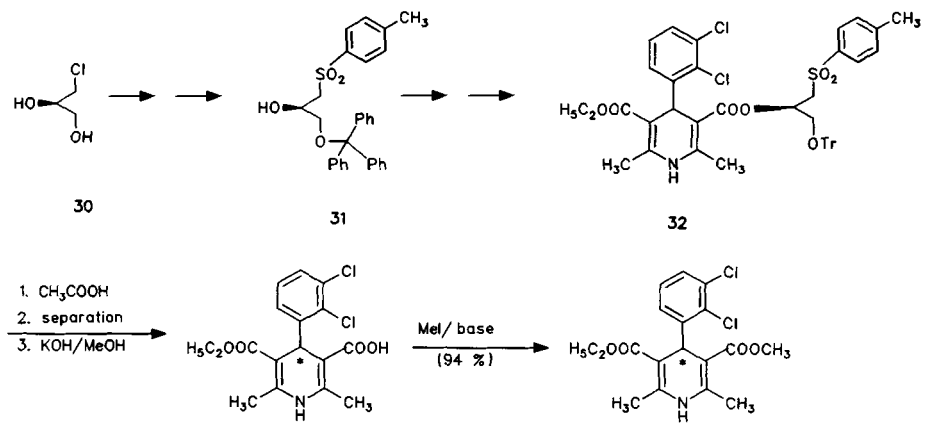

Scheme 5. Tr = trityl.

30 **31** **32** **33** **34**

Esters have also been successfully used as acidifying groups.[104] After esterification and protection of the amino group, threonine (**35**) is coupled via the corresponding acetoacetic ester to the dihydropyridine moiety of **37**. An advantageous feature of this method is the wide range of variation possible in the chiral threonine structure; thus, the best combination of substituents can be chosen for each separation problem. The diastereomers are separated by crystallization, chromatography, or Craig distribution. Finally, the threonine group is preferably removed with bases such as 1,8-diazabicyclo[5.4.0]undec-7-ene (DBU) or 1,5-diazabicyclo[4.3.0]non-5-ene (DBN) to give the dihydropyridinecarboxylic acid **38** in a yield of over 70%. This method was used to synthesize the enantiomers of nimodipine (**8**) in fairly large quantities for the first time.[105] Chiral trichloroethyl esters which can be removed by β elimination have also been used.[106]

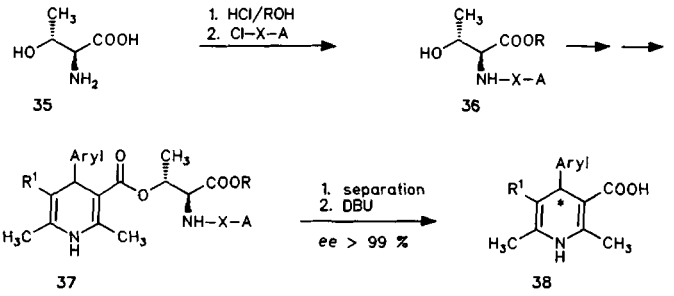

35 **36** **37** **38**

2.3.3. Removal by Hydrogenolysis

Another method for the preparation of enantiomeric dihydropyridines via diastereomeric esters involves the use of chiral benzyl esters, which can be removed regioselectively by hydrogenolysis after the enantiomer separation has been performed.[73, 107] The enantiomers of 1-phenylethyl ester **39** were separated by this method, the chiral carboxylic acid **40** being obtained by hydrogenolysis.

Once again, the chiral alcohol cannot be recycled. Moreover, the use of esterifying groups that can be removed by hydrogenolysis is severely limited by the ready hydrogenolysis of substituents often used in dihydropyridine chemistry. For example, the mandelic acid group cannot be removed from a felodipine precursor by hydrogenation without removal of the chlorine atoms.[103]

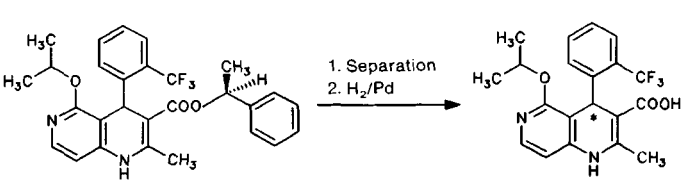

39 **40**

2.4. Enantioselective Synthesis of Special Dihydropyridines via Sulfoxides

Hantzsch dihydropyridine syntheses with chiral ester groups are only rarely diastereoselective, though one diastereomer is often formed in excess. However, a diastereoselective synthesis of the dihydropyridine sulfone **45** has recently been described.[108]

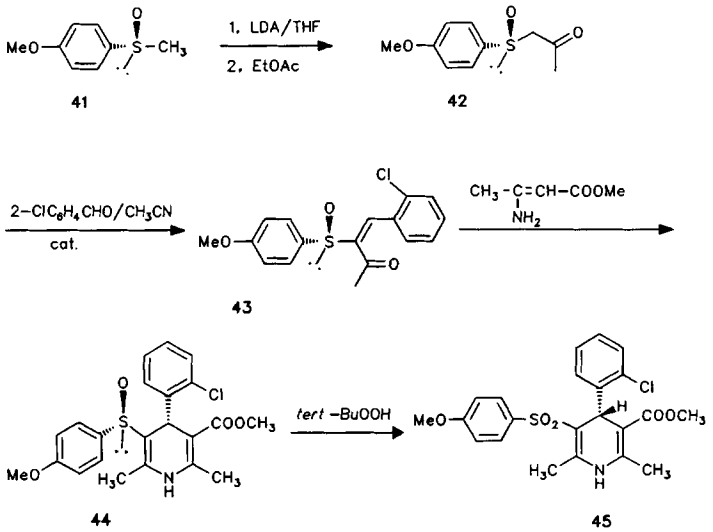

The Knoevenagel product **43** is obtained from the *R* sulfoxide **41** by *C*-acetylation (LDA = lithium diisopropylamide) followed by condensation with 2-chlorobenzaldehyde. Reaction with methyl 3-aminocrotonate then leads to the *S,S* diastereomer **44** in a yield of 48% (*de* = 94.0%). Oxidation of the sulfoxide yields the desired sulphone **45**.

2.5. Enantioselective Synthesis with Chiral Auxiliary Groups on the Nitrogen

Another possibility for the enantioselective synthesis of dihydropyridines is to attach the chiral auxiliary group (R*) to the nitrogen atom of the dihydropyridine ring (Scheme 6). However, difficulties arise in the preparation of the *N*-alkyldihydropyridines **48**, since reaction of **46** with **47** generally occurs preferentially at the methyl groups of the aminocrotonic esters to form the cyclohexene derivatives **49**. If the desired *N*-alkyldihydropyridines **48** are formed at all, the yields are poor.[5,10] Moreover, the chiral auxiliary group R* must still be removed. Both the need to remove the auxiliary group R* and the preparation of **48** can be avoided if the chiral auxiliary amine H_2NR^* is replaced by ammonia at the stage of the intermediate product **50** after the Michael addition of the enamine **46** to the benzylidene compound. However, this calls for high diastereoselectivity in the Michael addition **46** → **50**, since subsequent purification via diastereomers is not possible.

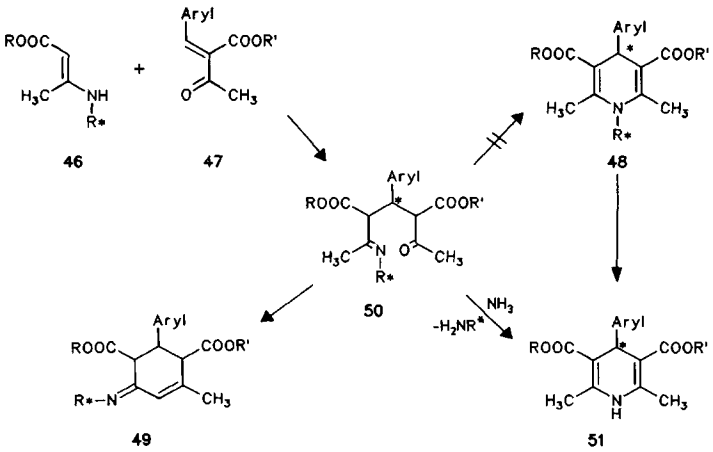

Scheme 6.

2.5.1. *Use of Chiral Hydrazones*

The reaction of acetoacetic ester **52** with the chiral hydrazine SADP yields the enamine **53**, from which the Michael addition product **54** is obtained after metalation with BuLi in THF at −78 °C and addition to benzylidene compounds having the *Z* configuration. Reaction with ammonium chloride in methanol leads to removal of SADP and formation of the desired dihydropyridine **55** with an enantiomeric excess of up to 90% in some cases.[109,110]

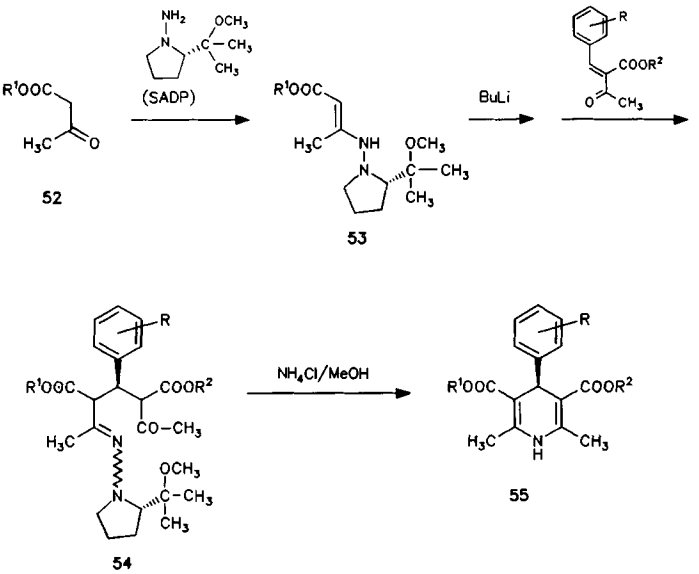

This method appears to produce particularly high enantiomeric excesses in the case of methoxy-substituted aromatic compounds and bulky *tert*-butyl esters.

2.5.2. *Use of Amino Acid Derivatives*

Variants of this method with amino acid derivatives as chiral auxiliary amines (Scheme 7) have been described, for example, for the preparation of the enantiomers of FRC 8411 (**58**) in enantiomerically pure form.[72,111,112] Valine *tert*-butyl ester (**56**) is converted into the chiral 3-aminocrotonic ester **57**. Metalation with LDA in THF under argon at −70 °C and reaction with the Michael acceptor

leads, after replacement of the valine ester with ammonia, to the (−) enantiomer **58** in a yield of almost 80% and with an enantiomeric excess of 94%.[111]

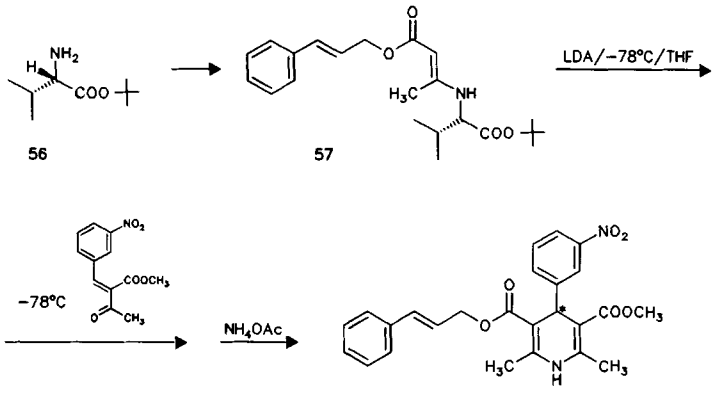

56 57 (−)-FRC 8411 58

Scheme 7.

The enantioselective dihydropyridine syntheses described above involve the use of chiral ligands that also have an additional oxygen ligand to fix the conformation of the anion. This could be a necessary condition for a diastereoselective Michael addition. Further support for this supposition is provided by the fact that for ligands without the additional complexing site (e.g., chiral esters of *N*-(1-phenylethyl)-3-aminocrotonic acid) the maximum optical yields obtainable were only 60%.[111, 113]

2.6. Chemoenzymatic Separation of Dihydropyridines

The stereoselective cleavage of simple prochiral dihydropyridinedicarboxylic diesters should be an effective method for the preparation of enantiomerically pure dihydropyridines. Initial successes have recently been achieved with the readily hydrolyzable *N*-benzyl-protected dihydropyridine derivative **59** (Bn = benzyl).[114]

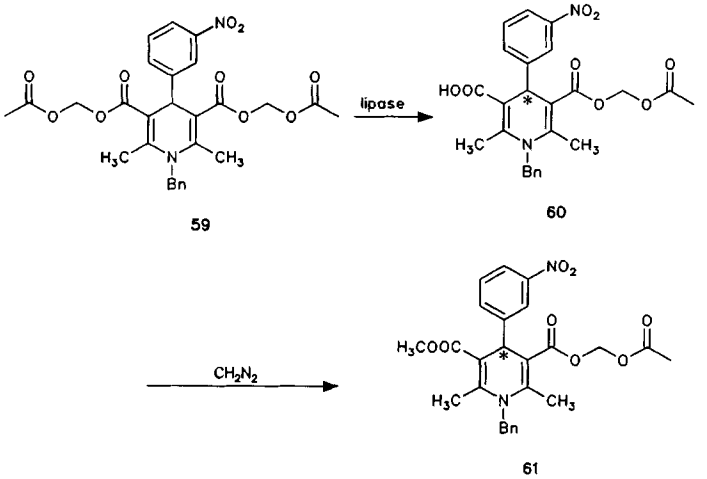

59 60 61

The monocarboxylic acid **60** was obtained by enzymatic hydrolysis of **59** with various lipases in a 10:1 mixture of *n*-butanol and water and was converted with diazomethane into the methyl ester **61**. Yields of up to 34% with an enantiomeric excess of *ee* = 88% were obtained with the lipase Pseudomonas P-30. Longer reaction times lead to higher enantiomeric excesses, but the chemical yields are markedly reduced.

2.7. Selective Reduction of Pyridines

The enantioselective reduction of pyridines would be an elegant route to optically active 1,4-dihydropyridines. Attempts to carry out the electrochemical reduction enantioselectively with ephedrinium bromide as an optically active conducting salt yielded only racemic 1,4-dihydropyridines.[115]

Since attack in position 4 by the bulky complex hydrides is particularly difficult in the case of 4-aryl-substituted pyridines, a fundamental drawback in such reductions is incorrect regioselectivity, leading to the formation of 1,2-dihydropyridines and reduction of the ester to the alcohol as a competing reaction.[116, 117] However, the addition of aryl anions to pyridines with no substituent in position 4, which is a basically similar route, has been successfully used for simple derivatives. Thus, in the case of **62** with chiral modification of the ester group, aryllithium can be added diastereoselectively in position 4 at −78 °C.[118]

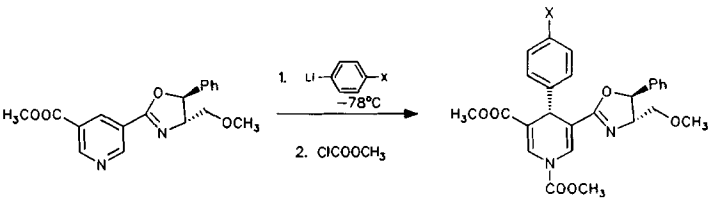

62 63

The diastereomeric excess is between 78% (X = H) and 90% (X = OMe). The addition of methyllithium is also highly diastereoselective.[119] It is doubtful whether the synthesis could be used for pharmacologically more important dihydropyridines with methyl substituents in positions 2 and 6, in view of the acidity of the methyl groups. The preparation of the pharmacologically important 4-aryldihydropyridines could also be limited by the difficulty in preparing suitable aryllithium reagents.

2.8. Chromatographic Separation of Enantiomers

The direct chromatographic separation of enantiomeric dihydropyridines on enantioselective chiral stationary phases has developed rapidly in recent years and is now one of the standard methods for the detection of the enantiomers in plasma and in tissue, for the verification of enantiomeric purity, and for the preparation of small quantities of enantiomers for initial pharmacological studies.

Optically active acrylamide polymers were already known in the mid-1980s[120] and were used for the resolution of racemic mandelic acid. Improved (meth)acrylamide poly-

mers were later used by *R. Grosser* et al. for the resolution of racemic dihydropyridines.[121, 122]

A large number of chiral stationary phases based on β-cyclodextrins,[123, 124] methacrylates,[125] glycoproteins,[126] and amylose and cellulose derivatives[127–131] are now available for the separation of enantiomeric dihydropyridines with various structures; these allow the determination of enantiomers in plasma in the nanogram range, as well as the resolution of racemates on the gram scale.

3. Influence of 1,4-Dihydropyridines on the Ca^{2+} Balance of the Cell

3.1. Importance of Ca^{2+} Ions in Contraction

Ca^{2+} ions play a fundamental role in the contraction of heart and smooth muscle cells. This was discovered by *Ringer* more than 100 years ago in experiments on spontaneously beating frog hearts.[132] He was able to show that the contractility of the hearts was greatly reduced in calcium-free solution, but returned to normal on addition of Ca^{2+} ions. The importance of Ca^{2+} ions to the contraction of the cell and the most important regulation mechanisms for the concentration of free Ca^{2+} ions are illustrated in Scheme 8.

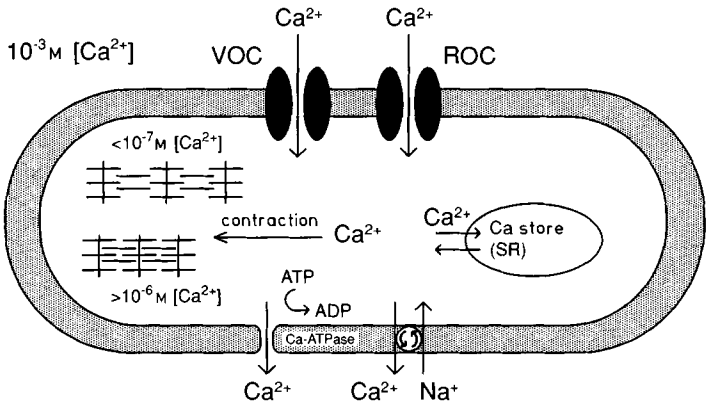

Scheme 8. The principal mechanisms for the regulation of the Ca^{2+} concentration in the heart cell. SR = sarcoplasmic reticulum, ROC = receptor-operated channels, VOC = voltage-operated channels.

The intracellular Ca^{2+} concentration is lower than the extracellular concentration by a factor of up to 10000 (10^{-7} to 10^{-6} M compared with about 10^{-3} M). At intracellular Ca^{2+} concentrations of $< 10^{-7}$ M, the filaments are fully dilated. When specific calcium channels in the cell membrane are opened for a short time, the calcium ion concentration in the cell increases. This triggers the release of Ca^{2+} ions from the intracellular calcium stores, mainly the sarcoplasmic reticulum (SR). The intracellular calcium ion concentration increases to $> 10^{-6}$ M and the filaments contract. The calcium ions are returned by transport mechanisms to intracellular storage (SR) or carried into the extracellular space (Ca-ATPase, Na^+/Ca^{2+} exchangers). When the Ca^{2+} concentration falls to less than 10^{-7} M, the filaments fully dilate and the original situation is restored. An increase in the Ca^{2+} concentration leads physiologically to an increase in the contractility of the heart and in the vascular tonus. The regulation of the intracellular Ca^{2+} concentration thus plays an important role in the contractility of the heart and the regulation of blood pressure.

3.2. Calcium Channels

Calcium channels can be classified according to how they are activated (Scheme 8, top):

1. *Receptor-operated channels* (ROC), which can be activated, for example, by catecholamines such as adrenaline or noradrenaline. These channels can be influenced pharmacologically, for example by α-receptor or β-receptor blockers.
2. *Voltage-operated channels* (VOC), which regulate the entry of calcium according to the membrane potential. These channels can be inhibited pharmacologically by so-called calcium antagonists belonging to various classes of compounds. These include the 1,4-dihydropyridines of the nifedipine type, benzylalkylamines of the verapamil type, and benzothiazepines such as diltiazem. The most potent are still the 1,4-dihydropyridines, which include not only derivatives that inhibit the entry of Ca^{2+} into the cell (calcium antagonists), but also others that increase it (calcium agonists). This class of compounds is therefore outstandingly suited for use in the investigation of calcium channels.

3.2.1. Characterization of the Voltage-Operated Calcium Channel (VOC)

Major advances have been achieved during recent years in the identification and characterization of the calcium channel proteins. Tritiated dihydropyridine ligands have been used to purify and identify the calcium channel proteins and to establish their primary structure.[133] The channel consists of four subunits, the α_1, α_2, β, and γ subunits, with molecular weights of 175, 170, 50, and 33 kD, respectively.[134–138] A 30-kD unit (δ unit) can be removed by reduction from the α_2 subunit, to which it is presumably attached through disulfide bridges. A proposal for the organization of these subunits (after Ref. [138]) is shown in Scheme 9. The α_1 unit contains the binding site for 1,4-dihydropyridines.[136, 138]

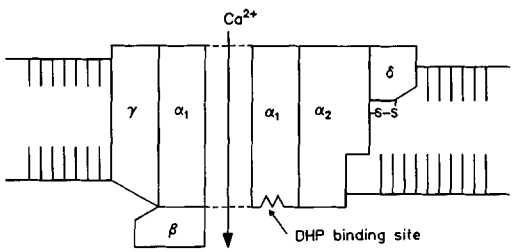

Scheme 9. Possible organization of the subunits of the Ca^{2+} channel (after [138]). DHP = 1,4-dihydropyridine.

The amino acid sequence of the α_1 unit exhibits similarities to the sequences of other ion channels, such as the extensively studied Na^+ channel.[133] As in the case of the Na^+ channel, various states are proposed for this channel (Scheme 10).

In the resting state (R) the channel is not conducting, but it can pass into the conducting open state (O) by depolarization. This depolarization can be achieved experimentally in vitro by increasing the extracellular K^+ concentration. From the open state, the channel can revert to the resting state (R) or switch over into the inactive state (I). Biologically, this inactivation is a sensible protection mechanism to safeguard the cell against Ca^{2+} overload. The inactive state has no ionic conductivity and *cannot* be activated by voltage changes. From this state the channel slowly returns to the resting state (R).

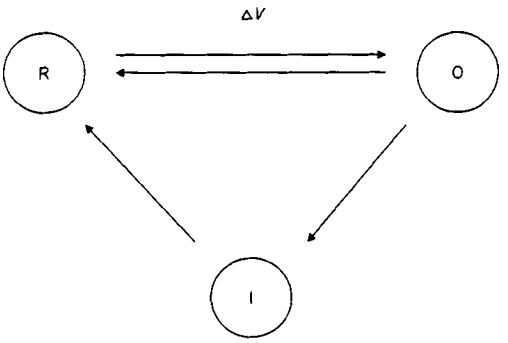

Scheme 10. Potential-dependent states of the Ca^{2+} channel (R = resting state, O = open state, I = inactive state).

Since membrane preparations are in a depolarized condition, the calcium channels are predominantly in the inactive state, so that binding data for 1,4-dihydropyridines refer to the inactive state. This is also shown by binding experiments on intact cells with calcium channels in working condition. These experiments confirm that depolarization of the cells with K^+ ions (concentration of the inactive state I increases) leads to a marked increase in the specific binding of 1,4-dihydropyridine calcium antagonists, with the result that it approaches the values found for membrane preparations.[139]

These investigations reveal that dihydropyridine calcium antagonists bind to and stabilize the inactive state of the calcium channel. Consequently, the number of channels capable of being activated (R) decreases and the entry of Ca^{2+} into the cell is reduced. Physiologically, this leads to a negatively inotropic effect on the heart and a decrease in the vascular tone, and hence in the blood pressure.

Ionic flux measurements on individual calcium channels provide evidence on how dihydropyridine calcium *agonists* act at the molecular level. Scheme 11 shows so-called patch-clamp recordings for groups of 12 individual channels in the absence (left) and in the presence of the calcium agonist BAY K 8644 at 5 μM concentration (right).[140]

It can be seen that the channel is closed at a membrane potential of -100 mV in the control (a). Changing the membrane potential to $+10$ mV occasionally causes the channel to open for a few milliseconds (downward deflections). Summation over many channels results in a calcium flux of the size found for intact cells. In the presence of BAY K 8644, the prototype calcium agonist, the channel is open for considerably longer (b), and this leads to a higher calcium flux on average (d). These results can be explained as arising from stabilization of the open state by calcium agonists.

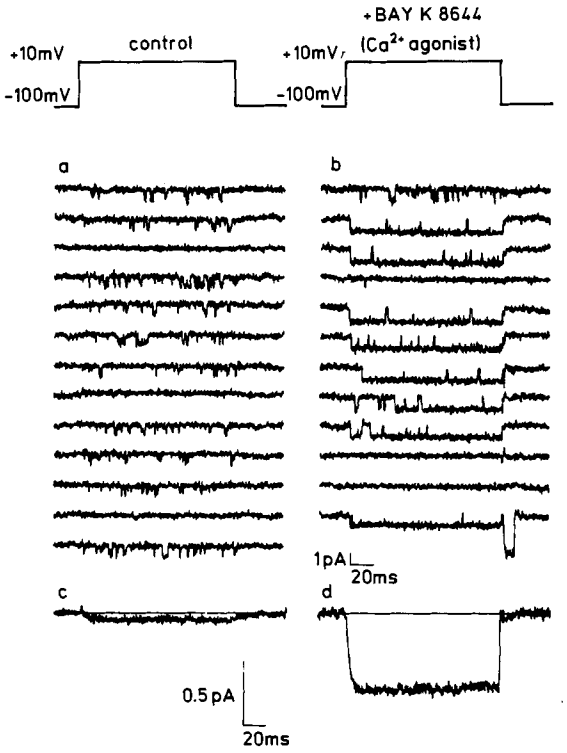

Scheme 11. Patch-clamp recording for individual Ca^{2+} channels in the absence (left) and in the presence (right) of a calcium agonist. Top: Course of the membrane potential with voltage jump from -100 mV to $+10$ mV. a,b: Measured single-channel activities; c,d: Averages of all measured single-channel activities. (After *Hess* et al. [140]).

The states R, O, and I describe only the function. The steric structures corresponding to these states can only be surmised, though the recent elucidation of the primary structure of the α_1 unit may lead to further advances in our understanding.[141] On the other hand, a large number of dihydropyridines have been synthesized over the last 20 years, so that inferences regarding the structure of the binding site ("lock") can be drawn from the shape of the "key". These aspects will be examined further in the following sections.

4. Conformational Aspects Relating to 4-Aryl-1,4-dihydropyridine-3,5-dicarboxylates

Dihydropyridines of the nifedipine type, **64**, are flexible molecules, in which the aryl ring and the ester groups can rotate and the conformation of the dihydropyridine ring can change.

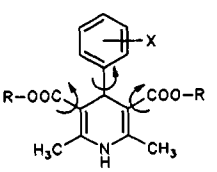

64

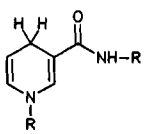

65

Since the discovery of the pharmacological effects of this class of substances, it has been of interest to know which conformation produces the optimum effect, and whether a

reversal of the pharmacological effect can be traced to changes in conformation.

A series of investigations on rigid dihydropyridines in recent years have yielded information on the "active conformation". This information has also been supported by theoretical calculations and X-ray structural analyses.

4.1. Conformations of the 1,4-Dihydropyridine Ring and Position of the 4-Aryl Substituent

In 1,4-dihydropyridines with no substituent in position 4, such as NADH model compounds of the type **65**, the dihydropyridine ring in the crystal is practically planar.[142-145] Ab initio calculations for the unsubstituted dihydropyridine ring also show only a minimal preference for a very flat boat conformation.[146]

A different picture is found for 4-aryl-substituted 1,4-dihydropyridines of the nifedipine type, **64**. Calculations for these compounds show a preference for the boat form,[147] and this has also been confirmed by numerous X-ray structural investigations. However, a boat conformation for the dihydropyridine ring has considerable consequences with regard to possible conformers. Thus, the 4-aryl substituent may occupy a pseudoaxial position as in **66**, or it may be equatorial as in **67** (Scheme 12). Interconversion between the two forms is possible by inversion of the dihydropyridine ring.

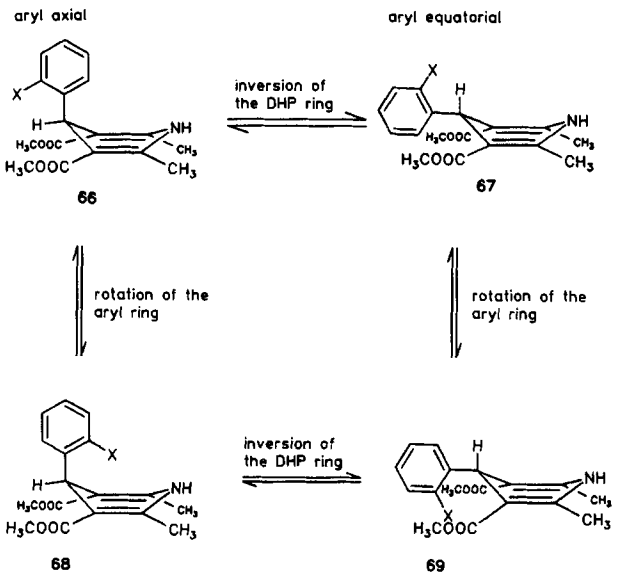

Scheme 12. Boat conformation of the 1,4-dihydropyridine ring and position of the 4-aryl substituent.

Further rotamers can be visualized if the 4-aryl substituent is substituted in the *ortho* or *meta* position (X ≠ H). The group X may then either be on the same side as the hydrogen, as in **66** (synperiplanar, *sp*), or, following rotation of the phenyl ring, it may lie above the dihydropyridine ring as in **68** (antiperiplanar, *ap*). These rotamers are also conceivable if the aryl substituent is in a pseudoequatorial position (**69** ⇄ **67**).

As was mentioned earlier, many X-ray structural analyses of dihydropyridines of the nifedipine type, **64**, show that the dihydropyridine ring is in fact in a flattened boat conformation, with the 4-aryl substituent in the pseudoaxial position and orthogonal to the plane of the dihydropyridine ring;[66,91,108,148-162] that is, the conformation **66** is favored in the crystal. It was postulated even in the early work that this orthogonal arrangement of the 4-phenyl substituent was important to the pharmacological activity,[10] since *ortho* substitution in the 4-phenyl ring gave particularly active derivatives and suggested an enforced orthogonal arrangement as in biphenyls.

A correlation was also found between the bulk of the *ortho* substituent X and the pharmacological effect.[163] Investigations on rigid dihydropyridines have shown that this orthogonal arrangement of the two rings is essential.[164,165] Compound **70a**, in which the aryl ring has been forced into an unfavorable conformation, is pharmacologically inactive. Only when the size of the lactone ring is increased to 12 members does the favorable orthogonal arrangement of the aryl group, as in **71b**, become possible, leading to active compounds.

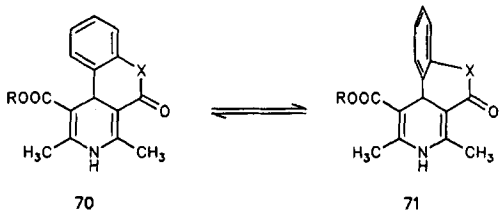

a X = -O-

b X = -O-(CH$_2$)$_5$-O-

The axial position of the 4-phenyl substituent in **66** also appears to be essential to the pharmacological activity of the compound. Thus, replacement of the C4 hydrogen with a methyl group (**72** → **73**) leads to a dramatic change in the conformation, as has been shown by AM1 calculations and X-ray structural analyses.[166] In the crystal, the phenyl substituent in **73** is no longer axial, but has moved into the equatorial conformation. The antihypertensive activity of **73** is three orders of magnitude weaker than that of **72**. Derivatives in which the axial conformation of **72** is fixed by a sulfur

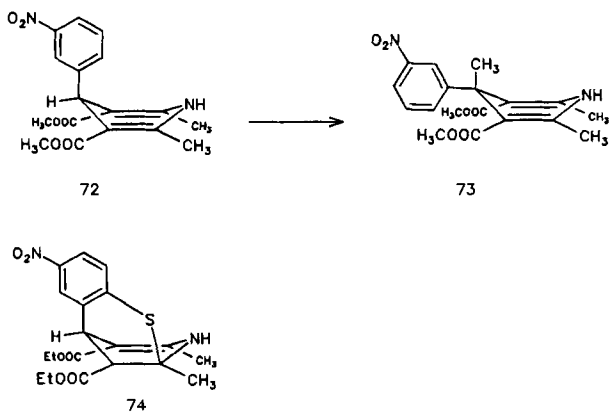

bridge (e.g., **74**) also exhibit excellent binding to dihydropyridine receptors and act as strong calcium antagonists,[167] though the Michael addition product **74** is no longer a dihydropyridine. This example demonstrates very impressively that with the correct steric arrangement of the necessary substituents, the dihydropyridine structure plays only a minor role in the biological activity.

Another aspect that has already been mentioned is the arrangement of the *ortho* or *meta* substituents X in the phenyl ring in relation to the dihydropyridine ring. Two rotamers are possible with orthogonal and axial arrangements of the phenyl ring. In the synperiplanar arrangement, the substituent X lies on the same side as the C4 hydrogen on the dihydropyridine ring (**66**), whereas rotation through 180° brings it above the plane of the dihydropyridine ring, antiperiplanar to the hydrogen (see Scheme 12).

In 9-arylfluorenes, **75**, which have a very similar structure, rotamers of this type are not only detectable by NMR spectroscopy, but can even be isolated in a few cases.[168–170] Isolation of rotamers is not possible for 1,4-dihydropyridines of type **66**. This points to a fast equilibrium, **66** ⇄ **68**, with a lower activation barrier than in the fluorenes **75**.

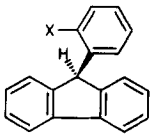

75

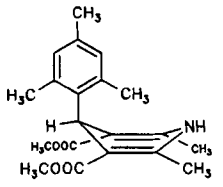

76

Hindered rotation has been demonstrated in one case for a derivative with extreme steric hindrance, **76**.[171] The NMR spectrum of **76** shows a broad singlet for the two *ortho* methyl groups. On cooling, coalescence occurs at $-18\,^{\circ}C$, and the signal splits into two singlets at $-50\,^{\circ}C$. The calculated activation energy, $\Delta G^{\neq} = 51\ kJ\,mol^{-1}$, correlates well with calculated values for similar compounds ($44\ kJ\,mol^{-1}$[172]).

With a few exceptions,[148, 154] the form **66** is favored in the crystalline state.[66, 91, 108, 149–162] Theoretical calculations[172–174] also indicate a preference for the *sp* conformer rather than the *ap* conformer. The calculated activation energy of $44\ kJ\,mol^{-1}$[172] also indicates that the equilibrium **66** ⇄ **68** is fast.

The thermodynamic preference for the *sp* conformation in solution can also be confirmed by NMR spectroscopy. By measurement of nuclear Overhauser effects of the hydrogen atom H_6 with H_4 in **77**, it can be shown that, for derivatives of the type **66** in comparison with **68**, the *sp* conformation is favored in solution.[171–175] On the other hand, it appears

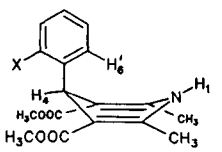

sp-77

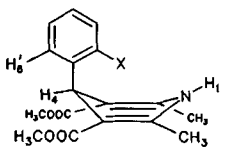

ap-77

from measurements on pharmacologically less active bicyclic dihydropyridines that the *ap* form is favored here.[176] It is also possible, by direct measurement of the two nuclear Overhauser effects, H_6/H_1 and H_6/H_4, to determine the thermodynamic distribution of the two conformers and hence to find the energy difference.[154]

Though the *sp* form is usually favored in the crystal and in solution, the energy differences are too small to rule out the possibility of interactions that favor other conformers at the site of biological action. However, this possibility does not arise in the case of the bridged derivatives **74** and **78**. The

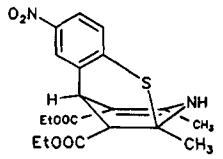

74

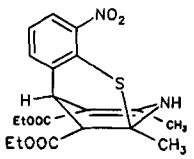

78

possible conformers *sp* and *ap* are immobilized here by a sulfur bridge. The calcium antagonist activity of **74**, with the forced *sp* arrangement of the nitro group, is two orders of magnitude greater than that of the *ap* form **78**.[167] The *sp* conformation **66** is thus probably essential at the site of action, at least in the case of the 3-nitrophenyl derivatives.

4.2. Influence of the Ester Groups on the Pharmacological Effect

The ester groups are of crucial importance to the pharmacological effect. Not only does variation of the ester groups lead to quantitative changes in the activity, but replacement of an ester group by other groups can also produce dramatic qualitative changes (Section 4.2.3). A method that has been adopted to distinguish clearly between the two sides of dihydropyridines is to regard the preferred conformation of the 1,4-dihydropyridine ring as a flattened boat (**79**) with C4 as the bow, the axial aryl ring as the bowsprit, and the nitrogen as the stern.[14]

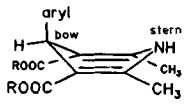

79

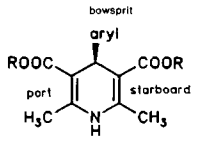

79a

The two sides of the dihydropyridine ring can then be referred to as the port side (left) and the starboard side (right).[177] This designation is more suitable for our discussion and less specialized than the *pro R/S* or the *re/si* nomenclature for enantiotopic sides.[178]

4.2.1. Conformation of the Ester Group

The "equatorial" arrangement of the ester groups, which is forced by sp^2 hybridization in the dihydropyridine **80**, is

essential to the pharmacological activity of the compounds, as is shown by **74** and **81**. The pharmacological activity of **81**, with the ester group in axial position, is weaker by two orders of magnitude than that of **74** or **80**.[167]

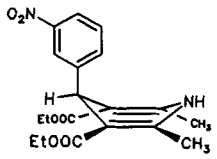

80

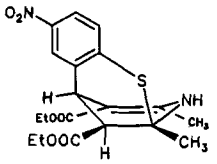

74

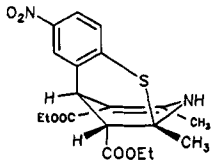

81

Another important aspect is the rotation of the ester group. Assuming a favored coplanar arrangement of the ester carbonyl with the double bond of the dihydropyridine ring, three conformations are possible in principle for the ester groups: *trans/trans*, in which the carbonyl groups of both esters are *trans* to the double bond of the dihydropyridine (**82a**), *cis/cis* with a *cis* arrangement of both carbonyl groups (**82c**), and enantiomeric *cis/trans* and *trans/cis* arrangements (**82b**). An analysis of the results of 26 X-ray structural investigations shows a preference for the *cis/trans* and *cis/cis* arrangements in the crystal (Table 1).[14]

Table 1. Conformations of the ester groups in compounds of type **82a–82c** as determined by X-ray structural analyses.

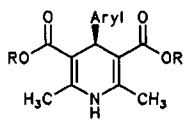

82a (*trans/trans*)

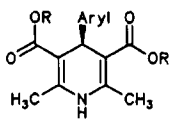

82b (*cis/trans*)

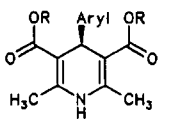

82c (*cis/cis*)

	82a	**82b**	**82c**
with *ortho* aryl substituent	0	3 out of 10	7 out of 10
without *ortho* aryl substituent	0	14 out of 16	2 out of 16

A preference for the *cis/cis* arrangement is found for *ortho*-substituted derivatives (7 out of 10), whereas the asymmetric *trans/cis* conformation is favored for derivatives without *ortho* substitution (14 out of 16). The *trans/trans* arrangement has not been observed and is also energetically unfavorable according to theoretical calculations.[179]

Fused 1,4-dihydropyridines also suggest that for a satisfactory calcium antagonist effect, at least one ester must be in the *cis* arrangement, since the compounds **83**,[61] **84**,[180] and **85**[181] may be regarded as derivatives with an immobilized ester group.[182]

The assumption that a *cis* arrangement of the ester group (see **86**) is necessary for hydrogen bonding to the receptor (Rec)[158, 179, 188] may also be valid for the imido analogues **84** and **85**, but less so for the thiophene derivative **83**. On the contrary, with the *cis* arrangement of the ester group, it appears to be more important that the bulky lipophilic alkyl chain should lie parallel to the aromatic ring. This is supported by the fact that the derivative **87**, in which the lipophilic chain of the ester group corresponds more to the *trans* arrangement of this group, is practically inactive.[61] A similar decrease in activity has also been found for the corresponding *N*-alkyl derivatives **88** of CI-951 (**84**).[189] The example **83** also shows on *which* side the ester group must have the *cis* conformation and can be replaced by the alkylthiophene group, since the absolute configurations of the enantiomers of **83** are known.[61]

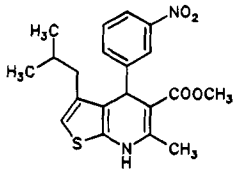

83

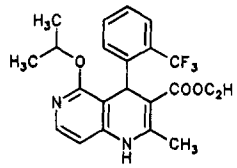

84

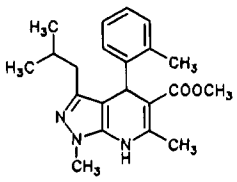

85

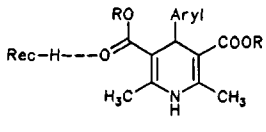

86

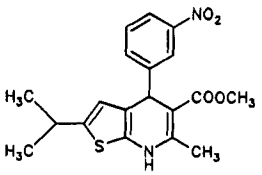

87

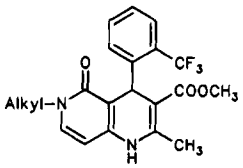

88

(*S*)-**83** is 50 times more active in the receptor binding test than (*R*)-**83**, and its calcium antagonist activity is 20 times stronger (Table 2). This shows, that for a good pharmacological effect, the ester group on the port side of the dihydropyridine ring must have the *cis* conformation, whereas replacement of the ester group on the starboard side with the alkylthiophene group has an adverse effect, as is shown by a comparison with the flexible diester **89**.[190, 191] The weak activity of (*R*)-**83** does not appear to be due to the enforced unfavorable *cis* arrangement of the ester group in (*R*)-**83**, since racemic **87** (and hence also (*R*)-**87** with the enforced

Table 2. Relative activities of the enantiomers of **83** ("immobilized" ester group) in comparison with the flexible diester **89**.

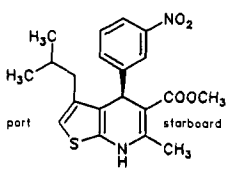

(*S*)-**83**

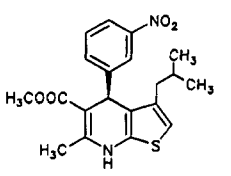

(*R*)-**83**

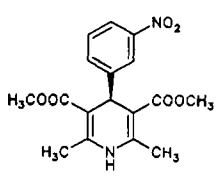

89

	(*S*)-**83**	(*R*)-**83**	**89**
[^{3}H] Nitrendipine displacement	50	1	50 [191]
Inhibition of the K^+-induced contraction (rabbit aorta)	20	1	5

trans arrangement) is inactive, but rather to the impossibility of additional hydrogen bonding on the starboard side.

4.2.2. *Influence of the Size of the Ester Groups*

Once the preparation of enantiomerically pure dihydropyridines had been established, it quickly became apparent that dihydropyridines with unsymmetrical ester substitution are generally more active pharmacologically than those with symmetrical substitution. The increase in activity is mainly associated with an increase in the size of the ester group on the port side, as can be seen from Table 3.

Table 3. Influence of the size of the ester group on the calcium antagonist activity.

Compound	Relative activity
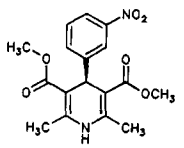 **89**	1
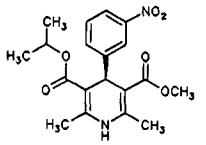 (*S*)-**90**	15
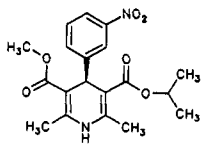 (*R*)-**90**	16

[a] Inhibition of the Ba^{2+}-induced contraction of aorta rings

Thus, in the flexible diester **89**, replacement of the methyl ester group on the left with isopropyl ((*S*)-**90**) increases the activity by a factor of 15, whereas replacement of the ester on the right with isopropyl ((*R*)-**90**) has little effect.[192] Numerous enantiomerically pure dihydropyridines with known absolute configurations[193] subsequently confirmed the discovery that for dihydropyridines with sterically different substituents, the enantiomer with the larger ester group on the port side is the more potent. Thus, for other mixed methyl/isopropyl esters such as **91** and **92** (Table 4), the enantiomers with the larger isopropyl ester group on the port side are the more active, and the same is true of the dihydropyridine analogue **94**. If an ester group is replaced by an oxadiazole group as in **93** or by an amide group as in **95**, the more active enantiomer has the larger substituent again on the port side.

This rule is also valid for nicardipine (**10**) and a series of analogues with a lipophilic ester group containing nitrogen (**96**–**101**). Example **102** appeared to be a puzzling exception, since the *R* enantiomer was described as the more active in this case;[74] however, subsequent checks showed that an error had been made in the assignment.[202]

An important published observation that does not agree with this reasoning is that the active enantiomer of amlodipine (**103**) has the larger group on the starboard side.[91] This could possibly be explained by the essential hydrogen bonding of the starboard ester group, which dominates in the case of amlodipine because of the free amino group and outweighs the influence of the relative sizes of the ester groups. If this is correct, the activity of amlodipine derivatives should be largely independent of the size of the ester groups. A similar explanation could apply to the phenylsulfone **104**.[108]

To summarize, it is possible to say that the two ester groups in calcium antagonists have different functions at the site of action. Whereas the smaller ester group on the starboard side (R_{St}) in **A** is important for the formation of a

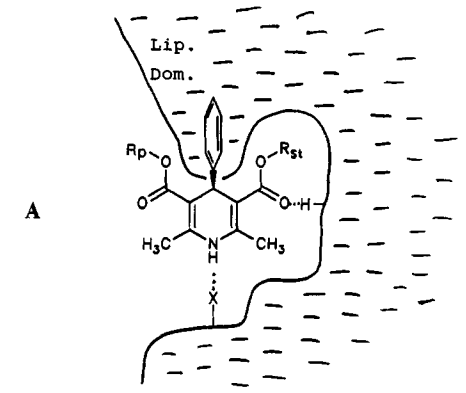

hydrogen bond with the binding site, the larger ester group on the port side with its lipophilic group (R_P) may occupy a lipophilic domain (Lip. Dom.) at the binding site. However, this binding cannot be very specific, since very different groups are tolerated.

4.2.3. *Reversal of the Pharmacological Activity by Replacement of the Ester Function*

The effects of the enantiomers of the dihydropyridinecarboxylic esters discussed in Section 4.1.2 differ in their intensity, but are qualitatively similar. However, there is another

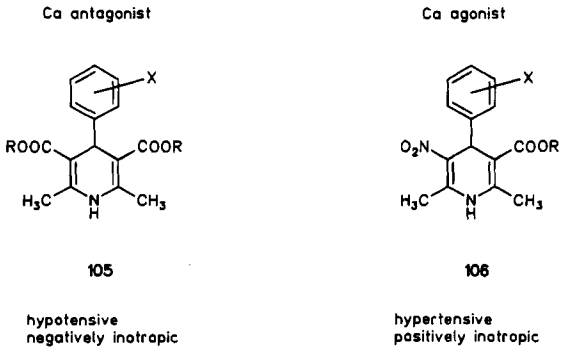

Table 4. Comparison of the activities of enantiomeric calcium antagonists with known absolute configurations.

More active enantiomer	Test	Activity index[a]	Ref.	More active enantiomer	Test	Activity index[a]	Ref.
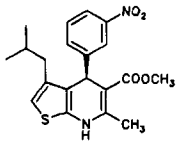 (+)-(S)-83	Displacement of tritiated ligands from the DHP receptor	55	[61]	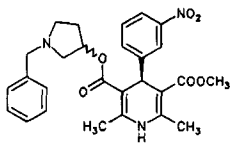 (S)-97	Displacement of tritiated ligands from the DHP receptor	20–70	[66]
	Inhibition of the K^+-induced contraction of aorta strips (rabbit)	20					
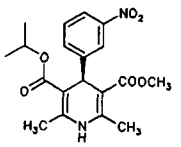 (-)-(S)-90	Inhibition of the K^+-induced contraction of aorta strips (rabbit)	100	[192]	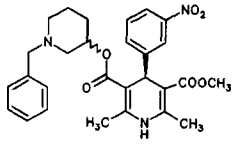 (S)-98	Blood pressure (rat)	ca. 30–100	[65]
	Inhibition of the Ba^{2+}-induced contraction of the ileum (guinea pig)	10					
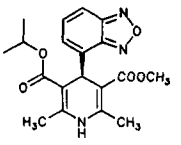 (+)-(S)-91	Blood pressure (cat)	100	[194]	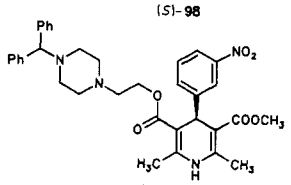 (+)-(S)-99	Blood pressure (rat)	30	[52]
	Inhibition of the K^+-induced contraction of aorta strips (rabbit)	160	[194]		Displacement of tritiated ligands from the DHP-receptor	80	
	Inhibition of the K^+ induced formation of inositol in brain membranes (rat)	20	[195]				
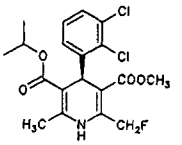 (+)-(S)-92	Blood pressure (dog)	(*S*) more active than (*R*)	[196]	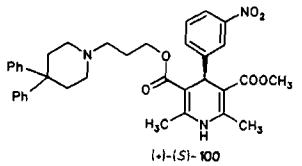 (+)-(S)-100	Displacement of tritiated ligands from the DHP receptor	40	[75] [201]
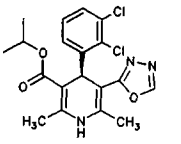 (+)-(S)-93	Displacement of tritiated ligands from the DHP-receptor	(*S*) more active than (R)	[197] [97]	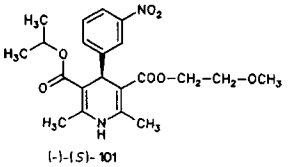 (-)-(S)-101	Inhibition of the K^+-induced contraction of aorta strips (rabbit)	5	[203]
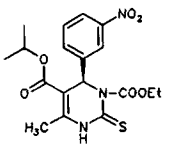 (-)-(R)-94	Inhibition of the K^+-induced contraction of aorta strips (rabbit)	ca. 1000	[198]	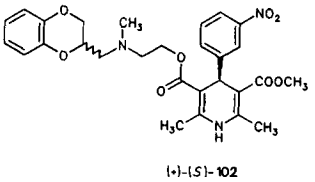 (+)-(S)-102	Displacement of tritiated ligands from the DHP receptor	55	[74]
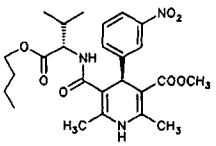 (R)-95	Blood pressure (dog)	(*R* more active than *S*)	[199] [200]	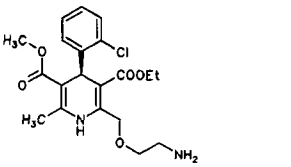 (-)-(R)-103	Inhibition of the K^+-induced contraction of aorta strips (rat)	800	[91]
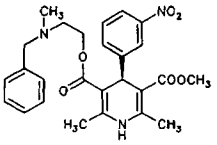 (+)-(S)-96	Displacement of tritiated ligands from the DHP receptor	14	[66]	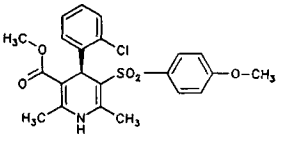 (+)-(S)-104	Blood pressure (rat)	10	[108]
	Blood pressure (dog)	3	[51]				

[a] The activity index indicates how many more times potent the active enantiomer is compared to the other enantiomer.

group of derivatives whose enantiomers have dramatically different pharmacological action profiles.[36] If one of the ester groups in 3,5-diesters (**105**) exhibiting calcium antagonist activity is replaced by a nitro group (**106**), the resulting compounds have exactly the opposite pharmacological effect.[204] Instead of blocking the entry of calcium into cardiac and vascular muscle, these derivatives enhance it. They thus increase the blood pressure and have a positively inotropic effect, and are therefore known as calcium agonists or calcium channel activators. In addition to the best-known

prototype BAY K 8644 (**107**), another nitro derivative, PN 202-791 (**108**), has also been reported to produce these effects[39] (Scheme 13).

The class of five-membered lactones also includes compounds having a similar effect,[36, 205] the most extensively studied of these being CGP 28-392 (**109**).[206] The same is true of the thiolactone derivative RS 30026 (**112**).[207, 208] Other calcium agonist prototypes are dihydropyridines in which one ester group has been replaced by hydrogen, such as H 160/51 (**110**)[36, 209] and the compound **111**.[210] The mixed ester/amide YC-170 (**113**)[211] has also been reported to exhibit calcium agonist properties, but these are considerably weaker than those of the prototypes mentioned above. Calcium agonist effects have also been reported for derivatives of the classes of compounds **114**,[36, 212] **115**,[36] **116**,[213] and **117**.[214]

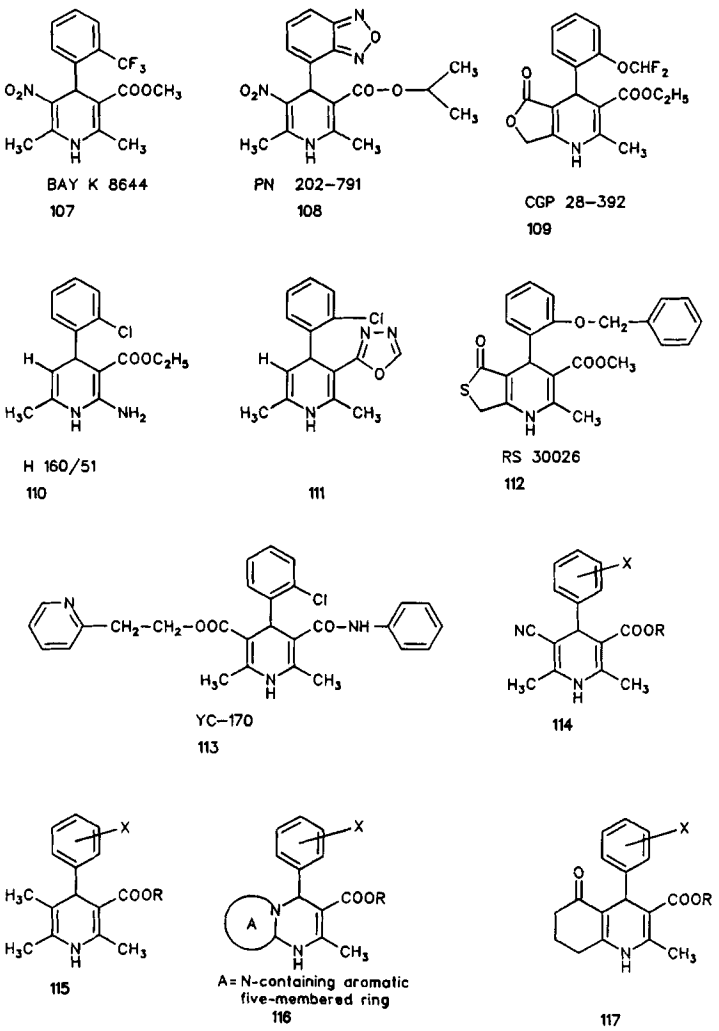

Scheme 13. Dihydropyridine calcium agonists.

If these structures are compared with those of the typical calcium antagonists, it is noticeable that one ester group has always been replaced by a relatively small group (except in the case of the weak calcium agonist YC-170). Obviously, since the two ester groups of the calcium antagonist diesters must satisfy different requirements in relation to the receptor, it is extremely important to know which of the two ester groups would have to be replaced by a nitro group in order to produce calcium agonist activity.

After separation of the enantiomers of **107**,[33] **108**,[39] and **110**,[215] it was found that only one enantiomer exhibited calcium agonist properties, whereas the other acted as a typical calcium antagonist. By determination of the absolute configurations of **107** and **108**, it was shown that only the replacement of the ester group on the port side by a nitro group leads to reversal of the activity, that is, to calcium agonist activity, whereas replacement of the ester group on the starboard side merely weakens the calcium antagonist activity (Scheme 14).

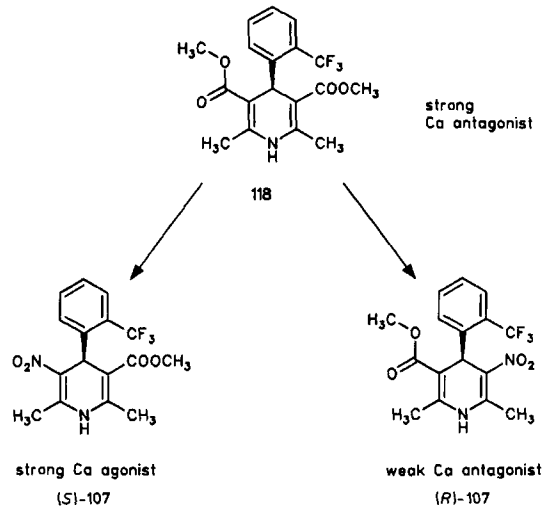

Scheme 14.

The same is true of the five-membered lactones. (*R*)-**119** (Scheme 15) is the calcium agonist enantiomer, whereas (*S*)-**119**, as expected, is found to be a weak calcium antagonist.[212]

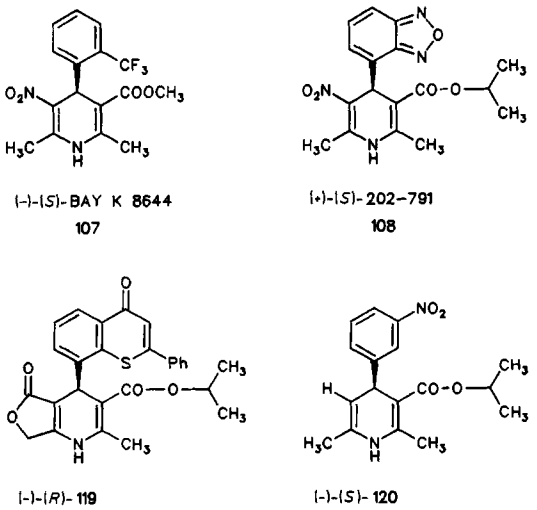

Scheme 15. Dihydropyridine calcium agonists having known absolute configurations (from X-ray structural data).

The smaller group in the calcium agonist enantiomer of **110** should also be on the port side. Though the absolute configurations of the enantiomers are unknown in this case,

they are known for the analogous derivative **120**,[216] whose *S* enantiomer, as expected, acts as an agonist. The same is true of the enantiomers of the nitriles **114**.[217, 218]

4.2.4. *Possible Reasons for the Calcium Agonist Activity*

If the structural requirements for a calcium antagonist (i.e., a larger ester group in the *cis* conformation on the port side; Scheme 16, **A**) are compared with those for a calcium agonist (Scheme 16, **B**), two striking differences are found:

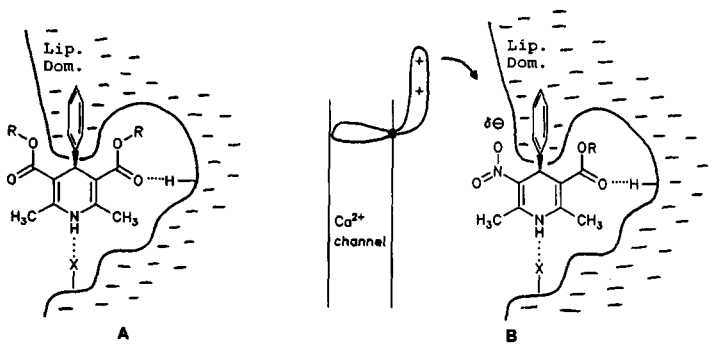

Scheme 16. Possible interactions of a typical calcium antagonist (**A**) and a typical calcium agonist (**B**) with a lipophilic domain and with a positively charged protein domain (case **B**).

the agonists lack the large lipophilic alkyl group on the port side and in its place they have a partial negative charge on the nitro group. Three possible interactions can therefore be considered:

1. The agonist cannot occupy lipophilic sites.
2. The negative charge on the *trans* oxygen of the nitro group may attract the positive charge of a protein (also through hydrogen bonding).
3. The agonist may repel negative charges in the protein.

It is conceivable, for example, that when the calcium channel is opened, a positively charged section of protein moves into the vicinity of the negative charge (Scheme 16, **B**) with the result that the open state is stabilized and the channel remains open longer. In contrast, the open time should be unchanged or may even be shortened by calcium antagonists. The function of the lipophilic group in the antagonists could be to produce stronger binding with the inactive state and hence to stabilize the latter.

The presence of the negative charge on the port side in the vicinity of the aromatic ring is understandable in nitro derivatives **107**, lactones **109**, and thiolactones **112**, but presents problems at first glance in the unsubstituted derivatives **110**/**111** or the methyl compounds **115**. However, calculations of surface potential show that negative potentials are also present in these molecules.[173] The reason is that the ester group on the starboard side is no longer present to shield the negative potential of the aromatic ring.

Scheme 17 shows the potential surfaces (blue = negative, red = positive) of three dihydropyridines viewed from the direction indicated by the arrows. The lactone **121** has a pronounced negative potential on the right due to the carbonyl group of the lactone; the H compound **122** has a smaller negative potential on the same side. In the calcium antagonist **123**, on the other hand, the positive potential of the isopropyl ester group can be seen on the lower right, shielding the negative potential from below.[219]

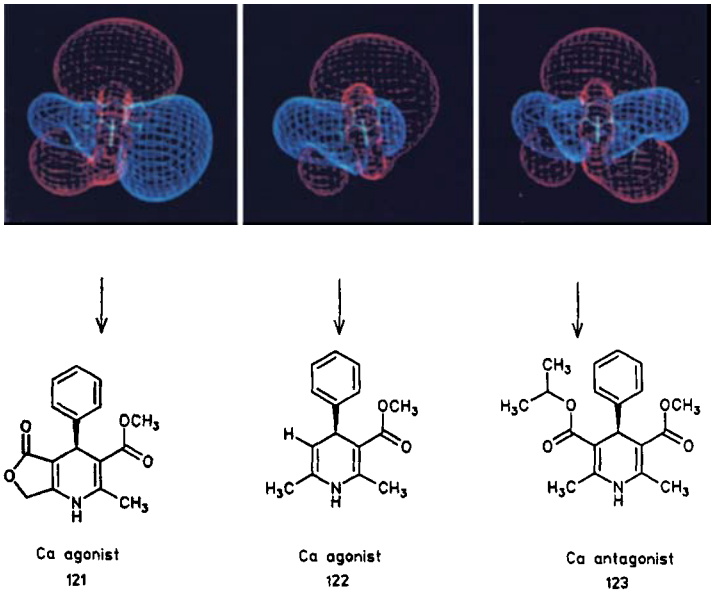

Scheme 17. Potential surfaces of an "active" calcium agonist, a "passive" calcium agonist, and a calcium antagonist. Blue = negative, red = positive.

Dihydropyridine calcium agonists can thus be divided into two classes:

1. *Active* calcium agonists, which bring with them a negative charge on the port-side substituent (nitro, lactone, thiolactone).
2. *Passive* calcium agonists, in which the negative potential of the π electrons of the aromatic ring on C4 is no longer shielded (H, CH_3).

This would mean that without the negative charge of the aromatic ring the *passive* calcium agonists would lose their agonist activity. The cyclohexyl derivatives **124**–**126** were used to test this hypothesis.

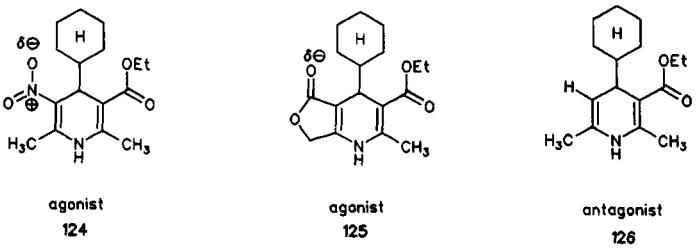

It was indeed found that only **124** and **125** are calcium agonists, whereas **126** exhibits typical calcium antagonist behavior.[216] A satisfactory explanation could even be provided for the very weak calcium agonist activity of YC-170 (**127**).

If the amide group, like the ester group, is in the *cis* conformation, the negative partial charge of the anilide could be responsible for the weak agonist activity. The calcium agonist enantiomer of **127** should thus have the *R* configuration.

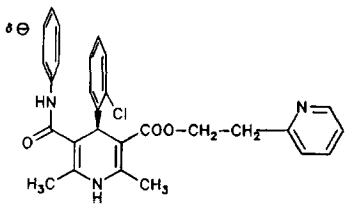

127

Calcium agonist activity has recently also been reported for compounds of the class of dihydropyridines in which positions 2 and 6 are unsubstituted (**128**).[208] A possible explanation for this observation is that the energy of the *trans* conformation of the ester group is reduced by the absence of steric interaction with the methyl group. Rotation of the port-side ester group from the possible "agonistic" *trans* conformation into the *cis* conformation, which would be more stable on the receptor, could also explain the observation that some calcium antagonist diesters may exhibit weak calcium agonist activity at lower concentrations.[220]

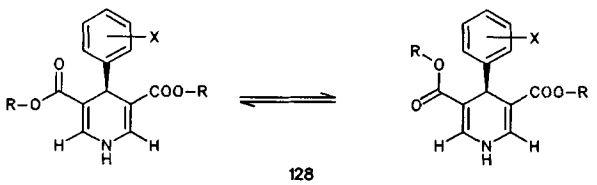

128

agonist conformation antagonist conformation

If this assumption is correct, this phenomenon should not be found with derivatives having an "immobilized" ester grouping, such as **83**. The calcium agonist effects of the dihydropyridines synthesized so far can be qualitatively explained by this model.

5. Summary and Outlook

4-Aryl-substituted 1,4-dihydropyridine-3,5-dicarboxylic esters of the nifedipine type have had an established place in the treatment of cardiovascular diseases for 15 years. In view of the extreme importance of the enantiomers of the 1,4-dihydropyridines, the existing methods for the preparation of the enantiomers have been discussed. The most important of these methods are the conventional resolution of racemic dihydropyridinemonocarboxylic acids and the cleavage of diastereomeric esters. A number of diastereoselective Michael additions with valine esters as optically active enamines exhibit high diastereoselectivity and appear very promising.

The pairs of enantiomeric 1,4-dihydropyridinedicarboxylic diesters exhibit both quantitative and qualitative differences in activity. Replacement of an ester grouping with a nitro group leads to derivatives with exactly the opposite pharmacological effect. Comparison of the absolute configurations has revealed, that in order to bring about this reversal of activity, it is important to determine which of the two ester groups in the calcium antagonist needs to be replaced by the nitro group. Substituents other than the nitro group are also able to produce this effect in a weaker form.

The switch from antagonism to agonism is produced by replacement of a larger lipophilic ester group with a smaller group having a negative potential (active agonists). Substituents with no negative potential of their own can also give rise to these effects, because they no longer shield the negative potential of the 4-aryl grouping (passive agonists). Many observed calcium agonist effects can be qualitatively explained by this model. It remains to be seen whether effects at the molecular biological level can be explained.

Our thanks are due to all those who have made their mark on dihydropyridine chemistry at Bayer during the last 25 years, particularly H. Meyer, E. Wehinger, and G. Franckowiak, as well as H. Böshagen, E. Schwenner, W. Seidel, and A. Straub. We are grateful to L. Born, R. Grosser, J. Kurz, V. Muschalek, P. Schmitt, and C. Wünsche for their analytical and spectroscopic support, and to M. Bechem, R. Gross, S. Hebisch, J. Hütter, M. Kayser, S. Kazda, A. Knorr, H. P. Rounding, M. Schramm, and G. Thomas for pharmacological tests and advise. We thank C. Lettner and E. Sauer for their patience in the preparation of this manuscript. Special thanks are due to F. Bossert and W. Vater for the discovery of the dihydropyridines as drugs exactly 25 years ago.

Received: April 24, 1991 [A 845 IE]
German version: *Angew. Chem. 103* (1991) 1587

[1] A. Hantzsch, *Justus Liebigs Ann. Chem. 215* (1882) 1–82.
[2] A. P. Philipps, L. D. Randall, US 2359329 (1943), Wellcome.
[3] C. P. Huttrer, E. Dale, *Chem. Rev. 48* (1951) 543–579.
[4] H. Haas, *Pharm. Ztg. 49* (1964) 1855–1862.
[5] F. Bossert, W. Vater, *Med. Res. Rev. 9* (1989) 291–324.
[6] F. Bossert, W. Vater, DE 1493677 (1964), Bayer AG.
[7] F. Bossert, W. Vater, *Naturwissenschaften 58* (1971) 578.
[8] B. Loev, R. E. Tedeschi, US 3511847 (1970), Smith Kline and French.
[9] B. Loev, S. J. Ehrreich, R. E. Tedeschi, *J. Pharm. Pharmacol. 24* (1972) 917–918.
[10] B. Loev, M. M. Goodman, K. M. Snader, R. Tedeschi, E. Macko, *J. Med. Chem. 17* (1974) 956–965.
[11] A. Fleckenstein, H. Tritthart, H. J. Döring, K. Y. Byon, *Arzneim. Forsch. 22* (1972) 22–33.
[12] A. Fleckenstein, G. Grün, *Arzneim. Forsch. 22* (1972) 334–344.
[13] V. Kastrons, R. Vitolins, G. Duburs, *Khim. Farm. Zh. 24* (1990) 14–21.
[14] D. J. Triggle, D. A. Langs, R. A. Janis, *Med. Res. Rev. 9* (1989) 123–180.
[15] "Drug action and cellular calcium regulation": R. A. Janis, P. Silver, D. J. Triggle, *Adv. Drug Res. 16* (1987) 309–591.
[16] M. Ohtsuka, M. Yokota, I. Kodama, K. Yamada, S. Shibata, *Gen. Pharmacol. 20* (1989) 539–556.
[17] A. Sausins, G. Duburs, *Heterocycles 27* (1988) 269–314.
[18] F. Bossert, H. Meyer, E. Wehinger, *Angew. Chem. 93* (1981) 755–763; *Angew. Chem. Int. Ed. Engl. 20* (1981) 762.
[19] D. M. Stout, A. I. Meyers, *Chem. Rev. 82* (1982) 223–243.
[20] J. Kuthan, A. Kurfürst, *Ind. Eng. Chem. Prod. Res. Dev. 21* (1982) 191–261.
[21] U. Eisner, J. Kuthan, *Chem. Rev. 72* (1972) 1–42.
[22] D. D. Freedman, D. D. Waters, *Drugs 34* (1987) 578–598.
[23] S. Kazda, R. Towart, *Br. J. Pharmacol. 72* (1981) 582P–583P.
[24] K. Tanaka, F. Gotoh, F. Muramatsu, Y. Fukuuchi, H. Okayasu, N. Suzuki, M. Kobari, *Arzneim. Forsch. 32* (1982) 1529–1534.
[25] S. Kazda, B. Garthoff, H. Meyer, K. Schlossmann, K. Stoepel, R. Towart, W. Vater, E. Wehinger, *Arzneim. Forsch. 30* (1980) 2144–2162.
[26] K. Stoepel, A. Heise, S. Kazda, *Arzneim. Forsch. 31* (1981) 2056–2064.
[27] J. E. Arrowsmith, S. F. Campbell, P. E. Cross, J. K. Stubbs, *Pharmacologist 27* (1985) 290; M. G. Dodd, I. Machin, J. R. C. Baird, *ibid. 27* (1985), 290; R. A. Burges, A. J. Carter, A. J. Higgins, D. G. Gardiner, K. J. Blackburn, *ibid. 27* (1985) 290.
[28] N. C. B. Nyborg, M. J. Mulvany, *J. Cardiovasc. Pharmacol. 6* (1984) 499–505.

[29] R. P. Hof, G. Scholtysik, R. Loutzenhiser, H. J. Vuorela, P. Neumann, *J. Cardiovasc. Pharmacol. 6* (1984) 399–406.
[30] K. Meguro, M. Aizawa, T. Sohda, Y. Kawamatsu, A. Nagaoka, *Chem. Pharm. Bull. 33* (1985) 3787–3797.
[31] T. Takenaka, S. Usuda, T. Nomura, H. Maeno, T. Sado, *Arzneim. Forsch. 26* (1976) 2172–2178.
[32] T. Furuta, S. Shibata, I. Kodama, K. Yamada, *J. Cardiovasc. Pharmacol. 5* (1983) 836–841.
[33] G. Franckowiak, M. Bechem, M. Schramm, G. Thomas, *Eur. J. Pharmacol. 114* (1985) 223–226.
[34] B. Loev, M. M. Goodman, *J. Heterocycl. Chem. 12* (1975) 363–365.
[35] E. Wehinger, F. Bossert, DE 2847237 (1980), Bayer AG.
[36] G. Franckowiak, H. Böshagen, F. Bossert, S. Goldmann, H. Meyer, E. Wehinger, J. Stoltefuss, M. Schramm, G. Thomas, R. Towart, DE 3130041 (1981), Bayer AG.
[37] H. Kühnis, DE 3445356 (1985), Ciba-Geigy AG.
[38] H. Meyer, E. Wehinger, F. Bossert, D. Scherling, *Arzneim. Forsch. 33* (1983) 106–112.
[39] R. P. Hof, U. T. Rüegg, A. Hof, A. Vogel, *J. Cardiovasc. Pharmacol. 7* (1985) 689.
[40] K. Suzuki, T. Shiraishi, Y. Yoshida, T. Matsumoto, M. Iwamoto, Y. Motoyoshi, H. Niwa, Y. Inoue, EP 118120 (1984), Nikken Chem.
[41] A. Vogel, DE 3320616 (1983), Sandoz.
[42] B. Kohl, W. R. Ulrich, D. Flockerzi, EP 394243 (1987), Byk Gulden Lomberg.
[43] J. J. Suh, Y. H. Hong, *Yakhak Hoechi 33* (4) (1989) 219–225; see also *Chem. Abstr. 112* (1990) 235135.
[44] J. J. Suh, Y. H. Hong, *Yakhak Hoechi 33* (2) (1989) 80–86; see also *Chem. Abstr. 112* (1990) 76894.
[45] C. A. Gandolfi, M. Frigerio, C. Riva, A. Zaliani, G. Long, R. Di Domenico, EP 383320 (1990), Boehringer Biochemia Robin.
[46] Y. K. Shim, S. H. Lee, J. S. Kang, W. J. Kim, *Taehan Hwahakhoe Chi 32* (2) (1988) 144–148; see also *Chem. Abstr. 110* (1989) 8013.
[47] "Hydrogenolyses of benzyl esters": E. Schwenner, J. Stoltefuss, unpublished.
[48] "Cleavage of β-silylethyl esters with fluoride ions": S. Goldmann, unpublished.
[49] M. Iwanami, T. Shibanuma, M. Fujimoto, R. Kawai, K. Tamazawa, T. Takenaka, K. Takahashi, M. Murakami, *Chem. Pharm. Bull. 27* (1979) 1426–1440.
[50] G. Genain, EP 273349 (1987), Syntex.
[51] T. Shibanuma, M. Iwanani, K. Okuda, T. Takenaka, M. Murakami, *Chem. Pharm. Bull. 28* (1980) 2809–2812.
[52] M. Kajino, Y. Wada, Y. Nagai, A. Nagaoka, K. Meguro, *Chem. Pharm. Bull. 37* (1989) 2225–2228.
[53] K. Kagara, S. Goshima, K. Mukai, JP 02117658 (1990), Fujisawa; see also *Chem. Abstr. 113* (1990) 132020.
[54] J. E. Arrowsmith, EP 331315 (1989), Pfizer Ltd.
[55] K. Tamazawa, T. Kojima, H. Arima, Y. Murakami, Y. Isomura, M. Okada, K. Takanobu, T. Takenaka, EP 160451 (1985), Yamanouchi.
[56] W. R. Ulrich, D. Flockerzi, K. Sanders, N. Kolassa, K. Klemm, H. Amschler, M. Eltze, C. Schudt, K. Eistetter, WO 8807531 (1988), Byk Gulden.
[57] Y. Shiokawa, K. Okumura, Y. Sato, JP 01052757 (1987), Fujisawa Pharm.; see also *Chem. Abstr. 111* (1989) 115050.
[58] K. Seto, R. Sakota, S. Tanaka, JP 62169796 (1987), Nissan Chem. Ind.; see also *Chem. Abstr. 107* (1987) 237011.
[59] D. Flockerzi, W. R. Ulrich, US 4975440 (1987), Byk Gulden.
[60] Y. Nakajima, T. Ogawa, A. Nakazato, M. Kawase, K. Soda, JP 63295560 (1988), Taisho Pharm.; see also *Chem. Abstr. 111* (1989) 39198.
[61] I. Adachi, T. Yamamori, Y. Hiramatsu, K. Sakai, S. Mihara, M. Kawakami, M. Masui, O. Uno, M. Ueda, *Chem. Pharm. Bull. 36* (1988) 4389–4402.
[62] J. P. Carter, W. J. Rzeszotarski, US 4975437 (1989), Marion Lab.
[63] K. Klemm, W. R. Ulrich, D. Flockerzi, K. Sanders, K. D. Beller, C. Schudt, R. Boer, K. Gietzen, WO 8907443 (1989), Byk Gulden.
[64] E. Wehinger, unpublished.
[65] K. Muto, T. Kuroda, H. Kawato, A. Karasawa, K. Kubo, N. Nakamizo, *Arzneim. Forsch. 38* (1988) 1662–1665.
[66] K. Tamazawa, H. Arima, T. Kojima, Y. Isomura, M. Okada, S. Fujita, T. Furuya, T. Takenaka, O. Inagaki, M. Terai, *J. Med. Chem. 29* (12) (1986) 2504–2511.
[67] H. Amschler, K. Eistetter, M. Eltze, D. Flockerzi, K. Klemm, N. Kolassa, K. Sanders, C. Schudt, W. R. Ulrich, EP 242829 (1987), Byk Gulden.
[68] D. Flockerzi, W. R. Ulrich, K. Sanders, K. D. Beller, K. Eistetter, M. Eltze, R. Boer, B. Kohl, H. Amschler, K. Klemm, EP 314038 = EP 393074 (1989), Byk Gulden.
[69] D. Flockerzi, W. R. Ulrich, K. Sanders, K. D. Beller, R. Boer, M. Eltze, K. Klemm, EP 336132 (1989), Byk Gulden.
[70] H. Amschler, D. Flockerzi, K. Klemm, B. Kohl, K. Eistetter, M. Eltze, N. Kolassa, K. Sanders, C. Schudt, W. R. Ulrich, EP 343193 (1988), Byk Gulden.
[71] H. Arima, K. Tamazawa, JP 62174071 (1987), Yamanouchi; see also *Chem. Abstr. 108* (1988) 131587.
[72] H. Ikawa, A. Kadoiri, Y. Sekine, EP 403957 (1990), Fujirebio.
[73] W. Herrmann, J. Kleinschroth, K. Steiner, EP 385423 (1990), Gödecke AG.
[74] G. Marciniak, A. Delgado, G. Leclerc, J. Velly, N. Decker, J. Schwartz, *J. Med. Chem. 32* (1989), 1402–1407.
[75] H. Amschler, B. Kohl, M. Eltze, D. Flockerzi, K. Klemm, N. Kolassa, K. Sanders, C. Schudt, W. R. Ulrich, EP 240828 (1987), Byk Gulden.
[76] H. Yamaguchi, H. Sugano, M. Hasegawa, K. Kataoka, Y. Okamya, S. Kishimoto, JP 01104046 (1989), Teijin Ltd.; see also *Chem. Abstr. 111* (1989) 173992.
[77] K. Muto, T. Kuroda, A. Karasawa, K. Yamada, N. Nakamizo, EP 106275 (1984), Kyowa Hakko Kogyo.
[78] C. Semeraro, D. Micheli, D. Pieraccioli, G. Gaviraghi, A. D. Borthwick, DE 3628215 (1987), Glaxo.
[79] K. Cooper, J. Steele, M. J. Fray, K. Richardson, EP 365140 (1990), Pfizer.
[80] B. Kamber, T. Leutert, H. Kühnis, K. Eichenberger, US 4616002 (1986), Ciba-Geigy.
[81] J. Stoltefuss, E. Schwenner, M. Bechem, C. Hirth, M. Kayser, M. Schramm, J. P. Stasch, EP 288758 (1988), Bayer AG.
[82] K. Tamazawa, H. Arima, M. Okada, Y. Isomura, K. K. Schmiegel, J. H. Wikel, CA 1273931 (1990), E. Lilly, Yamanoucchi.
[83] D. R. Holland, J. H. Wikel, R. F. Kauffman, J. K. Smallwood, K. M. Zimmerman, B. G. Utterback, J. A. Turk, M. I. Steinberg, *J. Cardiovasc. Pharmacol. 14* (3) (1989) 483–491.
[84] K. Seto, R. Sakoda, H. Matsumoto, Y. Kamikawaji, S. Tanaka, EP 260605 (1988), Nissan Chem. Ind.
[85] J. Robin, D. Pruneau, A. Bonenfant, FR 2577552 (1986), SORI; see also *Chem. Abstr. 107* (1987) 39787.
[86] H. Sugano, H. Yamaguchi, JP 61158962 (1986), Teijin Ltd.; see also *Chem. Abstr. 106* (1987) 32851.
[87] J. R. Kern, D. M. Lokensgard, T. Yang, *J. Chromatogr. 457* (1988) 309–316.
[88] P. J. Gris Seoane, J. M. Gonzalez Bosch, J. Boget Alemany, ES 2005543 (1989), Laboratorios Menarini; see also *Chem. Abstr. 113* (1990) 40468.
[89] M. Frigerio, A. Zaliani, C. A. Gandolfi, M. Germini, O. Tofanetti, S. Tognella, EP 272693 (1988), Boehringer Biochemia Robin.
[90] E. Wehinger, H. Meyer, F. Bossert, W. Vater, R. Towart, K. Stoepel, S. Kazda, DE 2935451 (1981), Bayer AG.
[91] J. E. Arrowsmith, S. F. Campbell, P. E. Cross, J. K. Stubbs, R. A. Burges, D. G. Gardiner, K. J. Blackburn, *J. Med. Chem. 29* (1986) 1696–1702.
[92] M. Kamikawaji, K. Seto, R. Sakota, JP 01113398 (1989), Nissan Chem. Ind.; see also *Chem. Abstr. 112* (1990) 25675.
[93] J. L. Peglion, Y. M. Gargouil, J. P. Vilaine, EP 406502 (1991), ADIR et Comp.
[94] A. Vogel, DE 3305577 (1983), Sandoz.
[95] H. Matsumoto, M. Kamikawa, K. Seto, R. Sakota, S. Tanaka, JP 02011592 (1990), Nissan Chem. Ind.; see also *Chem. Abstr. 113* (1990) 59536.
[96] G. Franckowiak, R. Grosser, G. Thomas, M. Schramm, R. Gross, DE 3447169 (1986), Bayer AG.
[97] K. Schönafinger, H. Bohn, P. A. Martorana, R. E. Nitz, DE 3431152 (1986), Cassella AG.
[98] S. Goldmann, H. Böshagen, DE 3714438 (1988), Bayer AG.
[99] G. Franckowiak, J. Stoltefuss, M. Bechem, R. Groß, M. Kayser, S. Hebisch, M. Schramm, EP 315018 (1989), Bayer AG.
[100] G. Franckowiak, J. Stoltefuss, M. Bechem, R. Groß, M. Kayser, S. Hebisch, M. Schramm, EP 315019 (1989), Bayer AG.
[101] S. Goldmann, J. Stoltefuss, unpublished.
[102] M. D. Taylor, R. J. Himmelsbach, B. E. Kornberg, J. Quin III, E. Lunney, A. Michel, *J. Org. Chem. 54* (1989) 5585–5590.
[103] B. Lamm, R. Simonsson, S. Sundell, *Tetrahedron Lett. 30* (1989) 6423–6426.
[104] J. Stoltefuss, M. Bechem, R. Groß, S. Hebisch, M. Schramm, EP 347678 (1989), Bayer AG.
[105] J. Stoltefuss, unpublished.
[106] A. J. G. Baxter, J. Dixon, K. J. Gould, T. McInally, A. C. Tinker, EP 125803 (1984), Fisons.
[107] H. Yamaguchi, M. Hasegawa, H. Sugano, JP 01029359 (1989), Teijin Ltd.; see also *Chem. Abstr. 111* (1989) 97095.
[108] R. Davis, J. R. Kern, L. J. Kurz, J. R. Pfister, *J. Am. Chem. Soc. 110* (1988) 7873–7874.
[109] E. Wehinger, H. Meyer, DE 3423105 (1986), Bayer AG.
[110] D. Enders, S. Müller, A. S. Demir, *Tetrahedron Lett. 29* (1988) 6437–6440.
[111] A. Kakuiri, H. Ikawa, N. Kobayashi, Y. Isowa, JP 63208573 (1988) Fujirebio; see also *Chem. Abstr. 110* (1989) 95014.
[112] K. Kataoka, H. Sugano, H. Yamaguchi, JP 2212474 (1990), Teijin Ltd.; see also *Chem. Abstr. 114* (1991) 143156.
[113] S. Goldmann, unpublished.
[114] X. K. Holdgrün, C. J. Sih, *Tetrahedron Lett. 32* (1991) 3465–3468.
[115] E. Wehinger, unpublished.

[116] E. Booker, U. Eisner, *J. Chem. Soc. Perkin Trans. 1 1975*, 929–931.
[117] S. Yamada, Y. Kikugawa, *Chem. Ind. (London) 1966*, 2169–2170.
[118] A. I. Meyers, T. Oppenlaender, *J. Chem. Soc. Chem. Commun. 1986*, 920–921.
[119] A. I. Meyers, T. Oppenlaender, *J. Am. Chem. Soc. 108* (1986) 1989–1996.
[120] G. Blaschke, F. Donow, DE 2500523 (1976), Merck Patent GmbH.
[121] U. Schwartz, R. Grosser, K. E. Piejko, B. Bömer, D. Arlt, DE 3532356 (1987), Bayer AG.
[122] R. Grosser (Bayer AG), private communication.
[123] D. W. Armstrong, T. J. Ward, R. D. Armstrong, T. E. Beesley, *Science (Washington DC) 232* (1986) 1130–1135.
[124] A. M. Stalcup, S. C. Chang, D. W. Armstrong, J. Pitha, *J. Chromatogr. 513* (1990) 181–194.
[125] Y. Tokuma, T. Fujiwara, H. Noguchi, *J. Pharm. Sci. 76* (1987) 310–313.
[126] E. Delee, I. Jullien, L. Le Garrec, *J. Chromatogr. 450* (1988) 191–197.
[127] Y. Okamoto, R. Aburatani, K. Hatano, K. Hatada, *J. Liq. Chromatogr. 11* (1988) 2147–2163.
[128] Y. Okamoto, K. Hatano, R. Aburatani, K. Hatada, *Chem. Lett. 1989*, 715–719.
[129] Y. Okamoto, R. Aburatani, K. Hatada, M. Honda, N. Inotsume, M. Nakano, *J. Chromatogr. 513* (1990) 375–378.
[130] V. Muschalek, V. Nickel, Bayer AG, unpublished.
[131] P. A. Soons, M. C. M. Roosemalen, D. D. Breimer, *J. Chromatogr. 528* (1990) 343–356.
[132] S. Ringer, *J. Physiol. 2* (1882) 380.
[133] T. Tanabe, H. Takeshima, A. Mikami, V. Flockerzi, H. Takahashi, K. Kangawa, M. Kojima, H. Matsuo, T. Hirose, S. Numa, *Nature (London) 328* (1987) 313–318.
[134] J. Galizzi, M. Borsotto, J. Barhanin, M. Fosset, M. Lazdunski, *J. Biol. Chem. 261* (1986) 1393.
[135] A. H. Sharp, T. Imagawa, A. T. Leung, K. P. Campbell, *J. Biol. Chem. 262* (1987) 12309.
[136] H. Glossmann, J. Striessnig, *ISI Atlas Sci. Pharmacol. 2* (1988) 202.
[137] P. L. Vaghy, E. McKenna, K. Itagaki, A. Schwartz, *Trends Pharmacol. Sci. 9* (1988) 398–402.
[138] W. A. Catterall, M. J. Seagar, M. Takahashi, *J. Biol. Chem. 263* (1988) 3535.
[139] X. Y. Wei, A. Rutledge, D. J. Triggle, *Mol. Pharmacol. 35* (1989) 541.
[140] P. Hess, J. B. Lansman, R. W. Tsien, *Nature (London) 311* (1984) 538.
[141] D. A. Langs, P. D. Strong, D. J. Triggle, *J. Comput.-Aided Mol. Des. 4* (1990) 215.
[142] I. L. Karle, *Acta Crystallogr. 14* (1961) 497.
[143] H. Koyama, *Z. Kristallogr. 118* (1963) 51.
[144] A. T. H. Lenstra, G. H. Petit, R. A. Dommisse, F. C. Alderweireldt, *Bull. Soc. Chim. Belg. 88* (1979) 133.
[145] A. Glasfeld, P. Zbinden, M. Dobler, S. A. Benner, J. D. Dunitz, *J. Am. Chem. Soc. 110* (1988) 5152–5157.
[146] H. J. Hofmann, R. Cimiraglia, *FEBS Lett. 241* (1988) 38.
[147] H. J. Hofmann, R. Cimiraglia, *J. Mol. Struct. THEOCHEM 205* (1990) 1.
[148] R. Fossheim, K. Svarteng, A. Mostad, C. Romming, E. Shefter, D. J. Triggle, *J. Med. Chem. 25* (1982) 126.
[149] A. Mishnev, A. E. Shvets, J. Bleidelis, G. Duburs, A. Sausins, V. Lusis, *Khim. Geterotsikl. Soedin 9* (1977) 1229.
[150] J. W. Krajewski, Z. Urbanczyk-Lipkowska, P. Gluzinski, *Cryst. Struct. Commun. 6* (1977) 787.
[151] A. Hempel, M. P. Gupta, *Acta Crystallogr. Sect. B34* (1978) 3815.
[152] A. M. Triggle, E. Shefter, D. J. Triggle, *J. Med. Chem. 23* (1980) 1442.
[153] R. Tacke, A. Bentlage, W. S. Sheldrick, L. Ernst, R. Towart, K. Stoepel, *Z. Naturforsch. B37* (1982) 443–450.
[154] G. Rovnyak, N. Andersen, J. Gougoutas, A. Hedberg, S. D. Kimball, M. Malley, S. Moreland, M. Porubcan, A. Pudzianowski, *J. Med. Chem. 31* (1988) 936–944.
[155] R. Fossheim, A. Joslyn, A. J. Solo, E. Luchowski, A. Rutledge, D. J. Triggle, *J. Med. Chem. 31* (1988) 300.
[156] A. Miyamae, S. Koda, Y. Morimoto, *Chem. Pharm. Bull. 34* (1986) 3071–3078.
[157] P. Berntsson, S. Wold, *Quant. Struct.-Act. Relat. 5* (1986) 45.
[158] R. Fossheim, *J. Med. Chem. 29* (1986) 305.
[159] R. Fossheim, *Acta Chem. Scand. Ser. B41* (1987) 581; *ibid. 40* (1986) 776–778.
[160] J. I. McKenna, L. Schlicksupp, N. R. Natale, R. D. Willett, B. E. Maryanoff, S. F. Flaim, *J. Med. Chem. 31* (1988) 473–476.
[161] D. A. Langs, P. D. Strong, D. J. Triggle, *Acta Crystallogr. Sect. C34* (1987) 707.
[162] D. A. Langs, D. J. Triggle, *Mol. Pharmacol. 27* (1985) 544.
[163] R. Rodenkirchen, R. Bayer, R. Steiner, F. Bossert, H. Meyer, E. Möller, *Naunyn-Schmiedeberg's Arch. Pharmacol. 310* (1979) 69–78.
[164] W. Seidel, H. Meyer, L. Born, S. Kazda, W. Dompert, *ACS 187th Natl. Meet. St. Louis 1984*, April 8–14, Med. Chem. Abstr. 14.
[165] W. Seidel, H. Meyer, L. Born, S. Kazda, W. Dompert in J. Seydel (Ed.): *QSAR Strategies Des. Bioact. Compd. Proc. Eur. Symp. Quant. Struct.-Act. Relat. 5th 1984*, VCH, Weinheim 1985, pp. 366–369.
[166] S. Goldmann, L. Born, S. Kazda, B. Pittel, M. Schramm, *J. Med. Chem. 33* (1990) 1413–1418.
[167] J. J. Baldwin, D. A. Claremon, P. K. Lumma, D. E. McClure, S. A. Rosenthal, R. J. Winquist, E. P. Faison, G. J. Kaczorowski, M. J. Trumble, G. M. Smith, *J. Med. Chem. 30* (1987) 690–695.
[168] T. H. Siddall III, W. E. Stewart, *J. Org. Chem. 34* (1969) 233–237.
[169] R. Saito, M. Oki, *Bull. Chem. Soc. Jpn. 55* (1982) 3273–3276.
[170] M. Nakamura, N. Nakamura, M. Oki, *Bull. Chem. Soc. Jpn. 50* (1977) 1097–1101.
[171] S. Goldmann, W. Geiger, *Angew. Chem. 96* (1984) 302; *Angew. Chem. Int. Ed. Engl. 23* (1984) 301.
[172] H. J. Hofmann, R. Cimiraglia, *Z. Chem. 28* (1988) 326–327.
[173] H. D. Höltje, S. Marrer, *J. Comput.-Aided. Mol. Des. 1* (1987) 23.
[174] P. Kovacic, W. D. Edwards, N. R. Natale, R. Sridhar, P. F. Kiser, *Chem. Biol. Interact. 75* (1990) 61.
[175] P. Berntsson, R. E. Carter, *Acta Pharm. Suec. 18* (1981) 221.
[176] U. Rose, *Chem. Ztg. 113* (1989) 85–86.
[177] H. Beard, R. McKie: *Sailing: a sailor's dictionary*, Workman, New York 1981.
[178] V. Prelog, G. Helmchen, *Helv. Chim. Acta 55* (1972) 2581–2598.
[179] M. Mahmoudian, W. G. Richards, *J. Chem. Soc. Chem. Commun. 1986*, 739–741.
[180] G. Satzinger, J. Hartenstein, K. Mannhardt, J. Kleinschroth, E. Fritschi, H. Osswald, G. Weinheimer, DE 3431303 (1986), Goedecke AG.
[181] G. F. DiFrancesco, M. A. Petty, EP 355234 (1990), Merrell Dow.
[182] Other derivatives of this structure type are known: S 830327 [183], MDL 143 [184], S 8363 [185], S 830256 [185], Goe 6070 [186], Y-19638 [187].
[183] I. Adachi, Y. Hiramatsu, M. Ueda, M. Kawakami, EP 207345 (1987), Shionogi Co.
[184] JP 59118786 (1984), Gruppo Lepetit SpA.
[185] I. Adachi, T. Yamamori, Y. Hiramatsu, K. Sakai, H. Sato, M. Kawakami, O. Uno, M. Ueda, *Chem. Pharm. Bull. 35* (1987) 3235–3252.
[186] G. Weinheimer, H. Osswald, *Naunyn-Schmiedeberg's Arch. Pharmacol. 340* (1989) R 55.
[187] N. Tsuda, T. Mishina, M. Obata, A. Inui, JP 61263977 (1986), Yoshitomi Pharm. Ind.; see also *Chem. Abstr. 106* (1987) 119901.
[188] D. A. Langs, D. J. Triggle, *Mol. Pharmacol. 27* (1985) 546.
[189] J. Kleinschroth, K. Mannhardt, J. Hartenstein, G. Satzinger, *IXth Int. Symp. Med. Chem. Berlin 1986*, Abstr. 2.1.6, p. 175.
[190] G. T. Bolger, P. Gengo, R. Klockowski, E. Luchowski, H. Siegel, R. A. Janis, A. M. Triggle, D. J. Triggle, *J. Pharmacol. Exp. Ther. 225* (1983) 291.
[191] The investigations were not carried out under exactly the same conditions and should therefore be treated with reservation.
[192] R. Towart, E. Wehinger, H. Meyer, *Naunyn-Schmiedeberg's Arch. Pharmacol. 317* (1981) 183–185.
[193] S. Goldmann, lecture at the conference *Neuere Entwicklungen in der Medizinischen Chemie*, Freiburg, October 1987.
[194] R. P. Hof, A. Hof, U. T. Rüegg, N. S. Cook, A. Vogel, *J. Cardiovasc. Pharmacol. 8* (1986) 221–226.
[195] G. Zernig, T. Moshammer, H. Glossmann, *Eur. J. Pharmacol. 128* (1986) 221–229.
[196] A. J. G. Baxter, J. Dixon, J. Fuher, K. J. Gould, T. McInally, C. N. Manners, D. W. Payling, *IXth Int. Symp. Med. Chem. Berlin 1986*, Abstr. 2.5.2, p. 310.
[197] K. Schönafinger, H. Bohn, lecture at the conference *Neuere Entwicklungen in der Medizinischen Chemie*, Freiburg, October 1987.
[198] K. S. Atwal, G. C. Rovnyak, S. D. Kimball, D. M. Floyd, S. Moreland, B. N. Swanson, J. Z. Gougoutas, J. Schwartz, K. M. Smillie, M. F. Malley, *J. Med. Chem. 33* (1990) 2629–2635.
[199] T. Leutert, B. Kamber, H. Fallert, M. Meier, H. Rogg, lecture at the conference *Neuere Entwicklungen in der Medizinischen Chemie*, Freiburg, October 1987.
[200] B. Kamper, T. Leutert, H. Kühnis, K. Eichenberger, EP 145956 (1985), Ciba-Geigy; see also *Chem. Abstr. 105* (1987) 43330; see also *Chem. Abstr. 106* (1987) 102094.
[201] R. Boer, A. Grassegger, C. Schudt, H. Glossmann, *Eur. J. Pharmacol. Mol. Pharmacol. Sect. 172* (1989) 131.
[202] Starting with (−)-(*R*)-**14** we obtained (+)-(S)-**118**. Therefore compound **6a**[74] must have the S,R configuration. S. Goldmann, J. Stoltefuss, unpublished results.
[203] R. Towart, E. Wehinger, H. Meyer, S. Kazda, *Arzneim. Forsch. 32* (1982) 338.
[204] M. Schramm, G. Thomas, R. Towart, G. Franckowiak, *Nature (London) 303* (1983) 535.
[205] S. Goldmann, F. Bossert, M. Schramm, G. Thomas, *VIIIth Int. Symp. Med. Chem. Uppsala 1984*, Proc. Vol. 1, p. 318.
[206] P. Erne, E. Bürgisser, F. R. Bühler, B. Dubach, H. Kühnis, M. Meier, H. Rogg, *Biochem. Biophys. Res. Commun. 118* (1984) 842–847.
[207] S. Goldmann, M. Schramm, G. Thomas, R. Gross, US 4642310 (1987), Bayer AG.
[208] L. Patmore, G. P. Duncan, B. Clarke, A. J. Anderson, R. Greenhouse, J. R. Pfister, *Br. J. Pharmacol. 99* (1990) 687–694.

[209] T. Beyer, P. Gjörstrup, U. Ravens, *Naunyn-Schmiedeberg's Arch. Pharmacol. 330* (1985) R 34.
[210] K. Schönafinger, H. Bohn, P. Martorana, R. E. Nitz, EP 183091 (1986), Cassella AG.
[211] H. Nakaya, Y. Hattori, N. Tohse, M. Kanno, *Naunyn-Schmiedeberg's Arch. Pharmacol. 333* (1986) 421–430.
[212] S. Goldmann, M. Schramm, G. Thomas, L. Born, unpublished.
[213] Y. Tsuda, T. Mishina, M. Obata, K. Araki, J. Inui, T. Nakamura, EP 217142 (1987), Yoshitomi Pharm. Ind.
[214] U. Rose, *Arch. Pharm. 323* (1990) 281.
[215] P. Gjörstrup, H. Harding, R. Isaksson, C. Westerlung, *Eur. J. Pharmacol. 122* (1986) 357–361.
[216] S. Goldmann, J. Stoltefuss, M. Bechem, S. Hebisch, unpublished.
[217] S. Goldmann, J. Stoltefuss, M. Bechem, M. Schramm, S. Hebisch, G. Thomas, unpublished.
[218] S. Goldmann, L. Born, unpublished.
[219] S. Goldmann, W. Röben, unpublished.
[220] G. Thomas, R. Gross, M. Schramm, *J. Cardiovasc. Pharmacol. 6* (1984) 1170–1176.

VCH Index Library

The electronic version can be read by all MS-DOS compatible computers. It is accessed by the Search module of the Literature Management Program VCH-Biblio.

ANGEWANDTE CHEMIE
A Journal of the Gesellschaft Deutscher Chemiker
International Edition in English

30 Year Index of Reviews
– in print or on diskette –

The reviews in Angewandte Chemie are amongst the most often cited chemical publications of each year. Many have become classics of the chemical literature. For thirty years they have been available in English as well as German. The 30 year review index now celebrates this anniversary by facilitating access to these important documents of the rapid development of our discipline. The index—both a chemical dictionary and a history book—offers you:

1. A list of all authors, indicating the main author and the title of the review.
2. A subject index giving the main author.
3. Both indexes provide complete information on date of issue and first and last page numbers of the German and English editions.

The electronic version of the index is available on 5¼" and 3½" diskettes.

If you order immediately, you save about 30% since the prepublication price is U.S. $44.00/£26.00 (plus postage) only until the end of January. Please order by telephone or in writing to **VCH, Software und Datenbanken, Postfach 10 11 61, D-W-6940 Weinheim, Tel. 0 62 01/6 02-2 71, Telefax 0 62 01/6 02-3 28.**

Silicon Nitride—From Powder Synthesis to Ceramic Materials

By Horst Lange,* Gerhard Wötting, and Gerhard Winter

Dedicated to Professor Karl Heinz Büchel on the occasion of his 60th birthday

Silicon nitride is a ceramic material of great interest to advanced engine construction and mechanical engineering owing to an outstanding combination of favorable properties like high mechanical strength at high temperatures, corrosion and wear resistance, great hardness, and low density. The material is based on high-quality Si_3N_4 powders, which are shaped and sintered to the ceramic component. This overview outlines the properties required for Si_3N_4 powders suitable for advanced ceramics. Processes in commerical use and those under development for the production of high quality Si_3N_4 powders are discussed as well as material manufacturing processes and material properties. By steadily improving powder quality, material properties, and the economy of powder and component production, chemistry and chemical technology play a major role in recent efforts to create a solid fundament for broad applications of silicon nitride ceramics.

"If one would surrender to geological phantasies, one could imagine that during the formation of our planet, when elements combined to the compounds making up its crust and mountain ranges, silicon reacted with nitrogen, and the still red-hot nitrogen-silicon, on contact with water, may have decomposed to silicic acid and ammonia. Thus, ammonia may have been formed originally and nitrogen thereby introduced into the forming organic compounds when living nature first started to appear."

H. Sainte-Claire Deville and F. Wöhler[**]

1. Introduction

Following speculations by *Deville* and *Wöhler*,[1] silicon nitride attracted attention for the first time as a possible raw material for the technical synthesis of ammonia. A series of patents from the period 1909–1918 describes the synthesis of ammonia by heating Si_3N_4 with solutions or dispersions of basic oxides, hydroxides, or salts, by treatment with hot water vapor, or by heating it in hydrogen atmosphere.[2–11] Because of the concurrent development of the Haber–Bosch process, these methods never gained any importance. It is not surprising, therefore, that this early interest in silicon nitride soon declined.

However, silicon nitride saw a remarkable renaissance after the discovery that it can be converted into a ceramic material. Silicon nitride ceramics significantly extend the limits of metallic materials under combined thermal and mechanical stress in corrosive environments.

2. Silicon Nitride as Ceramic Material

Silicon nitride is of great interest as a heavy-duty material for applications in chemical engineering, wear technology, metal working, energy technology, and especially in engine and turbine construction.[12–24] This broad interest arises from a favorable combination of great hardness, wear resistance, chemical stability, low density, and high mechanical strength at temperatures up to 1300 °C. The application of Si_3N_4 ceramic parts in combustion engines and gas turbines promises advantages like higher efficiency and better fuel use due to higher combustion temperatures, faster response of oscillating or rotating engine components (valves, pistons, turbocharger, and turbine rotors) due to low density, and longer service intervals due to a generally improved wear behavior.

Silicon nitride ceramics are produced either by nitriding silicon powder compacts or by sintering Si_3N_4 powder compacts.[25,26] The first method produces a porous, reaction-bonded material (RBSN, reaction-bonded silicon nitride) with almost negligible shrinkage; this material is used either directly or may be densified by a following sintering step (SRBSN, sintered RBSN).[25–30] The second method, which is covered comprehensively in this article, leads to Si_3N_4 ceramics of superior quality. These are of special interest to

[*] Dr. H. Lange
PK-F, Bayer AG
W-4150 Krefeld-Uerdingen (FRG)
Dr. G. Wötting
Cremer Forschungsinstitut
W-8633 Rödental (FRG)
Prof. Dr. G. Winter
Hermann C. Starck Berlin GmbH + Co KG
W-3380 Goslar (FRG)

[**] "Ueber die directe Bildung des Stickstoffsiliciums" in: *Ann. Chem. Pharm. 34* (1859) 248: "If one would surrender to geological phantasies, one could imagine that during the formation of our planet, when elements combined to the compounds making up its crust and mountain ranges, silicon reacted with nitrogen, and the still red-hot nitrogen-silicon, on contact with water, may have decomposed to silicic acid and ammonia. Thus, ammonia may have been formed originally and nitrogen thereby introduced into the forming organic compounds when living nature first started to appear.

advanced engine construction and advanced mechanical engineering.

To demonstrate their technological benefits reliably, Si_3N_4 components require a perfect and economical control of the entire manufacturing process, from the synthesis of the Si_3N_4 powder, its processing, forming, sintering to the precise finishing of the structural component (Fig. 1).

Nonuniformity of the starting powder—for example, even just a few extraneous particles, ill-defined particle clusters, or particle morphologies such as a mass of disordered, more or less agglomerated lumps, fibers, or whiskers, as well as extraneous particles or impurities dragged in through powder processing—induce fracture-causing structural defects, which cannot be remedied in the following manufacturing steps. Products of inferior quality and reliability are the result. Since powder-inherent sources of defects can hardly be eliminated by subsequent ceramic processing, the powder producer has a special responsibility to supply extremely well-defined, high-quality powders. To avoid environmental contamination by, say, dust particles, the transfer of powder processing, shaping, and sintering into clean rooms has been discussed.[31, 32] Repeatedly, this measure has been described to improve fracture strength and reliability.[33, 34] Furthermore, defects also arise during shaping, sintering, and finishing. These nowise trivial problems have to be solved convincingly to allow an economical, large-scale production of silicon nitride components. Here, chemistry plays an important role, since powder synthesis and component

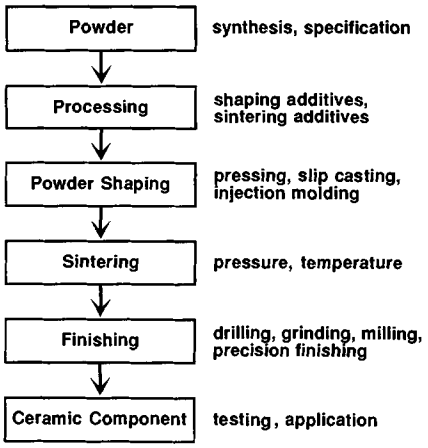

Fig. 1. Manufacturing process from powder to component.

manufacturing touch many problems of solid-state chemistry, surface chemistry, tribochemistry, and chemical engineering,[26, 35] some of which are fundamental.

3. The Structure of Silicon Nitride—Origin of Hardness, Durability, and Strength

Crystalline silicon nitride exists in two hexagonal modifications, α and β, which are built up from a three-dimensional

Horst Lange was born in 1957 in Enkhausen (Sauerland) and studied chemistry from 1975 to 1981 at the Universität Dortmund. In 1983 he received his Ph.D. under Prof. Nauman for work on perfluoroalkylzinc and -cadmium compounds and then worked for one year as a postdoc with Prof. Shreeve at the University of Idaho. Since 1985 he has worked at Bayer AG (Uerdingen) and since 1989 he has been leader of the engineering ceramics group.

Gerhard Wötting was born in 1951 in Markredwitz (Oberfranken) and studied Materials Science from 1969 to 1977 at the Fachhochschule Selb/Regensburg and the Technische Universität Berlin with emphasis on glass and ceramics. In 1982 he received his Ph.D. under Prof. Hausner for work on the sintering behavior of silicon nitride powders. From 1981 to 1987 he worked as a researcher at the Institut für Werkstoff-Forschung der Deutschen Forschungs- und Versuchsanstalt für Luft- und Raumfahrt in Cologne. Since 1987 he has been involved in developmental work in the area of materials technology/high-performance ceramics at the Cremer Forschungsinstitut, Rödental.

Gerhard Winter was born in 1937 in Klein-Mohrau (Sudetenland) and studied chemistry from 1957 to 1963 at the Universität Tübingen. He earned his doctorate in 1966 with a dissertation on graphite inclusion compounds under Prof. Rüdorff. In 1967 he began work at Bayer AG. Since 1986 he has taught at the Universität-Gesamthochschule Siegen. He currently heads research and development at Hermann C. Starck Berlin in Goslar and is the author of the book "Industrielle Anorganische Chemie".

network of SiN_4 tetrahedrons.[36, 37] Rigid structure and strong covalent bonds are the cause of the extraordinary hardness, durability, and mechanical strength of this material.

Figure 2 shows the crystal structure of β-Si_3N_4, which is built from a Si_6N_8 unit cell.[38] Along the crystallographic c axis, channels with a diameter of about 0.15 nm play a certain role in the diffusion of atoms, even large ones. α-Si_3N_4 is built from a $Si_{12}N_{16}$ unit cell;[24] since no channels occur in this structure, diffusion is much more difficult than in β-Si_3N_4 (Fig. 3).

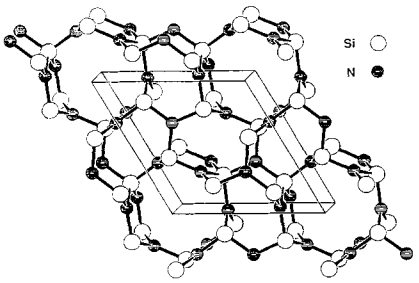

Fig. 2. Section of the crystal structure of β-Si_3N_4; view approximately along c.

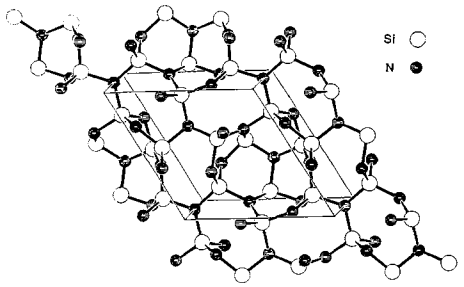

Fig. 3. Section of the crystal structure of α-Si_3N_4; view approximately along c.

Early work on the conditions leading to formation of either the α or β phase indicated that the α phase, assumed to be an oxygen-stabilized low-temperature modification with a narrow range of existence, has the empirical formula $Si_{11.4-11.5}N_{15}O_{0.3-0.5}$ (actually an oxinitride phase).[36, 40-42] However, the formation of the α phase required significantly less oxygen than presumed.[43] By chemical vapor deposition it was possible to produce α-Si_3N_4 single crystals extremely low in oxygen.[39, 44-47] Today α- and β-Si_3N_4 are regarded as polymorphic modifications; α-Si_3N_4 is the stable low-temperature modification, since the α-Si_3N_4 content of a powder increases as the temperature of synthesis decreases and since $\alpha \rightarrow \beta$ transformation occurs only at temperatures exceeding 1650 °C. Probably for kinetic reasons, a $\beta \rightarrow \alpha$ transformation has not yet been observed.

The α/β ratio of commercially available powders is usually determined by X-ray diffraction,[48, 49] but also IR[50-52] and ^{29}Si MAS NMR spectroscopy may be applied.[53-55] ^{29}Si MAS NMR spectroscopy is particularly useful since it can be employed to distinguish and quantify not only the crystalline phases but also amorphous Si_3N_4.[54] This method is also suitable for the study of sintering phenomena.[56, 57]

4. The Synthesis of Si_3N_4 Powders

For the technical synthesis of high-quality Si_3N_4 powders the three following methods are important (see Sections 4.2 to 4.4): nitridation of silicon powder [Eq. (a)],[58-61] carbothermal reduction of SiO_2 in the presence of nitrogen [Eq. (b)] or ammonia,[62-66] and ammonolysis of reactive silicon compounds [Eqs. (c) and (d)].[67-71]

$$3Si + 2N_2 \xrightarrow{1100-1400\,^\circ C} Si_3N_4 \quad (a)$$

$$3SiO_2 + 2N_2 + 6C \xrightarrow{1450-1600\,^\circ C} Si_3N_4 + 6CO \quad (b)$$

$$3SiCl_4 + 4NH_3 \xrightarrow{\text{ca. } 25-1400\,^\circ C} Si_3N_4 + 12HCl \quad (c)$$

$$3SiH_4 + 4NH_3 \xrightarrow{600-1400\,^\circ C} Si_3N_4 + 12H_2 \quad (d)$$

In contrast to direct nitridation or carbothermal reduction, ammonolysis does not yield crystalline Si_3N_4 directly. The reaction leads initially to extremely moisture-sensitive silicon diimide [Eq. (e)], which is then transformed by pyrolysis, via amorphous Si_3N_4, to α-Si_3N_4 [Eqs. (f) and (g)].[67-69, 72]

$$SiCl_4 + 6NH_3 \xrightarrow{\text{ca. } 25\,^\circ C} Si(NH)_2 + 4NH_4Cl \quad (e)$$

$$3Si(NH)_2 \xrightarrow{900-1200\,^\circ C} Si_3N_4 \text{ (amorphous)} + 2NH_3 \quad (f)$$

$$3Si_3N_4 \text{ (amorphous)} \xrightarrow{1300-1500\,^\circ C} \alpha\text{-}Si_3N_4 \quad (g)$$

Several other reactions [Eq. (h),[73-75] (i),[76] (j)[77, 78]] have not gained importance for technological or economical reasons, such as too great expense, too slow reaction kinetics, or the development of undesirable particle morphologies.

$$3SiS_2 + 4NH_3 \longrightarrow Si_3N_4 + 6H_2S \quad (h)$$

$$3SiC + 4NH_3 \longrightarrow Si_3N_4 + 3CH_4 \quad (i)$$

$$3SiO_2 + 4NH_3 \longrightarrow Si_3N_4 + 6H_2O \quad (j)$$

Furthermore, there have been numerous attempts to synthesize Si_3N_4 by pyrolysis or carbothermical reduction from silazanes [Eq. (k)] or siloxanes.[79] Because of the comparatively complicated and costly production and handling of silazanes, this method is less interesting for powder synthesis than for the manufacturing of Si_3N_4 fibers or coatings. Polymeric silazanes of suitable structure may be processed by spinning to produce fibers or by melt or solution coating; subsequent pyrolysis usually gives a 60–80% ceramic yield. There is also some fundamental interest in the use of silazanes as binders or plasticizers for silicon nitride powder molding by dry pressing or injection molding, since pyrolysis leaves nothing but Si_3N_4.

$$\frac{1}{n}[SiR_2 - NR]_n \xrightarrow[-RH,\ -H_2]{800-1400\,^\circ C,\ NH_3} Si_3N_4 \quad (k)$$

4.1. Required Powder Properties

A Si_3N_4 powder qualified for applications in advanced ceramics has to meet numerous demands regarding chemical

and physical properties. Important criteria for powder quality include purity, crystallinity, particle shape, particle size distribution, degree of particle agglomeration, and α/β ratio, as well as technological properties like good processing behavior in different powder shaping techniques and good sintering activity.

To minimize shrinkage and to avoid the development of density gradients during sintering, powder shaping has to aim at particle packing densities as high and as homogeneous as possible. This is achieved by defined particle size distributions, spherical particle shapes, mean particle sizes less than 1 μm, and exclusion of coarse or hard agglomerated particles. These factors, together with defined C and O contents, exclusion of extraneous particles, and a high α/β ratio, are important characteristics of powders with good sintering behavior and favor the development of a homogeneous grain structure during sintering. The spectrum of all these properties influences the general sintering activity of a powder. Roughly, sintering activity increases with decreasing particle size. However, powder processing becomes increasingly difficult (dust generation, bad densification behavior in dry pressing, high sintering shrinkage) as particle sizes decrease. Therefore, the search for universally applicable powders often requires a compromise between opposing demands. These circumstances, in turn, offer possibilities for special "powder designs", that is, tailor-made powders with special advantages in certain manufacturing processes. A free-flowing granulated Si_3N_4 powder, which will not crumble into dust particles but which is easy to densify, is favorable for charging automated dry presses and may illustrate this point.

Some powder properties, like the α/β ratio, have to be adjusted during the Si_3N_4 synthesis; others, like particle size, particle size distribution, or C and O content, may be influenced subsequently by suitable powder processing (e.g., milling, screening, or annealing). In order to minimize the efforts spent on powder processing, it is advantageous to adjust as many of the required properties as possible during the synthesis. To what extent this approach is technologically feasible and economically appropriate depends on the synthetic method chosen.

4.2. Si_3N_4 Synthesis by Direct Nitridation of Elemental Silicon

Direct nitridation of elemental silicon—the process used more than 80 years ago to show the correct stoichiometry of silicon nitride to be Si_3N_4[80]—is still the dominant procedure for the industrial synthesis of silicon nitride powders.[45-46] The main processing steps are nitridation of silicon powder, milling, and finally purification of the crude product (Fig. 4).

The selection of silicon powders of different purities strongly influences the impurity level of Si_3N_4. Besides commercially available, low-cost, metallurgical-grade silicon of different levels of purity, it is possible to use semiconductor-grade silicon as starting material of extremely high purity.[81]

For the actual synthesis, piles of silicon powder are allowed to react with nitrogen either discontinuously in chamber furnaces or continuously in conveyor-type pusher furnaces according to Equation (a) ($\Delta H = -750\ kJ\,mol^{-1}$). The reaction proceeds at a reasonable rate only above 1100 °C. Reaction rates strongly depend on particle size and chemical purity of the silicon powder.[60, 61, 82, 83] Especially traces of Fe catalyze the nitridation.[82, 84] Owing to its strong exothermal character the reaction has to be controlled carefully. Generally, low temperatures and the presence of hydrogen in the nitriding gas favor the formation of α-phase material.[60, 61, 85] Too high temperatures cause not only the formation of undesired β-Si_3N_4 but also strongly sintered agglomerates of Si_3N_4 primary particles, which finally require a more intensive milling process. Careful control of the exothermic reaction is also necessary to avoid an uncontrolled temperature rise exceeding the melting point of silicon in the powder bed.[60, 61, 82] The evolution of heat can be reduced by lowering the concentration of nitrogen in the nitriding atmosphere after onset of the reaction ("exothermal control"[86]). It may also be linited by a suitable, often empirically determined temperature control depending on nitridation kinetics, powder packing density, depth of powder bed, charge size, and type of furnace.[60, 61, 82]

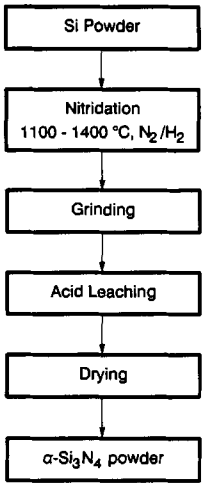

Fig. 4. Process for Si_3N_4 synthesis by direct nitridation.

After synthesis the sintered product is crushed and finally milled to the desired particle size. Depending on the powder processing, possible metallic impurities due to milling wear are removed by subsequent acid leaching.

A variation of the direct nitridation described here is the so-called SHS synthesis (self-propagating high-temperature synthesis[87-90]). Here the reaction proceeds very fast ("thermite-like") after local ignition under increased N_2 pressure.[91-95] Under these conditions the reaction zone moves with a speed of up to 0.1 $m\,sec^{-1}$ through the powder bed with temperatures often exceeding 1700 °C. The product is a high-β-phase material ($\beta > 95\%$), which requires the usual processing by milling and acid leaching.[95] So far the question whether high-β-phase Si_3N_4 powder is suitable for manufacturing advanced silicon nitride ceramics has been answered positively only sporadically;[96, 97] further investigation is required.[95] Other open questions in the further development of SHS synthesis, which may also be used for the production of other refractory compounds,[87-90, 94] concern the control of the α/β ratio and the mastery of cost-efficient, large-scale production. Whether SHS synthesis will

allow direct manufacturing of high-quality sintered components is another interesting issue.

4.3. Si_3N_4 Synthesis by Carbothermal Reduction

This method uses the reaction of SiO_2 powder with carbon at temperatures of about 1500 °C in a N_2 atmosphere, producing Si_3N_4 via a series of reactions [e.g., Eqs. (a), (l), and (m)]. The overall reaction is given by Equation (b).

$$SiO_2 + C \longrightarrow SiO + CO \quad (l)$$

$$SiO + C \longrightarrow Si + CO \quad (m)$$

$$3Si + 2N_2 \longrightarrow Si_3N_4 \quad (a)$$

$$3SiO_2 + 6C + 2N_2 \longrightarrow Si_3N_4 + 6CO \quad (b)$$

Since cheap and readily available silicate raw materials may be used, carbothermal reduction attracted early interest during the first attempts to synthesize Si_3N_4 as starting material for industrial-scale ammonia synthesis.[5-11, 98] There was no concern about chemical purity or particle morphology; reaction mixtures of quartz sand, silicates, carbon, and coke were even compounded with metal oxides to decrease the reaction temperature. Purification of the product from metallic impurities and nonreacted carbon was first achieved by acid leaching and oxidative treatment.[11]

Modern procedures ensure chemical purity by careful control of the purity levels of the starting materials. Besides high-purity, synthetic materials from pyrolysis[62] or sol–gel reactions,[63, 99, 100] natural products like quartz sand[98] and clay[101] may also be used, although at the expense of purity. Though stoichiometry requires a SiO_2/C ratio by weight of just 1:0.4 for a complete reaction, a considerable excess of carbon is required in practice. Usually, SiO_2/C ratios of 1:2 to 1:10 are employed.[62-66, 102, 103] Very good results yield extremely fine SiO_2 and C powders from, for example, gas-phase pyrolysis.[62, 103, 104] An intensive homogenization of the powders is necessary to ensure that the reaction is homogeneous and proceeds to completion. A very good alternative is provided by sol–gel-type methods, in which polycondensation of silicon halides with alcohols prone to polymerization (e.g., furfurol) yield easy-to-handle polymeric granules containing Si, O, and C in ultradisperse distribution. Thermal cracking yields an extremely homogeneous SiO_2/C mixture, which undergoes ready carbothermal reduction.[105]

Because carbothermal reduction may also proceed reversibly, CO formed in the course of the reaction has to be removed. In practice, the reaction is carried out either continuously in conveyor-type pusher furnaces or in chamber kilns, where the CO partial pressure is kept low by flowing N_2. Though Si_3N_4 formation generally increases with increasing temperature, increasing amounts of SiC, depending on CO partial pressure, are formed at temperatures exceeding 1450 °C; the SiC is practically inseparable from the Si_3N_4[65, 99, 106] (Fig. 5).

Particle size and particle morphology may be controlled by adding either crystalline spheroidal Si_3N_4 particles or Si_3N_4 whiskers as nuclei to the reaction mixture.[66] Since carbon acts also as a nucleation center for Si_3N_4 formation, its particle size influences Si_3N_4 powder characteristics as well. Very fine, high-surface carbon powders favor the formation of spheroidal Si_3N_4 particles; coarse, low-surface powders favor whisker formation.[99, 102]

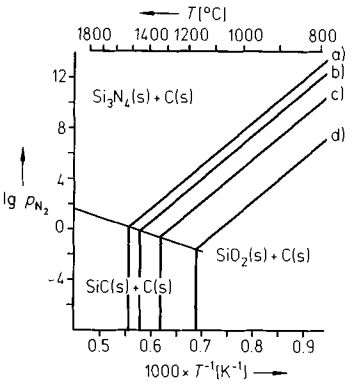

Fig. 5. Stability diagram for the system $SiC/Si_3N_4/SiO_2/C$ under varying CO partial pressures [106]. All compounds are present as solids. p_{CO}: a) 1 atm, b) 0.345 atm, c) 0.1 atm, d) 0.01 atm.

After synthesis the reaction product is milled to adjust the desired particle size and the particle size distribution (Fig. 6).

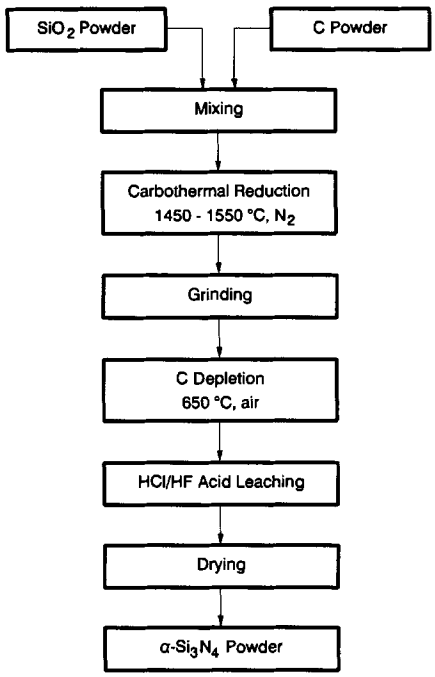

Fig. 6. Process for Si_3N_4 synthesis by carbothermal reduction.

By tempering in air,[66] NH_3, or chlorine-containing atmospheres[107, 108] at temperatures in the range of 600–800 °C excess carbon is removed. If required, incompletely reacted SiO_2 may be removed by HF leaching.

4.4. Ammonolysis of Reactive Silicon Compounds

4.4.1. Si_3N_4 Synthesis by Liquid-Phase Reaction of $SiCl_4$ and NH_3

The work on the liquid-phase reaction of $SiCl_4$ and NH_3 dates back to 1830, when *Persoz*[109] isolated a white precip-

itate, which he considered to be silicon tetraamide, $Si(NH_2)_4$. Subsequently, however, this precipitate was identified as silicon diimide, $Si(NH)_2$.[67-69, 110-114] Though this reaction may be described in its most simple form by Equation (e), further investigation showed a very complex

$$SiCl_4 + 6NH_3 \longrightarrow Si(NH)_2 + 4NH_4Cl \quad (e)$$

process, which led to differently polymerized, extremely moisture-sensitive $[Si(NH)_2]_x$.[112] Subsequent high-temperature pyrolysis leads to stable, processable α-Si_3N_4 via several intermediates and amorphous Si_3N_4 accompanied by NH_3 or N_2/H_2 liberation [Eq. (n)].[67-69, 112-117] The transformation of amorphous silicon nitride to crystalline α-Si_3N_4 proceeds above 1200 °C in a diffusion-controlled manner with an activation energy of 306 kJ mol^{-1}.[118]

$$\frac{3}{x}[Si(NH)_2]_x \xrightarrow{1200-1400\,^\circ C} \alpha\text{-}Si_3N_4 + N_2 + 3H_2 \quad (n)$$

It is remarkable that NH_4Cl still present from the $SiCl_4/NH_3$ reaction [Eq. (e)] influences the $Si(NH)_2$ pyrolysis.[115] In the absence of NH_4Cl, $Si(NH)_2$ is stable to 200 °C; it gradually loses NH_3 with increasing temperature, until finally amorphous Si_3N_4 is formed. However, thermal decomposition in the presence of NH_4Cl results in reaction of $Si(NH)_2$ and HCl to give a compound of the composition $Si_2N_3H_2Cl$, which decomposes to amorphous silicon nitride above 800 °C.

Pyrolysis of $Si(NH)_2$ at temperatures below 1200 K leads to the formation of an extremely fine, moisture-sensitive, amorphous Si_3N_4 powder showing primary particle sizes of about 10–30 nm and BET surfaces greater than 100 m^2 per g. Prolonged heating at temperatures of 1200 to 1400 °C induces crystallization of α-Si_3N_4 accompanied by particle coarsening. At temperatures exceeding 1500 °C mainly β-Si_3N_4 is formed.[69] Particle morphology, particle size, and α/β ratio are influenced by temperature, retention time, and impurities.[119, 120]

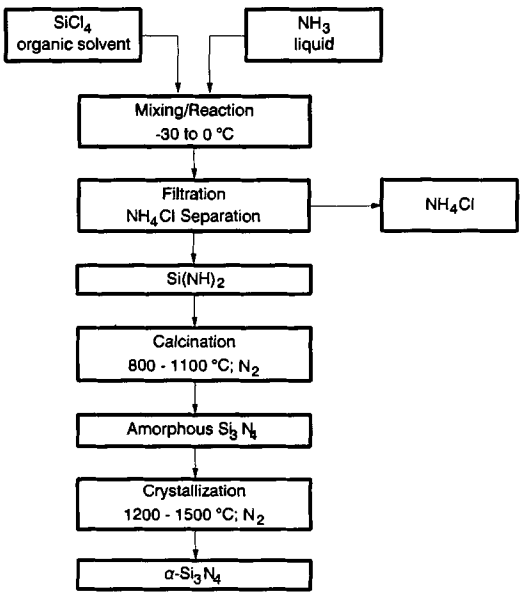

Fig. 7. Process for Si_3N_4 synthesis by $SiCl_4/NH_3$ liquid-phase reaction.

Since $SiCl_4/NH_3$ liquid-phase reaction allows the synthesis of a very pure and fine Si_3N_4 powder from easily purified and readily available starting materials, this method (often referred to as the *diimide process*) has been developed on a pilot scale (Fig. 7). The $SiCl_4/NH_3$ reaction is carried out in a two-phase system consisting of an organic solvent and liquid NH_3[72, 116, 117, 121] or by reacting $SiCl_4$ vapor with excess liquid NH_3,[122] thus dissolving the by-product NH_4Cl. The $Si(NH)_2$ precipitate is filtered and washed with liquid ammonia to remove residual NH_4Cl and finally calcined and crystallized to give α-Si_3N_4. In contrast to thermal NH_4Cl separation by sublimation, this procedure offers the technological advantage that no corrosive NH_3/HCl vapors are generated. However, upscaling has to take into consideration the large amount of NH_4Cl by-product, generated according to Equation (o). An economically favorable and ecologically safe application or disposal has yet to be found for this by-product.

$$3SiCl_4 + 16NH_3 \longrightarrow Si_3N_4 + 12NH_4Cl \quad (o)$$

4.4.2. Si_3N_4 Synthesis by Gas-Phase Reactions of $SiCl_4$ or SiH_4 with NH_3

Owing mainly to homogeneous nuclei formation, gas-phase reactions have a great potential for the production of extremely fine powders.[123] After formation and growth of nuclei in the reaction zone, particles cluster to aggregates and agglomerates, which may be separated as fine dust (Fig. 8).

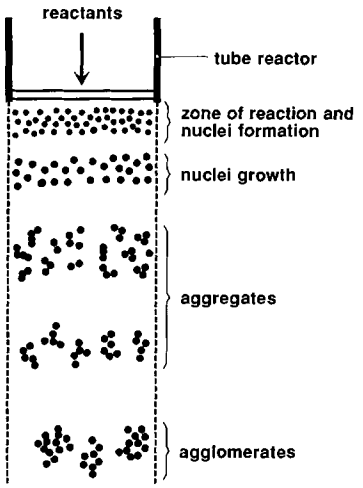

Fig. 8. Particle formation in gas-phase reactions [123].

For economical and technical reasons gas-phase reactions of $SiCl_4$ or SiH_4 with NH_3 are of special interest. From a technological point of view the use of cheap $SiCl_4$ requires the separation of the corrosive NH_4Cl by-product through either hot-gas filtration, extraction, or sublimation. Because of spontaneous ignition of SiH_4 in contact with air, however, the use of expensive SiH_4 requires extensive safety precautions. A technological advantage, though, is the formation

of hydrogen as gaseous by-product, which is easily separated. If $SiCl_4$ is used, reaction parameters may be adjusted to approach the stoichiometry of the reaction [Eq. (p)], thus

$$SiCl_4 + 2NH_3 \longrightarrow Si(NH)_2 + 4HCl \qquad (p)$$

keeping the amount of solid NH_4Cl by-product low compared to the corresponding liquid-phase reaction. Instead of using expensive pressure vessels, gas-phase reactions are run at atmospheric pressure in heated tube reactors (Fig. 9). Similar to industrial-scale synthesis of SiO_2 and TiO_2 powders, these reactions represent a good technological basis for a continuous, large-scale production of fine powders. As liquid-phase reactions, $SiH_4/SiCl_4$-NH_3 gas-phase reactions also yield amorphous Si_3N_4 precursors because of the short retention times of gas and particle streams in the hot reaction zone. These amorphous precursors have to be crystallized separately in a subsequent step.

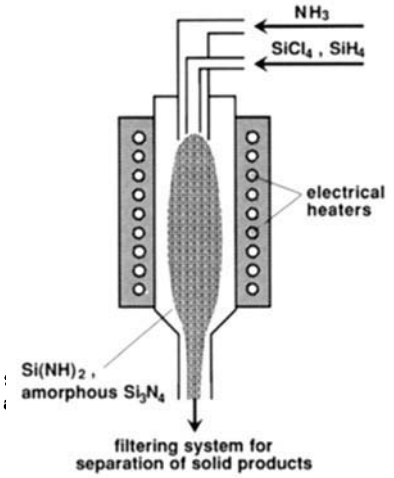

Fig. 9. Setup of a gas-phase reactor for the synthesis of Si_3N_4 from $SiCl_4$ and NH_3.

The reaction of SiH_4 and NH_3 in the temperature range of 500–900 °C yields amorphous powders with particle sizes of 30–200 nm and BET surfaces up to 26 $m^2 g^{-1}$.[70, 71] Our investigations on $SiCl_4/NH_3$ gas-phase reactions at temperatures of 300–1700 °C showed the formation of extremely fine, spheroidal and amorphous particles with BET surfaces up to 300 $m^2 g^{-1}$.[124, 125] Crystallization of these precursors induces particle coarsening; thus, the BET surface may be adjusted in the range of 2–20 $m^2 g^{-1}$.[70, 125]

Strict control of impurities, temperature, and retention time is important for the generation of very fine, uniform, high-α-phase Si_3N_4 particles by crystallization of amorphous Si_3N_4 (Fig. 10). The powders from $SiCl_4/NH_3$ gas-phase reactions require significantly less processing (Fig. 11) than products from direct nitridation or carbothermal reduction because of their inherent fine particle size and weak agglomeration. They are characterized by high chemical purity, good manufacturing properties, and high sintering activity.

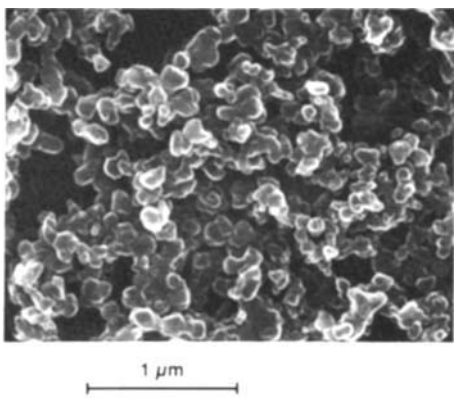

Fig. 10. α-Si_3N_4 powder by crystallization of amorphous Si_3N_4 from $SiCl_4/NH_3$ gas-phase reaction.

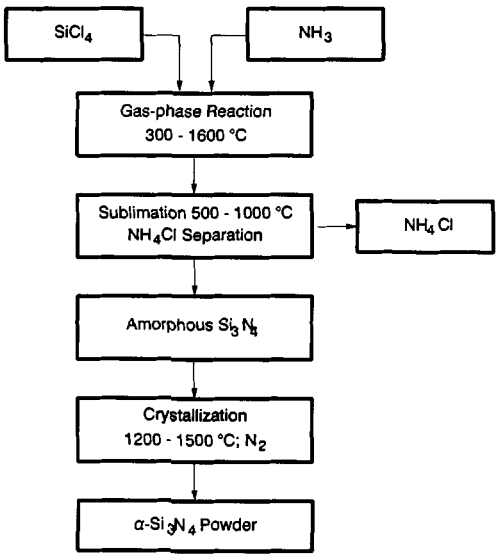

Fig. 11. Process for Si_3N_4 synthesis by $SiCl_4/NH_3$ gas-phase reaction.

4.5. Si_3N_4 Synthesis by Laser-Induced and Plasmachemical Reactions

The work on laser-induced[126–129] and plasmachemical reactions[130–134] as alternatives to "usual" thermal gas-phase reactions tries to avoid any heterogeneous nuclei formation due to contact of the reacting gases with hot reactor walls; thus, an extremely high degree of particle fineness and uniformity is guaranteed. Characteristic properties of both processes, which are based on chemical reactions already described above, are extremely fast heating and cooling rates of about 10^5 to 10^6 $K s^{-1}$ and fast reaction rates on the order of about 10^{-3} s. Figures 12 and 13 show experimental setups for laser-induced and plasmachemical Si_3N_4 synthesis from reactions of SiH_4 or $SiCl_4$ with NH_3. Particle size, crystallinity, α/β ratio, and stoichiometric composition of the reaction product are influenced by mass flow, pressure, stoichiometric ratio of reactants, and laser or plasmagenerator power output. A major problem of laser-induced synthesis is the small reaction diameter of the laser beam, which allows only product formation rates on the order of just a few grams per hour. Because of the extreme temperatures of several

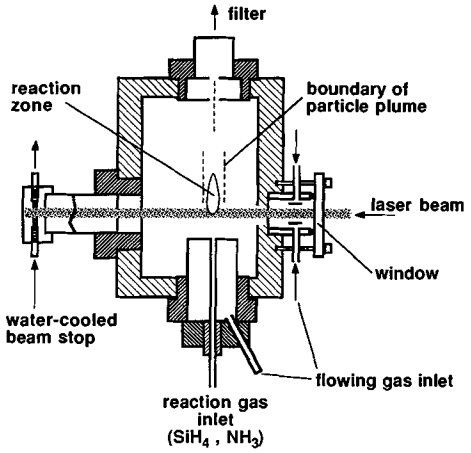

Fig. 12. Reactor for laser-induced Si_3N_4 synthesis from SiH_4 and NH_3 [126].

thousand K in plasmachemical reactions, the reactants are broken apart to different radicals, which may recombine in various ways in the temperature gradients of the reaction zone. Since fluid dynamics is also very important, it is very difficult to control the reaction precisely. Both laser-induced

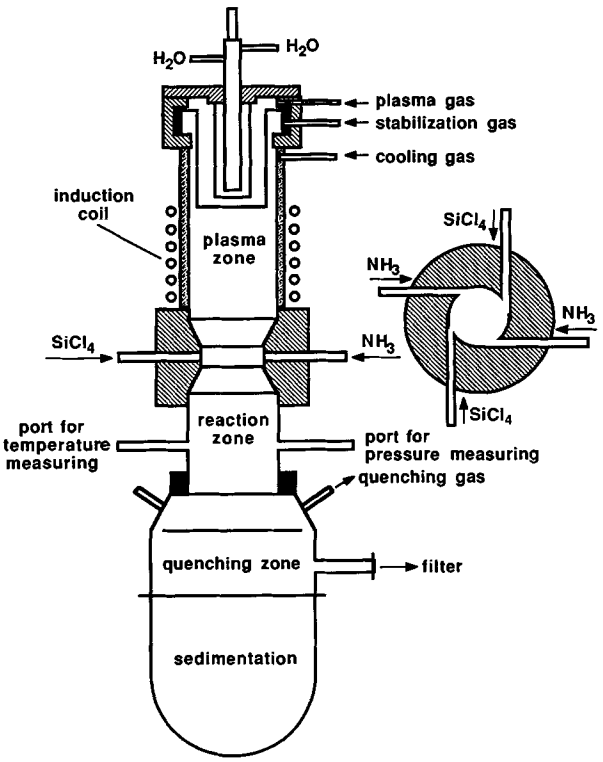

Fig. 13. Reactor for plasmachemical synthesis of Si_3N_4 from $SiCl_4$ and NH_3 [133].

and plasmachemical synthesis allow the generation of extremely fine powders with particle sizes of just 10–30 nm and BET surfaces greater than $100\,m^2g^{-1}$. However, the products often show incorrect stoichiometric composition, are amorphous, or possess changing, not exactly reproducible α/β ratios. Furthermore, they may contain free silicon as an undesired by-product from decomposition reactions. Because of these difficulties, laser-induced and plasmachemical reactions are not yet of importance to large-scale synthesis of Si_3N_4 powders, despite intense research.

5. Silicon Nitride Whiskers

After the discovery that crystal whiskers show unusual mechanical strength,[135] interest in the properties, production, and applications of ceramic whiskers grew.[136, 137] The use of whiskers to reinforce metallic or ceramic materials aims at improving fracture toughness or, more generally, mechanical properties of the matrix material. In spite of the strong general interest in ceramic whiskers, there are still problems in producing pure and uniform whiskers on a large scale in an economical way. The development of whisker production and processing methods especially has to take into account health precautions in order to exclude a potential hazard like that arising from asbestos fibers.[138, 139]

Chemically, the same methods as in the synthesis of spheroidal Si_3N_4 powder particles are used for the production of Si_3N_4 whiskers. However, additional measures are required in order to apply general techniques like vapor-phase transport or crystallization by vapor-liquid-solid (VLS) mechanisms to favor whisker formation.

5.1. Whiskers from the Reaction of Si and N_2

In direct nitridation of elemental silicon, Si_3N_4 whiskers are formed by reaction of silicon vapor and N_2. Figure 14 shows a simple experimental setup for this production method. Silicon is evaporated from a crucible at the bottom;

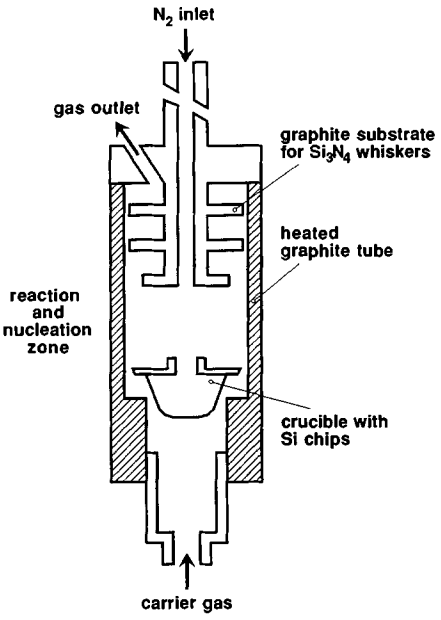

Fig. 14. Reactor for Si_3N_4 whisker synthesis from a Si/N_2 gas-phase reaction [140].

a stream of inert carrier gas is used to guide the Si vapor into a reaction zone in the upper part of the apparatus where it reacts with N_2 or NH_3. The Si_3N_4 whiskers precipitate onto graphite baffles from where they may be collected.

5.2. Whiskers from Carbothermal Reduction of SiO_2

This process, which may be run continuously in conveyor-type pusher furnaces, yields whiskers from the gas-phase reaction of SiO and N_2 or NH_3 in CO-containing atmospheres.[141-143] By adjusting stoichiometry, particle size, homogeneity, and packing density of the reaction mixture of silica and carbon raw materials, addition of silicon or metal oxides, and control of the reaction temperature, the amount of SiO generation and, consequently, Si_3N_4 whisker formation is optimized. Whisker formation is also favored if Si_3N_4 whiskers are added to the reaction mixture as growth nuclei.[143]

5.3. Whiskers from the Reaction of $SiCl_4$ with NH_3

As described above, the reaction of $SiCl_4$ with NH_3 leads to $Si(NH)_2$, which yields amorphous Si_3N_4 on calcination. If small amounts of Fe or SiO_2 are added to this material and the resulting mixture is heated to 1200–1500 °C in the absence of oxygen, Si_3N_4 whiskers are formed by a vapor-liquid-solid mechanism from Fe- or silicate-containing eutectic melt droplets[72, 143] (Fig. 15).

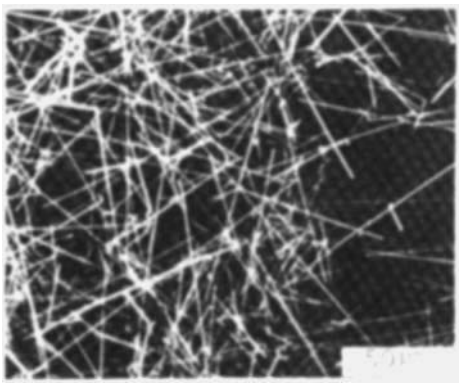

Fig. 15. α-Si_3N_4 whiskers by crystallization of amorphous Si_3N_4 [72].

5.4. Whiskers from the Reaction of SiS_2 with NH_3

Originally intended to produce high-purity Si_3N_4 powder, the reaction of SiS_2 with NH_3 offers a good way to produce Si_3N_4 whiskers.[73-75] In the first step, SiS_2 is synthesized by reaction of Si powder with H_2S at high temperature [Eq. (q)].

$$Si + 2H_2S \xrightarrow{900\,^\circ C} SiS_2 + 2H_2 \qquad (q)$$

The high vapor pressure of SiS, which forms on dissociation of SiS_2, leads to SiS_2 whisker growth by a VLS mechanism from eutectic droplets of SiS and sulfur vapor. Reaction of SiS_2 with NH_3 affords a $(Si\text{-}S\text{-}N\text{-}H)_x$ polymer, which thermally decomposes under NH_3 to amorphous silicon nitride [Eqs. (r) and (s)]. The amorphous silicon nitride is obtained in "spaghetti-like" morphology (Fig. 16) and may be crystallized to α-Si_3N_4 with retention of morphology.

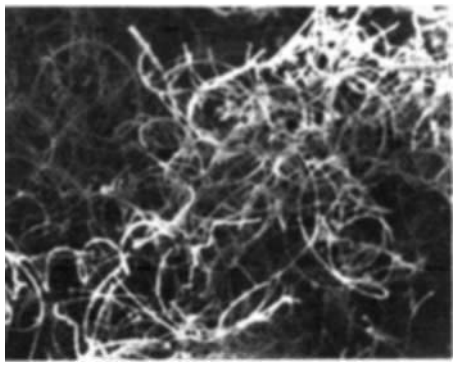

Fig. 16. Amorphous Si_3N_4 "spaghetti" from thermal decomposition of $(Si\text{-}S\text{-}N\text{-}H)_x$ polymers [74].

$$SiS_2 \xrightarrow[\text{ca. } 25-900\,^\circ C]{NH_3} (Si\text{-}S\text{-}N\text{-}H)_{polymer} \qquad (r)$$

$$(Si\text{-}S\text{-}N\text{-}H)_{polymer} \xrightarrow[900-1500\,^\circ C]{NH_3} Si_3N_4 \text{ (amorphous, crystalline)} \qquad (s)$$

5.5. Whiskers from the Reaction of SiC and NH_3

The reaction of SiC with NH_3 is remarkable since it leads to Si_3N_4 particles of unusual morphology. By heating a mixture of SiC and Fe powder in NH_3 to 1440 °C followed by a short-term temperature rise to 1480 °C, *Glemser* und *Horn*[76] obtained spiral-shaped α-Si_3N_4 whiskers (Fig. 17, left). Some of these spirals could be seen with the naked eye.

Recently, similar observations have been made in the investigation of vapor-phase deposition of Si_3N_4 from Si_2Cl_6,

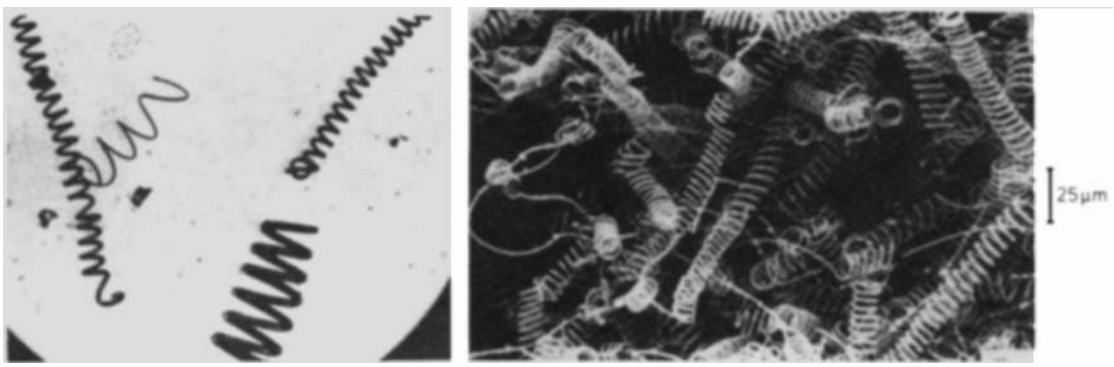

Fig. 17. Left: α-Si_3N_4 spirals from the reaction of SiC and NH_3 in presence of Fe [76]. Right: α-Si_3N_4 spirals by vapor-phase deposition from a mixture of Si_2Cl_6, NH_3, and H_2 onto a Fe-coated graphite substrate [144].

NH_3, and H_2 at 1200 °C onto a graphite substrate coated with Fe-containing compounds.[144, 145] The spiral-shaped whiskers (Fig. 17, right) are about 0.5–1.0 μm thick and consist of α-phase Si_3N_4 slightly contaminated by carbon and oxygen. They show a quite uniform morphology with a regular pitch of 3–5 μm, a spiral diameter of 5–10 μm, and a length of 50–100 μm. Obviously, spirals are formed only in a narrow fiber-diameter range of about 0.1–5 μm.

5.6. Properties of Si_3N_4 Whiskers

Some properties of commercially available Si_3N_4 whiskers are shown in Table 1. The principal problems in whisker production are the requirements of high chemical purity and uniform whisker morphology. Because of technological difficulties in producing a homogeneous distribution of Si_3N_4 whiskers in a matrix material, fracture-causing structural defects are often induced during material processing; in these cases, the originally intended toughening of the matrix actually turns out to be a weakening.[146, 147] Fundamental problems in whisker processing are often connected with shaping and sintering, since heaps of needlelike particles are much more difficult to compact by, say, dry pressing than heaps of spheroidal particles.

Table 1. Properties of commercially available Si_3N_4 whiskers.

Product	Tateho SNW [a]	Ube SN-W [b]
Synthetic method	carbothermal reduction	from amorphous Si_3N_4
Crystal phase	α	α
Diameter *d*	0.1–1.6 μm	0.1–0.4 μm
Length *l*	5–200 μm	5–20 μm
Aspect ratio *l*/*d*	3–2000	10–200
Density	3.18 $g cm^{-3}$	3.18 $g cm^{-3}$
Fe	max. 1000 ppm	4000–5000 ppm
Al	max. 2000 ppm	<100 ppm
Ca	max. 5000 ppm	<100 ppm
Mg	max. 2000 ppm	not specified
O	not specified	2–3%

[a] Tateho Chem. Ind., Japan [143]. [b] Ube Ind., Japan [72].

6. Remarks on the Procedures for Synthesis of Si_3N_4 Powders

A comparison of chemical and physical characteristics of powders from commercially used synthetic methods shows that direct nitridation, carbothermal reduction, and ammonolysis of reactive silicon compounds are principally able to furnish very fine, high-purity Si_3N_4 powders for applications in advanced ceramics (Table 2). Often variations of particle sizes, particle size distribution, and particle surface properties, which are important to ceramic processing, may be carried out after Si_3N_4 synthesis by suitable powder processing. Direct nitridation and carbothermal reduction use cheap raw materials and yield crystalline Si_3N_4 directly. However, the reaction products require extensive subsequent processing. On the other hand, ammonolysis of reactive silicon compounds yields moisture-sensitive products which require further thermal treatment for crystallization to yield α-Si_3N_4. Because of their inherent fine particle size and only weak particle agglomeration, the extent of subsequent powder processing is considerably reduced compared with direct nitridation and carbothermal reduction. Direct nitridation and $SiCl_4/NH_3$ gas-phase reactions seem to offer the best chances to furnish economically high-quality powders for the manufacturing of broadly applicable silicon nitride ceramics.

Table 2. Comparison of high-purity Si_3N_4 powders from different synthetic methods.

Powder type	DN 1 [a]	DN 2 [b]	GP [c]	FP [d]	CT [e]
Elemental analysis [wt %]					
N	38.2	38.2	38.5	>38.0	37.5
O	1.8–2.1	1.7–2.0	1.1–1.6	<2.0	2.0
C	<0.2	<0.2	<0.05	<0.2	0.9
Cl	<0.001	<0.001	<0.1	<0.01	[f]
Fe	<0.008	<0.03	<0.01	<0.01	0.007
Al	<0.005	<0.06	<0.004	<0.005	0.2
Ca	<0.002	<0.01	<0.002	<0.005	0.01
α-Si_3N_4	>92%	>94%	>90%	>95%	98%
Mean particle size d_{50} [μm]	0.6	0.8	0.5	0.5	0.9

[a] DN 1 = direct nitridation (LC 12 – SX, H. C. Starck, Berlin). [b] DN 2 = direct nitridation (LC 10, H. C. Starck, Berlin). [c] GP = $SiCl_4/NH_3$ gas-phase reaction (Grade GP, H. C. Starck, Berlin). [d] FP = $SiCl_4/NH_3$ liquid-phase reaction (SN E 10, Ube Ind., Tokyo). [e] CT = carbothermal nitridation (A 200, Toshiba Ceramics, Tokyo). [f] Not determined.

The production of Si_3N_4 whiskers is not yet commercially important, since Si_3N_4 whisker-reinforced materials have not found broad applications because of high costs and a lack of large-scale production methods for reliable components. For technological and economical reasons, especially carbothermal reduction and whisker growth from amorphous Si_3N_4 should be suited best to meet an eventually increasing demand.

7. The Manufacture of Sintered Si_3N_4 Ceramics

7.1. Fundamentals of Sintering and Structure Development

7.1.1. Physical and Chemical Aspects of Si_3N_4 Sintering

"Dry" sintering techniques used in densification of oxide ceramics cannot be applied to the sintering of Si_3N_4 powder compacts. Strong covalent Si–N bonds hinder useful mass transport through grain-boundary or lattice diffusion. The activation of diffusion by simply raising the sintering temperature is limited by ever-increasing thermal decomposition [Eq. (t)].

$$Si_3N_4\ (solid) \longrightarrow 3Si\ (liquid) + 2N_2\ (gas) \longrightarrow 3Si\ (gas) \qquad (t)$$

Since a N_2 partial pressure of 1 bar is reached at about 1900 °C, several precautions have to be taken in order to prevent excessive decomposition during sintering of Si_3N_4 at high temperatures. Most important is the addition of com-

pounds that form molten silicate phases and allow densification by liquid-phase sintering mechanisms. Well-suited additives include alkaline-earth oxides and rare-earth oxides either alone or in combination with Al_2O_3 or AlN.[148-152]

Above 1300 °C sintering additives react with SiO_2 or Si_2N_2O always present in Si_3N_4 powders to yield molten silicate phases. In the case of sufficient wetting and solubility of Si_3N_4, these silicate melts allow densification by capillary-force-induced particle rearrangements and dissolution/reprecipitation processes.

The efficiency of these mechanisms is illustrated by a model experiment using a presynthesized, nitrogen-saturated Mg-Al silicate glass as sintering additive (Fig. 18). At

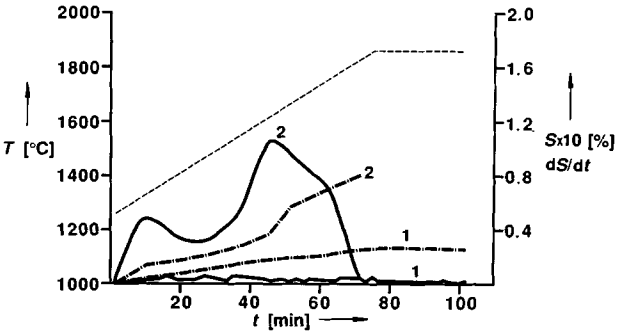

Fig. 18. Dilatometric investigation of Si_3N_4 sintering in the absence (1) and presence (2) of a nitrogen-saturated glass [153]. Temperature ----, dS/dt ——, shrinkage S -·-·-·-·-, dS/dt in [% min^{-1}].

1300 °C dilatometric monitoring of the process shows densification by capillary-force-induced particle rearrangement, since nitrogen saturation of the silicate glass does not allow further dissolution of N_2 or Si_3N_4. With increasing temperature Si_3N_4 solubility increases and densification via dissolution/reprecipitation is observed. A Si_3N_4 sample without sintering additives shows a completely unsatisfactory densification.

Another important precaution is sintering under high N_2 pressure to suppress decomposition according to Equation (t). Figure 19 shows that this technique significantly extends the temperature range of Si_3N_4 sintering.

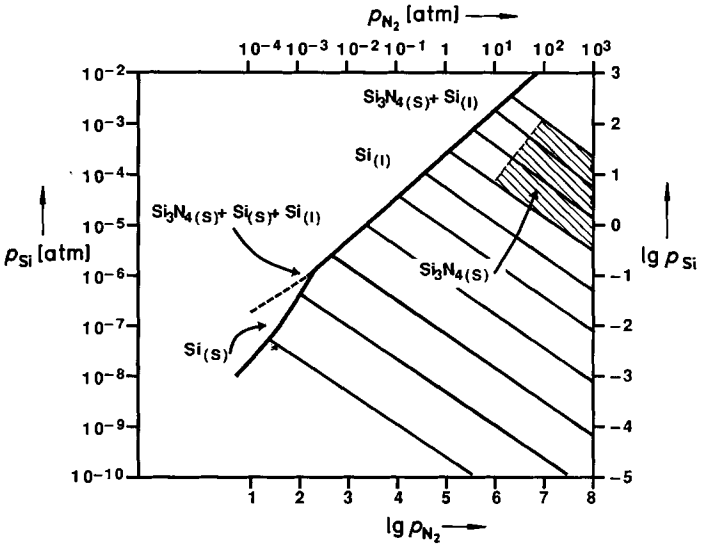

Fig. 19. Silicon vapor pressure in equilibrium with silicon nitride as a function of N_2 pressure and temperature [149]. The bold lines show temperature intervals of 100 K from 1300 °C to 2200 °C. The hatched region represents the range where sintering of Si_3N_4 takes place. The pressures were measured in Pa.

7.1.2. Structure Development

After particle rearrangement at low temperatures, which increases the packing density almost without influencing particle shape and particle size distribution, true sintering by dissolution/reprecipitation occurs at higher temperatures. At present, structure development is thought to depend on the kind of Si_3N_4 starting powder. Starting from α-Si_3N_4, reprecipitation of dissolved α-Si_3N_4 from almost saturated or slightly oversaturated solutions leads to crystallization of needle- or rodlike β-Si_3N_4 grains far from the energetic minimum.[154] Since a fine-grained, needlelike structure has a positive influence on fracture-mechanical properties ("in-situ whisker reinforcement") for numerous applications, this grain morphology is desired.[155, 156]. If β-Si_3N_4 powder is used, dissolution/reprecipitation occurs almost in equilibrium. The surface energy difference between small and large particles causes a continuous dissolution of small particles and their reprecipitation on large grains. This process allows grain growth with minimization of boundary surface energy

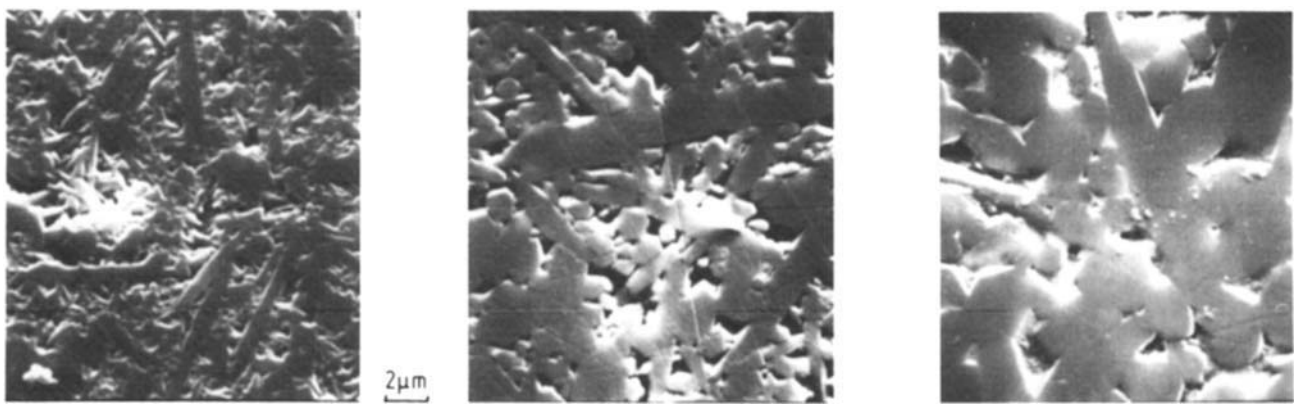

Fig. 20. Structure development in sintering of a Y_2O_3/Al_2O_3-doped Si_3N_4 powder [158]. Left: 1800 °C (10 min). Middle: 1800 °C (2 h), then 1820 °C (2 h). Right: 50 sintering cycles (see middle for conditions). Additives: 15 wt% Y_2O_3 + 3.4 wt% Al_2O_3.

leading to the development of approximately globular grains.[157]

Prolonged thermal treatment, far beyond the moment when densification is complete, favors grain growth by minimization of boundary energy ("Ostwald ripening") also in needle-grained structures and leads to grain coarsening with growth of spheroidal grains. In this case, structural development leads to the formation of globular grains, no matter whether α- or β-Si_3N_4 has been used as starting material. A study on structure development on prolonged heat treatment of α-phase Si_3N_4 is shown in Figure 20.

After sintering, all these materials contain an amorphous or semicrystalline secondary phase in between grain boundaries or in grain triple points (Fig. 21). Since especially

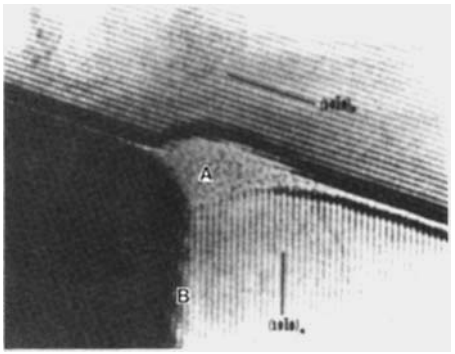

Fig. 21. Transmission electron microscopy (TEM) of amorphous secondary phase along grain boundaries in sintered Si_3N_4 [159]. The black lines show the direction $(10\bar{1}0)_\alpha$, A a grain triple point, B a grain boundary.

material properties at high temperatures are greatly influenced by the secondary phase, the reduction, modification, or complete elimination of this phenomenon is of major importance to the optimization of Si_3N_4 ceramic properties.[160]

7.1.3. Influence of Sintering Additives

The amount and chemistry of the molten silicate phase, which is formed by sintering additives, are of importance to the course of sintering, since they determine sintering kinetics. For example, the kinetics of MgO-doped systems are governed by dissolution, whereas the rate of diffusion is crucial in Y_2O_3-doped materials.[161] The influence of typical additives on sintering behavior is shown in Figure 22. For instance, the densification of Y_2O_3-doped Si_3N_4, which sinters at relatively high temperatures, may proceed at the low temperature level of ($MgO + Al_2O_3$)-doped materials if Al_2O_3 is added.

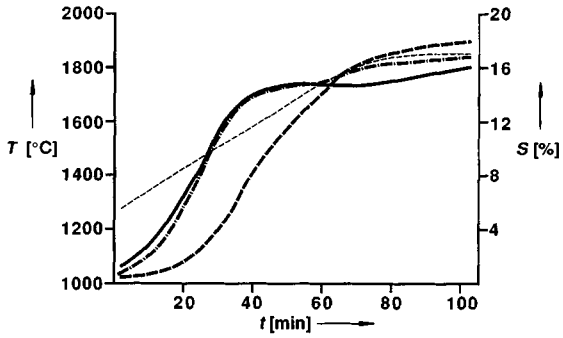

Fig. 22. Influence of type of additives on sintering behavior. ---- temperature, —— $MgO + Al_2O_3$, — • — $Y_2O_3 + Al_2O_3$, — — — Y_2O_3, S = shrinkage.

Different additive systems may form compounds of the type α'-$Me(Si,Al)_3(N,O)_4$ or β'-$Si_{6-x}Al_xO_xN_{8-x}$ with newly precipitated Si_3N_4 grains.[162, 163] The expectation that Si_3N_4 ceramics free of secondary grain-boundary phases can be produced by using this principle has only been fulfilled for Be-doped materials.[149, 160]

The amount and kind of additives also influence structure development and thus material properties. Fine-grained Si_3N_4 structures are favored in systems where the molten silicate phase shows a relatively high viscosity at sintering temperatures (e.g., systems doped with rare-earth oxides). The influence of additives is especially clear in the structure development of β'-SiAlON materials, where globular grains are favored. Figure 23 shows a comparison of these materials with a material sintered with MgO/Al_2O_3, which developed a needlelike structure. The exact reasons for this behavior are not yet completely understood.

7.1.4. Influence of Powder Characteristics

Besides the kind and amount of additives, the sintering behavior, structure development, and, finally, material properties depend strongly on the powder characteristics of the starting Si_3N_4 powder. Of further importance are the powder properties resulting from processing prior to shaping and sintering; in particular, it is necessary to break up particle agglomerates and to produce a homogeneous distribution of sintering additives. Relevant powder properties can be divid-

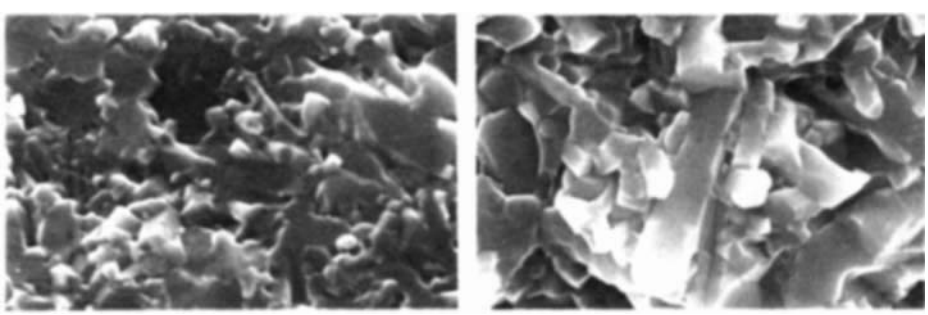

Fig. 23. Left: Globular structure in a β'-Si-Al-O-N material; right: needle-type structure in a MgO/Al_2O_3-doped material.

ed into physical, chemical, and technical characteristics, which together determine processing behavior and sintering activity in a complex way.

The influence of α/β-Si_3N_4 ratio has already been mentioned and is still a subject of intensive discussion.[54, 124, 155, 164, 165] A high α-phase content enhances sintering activity and favors the development of rodlike β-Si_3N_4 grains. With respect to sintering activity, amorphous Si_3N_4 would be of even greater advantage. However, its large-scale use is complicated owing to its sensitivity towards hydrolysis and its low powder-packing density, which results in enormous shrinkage during sintering.

Among chemical powder characteristics, the oxygen content is of special importance, since it influences the softening behavior and the amount and viscosity of the silicate phase formed on reaction with sintering additives. Although a great amount of low-viscosity silicate melt phase enhances sintering, it has a negative effect on the high-temperature properties of the material if the silicate phase remains as an amorphous, glassy grain-boundary phase. Thus, the oxygen content has to be adjusted to the amount of sintering additives required (or vice versa); it is a compromise between beneficial effects on sintering behavior and detrimental effects on high-temperature material properties. Usually, commercially available powders possess an oxygen content in the range of 1–2%.

Also the distribution of oxygen in the particle itself is of importance. If oxygen is concentrated on particle surfaces, it is directly available for silicate phase formation by reaction with sintering additives. In this way, surface oxygen improves sintering activity considerably.[166, 167] Therefore, high-quality Si_3N_4 powders usually possess oxygen-enriched particle surfaces, which allow fine-tuning of the amount of sintering additives required for complete densification and thereby result in improved material properties. The coating of a Si_3N_4 particle with an amorphous layer rich in oxygen is shown in Figure 24.[168]

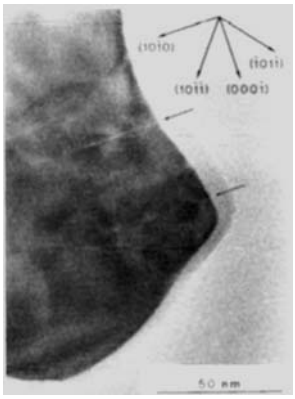

Fig. 24. TEM picture of the coating of a Si_3N_4 particle with an amorphous layer rich in oxygen [168]. Beam direction ($\bar{1}2\bar{1}0$). The arrows indicate Schottky partial dislocations.

Free carbon has a negative influence on sintering behavior, since it reduces the oxygen content of the powder with formation of volatile SiO and CO. The resulting ill-defined variations in silicate phase chemistry may cause incomplete sintering, undesired structure development, and, finally poor material properties.[153, 169] Chemically bonded carbon in the form of SiC is much less critical. Because of its inherent stability, this material may be considered as inert filler.[108, 147] The effects of other impurities have to be judged by their behavior in sintering; they may dissolve in the liquid phase with incorporation in the silicate structure or they may remain as particle inclusions with or without reaction with the Si_3N_4 matrix. Metal oxides and metal halides either evaporate during sintering or dissolve in the liquid phase, lowering its viscosity with the already discussed effects on sintering behavior, structure development, and material properties.

Metal particles like Fe, Mn, and Ti react with the Si_3N_4 matrix to form silicides or nitrides.[170] Compared to original particle sizes, inhomogeneities due to chemical reactions are larger[170] and thus generally detrimental to mechanical properties like fracture strength (Fig. 25).

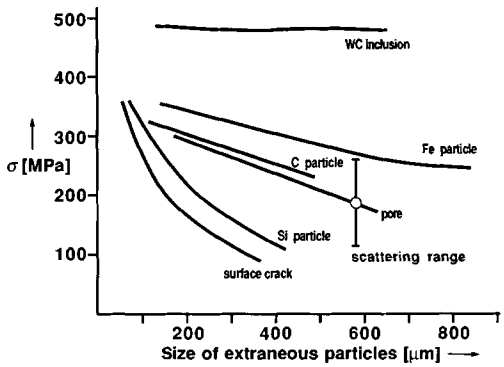

Fig. 25. Dependence of fracture stress σ on size of extraneous particles in Si_3N_4 sintered ceramics [171].

Granulometric powder properties, which involve particle size distribution, particle morphology, and particle agglomeration, influence processing behavior and the extent of powder processing required to produce an admixture of high sintering activity. Since sintering activity increases with increasing surface energy, "sub-μm" powders with a high content of particles less than 1 μm are advantageous. The amount of "coarse grains" attracts special attention, since these particles will dissolve in the silicate phase comparatively slowly. Therefore, sintering is slowed down and some particles may survive more or less unchanged to form structure inhomogeneities.

Whisker- or fiberlike Si_3N_4 particles cause similar effects, additionally making powder shaping more difficult. "Coarse grains" greater than 1 μm, as well as deviant particle morphologies, usually are not destroyed during powder processing to generate the sintering admixture. Powder processing has to guarantee that agglomerates of primary crystallites, which are principally present, are broken apart, since their size and the lack of sintering additives in their cores would induce very large defects and thus limit strength and reliability of the sintered component. Furthermore, the size and hardness of these agglomerates determine dispersibility and homogeneity of the sintering admixture; these properties are very important quality criteria. A qualitative and quantitative description of agglomeration mechanisms and agglom-

erate properties is steadily gaining importance as a goal of research.[172]

The shape—sharp-edged to spheroidal/globular—and the size distribution of primary crystallites determine also the limits of densification and the extent of sintering shrinkage. Green densities (i.e., the densities of the powder-shaped bodies prior to sintering) must be as high as possible to reduce the danger of critical tensions due to high shrinkage; these tensions would otherwise lead to cracks and fissures during temperature treatment.

Physical, chemical, and technological powder properties have a complex influence on sintering behavior, structure development, and final material properties. The relative influence of a single powder property may be estimated by means of statistical calculations.[167, 171]

7.2. Technological Aspects

7.2.1. Powder Processing

The processing of a Si_3N_4 powder to a highly sintering active admixture aims at breaking up particle agglomerates and distributing homogeneously the sintering additives. Wet processing in mills of high-energy density is well-suited for this purpose. However, attention has to be paid to the kind and amount of wear debris from these machines. Oxygen contamination due to partial hydrolysis of Si_3N_4 and carbon contamination are important if processing is done in either water- or organic-solvent-containing media. The extent of processing depends on starting powder quality, the desired powder shaping and sintering techniques, and the material property profile of the component to be manufactured. Since powder characteristics may vary considerably during processing, rigorous controls are necessary to ensure the highest possible uniformity of processing from lot to lot.

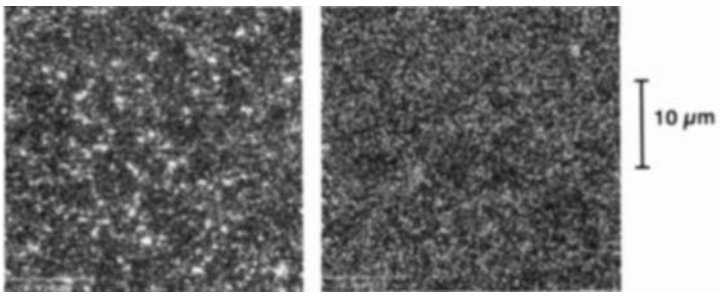

Fig. 26. Y distribution in Y_2O_3-doped Si_3N_4 sintering powder admixture. Left: By mechanical dispersal of Y_2O_3. Right: By precipitation of $Y(OH)_3$.

Extremely homogeneous distribution of sintering additives may be achieved far better by precipitation from solution than by intensive mechanical dispersion. Here, codrying of salt solutions and Si_3N_4 slips[153] has been investigated as well as precipitation of hydroxides from salt solutions[173] and precipitation by hydrolysis of metal alcoholates.[174, 175] Figure 26 shows that this approach leads to extremely homogeneous additive distributions.

7.2.2. Powder Shaping

Axial or isostatic dry pressing, extrusion, slip casting, or injection molding is used for powder shaping (Fig. 27). These procedures are well-known to the ceramic industry. Selection criteria depend on component complexity, on economics and, if required, on the feasibility of large-scale production. Dry pressing is used mainly for the production of

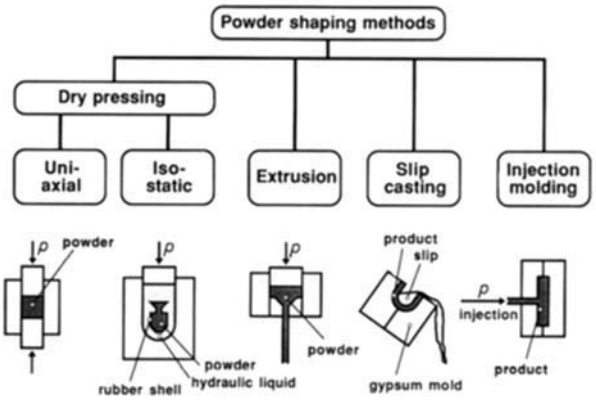

Fig. 27. Ceramic powder shaping methods. p = pressure.

components with simple geometry like plates, tubes, or cylinders. Slip casting and injection molding are favored to produce net-shape components of complex geometry on a large scale. All shaping techniques require certain, usually organic, processing additives. Binders ensure the stability of powder compacts in dry pressing, dispersion agents allow the production of highly particle-loaded, stable slips for slip casting, and plasticizers allow injection molding. Since especially injection molding promises an economical, large-scale production of complex components, its development has attracted worldwide attention.[176–178] All organic additives have to be burned out quickly and quantitatively prior to sintering without inducing defects like pores, cracks, or fissures. Because of the high amount of plasticizers, usually about 10–25 weight percent, this step is especially critical in injection molding. Although shaping is finished in a few seconds, plasticizer burnout requires several hours to several days depending on component thickness and kind of plasticizer. To improve this situation the development of new organic plasticizer systems, which may be decomposed either chemically or thermally after powder shaping, is of fundamental importance.

7.2.3. Sintering

The sintering techniques used for the manufacture of Si_3N_4 ceramics are compiled in Figure 28 together with process characteristics. Axial hot pressing in graphite matrices is used almost only for components of relatively simple geometry like rods, plates, or cylinders. Hot isostatic pressing (HIP), however, allows sintering of complex components.[179] Powder compacts are sealed gas-tight in metals or glasses of high melting point; plastic deformation of the softening material of the capsule results in uniform applica-

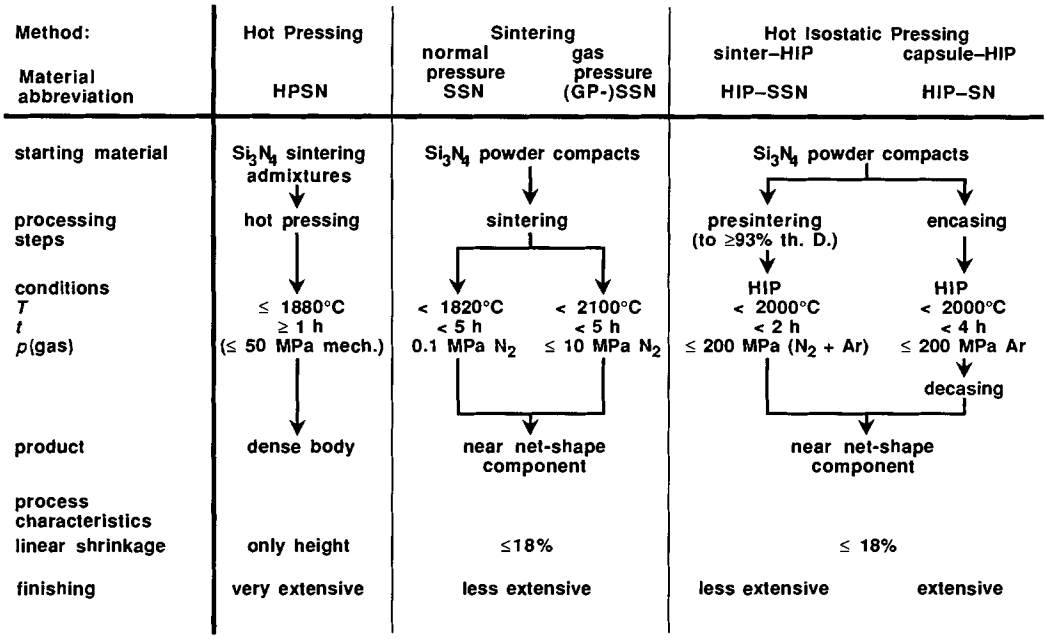

Fig. 28. Sintering processes for the manufacturing of dense Si_3N_4 components. mech. = mechanical, th. D. = theoretical density.

tion of the external gas pressure on the powder compact. Densification occurs with very precise retention of shape. After sintering is complete, the capsule is removed mechanically (sandblasting) or chemically (etching). Thus, this so-called capsule-hipping is an expensive and slow procedure not suited for low-cost mass production of ceramic components. Usually, it is applied for the production of components which are used under extreme conditions and would otherwise require an even greater effort for production.[180] However, "hipping" allows the manufacture of Si_3N_4 sintered materials with very good high-temperature properties due to the only very small amount—or even absence—of an amorphous grain-boundary phase.[181, 182] These developments, to date on laboratory scale, may gain importance for the manufacturing of Si_3N_4 components showing long-term mechanical strength at high temperatures.

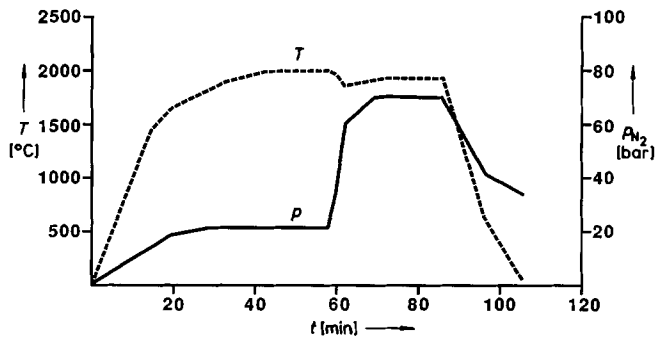

Fig. 29. Temperature–pressure–time profile during gas-pressure sintering of Si_3N_4 [149].

Cost-efficient mass production of near-finished Si_3N_4 components is possible by N_2 gas-pressure sintering, which was developed during the seventies and which is meanwhile industrially employed.[149] In this process a powder compact is heated to sintering temperature in a powder bed consisting of Si_3N_4 and BN. The course of temperature and pressure has to be adjusted to furnace geometry, sintering additives, and powder compact geometry (characteristic data in Fig. 28). Sintering under normal pressure limits the maximum temperature to about 1820 °C owing to the decomposition of Si_3N_4. However, sintering at increased N_2 pressure allows a further temperature increase and results in a pressure-assisted densification, which is effective only if the stage of closed porosity above 93% theoretical density was reached by normal pressure sintering. This method shortens the overall time required for complete densification; it even has a (limited) ability to increase strength and reliability of Si_3N_4 sintered components because of some defect healing. A typical course of temperature/pressure versus time in gas pressure sintering is shown in Figure 29.[149]

7.2.4. Finishing

Since sintered components are rarely used as fired, that is, without precise finishing, corrections of shape with adjustments of tolerances, as well as high-quality surface finishing, are required, especially for applications as engine or turbine components. Because of high hardness and comparatively high toughness of Si_3N_4 materials, these steps are time-consuming and expensive. Mainly cutting, grinding, honing, lapping, and ultrasonic erosion are used for finishing. Laser cutting and spark erosion are under development.[183, 184] Ultrasonic erosion is of special interest, since it allows the production of very complex components (e.g., gas turbine rotors) from simple monolithic shapes (Fig. 30). Generally, finishing has to be done extremely carefully in order to avoid strength and reliability deterioration by fracture-causing surface defects like cracks, fissures, and pits.

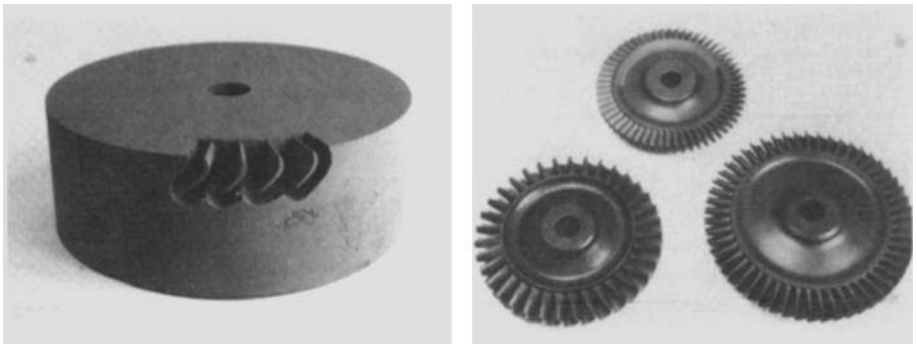

Fig. 30. Left: Manufacturing study for ultrasonic erosion of a turbine wheel from a hot-pressed Si_3N_4 monolith [185]. Right: Turbine wheels made of Si_3N_4 for applications in automotive gas turbines [186].

8. Physical and Chemical Properties

8.1. Physical Properties

Table 3 shows a compilation of important properties of completely densified Si_3N_4 ceramics. The scattering range of the data is mainly due to structural differences, which are influenced by starting powder characteristics, amount and kind of sintering additives, powder shaping, and sintering techniques as well as temperature, pressure, and soaking time during sintering. Fracture strength is surely the characteristic property determined most often; usually it is considered as a key criterion of quality. Some years ago, a significant dependence of material properties on the method of producing the starting powder was observed.[187] However, these differences almost vanished as a result of constant efforts to improve Si_3N_4 powder quality and production methods. The influence of sintering techniques on material properties is reflected in the so-called Weibull modulus (a statistical parameter to characterize a property distribution over a manifold of samples), which is used to characterize the scattering of fracture strength and thus the reliability of the material. The (limited) ability of a particular sintering process to anneal defects like pores, bubbles, internal cracks, and fissures is thereby quantified to a certain extent. The following values are typical for Weibull moduli of commercial materials: pressureless sintered Si_3N_4 >10; gas-pressure-sintered Si_3N_4 (GP-SSN) >15; isostatically hot-pressed Si_3N_4 (HIP-SSN), >20.

Table 3. Physical properties of dense Si_3N_4 material.

Property	Value
Decomposition temperature	2173 K
Theoretical density (th. D.)	α-phase: 3.168–3.118 $g cm^{-3}$ β-phase: 3.19–3.202 $g cm^{-3}$
Material density	95–100% th. D.
Thermal expansion coefficient (293–1473 K)	2.9–3.6 $10^{-6} K^{-1}$
Specific heat	700 $J K g^{-1} K^{-1}$
Electrical resistance [a]	10^{13} Ωcm
Microhardness (Vickers)	1400–1700 $MN m^{-2}$
Bending strength [a] [b]	600–1000 MPa
Fracture toughness [a]	5–8 $MPa m^{1/2}$
Elasticity modulus [a]	280–320 GPa
Thermal conductivity [a]	15–30 $W m^{-1} K^{-1}$
Critical temperature difference in thermal shock	600–800 K

[a] RT = room temperature. [b] Four-point bending

A general comparison of fracture strength is difficult, since materials for specialized applications have been developed. Here, the main criteria of quality include not only fracture strength, but also the strength level at temperatures greater than 1000 °C, fracture toughness, and hardness or wear resistance. Today, the state of the art is a strength level of 800–1000 MPa at room temperature; however, materials with fracture strengths exceeding 1000 MPa have been described.[188, 189]

By controlled structure development (in situ whisker reinforcement) it is possible to increase the fracture toughness of Si_3N_4 materials from a level of about 7 $MPa m^{1/2}$ to almost 10 $MPa m^{1/2}$;[190] a conventional material is compared to an "in situ whisker reinforced" material in Fig. 31.[191] The toughness level attained here could formerly be achieved only by reinforcement with extraneous particles (like whiskers or platelets).[192, 193]

At temperatures exceeding 1000 °C a decrease of strength in many materials is caused by slowly softening amorphous grain-boundary glass phases. The amount and kind of these phases determine creep and long-time fracture strength. All modifications of materials or technological processes to im-

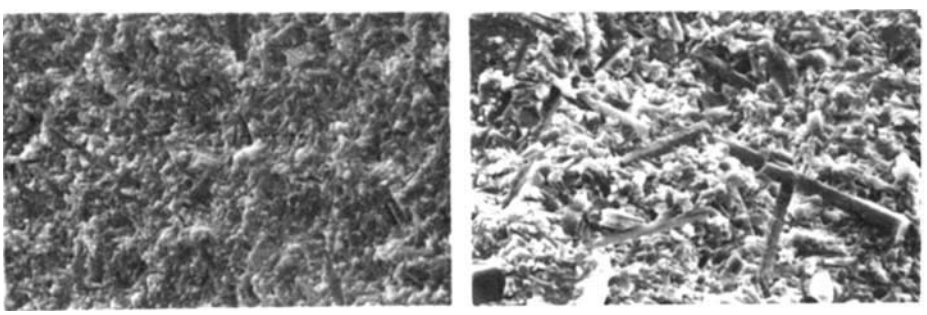

Fig. 31. Improving fracture toughness K_{Ic} by in situ whisker reinforcement [191]. Left: Structure of a conventional Si_3N_4 material ($K_{Ic} = 6.5$ $MPa m^{1/2}$). Right: Structure of an in situ whisker-reinforced material ($K_{Ic} = 9.5$ $MPa m^{1/2}$).

prove the dependence of fracture strength on temperature and to improve the strength level at high temperatures aim at reducing the amounts of amorphous grain-boundary glass phases or at generating higher refractory, crystallized grain-boundary phases together with optimization of structure. Recently, a successful realization of these concepts has been reported.[189]

An evaluation of a commercially available MgO-doped material is given in Figure 32.[194] Here, the failure probability resulting from Weibull analysis in the range of linear elastic stress up to 900 °C and probable reasons for positive or negative deviations caused by defect annealing or defect induction is shown. Figure 32 also shows the life expectancy of the material below short-time fracture load. To avoid

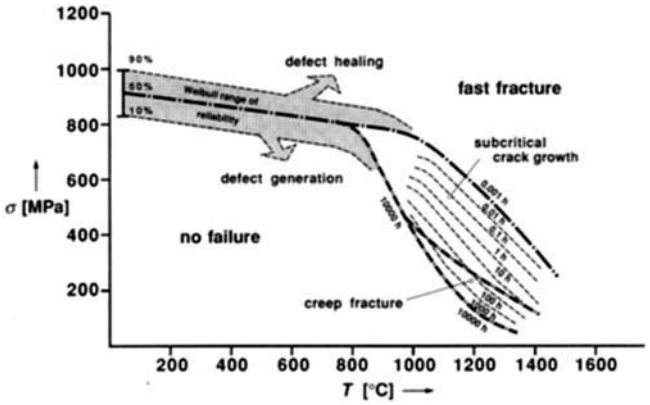

Fig. 32. Fracture strength of hot-pressed, MgO-doped Si_3N_4 as a function of temperature and time [164]. σ = flexural strength.

premature failure at a given temperature, the material should bear only considerably lower mechanical stresses than short-time fracture strengths would indicate.

8.2. Chemical Properties

Owing to the broad possible applications of sintered Si_3N_4, its chemical properties have been investigated with special regard to corrosive behavior.[195–198]

Silicon nitride is inert to numerous molten metals (e.g., Al, Zn, Sn, Pb, Cu, Ag, and Cd); however, in contact with molten transition metals like Fe, Co, Ni, V, and Cr, it reacts readily to form metal silicides and N_2. In contract with molten salts, oxidic slags, and glasses, only slow corrosion occurs. With the exception of hydrofluoric acid, Si_3N_4 ceramics are resistant to mineral acids. Mainly porous Si_3N_4 materials are attacked by hot strong caustic solutions or melts with formation of NH_3.

In the use of engine components made of Si_3N_4 (e.g., valves, turbocharger, gas turbines) the oxidation behavior of sintered Si_3N_4 is especially important. Since Si_3N_4 is coated with a thin protective layer of SiO_2 on heating in air, a good oxidation resistance is shown up to 1400 °C. In high-temperature oxidation two fundamentally different mechanisms of damage are observed.[196]

The first mechanism is based on the diffusion of sintering additives and impurities along grain boundaries owing to the higher oxygen potential at the surface of the material. Reaction with SiO_2 at the surface results in the formation of oxidic glass phases of low viscosity, which induce enhanced corrosion accompanied by N_2 formation. N_2 pores and modification changes of grain-boundary phases leading to different thermal expansion coefficients between glass phase and matrix material induce defects which lower the fracture strength of the material.

A second mechanism will lead to complete destruction if—depending on sintering additives—crystalline phases are formed during sintering, which are readily oxidized with concomitant volume expansion. Internal stress may build up so strongly, that the sintered component is completely destroyed in a short time. This phenomenon has been observed primarily in some ternary Y-Si-O-N and Ce-Si-O-N phases.[199] A suitable selection of sintering additives, the use of high-purity starting powders, and a reduction of additive and oxygen content are important in the development of high-temperature oxidation-resistant sintered Si_3N_4 materials.

9. Summary

Sintered silicon nitride is a promising material for applications in engine construction, mechanical engineering, wear and chemical technology, where high mechanical strength at high temperatures, corrosion and wear resistance, hardness, and low density are desired. Cutting tools, bearings, mill cladding, bearing gaskets, and engine components like valves, valve guides, turbocharger rotors, and gas turbines are prominent examples where this material is already used routinely or where it is being tested as a basic material.

To date, the required high-quality Si_3N_4 powders are commercially produced mainly by direct nitridation, to a lesser extent also by $SiCl_4/NH_3$ liquid-phase reaction (diimide process). Among processes under development, the $SiCl_4/NH_3$ gas-phase reaction seems to offer the best potential to furnish economically high-purity, highly sintering-active Si_3N_4 powders on a large scale.

Chemical and physical characteristics of the starting material, kind and amount of sintering additives, and sintering technique determine material properties. Their interdependence influences structure development as well as the kind and composition of silicate phases formed at grain boundaries.

Crystallization and reduction of the amount of these silicate phases are important to further improve material properties like fracture strength, creep, and corrosion resistance especially at high temperatures.

A flawless manufacturing process from powder synthesis to finished component is required to produce high-quality, reliable ceramic components. Injection molding, as a powder-shaping technology using cheap, high-quality, easily processible Si_3N_4 powders, has a great potential for the large-scale manufacturing of very complex components. Pressureless or low-pressure sintering is of great interest for the low-cost production of near-finished components. The development of economical methods for finishing sintered components of this very hard material is still necessary to decrease the very high finishing costs.

The work on economical methods to produce high-quality Si_3N_4 powders, to improve steadily powder and material

properties, and to manufacture reliably working ceramic components of superior quality should be viewed in its entirety as a necessary requirement for a broad application of silicon nitride advanced ceramics in the future.

Received: May 8, 1991 [A 844 IE]
German version: *Angew. Chem. 103* (1991) 1606

[1] H. Sainte-Claire Deville, F. Wöhler, *Ann. Chem. Pharm. 34* (1859) 248.
[2] DRP 236342 (1909); Zus.-Pat. 236892 (1909); Zus.-Pat. 241510 (1909), BASF.
[3] G. L. Williams, H. W. Campbell, US 1379668 (1918).
[4] H. Mehner, DRP 88999 (1899).
[5] A. S. Larsen, O. J. Storm, DRP 229638 (1909).
[6] BE 11091 (1913), Société Générale des Nitrures.
[7] A. R. Lindblad, US 1311568 (1918).
[8] A. S. Larsen, O. J. Storm, DRP 231090 (1910).
[9] DRP 234129 (1909), BASF.
[10] F. von Bichowsky, US 1415280 (1921).
[11] DRP 237436 (1909), BASF.
[12] E. M. Lenoe, R. N. Katz, J. J. Burke: *Ceramics for High Performance Applications III*, Plenum, New York 1979.
[13] F. L. Riley, *Sprechsaal 118* (1985) 225.
[14] W. Bunk, M. Böhmer, H. Kißler: *Keramische Komponenten für Fahrzeuggasturbinen II*, Springer, Berlin 1984.
[15] P. Walzer, M. Langer, *Motortech. Z. 44* (1983) 1.
[16] M. Taguchi, *Adv. Ceram. Mater. 2* (1987) 754.
[17] E. Gugel, *Keram. Z. 39* (1987) 698.
[18] K. H. Jack, *Endeavour 11* (1987) 80.
[19] F. Thümmler, G. Grathwohl, *Keram. Z. 40* (1988) 157.
[20] D. Fingerle, M. Fripan, U. Dworak, *ZWF Z. wirtsch. Fertigung 82* (1987) 392.
[21] J. Heinrich, J. Huber, P. Stingl, *ZWF Z. wirtsch. Fertigung 82* (1987) 487.
[22] H. Knoch, K. Hunold, *Tech. Mitt. 80* (1987) 31.
[23] D. Steinmann, *Chem. Anlagen + Verfahren, 1988*, 11.
[24] K. Uppenbrock, *Sprechsaal 121* (1988) 135; *ibid. 121* (1988) 494; *ibid. 122* (1989) 232.
[25] G. Ziegler, J. Heinrich, G. Wötting, *J. Mater. Sci. 22* (1987) 3041.
[26] C. Boberski, R. Hamminger, M. Peuckert, F. Aldinger, R. Dillinger, J. Heinrich, J. Huber, *Angew. Chem. Adv. Mater. 101* (1989) 1592; *Angew. Chem. Int. Ed. Engl. 28* (1989) 1560; *Adv. Mater. 1989*, 378.
[27] A. J. Moulson, *J. Mater. Sci. 14* (1979) 1017.
[28] L. Michalowsky, A. Rendtel, *Silikattechnik 38* (1987) 78.
[29] M. E. Washburn, W. S. Coblenz, *Am. Ceram. Soc. Bull. 67* (1988) 356.
[30] H.-J. Kleebe, *Dissertation*, Universität Köln 1988.
[31] H. Schubert, *Fortschrittsber. der Dtsch. Keram. Ges. 5* (1990) 29.
[32] J. R. Alcock, F. L. Riley, *J. Eur. Ceram. Soc. 6* (1990) 339.
[33] G. Bandyopadhyay, F. M. Mahoney, D. L. Sordelet, K. French in V. J. Tennery (Ed.): *Ceramic Materials and Components for Engines*, Am. Ceram. Soc. 1989, p. 1397ff.
[34] J. T. Neil, A. E. Pasto, L. J. Bowen, *Adv. Ceram. Mater. 3* (1988) 225.
[35] F. Aldinger, H.-J. Kaltz, *Angew. Chem. 99* (1987) 381; *Angew. Chem. Int. Ed. Engl. 26* (1987) 371.
[36] S. N. Ruddlesden, P. Popper, *Acta Crystallogr. 11* (1958) 465.
[37] S. Wild, P. Grieveson, K. H. Jack, *Spec. Ceram. 5* (1972) 385.
[38] R. Grün, *Acta Crystallogr. Sect. B35* (1979) 800.
[39] K. Kato, Z. Inoue, K. Kijima, I. Kawada, H. Tanaka, T. Yamane, *J. Am. Ceram. Soc. 58* (1975) 90.
[40] D. H. Hardie, K. H. Jack, *Nature 180* (1957) 323.
[41] K. Blegen, *Spec. Ceram. 6* (1975) 223.
[42] K. H. Jack in F. L. Riley (Ed.): *Progress in Nitrogen Ceramics*, Nijhoff, Leyden 1977, p. 45.
[43] US 1937792 (1976), Lucas Ind. Ltd.
[44] H. Haag, W. D. Glaser, B. Krismer in F. L. Riley (Ed.): *Progress in Nitrogen Ceramics*, Nijhoff, Leyden 1977, p. 315ff.
[45] I. Kohatsu, J. W. McCauley, *Mater. Res. Bull. 9* (1974) 917.
[46] K. Kijima, N. Setaka, H. Tanaka, *J. Cryst. Growth 24/25* (1974) 183.
[47] H. F. Priest, F. C. Burns, G. L. Priest, E. C. Skaar, *J. Am. Ceram. Soc. 56* (1973) 395.
[48] C. P. Gazzara, D. R. Messier, *Am. Ceram. Soc. Bull. 56* (1977) 777.
[49] K. Suzuki, Y. Kano, *Yogyo Kyokaishi 92* (1984) 101.
[50] J. P. Luongo, *J. Electrochem. Soc. 130* (1983) 1560.
[51] R. A. Andrievskii, M. A. Leontev, *Inorg. Mater. 20* (1984) 1786.
[52] T. K. Trout, J. M. Bellama, F. E. Brinckman, R. A. Faltynek, *J. Mater. Res. 4* (1989) 399.
[53] G. R. Hatfield, K. R. Carduner, *J. Mater. Sci. 24* (1989) 4209.
[54] K. R. Carduner, R. O. Carter, M. E. Milberg, G. M. Crosbie, *Anal. Chem. 59* (1987) 2794.
[55] K. R. Carduner, C. S. Blackwell, W. B. Hammond, F. Reidinger, G. R. Hatfield, *J. Am. Chem. Soc. 112* (1990) 4676.
[56] R. Dupree, M. H. Lewis, G. Leng-Ward, D. S. Williams, *J. Mater. Sci. Lett. 4* (1985) 393.
[57] K. R. Carduner, R. O. Carter, M. J. Kokosz, C. Peters, G. Crosbie, E. D. Stiles, *Chem. Mater. 1* (1989) 302.
[58] G. Schwier, G. Nietfeld, *Werkstoffe and Konstruktion 2* (1988) 149.
[59] G. Schwier, G. Nietfeld, *Sprechsaal 121* (1988) 174.
[60] G. Boden, S. Klemm, K. Quaritsch, *Silikattechnik 38* (1987) 161.
[61] G. Boden, R. Irmisch, G. Himpel, T. Reetz, *Sprechsaal 122* (1989) 224.
[62] Y. Tuohino, R. Laitinen, K. Torkell in G. L. Messing, S. Hirano, H. Hausner (Ed.): *Proc. 3rd Int. Conf. Powder Processing Sci.*, Am. Ceram. Soc. 1990, p. 337ff.
[63] K. Komeya, H. Inoue, *J. Mater. Sci. 10* (1975) 1243.
[64] H. Inoue, K. Komeya, A. Tsuge, *J. Am. Ceram. Soc. 65* (1982) 205.
[65] M. Mori, H. Inoue, T. Chirai in F. L. Riley (Ed.): *Progress in Nitrogen Ceramics*, Nijhoff, Den Haag 1983, p. 149ff.
[66] T. Ishii, A. Sano, I. Imai in S. Somiya, A. Mitomo, M. Yoshimura (Ed.): *Silicon Nitride – 1*, Elsevier Appl. Sci., London 1990, p. 59 ff.
[67] M. Blix, W. Wirbelauer, *Ber. Dtsch. Chem. Ges. 36* (1903) 4220.
[68] O. Glemser, P. Naumann, *Z. Anorg. Allg. Chem. 298* (1959) 134.
[69] K. S. Mazdiyasni, C. M. Cooke, *J. Am. Ceram. Soc. 56* (1973) 628.
[70] S. Prochazka, C. Greskovich, *Am. Ceram. Soc. Bull. 57* (1978) 579.
[71] W. M. Shen, EP 365295 (1989), Union Carbide Corp.
[72] Y. Kohtoku in S. Somiya, M. Nitomo, M. Yoshimura (Eds.): *Silicon Nitride – 1*, Elsevier Appl. Sci., London 1989, p. 71ff.
[73] P. E. D. Morgan, *U.S. Dept. of Energy, DOE-Report 83-004283* (1983).
[74] P. E. D. Morgan, E. A. Pugar, *J. Am. Ceram. Soc. 68* (1985) 699.
[75] P. E. D. Morgan, US 4552740 (1985).
[76] O. Glemser, H.-G. Horn, *Naturwissenschaften 49* (1962) 538.
[77] M. Hoch, K. Nair, *Bull. Am. Ceram. Soc. 58* (1979) 187.
[78] K. Komeya, H. Inoue, *J. Mater. Sci. 10* (1975) 1243.
[79] M. Peuckert, T. Vaahs, M. Bruck, *Adv. Mater. 2* (1990) 398.
[80] L. Weiss, T. Engelhardt, *Z. Anorg. Chem. 65* (1910) 38.
[81] A. Atkinson, A. J. Moulson, E. W. Roberts, *J. Am. Ceram. Soc. 59* (1976) 285.
[82] H. M. Jennings, *J. Mater. Sci. 18* (1983) 951.
[83] R. Pompe, L. Hermansson, T. Johansson, E. Djurle, D. E. Hatcher, *Mater. Sci. Eng. 71* (1985), 355.
[84] M. Mitomo, *J. Mater. Sci. 12* (1977) 273.
[85] H. M. Jennings, B. J. Dalgleish, P. L. Pratt, *J. Mater. Sci. 23* (1988) 2573.
[86] J. A. Mangels, *Am. Ceram. Soc. Bull. 60* (1981) 613.
[87] A. G. Merzhanov, P. Borovinskaja, *Dokl. Akad. Nauk SSSR 204* (1972) 366.
[88] V. Hlavacek, *Am. Ceram. Soc. Bull. 70* (1991) 240.
[89] Z. A. Munir, J. B. Holt, *J. Mater. Sci. 22* (1987) 710.
[90] A. G. Merzhanov, *Adv. Mater. 2* (1990) 570.
[91] K. Hirao, Y. Miyamoto, M. Koizumi, *J. Am. Ceram. Soc. 69* (1986) C 60.
[92] A. S. Muskasyan, V. M. Martynenko, A. G. Merzhanov, I. P. Borovinskaya, M. Yu. Blinov, *Fiz. Goreniya Vzryva 22* (1986) 43.
[93] K. Hirao, Y. Miyamoto, M. Koizumi, *Adv. Ceram. Mater. 2* (1987) 780.
[94] S. Kumar, J. A. Puszinski, V. Hlavacek in Z. A. Munir, J. B. Holt (Ed.): *Combustion and Plasma Synthesis of High Temperature Materials*, VCH Publishers, New York 1990.
[95] J. Lis, S. Majovrowski, J. A. Puszynski, V. Hlavacek, *Am. Ceram. Soc. Bull. 70* (1991) 244.
[96] M. Shimada, T. Okamoto, M. Koizumi, *Mem. Inst. Sci. Ind. Res., Osaka Univ. 41* (1984) 1.
[97] T. Nishioka, M. Myake, H. Matsumoto, M. Higuchi, JP 6389459 (1988).
[98] E. Friedrich, L. Sittig, *Z. Anorg. Allg. Chem. 143* (1925) 293.
[99] A. Szweda, A. Henry, K. H. Jack, *Proc. Br. Ceram. Soc. 31* (1981) 107.
[100] M. Mitomo, Y. Yoshioka, *Adv. Ceram. Mater. 2* (1987) 253.
[101] Y. Sugahara, J. Miyamoto, K. Kuoda, C. Kato, *Appl. Clay Sci. 4* (1989) 11.
[102] S. J. P. Durham, K. Shanker, R. L. Drew in H. Hausner, G. L. Messing, S. Hirano (Ed.): *Proc. 2nd Int. Powder Process. Sci. Conf.*, Deutsche Keramische Gesellschaft, Cologne 1988, p. 313ff.
[103] A. Hendry, K. H. Jack, *Spec. Ceram. 6* (1975) 199.
[104] K. Shanker, S. Grenier, R. A. L. Drew in G. L. Messing, S. Hirano, H. Hausner (Ed.): *Proc. 3rd Int. Powder Process. Sci. Conf.*, Am. Ceram. Soc. 1990, p. 329ff.
[105] W. Krumbe, B. Laubach, G. Franz, EP 362605 (1989), Bayer AG.
[106] A. Yamaguchi, *Refractories 38* (1986) 2. Engl. Transl., Tokyo 1986.
[107] W. Krumbe, B. Laubach, G. Franz, EP 237680 (1990), Bayer AG.
[108] L. Schönfelder, G. Franz, U. Wickel, G. Wötting, *Sci. Ceram. 14* (1988) 119.
[109] M. Persoz, *Ann. Chim. Phys. 44* (1830) 315.
[110] F. Lengfeld, *Am. Chem. J. 21* (1899) 52.1.
[111] E. Vigoureux, C. R. Hugot, *Hebd. Seances Acad. Sci. 136* (1903) 1670.
[112] M. Billy, *Ann. Chim. 4* (1959) 795.
[113] D. L. Segal, *Trans. J. Br. Ceram. Soc. 85* (1986) 184.
[114] O. Glemser, K. Beltz, P. Naumann, *Z. Anorg. Allg. Chem. 291* (1957) 51.
[115] M. Billy, M. Brossard, J. Desmaison, D. Giraud, P. Goersat, *J. Am. Ceram. Soc. 58* (1975) 254.
[116] US 4196178 (1980), Ube Industries.

[117] T. Yamada, T. Kawahito, T. Luai in S. Somiya, E. Kanai, K. Ando (Ed.): *Proc. 1st Int. Symp. Ceram. Components for Engines*, KTK Scientific Publ., Tokyo 1984, p. 333ff.
[118] R. Riedel, M. Seher, *J. Eur. Ceram. Soc. 7* (1991) 21.
[119] E. J. Jacquemij, P. J. van der Put, J. Schoonman, *High Temp. High Pressures 20* (1988) 31.
[120] J. Hojo, H. Maeda, A. Kato, *J. Ceram. Soc. Jpn. Int. Ed. 96* (1988) 820.
[121] Y. Kohtoku, T. Yamada, M. Migazaki, T. Iwai in W. Bunk, H. Hausner (Ed.): *Proc. 2nd Int. Symp. Ceram. Comp. for Engines*, Deutsche Keramische Gesellschaft 1986, p. 101ff.
[122] G. M. Crosbie, R. L. Predmedsky, J. M. Nicholson, E. D. Stiles, *Bull. Am. Ceram. Soc. 68* (1989) 1010.
[123] G. D. Ulrich, *Chem. Eng. News 1984*, 22.
[124] G. Franz, G. Schwier in Kursten: *Proc. 5th Int. Symp. on Raw Materials for New Technologies*, E. Schweizerbart'sche Verlagsbuchhandlung, Stuttgart 1990, p. 139ff.
[125] B. Laubach, G. Franz, U. Wickel, L. Schönfelder, DE 3536933 (1985), Bayer AG.
[126] W. R. Cannon, S. C. Danforth, J. H. Flint, J. S. Haggerty, R. A. Marra, *J. Am. Ceram. Soc. 65* (1982) 324.
[127] W. R. Cannon, S. C. Danforth, J. S. Haggerty, R. A. Marra, *J. Am. Ceram. Soc. 65* (1982) 330.
[128] Y. Kizaki, T. Kandori, Y. Fujitami, *Jpn. J. Appl. Phys. 24* (1985) 800.
[129] W. Ymons, K. J. Nilsen, S. C. Danforth in W. Bunk, H. Hausner: *Proc. 2nd Int. Symp. Ceram. Mater. Comp. for Engines*, Deutsche Keramische Gesellschaft, Cologne 1986, p. 39ff.
[130] J. Canteloup, A. Mocellin, *Proc. Br. Ceram. Soc. 6* (1975) 209.
[131] G. J. Vogt, C. M. Hollobaugh, D. E. Hull, L. R. Newkirk, J. J. Petrovic, *U.S. Dept. of Energy, DOE-Report 84-003774* (1984).
[132] G. J. Vogt, R. S. Vigil, L. R. Newkirk, M. Tikula in C. J. Timmermans (Ed.): *Proc. 7th Int. Symp. Plasma Chem., Vol. II*, IUPAC 1985, p. 657ff.
[133] O. Schulz, H. Hausner, *Elektrowaerme Int. Ed. B45* (1987) 174.
[134] N. Kubo, S. Futaki, K. Shiraishi in S. Somiya, M. Mitomo, M. Yoshimura: *Silicon Nitride - 1*, Elsevier Appl. Sci., London, p. 93ff.
[135] C. Herring, J. K. Galt, *Phys. Rev. 85* (1952) 1060.
[136] S. B. Hanna, F. F. Abdel-Mohsen, *Angew. Makromol. Chem. 133* (1985) 25.
[137] H. Grewe, K. Dreyer, J. Kolaska, *Ceram. Forum Intl., Ber. Dtsch. Keram. Ges. 1987*, 303.
[138] F. Pott, *Zentralbl. Bakteriol. Mikrobiol. Hyg. Abt. Orig. B184* (1987) 1.
[139] H.-G. Grimm, *Zentralbl. Arbeitsmed. Arbeitsschutz Prophyl. Ergon. 38 (Suppl. 1)* (1988) 2.
[140] A. L. Cunningham, L. G. Davis, *SAMPE J. 15* (1969) 120.
[141] R. C. Johnson, J. K. Alley, W. H. Warwick, R. H. Shell, US 3244480 (1966).
[142] M. Tanaka, T. Kawabe, JP 1324479 (1986).
[143] K. Niwano in S. Somiya, M. Mitomo, M. Yoshimura (Eds.): *Silicon Nitride - 1*, Elsevier Appl. Sci., London 1989, p. 117ff.
[144] *Techno Japan 22* (1979) 79.
[145] S. Motojima, H. Iwanaga, *Kinzoku 59* (1989) 47.
[146] G. Ziegler, *Ceram. Forum Intl., Ber. Dtsch. Keram. Ges. 68* (1991) 72.
[147] P. Greil, M. J. Hoffmann, K. L. Weisskopf, G. Petzow, *Fortschrittsber. Dtsch. Keram. Ges. 2* (1986/87) 27.
[148] G. R. Terwilliger, F. F. Langer, *J. Mater. Sci. 10* (1975) 1169.
[149] S. Prochazka, C. D. Greskovich, *U.S. Army Mater. and Mech. Res. Center Technical Report 78-32 (1978)*, SRD-77-178.
[150] J. T. Smith, C. L. Quackenbush in S. Somiya, S. Saito (Eds.): *Proc. Int. Symp. Factors in Densification and Sintering of Oxide and Nonoxide Ceramics*, Hakone 1978, p. 426ff.
[151] M. Mitomo, *J. Mater. Sci. 11* (1976) 1103.
[152] M. Mitomo in S. Somiya, M. Mitomo, M. Yoshimura (Eds.): *Silicon Nitride - 1*, Elsevier Appl. Sci., London 1990, p. 1ff.
[153] G. Wötting, *Dissertation*, TU-Berlin 1983.
[154] G. Wötting, G. Ziegler in S. Somiya (Ed.): *Proc. 1st Int. Symp. Ceram. Comp. for Engins*, KTK Scientific Publ., Tokio 1983, p. 412ff.
[155] F. F. Lange, *J. Am. Ceram. Soc. 62* (1979) 428.
[156] G. Himsoldt, H. Knoch, H. Hübner, F. W. Kleislein, *J. Am. Ceram. Soc. 62* (1979) 29.
[157] M. Mitomo, *J. Am. Ceram. Soc. 73* (1990) 2441.
[158] G. Wötting, G. Ziegler, *Fortschrittsber. Dtsch. Keram. Ges. 1* (1985) 33.
[159] D. R. Clarke in F. L. Riley (Ed.): *Progress in Nitrogen Ceramics*, Nijhoff, Leyden 1983, p. 341ff.
[160] P. Greil, *Sci. Ceram. 14* (1988) 645.
[161] S. Hampshire, *Proc. Br. Ceram. Soc. 31* (1981) 37.
[162] K. H. Jack in F. L. Riley (Ed.): *Progress in Nitrogen Ceramics*, Nijhoff, Brighton 1981, p. 109ff.
[163] Z.-K. Huang, P. Greil, G. Petzow, *J. Am. Ceram. Soc. Commun. 1983*, C69.
[164] V. K. Sarin, *Mater. Sci. Eng. A105/106* (1988) 151.
[165] G. Wötting, G. Ziegler, *Powder Met. Int 18* (1984) 18.
[166] M. Peuckert, P. Greil, *J. Mater. Sci. 22* (1987) 3717.
[167] G. Nietfeld, U. Wickel, G. Wötting in H. Hausner, G. L. Messing, S. Hirano (Ed.): *Proc. 2nd Int. Conf. Ceram. Powder Process. Sci.*, Deutsche Keramische Gesellschaft 1989, p. 795ff.
[168] G. Nabert, G. Ziegler, WF-Kolloquium, Werkstoff-Kolloquim des Instituts für Werkstoff-Forschung der Dtsch. Forschungsanstalt für Luft- u. Raumfahrt (DLR), Köln, 1990.
[169] H. Knoch, G. E. Gazza, *J. Am. Ceram. Soc. 62* (1979) 634.
[170] J. T. Neil, A. E. Pasto, L. J. Bowen, *Adv. Ceram. Mater. 3* (1988) 225.
[171] D. Munz, O. Rosenfelder, K. Goebbels, H. Reiter in W. Bunk (Ed.): *Keramische Komponenten für Fahrzeug-Gasturbinen III*, Springer, Berlin 1984, p. 513.
[172] R. A. Bauer, R. van Weeren, P. J. van der Put, F. E. Kruis, B. Scarlett, J. Schoonman in G. L. Messing, H. Hausner, S. Hirano (Ed.): *Proc. 3rd Int. Conf. Ceram. Powder Process. Sci.*, Am. Ceram. Soc., Westerville 1990, p. 259ff.
[173] J.-S. Kim, H. Schubert, G. Petzow, *J. Eur. Ceram. Soc. 1991*, in press.
[174] M. Kulig, W. Oroschin, P. Greil, *J. Eur. Ceram. Soc. 5* (1989) 209.
[175] R. de Jong, R. A. McCandey in G. de With, R. A. Terpstra, R. Metselaar (Ed.): *Proc. 1st Eur. Ceram. Soc. (ECerS) Conf.*, Elsevier Appl. Sci., London 1989, p. 1150-1154.
[176] M. J. Edirisinghe, J. R. G. Evans, *Int. J. High Tech. Ceram. 2* (1986) 1, 249.
[177] S. J. Stedmeyer, J. R. G. Evans, J. Woodthorpe, *Ceram. Int. 16* (1990) 107.
[178] U. Becker, *Kunststoffe 80* (1990) 575.
[179] B. Oberacker, A. Kühne, F. Thümmler, *Powder Met. Int. 19* (1987) 43.
[180] K. Hunold, *Ceram. Forum Intl., Ber. Dtsch. Keram. Ges. 60* (1983) 182.
[181] S. Kume, H. Yoshida, M. Machida, *J. Ceram. Soc. Jpn. Int. Ed. 95* (1987) 205.
[182] I. Tanaka, G. Pezzotti, T. Okamoto, Y. Miyamoto, *J. Am. Ceram. Soc. 72* (1989) 1656.
[183] W. König, M. Popp, J. Wemhöner in J. Kriegesmann (Ed.): *Technische Keramische Werkstoffe*, Deutscher Wirtschaftsdienst, Cologne 1989, Chapter 3.7.3.
[184] G. Spur, I. Subotka, T. H. Tio, U. E. Wunsch, *FBM-Fertigungstechnologie 64* (1987) 31; *ibid. 65* (1988) 28.
[185] E. Gugel, G. Leimer in W. Bunk (Ed.): *Keramische Komponenten für Fahrzeuggasturbinen III*, Springer, Berlin 1984, p. 133.
[186] K. D. Mörgenthaler in W. Bunk (Ed.): *Keramische Komponenten für Fahrzeuggasturbinen III*, Springer, Berlin 1984, p. 389.
[187] G. Ziegler, J. Heinrich, G. Wötting, *J. Mater. Sci. 22* (1990) 3041.
[188] K. Ueno, *J. Ceram. Soc. Jpn. Int. Ed. 97* (1989) 80.
[189] K. Komeya, *Proc. 7th CIMTEC*, Montecatini 1990, in press.
[190] Y. Tajima, K. Urashima, M. Watanabe, Y. Matsuo in G. L. Messing, F. Fuller, H. Hausner (Ed.): *Ceramic Transactions 1*, Am. Ceram. Soc., Westerville 1988, p. 1034ff.
[191] G. Wötting, G. Schwier, H. Lange in S. Hirano, H. Hausner, G. L. Messing: *Proc. 4th Int. Conf. Ceram. Powder Process. Sci.*, Nagoya 1991, in press.
[192] P. D. Stralek, *Am. Ceram. Soc. Bull. 65* (1986) 351.
[193] H. Kodama, T. Miyoshi, *Ceram. Eng. Sci. Proc. 10* (1989) 1072.
[194] G. D. Quinn, *J. Mater. Sci. 25* (1990) 4361.
[195] A. Rabenau, *Ber. Dtsch. Keram. Ges. 40* (1963) 6.
[196] G. Wötting, G. Ziegler, *Sprechsaal 123* (1990) 1102.
[197] H. Feld, E. Gugel, H. G. Nitzsche, *Werkst. and Korrosion 1969*, 671.
[198] R. E. Tressler, M. McNallun (Ed.): *Proc. Symp. Corrosion and Corrosive Degradation of Ceramics*, Am. Ceram. Soc., Westerville 1989.
[199] J. T. Smith, C. L. Quackenbush, *Am. Ceram. Soc. Bull. 59* (1980) 529.

Routes to New Aromatic Polycarbonates with Special Material Properties

By Dieter Freitag,* Gerd Fengler, and Leo Morbitzer

Polycarbonate together with the acrylonitrile/butadiene/styrene copolymers, and the polyamides constitute the leading groups of engineering thermoplastics; for polycarbonate in particular, continued dynamic growth is prophesized.

The underlying reason for this lies not only in its outstanding combination of technical properties and excellent price/performance balance, but also in the chemical and physical potential inherent in the basic structure of polycarbonate. The following review demonstrates with examples how this potential can be used in the development of new polycarbonates through the incorporation of alternative monomers, changes in the linear structure, end group variation, addition of special additives, and blending. The main emphasis of this article lies in the development of polycarbonates resistant to high temperature, with a good balance of technologically valuable properties. For scientific and practical interests a new criterion is offered for polycarbonates having both high-temperatures stability and impact strength.

"One must not only make a discovery, but also realize that a discovery has been made."
Hermann Schnell [1]

1. Introduction

Polycarbonate **1** from 2,2-bis(4-hydroxyphenyl)propane (Bisphenol A or BPA) has a worldwide consumption of ca. 595000 t (1989), along with the ABS-copolymers (1989 ca. 2000000 t) and polyamides (1989 ca. 800000 t in injection molding and extrusion grades, excluding fibers), forming the leading group of engineering thermoplastics (see Fig. 1). A segmental breakdown of the current polycarbonate market is shown in Table 1.[2] The major production sites are located in the USA, Western Europe, and Japan. The leading producers of polycarbonate are General Electric Corp. and Bayer AG.

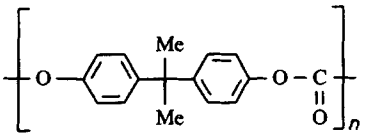

1

Due to the inherent chemical and physical potential of the basic structure of polycarbonate, a dynamic growth is still expected (polycarbonate consumption doubled between 1982 and 1988![2]) Polycarbonate has a good chance of surpassing polyamides (injection molding and extrusion grades, excluding fibers). It is predicted that in 1993 the polycarbonate consumption in the USA will be 385000 t, 30000 t higher than polyamide consumption (355000 t).[3] There are primarily three reasons for this outstanding "boost" in polycarbonate consumption (remembering that polycarbonate was first discovered in 1953,[1,4] nearly 20 years after the discovery of polyamides!):

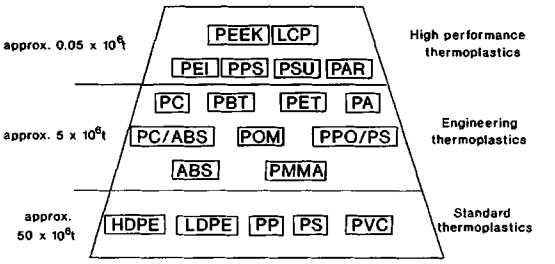

PEEK	Polyetheretherketone	PC/ABS	Polycarbonate/ABS-blend
LCP	Liquid crystalline polyester	POM	Polyoxymethylene
PEI	Polyetherimide	PPO/PS	Polyphenyleneoxide/polystyrene-blend
PPS	Polyphenylensulfide	ABS	Acrylonitrile/butadiene/styrene-copolymers
PSU	Polysulfone	PMMA	Polymethylmethacrylate
PAR	Polyarylate	HDPE	Polyethylene, high density
PC	Polycarbonate	LDPE	Polyethylene, low density
PBT	Polybutylene terephthalate	PP	Polypropylene
PET	Polyethylene terephthalate	PS	Polystyrene
PA	Polyamides	PVC	Polyvinylchloride

Fig. 1. Classification of the important thermoplastics and their consumption worldwide (1988).

Table 1. Industries which use polycarbonates and their shares of the market.

Industry	Examples	Market share [%]
Electric/Electronic	Housings for electrical household appliances, optical storage disks (CD)	49
Construction	Solid and twin-wall sheets	24
Automobile	Interior applications, lighting	8
Business Machines	Housings	6
Other	Packaging, medical applications, ophthalmic frames and lenses	13

[*] Dr. D. Freitag
Director of Research and Development,
Plastics Business Group, Bayer AG,
Rheinuferstrasse 7–9, W-4150 Krefeld (FRG)
Dr. G. Fengler
Research and Development,
Plastics Business Group, Bayer AG, W-4150 Krefeld (FRG)
Dr. L. Morbitzer
Central Research and Development,
Department of Polymer Physics,
Bayer AG, W-5090 Leverkusen (FRG)

a) In comparison to other engineering thermoplastics, polycarbonate possesses an outstanding combination of fundamental properties including transparency (BPA-polycarbonate is normally amorphous, i.e. optically homogeneous to visible light), relatively high temperature resistance (expressed by a glass transition temperature T_g of 150 °C, therefore maintaining its essential properties to near this temperature), outstanding toughness (i.e. high energy absorption capacity during impact), and blending potential (based on miscibility or at least partial miscibility of the polycarbonates with themselves or with various other polymers).
b) Excellent price/performance balance.
c) Technological exploitation of the chemical (structural modification) and physical potential of the polycarbonate structure has been more extensive compared to that of the other engineering thermoplastics, for example through i) incorporation of alternative monomers such as bisphenols (including telechelic phenols), which furnishes homopolycarbonates and both statistical and block copolycarbonates, ii) incorporation of tri- or polyfunctional monomers, which results in branching, iii) incorporation of aromatic dicarboxylic acids or hydroxycarboxylic acids instead of carbonic acid, which affords access to aromatic polyester carbonates, iv) variation of endgroups, v) the addition of special additives, and vi) the preparation of blends.

The following article focuses in particular on topic c), with emphasis on those developments in the polycarbonate field that, besides their scientific and economic importance, can serve as a model for further development of other thermoplastics.

2. New Aspects in the Commercial Production of Aromatic Polycarbonates

Of the various production methods, the interfacial polymerization process is currently employed almost exclusively for the production of polycarbonate (Scheme 1). The catalytic transesterification of diphenyl carbonate with bisphenol A and subsequent removal of phenol in the melt (Scheme 2), as well as the homogeneous polycondensation of bisphenol A with phosgene (pyridine process) have lost their earlier importance (a review of the commercial processes has been published[5]). Recently, the transesterification process in the melt has been given more recognition (laboratory and pilot

Dieter Freitag was born in 1939 in Offenbach, Germany. He studied chemistry at Freiburg and Frankfurt and received his doctoral degree with Professor Ried in Frankfurt. After postdoctoral studies with Professor Ried he joined Bayer AG in 1968 and did basic and polymer research in the Central Research and Development Department. In 1978 he joined the Plastics Business Group with responsibility for research in the field of new Engineering Thermoplastics and was later responsible for the research of all Bayer polycondensates. From 1986 to 1988 he led the development of high-performance engineering thermoplastics, thermosets, films, and additives in the applications department in Leverkusen. Since 1988 he has been director of Plastics Research, and is now head of the Plastics Research and Development Department.

Gerd Fengler, born 1943 in Stapelburg/Harz, studied chemistry in Braunschweig and in Hannover, where he received his doctorate in 1973 under the supervision of Professor E. Winterfeldt (TU Hannover). In 1974 he joined the Central Research Department of Bayer AG in Uerdingen. Since 1987 he has been with the Plastics Business Group, and in 1988 he became a group leader in the Plastics Research Department, which is currently the Plastics Research and Development Department.

Leo Morbitzer, born in 1934, graduated with a doctoral degree in physics at the Justus-Liebig-Universität in Giessen. In 1965 he joined Bayer AG in Leverkusen and was active in different fields of polymer physics. In the Central Research and Development Department he is now leader of a group concerned with the physics of thermoplastic multiphase polymers, theoretical aspects of polymer physics, and computer simulations.

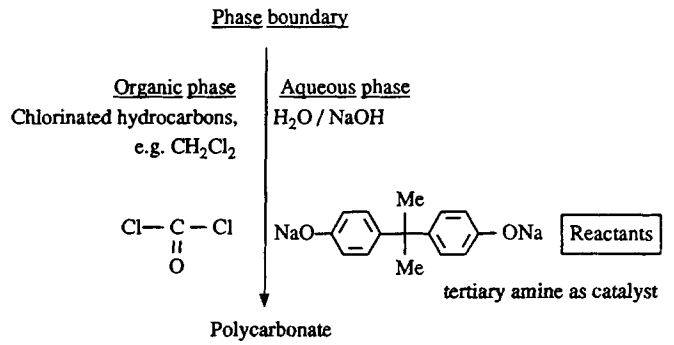

Scheme 1. Industrial manufacture of polycarbonate by interfacial polycondensation (interfacial process).

plant scale). The reason for this concern is on the one hand, the environment: the process requires no solvent such as dichloromethane and involves no waste water; no salt is formed (if the diphenyl carbonate salt-free process[6] is

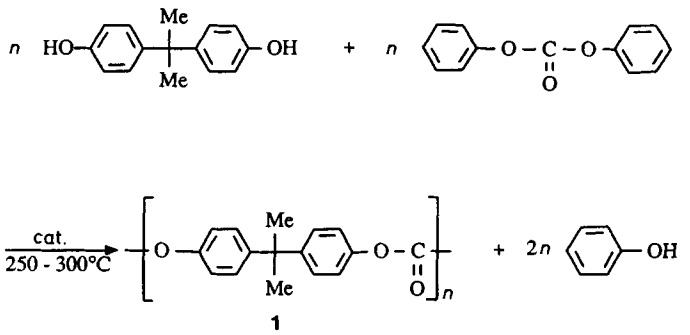

Scheme 2. Manufacture of polycarbonate by transesterification in the melt. cat. = catalyst.

used); this polycarbonate synthesis is phosgene free (if diphenyl carbonate is prepared phosgene-free e.g. by the reaction sequence (a), which is also salt free).

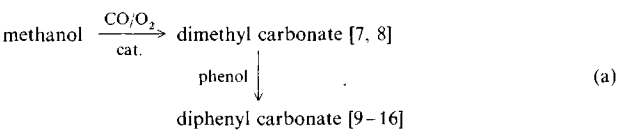

On the other hand not only can the starting materials (diphenyl carbonate, bisphenol A) be prepared in higher purity but also more reactive substituted diphenyl carbonates[17] and new catalyst systems[18-20] have become available; new reactors for high viscosity materials have been described;[21-25] variants of the process (e.g. intermediate isolation of oligocarbonates, crystallization, and subsequent solid-phase polycondensation of the crystallized oligocarbonate[26-28]) have been developed. Due to these innovations, side reactions previously associated with the melt transesterification process (which caused, for example, color problems) can be suppressed.

Variants of the transesterification process have also been described which use dialkyl carbonates (in particular dimethyl or diethyl carbonate)[29-34] instead of diphenyl carbonate. Dimethyl carbonate is currently produced in commercial quantities from CO and methanol using a phosgene-free process.[7, 8] However, the transesterification of dimethyl carbonate with bisphenol A to produce polycarbonate is not as simple as that with phenol to produce diphenyl carbonate, even if the catalysts that are successful in the latter reaction are used.

Semicrystalline polycarbonates, such as those prepared from bis(4-hydroxyphenyl)sulfane and (thermotropic[35-38]) aromatic polyester carbonates (see also Ref.[5]) are normally insoluble in conventional solvents. Therefore the melt transesterification process is the most practical way to produce high molecular weight polymers.

The direct reaction of bisphenols with carbon monoxide by catalysis to produce high molecular weight polycarbonates is still in an experimental stage. The large excess of catalyst (usually Pd compounds) and auxiliary base (sterically hindered tertiary amines) used in this process lead only to relatively low molecular weight polycarbonates ($M_n = 1700$–$11\,000\ g\,mol^{-1}$).[38-41, 43-46] Similar routes as for the coupling of bisphenols with carbon monoxide have also been described for the synthesis of diphenyl carbonate—the starting material in the melt process—from phenol and carbon monoxide.[38-43, 45-52]

An interesting polycarbonate production technique based on earlier studies[53, 54] of the catalyzed ring-opening polymerization of low viscosity cyclic oligocarbonates **2** to high molecular weight polycarbonates ($M_w = 200\,000$–$400\,000\ g \cdot mol^{-1}$) has recently been reported.[55-59] However the synthesis of the oligomers ((pseudo) dilution principle) as well as their processing, which is somewhat similar to reaction injection molding (RIM) is not yet commercially feasible.

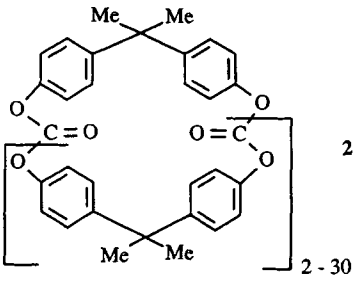

The use of this technique has in particular been proposed for the production of composites by polymerization of a mixture of cyclic oligomers and fillers such as glass or carbon fibers (prepregs). It is doubtful, however, whether polycarbonate will be a suitable matrix resin for composites, owing to its limited hydrolytic stability and—for this purpose—relatively low glass transition temperature (see also Refs.[60, 61]).

3. Modification of the Polycarbonate Structure

3.1. Homopolycarbonates and Copolycarbonates from Bisphenol A Derivatives and BPA-Copolycarbonates

In the course of polycarbonate research, numerous examples have been prepared from monomers of the bisphenol type. The driving force of these efforts was, on the one hand,

to overcome some of the inadequacies of BPA-polycarbonate (hydrolytic instability to bases, stress cracking on contact with many organic solvents); on the other hand, many of these efforts were directed at improving the properties of BPA-polycarbonate still further, and have in particular focused on raising its temperature resistance (expressed by T_g). However, temperature resistance can only be improved within certain limits if transparency, impact strength, melt flow, hydrolytic stability, and finally production costs are not to deviate too far from standard polycarbonate.

Of particular interest in this area are polycarbonates based on (substituted) alkylidene- and cycloalkylidene-bisphenols, and bisphenols containing cycloaliphatic ring systems. Tables 2 and 3 show the dependence of the T_g of some polycarbonates on the structure of the corresponding bisphenols (for a more detailed study see Ref.[5]). It is obvious that the main problem is not related to T_g, but in satisfying the other above-mentioned property limitations.

Table 2. Glass transition temperatures of polycarbonates from *o,o',o'',o'''*-tetrasubstituted bisphenols in comparison to polycarbonates from unsubstituted bisphenols.

Polycarbonate from HO–R–OH			Polycarbonate from		
R	T_g [°C]	Ref.	R'	T_g [°C]	Ref.
CH_2	147	[1,62–64]	Me	185	[66–68]
$C'Me_2$	149	[1,62–65]	Me	203	[66]
			Cl	230	[1,62–64,69,70]
			Br	265	[1,62–64,69,70]
Cyclohexylidene	179	[1,62–64]	Me	213	[66]
			Cl	290	[65]

Two especially informative developments (structural variations of BPA-polycarbonate) should help to demonstrate the underlying factors governing T_g and temperature resistance of polymers.

The temperature resistance of semicrystalline polymers is determined by the degree of crystallinity, crystal morphology, and by the magnitude of the melting point. With amorphous polymers such as the polycarbonates described here, the glass-transition temperature plays a decisive role in their temperature resistance. Only in the melt state (T_m) can the thermodynamic relationship described by the Gibbs–Helmholtz equation (b) have any physicochemical meaning. ΔH_m refers to the melt enthalpy and ΔS_m is the melt entropy. The magnitude of ΔS becomes smaller with increasing chain rigidity. Rigid chain polymers generally melt at higher temperatures.

$$T_m = \frac{\Delta H_m}{\Delta S_m} \qquad \text{(b)}$$

Unfortunately there is no thermodynamic equivalent in the sense of relationship (b) for the glass transition temperature, because the glass transition is a dynamic relaxation process. However, for many polymers, including polycarbonates, the empirical relationship $T_g \sim 2/3\ T_m$ holds. Polymers with increased chain rigidity or decreased chain mobility show, in general, a higher T_g than polymers with flexible chains. From earlier as well as on-going research, two developmental routes to polycarbonates with lower chain mobility and consequently higher temperature resistance (expressed as T_g) have been pursued:

- incorporation of 3,3′5,5′-tetramethyl bisphenol A (TMBPA) instead of bisphenol A
- full or partial substitution of BPA by a bisphenol based on hydrogenated isophorone (bisphenol TMC)

The replacement of BPA by TMBPA results in a polycarbonate, **3**, (space-filling model shown in Fig. 2) with a higher T_g (203 °C).[66] The reason for this increase in T_g (+ 53 °C higher than BPA-polycarbonate) is due to the hindered rotation about the phenyl–carbonate bond combined with the increased mass and volume of the monomer unit.

Table 3. Glass transition temperatures T_g of polycarbonates from bisphenols with cycloaliphatic ring systems.

Monomer	T_g [°C]	Ref.
HO–R–OH		
R =	224	[70]
R = 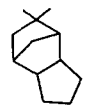	256	[70]
R = 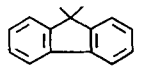	356, 275	[71–73]
R = 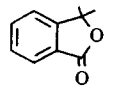	270	[74–76]
R =	290	[74,75]
R = 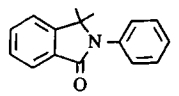	250	[74,75]
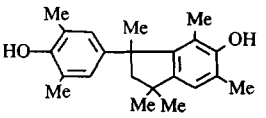	265	[77,78]
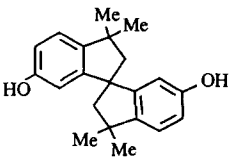	230	[79,80]

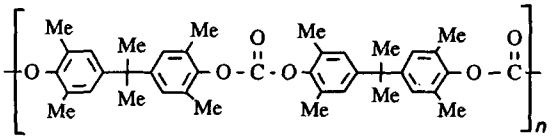

3

This polymer additionally exhibits a low melt viscosity (advantageous for processing!) and better stability towards hydrolysis. A severe disadvantage is, in addition to higher production costs, the loss in impact strength. It shows a brittle break behavior with low energy absorption capacity. These are the aspects that foil any large commercial success of TMBPA-polycarbonate.

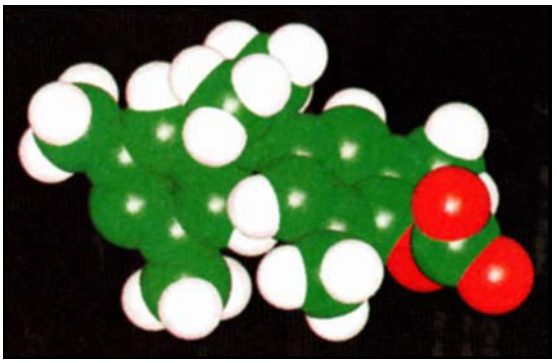

Fig. 2. Space-filling model of a unit of TMBPA-polycarbonate **3**.

How can this dramatic reduction in impact be explained? The modulus/temperature dependance of BPA- and TMBPA-polycarbonate as determined by dynamic mechanical analysis makes it possible to gain insights into the segmental motions of polymer chains. These segmental motions, which exist far below the glass transition, are the essential factors affecting the temperature-dependent polymer-relaxation processes in the solid state and are also responsible for possible macroscopic deformation under stress and consequently for the energy absorption capacity. It emerges (Fig. 3) that the replacement of BPA with TMBPA in polycarbonate not only raises the T_g to 203 °C, but also shifts the γ-relaxation maximum from −105 °C (BPA-polycarbonate) to +45 °C

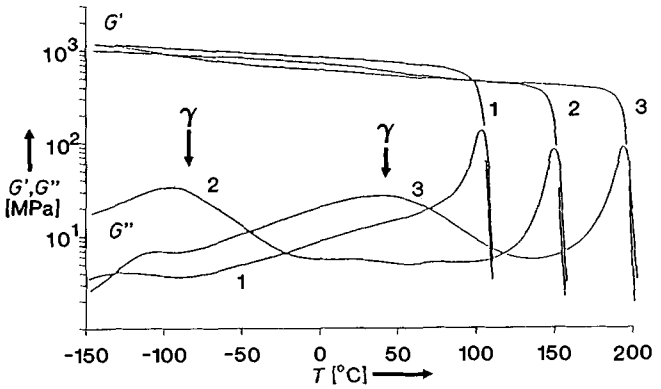

Fig. 3. Comparison of the modulus-temperature relationships of polystyrene (1), BPA-polycarbonate **1** (2), and TMBPA-polycarbonate **3** (3). G' = storage modulus, G'' = loss modulus.

(TMBPA-polycarbonate). Both effects are caused by steric hindrance exerted by the methyl groups which results in reduced rotational freedom of the phenyl–carbonate bond. It should be emphasized that the temperature shift in the γ-relaxation maximum is substantially larger than that for the glass transition. The decreased impact strength of TMBPA-polycarbonate can then be interpreted as a consequence of the shift in the γ-relaxation maximum (for a more detailed discussion see Ref.[81]).

These findings provide an important *new criterion* for the development of high temperature resistance, and at the same time sufficiently impact-resistant polycarbonates. The ratio of the glass transition temperature T_g to the temperature of the maximum of the γ-relaxation T_γ (in Kelvin, determined at 1 Hz) must be equal to or greater than the value of 2.52 determined for BPA-polycarbonate. By comparison T_g/T_γ for TMBPA-polycarbonate is 1.5, significantly lower than that for BPA-polycarbonate, i.e. a technologically valuable polycarbonate with high T_g must have a sufficiently low T_γ.

The comparison of such T_g/T_γ ratios for different polycarbonates assumes that the γ-relaxation intensities are similar. In addition T_g/T_γ is not a direct measure of impact strength because impact behavior is also influenced by other factors and occurs in the nonlinear deformation region.

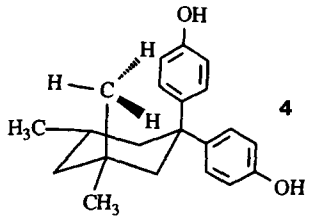

4

A real breakthrough in the solution to this problem (high T_g *and* good impact) was made in 1989 by the introduction of new (co)polycarbonates based on a bisphenol from hydrogenated isophorone (= bisphenol TMC) **4**.[82] The homopolycarbonate **5** (space-filling model shown in Fig. 4) ob-

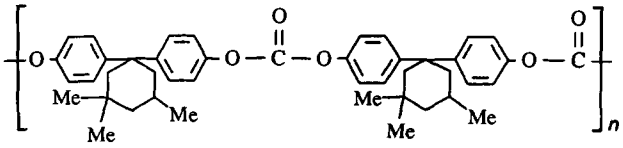

5

tained from **4** has a T_g of 239 °C and T_g/T_γ ratio of 3.1! The significance of this extremely high value can be seen in Table 4 when it is compared to other polycarbonates. How can such a high value of T_g/T_γ be explained? It can be assumed that the restriction in molecular mobility is due to the following additive effects (see the three-dimensional formula of **4**): a) restriction in the conformational mobility of the cyclohexane ring, and b) hindered rotational mobility of a phenyl ring through 1,3-diaxial interactions.

Since the mobility of the carbonate group is not affected ($T_\gamma = -108$ °C!), the polymer retains good impact strength. The T_γ of the bisphenol-TMC-polycarbonate is, in compari-

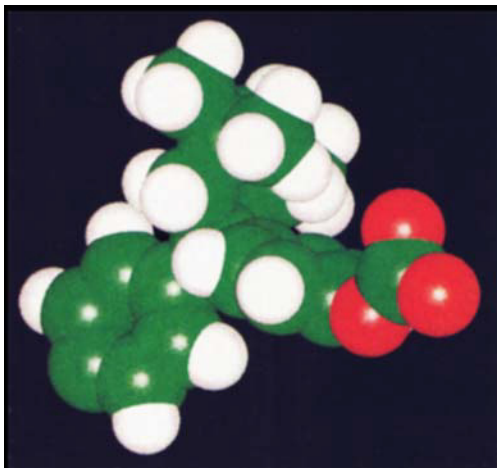

Fig. 4. Space-filling model of a unit of bisphenol-TMC-polycarbonate **5**.

Table 4. Comparison of the glass transition temperature and the temperature of the γ-relaxation maximum of bisphenol-TMC-polycarbonate with those of other polycarbonates and those of an aromatic polyester (based on BPA).

Polymer	T_g [°C]	T_γ [°C]	T_g/T_γ [a]
BPA-polycarbonate **1**	150	−105	2.52
Aromatic polyester	198	−90	2.57
TMBPA-polycarbonate **3**	203	45	1.50
Tetrabromobisphenol-A-polycarbonate	265	105	1.42
Bisphenol-Z-polycarbonate **6**	186	−58	2.13
Bisphenol-TMC-polycarbonate **5**	239	−108	3.10

[a] Temperatures in Kelvin.

son to the value of bisphenol-Z-polycarbonate, **6**, surprisingly low. A more detailed study and explanation of this effect will be published later.

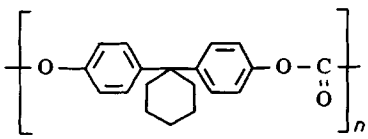

6

Bisphenol-TMC-polycarbonate can be produced in the same way as bisphenol-A-polycarbonate by the same interfacial polymerization process (from **4** and phosgene). Because the phenolic hydroxy groups of bisphenol-TMC have comparable reactivity with those of BPA, copolycarbonates in practically every ratio can be produced. In this way it is possible, depending on the comonomer ratio, to obtain copolycarbonates with T_g's between 150 °C and 239 °C.

The dependence of the glass transition temperature on the comonomer ratio is reflected quite well in the empirical Fox relationship $1/T_g = (C_1/T_{g1}) + (C_2/T_{g2})$ where T_{g1} and T_{g2} are the glass transition temperatures of the corresponding homopolymers, and C_1 and C_2 are the weight fractions of the corresponding bisphenols in the copolymer.

These copolycarbonates can be used as important vehicles in the study of molecular dynamics, particularly in studying low-temperature relaxation phenomena. As was previously mentioned, the maxima of the γ-relaxation for BPA- and TMBPA-polycarbonate are −105 °C and 45 °C respectively. To a first approximation, the positions of these maxima remain constant, independent of copolymer composition—only the peak intensities vary. New relaxation peaks of low intensity can be observed between the two γ-relaxation maxima. By systematic variation of the molecular structure of such polycarbonates it is possible to gain an insight into the length of those segments which are responsible for the low-temperature relaxation processes. Unfortunately the literature does not provide a complete picture of this situation.

BPA- and bisphenol-TMC-copolycarbonates show practically no impact problems while BPA/TMBPA copolycarbonates have serious deficiencies in impact strength. The main reason for these differences, as has already been mentioned, is that the γ-relaxation maxima of BPA- and BPTMC-polycarbonates are practically identical, while the γ-relaxation maximum for TMBPA-polycarbonate is shifted to a significantly higher temperature. Tables 5 and 6 show the basic properties of bisphenol-TMC-copolycarbonates in comparison to those of BPA-polycarbonate and other high-temperature-resistant amorphous thermoplastics.

While bisphenol-TMC-copolycarbonates have thermal stabilities comparable to those of aromatic polyester carbonates, their lower melt viscosity allows for better processibility. This processing advantage (due to lower melt viscosity) of bisphenol-TMC homo- and copolycarbonates as compared to other amorphous thermoplastics with similar temperature resistance can also be seen in Tables 5 and 6.

Table 5. Bisphenol-TMC-copolycarbonates in comparison to aromatic polyester carbonates and to bisphenol-A-polycarbonate.

	Content of **4**, [mol%]	T_g [°C]	Impact strength [kJ m^{-2}] [a]	Melt viscosity [Pa s] [b]	UV-stability
Polycarbonate from 65 mol% bisphenol A and 35 mol% **4**	35	187	n.b.	780	+
Polyester carbonate from 20 wt% BPA-carbonate and 80 wt% bisphenol-A-isoterephthalate (1:1)	–	184	n.b.	1600	–
Polycarbonate from 80 mol% BPA and 20 mol% **4**	20	174	n.b.	425	+
Polyester carbonate from 50 wt% BPA-carbonate and 50 wt% bisphenol-A-isoterephthalate (1/1)	–	172	n.b.	900	–
Polycarbonate from 100 mol% BPA	0	150	n.b.	200	–

[a] Determined according to ISO 180; n.b. = not broken. [b] Determined at 340 °C and a shear rate of 10 · s^{-1}.

Table 6. Comparison between bisphenol-TMC-polycarbonate, bisphenol-TMC-copolycarbonates, and other amorphous thermoplastics.

	Content of [mol%]	T_g [°C]	Impact strength [kJ m^{-2}] [a]	Melt viscosity [Pa s] [b]	UV-stability
Polycarbonate from 100 mol% **4**	100	239	8 × n.b. 2 × 150	400	+
Polyether imide	–	219	110	360	–
Polycarbonate from 45 mol% bisphenol A and 55 mol% **4**	55	205	n.b.	120	+
Polyarylate from bisphenol-A-iso/terephthalate (1/1)-	–	190	n.b.	300	–
Polysulfone from bisphenol A and 4,4'-dichlorodiphenyl sulfone	–	189	n.b.	270	–

[a] Determined according to ISO 180; n.b. = not broken. [b] Determined at 395 °C and a shear rate of 10 s^{-1}

These findings, high T_g and good impact strength combined with good melt flow, has not yet been obtained with any other aromatic polycarbonate. Another advantage of bisphenol-TMC-polycarbonates is their UV-stability, which is close to that of standard polycarbonate. Short term exposure of bisphenol-TMC-homopolycarbonate to temperatures of up to 400 °C (in air) results in only minimal discoloration. There is also a significant drop in the melt viscosity between 360 °C and 395 °C which can be used to increase product output (see Table 7).

Table 7. Melt viscosities [Pa s] at different shearing rates and temperatures.

	360 °C		395 °C	
Shear rate [s^{-1}]	100	1000	100	1000
BPA-polycarbonate **1** (η_{rel} = 1.32) [a]	139	116	91	83
Polyester carbonate from 50 wt % BPA-carbonate and 50 wt % bisphenol A-iso-/terephthalate (1/1), (η_{rel} = 1.30) [a]	256	261	131	111
Polyester carbonate from 20 wt % BPA -carbonate and 80 wt % bisphenol A-iso/terephthalate (1/1) (η_{rel} = 1.30) [a]	831	643	300	267
Bisphenol-TMC-polycarbonate **5** (η_{rel} = 1.296) [a]	1385	921	275	212

[a] η_{rel} = solution viscosity.

The starting materials are available in commercial quantities, and this together with the outstanding basic properties of these polycarbonates helps in commercializing the final products. The polymer precursor, bisphenol-TMC **4**, is produced in yields greater than 80 % by hydrogenation of isophorone and subsequent condensation of the resulting dihydroisophorone with phenol (Scheme 3).

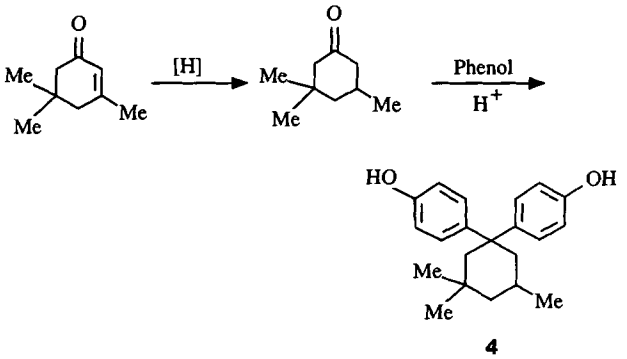

4

Scheme 3. Synthesis of **4** from isophorone.

To conclude this section some homo- or copolycarbonates will be described which can either supplement the inherent weaknesses of BPA-polycarbonate, or exhibit new properties such as liquid crystalline behavior (for a more detailed review see Ref.[5]).

a) Copolycarbonates of bisphenol A and tetrabromobisphenol A are of commercial importance. A small mol % of the comonomer enhances the flame resistance while having little effect on the standard property characteristics of BPA-polycarbonate (V 0/3.2 mm under UL 94 for transparent grades).

b) Polycarbonates with lower or zero birefringence are required for laser-optical data storage systems. One approach is to choose bisphenols which have built-in compensation of their birefringent components. The relatively high birefringence of BPA-polycarbonate can be attributed to the alignement of the phenyl rings "in series". Polycarbonates with low birefringence can be obtained from bisphenols containing bulky, polarizable side groups such as bisphenol AP (from acetophenone and phenol).[83, 83a] (For a review on "Polycarbonate and Light", see Ref.[83a]). An intramolecular compensation of birefringent components is also possible if both phenyl rings of the bisphenol are fixed perpendicular to each other via a spirocenter. An example of this type of structure is found for 6,6′-dihydroxy-3,3,3′,3′-tetramethyl-1,1-spiro(bisindane)polycarbonate.[80] The homopolymer is virtually birefringence-free, while the birefringence of the copolycarbonate with bisphenol A is dependent on the spiro(bisindane) content.

c) Fully aromatic copolycarbonates obtained by incorporation of at least 25 mol % 4,4′-dihydroxydiphenyl (based on the total bisphenol content) in combination with other bisphenols such as 4,4′-dihydroxydiphenyl ether surprisingly show thermotropic behavior.[84]

3.2. Block Copolycarbonates

By incorporating chemically different segments—for example flexible, hydrophilic, or hydrophobic blocks—in the polymer chain, it is possible to modify the property profile of polycarbonates (see also Ref.[5]). These segmented polycarbonates are preferably made as tri-block A–B–A, or multiblock ($(A\text{-}B)_n$) systems.

The synthesis of block copolycarbonates is best carried out in a homogeneous phase using inert solvents, or by interfacial polycondensation through the use of preformed mono- or bifunctional oligomers. By coupling equimolar amounts of bifunctional, reactive prepolymers, e.g. hydroxyl-terminated oligomers, and chloroformate-terminated oligomers, it is possible to obtain block copolycarbonates with an exact alternating sequence. On the other hand, the phosgenation of several hydroxyl-terminated species (bisphenols, oligomers) results in a nonuniform, more or less statistical arrangement. A completely random structure is only obtained when the hydroxyl-terminated components have the same reactivity toward phosgene. When the components differ in reactivity, fairly long sequences of the same structure are formed. The phosgenation of bisphenols of different acidities gives a block structure.[85]

3.2.1. Aromatic Poly(carbonate-cocarbonates)

These block copolymers are prepared by a two-stage interfacial process.[86, 87] Bisphenols used in this manner along with BPA include TMBPA,[88] 3,3′,5,5′-tetrabromobisphenol A, and 3,3′,5,5′-tetrachlorobisphenol A.[89, 90] These block copolymers have higher softening temperatures than the corresponding statistical copolymers.[89]

3.2.2. *Aromatic-Aliphatic Poly(carbonate-cocarbonates)*

For the preparation of mixed aromatic-aliphatic polycarbonates by the interfacial method, aliphatic hydroxyl groups have to be first converted into more reactive terminal groups (see also 3.2.3).

3.2.3. *Poly(ether-cocarbonates)*

The synthesis of poly(ether-cocarbonates) from poly(oxyethylene) glycol or poly(oxytetramethylene) glycol can be achieved using the corresponding bischlorocarbonates.[91] Under special conditions, the poly(ether)diols may also be incorporated directly by the interfacial method.[92] Through the incorporation of 20–30 wt. % of polyether blocks in BPA-polycarbonate as soft segments, a thermoplastic elastomer is obtained which is characterized by a remarkable combination of high strength and elastic recovery.[93, 94]

These block copolymers have been developed for use as oil-resistant elastomers and biocompatible membrane materials. The polar hydrophilic character of the flexible polyether segments is exploited in the separation of polar from nonpolar gases, microfiltration, ultrafiltration, electrophoresis, dialysis (blood purification), and reverse osmosis (desalination of seawater). The permeation properties are better than those of cellulose hydrate membranes.[5]

3.2.4. *Poly(ester-cocarbonates) with Aliphatic Polyester Segments*

These block copolymers, which, for example, contain dimeric acid[*]/hexanediol polyesters as soft segment, can be synthesized by interfacial polycondensation. Polycarbonate elastomers with a high content of dimeric fatty acid ester soft segments are expecially suitable as packaging materials for biological fluids. Block copolycarbonates containing less than 10 wt % dimeric acid, in comparison with the corresponding homopolycarbonate, have better low-temperature impact strength, better mold release properties, and higher stress-crack resistance to organic solvents.[95]

3.2.5. *Poly(siloxane-cocarbonates)*

Polysiloxane cocarbonates, in particular those based on polydimethylsiloxane and bisphenol A, count among the most investigated block copolymers. They are synthesized by cophosgenation of BPA with suitably terminated siloxane oligomers.

Exact alternating poly(siloxane-cocarbonates) of this type can be obtained by reaction of hydroxy-terminated oligocarbonates either with chlorine-terminated polysiloxanes in the presence of tertiary amines, or with dimethylamino-terminated polysiloxanes with elimination of dimethylamine by thermal cleavage.[87, 96–100] By suitable variation of stoichiometry or block lengths, it is possible to produce a wide variety of polymers representing the whole range of hardness and deformation, i.e. from an elastomer-modified thermoplastic to a thermoplastic elastomer. Their mechanical and optical properties are due to their two-phase nature caused by the formation of domains of different size and structure (microphase separation). Block copolymers with low polysiloxane content have outstanding low-temperature impact strength, while block copolycarbonates with a high polysiloxane content act as thermoplastic elastomers. In the latter case the dispersed polycarbonate domains can be thougth of as physical cross-links which allow the polysiloxane matrix to have a high elastic recovery across a broad temperature range.[101–104]

3.3. The Incorporation of Tri- or Higher Functional Monomers

In the melt, linear bisphenol A-polycarbonate exhibits Newtonian flow behavior up to high shear rates, i.e. the viscosity is nearly independent of shear rate. The incorporation of small amounts of tri- or multifunctional monomers gives branched polycarbonates exhibiting structural viscosity, i.e. non-Newtonian flow behavior (Fig. 5).

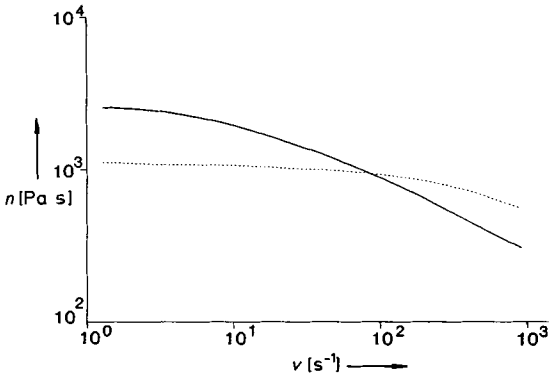

Fig. 5. Dependence of the melt viscosity η of linear (– – –) and branched (——) polycarbonates on shear rate ν at 300 °C.

From a commercial point view this means that branched polycarbonates are well suited for extrusion applications due to their high melt strength. In addition to the thermal stability of the branched junctions, the functional groups of the branching agent should have the same reactivity during the polymerization; 1,4-bis(4,4'-dihydroxytriphenylmethyl)benzene fulfills these conditions.[105] However nitrogen-containing branching agents have been described such as 3,3-bis(4-hydroxyphenol)-2-oxo-2,3-dihydroindole,[106] whose third functional group reacts after the branching agent has been incorporated into the polymer chain (→ long chain branching).

Branched BPA-polycarbonates are used primarily in the production of twin wall sheets, which is one of the largest growth areas for polycarbonate.[2] Twin wall sheets exhibit the following characteristics: excellent insulation, easy handling, high rigidity combined with good impact strength. In addition they are lightweight materials.

[*] Dimeric acids are dicarboxylic acids containing at least two side chains and one double bond which are obtained by dimerization of unsaturated fatty acids.

As a result, twin wall sheets can be used in applications such as glazing greenhouses, industrial windows, and dome construction. This effective control of melt viscosity behavior in BPA-polycarbonates has stimulated further, similar investigations on other industrial thermoplastics such as polyamides.

3.4. Modification of BPA-polycarbonate by Acid Moieties

Another way to improve the temperature resistance of BPA polycarbonate is through the incorporation of rigid aromatic ester units from terephthalic or isophthalic acid and BPA. The higher glass-transition temperatures of these polymers are due to the amount as well as the increased lengths of these rigid molecular units, i.e. the persistence length (Fig. 6). Even so, there is no severe restriction in the

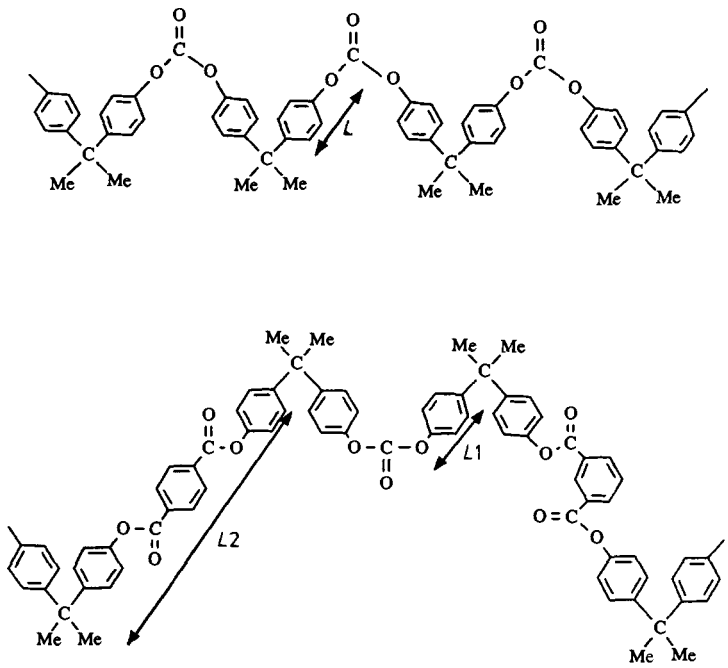

Fig. 6. Differences in the persistence lengths L in polycarbonates and aromatic polyester carbonates.

mobility of the carbonate group in aromatic polyester carbonates, as is observed in TMBPA-polycarbonate. Therefore these copolycarbonates have impact strengths similar to BPA-polycarbonate. Unfortunately, due to a stronger "physical cross-linking" effect (caused by higher entanglement density, see Ref.[81, 107–109]), aromatic polyester carbonates have higher melt viscosities than BPA-polycarbonate, which results in processing difficulties, particularly in molds containing long thin flow paths (see Tables 5–7).

Despite the higher melt viscosity, Bayer, General Electric, and Unitika (Japan) have commercialized aromatic polyester carbonates with glass-transition temperatures, depending on the aromatic ester content, of between 150 °C and approx. 190 °C. These materials have found typical applications in the electrical, electronic, lighting, automobile, and medical sectors, and in household appliances.

In nearly all of these market applications high temperature resistance, transparency, and impact strength are prerequisite.

This general concept of the incorporation of rigid units is currently being used also in the polyamide field (new aromatic-aliphatic polyamides from BASF, Ultramid T®, and Amoco, Amodel®).

Other polycarbonate modifications have been described in the literature such as partial replacement of the carbonate group by phosphonate groups thereby producing aromatic polyphosphonatocarbonates. These thermoplastic materials are inherently flame resistant and halogen-free,[5] however they are not commercially used because more effective alternatives for polycarbonate exist (see Section 5).

4. End-Group Variation

Typically, linear bisphenol A-polycarbonates of commercial significance have a molecular weight of ca. $M_w = 22000$ to $M_w = 35000\ g\,mol^{-1}$. The melt viscosity of these polycarbonates is relatively high, which means that the production of intricate molded parts, such as digital audio compact disks, is difficult.

In order to regulate the molecular weight and control the melt viscosity, phenol or *tert*-butylphenol are used as typical end groups. A reduction of the molecular weight to less than $M_w = 22000\ g\,mol^{-1}$ and a subsequent reduction in the melt viscosity, which is needed for compact disk production, is not possible without a corresponding loss in mechanical properties, particularly impact strength, when using the above-mentioned end groups.

The use of *p*-alkylphenols with branched alkyl groups containing eight or nine carbon atoms results in extremely high melt flow polycarbonates with a molecular weight of approx. $M_w = 18000\ g\,mol^{-1}$, which for all practical purposes have sufficient impact strength.[110] The improvement in toughness can be attributed to an additional relaxation process on the high-temperature shoulder of the γ-relaxation maximum.

These polycarbonates flow easily and uniformly, resulting in minimal entropy-elastic strain frozen into the material, and consequently lower optical birefringence. The relationship between mechanical properties, melt flow index (MFI),

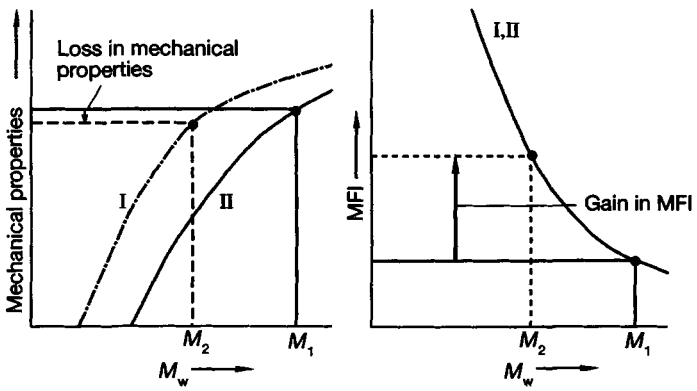

Fig. 7. Relationships between the general mechanical properties, the melt flow index MFI, and the molecular weight M_w for a CD-type (I) and standard polycarbonate (II).

and molecular weight for end-group-modified polycarbonate is shown in Figure 7.

Polycarbonates with branched long-chain *p*-alkylphenyl end groups are advantageous in the production of high-quality compact disks. Due to the lower optical birefringence of these disks the stored digital information can be read accurately by laser-optics. The digital information is precisely stored in cavities, the so-called pits, on the polycarbonate surface, which have a depth of approx. one quarter of the wavelength of the incident laser light (Fig. 8).

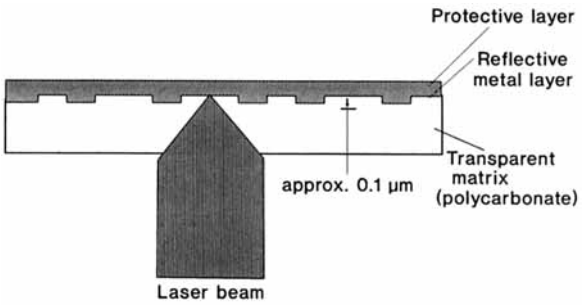

Fig. 8. Schematic model of a music-CD.

The cycle-time for producing a CD, a measure of productivity, which in 1984 was between 15 and 20 seconds, had in 1990 been reduced to approx. seven seconds. Accordingly, the recording industry has been revolutionized, replacing the PVC long-play disks by compact disks. Over 1.15 billion compact disks were produced in 1990 from approx. 23000 t polycarbonate.[2]

5. Property Modifications by Additives

Since the field of additives is so broad (for a comprehensive review see Ref.[5]), only flame retardant additives will be discussed here. The inherent flame resistance of BPA-polycarbonate (oxygen-index 26), as opposed to other engineering thermoplastics, is satisfactory enough for many applications.

The first generation of flame retardant additives for engineering thermoplastics were based on aromatic halogen compounds. For polycarbonate, tetrabromobisphenol-A-oligocarbonate is added either as an additive or directly as a copolycarbonate based on bisphenol A and tetrabromobisphenol A. This type of flame retardant technology has the disadvantage of producing hydrogen bromide (as well as other degradation products), which causes corrosion and introduces toxicity problems.

The second generation of flame retardant additives for polycarbonate employs additives free of chlorine and bromine, and the underlying principle may also be a key in solving the flame retardancy problems in other thermoplastics. In this technique, specific alkali salts of sulfonic acids and in particular the salts of perfluoroalkyl sulfonic acids[111] are used.

As little as 0.1 wt. % of such an additive is required for flame retardancy, which is low enough for the polycarbonate to remain transparent and to retain its mechanical properties.

The mechanism of flame retardancy by these additives is based on a Fries rearrangement of the aryl carbonate group, which results in the branching or cross-linking of the polycarbonate matrix at flame temperatures (see Scheme 4).[112, 113]

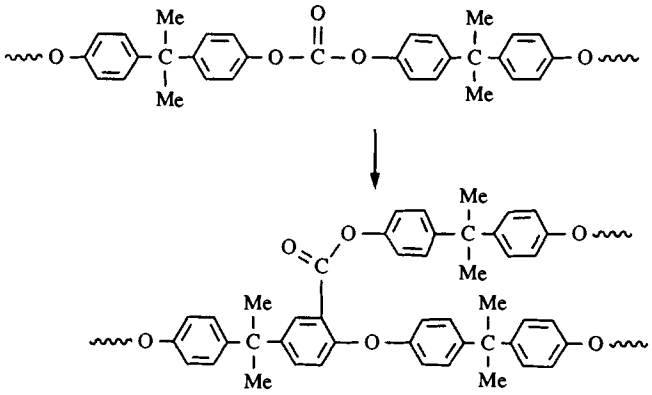

Scheme 4. The Fries rearrangement responsible for the flame-retarding action of alkali-metal sulfonates.

By this process, the melt behind the flame front is stabilized against burning drips, and also aids in the formation of a carbon protective layer. This flame retardancy effect can be improved by starting with branched, and therefore structurally viscous, polycarbonate.

6. Polycarbonate blends

Within the family of polycarbonates many interesting miscibility effects can be found (see also Ref.[5]).[114-116]

Miscibility is observed over the entire compositional range for the following binary systems: polycarbonates of TMBPA and BPA, TMBPA and bisphenol Z, TMBPA and bisphenol TMC, and BPA and bisphenol Z.

TMBPA-polycarbonate has in this respect the nature of a quasi-universal blending partner in producing single phase systems. This behavior is probably due to a steric shielding effect of the four methyl groups, which limits the interactions of parts of the TMBPA-polycarbonate molecules. This can be supported by the low cohesive energy-density of TMBPA-polycarbonate as compared to other polycarbonates.

Blends of BPA-polycarbonate and TMBPA-polycarbonates show, across the entire temperature spectrum, a similar relaxation behavior to the corresponding copolycarbonates: For both blend partners the typical γ-relaxation peaks vary in intensity with composition but the position of the γ-relaxation maxima remains constant. This suggests that the local segmental mobilities responsible for the γ-relaxation behavior are mainly of an intramolecular nature.

Two-phase systems with low partial miscibility are found for example, in the case of BPA-PC/BPTMC-PC blends. Blends from BPA- or BPTMC-polycarbonates and BPA/BPTMC-copolycarbonates with appropriate compositions are fully miscible, i.e. single-phase systems. These examples reflect the broad variability in structure/property relationships of blends in the "polycarbonate family."

Blends from polycarbonates and vinyl thermoplastics are also important from both a scientific as well as a commercial point of view. Table 8 shows some selected examples. Of these systems two have acquired special commercial importance: BPA-PC/SAN and BPA-PC/PBT (or BPA-PC/PET).

Table 8. Examples of blends from polycarbonates and vinyl thermoplastics.

Blend [a]	Remarks on miscibility (see also Ref. [115,116]) [b]
BPA-PC/PS	Two phases with marginal miscibility
BPA-PC/SAN 28 [c]	Two phases with increased partial miscibility
BPA-PC/PMMA	Two phases with significant partial miscibility, LCST [d] of approx. 180 °C
TMBPA-PC/PS	Complete miscibility with LCST [d] of approx. 240 °C [117]
TMBPA-PC/SAN	Extent of miscibility is controlled by the acrylonitrile content of the SAN blend partner
TMBPA-PC/SMA	Extent of miscibility is controlled by the maleic anhydride content of the SMA blend partner [e]
BPA-PC/PBT	Complete miscibility possible. The degree of miscibility is extremely dependent on the thermomechanical history of the blend. The degree of phase separation is driven by the ability of the PBT component to crystallize as well as by the degree of transesterification.
BPA-PC/PET	Not completely miscible as for BPA-PC/PBT
BPA-PC/poly-(ε-caprolactone)	Completely miscible as with many other aliphatic polyester

[a] For meaning of abbreviations see Figure 1; SAN = styrene/acrylonitrile copolymer, SMA = styrene/maleic anhydride copolymer. [b] According to typical compounding procedures followed by immediate quenching. [c] SAN with 28 wt% acrylonitrile. [d] LCST = Lower Critical Solution Temperature.

Both systems generally require the addition of an impact modifier, (for example, certain elastomers, from graft copolymers) to guarantee sufficient toughness, particularly in the low-temperature region, thus producing ternary or even quaternary systems of extreme complexity. Besides the partial miscibility of the blend components, which is required for their phase coupling, the deformation modes of the system are also dependent on the deformation mechanisms of the blend partners, (such as PC and SAN), as well as on the morphological architecture of the blend as a whole. In these blends, the polycarbonate component determines the character of the respective multi-phase systems.

6.1. Polycarbonate/ABS blends

Since their introduction in 1967, there has been a dramatic growth in the market volume of PC/ABS blends; in Western Europe, USA, and Japan it reached 29000 t by 1986. In 1996 the consumption of these blends is expected to reach 100000 t with a yearly growth of 12–13%, an overproportionate growth compared to even polycarbonate. The reason for this success is a better cost/performance balance. PC/ABS blends have found application in the automobile industry and in the electrical engineering and electronics sectors.

The outstanding characteristic of PC/ABS blends is their synergistic improvement of the notched impact strength at low temperature (Fig. 9). The aforementioned partial miscibility between BPA-polycarbonate and SAN is the main reason for this effect.[118]

Flame retardant PC/ABS blends are becoming more important (particularly those flame retardant grades which are chlorine- and bromine-free, which set the trend for the future). In these systems, flame retardancy is achieved through the combination of organic phosphates and finely dispersed polytetrafluoroethylene. This technology can serve as a model for the development of other flame retardant technical thermoplastics.

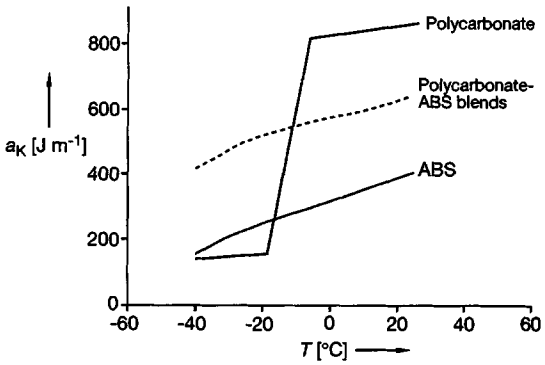

Fig. 9. Ductile–brittle transition of polycarbonate, ABS copolymers and polycarbonate-ABS blends (a_k = notched impact strength).

6.2. Polycarbonate-Polyester blends

The second most important class polycarbonate blends are the elastomer-modified polycarbonate/polyester blends, whose market volume in 1986 had reached 30000 t worldwide only six years after their introduction. In 1991 a market volume of approx. 70000 t is predicted.

This extraordinary growth can mainly be attributed to a combination of good temperature resistance, high toughness, and stress-crack resistance which are prerequisites for exterior applications in the automobile industry. These blends can be tailor-made for specific applications. For example, a blend from polycarbonate, polyethylene terephthalate, and an elastomer modifier has been developed for online paintable bumpers, which are stable towards benzene and can withstand an impact of up to 8 km h^{-1} down to −20 °C without irreversible deformation.

7. Outlook

The chemical and physical potential of the polycarbonate structure has by no means been exhausted, despite extensive application of fundamental polymer principles, as has been described in this article. On the contrary, new theoretical approaches are constantly being developed, such as computer simulation of the solid state (static as well as dynamic), which are more advanced for polycarbonates than for other engineering thermoplastics (see Ref.[120–122]). Through these methods, new insights into the microstructure of polycarbonates will be obtained which will act as guidelines for future chemical and technical developments.

We thank Dr. Lundy for assistance in translating the German text.

Received: April 15, 1991;
revised: August 2, 1991 [A 846 IE]
German version: *Angew. Chem. 103* (1991) 1626

[1] H. Schnell, *Angew. Chem. 68* (1956) 633–640.
[2] K. Kircher, *Kunststoffe 80* (1990) 1113–1117.
[3] A. S. Wood, *Mod. Plast. Int. 19* (1989), No. 12, pp. 39–42.
[4] D. N. Fox, *ANTEC-Paper*, Chicago 1985.
[5] D. Freitag, U. Grigo, P. R. Müller, W. Nouvertne: *Polycarbonates* (*Encycl. Polym. Sci. Eng. 11* (1988) 648–718).
[6] H.-J. Buysch, H. Krimm, DE-A 2447348 (1974), Bayer AG.
[7] U. Romano, R. Tesei, M. M. Mauri, P. Rebora, *Ind. Eng. Chem. Prod. Res. Dev. 19* (1980) 396–403.
[8] G. L. Curnutt, EP-A 269718 (= WO 87/07601) (1986), Dow Chem. Co.
[9] H. Krimm, H.-J. Buysch, H. Rudolph, EP-A 000879 (1977), Bayer AG.
[10] H. Krimm, H.-J. Buysch, H. Rudolph, EP-A 000880 (1977) Bayer AG.
[11] G. Illuminati, U. Ramano, R. Tesei, DE-A 2528412 (1974), Snamprogetti S.p.A.
[12] U. Romano, R. Tesei, DE-A 2552907 (1974), Anic S.p.A.
[13] J. E. Hallgren, DE-A 3308921 (1982), General Electric Co.
[14] V. Mark, DE-A 3445552 (1983), General Electric Co.
[15] V. Mark, DE-A 3445553 (1983), General Electric Co.
[16] Y. Kiso, Y. Matsunaga, EP-A 338760 (1988), Mitsui Petrochemical Industries, Ltd.
[17] D. J. Brunelle, *Makromolecular Reports A 28 (2)* (1991) 95–102.
[18] T. Sakashita, T. Shimoda, EP-A 351168 (1988), GE Plastics Japan Ltd.; EPA-A 360578 (1988) GE, Plastics Japan Ltd.
[19] D. J. Brunelle, US-A 4330664 (1979), General Electric Co.
[20] T. Horikawa, T. Takeda, Jpn. Kokai Tokkyo Koho 62158719 (1986), Daicel Chemical Industries Ltd.; *Chem. Abstr. 107* (1987) 237569 h.
[21] K. Tominari, A. Kanazawa, Y. Shigeta, Jpn. Kokai Tokkyo Koho 02153923 (1988), Nippon G. E. Plastics K. K.; *Chem. Abstr. 113* (1990) 133138 z.
[22] K. Tominari, A. Kanazawa, Y. Shigeta, Jpn. Kokai Tokkyo Koho 02153924 (1988), Nippon G. E. Plastics K. K.; *Chem. Abstr. 113* (1990) 133140 u.
[23] K. Tominari, A. Kanazawa, Y. Shigeta, Jpn. Kokai Tokkyo Koho 02153925 (1988), Nippon G. E. Plastics K. K., *Chem. Abstr. 113* (1990) 133165 f.
[24] K. Tominari, A. Kanazawa, Y. Shigeta, Jpn. Kokai Tokkyo Koho 02153926 (1988), Nippon G. E. Plastics K. K., *Chem. Abstr. 113* (1990) 133139 a.
[25] K. Tominari, A. Kanazawa, Y. Shigeta, Jpn. Kokai Tokkyo Koho 02153927 (1988), Nippon G. E. Plastics K. K.; *Chem. Abstr. 113* (1990) 133137 y.
[26] D. Morinaka, H. Imada, S. Kawase, Jpn. Kokai Tokkyo Koho 109591 (1977), Teijin Ltd.; *Chem. Abstr. 88* (1978) 74881 b.
[27] S. Fukuoka, T. Watanabe, T. Dozono, EP-A 338085 (1989), Asahi Chemical Industry Co. Ltd.
[28] I. Fukawa, S. Fukuoka, K. Komiya, Y. Sasahi, EP-A 403657 (= WO 90/7536) (1990), Asahi Chemical Industry Co. Ltd.
[29] D. J. Brunelle, W. E. Smith, DE-A 2950136 (1978), General Electric Co.
[30] H. Krimm, H.-J. Buysch, H. Rudolph, EP-B 39452 (1980), Bayer AG.
[31] D. A. Bolon, J. E. Hallgren, US-A 4452968 (1983), General Electric Co.
[32] B. Hudson, EP-A 299773 (1987), BP Chemicals Ltd.
[33] T. Watanabe, M. Chiyono, S. Shinsuke, Jpn. Tokai Tokkyo Koho 63205318 (1987), Asahi Chemical Industry Co. Ltd.; *Chem. Abstr. 110* (1989) 95991 a.
[34] T. Watanabe, M. Chono, S. Fukuoka, Jpn. Kokai Tokkyo Koho 63223035 (1987), Asahi Chemical Industry Co. Ltd.; *Chem. Abstr. 110* (1989) 155052 g.
[35] M. K. Akkapeddi, B. T. De Bona, Y.-C. Lai, D. C. Prevorsek, US-A 4398018 (1981), Allied Corporation.
[36] H. Brinkmeyer, M. Schmidt, H. Perry, A. El Sayed, EP-A 132637 (1986), Bayer AG.
[37] Y.-C. Lai, B. T. De Bona, D. C. Prevorsek *J. Appl. Polym. Sci 36* (1988) 819.
[38] J. E. Hallgren, DE-A 2738437 (1976), General Electric Co.
[39] A. J. Chalk, DE-A 2738487 (1976), General Electric Co.
[40] J. E. Hallgren, DE-A 2738488 (1976), General Electric Co.
[41] A. J. Chalk, DE-A 2815501 (1978), General Electric Co.
[42] J. E. Hallgren, DE-A 2815520 (1976), General Electric Co.
[43] J. E. Hallgren US-A 4349485 (1979), General Electric Co.
[44] D. A. Bolon, J. E. Hallgren, DE-A 3410428 (1983), General Electric Co.
[45] T. C. T. Chang, EP-A 350697 (1988), General Electric Co.
[46] T. C. T. Chang, EP-A 350700 (1988), General Electric Co.
[47] J. E. Hallgren, DE-A 2738519 (1976), General Electric Co.
[48] A. J. Chalk, DE-A 2738520 (1976), General Electric Co.
[49] J. E. Hallgren, DE-A 2815512 (1978), General Electric Co.
[50] J. E. Hallgren, DE-A 2949936 (1978), General Electric Co.
[51] D. A. Bolon, T. B. Gorczyca, J. E. Hallgren, US-A 4533504 (1982), General Electric Co.
[52] S. Fukuoka, H. Ogawa, T. Watanabe, Jpn. Kokai Tokkyo Koho 01165551 (1987), Asahi Chemical Industry Co. Ltd.; *Chem. Abstr. 112* (1990) 76618 j.
[53] H. Schnell, L. Bottenbruch, *Makromol. Chem. 57* (1962) 1–11.
[54] A. Horbach, H. Vernaleken, K. Weirauch, *Makromol. Chem. 181* (1980) 111–124.
[55] D. J. Brunelle, T. L. Evans, T. G. Shannon, E. P. Boden, K. R. Stewart, L. P. Fontana, D. K. Bonauto, *Polym. Prepr. Am. Chem. Soc. Div. Polym. Chem. 30* (1989) 567–570.
[56] E. P. Boden, D. J. Brunelle, T. G. Shannon, *Polym. Prepr. Am. Chem. Soc. Div. Polym. Chem. 30* (1989) 571–572.
[57] T. L. Evans, C. B. Berrnan, J. C. Carpenter, D. Y. Choi, D. A. Williams, *Polym. Prepr. Am. Chem. Soc. Div. Polym. Chem. 30* (1989) 573–574.
[58] K. R. Stewart, *Polym. Prepr. Am. Chem. Soc. Div. Polym. Chem. 30* (1989) 575–576.
[59] N. R. Rosenquist, L. P. Fontana, *Polym. Prepr. Am. Chem. Soc. Div. Polym. Chem. 30* (1989) 577–578.
[60] T. L. Guggenheim, S. J. McCormick, J. J. Kelly, D. J. Brunelle, A. M. Colley, E. P. Boden, T. G. Shannon, *Polym. Prepr. Am. Chem. Soc. Div. Polym. Chem. 30* (1989) 579–580.
[61] J. A. Cella, J. J. Talley, J. M. Fukuyama, *Polym. Prepr. Am. Chem. Soc. Div. Polym. Chem. 30* (1989) 581–582.
[62] H. Schnell, *Polym. Rev. 9* (1964).
[63] H. Schnell, *Ind. Eng. Chem. 51* (1959) 157.
[64] H. Schnell, *Plast. Inst. Trans. J. 28* (1960) 143.
[65] W. J. Jackson, Jr., J. R. Caldwell, *Ind. Eng. Chem. Prod. Res. Dev. 2* (1963) 246.
[66] V. Serini, D. Freitag, H. Vernaleken, *Angew. Makromol. Chem. 55* (1976) 175–189.
[67] V. Serini, F. Müller, W. Nising, H.-J. Buysch, D. Freitag, H. Kauth, EP-B 143386 (1984), Bayer AG.
[68] G. S. Kolesnikov, O. V. Smirnova, E. V. Korovina, N. M. Zimmer, *Vysokomol. Soedin. Ser. A 12* (1970) 1739–1744; *Chem. Abstr. 73* (1970) 110417 f.
[69] E. C. Gilbert, G. D. Brindell, *Coat Plast. Prepr. Pap. Meet. Am. Chem. Soc. Div. Org. Coat. Plast. Chem. 34* (1974) 136.
[70] H. Haupt, H. Vernaleken, K. Weirauch, U. Haberland, DE-A 2462470 (1974), Bayer AG.
[71] P. W. Morgan, *Macromolecules 3* (1970) 536.
[72] R. P. Kambour, J. E. Corn, S. Miller, G. E. Niznik, *J. Appl. Polym. Sci. 20* (1976) 3275.
[73] R. P. Kambour, W. V. Ligon, R. R. Russell, *J. Polym. Sci. Polym. Chem. Ed. 16* (1978) 327.
[74] M. S. Lin, E. M. Pearce, *J. Polym. Sci. Polym. Chem. Ed. 19* (1981) 2659.
[75] P. W. Morgan, *J. Polym. Sci. Part A Gen. Pap. 2* (1964) 437.
[76] J. McClendon, DE-A 2637003 (1977), Dow Chemical Co.
[77] V. Serini, G. Friedhofen, D. Freitag, J. Heuser, DE-A 2615038 (1976), Bayer AG.
[78] V. Serini, D. Freitag, L. Bottenbruch, H. Rudolph, DE-A 2901668 (1988), Bayer AG.
[79] K. C. Stueben, *J. Polym. Sci. Part A Gen. Pap. 3* (1965) 3209.
[80] G. R. Faler, J. C. Lynch, EP-A 287887 (1988), General Electric Co.
[81] L. Morbitzer, U. Grigo, *Angew. Makromol. Chem. 162* (1988) 87–107; G. Weymans, K. Berg, L. Morbitzer, U. Grigo, *ibid. 162* (1988) 109–121.
[82] D. Freitag, U. Westeppe, *Angew. Makromol. Chem. Rapid Commun. 12* (1991) 95–99.
[83] a) G. H. W. Buning, *Proc. Int. Symp. Optical Memory ISOM 1987* (Tokyo 1987), Poster WC 23; b) G. Kämpf, D. Freitag, W. Witt, *Angew. Makromol. Chem. 183* (1990) 243–272.
[84] H. R. Kricheldorf, D. Lübbers, *Macromolecules 23* (1990) 2656–2662.
[85] D. W. Fox, R. R. Gallucci, E. N. Peters, G. F. Smith, *Tech. Pap. Reg. Tech. Conf. Soc. Plast. Eng. Baltimore-Washington Sect. 1985*, 951.
[86] J. P. Critchley, V. C. R. McLoughlin, J. Thrower, I. M. White, *Chem. Ind. (London) 28* (1969) 934–936.
[87] A. Noshay, J. E. McGrath, Block Copolymers, Academic Press, Orlando, FL, USA, 1977.
[88] V. Serini, H. Vernaleken, H. Schnell, DE-A 2211956 (1972), Bayer AG.
[89] S. Kolesnikov, O. V. Smirnova, A. K. Mikitaev, V. M. Gladyshev, *Vysokomol. Soedin. Ser. A 12* (1970) 1424; *Chem. Abstr. 73* (1970) 56658 v.
[90] K. Kohyama, K. Nakamura, A. Matsuno, EP-B 61060 (1982), Mitsubishi Chemical Ind., Ltd.
[91] S. H. Merill, *J. Polym. Sci. 55* (1961) 343.
[92] M. Schreckenberg, R. Dhein, R. Lange, W. Waldenrath, DE-A 3408803 (1984), Bayer AG.
[93] E. P. Goldberg, *J. Polym. Sci. Part C Polym. Symp. 4* (1964) 707.
[94] S. H. Merill, S. E. Petrie, *J. Polym. Sci. Part A Gen. Pap. 3* (1965) 2189.
[95] R. Dhein, D. Nerger, M. Schreckenberg, L. Morbitzer, W. Nouvertné, *Angew. Makromol. Chem. 139* (1986) 157.
[96] H. A. Vaughn, Jr., US-P 3189662 (1961), General Electric Co.
[97] W. D. Merritt, Jr., J. H. Vestergaard, US-A 3821325 (1978), General Electric Co.
[98] W. D. Merritt, Jr., US-A 3832419 (1973), General Electric Co.
[99] W. Büchner, W. Noll, B. Bressell, DE-A 2162418 (1971), Bayer AG.
[100] D. W. Dwight, J. E. McGrath, A. R. Beck, J. S. Riffle, *Am. Chem. Soc. Div. Polym. Chem. Polym. Prepr. 29* (1979) 702.
[101] H. A. Vaughn, *J. Polym. Sci. Part B Polym. Lett 7* (1969) 569.

[102] D. G. LeGrand, *J. Polym. Sci. Part B Polym. Lett* 7 (1969) 579.
[103] R. P. Kambour, *J. Polym. Sci. Part B Polym. Lett* 7 (1969) 573.
[104] M. Narkis, A. V. Tobolsky, *J. Makromol. Sci. Phys. B4* (1970) 877.
[105] D. Freitag, U. Haberland, H. Krimm, DE-A 21 13347 (1972), Bayer AG.
[106] K. Idel, D. Freitag, W. Nouvertne, DE-A 2500092 (1976), Bayer AG.
[107] D. C. Prevorsek, B. T. De Bona, *J. Macromol. Sci. Phys. B19(4)* (1981) 605–622 and *ibid. B25(4)* (1986) 515.
[108] D. C. Prevorsek, Y. Kestan, B. T. De Bona, *Am. Chem. Soc. Div. Polym. Chem. Prepr. 20* (1979) 187–190.
[109] R. A. Mendelson, *Polym. Eng. Sci. 23* (1983) 79–85.
[110] D. Freitag, W. Nouvertne, K. Burkhardt, F. Kleiner, DE-A 2842005 (1980), Bayer AG.
[111] W. Nouvertne, DE-A 1930257 (1970), Bayer AG.
[112] R. P. Carter, G. E. Reinert, *Tech. Pap. Reg. Tech. Conf. Soc. Plast. Eng. N.Y. Sect. 1980*, 5–8.
[113] L. S. Thomas, S. A. Ogoe, *Techn. Pap. Reg. Tech. Conf. Soc. Plast. Eng. Baltimore-Washington Sect. 1985*, 1000–1002.
[114] R. Plaetschke, L. Morbitzer, U. Grigo, U. Westeppe: Mixing Aspects of Polycarbonates, an Important Class of Engineering Plastics, IUPAC-Conference, Montreal 1990.
[115] O. Olabisi, L. M. Robeson, M. T. Shaw: *Polymer-Polymer-Miscibility*, Academic Press, New York, 1979.
[116] L. A. Utracki, Polymer Alloys and Blends, Hanser, München 1989.
[117] R. Casper, L. Morbitzer, *Angew. Makromol. Chem. 58/59* (1977) 1–35.
[118] L. Morbitzer, H. J. Kress, C. Lindner, K. H. Ott, *Angew. Makromol. Chem. 132* (1985) 19–42.
[119] H. J. Kress, F. Müller, C. Lindner, H. Peters, J. Bueckers, DE-OS 3523314 (1987), Bayer AG.
[120] K. Sommer: Theoretisch-experimentelle Korrelation zwischen chemischer Primärstruktur und Eigenschaftsphänomenen bei Polykondensaten, Lecture at the 2nd. Symposium Material Science Research of the BMFT, Dresden, 1991.
[121] D. Theodoru, U. W. Suter, *Macromolecules 19* (1986) 397.
[122] W. Paul, K. Binder, D. W. Heermann, K. Kremer, *J. Phys. (Paris) II*, 1 (1991) 37.

Glycolipids as Immunomodulators: Syntheses and Properties

By Oswald Lockhoff*

Dedicated to Professor Karl Heinz Büchel on the occasion of his 60th birthday

Although the most successful vaccines still consist of attenuated or killed pathogens, it is evident that genetic engineering will eventually provide pure antigens in sufficient quantities. To achieve a protective effect, however, the immune response to these structures, which are only weakly immunogenic, must be activated by adjuvants. The discovery of chemically defined, well-tolerated, synthetic adjuvants is therefore especially important in effective immunoprophylaxis. A very promising class of compounds in this respect are synthetic glycosylamides, with two long alkyl chains consisting of alkylamines and fatty acids. Unlike natural glycolipids, which exert an immunosuppressive effect, the new glycolipid analogues described here show marked immunostimulation. In vaccination experiments with various antigens they provide efficient protection. Their mode of action, which differs from that of known adjuvants, makes glycolipid analogues particularly interesting for immunization of patients with defective T lymphocyte function, for example AIDS patients.

1. Introduction

One of the vital tasks of the mammalian immune system is to provide protection against infectious diseases. This is achieved by a network of interactions of various lymphoid cells (B and T lymphocytes) and phagocytic cells (monocytes, macrophages, granulocytes) through the formation and release of a number of activation, growth, and differentiation factors (interleukin I, interleukin II, tumour necrosis factor). Thus pathogens are selectively neutralized and eliminated, and the body itself remains unharmed.[1] Normally the immune system performs this task extremely well. In some cases, however, it is advisable to modulate the immune system pharmacologically, either by immunostimulation or by immunosuppression. Specific immunostimulation—enhancement of the immune response to specific exogenous structural elements (antigens)—is the aim of vaccination. Besides this there is now increasing interest in nonspecific immunostimulation, which uses a broad, nonantigen-dependent stimulus to elicit a more fundamental defensive response. The vaccination aspects will now be discussed in greater detail.

Most of the vaccines commonly used in human and veterinary medicine still consist of killed or weakened bacteria, viruses, or parasites. Although such vaccines have brought immense achievements to medicine, their potential applications have still not been exhausted. Currently under development are vaccines based on refined surface structures of pathogens (subunit vaccines) or on peptidic immunodominant epitopes hybridized with proteins. This trend has been enhanced by the availability of recombinant DNA technology[2] which makes it possible, for example, to express viral surface proteins in bacteria or cultures of animal cells. One of the great advantages of this approach is that it is much safer because the virulence of the pathogen is absent. However, it also poses the problem that these antigens are much less immunogenic in their pure form. To elicit an adequate protective effect they must be administered together with adjuvants that enhance the specific immune response to the antigens.[3,4]

In adjuvant research the separation of immunostimulation from inflammatory side effects is of central importance. Many adjuvants, such as the classic Freund's Complete Adjuvant (FCA, a water-in-oil emulsion with complete extracts of mycobacteria), are so poorly tolerated that they cannot even be used for veterinary vaccines. The only adjuvants registered for human use are inorganic gels such as aluminum hydroxide, a component of the first peptidic hybrid vaccine, which was tested against malarial diseases in humans.[5-7] In comparison with FCA, however, aluminum hydroxide exerts only weak activity and its use is therefore limited. Accordingly the search for well-tolerated, potent adjuvants has recently intensified enormously.[8]

There are numerous candidates, as described in several review articles:[9-14] metabolites such as interleukins, interferons, or peptide hormones, high molecular weight compounds of microbial origin, or chemically synthesized derivatives of numerous structural classes. Of particular interest are the low molecular weight adjuvants found in bacterial cell walls. These include compounds derived from the active component of mycobacteria (present in FCA), that is, muramyl dipeptide **1** (MDP),[15,16] such as murabutide, muroctasine, and muramyl tripeptide phosphatidylethanolamine (MTP-PE). Other potent adjuvants are compounds from the endotoxin family[17] whose active component is lipid A **2**.[18,19] Derivatives of this basic structure are lipid X or lipid Y, for example. Some of these compounds are undergoing clinical trials as vaccine components.

Modification of the basic structures of active compounds has shown that even tiny variations often lead to complete loss of biological activity. In many cases, however, it was possible to obtain highly active derivatives by covalent conjugation of the active basic structure with lipid residues, as in the examples above.

We have recently discovered a new class of conjugates of carbohydrates and lipids, which have adjuvant properties but are not derivatives of muramyl peptides or endotoxins. They are glycolipid analogues (GLAs), which offers an interesting alternative to existing structures.

[*] Dr. O. Lockhoff
Bayer AG
Zentrale Forschung
W-5090 Leverkusen 1 (FRG)

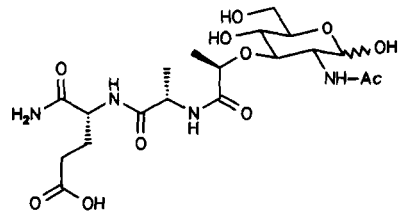

1

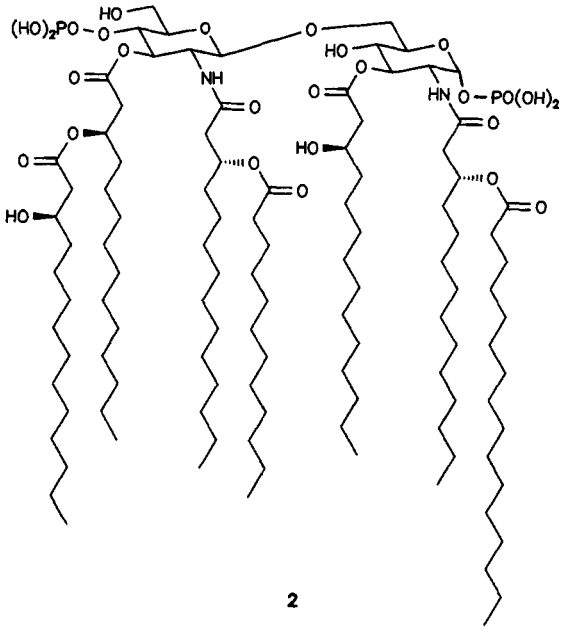

2

Fig. 1. Structural formulas of the immunomodulators muramyldipeptide **1** and lipid A **2**.

2. Glycosylamides as Glycolipid Analogues

Glycolipids are found at the surface of every cell. By virtue of their exposed position in the cell membrane, they serve as binding sites for lectins, antibodies, toxins, bacteria, or viruses and are therefore important in mediating the cell's communication with its external environment.[20-22]

Several hundred glycolipid structures on the mammalian cell surface are currently known. On the basis of their hydrophobic portion, they are divided into two classes, the glycosphingolipids **3** and the glycoglycerolipids **4**. The building blocks for glycosphingolipids are sphingosine, fatty acids, and carbohydrate residues and for glycoglycerolipids glycerol, fatty acids or fatty ethers, and carbohydrates. The sugar residues are *O*-glycosidically bonded.[23]

In view of the fundamental properties of this interesting class of cell wall components, their amphiphilic character conferred by the combination of lipophilic chains with hydrophilic carbohydrate head groups, and their immense biological importance, we began in the early 80s to investigate the chemistry of glycolipids and their simpler analogues in greater details. Our original aim was to synthesize simple

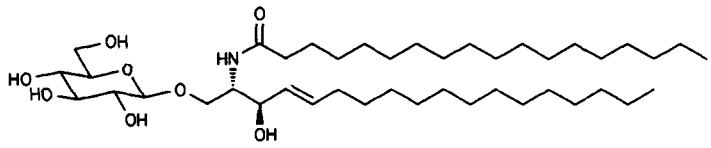

3 glycosphingolipids – glycosylceramides
– gangliosides
– sulfatoglycosphingolipids

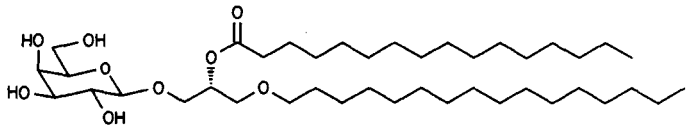

4 glycoglycerolipids – galactoglycerolipids
– sulfatogalactoglycerolipids

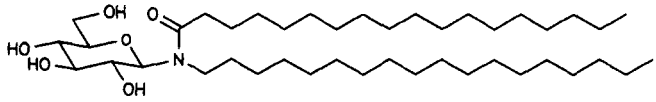

5 glycosylamides (glycolipidanalogues, GLA)

Fig. 2. Prototypes of the naturally occuring glycolipids **3** and **4** and of glycolipid analogues **5**. In **3** and **4** the monosaccharide moieties stand for mono- and oligosaccharides, which can contain *o*-sulfate esters.

glycosylamides such as **5** with long alkyl residues and variations in the polar region and to investigate the response these structures would elicit in biological systems. We expected lipophilic amide residues, formed from long-chain alkylamines and fatty acids and linked directly with the sugars

Oswald Lockhoff was born in 1949 in Cuxhaven, Germany. He studied chemistry at the University of Hamburg and was awarded his Ph.D. in 1980, having worked in the field of oligosaccharide synthesis under the supervision of Hans Paulsen. In the same year he joined Bayer AG as a research chemist in the Central Research Laboratories in Leverkusen and became a group leader in 1986. In 1988 he joined Bayer's Pharmaceutical Research Center in Wuppertal and in 1990 he returned to his position in Leverkusen. His research interests lie in the area of anti-infectives.

through the anomeric carbon atom, to mimic the functions of naturally occurring lipid residues.

2.1. Synthesis of Glycosylamides

Amides are not sufficiently basic to permit direct condensation with free sugars to form glycosylamides.[24] The use of the Hilbert–Johnson reaction[25] with *N*-alkylcarboxylic acid amides is also unsuitable because it produces only *N*-silylated derivatives which prevent *N*-glycoside synthesis.[26] The synthesis of glycosylamides is possible, though, if a two-step process is used.[27] The first step is the reaction of the free hydroxyl group on the anomeric C-atom of a sugar with an amine. This reaction leads to the glucopyranosylamine which, owing to the weak anomeric effect of the nitrogen atom, is obtained with an equatorial configuration.[28] The second step is the selective acylation of the basic nitrogen atom with an activated carboxylic acid derivative to form the glycosylamide.

A glycosylamine can be readily synthesized from a free sugar and ammonia or a short-chain aliphatic amine in a polar solvent at room temperature to give a crystalline product.[24] Owing to the differing solubilities of the free sugar and the fatty amine, however, this variant could not be used in our systems. Only at higher temperatures do the two components react to form glycosylamines. Under these conditions, however, increased quantities of by-products result from the irreversible degradation of the carbohydrates (browning reaction).[24, 29]

The synthesis of long-chain *N*-glycopyranosylamines is most successful if the free sugar such as D-glucose **6a** is warmed to 80 °C for about 15 min with stearylamine **7** (two to three molar excess) in an alcohol–water mixture or dimethylformamide (DMF). The excess of amine suppresses the formation of *N*,*N*-diglycosylamines.[30] Under these conditions the main product of the reaction is the β-glycosylamine **8a**, which precipitates together with the alkylamine **7** when the reaction mixture is cooled. Browning reactions occur to only a modest degree.

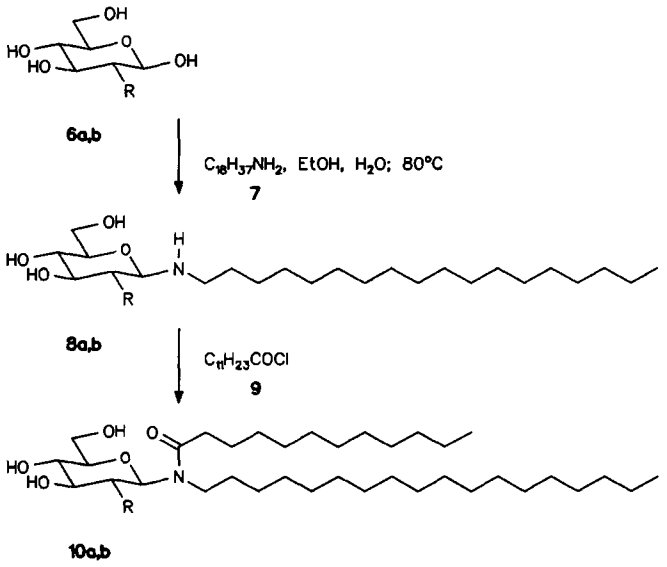

Fig. 3. Synthesis of simple glycosylamides. **a**: R=OH, **b**: R=NHAc.

The subsequent *N*-acylation of the amine mixture was possible in alcoholic solvents with an excess of activated fatty acid derivatives such as lauric acid chloride (**9**) or the mixed anhydride of lauric acid and ethyl chloroformate. This reaction gave a mixture of *N*-(β-D-glucopyranosyl)-*N*-stearyllauramide (**10a**) and *N*-stearyllauramide, from which the glycosylamide **10a** could be isolated chromatographically. Amide **10a** crystallizes from methanolic solution.

Other hexoses and pentoses can be converted to the corresponding glycosylamides under similar conditions. 2-Deoxy-D-glucose reacts with stearylamine **7** at 60 °C to give the corresponding glycosylamine within a few minutes, while the analogous reaction of *N*-acetylglucosamine **6b** with stearylamine **7** to give **8b** requires about 3 hours at 80 °C. Here too, higher temperatures lead to more browning products. Subsequent selective *N*-acylation of **8b** gives the *N*-(2-acetamino-2-deoxy-β-D-glucopyranosyl)-*N*-octadecylcarboxamide (**10b**).

Table 1. Comparison of the specific rotations of *N*-glycopyranosyl-*N*-octadecyldodecanoic acid amides **10**–**16**.

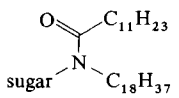

Compound	Sugar	$[\alpha]_D$	Solvent
10a	β-D-glucopyranosyl	8.6	CH_2Cl_2
10b	2-acetamino-2-deoxy-β-D-glucopyranosyl	13.9	THF
11	β-D-galactopyranosyl	11.4	CH_2Cl_2
12	β-D-mannopyranosyl	11.3	CH_2Cl_2
13	2-deoxy-β-D-glucopyranosyl	3.8	THF
14	α-D-arabinopyranosyl	−20.1	THF
15	α-L-arabinopyranosyl	20.0	THF
16	β-D-ribopyranosyl	4.2	THF

The analogous reactions of other hexoses and pentoses with stearylamine and lauric acid chloride gave the glycosylamides listed in Table 1, in yields of 50–70 %.[31]

2.2. Physical Properties of Glycosylamides

The synthesized glycosylamides are chromatographically pure and show small positive optical rotations (Table 1) which confirm the β-configuration.[32] For arabinose derivatives the α-configuration with an equatorial amide residue at C1 was the preferred derivative. The FAB mass spectra show distinct molecular peaks.

Both the ^1H and ^{13}C NMR spectra show the doubling of some signals which indicates the presence of two conformational isomers in solution. In the ^1H NMR spectrum the signals of the anomeric protons of **10a** are detectable at $\delta = 5.45$ and 4.84 with coupling constants of more than 8 Hz (solvent CD_3OD). In the ^{13}C NMR spectrum the signals of the anomeric carbon atoms appear at $\delta = 88.17$ and 84.28 in the intensity ratio 2:1 (solvent CD_3OD). ^{13}C NMR spectra of **10a** in [D_6]dimethyl sulphoxide at various temperatures show that the signals of the anomeric C atoms of this compound are well separated at 300 K ($\delta = 86.25$ and 81.90, intensity ratio 2:1), whereas at 353 K they coalesce. Other *N*-alkyl-*N*-glycosyl fatty acid amides of this class show simi-

lar behaviour. The phenomenon of signal doubling in the NMR spectra of glycosylamides is similar to that observed for analogous glycosylamides in the *N*-acetyl-*N*-(β-D-glucopyranosyl)-naphthylethylamine class, in which hindered rotation about the amidic C–N bond was investigated.[33]

A distinctive feature of amphiphilic molecules is the formation of high molecular weight aggregates above the critical concentration in aqueous media. The driving force is provided by the hydrophobic interactions between the alkyl chains, which in this arrangement are protected from interaction with water molecules.[34] The aggregates may form spherical, globular, oblate, or cylindrical micelles, single- or multi-walled vesicles (liposomes), double-layer lamellar phases, or inverted structures, in which the alkyl chains are parallel to each other. This parallel arrangement is also found in cell membranes, where the polar head groups of the phospholipids are at the membrane boundary and the alkyl chains point into the interior of the membrane.[35, 36]

The *N*-alkyl-*N*-glycosyl fatty acid amides also form aggregates in which the alkyl chains orient themselves parallel to each other. Evaluation of shear-area diagrams (Langmuir isotherms) of monomolecular films of these compounds at the water–air interface gave an area requirement of 40 Å^2 per molecule for each of the compounds **10a** and **12**.[37] This is consistent with the assumption of two parallel alkyl chains. By using small-angle X-ray scattering, it was shown that these compounds may form lamellar or hexagonal phases, depending on temperature.[38]

2.3. Adjuvant Effect of Glycosylamides

Investigation of *N*-alkyl-*N*-glycosyl fatty acid amides in immunological test systems surprisingly showed that several of these relatively simple compounds enhance the production of antibodies against various antigens. *N*-(β-D-Glucopyranosyl)-*N*-stearyllauramide (**10a**) was found to produce a dose-dependent increase in the formation of antibodies against sheep erythrocytes in vitro in the concentration range 3–100 μg mL^{-1}. Of particular interest was the finding that **10a** alone caused no mitogenic activity (induction of cell division): the formation of antibodies was detectable only in combination with an antigenic stimulus.[39] Thus **10a** acted like the known immunomodulators in the same dosage range, but evidently through a different, unknown mechanism. The immunological characterization of the glycosylamides is described in greater detail in Section 3. These findings motivated us to study the structure–activity aspects of this class of compounds more closely.

2.4. Chemical Optimization of the Basic Structure

We made modifications in the sugar residue, the lipophilic residues, and the branching region to investigate the influence of each of these substructures. Straight-chain alkylamines and aliphatic fatty acids were combined with hexopyranosyl and pentopyranosyl residues as shown in Figure 3. The effect on antibody synthesis in vitro depends on both the combination of alkyl chains and the nature of the carbohydrate components, the influence of the polar group being stronger. A β-D-glucopyranosyl residue has a strong effect similar to that of the 2-acetylamino-2-deoxy-β-D-glucopyranosyl residue and the β-D-mannopyranosyl residue; weaker activity was found for the β-D-galactopyranosyl residue. Pentopyranosyl and 2-deoxy-β-D-glucopyranosyl residues have little or no effect (Scheme 1).

Glycolipid	**10a**	**10b**	**11**	**12**	**13**	**14**	**15**	**16**
Antibody production	3	3	2	3	0	0	0	1

Scheme 1. Influence of the carbohydrate moiety on the primary immune response in vitro (murine spleen cells, antigen: sheep erythrocytes). The numbers indicate: 3 strong effect, 2 medium effect, 1 weak effect, 0 no effect.

In these in vitro models the biological effects are less dependent on the *n*-alkyl chains. However, each alkyl chain must be at least 12 carbon atoms long, since shorter chains lead to cytotoxic effects. The same has also been found for amphiphilic compounds comprising a pyranose residue and just one alkyl chain.

As a branching region, the amide grouping is also of great biological importance. Investigation of glycolipids with urethane, urea, thiolcarbamate, or allophanate groups **17**–**20**—obtained by reacting *N*-alkyl-*N*-β-D-glucopyranosylamines with alkyl chloroformates, alkyl isocyanates, alkylthiocarbonyl chlorides, or alkoxycarbonyl isocyanates—showed that, unlike glycosylamides, these compounds have only a slight effect on antibody production in vitro.

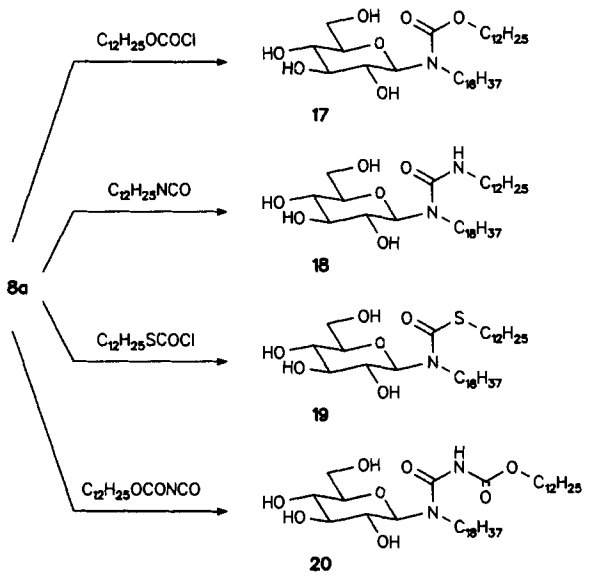

Fig. 4. Syntheses of glycosyl urethane **17**, urea **18**, thiocarbamate **19**, and allophanate **20** from **8a**.

The effect of increasing the lipophilicity of glycolipids was investigated by introducing a third alkyl chain into 2-amino-2-deoxy-D-glucose derivatives. Thus D-glucosamine hydrochloride **21** was reacted with octadecylamine in isopropanol at 65 °C to give *N*-(2-amino-2-deoxy-β-D-glucopyranosyl)-*N*-octadecylamine hydrochloride (**22**). Reaction with two equiv-

alents of stearoyl chloride gave *N*-(2-deoxy-2-octadecanoylamino-β-D-glucopyranosyl)-*N*-octadecyl-octadecanamide (**23**), which has three chains of 18 carbon atoms each. A derivative with three alkyl residues of different lengths on the glucosamine was produced as follows: acylation of the 2-amino group of glucosamine with dodecanoyl chloride gives 2-deoxy-2-dodecanoylamino-D-glucopyranose (**24**), *N*-glycosylation of which with dodecylamine provides *N*-(2-deoxy-2-dodecanoylamino-β-D-glucopyranosyl)-*N*-dodecylamine (**25**). Subsequent *N*-1-acylation of **25** with octadecanoyl chloride leads to *N*-(2-deoxy-2-dodecanoylamino-β-D-glucopyranosyl)-*N*-dodecyloctadecanamide (**26**). By using various alkylamines and acid chlorides a broad range of glucosamine derivatives with lipid residues with different chain lengths can be produced (Fig. 5).

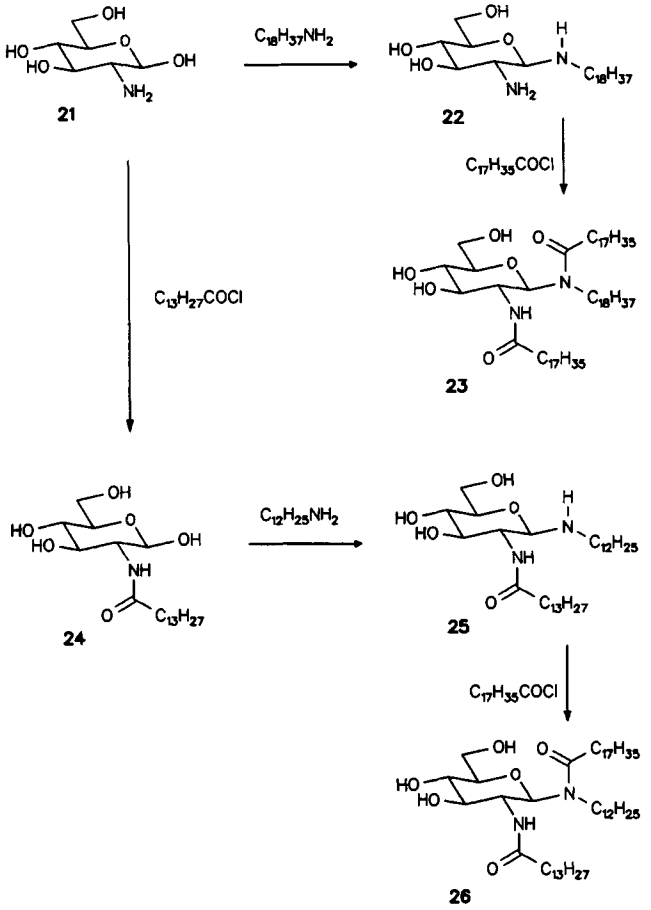

Fig. 5. Syntheses of glycolipids with three alkyl chains.

However, the investigations of compounds **23** and **26** and their homologues for biological activity proved very difficult because of their poor solubility in aqueous systems. The structure–activity relationships were not consistent, and so ultimately it was not possible to assess the biological effects of this subclass.

On the other hand, glycolipids with several hydroxyl groups or with charged functional groups should be much more solubile in water. With this aim we treated the disaccharides cellobiose, lactose, and maltose as well as the trisaccharide maltotriose successively with long-chain alkylamines and then fatty acid chlorides to give di- or trisaccharide lipids **27**–**30** (Fig. 6). These glycolipids are much more readily dispersible in water.

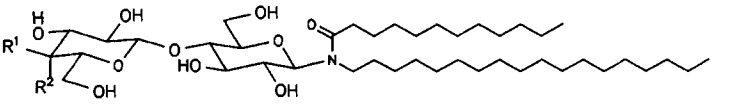

27 R^1 = OH, R^2 = H : β-cellobiosylamide
28 R^1 = H, R^2 = OH : β-lactosylamide

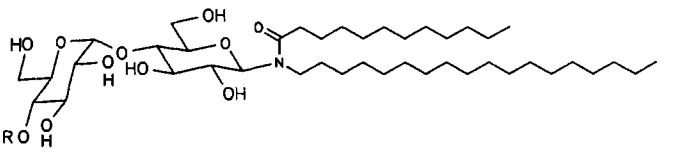

29 R = H: β-maltosylamide
30 R = α-D-glucopyranosyl: β-maltotriosylamide

Fig. 6. Glycosylamides of di- and trisaccharides.

Of particular interest were glycosylamides with phosphate ester groups. In immunomodulators derived from lipid A a phosphate ester group on the sugar is essential for biological activity; selective *O*-phosphorylation of lipids of monosaccharide amides was therefore investigated more closely.

We planned to achieve selective phosphorylation by exploiting increased nucleophilicity of the primary hydroxyl group at the C6 position. The reaction of **31** (obtained by a two-step reaction from D-galactose, dodecylamine, and stearoyl chloride) with dibenzylphosphoric acid chloride in the presence of pyridine leads to a phosphoric acid triester which, in the presence of palladium on carbon, can be hydrogenated to the 6-*O*-phosphorylated glycosylamide **32** (Fig. 7). This phosphorylation produced a qualitative change in the biological acitivity. Although **31** strongly stimulates antibody synthesis in vitro, this effect is somewhat less marked with **32**. However, **32** shows a significant antiviral activity against Herpes simplex virus type I (HSV I). This effect relies on the increase in the interferon titer induced by a virus infection.[40]

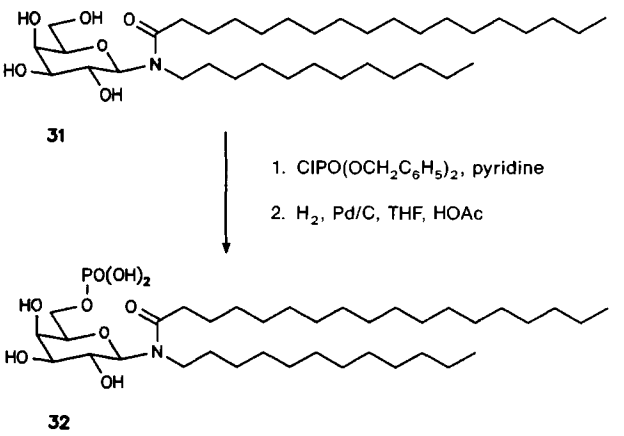

Fig. 7. Synthesis of an *O*-phosphorylated glycosylamide with antiviral activity.

2.5. Glycosylamides of Glucosamine

In order to introduce other charged functional groups in our studies of glycolipid derivatives, 2-amino sugars were investigated. Since glucosamine hydrochloride reacts with alkylamines to give *N*-alkyl-*N*-(2-amino-2-deoxy-β-D-glucopyranosyl)amine, the differentiation of the two amino functions is best achieved by blocking the amino group on the sugar. Since a benzyloxycarbonyl protecting group should offer the possibility of selective cleavage in the presence of a C1 amide function, D-glucosamine was converted to *N*-benzyloxycarbonyl derivative **33**. Compound **33** reacted with alkylamines in analogy to sugars with a 2-hydroxyl group, but much more slowly, to give glycosylamines. In DMF with tetradecylamine as the amine component glycosylamine **34** is obtained with a yield of 50–60 % after 4 h at 80 °C (Fig. 8). Owing to the longer reaction time the temperature- and time-dependent formation of by-products is more evident. The slow and incomplete course of the reaction is apparently due to the deactivating effect of the carbamate on the C2 of the sugar, which also improves the stability of the glycosylamine **34** against hydrolysis.

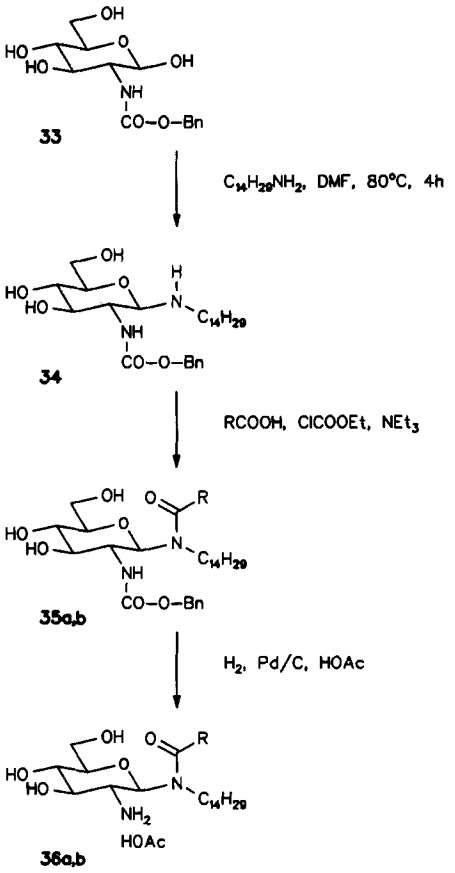

Fig. 8. Synthesis of 2-amino-2-deoxy-glycosylamides. Bn = benzyl, **a**: R = $C_{17}H_{35}$, **b**: R = $C_{11}H_{25}$.

Acylation of the C1 amino group of **34** with the mixed anhydride of stearic acid and ethyl chloroformate gives the glycosylamide **35a**, which after chromatographic purification can be readily hydrogenated to *N*-(2-amino-2-deoxy-β-D-glucopyranosyl)-*N*-tetradecyloctadecanamide (**36a**). Homologous compounds can be synthesized with other aliphatic amines and fatty acids.

As expected, the ammonium group in **36a** and its homologues enhances solubility in water. Solubility in water–ethanol (99:1 v/v) was determined by HPLC (Fig. 9).

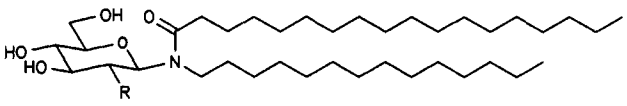

R	Solubility in water-ethanol 99:1 (v/v) [mg mL^{-1}]
OH	2.1
NH–Ac	2.0
NH_2 · HOAc	13.2

Fig. 9. Comparison of solubilities of glycosylamides with different C2-substituents on the glucose moiety.

The 2-amino-2-deoxy-glucosylamides have a marked effect on antibody synthesis in vitro and in vivo. The activities of several compounds, particularly **36a** and **36b**, are distinctly superior to that of **10a** and **10b**.

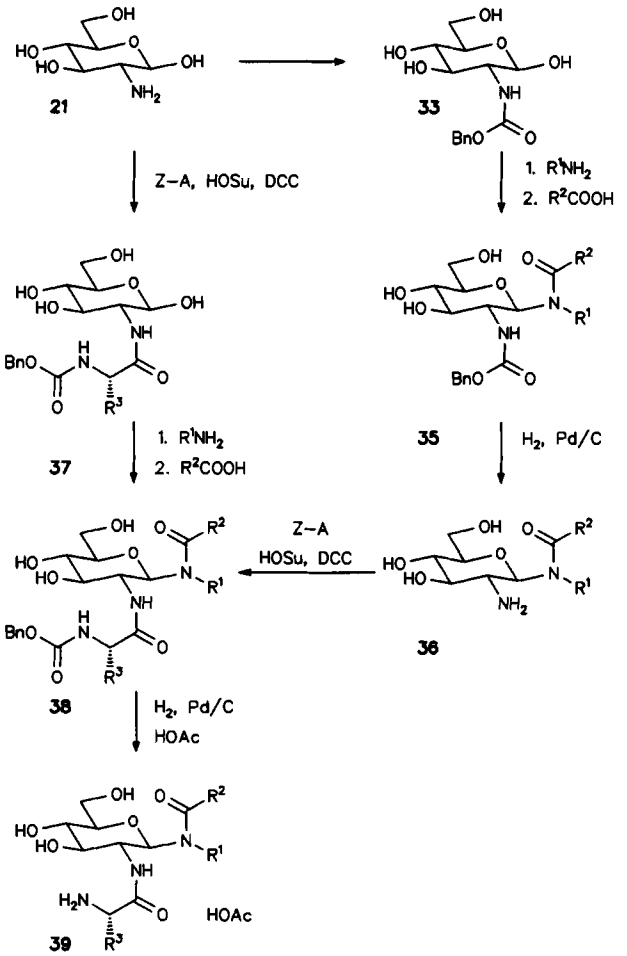

Fig. 10. Two routes to peptidoglycolipids. Z–A = benzyloxycarbonyl-protected amino acid, HOSu = *N*-hydroxysuccinimide, DCC = dicyclohexylcarbodiimide, R^1, R^2 = $C_{11}H_{23}$ to $C_{18}H_{37}$.

The compounds **36** and other homologues from this class permit further selective derivatization via the free amino function. Since previous findings suggested that glycolipids with ammonium groups in the head region would be of greatest interest, linkages with amino acids were targeted. The classic racemization-free condensation of **36** with protected amino acid *N*-hydroxysuccinimide esters provided *N*-(2-aminoacylamino-2-deoxy-β-D-glucopyranosyl)-*N*-alkyl fatty acid amides **38**, which can be deprotected by hydrogenolysis to the free amines **39** (Fig. 10). Thus, by combining aliphatic amines, fatty acids, and amino acids, a variety of glycolipids **39** with polar character could be produced.[41]

The synthesis of the peptidoglycolipids **39** was also achieved by a shorter route, with equally good results (Fig. 10). The first step was to produce the conjugate **37** from glucosamine and an *N*-benzyloxycarbonyl-protected amino acid. Compound **37** was treated with alkylamines and activated fatty acids in two steps, in the same way as *N*-acetyl-glucosamine, to give the blocked peptidoglycolipids **38**, which were deprotected to give **39**.

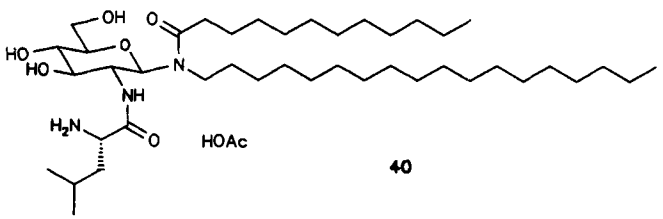

40

Fig. 11. Structural formula of BAY R 1005 (**40**).

From a variety of compounds of the type **39**, *N*-(2-deoxy-2-L-leucylamino-β-D-glucopyranosyl)-*N*-octadecyldodecanamide acetate (**40**, BAY R 1005) (Fig. 11) was selected for further biological development (see Section 3).

2.6. Lipophilic Glycosylamides of Muramyl Dipeptides

We were particularly interested in the linkage of the glycosylamide residue (as found in the GLA molecules) to muramyl dipeptide (MDP), **1**) and the effects such a modification would have on biological activity. MDP has already been linked with other lipophilic structures. Thus 6-*O*-mycolyl-MDP, 6-*O*-corynomycolyl-MDP,[42] and 6-*O*-ubiquinyl fatty acid esters of MDP[43] have been synthesized and have antitumour activity. Anti-infective or antitumour activity has also been found in MDP derivatives whose peptide segment is linked to a lipid residue by a covalent bond. Examples of this group are the conjugates of muramyl tripeptide and dipalmitoyl-phosphatidylethanolamine (CGP-19835A, MTP-PE)[44] or muramyl dipeptide and stearoyl-L-lysine (MDP-Lys (L18), muroctasine),[45] both of which are at an advanced stage of clinical development.[13]

The sugar element of MDP (**1**) is D-glucosamine. This structure also occurs in glycolipids of type *N*-(2-acetylamino-2-deoxy-β-D-glucopyranosyl)-*N*-alkylcarbonamide **41**. An attempt was therefore made to combine the two structural units in a single molecule in which the common element would be the amino sugar. In principle it ought to have been possible to synthesize the MDP lipids from muramyl dipeptide in two steps, by *N*-glycosylation followed by *N*-acylation. As expected, however, *N*-glycosidation of a 2-acetamino sugar entailed heavy losses, and it therefore seemed more economical to start from *N*-(2-acetylamino-2-deoxy-β-D-glucopyranosyl)-*N*-alkyl fatty acid amides **41**, introduce the 3-*O*-lactyl ether, and link with a dipeptide element. To introduce the lactyl ether residue at C3 of the sugar element **41**, the C4 and C6 hydroxyl groups were first blocked as benzylidene acetal. The compounds **42** were then isolated by crystallization (Fig. 12).

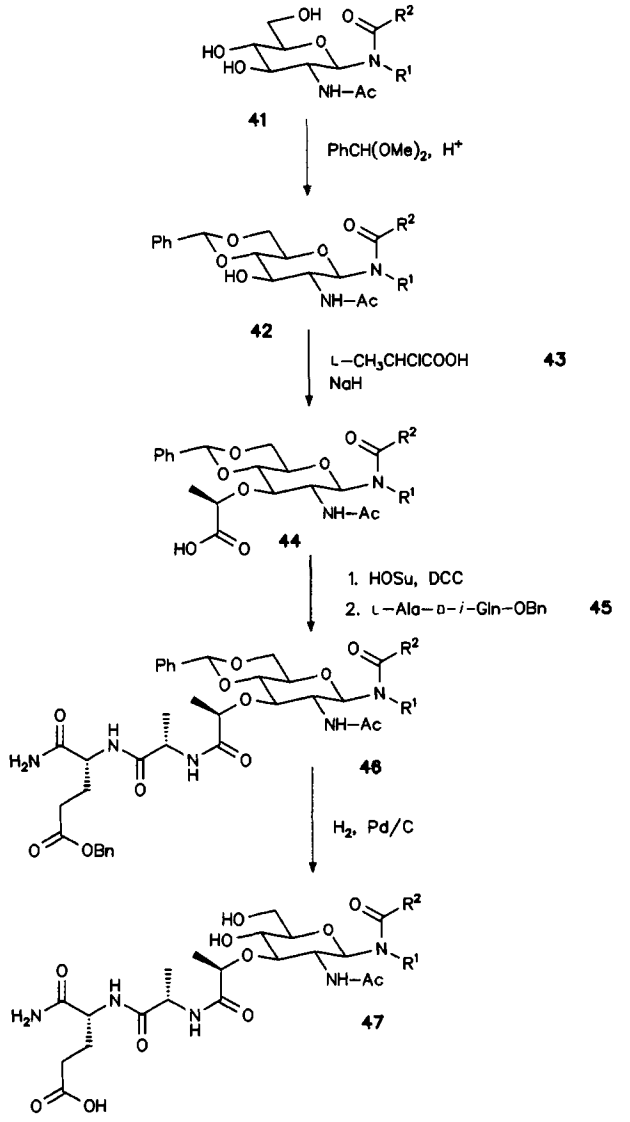

Fig. 12. Synthesis of *N*-glycosides of muramyldipeptide (MDP). R^1, R^2 = $C_{11}H_{23}$ to $C_{18}H_{37}$, *i*-Gln = isoglutamine.

The ^{1}H NMR spectra of the derivatives of **42** could be assigned completely. The amide rotamerism observed in the 4,6-unsubstituted glycolipids **41** is completely absent in **42**. Also in solution the compounds **42** are present in only a single conformation.

The alcohol function in **42** was then converted stereoselectively with L-chloropropionic acid **43** and sodium hydride to the lactyl ether derivative **44**.[46] The ether synthesis proceed-

ed with Walden inversion under conditions comparable to those reported for α-configured *O*-methyl glycosides.[47] No diastereomers were detectable by NMR spectroscopy. After activation of the carboxyl function as a hydroxysuccinimide ester, coupling with the dipeptide element[48] L-alanyl-D-isoglutamine benzyl ester **45** gave the protected MDP lipid derivative **46**, which could be converted into the free peptidoglycolipids **47** by hydrogenolysis.

As is often found in drug research the combination of two active structures into one molecule may result in a loss of activity. This proved also to be the case with the MDP glycolipids **47**, which induced little or no increase in antibody synthesis.

2.7. X-ray Crystallographic Studies

Knowledge of the conformation of lipids is key to understanding their mutual arrangement and their organization in a cell membrane. X-ray crystallographic studies of phospholipids[49–52] revealed that the two alkyl chains are arranged parallel to each other in an all-*trans* conformation with a spacing of 4.8 Å. The dihedral angle between the two planes is only a few degrees. The structure[53] of 1,2-dilauroyl-*sn*-*glycero*-3-phosphocholine **48** is shown in Figure 13.

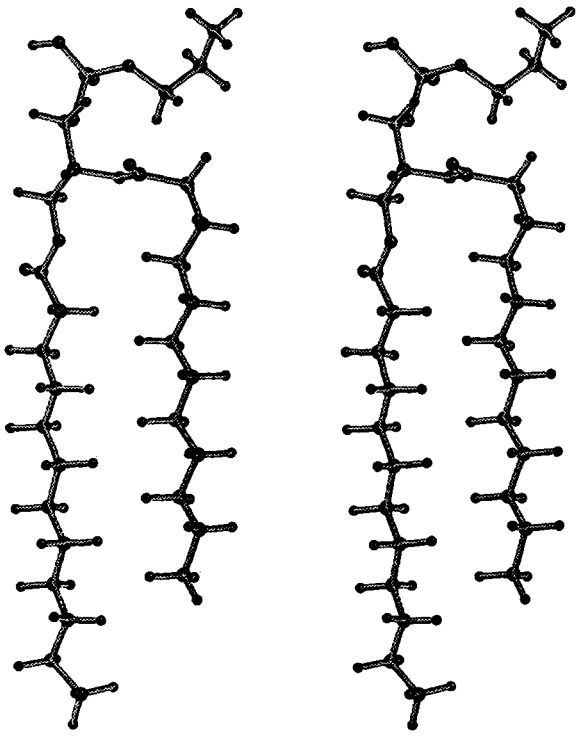

Fig. 13. Stereoplot of the structure of 1,2-dilauroyl-*sn*-*glycero*-3-phosphorylcholine **48** in the crystal [53].

No crystals suitable for X-ray structural analysis could be obtained from BAY R 1005 (**40**) itself, but this proved possible for a blocked precursor, the tri-*O*-acetate **49**, which crystallized in long needles from methanolic solution. Figure 14 shows the result of the X-ray crystallographic investigation.[54]

As expected, the sugar ring in **49** is present in the $^4C_1$-conformation with equatorial arrangement of all substituents. The lauric acid residue extends linearly into the plane of the sugar ring, while the alkyl chain of the alkylamine is situated above the plane of the ring. Also in this lipid derivative the two alkyl chains are parallel to each other with a mean separation of about 5 Å. A striking feature is the dihedral angle (ca. 90°) between the zigzag planes of the two alkyl chains which differs markedly from that of phospholipids. This arrangement is possible owing to two *gauche* conformations between C2–C3 and C3–C4 of the alkylamine fragment. The dihedral angle between C1–H1 in the sugar ring and the carbonyl group in the amide grouping at the anomeric carbon atom of the sugar is almost 0°.

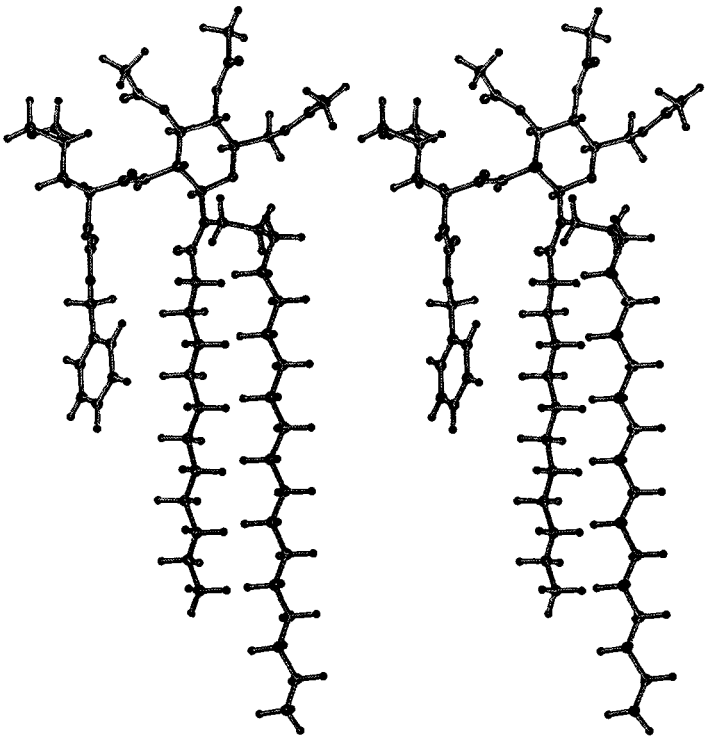

Fig. 14. Stereoplot of the structure of the glycosylamide **49** in the crystal.

Whether this orientation of the lipid residues relative to each other and relative to the sugar ring is also present in solution cannot be stated with certainty because this structure is probably favored by the parallel arrangement of the benzyloxycarbonyl protecting group in the crystal. However, ^{1}H NMR measurements indicate that **49** is present as a single conformer (without amide rotamerism) also in solution. This conformation must therefore be regarded as probable in the solution state as well.

After conversion of **49** to BAY R 1005 (**40**), amide rotamerism is again evident in the ^{1}H and ^{13}C NMR spectra, indicating that two different conformations are present in solution. The conformation found in the X-ray structural analysis may possibly be one of those that are present in BAY R 1005.

3. Adjuvant Activity

The biological activity profile of this new class of glycolipids is of extraordinary interest for vaccination. Both in vitro and in vivo they enhance the specific immune response (adjuvant effect), which we will now describe in more detail using the example of BAY R 1005 (**40**).

In the primary humoral immune response[55] (antibody synthesis of class IgM) of spleen cell cultures (mouse) to sheep erythrocytes as antigens in the presence of BAY R 1005 (**40**), this substance induces a dose-dependent increase in the number of antibody-forming cells in the concentration range 1–100 $\mu g\,mL^{-1}$. It is particularly important that this effect is completely independent of T lymphocytes and that the increase in antibody synthesis is strictly antigen-dependent and not the result of nonspecific polyclonal stimulation. Cultures that have not been stimulated with sheep erythrocytes show only a negligible increase in the number of antibody-forming cells in the presence of BAY R 1005 (**40**).[39, 56] Thus, unlike virtually all other adjuvants,[57, 58] GLAs show no mitogenic effect but act on B lymphocytes only when an antigenic stimulus is present. BAY R 1005 seems to act on populations of B lymphocytes as a second signal which is effective only if the primary signal of the antigen is sent first.

This adjuvant effect can also be reproduced in vivo in the immunization of mice. After the intraperitoneal administration of sheep erythrocytes and simultaneous subcutaneous administration of BAY R 1005 (**40**), a dose-dependent increase in the number of antibody-forming cells was detected (Fig. 15). Comparable increases in antibody titer were also observed after immunization with the soluble antigen ovalbumin.

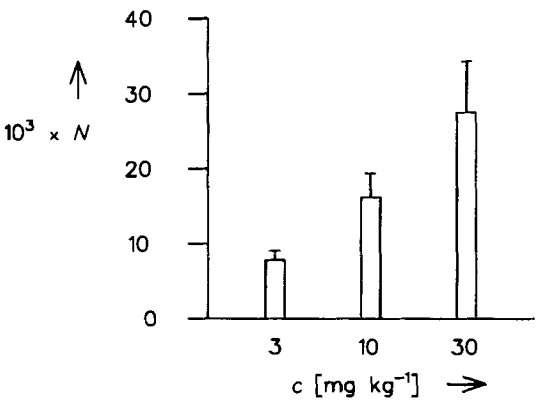

Fig. 15. Adjuvant effect of BAY R 1005 on the primary humoral immune response against sheep erythrocytes. An increasing dose c enhances the number N of antibody forming cells.

In vivo, BAY R 1005 (**40**) also induces an increase of antibody synthesis in response to viral vaccines administered in suboptimal concentrations.[59] By administering BAY R 1005 simultaneously, the protective effect of immunization with an inactivated pseudorabies virus vaccine was enhanced significantly. After the injection of infectious virus the survival rates and mean survival times were distinctly higher in the animals that had been additionally immunized with BAY R 1005 than in the controls (Table 2). Parallel to the protective effect, increased serum antibody titers with neutralizing properties were also detected. Conventional adjuvants led to no improvement in the protection of virus-infected mice.

BAY R 1005 is also effective in animals whose defense has been weakened. Restorative and adjuvant effects were observed in mice whose immune system had been suppressed by bacterial lipopolysaccharides or melanoma B_{16} tumors.

Table 2. Adjuvant effect of BAY R 1005 in CF-1 mice after immunization with pseudorabies virus inactivated with β-propiolactone in comparison to conventional adjuvants.

Treatment	Survival Rate [%] [a]
Control	
formulation (without immunization)	0
vaccine (without adjuvant)	60
Conventional adjuvants	
Freund's complete adjuvant [b]	60
$Al(OH)_3$ – saponin [b]	50
BAY R 1005 **40** [mg kg^{-1}]	
3	90
6	100
12	100

[a] Determined from tests with ten animals. [b] Mixed 1:1 with antigen.

All the data accumulated to date indicate that BAY R 1005, due to its efficacy and its mode of action, is a very interesting compound from a new class of adjuvants and is also very well tolerated both locally and systemically. Its effects on the immune system are very different from those of amphiphilic substances from other structural classes, which show strong immunosuppressive effects even at relatively low concentrations.[60] Its effects also differ significantly from the immunomodulatory properties of natural glycolipids from the glycosphingolipid class, which similarly suppress the response of lymphocytes to antigens in vitro.[61]

4. Summary and Prospects

The molecular mechanisms responsible for the immunological activity of glycolipid analogues are still largely unknown because of their complexity. According to the fluid mosaic model of membranes,[35] lipids play only a passive role in the stabilization of the cell membrane. But this model does not explain why nature synthesizes several hundred different lipids, expending considerable metabolic effort in doing so. Recent studies have shown that the lipid composition of a membrane influences the metabolic activity inside the cell. Even small structural changes in the polar head groups of glycolipids and phospholipids have strong effects on mutual miscibility in solid and liquid crystalline phases,[62] which in turn has an influence on membrane fluidity. Thus the conformation of proteins or receptors in the membrane can be affected.[63] Such a change in fluidity may perhaps be associated with the observed conformational isomer equilibria of glycolipids of the glycosylamide type. Also interesting in this context is the recent finding that cleavage products of sphingolipids, sphingosine, and lysosphingolipids can act as endogenous modulators of cell function by inhibiting protein kinase C.[64] The effect of BAY R 1005 (**40**) or of cleavage products possibly formed by lipases in the membrane on the second messenger systems has not yet been investigated.

In contrast to these speculations, the observed effects exerted by the glycolipids in our vaccination experiments are unequivocal. In combination with purified virus vaccines and subunit vaccines BAY R 1005 (**40**) leads to increased protection of virus-infected mice. Since preclinical trials in vivo in other animal species (pig, sheep, horse) and in vitro in isolated human blood cells[65] gave comparable results, use in veterinary and human medicine should be possible. In addition to the general efficacy of the substance, however, its mode of action deserves particular attention: the increase in antibody synthesis induced by BAY R 1005 (**40**) is specifically dependent on the antigen and is not the result of polyclonal stimulation. GLAs act on the proliferation of B lymphocytes as a second signal which has no effect until the antigen acts as a first signal. Since BAY R 1005 is capable of activating B lymphocytes without the helper function of T lymphocytes, it may prove very helpful as an adjuvant, particularly for the immunization of patients with diseases such as AIDS whose T lymphocytes function is defective.

This review contains results obtained by numerous colleagues who have been studying the chemical, physical, and biological aspects of these glycolipids. I am grateful for their commitment and persistence. The main synthetic work was done by P. Stadler, Y. Hayauchi, B. W. Krüger, and L. Röben. Physical aspects were studied by A. Zembrod and J. Goossens. The biological and mode of action studies and the evaluation of the glycolipids for vaccination were carried out by H. G. Opitz, K. G. Stünkel, G. Streissle, V. Klimetzek, and P. Thein. The spectroscopic structural analyses were performed by P. Schmitt, C. Wünsche, and D. Wendisch. I am grateful to L. Born for the X-ray structural analyses.

Received: August 14, 1991 [A 847 IE]
German version: *Angew. Chem. 103* (1991) 1639

[1] J. Klein, *Immunologie*, VCH Verlagsgesellschaft, Weinheim 1991.
[2] D. G. Kleid, *Annu. Rep. Med. Chem. 19* (1984) 223–230.
[3] A. C. Allison, N. E. Byars, *Bio/Technology 5* (1987) 1041–1045.
[4] H. S. Warren, L. A. Chedid, *Crit. Rev. Immunol. 8* (1988) 83–101.
[5] W. R. Ballou, S. L. Hoffman, J. A. Sherwood, M. R. Hollingdale, F. A. Neva, W. T. Hockmeyer, D. M. Gordon, I. Schneider, R. A. Wirtz, J. F. Young, G. F. Wasserman, P. Reeve, C. L. Diggs, J. D. Chulay, *Lancet 1987*, 1277–1281.
[6] D. A. Herrington, D. F. Clyde, G. Losonsky, M. Cortesia, J. R. Murphy, J. Davis, S. Baqar, A. M. Felix, E. P. Heimer, D. Gillessen, E. Nardin, R. S. Nussenzweig, V. Nussenzweig, M. R. Hollingdale, M. M. Levine, *Nature 328* (1987) 257–259.
[7] M. E. Patarroyo, R. Amador, P. Clavijo, A. Moreno, F. Guzman, P. Romero, R. Tacson, A. Franco, L. A. Murillo, G. Ponton, G. Trujillo, *Nature 332* (1988) 158–161.
[8] D. A. Eppstein, N. E. Byars, A. C. Allison, *Adv. Drug Delivery Rev. 4* (1990) 233–253.
[9] A. S. Fauci, S. A. Rosenberg, S. A. Sherwin, C. A. Dinarello, D. L. Longo, H. C. Lane, *Ann. Intern. Med. 106* (1987) 421–433.
[10] D. E. S. Stewart-Tull, M. Parant, *Ann. Immunol. Hung. 26* (1986) 197–223.
[11] V. Ruszala-Mallon, Y. I. Lin, F. E. Durr, B. S. Wang, *Int. J. Immunopharmacol. 10* (1988) 497–510.
[12] J. P. Devlin, K. D. Hargrave, *Tetrahedron 45* (1989) 4327–4369.
[13] G. Baschang, *Tetrahedron 45* (1989) 6331–6360.
[14] V. S. Georgiev, *Med. Res. Rev. 10* (1990) 371–409.
[15] A. Adam, E. Lederer, *Med. Res. Rev. 4* (1984) 111–152.
[16] P. Lefrancier, E. Lederer, *Pure Appl. Chem. 59* (1987) 449–454.
[17] J. A. Rudbach, J. Cantrell, J. T. Ulrich, M. S. Mitchell, *Adv. Exp. Med. Biol. 256* (1990) 665–676.
[18] O. Westphal, O. Lüderitz, *Angew. Chem. 66* (1954) 407–417.
[19] O. Lüderitz, C. Galanos, V. Lehmann, H. Mayer, E. T. Rietschel, J. Weckesser, *Naturwissenschaften 65* (1978) 578–585.
[20] S. Hakomori, *Annu. Rev. Biochem. 50* (1981) 733–764.
[21] T. Feizi, *Nature 314* (1985) 53–57.
[22] S. Hakomori, *Prog. Cancer Res. Ther. 32* (1985) 139–156.
[23] C. C. Sweeley, B. Siddiqui in M. I. Horowitz, W. Pigman (Eds.): *The Glycoconjugates, Vol. 1*, Academic, New York 1977, pp. 459–540.
[24] H. Paulsen, K.-W. Pflughaupt in W. Pigman, D. Horton (Eds.): *The Carbohydrates, Vol. 1B*, Academic, New York 1980, pp. 881–927.
[25] U. Niedballa, H. Vorbrüggen, *Angew. Chem. 82* (1970) 449–450; *Angew. Chem. Int. Ed. Engl. 9* (1970) 461–462.
[26] G. Snatzke, J. Vlahov, *Liebigs Ann. Chem. 1985*, 439–447.
[27] J. E. Hodge, B. F. Moy, *J. Org. Chem. 28* (1963) 2784–2789.
[28] H. Paulsen, Z. Györgydeak, M. Friedmann, *Chem. Ber. 107* (1974) 1590–1613.
[29] G. P. Ellis, *Adv. Carbohydr. Chem. 14* (1959) 63–134.
[30] H. S. Isbell, H. L. Frush, *J. Org. Chem. 23*, 1309 (1958).
[31] P. Stadler, O. Lockhoff, H. G. Opitz, K. Schaller, DE 3213650 (1982/1983), Bayer.
[32] G. P. Ellis, J. Honeyman, *Adv. Carbohydr. Chem. 10* (1955) 95–168.
[33] M. M. Vigdorchik, N. P. Kostyuchenko, R. P. Olad'ko, G. S. Mosina, Yu. N. Sheinker, N. L. Suvorov, *J. Org. Chem. USSR (Engl. Transl.) 9* (1973) 617–622.
[34] J. N. Israelachvili, S. Marcelja, R. G. Horn, *Q. Rev. Biophys. 13* (1980) 121–200.
[35] S. J. Singer, G. L. Nicolson, *Science 175* (1972) 720–731.
[36] H. Eibl, *Angew. Chem. 96* (1984) 247–262; *Angew. Chem. Int. Ed. Engl. 23* (1984) 257–271.
[37] B. Hagenhoff, M. Deimel, A. Benninghoven, H. O. Siegmund, D. Holtkamp, *J. Phys. D: Appl. Phys.* (1991), submitted.
[38] R. Zorn, M. Grünert, O. Lockhoff, G. Nimtz, *Biophys. J. 58* (1990) 1199–1206.
[39] K. G. Stünkel, O. Lockhoff, H. G. Opitz, V. Klimetzek, G. Streissle, A. Paessens, P. Stadler, H. D. Schlumberger, *Adv. Biosci. (Oxford) 68* (1988) 429–437.
[40] O. Lockhoff, B. W. Krüger, P. Stadler, A. Paessens, G. Streissle, P. Taylor, H. J. Zeiler, K. G. Metzger, DE 3403495 (1983/1985), Bayer.
[41] O. Lockhoff, Y. Hayauchi, P. Stadler, K. G. Stünkel, G. Streissle, A. Paessens, V. Klimetzek, H. J. Zeiler, K. G. Metzger, H. P. Kroll, H. Brunner, K. Schaller, DE 3521994 (1985/1987), Bayer.
[42] T. Shiba, S. Okada, S. Kusumoto, I. Azuma, Y. Yamamura, *Bull. Chem. Soc. Jpn. 51* (1978) 3307–3311.
[43] S. Kobayashi, T. Fukuda, I. Imada, M. Fujino, I. Azuma, Y. Yamamura, *Chem. Pharm. Bull. 27* (1979) 3193–3196.
[44] B. Lukas, K. H. Schmidt-Ruppin, DE 3326163 (1982/1984), Ciba-Geigy.
[45] T. Shiba, Y. Yamamura, O. Nagase, S. Kotani, H. Ogawa, US 4317771 (1982), Daiichi Seiyaku.
[46] O. Lockhoff, Y. Hayauchi, P. Stadler, H. Brunner, DE 3604681 (1986/1987), Bayer.
[47] Y. Matsushima, J. T. Park, *J. Org. Chem. 27* (1962) 3581–3583.
[48] S. Kusumoto, Y. Tarumi, K. Ikenaka, T. Shiba, *Bull. Chem. Soc. Jpn. 49* (1976) 533–539.
[49] P. B. Hitchcock, R. Mason, K. M. Thomas, G. G. Shipley, *Proc. Natl. Acad. Sci USA 71* (1974) 3036–3040.
[50] R. H. Pearson, I. Pascher, *Nature 281* (1979) 499–501.
[51] H. Hauser, I. Pascher, S. Sundell, *J. Mol. Biol. 137* (1980) 249–264.
[52] K. Harlos, H. Eibl, I. Pascher, S. Sundell, *Chem. Phys. Lipids 43* (1984) 115–126.
[53] M. Elder, P. B. Hitchcock, R. Mason, G. G. Shipley, *Proc. R. Soc. London A 354* (1977) 157–170.
[54] L. Born, O. Lockhoff, unpublished results.
[55] R. Mishell, R. W. Dutton, *J. Exp. Med. 126* (1967) 432.
[56] K. G. Stünkel, O. Lockhoff, G. Streissle, V. Klimetzek, A. Paessens, H. D. Schlumberger in J. C. Mani, J. Dornand (Eds.): *Lymphocyte Activation and Differentiation*, de Gruyter, Berlin 1988, pp. 421–425.
[57] J. Anderson, F. Melchers, C. Galanos, O. Lüderitz, *J. Exp. Med. 137* (1973) 943–953.
[58] C. Damais, M. Parant, L. Chedid, *Cell. Immunol. 34* (1977) 49–56.
[59] K. G. Stünkel, A. Paessens, G. Streissle, G. Hewlett, O. Lockhoff, H. D. Schlumberger in J. G. Kaplan, D. R. Green, R. C. Bleackley (Eds.): *Prog. Leukocyte Biol. 9 (Cellular Basis Immune Modulation)*, Liss, New York 1989, pp. 575–579.
[60] R. B. Ashman, R. V. Blanden, B. W. Ninham, D. F. Evans, *Immunol. Today 7* (1986) 278–283.
[61] D. M. Marcus, *Mol. Immunol. 21* (1984) 1083–1091.
[62] R. D. Koynova, H. L. Kuttenreich, B. G. Tenchov, H.-J. Hinz, *Biochemistry 27* (1988) 4612.
[63] I. Ishizuka, T. Yamakaiva in H. Wiegandt (Ed.): *Glycolipids*, Elsevier/Academic, New York 1985.
[64] Y. A. Hannun, R. M. Bell, *Science 243* (1989) 500–507.
[65] J. Bauer, K. G. Stünkel, *Biotechnol. Prog.*, in press.

Herbicides in Photosynthesis Research

By Wilfried Draber, Klaus Tietjen, Joachim F. Kluth, and Achim Trebst*

Dedicated to Professor Karl Heinz Büchel on the occasion of his 60th birthday

Photosynthesis and herbicide research have a long common history. Soon after the introduction of a new group of highly effective herbicides in 1956, the substituted aryl ureas, their mode of action was recognized to be the inhibition of light-driven electron flow and photosynthetic oxygen evolution. Many subsequent highly successful commercial herbicides, including those from other chemical classes, act by this mechanism. The study of their interaction with the photosynthetic system at the molecular level is a prime example of how rapidly advances in unraveling the mechanism of photosynthesis can be translated into practical uses. At the same time the herbicides continued to be valuable and efficient tools in photosynthesis research. In the past herbicides were instrumental in establishing many principal features of the biochemistry and biophysics of photosynthesis, in particular the role of plastoquinone, which is displaced from its binding pocket in one of the protein subunits of the photosystem II. Their further use in elucidating the molecular biology of photosynthesis is illustrated by the recent importance of herbicide-tolerant mutants for determining structural aspects of photosystem II. We will review the past and present state of the interaction of herbicide and photosynthesis research and will provide a model for the orientation of herbicides within the three-dimensional structure of their target, the D1 protein of photosystem II.

1. Introduction

A large number of commercial herbicides inhibit photosynthesis,[1-4] representing about 30% of the sales market in 1989. This report is concerned with those compounds that interfere with photosynthetic electron flow of photosystem II, which includes the majority of photosynthesis herbicides. The chemical structures of typical examples are shown in Figure 1. Their specific target has been identified as one of the protein subunits of photosystem II. Their mode of inhibition on PS II function is displacement of a plastoquinone (Q_B) from its binding site on that protein.[5] This herbicide-binding protein is now known to be one of the reaction-center polypeptides of PS II, called the D1 polypeptide subunit.

Rather early the correlation of the biochemistry of herbicides and their inhibitory pattern in photosynthesis with physicochemical descriptors of the compounds (QSAR studies, QSAR = Quantitative Structure–Activity Relationship) allowed the definition of basic chemical elements and substructures essential to their potency. This knowledge enabled specific biochemical and biophysical properties of the then hypothetical herbicide-binding protein to be recognized. It even became possible to determine the dimensions of the binding niche in the protein target required for good inhibition by inspecting the mirror image of the dimensions of the herbicide, before the binding protein had been identified in 1981. Thus research on the biochemistry and biophysics of PS II herbicides is at a more advanced stage than for most other types of herbicides.

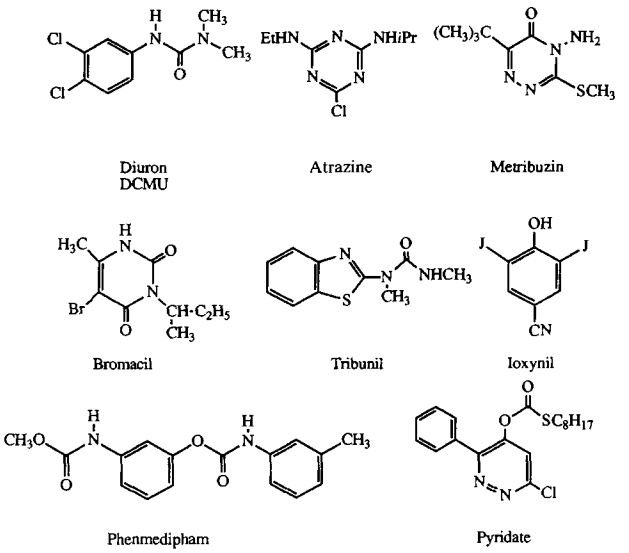

Fig. 1. Herbicides that inhibit photosystem II.

The identification of the herbicide-binding protein provided an important contribution in the biochemical and biophysical characterization of PS II. The decisive step in the elucidation of the structure of PS II was the X-ray structure analysis of the crystallized reaction center of purple bacteria,[6-8] which showed the homology of PS II to the photosystem of purple bacteria not only in function but also in structure and protein folding. However, a detailed understanding of PS II and its homology with the purple bacterial system would not have been possible without the use of inhibitors that are also herbicides.[9] This will be documented in this paper. The herbicide-binding protein was found to be a subunit of PS II as a result of experiments with radioactively labeled herbicides and of the sequencing of the *psb*A gene of herbicide-tolerant mutants. It is possible now to discuss the three-dimensional folding of the herbicide-binding

[*] Prof. Dr. A. Trebst
Lehrstuhl für Biochemie der Pflanzen
Ruhr-Universität
Postfach 102148, W-4630 Bochum 1 (FRG)
Dr. W. Draber, Dr. J. F. Kluth, Dr. K. Tietjen
Bayer AG
Sektor Landwirtschaft
Pflanzenschutzzentrum Monheim
W-5090 Leverkusen (FRG)

protein and the specific docking of a herbicide into its binding niche. The dimensions deduced from QSAR studies can now be equated with distances to amino acid residues in that niche.

2. The Electron-Flow System in the Photosynthesis Reaction Center

On illumination photosystem II oxidizes water to oxygen and reduces plastoquinone (PQ) to plastohydroquinone (PQH_2).[10, 11] The mechanism of this complex reaction sequence involves several electron carriers. The reaction center of PS II (RC) where the primary light event takes place consists of chlorophyll *a*, probably a dimer (P_{680}), that is bound via two histidines (His 198) to two homologous proteins about 32 kDa in size (the D1 and D2 polypeptides). When the reaction center P_{680} is excited, charge separation occurs, and in 10 psec the electron is passed from the excited primary electron donor P^*_{680} on to a primary electron acceptor, a pheophytin bound to the D1 protein subunit. The pheophytin in turn reduces the first plastoquinone in the electron-flow system (Q_A) in about one nsec. Q_A is reduced only to the semiquinone state, which remains bound tightly to the D2

Achim Trebst (born in Zeitz in 1929) graduated with a doctorate in Chemistry from the University Heidelberg in 1955 under F. Weygand and A. Wacker. After a brief interlude at the Technische Universität Berlin, he spent four years with D. I. Arnon in Berkeley, California, where he was introduced to the biochemistry of photosynthesis and of isolated chloroplasts. On his return he completed his habilitation under F. Weygand at the Technische Universität München. In 1963 he became Professor of the Biochemistry of Plants at the Universität Göttingen, and from 1967 he built up the chair of Biochemistry of Plants at the newly established Universität Bochum. He is member of the Leopoldina and Rheinisch-Westfälische Academy, honorary Doctor of the University of Stockholm and Purdue University, and E. and J. Michael Professor in the Weizmann Institute in Rehovot. His particular interest in the biochemistry of photosynthesis lies in the photosynthetic electron transport system and photophorylation in the thylakoid membrane of the chloroplasts.

Wilfried Draber was born in Schneidemühl in 1929 and studied in Kiel and Freiburg where he completed his doctorate under K. Wallenfels in 1960. He joined the Shell Basic Research in Birlinghoven and was transferred for a long period to the Agricultural Research Centre of Shell in Sittingbourne. From the end of 1966 he has worked in Pflanzenschutz-Forschung in Bayer AG. His particular interests involve the quantitative relationships between chemical structure and biological activity.

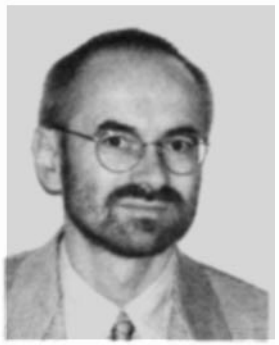

Klaus Tietjen was born in Cuxhaven in 1951 and studied chemistry in Freiburg. After obtaining his Diplom (1977) he worked in the Medizinische Universitätsklinik Freiburg on immunoassays for $1\frac{1}{2}$ years. He completed his doctorate at the Biologische Institute der Universität Freiburg under U. Matern in 1982 and pursued these studies in phytopathology as a postdoctoral fellow. In 1984 he became head of a laboratory investigating the biochemistry of herbicides and insecticides in the chemical research department of the Pflanzenschutzzentrum Monheim, Bayer AG.

Joachim Friedrich Kluth, born in Cologne in 1950, completed his Diplom in Chemistry there in 1975 and moved to the Max-Planck-Institute für Kohlenforschung, Mülheim/Ruhr. He obtained his doctorate from the University of Essen under P. Heimbach (1980) in the field of homogeneous transition-metal catalysis where he continued this research as Hochschulassistent. Since 1982 he has been in the chemical research of the Pflanzenschutzzentrum Monheim, Bayer AG.

protein subunit. The semiquinone (the radical anion $Q_A^{\bullet -}$) reduces the second plastoquinone Q_B, which is bound loosely to the D1 protein subunit. It is the Q_B reduction that is inhibited by the herbicides.

After charge separation the oxidized P_{680} is reduced to its initial state by the manganese complex of the oxygen-evolving system. A tyrosin participates in this reaction via a stabilized radical of Tyr 161 in a hydrophobic pocket in the D1 protein.[1,2] After four consecutive oxidation steps the manganese complex produces oxygen from water.

The primary charge separation in PS II occurs across the inner thylakoid membrane of the chloroplast. The reaction center P_{680} is oriented towards the lumen face of the thylakoid membrane. The plastoquinones that are reduced (Q_A and Q_B) are localized in the membrane to face the matrix space of the chloroplast. Therefore the electron released by the oxidation of P_{680} is moved quickly through ca. 30 Å, away from the positive, oxidized P_{680}. This slows down charge recombination in the reaction center and instead the oxidized P_{680} is reduced back to its original state by an electron from the water-splitting reaction. This is depicted in Figure 2. The result of the light-driven charge separation and the redox reaction across the membrane is that a more electronegative reducing equivalent (reduced quinone) has been generated from an electropositive electron donor (water).

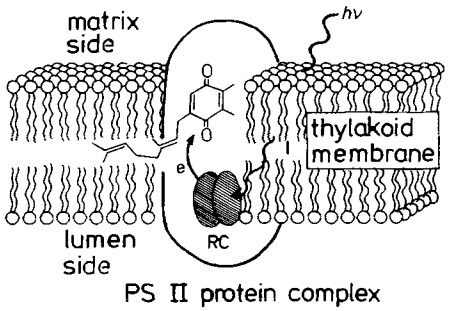

Fig. 2. Light-driven quinone reduction by photosystem II. An integral protein complex is embedded in the thylakoid membrane and orients the reaction center of PS II towards the lumen side of the membrane. On light excitation of the reaction center—depicted as a chlorophyll dimer P680—an ejected electron reduces plastoquinone, which is located on the opposite (matrix) side of the membrane. Herbicides displace this quinone.

After a second similar excitation cycle, Q_B accepts a second electron and becomes reduced to the hydroquinone state; the plastohydroquinone leaves the quinone binding pocket in the protein and equilibrates with a larger free plastoquinone/hydroquinone pool. A new plastoquinone moves into the D1 protein to become a new Q_B and the cycle continues. Two more excitations of P_{680}—i.e., 4 quanta in toto—are needed to oxidize the manganese complex (a cluster of four manganese atoms) to the redox state that produces one O_2 molecule from two water molecules (Fig. 3). The overall reaction of PS II leads to the formation of two stable products: plastohydroquinone and oxygen [Eq. (a)].

$$2H_2O + 4h\nu + 2PQ \longrightarrow 2PQH_2 + O_2 \qquad (a)$$

As Figure 3 also indicates, the protons in the water-splitting reaction are released into the inner lumen space of the thylakoid membrane, whereas the protons needed for hydroquinone formation are taken up from the matrix space. In this way a proton concentration gradient is established between the inner and outer space of the thylakoid, a consequence of vectorial electron flow across the membrane.

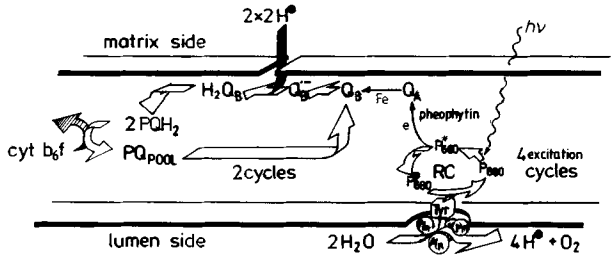

Fig. 3. Photosystem II and oxygen evolution. The reaction center P680 of PS II reduces plastoquinone Q_B via pheophytin and plastoquinone Q_A. Two excitation cycles are needed to reduce Q_B to the hydroquinone. Protons are taken up from the matrix space. The plastohydroquinone leaves the binding site on PS II and equilibrates with a larger plastoquinone/hydroquinone pool. Four excitation cycles through P680 are needed to oxidize the manganese complex via a tyrosine radical. The fully oxidized manganese complex oxidizes 2 molecules of water to evolve one O_2.

The free plastohydroquinones provided by photosystem II can move both laterally in the membrane and across it. They are oxidized by a cytochrome b_6/f complex, which transfers the electrons via plastocyanin (PC) to photosystem I (PS I). The protons liberated in the PQH_2 oxidation are released into the lumen space of the thylakoid, thus doubling the proton potential. Upon illumination photosystem I oxidizes plastocyanin and reduces $NADP^+$.

The photosynthetic electron transport chain causes oxygen evolution and provides the reducing power required for CO_2 assimilation in the form of NADPH (two NADPH are needed per CO_2 reduced or O_2 evolved). As this is an endergonic reaction, absorbed light quanta have to provide the driving force. The whole electron-flow system is depicted in Figure 4, which shows that the redox carriers of the electron-flow system are bound to three integral protein complexes (PS I, PS II, cytochrome b_6/f complex). Each complex spans the membrane and contains several carriers each oriented in or at the membrane by specific binding to the protein subunits of the complexes for optimal rates and directional electron flow. Peripheral proteins are connected to the integral complexes either on the lumen face of the membrane as, for example, the watersplitting system, or on the matrix face as for the $NADP^+$ reducing system via ferredoxin. The large integral complexes each consist of several hydrophobic protein subunits and are interconnected by carriers that can move laterally in or on the membrane: plastoquinone, plastocyanin, and ferredoxin. Figure 4 also indicates the site of inhibition for three types of inhibitors of photosynthetic electron flow: diuron inhibits photosystem II at the Q_B level, and dibromothymoquinone the cytochrome b_6/f complex at the FeS level; paraquat drains electrons from PS I and thus inhibits $NADP^+$ reduction.

In the mechanism of electron flow across the membrane, protons are taken up in certain redox reactions on the matrix side and released by others on the inside of the membrane. Together with the membrane potential of the electrogenic

steps (that is, steps that generate an electric field) of the charge separation in the two photosystems, these reactions result in a proton motive force that drives the proton-dependent adenine triphosphate (ATP) synthesis. ATP synthesis is catalyzed by the ATP synthase, a fourth transmembrane complex (Fig. 4).

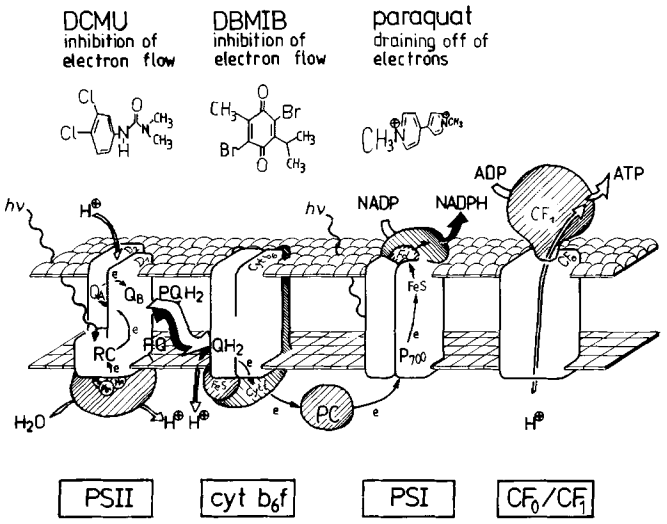

Fig. 4. Integral protein complexes and typcial inhibitors in photosynthetic electron flow and photophosphorylation. Photosystem I, photosystem II, and the cytochrome b_6/f complex contain several electron carriers bound to their polypeptide subunits. Mobile carriers like plastoquinone (PQ) and plastocyanin (PC) form the functional connection between the complexes. Peripheral polypeptides are attached to the integral complexes; for water-splitting on the lumen side of PS II and for $NADP^+$ reduction via ferredoxin (Fd) and bound FeS centers on the matrix side. The ATP synthase consists of a membrane-spanning proton channel (CF_0) and a peripheral CF_1 part. The complex uses the proton gradient, generated by proton liberation by the water-splitting and plastohydroquinone oxidation reaction, for ATP synthesis. Only the D1 and D2 subunits of PS II are indicated; the others (see text) are left out for clarity.

Equation (b) summarizes the generation of reducing power (NADPH) from water oxidation.

$$2H_2O + 2NADP^+ + 8h\nu \longrightarrow O_2 + 2NADPH + 2H^+ \qquad (b)$$

In an abbreviated flow system (Scheme 1) arrows indicate the transport of electrons from the donor to the acceptor electron carrier. Inhibitor sites are indicated.

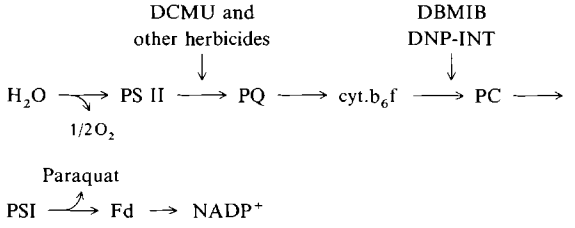

Scheme 1. Abbreviated reaction sequence for electron flow. Fd = ferredoxin, DNP-INT = dinitrophenyl ether of iodonitrothymol, Paraquat = methylviologen.

3. Comparison of the Structure and Function of Photosystem II to the Photosystem of Purple Bacteria

The oxygen-evolving PS II of plant photosynthesis shows homology in structure and function to the photosystem of purple bacteria.[13, 14] The crystallization and X-ray structure analysis of the latter[6-8] was a recent breakthrough in photosynthesis research.

3.1. Photosystem II

The integral membrane complex of photosystem II (Fig. 4) consists of at least ten protein subunits.[15] However all the electron-flow events in PS II take place via prosthetic groups bound to only two polypeptides, called D1 and D2. They form the actual reaction center of PS II. These two protein subunits of PS II are highly hydrophobic integral proteins of about 32 KDa in the thylakoid membrane. They contain the pigments, redox systems, and other components involved in the light-driven redox reaction across the membrane: P_{680}, two monomeric chlorophylls *a*, two pheophytins, two plastoquinones, and an iron ion bound via four histidines. Attached to these two polypeptides are two integral proteins of 47 and 43 kDa which carry about 30 core "antenna chlorophylls" to transfer excitation energy to chlorophyll in the reaction center.

In addition, preparations of a functional PS II contain two cytochrome b_{559} subunits.[16] Their function is still unclear, as is the role of the other smaller protein subunits. One small protein (4.8 kDa) always remains attached to a highly enriched, functional photosystem II, signalling a particular role, perhaps in conferring structural stability.[17] In the in

Table 1. Proteins, pigments, and redox carriers of plant and bacterial photosystems.

	photosystem II	photosystem of purple bacteria
polypeptides in the reaction center	D1 subunit D2 subunit	L subunit M subunit
further subunits	43 kDa (core antenna) 47 kDa (core antenna) products of the genes *psbH–psbN* two cytochrome b_{559} three peripheral proteins for Mn_4 stabilization	H subunit[a]
electron carriers	P680 chlorophyll dimer	P870 bacteriochlorophyll dimer
	two monomeric chlorophylls	two monomeric bacteriochlorophylls
	two pheophytins	two bacteriopheophytins
	two plastoquinones	two ubiquinones in *Rb. sphaeroides* one ubi- + one menaquinone in *Rps. viridis*
metal ions	one Fe four Mn Ca	one Fe
O_2 evolution	yes	no
electron donor	water	cytochrome c_2

[a] In *Rps. viridis* but not in the other purple bacteria an additional tetraheme protein is attached to the photosystem.

situ PS II complex, three hydrophilic peripheral polypeptides that stabilize the manganese complex of the water-splitting system are attached to the D1and D2 subunits.[18]

The amino acid sequences of all the protein subunits of PS II are known (Table 1). The major integral proteins are encoded in the chloroplast genome: the two reaction-center polypeptides D1 and D2 by the *psb*A and *psb*D gene and the 47 and 43 kDa polypeptides by the *psb*B and *psb*C, respectively.[19] However, the three peripheral polypeptides are en coded in the genome of the nucleus and are imported into the chloroplast.

The principal properties and mechanisms in electron flow through PS II have been known for a long time.[10, 11] Also long since recognized is the close similarity in the function of PS II with that of the reaction center of the photosynthetic purple bacteria[13] (whereas PS I is similar to the reaction center of some photosynthetic *green* bacteria). This homology of PS II to the photosystem of purple bacteria led to the breakthrough in understanding the structure of PS II.

3.2. The Photosystem of Purple Bacteria

The modern concept of the mechanism of plant photosynthesis as a water-splitting reaction accompanied by formation of a strong reductant was based on theoretical work by *van Niel* as early as 1941[20a] that recognized the similarities (rather than differences like the fact that bacteria cannot evolve oxygen) between plant and bacterial photosynthesis. This hypothesis was in contradiction to *Warburg's* notion of CO_2 splitting to oxygen and a "C" photolyte as the primary reaction.

Just how extensive the homology of photosynthetic electron flow in plants and purple bacteria is, became clear later. The carriers and the mechanisms of the electron flow in purple bacteria are very similar to those of PS II.[12-14, 21] Bacterial reaction centers (from *Rhodobacter sphaeroides*) contain four bacteriochlorophylls, among them a reaction center chlorophyll dimer P 870, two bacteriopheophytins, two bound ubiquinones, and iron ion bound to four histidines.[22] Exactly the same composition is found in PS II (Table 1). It is thus not surprising that a result in one system immediately stimulates research in the other. For example the concept of two bound quinones in the reaction center was established first in the bacterial system.[23] In agreement with this, terbutryn, a potent herbicidal inhibitor of photosystem II, is also an inhibitor of quinone reduction in purple bacteria.[24] The other herbicides, though, have little or no effect on bacterial photosynthesis.[24] The protein composition of the photosystem of purple bacteria is much simpler than that of PS II; it consists of only three protein subunits.[6, 22] The redox carriers of the photosystem are bound to two of them, called L and M. (Note that the reaction center of PS II is also bound to only two protein subunits.) Together with an H subunit they form the integral membrane complex in the bacterial system. The DNA sequences of the genes for the two proteins involved in the reaction center[22, 25] have a certain homology[25] to the amino acid sequences of the D1 and D2 subunits of PS II. After the X-ray structure of the photosystem of *Rhodopseudomonas viridis* became available,[6, 8] it was recognized that the folding of the protein sequences and therefore the structure of the reaction-center subunits of PS II and of the purple bacteria photosystem is also very similar indeed.[7, 26, 27]

The major difference between photosynthesis in bacteria and in plants is that bacteria cannot evolve oxygen. Instead they oxidize other inorganic or organic electron donors to generate the reducing power required for CO_2 assimilation. The electron donor for the bacterial reaction center is not a manganese complex but cytochrome c_2. The composition of plant and bacterial photosystems is summarized in Table 1.

Common to photosynthesis in bacteria and plants is that they can cycle electrons around a photosystem. Light excitation of the photosystem is the driving force for the charge separation across the membrane and vectorial electron flow. The ubiquinone pool reduced by the bacterial reaction center is oxidized back to the initial state by a cytochrome b/c_1 complex. This is analogous to the plastoquinone oxidation by the cytochrome b_6/f complex in the plant. In bacterial photosynthesis the electron is returned to the photosystem via a cytochrome c_2. This cytochrome is functionally homologous to plastocyanin, which is oxidized back by PS I. The vectorial redox reactions in bacterial systems also generate a proton potential that is used for ATP synthesis, as it is in plant photosynthesis. For this cyclic electron flow, bacteria need only one photosystem (Fig. 5). In the plant the generation of the reductant for CO_2 assimilation (NADPH) at the expense of water requires two photosystems.

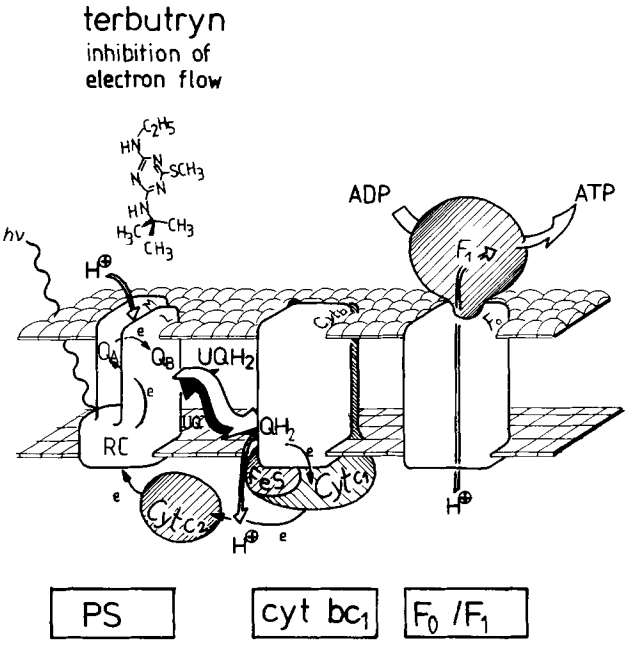

Fig. 5. Integral protein complexes and typical inhibitors in cyclic electron flow in purple bacteria. The integral complex of the photosystem and a cytochrome bc_1 complex participate in a cyclic system, in which ubiquinone mediates between the two complexes and pumps protons across the membrane. The ATP synthase is driven by the proton gradient.

The X-ray structure of the photosystem of purple bacteria of *Rhodopseudomonas viridis*[7, 8] and then of *Rhodobacter sphaeroides*[22] established the existence of five transmembrane helices each for the two reaction-center polypeptides L and M. It clearly indicated the orientation and binding to specific amino acids of the prosthetic groups (the reaction

center bacteriochlorophyll, bacteriopheophytins, Fe, and the two quinones) to these helices. Furthermore, the terbutryn orientation in the Q_B binding site was obtained directly by X-ray analysis after soaking the crystals with the herbicide.[7, 8] Thus the detailed structure of one photosystem was suddenly revealed and extrapolation to PS II could be attempted.

Accordingly it was proposed,[9, 26, 27] and subsequently experimentally verified,[16] that the D1 and D2 polypeptides are the reaction-center protein subunits of PS II. This was based not only on the (relatively low) amino acid sequence homology (about 27%) but more convincingly on their great folding homology to the L and M subunit of the bacteria according to hydropathy profile analysis.[26] Furthermore histidines for the binding of P_{680} and Fe in the D1 and D2 proteins of PS II were conserved at equivalent positions in the amino acid chains L and M[27] (as seen in the X-ray structure[6-8] of *R. viridis*), when the folding of the amino acids of these four polypeptides was aligned.

The key information that led to the proposal of the folding model for the PS II reaction-center polypeptides[26] was the identification of the amino acids in the D1 protein of plants and algae substituted in herbicide-tolerant mutants.[28] Equivalent amino acid substitutions occurred in purple bacteria resistant to the triazine herbicide terbutryn.[29] This surprisingly large homology in general, and even larger in the specific amino acid residues, permitted conclusions on the direct alignment of these amino acids in the vicinity of the Q_B sites. The terbutryn site is depicted in Figure 6 and will be explored in detail in Section 8.

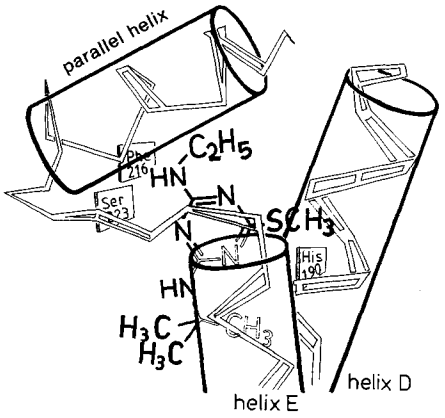

Fig. 6. The herbicide terbutryn in the L polypeptide subunit of the bacterial reaction center. The end of two transmembrane helices and a parallel helix are shown. They contain the Q_B- and herbicide-binding site according to [7]. Compare with Figure 11 for the binding of terbutryn in the equivalent D1 protein of PS II.

4. Photosynthesis and Herbicides

The first photosynthesis-inhibiting herbicides such as aryl urea (e.g. Diuron, DCMU) and triazine derivatives were identified 1956[1] even before the two light reactions and two photosystems were known and before plastoquinone had been discovered. Early on their mode of action was thought to involve the oxygen evolution system, but this could not be specified more closely at that time. When the two photosystems in plant photosynthesis were identified in 1960, the locus of herbicide action was narrowed down to photosystem II, which reduces plastoquinone (discovered in 1959). This progress in photosynthesis research now allowed a more detailed description of the biochemical and biophysical events in a photosystem and increased the usefulness of herbicidal inhibitors.

A prime example of the importance of this specific herbicide inhibition of a photosystem was the identification of quinones as the primary electron acceptor.[23, 30] Herbicides were also essential for the understanding of the features of a photosystem, such as the elucidation of the pathway of light excitation of PS II from varying antenna size and the accompanying fluorescence patterns and kinetics.[31, 32]

The concept of control of a reaction center's function by a hypothetical "state", called Q or A, was proposed by *Duysens*[31] and by *Butler*.[32] If the state Q is already reduced, it cannot accept an electron from the reaction center. As the photosystem is further excited, the excitation energy must be released and is observed as an increase in chlorophyll fluorescence. Herbicides prevent oxidation of the reduced state Q,[31] enhancing fluorescence. In this way the properties of PS II can be easily followed. The property of enhanced fluorescence upon addition of a herbicide is now often used as a convenient way of checking herbicide efficiency under field conditions.

The primary quencher Q of PS II, originally defined as a state rather than a specific compound, was identified ten years later to be a quinone by its absorption at 320 nm[30] and is now known to be the bound plastoquinone Q_A. The existence of two bound sites, Q_A and Q_B, in photosystem II was discovered after two quinones a were found in the bacterial system.[23] It became clear that a second bound quinone is necessary to transfer the electrons from the semiquinone of Q_A to the stable two-electron-accepting form: quinone Q_B (called a two-electron gate).[23]

Diuron and its class of herbicides were important not only for the characterization PS II, but also for identifying PS I reactions. Because the activity of PS I is not affected by these compounds its properties may be studied when PS II activity is inhibited by the presence of a herbicide.[33] Two other inhibitors, dibromothymoquinone (DBMIB)[34] and the dinitrophenyl ether of iodonitrothymol (DNP-INT),[35] were designed as possible PS II herbicides, and indeed turned out to be very potent quinone antagonists. Since they are also very effective in preventing plastohydroquinone oxidation, they became very important inhibitors of the cytochrome b_6/f complex[33] [see Fig. 4 and Equation (a)].

DBMIB was particularly instrumental in establishing the following facts: 1) there are two energy-conserving sites in the electron-flow system, that is, two proton transduction sites through the membrane that couple to ATP synthesis[36, 37] (shown in Figs. 2 and 4). 2) there is artificial proton pumping through the membrane possibly coupled to ATP formation.[38] This proved the existence of vectorial electron flow, which led to the final acceptance of the chemiosmotic theory of *P. Mitchell*, the major interest of photosynthesis research in the seventies.

The use of inhibitors (herbicides) continues unabated; their impact in recent years on the molecular biology of

photosynthesis is taken up again below. The number of papers in the literature on photosynthesis which use herbicides as convenient and powerful tools in photosynthesis research extends into the thousands.

5. The Chemistry and Biochemistry of Herbicides in Photosystem II

Advances in the understanding of photosynthetic mechanisms naturally gave strong impetus to industrial herbicide research as well. Photosynthetic assay systems are now routinely employed in industrial laboratories for a quick assay of the mode of action. The inhibitory potency of a herbicide, expressed by a pI_{50} value (= the negative logarithm of inhibitor concentration at which the photosynthetic activity is reduced by half) obtained in a cell-free system, that is, in isolated thylakoid membranes, is a direct measure of its primary action and is not complicated by secondary effects in the screening with intact plants, such as rate limitation by uptake, translocation, or degradation during transport to the target site. Important is the extrapolation to new chemical classes in the rational design of new compounds.

The correlation of inhibitory potency (as measured in isolated thylakoid membranes) to its descriptors in a group of herbicides (=QSAR), provides information on the possible contribution of electronic, steric, and lipophilicity parameters. These help to describe a mirror image of the binding pocket, from which its properties and dimensions and the interactions between the herbicide and amino acids may be deduced.

In 1961 already *Good*[39] suggested an interaction via hydrogen bonds of the essential element of the herbicide with specific peptide bonds in a hydrophobic pocket of the target protein. This concept turned out to be correct; these hydrogen bonds and the specific amino acids involved have now been identified and will be discussed in Section 8. The essential substructure in the classical type of PS II herbicides is considered to be an X=C−NH− group with an sp^2 hybridized carbon atom. This substructure is found in ureas, triazines, triazinones, carbamates and biscarbamates, pyridazinones, uraciles, anilides, and benzimidazoles. *Büchel* summarized the information in detail in 1972.[40] Classical and recent examples are shown in Figure 1 and Figure 7.

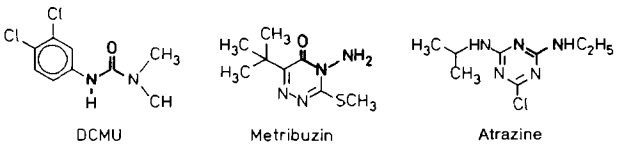

Fig. 7. The basic chemical unit in herbicides of the classical type (in boldface in the formulas). This element is essential for the binding to the protein of PS II.

Hansch and *Fujita*[41] introduced in 1964 a method for studying the correlation of chemical structure and biological activity by quantifying the biological potency with various physical parameters. This linear regression analysis method known as QSAR is applied to many pharmacologically active compounds and potential plant-protection agents. Photosynthesis inhibitors were among the first to be studied.[42, 43] The first QSAR study of arylureas by *Hansch* and *Deutsch*[43] led to Equation (c) in which the pI_{50} value is

$$pI_{50} = 4.183 + 1.290\,\pi + 0.544\,\sigma \qquad (c)$$

the easily determined negative logarithm of the concentration that inhibits 50% of photosynthesis activity in isolated thylakoids. The parameter π is proportional to the logarithm of the partition coefficient in octanol/water and σ is the Hammett constant. Later this QSAR was applied to many more ureas with other structures and to other photosynthesis herbicides.

At the photosynthesis meeting at Freundenstadt (1968) the QSAR of the just discovered 1,2,4-triazinone derivatives was reported.[44] The relatively simple equation has the form (d), where lg P is again the logarithm of the partition

$$pI_{50} = 4.608 + 1.959\,\lg P - 0.486\,(\lg P)^2 \qquad (d)$$

coefficient in octanol/water. The herbicide metamitron was developed as a result of this regression analysis. Other triazinones were analyzed and the QSAR published in 1979[45] even allowed a calculation of the dimensions in the binding niche (Fig. 8). The dimensions are now supported by computer modeling, as discussed below.

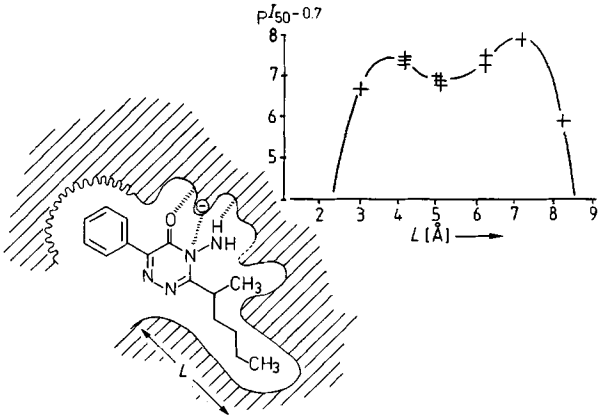

Fig. 8. Dimensions in the protein pocket binding of a triazinone herbicide. The dimensions were obtained in 1979 from QSAR studies on the correlation of the spatial parameters of a series of triazinone herbicides on the inhibitor potency in PS II [45]. These dimensions should be compared with those obtained after computer modeling in Figure 13. The inset shows the dependance of the inhibitory potency as pI_{50} on the chain length L of the 3-alkyl-4-amino-6-phenyl-1,2,4-triazin-5-ones, among them the commercial sugarbeet herbicide Goltix®.

6. Two Classes of Photosystem-II Herbicides in Overlapping Binding Sites

The "classical" herbicides of the urea and triazine type among others (Fig. 1) still dominate the field. But a second class of photosystem-II inhibitors with different chemical properties was recognized in 1979,[46] among them long-

known herbicides like dinoseb and ioxynil.[2, 3] They are, in the broadest sense of the term, phenolic inhibitors, for instance compounds like pyridate (Fig. 1) in which the effective form is the deacyl derivative, that is, a phenol. Nitrophenols, once thought to act by their uncoupling activity on respiratory phosphorylation, were shown to be very potent inhibitors of photosynthetic electron flow, like the cyanophenols (Fig. 9). Although they inhibit the PS II reaction somewhat differently from the classical PS II herbicides, they also interfere with Q_B function.[47]

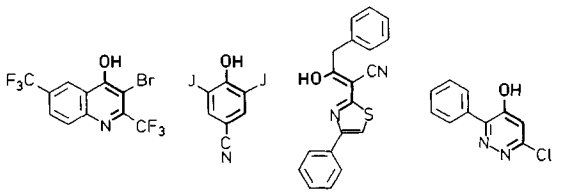

Fig. 9. The basic chemical unit in phenol type herbicides. A substituted quinoline, ioxynil, a ketonitril, and deacylpyridate are illustrated for comparison with the classical type herbicides in Figure 7.

The measurement of binding constants and studies of specific displacement of homologous inhibitors, introduced by *Tischer* und *Strotmann*,[48] indicated that phenol type herbicides also displace classical herbicides, although in a somewhat different way to the competitive displacement within the group of classical compounds.[49] A concept of overlapping binding sites in a common binding domain was developed[33, 46, 50] to accommodate different classes of chemical compounds in the same binding pocket of one protein (Fig. 10). Significantly phenol type compounds do

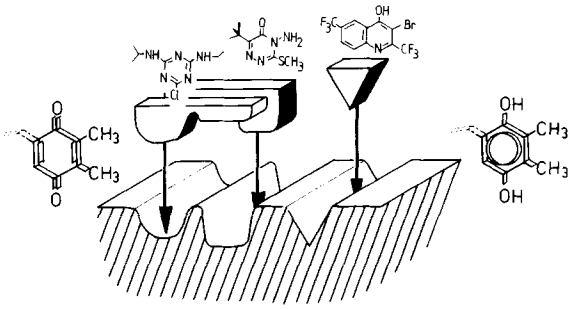

Fig. 10. Overlapping binding sites in the herbicide binding protein. Specific binding pockets were postulated for specific substituents of several herbicides in a common binding domain in order to explain different inhibition patterns of the two herbicide families that displace plastoquinone. Today this model from 1979 has given way to the postulate that different amino acid residues in the binding niche on the D1 protein are responsible for the binding of the herbicides as depicted in Figures 13 and 14.

not contain the essential structural element mentioned for ureas and classical herbicides. Furthermore, QSARs indicate a greater dependence on steric parameters, and those of *Verloop* in particular proved appropriate.[46] Molecular orbital calculations confirmed the very different charge distribution of the two groups,[51, 52] which, however, has not yet been incorporated into QSAR studies. In addition to nitro- and cyanophenols, more groups of compounds are known now to belong to the phenol type: hydroxyquinolines,[52] hydroxypyridines,[53] ketonitriles,[54] and the herbicide pyridate[55] in its deacyl form. Perhaps compounds in this class that are still under development will guide rational design into a new direction, because they show a different effect on regulatory processes in photosynthesis (Section 9).

7. Mutations in the *psb*A Gene in Herbicide-Tolerant Plants

The herbicide-binding protein D1 is encoded by the *psb*A gene in the chloroplast genome, sequenced first in 1982 by *Zurawski* et al.[56] A mutation in the *psb*A gene that led to atrazine tolerance in weeds growing close to maize or wheat fields[57] was shown to be due to an amino acid substitution in the D1 protein (Ser 264 → Gly).[58] This Ser 264 mutation has now been found in quite a number of higher plants that were exposed for longer periods to herbicides.[59] In nature only the Ser 264 to Gly change has been found. In cell cultures of higher plants Ser 264 to Thr[60] and to Asn[61] substitutions were also identified.

In green and blue-green algae (cyanobacteria) many more mutations can be produced, either by site-selected or site-directed mutageneses.[28] These algae have the same mechanism of photosynthesis as higher plants. Since the function and structure of the photosystems are the same, these algae are useful organisms for studying both photosynthesis and herbicides in the laboratory. As both cyanobacteria[62] and green algae[63] can now be transformed by mutagenized DNA, these organisms are very useful for genetic engeneering in herbicide research.

The significance of the mutations in the *psb*A gene and the resulting amino acid substitutions in the D1 protein (the herbicide-binding protein) is the identification of amino acid residues participating in herbicide binding in the protein target. Moreover, this is the basis for the future development and design of manipulated herbicide tolerance in crops. Altogether eight mutations that provide herbicide tolerance have now been identified by site-selected screening of natural mutants or mutants produced by mutagens.[64] They are Phe 211 to Ser, Val 219 to Ile, Ala 251 to Val, Phe 255 to Tyr, or Leu, Gly 256 to Asn or Glu, Ser 264 to Gly, Ala, or Thr, Asn 266 to Thr and Leu 275 to Phe. More recently site-directed mutagenesis (i.e. manipulating the DNA in vitro and then transforming cyanobacteria and green algae) has revealed many more amino acid substitutions in the D1 protein that can be analyzed for herbicide tolerance. The effect that conclusions from mutant studies have on computer modeling of protein folding and herbicide docking are discussed in Section 8.

Most of the mutants of the green algae *Chlamydomonas reinhardtii* tolerant to metribuzin are also resistant (cross resistance) to triazines, ureas, and other herbicides of the classical type (Fig. 1). To phenol type inhibitors (Fig. 9), however, these mutants show little tolerance or even hypersensitivity (or negative cross resistance).[65] These mutant studies show even more clearly that the classical and phenol type herbicides share some but not all of the amino acid binding sites of the Q_B binding pocket. Whereas the classical herbicides are bound to Ser 264 and Ala 251 (and therefore mutants become tolerant when these amino acids are

changed) phenols orient differently and do not change potency with a Ser 264 or Ala 251 mutation. The concept of overlapping binding sites[46, 50] has been replaced by computer models in which the correct orientation of each individual compound towards a particular amino acid residue in the binding domain of the Q_B site can be specified. Hypersensitivity to substituted triazinones was predicted[67] and in fact is found in certain mutants of *Chlamydomonas*.[66-68]

8. Topology of the Herbicide-Binding Niche in D1 Protein

The general topology of the D1 protein and the herbicide-binding site was proposed in 1986[26] after comparing its amino acid sequence and that of the L subunit of the purple bacteria. The first five mutants in herbicide-tolerant plants and algae known at that time agreed with the model because the amino acid substitutions could be well rationalized (see Section 1). For detailed modeling further information was used, such as results on natural or engineered mutants and from the cross resistance patterns.[65, 66, 68] The cross resistance of herbicides of different inhibitor families to different mutants is interpreted as reflecting different binding orientations. The two families of PS II herbicides were grouped as a serine- and a histidine-binding family.[69] Indeed this corresponded to the orientation of two inhibitors in the Q_B binding pocket of the photosystem of *Rps. viridis* observed by X-ray analysis.[7, 8] Recently the orientation of diuron in a diuron-sensitive mutant of *Rps. viridis* was also shown.[70] In this mutant the carbonyl group of diuron points towards a histidine. As diuron is a serine type inhibitor, but can point toward histidine as well, the classification is apparently not sufficient.

Photoaffinity labeling is another valuable technique for identifying amino acids in the herbicide-binding niche. When a radioactive azido derivative of the inhibitor is irradiated in the target pocket, it becomes covalently attached to the protein. In the first application *Pfister* and *Arntzen*[71] identified a 32 kDa protein as the herbicide-binding protein using azidotriazine. Proteolysis of the labeled protein indicated that Met 214 of the D1 protein was the binding site.[72] *Oettmeier* et al. sequenced the D1 protein after labeling it with azidomonuron[73] and azidocyanophenol.[74] They found that Tyr 237 and 254 and Val 246 were further aminoacids of the plant Q_B binding pocket.[73, 74]

With this information a number of herbicides were modeled in the Q_B binding niche of the reaction center polypeptide of PS II.[66, 68] Figure 11 shows schematically the binding of terbutryn in the D1 protein of PS II. In the analogous scheme for bacteria depicted in Fig. 6 terbutryn is bound to the L subunit of the photosystem. Figure 12 shows the part of the amino acid sequence of the L subunit of *Rps. viridis*[6-8] that is relevant for herbicide binding superimposed on the corresponding section of the D1 protein of PS II: the end of two transmembrane helices (IV and V), of a parallel helix and the connecting sequence. There are three additional amino acids in the D1 protein as can be seen in Fig. 12. The sequence from amino acid 222 to 247 in the D1 protein is omitted, as this has no homology to the L subunit of the bacterial system; the corresponding sequence of the L subunit therefore protrudes. The role of this sequence is discussed in Section 9, which deals with regulatory phenomena.

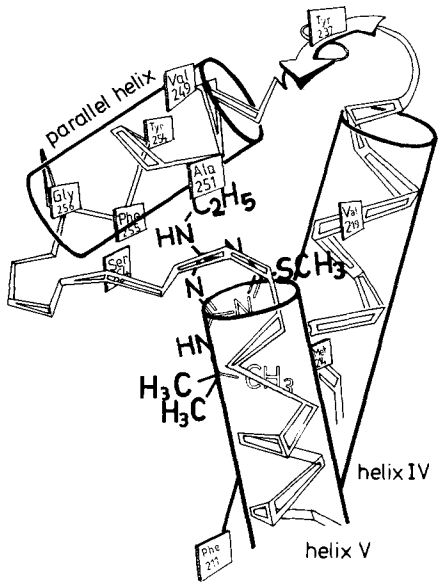

Fig. 11. The herbicide terbutryn in the D1 protein subunit of PS II. This computer model was constructed by using the homology with the folding of the L subunit in purple bacteria in Figure 6. Just the end of two transmembrane helices and the parallel helix participating in Q_B binding were involved. Aminoacids known to be involved in herbicide binding by amino acid substitutions in herbicide-tolerant plants (Phe 211, Val 219, Ala 251, Phe 255, Gly 256, Ser 264 and Leu 275) or tagged by photoaffinity labeling (Met 214, Tyr 237, Val 249, and Tyr 254) are marked.

To dock a herbicide into the Q_B binding pocket in the D1 protein, we used the data of cross resistance for a number of 3-alkyl derivatives of 4-amino-6-phenyl-1,2,4-triazin-5-ones, among them the sugarbeet herbicide metamitron (Goltix®, no. 2 in Table 2). The five mutations in *Chlamydomonas reinhardtii* are Val 219 to Ile, Ala 251 to Val, Phe 255 to Tyr, Ser 264 to Ala, and Leu 275 to Phe. The positions of these mutations in our model of the Q_B binding niche are depicted in Figure 13.

The inhibitor data for metamitron and six other 3-alkyl derivatives is given in Table 2. In the serine mutant the inhibitor potency of all triazinones is greatly reduced. This can be explained by the loss of a hydrogen bond between the hydroxyl group of serine and the triazinones. A detailed consideration of the possible spatial orientation indicates that a hydrogen atom of the free amino group of the inhibitor participates in the hydrogen bond to serine, whereas the carbonyl group of the triazinone participates in a hydrogen bond to the peptide group Phe 265 adjacent to serine. The phenyl ring of the triazinones accordingly points in the same direction as the isoprene side chain of plastoquinone. In this assumed basic orientation of the triazinones, the substituent R that we varied points to the direction of Ala 251, Ser 268 and finally Asn 247 (Fig. 13). The space for the side chain R is very similar to that proposed in 1978[45] from QSAR studies (compare Fig. 8 and Fig. 13).

There is a bottleneck between Ala 251 and Ser 268, which becomes narrower by the mutation of Ala 251 to Val. This

Fig. 12. Stereoplot of the protein folding of the Q_B binding pocket of the D1 protein of PS II (green)[68] superimposed on that of the L subunit of the bacterial photosystem (purple)[75]. The three-dimensional folding of the amino acid backbone is viewed perpendicular to the membrane plane, looking into the Q_B binding niche. To superimpose the D1 protein on the known folding of the L subunit, the four amino acids that have identical functions in both photosystems were brought into optimal correspondence. These are the two iron-binding histidine units 190 and 230 in the bacteria (215 and 272 in PS II) serine 223 (264 in plants) and phenylalanine 216 (255 in PS II), which is oriented behind the quinone ring. The D1 protein has more amino acids than the L subunit in this sequence: one between Ser 264 and transmembrane helix V and two between the parallel helix and the stretched sequence around Ala 263. Fourteen additional amino acids in the D1 protein between the parallel helix and transmembrane helix 4 have been omitted.

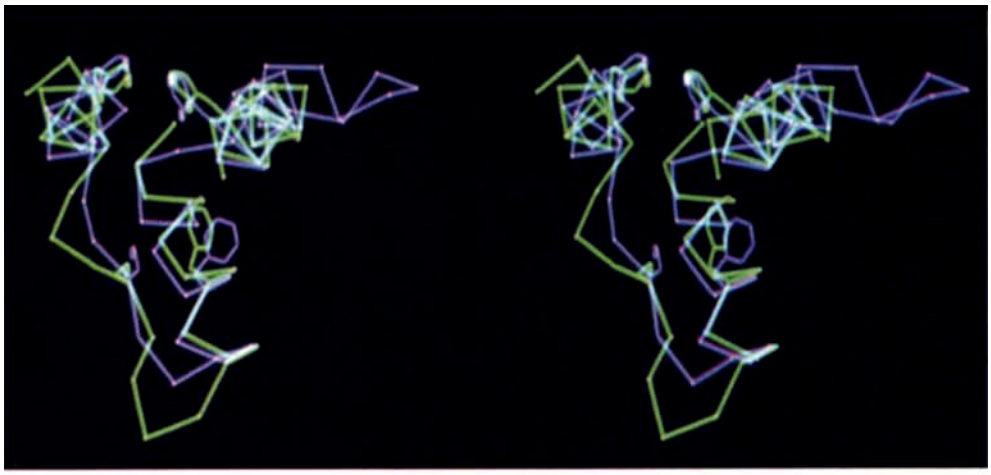

Fig. 12.

Fig. 13. Stereopicture of the orientation of an ethyl derivative of triazinone (compound 3 in Table 2, in red) in the Q_B binding pocket in the D1 protein of PS II (green). The protein folding of the D1 sequence in the Q_B site is viewed parallel to the membrane plane, that is, perpendicular to the view in Figure 12. Amino acid residues are indicated (in the atomic colors): Val 219*, Ala 251*, Phe 255*, Ser 264* and Leu 275*, Asn 247 and Ser 268. An asterisk indicates those that are substituted in herbicide-tolerant plants. A water molecule is postulated between Asn 247 and Ser 268.

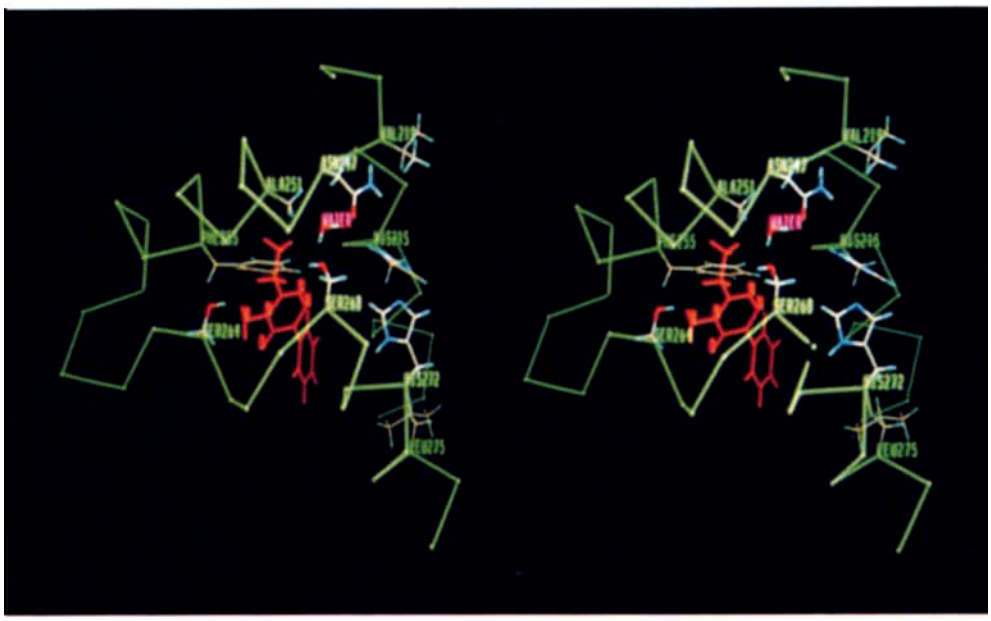

Fig. 13

Fig. 14. Stereopicture of the orientation of a pentyl derivative of triazinone (compound 6 in Table 2, in red) in the Q_B binding pocket in the D1 protein of PS II. The water molecule between Asn 247 and Ser 268 has been replaced by the herbicide and therefore the side chain of Ser 268 is turned sideways if compared with its orientation in Figure 13.

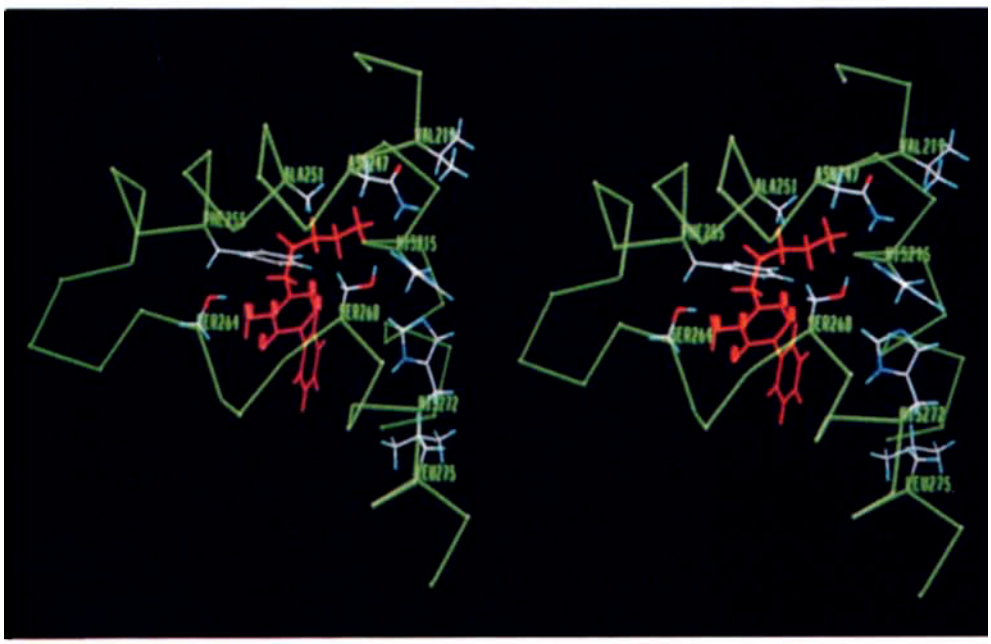

Fig. 14

feature which easily explains the strong decrease of the inhibitor values for the triazinones (Table 2). The decrease in inhibitor potency by increasing the chain length R of the triazinones indicates that the hexyl group extends to the end of the binding niche (Fig. 13). However, by compact folding of heptyl and octyl groups, these alkyl chains can also just be accommodated in the wild type (data not shown). Here the side chain of Asn 247 forms the bottom of the binding pocket. Though Val 219 is oriented behind Asn 247 and does not directly extend into the binding pocket, its mutation to the larger isoleucine further diminishes the space available by shifting Asn 247 into the binding area; the potency of the inhibitors falls.

Table 2. Inhibition of photosynthesis in wild type *Chlamydomonas reinhardtii* and five mutants by triazinones of type A.

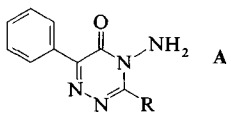

A

No.	R	pI_{50} wild type[a]	resistance factor for the mutants[b] Ser 264	Ala 251	Leu 275	Phe 255	Val 219
1	H	4.0	>1	>1	>1	0.5	>1
2	methyl	5.5	>30	130	6.3	0.3	1.3
3	ethyl	6.4	>250	100	6.3	0.2	16
4	propyl	5.2	>16	>16	4	0.1	1.6
5	butyl	6.0	>100	>100	10	0.16	2
6	pentyl	6.5	>320	>320	20	0.5	6.3
7	hexyl	4.0	>1	>1	>1	0.4	>1

[a] pI_{50} = negative logarithm of the molar concentration I_{50} of the inhibitor required to reduce the activity to half. [b] Resistance factor = I_{50} (mutant)/I_{50} (wild type).

Triazinones with a short substituent R (H, methyl, ethyl) only just reach Ala 251 (changed to Val in the mutant); surprisingly their potency is also lower. We conclude that in the mutant not only the local space for amino acid 251 is changed, but also the relative position of the parallel helix (position 247 to 258) towards Ser 264. Serine's hydrogen bonds dominate the overall binding affinity to triazinones. The triazinone with R = propyl exactly reaches the bottleneck between Ala 251 and Ser 268. A similar shift as in the Val 219 mutant will thus reduce its potency. The triazinones with larger substituents R like butyl and pentyl bind better to both wildtype and mutants than the propyl derivatives, possibly due to better spacefilling.

We further assume the presence of a water molecule between Ser 268 and Asn 247 in the wildtype (see Fig. 13), because the bacterial system contains a water molecule at an equivalent position.[7, 75-77] The displacement of the water molecule in the D1 protein by the Ala 251 and Val 219 mutations might explain the irregularities in the correlation of inhibitor potency with chain length (Table 2 and Fig. 8). Fig. 14 illustrates the binding of the pentyl derivative after the displacement of the water molecule visible in Figure 13.

All triazinone derivatives of Table 2 show higher inhibitor potency in the mutant Phe 255 to Tyr compared with the wildtype. The phenyl ring of Phe or Tyr 255 and the ring system of the triazinones are probably stacked with parallel ring orientations. The introduction of a hydroxyl group in the mutant should not disturb the stacking. As we see no possibility for an additional hydrogen bond between tyrosine and the triazinones, we cannot yet explain the increase in potency. As Leu 275 is not in direct contact with the triazinones, the inhibitor potency in the Leu 275 mutant is not affected.

9. Regulatory Phenomena Inhibited by PS II Herbicides

The mode of action of PS II herbicides was hitherto described as a competitive inhibition of Q_B function in the electron flow of PS II (i.e., arresting photosynthesis). An additional effect might have even more important consequences. This involves the inhibition of the fast degradation and biosynthesis (the rapid turnover) of the herbicide binding protein in the chloroplasts. Surprisingly, even under normal growth conditions the D1 polypeptide of PS II shows a much higher light-dependent degradation–biosynthesis turnover than all other thylakoid membrane proteins.[78, 79] It is thought that the rapid turnover is part of a repair mechanism.[5, 80] Apparently photosystem II is continuously deactivated by excess light, a process called photoinhibition.[80] The mechanism of deactivation is not yet defined but it appears to be due to damage in the amino acid sequence or a modification of the folding of the D1 protein. The damage to the D1 protein can be repaired only by displacement and complete resynthesis of the polypeptide and reassembly of photosystem II. This turnover and repair mechanism is prevented by most of the inhibitors of the Q_B site, such as diuron or atrazine,[78, 79, 81] but not by certain inhibitors of the phenol type, for example bromonitrothymol and ketonitrile.[82, 84] It might be significant that those inhibitors of PS II that inhibit turnover are also herbicides, whereas the others are not.

Interference of a herbicide with a regulatory process in photosynthesis might have much greater impact on the secondary response of the plant than mere interruption of the photosynthetic electron flow—after all, a plant survives extensive dark periods where no photosynthesis is possible. Interference with a repair process in photoinhibition would sustain and aggravate the inhibition of PS II.[66, 83, 84] Perhaps this provides a hint why the PS II herbicides do not destroy the plant just by starvation, but bleach it as well.[85]

The molecular basis for this interference with the light-dependent degradation of the D1 protein is slowly becoming clear. Apparently certain amino acids forming the Q_B binding pocket not primarily involved in electron flow participate in the photodegradation process. The primary cleavage site is close to Glu 240.[86, 87] A recognition sequence (PEST sequence) that would signal to a protease (Fig. 15) is postulated in a position just in front of Arg 238. As already mentioned, the photoaffinity technique tagged Tyr 237 with azidomonuron.[73] So this amino acid lies close to the cleavage site (Fig. 15). A substituent of a herbicide might extend into the extra loop in the amino acid sequence of the D1 protein that is specifically involved in regulatory processes in photoinhibition. In computer modeling (Figure 11–14) Tyr 237 can be placed close to Asn 247 and Val 219. Mutants have already shown that Val 219 is involved in herbicide binding. Thus it becomes conceivable that photoinhibition

and turnover processes are modulated by the redox and occupancy state of the Q_B site.[80, 84] Herbicides in the extra loop of the Q_B binding pocket interfere with the photodegradation, possibly by preventing necessary conformational changes involved in the cleavage process. In the vicinity of the protein cleavage site of the D1 protein in rapid turnover is Arg 238, a trypsin cleavage point. The behavior of Arg 238 toward trypsination mirrors that of the loop sequence toward photodegradation: the blocking of trypsination at Arg 238 by herbicides like DCMU and atrazine, but not by herbicides of the phenol class[84] is exactly analogous to the behavior of the two types of herbicides in photodegradation. The trypsination of the D1 protein has a long experimental history and actually led to the discovery of the protein site for herbicide binding to PS II.[88]

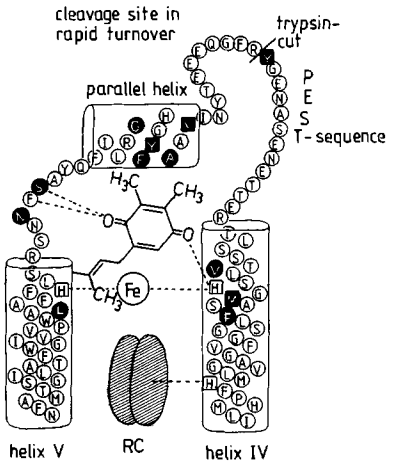

Fig. 15. Scheme of the folding of the amino acid sequence of protein D1 involved in herbicide binding and regulation (photodegradation). Broken lines represent interactions between plastoquinone and amino acid groups in the Q_B binding protein. Solid circles indicate amino acids substituted in mutants and blocks those tagged by photoaffinity labeling. A specific trypsin cut occurs at Arg 238 that is close to Tyr 237, tagged by azidomonuron. Amino acids 228 to 246 are significant for the cleavage of the D1 protein in its rapid turnover and in recognition of hypothetical protease (PEST sequence). This extra loop in the D1 protein of PS II (not present in the L subunit of bacteria) folds back over the Q_B site, probably placing Tyr 237 close to Asn 247 and Val 219. Certain herbicides in the Q_B site influence the rate of cleavage by an endogenous protease in rapid turnover, and by trypsin at Arg 238. (To compare this figure with the stereo plots in 12–14, helix V is drawn to the left of helix IV.) RC = reaction center.

Protein phosphorylation might play a role in control of photodegradation of the herbicide-binding protein, because the redox state of the plastoquinone pool also modulates the phosphorylation of a number of thylakoid proteins, among them the D1 polypeptide. This protein phosphorylation is inhibited by diuron,[89] another manifestation of herbicidal action. This is probably of great significance for understanding both the regulation of PS II and the mode of action of herbicides. The amino acid loop in the D1 protein from Arg 225 to Asn 247 has no equivalent in the otherwise homologous L subunit of the purple bacteria, which shows neither light-dependent protein turnover nor photoinhibition.

The recently recognized additional mode of action of the PS II herbicides will be a new field of mutual interest for photosynthesis and herbicide research. It promises insight into the molecular basis of the response of the photosynthetic electron-flow system to changes in physiological and light conditions as well as in stress situations.

10. Summary and Outlook

The original common goal of photosynthetic and herbicide research, namely the identification and both structural and functional characterization of the herbicide-binding protein, has been achieved. Surprisingly, it is a reaction-center polypeptide of photosystem II. Herbicide-tolerant mutants proved to be extremely useful in the construction of a three-dimensional model of the folding of this protein. Inhibitors can be modeled within the folded protein, and the amino acids involved in the binding (specific for individual herbicides) can be identified. The particular interactions can be approximated by force-field calculations. The rational design of chemically new photosynthesis inhibitors is no longer the limiting step in the development of a herbicide.

Knowledge of the binding of photosynthesis-inhibiting herbicides allows, in principle, the introduction of resistance on the primary function level by mutagenesis. The acceptance and economic viability of such a procedure is another question.

The knowledge of the three-dimensional folding of a membrane protein, first achieved through a crystal structure analysis by *Michel*, *Deisenhofer*, and *Huber*, gave research into photosynthesis an enormous thrust forward. Certain is that the nowhere near exhausted potential of the molecular genetic method will provide many more unsuspected and surprising insights. The elucidation of other, hitherto unknown regulatory phenomena, which probably also affect the herbicide-binding protein, will also give herbicide research new impetus. Even the properties of the D1 protein known at present, such as its turnover and its participation in protein phosphorylations, as well as the complicated control of the expression of its *psb*A gene, will challenge the molecular biologists for a long time. Photosynthesis and herbicide research promises to remain an outstanding example of cooperation between university and industry.

Received: June 14, 1991 [A 848 IE]
German version: *Angew. Chem. 103* (1991) 1650

[1] First report on the protosynthesis-inhibiting function of substituted aryl ureas: J. S. C. Wessels, R. van der Veen, *Biochim. Biophys. Acta 19* (1956) 548.
[2] C. Fedtke: *Biochemistry and Physiology of Herbicide Action*, Springer, Berlin 1982.
[3] J. R. Corbett, K. Wright, A. C. Baillie: *The Biochemical Mode of Action of Pesticides*, Academic Press, London 1984.
[4] D. E. Moreland, *Annu. Rev. Plant Physiol. 18* (1967) 365.
[5] Review: D. J. Kyle, *Photochem. Photobiol. 41* (1985) 106.
[6] J. Deisenhofer, H. Michel, *EMBO J. 8* (1989) 2149.
[7] J. Deisenhofer, H. Michel, *Angew.Chem. 101* (1989) 872; *Angew. Chem. Int. Ed. Engl. 28* (1989) 829.
[8] H. Michel, O. Epp, J. Deisenhofer, *EMBO J. 5* (1986) 2445.
[9] A. Trebst, W. Draber, *Photosynth. Res. 10* (1989) 381.
[10] For a recent review, see G. Renger, *Angew. Chem. 99* (1987) 660; *Angew. Chem. Int. Ed. Engl. 26* (1987) 643.
[11] For a recent review, see J. Barber, *Trends Biochem. Sci. 12* (1987) 321.
[12] R. J. Debus, B. A. Barry, G. T. Babcock, L. McIntosh, *Biochemistry 27* (1988) 9071.
[13] Review: L. Zimmermann, A. W. Rutherford, *Physiol. Veg. 23* (1985) 425.
[14] Review: M. Y. Okamura, R. J. Debus, D. Kleinfeld, G. Feher in B. L. Trumpower (Ed.): *Function of Quinones in Energy Conserving Systems*, Academic Press, New York 1982, p. 299.

[15] H. Koike, M. Ikeuchi, T. Hiyama, K. Mamada, Y. Inoue in M. Baltscheffsky (Ed.) *Current Research in Photosynthesis, Vol. 1*, Kluwer, Dordrecht 1989, p. 2351.
[16] O. Nanba, K. Satoh, *Proc. Natl. Acad. Sci. USA 84* (1987) 109.
[17] M. Ikeuchi, Y. Inoue, *FEBS Lett. 241* (1988) 99.
[18] N. Murata, M. Miyao, *Trends Biochem. Sci. 13* (1985) 122.
[19] J. D. Palmer, *Annu. Rev. Genet. 19* (1985) 325.
[20] a) C. B. van Niel, *Advan. Enzymol. Relat. Subj. Biochem. 1* (1941) 263; b) O. Wartung, *Angew. Chem. 69* (1957) 627; English version: *Science 128* (1958) 68.
[21] G. Feher, M. Y. Okamura in R. K. Clayton, W. Sistrom (Ed.): *The Photosynthetic Bacteria*, Plenum, New York 1978, p. 349.
[22] J. P. Allen, G. Feher, T. O. Yeates, H. Komiya, D. C. Rees, *Proc. Natl. Acad. Sci. USA 84* (1987) 5730.
[23] C. A. Wraight, *Photochem. Photobiol. 30* (1979) 767.
[24] R. R. Stein, A. Castellvi, J. P. Bogacz, C. A. Wraight, *J. Cell. Biochem. 24* (1984) 243.
[25] D. C. Youvan, E. J. Bylina, M. Alberti, H. Begusch, J. E. Hearst, *Cell (Cambridge, Mass.) 37* (1984) 949.
[26] A. Trebst, *Z. Naturforsch. C 41* (1986) 240.
[27] H. Michel, J. Deisenhofer, *Biochemistry 27* (1988) 1.
[28] J. D. Rochaix, J. Erickson, *Trends Biochem. Sci. 13* (1988) 56.
[29] M. L. Paddock, J. C. Williams, S. H. Rongey, E. C. Abresch, G. Feher, M. Y. Okamura, in J. Biggins (Ed.): *Progress in Photosynthesis Research Vol. III*, Nijhoff, Dordrecht 1989, p. 775.
[30] K. Witt, *FEBS Lett. 38* (1973) 116.
[31] L. N. M. Duysens, H. E. Sweers, *Stud. Microalgae Photosynth. Bact. 1963*, 353.
[32] W. L. Butler, *Biochim. Biophys. Acta 63* (1962) 309.
[33] A. Trebst, *Methods Enzymol. 69* (1980) 675.
[34] A. Trebst, E. Harth, W. Draber, *Z. Naturforsch. B 25* (1970) 1157.
[35] A. Trebst, H. Wietoska, W. Draber, H. J. Knops, *Z. Naturforsch. C 33* (1978) 919.
[36] J. M. Gould, D. Ort, *Biochim. Biophys. Acta 325* (1973) 157.
[37] A. Trebst, S. Reimer, *Biochim. Biophys. Acta 325* (1973) 546.
[38] A. Trebst, G. Hauska, *Naturwissenschaften 61* (1974) 308.
[39] N. E. Good, *Plant Physiol. 36* (1961) 788.
[40] K. H. Büchel, *Pestic. Sci. 3* (1972) 89.
[41] C. Hansch, T. Fujita, *J. Am. Chem. Soc. 86* (1964) 1616.
[42] C. Hansch in H. Metzner (Ed.): *Progress in Photosynthesis Research, Vol. III*, H. Laupp, Jr., Tübingen 1969, p. 1685.
[43] C. Hansch, E. W. Deutsch, *Biochim. Biophys. Acta 94* (1965) 381.
[44] W. Draber, K. H. Büchel, K. Dickoré, A. Trebst, E. Pistorius in H. Metzner (Ed.): *Progress in Photosynthesis Research, Vol. III*, H. Laupp, Jr., Tübingen 1969, p. 1789.
[45] W. Draber, C. Fedtke in H. Geißbühler (Ed.): *Advances in Pesticide Science Part 3*, Pergamon, Oxford 1979, p. 475.
[46] A. Trebst, W. Draber in H. Geißbühler (Ed.): *Advances in Pesticide Science, Part 2*, Pergamon, Oxford 1979, p. 223.
[47] W. Oettmeier, A. Trebst in Y. Inoue (Ed.): *The Oxygen Evolving System of Photosynthesis*, Academic Press Japan, Tokyo 1983, p. 411.
[48] W. Tischer, H. Strotmann, *Biochim. Biophys. Acta 460* (1977) 113.
[49] W. Oettmeier, C. Kude, H. J. Soll, *Pestic. Biochem. Physiol. 27* (1987) 50.
[50] C. J. Arntzen, C. L. Ditto, P. E. Brewer, *Proc. Natl. Acad. Sci. U.S.A. 76* (1979) 278.
[51] A. Trebst, W. Donner, W. Draber, *Z. Naturforsch. C 39* (1984) 405.
[52] W. Draber, B. Pittel, A. Trebst, in P. S. Magee, D. R. Henry, J. H. Block (Eds.): *Probing Bioactive Mechanisms (ACS Symp. Ser. 413* (1989) 215).
[53] A. Trebst, B. Depka, S. M. Ridley, A. F. Hawkins, *Z. Naturforsch. C 40* (1985) 391.
[54] U. Bühmann, E. C. Herrmann, C. Kötter, A. Trebst, B. Depka, H. Wietoska, *Z. Naturforsch. C 42* (1987) 704.
[55] J. Durner, A. Thiel, P. Böger, *Z. Naturforsch. C 41* (1986) 881.
[56] G. Zurawski, H. J. Bohnert, P. R. Whitfield, W. Bottomley, *Proc. Natl. Acad. Sci. USA 79* (1982) 7699.
[57] S. R. Radosevich, O. T. De Villiers, *Weed Sci. 24* (1976) 229.
[58] J. Hirschberg, L. McIntosh, *Science 222* (1983) 1346.
[59] J. Gressel, in S. O. Duke (Ed.): *Herbicide Physiology, Vol. II*, CRC Press, Boca Raton, Fl, USA 1985, p. 159.
[60] F. Sato, Y. Shigematsu, Y. Yamada, *MGG, Mol.* Gen. *Genet. 214* (1988) 358.
[61] A. Páy, M. A. Smith, F. Nagy, L. Márton, *Nucl. Acids Res. 16* (1988) 8176.
[62] J. Hirschberg, N. Ohad, I. Pecker, A. Rahat, *Z. Naturforsch. C42* (1987) 758.
[63] E. Przibilla, S. Heiss, U. Johanningmeier, A. Trebst, *Plant Cell 3* (1991) 169.
[64] A. Trebst in J. C. Caseley, G. W. Cussans, R. K. Atkin (Eds.): *Herbicide Resistance*, Butterworth-Heinemann, Oxford 1991, p. 145.
[65] G. F. Wildner, U. Heisterkamp, A. Trebst, *Z. Naturforsch. C45* (1990) 1142.
[66] A. Trebst, J. F. Kluth, K. Tietjen, W. Draber in H. Frehse (Ed.): *Pesticide Chemistry, Advances in International Research, Development and Legislation*, VCH, Weinheim 1991, p. 111.
[67] W. Oettmeier, K. Masson, C. Fedtke, J. Konze, R. R. Schmidt, *Pestic. Biochem. Physiol. 18* (1982) 357.
[68] K. Tietjen, J. F. Kluth, R. Andree, M. Haug, M. Lindig, K. H. Müller, H. J. Wroblowsky, A. Trebst, *Pestic. Sci. 31* (1991) 65.
[69] A. Trebst, *Z. Naturforsch. C42* (1987) 742.
[70] I. Sinning, H. Michel, P. Mathis, W. A. Rutherford, *FEBS Lett. 256* (1989) 192.
[71] K. Pfister, K. E. Steinback, G. Gardner, C. J. Arntzen, *Proc. Natl. Acad. Sci. USA 78* (1981) 981.
[72] P. K. Wolber, M. Eilmann, K. E. Steinback, *Arch. Biochem. Biophys. 248* (1986) 224.
[73] R. Dostatni, H. E. Meyer, W. Oettmeier, *FEBS Lett. 239* (1988) 207.
[74] W. Oettmeier, K. Masson, J. Höhfeld, H. E. Meyer, K. Pfister, H. P. Fischer, *Z. Naturforsch. C44* (1989) 444.
[75] H. Michel, J. Deisenhofer, R. Huber, entry in the Brookhaven Protein Data Bank under 1PRC (1989).
[76] M. L. Paddock, P. H. McPershon, G. Feher, M. Y. Okamura, *Proc. Natl. Acad. Sci. USA 87* (1990) 6803.
[77] E. Takahashi, C. A. Wraight, *Biochim. Biophys. Acta 1020* (1990) 107–120.
[78] A. K. Mattoo, H. Hoffmann-Falk, J. B. Marder, M. Edelman, *Proc. Natl. Acad. Sci. USA 81* (1984) 1380.
[79] J. B. Marder, P. Goloubinoff, M. Edelman, *J. Biol. Chem. 259* (1984) 3900.
[80] G. Schuster, R. Timberg, I. Ohad, *Eur. J. Biochem. 177* (1988) 403.
[81] A. K. Mattoo, J. B. Marder, M. Edelman, *Cell (Cambridge, Mass.) 56* (1989) 241.
[82] M. A. K. Jansen, S. Malkin, M. Edelman, *Z. Naturforsch. C45* (1990) 408.
[83] A. K. Mattoo, J. B. Marder, V. Gaba, M. Edelman in G. Akoyunogbu, H. Senger (Eds.): *Regulation of Chloroplast Differentation, Vol. 2*, Liss New York 1986, p. 607.
[84] A. Trebst, B. Depka, B. Kraft, U. Johanningmeier, *Photosynth. Res. 8* (1988) 163.
[85] D. E. Moreland, J. L. Hilton in L. J. Audus (Ed.): *Herbicides, Vol. 1*, Academic Press, London 1976, p. 493.
[86] A. Trebst, B. Depka, *Z. Naturforsch. C45* (1990) 765.
[87] B. M. Greenberg, V. Gaba, A. K. Mattoo, M. Edelmann, *EMBO J. 6* (1987) 2865.
[88] G. Renger, *Biochim. Biophys. Acta 440* (1976) 287.
[89] J. Bennett, E. K. Shaw, S. Bakr, *FEBS Lett. 210* (1987) 22.

Communications may be submitted in English *or* in German. Further details regarding the submission of communications can be found in the "Notice to Authors" reproduced in the January issue of the journal. Copies thereof may be obtained from the editorial office upon request.

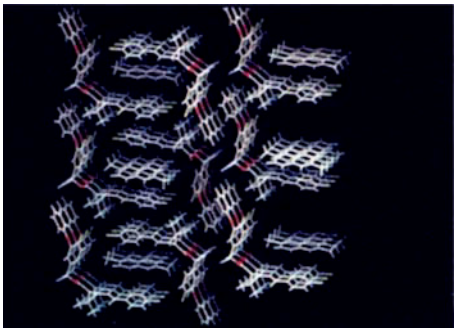

Fig. 1. Structure of the crystal lattice of the flumethrin inclusion compound **3**.

Diastereomer Separation by Formation of Inclusion Compounds: 2,6-Dimethylnaphthalene Complexes of Flumethrin

By *Liborius Born* and *Rainer Fuchs**

Dedicated to Professor Karl Heinz Büchel on the occasion of his 60th birthday

Flumethrin (**1**)[1] is a synthetic pyrethroid used in very small dosages to combat ticks of all types. It consists of 55–60% of the isomeric pair **1a**, (1*R*,3*S*,α*R*/1*S*,3*R*,α*S*), and 40–45% of isomeric pair **1b**, (1*R*,3*S*,α*S*/1*S*,3*R*,α*R*).

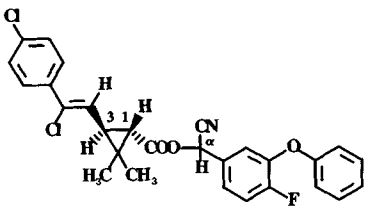

Flumethrin **1**

Some time after **1a**/**1b** is dissolved in a technical solvent, usually C_{11}–C_{13} alkyl naphthalenes, to prepare a commercial formulation (emulsion concentrate), the precipitation of crystals whose melting point (100 °C) is distinctly higher than that of **1a** (m. p. = 50 °C) or **1b** (waxy) is observed. Analyses by ^{1}H NMR spectroscopy, GC-MS, and HPLC show that the crystals contain a defined amount of 2,6-dimethylnaphthalene (**2a**), namely, two molecules of flumethrin (**1**) to one of **2a**. The analyses indicate further that the ratio **1a**:**1b** of 55:45 in the emulsion has changed in the crystalline precipitate to 96:4 (after recrystallization); that is, the crystals contain a much higher proportion of **1a**. The hypothesis that the isolated crystals were an inclusion compound of **1a** and **2a** was confirmed on warming 2 mol of **1a** and 1 mol of **2a** in 2-propanol to 50 °C to dissolve them, and cooling the solution to 20 °C. A crystalline inclusion compound (**3**) is obtained (m. p. 108 °C)[2] in 85–90% yield. In **3** the ratio **1a**:**2a** is also 2:1. To obtain more details on the structure of the crystalline inclusion compound **3**, an X-ray crystal analysis was undertaken.[3]

Figures 1 and 2 depict clearly[4] the role that **2a** plays in the lattice of **3**. The two isomers of **1a** form a pseudocycle that corresponds to a 32-membered macrocycle. This macrocycle encloses **2a** as guest[5] in such a way that the methyl groups are positioned in the gaps which remain when the host dimer forms its cavity. Thus **2a** interacts mainly with the chlorophenylvinyl residue of **1a**. This conclusion is supported by an analysis of the shorter heteromolecular distances (≤ 3.60 Å) between **1a** and **2a** which almost without exception involve the H atoms of the chlorophenyl groups. Electron donor/acceptor (EDA) interactions may therefore be the driving force for the formation of **3**.[6] The importance of potential EDA interactions on the formation of **3** is underlined by the fact that crystalline inclusion compounds are also obtained with the acid **4a** (see Table 1).

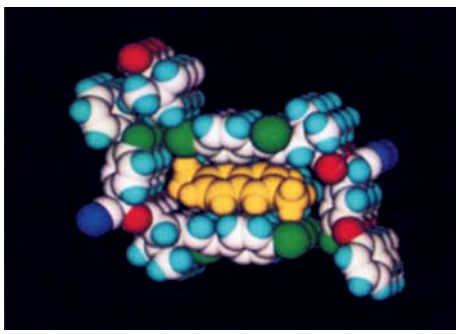

Fig. 2. Space-filling model of the flumethrin inclusion compound **3**.

The formation of flumethrin inclusion compounds is not limited to the guest molecule **2a**. The pseudocycle is large enough to accommodate anthracene (Table 1). The particular selectivity for **2a** is exemplified by the fact that the crystals formed from the technical solvent in which this effect was first noticed included exclusively **2a** as guest, although it represents only 4.8% of this mixture of naphthalene derivatives.[7]

Far more interesting than the separation of specific methylnaphthalenes is the diastereomeric separation on formation of the inclusion compound (Table 2). In contrast to common separations of stereoisomers of guest molecules,[8] the inclusion compounds described here cause the separation of diastereomers of the host molecule.

[*] Dr. R. Fuchs
Pflanzenschutzzentrum Monheim
Alfred-Nobel-Strasse 50, Geb. 6550
W-5090 Leverkusen-Bayerwerk (FRG)
Dr. L. Born
Zentrale Forschung der Bayer AG

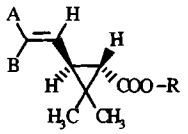

	A	B	R
4a		Cl	H
4b		Cl	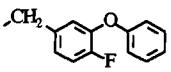
4c	Cl	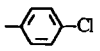	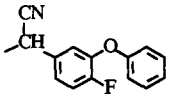
4d	Cl	Cl	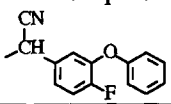
4e	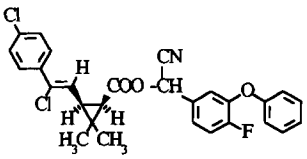		

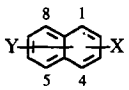

2a-i

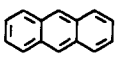

2j

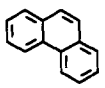

2k

Table 1. Formation of crystalline inclusion compounds with flumethrin or flumethrin derivatives.

host	guest	X	Y	molar ratio host:guest	m.p. [°C]
1a	**2a**	2-CH_3	6-CH_3	2:1	108
1a	**2j**	–		2:1	124 (decomp.)
1a	**2b**	2-CH_3	3-CH_3	2:1	90
1a	**2c**	2-CH_3	H	2:1	74
1a	**2k**	–		2:1	78
1a	**2d**	1-CH_3	H	[a]	
1a	**2e**	H	H	[a]	
1a	**2f**	2-OCH_3	H	[a]	
1a	**2q**	2-Cl	H	[a]	
1a	**2h**	2-NO_2	H	[a]	
1a	**2i**	2-OH	6-OH	[a]	
4a [b]	**2b**	2-CH_3	3-CH_3	1:1	132
4a [b]	**2j**	–		1:1	160 (decomp.)
4b [b]	**2a**	2-CH_3	6-CH_3	[a]	
4e [b]	**2a**	2-CH_3	6-CH_3	[a]	
4c [b]	**2a**	2-CH_3	6-CH_3	[a]	
4d [b]	**2a**	2-CH_3	6-CH_3	[a]	

[a] No inclusion compound. [b] **4a-e** were used as racemates.

Table 2. Separation of diastereomers of flumethrin by formation of inclusion compounds.

host		guest	inclusion compounds			
			1st cryst.		after recryst.	
1a	**1b**		**1a**	**1b**	**1a**	**1b**
55	45	**2a**	80	20	96	4
0	100	**2a**		no crystallization		
55	45	**2j**	71	29	92.5	7.5
55	45	**2b**			93	7
55	45	**2k**			92	8

[a] The crystalline inclusion compounds were prepared by mixing 1 mol of the host and 0.5 mol of the guest in 2-propanol. Recrystallization was from 2-propanol or toluene. The diastereomeric composition was determined by HPLC.

As shown in Figure 3, the two enantiomeric isomers of **1a** form a pseudocyclic dimer in which the CN groups are directed outwards. The isomers **1b** that are diastereomeric

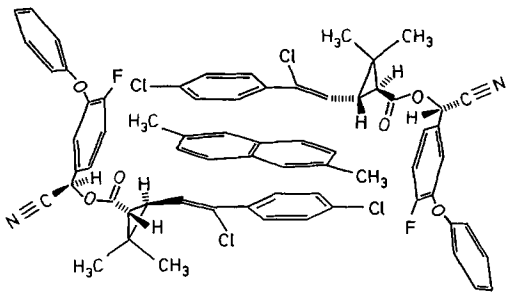

Fig. 3. Inclusion compound **3** with the isomeric pair **1a** (1*S*,3*R*,α*S*/1*R*,3*S*,α*R*). The CN groups point outward.

with **1a** were obtained by changing the configuration at the α-C atom. In this case (Fig. 4) if the rest of the molecular arrangement remained the same, the CN groups would point toward the carbonyl group, yielding a less favorable arrangement. Therefore the separation of the diastereomers may depend on the fact that only **1a** can adopt a configuration favorable for cavity formation and thus for the formation of a stable, well-crystalline inclusion compound. Cavity formation in the case of **1b** is less favorable and the inclusion compound less stable.

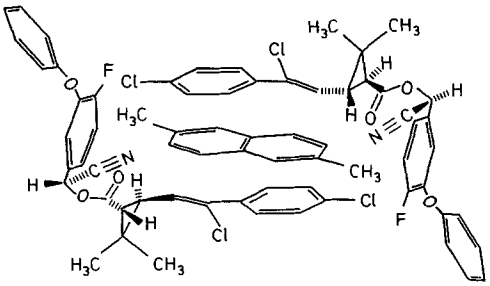

Fig. 4. By changing the configuration at the α-C atom, the inclusion compound with the isomer pair **1b** (1*S*,3*R*,α*R*)/1*R*,3*S*,α*S*) is obtained. The CN groups point inward.

Differentiation of diastereomers on formation of flumethrin–dimethylnaphthalene inclusion compounds has a parallel in the different insecticidal and acaricidal activity of flumethrin diastereomers. Only the isomer with the (1*R*,3*S*,α*S*) configuration is biologically active;[9] that is, it can adopt the correct configuration for its function. The elucidation of the structure of the stable flumethrin inclusion compound **3** might contribute to the understanding of the bonding of pyrethroids to receptor proteins. The observed separation of the flumethrin diastereomers also has a technically interesting aspect. In the technical isomeric mixture **1a**/**1b** the biologically active isomer is present in the pair **1b**. Selective precipitation and removal of the inactive isomeric pair by formation of a crystalline inclusion compound significantly increases the proportion of the active ingredient in the insecticide. This in turn reduces the dosage required for tick control, a desirable economical and ecological factor.

Received: August 1, 1991 [Z4846 IE]
German version: *Angew. Chem.* *103* (1991) 1699

CAS Registry numbers:
1a, 137330-26-8; **1a · 2a**, 137429-00-6; **1a · 2b**, 137429-02-8; **1a · 2c**, 137429-03-9; **1a · 2j**, 137429-01-7; **1a · 2k**, 137429-04-0; **1b**, 137330-27-9; **1b · 2a**, 137429-05-1; **2d**, 90-12-0; **2e**, 91-20-3; **2f**, 93-04-9; **2g**, 91-58-7; **2h**, 581-89-5; **2i**, 581-43-1; **4a · 2b**, 137330-24-6; **4a · 2j**, 137330-25-7; **4b**, 137232-96-3; **4c**, 69770-45-2; **4d**, 68359-37-5; **4e**, 69770-45-2.

[1] a) W. Stendel, R. Fuchs, *Vet. Med. Rev. 1982*, 115–129; b) R. Fuchs, I. Hammann, W. Stendel, DE-A 2730515 (July 6, 1977/January 18, 1979), Bayer AG.

[2] R. Fuchs, W. Stendel, DE-A 3629387 (August 29, 1986/March 3, 1988), Bayer AG.

[3] Crystal structure analysis of **3**: space group $P2_1/c$ (no. 14); $a = 2152.2(2)$, $b = 583.45(8)$, $c = 2388.9(3)$ pm, $\beta = 82.726(8)°$, Z(flumethrin) = 4, Z(2,6-dimethylnaphthalene) = 2, since this compound is situated on a symmetry center, $\rho_{calcd} = 1.314\ g\,cm^{-3}$. Enraf-Nonius CAD4 diffractometer, room temperature, $Cu_{K\alpha}$ radiation, 5054 independent reflections, empirical absorption correction, solution with direct methods. Refinement: anisotropic temperature factors for non-hydrogen atoms, isotropic temperature factors for hydrogen atoms; R (3263 reflections, 483 parameters) = 0.040. Further details of the crystal structure investigation may be obtained from the Fachinformationszentrum Karlsruhe, Gesellschaft für wissenschaftlich-technische Information mbH, W-7514 Eggenstein-Leopoldshafen 2 (FRG) on quoting the depository number CSD-55648, the names of the authors, and the journal citation.

[4] Drawn with the program SYBYL of Tripos Inc., St. Louis, USA, from X-ray crystallographic data.

[5] a) F. Vögtle, W. M. Müller, U. Werner, J. Franke, *Naturwissenschaften 72* (1985) 155; b) F. Cramer, *Angew. Chem. 68* (1956) 115.

[6] S. B. Ferguson, F. Diederich, *Angew. Chem. 98* (1986) 1127; *Angew. Chem. Int. Ed. Engl. 25* (1986) 1127.

[7] a) Composition [wt%] alkylbenzenes ($-C_{11}$) 23.4; naphthalene 14.2; 2-methylnaphthalene 29; 1-methylnaphthalene 13.9; 1,6-dimethylnaphthalene 5.2; 2,6-dimethylnaphthalene 4.8; other long-chain alkylnaphthalenes (12–13 C atoms); b) β-alkylated naphthalenes are also included preferentially within thiourea inclusion compounds: D. Montgomery, *J. Chem. Eng. Data 8* (1963) 432.

[8] a) D. Worsch, F. Vögtle, *Top. Curr. Chem. 140* (1987) 21–41; b) F. Toda, *ibid. 140* (1987) 43–69.

[9] K. Naumann in G. Haug, H. Hoffmann (Eds.): *Chem. Plant Prot. 4* ("Synthetic Pyrethroid Insecticides: Structures and Properties") (1990) 64–66.

Methyltrioxorhenium as Catalyst for Olefin Metathesis**

By *Wolfgang A. Herrmann,* Werner Wagner, Uwe N. Flessner, Ursula Volkhardt,* and *Hartmut Komber*

Dedicated to Professor Karl Heinz Büchel on the occasion of his 60th birthday

Methyltrioxorhenium (MTO, CH_3ReO_3) is the most easily accessible organometal oxide. It is prepared from dirhenium heptaoxide and tetramethyltin, may be conveniently purified by vacuum sublimation, is stable far above its melting point (m.p. 106 °C), dissolves in all organic solvents *and* water without decomposition, and is stable to air and acid.[1] In addition to these advantageous properties, MTO has exceptional catalyst qualities which we describe in this and the two subsequent communications.

[*] Prof. Dr. W. A. Herrmann, Dr. W. Wagner [+], U. N. Flessner, U. Volkhardt, Dr. H. Komber [++]
Anorganisch-chemisches Institut der Technischen Universität München
Lichtenbergstrasse 4, W-8046 Garching (FRG)

[+] New address: Consortium für Elektro-chemische Industrie GmbH
Zielstattstrasse 20
W-8000 München 70 (FRG)

[++] Alexander von Humboldt Fellow (1991). Permanent address: Institut für Technologie der Polymere, Hohe Strasse 6, O-8010 Dresden (FRG)

[**] Multiple Bonds between Main-Group Elements and Transition Metals, Part 100, first communication. (The second and third communications follow directly.) This work was supported by the Hoechst AG and the Fonds der Chemischen Industrie. Part 99: W. A. Herrmann, S. J. Eder, P. Kiprof, *J. Organomet. Chem. 412* (1991) 407–414.

The olefin metathesis is a reaction catalyzed by organometallic compounds, and its significance for the synthesis of basic and fine-chemical olefins as well as of polymers (polyalkenamers) is steadily increasing.[2,3] Variants, including both homogeneous and heterogenous catalysis, are presently used in eight technical processes,[2a,3] but the metathesis of *functionalized* olefins still presents problems (e.g., high catalyst concentrations, catalyst poisoning). In these cases cocatalysts (preferably alkyltin compounds) are essential, even for the more active systems (e.g. Re_2O_7/Al_2O_3).[2–4]

We have now discovered that the title compound MTO (**1a**) and higher homologues ($RReO_3$, R = alkyl, aryl) on acidic metal oxide supports form metathesis catalysts that are active without additives even for functionalized olefins.[5] The π complexes **1b, c** and the *N*-complex **1d** are, however, not suitable. The standard system MTO/Al_2O_3–SiO_2 (**I**) is simple to prepare and the most thoroughly studied. It catalyzes in particular the self-metathesis of allyl halides, ethers, silanes, and unsaturated carboxylates and nitriles, but also the ethenolysis of olefins with internal double bonds (Table 1). Catalyst **I** operates at room temperature and is also suitable for the metathesis of simple open-chain and cyclic olefins (Table 1 and 2). Otherwise frequent side reactions such as double-bond isomerization and olefin dimerization[2] are insignificant in the presence of **I**. The equilibrium in the metathesis of 1- and 2-hexene is established within minutes at 25 °C. For use with suspensions, the

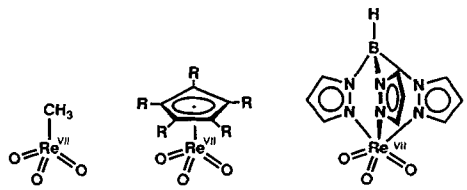

1a (MTO) **1b, R = H** **1c, R = CH_3** **1d**

Table 1. MTO-catalyzed self-metathesis and ethenolysis of open-chain olefins [a].

Starting olefin	Product olefin	Yield [%]
a) $CH_3CH{=}CHC_2H_5$	$[CH_3CH{=}]_2 + [C_2H_5CH{=}]_2$	100
b) $CH_3(CH_2)_3CH{=}CH_2$	$[C_4H_9CH{=}]_2 + CH_2{=}CH_2$	100 [b]
c) $Br(CH_2)_3CH{=}CH_2$	$[Br(CH_2)_3CH{=}]_2 + CH_2{=}CH_2$	63
d) $Br(CH_2)_4CH{=}CH_2$	$[Br(CH_2)_4CH{=}]_2 + CH_2{=}CH_2$	63
e) $(CH_3)_3SiCH_2CH{=}CH_2$	$[(CH_3)_3SiCH_2CH{=}]_2 + CH_2{=}CH_2$	80
f) $(CH_3)_3SiOCH_2CH{=}CH_2$	$[(CH_3)_3SiOCH_2CH{=}]_2 + CH_2{=}CH_2$	75
g) $C_2H_5OCH_2CH{=}CH_2$	$[C_2H_5OCH_2CH{=}]_2 + CH_2{=}CH_2$	56
h) $(CH_3)_2CHOCH_2CH{=}CH_2$	$[(CH_3)_2CHOCH_2CH{=}]_2 + CH_2{=}CH_2$	90
i) $BrCH_2CH{=}CH_2$	$[BrCH_2CH{=}]_2 + CH_2{=}CH_2$	90
k) $C_6F_{13}CH{=}CH_2$	$[C_6F_{13}CH{=}]_2 + CH_2{=}CH_2$	8
l) $C_6F_{13}CH_2CH{=}CH_2$	$[C_6F_{13}CH_2CH{=}]_2 + CH_2{=}CH_2$	20
m) $C_6F_{13}(CH_2)_2CH{=}CH_2$	$[C_6F_{13}(CH_2)_2CH{=}]_2 + CH_2{=}CH_2$	55
n) $C_2H_5O_2C(CH_2)_8CH{=}CH_2$	$[C_2H_5O_2C(CH_2)_8CH{=}]_2 + CH_2{=}CH_2$	41 [b]
o) $CH_3(CH_2)_7CH{=}CH(CH_2)_7COOCH_3$	$[CH_3(CH_2)_7CH{=}]_2 + [CH_3COO(CH_2)_7CH{=}]_2$	82
p) $CH_3(CH_2)_7CH{=}CH(CH_2)_7COOCH_3$ $CH_2{=}CH_2$	$CH_3(CH_2)_7CH{=}CH_2 + [CH_3COO(CH_2)_7CH{=}CH_2$	27 [b,c]

[a] Heterogeneous catalyst MTO on Al_2O_3–SiO_2 [5, 6]; room temperature. The equilibrium turnover is (absolute) 50% (= 100% of the theoretical turnover). With the exception of b) and n), closed systems were used. [b] Absolute yields with respect to the starting olefin. [c] Ethylene pressure: 7 bar.

solvents dichloromethane and chlorobenzene proved best. The volume of solvent used seemed not to affect the metathesis equilibrium.

Figures 1 and 2 show that **I** is a more efficient catalyst than Re_2O_7,[7] which for functionalized olefins is active only in the presence of organotin compounds. In the case of methyl

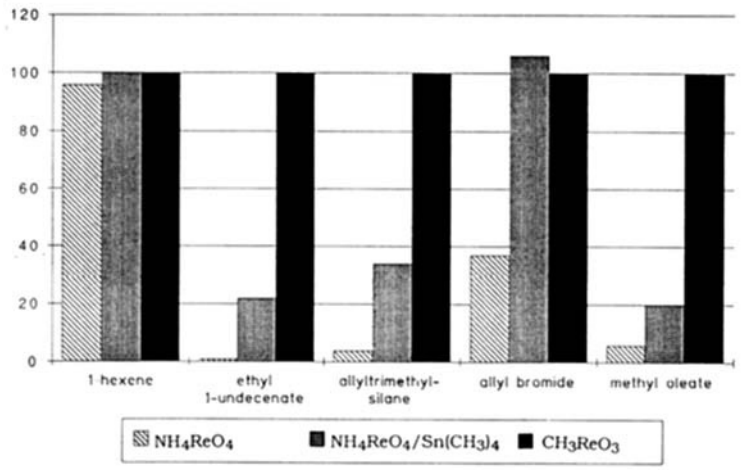

Fig. 1. Relative productivity of rhenium-containing heterogeneous metathesis catalysts, determined under standardized test conditions (25 °C, 60 min, carrier Al_2O_3–SiO_2 13/87, 3 wt% rhenium charge).

oleate, the conventional catalyst system prepared from NH_4ReO_4 approaches the activity of the new catalyst **I** only when the considerably higher maximum rhenium charge of about 10 wt% is employed.

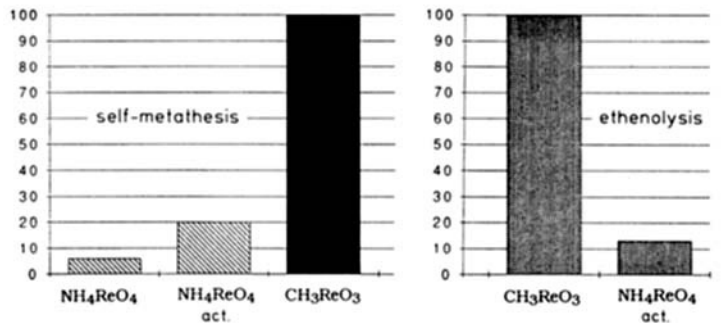

Fig. 2. Relative productivity of heterogeneous catalysts for the metathesis and ethenolysis of methyl oleate under standardized test conditions (25 °C, 60 min, support Al_2O_3–SiO_2 13/87, 3 wt% rhenium charge). Tetramethyltin was used for activation ("act.").

The special catalyst activity of MTO is lost when the methyl groups are cleaved. To avoid this degradation/deactivation reaction (which forms methane!), thermally pretreated carriers are required.[6] Besides Al_2O_3-containing systems, Nb_2O_5 is suitable.[8] Usually the catalyst loading rates are 1–3 wt% (ca. 13 g MTO per kg).

The following picture of the nature and mechanism of the MTO/Al_2O_3-SiO_2 system has been formed from physical studies of 900 metathesis experiments:

1) ESCA studies reveal that the metal oxidation state (Re^{VII}) is largely maintained on impregnation of the oxide support. Nevertheless, a very small proportion (not quantifiable by ESCA) of reduced species (Re^{VI}, Re^{V}) might be catalytically relevant.

2) MTO loses maximally 5% of the organic groups as methane and ethylene on the preparation of catalyst **I**. Use of CD_3ReO_3 (>99% D) confirmed the participation of metal-coordinated CD_3 groups in olefin metathesis (formation of $CD_2{=}CHC_2H_5$ and $CD_2{=}CH_2$ from 1-butene).

3) Free MTO cannot be separated from the carrier even under high vacuum at temperatures up to 150 °C. At higher temperatures decomposition accompanied by predominantly methane and ethylene evolution is observed. MTO can also not be removed from the carrier by solvents. We assume that MTO is fixed by condensation reactions such as that represented in the model equation (a).[9]

$$CH_3ReO_3 + HOCR_2CR_2OH \longrightarrow [CH_3ReO_2(OCR_2CR_2O)] + H_2O \quad (a)$$
$$R = CH_3$$

The condensation reaction increases the Lewis acidity of the rhenium, as is shown by solid state IR spectroscopy (diffuse reflectance):[10] the asymmetric ReO stretching band of catalyst **I** is shifted by up to 25 cm^{-1} to shorter wavelength relative to that of free MTO. This electronic change at the central atom is also reflected in the increased moisture sensitivity of catalyst **I**. Although free MTO is relatively stable in water and acid, the system MTO/Al_2O_3–SiO_2 is rapidly decomposed on hydrated surfaces to methane, ethylene, and perrhenate (GC, IR). Perrhenate bonded to the surface has been detected for the system Re_2O_7/Al_2O_3.[11]

MTO is also suitable for use in homogeneous catalyst systems for olefins that have no functional groups. Thus, the system MTO/R_nAlCl_{3-n} (**II**, R = CH_3, C_2H_5; n = 1, 2) is very efficient for the metathesis of 2-pentene at room temperature; equilibrium is achieved in less than 5 min (Re: olefin = 1:100).

Furthermore, *ring-opening polymerization* is catalyzed by the homogeneous catalyst **II**, as shown by the example of norbornene and some derivatives. Within minutes at room temperature polynorbornene of high molecular weight and medium polydispersity is formed [Equation (b) and Table 2].

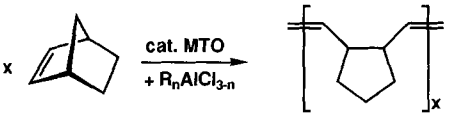

(b)

The products are very soluble and have a high proportion of *cis*-configurated moieties (up to 84%, Table 2). The *cis*-stereoselectivity can be controlled by the rhenium/cocatalyst ratio: an increase in the organoaluminum component yields a polymer with a higher proportion of *trans*-configuration. However, an eightfold excess of the cocatalyst causes low molecular weight products and insoluble polymers to form.[12]

Because practically all metathesis catalysts are based on oxides or halides of molybdenum, tungsten, and rhenium, MTO introduces—after 30 years of research in this field[2]—a new generation of structurally defined catalysts. Even though the mechanism (metal–carbene formation from MTO) has not been finally elucidated, the multifarious applications of the catalyst are already convincing. Still more important is the possibility of a designed catalyst optimization by variation of the alkyl groups on the metal. The activity and stability of the "classical" olefin metathesis catalyst

Table 2. MTO-catalyzed ring-opening polymerization of norbornene (25 °C, chlorobenzene, [Re]:[norbornene] = 1:500).

Cocatalyst	[Re]	[Al]	Polymer yield [%]	*cis*-Proportion of bonds [a] [%]	$\bar{M}_n$ [b] [g mol^{-1}]	$\bar{M}_w$ [b] [g mol^{-1}]	$\bar{M}_w/\bar{M}_n$
CH_3AlCl_2	1	2	75	84			
	1	4	94	84	490000	800000	1.6
$(CH_3)_2AlCl$	1	2	89	75	237000	800000	3.4
	1	4	94	47			
$CH_3CH_2AlCl_2$	1	2	99	81	710000	1020000	1.4
	1	4	79	62	142000	510000	3.6
$(CH_3CH_2)_2AlCl$	1	1	97	83			
	1	2	90	79	160000	370000	2.3
	1	4	92	66	348000	800000	2.3
	1	8	92	58			

[a] Determination by ^{13}C NMR. [b] Referred to polystyrene standard.

metals, molybdenum and tungsten, could also be optimized in this way. Moreover, catalytic properties are expected for the organic oxides of the neighboring element, osmium. Simple compounds such as $O{=}Os(CH_3)_4$ are known.[13]

Experimental Procedure

MTO as heterogeneous catalyst: MTO (**1a**, 1.25 g, 5.0 mmol) was dissolved in 50 mL of CH_2Cl_2 and added to a well-stirred suspension of the carrier material ([6], 130 g in 500 mL of CH_2Cl_2).

Metathesis of 1-hexene: CH_2Cl_2 (24.5 mL) was added to 1% of this contact suspension (3 wt% Re) in a 100 mL round-bottomed flask fitted with a nitrogen inlet and a reflux condenser. The mixture was treated with 1-hexene (5 mL, 40 mmol; Re:olefin = 1:800). The system was kept under slight positive pressure of dry nitrogen by means of a mercury check valve. (If the reaction was carried out under reflux to drive off the evolving ethylene, 93% of the initial olefin was converted after 30 min.) After fractional microdistillation of the reaction mixture 5-decene was isolated as *cis/trans* mixture. Yield: 2.0 g (77%).

Cometathesis of methyl oleate and ethylene: CH_2Cl_2 (35 mL) and methyl oleate (1.7 mL, 5 mmol) were added to 1% of the contact suspension (Re: olefin = 1:100) in a 1000 mL laboratory glass autoclave and pressurized with 7 bar ethylene. After 2 h at room temperature 27% of the starting material had reacted (see Table 1).

Norbornene polymerization: To a solution of MTO (6.3 mg, 2.5×10^{-2} mmol), chlorobenzene (3 mL), and CH_3AlCl_2 (100 µL of a 1 M solution in *n*-hexane) was added a solution of norbornene (1.2 g, 12.5 mmol) in 10 mL of chlorobenzene (Re:Al:olefin = 1:4:500). No starting material could be detected after 30 min. The reaction was stopped with 20 mL of methanol. A white polymer precipitated and was purified by dissolution in $CHCl_3$ and reprecipitation with CH_3OH. Yield: 1.1 g, 94%.

Received: July 19, 1991 [Z4805 IE]
German version: *Angew. Chem. 103* (1991) 1704

CAS Registry numbers:
Starting olefins of Table 2: a, 109-68-2; b, 592-41-6; c, 1119-51-3; d, 2695-47-8; e, 762-72-1; f, 18146-00-4; g, 557-31-3; h, 6140-80-3; i, 106-95-6; k, 25291-17-2; l, 80793-18-6; m, 27854-28-6; n, 68480-06-8; o, 2462-84-2. **1a**, 70197-13-6; Al_2O_3, 1344-28-1; SiO_2, 7631-86-9; $CH_2{=}CH_2$, 74-85-1; $MeAlCl_2$, 917-65-7; Me_2AlCl, 1184-58-3; $EtAlCl_2$, 563-43-9; Et_2AlCl, 96-10-6; NH_4ReO_4, 13598-65-7; $SnMe_4$, 594-21-4; (*Z*)-(BuCH$\ddagger_2$, 7433-78-5; (*E*)-(BuCH$\ddagger_2$, 7433-56-9; (MeCH$\ddagger_2$, 107-01-7; (EtCH$\ddagger_2$, 592-47-2; [Br(CH$_2$)$_3$CH$\ddagger_2$, 100960-98-3; [Br(CH$_2$)$_4$CH$\ddagger_2$, 137040-97-2; (TMSCH$_2$CH$\ddagger_2$, 3528-12-9; (TMSOCH$_2$CH$\ddagger_2$, 61549-43-7; (EtOCH$_2$CH$\ddagger_2$, 7250-85-3; (*i*PrOCH$_2$CH$\ddagger_2$, 88482-36-4; (BrCH$_2$CH$\ddagger_2$, 6974-12-5; (C_6F_{13}CH$\ddagger_2$, 56523-43-4; ($C_6F_{13}CH_2$CH$\ddagger_2$, 137091-62-4; [C_6F_{13}(CH$_2$)$_2$CH$\ddagger_2$, 137040-98-3; [EtCOO(CH$_2$)$_8$CH$\ddagger_2$, 137040-99-4; [Me(CH$_2$)$_7$CH$\ddagger_2$, 5557-31-3; [MeO$_2$C(CH$_2$)$_7$CH$\ddagger_2$, 13481-97-5; norbornene, 498-66-8; norbornene polymer, 25038-76-0; cyclopentane, 287-92-3.

[1] a) Review: W. A. Herrmann, *Angew. Chem. 100* (1988) 1297; *Angew. Chem. Int. Ed. Engl. 27* (1988) 1269; b) synthesis: W. A. Herrmann, J. G. Kuchler, G. Weichselbaumer, E. Herdtweck, P. Kiprof, *J. Organomet. Chem. 372* (1989) 351.

[2] a) J. C. Mol, J. A. Moulijn (*Catalytic Metathesis of Alkenes*) in M. Boudart (Eds.): *Catalysis–Science and Technology, Vol. 8*, Springer, Berlin 1987, p. 69ff. b) K. J. Ivin: *Olefin Metathesis*, Academic Press, New York 1983.

[3] Industrial applications: a) R. Streck, *Chem.-Ztg. 99* (1975) 397; b) S. Warwel, *Erdöl Erdgas Kohle 103* (1987) 238; c) R. F. Ohm, *CHEMTECH 10* (1980) 183; d) J. C. Mol, *ibid. 13* (1983) 250; e) W. A. Herrmann, *Kontakte (Darmstadt) 3* (1991) 29–52.

[4] W. A. Herrmann, J. G. Kuchler, J. K. Felixberger, E. Herdtweck, W. Wagner, *Angew. Chem. 100* (1988) 420; *Angew. Chem. Int. Ed. Engl. 27* (1988) 394.

[5] W. A. Herrmann, W. Wagner, U. Volkhardt, DOS-DE 3940196 (December 12, 1989/June 13, 1990), Hoechst AG; DOS-DE 3902357 (January 27, 1989/August 2, 1990), Hoechst AG; DOS-DE 4009910 (October 2, 1991), Hoechst AG.

[6] Al_2O_3–SiO_2 containing 13 wt% Al_2O_3 (grain size >15 µm) from Strem Chemicals Inc., Newburyport, MA, USA, was heated for 1 h at 550 °C in a stream of nitrogen and then doped with CH_3ReO_3. The catalyst must be handled in a dry atmosphere.

[7] S. Warwel, H. Ridder, G. Hachen, *Chem.-Ztg. 107* (1983) 115.

[8] R. Buffon, A. Choplin, M. Leconte, J.-M. Basset, W. Wagner, W. A. Herrmann, *J. Mol. Catal.*, in press.

[9] a) J. Takacs, P. Kiprof, J. Riede, W. A. Herrmann, *Organometallics 9* (1990) 783; b) W. A. Herrmann, P. Watzlowik, P. Kiprof, *Chem. Ber. 124* (1991) 1101.

[10] Cf. W. A. Herrmann, K. Rypdal, R. Tremmel, R. Blom, P. Kiprof, R. Alberto, J. Behm, R. W. Albach, H. Bock, B. Solouki, J. Mink, D. Lichtenberger, N. E. Gruhn, *J. Am. Chem. Soc. 113* (1991) 6527.

[11] a) K. P. J. Williams, K. Harrison, *J. Chem. Soc. Faraday Trans. 86* (1990) 1603; b) E. D. Hardcastle, J. E. Wachs, *J. Mol. Catal. 46* (1988) 15.

[12] K. I. Ivin, J. J. Rooney, C. D. Stewart, *J. Chem. Soc. Chem. Commun. 1978*, 603.

[13] W. A. Herrmann, S. J. Eder, P. Kiprof, K. Rypdal, *Angew. Chem. 102* (1990) 1460; *Angew. Chem. Int. Ed. Engl. 29* (1990) 1445.

Methyltrioxorhenium as Catalyst for Olefin Oxidation**

By *Wolfgang A. Herrmann,* Richard W. Fischer,* and *Dieter W. Marz*

Dedicated to Professor Karl Heinz Büchel on the occasion of his 60th birthday

The oxides of the neighboring elements of rhenium are active catalysts for olefin oxidation.[1] They depend, however, on different mechanisms for their activity: With hydrogen peroxide, molybdenum and tungsten oxides form "inorganic peroxides" of type L_nM–OOH, which have proved to be efficient epoxidation agents. Osmium tetroxide reacts with olefins *cis*-stereoselectively—in stoichiometric and catalytic processes—to yield vicinal diols, which are formed via structurally defined osmate esters.[1,2] However, no

[*] Prof. Dr. W. A. Herrmann, R. W. Fischer, Dr. D. W. Marz[+]
Anorganisch-chemisches Institut der Technischen Universität München
Lichtenbergstrasse 4, W-8046 Garching (FRG)

[+] New address: PCI Polychemie GmbH
Piccardstrasse 4, W-8900 Augsburg 1 (FRG)

[**] Multiple Bonds between Main-Group Elements and Transition Metals, Part 100, second communication. (The first and third communications precede and follow this paper.) This work was supported by the Hoechst AG and the Fonds der Chemischen Industrie. Part 99: W. A. Herrmann, S. J. Eder, P. Kiprof, *J. Organomet. Chem. 412* (1991) 407–414.

organorhenium oxidation catalyst displays a high enough activity and selectivity under practicable conditions. Even in the current literature, doubts about rhenium and its compounds' potential for catalysis of olefin oxidations are expressed.[1d, 3]

Although the simple rhenium oxides (such as Re_2O_7, ReO_3, and ReO_2), perrhenic acid, its inorganic esters (e.g. $(CH_3)_3SnOReO_3$), and the π complexes $[C_5H_5ReO_3]$ and $[\{C_5(CH_3)_5\}ReO_3]$[4] activate neither oxygen nor peroxides, alkylrhenium oxides $R_aRe_bO_c$ in general,[5] but especially the very stable, easily accessible methyltrioxorhenium (MTO, **1**), are highly active and selective catalysts for the oxidation of CC unsaturated compounds. In particular, **1** catalyzes the epoxidation of olefins with hydrogen peroxide. Both the alkene and the reaction temperature can be varied within a wide range (Table 1). The standard system MTO/H_2O_2/

Table 1. MTO-catalyzed epoxidation of olefins with H_2O_2.

	olefin	T [°C]	t [h]	product	yield [%] [a]
a)	propene	−10	12	propenoxide	50* [b]
				1,2-propanediol	50* [b]
b)	2-butene	−10	6	2,3-butanediol	100* [b]
c)	*cis*-2-pentene	25	3	2,3-pentanediol	10*
				cis-2,3-epoxypentane	90*
d)	2,3-dimethyl-2-butene	25	1	2,3-dimethyl-2,3-butanediol	75
e)	*trans*-4-octene	25	2	*trans*-4,5-epoxyoctane	95
f)	cyclohexene	82	0.1	*trans*-1,2-cyclohexanediol	97*
		10	5	1,2-epoxycyclohexane	90
g)	4-vinylcyclohexene	15	2	1,2-epoxy-4-vinyl-cyclohexane	50
				1,2-dihydroxy-4-vinylcyclohexane	40
h)	1-methylcyclohexene	25	2	1-methyl-1,2-cyclohexanediol	70
i)	1,4-cyclohexadiene	70	3	1,2,4,5-tetrahydroxycyclohexane	92
k)	*cis,cis*-1,5-cyclooctadiene	0	1.5	5,6-epoxycyclooctene	80
l)	cyclododecene	25	1	1,2-epoxycyclododecane	100*
m)	β-pinene	5	0.1	β-pinene oxide	40*
				β-pinane-1,2-diol	50*
n)	methyl oleate	25	24	methyl 9,10-dihydroxy-octadecanate	92
o)	allyl alcohol	25	10	2,3-epoxy-1-propanol	90
p)	crotylaldehyde	25	24	2,3-epoxybutaneal	60
q)	1,4-naphthoquinone	70	18	2,3-epoxy-1,4-naphthoquinone	64*
r)	pentafluorophenylethene	25	24	1,2-epoxy(pentafluorophenyl)ethane	38

[a] Those yields marked with an asterisk were determined by GC/MS. All others refer to isolated products. [b] Yields relative to reacted olefin (reaction at ambient pressure).

t-C_4H_9OH usually operates at room temperature with 0.1 to 1 mol% MTO with respect to the olefin. The yellow solution is stable for weeks below ca. 0 °C and need thus not be freshly prepared.

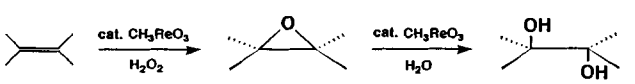

(a)

Depending on the constitution of the epoxide, a ring opening that is also catalyzed by MTO can take place to form *trans*-configurated 1,2-diols. In spite of the low pH of the catalyst solutions (pH ≈ 1–2) the activity of MTO can be traced not only to its Brønsted acidity but also to a metal effect.

Addition of an excess of amines such as 4,4'-dimethyl-2,2'-bipyridine, quinine, or cinchonine, suppresses the epoxide

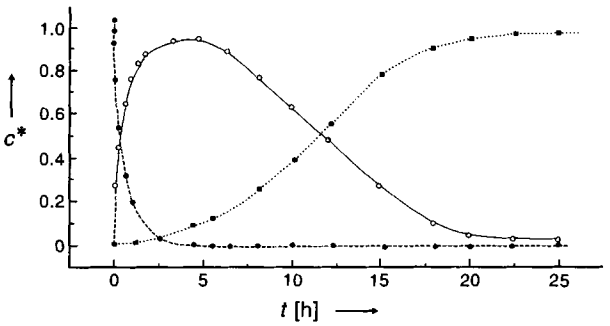

Fig. 1. Kinetics of the MTO-catalyzed cyclohexene oxidation. c^* = normalized concentration = c(starting material or product at $t = 0$)/c(cyclohexene at $t = 0$). ● c^*(cyclohexene); ○ c^*(1,2-epoxycyclohexane; ■ c^*(cyclohexane-1,2-diol)

ring opening even in 1,2-epoxycyclohexane, as a comparison of Figures 1 and 2 shows. Such amines lower the proton activity (pH ≈ 4) and form dissociation equilibria with the catalyst MTO[4,5] [Eq. (b)].

$$CH_3ReO_3 + n\,L \rightleftharpoons CH_3ReO_3(L)_n \qquad (b)$$

Besides *tert*-butyl alcohols, solvents such as tetrahydrofuran, ethyl acetate, toluene, and water may be used. Temperature control is essential for reactive olefins because of the high catalyst activity.

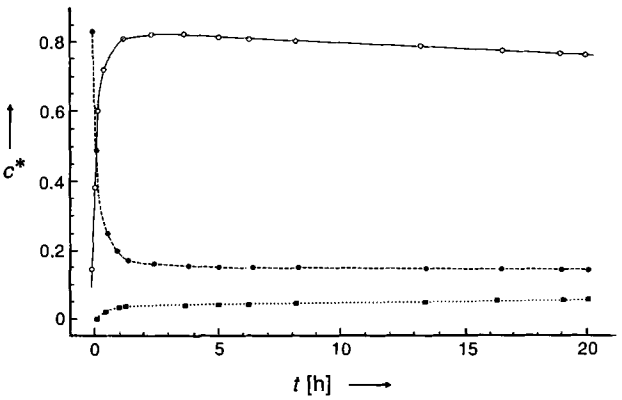

Fig. 2. Kinetics of the cyclohexene epoxidation with the MTO/coligand system. Labeling as in Fig. 1.

For storage a particularly stable form of MTO is easily prepared by warming a solution of MTO in distilled water, filtering the golden precipitate, washing with water, and drying in a vacuum. The solid is then pressed into 30–100 mg tablets. This procedure forms the first polymeric organometallic oxide:[7] it has the approximate empirical formula $\{CH_3ReO_3\}_\infty$, is in contrast to sublimable MTO no longer volatile, is stable to air and moisture, and is insoluble in all noncoordinating solvents but soluble in hydrogen peroxide. Polymer-MTO is very simple to dose in tablet form.

An immobilization of MTO can be achieved by the addition of polymeric materials that contain the required basic center for rhenium attachment, in particular amine- and amide-nitrogen atoms. Typical examples are the commercially available polyvinylpyridines which are charged with 1–10 wt% MTO. This procedure also lowers the volatility substantially: the monomers cannot be removed from the carrier even when heated to 150 °C under high vacuum. The advantage of this form of MTO lies in the easy recovery of the catalyst by filtration from the catalyst solution.

Although CH_3ReO_3 (MTO) and OsO_4 are isovalent molecules with similar structural and coordination chemistry—for instance, both yield stable adducts with amines like quinuclidine—they have different functions in the olefin/hydrogen peroxide system: in the first step OsO_4 forms osmate esters, which then undergo a stereoselective acid cleavage to afford vicinal *cis*-diols, whereas CH_3ReO_3 (unlike CH_3TcO_3[8]) reacts *not* with the olefin, but with H_2O_2 to be transformed in a multistep reaction into a hydroperoxo complex, probably of constitution **C** (Scheme 1), which is an exceptionally selective epoxidizing agent.

CH_3ReO_3 (a 14e compound) has a more pronounced Lewis-acidity than OsO_4 (a 16e compound). One may assume that this is responsible for the different catalytic mechanisms. Although the catalytic species has not yet been fully characterized, the alkyl groups of MTO and its derivatives are clearly indispensible: on one hand, monitoring the olefin oxidation by NMR spectroscopy shows that the methyl group of the catalyst remains coordinated to MTO; on the other hand addition of methyl-cleaving reagents halts the activity immediately. In this way inactive perrhenate is formed on addition of base [Eq. (c)].

$$CH_3ReO_3 + OH^- \longrightarrow CH_4 + [ReO_4]^- \qquad (c)$$

NMR and labeling experiments suggest the sequence of steps formulated in Scheme 1. There are *two* moles of H_2O_2 per mole of MTO required to form the active species **C** (δ_{CH3} = 2.6), which can be cleanly titrated against olefin. **C** can be extracted from MTO/perhydrol (a 30% H_2O_2 solution in water) into diethyl ether as a yellow complex and shows an IR band at 872 cm^{-1} typical for η^2-peroxo complexes, but it has so far eluded isolation. After prolonged reaction times, methanol is formed as a deactivation product of MTO.

tert-Butyl hydroperoxide is neither formed in the oxidation solution described here, nor can it be activated by MTO for olefin oxidations. Even after a pretreatment of MTO with H_2O_2, *t*-C_4H_9OOH does not function as a primary oxidizing agent.

The MTO/H_2O_2/*t*-C_4H_9OH system also oxidizes several alkynes: the major product from 3-hexyne is 4-hexen-3-one (*cis*/*trans*) in 55% yield; tolane yields 71% benzil. A catalytically accelerated Baeyer-Villiger oxidation can be performed with, for example, cyclobutanone.

The new class of oxidation catalysts is distinguished by a series of practical advantages: 1) High epoxide selectivity with the possibility of controlling the epoxide ring-opening kinetics through coligands, pH, and temperature; 2) high activity in a wide temperature range (−10− + 100 °C); 3) good stability of the oxidation-active system MTO/H_2O_2/*t*-C_4H_9OH at low temperatures (storable for months at −30 °C); 4) also active with electron-poor olefins (e.g. 2-bromo-2-butene) and simple gaseous olefins (e.g. propene, 2-butene); 5) use both as a homogeneous and a heterogeneous catalyst.

Furthermore, in no other epoxidation catalyst can the activity and selectivity be controlled as here by replacing the methyl groups with other alkyl groups. Important derivatives of the class of compounds have been described.[10] In particular, electron-withdrawing substituents promise further applications in catalytic oxidation as a result of the enhanced Lewis acidity of their metal center. The derivatization of MTO through the oxo groups is also known.[11] This also sets the new system aside from the "Milas reagents" (consisting of hydrogen peroxide and acidic metal oxides such as MoO_3, V_2O_5, and TiO_2), which have no constitutionally adjustable parameters.[12a]

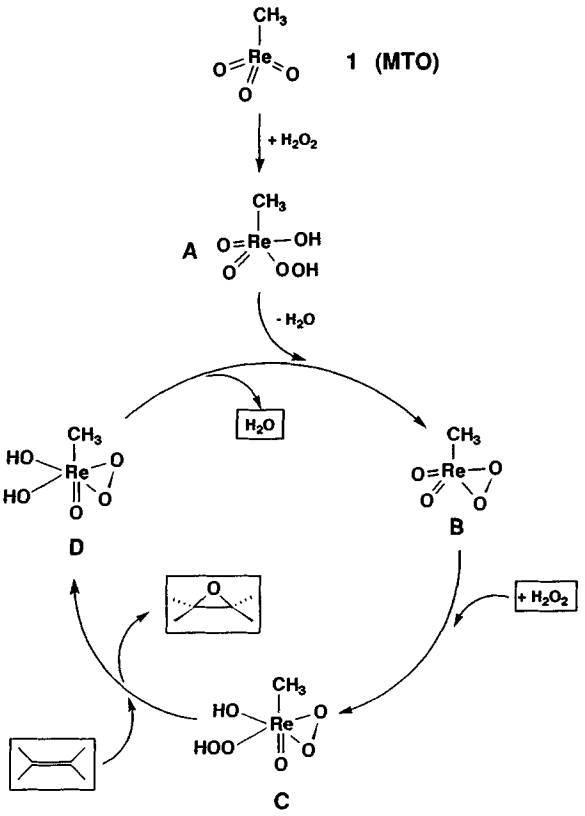

Scheme 1. Proposed mechanism for MTO-catalyzed epoxidation.

The oxidizing power of MTO/H_2O_2 is normally too weak for olefin cleavage, a reaction typical of ruthenium oxide catalysts;[11b] stilbene and some styrene derivatives alone are cleaved oxidatively. Re_2O_7 is said to catalyze the oxidative cleavage of cycloolefins by H_2O_2 to ω,ω'-dicarboxylic acids, but only in boiling glacial acetic acid.[12b]

Experimental Procedure

Oxidation solution: *tert*-Butyl alcohol (1 L) was kept at 30 °C and mixed with 0.3 L of perhydrol. The solution was stirred with anhydrous $MgSO_4$ (200 g) for 3 h and then filtered.

Catalytic olefin oxidation: Catalyst **1** (10–50 mg, 0.04–0.2 mmol) was dissolved in oxidation solution (3–30 mL, 6–60 mmol of H_2O_2). The olefin to be oxidized (5–25 mmol) was added to this yellow catalyst solution, which was either cooled by ice, held at a constant temperature of 10–20 °C, or allowed to react at ambient temperature. In the latter case the reaction mixture often reached boiling point (ca. 80 °C). At the end of the reaction, which was indicated by a decolorization of the solution, any remaining H_2O_2 was decomposed with a catalytic amount of MnO_2. The suspension was then filtered through a glass frit coated with celite, and the solvent removed under vacuum. The residue, a solid or a viscous mass, was either washed with or recrystallized from, common solvents (e.g. acetone, ethanol). Liquid products were distilled.

Oxidation of *cis*-1,4-dichloro-2-butene: MTO (0.3 g, 1.2 mmol) was dissolved in 100 mL oxidation solution (ca. 1.8 M in H_2O_2). *cis*-1,4-Dichloro-2-butene (15 mL, 0.14 mmol) was added dropwise to this yellow catalyst solution (molar ratio H_2O_2 : olefin : MTO = 150:120:1). The mixture was then stirred for 48 h at 25 °C. After the addition of manganese dioxide (0.5 g) the gray suspension was filtered over a glass frit coated with celite. The solvent was removed from the colorless filtrate under vacuum (oil pump). The crude product (ca. 80% 1,4-dichloro-2,3-epoxybutane and starting material) was purified by Vigreux distillation. Yield 14.52 g (74%).

Received: July 19, 1991 [Z4806 IE]
German version: *Angew. Chem. 103* (1991) 1706

CAS Registry numbers:
MTO, 70197-13-6; propene, 115-07-1, 2-butene, 107-01-7; *cis*-2-pentene, 627-20-3; 2,3-dimethyl-2-butene, 563-79-1; *trans*-4-octene, 14850-23-8; cyclohexene, 110-83-8; 4-vinylcyclohexene, 100-40-3; 1-methylcyclohexene, 591-49-1; 1,4-cyclohexadiene, 628-41-1; *cis*,*cis*-1,5-cyclooctadiene, 1552-12-1; cyclododecene, 1501-82-2; β-pinene, 1330-16-1, methyl oleate, 112-62-9; allyl alcohol,

107-18-6; crotyl aldehyde, 4170-30-3; 1,4-naphthoquinone, 130-15-4; pentafluorophenylethene, 653-34-9; propene oxide, 75-56-9; 1,2-propanediol, 57-55-6; 2,3-butanediol, 513-85-9; 2,3-pentanediol, 42027-23-6; *cis*-2,3-epoxypentane, 3203-99-4; 2,3-dimethyl-2,3-butanediol, 76-09-5; *trans*-4,5-epoxyoctane, 1689-70-9; *trans*-1,2-cyclohexanediol, 1460-57-7; 1,2-epoxycyclohexane, 286-20-4, 1,2-epoxy-4-vinylcyclohexane, 106-86-5; 1,2-dihydroxy-4-vinylcyclohexane, 31646-64-7; 1-methyl-1,2-cyclohexanediol, 6296-84-0; 1,2,4,5-tetrahydroxycyclohexane, 35652-37-0; 4-cyclohexene-1,2-diol, 117919-55-8; 5,6-epoxycyclooctene, 637-90-1; 1,2-epoxycyclododecane, 286-99-7; β-pinene oxide, 6931-54-0; β-pinane-2,10-diol, 2005-76-7; methyl 9,10-dihydroxyoctadecanoate, 1115-01-1; 2,3-epoxy-1-propanol, 556-52-5; 2,3-epoxybutanal, 52788-68-8; 2,3-epoxy-1,4-naphthoquinone, 15448-58-5; 1,2-epoxy(pentafluorophenyl)-ethane, 13561-85-8; *cis*-1,4-dichloro-2-butene, 1476-11-5; 1,4-dichloro-2,3-epoxybutane, 3583-47-9.

[1] Summaries: a) R. A. Sheldon, J. K. Kochi: *Metal-Catalyzed Oxidation of Organic Compounds*, New York 1981; b) W. J. Mijs, C. R. H. I. de Jonge (Eds.): *Organic Syntheses by Oxidation with Metal Compounds*, Plenum Press, New York 1986; c) R. A. Sheldon in R. Ugo (Eds.): *Aspects of Homogeneous Catalysis, Vol. 4*, Reidel, Dordrecht 1981, S. 3ff; d) H. A. Jørgensen, *Chem. Rev. 89* (1989) 431.

[2] a) R. Criegee, B. Marchand, H. Wannowius, *Liebigs Ann. Chem. 550* (1942) 99; b) Summary: M. Schröder, *Chem. Rev. 80* (1980) 187.

[3] Recently described Re^{V}-porphyrin complexes are active oxidizing agents: J. W. Buchler, S. Kruppa, M. Schmidt, G. Prescher, DOS-DE 3731689 (March 30, 1989) and DE 3731690 (January 19, 1989) DEGUSSA AG.

[4] Up-to date reviews: a) W. A. Herrmann, *Angew. Chem. 100* (1988) 1269; *Angew. Chem. Int. Ed. Engl. 27* (1988) 1297; b) W. A. Herrmann, *J. Organomet. Chem. 382* (1990) 1.

[5] W. A. Herrmann, DOS-DE 3902357 (January 27, 1989/August 2, 1990) Hoechst AG.

[6] W. A. Herrmann, J. G. Kuchler, G. Weichselbaumer, E. Herdtweck, P. Kiprof, *J. Organomet. Chem. 372* (1989) 351.

[7] W. A. Herrmann, R. W. Fischer, W. Scherer, unpublished results from 1991.

[8] W. A. Herrmann, R. Alberto, P. Kiprof, F. Baumgärtner, *Angew. Chem. 102* (1990) 188; *Angew. Chem. Int. Ed. Engl. 29* (1990) 189.

[9] W. A. Herrmann, G. Weichselbaumer, E. Herdtweck, *J. Organomet. Chem. 372* (1989) 371.

[10] Compounds $R-ReO_3$: a) W. A. Herrmann, C. C. Romao, R. W. Fischer, C. de Méric de Bellefon, P. Kiprof, *Angew. Chem. 103* (1991) 186; *Angew. Chem. Int. Ed. Engl. 31* (1991) 185. b) Also the aryl derivatives Aryl-ReO_3 are known: W. A. Herrmann, M. Ladwig, P. Kiprof, J. Riede, *J. Organomet. Chem. 371* (1989) C13; C. de Méric de Bellefon, W. A. Herrmann, P. Kiprof, C. Whitaker, *Organometallics*, in press. c) $(C_2H_5)C(CH_3)HCH_2-ReO_3$: W. A. Herrmann, Wang Mei, unpublished.

[11] $CH_3ReO_2(OR)_2$: a) J. Takacs, P. Kiprof, J. Riede, W. A. Herrmann, *Organometallics 9* (1990) 783; b) J. Takacs, P. Kiprof, J. G. Kuchler, W. A. Herrmann, *J. Organomet. Chem. 369* (1989) C1.

[12] a) N. A. Milas, S. Sussaman, *J. Am. Chem. Soc. 58* (1936) 1302; *ibid. 59* (1937) 2345; b) G. W. Parshall, US-Pat. 3646130 (February 29, 1972) DuPont.

Methyltrioxorhenium as Catalyst of a Novel Aldehyde Olefination**

By *Wolfgang A. Herrmann** and *Mei Wang*

Dedicated to Professor Karl Heinz Büchel on the occasion of his 60th birthday

One of the most important syntheses for olefins is the Wittig reaction.[1] Although restricted to the preparation of terminal double bonds, an organometallic variation that uses the organotitanium Tebbe–Grubbs reagent is a particularly efficient process for open-chain and cyclic enol ethers.[2] The driving force for this reaction is the high stability of the resulting TiO bond, which leads to drawbacks such as the necessity of stoichiometric quantities of the reagent. Here we describe the first aldehyde olefination catalyzed by a structurally defined organometallic compound.

Aldehyde **2** treated with diazoalkane **3** in the presence of an equimolar amount of a tertiary phosphane, preferably triphenyl- or tri-*n*-butylphosphane (**4a** or **4c**), affords the olefinic coupling product **5** according to Equation (a) if methyltrioxorhenium (MTO, **1a**)[3a] is used as catalyst. Although the scope of the applications of this olefin synthesis has not been exhaustively studied, the advantages of easily accessible reagents, simple procedures, mild reaction conditions (room temperature), and good yields are apparent. In particular, diazoacetates and -malonates may be transformed with saturated and unsaturated aliphatic and aromatic aldehydes into the olefins **5** containing terminal carboxyl groups. Neither by a Wittig reaction nor with Tebbe–Grubbs reagents can this class of compound be synthesized. In contrast to MTO (**1a**), the π complexes **1b,c**[3b] are not catalytically active.

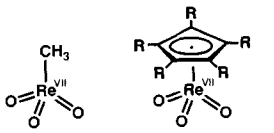

1a **1b**, R = H; **1c**, R = CH_3

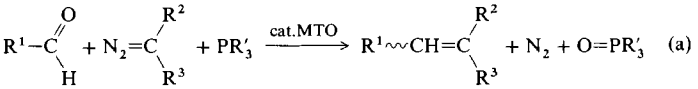

2 **3** **4** **5** (a)

2a, $R^1 = (CH_3)_2CH$
2b, $R^1 = C_6H_5CH{=}CH$ (*trans*)
2c, $R^1 = (CH_3)_2C{=}CH(CH_2)_2CH(CH_3)CH_2$
2d, $R^1 = (CH_3)_2C{=}CH(CH_2)_2C(CH_3){=}CH$
2e, $R^1 = C_6H_5$
2f, $R^1 = 4\text{-}BrC_6H_4$
2g, $R^1 = 4\text{-}NO_2C_6H_4$
3a, $R^2 = H$, $R^3 = CO_2C_2H_5$
3b, $R^2 = CO_2CH_3$, $R^3 = CO_2CH_3$
4a, $R' = (C_6H_5)$
4b, $R' = (m\text{-}C_6H_4SO_3^-Na^+)_3$
4c, $R' = (n\text{-}C_4H_9)$

The reaction is generally carried out at room temperature by adding the diazoalkane dissolved in benzene or tetrahydrofuran dropwise to a solution of stoichiometric amounts of aldehyde and triphenylphosphane and a catalytic amount of MTO (1–10 mol%) in the same solvent.[4] The reaction temperature (−20–+80 °C) has little effect on the product distribution. Minor products are formed in metal-catalyzed side reactions of the diazoalkane (formation of ketazines and olefins). Table 1 provides a preliminary summary of the scope of the new reaction. Existing double bonds or those being formed remain intact, because MTO does *not* catalyze cyclopropanation.[5]

If the molybdenum complex $[MoO_2\{S_2CN(C_2H_5)_2\}_2]$ is used in place of MTO, the olefins derived from diazomalonate according to Equation (a) are not obtained; instead stable phosphorus ylides are formed, which do not react with the aldehyde.[6]

[*] Prof. Dr. W. A. Herrmann, Dr. Mei Wang [+]
Anorganisch-chemisches Institut der Technischen Universität München
Lichtenbergstrasse 4, W-8046 Garching (FRG)

[+] Visiting scientist (1990/1991) from the Dalian Institute of Chemical Physics of the Academia Sinica (China).

[**] Multiple Bonds between Main-Group Elements and Transition Metals, Part 100, third communication. (The first and second communications precede this paper.) This work was supported by the Hoechst AG and the Alexander von Humboldt Foundation (scholarship for *M. W.*). We thank Dr. *J. K. Felixberger* for experimental assistance. Part 99: W. A. Herrmann, S. J. Eder, P. Kiprof, *J. Organomet. Chem. 412* (1991) 407–414.

Table 1. MTO-catalyzed aldehyde olefination [a].

no.	R^1CHO	$N_2=CR^2R^3$	phosphane	$R^1{\sim}CH=CR^2R^3$ (5) yield [%]	(*E*):(*Z*)
1	**2a**	**3a**	**4a**	82	85:15
2	**2a**	**3b**	**4a**	79	–
3	**2b**	**3a**	**4a**	97	60:40
4	**2c** [b]	**3a**	**4a**	89	45:55
5	**2d** [c]	**3a**	**4a**	91	43:57
6	**2d** [c]	**3b**	**4a**	75	–
7	**2e**	**3a**	**4a**	80	89:11
8	**2e**	**3b**	**4a**	90	–
9	**2f**	**3a**	**4a**	96	42:58
10	**2g**	**3b**	**4a**	87	–
11	**2g**	**3a**	**4a**	93	92:8
12	**2g**	**3a**	**4a**	78 [d]	92:8
13	**2g**	**3a**	**4b**	76 [e]	60:40
14	**2g**	**3a**	**4c**	98	97:3
15	**2g**	**3a**	**4c**	16	91:9

[a] Reaction conditions: 20 °C, 20 min, benzene, 10 mol% CH_3ReO_3; see [4]. [b] (*R*)-(+)-citronellal. [c] Citral. [d] 3 mol% CH_3ReO_3, 120 min. [e] Two-phase system C_6H_6/H_2O.

Both saturated and α,β-unsaturated aldehydes react, as well as benzaldehyde and its derivatives. Electron-withdrawing substituents on the aldehyde favor the olefination (Table 1). Some cycloketones undergo the reaction as well, although the yields and catalyst activities still need improvement: the olefin $(CH_2)_3C=CHCO_2C_2H_5$ is formed in ca. 45% yield from cyclobutanone and MTO/$P(C_6H_5)_3$ (20 °C, 2 h, 8 mol% MTO). The predominant side reaction here is a metal-catalyzed olefin formation from diazoalkane. An interesting variation with a two-phase water/benzene solvent system is possible for applications with the water-soluble phosphane **4b**; the workup then is limited to a simple phase separation, and phosphane and the rhenium catalyst remain in the aqueous phase. Tri(*n*-butyl)phosphine (**4**) is also suitable as cocatalyst.

The following has been established about the reaction mechanism of the new olefin synthesis:

1) MTO first forms the adduct $CH_3ReO_2 \cdot OP(C_6H_5)_3$ (**A'**) with the phosphane as formulated in Scheme 1. The adduct is known to afford complexes of the type CH_3ReO_2L (L = alkyne, for instance) under mild conditions.[7]
2) The isolated phosphane oxide adduct **A'** reacts with diazoalkanes to yield olefins. In the presence of aldehydes the formation of the symmetrical olefins (from diazoalkane) is suppressed in favor of the desired unsymmetrical olefins. Thus intermediate **A'** functions as a C–C coupling catalyst; in other words, the phosphane is necessary chiefly for aldehyde deoxygenation.
3) The stable phosphorus ylide $(C_6H_5)_3P=C(CO_2CH_3)_2$ does not even react with aldehydes in boiling benzene. At room temperature, but only in the presence of stoichiometric amounts of MTO, the olefins $R^1CH=C(CO_2CH_3)_2$ are formed (e.g., R^1 = 4-$NO_2C_6H_4$; ca. 80%). MTO (in benzene at 20 °C) does not catalyze olefin formation from ylides and phosphazines [Eq. (b) or (c)].
4) In the absence of phosphanes MTO acts as catalyst for diazoalkane decomposition: diazoacetate is transformed into fumarate and maleate at 20 °C *without formation of any side products* [Eq. (d)]. If aldehydes are added to such reactions, the product spectrum remains unchanged.
5) Stable five- and six-coordinate amine adducts of the type CH_3ReO_3L' (L' = quinuclidine; 2,2'-bipyridine)[8] react neither with aldehydes nor diazoalkanes. This shows that other complexes cannot be used instead of MTO.

Apparently the Lewis acidity of MTO and its reactivity with phosphanes is the determining factor for the olefin synthesis described here [Eq. (a)]. The phosphane-induced deoxygenation of MTO possibly enables a C–C bond to be formed between a metal-stabilized carbene species and the aldehyde, while the metal is oxidized back from Re^V to Re^{VII}. Although we have not yet isolated carbene complexes of type **B**, the nucleophilicity of the carbene ligands attached to metals in high oxidation states has been documented.[9,10] The C–C coupling step via metallaoxetane **C** formulated in Scheme 1 is not only plausible, but is also in accord with the observation that increasing the *C*-electrophilicity of the aldehyde employed increases the reaction rate and the yield. The

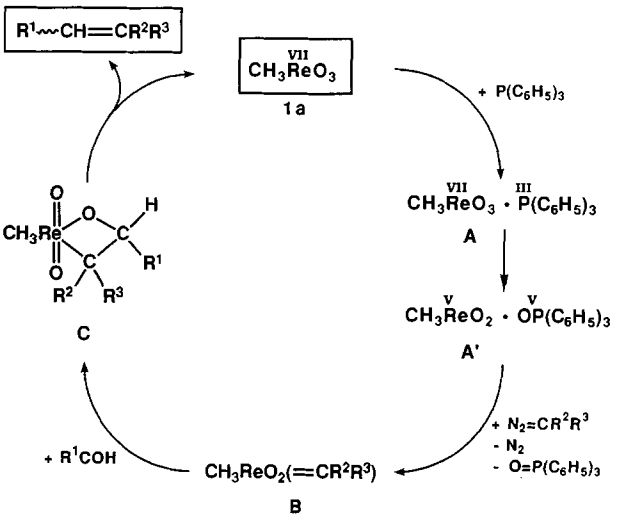

Scheme 1. Proposed mechanism of the olefination reaction according to Equation (a).

metal–carbene species **B** results from the displacement of the phosphane oxide by the diazoalkane, which thereby loses nitrogen (Scheme 1). Phosphorus ylides can be disregarded as carbene precursors, because carbenes do not even form from **3a** and **3b** under the reaction conditions. The reaction mechanism in Scheme 1 could be extended, however, if phosphazines are rapidly formed according to Equation (e); they also afford olefins **5** under the reaction conditions of Equation (a).

Thus rhenium-containing species are involved in every step of the catalytic cycle. Moreover, MTO implements the

$$2(C_6H_5)_3P=C(CO_2CH_3)_2 \xrightarrow{\text{cat. } CH_3ReO_3} \{CH(CO_2C_2H_5)\}_2 + 2P(C_6H_5)_3 \quad \text{(b)}$$

$$2(C_6H_5)_3P=N-N=C(CO_2CH_3)_2 \xrightarrow{\text{cat. } CH_3ReO_3} \{C(CO_2CH_3)_2\}_2 + 2P(C_6H_5)_3 + 2N_2 \quad \text{(c)}$$

$$2N_2=CH(CO_2C_2H_5) \xrightarrow{\text{cat. } CH_3ReO_3} \{CH(CO_2C_2H_5)\}_2 + 2N_2 \quad \text{(d)}$$

$$P(C_6H_5)_3 + N_2=C(C_6H_5)_2 \longrightarrow (C_6H_5)_3P=N-N=C(C_6H_5)_2 \quad \text{(e)}$$

$$(C_6H_5)_3P=C(CO_2CH_3)_2 + C_6H_5CHO + CH_3ReO_3 \longrightarrow C_6H_5CH=C(CO_2CH_3)_2 + O=P(C_6H_5)_3 \quad \text{(f)}$$

Wittig olefination of aldehydes with otherwise unreactive phosphorus ylides. Herein lies a potential extension of this important reaction [Eq. (f)]. Furthermore, a generalization of the catalytic diazoalkane decomposition according to Equation (d) is conceivable. Only the ketazine formation from aldehydes and diazoalkane, which can play a role with components other than **3a**, **b**, restricts the scope of the conversion formulated in Equation (a); ketazines are inert to MTO.

MTO is the first organometallic compound that enables catalytic olefin synthesis from easily accessible precursors. This property does not necessarily apply to other metal oxides: with the Mo^{VI} complex, $[MoO_2\{S_2CN(C_2H_5)_2\}_2]$, as catalyst the benzaldehyde/diazomalonate/triphenylphosphane system[6] affords predominantly the phosphorus ylide $(C_6H_5)_3P{=}C(CO_2R)_2$ ($R = C_2H_5$, 67%) even in boiling benzene, whereas MTO yields 90% of the desired olefin already at room temperature. The scope of the olefin synthesis described here should be able to be extended through designed exchange of the methyl groups of MTO for functionalized residues.[3c] In addition the search for analogous complexes of other cheaper metals with low coordination numbers and in high oxidation states will be worthwhile.

Received: July 19, 1991 [Z4807 IE]
German version: *Angew. Chem. 103* (1991) 1709

CAS Registry numbers:
1a, 70197-13-6; **2a**, 78-84-2; **2b**, 14371-10-9; **2c**, 2385-77-5; **2d**, 5392-40-5; **2e**, 100-52-7; **2f**, 1122-91-4; **2g**, 555-16-8; **3a**, 623-73-4; **3b**, 6773-29-1; **7a**, 603-35-0; **4b**, 63995-70-0; **4c**, 798-40-3; (*E*)-**5aa**, 15790-86-0; (*Z*)-**5aa**, 15790-85-9; **5ab**, 36825-11-3; (*E,E*)-**5ba**, 39806-16-1; (*E,Z*)-**5ba**, 38447-06-2; (*R,E*)-**5ca**, 137172-05-5; (*R,Z*)-**5ca**, 137170-91-3; (*E,X*)-**5da**, 137057-25-1; (*Z,X*)-**5da**, 137057-26-2; **5db**, 132549-07-6; (*E*)-**5ea**, 4192-77-2; (*Z*)-**5ea**, 4610-69-9; **5eb**, 6626-84-2; (*E*)-**5fa**, 24393-53-1; (*Z*)-**5fa**, 136265-11-7; (*E*)-**5ga**, 24393-61-1; (*Z*)-**5ga**, 51507-21-2; **5gb**, 6626-84-2; $(CH_2)_3C{=}CHCO_2Et$, 27741-65-7; cyclobutanone, 1191-95-3.

[1] Review: a) H.-J. Bestmann, O. Vostrowsky, *Top. Curr. Chem. 109* (1983) 85; H. Pommer, P. C. Thieme, *ibid. 109* (1983) 165; b) H.-J. Bestmann, R. Zimmermann in *Houben-Weyl, Methoden der Organischen Chemie, Vol. E1*, 4th. ed., Thieme, Stuttgart 1982, p. 616ff.
[2] a) K. A. Brown-Wensley, S. L. Buchwald, L. Cannizzo, L. Clawson, S. Ho, D. Meinhardt, J.-R. Stille, D. Straus, R. H. Grubbs, *Pure Appl. Chem. 55* (1983) 1733; b) J. Mulzer, H.-J. Altenbach, M. Braun, K. Krohn, H.-U. Reißig: *Organic Synthesis Highlights*, VCH Verlagsgesellschaft, Weinheim 1991, p. 192ff.
[3] a) W. A. Herrmann, J. G. Kuchler, G. Weichselbaumer, E. Herdtweck, P. Kiprof, *J. Organomet. Chem. 372* (1989) 351; b) W. A. Herrmann, R. Serrrano, H. Bock, *Angew. Chem. 96* (1984) 364; *Angew. Chem. Int. Ed. Engl. 23* (1984) 383; W. A. Herrmann, M. Taillefer, C. de Méric de Bellefon, F. Behn, *Inorg. Chem. 30* (1991) 3247; c) W. A. Herrmann, C. C. Romao, R. W. Fischer, P. Kiprof, C. de Méric de Bellefon, *Angew. Chem. 103* (1991) 183; *Angew. Chem. Int. Ed. Engl. 30* (1991) 185.
[4] Example (11 in Table 1): Ethyl diazoacetate (**3a**, 3.15 mL, 30 mmol) was added dropwise at room temperature to a solution of 4-nitrobenzaldehyde (**2g**, 4.53 g, 30 mmol), $P(C_6H_5)_3$ (**4a**, 7.90 g, 30.1 mmol), and MTO (**1**, 250 mg, 1 mmol) in 100 mL benzene. The mixture was stirred for 2 h, whereupon the solvent was removed under reduced pressure. The brown residue was taken up in *n*-hexane/ethyl acetate (6:1) and filtered over a SiO_2 column. The product precipitated from the yellow filtrate, and after recrystallizing it from dichloromethane/*n*-hexane we obtained 6.72 g (93%) of analytically pure $R^1CH{=}CHCO_2C_2H_5$ ($R^1 = 4\text{-}NO_2C_6H_4$) as a mixture of *E*/*Z* isomers (92:8).
[5] W. A. Herrmann, U. N. Flessner, unpublished.
[6] X. Lu, H. Fang, Z. Ni, *J. Organomet. Chem. 373* (1989) 77.
[7] W. A. Herrmann, J. K. Felixberger, J. G. Kuchler, E. Herdtweck, *Z. Naturforsch. B 45* (1990) 876.
[8] W. A. Herrmann, G. Weichselbaumer, E. Herdtweck, *J. Organomet. Chem. 372* (1989) 371.
[9] Reviews: a) R. R. Schrock, *Pure Appl. Chem. 19* (1986) 342; b) *J. Organomet. Chem. 300* (1986) 249; c) *Acc. Chem. Res. 12* (1979) 98.
[10] M. P. Doyle, *Acc. Chem. Res. 19* (1986) 348.
[11] Cf. deoxygenation of epoxides by organovanadium(III) complexes: J. Ruiz, M. Vivanco, C. Floriani, A. Chiesi-Villa, C. Guastini, *J. Chem. Soc. Chem. Commun. 1991*, 762.

Salt-free Synthesis of Azo and Hydrazone Dyes Under CO_2 Pressure

By *Roderich Raue*,* *Alfred Brack*, and *Karl H. Lange*

Dedicated to Professor Karl Heinz Büchel on the occasion of his 60th birthday

We present here a new method for the preparation of azo dyes in which the nitrous acid essential for the diazotization is liberated from its salts or esters by carbon dioxide at a pressure of 5 to 65 bar. Consequently, the amount of inorganic and organic salts produced as by-products is reduced considerably compared to the conventional procedure. This is of great ecological importance.

Azo dyes can be prepared in a two-step or single-step procedure. In the two-step process treatment of an amine with sodium nitrite in aqueous acidic solution leads to formation of a diazonium salt, which is subsequently treated with the coupling component.[1] In the one-step process diazotization in the presence of the coupling component provides the desired product.[2] Active methylene compounds as well as aromatics can be used as the nucleophilic coupling component.[3,4]

A disadvantage of both methods is the large amount of salts produced in the neutralization of the acid. Thus we sought to improve the procedure, by avoiding the formation of these by-products.

CO_2 is an inert, gaseous acid anhydride which can be easily removed from the hydration equilibrium by change of pressure or temperature. At atmospheric pressure an aqueous solution of carbon dioxide is only weakly acidic. Not unexpectedly, the passage of a vigorous CO_2 stream through a mixture of the aromatic amine, the coupling component, and an aqueous solution of sodium nitrite did not give even traces of an azo compound.

The apparent first dissociation equilibrium constant of carbonic acid has a pK of 6.46. This value is composed of the sum of the preceding hydration equilibrium constant of CO_2 ($pK = 3.16$) and the equilibrium constant of the true first dissociation step of carbonic acid ($pK_a = 3.3$).[5] It should be possible to shift the preceding hydration equilibrium of carbon dioxide by application of pressure such that the true first dissociation step of carbonic acid can be used for diazotization.

First we investigated the one-step synthesis of a precursor of hydrazone dyes [Eq. (a)].

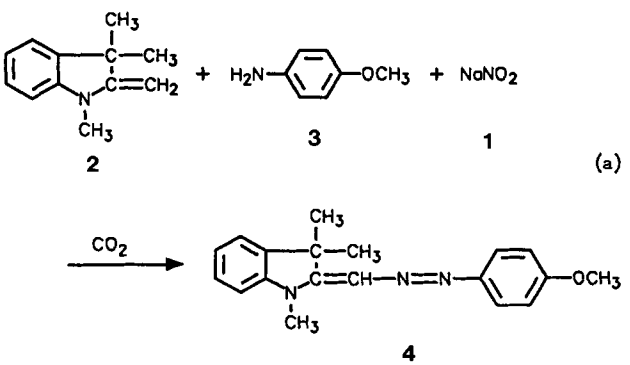

[*] Dr. R. Raue
B. von Suttnerstrasse 48, W-5090 Leverkusen 1 (FRG)
Dr. A. Brack, Dr. K. H. Lange
Farbenforschung 1
Bayer AG
W-5090 Leverkusen (FRG)

At a pressure of 5 bar a noticeable reaction took place, at 30 bar **4** was produced in >80% yield, and at 50 bar a complete conversion was achieved. Product yield and purity can be improved by employing mixtures of water and methanol as solvents. Not only the amines and coupling components, but also CO_2 is more soluble in methanol.[6] Because the dye **4** is obtained almost free of salt, the methylation to the *N*-alkyl-*N*-arylhydrazone dye could follow immediately. Instead of sodium nitrite esters of nitrous acid, for example, isoamyl nitrite (**5**) or methyl nitrite (**6**), can be used to avoid the formation of salt.[7]

This method has been used to prepare a large number of azo dyes. It is of particular interest that the one-step diazotization and coupling of heterocyclic amines with tertiary aromatic amines proceeded in quantitative yield. Usually heterocyclic amines can only be diazotized in concentrated acids by nitrosyl sulphuric acid. However, application of our procedure to the reaction of 3-amino-1,2,4-triazole (**7**), *N*-benzyl-*N*-ethyl-3-methylaniline (**8**), and isoamyl nitrite (**5**) in a mixture of methanol and water at a CO_2 pressure of 53.5 bar provided azo dye **9** in quantitative yield[7] [Eq. (b)].

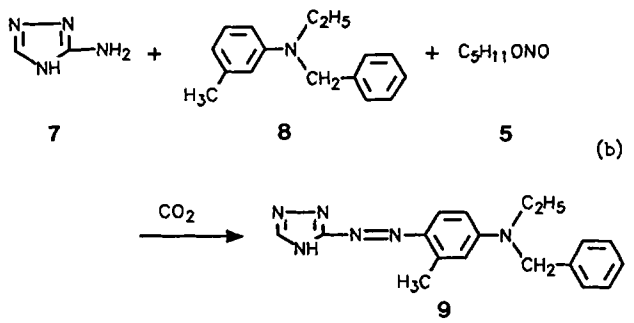

Experimental Procedure

2,3-Dihydro-1,3,3-trimethyl-indole-2-ylidenmethaneazo(4'-methoxybenzene) (**4**): 2,3-Dihydro-1,3,3-trimethyl-2-methyleneindole (**2**) (173 g, 1 mol), 4-methoxyaniline (**3**) (123 g, 1 mol), and a solution of sodium nitrite **1** (73 g, 1.06 mol) in 300 mL water were placed in an autoclave and CO_2 was introduced until a pressure of 50 bar was reached. The temperature then rose to 35 °C, and the pressure dropped. A pressure of 50 bar was maintained by further passage of CO_2 into the reaction vessel. After the reaction mixture was stirred at 35–40 °C for 3 h the autoclave was depressurized. The vented CO_2 can be recycled. The weakly alkaline suspension of the dye base was vacuum-filtered, washed to neutral pH, and dried. Yield: 301.2 g (98%) **4**; m.p.: 147–150 °C; correct C,H,N analyses; MS (EI, 70 eV): *m/z* 307 (M^+, 100%), 185 (39), 159 (92); IR (KBr) $\tilde{\nu}$[cm^{-1}] = 1585 (s), 1245 (s).

1,2,4-Triazolyl-3-azo-4'-*N*-ethyl-*N'*-benzyl-3'-methylaniline (**9**): In an autoclave were mixed **7** (16.8 g, 0.2 mol), **8** (45 g, 0.2 mol), **5** (30.4 g, 0.26 mol), 80 mL of methanol and 40 mL of water. CO_2 was introduced until a pressure of 53.5 bar was reached. The vessel was heated to 40 °C and for 3 hours the pressure was maintained by further passage CO_2 into the autoclave. After the reaction mixture was cooled to room temperature, the pressure was released. The vented carbon dioxide can be reused. The methanol was distilled off and the residue crystallized by treatment with saturated NaCl solution and some HCl. The dye was purified further by stirring with methylene chloride and was then dried. Yield: 61.4 g (100%) **9**; m.p.: 80–94 °C; correct C,H,N analyses; ^{1}H NMR ($CDCl_3$, 270 MHz): δ = 1.25 (t, 3H), 2.53 (s, 3H), 3.53 (q, 2H), 4.61 (s, 2H), 6.52 (s, 1H), 7.05–7.40 (several m, 7H), 7.78 (d, 1H), 8.26 (s, 1H); MS (EI, 70 eV): *m/z* 320 (M^+, 55%), 265 (8), 250 (9), 229 (M^+-C_7H_7, 26), 91 (100); IR (KBr): $\tilde{\nu}$[cm^{-1}] = 3430 (s), 1595 (s), 1230 (s).

Received: June 10, 1991 [Z 4691 IE]
German version: *Angew. Chem. 103* (1991) 1689
Publication delayed on authors' request

[1] K. Hunger, P. Mischke, W. Rieper, R. Raue, *Ullmann's Encycl. Ind. Chem., 5th ed, Vol. A3 1985*, pp. 245–324.
[2] J. W. Balon, DE-A 2139311 (1971), DuPont.
[3] R. Raue, DBP 1083000 (1957), Bayer.
[4] R. Raue, H.-P. Kühlthau, EP 42556 (1980), Bayer.
[5] H. R. Christen: *Grundlagen der allgemeinen und anorganischen Chemie*, 5th ed., Sauerländer, Aarau 1977, pp. 526–527.
[6] E. Hillenbrand, *Ullmann's Encykl. Tech. Chem., 4th ed., Vol. 14 1977*, pp. 569–581; S. Topham, *Ullmann's Encycl. Ind. Chem., 5th ed., Vol. A5 1986*, pp. 165–183.
[7] R. Raue, A. Brack, K. H. Lange, EP-A 91103 165.5 (1990), Bayer.

Synthesis and Structure of Ethynyl Isocyanide**

By *Michael Krüger, Helmut Dreizler,* Dagmar Preugschat,* and *Dieter Lentz**

Alkynyl isocyanides are a class of substances not previously accessible to experimental investigation. Here we report on the synthesis and gas-phase structure of the parent compound, ethynyl isocyanide (**1**),[1] which exhibits an unexpectedly high stability toward polymerization and isomerization. Whereas ethynyl cyanide (**2**), a constitutional isomer of **1**, was first described over 70 years ago[2] and, since its radioastronomic detection in interstellar space by *Turner*,[3] has been regarded as a "classical" interstellar molecule, all attempts so far to generate **1** have failed.[4] The synthesis of

HC≡C–N≡C **1** HC≡C–CN **2**

an ethynyl isocyanide ligand on a pentacarbonylchromium fragment by dehalogenation of pentacarbonyl(1,2-dichlorovinyl isocyanide)chromium (**3**) or by dehydrohalogenation of [Cr(CO)$_5$(CN–CCl=CH$_2$)] was also unsuccessful.[5]

In an investigation of the pyrolysis of partially halogenated (alkyl isocyanide)pentacarbonylchromium complexes by microwave spectroscopy, we were able to detect **2**. We suspected that it had arisen by isomerization[6] of **1**, and we therefore synthesized **3**[5a] as well as pentacarbonyl(1,1,2,2-tetrachloroethyl isocyanide)chromium (**4**).[7] Flash vacuum pyrolysis of **3** or **4** at 240 °C affords ethynyl isocyanide (**1**) (Scheme 1), which was characterized on the basis of its microwave spectrum and its gas-phase FT IR spectrum.

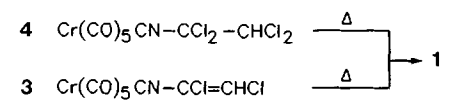

Scheme 1. Synthesis of **1**. Δ: temperature 240 °C, pressure 1–10 Pa.

Ethynyl isocyanide (**1**) can be prepared from **3** on a 10-mg scale. The synthesis from **4**, however, is accompanied by unavoidable partial isomerization of **1** to **2**. Compound **1** is

[*] Prof. Dr. H. Dreizler, Dipl.-Chem. M. Krüger
Institut für Physikalische Chemie,
Abteilung Chemische Physik der Universität
Ludewig-Meyn-Strasse 8, W-2300 Kiel 1 (FRG)
Priv.-Doz. Dr. D. Lentz, Dipl.-Chem. D. Preugschat
Institut für Anorganische und Analytische Chemie der Freien Universität
Fabeckstrasse 34–36, W-1000 Berlin 33 (FRG)

[**] This work was supported by the Fonds der Chemischen Industrie, the Deutsche Forschungsgemeinschaft, the Land Schleswig-Holstein, and the Graduiertenkolleg "Synthesis and Structural Elucidation of Low-Molecular-Weight Compounds" of the Freie Universität Berlin and the Technische Universität Berlin. We thank Prof. Dr. *H. Mäder*, Dr. *W. Stahl*, and Dr. *N. Heineking*, Kiel, for many encouraging discussions.

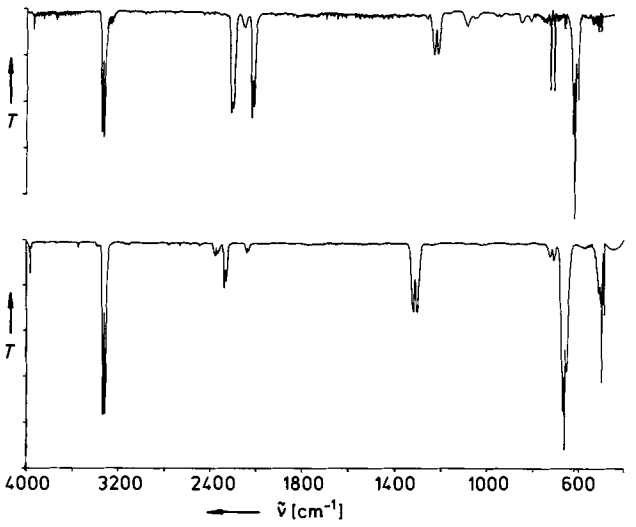

Fig. 1. Gas-phase FT IR spectra of H–C≡C–N≡C (**1**), top, and H–C≡C–C≡N, bottom. T = transmission.

stable for several weeks at −196 °C and for several days at room temperature in the gas phase at a partial pressure of a few torr. On slow thawing of the condensed phase, colorless **1** starts to turn brown above about −80 °C. The isocyanide is very volatile; thus, on fractional condensation in vacuum (1 Pa), it does not condense into a trap cooled to −120 °C. Compound **1** has the strong smell typical of isocyanides.

Figure 1 shows the gas-phase FT IR spectra of **1** and **2**. The spectra clearly differ with respect to the positions and intensities of the bands. The vibrational frequencies of **1** are in good agreement with the calculated data.[1a]

The Stark effect could be observed for the absorption lines corresponding to the rotational transitions $J' \leftarrow J = 3 \leftarrow 2$ and $4 \leftarrow 3$ in the continuous wave (CW) microwave spectrum[8] of **1**; the dipole moment of **1** was thus calculated to be $\mu = 2.93(4)$ D (Fig. 2)—in very good agreement with the

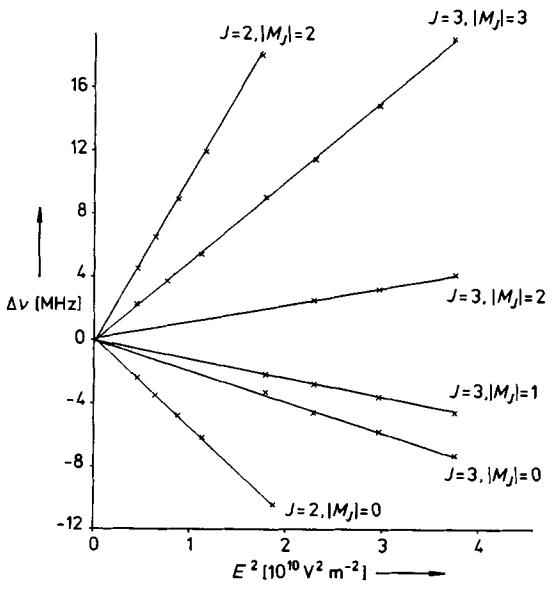

Fig. 2. Second-order Stark effect of **1**: frequency difference $\Delta\nu$ of the Stark components of the zero-field frequency as a function of the square of the electric field (E^2) for the rotational transitions $J+1 \leftarrow J$, $M_J \leftarrow M_J$ (J, rotational quantum number; M_J, projection quantum number). The dipole moment of **1** was calculated to be $\mu = 2.93(4)$ D. Calibration was carried out with carbonyl sulfide (OCS, $J' \leftarrow J = 3 \leftarrow 2$), $\mu = 0.715196(10)$ D [38].

results of ab initio calculations[9] ($\mu_e = 2.96$ D). The dipole moments of the isomer pair CH_3CN/CH_3NC are 3.925 D[10] and 3.83 D,[11] respectively; the perfluorinated derivatives have dipole moments of 1.262 D (CF_3CN)[12] and 1.153 D (CF_3NC).[13] The dipole moment of hydrogen cyanide is 2.985 D,[14] whereas isocyanic acid, HNC, exhibits a dipole moment of 3.05(10).[15] It is noteworthy that the dipole moments of the pairs of isomers discussed here are very similar, whereas the dipole moments of **1** and **2** (μ = 3.73171(1) D)[16] differ by 0.8 D.

To characterize **1** in greater detail by microwave spectroscopy, we measured the rotational transitions $J' \leftarrow J = 1 \leftarrow 0$ with a high-resolution[17] molecular-beam microwave FT spectrometer.[18] It was possible to observe, besides the main isotopomer, the species **1a–d** in natural abundance; these are the four conceivable isomers with a single isotopic heavy atom. Deuterated **3**[19] gave deuterated ethynyl isocyanide (**1e**), which was also characterized on the basis of its microwave spectrum. The rotational constants of **1–1e** are summarized in Table 1.

Table 1. Rotational constants of **1–1e** from the rotational transition $J' \leftarrow J = 1 \leftarrow 0$. Molecular beam measurement; errors in parentheses refer to the last digit.

Isotopomer		Rotational constant B_0 [MHz]
H–C≡C–N≡C:	**1**	4967.8370(3)
H–^{13}C≡C–N≡C:	**1a**	4813.1175(10)
H–C≡^{13}C–N≡C:	**1b**	4949.4452(7)
H–C≡C–^{15}N≡C:	**1c**	4944.7390(1)
H–C≡C–N≡^{13}C:	**1d**	4804.8725(3)
D–C≡C–N≡C:	**1e**	4598.2881(2)

The set of six rotational constants allows calculation of both an effective structure (r_0)[20, 21] and a complete substitution structure (r_s).[21, 22] In Table 2, the experimental r_s and r_0 values of **1** and **2** are compared with the ab initio equilibrium values (r_e).[1b] The C–C triple bond and the C–H bond

Table 2. Comparison of experimental and calculated bond lengths r [pm] of ethynyl isocyanide (**1**) [a] and ethynyl cyanide (**2**) [b]. Errors in parentheses refer to the last digit.

Compound	Bond	r_s	r_0	r_e [c]
1	C–H	105.5(1)	105.5(1)	106.5
1	C≡C	120.3(1)	120.2(1)	119.3
1	C–N	131.7(1)	131.8(1)	131.8
1	N≡C	117.5(1)	117.6(1)	117.3
2	C–H	105.8(2)	105.7(2)	106.6
2	C≡C	120.5(2)	120.3(2)	119.7
2	C–C	137.8(2)	138.2(2)	138.6
2	C≡N	115.9(2)	115.7(2)	115.3

[a] The uncertainties in the experimental bond lengths due to the errors in the rotational constants are far less than the errors given here. Methodical errors dominate [21]. [b] r_s and r_0 values of **2** from [32]. [c] SCF ab initio calculation with double zeta basis [1b].

are equally long in **1** and **2** within the limits of error; the bond lengths in acetylene[23] (120.3 and 106.1 pm) are also of nearly equal length. The length of the N–C triple bond of **1** is similar to the corresponding bond lengths in HNC (117.3 pm),[24] CH_3NC (116.6 pm),[25] CF_3NC (117.1 pm),[13] and the isocyanide triple-bond length in the recently prepared[26] and unequivocally identified[27] cyanoisocyanide (NC-CN,

Table 3. C–NC and C–CN single bond lengths in isocyanides and cyanides, respectively [pm].

Isocyanide	r (C–NC)	Ref.	Cyanide	r (C–CN)	Ref.
H_3C–NC	142.8(2)	[25]	H_3C–CN	145.8(3)	[33]
Ph–NC	141.0	[34]	Ph–CN	145.5(7)	[35]
H_2C=CH–NC	137.9(6)	[36]	H_2C=CH–CN	142.6(3)	[37]
NC–NC	131.60(26)	[28]	-		
HCC–NC	131.7(1)	This work	HCC–CN	137.8(2)	[32]

117.49(18) pm).[28] C–NC and C–CN single-bond lengths in isocyanides and cyanides, respectively, are compared in Table 3. The bond lengths strongly decrease in both classes of substance on going from the alkyl and aryl derivatives to the vinyl and, finally, the ethynyl compounds. The C–N single bonds in **1** and NC-NC[28] are the shortest bonds of this type so far found in isocyanides.

Since the microwave data of ethynyl isocyanide (**1**) are now known, it is possible to use radioastronomy to detect it in interstellar space, where its constitutional isomer **2** and its homologues $H-C\equiv C\!\left(-C\equiv C\right)_n CN$ (n = 1–4) are widely distributed.[29] In addition to HCN/HNC[30] and CH_3CN/CH_3NC,[31] this third nitrogen-containing isomer pair consisting of uncharged closed-shell molecules could further extend the radioastronomy studies on isomer relationships and contribute to the elucidation of interstellar chemistry.[39]

Experimental Procedure

1: **3** (440 mg, 1.7 mmol) was sublimed at ca. 1–10 Pa over 12 h through a Duran glass tube (30 × 2.5 cm) heated to 240 °C. Poorly volatile products were condensed in a trap cooled with dry ice/acetone. H–C≡C–N≡C (**1**) condensed in a trap cooled with liquid nitrogen and was pure according to the gas-phase IR spectrum. MS (80 eV): *m/z* 51 (M^+, 100%), 50 (M^+ – H, 17), 26 (M^+ – C_2H, 15); FT-IR (< 100 Pa): $\tilde{\nu}$[cm^{-1}] = 3345/3329 (C–H), 2223/2203 (C≡N), 2041/2024 (C≡C), 1237/1220, 730/713, 628/621/614/608; Molecular beam FT microwave spectrum (central frequencies $J' \leftarrow J = 1 \leftarrow 0$): ν[MHz] = 9935.6740(6), (**1**), 9626.2350(20) (**1a**), 9898.8904(15) (**1b**), 9889.4780(2) (**1c**), 9609.7450(6) (**1d**), 9196.5762(4) (**1e**).

Received: July 19, 1991 [Z 4802 IE]
German version: *Angew. Chem. 103* (1991) 1674

CAS Registry numbers:
1, 66723-45-3; **1a**, 66723-47-5; **1b**, 66723-48-6; **1c**, 66723-49-7; **1d**, 66723-50-0; **1e**, 66723-46-4; **3**, 137172-06-6; [D]**3**, 137091-63-5; **4**, 106065-00-3.

[1] Selected theoretical work on **1** and its properties: a) P. Botschwina, P. Sebald, *J. Mol. Spectrosc. 100* (1983) 1; b) N. N. Haese, R. C. Woods, *J. Phys. Chem. 73* (1980) 4521; Erratum: *ibid. 75* (1981) 3160; c) S. Wilson, *Astrophys. J. 220* (1978) 363; d) W. von Niessen, L. S. Cederbaum, J. Schirmer, G. H. F. Diercksen, W. P. Kraemer, *J. Electron. Spectrosc. Relat. Phenom. 28* (1982) 45; e) A. Greenberg, T. A. Stevenson, *J. Am. Chem. Soc. 107* (1985) 3488; f) M. Charton, A. Greenberg, T. A. Stevenson, *J. Org. Chem. 50* (1985) 2643.
[2] C. Moureu, J. C. Bongrand, *Ann. Chim. (Paris) 14* (1920) 14.
[3] B. E. Turner, *Astrophys. J. 163* (1971) L 35.
[4] M. Winnewisser, *Faraday Discuss. Chem. Soc. 71* (1981) 31.
[5] a) W. P. Fehlhammer, G. Beck, *J. Organomet. Chem. 379* (1989) 97; b) G. Beck, *Dissertation*, Freie Universität Berlin 1987, p. 25.
[6] C. Rüchardt, M. Meier, K. Haaf, J. Pakusch, E. K. A. Wolber, B. Müller, *Angew. Chem. 103* (1991) 907; *Angew. Chem. Int. Ed. Engl. 30* (1991) 893.
[7] W. P. Fehlhammer, F. Degel, G. Beck, *Chem. Ber. 120* (1987) 461.
[8] C. H. Townes, A. L. Schalow: *Microwave Spectroscopy*, Dover, New York 1975, Chap. 2, 10, 15.
[9] P. Botschwina (Universität Göttingen), private communication.
[10] S. A. Rackley, R. J. Butcher, M. Römheld, S. M. Freund, T. Oka, *J. Mol. Spectrosc. 92* (1982) 203.
[11] S. N. Ghosh, R. Trambarulo, W. Gordy, *J. Chem. Phys. 21* (1953) 308.
[12] B. P. Foreman, K. R. Chien, J. R. Williams, S. G. Kukolich, *J. Mol. Spectrosc. 52* (1974) 251.
[13] D. Christen, K. Ramme, B. Haas, H. Oberhammer, D. Lentz, *J. Chem. Phys. 80* (1984) 4020.
[14] W. L. Ebenstein, J. S. Muenter, *J. Chem. Phys. 80* (1984) 3989.
[15] G. L. Blackman, R. D. Brown, P. D. Godfrey, H. I. Gunn, *Nature (London) 261* (1976) 395.
[16] R. L. de Leon, J. S. Muenter, *J. Chem. Phys. 82* (1985) 1702.
[17] We will report in more detail elsewhere on the hyperfine structure in the microwave spectrum of **1**. Measurement in the millimeter-wavelength region to investigate centrifugal distortion and excited vibrational states are being carried out at present in Kiel.
[18] a) J.-U. Grabow, W. Stahl, *Z. Naturforsch. A 45* (1990) 1043; b) U. Andresen, H. Dreizler, J.-U. Grabow, W. Stahl, *Rev. Sci. Instrum. 61* (1990) 3694.
[19] Obtainable by using the deuterated chlorinated hydrocarbon in the synthesis of [D]**3**.
[20] Simultaneous fitting of all four bond lengths to the six effective rotational constants B_0 according to the least-squares procedure.
[21] W. Gordy, R. L. Cook: *Microwave Molecular Spectra*, Wiley, New York 1984, pp. 647–724.
[22] J. Kraitchman, *Am. J. Phys. 21* (1953) 17.
[23] W. J. Lafferty, R. J. Thibault, *J. Mol. Spectrosc. 14* (1964) 79.
[24] E. F. Pearson, R. A. Creswell, M. Winnewisser, G. Winnewisser, *Z. Naturforsch A 31* (1976) 1394.
[25] L. Halonen, I. M. Mills, *J. Mol. Spectrosc. 73* (1978) 494.
[26] T. van der Does, F. Bickelhaupt, *Angew. Chem. 100* (1988) 998; *Angew. Chem. Int. Ed. Engl. 27* (1988) 936; see also L. S. Cederbaum, F. Tarantelli, H.-G. Weikert, M. Scheller, H. Köppel, *ibid. 101* (1989) 770 and *28* (1989) 761.
[27] F. Stroh, M. Winnewisser, *Chem. Phys. Lett. 155* (1989) 21.
[28] M. C. L. Gerry, F. Stroh, M. Winnewisser, *J. Mol. Spectrosc. 140* (1990) 147.
[29] M. B. Bell, H. E. Matthews, *Astrophys. J. 291* (1985) L 63.
[30] See, for example, recent work on HCN and HNC: J. Harju, M. Sahu, C. Henkel, T. L. Wilson, K. C. Sahu, S. R. Pottasch, *Astron. Astrophys. 233* (1990) 197; C. Henkel, J. B. Whiteoak, L.-Å. Nyman, J. Harju, *Astron. Astrophys. 230* (1990) L 5; R. J. Sopka, H. Olofsson, L. E. B. Johannson, Nguyen-Q-Rieu, B. Zuckerman, *Astron. Astrophys. 210* (1989) 78.
[31] J. Cernicharo, C. Kahane, M. Guelin, J. Gomez-Gonzalez, *Astron. Astrophys. 189* (1988) L 1; D. J. DeFrees, A. D. McLean, E. Herbst, *Astrophys. J. 293* (1985) 236.
[32] M. D. Harmony, V. W. Laurie, R. L. Kuczkowski, R. H. Schwendeman, D. A. Ramsay, F. J. Lovas, W. J. Lafferty, A. G. Maki, *J. Phys. Chem. Ref. Data 9* (1979) 619.
[33] C. C. Costain, *J. Chem. Phys. 29* (1958) 864.
[34] B. Bak, B. P. van Eijck, C. Kierkegaard, *J. Mol. Struct. 18* (1973) 429.
[35] B. Bak, D. Christensen, W. B. Dixon, L. Hansen-Nygaard, J. Rastrup-Andersen, *J. Chem. Phys. 37* (1962) 2027.
[36] T.-A. Chang, M. D. Harmony, *J. Mol. Struct. 190* (1988) 17.
[37] C. C. Costain, B. P. Stoicheff, *J. Chem. Phys. 30* (1959) 777.
[38] K. Tanaka, H. Ito, K. Harada, T. Tanaka, *J. Chem. Phys. 80* (1984) 5893.
[39] Note added in proof (Nov. 4, 1991): Ethynyl isocyanide has recently been detected in TMC-1 (Taurus Molecular Cloud-1) using the above data: K. Kawaguchi, M. Ohishi, S. Ishikawa, N. Kaifu, *Astrophys. J.*, submitted.

A New Chromogenic β-Galactosidase Substrate: 7-β-D-Galactopyranosyloxy-9,9-dimethyl-9*H*-acridin-2-one **

By *Paul F. Corey**, *Robert W. Trimmer*, and *William G. Biddlecom*

Dedicated to Professor Karl Heinz Büchel on the occasion of his 60th birthday

The enzyme β-galactosidase (E.C. 3.2.1.23) has found wide use as an indicator enzyme for immunoassays[1] because of its relative stability and tolerance of conjugation to antibodies, other proteins, and solid supports, while retaining substantial activity. Derivatization of a phenolic chromogen or fluorogen with sugars such as β-galactose has been the basis for preparing indicating glycosidase substrates since *Aizawa*[2] introduced *p*-nitrophenyl β-D-galactopyranoside

[*] Dr. P. F. Corey, Dr. R. W. Trimmer, W. G. Biddlecom
Miles Inc., Diagnostics Division
P. O. Box 70, Elkhart, IN 46515 (USA)

[**] We thank Dr. *H. Arndt* for assistance in assigning the NMR spectra and Dr. *R. Carrico* for determining the enzyme kinetics of **10**.

in 1939. Over the years substrate derivatives of fluorescein, indoxyl, and methylumbelliferone have been synthesized, but their use has required coping with complex kinetics, poor solubility, and the need for expensive instrumentation.

The development of highly sensitive enzyme immunoassays that can be evaluated either visually or with simple instruments requires a chromogenic substrate that exhibits good aqueous solubility, a fast rate of enzymatic hydrolysis, a low Michaelis constant, and a large difference between the absorption maxima of the substrate and its hydrolysis product. Additionally, the hydrolysis product (chromogen) must have a pK_a below the pH optimum of the enzyme, an absorption maximum at long wavelength to assure minimal interference from colored constituents of the sample being evaluated (usually blood serum or urine), and a large extinction coefficient.

Only recently have long-wavelength β-galactosidase substrates been described that begin to satisfy these criteria. Resorufin β-galactoside[3] exhibits a 102 nm color shift (470 → 572 nm) upon hydrolysis, a Michaelis constant (K_m) of 0.38 mM, and fast turnover. But in our hands its solubility in 50 mM phosphate buffer (pH 8.0) is only 0.25–0.50 mM. Chlorophenol red β-galactoside[4] has a 160 nm color shift (414 → 574 nm) and excellent aqueous solubility, but we found its K_m to be more than twice as high as that reported for the resorufin substrate.

Our search for an improved long-wavelength β-galactosidase substrate led to the synthesis of the title compound **10**, a substrate with 20–25 mM solubility in 50 mM phosphate buffer (pH 8.0) and a 196 nm color shift (438 → 634 nm) as shown in Figure 1. β-Galactosidase cleaves the substrate

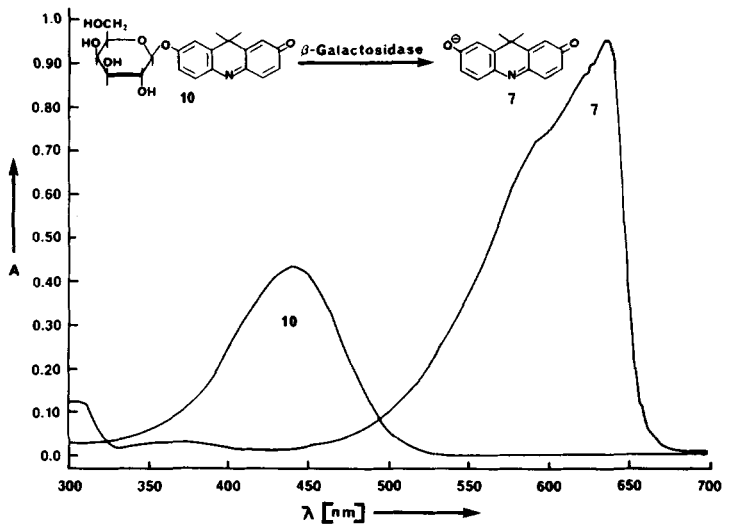

Fig. 1. The absorption spectra of solutions of **10** and **7** in sodium borate buffer (0.1 M, pH 10). A = Absorption in arbitrary units.

(k_{cat}) at the rate of 1.32×10^4 mol min^{-1} per mole of enzyme active site in a 50 mM phosphate buffer (pH 7.4) containing 5 mM $MgCl_2$, and exhibits a K_m of 0.17 mM. The absorbance of the deprotonated hydrolysis product at 634 nm (ε = 56000) is spectrally well removed from those of interfering colored sample constituents. Combined with good solubility, low K_m, fast turnover, and a large color shift, this makes **10** particularly well suited to immunoassays involving biological fluids. This substrate is presently used as the readout in an enzyme-labeled immunometric assay for measuring serum or plasma concentrations of the cardiac glycoside digoxin. In this assay[5] an excess of a monoconjugate of β-galactosidase with a Fab' fragment of an anti-digoxin mouse monoclonal antibody binds digoxin in the sample. The conjugate not bound to digoxin is then removed and the β-galactosidase activity of the assay solution is determined by using a dry reagent strip containing **10**. The test takes less than 15 min and can measure digoxin concentrations as low as 0.20 μg L^{-1}.

7-Hydroxy-9*H*-acridin-2-one (**7**) was first synthesized in 1928 by *Goldstein* and *Kopp*[6] and in 1970 by *Hill*, et al.[7] Poor yields from these procedures obligated us to work out the improved synthesis outlined in Scheme 1. Because commercially available 2,6-dichloroquinone-4-chloroimide (**2**) was used instead of the *p*-benzoquinone chloroimine employed in

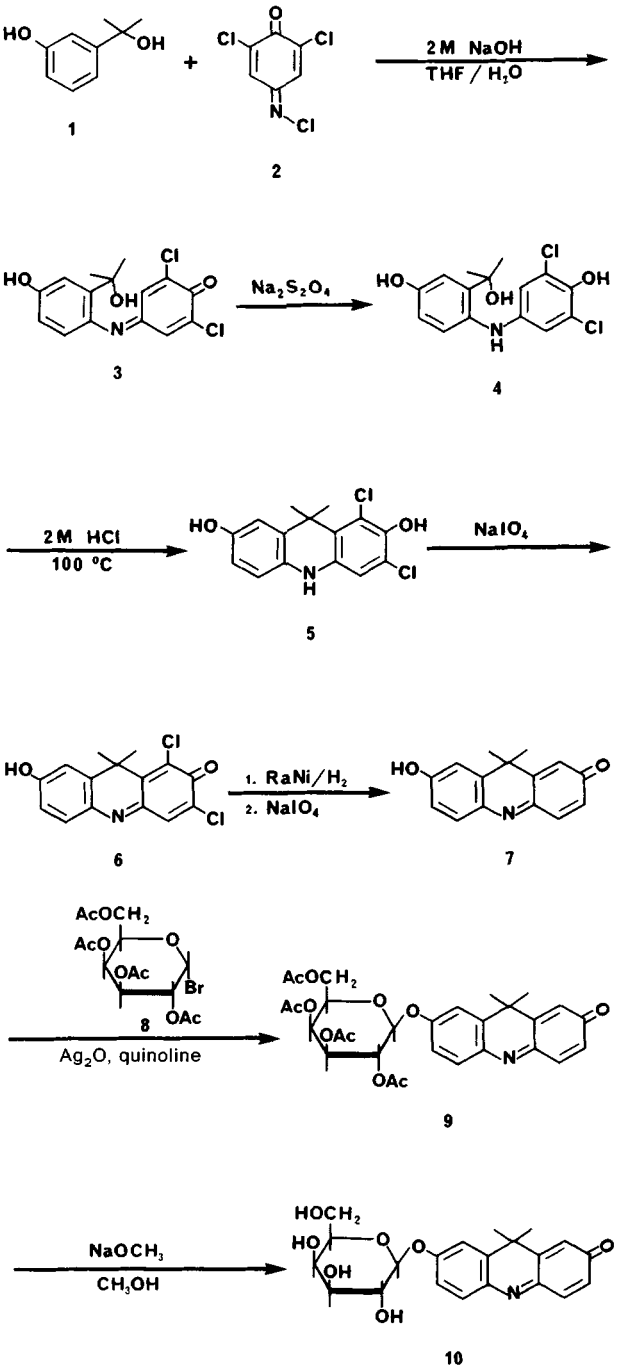

Scheme 1. Synthesis of 7-β-D-Galactopyranosylyloxy-9,9-dimethyl-9*H*-acridin-2-one (**10**).

Hill's procedure, it was possible to obtain the highly crystalline **6** in 82 % overall yield without isolation of every intermediate. The cyclization of dichloro compound **4** is more facile than that of the corresponding unchlorinated analogue and largely accounts for the improved yield of **6** with this process. Raney nickel dehalogenation of **6** followed by in situ oxidation gives **7** in 89 % yield.

Silver-promoted coupling of **7** with acetobromo-α-D-galactose (**8**) affords the bright yellow tetraacetate **9** in 80 % yield and deprotection of **9** gives the orange title compound **10** in 88 % yield.

Experimental Procedure

The ^1H and ^{13}C NMR spectra were recorded in $(CD_3)_2SO$ at 25 °C at 300.12 and 75.47 MHz, respectively.

6: A mixture of **1** [8] (1.52 g, 10.0 mmol) and **2** (2.10 g, 10.0 mmol) in THF (5 mL) was diluted with H_2O (5 mL) and cooled in ice. Aqueous 2 M NaOH (10.5 mL, 21 mmol) was added over 10 min. The deep blue reaction mixture was cooled at 0 °C for 1.5 h then blended into EtOAc (300 mL) and extracted twice with saturated aqueous NH_4Cl (350 mL). The resulting EtOAc solution of **3** was washed twice with a solution of $Na_2S_2O_4$ (25 g) in H_2O (250 mL) and once with saturated NaCl solution (brine), dried over Na_2SO_4, and concentrated to dryness to obtain crude **4**. A solution of **4** in MeOH (10 mL) was slowly blended into rapidly stirring, deoxygenated aqueous 2 M HCL (250 mL) at ambient temperature. The resulting suspension was heated in a 100 °C bath under Ar atmosphere for 1.25 h, during which time a gummy solid separated. The mixture was cooled, extracted twice with EtOAc (200 mL), and the combined extracts washed with brine (50 mL). The resulting solution was stirred vigorously for 15 min with a solution of $NaIO_4$ (3 g) in H_2O (100 mL) to oxidize **5**. The phases were then separated and the organic layer was washed with brine (100 mL), dried over Na_2SO_4, and concentrated to dryness. The residue was taken up in hot EtOH (500 mL) and concentrated to ca. 150 mL by boiling. Upon cooling **6** separated as black needles to afford, in 2 crops, 2.5 g (82 %). Recrystallization from EtOH gave the analytical sample (m.p. > 250 °C). ^1H NMR: $\delta = 7.76$ (s, 1H; C4-H), 7.50 (d, $J = 8.5$ Hz, 1H; C5-H), 7.06 (d, $J = 2.4$ Hz, 1H; C8-H), 6.84 (dd, $J = 8.5$, 2.4 Hz, 1H; C6-H), 3.32 (s, 1H; OH), 1.74 (s, 6H; 2 CH_3); ^{13}C NMR (assignment by ^1H-^{13}C correlation): $\delta = 172.1$ (C2), 162.7 (C7), 145.8 (C4a), 141.2 (C8a), 140.9 (C9a), 139.3 (C4), 134.9 (C1), 134.7 (C10a), 134.7 (C10a), 134.3 (C5), 132.6 (C3), 116.0 (C6), 114.2 (C8), 38.8 (C9), 26.3 (CH_3); UV/VIS (0.01 M NaOH) λ_{max} [nm] (ε) = 646 (42000). Correct C, H, N analyses.

7: A solution of **6** (2.0 g, 6.49 mmol) in 1 M NaOH (60 mL) and EtOH (40 mL) was treated with Raney Nickel 2800 (ca. 6 mL) and hydrogenated at 2.72 atm H_2 at ca. 70 °C for 5 h. After cooling to ambient temperature the reaction mixture was filtered through Celite, diluted with H_2O (500 mL), and exhaustively extracted with EtOAc. The combined EtOAc layers were vigorously stirred with a solution of $NaIO_4$ (4 g) in H_2O (300 mL) for 10 min at ambient temperature and then treated with 1 M HCl (100 mL). The phases were separated and the organic layer was washed with brine (50 mL), dried over $MgSO_4$, and concentrated to dryness to give **7** (1.38 g, 89 %). Crystallization from EtOAc/hexane (1:1), v/v) afforded **7** as ruby red needles identical to that prepared by the method of *Hill*, et al.[7] UV/VIS (0.01 M NaOH) λ_{max} [nm] (ε) = 634 (56000).

9: A mixture of **7** (1.57 g, 6.56 mmol), **8** (3.24 g, 7.87 mmol), Ag_2O (1.83 g, 7.87 mmol), and $CaSO_4$ (2.63 g) in EtOAc (31.65 mL) containing anhydrous quinoline (15.8 mL) was stirred for 19 h at ambient temperature in a closed flask protected from light. The reaction mixture was diluted with EtOAc (75 mL), filtered through Celite, extracted twice with aqueous 1.25 M HCl (75 mL), washed twice with brine (35 mL), extracted three times with 5 % aqueous $NaHCO_3$, washed again with brine (75 mL), dried over Na_2SO_4, and concentrated to dryness. The residue was taken up in EtOAc/hexane (3:2 v/v; 55 mL), stirred with Darco G-60 (4.78 g) at ambient temperature for 1 h, filtered through Celite, and concentrated to dryness. The residue was taken up in boiling EtOAc (5.5 mL), diluted with hexane (9 mL), and vigorously scratched; **9** separated upon cooling to yield 3.0 g (80 %) in two crops. Recrystallization from EtOAc/hexane (2:1 v/v) provided rosettes of fine yellow needles (m.p. = 156.5–158.0 °C). ^1H NMR: $\delta = 7.65$ (d, $J = 8.7$ Hz, 1H; C5-H), 7.44 (d, $J = 9.8$ Hz, 1H; C4-H), 7.29 (d, $J = 2.6$ Hz, 1H; C8-H), 7.04 (dd, $J = 8.7$, 2.6 Hz, 1H; C6-H), 6.82 (d, $J = 2.0$ Hz, 1H; C1-H), 6.63 (dd, $J = 9.8$, 2.0 Hz, 1H; C3-H), 5.75 (d, $J = 7.3$ Hz, 1H; C1′-H), 5.39 (d, $J = 2.1$ Hz, 1H; C4′-H), 5.32 (m, 1H; C3′-H), 5.29 (m, 1H; C2′-H), 4.54 (dd, $J = 7.0$, 5.2 Hz, 1H; C5′-H), 4.09 (m, 2H; C6′-H), 2.15 (s, 3H; $COCH_3$), 2.00 (s, 3H; $COCH_3$), 1.96 (s, 3H; $COCH_3$), 1.53 (s, 6H; CH_3); ^{13}C NMR (assignment by ^1H-^{13}C correlation): $\delta = 186.4$ (C2, C=O), 169.9 (OC=O), 169.5 (OC=O), 169.2 (OC=O), 158.1 (C7), 151.0 (C4a), 147.3 (C9a), 141.5 (C4), 139.6 (C8a), 137.3 (C10a), 133.1 (C5), 131.3 (C3), 127.5 (C1), 115.5 (C6), 113.8 (C8), 96.7 (C1′), 70.7 (C5′), 70.2 (C3′), 68.2 (C2′), 67.5 (C4′), 61.8 (C6′), 36.9 (C9), 32.3 (CH_3), 31.8 (CH_3), 20.6 ($COCH_3$), 20.5 ($COCH_3$), 20.4 ($COCH_3$); $[\alpha]_D$ + 37.3 ($c = 0.5$, $CHCl_3$). Correct C, H, N analyses.

10: A solution of **9** (5.3 g, 9.3 mmol) in warm MeOH (HPLC-grade, 250 mL) was cooled to ambient temperature and treated with NaOMe (0.106 g, 1.96 mmol). The hydrolysis reaction was monitored by TLC (silica gel; MeOH/$CHCl_3$ (15:85 v/v)) and was complete after 1.33 h, whereupon the reaction was quenched with HOAc (0.112 mL) and concentrated to dryness. The residue was dissolved in hot EtOH (75 mL), stirred for 10 min with Darco G-60, filtered through Celite, and concentrated in vacuo until the product began to separate. The solution was then further concentrated to a volume of 50 mL by boiling from which **10** separated upon cooling to yield 3.3 g (88 %) **10** in two crops. Recrystallization from EtOH followed by vacuum drying (1 h, 0.1 torr) at 132 °C gave the analytical sample which sinters at ca. 140 °C and melts with decomposition at 184–186 °C. ^1H NMR: $\delta = 7.59$ (d, $J = 8.7$ Hz, 1H; C5-H), 7.43 (d, $J = 9.8$ Hz, 1H; C4-H), 7.31 (d, $J = 2.6$ Hz, 1H; C8-H), 7.06 (dd, $J = 8.7$, 2.6 Hz, 1H; C6-H), 6.80 (d, $J = 2.1$ Hz, 1H; C1-H), 6.60 (dd, $J = 9.8$, 2.1 Hz, 1H; C3-H), 5.21 (d, $J = 5.1$ Hz, 1H; C2′-OH), 5.00 (d, $J = 7.7$ Hz, 1H; C1′-H), 4.91 (d, $J = 5.7$ Hz, 1H; C3′-OH), 4.68 (t, $J = 5.4$ Hz, 1H; C6′-OH), 4.54 (d, $J = 4.5$ Hz, 1H; C4′-OH), 3.38–3.73 (m, 6H; C2′–6′-H), 1.50 (s, 6H; CH_3); ^{13}C NMR (assignment by ^1H-^{13}C correlation): $\delta = 186.4$ (C2, C=O), 159.6 (C7), 150.3 (C4a), 147.5 (C9a), 141.5 (C4), 139.5 (C8a), 136.7 (C10a), 133.0 (C5), 131.0 (C3), 127.3 (C1), 115.4 (C6), 114.1 (C8), 100.4 (C1′), 75.8 (C5′), 73.4 (C3′), 70.2 (C2′), 68.2 (C4′), 60.5 (C6′), 37.1 (C9), 32.3 (CH_3), 31.9 (CH_3); UV/VIS (0.05 M phosphate pH 7.4) λ_{max} [nm] (ε) 438 (24700); $[\alpha]_D$ − 68.8° ($c = 1.3$, EtOH). Correct C, H, N analyses.

Received: May 27, 1991 [Z 4654 IE]
Publication delayed on authors' request
German version: *Angew. Chem. 103* (1991) 1694

CAS Registry numbers:
1, 7765-97-1; **2**, 101-38-2; **3**, 137041-53-3; **4**, 118290-03-2; **5**, 118290-04-3; **6**, 118290-05-4; **7**, 118290-06-5; **8**, 3068-32-4; **9**, 118290-07-6; **10**, 118290-08-7.

[1] M. J. O'Sullivan, J. W. Bridges, V. Marks, *Ann. Clin. Biochem. 16* (1979) 221.
[2] K. Aizawa, *Enzymologia 6* (1939) 321.
[3] J. Hofmann, M. Sernetz, *Anal. Chim. Acta. 163* (1984) 67.
[4] M. Kuhr, H. Batz, R. Herrmann, W. Kleeman, H. Buschek, *US Patent* 4668622 (1987) Boehringer Mannheim GmbH; *Chem. Abs. 104* (1986) 51076c.
[5] R. G. Sommer, T. L. Belchak, M. L. Bloczynski, S. J. Boguslawski, D. L. Clay, P. F. Corey, M. M. Foltz, R. A. Fredrickson, B. L. Halmo, R. D. Johnson, K. L. Marfurt, H.-V. Runzheimer, D. L. Morris, *Clin. Chem. 36* (1990) 201.
[6] H. Goldstein, W. Kopp, *Helv. Chim. Acta 11* (1928) 478.
[7] R. Hill, G. R. Bedford, B. R. Webster, *J. Chem. Soc. (C)* (1970) 2462.
[8] J. M. Bruce, P. Knowles, *J. Chem. Soc. (C)* (1966) 1627.

The Reaction of $PtCl_2$ with an *N,S,O*-Coordinated Calcium Complex: Synthesis and Structure of a Complexed CaPt Anion**

By *Matthew G. Davidson, Paul R. Raithby, Ronald Snaith, Dietmar Stalke,* and *Dominic S. Wright**

Recently we have described several aqua complexes of metalated organic molecules.[1] Most relevant here is $[Ox_2Ca(HMPA)_2(H_2O)_2]$ (**1**, Ox = 2-mercaptobenzoxazoyl), obtained from the reaction of 2-benzoxazolthione (OxH, 2 equiv), $Ca(OH)_2$ (1 equiv), and hexamethylphosphoric triamide (HMPA) (2 equiv). Complex **1** is easily dehydrated, giving $Ox_2Ca(HMPA)_2$ **2**.[1a] The key features of **1**

[*] Dr. D. S. Wright, M. G. Davidson, Dr. P. R. Raithby, Dr. R. Snaith, Dr. D. Stalke
University Chemical Laboratory
Lensfield Road, Cambridge CB2 1EW (UK)

[**] This work was supported by Gonville and Caius College, Cambridge (Research Fellowship for *D. S. W.*), and by the U.K. Science and Engineering Research Council and the Associated Octel Co. Ltd. (CASE Studentship for *M. G. D.*). We thank also Professor G. M. Sheldrick, University of Göttingen for financial support for *D. S.* (DAAD, NATO scholarship). All of the new work described is being patented by the Associated Octel Co., Ltd.

and **2** deserve note: In the anhydrous complex **2** the thioxo sidearms are coordinated to $Ca^{2\oplus}$; in complex **1**, however, the thioxo sidearms are displaced from the coordination sphere of the metal by the insertion of H_2O and participate in stabilizing the resulting H_2O complex by $S^{\delta\ominus} \cdots H_2O$ hydrogen bonds.

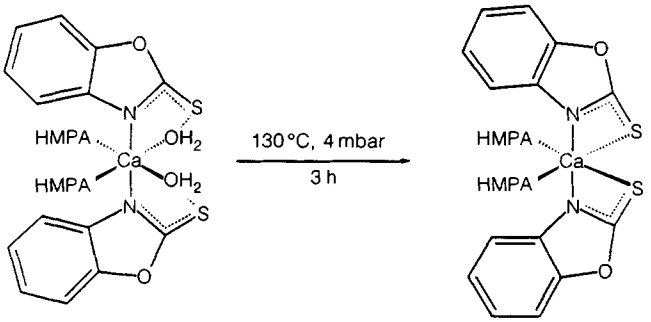

1 **2**

Encouraged by these results we postulated that chelate complexes like **2** might function as novel donor ligands to metal salts, MZ_n. The evidently weak Ca–S contacts in **2** could be disrupted and replaced by stronger M–S bonds (though maintaining the Ca–N coordinations) whilst the $Ca^{2\oplus}$ center of **2** could capture the salt anions, $Z^{\ominus}$. In hard/soft terms, $PtCl_2$ was an obvious choice for MZ_n since $Pt^{2\oplus}$ is compatible with $S^{\delta\ominus}$ and $Ca^{2\oplus}$ with $Cl^{\ominus}$. The idea works. Heating a mixture of complex **2** (3 equiv) with $PtCl_2$ (2 equiv) in toluene gives a bright yellow solution and a yellow powder, Ox_2Pt [Equation (a)]. After filtration, cooling of the solution gave golden yellow crystals of **3** in good yield.

$$\underset{\mathbf{2}}{3[Ox_2Ca(HMPA)_2]} + 2PtCl_2 \xrightarrow{C_6H_5CH_3} \underset{\mathbf{3}}{[(HMPA)_3Ca(\mu_2\text{-}Cl)_3Ca(HMPA)]^{\oplus}[Pt(Ox)_4CaCl]^{\ominus}} + Ox_2Pt \quad \text{(a)}$$

The solid-state structure of **3**, determined by X-ray crystallography,[2] consists of two Ca cations complexed by $Cl^{\ominus}$ and HMPA and a heteronuclear anionic complex. In addition, two toluene solvate molecules occupy general positions in the lattice, not interacting strongly with either the cation or the anion. The cation (Fig. 1, above) consists of two $Ca^{2\oplus}$ ions with pseudo-octahedral coordination geometries linked by three μ_2-$Cl^{\ominus}$ ions (mean Ca–Cl distance, 2.80(1) Å). Each Ca^{2+} ion is also complexed by three HMPA ligands [mean Ca–O distance, 2.27(2) Å]. This cation is apparently quite stable since it has been found in $CaCl_2(HMPA)_3$ which exists as $[(HMPA)_3Ca(\mu_2\text{-}Cl)_3Ca(HMPA)_3]^{\oplus}Cl^{\ominus}$.[3] Other cationic Ca_2-complexes are not known, although a magnesium analogue, $[Mg_2Cl_3(THF)_6]^{\oplus}[MoOCl_4(THF)]^{\ominus}$, has been reported.[4]

The structure of the anion of **3** (Fig. 1, below) lends credence to our initial musings. The $Pt^{2\oplus}$ center is coordinated by the four thioxo sidearms of four $Ox^{\ominus}$ ions (mean Pt–S distance, 2.32(2) Å) in the square-planar coordination geometry typical for Pt^{II} complexes[5a] (Pt deviates by 0.1 Å from the S_4 plane). The N centers of these $Ox^{\ominus}$ ions in turn bind to a $Ca^{2\oplus}$ center (mean Ca–N distance, 2.46(2) Å; cf 2.545(6) Å in **1**) which lies directly above Pt. The distance between Ca and Pt, 2.960(5) Å, precludes any interaction between the two atoms, because the sum of the radii of $Ca^{2\oplus}$ and $Pt^{2\oplus}$ is only ca. 1.8 Å.[5b]

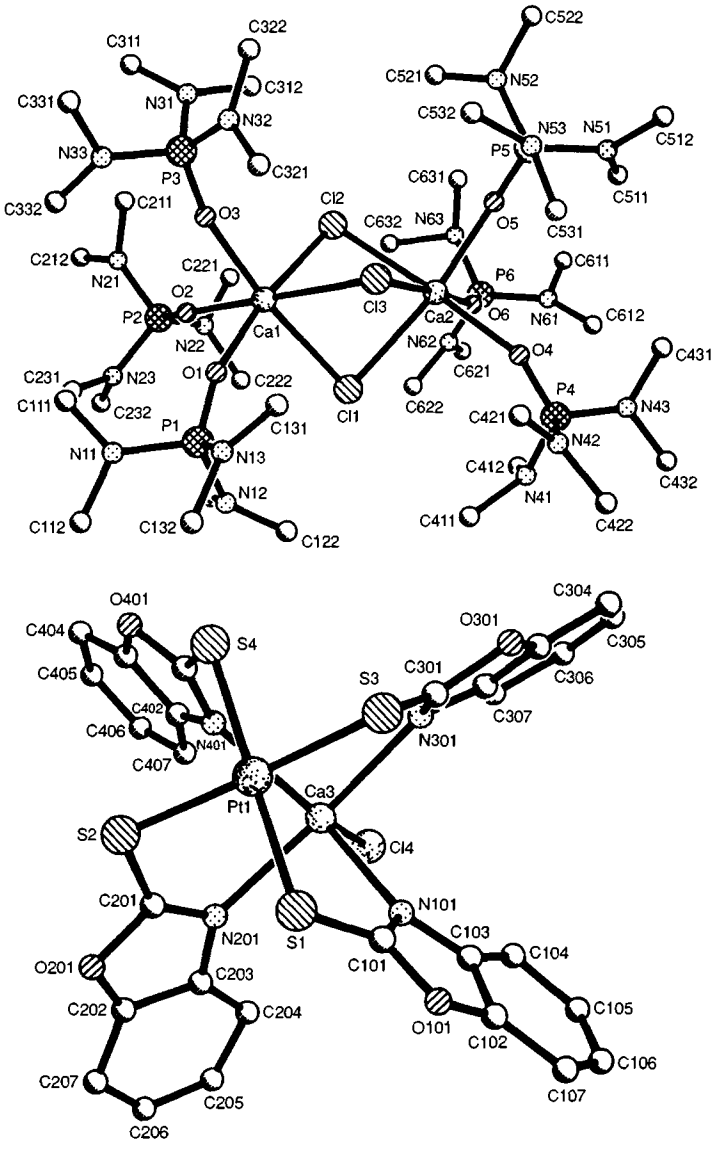

Fig. 1. Above: The structure of the cation of **3**. Below: The structure of the anion of **3**. The toluene molecules in the crystal have not been included.

A $Cl^{\ominus}$ ion completes the coordination of the $Ca^{2\oplus}$ ion as square-based pyramidal, to our knowledge a new geometry for this metal.[6] The anion of **3** can be viewed as a tetradentate $[Ox_4CaCl]^{3\ominus}$ ligand coordinated to a $Pt^{2\oplus}$ cation. In this way the $Pt^{2\oplus}$ and one $Cl^{\ominus}$ ion are built into the anion complex, while the second $Cl^{\ominus}$ from $PtCl_2$ is incorporated into the cation complex.

The results show that sidearm-donating complexes such as **2** can act as ligands to other metals. Indeed, a solution of **2** (or of the barium analogue $[Ox_2Ba(HMPA)_3]$ will react with other soft metal species, for example, $PdCl_2$, $CoCl_2$, $NiCl_2$, $SnCl_2$, resulting in crystalline products. The ligand precursor OxH can be described as Y–R–XH (Y = S, X = N). Since countless organic acids belong to this category, one might tailor Y–R–XH ligands (X, Y = O, S, N) using hard/soft concepts to give complexes with the general formula Y-R-XM′ which will react with MZ_n salts. For example, $[(C_6H_4OC(\cdots O)\cdots N)_2Ca(HMPA)_2]$, an analogue of **2** but with X,Y = N,O rather than N,S, reacts with $TiCl_3$ (containing the harder $Ti^{3\oplus}$ metal ion) to give a crystalline product containing both Ca and Ti whose structure is as yet unknown. Such ideas are relevant to metal–ion separation and

extraction, and to the development of heteronuclear catalysts. In addition, Pt–Ca co-complexes such as **3** could serve as models for complexes with deprotonated DNA bases as ligands since such bases also fit the Y–R–XH formula. (For C, G, and T, X = N and Y–R = C=O; for A, X = NH and Y–R = C=N.

Experimental Procedure

3: Platinum(II) chloride (0.266 g, 1 mmol) was added to a solution of $[Ox_2Ca(HMPA)_2]$ **2** (1.050 g, 1.5 mmol) in toluene (10 mL). The mixture was heated to 100 °C for 15 min whereupon all the $PtCl_2$ had reacted to give a yellow solution and a small quantity of yellow powder (Ox_2Pt). Filtration and cooling of the reaction mixture to 20 °C produced yellow cubic crystals of **3**. (Yield 0.660 g, 56%); m.p. 210–213 °C; correct C, H, N, Cl, P analyses; ^{1}H NMR [$(CD_3)_2SO$, 250 MHz, 20 °C] $\delta \approx 7.1$ (m, 26H, $Ox^{\ominus}$-*H*, $C_6H_5CH_3$), 2.53 (d, 108H, HMPA, $J = 9.5$ Hz), 2.30 (s, 6H, $C_6H_5CH_3$). Suitable crystals of **3** for X-ray diffraction were mounted under argon in a polyfluorinated hydrocarbon oil into Lindemann tubes.

Received: May 2, 1991
Revised: September 5, 1991 [Z 4608 IE]
German version: *Angew. Chem. 103* (1991) 1696

CAS Registry numbers:
2, 132461-58-6; **3**, 137057-16-0.

[1] a) P. Mikulcik, P. R. Raithby, R. Snaith, D. S. Wright, *Angew. Chem. 103* (1991) 452; *Angew. Chem. Int. Ed. Engl. 30* (1991) 428; b) D. Barr, P. R. Raithby, P. von R. Schleyer, R. Snaith, D. S. Wright, *J. Chem. Soc. Chem. Commun. 1990*, 643; c) D. R. Armstrong, D. Barr, P. R. Raithby, P. von R. Schleyer, R. Snaith, D. S. Wright, *Inorg. Chim. Acta 185* (1991) 163.

[2] X-ray crystal structure for **3** · 2 toluene ($C_{64}H_{124}Ca_3Cl_4N_{22}O_{10}P_6PtS_4 \cdot 2C_7H_8$), monoclinic, $P2_1/c$ (No. 14), $a = 19.750(4)$, $b = 24.223(4)$, $c = 24.379(5)$ Å, $\beta = 101.13(2)°$, $V = 11443.6$ Å^3, $M_r = 2317.31$, $Z = 4$, $\varrho_{calc} = 1.345$ g cm^{-3}, $F(000) = 4808$, $Mo_{K\alpha}$ radiation, $\lambda = 0.71069$ Å, $\mu(Mo_{K\alpha}) = 16.35$ cm^{-1}. The structure was solved by a combination of direct methods and Fourier difference techniques. Structure refined by blocked full-matrix least squares; Pt, Ca, Cl atoms anisotropic; H atoms not included in the refinement. High residuals because of 20% decomposition during data collection and severe positional disorder in HMPA ligands. 16540 reflections measured ($5 < 2\theta < 45°$), corrected for absorption and decay, 7508 unique observed reflections with $F > 5\sigma(F)$, $R = 0.097$, $R_w = 0.104$. Further details of the crystal structure investigation are available on request from the Director of the Cambridge Crystallographic Data Centre, University Chemical Laboratory, Lensfield Road, GB-Cambridge CB2 1EW (UK), on quoting the full journal citation.

[3] A. T. Brooker, P. R. Raithby, R. Snaith, D. S. Wright, unpublished results.

[4] P. Sobota, T. Phizinski, T. Lis, *Z. Anorg. Allg. Chem. 553* (1986) 215.

[5] a) N. N. Greenwood, A. Earnshaw: *Chemistry of the Elements*. Pergamon, Oxford 1984, p. 1070; b) p. 122 and 1333.

[6] For a review of the structures of alkaline earth complexes (especially Ca, Sr, Ba) see N. S. Poonia, A. V. Bajaj, *Coord. Chem. Rev. 87* (1988) 55.

Analysis of Polymer Latices by Small-Angle X-Ray Scattering

By *Ralf Grunder, Young Sam Kim, Matthias Ballauff,* Dietmar Kranz*, and *Hans-Georg Müller*

Dedicated to Professor Karl Heinz Büchel on the occasion of his 60th birthday

Polymer latices have found widespread use for a multitude of applications such as carpet backing, paper coating, protective or decorative coatings, dipped goods, textile pigment printing, leather finishing, nonwoven fabrics, and molded foam products. The structure of the latex particle determines the properties necessary for a given application. An important example of a heterogeneous structure of a latex particle is given by the core-shell morphology in which a spherical core of polymer A is enclosed by a shell of polymer B.[1] The analysis of such particles presents a difficult problem. Investigation by electron microscopy requires thin cuts and subsequent chemical staining of the polymeric phase by, for example, OsO_4.[2] It is obvious that this method only works for systems in which a contrast between the different phases can be effected. Small-angle neutron and small-angle X-ray scattering techniques,[3–5] however, give information on the morphology of latex particles without prior treatment. A necessary prerequisite is a sufficient contrast with regard to the scattering length density or the electron density between the different polymers and the dispersing medium. Here we present a small-angle X-ray (SAXS) analysis of core-shell particles composed of polystyrene (PS) and polymethylmethacrylate (PMMA). The particle size distribution of the latex necessary for the interpretation of the SAXS data has been determined by ultracentrifuge sedimention.[6, 7]

The intensity $I(q)$ of the scattered X-rays of spherical particles with equal diameter (normalized to the scattering intensity of a single electron) is given by Equation (a),[8] where $q(= 4\pi \sin(\theta/2)/\lambda; \theta =$ scattering angle) is the magnitude of the scattering vector and N the number of scattering particles per volume V. The scattering amplitude f is defined by Equation (b),[8] where $\rho_P(r)$ denotes the electron density of the particle as a function of the distance to the midpoint and ρ_S is the electron density of the dispersing agent. The form factor $P(q)$, which describes the intraparticle interferences, is characteristic of the internal structure of the particle. It is given by Equation (c).[8]

$$I(q) = (N/V) f^2 P(q) S(q) \quad \text{(a)}$$

$$f = 4\pi \int_0^\infty [\rho_P(r) - \rho_s] r^2 dr \quad \text{(b)}$$

$$P(q) = \{f^{-1} 4\pi \int_0^\infty [\rho_P(r) - \rho_S][\sin(q \cdot r)/q \cdot r] r^2 dr\}^2 \quad \text{(c)}$$

The structure factor $S(q)$ is related to the interparticle interferences at finite particle concentration.[8] $S(q)$ can be derived by Fourier transformation of the pair correlation function.[8]

Equation (a) holds true for a system of spheres uniform in diameter. For the interpretation of measurements on colloidal systems the size distribution of the particles must be taken into account explicitly. *Vrij* and co-workers[9, 10] were able to generalize Equation (a) to polydisperse systems. In particular, they were able to show that $S(q)$ can be calculated exactly for a system of hard spheres differing in size.

Figure 1 demonstrates the influence of the size distribution on the scattering intensities by displaying the form factor of homogeneous spheres under the assumption of a Gaussian size distribution (number average diameter 80 nm). The pronounced minima of the form factor of monodisperse spheres vanish with increasing nonuniformity (Fig. 1a). The marked influence of polydispersity must be taken into account for a quantitative evaluation of the SAXS experiment.

Since the SAXS experiment is done at finite concentrations, the structure factor $S(q)$ must not be disregarded.[11] Figure 1b shows $S(q)$ for a system of hard spheres at a volume fraction of the spheres of 0.2.[10] For monodisperse

[*] Prof. Dr. M. Ballauff, Dipl.-Chem. R. Grunder,
Dipl.-Chem. Y. S. Kim
Polymer-Institut der Universität
Kaiserstrasse 12, W-7500 Karlsruhe (FRG)
Dr. D. Kranz
Bayer AG, GB Kautschuk
W-4047 Dormagen (FRG)
Dr. H.-G. Müller
Bayer AG, ZF-TPP5
W-5090 Leverkusen (FRG)

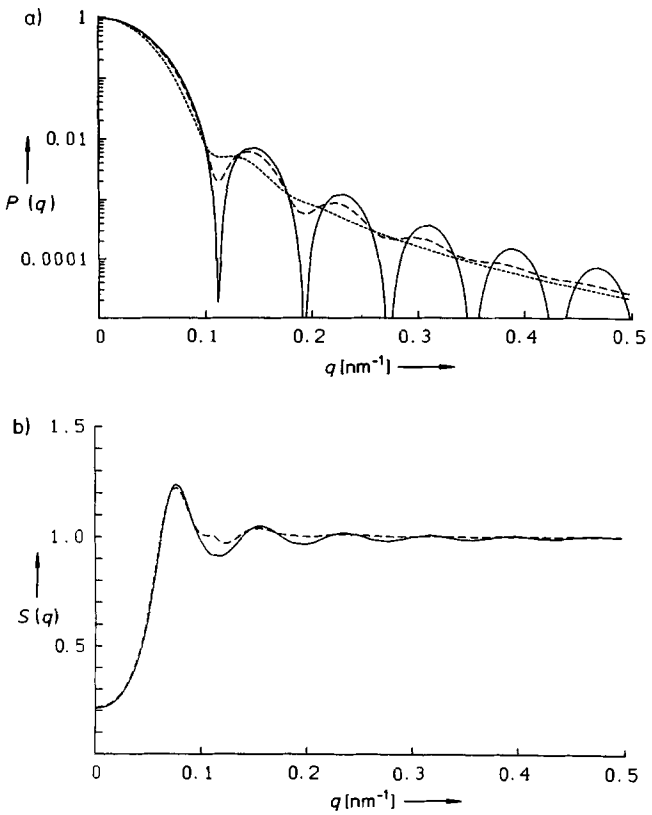

Fig. 1. a) Calculated form factor $P(q)$ [Eq. (c) and ref. [9]] for homogeneous spheres with a number average diameter of 80 nm and a Gaussian distribution of the diameters. ——, standard deviation $\sigma = 0$ nm (uniform size); — —, $\sigma = 6$ nm; - - - -, $\sigma = 12$ nm. b) Structure factor calculated according to [10]) for a system of hard spheres with a number average diameter of 80 nm and a Gaussian distribution of diameters. The volume fraction of the particles is 0.2. ——, standard deviation $\sigma = 0$ nm; — —, $\sigma = 6$ nm.

systems the structure factor differs from unity only below $q = 0.15$ nm^{-1}. Hence the scattering intensity in the region of higher q values is solely governed by the form factor $P(q)$. For polydisperse systems the oscillations of $S(q)$ are less pronounced. Here the influence of interparticle interferences is restricted to the region $q < 0.1$ nm^{-1}.

Figure 2 shows the experimental ("smeared") scattering intensities of the PS-latex forming the core and of the shell-core latex after adding the shell through subsequent polymerization of PMMA. The respective corrected ("desmeared") intensities are displayed in Figure 3.

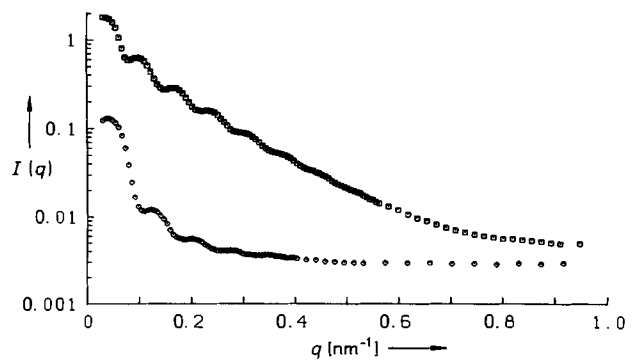

Fig. 2. Experimental (smeared) scattering intensities $I(q)$ of the shell-core latex (upper curve) and the polystyrene seed latex (lower curve). $I(q)$ in units of 10^5 impulses per 600 s.

An additional investigation of the region of smallest angles as a function of concentration showed that the scattering intensities above 0.1 nm^{-1} are solely determined by $P(q)$; that is, these data only refer to the internal structure of the particle. This finding is in accordance with the general discussion in Figure 1. Electron microscopy furthermore demonstrated that the PS seed latex, as well as the PS/PMMA shell-core latex, exhibits a spherical shape.

For a quantitative interpretation of the scattering intensities (Fig. 3) the size distribution was determined by ultracentrifuge sedimentation. The number distribution of the diameter d used for the SAXS analysis of the PS seed latex is shown in Figure 4. The theoretical form factor calculated for such a distribution is shown in Figure 3 as a solid line. The number average diameter of the particles resulting from this analysis is 80.2 nm. This value is higher than the diameter (71.5 nm) determined by sedimentation and electron microscopy. The reason for this discrepancy may be certainly traced back to the fact that the present fit does not take into account the soap molecules adsorbed on the surface of the PS particles. The emulgator used herein exhibits a pronounced electron density difference with regard to water as well as to the polymer. Its maximum length is 2.5 nm.[12, 13] Moreover, the surface of the

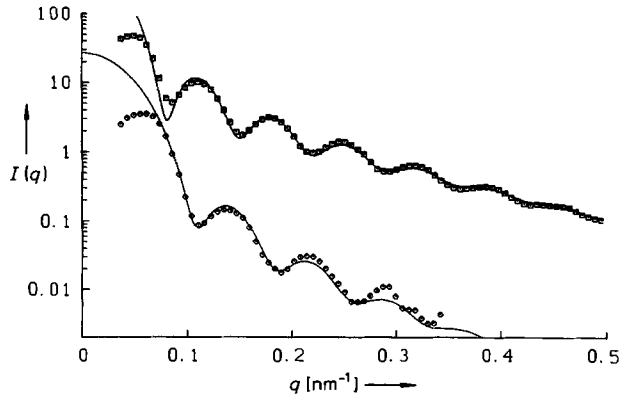

Fig. 3. Corrected (desmeared) intensities of the shell-core latex (upper curve) and of the polystyrene seed latex (lower curve). The solid lines represent the calculated form factors (see text for explanation). $I(q)$ in units of 10^5 e.u. per nm^3.

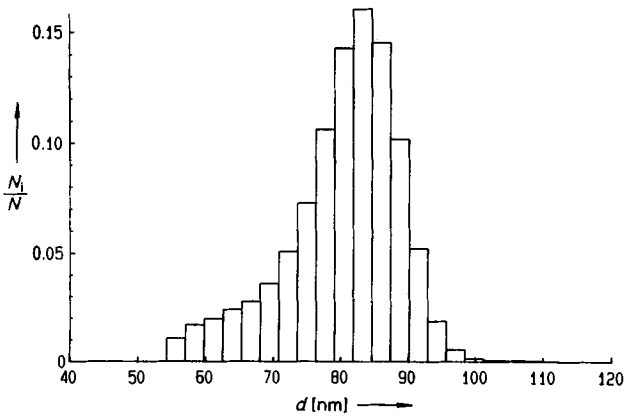

Fig. 4. Number distribution N_i/N of the diameters of the polystyrene seed latex used in the SAXS analysis (shape determined by ultracentrifuge sedimentation according to [6]).

particles contains sulfate end groups from the polymerization, which can also modify the interface between polymer and water.[14]

The experimental scattering intensities of the PS/PMMA latex were fitted by a shell-core model[15] consisting of a PS core (electron density difference to water: $\Delta\rho_e = 8\ e^-\ nm^{-3}$) with the shape of the size distribution identical to that in Figure 4. The PMMA shell ($\Delta\rho_e = 46.73\ e^-\ nm^{-3}$) was assumed to be of constant thickness (cf. also Ref. [5]). A fit of the experimental result based on the assumption of homogeneous spheres could not be achieved. The shell-core model yields 76.2 nm for the number average of the core diameter and 6.9 nm for the thickness of the shell. The resulting overall diameter is therefore 90 nm. The dimension of the shell compared favorably with the value of 6.25 nm deduced from mass balance. An investigation of the latex by rapid density gradient centrifugation showed that all particles have the same density. Thus, the size distribution could be determined by ultracentrifuge sedimentation and the number average diameter obtained is 90.2 nm.

The agreement between the different methods is excellent in the case of the PS/PMMA latex. It has to be noted, however, that the applied shell-core model leads to a slightly varying density of the particles. The effects of the sulfate end groups and of soap molecules adsorbed on the surface of the particles are less important in the case of the shell-core latex because of the much larger electron density difference between PMMA and water. All results clearly demonstrate that quantitative agreement between measured and calculated scattering intensities can be achieved if the size distribution of the latex particles is known accurately. Small-angle X-ray analysis therefore is a reliable method for the study of the morphology of polymer latices.

Experimental Procedure

Synthesis: The monomers styrene (Fluka, purum) and methyl methacrylate (Fluka, purum) were destabilized and distilled prior to use; the initiator potassium peroxodisulfate (Fluka, p.a.), the emulsifier (sodium *p*-dodecylbenzenesulfonate, Fluka, technical) and the inhibitor (*N,N*-diethylhydroxylamine (DEHA), Aldrich) were used without further purification; water used for polymerization was deionized and distilled in an apparatus made from quartz.

PS latex: Batch polymerization; heating of the mixture to 80 °C under nitrogen; start of the reaction by addition of initiator; reaction time 6 h with continuous stirring (300 rpm); termination of the reaction by addition of inhibitor; 525 g H_2O, 15 g 10 wt % emulsifier solution, 150 g styrene, 0.3 g $K_2S_2O_8$ in 6.0 g H_2O, addition of 15 g 10% emulsifier solution after 0.5 h, addition of 0.61 g 25 wt % DEHA solution after 6 h; conversion (of styrene) 93%.

PS/PMMA latex: Polymerization under starved conditions [16]; heating of the mixture to 80 °C under nitrogen, addition of initiator, addition of MMA (25 μL min^{-1}) over 7 h with continuous stirring at 300 rpm; termination of the reaction by addition of inhibitor; 79.36 g PS latex, 0.144 g $K_2S_2O_8$ in 9.92 g H_2O, 9.868 g MMA, addition of approximately 0.07 g 25 wt % DEHA solution after 7 h; conversion of MMA 100%.

Characterization: (1) Electron microscopy: transmission electron microscope Hitachi H700H; particle counter Zeiss TGZ-3; calibration of the magnification factor by internal standard PS latex (Balzers, $d = 313 \pm 2$ nm) and a grating replica (Balzers, 2160 lines mm^{-1}). (2) Ultracentrifuge: see [6]. (3) SAXS: Kratky-Kompakt-Kamera (A. Paar, Graz, Austria) with step scan device, recording of the intensity by a scintillation counter with pulse height discrimination, Nickel-filtered $Cu_{K\alpha}$ radiation ($\lambda = 0.154$ nm); determination of the primary intensity by the "moving slit" method [17]; width of the entrance slit; 20 μm; width of the detector slit, 50 μm; subtraction of the scattering intensities due to the empty capillary and to the electron density fluctuation of the samples (the latter correction according to [18] by determination of the background in the region of high angles); the correction of smeared intensity was done using the procedure of *Strobl* [19].

Received: June 20, 1991 [Z 4734 IE]
Publication delayed at authors' request
German version: *Angew. Chem. 103* (1991) 1715

[1] M. Okubo, *Makromol. Chem. Macromol. Symp. 35/36* (1990) 307.
[2] K. Kato, *Polym. Lett. 4* (1966) 35.
[3] J. W. Vanderhoff in G. E. Ham (Ed.): *Vinyl Polymerization, Vol. 1, Part II*, Dekker, New York 1969, and references cited therein.
[4] M. P. Wai, R. A. Gelman, M. G. Fatica, R. H. Hoerl, G. D. Wignall, *Polymer 28* (1987) 918; G. A. Bootle, J. E. Lye, R. Ottewill, *Makromol. Chem. Macromol. Symp. 35/36* (1990) 291.
[5] D. Hergeth, W. Lebek, W. D. Hergeth, K. Schmutzler, *Colloid Polym. Sci 268* (1990) 744.
[6] H.-G. Müller, *Colloid Polym. Sci. 267* (1989) 1113.
[7] H. Lange, *Colloid Polym. Sci. 258* (1980) 1077.
[8] A. Guinier, G. Fournet: *Small-Angle Scattering of X-Rays*, Wiley, New York, and Chapman and Hall, London 1955.
[9] J. Moonen, C. de Kruif, A. Vrij, *Colloid Polym. Sci. 266* (1988) 1068.
[10] A. Vrij, *J. Chem. Phys. 71* (1979) 3267.
[11] S. H. Chen, E. Y. Sheu in S. H. Chen, R. Rajagopalan (Eds.): *Micellar Solutions and Microemulsions*, Springer, New York 1990.
[12] P. C. Cabos, P. Delord, J. Rouvier, *J. Appl. Crystallogr. 10* (1977) 37.
[13] D. Cebula, R. K. Thomas, N. M. Harris, J. Tabony, J. W. White, *Faraday Discuss. Chem. Soc. 65* (1965) 76.
[14] L. A. Rosen, D. A. Saville, *J. Colloid Interface Sci. 140* (1990) 82.
[15] M. Kerker: *The Scattering of Light and Other Electromagnetic Radiation*, Academic Press, New York 1969.
[16] M. Okubo, A. Yamada, T. Matsumoto, *J. Polym. Sci. Polym. Chem. Ed. 16* (1980) 3219.
[17] H. Stabinger, O. Kratky, *Makromol. Chem. 179* (1978) 1655.
[18] R. J. Roe, *J. Appl. Crystallogr. 15* (1982) 182.
[19] G. R. Strobl, *Acta Crystallogr. Sect. A 26* (1970) 367.

Derivatives of 1,1″-Biferrocene with Sulfur and Selenium Bridges**

By *Max Herberhold,** *Hans-Dieter Brendel*, and *Ulf Thewalt*

Dedicated to Professor Erwin Weiss on the occasion of his 65th birthday

In view of the great amount of work on the lithiation of ferrocene,[1-5] it is surprising that nothing has been reported on the lithiation of 1,1″-biferrocene, $[Fe_2C_{20}H_{18}]$ (Fc-Fc) (**1**). Here we describe the preparation of a tetralithiated intermediate, **2**, and its reaction with sulfur and selenium.

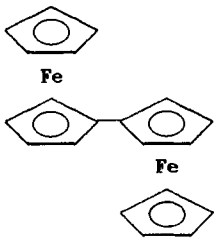

1

1: $[Fe_2C_{20}H_{18}]$ (Fc-Fc)
2: $[Fe_2C_{20}H_{14}Li_4 \cdot (tmeda)_n]$

tmeda = Me_2N–CH_2CH_2–NMe_2

In the presence of tetramethylethylenediamine (tmeda), ferrocene reacts with *n*-butyllithium to give the tmeda-stabilized 1,1′-dilithioferrocene **3**,[2,3] which reacts with sulfur in excess to give 1,2,3-trithia[3]ferrocenophane, $[FeC_{10}H_8S_3]$ (**4a**).[3,6]

The analogous lithiation of **1** with an excess of *n*-butyllithium in the presence of tmeda leads preferentially to the

[*] Prof. Dr. M. Herberhold, Dipl.-Chem. H.-D. Brendel
Laboratorium für Anorganische Chemie der Universität
Postfach 10 12 51, W-8580 Bayreuth (FRG)
Prof. Dr. U. Thewalt
Sektion für Röntgen- und Elektronenbeugung der Universität Ulm (FRG)

[**] This work was supported by the Deutsche Forschungsgemeinschaft and the Fonds der Chemischen Industrie.

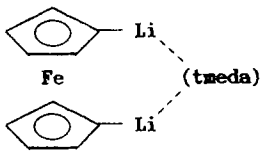

3

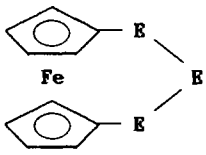

4a: E = S
4b: E = Se

tetralithiated product **2**, in which each of the four cyclopentadienyl rings is monolithiated and the fulvalene system contains the lithium substituents at positions 2 and 2″ (for numbering see Fig. 1). This was established by ^{1}H and ^{13}C NMR spectroscopy of the tetrasubstituted 1,1″-biferrocene derivatives **5** and **6**, obtained by reaction of **2** with excess Me_3SiCl and MeSSMe, respectively. Tetrasubstituted 1,1″-biferrocenes were previously unknown.

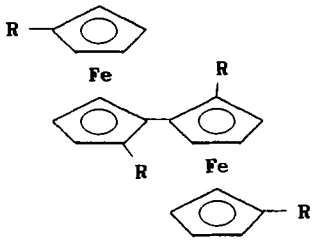

5: R = $SiMe_3$
6: R = SMe

Sulfurization of **2** with *cyclo*-octasulfur allows either two S_3 or two S_2 bridges to be introduced into **1**. A mixture of $[Fe_2C_{20}H_{14}(S_3)_2]$ (**7a**, side product) and $[Fe_2C_{20}H_{14}(S_2)_2]$ (**8a**, main product) is thereby formed. The selenium compounds $[FeC_{10}H_8(Se_3)]$ (**4b**)[6, 7] and $[Fe_2C_{20}H_{14}(Se_2)_2]$ (**8b**) are accessible in a corresponding way by reaction of **3** and **2**, respectively, with an excess of selenium; a selenium derivative analogous to **7a** was not obtained.

The NMR spectra of complexes **5**, **6**, **7a**, and **8a**,**b** confirm the presence of a tetrasubstituted 1,1″-biferrocene. In the ^{1}H NMR spectrum, two doublets of doublets and a triplet are observed for the fulvalene protons and four multiplets are found for the protons of the monosubstituted cyclopentadienyl rings. In the ^{13}C NMR spectrum, seven signals are observed for the carbon atoms bearing hydrogen atoms and three weaker-intensity signals for the C atoms at the substituted positions of the cyclopentadienyl rings. In the EI mass spectra, the molecular ion appears with high intensity, usually (except for **8b**) as the base peak.

According to the X-ray structure analysis,[8] the molecules of **7a** (Fig. 1, left) consist of two 1,2,3-trithia[3]ferrocenophane units; thus, the distances and angles in the S_3 chains correspond to those in **4a**.[9] In **8a**, the S_2 units bridge the two ferrocene moieties (Fig. 1, right). The molecules **7a** and **8a** are chiral; both compounds crystallize as racemates. Compound **7a** has no crystallographic symmetry, whereas **8a** displays crystallographic C_2 symmetry.

The molecular structures of **7a** and **8a** are shown in Figure 1 in such a way that the right (lower) ferrocene units of the 1,1″-biferrocene framework[10] have the same orientation; the central C1–C1″ bond of the fulvalene lies in the plane of the paper. The C1–C1″ distance in bridged $[Fe_2C_{20}H_{14}(S_2)_2]$ (**8a**) (1.459(4) Å) is hardly shorter than in $[Fe_2C_{20}H_{14}(S_3)_2]$ (**7a**) (1.479(7) Å); a value of 1.48(4) Å was given for 1,1″-biferrocene.[10c] The two five-membered ring planes of the fulvalene ligand are tilted toward each other by 23.3° in **7a** and 46.3° in **8a**. As in **4a**, the two five-membered

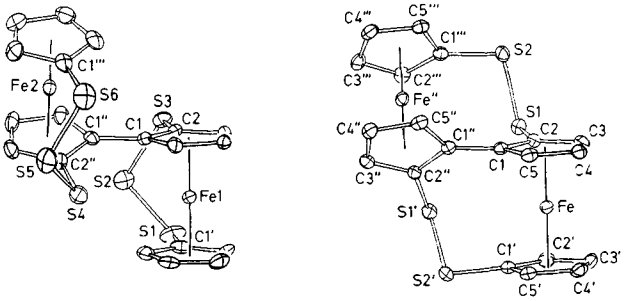

Fig. 1. Left: Molecular structure of $[Fe_2C_{20}H_{14}(S_3)_2]$ (**7a**) in the crystal. Selected bond lengths [Å] and angles [°]: S3-C2 1.755(5), S3-S2 2.052(2), S2-S1 2.045(2), S1-C1′ 1.754(6), C1-C1″ 1.479(7); C2-S3-S2 103.3(2), S1-S2-S3 105.1(1), C2″-C1″-C1-C2 23.2. Right: Molecular structure of $[Fe_2C_{20}H_{14}(S_2)_2]$ (**8a**) in the crystal. Selected bond lengths [Å] and angles [°]: S1-C2 1.751(3), S1-S2 2.066(1), S2-C1‴ 1.765(3), C1-C1″ 1.459(4); S2-S1-C2 100.3(1), S1-S2-C1‴ 103.8(1), C2″-C1″-C1-C2 46.3.

rings of the ferrocene units nearly eclipse each other; the deviations from the ideal eclipsed conformation (cf. Ref. [11]) are 0.08° in **4a**,[9] 0.4° and 1.7° in the Fe1 and Fe2 halves, respectively, of **7a**, and 9.5° in **8a**. For **1**, on the other hand, a twisting of 16–17°—between an eclipsed (0°) and a staggered (36°) conformation—has been reported.[10b, c] The rings of the ferrocene units lie practically parallel to each other; the tilting (i.e., the angle between the normals of the five-membered ring planes) is 2.85° in **4a**,[9] 1.5 and 1.9° in **7a**, and 2.0° in **8a**. The sulfur atoms are coplanar with the five-membered ring to which they are attached; the deviation of the sulfur atom from the ring plane is 0 Å in **4a**, <0.03 Å for all four relevant S atoms in **7a**, and 0.10 Å (away from Fe) in **8a**.

Experimental Procedure

2: *n*-Butyllithium (4.22 mL, 6.75 mmol) as a 1.6 M solution in hexane (Merck) was added to a solution of **1** (500 mg, 1.35 mmol) in 100 mL of hexane followed by addition of tmeda (1.01 mL, 6.75 mmol). The reaction mixture was heated at reflux for two days. The orange precipitate thereby formed contained **2**, which, after drying in a high vacuum, was dissolved in ether, THF, or toluene/THF and allowed to react directly with Me_3SiCl (at −78 °C), MeSSMe (at 0 °C), sulfur, or selenium (at 25 °C), each in excess.

5 and **6**: The reaction solution (50 mL of THF or diethyl ether) was stirred overnight, during which time it warmed to room temperature. It was then evaporated to dryness. Purification by chromatography on silica gel.

5: Elution with pentane; red-brown oil, which slowly crystallized on standing; yield 12%. ^{1}H NMR (C_6D_6, 25 °C): δ = 4.76 (dd, 2H), 4.12 (dd, 2H), and 4.31 (t, 2H) (fulvalene); 4.25, 4.14, 4.08 and 3.94 (each m, 2H) (cyclopentadienyl); 0.51 and 0.23 (each s, 18H) ($SiMe_3$ groups).

6: Elution with dichloromethane/pentane (1:4); light yellow powder; yield 16%. ^{1}H NMR (C_6D_6, 25 °C): δ = 4.79 (dd, 2H), 4.27 (dd, 2H), and 4.19 (t, 2H) (fulvalene); 4.43, 4.40, 4.30, and 4.22 (each m, 2H) (cyclopentadienyl); 2.15 and 1.72 (each s, 6H) (SMe-groups).

7a, **8a**: The reaction solution (50 mL of toluene/THF (1:1)) obtained from the reaction of **2** with sulfur (in five- to tenfold molar excess) was stirred at 25 °C for 48 h. After addition of 20 mL of water, the organic phase was separated and dried with Na_2SO_4 and the solvents were removed under vacuum. The residue was chromatographed on TLC plates (SiO_2). Development of the plates with pentane/dichloromethane (3:1) resulted in four orange zones, which contained **1** (small amount), $[Fe_2C_{20}H_{16}(S_3)]$ (small amount), $[Fe_2C_{20}H_{14}(S_3)_2]$ (**7a**), and $[Fe_2C_{20}H_{14}(S_2)_2]$ (**8a**). The zones were removed and the products, **7a** and **8a**, respectively, were purified again by TLC.

7a: Orange crystals, m.p. 194–197 °C; yield 8%. ^{1}H NMR (C_6D_6, 25 °C): δ = 4.30 (dd, 2H), 3.84 (dd, 2H), and 3.90 (t, 2H) (fulvalene); 4.26, 3.86, 3.79, and 3.46 (each m, 2H) (cyclopentadienyl).

8a: Orange crystals, darkening and decomposition above 180 °C; yield 23% based on **1**. ^{1}H NMR (C_6D_6, 25 °C): δ = 4.33 (dd, 2H), 4.24 (dd, 2H), and 3.84 (t, 2H) (fulvalene); 4.31, 4.08, 3.99, and 3.77 (each m, 2H) (cyclopentadienyl).

8b: TLC workup of the orange products obtained from the reaction of **2** with selenium (1:10) gave, besides $[Fe_2C_{20}H_{16}(Se_3)]$ (dec. 229 °C, yield 8%), $[Fe_2C_{20}H_{14}(Se_2)_2]$ (**8b**) as the main product: orange crystals, dec. 238 °C; yield

27%. ^{1}H NMR (C_6D_6, 25 °C): δ = 4.40 (dd, 2H), 4.20 (dd, 2H), and 3.84 (t, 2H) (fulvalene); 4.24, 4.10, 3.99, and 3.77 (each m, 2H) (cyclopentadienyl).

Received: July 11, 1991 [Z 4790 IE]
German version: *Angew. Chem. 103* (1991) 1664

[1] M. D. Rausch, G. A. Moser, C. F. Meade, *J. Organomet. Chem. 51* (1973) 1.
[2] M. D. Rausch, D. J. Ciappenelli, *J. Organomet. Chem. 10* (1967) 127.
[3] J. J. Bishop, A. Davison, M. L. Katcher, D. W. Lichtenberg, R. E. Merrill, J. C. Smart, *J. Organomet. Chem. 27* (1971) 241.
[4] I. R. Butler, W. R. Cullen, J. Ni, S. R. Rettig, *Organometallics 4* (1985) 2196.
[5] I. R. Butler, W. R. Cullen, *Organometallics 5* (1986) 2537, and references cited therein.
[6] R. Broussier, A. Abdulla, B. Gautheron, *J. Organomet. Chem. 332* (1987) 165.
[7] R. E. Hollands, A. G. Osborne, I. Townsend, *Inorg. Chim. Acta 37* (1979) L541; A. G. Osborne, R. E. Hollands, J. A. K. Howard, R. F. Bryan, *J. Organomet. Chem. 205* (1981) 395.
[8] X-ray structure analyses: $[Fe_2C_{20}H_{14}(S_3)_2]$ **7a**, orthorhombic, space group $Pca2_1$ (No. 29) with a = 13.383(2), b = 11.360(3), c = 12.983(3) Å; M = 558.38, Z = 4, ϱ_{calcd} 1.879 gcm^{-3}, $\mu(Mo_{K\alpha})$ = 20.0 cm^{-1}. Philips-PW-1100, graphite-monochromator $Mo_{K\alpha}$ radiation (λ = 0.71069 Å). Absorption correction applied as described by *F. Ugozzoli* [12]. 1438 unique reflections with $2\theta < 45°$ and $|F_0| > 1\sigma(F_0)$. Structure solution carried out using Patterson methods and refinement performed with anisotropic temperature factors and with the H atoms at fixed positions; R = 0.028, $R_w(F)$ = 0.030. SHELX 76 program package used [13]. Taking into account the anormal despersion, the values given for R and $R_w(F)$ support one (A) of two possible polarities of the structure. The R values are somewhat higher for the structure of opposite polarity (B). Since, in addition, chemically equivalent bond distances in B show slightly larger variations than in A, structure A apparently describes correctly the polarity of the crystal used.
$[Fe_2C_{20}H_{14}(S_2)_2]$ (**8a**), orthorhombic, space group *Pbcn* (No. 60) with a = 15.195(4), b = 9.564(4), c = 12.682(3) Å; M = 494.26, Z = 4, ϱ_{calcd} = 1.781 gcm^{-3}, $\mu(Mo_{K\alpha})$ 19.2 cm^{-1}. X-ray measurement and absorption as for **7a**. 1561 reflections with $2\theta < 50°$ and $|F_0| > 2\sigma(F_0)$, structure solution and refinement as described above. Further details on the crystal structure investigations are available on request from the Fachinformationszentrum Karlsruhe, Gesellschaft für wissenschaftlich-technische Information mbH, W-7514 Eggenstein-Leopoldshafen 2, (FRG), on quoting the depository number CSD-55646, the names of the authors, and the journal citation.
[9] B. R. Davis, I. Bernal, *J. Cryst. Mol. Struct. 2* (1972) 107.
[10] a) Z. L. Kaluskii, R. L. Avoyan, Y. T. Struchkov, *Zh. Struct. Khim. 3* (1962) 599; *J. Struct. Chem. USSR 3* (1962) 573; b) Z. L. Kaluskii, Y. T. Struchkov, R. L. Avoyan, *Zh. Strukt. Khim. 5* (1964) 743; *J. Struct. Chem. USSR 5* (1964) 683. c) A. C. McDonald, J. Trotter, *Acta Crystallogr. 17* (1964) 872.
[11] M. Herberhold, P. Leitner, U. Thewalt, *Z. Naturforsch. B45* (1990) 1503.
[12] F. Ugozzoli, *Comput. Chem. 11* (1987) 109.
[13] G. M. Sheldrick, SHELX-Program for Crystal Structure Determination, University of Cambridge, Cambridge, England (1976)

New Routes to the Synthesis of Polymers Containing Nitrile Groups**

By *Holger Brackemann, Michael Buback,* Frank Rindfleisch,* and *Stefan Rohde*

Dedicated to Professor Karl Heinz Büchel on the occassion of his 60th birthday

Demands for specialty elastomers are constantly increasing. In particular, low temperature flexibility and heat resistance are expected and considerable emphasis is placed on improving oil and aging resistance. A high-performance elastomer[1] was obtained by selective hydrogenation of nitrile rubber (butadiene/acrylonitrile copolymer). But this type of polymer modification is costly and alternative ways of producing polymers containing only C–C single bonds in the chain with nitrile substituents should therefore be investigated.

Hydrogenated nitrile rubber is formally a terpolymer consisting of units derived from ethene, acrylonitrile, and to a small extent 1-butene.[1] A corresponding material should thus be accessible by free-radical copolymerization of ethene (E) and acrylonitrile (AN) with small amounts of 1-butene.[2] The study of E/AN copolymerization, however, showed that the initiator consumption in this reaction is unexpectedly high and that adhesive products are formed. It is presumably on these grounds that direct chemically initiated copolymerization has not yet become a technical process.

During recent years considerable progress has been achieved in the field of free-radical polymerizations induced by excimer laser light.[3] A substantial advantage in these reactions relates to initiation being "nonmaterial" which allows the production of polymer free from initiator fragments. This aspect is especially important for reactions such as the E/AN copolymerization where initiator consumption is very high. Moreover, by variation of laser pulse energy and pulse repetition frequency, excimer laser-induced polymerizations may be easily and effectively controlled.

An alternative route to products similar to fully hydrogenated nitrile rubber might proceed from macromolecules with a polymer chain exclusively consisting of C–C single bonds. Appropriate substituents on the chain may be converted to nitrile groups. Both routes are outlined in the subsequent text.

The free-radical copolymerization of ethene and acrylonitrile induced by excimer laser light (KrF-line at 248 nm) has been studied in the temperature range of 423 to 523 K at pressures up to 2900 bar.[4, 5] Apart from the suggested prospects for polymer synthesis, the excimer laser offers unique possibilities for a detailed study of free-radical polymerization kinetics.[6] The reactivity ratio for ethene, r_E, was determined to be $r_E = 3.50 \exp[-2273\ (T/K)^{-1}]$ (at a constant pressure of p = 2450 bar). Taking the experimental uncertainty into account, r_E changes from 0.016 ± 0.003 at 423 K to 0.045 ± 0.008 at 523 K. While r_E is well below unity, the corresponding value for the reactivity ratio of acrylonitrile, r_{AN}, is close to 7.5. It follows from these r_E and r_{AN} values that at about 473 K and 2450 bar a monomer mixture containing 0.5 mol % AN produces (at differential conversion) a polymer containing approximately 15 mol % acrylonitrile units which is equivalent to 25 weight %. By applying the equations for ideal copolymerization kinetics to a copolymer system such as E/AN with this appreciable difference in the reactivity ratios, one can see that the polymerization rate is considerably slowed by low acrylonitrile monomer concentrations, for example of 0.5 mol %. This is simply because a free-radical chain end to which ethene has been added in the preceding step undergoes cross-propagation preferentially since $r_E \ll 1$. The subsequent addition of another acrylonitrile molecule, which is favorable because of $r_{AN} \gg 1$, is slow because the concentration of AN is very small. In addition, the rate coefficient for homopolymerization of AN is lower than for E. In contrast to chemically initiated polymerizations, the rate of laser-induced reaction can be accelerated by enhancing initiation without introducing considerable quantities of initiator fragments into the polymer. Along these lines, laser-induced high-pressure polymerization at 523 K has produced colorless, nonadhe-

[*] Prof. Dr. M. Buback, Dr. H. Brackemann, Dipl.-Chem. F. Rindfleisch, Dipl.-Chem. S. Rohde
Institut für Physikalische Chemie der Universität
Tammannstrasse 6, W-3400 Göttingen (FRG)

[**] This work was supported by Bayer AG. We thank Dr. *W. Obrecht* for valuable help.

sive E/AN copolymers with technically relevant AN contents up to 25 weight %.[5] It is difficult to increase the AN content further in experiments with excimer lasers, because the reacting system becomes inhomogeneous. Increasing the polymerization temperature or adding a solvent may extend the homogeneous region which offers the possibility of producing copolymers with even higher acrylonitrile content. The glass transition temperature of E/AN copolymers from laser-induced experiments is about 10 °C above T_g of corresponding material from the complete hydrogenation of butadiene–acrylonitrile rubber. By performing laser-induced E/AN polymerization in the presence of small amounts of 1-butene monomer, T_g should be lowered since the crystallinity due to ethylene sequences will be further reduced.

The difference in reactivity ratios for ethene/acrylic ester (AE) systems is less than that for E/AN. Starting from ethene/acrylic ester copolymers, which are more easily accessible, it seemed rewarding to study whether the ester group in a polymer modification reaction could be transformed into a nitrile group. The number of additional components required for this process should be as small as possible. Moreover, these components should be simple and easy to remove. In line with these prerequisites, the reaction of E/AE ester copolymer in dense fluid ammonia was investigated, in which NH_3 acts as reactant, dehydration agent, and solvent. The conversion to a copolymer of E/AN type proceeds via an intermediate copolymer of ethene/acrylamide (AA) type (Scheme 1). The first step in the reaction sequence with NH_3 dissolved in xylene and also with further auxiliary agents has already been investigated.[7, 8]

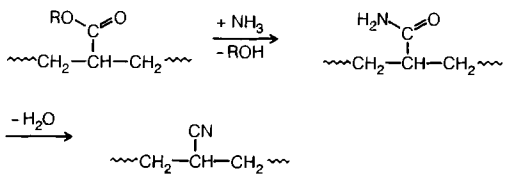

Scheme 1. Transformation of ester groups to nitrile functions in a polymer.

Polymer modification was studied at 1500 bar at temperatures between 448 and 523 K on ethene/butyl acrylate (BA) copolymer containing 7.8 mol % BA. At 523 K additional experiments were performed at 200 and 700 bar. Ammonia was employed in large excess. The ratio of NH_3 to BA groups at the beginning of the reaction was approximately 200 : 1. At specific reaction times the polymeric product was collected and the concentration of amide and nitrile functional groups was determined by IR analysis on polymer films. The concentration of ester groups in the polymeric material was obtained from the difference between the spectroscopically determined AA and AN concentrations and the known total concentration of functional groups. The spectroscopic determination was verified by elemental analysis. The IR analysis provides no indication of intra- or intermolecular reactions between polymeric functional groups. In preliminary tests, fully hydrogenated butadiene/acrylonitrile rubber with 34.9 mol % AN was kept in fluid ammonia at 523 K and 1500 bar for 24 hours. The IR spectra of polymer before and after this experiment did not indicate any reaction between nitrile groups.

In Figure 1 the fraction X of functional groups within the polymer (with $X = 100$ % referring to the absolute concentration of 7.8 mol % BA in the initial E/BA copolymer) is plotted versus reaction time for several reactions at 523 K and 1500 bar. The ester group (BA) reacts relatively rapidly.

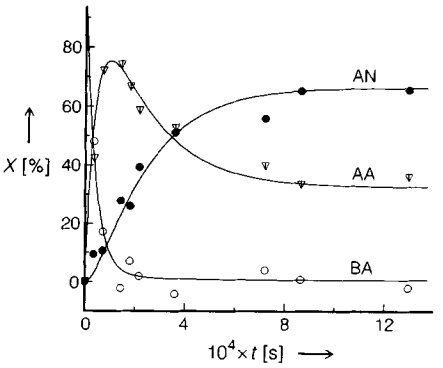

Fig. 1. Dependence of the fraction X of ester (BA), amide (AA), and nitrile (AN) functional groups in ethene/butyl acrylate copolymer (7.8 mol % BA) on reaction time t for polymer modification reactions with pure fluid ammonia at 523 K and 1500 bar. ($X = 100$ % refers to the total content of 7.8 mol % of functional groups.)

The amide group (AA) concentration passes through a pronounced maximum after a reaction time of about 3 hours and reaches a constant value at longer reaction times, as does the concentration of nitrile groups (AN). In the experiments at 523 K and 1500 bar the fraction of AN groups reaches a maximum value of about 70 %. Figure 2 shows corresponding data for 523 K and 200 bar. The intermediate maximum in AA concentration is less pronounced. In marked contrast to the reaction at 1500 bar (Fig. 1), the polymeric material contains ester groups in addition to nitrile and amide functional groups, even after long reaction times. The data in Figures 1 and 2 suggest that the polymer modification reaction should be treated as a consecutive-type reaction in which both steps are reversible.

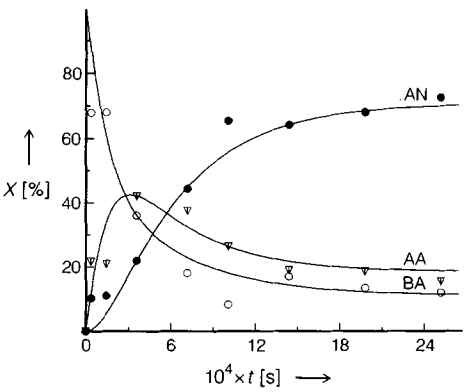

Fig. 2. Dependence of the fraction X of ester (BA), amide (AA), and nitrile (AN) functional groups in ethene/butyl acrylate copolymer (7.8 mol % BA) on reaction time t for polymer modification reactions with pure fluid ammonia at 523 K and 200 bar. ($X = 100$ % refers to the total content of 7.8 mol % of functional groups.)

The notations "ester (BA)", "amide", and "nitrile" in Scheme 2 denote the functional groups of the polymer. An analytical solution for this kinetic scheme is not available. Thus rate coefficients k_1 to k_4 are determined with an iterative computer program. The results are presented in Table 1. The forward reaction from ester to amide groups is treated

$$\text{ester (BA)} + NH_3 \underset{k_2}{\overset{k_1}{\rightleftharpoons}} \text{amide} + \text{butanol} \underset{k_3}{\overset{k_3}{\rightleftharpoons}} \text{nitrile} + H_2O$$

Scheme 2.

Table 1. Rate coefficients k of the polymer modification reaction of ethene/butyl acrylate copolymer (7.8 mol % BA) in dense fluid ammonia. The rate coefficients are assigned according to Scheme 2. (Mol % in k_2 and in k_4 refers to the concentration of amide and of nitrile functional groups in the polymer, respectively. The concentrations of the low molecular weight reactants, butanol and water, are determined, since only E/BA copolymer and pure NH_3 are employed in the experiments).

T [K]	p [bar]	$10^{-5} \times k_1$ [s^{-1}]	$10^{-5} \times k_2$ [s^{-1}(mol %)$^{-1}$]	$10^{-5} \times k_3$ [s^{-1}]	$10^{-5} \times k_4$ [s^{-1}(mol %)$^{-1}$]
448	1500	0.56	–	0.08	0.06
473	1500	2.87	–	0.30	0.18
498	1500	9.11	–	0.76	0.19
523	1500	24.30	–	2.66	0.25
523	700	6.48	0.65	3.70	0.21
523	200	3.66	0.32	1.92	0.09

as a pseudo-first-order reaction, as NH_3 is present in a large excess.

In the experiments up to 1500 bar, k_2 is too small to be reliably determined. The accuracy is assumed to be ± 10 % for k_1 and k_3 and ± 15 % for k_2 and k_4. Arrhenius plots for k_1 and k_3 are given in Figure 3. The data are well represented by a straight line. The activation energies (1500 bar) are 98 ± 9 kJ mol^{-1} for the ester to amide reaction (k_1), and 87 ± 8 kJ mol^{-1} for the amide to nitrile reaction (k_3). These values suggest that the reaction takes place in a homogeneous fluid phase. From the pressure dependence of k_1 an activation volume of $\Delta V^{\neq}(k_1) = -63 \pm 12$ cm^3 mol^{-1} is obtained. From the presently available experimental data activation energies for k_2 and k_4 and activation volumes for k_2, k_3, and k_4 cannot be determined to an accuracy of better than ± 40 %.

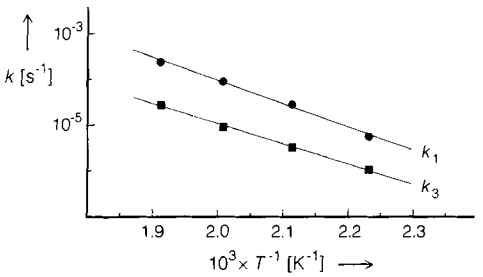

Fig. 3. Temperature dependence of the rate coefficients k_1 and k_3 (see Scheme 2).

The curves in Figures 1 and 2 have been calculated using the rate coefficients in Table 1. Based on the activation parameters, X–t diagrams may also be estimated for other temperatures and pressures. These data reveal the reaction time t after which the modification reaction has to be stopped in order to achieve a certain fraction of ester, amide, and nitrile groups (at fixed ethylene content). Moreover, the kinetic scheme allows an estimation of the reaction temperatures and pressure which are required to achieve a desired composition of functional groups (for high values of reaction time t). Because of the reversibility of all reaction steps (Scheme 2) polymers which have a broad distribution in the concentration of ester, amide, and nitrile groups can be converted into a chemically more uniform material.

With respect to the synthesis of polymers containing only nitrile functional groups, the results suggest that reaction be conducted in a countercurrent of pure fluid NH_3 or with the continuous removal of water from the system. As is to be expected, treating the product of a polymer modification reaction a second time with fluid ammonia increases the content of nitrile groups. But for technical purposes, the reaction times are too long (Figure 1 and 2). The modification reaction should thus be accelerated by applying still higher temperature or by using catalysts. The reaction rate should also increase when ethene/acrylic ester copolymers with an ester group smaller than in BA are employed.

In further experiments the modification reaction with fluid ammonia will be studied for ethene/acrylic ester compounds with higher ester content. In addition, larger quantities of polymeric material should be produced to enable a comprehensive characterization of product properties.

Received: June 20, 1991 [Z4735 IE]
Publication delayed on authors' request
German version: *Angew. Chem. 103* (1991) 1722

[1] W. Obrecht, H. Buding, U. Eisele, Z. Szentivanyi, J. Thörmer, *Angew. Makromol. Chem. 145/146* (1986) 161.
[2] R. E. Uschold, J. B. Finlay, *Appl. Polym. Symp. 25* (1974) 205.
[3] M. Buback, B. Huckestein, U. Leinhos, *Makromol. Chem. Rapid Commun. 8* (1987) 473; M. Buback, *Chem. Industrie, Düsseldorf 8* (1988) 44.
[4] H. Brackemann, M. Buback, Makromol. *Chem. 190* (1989) 3073; *Makromol. Chem. Rapid Commun. 10* (1989) 283.
[5] H. Brackemann, *Dissertation*, Göttingen 1989.
[6] M. Buback, J. Schweer, *Z. Phys. Chem. (Munich) 161* (1989) 153; M. Buback, B. Degener, B. Huckestein, *Makromol. Chem. Rapid Commun. 10* (1989) 311; M. Buback, *Makromol. Chem. 191* (1990) 1575.
[7] H. D. Anspon, US 3337517 (1967), Gulf Research & Development Company.
[8] G. Beau de Lomene, A. Armenaud, G. Houssard, J.-F. Boissel, M. de Haas, FR 1501193 (1967), Gulf Oil Corporation.

The X-ray Crystal Structure Analysis of a Fragmentable *N*-Acylpyridinium Ion**

By *Christian Lohse, Sandro Hollenstein,* and *Thomas Laube**

The catalytic effect of pyridines in acylation reactions is explained by the formation of an intermediate *N*-acylpyridinium ion **1**, which then undergoes nucleophilic attack by an alcohol or amine (Einhorn method, a variant of the Schotten–Baumann reaction).[1] The existence of this type of ion has been proven by NMR spectroscopy by *Olah* et al.[2] and by crystal structure analysis by *Jones* et al.[3] The molecular structure and crystal packing of **2**-BF_4 reported here allow conclusions regarding charge delocalization and the

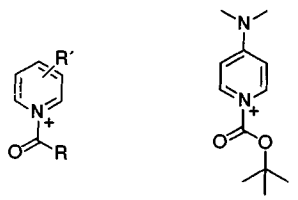

1 **2**

[*] Priv.-Doz. Dr. T. Laube, Dipl.-Chem. C. Lohse, Dipl.-Chem. S. Hollenstein
Laboratorium für Organische Chemie
der Eidgenössischen Technischen Hochschule
ETH-Zentrum, Universitätstrasse 16
CH-8092 Zürich (Switzerland)

[**] From the Diplomarbeit of *C. L.* This work was supported by the Schweizerischer Nationalfonds zur Förderung der wissenschaftlichen Forschung and the Fonds der Chemischen Industrie (Dozentenstipendium for *T. L.*).

two main reactions of **2**, namely, nucleophilic attack on the carbonyl C atom and fragmentation.

We attempted to obtain suitable crystals of several salts with cation **1** for X-ray structural analysis. *N*-Boc-4-dimethylaminopyridinium-tetrafluoroborate (**2**-BF_4), a reagent used for the transfer of Boc groups (Boc = *tert*-butoxycarbonyl), was prepared by the method of *Guibé-Jampel* and *Wakselman*.[4] Crystallization of **2**-BF_4 by isothermal distillation with acetonitrile/ether at room temperature led to partial decomposition, presumably to 4-dimethylaminopyridinium-tetrafluoroborate, producing crystals of **2**-BF_4 and the decomposition product.

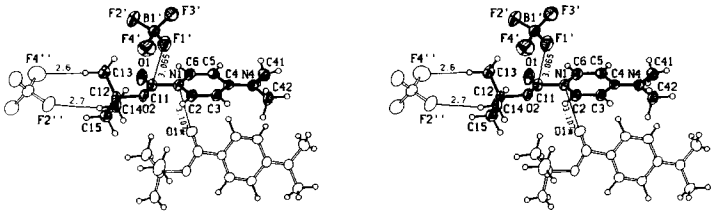

Fig. 1. ORTEP stereoview of the structure of **2**-BF_4 in the crystal. The ellipsoids are drawn at 50% probability; the H atoms are represented by spheres with a radius of 0.1 Å. One ion pair forms the asymmetric unit. Symmetry operations: ′ = $1-x, 2-y, -z$; ″ = $x-1, y, z-1$, * = $x, 1.5-y, z+0.5$.

Figure 1 shows the crystal structure of **2**-BF_4.[5] In cation **2**, which formally contains a urethane fragment, the carbonyl group, pyridine ring, and dimethylamino group are almost coplanar, making π interactions possible (see Table 1). The *tert*-butyl ester fragment, O1=C11−O2−*t*Bu,

Table 1. Selected distances [Å], angles, and torsion angles [°] for crystalline **2**-BF_4.

C11-N1 1.463(5)	C11-O1 1.191(5)	C11-O2 1.293(5)
O2-C12 1.523(5)	N1-C2 1.367(5)	C2-C3 1.347(5)
C3-C4 1.413(5)	C4-C5 1.421(6)	C5-C6 1.347(6)
C6-N1 1.351(5)	C4-N4 1.346(5)	
O1-C11-N1 119.6(4)	C11-O2-C12 121.1(3)	C11-N1-C2 122.3(4)
O1-C11-O2 130.9(4)	O2-C12-C13 109.7(3)	C11-N1-C6 118.1(4)
N1-C11-02 109.5(4)	O2-C12-C14 100.4(3)	C2-N1-C6 119.6(4)
	O2-C12-C15 108.0(4)	
O1-C11-O2-C12 − 2.5(7)	O1-C11-N1-C2 − 176.7(4)	C3-C4-N4-C41 + 179.9(5)
C11-O2-C12-C13 − 50.9(5)	O1-C11-N1-C6 + 3.0(6)	C3-C4-N4-C42 + 4.1(6)
C11-O2-C12-C14 − 167.6(4)	O2-C11-N1-C2 + 3.3(6)	C5-C4-N4-C41 − 0.9(7)
C11-O2-C12-C15 + 73.0(5)	O2-C11-N1-C6 − 177.0(4)	C5-C4-N4-C42 − 176.7(4)

displays the conformation typical for such esters.[6] The bond lengths in the pyridine ring of **2** systematically deviate from those of 4-dimethylaminopyridine.[7] In **2** the bonds N1−C2, N1−C6, C3−C4, and C2−C5 are 0.031(5), 0.015(5), 0.009(5), and 0.017(5) Å longer, while the bonds C2−C3, C5−C6, and C4−N4 are shorter by 0.031(5), 0.032(6), and 0.021(5) Å. These differences suggest a charge delocalization in the π system in accordance with the resonance structure **2′**.[8]

The deviations in the urethane-like part of **2** are more evident if one refers to the mean bond lengths of four *O-tert*-butylurethanes substituted on nitrogen with two sp^2 C atoms.[9] The N1−C11 and O2−C12 distances are 0.055(8) and 0.035(9) Å longer; the C11−O2 distance, 0.025(6) Å shorter; and the O1−C11−O2 angle, 4.3(6)° larger than expected. These deviations could be interpreted as proof of the contribution of resonance structures **2″** and **2′** to the overall description of **2**. This corresponds to a conjugation in the σ system (second-order hyperconjugation). These deviations are also in keeping with the reactions of **2**: the Boc group is easily transferred and under suitable conditions fragments to CO_2 and isobutylene.[10]

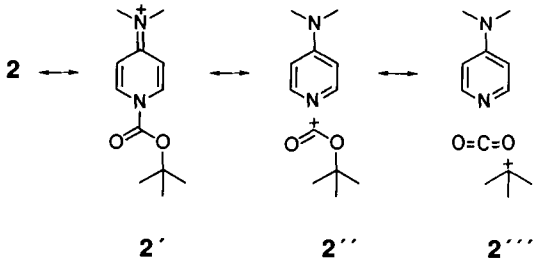

The counterion drawn with primed atom labels (Fig. 1) is in a favorable position for nucleophilic attack on C11 in the course of an acylation reaction.[11–13] The distance between C11 and F1′ is 3.065(5) Å (i.e. 0.085 Å less than the sum of the van der Waals radii); the O1=C11···F1′ angle is 109.1(3)°. The other face of the carbonyl C atom does not interact with a potential nucleophile. However, a carbonyl O atom, O1*, from another cation appears to have a purely electrostatic interaction with N1 (N1···O1* = 3.107(5) Å). In the crystal the *tert*-butyl group is surrounded by four BF_4 ions (shortest H···F distance, H132···F2′ = 2.5 Å). One of these anions is in a position favorable for the deprotonation of the *tert*-butyl group (antiperiplanar arrangement of N1−C11, O2−C12, and C−H; H143···F2″ = 2.7 Å; H133···F4″ = 2.6 Å). Thus **2** can be viewed as a model for **1**, and as a further example of hyperconjugation[14,15] and the correlation between chemical reactivity and crystal packing.[13]

Received: July 23, 1991 [Z4820 IE]
German version: *Angew. Chem. 103* (1991) 1678

CAS Registry number:
2, 65422-03-9.

[1] G. Höfle, W. Steglich, H. Vorbrüggen, *Angew. Chem. 90* (1978) 602–615; *Angew. Chem. Int. Ed. Engl. 17* (1978) 569.
[2] G. A. Olah, P. J. Szilagyi, *J. Am. Chem. Soc. 91* (1969) 2949–2955.
[3] P. G. Jones, K. Linoh, A. Blaschette, *Z. Naturforsch. B45* (1990) 267–270.
[4] E. Guibé-Jampel, M. Wakselman, *Synthesis 1977*, 772.
[5] Enraf-Nonius CAD4 diffractometer, $Mo_{K\alpha}$ radiation, graphite monochromator, measured at −30°C, space group $P2_1/c$, $a = 12.196(3)$, $b = 15.98(1)$, $c = 7.91(2)$ Å, $\beta = 106.8(4)°$, $V = 1477(4)$ Å^3; $\rho_{calc} = 1.395\ g\,cm^{-3}$, $Z = 4$, 2982 measured reflections with $\theta > 25°$, of these 1285 with $I > 3\,\sigma_I$. The structure was solved by direct methods (SHELXS-86, G. Sheldrick, Universität Göttingen, FRG, 1986) and refined with the full-matrix method first using unit weights, then with $w = \sigma_F^{-2}$ (SHELX-76, G. Sheldrick, University of Cambridge, UK, 1976), whereby the H atoms on C5, C14, and C41 were left free and all others were refined riding on their heavy atoms (H atoms on C42 with fixed $U = 0.08$ Å^2; 227 parameters, 5.7 reflections per parameter) : $R = 0.048$, $R_w = 0.043$. The graphics were prepared with ORTEP-II (C. K. Johnson, Oak Ridge National Laboratory, TN, USA, 1976). Further details of the crystal structure investigation may be requested from the director of the Cambridge Crystallographic Data Centre, University Chemical Laboratory, Lensfield Road, GB-Cambridge CB2 1EW on quoting the complete journal citation.
[6] W. B. Schweizer, J. D. Dunitz, *Helv. Chim. Acta 65* (1982) 1547–1554.
[7] U. Ohms, H. Guth, *Z. Kristallogr. 166* (1984) 213–217. Here we used the parameters obtained by averaging according in the C_{2v} symmetry.
[8] Other dimethylaminopyridinium ions display similar deviations; see for example S. G. DiMagno, K. C. Waterman, D. V. Speer, A. Streitwieser, *J. Am. Chem. Soc. 113* (1991) 4679–4681; S. Munavelli, E. J. Poziomek, C. S. Day, *Acta Crystallogr. Sect. C44* (1988) 272–275; M. Chao, E. Schempp, R. D. Rosenstein, *Acta Crystallogr. Sect. B33* (1977) 1820–1823.

[9] A. I. Meyers, D. G. Wettlaufer, *J. Am. Chem. Soc. 106* (1984) 1135–1136; D. Dhanak, S. Neidle, C. B. Reese, *Tetrahedron Lett. 26* (1985) 2017–2020; J. Symersky, P. Malon, L. Grehn, U. Ragnarsson, *Acta Crystallogr. Sect. A 46* (1990) 683–686.

[10] In Cambridge File (F. H. Allen, O. Kennard, R. Taylor, *Acc. Chem. Res. 16* (1983) 146–153) one finds another urethane similar to **2** (1-Boc-5-brom-2-methyl-4-nitro-1*H*-imidazol; J. D. Albright, D. B. Moran, *J. Heterocycl. Chem. 23* (1986) 913–919). This molecule may possibly dissociate heterolytically similar **2**. For a reference on the reactivity of heterocyclic amides see H. A. Staab, *Angew. Chem. 74* (1962) 407–432; *Angew. Chem. Int. Ed. Engl. 1* (1962) 351.

[11] C11 is planar-coordinated within the units of accuracy for measurement. (Sum of the angles is 360°).

[12] H. B. Bürgi, J. D. Dunitz, *Acc. Chem. Res. 16* (1983) 153–161.

[13] For other examples of interactions between carbocations and counter ions see T. Laube, *J. Am. Chem. Soc. 111* (1989) 9224–9232.

[14] T. Laube, *Angew. Chem. 98* (1986) 368–369; *Angew. Chem. Int. Ed. Engl. 25* (1986) 349–350.

[15] The σ conjugation observed here can be considered a further stereoelectronic effect in esters of the special type X–COOR (X = leaving group).

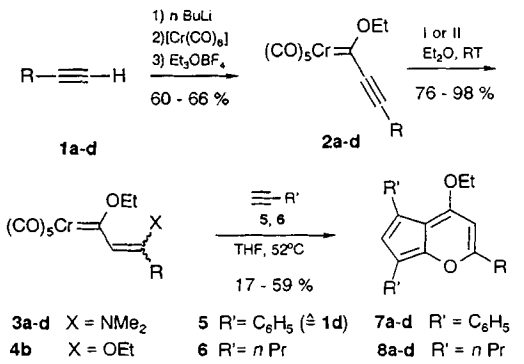

Scheme 1. Cyclopenta[*b*]pyrans **7** and **8** from 2-alkynylidenechromium complexes **2** (see Table 1 for yields). I: $HNMe_2$, 5 s; II: 5% EtONa/EtOH, 10 s. **1–8**: R = C_3H_5OEt (**a**), $C(CH_3)_2OEt$ (**b**), *t*-C_4H_9 (**c**), C_6H_5 (**d**). RT = room temperature.

Double Insertion of Alkynes into Chromium–Carbon Bonds of β-Donor-Substituted Vinylcarbene Complexes of Chromium—A Simple Route to Cyclopenta[*b*]pyrans*

By *Frank Stein, Michael Duetsch, Rolf Lackmann, Mathias Noltemeyer,* and *Armin de Meijere**

Dedicated to Professor Karl Heinz Büchel on the occasion of his 60th birthday

Fischer carbene complexes have now found application in preparative organic chemistry.[1] Of particular interest is the cycloaddition of α,β-unsaturated Fischer carbene complexes to alkynes, the so-called Dötz reaction, which, in the case of 1-alkoxycarbene complexes, leads to phenol or cyclohexadienone derivatives.[2] There have been numerous reports on the synthesis and chemical behavior of β-donor-substituted Fischer carbene complexes,[3] but not on their reactions with alkynes. We recently described the unusual behavior of β-(dimethylamino)vinylcarbene complexes of chromium on treatment with alkynes;[4] these complexes were easily obtained in excellent yields by Michael addition of dimethylamine to alkylvinylcarbene complexes. The cyclopentadiene products were obtained in good yields, however, only if a cyclopropyl substituent was also present at the β position. To determine whether the donor character of the cyclopropyl group exerts a significant effect in these reactions, we have now prepared the corresponding complex **3a** with a 1′-ethoxycyclopropyl group.

Compound **2a** was obtained in the usual way[3a, 5] from an alkyne[6] and hexacarbonylchromium followed by alkylation. Complex **3a** was then prepared in good yield by addition of dimethylamine to **2a** (Scheme 1). Surprisingly, reaction of **3a** with phenylacetylene (**5**) gave neither the corresponding cyclopentadiene[4] nor the expected cyclohexadienone product of the Dötz reaction.[2] Instead, a dark red solid was isolated in 17% yield. ^1H, ^{13}C NMR, and IR spectroscopy, as well as mass spectrometry, revealed that the product could only have arisen by incorporation of two alkyne molecules and a carbonyl ligand, and elimination of dimethylamine. An X-ray structure analysis established the identity of the product as the cyclopenta[*b*]pyran **7a** (Fig. 1).[7] Compound **7a** is a so-called pseudoazulene, a heterobicycle isoelectronic to azulene.[7, 8] Its skeleton deviates only slightly from planarity, the two rings forming an angle of 3.7°.

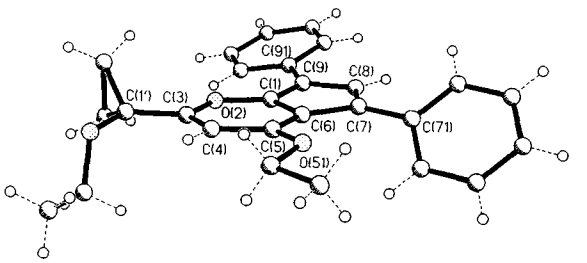

Fig. 1. Molecular structure of **7a** (SCHAKAL drawing)[9]. Important bond lengths [pm]: C(1)-O(2) 137.4(2), C(1)-C(6) 143.7(2), C(1)-C(9) 137.6(2), O(2)-C(3) 134.8(2), C(3)-C(4) 135.1(2), C(3)-C(1′) 148.3(2), C(4)-C(5) 142.0(2), C(5)-C(6) 138.0(2), C(5)-O(51) 133.7(2), C(6)-C(7) 144.7(2), C(7)-C(8) 138.0(3), C(7)-C(71) 147.5(2), C(8)-C(9) 143.7(2), C(9)-C(91) 146.5(3); angle between the planes C(1)-O(2)-C(3)-C(4)-C(5)-C(6) and C(1)-C(6)-C(7)-C(8)-C(9) 3.7°. The dotted atoms are oxygen atoms.

When an eightfold excess of alkyne **5** was used, **7a** could be obtained from **3a** in a yield of 41%. Since such pseudoazulenes, despite intensive research, were previously only accessible by multistep syntheses with in part strongly limited substitution patterns and/or in low yields,[7, 8] we examined whether this synthetic route could be generalized with respect to the alkynes employed, **1a–d**, as well as **5** and **6** (Scheme 1).

Indeed, the cyclopenta[*b*]pyrans **7b–d** and **8a–d** are also formed in the reaction of (β-dimethylaminovinyl)carbenechromium complexes **3a–d** with phenylacetylene (**5**) and with 1-pentyne (**6**). The best yields are obtained with complex **3b**, which contains a (2′-ethoxyprop-2′-yl) group and is particularly easy to prepare (see Table 1). In contrast to 2-cyclopropyl-substituted (2-ethoxyvinylcarbene) chromium complexes,[10] the ethanol adduct obtained from **2b** and **5** also reacts to give **7b**, albeit in lower yield. Accord-

[*] Prof. Dr. A. de Meijere, Dipl.-Chem. F. Stein, Dipl.-Chem. M. Duetsch
Institut für Organische Chemie der Universität
Tammannstrasse 2, W-3400 Göttingen (FRG)
Dr. R. Lackmann
Institut für Organische Chemie der Universität Hamburg (FRG)
Dr. M. Noltemeyer [+]
Institut für Anorganische Chemie der Universität Göttingen (FRG)

[+] Crystal structure analysis

[**] This work was supported by the Volkswagen-Stiftung and the Fonds der Chemischen Industrie. We thank Hoechst AG and Hüls AG for donations of chemicals. *R. L.* and *M. D.* thank the Studienstiftung des Deutschen Volkes and the Deutsche Forschungsgemeinschaft (Graduiertenkolleg: Kinetics and Selectivity of Chemical Processes in Dense, Liquid Phase), respectively, for doctoral fellowships.

ingly, only the quaternary group and the hetero substituent in the β position are responsible for the formation of cyclopenta[*b*]pyrans.

Table 1. Michael additions of $HNMe_2$ and HOEt to (alkynylethoxymethylene)chromium complexes **2** and reaction of 3-donor-substituted 1-chroma-2-ethoxydienes **3** and **4**[11] to give cyclopenta[*b*]pyrans **7** and **8**.

Starting complex	R	Michael adduct	X	Yield [%]	R'	Cyclopenta[*b*]-pyran	Yield [%]
2a		**3a**	NMe_2	95	Ph	**7a**	41
					*n*Pr	**8a**	17
2b	$C(CH_3)_2OEt$	**3b**	NMe_2	80	Ph	**7b**	51
					*n*Pr	**8b**	59 [a]
2c	*t*Bu	**3c**	NMe_2	84	Ph	**7c**	52
					*n*Pr	**8c**	43
2d [3a]	Ph	**3d** [3b]	NMe_2	86	Ph	**7d**	24
					*n*Pr	**8d**	19
2b	$C(CH_3)_2OEt$	**4b**	OEt	76	Ph	**7b**	27

[a] Yield after isolation: 66 %.

The mechanism of formation of **7** and **8** undoubtedly involves as the last step a 1,4 elimination of dimethylamine and ethanol, respectively, from the dihydro derivative **9**, which is presumably formed from a (trienylketene)tricarbonylchromium complex, **10**, by intramolecular [4 + 2] cycloaddition. Complex **10** results from CO insertion into a 1-chroma-(2 *Z*,4 *Z*)-octatetraene, **11**, which is formed, in turn, by double insertion of alkyne **5** or **6** into the chromium–carbon bond of **3** or **4**, respectively. The first insertion presumably leads primarily to (*Z*)-**12**, since otherwise, CO insertion and subsequent cyclization to the cyclohexadienone[12] could occur at this stage. The *Z* configuration of the newly formed

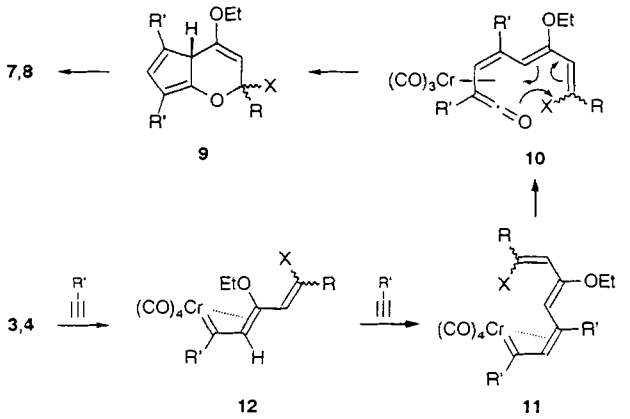

Scheme 2. Proposed mechanism for the formation of cyclopenta[b]pyrans **7** and **8** from **3** and **4**, respectively.

double bond in (*Z*)-**12** is probably due to the steric demand of the R group in 1-chroma-1,3-diene **3** or **4**, which, for *Z* configuration of the 3,4 double bond and assumed coplanarity, strives to attain the greatest possible separation from the 4-ethoxy group or the 3-H, respectively. NOE measurements[12] on **3b** established a *Z* configuration for the 3,4 double bond, whereas the dimethylamine and the ethanol adducts with (cyclopropylethynyl)pentacarbonylchromium complexes[4] exhibit *E* configurations. On the other hand, the ethanol adduct **4b**, prepared from **2b**, was obtained as an *E*/*Z* mixture (*E*/*Z* = 1.5:1).

Comparison of the absorption bands in the UV spectra of **7a** and **8a** with those of carbocyclic analogues is possible only qualitatively, since the correspondingly substituted azulenes are unknown. The spectra of **7a** and **8a**, however, are very similar to those of known pseudoazulenes:[8d-f] strong absorptions are observed at λ_{max} (log ε) = 204 (4.55), 233 (4.50), and 308 (4.53) for **7a** and 220 (4.22), 262 (3.98), and 3.41 (3.80) for **8a** and a very broad band is found in the visible region with a maximum at 484 (3.02) and 455 (2.52), respectively.

Table 2. Spectroscopic data for **3b** and **7b**[11].

3b: ^1H NMR (200 MHz, C_6D_6, also 1 D NOE): δ = 0.83 (t, ^3J = 7.0 Hz, 3 H; OCH_2CH_3), 1.02 (t, ^3J = 7.0 Hz, 3 H; OCH_2CH_3), 1.17 (s, 6 H; CH_3, {2-H}-CH_3 (+ 9.8 %)), 2.58 (s, 6 H; $N(CH_3)_2$), 2.76 (q, ^3J = 7.0 Hz, 2 H; OCH_2), 4.58 (q, ^3J = 7.0 Hz, 2 H; OCH_2), 6.32 (s, 1 H; 2-H). ^{13}C NMR (62.896 MHz, C_6D_6, DEPT): δ = 15.69 (+, OCH_2CH_3), 15.75 (+, OCH_2CH_3), 26.62 (+, CH_3), 45.08 (+, $N(CH_3)_2$), 59.02 (−, OCH_2), 72.76 (−, OCH_2), 78.74 (C_{quat}, $C(CH_3)_2$), 115.88 (C_{quat}, C-2), 165.71 (C_{quat}, C-3), 220.50, 224.55 (C_{quat}, C=O), 276.51 (C_{quat}, C-1). MS (EI, 70 eV): *m*/*z* 405 ($M^{\oplus}$, 3 %), 377 ($M-CO^{\oplus}$, 4 %), 349 ($M-2CO^{\oplus}$, 6 %), 321 ($M-3CO^{\oplus}$, 27 %), 293 ($M-4CO^{\oplus}$, 4 %), 265 ($M-5CO^{\oplus}$, 32 %), 177 (80 %), 124 (100 %), 52 ($Cr^{\oplus}$, 74 %). Correct C,H analysis.

7b: ^1H NMR (250 MHz, $CDCl_3$): δ = 1.25 (t, ^3J = 7.0 Hz, 3 H; OCH_2CH_3), 1.49 (t, ^3J = 7.0 Hz, 3 H; OCH_2CH_3), 1.66 (s, 6 H; $C(CH_3)_2$), 3.43 (q, ^3J = 7.0 Hz, 2 H; OCH_2), 4.28 (q, ^3J = 7.0 Hz, 2 H; OCH_2), 6.57 (s, 1 H; 6-H), 7.06–7.25 (m, 2 H; *para*-phenyl H), 7.28–7.48 (m, 4 H; *meta*-phenyl H), 7.38 (s, 1 H; 3-H), 7.60–7.69 (m, 2 H; *ortho*-phenyl H), 7.83–7.92 (m, 2 H; *ortho*-phenyl H). ^{13}C NMR (62.896 MHz, C_6D_6, DEPT): δ = 14.47 (+, OCH_2CH_3), 15.91 (+, OCH_2CH_3), 26.27 (+, CH_3), 59.09 (−, OCH_2), 64.95 (OCH_2), 76.72 (C_{quat}, $C(CH_3)_2$), 91.52 (+, C-6), 107.70 (C_{quat}), 108.78 (C_{quat}), 117.16 (C_{quat}), 124.23 (+, *para*-phenyl C), 124.74 (+, C-3), 124.85 (+, *para*-phenyl C), 125.40 (+, *meta*-phenyl C), 127.40 (+, *meta*-phenyl C), 128.54 (+, *ortho*-phenyl C), 129.20 (+, *ortho*-phenyl C), 135.64 (C_{quat}, phenyl C), 138.44 (C_{quat}, phenyl C), 148 (C_{quat}), 160.58 (C_{quat}), 168.10 (C_{quat}). MS (EI, 70 eV): *m*/*z* 400 ($M^{\oplus}$, 100 %), 372 ($M-C_2H_4^{\oplus}$, 26 %), 356 (9 %), 338 (18 %), 298 (8 %), 286 (10 %), 259 (22 %), 202 (11 %), 129 (22 %), 111 (7 %), 85 (7 %), 69 (4 %), 59 (13 %), 55 ($C_3H_3O^{\oplus}$, 6 %), 44 (14 %). Calculated for *m*/*z* ($M^{\oplus}$) 400.2038, found 400.2038.

Experimental Procedure

4-Ethoxy-2-(2′-ethoxyprop-2′-yl)-5,7-di-*n*-propylcyclopenta[*b*]pyran (**8b**): A solution of **3b** (304 mg, 0.75 mmol) and 1-pentyne (**6**; 410 mg, 6 mmol) in 15 mL of tetrahydrofuran was heated in a sealed Pyrex flask for 7 d at 52 °C. The reaction mixture was then filtered, the filtrate was concentrated to dryness, and the residue was chromatographed on 50 g of silica gel (pentane/diethyl ether 1:1, R_F = 0.66); 148 mg (59 %) of **8b** was obtained as red crystals, m.p. 132 °C; 28 mg (9 %) of the starting compound was recovered. The spectroscopic data for **3b** and **7b** are summarized in Table 2.

Received: June 7, 1991 [Z 4684 IE]
German version: *Angew. Chem. 103* (1991) 1669

CAS Registry numbers:
2a, 137124-98-2; **2b**, 137124-99-3; **2c**, 136918-95-1; **2d**, 36009-07-1; (*E*)-**3a**, 137124-95-9; (*Z*)-**3b**, 137124-96-0; **3c**, 137173-23-0; **3d**, 60349-49-7; (*E*)-**4b**, 137124-97-1; (*Z*)-**4b**, 137173-24-1; **5**, 536-74-3; **6**, 627-19-0; **7a**, 137124-87-9; **7b**, 137124-89-1; **7c**, 137124-91-5; **7d**, 137124-93-7; **8a**, 137124-88-0; **8b**, 137124-90-4; **8c**, 137124-92-6; **8d**, 137124-94-8.

[1] Reviews: a) K. H. Dötz, H. Fischer, P. Hofmann, F. R. Kreissl, U. Schubert, K. Weiss, *Transition Metal Carbene Complexes*, VCH, Weinheim 1983; b) K. H. Dötz, *Angew. Chem. 96* (1984) 573; *Angew. Chem. Int. Ed. Engl. 23* (1984) 587; c) W. D. Wulff, P.-C. Tang, K. S. Chan, J. S. McCallum, D. C. Yang, S. R. Gilbertson, *Tetrahedron 41* (1985) 5813; d) K.-S. Chan, G. A. Peterson, T. A. Brandvold, K. L. Faron, C. A. Challener, C. Hyldahl, W. D. Wulff, *J. Organomet. Chem. 334* (1987) 9; e) K. H. Dötz in A. de Meijere, H. tom Dieck (Eds.): *Organometallics in Organic Synthesis: Aspects of a modern Interdisciplinary Field*, Springer, Berlin 1988.

[2] a) K. H. Dötz, *Angew. Chem. 87* (1975) 672; *Angew. Chem. Int. Ed. Engl. 14* (1975) 644; b) K. H. Dötz, R. Dietz, A. von Imhof, H. Lorenz, G. Huttner, *Chem. Ber. 109* (1976) 2033; c) P.-C. Tang, W. D. Wulff, *J. Am. Chem. Soc. 106* (1984) 1132.

[3] a) E. O. Fischer, F. R. Kreissl, *J. Organomet. Chem. 35* (1972) C47; b) E. O. Fischer, H. J. Kalder, *ibid. 131* (1977) 57; c) R. Aumann, P. Hinter-

ding, *Chem. Ber. 123* (1990) 611; d) R. Aumann, P. Hinterding, C. Krüger, P. Betz, *ibid. 123* (1990) 1847; e) R. Aumann, P. Hinterding, *ibid. 123* (1990) 2047; f) L. Lattuada, E. Licandro, A. Papagni, S. Maiorana, A. C. Villa, C. Guastini, *J. Chem. Soc. Chem. Commun. 1988*, 1092.
[4] M. Duetsch, R. Lackmann, F. Stein, A. de Meijere, *Synlett 1991*, 324.
[5] E. O. Fischer, U. Schubert, W. Kleine, H. Fischer, *Inorg. Synth. 19* (1979) 164.
[6] H. C. Militzer, A. de Meijere, unpublished results; H. C. Militzer, *Dissertation*, Universität Hamburg 1990.
[7] To our knowledge, this is the first crystal structure analysis of a cyclopenta[*b*]pyran. The structure of a cyclopenta[*b*]thiapyran has been reported: Y. Hasegawa, Y. Kai, K. Miki, N. Tanka, N. Kasai, *Tetrahedron Lett. 22* (1981) 3065.
[8] a) G. V. Boyd, F. W. Clark, *J. Chem. Soc. (C) 1966*, 860; b) R. Matusch, K. Hartke, *Chem. Ber. 105* (1972) 2594; c) Y. Aso, M. Iyoda, S. Fujisawa, S. Yamaguchi, M. Nakagawa, *Tetrahedron Lett. 22* (1981) 3061; d) M. Iyoda, Y. Aso, M. Nakagawa, *Heterocycles 18* (1982) 137; e) H.-J. Timpe, A. V. El'cov, N. I. Rtiscev, *Chimia 28* (1974) 657; f) A. Olszowski, *Chem. Phys. Lett. 73* (1980) 256.
[9] Triclinic crystals of space group $P\bar{1}$, $Z = 2$, $a = 898.6(5)$, $b = 1106.9(7)$, $c = 1142.6(7)$ pm, $\alpha = 103.88(6)$, $\beta = 93.50(4)$, $\gamma = 98.26(4)°$, $\varrho_{calcd} = 1.22\ g\,cm^{-3}$, 3807 evaluated reflections with $2\theta \leq 45°$, $Mo_{K\alpha}$, $R = 0.0521$. Further details on the crystal structure investigation are available on request from Fachinformationszentrum Karlsruhe, Gesellschaft für wissenschaftlich-technische Information mbH, W-7514 Eggenstein-Leopoldshafen 2 (FRG), on quoting the depository number CSD-55781, the names of the authors, and the journal citation.
[10] R. Lackmann, M. Duetsch, F. Stein, A. de Meijere, unpublished results.
[11] All new compounds were characterized by spectroscopic methods (IR, ^1H NMR, ^{13}C NMR, MS) and their empirical formulas were confirmed by elemental analysis or high resolution mass spectroscopy.
[12] We thank Dr. *V. Sinnwell*, Universität Hamburg, for carrying out the NOE experiments.

Surface Organometallic Chemistry on Oxides: Selective Catalytic Low-Temperature Hydrogenolysis of Alkanes by a Highly Electrophilic Zirconium Hydride Complex Supported on Silica

By *Christine Lecuyer, Francoise Quignard, Agnès Choplin, Danielle Olivier,* and *Jean-Marie Basset**

The electrophilic activation of the C–H bond of alkanes on d^0 complexes of early transition metals (groups III–VI), lanthanides, and actinides is now well documented.[1] However, if one excludes H/D exchange between methane and deuterium,[2] no catalytic reaction involving a C–H activation step has been reported so far with d^0 metals. We report here the catalytic properties of a zirconium hydride supported on silica for the hydrogenolysis of neopentane, isobutane, and propane; the reaction forms isobutane, propane, and ethane respectively, together with methane.

Reaction of tetraneopentylzirconium ([$ZrNp_4$]) with the surface of silica previously dehydroxylated at 500 °C leads to the surface complex [($\equiv$SiO)$ZrNp_3$] (**1**), which has been characterized by elemental analysis, ^{13}C MAS NMR (MAS = magic angle spinning), in situ IR spectroscopy, and by its chemical reactivity with water.[3] A supported zirconium hydride **2** is obtained when **1** is reacted with molecular hydrogen (450 torr) at 150 °C.[4]

Hydride **2** has been qualitatively identified by in situ IR spectroscopy, and by its chemical reactivity with CH_3I and aqueous KOH.[5] Although this surface species is not yet fully characterized, the structure [($\equiv$SiO)$_3$ZrH] can be tentatively assigned to **2**. The only gaseous products detected on formation of **2** are methane and ethane. Therefore under these conditions, the neopentyl ligand, or the neopentane initially produced by cleavage of the neopentyl–zirconium bond, has undergone hydrogenolysis to yield as final products methane and ethane.

In effect, above 50 °C **2** catalyzes the hydrogenolysis of alkanes such as neopentane, isobutane, and propane. At 50 °C, neopentane ($p_{NpH} = 40$ torr, $p_{H_2} = 230$ torr) is totally converted in 100 hours. Up to a level of 50 % conversion, 85 % of the products are isobutane and methane (Fig. 1). At

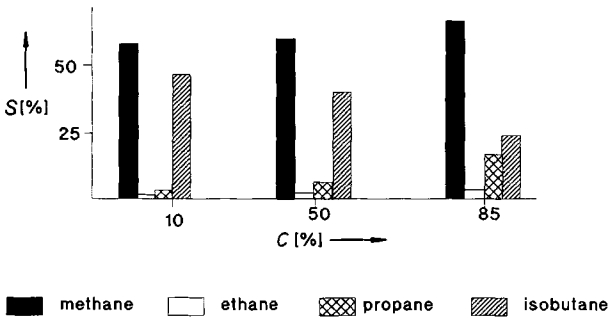

Fig. 1. Hydrogenolysis of neopentane: product distribution (S)/conversion (C) histograms ($T = 50$ °C, $p_{NpH} = 40$ torr, $p_{H_2} = 230$ torr, %Zr: 1.5 wt.%.)

higher conversion, isobutane is transformed into methane and propane, and the propane is subsequently transformed into methane and ethane. Interestingly, ethane does not undergo any significant further hydrogenolysis: this must have a mechanistic implication. Traces of 2-methylbutane are observed during the hydrogenolysis of neopentane.

When the reaction is performed at higher temperatures (e.g. 100 °C), the rate of hydrogenolysis is higher, but an increase in secondary reactions of the first-formed alkanes is observed: isobutane gives propane and methane and subsequently ethane and methane (Fig. 2). Hydrogenolysis of isobutane and propane has been carried out independently at 150 °C. The results confirm the relative simplicity of the reaction path observed with neopentane. In particular, hydrogenolysis of propane yields only methane and ethane at any conversion.

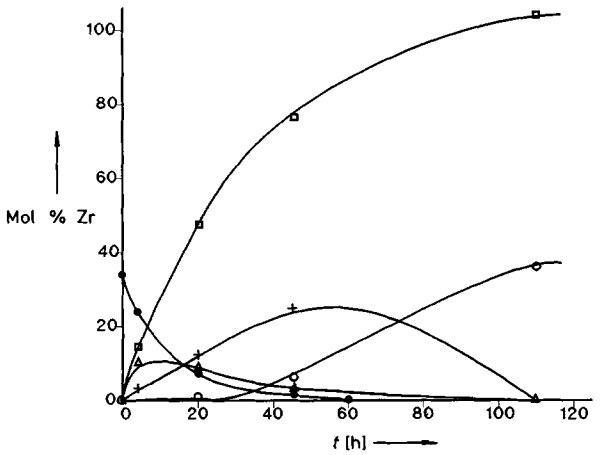

Fig. 2. Hydrogenolysis of neopentane at 100 °C. Concentration of the alkanes as a function of time ($p_{NpH} = 40$ torr; $p_{H_2} = 200$ torr). □ = methane, ○ = ethane, + = propane, △ = isobutane, ● = neopentane.

[*] Dr. J. M. Basset, C. Lecuyer, Dr. F. Quignard, Dr. A. Choplin, Prof. D. Olivier
Institut de Recherches sur la Catalyse,
2 Avenue Albert Einstein
F-69626 Villeurbanne Cedex (France)

[**] The financial support of the consortium ACTANE (Centre National de la Recherche Scientifique/French Industries) is gratefully acknowledged.

The mechanism proposed in Scheme 1 accounts for the products obtained from the hydrogenolysis of neopentane and lower alkanes. The first step is a C–H bond activation through σ bond metathesis[1e, 6, 7] on the surface zirconium hydride. It is deduced from a detailed investigation of the

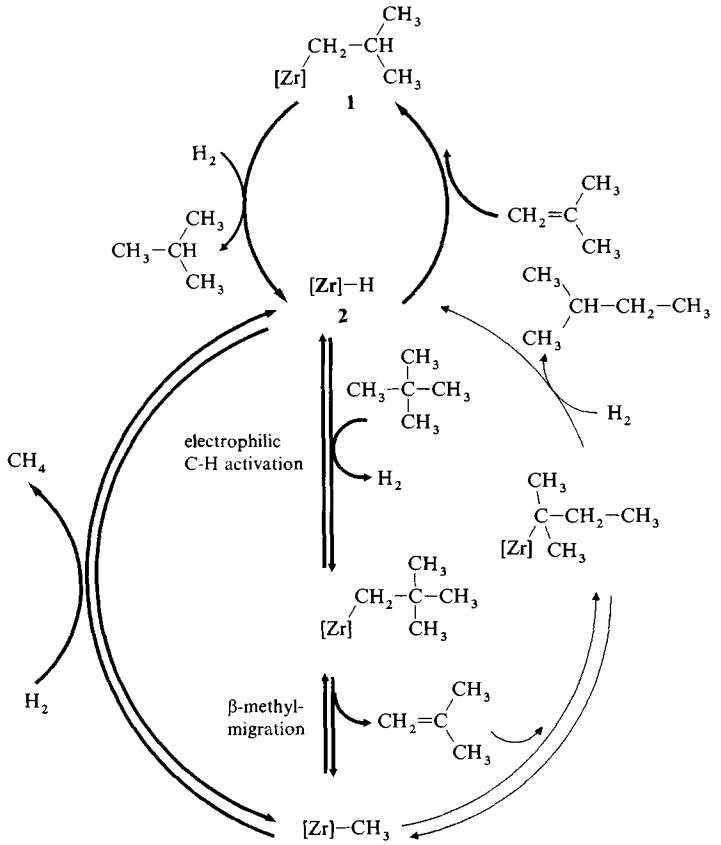

Scheme 1. **1**: [Zr] = (≡SiO)ZrNp$_2$, Np = neopentyl; **2** and following products: [Zr] = (≡SiO)$_3$Zr.

reactivity of **2** with cyclooctane and methane:[8] **2** reacts stoichiometrically to give the corresponding alkylzirconium complex and molecular hydrogen [Equation (a)]. This exchange reaction, which is believed to involve a four-center transition state with d^0 metals,[6, 7] occurs at 25 °C for cyclooctane and 150 °C for methane.[8]

$$[(\equiv SiO)_3ZrH] + RH \longrightarrow [(\equiv SiO)_3ZrR] + H_2 \qquad (a)$$
2

The surface hydride **2** is highly electrophilic: if one applies the Green formalism to oxide surfaces,[9] [(≡SiO)$_3$ZrH] can be considered an 8-electron d^0 species. Formation of molecular hydrogen and of a surface zirconium–neopentyl complex results from this first step.[8]

The next step is probably a β-methyl transfer leading to isobutene and a surface zirconium–methyl moiety.[10, 11] Hydrogenolysis of this latter fragment would then lead to methane. Isobutane would result from the hydrogenation of isobutene on a surface zirconium hydride.[4c] Formation of 2-methylbutane is easily explained by an anti-Markovnikov type addition of isobutene into the Zr–Me moiety followed by the hydrogenolysis of the Zr–alkyl bond. The reason why hydrogenolysis of ethane does not occur may be related to either the absence of a β-methyl group or the possible existence of an agostic interaction with the β-hydrogen as already observed on a scandium–ethyl fragment,[12] or both.

The results indicate clearly that an *immobilized* zirconium hydride is able to activate catalytically the C–H bonds of alkanes at low temperature, which has never been reported for any molecular analogue. Various reasons may be invoked for such a behavior:

- the zirconium hydride is very likely an 8-electron species which has, to our knowledge, no equivalent in molecular chemistry. Molecular zirconium(IV) hydrides are generally stabilized by two cyclopentadienyl ligands; they are thus 16-electron species and therefore less electrophilic than **2**.
- the extremely strong zirconium–oxygen bond which is responsible for the strong grafting of the transition metal to the support, does not allow any bimolecular deactivation as would certainly occur with a true molecular species.

Experimental procedure

Silica (Aerosil Degussa, 200 m^2 g^{-1}) was dehydroxylated under vacuum (500 °C, 16 h, 10^{-4} torr) and used in situ. [ZrNp$_4$] was synthesized following published procedures [13]. [ZrNp$_4$] was sublimed under vacuum (60 °C, 10^{-4} torr) on the freshly dehydroxylated silica; unreacted complex was removed by evacuation at the same temperature. The solid samples thus obtained were 1.5 wt% Zr. All gaseous reactants were carefully dried and deoxygenated over freshly regenerated molecular sieves (4 Å) and deoxo traps. All the catalytic tests were carried out in a pyrex batch reactor. The composition of the gas phase was followed by chromatography.

Received: July 15, 1991 [Z 4794 IE]
German version: *Angew. Chem. 103* (1991) 1692

CAS Registry numbers:
ZrNp$_4$, 38010-72-9; HZrNp$_3$, 137365-17-4; ZrH$_4$, 15457-96-2; neopentane, 463-82-1; 2-methylbutane, 78-78-4; isobutane, 75-28-5; propane, 74-98-6; methane, 74-82-8; ethane, 74-84-0.

[1] a) P. L. Watson, G. W. Parshall, *Acc. Chem. Res. 18* (1985) 51–56; b) I. P. Rothwell, *ibid. 21* (1988) 153–159; c) C. H. Hill, *Activation and Functionalization of Alkanes*, Wiley, New York 1989; d) C. M. Fendrick, T. J. Marks, *J. Am. Chem. Soc. 108* (1986) 425–437; e) M. E. Thompson, S. M. Baxter, A. R. Bulls, B. J. Burger, M. C. Nolan, B. D. Santarsiero, W. P. Schaefer, J. E. Bercaw, *ibid. 109* (1987) 203–219.
[2] A. M. Pyle, K. J. Jens, *J. Mol. Catal. 38* (1986) 337–339.
[3] The elemental analysis of the solid after reaction of [Zr(Np)$_4$] with silica dehydroxylated at 500 °C for 16 hours gave a C/Zr ratio of 16 instead of 15 expected for a [ZrNp)$_3$] moiety. Surface complex **1** reacts with water (22 torr) and liberates 3.15 mol of NpH per mole of grafted zirconium in agreement with the formulation of **1**. For a complete characterization of **1** see F. Quignard, C. Lecuyer, A. Choplin, C. Bougault, F. Lefebvre, F. D. Olivier, J. M. Basset, *Inorg. Chem.* submitted.
[4] Supported zirconium hydrides have already been reported. See, for example, a) V. A. Zakharov, V. K. Dudchenko, E. A. Paukshtis, L. G. Karakchiev, Y. I. Yermakov, *J. Mol. Catal. 2* (1977) 421–435; b) D. G. H. Ballard, *Adv. Catal 23* (1974) 263–325; c) J. Schwartz, M. D. Ward, *J. Mol. Catal. 8* (1980) 465–469; d) S. A. Vasnetsov, A. V. Nosov, V. M. Mastikhin, V. A. Zakharov, *ibid. 53* (1989) 37–41.
[5] ν(Zr-H): 1635 cm^{-1}. Surface hydride **2** reacts with water and liberates gaseous hydrogen; **2** reacts with CH_3I and liberates methane. A more complete characterization of the zirconium hydride will be described in F. Quignard, A. Choplin, C. Lecuyer, J. Corker, J. Evans, J. M. Basset, unpublished.
[6] H. Rabaa, J. Y. Saillard, R. Hoffmann, *J. Am. Chem. Soc. 108* (1986) 4327–4333.
[7] P. L. Watson, *J. Am. Chem. Soc. 105* (1983) 6491–6493.
[8] F. Quignard, A. Choplin, J. M. Basset, *J. Chem. Soc. Chem. Commun*, in press.
[9] A. Choplin, J. M. Basset, *J. Mol. Catal. 21* (1983) 95–108.
[10] W. Pfohl, *Justus Liebigs Ann. Chem. 629* (1960) 207.
[11] P. L. Watson, D. C. Roe, *J. Am. Chem. Soc. 104* (1982) 6471–6473.
[12] B. J. Burger, M. E. Thompson, W. D. Cotter, J. E. Bercaw, *J. Am. Chem. Soc. 112* (1990) 1566–1577.
[13] P. J. Davidson, M. F. Lappert, R. Pearce, *J. Organomet. Chem. 57* (1973) 269.

New Chiral Polyamide Stationary Phases for Chromatographic Enantiomer Separation

By *Dieter Arlt, Bruno Bömer, Rolf Grosser,* and *Walter Lange**

Dedicated to Professor Karl Heinz Büchel on the occasion of his 60th birthday

Many biologically active substances are now tested in their enantiomerically pure form. Chiral stationary phases (CSPs) can ensure not only reliable enantiomer analysis but also ready availability of the two enantiomers of a racemic active substance at a very early point in biological screening. Extensive use requires a range of CSPs which permit preparative separation at reasonable cost. Until now only a few types of CSPs could be considered: cellulose triacetate, cellulose tribenzoate,[1-3] and more recently cellulose urethanes,[4] *N*-(3,5-dinitrobenzoyl)amino acid phases,[5] and polyamide phases from optically active *N*-(meth)acryloyl monomers.[6-8] The present report concerns new, highly selective polyamide phases prepared from the optically active amino acid amides **1a–c** and **2a–c** for chromatographic separation of enantiomers.

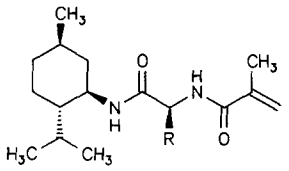

1a–c

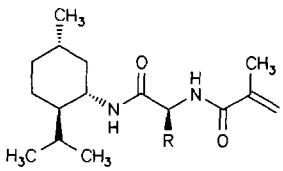

2a–c

a, R=CH_3; **b**, R=$CH_2CH(CH_3)_2$; **c**, R=(*S*)-$CH(CH_3)C_2H_5$

Since good separation results had been obtained with poly(meth)acrylamides, it was expected that new adsorbents of this type would extend the possibilities of direct enantiomer separation without prior derivatization. Besides the development of analytically useful HPLC phases,[9,10] these monomers should also make the synthesis of cross-linked bead polymers for preparative separations possible.[6-8] Poly(*N*-acryloyl-(*S*)-phenylalanine ethyl ester)[7] shows a good enantioselective separation of some racemates.[6,11] But more broadly applicable CSPs, distinguished by higher enantioselectivities particularly for the more polar, biologically active racemates, are also desirable.

It seemed necessary to us first of all to strongly restrict the conformative mobility of the monomer molecule by the incorporation of an additional amide group and a bulky residue. This reduces the number of energetically equivalent conformers which possibly have opposite effects on enantioselectivity. Secondly, the use of a rigid, bulky, and also chiral residue should enable a further increase in enantioselectivity through double stereodifferentiation.

Our new CSPs contain an amino acid structural unit which permits rational synthesis and fulfills the requirements mentioned. The increased rigidity in the immediate surroundings of the stereogenic center of the amino acid is ensured by a peptide bond. As the rigid bulky and additionally chiral group we chose optically active menthylamine, used in our earlier studies and available in both enantiomeric forms starting from (−)-menthone (**3**) or (+)-menthol.

(−)-Menthone (**3**) was converted into (−)-menthonoxime (**4**) with aqueous hydroxylamine solution in the presence of small quantities of an emulsifier at room temperature (Scheme 1). The highly diastereoselective reduction of the

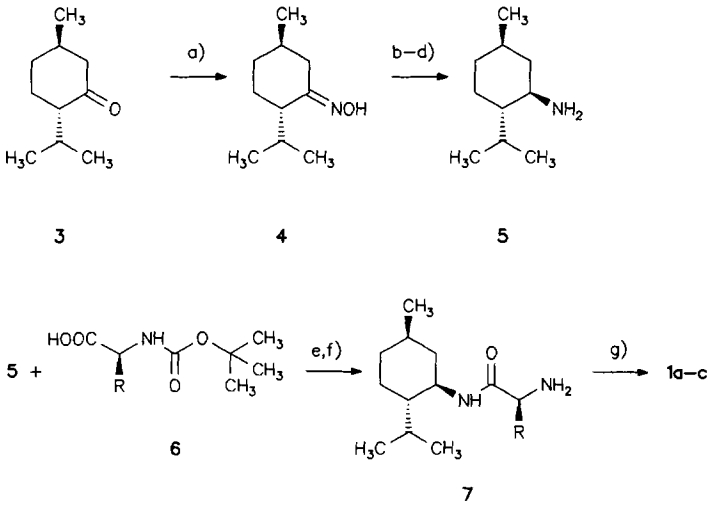

Scheme 1. Synthesis of optically active monomers. a) $NH_2OH \cdot HCl$, Na_2CO_3, sodium lauryl sulphate (15% in H_2O, catalytic amount), RT, 48 h, 95%; b) Na, EtOH, reflux; c) steam distillation, conc. HCl; d) NaOH, H_2O, 0 °C, 1 h, 75% for b–d; e) NEt_3, ClCOOEt, THF, −15 °C to RT, 30 min; 85–95%; f) CF_3COOH, CH_2Cl_2, 0 °C to RT, 2 h, NaOH, 90–95%; g) methacryloyl chloride, NEt_3, CH_2Cl_2, 0 °C to RT, 1 h, 75–85%).

oxime was possible even on a kg scale with sodium and ethanol under Wallach's conditions.[12] By recrystallization of the hydrochloride >98% epimerically pure (−)-menthylamine **5** was obtained. Linkage with an optically active amino acid, for example **6**, protected by a *N*-*tert*-butoxycarbonyl residue, was possible by activation of the carboxyl function as usual in peptide chemistry. The final products **1** were formed after removal of the protecting group with trifluoroacetic acid in dichloromethane, and subsequent treatment with methacryloyl chloride in the presence of triethylamine. Monomers **2** were prepared using an analogous reaction sequence starting from (+)-menthol. The diamides **1a–c** and **2a–c** were isolated by recrystallization with diastereomeric purity of >99:1.[13]

Analytical HPLC phases can be prepared from the optically active *N*-methacryloyl compounds by covalent bonding to modified silica gel under the conditions of radical polymerization (Scheme 2).

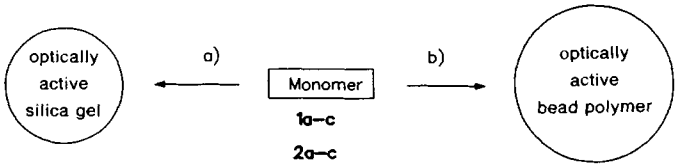

Scheme 2. Preparation of CSPs. a) Vinylsilica 5 μm: monomer = 1:1, azobis(isobutyronitrile) (AIBN, catalytic amount), toluene, 80 °C, 45 min or chloroform, reflux, 2 h; 10–15% polymer coating; b) monomer, 10–15% ethylene glycol dimethacrylate, chloroform, AIBN (catalytic amount), polyvinyl alcohol, water, 55 °C, 14 h; 75–93% beads with a particle size of 20–80 μm).

[*] Dr. W. Lange, Prof. Dr. D. Arlt, Dr. B. Bömer, Dr. R. Grosser
Bayer AG
Central Research and Development, ZF-FGF; Building Q 18
W-5090 Leverkusen (FRG)

The base can be a methacrylate-modified diol silica gel[9, 10, 14] or preferably vinylsilica.[15, 16] CSPs prepared in this way are not sensitive to pressure, extremely stable chemically, and can be used under any elution conditions without restriction. Bead polymerization in the presence of a crosslinking agent such as ethylene glycol dimethacrylate can be used to obtain CSPs for preparative purposes from methacrylamides.[7, 8, 13] The bead polymers are gels which work only under low-pressure conditions and are clearly superior to the HPLC phases in preparative separations because of their higher loadability and lower solvent requirements. For example, 0.4 g of **9** was separated completely into its enantiomers on 32 g of bead polymerizate derived from **2b** in one run.

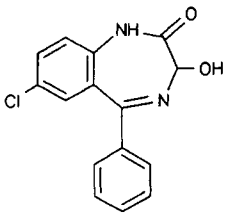

8

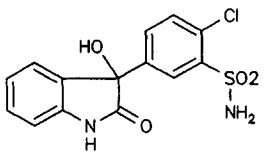

9

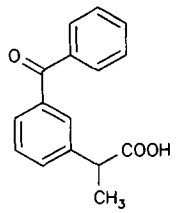

10

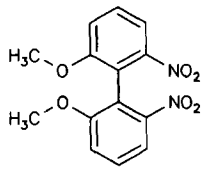

11

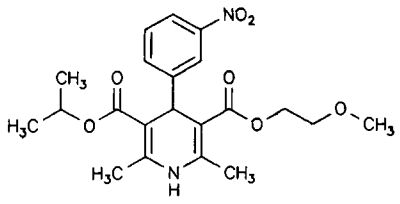

12

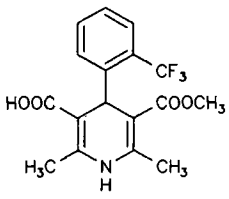

13

Table 1. Enantioselectivity values α [a] for racemates **8**–**13** [b] on CSPs [c] from monomers **1a**–**c**, **2a**–**c**, and (−)-menthylacrylamide. [17]

CSP from monomer	Amino acid	Menthyl group	**8**	**9**	**10**	**11**	**12**	**13**
1a	(*S*)-Ala	(−)	2.62	2.05	–	3.13	–	1.98
2a	(*S*)-Ala	(+)	1.34	1.56	1.29	–	–	–
1b	(*S*)-Leu	(−)	4.05	2.27	–	11.40	–	2.91
2b	(*S*)-Leu	(+)	1.68	2.34	1.14	6.12 [d]	1.11	2.60
1c	(*S*)-Ile	(−)	1.37	4.00	–	5.77	–	2.28
2c	(*S*)-Ile	(+)	2.60	3.31	1.18	3.56	1.26	1.89
(−)-menthylacrylamide	–	(−)	1.43	–	–	–	–	1.83

[a] $\alpha = (k'_2)(k'_1)^{-1}$, $k'_{1(2)} = (t_{1(2)} - t_0)(t_0)^{-1}$, t_0 = dead time. [b] The eluents were *n*-heptane/THF mixtures, in ratios of 1:2 for **8** und **9**, 3:2 for **10**–**12**, and 1:1 for **13**, to give a k'_1 value between 0.5 and 4. [c] 10–15% of optically active polymer on vinylsilica (5 μm) [16]. Columns: 25 × 0.46 cm; flow rate: 1 mL min^{-1}; T = 20 °C. [d] Flow rate: 2 mL min^{-1}.

Table 1 provides a review of the separation of various racemates on the new CSPs. It should be noted that these high enantioselectivities were obtained without arene interaction. This is an indication that the criteria outlined previously are valid for enantiomer discrimination.

The combined influence of the optically active menthyl residue and the stereogenic center of the amino acid led to substantially better separations in many cases. Thus, all the above-mentioned CSPs prepared from the (*S*)-(+) diastereomers **2a**–**c** separated ketoprofen **10** into its enantiomers, whilst this is not achieved on either the *S*-(−) CSPs derived from **1a**–**c** investigated previously or on the CSP from (−)-menthylacrylamide. For the biphenyl derivative **11** (Fig. 1) we have the opposite situation, namely that the

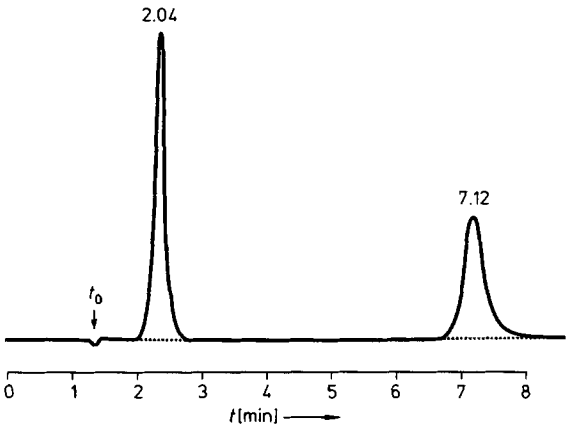

Fig. 1. Chromatographic enantiomer separation of **11** on the CSP prepared from **2b** (see Table 1).

enantioselective separations on the *S*-(−) CSPs were fundamentally superior to those on the *S*-(+) CSPs, although some of the latter also showed an outstanding selectivity for **11**. Such regularities were not observed in separations of racemic oxazepam **8** and chlorthalidone **9**, but at least one of the diastereomeric phases showed a clearly higher selectivity for these racemates than the simple polymer from (−)-

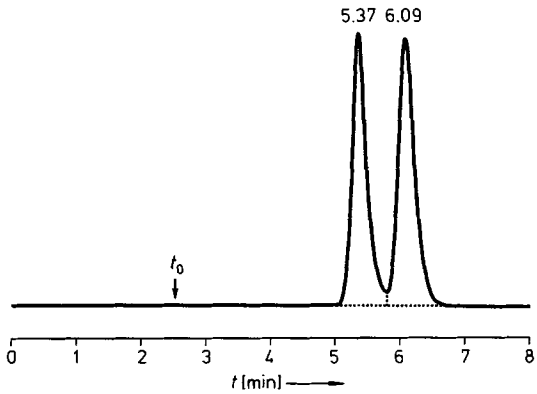

Fig. 2. Chromatographic enantiomer separation of **12** on the CSP prepared from **2c** (see Table 1).

menthylacrylamide. The separation of the nimodipine enantiomers **12** (Fig. 2) on the CSPs from the *S*-(+) diastereomers **2b** and **2c** with a larger amino acid alkyl residue was surprising, since the racemate **12** does not have

a good hydrogen bonding function in the vicinity of the stereogenic center.

Received: June 13, 1991 [Z 4704 IE]
German version: *Angew. Chem. 103* (1991) 1685
Publication delayed at authors' request

[1] G. Hesse, R. Hagel, *Chromatographia 6* (1973) 277–280.
[2] A. Mannschreck, H. Koller, R. Wernicke, *Kontakte (Darmstadt) 1985*, 40–48.
[3] E. Francotte, R. M. Wolf, *Chirality 3* (1991) 43–55.
[4] Review: Y. Okamoto, R. Aburatani, *Polym. News 14* (1989) 295–301.
[5] Review: W. H. Pirkle, T. C. Pochapsky, *Chem. Rev. 89* (1989) 347–362.
[6] Review: G. Blaschke, *Chromatogr. Sci. 40* (1988) 179–198.
[7] a) G. Blaschke, A. Schwanghart, *Chem. Ber. 109* (1976) 1967–1975; b) Sold as an analytical HPLC phase under the name Chiraspher® by E. Merck, Darmstadt.
[8] U. Schwartz, R. Grosser, K. E. Piejko, B. Bömer, D. Arlt, EP-B 218089 (1987), Bayer AG.
[9] G. Blaschke, W. Bröker, W. Fraenkel, *Angew. Chem. 98* (1986) 808–810; *Angew. Chem. Int. Ed. Engl. 25* (1986) 830–831.
[10] B. Bömer, R. Grosser, U. Schwartz, D. Arlt, K. E. Piejko, EP-B 282770 (1988), Bayer AG.
[11] a) D. Seebach, S. G. Müller, U. Gysel, J. Zimmermann, *Helv. Chim. Acta 71* (1988) 1303–1318; b) U. Gerlach, T. Haubenreich, S. Hünig, N. Klaunzer, *Liebigs Ann. Chem. 1989*, 103–104; c) A. Hallberg, R. Isaksson, A. R. Martin, J. Sandström, *J. Am. Chem. Soc. 111* (1989) 4387–4392.
[12] O. Wallach, *Justus Liebigs Ann. Chem. 276* (1893) 296–327.
[13] Examples of preparation: W. Lange, B. Bömer, R. Grosser, D. Arlt, EP-A 379917 (1990), Bayer AG.
[14] Suitable are e.g. LiChrosorb®-DIOL 5 μm from E. Merck, Darmstadt and Nucleosil®-OH 5 μm from Macherey and Nagel, Düren. For instructions see e.g. refs [9] and [13].
[15] H. Engelhardt, H. Löw, W. Eberhardt, M. Mauss, *Chromatographia 27* (1989) 535–543.
[16] We would like to thank Prof. Dr. *H. Engelhardt*, Dr. *H. Löw*, and Dipl. Chem. *W. Götzinger* of the University of Saarbrücken for discussions and providing vinylsilica.
[17] Preparation of vinylsilica: 10 g silica gel (Si 100, 5 μm) dried at 120 °C under high vacuum was suspended in 100 mL toluene, treated with 7 g trichlorovinylsilane, and heated at reflux. After the addition of 12.4 g triethylamine in 30 mL toluene the mixture was stirred for 16 h at 110 °C. The vinylsilica was washed with toluene, methanol, and dichloromethane and dried under high vacuum at 70 °C. Yield: 10.6 g; C,H analysis: 3% C, 0.8% H. Preparation of CSPs: 3 g monomer, 3 g vinylsilica, and 60 mg AIBN were stirred with 15 mL chloroform under nitrogen for 2 h at 65 °C. The product was filtered off under suction, washed with chloroform, dimethylformamide, and 2-propanol, and dried under high vacuum at 25 °C. Yield: 3.1–3.2 g; polymer coating 10–15%.

Diastereo- and Enantioselective Michael Addition Initiated Cyclizations to *trans*-Substituted Cyclopentanecarboxylates **

By *Dieter Enders,* Hermann J. Scherer,* and *Gerhard Raabe*

Dedicated to Professor Kurt Schaffner on the occasion of his 60th birthday

Intramolecular Michael additions are frequently used in the construction of cyclic systems (**A** → **B**).[1] If the primary addition product of an intermolecular Michael addition is intercepted with a tandem intramolecular reaction, cyclic products may be obtained too (**C** → **D**).[2,3] Because metalated SAMP/RAMP hydrazones (SAMP = (*S*)-1-amino-2-methoxymethylpyrrolidine, RAMP = (*R*)-1-amino-2-methoxymethylpyrrolidine) are proven chiral Michael donors,[4] asymmetric MIRC reactions (*M*ichael-*I*nitiated *R*ing *C*losure)[5] of the type **C** → **D** should be possible with high stereoselectivity. The 1,2-disubstituted cycloalkanes **D** with various nucleophile (Nu) and acceptor (Acc) functional groups in both side chains are important building blocks in the syntheses of bioactive compounds and natural products containing five-membered rings.[6]

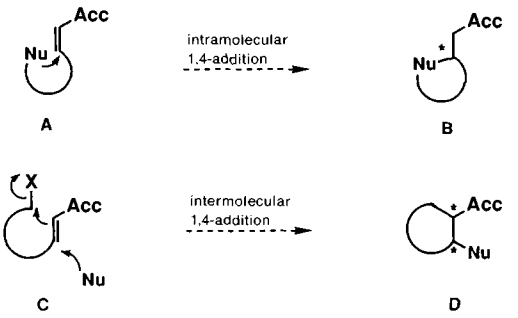

We report here the synthesis of highly diastereo- and enantiopure *trans*-disubstituted cyclopentanecarboxylates **4** by the MIRC reaction of SAMP/RAMP hydrazones **1** with methyl (*E*)-6-bromo-hex-2-enoate (**2**). SAMP hydrazones (*S*)-**1**, available from the corresponding methyl ketones, are metalated with lithium diisopropylamide at 0 °C and then treated with the ω-functionalized Michael acceptor at −78 °C. After workup the cyclized (*E*/*Z*)-hydrazones are

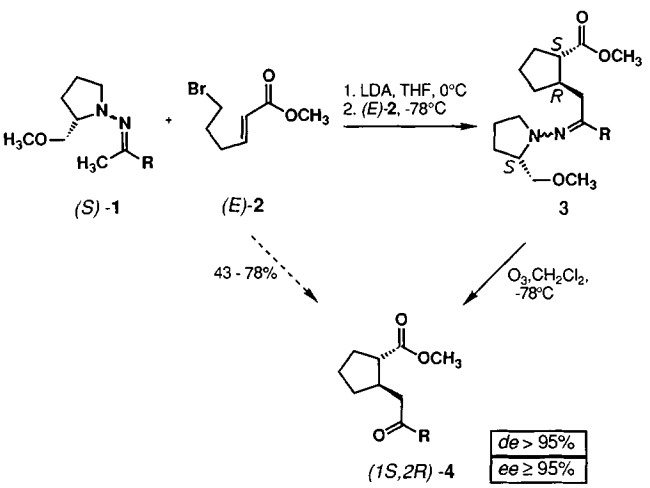

Scheme 1. LDA = lithium diisopropylamide. **a**, R = Me; **b**, R = *n*Bu; **c**, R = *i*Bu; **d**, R = Ph; **e**, R = *p*-BrC_6H_4.

obtained, which may be purified by chromatography and characterized. Usually the crude products **3** are converted directly to the final products (1*S*,2*R*)-**4** by oxidative cleavage with ozone. After chromatographic purification the *trans*-disubstituted cyclopentanecarboxylates **4** are obtained in 43–78% total yield and with high diastereomeric (*de* ≥ 95–99%) and enantiomeric excesses (*ee* ≥ 95–97%) (Table 1).

The *de* values for the cyclization products **3** and **4** were determined by ^{13}C NMR spectroscopy; the *ee* values for compounds **4a–c**, by gas chromatography with a chiral permethylated β-cyclodextrin stationary phase. The determination of the enantiomeric excesses of **4d, e** was possible by means of ^{1}H NMR experiments using the shift reagent

[*] Prof. Dr. D. Enders, Dipl.-Chem. H. J. Scherer, Dr. G. Raabe
Institut für Organische Chemie der Technischen Hochschule
Professor-Pirlet-Strasse 1, W-5100 Aachen (FRG)

[**] This work was supported by the Fonds der Chemischen Industrie. We thank Degussa AG, BASF AG, Bayer AG, and Hoechst AG for providing us with chemicals.

Table 1. *trans*-Disubstituted cyclopentanecarboxylates **4** obtained by asymmetric MIRC reaction.

4	R	yield [%] [a]	$[\alpha]_D^{RT}$ (*c*, $CHCl_3$)	*de* [%] [b]	*ee* [%] [b]
(1*S*,2*R*)-**4a**	Me	54	+51.1 (2.20)	>99	≥97
(1*S*,2*R*)-**4b**	*n*Bu	43	+39.7 (1.87)	>95 [c]	≥95
(1*S*,2*R*)-**4c**	*i*Bu	78	+47.4 (1.03)	>97	>96
(1*R*,2*S*)-**4c** [d]	*i*Bu	62	−47.6 (2.02)	>97	>96
(1*S*,2*R*)-**4d**	Ph	77	+63.8 (1.76)	>96 [c]	>96 [e]
(1*S*,2*R*)-**4e** [f]	*p*-BrC_6H_4	73	+48.3 (1.12)	>96 [c]	>95 [e]

[a] The yields are for the MIRC reaction and subsequent ozonolysis without isolation of the hydrazone intermediates **3**. [b] Determined by gas chromatography on a chiral stationary phase (permethyl-β-cyclodextrin, 115 °C, 1 bar H_2, see Fig. 1). [c] Determined by ^{13}C NMR spectroscopy. [d] RAMP was used as chiral auxiliary. [e] Determined by ^1H NMR Lanthanide Induced Shift (LIS) with $[Eu(hfc)_3]$. [f] M.p. = 46–47 °C.

$[Eu(hfc)_3]_3$. The racemic *trans*-cyclopentanecarboxylates, *rac*-**4a–e**, required for comparison were prepared in high diastereomeric purity from the corresponding dimethylhydrazone homocuprates according to the method previously described.[8]

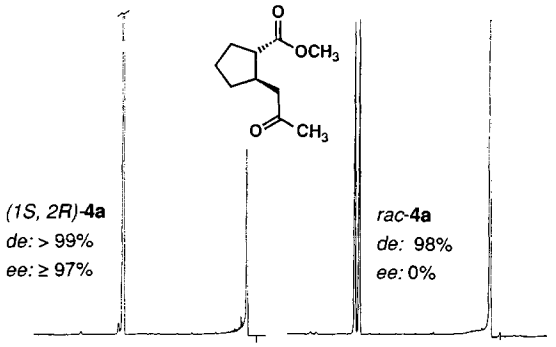

Fig. 1. Determination of diastereomeric and enantiomeric excesses by gas chromatography (fused silica capillary, heptakis(2,3,6-tri-*O*-methyl)-β-cyclodextrin in OV 1701, 115 °C, 1.0 bar H_2) [7].

The relative and absolute configurations of the cyclopentanecarboxylates were unambiguously assigned by X-ray structural analysis of compound **4e**.[9–12] This product obtained from the SAMP auxiliary was determined to have an (1*S*,2*R*) configuration. The simple change in auxiliaries from SAMP to RAMP affords access to the other enantiomer (Table 1). The absolute configuration (2*R*) of the stereogenic center generated in the first step of the 1,4-addition is in agreement with previous results of Michael additions with SAMP hydrazones [4] and the postulated mechanism of electrophilic substitutions with SAMP/RAMP hydrazones.[13]

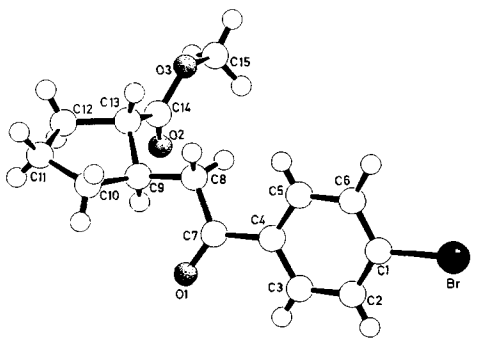

Fig. 2. X-ray crystal structure of (1*S*,2*R*)-**4e** [9].

The MIRC variation described here offers a direct and highly stereoselective approach to important synthetic building blocks.[14] Initial results show that this method can be applied in the syntheses of rings of other sizes (three-, six-, and seven-membered rings) as well as with other acceptors, for example sulfones.[15]

Experimental Procedure

To a stirred solution of 5.5 mmol lithium diisopropylamide [prepared from 0.78 mL diisopropylamine and 3.67 mL *n*-butyllithium solution (1.5 N in *n*-hexane)] at 0 °C under argon was added dropwise 5 mmol hydrazone **1**. The mixture was stirred 2 h at 0 °C and then cooled to −78 °C before a solution of 5 mmol (*E*)-**2** in 5 mL THF was added dropwise. The reaction mixture was stirred about 12 h during which time the temperature rose from −78 °C to 0–10 °C. After addition of 30 mL NH_4Cl solution and 50 mL ether, the phases were separated. The aqueous phase was extracted with ether (2 × 50 mL). The collected organic phases were washed with 10 mL saturated NaCl solution and dried over $Na_2SO_4/MgSO_4$. The solvent was removed under reduced pressure and the crude hydrazone was dissolved in 30 mL CH_2Cl_2 and cooled to −78 °C under argon. Ozone was then passed through the solution at this temperature until a blue-green color was observed. The excess ozone was dispelled by purging with an argon stream. Then the solvent was removed and the products were purified by column chromatography (ether/petroleum ether 1:3).

Received: July 30, 1991 [Z4842 IE]
German version: *Angew. Chem. 103* (1991) 1676

CAS Registry numbers:
1a, 65651-52-7; **1b**, 137057-38-6; *S*-**1c**, 137057-39-7; *R*-**1c**, 137057-40-0; **1d**, 89393-53-3; **1e**, 137057-41-1; (*E*)-**2**, 75424-49-6; **4a**, 135028-29-4; **4b**, 137057-34-2; (1*S*, 2*R*)-**4c**, 137057-35-3; (1*R*, 2*S*)-**4c**, 137170-92-4; **4d**, 137057-36-4; **4e**, 137057-37-5.

[1] a) D. A. Oare, C. H. Heathcock, *Top. Stereochem. 19* (1989) 227; b) E. Winterfeldt, *Kontakte (Darmstadt) 1987*, 37; c) G. Stork, N. A. Saccomano, *Tetrahedron Lett. 28* (1987) 2087; d) G. Berthiaume, J.-F. Lavalée, P. Deslongchamps, *ibid. 27* (1986) 5451; e) J.-F. Lavalée, G. Berthiaume, P. Deslongchamps, F. Grein, *ibid. 27* (1986) 5455; f) K. Shishido, Y. Sukegawa, K. Fukumoto, T. Kametani, *J. Chem. Soc. Perkin Trans. 1 1987*, 993.
[2] M. J. Chapdelaine, M. Hulce, *Org. React. (NY) 38* (1990) 225.
[3] a) T. Hudlicky, J. D. Price, *Chem. Rev. 89* (1989) 1467; b) M. P. Cooke, Jr., *Tetrahedron Lett. 1979*, 2199; c) G. H. Posner, J. J. Sterling, C. E. Whitten, C. M. Lentz, D. J. Brunelle, *J. Am. Chem. Soc. 97* (1975) 107; d) G. H Posner, J. P. Mallamo, A. Y. Black, *Tetrahedron 37* (1981) 3921; e) G. H. Posner, *Chem. Rev. 86* (1986) 831; f) R. D. Little, J. R. Dawson, *J. Am. Chem. Soc. 100* (1978) 4607; g) R. D. Little, R. Verhé, W. T. Monte, S. Nugent, J. R. Dawson, *J. Org. Chem. 47* (1982) 362; h) W. A. Nugent, F. W. Hobbs, Jr., *ibid. 48* (1983) 5364; i) W. A. Nugent, F. W. Hobbs, Jr., *ibid. 51* (1986) 3376; j) T. Uyehara, N. Shida, Y. Yamamoto, *J. Chem. Soc. Chem. Commun. 1989*, 113; k) M. Yamaguchi, M. Tsukamoto, I. Hirao, *Tetrahedron Lett. 26* (1985) 1723; l) Y. Inouye, S. Inamasu, M. Ohno, T. Sugita, H. M. Walborsky, *J. Am. Chem. Soc. 83* (1961) 2962; m) H. Hagiwara, T. Akama, A. Okano, H. Uda, *Chem. Lett. 1989*, 2149; n) S. Saito, Y. Hirohara, O. Narahara, T. Moriwake, *J. Am. Chem. Soc. 111* (1989) 4533; o) C. Fang, H. Suemune, K. Sakai, *Tetrahedron Lett. 31* (1990) 4751; p) A. I. Meyers, G. Licini, *ibid. 30* (1989) 4049; q) M. Yamaguchi, K. Hasebe, S. Tanaka, T. Minami, *ibid. 27* (1986) 959; r) C. R. Nevill, Jr., P. L. Fuchs, *Synth. Commun. 20* (1990) 761.
[4] a) D. Enders, K. Papadopoulos, *Tetrahedron Lett. 24* (1983) 4967; b) D. Enders, K. Papadopoulos, B. E. M. Rendenbach, R. Appel, F. Knoch, *ibid. 27* (1986) 3491; c) D. Enders, B. E. M. Rendenbach, *Tetrahedron 42* (1986) 2235; d) *Chem. Ber. 120* (1987) 1223; e) D. Enders, B. E. M. Rendenbach in R. Greengalph, T. R. Roberts (Eds.): *Enantioselective Synthesis of Bioregulators in Pesticide Science and Biotechnology*, Blackwell, Oxford 1987, p. 17; f) D. Enders, A. S. Demir, B. E. M. Rendenbach, *Chem. Ber. 120* (1987) 1731; g) D. Enders, A. S. Demir, H. Puff, S. Franken, *Tetrahedron Lett. 28* (1987) 3795; h) D. Enders, S. Müller, A. S. Demir, *ibid. 29* (1988) 6437.
[5] R. D. Little, J. R. Dawson, *Tetrahedron Lett. 21* (1980) 2609.
[6] a) L. A. Paquette, *Top. Curr. Chem. 119* (1984) 1; b) B. M. Trost, *Chem. Soc. Rev. 11* (1982) 141; c) B. M. Trost, *Angew. Chem. 98* (1986) 1; *Angew. Chem. Int. Ed. Engl. 25* (1986) 1; d) W. I. Taylor, A. R. Battersby (Eds.): *Cyclopentanoid Terpene Derivatives (Organic Substances of Natural Origin. Vol. 2)*, Dekker, New York 1969.
[7] A. Köhnes, *Dissertation*, Technische Hochschule Aachen 1991.
[8] E. J. Corey, D. Enders, *Chem. Ber. 111* (1978) 1337.
[9] Suitable crystals were obtained at −20 °C from petroleum ether. Orthorhombic, space group $P2_12_12_1$ (19) $a = 6.005(2)$, $b = 13.958(2)$, $c = 17.282(1)$ Å, $V = 1448.5$ Å^3, $M_{calc} = 325.2$, $Z = 4$, $F(000) = 664$, $\rho_{calc} = 1.491$ g cm^{-3}, $\mu = 30.11$ cm^{-1} (correction for spherical absorp-

tion), Enraf-Nonius four-circle diffractometer, $\omega/2\beta$ scans, 20 °C, $Mo_{K\alpha}$ radiation ($\lambda = 0.7169$ Å, graphite monochromator). 3336 independent reflections ($\pm h + k + l$), of which 2082 were observed [$I > 2\sigma(I)$, $R_m = 0.030$], $\sin\theta/\lambda_{max} = 0.6$ for solution and refinement. The structure was determined by the heavy atom method using the XTAL2.6 program package. Positions of hydrogen atoms calculated, 173 parameters refined, $R = 0.053$ ($R_w = 0.048$), residual electron density 0.7 e Å^{-3}. An enantiopole parameter[11,12] refined to 0.004 confirms the absolute configuration shown in Figure 2. Further details of the crystal structure may be obtained from the Fachinformationszentrum Karlsruhe, Gesellschaft für wissenschaftlich-technische Information mbH, W-7514 Eggenstein-Leopoldshafen 2, on quoting the depository number CSD-55614, the names of the authors, and the journal citation.

[10] S. R. Hall, J. M. Stewart (Eds.): *XTAL2.6 User's Manual*, Universities of Western Australia and Maryland 1989.

[11] H. D. Flack, *Acta Crystallogr. Sect. A 39* (1983) 876.

[12] G. Bernardinelli, H. D. Flack, *Acta Crystallogr. Sect. A 41* (1985) 500.

[13] a) D. Enders in J. D. Morrison (Eds.): *Asymmetric Synthesis Vol. 3*, Academic, Orlando 1984, p. 275; b) D. Enders, *Chem. Scripta 25* (1985) 139; c) D. Enders, G. Bachstädter, K. A. M. Kremer, M. Marsch, K. Harms, G. Boche, *Angew. Chem. 100* (1988) 1580; *Angew. Chem. Int. Ed. Engl. 27* (1988) 1522.

[14] All new compounds gave correct elemental analyses and spectra (NMR, IR, MS).

[15] D. Enders, H. Scherer, unpublished results; H. J. Scherer, *Dissertation*, Technische Hochschule Aachen 1991.

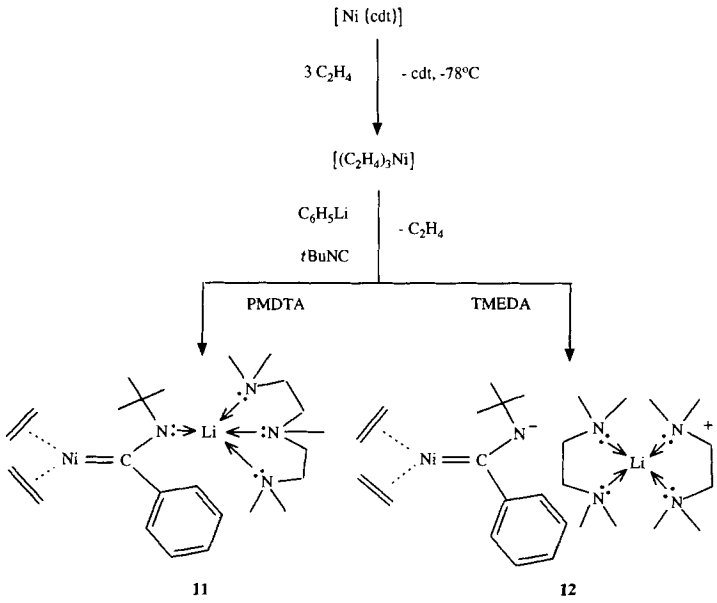

Nickel(0)-Carbene Complexes

By *Barbara Gabor, Carl Krüger, Bernd Marczinke, Richard Mynott*, and *Günther Wilke**

Dedicated to Professor Horst Prinzbach on the occasion of his 60th birthday

Isocyanides can be metalated, e.g. with *n*-butyllithium, in the α-position.[1] We were interested whether $[Ni(CNCH_3)_4]$ **1** reacts with *n*BuLi in the same way to give $[Ni(CNCH_2Li)_4]$ **2**. Compound **1**, which is insoluble in pentane, dissolves when treated in this solvent at −20 °C with four equivalents of *n*BuLi. No liberation of *n*-butane is observed, either immediately or upon subsequent hydrolysis. Apparently, *n*BuLi adds to the C=N bond, possibly with formation of $[Ni\{=C(C_4H_9)NLi(CH_3)\}_4]$ **3**, which, however, could hitherto not be isolated, since it undergoes secondary reactions.

Attempts to obtain **2** from $LiCH_2NC$ and $[Ni(cod)_2]$ led to displacement of 1,5-cyclooctadiene (cod) and loss of methylene to give $Li_4[Ni(CN)_4]$ **4**,[2] which reacts with $(CH_3)_3SiCl$ to the homoleptic complex of trimethylsilyl isocyanide $[Ni\{CNSi(CH_3)_3\}_4]$ **5**.[3] In a completely analogous way $[(tpp)_3NiCN][Li(thf)_2]$ **6** (tpp = triphenylphosphane) reacts with $(CH_3)_3SiCl$ to give $[(tpp)_3Ni\{CNSi(CH_3)_3\}]$ **7**. A compound analogous to **6** is formed from [Ni(cdt)] (cdt = all-*trans*-1,5,9-cyclododecatriene) and the addition products **8** of phenyllithium and *tert*-butyl isocyanide. Aside from benzene and isobutene, formation of an adduct of LiCN and [Ni(cdt)] is observed, in the presence of *N,N,N'N'*-tetramethylethylenediamine (TMEDA) $[(cdt)NiCN][Li(tmeda)_2]$ **9** and of pentamethyldiethylenetriamine (PMDTA) [(cdt)-NiCN][Li(pmdta)] **10**. According to the NMR spectra all three C=C bonds of cdt are coordinated to the Ni atom. **9** and **10** can also be prepared directly from [Ni(cdt)] and LiCN.[4]

$[Ni(C_2H_4)_3]$ forms well-defined complexes with organolithium[5] and organomagnesium compounds.[6] Metalated aldimines, such as the adduct **8** of phenyllithium and *tert*-butyl isocyanide, should likewise coordinate as masked acyl carbanions to nickel(0) complexes.[7] **8** reacts with $[Ni(C_2H_4)_3]$ in this sense in the presence of one equivalent of PMDTA with formation of **11** (yellow crystals).[8] With TMEDA, **12** is obtained.

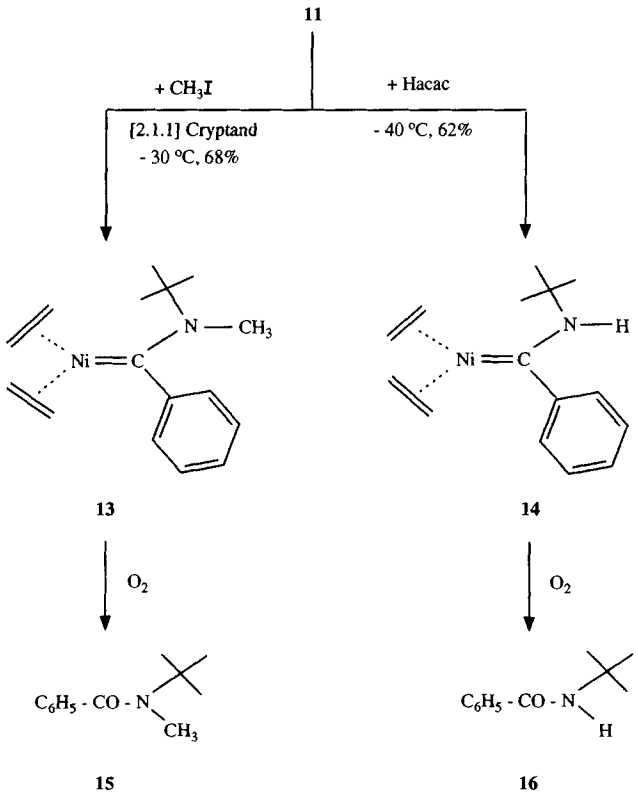

Whereas lithiumacetyl- and lithiumcarbamoylnickel(0) complexes cannot be converted into neutral nickel(0)-carbene complexes,[9] the alkylation of **11** with CH_3I in the presence of [2.1.1]cryptand successfully leads to formation of the neutral 16e nickel(0)-carbene complex **13**.[10] Without cryptand, only amorphous products are obtained. The protonation of **11** with acetylacetone (Hacac) in ether leads in a comparable way to **14**.[11] **13** and **14** precipitate in the form of orange-

[*] Prof. Dr. G. Wilke, B. Gabor, Prof. Dr. C. Krüger, Dr. B. Marczinke, Dr. R. Mynott
Max-Planck-Institut für Kohlenforschung
Kaiser-Wilhelm-Platz 1, W-4330 Mülheim a. d. Ruhr (FRG)

yellow crystals, which are readily soluble in ether and THF, but only sparingly soluble in pentane. **13** and **14** are the first 16e nickel(0)-carbene complexes; moreover, they contain only olefins as further ligands.

For chemical characterization, **13** and **14** were converted with oxygen into the acid amides **15** and **16**, respectively. **13** and **14** are stable up to about room temperature and could be characterized on the basis of NMR spectra. The 400-MHz ^{1}H NMR and 75.5-MHz ^{13}C NMR spectra of solutions of **13**[10] in [D$_8$]THF are temperature dependent. At -30 °C a sharp signal is observed at $\delta = 48.6$ for the ethene C atoms and an AA'BB' multiplet ($\delta_A = 2.38$, $\delta_B = 2.18$) for the diasterotopic geminal ethene protons. The signal for the carbene-C atom, with $\delta = 280.4$, lies in the range characteristic for aminocarbene complexes.[12] At -110 °C the rotation of the ethene ligand about the bond axis to the Ni atom is frozen, i.e. the ethene-C atom now affords two sharp signals at $\delta =$ 50.4 and 46.0.

An unequivocal proof of the structure was provided by a crystal structure analysis of **13** at -173 °C.[13]

It can be seen from Figure 1 that the ligands are arranged around the nickel atom in a trigonal planar fashion. Two

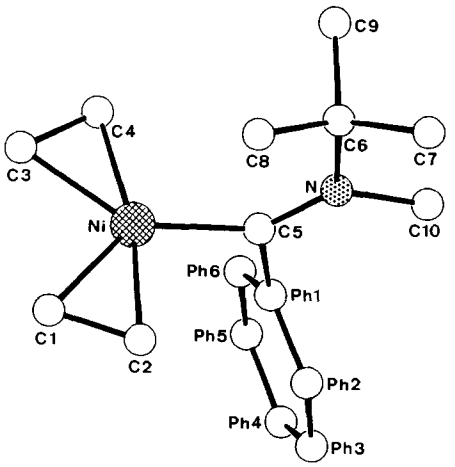

Fig. 1. Structure of **13** in the crystal. Selected bond lengths [Å] and angles [°]: Ni-C1 2.008(1), Ni-C2 2.008(1), Ni-C3 2.000(1), Ni-C4 1.999(1), Ni-C5 1.889(1), C5-N 1.320(1), C5-Ph1 1.503(1), C1-C2 1.392(2), C3-C4 1.398(2); Ph1-C5-N 115.3(1), Ph1-C5-Ni 108.7(1), N-C5-Ni 136.1(1) [13, 16].

coordination sites are occupied by the ethene units, the third by the planar aminocarbene ligand. The coordination plane of the metal (Ni, midpoint of C1–C2, midpoint of C3–C4) forms a dihedral angle of 81.3° with the plane of the carbene (N,C5,Ph1), the phenyl ring an interplanar angle of 74.3° with the latter plane. From the torsion angles (Ph1,C5,N,C6 $=180°$ and Ph1,C5,N,C10 $= 4.9°$) it follows that there is a flattening of the coordination geometry of the nitrogen atom and thus a demonstrated double bond character for C5–N (1.320(1) Å) that is typical of aminocarbene complexes.

By reaction of **14** with phosphanes PR_3 (R = Et, cyclohexyl (cHex), Ph) one or two ethene ligands can be displaced,

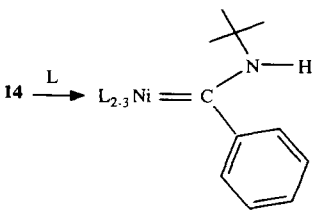

17, L = C_2H_4 + PEt_3
18, L = C_2H_4 + $PcHex_3$
19, L = C_2H_4 + PPh_3
20, L = 2 PPh_3
21, L = 3 CO

with formation of the monophosphane complexes **17**–**19** in good yields in the form of red crystals as well as of the bisphosphane complex **20**. Both in the case of **14** and **13**, reaction with CO leads to the tricarbonylnickel carbene complexes **21** and **22**, respectively, which are not accessible from [Ni(CO)$_4$] and organolithium compounds.

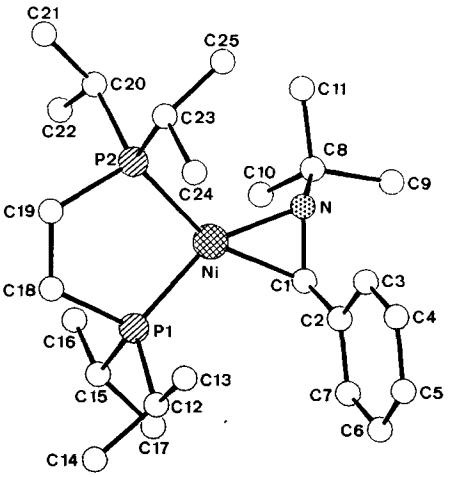

Fig. 2. Crystal structure of **23**. Selected bond lengths [Å] and angles [°]: Ni-P1 2.165(1), Ni-P2 2.188(1), Ni-N 1.915(3), Ni-C1 1.959(4), N-C1 1.375(5), C1-Ni-N 41.6(2), C1-Ni-P2 157.3(1), C1-Ni-P1 110.8(1), N-Ni-P2 116.7(1), N-Ni-P1 152.3(1), P2-Ni-P1 91.0(1) [15, 16].

Surprisingly, displacement of the ethene ligands from **14** takes a completely different course when chelate phosphanes $R_2PCH_2CH_2PR_2$ are employed. Between -20 °C and room temperature the complexes **23** and **24** are obtained in which imines are coordinated to nickel(0), i.e. a rearrangement takes place en route from **14** to **23** and **24**.[14] The structures follow unequivocally from the NMR spectra and a crystal structure analysis of **23** (Fig. 2).[15] Reaction of **14** with half an equivalent of $Ph_2PCH_2CH_2PPh_2$ affords a red, finely crystalline precipitate, whose composition and spectroscopic data are consistent with the presence of **25**.

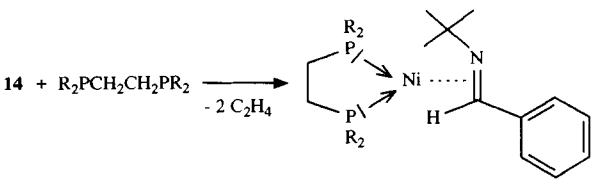

23, R = *i*Pr
24, R = cyclohexyl

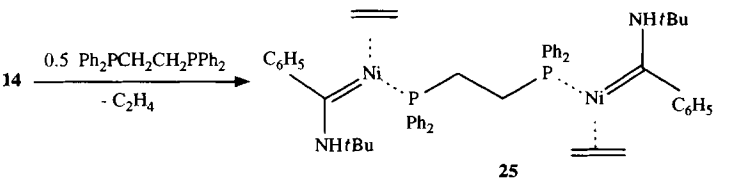

25

The results suggest a path by which the tetracarbenenickel(0) complex **3** might be formed.

Received: July 31, 1991 [Z 4840 IE]
German version: *Angew. Chem. 103* (1991) 1711

CAS Registry numbers:
11, 137057-22-8; **13**, 137041-55-5; **14**, 137041-54-4; **23**, 137041-56-6; [Ni(cdt)], 12126-69-1.

[1] U. Schöllkopf, F. Gerhart, *Angew. Chem. 80* (1968) 842; *Angew. Chem. Int. Ed. Engl. 7* (1968) 805.
[2] A. Mollbach, G. Wilke, unpublished.
[3] a) B. Marczinke, *PhD Thesis*, Universität Bochum 1988; b) E. Bessler, B. M. Barbosa, W. Miller, J. Weidlein, *Z. Naturforsch. B46* (1991) 490.
[4] K. R. Pörschke, unpublished.
[5] W. Kaschube, *Dissertation*, Universität Bochum 1987.
[6] K. R. Pörschke, G. Wilke, *Chem. Ber. 117* (1984) 56.
[7] G. E. Niznik, W. H. Morrison III, H. M. Walborsky, *J. Org. Chem. 39* (1974) 600.
[8] All the new compounds gave correct elemental analyses. Procedure for **11**: A solution of LiC_6H_5 (2.75 g, 30.6 mmol) in ether (100 mL) was treated with *t*BuNC (3.3 mL, 29.2 mmol) and PMDTA (9.0 mL) at −25 °C. After 20 min, an orange precipitate separated out from the deep-red solution which dissolved upon addition of a solution of $[Ni(C_2H_4)_3]$ prepared from [Ni(cdt)] (6.43 g, 29.1 mmol) in 50 mL of ether. After 12 h at −78 °C a yellow crystallizate was obtained which was isolated cold by suction, washed with cold ether, and dried at −30 °C in a high vacuum. Yield: 8.2 g (62%). ^{1}H NMR (200 MHz, [D$_8$]THF, −30 °C): δ = 1.27 (s, 9H; $C(CH_3)_3$), 1.93–2.09 (m, 8H; C_2H_4), 2.12 (s, 12H; $N(CH_3)_2$), 2.20 (s, 3H; NCH_3), 2.30–2.40 (m, 8H; NCH_2CH_2N), 6.96–7.13, 5H; C_6H_5). ^{13}C NMR (75.5 MHz, [D$_8$]THF, −30 °C): δ = 260.0 (Ni=C), 155.3, 123.8, 128.1, 124.3 (C_6H_5), 58.5, 56.3 (NCH_2CH_2N), 57.8 ($C(CH_3)_3$), 46.2 ($N(CH_3)_2$), 43.4 (C_2H_4), 32.1 ($C(CH_3)_3$), 44.2 (NCH_3).
[9] E. O. Fischer, F.R. Kreissl, E. Winkler, C. G. Kreiter, *Chem. Ber. 105* (1972) 588.
[10] Procedure for **13**: A solution of **11** (1.29 g, 2.82 mmol) in THF (20 mL) was treated at −30 °C with 0.75 mL (2.86 mmol) of 4,7,13,18-tetraoxa-1,10-diazabicyclo[8.5.5]eicosane (Kryptofix 211) and 395 mg (2.8 mmol) of CH_3I in 10 mL of ether. A yellow precipitate was formed. The mixture was warmed within 1 h to 0 °C and the ether removed in a high vacuum. The residue was taken up in pentane and filtered. On cooling the red filtrate to −78 °C orange-red prismatic crystals separated out; these were filtered off, washed with pentane, and dried in a high vacuum at 0 °C. 558 mg (68%). ^{1}H NMR (400 MHz), [D$_8$]THF, −30 °C): δ = 1.52 (s, 9H; $C(CH_3)_3$), 2.18, 2.39 (m, 8H; C_2H_4), 2.99 (s, 3H; NCH_3), 6.67–7.16 (m, 5H; C_6H_5). ^{13}C NMR (75.5 MHz, [D$_8$]THF, −30 °C): δ = 280.4 (Ni=C), 148.1, 120.5, 128.7, 124.6 (C_6H_5), 63.9 ($C(CH_3)_3$), 48.6 (C_2H_4), 38.4 (NCH_3), 29.4 ($C(CH_3)_3$). Mass spectrum (70 eV/50 °C): *m/z* 289 ($M^{\oplus}$) (calcd. 289 for ^{58}Ni).
[11] Procedure for **14**: A suspension of **11** (9.13 g, 20.1 mmol) in 80 mL of ether was treated at −40 °C with a solution of acetylacetone (2.1 mL, 20.4 mmol) in ether (20 mL) and warmed to 0 °C. After 30 minutes the precipitated lithium acetylacetonate was removed by filtration and the red solution cooled to −78 °C. The orange crystals that separated from the filtrate were recovered by filtration, washed with pentane, and dried at −20 °C in a high vacuum. **14** initially crystallized together with a half equivalent of PMDTA, which was removed by recrystallization from pentane. 3.44 g (62%). ^{1}H NMR (400 MHz, [D$_8$]THF, −30 °C): δ = 1.40 (s, 9H; $C(CH_3)_3$), 2.21–2.35 (m, 8H; C_2H_4), 7.0–7.18 (m, 5H; C_6H_5), 9.27 (s, 1H; NH). ^{13}C NMR (75.5 MHz, [D$_8$]THF, 40 °C): δ = 277.3 (Ni=C), 150.4, 123.4, 128.5, 127.4 (C_6H_5), 57.4 ($C(CH_3)_3$), 48.3 (C_2H_4), 30.1 ($C(CH_3)_3$). Mass spectrum (70 eV/40 °C): *m/z* 275 ($M^{\oplus}$) (calcd. 275 for ^{58}Ni).
[12] B. E. Mann, B. F. Taylor: *^{13}C-NMR-Data for Organometallic Compounds*, Academic Press, London 1981.
[13] Crystal structure analysis of **13** ($C_{16}H_{25}NNi$, M_r = 290.1): crystal dimensions 0.20 × 0.20 × 0.42 mm, a = 10.002(2), b = 11.949(2), c = 12.295(3) Å, β = 100.24(2)°, V = 1520.1 Å^3, T = −173 °C, ϱ_{calcd} = 1.27 g cm^{-3}, μ = 12.66 cm^{-1}, $F(000)$ = 624 e, Z = 4, monoclinic, space group $P2_1/a$ (No. 14), Enraf-Nonius CAD4 diffractometer, λ = 0.71069 Å, method of measurement ω-2θ, 19133 measured reflections ($+h, +k, +l$) [EDD determination, X-X], $[\sin\theta/\lambda]_{max}$ 0.90 Å^{-1}, analytical absorption correction (min: 1.253, max: 1.418), 9214 independent and 7121 observed reflections [$I > 2\sigma(I)$], 263 refined parameter; heavy atom method, H atom positions observed and included in the least squares refinement, R = 0.039, R_w = 0.035 $w = 1/\sigma^2$ (F_o), maximum residual electron density 0.91 eÅ^{-3}. See also Ref. [16].
[14] Procedure for **23**: A stirred solution of **14** (861.5 mg, 3.12 mmol) in toluene (25 mL) was treated at −78 °C with a solution of 0.95 mL (3.1 mmol) of dppe in 5 mL of toluene and the mixture warmed to −10 °C for 2 h. The solution was evaporated down in a high vacuum, and 20 mL of pentane was added. Within a day at −78 °C, crystals precipitate. They were separated off, washed with pentane, and dried at room temperature in an oil-pump vacuum. Yield: 927 mg (62%). M.p. 160 °C (decomp.). ^{1}H NMR (400 MHz, [D$_8$]THF, 27 °C): δ = 0.08–1.35 (m, 24H; $P(CH(CH_3)_2)$, 1.25 (s, 9H; $C(CH_3)_3$), 1.63–2.28 (m, 4H; $P(CH(CH_3)_2)$, 5.05 (d, 1H; CH=$NC(CH_3)_3$, 6.75–7.27 (m, 5H; C_6H_5). ^{13}C NMR (75.5 MHz), [D$_8$]THF, −30 °C): δ = 150.4, 124.9, 128.1, 121.9 (C_6H_5), 67.7 (CH=$NC(CH_3)_3$), 56.1 ($C(CH_3)_3$), 33.4 ($C(CH_3)$ 26.9, 26.5, 25.1, 23.2 ($PC(CH_3)_2$), 21.1, 21.0, 20.4, 20.0, 19.7, 18.8, 17.4, 16.7 ($PC(CH_3)_2$), 20.7, 20.1 (PCH_2CH_2P). ^{31}P NMR (32.4 MHz, [D$_8$]toluene, 38 °C): δ = 63.6, 65.8 (d; J_{PP} = 66.0 Hz). Mass spectrum (70 eV/120 °C): *m/z* 481 ($M^{\oplus}$) (calcd. 481 for ^{58}Ni).
[15] Crystal structure analysis of **23** ($C_{25}H_{47}NiNP_2$, M_r = 482.3): crystal dimensions 0.14 × 0.29 × 0.36 mm, a = 16.943(2), b = 17.420(2), c = 9.434(2) Å, β = 94.39(1)°, V = 2776.1 Å^3, ϱ_{calcd} = 1.15 g cm^{-3}, μ = 8.25 cm^{-1}, $F(000)$ = 1048 e, Z = 4, monoclinic, space group Cc (No. 9), Enraf-Nonius CAD4 diffractometer, λ = 0.71069 Å, method of measurement ω-2θ, 6267 measured reflections ($\pm h, \pm k, +l$), $[(\sin\theta/\lambda]_{max}$ 0.65 Å^{-1}, 3140 independent and 2509 observed reflections [$I > 2\sigma(I)$], 261 refined parameters, heavy-atom method, H atom positions calculated and not included int the least squares refinement, R = 0.031, R_w = 0.033 [$w = 1/\sigma^2$ (F_o)] maximum residual electron density 0.40 eÅ^{-3}. See also Ref. [16].
[16] Further details of the crystal structure analyses are available on request from the Fachinformationszentrum Karlsruhe, Gesellschaft für wissenschaftlich-technische Information mbH, W-7514 Eggenstein-Leopoldshafen 2 (FRG), on quoting the depository number CSD-55642, the names of the authors, and the journal citation.

Tetraalkoxytitanium-Carbene Complexes with Double Intramolecular Et_2Al Bridging

By *Carl Krüger, Richard Mynott, Carsten Siedenbiedel, Ludwig Stehling*, and *Günther Wilke**

Dedicated to Professor Kurt Schaffner on the occasion of his 60th birthday

During investigations of the vaporization of elemental titanium in ketone and aldehyde matrices we have observed C–C coupling with formation of titanium(II) diolates. They contain, in addition, end-on coordinated ketones or aldehydes. In the case of the di-*tert*-butyl ketone no coupling takes place, and only two ketone molecules are bound side-on per Ti atom.[1] The product of a vaporization of titanium in ketone surprisingly forms a catalyst with $AlEt_3$, with which high molecular weight polyethylene can be prepared. In this connection we have investigated the synthesis and the behavior of titanium(IV) bisdiolates as components of Ziegler catalysts. Already in 1956 *H. Martin*[2] was able to show that a catalyst is formed from $Ti(OnBu)_4$ and $AlEt_3$ which preferentially dimerizes ethene to butene at normal pressure, without significant amounts of polyethylene being formed. At the same time *Wilke* found[3] that butadiene affords high molecular weight 1,2-polybutadiene with this catalyst system.

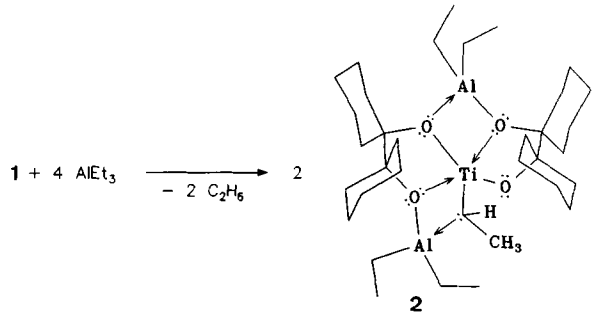

Scheme 1. **1** is a titanium bisdiolate (see Text).

When $Ti(OEt)_4$ is allowed to react with bicyclohexyl-1,1'-diol, ethanol can be removed, and a very sparingly soluble titanium bisdiolate **1** is obtained, which according to its mass spectrum is dimeric (*m/z* 880 ($M^{\oplus}$)). The product of the same

[*] Prof. Dr. G. Wilke, Prof. Dr. C. Krüger, Dr. R. Mynott, C. Siedenbiedel, L. Stehling [+]
Max-Planck-Institut für Kohlenforschung
Kaiser-Wilhelm-Platz 1, W-4330 Mülheim a. d. Ruhr (FRG)
[+] Deceased.

composition obtained from cyclohexanone and Ti atoms is extremely soluble even in pentane. Colorless **1** reacts with two equivalents of $AlEt_3$ per Ti atom in toluene at $-78\,^{\circ}C$ to $-30\,^{\circ}C$ with evolution of two equivalents of ethane to give a red solution. After removal of the toluene a red oil remains, which can be crystallized in pentane at $-78\,^{\circ}C$ (Scheme 1). The red crystals of **2** (40–50% yield) are stable at room temperature. According to elemental analysis **2** has the composition $C_{34}H_{64}O_4Al_2Ti$ (mass spectrum (70 eV/140 °C): m/z 638 ($M^{\oplus}$)). The structure of **2** could be elucidated on the basis of the NMR spectra[4] and a crystal structure analysis[5] (Fig. 1).

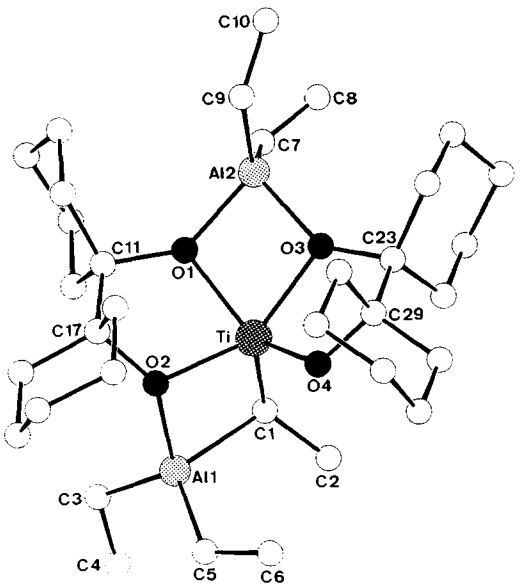

Fig. 1. Crystal structure of **2**. Selected bond lengths [Å] and angles [°]: Ti-O1 2.022(3), Ti-O2 1.960(3), Ti-O3 2.026(3), Ti-O4 1.801(3), Ti-C1 1.933(6), Al1-O2 1.872(3), Al1-C1 2.108(6), Al2-O1 1.853(3), Al2-O3 1.833(3), C1-C2 1.49(1); O2-Ti-C1 88.6(2), Ti-O2-Al1 93.9(1), O2-Al1-C1 86.0(2), Al1-C1-Ti 87.7(2), Al1-C1-C2 114.8(4), C2-C1-Ti 134.3(5).

The ^1H and ^{13}C NMR spectra show that **2** is present in solution in the form of two isomers in the ratio 3.3:1. The positions of the carbene C signals at $\delta = 202.1$ (major component) and 192.2 (minor component) are consistent with those of alkylidene-bridged heterobimetallic carbene complexes such as the structurally analogous Tebbe compounds.[6] Both compounds lack symmetry elements: All 34 C signals of the major component are observed. The occurrence of the two diastereomers can be formally explained in terms of an (*R**)- and an (*S**)-configurated carbene C atom.

The formation of the carbene ligand rests on the fact that two ethyl groups are transferred from the same side to the Ti atoms of **1** so that subsequently an α-H-elimination with cleavage of ethane can take place. As expected, the protolysis of **2** with 2-ethylhexanol affords five equivalents of ethane. With oxygen a product of the composition $C_{32}H_{60}O_9Al_2Ti$ is formed following reaction of all Al–C bonds and replacement of the carbene group by an O atom. The expected acetaldehyde could be detected only in traces under these conditions; in the oxidation with ozone, however we found 97% aldehyde.

Ethene cannot be polymerized with **2** alone; the polymerization takes place only upon addition of excess $AlEt_3$. With the strongly ring-strained 3,3-dimethylcyclopropene, however, **2** reacts in toluene already at room temperature. Addition takes place with ring-opening and formation of the carbene complex **3**. So far, it has not been possible to crystallize the red-brown product. The elemental composition corresponds to $C_{39}H_{72}O_4Al_2Ti$, and in the mass spectrum a peak was observed at m/z 706 ($M^{\oplus}$). The constitution could be ascertained on the basis of the NMR spectra.[7] As in the case of **2**, two isomers are observed which differ in the relative configuration of the carbene C atom. In the ^{13}C NMR spectrum the carbene C signal of the main component (87%) lies at $\delta = 214.9$ ($^1J_{C,H} = 102$ Hz). The double bond in the side chain is *trans*-configurated in both isomers. Remarkably, **3** reacts no further with excess dimethylcyclopropene, possibly on steric grounds.

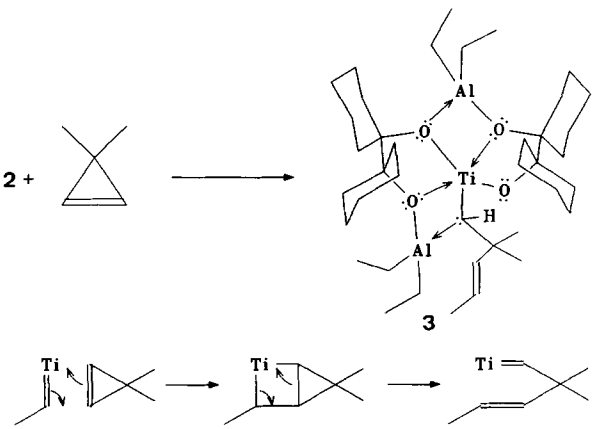

Scheme 2. Reaction of 3,3-dimethylcyclopropene with **2** to give **3**, including proposed mechanism.

To our knowledge **2** is the first example of a titanium-carbene complex, which is not derived from "titanocene" but from a titanium alkoxide, even though the analogy to a "Tebbe reagent"[6] is unmistakable. Also consistent with this is the reaction with 3,3-dimethylcyclopropene to give **3**, which may proceed according to the mechanism formulated in Scheme 2. So far, the titanium bicyclo[2.1.0]pentane intermediate could not be isolated, presumably since it immediately rearranges under the influence of the Et_2Al group; this would be consistent with observations made with corresponding titanocene derivatives.[8, 11]

Received: July 31, 1991 [Z 4841 IE]
German version: *Angew. Chem. 103* (1991) 1714

CAS Registry numbers:
1, 137257-96-6; **2**, 137257-97-7; **3**, 137257-98-8; $Ti(OEt)_4$, 3087-36-3; $AlEt_3$, 97-93-8; bicyclohexyl-1,1'-diol, 2888-11-1; 3,3-dimethylcyclopropene, 3907-06-0.

[1] W. Haaf, H. Schwager, C. Siedenbiedel, L. Stehling, W. Storm, G. Wilke, unpublished.
[2] H. Martin, *Angew. Chem. 68* (1956) 306.
[3] G. Wilke, *Angew. Chem. 68* (1956) 306.
[4] ^1H NMR (400 MHz, [D$_6$]benzene, 27 °C): **2** (major component, 77%): $\delta = 7.71$ (q, $^3J(H,H) = 7.4$ Hz, 1H; TiCH), 2.55 (d, $^3J(H,H) = 7.4$ Hz, 3H; TiCHCH_3); **2** (minor component, 23%): $\delta = 8.61$ (q, $^3J(H,H) = 8.5$ Hz, 1H; TiCH), 2.09 (d, $^3J(H,H) = 8.5$ Hz, 3H; TiCHCH_3). ^{13}C-NMR (100.6 MHz, [D$_6$]benzene, 27 °C): **2** (major component): $\delta = 202.1$ (d, $^1J(C,H) = 110$ Hz, 1C; TiCH), 96.9, 95.9, 93.5, 91.2 (each s, each 1C; (*OC*), 28.2 (q, $^1J(C,H) = 127$ Hz; TiCHCH_3); **2** (minor component): $\delta = 192.2$ (d, 1C; TiCH), 24.7 (q, $^1J(C,H) = 127$ Hz; TiCHCH_3).
[5] Crystal structure analysis of **2** ($C_{34}H_{64}O_4Al_2Ti$, $M_r = 638.7$): crystal dimensions $0.29 \times 0.47 \times 0.29$ mm, $a = 12.218(1)$, $b = 18.819(2)$, $c = 15.823(1)$ Å, $\beta = 92.40(1)^{\circ}$, $V = 3635.0$ Å^3, $\varrho_{calcd} = 1.17$ g cm^{-3}, $\mu = 3.11$ cm^{-1}, $F(000) = 1392$ e, $Z = 4$, monoclinic, space group $P2_1/n$ (No. 14), Enraf-Nonius CAD4 diffractometer, $\lambda = 0.71069$ Å, method of measurement ω-2θ, 8796 measured reflections ($\pm h, +k, +l$), $[\sin\theta/\lambda]_{max}$ 0.65 Å^{-1}, 8249 independent and 4659 observed reflections [$I > 2\sigma(I)$], 370 refined parameters, direct methods, H atom positions calculated

and not included in the least squares refinement, $R = 0.079$, $R_w = 0.069$ [$w = 1/\sigma^2(F_o)$], maximum residual electron density 0.82 e Å^{-3}. Further details of the crystal structure analysis are available on request from the Fachinformationszentrum Karlsruhe, Gesellschaft für wissenschaftlich-technische Information mbH, W-7514 Eggenstein-Leopoldshafen 2 (FRG), on quoting the depository number CSD-55643, the names of the authors, and the journal citation.

[6] F. N. Tebbe, G. W. Parshall, G. S. Reddy, *J. Am. Chem. Soc. 100* (1978) 3611.

[7] ^{1}H NMR (400 MHz, [D$_6$]benzene, 27 °C): **3** (major component, 87%): $\delta = 7.61$ (s, 1H; TiCH), 5.71 (dq, ^3J(H,H) = 15.4 Hz, 1H; $-CMe_2CH=$), 5.29 (dq, ^3J(H,H) = 15.4 Hz, $^3J(H,H_{Me}) = 6.4$ Hz, 1H; $=CHMe$); **3** (minor component, 13%): $\delta = 8.20$ (s, 1H; TiCH), 5.47 (dq, ^3J(H,H) = 15.4 Hz, 1H; $-CMe_2CH=$), 5.25 (dq, ^3J(H,H) = 15.4 Hz, 1H; $=CHMe$). ^{13}C NMR (100.6 MHz, [D$_6$]benzene, 27 °C): **3** (major component): $\delta = 214.9$ (d, ^1J(C,H) = 102 Hz, 1C, TiCH), 143.6 (d, ^1J(C,H) = 147 Hz, 1C; $CMe_2CH=$), 118.6 (d, ^1J(C,H) = 149 Hz, 1C; $=CHMe$), 97.2, 96.6, 93.7, 92.5 (je s, je 1C; *OC*), 49.3 (s, 1C; CMe_2), 32.4, 30.8 (q, ^1J(C,H) = 125 Hz, je 1C; $C(CH_3)_2$ 18.3 (q, ^1J(C,H) = 125 Hz, 1C; $=CHCH_3$); **3** (minor component): $\delta = 197.0$ (d; TiCH).

[8] S. L. Buchwald, R. H. Grubbs, *J. Am. Chem. Soc. 105* (1983) 5490.

[9] L. R. Gilliom, R. H. Grubbs, *Organometallics 5* (1986) 721.

[10] B. J. J. van Heisteeg, G. Schat, O. S. Akkerman, F. Bickelhaupt, *J. Organomet. Chem. 310* (1986) C25.

[11] P. Binger, P. Müller, R. Benn, R. Mynott, *Angew. Chem. 101* (1989) 647; *Angew. Chem. Int. Ed. Engl. 28* (1989) 610.

Novel Tetranuclear Iron–Hexapentaene Complexes: The First Examples of Poly-π-Allyl Complexes

By *Masahiko Iyoda,* Yoshiyuki Kuwatani, Masaji Oda, Kazuyuki Tatsumi,* and *Akira Nakamura*

Dinuclear iron complexes of [3]cumulenes (butatrienes) have received considerable attention because of their high stability and their unique twofold π-allyl structure **1** with an iron–iron bond.[1] Although tetranuclear π-allyl complexes of [5]cumulenes (hexapentaenes) with transition metals might have an interesting π-allyl complex chain structure **2**, transition metal complexes of [5]cumulenes have not yet been extensively studied.[2] Previously, the reaction of hexapentaene with [$Fe_3(CO)_{12}$] was reported to produce only deep purple-red crystals.[3] We reinvestigated the reactions of [5]cumulenes with [$Fe_3(CO)_{12}$] and found the formation of novel tetranuclear iron complexes **2** with iron–iron bonds.

1 **2**

Because of its instability, hexapentaene (C_6H_4) was generated in situ by the reduction of 1,6-dichloro-2,4-hexadiyne (**3**) with zinc.[4] Thus, **3** was treated with zinc in benzene–isooctane at 90–100 °C in the presence of [$Fe_3(CO)_{12}$] to give two isomeric iron–hexapentaene carbonyl complexes **4** (1.6%) and **5** (2%). These complexes are stable both in solid state and in solution. Interestingly, **4** isomerizes to **5** on either heating at 110 °C or irradiation (> 300 nm). In a similar manner treatment of **6** with zinc at 90–100 °C in the presence of [$Fe_3(CO)_{12}$] yielded complexes **7** (2%) and **8** (0.5%), together with the known **9**[2] (2%). The tetranuclear complexes **7** and **8** are less soluble than the dinuclear complex **9**. In particular, **8** is only slightly soluble in organic solvents, presumably due to its rigid molecular structure. Since **9** produces **7** (19%) and **8** (2%) in its reaction with [$Fe_3(CO)_{12}$] in refluxing isooctane, dinuclear complexes such as **9** can be regarded as precursors to the tetranuclear complexes **4** and **5** as well as **7** and **8**. Although isomer **7** was usually the major product, ultraviolet irradiation (> 300 nm) causes its isomerization to **8**.

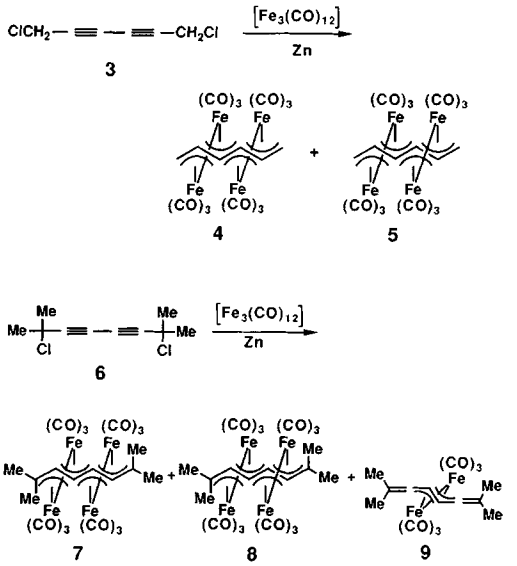

Table 1. Selected physical data of **4**, **5**, **7**, and **8**.

4: Dark red prisms (from pentane), m.p. = 130–133 °C (decomp.); MS: *m/z* (rel. int. [%]) 636 (38, M^+), 608 (30), 580 (10), 552 (15), 524 (12), 496 (32), 468 (100), 442 (75), 412 (34), 384 (44), 356 (51), 328 (56), 300 (67); ^{1}H NMR (270 MHz, $CDCl_3$): $\delta = 4.31$ (d, $J = 2.2$ Hz, 2H; CH_2), 4.82 (d, $J = 2.2$ Hz, 2H; CH_2); ^{13}C NMR (67.5 MHz, $CDCl_3$): $\delta = 68.5$ (d), 84.9 (s), 143.2 (s), 205.0 (s), 206.9 (br.s), 208.1 (s), 212.5 (s); UV/VIS (CH_2Cl_2): λ_{max} [nm] (lg ε) = 314 (4.20), 347 sh (4.07), 466 sh (3.52); IR (KBr): $\tilde{\nu}$ [cm^{-1}] = 2085, 2060, 2035, 1998, 1990, 1973 (C=O).

5: Dark violet fine needles (from CH_2Cl_2-hexane), m.p. = 150 °C (decomp.); MS: *m/z* (rel. int. [%]) 636 (54, M^+), 608 (21), 580 (9), 552 (17), 524 (18), 495 (48), 468 (100), 440 (65), 412 (30), 384 (43), 356 (48), 328 (60), 300 (71); ^{1}H NMR (270 MHz, $CDCl_3$): $\delta = 4.50$ (d, $J = 2.4$ Hz, 2H; CH_2), 4.97 (d, $J = 2.4$ Hz, 2H; CH_2); ^{13}C NMR (100 MHz, $CDCl_3$): $\delta = 70.4$ (d), 79.2 (s), 131.7 (s), 204.5 (s), 207.9 (s), 211.9 (s), 212.4 (s); UV/VIS (CH_2Cl_2): λ_{max} [nm] (lg ε) = 293 sh (4.18), 335 sh (4.02), 431 sh (3.51), 580 (3.51); IR (KBr): $\tilde{\nu}$ [cm^{-1}] = 2070, 2025, 1999, 1980 (C=O).

7: Dark red prisms (from pentane), m.p. = 150 °C (decomp.); MS: *m/z* (rel. int. [%]) 692 (45, M^+), 664 (20), 636 (10), 608 (20), 580 (15), 552 (60), 524 (100), 496 (85), 468 (45), 440 (35), 412 (55), 384 (55), 356 (75); ^{1}H NMR (270 MHz, $CDCl_3$): $\delta = 2.13$ (s, 6H; CH_3), 2.57 (s, 6H; CH_3); ^{13}C NMR (67.5 MHz, $CDCl_3$): $\delta = 28.8$ (q), 31.5 (q), 84.8 (s), 115.0 (s), 136.9 (s); UV/VIS (CH_2Cl_2): λ_{max} [nm] (lg ε) = 308 sh (4.23), 350 sh (4.02), 476 sh (3.45); IR (KBr): $\tilde{\nu}$ [cm^{-1}] = 2083, 2060, 2025, 1986, 1975, 1962 (C=O).

8: Dark violet fine needles (from CH_2Cl_2), m.p. = 170 °C (decomp.); MS: *m/z* (rel. int. [%]) 692 (46, M^+), 664 (33), 636 (15), 608 (24), 580 (22), 552 (67), 524 (100), 496 (91), 468 (48), 440 (37), 412 (74), 384 (46), 356 (48); ^{1}H NMR, (270 MHz, $CDCl_3$): $\delta = 2.19$ (s, 6H; CH_3), 2.56 (s, 6H; CH_3); ^{13}C NMR (100 MHz, $CDCl_3$): $\delta = 29.2$ (q), 32.3 (q), 79.9 (s), 117.3 (s), 127.1 (s); UV/VIS (CH_2Cl_2): λ_{max} [nm] (lg ε) = 274 sh (4.43), 341 sh (4.04), 435 sh (3.53), 580 (3.41); IR (KBr): $\tilde{\nu}$ [cm^{-1}] = 2058, 2025, 1986, 1970 (C=O).

[*] Prof. Dr. M. Iyoda[+], Dr. Y. Kuwatani, Prof. Dr. M. Oda
Department of Chemistry, Faculty of Science
Osaka University
Toyonaka, Osaka 560 (Japan)
Prof. Dr. K. Tatsumi [++], Prof. Dr. A. Nakamura
Department of Macromolecular Science, Faculty of Science
Osaka University

[+] New address: Department of Chemistry, Faculty of Science
Tokyo Metropolitan University
Hachioji, Tokyo 192-03 (Japan)

[++] New address: Department of Chemistry
Faculty of Engineering Science
Osaka University
Toyonaka, Osaka 560 (Japan)

The tetranuclear complexes exhibit characteristic electronic and NMR spectra (Table 1), the latter reflecting the highly symmetrical structures. The ^{1}H NMR spectra of **4** and **5** show two doublets at $\delta = 4.82$ and 4.31, and 4.97 and 4.50, respectively. The ^{1}H NMR spectra of **7** and **8** contain only two singlets of methyl groups at $\delta = 2.57$ and 2.13, and 2.56 and 2.19, respectively. The ^{13}C NMR spectra of **4** and **5** show three signals of carbon skeleton (**4**: $\delta = 143.2$, 84.9, 68.5; **5**: $\delta = 131.7$, 79.2, 70.4) besides carbonyl signals. The strong IR bands at 1970–2085 cm^{-1} arise from the stretching of the terminal carbonyl groups. None of the spectra show absorptions in the bridging carbonyl region. Interestingly, the mass spectra of these complexes reveal the stepwise elimination of twelve CO groups to $[R_4C_6Fe_4]^{\oplus}$ (R = H, CH_3). Similar fragmentation processes were reported in the mass spectra of the butatriene–iron carbonyl complexes $[(R_4C_4)Fe_2(CO)_6]$.[5, 6]

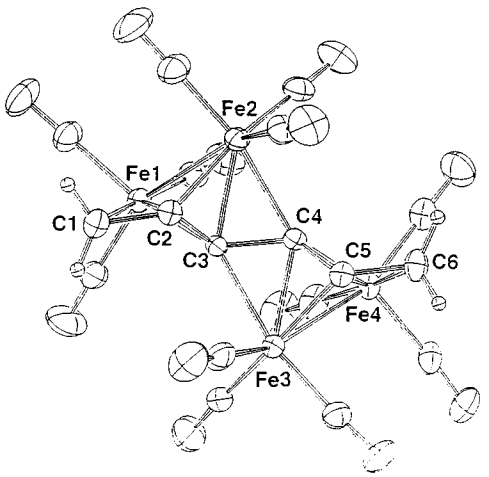

Fig. 1. X-ray crystal structure of **4**. Selected bond distances [Å] and angles [°]: Fe1-Fe2 2.5991(8), Fe3-Fe4 2.589(1), Fe1-C1 2.216(5), Fe1-C2 2.018(4), Fe1-C3 1.965(3), Fe2-C2 1.903(4), Fe2-C3 2.096(4), Fe2-C4 2.222(4), F3-C3 2.208(4), Fe3-C4 2.104(4), Fe3-C5 1.897(4), Fe4-C4 1.955(4), Fe4-C5 2.013(4), Fe4-C6 2.195(4), C1-C2 1.378(5), C2-C3 1.386(5), C3-C4 1.461(5), C4-C5 1.382(5), C5-C6 1.377(5); C1-C2-C3 126.1(4), C2-C3-C4 125.8(3), C3-C4-C5 124.9(3), C4-C5-C6 125.6(4).

The structures of **4** and **5** were determined by X-ray diffraction (Fig. 1 and 2).[7] As shown in Figure 1, **4** has an approximate C_2 symmetry with a twofold axis passing through the midpoint of the C3–C4 bond. The Fe–Fe and Fe–CO bond lengths are normal. The hexapentaene skeleton has a zig-zag configuration in which the average bond angle between each set of three carbon atoms is 125.6°. The atoms C1–C4 and C3–C6 lie in two planes which are twisted 79.6(5)° respective to each other. The dihedral angle between Fe2–C3–C4 and Fe3–C3–C4 is 155.0(1)°. Complex **5** has a crystallographic center of symmetry (Fig. 2) and the central four-membered ring consisting of Fe1–C1–Fe1*–C1* is exactly planar. The hexapentaene skeleton has a zig-zag configuration with bond angles of 124.1° and 127.9°. Of special note is the coplanarity of the six carbon atoms of the hexapentaene ligand (maximum deviation 0.02 Å).

The coordination geometry of each iron atom of **4** and **5** is best described as distorted octahedral. Each complex has two short (1.897–1.984 Å) and four long bonds (2.018–2.222 Å) between the iron atoms and the carbon atoms in the cumulene ligand. This bonding mode is analogous to that of butatriene[bis(tricarbonyliron)] complexes.[8]. It is noteworthy that the cumulenic carbons (C3 and C4 in **4** and C1 and

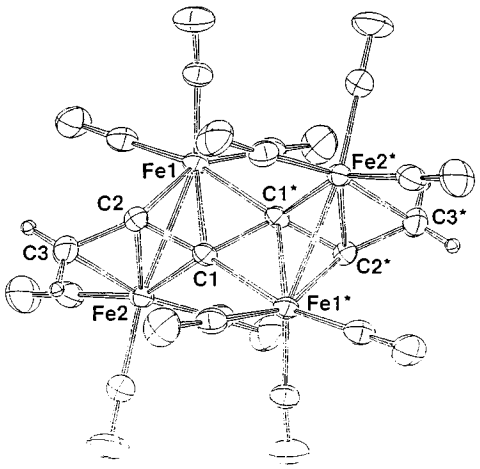

Fig. 2. X-ray crystal structure of **5**. Selected bond distances [Å] and angles [°]: Fe1-Fe2 2.577(1), Fe1-C1 2.096(5), Fe1-C2 1.927(5), Fe1-C1* 2.183(5), Fe2-C1 1.984(5), F2-C2 2.024(5), Fe2-C3 2.198(6), C1-C2 1.386(7), C2-C3 1.370(8), C1-C1* 1.454(9); C1*-C1-C2 124.1(6), C1-C2-C3 127.9(5).

C1* in **5**) form bonds to five other atoms. Thus, two π orbitals of these central carbon atoms are equally shared with two iron atoms (Fe2 and Fe3 in **4** and Fe1 and Fe1* in **5**). The double coordination on both sides of π bond causes the lengthening of the central bonds to 1.461(5) Å in **4** and 1.454(9) Å in **5**. Although similar coordination has been previously described in transition metal complexes of acetylenes,[9] this is new in the complexes of cumulenes. The four $Fe(CO)_3$ groups in each complex are aligned along the hexapentaene linkage with η^3-allyl-like coordination,[10] and make a π-allyl chain complex.

Extended Hückel calculations were performed on **4** and **5**.[11] Despite the substantial differences in their geometries, the two isomers were found to be comparable energetically; isomer **4** is calculated to be only 0.31 eV lower in energy. Also the calculated charge distribution (Q) as well as the Fe–C and C–C overlap populations (P) are remarkably similar, indicating that the nature of the Fe–hexapentaene bonds in **4** and **5** is essentially the same. The salient results of the population analyses are: 1) P(Fe1–C3) of 0.347 (**4**) and 0.340 (**5**) and P(Fe2–C2) of 0.369 (**4**) and 0.370 (**5**) are notably larger than the other Fe1(Fe2)–C overlap populations (0.058–0.168), because these bonds contain contributions from Fe–C σ-bonding in addition to the Fe–π-allyl type interactions. 2) The inner C3–C4 bond is evidently weaker than the outer C–C bonds; P(C3–C4) = 0.903 (**4**) and 0.915 (**5**) versus P(C1–C2), P(C2–C3) = 1.036–1.080. 3) The innermost carbons (C3 and C4) are highly positively charged; Q = +0.201e (**4**) and +0.187e (**5**). 4) The Fe–Fe bonding interaction is retained upon coordination to hexapentaene; P(Fe–Fe) = 0.187 (**4**) and 0.184 (**5**) versus 0.200 for $[Fe_2(CO)_6]^{2+}$. These theoretical results are consistent with our experimental findings.

Received: June 7, 1991 [Z 4687 IE]
German version: *Angew. Chem. 103* (1991) 1697

CAS Registry numbers:
3, 16266-59-6; **4**, 137123-38-7; **5**, 137252-32-5; **6**, 2431-48-3; **7**, 137123-39-8; **8**, 137172-95-3; **9**, 56126-35-3; $[Fe_3(CO)_{12}]$, 17685-52-8.

[1] *Gmelin Handbuch der Organischen Chemie: Organoiron Compounds, Part C3*, Springer, Berlin 1979, p. 10.
[2] R. B. King, C. A. Harmon, *J. Organomet. Chem. 88* (1975) 93.
[3] A. Nakamura, *Bull. Chem. Soc. Jpn. 38* (1965) 1868.

[4] See W. M. Schubert, T. H. Liddicoet, W. A. Lanka, *J. Am. Chem. Soc. 74* (1952) 569; *ibid. 76* (1954) 1929.
[5] R. B. King, *J. Am. Chem. Soc. 88* (1966) 2075; R. B. King, A. Efraty, *Org. Mass Spectrom. 2* (1969) 657.
[6] S. Otsuka, A. Nakamura, T. Yoshida, *Bull. Chem. Soc. Jpn. 40* (1967) 1266.
[7] Crystallographic data: Rigaku AFC-5R diffractometer, $Mo_{K\alpha}$ radiation ($\lambda = 0.71073$ Å, graphite monochromator), 23 ± 1 °C. Solution: direct methods (MITHRIL-based TEXRAY System). Refinement: all atoms including hydrogens were found; all non-H atoms were refined anisotropically and all H atoms, isotropically by full matrix least-squares procedures. **4**: $0.2 \times 0.35 \times 0.4$ mm^3, monoclinic, space group $C2/c$, $a = 13.952(4)$, $b = 10.566(5)$, $c = 30.690(4)$ Å, $\beta = 97.16(2)°$, $V = 4489(2)$ Å^3, $Z = 8$, $\rho_{calcd} = 1.88$ g cm^{-3}. 7219 reflections collected ($3° < 2\theta < 60°$); unique: 6294; observed: 3915 [$|F_o|^2 > 3\sigma(F_o^2)$]. $R = 0.039$, $R_w = 0.042$. 323 refined parameters. **5**: $0.15 \times 0.3 \times 0.3$ mm^3, triclinic, space group $P\bar{1}$, $a = 9.088(2)$, $b = 9.813(2)$, $c = 7.614(2)$ Å, $\alpha = 99.62(2)$, $\beta = 114.59(1)$, $\gamma = 108.94(1)°$, $V = 552.5(2)$ Å^3, $Z = 1$, $\rho_{calcd} = 1.91$ g cm^{-3}. 3424 reflections collected ($3° < 2\theta < 60°$); unique: 3236; observed: 1684 [$|F_o|^2 > 3\sigma(F_o^2)$]. $R = 0.042$, $R_w = 0.043$. 162 refined parameters. Crystallographic analysis performed by Molecular Structure Corporation, College Station, TX (USA). Further details of the crystal structure investigation are available on request from the Director of the Cambridge Crystallographic Data Centre, University Chemical Laboratory, Lensfield Road, GB-Cambridge CB2/EW (UK), on quoting the full journal citation.
[8] a) J. N. Gerlach, R. M. Wing, P. C. Ellgen, *Inorg. Chem. 15* (1976) 2959; b) D. Bright, O. S. Mills, *J. Chem. Soc. Dalton Trans. 1972*, 2465.
[9] L. F. Dahl, D. L. Smith, *J. Am. Chem. Soc. 84* (1962) 2450; B. F. G. Johnson, J. Lewis, B. E. Reichert, K. T. Schorpp, G. M. Sheldrick, *J. Chem. Soc. Dalton Trans. 1977*, 1417; E. Sappa, A. Tiripicchio, M. T. Camellini, *ibid. 1978*, 419; J. R. Fox, W. L. Gladfelter, G. L. Geoffroy, I. Tavanaiepour, S. Abdel-Mequid, V. W. Day, *Inorg. Chem. 20* (1981) 3230.
[10] A similar bond between butatriene and iron atoms has been suggested to be an η^3-allyl bond. [8a]
[11] Our calculations reasonably reproduced the main features of the X-ray derived structure of **4** and **5**. The extended Hückel parameters for Fe are the following: orbital exponents: 4s and 4p, 1.9; 3d, 5.35(0.5366) + 1.8(0.6678). H_{ii}: 4s, −9.17 eV; 4p, −5.37 eV; 3d, −12.7 eV. The parameters for C and H are the standard ones. Geometrical assumptions include the followings: C–C, 1.4 Å; C–H, 1.09 Å; Fe–Fe, 2.6 Å; Fe–C(carbonyl), 1.8 Å; C–O 1.13 Å; the center of Fe–Fe bond is situated 1.45 Å above the center of C2–C3 or C4–C5 bond.

$(NBu_4)[Mn_4O_2(H_2O)(O_2CPh)_9]$, a Butterfly Complex with Bound H_2O, and Its Use to Prepare Octanuclear and Undecanuclear Metal Complexes**

By *Sheyi Wang, John C. Huffman, Kirsten Folting, William E. Streib, Emil B. Lobkovsky,* and *George Christou**

Manganese chemistry at the higher metal oxidation states ($\geq$ II) is currently an area of great activity. One reason for this is the occurrence of Mn in biological systems,[1] particularly the Mn_4 aggregate in the photosynthetic water oxidation center (WOC).[2] To model the WOC, we have prepared complexes of formulation $[Mn^{III}_4O_2(O_2CR)_x(L\text{–}L)_2]^z$ ($x = 6$ or 7; L–L = a chelate ligand; $z = -1, 0, +1$) possessing the $[Mn_4(\mu_3\text{-}O)_2]^{8+}$ core with a butterfly disposition of Mn atoms.[3] Higher nuclearity Mn_y aggregates ($y \geq 6$) have also been attracting increasing interest, not least for their aesthetic qualities.[4–8] More importantly, however, these aggregates have displayed a propensity for large spin ground states.[4c, 8b, d] Only a limited number of higher nuclearity Mn aggregates are currently known, including various structural types and oxidation levels;[4–8] we have pointed out elsewhere the potential utility of discrete Mn aggregates with large spin ground states as precursors to molecular ferromagnets.[8b] We herein describe results of relevance to both the above areas: namely, the preparation of an Mn_4O_2 complex with a bound H_2O ligand, and its employment as a stepping-stone to new Mn_8 and Na_2Mn_9 aggregates.

The comproportionation between $[Mn(O_2CPh)_2] \cdot 2\,H_2O$ and NBu_4MnO_4 (Bu = *n*Bu) in an approximate 2.5:1 ratio in EtOH/MeCN yields dark red crystals of $(NBu_4)[Mn_4O_2(H_2O)(O_2CPh)_9]$ (**1**) in 90–95 % yield after recrystallization.[9] The structure[10] of the anion of **1** (Fig. 1) shows a butterfly $[Mn^{III}_4O_2]^{8+}$ core similar to that in, for example, $[Mn_4O_2(O_2CMe)_7(bpy)_2]^+$ and $[Mn_4O_2(O_2CMe)_7(pic)_2]^-$ (bpy = 2,2′-bipyridine; pic^- = 2-picolinate).[3] However, the absence of chelating bpy or pic has interesting consequences; Mn4 possesses instead an additional benzoate group in a rare asymmetrical chelating mode, where Mn4–O24 (2.373(11) Å) is much longer than Mn4–O22 (1.947(11) Å). There is also an additional benzoate group at Mn3 but this is ligated in a monodentate fashion; the remaining site is occupied by a terminal aqua ligand (O18), which is hydrogen-bonded to the unligated benzoate atom O25 (O18 ··· O25, 2.634(24) Å).

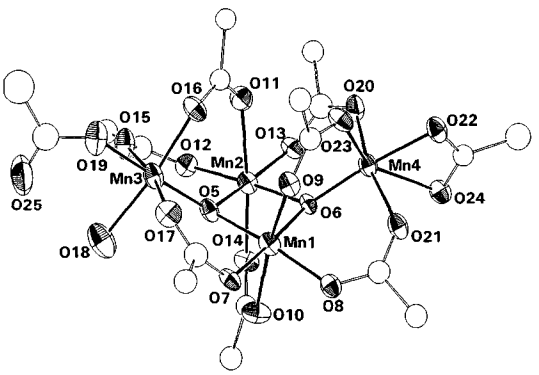

Fig. 1. ORTEP representation of the anion of complex **2**. For clarity, only one benzoate phenyl carbon atom is shown. Selected bond distances [Å]: Mn1 ··· Mn2, 2.816(4), Mn1 ··· Mn3, 3.367(4), Mn1 ··· Mn4, 3.296(4), Mn2 ··· Mn3, 3.302(4), Mn2 ··· Mn4, 3.365(4), O5-Mn1, 1.900(11), O5-Mn2 1.913(10), O5-Mn3 1.823(11), O6-Mn1 1.909(10), O6-Mn2 1.905(11), O6-Mn4 1.825(10), Mn1-O7, 1.946(11), Mn1-O8, 1.940(12), Mn1-O9, 2.206(11), Mn1-O10, 2.206(12), Mn2-O11, 2.202(12), Mn2-O12, 1.923(11), Mn2-O13, 1.973(11), Mn2-O14, 2.136(11), Mn3-O15, 2.136(12), Mn3-O16, 1.982(11), Mn3-O17, 2.111(12), Mn3-O18, 2.102(13), Mn3-O19, 1.903(13), Mn4-O20, 2.038(12), Mn4-O21, 2.037(12), Mn4-O22, 1.974(11), Mn4-O23, 2.016(12), Mn4-O24, 2.373(11), O18 ··· O25, 2.634(24).

Complex **1** represents important progress for our WOC modeling work since it possesses a water-binding site. The ligation of H_2O and its hydrogen bonding to a carboxylate group may be providing a glimpse into how the WOC binds its substrate H_2O and activates it to deprotonation, a necessary step in water oxidation. We are, therefore, studying the reactivity of **1**. Initial efforts have unearthed unusual products from the reactions with benzoyl peroxide and Me_3SiCl.

Attempted oxidation of **1** with equimolar amounts of $(PhCO)_2O_2$ in MeCN causes a darkening of color and crystallization of $[Na_2Mn_9O_7(O_2CPh)_{15}(MeCN)_2] \cdot 3$ MeCN (**2** · 3 MeCN) in 31 % yield after addition of $NaClO_4$.[11] The structure[12] of **2** (Fig. 2) comprises a mixed-metal undecanuclear $[Na_2Mn_9O_7]^{15+}$ core peripherally ligated by benzoate and MeCN groups; the two Na^+ ions are linked to the Mn atoms by both core oxide and benzoate bridges. Thus we

[*] Prof. Dr. G. Christou, S. Wang, Dr. J. C. Huffman, Dr. K. Folting, Dr. W. E. Streib, Dr. E. B. Lobkovsky
Department of Chemistry and the Molecular Structure Center
Indiana University
Bloomington, IN 47405 (USA)

[**] This work was supported by the U.S. National Institutes of Health (GM 39083).

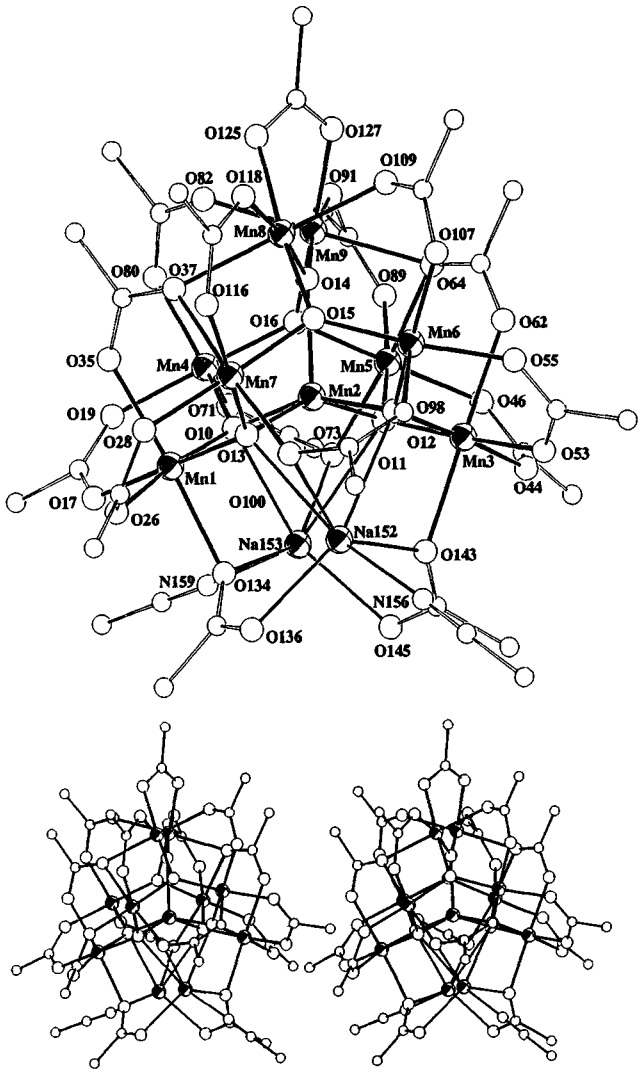

Fig. 2. ORTEP representation and stereoview of complex **2**. Only one phenyl carbon of the benzoate ligand is shown. Selected bond distances [Å]: Mn1···Mn2, 2.886(3), Mn2···Mn3, 2.871(3), Mn1···Mn4, 3.359(3), Mn1···Mn7, 3.318(3), Mn2···Mn4, 3.311(3), Mn2···Mn5, 3.241(3), Mn2···Mn6, 3.318(3), Mn2···Mn7, 3.261(3), Mn3···Mn5, 3.315(3), Mn3···Mn6, 3.358(3), Mn2···Mn8, 3.388(3), Mn2···Mn9, 3.393(3), Mn8···Mn9, 3.281(3), O10-Mn1, 1.893(4), O10-Mn2 1.934(4), O10-Mn4 1.888(4), O10-Na153, 2.537(5), O11-Mn2 1.906(4), O11-Mn3 1.884(4), O11-Mn5 1.858(4), O11-Na153, 2.824(5), O12-Mn2 1.927(4), O12-Mn3 1.895(4), O12-Mn6 1.891(4), O12-Na152, 2.610(5), O13-Mn1 1.892(4), O13-Mn2 1.911(4), O13-Mn7 1.890(4), O13-Na152, 2.596(5), O14-Mn2 2.111(4), O14-Mn8 1.851(4), O14-Mn9 1.859(4), O15-Mn6 1.845(4), O15-Mn7 1.872(4), O15-Mn8 1.884(4), O16-Mn4 1.849(4), O16-Mn5 1.886(4), O16-Mn9 1.889(4).

prefer a mixed-metal aggregate description to an ion-pairing description. The Mn atoms are all in the +III oxidation state as evidenced by interatomic distances and Jahn–Teller elongations; the Mn_9 portion of **2** is similar to that observed in $[Mn_9O_7(O_2CPh)_{13}(py)_2]$.[6b] It consists of two $[Mn_4O_2]^{8+}$ units (Mn(1,2,4,7) and Mn(2,3,5,6)) which share the square-pyramidal Mn2 atom and are capped by Mn8 and Mn9 through μ_3-oxides O14, O15, and O16. The complex has idealized C_2 symmetry. There were no changes in the metal's oxidation state in the conversion of **1** into **2**, so the precise function of the $(PhCO)_2O_2$ is unclear; however, the yield of **2** is only 31% and the presence of other products in the reaction filtrate is under investigation. The influence of experimental conditions on the reaction of **1** with $(PhCO)_2O_2$ is also being studied.

Carboxylate abstraction from complex **1** with 4 equiv of Me_3SiCl in CH_2Cl_2, followed by addition of Et_2O to the red-brown solution, produces a dark red precipitate. Recrystallization from CH_2Cl_2/Et_2O yields dark red crystals of the octanuclear Mn^{III} complex $(NBu_4)[Mn_8O_6Cl_6(O_2CPh)_7(H_2O)_2]\cdot x CH_2Cl_2$ (**3**, Bu = *n*Bu, 45–60% yield).[13] The structure[14] of the anion of **3** (Fig. 3) consists of an $[Mn_8O_6Cl_4]^{8+}$ core coordinated on its periphery to bridging $PhCO_2^-$, terminal Cl^-, and terminal H_2O ligands. As in **2**, the $[Mn_8O_6Cl_4]^{8+}$ core may again be conveniently considered to be constructed from the fusion of two $[Mn_4O_2]^{8+}$ butterfly units (Mn(1,2,4,7) and Mn(2,3,5,6)) sharing Mn2; this time there is only one capping Mn atom (Mn8) connected through O13 and O14. Moreover, the core now contains bridging Cl^- atoms. The core would possess C_{2v} symmetry and a C_2 axis passing through Mn2, the midpoint of the O13···O14 vector, and Mn8, except that the Mn8 lies off the C_2 axis to form a bond to Cl15. This converts Cl15 into an unusual example of a μ_4-Cl atom, bridging a nearly planar

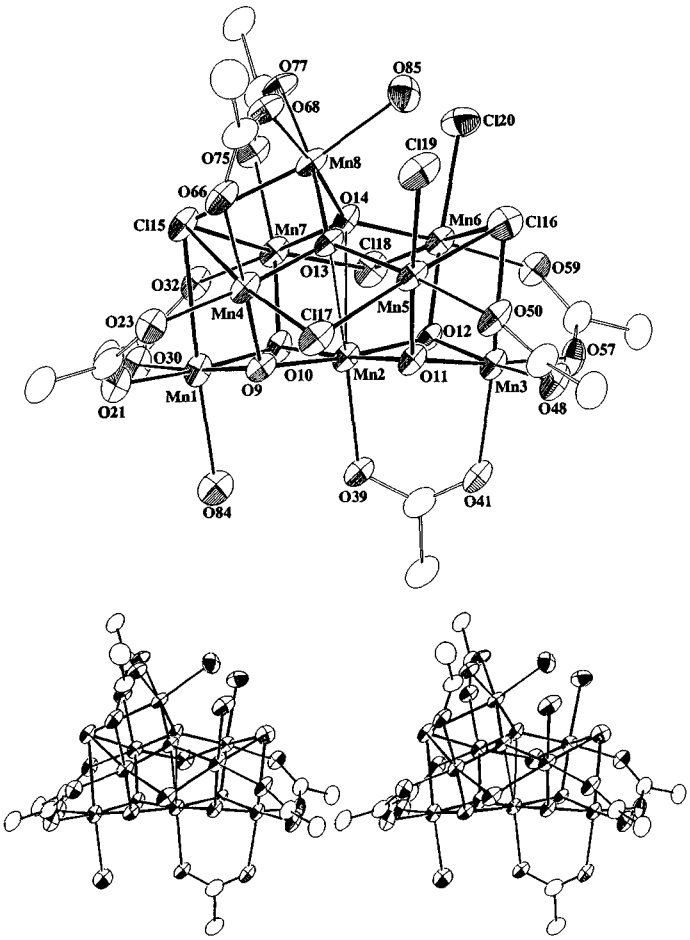

Fig. 3. Labeled ORTEP representation and stereoview of the anion of complex **3**. For clarity, only one phenyl carbon of each benzoate group is shown. Selected bond distances [Å]: Mn1···Mn2, 2.828(3), Mn1···Mn4, 3.145(2), Mn1···Mn7, 3.137(3), Mn2···Mn3, 2.791(3), Mn2···Mn4, 3.191(2), Mn2···Mn5, 3.218(2), Mn2···Mn6, 3.197(3), Mn2···Mn7, 3.180(3), Mn2···Mn8, 3.625(2), Mn3···Mn5, 3.141(2), Mn3···Mn6, 3.131(3), Mn4···Mn5, 3.171(3), Mn4···Mn8, 3.150(3), Mn5···Mn8, 3.493(3), Mn6···Mn7, 3.176(3), Mn6···Mn8, 3.508(3), Mn7···Mn8, 3.158(2), O9-Mn1 1.887(8), O9-Mn2 1.900(7), O9-Mn4 1.881(8), O10-Mn1 1.872(7), O10-Mn2 1.928(8), O10-Mn7 1.878(7), O11-Mn2 1.912(8), O11-Mn3 1.881(7), O11-Mn5 1.867(8), O12-Mn2 1.901(7), O12-Mn3 1.888(8), O12-Mn6 1.883(7), O13-Mn2 2.676(7), O13-Mn4 1.878(7), O13-Mn5 1.929(8), O13-Mn8 1.885(7), O14-Mn2 2.636(7), O14-Mn6 1.932(7), O14-Mn7 1.892(8), O14-Mn8 1.891(7), Cl15-Mn1 2.692(4), Cl15-Mn4 2.787(3), Cl15-Mn7 2.776(3), Cl15-Mn8 2.709(4), Cl16-Mn3 2.602(4), Cl16-Mn5 2.703(4), Cl16-Mn6 2.685(4), Cl17-Mn4 2.461(4), Cl17-Mn5 2.571(3), Cl18-Mn6 2.616(4), Cl18-Mn7 2.466(3), Mn5-Cl19, 2.263(4), Mn6-Cl20, 2.246(4), Mn1-O84, 2.191(9), Mn8-O85, 2.184(9).

Mn_4 unit. Another unusual structural feature is to be found at Mn2. The core structure as described above designates Mn2 as five-coordinate with square-pyramidal geometry as seen for Mn2 in complex **2**. It is clear, however, that Mn2 has two additional bonds to O13 and O14; these are long (average 2.656 Å) but they are real because Mn2 lies approximately in the plane containing O9–O12[15a] and not below it, as expected for sp geometry and seen in **2**, and because O13 and O14 are approximately trigonal planar, whereas the other bridging oxides are pyramidal. Indeed, O13 and O14 lie slightly out of their Mn_3 planes towards Mn2.[15b] Thus, Mn2 is best described as seven-coordinate, and O13 and O14 as four-coordinate trigonal pyramidal.

Very unusually for higher nuclearity Mn aggregates, complex **3** supports reversible redox processes. Shown in Figure 4 is the cyclic voltammogram in CH_2Cl_2. Both a reduction

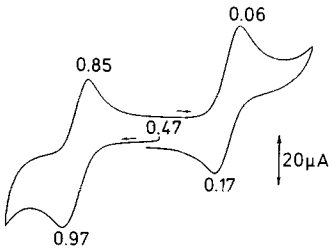

Fig. 4. Cyclic voltammogram at $50\,mVs^{-1}$ for complex **3** in CH_2Cl_2. The quoted potentials are referred to the ferrocene/ferricinium couple under the same conditions.

and an oxidation process are observed at potentials of 0.12 and 0.91 V vs. ferrocene, respectively. Complex **3** is thus the central member of the electron transfer series shown in Equation (a). While the oxidation is at a quite high potential,

$$\underset{7\,Mn^{III},Mn^{IV}}{[\,]} \overset{0.91\,V}{\rightleftharpoons} \underset{8\,Mn^{III}}{[Mn_8O_6Cl_6(O_2CPh)_7(H_2O)_2]^-} \overset{0.12\,V}{\rightleftharpoons} \underset{Mn^{II},7\,Mn^{III}}{[\,]^{2-}} \quad (a)$$

the reduction is much more facile. Attempts to generate and isolate both the neutral and dianionic forms are currently in progress; it will be interesting to determine the site of oxidation/reduction and any resulting structural perturbations.

In summary, the preparation of complex **1** is both important for continuing WOC modeling efforts and provides a new, easily prepared, and convenient starting point for the preparation of the new higher nuclearity Mn aggregates **2** and **3**.

Received: July 23, 1991 [Z 4818 IE]
German version: *Angew. Chem. 103* (1991) 1681

[1] a) K. Wieghardt, *Angew. Chem. 101* (1989) 1179; *Angew. Chem. Int. Ed. Engl. 28* (1989) 1153; b) J. B. Vincent, G. Christou, *Adv. Inorg. Chem. 33* (1989) 197.

[2] a) E. Renger, *Angew. Chem. 99* (1987) 660; *Angew. Chem. Int. Ed. Engl. 26* (1987) 643; b) G. T. Babcock in J. Amesz (Ed.): *New Comprehensive Biochemistry*, Vol 15, Elsevier, Dordrecht 1987, p. 125–158; c) G. W. Brudvig, R. H. Crabtree, *Prog. Inorg. Chem. 37* (1989) 99; d) D. Ghanotakis, C. F. Yocum, *Annu. Rev. Plant Physiol. Plant Mol. Biol. 41* (1990) 255.

[3] a) J. B. Vincent, C. Christmas, H.-R. Chang, Q. Li, P. D. W. Boyd, J. C. Huffman, D. N. Hendrickson, G. Christou, *J. Am. Chem. Soc. 111* (1989) 2086; b) G. Christou, *Acc. Chem. Res. 22* (1989) 328; c) E. Libby, J. K. McCusker, E. A. Schmitt, K. Folting, J. C. Huffman, D. N. Hendrickson, G. Christou, *Inorg. Chem. 30* (1991) 3486.

[4] Mn_6 complexes: a) A. R. E. Baikie, A. J. Howes, M. B. Hursthouse, A. B. Quick, P. Thornton, *J. Chem. Soc. Chem. Commun. 1986*, 1587; b) N. V. Gerbeleu, A. S. Batsanov, G. A. Timko, Y. T. Struchkov, K. M. Indirchan, G. A. Popovich, *Dokl. Akad. Nauk SSSR 294* (1987) 256; c) A. Caneschi, D. Gatteschi, J. Laugier, P. Rey, R. Sessoli, C. Zanchini, *J. Am. Chem. Soc. 110* (1988) 2795; d) A. R. Schake, J. B. Vincent, Q. Li, P. D. W. Boyd, K. Folting, J. C. Huffman, D. N. Hendrickson, G. Christou, *Inorg. Chem. 28* (1989) 1915; e) R. Bhula, S. Collier, W. T. Robinson, D. C. Weatherburn, *Inorg. Chem. 29* (1990) 4027.

[5] Mn_8 complexes: E. Libby, K. Folting, J. C. Huffman, G. Christou, *J. Am. Chem. Soc. 112* (1990) 5354.

[6] Mn_9 complexes: a) C. Christmas, J. B. Vincent, H.-R. Chang, J. C. Huffman, G. Christou, D. N. Hendrickson, *J. Am. Chem. Soc. 110* (1988) 823; b) D. W. Low, D. M. Eichhorn, A. Draganescu, W. H. Armstrong, *Inorg. Chem. 30* (1991) 877.

[7] Mn_{10} complexes: K. S. Hagen, W. H. Armstrong, M. M. Olmstead, *J. Am. Chem. Soc. 111* (1989) 774.

[8] Mn_{12} complexes: a) T. Lis, *Acta Crystallogr. Sect. B 36* (1980) 2042; b) P. D. W. Boyd, Q. Li, J. B. Vincent, K. Folting, H.-R. Chang, W. E. Streib, J. C. Huffman, G. Christou, D. N. Hendrickson, *J. Am. Chem. Soc. 110* (1988) 8537; c) D. Luneau, J.-M. Savariault, J.-P. Tuchagues, *Inorg. Chem. 27* (1988) 3912; d) A. Caneschi, D. Gatteschi, R. Sessol, A. L. Barra, L. C. Brunel, M. Guillet, *J. Am. Chem. Soc. 113* (1991) 5873.

[9] Correct elemental analysis for $C_{79}H_{83}NO_{21}Mn_4$; electronic spectrum in CH_2Cl_2: λ_{max} [nm] (ε_M [$L\,mol^{-1}\,cm^{-1}$]), 476 (11,560).

[10] Crystal data: $C_{79}H_{83}NO_{21}Mn_4$, monoclinic, $P2_1/c$, $T = -129\,°C$, $a = 17.394(3)$, $b = 19.040(3)$, $c = 25.660(5)$ Å, $\beta = 103.51(1)°$, $V = 8262.73$ Å^3, $Z = 4.6° \le 2\theta \le 45°$, 10788 unique, 4590 observed reflections, $F > 2.33\sigma(F)$. All non-hydrogen atoms were readily located. Due to the large number of independent atoms, only the Mn and O atoms were refined anisotropically. Hydrogen atoms, except those of the water molecule, were included in calculated positions as fixed contributors. Final $R = 0.0911$, $R_w = 0.0926$.

[11] The crystals lose MeCN on drying and appear to be hygroscopic. Correct elemental analysis for $C_{109}H_{84}N_2O_{38.5}Na_2Mn_9$ ($2 \cdot 1.5\,H_2O$).

[12] Crystal data: $C_{109}H_{84}N_2O_{38.5}Na_2Mn_9$, triclinic, $P\bar{1}$, $T = -170\,°C$, $a = 15.116(2)$, $b = 27.903(4)$, $c = 15.007(2)$ Å, $\alpha = 102.40(1)$, $\beta = 112.36(1)$, $\gamma = 84.17(1)°$, $V = 5715.26$ Å^3, $Z = 2.6° \le 2\theta \le 45°$. All non-hydrogen atoms were refined with anisotropic thermal parameters except those of the lattice solvent molecules; the latter were refined isotropically, as were the hydrogen atoms, which were included in calculated positions. $R = 0.0514$, $R_w = 0.0525$.

[13] The crystals lose CH_2Cl_2 on drying and the analysis shows no solvent of crystallization. Correct elemental analysis for $C_{65}N_{75}NO_{22}Cl_6Mn_8$; electronic spectrum in CH_2Cl_2: λ_{max} [nm] (ε_M [$L\,mol^{-1}\,cm^{-1}$]), 442 (4200), 488 (3510).

[14] Crystal data: $C_{65}H_{75}NO_{22}Cl_6Mn_8 \cdot x CH_2Cl_2$, triclinic, $P\bar{1}$, $T = -169\,°C$, $a = 16.104(4)$, $b = 21.501(6)$, $c = 14.843(4)$ Å, $\alpha = 94.24(1)$, $\beta = 105.96(1)$, $\gamma = 89.07(1)°$, $V = 4927.79$ Å^3, $Z = 2$, $6° \le 2\theta \le 45°$, 11794 unique, 10108 observed reflections, $F > 3\sigma(F)$; one butyl group and one phenyl group showed disordered C atoms; H atoms were included as fixed contributors, three CH_2Cl_2 groups were clearly observed but with approximately half occupancy; two additional peaks with low occupancy were also found that were lower occupancy CH_2Cl_2 groups or possibly H_2O groups. Final $R = 0.0912$, $R_w = 0.0944$. Further details of the crystal structure investigations are available on request from the Director of the Cambridge Crystallographic Data Centre, University Chemical Laboratory, Lensfield Road, GB-Cambridge, CB2 1EW (UK), on quoting the complete journal citation.

[15] a) Mn2 lies only 0.084 Å below the least-squares plane containing atoms O9–O12. b) O13 and O14 lie 0.104 and 0.129 Å, respectively, out of their Mn_3 planes towards Mn2.

Template-Controlled Formation of Cluster Shells or a Type of Molecular Recognition: Synthesis of $[HV_{22}O_{54}(ClO_4)]^{6-}$ and $[H_2V_{18}O_{44}(N_3)]^{5-}$

By *Achim Müller,* Erich Krickemeyer, Michael Penk, Ralf Rohlfing, Anja Armatage,* and *Hartmut Bögge*

Dedicated to Professor Karl Heinz Büchel on the occasion of his 60th birthday

In a recently published article[1] on the metal-chalcogenide clusters, the old problem was addressed that the possibilities of designing a directed synthesis for the sponta-

[*] Prof. Dr. A. Müller, E. Krickemeyer, Dipl.-Chem. M. Penk, Dipl.-Chem. R. Rohlfing, A. Armatage, Dr. H. Bögge
Lehrstuhl für Anorganische Chemie I
Fakultät für Chemie der Universität
Postfach 8640, W-4800 Bielefeld 1 (FRG)

neous formation of a cluster in solution are limited. Here it will be shown that by different types of linking of an inorganic basic unit—controlled by a central anionic template—one can influence the shape and size of cluster shells.[2] It is even possible to reach the region of "nanostructures",[3, 4a] bordering the domain of molecular and supramolecular designs.[4b] Herein, we report on the title compounds **1** and **2**, which contain a cluster shell structurally complementary to "guest" ions ClO_4^- and N_3^-, respectively. They were prepared as NEt_4^+ salts by oxidation of $[H_9V_{19}O_{50}]^{8-}$[5] in aqueous solution and characterized by elemental analysis (including manganometric V^{IV} determination), IR spectroscopy, and single-crystal X-ray structure analysis.[6]

$(NEt_4)_6[HV_{22}O_{54}(ClO_4)]$ **1** $(NEt_4)_5[H_2V_{18}O_{44}(N_3)]$ **2**

$[V_{34}O_{82}]^{10-}$ **3** $[HV_{18}O_{44}(NO_3)]^{10-}$ **4** $[H_9V_{19}O_{50}]^{8-}$ **5**

The anions of **1** and **2** (Fig. 1), which can be formally written as $[HV_8^{IV}V_{14}^{V}O_{54}(ClO_4)]^{6-}$ and $[H_2V_8^{IV}V_{10}^{V}O_{44}(N_3)]^{5-}$, form cluster shells with approximate D_{2d} and D_{2h} symmetry, respectively (without taking the H atoms in account). Compounds **1** and **2** are built up of edge- and corner-sharing tetragonal OVO_4 pyramids and encapsulate ClO_4^- and N_3^- ions, respectively.

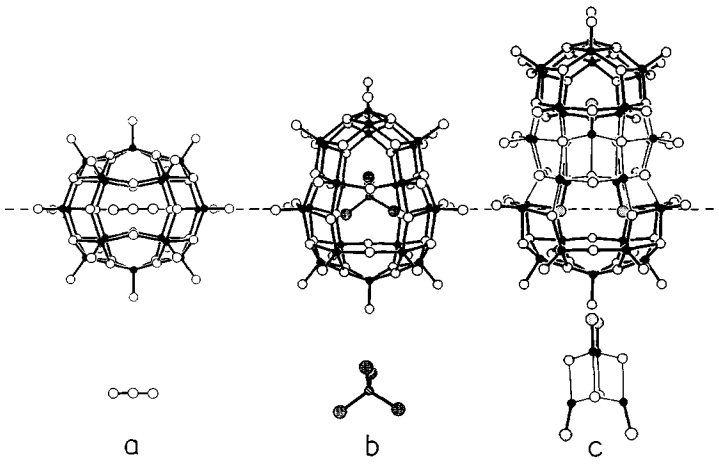

Fig. 1. Comparison of the structures of the ions a) $[H_2V_{18}O_{44}(N_3)]^{5-}$, b) $[HV_{22}O_{54}(ClO_4)]^{6-}$ and c) $[V_{34}O_{82}]^{10-}$ with their central units. The cluster shell of $[HV_{22}O_{54}(ClO_4)]^{6-}$ is formally formed from $[V_{34}O_{82}]^{10-}$ by removal of the two middle layers (thinly drawn bonds) and linking of the half-shells thus formed; $[H_2V_{18}O_{44}(N_3)]^{5-}$ is formed by penetration (condensation) of these half shells. The shape-determining templates are shown slightly enlarged and dotted. View perpendicular to the approximate S_4 axes in $[HV_{22}O_{54}(ClO_4)]^{6-}$ and $[V_{34}O_{82}]^{10-}$ and along a C_2-axis of $[H_2V_{18}O_{44}(N_3)]^{5-}$ (V = black, O = white, Cl = hatched; without protons).

The type of synthesis and structure of the novel cluster anions of **1** and **2** compared to some others such as those of **3** (with a central $\{V_4O_4\}O_4$ cluster with four terminal short V=O bonds and corresponding tetragonal $(O_t)_4$ disphenoid with D_{2d} symmetry;[3] Fig. 1), **4** (with an encapsulated NO_3^- ion[2]), and **5**[5] (with six very strong exchange-coupled V^{IV}–V^{IV} pairs that are structure-determining[3]), prove that the cluster shell formation is controlled via the molecular recognition of a template.

This can be substantiated in more detail as follows: There is a structural correlation between the shells of **1**, **2**, and **3** (Fig. 1); **3** consists of six almost planar V–O layers (with exception of the $\{V_3O_7\}$ units at the poles), which are oriented perpendicular to the S_4 axis. The layers correspond to a distorted section from an NaCl lattice, whereby some central positions in the layers neighboring the poles are not occupied. By formal removal of the two middle layers of **3** (a $\{V_{12}O_{28}\}$ fragment which contains the central $\{V_4O_4\}O_4$ cube) with subsequent linking of the remaining $\{V_{11}O_{27}\}$ half shells, the shell of **1** is formed, and the original (approximate) D_{2d} symmetry ($\bar{4}2m$) is retained (D_{2d} is a subgroup of T_d; cf. below). Hereby, a relatively close packing of O-atoms[7] seems to be decisive for the stability of **1** and **3**. Although the $O\cdots O$ distances in the central ClO_4^- ion in **1** (229–237 pm) are considerably shorter than the corresponding two $O_t\cdots O_t$ distances in the $\{V_4O_4\}(O_t)_4$ unit of **3** (332–336 pm), in both cases topologically equivalent half-shells are formed.

The formation of half-shells of **1** and **3** (and their contrarotation by 90°, whereby an S_4 axis results) distinctly follows after the recognition of the "$(O\cdots O)_2$-unit" (Fig. 2). The arrangement of the four shape-determining terminal O_t-atoms of the cube (tetragonal disphenoid) of **3** corresponds to that of the four O atoms of the ClO_4^- unit of **1**. The cluster shell of **2** (approximate symmetry D_{2h}) can formally be generated in a similar way by "condensation" of two $\{V_{11}O_{27}\}$ half-shells, the tendency of formation of which is obviously high (Fig. 1). The linear azide ion ($D_{\infty h}$) now acts as template (N(N)N instead of $(O\cdots O)_2$), such that the two shells are mirror images, i.e. are arranged without mutual rotation (as in **1** and **3**) and that the cluster shell thus has a more oblong shape, complementary to the azide ion. In **2**, the shortest $N\cdots O$ distances (305 pm!) are still significantly longer than the comparable distances between the cluster shell and the central unit in **1** and **4**.

That is, cluster shells can be generated by various types of linking of OVO_4 square-pyramids[8] (where however, weak metal-metal interactions can also play a role in the structure formation[9]). It is noteworthy here that the template ↔shell interaction can be extremely weak and so far is unique for molecular systems (anion in an anion!). The ions ClO_4^-, N_3^-, and NO_3^- (in **1** and **2** and **4**, respectively) formally appear to "hover", despite fixation (i.e. without disorder) in the cavity (Figs. 1 and 3), and are not an integral component of the cluster shell, e.g. by formation of (strong) covalent V–O (center) bonds,[10] as in classical hetero/isopolyanions[11] (proof: bond length data e.g. in Fig. 2, but also the small halfwidth of the $\nu_3(F_2) = \nu_{as}$(Cl–O) band and the extremely

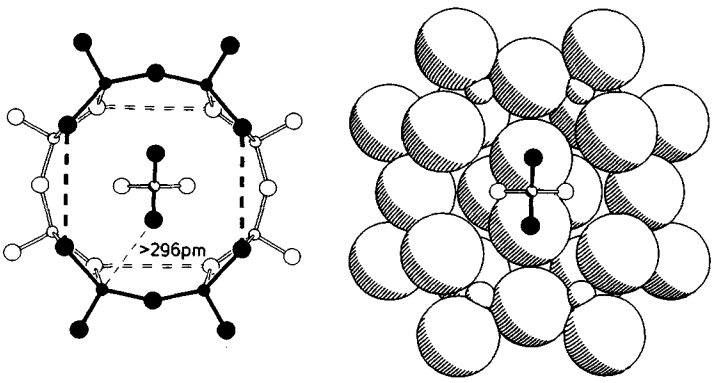

Fig. 2. The two middle layers perpendicular to the approximate S_4 axis with central ClO_4^- in the anion of **1**. Left: the atoms and bonds of the upper layer are shown in black, those of the lower layer, rotated by 90°, in white, and the central Cl shaded. Right: Space-filling model of the same atoms (Cl–O vectors of the central ClO_4^- ion marked as on the left).

small halfwidth of the $\nu_3(E'') = \nu_{as}(N-O)$ band in comparison to known data[12]). Also important in this connection is that the four terminal O_t atoms bound to the $\{V_4O_4\}$ cube ($V-O_t$: 161–166 pm) within the cluster shell or the $\{V_{11}O_{27}\}$-fragment cluster shells of **3** do not show any significant bonding to the V atoms of the shells ($V \cdots O > 254$ pm), since the $V-O_t$ bonds would otherwise be longer.

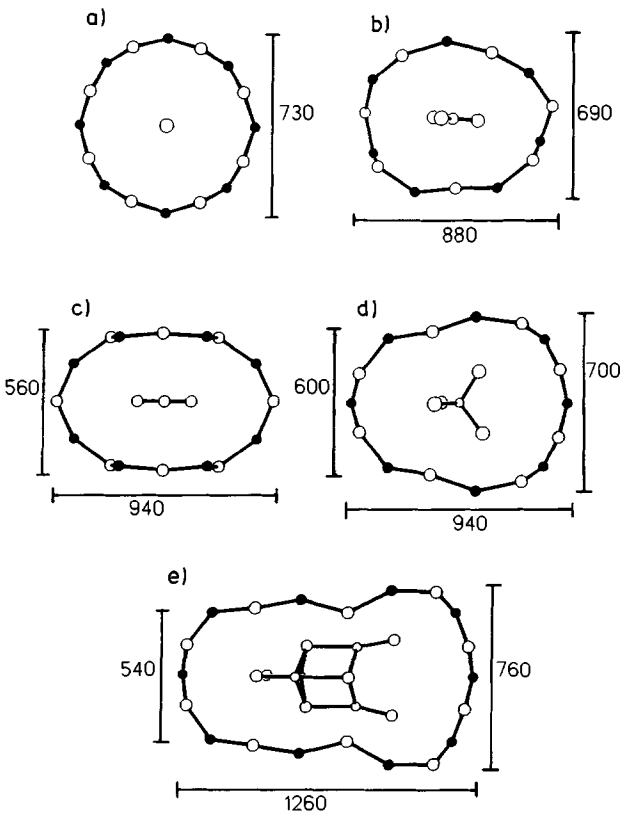

Fig. 3. Illustration of the template effect by simplified representation of the shape and size of some V–O cluster shells (with dimensions in pm). In these "cross-sections" the atoms in the chosen projection have the greatest distance from the "center". a) $[H_4V_{18}O_{42}(X)]^{9-}$, X = Cl, Br, I (A. Müller, M. Penk, R. Rohlfing, E. Krickemeyer, J. Döring, *Angew. Chem. 102* (1990) 927; *Angew. Chem. Int. Ed. Engl. 29* (1990) 926); b) $[HV_{18}O_{44}(NO_3)]^{10-}$ [2]; c) $[H_2V_{18}O_{44}(N_3)]^{5-}$ with view perpendicular to the "mirror plane of the half-shells"; d) $[HV_{22}O_{54}(ClO_4)]^{6-}$; e) $[V_{34}O_{82}]^{10-}$ (the covalent V–O bonds between the $\{V_4O_4\}O_4$ cube and the cluster shell have been omitted here).

Finally, it should be mentioned that the point group of the cluster shell of **1** and **2**, i.e. with highly symmetric template (e.g. with T_d and $D_{\infty h}$ symmetry, respectively) corresponds to a subgroup of the point group of the latter. The phenomenon discussed here has prompted us to speak cautiously of an "induced self-organization".[2, 13, 14] (See also [4b].)

Experimental

1: A solution of NEt_4ClO_4 (16.0 g, 69.65 mmol) in 250 mL of H_2O was treated with 6.6 g (3.11 mmol) of freshly prepared $(NH_4)_8[H_9V_{19}O_{50}] \cdot 11H_2O$ [5] and transferred to a 500 mL Erlenmeyer flask (wide-necked; covered with watch glass). The mixture was heated to 75 °C for 60 h without stirring on a hot plate. The precipitated black crystals of **1** were filtered off from the hot solution, washed with a little cold H_2O, air-dried on the filter paper, and stored under inert gas. Yield: 2.5 g (32.4% based on $(NH_4)_8[H_9V_{19}O_{50}] \cdot 11H_2O$). IR main absorption bands (solid/KBr pellet/[cm^{-1}]): $\tilde{\nu} = 1090$(m). (ν_{as}(ClO)), 992(vs) (ν(V=O_{term})), 825(m), 783(m), 720(s), 625(s)/614(sh) (ν_{as}(VOV)).

2: A solution of 4.0 g (18.43 mmol) of NEt_4BF_4 in 200 mL of H_2O was treated with 1.65 g (0.78 mmol) of freshly prepared $(NH_4)_8[H_9V_{19}O_{50}] \cdot 11H_2O$ [5] and 1.0 g (15.38 mmol) of NaN_3 and transferred to a 300 mL Erlenmeyer flask (wide-necked; covered with a watch glass). The mixture was kept at 75 °C without stirring for 16 h (in a fume cupboard, formation of HN_3!). The precipitated black crystals of **2** were filtered off and stored as described for **1**. Yield: 1.0 g (52.5% based on $(NH_4)_8[H_9V_{19}O_{50}] \cdot 11H_2O$). IR main absorption bands (solid/KBr/pellet/[cm^{-1}]): $\tilde{\nu} = 2019$(s). 2006(w) (ν_{as}(NNN)), 995(vs) (ν(V=O_{term})), 809(sh)/785(m), 698(s), 618(m) (ν_{as}(VOV)).

Received: July 5, 1991 [Z 4775 IE]
German version: *Angew. Chem. 103* (1991) 1720

CAS Registry numbers:
1, 137122-11-3; **2**, 137122-13-5; $(NH_4)_8[H_9V_{19}O_{50}]_8 \cdot 11H_2O$, 118069-97-9.

[1] S. C. Lee, R. H. Holm, *Angew. Chem. 102* (1990) 868; *Angew. Chem. Int. Ed. Engl. 29* (1990) 840.
[2] A. Müller, *Nature 352* (1991) 115.
[3] A. Müller, R. Rohlfing, J. Döring, M. Penk, *Angew. Chem. 103* (1991) 575; *Angew. Chem. Int. Ed. Engl. 30* (1991) 588.
[4] a) Perspectives for new molecular materials are recognizable in this connection (D. Gatteschi, L. Pardi, A. L. Barra, A. Müller, J. Döring, *Nature*, in press); cf. also J. Simon, J.-J. André, A. Skoulios, *New. J. Chem. 10* (1986) 295; J. Simon, F. Tournilhac, J.-J. André, *ibid. 11* (1987) 383; J. Simon, P. Bassoul, S. Norvez, *ibid. 13* (1989) 13. b) J.-M. Lehn, *Angew. Chem. 100* (1988) 91; *Angew. Chem. Int. Ed. Engl. 27* (1988) 89; *ibid. 102* (1990) 1347 and *29* (1990) 1304.
[5] A. Müller, M. Penk, E. Krickemeyer, H. Bögge, H.-J. Walberg, *Angew. Chem. 100* (1988) 1787; *Angew. Chem. Int. Ed. Engl. 27* (1988) 1719.
[6] Crystal structure analyses: **1**: space group $C2/c$, $a = 2092.4(8)$, $b = 2064.6(9)$, $c = 2396.2(9)$ pm, $\beta = 93.87(3)°$, $V = 10328 \times 10^6$ pm^3, $Z = 4$, $\mu = 19.4$ cm^{-1}, $\rho_{calcd} = 1.84$ $g cm^{-3}$, $R = 0.082$ for 4744 independent reflections ($F > 4\sigma(F)$). **2**: space group $P\bar{1}$, $a = 1382.5(3)$, $b = 1412.3(3)$, $c = 1421.1(2)$ pm, $\alpha = 119.04(1)$, $\beta = 92.93(2)$, $\gamma = 113.93(2)°$, $V = 2108 \times 10^6$ pm^3, $Z = 1$, $\mu = 19.2$ cm^{-1}, $\rho_{calcd} = 1.83$ $g cm^{-3}$, $R = 0.043$ for 6338 independent reflections ($F > 4\sigma(F)$). H atoms could not be localized. Siemens R3m/V-diffractometer, $Mo_{K\alpha}$ radiation, graphite monochromator. Further details of the crystal structure investigations are available on request from the Fachinformationszentrum Karlsruhe, Gesellschaft für wissenschaftlich-technische Information mbH, W-7514 Eggenstein-Leopoldshafen 2 (FRG), on quoting the depository number CSD-55644, the names of the authors, and the journal citation.
[7] A. Müller, M. Penk, J. Döring, *Inorg. Chem.*, in press.
[8] Completely different to the situation in the case of polyanions of molybdenum or tungsten, in which an octahedral coordination is preferred: M. T. Pope, A. Müller, *Angew. Chem. 103* (1991) 56; *Angew. Chem. Int. Ed. Engl. 30* (1991) 34.
[9] In the starting material **5**, twelve localized V^{IV} centers which are arranged to give six "very" strongly exchange-coupled pairs are structure determining[3,7]; in comparison, in the case of reduced clusters of 4d- and, above all, 5d-elements the electronic influence is always crucial; cf. A. Müller, E. Krickemeyer, M. Penk, V. Wittneben, J. Döring, *Angew. Chem. 102* (1990) 85; *Angew. Chem. Int. Ed. Engl. 29* (1990) 88. However as a result of the partial oxidation of **5**, this influence is limited. In **1** and **2** the antiferromagnetically coupled V^{IV} centers ($\mu_{eff}[\mu_B] = 4.5$ (**1**), 3.7 (**2**) at 25 °C), are no longer all localized (again unlike 5), as has been shown by calculations of the bond valence sums; cf. also A. Müller, J. Döring, H. Bögge, *J. Chem. Soc. Chem. Commun. 1991*, 273.
[10] In **1**, **2** and **4**, however, the central "anionic group" is remarkably *not* disordered; very weak interactions of the O and N atoms of the central unit with the V and O atoms of the shell "fix" the "guest" ion. The shortest $O \cdots O$ distances are longer than in a "Keggin-like" structure[11] and correspond, e.g., with 289.0(1) and 274.5(4) pm, to about the sum of the effective ionic radii of O^{2-} (140 pm, identical with the van-der-Waals radius of oxygen). A "rotation" of the central unit in **1** and **4** is not possible because the O–O contacts would become too short (cf. Fig. 2). Different attractive $V \cdots O$ (center) interactions are recognizable from the distances (> 296.0 pm in **1** and > 278.5 pm in **4**, but 218–246 pm in **5**), where stronger interactions are found with higher (more negative) charge on the central units. (On weak repulsive interactions between the negative shell and the negative template, see [2].)
[11] M. T. Pope: *Heteropoly and Isopoly Oxometalates*, Springer, Berlin 1983.
[12] The ν_3 band is, e.g., always split owing to the formation of ion pairs in aqueous solutions of nitrates (cf., e.g., Raman spectra in R. E. Hester, R. A. Plane, *Inorg. Chem. 3* (1964) 769). The results of the investigation of weak interactions between anions and cluster shells by Raman and IR measurements will be reported on elsewhere.
[13] The term (dissipative) self-organization usually refers to the formation of macroscopic structures—far apart from equilibrium—and also applies beyond the range of the sciences; see I. Prigogine: *From Being to Becoming—Time and Complexity in the Physical Sciences*, W. H. Freeman, New York 1980; A. Dress, H. Hendrichs, G. Küppers (Eds.): *Selbstorganisation*, Piper, München 1986. Various structure forming processes in the neigh-

borhood of equilibrium, e.g. phase transitions, can however be formally described in a similar way mathematically; see H. Haken, A. Wunderlin: *Die Selbststrukturierung der Materie*, Vieweg, Braunschweig 1991. In our view microscopic structure formation (self-organization) under the influence of a primarily formed matrix (as in the case of **3**[3]) and such that proceed via weak interactions with an external matrix have probably had importance in prebiotic elementary processes (formation of biopolymers) (cf. also the definitions "matrix" and "template" in O.-A. Neumüller: *Römpps Chemie-Lexikon*, Franckh'sche Verlagshandlung, Stuttgart 1985 and 1988, p. 2510 and 4152, respectively).

[14] A further future aspect emerges from the fact that in **1** and **2** not all positions in the two equivalent layers neighboring the polar $\{V_3O_7\}$ units are occupied, so that other units can also be encapsulated in the cluster shells. For example, in the cluster shell of **2** also a disordered NO_3^- ion can occur with one NO moiety replacing the N(N)N one: A. Müller, R. Rohlfing, unpublished results.

Synthesis and Structure of the First Tellurium(III) Radical Cation**

By *Már Björgvinsson, Thorsten Heinze, Herbert W. Roesky,* Frank Pauer, Dietmar Stalke,* and *George M. Sheldrick**

Dedicated to Professor Karl Heinz Büchel on the occasion of his 60th birthday

Although compounds with tellurium–nitrogen bonds have been used for some time in organic synthesis,[1] it is only in the last few years that they have been unambiguously structurally characterized.[2–12] Our interest in Te–N compounds was particularly stimulated by the isolation of the novel tricyclic tellurium nitride $(ClTeNSN)_3N \cdot 3\,DMF$.[10] In general, however, suitable stable precursors for the preparation of new Te–N compounds have been lacking. Recently, we prepared $Te(N(SiMe_3)_2)_2$ (**1**) in relatively good yields.[12] In our study of the coordination properties of **1** toward silver cations, we have isolated and structurally characterized the AsF_6^- salt of the first Te^{III} radical cation, $[Te(N(SiMe_3)_2)_2]^{\bullet+}$ ($\mathbf{2}^{\bullet+}$).

A dark blue solution of **3** was formed when a cold mixture (−78 °C) of **1** and $Ag^+AsF_6^-$ in CH_2Cl_2 was allowed to

$$\underset{\mathbf{1}}{Te(N(SiMe_3)_2)_2} + Ag^+AsF_6^- \xrightarrow[-Ag^0]{CH_2Cl_2} \underset{\mathbf{3}}{[Te(N(SiMe_3)_2)_2]^{\bullet+}[AsF_6]^-} \quad (a)$$

warm to room temperature [Eq. (a)]. Large crystalline blocks of **3** were isolated and its crystal structure was determined by low-temperature X-ray crystallography.[13] The crystals of **3** consist of monomer $\mathbf{2}^{\bullet+}$ coordinated by two AsF_6^- anions; thus, chains of alternating cations and anions are formed (Fig. 1).

The average Te–N distance of $\mathbf{2}^{\bullet+}$ (196.6(4) pm) is 8 pm shorter than that of its neutral analogue **1**,[12] indicating some multiple-bond character. Furthermore, the Si–N distances are longer, the average Si–N–Te bond angle is larger, the average Si–N–Si bond angle is smaller, and the pyramid formed from the N, Si, Si, and Te atoms is flatter than in **1**. These findings correlate well with the model of enhanced back-bonding of nitrogen-atom lone pairs to the positively charged tellurium atom of $\mathbf{2}^{\bullet+}$. Two long interionic Te···F contacts (318.6(1) (F2) and 317.9(1) (F6) pm), shorter than the van der Waals distance (355 pm[14] and 353 pm[15]) are present in **3** (Fig. 1).

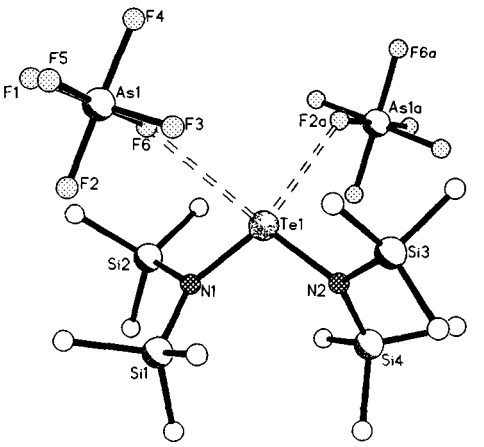

Fig. 1. Molecular structure of $\mathbf{2}^{\bullet+}$ and its nearest AsF_6^- neighbors (hydrogen atoms have been omitted). Broken lines show relatively short interionic contacts. Important distances [pm], bond angles [°], and torsional angles [°] for $\mathbf{2}^{\bullet+}$: Te1-N1 196.4(4), Te1-N2 196.8(4), N1-Si1 179.5(4), N1-Si2 180.0(4), N2-Si3 179.4(4), N2-Si4 179.2(4); N1-Te1-N2 106.8(1), Te1-N1-Si1 123.4(2), Te1-N1-Si2 114.6(2), Te1-N2-Si3 114.2(2), Te1-N2-Si4 122.5(2), Si1-N1-Si2 120.7(2), Si3-N2-Si4 121.3(2); N2-Te1-N1-Si1 51.7, N2-Te1-N1-Si2 −141.0, N1-Te1-N2-Si3 −139.3, N1-Te1-N2-Si4 56.3. For the AsF_6^- ion the bond distances and bond angles lie in the following ranges: As-F 165.9(5) −169.8(4) pm, F-As-F 87.2(4) −91.5(5)°, respectively. The fluorine atoms are disordered in the As–F1–F2–F3–F4 plane [13].

The solution ^1H NMR spectrum of **3** gave a relatively broad signal ($\Delta\nu_{1/2} = 18$ Hz), as expected for a radical. Only a single broad peak ($\Delta\omega_{1/2} \approx 15$ G) was observed in the ESR spectrum of **3** in $CDCl_3$, indicating a small spin density on the nitrogen atoms. Similar behavior has been observed for the isovalent pnictogen analogues of $\mathbf{2}^{\bullet+}$, $[P(N(SiMe_3)_2)_2]^{\bullet}$ ($\mathbf{4}^{\bullet}$) and $[As(N(SiMe_3)_2)_2]^{\bullet}$ ($\mathbf{5}^{\bullet}$).[16] It was further evident from the hyperfine coupling constants of $\mathbf{4}^{\bullet}$ and $\mathbf{5}^{\bullet}$ that the single electron was localized in a p orbital on the pnictogen atoms. Similar behavior is expected for $\mathbf{2}^{\bullet+}$. Thus, assuming an AX_2E_2 electron-pair arrangement around tellurium in **1**,[17] removal of an electron from **1** would result in a rehybridization of the tellurium atom such that a pair of electrons are in a sp^2 orbital and the single electron is in a p orbital.[18]

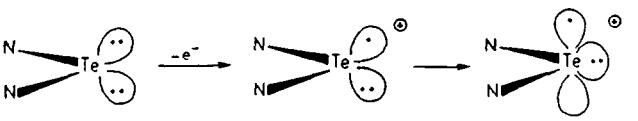

Scheme 1. Rehybridization of the tellurium orbitals on conversion of **1** to $\mathbf{2}^{\bullet+}$.

The bulky $N(SiMe_3)_2$ groups are expected to hinder the dimerization of $\mathbf{2}^{\bullet+}$. Furthermore, $\mathbf{2}^{\bullet+}$ is stabilized by the interionic $\mathbf{2}^{\bullet+} \cdots AsF_6^-$ contacts. By contrast, dimers with relatively short Te···Te contact distances are present in the crystals of the neutral compound **1**.[12] Dimerization of $\mathbf{2}^{\bullet+}$ is probably hindered owing to steric factors, which would reduce the energetically favorable ion-pair contacts, and electrostatic repulsion between the positively charged telluri-

[*] Prof. Dr. H. W. Roesky, Prof. G. M. Sheldrick, Dr. M. Björgvinsson, Dipl.-Chem. T. Heinze, Dr. F. Pauer, Dr. D. Stalke
Institut für Anorganische Chemie der Universität
Tammannstrasse 4, W-3400 Göttingen (FRG)

[**] This work was supported by the Deutsche Forschungsgemeinschaft (Leibniz-Programm), the Fonds der Chemischen Industrie, and the Alexander von Humboldt Foundation (award of a fellowship to *M.B.*). We wish to thank Dr. *D. Marsh* and *B. Angerstein* at the Max-Planck-Institut für Biophysikalische Chemie, Göttingen, for measuring the ESR spectra.

um atoms. Contact ion pairs are presumably also present in CH_2Cl_2 and $CHCl_3$ solvents since no sharp ^{19}F NMR resonances were observed in freshly prepared solutions of **3**. Concentrated solutions of **3** are only metastable at room temperature, however, their blue color disappearing after approximately one week.

The isolation of a Te^{III} radical cation and the determination of its detailed geometry affords a unique opportunity for a general study of the nature of related species. Furthermore, the unexpected oxidation of **1** by $Ag^+AsF_6^-$ strongly suggests that this synthetic method could be generalized to other tellurium compounds.

Experimental Procedure

All manipulations were performed under an inert atmosphere of dry nitrogen gas inside a drybox or on a glass vacuum line. The CH_2Cl_2 and $CHCl_3$ solvents were dried over P_4O_{10} and distilled and stored over molecular sieves (4 Å) prior to use. In a typical preparation, **1** (1.13 g, 2.51 mmol) and $Ag^+AsF_6^-$ (0.74 g, 2.50 mmol) were loaded into separate arms of an H-shaped glass reaction vessel (equipped with teflon valves and a glass frit). After dissolving the compounds in CH_2Cl_2 (30 ml) the solutions were thoroughly mixed at −78 °C and the yellow solution allowed to warm to room temperature. The resulting dark blue solution was then filtered from the white-grey silver metal powder and the solvent slowly condensed off to give large black crystalline blocks of **3**. ^1H NMR (80 MHz, $CDCl_3$, −50 °C, ext. TMS): $\delta = 0.45$ ($\Delta\nu_{1/2} = 18$ Hz). ESR ($CDCl_3$, 10 °C): $g = 2.0$ ($\Delta\omega_{1/2} = 15$ G). UV/VIS (CH_2Cl_2): λ_{max} [nm] = 615.

Received: March 4, 1991 [Z 4469 IE]
Publication delayed at the authors' request
German version: *Angew. Chem. 103* (1991) 1671

CAS Registry numbers:
1, 130497-87-9; **3**, 137300-30-2; $Ag^+AsF_6^-$, 12005-82-2.

[1] G. Kirsch, L. Christiaens in S. Patai (Ed.): *Chemistry of Selenium and Tellurium Compounds Vol. 2*, Wiley, New York, 1987, chapter 11, pp. 421–461.
[2] H. Hartl, P. Huppmann, D. Lentz, K. Seppelt, *Inorg. Chem. 22* (1983) 2183.
[3] V. Betini, P. Dapporto, F. Lucchesini, A. Sega, A. De Munno, *Acta Crystallogr. Sect. C 40* (1984) 653.
[4] R. Neidlein, D. Knecht, A. Gieren, C. Ruiz-Pérez, *Z. Naturforsch. B 42* (1987) 84.
[5] J. S. Thrasher, J. B. Nielsen, S. G. Bott, D. J. McClure, S. A. Morris, J. L. Atwood, *Inorg. Chem. 27* (1988) 570.
[6] E. Hey, C. Ergezinger, K. Dehnicke, *Z. Naturforsch. B 44* (1989) 205.
[7] J. Münzenberg, M. Noltemeyer, H. W. Roesky, *Chem. Ber. 122* (1989) 1915.
[8] J. P. Johnson, G. K. MacLean, J. Passmore, P. S. White, *Can. J. Chem. 67* (1989) 1687.
[9] A. Haas, R. Pohl, *Chimia 43* (1989) 261.
[10] H. W. Roesky, J. Münzenberg, M. Noltemeyer, *Angew. Chem. 102* (1990) 73; *Angew. Chem. Int. Ed. Engl. 29* (1990) 61.
[11] P. F. Kelly, A. M. Z. Slawin, D. J. Williams, J. D. Woollins, *Polyhedron 9* (1990) 2659.
[12] M. Björgvinsson, H. W. Roesky, F. Pauer, D. Stalke, G. M. Sheldrick, *Inorg. Chem. 29* (1990) 5140.
[13] Crystallographic data for **3** (−120 °C): orthorhombic, $a = 1137.6(2)$, $b = 1253.3(2)$, $c = 1844.1(3)$ pm, $V = 2.6292$ nm^3, space group $P2_12_12_1$, $Z = 4$, $\varrho_{calcd} = 1.61$ g cm^{-3}, 3365 unique reflections [$|F_0| > 3\sigma(|F_0|)$], $2\theta = 8$–$45°$ refined to $R = 0.0261$, $R_w = 0.0279$. The disordered fluorine atoms F 1–F 4 and F 1′–F 4′, with 63 % and 67 % occupancy, respectively, were refined with identical anisotropic displacement parameters for opposite fluorine atoms. All As–F distances in the disordered plane were restrained to the same value, and a separate restraint was applied to make As–F distances perpendicular to the plane equal to one another. In addition, all F ··· F distances involving one disordered fluorine and one nondisordered fluorine were restrained to be equal. Further details of the crystal structure investigation may be obtained from the Fachinformationszentrum Karlsruhe, Gesellschaft für wissenschaftlich-technische Information mbH, W-7514 Eggenstein-Leopoldshafen 2 (FRG), on quoting the deposit number CSD-55340, the name of the authors, and the journal citation.
[14] L. Pauling: *The Nature of the Chemical Bond*, 3rd ed., Cornell University Press, Ithaca, NY, USA 1960, chapter 7; *Die Natur der chemischen Bindung*, 3rd ed., Verlag Chemie, Weinheim 1968.
[15] A. Bondi, *J. Phys. Chem. 68* (1964) 441.
[16] M. J. S. Gynane, A. Hudson, M. F. Lappert, P. P. Power, H. Goldwhite, *J. Chem. Soc. Dalton Trans. 1980*, 2428.
[17] a) R. J. Gillespie: *Molecular Geometry*, van Nostrand London 1972; b) For a physical basis of VSEPR (valence shell electron pair repulsion) see R. F. Bader, R. J. Gillespie, P. J. McDougall in J. F. Liebmann, A. Greenberg (Eds.): *From Atoms to Polymers: Isoelectronic Analogies, Ser. 11*: VCH Publishers, New York 1989, pp. 1–51.
[18] As pointed out by one of the reviewers, an alternative rationalization would be that an electron is removed from a doubly occupied tellurium nonbonding p orbital (b_2), perpendicular to the TeN_2 plane. This model is analogous to the MO description of the oxygen-atom lone pair in H_2O. However, for a criticism of this description see [17b], p 32.

Tetrakis(dimethylamino)ethene: An Extremely Electron-Rich Molecule with Unusual Structure both in the Crystal and in the Gas Phase**

By *Hans Bock,* Horst Borrmann, Zdenek Havlas, Heinz Oberhammer,* Klaus Ruppert*, and *Arndt Simon**

Dedicated to Hans Georg von Schnering on the occasion of his 60th birthday

Which organic molecules possess such low first ionization energies that they approach those of the alkaline-metal atoms Li (5.40 eV) and Na (5.14 eV)? Only a few answers can be given to this question and one of them is tetrakis(dimethylamino)ethene ($IE_1^V = 6.13$ eV[1,a,b]). On dissolving in oxygen-free water, therefore, it forms a radical cation, presumably according to $M_{solv.} + H^{\oplus}_{solv.} \rightarrow 1/2\,H_2 + M^{\bullet\oplus}_{solv.}$ with H_2 evolution.[1c] Two-electron oxidation[1d] by halogens (X_2) yields the dication salt, the structure of which is characterized by a central CC single bond of 150 pm length and two cyanine-like molecular halves twisted relative to each other by up to 76°[1e] [Eq. (a)].

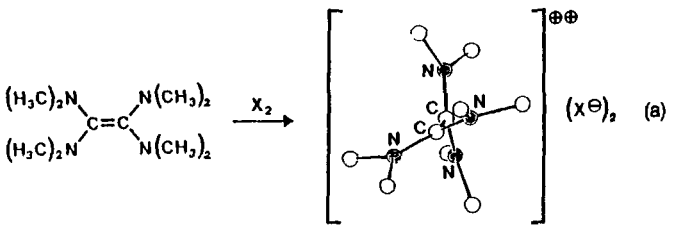

(a)

The electron richness of the readily oxidizable title compound[1f] is further illustrated by a comparison with the valence-isoelectronic hydrocarbon derivative, the tetraanion of tetraisopropylethene, $((H_3C)_2C^{\ominus})_2C{=}C(C^{\ominus}(CH_3)_2)_2$, taking into consideration the different effective nuclear charges

[*] Prof. Dr. H. Bock, Dr. Z. Havlas[+], Dipl.-Chem. K. Ruppert
Institut für Anorganische Chemie der Universität
Niederurseler Hang, W-6000 Frankfurt am Main 50 (FRG)
Prof. Dr. A. Simon, Dr. H. Borrmann
Max-Planck-Institut für Festkörperforschung
Heisenbergstrasse 1, W-7000 Stuttgart 80 (FRG)
Prof. Dr. H. Oberhammer
Institut für Physikalische und Theoretische Chemie der Universität
Auf der Morgenstelle 8, W-7400 Tübingen (FRG)
[+] Permanent address: Institute of Organic Chemistry and Biochemistry of the Czechoslovakian Academy of Sciences, Prague (CSFR)

[**] Structures of Sterically Overcrowded and Charge-Perturbed Molecules, Part 12. This work was supported by the Deutsche Forschungsgemeinschaft, the Fonds der Chemischen Industrie, and the State of Hesse. Part 11: H. Bock, *GIT Fachz. Lab. 35* (1991) 557.

($Z_{eff}(N) > Z_{eff}(C)$. In addition, this comparison accentuates the envelope of space-filling substituents, which can both stabilize charges in molecular ions by delocalization and distort considerably the bond skeletons in the neutral molecules,[2] as is observed especially for compounds with vicinal dialkyl or alkylaryl amino groups attached to CC multiple bonds[3] (Scheme 1). Thus, in tetrakis(dimethylamino)-*p*-

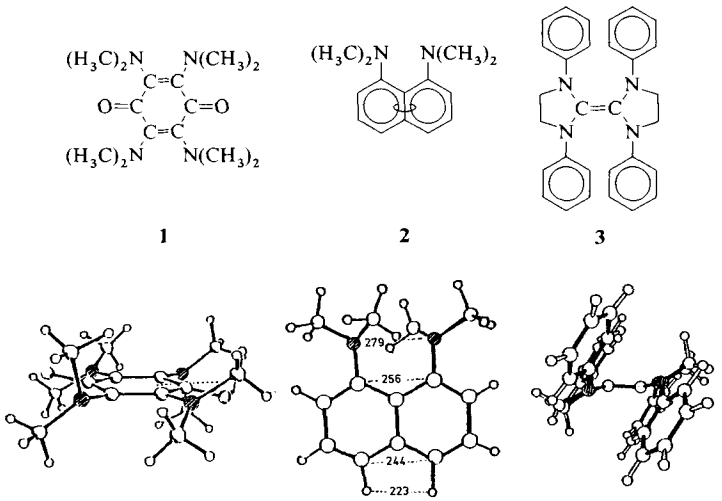

Scheme 1. Selected structures of sterically overcrowded, unsaturated nitrogen compounds (N centers hatched; distances in pm; cf. text).

benzoquinone (**1**) a chair conformation is enforced,[3a] in the proton sponge 1,8-bis(dimethylamino)naphthalene (**2**) the N···N distance is stretched by some 35 pm to 279 pm,[3b] and in the tetraphenylaminoethene derivative **3** the rings are arranged in two layers.[3c]

Which structure will the title compound with its extreme redox properties show? A totally geometry-optimized calculation for the 38-atom molecule using the well-tested semiempirical AM1 procedure,[4a] which was performed despite some objections concerning both the presumed violation of the parameter boundaries[4b] and the considerable number of degrees of freedom (108),[4c] predicts a planar $N_2C{=}CN_2$ skeleton with a C=C bond of 138 pm length and with all N lone pairs of the flattened $(H_3C)_2N$ groups in the central molecular plane. However, the calculated first ionization energy deviates by +2.7 eV,[3c] suggesting that only one of the numerous local total energy minima has been found.

The structure of air-sensitive tetrakis(dimethylamino)-ethene,[1f] which solidifies only at 273 K and decomposes above 373 K by loss of $(H_3C)_2NH$, was determined by single-crystal X-ray analysis[5] and, to avoid artifacts due to packing effects,[5] by electron diffraction in the gas phase[6] (Fig. 1). Indeed, the latter proved to be essential for the understanding of a structurally inconspicuous, but chemically significant disorder in the crystal.[7]

The solid-state structure of tetrakis(dimethylamino)-ethene[5] (Fig. 1a) reveals an unusual and chiral bond skeleton. The molecular halves on both sides of the C=C axis (stretched to 135 pm) are twisted relative to each other by 28° and each two opposite $(H_3C)_2N$ groups are either nearly planarized or seemingly fully planar ($\sum \sphericalangle$ CNC = 354° und 360°). Analysis of the radial distribution function, calculated by Fourier transformation from the scattering intensities,[6b] yields a gas-phase electron diffraction structure (Fig. 1b) with a twofold axis through the central C=C bond and confirms the basic X-ray structure data. For instance, the two $(R_2N)_2C$ molecular halves are also twisted by 28° in the gas phase and the R_2N groups are rotated relative to the CN_2 planes by 55°. In contrast to the structure in the crystal, however, all dimethylamino groups are pyramidal ($\sum \sphericalangle$ CNC = 351°) in the gas phase. A subsequently calculated disorder model for the crystal, on the other hand, also yields pyramidal R_2N substituents with angle sums of 351° and 353°. Both in the solid[5] and in the gas phase,[6] therefore, tetrakis(dimethylamino)ethene shows a surprising molecular structure, in which owing to steric overcrowding all four N lone pairs of the largely flattened dimethylamino substituents are twisted by torsion angles ω(CC-NC_2) of 55° out of their optimum π-interaction positions.

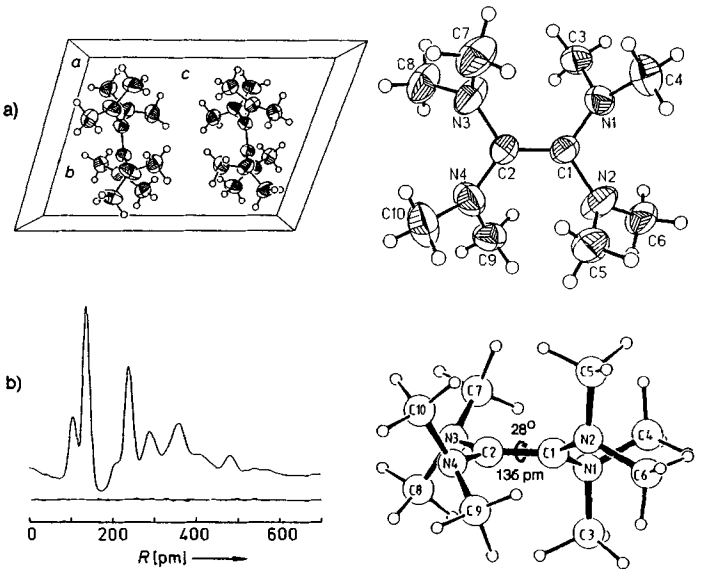

Fig. 1. Structure of $((H_3C)_2N)_2C{=}C(N(CH_3)_2)_2$. a) Results of the single-crystal structure analysis [5]. Left: Unit cell containing two molecules (intermolecular distances H···H > 243 pm); Right: Averaged molecular structure. Important distances [pm] for the averaged structure and, in curly brackets, for the one resolved using a disorder model [7]: C1-C2 135.1(2) {135.0(2)}, C1/C2-N 139.9(2) to 140.8(3) {141.7(3)}, N-C(H) 141.1(4) to 145.1(4) {144.0(3)}. Angle N_2C-CN_2 28.3° (ω = 0° would indicate a twisting of the dimethylamino groups to a position with the N lone pairs perpendicular to the CN_2 plane). For further details see [5, 7]. b) Structure analysis by electron diffraction in the gas phase [6]. Left: Radial distribution function: Right: Molecular structure; important distances [pm] and angles [°]: C1-C2 136, C1/C2-N 140, N-C 145, C-H 111, C2-C1-N 121, N-C1/C2-N 118, (H)C-N-C(H) 113, $\sum \sphericalangle$ CNC 351, N_2C-CN_2 28, C2C1-NC 55. For further details see [6b].

Comparison of these results with literature data confirms that the title compound is one of the most distorted simple ethylenes, $(R_nE)_2C{=}C(ER_n)_2$, even with respect to the record values[8] so far reported for sterically overcrowded fulvene and bis(fluorenylidene) derivatives, which exhibit C=C distances up to 141 pm and twist angles up to 40°. For instance, even the closest approaches to the still unknown tetrakis(*tert*-butyl)ethene, the fourfold 1-methylcyclopropyl- and trimethylsilyl-substituted hydrocarbons show a C=C bond of only 135 pm length and twist angles of only 20° and 29.5°, respectively. In contrast, the tetraisopropyl derivative, $((H_3C)_2HC)_2C{=}C(CH(CH_3)_2)_2$, which is valence-isoelectronic to $((H_3C)_2N)_2C{=}C(N(CH_3)_2)_2$, behaves rather normally ($d_{C=C}$ = 135 pm, ω = 0°).[8] This comparison, therefore, illustrates the spatial requirement of the N lone pairs (Scheme 1), which is evaded in tetrakis(dimethylamino)-ethene by the twisting of the N_2C-CN_2 skeleton and the flattening of the $(H_3C)_2N$ substituents as well as by their torsions around the C–N bonds.[3a, 9]

In conjunction with quantum-chemical calculations,[9] the unexpected structural data allow a plausible rationalization of the basic properties of the extremely electron-rich molecule tetrakis(dimethylamino)ethylene. Thus, its rather low first vertical ionization energy is readily explained by the considerably flattened dimethylamino pyramids – without any contradiction to the considerably reduced π interaction[1b] ($\cos^2 55° = 0.33$) caused by the ω(CC-NR_2) twisting. This interpretation is supported, for example, by the extremely low first vertical ionization energy of triisopropylamine (only 7.18 eV[2]), which is due to its almost planar NC_3 skeleton and is 1.26 eV below that of pyramidal $N(CH_3)_3$ with a CNC angle sum of 333°.[2] Additional AM1 calculations for tetrakis(dimethylamino)ethene starting from the solid-state and gas-phase structural data[9] result, as expected, in different local total energy minima and approximate its first ionization energy via Koopmans' correlation, $IE_n^V = -\varepsilon_j^{SCF}$, satisfactorily down to 7.2 eV. The observation[1f] that $((H_3C)_2N)_2C{=}C(N(CH_3)_2)_2$ exhibits a single ^{1}H NMR signal down to 220 K can be rationalized in terms of the low inversion barrier[10] of largely flattened dimethylamino groups, which together with the CN_2 librations (Fig. 1a) allows time-averaged equivalent positions of the methyl C centers. The tremendous structural change on oxidation to the dication [Eq. (a)] also seems to be "preprogrammed" by the molecular dynamics.

Despite its now-known ground-state structure, the extremely electron-rich title molecule still poses numerous problems. For instance, calculations for its radical cation[10] suggest that the positive charge might be lopsidedly distributed over the two molecular halves – in full agreement with the different ^{1}H coupling constants of 0.28 mT and 0.328 mT obtained by ESR and especially ENDOR spectroscopy, respectively.[1c, f]

Received: July 6, 1991 [Z 4779 IE]
German version: *Angew. Chem. 103* (1991) 1733

CAS Registry number:
tetrakis(dimethylamino)ethene, 996-70-3.

[1] Measurement using a high-performance Leybold Heraeus UPG 200 photoelectron spectrometer yielded 6.13 eV: H. Bock, B. Solouki, unpublished. b) Literature value: 5.95 eV (B. Cetinkaya, G. H. King, S. S. Krishnamurthy, M. F. Lappert, J. B. Pedley, *J. Chem. Soc. Chem. Commun. 1971*, 1370. c) H. Bock, B. Hierholzer, *Angew. Chem. 100* (1988) 1127; *Angew. Chem. Int. Ed. Engl. 27* (1988) 1069. d) H. Bock, D. Jaculi, *ibid. 96* (1984) 298, and *23* (1984) 305: The cyclic voltammogram in aprotic dimethylformamide solution shows an unstructured (two-electron) wave between $E_{pc} = -0.63$ V and $E_{pa} = -0.52$ eV. e) H. Bock, K. Ruppert, K. Merzweiler, D. Fenske, H. Goesmann, *ibid. 101* (1989) 1715, and *28* (1989) 1684. f) Review: N. Wiberg, *ibid. 80*, (1968) 809, and *7* (1968) 766, and references cited therein, especially N. Wiberg, J. W. Buchler, *Z. Naturforsch. B 19* (1964) 5; cf. also H. E. Winberg, D. R. Downing, D. D. Coffmann, *J. Am. Chem. Soc. 87* (1965) 2054 (^{1}H NMR).

[2] Cf., e.g., H. Bock, I. Göbel, Z. Havlas, S. Liedle, H. Oberhammer, *Angew. Chem. 103*, (1991) 193; *Angew. Chem. Int. Ed. Engl. 30* (1991) 187.

[3] a) H. Bock, K. Ruppert, C. Näther, Z. Havlas, *Angew. Chem. 103*, (1991) 1194, *Angew. Chem. Int. Ed. Engl. 30* (1991) 1180. b) H. Einspar, J.-B. Robert, R. E. Marsh, J. D. Roberts, *Acta Crystallogr. Sect. B 29* (1973) 1611. c) P. B. Hitchcock, *J. Chem. Soc. Dalton Trans. 1979*, 1314. d) An exception is hexakis(dimethylamino)benzene, $C_6(NR_2)_6$, which possesses approximately C_{6h} symmetry: J. M. Chance, B. Kahr, A. B. Buda, J. P. Toscano, K. Mislow, *J. Org. Chem. 53*, (1988) 3226.

[4] a) M. J. S. Dewar, E. G. Zoebisch, E. F. Healy, J. P. Stewart, *J. Am. Chem. Soc. 107* (1985) 3902; cf. also, e.g., M. J. S. Dewar, K. M. Dieter, *ibid. 108* (1986) 8075. b) For the simultaneous optimization of the C/H/N/O parameters over 120 molecules have been selected [4a]; however, none of them were chosen from the point of view of steric overcrowding and not a single one with more than one, always pyramidal $(H_3C)_2N$ group. c) We used the SCAMP Version 4.10 (Dr. *T. Clark*, Universität Erlangen) on an IBM RISC 6000/320 work station with 32-Mb CPU and needed about 8 h of computation time. Selected calculated structure parameters ([pm] or [°]): C=C 138, CN 144, CH 112, CCN 119 and 125, $\sum \sphericalangle$ CNC 338 and 344. Additional results: $\Delta H_f = 225$ kJ mol^{-1}; $\varepsilon_{42} = -8.7$ eV; $q_C = 0.04$; $q_N = -0.26$. Cf. also the MNDO results based on the assumption of pyramidal $(H_3C)_2N$ substituents [1e] as well as from calculations based on the structures determined [10].

[5] Crystal structure: $C_{10}H_{24}N_4$. The air-sensitive compound, which was purified by repeated fractional condensation at 10^{-5} mbar pressure, was placed in a Mark tube (about 2 cm full) and slowly cooled below its melting point of 0 °C. Cautious warming followed again by slow cooling afforded a single crystal (cf. A. Simon, H. Borrmann, *Angew. Chem. 100* (1988) 1386; *Angew. Chem. Int. Ed. Engl. 27* (1988) 1339). On further cooling of the crystal, several phase transformations were observed in Guinier investigations. Reflection data of the high-temperature phase were recorded both at 218 K and 243 K, but did not show any significant deviations on structure refinement. Data: $a = 771.4(2)$, $b = 826.8(2)$, $c = 1138.3(3)$ pm, $\alpha = 106.73(2)$, $\beta = 92.11(2)$, $\gamma = 108.44(2)°$, $V = 653.02 \times 10^6$ pm^3; measurement temperature 218 K, $M = 200.33$, $\rho_{calcd} = 1.02$ g cm^{-3}, $\mu(Mo_{K\alpha}) = 0.06$ mm^{-1}, triclinic $P\bar{1}$ (No. 2 Int. Tab.), $Z = 2$, Syntex $P2_1$ four-circle diffractometer, 3018 measured reflections within $4° < 2\theta < 55°$ ($\omega/2\theta$ scan), of which 2263 are independent with $F > 2\sigma(F)$; structure solved by direct methods (SHELXTL-Plus), 239 parameters, $R = 0.061$, $R_w = 0.063$ ($w = 1/\sigma^2(F) + 0.0001\,F^2$), Goof = 1.311, residual electron density +0.19/−0.15 e/Å^3, C and N atoms, including split positions [7], anisotropically refined, H positions found and refined isotropically applying a common C–H distance and the same temperature factor for each methyl group. Further details are available on request from the Fachinformationszentrum Karlsruhe, Gesellschaft für wissenschaftlich-technische Information mbH, W-7514 Eggenstein-Leopoldshafen 2 (FRG), on quoting the depository number CSD-55907, the names of the authors, and the journal citation.

[6] Electron diffraction in the gas phase. a) The air-sensitive $C_{10}H_{24}N_4$ was purified by distillation at 10^{-4} mbar and kept under Ar in the dark. The scattering intensities were recorded at two camera distances (25 and 50 cm) with a G2 gas diffractograph using an acceleration voltage of about 60 kV. The temperature of the sample was 345 K (vapor pressure between 2 and 3 mbar) and that of the inlet nozzle 350 K; no decomposition was observed. b) For the structure determination, several models with different orientation of the four dimethylamino groups, as well as planar or twisted C_2N_4 skeleton, were tested. Satisfactory agreement between calculated and experimental radial distribution functions (Fig. 1b) was only achieved using a model similar to the solid-state structure of C_2 symmetry with the axis along the C=C bond. The least-squares fit is based on the following assumptions: local C_{3v} symmetry for the CH_3 and C_s symmetry for the $N(CH_3)_2$ groups, each with the same geometric parameters. In the electron diffraction experiment, the C–C distance was insufficiently determined and was therefore set equal to the value from the crystal analysis. The following distances [pm] and angles [°] result (error limits are 3σ values and refer to the last digit): C-H 111.0(4), C=C 136 (assumed), C-N 140.3(4), N-C 145.2(3), N-C-N 118.4(8), C-N-C(H) 119.2, (H)C-N-C(H) 112.8(15), H-C-H 108.3(8), ω(C=C) 28(2), ω(C-N) 55(2) (twisting of the dimethylamino groups around the C–N bond: for $\omega = 0$, the N lone pairs are perpendicular to the CN_2 plane). The methyl groups are staggered with respect to the opposite N–C bond.

[7] Residual electron density within about 50 pm distance from N4 (Fig. 1a) indicates a partial inversion of the pyramids. The elongation of the thermal ellipsoids for N2 and N3 perpendicular to the NC_3 plane also points to a positional disordering, which could be due to the presence of some molecules in inverted orientation. Contrary to this assumption, however, N1 does not show disordering. For an individual disorder of the R_2N groups, a calculation with split positions for N2 (0.5:0.5), N3 (0.65:0.35), and N4 (0.85:0.15) improves the R value slightly from 0.064 to 0.061 and yields a pyramidal structure of all N centers with angle sums of 353° (N1), 352° (N2), 351° (N3), and 352° (N4). At this point we also want to express our gratitude to the "structure-competent" referee for his helpful critical comments.

[8] Review: W. Luef, R. Keese (Nonplanar Carbon-Carbon Double Bonds), *Top. Stereochem. 20* (1991) 231–318: Accordingly, the longest C=C bonds of 141 pm length are found in 1-(*N*-benzyl-1,2-dihydropyridinylidene)fulvenes, followed by the 139-pm-long ones in bis(1-isopropoxycarbonylfluorenylidene), which with a dihedral angle of 40° also exhibits the strongest twisting observed so far. Of the numerous reported ethylene derivatives (cf. e.g., J. Deuter, H. Rodewald, H. Irngartinger, T. Loerzer, W. Lüttke, *Tetrahedron Lett. 26* (1985) 1031), noteworthy are 1,1-di-*tert*-butyl-2,2-diphenylethene ($d_{C=C} = 136$ pm; $\omega = 24°$) and, as an example with an additional bending angle φ, octabromopentalene ($d_{C=C} = 139$ pm, $\omega = 37°$, $\varphi = 3°$). In tetrakis(trimethylsilyl)ethene (A. Sekiguchi, T. Nakanishi, C. Kabuto, H. Sakurai, *J. Am. Chem. Soc. 111* (1989) 3748), the molecular halves are twisted relative to each other by 29.5°.

[9] Additional AM1 calculations based on the crystal and gas-phase structural data, prove that, depending on the starting geometry, different local minima are approached. Thus, AM1 calculations proceeding from the crystal structure (Fig. 1a and [5]) yield $\varepsilon_{42} = -7.19$ eV, $q_C = +0.07$, $q_N = -0.25$, and an enthalpy of formation $\Delta H_f = 303$ kJ mol^{-1}, which is about 80 kJ mol^{-1} above that resulting from a complete geometry optimization

based on standard structure data [4]. In contrast, the C_2 gas-phase structure as an starting point leads to a geometry-optimized structure with $\omega(N_2C=CN_2) = 13°$ and $\varepsilon_{a2}^{AM1} = -8.2$ eV as well as $q_{C1} = 0.12$, $q_{C2} = 0.03$, $q_{N1/2} = -0.28$, and $q_{N3/4} = -0.31$, which add up to a dipole moment of 1.9 D. The calculated enthalpy deviates by only $+20$ kJ mol^{-1}. The enthalpy differences are due to numerous changes within the molecular skeleton, which can be analyzed based on additionally calculated force constants (kJ mol^{-1} pm^{-2} or kJ mol^{-1} degree^{-2}) and be classified according to C=C stretch (0.7) and angle changes, decreasing in the sequence CNC-angle widening (5.0) > N pyramidalization (1.0) > C=C rotation ≈ C-NC$_2$ rotation (0.1). All force constants are positive and therefore prove that the movements covered by them originate from a (local) minimum of the total energy. An additional ab initio SCF calculation employing a 4-31 G basis set predicts for a 28° twisting of ethylene an energy difference of $+48$ kJ mol^{-1}, which further illustrates the steric overcrowding in tetrakis(dimethylamino)ethene.

[10] A totally geometry-optimized AM1 calculation for the radical cation (H. Bock, Z. Havlas, unpublished) predicts $d_{C-C} = 151$ pm, $\omega(N_2C-CN_2) = 61°$, and $\sum \sphericalangle CNC = 360°$ and 349°. For the molecular half containing the cyanine-like flattened $(H_3C)_2N$ groups [cf. Eq. (a)] a total charge of $+0.85$ is calculated. Experiments to isolate a salt of the tetrakis(dimethylamino)ethene radical cation, $[(R_2N)_2^{\oplus}C\text{-}^{\bullet}C(NR_2)_2]X^{\ominus}$, are under way (H. Bock, I. Göbel, unpublished).

Synthesis of an Elicitor-Active Heptaglucan Saccharide for Investigation of Defense Mechanisms of Plants

By *Jens Peter Lorentzen,* Barbara Helpap,* and *Oswald Lockhoff*

Dedicated to Professor Karl Heinz Büchel on the occasion of his 60th birhday

Elicitors are substances that induce the defense reactions of plants by activating the biosynthesis of phytoalexins. In the soybean/*Phytophthora megasperma* host–parasite system the heptasaccharide **19** is the smallest strong elicitor-active unit[1] that binds to a receptor. This β-glucan structure is formed hydrolytically from the cell wall of the pathogen. The binding of the glucan fragment to a membrane protein of the host organism presumably induces the formation of a second messenger system. The signal chain ends with the biosynthesis of the phytoalexin glyceolin.[2]

The chemical synthesis of defined oligoglucan fragments should make the study of plant defense mechanisms possible starting, for example, from the mechanism of the photoelicitor–binding protein interaction and the resulting signal transmission to the biosynthesis of phytoalexin.

We report here a new and more efficient synthesis of heptasaccharide **19**. Our synthesis distinguishes itself from earlier preparations[3] by its small number of very efficient reaction steps. Outstandingly high yields (16% in 5 steps from **11** and **14**) of the carbohydrate sequence **19** have been obtained by a block synthesis using the thiotrisaccharide donor **11** and the glycosyl acceptor **14**.

The synthesis of thioglycoside **11** began with the preparation of disaccharide **3** (yield 35%, $[\alpha]_D^{20}$ $-28°$ ($c = 1.04$, CH_2Cl_2)). The reaction of penta-*O*-acetyl-β-D-glucopyranose **1** with the only somewhat reactive hydroxyl function of the 1,6-anhydro derivative **2**[4] to give coupling product **3** was possible with Lewis acid catalysis using trimethylsilyl trifluoromethanesulfonate.[5] In one reaction sequence **3** was hydrolyzed to **4**, which was then perbenzoylated to **5** and

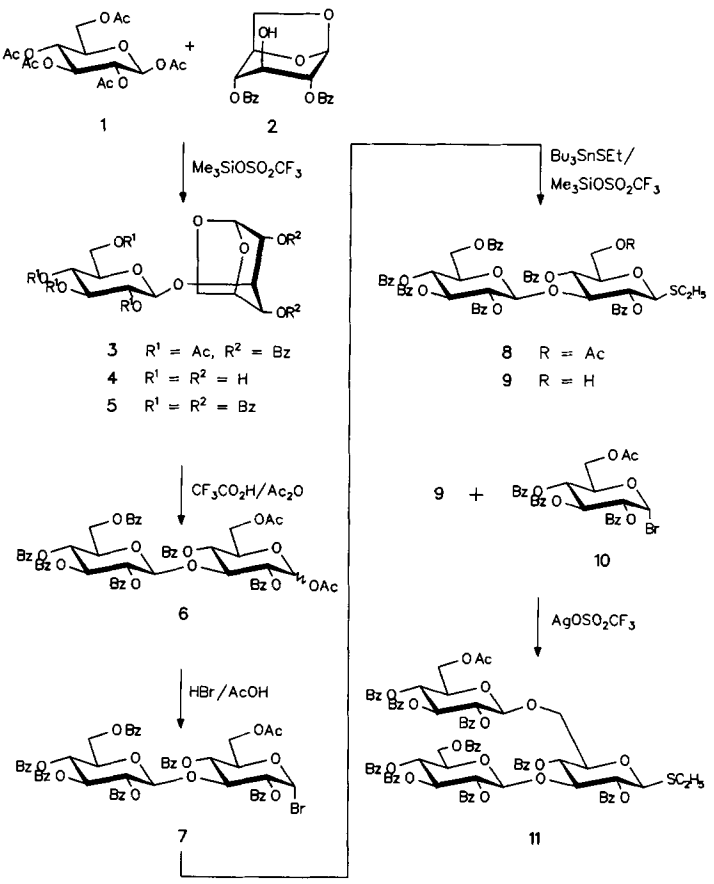

Scheme 1. Synthesis of trisaccharide–thioglycoside donor **11**. Ac = CH_3CO, Bz = C_6H_5CO.

cleaved to the diacetate **6** by acetolysis of the 1,6-anhydro ring. Bromide **7** was obtained from **6** under standard conditions and then converted to the thioethyl glycoside **8** in a reaction with ethyl tributylstannyl sulfide,[6] catalyzed by trimethylsilyl trifluoromethanesulfonate. The acetyl function of **8** was cleaved in very high yield with hydrogen chloride in methanol[7] in the presence of the benzoate protecting groups. The glycosyl bromide **10**[8] was a suitable building block for preparation of the trisaccharide–thioglycoside donor **11** (yield 50.5%, $[\alpha]_D^{20}$ $-25°$ ($c = 1.06$, CH_2Cl_2)), which can be obtained under modified Koenigs–Knorr conditions[9] with the aid of silver trifluoromethanesulfonate.

The ethylthio function of the anomeric center functions as a stable protecting group, but can also be activated selectively for further glycoside syntheses.[10] Accordingly, the trisaccharide donor **11** is a good starting material for oligosaccharide syntheses; after the acetyl function has been cleaved, chain lengthening is also possible.

Coupling to the tetrasaccharide **15** (yield 65%, $[\alpha]_D^{20}$ $-48°$ ($c = 0.98$, CH_2Cl_2)) was achieved without difficulty under alkylating conditions[10] with acceptor **14** (Scheme 2). Compound **14** was accessible from perbenzylated glucose **12** by selective acetolysis of the 6-*O*-benzylether followed by hydrolysis of the 6-*O*-acetate **13**. The deacetylation[7] of the primary hydroxyl function on **15** to **16** permitted a further chain extension with the trisaccharide donor **11**. The glycoside synthesis was carried out with methyl trifluoromethanesulfonate catalysis and led to the heptasaccharide **17** (yield 36%, $[\alpha]_D^{20}$ $-36°$ ($c = 0.99$, CH_2Cl_2)). The molecule was deprotected in two steps. Basic hydrolysis of the ester functions was followed under standard conditions by hydrogenation of the

[*] Dr. J. P. Lorentzen, Dr. B. Helpap, Dr. O. Lockhoff
Bayer AG
ZF-FWI, Building Q 18/6
Bayerwerk, W-5090 Leverkusen (FRG)

benzyl ether function to give the deprotected heptasaccharide **19** [yield 93.5%, $[\alpha]_D^{20}$ −19° (c = 0.69, H_2O); Lit. [3b]: $[\alpha]_D^{20}$ −12° (c = 0.5, H_2O)].

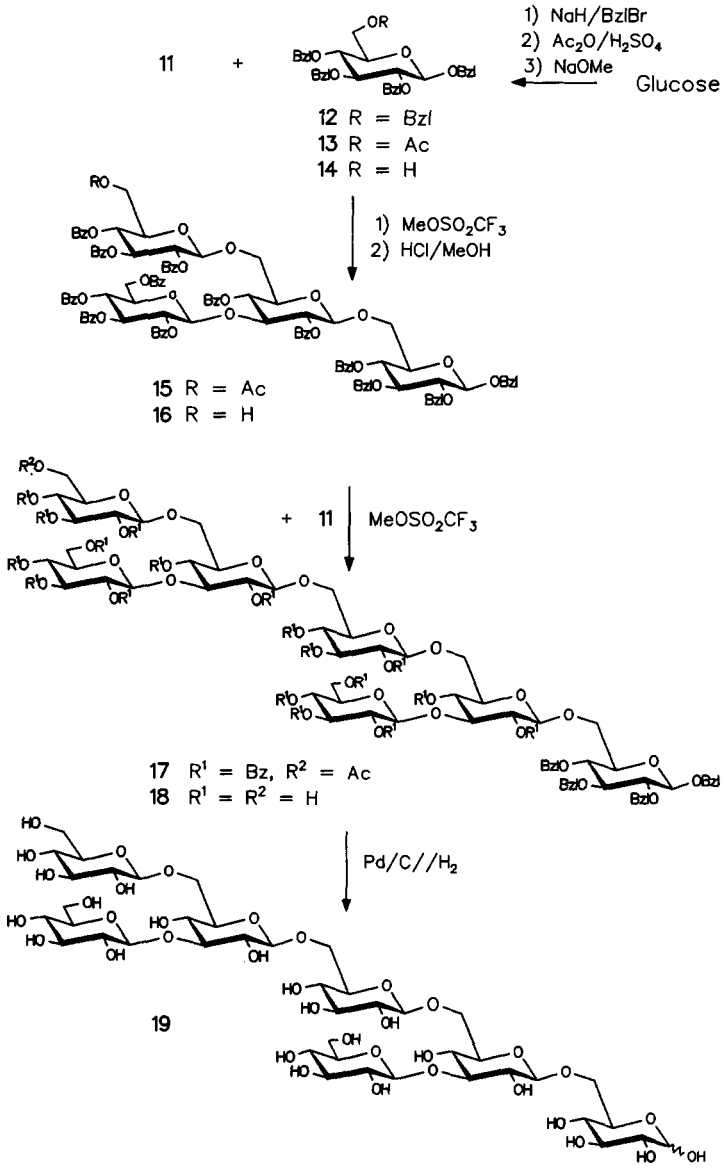

Scheme 2. Synthesis of heptasaccharide **19**. Bzl = $C_6H_5CH_2$.

Besides the desired heptasaccharide, homologous β-glucan fragments of variable chain length and branching points are obtainable by the efficient synthesis described here. These derivatives should make it possible to study structure–effect relationships.

Received: June 12, 1991 [Z 4698 IE]
German version: *Angew. Chem. 103* (1991) 1731
Publication delayed on author's request.

CAS Registry numbers:
1, 604-69-3; **2**, 57632-01-6; **3**, 137334-32-8; **4**, 137334-33-9; **5**, 137334-34-0; **6**, 137334-35-1; 7, 137334-36-2; **8**, 137334-37-3; **9**, 137334-38-4; **10**, 137334-39-5; **11**, 137334-40-8; **12**, 67890-29-3; **13**, 27851-30-5; **14**, 27851-29-2; **15**, 137334-41-9; **16**, 137334-42-0; **17**, 137334-43-1; **18**, 137334-44-2; **19**, 87102-55-4; glucose, 50-99-7.

[1] a) J. K. Sharp, M. McNeil, P. Albersheim, *J. Biol. Chem. 259* (1984) 11321; b) J. K. Sharp, P. Albersheim, P. Ossowski, A. Pilotti, P. Garegg, B. Lindberg, *ibid. 259* (1984) 11341.

[2] a) W. E. Schmidt, J. Elbel, *Proc. Natl. Acad. Sci. USA 84* (1987) 4117; b) E. G. Cosio, H. Pöpperl, W. E. Schmidt, J. Ebel, *Eur. J. Biochem. 175* (1988) 309.

[3] a) P. Ossowski, A. Pilotti, P. J. Garegg, B. Lindberg, *J. Biol. Chem. 259* (1984) 11337; b) P. Fügedi, W. Birberg, P. J. Garegg, A. Pilotti, *Carbohydr. Res. 164* (1987) 297; c) P. Fügedi, P. Garegg, *J. Carbohydr. Chem. 7* (1988) 389.

[4] J. S. Brimacombe, L. C. N. Tucker, *Carbohydr. Res. 40* (1975) 387.

[5] a) T. Ogawa, K. Beppu, S. Nakabayashi, *Carbohydr. Res. 93* (1981) C6; b) H. Paulsen, M. Paal, *ibid. 135* (1984) 53.

[6] T. Ogawa, M. Matsui, *Carbohydr. Res. 54* (1977) C17.

[7] N. E. Byramova, M. V. Ovchinnikov, L. V. Backinowsky, N. K. Kochetkov, *Carbohydr. Res. 124* (1983) C8.

[8] The first step in the preparation of glycosyl bromide **10** was perbenzoylation of glucosan. After acetolysis of the 1,6-anhydro ring the resulting diacetate can be converted to the halogenated compounds under standard conditions.

[9] S. Hanessian, J. Banoub, *Carbohydr. Res. 53* (1977) C13.

[10] a) H. Lönn, *Carbohydr. Res. 139* (1985) 105; b) H. Lönn, *ibid. 139* (1985) 115; c) F. Dasgupta, P. J. Garegg, *ibid. 202* (1990) 225.

Synthesis of Muropeptide Conjugates of 2,3-Dideoxy-β-D-*manno*-2-octulosonic Acid

By *Hans-Georg Lerchen** and *Hein-Peter Kroll*

Dedicated to Professor Karl Heinz Büchel on the occasion of his 60th birthday

Lipopolysaccharides (LPS) in the outer membrane of gram-negative bacteria play an important role in the growth and virulence of these cells.[1] One structural element in the inner core region specific to bacteria, yet found universally, is 3-deoxy-β-D-*manno*-2-octulosonic acid (KDO) (**1**). The inhibition of its biosynthesis is thus an attractive goal in drug research.[2] The key enzyme in the biosynthesis is cytidinemonophosphate-(CMP)-KDO-synthetase.[3] 2-Deoxy-β-KDO-derivatives like **2a** and **2b** have been described as potent enzyme inhibitors, but are not able to penetrate the bacterial membrane due to structural parameters.[4a] To solve this

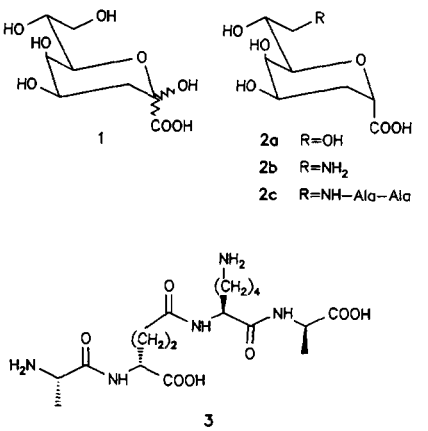

problem *Lartey* et al. as well as *Claesson* et al. synthesized the 8-amino-linked dipeptide conjugate **2c**,[4b,c] which is actively transported by peptide permeases into the bacterial cell.

[*] Dr. H.-G. Lerchen
Bayer AG, Zentrale Forschung, Q18
W-5090 Leverkusen (FRG)
Dr. H.-P. Kroll
Bayer AG, Institut für Chemotherapie
W-5600 Wuppertal (FRG)

Table 1. Linkage of 2-deoxy-β-KDO **2a** with protected peptide derivatives **4** producing **5** and subsequent deprotection to the free glycoconjugates **6** [a, b].

muropeptide derivatives	protected 2-deoxy-β-KDO conjugates	yield [%]	free glycoconjugates	yield [%]
4a H-Ala-D-*i*Gln-Bzl · HCl	**5a** 2d-β-KDO-Ala-D-*i*Gln-Bzl	89	**6a** 2d-β-KDO-Ala-D-*i*Gln	91
4b H-Ala-D-Glu(Bzl)-Bzl · TFA	**5b** 2d-β-KDO-Ala-D-Glu(Bzl)-Bzl	72	**6b** 2d-β-KDO-Ala-D-Glu	93
4c H-Ala-D-Glu(Lys(Z)-Bzl)-Bzl · TFA	**5c** 2d-β-KDO-Ala-D-Glu(Lys(Z)-Bzl)-Bzl	43	**6c** 2d-β-KDO-Ala-D-Glu(Lys)	82
4d H-Ala-D-Glu(Lys(Z)-D-Ala-Bzl)-Bzl · TFA	**5d** 2d-β-KDO-Ala-D-Glu(Lys(Z)-D-Ala-Bzl)-Bzl	75	**6d** 2d-β-KDO-Ala-D-Glu(Lys-D-Ala)	80
4e H-D-Glu(Lys(Z)-Bzl)-Bzl · TFA	**5e** 2d-β-KDO-D-Glu(Lys(Z)-Bzl)-Bzl	46	**6e** 2d-β-KDO-D-Glu(Lys)	80

[a] *i*Gln = isoglutamine, 2d-β-KDO = 2,3-dideoxy-β-D-*manno*-2-octulosonoyl, TFA = trifluoroacetic acid, Z = *N*-benzyloxycarbonyl. [b] Purity of the new compounds was assessed by ^1H and ^{13}C NMR spectroscopy.

There, **2c** is cleaved by peptidases with release of the enzyme inhibitor **2b**. However, in vivo this dipeptide cleavage may also be carried out by eukaryotic peptidases outside the bacterial cell.[5] To prove the therapeutic value of 2-deoxy-β-KDO derivatives, prodrugs of **2a** must be synthesized, which should be quite stable in vivo, releasing inhibitor **2a** only inside the bacterial cell.

We herein describe the synthesis of 1-carboxyl-linked peptide conjugates of 2-deoxy-β-KDO **2a**. Their stability can be varied by the introduction of different anchor groups at which cleavage could occur. We chose peptidic carriers derived from bacterial muropeptides, sequences which are taken up preferentially by bacteria during the course of peptidoglycan metabolism.[6] 2-Deoxy-β-KDO **2a** was linked to the terminal amino group of **3** or appropriate partial sequences. The suitably protected peptide derivatives **4** were prepared by known methods[7] (Table 1). The ammonium salts of the oligopeptide fragments **4** were attached efficiently to the carboxyl group of unprotected **2a** by the Wünsch–Weygand method[8] with dicyclohexylcarbodiimide (DCC)/*N*-hydroxysuccinimide (HOSu) in the presence of Hünig base. Hydrogenolysis of **5** provided the deprotected conjugates **6**.

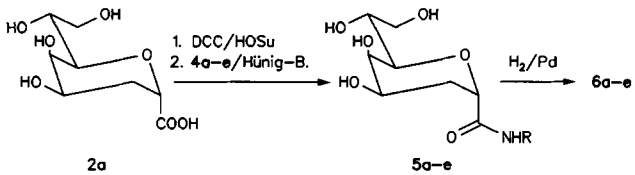

Scheme 1. Linkage of 2-deoxy-β-KDO **2a** with suitably protected peptide derivatives **4a–e** to the conjugates **5a–e** and complete deprotection to **6a–e** (Table 1).

All deprotected glycoconjugates **6** proved to be stable to peptidases. However, the release of the enzyme inhibitor inside the bacterial cell is an additional requirement for antibacterial activity of conjugates such as **6**, after their uptake through the membrane. To check the carrier potential of muropeptide fragments, cleavable anchor groups, for example, active esters[9] had to be introduced between carrier and drug.

The cesium salt method[10] effected the elegant transformation of the carboxyl function of **2a** into labile ester derivatives without the protection of the hydroxyl functions. The selective removal of protecting groups in the presence of activated ester bonds was thus avoided (Scheme 2).

The starting material cesium 2,3-dideoxy-β-D-*manno*-2-octulosonate **7** was obtained from the reaction of **2a** with Cs_2CO_3. Alkylation of **7** with α-benzyl-γ-chloromethyl Z-L-alanyl-D-glutamate[11] yielded the geminal diol ester derivative **8**, which was deprotected by hydrogenolysis providing **9**. The glycolic ester **10** was obtained by alkylation and hydrogenolysis in the same manner and can be modified broadly. Subsequent reactions with muropeptide fragments yielded 2-deoxy-β-KDO conjugates such as **11**, which was deprotected by hydrogenolysis to **12**.

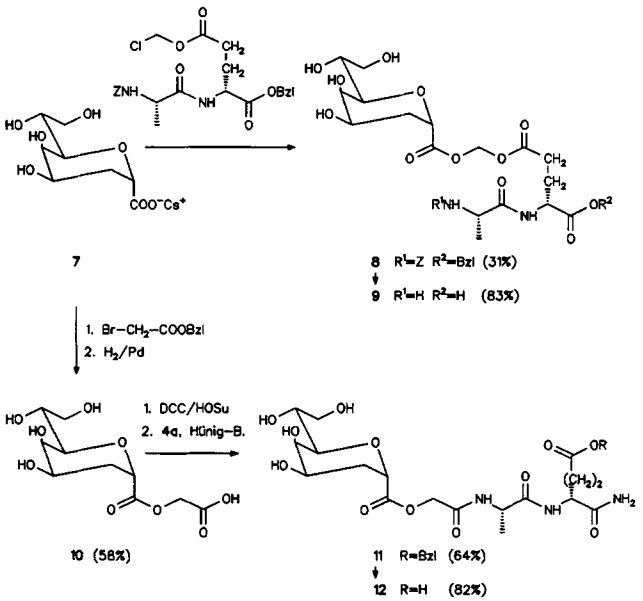

Scheme 2. Attachment of muropeptide derived fragments to **2a** by alkylation of cesium 2,3-dideoxy-β-D-*manno*-2-octulosonate.

Bacterial enzymatic cleavage was shown for the derivatives **9** and **12**.[13] The in vitro antibacterial activity measured for **9** verifies its uptake into the bacterial cell as well as the release of the enzyme inhibitor in the cytoplasm. Thus by different modifications of the 1-carboxyl-function of the 2-deoxy-β-KDO unit in **6**, **9**, and **12** a graduation in in vivo stability is realized with respect to a selective cleavage inside the bacterial cell.

Received: June 5, 1991 [Z 4679 IE]
German version: *Angew. Chem. 103* (1991) 1728

CAS Registry numbers:
2a, 107573-28-4; **4a**, 59524-62-8; **4b**, 66025-58-9; **4c**, 137040-40-5; **4d**, 137040-42-7; **4e**, 137040-44-9; **5a**, 137040-52-9; **5b**, 137040-53-0; **5c**, 137040-54-1; **5d**, 137040-55-2; **5e**, 137040-56-3; **6a**, 137040-57-4; **6b**, 137040-58-5; **6c**, 137040-59-6; **6d**, 137040-60-9; **6e**, 137040-61-0; 7, 137040-45-0; **8**, 137040-46-1; **9**, 137040-47-2; **10**, 137040-48-3; **11**, 137040-49-4; **12**, 137040-50-7; $BrCH_2COOBzl$, 5437-45-6; z-alanyl-D-glutamyl-α-benzyl-γ-chloromethylester, 137040-51-8.

[1] Review: O. Lüderitz, M. A. Freudenberg, C. Galanos, V. Lehman, E. T. Rietschel, D. H. Shaw, *Curr. Top. Membr. Transp. 17* (1982) 79.
[2] Review: F. Unger, *Adv. Carbohydr. Chem. Biochem. 38* (1981) 323.
[3] M. A. Ghalambor, E. C. Heath, *J. Biol. Chem. 241* (1966) 3216; W. E. Kohlbrenner, S. W. Fesik, *ibid. 260* (1985) 14695.

[4] a) A. Claesson, K. Luthman, K. Gustafsson, G. Bondesson, *Biochem. Biophys. Res. Commun. 143* (1987) 1063; b) R. Goldman, W. E. Kohlbrenner, P. Lartey, A. Pernet, *Nature 329* (1987) 730; c) A. Claesson, A. M, Jansson, B. C. Pring, S. M. Hammond, B. Ekström, *J. Med. Chem. 30* (1987) 2309.
[5] P. Lartey, *Drugs of the Future 13* (1988) 555.
[6] E. W. Goodell, *J. Bacteriol. 163* (1985) 305; E. W. Goodell, C. F. Higgins, *ibid. 169* (1987) 3861.
[7] Review: E. Wünsch in *Methoden Org. Chem. (Houben-Weyl) 15/1,2* (1974).
[8] E. Wünsch, F. Drees, *Chem. Ber. 99* (1966) 110; F. Weygand, D. Hoffmann, E. Wünsch, *Z. Naturforsch. B 21* (1966) 426.
[9] Review: H. Bundgaard in B. Roche (Eds.): *Bioreversible Carriers in Drug Design*, Pergamon, London 1987, p. 13–94.
[10] B. F. Gisin, *Helv. Chim. Acta 56* (1973) 1476; W. H. Kruizinga, B. Strijtveen, R. M. Kellogg, *J. Org. Chem. 46* (1981) 4321; H.-G. Lerchen, H. Kunz, *Tetrahedron Lett. 26* (1985) 5257.
[11] Preparation from Z-L-Ala-D-Glu(OH)-Bzl with chloromethylchlorosulfate under phase transfer conditions (see [12]). During the reaction with **7** cyclization of the glutamic acid unit to the imide occurs as a side reaction.
[12] B. Baltzer, E. Binderup, W. v. Daehne, W. O. Godtfredsen, K. Hansen, B. Nielsen, H. Sorensen, S. Vangedal, *J. Antibiot. 33* (1980) 1183.
[13] The enzymatic cleavage was detected in a CMP-KDO-synthetase assay. The derivatives **9** and **12** showed activity in this assay only after preincubation with bacterial cell lysate.
[14] A reduction of the bacterial cell counts of *Salmonella typhimurium* by 3.6 log units compared to the untreated control was measured 24 and 36 h after treatment with 2.2 μM **9**.

The Reaction-Accelerating Neighboring-Group Effects in the Reaction of Vinyl Bromides with Alkyl-Transition Metal Reagents**

By *Thomas Kauffmann** and *Dirk Stach*

Dedicated to Professor Karl Heinz Büchel on the occasion of his 60th birthday

In the alkylation and carbonyl-olefination of ketones with transition metal reagents, basic groups located in the α- or β-position to the keto group exercise a reaction-promoting[1–4] or reaction-inhibiting influence,[3, 4] which enables very selective ("chele-" and "anticheleselective"[3, 4]) alkylations (for example see Scheme 1) and carbonyl-olefinations.

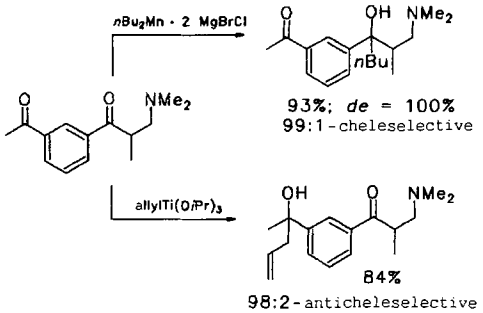

Scheme 1. Example of neighboring group effects in the alkylation and allylation of a diketone [5].

Such neighboring group effects are most probable in reactions, which already proceed rapidly at low temperature.[5] Following the finding that alkyliron and alkylcobalt reagents react rapidly at −78 °C with vinyl bromides with cross-coupling,[6, 7] we have checked by competition experiments with the substrates **1**–**5** (Scheme 2) according to Scheme 3 whether basic groups (OH, OMe, CN) in the α- or β-position to the Br atom of vinyl bromides influence the rate of cross-coupling.[8] We found this to be true on using Me_4FeLi_2, Me_4MnLi_2 and nBu_4MnLi_2 (Table 1), but not on using Me_4CoLi_2 and Me_2CuLi. The cobalt reagent is too reactive to be able to react selectively, while the copper reagent is almost completely deactivated by the functionalized vinyl bromides **2**–**5**. Diethyl ether was substantially more suitable as solvent than the strongly complexing tetrahydrofuran.

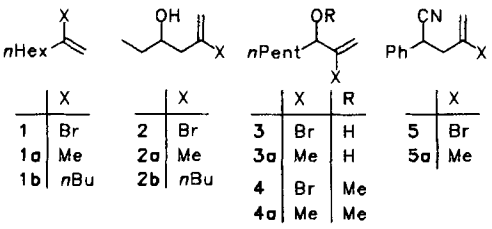

Scheme 2. Starting compounds **1**–**5** and products **a**, **b** of the competition experiments (*n*Hex = *n*-hexyl; *n*Pent = *n*-pentyl).

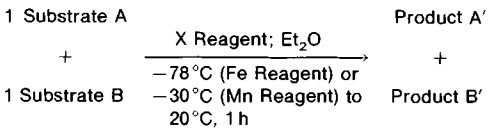

Scheme 3. Conditions in the competition experiments. The molar ratio is evidenced by the factors before the reagents.

Table 1. Competition reactions carried out according to Scheme 3.

Substrates		Mol. equiv. Reagent	Products and yields [%]				Product ratio	Recovery of substrates [a]	
1	**2**	0.66 Me_4FeLi_2	**1a**	6	**2a**	48	11:89	90	25
1	**2**	0.66 Me_4MnLi_2	**1a**	14	**2a**	78	15:85	73	15
1	**2**	1 nBu_4MnLi_2	**1b**	10	**2b**	74	12:88	66	17
1	**3**	1 Me_4MnLi_2	**1a**	<1	**3a**	67	1:99	71	13
1	**3**	0.5 Me_4FeLi_2	**1a**	5	**3a**	79	6:94	66	8
1	**4**	1 Me_4MnLi_2	**1a**	<1	**4a**	72	1:99	55	5
1	**5**	0.5 Me_4FeLi_2	**1a**	4	**5a**	76	5:95	81	0
1	**5**	1 Me_4MnLi_2	**1a**	0	**5a**	0	–	76	73
2	**3**	0.5 Me_4FeLi_2	**2a**	17	**3a**	73	10:90	64	7
2	**3**	0.5 Me_4MnLi_2	**2a**	32	**3a**	82	28:72	41	<1

[a] As percentage of material employed.

The reactions of the hydroxyvinyl bromides **2** and **3** with Me_4FeLi_2 (at −78 °C) and Me_4MnLi_2 (at −30 °C) were examined more closely. In 1 : 1 reactions one mole equivalent of CH_4 was formed in each case, and in the IR spectrum (at −20 °C) the OH-stretching vibration bands of **2** and **3** at 3473 and 3439 cm^{-1}, respectively, disappeared. It follows, therefore, that an Fe- or Mn-alkoxide, respectively, is most likely formed in the course of the reaction. The alkoxide is presumably formed before the cross-coupling, for which we consider, as far as educts **2** and **3** are concerned, the "insertion-deinsertion" mechanism formulated in Scheme 4A more likely than the mechanism formulated in Scheme 4B. Since, to our knowledge, only transition-metal reagents for the cross-coupling with vinyl bromides are suitable whose metal atom can assume a higher oxidation state (Ti^{IV} reagents are e.g. unsuitable), we assume a compound of the type **9** as intermediate of the insertion step **6** → **7**.

[*] Prof. Dr. T. Kauffmann, Dr. D. Stach
Organisch-chemisches Institut der Universität
Corrensstrasse 40, W-4400 Münster (FRG)

[**] Transition-Metal-Activated Organic Compounds, Part 36. This work was supported by the Volkswagenstiftung, the Deutsche Forschungsgemeinschaft, and the Fonds der Chemischen Industrie.—Part 35: T. Kauffmann, J. Jordan, J. Sander, *Chem. Ber.*, in press.

Due to opposing effects of ring strain and entropy, the series four-membered ring ≪ five-membered ring > six-membered ring generally holds true for the rate of ring formation. In the case of the mechanism of Scheme 4A it is therefore fully understandable that in competition reactions with the substrate pair **2**/**3** (Table 1) α-hydroxyvinyl bromide **3** reacts more rapidly in each case. In the mechanism of Scheme 4B rather the opposite would be expected, since **3** would react via a four-membered ring intermediate. The mechanism of Scheme 4A reveals, moreover, a clear parallel to the confirmed chelate mechanism of the methylation of the α-hydroxyketone benzoin with methyl-transition-metal reagents,[3, 9] in which the hydroxy group likewise exercises an accelerating neighboring effect.[1-3]

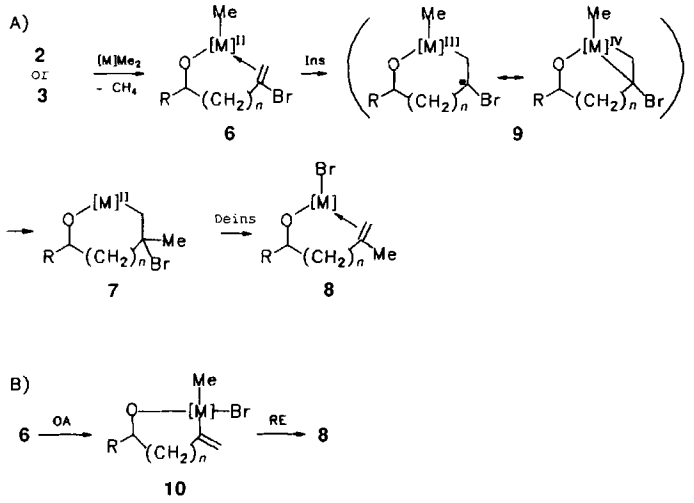

Scheme 4. Possible mechanism of the cross-coupling of the hydroxyvinyl bromides **2** and **3** (n = 0, 1; M = Fe, Mn, with additional ligands, which are omitted for simplification). A) Ins and Deins = insertion and deinsertion, respectively. b) OA and RE = oxidative addition and reductive elimination, respectively.

The acceleration of nucleophilic substitutions of sp^3-C-bound halogen atoms by neighboring groups[10] ("anchimeric" assistance[11]) is based on the fact that the neighboring groups assume a direct bond relationship to the reaction center and in this way stabilize transition states or intermediates (for example see Scheme 5). Another principle

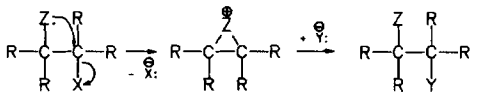

Scheme 5. Substitution of an sp^3-C-bound halogen atom with anchimeric assistance.

underlies the substitution of sp^2-C-bound halogen atoms accelerated by neighboring groups described here; it includes involvement of the neighboring group in a bonding relationship to the reaction center of the substitution and also of (in the case of **9** or **10**) the metal atom coordinated to the neighboring group.

Experimental

The methyl reagents, all of which are described in the literature as isolated complexes, were prepared in situ by reaction of four or two mole equivalents, respectively, of MeLi with $FeCl_2$ (conveniently obtainable by 1:1 reaction of $FeCl_3$ and MeLi), $MnBr_2$, $CoCl_2$ and CuI, respectively. nBu_4MnLi_2 was prepared analogously with *n*BuLi. The vinyl bromides used as starting compounds and their alkylation products required as reference substances, of which **3**, **4**, **5**, **2b**, and **4a** have still not been described, were synthesized on a preparative scale[12] (the methylation products by reaction of the vinyl bromides with Me_4CoLi_2). The evaluation of the competition experiments (identification and quantification of the products) was accomplished gas-chromatographically with the aid of authentic reference substances.

Received: July 5, 1991 [Z 4776 IE]
German version: *Angew. Chem. 103* (1991) 1683

[1] T. Kauffmann, T. Möller, H. Rennefeld, S. Welke, R. Wieschollek, *Angew. Chem. 97* (1985) 351; *Angew. Chem. Int. Ed. Engl. 24* (1985) 348.
[2] T. Kauffmann, K. Abel, W. Bonrath, M. Kolb, T. Möller, C. Pahde, S. Raedeker, M. Robert, M. Wensing, B. Wichmann, *Tetrahedron Lett. 27* (1986) 5351.
[3] T. Kauffmann in H. Werner, G. Erker (Eds.): *Organometallics in Organic Synthesis 2*, Springer, Berlin 1989, p. 161.
[4] T. Kauffmann in U. Schubert (Ed.): *Advances in Metal Carbene Chemistry*, Kluwer, Dordrecht 1989, p. 359.
[5] D. Schlosser, *PhD Thesis*, Universität Münster 1991.
[6] T. Kauffmann, B. Laarmann, D. Menges, K.-U. Voss, D. Wingbermühle, *Tetrahedron Lett. 31* (1990) 507.
[7] T. Kauffmann, G. Hopp, B. Laarmann, D. Stegemann, D. Wingbermühle, *Tetrahedron Lett. 31* (1990) 514.
[8] D. Stach, *PhD Thesis*, Universität Münster 1991.
[9] M. T. Reetz, R. Steinbach, J. Westermann, R. Urz, B. Wenderoth, R. Peter, *Angew. Chem. 94* (1982) 133; *Angew. Chem. Int. Ed. Engl. 21* (1982) 135.
[10] B. Capon, S. P. McManus: *Neighboring Group Participation, Vol. 1*, Plenum, New York 1976.
[11] S. Winstein, C. R. Lindegren, H. Marshall, L. L. Ingraham, *J. Am. Chem. Soc. 75* (1953) 147.
[12] T. Kauffmann, D. Stach, unpublished.

Enantioselective and Diastereoselective Total Synthesis of the Antimycotically Active Natural Product Chlorotetaine: Revision of the Relative Configuration**

By *Hanno Wild** and *Liborius Born*

Dedicated to Professor Karl Heinz Büchel on the occasion of his 60th birthday

In common with the longer known and related substance bacilysin,[1] the dipeptide chlorotetaine (recently isolated from the *Bacillus subtilis* strain BGSC 1E2), whose structure has been identified as **1**,[2] possesses interesting antimycotic properties.

[*] Dr. H. Wild
Bayer AG, Chemisch-wissenschaftliches Labor Pharma
Postfach 10 17 09, W-5600 Wuppertal 1 (FRG)
Dr. L. Born
ZF-DZA Structure Research, Bayerwerk
W-5090 Leverkusen (FRG)

[**] We wish to thank Prof. *Jung*, Tübingen, FRG for supplying a sample of natural chlorotetaine **1**.

Though three syntheses have been published for anticapsin,[3] the *C*-terminal amino acid of bacilysin, no stereoselective general approach to amino acids of this unusual type has been published so far. We report here the first total synthesis of chlorotetaine. Based on this work the natural compound was assigned structure **2** above, which is epimeric to structure **1** with an (*S*)-configurated C-atom in the cyclohexenyl residue. In planning the synthesis it had to be borne in mind that chlorotetaine is only stable in solution at a pH of about 5. Above pH 7 as well as below pH 5 the biological activity decreases rapidly, especially on heating.[2] The main reaction in alkaline media is the intramolecular 1,4-addition of the amide to the enone system, with formation of a 6-oxo-octahydroindole.[3b, c] Since the risk of this side reaction is present during all the intermediate steps of the synthesis as well, the enone should not be liberated until the latest possible moment. Scheme 1 shows the reaction sequence that should lead to the dipeptide **1**, the presumed chlorotetaine.

The cuprate of the bislactim ether **4**[4] reacted with dienone **3**[5] giving the desired diastereomerically pure 3-cyclohexenone derivative **5** from 1,6-addition in a 40% yield, in addition to 24% of the 1,4-adduct **6**. Compound **5** was then hydrogenated to cyclohexanone **7**. In the next step the desired configuration at C1′ was produced as described by *Koga* et al.[6] and *Simpkins* et al.[7] by diastereoselective deprotonation with lithium (*R,R*)-bis(phenylethyl)amide (**8**). By analogy with the reactions of simple 4-alkylcyclohexanones the principal diastereomer should possess the configuration indicated for **9**. To generate the necessary 2-chloroenone system, silyl enol ether **9** was first converted into diazo compound **10** via a *C*-trifluoroacetyl intermediate.[8] The reaction of **10** with phenylselenyl chloride at −5 °C was spontaneous, and subsequent oxidative elimination gave chloroenone **11**.[9] Before the hydrolysis of the bislactim ether, the ketone had to be reduced,[10] since acidic cleavage of **11** with subsequent liberation of the amine led to the already mentioned intramolecular 1,4-addition. Alcohol **12** yielded the dipeptide **13** without problems after hydrolysis and linkage with (*S*)-Boc-alanine. The product could be reoxidized to the cyclohexenone in a good yield by manganese dioxide. At this stage small quantities of the undesired diastereomer could easily be removed by chromatography.[11]

After cleavage of the Boc protecting group, the methyl ester was saponified with porcine pancreas lipase. Despite these mild conditions free dipeptide **1** was not obtained, but rather, a diastereomeric mixture of the octahydroindole arising from intramolecular 1,4-addition.

Scheme 2 shows the synthesis of dipeptide **2**, which is epimeric to **1**. Starting from cyclohexanone **7**, the protected dipeptide **16** was prepared in a reaction sequence completely analogous to that indicated in Scheme 1 and in a comparable yield.[11] The deprotonation of **7** in the presence of trimethylsilyl chloride by (*S,S*)-**8** yielded silyl enol ether **15**, epimeric to **9**, with the same selectivity. Cleavage of the Boc protecting group from **16**, followed by lipase-catalyzed saponification and reverse-phase chromatography to separate off decomposition products, yielded the dipeptide **2**, which

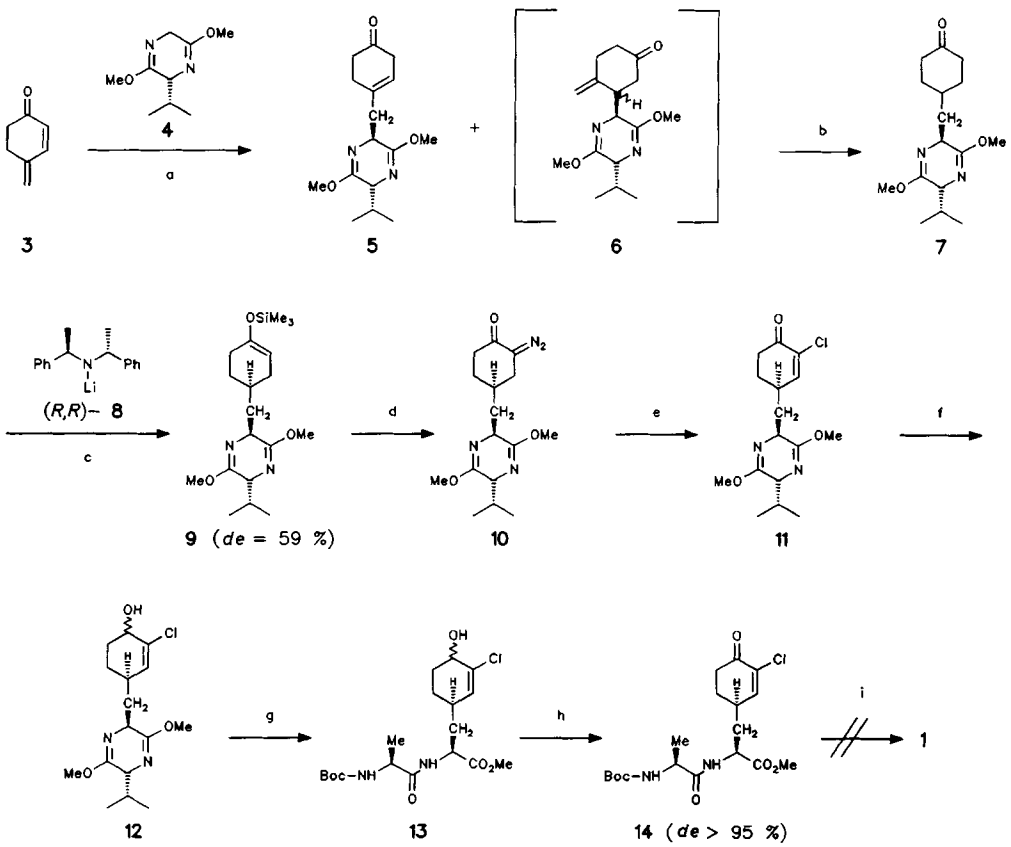

Scheme 1. a) **4**, *n*BuLi, THF, Me_2S, −78 °C; 0.5 equiv CuBr·Me_2S, 30 min, −40 °C; **3**, −78 °C; AcOH (**5**: 40 %, *de* > 95 %; **6**: 24 %, *de* (1,4) > 95 %, *de* (1,5) = 81 %; b) 3 atm H_2, Pd/C, ethyl acetate, 2 h (97 %); c) (*R,R*)-**8**, Me_3SiCl, THF, −78 °C, +7 (76 %); d) MeLi, THF, 0 °C; $CF_3CO_2CH_2CF_3$, −78 °C; TsN_3, NEt_3, CH_3CN, 2 h (66 %); e) PhSeCl, CH_2Cl_2, −5 °C; 3 equiv H_2O_2, pyridine, CH_2Cl_2, 1 h, 0 °C (67 %); f) $NaBH_4$, $CeCl_3$, MeOH (89 %); g) 2 equiv HCl, CH_3CN, H_2O, 2 h; saturated Na_2CO_3 solution; (*S*)-Boc-alanine, dicyclohexylcarbodiimide (DCC), hydroxybenzotriazole (HOBT), THF, 1 h (87 %); h) MnO_2, CH_2Cl_2, 6 h; chromatography on silica gel (59 %); i) CF_3CO_2H, anisole, 1 h, 0 °C; porcine pancreas lipase (Sigma: L 3126), buffer pH 7.5, 4 h.

 © VCH Verlagsgesellschaft mbH, W-6940 Weinheim, 1991 0570-0833/91/1212-1686 $ 3.50+.25/0 Angew. Chem. Int. Ed. Engl. 30 (1991) No. 12

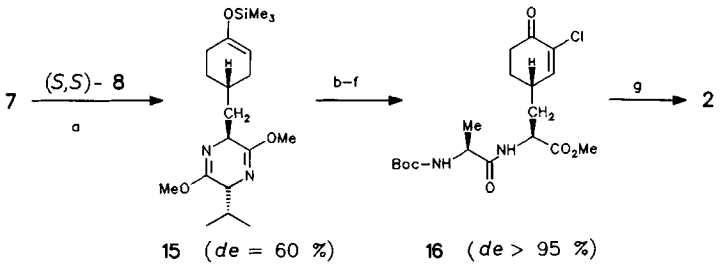

Scheme 2. a) (*S,S*)-**8**, Me_3SiCl, THF, $-78\,^{\circ}C$, $+7$ (71 %); b–f) see Scheme 1, **9** → **14**; g) CF_3CO_2H, anisole, 1 h, 0 °C; porcine pancreas lipase (Sigma: L 3126), buffer pH 7.5; purification on RP-8, Lobar with H_2O (52 %).

was in every respect (NMR, UV, DC, HPLC) identical to naturally occurring chlorotetaine.[12]

That the selective deprotonation of the cyclohexanone **7** had actually followed the expected course was demonstrated beyond question by a X-ray structure analysis of the *N*-trityl derivative **17** prepared analogously to **16** from silyl enol ether **15**. The asymmetric C atom in the cyclohexene ring of **17**, thus also in chlorotetaine **2**, was shown by this analysis to possess an (*S*)-configuration. The amino acid residue, at least in the crystal, is in the *axial* position (allylic 1,2-strain[14]). In the original determination of the configuration of chlorotetaine based on its circular dichroism (CD) spectrum, this group was presumed to be equatorial.

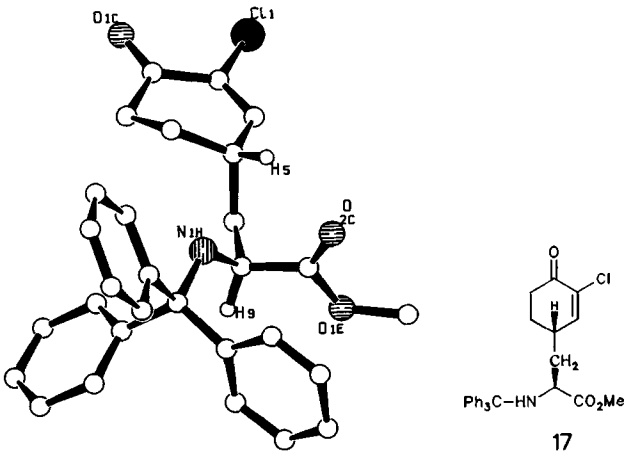

17

Fig. 1. Structure of **17** in the crystal (SCHAKAL representation) [13].

The higher stability of chlorotetaine **2** compared with that of epimer **1** is easy to explain: Whereas the cyclization of **1** leads to an octahydroindole with an *exo*-carboxyl substituent, the same reaction starting from **2** is made more difficult by the formation of a product with an *endo*-carboxyl residue.

Received: June 13, 1991
Revised: September 23, 1991 [Z 4703 IE]
German version: *Angew. Chem. 103* (1991) 1729

CAS Registry numbers:
1, 117985-03-2; **2**, 117985-03-2; **3**, 66629-58-1; **4**, 109838-85-9; **5**, 137232-86-1; **6**, 137232-87-2; **7**, 137232-88-3; (*R,R*)-**8**, 113680-88-9; (*S,S*)-**8**, 72659-60-0; **9**, 137232-89-4; **10**, 137232-90-7; **11**, 137232-91-8; **12** (isomer 1), 137232-92-9; **12** (isomer 2), 137330-23-5; **13** (isomer 1), 137331-07-8; **13** (isomer 2), 137232-95-2; **14**, 137232-93-0; **15**, 137330-21-3; **16**, 137330-22-4; **17**, 137232-94-1; (*S*)-Boc-alanine, 15761-38-3.

[1] J. E. Walker, E.-P. Abraham, *Biochem. J. 118* (1970) 563.
[2] a) C. Rapp, G. Jung, W. Katzer, W. Loeffler, *Angew. Chem. 100* (1988) 1801; *Angew. Chem. Int. Ed. Engl. 27* (1988) 1733; b) G. Jung, W. Loeffler, C. Rapp, W. Katzer, F. Petersen, DE-A 3834662 (1990).
[3] a) R. W. Rickards, J. L. Rodwell, K. J. Schmalzl, *J. Chem. Soc. Chem. Commun. 1977*, 849; b) B. C. Laguzza, B. Ganem, *Tetrahedron Lett. 22* (1981) 1483; c) M. Souchet, M. Baillarge, F. LeGoffic, *ibid. 29* (1988) 191; d) M. J. Crossley, T. W. Hambley, A. W. Stamford, *Aust. J. Chem. 43* (1990) 1827.
[4] U. Schöllkopf, D. Pettig, E. Schulze, M. Klinge, E. Egert, B. Benecke, M. Noltemeyer, *Angew. Chem. 100* (1988) 1238; *Angew. Chem. Int. Ed. Engl. 27* (1988) 1194.
[5] A. J. Birch, *J. Proc. R. Soc. N.S.W. 83* (1949) 245.
[6] R. Shirai, M. Tanaka, K. Koga, *J. Am. Chem. Soc. 108* (1986) 543.
[7] C. M. Cain, R. P. C. Cousins, G. Coumbarides, M. S. Simpkins, *Tetrahedron 46* (1990) 523.
[8] R. L. Danheiser, R. F. Miller, R. G. Brisbois, S. Z. Park, *J. Org. Chem. 55* (1990) 1959.
[9] D. J. Buckley, M. A. McKervey, *J. Chem. Soc. Perkin Trans 1 1985*, 2193.
[10] J.-L. Luche, L. Rodriguez-Hahn, P. Crabbe, *J. Chem. Soc. Chem. Commun. 1978*, 601.
[11] All new compounds gave satisfactory spectroscopic and mass spectrometric data. Selected physical data: **14**: $R_F = 0.32$ (Ether); ^1H NMR ($CDCl_3$): $\delta = 1.38$ (d, $J = 6.5$ Hz, 3H), 1.43 (s, 9H), 1.70–1.85 (m, 2H), 2.05–2.20 (m, 2H), 2.55 (dd, $J = 11$, 5 Hz, 1H), 2.62–2.78 (m, 2H), 3.58 (s, 3H), 4.13 (quint., $J = 6.5$ Hz, 1H), 4.74 (td, $J = 8.4$ Hz, 1H) 4.92 (br, 1NH), 6.72 (d, $J = 8$ Hz, 1NH), 7.17 (d, $J = 2.5$ Hz, 1H). **16**: $R_F = 0.40$ (Ether); ^1H NMR ($CDCl_3$): $\delta = 1.38$ (d, $J = 6.5$ Hz, 3H), 1.45 (s, 9H), 1.65–2.05 (m, 3H), 2.30–2.45 (m, 1H), 2.51 (dd, $J = 13$, 4 Hz, 1H), 2.62–2.78 (m, 2H), 3.56 (s, 3H), 4.12 (quint., $J = 6.5$ Hz, 1H), 4.75 (td, $J = 8$, 4 Hz, 1H), 4.92 (br, 1NH), 6.68 (d, $J = 8$ Hz, 1NH), 6.93 (d, $J = 3$ Hz, 1H).
[12] Crystal structure analysis of **17**: Space group $P2_12_12_1$ (No. 19); $a = 1010.9(4)$, $b = 1843.9(4)$, $c = 1335.2(3)$ pm, $Z = 4$, $\varrho_{calc.} = 1.265$ g cm^{-3}. Enraf-Nonius-CAD4 diffractometer, room temperature, CuKα radiation, 2585 independent reflections, empirical absorption correction, solution by direct and differential Fourier methods. Refinement: anisotropic temperature factors (nonhydrogen atoms), isotropic temperature factors (hydrogen atoms), R (1887 reflections, 420 parameters) = 0.041. Further details of the crystal investigation can be obtained from the Fachinformationszentrum Karlsruhe, Gesellschaft für wissenschaftlich-technische Information mbH, W-7514 Eggenstein-Leopoldshafen 2, by quoting the file number CSD-55831, the authors, and the journal reference.
[13] a) S. K. Malhotra, D. G. Moakley, F. Johnson, *J. Chem. Soc. Chem. Commun. 1967*, 448; b) F. Johnson, *Chem. Rev. 68* (1968) 375.

Tandem Silyl Migrations Leading to α,β-Bis-silylated Enals and Enones**

By *Bernd Mergardt, Klaus Weber, Gunadi Adiwidjaja,* and *Ernst Schaumann**

Dedicated to Professor Michael Hanack on the occasion of his 60th birthday

An α-silyl residue makes α,β-unsaturated carbonyl compounds universally modifiable Michael acceptors and, at the same time, prevents any otherwise ready polymerization.[1] We report here on the productive synthesis of α,β-bis-silylated compounds by two successive mechanistically remarkable silyl migrations.

Deprotonation of the readily accessible[2] 2-alkynyl silyl ether **1** with *n*BuLi affords carbanions, which lead by 1,2-O-C-silyl migration (silyl-Wittig or retro-Brook rearrange-

[*] Prof. Dr. E. Schaumann[+], Dr. B. Mergardt, Dipl.-Chem. K. Weber
Institut für Organische Chemie der Universität
Martin-Luther-King-Platz 6, W-2000 Hamburg 13 (FRG)
Dr. G. Adiwidjaja
Mineralogisch-Petrographisches Institut der Universität Hamburg
[+] New address:
Institut für Organische Chemie der Technischen Universität Clausthal
Leibnizstrasse 6, W-3392 Clausthal-Zellerfeld (FRG)

[**] This work was supported by the Fonds der Chemischen Industrie.

ment[3j]) and, when $R^2 = H$, also by 1,3-hydrogen shift to a complex equilibrium system.[4] We have now found that specific protonation to give the β-alkynols **2** silylated in the 1-position can be achieved by addition of trifluoroacetic acid at −78 °C (Table 1). This β-alkynol synthesis is comparable with the corresponding rearrangements of aryl silyl[3b] and allyl silyl ethers,[5] and in the present case leads to silyl-containing synthetic building blocks which are otherwise only accessible indirectly.[6]

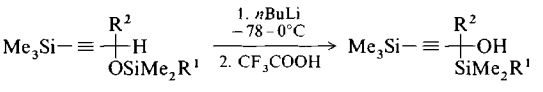

1 **2**

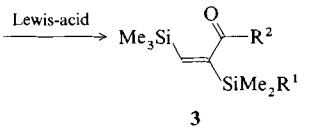

3

a: R^1 = Me, R^2 = H; **b**: R^1 = *t*Bu, R^2 = H; **c**: R^1 = CMe_2iPr, R^2 = H; **d**: $R^1 = R^2$ = Me.

Despite their number of functional groups the bis-*C*-silylated β-alkynols **2** are storable at 0 °C, and are also stable in benzene solution. In CH_2Cl_2 as solvent, on the other hand, an internal redox reaction to the α,β-unsaturated carbonyl derivatives **3** is observed,[7] which in the case of the silyl-free parent compounds must, as a rule, be catalyzed by metal complexes.[8] In the case of **2** the reaction is accelerated by Lewis acids (about 10 mol%) and is thus of preparative interest. The conversion of **2a**–**c** into **3a**–**c** with $TiCl_4$ or $FeCl_3$ as catalyst is complete within minutes, whereas with $ZnCl_2$ as catalyst the best yields are obtained after a much longer time (≈10 h). $MgCl_2$, on the other hand, is less effective; $CeCl_3$ and also *p*-toluenesulfonic acid lead to desilylation products. **2d** is converted into **3d** upon catalysis with $TiCl_4$ or BF_3 etherate.

In all cases only one diastereomer of **3** is formed, and according to the results of an X-ray structure analysis of the derivative **5**, the C=C-moiety is (*E*)-configurated.[9]

Table 1. Yields, physical data, and selected spectroscopic data of the products obtained.

Product	Yield [a]	B.p./*p* (m.p.) [b]	IR $\tilde{\nu}$ [c]	^{1}H NMR δ(CH≡C–CH) [d]	^{13}C NMR δ(C≡C–C) [e]
2a [6b]	78	80–83/10	3393, 2157	3.95 (s)	108.1, 91.7, 56.9
b	84	100–104/10	3417, 2157	4.12 (s)	108.6, 92.2, 55.4
c	88	140–142/10	3436, 2157	4.15 (s)	108.9, 92.1, 56.2
d	54	195 (11–13)	3435, 2152	–	111.6, 90.0, 61.3
3a	41	76–78/10 (28–30)	1677	10.18 (s), 7.37 (s)	195.8, 165.7, 163.4
b	58	105/10	1680	10.17 (s), 7.36 (s)	195.8, 167.8, 161.3
c	75	115/10	1681	10.22 (s), 7.43 (s)	196.0, 167.4, 163.1
d	74	95/20	1686	6.31 (s)	206.9, 168.7, 146.3
4	74	102/10	3426, 1249, 839	6.15 (d, ^4J = 1), 4.76 (dq, ^3J = 6.5, ^4J = 1)	169.8, 140.5, 73.3
5	92	(191)	3481, 3148, 1695, 1672, 1250, 837	8.22 (broad s), 6.74 (d, J = 0.9)	159.2 or 157.5, 152.1, 146.9
6	68	95/10	1713	9.08 (s), 7.56 (s)	186.3, 155.0, 139.0

[a] Yield in [%]. [b] B.p./*p* [°C/torr]; m.p. [°C]. [c] IR spectrum recorded as film or in KBr, $\tilde{\nu}$ [cm^{-1}]. [d] ^{1}H NMR (250 MHz, C_6D_6 ≙ δ = 7.16), J [Hz]. [e] ^{13}C NMR (100 MHz, C_6D_6 ≙ δ = 128.0).

Investigations on the reaction behavior of **3** show that the carbonyl group is attacked upon reaction with methylmagnesium iodide or semicarbazide, leading to formation of **4** and **5**, respectively, whereas the α-silyl group is substituted by bromine, leading to formation of **6** (Table 1).

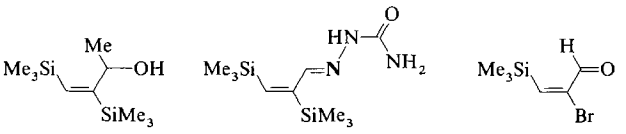

4 **5** **6**

Experimental

Silyl-Wittig rearrangement to **2a**–**c**: An *n*BuLi solution (2.3 M in hexane, 87 mL, 200 mmol) in tetrahydrofuran (200 mL) cooled to −78 °C was treated dropwise with **1** (200 mmol; cooled to temperatures below −50 °C). The mixture was stirred at −78 °C for 30 min and carefully neutralized with trifluoroacetic acid (15.3 mL, 200 mmol). After dilution with diethyl ether (200 mL), rapid washing with saturated NH_4Cl solution (1 ×), and with water (5 ×) for complete removal of THF, the solution was dried over $MgSO_4$ and then evaporated down in a water-jet vacuum and purified by Kugelrohr distillation, preferably in the presence of hydroquinone. The compounds **2a**–**c** are obtained as slightly yellow colored liquids (Table 1). For the preparation of **2d**, THF must be replaced by ether, and, before addition of the acid (at −78 °C), the solution must be stirred for ca. 15 h at room temperature.

Redox reaction to give **3**: A mixture of **2** (120 mmol) and $ZnCl_2$ (1.36 g, 10 mmol; for **3a**–**c**) or $TiCl_4$ (1.90 g, 10 mmol; for **3d**) in dichloromethane (120 mL) was stirred at room temperature; with **2a**–**c** as starting material, a color change from yellow to deep-brown was observed. After completion of the reaction (IR monitoring, about 10 h, see Table 1) the reaction solution was worked up and distilled as described above. Yellow colored liquids were obtained, which, after spinning band column distillation, were analytically pure.

Received: June 27, 1991 [Z 4750 IE]
German version: *Angew. Chem. 103* (1991) 1679

CAS Registry numbers:
1a, 50965-66-7; **1b**, 83578-59-0; **1c**, 137092-05-8; **1d**, 103620-64-0; **2a**, 112947-66-7; **2b**, 137092-06-9; **2c**, 137092-07-0; **2d**, 137092-08-1; **3a**, 137092-09-2; **3b**, 137092-10-5; **3c**, 137092-11-6; **3d**, 137092-12-7; **4**, 137092-13-8; **5**, 137092-14-9; **6**, 137092-15-0; $TiCl_4$, 7550-45-0; $FeCl_3$, 7705-08-0; $ZnCl_2$, 7646-85-7; $Et_2O \cdot BF_3$, 109-63-7.

[1] G. Stork, B. Ganem, *J. Am. Chem. Soc. 95* (1973) 6152; G. Stork, J. Singh, *ibid. 96* (1974) 6181; R. K. Boeckman, Jr., *ibid. 95* (1973) 6867; *ibid. 96* (1974) 6179; *Tetrahedron 39* (1983) 925.

[2] L. Brandsma, H. D. Verkruijsse: *Synthesis of Acetylenes, Allenes and Cumulenes*, Elsevier, Amsterdam 1981, p. 58; H. Wetter, K. Oertle, *Tetrahedron Lett. 26* (1985) 5515.

[3] a) T. Nakai, K. Mikami, *Chem. Rev. 86* (1986) 885; M. Schlosser, S. Strunk, *Tetrahedron 45* (1989) 2649; b) R. J. Linderman, A. Ghannam, *J. Am. Chem. Soc. 112* (1990) 2392.

[4] H. J. Reich, M. J. Kelly, *J. Am. Chem. Soc. 104* (1982) 1119; K. J. H. Kruithof, G. W. Klumpp, *Tetrahedron Lett. 23* (1982) 3101.

[5] J. S. Panek, M. A. Sparks, *Tetrahedron Lett. 28* (1987) 4649; R. L. Danheiser, D. M. Fink, K. Okano, Y.-M. Tsai, S. W. Szczepanski, *J. Org. Chem. 50* (1985) 5393; W. C. Still, T. L. Macdonald, *J. Am. Chem. Soc. 96* (1974) 5561.

[6] a) I. Kuwajima, M. Kato, *Tetrahedron Lett. 21* (1980) 623; M. Kato, A. Mori, H. Oshino, J. Enda, K. Kobayashi, I. Kuwajima, *J. Am. Chem. Soc. 106* (1984) 1773; M. E. Jung, B. Gaede, *Tetrahedron 35* (1979) 621; b) R. J. Linderman, Y. Suhr, *J. Org. Chem. 53* (1988) 1569.

[7] Similar compounds have been obtained as *E*/*Z*-mixtures by hydrosilylation of the corresponding alkynols: V. B. Pukhnarevich, I. I. Tsykhanskaya, M. G. Voronkov, *Izv. Akad. Nauk SSSR Ser. Khim. 1984*, 427; *Chem. Abstr. 100* (1984) 209970.

[8] D. Ma, X. Lu, *J. Chem. Soc. Chem. Commun. 1989*, 890; *Tetrahedron Lett. 30* (1989) 2109; A. Arcadi, S. Cacchi, F. Marinelli, D. Misiti, *ibid. 29* (1988) 1457; cf. also E. J. Corey, S. Terashima, *ibid. 1972*, 1815.

[9] Crystal structure analysis: Enraf-Nonius CAD4-SDP diffractometer, monochromatized $Cu_{K\alpha}$ radiation, measurement range $2° \leq \theta \leq 65°$; space group $Pna2_1$ (No. 33), a = 2068.6(2), b = 1200.3(2), c = 2053.1(1) pm; ϱ_{calcd} = 1.01 gcm^{-3}; Z = 12; 2682 reflections. Solution of structure: MULTAN, difference Fourier synthesis; R = 0.071, R_w = 0.069. Further details of the crystal structure investigation are available on request from the Fachinformationszentrum Karlsruhe, Gesellschaft für wissenschaftlich-technische Information mbH, W-7514 Eggenstein-Leopoldshafen 2 (FRG) on quoting the depository number CDS-55789, the names of the authors, and the journal citation.

Selective *p*-Chlorination of Biphenyl in L Zeolites**

By *Artur Botta,* Hans-Josef Buysch,* and *Lothar Puppe*

Dedicated to Professor Karl Heinz Büchel on the occasion of his 60th birthday

4,4'-Dichlorobiphenyl (**3**) is regarded as an interesting precursor for high performance polymers,[1, 2] but until now a simple process by which this compound could be synthesized directly on an industrial scale was not available.[3, 4] Conventional chlorination of biphenyl (**1**) with Lewis acid catalysis (Scheme 1) gives mixtures consisting mainly of *o*- and *p*-chloro isomers **2**, **4**–**6**, from which only small amounts of the desired product **3** can be isolated, and then only by laborious procedures. For this reason only polychlorinated biphenyls (PCBs) were used industrially as insulating and hydraulic fluids until their use was recently prohibited.

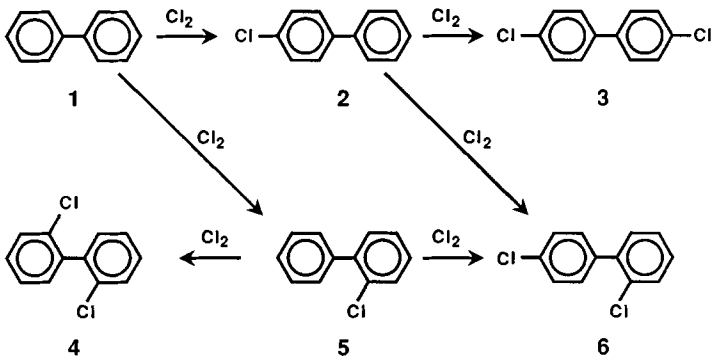

Scheme 1. Products of the chlorination of biphenyl (**1**).

It was thought that certain zeolites ought to be particularly suitable as catalysts for the desired dichlorination of biphenyl in view of their shape selectivity.[5] As compared with Fe catalysis, catalysis with several types of zeolites in the chlorination of substituted benzenes such as toluene and chlorobenzene with a variety of chlorinating agents shifts the isomer ratio more[6] or less[7] markedly towards *p*-substitution. This applies particularly to zeolite L (structure type LTL).[8] Zeolite-catalyzed chlorinations of **1** have not previously been described.

Chlorinations performed initially in molten **1** with acidic and metal-exchanged zeolites of various structure and pore diameters (see the selected list in Table 1) gave higher *p*-selectivity with respect to **1** than $FeCl_3$ or acidic phyllosilicates (e.g. Tonsil K 10®) and conversions of around 100%. We achieved product selectivities initially exceeding 60% for **3** with zeolite L. As the comparison of K-zeolite L with H-zeolite L shows (Table 1), the nature of the cation plays a crucial role.[9]

The results of the chlorine substitution of **1** in the presence of variously structured zeolites, especially zeolite L, with a variety of cations suggest that a new type of selectivity occurs in the zeolite-catalyzed chlorination of aromatic hydrocarbons. The concept of geometry-related "shape selectivity"[5] cannot be applied here (zeolites of similar pore diameter but of different types behave in different ways). Rather it would appear that the ionic radius, charge, and spatial arrangement of the cations and their force fields are responsible for the activation of the Cl_2 molecule. They are the factors that actually direct the substitution.

Table 1. Product distribution [wt%] for the chlorination of **1**, neat, 100% Cl_2.

Catalyst	1	5	2	4	6	3	other	Σ2 + 3
2 g $FeCl_3$	1.0	15.4	6.4	13.2	23.7	9.1	31.2	15.5
Tonsil K 10® [a]	0.1	18.1	4.0	7.4	31.8	26.5	12.1	30.5
Na-zeolite X	–	11.8	0.6	8.3	34.9	34.0	10.4	34.6
K-zeolite Ω	–	16.5	1.2	3.2	25.5	47.0	6.6	48.2
K,Na-zeolite T [b]	–	10.1	0.2	5.8	39.6	33.5	10.8	33.7
H-mordenite	–	13.4	3.1	2.4	27.6	45.0	8.5	48.1
H-zeolite L	–	7.5	2.9	6.5	25.4	45.8	11.9	48.7
Na, K-zeolite L	–	12.2	8.8	1.1	12.6	60.3	5.0	69.1
K-zeolite L	–	5.0	2.7	2.2	16.8	66.5	6.8	69.2
K-zeolite L + $ClCH_2COOH$ [c]	–	2.1	2.7	0.4	8.1	83.7	3.0	86.4

[a] Catalyst from Südchemie AG, Munich (FRG). [b] Mixed lattice. [c] 13% based on K-zeolite L.

Despite many attempts at improving the 4,4'-selectivity in the chlorination of neat **1** with K-zeolite L through the use of cocatalysts, reproducible results were achieved only with carboxylic acid derivatives.[6b, 9]. Chlorination with selectivity exceeding 80% was obtained in the particular case of chloroacetic acid (Table 1).

To investigate chlorination of **1** at lower temperatures it was necessary to use solvents. In dichloromethane (20–40 °C) with K-zeolite L as catalyst, product selectivities for **3** exceeding 90% were obtained for the first time.[10, 11, 12] Reactions in other inert solvents were not as selective. Even the use of solvents closely related to dichloromethane, for example tri- and tetrachloromethane or -ethane, reduced the conversion and also the 4,4'-selectivity below the values obtained in the neat chlorination (Table 2).

Table 2. Product distribution [wt%] for the chlorination of **1** in solution, K-zeolite L, 20 °C, 100% Cl_2.

Solvent	1	5	2	6	3	others	Σ2 + 3
CH_2Cl_2	–	1.9	3.0	4.9	89.0	1.2	92.0
$CHCl_3$	0.3	16.6	26.8	9.7	37.0	9.6	63.8
CCl_4	–	10.0	5.7	14.7	66.5	4.1	72.4
CH_3COOH [a]	2.7	28.9	31.9	8.8	13.0	14.7	44.9
nitrobenzene [a]	–	18.1	19.2	4.4	29.5	28.8	48.6
1,2-dichloropropane	0.7	10.1	35.9	5.4	39.7	8.9	75.6
1,1,1-trichloroethane	29.8	10.2	33.0	1.0	2.9	23.1	35.9

[a] 40 °C.

Dichloromethane evidently does not act simply as a diluent in the chlorination of **1**. Investigations still in progress suggest that the activation of the reactants and diffusion and transport processes in the zeolite channels[13]—the desired product **3** has poor solubility in dichloromethane—are influenced in a favorable manner. The activity- and selectivity-promoting influence of dichloromethane was found only in L zeolites. Further evidence of the favorable effect of dichloromethane, especially in chlorinations catalyzed by zeolite L are shown in Table 3.

Although H-zeolite L was unselective here, just as in neat chlorinations,[14] the alkaline and alkaline-earth metal-ex-

[*] Dr. A. Botta, Dr. H.-J. Busch
Bayer AG, ZF-FGF, R 79
W-4150 Krefeld 11 (FRG)
Dr. L. Puppe
Bayer AG, PK-F, R 20
W-5090 Leverkusen (FRG)

[**] The work reported here was supported by the Federal German Ministry of Research and Technology.

Table 3. Product distribution [wt%] for the chlorination of **1** in CH_2Cl_2, 40 °C, in the presence of various L zeolites.

Zeolite	% Cl_2	**1**	**5**	**2**	**6**	**3**	others	Σ**2** + **3**
H-L	100	–	29.3	23.1	17.2	22.0	8.4	45.1
H-L	110	–	27.1	18.4	20.0	25.2	9.3	43.7
Li-L	100	–	1.4	5.6	1.5	91.0	0.5	96.6
Li-L	110	–	0.3	–	2.7	96.7	0.3	96.7
Na-L	100	–	1.7	0.5	3.0	93.9	0.9	94.4
Na-L	110	–	0.2	0.2	4.7	94.4	0.5	94.6
K-L	100	–	1.6	7.2	1.7	89.0	0.5	96.2
K-L	110	–	1.0	–	2.4	96.4	0.2	96.4
Rb-L	100	–	1.8	18.4	1.8	76.8	1.2	95.2
Cs-L	100	0.1	4.2	22.1	3.2	66.6	3.8	88.8
Mg-L [a]	100	–	7.6	3.4	14.0	73.2	1.8	76.6
Ca-L	100	–	2.5	17.4	2.6	75.3	2.3	92.7
Ca-L	110	–	2.4	12.7	3.0	79.7	2.2	92.4
Sr-L	100	–	2.4	11.9	2.7	81.9	1.1	93.8
Sr-L	110	–	1.8	3.4	2.8	91.0	1.0	94.4
Ba-L	100	0.3	3.3	13.7	3.0	78.9	0.8	92.6
Zn-L	100	0.2	20.4	21.0	14.3	37.4	6.7	58.4
Zn-L	110	–	19.7	17.0	15.6	40.5	7.2	57.5
La-L	100	–	4.5	17.0	0.2	74.4	3.9	91.4
Ce-L	100	0.3	17.1	30.1	11.3	34.1	7.1	64.2
Ag-L	100	–	2.4	11.9	2.2	83.1	0.4	95.0
Ag-L	110	–	1.5	0.5	3.2	94.2	0.6	94.7
Pb-L	100	–	1.9	6.2	2.7	88.5	0.7	94.7

[a] 20 °C.

changed L types showed outstanding *p*-selectivity, which is demonstrated most clearly in the sum of the 4-mono and 4,4'-dichloro selectivities (see the final columns in Tables 1–3). Differences of activity (incomplete Cl_2-conversion) could be equalized by the use of approximately 10% excess chlorine. The yields of **2** and **3** were thus increased for catalysis with L zeolites with Li, Na, K, and Ag ions; however, excess chlorine had no positive effect on reactions with the H, Ca, and Zn type catalysts (Table 3). Thus optimal *p*-selectivities were obtained with L zeolites containing cations with an ionic radius of about 0.13 nm.[15] This applies not only to K, Rb, Sr, Ba, and La but also to Ag and Pb ions. The high degree of *p*-substitution in the chlorination of **1** in the presence of either Li- or Na-zeolite L (ionic radii 0.068 and 0.097 nm!)[15] does not conform to this rule, however.

Experimental Procedure

Neat process: Biphenyl (**1**) (77.1 g, 0.5 mol) was melted under N_2 in a stirring apparatus and catalyst in powder form (15 g) [16] and cocatalyst (if necessary) were added. Then, for 6 h, during which time the temperature was raised from 80 °C to 140 °C, Cl_2 (70.9 g, 1 mol) was introduced. N_2 was then passed through while stirring was continued for 30 min [17].

Solution process: Powdered catalyst [16] (15 g) was suspended in a solution of **1** (77.1 g, 0.5 mol) in dichloromethane (160 mL). Cl_2 (70.9 g, 1 mol or 78.0 g, 1.1 mol) was introduced for 6 h at 20 °C or 40 °C. Product **3** fell out of solution. Stirring was continued for 15 min, during which time N_2 was passed through [17].

Received: June 12, 1991 [Z 4699 IE]
German version: *Angew. Chem.* (1991) 1687
Publication delayed on authors' request

CAS Registry numbers:
2, 2051-62-9; **3**, 2050-68-2; **4**, 13029-08-8; **5**, 2051-60-7; **6**, 34883-43-7; CH_2Cl_2, 75-09-2; $ClCH_2CO_2H$, 79-11-8.

[1] *Ullmanns Encykl. Tech. Chem.*, 4th ed; 1972–1984, Vol. 9, pp. 515–517. *Ullmann's Encycl. Ind. Chem.*, 5th ed; 1986; Vol. A6, pp. 347–350.
[2] a) H. W. Hill, J. T. Edmonds, US-Pat 3396110 (1968), Phillips Petroleum Co. (*Chem. Abstr. 69* (1968) 60564w); b) S. Jinbo, M. Ito, K. Otomo, H. Hiraide, JP-B 61231030 (1986), Hodogaya Chem. Co., Ltd. (*Chem. Abstr. 106* (1987) 177103u).
[3] A. B. Goel, *Inorg. Chim. Acta 84* (1984) L25–L27.
[4] M. Uchiyama, T. Suzuki, Y. Yamazaki, *Chem. Lett. 1983*, 1165–1166.
[5] S. M. Csicsery, *Pure Appl. Chem. 58* (1986) 841–856.
[6] a) Y. Higuchi, T. Suzuki, EP-B 112722 (1984), Ihara Chem. Ind. Co., Ltd. (*Chem. Abstr. 101* (1984) 230115z); b) T. Suzuki, C. Komatsu, EP-B 154236 (1985), Ihara Chem. Ind. Co., Ltd. (*Chem. Abstr. 104* (1986) 148465s); c) K. Smith, M. Butters, *Synthesis 1985*, 1157–1158; d) T. Miyake, K. Sekizawa, T. Hironaka, M. Nakano, S. Fujii, Y. Tsutsumi, *Stud. Surf. Sci. Catal. (Amsterdam) 28* (1986) 747–754; e) K. Sekizawa, T. Miyake, M. Nakano ,T. Hironaka, S. Fujii, M. Kikuchi, *ibid. 44* (1989) 203–210.
[7] L. Delaude, P. Laszlo, *J. Org. Chem. 55* (1990) 5260–5269.
[8] R. M. Barrer, H. Villiger, *Z. Kristallogr. 128* (1969) 352.
[9] A. Botta, H.-J. Buysch, L. Puppe, EP-B 334097 (1989), Bayer AG (*Chem. Abstr. 112* (1990) 138722z).
[10] A. Botta, H.-J. Buysch, L. Puppe, EP-B 423479 (1991), Bayer AG.
[11] In analogy, *p*-terphenyl could be chlorinated with 97% selectivity to 4,4''-dichloro-*p*-terphenyl, in contrast to its *o*- and *m*-isomers.
[12] X-ray analysis of the catalyst after it had been used several times with undiminished activity showed no change.
[13] The assumption that the catalysis actually takes place inside the zeolite is supported by the fact that a sample of K-zeolite L whose external surface was sealed by trimethylsilyation also showed undiminished activity and selectivity (96%).
[14] This agrees with findings obtained for chlorination in the presence of zeolites of the Y series. The zeolites with high acidity lack *p*-selectivity [6d–e, 7].
[15] K.-H. Hellwege (Ed.): *Landolt-Börnstein*, 6th ed.; Springer Verlag, Berlin 1955; Vol. 1, Part 4, pp. 523–525.
[16] Before use all the zeolites were calcined at 400 °C for three hours (muffle furnace).
[17] The composition of the reaction mixture was determined by comparing their gas chromatograms with those of authentic samples.

Stereoselective Synthesis of Cyclic Dipeptide Hydroxyalkyl Isosteres via Metalated *N,N*-Dialkylcarbamate 2-Alkenyl Esters**

By *Rudolf Hanko*,* *Klaus Rabe*, *Robert Dally*, and *Dieter Hoppe**

Dedicated to Professor Karl Heinz Büchel on the occasion of his 60th birthday

Peptide isosteres,[1] generated by replacing an amide bond with a hydrolytically stable unit, are of increasing importance in medicinal chemistry for the development of protease inhibitors.[2] Hydroxyalkyl isosteres[3] have attracted our particular interest, because members of this group of peptide isosteres are known to be very potent inhibitors of aspartic proteases like renin[4] and HIV protease.[5] Whereas many strategies have been developed to synthesize noncyclic isosteres,[3, 6] the cyclic derivatives **1a** and **1b** (Scheme 1) have so far eluded every attempt at their stereoselective synthesis.[5, 7, 27] Here we describe the first stereoselective route to **1** via a highly diastereoselective synthesis of the key intermediates **2** and **3** and their transformation into **1a** and **1b**.

We reasoned that a retrosynthetic disconnection of **2** and **3** into amino aldehyde **A** and a homoenolate **B** should allow a highly convergent synthetic approach. Since metalated 2-alkenyl *N,N*-dialkylcarbamates are easily accessible and highly *anti*-diastereoselective synthetic equivalents[8] for homoenolates of type **B**, we examined the reaction of (1-cyclopentenyl)methyl carbamate **4** with protected amino alde-

[*] Prof. Dr. D. Hoppe, Dr. K. Rabe
Institut für Organische Chemie der Universität
Olshausenstrasse 40–60, W-2300 Kiel (FRG)
Dr. R. Hanko
Bayer AG, Chemisch wissenschaftliches Labor Pharma
Postfach 101709, W-5600 Wuppertal 1 (FRG)
R. Dally
Miles, Inc., 400 Morgan Lane
West Haven, CT 06516 (USA)

[**] This work was supported by the Deutsche Forschungsgemeinschaft and the Fonds der Chemischen Industrie.

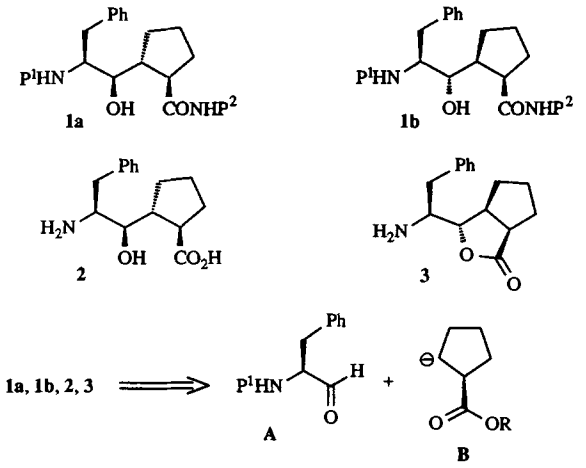

Scheme 1. P^1, P^2 = protecting groups.

hydes **6** (Scheme 2). The carbamate **5** (2.0 equiv.) was lithiated in ether, subjected to a metal exchange with titanium tetraisopropoxide, and then added to Cbz- or Boc-(*S*)-phenylalaninal, **6a** and **6b**,[9] respectively (Cbz = benzyloxycarbonyl, Boc = *tert*-butoxycarbonyl). In both cases, only the two expected,[10] easily separable (1 *Z*)-3,4-*anti* diastereomers[11-13] **7a** and **8a** (23 % + 50 %) or **7b** and **8b** (42 % + 50 %) were formed by stereospecific reagent-controlled addition of both enantiomers of the racemic allyl titanate.[8c].

Generation of the "Ψ-(*S*)" configuration at C-2 in dipeptide isosteres derived from precursors **7** requires a *cis* relationship of the substituents on the cyclopentane ring, which

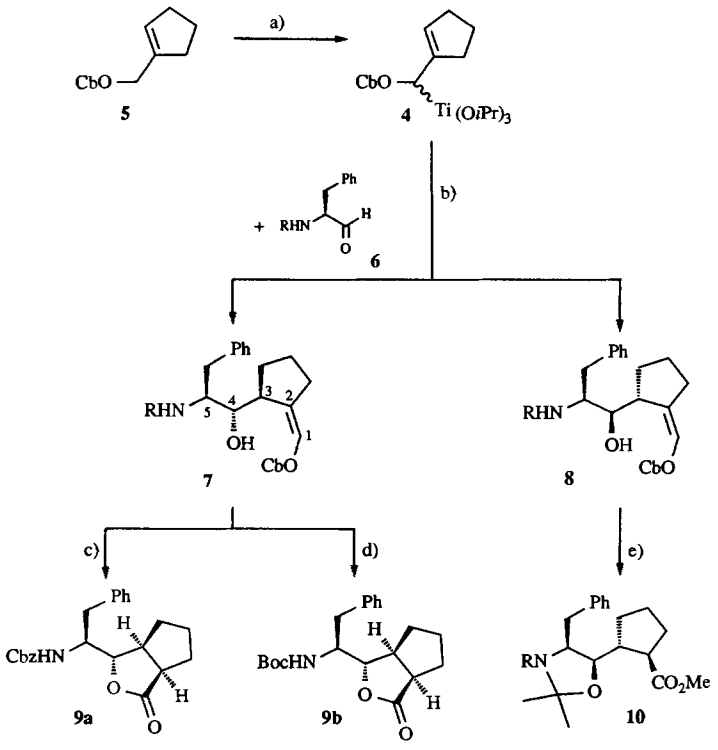

Scheme 2. **6**–**8**, **10**: R = CO_2Bn (Cbz) (**a**), CO_2tBu (Boc) (**b**). Cb = C(=O)N(*i*Pr)$_2$; P^1, P^2 = protecting groups; Bn = benzyl. a) 2.0 equiv. **5**; 2.2 equiv. *n*BuLi/*N*,*N*,*N*′,*N*′-tetramethylethylenediamine (TMEDA), ether, 0.5 h at −78 °C; 4 equiv. Ti(O*i*Pr)$_4$; b) **6**, 0.5 h at −78 °C → 0 °C; 2 N HCl. c) 0.1 equiv. $Hg(OAc)_2$, 2.0 equiv. $MeSO_3H$ in MeOH, 15 h at 0 °C → 20 °C; *m*-chloroperbenzoic acid (MCPBA), $BF_3 \cdot OEt_2$, CH_2Cl_2 [15a]. d) 2 equiv. $BH_3 \cdot Me_2S$, THF; 15 h at 0 °C → 20 °C; 30 % H_2O_2/NaOH; pyridinium dichromate (PDC). e) See a)–d) Scheme 3; only **8a** was transformed into **10a**.

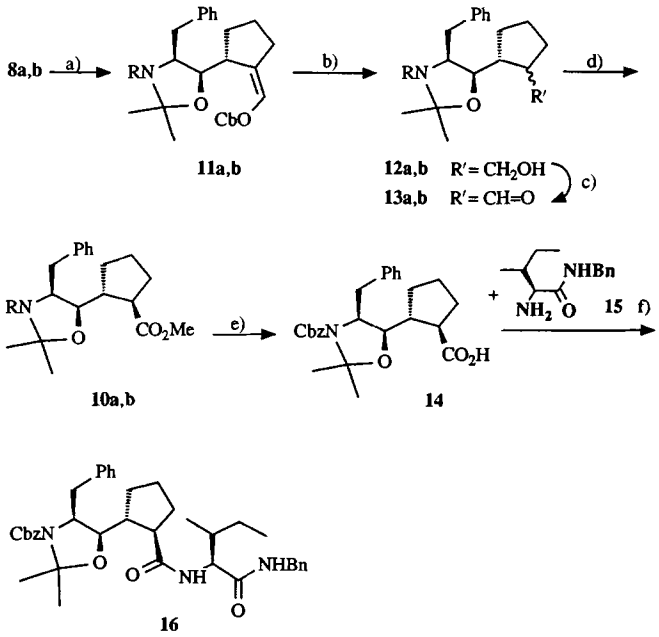

Scheme 3. **8**, **10**, **11**, **12**, **13**: R = Cbz (**a**), Boc (**b**). a) 2.5 equiv. 2-methoxypropene, cat. $POCl_3$, DMF, 15 h at 0 °C → 20 °C. b) 2 equiv. $BH_3 \cdot Me_2S$, THF, 15 h at 0 °C → 20 °C; 30 % H_2O_2/NaOH. c) PDC, CH_2Cl_2. d) 2 equiv. NaOMe, MeOH 15 h at 20 °C; 4 equiv. Br_2, 20 equiv. $NaHCO_3$, MeOH/H_2O, 5 h at 0 °C → 20 °C [16]. e) LiOH, THF/MeOH. f) DMF, PPA, Et_3N [17].

is ensured by lactone formation. Mercury(II) acetate-promoted methanolysis[15] of **7a**, followed by Grieco oxidation,[15b] afforded the Cbz-protected γ-lactone **9a**[11,12] (53 %) via the corresponding lactol ethers. The sequence failed with the acid-labile Boc derivative **7b**, which was therefore subjected to a hydroboration–oxidation sequence to yield the lactone **9b**[11,12] (48 %) via the lactol. For elaboration of the (2*R*) configuration in the (3*R*, 4*R*, 5*S*) diastereomer of **8a**, a thermodynamically driven epimerization to give an appropriate *trans*-disubstituted cyclopentane was envisaged. The hydroboration of the *N*,*O*-acetonides **11a**, **b**[11,12] proceeded via reductive elimination of the carbamoyloxy group and afforded in each case an epimeric mixture of the alcohols **12a**, **b**[11,12] (Scheme 3). The epimeric aldehydes **13a**, **b** obtained by PDC oxidation each formed a single diastereomer on treatment with methanolic sodium methoxide. Aldehydes **13a** and **13b** were subjected to an oxidative esterification under the conditions worked out by *Lichtenthaler*[16] and yielded the methyl esters[11,12] **10a** and **10b** in 39 % and 50 % yield, respectively (based on **11**). Thus, the suitably protected (2*R*, 3*S*, 4*S*, 5*S*) and (2*R*, 3*R*, 4*R*, 5*S*) diastereomers **9a**, **b** and **10a**, **b** of the dipeptide

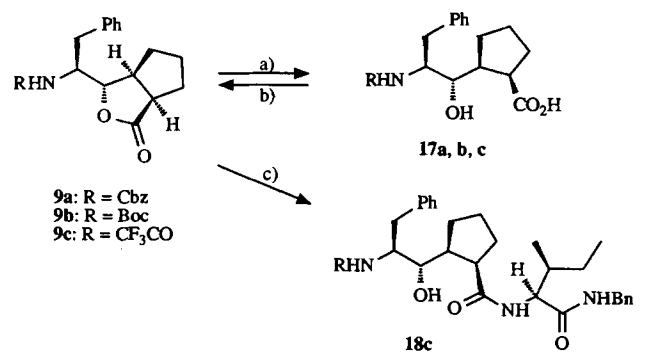

Scheme 4. a) LiOH, MeOH, H_2O. b) *tert*-Butyldimethylsilyl chloride (TBDMSCl), NEt_3. c) $AlMe_3$, **15**, Cl_3CCH_3.

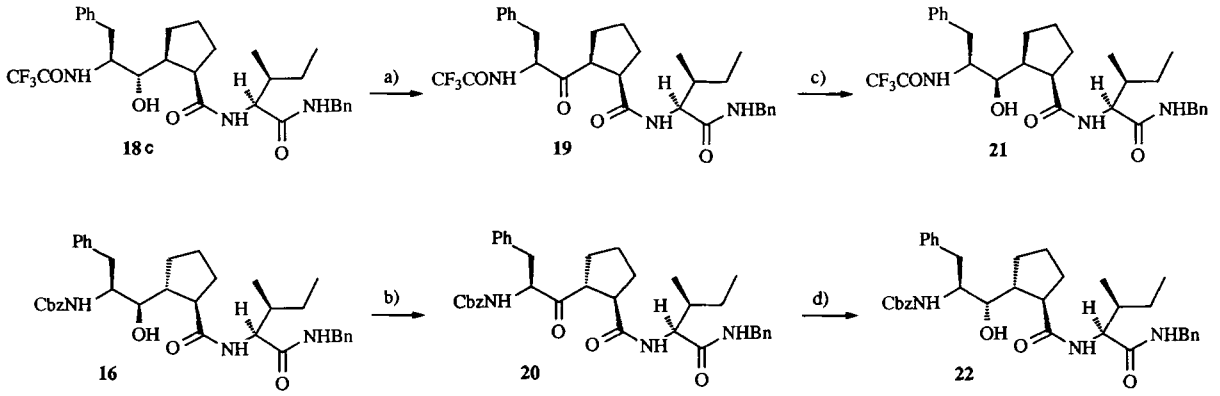

Scheme 5. a) 2.0 equiv. $K_2Cr_2O_7$, 0.1 equiv. Bu_4NHSO_4 in 30 % H_2SO_4 [21] in CH_2Cl_2, 20 min at 25 °C. b) 0.5 equiv. $K_2Cr_2O_7$, 0.1 equiv. Bu_4NHSO_4 in 30 % H_2SO_4 [22] in CH_2Cl_2, 30 min at 25 °C. c) 3.0 equiv. $LiBH_4$, THF [23], 2 h at −78 °C. d) 3.0 equiv. N-Selectride, THF [24], 3 h at −40 °C.

isosteres Phe-Ψ [CHOHCH]Pro are accessible from amino aldehydes **6a, b** in 12/20 % and 16/23 % overall yield; only one facile diastereomer separation is required.

The *trans* diastereomer **10a**, after transformation into the acid **14a**, was coupled with (*S*)-isoleucine benzylamide **15**[17] by PPA-coupling (PPA = propanephosphonic acid anhydride) to afford the tripeptide isostere **16** (59 %).[12]

The incorporation of the lactones **9** into peptide sequences is hampered by the pronounced tendency of bicyclic hydroxy acids like **17** to relactonize,[18] even if the hydroxyl group is silyl-protected (Scheme 4). A possible way to overcome this problem would be the Weinreb method[19] using dialkylaluminum amides as ring-opening reagents. To our knowledge, this procedure has not yet been used with amino acid derivatives **15** as amine components. Our initial attempts using lactone **9b**[20] together with (*S*)-isoleucine benzylamide (**15a**) in the presence of one equivalent of trimethylaluminum in 1,1,1-trichloroethane at 40 °C for 24 h did not lead to the desired product **18**. The unreacted starting materials were recovered in greater than 90 % yield. However, the desired product **18c**[12] is obtained in 72 % yield if excess trimethylaluminum is used (one equivalent for each acidic NH amide proton in the amino acid or the lactone moiety).

This method provides the first approach to *cis*-substituted cyclic hydroxyalkyl isosteres[7] of type **18** by ring opening of lactones **9**. Taken together with the homoaldol methodology, this approach easily affords *anti*-configurated spacers **16** and **18**. To obtain the corresponding *syn* adducts **21** and **22** as well, we developed the following efficient and stereoselective oxidation/reduction procedure (Scheme 5): Compound **18c** was readily oxidized under phase-transfer conditions[25] to yield 71 % of ketone **19**, which was reduced to the inverted isomer **21**[12] in 69 % yield by treatment with $LiBH_4$ in THF. There was no trace of **18** detectable by 300 MHz ^{1}H NMR spectroscopy or TLC. Similarly, **16** was oxidized to ketone **20** in 95 % yield. Stereoselective reduction of **20** to the epimer **22**[12] was accomplished by treatment with 3.0 equivalents of N-Selectride in THF at −40 °C for 3 h (81 % yield, no detectable trace of **16**).

This methodology thus allows the stereoselective synthesis of the four stereoisomeres **16**, **18c**, **21**, and **22** of the Phe-[CHOHCH]Pro spacer series.[12, 26] We are currently exploring the applicability of this synthetic sequence to spacers of different ring sizes and substitution patterns.

Experimental Procedure

18c: To a suspension of **9c** (102 mg, 300 μmol) in 200 μL of 1,1,1-trichloroethane (TCE) was added 150 μL of a 2 M solution of $AlMe_3$ in TCE at 20 °C. A suspension of **15** (132 mg, 600 μmol) in 150 μL of TCE in a dry reaction vessel under an atmosphere of argon was treated with 600 μL of 2 M $AlMe_3$ in TCE. The vessel was warmed to 60 °C for 1 h, then cooled to 20 °C. The lactone/$AlMe_3$ complex was added to the reaction vessel via syringe with stirring and the reaction solution was warmed to 60 °C until the lactone complex was consumed (about 4 h), The reaction was cooled to 0 °C and quenched by careful addition of AcOH (235 mg, 3.9 mmol). The resulting gel was dissolved in 20 mL of CH_2Cl_2 and washed with 10 mL of HCl solution (pH 4). The aqueous phase was extracted with 2 × 5 mL of CH_2Cl_2. The organic layers were combined and washed with 10 mL of saturated $NaHCO_3$. After evaporation of the solvent, the crude product was chromatographed on 20 cm^3 of silica gel (20 μm) with CH_2Cl_2/MeOH to yield 121 mg (72 %) of **18c**.

Received: June 14, 1991 [Z 4708/4709 IE]
Publication delayed at the authors' request
German version: *Angew. Chem. 103* (1991) 1725

CAS Registry numbers:
5, 87143-44-0; **6a**, 59830-60-3; **6b**, 72125-45-4; **7a**, 130398-74-2; **7b**, 130372-17-7; **8a**, 130466-41-0; **8b**, 130464-91-4; **9a**, 130372-26-8; **9b**, 130372-24-6; **9c**, 137143-94-3; **10a**, 137143-90-9; **10b**, 130372-23-5; **11a**, 137143-91-0; **11b**, 130464-93-6; **12a** (isomer 1), 137144-01-5; **12a** (isomer 2), 137252-34-7; **12b** (isomer 1), 130464-95-8; **12b** (isomer 2), 130464-96-9; **13a** (isomer 1), 137144-02-6; **13a** (isomer 2), 137252-35-8; **13b** (isomer 1), 130372-21-3; **13b** (isomer 2), 130464-97-0; **14**, 137143-92-1; **15**, 129253-02-7; **16**, 137143-93-2; **17a**, 137143-99-8; **17b**, 128211-08-5; **17c**, 137144-00-4; **18c**, 137143-95-4; **19**, 137143-96-5; **20**, 137143-97-6; **21**, 137252-33-6; **22**, 137143-98-7.

[1] a) M. Szelke, D. M. Jones, A. Hallet, B. J. Leckie, in V. J. Hruby, D. H. Rich (Eds.): *Peptides, Structures and Function (Proc. Am. Pept. Symp. 8th)* Pierce Chemical Co., Rockford, IL 1983, p. 579; b) D. H. Rich in *Comprehensive Medicinal Chemistry, Bd. 2*, Pergamon 1990, p. 391.
[2] Übersicht in: R. Henning, *Nachr. Chem. Tech. Lab. 38* (1990) 460.
[3] M. Shiozaki, T. Hata, Y. Furukawa, *Tetrahedron Lett. 30* (1989) 3669.
[4] P. Bühlmayer, A. Caselli, W. Fuhrer, R. Göschke, V. Rasetti, H. Rueger, J. L. Stanton, L. Criscione, J. M. Wood, *J. Med. Chem. 31* (1988) 1839.
[5] I. S. Sigal, J. R. Huff, P. L. Darke, J. P. Vacca, S. D. Young, S. J. Desolms, W. J. Thompson, T. A. Lyle, S. L. Graham, A. K. Ghosh, EP-A 0337714 (1989).
[6] a) T. Nishi, M. Kataoka, Y. Morisawa, *Chem. Lett. 1989*, 1993; b) P. Herold, R. Duthaler, G. Rihs, C. Angst, *J. Org. Chem. 54* (1989) 1178; c) P. K. Chakravarty, S. E. de Laszlo, C. S. Sarnella, J. P. Springer, P. F. Schuda, *Tetrahedron Lett. 30* (1989) 415; d) S. Thaisrivongs, D. T. Pals, L. T. Kroll, S. R. Turner, F.-S. Han, *J. Med. Chem. 30* (1987) 976; e) M. W. Holladay, F. G. Salituro, D. H. Rich, *ibid. 30* (1987) 374; f) D. J. Kempf, *J. Org. Chem. 51* (1986) 3921; g) A. H. Fray, R. L. Kaye, E. F. Kleinmann, *ibid. 51* (1986) 4828; h) B. E. Evans, K. E. Rittle, C. F. Homnick, J. P. Springer, J. Hirshfield, D. F. Veber, *ibid. 50* (1985) 4615; i) S. Kano, T. Yokomatsu, S. Shibuya, *Tetrahedron Lett. 32* (1991) 233, zit. Lit.
[7] a) G. B. Dreyer, B. W. Metcalf, T. A. Tomaszek, T. J. Carr, A. C. Chandler, L. Hyland, S. A. Fakhoury, V. W. Magaard, M. L. Moore, J. E. Strickler, C. Debouck, T. D. Meek, *Proc. Natl. Acad. Sci. USA 86* (1989) 9752; b) J. V. N. V. Prasad, D. H. Rich, *Tetrahedron Lett. 31* (1990) 1803; c) I. S. Sigal, EP-A 89303539.4 (1989); d) H.-E. Radunz, V. Eiermann, G. Schneider, A. Riethmüller, *Tetrahedron 47* (1991) 1887.
[8] a) D. Hoppe, R. Hanko, A. Brönneke, F. Lichtenberg, *Angew. Chem. 93* (1981) 1106; *Angew. Chem. Int. Ed. Engl. 20* (1981) 1024; b) R. Hanko. D. Hoppe, *ibid. 94* (1982) 378 *and 21* (1982) 372; c) T. Krämer, D. Hoppe, *Tetrahedron Lett. 28* (1987) 5149; Übersichten: d) D. Hoppe, *Angew. Chem. 96* (1984) 930; *Angew. Chem. Int. Ed. Engl. 23* (1984) 932; e) D. Hoppe, T. Krämer, J.-R. Schwark, O. Zschage, *Pure Appl. Chem. 62* (1990) 1999.
[9] a) J. A. Fehrentz, B. Castro, *Synthesis 1983*, 676; b) S. Nahm, S. M. Weinreb, *Tetrahedron Lett. 22* (1981) 3815.

[10] Apparently with no exception, (*E*)-2-alkenyl carbamates give exclusively (*Z*)-*anti* diastereomeres under these conditions [8].
[11] ^{1}H NMR and ^{13}C NMR spectra are in agreement with the proposed structures, although their significance is limited by line broadening. The new compounds gave satisfactory microanalyses (C,H ± 0.3 %).
[12] $[\alpha]_D^{20}$ (c = 1.0–2.0, CH_2Cl_2): **7a**, −63.2; **7b**, +16.8; **8a**, −96.5; **8b**, +94.2; **9a**, −16.0; **9b**, −4.8; **10a**, −51.6; **10b**, −65.0; **11a**, −81.3; **11b**, −97.6; **12a**, −53.6/−53.1; **16**, −60.7. $[\alpha]_D^{20}$ (c = 0.7–1.4, CH_2Cl_2): **18c**, −9.1. $[\alpha]_D^{20}$ (10 % MeOH/CH_2Cl_2): **21**, −32.7; **16**, −75.0; **22**, −57.0.
[13] The relative configuration at C-4 and C-5 was confirmed by transformation of the amino alcohols into 1,3-oxazolidin-2-ones [14]. The less polar 4,5-*anti* diastereomeres **7a, b** afforded the *trans* heterocycles [11] [^{1}H NMR (300 MHz), $^3J(4.5)$ = 5.1 Hz: $[\alpha]_D^{20}$ = +69.8 (c = 2.0, CH_2Cl_2)], whereas from **8a, b** the *cis* compound [11] [$^3J(4.5)$ = 6.7 Hz; $[\alpha]_D^{20}$ = −222.0, (c = 1.0–2.0, CH_2Cl_2); m.p. 149 °C (hexane)] was obtained.
[14] a) S. Kobayashi, T. Isobe, M. Ohno, *Tetrahedron Lett. 25* (1984) 5079; b) M. N. Dufour, P. Jouin, J. Poncet, A. Pantaloni, B. Castro, *J. Chem. Soc. Perk. Trans. 1 1986*, 1895; c) H. Harada, A. Tsubaki, T. Kamijo, K. Iizuka, Y. Kiso, *Chem. Pharm. Bull 37* (1989) 2570; d) R. Metternich, W. Lüdi, *Tetrahedron Lett. 29* (1988) 3923; e) M. Sakaitani, Y. Ohfune, *J. Am. Chem. Soc. 112* (1990) 1150.
[15] a) D. Hoppe, A. Brönneke, *Tetrahedron Lett. 24* (1983) 1687; b) P. A. Grieco, T. Oguri, Y. Yokoyama, *ibid. 1978* 419.
[16] D. R. Williams, F. D. Klingler, E. E. Allen, F. W. Lichtenthaler, *Tetrahedron Lett. 29* (1988) 5087.
[17] H. Wissmann, H.-J. Kleiner, *Angew. Chem. 92* (1980) 129 *Angew. Chem. Int. Ed. Engl. 19* (1980) 133.
[18] Treatment of **9a** with 1.05 equivalents of LiOH in MeOH/THF/H_2O (10 : 1 : 1) for 30 min at 20 °C gave **17a**. Attempted silylation of **17a** (imidazole, TBDMSCl, followed by treatment with H_2O/HOAc (10 : 1) in THF) gave **9a** in 90 % yield but no silylated acid.
[19] a) T. Hirabayashi, K. Itoh, S. Sakai, Y. Ishii, *J. Organomet. Chem. 25* (1970) 33; b) A. Basha, M. Lipton, S. M. Weinreb, *Tetrahedron Lett.* 1977 4171; c) R. S. Garigipati, D. M. Tschaen, S. M. Weinreb, *J. Am. Chem. Soc. 112* (1990) 3475; d) see also: Y. Yamamoto, T. Furuta *Chem. Lett. 1989*, 797.
[20] Compound **9c** was synthesized by hydrogenolysis of **9a** (10 % Pd/C, *i*PrOH/THF/H_2O (10 : 1 : 1), H_2 16 h, 25 °C, filtration over Celite and solvent removal) followed by reaction of the crude material with 1.2 equivalents of trifluoroacetic acid in CH_2Cl_2 in the presence of 1.5 equivalents of NET_3 to yield **9c** in 92 % yield after chromatography.
[21] The concentration of **12a** should not exceed 0.03 M and the reaction time should not exceed 20 min to avoid the formation of side products.
[22] The dichromate concentration should be around 0.025 M in H_2SO_4 and the concentration of **14a** in CH_2Cl_2 should be 0.03 M.
[23] The reaction was quenched at −76 °C with HOAc prior to workup.
[24] The reaction was quenched at −40 °C with HOAc prior to workup.
[25] D. Landini, F. Montanari, F. Rolla, *Synthesis 1979*, 134.
[26] The trifluoroacetyl group can be removed under the conditions described by F. Weygand, E. Frauendorfer, *Chem. Ber. 103* (1970) 2437.
[27] Note added in proof (November 9, 1991): another method based on allylsilanes was published after our manuscript had been submitted: J. V. N. V. Prasad, D. H. Rich, *Tetrahedron Lett. 32* (1991) 5857.

Isophlorins: Molecules at the Crossroads of Porphyrin and Annulene Chemistry **

By *Michael Pohl, Hans Schmickler, Johann Lex,* and *Emanuel Vogel* *

Dedicated to Professor Karl Heinz Büchel on the occasion of his 60th birthday

The porphyrin–isophlorin redox system, **1** ⇄ **2**, represents a challenge for porphyrin chemistry and is a prime example of the intertwined structural and chemical relationships between porphyrins and annulenes. Isophlorin (*N,N'*-dihydroporphyrin, **2**), which was discussed for the first time by *Woodward* in connection with the synthesis of chlorophyll[1] but has remained hypothetical up to now, constitutes a bridged [20]annulene with quinodimethane-like partial structures. In contrast to **1**, compound **2** very likely exhibits some deviation from planarity, since, on the basis of structural findings about protonated porphyrins,[2] the presence of four imino hydrogens should cause nonbonding H ··· H interactions in the center of the molecule.

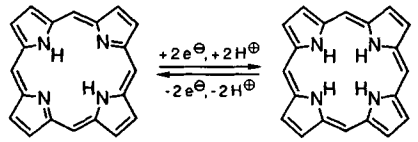

1 *hypothetical* **2**

Recent observations on the porphycene–*N,N'*-dihydroporphycene redox system,[3] which drew our attention to **1** ⇄ **2**, support the conjecture that **2** should readily undergo aromatization to give porphyrin (**1**), either by a sequence of two-electron oxidation and deprotonation or by another pathway.[1] This may explain why isophlorins have managed to defy not only synthesis but also the elucidation of their possible biological relevance. On the other hand, dianionic metal complexes derived from isophlorins are available from the corresponding metalloporphyrins by reduction with alkali metals and have been known for some time.[4]

It occurred to us that the search for **2**, currently pursued in this laboratory, should be paralleled by efforts to obtain tetraoxa-, tetrathia-, and *N,N',N'',N'''*-tetramethylisophlorin (**3**, **4**, and **5**, respectively), taking into account the multifaceted interest [20]annulenes of the isophlorin-type command (π-bonding relationships, dependence of paratropism on geometry, components of supramolecular structures, etc.). Having recently synthesized tetraoxaisophlorin (**3**), a model for a planar [4n]annulene of high symmetry, starting from the tetraoxaporphyrin dication,[5, 6] we have now succeeded in preparing the octaethyl derivative **7** of *N,N',N'',N'''*-tetramethylisophlorin.

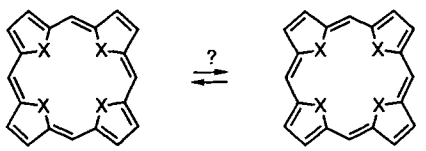

3: X = O
4: X = S
5: X = NCH$_3$

A promising synthetic pathway to **7**, analogous to the route to tetraoxaisophlorin (**3**), is offered by two-electron reduction—or four-electron reduction and subsequent partial reoxidation—of *Franck*'s *N,N',N'',N'''*-tetramethyloctaethylporphyrin dication[7] as its diperchlorate **6**.[8] The desired [20]annulene **7** was obtained by treatment of **6**, suspended in THF, for 30 min at −78 °C with a 0.15 molar solution of anthracene-sodium in THF (1.2-fold excess based on two-electron reduction). There was no evidence of overreduction to the potentially aromatic [20]annulene dianion. After excess reducing agent had been destroyed by oxygen, the reaction was worked up conventionally (addition of hydroquinone). Crystallization from ethanol/hexane (4:1) gave **7** as lustrous brown needles, which above 190 °C turned yellow and decomposed (yield 75 %). In contrast to the highly reactive tetraoxaisophlorin (**3**), **7** is moderately stable on exposure to air.

[*] Prof. Dr. E. Vogel, M. Pohl, Dr. J. Lex, Dr. H. Schmickler
Institut für Organische Chemie der Universität
Greinstrasse 4, W-5000 Köln 41 (FRG)

[**] This work was supported by the German Israeli Foundation for Scientific Research and Development (*G. I. F.*). We thank Prof. Dr. *F.-G. Klärner* (Universität Bochum), Priv.-Doz. Dr. *J. Hahn*, and Dipl.-Chem. *A. Hopp* (Universität Köln) for helpful discussions.

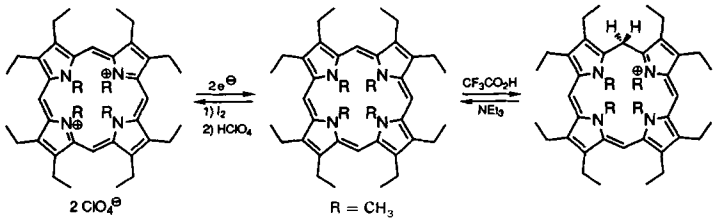

6 7 8

The structural assignment of **7** is based on the temperature-dependent ^{1}H NMR spectrum (Fig. 1). As indicated by the characteristic changes in line shape of the spectrum in the range from -72 °C to 104 °C, the molecule undergoes a rapid degenerate π-bond shift at room temperature in analogy to the behavior of other [4n]annulenes.[9] This dynamic process is sufficiently slow at -72 °C, so that the spectrum recorded corresponds to compound **7** with localized π bonds: a singlet at $\delta = 5.12$ (4H, *meso* H), two singlets at $\delta = 4.51$ and 3.74 (2×6H, *N*-CH_3^a and *N*-CH_3^b, respectively),[10] two quartets at $\delta = 2.63$ and 1.98 (2×8H, CH_2),[11] and two triplets at $\delta = 1.37$ and 1.00 (2×12H, CH_3). When the temperature is raised, the signal of the *meso* protons remains unchanged as expected, whereas the three pairs of signals for the protons involved in the exchange process each coalesce after initial line broadening (16 °C for *N*-CH_3). Raising the temperature still further (to 104 °C) results in the simple spectrum predicted for **7** when it undergoes rapid exchange; this consists of two singlets, one quartet, and a triplet (effective D_{2d} molecular symmetry).

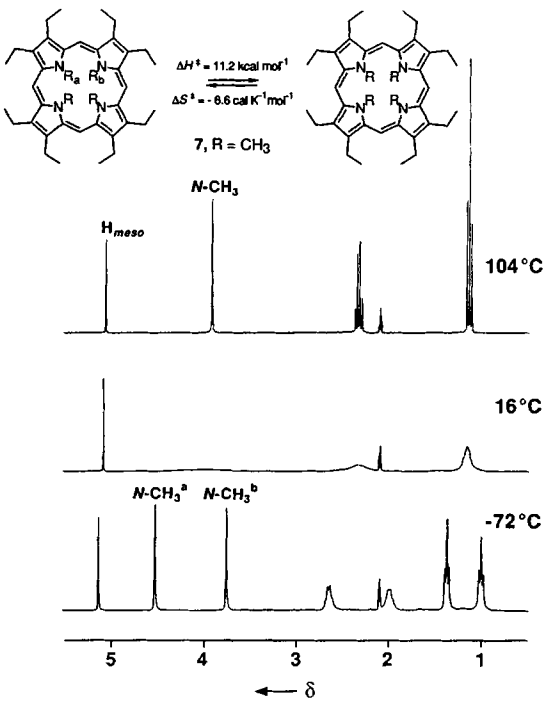

Fig. 1. Temperature dependence of the ^{1}H NMR spectrum (300 MHz, [D_8]-toluene) of **7**: -72 °C (region of slow exchange), 16 °C (coalescence range), and 104 °C (region of fast exchange).

Any discussion of the ^{1}H NMR spectrum must take into account the possible existence of stable conformers of **7** due to the spatial demands of the *N*-methyl groups. The number and kind of proton resonances reveal that **7** is present exclusively as one conformer, which must be either the all-*syn* or the *syn,anti,syn,anti* form (arrangement of the *N*-methyl groups with respect to the mean plane of the ring framework). Since **7** was obtained from **6**, which exists as the *syn,anti,syn,anti* conformer, and since conformational stability is very likely maintained in *N,N',N'',N'''*-tetramethylporphyrins even at higher temperature, **7** may also be assumed to exist as the *syn,anti,syn,anti* conformer. The notion that the π-bond shift in **7** is accompanied by a degenerate conformational change of the *N*-methyl groups that escapes detection by NMR spectroscopy is therefore unrealistic.

An X-ray structure analysis of **7**[12] established that, in the crystal, the compound is saddle-shaped with *syn, anti,syn,anti* conformation of the *N*-methyl groups (Fig. 2), as observed for its dicationic precursor **6**. However, whereas the heterocyclic five-membered rings in the aromatic **6** are equivalent, those in **7** are alternately pyrrole and pyrroline rings, as portrayed in the conventional structural formula (reduction of molecular symmetry from D_{2d} to C_{2v}). Because of the steric hindrance of the *N*-methyl groups, the pyrrole and pyrroline rings are tilted by 49° and 26°, respectively, out of the plane defined by the four *meso*-methine carbon atoms (the corresponding torsion angles C_β-C_α-C_m-C_α are 52° and 11°, respectively). The remarkably strong twisting of the pyrrole rings becomes understandable if one bears in mind that the interaction between the respective methyl groups is especially pronounced owing to the sp^2 hybridization of ni-

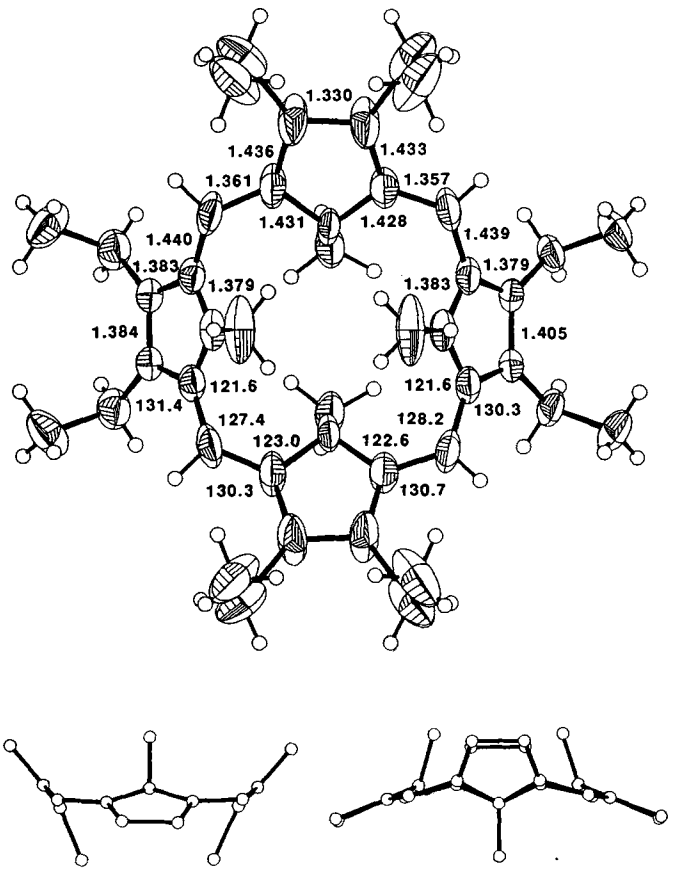

Fig. 2. Molecular structure of **7**. The molecule has approximate C_{2v} symmetry (exact C_s), as the three projections show. Above: Top view with bond lengths [Å] and angles [°]; standard deviations 0.009 Å and 0.5°. The thermal ellipsoids are drawn at 40% probability. Below: Side view (without substituents and H atoms): left, parallel to the crystallographic mirror plane; right, perpendicular to it.

trogen (the N-CH_3 bond forms an angle of only 20° with the pyrrole ring plane; sum of bond angles 356°) and the torsions only affect single bonds. In the case of the pyrroline rings, the nitrogen is sp^3-hybridized as expected (sum of bond angles 340°), since the *N*-methyl groups project by no less than 46° from the ring plane. With regard to the structural parameters of the five-membered rings, it is noteworthy that the pattern of bond lengths in the pyrrole rings does not correspond to that in porphyrins, but is comparable to that of the isolated pyrrole rings in *Franck's* *N,N',N'',N'''*-tetramethyloctakis-(carboxymethyl)porphyrinogen (N-C_α = 1.355 Å, C_α-C_β = 1.373 Å, C_β-C_β = 1.416 Å).[8]

Table 1. Dependence of the paratropism of isophlorins on geometry. ^{1}H NMR chemical shifts (δ values) of the *meso* protons in **3**, **7**, and **9** (vinylic hydrogen atoms), as well as of the *N*-CH_3 protons in **7** and **9** (each 300 MHz, [D_8]THF, −50 °C).

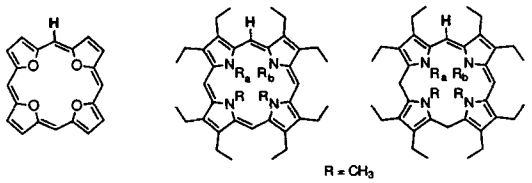

	3	**7**	**9**
H_{meso}	−0.30	4.95	5.32
N-CH_3^a	-	4.38	2.75
N-CH_3^b	-	3.48	1.41

The ^{1}H NMR spectrum of saddle-shaped **7**, when compared with the spectra of nearly planar tetraoxaisophlorin **3** and *N,N',N'',N'''*-tetramethyl-5,10-dihydroisophlorin (as octaethyl derivative **9**)[13] in which the cyclic conjugation is interrupted, is very informative since it reveals in a particularly striking way the dependence of paratropism of [4n]annulenes[14] on molecular geometry (Tables 1 and 2). On going from tetraoxaisophlorin (**3**) to the nitrogen compound **7**, the resonance of the *meso* protons is shifted by no less than $\Delta\delta$ = 5.3 to lower field, and thus comes close to the location of the resonances of the vinylic protons of **9**. Clearly, this shift difference indicates an almost complete geometry-induced loss of paratropism in **7**.[14, 15]

The other spectra of **7** are consistent with the properties of the compound so far determined. The ^{13}C NMR spectrum (at −60 °C) shows, complementarily to the low-temperature ^{1}H NMR spectrum, eleven signals, four of which correspond to quaternary carbon atoms. In the UV/VIS spectrum, a broad band is found at 356 nm (ε = 35000) with a shoulder at 516 nm (ε = 1440) extending beyond 700 nm. An IR band at 1601 cm^{-1} (no equivalent band in porphyrins) can, on the basis of comparisons,[4b, c, 16] be assigned with some certainty to the stretching vibration of the exocyclic C=C bonds at the α-pyrroline positions. In the mass spectrum, the molecular ion (100%) is accompanied by the doubly charged aromatic ion as a prominent peak (25%), a fact that underlines the [4n]annulene character of **7**.

Chemically, the [4n]annulene nature of **7** is reflected above all in its ready oxidizability. Even mild oxidizing agents like iodine, silver(I), and iron(III) ions transform **7** into the dication **6**, whereas bromine is necessary to convert *N,N',N'',N'''*-tetramethyloctaethylporphyrinogen into **6**.[7] On the other hand, reduction of **7** with alkali metals to give the 22 π dianion has not yet met with success,[17] even though there are precedents for the formation of nonplanar, aromatic [4n]-annulene dianions.[18] Reaction of **7** with trifluoroacetic acid in THF affords the protonation product, *N,N',N'',N'''*-tetramethyloctaethylphlorin cation **8** (Table 2), which is stable in solution and was identified by NMR spectroscopy; treatment of **8** with bases regenerates **7**.

The current discussion on the mechanism—particularly the geometry of the transition state—of the π-bond shift in cyclooctatetraenes[9b, 19] and other nonplanar 4n π-electron systems[9c, 20] prompted us to derive the activation parameters of the degenerate π-bond shift in **7** from the ^{1}H NMR spectrum (Fig. 1). To accomplish this, we recorded the spectrum at 17 temperatures from −72 °C to 104 °C[21] and calculated the rate constants by line-shape analysis of the *N*-CH_3 signals (DNMR5).[22] Evaluation of the kinetic data on the basis of the Eyring equation afforded the following parameters for the dynamic process in **7**: $\Delta H^{\neq}$ = 11.2 ± 0.2 kcal mol^{-1}, $\Delta S^{\neq}$ = − 6.6 ± 0.6 cal K^{-1} mol^{-1}, and thus $\Delta G^{\neq}_{298}$ = 13.2 kcal mol^{-1} (the error range results from the statistical standard deviation of the Eyring equation).

The saddle-shaped ring framework of the *N,N',N'',N'''*-tetramethylisophlorin **7** can accommodate a certain flattening, though not a complete planarization, if the pyrrole ring nitrogens also become pyramidalized. Accordingly, the activation energy of the π-bond shift in **7** is on the order of magnitude of that for other nonplanar [4n]annulenes, particularly that of cyclooctatetraene,[9b] whereas, in the case of the essentially planar **3**, it is so strongly lowered (< 3 kcal mol^{-1}) that its measurement verges on the limits of ^{1}H and ^{13}C NMR spectroscopy (the signal of the furanoid hydrogens in **3** remains sharp at −135 °C). A relationship to the dynamics of cyclooctatetraene appears to exist here insofar as *Ermer, Klärner*, et al. have suggested that the transition state of the π-bond shift in this annulene is not necessarily planar, but rather adopts the shape of a flattened saddle.[23] As *Paquette* et al. have convincingly demonstrated in recent investigations, it is justified for at least a number of bridged cyclooctatetraenes to assume such a nonplanar geometry in the transition state of the π-bond shift.[19] The appreciably negative activation entropy found for the double-bond shift in **7** indicates that, in the transition state of this degenerate process, degrees of freedom of internal motion are frozen by strong steric compression of the *N*-methyl groups.

Due to their chirality, singly *meso*-substituted *N,N',N'',N'''*- tetramethylisophlorins should permit the presumed conformational stability of the *N,N',N'',N'''*-tetramethylisophlorin macrocycle **7**—after separation into the enantiomers—to be reexamined. Whereas electrophilic substitutions at **7** have been unsuccessful so far, *N,N',N'',N'''*-tetramethyl-5-cyanooctaethylisophlorin (**11**) could easily be obtained starting from **6**. Reaction of **6** with sodium cyanide (excess) in ethanol (30 min) surprisingly leads not to the expected bisadducts (stereoisomeric *N,N',N'',N'''*-tetramethyl-5,10-dicyano-5,10-dihydroisophlorins), but instead to the air-stable nitrile **11** as the sole isolable product. Compound **11** was obtained, after conventional workup and crystallization from methanol, as green-black needles (m.p. 203 °C, yield 70%). Despite its lower symmetry compared with **7** (C_2 vs. C_{2v}), **11** is still able to undergo a degenerate π-bond shift, which is revealed in the corresponding temperature dependence of the NMR spectra (Table 2). It seems compelling to postulate the *N,N',N'',N'''*-tetramethylphlorin cation **10** as intermediate in the reaction of the dication **6** with cyanide ion to form **11**. That **10** would be deprotonated to **11** by cyanide ion was as unexpected as the transformation of **11** back to **6** by mineral acids.

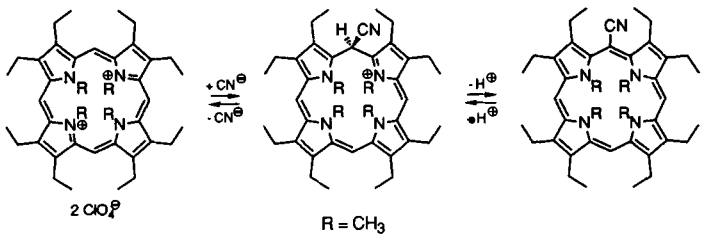

6 **10** **11**

The resolution of **11** did not prove necessary, since in this case, in contrast to that of **7**,[11] the diastereotopic methylene protons of the ethyl groups allowed the conformational stability of the *N*,*N*′,*N*″,*N*‴-tetramethylisophlorin macrocycle to be established unequivocally by NMR spectroscopy. Apparently, the local anisotropy of the nitrile group causes the diastereotopic methylene protons of the ethyl groups in neighboring position to the *meso* substituent to appear as a well-resolved multiplet, which forms the AB part of an ABX_3 system. When the sample is heated, this group of signals shows no tendency to collapse to a simple quartet, but rather remains sharp to 175 °C (the instrumental limit of measurement). Double resonance experiments,[24] moreover, gave no evidence of energy transfer between the methylene protons. The NMR spectroscopic results indicate that the energy barrier for the conformational change of the *N*-methyl groups in the *N*,*N*′,*N*″,*N*‴-tetramethylisophlorin macrocycle is at least 25 kcal mol^{-1}. The possibility that the π-bond shift in **7** and **11** is accompanied by such a conformational process can therefore be ruled out.

Table 2. Selected physical data for **7**–**9** and **11**.

7: ^{1}H NMR (300 MHz, $C_6D_5CD_3$, −72 °C): δ = 5.12 (s, 4H, H-*meso*), 4.51 (s, 6H, *N*-CH_3^a), 3.74 (s, 6H, *N*-CH_3^b), 2.63, 1.98 (2q, 16H, CH_2), 1.37, 1.00 (2t, 24H, CH_3). ^{1}H NMR (300 MHz, $C_6D_5CD_3$, 104 °C): δ = 5.05 (s, 4H, H-*meso*), 3.91 (s, 12H, *N*-CH_3), 2.32 (q, 16H, CH_2), 1.14 (t, 24H, CH_3). ^{13}C NMR (75.5 MHz, [D$_8$]THF, −60 °C): δ = 156.04, 138.60, 128.72, 128.03, 92.72, 40.79, 36.25, 19.01, 17.89, 16.53, 15.38. MS (EI, 70 eV): *m*/*z* 592 (M^+, 100%), 296 (M^{2+}, 25%). IR (CsI): $\tilde{\nu}$ [cm^{-1}] = 3100, 2964, 2930, 2870, 1601, 1459, 1395, 1357, 1316, 1261, 1191, 1054, 980, 961, 804, 745, 698, 667, 602. UV/VIS (THF): λ_{max} [nm] (ε) = 286 (22000), 356 (35000), 387 (25000) sh, 416 (1450).

8: ^{1}H NMR (300 MHz, [D$_8$]THF, CF_3CO_2H): δ = 6.68 (s, 2H, H-10,20), 5.42 (s, 1H, H-15), 3.84 (s, 2H, H-5), 3.61, 3.26 (2s, 12H, H-21,22,23,24), 2.65 (m, 4H, H-3a,7a), 2.62 (m, 4H, H-2a,8a), 2.50 (m, 4H, H-13a,17a), 2.44 (m, 4H, H-12a, 18a), 1.22 (t, 6H, H-2b,8b), 1.18 (t, 6H, H-3b, 7b), 1.17 (t, 6H, H-12b,18b), 1.13 (t, 6H, H-13b,17b). ^{13}C NMR (75.5 MHz, [D$_8$]THF, CF_3CO_2H): δ = 166.22, 154.79, 150.14, 146.56, 140.12, 128.19, 126.83, 126.28, 114.41, 86.21, 38.96, 35.43, 22.47, 19.09, 18.59, 18.04, 17.81, 16.57, 16.17, 15.63, 14.74. UV/VIS (THF/CF_3CO_2H): λ_{max} [nm] (ε) = 276 (17000), 341 (14000), 434 (20000), 771 (830).

9: ^{1}H NMR (300 MHz, [D$_8$]THF, 20 °C): δ = 5.33 (s, 2H, H-15,20), 3.90 (br. s, 4H, H-5,10), 2.88 (s, 3H, H-22), 2.79 (s, 6H, H-21,23), 2.50 (m, 4H, H-7a,8a), 2.45 (m, 4H, H-3a,12a), 2.40 (m, 4H, H-17a,18a), 2.35 (m, 4H, H-2a,13a), 1.51 (s, 3H, H-24), 1.15 (t, 6H, H-7b,8b), 1.13 (t, 6H, H-17b,18b), 1.10 (t, 6H, H-3b,12b), 1.05 (t, 6H, H-2b,13b). ^{13}C NMR (75.5 MHz, [D$_8$]THF): δ = 151.99, 137.89, 126.95, 126.48, 125.96, 122.71, 122.11, 121.35, 87.29, 32.97, 31.73, 31.56, 22.19, 19.22, 18.80, 18.60, 18.28, 17.47, 17.27, 16.10, 15.43. MS (EI, 70 eV): *m*/*z* = 594 (M^+, 100%). IR (CsI): $\tilde{\nu}$ [cm^{-1}] = 2962, 2929, 2870, 2612, 1453, 1371, 1314, 1263, 1054, 963, 745. UV/VIS ($CHCl_3$): λ_{max} [nm] (ε) = 250 (26000), 362 (14000), 401 (14000).

11: ^{1}H NMR (300 MHz, $CDCl_3$, −59 °C): δ = 5.30, 4.92 (2s, 2H, H-10,20), 4.96 (s, 1H, H-15), 4.25, 4.08, 3.51, 3.12 (4s, 12H, H-21,22,23,24), 2.4–2.7 (m, 4H, H-3a,7a), 2.1–2.4 (m, 12H, H-2a,8a,12a, 13a,17a,18a), 1.14–1.24 (m, 6H, H-3b,7b), 1.00–1.14 (m, 18H, H-2b,8b,12b,13b,17b,18b). ^{1}H NMR (300 MHz, $CDCl_3$, 59 °C): δ = 5.15 (s, 2H, H-10,20), 4.94 (s, 1H, H-15), 3.83, 3.74 (2br.s, 12H, H-21,22,23,24), 2.5–2.8 (m, 4H, H-3a,7a), 2.2–2.4 (m, 12H, H-2a,8a,12a,13a,17a,18a), 1.25 (t, 6H, H-3b,7b), 1.14, 1.12, 1.10 (3t, 18H, H-2b,8b,12b,13b,17b,18b). ^{13}C NMR (75.5 MHz, $CDCl_3$, −59 °C): δ = 163.79, 157.13, 155.77, 148.59, 142.84, 138.56, 137.97, 135.39, 130.09, 130.02, 128.37, 128.31, 127.42, 126.88, 126.56, 123.93, 121.24, 97.44, 94.00, 92.67, 70.74, 40.75, 37.47, 35.75, 34.82, 17.2–17.9 (br.), 16.30, 15.97, 15.68, 15.50, 15.32, 15.16, 14.73. MS (EI, 70 eV): *m*/*z* = 617 (M^+, 100%), 309 (M^{2+}, 50%). IR (CsI): $\tilde{\nu}$ [cm^{-1}] = 3019, 2966, 2933, 2184, 1605, 1560, 1528, 1458, 1056, 959, 798, 685. UV/VIS (hexane): λ_{max} [nm] (ε) = 313 (21000), 376 (36000), 404 (2500).

Received: June 28, 1991
Supplemented: September 24, 1991 [Z 4756 IE]
German version: *Angew. Chem. 103* (1991) 1737

CAS Registry numbers:
6, 124318-47-4; **7**, 136947-69-8; **8**, 136947-70-1; **9**, 136947-72-3; **11**, 136947-71-2.

[1] R. B. Woodward, *Angew. Chem. 72* (1960) 651; *Ind. Chim. Belg. 27* (1962) 1293; R. B. Woodward, W. A. Ayer, J. M. Beaton, F. Bickelhaupt, R. Bonnett, P. Buchschacher, G. L. Closs, H. Dutler, J. Hannah, F. P. Hauck, S. Itô, A. Langemann, E. Le Goff, W. Leimgruber, W. Lwowski, J. Sauer, Z. Valenta, H. Volz, *Tetrahedron 46* (1990) 7599. For phlorins discovered by *Woodward* in the course of the synthesis of chlorophyll, see also: D. Mauzerall, *J. Am. Chem. Soc. 84* (1962) 2437; *ibid. 82* (1960) 1832.

[2] A. Stone, E. B. Fleischer, *J. Am. Chem. Soc. 90* (1968) 2735; N. Hirayama, A. Takenaka, Y. Sasada, E.-I. Watanabe, H. Ogoshi, Z.-I. Yoshida, *J. Chem. Soc. Chem. Commun. 1974*, 330.

[3] E. Vogel, I. Grigat, M. Köcher, J. Lex, *Angew. Chem. 101* (1989) 1687; *Angew. Chem. Int. Ed. Engl. 28* (1989) 1655.

[4] a) G. L. Closs, L. E. Closs, *J. Am. Chem. Soc. 85* (1963) 818; b) J. W. Buchler, L. Puppe, *Liebigs Ann. Chem. 740* (1970) 142; c) A. Botulinski, J. W. Buchler, K.-L. Lay, H. Stoppa, *ibid. 1984*, 1259; d) A. M. Schul'ga, G. N. Sinyakov, G. P. Gurinovich, *Biofizika 23(1)* (1978) 5; *Chem. Abstr. 88* (1978) 202315j; e) R. Cosmo, C. Kautz, K. Meerholz, J. Heinze, K. Müllen, *Angew. Chem. 101* (1989) 638; *Angew. Chem. Int. Ed. Engl. 28* (1989) 604.

[5] E. Vogel, W. Haas, B. Knipp, J. Lex, H. Schmickler, *Angew. Chem. 100* (1988) 445; *Angew. Chem. Int. Ed. Engl. 27* (1988) 406.

[6] The very reactive **3** (black crystals) exhibits the following spectroscopic data: ^{1}H NMR (300 MHz, [D$_8$]THF, room temperature): δ = 2.47 (s, 8H, H-β), −0.15 (s, 4H, H-*meso*); ^{13}C NMR (75.5 MHz, [D$_8$]THF, room temperature): δ = 164.54 (C-α), 122.34 (C-β), 97.47 (C-*meso*); MS (EI 70 eV): *m*/*z* 316 ($M^{2\oplus}$, 100 %), 158 ($M^{2\oplus}$, 22 %); IR (KBr): $\tilde{\nu}$ = 3120, 1624, 1346, 1285, 1123, 1062, 1020, 978, 937, 888, 820, 784, 756, 723, 669, 608 cm^{-1}; UV/VIS (THF): λ_{max} [nm] (ε) = 315 (107000), 326 (92000) sh, 343 (124000), 368 (4800) sh, 402 (6000) sh, 408 (6200), 423 (7900), 430 (7000) sh, 452 (7000), 465 (4300) sh, 487 (5600), 620 (250) sh, 699 (340), 770 (350); P. Röhrig, *Dissertation*, Universität Köln 1991. The publication on **3**, which has been delayed by disorder problems in the structural-chemical investigations, is in preparation.

[7] *N*,*N*′,*N*″,*N*‴-Tetramethylporphyrin dications (as dibromides) were described for the first time by *B. Franck*: B. Franck, *Angew. Chem. 94* (1982) 327; *Angew. Chem. Int. Ed. Engl. 21* (1982) 343; R. Steinkamp, *Dissertation*, Universität Münster 1978.

[8] The X-ray structure analysis of the *N*,*N*′,*N*″,*N*‴-tetramethyloctaethylporphyrin dication as diperchlorate **6** has been carried out by us in connection with investigations on the tetrathiaporphyrin dication: E. Vogel, P. Röhrig, M. Sicken, B. Knipp, A. Herrmann, M. Pohl, H. Schmickler, J. Lex, *Angew. Chem. 101* (1989) 1683; *Angew. Chem. Int. Ed. Engl. 28* (1989) 1651; X-ray structure analysis of the *N*,*N*′,*N*″,*N*‴-tetramethyloctakis(carboxymethyl)porphyrinogen (as the dihydrate): G. Sawitzki, H. G. von Schnering, *ibid. 88* (1976) 616 and *15* (1976) 552.

[9] a) Cyclobutadiene: S. Masamune, *Pure Appl. Chem. 44* (1975) 861; G. Maier, *Angew. Chem. 100* (1988) 317; *Angew. Chem. Int. Ed. Engl. 27* (1988) 309; see also D. J. Cram, M. E. Tanner, R. Thomas, *Angew. Chem. 103* (1991) 1048; *Angew. Chem. Int. Ed. Engl. 30* (1991) 1024; b) cyclooctatetraene: F. A. L. Anet, *J. Am. Chem. Soc. 84* (1962) 671; J. F. M. Oth, *Pure Appl. Chem. 25* (1971) 573; c) bridged [12]annulenes: E. Vogel, H. Königshofen, K. Müllen, J. F. M. Oth, *Angew. Chem. 86* (1974) 229; *Angew. Chem. Int. Ed. Engl. 13* (1974) 281; H. Kohnz, B. Düll, K. Müllen, *ibid. 101* (1989) 1375 and *28* (1989) 1343.

[10] The assignment of *N*-CH_3^a and *N*-CH_3^b (in the region of slow exchange) was based on the fact that, in the case of **9**, the protons of the *N*-methyl group on the pyrrole nitrogen show resonance at lower field than those of the *N*-methyl group on the pyrroline nitrogen (Table 1).

[11] In **7**, the methylene protons of the ethyl groups are diastereotopic owing to the nonplanar conformation of the ring framework and thus form the AB part of an ABX_3 system; however, in toluene at lower temperature, the anticipated multiplet of the methylene protons has degenerated to a poorly resolved quartet. For the exploitation of diastereotopic methylene protons for the detection of dynamic processes by NMR spectroscopy, see K. M. Barkigia, M. D. Berber, J. Fajer, C. J. Medforth, M. W. Renner, K. M. Smith, *J. Am. Chem. Soc. 112* (1990) 8851; C. J. Medforth, M. D. Berber, K. M. Smith, J. A. Shelnutt, *Tetrahedron Lett. 31* (1990) 3719.

[12] $C_{40}H_{56}N_4$, dec. above 190 °C, crystals from acetonitrile; monoclinic space group $C2/m$, $Z = 4$; $a = 14.847(4)$, $b = 22.068(7)$, $c = 11.687(3)$ Å, $\beta = 110.10(2)°$; $\rho_{calcd} = 1.095$ g cm^{-3}; intensity measurements on a four-circle diffractometer (0 °C, $\lambda_{Mo} = 0.71069$ Å, $\theta_{Mo}(max) = 25°$); refinement (C,N anisotropic, H isotropic) taking into consideration 1397 reflections with $F_0 > 4\sigma(F_0)$, $R = 0.082$, $R_w = 0.089$ (under the conditions of measurement, the crystal slowly decomposed; further lowering of the temperature led to a phase change). Further details of the crystal structure investigation are available on request from the Fachinformationszentrum Karlsruhe, Gesellschaft für wissenschaftlich-technische Information mbH, W-7514 Eggenstein-Leopoldshafen 2 (FRG), on quoting the depository number CSD-55802, the names of the authors, and the journal citation.

[13] The dihydro compound **9** is formed from the *N,N',N'',N'''*-tetramethyloctaethylporphyrin dication **6** by reduction with $NaBH_4$ in methanol (10 min, room temperature). Conventional workup and crystallization from hexane/ethanol affords the dihydro compound **9** as yellow rods, which decompose above 250 °C; yield 80% (see Table 2 for spectral data).

[14] A pronounced geometry dependence of the paratropism in twisted phenanthrene dianions has been demonstrated recently: R. Frim, A. Mannschreck, M. Rabinovitz, *Angew. Chem. 102* (1990) 919; *Angew. Chem. Int. Ed. Engl. 29* (1990) 919.

[15] For a discussion of ring-current effects in [4n]annulenes, see: J. A. Pople, K. G. Untch, *J. Am. Chem. Soc. 88* (1966) 4811; R. B. Mallion, *Pure Appl. Chem. 52* (1980) 1541; A. Minsky, A. Y. Meyer, M. Rabinovitz, *Tetrahedron 41* (1985) 785.

[16] A comparable band is found for *N,N',N'',N'''*-tetramethyl-5,10-dihydrooctaethylisophlorin (**9**) (Table 2).

[17] The difficulty in reducing **7** to the dianion is also borne out by cyclic voltammetry. Two irreversible reduction waves are observed at very negative potentials (−2.42 and −2.69 V vs. the saturated calomel electrode, THF, nBu$_4$NPF$_6$, 100 mVs^{-1}).

[18] [12]Annulene dianion: J. F. M. Oth, G. Schröder, *J. Chem. Soc. B 1971* 904; 1,6-methano[12]annulene dianion: J. F. M. Oth, K. Müllen, H. Königshofen, M. Mann, Y. Sakata, E. Vogel, *Angew. Chem. 86* (1974) 232; *Angew. Chem. Int. Ed. Engl. 13* (1974) 284.

[19] L. A. Paquette, M. P. Trova, J. Luo, A. E. Clough, L. B. Anderson, *J. Am. Chem. Soc. 112* (1990) 228; L. A. Paquette, T.-Z. Wang, J. Luo, C. E. Cottrell, A. E. Clough, L. B. Anderson, *ibid. 112* (1990) 239; see also: K. Müllen, W. Heinz, F.-G. Klärner, W. R. Roth, I. Kindermann, O. Adamczak, M. Wette, J. Lex, *Chem. Ber. 123* (1990) 2349.

[20] In highly substituted heptalenes, the separation of the π-bond isomers and their resolution afforded definite proof that the π-bond shift proceeds via a nonplanar, helical-chiral transition state: K. Hafner, G. L. Knaup, H. J. Lindner, *Bull. Chem. Soc. Jpn. 61* (1988) 155.

[21] The measurement was carried out in degassed [D_8]toluene; the temperature calibration was accomplished with methanol and ethylene glycol.

[22] G. Binsch, H. Kessler, *Angew. Chem. 92* (1980) 445; *Angew. Chem. Int. Ed. Engl. 19* (1980) 411; DNMR 5: D. S. Stephenson, G. Binsch, *Quantum Chem. Progr. Exch. 10* (1978) 365.

[23] O. Ermer, F.-G. Klärner, M. Wette, *J. Am. Chem. Soc. 108* (1986) 4908.

[24] H. Günther: *NMR-Spektroskopie*, 2nd ed., Thieme, Stuttgart 1983.

Stereoselective Synthesis of Annelated Piperidines by Photochemical Cycloaddition and Iminium Ion–Allylsilane Cyclization**

By *Lutz F. Tietze** and *Josef R. Wünsch*

Dedicated to Professor Karl Heinz Büchel on the occasion of his 60th birthday

A general method for the synthesis of *N*-heterocycles **2** is the intramolecular cyclization of iminium ions **1**, which contain a vinyl or allylsilane group. The formation of the iminium ions **1** is usually carried out by condensation of an amine with an aldehyde or ketone, reduction of an imide, decarboxylation of α-amino acids, or cleavage of cyanide from α-amino nitriles or of amines from aminals.[1].

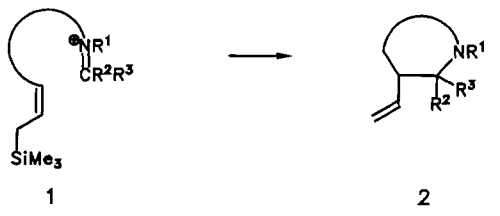

1 2

We have shown that iminium ions can also be formed from photochemically generated intermediates. For example, the photochemical cycloaddition of enamine carbaldehydes[2] such as **3** with alkenes such as **4** leads to 1,4-dihydropyridines **8**[3] (Scheme 1); the initially formed 2-hydroxytetrahydropyridine **6** undergoes acid-catalyzed dehydration, presumably via iminium ion **7**, to give the 1,4-dihydropyridine[4] **8**. In this communication we describe a consecutive sequence of reactions in which an iminium ion formed in this way is trapped by an allylsilane. This photochemical cycloaddition requires reactive alkenes containing an allylsilane moiety, which remains intact during the chemoselective reaction.

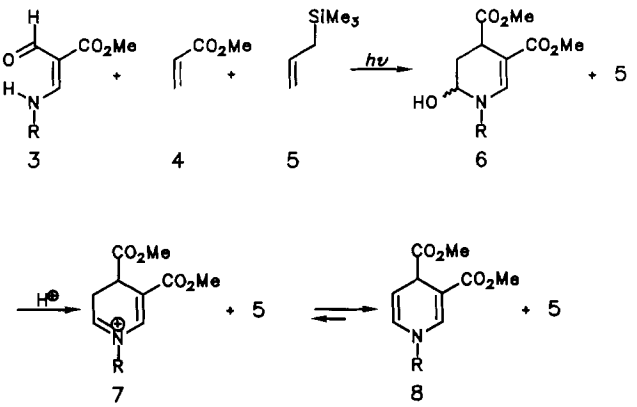

3 4 5 6 7 8

Scheme 1. **3**, **6**–**8**: R = *t*Bu (**a**), H (**b**), CH_3 (**c**), *p*-$MeOC_6H_4CH_2$ (**d**).

The investigations revealed that alkenes with electron-acceptor groups, such as **4**, undergo photochemical cycloaddition much faster than allylsilanes. Thus, irradiation of the enamine carbaldehydes **3** in the presence of a 50-fold excess of methyl acrylate (**4**) and the allylsilane **5** resulted exclusively in chemo- and regioselective formation of the 2-hydroxytetrahydropyridine **6**, which was not isolated but instead treated directly with trifluoroacetic acid to give, via **7**, the 1,4-dihydropyridine **8** in 81% yield (CH_2Cl_2, high-pressure Hg lamp, 500 W, $\lambda > 280$ nm, −40 °C, 18 h). Presumably, **3** and **4** react to form a cyclobutane system,[5] which then gives **6** via several still unknown intermediates.

For the consecutive reactions we used the configurationally uniform alkenes (2 *E*, 6 *Z*)-**13** and (2 *E*, 7 *Z*)-**14**, which are

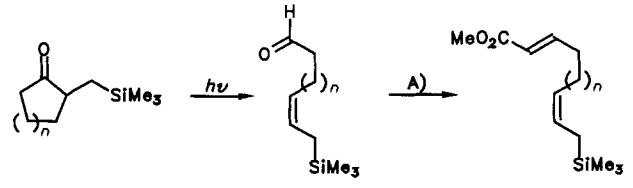

9: $n=1$ **11**: $n=1$ **13**: $n=1$
10: $n=2$ **12**: $n=2$ **14**: $n=2$

Scheme 2. A) = Horner–Wadsworth–Emmons modification of the Wittig reaction.

[*] Prof. Dr. L. F. Tietze, J. R. Wünsch
Institut für Organische Chemie der Universität
Tammannstrasse 2, W-3400 Göttingen (FRG)

[**] This work was supported by the Deutsche Forschungsgemeinschaft (SFB 93) and the Fonds der Chemischen Industrie.
J. R. Wünsch thanks the Fonds for a doctoral fellowship.

easily prepared in 63 and 88 % overall yield, respectively, by photochemical cleavage[6] of **9** and **10** to give **11** and **12**, respectively, followed by the Horner–Wadsworth–Emmons modification of the Wittig reaction[7] (Scheme 2). The configuration of the alkene involved in the photochemical cycloaddition has no influence on the stereoselectivity, because the reaction proceeds via a triplet state.[8].

The photochemical reaction of **3a–d** with a 40- to 50-fold excess of alkene **13** or **14** gives the 2-hydroxytetrahydropyridines **15b–d** or **16b–d**, respectively, which, after chromatographic separation of the excess alkene (column filtration), are transformed into the desired azabicycles **17b–d** or **18b–d**, respectively, by treatment with Brønsted or Lewis acids at −78 °C to −20 °C. The photochemical cycloaddition can also be carried out with a tenfold excess of **13** or **14** if **3a–d** is added in portions during the reaction (no product could be isolated with **3a**). The best yields (44–48 %) in the reaction of **15** were obtained when trifluoroacetic acid in CH_2Cl_2 was used; this also holds for the reaction of **16**, although, in this case, trifluoroacetic acid must be used as the solvent. However, since the esters are thereby partially solvolyzed, reesterification is necessary. This is accomplished, after removal of the trifluoroacetic acid, by refluxing the product in methanol/6 N HCl (5 mol %) for 4 h. The highest yields are obtained in the reaction of **16** (R ≠ H) with tin tetrachloride[8] as promoter in dichloromethane (Table 1).

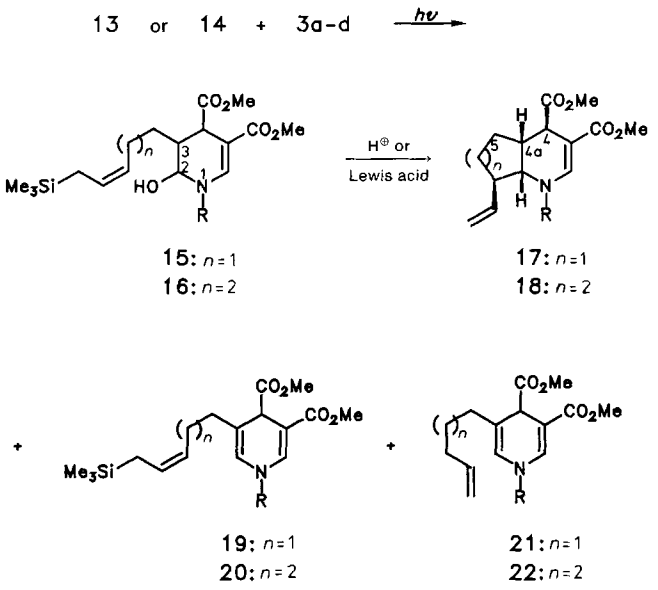

Table 1. Consecutive photochemical cycloaddition and iminium ion–allylsilane cyclization of the enamine carbaldehydes **3a–d** with the alkenes **13** and **14** to give **17** and **18**, respectively.

Enamine carbaldehyde	Alkene	Product	Promoter	Solvent	Overall yield [a]
3d	**13**	**17d**	4 equiv. CF_3COOH	CH_2Cl_2	44
3d	**13**	**17d**	1.1 equiv. Me_3SiOTf	CH_2Cl_2	31
3d	**13**	**17d**	1.1 equiv. Me_2AlCl	CH_2Cl_2	19
3d	**13**	**17d**	1.1 equiv. $TiCl_4$	CH_2Cl_2	9
3d	**13**	**17d**	$NBu_4^{\oplus}F^{\ominus}$	CH_2Cl_2	–
3b	**13**	**17b**	4 equiv. CF_3COOH	CH_2Cl_2	48
3c	**13**	**17c**	–	CF_3COOH	47
3b	**14**	**18b**	–	CF_3COOH	41
3b	**14**	**18b**	1.5 equiv. $SnCl_4$	CH_2Cl_2	26
3c	**14**	**18c**	–	CF_3COOH	45
3c	**14**	**18c**	1.5 equiv. $SnCl_4$	CH_2Cl_2	51
3a	**14**	**18a**	–	CF_3COOH	–
3d	**14**	**18d**	–	CF_3COOH	42
3d	**14**	**18d**	1.5 equiv. $SnCl_4$	CH_2Cl_2	46

[a] Total yield **3** → **17**/**18** [%].

The 1,4-dihydropyridines **19** and **20** and their protodesilylated derivatives **21** and **22** are formed as side products (10–19 %) in all the reactions. In the presence of trifluoroacetic acid it was also possible to cyclize the 1,4-dihydropyridines **19** and **20** to **17** and **18**, respectively. As expected, the reaction of **15** and **19**, as well as of **16** and **20**, with fluoride ions did not lead to the cyclized products **17** and **18**, respectively.

The photocycloaddition–iminium ion–allylsilane sequence proceeds with high diastereoselectivity. Thus, of the eight possible diastereomers, only the configurational isomers **17** or **18** were found in each case. We presume that intramolecular attack of the allylsilane group on C-2 in the iminium ion **23** occurs *anti* to the hydrogen on C-3. This is in accord with stereoelectronic control[10] of the addition. The *trans* arrangement of the substituents in **23** arises either directly in the photochemical cycloaddition and/or via an iminium–enamine isomerization.

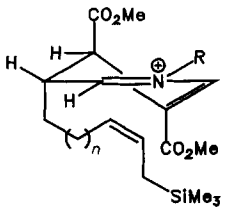

23

The *cis* linkage of the rings in **17** and **18** is revealed by the relatively small coupling constants of $J = 4.0–7.0$ Hz for the 4 a-H and 7 a-H signals and the 4 a-H and 8 a-H signals. The coupling of 7-H and 7 a-H, as well as of 8-H and 8 a-H, has a value of $J = 6.0–9.0$ Hz, that of 4-H and 4 a-H a value of $J = 5.5–9.0$ Hz. These values are only consistent with configurations such as those in **17** and **18**.

Experimental Procedure

A solution of enamine carbaldehyde **3** (1 mmol) and diene **13** or **14** (40–60 mmol) in 150 mL of CH_2Cl_2 was irradiated in a ring photoreactor at −40 °C with a high-pressure Hg lamp (500 W, Hanau) while a stream of argon was bubbled through the reaction solution. After complete conversion, the volatiles were removed under vacuum and the residue was separated from excess diene by flash chromatography on 50 g of basic Al_2O_3 with petroleum ether as eluent. The column was eluted with MeOH, the MeOH was completely removed under vacuum, and the residue was dissolved in 25 mL of CH_2Cl_2. The Brønsted or Lewis acid was then added to this solution at −78 °C, the solution was allowed to warm to 20 °C, the reaction was quenched with a saturated $NaHCO_3$ solution, and the product was purified on silica gel.

17d: ^{1}H NMR (200 MHz, $CDCl_3$, 25 °C): $\delta = 1.39–1.74$ (m, 2 H, 5-H), 1.75–2.06 (m, 2 H, 6-H), 2.21 (m, 1 H, 4 a-H), 2.56 (quin, J (H,H) ≈ 7.0 Hz, 1 H, 7-H), 3.15 (d, J (H,H) = 7.0 Hz, 1 H, 4-H), 3.17 (dd, J (H,H) ≈ 7.0 Hz, 1 H, 7 a-H), 3.67 (s, 3 H, OCH_3), 3.70 (s, 3 H, OCH_3), 3.80 (s, 3 H, Ph-OCH_3), 4.32 (d, J (H,H) = 15.0 Hz, 1 H, 1'-H), 4.46 (d, J, (H,H) = 15.0 Hz, 1 H, 1'-H), 5.02 (ddd, J (H,H) ≈ 10.0 Hz, J (H,H) ≈ 2.0 Hz, J (H,H) = 0.8 Hz, 1 H, 9 a-H), 5.07 (ddd, J (H,H) = 17.0 Hz, J (H,H) = 2.0 Hz, J (H,H) = 0.9 Hz, 1 H, 9 b-H), 5.75 (ddd, J (H,H) = 17.0 Hz, J (H,H) = 10.0 Hz, J (H,H) ≈ 8.0 Hz, 1 H, 8-H), 7.02 (AA'BB', analyzed as AB, $\Delta\nu_{AB} = 54.0$ Hz, J (H,H) ≈ 9.0 Hz, 4 H, Ph-H), 7.65 (d, $J = 0.9$ Hz, 1 H, 2-H). ^{13}C NMR (50.3 MHz, $CDCl_3$, 25 °C): $\delta = 27.54$ (C-5, C-6), 39.30 (C-4 a), 40.58 (C-4), 47.33 (C-7), 50.74 (OCH_3), 51.98 (OCH_3), 55.28 (Ph-OCH_3), 57.22 (C-1'), 61.60 (C-7 a), 92.15 (C-3), 114.2 (2 x C-4'), 115.5 (C-9), 128.4 (C-2'), 128.8 (2 x C-3'), 141.0 (C-8), 146.2 (C-2), 159.3 (C-5'), 168.2 (CO), 175.8 (CO).

18d: ^{1}H NMR (200 MHz, $C_2D_2Cl_4$, 100 °C): $\delta = 1.11–1.76$ (m, 6 H, 5-H, 6-H, 7-H), 2.05 (dddd, J (H,H) = 9.0 Hz, J (H,H) = 8.0 Hz, J (H,H) = 4.5 Hz, J (H,H) = 4.0 Hz, 1 H, 4 a-H), 2.26–2.43 (m, 1 H, 8-H), 2.92 (dd, J (H,H) = 9.0 Hz, J (H,H) = 4.5 Hz, 1 H, 8 a-H), 3.41 (d, J (H,H) = 9.0 Hz, 1 H, 4-H), 3.64 (s, 3 H, OCH_3), 3.67 (s, 3 H, OCH_3), 3.80 (s, 3 H, Ph-OCH_3), 4.29 (s, 2 H, 1'-H), 5.03 (ddd, J (H,H) = 17.0 Hz, J (H,H), = 2.0 Hz, J

(H,H) = 0.9 Hz, 1 H, 10 b-H), 5.07 (ddd, J(H,H) = 10.0 Hz, J(H,H) = 2.0 Hz, J (H,H) = 0.9 Hz, 1 H, 10 a-H), 5.75 (ddd, J (H,H) = 17.0 Hz, J (H,H) = 10.0 Hz, J (H,H) = 8.0 Hz, 1 H, 9-H), 7.02 (AA'BB', analyzed as AB, $\Delta\nu_{AB}$ = 54.0 Hz, J (H,H) = 9.0 Hz, 4 H, Ph-H), 7.54 (m, 1 H, 2-H). ^{13}C NMR (50.3 MHz, $C_2D_2Cl_4$, 100 °C): δ = 19.80* (C-6), 27.71* (C-5), 30.65 (C-7), 35.96 (C-4 a), 40.26 (C-4), 41.24 (C-8), 50.45 (OCH_3), 51.57 (OCH_3), 55.45 (Ph-OCH_3), 58.87 (C-1'), 59.73 (C-8 a), 93.47 (C-3), 114.6 (2 x C-4'), 115.8 (C-10), 128.8 (2 x C-3'), 129.1 (C-2'), 140.4 (C-9), 146.1 (C-2), 159.6 (C-5'), 167.9 (CO), 175.6. The asterisk indicates peaks that are not yet unambiguously assigned.

Received: April 4, 1991 [Z 4551 IE]
Publication delayed at the authors' request
German version: *Angew. Chem. 103* (1991) 1665

CAS Registry numbers:
3a, 93589-90-3; **3b**, 116952-07-9; **3c**, 116952-08-0; **3d**, 136953-20-3; **13**, 136953-19-0; **14**, 136953-18-9; **17b**, 136953-17-8; **17c**, 136953-12-3; **17d**, 136953-11-2; **18a**, 136953-15-6; **18b**, 136953-13-4; **18c**, 136953-14-5; **18d**, 136953-16-7.

[1] L. F. Tietze, M. Bratz, *Chem. Ber. 122* (1989) 997; *Liebigs Ann. Chem.* (1989) 559; S. D. Larsen, P. A. Grieco, *J. Am. Chem. Soc. 107* (1985) 1768; S. F. McCann, L. E. Overman, *ibid. 109* (1987) 6107; G. W. Daub, D. A. Heerding, L. E. Overman, *Tetrahedron 44* (1988) 3919; D. J. Hart, T. K. Yang, *J. Org. Chem. 50* (1985) 235; H. Hiemstra, M. H. A. M. Sno, R. J. Vijn, W. N. Speckamp, *ibid. 50* (1985) 4014; H. Rapoport, *Lect. Heterocycl. Chem. 4* (1978) 47; L. F. Tietze, G. Kinast, *Angew. Chem. 88* (1976) 261; *Angew. Chem. Int. Ed. Engl. 15* (1976) 239.
[2] L. F. Tietze, A. Bergmann, G. Brill, K. Brüggemann, U. Hartfiel, E. Voß, *Chem. Ber. 122* (1989) 83.
[3] L. F. Tietze, A. Bergmann, K. Brüggemann, *Synthesis 1986*, 190; L. F. Tietze, K. Brüggemann, *Angew. Chem. 94* (1982) 550; *Angew. Chem. Int. Ed. Engl. 21* (1982) 539; L. F. Tietze, A. Bergmann, *ibid. 97* (1985) 135 and *24* (1985) 127.
[4] A. Sausins, G. Duburs, *Heterocycles 27* (1988) 269; *ibid. 27* (1988) 291; D. M. Stout, A. I. Meyers, *Chem. Rev. 82* (1982) 223; F. Bossert, H. Meyer, E. Wehinger, *Angew. Chem. 93* (1981) 755; *Angew. Chem. Int. Ed. Engl. 20* (1981) 762.
[5] J. D. Winkler, P. M. Hershberger, *J. Am. Chem. Soc. 111* (1989) 4852.
[6] L. F. Tietze, M. Ruther, *Chem. Ber. 123* (1990) 1387; L. F. Tietze, J. R. Wünsch, *Synthesis 1990*, 985, 1204.
[7] M. W. Rathke, M. Nowak, *J. Org. Chem. 50* (1985) 2624.
[8] L. F. Tietze, K. Brüggemann, unpublished results.
[9] R. P. Polniaszek, S. E. Belmont, R. Alvarez, *J. Org. Chem. 55* (1990) 215; D. Schinzer (Ed.): *Selectivities in Lewis Acid Promoted Reactions*, Kluwer, Dordrecht 1989.
[10] P. Deslongchamps: *Stereoelectronic Effects in Organic Chemistry*, Pergamon, Oxford 1986.

Three- and Fourfold Bridgehead-Substituted Tribenzotriquinacenes**

By *Andreas Schuster* and *Dietmar Kuck**

Dedicated to Professor Michael Hanack on the occasion of his 60th birthday

The threefold benzo-stabilized triquinacene **1**, one of the three prototypic centrotriindanes, provides, in contrast to the parent compound, an opportunity to study reactions at the four bridgehead positions through the formation of stable, well-crystallizing compounds. As we were recently able to show in collaboration with *de Meijere* et al.,[2] the threefold benzoannelation in the case of **1** also contributes considerably to the stabilization of anionic and olefinic derivatives of this system. We now present the particularly stable olefin **3**, which is readily accessible from **1** and which affords a variety of novel bridgehead-substituted tribenzotriquinacenes in some, in part, unusual reactions.

The tribenzoquinacene **1** is accessible via two routes[2, 3] and, despite its extremely poor solubility, can be converted almost quantitatively into the C_{3v} symmetrically substituted tribromo derivative **2** (Scheme 1). Aminolysis of **2** with dimethylamine affords the tribenzodihydroacepentalene **3**, also in high yields. In contrast to the analogously prepared dihydroacepentalenes,[6] crystalline **3** is absolutely air-stable—a remarkable property in view of the two strongly pyramidalized olefinic atoms C1 and C10.[7, 8] The analogous bis(trimethylsilyl) compound is likewise accessible from **1**, but is far less stable than **3**.[2, 9]

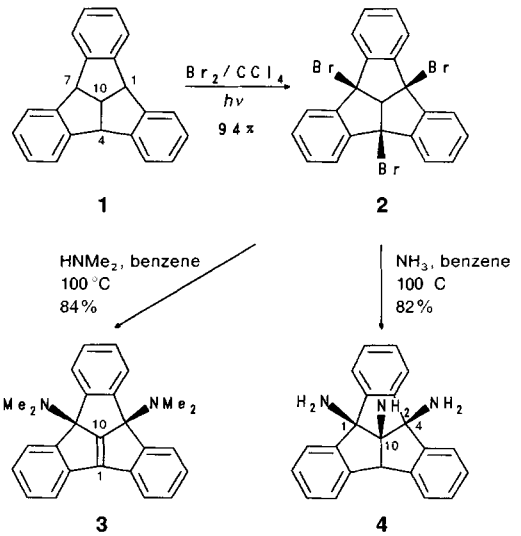

Scheme 1. Syntheses starting from tribenzotriquinacene **1**

Surprisingly, *ammonolysis* of **2** leads to the triamino compound **4** with C_s symmetric substitution. The constitution of this compound, which is also obtainable in good yields, is unequivocally confirmed by its NMR spectrum (Table 1). The 1,4,10-triamine is thus the first triquinacene with heterosubstitution at the central bridgehead to be obtained in a direct synthesis.[10, 11] Attempts to explain the unexpected reaction of **2** with ammonia by further experiments were hitherto not very successful.[12] The intermediary analogue of **3** (H instead of Me, **3'**) is, in contrast to **3**, apparently not sufficiently kinetically stabilized.[13]

Two of the reactions of **3** carried out with 1,3-dipolar agents deserve special mention, namely those with azides (Scheme 2). **3** reacts smoothly with phenyl azide to give the regioisomer **9**, a triquinacene substituted by nitrogen at all four bridgehead atoms. Presumably, steric factors are mainly responsible here for the high regioselectivity. On the other hand, with trimethylsilyl azide we could not isolate the expected cycloaddition products, despite all measures to exclude moisture. Instead the 1-azido-4,7-bis(dimethylamino) derivative **6** was obtained in good yields, once again as a well-crystallizing compound. The NMR data and thermolysis results indicate that the three outer bridgehead atoms carry substituents (Table 1);[14] conclusive chemical proof (Scheme 2) was provided by the reduction of **6** with $LiAlH_4$ to give **7**, and the subsequent methylation according to *Eschweiler* and *Clarke* to give 1,4,7-tris(dimethylamino)tribenzotriquinacene **8**, whose C_{3v} symmetric constitution unambiguously followed from the ^{1}H and ^{13}C NMR spectra (Table 1).

[*] Dr. D. Kuck, Dr. A. Schuster
Fakultät für Chemie der Universität
Universitätsstrasse 25, W-4800 Bielefeld 1 (FRG)

[**] Benzoannelated Centropolyquinanes, Part 10. This work was supported by the Deutsche Forschungsgemeinschaft.—Part 9: D. Kuck, A. Schuster, R. A. Krause, *J. Org. Chem. 56* (1991) 3472–3495.

A number of fourfold heterosubstituted tribenzotriquinacenes can be prepared from the olefin **3**. Thus **3** reacts at low temperatures with bromine to give the dibromide **10** (Scheme 2), which can be converted as expected with dimethylamine into the, once again, C_{3v} symmetric 10-bromo-1,4,7-tris(dimethylamino)tribenzotriquinacene **11**. All attempts at the solvolysis of the C10–Br bond have so far failed.[15]

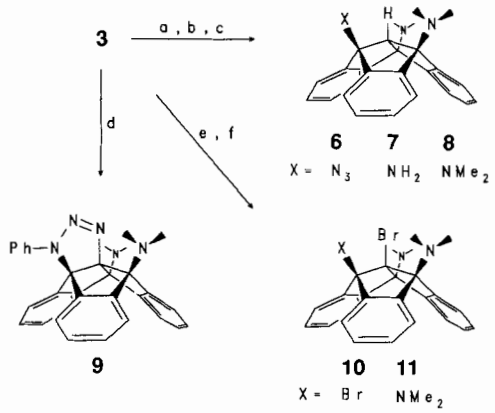

Schema 2. a) Me_3SiN_3/CH_2Cl_2, room temperature, 1 d (76 % **6**); b) $LiAlH_4$/THF, RT, 6 h (96 % **7**); c) $HCO_2H/CH_2O/H_2O$, 130 °C, 2 h (80 % **8**); d) PhN_3/CH_2Cl_2, RT, 1 d (94 % **9**); e) Br_2/CH_2Cl_2, −60 °C, addition over 6 h (85 % **10**); f) $HNMe_2/C_6H_6$, 100 °C, 1 d (54 % **11**).

Furthermore, we found an unexpected direct entry to 1,10-cyclopropa-annelated tribenzoquinacenes starting from **3**. Cyclopropatriquinacenes of type **15** are to our knowledge unknown so far; but several saturated derivatives have, however, been synthesized very recently from the dodecahedrane series.[16, 17] It therefore seemed interesting to check whether *tribenzo*triquinacene analogues are stable compounds despite the conjugation of the central cyclopropane ring with two π systems.[18]

The olefin **3** adds diazomethane and 2-diazopropane quantitatively with formation of the tetracyclic dihydropyrazoles **12** and **13**, respectively (Scheme 3). The similarly high yields and the almost identical NMR chemical shifts of the three *N*-substituted bridgehead atoms point to the same constitution of the two tetracyclic frameworks. Since considerable steric hindrance is assumed for the diazopropane adduct with a $C(CH_3)_2$ substituent on C10, **12** and **13** are assigned the structures shown, with a centro-N=N group.

Irradiation of a suspension of **12** in cyclohexane at room temperature (quartz filter) leads with complete deamination to the tetracycle **14**. Actually the product is formed in only 18 % yield, together with large amounts of polymeric material, but it can be isolated in pure form by medium pressure chromatography (MPLC) and slow crystallization. Surprisingly, it is very soluble compared to many other triben-

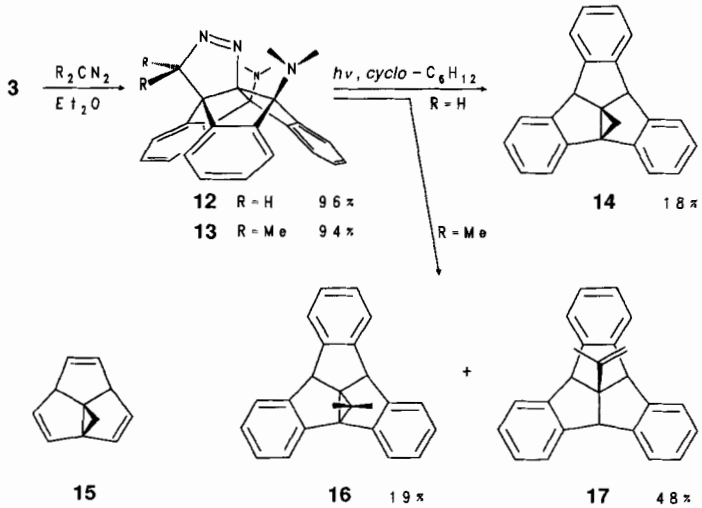

Scheme 3. Synthesis of cyclopropatriquinacenes.

Table 1. Physical data of selected compounds [IR(KBr), ^1H NMR ($CDCl_3$, 300 MHz), ^{13}C NMR ($CDCl_3$, 75 MHz), MS (EI, 70 eV)].

2: IR: $\tilde{\nu}$[cm^{-1}] = 3083, 3066, 3014, 1469, 1460, 1273, 1207; ^1H NMR: 3 AA'BB' spin systems δ_A = 7.68 (6 H), δ_B = 7.37 (6 H), δ = 5.58 (s, 1 H); ^{13}C NMR: δ = 143.6 (s), 130.6 (d), 125.1 (d), 89.2 (d), 67.1 (s); MS: *m/z* 435, 437, 439 ([*M* − Br]$^{\oplus}$; 51, 95, 51), 277 (78), 276 (68), 274 (21), 138 (100), 137 (33)

3: IR: $\tilde{\nu}$[cm^{-1}] = 3059, 2977, 2964, 2852, 2827, 2818, 1466, 1459, 1272, 1056; ^1H NMR: δ = 7.87 (d, 2 H, ^3J = 6.1 Hz), 7.57 (d, 2 H, ^3J = 6.4 Hz), AA'BB' spin system δ_a = 7.43 (2 H), δ_B = 7.20 (2 H), δ = 7.32–7.28 (m, 4 H), 2.56 (s, 12 H); ^{13}C NMR: δ = 164.1 (s), 154.4 (s), 153.8 (s), 144.1 (s), 139.3 (s), 127.8 (d), 126.7 (d), 126.6 (d), 124.8 (d), 122.2 (d), 78.2 (s), 41.5 (CH_3); MS: *m/z* 364 (*M*$^{\oplus}$, 1), 321 (14), 319 (8), 277 (26), 276 (100), 159 (2), 138 (9)

4: IR: $\tilde{\nu}$[cm^{-1}] = 3645, 3316 (br), 3064, 3025, 2872, 1476, 1453, 1219; ^1H NMR: δ = 7.64 (d, 2 H, ^3J = 6.8 Hz), AA'BB' spin system δ_A = 7.59 (2 H), $\delta_B \approx$ 7.25 (2 H, masked), δ = 7.40 (d, 2 H, ^3J = 6.7 Hz), 7.29–7.21 (m, 4 H), 4.48 (s, 1 H), 1.87 (br.s, 6 H, NH_2); ^{13}C NMR: δ = 148.1 (s), 146.7 (s), 142.0 (s), 129.0 (d), 128.7 (d), 128.1 (d), 124.1 (d), 123.9 (d), 83.3 (s), 75.2 (s), 64.0 (d); MS: *m/z* 325 (*M*$^{\oplus}$, 57), 308 (69), 307 (33), 291 (100), 280 (22), 265 (18), 231 (10)

6: Colorless crystals, m.p. 203–208 °C (from CH_2Cl_2/MeOH); IR: $\tilde{\nu}$[cm^{-1}] = 3073, 3034, 2984, 2950, 2861, 2821, 2091 (N_3), 1476, 1454, 1242, 1235, 1225; ^1H NMR: masked AA'BB' and ABCD spin systems δ = 7.63–7.59 (m, 2 H), 7.58–7.55 (m, 2 H), 7.53–7.50 (m, 2 H), 7.32–7.28 (m, 6 H), 4.32 (s, 1 H, 10-H), 2.26 (s, 12 H, CH_3); ^{13}C NMR: δ = 146.3 (s), 144.8 (s), 142.6 (s), 129.7 (d), 129.1 (d), 124.7 (d), 124.5 (d), 123.3 (d), 83.7 (s), 80.6 (s), 55.3 (d), 41.0 (CH_3); MS: *m/z* 407 (*M*$^{\oplus}$, 2), 364 (20), 362 (24), 319 (62), 291 (100), 290 (88), 276 (13)

8: IR: $\tilde{\nu}$[cm^{-1}] = 3069, 3030, 2988, 2930, 2817, 2781, 1474, 1452, 1228, 1060, 1011, 769; ^1H NMR: 3 AA'BB' spin systems δ_A = 7.53 (6 H), δ_B = 7.22 (6 H), δ = 4.37 (s, 1 H, 10-H), 2.35 (s, 18 H, CH_3); ^{13}C NMR: δ = 145.9 (s), 128.6 (d), 124.2 (d), 83.9 (s), 41.7 (CH_3); the signal for C10 presumably lies at δ = 77.8; MS (EI, 70 eV): *m/z* 409 (*M*$^{\oplus}$, 2), 365 (37), 364 (48), 321 (100), 320 (34), 277 (36), 276 (59), 160.5 (11), 138 (15)

9: IR: $\tilde{\nu}$[cm^{-1}] = 3089, 3067, 3029, 3005, 2986, 2940, 2875, 2840, 1596, 1488, 1473, 1462, 1270, 1224, 1003; ^1H NMR: δ = 7.57 (d, 2 H, ^3J = 7.9 Hz), AA'BB' spin system δ_A = 7.54 (2 H), $\delta_B \approx$ 7.30 (2 H), δ = 7.43 (d, 2 H, ^3J = 7.6 Hz), 7.39–7.23 (m, 5 H), 7.14 (s, 4 H), 2.83 (s, 6 H, CH_3), 2.37 (s, 6 H, CH_3); ^{13}C NMR: δ = 146.8 (s), 144.4 (s), 140.6 (s), 140.4 (s), 129.4 (d), 129.3 (d), 129.1 (d), 128.7 (d), 127.3 (d), 126.5 (d), 125.4 (d), 124.6 (d), 124.3 (d), 117.0 (s), 86.9 (s), 83.1 (s), 41.1 (CH_3), 39.7 (CH_3); MS: *m/z* 483 (*M*$^{\oplus}$, 5), 411 (16), 378 (100), 367 (84), 335 (40), 320 (20), 290 (24), 276 (49), 183.5 (7); UV/VIS (*n*-heptane, $c = 1.25 \times 10^{-4}$ M): λ_{max}[nm] (ε) = 295 (6280), 276 (8130), 268 (9180)

11: IR: $\tilde{\nu}$[cm^{-1}] = 3075, 3031, 2980, 2927, 2884, 2800, 1473, 1453, 1259, 1205, 1065, 757; ^1H NMR: 3 AA'BB' spin system δ_A = 7.42 (6 H), δ_B = 7.19 (6 H), δ = 2.73 (18 H, N-CH_3); ^{13}C NMR: δ = ca. 144 (s), 128.5 (d), 125.1 (d), 113.0 (s), 86.0 (s), 40.0 (CH_3); MS: *m/z* 487, 489 (*M*$^{\oplus}$; 16, 16), 443, 445 (21,20), 363 (10), 320 (23), 278 (17), 277 (21), 276 (53), 58 (100)

14: IR: $\tilde{\nu}$[cm^{-1}] = 3065, 3036, 3010, 2888, 1473, 1455, 1254, 1100, 755, 733; ^1H NMR: δ = 7.63–7.60 (m, 2 H), 7.53–7.50 (m, 2 H), 7.43–7.40 (m, 2 H), 7.21–7.14 (m, 6 H), 4.67 (s, 2 H), 1.69 (s, 2 H, CH_2); ^{13}C NMR: δ = 149.7 (s), 145.0 (s), 144.4 (s), 127.1 (d), 126.7 (d), 125.2 (d), 124.9 (d), 124.6 (d), 124.2 (d), 53.9 (d), 46.9 (s), 41.5 (s), 29.5 (t, CH_2); MS: *m/z* 292 (*M*$^{\oplus}$, 100), 291 (49), 289 (28), 280 (15), 276 (14), 215 (8), 146 (4), 138 (12); UV/VIS (*n*-heptane, $c = 4.45 \times 10^{-5}$ M): λ_{max}[nm] (ε) = 277 (2670), 270.5 (2760), ca. 264 (1800)

16: IR: $\tilde{\nu}$[cm^{-1}] = 3065, 3035, 3015, 2978, 2927, 2873, 1475, 1464, 1455, 752, 737, 721; ^1H NMR: AA'BB' spin system δ_A = 7.53 (2 H), $\delta_B \approx$ 7.15 (2 H, masked), δ = 7.43–7.40 (m, 4 H), 7.18–7.12 (m, 4 H), 4.52 (s, 2 H), 1.06 (s, 6 H); ^{13}C NMR: δ = 151.6 (s), 144.9 (s), 143.3 (s), 127.1 (d), 127.0 (d), 126.6 (d), 125.4 (d), 124.5 (d), 123.7 (d), 56.2 (s), 52.6 (d), 51.7 (s), 34.8 (s), 18.7 (CH_3); MS: *m/z* 320 (*M*$^{\oplus}$, 100), 305 (55), 289 (22), 279 (27), 278 (21), 277 (20), 276 (26), 178 (7), 144.5 (11), 138 (13); UV/VIS (*n*-heptane, $c = 5.0 \times 10^{-5}$ M): λ_{max}[nm] (ε) = 277 (3000), 270.5 (2740), ca. 264 (1920)

17: IR: $\tilde{\nu}$[cm^{-1}] = 3065, 3027, 2986, 2974, 2927, 1633, 1485, 1476, 1456, 1375, 875, 753, 733; ^1H NMR: 3 AA'BB' spin systems δ_A = 7.45 (6 H), δ_B = 7.18 (6 H), δ = 5.05 (s, 1 H), 4.92 (s, 3 H), 4.87 (s, 1 H), 1.90 (s, 3 H, CH_3); ^{13}C NMR: δ = 148.3 (s), 145.0 (s), 127.5 (d), 124.1 (d), 108.1 (t), 70.2 (s), 60.6 (d), 20.1 (CH_3); MS: *m/z* 320 (*M*$^{\oplus}$, 100), 305 (44), 290 (10), 289 (15), 279 (16), 278 (27), 277 (18), 276 (23), 178 (11), 145 (11) 138 (14)

zotriquinacenes.[2-5] The ^{1}H NMR, ^{13}C NMR, and mass spectra unequivocally confirm the structure of **14** (Table 1).

Under the same conditions the diazopropane adduct **13** furnishes the tetracycle **16** in 19% yield; the main product, however, is the ring-opened 10-(propen-2-yl)tribenzotriquinacene **17**. Also these two compounds are spectroscopically unambiguously identifiable (Table 1) and like **14** are very stable in crystalline form. **17** is the first triquinacene with an unsaturated substituent on the central C atom and ought to be convertible into further, interesting C10-substituted tribenzotriquinacenes.[4, 5, 19]

The photolytic deamination of the cycloadducts **12** and **13** is surprising.[20] In the tribenzotriquinacenes this process is possibly facilitated by radicals generated in the course of the deazotization and is additionally favored by the formation of highly conjugated isoindene intermediates. Also consistent with this hypothesis is the ring-opening of **13** to give **17**.

The diaminoolefin **3** and the bridgehead-substituted tribenzotriquinacenes presented here for the first time prompt further investigations. Thus, the strictly ecliptic orientation of up to four vicinal substituents on the convex side of the molecule with the rigid triquinacene framework could lead to concerted dipolar interactions. The consequences of the particular stereochemistry of such highly functionalized spherical molecules for structure and reactivity should be studied in more detail.

Experimental Procedure for Selected Compounds

2: A suspension of tribenzotriquinacene **1** (560 mg, 2.00 mmol) in tetrachloromethane (100 mL) was treated dropwise at 50 °C with 6.00 mL of a 1.0 M solution of bromine in tetrachloromethane (6.00 mmol). The suspension was additionally irradiated with a photolamp (500 W). After very rapid uptake of the bromine (effervescence!), the solvent was removed and the yellow-brown residue recrystallized from toluene. **2** (970 mg; 94%) was obtained in the form of brownish platelets; m.p. 320–325 °C (decomp.).

3: **2** (517 mg, 1.00 mmol) was frozen in anhydrous benzene (10 mL) in a test tube (180 mm × 22 mm) containing a small stirring rod. Dimethylamine (20 mL) was condensed into the tube which was then placed in a steel autoclave (190 mm × 26 mm, Roth); the autoclave was sealed tight and the reaction mixture stirred magnetically in an oil bath at 100 °C for 20 h. After the reaction mixture cooled, the excess amine was removed and the contents of the test tube were diluted with 20 mL of dichloromethane and 20 mL of water. After extractive workup with CH_2Cl_2, drying with Na_2SO_4, and removal of the solvent, a light-brown crystalline residue was obtained, which upon recrystallization from CH_2Cl_2/MeOH afforded 305 mg (84%) of **3** in the form of colorless needles; m.p. 231 °C.

4: As described for **3**, **2** (517 mg, 1.00 mmol) was allowed to react in benzene (precooled to −40 °C) with liquid ammonia (10 mL) in a sealed tube. After workup and recrystallization from CH_2Cl_2/*n*-heptane **4** (266 mg, 82%) was obtained in the form of very fine, colorless needles; m.p. 248 °C (decomp.).

9: A solution of **3** (364 mg, 1.00 mmol) in dichloromethane (10 mL) was treated with phenyl azide (300 mg, 2.50 mmol) and the mixture stirred for 24 h at room temperature. Methanol was then added and the solution slowly evaporated down in a rotary evaporator until crystallization started. **5** (514 mg, 94%) was obtained in the form of colorless crystals; m.p. 251 °C.

10: To a solution of **3** (364 mg, 1.00 mmol) in anhydrous dichloromethane precooled to −60 °C was added dropwise a 50.0 mM solution of bromine (1.00 mmol) in dichloromethane (20 mL) over 6 h using a fine-bore dropping funnel. After warming to room temperature, the suspension was evaporated down in vacuo to a volume of 10 mL and treated with an equal amount of anhydrous ethyl acetate. The precipitated crystals were recovered by suction and recrystallized from CH_2Cl_2/EtOAc. **10** (445 mg; 85%) was obtained in the form of yellow crystals; m.p. 216 °C (decomp.).

11: Aminolysis of **10** (131 mg, 250 mmol), analogously to the reaction of **2** with dimethylamine, afforded a crude product, which, after recrystallization from CH_2Cl_2/MeOH, furnished **11** (65 mg; 54%) in the form of colorless crystals; m.p. 278 °C (decomp.).

14, **16**, and **17**: The cycloadducts **12** (m.p. 272 °C) and **13** (m.p. 330 °C) were obtained from **3** by standard methods.—Photolysis: In a falling film photoreactor (Normag, 400 mL volume, quartz glass cooling and immersion tubes, Hanau T 718Z1, 500 W mercury vapor lamp) a suspension of 500 μmol of **12** (204 mg) or **13** (217 mg) in 350 mL of cyclohexane (Uvasol, Merck) was purged of dissolved oxygen by passage of nitrogen for 10 min. After tempering to 20 °C, the photoreaction was started; after about 10 min the reaction mixture clarified, and after a further 40 min a renewed yellowish clouding was observed. Optimal yields were achieved after radiation for 90 min. The reaction mixture was evaporated to dryness in a rotary evaporator.—Isolation of **14**: The yellow residue was taken up in a little dichloromethane and filtered through silical gel. Finally, the nonpolar components (hydrocarbons) were isolated by MPLC (LiChroprep Si60, 40–60 μm, Merck, *n*-hexane/dichloromethane 4/1) as a yellow oil. Subsequent vapor-diffusion crystallization furnished up to 26 mg of **14** (18%) in the form of very fine needles; m.p. 272 °C.—Isolation of **16** and **17**: The yellow residue was taken up in a little dichloromethane and filtered with dichloromethane/*n*-hexane (1/1) through silica gel. The mixture of isomers (MS; 120 mg, 75%) was separated by MPLC with *n*-hexane/dichloromethane (5/1): 30 mg (19%) of **16** was obtained in the form of colorless crystals (m.p. 242 °C) and 76 mg (48%) of **17** as colorless needles (m.p. 161 °C).—All the new compounds gave satisfactory elemental analyses.

Received: June 21, 1991;
Revised: September 12, 1991 [Z 4739, 4740 IE]
German version: *Angew. Chem. 103* (1991) 1717

CAS Registry numbers:
1, 120022-86-8; **2**, 137041-65-7; **3**, 137041-66-8; **4**, 137041-67-9; **6**, 137041-68-0; **7**, 137041-69-1; **8**, 137041-70-4; **9**, 137041-71-5; **10**, 137041-72-6; **11**, 137041-73-7; **12**, 137041-74-8; **13**, 137041-75-9; **14**, 137041-76-0; **16**, 137041-77-1; **17**, 137041-78-2; phenyl azide, 622-37-7; trimethylsilyl azide, 4648-54-8; diazomethane, 334-88-3; 2-diazopropane, 2684-60-8.

[1] D. Kuck in I. Hargittai (Ed.): *Quasicrystals, Networks, and Molecules of Fivefold Symmetry*, VCH Publishers, New York 1990, Chap. 19.
[2] D. Kuck, A. Schuster, B. Ohlhorst, V. Sinnwell, A. de Meijere, *Angew. Chem. 101* (1989) 626–628; *Angew. Chem. Int. Ed. Engl. 28* (1989) 595–597.
[3] D. Kuck, T. Lindenthal, A. Schuster, unpublished.
[4] The 10-methyl- and 10-ethyl-substituted tribenzotriquinacenes [3,5] are also readily substitutable threefold at the peripheral bridgehead atoms: A. Schuster, *Dissertation*, Universität Bielefeld 1991.
[5] D. Kuck, *Angew. Chem. 96* (1984) 515–516; *Angew. Chem. Int. Ed. Engl. 23* (1984) 508–509.
[6] a) H. Butenschön, A. de Meijere, *Tetrahedron Lett. 25* (1984) 1693–1696; b) *Helv. Chim. Acta 68* (1985) 1658–1669; c) H. Butenschön, *Dissertation*, Universität Hamburg 1983.
[7] Review of pyramidalized olefins: a) W. T. Borden, *Chem. Rev. 89* (1989) 1095–1109; b) P. M. Warner, *ibid. 89* (1989) 1067–1093; c) W. Luef, R. Keese, *Top. Stereochem. 20* (1991) 231–318; d) R. P. Johnson in J. F. Liebman, A. Greenberg (Eds.): *Molecular Structure and Energetics, Vol. 3*, VCH Publishers, Deerfield Beach 1986, Chap. 3; e) G. Szeimies in R. Abramovitch (Ed.): *Reactive Intermediates, Vol. 3*, Plenum, New York 1983, Chap. 5; f) A. Greenberg, J. F. Liebman: *Strained Organic Molecules*, Academic Press, New York 1978, Chap. 3.
[8] According to force field calculations (MM2 (87)) the pyramidalization angles [7a] in **3** are Φ(C1) = 39.3° and Φ(C10) = 40.6°.
[9] B. Ohlhorst, *Dissertation*, Universität Hamburg 1989.
[10] Perchlorotriquinacenes have already been described: a) I. T. Jacobsen, *Acta Chem. Scand. 21* (1967) 2235–2246; b) *ibid. 26* (1972) 2477–2493; c) *Chem. Scr. 5* (1974) 174–192.
[11] a) P. Bischof, *Angew. Chem. 88* (1976) 609–610; *Angew. Chem. Int. Ed. Engl. 15* (1976) 556; b) L. A. Paquette, S. V. Ley, S. Maiorana, D. F. Schneider, M. J. Broadhurst, R. A. Boogs, *J. Am. Chem. Soc. 97* (1975) 4658–4667; c) R. C. Bingham, P. von R. Schleyer, *ibid. 93* (1971) 3189–3199; d) L. A. Paquette, *Top. Curr. Chem. 79* (1979) 41–165.
[12] Attempts to add NH_3 to **3** in NH_4Cl/NH_3 were unsuccessful [4].
[13] We presume that **3'** forms a chelate complex **5** with $NH_4^{\oplus}$, in which the ammonium proton orientated to the 1,10 double bond attacks electrophilically at C1.

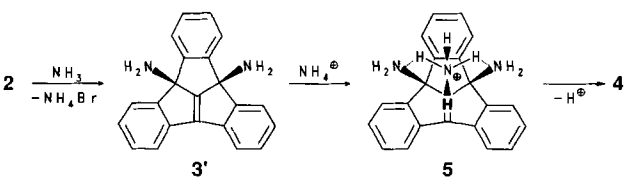

[14] D. Kuck, A. Schuster, unpublished.
[15] No reaction was observed upon heating **11** with NH_3/benzene in an autoclave at 100 °C and with KOH/triethyleneglycol up to 120 °C.
[16] a) L. A. Paquette, T. Kobayashi, J. C. Gallucci, *J. Am. Chem. Soc. 110* (1988) 1305–1307; b) L. A. Paquette, T. Kobayashi, M. A. Kesselmayr, J. C. Gallucci, *J. Org. Chem. 54* (1989) 2921–2930.
[17] a) R. Pinkos, J.-P. Melder, H. Fritz, H. Prinzbach, *Angew. Chem. 102* (1990) 102–105; *Angew. Chem. Int. Ed. Engl. 29* (1990) 92; b) J.-P. Melder, R. Pinkos, H. Fritz, H. Prinzbach, *ibid. 102* (1990) 105–109 and *29* (1990) 95.

[18] The *increase* in reactivity of centropolyquinanes by benzoannelation has already been reported: a) see Ref. [2], b) B. Paisdor, D. Kuck, *J. Org. Chem. 56* (1991) 4753–4759.

[19] C10-substituted triquinacenes: a) A. K. Gupta, G. S. Lannoye, G. Kubiak, J. Schkeryantz, S. Wehrli, J. M. Cook, *J. Am. Chem. Soc. 111* (1989) 2169–2179; b) A. K. Gupta, J. M. Cook, U. Weiss, *Tetrahedron Lett. 29* (1988) 2535–2538; c) X. Fu, J. M. Cook, *ibid. 31* (1990) 3409–3412; d) B. Bengtson, *Dissertation*, Universität Hamburg 1986.

[20] Similar reductive C–N cleavages have been observed in the photolytic decomposition of simple alkylamines: a) M. Mousson-Canet. J. C. Mani: *Photochemistry and Molecular Reactions*, Israel Program for Scientific Translations, Jerusalem 1972, p. 76; b) H. Dürr, W. Bujnoch, H. Kober, *Methoden Org. Chem. (Houben Weyl) 4th ed 1952–*, Vol.4/5b, p. 1076.

1,3-Dipolar Cycloaddition as the Key Reaction in the Synthesis of Potent Renin Inhibitors

By *Günter Benz,* Rolf Henning,* and *Johannes-Peter Stasch*

Dedicated to Professor Karl Heinz Büchel on the occasion of his 60th birthday

The renin–angiotensin system plays a central role in the pathogenesis of hypertension, mostly via the circulating vasoconstrictor angiotensin II. Although Angiotensin-Converting Enzyme Inhibitors (ACE Inhibitors) like captopril and enalapril[1] have already been introduced to therapy, emphasis has been directed toward renin inhibitors in recent years because of their supposedly better selectivity.[2] This increased interest has spurred synthetic work.

The most important reaction of renin is the proteolysis of the *N*-terminus of the globular protein angiotensinogen to the decapeptide angiotensin I. If the Leu-Val peptide bond in **1** cleaved in this reaction is replaced by an (*S*)-hydroxyethylene amide bond surrogate, renin inhibitors of the type **2** are obtained.[3] Because these molecules resemble the transition state for cleavage by aspartyl proteases they possess a high affinity for renin[4] but are not cleavable by the enzyme. Many renin inhibitors are rapidly degradated in vivo. This proteolysis should be hampered when the *C*-terminal amide bond is inverted. For this reason we propose renin inhibitors of the type **3** which has both modifications—the inverted peptide bond and the hydroxyethylene unit. To maintain the topology of the peptide chain the adjacent amino acid must have the D-configuration.

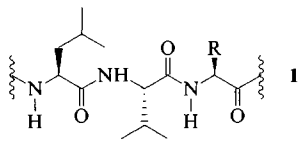

1

Leu Val

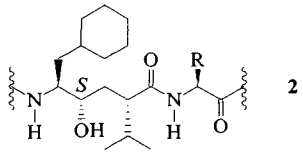

2

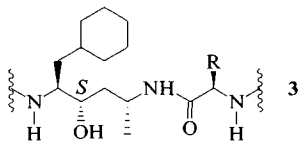

3

The 1,3-dipolar cycloaddition of allylamines with *N*-benzylnitrones[5] provides an easy access to this type of structure in which two stereocenters are generated early in the reaction sequence. The stereochemical course of the reaction can be influenced either by chiral nitrones[6] or by chiral allylamines.[7] The synthesis of the isoxazolidines and a potent renin inhibitor **14** is shown in Scheme 1.[8].

N-Boc-allylamine **4**[9] was prepared in four steps from *N*-Boc-phenylalanine. The subsequent reaction with benzylnitrone **5** at 140 °C in mesitylene led after 8 h to a mixture of four diastereomeric isoxazolidines **7**, in the ratio **7a** (1*R*, 3*S*, 4*S*) 0.75, **7b** (1*S*, 3*S*, 4*S*) 1.00, **7c** (1*S*, 3*R*, 4*S*) 0.60, **7d** (1*R*,

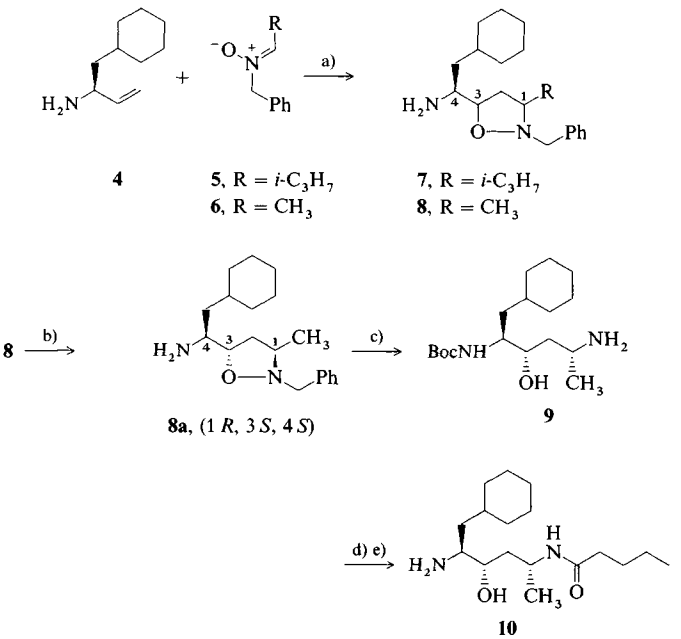

4 **5**, R = *i*-C_3H_7; **6**, R = CH_3 **7**, R = *i*-C_3H_7; **8**, R = CH_3

8a, (1*R*, 3*S*, 4*S*) **9** **10**

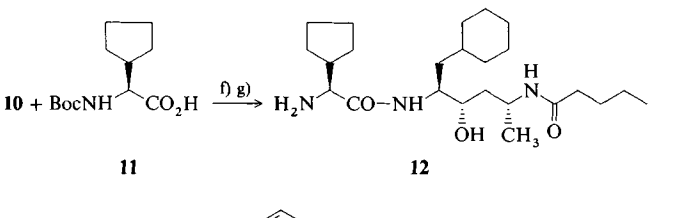

11 **12**

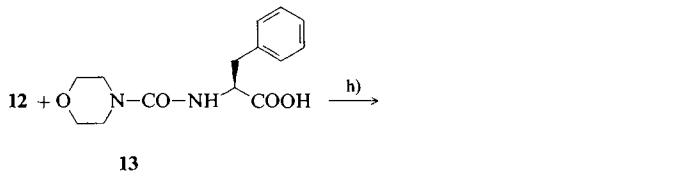

13

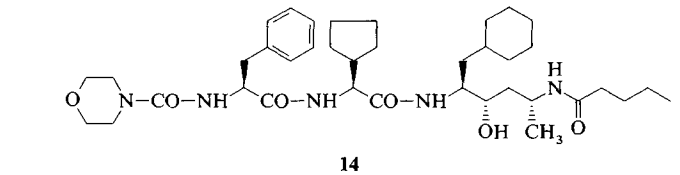

14

Scheme 1. a) Mesitylene, 140 °C, 8 h, 52% **7**; b) SiO_2, chromatography, *n*-hexane/ether 7:3; c) $NH_4^+HCO_2^-$, 10% Pd/C, CH_3OH, reflux, 60 min; d) $(n\text{-}C_4H_9CO)_2O$, NEt_3, CH_3OH; e) 4 N HCl, dioxane, 30 min; f) (*S*)-cyclopentylglycine **11**, dicyclohexylcarbodiimide (DCC), hydroxybenzotriazole (HOBT), diisopropylethylamine (DIPEA); g) 4 N HCl, dioxane, 30 min; h) morpholinocarbonyl-Phe **13**, DCC, HOBT, DIPEA.

[*] Dr. G. Benz
Miles Research Center, Department of Chemistry
400 Morgan Lane, West Haven, CT 06516-4175 (USA)
Dr. R. Henning, Dr. J.-P. Stasch
Bayer AG, PH-FE
Postfach 10 17 09, W-5600 Wuppertal 1 (FRG)

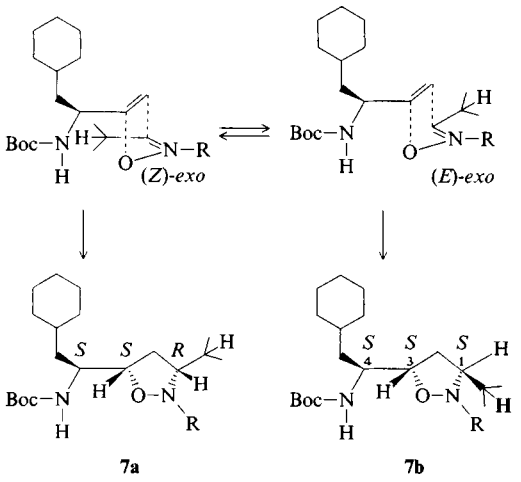

Scheme 2.

3*R*, 4*S*) 0.64 (HPLC analysis). Because of the allylic stereocenter, the attachment of the nitrone should be directed from the less hindered *Si* side. The variation of solvent (toluene, dimethoxyethane, dimethyl sulfoxide, dimethylformamide), temperature (40 °C–140 °C), and reaction time (30 min to 48 h) did not improve the stereoselectivity.

The generation of the preferred diastereomer **7b** is explained by an (*E*)-*exo* transition state (Scheme 2). The ground state *Z*-configured nitrones equilibrate to *E*-nitrones at higher temperatures[10] depending on substituents and solvent and react under kinetic control from the *exo* side. The configurations of the four diastereomers **7a–d** could be determined easily from the cyclic derivatives **17**[11] and **18** by NMR experiments (Scheme 3).

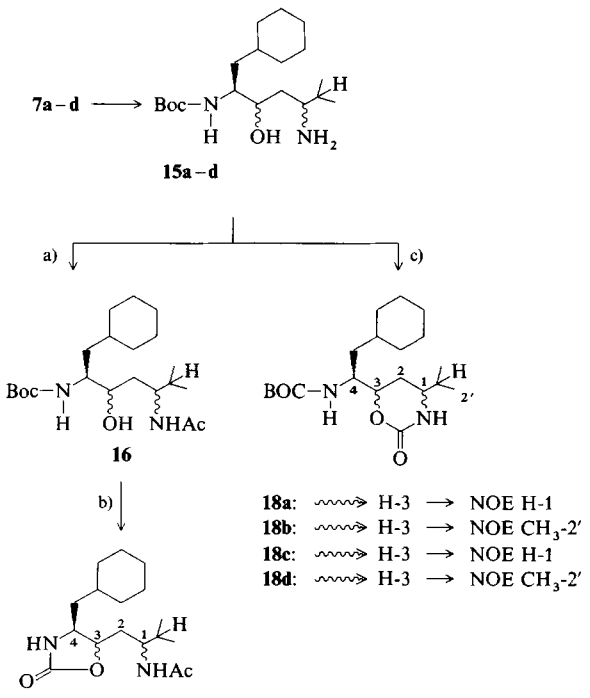

17a: $J_{3,4}$ = 5.2 Hz
17b: $J_{3,4}$ = 5.9 Hz
17c: $J_{3,4}$ = 7.2 Hz
17d: $J_{3,4}$ = 7.9 Hz

Scheme 3. a) AcOAc, CH_3OH, 20 min, room temperature; b) NaH, DMF, 60 min, room temperature; c) *N,N'*-carbonyldiimidazole, CH_2Cl_2, 60 min, *N*,*N*-dimethylaminopyridine, room temperature.

Vicinal coupling constants in **17** with values between 5 and 6 Hz suggest a 3,4-*threo* configuration (**17a,b**), between 7 and 8 Hz suggest a 3,4-*erythro* configuration (**17c,d**).[12] Based on the results of NOE NMR experiments a *trans* orientation of the substituents at C1 and C3 is proposed in oxazolones **18b,d** and a *cis* configuration in **18a,c**. From consideration of the absolute configuration at C4 (obtained from L-amino acid), the configuration of all centers C1, C3, C4 can be assigned with certainty.

With **7b** and the stereochemically identical (Cahn–Ingold–Prelog-sequence rule!) **8a** as a central intermediate, potent renin inhibitors as exemplified by **14** can be synthesized. Catalytic transfer hydrogenation on Pd/C led to the acyclic 1,3-aminoalcohol **9**, which after acylation was deprotected on the nitrogen terminus to **10**. Cyclopentylglycine **11**[13] and *N*-morpholinocarbonylphenylalanine **13**[14] were coupled under standard peptide coupling conditions. The resulting inhibitors were purified by silica gel chromatography. The renin inhibitors **19–21** were prepared by analogous routes. Their enzyme inhibitory activity against endogenous renin from human plasma[15] is shown in Table 1.

Table 1. Human plasma renin inhibition of selected renin inhibitors. For IC_{50} value see [15].

Structure	IC_{50} [nmol L^{-1}]
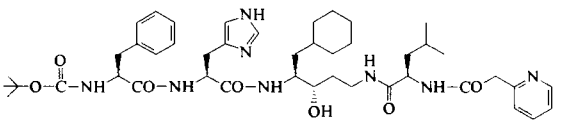 **19**	23
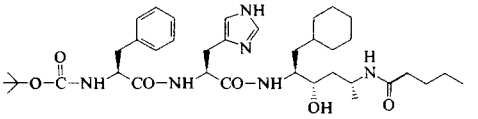 **20**	46
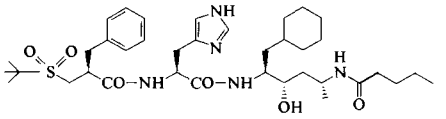 **21**	2.0
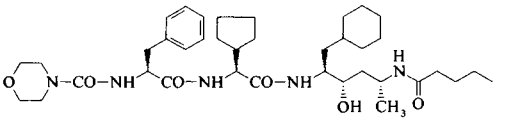 **14**	1.3

Experimental Procedure

7: In a three-necked 3 L flask equipped with a mechanical stirrer and a water separator *N*-Boc-allylamine **4** (202.4 g, 0.8 mol) was dissolved in mesitylene (1 L) and heated to 140 °C. At this temperature a mixture of *N*-benzylhydroxylamine (197 g, 1.6 mol) and 2-methylpropanal (115.2 g, 1.6 mol) in mesitylene (800 mL) was slowly added over 2 h. After 4 h the same amounts of *N*-benzylhydroxylamine, 2-methylpropanal, and mesitylene were added. After 4 h the solvent was evaporated. The residue was dissolved in diethyl ether and washed with 1 M $KHSO_4$ solution. The mixture of the diastereomers was purified on silica gel [eluent: *n*-hexane/diethyl ether (7:3)]. A second chromatographic separation provided the pure diastereomers: **7a** (34 g), **7b** (69 g), **7c** (10 g), **7d** (11 g), and 44 g mixed fractions. Total yield: 168 g (52.2%).

Received: July 25, 1991 [Z 4824 IE]
German version: *Angew. Chem. 103* (1991) 1735

CAS Registry numbers:
4, 104881-98-3; **5**, 115869-93-7; **6**, 20135-15-3; **7a**, 137435-18-8; **7b**, 137435-19-9; **7c**, 137435-20-2; **7d**, 137435-21-3; **8a**, 137435-22-4; **9**, 137435-23-5; **10**, 137435-24-6; **11**, 109183-72-4; **12**, 137435-25-7; **13**, 114457-62-4; **14**, 137435-26-8; **15a**, 137492-81-0; **15b**, 137492-82-1; **15c**, 137492-83-2; **15d**, 137492-84-3; **16a**, 137435-27-9; **16b**, 137492-85-4; **16c**, 137492-86-5; **16d**, 137492-87-6; **17a**, 137435-28-0; **17b**, 137435-29-1; **17c**, 137435-30-4; **17d**, 137435-31-5; **18a**, 137435-32-6; **18b**, 137492-88-7; **18c**, 137492-89-8; **18d**, 137492-90-1; **19**, 137435-33-7; **20**, 137464-51-8; **21**, 137435-34-8; $(n\text{-}C_4H_9CO)_2O$, 2082-59-9; renin, 9015-94-5; *N*-benzylhydroxylamine, 622-30-0; 2-methylpropanal, 78-84-2.

[1] M. J. Wyvratt, A. A. Patchett, *Med. Res. Rev. 5* (1985) 483.
[2] W. J. Greenlee, *Med. Res. Rev. 10* (1990) 173.
[3] P. Bühlmayer, A. Caselli, W. Fuhrer, R. Göschke, V. Rasetti, H. Rueger, J. L. Stanton, L. Criscione, J. M. Wood, *J. Med. Chem. 31* (1988) 1839.
[4] a) R. Wolfenden, *Acc. Chem. Res. 5* (1972) 10; b) G. E. Lienhard, *Science 180* (1973) 149; c) L. Pauling, *Chem. Eng. News 24* (1946) 1375.
[5] J. J. Tufariello in A. Padwa (Ed.): *1,3-Dipolar Cycloaddition Chemistry, Vol. 2*, Wiley, New York 1984, pp. 83–168.
[6] a) K. Kasahara, H. Iida, C. Kibayashi, *J. Org. Chem. 54* (1989) 2225; b) A. Vasella, *Helv. Chim. Acta 60* (1977) 426.
[7] S. Mzengeza, R. A. Whitney, *J. Org. Chem. 53* (1988) 4074.
[8] ^{1}H NMR, ^{13}C NMR, EI-MS, and FAB-MS spectra are consistant with the proposed structures of all compounds.
[9] a) Boc-Phe was hydrogenated over 5% Pd/C with 5 atm H_2. Subsequent coupling with *N*-methyl-*O*-methyl-hydroxylamine [9b] after activation with *N*-propylphosphonic acid anhydride [9c] provided an amino acid amide, which was reduced quantitatively with $LiAlH_4$ to the amino acid aldehyde [9d]. Wittig reaction with "instant ylide" (methyltriphenylphosphonium bromide and sodium amide) [9e] gave the *N*-Boc-allylamine **4** in 80% yield. b) S. Nahm, S. M. Weinreb, *Tetrahedron Lett. 22* (1981) 3815; c) H. Wissmann, H. J. Kleiner, *Angew. Chem. 92* (1980) 129; *Angew. Chem. Int. Ed. Engl. 19* (1980) 133; d) J. A. Fehrentz, B. Castro, *Synthesis 1983*, 676; e) M. Schlosser, B. Schaub, *Chimia 36* (1982) 36.
[10] R. Huisgen, H. Seidl, I. Bruning, *Chem. Ber. 102* (1969) 1102.
[11] J. R. Luly, J. F. Dellaria, J. J. Plattner, J. L. Soderquist, N. Yi, *J. Org. Chem. 52* (1987) 1487.
[12] S. Futagawa, T. Inui, T. Shiba, *Bull. Chem. Soc. Jpn. 46* (1973) 3308.
[13] D. Nisato, J. Wagnon, G. Callet, D. Mettefeu, J.-L. Assens, C. Plouzane, B. Tonnere, V. Pliska, J.-L. Fauchere, *J. Med. Chem. 30* (1987) 2287.
[14] J. J. Plattner, P. A. Marcotte, H. D. Kleinert, H. H. Stein, J. Greer, G. Bolis, A. K. L. Fung, B. A. Bopp, J. R. Luly, H. L. Sham, D. J. Kempf, S. H. Rosenberg, J. F. Dellaria, B. De, J. Merits, T. J. Perun, *J. Med. Chem. 31* (1988) 2277.
[15] Human plasma renin inhibition assay: Human plasma was stored at −20 °C after the addition of ethylenediaminetetraacetic acid (EDTA) as anticoagulant. The plasma renin activity (PRA) was determined as the rate of formation of angiotensin I from endogenous angiotensinogen and renin after incubation at 37 °C. The reaction solution contained 150 μL of plasma, 3 μL of 6.6% 8-hydroxyquinoline sulfate solution, 3 μL of 10% dimercaprol (2,3-dimercapto-1-propanol) solution, and 144 μL of sodium phosphate buffer (0.2 M; 0.1% EDTA; pH 5.6) with or without the test substances in various concentrations. The angiotensin I formed per time unit was determined with a radioimmunoassay (Sorin Biomedica, Italy). The percentage inhibition of plasma renin activity was calculated by comparison of the amount of angiotensin I with and without inhibitor.

A New Approach to 2-Equivalent Couplers for Color Photography

By *Peter Bergthaller*

Dedicated to Professor Karl Heinz Büchel on the occasion of his 60th birthday

Materials for today's color photography, which function almost exclusively according to the Fischer principle of chromogenic coupling (Scheme 1),[1] are increasingly produced using 2-equivalent couplers **1**. In contrast to 4-equivalent couplers **2**, 2-equivalent couplers consume two rather than four equivalents of silver halide[2] per dye molecule formed, which explains our economic motivation in this research.

[*] Dr. P. Bergthaller
Agfa-Gevaert AG, FE-CH
W-5090 Leverkusen-Bayerwerk (FRG)

The anions of diazoles and triazoles, cyclic dicarboximides, hydantoins, and phenols are classic nucleophilic leaving groups $X^{\ominus}$. They raise the acidity of the couplers and affect the kinetics of the coupling process. The leaving groups HX which have been split off can behave in two ways, being either photographically inert or intervening in the photographic process. They can, for example, deactivate existing development nuclei or produce new development nuclei, as a result of their redox or ligand properties. These photographic effects[3, 4] as well as their greater color yield make 2-equivalent couplers indispensable for modern color film.

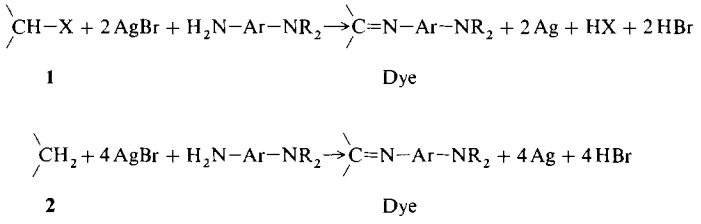

Scheme 1. Chromogenic coupling (Ar = aryl).

Both photographic and synthetic factors must be taken into account when choosing the optimum leaving group. The prerequisite for the linking of the 4-equivalent coupler and leaving group—both are nucleophiles—is that one of them can be converted into an electrophile. The introduction of the leaving group as an electrophile is only possible in thiol leaving groups by way of sulfenylation. N and O leaving groups cannot be introduced into the synthesis as electrophiles. For the acylacetanilides used as yellow couplers, this linkage problem can be solved by introducing a halogen atom into the coupling position. α-Chloro- and α-bromoacylacetanilides easily exchange the halogen atom for O or N nucleophiles under suitable reaction conditions.

This *umpolung* is no longer possible for the industrially used magenta couplers of the pyrazolone and pyrazoloazole classes. After introduction of a halogen atom the coupling position remains strongly nucleophilic. Thus, bromination continues in the case of the anilinopyrazolone **3** to the 4,4′-dibromo compound. Dihalogen-substituted pyrazolones are base-sensitive, however, and disintegrate with ring fission on contact with strong bases.[5] When attacked by basic nucleophiles, monohalogen pyrazolones easily disproportionate. Only with *N*-acyl protecting groups may they be converted to weak C-electrophiles.[6] In the cyan couplers from the phenol and naphthol classes, nucleophilic substitution of the chemically inert, aromatically bonded halogen at the coupling position by an imidazole or triazole residue is not at all possible.

In our attempts to find a preparative method for the direct bonding of 4-equivalent couplers with leaving groups from the classes of 1,2,3-triazoles, 1,2,4-triazoles, or benzotriazoles, we chose leaving groups which could be introduced as electrophiles. In the chemistry of the yellow couplers, this function is optimally fulfilled by Cl and Br. Lead(IV) acetate is a classic reagent for the *umpolung* of a C-nucleophile,[7] but its use in the introduction of leaving groups is greatly restricted due to its strong oxidizing effect. With suitable phenols, for example, it forms quinol acetates which trap nucleophiles, mainly by Michael addition, thus not directing them to the coupling position.[8] Iodophenyl chloride and 2-iodosobenzoic acid[9, 10] are unsuitable *umpolung* reagents for reasons of stability.

We found a preparatively useful system of reagents in the selenium(IV) compounds.[11] A predecessor to our reaction possibly operating on a principle of its own, is the reaction of acetophenones with seleninyl chloride,[12] in which isolable diphenacylselenium dichlorides are formed, which thermally dissociate to phenacyl chlorides[13] with selenium extrusion. This reaction cannot generally be applied to color couplers because seleninyl chloride is also a chlorinating agent. The selenium bromides, for example aryl selenyl bromides, aryl selenium tribromides, and diaryl selenium bromides, are also primarily brominating agents.

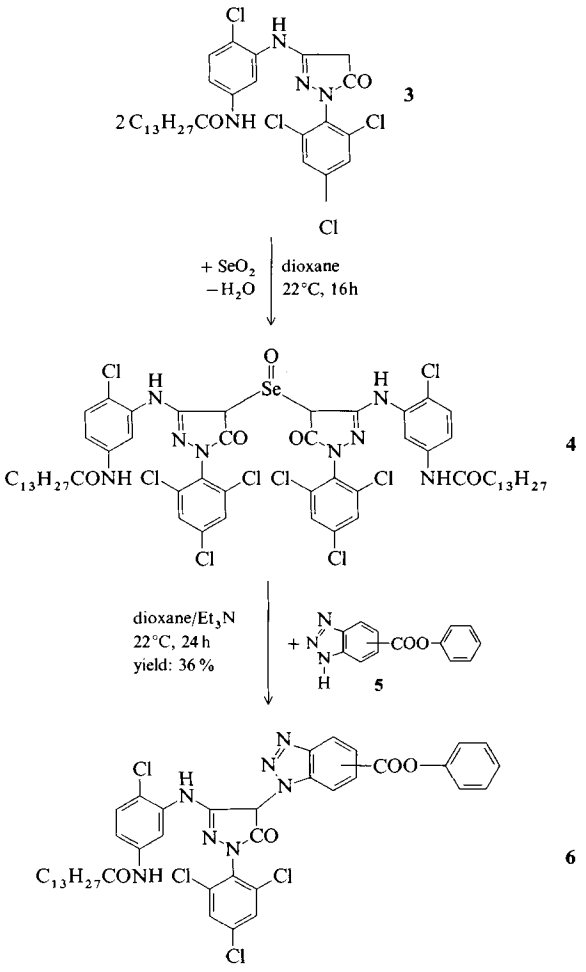

In contrast, the Lewis acids selenium dioxide and ditosylselenium diimine,[14] both difunctional electrophiles, attack highly reactive couplers, such as 3-anilinopyrazolone **3**. The hardly soluble and surprisingly stable primary product **4** (a bispyrazolyl selenium oxide according to elementary analysis) can itself be attacked by bases and adds the anions of benzotriazoles **5** in aprotic media. The dark red solution of the anions of **4** and **5** precipitates selenium while forming the 2-equivalent coupler **6** and yet unidentified by-products. Of two coupler molecules used, only one is converted to the desired 2-equivalent coupler. We have not yet established whether the fission of the adduct occurs as nucleophilic substitution with emission of a selenenate ion, which can itself disproportionate to elemental selenium, or as genuine extrusion. Direct substitution of the selenium oxide group by the triazolide ion can also not be ruled out.

Related experiments with the cyan coupler **7** from the class of 1-naphthol-2-carboxylic acid anilides were successful only with more active selenylation reagents. The course of the reaction could not be explained due to the instability of the intermediate stages. For example, when $SeCl_4$ is heated in chlorobenzene with *N*-trimethylsilyl-benzotriazoles at a molar ratio of 1:2, a nonuniform Se^{IV}-benzotriazolide **8** forms, which still demonstrates Lewis acid characteristics and forms a number of products with the cyan coupler, including an adduct of unknown structure. This adduct disintegrates

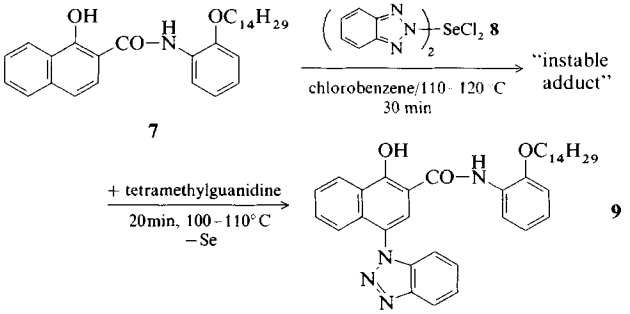

when attacked by the strong base tetramethylguanidine, releasing the 2-equivalent coupler **9**.

Experimental Procedure

6: To 6.14 g (10 mmol) commercial magenta coupler **3** in 100 mL dioxane was added 0.6 g (5.5 mmol) SeO_2 with stirring. The flask was sealed and agitated 6 h at 22 °C. The resultant dark green suspension of **4** was treated with 2.71 g (10 mmol) **5** and 5 mL triethylamine, and agitated further in a sealed flask. Within 3 h **4** had dissolved and the reaction mixture turned red. After 24 h the selenium was removed by filtration. The filtrate was concentrated under reduced pressure and then stirred with 25 mL acetic acid. Unreacted **5** was thus converted into the poorly soluble acetate and removed by filtration. The filtrate was concentrated under reduced pressure, recrystallized from 15 mL acetonitrile, and purified by column chromatography on 300 g silica gel (eluent: toluene/acetone gradient with increasing polarity). The polar fractions were stirred with acetonitrile, yielding 3.15 g **6** as gray crystals (m.p. = 145–150 °C). The thin-layer chromatogram shows **6** to be a mixture of two clearly separated isomers (eluent: toluene/ethylacetate/propanol/methanol 10:6:3:1; R_f values: 0.30 and 0.37). IR (KBr): $\tilde{\nu}$ [cm^{-1}] = 2920, 2850 (C–H), 1745 (C=O) ^{1}H NMR (200 MHz, [D_6] dimethyl sulfoxide, TMS): δ = 9.73 (2s), 8.87 (s), 8.08–8.4 (m, 2 H), 7.69–7.82 (m), 7.1–7.53 (m), 3.85 (s), 2.1–2.3 (2t, CH_2), 1.5–1.6 (2t, CH_2), 1.15–1.33 (m, CH_2), 0.82–0.9 (t, CH_3).

9: 1.92 g *N*-trimethylsilylbenzotriazole (10 mmol) and 1.1 g selenium tetrachloride (5 mmol) were heated at reflux in 20 mL dry chlorobenzene until the selenium tetrachloride dissolved. Then 4.71 g (10 mmol) **7** prepared by melting phenyl 1-naphthol-2-carboxylate with 2-aminophenyltetradecylether at 140 °C was added to the brown solution while stirring. The initially purple suspension turned brown and was heated at 115–120 °C for a further 30 min. After the addition of 1.6 mL 1,1,3,3-tetramethylguanidine, the reaction mixture was cooled and taken up in 200 mL ethyl acetate. 0.25 g Gray selenium was removed by filtration. The filtrate was washed with 100 mL water and 2 mL 35 % HCl, dried, and concentrated with a rotary evaporator. The residue was purified by column chromatography (70 g silica gel; eluent: cyclohexane with increasing toluene component). The polar fractions were concentrated and stirred with cyclohexane, providing 0.2 g **9** (m.p. = 110–112 °C from cyclohexane). IR (KBr): $\tilde{\nu}$ [cm^{-1}] = 3440 (N–H) 2920, 2850 (C–H), 1645 (C=O), 1550, 760, 742 (C=C). ^{1}H NMR (200 MHz, $CDCl_3$, TMS): δ = 14.06 (s, OH), 8.79 (s, NH), 8.6–8.66 (d, CH), 8.38–8.45 (d, CH), 8.2–8.26 (d, CH), 6.86–7.71 (m, CH), 4.0 (t, CH_2), 1.84 (m, CH_2), 1.0–1.24 (m, CH_2) 0.9 (t, CH_3).

Received: May 21, 1991
Revised: July 12, 1991 [Z 4635 IE]
German version: *Angew. Chem. 103* (1991) 1742

[1] R. Fischer, H. Siegrist, *Photogr. Korresp. 18* (1914) 208; *Chem. Abstr. 8* (1914) 1710.
[2] J. Fleckenstein in T. James (Ed.): *The Theory of the Photographic Process*, 4th ed., Macmillan, New York 1977, p. 355.
[3] C. R. Barr, J. R. Thirtle, P. W. Vittum *Photogr. Sci. Eng. 13* (1969) 74, 214; *Chem. Abstr. 70* (1969) 101 608e.

[4] E. Ranz, *Chem. Labor Betr. 30* (1979) 229.
[5] K. Kirschke, G. Lutze, E. Schmitz, *J. Prakt. Chem. 326* (1984) 367.
[6] K. Nakamura, S. Ichijima, N. Furutachi, Y. Kosuge, DE-A 2703589 (January 28, 1977): Fuji Photo Film; *Chem. Abstr. 87* (1977) P 169258x.
[7] E. Zbiral, *Synthesis 1972*, 285.
[8] F. Langer, F. Wessely, *Monatsh. Chem. 88* (1957) 298.
[9] O. Neilands, G. Vanags, *Dokl. Akad. Nauk SSSR 141* (1961) 872; *Chem. Abstr. 56* (1962) 12715d.
[10] T. Kappe, G. Korbuly, W. Stadlbauer, *Chem. Ber. 111* (1978) 3857.
[11] P. Bergthaller, DE-B 40404722 (December 18, 1990), Bayer AG.
[12] R. E. Nelson, R. N. Jones, *J. Am. Chem. Soc. 52* (1930) 1588.
[13] J. P. Schaefer, F. Sonnenburg, *J. Org. Chem. 28* (1963) 1128.
[14] K. B. Sharpless, T. Hori, L. K. Truesdale, C. O. Dietrich, *J. Am. Chem. Soc. 98* (1976) 269.

The Synthesis of the First Decametal Nitrido Cluster; X-Ray Structure Analysis and ^{14}N NMR Studies of $[(Ph_3P)_2N][Ru_{10}N(CO)_{24}]$**

By *Philip J. Bailey, Gráinne C. Conole, Brain F. G. Johnson, Jack Lewis,* Mary McPartlin,* Adrian Moule,* and *Della A. Wilkinson*

The chemistry of nitrido-metal clusters is of widespread interest because it provides model systems for study of the species formed during chemisorption of nitrogen and nitrogen compounds on bulk metal surfaces during heterogeneous catalysis.[1] Although several large nitrido clusters of cobalt and rhodium have been reported,[2] the synthesis of high-nuclearity nitrido-metal carbonyls of the iron triad has proved difficult because of the ease with which the CO ligands undergo scission to generate contaminating carbido analogues from which separation of the nitride is very difficult. We now report that the first decametal nitrido species, the monoanion $[Ru_{10}N(CO)_{24}]^-$ (**1**), has been isolated cleanly from redox condensation of the hexanuclear nitrido cluster $[Ru_6N(CO)_{16}]^-$ (**2**) with $[Ru_3(CO)_{12}]$ **3**. X-ray studies confirm that the $[Ru_6N]$ unit has remained intact, giving a nitrido cluster with the tetracapped octahedral metal framework previously only known for carbido or hydrido species.[3-5]

Our first synthesis of the the decanuclear nitrido monoanion **1** involved direct reaction of stoichiometric amounts of the azide salt $[(Ph_3P)_2N][N_3]$ with the triruthenium cluster **3** in diglyme under reflux at 162 °C (Scheme 1). This route gave moderate yields of **1** but proved unsatisfactory because it also gave significant quantities of the carbido monoanion $[HRu_{10}C(CO)_{24}]^-$ (**4**), from which the nitride could not readily be separated by chromatography, together with the carbido dianion $[Ru_{10}C(CO)_{24}]^{2-}$ (**5**). Deprotonation of the hydride **4** to to the dianion **5** followed by TLC enabled separation of the nitride **1**, but there always remained a weak hydride signal in the ^1H NMR spectrum, indicating residual traces of contamination by **4**.

The recent[4] report of the synthesis of the decaruthenium carbido dianion **5** by redox condensation of the interstitial carbido dianion $[Ru_6C(CO)_{16}]^{2-}$ with $[Ru_3(CO)_{12}]$ (**3**) prompted a new approach to the synthesis of the nitride $[Ru_{10}N(CO)_{24}]^-$ (**1**). The direct buildup of the decanuclear species from the known[6] preformed nitrogen-centered octahedral cluster $[Ru_6N(CO)_{16}]^-$ (**2**) on reaction with **3**, as shown in the Scheme 1, has now given **1** in good yield free from carbide contamination.

Single-crystal X-ray structure analysis of the $[(Ph_3P)_2N]^+$ salt of the nitride **1**[7] established its tetracapped octahedral framework (Fig. 1). The overall structure is almost indistinguishable from that observed in X-ray studies of the formally isoelectronic carbido monohydride $[HRu_{10}C(CO)_{24}]^-$ (**4**),[2] and there are no significant differences in lengths between equivalent bonds in the two isomorphous compounds. Initial evidence that the monoanion **1** was the nitride was based mainly on the nature of the synthetic route, and evidence from the X-ray study was consistent with this because refinement of the central atom as carbon, instead of nitrogen, led to an improbably low value for its thermal parameter.

Unequivocal confirmation of the presence of an interstitial nitride was obtained from the ^{14}N NMR spectrum[8] of $[(Ph_3P)_2N][Ru_{10}N(CO)_{24}]$, which consits of a singlet at $\delta = 410$, assigned to the nitride, and a second singlet at $\delta = 310$ due to the nitrogen atom of the counterion. The low-frequency shift of the interstitial nitride resonance, relative to that $[Ru_6N(CO)_{16}]^-$ (**2**) ($\delta = 538$),[6] follows a similar trend to that observed in the ^{13}C NMR spectra of the analogous carbido species $[Ru_{10}C(CO)_{24}]^{2-}$ ($\delta = 362$)[5] and $[Ru_6C(CO)_{16}]^{2-}$ ($\delta = 461.2$).[9]

Reaction of **1** with carbon monoxide (1 atm, 20 °C in CH_2Cl_2) results in quantitative conversion to $[Ru_5N(CO)_{14}]^-$ and $[Ru_3(CO)_{12}]$ (**3**) within five minutes (Scheme 1). It has previously been established that the precursor hexaruthenium nitride decomposes to these species in the presence of excess CO,[6] so it seems probable that $[Ru_6N(CO)_{16}]^-$ (**2**) is an intermediate in the decomposition to the pentanuclear species and that the synthesis of **1** is therefore reversible. Prompted by this, we subjected the decaruthenium analogue $[Ru_{10}C(CO)_{24}]^{2-}$ (**5**) to carbon monoxide under the same mild conditions and found that it also is completely degraded, giving $[Ru_6C(CO)_{16}]^{2-}$ and **3**; thus, the synthesis of **5** is also reversible. That the degradation of the decaruthenium

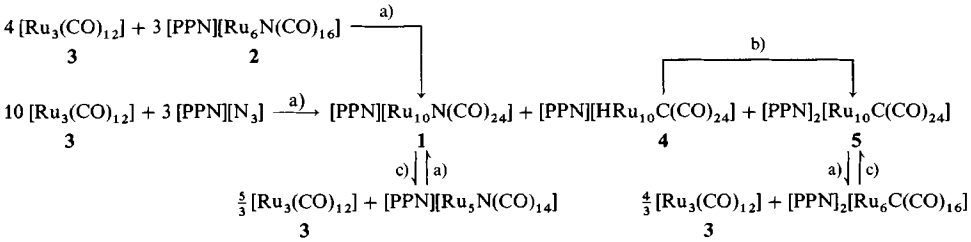

Scheme 1. a) Diglyme, 162 °C, 3 h. The decaruthenium clusters were obtained in variable proportions from this reaction. The origin of the hydrido ligand is unknown, but is assumed to be due to traces of water in the solvent. b) Diazobicyclo[5.4.0]undec-7-ene (DBU), CH_2Cl_2, 5 min. c) CO, 1 atm, 5 min, CH_2Cl_2. PPN = $[(Ph_3P)_2N]^+$.

[*] Prof. Lord Lewis, Dr. P. J. Bailey, Prof. B. F. G. Johnson, Dr. A. Moule, Dr. D. Wilkinson
University Chemical Laboratories
GB-Cambridge CB2 1EW (UK)
Prof. M. McPartlin, Dr. G. C. Conole
School of Chemistry, The Polytechnic of North London
Holloway Road, GB-London N7 8DB (UK)

[**] We thank the Science and Engineering Research Council (SERC) for studentships (*G. C. C., A. M., D. A. W.*).

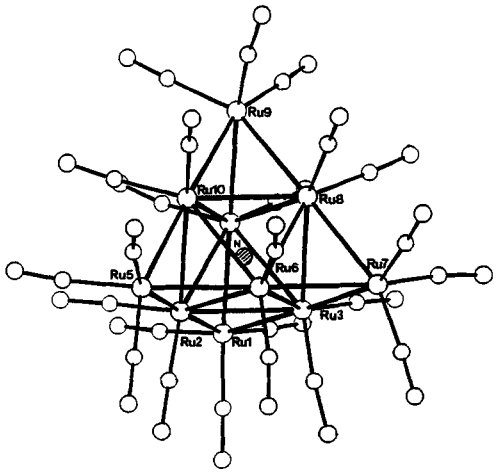

Fig. 1 Structure of the nitrido monoanion $[Ru_{10}N(CO)_{24}]^-$ (**1**). Principal Ru–Ru distances [Å] (maximum standard deviation 0.005 Å): Ru2-Ru3 2.884, Ru2-Ru4 2.854, Ru2-Ru6 2.849, Ru2-Ru10 2.845, Ru3-Ru4 2.846, Ru3-Ru6 2.855, Ru3-Ru8 2.862, Ru4-Ru8 2.864, Ru4-Ru10 2.861, Ru6-Ru8 2.855, Ru6-Ru10 2.856, Ru8-Ru10 2.842, Ru1-Ru2 2.761, Ru1-Ru3 2.790, Ru1-Ru4 2.767, Ru5-Ru2 2.789, Ru5-Ru6 2.774, Ru5-Ru10 2.791, Ru7-Ru3 2.773, Ru7-Ru6 2.778, Ru7-Ru8 2.781, Ru9-Ru4 2.780, Ru9-Ru8 2.787, Ru9-Ru10 2.783. Selected bond ranges Ru–C (carbonyl): 1.70–1.90(5), C-O 1.12–1.28(5), Ru-N (nitrido) 1.97(3)–2.08(2) Å.

carbide **5** does not continue to the pentanuclear stage is evidence of the superior ability of carbido ligands, compared to nitride, to maintain the integrity of a cluster, and it is relevant that severe conditions (90 atm, 100 °C) are required for the conversion of $[Ru_6C(CO)_{17}]$ to $[Ru_5C(CO)_{15}]$.[10] The behavior of these decaruthenium species is in marked contrast to that of the decaosmium cluster $[Os_{10}C(CO)_{24}]^{2-}$, with resists degradation by CO even under extreme conditions.[11]

The reaction of an interstitial hexaruthenium species with **3** has not proved to be generally applicable as a route to tetracapped octahedral clusters, as we have shown that reaction of the octahedral cluster hydride $[Ru_6H(CO)_{18}]^-$ with **3** gives $[H_2Ru_{10}(CO)_{25}]^{2-}$, which has a unique structure based on the capping of a polyhedron by fusion of an octahedron with a square pyramid, a structure which probably reflects the necessity of accommodating a further carbonyl ligand on the cluster surface, both this structure and the tetracapped octahedron having the same polyhedral electron count of 134.[12]

Received: July 19, 1991 [Z 4808 IE]
German version: *Angew. Chem. 103* (1991) 1672

[1] T. Pignet, L. D. Schmidt, *J. Catal. 40* (1975) 212; R. Eisenberg, D. E. Hendriksen, *Adv. Catal. 28* (1979) 79; A. Czaka, K. Aika, *Catal. Sci. Technol. 3* (1981) 87.

[2] S. Martinengo, G. Ciani, A. Sironi, *J. Chem. Soc. Chem. Commun. 1991*, 26, and references therein.

[3] P. F. Jackson, B. F. G. Johnson, J. Lewis, P. R. Raithby, M. McPartlin, W. J. H. Nelson, *J. Chem. Soc. Chem. Commun. 1980*, 224; *J. Chem. Soc. Dalton Trans. 1982*, 2099; P. F. Jackson, B. F. G. Johnson, J. Lewis, M.-C. Malatesta, M. McPartlin, *J. Chem. Soc. Chem. Commun. 1982*, 49; D. Braga, B. F. G. Johnson, J. Lewis, M. McPartlin, W. J. H. Nelson, M. D. Vargas, *ibid. 1983*, 241.

[4] T. Chihara, R. Komoto, H. Yamazaki, Y. Matsuura, *Inorg. Chem. 28* (1989) 964.

[5] P. J. Bailey, B. F. G. Johnson, J. Lewis, M. McPartlin, H. R. Powell, *J. Organomet. Chem. 337* (1989) C17; P. J. Bailey, M. J. Duer, B. F. G. Johnson, J. Lewis, G. C. Conole, M. McPartlin, H. R. Powell, C. E. Anson, *ibid. 383* (1990) 441.

[6] M. L. Blohm, W. L. Gladfelter, *Organometallics 4* (1985) 45.

[7] Crystal data for $[(Ph_3P)_2N][Ru_{10}N(CO)_{24}]$ **1**: $C_{61}H_{32}Cl_2N_2O_{24}P_2Ru_{10}$, $M = 2319.87$, space group $P2_1/c$, $a = 11.763(2)$, $b = 17.817(4)$, $c = 35.330(5)$ Å, $\beta = 94.33(2)°$. $V = 7383.38$ Å^3, $\varrho_{calcd} = 2.09$ g cm^{-3}, $Z = 4$, $\mu(Mo_{K\alpha}) = 19.72$ cm^{-1}, $F(000) = 4432$. Data were collected on a Philips PW1000 diffractometer in the θ range 3–25°, with a scan width of 0.90°, final $R = 0.0613$, $R_w = 0.0582$, using 2300 absorption-corrected data with $I/\sigma(I) \geq 3.0$. The nitrido N atom and all the atoms forming one of the virtual mirror planes of the monoanion are close to the *ac* face of the unit cell. This means that adjacent monoanions generated by the *c* glide are virtually related to each other by a noncrystallographic translation of *c*/2, resulting in all data with $l = 2n + 1$ being weak. Satisfactory refinement was achieved by refining the pseudosymmetry-related halves of the monoanion in alternate cycles.

[8] ^{14}N NMR spectrum recorded at 28.90 MHz from ca. 30 mg of $[(Ph_3P)_2N][Ru_{10}N(CO)_{24}]$ in CD_2Cl_2 (0.5 mL). Nitromethane was used as a secondary internal reference [$\delta(^{14}N, NH_3) = 0$].

[9] J. S. Bradley, *Adv. Organometal. Chem. 22* (1983) 1, and references therein.

[10] D. F. Farrer, P. F. Jackson, B. F. G. Johnson, J. Lewis, J. N. Nicholls, M. McPartlin, *J. Chem. Soc. Chem. Commun. 1981*, 415.

[11] P. F. Jackson, *Ph.D. Thesis*, Cambridge University 1980.

[12] P. J. Bailey, E. Charalambous, J. Hoyle, B. F. G. Johnson, J. Lewis, M. McPartlin, *J. Chem. Soc. Chem. Commun. 1990*, 1443.

Dilithiation of a Primary Amine: Synthesis and Structure of $[(\alpha\text{-Naphthyl-NLi}_2)_{10}(Et_2O)_6] \cdot Et_2O$, a Paramagnetic Li_{20} Aggregate**

By *David R. Armstrong, Donald Barr, William Clegg, Simon R. Drake, Richard J. Singer, Ronald Snaith,* Dietmar Stalke,* and *Dominic S. Wright*

Lithium amides $(RR'NLi)_n$ and their complexes $(RR'NLi \cdot xL)_n$ (L = Lewis base) are valuable deprotonating reagents in organic synthesis.[1] Many such reagents have been structurally characterized not only in the solid state[2] but also in solution (where they operate) chiefly by ^{6}Li, ^{7}Li, and ^{15}N NMR spectroscopy.[2b, 3] However, all this effort has centered on *N*-monolithiated species usually derived from secondary amines RR'NH with R, R' ≠ H (exceptions are $[2,4,6\text{-}tBu_3C_6H_2N(H)Li(OEt_2)]_2$[4a] and $[mesityl_2BN(H)Li(OEt_2)]_2$[4b]). Here we describe the first full investigation of the dilithiation of a primary amine, 1-aminonaphthalene, by *n*-butyllithium in diethyl ether. The high-yielding, crystalline product **1** of this reaction is paramagnetic. Its main structural element is an $N_{10}Li_{14}$ central cluster, to which six $[Li(Et_2O)]^+$ units are attached by coordination to the N atoms.

$[(1\text{-}C_{10}H_7NLi_2)_{10}(Et_2O)_6] \cdot Et_2O$ **1**

Ab initio MO calculations (3-21G basis set) were conducted to probe the possibilities in the dilithiation of naphthylamine. Three types of products were examined

[*] Dr. R. Snaith, Dr. D. Barr, Dr. R. J. Singer, Dr. D. Stalke, Dr. D. S. Wright
University Chemical Laboratory
Lensfield Road, GB-Cambridge, CB2 1EW (UK)
Dr. D. R. Armstrong
Department of Pure and Applied Chemistry
University of Strathclyde, GB-Glasgow, G1 1XL (UK)
Dr. W. Clegg
Department of Chemistry, University of Newcastle upon Tyne,
GB-Newcastle upon Tyne, NE1 7RU (UK)
Dr. S. R. Drake
Department of Chemistry, Imperial College of Science,
Technology and Medicine, GB-London SW7 2AY (UK)

[**] We thank the following for financial support: the Associated Octel Co. Ltd. (*D. B., R. S.*), the Science and Engineering Research Council and the Royal Society (*W. C.*), the Deutsche Akademische Austausch Dienst (Nato Fellowship for *D. S.*), and Gonville and Caius College, Cambridge (*D. S. W.*). Thanks are also given to Dr. *A. T. Brooker* for help with syntheses.

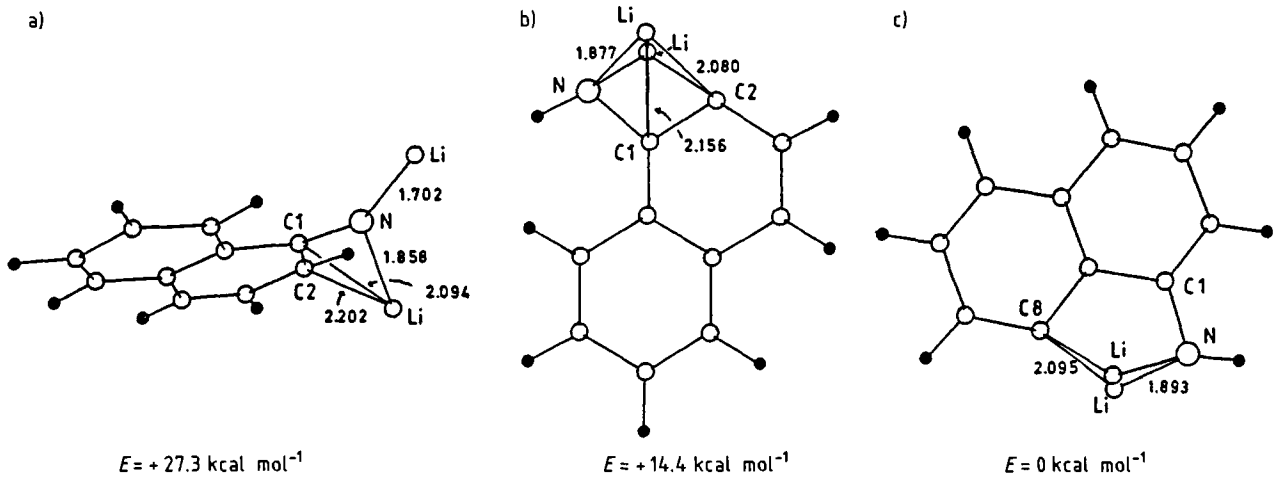

Fig. 1. Ab initio optimized geometries of the isomers of dilithiated α-naphthylamine. The most stable structures for the a) *N,N*-, b) *N,C*2-, and c) *N, C*8-dilithiated species (distances in Å). The ab initio optimized geometries described were obtained from the computer program GAMESS[8] using the 3-21 G basis set [9]. The absolute energies calculated for the optimized structures of dilithiated naphthylamine are −449.593006, −449.613554, −449.636457 Hartree.

resulting from *N,N*-dilithiation, *N*- and *C*2-dilithiation (*ortho*), and *N*- and *C*8-dilithiation (*peri*). For each of these Li_2 products several starting geometries were optimized without symmetry restrictions. Figure 1 illustrates the most stable optimized structure found for each type and notes their relative energies. The least stable structure (Figure 1a) displays *N,N*-dilithiation; here one Li atom also interacts with C1 and C2 while the other Li atom is bonded only to N. The product of *N*-, *C*2-dilithiation is more stable; in it, each Li atom is coordinated to N, C1, and C2 on opposite faces of the naphthyl ring (Figure 1b). The most stable structure found has *N*-, *C*8-dilithiation (Figure 1c), in which two Li atoms bridge N and C8. These initial calculations imply that dilithiation of a primary amine RNH_2 could well afford an N–Li/C–Li rather than an N–Li_2 species. This conclusion is not restricted to aromatic amines. Calculations for the products of the dilithiation of vinylamine $H_2C{=}CH{-}NH_2$ (at the higher 6-31G level, again without symmetry constraints) conclude that the most stable structure is CHLi=CH–NLi, in which both Li atoms bridge N and C2 above and below the nearly planar C=C–N moiety. The lowest energy structure of $CH_2{=}CH{-}NLi_2$, in which one Li atom bridges the CC double bond and the other is bound terminally on N, is 6.8 kcal mol^{-1} less stable. However, it must be stressed that all such calculations relate to isolated, monomeric molecules free of donating solvent interactions.

The dilithiated compound **1** was isolated as yellow cubic crystals. Its IR spectrum (Nujol mull) fails to reveal ν(N–H) stretches. These bands, which are strong in the spectrum of 1-$C_{10}H_7NH_2$ (at 3340, 3220 cm^{-1}), reappear on the slightest exposure of **1** to air (along with a ν(O–H) stretch at 3680 cm^{-1} for LiOH); **1** also turns black on contact with air. The ^{1}H NMR spectrum (in [D_8]dimethyl sulfoxide) shows the characteristic patterns for the naphthyl unit (7H) and for Et_2O ($\approx$5 H $\hat{=}$ $\frac{1}{2}$ Et_2O; the crystals lose ether rapidly). But there is no signal for the NH_2 groups (1-$C_{10}H_7NH_2$: δ = 5.77). ^{1}H NMR spectra measured in CD_3OD (which could react with **1** to give $LiOCD_3$ and 1-$C_{10}H_7ND_2$, 1-$C_{10}H_7NDH$, or 1-$C_{10}H_7NH_2$, depending on the identity of **1**) fail to reveal any NH protons.

The crystal structure of **1** ratifies these spectroscopic results.[5] Despite considerable disorder, which can be only partially resolved, the molecular structure is quite clear (Figure 2). Each naphthyl N^{2-} group interacts with four or six Li atoms in a central $N_{10}Li_{14}$ cluster, to which are attached six $(Et_2OLi)^+$ groups. Four of these are terminally bonded to one N each at the ends of the cluster; the other two are more centrally positioned and bridge two N atoms each. Thus every N atom is surrounded by either five or six closest Li neighbors, resulting in an overall neutral molecule. The

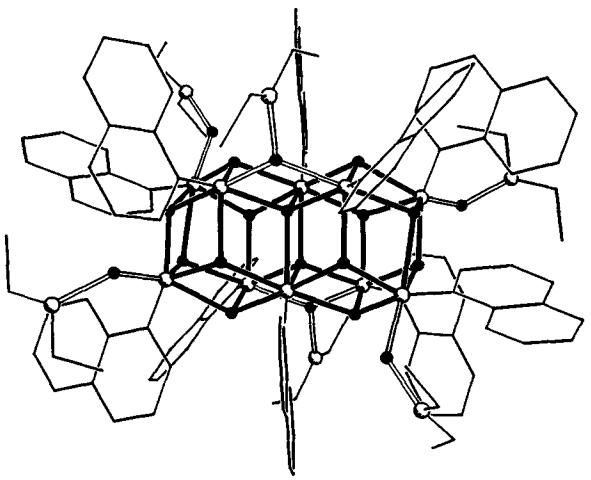

Fig. 2. Structure of **1** in the crystal (without H atoms and without the uncoordinated Et_2O molecule). Only one component of disordered groups is shown. Li atoms are shown as filled circles; O and N atoms, as open circles. Li-N bonds of the $N_{10}Li_{14}$ core are depicted as filled lines, bonds to the six surrounding $LiOEt_2$ groups (both terminal and bridging), as outlines. Key distances [Å]: N-Li 1.91(2)–2.25(2), O-Li 1.89(4)–2.00(3), Li···Li close contacts within the $N_{10}Li_{14}$ core 2.30(3)–2.56(4), Li···C (naphthyl) contacts 2.20(3)–2.49(3).

remaining ether isnot coordinated to Li but occupies a vacant lattice site. The coordination numbers of the Li centers range from 2 (for four Li atoms), to 3 (for fourteen), to 4 (for two). The central $N_{10}Li_{14}$ core consists of two rhombic dodecahedra sharing a common face which contains an inversion center. Li and N atoms occupy alternate vertices. Besides participating in Li–N and Li–O interactions, the Li centers are necessarily brought into close contact with the carbon and hydrogen atoms of the naphthyl groups. Other

highly-aggregated dilithiated organics akin to **1** include the nitrile dodecamer **2**[6a] and the sulfone hexamer **3**.[6b] It is also noteworthy that the core of **1** can be considered as belonging to the fluorite (CaF_2) structural type (N corresponding to Ca, Li to F) and that even the "external" Et_2O-complexed Li atoms fit this quasi-isomorphicity. Many AB_2 species, including alkali metal oxides and sulfides[7a] (and, indeed, Li_2NH[7b]), crystallize in this fluorite arrangement.

$[\{(Me_3SiCCN)Li_2\}_{12}(Et_2O)_6]$ **2**

$[\{(Me_3SiCSO_2Ph)Li_2\}_6Li_2O(THF)_{10}]$ **3**

An unexpected feature of **1** is that it is paramagnetic. The ^1H NMR signals found for **1** in benzene solutions are broad. The ^7Li NMR spectrum (139.97 MHz) of **1** in the same solvent at 25 °C shows (most unusually) three distinct resonances, centered at $\delta = 3.34$, 0.69, and -1.35 (the reference is PhLi in benzene); however, these signals are too broad to allow meaningful integration. The repeated ESR spectra of solid **1** (in a sealed tube under an inert atmosphere) measured between 4.5 K and room temperature consist of a single, slightly asymmetric signal, which can not be attributed to common impurities such as iron or oxygen. No hyperfine interaction could be resolved, though broadening in the shoulders of the signal may be associated with a nitrogen hyperfine interaction (if so, the nitrogen coupling constant would be ca. 15 G). The resonance has a g value of 2.0047 ± 0.0005 and a line width $\Delta H_{pp} = 17\ G \pm 0.5\ G$ and remains essentially unchanged at all temperatures. The g value is consistent with that of a low symmetry nitrogen radical with a p^5 configuration, though a neutral $(1\text{-}C_{10}H_7NLi_2)_{10}$ cluster requires all ten nitrogens to have p^6 configuration. Since we observed no signal attributable to a naphthyl radical anion, charge transfer from N to the naphthyl unit seems unlikely. At this stage we cannot deduce the number of unpaired electrons in the cluster.

The structure of **1** can be understood in terms of electrostatic bonding between Li^+ cations and organic anions. A RN^{2-} dianion will interact with as many Li^+ ions as is sterically possible. This leads to the formation of an aggregate or cluster, especially when R is a flat group such as naphthyl.

Experimental Procedure

1: *n*-Butyllithium (6.2 mL of a 1.6 M solution in hexane, 10 mmol) was added to a chilled (−40 °C) solution of 1-aminonaphthalene (0.715 g, 5 mmol) in diethyl ether (7.5 mL) under nitrogen. The reaction mixture displayed an initial green fluorescence and then turned red and finally orange. At ca. −20 °C a yellow powder precipitated which dissolved at ca. 0 °C. Refrigeration of this yellow solution afforded pale yellow cubic crystals of **1** (first batch yield, 68%); m.p. = 230 °C (decomp. to a red solid); correct C,H,N,Li-analysis; ^1H NMR (250 MHz, 25 °C, $(CD_3)_2SO$): $\delta = 8.03$ (s, 1H), 7.24 (d, 1H), 7.03 (t, 1H), 6.84 (t, 1H), 6.70 (t, 1H), 5.94 (d, 2H), 3.39 (q, ca. 2H), 1.11 (t, ca. 3H); ^1H NMR (250 MHz, 25 °C, CD_3OD) $\delta = 7.94$ (m, 1H), 7.68 (m, 1H), 7.37 (m, 2H), 7.20 (m, 2H), 6.78 (m, 1H), 3.36 (q, ca. 2H), 1.12 (t, ca. 3H)}.

Received: July 22, 1991 [Z 4810 IE]
German version: *Angew. Chem. 104* (1991) 1702

CAS Registry numbers:
1, 137259-14-4; 1-aminonaphthalene, dilithium salt, 137059-63-1.

[1] For accounts of the synthetic uses of lithium amides, see for example: a) M. Fieser: *Reagents for Organic Synthesis, Vol. 15*, Wiley-Interscience, New York 1990, as well as Vol. 1–14; b) J. L. Wardell in F. R. Hartley (Ed.): *The Chemistry of the Metal-Carbon Bond. Vol. 4 (The Use of Organometallic Compounds in Organic Synthesis)*, Wiley, Chichester 1987; c) L. Brandsma, H. D. Verkruijsse: *Preparative Polar Organometallic Chemistry, Vol. 1*, Springer, Berlin 1987.

[2] a) For a review of the crystal structures of lithiated organics in general: W. Setzer, P. von R. Schleyer, *Adv. Organomet. Chem. 24* (1985) 353; b) For a review of Li-N-species in particular: K. Gregory, P. von R. Schleyer, R. Snaith, *Adv. Inorg. Chem. 37* (1991), in press.

[3] For typical studies: a) D. Reed, D. Barr, R. E. Mulvey, R. Snaith, *J. Chem. Soc. Dalton Trans. 1986*, 557; b) L. M. Jackman, L. M. Scarmoutzos, *J. Am. Chem. Soc. 109* (1987) 5348; c) A. S. Galiano-Roth, E. M. Michaelides, D. B. Collum, *ibid. 110* (1988) 2658; d) J. S. DePue, D. B. Collum, *ibid. 110* (1988) 5518, 5524; e) D. R. Armstrong, D. Barr, W. Clegg, S. M. Hodgson, R. E. Mulvey, D. Reed, R. Snaith, D. S. Wright, *ibid. 111* (1989) 4719; f) A. S. Galiano-Roth, D. B. Collum, *ibid. 111* (1989) 6772.

[4] a) B. Cetinkaya, P. B. Hitchcock, M. F. Lappert, M. C. Misra, A. J. Thorne, *J. Chem. Soc. Chem. Commun. 1984*, 148; b) R. A. Bartlett, H. Chen, H. V. R. Dias, M. M. Olmstead, P. P. Power, *J. Am. Chem. Soc. 110* (1988) 446.

[5] **1**: $M_r = 2069.4$, monoclinic space group $P2_1/n$, $a = 14.111(2)$, $b = 14.270(3)$, $c = 28.866(5)$ Å, $\beta = 93.84(2)°$, $V = 5799.5$ Å^3, $Z = 2$, $\rho_{calcd.} = 1.185$ g cm^{-3}, $F(000) = 2188$, $Cu_{K\alpha}$-radiation, $\lambda = 1.54184$ Å, $\mu = 0.51$ mm^{-1}, $T = 150$ K, $2\theta_{max} = 110°$, 3902 unique observed reflections; $R = 0.18$, $R_w = 0.21$, $S = 1.93$ for 612 parameters. Disorder was resolved for one naphthyl and two ether groups in the asymmetric unit (half the molecular structure); naphthyl groups were treated as ideal rigid groups of two fused hexagons with sides 1.395 Å and angles 120° and with idealized H atoms; ether groups were refined with restrained geometry and no H atoms. Satisfactory models have not yet been found for other extensive disorder evident from the high apparent thermal motion parameters and high R. However, the basic molecular structure of **1** is clear. Further details of the crystal structure investigation can be obtained from the Director of the Cambridge Crystallographic Data Centre, University Chemical Laboratory, Lensfield Road, Cambridge, CB2 1EW (UK), by quoting the full journal citation.

[6] a) W. Zarges, M. Marsch, K. Harms, G. Boche, *Chem. Ber. 122* (1989) 1307; b) H.-J. Gais, J. Vollhardt, H. Günther, D. Moskau, H. J. Lindner, S. Braun, *J. Am. Chem. Soc. 110* (1988) 978.

[7] a) A. F. Wells: *Stuctural Inorganic Chemistry*, 5th ed., Oxford University Press, Oxford 1984, p. 252; b) R. Juza, K. Opp, *Z. Allg. Anorg. Chem. 266* (1951) 325.

[8] a) M. Dupuis, D. Spangler, J. J. Wendoloski, *GAMESS* (N. *R. C. C. Software Catalogue*) Program No. QGO1, Washington, D.C., USA, 1980, Vol. 1; b) M. F. Guest, J. Kendrick, S. A. Pope, *GAMESS Documentation*, Daresbury Laboratory, Daresburg, Great Britain 1983.

[9] J. S. Binkley, J. A. Pople, W. J. Hehre, *J. Am. Chem. Soc. 102* (1980) 939.

4-Acyl-2,3,4,5-tetrahydro-2-methyl-2,5-methanobenz-1,4-oxazepine, Derivatives of a New Heterocycle

By *Hans-Joachim Kabbe,* Helmut Heitzer,* and *Liborius Born*

Dedicated to Professor Karl Heinz Büchel on the occasion of his 60th birthday

In the context of an investigation into ion channel modulators[1, 2] the previously unknown heterocycle **1** was required. We planned a synthesis following the sequence **2** → **7** → **1**. Prerequisites for its successful implementation were: a) the availability of the chromanones **4**, which we hoped to obtain through the pyrrolidine-catalyzed reaction[3, 4] of the ketones **2** and **3**; b) the intramolecular addition of the amide group to the carbenium ion **6** to give **7**; and c) the selective nitration of **7** to give the target molecule **1**.

The reaction of aminoacetic acid with acetic anhydride under the standard conditions of the Dakin–West reaction gave the diacyl compound **3**,[5] which was converted to **4** via pyrrolidine-mediated cleavage of one of its acyl groups. Reduction

[*] Dr. H.-J. Kabbe, Dr. H. Heitzer, Dr. L. Born
Bayer AG, Zentrale Forschung
W-5090 Leverkusen 1 (FRG)

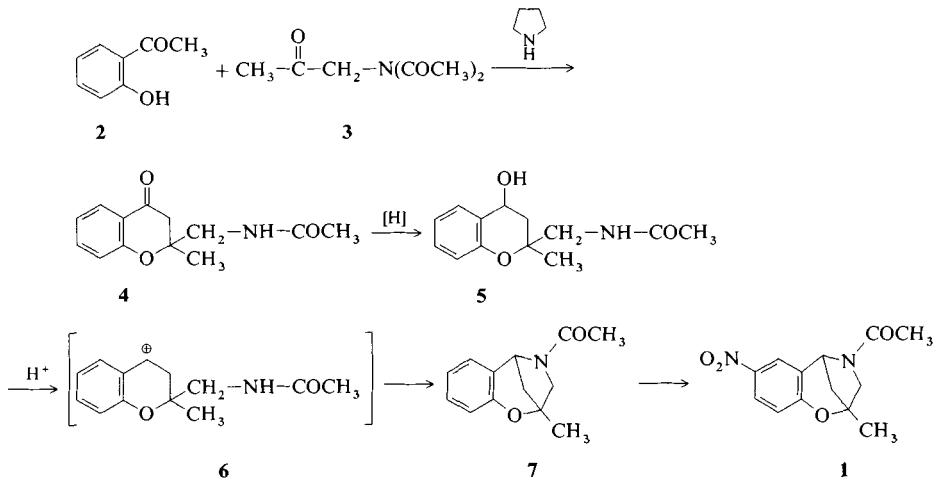

of **4** (excess sodium borohydride in methanol, 2 days, 25 °C) delivered **5** as a mixture of diastereomers. In the presence of anhydrous acid both isomers gave rise to the carbenium ion **6**, which underwent intramolecular reaction providing tricycle **7** (75% yield). Chromene **9** was produced as a side-product (ca. 10%). Nitration of **7** ($[Cu(NO_3)_2] \cdot 3H_2O$, acetic anhydride, 2 h, 55 °C) afforded the target molecule **1**.

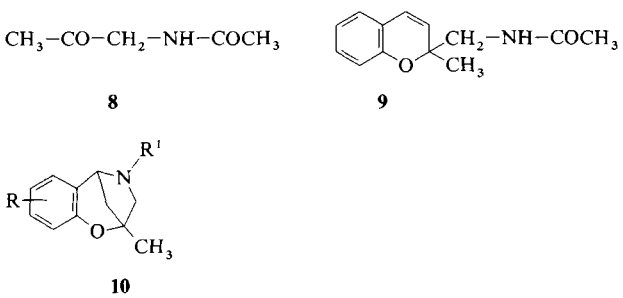

Variation of the starting materials allowed the preparation of other benzoxazepines **10**. Other new derivatives were simply obtained by hydrolysis of the *N*-acetyl compounds available from **8** followed by reacylation (e.g. to **10h**, Table 1). Isocyanates and sulfonyl chlorides gave ureas (**10g**) and sulfonamides (**10f**).

Table 1. Selected examples of **10**.

X	R	R¹	yield [a] [%]	m.p.
10a	H	CHO	41 [b]	103–105 °C
10b	H	C_6H_5CO	68 [b], 58 [c]	104–106 °C
10c	H	$C_6H_5CH_2CO$	73 [b]	86– 88 °C
10d	7-NO_2	C_2H_5CO	80 [b]	106–108 °C
10e	8-CH_3O	CH_3CO	83 [c]	132–134 °C
10f	H	$C_6H_5SO_2$	86 [b]	108–110 °C
10g	7-NO_2	CH_3NHCO	92 [b]	189–191 °C
10h	H	H	89 [d]	87– 89 °C

[a] Refers to the last step. [b] From reacylation of the corresponding amine. [c] Cyclization of analogues of **5**. [d] 10 h at reflux in dimethoxyethane/4 N NaOH.

The ^1H NMR spectra of compounds of type **7** show doubling of all the expected signals. At higher temperatures (DMF, DMSO, 120 °C) these signals did not coalesce. These observations suggest a strongly hindered amide bond rotation. Two methods of recrystallization allowed the isolation of two distinct crystal forms: a coarse modification from the melt (rotamer **1**) and a fine modification from solution (rotamer **2**). Subsequent X-ray crystallographic examination

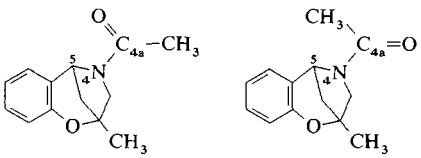

7, modification 1 **7**, modification 2

showed the carbonyl group in **7** to be pointing either towards or away from the aromatic ring. This is the first case known to us of two crystalline amide rotamers isolable at room temperature. This high stability is restricted to the solid state in which the two rotamers are ordered in different crystal lattices; the carbonyl group and the N4–C5 bond lie virtually in the same plane.[6] In solution (chloroform, DMSO, DMF)

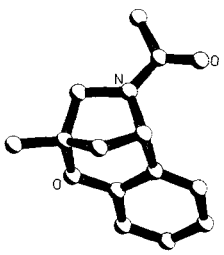

Fig. 1. X-ray crystal structure of compound **7**, modification 1.

the two crystal forms equilibrate within the time required for preparation of an NMR sample to the originally noted 1:1 mixture of rotamers. Consequently, separation by HPLC is not possible. As expected these isomeric mixtures are not present in the ureas (e.g. **10g**) or the sulfonamides (e.g. **10f**), and thus no doubling of their ^1H NMR signals is observed.

Experimental Procedure

4: To a solution of **3** (142 g, 0.88 mol) and **2** (120 g, 0.88 mol) in toluene (400 mL) was added pyrrolidine (185 mL). The mixture was stirred for 4 days at 25 °C. After successive washes with 2 N HCl, 2 N NaOH, and water the organic phase was evaporated in vacuo. Ether was added and 67.8 g of **4** precipitated (m.p. = 98–100 °C). The aqueous solutions were extracted with *n*-butanol. This organic phase was evaporated and the residue purified by

chromatography to give a further 69 g of the same chromanone. Yield: 136.8 g **4** (68%).

7: To a solution of **5** (50 g) in chlorobenzene (600 mL) heated to 90 °C was added cyclohexane (400 mL) and *p*-toluenesulfonic acid (3 g). The mixture was stirred at reflux for 25 minutes with continuous removal of water (Dean-Stark trap). The mixture was then poured into a sodium bicarbonate solution. The organic phase was washed with water, dried over Na_2SO_4, and evaporated under reduced pressure to give **7** (34.5 g, 75%), m.p. = 110–112 °C (The dehydration sometimes occurrs spontaneously and should be performed in a flask not more than half full). ^{1}H NMR (Varian XL-200, 200 MHz, $CDCl_3$, 25 °C, TMS): δ = 1.65 and 1.66 (2 singlets, CH_3, C2); 1.90 and 2.15 (2 singlets, acetyl CH_3); 2.1–2.3 (2 ABX systems, 2H, methano bridge); 3.5–3.8 (2 AB systems, 2H, C3); 4.81 and 5.37 (dd, 1H, C5); 6.8–7.3 (multiplet, 4H, aromatic H). IR (KBr): $\tilde{\nu}_{CO}$ = 1650 cm^{-1}.

10g: ^{1}H NMR ($CDCl_3$): δ = 1.70 (s, CH_3, C2); 2.2 (ABX multiplet, methano CH_2); 2.73 (d, NH-CH_3); 3.6 (AB quartet, 2H, C3); 4.63 (broad q, NH); 5.10 (H, C5); 6.8–8.2 (3 aromatic H: 6.81 (d), 8.02 (dd), 8.15 (d)).

Received: May 16, 1991 [Z 4632 IE]
German version: *Angew. Chem. 103* (1991) 1667
Publication delayed on authors' request

CAS Registry numbers:
2, 118-93-4; **3**, 51862-97-6; **4**, 137232-97-4; **5**, 137232-98-5; 7-MeO-**5**, 137232-99-6; **7**, 137233-00-2; **10a**, 137233-01-3; **10b**, 137233-02-4; **10c**, 137233-03-5; **10d**, 137233-04-6; **10e**, 137233-05-7; **10f**, 137233-06-8; **10g**, 137233-07-9; **10h**, 137233-08-0.

[1] V. A. Ashwood, F. Cassidy, M. C. Coldwell, J. M. Evans, T. C. Hamilton, D. R. Howlett, D. M. Smith, G. Stemp, *J. Med. Chem. 33* (1990) 2667.
[2] D. W. Robertson, M. I. Steinberg, *J. Med. Chem. 33* (1990) 1529.
[3] H. J. Kabbe, *Synthesis 1978*, 886.
[4] H. J. Kabbe, A. Widdig, *Angew. Chem. 94* (1982) 254; *Angew. Chem. Int. Ed. Engl. 21* (1982) 247.
[5] R. H. Wiley, O. H. Borum, *J. Am. Chem. Soc. 70* (1948) 2005.
[6] Crystal data of **7**. Modification 1: monoclinic, space group $P2_1/c$, N4–C4a = 134.6 pm, N4–C4a valency = 1.4 , C5-N4-C4a-O torsion angle = – 3.2°. Modification 2: triclinic, space group $P\bar{1}$, N4-C4a = 132.8 pm, N4-C4a valency = 1.55, C5-N4-C4a-O torsion angle = 173.5 °C. Further X-ray crystallographic data can be obtained from the Fachinformationszentrum Karlsruhe, Gesellschaft für wissenschaftlich-technische Information mbH, W-7514 Eggenstein-Leopoldshafen 2, by quoting the deposit number CSD-55553, the authors, and the literature reference.

Antibody Catalysis of Glycosidic Bond Hydrolysis**

By *Jean-Louis Reymond, Kim D. Janda,** and *Richard A. Lerner**

Monoclonal antibodies raised against transition state mimics have been shown to catalyze a number of chemical reactions[1] and for this reason have been called abzymes (*antibody enzymes*). Existing examples have focused on base-catalyzed transformations involving negatively charged transition states and to a lesser extent on electrocyclic and redox reactions. We report here the first antibody which catalyzes the acid-promoted hydrolysis of an activated glycosidic bond.[2]

The reaction which we chose to investigate was the hydrolysis of aryloxytetrahydropyran **1**. This type of acetal, although much more labile than a real glycoside, is a prototypical model for a glycosidic bond.[3a, b] Both the spontaneous and the acid-catalyzed cleavage involve rate determining heterolytic dissociation of the exocyclic carbon-oxygen bond.[3c] Due to stereoelectronic effects the reaction rate is conformation dependent; the axial chair conformer is the more labile form (Fig. 1).[3d] A detailed semi-empirical calculation of the transition state geometry suggests that the exocyclic C–O bond is approximately 1.8 to 2.2 Å in length.[4] We reasoned that piperidinium ions like **2** or **3**, with a carbon–nitrogen bond of approximately 1.5 Å, might be acceptable mimics for the proposed cationic transition state involved in the acid-catalyzed cleavage of **1**, provided that the benzylic nitrogen substituent could be constrained to the axial position. This was achieved by substituting the 3-position of **2** and **3** to form our antigens **4**, **5**, and **6**. In addition, a convenient handle was created for hapten–carrier protein immobilization (Fig. 1).

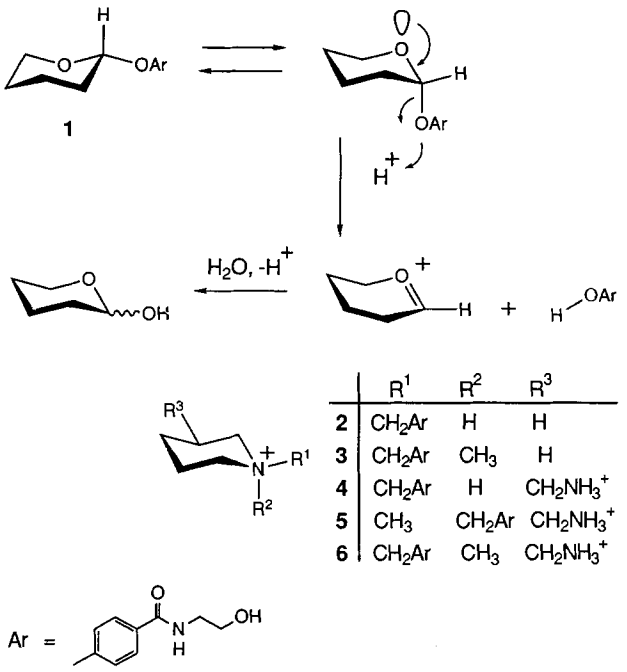

	R^1	R^2	R^3
2	CH_2Ar	H	H
3	CH_2Ar	CH_3	H
4	CH_2Ar	H	$CH_2NH_3^+$
5	CH_3	CH_2Ar	$CH_2NH_3^+$
6	CH_2Ar	CH_3	$CH_2NH_3^+$

Fig. 1. Above: Mechanism of the hydrolytic cleavage of 2-aryloxytetrahydropyrans. Below: Transition state models.

Hapten **4** was synthesized in 8 steps starting from 3-hydroxymethylpiperidine and 4-(chloromethyl)-*N*-(2′-hydroxyethyl)benzamide.[5] In a similar fashion, a 1:1 mixture of diastereoisomeric haptens **5** and **6** was obtained starting with *N*-methyl-3-hydroxymethylpiperidine. Both **5** and **6** were separated by reverse phase high performance liquid chromatography (RP-HPLC)[6a] and their relative configuration was assigned on the basis of the ^{1}H NMR spectrum of **5**.[6b] A linker was attached to **4**, **5**, and **6** to insure immunogenicity (5-[(2,5-dioxo-1-pyrrolidinyl)oxy]-5-oxopentanoyl chloride, Et(*i*Pr)$_2$N, dimethylformamide (DMF), –30 °C) and these activated haptens were coupled to the carrier proteins bovine serum albumine (BSA) and keyhole limpet hemocyanin (KLH). Balb/c mice were immunized with the KLH conjugates and antibodies were generated by standard protocols.[7] Monoclonal antibodies were purified from ascites fluid by anion exchange chromatography (16 antibodies were obtained from immunization with **4**, 26 from **5**, and 3 from **6**) and assayed against substrate **1** for production of 4-hydroxy-*N*-(2′-hydroxyethyl)benzamide.[8] Two monoclonal antibodies, both derived from immunization with hapten **5**, were found to be catalytic. After affinity chromatography

[*] Prof. K. D. Janda, Prof. R. A. Lerner, Dr. J.-L. Reymond
Departments of Molecular Biology and Chemistry
The Scripps Research Institute
10666 North Torrey Pines Road, La Jolla, CA 92037 (USA)

[**] This work was financially supported by the U.S. National Institute of Health (GM 43858, *K. D. J.*) and the Schweizerischen Nationalfonds zur Förderung der Wissenschaften (postdoctoral fellowship for *J.-L. R.*).

(protein G), antibody 14D9 was chosen for further characterization due to its rate of reaction and stereoselectivity.

The hydrolysis of **1** catalyzed by 14D9 initially followed Michaelis–Menten kinetics ($K_m = 100\ \mu M$, $k_{cat} = 7.8 \times 10^{-5}\ s^{-1}$).[9] Potent inhibition by hapten **3** was observed and this allowed quantitative titration of the catalytic activity.[10] At pH = 5.7, the abzyme reaction is approximately 70 times faster than the "background reaction". A pH–rate profile study (Fig. 2) indicated the rate of the background hydrolysis of **1** to be the sum of a pH-independent reaction ($k_0 = 4.8 \times 10^{-7}\ s^{-1}$) and a H^+-catalyzed reaction ($k_{H^+} = 0.33\ M^{-1} s^{-1}$). In contrast, the antibody-catalyzed reaction seems to be completely pH-dependent, and thus would appear to be an acid-catalyzed process. However, this must be viewed with caution because the pH range investigated was limited (Fig. 2).[11]

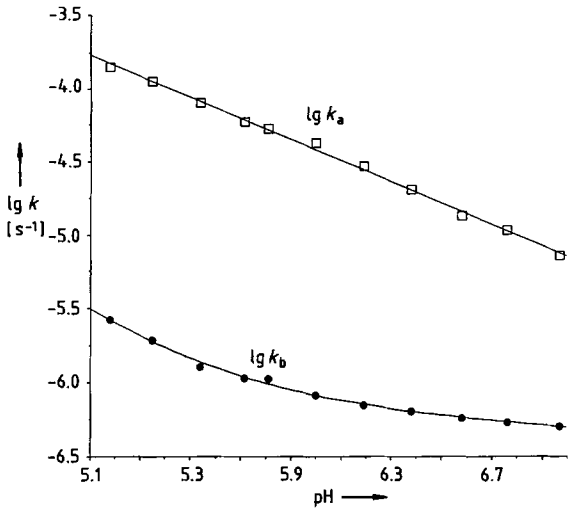

Fig. 2. Plot of $\lg k_a$ and $\lg k_b$ vs. pH. (□ antibody 14D9-catalyzed hydrolysis, • background hydrolysis of **1**). The assays were performed at 20 °C in solutions which were 50 mM in MES and 100 mM in NaCl. The upper trace is the result of the best linear fit of all the points. The lower line was calculated from the equation $k_{obsd} = k_0 + k_{H^+} \cdot [H^+]$.

To examine the hypothesis that the abzyme reacts with conformational selectivity, we synthesized diastereoisomers **7**–**10** (Fig. 3).[12] ^1H NMR spectra of these compounds in D_2O show them to have a chair conformation in solution. The phenolic leaving group is fixed either in the axial (**7** and **9**) or the equatorial (**8** and **10**) position. None of these compounds was accepted as a substrate,[13] but all competitively inhibited the reaction of **1** and 14D9 (Fig. 3). A clear selectivity was observed for the (2*S*,6*R*)-(−)-isomer **7**. This strongly

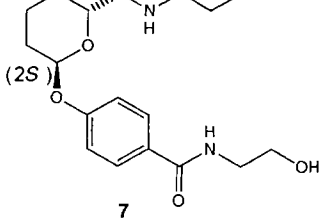

		K_i
7	(2*S*,6*R*) (−)	35 μM
8	(2*R*,6*R*) (+)	500 μM
9	(2*R*,6*S*) (+)	600 μM
10	(2*S*,6*S*) (−)	250 μM

Fig. 3. Stereoselective competitive inhibition of the antibody 14D9-catalyzed cleavage of **1**.

suggests that the immune response was directed to the corresponding enantiomer of our racemic hapten **5**, and that the stereochemical information concerning the axial placement of the phenolic leaving group was effectively transferred to the antibody binding pocket. This stereochemical selectivity probably allows the antibody to bind substrate **1** in the reactive axial chair conformation, and to achieve catalysis by a reaction pathway very similar to the well-characterized process in solution. However, we could not determine whether *both* enantiomers of the racemic substrate **1** actually reacted within the antibody binding pocket (Fig. 3). Interestingly, if only one enantiomer were a substrate, then the other would probably be quite a good inhibitor, which means that the observed catalytic rate with racemic **1** would not reflect the true catalytic rate for the reactive enantiomer.

To further characterize the specific interactions within our abzyme's binding pocket, we employed compounds **11**–**14**. These compounds, truncated versions of the tightly binding inhibitor **3**, competitively inhibited the hydrolysis of **1** by 14D9 (Fig. 4). From the weak inhibition observed with ben-

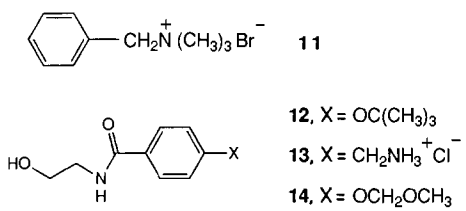

Fig. 4. Competitive inhibitors of antibody 14D9 (see text).

zyltrimethylammonium bromide (**11**, $K_i = 400\ \mu M$), it is apparent that the recognition of the aromatic side chain is an important factor in abzyme–antigen binding. Furthermore, the bulky, hydrophobic, *tert*-butyl ether **12** ($K_i = 5 \mu M$) is a much better inhibitor than either the charged primary benzylammonium salt **13** ($K_i = 90\ \mu M$) or the hydrophilic methoxymethyl ether **14** ($K_i = 600\ \mu M$). Abzyme–antigen binding thus appears to be mediated more efficiently by hydrophobic interactions between the abzyme binding pocket and the hydrocarbon envelope of the quaternary ammonium center than by coulombic interactions between the haptenic positive charge and the antibody.[14] Significant hydrophobic interactions are not surprising in an aqueous system and probably partly account for the low catalytic efficiency of 14D9 since the hydrolytic rate of **1**, as in many reactions involving charged transition states, strongly depends on solvent polarity.[15]

In summary, acid-mediated antibody-catalyzed cleavage of a prototypical activated glycosidic bond was achieved, and a first step toward the development of an antibody capable of glycosidic bond cleavage has been made. The results of this preliminary study point to the importance of stereochemical control in the haptenic design. The need to secure chemical catalysis within an antibody binding pocket is also evident. Future research will address this point.

Received: July 29, 1991 [Z 4836 IE]
German version: *Angew. Chem. 103* (1991) 1690

CAS Registry numbers:
1, 137364-79-5; **2**, 137364-80-8; **3**, 137364-81-9; **4**, 137364-82-0; **5**, 137364-83-1; **6**, 137364-84-2; **7**, 137364-85-3; **8**, 137490-30-3; **9**, 137490-31-4; **10**, 137490-32-5; **11**, 5350-41-4; **12**, 137364-86-4; **13**, 137364-87-5; **14**, 137364-88-6; activated

hapten a, 137364-89-7; activated hapten b, 137364-90-0; activated hapten c, 137364-91-1; 4-chloromethyl-*N*-(2-hydroxyethyl)benzamide, 137364-92-2; 5-[(2,5-dioxo-1-pyrrolidenyl)oxy]-5-oxopentanoylchloride, 117746-42-6; 3-hydroxymethylpiperidine, 4606-65-9.

[1] R. A. Lerner, S. J. Benkovic, P. G. Schultz, *Science (Washington D.C.) 252* (1991) 659.

[2] There is one report of antibody catalysis of an acid-catalyzed reaction, namely the hydrolytic cleavage of a trityl-protected primary alcohol: B. L. Iverson, K. E. Cameron, G. K. Jahangiri, D. S. Pasternak, *J. Am. Chem. Soc. 112* (1990) 5320.

[3] a) A. J. Kirby, *CRC Crit. Rev. in Biochem. 22* (1987) 283; b) M. L. Sinnott, *Chem. Rev. 90* (1990) 1171; c) An alternative pathway involving heterolytic cleavage of the endocyclic carbon–oxygen bond has been proposed for the lysozyme reaction (C. B. Post, M. Karplus, *J. Am. Chem. Soc. 108* (1986) 1317). Our substrate **1**, like the frequently employed *p*-nitrophenyl glycosides, is electronically imbalanced by the aromatic leaving group, and the possibility of a ring opening pathway is not relevant. d) Such stereoelectronic control does not necessarily apply to all glycopyranose derivatives; see: A. J. Bennet, M. L. Sinnott, *J. Am. Chem. Soc. 108* (1986) 7287.

[4] H.-B. Bürgi, K. C. Dubler-Steudle, *J. Am. Chem. Soc. 110* (1988) 7291.

[5] All new compounds were characterized by ^{1}H NMR and MS. Crystalline products gave satisfactory elemental analyses (±0.3%).

[6] a) Semi-preparative RP-HPLC (C-18 column, 0.1% HCl/H_2O, 1 mL min^{-1}): **5**: retention time, t_R = 15.0 min, **6**: t_R = 15.7 min; b) Nuclear Overhauser effects (NOE) (D_2O, 500 MHz): **5**: Irradiation of the CH_3-N$^+$ signal affected the piperidine ring protons $H_{eq}C(2) + H_{eq}C(6)$ (2.6%), $H_{ax}C(6)$ (4.5%) and $H_{ax}C(2)$ (4.5%); Irradiation of the signal at δ = 4.6 (Ar-CH-N$^+$) affected $H_{eq}C(2) + H_{eq}C(6)$ (2.1%), $H_{ax}C(3)$ (2.8%) and $H_{ax}C(5)$ (2.1%).

[7] a) G. Köhler, C. Milstein, *Nature (London) 256* (1975) 495; b) E. Enguall, *Methods Enzymol. 70* (1980) 419.

[8] 20 μM Antibody, 500 μM substrate **1**, 100 mM bis-tris pH 6.0, 100 mM NaCl. 20 °C. Formation of the phenol product was followed by RP-HPLC (C-18, CH_3CN/H_2O 20:80, 0.8 mL min^{-1}, t_R = 4.20 min) against an internal standard (2-acetamidophenyl-2′-hydroxyethylether, t_R = 7.41 min).

[9] Assay conditions: 2 to 15 μM antibody, 25 to 300 μM substrate **1**, 100 mM morpholinoethanesulfonic acid (MES), pH 5.7, 100 mM NaCl, 20 °C (see also ref. [8]). There was no difference in the observed rates with antibody 14D9 when tested at pH 6.0 in either bis-tris or MES (100 mM and 50 mM buffers).

[10] Potent inhibition by our hapten **3** was demonstrated by the following experiment: a 4 μM solution of 14D9 was completely inhibited by 10 μM of **3**. After 5 days of extensive dialysis at 37 °C, the inhibited antibody recovered only 40% of the activity of the noninhibited control sample.

[11] Antibody 14D9 was unstable below pH = 5.2.

[12] a) The key intermediate was 2-aminomethyl-3,4-dihydro-2*H*-pyran, which was resolved with mandelic acid. Absolute configuration was tentatively assigned by comparison of the optical rotation of its chloroacetamide derivatives with known γ-substituted valerolactone derivatives: W. H. Pirkle, P. E. Adams, *J. Org. Chem. 44* (1979) 2169.

[13] The lack of antibody catalysis on compounds **7** to **10** could result from nonproductive binding of the propanamidomethyl side chain, leading to an unreactive abzyme–substrate complex.

[14] a) Recent mutagenesis studies on the anti-phosphocholine antibody McPC603 suggested that binding of the alkyltrimethyl ammonium moiety is mediated by electrostatic interactions with two carboxylates on the protein. Van der Waals contacts to the alkyl groups were judged less important: R. Glockshuber, J. Stadlmüller, A. Plückthun, *Biochemistry 30* (1991) 3049.

[15] a) The rate for the H$^+$-catalyzed hydrolysis of **1** in 100% H_2O is 30 times the rate reported for the hydrolysis of *p*-(2-tetrahydropyranyloxy)benzoic acid in 50% aqueous dioxane ($k_2 = 9.2\ 10^{-3}$ M^{-1} s^{-1}): T. H. Fife, E. Anderson, *J. Am. Chem. Soc. 93* (1971) 6610.

Corrigendum

In the communication "Enzymatic Two-Step Synthesis of *N*-Acetylneuraminic Acid in the Enzyme Membrane Reactor" by U. Kragl, D. Gygax, O. Ghisalka, and C. Wandrey (*Angew. Chem. Int. Ed. Engl. 30* (1991) 827, the units of the time *t* on the abscissa of Figure 2 should be hours and not minutes.

Registered names, trademarks, etc. used in this journal, even when not marked as such, are not to be considered unprotected by law.

© VCH Verlagsgesellschaft mbH, W-6940 Weinheim, 1991. – Printed in the Federal Republic of Germany by Konrad Triltsch Druck- und Verlagsanstalt Würzburg.

All rights reserved (including those of translation into foreign languages). No part of this issue may be reproduced in any form — by photoprint, microfilm, or any other means — nor transmitted or translated into a machine language without written permission from the publishers. Only single copies of contributions, or parts thereof, may be made for personal use. This journal was carefully produced in all its parts. Nevertheless, authors, editors and publisher do not warrant the information contained therein to be free of errors. Readers are advised to keep in mind that statements, data, illustrations, procedural details or other items may inadvertently be inaccurate.

Valid for users in the USA: The appearance of the code at the bottom of the first page of an article (serial) indicates the copyright owner's consent that copies of the article may be made for personal or internal use, or for the personal or internal use of specific clients. This consent is given on the condition, however, that the copier pay stated per-copy fee through the Copyright Clearance Center, Inc. (CCC), for copying beyond that permitted by Sections 107 or 108 of the U.S. Copyright Law. This consent does not extend to other kinds of copying, such as copying, for general distribution, for advertising or promotional purposes, for creating new collective works, or for resale. For copying from back volumes of this journal see 'Permissions to Photo-Copy: Publisher's Fee List' of the CCC.

Editorial office: Postfach 10 11 61, W-6490 Weinheim, Federal Republic of Germany, Telephone (06201) 60 23 15, Telex 465 516 vchwh d, Telefax (06201) 602 328, E-Mail Z16@DHDURZ2 in Earn Bitnet.

Editor: *Peter Gölitz*

Associate editors: *R. H. Schmidt-Radde, K. J. Schneider, A. Stimson.* **Editorial assistant:** *E. Schweikart*

Publishers: VCH Verlagsgesellschaft mbH. (Managing Director: *Hans Dirk Köhler, Dr. Karl-Heinz Köpfer*), Pappelallee 3, W-6940 Weinheim, Federal Republic of Germany.

Advertising office (Advertising Manager *R. J. Roth*): Postfach 10 11 61, W-6940 Weinheim, Federal Republic of Germany, Telephone (0 62 01) 60 61 36, Telex 4 67 155, Telefax (0 62 01) 606 156.

AUTHOR INDEX [*Angew. Chem. Int. Ed. Engl. 30* (1991)]

The page numbers in square brackets refer to the German edition [*Angew. Chem. 103* (1991)] of Angewandte Chemie. Page numbers in round brackets indicate errata.

Abbenhuis, H. C. L. 996 [1046]
Adachi, T. 982 [1025]
Adam, W. 200, 1365 [187, 1395]
Adiwidjaja, G. 1687 [1679]
Aguilar, J. 555 [596]
Aguilar-Parrilla, F. 88 [88]
Ahlrichs, R. 832 [848]
Albano, V. G. 847 [895]
Almen, H. 561 [608]
Alt, H. G. 1119 [1139]
Altmann, K.-H. 1514 [1504]
Altmeyer, O. 1136 [1158]
Amann, R. 1320 [1373]
Amoroso, A. J. 107, 1505 [102, 1529]
Andersen, M. W. 97 [90]
Anderson, P. A. 1501 [1511]
Andersson, S. 754 [771]
Andler, S. 1365 [1395]
Ando, H. 446 [454]
Anelli, P. L. 1036 [1052]
Angermund, K. 1354 [1379]
Apeloig, Y. 1479 [1546]
Arai, Y. 446 [454]
Arlt, D. 1662 [1685]
Armaroli, N. 1333 [1367]
Armatage, A. 1674 [1720]
Armstrong, D. R. 1707 [1702]
Arnz, R. 683 [702]
Asfari, Z. 854 [887]
Asharin-Fard, S. 558 [614]
Ashton, P. R. 80, 1036, 1039, 1042 [96, 1052, 1055, 1058]
Attinà, M. 1457 [1527]
Atwood, D. A. 1143 [1164]
Atwood, J. L. 1141 [1163]
Auchter-Krummel, P. 1003 [996]
Auner, N. 444, 1132, 1151 [425, 1155, 1172]
Avnir, D. 1379 [1409]

Baceiredo, A. 1154 [1174]
Badía, J. 555 [596]
Baena, M. J. 711 [716]
Bailey, P. J. 1706 [1672]
Baker, G. R. 1176, 1178 [1205, 1207]
Baldus, H.-P. 605 [620]
Ballauff, M. 1650 [1715]
Balzani, V. 190, 1333 [186, 1367]
Bär, E. 88 [88]
Bär, M. R. 832 [848]
Bard, A. J. 836 [882]
Baret, P. 85 [75]
Barlos, K. 590 [572]
Barr, D. 82, 1501, 1707 [97, 1511, 1702]
Barron, A. R. 1353 [1403]
Barsacchi, M. 989 [992]
Barth, A. 303 [325]
Barth, T. 1028 [1006]
Bartley, S. L. 448 [447]
Bashall, A. 980, 1164 [1021, 1186]
Basset, J.-M. 1660 [1692]
Batail, P. 1498 [1508]
Batcheller, S. A. 902 [916]
Baudler, M. 580 [590]
Bauer, T. 561 [608]
Bauermeister, H. 191 [207]
Bayer, E. 113 [117]
Bayer, G. M. 961 [1012]
Beck, H. P. 824 [897]
Beck, J. 1128 [1149]
Beck, W. 168, 1467 [173, 1492]
Becke, A. D. 409 [421]
Becker, H. 130 [134]
Behera, R. K. 1176 [1205]
Behrendt, L. 1008 [991]
Behrens, U. 870 [847]
Beller, M. 868 [878]
Belluš, D. 1193, 1465 [1219, 1533]
Benn, R. 426 [436]
Bensch, W. 1183 [1197]
Benz, G. 1702 [1735]
Berger, U. 830 [857]
Bergsträsser, U. 207 [208]
Bergthaller, P. 1704 [1742]
Bernadou, J. 702 [718]
Bernardinelli, G. 1490 [1530]
Bernd, M. 712 [704]
Berndt, A. 594, 1479 [580, 1546]
Berrisford, D. J. 82 [97]
Bertrand, G. 1154 [1174]
Bestmann, H. J. 86 [78]
Bhula, R. 688 [715]
Biddlecom, W. G. 1646 [1694]
Biehler, K. 547 [601 (906)]
Bill, E. 1494 [1499]
Binger, P. 207, 310 [208, 316]
Binnewies, M. 745 [762]
Björgvinsson, M. 1677 [1671]
Blachnik, R. 605 [620]
Blake, A. J. 1139 [1161]
Blase, W. 326 [335]
Bläser, D. 173 [199]
Blechert, S. 412 [428]
Blocher, A. 1476 [1489]
Bo, Y. 687 [727]
Boche, G. 321, 1455 [338, 1497]
Bochkarev, M. N. 1149 [1170]
Bochmann, M. 973 [975]
Bock, Hans 187, 714, 1180, 1183, 1186, 1678 [193, 706, 1194, 1197, 1200, 1733]
Bock, Harald 414 [450]
Bodensieck, U. 1126 [1147]
Boese, R. 173, 971, 993, 1015, 1160, 1370, 1463, 1484, 1518 [199, 1027, 1032, 1029, 1179, 1374, 1542, 1495, 1544]
Bögge, H. 1512, 1674 [1501, 1720]
Böhme, D. K. 884, 1323 [898, 1396]
Bolm, C. 403, 542 [414, 556]
Bömer, B. 1662 [1685]
Bönnemann, H. 1312 [1344]
Bordoni, S. 847 [895]
Born, L. 1634, 1685, 1709 [1699, 1729, 1667]
Borrmann, H. 1678 [1733]
Bortlik, K. 1315 [1354]
Bortz, M. 883 [841]
Bosold, F. 1455 [1497]
Bott, S. G. 1141 [1163]
Botta, A. 1689 [1687]
Böttcher, F. 101 [79]
Bovin, J.-O. 864, 874 [891, 852]
Brachthäuser, B. 1488 [1552]
Brack, A. 1643 [1689]
Brackemann, H. 1654 [1722]
Braga, D. 847 [895]
Braude, V. 1479 [1546]
Braun, J. 852 [861]
Braun, M. 1318 [1369]
Breitmaier, E. 202 [189]
Brendel, H.-D. 1652 [1664]
Breuckmann, R. 683 [702]
Brijoux, W. 1312 [1344]
Brinkmann, R. 1312 [1344]
Bronger, W. 759 [776]
Brown, C. L. 1039, 1042 [1055, 1058]
Bryce, M. R. 871 [867]
Buback, M. 641, 1654 [658, 1722]
Buchholz, H. 1518 [1544]
Bühl, M. 1160 [1179]
Bujacz, G. 578 [604]
Bulach, V. 572 [611]
Burek, C. J. 1143 [1164]
Burgess, M. L. 704 (1192) [723 (1418)]
Burkhardt, A. 828 [850]
Burrell, A. K. 91 [83]
Bursten, B. E. 1069 [1085]
Buschmann, H. 477 [480]
Buschmann, J. 414 [450]
Busetto, L. 847 [895]
Buss, D. H. 1017 [1017]
Buss, V. 869 [889]
Butenschön, H. 880 [871]
Buttkus, U. 1514 [1504]
Buysch, H.-J. 1689 [1687]

Cabrera, I. 76 [106]
Cacace, F. 1457 [1527]
Calabrese, J. C. 450 [459]
Calderazzo, F. 102 [109]
Cammann, K. 516 [519]
Camps, F. 1470 [1540]
Canadell, E. 1498 [1508]
Carmona, D. 1171 [1192]
Carneiro, J. W. de M. 683 [702]
Carter, R. L. 293 [298]
Cayton, R. H. 862 [893]
Chadha, R. K. 598 [592]
Chan, C. 1337 [1389]
Chi, K.-M. 194 [196]
Chiang, Y. 1356, 1366 [1391, 1407]
Chisholm, M. H. 673, 862 [690, 893]
Chmielewski, D. 1343 [1361]
Choplin, A. 1660 [1692]
Christmas, C. A. 598 [592]
Christou, G. 305, 1672 [314, 1681]
Chrystal, E. J. T. 1039, 1042 [1055, 1058]
Clegg, W. 1707 [1702]
Cockcroft, J. K. 101 [79]
Coffin, M. A. 871 [867]
Cohen, H. 1158 [1177]
Coleman, A. P. 973 [975]
Conole, G. C. 1706 [1672]
Consiglio, G. 989 [992]
Constable, E. C. 407, 1363, 1450 [418, 1401, 1482]
Contreras, L. 1143 [1164]
Corbelin, S. 825 [875]
Corbett, J. D. 856 [842]
Cordier, G. 326 [335]
Corey, E. J. 455 [469]
Corey, P. F. 1646 [1694]
Corradini, R. 1348 [1363]
Corriu, R. 1130 [1153]

Coulon, C. 1498 [1508]
Cowley, A. H. 1141, 1143 [1163, 1164]
Cozens, F. 1337 [1389]
Crabtree, R. H. 193 [205]
Craig, D. C. 704 (1192) [723 (1418)]
Cram, D. J. 1024 [1048]
Crespo, M. I. 74 (216) [85 (222)]
Cyr, M. J. 91 [83]

Dahan, F. 1154 [1174]
Dai, W.-M. 1032, 1387 [1034, 1453]
Dally, R. 1690 [1725]
Danovich, D. 1479 [1546]
Davidson, M. G. 1648 [1696]
Day, V. W. 422 [426]
de Delgado, G. C. D. 420 [438]
de Meijere, A. 1361, 1518, 1658 [1350, 1544, 1669]
de Mendoza, J. 1331 [1365]
de Meric de Bellefon, C. 185 [183]
DeCian, A. 838 [884]
Declercq, J.-P. 994 [1044]
Defaye, J. 78 [94]
Degroot, D. C. 1325 [1404]
Dehnicke, K. 577 [564]
Dehnicke, S. 1349 [1371]
Della Védova, C. O. 1145 [1166]
Denis, J. M. 196 [191]
Deslongchamps, G. 858 [880]
Diederich, F. 678, 698 [695, 708]
Dietrich, H. 1328 [1348]
Dietrich, M. 205 [215]
DiMaio, A.-J. 194 [196]
Dinges, J. 1339 [1385]
Dinjus, E. 1312 [1344]
Dittmer, M. 436 [431]
Dittrich, A. 76 [106]
Dohmeier, C. 564 [594]
Dolg, M. 1186 [1200]
Donald, D. 954 [968]
Dörges, C. 106 [82]
Döring, J. 210, 588 [203, 575]
Draber, W. 1621 [1650]
Drake, S. R. 1707 [1702]
Drauz, K. 712 [704]
Dreizler, H. 1644 [1674]
Drewlies, R. 103 [76]
Dreyer, M. 555 [596]
Driess, M. 1022 [979]
Dubourg, A. 994 [1044]
Duetsch, M. 1658 [1669]
Dunbar, K. R. 448 [447]
Duthaler, R. O. 705 [729]

Ebihara, M. 856 [842]
Echegoyen, L. 838 [884]
Eck, W. 414 [450]
Edelmann, F. T. 693 [720]
Edwards, P. P. 1501 [1511]
Effenberger, F. 873 [866]
Eger, R. 1188 [1210]
Egert, E. 964 [1008]
Ehrenberg, S. 334 [320]
Eicher, T. 130 [134]
Ellestad, G. 418 [462]
Ellis, J. E. 194 [196]
Ellwood, P. 80 [96]
Elschenbroich, C. 547 [601 (906)]
Enders, D. 1664 [1676]
Enders, M. 84 [80]
Englert, U. 313, 690, 1377 [329, 732, 1357]
Englisch, U. 613 [629]
Enkelmann, V. 1121 [1142]
Eppley, D. F. 584 [616]
Erker, G. 1349 [1371]
Ernst, B. 1465 [1533]
Espinet, P. 711 [716]
Esser, P. 477 [480]
Estermaier, L. M. 1314 [1353]
Etzbach, T. 580 [590]
Eugster, C. H. 654 [671]
Evans, J. S. O. 1156 [1175]

Famulok, M. 858 [880]
Farin, D. 1379 [1409]
Farshchi, H. 600 [619]
Fehlhammer, W. P. 88 [88]
Feiken, N. 996 [1046]
Felix, D. 1008 [991]
Fengler, G. 1598 [1626]
Ferrer, J. 1171 [1192]
Fessner, W.-D. 555, 1020 [596, 985]
Filali, A. 560 [563]
Filippou, A. C. 1167 [1188]
Fischer, H. 998 [1013]
Fischer, J. 838 [884]
Fischer, R. W. 185, 1638 [183, 1706]
Fitjer, L. 436, 1492 [431, 1534]
Flad, J. 409 [421]
Fleischer, F. 1484 [1495]
Flessner, U. N. 1636 [1704]
Folting, K. 305, 1672 [314, 1681]
Fontecave, M. 1135 [1151]
Foxman, B. M. 420 [438]
Freitag, D. 1598 [1626]
Frenking, G. 577, 1001, 1146 [564, 1038, 1167]
Frerichs, S. R. 194 [196]
Frijns, J. H. G. 1152 [1181]
Fuchs, J. 88 [88]
Fuchs, R. 1634 [1699]
Fukuda, Y. 1339 [1385]
Furber, M. 954 [968]

Gabor, B. 1666 [1711]
Gade, L. H. 107, 1164 [102, 1186]
Gadelle, A. 78 [94]
Gaillard, J. 1135 [1151]
Gallagher, M. J. 704 (1192) [723 (1418)]
Gamper, S. 1132 [1155]
García, G. 716 [733]
García, J. 716 [733]
Gassmann, R. 1514 [1504]
Gatos, D. 590 [572]
Gauss, D. H. 613 [629]
Ge, L. 296 [301]
Gellon, G. 85 [75]
Gerez, C. 1135 [1151]
Gerke, R. 964 [1008]
Gerner, R. 1017 [1017]
Gersdorff, J. von 1461 [1536]
Ghisalba, O. 827 (1713) [854]
Gibson, V. C. 980 [1021]
Gier, T. E. 1169 [1191]
Giese, B. 600 [619]
Giroud-Godquin, A.-M. 375 [370]
Gleiter, R. 205, 681, 1518 [215, 699, 1544]
Glemser, O. 1017 [1017]
Gobbi, A. 1001 [1038]
Göbel, I. 187 [193]
Goddard, R. 1124 [1145]
Goldmann, S. 1559 [1587]
Gompper, R. 332, 334 [318, 320]
Gonda, J. 1465 [1533]
Goodnow, T. T. 1039 [1055]
Goto, T. 17 [17]
Gowik, P. 1485 [1490]
Graczyk, P. 578 [604]
Grant, A. S. 1366 [1407]
Grasser, F. 1311 [1346]
Graulich, J. 547 [601 (906)]
Grevels, F.-W. 1343 [1361]
Gries, S. 565 [595]
Grimme, W. 205 [215]
Grosser, R. 1662 [1685]
Grossman, S. H. 1178 [1207]
Grove, D. M. 996 [1046]
Grover, N. 1517 [1525]
Grunder, R. 1650 [1715]
Grünleitner, W. 1167 [1188]
Grützmacher, H. 709, 1017 [721, 976]
Gudat, A. 199 [217]
Gudat, D. 217 [251]
Guenot, P. 196 [191]
Guillemin, J. C. 196 [191]
Gütlich, P. 975 [1015]
Gygax, D. 827 (1713) [854]

Haaf, K. 893 [907]
Haag, S. 831 [874]
Haag, T. 1487 [1550]
Haarer, D. 540 [553]
Haarman, H. F. 996 [1046]
Haas, J. 310 [316]
Hadjiarapoglou, L. 200 [187]
Hagen, P. M. 598 [592]
Haggerty, B. S. 194 [196]
Hahn, F. E. 203 [213]
Hahn, U. 343 [351]
Handel, H. 560 [563]
Hanko, R. 1690 [1725]
Hans, J. 878 [845]
Hansen, H.-P. 1377 [1357]
Harlow, R. L. 450 [459]
Harms, K. 321, 1455, 1472, 1474 [338, 1497, 1515, 1517]
Harris, P. R. 1143 [1164]
Harrison, W. T. A. 1169 [1191]
Harrowfield, J. M. 854 [887]
Hartl, H. 328 [311]
Hartmann, G. R. 1314 [1353]
Hartmanns, J. 600 [619]
Harvey, D. F. 598 [592]
Hassler, C. 436 [431]
Häussling, L. 569 [568]
Havlas, Z. 187, 714, 1180, 1183, 1678 [193, 706, 1194, 1197, 1733]
Hawthorne, M. F. 1507 [1519]
Hayashi, M. 1496 [1513]
Heckmann, G. 553, 850, 852 [562, 860, 861]
Heibel, G. E. 1345 [1381]
Heil, M. 1365 [1395]
Heimgartner, H. 238 [271]
Heinemann, U. 343 [351]
Heinze, J. 170, 205, 1361 [175, 215, 1350]
Heinze, T. 1677 [1671]
Heitzer, H. 1709 [1667]
Helbing, J. 423 (892) [456 (1066)]
Helpap, B. 1681 [1731]
Hendrickson, D. N. 305, 598 [314, 592]
Henin, F. 416 [460]
Henk, P. 681 [699]
Henkel, G. 769 [785]
Henney, R. P. G. 1363 [1401]
Henning, R. 1702 [1735]
Hentrich, F. 440 [429]
Herberhold, M. 1652 [1664]
Herberich, G. E. 313, 690 [329, 732]

Herdtweck, E. 430, 444, 1132, 1151 [446, 425, 1155, 1172]
Hermoso, J. A. 716 [733]
Herpers, E. 1018 [989]
Herrmann, A. T. 310 [316]
Herrmann, E. 969 [1023]
Herrmann, W. 426 [436]
Herrmann, W. A. 185, 818, 1636, 1638, 1641 [183, 835, 1704, 1706, 1709]
Heywang, G. 176 [201]
Hildebrandt, B. 97 [90]
Hiller, W. 179, 324 [182, 339]
Hirsch, A. 1309 [1339]
Hirschmann, R. 1278 [1305]
Hitchcock, P. B. 438 [439]
Hoffmann, J. 207 [208]
Hoffmann, N. 477 [480]
Hoffmann, R. 1 [1]
Hoffmann, R. W. 97 [90]
Hofmann, J. 998 [1013]
Hofmann, P. 313 [329]
Hofmeister, J. 1030 [1003]
Höfner, A. 594 [580]
Höhn, P. 831 [874]
Hollenstein, S. 1656 [1678]
Honert, D. 1372 [1376]
Hönle, W. 828, 1183 [850, 1197]
Hope, H. 691 [726]
Hopf, H. 432, 1117, 1127 (1386) [441, 1137, 1148 (1418)]
Hoppe, D. 321, 1690 [338, 1725]
Horchler von Locquenghien, K. 1154 [1174]
Horn, E. 996 [1046]
Horton, A. D. 1152 [1181]
Horváth, I. T. 1009 [1042]
Hrušák, J. 884, 1323 [898, 1396]
Huan, G. 422 [426]
Hübel, M. 103 [76]
Hübner, K. 860 [856]
Huffman, J. C. 862, 1672 [893, 1681]
Huffman, M. A. 1463 [1542]
Hühnerfuss, H. 320 [328]
Hunger, M. 686 [728]
Hünig, S. 561, 563 [608, 610]
Hunold, R. 594 [580]
Hunter, W. N. 1254 [1280]
Hursthouse, M. B. 871, 973 [867, 975]
Hutchinson, J. 299 [304]
Huttner, G. 303 [325]
Hwang, C.-K. 299, 1032 [304, 1034]

Ibers, J. A. 91 [83]
Ikebe, M. 177 [178]
Impellizzeri, G. 1348 [1363]
Irngartinger, H. 565 [595]
Isagawa, K. 984 [1000]
Isshiki, K. 418 [462]
Iwaki, D. 1173 [1202]
Iyoda, M. 1670 [1697]

Jacke, J. 1343 [1361]
Jacob, M. 754 [771]
Jacobson, A. J. 422 [426]
Jaeger, R. 103 [76]
Jakubke, H.-D. 1437 [1440]
Janati, T. 196 [191]
Janda, K. D. 1711 [1690]
Jansen, M. 329, 883, 1510, 1547 [327, 841, 1506, 1574]
Jaun, B. 1315 [1354]
Jehoulet, C. 836 [882]
Jeong, K.-S. 858 [880]
Jerzembeck, M. 745 [762]
Jeske, G. 1017 [1017]
Jiménez, J. 198 [190]
Johnson, A. L. 1176 [1205]
Johnson, B. F. G. 107, 1164, 1505, 1706 [102, 1186, 1529, 1672]
Jones, P. G. 198, 1127 (1386) [190, 1148 (1418)]
Jones, R. A. 1141, 1143 [1163, 1164]
Jones, R. O. 630 [647]
Jordan, J. 1138 [1160]
Jordan, S. 423 (892) [456 (1066)]
Joussen, T. 1312 [1344]
Jung, G. 1051 [1067]
Justus, K. 436 [431]

Kabbe, H.-J. 1709 [1667]
Kador, L. 540 [553]
Kai, Y. 446 [454]
Kaifer, A. E. 1039 [1055]
Kalinowski, H.-O. 1484 [1495]
Kallenborn, R. 320 [328]
Kalsbeck, W. A. 1517 [1525]
Kambe, N. 177 [178]
Kämmerling, H. T. 205 [215]
Kanatzidis, M. G. 1325 [1404]
Kanehisa, N. 446 [454]
Kannewurf, C. R. 1325 [1404]
Karbach, D. 575 [582]
Kasai, N. 446 [454]
Kauffmann, T. 1138, 1684 [1160, 1683]
Kaufmann, F.-P. 1479 [1546]
Kawanishi, S. 1351 [1343]
Kawano, Y. 843 [877]
Kawazu, K. 982 [1025]
Keck, H. 318 [331]
Kee, T. P. 980 [1021]
Kehr, G. 1370 [1374]
Kennard, O. 1254 [1280]
Kessler, H. 954, 1329 [968, 1341]
Khan, M. I. 210 [203]
Kiedrowski, G. von 423 (892), 822 [456 (1066), 839]
Kielhorn, S. 1017 [1017]
Kim, Y. S. 1650 [1715]
Kiprof, P. 185, 1167 [183, 1188]
Kirmse, W. 1018 [989]
Kitamura, M. 49 [34]
Klabunde, K.-U. 172 [198]
Klaff, N. 690 [732]
Klapötke, T. M. 1485 [1490]
Klärner, F.-G. 683 [702]
Klaus, C. B. A. 1314 [1353]
Klein, T. 303 [325]
Kleine-Klausing, A. 412 [428]
Klenk, H. 712 [704]
Klinkhammer, K.-W. 179 [182]
Klopp, I. 1354 [1379]
Klug, W. 683 [702]
Kluth, J. F. 1621 [1650]
Kneifel, H. 202 [189]
Kniep, R. 199, 831 [217, 874]
Knieriem, B. 964 [1008]
Knobler, C. B. 698, 1507 [708, 1519]
Knoch, F. 552, 1311, 1477 [599, 1346, 1493]
Knops, P. 958 [972]
Kobuke, Y. 1496 [1513]
Koelliker, R. 707 [724]
Köhler, K. F. 577, 1146 [564, 1167]
Kölle, U. 690, 956 [732, 970]
Komber, H. 1636 [1704]
Kondo, T. 17 [17]
König, B. 1361 [1350]
König, W. A. 320 [328]
Kooijman, H. 996 [1046]
Kopf, J. 825 [875]
Korall, B. 1312 [1344]
Kornick, A. 745 [762]
Kossakowski, J. 690 [732]
Kottenhahn, M. 712 [704]
Kragl, U. 827 (1713) [854]
Krämer, A. 84 [80]
Krämer, R. 1467 [1492]
Kranz, D. 1650 [1715]
Krätschmer, W. 884 [898]
Kräutler, B. 1315 [1354]
Krebs, B. 769 [785]
Kremer, M. 1186 [1200]
Kremer, R. 303 [325]
Kremer, R. K. 1188 [1210]
Kresge, A. J. 1356, 1366 [1391, 1407]
Kreutzer, M. 1127 (1386) [1148 (1418)]
Krickemeyer, E. 1512, 1674 [1501, 1720]
Krieger, C. 1028, 1030 [1006, 1003]
Kroll, H.-P. 1682 [1728]
Kroon, J. 1358 [1398]
Krüger, C. 310, 1124, 1349, 1354, 1666, 1668 [316, 1145, 1371, 1379, 1711, 1714]
Krüger, M. 1644 [1674]
Kuchen, W. 318 [331]
Kuck, D. 1699 [1717]
Kunz, G. 964 [1008]
Kunz, H. 694 [712]
Kunze, K. 95 [92]
Kupčik, V. 561, 964 [608, 1008]
Kurreck, H. 1461 [1536]
Kurz, M. 1329 [1341]
Kuwatani, Y. 1670 [1697]

Laatsch, H. 866 [858]
Lackmann, R. 1658 [1669]
Laguna, A. 198 [190]
Laguna, M. 198 [190]
Lahav, M. 696 [698]
Lahoz, F. J. 1171 [1192]
Lange, H. 1579 [1606]
Lange, K. H. 1643 [1689]
Lange, W. 1662 [1685]
Langer, M. 681 [699]
Langhauser, F. 310 [316]
Langohr, U. 561 [608]
Lanneau, G. 1130 [1153]
Lappert, M. F. 438 [439]
Laszlo, P. 1 [1]
Latour, J.-M. 1135 [1151]
Laube, T. 1656 [1678]
Laue, T. 432 [441]
Layh, M. 324 [339]
Lechner, P. 552 [599]
Lecuyer, C. 1660 [1692]
Lehn, J.-M. 190, 838, 1331 [186, 884, 1365]
Lehnert, A. 874 [852]
Lehr, J. 1015 [1029]
Leis, C. 1132 [1155]
Leiserowitz, L. 696 [698]
Lemke, M. 1512 [1501]
Lemke, U. 516 [519]
Lendzian, F. 1461 [1536]
Lentz, D. 1644 [1674]
Lerchen, H.-G. 1682 [1728]
Lerner, R. A. 1711 [1690]
Lewis, J. 107, 1164, 1505, 1706 [102, 1186, 1529, 1672]
Lex, J. 205, 681, 1693 [215, 699, 1737]
Li, Q. 1309 [1339]
Lichtenthaler, F. W. 1339 [1385]

Lidin, S. 754 [771]
Liebmann, A. 1375 [1358]
Liedle, S. 187 [193]
Lilienbaum, D. 1331 [1365]
Limbach, H.-H. 88, 1372 [88, 1376]
Lingens, F. 1487 [1550]
Link, R. 1372 [1376]
Livage, C. 1498 [1508]
Lobkovsky, E. B. 862, 1672 [893, 1681]
Lockhoff, O. 1611, 1681 [1639, 1731]
Loebel, J. 435, 1149 [444, 1170]
Lohrenz, J. 1455 [1497]
Lohse, C. 1656 [1678]
Lönnecke, P. 605 [620]
López, G. 716 [733]
Lorentzen, J. P. 1681 [1731]
Lorenzen, N. P. 825 [875]
Lowack, R. H. 1162 [1183]
Lüer, I. 1333 [1367]
Luger, P. 414 [450]
Luo, X.-L. 193 [205]
Lurz, C.-J. 1494 [1499]
Lüttke, W. 964 [1008]
Lynch, V. 977 [1018]

Maas, G. 207, 306 [208, 312]
McBride, J. M. 293 [298]
Maccarrone, G. 1348 [1363]
McClelland, R. A. 1337 [1389]
McCusker, J. K. 305, 598 [314, 592]
MacDougall, P. J. 1001 [1038]
McGhee, E. 91 [83]
McIntyre, G. J. 1164 [1186]
Mack, H.-G. 1145 [1166]
McPartlin, M. 980, 1164, 1706 [1021, 1186, 1672]
Madaule, Y. 994 [1044]
Mahjoub, A. R. 323, 876 [309, 844]
Mahr, G. 1477 [1493]
Mahrwald, R. 593 [577]
Maier, G. 1484 [1495]
Maier, W. F. 1509 [1523]
Maier-Greiner, U. H. 1314 [1353]
Maitlis, P. M. 375 [370]
Makryaleas, K. 712 [704]
Maligres, P. 418, 1032 [462, 1034]
Malm, J.-O. 874 [852]
Mandon, D. 572 [611]
Männle, F. 1372 [1376]
Mannschreck, A. 602 [588]
Marchelli, R. 1348 [1363]
Marczinke, B. 1666 [1711]
Mardones, M. A. 1141 [1163]
Märki-Fischer, E. 654 [671]
Märkl, G. 106 [82]
Marsch, M. 321, 1455 [338, 1497]
Marsmann, H. 834, 962 [873, 978]
Martin, J. D. 1498 [1508]
Martínez-Ripoll, M. 716 [733]
Maruyama, K. 582 [579]
Marz, D. W. 1638 [1706]
Masamune, S. 902 [916]
Massa, W. 547, 594 [601 (906), 580]
Matile, P. 1315 [1354]
Matsugo, S. 1351 [1343]
Matsuura, T. 1351 [1343]
Mattausch, H. 1188 [1210]
Mattay, J. 1336 [1352]
Matzen, M. 423 (892) [456 (1066)]
Mäurer, M. 602 [588]
Mauz, E. 998 [1013]
Maynard, G. D. 1368 [1392]
Mazid, M. 871, 973 [867, 975]
M'boungou-M'passi, A. 416 [460]
Mecati, A. 190 [186]
Medici, L. 989 [992]
Meerholz, K. 1361 [1350]
Meier, B. 686 [728]
Meier, M. 893 [907]
Méndez, L. 82 [97]
Mendoza, A. 1171 [1192]
Menger, F. M. 1086 [1104]
Mennekes, T. 173 [199]
Mergardt, B. 1687 [1679]
Mertesdorf, C. 1375 [1358]
Mesa, E. 1331 [1365]
Metternich, H. J. 312 [336]
Metz, B. 547 [601 (906)]
Metzenthin, T. 561, 563 [608, 610]
Metzger, J. O. 600 [619]
Meunier, B. 702 [718]
Meyer, K. 561 [608]
Meyerstein, D. 1158 [1177]
Michel, B. 569 [568]
Michenfelder, A. 596 [617]
Miehe, G. 964 [1008]
Mierke, D. F. 954 [968]
Mikołajczyk, M. 578 [604]
Mikulcik, P. 428 [452]
Milius, W. 831 [874]
Miller, J. S. 450 [459]
Miller, L. L. 986 [1002]
Milne, P. E. Y. 1139 [1161]
Milstein, D. 707 [724]
Minkwitz, R. 328 [311]
Mitchell, R. H. 1013 [1031]
Mizuno, K. 984 [1000]
Möbius, K. 1461 [1536]
Modro, A. 1337 [1389]
Moll, M. 552, 1311 [599, 1346]
Moorefield, C. N. 1176, 1178 [1205, 1207]
Morbitzer, L. 1598 [1626]
Moretó, J. M. 1470 [1540]
Mori, T. 984 [1000]
Morishima, T. 977 [1018]
Mosandl, T. 200 [187]
Moule, A. 1706 [1672]
Müllen, K. 1003 [996]
Müller, A. 34, 210, 588, 1512, 1674 [56, 203, 575, 1501, 1720]
Müller, B. 893 [907]
Müller, F. 1336 [1352]
Müller, H.-G. 1650 [1715]
Müller, J. 175, 1377 [201, 1357]
Müller-Buschbaum, Hk. 723 [741]
Mulzer, J. 414, 1452 [450, 1484]
Munschauer, R. 306 [312]
Murata, I. 172, 1174 [198, 1203]
Mutter, M. 1514 [1504]
Muzart, J. 416 [460]
Mynott, R. 1666, 1668 [1711, 1714]

Nagata, T. 582 [579]
Nakahira, H. 177 [178]
Nakajima, S. 582 [579]
Nakamura, A. 1670 [1697]
Nakasuji, K. 172 [198]
Näther, C. 1180 [1194]
Nesper, R. 409, 789 [421, 805]
Nessel, A. 1006 [999]
Neugebauer, F. A. 1028 [1006]
Newkome, G. R. 1176, 1178 [1205, 1207]
Nicolaou, K. C. 299, 418, 585, 1032, 1100, 1387 [304, 462, 566, 1034, 1119, 1453]
Niecke, E. 90, 217, 312, 1136 [103, 251, 336, 1158]
Nieger, M. 90, 964, 1136 [103, 1008, 1158]
Niemeyer, C. M. 1472, 1474 [1515, 1517]
Niemeyer, M. 964 [1008]
Niessner, R. 466 [542]
Nolte, M. 1349, 1354 [1371, 1379]
Noltemeyer, M. 436, 860, 866, 1492, 1658 [431, 856, 858, 1534, 1669]
Norrestam, R. 864 [891]
Nowicki, J. 328 [311]
Nowotny, M. 547 [601 (906)]
Noyori, R. 49 [34]
Nubbemeyer, U. 1465 [1533]
Nürnberg, O. 1006 [999]
Nygren, M. 864 [891]

Oberhammer, H. 187, 1145, 1678 [193, 1166, 1733]
Oda, M. 1670 [1697]
Oehme, M. 969 [1023]
Ogden, M. I. 854 [887]
Ogilvie, W. W. 299 [304]
Ogino, H. 843 [877]
Ogoshi, H. 1496 [1513]
O'Hare, D. 1156 [1175]
Öhrlein, R. 1465 [1533]
Okuda, J. 430 [446]
Oliver, A. M. 1358 [1398]
Olivier, D. 1660 [1692]
Oltra, H. M. 1492 [1534]
Ooka, T. 1173 [1202]
Oro, L. A. 1171 [1192]
Ostoja Starzewski, K. A. 961 [1012]
Osuka, A. 582 [579]
Otsuji, Y. 984 [1000]

Pace, C. N. 343 [351]
Paddon-Row, M. N. 1358 [1398]
Paetzold, P. 173, 175, 544, 1377 [199, 201, 559, 1357]
Pakusch, J. 893 [907]
Palazzi, A. 847 [895]
Pampaloni, G. 102 [109]
Paquette, L. A. 1368 [1392]
Park, Y. 1325 [1404]
Parkin, S. S. P. 1498 [1508]
Parry, K. P. 1039, 1042 [1055, 1058]
Pauer, F. 1677 [1671]
Payne, M. W. 856 [842]
Penk, M. 588, 1674 [575, 1720]
Penneau, J.-F. 986 [1002]
Pestana, D. C. 691 [726]
Petasis, N. A. 1100 [1119]
Pete, J.-P. 416 [460]
Peters, K. 326 [335]
Petrucci, G. 989 [992]
Petzoldt, J. 849 [870]
Philipp, U. C. 86 [78]
Pickardt, J. 550 [586]
Pierre, J. L. 85 [75]
Pietraszkiewicz, M. 1042 [1058]
Piguet, C. 1490 [1530]
Pitié, M. 702 [718]
Plesnivy, T. 1375 [1358]
Plitt, H. S. 832 [848]
Plückthun, A. 296 [301]
Poganiuch, P. 975 [1015]
Pohl, M. 1693 [1737]
Pohl, S. 834, 881, 962 [873, 869, 978]
Polborn, K. 332, 334 [318, 320]
Polk, M. 1015 [1029]
Pope, M. T. 34 [56]
Poszich-Buscher, C. 202 [189]
Power, M. B. 1353 [1403]

Power, P. P. 330, 691 [308, 726]
Prasad, C. V. C. 299 [304]
Pratviel, G. 702 [718]
Prenzel, A. 550 [586]
Preugschat, D. 1644 [1674]
Preuss, H. 409 [421]
Preuss, H.-W. 1186 [1200]
Priou, C. 1130 [1153]
Pritzkow, H. 84, 709, 1017 [80, 721, 976]
Probst, R. 1132 [1155]
Prout, C. K. 1156 [1175]
Pruszynski, P. 1356, 1366 [1391, 1407]
Puder, P. 436 [431]
Puppe, L. 1689 [1687]
Pyykkö, P. 604 [622]

Quignard, F. 1660 [1692]

Raabe, G. 1664 [1676]
Rabe, K. 1690 [1725]
Rabenau, A. 199 [217]
Raithby, P. R. 107, 428, 1011, 1363, 1505, 1648 [102, 452, 1040, 1401, 1529, 1696]
Ramarohetra, M. 994 [1044]
Ramos Tombo, G. M. 1193 [1219]
Ramphal, J. Y. 1100 [1119]
Rau, D. 870 [847]
Rau, H. 416 [460]
Raue, R. 1643 [1689]
Rauschenbach, A. 714 [706]
Rebek, J., Jr. 858 [880]
Recknagel, A. 693 [720]
Reed, D. 1011, 1459 [1040, 1539]
Reetz, M. T. 103, 1146, 1472, 1474, 1531 [76, 1167, 1515, 1517, 1559]
Regitz, M. 207, 674 [208, 691]
Rehder, D. 148 [152]
Rehr, A. 329, 1510 [327, 1506]
Reichardt, C. 558 [614]
Renneberg, H. 318 [331]
Reschetilowski, W. 686 [728]
Reuter, H. 1482 [1487]
Reyes, J. 1171 [1192]
Reymond, J.-L. 1711 [1690]
Rheingold, A. L. 194 [196]
Ricart, S. 1470 [1540]
Ricci, A. 1457 [1527]
Richter, M. 607 [606]
Riechers, H. 191 [207]
Rieder, H. 561 [608]
Rieger, D. 88 [88]
Riess, J. G. 567 [584]
Rindfleisch, F. 1654 [1722]
Ringsdorf, H. 76, 315, 569, 1375 [106, 323, 568, 1358]
Rissanen, K. 1331 [1365]
Ritter, H. 677 [694]
Rittich, S. 202 [189]
Rizzarelli, E. 1348 [1363]
Robinson, O. B. 980 [1021]
Robl, C. 564 [594]
Rocchi, L. 102 [109]
Rodriguez, J. 993 [1032]
Rodriguez, M. 1020 [985]
Rodríguez-Ubis, J.-C. 1331 [1365]
Roesky, H. W. 860, 1677 [856, 1671]
Rohde, S. 1654 [1722]
Rohen, A. 516 [519]
Rohlfing, R. 588, 1674 [575, 1720]
Rohr, J. 183 [211]
Rohrer, H. 569 [568]
Romao, C. C. 185 [183]
Ros, M. B. 711 [716]
Roth, S. 176 [201]
Rotter, H. 1372 [1376]
Rubin, Y. 698 [708]
Rüchardt, C. 893 [907]
Rück, K. 694 [712]
Rüdiger, W. 1216 [1242]
Ruiz, J. 716 [733]
Rump, M. 1349 [1371]
Runsink, J. 175 [201]
Ruppert, K. 714, 1180, 1183, 1678 [706, 1194, 1197, 1733]
Ryabov, A. D. 931 [945]
Ryu, I. 177 [178]

Saak, W. 834, 881, 962 [873, 869, 978]
Saalfrank, R. W. 1494 [1499]
Sabbatini, N. 190 [186]
Sacha, H. 1318 [1369]
Saenger, W. 343 [351]
Saha-Möller, C. R. 200 [187]
Saitho, Y. 1173 [1202]
Saito, I. 1351 [1343]
Saito, J. 1174 [1203]
Sakaguchi, M. 446 [454]
Sakai, A. 446 [454]
Sánchez, G. 716 [733]
Sander, J. 516 [519]
Santaella, C. 567 [584]
Sasaki, N. 982 [1025]
Sasaki, S. 172 [198]
Sauer, W. 547 [601 (906)]
Sauerbrei, B. 1503 [1521]
Saunders, M. J. 1178 [1207]
Savignac, P. 196 [191]
Savin, A. 409 [421]
Schäfer, A. 834, 962 [873, 978]
Schäfer, M. 860 [856]
Schäfer, W. 590 [572]
Schaffner, K. 1343 [1361]
Scharf, H.-D. 477 [480]
Schaumann, E. 1687 [1679]
Scheer, M. 969 [1023]
Scheffler, K. 602 [588]
Schellenberg, M. 1315 [1354]
Schellenberger, V. 1437 [1440]
Schepp, N. P. 1356, 1366 [1391, 1407]
Scherer, H. J. 1664 [1676]
Scherer, O. J. 553, 850, 852 [562, 860, 861]
Schick, H. 593 [577]
Schindler, J. 1325 [1404]
Schinzer, D. 687 [727]
Schleimer, M. 987 [994]
Schleyer, P. von R. 1160 [1179]
Schlögl, R. 967 [983]
Schlüpmann, J. 1461 [1536]
Schmalstieg, L. 681 [699]
Schmalz, M. 967 [983]
Schmalzing, D. 987 [994]
Schmickler, H. 683, 1693 [702, 1737]
Schmid, G. 874, 1015 [852, 1029]
Schmidbaur, H. 433, 1488 [442, 1552]
Schmidpeter, A. 308 [333]
Schmidt, A. J. 866 [858]
Schmidt, B. 99, 1321 [100, 1383]
Schmidt, R. R. 1328 [1348]
Schmieder, P. 1329 [1341]
Schmitt, E. A. 305 [314]
Schmittel, M. 999 [981]
Schmock, F. 577 [564]
Schneider, A. 555 [596]
Schneider, D. 700 [710]
Schneider, H.-J. 1417 [1419]
Schneider, J. J. 1124 [1145]
Schneider, R. 207 [208]
Schnering, H. G. von 326, 409, 1183 [335, 421, 1197]
Schnick, W. 830 [857]
Schnöckel, H. 564, 832 [594, 848]
Schobert, K. 1494 [1499]
Schöllhorn, R. 967 [983]
Scholz, A. 435 [444]
Scholz, J. 435 [444]
Schomburg, D. 191 [207]
Schönewolf, M. 183 [211]
Schramm, H. O. 1509 [1523]
Schreiner, E. P. 585 [566]
Schröder, A. 575 [582]
Schröder, D. 991 [987]
Schuchmann, H.-P. 1229 [1255]
Schulte, G. 193 [205]
Schulz, G. E. 555 [596]
Schulz, M. 596 [617]
Schumann, H. 435, 1149 [444, 1170]
Schurig, V. 987 [994]
Schuster, A. 1699 [1717]
Schuster, D. I. 1345 [1381]
Schütz, J. U. von 561 [608]
Schwarz, H. 820, 884, 991, 1323 [837, 898, 987, 1396]
Schweiger, A. 265 [223]
Schwesinger, R. 1372 [1376]
Seebach, D. 99, 1008, 1321 [100, 991, 1383]
Seel, C. 442 [433]
Seggern, H. von 999 [981]
Seidenschwarz, C. 444, 1151 [425, 1172]
Seifert, C. 332 [318]
Sellmann, D. 552, 1311, 1477 [599, 1346, 1493]
Seppelt, K. 323, 361, 876 [309, 399, 844]
Serhan, C. N. 1100 [1119]
Serrano, J. L. 711 [716]
Sessler, J. L. 91, 977 [83, 1018]
Sewald, N. 444 [425]
Shaw, A. 980 [1021]
Sheldrick, G. M. 1677 [1671]
Shibata, M. 446 [454]
Shoner, S. C. 330 [308]
Siebert, W. 84 [80]
Siedenbiedel, C. 1668 [1714]
Siehl, H.-U. 1479 [1546]
Sieler, J. 969 [1023]
Sime, R. L. 942 [956]
Simon, A. 101, 1188, 1678 [79, 1210, 1733]
Sinerius, G. 555 [596]
Singer, R. J. 1707 [1702]
Sitzmann, H. 971 [1027]
Slawin, A. M. Z. 82, 1036, 1039 [97, 1052, 1055]
Smith, A. L. 1032 [1034]
Smola, A. 435 [444]
Snaith, R. 82, 428, 1011, 1648, 1707 [97, 452, 1040, 1696, 1702]
Snider, B. B. 420 [438]
Somer, M. 326 [335]
Sonntag, C. von 1229 [1255]
Sonoda, N. 177 [178]
Sotiropoulos, J.-M. 1154 [1174]
Sousa, L. R. 1363 [1401]
Spek, A. L. 996 [1046]
Spencer, N. 1036, 1039, 1042 [1052, 1055, 1058]
Spijker, N. M. 180 [179]
Spitzner, D. 1320 [1373]
Srinivas, R. 1323 [1396]
Staab, H. A. 1028, 1030 [1006, 1003]

Stach, D. 1684 [1683]
Stahl, W. 585 [566]
Stalke, D. 1459, 1648, 1677, 1707 [1539, 1696, 1671, 1702]
Stamatis, N. 1479 [1546]
Stang, P. J. 1469 [1549]
Stasch, J.-P. 1702 [1735]
Staton, I. 80 [96]
Staunton, J. 1302 [1331]
Steenken, S. 1337 [1389]
Stegmann, H. B. 602 [588]
Stehling, L. 1668 [1714]
Steigelmann, O. 433, 1488 [442, 1552]
Stein, F. 1658 [1669]
Steinke, T. 1160 [1179]
Stelzer, U. 873 [866]
Stenzel, J. R. 194 [196]
Steudel, R. 550 [586]
Stoddart, J. F. 70, 80, 82, 1036, 1039, 1042 [71, 96, 97, 1052, 1055, 1058]
Stoeckli-Evans, H. 1126 [1147]
Stoltefuss, J. 1559 [1587]
Strähle, J. 102 [109]
Streib, W. E. 305, 1672 [314, 1681]
Streubel, R. 90 [103]
Strittmatter, R. J. 1069 [1085]
Struck, O. 1494 [1499]
Stucky, G. D. 1169 [1191]
Sugihara, Y. 1174 [1203]
Sugimoto, T. 446 [454]
Sugita, H. 984 [1000]
Sugiyama, H. 1351 [1343]
Sumida, Y. 1496 [1513]
Süsse, P. 964 [1008]
Süss-Fink, G. 72, 1126 [73, 1147]
Suter, U. W. 989 [992]

Tacke, M. 564 [594]
Tamm, M. 203 [213]
Tanner, M. E. 1024 [1048]
Tatsumi, K. 1670 [1697]
Tattershall, B. W. 605 [620]
Terasaki, O. 754 [771]
Terlouw, J. K. 318 [331]
Thewalt, U. 1652 [1664]
Thiele, G. 1372 [1376]
Thiele, K.-H. 435 [444]
Thiele, M. 308 [333]
Thiem, J. 1163, 1503 [1184, 1521]
Thomas, R. 1024 [1048]
Thornton, P. 1139 [1161]
Thorp, H. H. 1517 [1525]
Thümmler, F. 1216 [1242]
Tietjen, K. 1621 [1650]
Tietze, L. F. 868, 1697 [878, 1665]
Tillmanns, E. 561 [608]
Tobita, H. 843 [877]
Torisawa, Y. 1032 [1034]
Toriumi, K. 582 [579]
Tornieporth-Oetting, I. C. 1485 [1490]
Toyoda, J. 172 [198]
Trautwein, A. X. 1494 [1499]
Trebst, A. 1621 [1650]
Tremel, W. 840 [900]
Trifonov, A. A. 1149 [1170]
Trimmer, R. W. 1646 [1694]
Tschierske, C. 440 [429]
Tsumuraya, T. 902 [916]

Uhl, W. 179, 324 [182, 339]
Ullmann, J. 1469 [1549]
Unger, B. 686 [728]
Usón, R. 198 [190]

van Boeckel, C. A. A. 180 [179]
van de Loosdrecht, J. 190 [186]
Van Duyne, G. D. 584 [616]
van Eldik, R. 1158 [1177]
van Koten, G. 996 [1046]
van Pée, K.-H. 1487 [1550]
Vasisht, S.-K. 93 [105]
Vázquez, P. 1331 [1365]
Veale, C. A. 299 [304]
Vecchio, G. 1348 [1363]
Veciana, J. 74 (216) [85 (222)]
Vegas, A. 716 [733]
Veith, M. 95, 878 [92, 845]
Venzmer, J. 315 [323]
Verhoeven, J. W. 1358 [1398]
Vicens, J. 854 [887]
Vierling, P. 567 [584]
Viñas, J. M. 1470 [1540]
Visser, H. C. 318 [331]
Vogel, E. 681, 683, 1693 [699, 702, 1737]
Vogel, S. 303 [325]
Vögtle, F. 442, 575, 958, 1331, 1333 [433, 582, 972, 1365, 1367]
Volkhardt, U. 1636 [1704]
Völkl, C. 1167 [1188]
Vollhardt, K. P. C. 993, 1463 [1032, 1542]
Voss, K.-U. 1138 [1160]

Wachter, J. 1120 [1140]
Wagner, H.-U. 332, 334 [318, 320]
Wagner, J. 179 [182]
Wagner, W. 1636 [1704]
Waldmann, H. 1306 [1335]
Walther, P. 852 [861]
Wandrey, C. 827 (1713) [854]
Wang, J.-L. 696 [698]
Wang, M. 1641 [1709]
Wang, S. 305, 1672 [314, 1681]
Warhurst, N. J. W. 438 [439]
Washausen, P. 191 [207]
Weatherburn, D. C. 688 [715]
Webb, K. J. 973 [975]
Weber, K. 1687 [1679]
Wedig, U. 828 [850]
Weidenbruch, M. 834, 962 [873, 978]
Weidenhiller, G. 433 [442]
Weiske, T. 884 [898]
Weiss, E. 825 [875]
Weiss, R. 572, 1162 [611, 1183]
Wendeborn, S. V. 418, 1032 [462, 1034]
Wendlandt, K.-P. 686 [728]
Wendorff, J. H. 405, 1375 [416, 1358]
Werner, B. 553 [562]
Werner, H. 596, 700, 1006 [617, 710, 999]
Werner, S. 1124, 1349 [1145, 1371]
Wesemann, L. 313, 690 [329, 732]
Wettling, T. 207 [208]
Wey, H. G. 880 [871]
Wheeler, K. A. 420 [438]
Whetten, R. L. 678 [695]
White, A. H. 854 [887]
Wiberg, N. 93 [105]
Wieczorek, M. W. 578 [604]
Wiedorn, M. 1509 [1523]
Wiemann, T. 1163 [1184]
Wild, D. 200 [187]
Wild, H. 1685 [1729]
Wiley, D. W. 450 [459]
Wilhelm, D. 824 [897]
Wilke, G. 1666, 1668 [1711, 1714]
Wilken, H. 516 [519]
Wilkinson, D. A. 1706 [1672]
Willershausen, P. 594 [580]
Williams, A. F. 1490 [1530]
Williams, D. J. 82, 1036, 1039 [97, 1052, 1055]
Wilmes, O. 681 [699]
Windscheif, P.-M. 1331 [1365]
Winnik, F. M. 315 [323]
Winpenny, R. E. P. 1139 [1161]
Winter, B. 516 [519]
Winter, G. 1579 [1606]
Winter, R. 850 [860]
Winterfeldt, E. 191 [207]
Wirz, J. 1356, 1366 [1391, 1407]
Wiseman, P. J. 1156 [1175]
Wittneben, V. 210, 1512 [203, 1501]
Wlotzka, B. 423 (892) [456 (1066)]
Wolber, E. K. A. 893 [907]
Wolczanski, P. T. 584 [616]
Wolf, H. C. 561 [608]
Wolf, J. 1006 [999]
Wolf, J.-G. 994 [1044]
Wolmershäuser, G. 553, 850, 852 [562, 860, 861]
Wong, W.-T. 107, 1505 [102, 1529]
Woning, J. 1345 [1381]
Wötting, G. 1579 [1606]
Wrackmeyer, B. 1370 [1374]
Wright, D. S. 82, 428, 1011, 1459, 1648, 1707 [97, 452, 1040, 1539, 1696, 1702]
Wudl, F. 1309 [1339]
Wulff, G. 849 [870]
Wünsch, J. R. 1697 [1665]
Wurst, K. 102 [109]

Yamamoto, A. 982 [1025]
Yamamoto, K. (Kyoto) 1351 [1343]
Yamamoto, K. (Osaka) 1173 [1202]
Yang, X. 1507 [1519]
Yaouanc, J.-J. 560 [563]
Yoshida, T. 982 [1025]
Yoshida, Z. 446 [454]

Zander, M. 432 [441]
Zanotti, V. 847 [895]
Zaschke, H. 440 [429]
Zein, N. 418 [462]
Zeller, K.-P. 1476 [1489]
Zhao, Y.-F. 604 [622]
Zhou, P. 1013 [1031]
Ziegler, B. 594 [580]
Ziessel, R. 190, 844, 1331 [186, 863, 1365]
Zimmer, M. 193 [205]
Zimmermann, K. H. 430 [446]
Zinsmeister, H. D. 130 [134]
Zöllner, S. 1518 [1544]
Zschage, O. 321 [338]
Zsolnai, L. 303 [325]
Zulauf, P. 1455 [1497]
Zurmühlen, F. 207 [208]
Zybill, C. 1132 [1155]

INDEX OF AUTHORS AND REVIEWERS OF BOOKS

This index lists separately the names of Authors/Editors and Reviewers, respectively, of books reviewed in *Angew. Chem. Int. Ed. Engl. 30* (1991).

Bookauthors

Abramovicz, D. A. 1529
Adams, R. D. 337
Almond, M. J. 610
Anpo, M. 111
Atkins, P. W. 609
Baggott, J. 1526
Baranowski, B. 110
Bencini, A. 340
Bernstein, E. R. 1382
Betina, V. 214
Bleha, T. 341
Block, E. 1190
Boyd, D. B. 452
Casey, M. 213
Christoffersen, R. E. 1523
Constable, E. C. 1384
Conway, W. D. 892
Davies, J. A. 1527
Doi, Y. 1525
Dötz, K. H. 1520
Downs, A. J. 610
Drayton, C. J. 890
Emmett, J. C. 888
Ermolenko, I. N. 213
Field, L. D. 721
Friebolin, H. 1383
Gatteschi, D. 340
Giese, B. 611
Gilbert, A. 1526
Göpel, W. 110
Greenberg, A. 1527
Gulko, N. V. 213
Haasen, P. 1521
Hargittai, I. 1382
Hart, J. P. 1049
Hartley, F. R. 1046
Hattori, H. 720
Haufe, G. 1191
Hesse, J. 110
Hoffmann, R. W. 1520
Janson, J.-C. 212
Jurczac, J. 110
Kaesz, H. D. 337
Karlson, P. 891
Kaye, B. H. 339
Kennewell, P. D. 886
Klamann, D. 1524
Krätz, O. 1046
Lazár, M. 341
Lee, S. M. 609
Leigh, G. J. 721
Leonard, J. 213
Ley, S. V. 1386
Liebman, J. F. 1527
Lipkowitz, K. B. 452
Lis, H. 338
Low, C. M. 1386
Lygo, B. 213
Lyubliner, I. P. 213
Mann, G. 1191
Mann, S. 214
Mason, T. J. 1385
Matsuura, T. 111
Misono, M. 720
Mukaiyama, T. 1381
Naumann, K. 453
Ono, Y. 720
Ozawa, L. 1048
Patai, S. 718, 719
Pileni, M. P. 339
Plesch, P. H. 1522
Procter, G. 213
Ramsden, C. A. 889
Rees, M. H. 1529
Regitz, M. 611, 1047
Rogers, D. W. 1384
Rychlý, J. 341
Rydén, L. 212
Sammes, P. G. 887
Scherer, O. J. 1047
Schomburg, G. 1050
Seeman, J. I. 1190
Senechal, M. 1525
Serratosa, F. 340
Sharon, N. 338
Shriver, D. F. 337
Sternhell, S. 721
Tanabe, K. 720
Taylor, J. B. 889
Taylor, R. 337
Vögtle, F. 215
Watson, P. L. 1527
Webb, J. 214
Wendisch, D. A. W. 1381
Williams, R. J. P. 214
Williams, T. I. 1049
Zemel, J. N. 110

Reviewers

Ahr, H.-J. 889
Anke, T. 214
Boudjouk, P. 1385, 1386
Braun, R. W. 887
Brückner, R. 215
Bürger, H. M. 1525
Butenschön, H. 1520
Butler, J. E. 886
Cammann, K. 110
Cavanagh, J. 1383
Cramer, F. 891
Dalhoff, A. 887
Edelmann, F. T. 1522
Feltkamp, H. 892
Fessner, W.-D. 611, 1529
Frenking, G. 452
Friedl, A. 888
Gabius, H.-J. 338
Griesbeck, A. G. 1526
Griesinger, C. 1381
Gross, R. 886
Gruenewaldt, G. 886
Grützmacher, H. 1190
Günther, J. 889
Hartwig, W. 890
Hebisch, S. 888
Hecker, G. 888
Herges, R. 1384
Hoffmann, R. 1046
Hofmann, P. 1527
Hopf, H. 1190
Kador, L. 1048
Kaim, W. 1384
Kauffman, G. B. 721
Kaupp, G. 111
Keese, R. 1191
Klotzbücher, W. E. 610
Kniep, R. 1521
Knölker, H.-J. 213
Koch, W. 1523
Kogler, H. 721
Krampitz, G. 214
Krause, H.-P. 889
Lange, T. 1382
Laschewsky, A. 339
Lidin, S. 1382
Luef, W. 1191
McBride, J. M. 1525
Maier, W. F. 720
Martin, T. P. 1382
Matlin, S. A. 1050
Meyer, G. 110
Meyer, W. 213
Möller, E. 889
Müller, H.-M. 1525
Mulzer, J. 453
Neier, R. 340, 1381
Nuyken, O. 341
Pawson, S. 1529
Power, P. P. 1047
Reichardt, C. 337
Robens, E. 339
Rounding, P. 886
Ruland, W. 609
Schank, K. 718, 719
Schmidt, D. 887
Schmitz, E. 1524
Schmutzler, R. 1046
Seipke, G. 212
Sommermeyer, H. 888
Stasch, H.-P. 888
Süss-Fink, G. 337
Todd, A. R. 1049
Unterbeck, A. 886
Wang, J. 1049
Weihrauch, T. 886
Wohlfeil, S. 887

SUBJECT INDEX

(A second page number to an entry indicates an erratum to the corresponding article.)

(R) = Review Article (H) = Highlights (C) = Short Communication (B) = Book Review (L) = Correspondence

Ab initio calculations
- Ab initio Calculations on the $(ClAuPH_3)_2$ Dimer with Relativistic Pseudopotential: Is the "Aurophilic Attraction" a Correlation Effect? (C) 604
- Basic Principles and Techniques of Molecular Quantum Mechanics (B) 1523
- $[Cu(\eta^2\text{-}H_2)Cl]$, a Model Compound for H_2 Complexes. Ab Initio Calculations and Identification by IR Spectroscopy (C) 832
- Dilithiation of a Primary Amine: Synthesis and Structure of $[(\alpha\text{-Naphthyl-}NLi_2)_{10}(Et_2O)_6] \cdot ET_2O$, a Paramagnetic Li_{20} Aggregate (C) 1707
- On the Origin of π-Facial Diastereoselectivity in Addition Reactions of Cyclohexane-Based Systems (C) 1146
- Solvation Effects on Geometry and Chemical Shifts. An Ab Initio/IGLO Reconciliation of Apparent Experimental Inconsistencies on $H_3B \cdot NH_3$ (C) 1160
- The Radical Cations of Silaketene and Several Isomers of $[C,H_2,Si,O]^{\bullet\oplus}$: An Ab Initio MO Investigation (C) 1323
- The Structure of the Trimethylenemethane Dianion and the Question of Y-Aromaticity (C) 1001

Abzyms
- Antibody Catalysis of Glycosidic Bond Hydrolysis (C) 1711

Acenaphthylenes
- σ-Homoacenaphthylene and π-Homoacenaphthene (C) 683

Acetals
- Stereoselective Synthesis of Acetal-β,β-diglucosides, a Novel Class of Glycosides and Chiral Acetals (C) 868

Acetoxyalkynes
- Palladium(II)-Induced Conversion of α-Acetoxyalkynes into α,β-Unsaturated α-Acetoxyketones; a Novel Access to α-Diketones (C) 593

ACRL Toxin I
- ACRL Toxin I: Convergent Total Synthesis of Its 3-Methyl Enol Ether from D-Glucose (C) 1339

Actinide compounds
- Cyclopentadienyl-Actinide Complexes: Bonding and Electronic Structure (R) 1069

Adamantanes
- $Li_{10}P_4N_{10}$—A Lithium Phosphorus(v) Nitride Containing the New Complex Anion $P_4N_{10}^{10\ominus}$ (C) 830

1,4 Additions
- β-Alkyl and β-Alkyl-α-Hydroxy Carboxylic Acid Derivatives from Radical or Ionic 1,4 Addition of Dialkylaluminum Chlorides to α,β-Unsaturated *N*-Acyl Urethanes (C) 694

Aerosols
- Chemical Characterization of Aerosols: On-Line and In Situ (R) 466

Aldol reactions
- Diastereoselective Enzymatic Aldol Additions: L-Rhamnulose and L-Fuculose 1-Phosphate Aldolases from *E. coli* (C) 555
- *Anti*-Selective and Diastereofacially Selective Aldol Reactions with (*R*)-2-Siloxy-1,2,2-triphenylethyl propionate (C) 1318

Alicyclic compounds
- Chemistry of Alicyclic Compounds. Structure and Chemical Transformations (B) 1191

Alkali metal compounds
- η^1-(1*S*,2*E*)-1-(*N*,*N*-diisopropylcarbamoyloxy)-3-trimethylsilylallyllithium · (−)-Sparteine: Structure of a Chiral, Carbamoyloxy-substituted Allyllithium Compound (C) 321
- Dilithiation of a Primary Amine: Synthesis and Structure of $[(\alpha\text{-Naphthyl-}NLi_2)_{10}(Et_2O)_6] \cdot ET_2O$, a Paramagnetic Li_{20} Aggregate (C) 1707
- $LiClO_4$ in Ether—an Unusual Solvent (H) 1306
- (2-Lithio-3-bromobenzofuran · Diisopropyl Ether)$_2$ and 1-Phenylsulfonyl-2-lithio-3-fluorobenzene Pentamethyldiethylenetriamine: Crystal Structures of Compounds with Lithium and Halogen on Neighboring Carbon Atoms (C) 1455
- 5-Lithio-2*H*-tetrazolium Carbenoids: NMR Spectroscopic Detection and Reactions with Nitrogen Electrophiles (C) 1162
- Mixed-Anion Aggregates of Metalated Organics: Preparation and Structure of the Mixed-Anion Tetramer $(PhO^{\ominus}Li^{\oplus} \cdot HMPA)_3(\mu_3\text{-}HMPA \cdot Li^{\oplus})NCS^{\ominus}$ (C) 1011
- Observation of a Direct Sn–Li Bond; The Crystal and Molecular Structure of Monomeric $[Ph_3SnLi \cdot PMDETA]$ and the Detection of $^{119,117}Sn\text{–}^7Li$ NMR Coupling in Solution (C) 1459
- On the Electrochemical Oxidation of $Cs^{\oplus}$ and Other Alkali-Metal Ions in Liquid Sulfur Dioxide and Acetonitrile (C) 836
- Phenylsodium Compounds with η^3-Allyl or η^6-Phenyl Coordination (C) 825
- Solvated Electron in the Synthesis of Ionic Clusters in Zeolites (C) 1501
- Solvent-free Tris(trimethylsilyl)methyllithium (C) 324
- Synthesis and Structure of the Potassium Salts of 1,3,2-Diazaboroles (C) 1015
- The Two-Electron Reduction of 1,1′-Diphenylethene by Lithium or Sodium to Different 1,1,4,4-Tetraphenylbutane-1,4-diide Salts via C—C Bond Formation—A Monomeric Dilithium Contact Ion Triple and a Polymer String of "Hydrocarbon Oysters Containing Solvated Sodium Pearls" (C) 1183
- Volume Effect or Paddle-Wheel Mechanism—Fast Alkali-Metal Ionic Conduction in Solids with Rotationally Disordered Complex Anions (R) 1547

Alkaline earth metal compounds
- Alkaline Earth Metal Complexes Containing Deprotonated Organic Acids and Water: Preparation, Structures and a New Synthetic Strategy (C) 428
- The Synthesis and Structure of Some New Sodalites: The Lithium Haloberyllophosphates and -arsenates (C) 1169

Alkanes
- Surface Organometallic Chemistry on Oxides: Selective Catalytic Low-Temperature Hydrogenolysis of Alkanes by a Highly Electrophilic Zirconium Hydride Complex Supported on Silica (C) 1660

Alkene complexes
- *mer*-$[Cr(CO)_3(\eta^4\text{-norbornadiene})(\eta^2\text{-ethene})]$: A Key Compound in Understanding the Mechanism of the Photocatalytic Diene Hydrogenation with Chromium Carbonyl Complexes (C) 1343
- Nickel(0)-Carbene Complexes (C) 1666

Alkenes
- Methyltrioxorhenium as Catalyst for Olefin Oxidation (C) 1638
- Methyltrioxorhenium as Catalyst of a Novel Aldehyde Olefination (C) 1641
- Tetraethynylethene (C) 698
- The Reaction-Accelerating Neighboring-Group Effects in the Reaction of Vinyl Bromides with Alkyl-Transition Metal Reagents (C) 1684

Alkyne complexes
- Unique Reactivity of Heterodinuclear Pentacarbonyl(Fulvalene)Molybdenumruthenium with Alkynes: Fluxionality, Rearrangements, Structures, and First Reversible Conversion of a "Side-on"- to a Semi-Bridging Alkenylidene Ligand (C) 1463

Alkynes
- Flash Photolytic Generation and Study of Ynamines. First Observation of Primary and Secondary Ynamines in Solution (C) 1356
- Synthesis and Characterization of Radical-Substituted Diacetylene Derivatives (C) 450
- Tetraethynylethene (C) 698

Allyl sulfides
- 1,2-Asymmetric Induction in the Ketene Claisen Rearrangement of Allyl Sulfides (C) 1465

Aluminum compounds
- $[InAs_3]^{6\ominus}$ and $[AlSb_3]^{6\ominus}$, Trigonal Planar Anions in Cs_6InAs_3 and Cs_6AlSb_3 (C) 326
- $K_2[Al_{12}iBu_{12}]$, a Compound with Al_{12} Icosahedra (C) 179
- Monovalency of the Third Main-Group Elements: News from EX-Type Compounds (H) 544
- Tetraalkoxytitanium-Carbene Complexes with Double Intramolecular Et_2Al Bridging (C) 1668
- Tetrameric Gallium and Aluminum Chalcogenides, $[t\text{BuME}]_4$ (M = Al,Ga; E = S,Se,Te). A New Class of Heterocubanes (C) 1143
- The Tetrameric Aluminum(I) Compound $[\{Al(\eta^5\text{-}C_5Me_5)\}_4]$ (C) 564

Amines
- Dilithiation of a Primary Amine: Synthesis and Structure of $[(\alpha\text{-Naphthyl-}NLi_2)_{10}(Et_2O)_6] \cdot ET_2O$, a Paramagnetic Li_{20} Aggregate (C) 1707
- Stereoselective Synthesis of Vicinal Diamines (C) 103
- Synthesis of a Novel Macrobicyclic Cavity Possessing Six Convergent Hydroxyl Groups and Acting as a Siderophore (C) 85

Amino acids
- 3-Amino-2*H*-Azirines. Synthons for α,α-Disubstituted α-Amino Acids in Heterocycle and Peptide Synthesis [New Synthetic Methods (84)] (R) 238

- Chemoenzymatic Syntheses of ω-Ureido D-Amino Acids (C) 712
- 6-Deoxy-6-*N*-histamino-β-cyclodextrin Copper(II) Complex, a New Enantioselective Receptor for Aromatic Amino Acids (C) 1348
- New Approaches to the Use of Amino Acids as Chiral Building Blocks in Organic Synthesis [New Synthetic Methods (85)] (R) 1531
- Synthesis of β,γ-Unsaturated D-α-Amino Acids from L-Cysteine (C) 705

Amino sugars
- Amino-substituted β-Benzyl-*C*-glycosides; Novel β-Glycosidase Inhibitors (C) 1328
- Enzymatic Two-Step Synthesis on *N*-Acetylneuraminic Acid in the Enzyme Membrane Reactor (C) 827 (1713)

Ammonia
- Facile N–H Cleavage of Ammonia (C) 707

Analytical methods
- Chemical Characterization of Aerosols: On-Line and In Situ (R) 466
- Electroanalysis of Biologically Important Compounds (B) 1049
- Pulsed Electron Spin Resonance Spectroscopy: Basic Principles, Techniques, and Examples of Applications [New Analytic Methods (43)] (R) 265
- Ultramicroelectrodes—a New Dimension in Electrochemistry? (H) 170

Annulenes
- [14]Annulenequinones with Anthraquinone Periphery: "Isopyrenequinone" (C) 681
- Conversion of a Diatropic Bridged Annulene into a Paratropic Species on Metal Complexation (C) 1013
- Isophlorins: Molecules at the Crossroads of Porphyrin and Annulene Chemistry (C) 1693

Anomeric effect
- Conformational Preference of 2-Triphenylphosphonio-1,3-dithianes: Competition between Steric and Anomeric Effects (C) 578

Anthocyanins
- Structure and Molecular Stacking of Anthocyanins—Flower Color Variation (R) 17

Antibiotics
- Chemistry and Biology of the Enediyne Anticancer Antibiotics (R) 1387
- Lantibiotics—Ribosomally Synthesized Biologically Active Polypeptides containing Sulfide Bridges and α,β-Didehydroamino Acids (R) 1051
- Synthetic Strategy for the Coupling of the Calicheamicin Oligosaccharide with Aglycons: Synthesis of Dynemicin A-Calicheamicin Hybrid Structures (C) 585

Antibodies
- Antibody Catalysis of Glycosidic Bond Hydrolysis (C) 1711

Antimony compounds
- Synthesis and Structure of an N_2Sb_2 Ring with Different Types of Coordination for Antimony Atoms (C) 860

Antitumor agents
- Chemoenzymatic Syntheses of ω-Ureido D-Amino Acids (C) 712
- Enediyne Compounds Equipped with Acid-, Base- and Photo-Sensitive Triggering Devices. Chemical Simulation of the Dynemicin A Reaction Cascade (C) 1032

Arene complexes
- Ring Opening of a Cyclobutabenzene Complex under Very Mild Conditions (C) 880
- The Reduction of the NbX_5/AlX_3 System with Aluminum in the Presence of Aromatic Hydrocarbons: An Approach to Niobium(II), Niobium(I), and Niobium(0) Organometallics (C) 102

Arenes
- A General Entry to Rigid Systems with Alternatingly Orthogonal Arene Units via Diels–Alder Reactions (C) 1361
- A Homogeneous Platinum Catalyst in the Stationary $BF_3 \cdot H_2O$ Phase for the Hydrogenation of Arenes (C) 1009
- Aromatic Systems with Polymethine-like Structures: A Structural Comparison of Bis- and Tris(dimethylamino)-phenalenium Ions (C) 1030
- Bryophytes, a Source of Biologically Active, Naturally Occurring Material? (R) 130
- Ring Inversion in Sterically Hindered Arenes (C) 1484
- Stereoselective Synthesis of Annelated Piperidines by Photochemical Cycloaddition and Iminium Ion–Allylsilane Cyclization (C) 1697
- 1,4,5,8-Tetrakis(dimethylamino)naphthalene: Synthesis, Structure, "Proton Sponge" and Electron Donor Properties (C) 1028

Aromatic substitution
- Electrophilic Aromatic Substitution (B) 337

Aromaticity
- 2,3a,5,6a-Tetraazapentalene Dications and Tetraamino-1,3,5,7-tetrazocine (C) 334
- [14]Annulenequinones with Anthraquinone Periphery: "Isopyrenequinone" (C) 681
- Conversion of a Diatropic Bridged Annulene into a Paratropic Species on Metal Complexation (C) 1013
- σ-Homoacenaphthylene and π-Homoacenaphthene (C) 683
- Synthesis of a Highly Amphoteric *s*-Indaceno[1,2,3-*cd*:5,6,7-*c'd'*]diphenalene: Switching between Diatropism and Paratropism Due to Changes in Oxidation Level (C) 172
- Tercalicene and Quatercalicene (C) 446
- 1,3,5,7-Tetrakis(diethylamino)-*s*-indacenediylium bis(tetrafluoroborate)—a Stable *s*-Indacene Dication (C) 332
- 2,3,6,7-Tetramethoxythianthrene Dication: An "Aromatic" π System "Gives Up the Ghost" (C) 714
- The Structure of the Trimethylenemethane Dianion and the Question of Y-Aromaticity (C) 1001

Arsenic compounds
- Arsenic Compounds in Organic Synthesis: Pentamethinium Salts from Aminoarsanes and Pyrylium Salts (C) 994
- Do Partial Charges Alone Govern the Relative Stability of the Isomeric Heptaheteronortricyclane Anions $[P_{7-x}As_x]^{3\ominus}$? (C) 828

Arynes
- (2-Lithio-3-bromobenzofuran · Diisopropyl Ether)$_2$ and 1-Phenylsulfonyl-2-lithio-3-fluorobenzene Pentamethyldiethylenetriamine: Crystal Structures of Compounds with Lithium and Halogen on Neighboring Carbon Atoms (C) 1455

Asymmetric protonations
- Enantioselective Protonation of a Simple Enol: Aminoalcohol-Catalyzed Ketonization of a Photochemically Produced 2-Methylinden-3-ol (C) 416

Asymmetric syntheses
- η^1-(1*S*, 2*E*)-1-(*N*,*N*-diisopropylcarbamoyloxy)-3-trimethylsilylallyllithium · (−)-Sparteine: Structure of a Chiral, Carbamoyloxy-substituted Allyllithium Compound (C) 321
- Addition of Chiral Nucleophiles to Pyridine Compounds: Total Synthesis of (−)-Isovallesiachotamine and (+)-Vallesiachotamine (C) 1320
- 1,2-Asymmetric Induction in the Ketene Claisen Rearrangement of Allyl Sulfides (C) 1465
- Bis(4,5-dihydrooxazolyl) Derivatives in Asymmetric Catalysis (H) 542
- Catalytic and Stoichiometric Enantioselective Addition of Diethylzinc to Aldehydes Using a Novel Chiral Spirotitanate (C) 99
- Catalytic Enantioselective Epoxidations of Simple Olefins (H) 403
- Chirality and Crop Protection (R) 1193
- Diastereo- and Enantioselective Michael Addition Initiated Cyclizations to *trans*-Substituted Cyclopentanecarboxylates (C) 1664
- 2,2-Dimethyl-α,α,α',α'-tetrakis(β-naphthyl)-1,3-dioxolan-4,5-dimethanol (DINOL) for the Titanate-Mediated Enantioselective Addition of Diethylzinc to Aldehydes (C) 1321
- Double Stereodifferentiation in Carbohydrate Coupling Reactions: The Mismatched Interaction of Donor and Acceptor as an Unprecedented Factor Governing the α/β Ratio of Glycoside Formation (C) 180
- Efficient Stereoselective Total Synthesis of Denticulatins A and B (C) 97
- Enantioselective Addition of Organometallic Reagents to Carbonyl Compounds: Chirality Transfer, Multiplication, and Amplification [New Synthetic Methods (83)] (R) 49
- Importance of Oxyanion Orientation to the Stereochemical Control of Anionic Oxy-Cope Rearrangements (C) 1368
- Intramolecular Diels–Alder Reactions: Diastereofacial Selectivity and Coupling with an Aliphatic Claisen Rearrangement (C) 414
- New Approaches to the Use of Amino Acids as Chiral Building Blocks in Organic Synthesis [New Synthetic Methods (85)] (R) 1531
- *Anti*-Selective and Diastereofacially Selective Aldol Reactions with (*R*)-2-Siloxy-1,2,2-triphenylethyl propionate (C) 1318
- Stereoselective Synthesis of Cyclic Dipeptide Hydroxyalkyl Isosteres via Metalated *N*,*N*-Dialkylcarbamate 2-Alkenyl Esters (C) 1690
- Stereoselective Synthesis of Vicinal Diamines (C) 103
- The Isoinversion Principle—a General Model of Chemical Selectivity (R) 477
- Titanate-Catalyzed Enantioselective Addition of Dialkylzinc Compounds—Generated in situ from Grignard Reagents in Ether—to Aldehydes (C) 1008

Aurophilicity
- Ab initio Calculations on the $(ClAuPH_3)_2$ Dimer with Relativistic Pseudopotential: Is the "Aurophilic Attraction" a Correlation Effect? (C) 604
- Direct Observation of the Central Atom in $[C(Au\{P(C_6H_5)_2(p\text{-}C_6H_4NMe_2)\})_6](BF_4)_2$ by ^{13}C NMR Spectroscopy (C) 1488
- Triaurated Phosphonium Cations $[RP(AuPPh_3)_3]^{\oplus}$ and the Electron-deficient, Hypercoordinated Phosphonium Dication $[P(AuPPh_3)_5]^{2\oplus}$ (C) 433

Autobiographies
- Profiles, Pathways and Dreams. Autobiographies of Eminent Chemists (B) 1190
Azadodecaborane
- *closo*-Azadodecaborane, $NB_{11}H_{12}$ (C) 175
Azarhoda-*closo*-dodecaborane (C) 1377
Azirines
- [3 + 2] Cycloadditions with Azirine Radical Cations: A New Synthesis of *N*-Substituted Imidazoles (C) 1336
- 3-Amino-2*H*-Azirines. Synthons for α,α-Disubstituted α-Amino Acids in Heterocycle and Peptide Synthesis [New Synthetic Methods (84)] (R) 238
Azo dyes
- A New Approach to 2-Equivalent Couplers for Color Photography (C) 1704
- Salt-free Synthesis of Azo and Hydrazone Dyes Under CO_2 Pressure (C) 1643
Azobenzene
- Reduction of Azobenzene by Naphthaleneytterbium: A Tetranuclear Ytterbium(III) Complex Combining 1,2-Diphenylhydrazido(2−) and Phenylimido Ligands (C) 1149
Azomethines
- Effects of Perturbed Symmetry: Low-Melting Stable Mesogens Based on *ortho*-Palladated Imines (C) 711

Beckmann rearrangements
- Synthesis of Heterocycles by Tandem Reactions: Beckmann Rearrangements/Allylsilane Cyclizations (C) 687
Benzene isomers
- Tricarbonyl-η^6-(3,4-dimethylenecyclobutene)chromium(0), a Second Isomer of [(Benzene)Cr(CO)$_3$] (C) 870
Benzilic acid
- The Structure of "Organic Permanganate" (C) 704 (1192)
Benzobicyclooctenes
- *syn*-Sesqui- and -Sesterbenzobicyclo[2.2.2]octene, Molecules with Stacked Benzene Rings (C) 205
Benzonitriles
- Extension of Free Energy Correlations to Gas-Phase Ionic Reactions. Competitive Alkylation of Substituted Benzonitriles by $(CH_3)_2Cl^+$ Ions (C) 1457
Benzoxazepines
- 4-Acyl-2,3,4,5-tetrahydro-2-methyl-2,5-methanobenz-1,4-oxazepine, Derivatives of a New Heterocycle (C) 1709
Benzyl cation
- Laser Flash Photolysis Generation, Spectra, and Lifetimes of Phenylcarbenium Ions in Trifluoroethanol and Hexafluoroisopropyl Alcohol. On the UV Spectrum of the Benzyl Cation (C) 1337
Betaine dyes
- Chromoionophoric Pyridinium-*N*-phenolate Betaine Dyes (C) 558
Biocatalysis (B) 1529
Biochemistry
- Chemistry and Biology of the Enediyne Anticancer Antibiotics (R) 1387
- Chemistry of Plant Protection. Vol.4: Synthetic Pyrethroid Insecticides (B) 453
- Lantibiotics—Ribosomally Synthesized Biologically Active Polypeptides containing Sulfide Bridges and α,β-Didehydroamino Acids (R) 1051
- Lectins (B) 338
- Lipoxins and Related Eicosanoids: Biosynthesis, Biological Properties, and Chemical Synthesis (R) 1100
- Parabolic Growth of a Self-Replicating Hexadeoxynucleotide Bearing a 3'-5'-Phosphoamidate Linkage (C) 423 (892)
- The Extraordinary Enzymes Involved in Erythromycin Biosynthesis (H) 1302
- The Rationality of Random Screening—Efficient Methods of Selection of Peptides and Oligonucleotide Ligands (H) 296
Bioinorganic chemistry
- Functional Modeling of Ni,Fe Hydrogenases: A Nickel Complex in an *N,O,S* Environment (C) 193
- Intermediates in Nitrogenase Models: N_2H_3 and N_2H_4 as η^2-Coordinated Ligands (C) 303
- $[Mo(CO)_2(^{tbu}S'_2)_2]$ and $[MoCO(PPh_3)(^{tbu}S'_2)_2]$: CO Coordination at [Mo—S] Centers Where Mo Is in a High Oxidation State (C) 1311
- The Bioinorganic Chemistry of Vanadium (R) 148
- The Neutral Transition Metal Thiolates $[M(SAr)_2]_2$ (M = Mn, Fe or Co, Ar = 2,4,6-*t*-Bu$_3$C$_6$H$_2$) (C) 330
- Transition-Metal Thiolates: From Molecular Fragments of Sulfidic Solids to Models for Active Centers in Biomolecules (R) 769
Biomembranes
- Interaction of Hydrophobically-Modified Poly-*N*-isopropylacrylamides with Model Membranes—or Playing a Molecular Accordion (C) 315
Biomineralization
- Biomineralization, Chemical and Biochemical Perspectives (B) 214
Biopolymers
- Microbial Polyesters (B) 1525
- Novel Polymeric Materials from Monodisperse Copolypeptides by Biotechnological Methods (H) 677
Biosensors
- Chemical Sensors and Biosensors—Principles and Applications (R) 516
Biphenyls
- Selective *p*-Chlorination of Biphenyl in L Zeolites (C) 1689
Biradicals
- The Mechanism of Interaction of Triplet 3-Methylcyclohex-2-en-1-one with Maleo- and fumarodinitrile: Evidence for Direct Formation of Triplet 1,4-Biradicals in [2 + 2] Photocycloadditions without the Intermediacy of Exciplexes (C) 1345
Bismuth compounds
- $Ag_{25}Bi_3O_{18}$, a Potentially Valence-Unstable Bi^{III}/Bi^{V} Compound (C) 883
Bistable molecules
- Energetic and Constitutional Hysteresis in Bistable Molecules (H) 956
- Thermal and Light-Induced Spin Crossover to a Metastable Low-Spin State in $[Fe(mtz)_6](CF_3SO_3)_2$ (C) 975
Boron compounds
- A Cyclic Methyleneborane with Trapezoidal Geometry (C) 594
- *closo*-Azadodecaborane, $NB_{11}H_{12}$ (C) 175
- Azarhoda-*closo*-dodecaborane (C) 1377
- $BPh_4^{\ominus}$ as a Ligand in Cationic Zirconium Complexes: Novel Bonding Mode and Fluxionality (C) 1152
- π-Coordination of Diorganotin Dications (C) 1370
- Crown Ethers with a Lewis Acidic Center: A New Class of Heterotopic Host Molecules (C) 1472
- Heterotopic Host Molecules for Binding Two Different Guests (C) 1474
- "[12]Mercuracarborand-4", the First Representative of a New Class of Rigid Macrocyclic Electrophiles: The Chloride Ion Complex of a Charge-Reversed Analogue of [12]Crown-4 (C) 1507
- Metal-assisted Organization rather than Preorganization for the Design of Macrocyclic Hosts (C) 1496
- Monovalency of the Third Main-Group Elements: News from EX-Type Compounds (H) 544
- Solvation Effects on Geometry and Chemical Shifts. An Ab Initio/IGLO Reconciliation of Apparent Experimental Inconsistencies on $H_3B \cdot NH_3$ (C) 1160
- Synthesis and Structure of the Potassium Salts of 1,3,2-Diazaboroles (C) 1015
- Synthesis, Structure, and Rearrangement of 1,3-Dibora[5]radialenes (C) 84
- Tetra-*tert*-butyltetraboratetrahedrane (C) 173
Bredt rule
- An Exception to the Bredt Rule in the Photoenolization of 4-Benzoyl[2.2]paracyclophane (C) 432
Brevetoxin A
- Novel Strategies for the Construction of Complex Polycyclic Ether Frameworks. Stereocontrolled Synthesis of the FGHIJ Ring System of Brevetoxin A (C) 299
Bridging ligands
- A Cluster with the Triply Facially Bridging Trimethylenemethane Ligand: Structure and Bonding of $[\{Rh(cod)\}_3(\mu_3\text{-}H)\{\mu_3\text{-}C(CH_2)_3\}]$ (C) 313
- $[Cp_2Fe_2(CO)_3(\mu\text{-}SitBu \cdot NMI)]I$: The First Silanetriyldiiron Complex (C) 843
- Derivatives of 1,1''-Biferrocene with Sulfur and Selenium Bridges (C) 1652
- Dinuclear Cyanoalkylidene Complexes of Iron (C) 847
- Formation of Doubly Vinyl-Bridged Binuclear Iridium Complexes by C-H Activation (C) 1006
Butenandt
- Adolf Butenandt. Biochemiker, Hormonforscher, Wissenschaftspolitiker (B) 891
Butenolides
- A Simple Way to Predict the Products of Topochemical Photoreactions on the Basis of Force Field Calculations (C) 1354

C_1 building blocks
- Designed Coupling of C_1 Ligands: Organometallic Model Reactions (H) 1119
C_4 building blocks
- Enzymatic Synthesis of Chiral C_4 Building Blocks from *meso*-Tartaric Acid (C) 86
Cadmium compounds
- Synthesis of Sterically Hindered Tellurophenols and the Structure of $[Cd(\mu\text{-}TeC_6H_2Me_3)_2]_\infty$ (C) 973
Cage compounds
- Inclusion of Metal Ions within a Tin–Oxygen Cage Stabilized by Organic Residues: Crystal Structure of $[(i\text{PrSn})_{12}O_4(OH)_{24}][Ag_7I_{11}] \cdot NaCl \cdot H_2O \cdot 10\,DMSO$ (C) 1482
Calcium antagonists
- 1,4-Dihydropyridines: Effects of Chirality and Conformation on the Calcium Antagonist and Calcium Agonist Activities (R) 1559
Calcium compounds
- The Reaction of $PtCl_2$ with an *N,S,O*-Coordinated Calcium Complex: Synthesis and Structure of a Complexed CaPt Anion (C) 1648
Calicenes
- Tercalicene and Quatercalicene (C) 446

Calicheamicins
- Chemistry and Biology of the Enediyne Anticancer Antibiotics (R) 1387
- Synthetic Strategy for the Coupling of the Calicheamicin Oligosaccharide with Aglycons: Synthesis of Dynemicin A-Calicheamicin Hybrid Structures (C) 585
Calixarenes
- Triple Inclusion by a Calixarene: the Crystal Structure of the Europium(III) Complex of Bis(homooxa)-*p*-*tert*-butylcalix[4]arene (C) 854
Carbamic acids
- Stereoselective Synthesis of Cyclic Dipeptide Hydroxyalkyl Isosteres via Metalated *N*,*N*-Dialkylcarbamate 2-Alkenyl Esters (C) 1690
Carbanions
- (2-Lithio-3-bromobenzofuran · Diisopropyl Ether)$_2$ and 1-Phenylsulfonyl-2-lithio-3-fluorobenzene Pentamethyldiethylenetriamine: Crystal Structures of Compounds with Lithium and Halogen on Neighboring Carbon Atoms (C) 1455
- Phenylsodium Compounds with η^3-Allyl or η^6-Phenyl Coordination (C) 825
- The Two-Electron Reduction of 1,1′-Diphenylethene by Lithium or Sodium to Different 1,1,4,4-Tetraphenylbutane-1,4-diide Salts via C–C Bond Formation—A Monomeric Dilithium Contact Ion Triple and a Polymer String of "Hydrocarbon Oysters Containing Solvated Sodium Pearls" (C) 1183
Carbene complexes
- Coupling of Alkynes with Carbene Ligands to Tungsten-coordinated Cyclopropenes and Their Stereoselective Isomerization to Vinylcarbene Complexes (C) 998
- Dinuclear Cyanoalkylidene Complexes of Iron (C) 847
- Double Insertion of Alkynes into Chromium–Carbon Bonds of β-Donor-Substituted Vinylcarbene Complexes of Chromium—A Simple Route to Cyclopenta[*b*]pyrans (C) 1658
- Fischer Carbene Complexes Facilitate the Intramolecular Pauson-Khand Reaction (C) 1470
- Mononuclear Silylvinylidene Rhodium Complexes from Silylalkynes: The $SiMe_3$ Migration as an Alternative to the [1,2]-H Shift (C) 700
- Nickel(0)-Carbene Complexes (C) 1666
- Tetraalkoxytitanium-Carbene Complexes with Double Intramolecular Et_2Al Bridging (C) 1668
Carbenes
- 5-Lithio-2*H*-tetrazolium Carbenoids: NMR Spectroscopic Detection and Reactions with Nitrogen Electrophiles (C) 1162
- Stable Carbenes—Illusion or Reality? (H) 674
- The Mechanism of Acylcarbene Insertion into O–H Bonds—Direct Observation of the Enol of a Carboxylic Acid Ester in Aqueous Solution (C) 1366
- Unusual Mode of Addition of 1,2-Alkadienylidene Carbenes to 1,3-Dienes: 1,4 Addition to Rigid and Flexible 1,3-Dienes (C) 984
Carbocations
- Direct Observation of the Central Atom in $[C(Au\{P(C_6H_5)_2(p\text{-}C_6H_4NMe_2)\})_6](BF_4)_2$ by ^{13}C NMR Spectroscopy (C) 1488
- $[FCNF]^+[AsF_6]^-$, a Salt of the Linear 22-Valence Electron Cation $[FCNF]^+$ (C) 1485
- Laser Flash Photolysis Generation, Spectra, and Lifetimes of Phenylcarbenium Ions in Trifluoroethanol and Hexafluoroisopropyl Alcohol. On the UV Spectrum of the Benzyl Cation (C) 1337
- Recombination of Carbocation-Sulfinate Ion Pairs (C) 1018
- 1,3,5,7-Tetrakis(diethylamino)-*s*-indacenediyliumbis(tetrafluoroborate)—a Stable *s*-Indacene Dication (C) 332
- The First Persistent β-Silyl-Substituted Vinyl Cation (C) 1479
Carbohydrates
- Antibody Catalysis of Glycosidic Bond Hydrolysis (C) 1711
- Chemoenzymatic Syntheses of Sialyloligosaccharides with Immobilized Sialidase (C) 1503
- Direct Assignment of Absolute Configuration of Chiral Alkyl Gluconamides by Wettability Measurements (C) 696
- Double Stereodifferentiation in Carbohydrate Coupling Reactions: The Mismatched Interaction of Donor and Acceptor as an Unprecedented Factor Governing the α/β Ratio of Glycoside Formation (C) 180
- Galactosyltransferase-Catalyzed Synthesis of 2′-Deoxy-*N*-acetyllactosamine (C) 1163
- Selective Halogenation at Primary Positions of Cyclomaltooligosaccharides and a Synthesis of Per-3,6-anhydro Cyclomaltooligosaccharides (C) 78
- Stereoselective Synthesis of Acetal-β,β-diglucosides, a Novel Class of Glycosides and Chiral Acetals (C) 868
- Synthesis and Characterization of Per-3,6-anhydro Cyclodextrins (C) 80
- Synthesis of an Elicitor-Active Heptaglucan Saccharide for Investigation of Defense Mechanisms of Plants (C) 1681
Carbon fibers
- Chemically Modified Carbon Fibers and their Applications (B) 213
Carbon–carbon linkage
- Designed Coupling of C_1 Ligands: Organometallic Model Reactions (H) 1119
- 2,2-Dimethyl-$\alpha,\alpha,\alpha',\alpha'$-tetrakis($\beta$-naphthyl)-1,3-dioxolan-4,5-dimethanol (DINOL) for the Titanate-Mediated Enantioselective Addition of Diethylzinc to Aldehydes (C) 1321
- Double Insertion of Alkynes into Chromium–Carbon Bonds of β-Donor-Substituted Vinylcarbene Complexes of Chromium—A Simple Route to Cyclopenta[*b*]pyrans (C) 1658
- β-Lithio Ketone Enolates: Generation and Reactions with Electrophiles (C) 177
- Metal-Centered Coupling of Two Carbyne Ligands To Form an Alkyne Ligand (C) 1167
- Methylating Reductive Dimerization of Aromatic Carbonyl Compounds, a Novel Organometallic Reaction (C) 1138
- Methyltrioxorhenium as Catalyst of a Novel Aldehyde Olefination (C) 1641
- Reactions of Substituted Alkynes at a Conformationally Rigid (Olefin)cobalt Fragment (C) 430
- Stereospecific γ-Ray-Induced Trimerization of Crystalline Sodium *trans*-2-Butenoate (C) 420
- The Reaction-Accelerating Neighboring-Group Effects in the Reaction of Vinyl Bromides with Alkyl-Transition Metal Reagents (C) 1684
- The Two-Electron Reduction of 1,1′-Diphenylethene by Lithium or Sodium to Different 1,1,4,4-Tetraphenylbutane-1,4-diide Salts via C–C Bond Formation—A Monomeric Dilithium Contact Ion Triple and a Polymer String of "Hydrocarbon Oysters Containing Solvated Sodium Pearls" (C) 1183
- Titanate-Catalyzed Enantioselective Addition of Dialkylzinc Compounds—Generated in situ from Grignard Reagents in Ether—to Aldehydes (C) 1008
- Unusual Mode of Addition of 1,2-Alkadienylidene Carbenes to 1,3-Dienes: 1,4 Addition to Rigid and Flexible 1,3-Dienes (C) 984
Carbonyl complexes
- *mer*-$[Cr(CO)_3(\eta^4\text{-norbornadiene})(\eta^2\text{-ethene})]$: A Key Compound in Understanding the Mechanism of the Photocatalytic Diene Hydrogenation with Chromium Carbonyl Complexes (C) 1343
Carbonylation
- Syndiotactic Poly(1-oxo-2-phenyltrimethylene): On the Mode of the Chain Growth under Palladium Catalysis (C) 989
Carbonylmetalates
- Direct Location of the Hydrido Ligands in the Dianion $[H_4Os_{10}(CO)_{24}]^{2-}$ by a Neutron Diffraction Study of Its $[(Ph_3P)_2N]^+$ Salt at 20 K (C) 1164
- Eight-Coordinate Metal Carbonyls Containing Only Monodentate Ligands. Syntheses and Structural Characterization of $[nPr_4N]_2[(Ph_3Sn)_4M(CO)_4]$, M = Zr, Hf (C) 194
- Highly Reduced Metal Carbonyls (H) 168
- Synthesis and Characterization of a New Binary Deca-osmium Carbonyl Cluster Anion—An Intermediate in the Formation of Other High-nuclearity Osmium Carbonyl Clusters; Crystal and Molecular Structure of $[Ph_4P]_2[Os_{10}(CO)_{26}]$ (C) 1505
- The Synthesis of the First Decametal Nitrido Cluster; X-Ray Structure Analysis and ^{14}N NMR Studies of $[(Ph_3P)_2N][Ru_{10}N(CO)_{24}]$ (C) 1706
Carbyne complexes
- Designed Coupling of C_1 Ligands: Organometallic Model Reactions (H) 1119
- Metal-Centered Coupling of Two Carbyne Ligands To Form an Alkyne Ligand (C) 1167
Carcinogenicity
- Synthesis of the 2,3-Epoxy-2,3-dihydro-2,3-dimethylbenzo[*b*]furan, the Proposed Ultimate Mutagen of the Benzofuran Dioxetanes (C) 200
Carotenoids
- The Chemistry of Rose Pigments (R) 654
Catalysis
- A Homogeneous Platinum Catalyst in the Stationary $BF_3 \cdot H_2O$ Phase for the Hydrogenation of Arenes (C) 1009
- Antibody Catalysis of Glycosidic Bond Hydrolysis (C) 1711
- Biocatalysis (B) 1529
- Blocking of Acidic Centers upon Hydrothermal Dealumination of ZSM-5 Zeolites (C) 607
- Catalytic Enantioselective Epoxidations of Simple Olefins (H) 403
- *mer*-$[Cr(CO)_3(\eta^4\text{-norbornadiene})(\eta^2\text{-ethene})]$: A Key Compound in Understanding the Mechanism of the Photo-

catalytic Diene Hydrogenation with Chromium Carbonyl Complexes (C) 1343
- Formation of Colloidal Transition Metals in Organic Phases and Their Application in Catalysis (C) 1312
- Methyltrioxorhenium as Catalyst for Olefin Metathesis (C) 1636
- Methyltrioxorhenium as Catalyst for Olefin Oxidation (C) 1638
- Methyltrioxorhenium as Catalyst of a Novel Aldehyde Olefination (C) 1641
- Microporous Silica Films (C) 1509
- Photocatalysis of the Homogeneous Water-Gas Shift Reaction under Ambient Conditions by Cationic Iridium(III) Complexes (C) 844
- Surface Organometallic Chemistry on Oxides: Selective Catalytic Low-Temperature Hydrogenolysis of Alkanes by a Highly Electrophilic Zirconium Hydride Complex Supported on Silica (C) 1660
- Syndiotactic Poly(1-oxo-2-phenyltrimethylene): On the Mode of the Chain Growth under Palladium Catalysis (C) 989
- Synthesis and Characterization of P-containing ZSM-5 Zeolites (C) 686
- Tetraalkoxytitanium-Carbene Complexes with Double Intramolecular Et_2Al Bridging (C) 1668
- Titanate-Catalyzed Enantioselective Addition of Dialkylzinc Compounds—Generated in situ from Grignard Reagents in Ether—to Aldehydes (C) 1008

Catenanes
- Molecular Trains: The Self-Assembly and Dynamic Properties of Two New Catenanes (C) 1042
- Self-Assembling [3]Catenanes (C) 1039

Ceramics
- Silicon Nitride—From Powder Synthesis to Ceramic Materials (R) 1579

C-H activation
- Activation of Methane (H) 820
- Formation of Doubly Vinyl-Bridged Binuclear Iridium Complexes by C-H Activation (C) 1006
- Oxidation of Alkanes by $[Fe(O)OH]^{\oplus}$ in the Gas Phase—the Role of Iron Oxidation State in C–H Activations (C) 991
- Selective Hydrocarbon Activation. Principles and Progress (B) 1527
- Surface Organometallic Chemistry on Oxides: Selective Catalytic Low Temperature Hydrogenolysis of Alkanes by a Highly Electrophilic Zirconium Hydride Complex Supported on Silica (C) 1660

Chalcogen compounds
- Tetrameric Gallium and Aluminum Chalcogenides, $[t\mathrm{BuME}]_4$ (M = Al,Ga; E = S,Se,Te). A New Class of Heterocubanes (C) 1143

Charge separation
- Solvent Dependence of Photoinduced Intramolecular Electron Transfer: Criteria for the Design of Systems with Rapid, Solvent-Independent Charge Separation (C) 1358

Charge transfer complexes
- A Distorted *anti*-Perovskite Structure in Ternary Tetrathiafulvalenium Salts: Construction, Distortion, and Antiferromagnetic Ordering (C) 1498
- Benzene Bis(diazocyanides)—the First Acceptors of the Inverse Wurster Type for Conductive Organic Materials (C) 561
- Novel Building Blocks for the Synthesis of Organic Metals (H) 1121
- $[\{Re_2Cl_4(dppm)_2\}_2(\mu\text{-TCNQ})]$, a Novel Charge Transfer Complex Derived from a Donor with a Metal-Metal Multiple Bond (C) 448

Chelate ligands
- Chelate Complexes with Triisocyanide Ligands (C) 203
- Cp'_2TiS_5O and Cp'_2TiOS_5—Isomeric Titanocene Complexes with Two Novel S-O Chelate Ligands ($Cp' = \eta^5\text{-}CH_3C_5H_4$) (C) 550
- Hexanuclear Ferric Complex with a Novel $S = 5$ Ground State (C) 598

Chemical bonding
- Bonding Patterns in Intermetallic Compounds (R) 789

Chemical structures
- Representation in Chemistry (R) 1

Chemical systems
- Groups of Organic Molecules That Operate Collectively (R) 1086

Chiral auxiliaries
- β-Alkyl and β-Alkyl-α-Hydroxy Carboxylic Acid Derivatives from Radical or Ionic 1,4 Addition of Dialkylaluminum Chlorides to α,β-Unsaturated *N*-Acyl Urethanes (C) 694
- Catalytic and Stoichiometric Enantioselective Addition of Diethylzinc to Aldehydes Using a Novel Chiral Spirotitanate (C) 99
- 2,2-Dimethyl-α,α,α′,α′-tetrakis(β-naphthyl)-1,3-dioxolan-4,5-dimethanol (DINOL) for the Titanate-Mediated Enantioselective Addition of Diethylzinc to Aldehydes (C) 1321
- Enantioselective Addition of Organometallic Reagents to Carbonyl Compounds: Chirality Transfer, Multiplication, and Amplification [New Synthetic Methods (83)] (R) 49
- *Anti*-Selective and Diastereofacially Selective Aldol Reactions with (*R*)-2-Siloxy-1,2,2-triphenylethyl propionate (C) 1318

Chirality
- Chirality and Crop Protection (R) 1193
- Dyes for Visual Distinction between Enantiomers: Crown Ethers as Optical Sensors for Chiral Compounds (H) 958
- Helical Semiquinones: Proof of Chirality by ENDOR Spectroscopy (C) 602
- Optically Active "Stereocomplexes" of Isotactic Poly(methyl methacrylates) with Main-Chain Chirality (C) 849
- Recombination of Carbocation-Sulfinate Ion Pairs (C) 1018
- Spontaneous Resolution by Stirred Crystallization (H) 293

Chlorinated hydrocarbons
- Enantioselective Metabolism of (±)-α-1,2,3,4,5,6-Hexachlorocyclohexane in Organs of the Eider Duck (C) 320

Chlorinations
- Selective *p*-Chlorination of Biphenyl in L Zeolites (C) 1689

Chlorine dioxide
- Crystal Structure of Chlorine Dioxide (C) 1510

Chlorophyll
- On the Enigma of Chlorophyll Degradation: The Constitution of a Secoporphinoid Catabolite (C) 1315

Chlorotetaine
- Enantioselective and Diastereoselective Total Synthesis of the Antimycotically Active Natural Product Chlorotetaine: Revision of the Relative Configuration (C) 1685

Chromatography
- Countercurrent Chromatography (B) 892
- 6-Deoxy-6-*N*-histamino-β-cyclodextrin Copper(II) Complex, a New Enantioselective Receptor for Aromatic Amino Acids (C) 1348
- Dynamic HPLC: A Method for Determining Rate Constants, Energy Barriers, and Equilibrium Constants of Molecular Dynamic Processes (C) 74 (216)
- Enantiomer Separation on Immobilized Chirasil-Metal and Chirasil-Dex by Gas Chromatography and Supercritical Fluid Chromatography (C) 987
- Gas Chromatography—A Practical Course (B) 1050
- New Chiral Polyamide Stationary Phases for Chromatographic Enantiomer Separation (C) 1662

Chromium compounds
- *mer*-$[Cr(CO)_3(\eta^4\text{-norbornadiene})(\eta^2\text{-ethene})]$: A Key Compound in Understanding the Mechanism of the Photocatalytic Diene Hydrogenation with Chromium Carbonyl Complexes (C) 1343
- Double Insertion of Alkynes into Chromium–Carbon Bonds of β-Donor-Substituted Vinylcarbene Complexes of Chromium—A Simple Route to Cyclopenta[*b*]pyrans (C) 1658
- Reversible Intramolecular Base Stabilization of a Low-Coordinate Silicon Atom in the Silanediyl Complex $[(o\text{-}Me_2NCH_2C_6H_4)_2Si = Cr(CO)_5]$ (C) 1132
- Ring Opening of a Cyclobutabenzene Complex under Very Mild Conditions (C) 880
- Tricarbonyl-η^6-(3,4-dimethylenecyclobutene)chromium(0), a Second Isomer of [(Benzene)$Cr(CO)_3$] (C) 870

Chromoionophores
- Chromoionophoric Pyridinium-*N*-phenolate Betaine Dyes (C) 558
- Dyes for Visual Distinction between Enantiomers: Crown Ethers as Optical Sensors for Chiral Compounds (H) 958

Circular dichroism
- Circular Dichroism of a Chiral Cyanine Dye Dimer Trapped in γ-Cyclodextrin (C) 869

Circulenes
- [7.7]Circulene, a Molecule Shaped Like a Figure of Eight (C) 1173

Claisen rearrangements
- 1,2-Asymmetric Induction in the Ketene Claisen Rearrangement of Allyl Sulfides (C) 1465
- Intramolecular Diels–Alder Reactions: Diastereofacial Selectivity and Coupling with an Aliphatic Claisen Rearrangement (C) 414

Clusters
- A Novel Oligomer of Condensed Metal Atom Clusters in $[Y_{16}Ru_4I_{20}]$ (C) 856
- An Unusual Polyoxovanadium Organophosphonate Anion, $[H_6(VO_2)_{16}(CH_3PO_3)_8]^{8\ominus}$ (C) 422
- $[As^{V}V^{V}_{12}V^{IV}_{2}O_{40}]^{7\ominus}$, a Topologically Interesting, Mixed Valence Cluster as Model for Vanadium Minerals Formed by Weathering (C) 210
- Atomic and Molecular Clusters (B) 1382
- *closo*-Azadodecaborane, $NB_{11}H_{12}$ (C) 175
- $(n\mathrm{Bu}_4\mathrm{P})_2[Os_{20}(CO)_{40}]$, a Thermolytically Generated High-Nuclearity Cluster with a Tetrahedral Cubic-Close-Packed Metal Core (C) 107
- Direct Location of the Hydrido Ligands in the Dianion $[H_4Os_{10}(CO)_{24}]^{2-}$ by a Neutron Diffraction Study of Its $[(Ph_3P)_2N]^+$ Salt at 20 K (C) 1164

- Formation of a Cluster Sheath around a Central Cluster by a "Self-Organization Process": the Mixed Valence Polyoxovanadate $[V_{34}O_{82}]^{10\ominus}$ (C) 588
- Isolated and Condensed Ta_2Ni_2 Clusters in the Layered Tellurides $Ta_2Ni_2Te_4$ and $Ta_2Ni_3Te_5$ (C) 840
- $K_2[Al_{12}iBu_{12}]$, a Compound with Al_{12} Icosahedra (C) 179
- Molecular Systems with Perfect Metal Structure (H) 72
- $(NBu_4)[Mn_4O_2(H_2O)(O_2CPh)_9]$, a Butterfly Complex with Bound H_2O, and Its Use to Prepare Octanuclear and Undecanuclear Metal Complexes (C) 1672
- Polyoxometalate Chemistry: An Old Field with New Dimensions in Several Disciplines (R) 34
- Spontaneous Self Assembly of an Octanuclear Iron-Nickel Cluster by Reaction of $[Fe_6S_6I_6]^{2\ominus}$ with $[NiI_4]^{2\ominus}$ (C) 881
- Synthesis and Characterization of a New Binary Deca-osmium Carbonyl Cluster Anion—An Intermediate in the Formation of Other High-nuclearity Osmium Carbonyl Clusters; Crystal and Molecular Structure of $[Ph_4P]_2[Os_{10}(CO)_{26}]$ (C) 1505
- Template-Controlled Formation of Cluster Shells or a Type of Molecular Recognition: Synthesis of $[HV_{22}O_{54}(ClO_4)]^{6-}$ and $[H_2V_{18}O_{44}(N_3)]^{5-}$ (C) 1674
- $Th_6Br_{15}H_7$—Stabilization of a Th_6Br_{12} Cluster by Seven Hydrogen Atoms (C) 101
- The Chemistry of Metal Cluster Complexes (B) 337
- The Cluster Anion $[Ru_6H(CO)_{15}S_3]^-$: A Planar Hexanuclear Metal Framework with Almost Perfect C_{3v} Symmetry (C) 1126
- The Synthesis of the First Decametal Nitrido Cluster; X-Ray Structure Analysis and ^{14}N NMR Studies of $[(Ph_3P)_2N][Ru_{10}N(CO)_{24}]$ (C) 1706

Cobalt compounds
- Intermediates in Nitrogenase Models: N_2H_3 and N_2H_4 as η^2-Coordinated Ligands (C) 303
- New Discoveries in the Realm of Metal-Metal Multiple Bonds: $[\eta^5$-$C_5Me_5)_2Co_2]$, the First Organometallic Multiple-Bond Complex without Bridging Ligands (H) 1120
- Pressure-Assisted Formation of a Cobalt–Carbon σ Bond: A High-Pressure Pulse Radiolysis Study (C) 1158
- Reactions of Substituted Alkynes at a Conformationally Rigid (Olefin)cobalt Fragment (C) 430
- Reactivity of Cobalt Atoms towards 1,2,3,4,5-Pentamethylcyclopentadienyl: Synthesis and Structure of Bis(η^5-pentamethylcyclopentadienyl)-(μ_2-η^5:η^5-pentamethylcyclopentadienyl)dicobalt and Bis(η^5-pentamethylcyclopentadienyl)dicobalt (C) 1124
- Structure of a Self-assembling Triple-helical Complex containing two Cobalt^{II} Ions (C) 1490

Colloids
- Formation of Colloidal Transition Metals in Organic Phases and Their Application in Catalysis (C) 1312
- Ligand-Stabilized Bimetallic Colloids Identified by HRTEM and EDX (C) 874

Complexes with arsenic ligands
- *cyclo*-As_8 as Complex Ligand (C) 850

Complexes with carbon ligands
- Mononuclear Silylvinylidene Rhodium Complexes from Silylalkynes: The $SiMe_3$ Migration as an Alternative to the [1,2]-H Shift (C) 700
- Novel Tetranuclear Iron–Hexapentaene Complexes: The First Examples of Poly-π-Allyl Complexes (C) 1670
- Reactions of Substituted Alkynes at a Conformationally Rigid (Olefin)cobalt Fragment (C) 430

Complexes with chalcogen ligands
- The Synthesis and Structure of the Yellow and Green Forms of $[Nb(O)Cl_3(PMe_3)_3]$ and the Orange and Green Forms of $[Nb(S)Cl_3(PMe_3)_3]$; Examples of Perfectly Matched Bond-Stretch Isomers? (C) 980

Complexes with diene ligands
- $[Cp_2^*La(thf)(\mu$-η^1,η^3-$C_4H_6)LaCp_2^*]$: Synthesis and Structure of a Butadiene-Lanthanoid Complex (C) 435

Complexes with hydrido ligands
- Direct Location of the Hydrido Ligands in the Dianion $[H_4Os_{10}(CO)_{24}]^{2-}$ by a Neutron Diffraction Study of Its $[(Ph_3P)_2N]^+$ Salt at 20 K (C) 1164
- $Th_6Br_{15}H_7$—Stabilization of a Th_6Br_{12} Cluster by Seven Hydrogen Atoms (C) 101
- The Cluster Anion $[Ru_6H(CO)_{15}S_3]^-$: A Planar Hexanuclear Metal Framework with Almost Perfect C_{3v} Symmetry (C) 1126

Complexes with hydrogen ligands
- $[Cu(\eta^2$-$H_2)Cl]$, a Model Compound for H_2 Complexes. Ab Initio Calculations and Identification by IR Spectroscopy (C) 832

Complexes with nitrogen ligands
- Alkaline Earth Metal Complexes Containing Deprotonated Organic Acids and Water: Preparation, Structures and a New Synthetic Strategy (C) 428
- Bis(4,5-dihydrooxazolyl) Derivatives in Asymmetric Catalysis (H) 542
- Effect of Intramolecular Coordination on Tantalum-Alkylidene-Centered Reactions: Synthesis and Structure of a Tantalum-Olefin Adduct and a Tantalum-Zinc-Alkylidene Complex (C) 996
- Intermediates in Nitrogenase Models: N_2H_3 and N_2H_4 as η^2-Coordinated Ligands (C) 303
- Metal-Ion Dependent Regioselectivity in Cyclometalation Reactions (C) 1363
- Nickel-catalyzed Cyclotrimerization of Malononitrile: The Dicyanomethanide-bridged, Anionic Ni^{II} Complex $[\{Ni(C_5F_5)_2(\mu$-$NCCHCN)\}_2]^{2\ominus}$ (C) 716
- Oxidative Cleavage of Triethylenetetramine (trien) to Yield Diethylenetriamine (dien): Structure of the Mn^{II}/Mn^{III} Heptanuclear Complex $[Mn_7(trien)_2(dien)_2O_4(OAc)_8](PF_6)_4 \cdot 2H_2O$ (C) 688
- Reduction of Azobenzene by Naphthaleneytterbium: A Tetranuclear Ytterbium(III) Complex Combining 1,2-Diphenylhydrazido(2−) and Phenylimido Ligands (C) 1149
- The High-Yield Synthesis and Characterization of the First Porphyrin-Cyclam Dinucleating Ligand and Its Iron(III)/Copper(II) Complex (C) 572
- The Synthesis of the First Decametal Nitrido Cluster; X-Ray Structure Analysis and ^{14}N NMR Studies of $[(Ph_3P)_2N][Ru_{10}N(CO)_{24}]$ (C) 1706

Complexes with oxygen ligands
- Alkaline Earth Metal Complexes Containing Deprotonated Organic Acids and Water: Preparation, Structures and a New Synthetic Strategy (C) 428
- Chloride-Induced Conversion of $[Mn_4O_2(OAc)_6(py)_2(dbm)_2]$ to $[Mn_4O_3Cl(OAc)_3(dbm)_3]$: Potential Relevance to Photosynthetic Water Oxidation (C) 305
- Oxidative Cleavage of Triethylenetetramine (trien) to Yield Diethylenetriamine (dien): Structure of the Mn^{II}/Mn^{III} Heptanuclear Complex $[Mn_7(trien)_2(dien)_2O_4(OAc)_8](PF_6)_4 \cdot 2H_2O$ (C) 688

Complexes with phosphorus ligands
- A Cp_2Zr Complex of a Phosphaalkyne Dimer as Educt in the Synthesis of Cyclic Phosphorus Compounds (C) 207
- Bicyclic P_6 as Complex Ligand (C) 553
- Carbonyl(pentaphosphacyclopentadienyl)-Transition Metal Complexes (M = Cr, Mo, W, Mn) through Directed Syntheses with *cyclo*-$P_5^{\ominus}$ (C) 580
- Direct Observation of the Central Atom in $[C(Au\{P(C_6H_5)_2(p$-$C_6H_4NMe_2)\})_6](BF_4)_2$ by ^{13}C NMR Spectroscopy (C) 1488
- Phosphorus Monoxide (PO) as Complex Ligand (C) 852
- The First Metallobis(methylene)phosphoranes—Unexpected Isomerization to a Phosphaferrocene (C) 312
- The *cyclo*-P_4 Ligand as 12-Electron Donor (C) 969

Complexes with silicon ligands
- $[Cp_2Fe_2(CO)_3(\mu$-Si*t*Bu · NMI)]I: The First Silanetriyldiiron Complex (C) 843
- Intramolecular Base Stabilization of Si = N and Si = P Compounds and Related Transition-Metal Silanediyl Complexes (C) 1130
- Reversible Intramolecular Base Stabilization of a Low-Coordinate Silicon Atom in the Silanediyl Complex $[(o$-$Me_2NCH_2C_6H_4)_2Si = Cr(CO)_5]$ (C) 1132

Complexes with sulfur ligands
- Cp'_2TiS_5O and Cp'_2TiOS_5—Isomeric Titanocene Complexes with Two Novel S-O Chelate Ligands ($Cp' = \eta^5$-$CH_3C_5H_4$) (C) 550
- $[\{Fe(\mu$-$'S_4')\}_2(\mu$-$S_2)\}$: A Model Complex for [Fe–S] Enzymes with a New Type of [2Fe–2S] Center (C) 1477
- $[Mo(CO)_2(^{t}buS'_2)_2]$ and $[MoCO(PPh_3)(^{t}buS'_2)_2]$: CO Coordination at [Mo—S] Centers Where Mo Is in a High Oxidation State (C) 1311
- Proof of Strong S−H···S Bridges in $[Ru(SH_2)(PPh_3)('S_4')] \cdot THF$, the First H_2S Complex Characterized by X-Ray Crystallography (C) 552
- $[Re_2S_{16}]^{2-}$, a Soluble Metal Sulfide with Interesting Electronic Properties and Unusual Reactivity (C) 1512
- Spontaneous Self Assembly of an Octanuclear Iron-Nickel Cluster by Reaction of $[Fe_6S_6I_6]^{2\ominus}$ with $[NiI_4]^{2\ominus}$ (C) 881
- The Neutral Transition Metal Thiolates $[M(SAr)_2]_2$ (M = Mn, Fe or Co, Ar = 2,4,6-*t*-$Bu_3C_6H_2$) (C) 330
- The Reaction of $PtCl_2$ with an *N,S,O*-Coordinated Calcium Complex: Synthesis and Structure of a Complexed CaPt Anion (C) 1648
- Transition-Metal Thiolates: From Molecular Fragments of Sulfidic Solids to Models for Active Centers in Biomolecules (R) 769

Complexes with tin ligands
- Eight-Coordinate Metal Carbonyls Containing Only Monodentate Ligands. Syntheses and Structural Characterization of $[nPr_4N]_2[(Ph_3Sn)_4M(CO)_4]$, M = Zr, Hf (C) 194

Composites
- International Encyclopedia of Composites. Volumes 1 and 2 (B) 609
Computer
- Computational Chemistry Using the PC (B) 1384
- Reviews in Computational Chemistry (B) 452
Configuration
- Direct Assignment of Absolute Configuration of Chiral Alkyl Gluconamides by Wettability Measurements (C) 696
Conformation
- Conformational Preference of 2-Triphenylphosphonio-1,3-dithianes: Competition between Steric and Anomeric Effects (C) 578
- Light Absorption as well as Crystal and Molecular Structure of *N,N'*-Dimethylindigo: An Example of the Use of Synchrotron Radiation (C) 964
- Ring Inversion in Sterically Hindered Arenes (C) 1484
- Switch Peptides: pH-Induced α-Helix to β-Sheet Transitions of Bis-amphiphilic Oligopeptides (C) 1514
Coordination
- A Complex with Three-Coordinate Tungsten Atom: $[(silox)_2W = NtBu]$ (silox = tBu_3SiO) (C) 584
- A New Macrobicyclic Tris-bipyridine Ligand and Its Cu^I_2 and Ag^I_3 Complexes (C) 1331
- $BPh_4^{\ominus}$ as a Ligand in Cationic Zirconium Complexes: Novel Bonding Mode and Fluxionality (C) 1152
- π-Coordination of Diorganotin Dications (C) 1370
- Different Reaction Behavior of Lead Bis(tri-*tert*-butoxygermanate) and Lead Bis(tri-*tert*-butoxystannate) towards Nonacarbonyldiiron (C) 878
- Endoreceptors with Convergent Phenanthroline Units: A Molecular Cavity for Six Guest Molecules (C) 1333
- Intramolecular Base Stabilization of Si = N and Si = P Compounds and Related Transition-Metal Silanediyl Complexes (C) 1130
- *trans*-[Mo(η^2-*O,C*-PhNCO)(η^2-*C,N*-PhNCO)(*syn*-Me_8[16]aneS$_4$)]; Novel Discrimination of the C=O and C = N Bonds of PhNCO at Stereochemically Different Axial Sites (C) 982
- Phenylsodium Compounds with η^3-Allyl or η^6-Phenyl Coordination (C) 825
- Synthesis and Structure of an N_2Sb_2 Ring with Different Types of Coordination for Antimony Atoms (C) 860
- The *cyclo*-P_4 Ligand as 12-Electron Donor (C) 969
- The Structure of $IF_8^{\ominus}$ (C) 876
Copper compounds
- [Cu(η^2-H_2)Cl], a Model Compound for H_2 Complexes. Ab Initio Calculations and Identification by IR Spectroscopy (C) 832
- Heterometallic Compounds Involving d- and f-Block Elements: Synthesis, Structure, and Magnetic Properties of Two New Ln_xCu_4 Complexes (C) 1139
- $K_2Cu_5Te_5$, a Novel Mixed-Valence Layered Compound with Metallic Properties (C) 1325
- New Intermediate Phases of the Composition $La_{2n+2}Cu_{n+4}O_{4n+7}$ in the La–Cu–O System: the Crystal Structure and Thermal Stability of $La_2Cu_2O_5$ (C) 864
- The Crystal Chemistry of Copper Oxometalates (R) 723
Correspondence (L) 1192
Corrigenda 216, 892, 1386, 1713
Cram
- Profiles, Pathways and Dreams. Autobiographies of Eminent Chemists (B) 1190
Crown ethers
- Aggregation of Aza Crown Ethers by Metalation: Synthesis and Crystal Structure of 1-Lithio-1,7-diaza[12]-crown-4—The First Lithiated Crown Ether (C) 82
- Chromoionophoric Pyridinium-*N*-phenolate Betaine Dyes (C) 558
- Crown Ethers with a Lewis Acidic Center: A New Class of Heterotopic Host Molecules (C) 1472
- Heterotopic Host Molecules for Binding Two Different Guests (C) 1474
- Stoichiometric Mono *N*-Functionalization of Tetraazamacrocycles via Phosphoryl-Protected Intermediates (C) 560
Cryptates
- A New Macrobicyclic Tris-bipyridine Ligand and Its Cu^I_2 and Ag^I_3 Complexes (C) 1331
- Cryptatium: A Species of Expanded Atom/Radical Ion Pair Type from Electroreductive Crystallization of the Macrobicyclic Sodium Tris(Bipyridine) Cryptate (C) 838
Crystallization
- Spontaneous Resolution by Stirred Crystallization (H) 293
Crystallography
- Crystalline Symmetries. An Informal Mathematical Introduction (B) 1525
Cubanes
- Tetrameric Gallium and Aluminum Chalcogenides, $[t$BuME$]_4$ (M = Al,Ga; E = S,Se,Te). A New Class of Heterocubanes (C) 1143
Cumulenes
- Novel Tetranuclear Iron–Hexapentaene Complexes: The First Examples of Poly-π-Allyl Complexes (C) 1670
Cyanamide
- Herbicide Resistance in Transgenic Plants through Degradation of the Phytotoxin to Urea (C) 1314
Cyanides
- The Isocyanide–Cyanide Rearrangement; Mechanism and Preparative Applications (R) 893
Cyanines
- Arsenic Compounds in Organic Synthesis: Pentamethinium Salts from Aminoarsanes and Pyrylium Salts (C) 994
- Circular Dichroism of a Chiral Cyanine Dye Dimer Trapped in γ-Cyclodextrin (C) 869
- Structural Changes on Twofold Oxidation of Tetrakis(dimethylamino)-*p*-benzoquinone: A Sterically Overcrowded Electron-Rich "Chair" Compound Turns into a "Twist" Dicyanine Salt (C) 1180
Cyclic voltammetry
- Cyclooctatetraenylene Vinylene (C) 1003
- On the Electrochemical Oxidation of $Cs^{\oplus}$ and Other Alkali-Metal Ions in Liquid Sulfur Dioxide and Acetonitrile (C) 836
Cyclizations
- Synthesis of Heterocycles by Tandem Reactions: Beckmann Rearrangements/Allylsilane Cyclizations (C) 687
Cycloadditions
- [3 + 2] Cycloadditions with Azirine Radical Cations: A New Synthesis of *N*-Substituted Imidazoles (C) 1336
- A Simple Way to Predict the Products of Topochemical Photoreactions on the Basis of Force Field Calculations (C) 1354
- Chemo- and Stereoselective Cobalt-Mediated [2 + 2 + 2]Cycloaddition of Alkynes with Uracil Derivatives. A Novel Synthetic Entry to Modified Nucleosides (C) 993
- 1,3-Dipolar Cycloaddition as the Key Reaction in the Synthesis of Potent Renin Inhibitors (C) 1702
- Novel Naphthalene- and Cyclohexa-1,3-diene–Silene Cycloadducts (C) 444
- Novel Reactions of Disubstituted 1,2-Dioxetanes with Olefins as π-Nucleophiles: Cycloadditions via 1,6-Dipoles (C) 1365
- Stereoselective Synthesis of Annelated Piperidines by Photochemical Cycloaddition and Iminium Ion–Allylsilane Cyclization (C) 1697
- The Mechanism of Interaction of Triplet 3-Methylcyclohex-2-en-1-one with Maleo- and fumarodinitrile: Evidence for Direct Formation of Triplet 1,4-Biradicals in [2 + 2] Photocycloadditions without the Intermediacy of Exciplexes (C) 1345
- Unusual Mode of Addition of 1,2-Alkadienylidene Carbenes to 1,3-Dienes: 1,4 Addition to Rigid and Flexible 1,3-Dienes (C) 984
Cyclobutadiene
- Incarcerated Atoms and Reactive Molecules (H) 1117
- The Taming of Cyclobutadiene (C) 1024
Cyclodextrins
- Circular Dichroism of a Chiral Cyanine Dye Dimer Trapped in γ-Cyclodextrin (C) 869
- 6-Deoxy-6-*N*-histamino-β-cyclodextrin Copper(II) Complex, a New Enantioselective Receptor for Aromatic Amino Acids (C) 1348
- Enantiomer Separation on Immobilized Chirasil-Metal and Chirasil-Dex by Gas Chromatography and Supercritical Fluid Chromatography (C) 987
- Synthesis and Characterization of Per-3,6-anhydro Cyclodextrins (C) 80
Cyclohexanones
- On the Origin of π-Facial Diastereoselectivity in Addition Reactions of Cyclohexane-Based Systems (C) 1146
Cyclooctatetraenes
- Cyclooctatetraenylene Vinylene (C) 1003
Cyclopentadienyl complexes
- Cyclopentadienyl-Actinide Complexes: Bonding and Electronic Structure (R) 1069
Cyclopentadienyl radicals
- Synthesis and Structure of the Pentaisopropylcyclopentadienyl Radical (C) 971
Cyclopentane carboxylic acids
- Diastereo- and Enantioselective Michael Addition Initiated Cyclizations to *trans*-Substituted Cyclopentanecarboxylates (C) 1664
Cyclopentenones
- Fischer Carbene Complexes Facilitate the Intramolecular Pauson-Khand Reaction (C) 1470
Cyclophanes
- A General Entry to Rigid Systems with Alternatingly Orthogonal Arene Units via Diels–Alder Reactions (C) 1361
- An Exception to the Bredt Rule in the Photoenolization of 4-Benzoyl[2.2]paracyclophane (C) 432
- Derivatives of 1,1''-Biferrocene with Sulfur and Selenium Bridges (C) 1652
- Molecular Trains: The Self-Assembly and Dynamic Properties of Two New Catenanes (C) 1042
- Self-Assembling [3]Catenanes (C) 1039

- Self-Assembling [2]Pseudorotaxanes (C) 1036

Cyclopropenes
- Coupling of Alkynes with Carbene Ligands to Tungsten-coordinated Cyclopropenes and Their Stereoselective Isomerization to Vinylcarbene Complexes (C) 998

Cyclopropylidenes
- 7,7'-Bi(dispiro[2.0.2.1]heptylidene)—the Perspirocyclopropanated Bicyclopropylidene (C) 1518

Cysteine
- Synthesis of β,γ-Unsaturated D-α-Amino Acids from L-Cysteine (C) 705

Data transmission
- Chemical Reactions in the Manufacture of Waveguides for Long Distance Optical Data Transmission (R) 745

Dealumination
- Blocking of Acidic Centers upon Hydrothermal Dealumination of ZSM-5 Zeolites (C) 607

Deformation isomerism
- Dichloro(pentamethylcyclopentadienyl)-ruthenium—Novel Dichotomy in a Molecular Structure (C) 690
- The Synthesis and Structure of the Yellow and Green Forms of $[Nb(O)Cl_3(PMe_3)_3]$ and the Orange and Green Forms of $[Nb(S)Cl_3(PMe_3)_3]$; Examples of Perfectly Matched Bond-Stretch Isomers? (C) 980

Dendrimers
- Alkane Cascade Polymers Possessing Micellar Topology: Micellanoic Acid Derivatives (C) 1176
- Surface Fractality of Dendrimers (C) 1379
- Unimolecular Micelles (C) 1178

Density functional calculations
- Molecular Structures from Density Functional Calculations with Simulated Annealing (R) 630

Denticulatins
- Efficient Stereoselective Total Synthesis of Denticulatins A and B (C) 97

Diamines
- Stereoselective Synthesis of Vicinal Diamines (C) 103

Diastereomeric resolution
- Diastereomer Separation by Formation of Inclusion Compounds: 2,6-Dimethylnaphthalene Complexes of Flumethrin (C) 1634

Diazaboroles
- Synthesis and Structure of the Potassium Salts of 1,3,2-Diazaboroles (C) 1015

Diazo compounds
- 1,3-(C → O) Silyl Shift in α-Diazo α-Silyl Ketones: Cycloaddition Reactions and Kinetic Proof for the β-Siloxydiazoalkene Intermediate (C) 306
- Reactivity of a (Diazomethylene)phosphorane with Alkylating Agents and Lewis Acids; Synthesis of the First α-Diazoalkylborates (C) 1154

Diazocyanides
- A New Route to Aromatic Diazocyanides (C) 563
- Benzene Bis(diazocyanides)—the First Acceptors of the Inverse Wurster Type for Conductive Organic Materials (C) 561

Dictionary
- Acronyms and Abbreviations in Molecular Spectroscopy. An Encyclopedic Dictionary (B) 1381

Didemnenones
- A Short and Flexible Enantioselective Synthesis of the Didemnenones (C) 191

Diels–Alder reactions
- A General Entry to Rigid Systems with Alternatingly Orthogonal Arene Units via Diels–Alder Reactions (C) 1361
- Ammoniumyl Salt-Induced Diels-Alder Reaction of Ketenes—Control of [2 + 2] vs. [4 + 2] Selectivity (C) 999
- Intramolecular Diels–Alder Reactions: Diastereofacial Selectivity and Coupling with an Aliphatic Claisen Rearrangement (C) 414

Dihydropyridines
- 1,4-Dihydropyridines: Effects of Chirality and Conformation on the Calcium Antagonist and Calcium Agonist Activities (R) 1559

Diketones
- Palladium(II)-Induced Conversion of α-Acetoxyalkynes into α,β-Unsaturated α-Acetoxyketones; a Novel Access to α-Diketones (C) 593

Dimethylenecyclobutene
- Tricarbonyl-η^6-(3,4-dimethylenecyclobutene)chromium(0), a Second Isomer of $[(Benzene)Cr(CO)_3]$ (C) 870

Dinaphthofurofurans
- 2,2'-(Ethynediyl)bis(4-alkoxy-1-naphthols) and Dinaphthofuro[3,2-*b*]furans—Substances with Unusual Photoreactivity and Photochromic Behavior (C) 866

Dioxetanes
- Novel Reactions of Disubstituted 1,2-Dioxetanes with Olefins as π-Nucleophiles: Cycloadditions via 1,6-Dipoles (C) 1365
- Synthesis of the 2,3-Epoxy-2,3-dihydro-2,3-dimethylbenzo[*b*]furan, the Proposed Ultimate Mutagen of the Benzofuran Dioxetanes (C) 200

Diphosphirenes
- Formation of a *trans*-1,2,4,5-Tetraphosphatricyclo[3.1.0.$0^{2,4}$]hexane by [2 + 2] Cyclodimerization of a 3*H*-Diphosphirene (C) 90

1,6-Dipoles
- Novel Reactions of Disubstituted 1,2-Dioxetanes with Olefins as π-Nucleophiles: Cycloadditions via 1,6-Dipoles (C) 1365

Divinyldisiloxane
- Synthesis and Structure of a *rac*-Tris(divinyldisiloxane)diplatinum(0) Complex and its Reaction with Maleic Anhydride (C) 438

Djerassi
- Profiles, Pathways and Dreams. Autobiographies of Eminent Chemists (B) 1190

DNA
- Chemically Modified Oligonucleotides as Probes and Inhibitors (R) 613
- Single-Crystal X-Ray Diffraction Studies of Oligonucleotides and Oligonucleotide–Drug Complexes (R) 1254

DNA cleavage
- Bis(hydroperoxy)naphthaldiimide as a „Photo-Fenton Reagent": Sequence-Specific Photocleavage of DNA (C) 1351
- Enediyne Compounds Equipped with Acid-, Base- and Photo-Sensitive Triggering Devices. Chemical Simulation of the Dynemicin A Reaction Cascade (C) 1032
- Furfural as a Marker of DNA Cleavage by Hydroxylation at the 5' Carbon of Deoxyribose (C) 702
- Photolytic Cleavage of DNA by $[Pt_2(P_2O_5H_2)_4]^{4-}$ (C) 1517
- Selectivity and Mechanism of Action of Novel DNA-Cleaving Sulfones (C) 418

Drug design
- Comprehensive Medicinal Chemistry. Volume 4: Quantitative Drug Design (B) 889

Drugs
- Comprehensive Medicinal Chemistry. Volume 6: Cumulative Subject Index and Drug Compendium (B) 890

Dyes
- A New Approach to 2-Equivalent Couplers for Color Photography (C) 1704
- Salt-free Synthesis of Azo and Hydrazone Dyes Under CO_2 Pressure (C) 1643

Dynamic HPLC
- Dynamic HPLC: A Method for Determining Rate Constants, Energy Barriers, and Equilibrium Constants of Molecular Dynamic Processes (C) 74 (216)

Dynemicin A
- Enediyne Compounds Equipped with Acid-, Base- and Photo-Sensitive Triggering Devices. Chemical Simulation of the Dynemicin A Reaction Cascade (C) 1032

Ecology
- Chemical Characterization of Aerosols: On-Line and In Situ (R) 466
- Enantioselective Metabolism of (±)-α-1,2,3,4,5,6-Hexachlorocyclohexane in Organs of the Eider Duck (C) 320
- The Diels–Alder Dimer of 6-Hydroxy-2,6-dimethylcyclohexa-2,4-dienone, an Unusual Metabolite in the Bacterial Degradation of 2,6-Xylenol (C) 202

Eicosanoids
- Lipoxins and Related Eicosanoids: Biosynthesis, Biological Properties, and Chemical Synthesis (R) 1100

Elastomers
- New Routes to the Synthesis of Polymers Containing Nitrile Groups (C) 1654

Electroanalysis
- Electroanalysis of Biologically Important Compounds (B) 1049

Electrochemistry
- Ultramicroelectrodes—a New Dimension in Electrochemistry? (H) 170

Electron beam
- Cathodoluminescence. Theory and Applications (B) 1048

Electron localization
- A New Look at Electron Localization (C) 409

Electron transfer
- Investigation of the Light-Induced Charge Transfer between Covalently Linked Porphyrin and Quinone Units by Time-Resolved EPR Spectroscopy (C) 1461
- Solvent Dependence of Photoinduced Intramolecular Electron Transfer: Criteria for the Design of Systems with Rapid, Solvent-Independent Charge Separation (C) 1358

Electronic structure
- Thermal and Light-Induced Spin Crossover to a Metastable Low-Spin State in $[Fe(mtz)_6](CF_3SO_3)_2$ (C) 975

Elicitors
- Synthesis of an Elicitor-Active Heptaglucan Saccharide for Investigation of Defense Mechanisms of Plants (C) 1681

Eliel
- Profiles, Pathways and Dreams. Autobiographies of Eminent Chemists (B) 1190

β-Eliminations
- (2-Lithio-3-bromobenzofuran · Diisopropyl Ether)$_2$ and 1-Phenylsulfonyl-2-lithio-3-fluorobenzene Pentamethyldiethylenetriamine: Crystal Structures of Compounds with Lithium and Halogen on Neighboring Carbon Atoms (C) 1455

Enantiomeric resolution
- 6-Deoxy-6-*N*-histamino-β-cyclodextrin Copper(II) Complex, a New Enantioselective Receptor for Aromatic Amino Acids (C) 1348
- Enantiomer Separation on Immobilized Chirasil-Metal and Chirasil-Dex by Gas Chromatography and Supercritical Fluid Chromatography (C) 987
- New Chiral Polyamide Stationary Phases for Chromatographic Enantiomer Separation (C) 1662
- Spontaneous Resolution by Stirred Crystallization (H) 293

Enantioselective complexation
- Enantioselective Complexation of Flexible and Rigid Substrates through Molecular Recognition (C) 858

ENDOR spectroscopy
- Helical Semiquinones: Proof of Chirality by ENDOR Spectroscopy (C) 602

Endoreceptors
- Endoreceptors with Convergent Phenanthroline Units: A Molecular Cavity for Six Guest Molecules (C) 1333

Enediynes
- Chemistry and Biology of the Enediyne Anticancer Antibiotics (R) 1387
- Enediyne Compounds Equipped with Acid-, Base- and Photo-Sensitive Triggering Devices. Chemical Simulation of the Dynemicin A Reaction Cascade (C) 1032
- Synthetic Strategy for the Coupling of the Calicheamicin Oligosaccharide with Aglycons: Synthesis of Dynemicin A-Calicheamicin Hybrid Structures (C) 585

Enols
- Enantioselective Protonation of a Simple Enol: Aminoalcohol-Catalyzed Ketonization of a Photochemically Produced 2-Methylinden-3-ol (C) 416
- The Mechanism of Acylcarbene Insertion into O–H Bonds—Direct Observation of the Enol of a Carboxylic Acid Ester in Aqueous Solution (C) 1366

Enones
- Tandem Silyl Migrations Leading to α,β-Bis-silylated Enals and Enones (C) 1687

Enzymatic catalysis
- A Metal-Ion- and Cofactor-independent Enzymatic Redox Reaction: Halogenation by Bacterial Nonheme Haloperoxidases (C) 1487
- Chemoenzymatic Syntheses of Sialyloligosaccharides with Immobilized Sialidase (C) 1503
- Chemoenzymatic Syntheses of ω-Ureido D-Amino Acids (C) 712
- Diastereoselective Enzymatic Aldol Additions: L-Rhamnulose and L-Fuculose 1-Phosphate Aldolases from *E. coli* (C) 555
- Enzymatic Synthesis of Chiral C_4 Building Blocks from *meso*-Tartaric Acid (C) 86
- Galactosyltransferase-Catalyzed Synthesis of 2′-Deoxy-*N*-acetyllactosamine (C) 1163
- Protease-Catalyzed Kinetically Controlled Peptide Syntheses (R) 1437
- The Biochemical Reactions of Organometallics with Enzymes and Proteins (R) 931

Enzyme membrane reactor
- Enzymatic Two-Step Synthesis on *N*-Acetylneuraminic Acid in the Enzyme Membrane Reactor (C) 827 (1713)

Enzymes
- A New Chromogenic β-Galactosidase Substrate: 7-β-D-Galactopyranosyloxy-9,9-dimethyl-9*H*-acridin-2-one (C) 1646
- Comprehensive Medicinal Chemistry. Volume 2: Enzymes and other Molecular Targets (B) 887
- Reduction of the Small Subunit of Ribonucleotide Reductase by Diimide: Evidence for the Formation of the Mixed-Valence Fe^{II}–Fe^{III} Center (C) 1135
- The Extraordinary Enzymes Involved in Erythromycin Biosynthesis (H) 1302

Epoxidations
- Catalytic Enantioselective Epoxidations of Simple Olefins (H) 403

Erythromycins
- Erythromycin Synthesis—A Never-ending Story? (H) 1452
- The Extraordinary Enzymes Involved in Erythromycin Biosynthesis (H) 1302

ESR spectroscopy
- EPR of Exchange Coupled Systems (B) 340
- Investigation of the Light-Induced Charge Transfer between Covalently Linked Porphyrin and Quinone Units by Time-Resolved EPR Spectroscopy (C) 1461
- Pulsed Electron Spin Resonance Spectroscopy: Basic Principles, Techniques, and Examples of Applications [New Analytic Methods (43)] (R) 265

Ethenyl(phenyl)iodonium triflate
- Synthesis of Ethenyl(phenyl)iodonium Triflate, $[H_2C=CHIPh][OSO_2CF_3]$, and Its Application as a Parent Vinyl Cation Equivalent (C) 1469

Ethynyl isocyanide
- Synthesis and Structure of Ethynyl Isocyanide (C) 1644

Felkin-Anh model
- On the Origin of π-Facial Diastereoselectivity in Addition Reactions of Cyclohexane-Based Systems (C) 1146

Fenton reagent
- Bis(hydroperoxy)naphthaldiimide as a „Photo-Fenton Reagent": Sequence-Specific Photocleavage of DNA (C) 1351

Fischer-Tropsch synthesis
- Designed Coupling of C_1 Ligands: Organometallic Model Reactions (H) 1119

Flower colors
- Structure and Molecular Stacking of Anthocyanins—Flower Color Variation (R) 17

Fluid phases
- Spectroscopy of Fluid Phases—The Study of Chemical Reactions and Equilibria up to High Pressures (R) 641

Flumethrin
- Diastereomer Separation by Formation of Inclusion Compounds: 2,6-Dimethylnaphthalene Complexes of Flumethrin (C) 1634

Fluorides
- Stable Phosphazenium Ions in Synthesis—an Easily Accessible, Extremely Reactive „Naked" Fluoride Salt (C) 1372

Fluorine compounds
- Bis(fluorocarbonyl) Peroxide; an Unusual Molecular Structure (C) 1145
- $[FCNF]^+[AsF_6]^-$, a Salt of the Linear 22-Valence Electron Cation $[FCNF]^+$ (C) 1485
- Fluorine-Stabilized Sulfur–Carbon Multiple Bonds (R) 361
- Highly Stable Liposomes Derived from Perfluoroalkylated Glycerophosphocholines (C) 567

Fractals
- A Random Walk Through Fractal Dimensions (B) 339
- Surface Fractality of Dendrimers (C) 1379

Fullerenes
- C_{60}: From Soot to Superconductors (H) 678
- Endohedral Cluster Compounds: Inclusion of Helium within $C_{60}^{\bullet\oplus}$ and $C_{70}^{\bullet\oplus}$ through Collision Experiments (C) 884
- Globe-trotting Hydrogens on the Surface of the Fullerene Compound $C_{60}H_6(N(CH_2CH_2)_2O)_6$ (C) 1309
- Incarcerated Atoms and Reactive Molecules (H) 1117
- The Third Allotropic Form of Carbon (H) 70

Fulvalenes
- On a Metathesis Reaction of Tetrathiafulvalene (TTF) (C) 1127 (1386)
- Unique Reactivity of Heterodinuclear Pentacarbonyl(Fulvalene)Molybdenumruthenium with Alkynes: Fluxionality, Rearrangements, Structures, and First Reversible Conversion of a "Side-on"- to a Semi-Bridging Alkenylidene Ligand (C) 1463

Fungicides
- Chirality and Crop Protection (R) 1193

Furanes
- A General Entry to Rigid Systems with Alternatingly Orthogonal Arene Units via Diels–Alder Reactions (C) 1361

Furfural
- Furfural as a Marker of DNA Cleavage by Hydroxylation at the 5′ Carbon of Deoxyribose (C) 702

β-Galactosidase
- A New Chromogenic β-Galactosidase Substrate: 7-β-D-Galactopyranosyloxy-9,9-dimethyl-9*H*-acridin-2-one (C) 1646

Gallium compounds
- A Novel Gallium–Phosphorus Cage Compound (C) 1141
- Synthesis and Structure of the Novel Ga_3P_3 Ring Compound $[(2,4,6\text{-}Ph_3C_6H_2)GaP(cyclo\text{-}C_6H_{11})]_3$ (C) 691
- Tetrameric Gallium and Aluminum Chalcogenides, $[t\text{BuME}]_4$ (M = Al,Ga; E = S,Se,Te). A New Class of Heterocubanes (C) 1143
- The Interaction of Tri-*tert*-butylgallium with White Phosphorus: Isolation of an Unusual Gallium Phosphorus Cluster (C) 1353

Gas-phase reactions
- Extension of Free Energy Correlations to Gas-Phase Ionic Reactions. Competitive Alkylation of Substituted Benzonitriles by $(CH_3)_2Cl^+$ Ions (C) 1457
- RS–P=S in the Gas Phase—First Generation of (Organothio)thioxophosphanes (C) 318

Gene technology
- Herbicide Resistance in Transgenic Plants through Degradation of the Phytotoxin to Urea (C) 1314

Germanium compounds
- Strained-Ring and Double-Bond Systems Consisting of Frameworks of the Group 14 Elements Si, Ge, and Sn (R) 902

Glass fibers
- Chemical Reactions in the Manufacture of Waveguides for Long Distance Optical Data Transmission (R) 745

Glycerinopyrin
- Biogenesis of the Carbon Skeleton of Glycerinopyrin: A New Biosynthetic Pathway for Pyrroles (C) 183

Glycolipids
- Glycolipids as Immunomodulators: Syntheses and Properties (R) 1611

Glycoproteins
- Chemoenzymatic Syntheses of Sialyloligosaccharides with Immobilized Sialidase (C) 1503
Glycoside synthesis
- Double Stereodifferentiation in Carbohydrate Coupling Reactions: The Mismatched Interaction of Donor and Acceptor as an Unprecedented Factor Governing the α/β Ratio of Glycoside Formation (C) 180
Glycosides
- Amino-substituted β-Benzyl-*C*-glycosides; Novel β-Glycosidase Inhibitors (C) 1328
- Stereoselective Synthesis of Acetal-β,β-diglucosides, a Novel Class of Glycosides and Chiral Acetals (C) 868
Gold compounds
- A Mixed-Valent Pentanuclear Gold Complex Containing a Linear $Au_5^{9\oplus}$ Chain (C) 198
- Ab initio Calculations on the $(ClAuPH_3)_2$ Dimer with Relativistic Pseudopotential: Is the "Aurophilic Attraction" a Correlation Effect? (C) 604
- Direct Observation of the Central Atom in $[C(Au\{P(C_6H_5)_2(p\text{-}C_6H_4NMe_2)\})_6](BF_4)_2$ by ^{13}C NMR Spectroscopy (C) 1488
- Ligand-Stabilized Bimetallic Colloids Identified by HRTEM and EDX (C) 874
- Metal-Ion Dependent Regioselectivity in Cyclometalation Reactions (C) 1363
- Triaurated Phosphonium Cations $[RP(AuPPh_3)_3]^{\oplus}$ and the Electron-deficient, Hypercoordinated Phosphonium Dication $[P(AuPPh_3)_5]^{2\oplus}$ (C) 433
Graphical representations
- Representation in Chemistry (R) 1

Halogen compounds
- $(I_3O_6)^{\oplus}$, a Novel Polyoxo Cation of Iodine (C) 329
- SiI_2—A Novel Triatomic Molecule with a Relativistic Touch (C) 1186
- Synthesis and Crystal Structure of $Br_5^{\oplus}MF_6^{\ominus}$ (M = As, Sb) (C) 328
- $Th_6Br_{15}H_7$—Stabilization of a Th_6Br_{12} Cluster by Seven Hydrogen Atoms (C) 101
- The Structure of $IF_6^{\ominus}$ (C) 323
- The Structure of $IF_8^{\ominus}$ (C) 876
Halogenations
- A Metal-Ion- and Cofactor-independent Enzymatic Redox Reaction: Halogenation by Bacterial Nonheme Haloperoxidases (C) 1487
- Selective Halogenation at Primary Positions of Cyclomaltooligosaccharides and a Synthesis of Per-3,6-anhydro Cyclomaltooligosaccharides (C) 78
Helices
- Helices, Supramolecular Chemistry, and Metal-directed Self-Assembly (H) 1450
- Structure of a Self-assembling Triple-helical Complex containing two Cobalt^{II} Ions (C) 1490
Heptaheteronortricyclanes
- Do Partial Charges Alone Govern the Relative Stability of the Isomeric Heptaheteronortricyclane Anions $[P_{7-x}As_x]^{3\ominus}$? (C) 828
Herbicides
- Chirality and Crop Protection (R) 1193
- Herbicide Resistance in Transgenic Plants through Degradation of the Phytotoxin to Urea (C) 1314
- Herbicides in Photosynthesis Research (R) 1621
Heteroarenes
- Double Insertion of Alkynes into Chromium–Carbon Bonds of β-Donor-Substituted Vinylcarbene Complexes of Chromium—A Simple Route to Cyclopenta[*b*]pyrans (C) 1658
- Synthesis of the 2,3-Epoxy-2,3-dihydro-2,3-dimethylbenzo[*b*]furan, the Proposed Ultimate Mutagen of the Benzofuran Dioxetanes (C) 200
- 2,4,6-Triaryl-1,3,5λ^3-diazaphosphinines (C) 106
Heteroatom chemistry
- Heteroatom Chemistry (B) 1190
Heterobenzenes
- Synthesis and Structure of the Novel Ga_3P_3 Ring Compound $[(2,4,6\text{-}Ph_3C_6H_2)GaP(cyclo\text{-}C_6H_{11})]_3$ (C) 691
Heterocycles
- A Novel Gallium–Phosphorus Cage Compound (C) 1141
- A Telluradistannirane and a 1,3-Ditelluradistannetane by Stepwise Addition of Tellurium to a Distannene (C) 834
- 2,3a,5,6a-Tetraazapentalene Dications and Tetraamino-1,3,5,7-tetrazocine (C) 334
- 3-Amino-2*H*-Azirines. Synthons for α,α-Disubstituted α-Amino Acids in Heterocycle and Peptide Synthesis [New Synthetic Methods (84)] (R) 238
- Conformational Preference of 2-Triphenylphosphonio-1,3-dithianes: Competition between Steric and Anomeric Effects (C) 578
- Cooligomerization of Phosphaalkynes and Alkynes in the Coordination Sphere of Rhodium Complexes (C) 310
- Diphosphonio Isophosphindoles, Phospholes with a Planar Phosphorus (C) 308
- Naphtho[2,3-*d*][1,2,3]oxadiazole (C) 1476
- Novel Naphthalene- and Cyclohexa-1,3-diene–Silene Cycloadducts (C) 444
- Synthesis and Structure of an Azadistanniridine (C) 1017
- Synthesis of Heterocycles by Tandem Reactions: Beckmann Rearrangements/Allylsilane Cyclizations (C) 687
- The Chemistry of Organophosphorus Compounds. Vol. 1: Primary, Secondary, and Tertiary Phosphines, Polyphosphines, and Heterocyclic Organophosphorus(III) Compounds (B) 1046
Heteropolyanions
- Polyoxometalate Chemistry: An Old Field with New Dimensions in Several Disciplines (R) 34
Heterotopic molecules
- Crown Ethers with a Lewis Acidic Center: A New Class of Heterotopic Host Molecules (C) 1472
- Heterotopic Host Molecules for Binding Two Different Guests (C) 1474
High-nuclearity clusters
- $(nBu_4P)_2[Os_{20}(CO)_{40}]$, a Thermolytically Generated High-Nuclearity Cluster with a Tetrahedral Cubic-Close-Packed Metal Core (C) 107
- Direct Location of the Hydrido Ligands in the Dianion $[H_4Os_{10}(CO)_{24}]^{2-}$ by a Neutron Diffraction Study of Its $[(Ph_3P)_2N]^+$ Salt at 20 K (C) 1164
- Molecular Systems with Perfect Metal Structure (H) 72
- $(NBu_4)[Mn_4O_2(H_2O)(O_2CPh)_9]$, a Butterfly Complex with Bound H_2O, and Its Use to Prepare Octanuclear and Undecanuclear Metal Complexes (C) 1672
- Synthesis and Characterization of a New Binary Deca-osmium Carbonyl Cluster Anion—An Intermediate in the Formation of Other High-nuclearity Osmium Carbonyl Clusters; Crystal and Molecular Structure of $[Ph_4P]_2[Os_{10}(CO)_{26}]$ (C) 1505
- The Synthesis of the First Decametal Nitrido Cluster; X-Ray Structure Analysis and ^{14}N NMR Studies of $[(Ph_3P)_2N][Ru_{10}N(CO)_{24}]$ (C) 1706
High-pressure chemistry
- New Routes to the Synthesis of Polymers Containing Nitrile Groups (C) 1654
- Spectroscopy of Fluid Phases—The Study of Chemical Reactions and Equilibria up to High Pressures (R) 641
High-pressure synthesis
- High Pressure Chemical Synthesis (B) 110
High-spin complexes
- Hexanuclear Ferric Complex with a Novel $S = 5$ Ground State (C) 598
High-vacuum techniques
- High Vacuum Techniques for Chemical Synthesis and Measurements (B) 1522
History of chemistry
- Adolf Butenandt. Biochemiker, Hormonforscher, Wissenschaftspolitiker (B) 891
- Faszination Chemie. 7000 Jahre Kulturgeschichte der Stoffe und Prozesse (B) 1046
- Lise Meitner and Fission: Fallout from the Discovery (R) 942
- Profiles, Pathways and Dreams. Autobiographies of Eminent Chemists (B) 1190
- Representation in Chemistry (R) 1
- Robert Robinson—Chemist Extraordinary (B) 1049
Homocycles
- 7,7'-Bi(dispiro[2.0.2.1]heptylidene)—the Perspirocyclopropanated Bicyclopropylidene (C) 1518
- Hexaspiro[3.0.3.0.3.0.3.0.3.0.3.0]tetracosane ([6.4]Rotane) (C) 436
Host–guest chemistry
- A New Macrobicyclic Tris-bipyridine Ligand and Its Cu_2^I and Ag_3^I Complexes (C) 1331
- Aggregation of Aza Crown Ethers by Metalation: Synthesis and Crystal Structure of 1-Lithio-1,7-diaza[12]-crown-4—The First Lithiated Crown Ether (C) 82
- Crown Ethers with a Lewis Acidic Center: A New Class of Heterotopic Host Molecules (C) 1472
- Cryptatium: A Species of Expanded Atom/Radical Ion Pair Type from Electroreductive Crystallization of the Macrobicyclic Sodium Tris(Bipyridine) Cryptate (C) 838
- Diastereomer Separation by Formation of Inclusion Compounds: 2,6-Dimethylnaphthalene Complexes of Flumethrin (C) 1634
- Dyes for Visual Distinction between Enantiomers: Crown Ethers as Optical Sensors for Chiral Compounds (H) 958
- Endohedral Cluster Compounds: Inclusion of Helium within $C_{60}^{\oplus}$ and $C_{70}^{\oplus}$ through Collision Experiments (C) 884
- Endoreceptors with Convergent Phenanthroline Units: A Molecular Cavity for Six Guest Molecules (C) 1333
- Helices, Supramolecular Chemistry, and Metal-directed Self-Assembly (H) 1450
- Heterotopic Host Molecules for Binding Two Different Guests (C) 1474
- Incarcerated Atoms and Reactive Molecules (H) 1117
- Mechanisms of Molecular Recognition: Investigations of Organic Host–Guest Complexes (R) 1417

- "[12]Mercuracarborand-4", the First Representative of a New Class of Rigid Macrocyclic Electrophiles: The Chloride Ion Complex of a Charge-Reversed Analogue of [12]Crown-4 (C) 1507
- Metal-assisted Organization rather than Preorganization for the Design of Macrocyclic Hosts (C) 1496
- Strategy for the Synthesis of Tube-Shaped Molecules (C) 575
- Structure of a Self-assembling Triple-helical Complex containing two Cobalt^{II} Ions (C) 1490
- Template-Controlled Formation of Cluster Shells or a Type of Molecular Recognition: Synthesis of $[HV_{22}O_{54}(ClO_4)]^{6-}$ and $[H_2V_{18}O_{44}(N_3)]^{5-}$ (C) 1674
- The Taming of Cyclobutadiene (C) 1024
- Triple Inclusion by a Calixarene: the Crystal Structure of the Europium(III) Complex of Bis(homooxa)-*p*-*tert*-butylcalix[4]arene (C) 854

Houben-Weyl
- Houben-Weyl. Methoden der Organischen Chemie. Band E 19a, Teil 1 und 2. C-Radikale (B) 611
- Houben-Weyl. Methoden der Organischen Chemie. Volume E16a, Parts 1 and 2: Nitrogen Compounds I (B) 1524

Hydantoins
- Chemoenzymatic Syntheses of ω-Ureido D-Amino Acids (C) 712

Hydrides
- Complex Transition Metal Hydrides (R) 759

Hydrogen bonds
- 1,4,5,8-Tetrakis(dimethylamino)naphthalene: Synthesis, Structure, "Proton Sponge" and Electron Donor Properties (C) 1028

Hydrogen bridges
- Enantioselective Complexation of Flexible and Rigid Substrates through Molecular Recognition (C) 858
- Molecular and Ionic Hydrogen Isocyanide (CNH) Adducts with N-H···O- and "Super-Short" N-H···N-Hydrogen Bridges: Metal-Stabilized Hydrogen Bisisocyanides (C) 88
- Proof of Strong S–H···S Bridges in $[Ru(SH_2)(PPh_3)('S_4')]\cdot THF$, the First H_2S Complex Characterized by X-Ray Crystallography (C) 552

Hydrogen isocyanide
- Molecular and Ionic Hydrogen Isocyanide (CNH) Adducts with N-H···O- and "Super-Short" N-H···N-Hydrogen Bridges: Metal-Stabilized Hydrogen Bisisocyanides (C) 88

Hydrogen migration
- Globe-trotting Hydrogens on the Surface of the Fullerene Compound $C_{60}H_6(N(CH_2CH_2)_2O)_6$ (C) 1309

Hydrogenases
- Functional Modeling of Ni,Fe Hydrogenases: A Nickel Complex in an *N,O,S* Environment (C) 193

Hydrogenation
- A Homogeneous Platinum Catalyst in the Stationary $BF_3\cdot H_2O$ Phase for the Hydrogenation of Arenes (C) 1009
- *mer*-[$Cr(CO)_3(\eta^4$-norbornadiene)(η^2-ethene)]: A Key Compound in Understanding the Mechanism of the Photocatalytic Diene Hydrogenation with Chromium Carbonyl Complexes (C) 1343

Hydrosilylation
- Synthesis and Structure of a *rac*-Tris(divinyldisiloxane)diplatinum(0) Complex and its Reaction with Maleic Anhydride (C) 438

Hydroxy carboxylic acids
- β-Alkyl and β-Alkyl-α-Hydroxy Carboxylic Acid Derivatives from Radical or Ionic 1,4 Addition of Dialkylaluminum Chlorides to α,β-Unsaturated *N*-Acyl Urethanes (C) 694

Hyperconjugation
- The First Persistent β-Silyl-Substituted Vinyl Cation (C) 1479
- The X-ray Crystal Structure Analysis of a Fragmentable *N*-Acylpyridinium Ion (C) 1656

Imidazoles
- [3 + 2] Cycloadditions with Azirine Radical Cations: A New Synthesis of *N*-Substituted Imidazoles (C) 1336

Iminophosphanes
- Iminophosphanes: Unconventional Compounds of Main Group Elements (R) 217

Immuno assays
- A New Chromogenic β-Galactosidase Substrate: 7-β-D-Galactopyranosyloxy-9,9-dimethyl-9*H*-acridin-2-one (C) 1646

Immunostimulation
- Glycolipids as Immunomodulators: Syntheses and Properties (R) 1611

Immunosuppression
- Toward the Understanding of Immunosuppression (H) 954

Indacenes
- Synthesis of a Highly Amphoteric *s*-Indaceno[1,2,3-*cd*:5,6,7-*c'd'*]diphenalene: Switching between Diatropism and Paratropism Due to Changes in Oxidation Level (C) 172
- 1,3,5,7-Tetrakis(diethylamino)-*s*-indacenediyliumbis(tetrafluoroborate)—a Stable *s*-Indacene Dication (C) 332

Indenes
- 2-Triphenylmethyldicyclohept[*cd*,*g*]-indene: A Novel *cata-peri* Condensed Nonalternant Hydrocarbon (C) 1174

Indigo
- Light Absorption as well as Crystal and Molecular Structure of *N,N'*-Dimethylindigo: An Example of the Use of Synchrotron Radiation (C) 964

Indium compounds
- $[InAs_3]^{6\ominus}$ and $[AlSb_3]^{6\ominus}$, Trigonal Planar Anions in Cs_6InAs_3 and Cs_6AlSb_3 (C) 326
- In_7Cl_9—A New "Old" Compound in the System In-Cl (C) 824
- On the Differing Lewis Basicity of In^I Compared with Sn^{II} in Molecular Indium-Tin and Thallium-Tin Alkoxides (C) 95

Indole alkaloids
- Addition of Chiral Nucleophiles to Pyridine Compounds: Total Synthesis of (−)-Isovallesiachotamine and (+)-Vallesiachotamine (C) 1320

Information storage
- Thermally Irreversible Photochromic Liquid Crystal Polymers (C) 76

Inhibitors
- Amino-substituted β-Benzyl-*C*-glycosides; Novel β-Glycosidase Inhibitors (C) 1328
- Chemically Modified Oligonucleotides as Probes and Inhibitors (R) 613
- 1,3-Dipolar Cycloaddition as the Key Reaction in the Synthesis of Potent Renin Inhibitors (C) 1702
- Stereoselective Synthesis of Cyclic Dipeptide Hydroxyalkyl Isosteres via Metalated *N,N*-Dialkylcarbamate 2-Alkenyl Esters (C) 1690
- Synthesis of Muropeptide Conjugates of 2,3-Dideoxy-β-D-*manno*-2-octulosonic Acid (C) 1682
- Toward the Understanding of Immunosuppression (H) 954

Insecticides
- Chemistry of Plant Protection. Vol.4: Synthetic Pyrethroid Insecticides (B) 453
- Chirality and Crop Protection (R) 1193

Intercalation compounds
- Structure of an Organometallic Intercalate: Single Crystal X-Ray and Powder Neutron Diffraction Study of $[SnS_2\{Co(\eta\text{-}C_5H_5)_2\}_{0.31}]$ and $[SnS_2\{Co(\eta\text{-}C_5D_5)_2\}_{0.31}]$ (C) 1156

Interhalogen compounds
- The Structure of $IF_8^{\ominus}$ (C) 876

Intermetallic compounds
- Bonding Patterns in Intermetallic Compounds (R) 789

Interstellar chemistry
- Synthesis and Structure of Ethynyl Isocyanide (C) 1644

Iodine compounds
- Synthesis of Ethenyl(phenyl)iodonium Triflate, $[H_2C=CHIPh][OSO_2CF_3]$, and Its Application as a Parent Vinyl Cation Equivalent (C) 1469

Ionic clusters
- Solvated Electron in the Synthesis of Ionic Clusters in Zeolites (C) 1501

Ionic conductors
- Volume Effect or Paddle-Wheel Mechanism—Fast Alkali-Metal Ionic Conduction in Solids with Rotationally Disordered Complex Anions (R) 1547

Iridium compounds
- Facile N–H Cleavage of Ammonia (C) 707
- Formation of Doubly Vinyl-Bridged Binuclear Iridium Complexes by C-H Activation (C) 1006
- Metal Carbonyl Complexes of Sapphyrins (C) 91
- Photocatalysis of the Homogeneous Water-Gas Shift Reaction under Ambient Conditions by Cationic Iridium(III) Complexes (C) 844
- Reversible Isomerization of the Dinuclear Complex [(η^6-*p*-cymene)RuCl(μ-pz)$_2$Ir(CO)$_2$] with Formation of a Ruthenium-Iridium Bond (C) 1171

Iron compounds
- Conversion of a Diatropic Bridged Annulene into a Paratropic Species on Metal Complexation (C) 1013
- $[Cp_2Fe_2(CO)_3(\mu\text{-}SitBu\cdot NMI)]I$: The First Silanetriyldiiron Complex (C) 843
- Derivatives of 1,1''-Biferrocene with Sulfur and Selenium Bridges (C) 1652
- Different Reaction Behavior of Lead Bis(tri-*tert*-butoxygermanate) and Lead Bis(tri-*tert*-butoxystannate) towards Nonacarbonyldiiron (C) 878
- Dinuclear Cyanoalkylidene Complexes of Iron (C) 847
- $[\{Fe(\mu\text{-}'S_4')\}_2(\mu\text{-}S_2)\}$: A Model Complex for [Fe–S] Enzymes with a New Type of [2Fe–2S] Center (C) 1477
- Hexanuclear Ferric Complex with a Novel $S = 5$ Ground State (C) 598
- $Li_4[FeN_2]$: A Nitridoferrate(II) with Anions Isosteric with CO_2. A Defect Variant of the Li_3N Type Structure (C) 199
- Novel Tetranuclear Iron–Hexapentaene Complexes: The First Examples of Poly-π-Allyl Complexes (C) 1670
- Oxidation of Alkanes by $[Fe(O)OH]^{\oplus}$ in the Gas Phase—the Role of Iron Oxidation State in C–H Activations (C) 991
- Reduction of the Small Subunit of Ribonucleotide Reductase by Diimide: Evidence for the Formation of the Mixed-Valence Fe^{II}–Fe^{III} Center (C) 1135

- Sandwiches Bring a New Element to Molecular Recognition (H) 407
- Spontaneous Self Assembly of an Octanuclear Iron-Nickel Cluster by Reaction of $[Fe_6S_6I_6]^{2\ominus}$ with $[NiI_4]^{2\ominus}$ (C) 881
- $Sr_2Li[Fe_2N_3]$ and $Ba_2Li[Fe_2N_3]$: Nitridoferrate(II) Isotypes with $^1_\infty[(FeN_{3/2})_2^{5\ominus}]$ Anions (C) 831
- Synthetic Siderophores of the Tetrazolenol Type: Iron(III) Complexes and Two-dimensional Iron(II) Coordination Polymers (C) 1494
- The First Metallobis(methylene)phosphoranes—Unexpected Isomerization to a Phosphaferrocene (C) 312
- Thermal and Light-Induced Spin Crossover to a Metastable Low-Spin State in $[Fe(mtz)_6](CF_3SO_3)_2$ (C) 975

Isocyanates
- *trans*-[Mo(η^2-*O,C*-PhNCO)(η^2-*C,N*-PhNCO)(*syn*-Me_8[16]aneS$_4$)]; Novel Discrimination of the C=O and C=N Bonds of PhNCO at Stereochemically Different Axial Sites (C) 982

Isocyanides
- Chelate Complexes with Triisocyanide Ligands (C) 203
- Synthesis and Structure of Ethynyl Isocyanide (C) 1644
- The Isocyanide–Cyanide Rearrangement; Mechanism and Preparative Applications (R) 893

Isoinversion principle
- The Isoinversion Principle—a General Model of Chemical Selectivity (R) 477

Isomerization
- Energetic and Constitutional Hysteresis in Bistable Molecules (H) 956
- Reversible Isomerization of the Dinuclear Complex [(η^6-*p*-cymene)RuCl-(μ-pz)$_2$Ir(CO)$_2$] with Formation of a Ruthenium-Iridium Bond (C) 1171
- Ring Opening of a Cyclobutabenzene Complex under Very Mild Conditions (C) 880
- Synthesis and Interconversion of New $(CH)_{14}$ Isomers (C) 1020
- Synthesis, Structure, and Isomerization of the (*E*)- and (*Z*)-Isomers of a Diphosphene (C) 1136

Isophlorins
- Isophlorins: Molecules at the Crossroads of Porphyrin and Annulene Chemistry (C) 1693

Isopyrenequinone
- [14]Annulenequinones with Anthraquinone Periphery: "Isopyrenequinone" (C) 681

Isoselectivity
- Isoselective Relationship for the Stereoselectivity of the Transfer of Hydrogen Atoms to Cyclic Alkyl Radicals (C) 600

Isotacticity
- Optically Active "Stereocomplexes" of Isotactic Poly(methyl methacrylates) with Main-Chain Chirality (C) 849

Ketenes
- Ammoniumyl Salt-Induced Diels-Alder Reaction of Ketenes—Control of [2 + 2] vs. [4 + 2] Selectivity (C) 999

Laboratory practice
- High Vacuum Techniques for Chemical Synthesis and Measurements (B) 1522

Lactols
- A Short and Flexible Enantioselective Synthesis of the Didemnenones (C) 191

Lanthanoid compounds
- A Novel Oligomer of Condensed Metal Atom Clusters in $[Y_{16}Ru_4I_{20}]$ (C) 856
- Heterometallic Compounds Involving d- and f-Block Elements: Synthesis, Structure, and Magnetic Properties of Two New Ln_xCu_4 Complexes (C) 1139
- Luminescence Properties of $Eu^{3\oplus}$ and $Tb^{3\oplus}$ Complexes of Branched Macrocyclic Ligands Containing Four 2,2'-Bipyridine Units (C) 190
- One-Step Synthesis of Organolanthanide(II) Complexes from the Metal (C) 693
- Reduction of Azobenzene by Naphthaleneytterbium: A Tetranuclear Ytterbium(III) Complex Combining 1,2-Diphenylhydrazido(2−) and Phenylimido Ligands (C) 1149
- Superconductivity in Layered Structures of Rare-Earth Carbide Halides (C) 1188
- Triple Inclusion by a Calixarene: the Crystal Structure of the Europium(III) Complex of Bis(homooxa)-*p*-*tert*-butylcalix[4]arene (C) 854

Lanthanum compounds
- [Cp^*_2La(thf)(μ-η^1,η^3-C_4H_6)LaCp^*_2]: Synthesis and Structure of a Butadiene-Lanthanoid Complex (C) 435
- New Intermediate Phases of the Composition $La_{2n+2}Cu_{n+4}O_{4n+7}$ in the La–Cu–O System: the Crystal Structure and Thermal Stability of $La_2Cu_2O_5$ (C) 864

Lantibiotics
- Lantibiotics—Ribosomally Synthesized Biologically Active Polypeptides containing Sulfide Bridges and α,β-Didehydroamino Acids (R) 1051

Latex
- Analysis of Polymer Latices by Small-Angle X-Ray Scattering (C) 1650

Lead compounds
- Different Reaction Behavior of Lead Bis(tri-*tert*-butoxygermanate) and Lead Bis(tri-*tert*-butoxystannate) towards Nonacarbonyldiiron (C) 878

Lectins (B) 338

Lewis basicity
- On the Differing Lewis Basicity of In^I Compared with Sn^{II} in Molecular Indium-Tin and Thallium-Tin Alkoxides (C) 95

Ligand reactivity
- Metals and Ligand Reactivity (B) 1384

Liposomes
- Highly Stable Liposomes Derived from Perfluoroalkylated Glycerophosphocholines (C) 567
- Interaction of Hydrophobically-Modified Poly-*N*-isopropylacrylamides with Model Membranes—or Playing a Molecular Accordion (C) 315

Lipoxins
- Lipoxins and Related Eicosanoids: Biosynthesis, Biological Properties, and Chemical Synthesis (R) 1100

Liquid crystals
- Bolaamphiphilic Polyols, a Novel Class of Amphotropic Liquid Crystals (C) 440
- Complexation of Transition Metal Ions with Substituted Aza Macrocycles: Induction of Columnar Mesophases by Molecular Recognition (C) 1375
- Effects of Perturbed Symmetry: Low-Melting Stable Mesogens Based on *ortho*-Palladated Imines (C) 711
- Metallomesogens: Metal Complexes in Organized Fluid Phases (R) 375
- Piezoelectric Liquid-Crystalline Elastomers (H) 405
- Thermally Irreversible Photochromic Liquid Crystal Polymers (C) 76

Lithio ketone enolates
- β-Lithio Ketone Enolates: Generation and Reactions with Electrophiles (C) 177

Lithium amides
- Aggregation of Aza Crown Ethers by Metalation: Synthesis and Crystal Structure of 1-Lithio-1,7-diaza[12]-crown-4—The First Lithiated Crown Ether (C) 82

Lithium perchlorate
- $LiClO_4$ in Ether—an Unusual Solvent (H) 1306

Low-coordinate transition metals
- A Complex with Three-Coordinate Tungsten Atom: [(silox)$_2$W = N*t*Bu] (silox = tBu$_3$SiO) (C) 584

Low-valent compounds
- A Stable Os^0 16-Electron Complex: Synthesis and Structure of [OsCl(NO)-(P*i*Pr$_3$)$_2$] (C) 596
- Different Reaction Behavior of Lead Bis(tri-*tert*-butoxygermanate) and Lead Bis(tri-*tert*-butoxystannate) towards Nonacarbonyldiiron (C) 878
- Monovalency of the Third Main-Group Elements: News from EX-Type Compounds (H) 544
- One-Step Synthesis of Organolanthanide(II) Complexes from the Metal (C) 693
- The Tetrameric Aluminum(I) Compound [{Al(η^5-C_5Me_5)}$_4$] (C) 564

Luminescence
- Cathodoluminescence. Theory and Applications (B) 1048

Luminescent materials
- Luminescence Properties of $Eu^{3\oplus}$ and $Tb^{3\oplus}$ Complexes of Branched Macrocyclic Ligands Containing Four 2,2'-Bipyridine Units (C) 190

Macrobicycles
- A New Macrobicyclic Tris-bipyridine Ligand and Its Cu^I_2 and Ag^I_3 Complexes (C) 1331
- Endoreceptors with Convergent Phenanthroline Units: A Molecular Cavity for Six Guest Molecules (C) 1333
- Molecular Recognition and Transport of Nucleobases—Superiority of Macrobicyclic Host Molecules (C) 442

Macrocycles
- Complexation of Transition Metal Ions with Substituted Aza Macrocycles: Induction of Columnar Mesophases by Molecular Recognition (C) 1375
- Luminescence Properties of $Eu^{3\oplus}$ and $Tb^{3\oplus}$ Complexes of Branched Macrocyclic Ligands Containing Four 2,2'-Bipyridine Units (C) 190
- Mechanisms of Molecular Recognition: Investigations of Organic Host–Guest Complexes (R) 1417
- Metal-assisted Organization rather than Preorganization for the Design of Macrocyclic Hosts (C) 1496
- Stoichiometric Mono *N*-Functionalization of Tetraazamacrocycles via Phosphoryl-Protected Intermediates (C) 560
- Strategy for the Synthesis of Tube-Shaped Molecules (C) 575
- Synthesis of a Novel Macrobicyclic Cavity Possessing Six Convergent Hydroxyl Groups and Acting as a Siderophore (C) 85

Magnetic properties
- Dilithiation of a Primary Amine: Synthesis and Structure of [(α-Naphthyl-$NLi_2)_{10}(Et_2O)_6$] · ET_2O, a Paramagnetic Li_{20} Aggregate (C) 1707
- Heterometallic Compounds Involving d- and f-Block Elements: Synthesis, Structure, and Magnetic Properties of Two New Ln_xCu_4 Complexes (C) 1139

Malononitrile
- Nickel-catalyzed Cyclotrimerization of Malononitrile: The Dicyanomethanide-bridged, Anionic Ni^{II} Complex $[\{Ni(C_5F_5)_2(\mu\text{-}NCCHCN)\}_2]^{2\ominus}$ (C) 716
Maltooligosaccharides
- Selective Halogenation at Primary Positions of Cyclomaltooligosaccharides and a Synthesis of Per-3,6-anhydro Cyclomaltooligosaccharides (C) 78
Manganese compounds
- Chloride-Induced Conversion of $[Mn_4O_2(OAc)_6(py)_2(dbm)_2]$ to $[Mn_4O_3Cl(OAc)_3(dbm)_3]$: Potential Relevance to Photosynthetic Water Oxidation (C) 305
- d-Electron Density in Formal d^0 Systems from Multiplet Splitting in the Photoelectron Spectrum of Permanganates (C) 967
- Furfural as a Marker of DNA Cleavage by Hydroxylation at the 5′ Carbon of Deoxyribose (C) 702
- $(NBu_4)[Mn_4O_2(H_2O)(O_2CPh)_9]$, a Butterfly Complex with Bound H_2O, and Its Use to Prepare Octanuclear and Undecanuclear Metal Complexes (C) 1672
- Oxidative Cleavage of Triethylenetetramine (trien) to Yield Diethylenetriamine (dien): Structure of the Mn^{II}/Mn^{III} Heptanuclear Complex $[Mn_7(trien)_2(dien)_2O_4(OAc)_8](PF_6)_4 \cdot 2H_2O$ (C) 688
Mass spectrometry
- Activation of Methane (H) 820
- Endohedral Cluster Compounds: Inclusion of Helium within $C_{60}^{\bullet\oplus}$ and $C_{70}^{\bullet\oplus}$ through Collision Experiments (C) 884
- Oxidation of Alkanes by $[Fe(O)OH]^{\oplus}$ in the Gas Phase—the Role of Iron Oxidation State in C–H Activations (C) 991
Materials science
- Materials Science and Technology (A Comprehensive Treatment). Volume 5: Phase Transformations in Materials (B) 1521
- Routes to New Aromatic Polycarbonates with Special Material Properties (R) 1598
- Silicon Nitride—From Powder Synthesis to Ceramic Materials (R) 1579
Matrix isolation
- Spectroscopy of Matrix Isolated Species (B) 610
Mechanistic studies
- Pressure-Assisted Formation of a Cobalt–Carbon σ Bond: A High-Pressure Pulse Radiolysis Study (C) 1158
Medicinal chemistry
- Comprehensive Medicinal Chemistry. Volume 5: Biopharmaceutics (B) 889
- Comprehensive Medicinal Chemistry. Volume 6: Cumulative Subject Index and Drug Compendium (B) 890
- Comprehensive Medicinal Chemistry. Volume 2: Enzymes and other Molecular Targets (B) 887
- Comprehensive Medicinal Chemistry. Volume 1: General Principles (B) 886
- Comprehensive Medicinal Chemistry. Volume 3: Membranes and Receptors (B) 888
- Comprehensive Medicinal Chemistry. Volume 4: Quantitative Drug Design (B) 889
Meitner
- Lise Meitner and Fission: Fallout from the Discovery (R) 942
Membranes
- Comprehensive Medicinal Chemistry. Volume 3: Membranes and Receptors (B) 888
- Highly Stable Liposomes Derived from Perfluoroalkylated Glycerophosphocholines (C) 567
Mercury compounds
- "[12]Mercuracarborand-4", the First Representative of a New Class of Rigid Macrocyclic Electrophiles: The Chloride Ion Complex of a Charge-Reversed Analogue of [12]Crown-4 (C) 1507
Metabolism
- Enantioselective Metabolism of (±)-α-1,2,3,4,5,6-Hexachlorocyclohexane in Organs of the Eider Duck (C) 320
Metalates
- Eight-Coordinate Metal Carbonyls Containing Only Monodentate Ligands. Syntheses and Structural Characterization of $[nPr_4N]_2[(Ph_3Sn)_4M(CO)_4]$, M = Zr, Hf (C) 194
- Highly Reduced Metal Carbonyls (H) 168
Metallacycles
- Competing Occurrence of Isomeric (Dialkyltartrato)zirconocene Dimers with Dimetallatricyclic and Ten-Membered Dimetallamonocyclic Frameworks (C) 1349
- Metal-Ion Dependent Regioselectivity in Cyclometalation Reactions (C) 1363
Metalla-enes
- Metalla-enes and Metalla-ynes—from Small Molecules to Infinite Polymers (H) 673
Metallomesogens
- Metallomesogens: Metal Complexes in Organized Fluid Phases (R) 375
Metathesis
- Methyltrioxorhenium as Catalyst for Olefin Metathesis (C) 1636
- On a Metathesis Reaction of Tetrathiafulvalene (TTF) (C) 1127 (1386)
Methane
- Activation of Methane (H) 820
Methionine
- A Metal-Ion- and Cofactor-independent Enzymatic Redox Reaction: Halogenation by Bacterial Nonheme Haloperoxidases (C) 1487
Methylation
- Methylating Reductive Dimerization of Aromatic Carbonyl Compounds, a Novel Organometallic Reaction (C) 1138
Methylene phosphonium ions
- Methylene Phosphonium Ions (C) 709
Methyleneboranes
- A Cyclic Methyleneborane with Trapezoidal Geometry (C) 594
Methylindenol
- Enantioselective Protonation of a Simple Enol: Aminoalcohol-Catalyzed Ketonization of a Photochemically Produced 2-Methylinden-3-ol (C) 416
Methyltrioxorhenium
- Methyltrioxorhenium as Catalyst for Olefin Metathesis (C) 1636
- Methyltrioxorhenium as Catalyst for Olefin Oxidation (C) 1638
- Methyltrioxorhenium as Catalyst of a Novel Aldehyde Olefination (C) 1641
Micelles
- Alkane Cascade Polymers Possessing Micellar Topology: Micellanoic Acid Derivatives (C) 1176
- Groups of Organic Molecules That Operate Collectively (R) 1086
- Structure and Reactivity in Reverse Micelles (B) 339
- Unimolecular Micelles (C) 1178
Michael additions
- Diastereo- and Enantioselective Michael Addition Initiated Cyclizations to *trans*-Substituted Cyclopentanecarboxylates (C) 1664
- Tandem Silyl Migrations Leading to α,β-Bis-silylated Enals and Enones (C) 1687
Mixed-valent compounds
- A Mixed-Valent Pentanuclear Gold Complex Containing a Linear $Au_5^{9\oplus}$ Chain (C) 198
- $Ag_{25}Bi_3O_{18}$, a Potentially Valence-Unstable Bi^{III}/Bi^{V} Compound (C) 883
- $[As^{V}V^{V}_{12}V^{IV}_{2}O_{40}]^{7\ominus}$, a Topologically Interesting, Mixed Valence Cluster as Model for Vanadium Minerals Formed by Weathering (C) 210
- Formation of a Cluster Sheath around a Central Cluster by a "Self-Organization Process": the Mixed Valence Polyoxovanadate $[V_{34}O_{82}]^{10\ominus}$ (C) 588
- $K_2Cu_5Te_5$, a Novel Mixed-Valence Layered Compound with Metallic Properties (C) 1325
- Reduction of the Small Subunit of Ribonucleotide Reductase by Diimide: Evidence for the Formation of the Mixed-Valence Fe^{II}–Fe^{III} Center (C) 1135
Modhephene
- Synthesis, Absolute Configuration and Specific Rotation of (+)- and (−)-Modhephene (C) 1492
Molecular dynamics
- Molecular Structures from Density Functional Calculations with Simulated Annealing (R) 630
Molecular recognition
- Complexation of Transition Metal Ions with Substituted Aza Macrocycles: Induction of Columnar Mesophases by Molecular Recognition (C) 1375
- Direct Observation of Streptavidin Specifically Adsorbed on Biotin-Functionalized Self-Assembled Monolayers with the Scanning Tunneling Microscope (C) 569
- Enantioselective Complexation of Flexible and Rigid Substrates through Molecular Recognition (C) 858
- Molecular Recognition and Transport of Nucleobases—Superiority of Macrobicyclic Host Molecules (C) 442
- Sandwiches Bring a New Element to Molecular Recognition (H) 407
Molecular sieves
- The Synthesis and Structure of Some New Sodalites: The Lithium Haloberyllophosphates and -arsenates (C) 1169
Molybdenum compounds
- A Distorted *anti*-Perovskite Structure in Ternary Tetrathiafulvalenium Salts: Construction, Distortion, and Antiferromagnetic Ordering (C) 1498
- $[Mo(CO)_2(^{tbu}S'_2)_2]$ and $[MoCO(PPh_3)(^{tbu}S'_2)_2]$: CO Coordination at [Mo–S] Centers Where Mo Is in a High Oxidation State (C) 1311
- Mo–Mo Quadruple Bonds Bridged by 1,8-Naphthyridinyl-2,7-Dioxide: an Insight into the Nature of a Parallel-Linked Stiff-Chain Polymer: $+M^nM\sim M^nM+_x$ (C) 862
- *trans*-[Mo(η^2-*O,C*-PhNCO)(η^2-*C,N*-PhNCO)(*syn*-Me_8[16]aneS$_4$)]; Novel Discrimination of the C=O and C=N Bonds of PhNCO at Stereochemically Different Axial Sites (C) 982
- Synthesis, Structure, and Rearrangement of 1,3-Dibora[5]radialenes (C) 84
- Unique Reactivity of Heterodinuclear Pentacarbonyl(Fulvalene)Molybdenum-ruthenium with Alkynes: Fluxionality, Rearrangements, Structures, and First Reversible Conversion of a "Side-on" to a Semi-Bridging Alkenylidene Ligand (C) 1463

Mosses
- Bryophytes, a Source of Biologically Active, Naturally Occurring Material? (R) 130
Multiple bonds
- Fluorine-Stabilized Sulfur–Carbon Multiple Bonds (R) 361
- Iminophosphanes: Unconventional Compounds of Main Group Elements (R) 217
- Intramolecular Base Stabilization of Si = N and Si = P Compounds and Related Transition-Metal Silanediyl Complexes (C) 1130
- Metalla-enes and Metalla-ynes—from Small Molecules to Infinite Polymers (H) 673
- Mo–Mo Quadruple Bonds Bridged by 1,8-Naphthyridinyl-2,7-Dioxide: an Insight into the Nature of a Parallel-Linked Stiff-Chain Polymer: $+M^nM{\sim}M^nM+_x$ (C) 862
- Multiple Bonds and Low Coordination in Phosphorus Chemistry (B) 1047
- New Discoveries in the Realm of Metal-Metal Multiple Bonds: $[\eta^5\text{-}C_5Me_5)_2Co_2]$, the First Organometallic Multiple-Bond Complex without Bridging Ligands (H) 1120
- Reactivity of Cobalt Atoms towards 1,2,3,4,5-Pentamethylcyclopentadienyl: Synthesis and Structure of Bis(η^5-pentamethylcyclopentadienyl)-(μ_2-η^5:η^5-pentamethylcyclopentadienyl)dicobalt and Bis(η^5-pentamethylcyclopentadienyl)dicobalt (C) 1124
- $[\{Re_2Cl_4(dppm)_2\}_2(\mu\text{-TCNQ})]$, a Novel Charge Transfer Complex Derived from a Donor with a Metal-Metal Multiple Bond (C) 448
- $[Re_2S_{16}]^{2-}$, a Soluble Metal Sulfide with Interesting Electronic Properties and Unusual Reactivity (C) 1512
- Strained-Ring and Double-Bond Systems Consisting of Frameworks of the Group 14 Elements Si, Ge, and Sn (R) 902
- Synthesis, Structure, and Isomerization of the (*E*)- and (*Z*)-Isomers of a Diphosphene (C) 1136
- Unsaturated Tin Compounds: Generation and Reactivity of $Me_2Sn{=}C(SiMe_3)_2$ and $Me_2Sn{=}N(SitBu_2Me)$ (C) 93
Mycotoxins
- Mycotoxins. Chemical, Biological and Environmental Aspects (B) 214

Naphthalines
- Solvent Dependence of Photoinduced Intramolecular Electron Transfer: Criteria for the Design of Systems with Rapid, Solvent-Independent Charge Separation (C) 1358
Natural products
- A Short and Flexible Enantioselective Synthesis of the Didemnenones (C) 191
- ACRL Toxin I: Convergent Total Synthesis of Its 3-Methyl Enol Ether from D-Glucose (C) 1339
- Biogenesis of the Carbon Skeleton of Glycerinopyrin: A New Biosynthetic Pathway for Pyrroles (C) 183
- Bryophytes, a Source of Biologically Active, Naturally Occurring Material? (R) 130
- Efficient Stereoselective Total Synthesis of Denticulatins A and B (C) 97
- Enantioselective and Diastereoselective Total Synthesis of the Antimycotically Active Natural Product Chlorotetaine: Revision of the Relative Configuration (C) 1685
- Erythromycin Synthesis—A Never-ending Story? (H) 1452
- Lipoxins and Related Eicosanoids: Biosynthesis, Biological Properties, and Chemical Synthesis (R) 1100
- Mycotoxins. Chemical, Biological and Environmental Aspects (B) 214
- Novel Strategies for the Construction of Complex Polycyclic Ether Frameworks. Stereocontrolled Synthesis of the FGHIJ Ring System of Brevetoxin A (C) 299
- Structure and Molecular Stacking of Anthocyanins—Flower Color Variation (R) 17
- Synthesis, Absolute Configuration and Specific Rotation of (+)- and (−)-Modhephene (C) 1492
- Synthesis of a Biologically Active Taxol Analogue (C) 412
- The Bioinorganic Chemistry of Vanadium (R) 148
- The Chemistry of Rose Pigments (R) 654
Neighboring-group effects
- The Reaction-Accelerating Neighboring-Group Effects in the Reaction of Vinyl Bromides with Alkyl-Transition Metal Reagents (C) 1684
Neuraminic acid
- Enzymatic Two-Step Synthesis on *N*-Acetylneuraminic Acid in the Enzyme Membrane Reactor (C) 827 (1713)
Nickel compounds
- Functional Modeling of Ni,Fe Hydrogenases: A Nickel Complex in an *N,O,S* Environment (C) 193
- Isolated and Condensed Ta_2Ni_2 Clusters in the Layered Tellurides $Ta_2Ni_2Te_4$ and $Ta_2Ni_3Te_5$ (C) 840
- Nickel(0)-Carbene Complexes (C) 1666
- Nickel-catalyzed Cyclotrimerization of Malononitrile: The Dicyanomethanide-bridged, Anionic Ni^{II} Complex $[\{Ni(C_5F_5)_2(\mu\text{-NCCHCN})\}_2]^{2\ominus}$ (C) 716
- Spontaneous Self Assembly of an Octanuclear Iron-Nickel Cluster by Reaction of $[Fe_6S_6I_6]^{2\ominus}$ with $[NiI_4]^{2\ominus}$ (C) 881
Niobium compounds
- *cyclo*-As_8 as Complex Ligand (C) 850
- The Reduction of the NbX_5/AlX_3 System with Aluminum in the Presence of Aromatic Hydrocarbons: An Approach to Niobium(II), Niobium(I), and Niobium(0) Organometallics (C) 102
- The Synthesis and Structure of the Yellow and Green Forms of $[Nb(O)Cl_3(PMe_3)_3]$ and the Orange and Green Forms of $[Nb(S)Cl_3(PMe_3)_3]$; Examples of Perfectly Matched Bond-Stretch Isomers? (C) 980
Nitrides
- $Li_{10}P_4N_{10}$—A Lithium Phosphorus(V) Nitride Containing the New Complex Anion $P_4N_{10}^{10\ominus}$ (C) 830
- Se_4N_2, a Novel Selenium Nitride (C) 577
Nitridoferrates
- $Sr_2Li[Fe_2N_3]$ and $Ba_2Li[Fe_2N_3]$: Nitridoferrate(II) Isotypes with $^1_\infty[(FeN_{3/2})_2^{5\ominus}]$ Anions (C) 831
Nitrogen compounds
- Aromatic Systems with Polymethine-like Structures: A Structural Comparison of Bis- and Tris(dimethylamino)phenalenium Ions (C) 1030
- Complexation of Transition Metal Ions with Substituted Aza Macrocycles: Induction of Columnar Mesophases by Molecular Recognition (C) 1375
- Houben-Weyl. Methoden der Organischen Chemie. Volume E16a, Parts 1 and 2: Nitrogen Compounds I (B) 1524
- $Li_4[FeN_2]$: A Nitridoferrate(II) with Anions Isosteric with CO_2. A Defect Variant of the Li_3N Type Structure (C) 199
- 5-Lithio-2*H*-tetrazolium Carbenoids: NMR Spectroscopic Detection and Reactions with Nitrogen Electrophiles (C) 1162
- Stoichiometric Mono *N*-Functionalization of Tetraazamacrocycles via Phosphoryl-Protected Intermediates (C) 560
- Synthesis and Structure of an Azadistanniridine (C) 1017
- 1,4,5,8-Tetrakis(dimethylamino)naphthalene: Synthesis, Structure, "Proton Sponge" and Electron Donor Properties (C) 1028
- 2,4,6-Triaryl-1,3,5λ^3-diazaphosphinines (C) 106
- Triisopropylamine: A Sterically Overcrowded Molecule with a Flattened NC_3 Pyramid and a "p-Type" Nitrogen Electron Pair (C) 187
NMR spectroscopy
- Analytical NMR (B) 721
- Basic One- and Two-Dimensional NMR Spectroscopy (B) 1383
- Characterization of Intermediate Steps in the Polymerizations with Ziegler Catalysts on MgH_2 by CP/MAS NMR Spectroscopy (C) 426
- Direct Observation of the Central Atom in $[C(Au\{P(C_6H_5)_2(p\text{-}C_6H_4NMe_2)\})_6](BF_4)_2$ by ^{13}C NMR Spectroscopy (C) 1488
- HETLOC, an Efficient Method for Determining Heteronuclear Long-Range Couplings with Heteronuclei in Natural Abundance (C) 1329
- Observation of a Direct Sn–Li Bond; The Crystal and Molecular Structure of Monomeric $[Ph_3SnLi \cdot PMDETA]$ and the Detection of $^{119,117}Sn$–^7Li NMR Coupling in Solution (C) 1459
- Solvation Effects on Geometry and Chemical Shifts. An Ab Initio/IGLO Reconciliation of Apparent Experimental Inconsistencies on $H_3B \cdot NH_3$ (C) 1160
Nobel Lecture
- The Logic of Chemical Synthesis: Multistep Synthesis of Complex Carbogenic Molecules (Nobel Lecture) (R) 455
Nomenclature
- Nomenclature of Inorganic Chemistry: Recommendations 1990 (B) 721
Nonalternant hydrocarbons
- 2-Triphenylmethyldicyclohept[*cd,g*]indene: A Novel *cata-peri* Condensed Nonalternant Hydrocarbon (C) 1174
Nuclear fission
- Lise Meitner and Fission: Fallout from the Discovery (R) 942
Nucleobases
- Molecular Recognition and Transport of Nucleobases—Superiority of Macrobicyclic Host Molecules (C) 442
Nucleosides
- Chemo- and Stereoselective Cobalt-Mediated [2 + 2 + 2]Cycloaddition of Alkynes with Uracil Derivatives. A Novel Synthetic Entry to Modified Nucleosides (C) 993

Oligonucleotides
- Chemically Modified Oligonucleotides as Probes and Inhibitors (R) 613
- Light-Directed Parallel Synthesis of Up to 250000 Different Oligopeptides and Oligonulceotides (H) 822
- Parabolic Growth of a Self-Replicating Hexadeoxynucleotide Bearing a 3′-5′-Phosphoamidate Linkage (C) 423 (892)

- Single-Crystal X-Ray Diffraction Studies of Oligonucleotides and Oligonucleotide–Drug Complexes (R) 1254
- The Rationality of Random Screening—Efficient Methods of Selection of Peptides and Oligonucleotide Ligands (H) 296

Oligopeptides
- Switch Peptides: pH-Induced α-Helix to β-Sheet Transitions of Bis-amphiphilic Oligopeptides (C) 1514

Optical waveguides
- Chemical Reactions in the Manufacture of Waveguides for Long Distance Optical Data Transmission (R) 745

Organic chemistry
- Houben-Weyl. Methoden der Organischen Chemie. Band E 19a, Parts 1 and 2. C-Radikale (B) 611
- Houben-Weyl. Methoden der Organischen Chemie. Volume E16a, Parts 1 and 2: Nitrogen Compounds I (B) 1524
- Reizvolle Moleküle der Organischen Chemie (B) 215

Organic conductors
- An Imide Radical Anion which Assembles into π-Stacks in Solution (C) 986
- Benzene Bis(diazocyanides)—the First Acceptors of the Inverse Wurster Type for Conductive Organic Materials (C) 561
- Novel Building Blocks for the Synthesis of Organic Metals (H) 1121
- Radical Cation Salts of 1,3,6,8-Tetrakis(methylthio)pyrene—New Easily Accessible Compounds with High Electrical Conductivity and Excellent Stability (C) 176
- *syn*-Sesqui- and -Sesterbenzobicyclo-[2.2.2]octene, Molecules with Stacked Benzene Rings (C) 205

Organic permanganate
- The Structure of "Organic Permanganate" (C) 704 (1192)

Organic synthesis
- Advanced Practical Organic Chemistry (B) 213
- Challenges in Synthetic Organic Chemistry (B) 1381
- Chemistry and Biology of the Enediyne Anticancer Antibiotics (R) 1387
- Enediyne Compounds Equipped with Acid-, Base- and Photo-Sensitive Triggering Devices. Chemical Simulation of the Dynemicin A Reaction Cascade (C) 1032
- Erythromycin Synthesis—A Never-ending Story? (H) 1452
- Lipoxins and Related Eicosanoids: Biosynthesis, Biological Properties, and Chemical Synthesis (R) 1100
- Organic Chemistry in Action. The Design of Organic Synthesis (B) 340
- Organic Synthesis via Organometallics (B) 1520
- Synthetic Strategy for the Coupling of the Calicheamicin Oligosaccharide with Aglycons: Synthesis of Dynemicin A-Calicheamicin Hybrid Structures (C) 585
- The Logic of Chemical Synthesis: Multistep Synthesis of Complex Carbogenic Molecules (Nobel Lecture) (R) 455

Organometallic biochemistry
- The Biochemical Reactions of Organometallics with Enzymes and Proteins (R) 931

Organometallic reagents
- Enantioselective Addition of Organometallic Reagents to Carbonyl Compounds: Chirality Transfer, Multiplication, and Amplification [New Synthetic Methods (83)] (R) 49

Osmium compounds
- A Stable Os^0 16-Electron Complex: Synthesis and Structure of $[OsCl(NO)(PiPr_3)_2]$ (C) 596
- $(nBu_4P)_2[Os_{20}(CO)_{40}]$, a Thermolytically Generated High-Nuclearity Cluster with a Tetrahedral Cubic-Close-Packed Metal Core (C) 107
- Direct Location of the Hydrido Ligands in the Dianion $[H_4Os_{10}(CO)_{24}]^{2-}$ by a Neutron Diffraction Study of Its $[(Ph_3P)_2N]^+$ Salt at 20 K (C) 1164
- Synthesis and Characterization of a New Binary Deca-osmium Carbonyl Cluster Anion—An Intermediate in the Formation of Other High-nuclearity Osmium Carbonyl Clusters; Crystal and Molecular Structure of $[Ph_4P]_2[Os_{10}(CO)_{26}]$ (C) 1505

Oxadiazoles
- Naphtho[2,3-*d*][1,2,3]oxadiazole (C) 1476

Oxazepines
- 4-Acyl-2,3,4,5-tetrahydro-2-methyl-2,5-methanobenz-1,4-oxazepine, Derivatives of a New Heterocycle (C) 1709

Oxidations
- Methyltrioxorhenium as Catalyst for Olefin Oxidation (C) 1638
- On the Electrochemical Oxidation of $Cs^{\oplus}$ and Other Alkali-Metal Ions in Liquid Sulfur Dioxide and Acetonitrile (C) 836
- Oxidative Cleavage of Triethylenetetramine (trien) to Yield Diethylenetriamine (dien): Structure of the Mn^{II}/Mn^{III} Heptanuclear Complex $[Mn_7(trien)_2(dien)_2O_4(OAc)_8](PF_6)_4 \cdot 2H_2O$ (C) 688
- Palladium(II)-Induced Conversion of α-Acetoxyalkynes into α,β-Unsaturated α-Acetoxyketones; a Novel Access to α-Diketones (C) 593
- Structural Changes on Twofold Oxidation of Tetrakis(dimethylamino)-*p*-benzoquinone: A Sterically Overcrowded Electron-Rich "Chair" Compound Turns into a "Twist" Dicyanine Salt (C) 1180

N-oxides
- Synthesis and Characterization of Radical-Substituted Diacetylene Derivatives (C) 450

Oxy-Cope rearrangements
- Importance of Oxyanion Orientation to the Stereochemical Control of Anionic Oxy-Cope Rearrangements (C) 1368

Oxygen compounds
- Bis(fluorocarbonyl) Peroxide; an Unusual Molecular Structure (C) 1145

Palladium compounds
- Effects of Perturbed Symmetry: Low-Melting Stable Mesogens Based on *ortho*-Palladated Imines (C) 711

Paramagnetism
- EPR of Exchange Coupled Systems (B) 340
- Organic Chemistry in Action. The Design of Organic Synthesis (B) 340

Pauson–Khand reaction
- Fischer Carbene Complexes Facilitate the Intramolecular Pauson-Khand Reaction (C) 1470

Pentacene
- Optical Detection of Single Molecules in a Solid: A New Frontier in Optical Spectroscopy? (H) 540

Pentaisopropylcyclopentadienyl radical
- Synthesis and Structure of the Pentaisopropylcyclopentadienyl Radical (C) 971

Pentalenes
- 2,3a,5,6a-Tetraazapentalene Dications and Tetraamino-1,3,5,7-tetrazocine (C) 334

Peptide conjugates
- Synthesis of Muropeptide Conjugates of 2,3-Dideoxy-β-D-*manno*-2-octulosonic Acid (C) 1682

Peptide isosters
- 1,3-Dipolar Cycloaddition as the Key Reaction in the Synthesis of Potent Renin Inhibitors (C) 1702
- Stereoselective Synthesis of Cyclic Dipeptide Hydroxyalkyl Isosteres via Metalated *N,N*-Dialkylcarbamate 2-Alkenyl Esters (C) 1690

Peptide syntheses
- Directed Synthesis of Peptides from α-Amino Acid Esters at Metal Centers (C) 1467
- Protease-Catalyzed Kinetically Controlled Peptide Syntheses (R) 1437
- Synthesis of Prothymosin α (ProTα)—a Protein Consisting of 109 Amino Acid Residues (C) 590

Peptides
- 3-Amino-2*H*-Azirines. Synthons for α,α-Disubstituted α-Amino Acids in Heterocycle and Peptide Synthesis [New Synthetic Methods (84)] (R) 238
- Lantibiotics—Ribosomally Synthesized Biologically Active Polypeptides containing Sulfide Bridges and α,β-Didehydroamino Acids (R) 1051
- Light-Directed Parallel Synthesis of Up to 250000 Different Oligopeptides and Oligonulceotides (H) 822
- Medicinal Chemistry in the Golden Age of Biology: Lessons from Steroid and Peptide Research (R) 1278
- Novel Polymeric Materials from Monodisperse Copolypeptides by Biotechnological Methods (H) 677
- Switch Peptides: pH-Induced α-Helix to β-Sheet Transitions of Bis-amphiphilic Oligopeptides (C) 1514
- The Rationality of Random Screening—Efficient Methods of Selection of Peptides and Oligonucleotide Ligands (H) 296

Peroxyl radicals
- The Elucidation of Peroxyl Radical Reactions in Aqueous Solution with the Help of Radiation-Chemical Methods (R) 1229

Pharmaceutics
- Comprehensive Medicinal Chemistry. Volume 5: Biopharmaceutics (B) 889
- 1,4-Dihydropyridines: Effects of Chirality and Conformation on the Calcium Antagonist and Calcium Agonist Activities (R) 1559
- 1,3-Dipolar Cycloaddition as the Key Reaction in the Synthesis of Potent Renin Inhibitors (C) 1702
- Glycolipids as Immunomodulators: Syntheses and Properties (R) 1611
- Medicinal Chemistry in the Golden Age of Biology: Lessons from Steroid and Peptide Research (R) 1278
- Single-Crystal X-Ray Diffraction Studies of Oligonucleotides and Oligonucleotide–Drug Complexes (R) 1254
- Synthesis of Muropeptide Conjugates of 2,3-Dideoxy-β-D-*manno*-2-octulosonic Acid (C) 1682

Phase transformations
- Materials Science and Technology (A Comprehensive Treatment). Volume 5: Phase Transformations in Materials (B) 1521

Phenalenes
- Synthesis of a Highly Amphoteric *s*-Indaceno[1,2,3-*cd*:5,6,7-*c'd'*]diphenalene: Switching between Diatropism and Paratropism Due to Changes in Oxidation Level (C) 172

Phenols
- The Diels–Alder Dimer of 6-Hydroxy-2,6-dimethylcyclohexa-2,4-dienone, an Unusual Metabolite in the Bacterial Degradation of 2,6-Xylenol (C) 202
Phosphaalkynes
- A Cp_2Zr Complex of a Phosphaalkyne Dimer as Educt in the Synthesis of Cyclic Phosphorus Compounds (C) 207
- Cooligomerization of Phosphaalkynes and Alkynes in the Coordination Sphere of Rhodium Complexes (C) 310
- Synthesis of Nonstabilized Phosphaalkynes by Vacuum Gas-Solid HCl Elimination (C) 196
Phosphabenzene
- Bis(η^6-phosphabenzene)vanadium: Synthesis, Structure, Redox Properties and Conformational Flexibility (C) 547
Phosphaferrocenes
- The First Metallobis(methylene)phosphoranes—Unexpected Isomerization to a Phosphaferrocene (C) 312
Phosphazenium ions
- Stable Phosphazenium Ions in Synthesis—an Easily Accessible, Extremely Reactive „Naked" Fluoride Salt (C) 1372
Phospholes
- Diphosphonio Isophosphindoles, Phospholes with a Planar Phosphorus (C) 308
Phosphonium cations
- Triaurated Phosphonium Cations $[RP(AuPPh)_3]^{\oplus}$ and the Electron-deficient, Hypercoordinated Phosphonium Dication $[P(AuPPh_3)_5]^{2\oplus}$ (C) 433
Phosphorus compounds
- A Novel Gallium–Phosphorus Cage Compound (C) 1141
- A Novel Phosphorus Chalcogenide: P_2Se_5 (C) 605
- Bicyclic P_6 as Complex Ligand (C) 553
- Carbonyl(pentaphosphacyclopentadienyl)-Transition Metal Complexes (M = Cr, Mo, W, Mn) through Directed Syntheses with *cyclo*-$P_5^{\ominus}$ (C) 580
- Do Partial Charges Alone Govern the Relative Stability of the Isomeric Heptaheteronortricyclane Anions $[P_{7-x}As_x]^{3\ominus}$? (C) 828
- Formation of a *trans*-1,2,4,5-Tetraphosphatricyclo[3.1.0.$0^{2,4}$]hexane by [2 + 2] Cyclodimerization of a 3*H*-Diphosphirene (C) 90
- Iminophosphanes: Unconventional Compounds of Main Group Elements (R) 217
- $Li_{10}P_4N_{10}$—A Lithium Phosphorus(v) Nitride Containing the New Complex Anion $P_4N_{10}^{10\ominus}$ (C) 830
- Methylene Phosphonium Ions (C) 709
- Multiple Bonds and Low Coordination in Phosphorus Chemistry (B) 1047
- Reactivity of a (Diazomethylene)phosphorane with Alkylating Agents and Lewis Acids; Synthesis of the First α-Diazoalkylborates (C) 1154
- RS–P=S in the Gas Phase—First Generation of (Organothio)thioxophosphanes (C) 318
- Synthesis and Structure of the Novel Ga_3P_3 Ring Compound [(2,4,6-$Ph_3C_6H_2$)GaP(*cyclo*-C_6H_{11})]$_3$ (C) 691
- Synthesis, Structure, and Isomerization of the (*E*)- and (*Z*)-Isomers of a Diphosphene (C) 1136
- The Chemistry of Organophosphorus Compounds. Vol. 1: Primary, Secondary, and Tertiary Phosphines, Polyphosphines, and Heterocyclic Organophosphorus(III) Compounds (B) 1046
- The Interaction of Tri-*tert*-butylgallium with White Phosphorus: Isolation of an Unusual Gallium Phosphorus Cluster (C) 1353
- 2,4,6-Triaryl-1,3,5λ^3-diazaphosphinines (C) 106
- 1,2,3-Triphospha-4-silabicyclo[1.1.0]butanes from Activated, Stable Phosphasilenes and White Phosphorus (C) 1022
Phosphorus monoxide
- Between Stars and Metals: Phosphorus Monoxide, PO (H) 818
- Phosphorus Monoxide (PO) as Complex Ligand (C) 852
Photochemistry
- A Simple Way to Predict the Products of Topochemical Photoreactions on the Basis of Force Field Calculations (C) 1354
- *mer*-[Cr(CO)$_3$(η^4-norbornadiene)(η^2-ethene)]: A Key Compound in Understanding the Mechanism of the Photocatalytic Diene Hydrogenation with Chromium Carbonyl Complexes (C) 1343
- Essentials of Molecular Photochemistry (B) 1526
- Flash Photolytic Generation and Study of Ynamines. First Observation of Primary and Secondary Ynamines in Solution (C) 1356
- Laser Flash Photolysis Generation, Spectra, and Lifetimes of Phenylcarbenium Ions in Trifluoroethanol and Hexafluoroisopropyl Alcohol. On the UV Spectrum of the Benzyl Cation (C) 1337
- Photochemistry on Solid Surfaces (B) 111
- The Mechanism of Acylcarbene Insertion into O–H Bonds—Direct Observation of the Enol of a Carboxylic Acid Ester in Aqueous Solution (C) 1366
- The Mechanism of Interaction of Triplet 3-Methylcyclohex-2-en-1-one with Maleo- and fumarodinitrile: Evidence for Direct Formation of Triplet 1,4-Biradicals in [2 + 2] Photocycloadditions without the Intermediacy of Exciplexes (C) 1345
Photochromicity
- 2,2′-(Ethynediyl)bis(4-alkoxy-1-naphthols) and Dinaphthofuro[3,2-*b*]furans—Substances with Unusual Photoreactivity and Photochromic Behavior (C) 866
Photochromism
- Thermally Irreversible Photochromic Liquid Crystal Polymers (C) 76
Photoelectron spectroscopy
- d-Electron Density in Formal d^0 Systems from Multiplet Splitting in the Photoelectron Spectrum of Permanganates (C) 967
- SiI_2—A Novel Triatomic Molecule with a Relativistic Touch (C) 1186
Photoenolizations
- An Exception to the Bredt Rule in the Photoenolization of 4-Benzoyl[2.2]paracyclophane (C) 432
Photography
- A New Approach to 2-Equivalent Couplers for Color Photography (C) 1704
Photosynthesis
- A 1,2-Phenylene-Bridged Porphyrin Dimer—Synthesis, Properties, and Molecular Structure (C) 582
- Chloride-Induced Conversion of $[Mn_4O_2(OAc)_6(py)_2(dbm)_2]$ to $[Mn_4O_3Cl(OAc)_3(dbm)_3]$: Potential Relevance to Photosynthetic Water Oxidation (C) 305
- Herbicides in Photosynthesis Research (R) 1621
- Phytochrome, the Visual Pigment of Plants (R) 1216
Phytoalexins
- Synthesis of an Elicitor-Active Heptaglucan Saccharide for Investigation of Defense Mechanisms of Plants (C) 1681
Phytochrome
- Phytochrome, the Visual Pigment of Plants (R) 1216
Piezoelectricity
- Piezoelectric Liquid-Crystalline Elastomers (H) 405
Piperidines
- Stereoselective Synthesis of Annelated Piperidines by Photochemical Cycloaddition and Iminium Ion–Allylsilane Cyclization (C) 1697
Platinum compounds
- Photolytic Cleavage of DNA by $[Pt_2(P_2O_5H_2)_4]^{4-}$ (C) 1517
- Synthesis and Structure of a *rac*-Tris(divinyldisiloxane)diplatinum(0) Complex and its Reaction with Maleic Anhydride (C) 438
- The Reaction of $PtCl_2$ with an *N,S,O*-Coordinated Calcium Complex: Synthesis and Structure of a Complexed CaPt Anion (C) 1648
Polyacetylenes
- Polyacetylene in Polyacrylonitrile Matrix: Novel Soluble Matrix Polyacetylenes by Ylide-Nickel Catalysis (C) 961
Polyamides
- New Chiral Polyamide Stationary Phases for Chromatographic Enantiomer Separation (C) 1662
Polycarbonates
- Routes to New Aromatic Polycarbonates with Special Material Properties (R) 1598
Polycations
- A Polymeric Tellurium Cation by Oxidation of Tellurium with Tungsten Bromides (C) 1128
Polycycles
- [7.7]Circulene, a Molecule Shaped Like a Figure of Eight (C) 1173
- Hexaspiro[3.0.3.0.3.0.3.0.3.0.3.0]tetracosane ([6.4]Rotane) (C) 436
- Novel Strategies for the Construction of Complex Polycyclic Ether Frameworks. Stereocontrolled Synthesis of the FGHIJ Ring System of Brevetoxin A (C) 299
- *syn*-Sesqui- and -Sesterbenzobicyclo[2.2.2]octene, Molecules with Stacked Benzene Rings (C) 205
- Strategy for the Synthesis of Tube-Shaped Molecules (C) 575
- Synthesis and Interconversion of New $(CH)_{14}$ Isomers (C) 1020
- Tercalicene and Quatercalicene (C) 446
Polyenes
- [7.7]Circulene, a Molecule Shaped Like a Figure of Eight (C) 1173
- Cyclooctatetraenylene Vinylene (C) 1003
- 2,2′-(Ethynediyl)bis(4-alkoxy-1-naphthols) and Dinaphthofuro[3,2-*b*]furans—Substances with Unusual Photoreactivity and Photochromic Behavior (C) 866
- 2-Triphenylmethyldicyclohept[*cd,g*]indene: A Novel *cata-peri* Condensed Nonalternant Hydrocarbon (C) 1174
Polyesters
- Microbial Polyesters (B) 1525
Polymer chemistry
- Chemical Reactions of Natural and Synthetic Polymers (B) 341
Polymerization
- Characterization of Intermediate Steps in the Polymerizations with Ziegler Catalysts on MgH_2 by CP/MAS NMR Spectroscopy (C) 426

- Polyacetylene in Polyacrylonitrile Matrix: Novel Soluble Matrix Polyacetylenes by Ylide-Nickel Catalysis (C) 961
- Syndiotactic Poly(1-oxo-2-phenyltrimethylene): On the Mode of the Chain Growth under Palladium Catalysis (C) 989

Polymers
- Analysis of Polymer Latices by Small-Angle X-Ray Scattering (C) 1650
- Interaction of Hydrophobically-Modified Poly-*N*-isopropylacrylamides with Model Membranes—or Playing a Molecular Accordion (C) 315
- Metalla-enes and Metalla-ynes—from Small Molecules to Infinite Polymers (H) 673
- New Routes to the Synthesis of Polymers Containing Nitrile Groups (C) 1654
- Piezoelectric Liquid-Crystalline Elastomers (H) 405
- Routes to New Aromatic Polycarbonates with Special Material Properties (R) 1598

Poly(methyl methacrylates)
- Optically Active "Stereocomplexes" of Isotactic Poly(methyl methacrylates) with Main-Chain Chirality (C) 849

Polyols
- Bolaamphiphilic Polyols, a Novel Class of Amphotropic Liquid Crystals (C) 440

Polyoxometalates
- $Ag_{25}Bi_3O_{18}$, a Potentially Valence-Unstable Bi^{III}/Bi^{V} Compound (C) 883
- An Unusual Polyoxovanadium Organophosphonate Anion, $[H_6(VO_2)_{16}(CH_3PO_3)_8]^{8\ominus}$ (C) 422
- $[As^{V}V^{V}_{12}V^{IV}_{2}O_{40}]^{7\ominus}$, a Topologically Interesting, Mixed Valence Cluster as Model for Vanadium Minerals Formed by Weathering (C) 210
- Formation of a Cluster Sheath around a Central Cluster by a "Self-Organization Process": the Mixed Valence Polyoxovanadate $[V_{34}O_{82}]^{10\ominus}$ (C) 588
- New Intermediate Phases of the Composition $La_{2n+2}Cu_{n+4}O_{4n+7}$ in the La–Cu–O System: the Crystal Structure and Thermal Stability of $La_2Cu_2O_5$ (C) 864
- Polyoxometalate Chemistry: An Old Field with New Dimensions in Several Disciplines (R) 34
- Template-Controlled Formation of Cluster Shells or a Type of Molecular Recognition: Synthesis of $[HV_{22}O_{54}(ClO_4)]^{6-}$ and $[H_2V_{18}O_{44}(N_3)]^{5-}$ (C) 1674
- The Crystal Chemistry of Copper Oxometalates (R) 723

Porphyrinoids
- Isophlorins: Molecules at the Crossroads of Porphyrin and Annulene Chemistry (C) 1693
- On the Enigma of Chlorophyll Degradation: The Constitution of a Secoporphinoid Catabolite (C) 1315
- Rubyrin: A New Hexapyrrolic Expanded Porphyrin (C) 977

Porphyrins
- A 1,2-Phenylene-Bridged Porphyrin Dimer—Synthesis, Properties, and Molecular Structure (C) 582
- Investigation of the Light-Induced Charge Transfer between Covalently Linked Porphyrin and Quinone Units by Time-Resolved EPR Spectroscopy (C) 1461
- Metal Carbonyl Complexes of Sapphyrins (C) 91
- The High-Yield Synthesis and Characterization of the First Porphyrin-Cyclam Dinucleating Ligand and Its Iron(III)/Copper(II) Complex (C) 572

Protein folding
- Ribonuclease T1: Structure, Function, and Stability (R) 343

Proteins
- Chemically Modified Oligonucleotides as Probes and Inhibitors (R) 613
- Protein Purification. Principles, High Resolution Methods and Applications (B) 212
- Ribonuclease T1: Structure, Function, and Stability (R) 343
- Synthesis of Prothymosin α (ProTα)—a Protein Consisting of 109 Amino Acid Residues (C) 590
- Towards the Chemical Synthesis of Proteins (R) 113

Prothymosin
- Synthesis of Prothymosin α (ProTα)—a Protein Consisting of 109 Amino Acid Residues (C) 590

Proton sponge
- 1,4,5,8-Tetrakis(dimethylamino)naphthalene: Synthesis, Structure, "Proton Sponge" and Electron Donor Properties (C) 1028

Pyranes
- Double Insertion of Alkynes into Chromium–Carbon Bonds of β-Donor-Substituted Vinylcarbene Complexes of Chromium—A Simple Route to Cyclopenta[*b*]pyrans (C) 1658

Pyrenes
- Radical Cation Salts of 1,3,6,8-Tetrakis(methylthio)pyrene—New Easily Accessible Compounds with High Electrical Conductivity and Excellent Stability (C) 176

Pyridazines
- Ring Inversion in Sterically Hindered Arenes (C) 1484

Pyridines
- Addition of Chiral Nucleophiles to Pyridine Compounds: Total Synthesis of (−)-Isovallesiachotamine and (+)-Vallesiachotamine (C) 1320
- Nickel-catalyzed Cyclotrimerization of Malononitrile: The Dicyanomethanide-bridged, Anionic Ni^{II} Complex $[\{Ni(C_5F_5)_2(\mu\text{-NCCHCN})\}_2]^{2\ominus}$ (C) 716
- The X-ray Crystal Structure Analysis of a Fragmentable *N*-Acylpyridinium Ion (C) 1656

Pyrroles
- Biogenesis of the Carbon Skeleton of Glycerinopyrin: A New Biosynthetic Pathway for Pyrroles (C) 183

Quasicrystals
- Crystalline Symmetries. An Informal Mathematical Introduction (B) 1525
- On the Quasicrystalline State (R) 754
- Quasicrystals, Networks, and Molecules of Fivefold Symmetry (B) 1382

Quinodimethanes
- The Structure of "Organic Permanganate" (C) 704 (1192)

Quinones
- [14]Annulenequinones with Anthraquinone Periphery: "Isopyrenequinone" (C) 681
- Investigation of the Light-Induced Charge Transfer between Covalently Linked Porphyrin and Quinone Units by Time-Resolved EPR Spectroscopy (C) 1461
- Naphtho[2,3-*d*][1,2,3]oxadiazole (C) 1476
- Structural Changes on Twofold Oxidation of Tetrakis(dimethylamino)-*p*-benzoquinone: A Sterically Overcrowded Electron-Rich "Chair" Compound Turns into a "Twist" Dicyanine Salt (C) 1180

Radialenes
- Synthesis, Structure, and Rearrangement of 1,3-Dibora[5]radialenes (C) 84

Radical anions
- An Imide Radical Anion which Assembles into π-Stacks in Solution (C) 986

Radical cations
- [3 + 2] Cycloadditions with Azirine Radical Cations: A New Synthesis of *N*-Substituted Imidazoles (C) 1336
- A Distorted *anti*-Perovskite Structure in Ternary Tetrathiafulvalenium Salts: Construction, Distortion, and Antiferromagnetic Ordering (C) 1498
- Ammoniumyl Salt-Induced Diels-Alder Reaction of Ketenes—Control of [2 + 2] vs. [4 + 2] Selectivity (C) 999
- Cryptatium: A Species of Expanded Atom/Radical Ion Pair Type from Electroreductive Crystallization of the Macrobicyclic Sodium Tris(Bipyridine) Cryptate (C) 838
- Synthesis and Structure of the First Tellurium(III) Radical Cation (C) 1677
- The Radical Cations of Silaketene and Several Isomers of $[C,H_2,Si,O]^{\bullet\oplus}$: An Ab Initio MO Investigation (C) 1323

Radicals
- A Tetrathiotrimethylenemethane Derivative (C) 871
- Bis(hydroperoxy)naphthaldiimide as a „Photo-Fenton Reagent": Sequence-Specific Photocleavage of DNA (C) 1351
- Houben-Weyl. Methoden der Organischen Chemie. Band E 19a, Parts 1 and 2. C-Radikale (B) 611
- Isoselective Relationship for the Stereoselectivity of the Transfer of Hydrogen Atoms to Cyclic Alkyl Radicals (C) 600
- Pressure-Assisted Formation of a Cobalt–Carbon σ Bond: A High-Pressure Pulse Radiolysis Study (C) 1158
- Synthesis and Characterization of Radical-Substituted Diacetylene Derivatives (C) 450
- Synthesis and Structure of the Pentaisopropylcyclopentadienyl Radical (C) 971
- The Elucidation of Peroxyl Radical Reactions in Aqueous Solution with the Help of Radiation-Chemical Methods (R) 1229

Random screening
- The Rationality of Random Screening—Efficient Methods of Selection of Peptides and Oligonucleotide Ligands (H) 296

Reaction mechanisms
- Dynamic HPLC: A Method for Determining Rate Constants, Energy Barriers, and Equilibrium Constants of Molecular Dynamic Processes (C) 74 (216)
- Extension of Free Energy Correlations to Gas-Phase Ionic Reactions. Competitive Alkylation of Substituted Benzonitriles by $(CH_3)_2Cl^+$ Ions (C) 1457
- The Elucidation of Peroxyl Radical Reactions in Aqueous Solution with the Help of Radiation-Chemical Methods (R) 1229
- The Mechanism of Interaction of Triplet 3-Methylcyclohex-2-en-1-one with Maleo- and fumarodinitrile: Evidence for Direct Formation of Triplet 1,4-Biradicals in [2 + 2] Photocycloadditions without the Intermediacy of Exciplexes (C) 1345

Reactive intermediates
- 1,3-(C → O) Silyl Shift in α-Diazo α-Silyl Ketones: Cycloaddition Reactions and Kinetic Proof for the β-Siloxydiazoalkene Intermediate (C) 306

- Stable Carbenes—Illusion or Reality? (H) 674

Reagents
- A New Chromogenic β-Galactosidase Substrate: 7-β-D-Galactopyranosyloxy-9,9-dimethyl-9*H*-acridin-2-one (C) 1646
- $LiClO_4$ in Ether—an Unusual Solvent (H) 1306
- Organic Synthesis via Organometallics (B) 1520
- Stable Phosphazenium Ions in Synthesis—an Easily Accessible, Extremely Reactive „Naked" Fluoride Salt (C) 1372
- The Reaction-Accelerating Neighboring-Group Effects in the Reaction of Vinyl Bromides with Alkyl-Transition Metal Reagents (C) 1684

Rearrangements
- Importance of Oxyanion Orientation to the Stereochemical Control of Anionic Oxy-Cope Rearrangements (C) 1368
- Recombination of Carbocation-Sulfinate Ion Pairs (C) 1018
- Tandem Silyl Migrations Leading to α,β-Bis-silylated Enals and Enones (C) 1687
- The Isocyanide–Cyanide Rearrangement; Mechanism and Preparative Applications (R) 893

Reductions
- The Reduction of the NbX_5/AlX_3 System with Aluminum in the Presence of Aromatic Hydrocarbons: An Approach to Niobium(II), Niobium(I), and Niobium(0) Organometallics (C) 102

Renin
- 1,3-Dipolar Cycloaddition as the Key Reaction in the Synthesis of Potent Renin Inhibitors (C) 1702

Retrosynthesis
- The Logic of Chemical Synthesis: Multistep Synthesis of Complex Carbogenic Molecules (Nobel Lecture) (R) 455

Rhenium compounds
- Alkyl- and Arylrhenium Trioxides (C) 185
- Methyltrioxorhenium as Catalyst for Olefin Metathesis (C) 1636
- Methyltrioxorhenium as Catalyst for Olefin Oxidation (C) 1638
- Methyltrioxorhenium as Catalyst of a Novel Aldehyde Olefination (C) 1641
- $[\{Re_2Cl_4(dppm)_2\}_2(\mu\text{-TCNQ})]$, a Novel Charge Transfer Complex Derived from a Donor with a Metal-Metal Multiple Bond (C) 448
- $[Re_2S_{16}]^{2-}$, a Soluble Metal Sulfide with Interesting Electronic Properties and Unusual Reactivity (C) 1512

Rhodium compounds
- A Cluster with the Triply Facially Bridging Trimethylenemethane Ligand: Structure and Bonding of $[\{Rh(cod)\}_3(\mu_3\text{-H})\{\mu_3\text{-C}(CH_2)_3\}]$ (C) 313
- Azarhoda-*closo*-dodecaborane (C) 1377
- Cooligomerization of Phosphaalkynes and Alkynes in the Coordination Sphere of Rhodium Complexes (C) 310
- Directed Synthesis of Peptides from α-Amino Acid Esters at Metal Centers (C) 1467
- Metal Carbonyl Complexes of Sapphyrins (C) 91
- Mononuclear Silylvinylidene Rhodium Complexes from Silylalkynes: The $SiMe_3$ Migration as an Alternative to the [1,2]-H Shift (C) 700

Ribonuclease
- Ribonuclease T1: Structure, Function, and Stability (R) 343

Roberts
- Profiles, Pathways and Dreams. Autobiographies of Eminent Chemists (B) 1190

Robinson
- Robert Robinson—Chemist Extraordinary (B) 1049

Rose pigments
- The Chemistry of Rose Pigments (R) 654

Rotanes
- Hexaspiro[3.0.3.0.3.0.3.0.3.0.3.0]tetracosane ([6.4]Rotane) (C) 436

Rotaxanes
- Self-Assembling [2]Pseudorotaxanes (C) 1036

Rubyrin
- Rubyrin: A New Hexapyrrolic Expanded Porphyrin (C) 977

Ruthenium compounds
- A Novel Oligomer of Condensed Metal Atom Clusters in $[Y_{16}Ru_4I_{20}]$ (C) 856
- Dichloro(pentamethylcyclopentadienyl)-ruthenium—Novel Dichotomy in a Molecular Structure (C) 690
- Energetic and Constitutional Hysteresis in Bistable Molecules (H) 956
- Proof of Strong S–H···S Bridges in $[Ru(SH_2)(PPh_3)('S_4')]\cdot THF$, the First H_2S Complex Characterized by X-Ray Crystallography (C) 552
- Reversible Isomerization of the Dinuclear Complex $[(\eta^6\text{-}p\text{-cymene})RuCl(\mu\text{-pz})_2Ir(CO)_2]$ with Formation of a Ruthenium-Iridium Bond (C) 1171
- The Cluster Anion $[Ru_6H(CO)_{15}S_3]^-$: A Planar Hexanuclear Metal Framework with Almost Perfect C_{3v} Symmetry (C) 1126
- The Synthesis of the First Decametal Nitrido Cluster; X-Ray Structure Analysis and ^{14}N NMR Studies of $[(Ph_3P)_2N][Ru_{10}N(CO)_{24}]$ (C) 1706
- Unique Reactivity of Heterodinuclear Pentacarbonyl(Fulvalene)Molybdenum-ruthenium with Alkynes: Fluxionality, Rearrangements, Structures, and First Reversible Conversion of a "Side-on"- to a Semi-Bridging Alkenylidene Ligand (C) 1463

Sandwich complexes
- Bis(η^6-phosphabenzene)vanadium: Synthesis, Structure, Redox Properties and Conformational Flexibility (C) 547
- Cyclopentadienyl-Actinide Complexes: Bonding and Electronic Structure (R) 1069
- Derivatives of 1,1″-Biferrocene with Sulfur and Selenium Bridges (C) 1652
- Reactivity of Cobalt Atoms towards 1,2,3,4,5-Pentamethylcyclopentadienyl: Synthesis and Structure of Bis(η^5-pentamethylcyclopentadienyl)-(μ_2-η^5:η^5-pentamethylcyclopentadienyl)dicobalt and Bis(η^5-pentamethylcyclopentadienyl)dicobalt (C) 1124
- Sandwiches Bring a New Element to Molecular Recognition (H) 407
- Structure of an Organometallic Intercalate: Single Crystal X-Ray and Powder Neutron Diffraction Study of $[SnS_2\{Co(\eta\text{-}C_5H_5)_2\}_{0.31}]$ and $[SnS_2\{Co(\eta\text{-}C_5D_5)_2\}_{0.31}]$ (C) 1156
- The Biochemical Reactions of Organometallics with Enzymes and Proteins (R) 931

Sapphyrins
- Metal Carbonyl Complexes of Sapphyrins (C) 91

Scanning tunneling microscopy
- Direct Observation of Streptavidin Specifically Adsorbed on Biotin-Functionalized Self-Assembled Monolayers with the Scanning Tunneling Microscope (C) 569

Selectivity
- Isoselective Relationship for the Stereoselectivity of the Transfer of Hydrogen Atoms to Cyclic Alkyl Radicals (C) 600
- The Isoinversion Principle—a General Model of Chemical Selectivity (R) 477

Selenium compounds
- A Novel Phosphorus Chalcogenide: P_2Se_5 (C) 605
- Se_4N_2, a Novel Selenium Nitride (C) 577

Self-assembly
- Groups of Organic Molecules That Operate Collectively (R) 1086
- Helices, Supramolecular Chemistry, and Metal-directed Self-Assembly (H) 1450
- Molecular Trains: The Self-Assembly and Dynamic Properties of Two New Catenanes (C) 1042
- Self-Assembling [3]Catenanes (C) 1039
- Self-Assembling [2]Pseudorotaxanes (C) 1036
- Structure and Molecular Stacking of Anthocyanins—Flower Color Variation (R) 17
- Structure of a Self-assembling Triple-helical Complex containing two $Cobalt^{II}$ Ions (C) 1490

Self-replicating systems
- Parabolic Growth of a Self-Replicating Hexadeoxynucleotide Bearing a 3′-5′-Phosphoamidate Linkage (C) 423 (892)

Semiquinones
- Helical Semiquinones: Proof of Chirality by ENDOR Spectroscopy (C) 602

Sensors
- Chemical Sensors and Biosensors—Principles and Applications (R) 516
- Dyes for Visual Distinction between Enantiomers: Crown Ethers as Optical Sensors for Chiral Compounds (H) 958
- Sensors—A Comprehensive Survey. Vol. 1 + 5 (B) 110

Sialidase
- Chemoenzymatic Syntheses of Sialyloligosaccharides with Immobilized Sialidase (C) 1503

Siderophores
- Synthesis of a Novel Macrobicyclic Cavity Possessing Six Convergent Hydroxyl Groups and Acting as a Siderophore (C) 85
- Synthetic Siderophores of the Tetrazolenol Type: Iron(III) Complexes and Two-dimensional Iron(II) Coordination Polymers (C) 1494

Silaketene
- The Radical Cations of Silaketene and Several Isomers of $[C,H_2,Si,O]^{+\bullet}$: An Ab Initio MO Investigation (C) 1323

Silanetriyl complexes
- $[Cp_2Fe_2(CO)_3(\mu\text{-Si}t\text{Bu}\cdot NMI)]I$: The First Silanetriyldiiron Complex (C) 843

Silicon compounds
- 1,3-(C → O) Silyl Shift in α-Diazo α-Silyl Ketones: Cycloaddition Reactions and Kinetic Proof for the β-Siloxydiazoalkene Intermediate (C) 306
- Facile Synthesis of Si-Functional Silacyclobutenes (C) 1151
- Intramolecular Base Stabilization of Si=N and Si=P Compounds and Related Transition-Metal Silanediyl Complexes (C) 1130
- Microporous Silica Films (C) 1509
- Novel Naphthalene- and Cyclohexa-1,3-diene–Silene Cycloadducts (C) 444
- SiI_2—A Novel Triatomic Molecule with a Relativistic Touch (C) 1186
- Strained-Ring and Double-Bond Systems Consisting of Frameworks of the Group 14 Elements Si, Ge, and Sn (R) 902

- Synthesis and Structure of a *rac*-Tris(divinyldisiloxane)diplatinum(0) Complex and its Reaction with Maleic Anhydride (C) 438
- The Radical Cations of Silaketene and Several Isomers of $[C,H_2,Si,O]^{\bullet\oplus}$: An Ab Initio MO Investigation (C) 1323
- 1,2,3-Triphospha-4-silabicyclo[1.1.0]-butanes from Activated, Stable Phosphasilenes and White Phosphorus (C) 1022

Silicon nitride
- Silicon Nitride—From Powder Synthesis to Ceramic Materials (R) 1579

Silver compounds
- A New Economical Process for the Preparation of Silver(I,III) Oxide, AgO (C) 1017
- $Ag_{25}Bi_3O_{18}$, a Potentially Valence-Unstable Bi^{III}/Bi^{V} Compound (C) 883
- Inclusion of Metal Ions within a Tin–Oxygen Cage Stabilized by Organic Residues: Crystal Structure of $[(i\mathrm{PrSn})_{12}O_4(OH)_{24}][Ag_7I_{11}]\cdot NaCl\cdot H_2O\cdot 10\,DMSO$ (C) 1482

Small-angle X-ray scattering
- Analysis of Polymer Latices by Small-Angle X-Ray Scattering (C) 1650

Sodalites
- The Synthesis and Structure of Some New Sodalites: The Lithium Haloberyllophosphates and -arsenates (C) 1169

Sodium *trans*-2-Butenoate
- Stereospecific γ-Ray-Induced Trimerization of Crystalline Sodium *trans*-2-Butenoate (C) 420

Solid acids
- New Solid Acids and Bases (B) 720

Solid bases
- New Solid Acids and Bases (B) 720

Solid-phase synthesis
- Towards the Chemical Synthesis of Proteins (R) 113

Solid-state chemistry
- A Simple Way to Predict the Products of Topochemical Photoreactions on the Basis of Force Field Calculations (C) 1354
- Stereospecific γ-Ray-Induced Trimerization of Crystalline Sodium *trans*-2-Butenoate (C) 420
- Volume Effect or Paddle-Wheel Mechanism—Fast Alkali-Metal Ionic Conduction in Solids with Rotationally Disordered Complex Anions (R) 1547

Solid-state spectroscopy
- Optical Detection of Single Molecules in a Solid: A New Frontier in Optical Spectroscopy? (H) 540

Soluble polymers
- Polyacetylene in Polyacrylonitrile Matrix: Novel Soluble Matrix Polyacetylenes by Ylide-Nickel Catalysis (C) 961

Solvatochromism
- Chromoionophoric Pyridinium-*N*-phenolate Betaine Dyes (C) 558

Sonochemistry
- Sonochemistry: The Uses of Ultrasound in Chemistry (B) 1385
- Ultrasound in Synthesis (B) 1386

Spectroscopy
- Acronyms and Abbreviations in Molecular Spectroscopy. An Encyclopedic Dictionary (B) 1381
- Light Absorption as well as Crystal and Molecular Structure of *N,N'*-Dimethylindigo: An Example of the Use of Synchrotron Radiation (C) 964
- Optical Detection of Single Molecules in a Solid: A New Frontier in Optical Spectroscopy? (H) 540
- Spectroscopy of Fluid Phases—The Study of Chemical Reactions and Equilibria up to High Pressures (R) 641
- Spectroscopy of Matrix Isolated Species (B) 610

Spin crossover
- Thermal and Light-Induced Spin Crossover to a Metastable Low-Spin State in $[Fe(mtz)_6](CF_3SO_3)_2$ (C) 975

Spiro compounds
- 7,7'-Bi(dispiro[2.0.2.1]heptylidene)—the Perspirocyclopropanated Bicyclopropylidene (C) 1518

Spiropentenes
- Difference Electron Densities in a Spiropentene (C) 565

Stereochemistry
- On the Origin of π-Facial Diastereoselectivity in Addition Reactions of Cyclohexane-Based Systems (C) 1146

Steroids
- Medicinal Chemistry in the Golden Age of Biology: Lessons from Steroid and Peptide Research (R) 1278

Stiff-chain polymer
- Mo–Mo Quadruple Bonds Bridged by 1,8-Naphthyridinyl-2,7-Dioxide: an Insight into the Nature of a Parallel-Linked Stiff-Chain Polymer: $\{M^nM\sim M^nM\}_x$ (C) 862

Strained rings
- 7,7'-Bi(dispiro[2.0.2.1]heptylidene)—the Perspirocyclopropanated Bicyclopropylidene (C) 1518
- Difference Electron Densities in a Spiropentene (C) 565
- Facile Synthesis of Si-Functional Silacyclobutenes (C) 1151
- Strained-Ring and Double-Bond Systems Consisting of Frameworks of the Group 14 Elements Si, Ge, and Sn (R) 902
- Tetra-*tert*-butyltetraboratetrahedrane (C) 173
- The Interaction of Tri-*tert*-butylgallium with White Phosphorus: Isolation of an Unusual Gallium Phosphorus Cluster (C) 1353
- The Taming of Cyclobutadiene (C) 1024
- Thiadistannirane, 1,2-Dithiadistannetane, and Selenadistannirane: Small Rings with Tin–Tin Bonds (C) 962
- Three- and Fourfold Bridgehead-Substituted Tribenzotriquinacenes (C) 1699
- 1,2,3-Triphospha-4-silabicyclo[1.1.0]butanes from Activated, Stable Phosphasilenes and White Phosphorus (C) 1022

Streptavidin
- Direct Observation of Streptavidin Specifically Adsorbed on Biotin-Functionalized Self-Assembled Monolayers with the Scanning Tunneling Microscope (C) 569

Structure elucidation
- Aromatic Systems with Polymethine-like Structures: A Structural Comparison of Bis- and Tris(dimethylamino)-phenalenium Ions (C) 1030
- Bis(fluorocarbonyl) Peroxide; an Unusual Molecular Structure (C) 1145
- Crystal Structure of Chlorine Dioxide (C) 1510
- Difference Electron Densities in a Spiropentene (C) 565
- $[InAs_3]^{6\ominus}$ and $[AlSb_3]^{6\ominus}$, Trigonal Planar Anions in Cs_6InAs_3 and Cs_6AlSb_3 (C) 326
- $(I_3O_6)^{\oplus}$, a Novel Polyoxo Cation of Iodine (C) 329
- $Li_4[FeN_2]$: A Nitridoferrate(II) with Anions Isosteric with CO_2. A Defect Variant of the Li_3N Type Structure (C) 199
- Light Absorption as well as Crystal and Molecular Structure of *N,N'*-Dimethylindigo: An Example of the Use of Synchrotron Radiation (C) 964
- On the Enigma of Chlorophyll Degradation: The Constitution of a Secoporphinoid Catabolite (C) 1315
- Ribonuclease T1: Structure, Function, and Stability (R) 343
- Single-Crystal X-Ray Diffraction Studies of Oligonucleotides and Oligonucleotide–Drug Complexes (R) 1254
- Synthesis, Absolute Configuration and Specific Rotation of (+)- and (−)-Modhephene (C) 1492
- Synthesis and Crystal Structure of $Br_5^{\oplus}MF_6^{\ominus}$ (M = As, Sb) (C) 328
- Tetrakis(dimethylamino)ethene: An Extremely Electron-Rich Molecule with Unusual Structure both in the Crystal and in the Gas Phase (C) 1678
- The Structure of $IF_6^{\ominus}$ (C) 323
- The X-ray Crystal Structure Analysis of a Fragmentable *N*-Acylpyridinium Ion (C) 1656
- Triisopropylamine: A Sterically Overcrowded Molecule with a Flattened NC_3 Pyramid and a "p-Type" Nitrogen Electron Pair (C) 187

Structure predictions
- Molecular Structures from Density Functional Calculations with Simulated Annealing (R) 630

Sulfones
- Selectivity and Mechanism of Action of Novel DNA-Cleaving Sulfones (C) 418

Sulfonyloxynitriles
- Synthesis and Stereoselective Reactions of (*R*)-α-Sulfonyloxynitriles (C) 873

Sulfur compounds
- A Tetrathiotrimethylenemethane Derivative (C) 871
- Conformational Preference of 2-Triphenylphosphonio-1,3-dithianes: Competition between Steric and Anomeric Effects (C) 578
- Fluorine-Stabilized Sulfur–Carbon Multiple Bonds (R) 361
- Radical Cation Salts of 1,3,6,8-Tetrakis(methylthio)pyrene—New Easily Accessible Compounds with High Electrical Conductivity and Excellent Stability (C) 176
- Recombination of Carbocation-Sulfinate Ion Pairs (C) 1018
- RS−P=S in the Gas Phase—First Generation of (Organothio)thioxophosphanes (C) 318
- Synthesis and Stereoselective Reactions of (*R*)-α-Sulfonyloxynitriles (C) 873

Sulphenic acids
- The Chemistry of Sulphenic Acids and their Derivatives (B) 718

Sulphinic acids
- The Chemistry of Sulphinic Acids, Esters and their Derivatives (B) 719

Superconductors
- C_{60}: From Soot to Superconductors (H) 678
- d-Electron Density in Formal d^0 Systems from Multiplet Splitting in the Photoelectron Spectrum of Permanganates (C) 967
- New Intermediate Phases of the Composition $La_{2n+2}Cu_{n+4}O_{4n+7}$ in the La–Cu–O System: the Crystal Structure and Thermal Stability of $La_2Cu_2O_5$ (C) 864
- Superconductivity in Layered Structures of Rare-Earth Carbide Halides (C) 1188
- The Crystal Chemistry of Copper Oxometalates (R) 723

Surface chemistry
- Photochemistry on Solid Surfaces (B) 111
Syndiotactic polymers
- Syndiotactic Poly(1-oxo-2-phenyltrimethylene): On the Mode of the Chain Growth under Palladium Catalysis (C) 989
Synthetic methods
- 3-Amino-2*H*-Azirines. Synthons for α,α-Disubstituted α-Amino Acids in Heterocycle and Peptide Synthesis [New Synthetic Methods (84)] (R) 238
- Arsenic Compounds in Organic Synthesis: Pentamethinium Salts from Aminoarsanes and Pyrylium Salts (C) 994
- Enantioselective Addition of Organometallic Reagents to Carbonyl Compounds: Chirality Transfer, Multiplication, and Amplification [New Synthetic Methods (83)] (R) 49
- β-Lithio Ketone Enolates: Generation and Reactions with Electrophiles (C) 177
- New Approaches to the Use of Amino Acids as Chiral Building Blocks in Organic Synthesis [New Synthetic Methods (85)] (R) 1531
- Novel Strategies for the Construction of Complex Polycyclic Ether Frameworks. Stereocontrolled Synthesis of the FGHIJ Ring System of Brevetoxin A (C) 299
- The Isocyanide–Cyanide Rearrangement; Mechanism and Preparative Applications (R) 893

Tantalum compounds
- Effect of Intramolecular Coordination on Tantalum-Alkylidene-Centered Reactions: Synthesis and Structure of a Tantalum-Olefin Adduct and a Tantalum-Zinc-Alkylidene Complex (C) 996
- Isolated and Condensed Ta_2Ni_2 Clusters in the Layered Tellurides $Ta_2Ni_2Te_4$ and $Ta_2Ni_3Te_5$ (C) 840
Taxanes
- Synthesis of a Biologically Active Taxol Analogue (C) 412
Tellurium compounds
- A Polymeric Tellurium Cation by Oxidation of Tellurium with Tungsten Bromides (C) 1128
- A Telluradistannirane and a 1,3-Ditelluradistannetane by Stepwise Addition of Tellurium to a Distannene (C) 834
- Isolated and Condensed Ta_2Ni_2 Clusters in the Layered Tellurides $Ta_2Ni_2Te_4$ and $Ta_2Ni_3Te_5$ (C) 840
- $K_2Cu_5Te_5$, a Novel Mixed-Valence Layered Compound with Metallic Properties (C) 1325
- Synthesis and Structure of the First Tellurium(III) Radical Cation (C) 1677
- Synthesis of Sterically Hindered Tellurophenols and the Structure of $[Cd(\mu\text{-}TeC_6H_2Me_3)_2]_\infty$ (C) 973
Tentacle polymers
- Towards the Chemical Synthesis of Proteins (R) 113
Terpenes
- Bryophytes, a Source of Biologically Active, Naturally Occurring Material? (R) 130
Tetraethynylethene (C) 698
Tetrahedranes
- Tetra-*tert*-butyltetraboratetrahedrane (C) 173
Tetrakis(dimethylamino)ethene
- Tetrakis(dimethylamino)ethene: An Extremely Electron-Rich Molecule with Unusual Structure both in the Crystal and in the Gas Phase (C) 1678
Tetrathiafulvalenes
- A Distorted *anti*-Perovskite Structure in Ternary Tetrathiafulvalenium Salts: Construction, Distortion, and Antiferromagnetic Ordering (C) 1498
- On a Metathesis Reaction of Tetrathiafulvalene (TTF) (C) 1127 (1386)
Textbooks
- General Chemistry. International Student Edition (B) 609
- Physics and Chemistry of the Upper Atmosphere (B) 1529
Thallium compounds
- On the Differing Lewis Basicity of In^I Compared with Sn^{II} in Molecular Indium-Tin and Thallium-Tin Alkoxides (C) 95
Theoretical chemistry
- A New Look at Electron Localization (C) 409
- Basic Principles and Techniques of Molecular Quantum Mechanics (B) 1523
- Molecular Structures from Density Functional Calculations with Simulated Annealing (R) 630
- Reviews in Computational Chemistry (B) 452
Thianthrenes
- 2, 3, 6, 7 - Tetramethoxythianthrene Dication: An "Aromatic" π System "Gives Up the Ghost" (C) 714
Thin films
- Microporous Silica Films (C) 1509
Thiocyanates
- Mixed-Anion Aggregates of Metalated Organics: Preparation and Structure of the Mixed-Anion Tetramer $(PhO^{\ominus}Li^{\oplus} \cdot HMPA)_3(\mu_3\text{-}HMPA \cdot Li^{\oplus})NCS^{\ominus}$ (C) 1011
Thiolates
- Transition-Metal Thiolates: From Molecular Fragments of Sulfidic Solids to Models for Active Centers in Biomolecules (R) 769
Thorium compounds
- Bicyclic P_6 as Complex Ligand (C) 553
- $Th_6Br_{15}H_7$—Stabilization of a Th_6Br_{12} Cluster by Seven Hydrogen Atoms (C) 101
Tin compounds
- A Telluradistannirane and a 1,3-Ditelluradistannetane by Stepwise Addition of Tellurium to a Distannene (C) 834
- π-Coordination of Diorganotin Dications (C) 1370
- Inclusion of Metal Ions within a Tin–Oxygen Cage Stabilized by Organic Residues: Crystal Structure of $[(i\text{PrSn})_{12}O_4(OH)_{24}][Ag_7I_{11}] \cdot NaCl \cdot H_2O \cdot 10\,DMSO$ (C) 1482
- Observation of a Direct Sn–Li Bond; The Crystal and Molecular Structure of Monomeric $[Ph_3SnLi \cdot PMDETA]$ and the Detection of $^{119,117}Sn$–^7Li NMR Coupling in Solution (C) 1459
- On the Differing Lewis Basicity of In^I Compared with Sn^{II} in Molecular Indium-Tin and Thallium-Tin Alkoxides (C) 95
- Strained-Ring and Double-Bond Systems Consisting of Frameworks of the Group 14 Elements Si, Ge, and Sn (R) 902
- Synthesis and Structure of an Azadistanniridine (C) 1017
- Thiadistannirane, 1,2-Dithiadistannetane, and Selenadistannirane: Small Rings with Tin–Tin Bonds (C) 962
- Unsaturated Tin Compounds: Generation and Reactivity of $Me_2Sn{=}C(SiMe_3)_2$ and $Me_2Sn = N(Si\text{t}Bu_2Me)$ (C) 93
Titanium compounds
- Catalytic and Stoichiometric Enantioselective Addition of Diethylzinc to Aldehydes Using a Novel Chiral Spirotitanate (C) 99
- Cp'_2TiS_5O and Cp'_2TiOS_5—Isomeric Titanocene Complexes with Two Novel S-O Chelate Ligands ($Cp' = \eta^5\text{-}CH_3C_5H_4$) (C) 550
- Tetraalkoxytitanium-Carbene Complexes with Double Intramolecular Et_2Al Bridging (C) 1668
Total syntheses
- ACRL Toxin I: Convergent Total Synthesis of Its 3-Methyl Enol Ether from D-Glucose (C) 1339
- Enantioselective and Diastereoselective Total Synthesis of the Antimycotically Active Natural Product Chlorotetaine: Revision of the Relative Configuration (C) 1685
Transition metals
- Formation of Colloidal Transition Metals in Organic Phases and Their Application in Catalysis (C) 1312
Transition-metal hydrides
- Complex Transition Metal Hydrides (R) 759
Transition-metal thiolates
- Transition-Metal Thiolates: From Molecular Fragments of Sulfidic Solids to Models for Active Centers in Biomolecules (R) 769
Transmission electron microscopy
- Ligand-Stabilized Bimetallic Colloids Identified by HRTEM and EDX (C) 874
Triethylenetetramine
- Oxidative Cleavage of Triethylenetetramine (trien) to Yield Diethylenetriamine (dien): Structure of the Mn^{II}/Mn^{III} Heptanuclear Complex $[Mn_7(trien)_2(dien)_2O_4(OAc)_8](PF_6)_4 \cdot 2H_2O$ (C) 688
Triisopropylamine
- Triisopropylamine: A Sterically Overcrowded Molecule with a Flattened NC_3 Pyramid and a "p-Type" Nitrogen Electron Pair (C) 187
Trimethylenemethane
- A Cluster with the Triply Facially Bridging Trimethylenemethane Ligand: Structure and Bonding of $[\{Rh(cod)\}_3(\mu_3\text{-}H)\{\mu_3\text{-}C(CH_2)_3\}]$ (C) 313
- The Structure of the Trimethylenemethane Dianion and the Question of Y-Aromaticity (C) 1001
Trimethylenemethanes
- A Tetrathiotrimethylenemethane Derivative (C) 871
Triquinacenes
- Three- and Fourfold Bridgehead-Substituted Tribenzotriquinacenes (C) 1699
Tris(trimethylsilyl)methyllithium
- Solvent-free Tris(trimethylsilyl)methyllithium (C) 324
Tungsten compounds
- A Complex with Three-Coordinate Tungsten Atom: $[(silox)_2W = N\text{t}Bu]$ (silox = $t\text{Bu}_3SiO$) (C) 584
- A Polymeric Tellurium Cation by Oxidation of Tellurium with Tungsten Bromides (C) 1128
- Coupling of Alkynes with Carbene Ligands to Tungsten-coordinated Cyclopropenes and Their Stereoselective Isomerization to Vinylcarbene Complexes (C) 998
- Metal-Centered Coupling of Two Carbyne Ligands To Form an Alkyne Ligand (C) 1167
- Methylating Reductive Dimerization of Aromatic Carbonyl Compounds, a

Novel Organometallic Reaction (C) 1138
- The *cyclo*-P_4 Ligand as 12-Electron Donor (C) 969

Ultramicroelectrodes
- Ultramicroelectrodes—a New Dimension in Electrochemistry? (H) 170

Ultrasound
- Sonochemistry: The Uses of Ultrasound in Chemistry (B) 1385
- Ultrasound in Synthesis (B) 1386

Unsaturated amino acids
- Synthesis of β,γ-Unsaturated D-α-Amino Acids from L-Cysteine (C) 705

Unstable molecules
- Synthesis and Structure of Ethynyl Isocyanide (C) 1644

Upper atmosphere research
- Physics and Chemistry of the Upper Atmosphere (B) 1529

Uracil derivatives
- Chemo- and Stereoselective Cobalt-Mediated [2 + 2 + 2]Cycloaddition of Alkynes with Uracil Derivatives. A Novel Synthetic Entry to Modified Nucleosides (C) 993

Valence tautomerism
- σ-Homoacenaphthylene and π-Homoacenaphthene (C) 683

Vanadium compounds
- An Unusual Polyoxovanadium Organophosphonate Anion, $[H_6(VO_2)_{16}(CH_3PO_3)_8]^{8\ominus}$ (C) 422
- $[As^{V}V^{V}_{12}V^{IV}_{2}O_{40}]^{7\ominus}$, a Topologically Interesting, Mixed Valence Cluster as Model for Vanadium Minerals Formed by Weathering (C) 210
- Bis(η^6-phosphabenzene)vanadium: Synthesis, Structure, Redox Properties and Conformational Flexibility (C) 547
- Formation of a Cluster Sheath around a Central Cluster by a "Self-Organization Process": the Mixed Valence Polyoxovanadate $[V_{34}O_{82}]^{10\ominus}$ (C) 588
- Template-Controlled Formation of Cluster Shells or a Type of Molecular Recognition: Synthesis of $[HV_{22}O_{54}(ClO_4)]^{6-}$ and $[H_2V_{18}O_{44}(N_3)]^{5-}$ (C) 1674
- The Bioinorganic Chemistry of Vanadium (R) 148

Vinyl cations
- Synthesis of Ethenyl(phenyl)iodonium Triflate, $[H_2C{=}CHIPh][OSO_2CF_3]$, and Its Application as a Parent Vinyl Cation Equivalent (C) 1469
- The First Persistent β-Silyl-Substituted Vinyl Cation (C) 1479

Visual pigment
- Phytochrome, the Visual Pigment of Plants (R) 1216

Water-gas shift reaction
- Photocatalysis of the Homogeneous Water-Gas Shift Reaction under Ambient Conditions by Cationic Iridium(III) Complexes (C) 844

Wettability measurements
- Direct Assignment of Absolute Configuration of Chiral Alkyl Gluconamides by Wettability Measurements (C) 696

2,6-Xylenol
- The Diels–Alder Dimer of 6-Hydroxy-2,6-dimethylcyclohexa-2,4-dienone, an Unusual Metabolite in the Bacterial Degradation of 2,6-Xylenol (C) 202

Ynamines
- Flash Photolytic Generation and Study of Ynamines. First Observation of Primary and Secondary Ynamines in Solution (C) 1356

Zeolites
- Blocking of Acidic Centers upon Hydrothermal Dealumination of ZSM-5 Zeolites (C) 607
- Selective *p*-Chlorination of Biphenyl in L Zeolites (C) 1689
- Solvated Electron in the Synthesis of Ionic Clusters in Zeolites (C) 1501
- Synthesis and Characterization of P-containing ZSM-5 Zeolites (C) 686

Ziegler catalysts
- Characterization of Intermediate Steps in the Polymerizations with Ziegler Catalysts on MgH_2 by CP/MAS NMR Spectroscopy (C) 426

Zirconium compounds
- A Cp_2Zr Complex of a Phosphaalkyne Dimer as Educt in the Synthesis of Cyclic Phosphorus Compounds (C) 207
- $BPh_4^{\ominus}$ as a Ligand in Cationic Zirconium Complexes: Novel Bonding Mode and Fluxionality (C) 1152
- Competing Occurrence of Isomeric (Dialkyltartrato)zirconocene Dimers with Dimetallatricyclic and Ten-Membered Dimetallamonocyclic Frameworks (C) 1349
- Surface Organometallic Chemistry on Oxides: Selective Catalytic Low-Temperature Hydrogenolysis of Alkanes by a Highly Electrophilic Zirconium Hydride Complex Supported on Silica (C) 1660